World Renewable Energy Congress – Sweden

8–13 May, 2011
Linköping, Sweden

Editor

Professor Bahram Moshfegh

Copyright

Linköping Electronic Conference Proceedings, 57
Linköping University Electronic Press
Linköping, Sweden, 2011

http://www.ep.liu.se/ecp_home/index.en.aspx?issue=057
ISBN: 978-91-7393-070-3
ISSN 1650-3740 (online)
ISSN 1650-3686 (print)

Table of Contents

Bioenergy Technology

Climate Change Issues

Energy End-Use Efficiency Issues

Fuel Cells

Geothermal Applications

Hydropower Applications

Industrial Energy Efficiency

Low-Energy Architecture

Marine and Ocean Technology

Policy Issues

Photovoltaic Technology

Sustainable Cities and Regions

Sustainable Transport

Solar Thermal Applications

Wind Energy Applications

Volume 1

Bioenergy Technology

Fuel supplier selection for large scale UK bioenergy schemes

James A. Scott[1,*], William Ho[1], Prasanta Kumar Dey[1]

[1] *Aston University, Birmingham, UK*
** Corresponding author. Tel: +44 121 204 3210 Fax: +44 121 204 3326, E-mail: scottja1@aston.ac.uk*

Abstract: This article presents a potential method to assist developers of future bioenergy schemes when selecting from available suppliers of biomass materials. The method aims to allow tacit requirements made on biomass suppliers to be considered at the design stage of new developments. The method used is a combination of the Analytical Hierarchy Process and the Quality Function Deployment methods (AHP-QFD). The output of the method is a ranking and relative weighting of the available suppliers which could be used to improve optimization algorithms such as linear and goal programming. The paper is at a conceptual stage and no results have been obtained. The aim is to use the AHP-QFD method to bridge the gap between treatment of explicit and tacit requirements of bioenergy schemes; allowing decision makers to identify the most successful supply strategy available.

Keywords: *AHP, QFD, Bioenergy, supplier selection*

1. Introduction

The UK Bioenergy industry is expected to undergo significant growth over the coming decade as utilities and government aim to reach renewable energy targets by 2020. This expected growth is due to increasing installations of biomass heating, biofuel production for transport, biochemical for oil substitution, combined heat and power production and centralized electricity generation from biomass. For the sector to succeed the rapid development of demand for biomass resources must be matched by a sustainable supply. The various different bioenergy conversion processes that can be used to supply this range of lower carbon products brings a diverse set of material suppliers to the attention of project developers and procurement managers.

These fuels are likely to arise from a wide variety of sources and will have greatly differing properties and characteristics such as varying moisture or energy content. Additionally there are likely to be both positive and negative impacts associated with deciding to use a particular supplier. These impacts are less well defined when compared to the explicitly expressed measures of material properties and cost. The more tacit properties of a biomass fuel could include labor hours, CO_2 emissions, air water and noise pollution, job creation, waste diverted from landfill, price fluctuation and reliability of supply are all examples of impacts a bioenergy scheme may have upon wider society and the environment. The challenge for the procurement manager is to decide which sources of materials to select and how much of each material to purchase from each supplier, thus creating a supply strategy.

Most conversion plants will have some technical parameters to which the input feedstock blend should comply with; these parameters define the desired fuel specification required of the blend. The problem of which blend to use lends itself well to goal programming techniques as the relationships are linear and the optimal blend can be expected to be a mixture of materials from different sources. Several methods have previously been successfully applied to the optimization of the bioenergy supply chain under various contexts. For instance for a multi-fuel problem and maximizing some objective function; energy efficiency, net CO_2 emissions, or labor hours [1]. The output of such decision models is to

give recommendations on the optimal location and capacity of new bioenergy plants, or to suggest an optimal supply or logistics strategy.
Previous research on the tacit impacts of a bioenergy system also exists. Often these tacit requirements are described in the context of sustainability metrics described as social and environmental impacts. Key sustainability constraints for UK bioenergy schemes have been identified as greenhouse gas savings, land availability, air quality, and problems associated with facility siting [2]. In a study on decision making for sustainable energy schemes some assessment criteria were identified and categorized as ecological, social and economic and included factors such as *employment rate*, *land competition* and *supply security* [3]. Indeed the study of sustainability regarding biomass grown for energy use has attracted a great amount of academic and public attention over the past decade.

The understanding of these two sides of the supplier selection problem is fairly robust considering the relative immaturity of the sector and the small number of commercially operating schemes. There is a gap in the treatment of the supplier selection problem however and more widely in the design of the biomass supply chain. The existing studies are unable to fully combine the optimization algorithms used for explicit aspects with knowledge of tacit requirements made of suppliers. This work presents a possible method to bridge this gap between the treatment of tacit and explicit requirements. The output of the work will be a structured process for developers to follow which will allow a score to be generated for each supplier given the extent to which that supplier meets the requirements of the development and any identified critical stakeholders.

The method behind the proposed framework is the combined AHP-QFD supplier selection method [4]. The hypothesis is that by selecting biomass suppliers using the AHP-QFD method a combination of suppliers can be selected to provide a supply which more effectively meets the needs of the conversion facility whilst remaining within the feasible region of cost and technical requirements.

This approach allows developers to move their procurement strategy beyond the model of transaction cost theories which are not suitable for the non-commodity market faced by the bioenergy industry sector at present. Building relationships between suppliers and conversion facilities will allow suppliers to better understand and meet the requirements of the conversion facility. Increasing the degree to which requirements are satisfied and maintaining a competitive cost for the fuel compared to other supply options. This is expected to be a better model for all parties than either the transaction cost model or the vertically integrated supply chain model.

2. Methodology

The AHP-QFD method has been applied in several previous cases for the selection problem under various multi-criteria conditions. The AHP-QFD method has been frequently applied in the manufacturing sector to select engineering projects [5] and more commonly to the area of product design [6, 7] that QFD was initially developed for. Elsewhere the method has also been applied to selecting budgets, teams and facility locations within logistics problems.
Current practice is for developers to select supply blends based on a mixture of experience and market knowledge as well as the price of each supply. The AHP-QFD method will be used to generate a recommended supply blend for a given scheme with a supply blend designed using current practice. The two recommended supply blends will then be compared with one another to determine the extent to which key tacit requirements are met by each approach.

2.1. The QFD Method

Quality Function Deployment (QFD) allows the requirements of a customer to be mapped against the characteristics of a product. The House of Quality technique is closely associated with QFD and allows for this translation or mapping to be done systematically. The method uses one or more interrelationship matrices to relate the properties of the product to the requirements of the customer. The customer requirements are given a weighting related to its importance to the customer. The person or team of people completing the matrix is required to judge to what extent each requirement is met by each product characteristic. The output of the process is an importance score for each of the product characteristics.

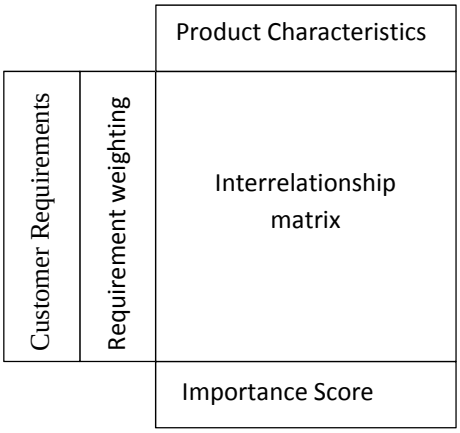

Fig. 1. A typical construction of a product HoQ.

The great advantage of the HoQ and QFD method is that each product characteristic is given a relative importance related to the degree to which that characteristic meets the customers' requirements. The weakness of the method is that the assigned importance is heavily reliant upon accurate completion of the interrelationship matrix. Any inconsistency or inaccuracy in this part of the HoQ process will lead to misleading final importance scores. Obtaining accurate weightings for the customer requirements is also important. This weakness is overcome when the Analytical Hierarchy Process (AHP) is applied.

2.2. The AHP-QFD Method

This section describes the steps used to determine the relationship weightings between the list of product characteristics and the customer requirements thus completing the interrelationship matrix. The following steps describe the AHP for use in a House of Quality.

Step 1: Construct a comparison matrix A with a customer requirement for each row and a product characteristic for each column.

$$A = \begin{bmatrix} a_{11} & a_{12} & \cdots & a_{1n} \\ a_{12} & a_{22} & \cdots & a_{2n} \\ \vdots & \vdots & \ddots & \vdots \\ a_{n1} & a_{n2} & \cdots & a_{nn} \end{bmatrix}, \qquad (1)$$

Where n is the number of elements in the top array (Product Characteristics), and a_{ij} is the comparison of element i to element j using a 9-point scale shown in table 1.

Step 2: AHP Synthesization
Divide each entry of the matrix A by the column total. This creates a normalized comparison matrix *A'*.

$$A' = \begin{bmatrix} \frac{a_{11}}{\sum_{i \in R} a_{i1}} & \cdots & \frac{a_{1n}}{\sum_{i \in R} a_{in}} \\ \vdots & \ddots & \vdots \\ \frac{a_{n1}}{\sum_{i \in R} a_{i1}} & \cdots & \frac{a_{nn}}{\sum_{i \in R} a_{in}} \end{bmatrix}, \quad (2)$$

Where R is a set of customer requirements $R = \{1, 2, \ldots, n\}$.

Step 3: Create a column vector *C* from the averages of each row of matrix *A*'.

$$C = \begin{bmatrix} c^{1}_{1k} \\ \vdots \\ c^{1}_{nk} \end{bmatrix} = \begin{bmatrix} \frac{\left(\frac{a_{11}}{\sum_{i \in R} a_{i1}} + \frac{a_{12}}{\sum_{i \in R} a_{i2}} + \cdots + \frac{a_{1n}}{\sum_{i \in R} a_{in}} \right)}{n} \\ \vdots \\ \frac{\left(\frac{a_{n1}}{\sum_{i \in R} a_{i1}} + \frac{a_{n2}}{\sum_{i \in R} a_{i2}} + \cdots + \frac{a_{nn}}{\sum_{i \in R} a_{in}} \right)}{n} \end{bmatrix}, \quad (3)$$

Where c^{1}_{ik} denotes the relationship weightings between the product characteristics *i* and the corresponding customer requirement *k*.

Step 4: Verify Consistency of AHP
To ensure that the respondent has assigned values from table 1 in a consistent way a consistency test should be carried out. Create a further column matrix by multiplying each entry in column *i* of matrix *A* by the column vector c^{1}_{ik} from step 3 then divide by the sum of values in each row *i* by c^{i}_{ik}.

$$\overline{C} = \begin{bmatrix} \overline{c}^{-1}_{1k} \\ \vdots \\ \overline{c}^{-1}_{nk} \end{bmatrix} = \begin{bmatrix} \frac{c^{1}_{1k} a_{11} + c^{1}_{2k} a_{12} + \ldots + c^{1}_{nk} a_{1n}}{c^{1}_{1k}} \\ \vdots \\ \frac{c^{1}_{1k} a_{n1} + c^{1}_{2k} a_{n2} + \ldots + c^{1}_{nk} a_{nn}}{c^{1}_{nk}} \end{bmatrix}, \quad (4)$$

Where $\bar{C}$ is a weighted sum vector.

Table 1. AHP scale for completing the HoQ comparison matrix.

Intensity	Importance	Explanation
1	Equal	Two activities are equally important
3	Moderate	One is slightly more important than the other
5	Strong	One is strongly more important than the other
7	Very Strong	One is dominant of the other
9	Extreme	Highest possible affirmation of evidence favoring one over another.
2,4,6,8	Intermediate	Used for compromise when desired value falls between above scales
Reciprocals of the above numbers		Used for inverse relationships

Step 5: Calculate the averages of values in vector $\bar{C}$ to give the maximum Eigenvalue (λ_{max}) of matrix *A*.

$$\lambda_{\max} = \frac{\sum_{i \in R} \bar{C}_{ik}}{n}, \tag{5}$$

Step 6: Calculate the consistency index.

$$CI = \frac{\lambda_{\max} - n}{n-1}, \tag{6}$$

Step 7: Compute the consistency ratio,

The consistency ratio is based on RI(n), a random index taken from table 2 based on the value of n.

$$CR = \frac{CI}{RI(n)}, \tag{7}$$

The consistency ratio is a measurement of consistent responses when completing the relationship matrix. If the measurement is greater than 0.10 the process is considered inconsistent and should be repeated in the hope of realizing a more consistent response. This measurement of consistency gives greater confidence when using the AHP-QFD method over the QFD method alone.

Table 2: List of Random Index values

n	2	3	4	5	6	7	8	9
RI(n)	0	0.58	0.90	1.12	1.24	1.32	1.41	1.45

Assuming consistency is acceptable the matrix will be populated with relationship weightings that link the top matrix with the left hand side matrix (Product characteristics with Customer Requirements from Fig. 1). The importance rating of each product characteristic can then be calculated.

Step 8: Compute importance rating

$$w_i^1 = \sum_{k \in S} p_k c_{ik}^1, \tag{8}$$

Where S denotes the set of customer requirements $S=\{1, 2, \ldots, m\}$, and p_k denotes the importance rating given to that requirement.

The result of step 8 is an importance score for each product characteristic which has been obtained from the requirements of customers. The AHP-QFD method can also be applied to a selection problem. By using the QFD to link the requirements made on a supplier, to the characteristics displayed or possessed by any given supplier, qualitative aspects of supplier selection can be managed in a systematic and robust way.

2.3. The AHP-QFD approach for bioenergy suppliers

The QFD method can deal with both qualitative and quantitative aspects of a product or service [7], several other techniques are available for the explicit optimization of fuel blends, therefore the QFD-AHP process will be used to better analyze and understand the qualitative requirements made of suppliers. The method is intended to be applied from a developer perspective as it is the developer that will make the initial decisions on the supply strategy for the scheme. Therefore rather than customer requirements being used as the success criteria the requirements of the developer and the scheme should be identified and weighted.

Many of the requirements of a good biomass supplier are likely to be in line with the requirements on suppliers from other industries. Reliability, company size, responsiveness and quality control are likely to be important tacit requirements. Other requirements may be more unusual and regard the material itself such as accreditation by sustainable forestry bodies, the local or national sourcing of waste, compliance with best practice and the method of delivery may be important aspects not covered by the technical fuel specification.

Having identified the requirements the developer places upon potential suppliers the relative importance of each requirement should be identified. This is done using the first HoQ matrix. The developer is likely to consist of several teams or members of staff with different perspectives on the project. These different teams will place differing importance weightings on different requirements. In this case the developer teams are considered to be equally important, typical developer teams may consist of planning, technical/design teams and finance teams.

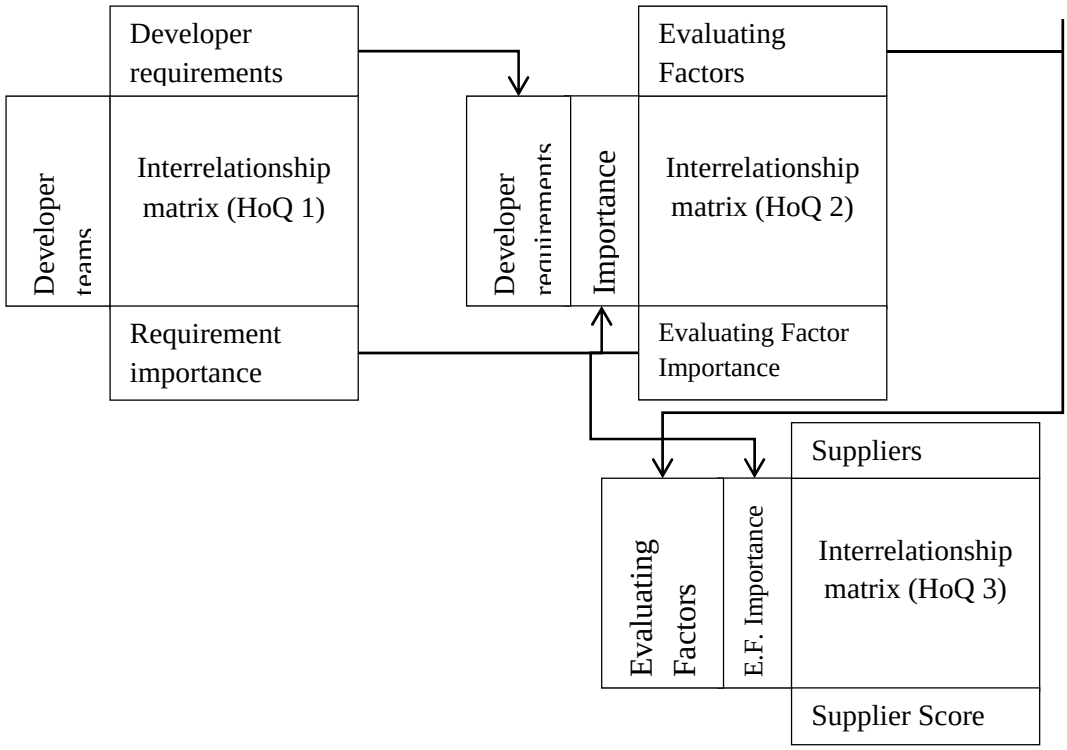

Fig. 2. HoQ 1 giving the importance of each requirement as determined by the developer. HoQ 2 linking the developer requirements with available evaluating factors for potential suppliers and HoQ 3linking those evaluating factors with the available suppliers to the bioenergy scheme.

The output of HoQ 1 is then used in HoQ 2 which links the developer requirements to externally observable characteristics possessed by the suppliers. These characteristics take the place of product characteristics and allow the decision maker to determine to what extent each requirement would be met by certain aspects of a supplier. For instance a requirement for sustainable fuel would be significantly met by a supplier approved by some sustainable forestry stewardship scheme. The use of organic wastes may be negatively related to a requirement to keep site odors to a minimum whilst a guarantee to deliver at within a narrow band of moisture content may score highly against a requirement for consistent fuel characteristics.

A final House of Quality table HoQ 3 can then be constructed which links the evaluating factors and their relative importance with the suppliers available. Here the decision maker must decide to what extent each supplier matches the evaluating factors identified. The output of HoQ 3 is a score for each supplier based on the ability of that supplier to meet the tacit requirements of the developer. Those suppliers that score highest should be favored.

3. Discussion

The weighted ranking score of each supplier assists decision makers in determining which suppliers to use when creating a strategy for biomass supply to large scale facilities. The massive quantity of materials required for large scale conversion facilities mean supply chain managers are forced to source from a range of materials and sources. The objective function for optimization algorithms can, using the presented method, incorporate the tacit requirements made on suppliers to create a model constrained by the explicit requirements of material specification imposed by equipment specifications. The objective function therefore could take a form similar that shown in equation (9).

$$\max\left(w_1 S_1 + w_2 S_2 + \ldots w_m S_m\right) \quad (9)$$

Where w_m denotes the score for each supplier S_m for m different suppliers. This approach would ensure the resulting suggested strategy is technically feasible, whilst also ensuring the best possible combination of suppliers is contracted.

The AHP-QFD method is suitable for application within developing companies as it is simple to apply and gives predictable and clear outputs for the decision maker. An inherent weakness of the approach is the subjective viewpoint of the decision maker compiling the list of requirements. In this application this weakness is minimized by considering only requirements of the teams within the developer company, not the wider stakeholder group. The AHP-QFD method also has an advantage over other weighting or ranking methods that could be incorporated into the objective function as it directly translates the requirements made on suppliers into their performance score using a robust method rather than a user estimate.

As the research develops more stakeholders could be interviewed for requirements and asked to complete the AHP-QFD process. This would allow developers to gain insight into the requirements that should be satisfied to make the scheme more successful from the perspective of other development stakeholders. As the framework is applied to different stakeholders a database of requirements can be constructed showing global and scheme specific requirements of different stakeholders.

This work is part of a CASE studentship PhD awarded by the ERSC and the authors are grateful for support from Express Energy Holdings UK.

References

[1] N. Ayoub, E. Elmoshi, H. Seki and Y. Naka, Evolutionary algorithms approach for integrated bioenergy supply chains optimization, Energy Conversion and Management, 50, 2009.

[2] P. Thornley, P. Upham and J. Tomei, Sustainability constraints on UK bioenergy development, Energy Policy, 37, 2009, pp. 5623-5635.

[3] T. Buchholz, E. Rametsteiner, T. Volk and V. Luzadis, Multi Criteria Analysis for bioenergy systems assessments, Energy Policy, 37, 2009, pp. 484-495.

[4] W. Ho, An integrated analytical approach for selecting suppliers strategically, 3rd World Conference on Production and Operations Management, 2008, CD-ROM.

[5] N. Hanumaiah, B. Ravi and N. P. Mukherjee, Rapid hard tooling process selection using QFD-AHP methodology, Journal of Manufacturing Technology Management, 17, 2006, pp. 332 - 350.

[6] S. Myint, A framework of an intelligent quality function deployment (IQFD) for discrete assembly environment, Computers & Industrial Engineering, 45, 2003, pp. 269-283.

[7] C. N. Madu, C. Kuei and I. E. Madu, A hierarchic metric approach for integration of green issues in manufacturing: a paper recycling application, Journal of Environmental Management, 64, 2002, pp. 261-272.

Bioenergy Decision Support Systems: Worth the Effort?

Daniel Wright[1,*], Prasanta Dey[1], John Brammer[1], Phil Hunt[2]

[1] *Aston University, Birmingham, UK*
[2] *Enco Energy Limited, UK*
* *E-mail: Wrightd1@Aston.ac.uk*

Abstract: The purpose of this research is to explore the disparity between the existing model-orientated bioenergy decision support system (DSS) functions and what is desired by practitioners, in particular bioenergy project developers. This research has compiled the published bioenergy project development models, to highlight the characteristics emphasised by academics. When contrasted against a UK practitioner's perspective through the administration of a Likert style questionnaire, it is clear that the general DSS issues still persist. Finally, the research suggests how this 'theory-practice' divide could be addressed. The research contributes by giving a unique insight into the demands of a practitioner, but is currently limited by a small sample size.

Keywords: *Decision Support System, Bioenergy Project Development, Theory-Practice Divide*

1. Introduction

Developing a bioenergy project requires large volumes of complex information to be gathered and processed by project developers. This information tends to be fairly structured and accessible; although, often not easily retrievable for use in a timely manner [1]. The difficulties faced in progressing through the necessary phases in bioenergy project development encourage a dependence on experts, which restricts knowledge transfer and non-expert project developers entering the industry – ultimately constraining sector growth. This could be one explanation why growth in the UK bioenergy market, in particular has been slower than expected, with some referring to growth as 'slight' [2].

Academic literature supports the use of model-oriented decision support systems as a proven method to aid both expert and non-expert decision-makers [3], with a substantial amount of bioenergy support systems being assembled to address a multitude of development problems in countries such as: Japan, Greece and Italy. Although, this literature rarely considers the most critical issue; the theory-practice divide in DSS research [4]. At present, there is no research to understand the lack of practical application of decision support tools in the bioenergy sector. With the dire need for bioenergy project support tools to aid decision-making and in turn sector growth in the UK, but with a persistent disconnect between theory and practice [4, 5], a lack of relevance [5] and little evidence to show that these tools are ever really adopted [6] – can a decision support system really ever have a pragmatic contribution.

1.1. Objectives

The research objectives are to ascertain whether bioenergy DSS are worth the effort, by:

- reviewing published bioenergy project development DSS models;
- critically comparing these models to the requirements of the industry practitioner;
- discussing how future research could be more applicable to the practitioner.

1.2. Contribution

The contribution of this research is two-fold: it is the first paper to analyse the characteristics of all existing model-orientated DSS papers in developing bioenergy projects; and it increases understanding of the theory-practice gap by assessing these characteristics against a practitioner's perspective.

2. Developments and Issues with Decision Support Systems

Since the term decision support system' was coined by Gorry and Scott-Morton [7] when suggesting a framework for improving management information systems (MIS), there have been many developments in this discipline. One of the most successful attempts to classify the characteristics of a DSS was by Alter [8] who created a taxonomy of seven categories, which could be further condensed down to two: data-orientated or model-orientated support systems. The bioenergy DSS models reviewed in this research are all model-orientated, spanning the *representation* and *optimisation* categories in Alter's [8] classification, most support systems in use today are in these two categories [4]. Model-orientated decision support systems are typified by their user(s) and whether they integrate knowledge. This can be seen in the table below:

Table 1. DSS types [9].

Type	Description
Personal DSS (PDSS)	Small-scale systems that are normally developed for one manager, or a small number of independent managers, for one decision task.
Group support systems (GSS)	Decision responsibility is shared by a number of managers and a number of managers need to be involved in the decision process.
Intelligent DSS (IDSS) / knowledge-based DSS	Intelligent DSS can be classed into two generations: the first involved the use of rule-based expert systems and the second generation uses neural networks, genetic algorithms and fuzzy logic [Turban et al., 2005 cited 9].
Knowledge management-based DSS	Involves the combination of several areas including IT, organizational behaviour, organizational structure, economics and organizational strategy.

Table 1, also illustrates the chronological order in which the field has developed. The earlier PDSS were intended for a single decision-maker or user. As the field developed, multiple decision-makers were accounted for in the DSS design. More recently, in the last two decades researchers have built in expertise to support systems to further support decision-making.

Decision support systems have been extensively applied to a myriad of industries and problems over the past four decades, with Eom [4] reviewing over 25,000 published articles; however, he concluded theory-practice divide issues still persist. A paper by Arnott and Pervan [5] reduced the field's problems to eight issues, of which the research has selected four relating to the theory-practice divide have been selected, listed in table 2:

Table 2. DSS discipline key issues [adapted from 5].

Key Issue	Comments
Professional relevance	Most DSS research is disconnected from practice.
Research methods and paradigms	DSS is more dominated by positivism than general IS [information systems]. Case study research is under represented. A long history of design science research could contribute methodologically to IS research.
Theoretical foundations	Around half of the papers have no explicit foundation in judgement and decision-making. Much DSS research is based on a relatively old theoretical foundation.
Inertia and conservatism	The relatively older types of PDSS and GSS still dominate research agendas.

The first and foremost issue is 'professional relevance', Arnott and Pervan [5] found "only 10.1% of research is regarded as having high or very high practical relevance. On the other hand, 49.2% of research was regarded as either having low practical relevance or none at all". Two of the papers, Hirschheim and Klein [10] and Banbasat and Zmud [11], which are cited in the focal article as giving possible explanations, point toward the disconnect between these two groups; both articles focus on the researcher and academia as the cause of the divide. With Hirschheim and Klein [10], in particular, analysing the performance of the discipline from an external, management viewpoint. They show how the practitioners' expectations were not fulfilled – no matter how unrealistic. The issue with this defence is that it is bias and fails to consider, the practitioners' role in this 'disconnect'.

There are a variety of possible explanations why decision support systems fail to get adopted by practitioners. The first being given by Rizzoli and Young [12] who found that decision-makers lack trust in a DSS even if it is proven to be effective, opting for their own often sub-optimal decisions. A case in point is a study of forestry operations decision-makers in Canada, who would rather rely on their own ability than computer software's [Rooney, 1996 cited 1]. This was also found by Wierzbicki and Wessels [13:37] who discovered "the higher the level and experience of a decision-maker, the less inclined she/he is to trust in various tools and methods of decision analysis and support". The second explanation may be as Brown and Vari [6] suggested "the practical impact of decision aids on business decisions is less easy to establish, due to the cloak of commercial secrecy…" with the successful DSS being used to achieve a competitive advantage rather than for publication.

The second issue shown in table 1 is the research method and paradigm typically applied in DSS research. Arnott and Pervan [5] found that the discipline is still overwhelmingly positivist, their conclusion to remedy this was a greater reliance on case study research, and adoption of the interpretive paradigm. This issue is inextricably linked to 'practical relevance', possibly because academia has been guilty of pursuing 'rigour over relevance'[11], and the classical hypothetico-deductive positivist paradigm is the most suitable method for achieving this rigour. Although, an interpretive case study would increase the practical relevance of a DSS publication, it is not necessarily the only method of addressing this issue. It is possible to increase relevance without requiring a paradigm shift; an experimental positivist or post-positivist DSS could increase practical relevance with the empirical testing of the model(s) through actual cases application.

The third and forth issues follow on from the preceding problems in the general discipline. Arnott and Pervan [5] classified a paper as having a theoretical foundation if there was theory cited in the research design and result interpretation, they stated that the results in general DSS research was quite alarming, after finding just under half of all papers reviewed (47.8%) lacking a theoretical foundation. Additionally, they discovered that the older – more popular – types of DSS (PDSS and GSS) performed better than other DSS types. Finally, their research found that inertia and conservatism in the discipline, even accounting for the publication lag, meant that the newer types of DSS were not being fully adopted by academia.

These four issues in the general decision support system field are still present, and have not been fully addressed over the past four decades. It is unclear who is at fault: practitioners, academia, or both. However, it is clear in the context of this research problem, that if these issues are addressed by the bioenergy industry, their use and contribution will greatly increase.

3. Decision Support Systems in the Bioenergy Industry

There have been many bioenergy decision support systems created for academic papers which address different issues in developing bioenergy projects. The research has excluded a small group of sustainability DSS papers, as they are beyond the scope of this research. A timeline of all the relevant bioenergy DSS literature has been compiled in figure 1; this is a substantial number of research papers considering this is a relatively new academic field. The extent to which DSS tools have been utilised in academic journals could be attributed to the complexity of effectively making decisions in the energy sector, making it is necessary to utilise some form of support model [14].

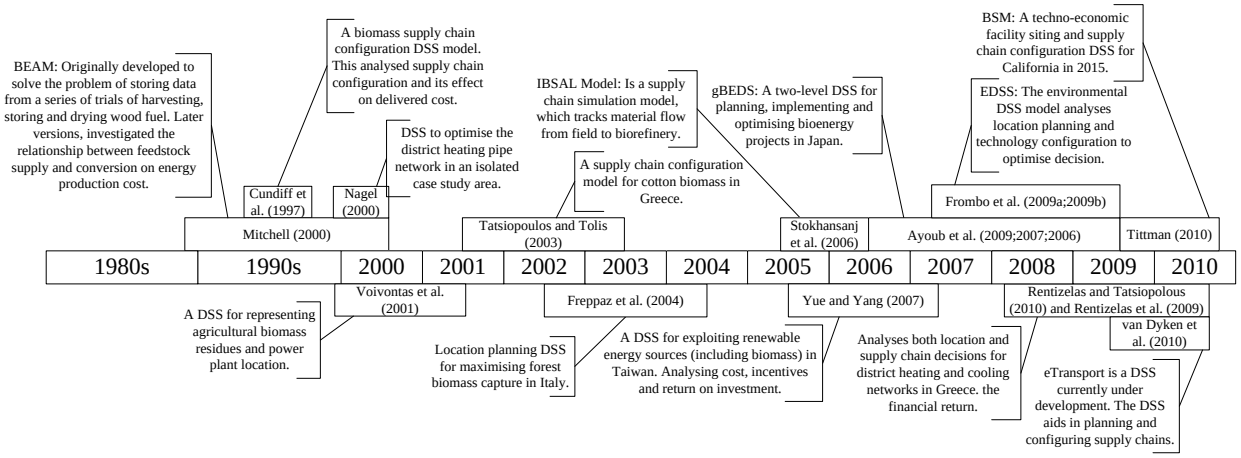

Fig. 1. Annotated timeline of model-oriented bioenergy DSS research.

The timeline highlights 13 DSS models created for developing bioenergy projects, primarily spanning two decades, with most models being created in the last 10 years. The timeline gives a brief overview of each DSS and shows the publication lag, or when explicitly stated in the article, when research began.

4. Methodology

The paper gives an exploratory insight into what a bioenergy project developer requires from a DSS. The primary data for this research was gathered by creating a questionnaire for practitioners, which analyses their opinion on the existing bioenergy research papers traits.

From the descriptive statistics gathered from the analysis of the DSS characteristics (table 3), a scale of importance was attributed to each characteristic. The frequency ranking scale was: low (0-2 articles); medium (3-5 articles); high (6-8 articles); very high (9 or more articles).

4.1. Bioenergy DSS Characteristics

Before it is possible to assess the focus of bioenergy decision support systems, it is necessary to analyse their characteristics. To achieve this key attribute categories have been created, some relate to the configuration of the DSS, such as: type of DSS, intended user(s), research paradigm etc; whereas, the remaining characteristics relate to the professional relevance and model application. The scales attributed to each of the characteristics varies, most are non-parametric nominal scales. In some cases a simple dichotic yes/no choice was utilised, as seen in table 3.

Table 3. DSS Characteristic Classifications.

Category	Classification
Type of DSS	This characteristic refers to the DSS design. The bioenergy DSS models are categorised as: personal (PDSS), group (GSS), intelligent or knowledge-based, or knowledge management-based.
User(s)	The categories for this measure are: national or regional planners/developers, local developers, investors and not stated. Importantly, if the intended user of the decision support tool is not explicitly stated in the research paper then they are categorised as not stated.
Research method	The research method and paradigm categories are based on the Arnott and Pervan [5] classification: non-empirical conceptual, illustrative or applied concepts; empirical objects or events and processes.
Practical relevance	This is the foremost issue with decision support systems. As the Arnott and Pervan [5] paper utilised a subjective scale, administered by a group of experts to judge whether the article had practical relevance (none, low, medium, high, very high). It was important to implement a similar system, with a less interpretive grounding. Table 4 applies a measure for each existing bioenergy articles.
Theoretical foundation	The method of judging whether a bioenergy DSS paper has a theoretical foundation will be the same as applied in Arnott and Pervan [5]. They distinguished between only citing other theory in the introductory chapters and citing theory in the method and discussion sections, as no theoretical foundation or having a theoretical foundation respectively.
Project lifecycle	The research also categories the DSS models by the targeted phase in the bioenergy project lifecycle, the phases are: planning, construction and operation [15]. As decisions are made throughout a project's lifecycle phases, it was important to ascertain where the current support systems focused.
Model output	The bioenergy model output(s) were also recorded as: financial, non-financial or multiple.

As the theory-practice divide and whether decision support systems are worth the effort, is the primary focus of this research, emphasis has been placed on creating a practical relevance scale, as seen in the table below:

Table 4. Scale for establishing practical relevance.

Relevance	Measure
Low	Hypothetical case
Medium	Single application or case study
High	Multiple practical uses
Very high	Multiple practical uses and application examples

This research argues that a DSS which is possesses multiple practical uses; meaning it can be applied to multiple cases to solve problems (generalisable), will have the highest practical relevance. Moreover, if this is also demonstrated in the academic article, as opposed to merely stating a support system's generalisability, then this achieves 'very high' practical relevance.

4.2. Practitioner Questionnaire

A simple closed choice questionnaire, with a five-point Likert style scale for importance (none, low, medium, high, very high) was designed to explore whether bioenergy project developers placed similar emphasis on the characteristics in the existing bioenergy support systems. Due to the constraints of the research paper, the questionnaire is not included, but is available on request. The results of the questionnaire can be seen in table 5. The respondent organisation is a SME developer of biomass combined heat and power projects in the UK.

4.3. Research Limitations

The research is currently limited to one organisation, but this is because the research is on-going. Although, this is presently a limited sample size, its contribution remains as the first study to explicitly state the practitioner's view.

5. Results

The results table (5) below, illustrates the comparisons between the academic and practitioner weighting:

Table 5. Results table.

Characteristic	Application	Academic Weighting (no.)	Practitioner Weighting
Type of DSS	PDSS	Very high (10)	High
	GSS	Low (0)	High
	Knowledge-based	Medium (3)	Very high
	Knowledge mgmt' based	Low (0)	Low
User(s)	National or regional	Low (1)	Very high
	Local	Low (0)	Very high
	Investor	Low (1)	Very high
	Implied/not stated	Low importance (10)	Very important
Method	Empirical	High (7)	High
	Non-empirical	High (6)	Low
Practical relevance	Low/med (single application)	Very high (10)	High
	High/v.high (multiple applications)	Medium (3)	Very High
Theoretical foundation	Yes	Low (2)	Very high
	No	Very high (11)	-
Bioenergy lifecycle phase	Planning	Very high (13)	Very high
	Construction	Low (0)	Very high
	Operation	Low (0)	Very high
Model output	Financial	High (7)	Very high
	Non-financial	Low (2)	High
	Both	Medium(4)	-

5.1. Analysis

The results highlighted that the foremost issue of practical relevance in the bioenergy sector was an improvement on the Arnott and Pervan [5] findings, with 3 models or 23.1% classified as having a high or very high practical contribution, as opposed to only 10.1% of their sample were categorised as such. Although, it is not possible to truly know if the criteria

for assessing this were exactly the same, this verifies the research paper's interpretation of the practical relevance scale.

Moreover, the user(s) of the bioenergy DSS tended not to be mentioned or explicitly stated (76.9%) in the bioenergy publications, this can only support the argument for the lack of relevance, as the user is most likely the practitioner. This is something that the respondent organisation felt particular strong about, stating that it is very important to target each user group, and to explicitly tailor a DSS to their requirements. However, there is a general agreement between the academic and practitioner viewpoint on the most suitable output of the model, with the most emphasis placed on financial performance measures.

The bioenergy lifecycle phase results are also particularly interesting, as all of the 13 bioenergy models supported decision-making in the planning phase: in supply chain planning, location planning or both. None of the existing models supported the decision-maker in the later phases of a project's lifecycle; this highlights a need for further work considering that the respondent classified all phases as equally important.

The second issue raised was the lack of case study research and positivist paradigm dominance in the general DSS field. This was found to still be present in the bioenergy development models, with all papers reviewed having a positivist paradigm. Although, there was a high level of case study research found, with more than half of the bioenergy support systems possessing empirical data from case studies. This importance was also expressed in the respondent organisation's support for empirically grounded case studies.

The existing bioenergy research performed worse than the general discipline with regard to the theoretical foundation. This category classified 11 of the 13 models as not having a theoretical foundation in the model development and result analysis sections of the academic paper, this is considerably higher than the 47.8% found by Arnott and Pervan [5]. Furthermore, PDSS represented the majority of existing models, illustrating the inertia and conservatism within the discipline; although, it can be seen that group support systems were not adopted, the more recent knowledge-based DSS did quite well in this sector (23.1%).

6. Conclusion

From analysing the current issues in general DSS research (section 2), it is clear that the four issues relating to the theory-practice divide are interlinked; what wasn't clear was whether the bioenergy DSS research suffered from the same shortcomings. The bioenergy article analysis and the primary research in this paper have shown that for the most part they are still present. This could, therefore, explain why there is little evidence of practical adoption.

Arguably, if the purpose of building a DSS is to support decision-making, then practical application has to be regarded as the most important parameter. The most suitable way of addressing this issue is to design a system tailored to the decision-maker – this does not appear to be a priority of the existing research. Acknowledging and explicitly integrating the requirements of the user into the model building and testing stages will undoubtedly increase adoption. Furthermore, if generalisable model-orientated support systems have the highest level of practical relevance, then where possible they should take preference over a single use model. Finally, creating knowledge-based or intelligent DSS models which allow for group decision-making will not only reduce the conservatism issue but also allow for a potentially greater contribution. Addressing the issues raised in this paper is undoubtedly the first barrier to realising the full potential of decision support systems in the bioenergy industry.

6.1. Further Work

Firstly, as the research presented is at an early stage, the next step is to increase the respondent sample size to include national and regional developers and investors, to better ascertain what functionality bioenergy project developers require. Moreover, a larger sample size would allow for inferential statistical analysis, adding a greater level of depth to the research. Secondly, as there is no research into decision support models for the latter phases of a bioenergy lifecycle, this presents an interesting new avenue of enquiry.

References

[1] C. P. Mitchell, Development of decision support systems for bioenergy applications, Biomass and Bioenergy, 18, 2000, pp. 265-278.

[2] R. Slade, C. Panoutsou and A. Bauen, Reconciling bio-energy policy and delivery in the UK: Will UK policy initiatives lead to increased deployment?, Biomass and Bioenergy, 33, 2009, pp. 679-688.

[3] D. J. Power, Decision Support Systems, Greenwood Pressed, 2002.

[4] S. B. Eom, The Development of Decision Support Systems Research, The Edwin Mellen Press Ltd, 2nd ed, 2007.

[5] D. Arnott and G. Pervan, Eight key issues for the decision support systems discipline, Decision Support Systems, 44, 2008, pp. 657-672.

[6] R. Brown and A. Vari, Towards a research agenda for prescriptive decision science: The normative tempered by the descriptive, Acta Psychologica, 80, 1992, pp. 33-47.

[7] G. A. Gorry and S. S. Scott-Morton, a framework for management information systems, Sloan Management Review, 13, 1971, pp. 55 - 70.

[8] S. Alter, Decision Support Systems: Current Practice and Continuing Challenges Addison Wesley Longman ed, 1980.

[9] D. Arnott and G. Pervan, A critical analysis of decision support systems research, Journal of Information Technology, 20, 2005, pp. 67-87.

[10] R. A. Hirschheim and H. K. Klein, Crisis in the IS field? A critical reflection on the state of the discipline, Journal of the Association for Information Systems, 4, 2003, pp. 237-293.

[11]I. Benbasat and R. W. Zmud, Empirical research in information systems: the practice of relevance, MIS Q., 23, 1999, pp. 3-16.

[12]A. E. Rizzoli and W. J. Young, Delivering environmental decision support systems: software tools and techniques, Environmental Modelling & Software, 12, 1997, pp. 237-249.

[13]A. P. Wierzbicki and J. Wessels, The modern decision maker, In: J. Wessels, Model-based decision support methodology with environmental applications, Kluwer Academic Publishers, 2000.

[14] M. Simo, L. Risto, A. Anna-Maria and J. Antti, Multi-criteria decision support in the liberalized energy market, Journal of Multi-Criteria Decision Analysis, 12, 2003, pp. 27-42.

[15] R. M. Carlos and D. B. Khang, A lifecycle-based success framework for grid-connected biomass energy projects, Renewable Energy, 34, 2009, pp. 1195-1203.

Options for Increased Use and Refining of Biomass – the Case of Energy-intensive Industry in Sweden

Hanna Ljungstedt[1,*], Daniella Johansson[1], Maria T Johansson[2], Kersti Karltorp[1]

[1] *Department of Energy and Environment, Chalmers University of Technology, Gothenburg, Sweden*
[2] *Department of Management and Engineering, Linköping University, Linköping, Sweden*
** Corresponding author. Tel: +46 317728534 Fax: +46 317721152, E-mail:hanna.ljungstedt@chalmers.se*

Abstract: Events in recent decades have placed climate change at the top of the political agenda. In Sweden, energy-intensive industries are responsible for a large proportion of greenhouse gas emissions and their ability to switch to renewable energy sources could contribute to the transition to a decarbonised economy. This interdisciplinary study has its starting point in three energy-intensive industries' opportunities to take part in the development towards increased refining and use of biomass. The study includes the pulp and paper industry, the iron and steel industry and the oil refining industry, each exemplified by a case company. It can be concluded that there are several technological options in each industry. On the other hand, implementing one option for increased use of biomass in each case company could demand up to 34% of the estimated increase in Swedish biomass supply, in 2020. Additionally, in a longer time perspective none of the case companies believes that the amount of biomass in the Swedish industrial energy system have the possibility to increase significantly in the future.

Keywords: *Biomass, Energy-intensive industry, CO_2 emissions, Case study.*

1. Introduction

Increased awareness of the effects of climate change has placed mitigation of greenhouse gas emissions at the top of the political agenda, urging a transition to a decarbonised economy. Sweden has taken a prominent position in the international discussions about this transition and is simultaneously creating national policies to mitigate climate change, for example the green certificates for generation of electricity from renewable energy sources. In Sweden, the industrial sector represents one third of the total energy use and in 2008 this sector used 151 TWh [1]. The Swedish pulp and paper, iron and steel and oil refining industry accounted for more than 70% of the energy use (50%, 15%, 7% resp.) in the industrial sector and were responsible for 44% of the CO_2 emissions from Swedish companies (that are a part of the European Emission Trading Scheme) in 2008 [2]. Therefore their ability to switch to renewable energy sources could contribute to mitigate climate change effects. Since a large part of Sweden is covered by forest or agricultural land, biomass has the potential to be one of these renewable sources.

Several studies have analysed the options for biomass use in Sweden [3; 4]. More specifically, the potential for increased biomass use and refining in the pulp and paper industry is analysed by e.g. Andersson [5]. Berntsson et al [6] and Johansson et al. [7] analyses the biomass use in the oil refining industry and Norgate and Landgate [8] investigates the same issue for the iron and steel industry. This study includes these three industries in order to get a comparative view on the potential for biomass use and refining in Swedish energy-intensive industry. However, it is important when studying these industries jointly to take into account their different prerequisites for use and refining of biomass, regarding current feedstock as well as processes. The aim of the study is to investigate how these industries can contribute towards a future increased use and refining of biomass. A case study approach is used and three case companies are studied, one for each industry. The aim of the study is evaluated through three research questions; 1) What are the possible technological options for increased use and refining of biomass for the studied industries? 2) If implemented in the case companies, what

amount of biomass would these technological options require compared to the potential of increased biomass supply in Sweden 2020? 3) What possibilities and obstacles do the case companies recognize for increased use and refining of biomass in their industry?

2. Methodology

This interdisciplinary study illuminates both technological options and business strategies, revealing conflicting and co-operational interests and creates the potential for a profound understanding of sustainable future development in this area. The study is based on a case study approach and both interviews and literature surveys are used to collect data. For research question 2 and 3 each industry is represented by a case company, which are presented at the end of this section. The case companies are chosen since they all have an ambitious attitude to climate change mitigation activities and have shown interests in collaborations with universities.

The first research question is answered by a literature survey, in which the following commercial technologies are included; pyrolysis, catalytic cracking, hydro cracking and production of wood-fuel pellets. Not commercially available technologies included are second generation ethanol fermentation, biomass gasification, lignin extraction and black liquor gasification.[1] Technologies in an early stage of development or with a limited potential to increase the use and refining of biomass in the industrial sectors were not included in this study. The included technologies are based on wood and agricultural biomass and do not compete with the core capabilities of the case companies. For the second research question the result of the first is combined with the different preconditions at the case companies and the potential future biomass demand. However, only technologies that are possible to implement at each case company are evaluated. The results for the third research question are based on qualitative and semi-structured interviews. Two representatives for each case company were interviewed, one at corporate group level and one at facility level.

In this study biomass is considered to be a limited resource. The biomass required to implement a technology is therefore compared to the future potential of increased biomass supply in Sweden. Several studies have estimated the increase in supply of wood and agricultural biomass, in Sweden. In this study a moderate increase of biomass supply has been used, estimated of 38 TWh/year in 2020 in reference [9].

The studied case companies are; Södra Cell for the pulp and paper industry, SSAB for the iron and steel industry and Preem AB for the oil refining industry. For the calculations in research question 2, the following specific facilities are used; Södra Cell Värö that produced 380 ktonnes of kraft pulp [10], SSAB Strip Products in Luleå that produced around 2.2 Mtonnes of steel slabs and 750 ktonnes of coke [11] and Preem's refineries in Lysekil and Gothenburg with annual oil refining capacities of 11.4 Mtonnes and 5 Mtonnes of crude oil respectively in 2008[12]. The choice of facilities limits the study to kraft pulp mills[2] for the pulp and paper industry and to integrated steel plants[3] for the iron and steel industry. Additionally, the refinery in Gothenburg is smaller and less complex than the refinery in Lysekil.

[1] More information about these biorefining technologies can be found in Johansson et al [13].
[2] Chemical pulp and not paper is the final product.
[3] The processes are based on iron ore.

3. Results

This section presents opportunities for increased use and refining of biomass in the three energy-intensive industries studied. Furthermore, the amount of biomass required for the options are related to the estimated increase in biomass supply in Sweden in 2020. Additionally, the case companies' views on future increased use of biomass in their industry are presented. To distinguish the results based on interview outcomes from results based on calculations or literature studies all interview references are marked with an asterisk.

3.1. Pulp and paper industry

For the pulp and paper industry, with its wood biomass based processes and extensive experience of logistics of timber, the increased demand for biomass has lead to increased competition for the industry's raw material but also opened new opportunities for increased refining of intermediate and by-products. The existing infrastructure for transportation of raw materials, storage possibilities on site and knowledge of handling of biomass can facilitate increased import of biomass as well as export of products based on biomass.

Like the industry in general, the case company Södra Cell is affected by the changes in its environment. The price of biomass, chemicals and energy affect the production cost, on the other hand energy prices also affect Södra Cell's incomes positively [14]*. Södra Cell's strategy is to increase energy efficiency in order to minimise purchased energy so that only raw material is bought and additionally the company wishes to become independent from fossil fuel [14]*. This is achieved by increasing the efficiency of the production processes, through technological choices adapted to the different prerequisites at Södra Cell's three Swedish mills. The mill in Mönsterås has invested in a condensing turbine to increase electricity production, Södra Cell Mörrum is planning a LignoBoost[4] process and Värö's mill installed a bark drier during 2009. The company is interested in using new technologies for producing non-cellulose-based products, e.g. district heating, electricity, lignin or tall oil, but only as long as these are produced from residues and thus do not compete with pulp production [14]*. All these alternatives offer the possibility of increased export of energy products without increasing the total import of biomass to the facilities. Policies, particularly the green certificates for electricity, have contributed to justify activities that improve energy efficiency and investment in new technologies.

In the case of replacement of the recovery boiler or increase in production capacity in a kraft pulp mill, gasification of black liquor could be an interesting alternative. The technology is currently at the demonstration plant level and it is argued by Pettersson and Harvey that a large scale implementation is unlikely to occur before 2020 [15]. Their conclusions are based upon a study of energy and material balance consequences of implementation of black liquor gasification for production of DME in a model mill. They argue that pulp mills will be more energy efficient by 2020 (using best available technology of today). The study shows that one consequence would be an increased biomass demand that, in the case of Södra Cell Värö would correspond to about 700 GWh/year. Södra Cell claims that the main barrier for implementing this technology is the high investment cost of the gasifier [14]*. Ekbom et al. [16] estimated the investment cost for a large scale gasifier to be more than twice the cost for a recovery boiler with the same capacity. Furthermore, the technology would also compete for biomass feedstock with the LignoBoost process [14]*. Finally, a sign of another path of development with a slightly different character is Södra Cell's research on green chemicals,

[4] A process for separating lignin from black liquor. The lignin is sold as high value fuel.

which is conducted at the headquarters in Växjö by an R&D team of 50 peoples based in Värö [14]*.

3.2. Iron and steel industry

The spectrum of options to increase use and refining of biomass in an integrated steel plant is narrow, but the existing options have great potentials to reduce the industry's CO_2 emissions. An integrated steel plant can replace some of the coke used as reducing agent in the blast furnace, with biomass derived products such as charcoal, syngas, methane and ethanol. However, it is not possible to substitute all the coke in the blast furnace as coke acts as a physical support material and hence ensures correct gas permeability, process temperature and process drainage. Moreover, gasified biomass can be used as fuel in the steel plant's heating furnaces and replace the fossil fuel used today. Another option for an integrated steel plant is a partnership in an industrial symbiosis together with a biorefinery. For example, excess heat from the steel plant can be used by an ethanol plant and the ethanol can be used as reducing agent in the blast furnace or as transportation fuel in the steel plant's vehicles. Furthermore, an integrated steel plant can cooperate with a gasification plant and a Direct Reduced Iron (DRI) plant. The DRI plant can use syngas from the gasifier together with coke oven gas as reducing agent and DRI can be charged into the blast furnace or into the converter.

The interviewed representatives at the case company SSAB Strip Products state that a large scale replacement, of for example coke with products derived from biomass in the blast furnace, would need an extensive amount of biomass which makes it unlikely to be realized [17]*. Calculations for SSAB Strip Products demonstrate that a replacement of the pulverised injection coal with pulverised charcoal would demand approximately 4.4 TWh/year[5] of dry wood. If instead bio-methane was considered for injection, it would be possible to replace one third of the injection coal without affecting the blast furnace process [17]*, which would demand approximately 1.5 TWh/year of methane. If the methane is produced through gasification of biomass it would demand about 2.5 TWh/year[6] of dry wood. However, SSAB Strip Products identifies a risk in substituting coke with products derived from biomass as a substitution could affect the quality of the products, before the process is optimised, which could reduce the company's competitiveness [17]*.

The development of CO_2 prices and the global raw material markets will probably have the greatest impact on SSAB Strip Products' choice of future development path [17]*. Currently, energy-rich process gases are exported from SSAB Strip Products and used as fuel in a combined heat and power (CHP) plant. With regard to biomass use, the representatives from SSAB Strip Products consider it a better option to investigate possibilities to use excess energy-rich gases from the steel production internally at SSAB Strip Products and use biomass in a CHP plant [17]*. As a result of this line of reasoning, the company is increasing the efficiency of its energy system and aims at reducing its CO_2 emissions by 2% by 2012, which corresponds to 130,000 tonnes of CO_2 [11].

3.3. Oil refining industry

In a transition to more sustainable production and use of fuels the oil refining industry could play an important role with its extensive experience in processing and converting petroleum oil products into valuable fuels. The oil refining industry has the opportunity to use existing equipment for refining of biomass. By using the existing catalytic cracking unit or the

[5] Calculations were based upon a biomass-carbonisation kiln with a weight-basis yield of 37%.
[6] In the calculations, a gasification plant with a biomass to SNG conversion efficiency of 60% is used.

hydrotreating unit bio-oils can be upgraded to transport fuels that meet the existing fuel standards. At present, there is an increasing demand of hydrogen in the oil refining industry which is due to a process change into more valuable products, e.g. diesel, aviation fuel etc. This increasing demand can be supplied by production of hydrogen trough gasification of biomass. Moreover, hydrogen could also be produced by natural gas steam reforming and indirect use of biomass via production of synthetic natural gas (SNG). Another option for utilisation of biomass in the oil refining industry is gasification followed by Fischer Tropsch synthesis. This process could be placed on-site at the refinery or off-site, closer to the biomass feedstock. To maximise the production of Fisher Tropsch diesel and improve the efficiency, the by-products from the process, naphtha and wax, could be further utilised in existing refinery processes.

Results from the interview with the case company for the oil refining industry, Preem AB, show that they considers biomass as a raw material that could be used in their processes, since this offers a new business opportunity and the company seems eager to be an early mover in the market for green diesel [18]*. On the other hand this can also be regarded as a matter of survival for Preem AB, since many European oil refineries of the same size as Preem AB's refinery in Gothenburg have faced bankruptcy lately [18]*. Preem's strategy for the future consists of two parallel paths: developing the Gothenburg refinery towards the production of green diesel and increasing the complexity of the Lysekil refinery for refining of crude oil [18]*. This strategy includes a recently started biomass-based hydrotreating process in Gothenburg, which is regarded as a step between the first and second generation renewable fuel, i.e. fuel production based on gasification. Karlsson and Nyström [18]* explain that regarding the development of gasification, they consider cleaning after the process as a huge challenge which demands co-operation by industry, universities and the government, in order to reduce risks and exchange competencies.

Calculations for Preem AB´s refineries in Sweden show that replacement of the total hydrogen demand through gasification[7] of solid biomass would demand approximately 1.2 TWh/year at Gothenburg refinery and 6.60 TWh/year at Lysekil refinery. However, if hydrogen is produced through gasification of pyrolysis oil, i.e. including a pyrolysis pre-treatment step for the biomass, biomass requirements of 1.7 TWh/year in Gothenburg and 9.2 TWh/year in Lysekil are needed. With regard to hydrogen production trough steam reforming of SNG, supplying Preem's refineries in Gothenburg and Lysekil would require approximately 1.8 and 9.5 TWh/year biomass respectively. It is important to stress that these requirements are based on the current total hydrogen demand and on the assumption that it is possible to replace the whole demand. More detailed calculations about biomass gasification in Gothenburg are found in Johansson et al. [7].

The adjustment of the refinery in Lysekil for optimal use of crude oil, is motivated by the belief that there will continue to be a market for liquid fuel from crude oil, due to crude oil's efficiency as an energy carrier and its relative low cost [18]*. Since biomass is a limited resource Preem AB's plan is a 30% blend of green diesel into fossil diesel. Calculations shows that the production of 100 000 m^3 diesel, with a 30% renewable content, will at the refinery in Gothenburg refinery demand 1.15 TWh/year of raw tall oil, requiring 55% of the total Swedish raw tall oil production. Although tall oil is the first biomass-based raw material Preem AB is investigating other options are for example used oils and oil from algae [18]*.

[7] Calculations are based on assumptions presented in [13] and for gasification for hydrogen production updated with result from [7].

3.4. Future prospective

Even though current policies try to stimulate use of biomass as a source of energy and several technological options are possible, none of the case companies believes that biomass will increase significantly in the Swedish industrial energy system over a longer time perspective. The reason for this is that biomass is regarded as a limited resource and neither SSAB Strip Products nor Preem believe that biomass could represent a large-scale substitute for the currently used fossil fuel. The case companies' views on biomass as a limited resource are in line with the result that is obtained when calculating the biomass demand from the previous described technologies in comparison with the future increase in biomass supply in Sweden until 2020.

The biomass demand for the technological options that can be seen in Fig. 1 show a large share of the biomass considered to be available for new actors in 2020. However, it is important to note that the potential described above is the highest possible demand; some of the technologies may be implemented in a smaller scale, needing less biomass. Furthermore, it is not possible to implement all technologies described in section 3.1-3.3 in one facility within the case company at the same time as some of them compete for the same resources or supply the same feedstock.

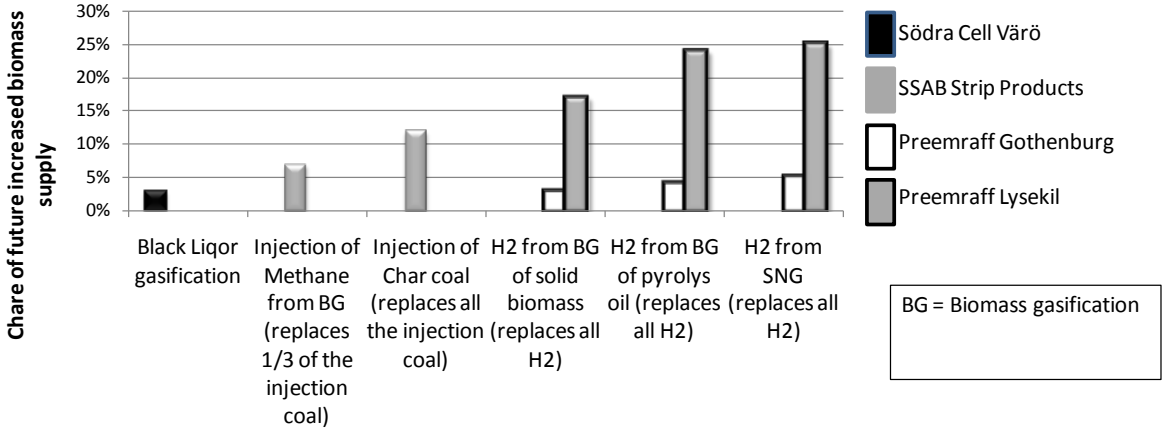

Fig. 1. The share of future increase in biomass supply that is needed if a technology to increase biomass use/refining would be implemented at each case company. Note that this is the highest biomass demand. Options not requiring increased import of biomass or do not significantly affecting the CO_2 balance at the case company are not included.

Adding the biomass demand for hydrogen production from biomass gasification at Preemraff Lysekil and Gothenburg, injection of pulverised charcoal at SSAB Strip Products and black liquor gasification at Södra Cell Värö would require 34 % of the total increase of biomass supply in 2020 (38 TWh/year [9]). For the pulp and paper industry the only option that requires increased import of biomass is included, in the oil-refining industry the hydrogen production alternative with the most efficient use of biomass is included and for the iron and steel industry the option substituting the largest amount of fossil fuel is included.

Despite the somewhat pessimistic view of biomass potential as a future feedstock the representatives we met at both Södra and Preem appreciate that the companies they represent have chosen to become actively involved in environmental issues. In a longer perspective, Södra hopes that they still can use biomass for their current core business, pulp production,

and additionally for production of e.g. composite material, cloths, chemicals or medicine [14]*. SSAB Strip Products does not believe that any biomass technology will be implemented at their facility. Instead they believe that available excess heat will be integrated with surrounding energy systems, in which biomass could be one of several feedstocks [17]*. In contrast, Preem´s strategy for the refinery in Gothenburg to remain competitive is to modify existing infrastructure for production of both renewable and fossil diesel. Preem fears that competition for biomass as a feedstock between different industrial sectors will be more important in a longer perspective than competition within the oil refining industry [18]*.

4. Discussion and Conclusions

The study shows several possibilities for increased use and refining of biomass in the three industries studied: Kraft pulp mills can export by-products either unrefined or refined into higher value added products. Additionally, oil refineries can import biomass feedstocks for the production of green diesel or hydrogen and integrated steel plants can use biomass-derived products as reducing agent in the blast furnace. Finally, all three industries have options to export excess heat to biorefineries with demand for heat.

This study shows that technologies for increased use and refining of biomass implemented at three energy-intensive industries would require up to 34% of the Swedish potential for increased supply of biomass in 2020. Although estimations of the increase in biomass supply is very uncertain, the fact that biomass is a limited resource have been recognized by the case companies. Hence, it is important to evaluate the options in relation to alternative scopes of use for the biomass before any new investments are made. One important issue to address is how the biomass is most efficiently used in order to reduce CO_2 emissions. Furthermore, the market for biomass is global and biomass price and expected profits for the purchaser will probably have an impact on where the biomass will be used in the future. There are large differences in required amounts of biomass for the different industry sectors, which could affect the probability of realization of the options. Companies located near harbours may have a financial advantage on the global biomass market since transportation costs can be reduced. Finally, it is vital from an environmental point of view that the biomass resources are exploited in a sustainable way with re-planting and responsible land-use.

Regarding the case companies, both Södra Cell and Preem are investigating possibilities to introduce new technologies for increased use and refining of biomass and have identified this as a new business opportunity. On the other hand, SSAB Strip Products considers biomass a too limited resource, especially compared to coal and coke, which the company uses today, and is not interested in investing in facilities not related to its core capabilities. The interview results for Södra and SSAB Strip Products are in line with the results from the calculations. For Preem, the calculations indicate that a large amount of biomass would be required for the different options (see Fig 1), which would constitute a barrier for implementation. In the interviews the company has an optimistic view on implementing options for increased use and refining of biomass. However, these options are based on using existing infrastructure but adopting it to biomass based feedstock and are thus not the same technologies as in our calculations.

This study concludes that opportunities for Swedish energy-intensive industry to increase use and refining of biomass exist, but with many potential barriers for implementation. However, the study points towards a trend in Swedish energy-intensive industries; the industries are more aware of their CO_2 emissions and seek options to be more climate neutral.

References

[1] Swedish Energy Agency, Energy in Sweden 2009 Facts and Figures, Energimyndighetens publikationsservice, 2009.

[2] Swedish Environmental Protection Agency, Register of emissions and allocation 2008, 2008, (in Swedish).

[3] G. Berndes, and L. Magnusson, The future of bioenergy in Sweden – Background and summary of outstanding issues, 2006.

[4] K. Ericsson and P. Börjesson, Potential disposition of biomass for production of electricity, heat and fuels including energy combines, The Faculty of Engineering at Lund University, 2008 (In Swedish).

[5] E. Andersson, Benefits of Integrated Upgrading of Biofuels in Biorefineries – Systems Analysis, Doctoral Thesis, Chalmers University of Technology, 2007.

[6] T. Berntsson, et al, Towards a sustainable Oil Refinery, Chalmers EnergiCentrum, 2008, CEC2008:1.

[7] D. Johansson, PÅ. Franck, T. Berntsson, A process integration analysis of hydrogen production from biomass in the oil refining industry, Proceeding of the 19th International Congress of Chemical and Process Engineering and 7th Congress of Chemical Engineering 2010.

[8] T. Norgate and D. Langberg, Environmental and Economic Aspects of Charcoal Use in Steelmaking. ISIJ International 2009:49(4) pp. 587-595.

[9] Förnybart.nu, Renewable energy and energy efficiency – potential for 2020, 2009 (In Swedish).

[10] Södra Cell Värö. Environmental information 2006-2009, 2010,http://www.sodra.com

[11] SSAB Strip Products. Environmental report 2008, SSAB Strip Products, Luleå (Miljörapport 2008,SSAB Tunnplåt AB, Luleå), 2009, www.ssab.com

[12] Preem, 2009, www.preem.se

[13] D. Johansson, M. Johansson, K. Karltorp, H. Ljungstedt, J. Schwabecker, Pathways for Increased Use and Refining of Biomass in Swedish Energy-Intensive Industry, ISSN 1403-8307, Energy Systems Programme, Linköping University, 2009.

[14] A. Andersson, Interview, 2009, Energy Coordinator at Södra in Växjö.

[15] K. Pettersson, S. Harvey, The Effect of Increased Heat Integration of the Cost for Producing DME via Black Liquor Gasification, Proceedings of 22nd International Conference onEfficiency, Cost, Optimization, Simulation and Environmental Impact of Energy Systems 2009.

[16] Ekbom T, Berglin N, Lögdberg S. Black liquor gasification with motor fuel production – BLGMF II, Swedish Energy Agency, Nykomb Synergetics, 2005.

[17] N. Edberg, K. Kärsrud, Interview, 2009, Manager Raw materials and energy at

SSAB Strip Products iectively Director of Environmental Affairs at SSAB.

[18] S. Nyström, B. Karlsson, Interview, 2009, Refinery Development respectively Manager Buiness Development at Preem AB, Gothenburg.

Is Bioenergy the Big Bad Wolf in the Forestry Sector? A discussion about the sustainable supply chain management role in bioenergy systems

Alessandro Sanches Pereira

PhD Student at Energy and Climate Studies Division, ITM/KTH, Stockholm, Sweden
Tel: +46 8 790 74 31, Fax: +46 8 20 41 61, E-mail: alessandro.sanches.pereira@energy.kth.se

Abstract: The paper's aim is to use a bioenergy supply chain management approach in order to reinforce sustainable development in a likely scenario of competition between bioenergy and the production of other goods extracted from wood. This competition is perceived as a threat because it may lead to an increase in raw material and energy prices and reduce the competitiveness of the European pulp & paper industry compared to other regions of the world. The key question is then: is bioenergy the big bad wolf in the forestry sector or an opportunity for improving the sustainability of biomass-based supply chains? The work assumes bioenergy as an opportunity because a systemic approach to bioenergy systems' optimization can lead to performance improvement beyond the boundaries of a single company and increase the sustainability aspects of the entire network. The results are based on content analysis conducted by a literature review and information gathering from relevant publications in the field.

Keywords: *Bioenergy Systems, Sustainable Supply Chain Management, Systems Analysis.*

1. Why sustainable supply chain management is important?

The energy price shocks of the 1970s served as a major incentive to revisit energy practices. As a result, several nations launched efficiency programs and tried to develop solutions to replace hydrocarbon fuels. However, for some time low oil prices has been a barrier and preventing renewable energy from taking up on large commercial scale [1]. More recently, renewables gained new momentum as a result of favorable policies, such as in the EU where the target is to reach 20% of renewables by 2020. Nevertheless, the development of renewables is by no means given. The increasing availability of gas and the delayed removal of fossil fuel subsidies could again hamper the competitiveness of renewables for many years to come [2].

At present, we are facing a new crisis based on the depletion of natural resources, expected scarcity of fossil fuels, increasing energy prices worldwide, increasing global competition for fuels, and global efforts to reduce greenhouse gas emissions. In this context, energy from renewable sources remains a key component to mitigate environmental risks and increase energy security. According to the International Energy Agency, renewable energy sources – such as wind power, solar energy, hydropower and biomass – responded for only 12.9% of the global primary energy supply and 18.7% of the global electricity production in 2008. IEA calculates that, without new policies in place, global primary energy demand could increase by 45% by 2030 compared to 2006 levels. Transportation could account for 57% of the global primary oil consumption, compared with 52% now and 38% in 1980. The agency emphasizes the need for policy actions in order to change the so-called *"business-as-usual"* scenario and foster an increased share of renewables in the future global energy mix [3].

Certainly, the need to shift energy systems towards renewable sources is well recognized. This tends to put a lot of emphasis on technology development. However, intensifying the use of renewable energy systems is not only a technological challenge. To optimally explore constrained renewable resources (e.g., forest-based biomass), technological management challenges have to be faced. This paper assumes that a strategic use of bioenergy supply

chains, in particular the use of the concept of sustainable supply chain management in the forest-based bioenergy systems can improve the sustainability aspects throughout the chain.

1.1. Sustainable Supply Chain Management

Lambert *et. al.* (1998, p.1) describes supply chain management (SCM) as *"the integration of key business process from end-user through original suppliers, that provides products, services and information that add value for customers and other stakeholders"* [4]. In 2001, Mentzer *et. al.* (2001, p.18) has outlined a complementary definition that defines SCM as *"the systemic , strategic coordination of the traditional business functions and the tactics across these business functions within a particular company and across businesses within the supply chain, for the purposes of improving the long-term performance of individual companies and the supply chain as a whole"* [5]. Nowadays, the Council of Supply Chain Management Professionals (CSCMP) describes supply chain management as *"the planning and management of all activities involved in sourcing and procurement, conversion, and all logistics management activities. Importantly, it also includes coordination and collaboration with channel partners, which can be suppliers, intermediaries, third party service providers, and customers. In essence, supply chain management integrates supply and demand management within and across companies"* [6]. Svensson (2007, p.263) and Cater & Rogers (2007, p.368) argue that in order to SCM become sustainable it should integrate and equalize economic profit, environmental and social goals to long-term performance of individual companies as well as their supply chains [7] [8].

In this context, the sustainable supply chain management concept in general is understood as the management of services, products and raw materials along the chain – from suppliers to manufacturer and/ service provider to final consumer and back again in the cycle – with improvements to the environmental and social goals. The interaction between suppliers and consumers is understood by this work as the flows of energy, materials, and greenhouse gases emissions from suppliers to consumers.

This study assumes that if forest-based biomass is to compete with fossil fuels, there is a need to create more reliable and constant supplies of bioenergy on a long-term basis and a more efficient distribution to points of consumption in more sustainable ways.

1.2. Methodological approach

The paper's originality is the use a bioenergy supply chain management approach instead of the commonly used *"Command & Control"* mechanisms (i.e., legal standards, taxation and/or subsidies) in order to reinforce sustainable development in a likely scenario of competition between bioenergy transformation (e.g., heat and electricity) and the production of other goods extracted from forest-based biomass.

In order to complete this work, the methodological approach was based on a content analysis conducted by a literature review and information was gathered from relevant publication found on hard copy publications and electronic journals provided by well-known publishers (e.g., Willey and Elsevier).

1.3. Work Structure

This paper is divided into 4 main sections. First section has introduced the sustainable supply chain management concept used in the paper and background information about the management challenge and the methodology used in the study. Second section presents the findings related to biomass as an important renewable source and the significance of adding

value along its production chains. The third section discusses the need to understand the re-distribution of available resources in an increasing competitive environment. Finally, the forth section indicates an option to shift from the perspective of bioenergy as a threat to the perception of opportunity in the forest-based supply chain.

2. Forest-based biomass: now and beyond

The EU RES Directive aims to promote the use of energy from renewable sources. Each Member State has to achieve a specific target so that, as a whole, the EU shall have 20% of the total energy based on renewables by the year 2020. The Directive sets a common vision for the EU. It also contains a roadmap to cut down 20% of the EU greenhouse gases emissions [9]. The Directive sets an important framework alongside with the European Strategic Energy Technology Plan (SET-Plan) for reducing the EU's oil dependence, which is also illustrated by the target set for the transport sector: 10 % biofuels by 2020. Although the EU is expected to fall short on the 2010 target of 5.75% biofuels, it is expected to reach beyond the 2020 target.

In this context, renewable energy is assuming an increased prominence among Member States, mostly motivated by security of supply as well as greenhouse gases emissions reduction objectives. Among the Member Countries, Sweden is often regarded as one of the frontrunners concerning the development, promotion and implementation of renewable energy policy and technology. The Swedish mandatory target for the share of energy from renewable source in gross final consumption of energy in 2020 is 49%. On the other hand, the proportion that is forecasted by the Swedish Energy Agency (SEA) sums up to 50.2% in the same period. This means that Sweden shall reach beyond the binding national target by 1.2% and this trend can be traced in the considerable expansion of renewable energy of the last years [10].

In 2008, the Swedish share of renewables was 44.1%. This corresponds to an excess of approximately 2.5% already above the indicated trajectory for 2011-2012 period [11]. A very important part of this success lies on the national expansion of the bioenergy sector during the last few decades [12].

The RES Directive is not the only driving force affecting bioenergy utilization. Ling and Silveira (2005) consider that current policies being applied in the EU enhance the condition but there are also other important forces such as internationalization of the bioenergy segment, integration of bioenergy systems with other transformation processes, and the fact that bioenergy is becoming a mainstream alternative. In line with this perception, a biomass study carried out by McKinsey and Pöyry for the Confederation of European Paper Industries (CEPI) indicates that meeting bioenergy targets set by the RES Directive could lead to a wood deficit of 200 up to 260 million m^3 in Europe by 2020. This has worried, for example, the pulp & paper sector which is afraid of potential competition in the markets for raw materials [13].

Bioenergy contribution has grown from the second largest source of energy in 2003 to the leading position in the final energy use in Sweden. In the last couple of years, the bioenergy share has increased from 28.6% in 2007 to 31.7% in 2009 and it is still growing. As a result, biomass is not just an alternative but has turned into a major reliable energy source [11].

An important aspect of the bioenergy segment in Sweden is the fact that most of the biomass used for heat and electricity generation in the country comes from forests. Despite of its importance in the transition to a long-term sustainable energy system, the strategic use of

bioenergy supply chain management and its overall impacts in the forestry sector are still very much restricted to cost effectiveness and excellence in customer service in pursuit of profit and competitive advantage [14] [15] [16] [7]. As a result, the majority of the current models for analyzing it do not consider the overall value of a supply chain [17]. They frequently focus on improving the individual performance of the various actors along the chain (e.g., company level approach). This is because there are a variety of flow structures and each one of them has a direct impact in the supply chain organization, which makes difficult to foster overall performance. Figure 1 presents a variety of flows based on the work of Haartveit *et al.* (2004) and their specific characteristics that directly define supply chain structure configuration and its complexety [18].

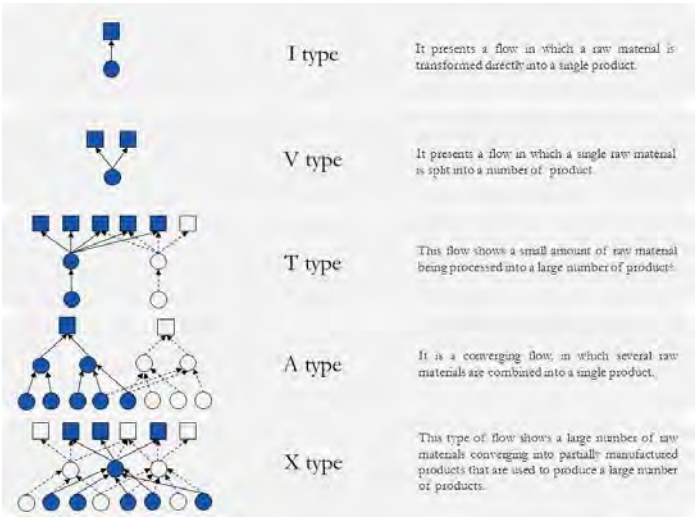

Fig. 1. Types of flows structures within a supply chain adapted from Haartveit et.al.(2004)

Independent from its configuration, the supply chain concept intuitively implies a network of actors divided into a variety of organizational structures operating at different stages/structures/levels and combining efforts in order to deliver products to customers. This means that management and control of flows involve collaboration among actors and, as any complex system structure, the supply chain might need several strategies and information flows operating at different structure levels. At an overarching level, this includes general information such as inventories, statistics, policy targets, etc. This information could be in the public domain while specific information (e.g., detailed information about a region) may require further investigation. At the company level, there are strategies related to the business model, market competition, planned production, price mechanisms, etc. These strategies are not in the public domain but reflect the response of various actors to opportunities in the market [17] [18]. As a result, an effective strategy for supply chain management depends on the specific characteristics and complexity of the chain under study.

It is clear that a renewable energy source can play a major role in addressing environmental degradation at large. This is because a renewable source such as biomass, if used in a sustainable way, is not depletable and produces less greenhouse gases emissions than fossil fuels. However, an important finding was that supply management improvements could add value along various production chains to reinforce, optimize, and operate the whole network and achieve a sustainable development.

3. From threat to opportunity: a discussion

Among the renewable energy resources, wood is one of the most important renewable sources for achieving the 2020's target in the EU. Today in Europe, wood already represents over 50% of the total renewables [19]. In addition, wood is expected to continue playing a key role in the development of renewables in the continent. However, increasing extraction of forest biomass for energy purposes could have impacts on other segments of the forestry sector as a whole. The current perception among some market actors is that meeting bioenergy targets set by EU will only be possible by increasing the biomass extraction from forest [20].

In the short term, strategies endorsing *status quo* practices could lead to enlarged extraction of forest resources. Although this could result in immediate direct positive benefits in the local economy (e.g., work generation and income), it could also lead to loss of biodiversity as well as environmental impacts on soil and water that can compromise the total resource productivity in the long run.

In the middle run, competition between bioenergy use and the production of other goods extracted from wood may induce to an increase in raw material and energy prices and reduce the competitiveness of the European pulp & paper industry compared to other regions of the world (e.g., South America, especially Chile and Brazil).

In the long term, intensified competition among different segments of the forest-based industry could lead to the closing down of industrial plants following on production relocations. This implies lay-offs, initially to rescue companies' productivity levels, but eventually to deal with competitiveness at an international scale.

By being a traditional and well-established sector from the start, the forestry sector – especially the pulp & paper companies – perceives bioenergy targets more as a threat than an opportunity. In this perspective, the RES Directive and, especially, forest-based bioenergy becomes *the big bad wolf in the forest*. If perceived negatively, there is risk that administrative barriers more than financial and technical obstacles may hold back or – at the least – delay further bioenergy development, above all in the pulp & paper segment.

Considering that a *"sustainable energy solution needs to be motivated beyond their technical performance and economic efficiency, and become attractive in the context of regional development, environmental and social benefits"* [21]. It is necessary to understand the re-distribution of available resources and the process along the bioenergy value chain network in order to tackle the potential obstacles (i.e., administrative barriers in the pulp & paper sector).

New actors and new configurations of value chains can be perceived as a threat by conservative segments because they can – in a very short time – increase the demand of raw materials, increase competition in an already aggressive environment, change land use, and create an uneven biomass supply. However, this is also an opportunity for creating new alliances, facilitating transitions, and opening new markets. In order to shift from the perspective of threat to the perception of opportunity, it is necessary to understand the process along the bioenergy value chain network and re-distribution of available resources. This is because a performance frontier of any given supply chain should be understood as a system performance due to its complexity and interconnected nature (see Figure 2). In doing so, the real competitive position or the performance frontier of a supply chain becomes based on the supply chain's weakest link [17].

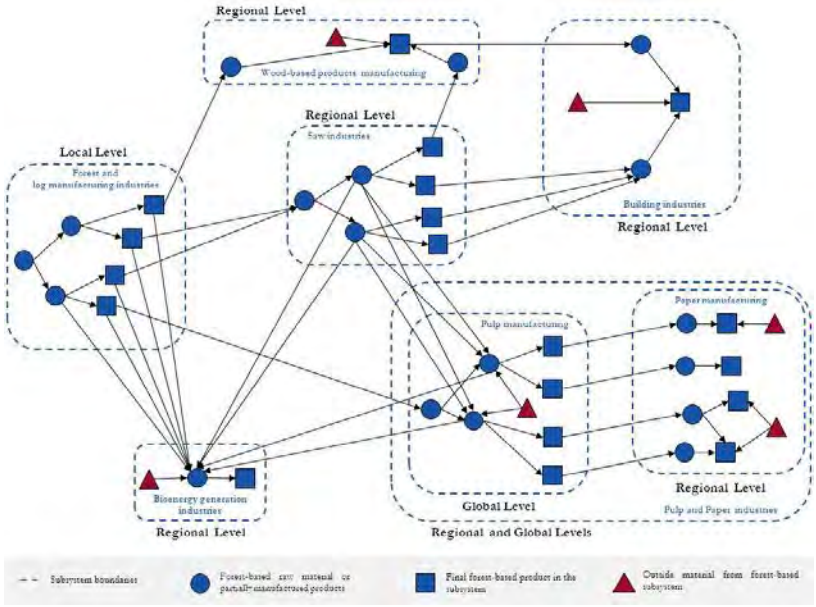

Fig. 2. Generalized structure of the forestry industry supply chain

As the Figure 2 has presented, the forestry industry supply chains are complex and characterized by multitude of flows resulting in many products and services, as well as by-products along the chain. In addition, Haartveit *et al.* (2004) describes that the roles of individual actors in the supply chain are highly dependent on the supply chain own structure and specific characteristics. This is because material and information flows, as well as the product flow can vary in levels (i.e., from local to regional and/or global levels) and structure.

The initial question is bioenergy is the big bad wolf in the forestry sector or an opportunity for expansion, given the uncertainty of future costs of oil. In any case – threat or opportunity – , it is clear that a systemic approach in such complex network makes the strategic configuration of the bioenergy supply chain a critical task for management decisions and a major administrative challenge [16] [7] (22].

4. Conclusion remarks: a way of getting through

The rapid expansion in global trade of biomass (i.e., wood pulp) is expected to continue over the next years. On the other hand, a likely new international biomass commodity (i.e., wood chips and pellets) could also rise as direct result of more countries favoring renewable energy and relatively inexpensive local supplies of biomass reaching their limits. In this respect, the new competition may well rearrange the forestry industry supply chain structure presented in Figure 2 by redefining the boundaries' levels.

In short, the devil is in the details. This is because forthcoming competitions will strength the need for actions. At the same time, external triggers (i.e., environmental and social standards) placed by governmental agencies, stakeholders and consumers are going to continue playing a major role. By doing so, a sustainable bioenergy system has to become focused more in a systemic approach process and less in single individuals' efficiency, which is currently in place. In other words, a systemic approach means that bioenergy systems' optimization must aim at the overall supply chain by asking for performance improvement beyond the boundaries of the single company in order to improve the sustainability aspects of the entire network. An increased system understanding will allow not only a better estimation of the potential effects of the RES Directive on existing supply chains but also an evaluation of the improvements that are necessary while planning future bioenergy supply chains. Moreover, it

would assist us in identifying challenges in the bioenergy sector and leverage points in its system that could be used to foster climate change mitigation and energy security.

This study is the starting point of the author's doctoral research and for that reason has its limitations which open opportunities for future research. Like all content analysis the empirical validity of the bioenergy as an opportunity to the forestry industry needs to be tested in case studies. Future studies should examine not only operations, logistics, structures and other activities but also the flows of material, energy and greenhouse gases emissions to comprehend if there are other important aspects to be considered by a sustainable supply chain management for bioenergy systems.

Acknowledgement

I wish to thank my supervisor *Professor Semida Silveira* for truly understanding and supporting me during this moment in my life as a new member of Energy and Climate Studies Division at KTH. Many thanks go also to my former supervisor in Brazil *Professor Emília Wanda Rutkowski* for guidance and the *Erasmus Mundus External Cooperation Window EU-Brazil StartUP Programme* for the financial aid.

Reference

[1] Fondation Euractiv. EU Renewable Energy Policy. EurActive.com. [Online] 2010. [Cited: 10 18, 2010.] http://www.euractiv.com/en/energy/eu-renewable-energy-policy/article-117536.

[2] International Energy Agency. World Energy Outlook 2010. s.l. : OECD/IEA, 2010a. ISBN 978-92-64-08624-1.

[3] —. 2010 Key world energy statistics. Paris : OECD/IEA, 2010b.

[4] Lambert, D. M., Cooper, M. C. and Pagh, J. D. Supply chain Management: implementation issues and research opportunities. The International Journal of Logistics Management. 1998, Vol. 9, 2.

[5] Mentzer, J. T., et al. Defining Supply Chain Management. Journal of Business Logistics. 2001, Vol. 22, 2.

[6] Council of Supply Chain Management. Supply Chain Management Definition. [Online] [Cited: January 8, 2011.] http://cscmp.org/aboutcscmp/definitions.asp.

[7] Svensson, G. Aspects of sustainable supply chain management (SSCM): conceptual framework and empirical example. Supply Chain Management: An International Journal. 2007, Vol. 12, 4, pp. 262-266.

[8] Carter, C. R. and Rogers, D. S. A framework of sustainable supply chain management: moving toward new theory. International Journal of Physical Distribution & Logistics Management. 2008, Vol. 38, 5.

[9] European Union. Directive 2009/28/EC. Promotion of the use of energy from renewable sources and amending and subsequebtly repealing Directives 2001/77/EC and 2003/30/EC. Brussel : Official Journal of the European Union, 2009. Vol. L 140/16 EN, 5.6.2009.

[10] Swedish Energy Agency. Special forecast document for Sweden under Article 4(3) of Directive 2009/28/EC. Stockholm, Sweden : Swedis Energy Agency, 2009a. Interim report on Swedish Energy Agency mandate 13 under the 2009 letter of regulation on the basis for the Swedish national renewable energy action plan.

[11] —. Energiläget i siffror 2009/Energy in Sweden Facts and figures. Energimyndigheten. [Online] 2009b. [Cited: October 20, 2010.] http://213.115.22.116/System/TemplateView.aspx?p=Energimyndigheten&view=default&cat=/Broschyrer&id=d65d018c86434ed2ae31baeba2456872.

[12] Ling, E & Silveira, S. New challenges for bioenergy in Sweden. [ed.] S. Silveira. Bioenergy: realizing the potential. Stockholm, Sweden : Swedish Energy Agency & Elsevier B.V., 2005, pp. 31-57.

[13] Galembert, B. Bio-energy and wood mobilization. Proceedings from a Seminar during the European Paper Week 2007. Brussels : EUBIONET - European Bioenergy Networks, November 28, 2007.

[14] Christopher, M. Logistics and supply chain management: strategies for reducing cost and improving service. 2nd. London : Pitman Publishing, 1998. DOI: 10.1080/13675569908901575.

[15] Bowersox, D.J. & Closs, D.J. Logistical Management: the Integrated Supply Chain Process. 3rd. New York : McGraw-Hill Companies, 1986. ISBN: 0070068836.

[16] Srivastava, S.K. Green supply-chain management: a state-of-the-art literature review. International Journal of Management Reviews. 2007, Vol. 9, 1, pp. 53-80.

[17] Seuring, S. The product-relationship-matrix as framework for strategic supply chain design based on operations theory. International Journal of Production Economics. July 2009, Vol. 120, 1, pp. 221-232.

[18] Haartveit, E.Y., Kozak, R.A. & Maness, T.C. Supply Chain Management Mapping for the Forest Products Industry: Three Cases from Western Canada. Journal of Forest Products Business Research. 2004, Vol. 1.

[19] Bosch, J., et al. Panorama of energy: energy statistics to support EU policies and solutions. [ed.] J. Bosch & R. Mertens. Eurostat Statistical Books. Luxembourg : Eurostats, European Communities, Office for Official Publications of the European Communities, 2007, pp. 1-178.

[20] Werhahn-mees, W., et al. Sustainability impact assessment of increasing resource use intensity in forest bioenergy production chains. Global Change Biology: Bioenergy. 2010, Vol. 2, 4.

[21] Silveira, S., [ed.]. Bioenergy - Realizing The Potential. 1st. Oxford : Elsevier Ltd, 2005. ISBN: 0-080-44661-2.

[22] Lee, H., Padmanabhan, V. and Whang, S. The bullwhip effect in supply chains. MIT Sloan Managment Review. 1997, Vol. 38, 3, pp. 93-112.

Bioenergy production in the Toruń biogas plant (Poland)

Bartłomiej Igliński[1*], Jerzy Sobólski[2]

[1] *Nicolaus Copernicus University, Toruń, Poland*
[2] *Biogaz Inwestor Co., Toruń, Poland*
** Corresponding author. Tel: +48 0566114331, Fax: +48 0566542477, E-mail: iglinski@chem.umk.pl*

Abstract: This paper describes the work of the biogas plant in Toruń (Poland). Biogas has been obtained from municipal waste since 1998 at the Municipal Waste Landfill Site in Toruń. Biodegradable waste constitutes about 45-50% of the waste dumped into the site. These municipal wastes have been disposed of at this site since 1964. Biogas is obtained during approximately 8000 hours per year from 62 wells. The highest methane contents in biogas (>60%) were achieved between 2000-2003 and in 2008. As a result of biogas combustion, thermal and electrical energy is produced. The total quantity of energy produced during a year is 11 000 MWh, but higher amounts were achieved in 2004 and 2008 (nearly 12 500 MWh). The heat and electrical energy obtained is supplied to the city inhabitants by the Power Station Toruń S.A. and the Thermal Energy Station Toruń Co. Ltd.

Keywords: *bioenergy, biogas, Toruń, municipal wastes*

1. Introduction

Biogas is one of the most important renewable energy sources [1,2]. Known also as a waste site gas, biogas is heavier than air. Regardless of the substrate, it has two major components – methane and carbon dioxide. Biogas is obtained from waste biomass [3,4]. This covers a wide and difficult to manage range, starting from forest and farming wastes (including fermented liquid manure) through sewage sludge to municipal wastes [5,6].

The Municipal Waste Landfill Site in Toruń (Fig. 1) is designated, mostly, for municipal wastes. The site is located in the northern part of the city, in the industrial district, 10 km away from the city centre. The location complies with the local spatial management plan -in the area designated for the municipal waste disposal complex. The site is located on a plain with little altitude differences, with ground declination toward the south and the current Vistula Valley, located 3.5 km away.

Fig.1. Location of biogas installation.

The wastes have been disposed of at the site since 1964. Originally solid and liquid wastes were dumped without any formal or legal agreement in an unregulated manner. Since its

modernisation in 1993, the waste landfill site has been functioning as a legally sanctioned waste site for the city of Toruń.
The total area of the site is 12.1 ha, including:

- two landfill sections of total area of 8.5 ha, exploitation time 1964/86 and 1992/95 – there are no safeguards against leaches to underground waters; these are the areas the waste site gas-biogas is obtained from,
- post-discharge terrace of total area of 1.7 ha; until 1991 in this area there used to function two partially proofed landfill sections for industrial post-discharge sludge,
- landfill section of area of 1.9 ha, used since 1995, so called "basin" – proofed with geo-membrane HDPE 1.5 mm with a built-up sewage drainage system.

On December 31st 2009 the waste site was closed. It is estimated that biogas from the dumped waste will be exploited for the next 15-20 years. In the near future a further biogas installation is to open at a new, nearby waste site.

1.1. The type and amount of waste dumped at the site

The landfill waste site in Toruń is a target place for municipal waste disposal as well as the disposal of industrial waste, qualified to be disposed there, as a result of the decisions of the competent administration authorities. At the site there are no wastes considered to be dangerous substances according to environmental protection regulations. Table 1 shows the composition of wastes. The major components of municipal waste are organic wastes, which are subject to the natural process of biodegradation. In Toruń biogas is obtained from non-segregated waste, which is a result of the lack of pro-ecological management in the 1970s in Poland. The biodegradable wastes constitute about 45-50% of the stream of municipal wastes. The amount of dumped waste is estimated at 2 500 000 Mg.

Table 1. The composition of municipal waste of the city of Toruń (%).

Fraction	Year		
	1991	2000	2009
Plant food waste	25.2	14.8	14.4
Animal food waste	4.3	1.0	0.0
Other organic waste	3.4	8.8	14.2
Paper and cardboard	13.4	18.7	12.3
Plastics	5.1	19.9	11.2
Textile waste	4.4	3.5	2.5
Glass	6.9	12.0	7.6
Metals	3.4	2.8	5.4
Other mineral waste	6.9	4.7	3.4
Fraction < 10 mm	27.0	13.8	29.0

2. The system for obtaining biogas in the Toruń biogas plant

In 1991-1992, within the framework of the programme to improve the natural environment, research was conducted in Poland to examine 15 municipal waste landfill sites in order to check the amount and quality of biogas. At the waste site in Toruń, 6 gas wells were built that ran 16 m deep into the bowl of the site. After 800 hours of work, the mean parameters of obtained biogas were satisfactory (61.1% CH_4, 28.8 CO_2, 0.1% O_2). The initial analysis, as well as the further research, confirmed that the biogas produced at the municipal waste landfill site in Toruń is adequate for commercial use.

In 1993 a request was made for financial support from the Thermie programme in order to build a pioneering installation for obtaining and utilising waste site gas in Toruń. With the support of the European Union Commission, a contract was signed to realise this project and to finance it at 30% of net costs. In order to build and operate a modern waste site gas utilisation unit, a new company was established – Biogas Investor Co. Ltd. The investment was partially financed by the National and Voivodship Environmental Protection Fund as well as by 30% subvention from the European Union, allocated as a part of the Thermie programme.

The gas from waste landfill piles started being used on 10 September 1997. On 10 September 1999 additional works were finished and a use permit was obtained. In 2001 the maximum technical and production parameters were achieved. The gas production covered 11 ha of the waste site near Kociewska Street in Toruń. In this area 40 gas wells were drilled (Fig. 2), which are boreholes 16 m deep and suction pipes were laid. The system is equipped with a technical biogas suction apparatus (MPR), gas mains, thermal-electric mains (CHP) of power 550 kW_e and 770 kW_t. The thermal-electric power station is connected to the heating and power network. The whole system is totally automatic and computer directed. In April 2002 a further 3 ha of the waste landfill site were covered by degassing equipment as 12 new biogas wells were built and utilised as a part of the system.

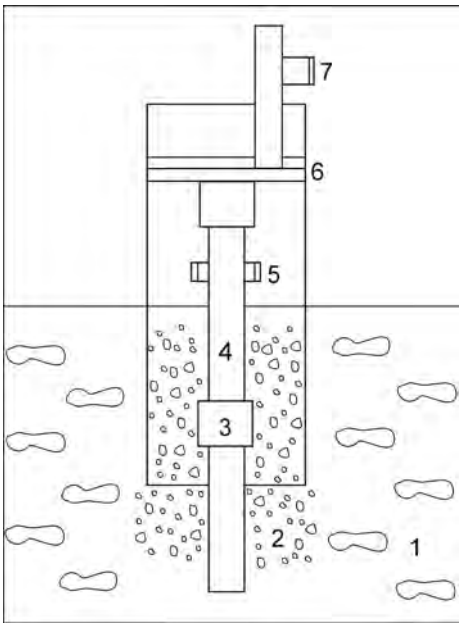

Fig. 2. Construction of wells: 1 – waste, 2 – gravel, 3 – plug-in muff, 4 – degassing pipe, 5 – gas intake, 6 – gas proof cover, 7 – pipe line.

In January 2004 the second power-producing unit of power 324 kW_e was opened, which marked the end of the first stage of development of the system for obtaining and utilisation of waste site gas. During this stage, 12 wells, 2 788 m of gas pipes, a transformer station, wire line NN were built and a power-generating system was bought. Since 1 March 2004 the biogas system has been working at the power of 698 kW_e and 770 kW_t – utilising 440 Nm^3/h of waste site gas obtained from municipal waste piles of 16 m height and 14 ha base.
In 2007 and 2009 respectively 17 and 5 new wells were built. In 2009 12 wells of low efficiency were closed. Currently, biogas is obtained from 62 wells.

3. Biogas production in the Toruń biogas plant

The biogas obtained from the degassing wells is transported via gas pipes to an MPR module, where suction and pumping equipment, a gas composition analyser and flow meters showing the flow in particular gas wells**.** Transported from an MPR module by a common pipe, gas from individual wells is then sent to the decanter, where water contained in the biogas is outdropped. After drying, depending on the requirements, biogas is directed to the module generating electrical power and heat or to the power generating system operating since 2004.
The composition of gas taken from each well is constantly monitored using the stationary analyser SATGAS 800 (S.A. TechnikAS, Denmark). The content of CH_4, CO_2 and O_2 is analysed, the remaining part is assumed to be N_2. The collection of biogas is fully controlled: in situations where the methane concentration decreases below 40% or oxygen concentration increases above 0.3%, the well is closed.

Fig. 3 represents the amount of biogas obtained between 1998 and 2009. The least amount of biogas was obtained at the first start-up (1998), and in 2002 when maintenance work was carried out. Since 2003 when 12 new wells were opened, the amount of obtained biogas has risen by 50%. The highest methane content in biogas (>60%) was achieved in 2000-2003. Since 2004 a decrease in methane content has been observed, which is contributed to the ageing of resources from which biogas is obtained. This phenomenon is partially caused by the common use of virtually non-degradable foil bags for rubbish collection in Poland. Having arrived at the site, these bags create a specific geo-membrane, making it difficult for nutrients and water to penetrate into deeper parts of the waste site. Water content is essential to the development of microorganisms. When the content of dry matter is higher than 40%, the life processes of microorganisms are disturbed, which leads to a lower methane content of the biogas and smaller quantities of biogas produced. One of the solutions aimed at avoiding the geo-membrane issues created by the waste foil is to use a mill to crush waste prior to dumping it onto the waste site. When the methane content drops below 40%, it is planned to use natural gas to aid the biogas stream fed into the engine. This will make the combusted gas more calorific and extend the working lifetime of the biogas site. It will also mean that the power of installed equipment is fully used. Opening new wells as well as closing the inefficient ones leads to increased methane content in biogas.

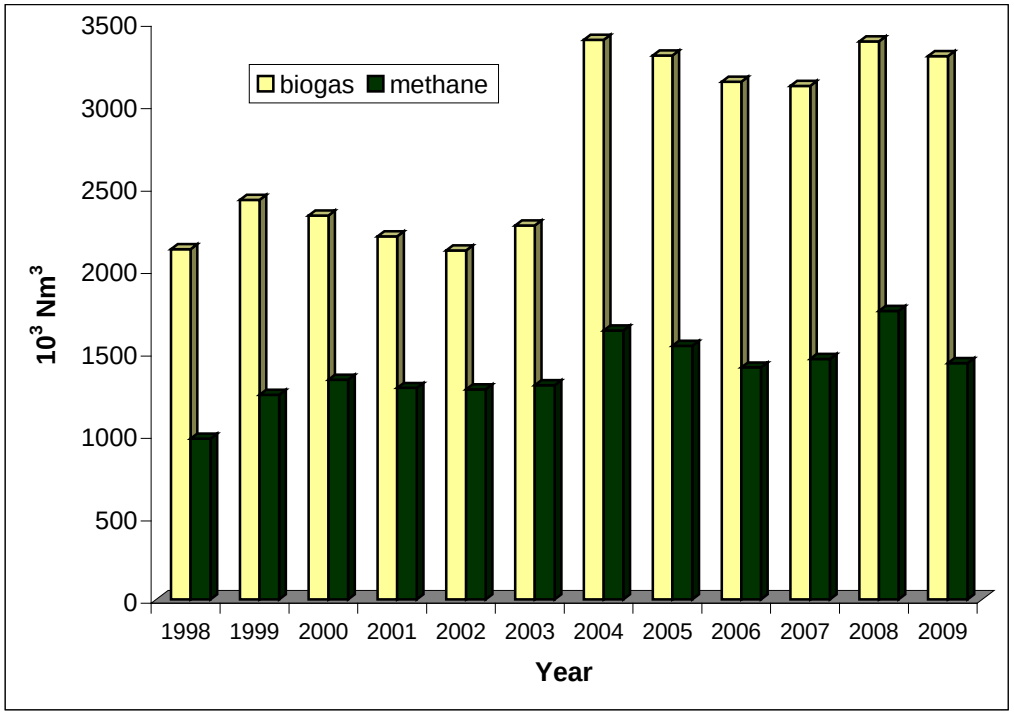

Fig. 3. The amount of biogas and methane obtained in 1998-2009.

Biogas is obtained during 8 000 hours annually. The highest mean electric power generated was achieved during the last six years, which was influenced by the new wells and the second power-generating system being opened. Apart from the first year of start-up (1998), the mean thermal power has remained at the same level. The amount of heat produced was 25% higher than the amount of electrical power over the years 1998-2007. Since 2008 the amounts of heat produced and electric power have been at a similar level (6000 MWh).
The total amount of energy produced over a year stays at the level of 11 000 MWh (Fig. 4), but the highest amounts were achieved in 2004 and 2008 (nearly 12 500 MWh). The obtained heat and electric energy is supplied to the city inhabitants by the Power Station Toruń S.A. and the Thermal Energy Station Toruń Co. Ltd.

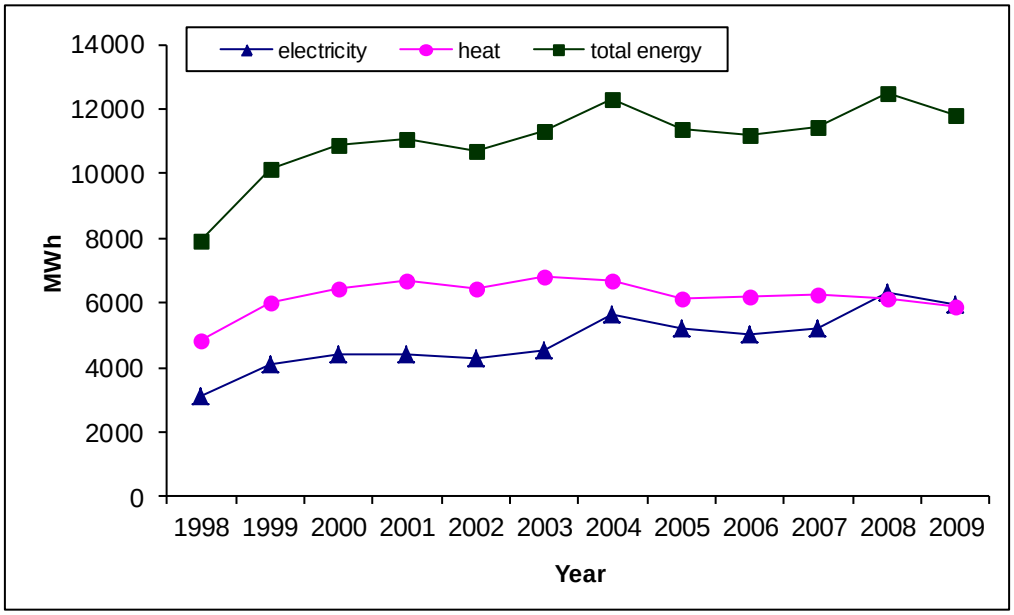

Fig. 4. Electricity and heat prduction in 1998-2009.

4. Perspectives of biogas production in biogas plant in Toruń

During most of the operation time of Toruń landfill installation there was no record of waste deposited there. Apart from the municipal waste, the industrial (hazardous) waste was also deposited, including bricks, tires and chemical waste. Thus, it is only possible to estimate the amount of biogas and methane content in landfil gas using the results obtained so far. Currently, the next twenty wells are to be built at the landfill site in 2011, which is going to increase the amount and quality of biogas in comparison to the previous years (Fig. 3). Within the following years (after 2011) the quality of biogas as well as methane content in LFG will continue to deplete and biogas parameters will be gradually decreasing. In the near future a new biogas installation will operate at a new municipal landfill site in Toruń.

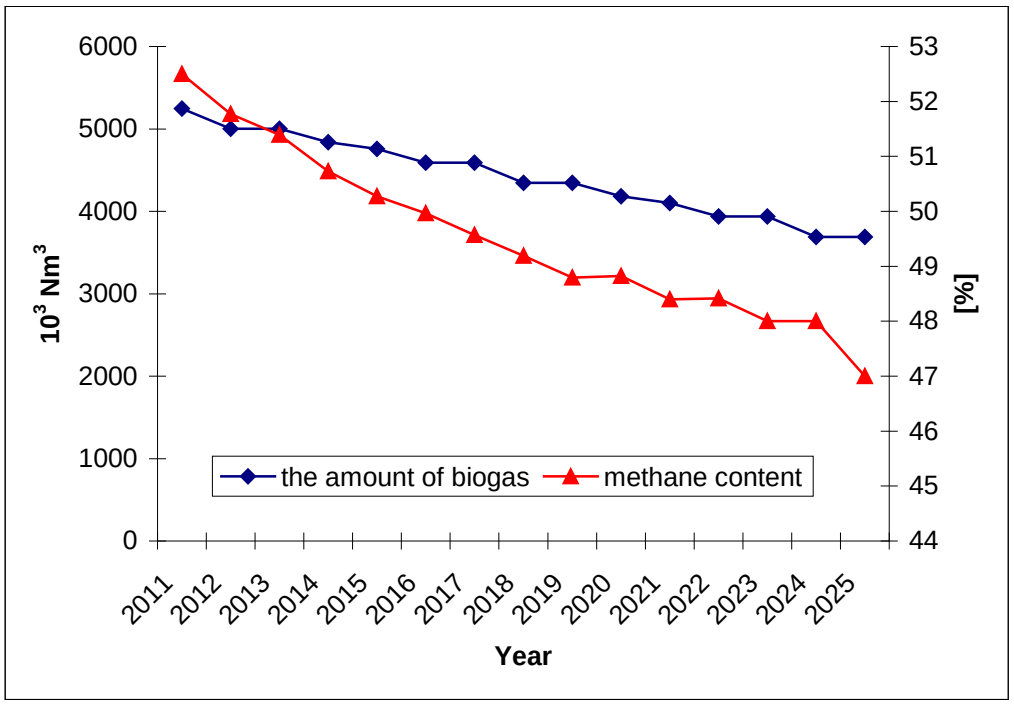

Fig. 5. Estimated amount of biogas and methane content.

5. Ecological effect of biogas production

The biogas installation in Toruń ensures the utilisation of biogas created at the municipal waste landfill site. The major component of biogas – methane – is a highly flammable and explosive gas. A fire at the waste site could be very difficult to control and could last over months, emitting during this time considerable amounts of CO_2, CO, dioxins, furans and soot. Methane is one of the gases with a strong impact on the green house effect. Research has shown [9] that methane emission from waste landfill sites causes the green house effect 25 times higher than that caused by carbon dioxide [10].

Between 1998-2009, 33095283 m^3 of biogas was utilised, including 16626081 m^3 of methane, which corresponds to 75 213 Mg of lignite ("brown coal") or 30815 Mg of hard coal. Combustion of such an amount of coal would lead to the emission of CO_2, CO, SO_2, NO_x and of dusts. Obtained biogas is burnt at the location where it is produced (Toruń), whereas hard coal needs to be transported from the mines (Upper Silesia – 300-400 km), which also involves the emission of harmful gases and increases the cost of its production [11,12].
In the near future it is planned for all the public transport vehicles and the Municipal Waste Management Services vehicles to be fuelled by natural gas with the addition of treated biogas.

The Gas Fuels Station in Toruń was opened in 2008 for this purpose and the first buses are now testing the gas fuel [2,13].

6. Conclusions

Toruń waste site gas recovery and utilisation installation, combines the production of electrical and thermal energy, it is the first one in this part of Europe to be equipped with such modern technology. It eliminates the negative impact of waste site gas emission, which would enhance the greenhouse effect and contribute to ozone layer destruction. Additionally it also produces green thermal and electrical power, which improves the environment of historic Toruń, the Old Town of which is on the UNESCO heritage list [13].
Summing up the possibilities offered by alternative energy sources, it must be stressed that their use seems essential to the country that wants to lead a policy of balanced development. Before we ask how many new coal power plants to build and whether nuclear energy should be developed, we should try to answer the alternative questions – what resources there are in rationalization and how much energy can be provided by renewable, environmentally friendly energy sources.

References

[1] P. Weiland, Biogas production: current state and perspectives, Applied Microbiology and Biotechnology 85, 2010, pp. 849-860.

[2] B. Igliński, R. Buczkowski, M. Cichosz, Bioenergy technologies, Nicolaus Copernicus University Publishing, 2009, pp. 255-298.

[3] J.D. Murphy, E. McKeogh, G. Kiely, Technical/economic/environmental analysis of biogas utilisation, Applied Energy 77, 2004, pp. 407-427.

[4] J.D. Murphy, E. McKeogh, Technical, economic and environmental analysis of energy production from municipal solid waste, Renewable Energy 29, 2004, 1043-1057.

[5] R. Buczkowski, A. Iglińska, B. Igliński, The possibilities of obtaining biomass for biogas production in the region of Toruń, Chemistry for Agriculture 7, 2006, pp. 865-869.

[6] R. Kothari, V.V. Tyagi, A. Pathak, Waste-to-energy: A way from renewable energy sources to sustainable development, Renwable and Sustainable Energy Reviews 14, 2010, pp. 3164-3170.

[7] U. Desideri, F. Di Maria, D. Leonardi, S. Proietti, Sanitary landfill energetic potential analysis: a real case study, Energy Conversation and Management 44, 2003, pp. 1969-1981.

[8] R. Arthur, M.F. Baidoo, E. Antwi, Biogas as a potential renewable energy source: A Ghanaian case study, Renewable Energy 36, 2011, pp. 1510-1516.

[9] Website: http://www.ipcc.ch/pdf/assessment-report/ar4/wg1/ar4-wg1-chapter2.pdf

[10] C. Cornejo, A.C. Wilkie, Greenhouse gas emission and biogas potential from livestock on Ecuador, Energy for Sustainable Development 14, 2010, pp. 256-266.

[11] L.J. Nilsson, M. Pisarek, J. Buriak, A. Oniszk-Popławska, P. Bućko, K. Ericsson, Ł. Jaworski, Energy policy and the role of bioenergy in Poland, Energy Policy 34, 2006, pp. 2263-2278.

[12] J. Paska, M. Salek, T. Surma, Current status and prospectives of renewable energy sources in Poland, Renewable and Sustainable Energy Reviews 13, 2009, pp. 142-154.

[13] B. Igliński, W. Kujawski, R. Buczkowski, M. Cichosz, Renewable energy in Kujawsko-Pomorskie Voivodeship(Poland), Renewable and Sustainable Energy Reviews 14, 2010, pp. 1336-1341.

Influence of different cell disruption techniques on mono digestion of algal biomass

Sebastian Schwede[1,*], Alexandra Kowalczyk[1], Mandy Gerber[1], Roland Span[1]

[1] *Ruhr-Universität Bochum, Thermodynamics, Bochum, Germany*
** Corresponding author. Tel: +49 234 32 26390, Fax: +49 234 32 14163, E-mail:s.schwede@thermo.rub.de*

Abstract: Due to high growth rates microalgae provide an enormous potential as a source for biomass besides conventional energy crops. The algal biomass can be used for bioenergy production. Anaerobic digestion to biogas is one of the most energy-efficient and environmentally beneficial technologies for alternative energy carrier production. The resistance of the algal cell wall is generally a limiting factor for cell digestibility. In the present work different cell disruption techniques (microwave heating; heating for 8 hours at 100°C; freezing over night at -15°C; French press; ultrasonic) on algal biomass of *Nannochloropis salina* were carried out. The disrupted material was digested to biogas in batch experiments according to VDI 4630. The results indicate that hydrolysis of algal cells is the rate-limiting step in anaerobic digestion of algal biomass. Cell disruption by heating, microwave and French press show a considerable increase in specific biogas production and degradation rate. Compared to the untreated sample the specific biogas production was increased for the heating approach by 58 %, for the microwave by 40 % and for the French press by 33 %.

Keywords: *Anaerobic digestion, Microalgae, Cell disruption, Specific biogas production, Pretreatment*

1. Introduction

Microalgae are microscopic algae and cyanobacteria, which use sunlight and atmospheric carbon dioxide for growth by photosynthesis. The common doubling time is 3.5 to 24 hours in the exponential growth phase [1]. Compared to terrestrial plants with biomass production rates of 20 to 25 tons per ha and year, production rates of more than 100 tons per ha and year have been obtained for microalgae in photobioreactors or in high-rate raceway ponds [2]. Besides the reduction of carbon dioxide emission by using algae as source for biofuels, the production of algal biomass is not competing with conventional agriculture for resources [3], [4].

Anaerobic digestion of biomass to produce biogas is, concerning the multiple utilization, a promising technology for bioenergy production [5]. The fermentation process of organic matter is divided into four steps conducted by different consortia of microorganisms and leads to a gas, which mostly consists of methane and carbon dioxide. The rate of organic degradation depends on the particle size and the access of the microorganisms to the particular components of the substrate at hydrolysis step. For substrates with high amounts of complex biopolymers like lipids, cellulose and proteins the hydrolysis is the rate-limiting step. For easily biodegradable material like dissolved carbohydrates (e.g. glucose) methanogenesis and acetogenesis are rate-limiting due to lower growth rates of the involved bacteria. Algal biomass contains high amounts of lipids and proteins and the resistance of the cell wall is one of the limiting factors for cell digestibility [6]. Many green microalgae possess a thin trilaminar outer wall (TLS) with a very high resistance to chemical and enzymatic degradation based on the incorporation of insoluble, non-hydrolysable aliphatic biomacromolecules called algeanans [7, 8]. For *Nannochloropsis salina* (*N.salina*), a unicellular marine eustigmato-phyceae, 1-2% of dry matter was detected as algeanans [8].

Aim of the current work was to show one of the two bottlenecks of *N.salina* biomass as mono-substrate in anaerobic digestion processes: the resistance of algal cell walls to

enzymatic hydrolysis beside the unbalanced chemical composition due to low C/N-ratio. Batch experiments of physically disrupted cell material were carried out in comparison to untreated algal cells.

2. Methodology

2.1. Substrate

As substrate for the batch tests algal biomass from *N.salina* was used. Algal biomass was taken from Phytolutions Ltd., Bremen. Algal sludge was harvested by centrifugation to dry matter content of 35 wt%. For disruption the algal biomass was suspended in tap water. The content of total solids (TS) and volatile solids (VS) before and after digestion was determined according to DIN 12879 and DIN 12880 [9, 10].

2.2. Cell disruption

Cell disruption of algal biomass was performed by different physical methods. Experimental conditions were optimized according to different sources (e.g. protein purification, lipid extraction), since less data for pretreatment of algae in biogas fermentation is available [11-14]. The influence of temperature was examined by freezing over night at -15°C, heating for 8 hours at 100°C in a compartment dryer (Function line, Heraeus) and by microwave heating (five times until boiling at 600 W and 2450 MHz; Inverter Grill, Panasonic). For ultrasonic treatment the cell suspension was disrupted three times for 45 seconds at 200 W with 30 kHz output (Sonifier 250, Branson). Influence of high pressure homogenization was examined by French press (French pressure cell press, TermoSpectronic). Two runs at 10 MPa were conducted for each sample.

To validate the disruption success the absorption of centrifuged samples (3 min at 13400 rpm; dilution 1/10) were photometrically measured. The three aromatic amino acids phenylalanine, tyrosine and thyptophan show maximal absorption at 280 nm. These values correlate with the amount of released protein.

2.3. Anaerobic digestion experiments

Anaerobic digestion of *N. salina* was carried out as batch tests according to VDI 4630 [15]. Digestate from a biogas plant (input material maize silage and cattle dung) was taken as inoculum in a ratio of 2/1 compared to the substrate. 7 g VS were appointed from the digestate, 3.5 g VS from the algal biomass. The difference to 400 ml (sample volume) was filled up with tap water. In addition the inoculum was mono-digested. All approaches were investigated in triplicate batch tests at 38°C about a period of 40 days. The produced biogas volume was recorded by measurement of the displacement of a seal liquid (55.2 g/l sulphuric acid; 200 g/l sodium sulphate decahydrate) in 400 ml eudiometers. Dry gas volumes were corrected to standard temperature and pressure conditions (STP: 0°C, 1013 hPa).For calculation of the biogas volume produced by the algal biomass, the inoculum gas volume was deducted.

2.4. Regression equation

An equation (Eq. (1)) was fitted to every sample to illustrate the daily gas production over retention time.

$$V_{STP,dr}(t) = a + \frac{b}{2} \cdot (\tanh(c \cdot (t - d)) + 1) + \frac{e}{2} \cdot (\tanh(f \cdot (t - g)) + 1) \qquad (1)$$

where $V_{STP,dr}$ is the dry biogas volume under standard temperature and pressure conditions, *t* is the time and *a* to *g* are fitting parameters used to describe the progression. Eq. (1) was used to combine the triplicate approaches and to deduct the gas production of the inoculum.

3. Results

All exerted disruption techniques were successful and showed higher absorption compared to the untreated sample (Figure 1). Photometrical measurement due to released cytosolic protein by cell wall deletion was highest in French press treated samples (2.18). Decreasing amounts were detected in high temperature (1.74) and microwave (1.3) samples. Cell disruption in ultrasonic (0.79) and frozen (0.31) samples was less successful.

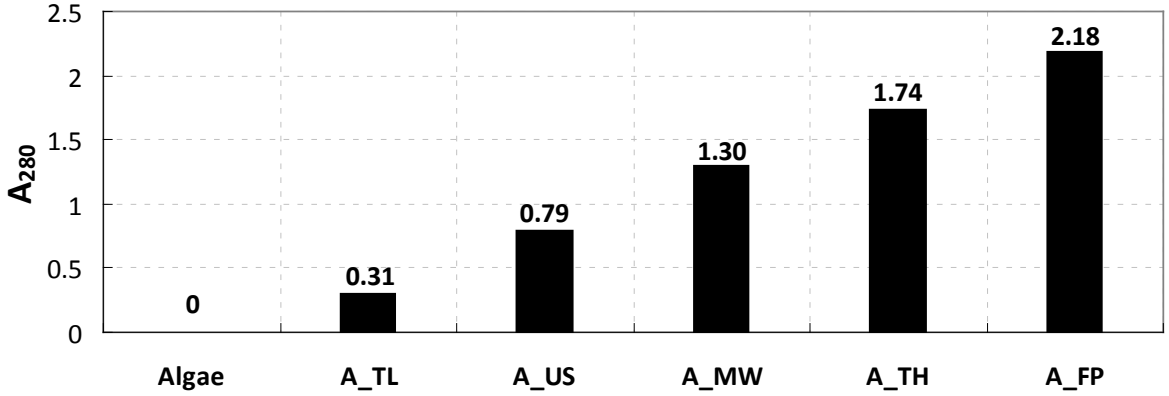

Fig. 1. Absorption at 280 nm (A_{280}) of disrupted cell suspensions compared to the untreated sample (Algae). (A_TL) = low temperature, (A_US) = ultrasonic, (A_MW) = microwave, (A_TH) = high temperature and (A_FP) = French press.

VS were determined before and after anaerobic digestion. The VS degradation was calculated for the substrate (Figure 2). For all disrupted samples the VS degradation was higher than for the untreated sample (25.2%). High temperature (53.8%), French press (54.5%) and microwave (58.7%) were in the same range between 50 and 60%. Lower degradation rates were determined for ultrasonic (41.4%) and the frozen sample (35.4%).

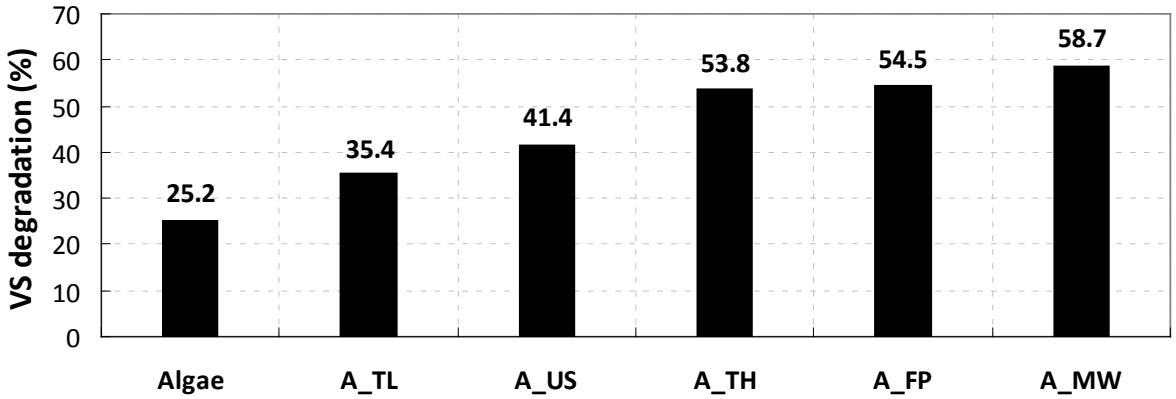

Fig. 2. Volatile solid (VS) degradation of disrupted samples compared to the untreated sample (Algae). (A_TL) = low temperature, (A_US) = ultrasonic, (A_MW) = microwave, (A_TH) = high temperature and (A_FP) = French press.

To compare the digestion progression of the different samples the determined biogas volume was calculated by regression analysis (Eq. (1)). The biogas produced by the inoculum was

deducted (Figure 3). High temperature (A_TH) and microwave (A_MW) disruption showed the highest biogas volume and exhibited a saturation curve, where biogas volume of A_TH (2150 mL) was above A_MW (1900 mL). Biogas volume of the French press sample (A_FP; 1800 mL) was highest during the first 13 days and dropped then below A_TH and A_MW. The untreated sample (Algae; 1265 mL) exhibited a plateau after ten days and reached saturation after 30 days. The progression of produced biogas volume for ultrasonic (A_US) and the frozen sample (A_TL) are similar to the untreated sample. Evolved biogas was for A_US (1080 mL) at the beginning higher and at the end below the Algae, whereas the produced biogas volume for A_TL (920 mL) was below the untreated sample for the whole experiment.

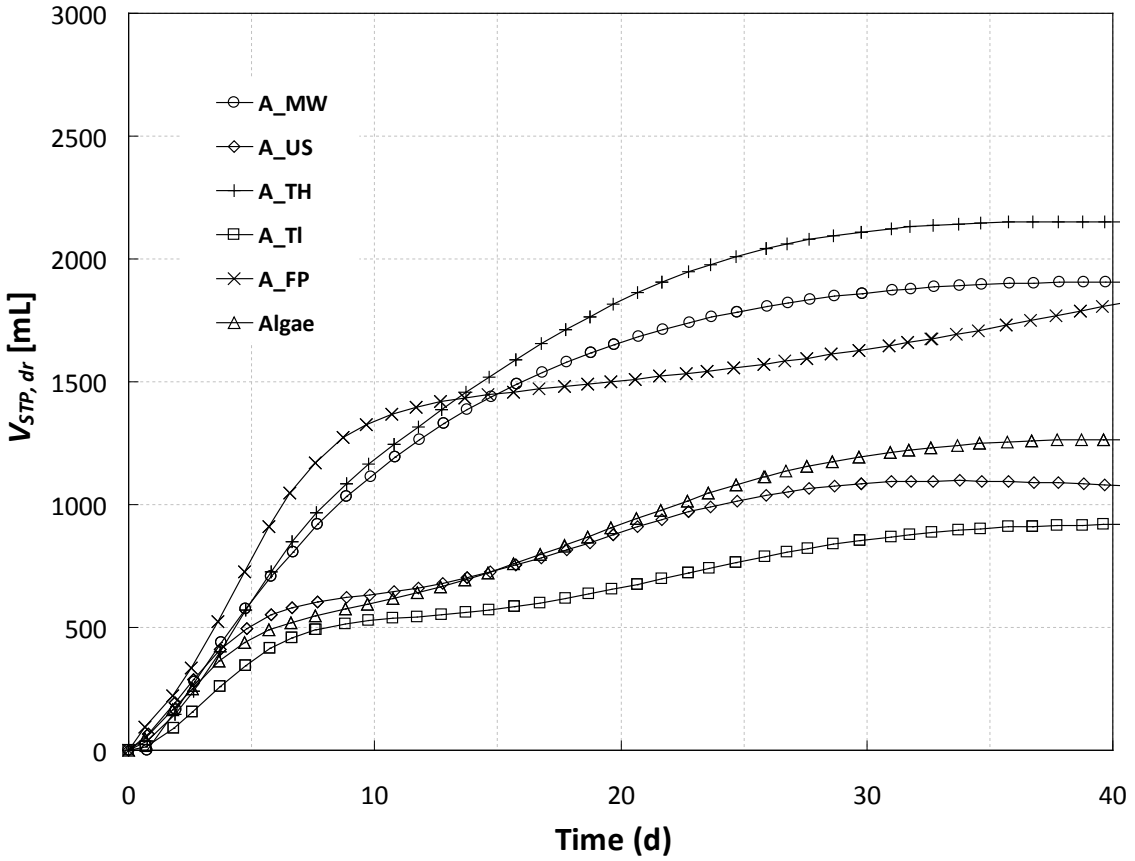

Fig. 3. Biogas production. Biogas volume is indicated in mL as dry gas under standard temperature and pressure conditions (STP, dr). High temperature (A_TH), microwave (A_MW) and French press (A_FP) show different progression and higher biogas volume compared to the untreated sample (Algae). The biogas production progression for ultrasonic (A_US) and the frozen sample (A_TL) is similar, the biogas volume lower as in the untreated sample. VS content was from 3.7 to 3.9 g.

Specific biogas production referred to the added amount of VS was determined for comparability (Figure 4). Compared to the untreated sample (Algae; 347 $mL_{STP,dr}$/g VS) frozen (A_TL; 233 $mL_{STP,dr}$/g VS) and ultrasonic (A_US; 247 $mL_{STP,dr}$/g VS) samples showed lower specific biogas production. In French press (A_FP; 460 $mL_{STP,dr}$/g VS), microwave (A_MW; 487 $mL_{STP,dr}$/g VS) and high temperature (A_TH; 549 $mL_{STP,dr}$/g VS) treated samples the biogas yield was higher than in untreated samples. Due to similar VS content order of specific biogas production is comparable to produced biogas volume stated above.

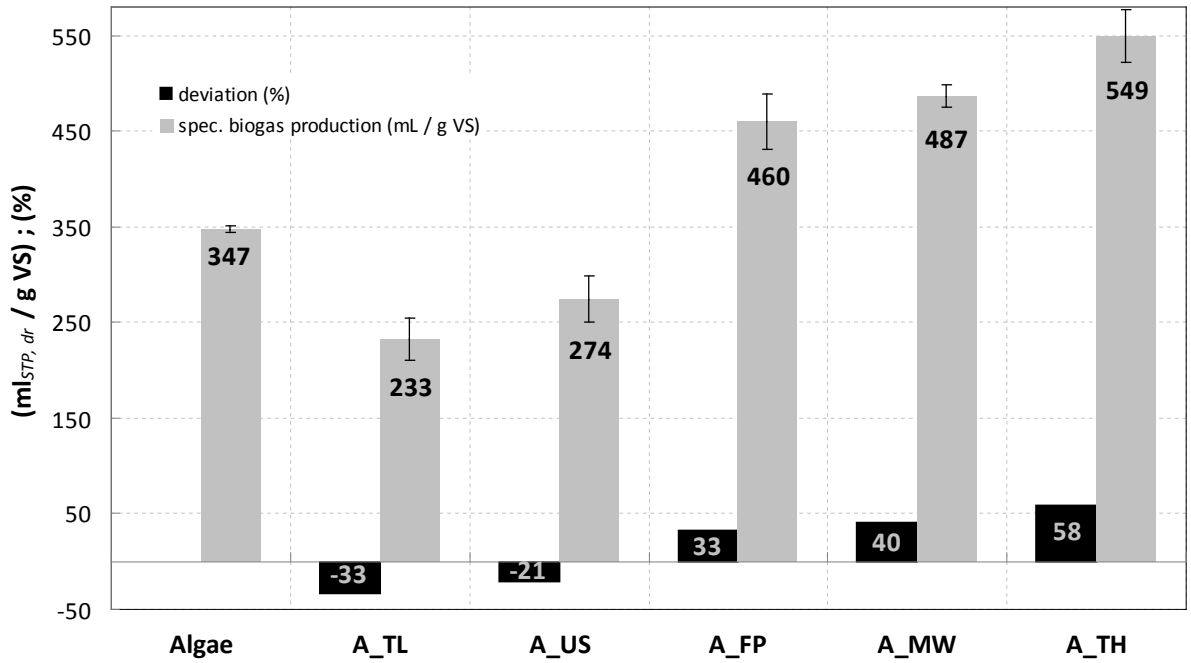

Fig. 4. Specific biogas production of disrupted samples in comparison to the untreated sample (Algae). The freezing (A_TL) and ultrasonic treatment (A_US) showed lower specific biogas production. Increasing biogas yields were determined for French press (A_FP), microwave (A_MW) and high temperature (A_TH) samples. In addition deviation of specific biogas production from the untreated sample was stated.

4. Discussion and conclusions

The results indicate that effectively cell wall degradation is a limiting factor in anaerobic mono-digestion processes of *N.salina* biomass. The validation of cell disruption efficiency shows enhancement for all disruption techniques. Higher VS degradation and lower specific biogas production for the frozen (A_TL) and the ultrasonic (A_US) treated samples are a sign for loss of volatile organic material during cell disruption. Gas bubbles due to cavitation in ultrasonic samples were not yet examined. Microwave (A_MW) and French press (A_FP) samples showed higher VS degradation than high temperature samples (A_TH) with less specific biogas production. Organic material must have been lost in these processes, too.

The appropriated cell disruption techniques showed different efficiency and effects on anaerobic digestion. Thermal pretreatment exhibited the best results as indicated by Chen and Oswald in previous studies, where methane formation efficiency was improved by up to 33% [11]. Ultrasonic treatment improved substrate solubility, whereas a negative effect on specific biogas production was observed as indicated by Samson and LeDuy for *Spirulina maxima* algal biomass [12]. The effect was explained by changes in the chemical composition of the culture media due to cell disruption. VS degradation was differently to the data obtained in this work below the untreated sample. Sonification and high pressure homogenization (French press) are standard methods for disruption of algal and bacterial cells in protein purification. Microwave irradiation gains significance in lipid extraction from algae for biofuel production [13, 16]. For French press and microwave no comparative data of algal fermentation after cell disruption is available.

In this work one major limiting factor for *N.salina* mono-digestion was revealed: the resistance of the algal cell wall against enzymatic hydrolysis. Mussgnug et al. showed that

without pretreatment the accessibility to cell disintegration is a Major factor for efficiency of fermentative biogas production [17]. Easy degradable microalgae were found to have no cell wall (*Dunaliella salina*) or a protein-based cell wall without cellulose or hemicellulose (*Chlamydomonas reinhardtii*). Specific biogas production of untreated *D.salina* (505 $mL_{STP,dr}$/g VS) and *C.reinhardtii* biomass (587 $mL_{STP,dr}$/g VS) was in the range of high temperature samples (549 $mL_{STP,dr}$/g VS) with highest specific biogas production after pretreatment in this work. The cell degradation was 100% for *D.salina* and 70% for *C.reinhardtii*. After pretreatment of *N.salina* a maximum of about 60% (A_MW) degraded VS were determined. Consequently, *N.salina* cell wall is resistant against enzymatic hydrolysis and degradability was improved by physical pretreatment. Whether the cell wall is partly resistant against the different disruption techniques or other limitations like low C/N-ratio or ammonia-inhibition affect the low degradability after pretreatment, is ambiguous. A control with 100% cell disintegration was not conducted in this work.

The potential of microalgae for biogas production is depending on the selected strain [17]. Besides the cell disintegration due to cell wall structure, factors like growth kinetics, biochemical composition or biomass yield are important selective parameters for evaluation. Combined biorefinery concepts can be a possible solution to reduce the influence of cell wall hydrolysis. Anaerobic digestion of pretreated microalgae after lipid extraction for biodiesel production can be the key process to make microalgae sustainable as a source for biofuels by nutrition and energy recovery [6].

In further studies the rated ranges with positive effects have to be investigated for the different disruption approaches. Energy balances with regard to commercial applications have to be examined.

Acknowledgements

We thank RWE Innogy GmbH for supporting the project and Phytolutions Ltd. for providing the algal biomass. This work was partly supported with a grant by the Graduate School of Energy Efficient Production and Logistics.

References

[1] Y. Chisti, Biodiesel from microalgae, Biotechnology Advances 25, 2007, pp. 294–306.

[2] A. S. van Carlsson, J. B. Beilen, R. Möller, D. Clayton, Micro- and macroalgae utility for industrial applications. Outputs from the EPOBIO project. D. Bowles. York, UK, 2007.

[3] V. Patil, K. Tran, H. R. Giselrød, Towards sustainable production of biofuels from microalgae, International Journal of Molecular Sciences 9, 2008, pp. 1188–1195.

[4] L. Rodolfi, G. Chini Zittelli, N. Bassi, G. Padovani, N. Biondi, G. Bonini, M. R. Tredici, Microalgae for oil: Strain selection, induction of lipid synthesis and outdoor mass cultivation in a low-cost photobioreactor, Biotechnology and Bioengineering 102, 2009, pp. 100–112.

[5] P. Weiland, Biogas production: current state and perspectives, Applied Microbiology and Biotechnology 85, 2010, pp. 849–860.

[6] B. Sialve, N. Bernet, O. Bernard, Anaerobic digestion of microalgae as a necessary step to make microalgal biodiesel sustainable, Biotechnology advances 27, 2007, pp. 409–416.

[7] S. Derenne, C. Largeau, C. Berkaloff, B. Rousseau, C. Wilhelm, P. G. Hatcher, Non-hydrolysable macromolecular constituents from outer walls of *Chlorella fusca* and *Nanochlorum eucaryotum*, Phytochemistry 31, 1992, pp. 1923–1929.

[8] F. Gelin, I. Boogers, A. A. M. Noordeloos, J. S. S. Damste, R. Riegman, J. W. de Leeuw, Resistant biomacromolecules in marine microalgae of the classes Eustigmatophyceae and Chlorophyceae: Geochemical implications, Organic Geochemistry 26, 1997, pp. 659–675.

[9] DIN EN 12880, Bestimmung des Trockenrückstandes und des Wassergehalts, 2001.

[10] DIN EN 12879, Bestimmung des Glühverlustes der Trockenmasse, 2000.

[11] P. H. Chen, W. J. Oswald, Thermochemical treatment for algal fermentation, Environment International 24, 1998, pp. 889–897.

[12] R. Samson, A. Leduy, Influence of mechanical and thermochemical pretreatments on anaerobic digestion of *Spirulina maxima* algal biomass, Biotechnology Letters 5, 1983, pp. 671–676.

[13] J. Lee, C. Yoo, S. Jun, C. Ahn, H. Oh, Comparison of several methods for effective lipid extraction from microalgae, Bioresource Technology 101, 2010, pp. 75-77.

[14] K. Cormann, M. Ikeuchi, M. Rögner, M. Nowaczyk, R. Stoll, Sequence-specific ^{1}H, ^{13}C, and ^{15}N backbone assignment of Psb27 from *Synechocystis* PCC 6803, Biomolecular NMR Assignments 3, 2009, pp. 247-249.

[15] VDI 4630, Vergärung organischer Stoffe, 2005.

[16] S. Balasubramanian, J. D. Allen, A. Kanitkar, D. Boldor, Oil extraction from *Scenedesmus obliquus* using a continuous microwave system - design, optimization, and quality characterization, Bioresource Technology 102 , 2011, pp. 3396-3403.

[17] J. H. Mussgnug, V. Klassen, A. Schlüter, O. Kruse, Microalgae as substrates for fermentative biogas production in a combined biorefinery concept, Journal of Biotechnology 150, 2010, pp. 51-56

Scale up of laboratory scale to industrial scale biogas plants

Alexandra Kowalczyk[1,*], Sebastian Schwede[1], Mandy Gerber[1], Roland Span[1]

[1] *Ruhr-University Bochum, Institute of Thermo and Fluid Dynamics, Bochum, Germany*
** Corresponding author. Tel: +49 234 32 26409, Fax: +49 234 32 14163, E-mail: a.kowalczyk@thermo.rub.de*

Abstract: Industrial biogas plants often do not operate in their optimum. To investigate limits of anaerobic digestion processes experiments are necessary. Economically it would be feasible to perform these tests at laboratory scale, if the tests could be transferred to industrial scale. This work presents a preliminary study, in which two different scales of laboratory digesters are compared and reproducibility of tests is investigated.
Therefore, three identical glass digesters with a liquid volume of up to 22 liter and a steel-digester with a liquid volume of 390 liter were used. All digesters were started up with digestate from an industrial biogas plant, were fed with cow manure and corn cob mix, and were operated at the same process parameters like temperature, organic loading rate and retention time. Gas volumes were measured continuously. Twice a day the composition of the biogas was analyzed. Dry matter and volatile solids were quantified once a week.
The presented data show a good reproducibility between biogas plants of the same scale. The transferability to a bigger scale is in an acceptable range, but depending on the organic loading rate the deviation between the different scales varies.

Keywords: *biogas plant, laboratory scale, comparison, reproducibility, transferability*

1. Introduction

Sources for renewable energy become more and more important. Among the renewable energies biogas has the advantage that it is a not fluctuating source. When being used in the existing pipeline infrastructure, it can even be stored to compensate for fluctuations in consumption. Storage for short periods is possible directly in most plants. Biogas can be gained in an anaerobic digestion process from different organic substances, e.g. from energy crops, agricultural waste or municipal organic waste.

Industrial biogas plants often do not operate in their optimum. To reach a higher efficiency for biogas plants it is necessary to know the limits for the anaerobic digestion process. These limits have to be identified in experiments. Economically it is not feasible to perform these tests on an industrial scale biogas plant since they involve the risk of long lasting production curtailments. Therefore, experiments at laboratory scale are the most common way to study the anaerobic digestion process. To use the results of laboratory scale experiments, it is essential to know whether the results are transferable to industrial scale and whether the experiments are reproducible.

To answer these questions it is necessary to use exactly the same inoculums for all digesters used in one test series and the same substances for feeding, because the anaerobic digestion process is a strongly dynamical process and depends very much on the used material. Furthermore, all digesters investigated should be operated with the same process parameters such as temperature, organic loading rate (OLR), hydraulic retention time and liquid volume for studies on reproducibility. For transferability studies only the liquid volume is allowed to vary. Transferability and reproducibility were investigated by Brunn et al. [1] with a non identical OLR for the different scales. Gallert et al. [2] operated their digesters with different OLR and hydraulic retention times. This work presents results of a pre study in which two different scales of laboratory digesters are compared keeping all process parameters as equal as possible. Furthermore, a reproducibility test was carried out with identical digesters. In coming tests a laboratory scale digester will be compared with an industrial scale biogas plant.

2. Methodology

To prove the reproducibility of experiments on the anaerobic digestion process, three identical continuous (22 liter laboratory) digesters were used. The transferability of experimental results to different scales was investigated comparing the 22 liter digesters to a 390 liter continuous digester.

2.1. Experimental setup

One of the three identical digesters with a liquid volume of 22 liter is shown in Fig. 1. The double glass shell of the digester is used for heating and gives the possibility to observe mixing and liquid level. Mixing is realized by a central stirring system with three mixing elements. These are propeller mixers with three blades for every mixing element. At the bottom a ball valve allows to discharge the digester or to take samples. For feeding a ball valve connected with the lid is used. From the top of the digester a gas-pipe leads to a 5 liter gas sampling bag. The gas sampling bag is necessary, to avoid low pressure by draining during feeding or taking samples. From the gas sampling bag a heated pipe leads to a drum type gasmeter (TG 05; Ritter). The gasmeter has a PT-100 thermometer and a manometer to be able to calculate the standard volume flow.

Fig. 1. Left: One of the three continuous 22 l digesters; Right: continuous 390 l digester.

Two identical gas chromatographs (GC) (Focus GC, Thermo Electron Corporation, Axel Semrau) are used to analyze the gas composition. One is equipped with a thermal conductivity

detector (Thermo Fisher Scientific, Axel Semrau) with a micropacked column (ShinCarbon ST 100/120, Restek) for analyzing methane (CH_4), carbon dioxide (CO_2), oxygen (O_2) and nitrogen (N_2). The other GC is connected to a mass spectrometer (DSQ II, Thermo Electron Corporation, Axel Semrau) with a capillary column (GS-GasPro, J&W Scientific Products) for hydrogen sulfide (H_2S). Furthermore a variable over pressure function is connected to the top. To determine the temperature in the digester a PT-100 thermometer is used.

The biogas plant with a liquid volume of 390 liter is shown in Fig. 1. It is made of stainless steel. The geometry of the digester is a scale-down of an industrial plant with 3000 m^3 liquid volume. The gas flow is much higher in the 390 liter digester. Therefore, no problems with low pressure occur during feeding or taking samples and a gas sampling bag is not needed. A constant liquid level is held due to a siphon which connects the digester with a storage tank. The digester is mixed by a central stirring system with three mixing elements. These are pitched blade impellers with two blades. This means, that they differ in their geometry compared to the ones of the 22 liter digesters. Temperature is measured on three levels. The digester is equipped with the same metrology as the smaller digesters. The measured quantities and their uncertainties are summarized in Table 1.

Table 1. Measured quantities and their uncertainties.

T	p	$\dot{V}$	CH_4	CO_2	O_2	N_2	H_2S
(mK)	(mbar)	(%)	(mol-%)	(mol-%)	(mol-%)	(mol-%)	(ppm)
± 31,0	± 1,5	± 0,2	± 4,0	± 3,4	± 0,2	± 0,3	± 615,3

2.2. Experimental performance

All four digesters were filled with digestate from an industrial biogas plant (fed with maize silage (MS), corn cob mix (CCM) and cow manure (CM)) at the beginning. During the test period of 40 days the digesters were run at the same temperature level of ca. 38°C. The test period of 40 days was considered to be sufficient, after the digesters showed a good reproducibility and transferability even with changing organic loading rates (OLR). Once a day they were fed with the same mixture of CCM and CM, which was mashed with digestate. CM was chosen because of its good buffer capacity. CCM and CM are, compared e.g. to MS, very homogeneous and well suited for reproducibility and transferability tests. The chosen feeding rates ensured the same OLR for all digesters. The OLR is calculated according to

$$OLR = \frac{\dot{m}_{VS}}{V_{liq}} \qquad (1)$$

where $\dot{m}_{VS}$ is the input mass flow of volatile solids (VS) and V_{liq} the liquid volume of the respective digester. The OLR was increased from 0.20 to 2.54 $kg_{VS}m^{-3}d^{-1}$ during the test period. The steps are shown in Fig. 2.

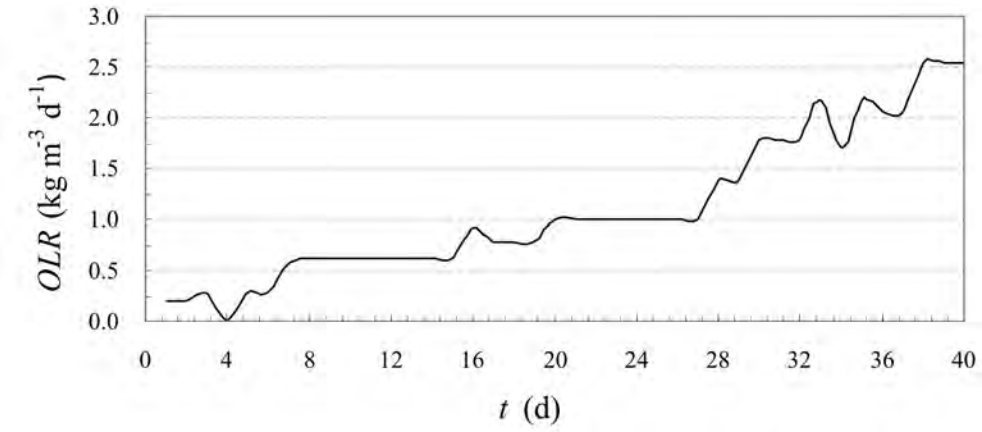

Fig. 2. OLR over test period for all digesters.

Before and after feeding gas samples were taken for gas quality analysis. During the whole test period the gas flow was measured continuously and the digesters have been stirred without any interruptions. Six times during the test period of 40 days dry matter (DM) and volatile solids (VS) where determined according to DIN 12879 [3] and DIN 12880 [4], respectively.

3. Results

During the test period the four plants showed a good agreement with respect to the analyzed parameters. Fig. 3 and Fig. 4 give an overview of the performance for two different days. The diagrams show the standard volume flow reduced by the liquid volume of the digester over one day. The reduction is necessary, because otherwise it would not be possible to compare the 22 liter digesters to the 390 liter digester. The drop in Fig. 3 and at 05:00 and 08:00 o'clock in Fig. 4 result from sampling for gas analysis. The fluctuations between 10:00 and 15:00 o'clock are caused by feeding and taking samples for gas analysis.

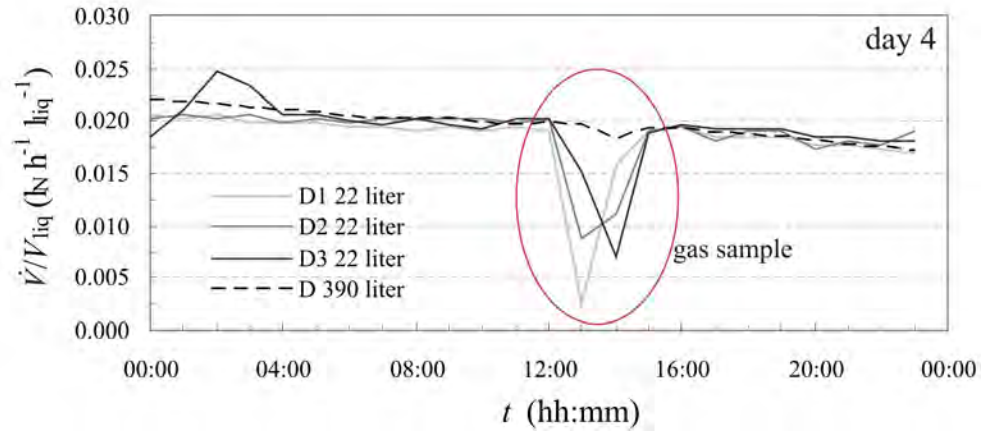

Fig. 3. Volume flow referring to the filling volume for fourth day (D: Digester).

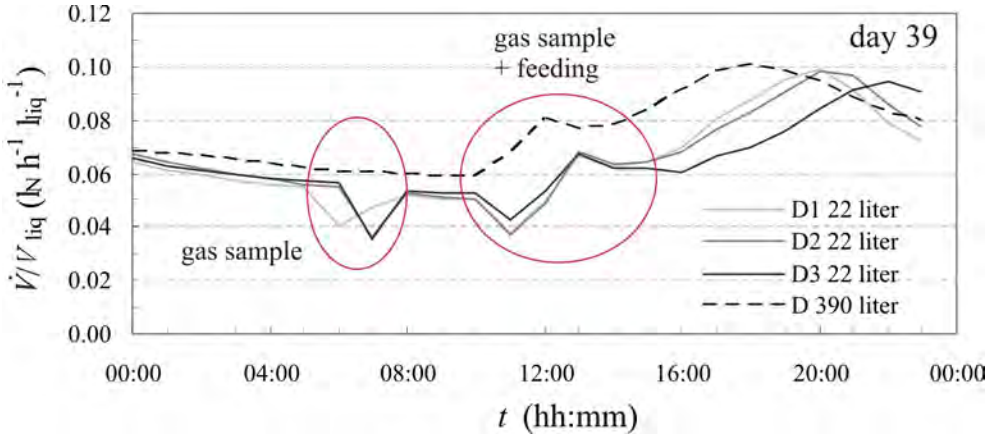

Fig. 4. Volume flow referring to the liquid volume for 39th day (D: Digester).

Fig. 3 shows a nearly identical shape of the curve with very similar results for all four digesters. In Fig. 4 the curve of the 390 l digester deviates from the ones of the 22 l digesters. The trends at the two different scales are comparable at any time, for derivates. In this example the curve of the third 22 liter digester is displaced on the time-line, but shows the same trends.

Fig. 5 shows the daily average of the absolute standard deviation for the 22 liter digesters, as well as the daily average of the absolute deviation between the 390 liter digester and the average of the three 22 liter digesters. To calculate the deviation the values during feeding or taking gas samples, as described in Fig. 3 and Fig. 4, and outliers were excluded. On the second axis the average of the daily gas volume flow to the liquid volume of the digesters is shown. Here the outliers are excluded as well.

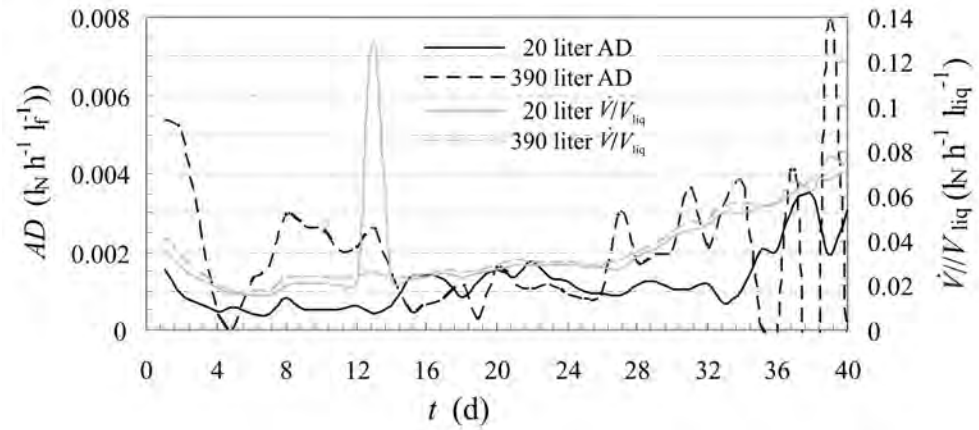

Fig. 5. Daily average of the absolute standard deviation (AD) for the three 22 liter digesters and daily average of the absolute deviation (AD) between 390 liter digester. Also the average of the three 22 liter digesters and the daily average of the gas volume flow reduced by the liquid volume for 22 liter and 390 liter digesters.

Fig. 5 shows a good reproducibility of the three 22 l digesters among each other. The relative standard deviation is between 1.42 and 5.96 % (excluded one outliner with 21.58 % on day 13) for the 22 liter digesters among each other. Comparing the average of the 22 l digesters to the 390 l digester the relative deviation is between 0.68 and 18.07 %. This and the shape of the curves for the gas volume flow in Fig. 5 for both digester scales are an evidence for a possible transferability of experimental results in different scales.

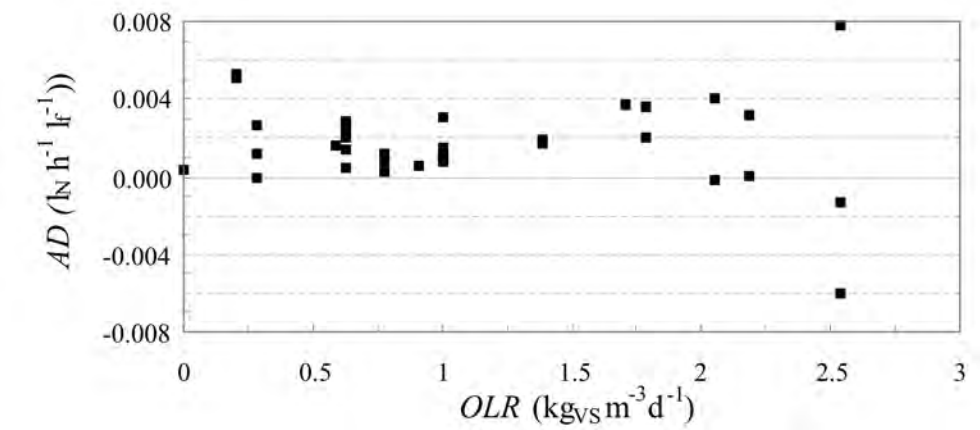

Fig. 6. Absolute deviation (AD) of the 390 liter digester to the average of the 22 liter digesters over OLR.

Fig. 6 shows the absolute deviation of 390 liter to 22 liter digesters (referring to gas volume flow to liquid volume) over OLR. For each OLR, expect 2.53 $kg_{VS}m^{-3}d^{-1}$, the deviation is between 0.0002 and 0.0053 $l_N h^{-1} l_f^{-1}$. For an OLR of 2.53 $kg_{VS}m^{-3}d^{-1}$ the absolute deviation is between -0.0061 and 0.0078 $l_N h^{-1} l_f^{-1}$.

To compare the biogas quality, Fig. 7 shows the plot of the measured methane concentration. Expect for the curve of the first 22 liter plant at days 14-18 and a single peak of the 390 l digester at the end of the test period, all curves show a good agreement. The difference between the two scales till day 6 results from the gas sampling bags used for the 22 liter digesters, which contain air at start up.

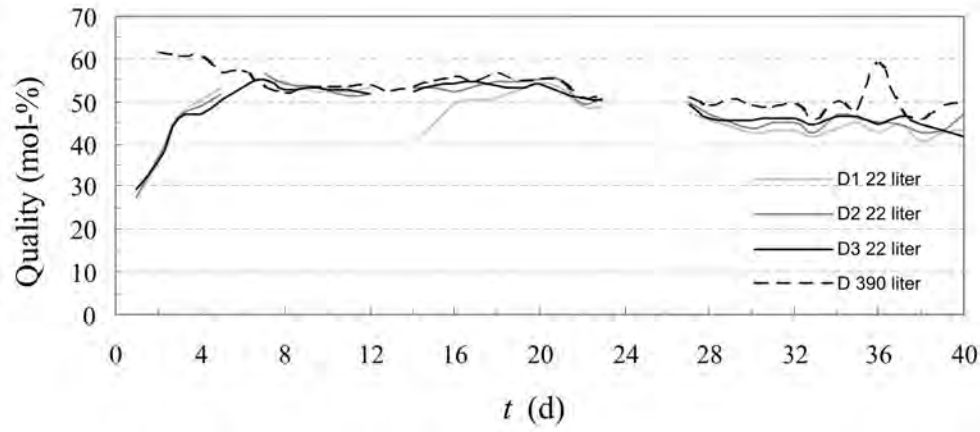

Fig. 7. Methane-rate over test period.

Table 2 shows results for DM and VS determined during the test. Day 0 represents the starting point, at which all digesters have been filled with the same inoculum. After the first week the DM in the 390 l digester decreases more than in the smaller digesters. This indicates a higher conversion of the substrates to biogas. This is also shown in Fig. 5, where the production rate of the 390 liter digester is always above the one of the 22 liter digesters.

Table 2. Dry matter (DM) and organic dry matter (VS) of all digesters through the test period.

t	(d)		0	7	16	23	29	36
DM	(% FM*)	BP1 22 l	8,37	8,10	7,85	7,61	7,47	7,63
		BP2 22 l	8,37	8,30	7,67	7,42	7,67	7,81
		BP3 22 l	8,37	8,33	7,55	7,37	7,48	7,61
		BP 390 l	8,37	7,72	7,38	7,11	7,11	7,57
VS	(% FM*)	BP1 22 l	6,47	6,00	5,65	5,50	5,64	5,76
		BP2 22 l	6,47	5,83	5,56	5,53	5,47	5,88
		BP3 22 l	6,47	6,00	5,65	5,39	5,45	5,73
		BP 390 l	6,47	5,92	5,63	5,43	5,43	5,76

* fresh mass

4. Conclusion and Outlook

The presented results show a high degree of reproducibility at equal experimental conditions. During the test period the daily relative standard deviation of the three 22 liter digesters is between 1.42 and 5.96 %. Reasons for this deviation are the heterogeneity of the fed substrates and small differences in liquid volume and digester temperature.

The relative deviation of the 390 l digester to the three 22 liter digesters is between -6.92 and 18.07 % with an average of 6.33 %. This is not caused by the OLR, which was varied during the test. The reasons for the deviation have to be searched in the same causes as the ones for the reproducibility. Additional reasons are the differences in geometry, in materials used for the digesters and in mixing.

Good correspondence between a laboratory scale digester and a full scale digester was observed by Gallert et al. [2]. This is a good indicator, that experiments in laboratory scale can be transferred to industrial scale. Aivasidis and Wandrey [5] concluded, that it is possible to scale up anaerobic digesters and that experiments in laboratory and pilot scale can provide data to design an industrial scale digester.

Also Brunn et al [1] figured out a good reproducibility for digesters of the same scale, but not for transferability. The industrial scale digester produces 36% more gas, compared to the used laboratory scale digester. As explained by Brunn et al. this causes in different feeding schedules and substrates (substrates for the laboratory digester were taken once a week). This shows the importance of similar process parameters for tests relating to reproducibility and transferability.

The next step in studying the transferability of experimental results should be a comparison between a digester at laboratory scale with one at industrial scale. All process parameters have to be chosen as identical as possible, as the presented results underline the importance of synchronicity of all process parameters. Currently the industrial biogas plant is being equipped with the necessary measure devices.

Acknowledgements

We thank RWE Innogy GmbH for supporting the presented work.

References

[1] L. Brunn, C. Dornack, B. Bilitewski, Application of laboratory scale experiments to industrial scale in case of anaerobic waste treatment, Fresenius Environmental Bulletin 18 (2), 2009, pp. 196-203

[2] G. Gallert, A. Henning, J. Winter, Scale-up of anaerobic digestion of the biowaste fraction from domestic wastes, Water Research 37, 2003, pp. 1433-1441

[3] DIN EN 12879, Characterization of sludges - Determination of the loss on ignition of dry mass, 2001

[4] DIN EN 12880, Characterization of sludges - Determination of dry residue and water content, 2001

[5] A. Aivasidis, C. Wandrey, Development and Scaleup of a high-rate biogas process for treatment of organically polluted effluents, Annals of the New York Academy of Sciences 589, 1990, pp 599-615

The effect of distinct operational conditions on organic material removal and biogas production in the anaerobic treatment of cattle manure

Neslihan Manav Demir, Tamer Coşkun, Eyüp Debik*

Yildiz Technical University, Environmental Engineering Department, Istanbul, Turkey
** Corresponding author. Tel: +90 212 3835369, Fax: +90 212 3835358, E-mail: debik@yildiz.edu.tr*

Abstract: Although very difficult to treat due to their complicated composition, the increasing amounts of cattle manure generation makes their purification a compulsory task for environmental engineers to prevent their adverse environmental impacts. Historically, these wastes have been used as a fuel or a soil fertilizer. The generation of cattle manure even in increasing amounts in Turkey, however, makes this kind of use unfeasible. Therefore, new methods to dispose of these wastes are required. This study focuses on the anaerobic digestion process for the treatment of cattle manure. In the study, two lab-scale anaerobic reactors were employed to investigate the effects of different operating temperatures (35 ºC and 55 ºC), of different total suspended solids concentrations (%5 and 10%), of different hydraulic retention times (20 days and 40 days), and of the addition of corn silage on the treatment performance. The performance of the reactor was evaluated with respect to total solids (TS), volatile solids (VS) and biogas production. The results of the study suggested that the thermophilic reactor showed a good treatment performance (59% VS removal and 0.29 L methane per VS added) when the cattle manure of 10% solids content together with corn silage were fed. Besides, it was concluded that the addition of corn silage to the reactors improved the treatment efficiencies and that the addition of irrigational organic materials increases biogas production rate. The results of the study point out that anaerobic digestion process is a viable option for cattle manure stabilization and valuable gas production.

Keywords: *Anaerobic Digestion, Cattle Manure, Biogas, Methane*

Nomenclature

TS	*total solids..... mg.kg^{-1}*	*TOC*	*total organic carbon.....mg.kg^{-1}*
VS	*volatile solids ..... mg.kg^{-1}*	*COD*	*chemical oxygen demand..... mg.L^{-1}*
HRT	*hydraulic retention times ..... day*	*cfu*	*colony forming unit .....*

1. Introduction

The number of cattles have shown an increasing trend in Turkey. In 2007, the capacity of cattles in Turkey reached over 11 millions [1]. This increase, unfortunately, led to an increase in the environmental problems caused by inappropriate disposal of cattle manures into the environment, due to which the proper treatment of these wastes gained attraction in last years. Current disposal methods (burning and using as fertilizer) have proven to be inadequate and research is ongoing for new treatment methods.

Cattle manure can be as harmful as other industrial wastes in environmental aspects. Therefore, development of new treatment methods for the safe disposal of these wastes would prevent endangering the public health. Besides, the end product of the anaerobic digestion process could easily be used as an organic fertilizer and this use would contribute to sustainable development strategies.

In addition to the severe environmental impacts caused by the uncontrolled disposal of cattle manure, possible future energy crisis makes the environmental engineers to provide solutions both economically and environmentally sound. Production of energy through biomass along with a by-product that can be used as a natural fertilizer are the major advantages of this process.

Although being a very complicated process, anaerobic digestion simply involves three stages as (1) the conversion of high-density organic materials into low-density materials by hydrolysis, (2) the conversion of low-density organics into acetate by acid bacteria, and (3) methane production by methane bacteria by consuming acetate, carbon dioxide and hydrogen [2]. Coskun et al. (2009) listed the factors affecting the anaerobic digestion of cattle manure as (1) solids content and hydraulic retention time, (2) pH and alkalinity, (3) trace elements and nutrients, (4) temperature, (5) toxic content of the waste, (6) C/N ratio, and (7) dilution ratio of the waste [3].

This study aims at the evaluation of anaerobic digestion alternatives for cattle manure treatment with differing hydraulic retention times, feed contents and feed solids contents. The investigation involved the determination of the most feasible anaerobic digestion method for the treatment of cattle manure in Turkey.

2. Methodology

2.1. Characterization of cattle manure

Cattle manure contains insoluble organic materials as well as soluble organics such as polysaccharides, fats, and volatile fatty acids. Their high chemical oxygen demand (COD), ammonia and phosphorous content make them very complicated and extremely difficult to treat [4]. The cattle manure used in this study was obtained from Gebze District of Kocaeli of Turkey and the characteristics of the waste are given in Table 1.

Table 1. General characteristics of the raw cattle manure (Gebze-Kocaeli)

Parameter	Unit	Value
pH	-	7.41
Moisture	%	80.98
Volatile solids (VS)	%	73.58
Ash	%	5.12
C	%	39.12
N	%	1.35
C:N	-	28.94
P	%	0.96
H	%	5.01
S	%	0.40

2.2. Measurement methods

TS, VS, total organic carbon (TOC), biogas production and methane content of the biogas were continuously monitored during the study. For TS and VS, the method “DS/EN 12879 Characterization of sludges” was followed. TOC analyses were conducted using Hach-Lange IL 550 TOC/TN device. TOC analyses were conducted in the effluents from the reactors starting from the sixth week of the study. The biogas production was measured daily via a Ritter Drum-type gasmeter and LMSx Multigas Analyser was used to assess the biogas composition. *Salmonella spp.* was measured according to “ISO 6579/April, 1996 Salmonella measurement methods” while “NF-ISO 166492 (June 2001) Horizontal method for the enumeration of glucuronidase-positive Escherichia coli β – Part 2: Technique of colony count at 44 °C by means of 5-bromo-4-chloro-3-indolyl-β-D-glucuronate acid (IC: V08-031-2)” was used for E.coli measurement.

2.3. Experimental setup

Two lab-scale, completely mixed, stainless-steel, cylindrical anaerobic reactors with 10 L of active volumes were operated at 35 ºC and 55 ºC, simultaneously, for the treatment of cattle manure. The solids contents of 5% and 10% along with the hydraulic retention times of 20 days and 40 days were used during the study. Solids content of the manure was set to 5% or 10% with tap water before feeding. Further, mixtures of cattle manure and corn silage were fed to determine the effects of the use of a supplementary organic material. The reactor performances were evaluated with respect to TS, VS, *Salmonella spp.*, and E.coli removal efficiencies as well as biogas production rate. The experimental setup is shown in Figure 1.

Fig. 1. Lab-scale anaerobic treatment system [3].

3. Results

3.1. Cattle manure feed at 5% solids content

First of all, the reactors were fed with only cattle manure of 5% solids content and were operated at 20 days of hydraulic retention time (HRT) at 35 ºC (mesophilic range) and 55 ºC (thermophilic range), respectively. After 10 weeks of successful operation, the retention times were increased to 40 days. Figure 2 shows the change of TS, VS and TOC when only cattle manure of 5% solids content was fed to the reactors.

The TS concentration in the effluent of mesophilic reactor at HRT=20 days changed between 39,000 and 43,000 mg/kg while values of same range were obtained in the effluent of thermophilic reactor. The TS removal efficiency of the mesophilic reactor was calculated between 14% and 21% while that of thermophilic one ranged between 10% to 21%. After increasing the HRT to 40 days, the TS content of the effluents were increased first and then decreased to 31,000 mg/kg for mesophilic reactor and 32,000 mg/kg for thermophilic one in 16^{th} week. At the end of the study, the TS removal efficiencies reached to about 38% and 36% for mesophilic and thermophilic reactors, respectively. The reason for the TS removal efficiency to drop first when the HRT was increased from 20 days to 40 days is the reaction of microorganisms to the changing environmental conditions [3].

During the study, VS concentration of the waste was determined to be 38,800 mg/kg. For HRT=20 days, effluent VS concentrations ranged from 27,000 to 30,000 mg/kg and from 28,000 to 31,000 mg/kg for mesophilic and thermophilic reactors, respectively. The VS removal efficiencies ranged from 23% to 30% and from 20% to 29%, respectively. After increasing the HRT to 40 days, the effluent VS concentrations increased first and decreased to around 23,000 mg/kg for both reactors. At the end of the study, the VS removal efficiencies were about 41% for both reactors.

TOC concentration of the waste was measured as approximately between 15,600 and 19,900 mg/kg. For HRT=20 days, average effluent TOC concentrations were around 11,700 mg/kg and 12,300 mg/kg for mesophilic and thermophilic reactors, respectively. After increasing the HRT to 40 days, average effluent TOC concentrations were increased to about 12,000 and 13,300 mg/kg, respectively. The effluent TOC concentrations averaged over the whole study were 11,900 and 13,000 mg/kg for mesophilic and thermophilic reactors, respectively, and average TOC removal efficiencies of the reactors were calculated as 32.8% and 25.4%, respectively.

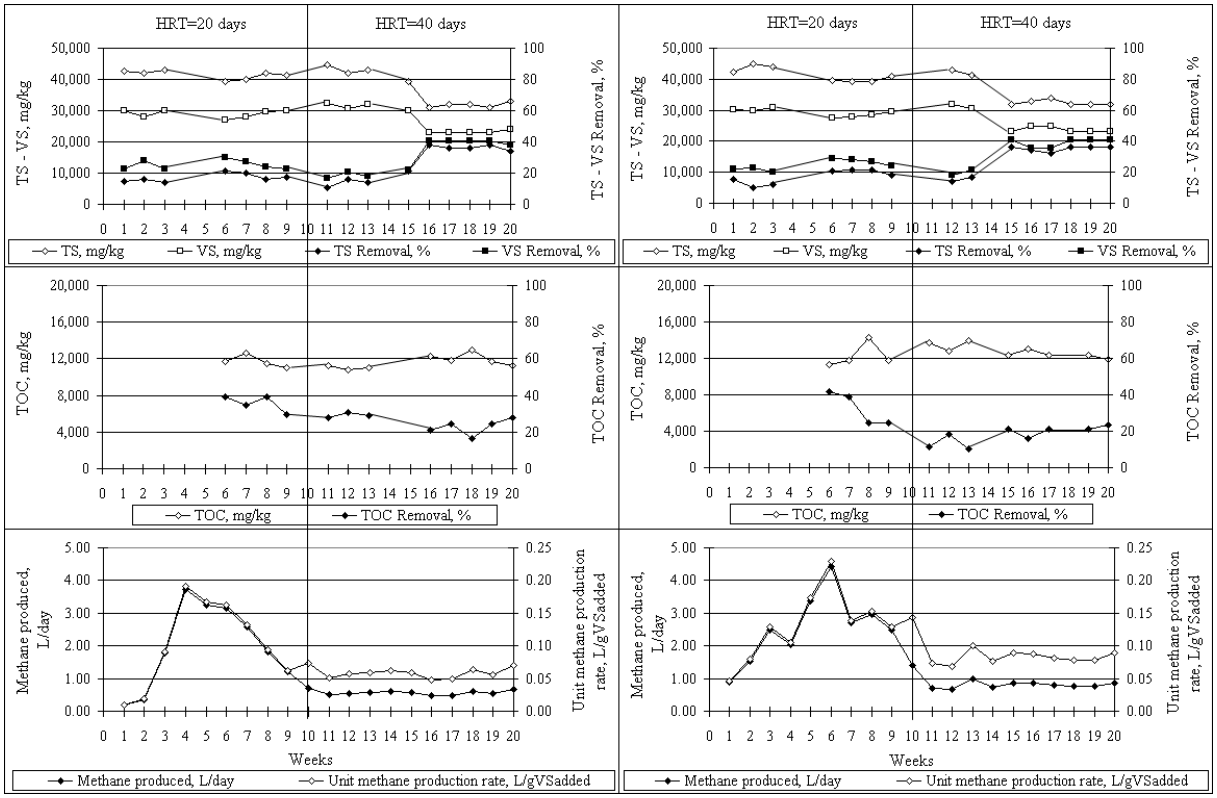

Fig. 2. TS, VS and TOC concentrations in the effluents from mesophilic (A) and thermophilic (B) reactors when only cattle manure of 5% solids content was fed.

Starting with the second week of the study, biogas production rate showed an increasing trend for both reactors. However, the rate was decreased after increasing the HRT. The biogas production rate was measured as between 0.10 and 0.34 L_{biogas}/ gVS_{added}, and between 0.15 and 0.41 L_{biogas}/ gVS_{added} for mesophilic and thermophilic reactors according to the HRTs of 20 days and 40 days, respectively. During the whole study, methane content of the biogas was between 45% and 55% for both reactors. Therefore, the methane production rates for mesophilic and thermophilic reactors ranged from 0.06 to 0.19 $L_{methane}$/ gVS_{added} and from 0.08 to 0.23 $L_{methane}$/ gVS_{added}, respectively.

Salmonella spp. was not detected in both effluents during the whole study. For thermophilic reactor, E. coli was determined to be 10 cfu/kg while this value reached up to 1,000 cfu/kg for mesophilic one. The results showed that the mesophilic range of operating temperature (35 °C) was less effective in E.coli removal while they are completely removed in thermophilic temperature (55 °C).

3.2. Cattle manure feed at 10% solids content

In this stage of the study, the solids content of the raw waste was increased to 10% and the reactors were operated at HRT of 40 days. Average concentrations of TS, VS, and TOC in the raw waste were determined to be 100,000 mg/kg, 82,400 mg/kg, and 36,400 mg/kg, respectively. The results of TS, VS, and TOC analyses in the effluents are shown in Figure 3. For mesophilic reactor, TS, VS, and TOC removal efficiencies were around 20.3%, 23.8%, and 21.3%, respectively. The removal efficiencies for the thermophilic reactor were calculated as 24.9%, 28.3%, and 22.1%, respectively.

In this stage, the mesophilic and thermophilic reactors produced 0.12 to 0.23 L_{biogas}/gVS_{added} and 0.16 to 0.32 L_{biogas}/gVS_{added} of biogas, respectively. The methane production rates were measured as between 1.17 to 2.16 L/day and 1.47 to 2.89 L/day, respectively. In terms of VS fed to the reactors, mesophilic reactor produced 0.06 to 0.10 L methane per gVS_{added} while the rate for thermophilic one was measured as between 0.08 and 0.14 $L_{methane}/ gVS_{added}$.

In the aspect of *Salmonella spp*. removal, both reactors produced perfect effluents. However, this was not the same for E.coli. E.coli was not detected in the effluent from the thermophilic reactor while the mesophilic one was less effective in E.coli removal.

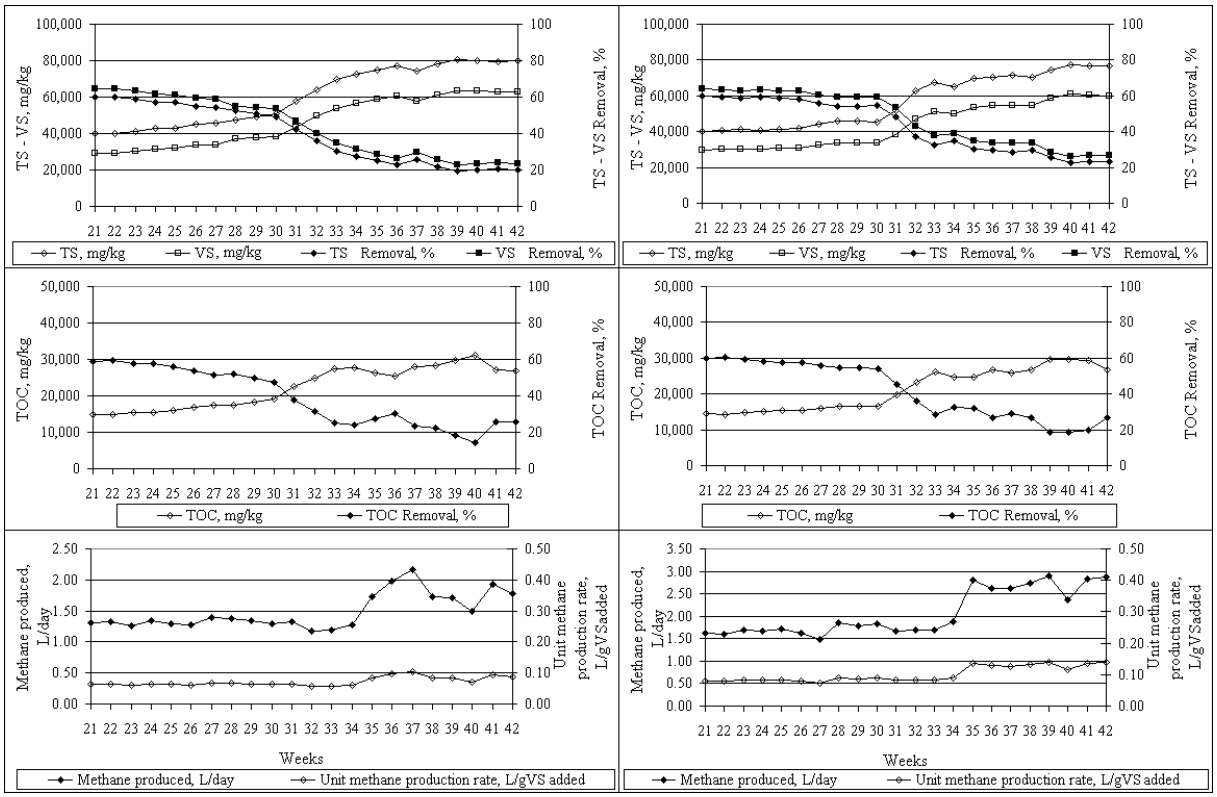

Fig. 3. TS, VS and TOC concentrations in the effluents from mesophilic (A) and thermophilic (B) reactors when only cattle manure of 10% solids content was fed.

3.3. Mixture of cattle manure and corn silage feed at 10% solids content

In this stage of the study, anaerobic digestion of cattle manure along with corn silage as supplementary organic waste was investigated. In this stage of the study corn silage was added to cattle manure of 10% solids content and the reactors were operated at an HRT of 40 days. TS, VS, and TOC concentrations of the corn silage were measured as 230,000 mg/kg, 205,000 mg/kg, and 83,000 mg/kg, respectively. Those of the mixture of cattle manure and

corn silage were determined to be 161,600 mg/kg, 140,600 mg/kg, and 58,400 mg/kg, respectively. TS, VS, and TOC concentrations measured in the effluents from the reactors are shown in Figure 4.

TS removal efficiencies of the reactors were calculated as around 47.5% for mesophilic one and around 51.4% for thermophilic one while VS removal efficiencies were observed as about 53% and about 59%, respectively. 49% and 52.4% of TOC removal efficiencies were obtained for mesophilic and thermophilic reactors, respectively.

After feeding the mixture of cattle manure and corn silage together, the biogas production rate was measured as between 0.16 and 0.37 L_{biogas}/gVS_{added} for mesophilic reactor and between 0.31 and 0.54 L_{biogas}/gVS_{added} for thermophilic reactor. For mesophilic and thermophilic reactors, methane production rates were observed to range from 0.08 to 0.19 $L_{methane}/gVS_{added}$ and from 0.15 to 0.29 $L_{methane}/gVS_{added}$, respectively.

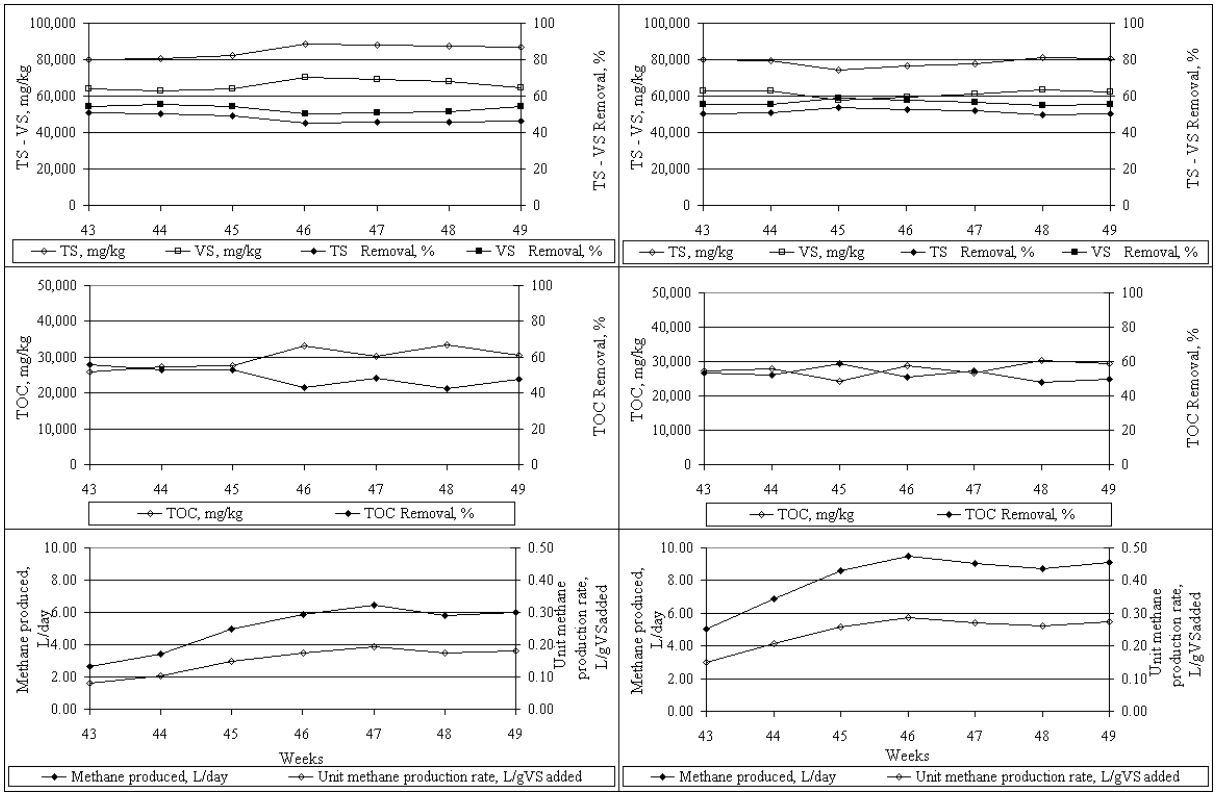

Fig. 4. TS, VS and TOC concentrations in the effluents from mesophilic (A) and thermophilic (B) reactors when a mixture of cattle manure and corn silage of 10% solids content was fed.

Although the removal efficiency in mesophilic reactor increased considerably by the use of corn silage as a supplementary organic waste, the reactor was still less effective in E.coli removal than thermophilic reactor which completely removed E.coli and *Salmonella spp*.

4. Discussion

The results from the both reactors, which are used to treat cattle manure of 5% and 10% solids content anaerobically, suggests that TS, VS, and TOC removal efficiencies as well as biogas and methane production rate per gram VS added were quite similar. The highest removal efficiencies and the highest biogas/methane production rates were obtained in the stage in which cattle manure and corn silage were mixed to obtain 10% of solids content. The results from this stage were compared to the literature data (Table 2). The results shown in Table 2

suggest that study results (VS removal efficiency and methane production rate) are satisfactory compared to literature data. Finally, it is necessary to state that the thermophilic reactor was successful in both *Salmonella spp.* and E.coli removal in stages of the study while mesophilic one was not satisfactory in E.coli removal although it successfully removed *Salmonella spp*. Related Turkish legislation suggests that *Salmonella spp*. and E.coli must not be detected in the effluent [5].

Table 2. Comparison of the study results with literature data.

Reference	Reactor type	VS removal (%)	Methane production ($L_{methane}/gVS_{added}$)
Current study*	Complete mix	59	0.15 – 0.29
[6]	Fill-decant anaerobic	48 – 53.6	0.24 – 0.25
[7]	Anaerobic hybride	59 – 68	0.19
[8]	Two-phase anaerobic digester	30.3 – 62.4	0.07 – 0.24
[9]	Temperature-phased anaerobic digester (TPAD)	37 – 41.5	0.15 – 0.22
[10]	Complete mix	28	0.20
[11]	Temperature-phased anaerobic digester (TPAD)	42.6	0.23
[12]	Anaerobic SBR	22	0.07 – 0.15
[13]	Complete mix	38.4	0.25
[14]	Fill-decant type	42 – 52	0.17 – 0.22
[15]	Complete mix	24.7	0.09

*Cattle manure of 10% solid content mixed with corn silage

5. Conclusions

The performance of anaerobic digestion process for the treatment of cattle manure was investigated in this study. The results of the study, in which the effects of different operational temperatures (35 ºC and 55 ºC), different solids content of the feed (5% and 10%), different hydraulic retention times (20 and 40 days) and the addition of corn silage to the feed on the TS and VS removal performances of the reactors and on the biogas production, suggests

- that cattle manure is possible to treat by both feeding alone and feeding mixed with an organic supplementary material (corn silage for the case),
- that the addition of corn silage to the cattle manure increases the treatment efficiency in both reactors,
- that higher VS removal efficiencies and higher methane production were observed if corn silage are provided to the feed,
- that the thermophilic range of operational temperature shows higher performance in the aspects of both methane production and pathogen removal,
- and that cattle manure can be stabilized by anaerobic digestion in an economical and environmentally beneficial way.

Considering all results from the study, it was concluded that thermophilic reactor was satisfactorily effective in pathogen microorganisms removal and VS stabilization. Besides during the stabilization process the use of a supplementary organic material (corn silage) was proven to sustain high energy production potential.

Acknowledgement

The data presented in this paper was derived from the results of the project 106G026

financially supported by TUBİTAK under the title of "Public Foundations Research and Development Projects." The authors would like to thank TUBİTAK for financial support.

References

[1] TUIK(http://tarimsalbilgi.bloggum.com/yazi/tuikden-hayvansal-urunler-tablosu.html)

[2] R.E. Speece, Anaerobik Biotechnology for Industrial Wastewater, Vanderbilt University, 1995, Tennessee.

[3] T. Coşkun, N. Manav, E. Debik, M.S. Binici, C. Tosun, E. Mehmetli, A. Baban, Anaerobic digestion of cattle manure", Sigma Journal of Engineering and Natural Sciences, article in press, in Turkish.

[4] A. Keshtkar, H. Ghaforian, G. Abolhamd and B. Meyssami, Dynamic Simulation of Cyclic Batch Anaerobic Digestion of Cattle Manure, Bioresource Technology 80, 2001, pp. 9-17.

[5] Turkish legislation on production, import, export, supply, and audit of irrigational supplies with organic, organomineral, microbial and enzyme content. Official Print No. 25452 on May 4, 2004, Article 6.

[6] E. Sanchez, R. Borja, P. Weiland, L. Travieso and A. Martin, Effect of temperature and pH on the kinetics of methane production, organic nitrogen and phosphorus removal in the batch anaerobic digestion process of cattle manure, Bioprocess Eng. 22, 2006, pp. 247–252.

[7] G. Demirer and S. Chen, Anaerobic Digestion of Dairy Manure in a Hybrid Reactor With Biogas Recirculation, World Journal of Microbiology and Biotechnology 21, 2005, pp. 1509-1514.

[8] G. Demirer and S. Chen, Effect of Retention Time and Organic Loading Rate on Anaerobic Acidification and Biogasification of Dairy Manure, Journal of Chemical Technology and Biotechnology 79 (12), 2004, pp. 1381-1387.

[9] A. Sung and H. Santha, Performance of temperature-phased anaerobic digestion (TPAD) system treating dairy cattle wastes, Water Res. 37, 2003, 1628–1636.

[10] B.K. Ahring, A.A. Ibrahim and Z. Mladenovska, Effect of temperature increase from 55 to 65°C on performance and microbial population dynamics of an anaerobic reactor treating cattle manure, Wat. Res. 35 (10), 2001, pp. 2446- 2452.

[11] S. Sung and H. Santha, Performance of Temperature-Phased Anaerobic Digestion (TPAD) System Treating Dairy Cattle Wastes, Tamkang Journal of Science and Engineering 4 (4), 2001, 301-310.

[12] P.N. Dugba and R. Zhang, Treatment of Dairy Wastewater with Two-Stage Anaerobic Sequencing Batch Reactor Systems - Thermophilic Versus Mesophilic Operations, Bioresource Tehnology 68 (3), 1999, pp. 225-233.

[13] A. Singh, G. Giridhar, M. Madan and P. Vasudevan, Anaerobic digestion: an appropriate process for integrated utilization of biomass from non-conventional sources, Proc Fifth Int Symp on Anaerobic Digestion, 1988, pp. 943–946.

[14] S.J. Hall, D.L. Hawkes, F.R. Hawkes and A. Thomas, Mesophilic anaerobic digestion of high solids cattle waste in a packed bed digester, J Agr Eng Res 32, 1985, pp.153–162.

[15] D.J. Hills, Methane gas production from dairy manure at high solids concentrations, T. ASAE 23, 1980, pp. 122–126.

Slaughterhouse waste co-digestion - Experiences from 15 years of full-scale operation

A.E.W. Ek[1], S. Hallin[2], L. Vallin[2], A. Schnürer[3], M. Karlsson[2, 4, *]

[1] *Swedish Biogas International Korea Co., Ltd, Totaleco B/D 1302-7, Seocho-Dong, Seocho-Gu, Seoul, Republic of Korea.*
[2] *Dept. of Biogas R & D, Tekniska Verken i Linköping AB, Sweden.*
[3] *Dept. of Microbiology, Swedish University of Agricultural Sciences, Uppsala, Sweden.*
[4] *Dept. of Physics, Chemistry and Biology, Linköping University, Linköping, Sweden*
** Corresponding author: Tel: +46 13308419, E-mail: martin.karlsson@tekniskaverken.se, marka@ifm.liu.se*

Abstract: At Tekniska Verken in Linköping AB (TVAB) there is a long time experience of handling and producing biogas from large volumes of slaughterhouse waste. Experiences from research and development and plant operations have lead to the implementation of several process improving technological/biological solutions. We can in this paper describe how the improvements have had several positive effects on the process, including energy savings, better odor control, higher gas quality, increased organic loading rates and higher biogas production with maintained process stability. In addition, it is described how much of the process stability in anaerobic digestion of slaughter house waste relates to the plant operation, which allow the microbiological consortia to adapt to the substrate. Since digestion of proteinaceous substrates like slaughterhouse waste lead to high ammonia loads, special requirements in ammonia tolerance are placed on the microbiota of the anaerobic digestion. Biochemical assays revealed that the main route for methane production proceed through syntrophic acetate oxidation, which require longer retention times than methane production by acetoclastic methanogens. Thus, the long retention time of the plant, accomplished by a low dilution of the substrate, is a vital component of the process stability when treating high protein substrates like slaughterhouse waste.

Keywords: *Anaerobic digestion, co-digestion, full-scale, slaughterhouse waste, syntrophic acetate oxidation*

1. Introduction

Slaughterhouse waste is the very energy-rich waste stream of meat industry [1]. As such, it is an attractive material to treat through anaerobic digestion for the production of biogas. However, there are many potential technical and microbiological problems associated with anaerobic digestion of slaughterhouse waste. These include the practical handling according to European Union Animal By-Products (ABP) Regulation [2], protein content [3] and high degradation and volatile fatty acid (VFA) formation rates [4,5]. Reported here are the experiences, production results and R & D activities at the full scale co-digestion biogas plant treating slaughterhouse waste in Linköping, Sweden, for the period 1997-2010.

1.1. Anaerobic digestion of protein-rich substrate

Anaerobic digestion of organic material is a complex microbiological process requiring the combined activity of several groups of microorganisms with different metabolic capacities which need to work in a synchronized manner in order to obtain a stable biogas process [6]. One type of key organisms are the methanogens, producing methane mainly from acetate or hydrogen and carbon dioxide. Protein-rich substrate, such as slaughterhouse waste, is a well-known source of sulfide formation during anaerobic degradation. The increased concentration of sulfides in the digester lead to higher concentrations of corrosive H_2S in the biogas and can further lead to sulfide inhibition of the methanogens [7,8]. When the proteins in slaughterhouse waste are degraded, not only sulfides are formed but also ammonia [3]. The released ammonia increases the pH in the digester and with a large ratio of slaughterhouse waste in the substrate mixture, the pH tends to reach over 8.0, which can be growth limiting for some VFA consuming methanogens [9]. The above optimal pH, together with a high

fermentation rate of proteins and fats in the slaughterhouse waste can lead to an accumulation of fatty acids. Thus, if the organic load to the digester is not decreased at that point, the process overload can lead to increasing concentrations of process inhibiting fatty acids, the consequential pH drop and finally to a total inhibition of methanogenesis and process collapse will follow. The released ammonia (NH_3) from protein degradation is in equilibrium with the less harmful ionized ammonium species (NH_4^+). However, the non-ionized form is itself also a source of inhibition of microorganisms, since the neutral NH_3 can easily pass through cell membranes of bacteria and archaea and upon entering the cell disrupt *e.g.* intra-cellular pH and concentrations of other ions [8]. Thus, methods to lower ammonia levels in anaerobic digesters treating high-protein substrates are desirable and subject to active research [10,11]. Furthermore, at increased pH and temperature, the equilibrium is shifted towards the toxic ammonia, resulting in a positive correlation between toxicity effects and increasing pH and temperature [12]. Among the methanogens, the acetate-utilizing methanogens have been suggested to be responsible for 70-80 % of the methane produced [6]. However, recent results suggest that an alternative methane producing pathway is activated at elevated levels of ammonia [13]. In this pathway, acetate is converted to hydrogen and carbon dioxide by syntrophic acetate oxidizers (SAO), followed by the subsequent reduction of carbon dioxide to methane by hydrogen utilizing methanogens, *i.e.* by this pathway methane is produced by hydrogenotrophic methanogens only. Development of SAO has been shown to occur due to a selective inhibition of acetate-utilizing methanogens by ammonia, released *e.g.* during the degradation of proteins [13].

1.2. Co-digestion plant design and operation

The plant for co-digestion of slaughterhouse waste started operation in 1996. The plant is operated by the company Svensk Biogas AB (SvB), a subsidiary to TVAB, and has since start-up continuously supplied upgraded vehicle-fuel quality biomethane. TVAB has an in-house Biogas R & D department, which continuously work to support production and improve plant performance. Biogas process research is further conducted in collaboration with Linköping University and the Swedish University of Agricultural Sciences [14,15].

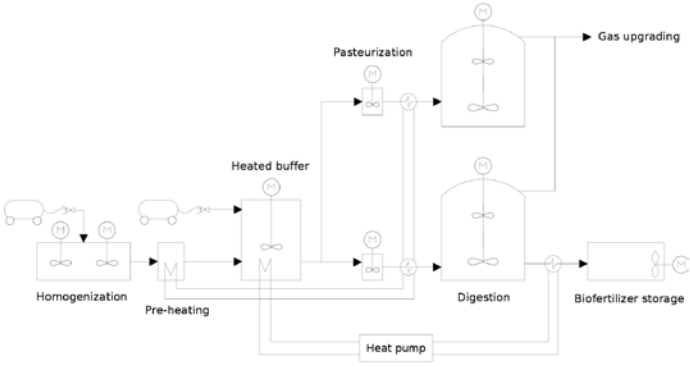

Figure 1. Schematic diagram of the process at Linköping Biogas plant.

The co-digestion plant consists of three basic parts: 1) substrate reception and storage, 2) pasteurization equipment, and 3) anaerobic digesters (Fig. 1). Yearly capacity of the plant is 55 000 metric tons, and the proportion of slaughterhouse waste in the total substrate mixture has varied between 35 and 75 % (w/w, yearly average). During 2010, the capacity of the plant was expanded to 100 000 tons/year.

Slaughter house waste is treated with formic acid at the slaughter house and all waste is delivered to the plant by closed trucks in a grinded (≤ 12 mm) pumpable form and is either

transferred into a combined homogenization and buffer tank or directly into a second, heated buffer tank. After homogenization the substrate mixture is continually pumped to the second heated buffer tank. The target temperature of the second buffer tank is above 75 °C to avoid foaming, to pre-heat the material before pasteurization and to provide a stable thermal disintegration of the substrate. Substrate which is delivered warm is pumped directly to the heated buffer tank to save energy on substrate heating. Before loading of the digesters, the substrate is pasteurized in a batch process for one hour at 70 °C, to fully comply with the EU ABP regulation for category three materials [2]. The anaerobic digestion takes place at mesophilic conditions (38 °C) and the process heat is supplied through the city's waterborne district heating system. The two digesters are continuously stirred tank reactors (CSTR) run in parallel, with a total volume of 7400 m^3 and a hydraulic retention time (HRT) of 45-55 days. The gas composition is, on average, 68 % CH_4, 31 % CO_2 and <100 ppm H_2S. No significant modification to the plant has been necessary, as a consequence of ABP regulation implementation, since the plant was already equipped with the required pasteurization function. However, the precise categorization of different substrates of animal origin has changed over the years, as legislation and its interpretation have changed.

2. Materials and methods

2.1. Operation and analysis data

Operational data on biogas production, biogas composition and the amount and type of incoming substrates were collected from the plant's SCADA-system. pH was analyzed with a WTW 526 pH meter (WTW Inolab, USA), according to Swedish Standard SS 028122:2. Partial (bicarbonate) alkalinity was analyzed by titration to pH 5.4, with simultaneous removal of CO_2, in accordance with Swedish standard SS-EN ISO 9963 Part 2.

Total solids (TS) and volatile solids (VS) were analyzed according to Swedish Standard SS 028113. VFAs were analyzed with a modified spectroscopic HACH method (HACH no. 8196). Dissolved free ammonium nitrogen was analyzed according to FOSS Tecator's Kjeltec method, on a Kjeltec 2200 (Foss Tecator, Denmark). The method gives the concentration of total dissolved free ammonium including a minor fraction of dissolved ammonia nitrogen. (NH_4^+-N (aq) + NH_3-N (aq)).

2.2. Labeling experiments

Inoculation of digester samples with isotopically labeled acetate was performed in order to distinguish between methane formation by acetate utilizing methanogens or via syntrophic acetate oxidation and hydrogenotrophic methanogens. Aliquots of digester content (20 ml) were transferred during flushing with N_2/CO_2 (80/20 percent) to sterile serum vials (118 ml). The bottles were closed with butyl rubber stoppers and aluminum caps and the labeling studies were started by the addition of (2-^{14}C)-acetate (Amersham, England) to a final concentration of 10 kBq/ml. The culture was incubated at 37 °C and the degradation of (2-^{14}C)-acetate and the concomitant formation of $^{14}CH_4$ and $^{14}CO_2$ were determined by scintillation counting. The labeling pattern was analyzed when approximately 90 % of the labeled acetate had been converted. Finally, the ratio of $^{14}CO_2/^{14}CH_4$ was determined and values above 1 were considered as evidence for SAO.

3. Results

3.1. Operational strategy development

During the two first years of operation about 50 % (w/w) of the substrate consisted of cattle manure. This is a common way to avoid problems with process overloading,

nitrogen/ammonia inhibition and micronutrient deficiency [16,17]. However, diluting the substrate mixture with manure has the negative effect of decreasing the amount of methane produced per reactor volume, since the methane yield of manure is far lower than that of slaughterhouse waste [18]. To increase the profitability of the plant, and to meet the increased demand for biomethane as a vehicle fuel, a gradual replacement of manure with more slaughterhouse and other organic wastes with higher methane potential have been implemented (fig. 2B).

3.1.1. Organic load of digesters and biogas production

At start-up, the plant was designed for a substrate mixture with a TS maximum of 8 %. However, as a result of the constant endeavor to increase the organic load and thereby methane production, the TS of the incoming substrate mixture, sampled in the heated buffer tank, has during 2009/2010 reached a TS of 17 % as a yearly average (Fig. 2A), with individual samples during 2009/2010 sometimes reaching 20 %. A replacement of steam injection with district heating for pasteurization in 2007, also led to a thicker substrate mixture, since added water no longer enter the system through the steam.

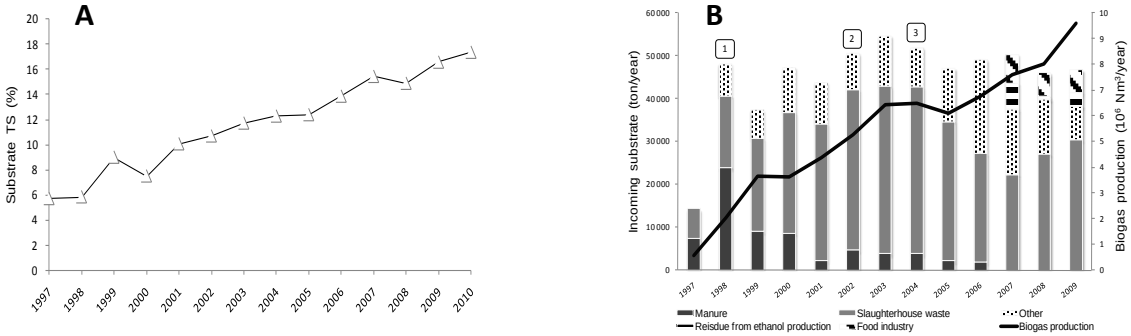

Figure 2. A) Total solids (TS) of incoming substrate (yearly average) during 1997-2010 (data for 2010 up until 2010-05-06), sampled in the heated buffer tank. B) Annual amount of substrate, substrate composition and biogas production during 1997 - 2009. Number captions denote implementation of process additives: [1] $FeCl_2$; [2] hydrochloric acid; [3] KMB1.

As can be seen in Fig. 2B, the plant has experienced an almost unbroken increase of yearly biogas production. In 2009 the average volumetric biogas production reached an average of 3.6 $Nm^3/(m^3\_R \cdot d)$ and a yearly total production of 9.6 million Nm^3.

3.2. Main achievements in process stabilization and optimization

The cut down in manure usage put a focus on process development, which was facilitated by three main appendages to the operational strategy of the plant; 1) addition of ferrous chloride, 2) addition of hydrochloric acid and 3) addition of the process additive KMB1 (Fig. 2B).

3.2.1. Addition of ferrous chloride

Sulfide-associated problems, such as corrosive H_2S in the biogas and sulfide-inhibition of the methanogenesis are both reduced by precipitation of sulfides with Fe(II). At the plant, the addition of ferrous chloride to the homogenization and pasteurization tanks commenced in May 1998 and as a result, the sulfide concentration in the digesters and the concentration of H_2S in the biogas were reduced, as well as the sulfur load on the water scrubbers [19]. The use of ferrous chloride has continued since 1998 and because the addition of the precipitant is made already in the homogenization and pasteurization tanks, the H_2S-induced odors from the buffer and pasteurization tanks are also reduced.

3.2.2. Addition of hydrochloric acid

Laboratory tests, with addition of hydrochloric acid to co-digestion reactors operated under mesophilic conditions were performed in 1999-2000 [20]. Positive effects on volumetric gas production and VFA levels were noted in the digesters where pH was lowered with hydrochloric acid and full-scale acid addition was started at the plant in March 2002. On comparison of the operation performance of the plant in 2000-2001 with 2002-2003, the following direct and indirect effects were observed [19]: digester loading rate could be increased with 70 % on VS basis, gas production increased, acetate concentration decreased by 43 % and partial alkalinity concentration increased from 11 000 mg/L to 17 000 mg/L. On average, between the two periods, the amount of material increased by 20 % (fig 2B) whereas the dry substance of the material increased with 26 % during the same period (fig. 2A). Since also the percentage of slaughter house waste increased from 59 to 72 % in the material, the VS percentage of TS increased. Thus, the gas production increase was a result of the increased loading rate since the specific methane yield per kg VS was unchanged.

3.2.3. Addition of process additive KMB1

To further enhance process stability, and to increase the efficiency of the plant, a process additive known as KMB1 was developed at TVAB [21]. The main effects of the additive were: (1) more stable production, enabling (2) higher organic loading rate without process disturbances and heavy foaming [19], leading to (3) higher methane production. Also, the additive enabled the decrease and final removal of manure in the substrate mixture, and has been added to the plant since November 2003.

3.3. Plant performance after process improvements

After implementation of the three process improving additives mentioned above, a closer study of the process reveal the positive effects (data from 2004-2005). In the heated buffer tank the VFA levels fluctuate to a great extent and can occasionally get very high (up to 16 000 mg/L) while the pH is low (Fig. 3A). However, even though the buffer tank substrate display a low pH and high, fluctuating VFA concentrations (average 8400 mg/L, pH 5.5), the concentration of VFA in the digester is low and stable (average 1600 mg/L, max 2800 mg/L) and the digester fluid has a stable pH of 8.0 (7.9-8.1).

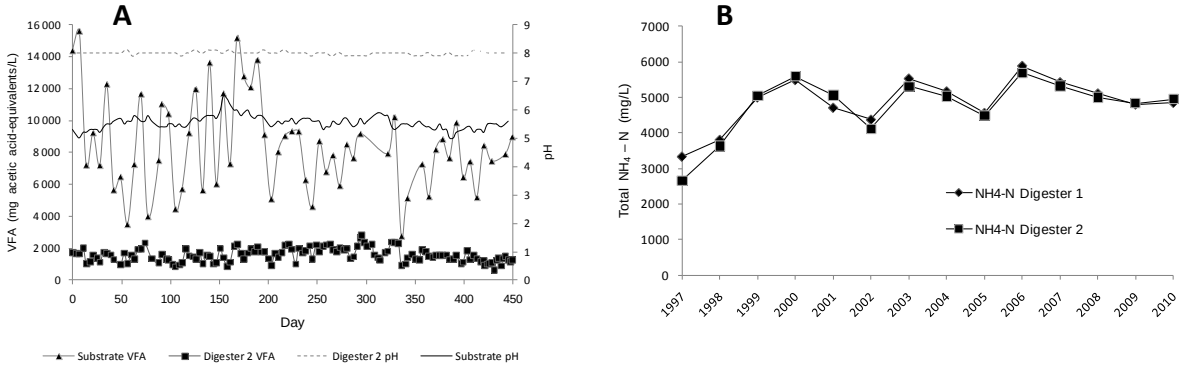

Figure 3 A). Volatile fatty acid (VFA) concentrations (mg acetic acid-equivalents/L) and pH levels in the heated buffer tank (denoted: substrate) and in the biogas digester (data from 2004-2005). B) Total ammonium (NH_4^+-N (aq) + NH_3-N (aq)) concentrations (mg/L) in the digesters during 1997-2010.

Since the plant's early years of operation, the total NH_4-N concentration has been high. The average for both digesters during 1999-2010 has been 5060 mg/L, with a maximum yearly

average of 5880 mg/L (digester 1, 2006) and a minimum yearly average of 4120 (digester 2, 2002) (Fig. 3B). Labeling experiments were performed in 2008 to establish what type of methane formation pathway is prevalent – methane formation by acetate utilizing methanogens or via syntrophic acetate oxidation and hydrogenotrophic methanogens?

The labeling analysis showed production of high levels of labeled carbon dioxide in relation to labeled methane. The $^{14}CO_2/^{14}CH_4$ quota was determined to be 16; clearly showing that methane production in the digester occurred mainly through syntrophic acetate oxidation and hydrogenotrophic methanogenesis. Since the digester is operated at high ammonium levels (5300 mg NH_4^+-N/L at the time of sampling) this is a result that was expected and in accordance with the previous studies that have shown development of SAO in response to increasing ammonia levels[13]. The development of this prevailing metabolic pathway is likely the explanation to the stable operation of the process even at high ammonia levels. Given that methanogenesis via syntrophic acetate oxidation involves a hydrogenotrophic methanogen, that tolerates higher levels of ammonia than acetoclastic methanogens, methane production from acetate can still proceed even though the acetoclastic methanogens are inhibited. Furthermore, isolation and characterization of several ammonia tolerant hydrogen utilizing methanogens, as well as ammonia tolerant syntrophic acetate oxidizing bacteria, support this suggested mechanism for ammonia adaptation in biogas processes [22-24]. However, the generation time of a SAO culture was calculated to be approx. 28 days [13] which can be compared with the times of around 2 - 12 day for acetate utilizing methanogens [25]. Thus, the long retention time would seem to be a prerequisite to allow SAO to establish in the digester.

3.4. Practical experiences

The general plant operation experiences of anaerobic digestion of slaughterhouse waste concern two main themes: 1) logistics and transportation and 2) process and technology. At the slaughterhouse, the waste is grinded to ≤12 mm and treated with formic acid. The grinding at the slaughterhouse allows for transportation of the substrate in slurry form, and thereby a closed-system handling at the biogas plant, which prevents odor problems. Treatment with formic acid prevents foaming which would otherwise cause significant problems during transport and storage at the biogas plant. The thermal disintegration of the substrate in the heated buffer tank, and the fact that the substrate temperature is over 70 °C in large parts of the system, reduces potential problems with clogging and eases pumping of the substrate due to reduced viscosity. Furthermore, to achieve a stable process the type of material co-digested with the slaughterhouse waste is important, and the complimentary substrates should work well in the plant, both from a practical and a process point of view, which will lead to an even substrate mixture over time and thus an even organic loading rate and a stable biogas process.

4. Conclusions

From the long time experiences the following conclusions are established:

- It is possible to operate CSTR co-digestion of slaughterhouse waste, at substrate TS levels significantly over the original design level.
- The plant is operating well at high levels of ammonium, and the long HRT (45-55 day) enables establishment of a mesophilic syntrophic acetate oxidizing culture.
- With optimization of process parameters, substrate composition and through the addition of process additives, it has for 15 years been possible to achieve a continued increase of the biogas production, with basically the original plant capacity.

References

[1] Edström M., Nordberg Å., Thyselius L. Anaerobic treatment of animal byproducts from slaughterhouses at laboratory and pilot scale. Applied Biochemistry and Biotechnology, 109 (13), 2003, pp. 127 - 138.

[2] European Community. Regulation (EC) No. 1774/2002 of the European Parliament and of the Council laying down health rules concerning animal by-products not intended for human consumption. Official Journal, L 273, 2002, pp. 1 - 95.

[3] Hejnfelt A. and Angelidaki, I. Anaerobic digestion of slaughterhouse by-products. Biomass and Bioenergy 33 (8), 2009, pp. 1046 - 1054.

[4] Salminen E., Einola J., Rintala J. Characterisation and anaerobic batch degradation of materials accumulating in anaerobic digesters treating poultry slaughterhouse waste. Environ. Technol. 22 (5), 2001, pp. 577 - 585.

[5] Salminen E. and Rintala J. Semi-continuous anaerobic digestion of solid poultry slaughterhouse waste: effect of hydraulic retention time and loading. Water Research 36 (13), 2002, pp. 3175 - 3182.

[6] Zinder S. H. Microbiology of Anaerobic Conversion of Organic Wastes to Methane: Recent Developments. ASM news, 50 (7), 1984.

[7] Ochieng' Otieno F. A. Anaerobic digestion of wastewaters with high strength sulphates. Discovery and Innovation 8 (2), 1996, pp. 143 - 150.

[8] Chen Y., Cheng J. J., Creamer K. S. Inhibition of anaerobic digestion process: A review. Bioresource Technology 99 (10), 2008, pp. 4044 - 4064.

[9] Jiunn-Jyi L., Yu-You L., Noike, T. Influences of pH and moisture content on the methane production in high-solids sludge digestion. Water Research 31 (6), 1997, pp. 1518 - 1524.

[10] Tada C., Yang Y., Hanaoka T., Sonoda A., Ooi K., Sawayama S. Effect of natural zeolite on methane production for anaerobic digestion of ammonium rich organic sludge. Bioresource Technology 96 (4), 2005, pp. 459 - 464.

[11] Nordell E., Hallin S., Johansson M., Karlsson M. The diverse response on degradation rate of different substrates upon addition of zeolites. Third International Symposium on Energy from Biomass and Waste, Venice, Italy, 2010. ISBN 978-88-6265 -008-3.

[12] Siegrist H., Vogt D., Garcia-Heras J.L., Gujer W. Mathematical model for meso- and thermophilic anaerobic sewage sludge digestion. Environmental Science and Technology, 36 (5), 2002, pp. 1113 - 1123.

[13] Schnürer A. and Nordberg Å. Ammonia, a selective agent for methane production by syntrophic acetate oxidation at mesophilic temperature. Water Science and Technology 57 (5), 2008, pp. 735 - 740.

[14] Hellman J., Ek A. E. W., Sundberg C., Johansson M, Svensson B. H. and Karlsson M. Mechanisms of increased methane production through re-circulation of magnetic biomass carriers in an experimental continuously stirred tank reactor. 12th World Congress on anaerobic digestion, Guadalajara, Mexico, 2010.

[15] URL: http://microdrive.phosdev.se/index.php?page=Companies

[16] Tafdrup S. Centralized biogas plants combine agricultural and environmental benefits with energy production. Water Science and Technology 30 (12), 1994, pp. 133 - 141.

[17] Alvarez R. and Lidén G. Semi-continuous co-digestion of solid slaughterhouse waste, manure, and fruit and vegetable waste. Renewable Energy 33 (4), 2008, pp. 726 - 734.

[18] Deublein D. and Steinhauser A. Biogas from waste and renewable sources. Weinheim, Germany. Wiley-VCH, 2008.

[19] Vallin L, Christiansson A., Arnell M., Undén P. D2.2 Operational experiences of cost effective production in Linköping, Sweden. Biogasmax Integrated Project No. 019795, 2007.

[20] Ejlertsson J. (2005). Swedish Patent No SE 525 313.

[21] Holm S., Ejlertsson J., Carlson B. (2005). Swedish Patent No SE 526 875.

[22] Schnürer A., Schink B., Svensson B.H. *Clostridium ultunense* sp. nov., a mesophilic bacterium oxidizing acetate in syntrophic relationship with a hydrogenotrophic methanogenic bacterium. International Journal of Systematic Bacteriology 46 (4), 1996, pp. 1145 - 1152.

[23] Schnürer A., Zellner G., Svensson B.H. Mesophilic syntrophic acetate oxidation during methane formation in different biogas reactors. FEMS Microbiology Ecology 29, 1999, pp. 249 - 261

[24] Karlsson M., Roos S., Schnürer A. Description of '*Candidatus Syntrophicus schinkii*' an anaerobic, syntrophic acetate-oxidizing bacterium isolated from mesophilic digester operating at high concentration of ammonia. FEMS Microbiology Letters, 309 (1), 2010, pp. 100 – 104.

[25] Jetten M. S. M., Stams A. J. M., Zehnder A. J. B. Methanogenesis from acetate: A comparison of the acetate metabolism in *Methanothrix soehngenii* and *Methanosarcina* spp. FEMS Microbiology Letters, 88 (3-4), 1992, pp. 181 - 197.

Development of Process Technology to Produce Low Cost Biofuel I - Minimization of Operating Parameters during Preparation of Biodiesel

Soumya Parida, Sunasira Misra, Debendra Kumar Sahu*

Dept. of Chemistry, C.V. Raman College of Engineering, Bidyanagar, Mahura, Janla, Bhubaneswar-752054, India
** Corresponding author. Tel: 91-674 2460043, Fax: 91-674 2460093,Mobile: 91-9937141191, E-mail: drdksahu62@rediffmail.com*

Abstract: Fatty acid methyl ester (FAME), a renewable liquid biofuel popularly known as biodiesel, is emerging as a suitable replacement to common diesel fuel (CDF) in unmodified Compression Ignition (CI) engine. Present article reports the development of a process to reduce the operating cost during the conversion of vegetable oil to biodiesel through the application 1kW sonication techniques at various stages of the composite process. Around 98 % yield was achieved by employing minimum quantity of excess alcohol and alkali catalyst in transesterification reaction. After the completion of reaction, instantaneous separation of FAME from glycerol is a noticeable advantage. Its reaction parameters such as time and temperature have been reduced drastically. The ultrasound energy had also produced excellent benefit during purification of crude FAME through the efficient removal of mono and diglyceride from FAME. The analysis of the products was done as per ASTM methods and its fuel characteristics were evaluated using a research engine.

Keywords: *FAME, Biodiesel, Transesterification, Ultrasonication, Compression Ignition engine*

1. Introduction

Stupendous efforts have been made during the last few decades on bio-fuel chemistry. Amongst these, biodiesel in particular, has captured the world attention as an impressive substitute to common diesel fuel (CDF). It is the monoalkyl esters of long chain fatty acids (FAME) derived from vegetable oil and animal fats. The feedstock composed of mainly triglycerides with high viscosity, very low vapor pressure and impurities like free fatty acid (FFA), phospholipids, moisture, vegetable sediments and gum hence cannot act as ideal fuel for CI engine [1]. On being converted to FAME (having both carbon and viscosity equivalent to CDF) through a chemically reversible reaction called transesterification [1, 2], it becomes suitable to replace CDF, hence called biodiesel. Transesterification reaction is the vital step of the composite process where the vegetable oil (triglyceride) is treated with a short chain alcohol viz. methanol, in presence of a catalyst (acidic/basic) at a suitable temperature and reaction time to produce corresponding FAME as per gross reaction (1). It is renewable, biodegradable with relatively less emission profile, admissible viscosity, flash point and a high cetane number [3].

Triglycerides + 3 CH_3OH -→ Glycerol + FAME (1)

Even though the synthesis of FAME from vegetable oil is relatively facile its economization is challenging. The major drawback of the composite process lies largely on the costly feedstock, inefficient extraction of oil from seed, complicated purification of crude oil and product, high reaction parameters of transesterification, ineffective separation of products and loss of homogeneous catalyst. The difficulty involved with purification step of FAME comprises utilization of vast quantity of fresh water, loss of small quantity of the product with water followed by waste water treatment.

The present paper attempts to develop a process to produce biodiesel from refined soybean oil and sunflower oil by overcoming major hurdles involved in both transesterification and

purification steps. Reduction of reaction parameters and other improvements in the various working steps have been tried with the help of ultrasonic waves [4, 5]. The purified biodiesel was subjected for exploration of its fuel characteristics in an unmodified CI engine.

2. Materials and methods

2.1. Materials

Refined soybean oil of nature fresh brand and sunflower oil of fortune brand were procured from local dealers. Anhydrous methanol (MeOH) (99.5%) and sodium hydroxide (NaOH) pellets were procured from M/s Finar, Ahmedabad. Fatty acid profile of the feedstock was evaluated by Gas Chromatography while moisture by using Karl Fischer (Systronics make) and phospholipids by classical method. Refined vegetable oil are found to contain negligible quantity of free fatty acid, moisture phospholipids, and used as feedstock for biodiesel preparation without further purification. The Ultrasonic Processor of Sonapros PR-1000 model of 1kW was used to generate sonication in a special designed three necked glass reaction vessel housed in a sound dampener. Gas Chromatograph of model CERES 800 plus of M/s Thermo Electron LLS Pvt. Ltd was used for the analysis of glycerol, monoglycerides, diglycerides, triglycerides, methyl esters of various fatty acids. Kirloskar make compression ignition engine with variable compression ratio was procured to study its performance with different biodiesel and evaluate their respective fuel properties.

2.2. Method

2.2.1. Transesterification reaction for the conversion of vegetable oil to FAME

All the ingredients of transesterification such as vegetable oil, anhydrous methanol was kept over freshly dried anhydrous sodium sulphate for over 10hours before use. Clearly homogeneous stock solution of desired strength of sodium hydroxide-methanol was prepared and also stored over freshly dried anhydrous sodium sulphate to remove any possibility of moisture formation. Exactly weighed quantity of vegetable oil was taken in the sonication vessel and preheated to a temperature 5^{o}C below the operating temperature. Methanol-sodium hydroxide catalyst solution was added into the sonication vessel very slowly without lowering the pre set temperature of the vessel. Appropriate horns/probes of the ultrasonic processor were inserted into the sonicator vessel so that its tip dips about 5mm into the alcohol phase. Reflux condenser, thermocouple, and dropper to draw sample time to time were placed with the reactor and appropriate sonication energy was applied. The experiments were conducted over wide range of methanol and oil molar ratio between 3:1 to 15:1, varying quantity of sodium hydroxide catalyst ranging from 0.1% to 1.5% with respect to oil and reaction times varying from 5 minutes to 45 minutes as well as wide temperature range of 30 to 70°C. After the completion of the reaction, heavier glycerol was gravity separated instantaneously from the reacted mixture leaving FAME as upper layer in a separating funnel.

2.2.2. Purification of Products

Crude FAME containing free glycerol, small amount of alkali and partial unconverted portion of triglycerides usually are usually done complicated water washing or vacuum distillation methods [6]. Disadvantages associated with such classical process is the partial loss of biodiesel and poisonous methanol, total loss of costly homogeneous catalyst, use of large quantity of fresh water followed by adopting costly waste water treatment process. While purification through distillation under reduced pressure was found to make partial oxidation of biodiesel due to the presence of double bond with fatty acids of FAME. Moreover, both methods failed to reduce mono- and diglycerides impurities from it [7]. In order to overcome the difficulties a novel method was adopted to purify FAME after its separation from reaction

mixture. The neutralization of the alkali content of the product was done with dilute sulphuric acid [8] followed by counter current water washing to remove entire unreacted alcohol and residual free glycerol. By this way the requirement of fresh water was reduced to only 2 liters per litre of FAME in compare to large quantity of water utilized earlier [9]. The methanol was recovered from the waste water by distillation. About 90% methanol content of washed water was recovered by distillation. The waste of small quantity of FAME through washed water was minimized by reusing the distillate as washing fluid. The purified product was dried under by purging dried air. The mono- and diglycerides were reduced from the product by treating with silica gel of particular surface property and of particular mesh size under ultrasonication for 15-20 minutes. This purification method without thermal treatment prevents partial decomposition of the relatively unstable FAME containing un-conjugated double bonds.

2.2.3. Analysis of biodiesel

The ester content of soybean oil methyl ester and sunflower oil methyl ester was determined using Gas Chromatography with Flame Ignition Detector (FID), % yield was calculated following ASTM: D 6584-00 and moisture, viscosity, flash-fire point, density, etc as per the ASTM6547 method and GC graph is shown in Fig. 1.

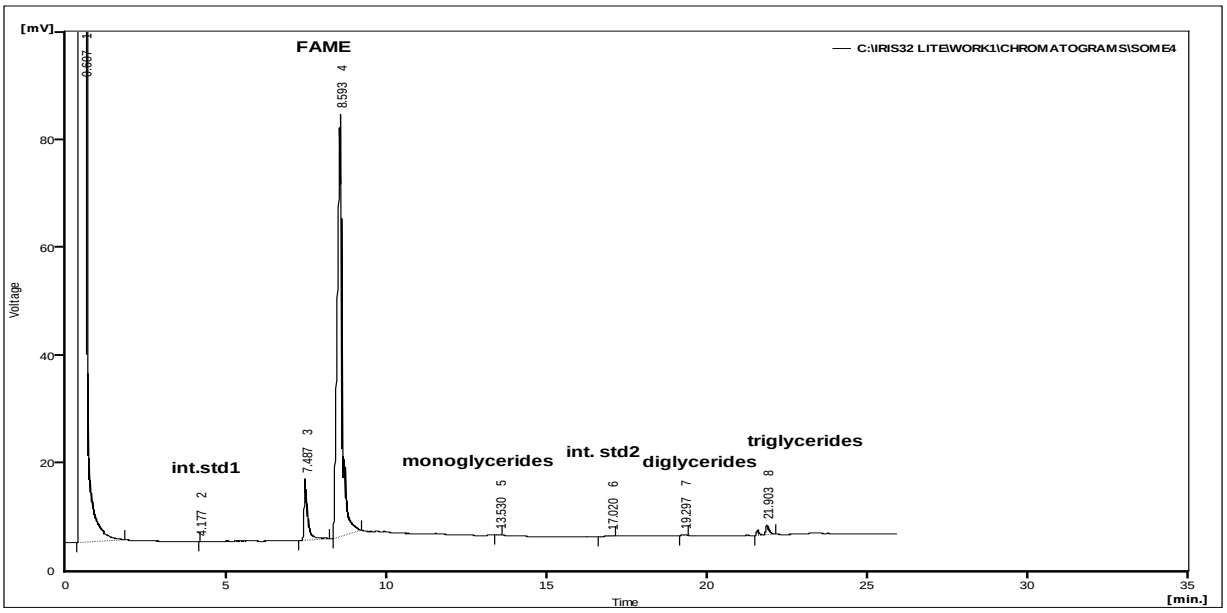

Fig. 1. Soy-FAME Gas Chromatogram

3. Results and Discussion

3.1. Effect of alcohol oil molar ratio:

The theoretical molar ratio of alcohol to oil in the transesterification reaction is 3:1. The higher molar ratio of methanol to oil is involved with catalytic braking of carbonyl bond with glycerides under strong thermal turbulence created by sonication. Availability of more solvent brings poorly soluble oil slowly into the homogeneous reaction phase. The nascent fatty acids after its liberation from glyceride are highly acidic for esterifiation with vast quantity of methanol available as medium. The presence of alkali catalyst in the reaction mixture probably helps the esterification. It is observed that with 5:1 to 9:1 molar ratio of alcohol-oil, ester formation (shown in Fig. 2) is more than 98%. When it is increased to 15:1 the yield of esters dropped to 80%. Such higher molar ratio of alcohol to oil probably reduces the

adequate homogeneous catalytic concentration by dilution as well as interferes with the separation of glycerin as it is dispersed in large volume of solution thereby lowers the yield of esters. FAME yield is drastically reduced when molar ratio goes down from 5:1 which may be due to the fact that insufficient solvent fails to bring poorly soluble oil for reaction zone. Sonication technique proved to be more beneficial leading to an enhancement in the yield.

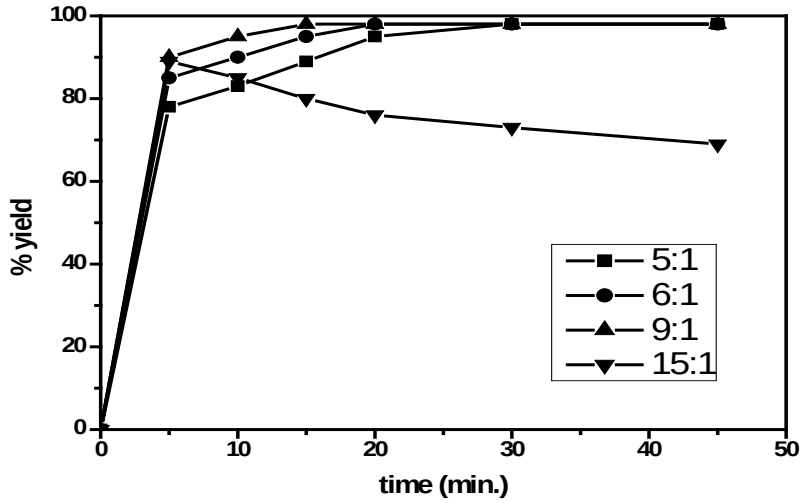

Fig. 2. Percentage yield of soy-FAME at varied methanol-oil molar ratios and different interval

3.2. Effect of catalyst concentration:

Methanolysis of soybean and sunflower oil is done by taking low cost NaOH as catalyst over the concentration range of 0.3 to 1.2 % wt with respect to oil. With alcohol-oil molar ratio 6:1 and temperature 60°C the product is analyzed at different time intervals starting from 5 min to 45 minutes. The results are displayed in Fig. 3. It is observed that the reaction has shown a yield of around 85% even with a low catalyst concentration of 0.3% in 45 minutes. Unlike the mechanical stirring method where the yield of products with low catalyst concentration is quite low, the sonication technique proved to be more beneficial leading to an enhanced increase in yield of methyl esters. However the maximum 98% yield is obtained at catalyst concentration of 1% wt. of oil in less than 15 minutes time. Longer reaction time found to increase the viscosity of FAME may be due to back reaction of FAME with glycerol.

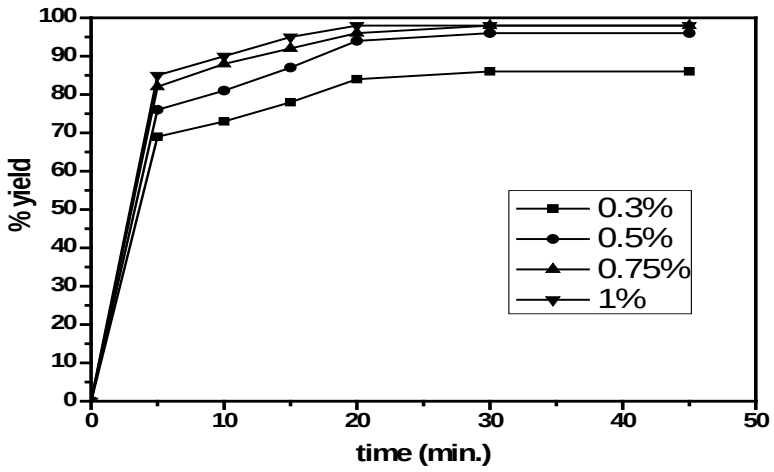

Fig. 3. Percentage yield of soy-FAME at varied catalyst concentrations and different time intervals

3.3. Effect of temperature:

It is observed that transesterification under sonication is temperature dependent. At temperature 60-65°C more than 90% conversion is achieved in just 5 min (shown in Fig. 4). The gas chromatogram for this conversion is shown in Fig. 1. The ultrasound technique involves the formation of a fine dispersion between oil and alcohol due to micro-turbulence generated by cavitations bubbles creating enormous interfacial area. Thermal input between two immiscible liquids under sonication forms more dispersion and thus accelerates chemical reactions especially between two immiscible ingredients.

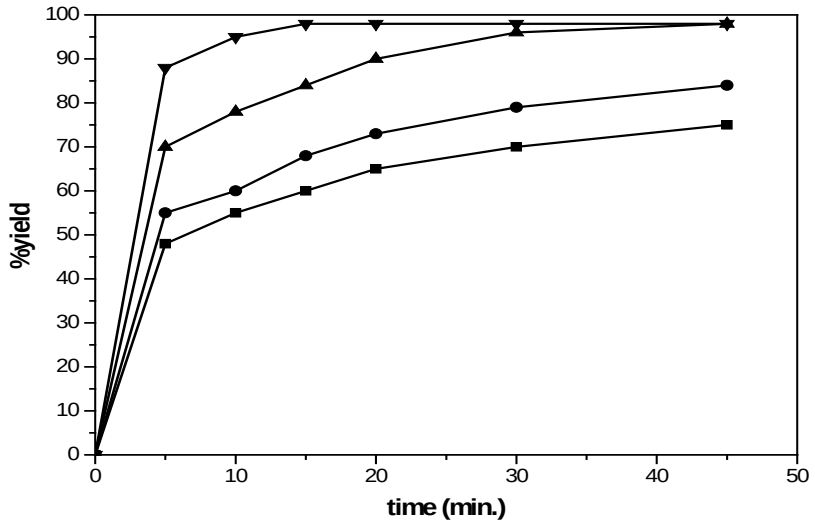

Fig. 4. % yield of soybean oil methyl ester at varied temperature and different time intervals

3.4. Performance of biodiesel in IC engine

The biodiesel with maximum conversion (98%) after purification and analysis is taken up for the evaluation of its fuel properties in a CI research engine. Due to low vapour pressure of FAME the flash point is found to be more than 130^0C. Hence it cannot be used as a direct fuel in the unmodified CI engine. Hence, FAME is blended with CDF in the proportion of 5% and 10%, called as B-05 and B-10 and used as fuel [6] in the unmodified CI engine.

The density and kinematic viscosity of FAME is equivalent to CDF. The gross calorific value (GCV) is 1-2% lower than diesel. The brake specific fuel consumption (BSFC) i.e. the ratio of fuel mass flow of an engine to its output power were drawn for soybean FAME-CDF blended B-05 and B-10 at low engine load under variable compression ratio (CR). BSFC is found to be higher at lower loads and as the load increased its value decreased. It is also noticed that the BSFC for B-05 is greater than that of B-10. The difference between BSFC values for both the blends is reduced with rise in load (Fig. 5 & 6). Due to higher flash point and lower calorific value, the BSFC should rise with biodiesel content in the biodiesel-diesel blended fuel, but at lower loads this does not happen. It may be due to the presence of oxygen (attached to carbonyl carbon) content in biodiesel as well as its better spray characteristics (due to its lower viscosity) and comparable energy density for which the brake power is improved [10]. Overall, BSFC of biodiesel is at par with CDF, may be due to the presence of un-conjugated double bonds with fatty acids of FAME.

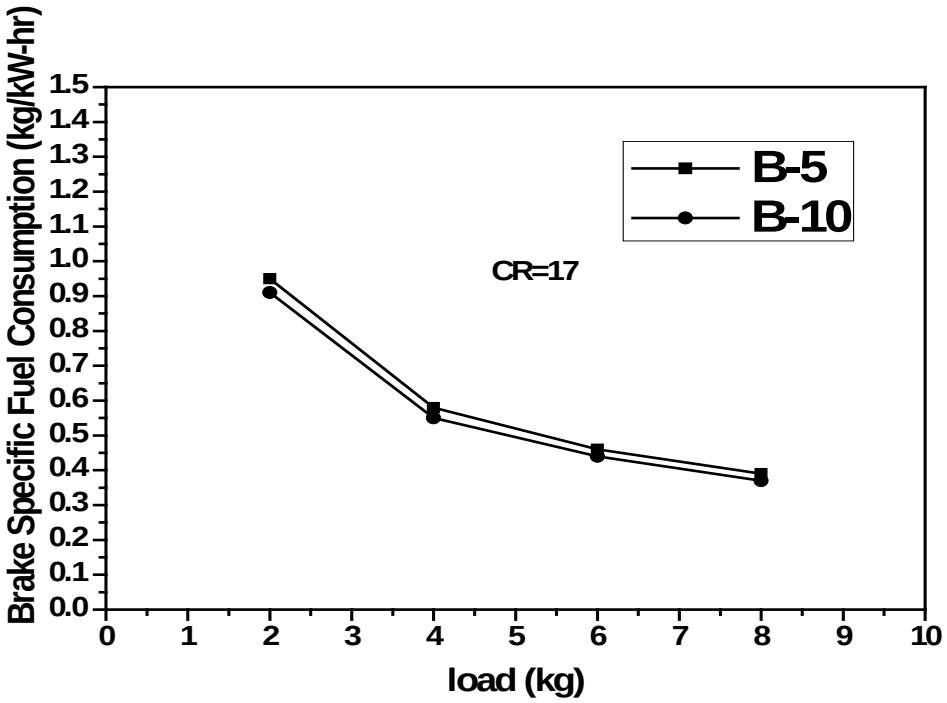

Fig. 5. Variation of Brake Specific Fuel Consumption with different loads at CR of 17 for B-05 & B-10

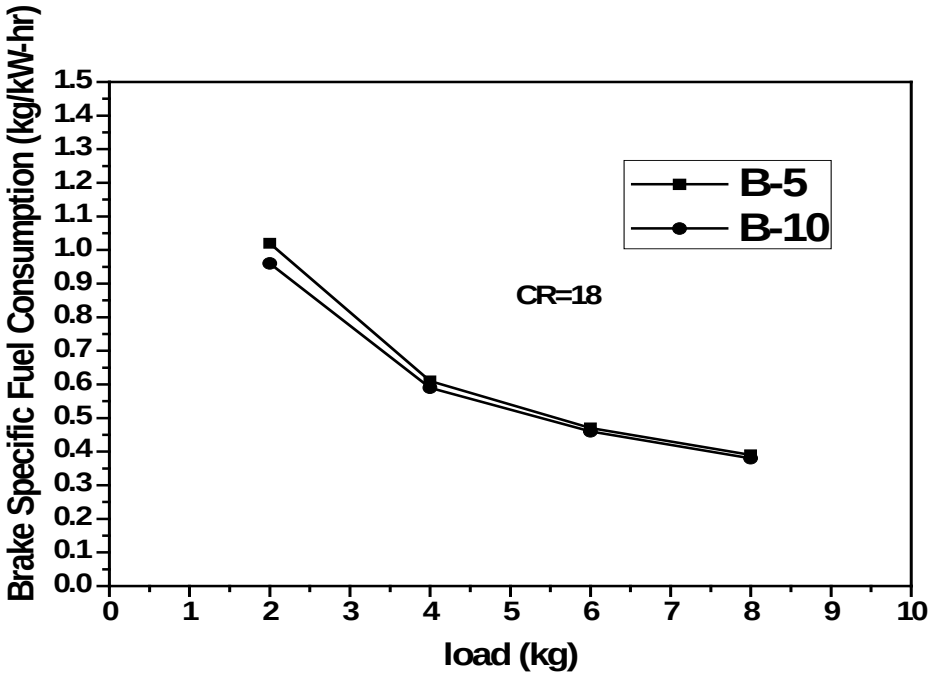

Fig. 6. Variation of BSFC with different loads at compression ratio 18 for B-05 & B-10

4. Conclusion

The paper puts up a composite process to produce biodiesel from vegetable oil with reduced operating parameters such as the reduction of reaction time, reaction temperature, reduction in quantity of unrecoverable homogeneous catalyst, utilization of lesser amount of excess methanol for achieving excellent yield by the application of low energetic (1kW) ultrasonication. However, the transesterification reaction under sonication is found to be

temperature dependent. The separation of FAME from glycerol under the present working condition is instantaneous. The complicated purification step has been simplified. Use of silica gel along with sonication found to reduce the impurities of crude FAME such as free glycerol, mono and diglycerides. Hence, the application of sonication is found to be beneficial with composite process of synthesizing biodiesel from refined vegetable oil. Brake Specific Fuel Consumption of biodiesel prepared through the application of ultrasonication found to be at par with that of Common Diesel Fuel although the gross calorific value of biodiesel is 1.5% lower than CDF, which may be due to the presence of un-conjugated double bonds with many fatty acids of FAME that could replace it in CI engine.

References

[1] Ma F., Hanna M.A., Biodiesl production: A review, Bioresour Technol.70, 1999, pp.1-15

[2] Meher L.C.,Vidyasagar D,Naik S.N. Technical aspects of biodiesel production by transesterification-a review, Renewable and Sustainable Energy Reviews 10, 2006, pp. 248-268

[3] Toda, M; Takagaki A, Okamura M, Kondo J.N., Hyashi S, Domen K, Hana M.; Biodiesel made with sugar catalyst, Nature 438, 2005, pp. 178

[4] Karaosmanoglu F, Cigizoglu K.B.,Tuter M,Ertekin S. Investigation of refining steps of biodiesel production, Energy and Fuels 10, 1997, pp. 890-895

[5] Sahu D.K. and Parida S., A Process Technology for the Production of Low Cost Biodiesel, Indian Patent Application no- 165/KOL/2009 of dated 29.01.2009,

[6] Yori J.C., D'Ippolit S.A., Pieck C.L., Vera C.R., Deglycerolyzation of biodiesel streams by adsorption over silica beds, Energy & Fuels 21, 2007, pp. 347-353

[7] Sahu, D.K. and Parida, S., Application of process of sonoication for single phase stability of straight vegetable oil-diesel blended fuel, WREC2009-Asia, pp. 56

[8] Naik M., Meher L.C., Naik S.N., Das L.M., Production of biodiesel from high free fatty acid Karanja (Pongamia pinnata) oil, Biomass and Bioenergy 32, 2008, pp. 354-357

[9] Issariyakul T., Kulkarni M.G., Meher L.C., Dalai A.K., Bakhshi N.N., Chemical Engg. Journal 140, 2008, pp. 77-85

[10] Raheman H. and Ghadge S.V. Performance of Diesel engine with biodiesel at varying compression ratio and ignition timing, Fuel 87, 2008, pp. 2659-66

Orthogonal array design for biodiesel production optimization - using ultrasonic-assisted transesterification of *Camelina sativa* L. Crantz oil

WU Xuan[1,*], LEUNG Y.C., Dennis[1]

[1] *Department of Mechanical Engineering, The University of Hong Kong, Hong Kong, China*
** Corresponding author. Tel: +852 51363280, E-mail:wuxuan@hku.hk*

Abstract: Camelina seed oil has recently attracted great interest as a low-cost feedstock for biodiesel production because of its high oil content and environmental benefits. In the present study, an orthogonal array design was used to optimize the biodiesel production from camelina seed oil using ultrasonic-assisted transesterification. Four relevant factors are investigated: methanol to oil ratio, catalyst concentration, reaction time and temperature to obtain maximum fatty acid methyl ester (FAME) yield of biodiesel. An OA_{25} matrix was employed to study the effect of the four factors, by which the effect of each factor was estimated using statistical analysis. Based on the results of the statistical analysis after the orthogonal experiments, maximal biodiesel FAME yield (98.6 %) was obtained under the conditions of 8:1 methanol to oil molar ratio, 1.25 wt.% catalyst concentration (KOH), 50 min reaction time, and 55 ℃ reaction temperature. Other properties of the optimized biodiesel, including density, kinematic viscosity, and acid value, were conformed to the relevant ASTM and EN biodiesel standards and thus the optimized biodiesel from camelina oil basically qualified to be used as diesel fuel.

Keywords: Biodiesel, Orthogonal experiment, Optimization, Ultrasonic-assisted, Camelina oil.

1. Introduction

In recent years, biodiesel, as a low-emission renewable fuel, has attracted great public interest and there is a huge demand for biodiesel in the renewable fuel market. At present, most ~~of~~ biodiesel is produced from vegetable oils, such as soybean and rapeseed [1]. However, many vegetable oils for biodiesel production are edible and compete with the edible oil market. It will increase the cost of vegetable oils and cause deforestation since a lot of forests have to be felled for plantation purposes [2]. Moreover, the cost of raw materials accounts for 60-80 % of total biodiesel production [3]. Increasing cost of vegetable oils also causes the cost of biodiesel production higher. Therefore, many researchers focus on di fferent feedstocks of biodiesel and explore non-edible vegetable oils for biodiesel production, such as jatropha curcas oil and algae oil [4].

Camelina (*Camelina sativa* L. Crantz), is a spring annual oilseed plant originated in Germany in about 600 B.C.. It grows well in temperate climates and matures earlier than other oilseed crops [5]. In comparison with common oilseed crops, camelina has lower agriculture inputs, such as lower water, pesticide and fertilizer requirements, and higher cold-weather tolerance. Therefore, camelina may avoid deforestation in certain extent since it can be cultivated in agriculturally undesirable lands which are not suitable for normal crops, hence improving the quality of lands [6]. Furthermore, camelina seeds have an oil content as high as 28 to 40 %, which makes camelina a high oil-bearing crop [7]. Therefore, the use of camelina oil as feedstock for biodiesel production can greatly reduce the production cost of biodiesel and offer some environmental benefits.

Frohlich and Rice [8] already evaluated the possibility of using camelina oil as a source for biodiesel production and Patil et al. [9] also tried to produce biodiesel from camelina oil using supercritical and subcritical methanol with cosolvents. Although there are some studies related to biodiesel produced from camelina oil, the optimal production conditions have never been investigated. Most optimal conditions were attained using a stepwise approach, which examined one process condition at a time [10]. This method was time-consuming and might

not get the right optimal conditions because some process conditions affect the yield of biodiesel simultaneously. This paper used an orthogonal array experimental design to optimize the biodiesel production conditions from camelina seed oil in order to avoid these problems. The use of the chemometric method: Orthogonal Array Experimental Design for process optimization has already found many applications elsewhere. It involves the selection of some representative combinations of factors and levels for the experiments to reflect the situation of the whole selected examined area. It is a cost-effective optimization strategy that can obtain the optimal level of each factor in a limited number of experimental trials [11]. This paper discussed the main process conditions in the transesterification reaction using orthogonal array experiments to optimize biodiesel production. To confirm whether or not the final product can be used as a qualified fuel, this study ~~will~~ also examined its compliance with international biodiesel standards.

Normally, a stirred reactor is used as the reaction vessel for continuous alkali-catalyzed biodiesel production. However, ultrasonic irradiation has proved to be a useful tool for strengthening the mass transfer of immiscible liquids. It can cause cavitation of bubbles near the phase boundary between immiscible liquid phases and then the asymmetric collapse of the cavitations bubbles disrupts the phase boundary and causes emulsification. Micro jets, which are formed by impinge one liquid to another, lead to intensive mixing of the system near the phase boundary and thus reactants can be produced more quickly [12, 13]. Therefore, assisted with ultrasound, the reaction time may be reduced dramatically and the high reaction temperature may be lower than in traditional mechanical stirring production process. That would reduce the production cost of biodiesel and save more energy.

2. Methodology

Reagents and catalysts

Cold-pressed camelina seed oil, obtained from Campressco Products Inc. (Saskatchewan, Canada), was used for the experiments. The main chemical compositon of the oil was, expressed in wt.%, 5 % palmitic acid, 16.7 % oleic acid, 16.9 % linoleic acid, 16.1 % cis-11-eicosenoic acid and 38.1 % linolenic acid. Analytical grade methanol (99.9 %) was used in the experiments and potassium hydroxide (>85 %) in pellet form was used as the catalyst for the alkaline transesterification reaction.

2.1. Experimental process

Around 100 g (±0.1) of camelina oil was weighted and placed in a 250 ml glass bottle. The amount of methanol used was calculated based on its molar ratio with oil. The catalyst was first dissolved completely in methanol with a prefixed amount using a standard mixer, and then the mixture was added into the oil. The whole reaction was carried out in an ultrasonic bath obtained from Jeio Tech Co., Ltd. (model: US-05; frequency: 40 KHz; volume: 5L) and operated at 40 KHz. To enhance mass transfer and the reaction rate, the bottle was shaken for about 20 seconds by hand for every 10 minutes. Until reaching the preset reaction time, the glass bottle was then removed from the bath and the products of the reaction were settled down overnight at the room temperature. Two major products was observed in the bottle: crude biodiesel phase at the top and glycerol phase at the bottom. These two phases were separated by centrifugation (rotating speed: 8000 rpm; time: 5 min). After that the crude biodiesel was washed several times by deionized water assisted with ultrasound to remove the impurities and unreacted catalyst. The use of ultrasound reduced the washing times.

2.2. Orthogonal experiment design

In the study, the experiments were based on an orthogonal array experimental design (OA_{25} matrix) where the following four variables were analyzed: methanol to oil molar ratio (factor A), catalyst concentration (factor B), reaction time (factor C) and reaction temperature (factor D). These variables were identified to have significant effects on the yield of biodiesel produced from other feedstocks [10]. An OA_{25} matrix was employed to assign the considered factors and levels as shown in Table 1. Twenty-five trials were carried out according to the OA_{25} matrix to complete the optimization process. Each row of orthogonal array represents a run, which is a specific set of factor levels to be tested. The run order of the trials was randomized to avoid any personal or subjective bias. Here the matrix denotes four factors each with five levels and the extra column remained could be used as experimental error to indicate the reliability of the whole experiments. Statistical analysis was carried out to reflect the optimal reaction conditions and their magnitudes.

Table 1 Levels and factors affecting the FAME yield of biodiesel.

	Factors			
Level	Alcohol quantity (Molar ratio) A	Catalyst concentration (wt.%) B	Reaction time /min C	Reaction temperature /℃ D
1	2:1	0.75	10	25
2	4:1	1	30	35
3	6:1	1.25	50	45
4	8:1	1.5	70	55
5	10:1	1.75	90	65

2.3. Fuel properties of biodiesel

The whole experiments of biodiesel were aimed at increasing the fatty acid methyl ester (FAME) yield. This yield determines the quality of the biodiesel product and indicates the efficiency of oil conversion. The EN standard (EN14214) requires FAME content of biodiesel to be over 96 % [14]. In the present study, the FAME yield was analyzed by a Hewlett-Packard 6890 Series gas chromatograph (Palo Alto, USA) according to the AOCS official methods Ce 1-62 [15], equipped with a flame ionization detector (FID) operating at 300 ℃ and a capillary injection system operating at 250 ℃. The carrier gas was high-purity helium, with a constant flow of 1.0 ml/min, and samples of 1 μL were injected in split mode with a split ratio of 80:1. The column was a BD-EN14103 HP-INNOWax column (J&W Scientific, USA) with 30 m in length, 0.32 mm internal diameter and 0.25 μm film thickness. To minimize the experimental error, a known amount of a specific component methyl nonadecanoate (C19:0), used as the internal standard, was added into the sample prior to the GC injection. Other properties of the final biodiesel product, including density, kinematic viscosity and acid value, were determined in order to evaluate its suitability as diesel fuel substitute. The density was determined at the room temperature by using a density bottle while its kinematic viscosity was determined with an ubbelohde glass capillary kinematic viscometer according to the ASTM D445 method. The acid value (AV) was calculated according to the ASTM D644 method. All data reported were arithmetic means of triplicate assays.

2.4. Statistical analysis of orthogonal experiments

The statistical analysis included a range analysis and an analysis of variance (ANOVA). Range analysis was used to indicate the effect of each factor and determine the optimal level

of different factors. The mean value of the sum of the evaluation indexes of all levels in each factor ($\overline{K_{ji}}$) was used to determine the optimal level and the optimal combination of factors. The range (R_j) was defined as the range between the maximum and minimum value of the mean values and used to evaluate the importance of the factors. The optimal level for each factor could be obtained when $\overline{K_{ji}}$ is the largest and larger R_j means greater significance of the factor [16]. Although the optimal value of different factors can be easily determined by the range analysis, this method cannot distinguish whether the difference between the data fluctuation of each factor level was caused by experimental conditions or by experimental errors. Due to the limitation of the range analysis, analysis of variance was necessary to obtain the magnitudes of the factor affecting the result [17]. In the ANOVA, the data were analyzed by a F-test. The F value of each factor (F_j) implies the ratio of the variance for the each factor (V_j) to that of the experimental error (V_e) [16, 18]. During the F-test, F_α was a constant and defined as a critical value of the F-value for different inspection levels and can be found from the distribution table of the F-values [18]. When F_j is larger than F_α, the factor effect for the results is prominent; otherwise the factor effect for the results is not prominent. Moreover, the percentage contribution of each factor (P_j) was the percentage of the purified sum of square deviation for each factor (SS_j') in the total sum of square deviation (SS_T). It reflects the factor's influence and the percentage contribution due to experimental error providing an estimate of the adequacy of the whole experiments. Larger percentage contribution means more significant factor influence. When the percentage contribution due to error is low, say 15 % or less, it can be assumed that no important factor has been omitted and the whole experimental results are reliable [18, 19].

3. Results and discussion

3.1. Fatty acid methyl ester yield and statistical analysis

According to the OA_{25} matrix, twenty-five experiments were carried out and the results were shown in Table 2. As mentioned before, the extra column was used as the experimental error to indicate the reliability of the whole experiments. These data were taken as the original data and used in the statistical analysis.

The mean values ($\overline{K_{ji}}$) and the relative data of range analysis were shown in Table 3. The highest FAME yield of each level was clearly distinguished when methanol to camelina seed oil molar ratio was 8:1 (93.4 %), catalyst concentration was 1.25 wt.% (89.5 %), reaction time was 50 minutes (87.8 %) and reaction temperature was 55 ℃ (86.9 %) since $\overline{K_{ji}}$ at these combinations ($A_4B_3C_3D_4$) was the highest. Since larger R_j means bigger impact on the product yield, compared with the range values of different factors (R_j), the order of significant factors was: methanol to oil ratio (36.9) > catalyst concentration (14.8) > reaction time (10.3) > reaction temperature (7.3). The mean values of each factor ($\overline{K_{ji}}$) were shown in Fig.1. It should be noted that these lines were only used to show the trend of each factor, not for predicting other values that were not experimented [20]. Based on the changes of $\overline{K_{ji}}$, it can be observed that the FAME yield was dramatically increased from 56.5 % to 93.4 % with the ratio of methanol to oil increased from 2:1 to 8:1, and then slightly decreased. It indicated that increasing methanol amount immediately speeded up the transesterification reaction and shifted the reaction equilibrium toward the product side to form more FAME. However, further increasing the methanol amount beyond the optimal ratio reduced the yield since methanol also acts as an emulsifier that enhances emulsion. This caused a drop in FAME yield and complicated the washing process. The FAME yield increased with increasing catalyst concentration and reached maximum (89.5 %) at 1.25 wt.%. Beyond the optimal point, the yield slightly decreased to 86 %. It indicated that sufficient amount of catalyst was

required for complete conversion but excessive catalyst might activate the oil to react with the alkali catalyst, and thus formed more soaps and reduced the FAME yield. For reaction time, the FAME yield increased steadily first, and reached a maximum (87.8 %) at 50 min, and then the yield reduced slightly. Theoretically, FAME conversion would increase with reaction time. However, beyond the optimal time, the FAME yield slightly reduced because of the backward reaction and the saponification reaction [10]. Finally, reaction temperature seems to have little effect on the FAME yield with a change from 79.7 % to 86.9 %. Since the reaction was carried out in an ultrasonic bath, the cavitation led to a localized increase in temperature at the phase boundary and thus the influence of reaction temperature was small.

Table 2 FAME yield of biodiesel in OA_{25} matrix.

Trial no.	Factors				Results	
	A	B	C	D	Experimental error level	FAME yield (wt.%)
1	2:1	0.75	10	25	1	28.5
2	2:1	1.00	30	35	2	53.6
3	2:1	1.25	50	45	3	68.4
4	2:1	1.50	70	55	4	67.6
5	2:1	1.75	90	65	5	64.2
6	4:1	0.75	30	45	4	84.1
7	4:1	1.00	50	55	5	93.4
8	4:1	1.25	70	65	1	95.2
9	4:1	1.50	90	25	2	90.5
10	4:1	1.75	10	35	3	85.9
11	6:1	0.75	50	65	2	88.5
12	6:1	1.00	70	25	3	91.6
13	6:1	1.25	90	35	4	95.8
14	6:1	1.50	10	45	5	92.5
15	6:1	1.75	30	55	1	96.2
16	8:1	0.75	70	35	5	88.5
17	8:1	1.00	90	45	1	94.6
18	8:1	1.25	10	55	2	93.6
19	8:1	1.50	30	65	3	96.9
20	8:1	1.75	50	25	4	93.3
21	10:1	0.75	90	55	3	83.8
22	10:1	1.00	10	65	4	87.1
23	10:1	1.25	30	25	5	94.4
24	10:1	1.50	50	35	1	95.6
25	10:1	1.75	70	45	2	90.3

Table 3 Range analysis data of biodiesel FAME yield.

	Alcohol quantity (Molar ratio) A	Catalyst concentration (wt.%) B	Reaction time /min C	Reaction temperature /℃ D
$\overline{K_{i1}}$	56.5	74.7	77.5	79.7
$\overline{K_{i2}}$	89.8	84.1	85.0	83.9
$\overline{K_{i3}}$	92.9	89.5	87.8	86.0
$\overline{K_{i4}}$	93.4	88.6	86.6	86.9
$\overline{K_{i5}}$	90.2	86.0	85.8	86.4
R_j	36.9	14.8	10.3	7.3

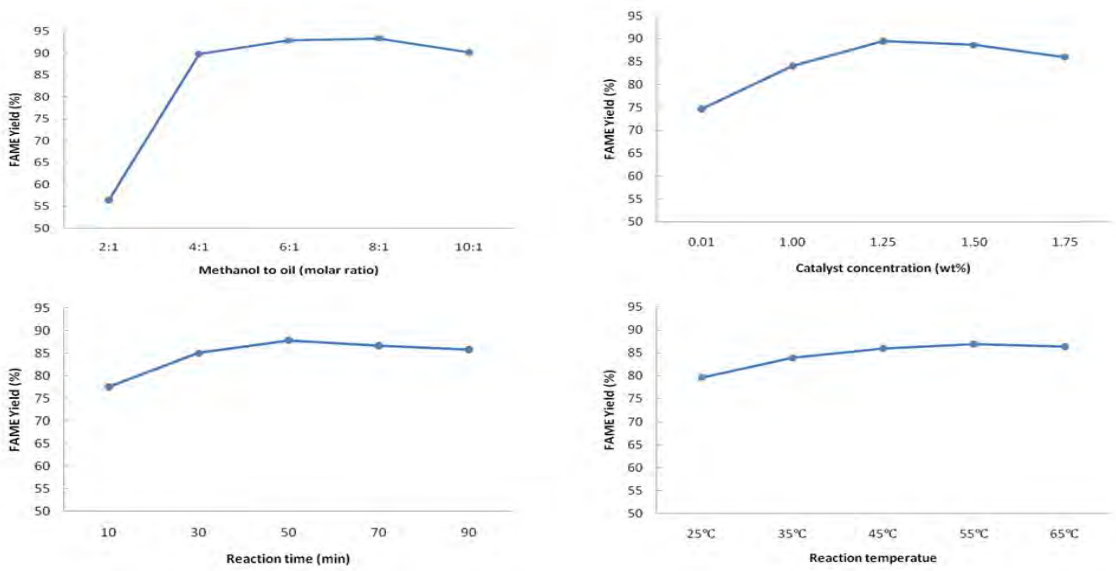

Fig.1. Relationship between the mean values of various influence factor and FAME yield.

The data of ANOVA for the FAME yield was shown in Table 4. For the inspection level, α=0.05, the critical value can be found from the distribution table of F-value: $F_a(4,4) = 6.39$. It was obvious that $F_A\,(72.2) > F_a$, $F_B\,(10.2) > F_a$. It indicated that methanol to oil ratio and catalyst concentration were the prominent factors affecting the FAME yield of biodiesel, when the regression curve and analysis were within a 95 % confidence level. Furthermore, from the percentage contribution, it was deduced that the most important factor contributing to the product yield was factor A (methanol to oil ratio, 78.5 %), followed by factor B (catalyst concentration, 10.1 %), whereas factors C (reaction time, 4.2 %) and factor D (reaction temperature, 1.7 %) were not the significant factors for the change of FAME yield. Since the percentage contribution due to error was low (5.5 %), it was assumed that no important factor had been omitted and the whole experimental results were reliable.

Table 4 ANOVA results of the FAME yield in OA_{25} matrix.

Source	SS_j	df	V_j	F_j	$F_a(4,4)=6.39$	SS_j'	P_j (%)
A	4986.1	4	1246.5	72.2	>	4917	78.5
B	702.9	4	175.7	10.2	>	633.8	10.1
C	331.8	4	83.0	4.8	<	262.7	4.2
D	176.9	4	44.2	2.6	<	107.8	1.7
e	69.1	4	17.3	—		345.5	5.5
T	6266.8	20				6266.8	100

3.2. Optimization of the experimental conditions

According to the statistical analysis, the four experimental conditions affected the FAME yield of biodiesel differently. The amount of methanol and catalyst influenced dramatically the FAME yield and reaction temperature had a few effect on the FAME yield. The results indicated that increasing the level of these factors speeded up the reaction and the FAME conversion. However, beyond the optimal level, the FAME yield slightly reduced because of the backward reaction, such as emulsion and saponification. On the other hand, reaction temperature had little effect on the FAME yield since assisted with ultrasound already led to a localized increase in temperature at the liquid phase boundary.

Finally, the experiment was repeated under the optimal process conditions to confirm the validity of the optimization. A FAME yield of 98.6 % was obtained, which was higher than any former orthogonal experimental result. Compared with the data of the Trial 18 experiment, it was obvious that there was slight difference in the FAME yield (93.6 %) because of the influence of reaction time (10 min in Trial 18 and 50 min under optimal conditions). This result was consistent with that of the statistical analysis. And compared with the results of the traditional mechanical stirring production process, the FAME yield under optimal conditions with ultrasonic-assisted was much higher. Both the reaction time and the amount of catalyst used were reduced [8]. Other properties of biodiesel produced under the optimal conditions were also measured. The density of biodiesel was 0.882 g/cm^3, while the kinematic viscosity was 3.66 cst at 40℃, and the acid value was 0.217 mg KOH/g. Compared with the ASTM D6751 and EN 14214 standards, all the tested fuel properties of biodiesel produced under the optimal production conditions met the requirements. Therefore, optimized biodiesel basically qualified to be used as the diesel fuel.

4. Conclusions

In this research, the alkali-catalyzed ultrasonic-assisted transesterification reaction of camelina seed oil was studied and optimized through the orthogonal experiments with an OA_{25} matrix and a statistical analysis. According to the range analysis, the FAME yield of biodiesel increased sharply with increasing the amount of methanol used and catalyst concentration but was slightly reduced after the optimal point. The FAME yields also increased with increasing reaction time and temperature but the change was small. According to the ANOVA, the amount of methanol and catalyst used were significant factors for the FAME yield. After the whole statistical analysis, the optimal FAME yield of biodiesel (98.6 %) was obtained to be methanol to oil molar ratio of 8:1, catalyst concentration of 1.25 wt.%, reaction time of 50 min and reaction temperature of 55 ℃. Since the tested fuel properties of biodiesel conformed to the ASTM D6751 and EN 14214 standards, camelina seed oil biodiesel produced under the optimal conditions basically can be used as a qualified fuel.

Acknowledgement

The authors would like to acknowledge the support of the ICEE and the University Development Fund of the University of Hong Kong.

Reference

[1] P.D. Patil, S. Deng, Optimization of biodiesel production from edible and non-edible vegetable oils, Fuel 2009, pp. 1302-6.

[2] D.Y.C. Leung, X. Wu, M.K.H. Leung, A review on biodiesel production using catalyzed transesterification, Applied Energy 2010, pp. 1083-95.

[3] M.M. Gui, K.T. Lee, S. Bhatia, Feasibility of edible oil vs. non-edible oil vs. waste edible oil as biodiesel feedstock, Energy 2008, pp. 1646-53.

[4] A. Demirbas, M. Fatih Demirbas, Importance of algae oil as a source of biodiesel, Energy Conversion and Management 2011, pp. 163-70.

[5] J. Budin, W. Breene, D. Putnam, Some compositional properties of camelina (camelina sativa L. Crantz) seeds and oils, Journal of the American Oil Chemists' Society 1995, pp. 309-15.

[6] B.R. Moser, S.F. Vaughn, Evaluation of alkyl esters from Camelina sativa oil as biodiesel and as blend components in ultra low-sulfur diesel fuel, Bioresource Technology 2010, pp. 646-53.

[7] B.R. Moser, S.F. Vaughn, Evaluation of alkyl esters from Camelina sativa oil as biodiesel and as blend components in ultra low-sulfur diesel fuel, Bioresource Technology pp. 646-53.

[8] A. Frohlich, B. Rice, Evaluation of Camelina sativa oil as a feedstock for biodiesel production, Industrial Crops and Products 2005, pp. 25-31.

[9] P.D. Patil, V.G. Gude, S. Deng, Transesterification of Camelina Sativa Oil using Supercritical and Subcritical Methanol with Cosolvents, Energy & Fuels 2009, pp. 746-51.

[10] D.Y.C. Leung, Y. Guo, Transesterification of neat and used frying oil: Optimization for biodiesel production, Fuel Processing Technology 2006, pp. 883-90.

[11] C.Y. Zhou, M.K. Wong, L.L. Koh, Y.C. Wee, Orthogonal array design for the optimization of closed-vessel microwave digestion parameters for the determination of trace metals in sediments, Analytica Chimica Acta 1995, pp. 121-30.

[12] F.F.P. Santos, S. Rodrigues, F.A.N. Fernandes, Optimization of the production of biodiesel from soybean oil by ultrasound assisted methanolysis, Fuel Processing Technology 2009, pp. 312-6.

[13] C. Stavarache, M. Vinatoru, R. Nishimura, Y. Maeda, Fatty acids methyl esters from vegetable oil by means of ultrasonic energy, Ultrasonics Sonochemistry 2005, pp. 367-72.

[14] EN, The EN 14214 Standard-Specifications and Test Methods. 2003.

[15] AOCS, Fatty Acid Composition by Gas Chromatography. AOCS Official Method Ce 1-62, 1997.

[16] C. Chuanwen, S. Feng, L. Yuguo, W. Shuyun, Orthogonal analysis for perovskite structure microwave dielectric ceramic thin films fabricated by the RF magnetron-sputtering method, Journal of Materials Science: Materials in Electronics 2009, pp. 349-54.

[17] D.P. Zhang, Y.L. Luo, Applied Probability and Statistics, Beijing: Higher Education Press, 2000.

[18] P.J. Ross, Taguchi techniques for quality engineering : loss function, orthogonal experiments, parameter and tolerance design, New York, 1988.

[19] A.S. Hedayat, N.J.A. Sloane, J. Stufken, Orthogonal Arrays: Theory and Applications, New York: Springer, 1999.

[20] F. Farahmand, D. Moradkhani, M.S. Safarzadeh, F. Rashchi, Brine leaching of lead-bearing zinc plant residues: Process optimization using orthogonal array design methodology, Hydrometallurgy 2009, pp. 316-24.

Lipase catalyzed transesterification of tung and palm oil for biodiesel

Ya-Nan Wang[1,2], Ming-Hsun Chen[2], Chun-Han Ko[2,3,*], Pei-Jen Lu[4], Jia-Ming Chern[4], Chien-Hou Wu[5], Fang-Chih Chang[6]

[1] *The Experimental Forest, National Taiwan University, Nan-Tou, Taiwan, R.O.C.*
[2] *School of Forestry and Resource Conservation, National Taiwan University, Taipei, Taiwan, R.O.C.*
[3] *Bioenergy Research Center, National Taiwan University, Taipei, Taiwan, R.O.C.*
[4] *Department of Chemical Engineering, Tatung University, Taipei, Taiwan, R.O.C.*
[5] *Department of Biomed. Engr. & Env. Sci., National Tsing Hua Univ., Hsin-Chu, Taiwan, R.O.C.*
[6] *The Instrument Center, National Cheng Kung University, Tainan, Taiwan, R.O.C.*
* *Corresponding author. Tel: +886 2 33664615, Fax: +886 2 26454520, E-mail: chunhank@ntu.edu.tw*

Abstract: The tung oil and palm oil were subjected to enzymatic transesterification. Immobilized lipase (Novozyme 435) was used at 10 % w/v vs. oil. The reactions were conducted at 40°C to 60°C with methanol and ethanol at a molar ratio of 1:3 for 24 hours. Temperature was found critical for the conversion efficiencies. Under 55°C after 24 hour, the optimal conversions of tung oil and palm oil fatty acid methyl esters (FAMEs) were 48 % and 63 %. The optimal conversions for tung oil and palm oil fatty acid ethyl esters (FAEEs) at 50°C were 20 % and 55 % respectively at 50°C. It was found the effciencies of FAEEs conversion were lower than the ones of FAMEs conversion. It was found that the tung oil consisted of 80 % unsaturated fatty acids, and palm oil consisted by just over 50% saturated fatty acids, by contrast. The results showed that the fatty acid composition of oil could directly impact on the efficiencies of enzymatic transesterification. A numerical model was derived to describe the reaction in this two-phase system. It was found that fitted mass transfer coefficients and rate constants of the pseudo-steady-state second order reaction were consistent to experimental results.

Keywords: *Biodiesel, Lipase, Palm oil, Transesterification, Tung oil.*

1. Introduction

Tung Tree (*Vernicia fordii*) is widely distributed in Taiwan, as well as in southern China, Burma, and northern Vietnam. Its seed oil, as known as tung oil, had been conventionally used in lamps for lighting, as well as an ingredient for wood paint and varnish. Currently, non-edible oils have been more favourable to serve as biodiesel feedstocks to avoid competitions with food sources under increasing population pressures. The utilization of seed oil from tree sources can have synergistic benefits with afforestation, like carbon sequestration and climate mitigation. Lipase transesterification of triglycerides is an eco-friendly alternative to chemical process due to a lower process temperature and an improved selectivity [1, 2]. In addition, many operational advantages of using immobilized lipase were reported [3, 4]. Few catalytic transesterification of tung oil were reported [5], and even fewer lipase transesterification of tung oil for biodiesel production was reported [6].

In order to characterize the enzymatic transesterification for tung oil, various temperatures were employed with methanol and ethanol. The results were compared to the ones of the palm oil. In contrast to mono-phase three-step reactions [7-9], fewer models were considering two-phase mass transfers for immobilized lipases [10, 11]. A numerical model, considering dual phase mass transfer coefficients and rate constants of the pseudo-steady-state second order reaction, was derived to describe the reaction in this two-phase system. No other published studies compared the differences for transesterification by immobilized lipases between two plant oils with different degree of unsaturation in a two-phase system.

2. Methodology

2.1. Experimental

2.1.1. Materials and analytical methods

The locally obtained tung and palm oils were de-waxed by dichloromethane [12]. Their fatty acid contents were verified using a G C/MS following protocols described by Chinese National Standard (CNS) 15051 (2007) and ISO 5508 (1990). The composition is listed in Table 1. Lipase immobilized onto catalytic exchange resins (Novozyme 435, B aesvegard, Denmark) was used without further treatments.

Table 1. Fatty acids composition of tung oil and palm oil.

Plants	C16:0	C18:0	C18:1	C18:2	C18:3$^{\Delta 9,11,13}$
Tung oil	2.67	2.4	7.88	6.6	80.46
Palm oil	52.71	3.8	36.73	6.7	--

2.1.2. Reaction Conditions

Tung and palm oils were subjected to enzymatic transesterification, with parameters from the studies cited in a recent review [13]. Immobilized lipase was used at 10 % w/v vs. oil [14]. The reactions were conducted at the oil to alcohol molar ratio for 1:3. The reaction temperature was set at 40^{o}C, 45^{o}C, 50^{o}C, 55^{o}C, 60^{o}C with methanol for 24 hours. A stirring rate of 700 rpm was applied. Conversions by enzymatic transesterification were also quantified using a GC/MS based on the above protocols.

2.2. Numerical model

2.2.1. Mass transfer

Lipase was a water-soluble enzyme, and the catalyst particles are surrounded by a hydrophilic film consisting of methanol/ethanol and glycerol. The immiscible mixture of methanol/ethanol and tung/palm oil formed a film consisting mass transfer resistance:

$$-\frac{dC_A}{dt} = k_1(C_A - C_{As}) \quad (1)$$

where k_1 was the mass transfer coefficients of tung/palm oils; C_A and C_{AS} were the tung/palm oil concentrations in the oil phase and on the interfacial area, respectively, and t was time. In a mass-transfer limiting case, C_{AS} could be ignored:

$$-\frac{dC_A}{dt} = k_1 C_A \quad (2)$$

$$-\frac{dC_{A0}(1-X_A)}{dt} = k_1 C_{A0}(1-X_A) \quad (3)$$

$$\frac{dX_A}{dt} = k_1(1-X_A) \quad (4)$$

X_A was the conversion of tung/palm oils.

2.2.2. Pseudo steady-state second order reaction

After mass transfer resistance was overcome, a pseudo steady-state second order reaction was assumed:

$$-\frac{dC_A}{dt} = k_2 C_A{}^2 \tag{5}$$

$$-\frac{dC_{A0}(1-X_A)}{dt} = k_2 C_{A0}^2 (1-X_A)^2 \tag{6}$$

$$\frac{dX_A}{dt} = k_2 C_{A0} (1-X_A)^2 \tag{7}$$

k_2 was the rate constant of the pseudo-steady-state second order reaction; C_A and C_{A0} were the tung/palm oil concentrations at $t = t$ and $t=0$.

2.2.3. Numerical procedures

The parameters k_1 and k_2 were obtained from non-linear regression of the experimental oil conversion versus time data using Eq. (1-7) using SigmaPlot for Windows Version 10.0.

3. Results and Discussions

3.1. Effect of Alcohols

Figure 1 shows the effect of alcohols on the conversions of tung and palm oils at 50°C. The model fitted well with the experimental data. Conversions of tung oils at 24 hours were very sensitive to alcohol used in the transesterification: 40 % with methanol and 18 % with ethanol. Although conversions of palm oils at 24 hours were not very sensitive to alcohol used, the system using methanol demonstrated greater initial conversions for the first 12 hours than the one using ethanol.

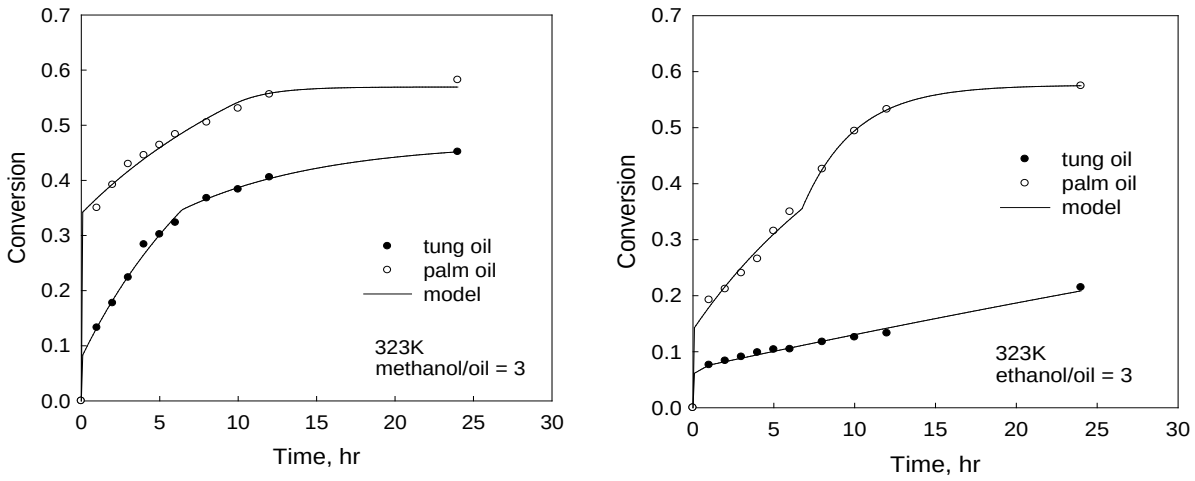

Fig. 1. Effect of alcohols on the conversions of tung/palm oils at 50°C. Left panel: methanols; right panel: ethanol.

3.2. Effect of Temperature

3.2.1. Reaction with methanol

Figure 2 shows the effect of temperature on the conversions of tung/palm oils using methanol from 45 to 55°C. The model fitted well with the experimental data. Conversions of both oils at 24 hours were slightly increased with this temperature increment. Again, greater initial conversions for the first 12 hours were shown for both oils.

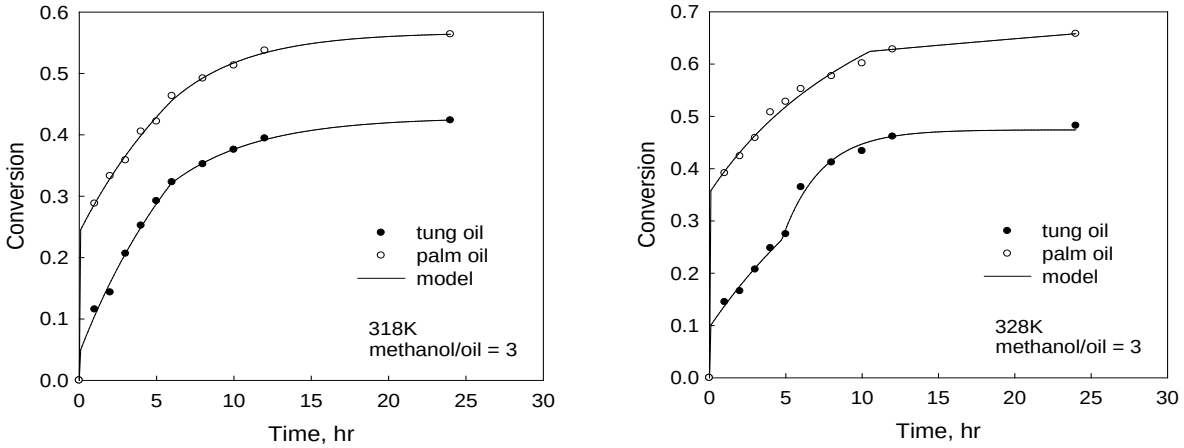

Fig. 2. Effect of temperature on the conversions of tung/palm oils using methanol. Left panel: 45°C; right panel: 55°C.

3.2.2. Reaction with ethanol

Figure 3 shows the effect of temperature on the conversions of tung/palm oils using ethanol from 40 to 50°C. The model fitted well with the experimental data. Conversions of both oils at 24 hours were increased with this temperature increment. Grater initial conversions for the first 12 hours were shown for both oils.

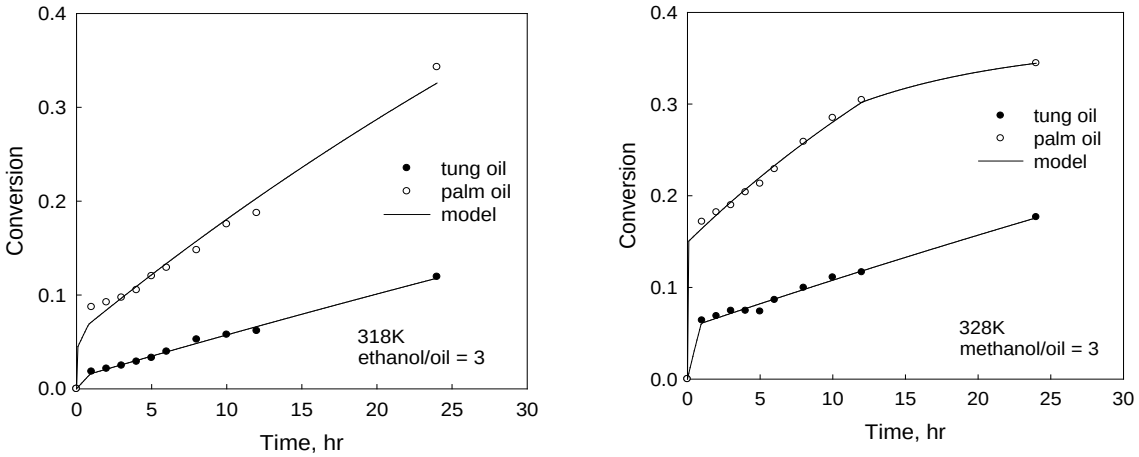

Fig. 3. Effect of temperature on the conversions of tung/palm oils using ethanol. Left panel: 45°C; right panel: 55°C.

3.3. Comparison of the kinetic parameters

Shown by Figure 1 to 3, the model fitted well with the experimental data for all cases. Trends of the obtained kinetic parameters were consistent to the conversions of experimental data. Then the physical meanings of the obtained kinetic parameters could be further discussed. Effect of reaction temperatures on the obtained kinetic parameters are listed in Table 2.

Table 2. Effect of reaction temperatures on the obtained kinetic parameters

T (°C)	Tung oil				Palm oil			
	Methanol		Ethanol		Methanol		Ethanol	
	k_1 (h^{-1})	k_2 ($M^{-1}h^{-1}$)	k_1 (h^{-1})	k_2 ($M^{-1}h^{-1}$)	k_1 (h^{-1})	k_2 ($M^{-1}h^{-1}$)	k_1 (h^{-1})	k_2 ($M^{-1}h^{-1}$)
40	214	0.050	0.0052	0.0076	--	--	--	--
45	378	0.072	8.6E-06	0.018	939	0.087	315	0.037
50	508	0.070	0.0391	0.019	1153	0.067	692	0.058
55	570	0.073	5.6E-06	0.068	1182	0.100	719	0.071
60	770	0.088	7.8E-06	0.041	915	0.093	250	0.061

The mass transfer coefficients (k_1) of tung oil with methanol were from 214 to 770 h^{-1}, generally less than 915 to 1182 h^{-1} of palm oil system. The highest mass transfer coefficients (k_1) of tung oil and palm oils were exhibited at 60 and 55°C, respectively. The mass transfer coefficients (k_1) of ethanol system were generally less than the ones of methanol system for both oils. The magnitude of order was similar for mass transfer coefficients (k_1) of palm oils but the differences between using methanol and ethanol were much greater for tung oils. The above finding for the difference caused by different alcohols was consistent to previous work using waste animal fats [15].

The reaction rate constants (k_2) of tung oil system using methanol were much greater than the ones using ethanol. However, the values in Table 2 for tung oils were of same magnitude of order. In the other hand, the reaction rate constants (k_2) of palm oil showed the same trend as tung oils. And the differences for palm oils were even smaller between methanol and ethanol. The above results implied that the safer ethanol could be employed for enzymatic transesterification.

The above finding suggested that the mass transfer of triglycerides into the surface of the immobilized lipase could play a deciding role for reduced conversions shown by Tung oils. The majority of highly unsaturated chain of Tung oils fatty acids may contribute higher affinities among tung oil triglycerides.

4. Conclusions and Recommendations

The present study showed that the fatty acid composition of oil could directly impact on the efficiencies of enzymatic transesterification. A numerical model with mass transfer coefficients and rate constants of the pseudo-steady-state second order reaction were successfully employed to describe the conversion. It was found that the mass transfer played a more important role than the one by reaction during enzymatic transesterification. The above finding suggested that the increased mixing could improve the processes for biodiesel conversion from tung oils.

References

[1] E. Hernandez-Martin, C. Otero, Different enzyme requirements for the synthesis of biodiesel: Novozym 435 and Lipozyme TL IM. Bioresource Technology 99, 2008, pp. 277-286.

[2] S. V. Ranganathan, S. L. Narasimhan, K. Muthukumar, An overview of enzymatic production of biodiesel, Bioresource Technology 99, 2008, pp. 3975-3981.

[3] V. M. Balcao, A. L. Paiva, F. X. Malcata, Bioreactors with immobilized lipases: state of the art, Enzyme and Microbial Technology 18, 1996, pp. 392-416.

[4] J. W. Chen, W. T. Wu, Regeneration of immobilized *Candida antarctica* lipase for transesterification, Journal of Bioscience and Bioengineering 95, 2003, pp. 466-469.

[5] J, Park, D. Kim, Z. Wang, P. Lu, S. Park, J. Lee, Production and characterization of biodiesel from tung oil, Biotechnology for Fuels and Chemicals 148, 2008, pp. 109-117.

[6] G. Z. Xu, B. L. Zhang, H. L. Liu, A study on immobilized lipase catalyzed transesterification reaction of tung oil, Agricultural Science in China 39, 2006, pp. 2089-2094.

[7] H. Noureddini, D. Zhu, Kinetics of transesterification of soybean oil, Journal of the American Oil Chemists' Society 74, 1997, pp. 1457-1463.

[8] D. Darnoko, M. Cheryan, Kinetics of palm oil transesterification in a batch reactor, Journal of the American Oil Chemists' Society 77, 2000, pp. 1263-1267.

[9] B. Freedman, R. O. Butterfield, E. H. Pryde, Transesterification kinetics of soybean oil, Journal of the American Oil Chemists' Society, 1986, 63, pp. 1375-1380.

[10] V. Calabro, E. Ricca, M. G. De Paola, S. Curcio, G. Iorio, Kinetics of enzymatic transesterification of glycerides for biodiesel production, Bioprocess and Biosystems Engineering, 2010, 33, pp. 701-710.

[11] S. Hari Krishna, N. G. Karanth, Lipases and lipase-catalyzed esterification reactions in nonaqueous media, Catalysis Reviews, 2002, 44, pp. 499-591.

[12] A. Randunz, G. H. Schmid, Wax esters and triglycerides as storage substances in seed of *Buxus sempervirens*, 2000, European Journal of Lipid Science and Technology, 102, pp. 734-738.

[13] S. V. Ranganathan, S. L. Narasimhan, K. Muthukumar, An overview of enzymatic production of biodiesel, Bioresource Technology, 2008, 99, pp. 3975-3981.

[14] S. Shah, M. N. Gupta, Lipase catalyzed preparation of biodiesel from Jatropha oil in a solvent free system, Process Biochemistry, 2007, 42, pp. 409-414.

[15] Y. Liu, H. Tan, X. Zhang, Y. Yan, B.H. Hameed, Effect of monohydric alcohols on enzymatic transesterification for biodiesel production, Chemical Engineering Journal, 2010, 157, pp. 223–229.

Study on Reaction Conditions in Whole Cell Biocatalyst Methanolysis of Pretreated Used Cooking Oil

Mohammad. Pazouki[1*], Farzane Zamani[1], Seyed Amir Hossein. Zamzamian[1], Ghasem. Najafpour[2]

[1] *Materials and Energy research center, Meshkindasht, Karaj, Iran*
[2] *Faculty of Chemical Engineering, Babol Noshirvani University of Technology, Babol, Iran*

** Corresponding author. Tel: +98 2616280031, Fax: +98 261 6280030, E-mail: mpazouki@merc.ac.ir*

Abstract: Biodiesel fuel (fatty acid methyl esters; FAMEs) can be produced by methanolysis of waste edible oil with a whole cell biocatalyst which is an attractive alternative to fossil fuel because it is produced from renewable resources. Utilizing whole cell biocatalyst instead of free or immobilized enzyme is a potential approach to reduce the cost of catalyst in lipase-catalyzed biodiesel production. *Rhizopus oryzae* (*R. oryzae*) PTCC 5174 cells were cultured with polyurethane foam biomass support particles (BSPs) and the cells immobilized within BSPs were used for the methanolysis of pretreated used cooking oil (UCO) for biodiesel production in this research. UCO is the residue from the kitchen, restaurant and food industries which promotes environmental pollution and human health risks. The inhibitory effect of undissolved methanol on lipase activity was eliminated by stepwise addition of methanol to the reaction mixture. The optimum conditions for the reaction were as follows: 50 BSPs, molar ratio of methanol to UCO 3:1, 15.54% (wt) water (in the form of buffer phosphate with pH= 6.8) based on UCO weight and temperature 35°C in three-step addition of methanol. The maximum methyl ester yield of 98.4% was obtained after 72 h of reaction in a shaken Erlenmeyer at mentioned conditions.

Keywords: *Biodiesel, Whole-cell biocatalyst, Methanolysis, Pretreated UCO*

1. Introduction

With the reduction of energy sources from fossil fuels, increase of the crude petroleum price and public awareness on impacts of its emissions on environment and their potential health hazards have created an interest for alternative fuel sources. Biodiesel is renewable, biodegradable, non-inflammable and non-toxic and it also has a favorable combustion emission profile, producing much less carbon monoxide, sulfur dioxide and unburned hydrocarbons than petroleum based diesel. The biodiesel fuel (fatty acid methyl esters), is defined as the mono-alkyl esters of fatty acids produced by transesterification of triglycerides [1-6] obtained from vegetable oils like soybean oil, jatropha oil, rapeseed oil, palm oil, sunflower oil, corn oil, peanut oil, canola oil and cottonseed oil [7]. Apart from vegetable oils, biodiesel can also be produced from other sources like animal fat (beef tallow, lard), waste cooking oil, greases (trap grease, float grease) and algae [8]. Because of the high price of high-quality virgin oils, the cost of biodiesel from these resources is higher than petroleum-based diesel [9]. The increasing of production of UCO from household, restaurants and industrial sources and to pour down it into drain has resulted in problems. The production of biodiesel from waste cooking oil to partially substitute petroleum diesel is one of the measures for solving the twin problems of environment pollution and energy shortage [10].

A number of processes have been developed for biodiesel-Production involving chemical or enzyme catalysis or Critical alcohol treatment [11-14]. Presently, industrial production of biodiesel from waste cooking oil is performed by chemical alkaline or acidic processes. Chemical catalysts including alkaline have been employed most widely since they give a high conversion of triglycerides to methyl esters in a short reaction time. However, chemical transesterification has some unavoidable drawbacks such as high energy and methanol

consumption, difficulty in glycerol recovery, the need to eliminate the catalyst and salt and a large amount of alkaline wastewater from the catalyst [15-18]. In the case where supercritical alcohol was used, higher rates of reaction were observed when it was compared to conventional transesterification. However, the requirements of high temperature, high pressure and high molar ratio of alcohol to oil make the process costly for industrial scale [8].

In recent times, there has been a growing interest in the use of enzymes such as lipases as biocatalyst for biodiesel production. Some advantages of lipase biocatalyst over the chemical-catalyzed reactions include the generation of no by-products, easy product removal mild reaction conditions (reaction temperature of 35-45°C) and catalyst recycling [19]. It has been reported that enzymatic reactions are insensitive to FFA and water content in waste cooking oil [19-21]. Hence, enzymatic reactions can be used in transesterification of used cooking oil [22]. But the cost of enzyme remains as a challenge for its industrial implementation. In order to enhance the cost effectiveness of the process, the enzyme (both intracellular and extracellular) is reused by immobilizing in a suitable biomass support particles of polyurethane that has resulted in considerable improvements in process efficiency [18].

In this work, waste edible oils obtained from MERC restaurant was used to produce biodiesel employing immobilized *R. oryzae* cells within biomass support particles of polyurethane foam. Furthermore, The effect of several parameters such as the molar ratio of methanol to UCO, water content, the enzyme content with the BSPs content and reaction temperature in three-step addition of methanol was determined on enzymatic methanolysis of pretreated UCO in a shaken Erlenmeyer for 72 h.

2. Methodology

2.1. Procedure of immobilization

All lipase catalyzed experiments were carried out using the filamentous fungus *R. oryzae* PTCC5174. Basal medium for growth of *R. Oryzae* which contained of polypepton 70 g; NaNO3 1.0 g; KH2PO4 1.0 g; MgSO4·7H2O 0.5 g and olive oil 30 g in 1 l of distilled water). Erlenmeyer (500 ml) containing 100 ml of the basal medium with biomass support particles (BSPs) were inoculated by aseptically transferring spores from a fresh agar slant using from 4% potato dextrose agar and 2% potato dextrose agar, and incubated at 30°C for 90h on a reciprocal shaker (150 oscillations/min, amplitude 70 mm). The *R. oryzae* cells became well immobilized within the BSPs as a natural consequence of their growth during shake-flask cultivation. Immobilization was effected by placing 150 particles inside an Erlenmeyer together with the medium, subjected to prior sterilization. The pH of the medium was initially adjusted to 5.6 and then allowed to follow its natural course. Reticulated polyurethane foam with a particle voidage of more than 97% and a pore size of 50 pores per linear inch (ppi) was cut into 6mm×6mm×3mm cuboids. After cultivation, the BSP-immobilized cells were separated from the culture broth by filtration, washed with tap water, and dried at room temperature for around 24h. To stabilize the lipase activity, the dried cells were treated with a 0.1% (v/v) glutaraldehyde solution at 25°C for 1h, washed with tap water, dried at room temperature for more than 24h, and then used as whole-cell biocatalyst for methanolysis reaction [23-24].

2.2. Methanolysis reaction

Methanolysis reaction was carried out in a 50 ml Erlenmeyer flask while incubated on a reciprocal shaker (150 oscillations/ min, amplitude 70 mm) at the temperature range of 25°C

to 45°C for 72 h. First, raw UCO was filtered by applying a reduced pressure system using a filter paper (Whatman42) to eliminate the indiscerptible impurities and was heated for 15 min at temperature of 90-110°C to eliminate extra water that has an influence on the transestrification reactions yield with methanol as an alcohol. The reaction mixture UCO 9.65 g, 0.1M phosphate buffer (pH 6.8) 0.5-3.5 ml and molar ratio of methanol to UCO 2-9:1 (one molar methanol (0.35 g) equivalent to 9.65 g UCO) was dispensed with 30-90 BSPs into an Erlenmeyer. The total of methanol was equally added to the reaction mixture at 0, 24 and 48 h reaction time. After the reaction, the whole cell biocatalyst was separated from the reaction mixture by filtration. Samples (200 µl) were withdrawn from the reaction mixture at specified time, centrifuged at 12,000 rpm for 5 min, to obtain the upper layer and were analyzed by capillary gas chromatography.

2.3. Gas chromatography (GC) analysis

The methyl esters content in the reaction mixture were quantified by using a gas chromatography/mass spectrometer (GC–MS) which was equipped with a HP-5 column with 30 meter long, internal diameter 0.25 millimeter. The column temperature was held at 160°C for 2 min, heated to 300°C with rate 8ºC/min and then maintained for 5min. The temperatures of the injector and detector were set at 280 and 230ºC; respectively. The total time of the process is 29.5 minute. For GC-MS analysis, 5µl of the aforementioned mixture and 300 µl of 1.4 mmol/l heptadecanoic acid methyl ester (hexane as the solvent) which is served as the internal standard were precisely measured and mixed thoroughly. A 1.0 µl of the treated sample was injected into a gas chromatograph column.

3. Results

Figure 1(a, b) and (c, d) shows the SEM micrographs of polyurethane foam particles surface with 2 magnifications before and after cell immobilization. The images are shown that the immobilization process was successfully preformed. Also, the weight of polyurethane foam particle after immobilization has increased almost twice. The efficiency of the process was checked by employing GC-Mass analysis of biodiesel product.

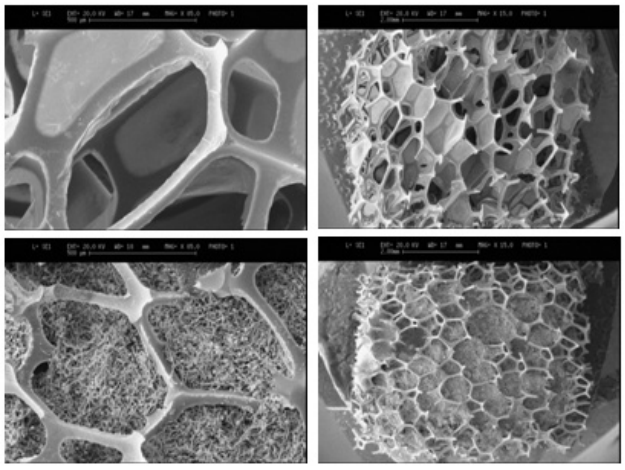

Fig. 1. SEM micrograph of foam particles: a. low magnification and b. high magnification, before immobilization; c. low magnification and d. high magnification, after immobilization.

3.1. Effect of temperature on the reaction

The reaction temperature is an important parameter in enzymatic catalysis. Higher temperatures can give a faster transformation, but too high temperature will lead to enzyme denaturing [25]. The effect of temperature on the lipase activity was examined by using a

temperature range of 25°C to 45°C as shown in Fig. 2 with a constant content of 50 BSPs, molar ratio of methanol to UCO 3:1, 15.54% (wt) water based on UCO weight, the reaction time of 72 h and in three-step addition of methanol. The lipase activity increased sharply when temperature enhanced from 25°C to 35°C, The highest yield was observed at 35°C. However, a further increase above 35°C in temperature leads to decrease in the reaction yield. This decrease in methyl ester yield can be explained by enzyme thermal denaturation.

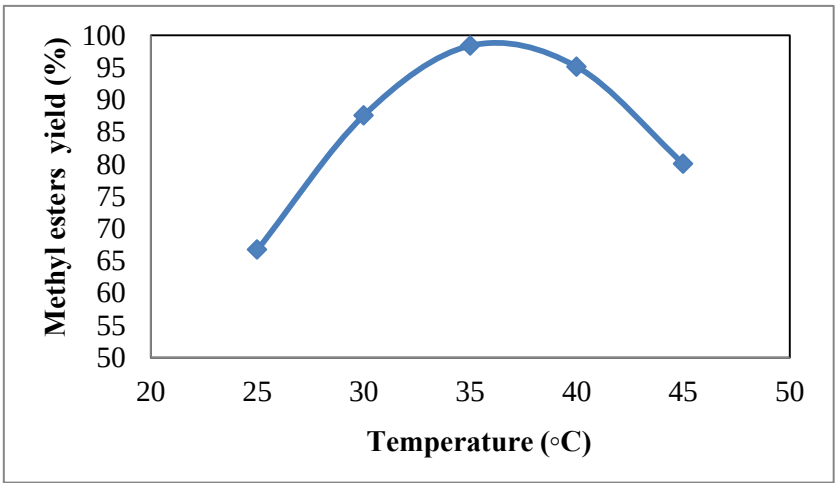

Fig.2. Effect of temperature on lipase-catalyzed methanolysis reaction. Reaction conditions: 50 BSPs, molar ratio of methanol to UCO 3:1, temperature of 25°C to 45°C,15.54% (wt) water based on UCO weight, the time of 72 h and in three-step addition of methanol.

3.2. Effect of water content on the reaction

It is well known that lipase, as a form of protein, requires the presence of water to maintain its live structure, and the activity of the enzyme in non-aqueous media is affected by the water content [10]. The reaction was examined in cases of water content (in the form of phosphate buffer with pH= 6.8) ranging from 5.18% to 36.27% (wt) water based on UCO weight, 50 BSPs, temperature 35°C, molar ratio of methanol to UCO 3:1, the reaction time of 72 h and in three-step addition of methanol. The result is shown in Fig. 3. As indicated in Fig. 3, the FAME content rose gradually as water content increased from 5.18% to 15.54% (wt) water based on UCO weight, and then declined as water content rose from 15.54% to 36.27%. This result indicates that the excessive water content affects the mass transfer of the oil phase of the reaction product, and inhibits esterification. It was observed that the FAME content reached its maximum at a water content of 15.54 wt% which was about 32.4% higher than water content of 5.18 wt%.

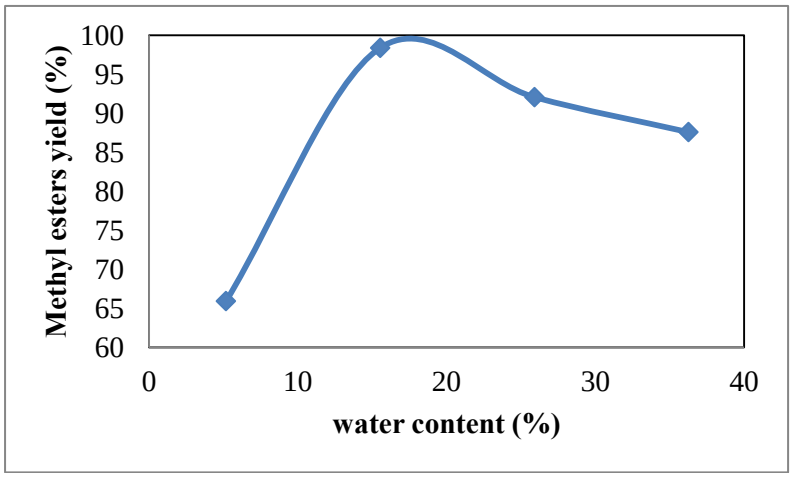

Fig. 3. Effect of water content on lipase-catalyzed methanolysis reaction. Reaction conditions: 50 BSPs, temperature 35°C, molar ratio of methanol to UCO 3:1, 5.18% to 36.27% (wt) water based on UCO weight, the time of 72 h and in three-step addition of methanol.

3.3. Effect of immobilized microorganism on the reaction

The enzyme activity produced of immobilized microorganism within BSPs increases with the immobilized microorganism content [10]. The effect of enzyme content on the transesterification reaction was examined with the BSPs content range from 30 to 90, temperature 35°C, molar ratio of methanol to UCO 3:1, 15.54% (wt) water based on UCO weight, the reaction time of 72 h and in three-step addition of methanol. As shown in Fig. 4, the FAME content increased along with the increase in enzyme content, because the more lipase available, the more substrate molecules were absorbed into the active center of the lipase, but the increase rate of FAME content declined as BSPs rose from 50 to 90. This phenomenon can be explained that the UCO content was excessive when enzyme content was under 50, and that as the enzyme content rose to become sufficient from 50 to 90, the FAME content increased only 0.88%. From an economic point of view, 50 BSPs is the most feasible content level for lipase in reaction of biodiesel synthesis from UCO.

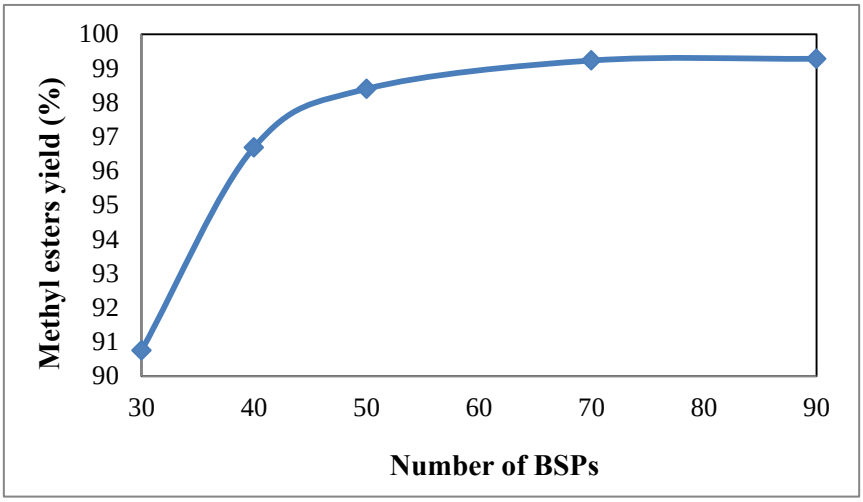

Fig. 4. Effect of BSPs content on lipase-catalyzed methanolysis reaction. Reaction conditions: BSPs content range from 30 to 90, temperature 35°C, molar ratio of methanol to UCO 3:1, 15.54% (wt) water, the reaction time of 72 h and in three-step addition of methanol.

3.4. Effect of Molar Ratio of Substrates on the Reaction

Methanolysis reaction was performed by using different substrate molar ratios of methanol to oil varying in the range of 2–9. The results (Fig.5) demonstrate that the methyl esters yield initially increases with increasing the methanol to oil molar ratio from 2 to 3 and reaches to its maximum at 3. However, a further increase in the methanol to oil molar ratio leads to decrease in the reaction yield. The highest methyl ester yield of 98.4% was achieved at a methanol to oil molar ratio of 3:1, and decreased to 50.68% when the molar ratio of 9:1 was utilized. This is in agreement with the earlier observation that excessive methanol concentration lead to lipase enzyme inactivation. The addition of methanol more than stoichiometric amounts exerts an inhibitory effect on enzyme performance. This could be due to the fact that the immiscible methanol was accumulated around the lipase structure including its active sites, reaching a concentration level sufficient to cause a denaturation of the protein. This phenomenon might lead to enzyme inactivation [24].

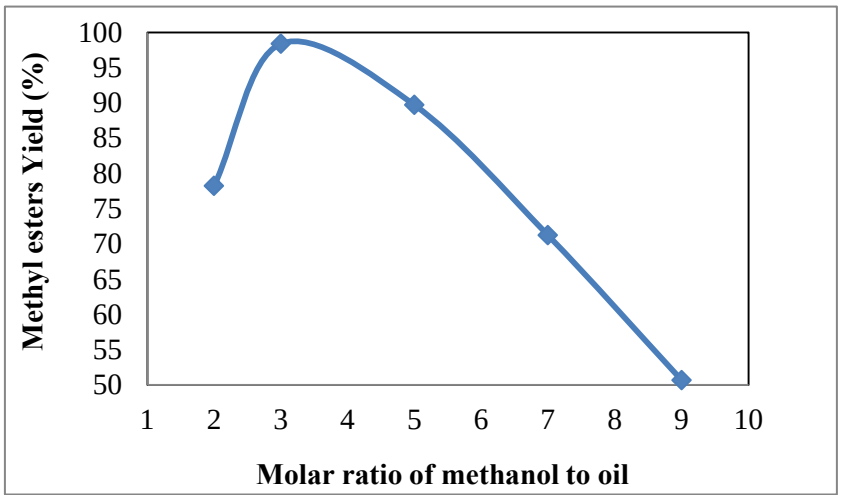

Fig. 5. Effect of methanol to oil molar ratio on lipase-catalyzed methanolysis reaction. Reaction conditions: 30 BSPs, temperature 35°C, molar ratio of methanol to UCO 2-9:1, 15.54% (wt) water, the reaction time of 72 h and in three-step addition of methanol.

3.5. Product analysis

The result of GC-Mass analysis indicated that the main components In the UCO-derived biodiesel were methyl octadecenoate, methyl hexadecenoate, methyl octadecadienoate, methyl octadecanoate, methyl tetradecanoate, methyl heptadecanoate, methyl dodecanoate and methyl pentadecanoate. These components account for 98.4% of the FAME.

3.6. Conclusions

The study shows that pretreated used cooking oil (UCO) can be efficiently converted to biodiesel fuel in a shaking Erlenmeyer methanolysis reaction using immobilized *Rhizopus Oryzae* (PTCC 5174) on polyurethane foam biomass support particles (BSPs). Therefore, this is an effective approach to reduce the cost of biodiesel feedstock and pollution problems.The optimum reaction conditions for the reaction were as follows: 50 BSPs, molar ratio of methanol to UCO 3:1, 15.54% (wt) water (in the form of buffer phosphate with pH= 6.8) based on UCO weight and temperature 35°C in three-step addition of methanol. The maximum methyl ester yield of 98.4% was obtained after 72 h of reaction in a shaken Erlenmeyer at mentioned conditions.

Based on GC-Mass analysis, the main components in UCO-derived biodiesel are methyl octadecenoate, methyl hexadecenoate, methyl octadecadienoate, methyl octadecanoate,

methyl tetradecanoate, methyl heptadecanoate, methyl dodecanoate and methyl pentadecanoate, which are the most compositions of FAME.

References

[1] G.M. Tashtoush, M.I. Al-Widyan and A.O. Al-Shyoukh, Experimental study on evaluation and optimization of conversion of waste animal fat into biodiesel, Energy Conversion and management 45, 2004, pp. 2679-711.

[2] S. Geyae, M. Jacobus and S. Letz, Comparison of diesel engine performance and emissions from heat and transesterified vegetable oil, Transactions of the ASAE 27(2), 1984, pp. 375-81.

[3] L.C. Meher, D.V. Sagar and S.N. Naik, Technical aspects of biodiesel production by transesterification-a review, Renewable and Sustainable Energy Reviews 10, 2006, pp. 48-68.

[4] F.R. Ma, and M.A. Hanna, Biodiesel production: a review, Bioresource Technology 70, 1999, pp. 1-15.

[5] G. W. Huber, S. lborra, A. Corma, Synthesis of transportation fuels from biomass: Chemistry, Catalysts, and engineering, Chemical Review 106 (9), 2006, pp. 4044-4098.

[6] S. Al-Zuhair, Production of biodiesel possibilities and challenges, Biofuels, Bioproducts and Biorefining 1 (1), 2007, pp. 57-66.

[7] C.L. Peterson, Vegetable oil as a diesel fuel: Status and research priorities, Transactions of the ASABE 29(5), 1986, pp. 1413-1422.

[8] G.G. Pearl, Animal Fat Potential for Bioenergy Use, Bioenergy 2002, The Biennial Bioenergy Conference, Boise, ID, September 2002, pp. 22-26.

[9] S. Zheng, M. Kates, M.A. Dubé and D.D. Mclean, Acid-catalyzed production of biodiesel from waste frying oil, Biomass and Bioenergy 30, 2006, pp. 267-72.

[10] Y. Chen, B. Xiao, J. Chang, Y. Fu, P. Lv and X. Wang, Synthesis of biodiesel from waste cooking oil using immobilized lipase in fixed bed reactor, Energy Conversion and Management 50, 2009, pp. 668-673.

[11] Y. Zhang, M.A. Dube, D.D. McLean and M. Kates, Biodiesel production from waste cooking oil: 1. Process design and technological assessment, Bioresource Technology 89, 2003, pp. 1-16.

[12] H. Fukuda, A. Kondo, H. Noda, Biodiesel fuel production by transesterification of oils, Journal of bioscience and bioengineering 92, 2001, pp. 405-416.

[13] Y. Warabi, D. Kusdiana, S. Saka, Reactivity of triglycerides and fatty acids of rapeseed oil in supercritical alcohols , Bioresource Technology 91, 2004, pp. 283–287.

[14] D. Kusdiana, S. Saka, Effects of water on biodiesel fuel production by supercritical methanol treatment, Bioresource Technology 91, 2004, pp. 289–295.

[15] M. J. Haas, P.J. Michalski, S. Runyon, A. Nunez and K.M. Scott, Production of FAME from acid oil, a by-product of vegetable oil refining, Journal of American Oil Chemists' Society 80, 2003, pp. 97-102.

[16] Q. He, Y. Xu, Y. Teng and D. Wang, Biodiesel production catalyzed by whole-cell lipase from Rhizopus chinensis, Chinese J. Catalysis 29, 2008, pp. 41-46.

[17] J. Lu, K. Nie, F. Xie, F. Wang and T. Tan, Enzymatic synthesis of fatty acid methyl esters from lard with immobilized Candida sp 99-125, Process Biochemistry 42, 2007, pp. 1367-1370.

[18] S. V. Ranganathan, S.L. Narasimhan and K. Muthukumar, An overview of enzymatic production of biodiesel, Bioresource Technology 99, 2008, pp. 3975-3981.

[19] W.H. Wu, T.A. Foglia, W.N. Marmer and J.G. Phillips, Optimizing production of ethyl esters of grease using 95% ethanol by response surface methodology, Journal of the American Oil Chemists' Society 76 (4), 1999, pp. 571-621.

[20] M.G. Kulkami, and A.K. Dalai, Waste cooking oil-an economical source for biodiesel: a review, Industrial and Engineering Chemistry Research 45, 2006, pp. 2901-13.

[21] A. Hsu, K.C. Jones and W.N. Marmer, Production of alkyl esters from tallow and grease using lipase immobilized in pyllosilicate sol-gel, Journal of American Oil Chemists' Society 78 (6), 2001, pp. 585-8.

[22] A. Hsu, K.C. Jones, T.A. Foglia and W.N. Marmer, Immobilized lipase-catalyzed production of alkyl esters of restaurant grease as biodiesel, Applied Biochemistry 36 (3), 2002, pp. 181-6.

[23] K. Ban, S. Hama, K. Nishizuka, M. Kaieda, T. Matsumoto, A. Kondo, H. Noda and H. Fukuda, Repeated use of whole-cell biocatalysts immobilized within biomass support particles for biodiesel fuel production, Journal of Molecular Catalysis B: Enzymatic 17, 2002, pp. 157-165.

[24] S. Hama, H. Yamaji, T. Fukumizu, T. Numata, S. Tamalampudi, A. Kondo, H. Noda and H. Fukuda, Biodiesel-fuel production in a packed-bed reactor using lipase-producing *Rhizopus oryzae* cells immobilized within biomass support particles, Biochemical Engineering Journal 34, 2007, pp. 273-278.

[25] N. Kaile, X. Feng, F. Wang, T. Tianwei, Lipase catalyzed methanolysis to produce biodiesel: Optimization of the biodiesel production, Journal of Molecular Catalysis B: Enzymatic 43, 2006, pp. 142-147.

EN 14103 adjustments for biodiesel analysis from different raw materials, including animal tallow containing C17

Fabrícia Gasparini[1], José Renato de O. Lima[1], Yussra A. Ghani[1], Rafael R. Hatanaka[1], Rodrigo Sequinel[1], Danilo L. Flumignan[1,2], José Eduardo de Oliveira[1*]

[1] Center for Monitoring and Research of the Quality of Fuels, Biofuels, Crude Oil and Derivatives – CEMPEQC - Organic Chemistry Department, Institute of Chemistry, , São Paulo State University – UNESP, R. Prof. Francisco Degni s/n, Quitandinha, 14800-900, Araraquara, São Paulo, Brazil.

[2] São Paulo Federal Institute of Education, Science and Technology – IFSP, Campus Avançado Matão, Rua José Bonifácio, 1176, Centro, 15990-040, Matão, São Paulo, Brazil

**Corresponding author: Tel: +55 16 3301 9666, Fax: +55 16 3301 9693, E-mail: jeduardo.unesp@yahoo.com.br*

Abstract: EN 14103 is suitable to quantify the ester content in biodiesel free of heptadecanoate ester (C17:0), because it is employed as internal standard (IS). But EN 14103 cannot be applied to the analysis of tallow biodiesel because C17:0 is found in animal fats. This work proposes an improved method, based on EN 14103 capable to determine ester content in tallow biodiesel. Twenty samples from tallow, soybean, babassu and palm biodiesels and its blends were used to carry out the analysis. Chromatograms of ethylic biodiesel were analyzed using separately methylic and ethylic C17:0 (IS). The results showed that some peaks from tallow biodiesel co-eluted with both IS peaks, confirming the impossibility to quantify ethylic esters using those standards. Despite this, in all analyzed samples it was observed a constant relationship between two neighbor peaks occurring naturally in the tallow samples. The rate between them was measured and applied as a correction factor to measure the real influence, caused on methylic C17:0 IS by natural C17:0. As a result, the original equation from EN 14103, modified by the introduction of a correction factor (F), resulted in another equation more adequate to analyze the ester content in tallow biodiesel and its blends. Pure tallow biodiesel presented ester content around 4.3% greater, when quantified using the equation containing the correction factor, instead of the original equation.

Keywords: *EN 14103, Tallow Ethylic Biodiesel, Heptadecanoate.*

1. Introduction

Biodiesel is a biofuel produced worldwide from several oils and fats, obtained from both vegetable and animal sources. This fuel is capable to work in diesel engines and hence be mixed to mineral diesel or replace it completely [1, 2]. Many countries around the world produce, import and/or export fuels, thus it is necessary to promote the internationalization of standards that specify the methods of analysis and maximum/minimum limits for quality parameters in order to allow a technically effective commerce worldwide. Technical data are used to set those limits. To harmonize the biodiesel specifications, the limits set in a global standard need to be carefully considered, since specification limits have arisen based in different utilization contexts [3]. Currently the evaluation of the biodiesel quality is a global concern. In this way experts from standards elaboration organizations from Brazil, United States and European Union, have participate of meetings with the objective of discuss standards for the evaluation of biodiesel quality.

The ester content is the most important biodiesel quality parameter, since the ester is the biodiesel itself. EN 14103 is a standard that evaluates chromatographically the ester content of biodiesel [4] and was developed for analysis of methylic biodiesel obtained from vegetable oils predominantly found in Europe. So this standard contemplates only methyl biodiesel obtained from oils which composition has the majority of carbon chains from C14:0 to C24:1 and which does not contain C17:0 in its composition. The wide feedstock diversity used to

produce biodiesel around the world [5] makes the use of EN 14103 inadequate not only when we consider the composition of the oils, but also the choice of applied alcohol. That standard can be useful to measure the ester content of soybean, sunflower, rapeseed and other methylic biodiesels, but do not makes mention to ethylic biodiesel and is not capable to measure the ester content of tallow biodiesel itself or when present in blends.

Biodiesel from tallow has C17:0 in its composition. This represents a major concern in Brazil in relation to assessment of its quality, once biodiesel from tallow is already inserted in the national and international market [6].

One Brazilian solution to overcome the limitations of EN 14103 was the development of NBR 15764 [7]. This standard allows biodiesel quantification produced from different types of oils fats and alcohols, using external standardization. However this method has a weakness even more critical when compared with all the EN 14103 limitations. The NBR 15764 states the use of chloroform as solvent. This solvent is incompatible with the (GC-FID) detector since it promotes corrosion of the detector during use with the consequent loss of sensitivity. Compounds containing chlorine atoms in its structure, when burned in the detector flame, produce hydrochloric acid, promoting the corrosion of the detector, and can infer the reliability of analysis results [8].

A large number of biodiesels from different raw materials are produced around the world and being marketed pure or as blends. Tallow biodiesel is possibly present in those blends. The possibility of using ethanol as reactant is another important factor that must to be taken in account because its choice for biodiesel preparation makes the analysis of ester content particularly impaired.

Thus, this paper proposes an evaluation and adjustment of the EN 14103 analytical conditions in order to quantify adequately total ester content not only from methylic but also ethylic biodiesel, even in matrices containing the C17:0 in its composition, taking in to account that the global trends are the commercialization of biodiesel "blends". The biodiesels used in this approach were prepared from soybean, palm, babassu oils and bovine tallow, the mostly used raw materials in Brazil.

2. Methodology

2.1. Raw materials, solvents and standards

Four different types of raw materials were used: soybean, palm, babassu oil and bovine tallow. Industrialized oils purchased in local shops were used and the tallow experienced craft process of grinding and frying before being used. Anhydrous ethanol was synthesis grade (Synth, lot 118784) Internal standards (IS) were methyl myristate (C14:0), methyl nervonate (C24:1), methylic and ethylic heptadecanoate (C17:0) (Nu-Chek, >99%). Heptane (Vetec-0803307) HPLC grade was used for sample dilutions.

2.2. Biodiesel

Eight ethylic biodiesels were prepared, by transesterification, two from each oil and fat selected. The preparations were performed in two conditions: varying the key variables responsible for the total or partial conversion into esters. Four biodiesel were made under conditions that present high conversion rate with the heating time of 120 min, molar ratio alcohol/oil 9:1 and 1% of catalyst. The other four biodiesel, were made under conditions to present low conversion rates with heating time of 30 min, molar ratio alcohol/oil 6:1 and 0,3%

of catalyst. All biodiesels were prepared at 75 °C, next to the boiling point of ethanol. The choice of conditions was performed according to a review of the literature [9-12]. The transesterification reactions were performed using ethanol and catalyzed by sodium hydroxide.

2.2. Blends

The eight biodiesel were mixed forming blends with different levels of esters, totalizing 20 samples. 10 mL of each sample was prepared containing equal volumes of each biodiesel with the aid of a micropipette.

2.3. Analysis of samples

The quantifications of ester content in biodiesel samples were performed, in triplicates, according to EN 14103 [Fat and oil derivatives - Fatty Acid Methyl Esters (FAME) - Determination of Ester and linolenic acid methyl esters contents] in a Shimadzu GC 2010 gas chromatograph with flame ionization detector (GC-FID). The chromatograph was configured with injector in split mode coupled to auto-sampler AOC 5000 for liquid samples. EN 14103 establishes the chromatographic conditions used in the quantification of fatty acid esters: sample injection volume = 1 mL, split = 1:20, injector and detector temperatures = 250 °C, isothermal oven temperature = 210 °C, pressure of helium carrier gas = 83 kPa due to "split" or adjusted to visualize clearly the peak of the methyl standard C24:1. Because of difficulties in visualize clearly the peak of the methyl standard C24:1, under isothermal conditions, in this study the isothermal condition of the oven was replaced by programmed temperature conditions. 120 °C for 2 minutes, heating rate 10 ºC/min to a temperature of 180 °C, where it remained for three minutes, new heating rate of 5 ºC/min until 240 ºC where it remained for 10 minutes. The capillary column used was a Restek-Carbowax 30 m long, 0.25 mm internal diameter and 0.25 mm stationary phase thickness.

2.4. Quantification of ester contents

20 mg/mL stock solutions of methyl myristate (C14:0) and methyl nervonate (C24:1) standards were prepared, while methylic and ethylic heptadecanoate standards were prepared in 10 mg/mL stock solutions. Methyl esters standards C14:0 and C24:1 were used to identify the range of integration. In addition, we used the methylic and ethylic (C17:0) esters as IS. The ester contents were obtained by integrating the peak areas ranging from C14:0 to C24:0 and subtracting heptadecanoate area, as showed in Eq. (1).

$$\%\ \mathbf{Ester} = \frac{\Sigma_A - A_{C17\,IS}}{A_{C17\,IS}} + \frac{(C_{EI} * V_{EI})}{m} * 100 \qquad (1)$$

where:

$\sum A$ = sum of areas of all peaks ranging from C14:0 and C24:0
$A_{C17\,IS}$= C17:0 IS area
C_{EI} = concentration (mg/mL) of C17:0 solution
V_{EI} = volume of C17:0 solution added to sample
m = mass of the sample (mg).

3. Results and Discussion

3.1. EN 14103 for ethylic biodiesel

To quantify ethyl esters in biodiesel according to EN 14103, a study was conducted using methyl and ethyl standards under the conditions described in 2.4. The retention times (RT) of methyl and ethyl standards were: methyl C14:0 (8.6 min), ethyl C14:0 (9.2 min), methyl C24:1 (26.5 min) and ethyl C24:1 (27.2 min). From these results is possible to note that there is only a small variation on the beginning and the end of integration intervals. It was not observed any new peak in both intervals; hence the ester quantification accuracy will be not affected by using methyl standards to analyze ethyl esters. The 20 samples of biodiesel used in this study were quantified using the method 1 (EN 14103) and method 2 (conditions of EN 14103 unchanged, except for the integration of the ester peaks performed using the ethyl standards RT). The results were compared using the Student T test. The value of t-calculated to a limit of 95% of confidence was 0.81 while the theoretical value is 1.98, meaning that there is no significant difference between the two methods of quantification. Furthermore, in both cases the ester content results variation were below the method repeatability, that is 1.6 % m/m.

3.2. EN 14103 applied to biodiesel containing C17

Biodiesels containing heptadecanoate (C17:0) in their composition, (e.g. beef tallow), needs two chromatographic runs to be analyzed; one with IS and another without the addition of the C17:0 IS. The reason for this is that C17:0 IS is necessary to assist the quantification, but if C17:0 is already present in the sample (e.g. tallow biodiesel) the C17:0 of the standard co-elutes and consequently presents an area bigger than that corresponds to itself. Looking at the chromatogram of a sample without C17:0 IS (Figure 1), it is possible to found the co-eluted peaks (A when using methylic IS and B if it is used ethylic IS). Therefore it is necessary to run another chromatogram without IS. After that, the peak area at the same retention time of C17:0 IS must be subtracted from it and included in the total peaks sum.

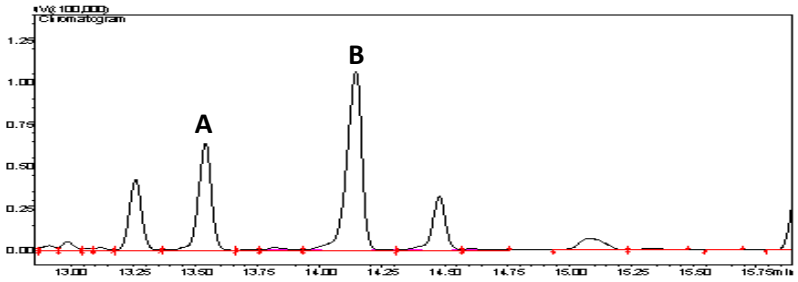

Fig. 1. Chromatogram window of a biodiesel blend showing the peaks A and B (A co-elutes with methylic C17:0 and B co-elutes with ethylic C17:0

During the development of the procedure, to overcome the need of two chromatographic runs, firstly, two chromatograms of ethyl and methyl C17:0 standards were obtained. The RTs were 13.5 min for methylic and 14.2 min for ethylic standards. The biodiesels of soybean, palm and babassu were diluted in heptane (without addition of C17:0 IS) in order to verify the occurrence of peaks in the RT 13.5 and 14.2 min. These chromatographic runs were successful, since they did not show any peaks in the regions of those RT. This fact showed the possibility of using both IS for ester quantification in the studied biodiesels samples.
Beef tallow biodiesel was then diluted with heptane and its chromatogram was compared with C17:0 standards methyl and ethyl chromatograms. Both, the methyl and ethyl standards co-elute with peaks of esters present in tallow biodiesel (Fig. 2).

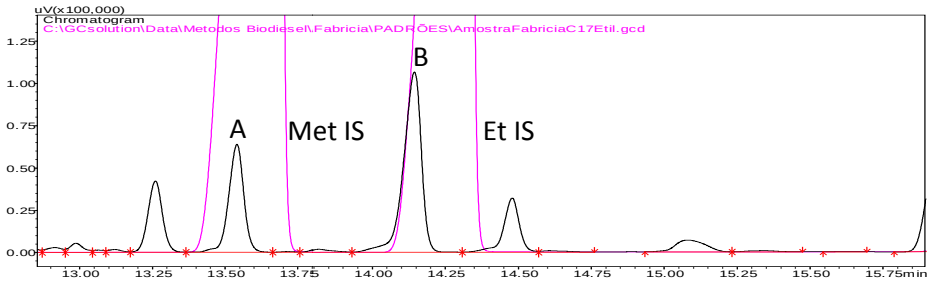

Fig. 2. Chromatogram window showing methyl (Met IS – black colour) and ethyl (Et IS - pink colour) IS peaks that co-elutes with A and B peaks from tallow biodiesel, respectively.

Thus, it is not possible to quantify correctly the ester content in tallow biodiesel or its blends using methylic or ethylic C17:0 IS. But, an accurate analysis of the chromatograms, allow to perceive a constant ratio between the two peaks areas A and B, that co-elute with C17:0 IS. To confirm how useful and confident would be this relationship between A and B peak area, a C17 external calibration curve was performed intending to support the quantification of C17 from samples. A seven point curve was produced using concentrations from 0.5 to 5 percent of ethylic C17 in heptane. Chromatographic conditions were similar to those used for ester content analysis official method EN 14103. Equation 2 is the curve calibration equation used to calculate A and B peak areas of the samples (R^2 = 0.9999). After that, seven biodiesel samples were analyzed from which five were mix of soybean and commercial beef tallow biodiesel and two of them were samples were pure biodiesel of soybean and beef tallow.

$$\%_{C17} = A_{peak} * 1{,}24638^{-7} + 1{,}59447^{-2} \quad (2)$$

Table 1 presents the percentage of tallow biodiesel in blends, C17 content into each sample and the ratio A/B results for every blend. The A and B peaks were quantified using the external calibration curve.

Table 1. Blends of tallow biodiesel with soybean, the % C17 found and ratio A/B peak.

	Mix 0 (0%)	**Mix 1 (5%)**	**Mix 2 (25%)**	**Mix 3 (45%)**	**Mix 4 (65%)**	**Mix 5 (85%)**	**Mix 6 (100%)**
Tallow Biodiesel	0	5	25	45	65	85	100
Soybean Biodiesel	100	95	75	65	45	15	0
%C17	-	0.021	0.028	0.328	0.0386	0.0451	0.049
A/B ratio	-	0.15	0.30	0.41	0.44	0.46	0.46

In the Graph 1 we can observe the behavior of A/B ratio related to C17 percentage. They are much correlated, especially when tallow biodiesel percentage is above fifty percent. In other hand, for pure tallow biodiesel or rich blends A/B variation curve is practically stable what shows that is possible to use an average A/B ratio value in order to correct the ester content analysis results without needs to proceed another GC analysis.

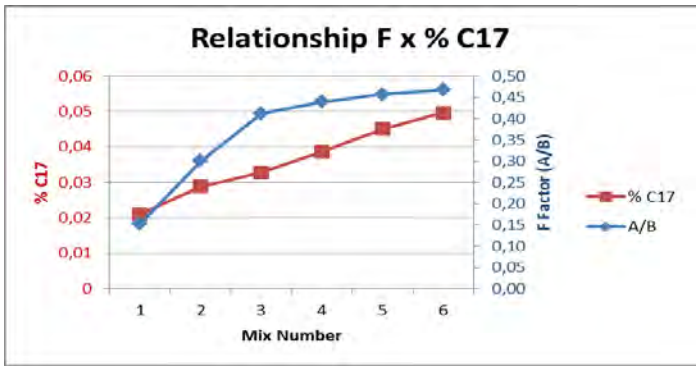

Graph 1. Behavior of A/B ratio related to C17 percentage in samples

Taking into account the relationship between the A and B peak areas and C17 percentage of pure beef tallow biodiesel (Graph 1), it was possible to establish a correctional factor that should be introduced into original formula of EN 14103 for quantify the ester content. The value adopted was the average of A/B ratio considering samples Mix 3, Mix 4, Mix 5 and Mix 6. That way we recommend to use 0,45 as a correctional factor "F".

For this, the area of methylic C17:0 IS used in Eq. 1 was replaced by other term containing F (A/B). In this new term, the methylic C17:0 IS area was subtracted of: ethylic C17:0 IS area (RT 14.2 min.) multiplied by F. Moreover, this last product represents the peak co-eluted with methylic IS, so it was added to total peak sum. Thus, for quantification of samples containing beef tallow biodiesel, the Eq.(1), was replaced by Eq. (3).

In Eq. (2) the $A_{C17\,IS}$ was replaced by $A_{C17\,IS} - (A_{C17et} * F)$.

$$\%\ \mathbf{Ester} = \frac{[(\Sigma_A + (A_{C17et} * F)) - (A_{C17\,IS} - (A_{C17et} * F))]}{A_{C17\,IS} - (A_{C17et} * F)} + \frac{(C_{EI} * V_{EI})}{m} * 100 \qquad (3)$$

where:

A_{C17Et}= Area of C17:0 ethylic present in the sample.

F = Correction factor

The mean value of F found was applied in the further experiments. Table 2 shows the study of F behavior to several samples of tallow biodiesel pure and its blends with soybean, babassu and palm oil biodiesel. Those samples were designed to present different ester levels intending to confirm F efficiency when applied to any matrix.

Although the t test did not show significant differences (t-calculated 0.78 and theoretical 1.03) for the sample of beef tallow biodiesel when using Eq. (1) and (3), the difference between results reach value bigger than the repeatability (1.6% m/m) of the method. A difference of 2.5% for beef tallow biodiesel was detected in its ester content. This difference is bigger than C17 ester content found by some authors [13] (1,7% of C17), however the complex biosynthesis of fatty acid can provide different level of this bioproducts available on fatty issue. Other works [6] presumes levels that can reach almost 5% of C17.

Table 2. Study of F behavior in different tallow biodiesel samples and blends.

Samples containing tallow	% ester no using F correction	% ester with F correction
Tb^{a}	7,4	7,5
$Tb^{c/a}$	46,3	46,5
$Tb^{d/a}$	52,8	53,0
$Tb^{e/a}$	49,6	49,7
Tb^{b}	91,6	93,1
$Tb^{c/b}$	96,8	98,9
$Tb^{d/b}$	97,1	99,2
$Tb^{e/b}$	94,2	96,3

a) Tallow biodiesel type low ester content; b) Tallow biodiesel type high ester content; c) soybean biodiesel type; d) babassu biodiesel; e) palm oil biodiesel.

In this sense, it was necessary to identify what substance is assigned to A peak. Since B is heptadecanoate. Some studies [6,13] concludes that A peak can be isomers of C17:0, like heptadecenoate and/or branched C17:0 fatty acid esters. Therefore, is comprehensible the fact of A and B present a regular proportion.

Within this context, we note that the difficulty in using the EN 14103 to quantify the levels of esters in biodiesel produced from different matrices was overcome. These achievements support us to propose the results of this work as a new standard, since the NBR 15764 is not suitable for quantifying the ester content in biodiesel.

4. Conclusions

Through an evaluation and adaptation of EN 14103, the limitations on feedstock and alcohol used in the production of biodiesel were effectively circumvented. Analyses performed using methyl and ethyl IS showed that there were no significant differences when comparing the results of ester content using both types of standards (methods 1 and 2). So ethyl and methyl biodiesel can be quantified using both methyl and ethyl IS using EN 14103 conditions.

For the ester quantification of ethyl beef tallow biodiesel, is necessary to introduce a correction factor (F) in the original equation of EN 14103 (Eq. 3), keeping the methylic standard C17:0 established by original method. In the cases when methylic beef tallow biodiesels are analyzed, it is necessary to do another few adjusts, however it should be used a similar procedure. Thus, it was possible to quantify adequately all peaks related to the esters in beef tallow ethylic biodiesel. In the other samples (soy, sunflower, rapeseed, babassu and palm biodiesels), there is no problem in using Eq. 3 because the final result will be equal. We recommend a study about composition of other fats in order to confirm existence and proportionality between A and B peaks.

References

[1] White Paper. Internationally compatible biofuel Standards. Tripartite task force Brazil, European Union & United States of America. 95, 2007, f. 31.

[2] Lima, J. R. O.; Silva, R. B.; Silva, C. C. M.; Santos, L. S. S.; Santos-Junior, J. R.; Moura E. M.; Moura, C. V. R. Biodiesel de babaçu *(Orbignya SP.)* obtido por via etanólica. Química Nova, v. 30, n. 3, 2007, pp. 600-603.

[3] Alleman, T.L. Harmonization of biodiesel specifications, Lipid Technology, v. 20, n. 02, 2008, pp. 40-42.

[4] EN 14103 DEUTSCHES INSTITUT FÜR NORMUNG. EN 14103: fat and oil derivatives – fatty acid methyl esters (FAME) – determination of ester and Linolenic acid methyl ester contents. Germany, 2003. 10 p.

[5] Atadashi, I.M.; Aroua, M.K.; Aziz, A.A. High quality biodiesel and its diesel engine application: A review. Renewable and Sustainable Energy Reviews, v.14, 2010, pp. 1999‑2008.

[6] MCT - AGÊNCIA NACIONAL DO PETRÓLEO, GÁS NATURAL E BIOCOMBUSTÍVEIS. Superintendência de Biocombustíveis e de Qualidade de Produtos. Centro de Pesquisas e Análises Tecnológicas. Comparação inter-laboratorial para análise de teor de ésteres em biodiesel de sebo bovino. Rio de Janeiro, 2009. 25 f.

[7] ASSOCIAÇÃO BRASILEIRA DE NORMAS TÉCNICAS. Biodiesel – determinação do teor total de ésteres por cromatografia gasosa. Homologação e publicação de normas brasileiras. Disponível em: <http://www.abnt.org.br/imagens/normalizacao_homologacao/lista_de_publicacao_-_2009.10.06_a_2009.10.30.pdf>. Acesso em: 05 abr. 2010.

[8] Ciola, R. Fundamentos da Cromatografia a Gás. São Paulo: Edgard Blucher, 1985.

[9] Tippayawong, N.; Kongjareon, E.; Jompakdee, W. Ethanolisys of soybean oil into biodiesel: process optimization via central composite design. Journal of Mechanical Science and Technology, v. 19, n. 10, 2005, pp. 1902-1909.

[10] Encimar, J. M.; Gonzlez, J. F.; Rodriguez, J. J.; Tejedor, A. Biodiesel fuels from vegetable oils: transesterification of *Cynara cardunculus* L. oils with ethanol. Energy and Fuels, v.16, n. 2, 2002, pp. 443-450.

[11] BRASIL. Portal do Biodiesel. Biogasolina: produção de éteres e ésteres da glicerina. Disponível em: <http://www.biodiesel.gov.br/docs/congressso2006/Co-Produtos/Biogasolina3.pdf> Acesso em: 20 fev. 2010.

[12] Rashid, U.; Anwar, F.; Knothe, G. Evaluation of biodiesel obtained from cottonseed oil. Fuel Processing Technology, v. 90, n. 9, 2009, pp. 1157-1163.

[13] CUNHA, M. E. Caracterização de biodiesel produzido com misturas binárias de sebo bovino, gordura de frango e óleo de soja. Dissertação de mestrado. Universidade Federal do Rio Grande do Sul, Porto Alegre, 2008, p. 55.

Indian-nut (*Aleurites moluccana*) and tucum (*Astrocaryum vulgare)*, non agricultural sources for biodiesel production using ethanol: composition, characterization and optimization of the reactional production conditions

José Renato de O. Lima[1], Fabricia Gasparini[1], Nadia de L. Camargo[1], Yussra A. Ghani[1], Rondenelly B. da Silva[2], José E. de Oliveira[1,*]

[1] *Center for Monitoring and Research of the Quality of Fuels, Biofuels, Crude Oil and Derivatives – CEMPEQC - Organic Chemistry Department, Institute of Chemistry, , São Paulo State University – UNESP, R. Prof. Francisco Degni s/n, Quitandinha, 14800-900, Araraquara, São Paulo, Brazil.*

[2] *Chemistry Department, Piauí Federal University – UFPI, Campus Ministro Petrônio Portela, Ininga, 64049-550, Teresina, Piauí, Brazil.*

** Corresponding author. Tel: +55 (16) 3301 9666, Fax: +55(16) 3301 9814, E-mail: jeduardo.unesp@yahoo.com.br*

Abstract: Indian-nut (*Aleurites moluccana*) and tucum (*Astrocaryum vulgare)* are oleaginous non eatable that present excellent oil content (about 60% and 30%, respectively) compared to soy bean grains (20%). Biodiesel production from these oils, using bioethanol as reactant, is an alternative for renewable energy source. In this paper, experimental design was used to determine the influence of these different kinds of oils on the transesterification reaction in order to evaluate the viability of biodiesel production process using ethanol as reactant. The most influential variables on the transesterification reaction yield were: alcohol to oil molar ratio, mass of catalyst, temperature and reaction time. In this paper, the variables was operated using experimental design with central composite. Compositional difference between both tucum and *Aleurites* oil has been verified by ^{1}H-NMR and GC analysis. Physicochemical properties presented by *Aleurites* biodiesel are in accordance with ANP Regulation n. 07. On the other hand, the same conditions were not adequate to achieve a high transesterification yield from handmade *Astrocaryum* oil. In this case, better conditions were only obtained from refined oil. The reactional conditions optimized based on a kind of oil sometimes can't be suitable for any biodiesel production reaction.

Keywords: *Biodiesel, Bioethanol, Aleurites, Optimization, Experimental design.*

1. Introduction

Vegetable oils are one of the most commonly used biofuels raw materials. The main reason is their great versatility in the industrial transformation and environmental gains of their processing, in relation to petroleum, due to the absence of sulfur and heavy metals in their composition [1]**.** In this way, vegetable oils enable the production of biodiesel, a biofuel with very similar features as petrodiesel. The biodiesel is obtained from the chemical transformation of the oils (glycerides) by a transesterification process. In this case, the glycerides react with an alcohol of short carbon chain in the presence of a strong acid ou alkaline catalyst, to produce a mixture of fatty acid alkyl esters and glycerol [2].

The alcohol generally employed in transesterification reactions to biodiesel production is methanol, however, it presents some disadvantages, such as: mostly of it is obtained from non-renewable sources, presents high toxicity and Brazil do not produces sufficient amount for internal consumption. In other hand, ethanol, even deprecated due some reactional inconveniences, becomes very attractive under economic, strategic and environmental points of view; presents low toxicity and can be produced from sugar-cane, a highly renewable source. Brazil is currently the world's leader in bioethanol production obtained from sugarcane. Because of government subsidies, large sugarcane crops, and high sales taxes on gasoline, Brazil has built a profitable national bioethanol industry. Sugarcane is grown in the

country as the climate presents perfect conditions for its cultivation and production. It is very easily converted to ethanol, and provides Brazil with huge supplies of bioethanol [3,4].

Lima *et al.* (2007; 2008) used bioethanol to prepare biodiesel from glycerides abundant in vegetable sources present in Brazil Midwest, North and Northeast regions, by homogenous catalysis reaching quantitative yield on catalytic process. These results became the motivation for a research aiming to overcome the reactional limitations for bioethanol and to improve its insertion into biodiesel energetic matrix.

Brazil has a lot of oleaginous vegetables with huge potential to produce biodiesel. The *Aleurites moluccana* seeds (so called indian nut or "noz-da-índia" in Brazil or "nogueira-de-iguapé") has been employed as an oil source for several years. *Aleurites* is original from tropical Asia and pacific islands; In Brazil, it is broadly spread in Atlantic Forest. The species is a tree with 10 m eter height, that produces green fruits having one or two seeds. The percentage of oil extracted from *Aleurites* seeds is higher than soy bean grains, for example. It is about 63% composed of oleic glycerides that have excellent properties for biodiesel production. The oil obtained from *Aleurites* seeds is mostly used to make soaps, candles and varnish [6] and was already used to produce methylic biodiesel [7] but, to the best of our knowledge, there are no reports on its use to produce ethylic biodiesel.

There is a great biodiversity of palm trees in Brazil and among them there is a palm tree, *Astrocaryum vulgare,* Mart. (popularly known as "tucum" or "tucumã" in Brazil) not used as a source of oil for biodiesel production. The "tucum" is a palm tree that grows up to 10 m high, in a highly dry soil and those that floods occasionally. The almond supplies eatable white grease used to produce soaps, cosmetics and medicines. The fruits are very appreciated and the fruition occurs between November and May [8]. The "tucum's" mature fruits are yellow and consist of the pulp and the almond that correspond respectively to about 53.2% and 24.5% of the fruit weight [9]. The pulp produces orange oil (18.18% w/w) in which polyunsaturated fatty acids predominate and the almond produces a white grease (29.59%) rich in lauric and myristic fatty acids. In Brazil it is possible to found the "tucum" tree in the Amazon and Northeast regions. The majority of its fatty acids consist of short chain, mainly lauric (52.51%) and myristic (25.04%). This property facilitates the kinetic of the transesterification reaction for biodiesel production leading to a product with more oxidative and thermal stabilities than biodiesel obtained from other oils, such as soybean [9].

As discussed earlier, nowadays, the optimization of biodiesel production mainly applying ethylic route, is of great relevance. The use of experimental design is a powerful tool to process optimization. The experimental design is a technique able to rationalize the application of experiments, to investigate, simultaneously, all potential variables that affect the results of a process. The advantages of working with experimental design are the achievement of more information using a smaller number of experiments, to perform studies about individual effect of each variable, how these variables interact independently and more than this, to analyze the results with a model that allows previsions of what will happen for any experiment into studied range. The response surface methodology, also, is a statistic tool for optimization based on factorial designs, to denote the response of the system, under study, with alterations in the variables [10].

According to Sarin *et al*. (2010), the properties of a biodiesel are influenced by the structure and amount of the component fatty acid esters, which depends on the oil source. So, the main objective of this work is to discuss the application of experimental design based on a specific

oil to a different oil, for the production of biodiesel. Moreover, we intend to propose "tucum" and indian nut oils as raw materials for biodiesel production using the ethylic route. In such way we intend to improve the reactional conditions, using experimental design, to obtain biodiesel from indian nut seeds oil, by ethylic route (NaOH as catalyst). Then, the best conditions should be applied to prepare biodiesel from almond oil of "tucum". Ester content, and other physico-chemical properties established by Resolution n. 07/2008, from Brazilian Regulatory Crude Oil, Natural Gas and Biofuels Agency [12], will be the principal reference parameters to verify the efficiency of reactional conditions obtained from experimental design.

2. Methodology

2.1. Experimental design for ethylic biodiesel preparation from Aleurites oil.

In order to obtain the response surface, it was applied an experimental design with central composite design. All variables: heating time, temperature, ethanol/oil molar ratio and mass of catalyst, were evaluated under five levels. These variables are shown in Table 1, together with their respective levels. A total of twenty six experiments were predicted. The results were analyzed using the software Statistica 7.0 [13].

Table 1. Variables and studied levels for the preparation of biodiesel from Aleurites seeds oil and ethanol (NaOH catalyst).

Variables	**Level**				
	-1,41	-1	0	+1	+1,41
Heat time /min.	50	70	90	110	130
Molar ratio /ethanol/oil	6:1	7:1	8:1	9:1	10:1
Temperature /°C	40	50	60	70	80
Catalyst /% w/w	0.6	0,7	0,8	0,9	1,0

2.2. Materials, methods and instruments

Ethanol (Synth, lot 118784) and sodium hydroxide (Qhemis, lot Q0011) of analytical grade were used without additional purification. Indian nut seeds were gathered at the city of Araraquara-SP, Brazil. The oil was obtained by milling the seeds and extracting the resulting material with hexane in a Soxhlet system during 10 hours. The yield was calculated dividing the final mass of oil extracted by the mass of the milled seeds. The "tucum" oil was obtained from the municipal district of Altos, PI, Brazil, and extracted by handmade way, in other words, it was extracted by milling and heating in water.

2.3. Preparation of the tucum and Indian-nut biodiesel

The transesterification of oils with ethanol, catalyzed by sodium hydroxide, were made using a three necked flask over a heating plate with magnetic stirrer. A condenser and a thermometer were connected to the flask. The third neck was closed with a rubber septum, through which the catalyst solution in ethanol was introduced using a syringe with a long needle under the heated ethanol/oil mixture surface. The reaction time began to be counted from this moment. The reaction mixture was kept in the flask under magnetic stirring. After the reaction time be completed, the final products were separated by centrifugation and the biodiesel (upper phase) was washed with distilled water. The biodiesel was, then, dried by heating at 60 ºC about 40 minutes under argon flow.

2.4. Physicochemical characterization of the tucum and Indian-nut biodiesel

The "tucum and Indian nut biodiesels were characterized by: visual aspect; ^{1}H NMR spectra; viscosity at 40 ºC (ASTM D445), specific gravity at 20 ºC (ASTM D4052), cupper corrosivity (3h at 50 ºC - ASTM D130); cold filter plugging point (ASTM D6371), acidity index (ASTM D664); ester content (EN/ISO 14103); free and total glycerol and glycerides index (EN 14105); iodine index (EN 14111), water content measured by the Karl Fisher method (ASTM D6304), content of sodium, potassium, calcium, magnesium and phosphorus (ICP-OES - NBR 15553) and oxidative stability analysis (Rancimat - EN 14112).

^{1}H NMR spectra were obtained in a equipment Varian Inova of 500MHz. $CDCl_3$ was applied as solvent (30 µL of sample and 600 µL of solvent). ^{1}H NMR spectrum was obtained at 300K temperature using 64000 acquisitions with pulse standard (s2pul), and tetramethylsilane TMS as reference. The spectral profile was used to observe the conversion of oil to biodiesel and to verify the oils composition.

3. Results / Discussion

Aleurites moluccana presented fruits with a high content of oil (60 %), such as found in other researches [7]. Tucum, how presented in the introduction [9], can produce around 30% of oil. This yield is better than soybean that shows an oil content around 25%, for example.

3.1. Experimental design for Aleurites biodiesel synthesizes

After all of the twenty six experiments and measure the ester content were done, were built six surface designs where the Y axis represents the percentage of ester content. The best results was obtained employing heat time about 90 minutes, molar rate alcohol/oil 8:1, temperature of 60 ºC and 0.8% of catalyst. Was reached more than 99% of conversion. However, we can see other conditions that could be applied considering the little difference at the final results. In other words, when employed 70 minutes; 9:1 molar rate; 60 °C and 0.8 % of catalyst we achieved nearby 100% of yield. These conditions were used to synthesize both Indian-nut and Tucum biodiesel.

3.1.1. Preparation of the tucum and Indian-nut biodiesel

It is necessary remember that the oils are from different sources and they were obtained by different process too. The optimization process has been done employing Indian-nut oil only. Exactly 100 g of oil was put into a flask and heated until 60 °C. After then, was added the ethylic alcohol containing the total mass of catalyst. There were not troubles during the reactional time. The purification process was done using distillate water at room temperature. It was around 30 °C. No special process was necessary to segregate the glycerin phase.

3.2. Physico-chemical characterization of the tucum and Indian-nut biodiesel

Physico-chemical properties showed that both biodiesel were very similar at rheological viewpoint, because their viscosity and density are practically equals. Table 2 shows analysis results. The water content proves the efficiency of drying process using argon gas. It was below the maximum limit of 500 ppm. Some ions level like sodium, potassium, calcium, magnesium and phosphorus are below quantification limit of ICP equipment. That way, the biodiesel are in accordance to ANP Resolution. The tucum biodiesel's low iodine index (14.6 g/100g) denotes his saturated character and hence his cloud point (5.0 °C) will be bigger than *Aleurites* biodiesel (-5.0 °C). The iodine index of *Aleurites* biodiesel (150.36 g/100g) reflects a high level of unsaturated chains on his composition. These unsaturated chains can resist lower temperatures than the saturated compounds without freezing.

Table 2. Aleurites and Tucum biodiesel physicochemical parameters.

PARAMETERS	UNIT	LIMIT	METHOD	RESULTS	
				Tucum	Aleurites
Aspect	-	LII*	Visual	LII	LII
Density at 20º C	kg/m3	850-900	ASTM D4052	0,8770	0,8789
Kinematic viscosity at 40ºC	mm2/s	3,0-6,0	ASTM D445	4,54	4,12
Water mass, max.	mg/kg	500	ASTM D6304	261,6	160,1
Sodium + Potassium, max.	mg/kg	5	NBR 15553	<LQ**	<LQ
Calcium + Magnesium, max.	mg/kg	5	NBR 15553	<LQ	<LQ
Phosphorus, max.	mg/kg	10	NBR 15553	<LQ	<LQ
Cupper corrosivity, 3h a 50 ºC, max.	-	1	ASTM D130	1 a	1 a
Cloud filter point pour, max.	ºC	19	ASTM D6371	5,0	-5,0
Iodine índex	g/100g	Anotate	EN 14111	14,67	150,36
Free glycerin	% mass	0,02	EN 14105	0,00	0,00

* Impurities free and limpid.; ** LQ: Quantification limit.

Total glycerin and glycerides content are not displayed because they are a parameter directly linked to ester content. Thus, in the tucum biodiesel we can not expect them are according to maximum limit due tucum ester content is only 79.8%. In other hand, total glycerin of *Aleurites* biodiesel (0.075%) was completely in agreement with that limit which can not be more than 0.25% of total glycerin. Free glycerin is an important parameter, especially in order to provide information about purification process. In this case, two biodiesel presented non quantitative mass of glycerin due to efficient washes.

3.3. ^{1}H NMR biodiesel analysis

When comparing indian nut and "tucum" biodiesels ^{1}H NMR spectra (e.g. Fig. 1 and 2) is possible to see differences, such as unsaturation level and compositional profile. Absence of representative peaks around 2.1 ppm in "tucum" spectrum, assigned to the methylene protons attached to the unsaturated carbon, shows its high degree of saturation.

Beyond this, near to 5.3 ppm the peak assigned to the H from CH unsaturated is in agreement with the previous observation about pi bonds. In the Glycerides chains presents in tucum biodiesel there is almost none pi bond beyond those of carbonyl groups. Observing chromatograms overlap (e.g. Fig.3), we can note the real composition`s difference between both oils and biodiesel from tucum and *Aleurites*.

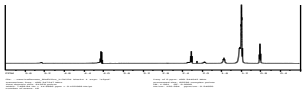

Figure 1. ^{1}H NMR Aleurites biodiesel spectrum.

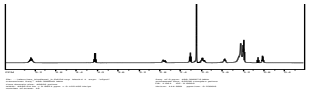

Figure 2. ^{1}H NMR "tucum" biodiesel spectrum.

3.4. Ester content

One of the most important reactional results is the ester content. This parameter represents how efficient was the reactional process. The principal target of this paper is to show how useful can be the optimization from an experimental design in order to apply it to others oils with different properties. If the ester contents yield are similar, so these same conditions could be applied. The *Aleurites* biodiesel synthesize presented yield about 99%. This result is almost the same as the one previously obtained during the optimization process. When those reactional conditions were applied to synthesize ethylic tucum biodiesel, the result achieved was only 79.8% for ester content. The minimum level described on Brazilian national legislation is 96.5%.

The chromatograms superimposed, e.g. Fig. 3, shows the composition differences between biodiesels from "tucum" and indian nut in terms of carbon chain length. In order to prove this, some ethylic ester standards were run on GC and their retention time (RT) were registered: C8:0, RT= 2.5 min; C12:0, RT=7.0 min; C14:0, RT= 8.0 min; C17:0, RT=14.2 and C24:1, RT=25.4 min. With this data, we can prove the saturated character of tucum oil. In the chromatogram could be seen that the majority of compounds from tucum biodiesel are between 2.5 and 15.0 minutes. In this interval there are C8:0, C10:0, C12:0, C14:0 and C16. Even a little after that, there are some peaks attributed to C18:0, or a small peak assigned to C18:1, but nothing after 17.5 minutes. Regarding *Aleurites*, most peaks are above 12.0 min and below 18 min. That interval covers saturated and unsaturated chains like C16:0, C18:0, C18:1, C18:2 and C18:3. Among those peaks, majority lies above 15.0 minutes, region of occurrence of peaks corresponding to esters with more than 17 carbons.

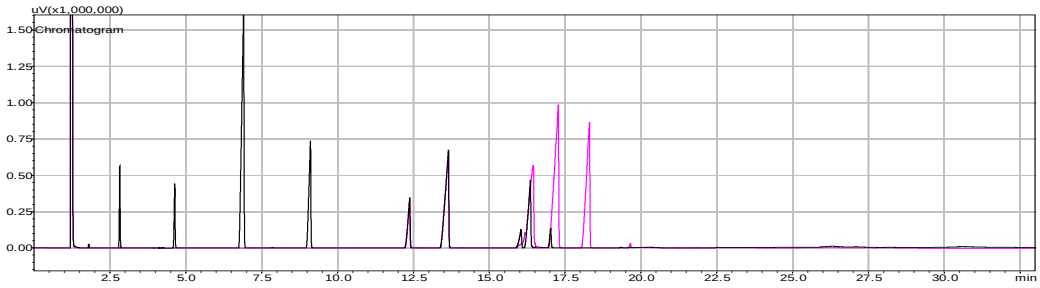

Figure 3. Superimposed "tucum" and indian nut biodiesels chromatograms (pink: Indian-nut biodiesel; black: tucum biodiesel.

3.5. "Tucum" biodiesel preparation yield under the best conditions found to indian nut biodiesel preparation.

The yield achieved to "tucum" biodiesel prepared, applying the best conditions developed by experimental design on indian nut oil, was very low. The preparation procedures were the same to both oils. Only during work up procedures there were some differences between them. Because of the acidity presented by "tucum" oil (soap generation) and its shorter carbon chains, the washing process generated more emulsions than during indian nut biodiesel work up; "tucum" biodiesel was washed much more times to remove soap excess and to break any emulsions. This can be one of the causes for the low yield of esters obtained from "tucum" oil. Other causes for the unsuitable behavior of "tucum" oil under the best experimental conditions developed for indian nut oil conversion to biodiesel may be its impurities, not removed during manual oil extraction process, and the manual oil extraction itself.

4. Conclusions

The oil content of "tucum" and indian nut seeds is greater than soybean grain. Ethanol showed technically suitable as a reagent to biodiesel production from indian nut and "tucum" oils. Indian nut oil has considerably more unsaturated esters than "tucum" oil, what explains its lower resistance to oxidation. Experimental central compound design and surface response methodology were efficient for optimization of the reactional conditions (time, temperature, molar ratio ethanol/oil and mass of catalyst) to obtain biodiesel from ethanol and indian nut oil. The optimized conditions led to an almost stoichiometric yield of biodiesel confirming the forecast of the technological viability of indian nut oil to obtain high yields of ethylic biodiesel. The same optimized conditions did not apply for "tucum" oil. Further experiments with "tucum" oil obtained by the same extraction procedure used to indian nut oil are necessary. Experimental design is an important tool to optimize chemical preparations. However, its relationship with raw materials characteristics must be carefully observed.

References

[1] Lee, S. W.; Herage, T.; Young, B. Emission reduction potential from the combustion of soy methyl ester fuel blended with petroleum distillate fuel. Fuel (83), 2004, pp. 1607-1613.

[2] Lima, J.R.O., Silva, R.B., Silva, C.C.M., Santos, L.S.S., Santos Jr, J.R., Moura, E.M., Moura, C.V.R. Biodiesel de babaçu (Orbignya sp.) obtido por via etanólica. Quimica nova 30 (3), 2007, pp. 600-603.

[3] BRASIL. Serviço Brasileiro de Apoio ás Micro e Pequenas Empresas (SEBRAE). Cartilha Biodiesel 2009. Available from: http://www.biodiesel.gov.br/docs/Cartilha_Sebrae.pdf.

[4] http://www.energyrefuge.com/archives/largest-ethanol-producer.htm, accessed in December 13, 2010

[5] Lima, J.R.O., Silva, R.B., Moura, E.M., Moura, C.V.R. Biodiesel of tucum oil, synthesized by methanolic and ethanolic routes. Fuel (87), 2008, pp. 1718–1723.

[6] Ojasti, J; Jiménez, E.G., Otahola, E.S., Román, L.B.G. Informe sobre las Especies Exóticas em Venezuela. Caracas, Venezuela, Ministerio del Ambiente y de los Recursos Naturales. 2001. A vailable from: www.institutohorus.org.br/download/fichas/Aleurites_moluccana.htm.

[7] Azam, M.M., Waris A., Nahar N.M. Prospects and potential of fatty acid methyl esters of some non-traditional seed oils for use as biodiesel in India. Biomass & Bioenergy (29), 2005, pp. 293-302.

[8] http://www.vivaterra.org.br/palmeiras_nativas.htm#tucuma, accessed in December 13, 2010

[9] Mambrim M.C.T, Arellano D.B. Caracterización de aceites de frutos de palmeras de la región amazónica del Brasil. Grasas y Aceites 48 (3), 1997, pp. 154-158.

[10] Baptista, P., Felizardo, P., Menezes, J.C., Correia, M.J.N. Multivariate near infrared spectroscopy models for predicting the methyl esters content in biodiesel. Analitica Chimica Acta (607), 2008, pp. 153-159.

[11] Sarin, R., Sharma, M., Khan, A.A., 2010. Terminalia belerica Roxb. seed oil: A potential biodiesel resource. Bioresource Technology (101), 2010, pp. 1380–1384.

[12] AGÊNCIA NACIONAL DO PETRÓLEO., 2008. Resolução ANP nº. 07. Diário Oficial da União (DOU), 20 mar. de 2008.

[13] Ryan, T. P. Modern Experimental Design. John Wiley & Sons. New Jersey, 2007.

A bubbling fluidized bed combustion system for forest residues

Anthony Goncalves[1,2], Laszlo Kiss[2], Marie-Isabelle Farinas[2], Daniel Rousse[1,*]

[1] *t3e Industrial research chair, École de technologie supérieure, Montréal, Canada*
[2] *GRIPS, Université du Québec à Chicoutimi, Chicoutimi, Canada*
** Corresponding author. Tel: +1 (418) 833-2110, Fax: +1 (514) 396-8950, E-mail: daniel@t3e.info*

Abstract: The main objective of the project was to develop or adapt a combustion technology that would permit a stable operation of a boiler fed with a combustible with a high level (50%) of humidity. The size of the unit was determined by the heating demand of a lacto-serum plant. Computer simulations and small scale laboratory experiments were used to design a fluidized bed, then fluid flow and heat transfer calculations were carried out to verifiy the heat balance (or energy balance) of an existing fixed boiler to be converted into à fluidized bed one. A grid involving 130 nozzles with 6 equally distributed holes (10 mm) was designed. The intake has a 23.37 mm I.D. It has been in operation for more than a year now and operation results are presented. It was found that the key aspect of the combustion process in such boilers is the homogeneity of the fluidized bed and the temperature control. We are now working on a way to broaden the range of type of wood and humidity levels.

Keywords: *Renewable energy source, Boiler, Bubbling fluidized bed*

Nomenclature

ΔP	*effective pressure drop across the bed*	*Pa*
A	*area of the bed*	m^2
Ar	*Archimedes number*	-
D	*particle diameter*	*m*
g	*gravity*	$m \cdot s^{-2}$
h	*convective transfer coefficient*	$W\ m^{-2}\ K^{-1}$
H	*height of the bed*	*m*
K	*fluidized bed constant, usually 5*	-
Nu	Nusselt number	-
Pr	Prandtl number	-
Re	*Reynolds number*	-
S	*surface to volume ratio*	-
T	*temperature*	*K*
U	*fluidization velocity*	$m \cdot s^{-1}$

Greek symbols

ρ	*density*	$kg \cdot m^{-3}$
λ	*thermal conductivity*	$W\ m^{-1}\ K^{-1}$
μ	*dynamic viscosity*	$kg \cdot m \cdot s^{-1}$
ε	*bed porosity*	-

Indices

mf	*minimum fluidization*
g	*gaz*
p	*solid particles*
r	*radiation*

1. Introduction

1.1. Context

The ever increasing level of greenhouse gas emissions combined with the overall rise in fuel prices (although fluctuations occur) are the main reasons behind efforts devoted to improve the use of various sources of energy. Economists, scientists, and engineers throughout the world are in search for: (1) strategies to reduce the demand; (2) methods to ensure the security of the supplies; (3) technologies to increase the energy efficiency of power systems; and (4) new and renewable sources of energy to replace the limited and harmful fossil fuels.

Nowadays, biomass (organic wastes) receives an ever increasing interest for energy production because this renewable source of energy:

- reduces the demand of fossil fuels,
- diversifies the sources of traditional energy,
- ensures the supplies at a local level,
- is carbon neutral?

Fluidized beds found several industrial applications such as coal and biomass combustion. Boilers involving such a technology are generally more efficient that their counterparts with fixed or mobile grids and this is why bubbling fluidized beds combustors (BFBC) are often selected to transform waste into energy. An efficient combustion for low calorific power fuels is possible with appropriate controls: according to Oka [1], it could reach up to 99%. Moreover, bubbling fluidized bed combustion of solid residues also becomes attractive for thermal steam generators because it can allow for variations in the regime by up to 4% per minute [2].

1.2. Fluidized beds combustion

Fluidization refers to the conditions for which a granular material behaves such as a fluid. To obtain fluidization, a gas (generally air) crosses a bed of particles with an appropriate upward flow rate to create forces that separate particles: the result is a turbulent mixing of gas and solids. The key idea is to obtain the highest mixing rate possible. In practice, the mass flow rate must be high enough to ensure an appropriate mixing and low enough to keep the particles in the mixing. The rationale behind this technology is that the tumbling action provides more effective chemical reactions and heat transfer in the solid fuel particles that are added to the bed.

In this paper, the process involves BFBC. During preheating, the bed is heated up with an auxiliary source (here natural gas). Then, the process is fed with biomass. This initialization process is critical to ensure proper operation. During combustion, part of the ashes and fine particles must be collected with a cyclone. The other part of the ashes is recovered through the sand circulation. The bed temperature – which influences the stability of combustion, the efficiency of the steam generator, and the rate of pollutants are the preponderant factors for this type of system.

1.3. Process characteristics

BFBC boilers operate at lower temperature than other types of boilers (800-850°C). This may lead to less NOx emissions. However, burning at low temperatures also causes increased polycyclic aromatic hydrocarbon emissions. The temperature upper limit is intrinsically due to the melting point of the most commonly used solid particle: sand. The development of eutectic within the sand is a crucial phenomenon to avoid. The creation of agglomerates will seriously impact the efficiency and may stop fluidization and, eventually, the whole process. The melting point of silica diminishes when it is mixed with ashes and eutectics are formed when hot spots occur in the bed. BFBC reduces the amount of sulfur produced in the form of SOx.

1.4. Overview of the installation

The whole factory into which the boiler is installed produces lactoserum which requires 6MWth and electricity (1MWe). The boiler produces 10T/h at 32 bars and 315^{o}C. The whole plant is shown in Fig. 1. On the left-hand side the storage and feeding systems (a) are shown while the boiler (b) is located in the center of the right-hand side of Fig. 1. The feeding system is a key element of the design as the process is continuous and cannot be stopped. The homogenization of the bark in terms of size and humidity is another key aspect. In Fig.1, the fuel is grabbed and thrown into the feeding system where some sorting occurs to avoid having large chunks of wood to get into the 40 cm worm gear. This gear feeds the combustion chamber. The fluidization grid is another key aspect of the process. The shape and size of the nozzles, the numbers and diameters of the orifices as well as the air outlet

velocity have to be selected to maximize the homogenization. The height of the bed and the pressure drop are other key parameters [3,4] discussed in subsequent sections.

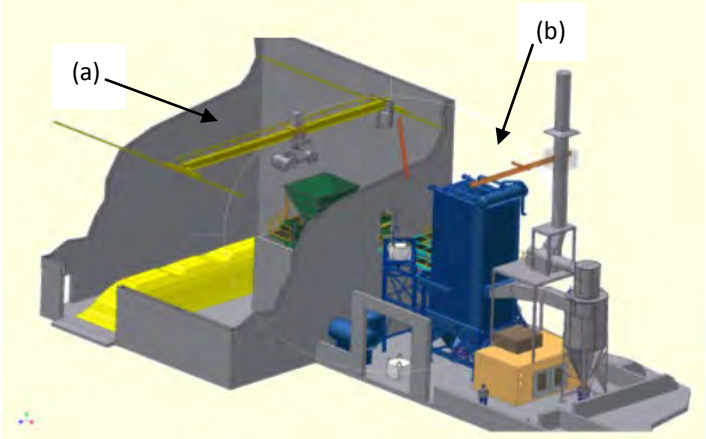

Fig. 1: Layout of the complete plant with: (a) Feeder and storage; (b) boiler, turbine and stack.

1.4.1. The storage system

In this area of the plant, the raw material is treated to maximize homogeneity in size, calorific power, and humidity. A mechanical treatment is applied to tear the biggest chunks of wood this to avoid mechanical failure of the feeding system. During winter, humidity and ice were initially found to cause mechanical blocking along the conveyors. Nowadays, by use of specific materials and appropriate controls of the feeding system, this problem vanished. Several tons of material can be stored in the area.

1.4.2. The feeding system

The feeding system has been designed for a rate of 4 tons per hour. Initially, the rough surface of the drop feed, made of refractory, involved too much friction. Suddenly, clusters of bark accumulated in the drop feed were inappropriately falling in the bed. A defluidization was occurring followed by several local hot spots in the bed. There was a high potential for eutectic formation. The refractory has been replaced to solve the problem.

1.4.3. The boiler

The Falmec boiler (B.F.I) was originally designed for a fixed grid (water tubes type). The main design limitation was then the size of the combustion chamber itself which limited the width of the fluidized bed. The overall area of the bed, *A*, was hence predetermined (2,3m x 2 m) and thus the imposed the minimal fluidization velocity (which also depends upon the particles size): U_{mf} =1,5 m/s. The primary fan delivers 75 kW with a pressure of 1,27 m CE (or 0,12 bars) during normal operation. This pressure allows for the circulation of the air through the sand bed. The secondary fan as a power of 30 kW with a pressure of 0,38 m CE (or 0,04 bars).

1.5. Start-up and control specifications

1.5.1. Start up

As mentioned earlier, during the start-up, the bed is preheated with an auxiliary burner then the biomass is fed-in. The crucial steps of this initialization process are: (1) verification of the minimal sand thickness of height; (2) start of the primary fan (to initiated fluidization); (3) start of the auxiliary burner; (4) heating of the sand until auto-ignition temperature (about

700°C); (5) low speed feeding; (6) progressive increase of the biomass flow rate to reach the appropriate average temperature of 850°C.

In the proposed boiler, the main difficulty with the auxiliary burner is that it is located above the bed and this causes poor heat transfer to the bed (between the flame and the sand). Afterwards, we realized that, due to its position, the auxiliary burner was undersized slightly. Moreover, the fluidization (process) air should have been heated to shorten the start-up procedure. One way to enhance the start-up process was to add oil (on a temporary basis) in attempts to improve it. Since then, we rely on drier bark at the beginning.

1.5.2. Controls

The control of a steam generator is largely documented [5,6] while that of fluidized beds is also quite documented [7, 8]. Start-up procedures are also documented [2]. The main parameters to control are the flow rates of the two fans, the stability of the combustion, and the bed temperature, with emphasis on the latter. An increase of the mass flow rate of fluidization air increases the temperature (increase in the combustion rate, internal heat release) and inversely [9, 1]. This indicates that the combustion takes place partly within the bed and partly above the bed (appearance of flames above the bed) in the combustion chamber. Several methods allowing for the control of the fluidization regime with primary air and bed temperature measurements could be carried-out but these methods have not been considered in our installation. It is the variation of the bark or wood chunks humidity, needed at about 50%, which was found to require a rigorous control and measurement here.

The system was started during winter 2009 and a data acquisition system permitted the continuous recording of the most important variables: (1) three thermocouples immersed in the bed; (2) the fan speed (primary, secondary, exhaust); (3) percentage of oxygen in the combustion products; (4) steam pressure. In this study, the fluidization regime was said to be in steady state when the three thermocouples showed similar temperatures (Fig.3 and 4).

2. The fluidized bed design and method

2.1. The pressure drop and critical velocity

The fluidization velocity is a basic parameter but its evaluation is rather complicated. Several correlations based on the pressure drop across the bed are available and this pressure drop varies linearly or nearly linearly with the fluidization velocity. In the case of a turbulent flow, Ergun [10] proposed the following expression:

$$\frac{-\Delta P}{H} = 150\frac{(1-\varepsilon)^2}{\varepsilon^3}\frac{\mu U_g}{D^2} + 1.75\frac{(1-\varepsilon)}{\varepsilon^3}\frac{\rho_g U_g^{\,2}}{D} \tag{1}$$

In the fluidization regime, the pressure drop in the bed corresponds to the weight of the particles minus the Archimedes force divided by the surface area of the bed. Since the solid volume is H x A x (1-ε), this yields:

$$-\Delta P = \frac{HA(1-\varepsilon)(\rho_p - \rho_g)g}{A} \tag{2}$$

It is possible to obtain the minimal fluidization velocity when the pressure drop, eq. 2. is inserted into eq.1, yielding:

$$(1-\varepsilon)(\rho_p-\rho_g)g = 150\frac{(1-\varepsilon)^2}{\varepsilon^3}\frac{\mu U_g}{D^2} + 1.75\frac{(1-\varepsilon)}{\varepsilon^3}\frac{\rho_g {U_g}^2}{D} \quad (3)$$

Introducing the relevant Archimedes and Reynolds numbers gives:

$$\mathrm{Ar} = 150\frac{(1-\varepsilon)}{\varepsilon^3}\mathrm{Re}_{mf} + 1.75\frac{1}{\varepsilon^3}{\mathrm{Re}_{mf}}^2 \quad (4)$$

Several researchers tried to correlate their results with this expression to evaluate the minimal fluidization velocity:

$$U_{mf} = \frac{\mu\left[\left(C_1^2 + C_2 * \mathrm{Ar}\right)^{0.5} - C_1\right]}{D * \rho_g} \quad (5)$$

where C_1= 27.2 and C_2= 0.0408 according the results of Grace [11].

2.2. Heat transfer and energy balance

First, the heat transfer characteristic into the fluidized bed
The predominant parameters which influence the heat transfer coefficient are the fluidization velocity, the particle size and the temperature. The Nusselt number for a fixed object immersed in a particle bed was correlated by several researchers. For particle size lower than one millimeter, the refined correlation proposed by Baskakov [12] was used:

$$\mathrm{Nu} = 0.85\mathrm{Ar}^{0.19} + 0.006\mathrm{Ar}^{0.5}\,\mathrm{Pr}\,0.33 + \frac{h_r D}{\lambda_g} \quad (6)$$

This equation stands for an Archimedes number ranging between 10^2 and 10^9 and involves the radiative component of heat transfer calculated with respect to the bed and wall temperatures.
The overall energy balance was established to ensure that the existing boiler combined with the fluidized bed could reach the expected parameters (flow, temperature, pressure). A code was developed based on the temperature of the bed for overall balance calculations. The heat transfer by convection, radiation, and conduction was taken into account. This code permits to show that the combustible moisture level of 50% should be respected to ensure a proper operation in term of bed temperature.

2.3. The nozzles design

The Ergun software [13] has been used to design the bed. The software allows to obtain the suitable air velocities as a function of the fluidization regime, the temperature, the particle size, the height of the bed, and the heat transfer. It enables one to account for pressure drops and homogenization of fluidization. Although not straightforward to use, Ergun permits to correlate the number of holes in the nozzle, the diameter, the minimal fluidization velocity, and the exit nozzle velocity. Whereas several installations may use a perforated plate at the bottom, our combustion calls for a continuous ashes recovery. Hence, fluidization nozzles where used.

Fifteen different nozzles where designed, built, and investigated (two of them are shown in Fig.2a). All were satisfying the design constraints and criteria. The one respecting the

minimum pressure drop required to ensure a stable and homogeneous fluidization was ultimately selected. The tests were then carried out in the lab without combustion in a cylindrical sand bed (Fig. 2b).

(a) (b)

Fig. 2: (a) Two of the eight nozzles that were simulated. (b) The laboratory test bench.

Four different sizes of sand particles, ranging from 1 to 2mm, 0.841 to 1mm, 0.500 to 1mm, and 250 to 500µm were tested. Mixing was also carried out with bark samples of about 1 cm by 2 cm. We found that the bark size did not matter and that the mixing was occurring only in the upper level of the bed, close to the surface. It is however important to note that the cold tests were quite different than the flowing full-scale results.

Finally, a bed involving 130 nozzles (Fig. 3) with 6 equally distributed holes (10 mm) was selected. The intake has a 23.37 mm I.D. The pressure loss is 5kPa when the flow rate is maximum. This flow rate varies from 0.0185 m³/mn at 20ºC. 300 mm of sand was found to be the lowest limit for an homogeneous distribution of air while 600 mm was identified as the upper limit to avoid the over sizing of the fan.

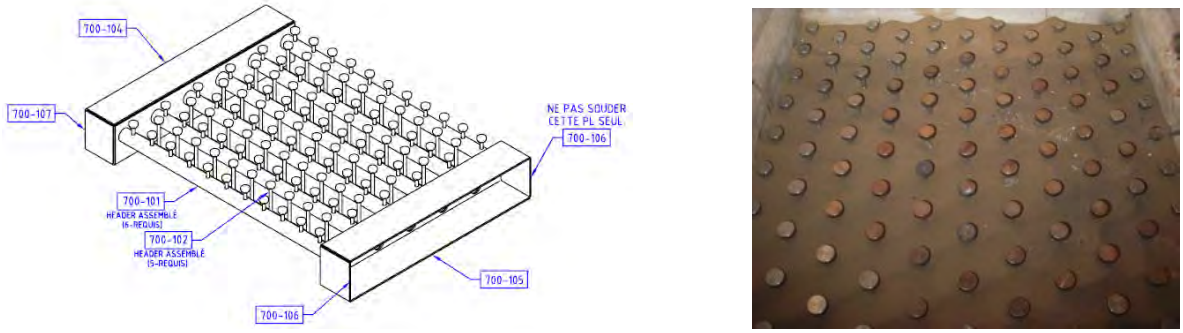

(a) (b)

Fig. 3: The fluidized bed: (a) Full scale model; (b) Actual bed with uncovered heads.

3. Results

Several preliminary tests (not reported here) were needed to fine-tune the operations at the beginning. We worked until uniform temperatures were obtained, thus obtaining a suitable fluidization regime. We also found out that the content of oxygen remained constant with the temperature increase which in turn was proportional to an increase in the mass flow rate of combustible. We noticed that the biomass (fir bark) involved sand that progressively increased the level of the bed (after 10-12 hours of operations) which had to be lowered (by a simple control of the sand circulation). Our first series of tests showed a temperature

variation between 730°C and 838°C. The content in oxygen varied from 1% to 13%. A high content (near 21%) indicates that the combustion is almost completed while à low content shows that there is a high combustion.

Fig. 4 presents two test cases at two different temperatures and same pressure levels. Temperature and boiler pressure are indicated on the left axis (0-1000 range) while the oxygen content and the fan speed is reported in % on the right axis (0-100% range). The abscissa is time in hours.

Fig.4a shows, over a period of about one hour, that the control system maintains the steam pressure (represented by ×) constant at about 350 PSI (the set-point). Indeed, the pressure varied between 320 and 356 PSI (± 9%). In Fig. 4, decreases in the pressure occur with increases in the primary fan velocity (represented by ✳). This corresponds to a simultaneous increase in combustion as the content in oxygen (left axis, represented by Δ) decreases. This content is always below 16%, which is excellent. The temperature here varied from 650ºC to 785ºC.

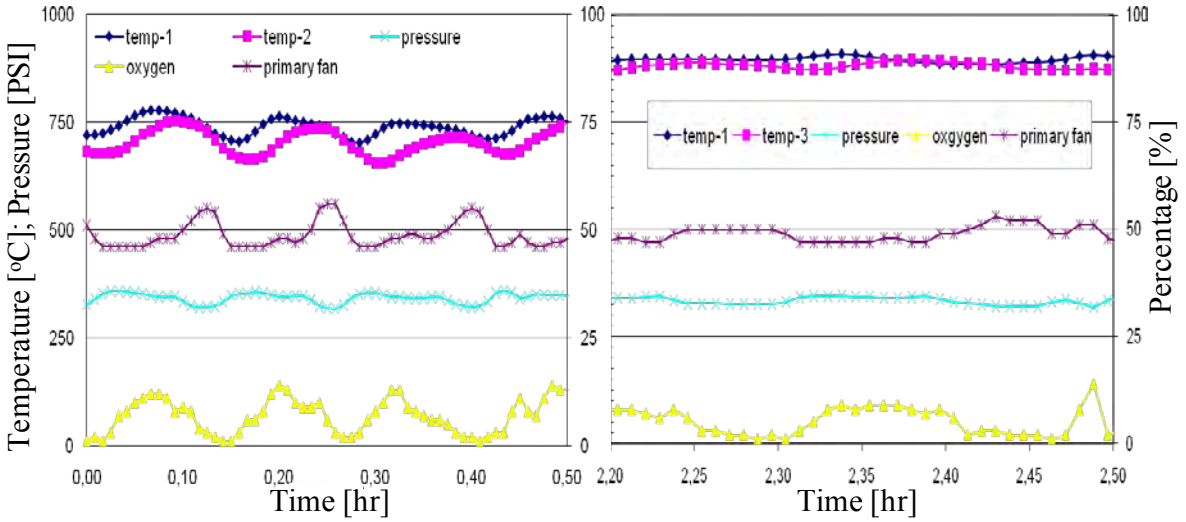

Fig. 4: Temperature, pressure, oxygen content and primary fan power as functions of time: (a) lower regime; (b) higher regime.

Fig. 4b illustrates, over a period of about one quarter of an hour, that the control system maintains the steam pressure constant at about 340 PSI (± 7%): A more stable regime is shown. In Fig. 4b, the trends are similar to those reported in its twin but the regime is higher with temperature ranging between 865ºC and 915ºC. This indicates a higher combustion regime also shown by a lower content in oxygen for the period. The temperature is also more homogeneous in this test case as the control loop improved with time and experience with the boiler.

An interesting feature of the installation is that the pressure settings remained constant during the test showing no need for manual adjustments after the tuning of controls.

4. Conclusion

A bubbling fluidized bed for the combustion of moist wood residues has been designed for an existing steam generator originally involving a fixed grid. The objective was to allow this generator to accept combustibles with a high level of humidity with no compromise over

performance. This paper first presented the complete installation and insisted on a few design parameters and issues that pertain to the bed nozzles and lay-out. The format of the paper cannot permit to provide all relevant details.

When applied to the combustion of forest residues, the key aspects to address were found to be the proper size and humidity of the feed stock. And here, not only on an average basis: a homogeneous mixture ensures a stable process which avoids the generation of local hot spots that could provoke eutectics (agglomerates) and force the shut-down.

The positive points:

- The flexibility in terms of steam demand;
- The combustion efficiency (up to 99%);
- The low maintenance (changes of the sand) requirements.

The need for improvements:

- The design calls for a deep knowledge of fluidization which is not the case with other (simpler) technologies such as fixed grid boilers;
- The acceptance of a w ider range of humidity variation of the feed stock;
- The training of the personnel.

The BFBC is nevertheless an excellent solution to burn humid residuals and recover the energy because of its flexibility, its efficiency, and its cleanness.

References

[1] S.N. Oka, Fluidized Bed Combustion, Marcel Dekker, Inc., New York 2004.

[2] P. Basu, Combustion and Gasification in Fluidized Bed, CRC Press, 2006.

[3] A. Delebarre, J-M. Morales, L. Ramos, Influence of the bed mass on its fluidization characteristics, Chemical Enginnering Journal, 98, 2004, pp.81-88

[4] A. Hepbsali, Estimation of bed expansion in a freely-bubbling three dimensional gas-fluidized bed, Int. J. Energy Res., 22, 1998, pp.1365-1380

[5] G.F. Gilman, Boiler Control Systems Engineering, 2005

[6] Stulz et Kitto, Steam-its generation and use, Babcock and Wilcox, 40th edition, 1992, pp.16-17

[7] D. Geldart, Gas fluidization technology, Ed. John Wiley & sons, 1986

[8] A.J Croxford, M.A. Gliberston, Control of the state of a bubbling fluidized bed, Chemical Engineering Science. 61, 2006, pp.6302-6315

[9] D.L. Kraft, Bubbling Fluid Boiler Emissions Firing Bark & Sludge, TAPPI Engineering Conference, 1998.

[10] S. Ergun, Fluid flow through packed columns, Chem. Eng. Prog, 48. 1952, pp.89-94

[11] J. R. Grace, Fluidized bed hydrodynamics, In Handbook of Multiphase Systems, Hestroni, G., Ed., Hemisphere, Washington, DC, chap.8.1, 1982

[12] A. P. Baskakov et al., Heat transfer to objects immersed in fluidized beds, powder technol.8, 1973, pp.273-282

[13] Khali Shakourzadeh, Ergun software – Instruction manual, University of Compiegne (UTC), Paris, France.

Assessment of the energetic efficiency of a continuously operating plant for hydrothermal carbonisation of biomass

Jan Stemann[1,*], Felix Ziegler[1]

[1]*Technische Universität Berlin, Institute of Energy Engineering, Germany*
** Corresponding author, Tel: +49 30 314 28483, Fax: +49 30 314 22253, E-mail: jan.stemann@tu-berlin.de*

Abstract: To date wet lignocellulosic biomass cannot be used efficiently for energy production. By hydrothermal carbonisation (HTC) wet biomass may be efficiently transformed to a solid, lignite-like fuel with good dewatering and grinding properties and a high calorific value. Energetic yields of the HTC reaction can be derived from lab scale experiments. However, for the assessment of energetic efficiencies of a HTC plant the amount of external energy consumption needs to be calculated. A model of a semi-continuously HTC plant is presented with a heat recovery system which is based on recycling of hot compressed water. Results of simulations with the program Engineering Equations Solver show that energy consumption can be significantly reduced by internal heat recovery. Efficiencies of a HTC plant model are presented based on experiments with beech wood chips as a model biomass. A sensitivity analysis of the water content of the biomass and the heat of reaction is presented.

Keywords: *Hydrothermal carbonisation, biomass, heat recovery, efficiency*

1. Introduction

Hydrothermal carbonisation (HTC) is a pretreatment process of biomass in hot compressed water at around 200°C. Thereby the carbon content and higher heating value (HHV) is increased[1,2]. Apart from application as a soil ameliorant it therefore has been discussed as fuel[3]. The product (related to as "hydrochar" or "char") leaves the reactor as a slurry and must be mechanically dewatered and dried for combustion. By removing water and further compression an energetically dense fuel can be formed facilitating transportation and storage. Good grinding properties make it applicable for gasification and further refining. Energetic yields of the solid of 75-90 % for the HTC process with regards to the HHV can be expected, because the whole fraction of lignocellulose is converted. The HHV of the solid increases when higher temperatures are applied. Yet, the energetic yield decreases for higher temperatures because of a decrease of the solid yield[2,3,4]. Potential feedstock includes digestate, municipal waste, grass, leaves, bagasse and wood[5]. Mass and energetic yields in this contribution are derived from lab scale and pilot scale experiments.

However, in order to assess the energetic efficiency of a HTC plant also external energy consumption must be taken into account - especially for heating the biomass to reaction temperature, for mechanical dewatering of the hydrochar slurry and for drying. The amount of energy needed to heat biomass with a water content of 80% to reaction temperature is app. 24% of the energy of the hydrochar. For drying of char with a water content of 30% app. 4% of its energy is needed. This shows that external energy consumption may decrease the efficiency of a HTC plant significantly and that heat recovery within an elaborated heat regime is crucial. In prior works it was shown that the use of flash steam from expansion of the hot slurry can significantly increase the efficiency of the process[6,7]. But release of pressure and the mixing of steam with colder water necessarily results in a loss of exergy, compared to direct recycling of hot compressed water which is proposed here.

1.1. Semi-continuous biomass feeding

Generally batch or continuous systems are applicable for a HTC plant. Yet, for continuous or semi-continuous systems, reaction heat can be used more efficiently. Also adjacent equipment can be utilized more efficiently and pressure changes in the reactor can be avoided. However, feed systems for solid matter against pressure are challenging – especially for heterogeneous biomass. Piston pumps usually can only pump biomass with a water content of 90%. For dry matter lock hopper systems are widely used, although they come along with a loss of gas for every cycle. Yet for the case of HTC this does not necessarily need to be a disadvantage because reaction gas needs to be discharged from a continuous reactor. Lock hopper valves are prone to abrasion and plugging. Here ball segment valves with a nominal diameter of up to 600 mm made of ceramic may be appropriate[8]. In order to reduce the loss of gas, further feeding systems have been developed including rotary feeders, plug-forming feeders, non-plug-forming feeders[9]. In this contribution we will present a model of a semi-continuously operating system with a lock-hopper feeding system.

1.2. Heat recovery

For a HTC plant an efficient processing of heat will be crucial. In a continuous HTC plant there are three mechanisms which require most of the energy and which are addressed by the plant model: (1) Much water along with the biomass needs to be heated to reaction temperature. This can be reduced if relatively dry biomass is fed via a lock hopper system. Additional water to fully cover biomass in the reactor and enhancing the reaction may be hot compressed process water which is recycled. However this requires mechanical dewatering of the hydrochar slurry after the reaction at elevated temperature and pressure. (2) Additional energy is used for drying wet hydrochar, which requires that the product is mechanically dewatered as well as possible. By dewatering at reaction temperature, a significantly lower water content can be expected. This is because of lower surface tension, density and viscosity of hot water, as was practically examined and realized for mechanical-thermal dewatering of lignite[10,11]. (3) By discharging reaction gas from the reactor a significant amount of steam is discharged as well. By increasing the absolute pressure in the reactor and hence the partial pressure of reaction gases, the loss of vapour can be decreased.

The model aims at using only internal heat sources for preheating of biomass and for drying. Only for the highest temperature level before the entrance of biomass in the reactor external energy is used for the supply of steam.

2. Modelling

For the simulation the program Engineering Equation Solver (EES) is used. Mass and enthalpy balances were entered for all mass flows. Enthalpy of components (except for steam) is set to zero for 0°C. The process is modelled in a steady state although lock hopper and piston press work semi-continuously in reality. Indirect heat transfer to solids or slurries is difficult and fouling on heat exchangers may increase considerably above 100°C[7]. Therefore in the model it is assumed that indirect heat transfer is only feasible up to a temperature of 100°C. The model assumes a capacity of the plant of 2000 kg/h of dry biomass. Below the model is described in detail and is depicted in Fig. 1.

2.1. Preheating of biomass

Biomass with a water content of 0.6 is heated by indirect heat transfer by low temperature waste water and vapour to 100°C at atmospheric pressure. The heat capacity of dry biomass and hydrochar is 1.6 $kJ/kg \cdot K^{-1}$ and 1.45 $kJ/ kg \cdot K^{-1}$ respectively. After preheating at

atmospheric pressure biomass is fed to the lock hopper and is mixed with internal steam from the first flash tank. Then it is mixed with hot compressed water and is finally mixed with external steam from a steam generator until it reaches the necessary temperature and water to biomass ratio of 7:1. External steam is produced by a steam generator operated with natural gas with an efficiency of 0.9.

2.2. HTC reaction

The heat of reaction was measured by differential scanning calorimetry (PerkinElmer DSC-7). 4 mg of ground poplar wood were heated with 20 mg of de-ionized water to 220°C in stainless steel high pressure capsules. In the reference capsules only de-ionized water was used. The experiments were conducted according to ISO 11357-1:1997 and ISO 11357-5:1999. In [12] the applicability and uncertainty of this method for long lasting heat flows is discussed in detail. The mean heat released by the reaction within the first 4 hours was 500 J/g of dry biomass. The uncertainty of the experiments was 30% but could be higher if process water was recycled and therefore in the sensitivity analysis it is altered from 200 to 800 J/g.

In the model the biomass enters the reactor where it reaches the reaction temperature of 210°C by heat of reaction. Heat equilibration is assumed to be dominated by evaporation of water at superheated areas at the bottom of the reactor and condensation at relatively cold biomass on the top. Heat losses of the reactor were assessed to be 5-20 kW depending on insulation which accounts for 0.2% of the system power of the HTC plant. This shows that heat losses in an industrial scale may play a minor role which is not the case for lab experiments which require constant heating in order to maintain a certain temperature. In the model an overall heat loss of 20 kW is assumed and is completely attributed to the reactor.

The model uses experimental mass and energy balances of the HTC reaction. Solid yield, gas yield and heating values are derived from lab experiments with beech wood chips in a 200 mL reactor which could also be reproduced in a 250 L pilot scale reactor. The experiments were performed at the same conditions which are assumed in the model (reaction temperature 210°C, reaction time 4h, water to biomass ratio 7:1). The main results of the experiments which are used in the model are depicted in Table 1.

Table 1. Mass and energy balances of lab and pilot scale experiments with uncertainties shown in parenthesis.

	$wood_{dry}$	$char_{dry}$	solid yield	gas	gas yield	HHV	LHV	energetic $yield_{HHV}$
	mass(g)	mass(g)	(-)	mass(g)	(-)	(MJ/kg)	(MJ/kg)	(-)
Lab scale	19.98 (0.03)	12.88 (0.09)	0.644 (0.003)	0.69 (0.01)	0.035 (0.001)	23.27	22.01	0.781[1]
Pilot scale	14710 (120)	9980 (860)	0.680 (0.064)	-		22.88	21.53	0.808[1]

[1] HHV_{wood} =19.20 MJ/kg, LHV_{wood}=18.06 MJ/kg

Mass and energy yields could be well reproduced for lab experiments. Mass yields from pilot scale experiments altered mainly because the reactor could not be flushed as well. Solid and energetic yields are slightly lower and HHV is slightly higher than reported earlier for experiments at similar temperatures[3,4]. This can be explained by application of higher water to biomass ratio and longer reaction time in the experiments presented above, which will be discussed in detail elsewhere.

The ratio of reaction water and solved organic substances to biomass is 0.32 according to the experiments, yet in the model thermodynamic properties of pure water are assumed. It is assumed that reaction gas only consists of carbon dioxide. The partial pressure of the reaction gas in the reactor is assumed to be 0.9 MPa in order to be completely removed by gas loss of the lock hopper.

2.3. Mechanical dewatering and drying:

Electricity consumption of the piston press is calculated in two steps. First the char is dewatered to a water content of 0.6 with a pressure of 3 MPa. Then the char is dewatered to a final water content of 0.3 by a pressure of 10 MPa. The work is calculated by multiplying the volume of the displaced water with the respective pressure and assuming an efficiency of 0.9. The primary energy consumption of the piston press PEC_{press} is calculated by multiplying the electricity consumption with a primary energy factor. A factor of 2.5 is applied assuming an energy conversion efficiency of the char of 40% in a thermal power plant and thus resulting in a primary energy consumption of the piston press of 0.163 GJ/h.

The water content of the hydrochar after mechanical dewatering is assumed to be 30% corresponding to 31% achieved by pilot scale mechanical-thermal dewatering of lignite at 200°C[10,11]. After dewatering the pressure of the piston is released. In the model it is assumed that this results in evaporation of residual water and cooling to 105°C. Further assuming adiabatic conditions this results in drying to 22% water content which compares to 24% achieved at 200°C[10,11]. Relaxation steam is used for preheating biomass. Afterwards biomass is dried in a rotary drier using steam at 130°C from the second flash tank and abstracted reaction gas and steam from the reactor. Values for desorption heat of lignite[10] are used for the simulation of drying and no external energy is used for drying.

The efficiency of the plant in Table 2&3 is calculated according to Eq. (1):

$$efficiency_{HHV/LHV} = \frac{energy_{hydrochar,HHV/LHV}}{energy_{biomass,HHV/LHV} + energy_{natural\ gas} + PEC_{press}} \quad (1)$$

3. Results

3.1. Simulation results

In Fig. 1 the model as presented before is depicted including mass flows and state variables. The biomass is heated by steam from the first flash tank to 156°C and then is mixed with the hot compressed water from the piston press.

This way the slurry reaches 196°C and only a limited amount of external heat is needed to finally heat biomass and water to 205°C. The amount of external energy needed for this step is 1.03 GJ/h which is 2.7% of the energy of the biomass and 3.4% of the energy of the hydrochar. Heat of reaction then is sufficient to heat biomass to reaction temperature of 210° and to make up for heat losses and gas losses via the lock hopper. The temperature of the waste water is 105°C and cannot be further used at this temperature level. The char can be dried to a water content of 7% by using only internal heat.

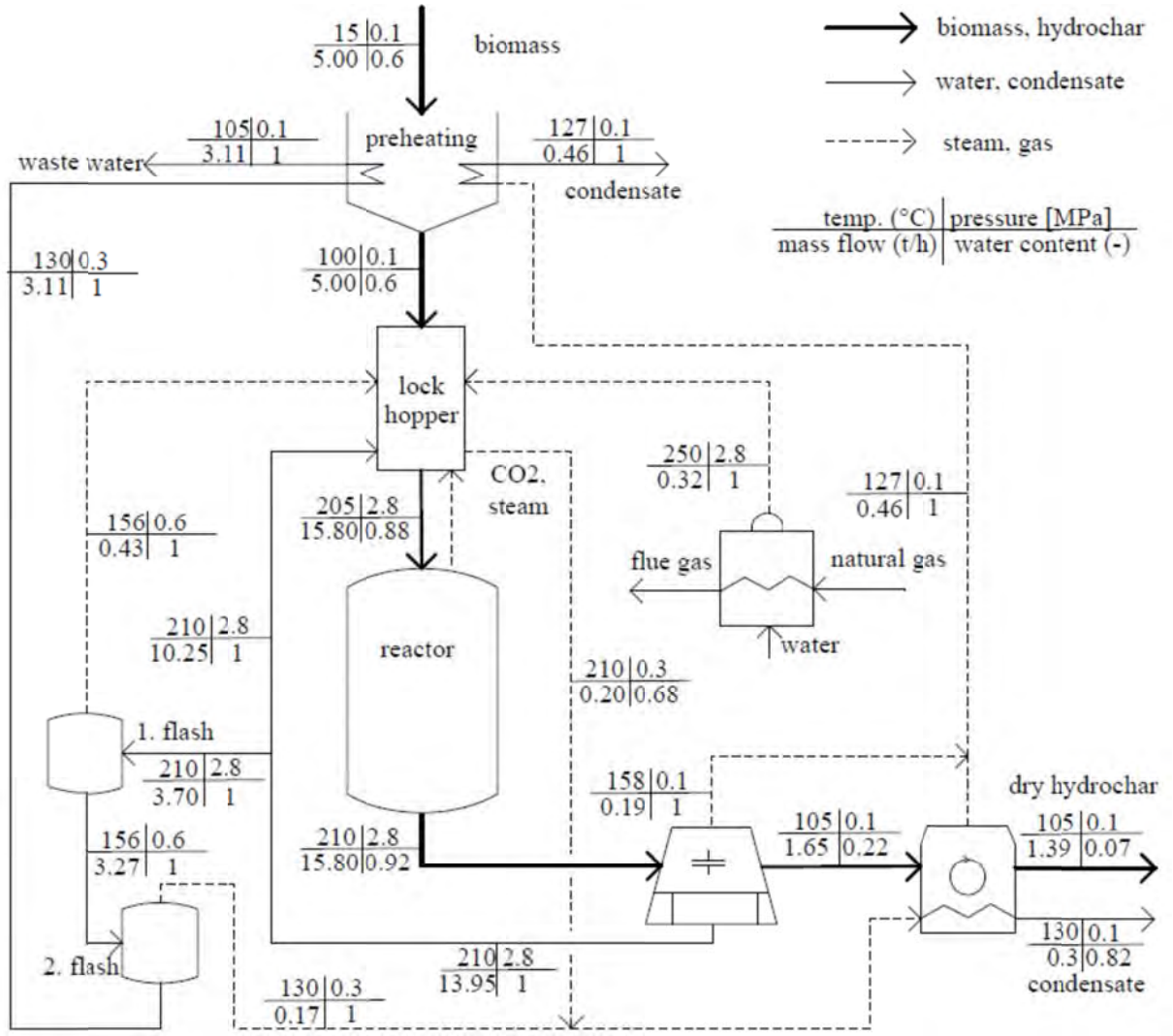

Fig. 1. Model of HTC plant with mass flows and state variables.

3.2. Sensitivity analysis

The water content of the biomass significantly determines the amount of energy needed to heat the biomass to reaction temperature. Therefore it was varied as an input parameter in the simulation from 0.5-0.75 and results are depicted in Table 2. For a higher water content the amount of natural gas needed increases and makes up between 2.2 % and 7.3 % of the energy of the hydrochar. On the other hand the water content of the dried char decreases significantly. This is because less water can be recycled allowing for a higher amount of steam from the second flash tank to be used for drying. The efficiency is calculated both on basis of the HHV and LHV. The efficiency of the HTC plant decreases with a rising water content on the basis of the HHV because more external energy is required. The efficiency of the plant increases on a LHV basis because the lower heating value of the biomass decreases significantly with a higher water content.

Table 2. Results from the variation of the water content of biomass.

water content			energy (GJ/h)				efficiency	
biomass (-)	char (-)	natural gas	biomass (HHV)	biomass (LHV)	char (HHV)	char (LHV)	(HHV) (-)	(LHV) (-)
0.5	0.104	0.650	38.40	31.24	30.06	28.07	0.767	0.876
0.55	0.088	0.819	38.40	30.16	30.06	28.13	0.763	0.903
0.6	0.069	1.032	38.40	28.80	30.06	28.20	0.759	0.940
0.65	0.044	1.307	38.40	27.06	30.06	28.29	0.754	0.992
0.7	0.011	1.675	38.40	24.73	30.06	28.40	0.747	1.069
0.75	0.000	2.191	38.40	21.47	30.06	28.43	0.738	1.193

For a very wet feedstock it may be favourable to mechanically dewater biomass before feeding it to the HTC plant. This would drastically decrease the amount of waste water by recycling a larger part of the water. Therefore it would also decrease the amount of energy needed to heat biomass to reaction temperature. Assuming a decrease of water content of 0.15 in a screw extruder and an electricity demand of 50 kWh/t_{DM}[13] and a primary energy factor of electricity of 2.5 the energetic breakeven point would be at a water content of 0.71 of the biomass.

The heat of reaction was varied in the model between 200 and 800 J/g while the water content of the biomass is set constant to 0.6. The results are depicted in Table 3. With increasing heat of reaction the amount of natural gas needed decreases significantly and would be zero for 840 J/g for the heat of reaction. As less external heat is consumed for heating the biomass, slightly more internal water is recycled. Therefore, less internal steam is available for drying the char, resulting in a small increase of the water content.

Table 3. Results from variation of reaction heat.

reaction heat	water content char	energy (GJ/h)	efficiency (-)	
(J/g)	(-)	natural gas	(HHV)	(LHV)
200	0.054	1.946	0.742	0.914
300	0.059	1.641	0.748	0.923
400	0.064	1.336	0.754	0.931
500	0.069	1.032	0.759	0.940
600	0.074	0.728	0.765	0.949
700	0.078	0.425	0.771	0.958
800	0.083	0.122	0.777	0.968

In the past it was disputed if a self sustaining heat regime was achievable for a HTC plant. As shown above heat demand both depends on the water content of the biomass and the heat of reaction. This means that at a certain water content the heat of reaction would have to be above a certain value. Eq. (2) describes the cases in which the condition of a self sustaining heat regime would be fulfilled for the configuration presented above:

$$h_{reac} \geq 245 * e^{2.1*WC} \qquad (2)$$

where h_{reac} is the heat of reaction (J/g) and WC is the water content (-).

4. Discussion & Conclusion:

It is shown that external energy consumption of a HTC plant can be significantly reduced by addressing the most energy consuming processes of biomass preheating, char drying and reaction gas abstraction. By recycling of hot compressed water efficient heat recovery can be achieved. By using internal heat only, biomass can be heated to 196°C and hydrochar can be dried to 7% water content. External primary energy is needed to further heat biomass to reaction temperature. Electricity is consumed for mechanical dewatering of the char. The total amount of external primary energy for the base case is 4% of the energy of the char which is about half as much as calculated earlier[6]. Depending on the amount of water content and heat of reaction it varies between 1-8%.

Efficiencies for the HHV of the presented HTC plant range from 74-78% based on lab experiments with beech wood chips. Further studies on energetic yields of the HTC reaction are necessary for different feedstock and reaction conditions. However, it can be assumed that external primary energy consumption mainly depends on the plant set up and on the water content of the biomass and the heat of reaction.

In previous publications the intensity of the heat of reaction was overestimated considerably by theoretical considerations. Here values from calorimetric measurements are used and it is shown that it is an important parameter for the assessment of the efficiency of a HTC plant. Therefore additional research is necessary for a better understanding of this parameter.

Recycling of process water is favourable because the amount of waste water can be reduced and heat can be recovered. It is shown that mechanical dewatering of biomass before the HTC reaction can reduce primary energy consumption for wet biomass. In addition a higher amount of recycled water may also slightly increase the energetic yield of the hydrochar because parts of the organic substances in the water may polymerize further. For quantification of this effect further studies are necessary which require extensive dewatering of samples after reaction. Also by further decreasing the ratio of water to biomass the solid yield can be increased. Both effects may increase the solid yield by a few percent.

Acknowledgements

This work has been funded by the German Federal Ministry of Education and Research as part of the joint research project 01LS0806B. We would like to thank Suncoal Industries GmbH for the opportunity to do experiments at their facilities.

References

[1] F. Bergius, Die Anwendung hoher Drucke bei chemischen Vorgängen und eine Nachbildung des Entstehungsprozesses der Steinkohle, Wilhelm Knapp, 1913, pp. 33–58.

[2] S. Inoue, T. Hanaoka, T. Minowa, hot compressed water treatment for production of charcoal from wood, Journal of Chemical Engineering of Japan 10, 2002, pp. 1020-1023.

[3] W. Yan, J. Hastings, T. Acharjee, C. Coronella, V. Vásquez, Mass and energy balances of wet torrefaction of lignocellulosic biomass, Energy Fuels 24, 2010, pp. 4738-4742.

[4] W. Yan, T. Acharjee, C. Coronella, V. Vásquez, Thermal Pretreatment of Lignocellulosic Biomass, Environmental Progress and Sustainable Energy, 28, 3, 2009, pp. 435-440

[5] C. Grimm, Fördervorhaben der DBU zur Hydrothermalen Karbonisierung – Ziele und Stand, Gülzower Fachgespräche 33, Fachagentur Nachwachsende Rohstoffe (FNR), 2010, pp. 37-40.

[6] B. Erlach, G. Tsatsaronis, Upgrading of biomass by hydrothermal carbonisation: analysis of an industrial-scale plant design. Proceedings of 23rd International Conference on Efficiency, Cost, Optimization, Simulation and Environmental Impact of Energy Systems. Lausanne, Switzerland, 14–17 June 2010.

[7] S. Hägglund, (ed.), Vatkolning av Torv AB, Technical Report, Svensk Torvförädling, Lund, Sweden, 1960, p 188.

[8] J. Daniel, pers. comm. [distribution of special valves, Cera System, Hermsdorf] 21.07.2010.

[9] M. Swanson, M. Musich, D. Schmidt, J. Schultz, feed system innovation for gasification of locally economical alternative fuels, final report, energy & environmental research center, University of North Dakota (2002), pp. 77-109.

[10] S. Berger, Entwicklung und technische Umsetzung der Mechanisch/Thermischen Entwässerung zum Einsatz als Vortrocknungsstufe in braunkohlegefeuerten Kraftwerken, Berichte aus der Verfahrenstechnik, Shaker Verlag, Aachen, 2002, pp. 8, 63-112.

[11] C. Bergins, Mechanismen und Kinetik der Mechnisch/Thermischen Entwässerung von Braunkohle, Berichte aus der Verfahrenstechnik, Shaker Verlag, Aachen, 2001, pp. 39-58.

[12] A. Funke, F. Ziegler, Propagation of uncertainties and systematic errors in the measurements of long-lasting heat flows using differential scanning calorimetry, accepted for publication in Journal of Thermal Analysis and Calorimetry.

[13] V. Scholz, W. Daries, R. Rinder, Mechanische Entwässerung von Silage, Landtechnik 5, 2009, pp. 333-335.

Minimization of exergy losses in combustion processes with an illustration of a membrane combustion

Markku J. Lampinen*, Ralf Wiksten, Arto Sarvi, Kari Saari and Marjut Penttinen

Aalto University, Department of Energy Technology, Applied Thermodynamics, Sähkömiehentie 4J, P.O. Box 14400, FI-00076 Aalto, Finland
** Corresponding author. Tel: +358-9-47023582, +358-500-448418, E-mail: Markku.Lampinen@tkk.fi*

Abstract: The efficiency of internal combustion engines and gas turbine processes are free from Carnot limitations as they are not performing cycle processes – the initial state of the thermodynamic system is the fuel with air, whereas the final state is the flue gas, whose chemical composition is different than fuel and air. Therefore, as we show here, the theoretical thermodynamic efficiencies of ideal combustion engines and gas turbine processes can be very high, the same as it is for fuel cells. The entropy generation analysis, what we have done for the internal combustion engines and gas turbines, shows that they suffer for relatively low efficiencies because of the exergy losses in the combustion processes, i.e. for the reason that the combustion reaction takes place quite far from the equilibrium state. We have studied several different combustion processes in the Exergy-project of MIDE-program to find a method for decreasing the entropy generation in the combustion. If the entropy generation can be reduced, by any means, then as a "reward", we get the outlet pressure of the flue gas higher than the inlet air pressure without using any compressor which in turn would then increase the efficiency essentially. We present here a theoretical description of a membrane combustion method which, with the aid of gasification, suits for bioenergy. Shortly, it can be described as a molecular scale oxygen gas compressor driven by the combustion reaction, where the affecting force is amplified by the electric field across the membrane.

Keywords: *Entropy, exergy, combustion, membrane, efficiency, combustion engine, gas turbine process*

1. Introduction

In adiabatic combustion process the outlet temperature of the flue gas depends on the air factor λ and the fuel. It does not depend on the pressure as far as we consider the flue gas as an ideal gas, because then the specific enthalpy of the species (i) depends only on its temperature: $h_i = h_i(T)$. In very high pressures near to the critical pressure, where the ideal gas assumption is no longer valid, the pressure affects also on the specific enthalpy.

Hence, the pressure of the outflow gas does not follow from the energy balance, but it depends on the manner how the combustion process is realized. So we need the second law of thermodynamics to analyze this. The specific entropy of the gas species (i) depends on the temperature T, and also on its partial pressure p_i, i.e. according to the ideal gas model $s_i(T, p_i) = s_i(T, p_0) - R\ln(p_i / p_0)$, which shows that the higher the pressure p_i the smaller is the entropy s_i. Here the reference pressure $p_0 = 1\,bar$ and the gas constant $R = 8.314\ J/molK$. The entropy generation in the adiabatic combustion is

$$\sigma_{irr} = \sum_{out} n_i s_i - \sum_{in} n_j s_j \geq 0, \qquad (1)$$

from which we see that the higher is the outlet pressure, the smaller is the entropy generation σ_{irr}. Instead of the entropy generation we may as well speak of the exergy loss defined as

$$T_{(-)}\sigma_{irr} = exergy\ loss, \qquad (2)$$

which describes the loss of mechanical work in chemical combustion reaction, or the loss to increase the pressure of the flue gas by the chemical reaction. Temperature $T_{(-)}$ is defined with the aid of the real final state (B) and the ideal isentropic final state (B_s) as follows [1]:

$$T_{(-)} \equiv \frac{H(B_s) - H(B)}{S(B_s) - S(B)} \tag{3}$$

Usually the flue gases from the combustion chambers in the gas turbine processes flow out approximately at the same pressure as the inlet flow of the air, and we speak then about combustion at constant pressure. In our earlier paper [2] we have shown that in the conventional combustion with constant pressure the entropy generation is very high and the exergy loss $(T_{(-)}\sigma_{irr})$, depending on the air factor and the fuel, is about half of the heat value of the fuel.

In the classical form of the Guoy-Stodola, the exergy loss is defined as $T_o\sigma_{irr}$, where T_o is the lowest temperature of the surroundings with which the system is in thermal contact. As we have shown in our earlier paper [2] the choice of the temperature T_o for Eq.(2) does not give the accurate value for the lost of the work and for the efficiency of combustion engines (for Eq.(4) below), only an upper limit, and therefore, as shown in [2] we use the correct temperature $T_{(-)}$ instead of T_o.

2. Isentropic combustion

The ideal adiabatic combustion process is such that there is no entropy generation, $\sigma_{irr} = 0$. In the language of thermodynamics it is called an isentropic combustion, and it means a combustion process which proceeds via equilibrium states. In the following we discuss how important for the efficiency it is to keep the entropy generation σ_{irr} as small as possible in order to have a good efficiency.

2.1. Combustion engine

For the combustion engine the following general equation for the efficiency can be derived [1]

$$\eta = 1 - \frac{T_{(-)}\sigma_{irr}}{-[H(B_s) - H(A)]} \tag{4}$$

where σ_{irr} is the generation of entropy in the whole combustion engine process and $-[H(B_s) - H(A)]$ is the heat value of the isentropic combustion process from A to B_s, which is defined so that $S(A) = S(B_s)$. In the denominator of Eq.(4) there is the enthalpy difference $-[H(B_s) - H(A)]$ because our system is a closed system which makes transformation process in the engine during 720^o degrees of rotation of the crank shaft. The entropy generation σ_{irr} (J/K) means correspondingly the entropy generation during 720^o degrees of rotation.

We studied [1] the exergy losses of the diesel engine process, shown in Fig.1, and we found that 79% of all exergy losses took place between the combustion process steps 4-5-6-7. The whole efficiency of the diesel engine was 47.5%. Therefore, if we could eliminate the exergy losses of combustion, then the exergy losses left were 21% x 52.5% = 11% and the efficiency of the diesel engine would be $\eta = 89\%$. It can be so high as the theoretical efficiency can be even one as we see from Eq.(4). The reason for that is that the efficiency is not limited by Carnot formulae because the process is not a cycle process. The efficiency is under the same type of limitations as fuel cells, but for the combustion engine the reference process is an ideal reversible adiabatic process whereas for the fuel cells it is an ideal reversible isothermal process. Therefore, the maximum work out here is $-\Delta H(S = const)$, whereas for the fuel cell it is $-\Delta G(T = const, p = const)$.

How would then the ideal process without any exergy losses in the combustion steps look like compared to Figure 1a? First of all, the engine would be then a two stroke engine, but without having any dead volume. Suppose first that the piston is at left (with volume=0) and the hot flue gas starts to fill the cylinder by pushing the piston to the right in Fig.1b by constant pressure (say at 230 bar as in Fig.1a) from the point 4* to the point 5*. At that point the inlet valve is closed and the isentropic expansion process starts, during which the pressure and the temperature become lower. The length of the piston stroke is such that the point 9* is reached. After that the outlet valve is opened and the flue gas is flowing out to the turbocharger at constant pressure (3 bar in Figs.1a and 1b). All the flue gas is pushed off at constant pressure to the zero dead volume and then the process is repeated by filling the cylinder again by hot flue gas with a high pressure. The turbine unit of the turbocharger is rotating the shaft of the compressor which is feeding air into the special external membrane combustion chamber. That external membrane combustion chamber is assumed to produce the flue gas out at high pressure without any remarkable additional work (only the compression work for fuel feeding) and theoretically with zero entropy generation.

The efficiency of this type of a combustion engine shown Fig.1b is much higher than the engine in Fig.1a because the compression work (3-4 in Fig.1a) is not needed and because the expansion (point 8) continues down to 3 bar whereas it stops now (Fig.1a) at 12 bar, which means that more expansion work can be taken out to the crank shaft by the process.

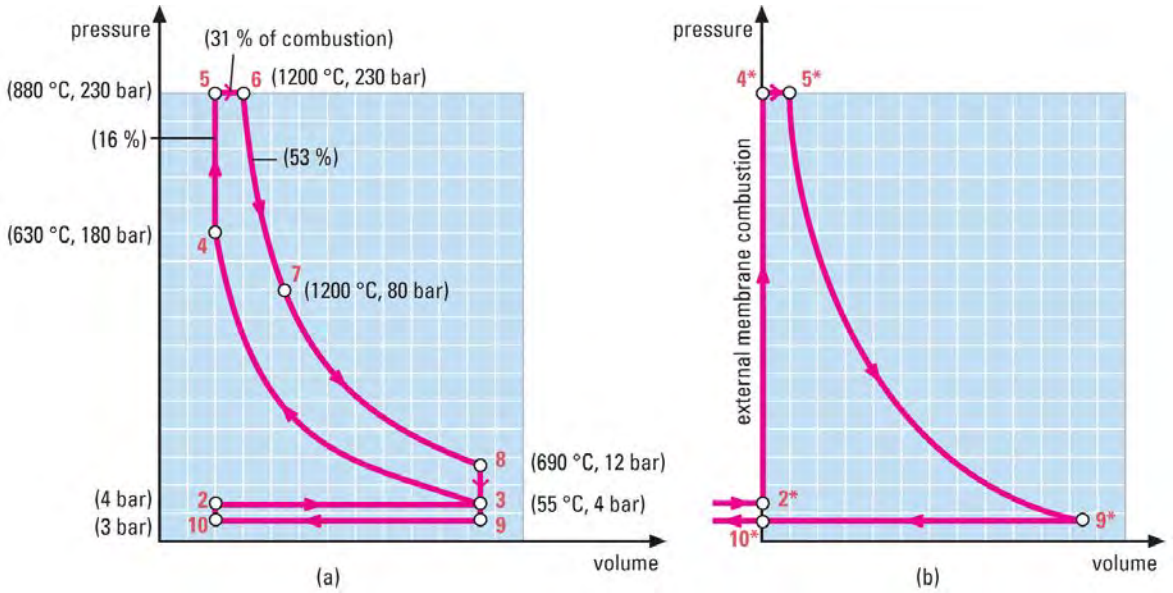

Fig. 1a. Turbocharged diesel engine process. Combustion takes place between 4-5-6-7.
1b. Turbocharged external membrane combustion engine. Combustion only between 2-4*.*

2.2. Gas turbine process

Also for the gas turbine processes the exergy losses in the combustion chamber are of crucial importance. In a methane gas driven power plant in Finland the gas turbine gives out 94 MW of shaft power with the flue gas inlet at 1100 ^{o}C and pressure 11 bar (abs). The compressor driven by the gas turbine takes 54MW which means that the shaft power delivered to the generator is 94 MW – 54 MW = 40 MW. By reducing sufficiently the entropy generation in the combustion unit the outlet pressure of 11 bar could be achieved without using the compressor at all, and thus the whole turbine power could be transferred to the generator which of course, would increase the efficiency essentially. The principal power process based on the use of the theoretical isentropic combustion chamber is shown in Fig.2.

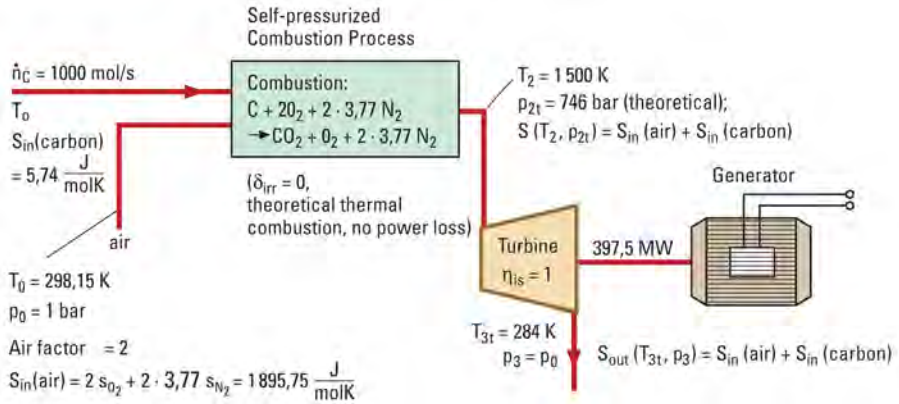

Fig. 2. Illustration of an ideal theoretical gas turbine process where the combustion takes place isentropically [1].

Figure 2 shows the theoretical limits for the gas turbine process if the entropy generation is zero in the combustion chamber and also in the turbine. If $\sigma_{irr} = 0$ in the combustion chamber, then as shown in Fig.2, the outlet pressure will be as high as $p_{out} = 746\ bar$. This is, of course just a theoretical number, but it shows that there is a great potential to improve the conventional combustion process. For instance, to achieve pressure ratio $p_{out} / p_{in} = 11$ in the

combustion chamber with carbon as fuel and with λ=1, we need to decrease entropy generation from $\sigma_{irr} = 366\ J/molK$ only to $\sigma_{irr} = 270\ J/molK$. In the following we will shortly discuss how we could do this by a membrane combustion.

3. Principle of semipermeable membrane combustion

Ceramic membranes made of yttria-stabilized zirconia (in Fig.3: ZrO_2/Y_2O_3) has the property that in sufficient high temperatures (800-1000 ^oC) they start to conduct oxygen ions (O^{2-}). The ionic conductivity depends on the amount of yttria in the structure. Approximately half of the amount of yttria atoms in the crystalline structure can offer vacancies to be occupied by "hopping" oxygen ions. These materials are well known from Solid Oxide Fuel Cells and from lamda-sensors used in cars for measuring the oxygen concentration in flue gases.

As shown in Fig.3, the oxygen gas is consumed on the surface of the combustion side and therefore, the partial pressure of oxygen gas becomes there lower than on the surface of the airside. Because of the ionic form of oxygen, the difference of partial pressures generates a potential difference, which can be estimated by Nernst equation (see Fig.3). The electric field performed by the potential difference is the driving force for the oxygen transport through the membrane. Depending on the concentration of oxygen ions, the electric volumetric force field (ion charge density x electric field, N/m^3) can be amplified to several magnitudes higher than the partial pressure gradient of oxygen gas.

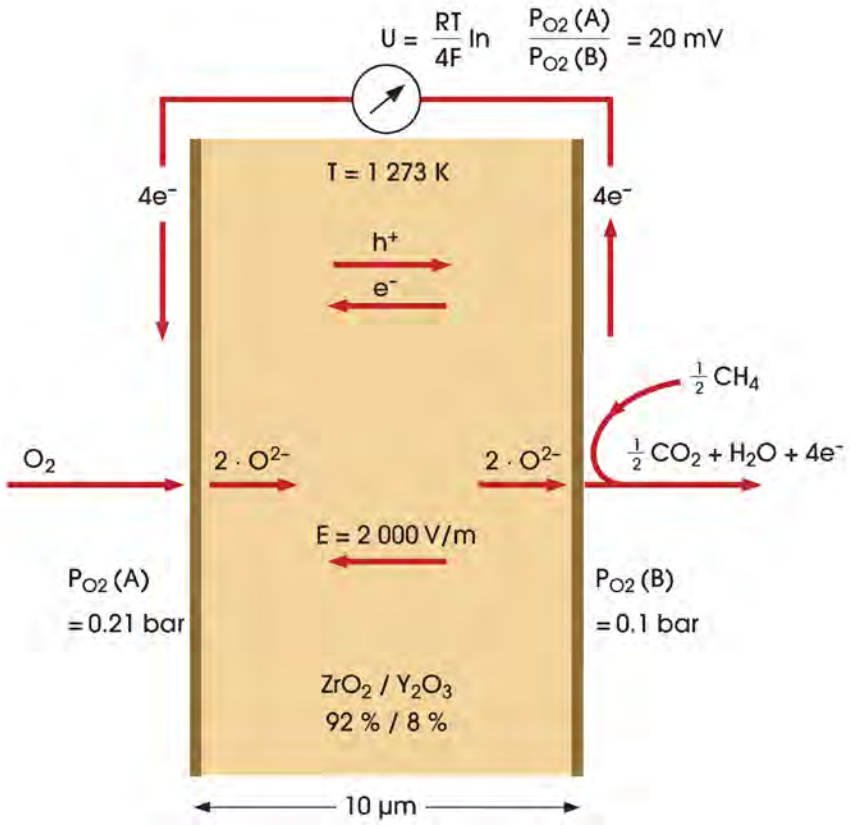

Fig. 3. Semipermeable oxygen gas membrane. Electric potential difference across the membrane is illustrated by assuming that the partial pressures of oxygen are 0.21 bar (on the air side) and 0.1 bar (on the flue gas side). The total pressure of the flue gas p(B) is kept higher than the total pressure of air p(A) by adjusting the outlet flow of flue gas accordingly.

Recently, it has been studied the ionic and electronic charge transport for single crystals of yttria-stabilized zirconia with additional nitrogen doping, e.g. [3] and [4]. At temperatures above 850 ^{o}C, even in the presence of a very small oxygen concentration in the surrounding gas phase, the nitrogen ion dopant becomes highly mobile, and thus diffuses to the surface where it is oxidized to gaseous N_2(g). The technical motivation for that study [3] has been to achieve sufficient nitrogen ion conductivity for the development of a nitrogen sensor or nitrogen pumps. In the membrane combustion the driving force for the nitrogen transportation comes also from the electric field generated by the oxidation of the fuel. The flow of nitrogen gas lowers the temperature of the membrane, which merely by oxygen combustion would be too high. A construction using nitrogen and oxygen gas semipermeable membranes is shown in Fig.4.

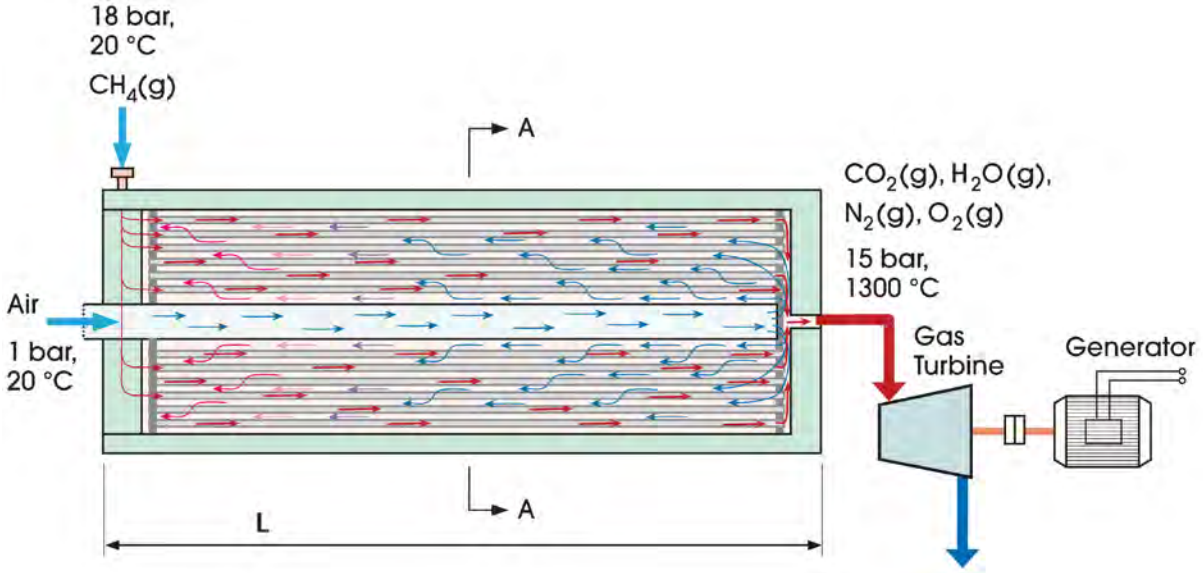

Fig. 4. Hollow ceramic fibers used in the membrane combustion. Fuel (here the methane gas) is fed in the fibers and air outside of the fibers.

4. Discussion

We have discussed here that the entropy generation in the combustion processes is the crucial point that reduces the efficiencies of combustion engines and gas turbine processes. We have presented here an illustration of a membrane combustion method which, with the aid gasification is quite suitable for bioenergy, and which can reduce the entropy generation by pressurizing the combustion chamber without using any external work. Shortly, it can be described as a molecular scale gas compressor driven by the combustion reaction, where the affecting force is amplified by the electric field across the membrane.

Acknowledgements

This study was supported and financed by the MIDE-program of Aalto University. We wish to thank prof. Yrjö Neuvo and Dr. Sami Ylönen for the kind support to this work. The authors wish to acknowledge also prof. Frank Pettersson and prof. Ron Zevenhoven from Åbo Akademi for many useful discussions.

References

[1] M.J. Lampinen, R. Wiksten, A. Sarvi, K. Saari and M. Penttinen: Minimization of exergy losses in combustion processes and its consequences. XXII Sitges Conference on Statistical Mechanics. Energy Conversion: From Nanomachines to Renewable Sources. Sitges, Barcelona, Spain, 7-11, June 2010.

[2] M.J. Lampinen and R. Wiksten, Theory of effective heat-absorbing and heat-emitting temperatures in entropy and exergy analysis with applications to flow systems and combustion processes. Journal of Non-Equilibrium Thermodynamics 31, 2006, pp. 257-291.

[3] I. Valov, V. Ruhrup, R. Klein, T.-C. Rödel, A. Stork, S. Berendts, M. Dogan, H.-D. Wiemhöfer, M. Lerch, J. Janek, Ionic and electronic conductivity of nitrogen-doped YSZ single crystals. Solid State Ionics 180, 2009, pp. 1463-1470.

[4] M. Lerch, J. Janek, K.D. Becker, S. Brendts, H. Boysen, T. Bredow, R. Dronskowski, S.G. Ebbinghaus, M. Kilo, M.W. Lumey, M. Martin, C. Reimann, E. Schweda, I. Valov, H.D., Wiemhöfer, Oxide nitrides: From oxides to solids with mobile nitrogen ions Progress in Solid State Chemistry 37, 2009, pp. 81-131.

Sugar Cane Trash Pyrolysis for Bio-oil Production in a Fluidized Bed Reactor

Wasakron Treedet [1] and Ratchaphon Suntivarakorn [2*]

Department of Mechanical Engineering, Faculty of Engineering, Khon Kaen University, Khon Kaen, Thailand
[1] Email: me-kku@hotmail.com, Tel: +66 819745248, Fax: +66 43347879
** Corresponding author, [2] E-mail: ratchaphon@kku.ac.th, Tel: +66 819891983, Fax: +66 43347879*

Abstract: The objective of this work was to study bio-oil production from sugar cane trash by a pyrolysis process in fluidized bed reactor. The experiments were carried out at different temperatures ranging from 460 – 540 ^{o}C and at different medium gas flow rates between 120 -160 cc.s^{-1}. Two different gases, Nitrogen (N_2) and air, were used as the fluidizing medium in order to study the effect of a different medium on the yield and properties of the bio-oil. The experimental result showed that the maximum bio-oil yields of 46.2 wt% and 31.95 wt% were obtained at 500 ^{o}C and 160 cc.s^{-1} for air and Nitrogen medium, respectively. The bio-oil yield obtained when using air as a medium was higher than that when using Nitrogen medium. This was a result of the higher quantity of water content in the air. The properties of bio-oil were determined and the result showed that its heating value, dynamic viscosity, density, water content, and pH were 15.48 MJ.kg^{-1}, 2.31 cSt 1,019 kg.m^{-3}, 52 wt% and 3, respectively. By dehydration of the obtained bio-oil, the heating value, viscosity and density were increased to 19.81 MJ.kg^{-1}, 57.66 cSt and 1,260 kg.m^{-3}, respectively. These results show that the bio-oil can be used as a fuel oil for combustion in a boiler or a furnace without any modification. Furthermore, the energy consumption of the pyrolysis process was analyzed.

Keywords: *Sugar cane trash, Bio-oil, Pyrolysis, Fluidized bed reactor.*

1. Introduction

Biomass is widely considered as a major potential for renewable energy in the future. Residual biomass and renewable materials can be converted by a pyrolysis process to a combustible liquid usually termed as bio-oil. Bio-oil is renewable and biodegradable and has some advantages in transport, storage, combustion, retrofitting and flexibility in production and marketing. The bio-oil can be used in engines, turbines and furnaces for power generation. The bio-oil obtained from agricultural residuals is a form of renewable energy. In principle, utilizing this energy, in contrast to fossil fuels, does not add carbon dioxide, a greenhouse gas, to the atmospheric environment. Therefore, bio-oil can be recognized as a potential source of renewable energy based on the benefits of both energy recovery and environmental protection. Due to the lower contents of sulfur and nitrogen in agricultural residuals, its energy utilization also creates less environmental pollution than fossil fuel combustion.

Sugar cane trash from agricultural residues is abundant in Thailand which has an annual production of more than 10 million-tons [1]. Traditional methods such as composting and incineration are not suitable to process these organic solid wastes, as they contain small concentrations of N_2 for composting and smoke would be released to pollute the environment during incineration. Therefore, a practical method would be to pyrolyze cane trash to provide bio-oil. Currently, the potential of pyrolysis conditions for bio-oil production have been investigated. Asadullah et al. [2] has studied the pyrolysis of jute stick for bio-oil production in a continuous feeding fluidized bed reactor. The experimental results showed that the maximum yield of bio-oil was 66.7 wt% at 500 ºC. Ji-lu et al. [3] pyrolyzed cotton stalk in a fluidized bed using nitrogen as the carrier gas to fluidize the cotton stalk with sand. From the experiment, the yield of bio-oil first increased and then decreased as a function of the combustion temperature and the maximum yield of bio-oil was 55 wt% obtained at 510 ºC.

Furthermore, bio-oil production from many kinds of biomass, such as China Fir, Manchurian ash, Padauk wood, rice straw and rice husk has been performed in a fluidized bed reactor by fast pyrolysis [4-5]. The experimental results showed that the yield of bio-oil varied with combustion temperature, heating rate and volumetric flow-rate of nitrogen gas. Besides, using a fluidized bed reactor for bio-oil production, a fixed bed reactor and an induction-heating reactor have also been investigated [6-8]. From the experiment, it was found that the temperatures, nitrogen flow rates, heating rates and particle sizes play the roles of important parameters for the yield of bio-oil production.

However, at present, there has not been comprehensive research about the bio-oil production from sugar cane trash. The fast pyrolysis of cane trash in a fluidized bed reactor under different conditions was performed in order to know the suitable conditions of the parameters to produce the maximum bio-oil production and to determine the properties of bio-oil obtained. The effects of combustion temperature, flow rate of carrier gas and type of fluidizing medium were investigated. Furthermore, the energy consumption for bio-oil production was also analyzed.

2. Experimental material, device, method and procedure

2.1. Experimental material

The experimental materials include cane trash, sand, air and nitrogen (N_2). The physical properties of the cane trash and sand, such as density, porosity and diameter, are listed in Table 1. The proximate analysis and ultimate analysis of the cane trash are listed in Table 2 and Table 3, respectively. The sugar cane trash had dimensions of 1 x 3 mm and 5.94 wt% of moisture content in feedstock. Sand was used as the thermal carrier to transfer heat quickly from the hot N_2 (or air) to the cane trash. N_2 (or air) was used as the carrier gas to fluidize the cane trash with sand in the fluidized bed reactor.

Table 1. Physical properties of experimental material.

Physical properties	Cane trash	Sand
Density ($kg.m^{-3}$)	347.61	3,793.27
Porosity (%)	50.72	41.31
Diameter (mm)	1-3	0.332

Table 2. Proximate analysis of sugar cane trash.

Properties	Value
Fixed carbon (wt%)	21.26
Volatile matter (wt%)	70.86
Moisture content (wt%)	4.55
Ash (wt%)	3.33
Heating Value ($MJ.kg^{-1}$)	18.3

Table 3. Ultimate analysis of sugar cane trash.

Properties	Value (wt%)
C	51.21
H	5.16
N	1.93
O	40.33
S*	1.37

* Sulfur calculated by difference.

2.2. Experimental set-up

As shown in Fig. 1, the experimental device consisted mainly of a hopper, two cyclones and a condenser as well as seven thermocouples. The hopper was used to contain feedstock such as cane trash. The two screw feeders had the same configuration and size; the first one was used to control the feeding rate and the second one operated at a relatively high speed to prevent jamming the feeding system. The fluidized bed reactor operated at atmospheric pressure using N_2 (or air) as the fluidizing medium gas. The reactor had a height of 1.54 meter and a diameter of 10 cm in which the cane trash was rapidly heated for pyrolysis. The 6,000 W electric heater was able to pre-heat the N_2 (or air) to a temperature range of 500 ºC - 620 ºC before entering the fluidized bed reactor. The two cyclones were used to separate solid particles, such as charcoal and ash, from the hot gas. The condenser was equipped with copper pipes and a cooling tank. The condenser was able to quickly cool the cleaned hot gas into a liquid. Thermocouples were used to monitor and control the pyrolysis system. The locations of all measurement sensors, including the seven thermocouples are shown in Fig. 1. The specification of the thermocouples is K Type, made from an alloy of chromel - alumel, measurement range from -200 ºC to 1,372 ºC with measurement accuracy of the thermocouples of ±2 ºC. The Fuzzy+PID logic was used in the temperature control system.

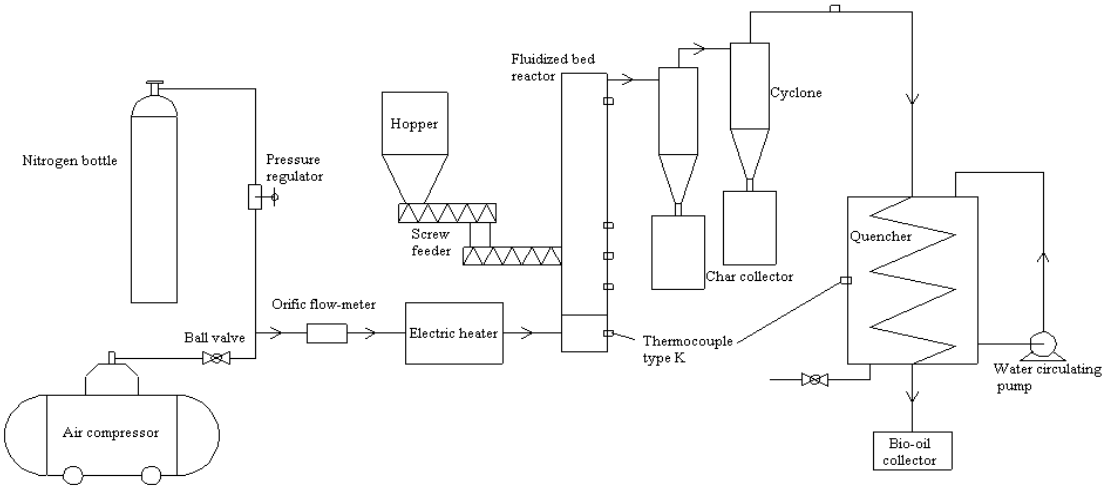

Fig. 1. The experimental set-up.

2.3. Experimental method

The experiment device was originally set up at Khon Kaen University in 2010 and presently scaled up to a cane trash feeding rates of 10 $kg.h^{-1}$. The cane trash powder had dimensions between 1 – 3 mm and was fed continuously into the reactor. The pyrolysis experiments using cane trash were performed at flow-rates of 120 $cc.s^{-1}$,160 $cc.s^{-1}$ and 200 $cc.s^{-1}$ while the temperature was ranged from 460 ºC – 540 ºC under N_2 atmosphere., The pyrolysis experiments using cane trash were also performed in a different medium gas at a flow-rate of 160 $cc.s^{-1}$ while the temperature was ranged from 460 ºC – 530 ºC under air static atmosphere. The yield of the bio-oil was heavily impacted by the rate of cooling in condenser. The cooling must be quick; otherwise, some condensable gas will be converted into non-condensable gas (NCG) [5]. Thus, in our experiment, the heat exchanger was operated in cool water and ice with a condensation temperature of - 4 ºC.

Besides bio-oil, two byproducts, namely charcoal and NCG, can also be obtained when cane trash is pyrolyzed. The yield of the bio-oil can be determined from the condensed liquid and the feedstock used. The yield of the charcoal can be calculated by dividing the ash contents in

the feedstock with that in the charcoal. The yield of NCG can be determined from the fact that the sum of the three product yields should equal 100%.

2.4. Experimental procedure

1. Turn on the electric heater and turn on the 1st motor of the feeder to prevent jamming the feeding system.
2. Transport N_2 into the pyrolysis system with a flow rate of 120 $cc.s^{-1}$.
3. When the temperature of the fluidized bed reactor reaches the expected temperature, turn on the 2nd motor of the feeder to transport1 kg of cane trash into the fluidized bed reactor. The expected temperature was varied from 460 – 540 ºC.
4. After 45 minutes, stop transporting cane trash into the fluidized bed reactor.
5. Turn off the electric heater and the water circulating pump.
6. Then, stop transporting N_2 into the pyrolysis system.
7. Collect the bio-oil and charcoal for the experiment.
8. Perform the experimental steps (1)-(7) again by varying the flow rate of N_2 from 120 $cc.s^{-1}$ to 160 $cc.s^{-1}$ and 200 $cc.s^{-1}$, respectively.
9. Perform the experimental steps (1)-(8) again by changing the fluidizing medium from N_2 to air.

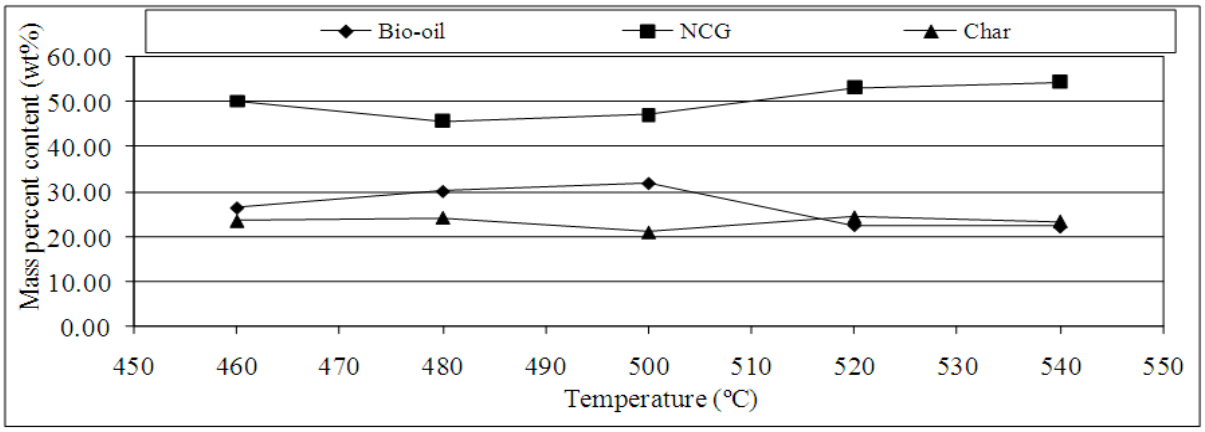

Fig. 2. Relationship between pyrolysis temperature and product yields for N_2 medium at flow-rate of 160 $cc.s^{-1}$ and temperature between 460 ºC – 540 ºC.

3. Results and discussions

3.1. Effect of temperature on the product distribution

Our preliminary experiments show that a N_2 temperature below 460 ºC is not sufficient for pyrolysis, as some cane trash was found in the charcoal and ash. In contrast, N_2 temperatures above 540 ºC are too high, as the yield of bio-oil is quickly reduced. Therefore, for these particular materials, the optimum temperature for pyrolysis seems to be within the range of 460 ºC – 540 ºC. The relationship between the yields of the three products and the pyrolysis temperature at 160 $cc.s^{-1}$ of N_2 volumetric flow rate is shown in Fig. 2.

From Fig. 2, it can be found that: (1) bio-oil yields first increase and then decrease with an increasing in N_2 temperature and the highest yield for cane trash is 31.95 wt% at 500 ºC, (2) NCG yields always increase with an increase in N_2 temperature and (3) charcoal yields always decrease with an increase in N_2 temperature. The influence of pyrolysis temperature is the same as the results of Z. Ji-lu et al. [3], S. Wang et al. [4] and Z. Ji-lu. [5], but the maximum yield of the bio-oil in their experiments is not equal to our experimental results.

The influence of pyrolysis temperature and the yield of the three products in air medium are shown in Fig. 3. It can be found that: the highest bio-oil yield of 46.2 wt% was obtained at an air temperature of 500 ºC and a volumetric air flow rate of 160 cc.s^{-1}. The function of the air temperature to the product yields is similar to the function of N_2 temperature. The result showed that the yield of bio-oil from air medium was higher than the yield of bio-oil from N_2 medium. This is caused by the higher water content in the air.

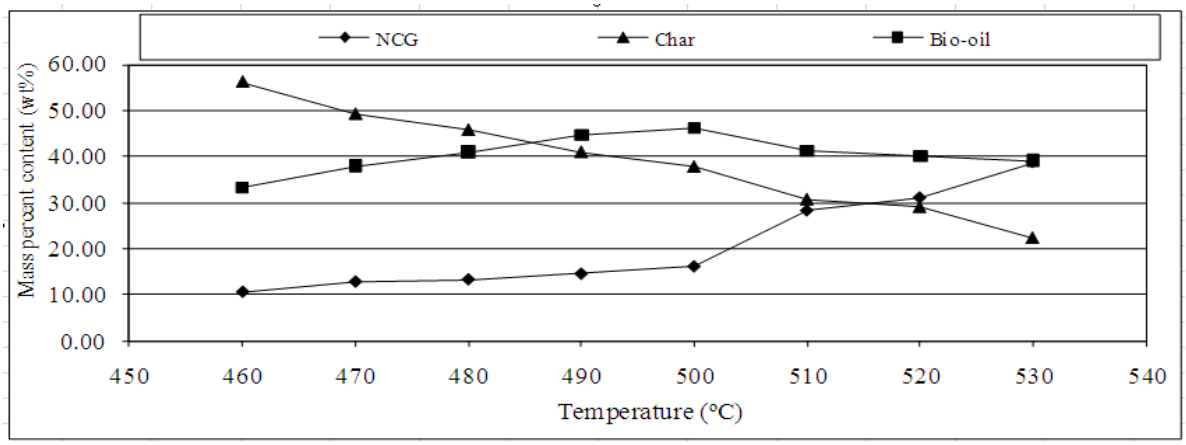

Fig. 3. Relationship between pyrolysis temperature and product yields for air medium at flow-rate of 160 cc.s^{-1} and temperature between 460 ºC – 530 ºC.

3.2. Effect of flow rate on product distribution.

It is known that sweeping the reactor with N_2 could increase the oil yield because sweeping the environment shortens the residence time of volatiles and reduces their chances of being involved in char and radical forming secondary reactions [6]. Fig. 4 shows the effect of the flow rate of N_2 on the production yield from cane trash pyrolysis. at a temperature of 500 ºC. The relationship between the N_2 flow-rate and the production yield shows that: (1) bio-oil yields first increase and then decrease with an increase in flow-rate and the highest yield for cane trash is 31.95 wt% at 160 cc.s^{-1}, (2) NGC yields always decrease with an increase in flow-rate and (3) charcoal yields always increase with the increase in flow-rate. This influence of the N_2 flow-rate is the same as the experimental result of M. F. Parihar et al. [6].

The decrease in bio-oil yields when flow-rate is increased may be due to the very short residence time of the vapors in the condenser and vapors unable to condense due to higher percentage of NGC. Furthermore, the increase in char yields when the flow-rate is increased may be due to un-burned cane trash in the reactor.

3.3. Effect of fluidizing medium gas on the products distribution.

Pyrolysis is a thermal decomposition occurring in the absence or less than 30% theory of air [9]. Bio-oil has a water content as high as 15 - 45 wt% derived from the original moisture in the feedstock and produced by the dehydration of air during the pyrolysis reaction and during storage. The presence of water lowers the heating value and the flame temperature, but on the other hand, water reduces the viscosity and enhances the fluidity, which is good for the atomization and combustion of bio-oil in the engine. Furthermore, the presence of oxygen creates the primary issue for the differences between bio-oils and hydrocarbon fuels. The high oxygen content leads to an energy density lower than that of conventional fuel by 50% and also an immiscibility with hydrocarbon fuels. In addition, the strong acidity of bio-oils makes

them extremely unstable. Therefore, the use of air as the fluidizing medium has an effect on the yield and properties of the bio-oil.

From the bio-oil production experiment using a different fluidizing medium, either air or N_2, the result showed that using air medium can produce a higher yield of bio-oil than that with N_2 medium, about 9.25 %wt at pyrolysis temperature of 500 ºC and a flow rate of 160 cc.s^{-1}. In addition, the bio-oil production from air medium had a high moisture content of 81.11 %wt while the bio-oil production from N_2 medium had a moisture content of 52.14 %wt. This result revealed that the air medium has a higher water content which has the advantage of reducing the viscosity of the bio-oil, but also the disadvantage of causing a lower heating value.

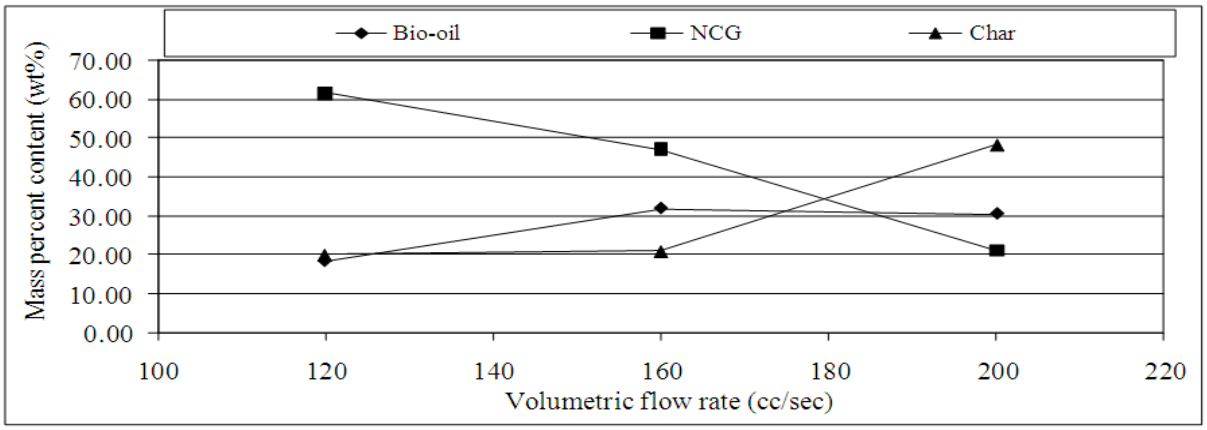

Fig. 4. Effect of flow rate on product yields from cane trash pyrolysis at temperature of 500 ºC and varying flow-rate of 120 cc.s^{-1},160 cc.s^{-1} and 200 cc.s^{-1}

3.4. Properties of the bio-oil.

The main properties of the bio-oil from cane trash are shown in Table 4. The low heating value (LHV) of bio-oil production from N_2 medium is higher than that from air medium because the air has a higher quantity of water content. Furthermore, the density, viscosity and pH of bio-oil production from N_2 medium and air medium are very comparable. To increase the heating value of the bio-oil, the water content in the bio-oil was dehydrated. The properties of the bio-oil after dehydration are shown in Table 5. The heating value, density and viscosity were increased while the pH was decreased for both N_2 and air medium.

Table 4. Main properties of bio-oil from cane trash.

Physical properties	Nitrogen medium	Air medium
Heating value (MJ.kg^{-1})	15.48	1.36
Density (kg.m^{-3})	1019.20	1010.12
Water content (wt%)	52.14	81.11
Viscosity (cSt) at 40 ºC	2.31	Similar to water
pH	3	3

Table 5. Main properties of bio-oil after dehydration.

Physical properties	Nitrogen medium	Air medium
Heating value (MJ.kg^{-1})	19.81	16.55
Density (kg.m^{-3})	1260	1230
Viscosity (cSt) at 40 ºC	57.66	-
pH	2	2

3.5. The energy consumption of the pyrolysis process.

The energy consumption of the bio-oil production using both N_2 and air as a medium was analyzed, and the results are shown in Table 6. The energy consumption was divided into two time periods which are during the pre-heating process and during the combustion process. During the pre-heating process, the reactor and fluidizing medium were heated by using a 6 kW heater and the fluidizing medium was transported by using an 15 hp air compressor. During the combustion process, the additional energy consumption was obtained from the use of two 120 W screw feeders for transporting the cane trash. To determine the energy consumption, the electric power was measured by watt meter and the working time of the process was recorded. The electric energy consumption *($MJ.kg^{-1}_{sugarcane\ trash}$)* was calculated by multiplication of the electric power (kW) by the number of working hours (h). From the calculation, the energy consumption of the bio-oil production was 131.14 $MJ.kg^{-1}_{sugarcane\ trash}$ and 143.52 $MJ.kg^{-1}_{sugarcane\ trash}$ for N_2 and air medium, respectively. The energy consumption when using N_2 medium was less than that when using air medium because the air compressor was not used when using N_2 as a medium. It was noted that the total energy consumption of bio-oil production from N_2 medium was 12.38 $MJ.kg^{-1}_{sugarcane\ trash}$ less than that when using air medium.

Table 6. The energy consumption of the pyrolysis process.

Energy consumption ($MJ.kg^{-1}_{sugarcane\ trash}$)	N_2 medium	Air medium
Electric energy from heater during pre-heating process	64.15	64.15
Electric energy from feeder during pre-heating process	0.97	0.97
Electric energy from air compressor during pre-heating process	55.58	55.58
Electric energy from heater during combustion process	10.15	10.15
Electric energy from feeder during combustion process	0.29	0.29
Electric energy from air compressor during combustion process	-	12.38
Total energy	131.14	143.52

4. Conclusion

Bio-oil production from sugar cane trash by a pyrolysis process was conducted in a fluidized bed reactor. The effects of the pyrolysis temperature, flow rate, different fluidizing medium on the yield of bio-oil production were investigated. The properties of the bio-oil and the energy consumption were also studied. The experiments were performed by varying the temperature from 460 ºC – 540 ºC and at flow rates of 120 $cc.s^{-1}$, 160 $cc.s^{-1}$ and 200 $cc.s^{-1}$ under air and N_2 atmosphere. From the experiment, sugar cane trash can be pyrolyzed into bio-oil. The experimental result showed that the maximum yields of bio-oil were 46.2 wt% and 31.95 wt% obtained at 500 ºC and 160 $cc.s^{-1}$for air and N_2 medium, respectively. The bio-oil yield obtained from using air as a medium was higher than that when using N_2 as a medium because of the presence of water content in the air. The result also revealed that the yield of bio-oil varied with the combustion temperature and volumetric flow-rate of the fluidizing medium.

The properties of the obtained bio-oil were determined. It was found that the heating value of bio-oil using N_2 medium was higher than that using air medium because air had a higher water content. Furthermore, the density and pH of the bio-oil production from both N_2 and air medium are very comparable. The heating value, viscosity and density of the bio-oil obtained from both N_2 and air medium, were increased by dehydration. The energy consumption of the bio-oil production was 131.14 $MJ.kg^{-1}_{cane\ trash}$ and 143.52 $MJ.kg^{-1}_{cane\ trash}$ for N_2 and air medium, respectively. This was indicated that the energy consumption for bio-oil production

was more than the energy obtained from the bio-oil. Considering the equipment that consumed the energy, it was found that the electric heater and air compressor consumed the most energy with 83.43 - 91.12% of the total energy consumption. However, the energy consumption can be reduced by using 2 hp of high pressure blower instead of the 15 hp of air compressor and adding heat recovery system to heat the medium gas before entering to the reactor. According to the energy saving measure, the energy cost will be lower and worthwhile for investment. From the above results, the obtained bio-oil can be used as a fuel oil for combustion in a boiler or a furnace without any modification.

Acknowledgement

The authors acknowledge the grant from Energy Management and Conservation Office (EMCO) and Engineering Faculty Research Fund to financially support the project reported in this paper. The authors are also grateful to acknowledge the Department of Mechanical Engineering, Faculty of Engineering, Khon Kaen University for supporting the tools and the equipment used in this research.

References

[1] NEPO (National Energy Policy Office) Journal Volume 50 [online] 2000 [cited 2009 Dec. 7]. Available from : http://www.eppo.go.th/vrs/VRS50-03- FutureFuel.html

[2] M. Asadullah, M.A. Rahman, M.M. Ali, M.A. Motin, M.B. Sultan, M.R. Alam and M.S. Rahman, Jute stick pyrolysis for bio-oil production in fluidized bed reactor, Bioresource Technology 99, 2008, pp. 44-50.

[3] Z. Ji-lu, Y. Wei-ming and W. Na-na, Bio-oil production from cotton stalk, Energy Conversion and Management 49, 2008, pp.1724–1730.

[4] S. Wang, M. Fang, C. Yu, Z. Luo and K. Cen, Flash Pyrolysis of biomass particles in fluidized bed for bio-oil production, China Particuology 3 (1-2), 2005, pp.136 – 140.

[5] Z. Ji-lu, Bio-oil from fast pyrolysis of rice husk: Yields and related properties and improvement of the pyrolysis system, Journal of Analytical and Applied Pyrolysis 80, 2007, pp.30 – 35.

[6] M.F. Parihar, M. Kamil, H.B. Goyal, A.K. Gupta and A.K. Bhatnagar, An experimental study on pyrolysis of biomass, Trans IChemE Part B 85, 2007, pp.458–465.

[7] M. Asadullah, M.A. Rahman, M.M. Ali, M.S. Rahman, M.A. Motin, M.B. Sultan and M.R. Alam, Production of bio-oil from fixed bed pyrolysis of bagasse, Fuel 86, 2007, pp. 2514-2520.

[8] S. Sensoz, D. Angin, Pyrolysis of safflower (Charthamus tinctorius L.) seed press cake in a fixed-bed reactor: Part 2. Structural characterization of pyrolysis bio-oils, Bioresource Technology 99, 2008, pp.5498 – 5504.

[9] A.V. Bridgwater, Biomass fast pyrolysis, Thermal Science 8(2), 2004, pp.21-49.

Combustion of some Thai agricultural and wood residues in a pilot swirling fluidized-bed combustor

Vladimir I. Kuprianov[1,*], Porametr Arromdee[1], Songpol Chakritthakul[1], Rachadaporn Kaewklum[2], Kasama Sirisomboon[3]

[1] *School of Manufacturing Systems and Mechanical Engineering, Sirindhorn International Institute of Technology Thammasat University, Pathum Thani 12121, Thailand*
[2] *Department of Mechanical Engineering, Faculty of Engineering, Burapha University Chonburi 20131, Thailand*
[3] *Department of Mechanical Engineering, Faculty of Engineering and Industrial Technology Silpakorn University, Nakhon Pathom, 73000, Thailand*
** Corresponding author. Tel: +66 2 986 9009x2208, Fax: +66 2 986 9212, E-mail: ivlaanov@siit.tu.ac.th*

Abstract: This paper reports a comparative study of burning Thai rice husk, sunflower shells and fine rubberwood sawdust as well as co-firing of the sawdust and shredded eucalyptus bark in the swirling fluidized-bed combustor (SFBC). All experiments for firing individual fuels were performed for the combustor heat input of ~300 kW_{th}. However, in the co-firing tests, the fuel mixture was delivered at a fixed feedrate, while ranging mass fraction of the blended fuels. For each fuel option, excess air was varied from 20% to 80%, while a flowrate of secondary air was constant. Temperature and gas concentrations (O_2, CO and NO) were measured in axial directions in the reactor, as well as at stack. Axial profiles of these variables were compared between the fuel options for selected operating conditions. The axial temperature profiles were weakly dependent on operating conditions, whereas the axial gas concentration profiles were apparently affected by fuel properties, excess air and secondary air injection. The behavior of CO and NO indicated the occurrence of three (or four) specific regions along the combustor height. As revealed by the experimental results, CO and NO emissions from the combustor can be controlled meeting the national emission standard, via maintaining excess air at ~55%, for all the fuel options. At this excess air, high, 99.1–99.9%, combustion efficiency is achievable when burning these fuels in the SFBC. However, the best combustion and emission performance for the co-firing of rubberwood sawdust and eucalyptus bark can be ensured at 85% sawdust contribution to the combustor heat input.

Keywords: *Biomass Residues, Swirling Fluidized-Bed Combustor, Emissions, Combustion Efficiency*

1. Introduction

Biomass is an important source of energy in Thailand. Some agricultural and forest-related residues collected on a large scale (such as rice husk, sugar cane bagasse, wood sawdust and chips) are widely used in this country as biomass fuels for heat and power generation. However, the domestic agricultural and industrial sectors generate a variety of residues and/or byproducts potentially considered as fuels due to their excellent combustion properties.

The fluidized bed-combustion technology is proven to be effective for conversion of energy from biomass. A large number of studies have been devoted to bubbling, vortexing and circulating fluidized-bed combustion systems firing conventional biomass fuels [1–4]. Some authors pointed out difficulties in achieving high combustion efficiency when firing high-ash biomass fuels [1,2], while the others highlighted ash-related operational problems caused by alkali-based compounds in biomass ashes [1,5]. These studies revealed that the combustion of most conventional biomass fuels is accompanied by substantial gaseous emissions [1–4].

During the past decade, a growing attention has been paid to the feasibility of effective utilization of various unconventional biomass fuels (from fibrous fuels to fruit stones and shells), basically, through their burning in bubbling and circulating fluidized-bed combustion systems. As shown in relevant pioneering works, combustion efficiency of these systems

firing unconventional fuels is comparatively low and strongly affected by fuel properties, whereas gaseous emissions can be controlled at levels typical for conventional fuels [6–8].

Due to some specific hydrodynamic features, an innovative swirling fluidized-bed combustor (SFBC) with a cone-shaped bed seems to be a promising multi-fuel combustion technique for effective firing of various biomass fuels with significantly different fuel properties and characteristics. A swirling gas–solid fluidized bed is reported to ensure the flexibility in fuel particle size and shape, and, also, prevent the growth of large bubbles in the bed [9].

This work was aimed at comparing the combustion and emission performance of the SFBC between different fuel options: (1) individual burning of Thai rice husk, sunflower shells and fine rubberwood sawdust, and (2) co-firing of the sawdust and eucalyptus bark. Effects of fuel properties and operating conditions on major (CO and NO) emissions, as well as on combustion efficiency of the SFBC, were the main focus of this study.

2. Materials and Methods

2.1. Experimental set-up

Fig. 1 depicts the schematic diagram of an experimental set-up with the SFBC. The combustor consisted of six refractory-lined steel modules: a conical section with a 40° cone angle and an inner diameter of d_0 = 0.25 m at the bottom plane, and five cylindrical sections of 0.5 m height and 0.9 m inner diameter. Quartz sand of 0.5–0.6 mm particle size and 30 cm static bed height was used as the inert bed material to ensure stable swirling fluidized-bed regime [9].

An annular spiral air distributor arranged at the bottom of the conical section was used as the swirler of the bed. A 25-horsepower blower delivered primary air to the combustor. For firing

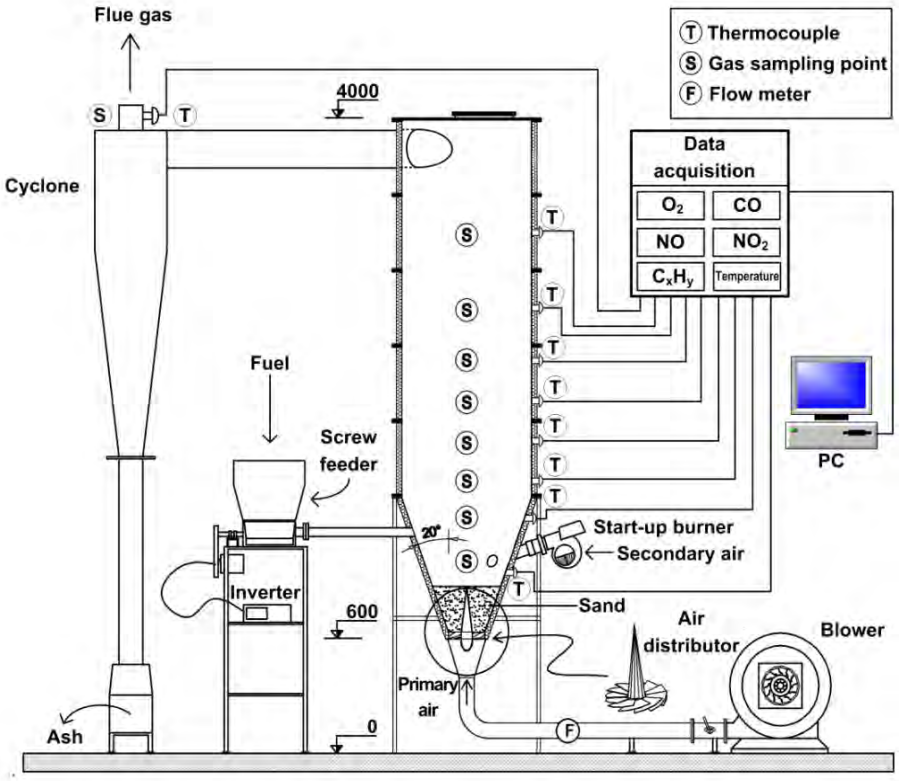

Fig. 1. Schematic diagram of the experimental set-up with the swirling fluidized-bed combustor.

rice husk and sunflower shells, the air distributor was made up of 11 straight steel vanes, each vane being with a length of L = 0.09 m and a swirl angle of β = 76° (or 14° to the horizontal). However, for the (co-)firing tests with rubberwood sawdust, the SFBC was equipped with a 22-vane air distributor assembled from the straight steel vanes with L = 0.085 m and β = 79°. The swirl number of both axial-flow swirlers used in this study was estimated by Ref. [10]:

$$S = \frac{2}{3}\left[\frac{1-(d_h/d_0)^3}{1-(d_h/d_0)^2}\right]\tan\beta \qquad (1)$$

where d_h is the hub diameter of the swirler: $d_h = d_0 - 2L$.

A diesel-fired burner (model "Press G24" from Riello Burners Co.) was used to preheat sand during the combustor start-up. This start-up burner was fixed at a 0.5 m level above the air distributor and inclined at a −30° angle to the horizon. When the bed temperature attained ~700 °C, a diesel pump of the burner was turned off, and the combustor load was sustained by feeding biomass fuel. A screw-type feeder delivered the fuel over the bed at a 0.6 m level above the air distributor. During the combustion tests, the burner fan remained to operate injecting secondary air tangentially into the bed splash zone at a constant flowrate of Q_{ba} = 0.024 Nm^3/s required to protect the burner head against overheating and impacts from solids.

A "Testo-350XL" gas analyzer was used to measure temperature and gas concentrations (O_2, CO and NO) along the axial direction (Z) in the reactor space, as well as at the cyclone exit.

2.2. The fuels

Table 1 shows the ultimate and proximate analyses as well as lower heating value (LHV) of rice husk, sunflower shells, rubberwood sawdust and eucalyptus bark used in this study. Except eucalyptus bark with its high moisture content (W), the biomass residues were, in effect, high-volatile (VM), low-S fuels. Meanwhile, rice husk included an elevated proportion of fuel ash (A) affecting LHV and fuel devolatilization rate. The average dimensions of rice husk particles were (on average) 2 mm wide, 0.5 mm thick and 10 mm long. On the contrary, sunflower shells were characterized by rather low fuel-ash but medium fuel-N contents, and individual particles of this biomass fuel were a width of 6 mm, a thickness of 0.7 mm, and a length of 10 mm (on average). The main features of rubberwood sawdust were elevated fuel-N but rather low fuel-ash, as well as small particle size (of ~200 μm dominant size). Eucalyptus bark had significant fuel moisture but rather low contents of fixed carbon (FC), fuel-N, fuel-S and fuel-ash. Note that the large size and hard structure of eucalyptus bark particles caused significant problems with fuel feeding when using the above screw-type feeder. It was therefore decided to burn the bark as shredded fuel co-fired with fine rubberwood sawdust.

Table 1. Properties of biomass fuels used in the combustion tests

Biomass fuel	Ultimate analysis (wt.%, as-received basis)					Proximate analysis (wt.%, as-received basis)				
	C	H	O	N	S	W	A	VM	FC	LHV (kJ/kg)
Rice husk	40.5	4.1	28.7	0.3	0.03	8.4	18.0	58.0	15.6	14,620
Sunflower shells	52.2	5.6	29.7	0.6	0.10	9.1	2.7	65.6	22.6	17,150
Rubberwood sawdust	46.7	5.7	33.5	1.8	0.04	6.6	5.7	61.5	26.2	17,070
Eucalyptus bark	25.8	2.9	19.2	0.2	0.02	47.5	4.4	41.5	6.6	8 320

2.3. Experimental planning

Two test series were carried out on the conical SFBC: (1) for firing rice husk and sunflower shells using an 11-vane swirler, and (2) for firing rubberwood sawdust, and also its co-firing with eucalyptus bark using a 22-vane swirler. In the first test series, to ensure similar heat inputs to the combustor (~300 kW_{th}), the fuel feedrate was different: 80 kg/h for firing rice husk, and 60 kg/h for firing sunflower shells. For these two fuel options, axial temperature and gas concentration profiles were compared between two values of excess air (EA): 40% and 80%. However, in the second test series, when a priority was given to the effects of fuel properties, the axial profiles were compared between the energy fractions of the sawdust in the fuel blend (EF_{sd}), while maintaining the fuel feedrate and excess air to be constant: 60 kg/h and 40%, respectively. The trials of the second test series were therefore performed for three sawdust energy fractions: EF_{sd} = 1 (firing pure sawdust at heat input of ~300 kW_{th}), EF_{sd} = 0.85 and EF_{sd} = 0.75.

For all the fuel options, CO and NO emissions and combustion efficiency of the SFBC were quantified for four values of EA: 20%, 40%, 60% and 80%. For each test run, excess air and heat losses (due to unburned carbon and incomplete combustion) were predicted together with combustion efficiency by Ref. [10]. The unburned carbon content in fly ash was determined by laboratory analysis with the aim to estimate associated heat loss (when it was sensible).

3. Results and Discussion

3.1. Axial temperature and gas concentration profiles in the SFBC

Fig. 2 shows the axial temperature as well as O_2, CO and NO concentration profiles in the SFBC firing rice husk and sunflower shells for two EA values: ~ 40% and ~80%. The

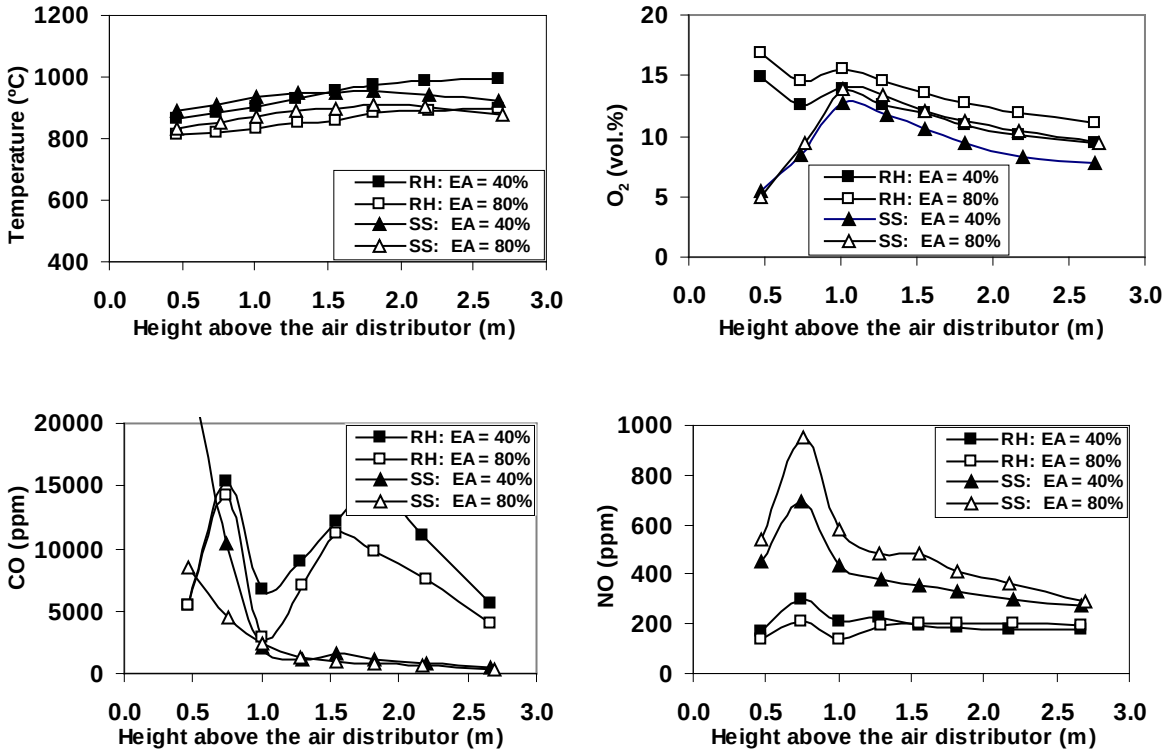

Fig. 2. Effects of excess air on the axial temperature as well as O_2, CO and NO concentration profiles in the conical SFBC firing rice husk (RH) and sunflower shells (SS) at similar heat inputs of ~300 kW_{th}.

temperature profiles were rather uniform, indicating the highly intensive heat-and-mass transfer in the reactor. For both fuels fired at similar EA, the temperatures at different points in the reactor were nearly the same due to similar heat inputs. An increase in EA resulted in some reduction of temperature at any given point, mainly, because of the air dilution effects. However, the axial gas concentration profiles in Fig. 2 exhibit strong effects of fuel properties and secondary air injection as well as the noticeable influence of excess air. In the dense bed region ($0 < Z < 0.5$ m), the rate of O_2 consumption for firing sunflower shells was significantly greater than that for rice husk, mainly, due to the coarser particles, higher VM and lower ash content in sunflower shells. In the next region (up to $Z = 1$ m), O_2 increased along the reactor centerline due to the injection of secondary air. In the combustor freeboard ($Z > 1$ m), O_2 gradually diminished along the centerline showing an apparent influence of excess air.

Like O_2, the CO behavior along the combustor height was quite different in various regions. When firing high-ash rice husk, CO formation in the dense bed occurred at a moderate rate, since some amounts of fuel-C and VM retained in the chars were carried over from this region. However, for firing sunflower shells with higher VM and substantially lower fuel-ash contents, CO formed in the dense bed at a quite significant rate, resulting in higher CO at all points along the reactor axis. In the upper region, up to $Z = 1$ m, CO was characterized by a significant negative gradient along the axial distance caused by the secondary air injection. When burning rice husk, due to the carryover of char-C and VM, CO exhibited a substantial axial increase in the region of $1.0 \text{ m} < Z < 1.8$ m due to oxidation of combustibles, followed by rapid decomposition of CO at the reactor top. However, CO was much lower at all locations in the freeboard when firing sunflower shells for the range of EA (see Fig. 2).

The axial NO concentration profiles in the combustor were found to exhibit four regions. At the combustor bottom, the rate of NO formation from nitrogenous volatile species (mainly, NH_3 [1]) prevailed the rate of NO decomposition. At $Z \approx 0.8$ m, NO attained the maximum, which was quite different for rice husk and sunflower shells, and affected by EA. Due to higher fuel-N, the NO maximum for firing sunflower shells was substantially greater than that for burning rice husk at similar EA. At $0.8 \text{ m} < Z < 1$ m, due to (i) catalytic reduction of NO by CO and (ii) reactions of NO with NH_3 and C_xH_y [1], NO exhibited some reduction in the axial direction. In the freeboard, the rates of NO formation and decomposition were quite low. For firing rice husk, these rates were nearly the same, resulting in rather stable values of NO along the centerline. However, for burning sunflower shells, the NO decomposition rate at the combustor top was greater than that of NO formation, which led to diminishing of NO along the combustor height. Effects of EA on the behavior of NO in the axial direction were rather weak for firing rice husk; however, the effects were substantial for burning sunflower shells.

Attempts to burn fine rubberwood sawdust in this combustor with the 11-vane air distributor, characterized by a swirl number of $S = 2.9$ (as estimated by Eq. (1)), failed in preliminary tests because of the dramatic carryover of light fuel/char particles from the combustor into the cyclone. To increase the residence time of the sawdust char particles in the reactor space, the SFBC was equipped with the 22-vane air distributor with a greater swirl number, $S = 3.6$.

Fig. 3 depicts the axial temperature as well as O_2, CO and NO concentration profiles in the SFBC for (co-)firing fine rubberwood sawdust and eucalyptus bark at different energy fractions of sawdust in the fuel blend at similar EA (of ~40%). Despite the substantial difference in S, the profiles in Fig. 3 exhibit the behaviors and trends similar to those of respective dependencies in Fig. 2. Thus, the axial temperatures for firing sawdust seen to be nearly the same as those for firing rice husk and sunflower shells, and this fact can be explained by similar heat inputs to the

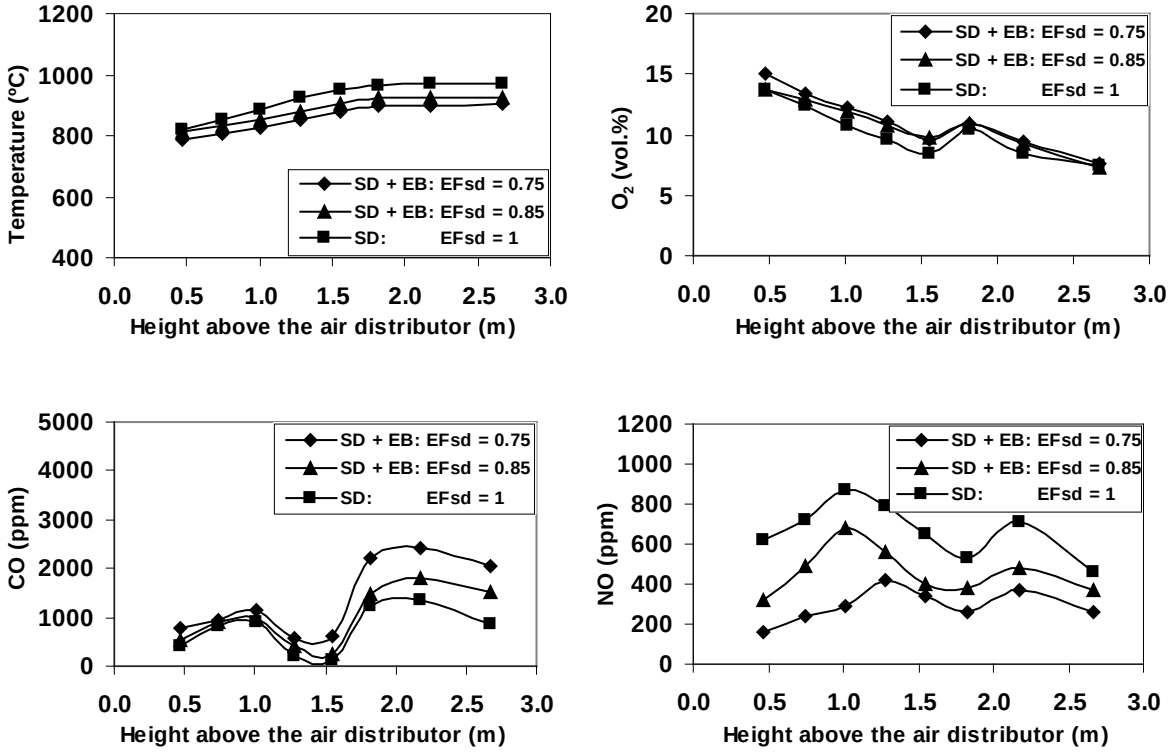

Fig. 3. Effects of the sawdust energy fraction in the fuel mixture on the axial temperature as well as O_2, CO and NO concentration profiles in the conical SFBC firing fine rubberwood sawdust (SD) or co-firing its mixture with eucalyptus bark (SD + EB) at similar excess air value of ~40%.

combustor. However, for the co-firing tests at EF_{sd} = 0.85 (corresponding to the sawdust mass fraction of $MF_{sd} \approx 0.73$) and EF_{sd} = 0.75 (at $MF_{sd} \approx 0.60$), the temperatures at all locations in the combustor volume where somewhat lower, mainly, due to increased moisture content in the blend. It can be seen in Fig. 3 that the effects of secondary air on the axial gas concentration profiles were shifted upward, as compared to the results for firing rice husk and sunflower shells. The carryover of light fuel/char particles of sawdust (or fuel blend) led to the elevated CO and NO concentrations in the freeboard, exhibiting secondary peaks of CO and NO at $Z \approx 2.2$ m. In the meantime, an increase in the mass fraction of eucalyptus bark in the mixture resulted in the higher concentration of CO at all locations along the centerline, mainly, due to the enhanced rate of carbon-C "wet" oxidation despite the reduction in temperature. Elevated CO, together with the reduction in fuel-N and combustion temperature, led to the lower NO concentrations with increasing the mass/energy fraction of eucalyptus bark in the fuel blend.

3.2. Emissions

Fig. 4 shows the CO and NO emissions from the SFBC firing rice husk and sunflower shells for the range of EA compared in the graphs with the Thai emission standards for biomass-fuelled industrial applications [11], all on 6% O_2 dry gas basis. As seen in Fig. 4, at EA of ~20%, the CO emission from the combustor was very high: ~4200 ppm for rice husk, and ~2700 ppm for sunflower shells. By increasing EA, the CO emission can be significantly reduced to a quite low level. However, with higher excess air, the NO emission was found to be increased, thus, indicating the fuel-NO formation mechanism [1]. An excess air of ~55% seems to be the best option at which both CO and NO emissions from this SFBC firing rice husk and sunflower shells comply with the corresponding national emission standards. Fig. 5

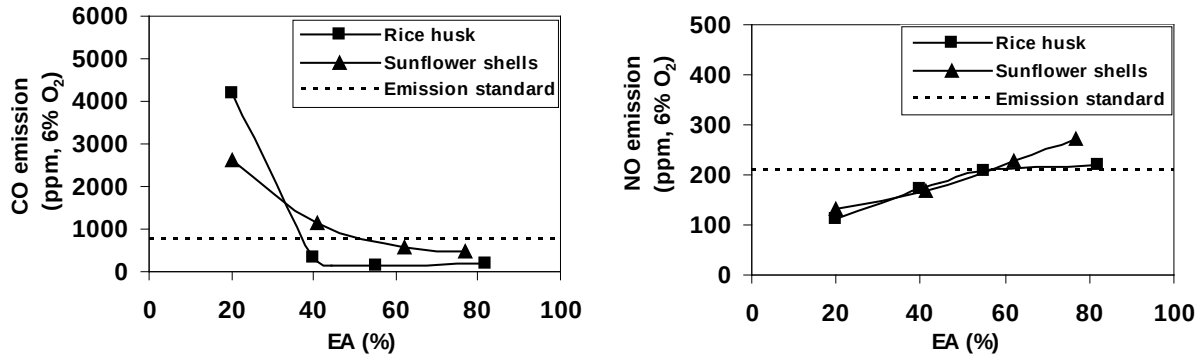

Fig. 4. Effects of excess air on the CO and NO emissions from the conical SFBC firing rice husk and sunflower shells at similar heat inputs of ~300 kW_{th}.

depicts the CO and NO emissions versus EA for (co-)firing rubberwood sawdust and eucalyptus bark for variable EF_{sd}. As seen in Fig. 5, to meet the emission standards, the SFBC should be fired at $EF_{sd} \approx 0.85$ (or SD/EB ≈ 73/27, by weight) maintaining excess air at ~55%.

3.3. Combustion efficiency

For all the fuel options, heat loss due to unburned carbon was found to be weakly dependent on EA and estimated as quite low (0.49–0.74% for firing rice husk, and ~0.15% for firing sunflower shells) or negligible (for firing rubberwood sawdust or its co-firing with eucalyptus bark). In the meantime, heat loss due to incomplete combustion was at a rather low level as well (<1%, for excess air of 40–80%). As the result, at 40–80% excess air values, the total combustion heat losses were estimated to be below 1%, which resulted in the high magnitudes of combustion efficiency, 99.1–99.9%, for all the fuels used. At excess air of ~55% ensuring best emission performance of the SFBC, the combustion efficiency was: 99.4% for rice husk, 99.5% for sunflower shells, 99.9% for rubberwood sawdust, 99.6% for the sawdust–bark mixture at $EF_{sd} = 0.85$, and 99.1% for the sawdust–bark mixture at $EF_{sd} = 0.75$.

4. Conclusions

In this comparative study, a swirling fluidized-bed combustor have been successfully tested for different fuel options: firing rice husk, sunflower shells and fine rubberwood sawdust, as

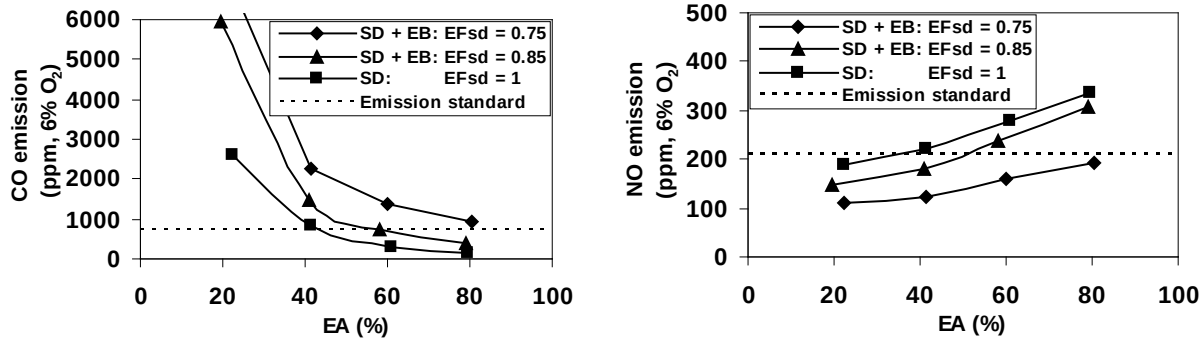

Fig. 5. Effects of excess air and sawdust energy fraction on the CO and NO emissions from the SFBC firing fine rubberwood sawdust (SD) or co-firing its mixture with eucalyptus bark (SD + EB).

well as co-firing the sawdust and eucalyptus bark at variable energy fraction of sawdust in the fuel blend. Substantial differences in properties of the selected fuels/blends (especially, in volatile matter, fuel-N and fuel-ash contents), as well as in the fuel particle size, affect significantly formation and decomposition of CO and NO in various regions of the combustor. For all the fuel options, CO emission can be effectively controlled by tangential injection of secondary air into the bed splash zone of the reactor. With higher excess air, NO emission from the combustor increases substantially in accordance with the fuel-NO formation mechanism. Through co-firing of rubberwood sawdust and high-moisture eucalyptus bark, NO emission from the combustor can be noticeably reduced, which is, however, accompanied by an increase in CO emission. Excess air of ~55% seems to be an optimal value ensuring high, 99.1–99.9%, combustion efficiency for the fuel range. At this excess air, CO and NO emissions can be controlled meeting corresponding national emission standards. For the co-firing, the best result is achievable when the sawdust energy fraction in the fuel blend is ~0.85.

Acknowledgement

The authors would like to acknowledge the financial support from the Thailand Research Fund (Contract No. BRG 5380015).

References

[1] J. Werther, M. Saenger, E.-U. Hartge, T. Ogada, Z. Siagi, Combustion of agricultural residues, Progress in Energy and Combustion Science 26, 2000, pp. 1–27.

[2] W. Permchart, V.I. Kouprianov, Emission performance and combustion efficiency of a conical fluidized-bed combustor firing various biomass fuels, Bioresource Technology 92, 2004, pp. 83–91.

[3] C.S. Chyang, K.W. Wu, C.S. Lin, Emission of nitrogen oxides in a vortexing fluidized bed combustor, Fuel 86, 2007, pp. 234–243.

[4] M. Fang, L. Yang, G. Chen, Z. Shi, Z. Luo, K.F. Cen, Experimental study on rice husk combustion in a circulating fluidized bed, Fuel Processing Technology 85, 2004, pp. 1273–1282.

[5] B.M. Jenkins, L.L. Baxter, T.R. Miles (Jr.), T.R. Miles, Combustion properties of biomass, Fuel Processing Technology 54, 1998, pp. 17–46.

[6] Kaynak B, Topal H, Atimtay AT, Peach and apricot stone combustion in a bubbling fluidized bed, Fuel Processing Technology 2005, 86: 1175–1193.

[7] M. Varol, A.T. Atimtay, Combustion of olive cake and coal in a bubbling fluidized bed with secondary air injection, Fuel 86, 2007, pp.1430–1438.

[8] H. Topal, A.T. Atimtay, A. Durmaz, Olive cake combustion in a circulating fluidized bed, Fuel 82, 2003, pp. 1049–1056.

[9] R. Kaewklum, V.I. Kuprianov, P.L. Douglas, Hydrodynamics of air–sand flow in a conical swirling fluidized bed: A comparative study between tangential and axial air entries, Energy Conversion and Management 50, 2009, pp. 2999–3006.

[10] P. Basu, K.F. Cen, L. Jestin, Boilers and Burners, Springer, New York, 2000.

[11] Pollution Control Department, Ministry of Natural Resources and Environment, Thailand. Air pollution standards for industrial sources. http://www.pcd.go.th/info_serv/reg_std_airsnd03.html.

Bioethanol production from cotton stalks or corn stover? A comparative study of their sustainability performance

Costas P. Pappis[1,*], Evangelos C. Petrou[1]

[1] *University of Piraeus, Department of Industrial Management and Technology, 80 Karaoli and Dimitriou Street, 18534, Piraeus, Greece*
** Corresponding author. Tel: +30 2104142150, Fax: +30 2104142342, E-mail:pappis@unipi.gr, epetrou@unipi.gr*

Abstract. The production of second generation biofuels (ones produced from lignocellulosic materials) has not yet been developed in a full commercial scale. However, a considerable number of pilot and demonstration plants have been announced or set up in recent years, with research activities taking place mainly in North America, Europe and a few other countries (e.g. Brazil, China, India etc). At the same time their environmental and economic performance are under examination. These performance issues are very sensitive on a variety of parameters such as feedstock material, production technology, logistics involved etc. In this study the sustainability performance of two alternative bioethanol's production systems, namely, one using cotton stalks and a second one using corn stover feedstock, are examined and compared using the Analytic Hierarchy Process method. Life Cycle Impact Assessment is used in order to evaluate each alternative's environmental performance. For this purpose, a modern powerful and state of the art software (SimaPro) is used. The systems' economic performance is based on cost/ benefit calculations.

Keywords: *Bioethanol, Analytical Hierarchy Process, Life Cycle Impact Assessment*

1. Introduction

Lignocellulosic materials, particularly agricultural residues, seem to be a very attractive source for bio-fuels' production (second generation biofuels) as indicated in recent literature [1],[2],[3]. The reasons for this are, first, they have a big potential, second, they have no adverse effect on food production, and, third, they have the least negative impacts (economic, environmental and social) to human systems compared to energy plant cultivations. Although the production of such biofuels has not yet been developed in a full commercial scale, several pilot and demonstration plants have been announced or set up. Relevant research activities, including performance issues such as environmental and economic ones, are taking place, mainly in North America, Europe and a few other countries [4],[5]. In general, the performance of such materials when used for the production and supply of biofuels depends on a variety of parameters such as kind of feedstock material, production technology, logistics involved etc. The evaluation of such performance is not straightforward, particularly in cases where multiple unrelated objectives or attributes have to be taken into account in the decision making process. In such cases, Operational Research methodologies have to be employed in order to arrive at safe conclusions. In this study the sustainability performance of two candidate alternative bioethanol's production systems, namely, one using cotton stalks and a second one using corn stover feedstock, are examined and compared using the Analytic Hierarchy Process method. Sustainability is meant to be composed of two criteria, namely the economic and the environmental ones, which have been taken into account for the final evaluation. Life Cycle Impact Assessment and, more specifically, the Eco-Indicator 99 method is used in order to evaluate each alternative's environmental performance. For this purpose, a modern powerful and state of the art software (SimaPro) is employed, while cost/ benefit calculations are used for the evaluation of the systems' economic performance. The result in the present case study is that corn stover is always preferable as a feedstock material.

2. Methodology

The methodology employed in this case study is as follows:
The sustainability performance of each bioethanol production system is expressed as a performance index combining the environmental and economic criteria and is calculated using the Analytic Hierarchy Process [6]. Cost/ benefit calculations are used for the evaluation of the systems' economic performance, while the environmental performance is evaluated by the Eco-Indicator 99 (EI 99) method. The combined performance index is then used for the selection of the best scenario from a sustainability perspective. A popular and state of the art software (SimaPro-Version 7.1) is used to determine the environmental performance of each scenario. SimaPro is a professional tool for collecting, analyzing and monitoring the environmental performance of products and services, following the ISO 14040 series recommendations. Amongst the Life Cycle Impact Assessment methods used by this software EI 99 is selected, since it is used extensively in similar evaluations and, in addition, it includes the land use impact category, which is important in agricultural production systems (as in the case of cotton and corn cultivation). The 2002 National Renewable Energy Laboratory's (NREL) report, referring to the design of the ethanol production system based on corn stover biomass, was used as a standard for the description of the production systems under evaluation [7]. Also data concerning the unit processes describing each production system were gathered by field research in Greece. Where no data were available proper assumptions were made. The economic performance of each alternative was measured in terms of total supply chain cost, in particular operational cost from field to distillery as the other costs are the same for both alternatives. The plant is assumed to be situated in the district of Thessaly since it can provide either the whole needed biomass quantity (in the case of corn stover) or the major part of it (in the cotton stalks case). The selected unit basis is 1 Kg EtOH (95% in water) at the distillery.

3. The alternative systems

Both alternative systems are evaluated in respect to the "field to distillery" bioethanol production, which includes the following stages: feedstock harvesting from fields; transport and feedstock storage & handling (size reduction etc); pretreatment and hydrolyzate conditioning process; saccharification and co-fermentation process; product, solids and water recovery stage (distillation, dehydration, evaporation and solid-liquid separation); wastewater treatment; product storage; power co-generation (by-product combustion for steam and electricity generation).

Alternative system A: Ethanol production from corn stover

The system is fed with corn stover harvested in Greece (Thessaly district). Key figures of the production system are presented in Table 1.

Table 1: Key figures for ethanol production from corn stover

	Value	**Note**
Feedstock quantity (t corn stover on a dry basis/yr)	750,000	
Harvested area (ha)	125,000	
Average distance for feedstock transportation (km)	70	5 km by tractor+ rail and 65 Km by lorry 28t
Capacity (t ethanol/yr)	213,300	
Power co-generated (Mwh/yr)	160.000	2.28 KWh/gal EtOH according to NREL report

The total feedstock quantity needed comes from Thessaly. The industrial process yield in the distillery is 284.4 g/Kg of dry feedstock. This value is 80% of the theoretical yield based on the chemical composition of corn stover as provided by NREL measurements [7] (measurements refer to the US). Corn stover is composed of glucan (37.4%), xylan (21.1%), lignin (18.0%) arabinan (2.9%), galactan (2.0%), mannan (1.6%), ash (5.2%), acetate (2.9%), protein (3.1%), extractives (4.7%) and unknown soluble solids (1.1%) (composition in % w/w on a dry basis). Since similar data for Greek corn stover are not available, we assume that their composition, and thus the yield of the industrial process, is identical to those of the US case.

Alternative system B: Ethanol production from cotton stalks

The system is fed with cotton stalks harvested in Greece (Thessaly and Macedonia districts). Key figures of the system are presented in Table 2.

Table 2: Key figures for ethanol production from cotton stalks

	Value	**Note**
Feedstock quantity (t cotton stalks on a dry basis/yr)	750,000	
Harvested area (ha)	300,000	
Average distance for feedstock transportation (km)	226	*16 km by tractor+ rail and 210 Km by lorry 28t*
Capacity (t ethanol/yr)	134,025	
By-product electricity (Mwh/yr)	269,000	*Proportional to lignin concentration of feedstock*

60% of needed feedstock is assumed to come from Thessaly and the rest from Macedonia. The industrial process yield in the distillery is assumed to be 80% of the theoretical yield based on cotton stalks chemical composition as in the case of corn stover ethanol production. Since chemical composition data for the Greek cotton stalks are not available, data from the literature were used [8]. Cotton stalks are composed of glucan (31,1%), xylan (8,3%), lignin (30.1%) arabinan (1.3%), galactan (1.1%), ash (6.0%), extractives (9.0%), and others (13.1%) (composition in % w/w on a dry basis). The aforementioned yield is based on the chemical composition mentioned above and is 178.7 g/kg of dry feedstock.

4. Results

4.1. Environmental criteria

The environmental performance of each of the alternatives was assessed using Life Cycle Impacts Analysis (realized by Sima-Pro). The following impact categories are selected as environmental criteria: Carcinogens, Respiratory organics effects, Respiratory inorganics effects, Climate change, Radiation effects, Ozone layer depletion, Ecotoxicity, Acidification / eutrophication, Land use, Minerals and Fossil fuels. No uncertainty evaluation was performed in this study.

4.1.1. Alternative's A Environmental Performance

For the evaluation of the environmental impacts, data from the Ecoinvent Report n.17 [9] about the inventory and the emissions, in addition to those of the NREL report [7], and data collected through field research were used. Some indicative emissions, in terms of volume produced per unit, are presented in Table 3.

Table 3: Indicative emissions from the corn stover ethanol production system

	Value	**Note**
CO_2 biogenic (Kg/Kg EtOH)	2.93	Emissions to air
Heat waste emissions (MJ/kg EtOH)	25.85	Emissions to air
CO (Kg/Kg EtOH)	0.000497	Emissions to air
Methane biogenic (Kg/Kg EtOH)	$3.0*10^{-5}$	Emissions to air
Mineral oil (Kg/Kg EtOH)	0.000426	Disposal

The resultant value for EI 99 of alternative A is 0.157. The system's performance per impact category is presented in Table 4. For reasons of comparison, the performance of the system "ethanol 95% in water from wood in distillery, CH'' (which describes the ethanol production system from residual wood in Switzerland and is included in the Ecoinvent Database [10]), is given in the same Table.

Table 4: Environmental Performance of the production systems under evaluation

	EtOH$^{(*)}$ from corn stover	**EtOH$^{(*)}$ from cotton stalks**	**EtOH$^{(*)}$ from wood**
Carcinogens	0.00449	0.00766	0.00252
Respir. Organics effects	$2.89*10^{-5}$	$7.51*10^{-5}$	$1.89*10^{-5}$
Respir. Inorganics effects	0.0266	0.0629	0.012
Climate change	0.0122	0.0333	-0.00557
Radiation	$3.49*10^{-5}$	$8.5*10^{-5}$	$1.78*10^{-5}$
Ozone layer depletion	$1.42*10^{-6}$	$3.81*10^{-6}$	$1.11*10^{-6}$
Ecotoxicity	0.00667	0.0122	0.00251
Acidification/Eutrophication	0.00548	0.0106	0.00186
Land use	0.0639	0.126	0.0423
Minerals	0.00138	0.00446	0.00083
Fossil fuels	0.00138	0.0967	0.0293
Environmental Index 99 (EI 99)	0.157	0.354	0.0858

$^{(*)}$: 1 Kg EtOH 95% in water in distillery

4.1.2. Alternative's B Environmental Performance

Data from field research and data from the Ecoinvent Report n.17 were used for the evaluation of the environmental impacts of this system. Where data were not available, reasonable assumptions were made in order to calculate the missing inventory data or emissions. Some indicative emissions, in terms of volume produced per unit, are presented in Table 5. The resultant value Eco-Indicator 99 of alternative A is 0.354. The system's performance per impact category is presented in Table 4.

Table 5: Indicative emissions from the cotton stalks ethanol production system

	Value	**Note**
CO_2 biogenic (Kg/Kg EtOH)	5.93362	Emissions to air
Heat waste emissions (MJ/kg EtOH)	45,36	Emissions to air
CO (Kg/Kg EtOH)	0.000833	Emissions to air
Methane biogenic (Kg/Kg EtOH)	$5.1*10^{-5}$	Emissions to air
Mineral oil (Kg/Kh EtOH)	0.000426	Disposal

4.2. Economic Performance

The criterion used for assessing the economic performance of each alternative is the economic performance (net economic benefit) of each alternative. A measure of the economic performance is the operation cost of each production system, including costs for feedstock, labour, maintenance, insurance & taxes, depreciations and secondary materials. The income from the excess electricity produced is also taken into account (negative cost). The income from ethanol produced is not taken into account for the economic performance evaluation since the calculation basis is 1 Kg EtOH and thus is the same for both alternatives. The operation cost of each of the alternatives is presented in Table 6. As the excess electricity generated by the cotton stalks' ethanol system is greater in relation to the corn stover ethanol system, this leads to a decreased operational cost in the former case.

Table 6: Alternatives' operation cost

	Cost of EtOH from corn stover production system (€/Kg EtOH)	**Cost of EtOH from cotton stalks production system (€/Kg EtOH)**
Feedstock	0.1232	0.1958
Other variable cost (cost for other raw and secondary materials)	0.0889	0.1415
Labor	0.0105	0.0168
Maintenance	0.0115	0.0183
Insurance & Taxes	0.0850	0.0135
Depreciations	0.0041	0.0651
Excess electricity sales	-0.1312	-0.3510
Total	0.1155	0.1000

4.3. Sustainability Performance

According to the preceding analysis, the corn stover ethanol production system is preferable from an environmental performance perspective while the cotton stalks' ethanol system is preferable from an economic perspective. AHP may be used for the purpose of selecting the best alternative based on both criteria, by aggregating the performance of each of the alternatives in terms of both criteria and thus determining an overall index U for each of the alternatives. Making the best choice is then straightforward. Table 7 summarizes the performance of each alternative in terms of both criteria. These performance values are the inverse absolute values of the EI 99 index and the total operation cost, respectively (values in parentheses). This adjustment is necessary in order for the following condition to be fulfilled:

Alternative A is preferable than B iff $x_{Aj} > x_{Bj}$, j=1,2 (x_{Aj} denotes the performance of alternative A in respect to criterion j)

Table 7: Alternatives' performance on environmental an economic criteria

Alternative	**Environmental criterion (EI 99)**	**Economic criterion (operation cost)**
EtOH from corn stover (alternative A)	$X_{A1:}$ 6.37(0.157)	$X_{A2:}$ 8.66 (0.1155)
EtOH from cotton stalks (alternative B)	$X_{B1:}$ 2.82 (0.354)	$X_{B1:}$ 10 (0.1000)

Following the AHP method, two pair-wise comparison matrices must be constructed (one for each criterion) for the determination of each alternative's score against each criterion. The values in these matrices show the decision maker's strength of preference between the two alternatives if only one criterion is taken into consideration. Based on the values presented in Table 7 the matrices are as in Table 8.

Table 8: Pairwise comparison matrices for score determination

	Environmental performance		**Economic benefit**	
	ALTERNATIVE A	ALTERNATIVE B	ALTERNATIVE A	ALTERNATIVE B
ALTERNATIVE A	1	5	1	1/3
ALTERNATIVE B	1/5	1	3	1

The calculated score values of each alternative on the selected criteria are shown in Table 9.

Table 9: Alternative scenarios' performance values

	Criteria	
Scenarios	Environmental Performance	Economic benefit
ALTERNATIVE A	0.83	0.25
ALTERNATIVE B	0.17	0.75

The pairwise comparison matrix for the determination of criteria weights is presented in Table 10. It is assumed that the environmental performance is "weekly more important" than the economic benefit criterion. This is a reasonable assumption, since biofuels come to serve environmental issues at least as much as economics considerations.

Table 10: Pairwise comparison matrix for criteria weights determination

	Environmental performance	Economic benefit
Environmental performance	1	2
Economic benefit	1/2	1

Thus the calculated weights for the environmental performance criterion w_1 and for the economic benefit criterion w_2 are 0.66 and 0.34, respectively. The resulting overall performance (sustainability index) of each alternative is:

$$U_A=0.66*0.83+0.34*0.25=0.6328$$
$$U_B=0.66*0.17+0.34*0.75=0.3672.$$

Thus alternative A must be chosen.

5. Discussion and Conclusions

In the present study the sustainability of two ethanol production systems was evaluated. The systems chosen will be located in Greece and use corn stover (alternative A) or cotton stalks (alternative B) as a raw material. The technology used (introduced by NREL, USA) includes prehydrolysis of raw material, simultaneous saccharification and co-fermentation process, and product, solids and water recovery stages. In addition, power is generated which is used for covering systems' needs and the excess is sold in the grid. For the sustainability evaluation, the environmental and economic performances of the alternatives were determined. It has been shown that ethanol made of corn stover has a better environmental performance than ethanol made of the cotton stalks. This is mainly due to the former's higher process production yield (in the plant) and to higher raw material yield (in the field). On the other hand, the cotton stalks ethanol system has a better economic performance than the corn stover

one, due to the bigger excess electricity produced by the former, which is sold to the grid, providing more income. The Analytic Hierarchy Process method was used in order to aggregate the environmental and economic performances of each of the alternatives into an overall (sustainability) index. The analysis has shown that, conditioned to the assumptions made, the corn stover ethanol system is preferable. In the study no uncertainty analysis was performed. It is worthy noting that:

- Ethanol production systems from lignocellulosic materials are a promising technology which is getting more mature nowadays. In Greece there exists adequate biomass potential for the development of such systems.
- The environmental performance of both corn stover and cotton stalks ethanol systems is generally good but it is worse in comparison to ethanol produced from wood.
- The cotton stalks ethanol system has a poorer environmental performance (especially regarding the land use impact category) in relation with the corn stover one, because of its low production yield in ethanol (as a consequence of cotton stalks' low concentration in cellulose) and its low raw material production yield in cotton fields.

Further research in the area of this study must cover:

- uncertainty issues in order for the critical values for a confident decision making process to be determined
- the way the plant's production capacity affects the sustainability of the system
- the exact determination of the chemical composition of Greek agricultural residues.

References

[1] Petrou E.C.; Pappis C. P. Biofuels: A Survey on Pros and Cons. Energy Fuels, 2009, 23 (2), 1055–1066.

[2] P. Sassner, M. Galbe, G. Zacchi. Techno-economic evaluation of bioethanol production from three different lignocellulosic materials. Biomass and Bioenergy, Vol 32, issue 5, May 2008, 422-430

[3] H von Blottnitz M. A Curan. A review of assessments conducted on bio-ethanol as a transportation fuel from a net energy, greenhouse gas, and environmental life cycle perspective. Journal of Cleaner Production, Volume 15, Issue 7, 2007, 607-619

[4] http://www.biolyfe.eu

[5] http://www.nile-bioethanol.org

[6] Winston W. Operations research. Application and Algorithms. Duxbury Press. Belmond, California. 1994.

[7] Aden A.; Ruth M.; Ibsen K.; Jechura J.; Neeves K.; Sheehan J.; Wallace B.; Montague L.; Slayton A.; Lukas J. Lignocellulosic Biomass to Ethanol Process Design and Economics Utilizing Co-Current Dilute Acid Prehydrolysis and Enzymatic Hydrolysis for Corn Stover. NREL, 2002.

[8] Silverstein RA; Chen Y; Sharma-Shivappa RR; Boyette MD; Osborne J. A comparison of chemical pretreatment methods for improving saccharification of cotton stalks. Bioresource Technol. 2007; 98:3000–3011.

[9] Jungbluth N.; Chuadacoff M.; Dauriat A.; Dinkel F.; Doka G.; Faist Emmenegger M.; Gnansounou A.; Shleiss K.; Spielmann M.; Stettler C.; Sutter J. 2007: Life Cycle Inventories for Bioenergy. Ecoinvent report No 17. Swiss Centre for Life Cycle Inventories. Dubendorf, CH.

[10] http://www.ecoinvent.org/database

Assessing the Environmental Performance of Integrated Ethanol and Biogas Production

Michael Martin*, Niclas Svensson, Jorge Fonseca

Linköping University, Environmental Technology and Management, Linköping, Sweden
** Corresponding author. Tel: +46 13281132, E-mail: michael.martin@liu.se*

Abstract: As the production of biofuels continues to expand worldwide, criticism about, e.g. the energy output versus input and the competition with food has been questioned. However, biofuels may be optimized to increase the environmental performance through the concepts of industrial symbiosis. This paper offers a quantification of the environmental performance of industrial symbiosis in the biofuel industry through integration of biogas and ethanol processes using a life cycle approach. Results show that although increasing integration is assumed to produce environmental benefits in industrial symbiosis, not all impact categories have achieved this and the results depend upon the allocation methods chosen.

Keywords: *Ethanol, Biogas, Industrial symbiosis, Environmental impacts, Biofuel*

1. Introduction

The production of biofuels for transport has seen a large increase in the past few years to meet the onset of policies for increased production and use worldwide. However, with this onset, biofuels have met much criticism [1,2] which ranges from debates about the competition with food to the energy used to produce the biofuels [3]. Dissimilarities and criticism result primarily from different assumptions made, system boundaries used, technologies and the reference energy systems used in life cycle assessment of biofuel systems [4]. However, biofuel production encompasses large quantities of inputs and outputs and therefore, consideration must be made for the efficient use of resources for biofuel production industries [2] for which the environmental performance may be bettered and the flows of material and energy optimized [5]. One approach to do this is by employing concepts from industrial symbiosis.

Industrial symbiosis is a branch of industrial ecology focusing upon the inter-firm interactions aiming to engage traditionally separate industries to cooperate in a collective approach to create competitive advantages through resource exchanges and synergistic possibilities [6]. However in industrial symbiosis, benefits have rarely been quantified in the literature [7].

On the island of Händelö in Norrköping, Sweden, a unique bioenergy complex of symbiotic activities between the ethanol, biogas and energy system takes place [5]. However, using the concept of industrial symbiosis, these symbiotic activities could be further improved and more synergies could occur [5]. Could these synergies therefore lead to improved environmental performance and can they be quantified?

The aim of this research paper is to outline and present the environmental impacts and performance of several symbiotic activities, i.e. integrated scenarios, between the biogas and bioethanol facilities located on the island of Händelö, Norrköping. Using exchanges (i.e. synergies) between the biogas and bioethanol facilities, the environmental performance will be quantified using a life cycle approach of the synergies for different scenarios with increasing degrees of integration.

2. Methodology

The environmental performance, i.e. environmental impacts, of symbiotic activities between biogas and ethanol production plants will be assessed by comparing different scenarios. Different degrees of integration will be tested from no integration at all (default) to all by-product residues from the ethanol plant used in the biogas plant, as described in the subsequent section entitled, *The Scenarios.*

2.1. System Description

The production of biofuels takes place on the island of Händelö in Norrköping, Sweden. Ethanol is produced from a combination of wheat, barley and rye resulting in a number of by-products such as Dried Distillers Grains with Solubles (DDGS), syrup and impurities. Biogas is produced through the anaerobic digestion of organic matter, in the scenarios e.g. wheat and barley and by-products of the ethanol facility. Conversion technologies and performance for the anaerobic digestion and fermentation processes have been obtained from the companies, along with material and energy flows [5,8-10].

The assessment takes the ethanol plant as starting point and keeps the ethanol fuel output static whereas all of the other inputs and outputs for that plant and the biogas plant are allowed to vary in accordance with the scenarios described below. This approach was chosen in order to reflect upon the importance of size differences between the plants but also of the potential implications of larger by-product exchanges between the two plants.

2.2. Tools and Impact Categories

A life cycle approach is applied to each scenario separately from a cradle-to-gate perspective. All life cycle assessment calculations of environmental impacts have been performed using the software package SimaPro v. 7.2. The life cycle impact assessments have been conducted using the EPD 2007 [11] method. This method was chosen due to its recommendation by the Swedish Environmental Management Council and providing a wide array of environmental impact categories, e.g. global warming potential (GWP), acidification, eutrophication and the use of non-renewable resources.

2.3. Allocation Procedures

By-products and the energy and emissions associated with their use have been taken care of by the use of two separate methods in this paper, including energy allocation and system expansion [4,8]. The energy content of these by-products has been computed for the lower heating value of the DM contained in each fraction. Energy allocation figures used for each scenario can be seen in Tables 1-2.

Table 1: Ethanol Production Allocation for Major Products and By-Products [8]

Product/ By-Product	DM Content (%)	Default Scenario	Existing Scenario	Scenario 1	Scenario 2	Scenario 3
Ethanol	-	70,7%	70,7%	70,7%	60,3%	60,3%
DDGS	90	21,7%	21,7%	21,7%	-	-
Syrup	27	5,6%	5,6%	5,6%	-	-
Impurities	86	2,0%	2,0%	2,0%	-	-
Stillage	16	-	-	-	39,7%	39,7%

Table 2: Biogas Production Allocation for Major Products and By-Products [8]

Product/ By-Product	Default Scenario	Existing Scenario	Scenario 1	Scenario 2	Scenario 3
Biogas	31,3%	35,7%	35,7	35,7%	33,7%
Biogas to Ethanol	-	-	-	-	2,0 %
Biofertilzer	68,7%	64,3%	64,3	64,3%	64,3%

System expansion, also known as substitution, has also been conducted to account for the replacement of by-products produced [4]. System expansion for the default and existing scenarios of the ethanol plant include the use of stillage products for fertilizers and animal fodder applications. Fodder replacement by DDGS and syrup in dry matter content (DM) has been assumed to replace Brazilian soy meal and European barley in the amounts of 0,4 kg DM and 0,6 kg DM [2]. Fertilizer nutrients replaced by biogas digestate per ton is assumed to replace 8 kg N, 5 kg NH_4, 1 kg P and 1,5 kg K per ton of produced digestate [8]. Furthermore, the lower heating value (LHV) for dried stillage has been assumed to be the same as that for the digestate [3] due to limited data availability.

2.4. The Scenarios

Scenarios have been produced to test and quantify the environmental performance of several different material and energy exchanges between the bioethanol and biogas production plants as aforementioned. Each scenario is tested using both the energy allocation and system expansion methods to account for energy and replacement of processes from the by-products [12,13]. The outputs have been expressed using the LHV for both biogas and ethanol, 50MJ/kg and 28,87 MJ/kg respectively.

2.4.1. Default Scenario

The default scenario will show the impacts of two stand alone plants with no integration. The two plants use respective inputs of wheat, barley and triticale for their production processes. In terms of biofuel production output, the main products are 17 TJ of biogas and 1 314 TJ of ethanol. All inputs and outputs of raw material, by-products, etc. are based on the aforementioned biofuel outputs [8]. The default scenario has been used to compare to the existing scenario in order to compare the environmental impacts of current practice with that of a stand alone system.

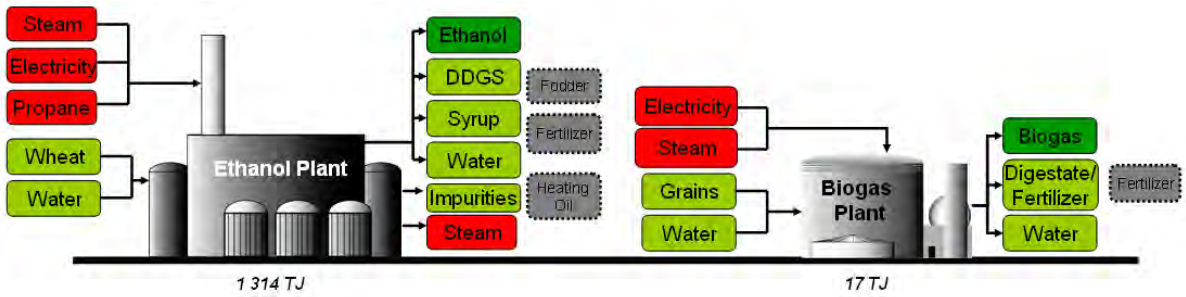

Fig. 1: Default Scenario. Note the avoidance of fodder and fertilizers from the ethanol and biogas plants for the system expansion have been included [8].

2.4.2. Existing Scenario and Scenario 1

The existing scenario is similar to the production process used pre-2009 on the island of Händelö. The exchange of thin stillage is used to produce biogas at the neighboring biogas plant. Furthermore, as the thin stillage is sent to the biogas plant at a temperature of around 70°C, it must be cooled to around 38°C for anaerobic digestion and thus electrical fans are used to cool the substrate and no external process heat is required [14,15]. The output of the system in biofuel is again 17 TJ of biogas and 1 314 MJ of ethanol for which all inputs and outputs are based [8]. Scenario 1 is similar to the existing scenario, however in Scenario 1 the impurities (consisting primarily of husks and filtered grains) are also sent to produce biogas. This therefore raises the output of biogas production and digestate, requiring more electricity and water for the digestion and upgrading processes respectively (ibid.).

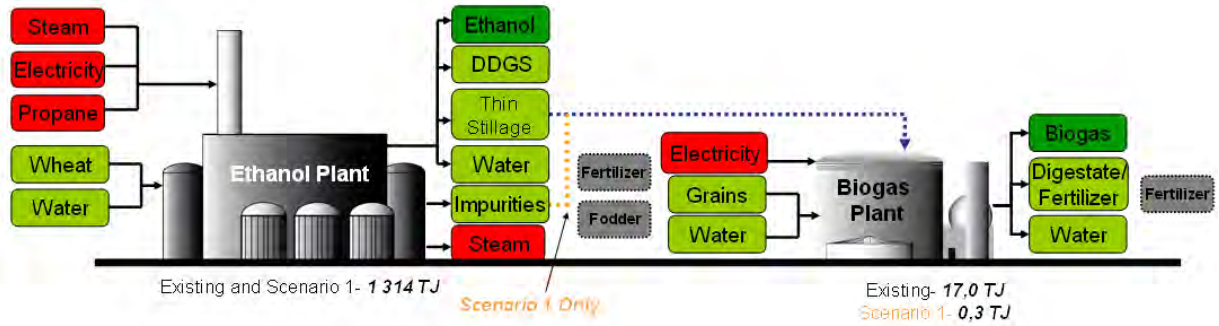

Fig. 2: Existing Scenario and Scenario 1. Note the avoidance of fodder and fertilizers for the system expansion have been included [8].

2.4.3. Scenarios 2 and 3

In Scenarios 2 and 3, it is assumed that all the stillage is sent to the biogas plant for anaerobic digestion. By doing so the ethanol plant can save a large input of energy, roughly 35% less energy [16] from the dryers and handling equipment for fodder production. Scenario 2 and 3 are similar, in that they both use stillage for biogas production. However, Scenario 3 differs in the fact that biogas replaces propane in the ethanol production plant for odor control [14]. Similar to the existing scenario, the stillage is sent to the biogas plant at a higher temperature than necessary for the process and electrical fans are used to cool the substrate, requiring no external process heat. The production of biogas has now been increased to 464 TJ in Scenario 2 and 438 TJ in Scenario 3 (accounting for the use of 26 TJ of biogas for ethanol production) while the production of ethanol remains the same as in the default and existing scenarios [8].

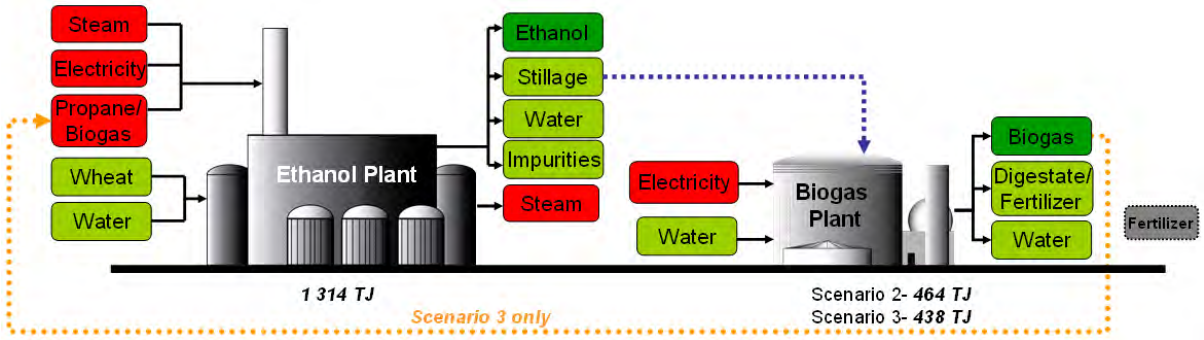

Fig. 3: Scenarios 2 & 3. Note that in Scenario 3, the biogas is used in place of propane (denoted by an orange dashed line). The figure also includes avoided fertilizers for the system expansion method [8].

2.5. Data Inventory

Data has been obtained from the biofuel production firms of Händelö, Norrköping in Sweden. Production figures are relevant for pre-2009 conditions for the default and existing scenarios [8-10,14,15]. When data has been limited or unavailable, comparable data from the Ecoinvent database v. 2.1 has been used for e.g. specific cultivation, fertilizers and transportation data. Energy for the system is provided from the Swedish electricity production system based primarily upon hydropower and nuclear power [17]. Process heat, in the form of steam is provided from a neighboring combined heat and power plant fueled by biomass [8,9,18]. Grains are transported within the Östergötland County to the island of Händelö, with an average distance of 100 km. Transportation of the various raw materials between the neighboring biogas and ethanol production firms is assumed to have an average distance of 5 km. The biofertilzer transport has been assumed to be on average 33 km [8].

3. Results and Discussion

The environmental performance of the integrated systems from the aforementioned scenarios can be seen in Figs. 4-6. These figures show the global warming potential, impacts from acidification and eutrophication as well as the use of non-renewable fuel. A discussion of the results will follow each figure in the subsequent sections. Further details can be found in Martin et al. [8]. The following notation has been used to describe each scenario in the figures:

D-EA: Default Scenario (Energy Allocation)
D-SE: Default Scenario (System Expansion)
E-EA: Existing Scenario (Energy Allocation)
E-SE: Existing Scenario (System Expansion)
1-EA: Scenario 1 (Energy Allocation)
1-SE: Scenario 1 (System Expansion)
2-EA: Scenario 2 (Energy Allocation)
2-SE: Scenario 2 (System Expansion)
3-EA: Scenario 3 (Energy Allocation)
3-SE: Scenario 3 (System Expansion)

3.1. Global Warming Potential

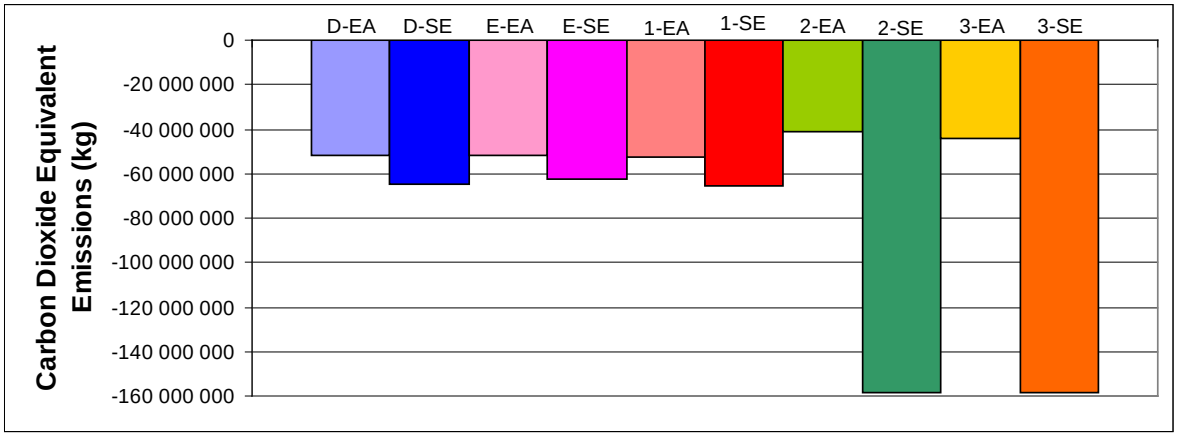

Fig. 4: Global Warming Potential of the different Scenarios measured in kg of CO_2-equivalent. [8]

From Fig. 4 it is apparent that there are some differences between each scenario, with the system expansion method producing the largest variations. The benefits related to the global warming potential from the energy allocation method do not to follow the trend found in the system expansion method with increasing integration of the biogas and ethanol systems, i.e. increased benefits with increasing integration. It can be seen that the systems with the largest integration also have a lower share of the impacts and benefits associated with their outputs

based on how the energy is allocated between the products and by-products. This means that while the systems may be increasingly integrated, the outputs receive a lower share of the benefits [8]. Furthermore, when all stillage is used for biogas production this increases the production of biogas thus increasing the use of electricity, water and transportation of biofertilizer and the stillage to and from the biogas facility. These increases therefore lead to reduced benefits for Scenarios 2 and 3 in the energy allocation. With increasing integration of the systems there are also larger impacts associated with increased transportation and electricity consumption (ibid.) thus decreased.

In the system expansion method, all benefits and burdens from the systems are allocated to the main outputs, ethanol and biogas. However, the use and substitution of processes associated with the by-products are also taken into account. Increasing integration tends to therefore produce larger benefits to the system with increasing integration, with exception to the existing scenario. This is primarily a result of the increase in biofertilizer replacing conventional fertilizers, though the biofertilizer production is reduced slightly in the existing scenario. When comparing the existing scenario with the default scenario, the default scenario has a larger benefit due to a larger input of grains. With the current system boundaries, cradle-to-gate, the grain thus sequestrates a large amount of carbon dioxide [8]. Consistent with the energy allocation methods, increasing integration of the systems leads to larger impacts associated with increased transportation and electricity consumption. Nonetheless, these increased impacts are consumed by the benefits to the system from the system expansion (ibid.). In Scenarios 2 and 3, by using the stillage and not adding extra heat for e.g. drying for DDGS production, these scenarios gain further benefits from less heat and water use. Scenario 3 can be seen to have slightly higher benefits in both allocation methods due primarily to the replacement of propane with biogas.

3.2. Non-Renewable Energy Consumption

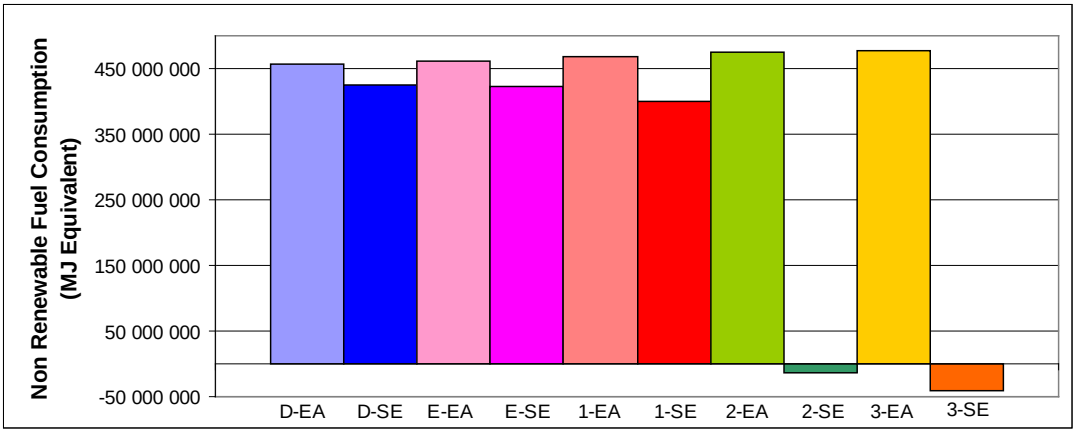

Fig. 5: Consumption of Non-renewable Energy in MJ-equivalent for the different scenarios. [8]

Another important aspect to show is the consumption of nonrenewable energy. The general trend for the consumption of non-renewable fuels for increasing integration is an increase in the energy allocation scenarios and a decrease in the system expansion method. An increase in the energy allocation scenarios is due to increased transportation of stillage and biofertilizer. The decrease of non-renewable fuel consumption with increasing integration in the system expansion scenarios arises from the enhanced quantities of biofertilzer produced, thus replacing conventional fertilizers.

3.3. Acidification and Eutrophication

In order to show an array of local and global impacts, the acidification and eutrophication impacts have also been documented in Fig. 6.

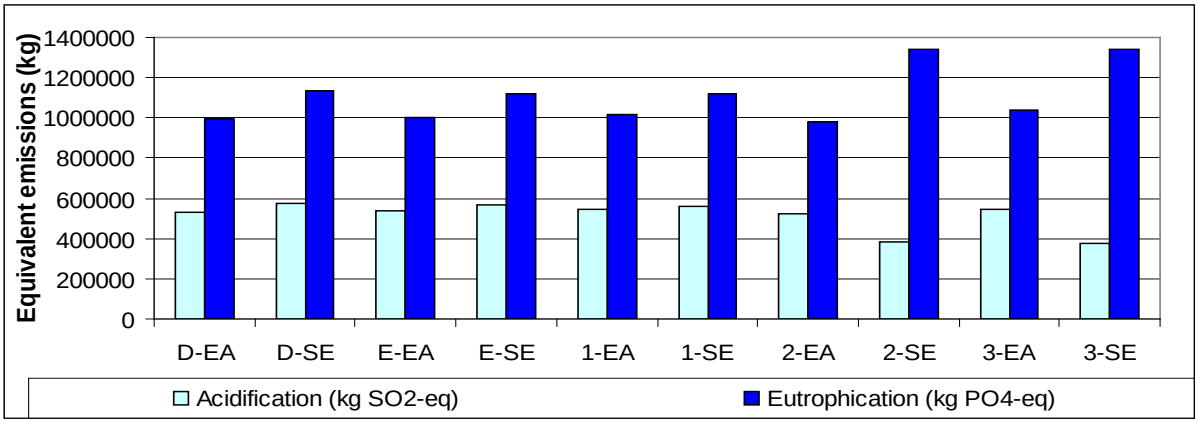

Fig. 6: Impacts in kilograms of equivalent SO_2 and PO_4 for Acidification and Eutrophication. [8]

Fig. 6 shows the Eutrophication potential for the allocation methods of each scenario. The increased integration of biogas and ethanol from the default scenario to the full use of stillage tends to correspond to larger eutrophication impacts in all cases except for the energy allocation method in Scenario 2 and when accounting for the use of biogas instead of propane in the system expansion method for Scenario 3. Once again this is primarily a result of the increase in transportation required with increased integration [8].

Correspondingly the impacts from acidification tend to increase slightly using energy allocation, with exception to Scenario 2. This stems from a slightly reduced impact from the transportation and cultivation of grains in this scenario while Scenario 3 thereafter increases. There is a general decrease in emissions of equivalent SO_2 for the system expansion method due to the reduction of fertilizer by increasing integration, and correspondingly increasing biofertilizer production, replacing conventional fertilizers [8].

4. Conclusions

The integration of biogas and ethanol production can be seen from this paper as a complex system. Although the CO_2-equivalent emissions may be further reduced by increasing the integration of the biofuel plants in the system expansion case, the energy allocation method proves opposite results. Furthermore local impacts such as acidification and eutrophication should be considered, which may increase with increasing integration. Therefore the allocation method chosen is crucial for taking into account energy and impacts embodied in by-products and replaced processes and may lead to converse results. The removal and addition of processes, materials and energy can have both improvements and rebound effects for the system. These impacts could possibly be resolved in the biogas plant by more efficient upgrading processes, transportation of stillage by pipeline and a more efficient cooling system for the incoming stillage as well as internal optimization at the ethanol plant.

This report thus shows that there is a need to understand the impacts produced from biofuel production and industrial symbiosis activities. Symbiotic activities may lead to environmental performance benefits, though the choice of impact category and allocation method is crucial when comparing local vs. global impacts. Nonetheless, this study may open for further work on the quantification of integrated biofuel production processes and other symbiotic activities.

References

[1] J.W. Ponton, Biofuels: Thermodynamic sense and nonsense, Journal of Cleaner Production, 17, 2009, pp.896-9.

[2] P. Börjesson, Good or bad bioethanol from a greenhouse gas perspective - What determines this? Applied Energy, 86, 2009, pp.589-94.

[3] P. Börjesson, L.M. Tufvesson, Agricultural crop-based biofuels – resource efficiency and environmental performance including direct land use changes, Journal of Cleaner Production, In Press, Corrected Proof, 2010.

[4] E. van der Voet, R.J. Lifset, L. Luo, Life-cycle assessment of biofuels, convergence and divergence, Biofuels, 1, 2010, pp.435-49.

[5] M. Martin, Industrial Symbiosis for the Development of Biofuel Production, Licentiate Thesis, 2010, pp.1-53.

[6] M.R. Chertow, Industrial symbiosis: Literature and taxonomy, Annual Review of Energy and the Environment, 25, 2000, pp.313-37.

[7] M. Karlsson, A. Wolf, Using an optimization model to evaluate the economic benefits of industrial symbiosis in the forest industry, Journal of Cleaner Production, 16, 2008, pp.1536-44.

[8] M. Martin, J. Fonseca, N. Svensson, A. Helgstrand, Assessing the Environmental Performance of Integrated Biogas and Ethanol Production: Quantifying Industrial Symbiosis in the Biofuel Industry, LIU-IEI-R-- 10/0115--SE, 2010, pp.1-50.

[9] Lantmännen Agroetanol AB, Lantmännen Agroetanol AB Homepage, 2009.

[10] Svensk Biogas AB, Svensk Biogas AB Homepage, 2009.

[11] Environdec, The international EPD system- a communication tool for international markets, 2009.

[12] European Union, Directive 2009/28/EC of the European Parliament and of the Council of 23 April 2009 on the promotion of the use of energy from renewable sources and amending and subsequently repealing Directives 2001/77/EC and 2003/30/EC, L140/16-62: Official Journal of the European Union, 2009.

[13] ISO, ISO 14040:2006 Environmental management-life cycle assessment-principles and framework ISO 14044: 2006, Environmental Management-Life Cycle Assessment-Requirements and Guidelines, 2006.

[14] P. Paulsson, Energianalys av etanolproduktion, Master of Science Thesis, SLU, 2007.

[15] J.A. Fonseca, Assessing the Environmental Impacts of Synergies between the Ethanol and the Biogas Industries, Master of Science Thesis, Linköping University, 2010.

[16] J.D. Murphy, N.M. Power, How can we improve the energy balance of ethanol production from wheat? Fuel, 87, 2008, pp.1799-806.

[17] S. Bernesson, D. Nilsson, P. Hansson, A limited LCA comparing large- and small-scale production of ethanol for heavy engines under Swedish conditions, Biomass and Bioenergy, 30, 2006, pp.46-57.

[18] E.ON Värme Sverige, E.ON i världsunikt energikombinat, 2009.

Evaluation of bamboo as a feedstock for bioethanols in Taiwan

Ya-Nang Wang[1,2], Chun-Han Ko[2,3,*], Chih-Yuan Lee[2], Heng-Ping Tsai[2], Wen-Hua Chen[4], Wen-Song Hwang[4], Ming-Jer Tsai[1,2], Fang-Chih Chang[5]

[1] *The Experimental Forest, National Taiwan University, Nan-Tou, Taiwan, R.O.C.*
[2] *School of Forestry and Resource Conservation, National Taiwan University, Taipei, Taiwan, R.O.C.*
[3] *Bioenergy Research Center, National Taiwan University, Taipei, Taiwan, R.O.C.*
[4] *Cellulose Ethanol Program, Institute of Nuclear Energy Research, AEC, Taoyuan, Taiwan, R.O.C.*
[5] *The Instrument Center, National Cheng Kung University, Tainan, Taiwan, R.O.C.*
** Corresponding author. Tel: +886 2 33664615, Fax: +886 2 13211001, E-mail: chunhank@ntu.edu.tw*

Abstract: The bamboo covers 152,300 ha in Taiwan, roughly of 7.2 % the overall forest area. This study evaluated Ma bamboo (*Dendrocalamus latiflorus* Munro) as a feedstock for bioethanols in Taiwan. Acidic steam explosion was employed to prepare Ma bamboo chips, as well as alkaline steam explosion, bleached and unbleached kraft pulps. For the saccharification of pretreated bamboo biomaterials, cellulase formulations were applied with three dosages: 2, 6, 12 percents weights to dried pulps. For acidic exploded pulp, the optimal yields were 348.92 ± 39.76 mg/ g o. d. pulp, 68% of pulp alpha cellulose contents. The hydrolysis efficiencies were negatively impacted by lignin and xylan contents of pretreated bamboo biomaterials. Simultaneous saccharification and fermentation (SSF) were also conducted using *Saccharomyces cerevisiae* D5A under 38°C and pH 5 at shake flask level. After 96 hours, 91.8 mg ethanol per g of α-cellulose was obtained for acid exploded pulp; 176.3 mg ethanol per g of α-cellulose was obtained for alkaline exploded pulp; 537.6 mg ethanol per g of α-cellulose was obtained for bleached bamboo pulp. Based on the experimental data, up to 10,700 tons of bioethanols could be produced annually by acidic steam explosion.

Keywords: *Bamboo, Bioethanol, Simultaneous hydrolysis and fermentation, Steam explosion*

1. Introduction

Bamboo stands cover 152,300 hecacres, roughly of 7.2 % the overall forest area in Taiwan [1]. Bamboos are endemic in south and east Asia. Bamboo biomass is accumulating daily, but little of them has been used (edible bamboo shoots and inedible part as materials) and most of them are wasted without utilizing. Its accumulation is about 26.1 tons/ha, with annual growth around 13.84 tons/ha under 5 year rotation cutting. Its fast growth and adaptability toward various soil and climate conditions make the bamboo a good candidate for a renewable resource. Bamboo had been conventionally used as the raw materials for producing artefacts, utensils, plywood, fiberboard, and decorated multi-layered panels in Taiwan and many Asian countries. Recently, more attention was paid for bamboo biomass as biofuel feedstock, *e. g.*, steam-exploded bamboo was employed for methane production [2].

Simultaneous saccharification and fermentation (SSF) processes were firstly described by Takagi *et al.* [3]: it combined enzymatic hydrolysis of cellulose and simultaneous fermentation of the fermentable sugars together to obtain ethanol. In the SSF process, the conditions are nearly the same as in separate hydrolysis and fermentation systems (SHF), just one different is that saccharification and fermentation are performed in the same reactor. Thus, put the yeast and the cellulolytic enzyme complex together reduces the accumulation and inhibition of sugars in the reactor which increasing ethanol yield and hydrolysis rate with respect to separate hydrolysis and fermentation [4]. Another advantage of SSF is that used one fermenter throughout the whole process reducing the facilities costs. This study evaluated Ma bamboo (*Dendrocalamus latiflorus* Munro) as a feedstock for bioethanols in Taiwan. Acidic and alkaline steam exploded bamboo biomass, as well as unbleached and bleached kraft bamboo pulps, were employed as raw materials to investigate the impact of lignin on SSF efficiencies.

2. Methodology

2.1. Materials

The Ma Bamboo (*Dendrocalamus latiflorus* Munro) sample, approx. 4-year-old Ma Bamboo culms, was collected from the Experimental Forest of National Taiwan University. The stem was chopped into 6 × 3 cm (length × width), then air dried for a mouth.

2.2. Steam-explosion

Air-dried bamboo sample was soaked into 1.5% H_2SO_4 solution or 1.5% NaOH & Na_2SO_3 solution for a week. Steam explosion conditions were: solid/liquid ratio=1:7; temperature and pressure of alkali-treated samples were held at 180, 190 and 200°C from 10 to 20 minutes. Acid-treated sampled were held at 190°C for 10 minutes. Samples were then washed by tap water on 200 mesh screen until neutral, then kept in 4 °C.

2.3. Kraft pulping and bleaching

Ma bamboo air-dried kraft pulp was cooked by M/K digester with wood to liquid ratio = 1/4 (w/v), 25% sulfidity and 17% active alkali. H-factor is about 650, with temperature raised at 1.5°C/min to 160 °C in 90 min, then kept at 160 °C for another 90 min. After washing and screening, then keep in 4 °C refrigerator. Bleached pulps were prepared by a commercial DEDD bleaching sequence [5], and then washed and kept in 4 °C refrigerator. "D" and "E" stand for chlorine dioxide and alkali extraction stages.

2.4. Enzyme hydrolysis

Acid and alkali steam-exploded bamboo pulps (biomass) were hydrolyzed with cellulases complex 50010 and 50013 (containing xylanase) from Novozymes®. Three enzyme loadings were equivalent to 1.5, 4.5, 9 IU endoglucanase (CMCase)/mL, 0.15, 0.44, 0.89 IU cellobiohydrolases/mL, and 1.2, 2.4, 7.1 IU xylanase/mL in reaction solutions. Hydrolysis was conducted in a total volume of 200 mL liquid with 0.05 M citrate buffer (pH 5), 2.5% (w/v) samples in a 250mL conical flask. The flasks was water bathed at 50°C, shaken at 100 rpm for 96 h, and the samples were analyzed every 12h.

2.5. Simultaneous saccharification and fermentation (SSF)

100 mL reaction solution, with 5% (w/v) steam-exploded bamboo, 1 % (w/v) yeast extract and 2 % (w/v) peptone, was subject to 38°C and pH 5 in a 250 mL conical flask. The sterilized reaction solution was inoculated with 5% (v/v) *Saccharomyces cerevisiae* D5A culture solutions with optical density at 0.1. The culture solution was prepared by was cultivated with yeast extract 10 g/L, peptone 20 g/L, dextrose 20 g/L for 18 h at 100 rpm, 38 °C on a rotary shaker. The enzymes were added into reaction solutions with endoglucanase 9 IU/mL, cellobiohydrolases 0.89 IU/mL and xylanase 7 IU/mL at 38°C for 96 h, then the samples were analyzed every 12h.

2.6. Analytical methods

Ma bamboo chip and steam exploded samples oven-dried and hand-kneaded, screened to 40-60 mesh before the compositional analyses: ash (TAPPI T211 om-07), acid-insoluble lignin (TAPPI T222 om-06), cellulose and α-cellulose (TAPPI T203 cm-09). Enzymatic hydrolysate and SSF samples were analyzed by high performance liquid chromatography (HPLC) using a ICSep ION-300 column and a RI detector for identifying organic acids, alcohols and mono sugars at 70 °C; mobile phase was 0.0085 N sulfuric acid at flow rate 0.4 mL / min. Error bars indicates the standard deviations from triplicate experiments.

3. Results and discussion

3.1. Compositional analysis

Various yields from pretreatment were obtained (on dried bamboo basis): 57 % for acid steam explosion, 58 % (200°C-10min) to 83% (180°C-10min) for acid steam explosion, 40 % for kraft pulping and 39.8% for bleaching.

Table 1. Compositional analysis of Ma bamboo samples. Units are mg/g dried wood.

Composition	ash	lignin	holocellulose	α-cellulose
Raw Ma bamboo	17±4.36	227.7±39.6	722±66.4	427.7±41.2
Alkali steam-explosion *				
180°C-10min	65±11	160±14.1	703±44	480±20.5
190°C-5min	54±13	148±21.8	820±81.7	598±69.7
190°C-10min	70±18.5	175±31.9	644±98.6	473±117.4
190°C-20min	46±8.1	171±44.1	702±35.2	550±49.1
200°C-10min	63±8.5	180±29.8	690±22.5	525.5±44.1
Acidic steam-explosion*	7.6±0.5	339±44.7	526±82.9	260±63.3
Kraft pulp	6.4±1.7	25.5±3.6	928±36.8	847±41.2
Bleached pulp	9±2.1	<2	966±28.9	869±43.5

** acid steam-exploded: 190°C held for 10 mins at 1.26 MPa*
** alkali steam-exploded: 180°C to 200°C and 0.99 MPa to 1.53 MPa of 5 samples * N.D.: not detected.*

Compositional analysis of raw material bamboo and pretreated samples were listed in Table 1. Great varieties of holocellulose contents were demonstrated for alkali steam exploded pulps. Generally, the lignin contents of alkali steam exploded pulps were lower then the ones of acidic steam exploded pulps. Holocellulose contents were highest for kraft pulp and bleached pulps. Acidic conditions might oxidize the cellulosic components and reduced the holocellulose of the pulps. In addition, the greater incomplete closure of compositional analysis for acidic steam exploded pulps, with its greater lignin content, was consistent to the above assumption. Lignin contents of alkali exploded pulps were increased with increasing treatment times. Although alkali would soften lignin in higher temperatures, soften lignin might melt onto cellulose fibrils; and lignin condensation [2] would contribute the increasing lignin contents among alkali steam exploded pulps.

3.2. Enzyme hydrolysis

Enzyme hydrolysis for pretreated samples was depicted in Fig.1. Enzyme loading was 9 IU endoglucanase/mL, 0.89 IU cellobiohydrolases/mL, and 7.1 IU xylanase/mL in reaction solutions. Conversions for sugar were based on dried weight of samples. 190°C-10min was chosen for alkali steam-exploded bamboo in Figure 1.

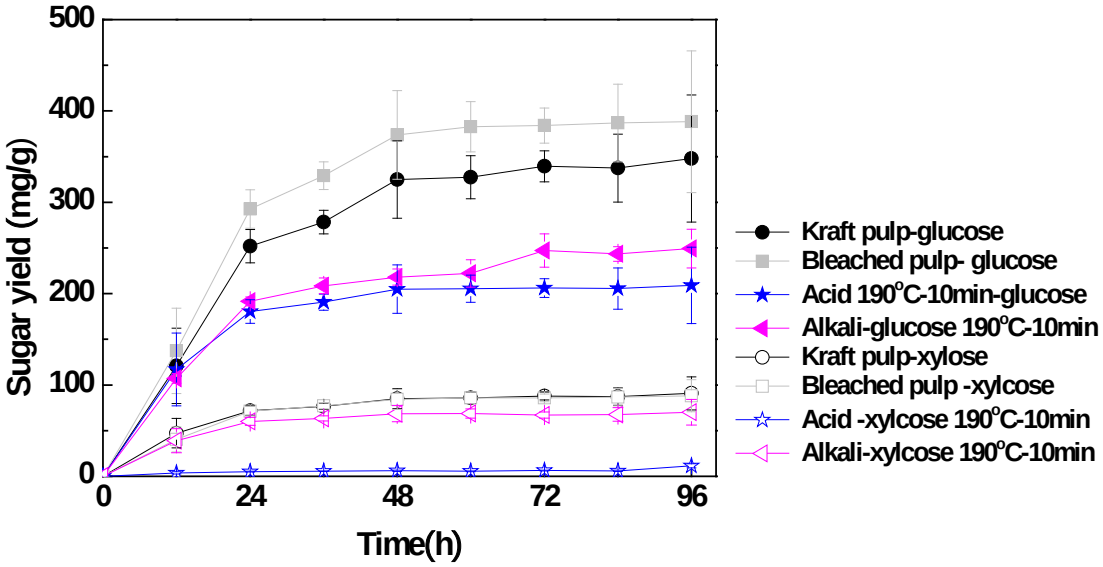

Figure 1. Enzyme hydrolysis to sugar conversion of pretreated bamboo samples with respect to time.

Glucose and xylose increased steadily prior to the first 24 h for all pulps, and the saturation was then reached at approx. 48 hours. At 96 h, the bleached pulp showed a optimal y 388.2 ± 69 mg/g, kraft pulp 347.8 ± 77 mg/g, alkali steam-exploded (190°C-10min) 249.3 ± 21 mg/g and acid steam-exploded 209.1±41 mg/g.

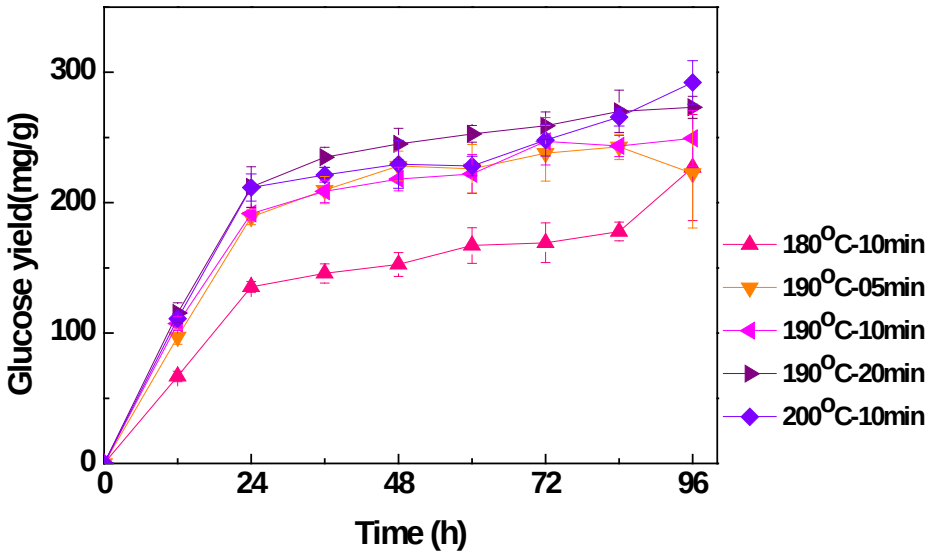

Figure 2. Enzyme hydrolysis to sugar conversion of alkali steam-exploded bamboo samples with respect to time.

Fig. 2 showed hydrolysis for 5 alkali steam-exploded samples, with other conditions as same as Figure 1. Except for the pulp for 180°C-10min, the other pulps have similar glucose yields at around 250 mg glucose per gram dried bamboo. Interestingly, the yields of 200°C-10min pulp were still slightly growing after 48 hours.

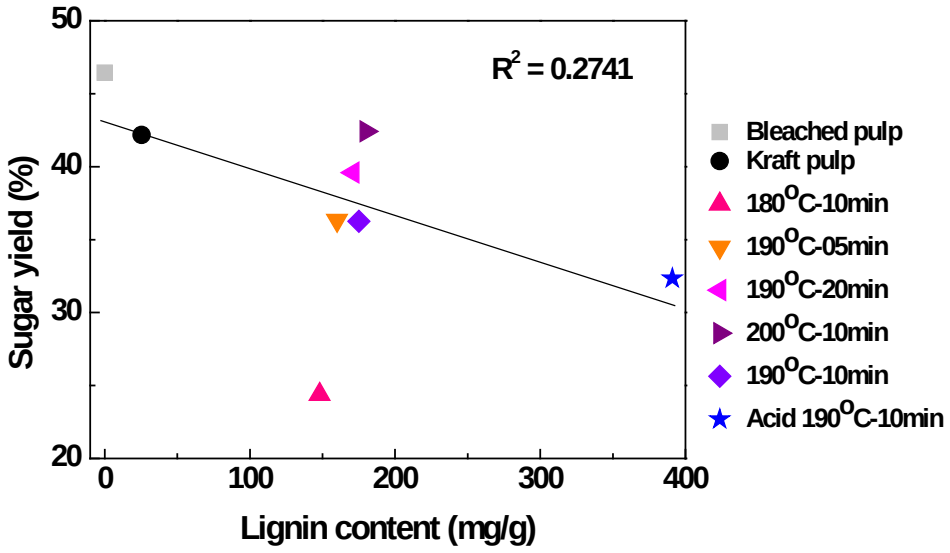

Figure 3. Correlation between pulp lignin contents and sugar yield during enzyme hydrolysis.

Effects of lignin contents on sugar yield during enzyme hydrolysis were shown by Figure 3. The trend was clearly shown, although the correlation was not clear. If the 180°C-10min pulp were removed, the correlation would be more obvious. There was almost no correlation for lignin contents and sugar yield among all alkali steam-exploded samples. The lowest sugar yield of 180°C-10min pulp suggested that other factors, like fiber dimensions, might also play important roles during enzyme hydrolysis. Since the mechanical separation of 180°C-10min pulp during alkali steam explosion should be the least.

3.3. Simultaneous saccharification and fermentation (SSF)

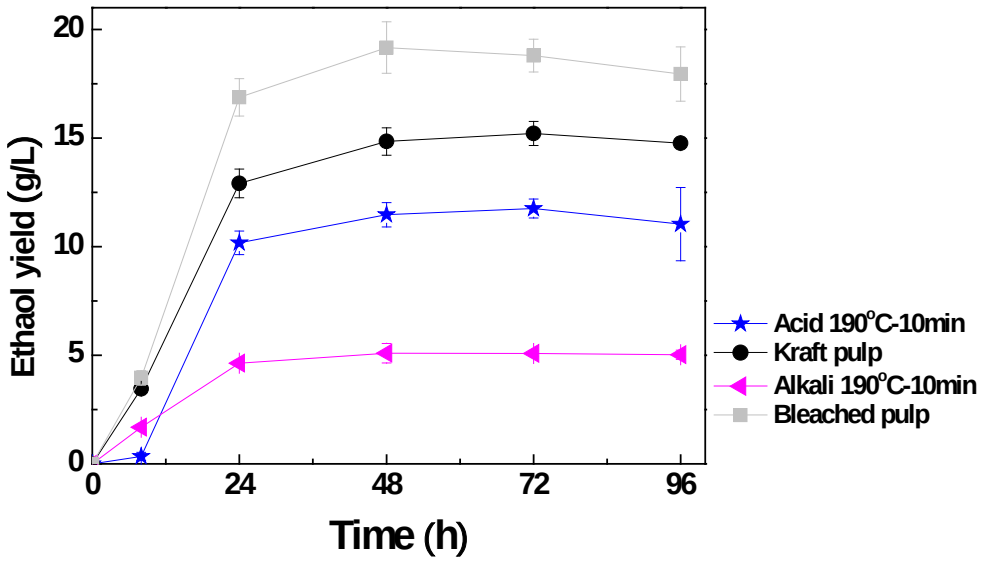

Figure 4. Ethanol yields for acid, alkali (190°C-10min) steam-exploded pulp, kraft and bleached pulps by SSF.

Ethanol yields for acid, alkali steam-exploded pulp, kraft and bleached pulps by SSF were shown by Figure 4. As expected, the ethanol yields of bleached and kraft pulps were higher than the values of acid and alkaline (190°C-10min) steam exploded pulps. Although the lignin content of alkaline 190°C-10min pulp was lower than the value of acid steam exploded pulps, melted lignin in alkali conditions might further hamper enzyme hydrolysis and fermentation.

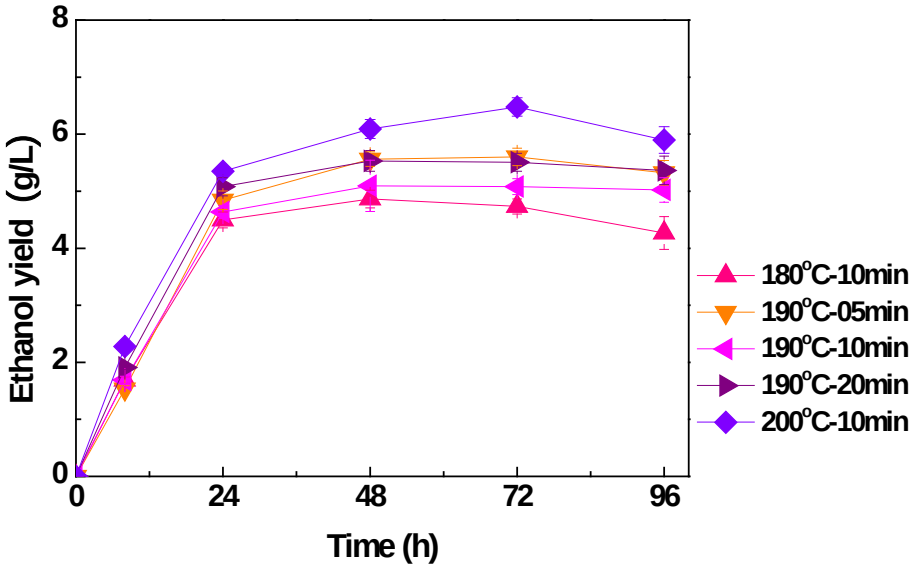

Figure 5. Ethanol yields for five alkali steam-exploded pulps by SSF.

Ethanol yields for five alkali steam-exploded pulps by SSF were shown by Figure 5. The yields increased steadily for the first 24 hours; then the optimal yields were reached after the next 48 hours. The yield from 200 °C-10min pulp was the most, and the yield from 180 °C-10min pulp was the least. With the respect of results from Table 1, lignin contents were not the deciding factor for the above observation.

3.4. Estimated of ethanol yields from bamboo in Taiwan

The bamboo covers 152,300 ha, with overall volume of 535,000 m^3 in Taiwan [1]. Its mass growth were estimated at 10~25 %. Assuming 160,000 m^3 (80,000 ton) of bamboo were harvested annually, Table 2 lists annual ethanol production from bamboo estimated by SSF following different pretreatments.

Table 2. Annual ethanol production from bamboo estimated by SSF following different pretreatments.

	Pretreatment yield (%)	Ethanol yield (g EtOH / g pulp)	Raw material to ethanol (%)	Estimate yield (10^4 tons/Yr)
Acid	57	0.23	13.40	1.07
180°C -10 min	83	0.10	8.07	0.64
190°C-05 min	80	0.11	8.96	0.72
190°C-10 min	76	0.10	7.73	0.61
190°C-20 min	63	0.11	6.97	0.55
200°C-10 min	58	0.13	7.51	0.60
Kraft pulp	40	0.30	12.16	0.97
Bleached pulp	39.8	0.38	15.25	1.22

3.5. Energy balance estimation

Energy balance estimation for bamboo ethanol, expressed by MJ per liter ethanol, were listed in Table 3. Energy consumption analyses for production of fuel ethanol from lignocellulosic biomass [6] and pulp/paper processing [7] were followed by this study. Table 3 showed that the net energy gains could be achieved for the processes with greater ethanol yields: acid steam explosion and fully bleached pulps. But net energy gains must include the utilization for combustion of the fermented waste, lignin.

Table 3. Energy balance estimation for bamboo ethanol (MJ per liter ethanol produced)

Process	Energy Input					Energy Output		Net
	Stock preparation	Pretreatment	SSF	Distillation, dehydration, purification	Total input	Lignin power	Ethanol	Energy gain
Acid explo.	2.483	35.16	13.93	13.7	65.27	48.7	21.2	4.62
180 ^{o}C -10 min	4.124	60.84	15.62	28	108.6	60.9	21.2	-26.49
190 ^{o}C -05 min	3.714	52.80	15.43	27.4	99.54	60.1	21.2	-17.33
Bleached pulp	2.182	34.64	11.73	11	59.55	40.6	21.2	2.24

4. Conclusions

Biomass derived by photosynthesis has strong potentials from bioethanol production. The present study demonstrated bamboo in Taiwan was a source couldn't be ignored for bioethanol production. Bamboos are some of the fastest growing plants in the world. Planned harvesting for will maximize its carbon sequestration potential without ecological damage. As much as 10,700 tons of bioethanols could be produced annually by acidic steam explosion.

References

[1] Taiwan Forestry Bureau, The Third Survey of Forest Resources and Land Use in Taiwan, Forestry Bureau of Council of Agriculture Executive Yuan, Taiwan, R.O.C., 1995.

[2] F. Kobayashi, H. Take, C. Asada and Y. Nakamura, Methane production from steam-exploded bamboo. Journal of bioscience and bioengineering 97(6), 2004, pp. 426-428.

[3] M. Takagi, S. Abe, S. Suzuki, G.H. Emert and N. Yata, A method for production of alcohol directly from cellulose using cellulase and yeast, In: Ghose, T.K. (Ed.), Proceedings of Bioconversion of cellulosic substances into energy, chemicals and microbial protein. I.I.T., New Delhi, 1977, pp. 551–571.

[4] C. Wyman and N. Hinman, Ethanol: fundamentals of production from renewable feedstocks and use as a transportation fuel. Applied Biochemistry and Biotechnology 24-25, 1988, pp735–742.

[5] CH Ko, ZP Lin, J Tu, CH Tsai, CC Liu, HT Chen, TP Wang, Xylanase production by Paenibacillus campinasensis BL11 and its pretreatment of hardwood kraft pulp bleaching, Int Biodeterior Biodegrad 64, 2010, pp13-19.

[6] C. A. Cardona and T. Sanchez, Energy consumption analysis of integrated flowsheets for production of fuel ethanol from lignocellulosic biomass. Energy 31(13), 2006, pp 2447-2459.

[7] M. Ruth, Jr T. Harrington, Dynamics of material and energy use in US pulp and paper manufacturing, Journal of Industrial Ecology 1(3), 1997, pp147-168.

Production of microalgae biomass and biohydrogen in solar bioreactors

Rodrigo Patiño[1,*], Daniel Robledo, Julia S. Martín del Campo

[1] *Departamento de Física Aplicada - Cinvestav, Mérida, México*
[2] *Departamento de Recursos del Mar - Cinvestav, Mérida, México*
** Corresponding author. Tel: +52 999 9429438, Fax: +52 999 9812917, E-mail: rtarkus@mda.cinvestav.mx*

Abstract: Only water hydrolysis with renewable energies is a sustainable process for hydrogen production. Biohydrogen production is an interesting alternative that is being explored at the scientific level. The microalgae *Chlamydomonas reinhardtii* has been extensively studied and used as a model for the photo-production of H_2. The aim of this proposal is to develop a sustainable bioprocess for the production of H_2 from *C. reinhardtii* and just preliminary results are shown here. For the first step, solar bioreactors have been tested. The biomass is recovered and suspended in another culture media with restricted concentrations of sulphur. The culture is maintained in a closed photobioreactor with magnetic stirring and 24-h illumination with fluorescent lamps. Hydrogen is produced continuously reaching maximal durations of about 20 days. Solar light should be tested in order to avoid energy requirements from artificial illumination during hydrogen production. Coupling the production system to a hybrid electric station, the process would be more sustainable. However, a lot of research must be developed before this technology would allow scale the hydrogen production to a pilot plant in order to be used in rural communities as a source of energy and as an alternative economic activity.

Keywords: *Microalgae, Chlamydomonas reinhardti, Biohydrogen, Photobioreactor, Sustainability*

1. Introduction

At this moment, none of the sustainable ways to produce energy can completely replace fossil fuels [1]. Nuclear and hydroelectric processes have been proposed some decades ago to solve some energetic demands, but they are controversial regarding sustainability. Alternatively, solar and wind systems are starting to offer technologic solutions at different energy consumption levels. In addition, biofuels are intended to slowly replace fossil fuels, but our knowledge still requires an improvement in the massive methods to produce them. On the other hand, hydrogen (H_2) has been proposed as an alternative fuel with a number of advantages [2]. Being a gas, molecular hydrogen is an attractive substance since it can be transformed to mechanical, thermal or electrical energies involving free-carbon processes. A clean combustion is possible with hydrogen, which involves environmental advantages over the common fossil fuels and even the biofuels. Moreover, future technologies for nuclear fusion could transform hydrogen to clean energy, emulating the processes in the Sun and the other stars.

Hydrogen is the most abundant element in the Universe; in the Earth, water and organic matter include hydrogen as a part of their composition [2]. Nevertheless, molecular hydrogen is not present in Nature and all its commercial production is not only more expensive than fossil fuels but also produce more pollution [3-5]. More than 90 % of the hydrogen production in the world depends on carbon compounds, principally fossil fuels, and its use as energy carrier is only justified in some applications as fuel for spaceships or demonstrative buses or cars. Renewable energies are being proposed to produce sustainable hydrogen in commercial processes: electrolysis units coupled to wind turbines, photovoltaic modules or hydropower systems [6]. Nevertheless, biohydrogen production is also an interesting alternative that is being explored at the scientific level, focusing on three microbial systems: bacterial fermentation, nitrogen fixation in photosynthetic cyanobacteria and photoproduction in green microalgae [7]. Another interesting bioprocess is the use of *in vitro* enzymatic cocktails [8].

The microalgae *Chlamydomonas reinhardtii* have been extensively studied and used as a model for the photo-production of H_2. Light is used through the photosynthesis as the primary energy source for biomass and bio-hydrogen production. The biomass is normally produced in aerobic systems through the well-known photosynthetic pathway. However, after a period of anaerobiosis, the electrons normally generated in the photosystem II are redirected to produce molecular hydrogen in a step catalyzed by a Fe-hydrogenase. Both the genetic expression of the enzyme and its activity are importantly inhibited with small quantities of oxygen [9]. However, only experiments with temperature control and fluorescent illumination are reported for these processes, resting sustainability to the hydrogen production.

The aim of this work is to develop a sustainable bioprocess to produce H_2 from *C. reinhardtii*. The process is separated in three steps: (i) aerobic cultures for biomass production, (ii) recuperation of the biomass and (iii) anaerobic systems for biohydrogen production. The production of biomass and biohydrogen should be performed in bioreactors with natural solar illumination and at environmental temperature. The integration of these steps with a hybrid electric station is planned in order to add sustainability to the process. However, it should be noted that only preliminary results are shown in this work, since more research is being performed before proposing energy balances or economical feasibility.

2. Methodology

2.1. Algal cultures

The strain CC-124 of *Chlamydomonas reinhardtii* (Chlamydomonas Center, USA) was used in this work. Three culture media have been tested for biomass production [10]: (i) Sueoka's High Salt (SHS) medium, as recommended by the strain provider, (ii) Tris-Acetate-Phosphate (TAP) medium, commonly used for hydrogen bioproduction [9], and (iii) a modified TAP medium without acetates (TP) in order to avoid bacterial contaminations during algae growth. The media were sterilized by vacuum filtration (Whatman, GFC, 0.2 μm) but the containers were only washed with household bleach (commercial sodium hypochlorite solution) and distilled water. Stocks are maintained with the SHS medium in Roux bottles with 24-h fluorescent illumination. Pre-cultures for inoculation in reactors were prepared with the corresponding medium during three to five days in Roux cultures with continuous artificial illumination and with bubbling from small air pumps.

2.2. Biomass characterization

Cellular counts were performed with an optical microscope (Olympus, CH-2) and correlated with optical density and with dry weight. Optical density was measured through a portable spectrophotometer (StellarNet, EPP2000) at 640 nm of wavelength. Dry weight was obtained with vacuum filtration of 10 ml of culture sample through membranes (Whatman, GFC 0.2 μm) and the same volume of culture medium to wash. Before and after filtration, the membranes were dried in a microwave oven (15 min, 10 W) and stabilized in a dissicator for 30 min in order to quantify the mass with an analytical balance (Ohaus Adventurer, ARx). Chlorophyll *a* was quantified directly on cellular samples with a fluorometer (Varian, CARY Eclipse), with an excitation wavelength at 432 nm and an emission wavelength at 668 nm. Calibration was previously performed with stock chlorophyll solutions at different concentrations.

2.3. Biomass production

2.3.1. Reactors

Two designs were tested for production of biomass in solar photobioreactors (Fig. 1). Vertical tubular reactors (VTR) were made on acrylic tubes (wall-thick: 25 mm, height: 90 cm) of different internal diameters: 70, 95 and 120 mm. The low part of the tubes was sealed with acrylic, allowing the air inlet through small holes (~1 mm i.d.). The operation volumes of the VTR were 3, 6 and 9 L, respectively. A flat panel reactor (FPR) was also made with acrylic walls (thick: 50 mm), and dimensions of 50 cm length, 50 cm height and 10 cm thick. The operation volume of the FPR was 20 L with air inlet in the low part of the box through porous stones. Both VTR and FPR have acrylic taps with an air outlet. The air inlet comes from a blower and it is passed through a humidifier before going into the reactors; air flux is controlled at 1 $L \cdot min^{-1}$ per liter of culture. Natural illumination was used, with solar radiation marked by days and nights. At least 14 batch experiments were performed with the VTR and two with the FPR.

Fig 1. Pictures showing two different types of solar photobioreactors for the production of microalgal biomass at external conditions: flat panel reactor and vertical tube reactors.

2.3.2. Off-line and on-line monitoring

Daily samples were analyzed with optical density, dry weight and fluorometry. Dry weight was used to evaluate the biomass growth kinetics and the maximal cellular density. Automatic measurements of temperature and illuminance were performed with programmable data loggers (Onset, HOBO Pendant UA-002-64). In addition, on-line monitoring of the pH and pO_2 was possible in the FPR with the corresponding probes (Sensorex) connected to a power supply and an interface (National Instruments, cDAQ-1972 chassis, NI9203 and NI9205 modules). The interface is connected to a personal computer in which data are automatically registered with the Signal Express (National Instruments) software.

2.3.3. Batch algae growth experiments

A number of 12 experiments were performed in the VTR with different conditions: two culture media (SHS and TP), three tube diameters (70, 95 and 120 mm) and two annual seasons (Winter and Spring). Later, one experiment was performed in two VTR with the same diameter (95 mm) and the same meteorological conditions, but with two culture media (SHS and TP). Finally, one experiment more was performed with three VTR at the same conditions (SHS, 95 mm) in order to verify the reproducibility of the growth. Two more experiments were performed with the FPR and the HSS medium at similar meteorological conditions. Other experiments are planned with different concentrations of CO_2 mixed with air.

2.4. Biomass separation

In order to change the culture medium of the microalgae, two low-cost processes have been tested. A separation column with packed cotton wool showed good results with the retention of the biomass. A number of packing densities and designs were essayed in order to optimize the biomass separation. After being washed with the new medium TAP-S (TAP with minimal concentrations of sulphur), the cotton wool is pressed in order to recover the biomass, which is re-suspended in the TAP-S medium at a defined cellular density. The second process uses the same VTR in which the biomass is grown. Polymeric hydrogel is added to the culture with air bubbling and the medium is absorbed and retained in the hydrogel structure. The concentrated culture is re-suspended in the TAP-S medium at a defined cellular density. The hydrogel does not absorb algal cells, it can be dried in a solar system and reused for subsequent culture absorption processes.

2.5. Biohydrogen production

Just preliminary experiments have been performed to test the production of hydrogen from microalgae in VTR with 24-h fluorescent illumination (~100 μE) in a laboratory with controlled temperature (298-300 K) and constant magnetic stirring (Fig. 2). The VTR are made in acrylic tubes (70 mm i.d.) as described previously, with a high of 30 cm and an operation volume of 1 L. The base of the tube is sealed in acrylic and the tap is made in Teflon with an o-ring to seal the system and with a gas outlet. This outlet is connected to a hydrogen PEM-FC (Polymeric Electrochemical Membrane Fuel Cell), which uses oxygen from air to produce water and electricity. The pH and the voltage of the fuel cell are registered on-line with the interface described in section *2.3.2.* and related with the production of hydrogen in the system. The temperature and the illuminance in the reactor are automatically registered with the data logger described in the same section. At the moment, four experiments have been performed with different biomass concentrations: 48, 71, 164 and 248 mg/L. Experiments with light/dark cycles and with natural solar illumination are planned.

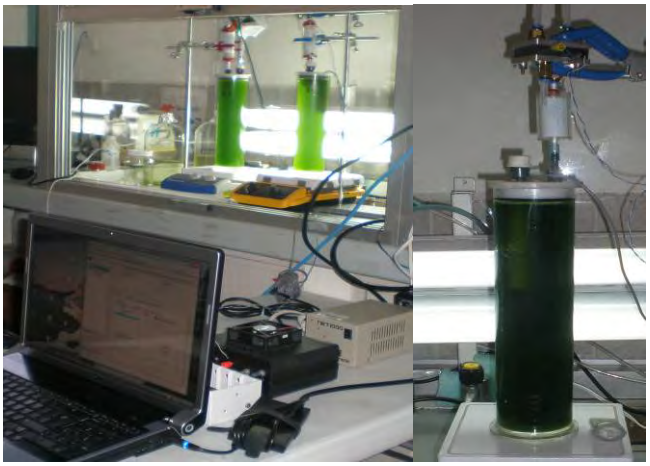

Fig. 2. Pictures showing the reactors for biohydrogen production with microalgae under laboratory conditions.

2.6. Hybrid electric station

The electrical requirements to perform the three processes, basically for air bubbling in the biomass production and separation, and for mixing in the biohydrogen production, may be obtained from a hybrid electric station. At the moment (Fig. 3), four polycrystalline photovoltaic panels (Yingli Solar, 110 W) and one wind turbine (Whisper 200, 1000 W) are installed with four acid lead batteries (Rolls Surette, 6 V) and an electrical inverter (Xantrex, DR1524) from DC (24 V) to AC (120 V). This installation is placed in the Cinvestav Marine

Station at Telchac Port, Yucatan (5 m AMSL, LAT: 21º20'28" N, LONG: 89º18'21" W). Electricity production from the hybrid station will be correlated with the meteorological conditions. The meteorological system (Davis, Vantage Pro 2 Plus) is installed in the Marine Station and has an automatic data registration every 10 min. Wind speed and orientation, solar radiation and temperature are some of the data which are obtained. The energetic fluxes in the hybrid plant will be registered in real time through and interface (National Instruments, Field Point).

Fig. 3. Pictures showing the hybrid electric station installed in Telchac Port, Yucatan, Mexico

3. Results

A typical biomass growth curve for the microalgae in the solar photobioreactors is shown in Fig. 4. The kinetics of the growth does not fit the Monod model; actually, the Gompertz model fits better with the experimental results (Fig. 5) [11,12]. In Table 1, 12 experiments in the VTR are compared in relation with the maximal cellular density, the specific growth rate and the residence time as a function of the medium (SHS or TP), the reactor diameter (70, 95 or 120 mm) and the annual season (winter or spring). The specific growth rate was computed as the slope from a linear correlation with the corresponding Gompertz equation as a function of the time; the lineal correlation had always a value $r^2 > 0.9$. The residence time was calculated as the surface below the curve in a graphic with the inverse of the instant growth rate *versus* the biomass concentration for everyday during the experiments [13]. Experiments 1 to 6 were performed during the Winter, the coolest season in Yucatan (Mexico), with an average temperature of 298 K and illuminance average values below 10 klux. In contrast, the experiments 7 to 12 were performed during the Spring, the hottest period in the year, with an average temperature of 303 K and illuminance averages values over 10 klux. Similar results were obtained in other experiments with both VTR and FPR. In addition, pH and pO_2 do not change importantly during the biomass growth.

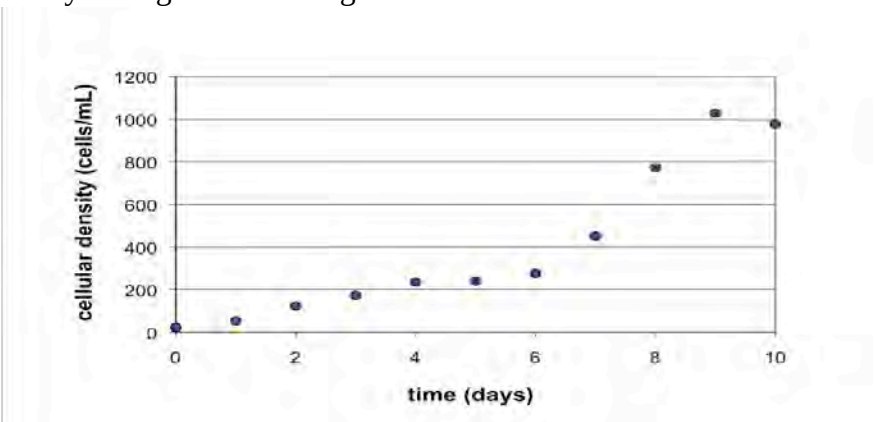

Fig. 4. Typical biomass growth of the microalgae in solar photobioreactors as followed by optical density.

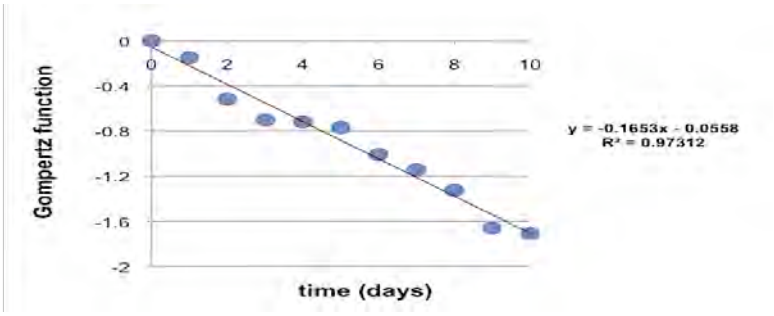

Fig. 5. Fit of the Gompertz model to the experimental cellular growth followed with dry biomass.

Table 1. The compared results for 12 experiments in vertical tubular reactors with three different diameters (d), two culture media and two annual seasons. Maximal cellular density as dry weight (D), specific growth rate (μ) and residence time (T) are reported.

Experiment number	Annual season	Culture medium	d (mm)	D (g/L) ±0.01	μ (day^{-1})	T (day) ±1.0
1	Winter	SHS	70	0.63	0.22 ± 0.02	8.5
2	Winter	SHS	95	0.64	0.30 ± 0.02	7.8
3	Winter	SHS	120	0.60	0.21 ± 0.01	9.8
4	Winter	TP	70	0.31	0.42 ± 0.05	5.2
5	Winter	TP	95	0.47	0.49 ± 0.03	3.4
6	Winter	TP	120	0.45	0.41 ± 0.04	4.1
7	Spring	SHS	70	0.34	0.09 ± 0.01	9.2
8	Spring	SHS	95	0.52	0.17 ± 0.01	7.2
9	Spring	SHS	120	0.44	0.16 ± 0.01	8.0
10	Spring	TP	70	0.33	0.49 ± 0.03	5.0
11	Spring	TP	95	0.39	0.48 ± 0.01	3.8
12	Spring	TP	120	0.35	0.41 ± 0.03	4.5

For the hydrogen production, the calibration of the fuel cell is being performed, where the voltage change is related with the hydrogen produced by the microalgae. In a graphic of measured voltage *versus* time, the surface below the curve is proportional to the total hydrogen production in the experiments. It is possible to see some preliminary results in Table 2 at different initial biomass concentrations. In general, the hydrogen production rate grows gradually during the first 30 hours and then it is maintained more or less constant for a certain period before going down to the base line. The length of this stationary production is directly related with the concentration of the initial biomass concentration with a maximal duration of 20 days for the biggest value of biomass. However, the production rate does not change between 71 and 439 mg/L of initial biomass concentration. The pH neither does change importantly during the experiments. However, the culture illuminances inside the reactor were found to decrease with time, and temperatures were found to be always lower than room temperature, principally at the beginning of the experiments when the biomass concentration is minimal.

Table 2. Biohydrogen production as a function of initial biomass concentration, at T = 298 K and atmospheric pressure. The maximal hydrogen production rate (ΔV_{max}) and the total hydrogen production (THP) are reported. The experiment with initial biomass concentration of 164 mg/L was cut before finishing the hydrogen production.

Initial biomass concentration (mg/L)	Final biomass concentration (mg/L)	ΔV_{max} (mV)	THP (V.h)
48	79	134	10,166
71	219	210	195,524
164	-	197	-
349	835	220	614,030

4. Discussion

The maximal concentration biomass has been obtained after 6 to 12 days of external cultures in solar photobioreactors. The VTR are easy to construct and manipulate, allowing to compare different culture conditions; they are very useful for research work. In general, for the experiments reported in Table 1, the reactor with 95 mm of internal diameter show a better performance for the production of biomass. The meteorological conditions influence significantly on this production, being Winter much better than Spring. Finally, it is possible to see that the TP medium gives the biggest values of the specific growth rate and the lowest values of the residence time, while the SHS medium gives the biggest cellular yields. These results show that the composition in the medium is important to regulate both the kinetics and the maximal biomass production. In particular, the SHS medium has important limitations of calcium and manganese, while the phosphate concentration is extremely low in the TP medium.

On the other hand, the FPR allow bigger production volumes and can soften temperature variations or extreme illuminances. A previous work reports that the raise of the temperature inside the FPR can be diminished when the biggest walls of the reactor are not exposed directly to solar radiation [11]. In general, both VTR and FPR show similar results for the biomass growth. This biomass production must be increased in order to find the economical feasibility and the sustainability of the process. This can be reached improving different operation conditions. By instance, a better system for gas/liquid interchanges, a different air bubbling flux or adding carbon dioxide to the air, could increase the yield of the production [12]. Additionally, it is necessary to reduce costs of the culture media and new compositions should be tested using alternative sources as wastewaters. With respect to the reactors, cheaper materials, as plastic bags, should be used instead of acrylic. It was also found that carbon dioxide in the air is minimally used when bubbled and the height of the reactors may be considerably increased. It is also important to test with a continuous or semi-continuous operation instead of the batch reactors.

For the biomass separation, the filtration with cotton wool is technically complicated and the risk of contamination is important. The medium absorption with hydrogel is much easier and cleaner, although the kinetics of the process should be standardized. The recycling of both hydrogel and medium is important to gain sustainability in the process. In relation with the biohydrogen production, much more work should be performed. It is very important to calibrate the performance of the fuel cell in order to have a true representation of the hydrogen production in the systems. The influence of the initial biomass concentration in the hydrogen production should be completely specified, as well the influence of the illuminance and the light/dark cycles, in order to scale the process in a solar photobioreactor.

5. Conclusions

Only partial results are shown here and more work is being performed to complete the project. It has been demonstrated that *Chlamydomonas reinhardtii* can be growth at external conditions in Yucatan (Mexico) using solar photobioreactors, both VTR and FPR. The production of biohydrogen in external reactors with solar illumination and no control of the temperature must be tested. The integration of all the processes with the hybrid electric station would allow knowing the feasibility of the hydrogen production as a sustainable process.

References

[1] B. Sorensen, Renewable energy; its physics, engineering, environmental impacts, economics & planning. Elsevier, 3 ed, 2004, 928 pp.

[2] B. Sorensen, Hydrogen and fuel cells: emerging technologies and applications. Elsevier, 450 pp.

[3] L. Barelli, G. Bidini, F. Gallorini, and S. Servili, Hydrogen production through sorption-enhanced steam methane reforming and membrane technology: A review, Energy 33, 2008, pp. 554-570.

[4] M. Balat, Potential importance of hydrogen as a future solution to environmental and transportation problems, International Journal of Hydrogen Energy 33, 2008, pp. 4013-4029.

[5] M. Balat, and M. Balat, Political, economic and environmental impacts of biomass-based hydrogen, International Journal of Hydrogen Energy 34, 2009, pp. 3589-3603.

[6] P. A. Pilavachi, A. I. Chatzipanagi, and A.I. Spyropoulou, Evaluation of hydrogen production methods using the Analytical Hierarchy Process, International Journal of Hydrogen Energy 34, 2009, pp. 5294-5303.

[7] M. L. Ghirardi, A. Dubini, J. Yun, and P. Maness, Photobiological hydrogen-producing systems, Chemical Society Reviews 38, 2009, pp. 52-61.

[8] X. Ye, Y. Wang, R. C. Hopkins, M. W. Adams, V. R. Evans, J. R. Mielenz, and Y.-H. P. Zhang, Spontaneous high-yield production of hydrogen from cellulosic materials and water catalyzed by enzyme cocktails, ChemSusChem 2, 2009, pp. 149-152.

[9] A. Hemschemeier, A. Melis, and T. Happe, Analytical approaches to photobiological hydrogen production in unicellular green algae, Photosynthesis Research 102, 2009, pp. 523-540.

[10] Chlamydomonas Center, Recipes for commonly used culture media, 2010, www.chlamy.org.

[11] P. Castorina, P.P. Delsanto and C. Giot, Classification scheme for phenomenological universalities in growth problems in physics and other sciences, Physical Review Letters 96, 2006, pp. 188701(1-4).

[12] P. Castorina, T.S. Deisboeck, P. Gabriele and C. Giot, Growth laws in cancer: implications in radiotherapy. Radiation Research Society 168, 2007, pp. 349-356.

[13] J.M. Lee. Biochemical engineering, Prentice-Hall, 2001, Chapter 6.

[14] L. Pantí, P. Chávez, D. Robledo and R. Patiño, A solar photobioreactor for the production of byohydrogen from microalgae, Solar Hydrogen and Nanotechnology Proc. of SPIE, 2007, pp. 66500Z1-66500Z9.

[15] H.J. Ryu, K.K. Oh and Y.S. Kim, Optimization of the influential factors fo the improvement of CO_2 utilization efficiency and CO_2 mass transfer rate, Journal of Industrial and Engineering Chemistry 15, 2009, pp.471-475.

Improvement of enzymatic hydrolysis of a marine macro-alga by dilute acid hydrolysis pretreatment

Parviz Yazdani [1*], Keikhosro Karimi [1,2], Mohammad J. Taherzadeh[2]

[1] *Department of Chemical Engineering, Isfahan University of Technology, Isfahan, 84156-83111, Iran*
[2] *School of Engineering, University of Borås, Borås 501 90, Sweden.*
** Corresponding author. Tel: +983113915623, Fax: +983113912677, E-mail: p.yazdani@ce.iut.ac.ir*

Abstract: The marine macro-alga *Nizimuddinia zanardini* was harvested from Persian Gulf to assess its biomass for fermentable sugar production. Hydrolysis of the macro-alga was investigated in two stages to evaluate the conversion of cellulose and hemicelluloses in biomass to corresponding monomeric sugars. The biomass was first subjected to dilute sulfuric acid pretreatments at 121 °C and then to enzymatic saccharification (45°C, pH 4.8) at different retention times. The results showed the ability of the first stage hydrolysis in depolymerization of xylan to xylose with a maximum yield of 64% (based on total xylose content) at 7% (w/w) acid concentration for 60 min. However, the yield of glucose from glucan was relatively low in the acid hydrolysis with a maximum of 14.4% (based on total glucan content) at 7% (w/w) acid concentration for 60 min. Under these conditions, no hydroxymethyl furfural (HMF) produced. Formation of furfural depended on the retention time and acid concentration, whereas the concentration of acetic acid was almost constant at retention times higher than 45 min and acid concentration of 7 %.The solid residuals were then subjected to enzymatic hydrolysis. The maximum yield of glucose from the macro-alga by enzymatic saccharification (45°C, pH 4.8, 24 h), using cellulase and *β*-glucosidase, was 70.2 g/kg (70.2% yield based on total glucan content).

Keywords: *Enzymatic hydrolysis, Dilute-acid hydrolysis, Macro-alga, Pretreatment.*

1. Introduction

Considering the expected decline in production of crude oil within a few years and growing concerns about enhanced global warming, production of non-fossil fuels that can cover the crude oil deficit is desirable. One such sources of energy are biofuels which can be produced by fermentation of sugar by microorganisms. Raw materials for these processes are usually obtained from agricultural products. However, if the biofuel industry is to expand in a near future, it is widely recognized that nonfood resources should be used [1].

The production of ethanol from feedstock, other than agriculture materials, has been developed in recent years and third generation biofuels are considered to be technically viable alternative bioenergy resource that is devoid of the major drawbacks. Marine resources have played an important role in biotechnology, particularly in the past decade. Previous studies of algal biofuel production have largely focused on microalgae [1], although there are several macro-algae which contain intracellular carbohydrates and have a potential for production of biofuels e.g. bioethanol and bio-oil. Nizimuddinia zanardini is among the macro-algae which contains appreciating amounts of cellulose. However, cellulose is a high molecular weight crystalline polymer which is highly stable and recalcitrant to enzymatic hydrolysis. Therefore, a pretreatment process is typically necessary for efficient conversion of cellulose to sugars. Dilute-acid treatment has been successfully developed for pretreatment of cellulosic materials. The pretreatment can enhance the carbohydrates available for enzymatic hydrolysis and fermentation. Aqueous pre-treatment at elevated temperatures result in an insoluble cellulose-rich fraction and a soluble fraction, containing hemicelluloses sugars and degradation products. It results in enrichment of the hard to digest materials in hydrolysate, and improves the yield of ethanol from the substrate [2].

2. Methodology

2.1. Nizimuddinia zanardini

Nizimuddinia zanardini used in all the experiments which was obtained from Persian Gulf (Chabahar Coastline, Iran). It was dried at 45°C for 24 hour and milled in a hammer mill to pass through a 1.27 mm screen. The milled macro-alga was stored at -5°C.

2.2. Hydrolysis

Prior to the hydrolysis experiments, 5 gram of the biomass was soaked in 100 ml dilute H_2S0_4 (7%, 3.5%, and 0.5%w/w) and pretreated in an autoclave at 121°C for different retention times (30, 45, and 60 min). It was then cooled and the liquor was drained. The dilute acid treated solid materials were then subjected to enzymatic hydrolysis using commercial cellulase (15 FPU/g dry biomass) and β-glucosidase (45 IU/g dry biomass) in 75 ml citrate buffer (PH=4.8) for 24 and 48 hours.

2.3. Analysis

All the liquids were analyzed by high-performance liquid chromatography (HPLC), equipped with UV/VIS and RI detectors (Jasco International Co., Tokyo, Japan). Glucose and xylose were determined by an Supelcogel Pb HPLC column at 80 °C. Deionized water was used as eluent at a flow rate of 0.6 ml/min. Acetic acid, furfural, and HMF were analyzed on an Aminex HPX-87H column (Bio-Rad) at 60 °C with 0.6 ml/min eluent of 0.005M sulfuric acid. Concentrations of glucose, xylose, and acetic acid were determined by RI detector, while furfural and HMF were quantified on UV chromatograms at 210 nm.
The macro-alga was also analyzed for glucan and xylan following the procedure described in NREL Chemical Analysis & Testing Procedure [3] and the results are summarized in (Table 1).

Table 1. Composition of Nizimuddinia zanardini.

Carbohydrate	(g/Kg dry substrate)
Glucan	100
Xylan	30
Galactan	70
Mannitol	150
Fructosan	50
Arabinan	15

3. Results and discussion

There are a few research has been performed on the pretreatment and enzymatic saccharification of marine macro-algae [4]. During pretreatment, it is possible to solubilize the hemicellulose to fermentable sugars [5]. However, depending on the temperature, the pretreatment usually produces sugar degradation products such as furfural and HMF, which known to be sever inhibitors for fermentative microorganisms [6,7]. Dilute acid pretreatment can be used for improvement of enzymatic saccharification beside the hydrolysis of hemicelluloses.

Dilute acid hydrolysis of macro-alga was performed at different acid concentration of 7, 3.5, and 0.5% at 120 °C. The most important results of the acid hydrolysis were summarized in Figs. 1-6.

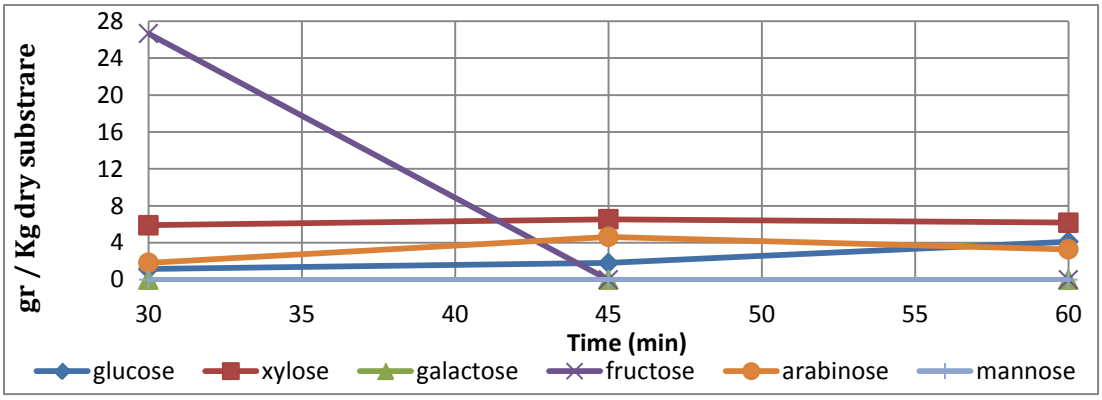

Fig. 1. The effect of retention time on the yields of glucose, xylose, galactose, fructose, arabinose and mannose production with 0.5% H_2SO_4.

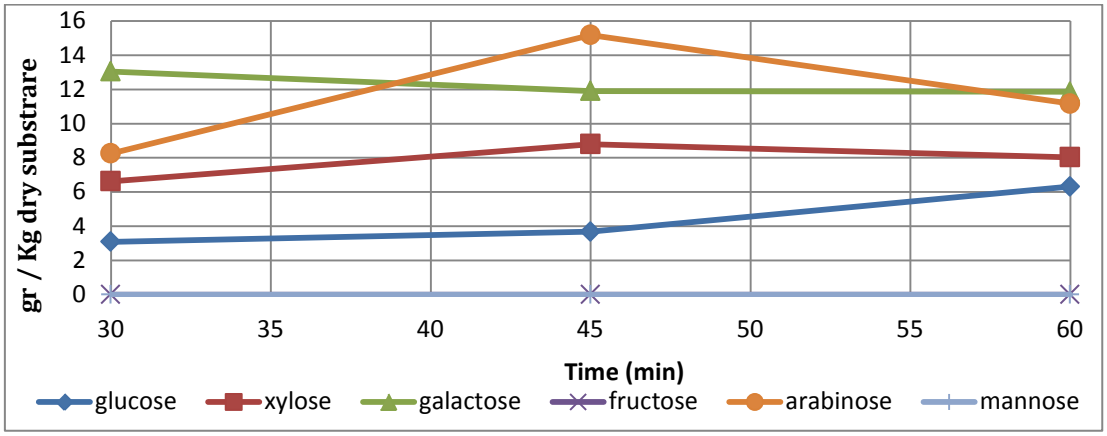

Fig.2. The effect of retention time on the yields of glucose, xylose, galactose, fructose, arabinose, and mannose production with 3.5% H_2SO_4.

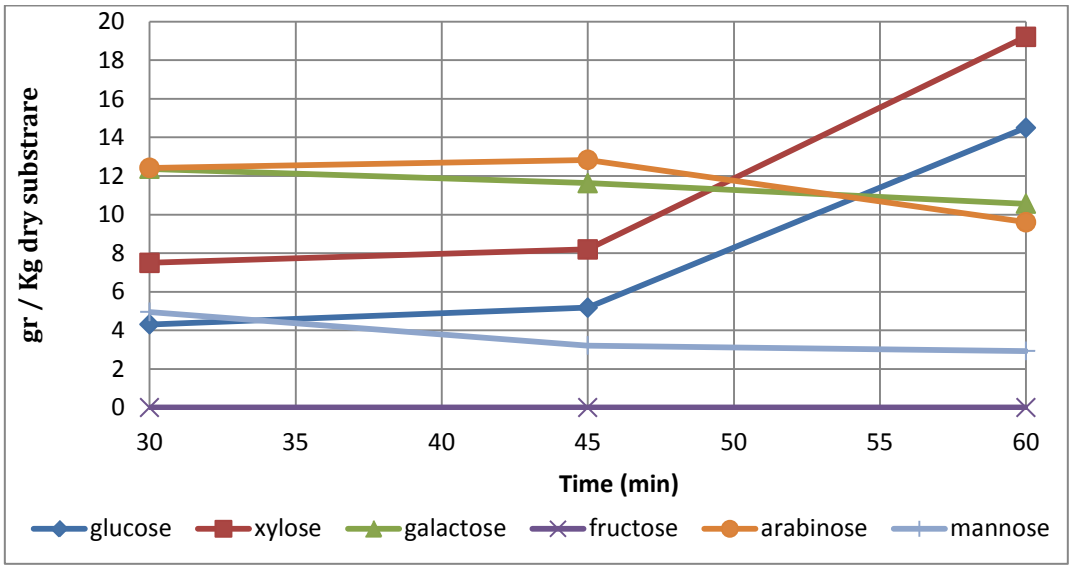

Fig. 3. The effect of retention time on the yields of glucose, xylose, galactose, fructose, arabinose and mannose production with 7% H_2SO_4.

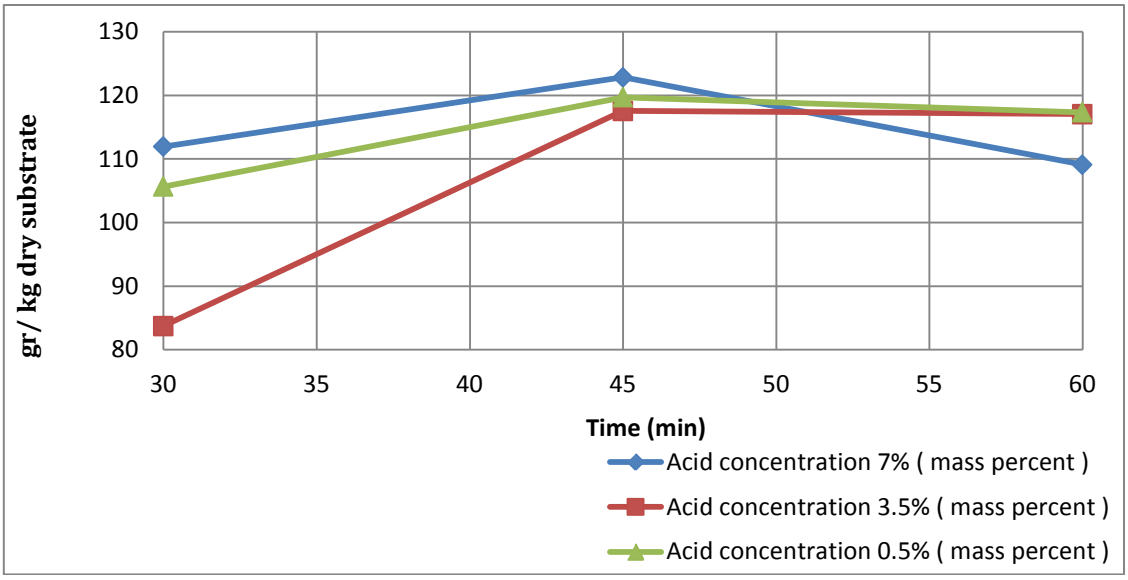

Fig. 4. The effect of retention time on the yields of mannitol by 7%, 3.5% and 0.5% H_2SO_4 .

A comparison of the maximum yields of xylose and glucose (fig. 3) with the xylan and glucan content of the macro-alga (Table. 1) showed the ability of the first stage hydrolysis to depolymerize xylan and glucan to maximum yields of 64% and 14.7% of the theoretical xylan and glucan contents, respectively. Theoretical xylose and glucose yields were calculated based on the total content of xylan and glucan in the macro-alga.

Increasing the retention time of hydrolysis from 30 to 45 min showed negligible effects on formation of glucose, but the yields of xylose, mannitol, galactose, furfural, and acetic acid were significantly affected (Fig. 1-6). It indicated that 30 min hydrolysis at 0.5-7% acid concentration is not enough to depolymerize the hemicelluloses of the biomass. On the other hand, since the concentration of acetic acid reached the maximum concentration (31.8 g/kg) in 60 min hydrolysis at 7% acid concentration, it in dicated complete hydrolysis of the hemicellulose within 60 min, and the optimum retention time should be sometimes between 45 and 60 min (Fig. 5).

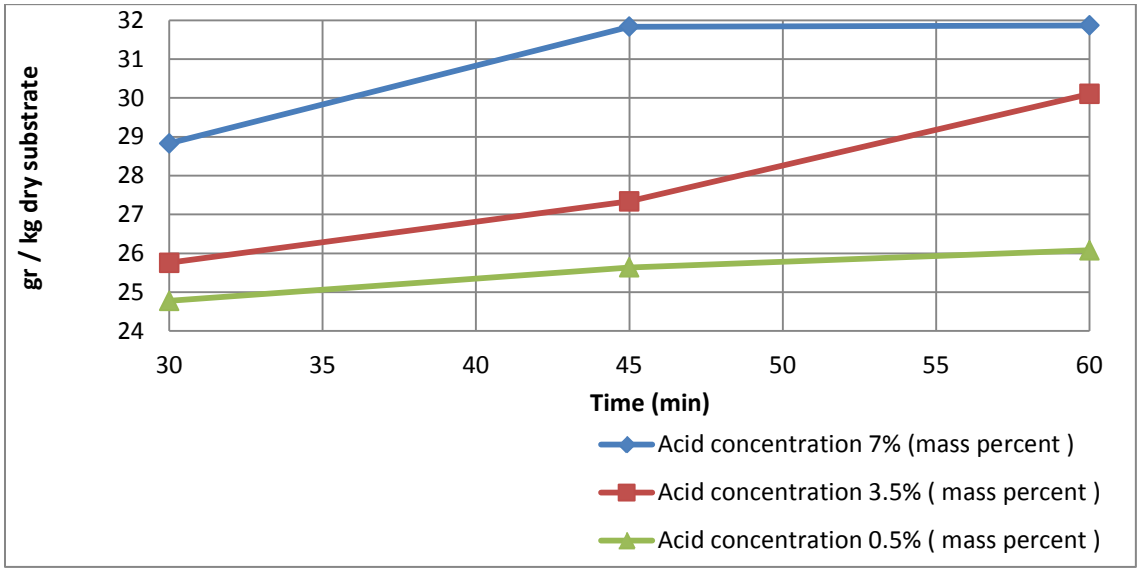

Fig. 5. The effect of retention time on the yields of acetic acid production with 7% , 3.5% and 0.5% H_2SO_4.

Furans, i.e. furfural and hydroxymethyl furfural (HMF), have inhibitory effect on ethanol production yields by fermentation. In this work, maximum yield of furfural was observed at 7% acid concentration and 60 min retention time, while HMF was not detected during all experiments (Fig. 6).

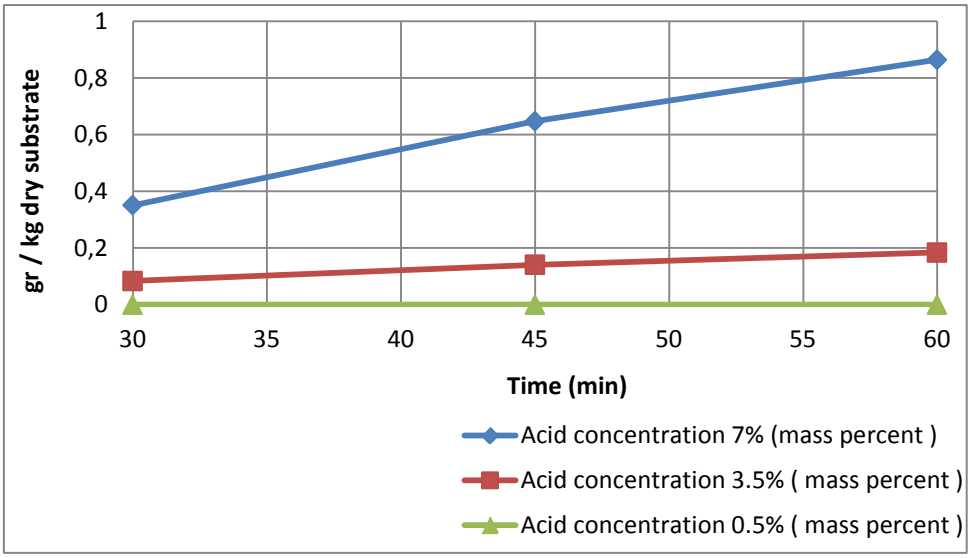

Fig. 6. The effect of retention time on the yield of furfural formation with 7%, 3.5% and 0.5% H_2SO_4.

At the second stage hydrolysis, the residual solids (Table. 2) subjected to enzymatic scarification by cellulase and β-glucosidase.

Table 2. The residual solids remaining after dilute acid hydrolysis.

Test case	Mass of substrate (g)
7%, 60 min	0.8043
7%, 45 min	1.2497
7%, 30min	1.2509
3.5%, 60 min	0.8135
3.5%, 45 min	0.9158
3.5%, 30min	1.2326
0.5%, 60 min	1.1850
0.5%, 45 min	1.2627
0.5%, 30min	1.4077

The yield of substrate without pretreatment for glucose after 24 hour incubation was only 2.98% of the dry substrate (Table. 3).

Table 3. Enzymatic hydrolysis results without pretreatment

Sugar	yield (g / kg of dry substrate)
Glucose	29.8
Xylose	10.05
Galactos	4.72
Mannitol	38.4
Mannose	1.0
Fructose	0
Arabinose	3.51

Among the all experiments, pretreatment with 7% sulfuric acid for 45 min and 24 hours enzymatic hydrolysis yielded the highest glucose in the enzymatic hydrolysates (Fig 7).

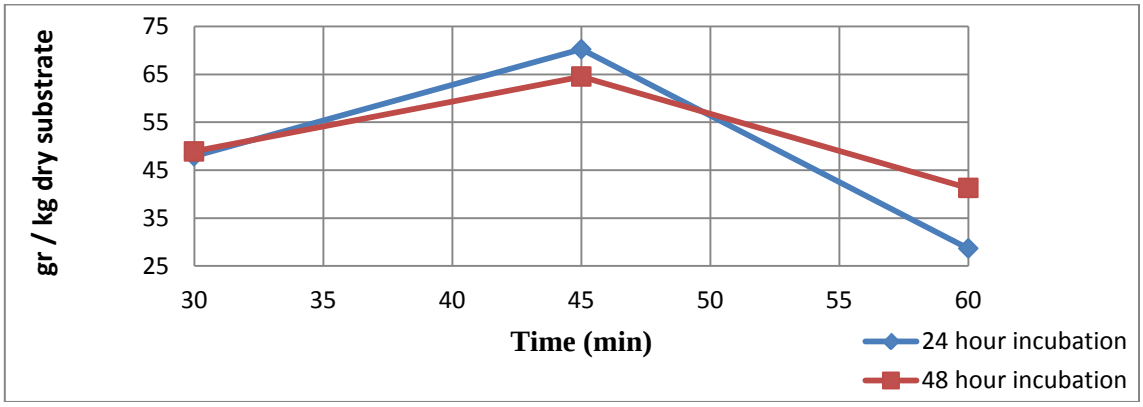

Fig. 7.The effect of retention time on the yields of glucose by enzymatic hydrolysis after pretreatment with 7% dilute acid for 30, 45, 60 min retention times.

4. Conclusions

It is possible to solubilize the hemicellulose to fermentable sugars by dilute acid hydrolysis.
The results of this study indicated that 7% (w/w) H_2SO_4 is a promising pretreatment in order to obtain high yields of sugars without sugar degradation products formation.
It is possible to obtain a saccharification yield of 70.2% (70.2 g/kg), based on the glucose content, by using 7% (w/w) acid at 120°C for 45 min and saccharification with two commercial enzymes, where the yield was only 29.8% without pretreatment.
The hydrolyzate of 7% (w/w) acid pretreatment at 120°C for 45 min contains mainly mannitol, which can be a suitable source for ethanol production. The hydrolyzates contains very low concentration of fermentation inhibitors.

References

[1] L. Brennan, P. Owende, Biofuels from microalgae—A review of technologies for production, processing, and extractions of biofuels and co-products, Renewable and Sustainable Energy Reviews 14, 2010, pp. 557–577

[2] M J. Taherzade, K. Karimi, Acid-base hydrolysis processes for ethanol from lignocellulosic material: a review, Bioethanol review, 2007, bioresources 2(3), pp. 472-499

[3] R. Ehrman, determination of carbohydrate in biomass by high performance liquid chromatography, Chemical analysis & testing task: NREL, LAP 002; 1996.

[4] X. Wang, X. Liu, G. Wang, Two-stage Hydrolysis of Invasive Algal Feedstock for Ethanol Fermentation, Journal of Integrative Plant Biology, no. doi : 10.1111/j.1744-7909.2010.01024.x.

[5] B. Saha, L. lten, M. Cotta, Y. Wu, Dilute Acid Pretreatment, Enzymatic Saccharification, and Fermentation of Rice Hulls to Ethanol, Biotechnol. Prog, 2005, 21, pp. 816-822

[6] B.Saba, K. Hayashi, Lignocellulose biodegradation and applications in biotechnology, In Lignocellulose Biodegradation, American Chemical Society: Washington, DC, 2004, pp. 2-34.

[7] C. Saha, J. Bothast, Pretreatment and Enzymatic Saccharification of Corn Fiber, Applied Biochemistry and Biotechnology, Vol. 76, 1999,pp. 65-77

Biodiesel from Microalgae as a solution of third world energy crisis

Md.Imran Kais[1,*], Farsad Imtiaz Chowdhury[2], Kazy Fayeen Shahriar[3]

[1] *Square Group,Dhaka,Bangladesh*
[2] *Rahimafrooz,Dhaka,Bangladesh*
[3]*Islamic University of Technology,Gazipur,Bangladesh*
** Corresponding author. Tel: +8801713337499, E-mail: kais@squaregroup.com*

Abstract: The world is heading towards the crisis of petro fuel. The excessive use of petrofuel is causing global warming. Now it is high time to search for alternative fuel source that will be environment friendly. The crisis for energy is more acute in Bangladesh, as there is no petrofuel source but only natural gas, the reserve has also dropped down to an alarming level. Again the global warming is threatening Bangladesh to be climate change victim. So there is no alternative for Bangladesh rather than renewable energy sources. Biofuel from microalgae can be a solution of this problem. Oil from the algae lipid can be turned into biodegradable and carbon neutral Biodiesel. Use of this diesel can reduce air pollution at remarkable level. This study focuses on algae cultivation in Bangladesh. A lab scale production of *Chlorella* and B*otroyococcus braunii* was executed in open pond and bioreactor system. Then diesel was produced by transesterification from collected algae oil. Later data was collected from this experiment. Cost analysis was prepared to get a clear concept of the actual scenario of algae fuel probability. This study indicates high potentiality of algae based fuel to be used in Bangladesh replacing diesel for energy production. It can be a model for any third world country to mitigate the energy crisis with a greener solution.

Keywords: *Transesterification, Biofuel, Microalgae ,Lipid*

1. Introduction

Our world is heading towards a severe dilemma of petrofuel usage for the next decades. The price of petrofuel is hiking up rapidly. On the other hand, the supply of fossil fuel will come to an end by 2050 considering a 5% flat increase in demand. Even though, if we can get, we cannot use those because excessive use of fossil fuel causes CO_2 increase in atmosphere and we are already facing tremendous effect of this, vicious change of climate. With the rapid growth of technology and civilization spreading over the world, from 1955 to 2005 the emission of CO_2 at atmosphere simply got twice from 3 billion tons of Carbon to 6 billion tons of Carbon, which certainly results in temperature increase, sea level hike, deviation of biodiversity and ecological imbalance. Most of the CO_2 emission is caused by USA, China and EU countries, but the high risked counties of the impact of this phenomenon are underdeveloped countries like Bangladesh, where Bangladesh causes less than 0.1 tons of Carbon emission/Person compared to almost 6 tons of Carbon emission/Person of USA. The production of natural gas is 100% domestic and the oil supply totally depends on import in Bangladesh. Major of 1961 MMCFD gas produced locally is consumed for power generation and rapidly growing industries. 96.7% of its 5271 MW power generation depends upon fossil fuels. The requirement of natural gas in Bangladesh is 1.5 times higher than the actual production.

Biodiesel can be a strong and ultimate solution to overcome this problem for Bangladesh. This carbon neutral fuel stops CO_2 increase rate in atmosphere and lowers pressure on fossil fuel. Microalgae are one of the sources of biodiesel that can be a major source of energy for future rather than Soya bean and Sugarcane. Microalgae are rich in lipid which can be used for producing Biodiesel.

The paper studies the probability of algae oil as an alternative of fossil fuel in Bangladesh. In particular, different species of algae were investigated for cultivation in different suitable

process, diesel was produced from algae lipid by transesterification, their fuel and chemical properties were analyzed. Also we analyzed data for productivity, practicality and potentiality to gain a cost benefit analysis for the commercialization of algae oil production in Bangladesh perspective.

2. Methodology

2.1. Potentiality of microalgae biodiesel in Bangladesh

The amount of diesel run Power plant in Bangladesh is 4% of its Total 5271 MW generation. to replace this by biodiesel of different sources, the amount of land required is shown in Table-1. From the table we can see, microalgae give us highest amount of oil. If we go for harvesting other oilseeds like soyabean, mustard oil and others these will occupy almost 30% of our available land for harvesting. Suppose, to get biodiesel from mustard oil it will require 1.28 M Ha land which is 3.6 times of the available land for mustard oil seed being harvested at present. So, this type of biodiesel production will create an immense pressure on the land available for harvesting in Bangladesh to mitigate its food crop demand.

Table 1: Comparison of sources of Biodiesel in Bangladesh for diesel supply of 230 MW power generations:

Crop	Percentage of Oil %	Oil yield (L/Ha)	Land required (Million Hectare)	Land at present (Million Hectare)
Mustard Oil	39-44	91.5	1.28	0.35
Ground Nut	48-50	156.0	0.75	0.087
Sesame	42-44	55.2	2.13	0.076
Soyabean	19-20	52.0	2.26	0.530
Sunflower	42-44	91.0	1.25	0.042
Microalgae	70	136900	0.00086	-
Microalgae	50	58700	0.002	

Source: Bangladesh Oilseed Harvesting Instruction, DAE and FAO/UNDP Project

This scarcity can be mitigated dramatically if we think of microalgae. These can contain up to 70% of their weight as lipid oil and the oil yield per Hectare is extremely high compared to other oil sources. Oil content of microalgae varies according to the species but most of them contain enough lipid oil to produce biodiesel from it. From Table -2 we can get an idea of the lipid oil content of different microalgae. Again microalgae grow almost twice in amount in every 24 hour in Bangladesh climate. So, thinking microalgae as a source of alternative fuel for Bangladesh can mitigate its continuous fuel crisis.

Table 2: Oil contents of microalgae species:

Microalgae species	Oil content(% of Dry Mass)
Botroyococcus braunii	25-75
Chlorella sp.	28-32
Crypthecodinium cohnii	20
Cilindrotheca sp.	16-37

Source: (Chisti, 2007; Mathew, 2008)

Producing microalgae in an expensive method compared to general crop production. The basic requirements for microalgae production are light, CO_2, water and nutrients. Nutrients include Nitrogen (N), Phosphorus (P), Iron and Silicon. These growth nutrients are relatively less expensive. The Carbon that is contained in dry Biomass of algae (almost 50% of total weight) is collected from atmosphere by the following reaction:

$$6CO_2 + H_2O \longrightarrow C_6H_{12}O_6+6O_2+6H_20$$

Producing 1 Ton of algae biomass requires 1.83 ton of CO_2. It can be incorporated with the power plant flue gas. This will reduce air pollution and also will minimize the cost of the algae production. Thus the algae production is carbon neutral, can retain the amount of carbon from the atmosphere.

The water required for microalgae can be used from any source, even the wastewater from our industrial or domestic use. The waste water already contains N or P for algae. Thus this can minimize the production cost as well as mitigates the environment pollution.

Adequate light is another requirement for high rate of Microalgae production. Throughout the year, except some cloudy days in rainy season, sunlight is quite sufficient in Bangladesh for microalgae production.

Space is another requirement for algae production which is largely available in Bangladesh. At present there are 0.73 million Hectare of (Table-3) land those are not suitable for any crop production and instantly can be used for algae production. Also the saline lands can be used for algae production.

Table 3: Type of land in Bangladesh

Type of Land	Amount (Million Hectare)
Dry land	0.73
Ponds	0.31
Low marshy land	3.16
Coastal saline land	0.218

Source: 1. DAE and Agriculture Ministry, 2004 2.Fisheries Department, 2007

The only two practical methods that we have applied for microalgae production in lab is raceway pond and photo bioreactor. We have produced *Chlorella* and *Botroyococcus braunii* in natural environment of Bangladesh to expedite our experiment.

2.2. Raceway Pond

It is made of closed loop water channel. The material may be anything like concrete, plastic or compacted earth with a paddlewheel for proper mixing and circulation of water. During daylight, the culture must be fed in front of the paddlewheel. CO_2 generally collected from the environment, but for better production rate CO_2 can be circulated against the flow of water for the photo biosynthesis. Temperature control of the water totally depends on nature by evaporation. For better production temperature must be maintained from 20^o C to 30^o C.

Figure1: Raceway pond setup


Figure2: Raceway pond setup (Top view)

In our experiment we constructed a low cost raceway pond system. The base body was constructed with 3 inch radius PVC pipe, bends are PVC bends jointed to liner section of pipes together. We put a simple paddlewheel electrically operated for circulation of water. The total amount of water contained in the raceway is 1.5 ft^3. Nutrients are fed into the pond at regular interval manually.CO_2 is naturally taken from air. The setup was successful to produce algae at a satisfactory level.

2.3. Photobioreactor

Tubular photobioreactor consists of solar collectors, where algae collect energy from the Sun. (Figure 3)

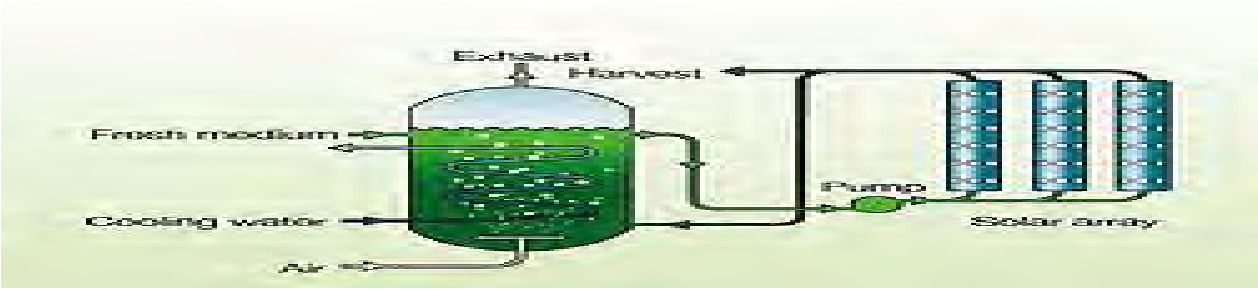

Figure 3: Conventinal PhotoBioreactor

This is generally made of plastic or glass. Tube diameter is limited to maintain proper penetration of sunlight. From the feeding vessel the flow progresses through a mechanical or diaphragm pump. Algae are collected from the vessel. The remaining algae pass through the closed loop. The solar collectors are oriented parallel to each other and flat above the ground to maximize the sunlight availability. The ground may be white painted or Alu foils may be used to maximize the sunlight capture. Biomass sedimentation can be prevented by using mechanical pump, airlift pump, diaphragm pump or peristaltic pump. To minimize higher concentration of O_2, at feeding vessel air is purged through the bottom. The cooling of the system can be maintained by heat exchanger at the feeding vessel.

Figure 4 and 5 shows the setup of low cost photobioreactor that we made at our Lab. Each of the three solar collectors is 9 inch long and diameter is 1.5 inch. Unit capacity is 0.0276ft^3 .Surface area is 0.88 ft^2 . The solar collectors are made of plastic tubes. The feeding vessel is 2 L HDP container. A small scale peristaltic pump is used for flow turbulence .There are three tubes fed into the feeding vessel, outlet and inlet from solar collectors and other for supplying air and CO_2 at the bottom of the vessel.

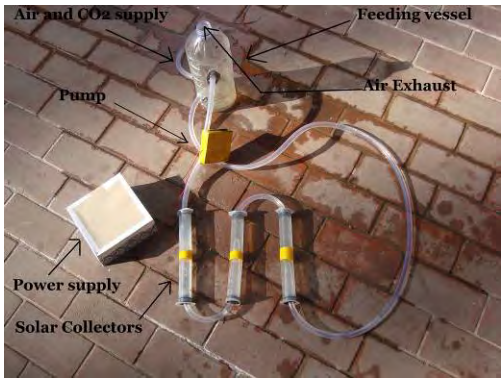

Figure 4: Details of PBR set up

Figure 5: Side view of PBR set up

2.4. Biodiesel Production

We collected set samples of Algae *(Chlorella 30 gm* and *Botroyococcus braunii 28 gm)* from and carried out the experiment at Chemistry Lab, Islamic University Of technology (IUT), Dhaka. Algae were ground by hand motor and pestle. The oil was extracted from the dry mass by drying the algae for 30 Minutes in 80^{o}C. Ether solution and Hexane was mixed to algae and the mixture was kept 24 hours for settling. Then by filtration the biomass was collected and oil was evaporated. A mixture of NaOH (0.25 gm) and 25 ml methanol was poured into a conical flask with the algae oil. The process than converts the algae oil into Biodiesel is called transesterification. It requires 3 mol of alcohol for each mole of triglyceride to produce 1 mol of glycerol and 3 mol of methyl esters. The conical flask is shaken for 4 hours at electric shakers.

$$\begin{array}{l} CH_2\text{-}OCOCR_1 \\ CH\text{-}OCOCR_2 \\ CH_2\text{-}OCOCR_3 \end{array} + 3CH_3OH \rightleftharpoons \begin{array}{l} CH_2\text{-}OH \\ CH\text{-}OH \\ CH_2\text{-}OH \end{array} + \begin{array}{l} R_1\text{-}COOCH_3 \\ R_2\text{-}COOCH_3 \\ R_3\text{-}COOCH_3 \end{array}$$

Triglyceride Methanol Glycerol Methyl Ester (Biodiesel)

After this reaction the solution was given time in idle for 20 Hours to settle the sediment layer to pour out the biodiesel. Then it is washed by 5% Water and dried under fan for 18 hours.

3. Results ad Discussions

3.1. Comparison between Raceway pond and Photobioreactor system lab experiment

Considering the productivity both by volume and area our experimental algae production from the PBR and raceway pond shows that (table 4), raceway pond system's productivity is lower than the PBR productivity by 11 times. But CO_2 consumption for both systems is almost same. It is possible to obtain more oil/ Hectare from PBR system rather than raceway

pond. As the biomass concentration is higher in PBR (21.97 times), so we can extract more biomass in the same time from PBR and less from Raceway pond.

Table 4: Lab experiment result of algae production scaled up to 100000 kg production:

Parameters	Raceway Pond	Photobioreactor
Annual biomass production(kg)	100000	100000
Volumetric productivity($kgm^{-3}d^{-1}$)	0.103	1.1
Areal Productivity($kgm^{-2}d^{-1}$)	0.029	0.034
Biomass concentration($kgm^{-3}\ d^{-1}$)	0.137	3.01
Dilution Rate(per day)	0.22	0.275
Oil yield(L/H)	99400	136900
Annual CO_2 consumption(Kg)	183300	183300

3.2. Comparison of Oil extracted from Chlorella and Botroyococcus braunii

Table 5: Measurement of gross and dry weight, extracted oil and biomass of algae:

Specimens	Gross wt(g)	Dry Weight(g)	Oil(g)	Biomass(g)
Chlorella	30	9	1.86	4.05
		30%	6.2%	45%
Botroyococcus braunii	28	12.6	7.56	5.29
		45%	27%	41.9%

Source: Author's Lab Experiment

Percentage of dry weight algae is higher in *Botroyoccus braunii* than in *Chlorella* (Table -5). Oil extracted from *Botroyoccus braunii* also at higher percentage rate as we found in table 2. After extraction Biomass was found lower in *Botroyoccus braunii* than *Chlorella*

3.3. Properties of Microalgae Biodiesel over Diesel

Table 6:

Properties	[1]Microalgae Biodiesel	[2]Diesel
Density	0.864kg/L	0.838Kg/L
Viscosity	5×10^{-4} Pa s at 40°C	1.9×10^{-4} Pa s at 40°C
Flash Point	75°C	75 °C
Heating value	0.35 MJ kg^{-1}	0.5 MJ kg^{-1}

Source: 1.Author's Lab experiment 2.PetroBangla Ltd

3.4. Cost Analysis of a project to run the 480 KW diesel generator of IUT (Islamic University of Technology, Dhaka) with biodiesel:

*Required diesel per hour at full load=120 L
*Total diesel required for 171 working days@ 6 hours time= 171 x 120 x 6=123120 L
*Total biodiesel B20 (20% Biodeisel-80 % Petrodiesel) = 24624 L=21275 Kg (table 6)
*Algae production required/day at 70 % oil Content=30390 Kg/year
*CO_2 produced by generator =278 Ton, CO_2 is fed into the algae production.
*CO_2 Consumed /year by the algae=30390 x 1.83 kg =55613.7 kg =55.6137 Ton
*Daily production required =83 Kg of Algae

*Required land=3000 Sqm at raceway pond system, productivity rate 0.103 kg/m^3/day and raceway depth 0.3 m.Total land with open spaces between the ponds=6000 Sqm.
*At a rate 560 Taka/Sqm (pipe, bends, cement, adhesive, paddlewheel, motor and other materials, labor and electricity) the total cost (fixed and variable) for 6000 Sqm stands =3360000 Taka=46666 USD. 1 Liter Oil price= (46666/24624) USD=1.88 USD

The cost for per Liter micro algae oil goes up to 136 taka or 1.88 USD at our project. The price is higher than diesel price (55 taka/L). The price can be reduced by attaining better efficiency and algae concentration in production. Also the pricing of microalgae oil can be bring in a relation with the crude oil price, so that it can be affordable to the limit of diesel price:

$C_{algae\ oil}=6.9 \times 10^{-3}\ C_{petroleum}$

4. Conclusion

As discussed here, we see that, microalgae oil is technically compatible like diesel. From Table -6 we find the properties are quite similar to diesel properties. So, similar engines or machines can be driven by microalgae oil instead of diesel .From Table-4, a comparative statement of both raceway pond and PBR is clear to us and surely this will encourage us for more diversified research on PBR in Bangladesh. From table-5, we understand which species of microalgae should be emphasized for biodiesel production at lower cost and higher efficiency. From earlier discussions it is clear that Bangladesh has a huge potentiality to produce microalgae as we still have available land and cheap labor for this. Both raceway pond and photobioreactor is possible in Bangladesh, but raceway pond can be introduced by mass level people in villages as the cost is lower and a huge supply of microalgae can be made available from this source and thus a revolution in energy sector can be ignited. Now we are working to find out the suitable, efficient and cost effective way for replacing the diesel that is being used in national energy production by scaling up the pilot work of microalgae oil use in IUT power generation. The most challenging part of this will be to reduce the price as lower as diesel or. Extensive researches need to be carried out for this work. Thinking of a better and greener Bangladesh, we must now rush towards this research more deeply and establish microalgae oil as a substitute of conventional diesel. This research can be implemented for third world countries to produce large scale microalgae oil and lessen the load from petrofuel.

Reference

[1] *Directory:Biodiesel from Algae Oil - PESWiki*. Retrieved on June 26th, 2007 from http://peswiki.com/index.php/Directory:Biodiesel_from_Algae_Oil

[2] *An in-depth look at biofuels from algae*. Retrieved on June 26th, 2007 from http://biopact.com/2007/01/in-depth-look-at-biofuels-from-algae.html

[3] *Algaculture - Wikipedia, the free encyclopaedia*. Retrieved on June 26th, 2007 from http://en.wikipedia.org/wiki/Algaculture

[4] *A Look Back at the U.S. Department of Energy's Aquatic Species Program: Biodiesel from Algae* by the National Renewable Energy Laboratory. Retrieved on June 26th, 2007 from http://www1.eere.energy.gov/biomass/pdfs/biodiesel_from_algae.pdf

[5] Acedo, I.D.C. Energy from biomass and wastes. Biomass Bioenergy, 1993: 77-80.

[6] Shay, E.G., Diesel fuel from vegetable oils: Status and Opportunities. Biomass Bioenergy, 1993: 227-242.

[7] Thomas, F.R., Algae for liquid fuel production Oakhaven Permaculture center, Permaculture Activist, Retrieved on 2006-12-18',9: 1-2.

[8] Roessler, P.G., L.M. Brown, T.G. Dunahay, D.A. Heacox, E.E. Jarvis and J.C. Schneider. Genetic-engineering approaches for enhanced production of biodiesel fuel from microalgae. 1994, ACS Symp Ser. 566: 255-270.

[9] Lorenz RT, Cysewski GR. Commercial potential for Haematococcus microalga as a natural source of astaxanthin. Trends Biotechnol, 2003,18:160–7.

[10] Molina Grima E, Acién Fernández FG, García Camacho F, Camacho Rubio F, Chisti Y. Scale-up of tubular photobioreactors. J Appl Phycol 2000,12:355–68.

[11] Molina Grima E, Fernández J, Acién Fernández FG, Chisti Y. Tubular photobioreactor design for algal cultures. J Biotechnol 2001,92: 113–31.

[12] Molina Grima E, Belarbi E-H, Acién Fernández FG, Robles Medina A, Chisti Y. Recovery of microalgal biomass and metabolites: process options and economics. Biotechnol Adv 2003, 20:491–515.

[14] Moo-Young M, Chisti Y. Considerations for designing bioreactors for shear-sensitive culture. Biotechnology 1988, 6:1291–6.

[15] Munoz R, Guieysse B. Algal–bacterial processes for the treatment of hazardous contaminants: a review. Water Res 2006, 40:2799–815.

[16] Nagle N, Lemke P. Production of methyl-ester fuel from microalgae. Appl Biochem Biotechnol 1990, 24–5:355–61. Nedbal L, Tichý V, Grobbelaar JU, Xiong VF, Neori

[17] Website: www.bpdb.bd.gov, www.petrobangla.org.bd

Preliminary study of hydrogen production from local arid area algae in a bubble column

M. W. Naceur[1*], F. Kaidi[2], R. Rihani[2] and N. Ait Messaoudene[3]

[1] *Laboratoire des Applications Energétiques de l'Hydrogène (LApEH); University Saad Dahlab of Blida. PO Box 270. Blida. Algeria*
[2] *Centre de Développement des Energies Renouvelables, Division Bioénergie et Environnement BP.62. Route de l'Observatoire - Bouzaréah. Algérie*
[3] *Department of Mechanical Engineering, Faculty of Engineering; University of Hail. Saudi Arabia*
** NACEUR M.W. Tel: +21325433631, Fax: +21325433631, E-mail:wnaceur@hotmail.com*

Abstract: Fighting climate change and ensuring sustainable development is one of the greatest concerns nowadays. In this regard, energy production from biomass is already a reality and presents tremendous possibilities of use as an alternative source. Among the various technologies, hydrogen production from microalgae is a promising clean energy alternative. Indeed, some unicellular green algae have the ability to produce hydrogen simply in the presence of water and light. However, an important factor governing the efficiency of hydrogen production by microalgae depends on the method of production. Designing a suitable bioreactor is therefore very important in order to control the main production parameters. Hence, a suitable bubble agitation system, with proper bubble size, that keeps algal cells in suspension is proposed.
The present work foresees a tentative method of hydrogen production from *Chlamydomonas sp*, a local alga from the arid area of Adrar (southern Algeria). This is performed in a photobioreactor of the type of a bubble column. It should be noted that a hydrodynamic study of the bubble column has been previously conducted. This has led to a proper choice of the diffuser and an approximate assessment of microalgae culture parameters. Moreover, various process parameters were monitored under a given light intensity, namely: pH, temperature, dissolved oxygen, etc. The observations show massive growth of the algae biomass which indicates a good adaptation of this type of photobioreactors for microalgae production, and subsequently hydrogen production as long as low rates are required.

Keywords: *Renewable Energy, Hydrogen, Microalgae, Photobioreactor, Bubble column.*

1. Introduction

World energy consumption can only grow given the accelerated growth of the population. It is largely dominated by fossil fuels (oil, natural gas and coal) as the sole energy source. Moreover, their massive use exposes the planet to two major problems: a devastating pollution caused by the emission of greenhouse gases and the depletion of fossil fuel reserves. The growing awareness about the risks of climate change and the conditions for sustainable development of the planet led to the search for alternative energy sources more environmentally friendly as substitute for fossil fuels. Ultimately, renewable energies are the best alternative. However, they have the disadvantage of not being competitive yet for many applications. More specifically, hydrogen appears to be the ideal alternative energy source and represents a serious hope to achieve an industrial era with considerably lower carbon dioxide emission. Indeed, it is considered as a viable alternative and as "the energy carrier of the future. Biologically produced hydrogen is a promising alternative to produce clean energy as it shares both advantages of being renewable and nonpolluting. In fact, from just water and solar energy, some unicellular green algae or cyanobacteria are known for their ability to provide hydrogen by photosynthesis [1]. However, for purely economic reasons, it is difficult to accept that biologically produced hydrogen may compete with other modes of production [2]. Bubble column reactors are mainly used in various industries such as: chemical, petrochemical, biological, bioenergetic…etc, due to their simple construction and their low operating costs. The gas holdup and the bubble size constitute important parameters for the study of the flow patterns in a bubble column. In addition, bubble size distribution, as well as

the gas holdup depends on some parameters such as: column geometry, operating conditions, physicochemical properties of the two phases put in contact and the type of gas sparger [3]. The liquid is assumed to be mixed by the motion of gas bubbles in it. However, the use of a gas sparger which generates small bubbles distributed with homogeneous way throughout the column ensures a better mixture [4].

The aim of the present work is to undertake preliminary test of photobiological production of hydrogen from microalgae strains isolated locally in Algeria. A Pyrex made bubble column type photobioreactor has been designed for this purpose with the possibility of controlling some of the culture parameters such as light intensity, thus allowing the optimization of certain operating conditions. To the dispersion of the gas phase, the total gas holdup , the bubble size distribution within the column are studied. So, the bubble diameter was measured by using a photographic method, with the help of a millimetre.

2. Methodology

2.1. Material and methods

2.1.1. Strain and culture medium used

Microalgae used in this study were isolated from freshwater samples collected from southern Algeria. The microalgal species used is a locally isolated *Chlamydomonas sp*. The culture medium used is tri-acetate phosphate (TAP) which is adjusted to pH 7.2. This medium is widely used for cultivation of microalgae for the purpose of hydrogen production.

2.1.2. Experimental set-up

The experimental set-up used in this study is a cylindrical Pyrex column of 0.04m internal diameter and 0.86m height, provided with several lateral pipes (Figure 1). Stirring provided by injecting air through a porous sintered glass diffuser of porosity 40µm, which is placed at the bottom of the column. The airflow is controlled by a flowmeter. It should be noted that a preculture is first prepared and inoculated in the column in 900 ml of culture medium. Bubbling with nitrogen is recommended to create anoxia (low dissolved oxygen) and counteract the inhibition of hydrogen production.

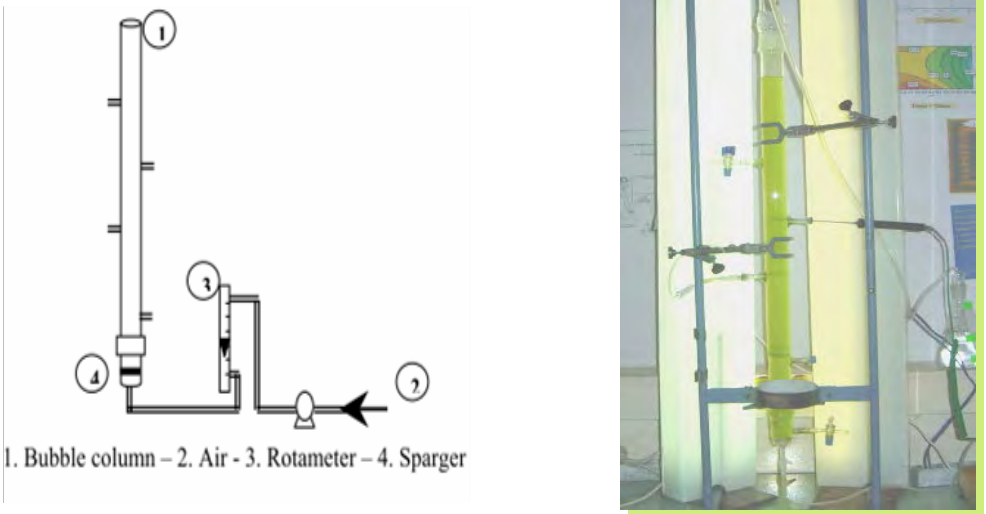

Fig. 1. Experimental set-up

2.1.3. Microalgae growth

The growth of microalgae is favorable in the presence of a culture medium rich in nutrients and exposed to sufficient luminous intensity. Different factors may influence the growth and the production of hydrogen from microalgae [5]. The experiments were performed in the bubble column inoculated with a preculture of *Chlamydomonas sp*, which allowed us to follow the temporal evolution of biophysical parameters such as: dissolved oxygen, pH and Temperature, etc. Microalgal cell count was performed using a microscope. The count is carried out with a cell count, which allows us to check any contamination present in the medium. An average of three samples is performed for each test.

2.1.4. Gas retention

The gas retention is given according to superficial gas velocity and the type of the sparger. For bubble columns the gas holdup, ε_g, is given by the following relation:

$$\varepsilon_G = \frac{\Delta H}{\Delta H + H_L} \quad (1)$$

Where:

H_L: Height of the liquid before injection of gas.
ΔH: Increase in the level of the liquid after gas expansion.

2.1.5. Bubble diameter

The average diameter of the bubbles is measured by a photographic method. The pictures of the bubbles were taken at a certain distance to the bottom of the column where the distribution of the bubbles is uniform with a using numerical photograph (SONY). Then, the photographs are treated and the diameter of the bubble is calculated using the software Matlab 6.5. The shape of the bubbles is generally ellipsoidal.

The local bubble diameter was calculated using the following relationship:

$$d_i = \sqrt[3]{a^2\, b} \quad (2)$$

Where a and b are the diameter and the width of the ellipsoid respectively.

For each gas velocity, the average Sauter diameter is calculated from the following relation:

$$d_{32} = \frac{\sum_i n_i . d_i^3}{\sum_i n_i . d_i^2} \quad (3)$$

n_i : the number of the bubbles with an individual diameter d_i.

2.1.6. Axial dispersion

The model employed is the one used to characterize flows in tubular engines. It takes into account two effects: convection, which represents the flow in block, and dispersion, which results from the molecular and turbulent diffusion. There are two types of contributions to dispersion: radial and axial [6]. The radial effect is negligible compared to the axial effect

when the ratio L/D is greater than 4. With these considerations, the transient matter assessment in the tracer is written as:

$$\frac{\partial C}{\partial t} = D_z \frac{\partial^2 C}{\partial z^2} - u\frac{\partial C}{\partial z} \qquad (4)$$

Where C is the concentration of the tracer, u the speed of the fluid, D_Z the axial dispersion coefficient, z the axial co-ordinate and t, the time

The solution of equation (4) is then:

$$\frac{c(t,z)}{c_E} = 1 + \frac{2L}{\pi\beta}\sum_{n=1}^{\infty}\left\{\frac{1}{n}\sin\left(\frac{n\pi}{L}\beta\right)\cos\left(\frac{n\pi}{L}z\right)\exp\left[-\left(\frac{n\pi}{L}\right)^2 D_z t\right]\right\} \qquad (5)$$

3. Results and discussions

3.1. Gas retention

The mixing of the liquid phase is ensured by the injection of gas. The study of the dispersion of the gas phase can bring information on the flow within the column. The gas retention εg, which is one of the most important parameters characterising the hydrodynamics of the bubble column reactors, depends mainly on the superficial gas velocity and the type of gas sparger. According to M.S. Michaud, 2001 [4], there is no significant difference in the value of gas retention according to the type of sparger used.

Our results, presented in figure 2, show clearly the influence of the type of sparger on the gas holdup. According to this figure, we observe that for superficial gas velocity lower than 0.03 m/s, the gas retention is similar for the two spargers. For high superficial gas velocity, however, the gas holdup obtained for sparger 1 is higher than that obtained in sparger 2. So the type of sparger does influence the gas holdup for high gas regimes. Indeed, sparger 1 (150 µm) generates large bubbles and thus increases the gas retention in the whole column. Moreover, the gas retention increases with increasing gas velocity, which is in agreement with the observations of Thomas et al. (1989) [7].

The dependence of the gas holdup on the superficial gas velocity v_g , can be written as:

$\varepsilon_g = C.\ (v_g)^{\alpha}$

The experimental values of C and α obtained in this work are: C=12.091 and α=0.747 for the sparger 1(150µm), which is in agreement with the work of Shah and al, 1982 [9]. According to this author, the exponent α varies usually from 0.7 to 1.2 for bubbly flow. As for sparger 2 (40µm), the constant C was 7.1511 and α was 0.6775 which corresponds to a heterogeneous flow where the exponent α ranged from 0.4 to 0.7 according to the same author. Figure 3 illustrates the experimental results compared to those found in the literature. For low superficial gas velocities our experimental results are in good agreement with those from the literature. However, for high gas velocities, the results diverge due mainly to the operating conditions and to the type of spargers used.

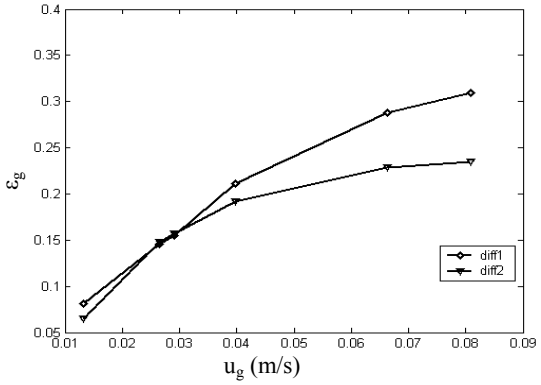

Fig. 2. Gas retention vs superficial gas velocity

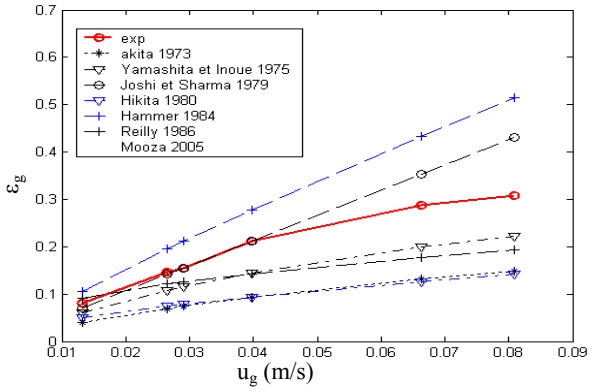

Fig. 3. Gas retention vs superficial velocity compared with the literature data

3.2. Bubble diameter

Bubble size is a very significant parameter for better understanding the gas dispersion within the column. In bubble column reactors, the variations of the average diameter of the bubbles depends on the type of gas sparger [8], and the Sauter diameter increases slightly with the increase of superficial gas velocity. For our study, the variation of the bubble size according to the superficial gas velocity is represented in figure 4, we notice that the average diameter of the bubbles increases with increasing gas velocity. We also observe a coalescence of the bubbles beyond a gas velocity of 0.033 m/s; at which point, the size of the bubbles becomes difficult to determine. The bubbles are generally ellipsoidal and for the porous spargers used, the bubble diameter ranges from 2,5 m m to 8,5 m m. For the two spargers, The Sauter diameter varies similarly according to the superficial gas velocity (Figure 5). However, for sparger 1, the Sauter diameter is about 5mm, while for sparger 2, the Sauter diameter is 7.5mm.

We also represent in the figure 4 and 5 the Sauter diameter and the average diameter for the two spargers. We note that the variation follows the same increasing pattern. However, sparger 1 presents larger bubbles than those generated by sparger 2.

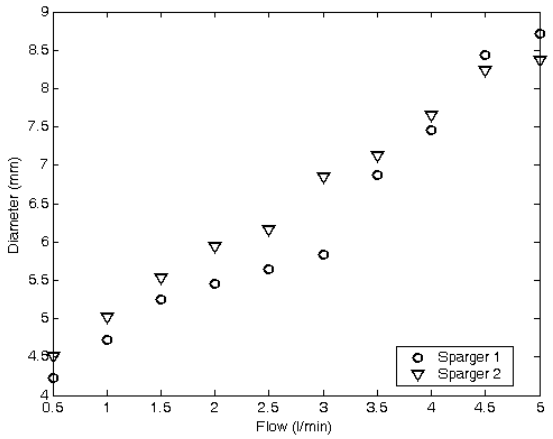

Fig. 4. Mean bubble diameter versus the injection gas velocity.

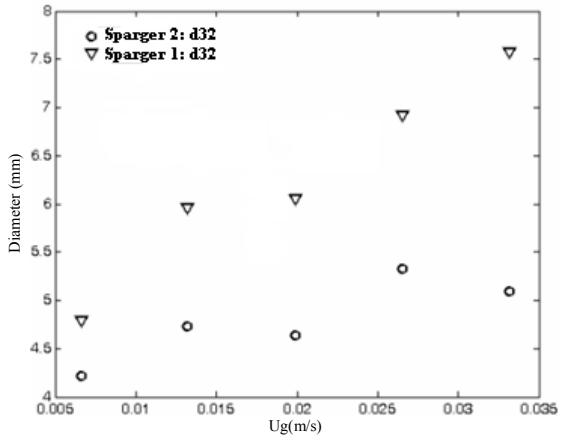

Fig. 5. Sauter diameter vs superficial gas velocity

3.3. Modelling of the column

The computed curves are generated using a model with axial dispersion. The results obtained are represented in figure 6 and 7 for each flow and each type of diffuser. The experimental data points are represented and compared with the model of axial dispersion. The parameters of the model are adjusted in order to obtain a good adjustment of the model to the experimental data using MATLAB 6.5. We note that for a bubble column in batch mode, the SDR fits the model of axial dispersion almost perfectly. The expression used is that of Eq. 5 and the results of this model seem to be in agreement with the experimental data. Figure 7 represent the exit of the tracer for diffuser 1 (150µm) for flow gas of Q_G =3l/min.

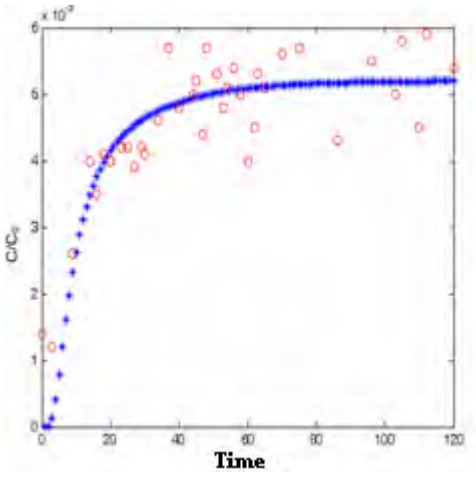

Fig. 6. Exit-tracer concentration in batch mode (D=150µm , Q_G =1 l/min)

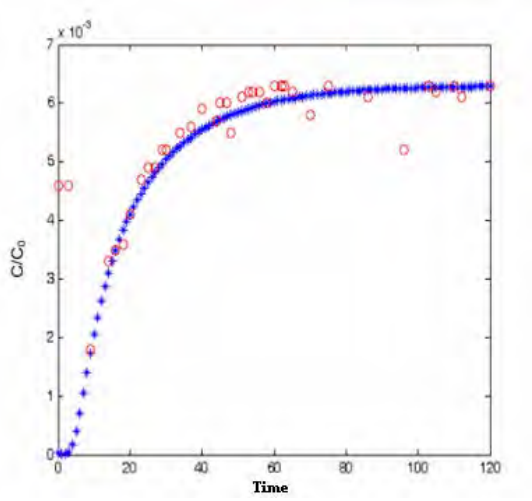

Fig. 7. Exit- tracer concentration in batch mode (D= 150µm, Q_G=3l/min)

3.4. Microalgae growth

For a light intensity of 7800 lux, a considerable evolution of microalgal biomass is observed over time. Figure 8 shows the change in optical density vs. time and informs us about the temporal evolution of the growth of microalgae. It is noted that this curve actually reflects the growth kinetics of the *Chlamydomonas sp*. Strain, reaching a maximum after 98 hours of cultivation, then a stationary phase where the concentration of biomass is stable

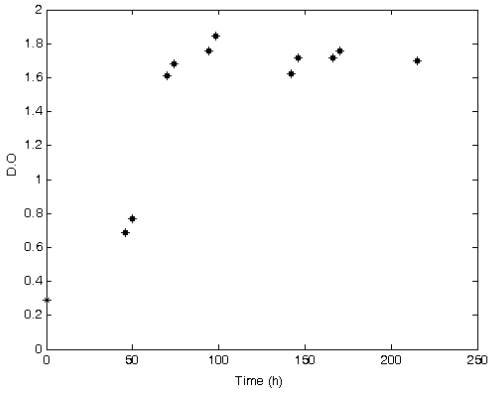

Fig . 8. Evolution of optical density vs Time

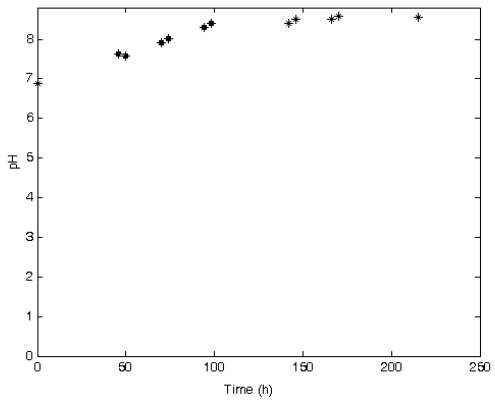

Fig. 9. pH vs time in growth algae

An increase of pH, while remaining within the range of 6.9 and 8.5, is also observed during growth (Figure 9). This increase reflects the growth of microorganisms. The pH increase is due to the microalgae photosynthetic activity. Given the fact that microalgae absorb CO_2 very

rapidly, the pH of the medium moves to values above 7.5 in the case where CO_2 demand of microalgae is higher than its supply to the middle. The variation of dry matter is shown in Figure 10 an increase in dry matter over time is observed, reflecting the concentration in the cell culture medium. However, a decrease of dry matter towards the end of growth is noted. The evolution of dissolved oxygen during growth is also monitored. Overall, dissolved oxygen increases over time during the period of illumination.

This also reflects the photosynthetic activity and hence the growth of microalgae (Fig. 11). The measured dissolved oxygen concentrations are in the range of 2.9 to 11.7mg/L.

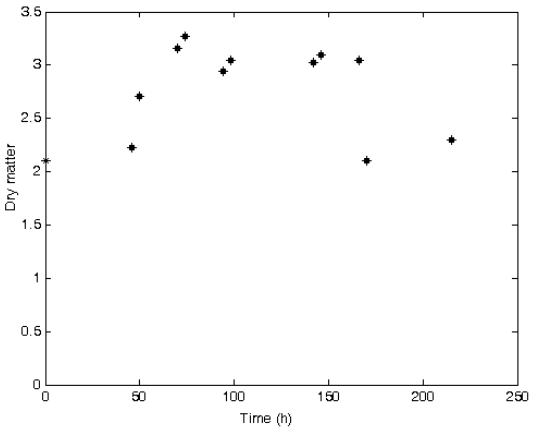

Fig. 10. Dry matter vs time

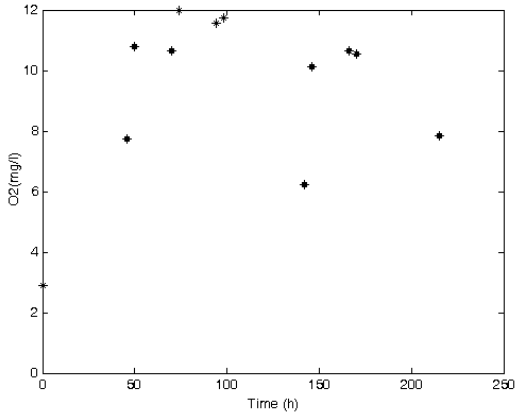

Fig. 11. Dissolved oxygen vs time

Preliminary tests of hydrogen production by the ***Chlamydomonas sp.*** strain are undertaken in the bubble column serving as a photobioreactor. The column is equipped with a mechanical agitation system to keep algal cells in suspension and prevent them from settling. It is noteworthy that during the hydrogen production testing, nitrogen bubbling is performed to achieve anoxia and induce the production of hydrogen [9, 10]. At the beginning of culture, the dissolved oxygen content is relatively constant. Beyond 20 m inutes, it increases due to photosynthesis (O_2 release). However, a short period after the cultivation initiation, we note the formation of small bubbles through the capillary tube leaving the bubble column type photobioreactor (gas trapping system). This can be explained by the fact that culture was in anoxia which favored the production of hydrogen (transcription of the Fe-hydrogenase). This is followed by an increase of oxygen dissolved in the medium which inhibits the production since bubbles are no longer observed. These observations are consistent with those reported by [11].

4. Conclusion

Bubble columns equipped with porous spargers offer a greater gas-liquid contact area as bubbles created by this type of spargers are numerous and far smaller. The use of porous spargers seems to be advantageous compared to the other types because of the multiple points of injection. According to the experimental results obtained, the type of sparger influences the gas retention for high superficial gas velocities. Moreover, the diameter of the bubbles increases with increasing gas velocity. We also note that the gas holdup and the Sauter diameter agree well with results reported in the literature. In the present study, the culture of locally isolated microalgae in a bubble column type photobioreactor is tested; followed by a preliminary investigation of hydrogen production.

The growth and massive evolution of algal biomass in this reactor type demonstrate the suitability of this type of reactor for the cultivation of microalgae. Subsequently, preliminary tests of the biological production of hydrogen by microalgae show that anoxia is achieved by nitrogen bubbling in the culture medium; which allowed observation a hydrogen production but for a short period of time only.

Thus, the preliminary tests of photobiological production of hydrogen by an algal strain and in a bubble column remain conclusive despite its transient character under the present conditions. The question that arises is how to maintain the conditions of the onset of hydrogen production for longer periods of time so to make it economically viable.
In order to elucidate a number of phenomena hitherto unexplained, this work is to be pursued and deepened to address these questions and more particularly in regard to the implementation of more adapted micro algal strains for hydrogen production in photobioreactors

References

[1] H. Gaffron, J. Rubin, Fermentative and photochemical production of hydrogen in algae, J Gen Physiol, 1942, 26: 219–240

[2] I. Akkerman, M. Janssen, J. Rocha, R. H. Wijffels, Photobiological hydrogen production : photochemical efficiency and bioreactor design", International Journal of Hydrogen Energy, 2002, 27 :1195–1208

[3] E. Camarasa, C.Vial, S. Poncin, G. Wild, N. Midoux, J. Bouillard, Influence of coalescnece behaviour of the liquid year D of gas sparging one hydrodynamics and bubble characteristics in A bubble column. Chemical Engineering and Processing, 1999, 38, 329-344

[4] M.S. Michaud, Hydrodynamic and biological study of one proceeds of methanisation has biofilm: the engine has turbulé bed opposite. Thesis of doctorate, I.N.S.A. France, 2001

[5] M. J. G. V. Barbosa, Microalgal photobioreactors: scale up a nd optimization, Thesis, Wageningen University, Wageningen, The Netherlands, 2003

[6] A. Behkish, Hydrodynamic and mass transfer parameters in large-scale slurry bubble column reactors, Ph.D. University of Pittsburgh, School of engineering, 2004

[7] D. Thomas, A. Bernis, Incidence of the aptitude for the coalescence of the fluid on t he hydrodynamics of the bed fluidized triphasic reverse functioning with counter-current; Recent Progress in Genius of the Processes, 1989 3(89), 161-166

[8] Y.T. Shah, B.G. Kelkar, S.P. Godbole, W-D. Deckwer, Design parameters estimates for bubble column reactors. A.I.Ch.E. Newspaper, 1982, 28, 353 –379

[9] S. Fouchard, A. Hemschemeier, A. Caruana, J. Pruvost, J. Legrand, T. Happe, G. Peltier, L. Cournac, Autotrophic and Mixotrophic Hydrogen Photoproduction in Sulfur-Deprived Chlamydomonas Cells, *Applied and Environmental Microbiology*, 2005, p. 6199–6205

[10] S.A. Markov, E.R. Eivazova, J. Greenwood, Photostimulation of H_2 production in the green alga Chlamydomonas reinhardtii upon pho toinhibition of itsO_2-evolving system, International Journal of Hydrogen Energy, 2006, V. 31, 1314 – 1317

[11] A. Melis, L. Zhang, M. Forestier, ML. Ghirardi, M. Seibert, Sustained photobiological hydrogen gas production upon r eversible inactivation of oxygen evolution in the green alga Chlamydomonas reinhardtii, Plant Physiol; 2000, V. 117, n°1, 29 – 39

Short Rotation Coppice in Italy: a model to asses economic, energetic and environmental performances of different crop systems

Bacenetti Jacopo[1*], Fiala Marco[1]

[1] *Department of Agricultural Engineering, Milan, Italy*
**Corresponding author. Tel: +39 0250316869, Fax: +39 0250316845, E-mail: jacopo.bacenett@unimi.it*

Abstract: In the near future, the role that renewable energies can play in order to achieve the ambitious objectives fixed by the European Union is decisive. Besides economic aspect also energetic and environmental issues of agro-energy chains must be carefully evaluated. We developed a software tool able to assess economic, energetic and environmental performance of renewable energy from biomass. The aim of this paper is present the software and its application about one of the most promising energy crop in Italy: Short Rotation Coppice (SRC) based on poplar clones.

SRC, subdivided into SRF – plantation with a short cutting frequency (1 or 2 yrs) and in MRF – plantation with a medium cutting time (5 yrs), takes up about 7,000 hectares in Italy. Twenty years after their introduction, in bibliography the information concerning this crop is not always clear and unanimous. On the basis of the cultivation technique carried out in Northern Italy, an economic, energetic and environmental (EEE) evaluation of the poplar SRC (SRF and MRF) has been carried out. The analysis is focused on field and transport phases of the agro-energy chain.

Keywords: *Short Rotation Coppice (SRC), Poplar, Energy Crops, Energy balance, Sustainability, CO_2 balance*

1. Introduction

In Italy, the contribution of agro-energy to national energy demand is still moderate; nevertheless, even if slowly contributing, its relevance has increased in recent years. Agro-energy seems like a possible and, theoretically, interesting alternative to traditional crops, allowing a diversification of income sources. Compared with other energy sources, the dedicated crops offer the advantage of extremely intense field management that ensures the highest yield as well as the shortest wait time. Cultivation of biomass crops on arable lands allows for increased energy production and should be quite profitable for the environment (groundwater protection, ecological planning, phyto-remediation, and Green House Gases absorption, among other options). This is especially true in the case of woody crops, including Short Rotation Coppice (SRC). Over the last 20 years in Italy, supported by favorable public grant programs, SRC has grown to comprise about 6,500 ha, mainly in the Po Valley area. Leaders in the Lombardy and Veneto Regions have been the first to give subsidies for SRC, and the planting areas in these regions now account for almost all the Italian land area dedicated to this energy crop, 4,000 and 1,300 ha, respectively.

In Italy, the woody species suitable for SRC are *Populus* spp, *Salix* spp, black locust, and eucalyptus; however, most plantations consist of specific poplar clones. This arboreus species is historically well-known by Italian farmers and has proven the most adaptable for bio-fuel production. Over the years, the development of new specific clones for biomass production (at the moment, the most important are AF2, Monviso, and Pegaso) and improvement in cultivation techniques have made it possible to obtain remarkable yield increases. Regarding the crop management, several systems with different cutting times have been used: first 1-year, and later, 2-year and 5- to 6-year. Different cutting times require different plant densities and different lane widths. The SRC thus can be subdivided into Short Rotation Forestry SRF – plantations with short cutting frequency (1 or 2 years) and (Medium Rotation Forestry) MRF – plantations with medium cutting frequency (> 5 years). Planting systems are different, too, with highly variable plant density: 10,000 to 14,000 plants/ha (annual plantation with

twin rows), 5,000 to 6,000 plants/ha (biennial plantation with single rows) and 1,000 - 1,800 plants/ha (in MRF). In plantations with medium cutting times, the distance between stumps in the row is quite similar to the width of lanes.

At present, even if the best quality bio-fuel comes from 5-year plantations, the larger part of Italian SRC is based on 2-years cuts. In the near future, MRF plantations will be more widespread because of the better quality of chips (mainly due to lower ash content).

Wood chips produced from SRC are a raw material with a low market value (sale prices range from 60 to 110 €/ t_{dm}); the economic sustainability of this crop is highly dependent on reduction of production costs. This aim can be reached through high yields as well as through the complete mechanization of all field operations. Among the field operations the harvest is the most difficult because of new, sophisticated equipment with high operating costs. The need for high yield requires high input during the crop cycle that can lessen both energetic and environmental sustainability.

In addition to economic sustainability, energetic and environmental aspects must be considered. Taking into account the considerable public grants given to the main agro-energy chains, researchers should evaluate not only economic sustainability (often achieved by means of public subsidies) but also energetic and environmental sustainability. In this way, a Comprehensive Sustainability could be estimated. Nevertheless, though experts in provide information about this wood-crop, the information is not always clear and unanimous. Regarding SRC energy performances, several values of woody biomass production have been reported [3, 6, 8, 12, 14] . Discrepancies in results can be attributed mainly to differences in the following factors: species cultivated, calculation methodology, cultivation techniques (i.e., field operations, type, and rate of fertilizers/herbicides), biomass yield, selection of agro-energy chain phases/operations (i.e., storage, transport, drying, conversion process).

Few studies have been conducted to investigate the environmental aspects of energy-crop cultivations, but a number of software tools to assess economic and energy performance of bio-energy production recently have been developed. Nevertheless, most of these tools lack flexibility; their analysis often is restricted to a single type of bio-energy chain or only the main operations of a chain. This makes application of them difficult for the several agro-energy chains actually in use.

Moreover in the future, evaluating the energy-environmental sustainability of each bio-energy chain will become more and more important. Already, before allowing public subsidies, leaders in several Italian regions are calling for energy and environmental evaluations of some bio-energy chains.

In order to overcome the above-mentioned limitations, we have developed a specific tool to assess the comprehensive sustainability of renewable energy produced by farms and easily are able to compare different agro-technical solutions. The software is capable of providing unbiased information on these three aspects (economic, energetic and environmental) of "Comprehensive Sustainability" of this bio-energy chain.

The aim of this work is to show the software tool and present an application regarding Short Rotation Coppice in Italy in order to clarify, 20 years after their introduction, the economic, energetic, and environmental sustainability of SRF and MRF with poplar in northern Italy.

2. Methodology

The software tool works on a farm scale, and the boundaries of the system analyzed are - at the moment - limited to the farm and transport phase of the chain and does not take into account the conversion process. The functional unit is 1 t_{dm} of biomass. Input required by the software are details of: (a) farm (area, agricultural machinery fleet, crop system); (b) cultivation technique (mechanization operations and sequence; input rate and market prices, energetic and carbon equivalent); and (c) the characteristics of products and byproducts (yields, market prices, lower heating value, and moisture content).

For the economic evaluation, the method of *fixed and variable costs* [11] is used, while for energy balance computation, the software uses the *Gross Energy Requirement* (GER) methodology [13]. The environmental analysis takes into account the same input considered in the energy evaluation and assesses the amount of GHG emitted according to guidelines of IPCC [9]. The mass and energy flow between the different operations of the supply chain are converted in economic, energetic, and environmental values, respectively, by using, for each used production factor, the price (P, €/kg or €/m^3), the energy equivalent (EE, MJ/kg or MJ/m^3), and the emission factor (FE, kg CO_2equivalent/kg or kgCO_2eq/m^3) [10].

For *direct input*, the economic, energetic, and environmental load of the production factors is accomplished easily by multiplying the quantity used (Q; kg or m^3) during the chain as showed in the following equations:

$$C_{ECO} = Q \cdot P \qquad [€]$$

$$C_{ENE} = Q \cdot EE \qquad [MJ]$$

$$C_{ENV} = Q \cdot EF \qquad [kgCO_2eq]$$

where C_{ECO}, C_{ENE}, C_{ENV} are, respectively, the economic, energetic, and environmental costs linked to the different production factors.

In addition to direct input during the cycles of production, others goods are required in order to allow the production of the biomass. These goods are not consumed completely when employed and can be used for several cycles of production. For these production factors, called *indirect input*, the economic, energetic and environmental cost (EEE cost) (C_{ECO}, C_{ENE}, C_{ENV}) is assessed using the same equations adopted for direct input but subdividing their value, the energy, and the greenhouse gases embedded for the overall hours of use and taking into account their economic life (years) and the annual employment (hours).

Therefore, for each production factor, the software computes an EEE cost that summarizes the "load" on the three levels of the analysis. The sum of all the EEE costs allows us to calculate the overall EEE cost for the produced biomass.

To calculate economic net income, the software considers chip-wood selling as well as public subsidies coming from the Rural Development Program (RDP) and Common Agricultural Policy (CAP). Regarding energy aspects, the Lower Heating Value (LHV) of biomass harvested is taken into account to assess the output of these phases of the agro-energy chain. Because the carbon absorbed and stored in the biomass will be oxidized when it will be utilized for energy purposes, this amount cannot be counted as one environmental output. Regarding the C cycle, the agro-energy chain is supposed to be neutral. The environmental output for the GHG issue must be assessed by comparing the emissions for the energy produced with the agro-energy chain with the emissions of a proper reference system (for

example, energy produced by a fossil fuel chain). Since at the moment, the software has not yet been implemented with the last phase of the chains, the environmental output cannot be calculated, and the analysis shows just the environmental production cost of the biomass ($kgCO_2eq/t_{dm}$). For the functional unit, the software assesses economic, energetic, and environmental cost (EEE Cost), economic and energetic revenues and gains, and the economic and energy ratios (between revenue and cost economic and between output and input energetic, respectively).

By means of the integration of the three EEE costs, the software computes a synthetic index, the Global Sustainability Index (GSI), which summarizes the results achieved on the three levels of the analysis.

3. Case Studies

In order to show its applicability, the software was used to evaluate the economic, energetic, and environmental performances of Short Rotation Coppice with poplar in Northern Italy. Two case studies are reported and compared: Short Rotation Forestry (SRF) with 2 years' cutting time and Medium Rotation Forestry (MRF) with 5 years' cutting time.

In both the cases, the crop duration is 10 years, with 2- and 5-year harvests for SRF and MRF, respectively. With respect to the operating conditions of the Po Valley area, the results concerning the conversion from cereals (maize) to poplar for biomass of 40 ha (50% of total farm AUA – Agricultural Used Area) are reported.

Table 1 shows the operations required during the entire SRF and MRF poplar cultivation-cycle. Table 2 shows the rates for the various production factors. Market prices and energy and environmental equivalents are deduced by bibliography [1, 2, 4, 5, 6, 7, 10].

In the study case, the software tool considers the following: (a) a biomass yield of 40 $t_{wb}/ha{\cdot}yr$ for SRF and equal to 40 $t_{wb}/ha{\cdot}yr$ for MRF (moisture content = 55%, LHV = 18.5 GJ/t_{dm} or 6.9 GJ/t_{wb}); (b) a chip-wood sale price of 35 €/t_{wb}; and for public grants: the decoupling cap (400 €/ha·yr) and the planting subsidy provided by leaders in the Lombardy Region (1000 €/ha).

The transport of the chip wood is carried out by a lorry (load volume: 96 m^3, 54000 km/year, 3 km/kg of gasoline, bulk density of the chips = 0,3 t/m^3, carriage price = 1,7 €/km). The lorry never travels empty, so the global coefficient of load for a round trip is equal to 100%. We considered two different transport distances of 70 and 450 km in order to take into account both small- to medium-sized plants in which the biomass supply is prevalently local and large-sized plants in which biomass is collected in a larger area.

4. Results

Table 3 shows the EEE Cost for the field phase of the agro-energy chain, with an overall price (selling price is more than public grants) equal to 109.5 and 105.6 €/t_{dm}, respectively, for SRF and MRF, and the energy crop allows the farmer a gain of 18,84 €/t_{dm} (265 €/ha·year) for poplar plantations with 2-year cutting times and of 46.1 €/t_{dm} (829 €/ha·year) for those with 5-year cutting time. Consequently, the ratio between economic cost and revenue is equal to 1,18 for SRF and 1,77 for MRF. The energetic aspect of the production cost represents approximately the 6.6% (for SRF) and the 4.3% (for MRF) of the LHV (MJ/kg_{wb}) of the biomass.

Table 1: Machines and mechanization planning on surface intended for SRC (SRF and MRF) and for traditional crops [4, 5]

OPERATION	MACHINE		COOPLING TYPE, MACHINE SIZE	WORKING YEARS [TIMES PER YEAR]		
				SRF	MRF	MAIZE
Pre-planting Fertilization	Manure Spreader	Agricultural Machinery Fleet	TP, 10 t, 10 m^3	1 **[1]**	1 **[1]**	From 1 to 10 **[1]**
Primary soil cultivation	Plough	Agricultural Machinery Fleet	P, double-shovel	1 **[1]**	1 **[1]**	From 1 to 10 **[1]**
Secondary soil cultivation	Rotary harrow	Agricultural Machinery Fleet	PP, 2,40 m	1 **[1]**	1 **[1]**	From 1 to 10 **[1]**
Transplanting	Planting Machine	Contractor	T, bifilar	1 **[1]**	1 **[1]**	-
Chemical Weed Control	Spraying machine	Agricultural Machinery Fleet	PP, 15 m, 1000 dm^3	1-3-5-7-9 **[1]**	1-6 **[2]** 2-7 **[1]**	From 1 to 10 **[1]**
Pests and Diseases Management	Spraying machine	Agricultural Machinery Fleet	PP, 15 m, 1000 dm^3	1-3-5-7-9 **[1]**	1-2-6-7 **[1]**	
Cover Fertilization	Fertilizer Spreader	Agricultural Machinery Fleet	PP, 1500 dm^3	3-5-7-9 **[1]**	6 **[1]**	From 1 to 10 **[1]**
Mechanical Weed Control	Rotary harrow	Agricultural Machinery Fleet	PP, 2,40 m	1-3-5-7-9 **[1]**	1-2-6-7 **[2]** 3-8 **[1]**	-
Harvest Operations	Harvester, Chipper, Trailer	Contractor	SPM, T, PP	2-4-6-8-10 **[1]**	5-10 **[1]**	-
Soil Final Restoration	Hoeing Machine	Contractor	P, 1,2 m	10 **[1]**	10 **[1]**	-

Table 4 shows the EEE cost for transport phase of the chain. Since the characteristics of the biomass are supposed to be unvaried for chips from both SRF and from MRF, the EEE cost for this phase is the same for both types of poplar plantations.

Summing the EEE cost for field and transport phase is possible to calculate the EEE cost for the biomass at the plant mouth of energetic conversion. This cost depends on the cutting time of the plantation as well as on the transport distance between the farm and the conversion plant.

After the field and transport phase, the EEE cost for the SRF plantations is equal to 96.8 €/t_{dm}, 499.1 MJ/t_{dm}, and 65.5 kg CO_2eq/t_{dm} if the distance between the farm and the conversion plant is 70 km, while for longer distances (450 km), this cost is significantly higher and reaches 151.7 €/t_{dm}, 1058.9 MJ/t_{dm}, and 120.8 kgCO_2eq/t_{dm}. In the case of medium rotation forestry, for the shorter distance, the EEE cost is 63.3 €/t_{dm}, 343,1 MJ/t_{dm}, and 44.2 kgCO_2eq/t_{dm} and equal to 118.5 €/t_{dm}, 902.9 MJ/t_{dm}, 99.4 kgCO_2eq/t_{dm} when the distance is 450 km. At the end of the transport operations, the energetic cost represents a variable share of the LHV (MJ/kg_{wb}) of the biomass: 15,3% for SRF in which the biomass is transported for a long distance, 7.2% for SRF when the product is destined to supply small plants, and 13.0% (d = 450 km) and 4.9% (d = 70 km) if the wood chips come from MRF.

Table 2: Production factors utilized within simulation on SRF and MRF [4, 5]

PRODUCTION FACTORS	QUANTITY		
	Unit	SRF	MRF
Planting material	cuttings/ha plant rod/ha	5560	1150
Organic Manure	t/ha	50	50
N fertilizer (covering)	kg/ha	320	200
Herbicide	kg/ha	20	12
Pesticide (pyrethroid)	kg/ha	10	4
Water	m^3/ha	2000	1600

Table 3: Field phase; EEE costs for two different cutting time

EEE COSTS FIELD PHASE	Unit	SRF	MRF
Economic	€/t_{dm}	92,4	59,5
Energetic	MJ/t_{dm}	456	301
Environmental	kg CO_2eq/t_{dm}	61,5	40,1

Table 4: Transport phase; EEE costs for two different distances

EEE COSTS TRANSPORT PHASE	Unit	Chip Wood	
		d = 70 km	d = 450 km
Economic	€/t_{dm}	4,13	59,0
Energetic	MJ/t_{dm}	42,1	601,9
Environmental	kg CO_2eq/t_{dm}	4,15	59,1

Comprehensive Sustainability is expressed by all 3 results obtained by the simulation. The smaller the area of the triangle identified by the three costs (economic, energetic, and environmental), the higher the energy-crop sustainability. Figure 1 shows the EEE cost for the different technical solutions studied; in blue are the results for SRF, while MRF results are shown in orange. Regarding the two different transport distances, on the left are shown the results for d = 70 km, and on the right are shown the results for d = 450 km.

The *Global Sustainability Index*, represented by the triangular area, can be calculated by means of Heron's formula. The highest is the GSI, and the lower is the global sustainability of the solution studied. The GSI is 348 and 838 for SRF, while it reaches 617 and 191 for MRF, for short and long transport distances, respectively.

5. Discussion and Conclusions

In the near future, the role that renewable energies can play in order to achieve the ambitious objectives fixed by the European Union is decisive; among the renewable energies, the agro-energy chains appear to be one of the most promising. On the other hand, the development of energy production in agriculture is linked strongly to the possibility that farmers can obtain satisfactory economic results. For this reason, in recent years, several kinds of public grants have been foreseen in order to induce farmers to plant energy crops. In addition to the economic aspects, the energetic and environmental issues also must be taken into account in order to avoid the diffusion of agro-energy chains that are effective from a monetary point of view but not functional regarding the others two topics that determine the Global Sustainability of the chain.

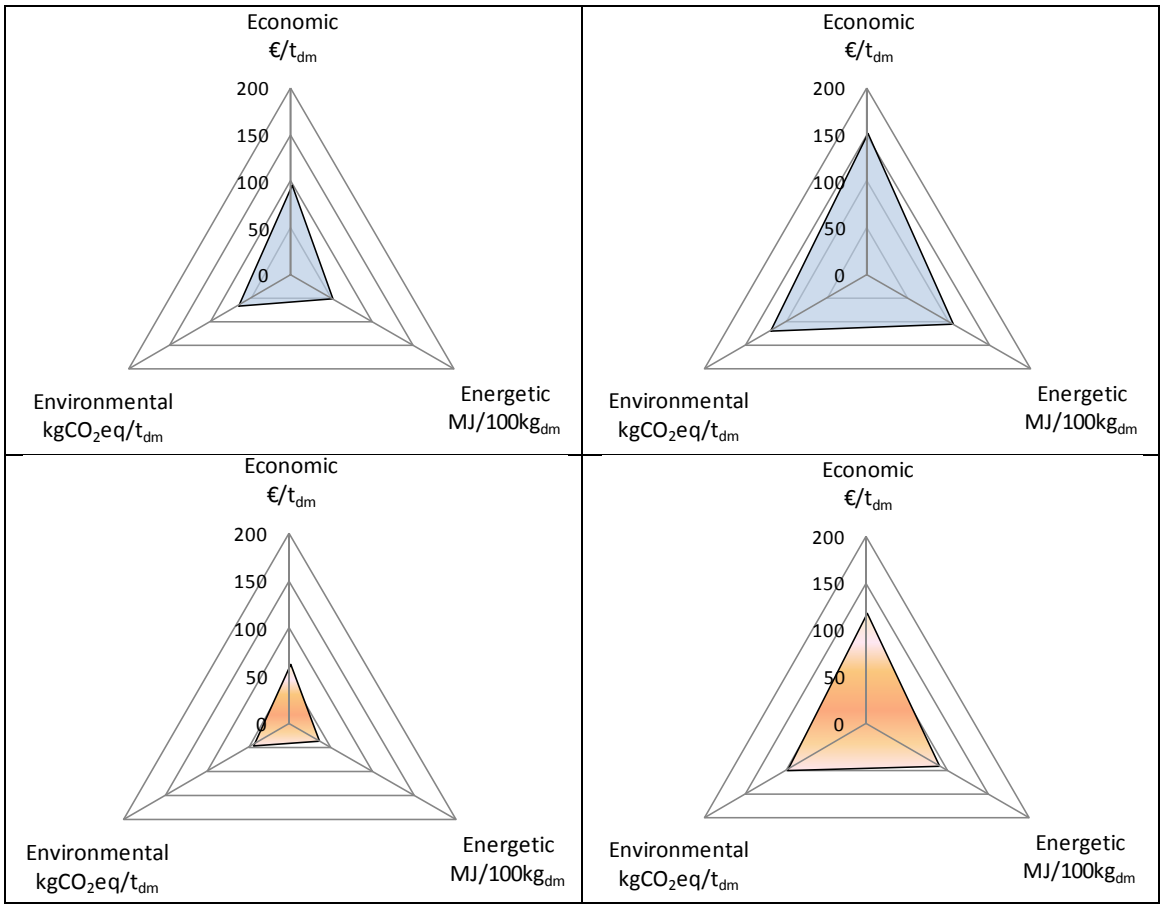

Figure 1 – EEE cost at plant mouth for the different scenarios analyzed

In Italy, good results have been achieved for wood energy crops, and today, a large area of SRC is cultivated. Nevertheless, two different kinds of poplar plantations are still practiced: SRF with short intervals between two harvests and MRF in which the harvests are separated by at least 4 to 5 years. Considering that the production and the transport to the conversion plants are the more energy intensive operations of the agro-energy chains, the present work is focused on the analysis of the economic, energetic, and environmental performances of these phases of the chains, comparing the results between SRF and MRF.

The analysis has been carried out to show that MRF, as compared with SRF, allows farmers to reach better results on all three levels studied. For the MRF, the higher yield and the lower level of input used during the crop cycle (such as nitrogen fertilization) allow the farmer to obtain a better EEE Cost and, consequently, a higher global sustainability.

Regarding transport, the distance between farm and conversion plant must be evaluated carefully; the EEE cost at plant mouth is significantly higher if the biomass transformation takes place in big plants far from the production area. In this analysis, we supposed that the lorry never travels empty, thus the reduction of the transport cost can be achieved only by the reduction of the distance. Accordingly, the development of several small and medium plants is preferable as opposed to the growth of a few large plants with a very large supply area.

The developed software is a useful tool in order to assess the EEE performances of the different agro-energy chains. Implementation of the last phase of the chains (conversion operations) will allow us to determine not only the agro-energy chain costs but also the output and benefits for the three levels considered.

References

[1] Bini G., Magistro S., Manuale dei fattori di emissione nazionali, Centro Tematico Nazionale Atmosfera Clima ed Emissioni Aria, Bozza Rapporto n.1, 2002, p. 1-193.

[2] Borjesson P., Energy analysis of biomass production and transportation. Biomass & Bioenergy, 1996, 11 (4), p. 305-314.

[3] Dubuisson X., Sintzoff I., Energy and CO_2 balances in different power generation routes using wood fuel from short rotation coppice. Biomass&Bioenergy, 1998, 15, p. 79-390

[4] Fiala M. et altri, Short Rotation Coppice in northern Italy: comprehensive sustainability, 18° European Biomass Conference, Lyon, 3-8 may 2010.

[5] Fiala M., Bacenetti J., Pioppo da biomassa in rotazione biennale,Sherwood, 2010,165.

[6] Heller et al., Life cycle assessment of a willow bioenergy cropping systems. Biomass & Bioenergy, 2003, 25, p. 147-165.

[7] Jarach M., Sui valori di equivalenza per l'analisi e il bilancio energetici in agricoltura. Rivista di Ingegneria Agraria, 1985, 2, p. 102-114.

[8] Koeleian G., Renewable energy from willow biomass crops: Life cycle energy, environmental and economic performance. Critical Reviews in Plant Sciences, 2005, p. 1-23

[9] IPCC, Guidelines for National Greenhouse Gas Inventories—Workbook, 1997.

[10] Lai R., Carbon emission from farm operations. Environment International, 2004, 30, p. 981-990.

[11] Lazzari M., Prontuario di Meccanica Agraria e Meccanizzazione, REDA, 2005.

[12] Matthews R., Modelling of energy and carbon budgets of wood fuel coppice systems. Biomass & Bioenergy, 2001, 21, p. 1-19.

[13] Slesser M., Wallece I., Energy consumption per tonne of competing agricultural products available to the EC (Commission of the European Communities, ed.), Information on Agriculture, 1982, 85, p. 168.

[14] Walle I.V. et al., Short-rotation forestry of birch, maple, poplar and willow in Flanders (Belgium) II. Energy production and CO2 emission reduction potential. Biomass and Bioenergy, 2007, 31, p. 276-283.

Integral analysis of feedstocks and technologies for Biodiesel production in tropical and subtropical countries

Carlos Ariel Cardona[1,*], Luis Eduardo Rincón[1], Juan Jacobo Jaramillo[1]

[1] *Universidad Nacional de Colombia sede Manizales, Colombia*
** Corresponding author. Tel: +57 3116007411, Fax: +57 68863220, E-mail: ccardonaal@unal.edu.co*

Abstract: In this work different methodologies from process engineering based on conceptual design and process simulation with ASPEN PLUS, life cycle assessment and waste reduction algorithm are used for energy, and environmental impact assessment of 5 different feedstocks (Palm, Jatropha, Microalgae, Tallow, Waste Cooking Oil) using 3 different technological configurations from industry, such processes with acid catalysis, basic catalysis and cogeneration, at Colombian and Peruvian context. It was found how productivities for process catalyzed with NaOH are comparatively higher (1.007-1.014 kg of Biodiesel per kg of Crude Oil), than those catalyzed with H_2SO_4 (0.845-0.949 kg of Biodiesel per kg of Crude Oil). The Production costs for basic catalyzed processes (USD/L 0.408-0.505) were higher than those for acid catalyzed processes (USD/L 0.219-0.257). The PEI (Potential Environmental Impact) generated for basic catalyzed, had a PEI per kg between -0.078 and -0.033, while acid catalyzed -0.031 and -0.025. Finally LCA for jatropha and palm oil process, evidence Ecosystem Quality damage, a Resources damage, a Human Health damage lower for Jatropha oil in comparison to Palm oil. The Jatropha oil, in a basic catalyzed configuration with energy cogeneration is the best alternative of process, environmental and economics by biodiesel production.

Keywords: *Integral Analysis, Biodiesel, WAR algorithm, LCA, Economic Evaluation*

1. Introduction

Biodiesel is produced from various fat and oils with vegetable, animal or algae origin. These Feedstocks (mainly composed by triglycerides), through transesterification reaction with short chain alcohols and in presence of catalyst, yields to fatty alkyl esters and glycerol as byproduct [1]. Almost 95% of vegetable oils used in biodiesel production are edible (palm, soybean, rapeseed oils). Different positive characteristics are related to Biodiesel: improvement of the environment, reduction of foreign oil imports, increase in rural job and energy self-sufficiency in rural areas. However, not all the above mentioned advantages are reached for all biodiesel feedstocks. Edible crops have food competition; possibly leading to food shortages and increase in their prices. Moreover, an expansion of these crops could require monoculture plantation, affecting water resources and biodiversity. Tropical and subtropical countries are called to be the future world suppliers of feedstocks and biodiesel given the high productivity in crops and algae. Most of these countries are involved in a difficult decision of what kind of feedstock should be used, and then the policies to be developed for encouraging new projects, with new feedstocks. Non-edible oils (jatropha and microalgae oil), allows the employment at massive scale of agricultural/degraded/waste lands, preserving most productive lands for food production. Animal fat (tallow oil) and waste cooking oil are valuable alternatives due their low market prices and availability. Additionally, aiming to increase competitiveness of oilseed based biodiesel plants is an actual trend to use cogeneration plants. Last allows the satisfaction of local heat and power requirements, while surplus electricity is sold to central grid [2]. In this work different methodologies from conceptual design and process simulation with ASPEN PLUS, life cycle assessment and waste reduction algorithm are used for energy, and environmental impact investigation of 5 different feedstocks using 3 different technological configurations from industry, such as process with acid catalysis, basic catalysis and cogeneration. The study was developed in the framework of two countries Colombia and Peru. As a result, two feedstocks

and one technological configuration are defined as the more convenient for biodiesel production in these countries.

2. Feedstocks for biodiesel production

In this work five feedstocks for biodiesel production, are analyzed, which can be potentially used in tropical and subtropical countries. i) **Oil Palm,** is one of the largest supply of edible oil in the world, extended throughout tropics, among major producers are Malaysia, Indonesia and Colombia with 83% of global production [3]. It is a high yield crop that requires small areas to be cultivated. ii) **Jatropha Curcas**, a Native American tropical crop, is a small tree belonging to the family of *Euphorbiaceae*. This crop is highly resistant plant capable of surviving in fallowed agricultural lands and low to high rainfall areas, being easily cultivated with little effort to sustain [4]. iii) **Microalgae**, is a promising feedstock, due to its ability to accumulate lipids and their high photosynthetic yields. Those used in biodiesel production are comprised by up to 40% of overall mass by fatty acids, among its representative species are: *Chlorella, Spirulina maxima,* and *Nannochloropsis sp.* They are fast growers in aquatic habitats, under autotrophic and heterotrophic conditions [5]. iv) **Waste oil**, includes residues from frying oils, soap stocks, yellow and brown greases, obtained from restaurants, hotels and industries; Their Free fatty acid content range between 10 and 25%, as result of frying process where heating in presence of air and light increase viscosity and specific heat, also changing surface tension, color and tendency to fat formation. This feature makes necessary a pretreatment stage before be converted in biodiesel [6]. Finally, v) **Tallow oil**, is a term referred to those fat and greases obtained in slaughter processing facilities from animals. Human consumption of tallow oil is low due its effect on health, finding its main use in the soap industry. However, when its market is overloaded, this oil is incinerated or disposed in landfills [7]. Because of that its use as biodiesel feedstock, is an attractive alternative due its easy availability and historical low prices.

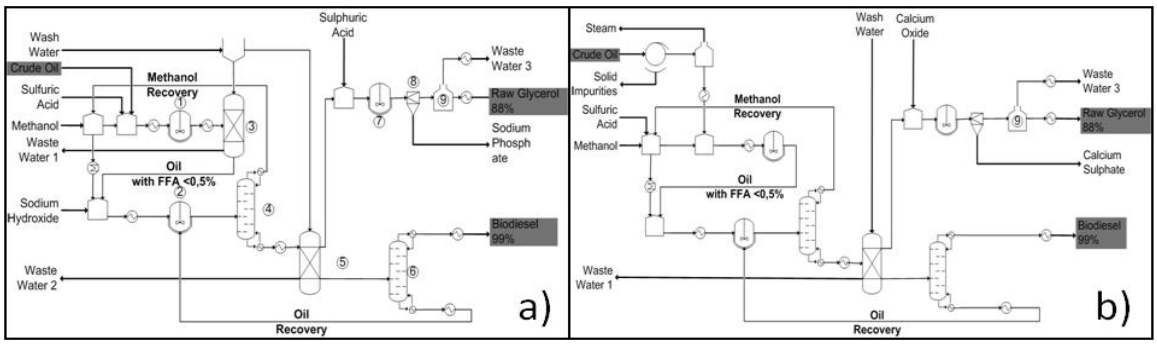

Fig. 1. Process flow diagram for Biodiesel production Using: a) Acid Catalysis; b) Basic Catalysis.

3. Technologies for Biodiesel Production

Biodiesel production can be described, in a general way, by three main sequential stages: i) **Pretreatment,** where undesired elements content in feedstock oil are withdraw. Particles, colloidal mater, pigment, extraction residues and other impurities can be removed using filtration. When water content (>0,06%) and free fatty acid (FFA) content (>4%), a saponification reaction can be induced, generating a gel soap instead of biodiesel. To avoid this is necessary dry the oil, and eliminate free fatty acids, using: Presterification or neutralization. ii) **Reaction,** in this stage, the oils suffer a transesterification reaction. Methanol is the most extensively used alcohol because its low cost and physical and chemical properties. The main catalysts, employed in transesterification process are: acids (sulphuric, phosphoric) or bases (sodium and potassium hydroxide) [8]. iii) **Separation and Purification**

stage is employed to produce biodiesel with high quality requirements. Biodiesel purification is performed by either of two main routes: 1) separating first esters and glycerin, before recover non c onverted alcohol or 2) using vacuum distillation to separate non c onverted alcohol, using then a decanter to separate glycerin and biodiesel [8]. Obtained biodiesel is then purified, removing excess of alcohol, catalyst, neutralization salts and possible soaps formed. The Selected technology for biodiesel production determines main process variables, such as: reaction time, phase, catalyst, as well as energy consumption (see Fig 1).

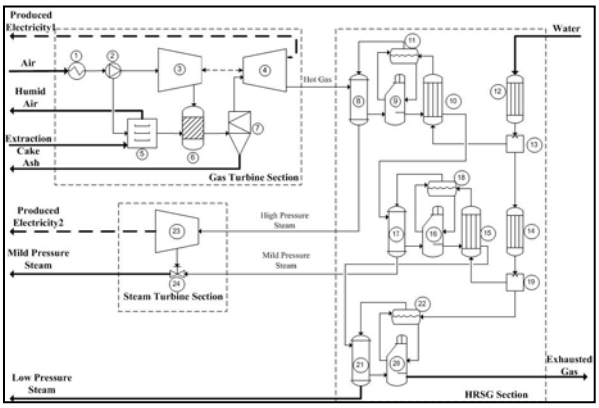

Fig. 2. Process flow diagram for Cogeneration system based on extraction cake residues

Cogeneration plants integrated to biodiesel production facilities usually employs extraction cakes and other biomass residues as fuel in a configuration called biomass fired cogeneration. Combined production of mechanical and thermal energy has remarkable cost and energy savings. Among available technologies for biomass fired cogeneration, the combined cycle gas turbine (CCGT), is considered as the most energy efficient. CCGT configurations are composed by: Gas Turbine, Heat steam recovery generator (HSRG) and Steam Turbine (see Fig. 2) [9].

4. Methodology

The simulations of biodiesel production and heat and power cogeneration were carried out in Aspen Plus 2006.5 (Aspen Technologies Inc., USA). This scheme allows obtaining data of mass and energy balances; as well as, basic engineering estimations of equipment size and its energy consumption. Feedstocks (Palm, Jatropha, Microalgae, Tallow and Waste cooking oils) for biodiesel production, were modeled as a sort of pseudocomponents, created to represent triglycerides and methyl esters; according to Chang and Liu methodology [10]. Conversely, Palm oil cake, jatropha oil cake and microalgae paste were introduced to simulator database as non conventional components according to its elemental and immediate analysis. Physicochemical properties for pseudocomponents, were estimated using the Marrero and Gani Method [11]. UNIFAC Dortmund for liquid phase, Soave Redlich Kwong with the Bosto Mathias modification for the vapor phase; water enthalpy calculated with NBS steam tables, were used as base methods. The Kinetic model for acid and basic catalysis, employed in this work, was reported by Granjo et al. [12], as first order and second order expressions, respectively. Biodiesel simulated process use a same flow rate input of 1000 kg/h, to make a comparison among yields for all processes. Additionally, from these values, was calculated a residue flow rate for palm oil cake, jatropha oil cake and microalgae paste; using it as input for the biomass fired cogeneration system. The economic analysis was performed using Aspen Icarus Process Evaluator package (Aspen Technology, Inc., USA), to calculate a mean cost in US dollar per liter for biodiesel produced with the selected feedstocks. This analysis was performed using the design information provided by Aspen

Plus, under the economic conditions of Colombia (annual interest rate of 17% and tax rate of 33%) and Peru (annual interest rate of 18% and tax rate of 30%). A straight Line depreciation method, at 12 year of analysis period, was considered. For feedstock prices, were employed the international reports from ICIS pricing; while, operative charges such operator and supervisor labor cost were defined for both countries at USD 2.14/h and USD 4.29/h, respectively. Electricity, potable water, low and high steam pressure costs were USD 0.0304/kWh, USD 1.25/m^3, USD 8.18/ton. The environmental impact was assessed with WAR, Waste Reduction algorithm (EPA, USA), to estimate the potential environmental impact (PEI) generated in the biodiesel production process. Considering eight environmental impact categories: Human toxicity potential by ingestion (HTPI), Human toxicity potential by exposure both dermal and inhalation (HTPE), Terrestrial toxicity potential (TTP), Aquatic toxicity potential (ATP), Global warming potential (GWP), Ozone depletion potential (ODP), Photochemical oxidation potential (PCOP), and Acidification potential (AP). The mass flow rate of each component in the process streams is multiplied by its chemical potency; determining its contribution to the potential environmental impact categories [13]. To compare the environmental profiles for all process, total PEI was determined by the sum of all (eight) potential environmental impact categories as follows:$\sum_{i=1}^{n} \propto_i \varphi_i$, where α_i is the weighting factor for potential environmental impact category *i*, and φ_i represents the potential environmental impact for category *i*. In this work all of the weighting factors were set equal to 1. Finally, Life cycle assessment was performed for those process with a potential impact in land change use (LCU), such palm and jatropha; using a demo version of SimaPro 7, with Eco-indicator 99 (E) as base method. The LCA study consists of four steps: Defining the goal and scope of the study; making a model of the product life cycle with all the environmental inflows and outflows; understanding the environmental relevance of all the inflows and outflows and finally the interpretation of the study [14].

Table 1. Simulation Results for Biodiesel Production using Basic or Acid Catalysis

	Basic Catalysis			**Acid Catalysis**	
	Palm Oil	**Jatropha Oil**	**Microalgae Oil**	**Tallow Oil**	**Waste Cooking Oil**
Materials (kg/h)					
Crude Oil	1000.00	1000.00	1000.000	1000.00	1000.00
FFA content (% wt)	6%	4%	4%	15%	10%
Water content (% wt)	0%	0%	0%	8%	12%
Methanol	160.21	214.75	207.77	1579.07	1772.44
NaOH	9.40	9.60	9.29	-	-
Water	1400.00	1400.00	1400.00	1250.00	1400.00
H_2SO_4	21.00	21.45	20.75	35.00	41.20
CaO	-	-	-	30.00	29.60
Products (kg/h)					
Biodiesel @>99% wt	1007.46	1009.69	1014.62	949.85	847.63
Glycerol @>88% wt	113.05	117.34	127.33	81.95	82.07
Waste Water	1010.95	942.77	1062.20	2163.03	1836.84
$CaSO_4$	-	-	-	104.51	95.27
Na_2SO_4	10.64	17.03	17.03	-	-

5. Results

In the simulation of biodiesel production for acid and basic catalyzed processes using palm, jatropha, microalgae, tallow and waste cooking oils, as feedstocks (see Table 1), was found

how productivities for process catalyzed with NaOH are comparatively higher (1.007-1.014 kg of Biodiesel/kg of Crude Oil), than those catalyzed with H_2SO_4 (0.848-0.949 kg of Biodiesel/kg of Crude Oil). Otherwise, Methanol consumption as well as global energy consumption (heating and electricity) is higher for acid catalyzed process, requiring 1.579-1.772 kg of Methanol/kg of crude oil and heating of 53.389 - 69.112 MW respectively. About process residues, acid catalyzed processes also have higher production rates for waste water (1.863-2.163 kg of Water/kg of crude oil). Simulation results for the biomass fired cogeneration plant using palm oil cake, jatropha oil cake and microalgae paste as fuels (see Table 2), reveals how heating energy production from jatropha cake (31.34 MW) is higher than produced with Microalgae paste (33.82 MW) and palm oil cake (20.61 MW). Consequently, only heating requirements for biodiesel production from jatropha (26.59 MW) are fully satisfied. Biodiesel from palm oil and microalgae oil meet only 68.13% and 74.15%, respectively of its Heating requirements. Regard to electricity, all cogeneration processes cover at 100% biodiesel plant requirements, with a surplus able to be sold. However, among three residues consider, was microalgae paste who cogenerates more electricity (8.34 MW) than jatropha oil cake (7.06 MW) and Palm Oil Cake (4.88 MW).

Table 2. Cogeneration Results for Extraction residues Based Biomass fired cogeneration system

	Jatropha Oil Cake	**Palm Oil Cake**	**Microalgae Oil Paste**
Available Residue [kg/h]	3092	2304	3964
Calorific Value [MJ/kg]	15.77	12.32	14.21
Total Cogenerated Heating [MW]	31.34	20.61	33.83
Total Cogenerated Electricity [MW]	7.66	4.88	8.34

Table 3. Economic Evaluation Results for Biodiesel Production using Basic Catalysis

	Jatropha Oil	**Palm Oil**	**Microalgae Oil**	**Waste Cooking Oil**	**Tallow Oil**
	USD/L	USD/L	USD/L	USD/L	USD/L
Raw material Cost	0.325	0.426	4.646	0.139	0.186
Total utilities Cost	0.022	0.021	0.022	0.052	0.044
Operating Labor	0.008	0.008	0.008	0.009	0.008
Maintenance	0.005	0.004	0.005	0.002	0.002
Operating Charges	0.002	0.002	0.002	0.002	0.002
Plant Overhead	0.006	0.006	0.006	0.006	0.005
General and Administrative Cost	0.039	0.037	0.038	0.008	0.010
Subtotal Cost	0.408	0.505	4.727	0.219	0.257
Credit by electricity selling	- 0.252	- 0.168	- 0.278	0.000	0.000
Total Cost with Cogeneration	0.157	0.337	4.449	0.219	0.257

Results of economic evaluation for biodiesel production under Colombian and Peruvian contexts were quite similar and because of that, in table 3, average results are presented. As highlights results, Raw material cost for basic catalyzed processes (USD 0.325-4.646/L) were higher than those for acid catalyzed processes (USD 0.139-0.186/L). Otherwise, Utilities costs for acid catalyzed processes (USD 0.044-0.052/L) were higher than basic catalyzed process (USD 0.021-0.022/L). Remaining cost, for both processes were similar. As result, Production costs for basic catalyzed processes (USD 0.408-0.505/L) were higher than those for acid catalyzed processes (USD 0.219-0.257/L). However, considering Potential income for electricity selling at average price between Colombia and Peru, can be seen how total

production cost for jatropha, palm and microalgae biodiesels were reduced to 0.157 USD/L, 0.337 USD/L and 4.449 USD/L, respectively.

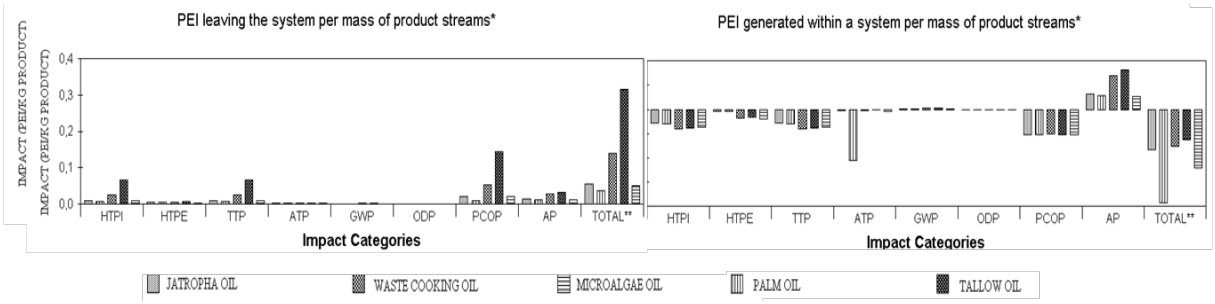

Fig. 3. PEI (Potential Environmental Impact) Analysis for Biodiesel Production from different feedstocks.

Regarding to environmental analysis; WAR analysis results of 5 biodiesel feedstocks, stated analyzing by process, how basic catalyzed had a PEI per kg of product ranging between 0.037 and 5.518e-2, while acid catalyzed catalysis between 0.139 and 0.317 for emissions output. Furthermore, when these feedstocks were analyzed by emission generation, basic catalyzed raw materials, had a PEI per kg between -0.078 and -0.033, while acid catalyzed -0.031 and -0.025 (see Fig. 3). Finally LCA analysis performed with SimaPro 7, for jatropha and palm oil process, evidence a Ecosystem Quality damage of 0.062 and 0.087 PDF*m^2*yr. Besides of a Resources damage of 1.07 and 1.49 MJ surplus, while Human Health damage was of 1.96e-6 y 2.73e-6 Daly, respectively.

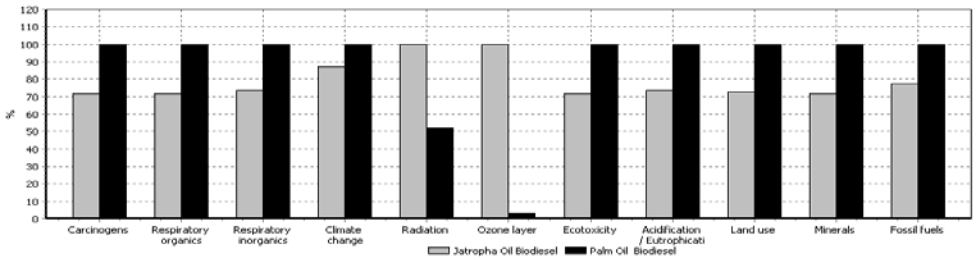

Fig. 4. LCA for Biodiesel Production from Jatropha oil and Palm oil

6. Discussion and Conclusions

In this work, the obtained results reveal how with selected five feedstocks is possible to obtain high quality biodiesel (>99 wt); besides, raw glycerol (88%wt). Among results for chemical processes simulation, can be seen how basic catalyzed processes have higher biodiesel yields (74-78%), than acid catalyzed ones (54-63%), with the consequent reduction in the total biodiesel produced. These results are lower compared with values between 90-95% reported from biodiesel simulations, on literature [15]. This fact can be explained by the lower quality of feedstocks considered, especially tallow and waste cooking oil, where a high FFA content and impurities presence; which, although increase the simulation quality, reduces the amount of initial reactant available for transesterification reaction, reducing also biodiesel produced.

Regard to cogeneration results, these gave an advantage to basic catalyzed processes due to the possibility of employ its extraction residues to generate heat and power. The bigger amount of heating potential was released by jatropha oil cake; while the higher power potential by microalgae oil paste. This result can be partially explained by the high calorific value and available flow of these residues, which increase its potential to generate steam and consequently produce heat and power (see Table 2). Jatropha oil cake results were the best,

due its capacity to meet heating requirements of the biodiesel plant generating also an important amount of electricity able to be selling to central grid.

Economic evaluation of biodiesel production process, without cogeneration, shows how production cost for basic catalyzed processes initially were higher than acid catalyzed, despite high methanol consumption of this last. These results were agreed with those reported on literature where biodiesel production cost range between USD $ 0.30 – 0.6/L [16]. The main component of this production cost was the raw material price, which is higher for vegetable oils (jatropha and palm) than for residual oils (waste cooking and tallow), explaining their lower production cost. However, when a cogeneration scheme is included for processes based on vegetable oils, which can employs its extraction residues as fuel in a biomass fired scheme, the total production cost of basic catalyzed process is reduced (see Table 3). Apart mention, deserves microalgae oil, which price as feedstock still today is higher, mainly due the high energy consumption in its processing, either in open pounds or bioreactors; in the future is expected is expected a reduction in its price using better microalgae oil production technologies.

The Environmental analysis results, reveals with WAR algorithm, how despite all processes had a positive PEI, still all of them can generate acid rain because its positive acidification potential produced by the sulphuric acid. In these sense, acid catalyzed processes had more polluting waste streams than basic catalyzed. Particularly, output emissions from process waste streams for waste cooking oil, had the more positive PEI among all simulated processes. This effect could be explained by the substances contained in its process residues, which had a high degree of potential PCOP influenced by acid catalysis, increasing the total values. Otherwise, palm and jatropha oils had the comparatively lesser PEI, revealing them as environmentally friendly feedstocks; because, they are converted to high value products in a cleaner process (basic catalysis) being more environmentally favorable, reducing significantly the aquatic toxicity potential. Regard to LCA analysis performed to jatropha and palm oils as best WAR results, was found that most promising feedstock was the jatropha oil because its comparatively low land use than the palm and its possibility of growth in fallow agricultural lands. Also, its impact on climate change and emissions were lower than palm at every stage, from cultivation to waste scenarios.

In conclusion, the more convenient configuration for biodiesel production in tropical and subtropical countries is employ jatropha oil in a basic catalyzed scheme, integrated to a cogeneration plant fired with jatropha oil cake. This configuration is able to produce high rates of biodiesel with the lower production cost, improved by electricity selling. Also, this configuration proves, be the most environmentally friendly with lesser potential emissions and climate change effect, as well as reduced land use by its ability to be growth in marginal lands.

Acknowledgements

The authors express their acknowledgments to the Colombian Institute for Development of Science and Technology (Colciencias) and Universidad Nacional de Colombia sede Manizales, for the financial support of this work.

References

[1]. Martín, C., et al., Fractional characterisation of jatropha, neem, moringa, trisperma, castor and candlenut seeds as potential feedstocks for biodiesel production in Cuba. Biomass and Bioenergy, 2010. **34**(4): p. 533-538.

[2]. Reith, J.H., et al., Co-production of bio-ethanol, electricity and heat from biomass residues, in 12th European Conference and Technology Exhibition on Biomass for Energy, Industry and Climate Protection. 2002: Amsterdam, the Netherlands.

[3]. Hoh, R., Malaysia Biofuels Annual Report 2010, G.A.I. Network, Editor. 2010, USDA Foreign Agricultural Service: Kuala Lumpur.

[4]. Sysaneth, S. and L. Duangsavanh, Impacts of Jatropha Plantation on Smallholders, T.S.M.R. Network, Editor. 2009, National Agriculture and Forestry Research Institute.

[5]. Lardon, L., et al., Life-Cycle Assessment of Biodiesel Production from Microalgae. Environmental Science & Technology, 2009. **43**(17): p. 6475-6481.

[6]. Phan, A.N. and T.M. Phan, Biodiesel production from waste cooking oils. Fuel, 2008. **87**: p. 3490-3496.

[7]. da Cunha, M.E., et al., Beef tallow biodiesel produced in a pilot scale. Fuel Processing Technology, 2009. **90**(4): p. 570-575.

[8]. Ma, F., L.D. Clements, and M.A. Hanna, Biodiesel Fuel from Animal Fat. Ancillary Studies on Transesterification of Beef Tallow. Industrial & Engineering Chemistry Research, 1998. **37**(9): p. 3768-3771.

[9]. Uddin, S.N. and L. Barreto, Biomass-fired cogeneration systems with CO2 capture and storage. Renewable Energy, 2007. **32**(6): p. 1006-1019.

[10]. Chang, A.-F. and Y.A. Liu, Integrated Process Modeling and Product Design of Biodiesel Manufacturing. Industrial & Engineering Chemistry Research, 2009. **49**(3): p. 1197-1213.

[11]. Marrero, J. and R. Gani, Group-contribution based estimation of pure component properties. Fluid Phase Equilibria, 2001. **183-184**: p. 183-208.

[12]. Granjo, J.F.O., B.P.D. Duarte, and N.M.C. Oliveira, Kinetic Models for the Homogeneous Alkaline and Acid Catalysis in Biodiesel Production, in Computer Aided Chemical Engineering, C.A.O.d.N. Rita Maria de Brito Alves and Evaristo Chalbaud Biscaia, Jr., Editors. 2009, Elsevier. p. 483-488.

[13]. Young, D., R. Scharp, and H. Cabezas, The waste reduction (WAR) algorithm: environmental impacts, energy consumption, and engineering economics. Waste Management, 2000. **20**(8): p. 605-615.

[14]. Mata, T.M., Young, D.M., and Costa C., Life Cycle Assessment of Gasoline Blending Options. Environmental Science Technology, 2003. **37**: p. 3724 3732.

[15]. Zhang, Y., et al., Biodiesel production from waste cooking oil: 1. Process design and technological assessment. Bioresource Technology, 2003. **89**(1): p. 1-16.

[16]. Chisti, Y., Biodiesel from microalgae. Biotechnology Advances, 2007. **25**(3): p. 294-306.54

Evaluation of the factors that affect the lignin content in the reed canarygrass (*Phalaris arundinacea* L.) in Latvia

Liena Poiša[1,*], Aleksandrs Adamovičs[1], Rasma Platače[2], Ērika Teirumnieka[2]

[1] *Institute of Agrobiotechnology, Latvia University of Agriculture, Jelgava, Latvia*
[2] *Rezekne Higher Education Institutions, Rezekne, Latvia*
** Liena Poiša. Tel: +26807673, Fax: +37163005682, E-mail: lienapoisa@inbox.lv*

Abstract: In the production of granules from plants the cohesive substance lignin has a great importance, as it holds the granule together and does not allow it to disintegrate. The objective of this research was to evaluate the influencing factors of lignin content in reed canarygrass (*Phalaris arundinacea* L.) crop yield. In this research the varieties of reed canarygrass 'Marathon' and 'Bamse' were analysed for yields of first and second year. The lignin content of the samples was established by Classon's method. Arsenic (As), Cadmium (Cd), and Lead (Pb) and other chemical elements were established in the reed canarygrass samples with the spectrometer Optima 2100DV. The reed canarygrass second year crop yield was 3-4 times greater than the first year crop yield. A significantly correlation ($p<0.05$) was established in the first crop yield October samples between lignin and natrium (Na). Some correlation relationships are contradictory, which confirms that within the plant growth period the meteorological conditions are of great importance. Analysing the determining factors of lignin content it can be seen that they were influenced by the interaction of various factors - the sowing and growing period, the variety and the N-fertilizer rate application.

Keywords: *Ashes, Heavy Metal, Lignin, N-fertilizer Rate, Phalaris arundinacea L., Yield*

Nomenclature

A	*area of the plots* ..... m^2	*DM*	*dry matter* ..... $t \cdot ha^{-1}$
R	*rainfall* ..... *mm*	*N*	*nitrogen fertilizer rate* ..... $kg \cdot ha^{-1}$
H	*plant height* ..... *m*	*Hv*	*heating value* ..... $MJ \cdot kg^{-1} DM$
L	*lignin content* ..... $g \cdot kg^{-1}$		
T	*mean temperature* ..... *K*		

1. Introduction

The most common natural polymer is cellulose, which with lignin and hemicellulose are the main components of plants (Gosselink et al., 2004; Lignin…, 2009). Cellulose pulp is considered as the first depositary of the sun's energy (Gosselink et al., 2004). In nature lignin is very resistant to degradation, as it has strong chemical bonds (McCrady, 1991).

Lignin first appeared hundreds of millions years ago, when plants started to grow vertically upwards. Lignin can be found in all caulescent plants, mainly in the cells and cellwalls. It regulates the transportation of liquid in plant cells (partly strengthening the cell walls, partly regulating the flow of liquid) also it a llows plants to grow longer to better compete for sunlight (McCrady,1991; Rouhi, 2000; Lignin…, 2009).

Lignin which is found in a natural state (protolignin) is of various types, which are common to deciduous trees, conifer trees and stemgrasses. Each type has a lot of variations; lignin can vary with each variety, each plant group, and at the same time even within one cell, and also according to the age of the plant (McCrady, 1991; Zaķis, 2008; Lignin…, 2009).

The technical lignin is used as a bonding material, a surfactant, growth enhancer, a supplementary substance for composite materials and other uses (Skudra et al., 2010). Up to

now only 2% of lignin had been used in cellulose and paper production (Gosselink et al., 2004). Products from lignin could be used to replace fossil resources (Gosselink et al., 2004). Also it must be noted, that low lignin content helps animals digest fodder. If the biosynthesis of lignin is complete, then the cell dies (Rouhi, 2000).

Today there are many studies concerning lignin as a by-product of wood-pulp processing. In Latvia it is traditional to produce energy from forestry products, but due to the sharp increase in price for fossil energy, it has become profitable to produce energy from agricultural biomass production. Reed canary grass is suitable for the Latvian agricultural climatic and growth conditions and can be used as a local resource for obtaining renewable energy.

Lignin is used variously, for instance in the production of materials (polymer, glue) and specific chemical substances (concrete additives, emulsifiers, binding materials) (Gosselink et al., 2004). In granule production chemical additives are not desirable (glue, lacquer, etc.) therefore the binding material lignin is important, which holds the granule together and does not allow it to disintegrate. Lignin improves the thermochemical energy transformation effectiveness (Boateng et al., 2006).

The objective of this research: to evaluate the influencing factors of lignin content in reed canarygrass (*Phalaris arundinacea* L.) crop yield.

2. Methodology

2.1. Field trials

The object of the research is reed canarygrass (*Phalaris arundinacea* L.). Three repeat experiments in the field with reed canarygrass varieties 'Marathon' and 'Bamse' were carried out in sod-podzolic loamy soil (the organic content of the soil - 5.2%, pH KCl - 5.8, P_2O_5 - 20 $mg \cdot kg^{-1}$, and K_2O - 90 $mg \cdot kg^{-1}$ of the soil).

The area of the plots was 16 m^2, the location of the plots was randomised. The reed canarygrass was sown after bare follow. Before sowing a complex fertiliser was applied N:P:K - 5:10:25 - 400 $kg \cdot ha^{-1}$. The nitrogen supplementary fertiliser rates: N0 - control, treatments - N30, N60, N90 $kg \cdot ha^{-1}$. Reed canarygrass variety 'Marathon' was sown on the 12th August in 2008 (henceforth 'Marathon' 08) and varieties "Marathon' and 'Bamse' - on 29th April in 2009 (henceforth 'Marathon' 09 and 'Bamse' 09). Nitrogen (N) supplementary fertiliser was given to 'Marathon' 08 on the 20th May 2009, and on the 22nd July 2009 for 'Marathon' 09 and 'Bamse' 09. On the 13th April 2010 the reed canarygrass plant growth was renewed. N fertiliser (ammonium nitrate) was applied at 21st April 2010.

The plant length was determined for five plants on each repeat occasion (for all plant stalks). The reed canarygrass samples were taken on the 12th October 2009 and the 4th April, 7th September, 6th October, 7th November 2010. The dry matter (DM) samples were taken from 0.25 m^2 areas on three occasions on the 12th October 2009, and the 4th April, 6th October 2010.

2.2. Laboratory work

Arsenic (As), cadmium (Cd), lead (Pb), titanium (Ti), potassium (K), calcium (Ca), magnesium (Mg), sodium (Na) and silicon (Si) concentrations in the reed canarygrass samples were established with the inductively coupled plasma optical emission spectrometer Perkin Elmer Optima 2100 DV. The heating value in the samples was established with the

calorimeter IKA C 5003. The ash content (three replications) was established with the accelerated standard method. Lignin content (three replications) in samples was determined using the method of Classon (Zaķis, 2008).

2.3. Meteorological conditions

The meteorological conditions were different in both trial years (Fig. 1.) The meteorological conditions for agriculture during 2009 the plant growth period had a significant deficit in rainfall. The temperature was in compliance with the long term yearly long-term average. In the winter of 2009/2010 snow was observed to be greater and the temperature was lower than the long term yearly long-term average.

On the 23rd and 24th of April 2010 there was snow and hail. The plant growth period in 2010 was characterized by higher temperatures and a lack of precipitation in April, July, August and September.

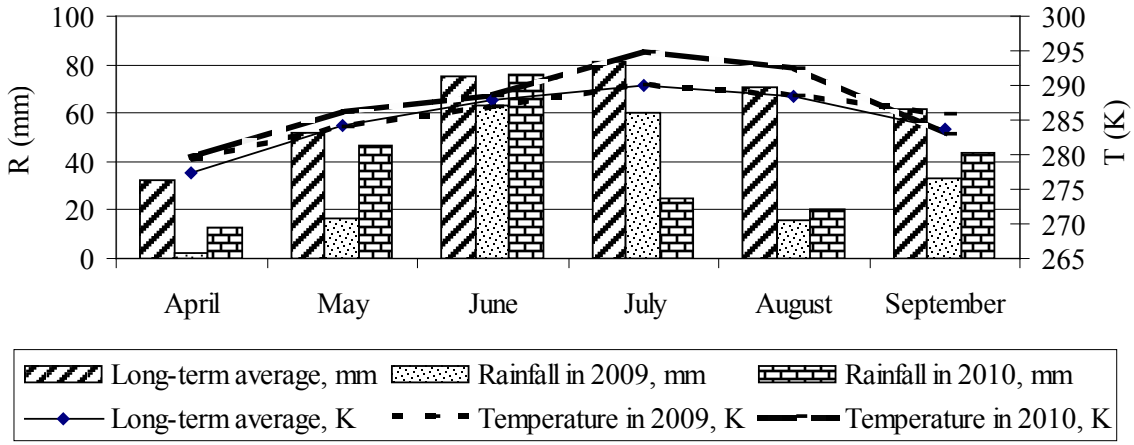

Fig. 1. Mean air temperature and sum of precipitation in 2009 and 2010 growing period.

2.4. Data analysis

The trial data were processed using correlation and variance analyses of two and three factors (ANOVA) and descriptive statistics. The means are presented with their LSD test. Representative average samples of the indicators were used in the calculations.

3. Results

The reed canary grass varieties sown in 2009, had a crop yield 3 - 4 times greater in the following year compared to the first year crop, but the 2008 sowing only produced a 2 times greater yield (Table 1). Two two-factor variance calculations showed, that the variety 'Marathon' had its crop yield for October 2010 influenced ($p<0.05$) by the sowing period ($\eta=62.5\%$) and N fertiliser rates($\eta=19.8\%$), but for both varieties 'Marathon' and 'Bamse' a significantly influence ($p<0.05$) was established for the variety($\eta=70.7\%$) and N fertiliser rates($\eta=10.8\%$). 'Marathon' 09 in the 2010 plant growth period grew three times longer compared to the year 2009, which was most influenced by N fertiliser rates ($p<0.05$).

Table 1. Reed canarygrass dry matter yield and plant length in the second crop year.

Varieties Sowing time	Fertilizer rate ($kg \cdot ha^{-1}$)	Dry matter, ($t \cdot ha^{-1}$)	Increase in comparison to the 2009 October crop yield (%)	Increase in comparison to the 2009 April crop yield (%)	Plant height (m)
'Bamse'	N0	9.80	437	456	1.548
29th April in 2009	N30	10.25	420	465	1.515
	N60	10.27	370	465	1.533
	N90	11.79	390	546	1.452
'Marathon'	N0	8.61	424	620	1.453
29th April in 2009	N30	8.94	422	493	1.566
	N60	8.87	394	406	1.527
	N90	8.57	371	384	1.485
'Marathon'	N0	8.98	196	201	1.443
12th August in 2008	N30	10.18	218	220	1.566
	N60	10.77	227	230	1.590
	N90	10.45	216	232	1.578
$LSD_{0.05varieties}$		0.19			0.024
$LSD_{0.05sowing\ time}$		0.18			0.036

A fundamental correlation ($p<0.05$) was established for the samples from the October first year crop between lignin and natrium (Na) (Fig. 2). During the investigation the significantly relationship ($p<0.05$) between the content of lignin and content of heavy metals in the reed canary grass plants was not established. Revealed a few trends ($p>0.05$), when increase lignin content in plants, decreases amount of Ca, Cd, but the amount of Si increase in plants.

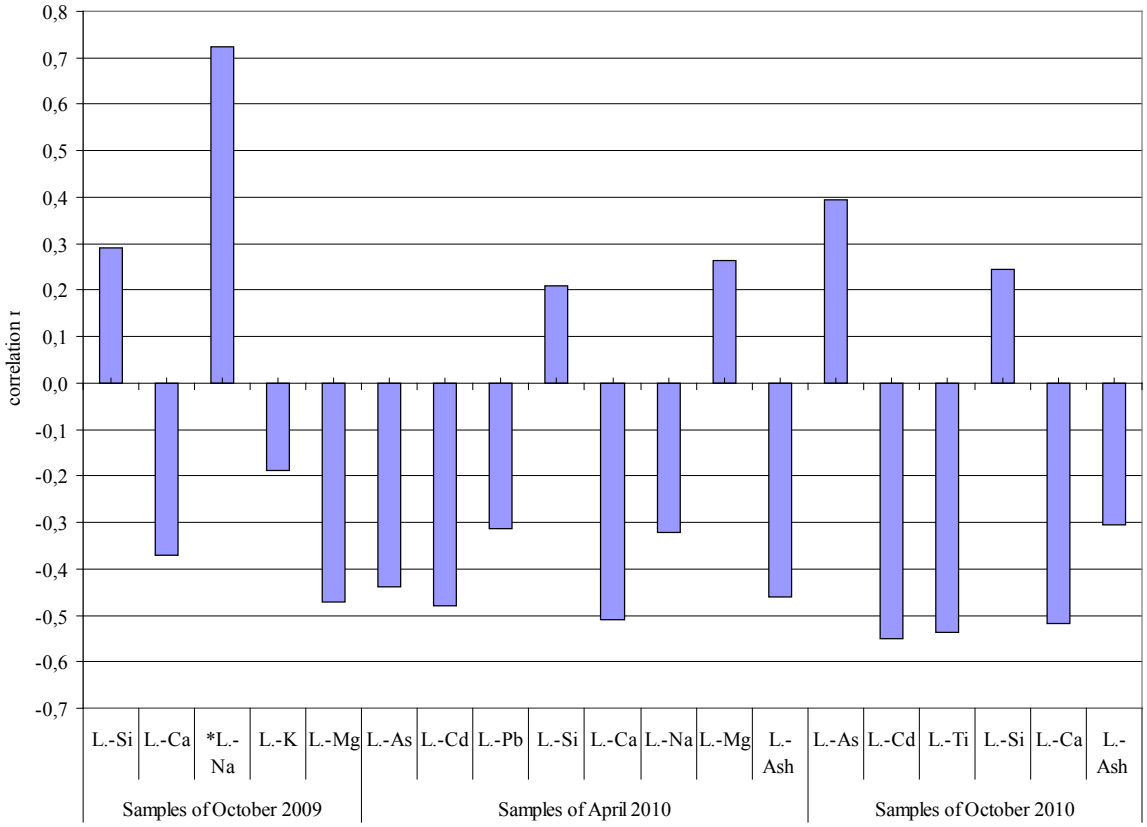

*Fig. 2. Relationship between lignin content (L.) and content of the metals in reed canary grass plants: *(p<0.05).*

Regression analysis for the samples taken in autumn 2010 shows that between lignin (y) and ash (x) content there is a significant connection (n=36; p=0.0036<0.05) which means, that between these indicators there is a linear connection.

The lignin content in the October samples from the 1st year crop yield was 140 - 210 $g \cdot kg^{-1}$, for the April samples it was 200 - 270 $g \cdot kg^{-1}$, but in the 2nd year crop yield it was from 179 $g \cdot kg^{-1}$ to 269 $g \cdot kg^{-1}$ (Fig. 3). Taking two 3-factor dispersion calculations, it can be seen, that the period when the samples are taken (η=70.1%) and the amount of the N fertiliser rate (η=14.7%) are of significant importance ($p<0.05$), but the sowing period (η=0.6%) and the chosen variety (η=3.9%) have no significant importance. The research has brought up contradictory results; in the 2009 sown varieties had the smallest lignin content using N fertiliser rate N30 $kg \cdot ha^{-1}$, but the lignin content was the largest for the 2008 sown variety 'Marathon', using N fertiliser rate N30 $kg \cdot ha^{-1}$. The polynomial equation shows lignin content depending on the sampling time (Fig. 3).

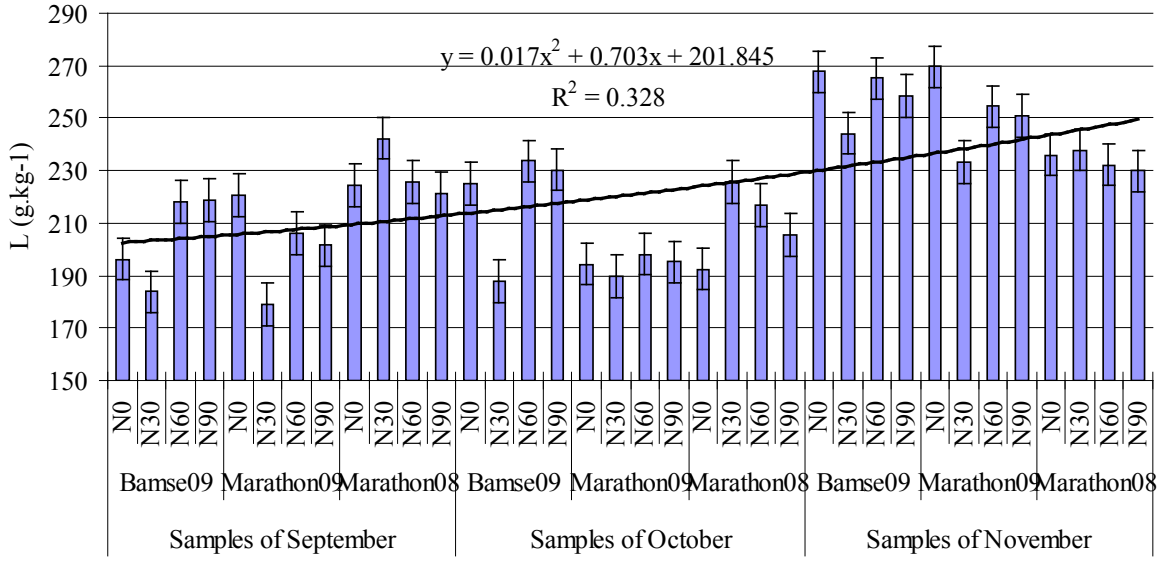

Fig. 3. Lignin content in reed canary grass 2nd year swards in 2010 (g·kg-1).

Heating value for the reed canary grass samples for the variable N90 varied from 17.16 to 18.13 MJ·ha^{-1} DM (Fig.4). A significant correlation between reed canary grass lignin content and the heating value was not established.

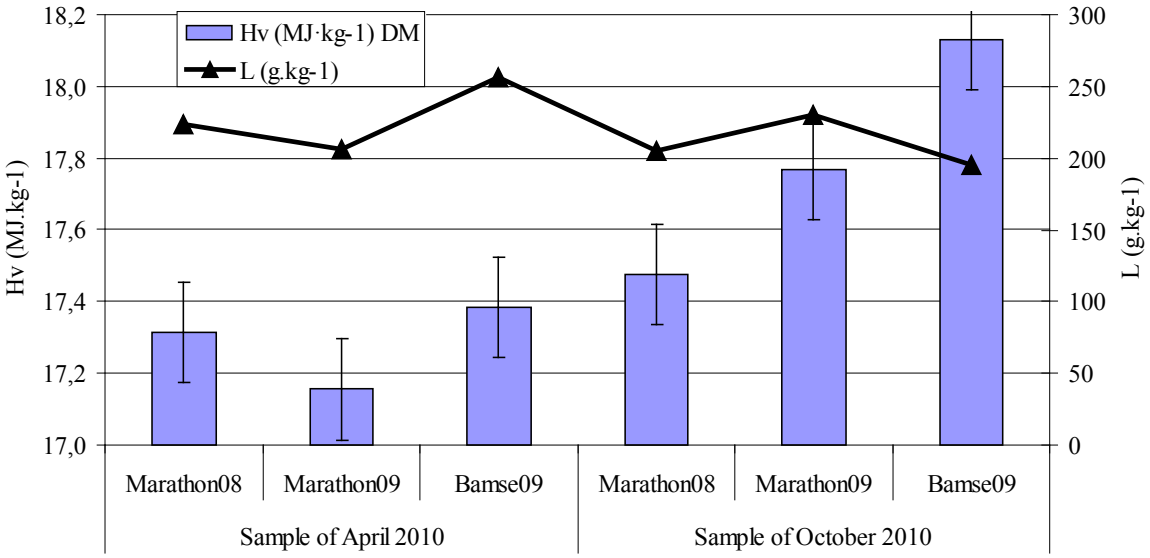

Fig. 4. Reed canary grass sample heating value and lignin content (N 90 kg·ha^{-1}).

The study will continue, because in this article is only the first and the second year yields lignin content analysis, which can vary when reed canarygrass seed get older, because now there are differences in quality indicators between the first and the second year samples.

4. Discussion and conclusion

An extended period with a precipitation deficit and air temperature above the yearly long-term average, get a negative impact on reed canarygrass productiveness during the 2010 plant growth period. Comparing lignin content correlations in relationship with various indicators

for the reed canarygrass crop yield for the 1st year, it can be seen, that for the samples these relationships are not fundamental. Data show, that great importance should be attached to the chemical composition of the plant, which can be manifested also in the genetic characteristics. A few correlative connections are contradictory, which confirms that within the plant growth period the meteorological conditions are of great importance.

Analysing the determining factor of lignin content it can be seen that they were influenced by the interaction of various factors-when the samples were taken, the sowing period, the variety and the N-fertilizer rate application. That is confirmed by other researchers, that the genetic biomass plant background, the period when samples are taken and the growing environment, influence the lignin content in plants (Boateng et al., 2006). The lignin content is significantly influenced by the age of reed canarygrass (McCrady, 1991; Zaķis, 2008; Lignin…, 2009). That means that for lignin extraction reed canary grass harvesting needs to take place as far as possible at the later stages of growth.

In the conclusion of study concluded that on the lignin content in reed canarygrass samples affect the agronomic factors - time of sowing, N fertilizer rate and harvest time. On the lignin content does not affect amount of heavy metals and other chemicals elements in plants. In study was not found that the lignin content affect on the solid fuel parameters such as ash content and heating value.

Acknowledgements

This publication has been prepared within the framework of the ESF Project „Attraction of human resources to the research of the renewable energy sources", Contract Nr. 2009/0225/1DP/1.1.1.2.0/09/APIA/VIAA/129. Thanks to Vītols Fund and the LAB-AN (Latvian Agronomic Society – Foreign Department) for granting me (L. Poiša) a bursary. The authors would like to thank L&T "Latgales lauksaimniecības zinātnes centrs" for arranging the trials of reed canarygrass; the Rezekne Higher Education Institution of Chemistry Laboratory assistants S. Augule and A. Meinerte for the help with the metal and lignin analysis; the Klaipeda University of Air Pollution from Ships study laboratory for help in determining the heating values.

References

[1] A. A. Boateng, H. G. Jung, P. R. Adler, Pyrolysis of energy crops including alfalfa stems, reed canarygrass, and eastern gamagrass, Fuel 85, 2006, pp. 2450–2457.

[2] R. J. A. Gosselink, E. de Jong, B. Guran, A. Abächerli, Co-ordination network for lignin — standardisation, production and applications adapted to market requirements (EUROLIGNIN), Industrial Crops and Products 20, 2004, pp. 121–129.

[3] Lignin and Ligninas: Advances in Chemistry, Ed. C.Heitner, D. R. Dimmel, J. A. Schmidt, Taylor and Francis, 2009, 1000 p.

[4] E. McCrady, The Nature of Lignin, Alkaline Paper Advocate 4, 1991, [20 Nov. 2010], http://cool.conservation-us.org/byorg/abbey/ap/ap04/ap04-4/ap04-402.html.

[5] A. M. Rouhi, Lignin and lignan biosynthesis, Chemical & Engineering News 78, 2000, pp. 29 – 32.

[6] S. Skudra, V. Shakels, B. Neiberte, G. Shulga, S. Reihmane, No Kehras celulozes un papīra rūpnīcas "Horizon" melnā atsārma iegūta sulfātlignīna fizikāli ķīmiskais

raksturojums, RTU zinātniskie raksti 1, Materiālzinātne un lietišķā ķīmija 22, 2010, pp. 38 - 43.

[7] G. Zaķis, Koksnes ķīmijas pamati, LV Koksnes ķīmijas institūts, 2008, 199 p.

Integrated Research on *Jatropha curcas* Plantation Management

Penjit Srinophakun[*1,2], Anna Saimaneerat[1], Isara Sooksathan[1], Niphon Visarathanon[1], Savitree Malaipan[1], Kosol Charernsom[1], Wiboon Chongrattanameteekul[1]

[1]*KU-biodiesel Project, Center of Excellent for Jatropha, Kasetsart University, Bangkok, Thailand*
[2]*Center of Excellent for Petroleum, Petrochemicals, and Advanced Materials, Department of Chemical Engineering, Faculty of Engineering, Kasetsart University, Bangkok, Thailand*
**Corresponding author. Tel: +66 2 9428555, Fax: +66 2 5614621, E-mail: penjit2004@yahoo.com*

Abstract: This paper will present the interactive research of expert team on *Jatropha curcas* plantation management to obtain high productivity in terms of dry seed weight per cultivation area. Set of experiments were designed and performed on randomize central block design and triplicate data were collected. The spacing was the important factor along with the cutting management program for long time cultivation. Therefore, the 3 different spacing (2x2, 2x3 and 3x3) were tested. The results show that 2x3 and 3x3 m spacing gave high yield of 129.2 and 127.1 kg/rai for the first cultivation year. In addition, types of insect and pest were surveyed in the Jatropha plantations and the ranking of the most found insect and pest was proposed. Mealy bug, Aphids and coccus were the most found insects in the Jatropha plantation. In the mean time, leaf spot, fungus infection, was the most sever in many areas in Thailand. Then the harmless chemical and biological treatments were tested to control those insects. The harmless chemical such as sodium lauryl sulphate and consumable products (tooth paste, shampoo etc) were used. In case of biological control, the natural predator, green lace wing, of the first top three insects was introduced and tested in the field. On the other hand, the number of insect pollinator was recorded at the Jatropha plantation responding to the Sun direction and time of the day. Interestingly, pollen germination also depends on the Sun direction. On the other hand, Box-Behnken design was used to optimize the transesterification of Jatropha oil to obtain the high fatty acid methyl ester (FAME) percentage. The results show that at the mole ratio of methanol and oil of 9:1, catalyze of 1.5%, reaction time of 72 min and temperature of 60 ^{o}C was the optimum condition and 99.0% of FAME was obtained. For the seed cake utilization, different rates of the seed cake (1,600, 800, 400 kg/rai) were applied to the cultivation of Chinese kale, tomato and potato. It was understandable that the mix of chemical fertilizer and Jatropha seed cake (1,600 kg/rai) gave the highest plant performance and no phorbol ester residue left in the cultivation soil and harvested vegetable.

Keywords: *Jatropha curcas, Plantation management, Jatropha insect and pest, Jatropha polinator*

1. Introduction

Jatropha curcas Linn. is perennial shrub belongs to Euphorbiaceae family same as rubber tree and cassava [1]. Originally, *Jatropha curcas* was native tree in South America and was induced to Thailand about 200 years ago by Portuguese who produced soap from Jatropha oil. Generally, Jatropha tree is 3-5 meter tall, smooth grey bark, having latex and heart green leaf. The flowers are small in size, white color and much more male flowers than female ones. Flowering occurs at the branch terminal. The fruit is green at the beginning and then turns to yellow and dark brown at the ripen stage. The fruit composes of 2-3 seeds. The seed is black, oval shape and one white point at the top. Oil content in the seed is about 30-40% [2, 3]. However, without the seed coat the oil content increases to 50-54%. Oil is non-edible, high unsaturated fatty acid with the same heating value as other vegetable oil. Jatropha can grow in many types of soil including marginal land which is not suitable land for food crop cultivation. This reduces the conflict of food/feed/fuel issue in some countries. Nevertheless, many products can be produced from Jatropha residues such as fertilizer from the seed cake (this work), pesticides and medical bio-active compounds from Jatropha extract [4, 5].

Jatropha curcas has great potential as energy crop as above mentioned. However, low yield seed is the burden and challenging for the researchers to overcome. Therefore, there have been many findings conducting to improve yield of Jatropha. As a wild crop the knowledge of Jatopha plantation management is little known and slowly developed. To accelerate the

research investigation under limited human resources and budget, the integrated research at the plantation level is desired. This paper shows how different discipline approaches to one goal of Jatropha yield improvement.

2. Methodology

This content will be divided to 5 sections according to the discipline and experimental set up. The five sections are agronomy, plant pathology, entomology, engineering and seed cake utilization.

2.1. Agronomy

To obtain the objective of Jatropha high yield, the optimum spacing and level of fertilizer was investigated. This experiment has been taken at 2 plantations. The first plantation aimed to conduct the investigation of the spacing (2x2; 2x3; 3x3 m) and the second plantation was to observe the effect of fertilizer (high, medium, low and none inputs) to the Jatropha performance. Note that high input means chemical (15-15-15 and 50 kg/rai) and organic fertilizer (500 kg/rai), medium means only chemical fertilizer (50 kg/rai), low means only organic fertilizer (500 kg/rai) and none is no fertilizer. Note that 6.5 rais equal 1 hectare. There is only 1 variety, TH1 (plant form seed) reported in this paper. The collected data are the seed yield, number of fruit, weight of 100 seed, plant height, and canopy width during one year cultivation time.

2.2. Plant pathology

The survey has been conducted across the Kingdom of Thailand to collect the specimen such as leaf or stem or confected part of Jatropha tree. The severity of pest was ranking and the specimens were then taken from the plantation to the laboratory for the biological assay. The symptom finally was identified.

2.3. Entomology

There are three investigations in this area namely insect, nature predator of Jatropha insects and pollinator. Each investigation was separately carried on by different researcher. For the insect, mealy bug, was controlled by household chemical and natural predator (green lace wing). In fact, green lace wing is effective natural predator not only for mealy bug but also aphids and coccus. This paper did the mass cultivation of green lace wings and their eggs were packed in the capsules and tested in the Jatropha plantation. Concerning the pollinator, the percentage of pollinator visiting to 1,500 flowers was recorded during the dry and wet season at different time of the day. Then the pollen was collected from the Jatropha canopy and germinated in the laboratory to check germination percentage.

2.4. Engineering (biodiesel production)

After the Jatropha seeds were collected from the field, the shells have been cracked by machine and oil was expelled using the oil expeller. The expelled oil was filtered to remove the solid residue and oil was used for biodiesel production using transestification technique and KOH was used as catalyst. The condition of biodiesel production namely mole ratio of methanol to oil (3-9), catalyst concentration (0.5-1.5%), reaction time (60-120 min) and reaction temperature (30-60 ^{o}C) was optimized by experimental Box-Behnken design. Then percentage of fatty acid methyl ester (%FAME) was analyzed by gas chromatography.

2.5. Seed cake Utilization

As known that one liter of Jatropha oil comes from about 4 kg of seed which will give about 3 kg of the seed cake. The objective of this section was to utilize the seed cake as fresh fertilizer to the vegetable cultivation. The experiment was conducted and applied to three types of vegetables namely Chinese kale, tomato and potato which represented the fresh consumed vegetables, fruit plants and root plants. Three level of seed cake was applied to those plants as high (1,600 kg/rai: 6.5 rais = 1 ha), medium (800 kg/rai) and low rates (400 kg/rai). Nevertheless, sole chemical fertilizer (recommended rate), sole organic fertilizer and half mixed of the seed cake (three doses) and chemical fertilizer or organic fertilizer were applied. Twelve treatments in total were carried out including the control (without fertilizer). The growth of plants was recorded. However, in this paper only the results of Chinese kale were reported. Samples were taken from the leaf and cultivation soil to check the phorbol ester residue. HPLC and LC-MS/MS were used to analyze phorbol ester content using TPA as external standard.

3. Result and Discussion

The results and discussion are divided into 5 parts according to the methodology as following.

3.1. Agronomy

As can be seen in Table 1, 2x2 and 2x3 spacing gave the high seed yield of 129.2 and 127.1 kg/rai respectively. Number of fruit and 100 seed weight responded directly to the seed yield. Even though the plant height is the same but the canopy width clearly relates to the spacing. The larger spacing of 3x3 comparing to the narrower ones gives the wider canopy width.

Table 1. Effect of spacing on Jatropha performance of TH1 variety.

Spacing	Seed yield (kg/rai)	number Fruit/rai	100 seed weight (g)	Plant height (m)	Canopy width (m)
2x2	129.2	55,804	86.3a	2.7	1.6b
2x3	127.1	56,698	84.4b	2.7	1.9a
3x3	97.9	44,498	84.2b	2.7	2.0a
F-test (a)	ns	ns	**	ns	**
LSD (0.05a)	-	-	0.6	-	2.7

Table 2. Effect of fertilizer on Jatropha performance of TH1 variety.

Input	Seed yield (kg/rai)	number Fruit/rai	100 seed weight (g)	Plant height (m)	Canopy width (m)
High	182.3a	80,455a	85.5	276.0a	187.5a
Medium	132.1b	58,826b	85.1	276.5a	188.6a
Low	98.6c	43,530c	85.2	264.1ab	183.6a
None	59.1d	26,524d	84.1	256.6b	163.5b
F-test (b)	**	**	ns	*	*
LSD (0.05b)	29.5	12892	-	13.3	17.8
Spacing x fertilizer	ns	ns	ns	ns	ns
CV (%)	25.3	24.9	3.6	5.0	9.9

3.2. Plant pathogen

The specimens (Fig 1.1) from the plantation were assayed for the microbial type. Leaf spot was the top ranking severity in the plantation as shown in Table 3. Fungal infection was the

most found particularly at the moderate temperature and high humidity. Fig. 1 shows the fascicles of conidiospores and conidium of *Pseudocercospora* sp. causing leaf spot.

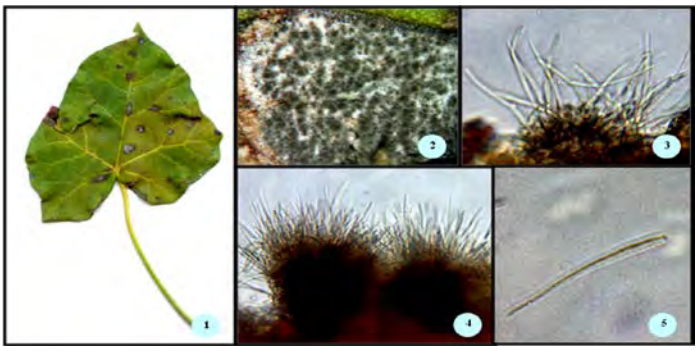

Fig.1. Leaf spot infected by Pseudocercospora sp. 1) disease symptom on leaf; 2) fungal fruiting structure under stero-microscope; 3, 4) fascicles of conidiophores; 5) conidium

Table 3. Diseases and severity in the Jatropha plantation.

Diseases	Severity
Leaf spot (*Pseudocercospora* sp.)	++++
Leaf spot (*Pestalotiopsis* sp.)	++
Leaf spot (*Phoma* sp.)	++
Leaf spot (*Alternaria brassicicola*)	+

3.3. Entomology

There are three different investigation in entomology namely Jatropha insect, natural predator and pollinator.

3.3.1. Jatropha Insect

From the field survey, it was obvious that mealy bug was the most found insect in many areas of Thailand. The second and third populations of insect found were aphids and coccus. Fig. 2 shows the mealy bug before and after the treatment of sodium lauryl sulfate (SLS). As can be seen in Fig.2b SLS dissolve wax on the mealy bug's body.

a *b*

Fig. 2. Mealy bug on the Jatropha tree a) before b) after treating with SLS

3.3.2. Natural predator

The survey of prime natural predators of Jatropha insect particularly mealy bug, aphids and coccus has been done intensively. Green lace wing was found to be the effective natural predator of those insects. This natural predator has potential for mass production. Therefore, it was selected for further study. Table 4 shows the longevity and number of egg collecting from the laboratory. Comparing of different starting egg numbers of 50, 100 and 200 eggs, starting with 50 eggs give the highest ratio of egg/longevity and reasonable daily egg number. As the result this number is used for finding the suitable food composition for egg production (Table

5). Bee pollen and honey food mixed was selected as it gave the highest ratio of egg/longevity and daily egg obtained.

Table 4. Number of eggs of Plesichrysa ramburi and its adult longevity from various number of starting adults at 27 °C and 70% RH.

No of starting	Ratio of egg/longevity	Mean longevity (day)	Daily obtained egg
50	2,080a	22.33c	94.12
100	3,590b	20.67b	180.40
200	4,565c	14.67a	323.78
CV (%)	2.98	3.11	-

Table 5. Number of eggs obtained from 50 starting aduls in different food composition.

Food composition	Ratio of egg/longevity	Mean longevity (day)	Daily obtained egg
Yeast & honey	1,708	14.00	122.00
Bee pollen & honey	1,891	13.67	138.37
CV (%)	5.25	14.95	-

After eggs were mass produced in the laboratory, 300 eggs were packed in the plastic tube and tested at the field sites for 1, 2 and 3 weeks including the control (no egg pack). Unfortunately, during the experiment, there were not many insects as expected. Therefore, we could not observe the different numbers of the predator and insects before and after treatment. This field experiment is needed to re-perform later.

3.3.3. Pollinator

The number of pollinator during the dry and wet seasons was recorded as shown in Fig 3. As can be seen in Fig 3, it is noticeable that the female flower is more preferable as the number of pollinator visiting is higher than male flower particularly in the morning. Fig 4 shows the percentage of pollen germination at different direction and time of the day. In the morning the high percentage of pollen germination is found in the direction exposing to the Sun. Correspondingly, in the late afternoon the higher percentage of pollen germination is found in the Southern west where the Sun is.

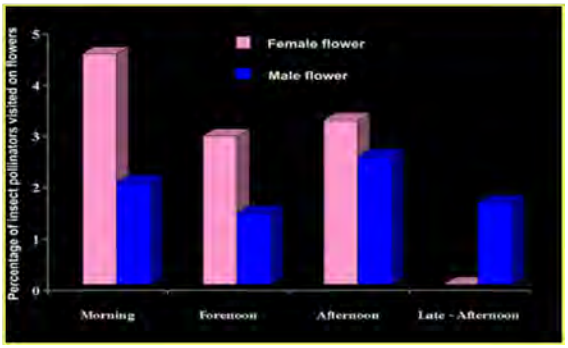

Fig. 3. The percentage of pollinator visiting female (first) and male flower (second) in the morning, late morning, afternoon and late afternoon

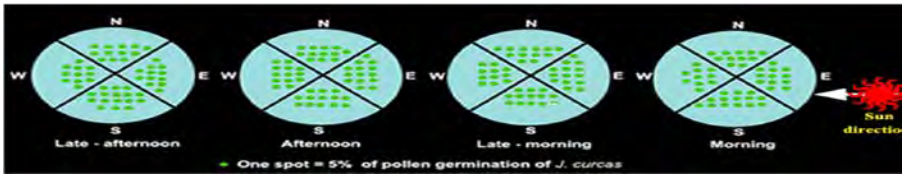

Fig. 4. The percentage of pollen germination according to the direction

3.4. Engineering

From the Box-Behnken design of experiment with three levels, 35 experiment runs were designed. The data was analyzed using Minitab software to construct the contour as in Fig 5. As can be seen in Fig 5, the effect of reaction temperature and time has more influence on % fatty acid methyl ester (FAME) (Fig 5a). While the effect of mole ratio of methanol to oil, and %KOH has greater effect than reaction temperature (Fig 5b & 5c). The optimum condition for transesterification from Jatropha oil suggested by the model was 9:1 mole ratio, 1.5% KOH, 72 min reaction time and 60 ^{o}C reaction temperature and 99.0% FAME was obtained at this optimum condition.

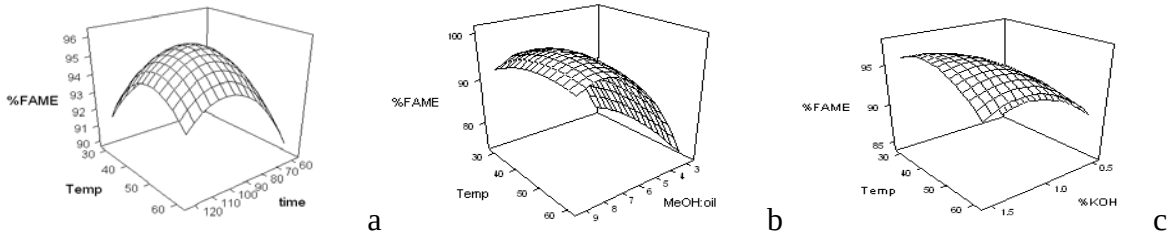

Fig. 5. Surface plot of %FAME and a)reaction temperature and time b) reaction temperature and mole ratio c) reaction temperature and %KOH (catalyst).

3.5. Seed cake utilization

Table 6 shows the growth performance of Chinese kale of twelve fertilizer treatments. Pure chemical fertilizer and half dose of chemical fertilizer plus high rate of Jatropha seed cake give the highest Chinese kale yield of 9.87 and 9.08 t/ha. Note that 4 kg of Jatropha seed will give approximately 1 kg of oil and 3 kg of seed cake. From the phorbol ester analysis, the residue of phorbol ester both in the Chinese kale and cultivation soil was not found.

Table 6. Average growth characteristic of Chinese kale (a, b, c show statistical significant).

Treatment	Leaf length (cm)	Leaf width (cm)	Plant height (cm)	Canopy height (cm)	Canopy width (cm)	Total yield (t/ha)
Without fertilizer	10.87c	8.70b	7.39b	19.83c	13.27cd	4.12c
CF	14.83a	12.26a	15.83a	29.27a	21.27a	9.87a
OF	11.18c	8.58b	7.73b	20.47c	17.00bc	2.02e
SF (400 kg/rai: H)	9.75c	7.05b	7.26b	18.37c	13.57cd	1.77e
SF (800 kg/rai: M)	9.63c	7.04b	7.83 b	17.60c	12.33d	4.08c
SF (1,600 kg/rai: L)	11.35bc	9.63ab	9.06b	22.91bc	14.42cd	3.77cd
0.5CF + SF (H)	12.10abc	10.03ab	10.13b	20.90c	14.23cd	7.07b
0.5CF + SF (M)	9.76c	8.00b	8.33b	19.07c	12.60cd	4.55c
0.5CF + SF (L)	14.23ab	12.40a	10.57b	27.87ab	19.67ab	9.08a
0.5OF + SF (H)	10.43ac	7.63b	8.05b	20.77c	15.40cd	2.60de
0.5OF + SF (M)	12.07abc	8.267b	9.60b	23.27bc	15.23cd	4.12c
0.5OF + SF (L)	11.50bc	9.16b	8.85b	23.30bc	15.20cd	3.99c

Please note that CF is the chemical fertilizer, OF is organic fertilizer and SF is Jatropha seed cake fertilizer,

4. Conclusion

This paper shows the multidisciplinary research work of Jatropha in the plantation level. The results of this preliminary investigation are the important basic knowledge to increase the Jatropha yield. The actual work has been done intensively in the plantation level to make sure that the developed technology is practical and useful for the future users. It is clear that Jatropha yield improvement is the challenge and it needs the integrated research of agriculture, engineering and science.

5. Acknowledgement

The authors would like to thank KURDI (Kasetsart University Research and Development Institute) and Toyota Motor Thailand Co., Ltd for the financial support.

References

[1] N. Carels, *Jatropha curcas*: A Review, Adv. Biot. Res. 2009, 50, pp. 39-86.

[2] D. Fairless, The Little Shrub that could-may be, 2007, Nature, 449, pp. 652—655.

[3] J. B. Kandpal and M. Madan, *Jatropha curcas*-a renewable source of energy for meeting future energy needs, 1995, Renew Energy, 6, pp. 159-160.

[4] A. Kumar and S. Sharma, An Evaluation of Multipurpose Oil Seed Crop for Industrial Uses (*Jatropha curcas* L.): A review Ind. Crops Prod., 2008, 28, pp.1-10.

[5] H. R. S. Makkar and K. Beckar, *Jatropha curcas*, a promising crop for the generation of biodiesel and value-added coproducts, 2009, Eur. J. Lipid Sci. Technol., 111, pp. 773-787.

Biomass waste – a source of raw materials and new energy source

Matjaž Kunaver[1, 4*], Edita Jasiukaitytė[1, 4], Nataša Čuk[1], Sergej Medved[2], Samuel Rodman Oprešnik[3], Tomaž Katrašnik[3]

[1]*National Institute of Chemistry, Ljubljana, Slovenia,*
[2]*University of Ljubljana, Biotechnical Faculty, Ljubljana, Slovenia*
[3]*University of Ljubljana, Faculty of Mechanical Engineering, Ljubljana, Slovenia*
[4] *Center of Excellence for Polymer Materials and Technologies, Tehnološki park 24, 1000 Ljubljana, Slovenia*
** Corresponding author: Matjaž Kunaver,Tel:+38614760363, Fax:+38614760300, e-mail: matjaz.kunaver@ki.si*

Abstract: Agricultural crop residues, such as straw, corn stover and wood wastes such as leftovers from timber cutting, broken furniture, sawdust, residues from paper mills etc. contain appreciable quantities of cellulose, hemicelluloses and lignin. Much effort has been devoted to convert these types of biomass into useful industrial and commercially viable products.
During liquefaction, lignocellulosic components are depolymerised to low molecular mass compounds with high reactivity and high hydroxyl group content. We have used a high energy ultrasound as an energy source to speed up the liquefaction process in our research. The liquefied biomass was used as a feedstock in synthesis of polyesters, polyurethane foams and adhesives. Adhesives for the wood particle boards with incorporated liquefied lignocellulosic materials emit less formaldehyde and products have the same or even better mechanical and physical properties.
A special attention was given to the utilization of the liquefied lignocellulosic materials as a new energy source with high heating value. It was found that the combustion efficiency of lignocellulosic liquid fuel is comparable to the combustion efficiency of Diesel fuel although it has much higher content of cyclic hydrocarbons. The emissions are within the range of the European emission regulations.
The utilization of liquefied lignocellulosic materials can at least partially reduce the crude oil consumption, thus increasing the use of the renewable resources in large extent.

Keywords: *biomass liquefaction, polyester synthesis, adhesives, fuel*

1. Introduction

Biomass based materials and wood in particular are among the most abundant renewable resources. Much effort has been devoted to convert these types of biomass into useful industrial and commercially viable products. One of the possible routes to achieving this is through **liquefaction** where wood or lignocellulosic materials, such as waste paper, starch, etc. reacts with phenol or multifunctional alcohols to yield low molecular mass, liquid products that can be used for polymer synthesis [1,2,3,].

In our research native hardwood and softwood as well as paper and different wood based waste materials were liquefied with different glycols and with a minor addition of p-toluene sulphonic acid as catalyst.

However, a novel approach to a very efficient energy input during the thermochemically conversion of lignocellulosic biomass into liquefied depolymerized products is the use of ultrasound power. Sonochemistry is nowadays an excellent tool in chemical, physical and biological processes. The irradiation with ultrasound can be regarded as a special type of energy input into the system. The range from 20 kHz to 1MHz is used in chemistry while higher frequencies are used in medical and diagnostic applications. The high frequency mechanical vibrations are transferred into the medium by titanium made horn, in different sizes and shapes. Ultrasound is transmitted through a medium via pressure waves and the main advantage is directly related to the physical effect of acoustic cavitation. Acoustic waves

can break the cohesion of a liquid and create micro cavities. The cavity is actually a micro bubble which corresponds to the sound wave by growing till becoming unstable. At that point bubbles collapse violently creating drastic conditions inside the medium for a very short time: temperatures of 2000-5000K and pressures up to 1800 a tm inside the collapsing cavity. Consequently, under such extreme conditions volatile molecules vaporize and form free radicals as was proved in extensive studies of the sonification of water. Radicals cause fragmentation of large molecules, stripping off the ligands and oxidation. Shaw and Lee [6] exposed the effluent from pulp and paper kraft mill to power ultrasound and efficiently reduced the chemical oxygen demand (COD) and effluent turbidity. Shock waves, generated at the collapse of cavities induce mechanical effects, such as splitting large molecules to smaller fragments, particle size reduction, surface cleaning and intensive mixing and heating. The later are used for the formation of stable emulsions in liquid-liquid systems.

Sonochemical methods are used also in carbohydrate chemistry [7]. Hydrolysis and clevage of di- and polysaccharides were quantitatively proved with starch, dextran, cellulose derivatives and other polysaccharides. In our research we have utilized high energy ultrasound for depolymerization and liquefaction of different lignocellulosic materials. It was found, that the reaction yield was in all experiments almost 100% and the reaction time grossly reduced.

Liquefied wood can be considered to be a polyhydric alcohol. After the liquefaction process, the presence of hydroxyl group-containing species in the wood components can be used as polyols for several different purposes. The hydroxyl value of the liquefied wood has been determined to be between 500 a nd 1000 m g of KOH/g. This high number means that the products can be used as the hydroxyl component in complex polyester synthesis [4]. Some benefits could be expected from such systems. These include the incorporation of the biomass components into the polymeric compositions and consequently, the provision of a certain degree of biodegradability. Esterification of a proportion of the hydroxyl groups reduces the reactivity of the liquid wood, a feature that is sometimes desired in polyurethane synthesis.

It was found during initial experiments that a mixture of liquefied wood with melamine-formaldehyde or melamine-urea-formaldehyde resin can react at elevated temperatures forming a solid crosslinked product that was suitable for the use in wood furniture industry. Such an adhesive has lower formaldehyde content than the standard melamine-formaldehyde or melamine-urea formaldehyde adhesives [5]. In the condensation – elimination reaction, the methylol groups of the melamine-formaldehyde resins precursors react with the hydroxyl groups on the liquefied wood, eliminating water or methanol. The acid catalyst which is present in the liquefied wood additionally speeds up the reaction.

In our research we have utilized high energy ultrasound for depolymerisation and liquefaction of different lignocellulosic materials, wood wastes in particular. A town with 350.000 inhabitants generate 5.700 tons of different wood waste materials per year, mainly broken furniture and packaging materials. Besides that, 2.300 tons of forest residues are deposited, manly tree branches, bark and larger pieces of timber. The aim of this study was to find a highly efficient way to transform this biomass waste into valuable chemicals and as a n ew energy source. It was found, that the reaction yield in all experiments was almost 100% and the reaction time grossly reduced.

The first objective of this study was to synthesize a liquefied wood that contained high hydroxyl group content, with a good yield in the liquefaction reaction. The second goal was to achieve the utilization of liquefied wood in the synthesis of polyester-polyols. These polyols were successfully utilized in polyurethane foam production. The third goal was to establish

the criteria for creating a melamin-fomaldehyde or a m elamine-urea-formaldehyde resin precursor that would react at elevated temperature with liquefied wood and could be used as an adhesive. The fourth objective was to utilize the liquefied wood as an energy source with high heating value. Most of liquefied products have a heating value higher than 22 KJ/kg, that is in the range of pure ethanol and higher than brown coal. Initial tests have indicated that these products could also be used as a motor fuel. Since the production of such liquid fuel utilizes a huge variety of lignocellulosic wastes and takes place under very mild reaction conditions, an overall energy output is high. Several possible applications in energy production were identified and explored by our group.

The utilization of liquefied lignocellulosic materials can at least partially reduce the crude oil consumption, thus increasing the use of the renewable resources in large extent.

2. Materials And Methods

The most common wood waste materials such as medium density fibreboard (MDF), veneered particleboard, particleboard, oriented strand board (OSB), plywood and wheat straw were milled on ROTSCH SM-2000 mill. All meals (flours) including spruce (*Picea spp.*) sawdust were sieved through a 2 mm screens and dried at room temperature to constant water content.

All chemicals were of synthesis grade (Merck) and were used without further purification.

2.1. Experimental setup

The liquefaction was carried out in a 1000mL three-neck glass reactor, equipped with the mechanical stirrer and condenser.

The ultrasonic device was UP400S processor, produced by Hielscher Ultrasonics GmbH, Warthestrasse 21, 14513 Teltow, Germany. The high frequency (24 kHz) power output can be regulated by adjustment of amplitude from 20% to 100% of the nominal power of 400W. The high frequency output is transferred through titanium cylindrical horn, introduced into the reactor through the side neck and submerged 20mm into the reaction mixture. The horn had diameter of 22 mm, with the calculated power output (at the maximum amplitude) 105Wcm^{-2}.

The experimental setup is shown in Figure 1.

2.2. Biomass (wood waste) liquefaction

The reactor was charged with 140g of biomass and 700g of glycol. 21g of p-toluenesulfonic acid was added. The liquefaction of different wood waste materials was governed in diethylene glycol: glycerol = 1:4 mixtures.

The mixture was heated for maximum of 2 hours at 180 °C while being constantly stirred.

The ultrasound was switched on when the temperature of the reaction mixture reached 160^{o}C. The energy input was controlled by the amplitude of the ultrasound. Ultrasound of amplitude from 20% to 100% was used for waste wood liquefaction.

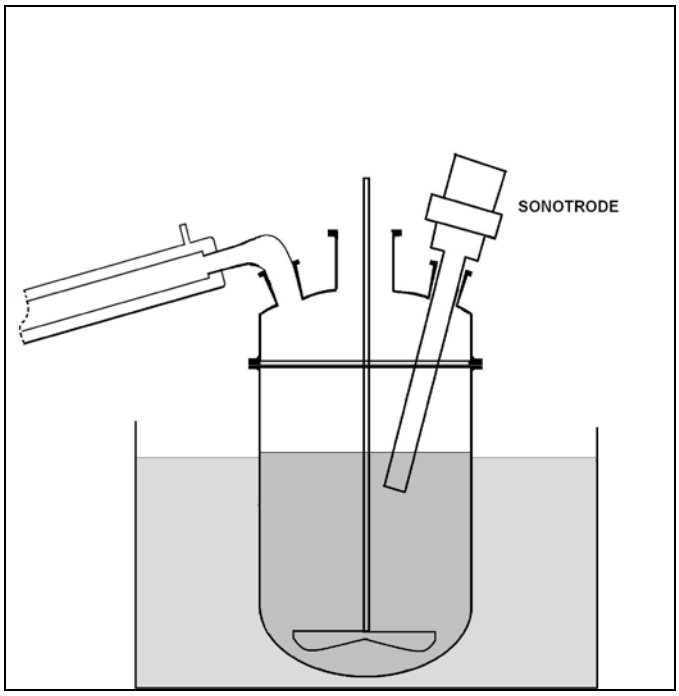

Fig. 1: Glass reactor with external heater, mixer and ultrasound sonotrode

2.3. Polyester polyols from the liquefied wood (LW)

Three different formulations with two different dibasic organic acids were used in order to study the differences in the physical and the chemical properties of the final products. 300 g of liquefied wood were used in combination with 60 g of adipic acid; the resulting polyester was identified as P1. With 60 g of phthalic acid anhydride, the product was identified as P2. With 30 g of adipic acid and 30 g of phthalic acid anhydride, the resulting polyester was identified as P3.

The liquefied wood was introduced into the four-necked 1000 cm^3 glass reactor, equipped with a water condenser and mechanical stirrer. The reactor was placed in an electric jacket heater. Adipic acid and/or phthalic acid anhydride were added when the liquefied wood reached 180^oC. Dibutyl tin oxide (0.2% w/w) was added as the sterification/transesterification catalyst. The mixture was heated gradually up to 200^oC, under stirring and was held at this temperature. Water was continuously distilled from the reaction system. A slight stream of nitrogen was introduced into the reactor for easier transport of water vapor into a condenser. A sample was withdrawn periodically from the reaction system and its acid value was determined. The total reaction time was between 160 minutes and 180 minutes. After completion of the reaction, when the acid value was reduced to less than 30 mgKOH/g, the reaction mixture was cooled to ambient temperature.

1.1. Product characterization

Hydroxyl values were determined by standard ASTM Standard D4274-05 (2005) method.
The extent of liquefaction was evaluated by determining the residue after the washing out the sample with dioxane and water (4:1 v/v). The residue was dried in an oven at 105^oC to constant weight. The conversion yield was calculated as the weight percentage based on the starting wood material.

3. Results and Discussion

3.1. The efficiency of the ultrasound

Initial experiments were dedicated to determining the influence of the ultrasound to the speed of the liquefaction reaction. The increase of the ultrasound amplitude reduces liquefaction time needed to achieve the same liquefaction residue amounts. The efficiency of the ultrasound is illustrated in Figure 2, where the liquefaction process without the use of the ultrasound needs 120 minutes to achieve the total liquefaction while with the ultrasound at the minimal amplitude of 20% only 80 minutes. Accordingly, the use of the ultrasound with 60% amplitude completes liquefaction in 60 minutes that represents only half of the time which is consumed in order to achieve the same liquefaction extent without ultrasound.

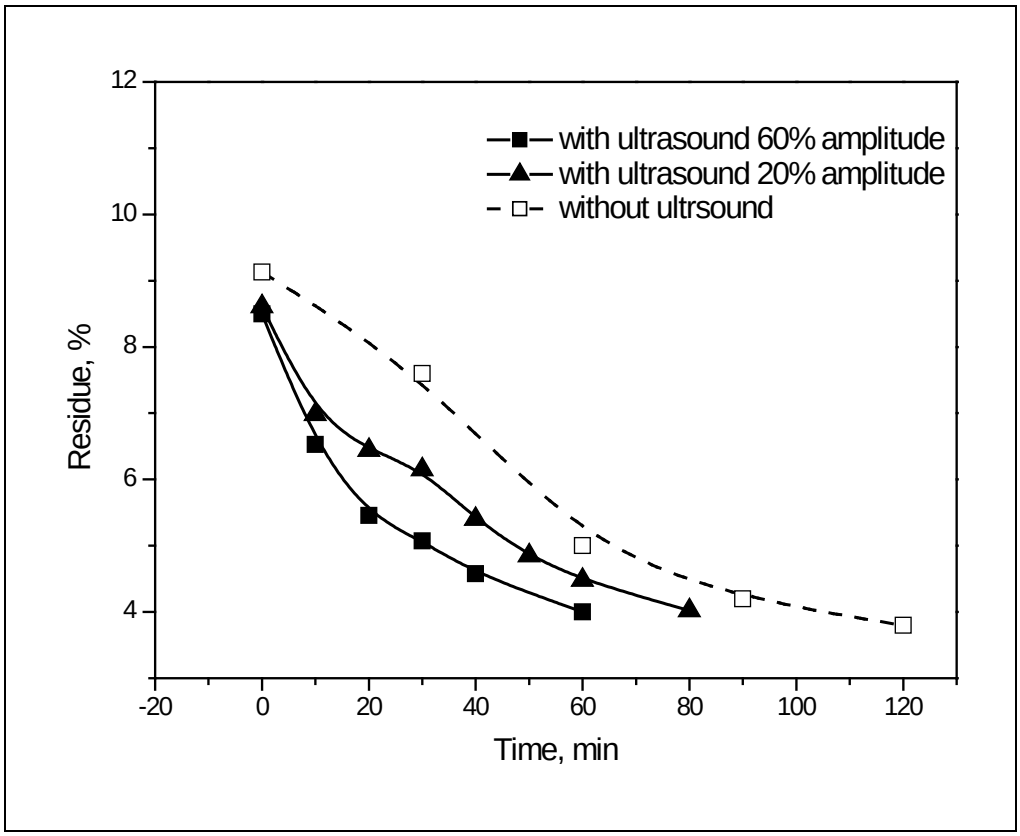

Fig. 2: The decrease of the wood residue in % during the liquefaction with ultrasound 60% amplitude (squares), 20% amplitude (triangles) and without ultrasound (empty squares). (Values at 0 min represent residue % of the samples taken after the reaction mixture achieved 160 °C and in case of ultrasonically assisted liquefaction - when the ultrasound was switched on.)

The powerful energy input through the cavitation effect is demonstrated in the reduction of the biomass particles size and through the depolymerization of the large biopolymers. The size reduction is visible by naked eye since after initial few minutes the reaction mixture becomes homogeneous dispersion. The process continues till all the biomass is completely dissolved and a dark brown liquid is formed with particles sizes less than 1μm.

3.2. Polyester polyols from liquefied wood

Liquefied wood was used as a component in polyester synthesis due to the large number of hydroxyl groups that are available in the liquefied wood. The liquefied wood was used as a substitute for part of the polyhydroxy alcohols that are standard raw material in polyester formulation. Polyester polyols were prepared by using adipic acid and/or phthalic acid anhydride in a high temperature polycondensation/esterification reaction. The polyesters were prepared under the standard high temperature polycondensation conditions, confirming the use of the liquefied wood as a raw material in polyester synthesis. The products were characterized using FTIR, GPC/SEC and viscosity measurements showing similar properties to those possessed by equivalent commercial polyesters. The characteristic data are presented in Table 1.

Table 1: Characteristic data of polyesters and the initial liquefied wood

	Mn(Av.) g/mol	MW(Av.) g/mol	PDI	OH value mgKOH/g	Viscosity kPa.s	% of wood (w/w)
LW	4790	19400	4.0	1043	2.8	28
P-1	10300	39900	3.9	798	1.9	22
P-2	4590	60000	13.1	378	1.9	23
P-3	7980	79500	10.0	437	2.2	23

A rise of the average molar mass was achieved together with a reduction of the hydroxyl group content. Such a modification of the polyester reactivity and complexity is favorable for further utilization in polyurethane synthesis. The final OH values of the polyesters were in the range of saturated polyesters that are used in polyurethane production. The viscosity is grossly dependent on the type of the glycol used for the liquefaction and on the wood glycol ratio. The use of wood in these experiments replaced up to 23% of polyhydroxy alcohols in polyester formulations. This amount varies according to product requirements and can be increased significantly.

3.3. Liquefied Wood As A New Particle Board Adhesive System

The OH groups in the liquefied wood, including those of the remaining unreacted glycols were available for the condensation reactions with different melamine-formaldehyde and melamine-urea-formaldehyde resin precursors. By measuring the mechanical properties of selected particle boards and by measuring the formaldehyde release, it was found, that a 50% addition of the liquefied wood met the European standard quality demands for particle boards. Formaldehyde release was lower than 8mg/100g in all experiments due to the positive influence of the liquefied wood components. It can be concluded that the products of the liquefied lignin with their aromatic character behaved as a formaldehyde scavenger. Lower formaldehyde emissions from particle boards due to the use of the liquefied wood, are extremely important in the provision of better quality of life. The properties of particle boards made with the mixture of the liquefied spruce wood and the melamine-urea-formaldehyde resin precursor Meldur H97 and melamine-formaldehyde resin precursor MS-1 were within the European standard EN 312 (2003), type P2 limitations..

On the basis of the presented values one can conclude that liquefied woods can be used as a substitute for synthetic resin precursors in adhesives that are used for particle board production.

3.4. Liquefied biomass as a fuel

A special attention was given to the utilization of the liquefied lignocellulosic materials as a new energy source with high heating value. Most of liquefied products have a heating value higher than 22 KJ/kg, that is in the range of pure ethanol and higher than brown coal. Initial tests have indicated that these products could also be used as a motor fuel. Since the production of such liquid fuel utilizes a huge variety of lignocellulosic wastes and takes place under very mild reaction conditions, an overall energy output is high. The viscosity of the liquefied biomass depends on the biomass content in the formulation and can be between 149 kPa.s to 2 kPa.s. However, if it is applied at higher temperatures, the viscosity is reduced to 100 Pa.s and can be directly introduced into the burner. The sulphur content is less than 0.3%. The carbon monoxide, nitrogen oxides and solid particles emission were within the range of the European emission regulations for heavy duty diesel engines.

Preliminary test were carried out in a prototype gas turbine, where efficiency, power output, exhaust emissions as well as wear and durability of components were examined. These results were compared to the results obtained during the tests with Diesel fuel. Due to high viscosity of the lignocellulosic liquid fuel, a new fuel injection system was designed and manufactured to allow injection of heated and pressurized fuel.

It was found that the combustion efficiency of lignocellulosic liquid fuel is comparable to the combustion efficiency of Diesel fuel although it has much higher content of cyclic hydrocarbons. It was also proven that utilization of lignocellulosic liquid fuel in the prototype gas turbine complies with current emission regulations for electric power generation. Differences in exhaust emissions while utilizing lignocellulosic liquid fuel and Diesel fuel were analyzed and interpreted. It was found that total hydrocarbon emissions are higher than those of Diesel fuel; however the difference diminishes for high air-fuel ratios, high combustion chamber air inlet temperature, and high fuel temperatures. All effects enhance evaporation of fuel with high viscosity thereby additionally enabling higher conversion rate of cyclic hydrocarbons. It was also found that NO_x emission increased slightly at the same enthalpy of exhaust gasses while using lignocellulosic liquid fuel, which could be attributed to high oxygen content of the fuel. Influence of utilizing lignocellulosic liquid fuel on wear and durability of components of the gas turbine and its fuel injection system is currently examined.

4. Conclusions

Different lignocellulosic materials were liquefied with yields higher than 95% and with additional use of the ultrasound the reaction times could be reduced for more than 50%.

Polyesters were synthesized using liquefied wood and other lignocellulosic materials as a replacement for a certain amount of polyhydric alcohols – produced from crude oil. The chemical and physical properties of such polyesters are favorable for their use in polyurethane synthesis. The use of wood in these experiments replaced up to 23% of polyhydroxy alcohols in polyester formulations.

Liquefied lignocellulosic materials were also used as adhesives for particle boards production – with reduced formaldehyde emission and excellent mechanical properties. By measuring the

mechanical properties of selected particle boards and by measuring the formaldehyde release, it was found, that a 50% addition of the liquefied wood met the European standard quality demands for particle boards. It can be concluded that the products of the liquefied lignin with their aromatic character behaved as a formaldehyde scavenger. Lower formaldehyde emissions from particle boards due to the use of the liquefied wood, are extremely important in the provision of better quality of life.

The liquefied biomass has high heating value. The residual particles have low average diameter and the liquefied biomass has low viscosity. These are the properties, favorable to its utilization as the liquid fuel in traditional oil burners and in diesel engines. The emissions are within the range of the European emission regulations. Successfully completed initial test thus pave the way for utilization of a new renewable fuel in gas turbines, which are known for their high efficiency, high power density, high reliability, technology availability and affordability. Overall energy conversion efficiency will be increased by utilizing co- or tri-generation power plants. The key achievement arises from the fact that the fuel is produced from mainly unused renewable source and from the fact that its use has very low carbon footprint.

References

[1] Lin L., Yoshioka M., Yao Y. and Shirashi N. Liquefaction of Wood in the Presence of Phenol Using Phosphoric Acid as a Catalyst and the Flow Properties of the Liquefied Wood. Journal of Applied Polymer Science 52, 1994, pp.1629-1636.

[2] Yamazaki J., Minami E., Saka S. Liquefaction of beech wood in various supercritical alcohols. Journal of Wood Science 52, 2006, pp.527-532

[3] Kržan A. and Kunaver M. Microwave heating in wood liquefaction. Journal of Applied Polymer Science 101 (2), 2006. pp.1051-1056

[4] Kunaver M., Jasiukaityte E., Čuk N. Guthrie J.T. Liquefaction of wood, synthesis and characterization of liquefied wood polyester derivatives. Journal of Polymer Science 115, 2010, pp.1265-1271

[5] Kunaver M., Medved S., Čuk N., Jasiukaityte E., Poljanšek I., Strnad T. Application of liquefied wood as a new particle board adhesive system. Bioresource Technology, 101, 2010, pp.1361-1368

[6] Shaw L.E. and Lee D. Sonication of pulp and paper effluent. Ultrasonic Sonochemistry 16, 2009, pp. 321-324

[7] Kardos N. and Luche J.L. Sonochemistry of carbohydrate compounds. Carbohydrate Research 332, 2001, pp. 115-131

Sustainable energy from dairy farm waste using a Microbial Fuel Cell (MFC)

XiaoNan Zhang, Laura Porcu, John M. Andresen*

Department of Chemical and Environmental Engineering, University Park, Nottingham, NG7 2RD
** Corresponding author. Tel: +44 115 951 4640, Fax: +44 115 951 4115,*
E-mail: enzjma@exmail.nottingham.ac.uk

Abstract: A dairy farm waste which include milk waste, unconverted feed and bedding, cow manure and cow slurry water have been applied as raw materials to produce renewable energy using a continuous flow membrane-less microbial fuel cell (MFC). The COD content decreased with 98% from 33,600 J/L to 558 J/L within 6 days by turning the organic content into electricity and hydrogen. The voltage generated reached a peak of 1.6136mV, which indicating that dairy farm waste can be an appropriate resource for MFC. The total energy of hydrogen gas was 38,338J/L on the sixth day, which suggesting that about 80% of the energy stored in the COD was transferred into hydrogen gas. The nitrogen content of the farm waste slurry also decreased 20% during the first 24 hours indicating that MFC can be used for nitrogen harvesting.

Keywords: *1. Biomass fuel; 2. Renewable energy; 3. Dairy farm; 4. MFC; 5. hydrogen production*

1. Introduction

There are close to 2 million dairy cows in the UK producing an estimate of 70 million m^3 of slurry annually. Since each m^3 of slurry contains 200-250kwh, it can be considered as one of the largest sustainable energy resource in the UK. Due to increasing use of intensive farming methods, agriculture derived wastes will continue to increase, especially within the livestock farming. From 1961 to 1999, there was a 34% increase of the total livestock numbers in UK (BERR & DEFRA, 2003). Farm wastes, such as slurry, dirty water, silage liquor and manure, need to be treated and disposed in an environmentally appropriate way. For dairy farms, most of the slurry wastes are used as fertilizer to grow winter feed crops for the animals. However, there are future logistical and economic constraints, such as for nitrate vulnerable zones were spreading is limited to 170kg/ha (Cinar et al., 2004). The restriction is to stop nutrients run-off into surrounding ground water from manure spread on the fields. Removal of nitrate is an option, but it is not easy to completely remove ammonia and other nitrogen compounds from wastewater or slurry water by conventional wastewater treatment technologies (Jetten et al., 2002). There are significant hazardous environmental impacts of nitrogen. For example, due to bacteria oxidation into nitrate, depletion of dissolved oxygen in receiving streams and promotion of eutrophication that are toxic to most aquatic organisms. Moreover, high concentration of nitrate in groundwater is also harmful to human health, because some diseases could occur, such as gastric cancers and infant methaemoglobinemia (Jetten et al., 2002). Therefore, there is a great potential for nitrate rich dairy farm waste to be used as feedstock in microbial fuel cells. In these processes, the available nutrients can be converted into energy resulting in reduced environmental impact and lowered energy cost for conventional dairy farms could be offset (Young and Pian, 2003).

2. Methodology

The Microbial Fuel Cell is a technology that can be used to generate electricity from waste water or animal slurry water by employing microorganisms to digest inorganic and organic compounds (Liu and Logan, 2004). The catalytic reaction of bacteria produces electrons which are transferred to the anode, i.e. the negative terminal, directly or by electron mediators (Liu and Logan, 2004). The microbes also produce protons that travel from the anode

chamber to the cathode chamber. The electrons from the anode travel through an external load and recombine with the protons at the cathode to form electric current and hydrogen.

In this study, a continuous flow membrane-less $1m^3$ MFC was used at 25° C temperature with a flow rate of 0.8L/min. The MFC pilot plant was located at the Sutton Bonington campus of the University of Nottingham (Figure 1). The microbial culture available in the liquid cow manure from a 3 million L storage tank at the Sutton Bonington Campus was used as inoculums.. A HACH spectrophotometer DR2500 (Inc.US) was used to conduct COD tests. An HPR-20 MS was used to quantify the hydrogen produced. The total nitrogen removal was been determined by the Kjeldahl method..

Figure 1MFC pilot plant of the University of Nottingham

3. Results

The COD value decreased rapidly during the first 2 days and then slightly decreased until the sixth day, as shown in Figure 2. The initial COD energy level was 33,600 J/L, and finally reached 558 J/L after 6 days. The overall removal of initial COD energy was 98%. This indicates that the microbial fuel cell is very active during the initial stage where nutrients, such as nitrates, are abundant.

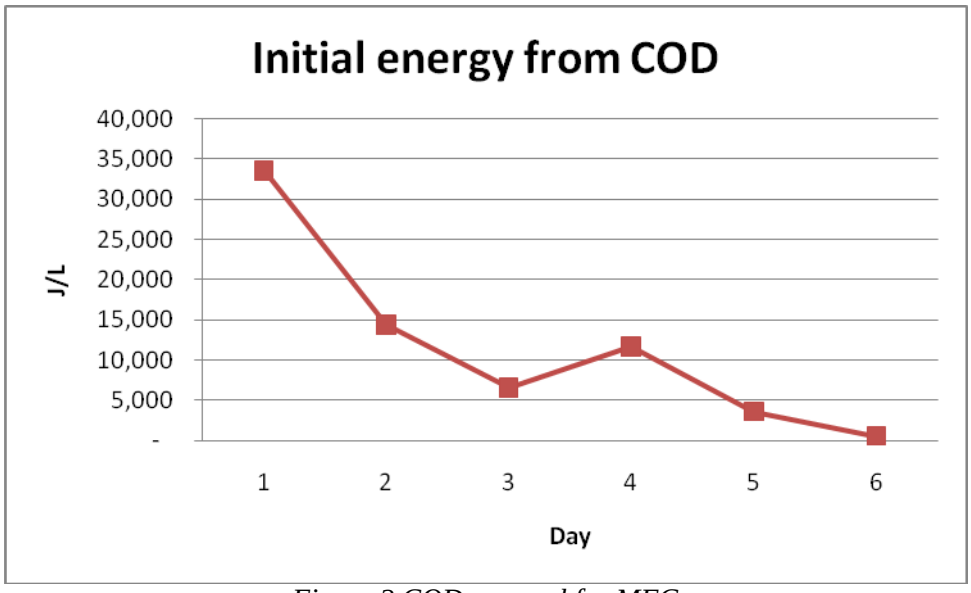

Figure 2 COD removal for MFC

Figure 3 shows the voltage variation between day 1 (0) to day 6 (5). The initial voltage increased from 1.2 mV to 1.6 mW within two days. Correspondingly, the largest amount of COD was removed from the first day to the third day. Therefore, the voltage achieved the highest value (1.6mV) on the third day and stayed stable until the end of forth day. As the COD energy is depleted, the voltage decreases on the sixth day.

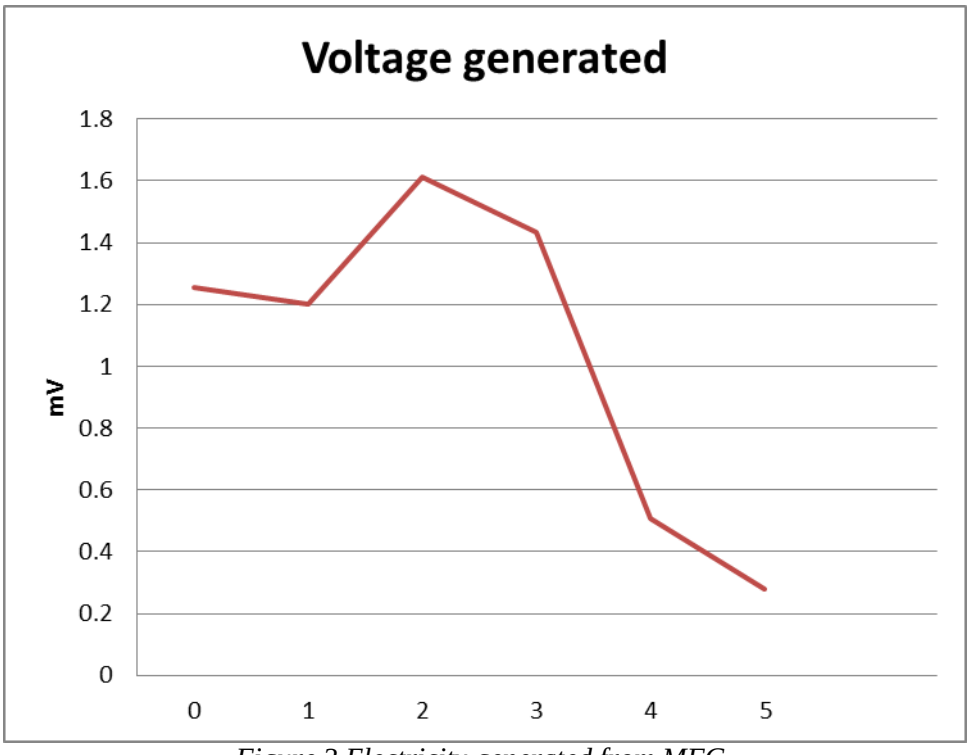

Figure 3 Electricity generated from MFC

Figure 4 shows the hydrogen production variation between day 1 (0) to day 6 (5). There was a rapid increase in the hydrogen produced within the first two days corresponding with the rapid fall in COD and increase in voltage generated. The energy content of hydrogen was

increasing continuously and finally achieved 38,333 J/L, which indicated that 80% of the COD energy was transferred to hydrogen gas.

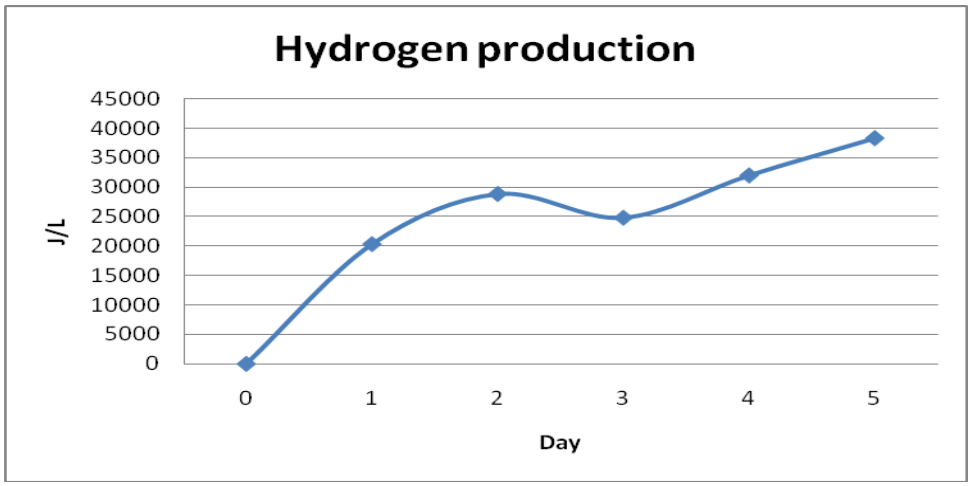

Figure 4 Energy to hydrogen production

According to the analysis, the content of nitrogen was decreasing continuously. There were 20% total nitrogen removals during the first 24 hours. That means organic nitrogen have been removed from liquid manure effectively by MFC, and stored in the MFC micro-organisms. The depletion of nitrate may also result in decreased microbial activity after day 4.

4. Conclusions

The overall COD removal from dairy farm waste using a microbial fuel cell was 98% after 6 days. The highest value of voltage generated was 1.6136mV indicating that dairy farm slurry waste is an appropriate resource for MFC. It could supply certain amount energy for the dairy farm, and also, the carbon emission and the disposal charging could be reduced. There is also bio-hydrogen produced by MFC where 80% of the COD energy has been transferred to hydrogen gas. Moreover, there were 20% nitrogen removals in the MFC during the first 24 hours. The most of nitrogen content of liquid slurry were immobilized in microbes indicating that available nitrate is a key for strong MFC activities.

References

[1] BERR& DEFRA, Energy White Paper. Our Energy Future—Creating a Low Carbon Economy, TSO, 2003.

[2] S. Cinar, T.T. Onay, A. Erdincler, Co-disposal alternatives of various municipal wastewater treatment-plant sludges with refuse. Advances in Environmental Research 8, 2004, pp. 477-482.

[3] M. Jetten, M. Schmid, I. Schmidt, M. Wubben, U. van Dongen, W. Abma, et al., Improved nitrogen removal by application of new nitrogen cycle bacteria, Rev Environ Sci Bio Technol 1, 2002, pp. 51– 63.

[4] L. Young, C.C.P. Pian, High-temperature, air-blown gasification of dairy-farm wastes for energy production, Energy 28, 2003, pp. 655–672.

[5] H. Liu, and B. E. Logan, Electricity generation using an air-cathode single chamber microbial fuel cell in the presence and absence of a proton exchange membrane, Environ. Sci. Technol., 38(14), 2004, pp.4040-4046.

Comparison of the combustion behaviors of agricultural wastes under dry air and oxygen

Hanzade Haykiri-Acma[1,*], Serdar Yaman[1]

[1] *Department of Chemical Engineering, Istanbul Technical University, Istanbul, Turkey*
** Corresponding author. Tel: +90 2122856291, Fax: +90 2122852925, E-mail:hanzade@itu.edu.tr*

Abstract: Burning tests of some agricultural waste biomass materials such as sunflower seed shell (SSS), hazelnut shell (HS), rice hull (RH), and olive refuse (OR) were performed in order to compare the combustion reactivities of these materials under dry air and oxygen. For this purpose, these samples were burned in a thermal analyzer to obtain TGA (Thermogravimetric Analysis), DTG (Derivative Thermogravimetry), DTA (Differential Thermal Analysis), and DSC (Differential Scanning Calorimetry) thermograms under both conditions. Initial sample mass was approximately 10 mg for each sample which has a particle size of <0.25 mm, and temperature was raised from ambient to 900°C with a linear heating rate of 40°C/min under gas flow rate of 100 mL/min. No hold time was allowed at the final temperature. The results of this study showed that the thermal reactivities of biomass species change in a wide region, and the type of the oxidative medium plays very important effects on the burning parameters such as the ignition point, maximum rate of combustion and its temperature, as well as the end point of burning. On the other hand, macromolecular ingredients of biomass such as hemicellulosics, celluloses, and lignin have significant effects on the combustion behavior of biomass.

Keywords: *Biomass, Agricultural Wastes, Combustion, Dry Air, Oxygen*

1. Introduction

There are several methods to control CO_2 emissions emitted from power plants including pre-combustion capture, post-combustion capture, and oxy-fuel combustion. Pre-combustion capture is also called as gasification or partial reforming for which fuel is reacted with air, oxygen, or steam to produce gaseous products. Post-combustion techniques are based on scrubbing of CO_2 from the flue gas. In oxy-fuel or O_2/CO_2 recycle combustion method, nitrogen is excluded using pure O_2 instead of air [1,2]. In oxy-fuel technique, the diluting effect of nitrogen in the flue gas does not take place, and the concentration of CO_2 becomes likely high which is suitable for CO_2 capture and storage (CCS) techniques [3]. That is, the concentration of CO_2 in the flue gas from conventional coal-fired boilers typically changes in the range of 4-14 vol % [1], whereas in case of oxy-fuel its concentration increases to 55-65 vol %. Then, cooling and condensing of water vapor leads to increase in the CO_2 concentration to around 96 vol % [4].

On the other hand, high concentrations of CO_2 in the combustion medium alter the combustion properties compared to N_2-rich combustion medium. Ignition temperature, burner stability, flame propagation, gas temperature, the char burnout, the radiating properties of the flame, the efficiency of the boiler, and the evolution of pollutants are closely affected from the high concentration of CO_2 [5]. Some of these alterations are directly associated with the increasing radiative properties and the thermal capacity of the mixture of CO_2 and water vapor compared to N_2. Combustion kinetics also changes considerably under high CO_2 concentration [6]. From this point of view, combustion characteristics of a given fuel species should be evaluated depending on the type of oxidizer.

So the aim of this paper is to investigate the differences in the combustion properties of some agricultural wastes using dry air or pure oxygen. For this purpose, sunflower seed shell, hazelnut shells, rice husks, and olive refuse have been selected as the model biomass species,

all of which are abundant in Turkey and they have already been used for energy resources for a long time.

2. Methodology

Agricultural biomass energy resources such as sunflower seed shell (SSS), hazelnut shells (HS), rice husks (RH), and olive refuse from milling (OR) used in this study are Turkish origin. These renewable energy sources were not dried in oven to avoid any modification in their original structure due to rapid drying, and they were kept at laboratory medium for 15 days to allow removal of the free moisture. Then, air-dried samples were milled and screened through a sieve having an opening of 250 μm. The proximate analysis and the gross calorific value measurements of the biomass species were carried out according to ASTM standards, and the ultimate analyses were performed by an elemental analyzer (EuroEA3000 model). These tests were repeated several times to check the reproducibility of the results.

The main ingredients of biomasses such as holocellulose (hemicellulosics + cellulose forms), lignin, and extractive matter were determined by analytical methods according to the following procedures. In order to remove the extractives and to obtain extractives-free samples, benzene-ethyl alcohol extraction procedure was applied according to ASTM D1105 standard.

The extractives-free bulk was then used as feedstock to isolate each of holocellulose and lignin. Isolation of holocellulose was performed with the mixtures of $NaClO_2$, acetic acid, and water. Whereas, the isolation of lignin was carried out by van Soest method in which extractives-free sample was treated with 72 vol % sulphuric acid to hydrolyze the cellulosics and to isolate the lignin [7]. The content of acid insoluble lignin which is called as “Klason Lignin” was determined by drying and ashing of the neutralized bulk.

Combustion tests of the samples were performed using a TA Instruments SDTQ600 model thermogravimetric analyzer with a differential scanning calorimetry detector. TGA (Thermogravimetric Analysis), DTG (Derivative Thermogravimetry), DTA (Differential Thermal Analysis), and DSC (Differential Scanning Calorimetry) thermograms were obtained using dry air or oxygen at flow rates of 100 mL/min, and the initial weights of the samples were around 10 mg. Temperature was increased from ambient to 900°C by a heating rate of 40°C/min, and no hold time was allowed.

3. Results and Discussion

Analysis results of the samples are seen in Table 1. According to data given in Table 1, it can be said that all the biomass species are rich in volatiles and their fixed carbon contents are considerably lower than the contents of volatiles. In fact, such a distribution of the contents of volatile matter and fixed carbon is typical for most biomass species [8]. SSS is the biomass material that contains the highest volatiles among the samples. Ash contents of the samples varies in a so wide range that the ash content of SSS is only 2.7 % while the ash content of RH reaches 23.8 %. Sulfur contents of the biomass species are very low regarding the ash contents of the low rank coals in general. On the other hand, hydrogen and nitrogen contents of all the samples are very close to each other.

Lignin contents of the biomass materials are also very close to each other except for HS. Although, the lignin contents of SSS, RH, and OR changes between 31.4 and 34.8 %, HS which has a woody structure contains higher lignin content as much as 51.5 %. Besides, SSS

which gives the highest volatiles yield also contains the highest holocellulose content. In addition, the lowest calorific value belongs to RH that is rich in ash forming mineral matter.

Table 1. Analysis results of the biomass species

		SSS	HS	RH	OR
Proximate Analysis (%, dry basis)	Volatiles	83.7	72.0	66.2	71.2
	Fixed Carbon	13.6	21.0	10.0	14.6
	Ash	2.7	7.0	23.8	14.2
Ultimate Analysis (%, dry-ash-free basis)	C	47.8	54.8	44.8	49.3
	H	6.1	6.7	6.3	6.2
	N	1.2	1.0	0.9	1.7
	S	0.3	0.1	0.1	0.1
	O*	44.6	37.4	47.9	42.7
Structural Analysis (%, dry basis)	Extractives	13.8	6.2	9.8	13.6
	Lignin	31.4	51.5	34.8	34.7
	Holocellulose	62.5	38.6	44.9	40.0
Calorific Analysis	Higher Calorific Value (MJ/kg)	17.7	18.2	13.9	17.2

* calculated by difference

DTG and DSC curves obtained from non-isothermal thermal analyses of the biomass samples under dry air are illustrated in Fig.1.

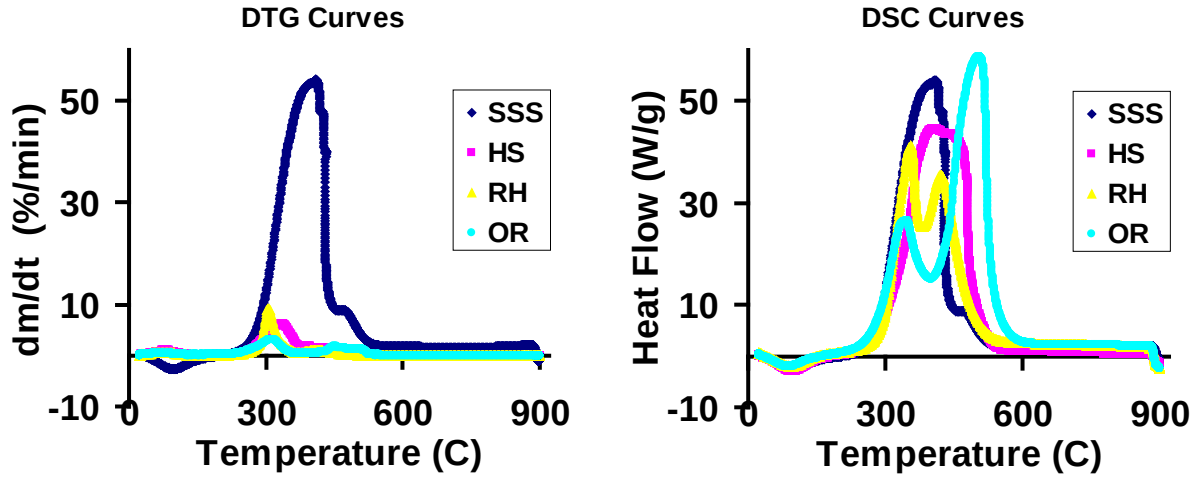

Fig. 1. DTG and DSC curves obtained from burning with dry air.

DTG curves which are seen on the left hand side of Fig.1 show the relation between temperature and the rates of the mass losses from the biomass samples. These curves indicated that the thermal decomposition and the burning of SSS have such a characteristics that it losses the weight so rapidly that its maximum rate of burning reaches 53.6 %/min at

413ºC. Besides, the maximum burning rates for the other samples could not be at this level that they were 8.2 %/min at 320 ºC for RH, 6.3 %/min at 307 ºC for HS, and 3.2 %/min at 314 ºC for OR. Although the mass losses from the samples continued as temperature increases up to the final temperature, they are negligible beyond 600ºC. The high thermal reactivity and the very high rates of mass losses from SSS can be attributed to the high contents of volatiles in this sample. In fact, high contents of holocellulose which is sum of hemicellulosics and cellulosics contribute to the formation of volatiles [9]. These constituents which are rich in weak ether bonds are thermally unstable and they produce volatile species. Of which, combustible volatiles are able to burn in the gaseous phase as homogeneous combustion. Elimination of the volatiles from the solid matrix leads to the formation of porous remnant and then burning of the char takes place firstly on the surface which is followed by diffusion of oxygen into the pores and complete burning of the particles. The latter is generally called as the heterogeneous burning stage [10]. Thus, all the organic part of the samples could be oxidized until the end of the burning experiment since the final temperature was high enough for combustion of most biomass materials.

On the other hand, the heat flows which are shown as DSC curves on the right hand side of Fig.1 predicts that the huge rates of mass losses in the DTG curve for SSS could not contribute to the exothermic performance of this sample at expected level. This is because the most of the mass losses are formed from the elimination of the volatiles such as carbon dioxide which play no important role on the calorific output. The exothermic regions for all the samples either comprised of two different parts or a unique broad peak having a shoulder, representing the effects of both homogeneous combustion of volatiles and char burning.

In order to investigate the individual effects of biomass ingredients on burning, each of the isolated ingredients including holocellulose, lignin, and extractive-free samples were burned under dry air condition. Fig.2 represents the burning characteristics of the ingredients of sunflower seed shell and rice husk, the burning properties of which were highly different in their parent samples.

The ingredients for both samples showed similar trends below 250°C that almost all of the ingredients lost the same weight in this stage. Increasing temperature affected the weight losses in different way that holocellulose and extractives-free sample of SSS rapidly lost weight while higher temperatures necessitated getting the similar decomposition yield for the lignin content of SSS. On the other hand, decompositions of holocellulose and lignin contents for RH exceeded the decomposition of extractives-free sample from 250°C to the end of the experiment. In this context, the high ratio of ash for RH is effective at this point, since most of the ash forming minerals still exist after treatment with benzene-ethyl alcohol. Accordingly, it is possible to conclude that the burning yields for the ingredients of SSS are higher than those for RH. This shows that the complex structure of biomass which is comprised of mainly from the major macromolecular ingredients are closely affected from the individual behaviors of the each ingredient during thermal process.

DTG and DSC curves obtained from the burning experiments in which oxygen were used instead of dry air are given in Fig.3.

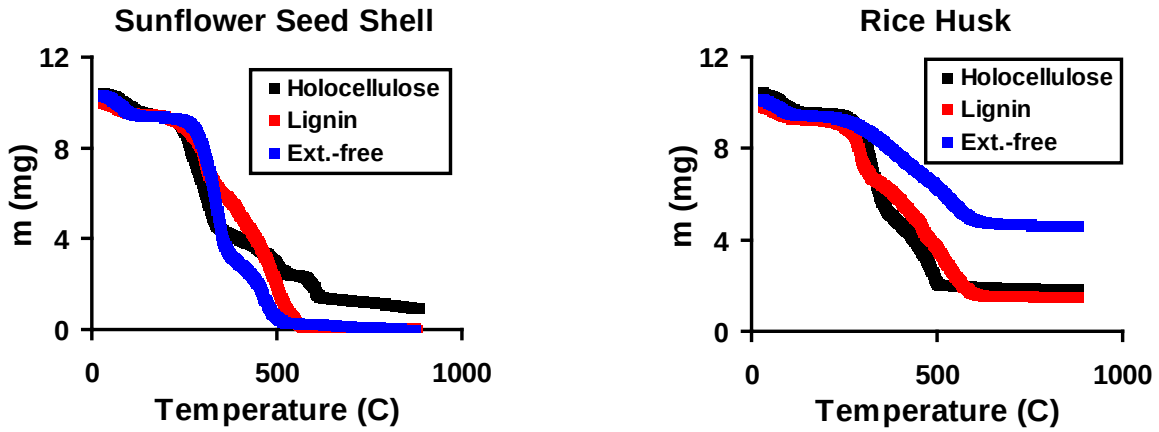

Fig. 2. TGA curves for the Ingredients of SSS and RH under dry air.

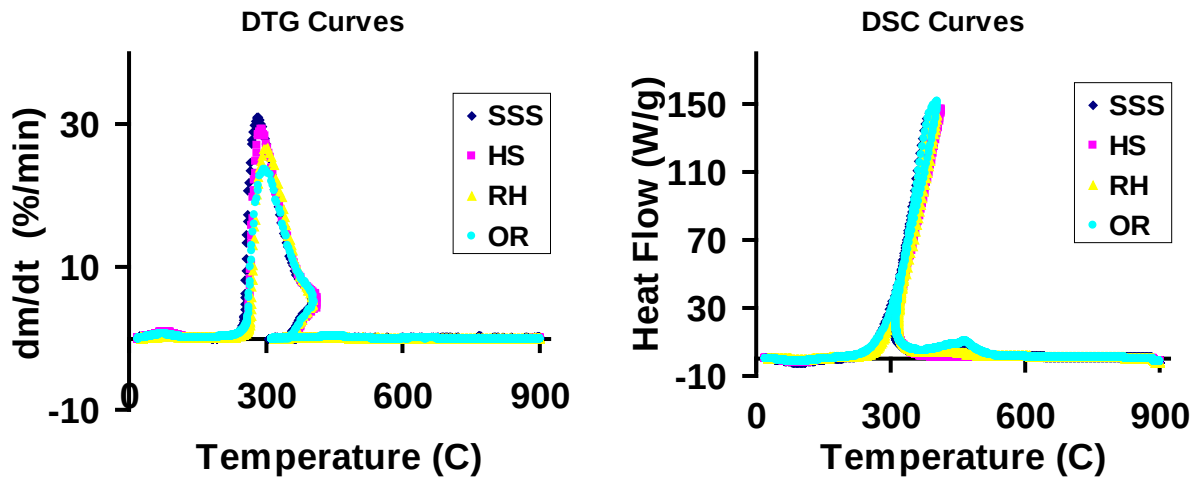

Fig. 3. DTG and DSC curves obtained from burning with oxygen

At the first sight it is likely to conclude that the difference among the DTG curves of the biomass species encountered for burning using dry air wholly disappeared, and the DTG curves almost overlapped in case of oxygen. Also, the burning rates for all the biomass samples except SSS increased more than three-folds when oxidizing gas changed from dry air to oxygen. This shows that usage of pure oxygen during burning of biomass so augmented the thermal reactivity that very different burning profiles could be obtained. Furthermore, the combustion process ended at lower temperatures. These findings can be supported by the results found from the DSC curves. That is, usage of pure oxygen so changed the shapes of the heat flow curves that they almost became very sharp peaks in contrast to the shapes of DSC curves for dry air which had some apparent regions in which heat flows take place. The exothermic heat flows occurred in so narrow temperature intervals that the temperatures of the

lower and upper limits of these regions are very close to each other. Therefore, it is very difficult to distinguish the individual DSC curves as well as DTG profiles. These results predict that not only the rates of the mass losses but also the heat flows are seriously influenced from the type of the oxidizer medium. Increase in the concentration of oxygen caused variations in thermal behavior of biomass in the favor of increasing reactivity.

4. Conclusions

Burning characteristics of some agricultural waste biomass species such as sunflower seed shell, hazelnut shell, rice husk, and olive refuse have been tested under dynamic flows of dry air or oxygen under relatively slow heating conditions in a thermal analyzer. These tests indicated that both the rates of the mass losses from the biomass samples and the heat flow properties are obviously different for each biomass material under dry air. For an example, sunflower seed shell showed such a different weight loss character from the other biomass samples under dry air that it is possible to say that its thermal reactivity is extremely higher than that for the other samples under investigated conditions. Despite this big difference in weight loss characteristics of SSS, heat flow properties determined from DSC curves could not monitored at expected level, and all the samples showed similar heat flow characteristics to some extent. The major ingredients of biomass samples including holocellulose and lignin plays a significant role on the thermal reactivity and the exothermic characteristics of the burning process.

On the other hand, a different situation was detected in the DTG and DSC curves obtained under pure oxygen. That is, almost all the DTG curves for the samples overlapped to form a unique peak as well as the DSC curves. This shows that usage of oxygen instead of dry air eliminated the differences in the thermal reactivity and the burning features of the biomass species under investigated conditions. Also, thermal reactivities of biomasses seriously increased in case of oxygen usage.

References

[1] J. Davison, K. Thambimuthu, Technologies for capture of carbon dioxide, in: Greenhouse Gas Control Technologies, Vol.I, Elsevier, 2005, pp. 3-13.

[2] R. Allam, V. White, N. Ivens, M. Simmonds, Heaters and boilers to oxyfiring by cryogenic air separation and flue gas recycle, in : Carbon Dioxide Capture for Storage in Deep Geologic Formations, Vol. 1, Elsevier, 2005, pp.451-475.

[3] G. Pipitone, O. Bolland, Power generation with CO_2 capture: Technology for CO_2 purification, International Journal of Greenhouse Gas Control 3, 2009, pp. 528–534.

[4] I. Hadjipaschalis, G. Kourtis, A. Poullikkas, Assessment of oxyfuel power generation technologies, Renewable and Sustainable Energy Reviews 13, 2009, pp. 2637–2644.

[5] P.A. Bejarano, Y.A. Levendis, Single-coal-particle combustion in O_2/N_2 and O_2/CO_2 environments, Combustion and Flame 153, 2008, pp. 270–287.

[6] T. Wall, Y. Liu, C. Spero, L. Elliott, S. Khare, R. Rathnam, F. Zeenathal, B. Moghtaderi, B. Buhre, C. Sheng, R. Gupta, T.Yamada, K. Makino, J. Yu, An overview on oxyfuel coal combustion—State of the art research and technology development, Chemical Engineering Research and Design 87, 2009, pp. 1003–1016.

[7] P.J. Van Soest, Use of detergents in the analysis of fibrous feeds. II. A rapid method for the determination of fiber and lignin. Journal of Association of Official Analytical Chemistry. 46, 1963, pp. 829-835.

[8] D.L. Klass, Biomass for renewable energy, fuels, and chemicals, Academic Press, 1998, pp. 237-239.

[9] R.Kandiyoti, A.Herod, K.Bartle, Solid fuels and heavy hydrocarbon liquids; thermal characterization and analysis, Elsevier, 2006, p.38.

[10] B.G.Miller, D.A. Tillman, Combustion engineering issues for solid fuel systems, Elsevier, 2008, pp.17-21.

Nigeria's Bio-Ethanol: Need for Capacity Building Strategies to prevent Food Crises

O. Phillips Agboola[1,*], O. Mary Agboola[2]

[1] *Mechanical Engineering Department, Eastern Mediterranean University, Famagusta, via Mersin 1o, Turkey*
[2] *Economics Department, Eastern Mediterranean University, Famagusta, via Mersin 1o, Turkey*
** Corresponding author. Tel:+903926301160, Fax:* +90 392 365 3715, *E-mail: phillips.agboola@cc.emu.edu.tr*

Abstract: This work reviews current bio-ethanol developments in Nigeria and offers recommendations to help sustains this trend of development. The use of staple crops, such as cassava for bio ethanol production is generating mixed reactions among the populace who depend largely on these crops for food due to poor living conditions in the country. This paper reports that while there is a target of 1.27 billion litres of ethanol per year to be blended with petroleum, the government is doing little to increase cassava production and cassava extraction efficiency. The current average yield of Nigeria's cassava stands at 15 tonnes per hectare compared to countries like Brazil with an average of 35 tonnes per hectare. Furthermore agricultural research and development in the country is underfunded, a situation which hampers innovation and growth in the agricultural sector. The need to concentrate efforts on increasing the average yield of cassava is emphasised in this work. This study could not explore the technical aspect of the cellulosic feedstock for bio-ethanol due to the non-standardization of the techniques coupled with the fact that the bio-ethanol industry in Nigeria is still at its infancy. It is obvious that the government lacks comprehensive policies to tackle the challenges that ethanol development will pose to the citizenry. Therefore this paper provides recommendations for policy makers to aid in formulating a sustainable bio-ethanol policy for Nigeria.

Keywords: *Ethanol, Biofuel, Energy crops, Food crise,Cassava*

1. Introduction

Environmental concerns and crude oil price volatility are creating market gaps between conventional and renewable energy sources. The conventional sources of energy are currently being supplemented by renewable energies to reduce and accommodate the high fluctuations in the price of oil in recent years. Bio fuel among other forms of renewable energy is attracting attention globally especially in Brazil and United State of America. It is being touted as the future supply of energy in transportation and electricity generation. Africa, the second largest continent in the world, host 13% of world's populations and 10% of the world crude oil reserves [1]. Africa's energy consumption is less than 5% of global consumption therefore African countries are categorised as poor based on energy consumption, a major developmental index. Bio fuel is not a recent development in a number of African countries like Zimbabwe, Malawi and Kenya as they started blending programmes in the 1980's. In Nigeria, bio-ethanol production is still in its infancy and requires attention from policy makers and financial institutions to develop and build the industry. In many African countries uncertainty exists on the massive utilization of bio-ethanol due to the possible risks of food scarcity. The use of bio-ethanol blend in Nigeria transportation fuel (E10) has triggered sharply polarized views among agricultural scientists, food engineers, policy-makers and the general public. Nigeria in an effort to minimise carbon emissions, energy insecurity and take advantage of renewable energy is investing in bio-ethanol technology in partnership with Brazil. One major concern shared by many on Nigeria's ethanol blend is her capacity to prevent food crises while achieving energy security. Bio-ethanol production in Nigeria adopts the use of cassava (majorly), sweet sorghum and sugarcane as feed stock knowing that these staple crops are the major food crops in Nigeria. Although Nigeria is the largest producer of cassava in the world, but more than 90% of cassava production in Nigeria is used for domestic

food consumption. The government's road map for achieving the bio-ethanol target of 1.27 billion litres/year distances itself from how this will not lead to food shortage in Nigeria. It is obvious that the bio-ethanol target of Nigeria is achievable due to the size of useful land available in the country but there is need for capacity building strategies to sustain bio-ethanol production. Nigeria's size and land usage are presented in Table 1.

Table 1: Nigeria's Size and Land use Parameters [2]

Nigeria	**Percentage (%)**	**Quantity (Million ha)**
A. SIZE		
Total Area	100.0	92.4
Land area	85.9	79.4
Water bodies	14.1	13.0
B. LAND USE		
Agricultural land	**77.8**	**71.9**
Arable cropland	30.5	28.2
Permanent cropland	2.7	2.5
Pasture land	30.6	28.3
Forest and woodland	11.6	10.9
Fadama	2.2	2.0
Other land	8.1	7.5

There is huge potential for bio-ethanol in Nigeria as can been seen from Table 1. Nigeria's total area is 92.4 million hectares out of which 79.4 million and 13.0 million hectares are occupied by land and water bodies respectively. Agricultural land occupies 71.9 million hectares making Nigeria one of the top bio-fuel potential countries in the world. In Nigeria 94% of households engage in crop farming while about 68% of households engage in livestock farming [3]. This work will attempt to review government's effort to advance bio-ethanol in Nigeria, assess the risk of using food crop for ethanol production and recommend policy to help in safe-guarding food security in the country.

2. Nigeria's Bio-Ethanol Feedstock and Industries

Nigeria bio-ethanol production like most countries in the world comes from first generation feedstock like cassava, sugarcane and sorghum. Cassava is the main feedstock for Nigeria's bio-ethanol because the country imports about 50% of its sugar consumption. The world annual cassava production is estimated at 208 million tones per year with about 60% grown in Africa. Figure 1 shows cassava production in some selected countries with Nigeria leading the production chart. Nigeria produces more than 40 million tonnes of cassava yearly with the average yield of 15 tons/hectare as compared to 25-30 tons/hectare obtainable in other countries. Nigeria has more than a million hectares of land that could support cassava commercial plantation if financial institutions will invest adequately [3]. The key driver's of Nigeria's bio-ethanol are 1) urgent need to reduce energy insecurity 2) increase electricity accessibility 3) need to raise GDP from 3.5% to 8% per annum and 4) maximise the use of available resources. The plan to blend ethanol with petroleum for domestic use is driven by

the need to reduce the cost of fuel importation, since Nigeria's refineries are not working at optimum capacity and to respond to climate change. Elijah I. Ohimain stated that, an investment of over $3.86 billion has already been committed to the construction of 19 ethanol bio refineries, 10,000 units of mini-refineries and feedstock plantations for the production of over 2.66 billion litres of fuel grade ethanol per annum. Also an additional 14 new projects are in the offing. Of the 20 pioneer projects, 4 are at the conception phase, 8 are in the planning phase, and 7 are under construction with only 1 operational. Many have argued that a sustainable bio-fuel policy will be needed to regulate sales, use and production [4-6].

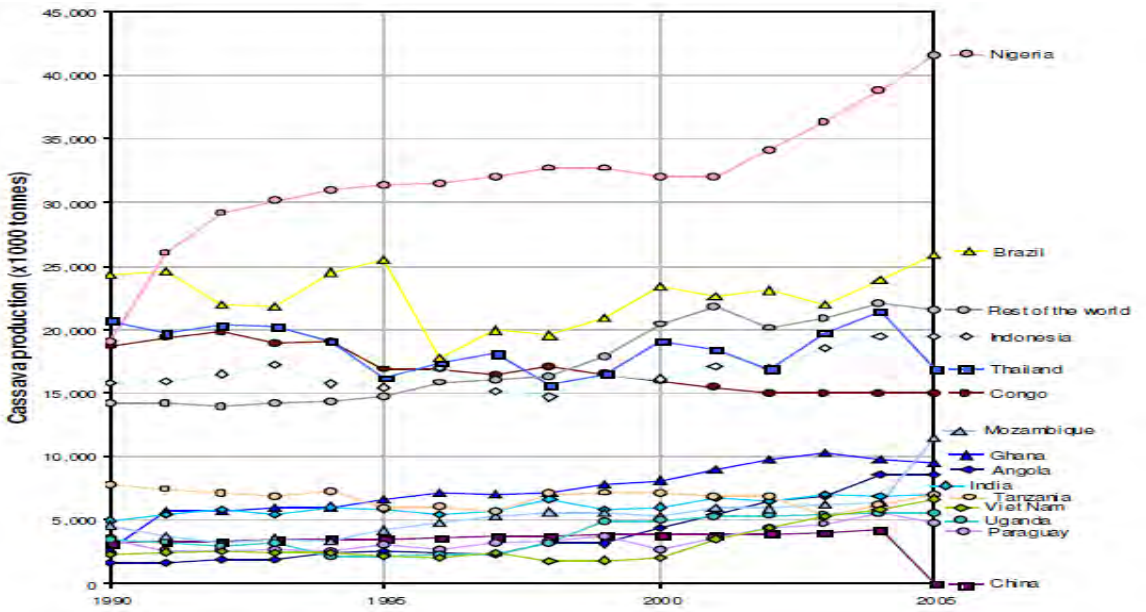

Fig. 1. Cassava production in selected countries 1990- 2005 (Source: F AO, 2007)

Table 2. Some Selected Ethanol Plant in Nigeria

Name of Company	Plant Location	Feed stock	Installed capacity (million litres/year)
Dura Clean	Bacita	Molasses/Cassava	4.4
AADL	Sango Ota	Cassava	10.9
CrowNek	Ekiti	Cassava	64.0
BV Energy Company	Bayelsa	Cassava	75.0
Akoni	Lagos	Cassava	53.0

Table 3. Some Selected Proposed Plants

No	Name of Company	Project information	Budget
1	Jigawa,Benue, Anambra and Ondo State	Integrated bio-ethanol refinaries and sugarcane farm	$4 Billion
2	Nasarawa State	Integrated bio-ethanol refinary and cassava farm	$27 Million
3	Casplex	Ethanol refinary and cassava farm	NA
4	Ekiti State	Integrated bio-ethanol refinary and cassava farm	$100Million
5	Petrobras	Ethanol plant	$200 Million
6	Kogi State	Ethanol plant	$1 Million
7	Taraba state	Ethanol plant	$115 Million
8	Niger State	Ethanol plant	$314 Million
9	lemna	Ethanol plant	$50 Million

Production of bio-ethanol from non-edible crops/oil seed and cellulosic substances are going to create a new window of opportunity for agriculture, mitigate green house emissions and end Fuel-Food debate. The entire supply chain and process of the first generation feedstock (e.g. Cassava) needs to be re-evaluated to derive added value from bio-ethanol. Currently bio-ethanol from energy crops grown for traditional markets is too expensive for use as fuel and this is causing rising cost of food especially in Nigeria where government regulations is ineffective. Table 2&3 shows bio-ethanol plants in Nigeria requiring mostly cassava as feedstock.

3. Cassava: Feedstock versus Staple Food

Nigeria produces more cassava than any other country in the world followed by Brazil. Nigeria's cassava production is almost double the production of Indonesia and Thailand. Cassava is a very versatile commodity with numerous uses and by products. The crop is abundant in 24 of the 36 states, requires minimum labour input, and remains the most important food security crop for millions of Nigerians. The leaves can serve as vegetables; the stem is used for plant propagation and grafting while the roots are typically processed for human and industrial consumption. Cassava flour has applications in the biscuits and confectionary industry, dextrin pre-gelled starch for adhesives, starch and hydrolysates for pharmaceuticals, and seasonings. Table 4 show Cassava production from 1990 -2005.

Nigeria's Cassava is traditionally processed into food products like, gari (roasted cassava granules),cassava chips and pellets, fufu flour, starch, cassava flour (lafun and elubo), etc consumed by the populace. Cassava in Nigeria is consumed mostly as gari in almost every part of the country. In some places the cassava root is a major staple while in other areas (especially in the south west) cassava leaves serve as vegetables. Since the populace is highly dependent on this crop, its use for bio-ethanol will lead to food crises. Already over 60% of the population is poor and survive with less than a dollar per day. The use of cassava for monosodium glutamate, glues/adhesives is also common but in small quantities when compared with its use for food. The ethanol content of cassava root depends on yield per hectare, technology used in the extraction and the variety of the cassava. A conservative average for a ton of cassava will be about 100 litres of ethanol [7-9]. The government target is to blend ethanol with PMS using a ratio of 9:1 meaning the government is adopting E10. Using the 2010 PMS consumption as baseline, total PMS consumption stood at 12.775×10^9 litres where over 60% was imported due to the poor state of the refineries in Nigeria. The drive to produce 1.2775×10^9litres (or 1.2775×10^6 m^3) of ethanol from cassava will require about 12.8 million tones of cassava. The average per capita food consumption in Nigeria is about 600 calories per capita per day where more than 300 calories per capita per day is from cassava in different forms. The consumption of gari may account for more than 70% of cassava consumption in Nigeria [10]. If the same cassava is to be used as feedstock for ethanol, it means that about 30% of total cassava production in Nigeria will not be available for the production of daily calories per capital per day.

Converting 30% of cassava production in Nigeria into ethanol will mean that around 3.83 million tonnes of gari will be lost in circulation thereby increase gari scarcity and threatening food security. The argument is that for every $1m^3$ of ethanol produced for fuel from cassava root, about 3 tones of gari are lost. According to Phillips et al [7] 16% of cassava produced is used in industries (excluding ethanol based industries) as raw materials, a value that must have increased since 2001. Since there is no data on the current percentage, if we assume 25% at the end of 2010 and allowing 10% for post harvest losses and wastes, it means just around

65% of cassava production will be left for other uses including food production and ethanol production).

According to the estimate revealed in this paper about 30% of cassava production is needed by the ethanol plants to deliver the 10% blended needed for the E10 in transportation. It is very obvious that 35% of the remaining cassava production can not feed the Nigeria populace of about 150 million who depend heavily on cassava products for survival due to its low cost availability and traditions. The daily consumption of ethanol in this paper does not include ethanol for cooking, a scheme the government is also seriously considering. This will increase the ethanol need as calculated in this study and will increase the need for cassava. Also the informal exportation of cassava to some neighbouring countries like Niger is not accounted for in this study. It is obvious that there is the danger of food insecurity in the country if she continues to pursue her cassava based ethanol policy without looking into other substitute energy crops.

Furthermore there is the need for second generation feedstock for Nigeria's ethanol needs. This can be obtained from the waste from wood industries, bamboo etc. Table 4 shows the production of cassava and yearly yield in Nigeria. it will be observed that the cassava production yield fluctuates without an trend of definite increment. The current yield stands at 15 tonnes / hectare.

Table 4: Levels of Cassava Production from 1990-2003 (tonnes)

Year	Production	Yield
1990	19,043,008	11.65
1991	26,004,000	10.19
1992	29,184,000	10.59
1993	30,128,000	10.59
1994	31,005,000	10.59
1995	31,404,000	10.68
1996	32,050,000	10.66
1997	32,695,000	11.88
1998	32,698,000	10.75
1999	32,070,000	10.64
2000	32,810,000	10.64
2001	32,586,000	10.80
2002	34,476,000	9.98
2003	33,379,000	10.92
2004	38,211,000	11.60
2005	42,012,000	11.60

Source: FAO (2004) &Authors

4. Capacity Building Strategies

Ethanol production in Nigeria has the potential to radically change the economic condition of the country which presently relies solely on the exportation of crude oil. The Nigerian agricultural sector which is currently dedicated only to food production, will also receive a boost. The construction of Ethanol plants in Nigeria is taking place within a non-consolidated governmental policy framework, though there are efforts to address this situation. The political environment in Nigeria is known to have lots of challenges, and the bio-ethanol

industry is no exception. No adequate policy framework exist that directly addresses the challenges and peculiarities of the bio-ethanol industry in Nigeria; however, this work will provide recommendations and capacity building strategies to sustain current developments in the Ethanol industry in Nigeria.

4.1 Research and Development Centres

One key attribute of the success of the Brazilian ethanol industry was the huge investment in agricultural research and development by both the government and the private sector. The results of most of the research carried out by some government owned agencies (like EMBRAPA) together with universities have allowed Brazil to play a major role in Bio-ethanol technology [11, 12]. There is need for Nigeria to learn from countries like Brazil and US on how to efficiently utilize agricultural land for optimum yield. Nigeria produces more than 40 million tonnes of cassava yearly with an average yield of about 15 tons/hectare as compared to 25-30 tons/hectare obtainable in other countries. Increasing efficiency of inputs and processes to optimize output per hectare of feedstock comes only through research. The growth rate in Brazil's efficiency in ethanol production is about 4% per year. Innovations in the industrial process of cassava (saccharification and fermentation) will allow an increase in carbohydrate extraction from the cassava root up to 70 %. The government's budget and policies have not laid emphasis on research and development but more on ethanol plant construction and cassava plantations. There are more than 70 universities in Nigeria and more than 4 of the Universities are Universities of Agriculture, well equipped to carry out research on the second generation feedstock for ethanol, but the government has consistently ignored the role of research institutions in its Bio-ethanol development. The government needs to empower the Universities through its various agencies to carry out substantial research to aid the development of a more sustainable ethanol technology.

4.2 Financial Institutions, Private Investments and government incentives

Nigeria's bio-ethanol feedstock production is government led and has little input from private firms. The industry needs more participation from commercial agricultural firms and support by financial institutions. Government intervention at the initial phase of bio-ethanol production is necessary but access to finance and availability of affordable loans should be encouraged. In Nigeria for instance, no insurance or commercial bank gives soft loans for the cultivation of cassava for bio-ethanol production. The banks are unwilling to provide finance due to market uncertainties and perceived high risks. The lack of adequate data to guide financial institutions and insurance firms in taking decisions are due to gross variations in the data obtained from the government and the private sector. There are a number of incentives the government can deploy to stimulate the Nigeria's bio-ethanol industry [13]. These include:

- **Pioneer Status**: All registered businesses engaged in activities related to biofuels production and/or the production of feedstock for the purpose of biofuel production and co-generation within the country shall be accorded Pioneer Status within the provisions of the Industrial Development (Income Tax Relief) Act.
- **Withholding tax on interest, dividends, etc**.: Biofuel companies shall be exempted from taxation, withholding tax and capital gains tax imposed under sections 78, 79, 80 and 81 of the Companies Income Tax Act in respect of interest on foreign loans, dividends, and services rendered from outside Nigeria to biofuel companies by foreigners
- **Waiver on import and customs duties:** Biofuel companies shall be exempted from the payment of customs duties, taxes and all other charges of a similar nature.

- **Waiver on Value Added Tax: T**his shall also apply to all Biofuel companies operating in Nigeria.
- **Long term preferential loans:** Preferential loan arrangements will be made available to investors in the biofuel industry to aid the development of large scale outgrower schemes and large scale integrated operations, including plantation, plant, and within the gate co-located power generation plants. An Environmental Degradation Tax shall be charged on oil and gas upstream operations to provide a source of funding for preferential loans.

5. Policy Recommendations

The development of bio-ethanol in Nigeria is a welcome idea coupled with the benefit of job employment and increased revenue for the government. The sustainability of bio-ethanol implies that government needs to improve on their present commitment and learn from the success stories of countries like Brazil and inculcate suggestions that will help to sustain the bio-ethanol development in Nigeria. In lieu of that the following recommendations are given:

(i) Effective and robust loan facilities: There is the need for long term loan facilities to motivate farmers into practicing commercialized farming. Agricultural incentives like little or no interest rates on short term loans, low interest on long term loans should be made available to farmers. The recapitalization of banks in Nigeria was to allow cash flow to small business but this is not the case.
(ii) The land use act: There are so many flaws in the land use act that needs to be amended, the land use acts needs to favour land for agriculture purposes.
(iii) Tax exception: Tax incentives should be given to private investors willing to invest in the bio-fuel feedstock.
(iv) Export and import duties: The waiver of duties on imports and exports related to bio-fuel should be considered by the government to kick start her ambition in the bio-ethanol field. Since the government has a poor record in the management of bio-ethanol blend. The management of bio- ethanol blend should be private sector driven
(v) Well equipped R&D: The technology of bio-ethanol in Nigeria should have indigenous perspectives, the government and the private sector should jointly fund research both at home and abroad to validate their outcomes at every point. Bio-fuel industry comes with new technology. The Universities of Agriculture in conjunction with Universities of Technology available in the country should be given the responsibility of pioneering this research.
(vi) Bio-fuel policy and legislature: Nigeria's bio-fuel policy at the moment is still sketchy and need thorough work to establish a frame work and legislature for industry. Clean energy and techniques should be well promoted and the consequences of breaking the law should be severe. The law to govern the bio-fuel industry should be corruption proof.
(vii) Promoting the use of second generation feed stocks: This will reduce the risk and threat to food security especially in Nigeria where the first generation feed stocks are the main source of food.
(ix) Setting up a Bio-fuel Feedstock regulatory body: A body like this will be given the responsibilities to oversee the sale, price and consumption of feedstock for domestic consumption and for the bio-fuel industry
(x) Brazil and the US partnership: The government should involve the two leading countries in bio-fuels to shape its bio-fuel policy and technology.

6. Conclusion

The development of the bio-ethanol industry in Nigeria is an important milestone in achieving energy self-sufficiency and sustainable development, especially in the transportation sector.

This paper has reviewed efforts of the Nigerian government towards bio-ethanol blend in the country, the risks and dangers involved in kick-starting ethanol production without proper policy and developmental frameworks to increase cassava production and yield. Commercial agriculture must play a pivotal role in this development of bio-ethanol without leading to food insecurity. There is need for the government to encourage and give incentive for cassava production in the country. The need for government to involve research institutions in the development of bio-ethanol and cassava cannot be over emphasis. The government also has to design incentives for financial institutions to grant soft loans for the purpose of cassava cultivation on a large scale. The government's ambition to advance bio-ethanol technology in Nigeria poses a threat to its populace of about 150 million if adequate frameworks are not put in place as recommended in this work. If the government wants to continue its bio-ethanol technology the paper recommends that the decision makers should carefully review the policy recommendations in this work.

References

[1] Bugaje IM and Mohammed IA. Biofuels Production Technology. Publisher - Science and Technology Forum, Nigeria. ISBN: 978-057-061-8 (2008)

[2] Ohimain, E.I., Emerging bio-ethanol projects in Nigeria: Their opportunities and challenges. Energy Policy (2010).

[3] Awoyinka, Y.A., 2009. Cassava marketing: options for sustainable agricultural development in Nigeria. Ozean Journal of Applied Science 2 (2), 175–183.

[4] Energy Commission of Nigeria (2005) Renewable Energy Master Plan. Abuja.

[5] www.pppra-nigeria.org.

[6] Azih, I., 2007. Biofuels demand: opportunities for rural development in Africa (Nigerian case study). In: Proceedings of the second European Forum on Sustainable Development, Berlin, Germany, 18–21 June 2007.

[7] Phillips TP, Taylor DS, Sanni L, Akoroda MO (2004). A cassava industrial revolution in Nigeria: The potential for a new industrial crop [Online].

[8] Atthasampunna S, Somchai P, Eur-aree A, Artjariyasripong S (1987). Production of fuel ethanol from cassava. World Journal of Microbiology and Biotechnology Volume 3, Number 2, pg135-142

[9] Export Wang W (2002). Cassava production for industrial utilization in China – Present and future perspectives [Online]. http://www.ciat.cgiar.org

[10] S.O Adamu, Trend and prospects of Cassava in Nigeria. Proceedings of a workshop on trend and prospects of cassava in the third World. IFPRI, Washington D.C. July 1989.

[11] Export Opportunities and Barriers in Africa-Growth and Opportunity Act-eligible countries U.S Trade Commission Investigation No. 332-464, 2005.

[12] Balat, M., Balat, H., Oz, C., 2008. Progress in bio-ethanol processing. Progress in Energy and Combustion Science 34, 551–573.

[13] NNPC, 2007a. Draft Nigerian Bio-fuel policy and incentives. Nigerian National Petroleum Corporation, Abuja.

Planting sweet sorghum under hot and dry climatic condition for bioethanol production

A. Almodares*, M.S. Hatamipour

University of Isfahan, Isfahan, Iran
** Corresponding author. Tel: +98-311-2369005, Fax: +98-311-2344761, E-mail: aalmodares@yahoo.com*

Abstract: Plants are the best choice for meeting the projected bio-ethanol demands.For this scope, a comparative analysis of the technological options using different feed stocks should be performed. Sweet sorghum can be used as a feedstock for ethanol production under hot and dry climatic conditions. Because, it has higher tolerance to salt and drought comparing to sugarcane and corn that are currently used for bio-fuel production in the world. In addition, high carbohydrates content of sweet sorghum stalk are similar to sugarcane but its water and fertilizer requirements are much lower than sugarcane. Also, sugarcane is not a salt tolerant plant. On the other hand, high fermentable sugar content in sweet sorghum stalk makes it to be more suitable for fermentation to ethanol.In this work, planting sweet sorghum in hot and dry provinces of Iran generally produced 80 tons stalks, 5 tons grains and 15 tons green leaves per hectare. However comparison among 29 sweet sorghum cultivars and lines showed that Rio had higher biomass (117.14t/ha), stalk yield (95.00t/ha), grain yield (5.00t/ha) and leaves (17.00 t/ha). It is interesting to point out that sweet sorghum could be cultivated in southern parts of Iran 3-4 times per year. Based on these results it is more economical to plant sweet sorghum for bio-ethanol production in hot and dry regions of the world.

Keywords: Sweet sorghum, carbohydrate, bio-ethanol, bio-fuel.

1. Introduction

Due to the diminishing fossil fuel reserves, alternative energy sources need to be renewable, sustainable, efficient, cost effective and safe [1]. Ethanol is one of the best renewable source that has all the above characteristics. Ethanol produced from starch hydrolysis and sugar fermentation from biomass is called bio-ethanol. The raw materials used in the ethanol production by fermentation can be classified into three main types of materials, which are sugars, starches and ligno-cellulose. Sugar can be converted into ethanol directly. Starch could be hydrolyzed to fermentable sugars by enzymes; and lingo-cellulose following pre-treatment by acids or alkali could be hydrolyzed to sugars. Industrial bio-ethanol is produced from various crops like sugarcane or sugar beet molasses, corn starch, sweet sorghum, tapioca etc. Among them sweet sorghum has been considered as one of the most promising crop for energy and industry in hot and dry climates. Sweet sorghum (*Sorghum bicolor* L.Moench) is a C_4 plant characterized by high biomass and sugar –yielding and a high photosynthetic efficiency [2,3]. It also has a rapid growth rate as it has a shorter growing season than sugarcane and therefore suitable to be grown in most parts of the world. It is well adapted to drought [4] and has the capability of remaining dormant during the driest period Sweet sorghum is the only plant that all parts of plant can be used for bio-ethanol production. Its stalk has sucrose, glucose and fructose readily fermented to ethanol. Its grain flowing starch hydrolysis to glucose could be fermented to ethanol. Sweet sorghum leaves and bagasse as lingo-cellulosic feed-stocks have the greatest potential to be used as second generation of biofuel production. The conversion of sweet sorghum leaves and bagasse to bio-ethanol requires pretreatment to break down the lingo-cellulosic structure, remove lignin and hydrolyze the cellulose and hemicellulose components to sugars. Sugars are converted to bio-fuel through fermentation. However conversion of lingo-cellulosic feed-stocks to bio-ethanol is not commercialized yet and it is a renewable energy for the future.Most part of Iran has hot and dry climatic condition and due to this condition, corn and wheat is imported. Sugar beet and sugar cane molasses are not in large quantities so the ethanol produced from these

substrates is supplied by industries. The purpose of this study was to plant sweet sorghum under Iran hot and dry climatic condition and produce bio-ethanol to be mixed with fuel.

2. Comparisons among sweet sorghum cultivars and lines

The purpose of this experiment was to determine the most adapted sweet sorghum cultivars and lines under hot and dry condition. 29 sweet sorghum cultivars and lines were compared in a randomized complete block design at the University of Isfahan Experiment Station and University of Isfahan Chemical engineering Lab. Plots consisted of 4 rows, 10 m apart and 0.75m apart. Plots received 300 kg/ha of di-ammonium phosphate and 100 kg/ha of urea disked into the soil before planting. Water was applied as needed. When kernels were at physiological maturity, three meters form two central rows were harvested. Biomass and stripped stalks were determined. The fresh stalk, after removing the leaves was crushed in a sugarcane crusher to extract the juice. After filtration through a sieve to remove the chaff etc. the soluble solids (brix), sucrose (pol%) and the purity of the juice were measured according to Varma [5]. Statistical analyses were performed using Statistical Analysis System (SAS) computer program. The means were compared according to Turkey's test.

3. Results and Discussion

3.1. Weather Information.

Iran has an arid climate with average annual precipitation of 250 mm or less.There is no summer rain and this low amount of rain precipitates from October to April when sugar crops such as corn, sorghum, sugar beet and sugar cane are not growing. Therefore all these crops should be irrigated from planting to harvest. Optimum temperature for sweet sorghum germination and growth is above 18 oC. Since sweet sorghum is a warm season crop, so its growth will be reduced considerably when temperature falls below 5 degree centigrade. Table 1 shows the planting date of different provinces of Iran. Sweet sorghum duration from planting to harvest is 120-150 days. So in Southern part of Iran when the growing season is long (Table2), sweet sorghum can be planted two to three times per year.

3.2. Comparison among sugarcane, sugar beet and sweet sorghum.

Among sugar and starch crops that is used for ethanol production in other countries, in Iran ethanol only is produced from sugarcane and sugar beet molasses.

In comparison to other two crops, sweet sorghum has the least crop duration, growing season, soil water requirements, water management and crop management (Table 3). Under Iran climatic condition sweet sorghum has similar biomass, sugar content, sugar yield and ethanol production to sugar cane. It should be mentioned that sugar cane can only be grown in the sought where there is no freeze temperature, whereas sweet sorghum is grown in most part of the country. Based on the above results it is recommended to plant sweet sorghum for ethanol production [6].

Table 1. The planting date of different provinces of Iran for sweet sorghum

State	Above 15 ^{o}C	Less than 0 ^{o}C
Bandar Abbas	Feb.	-
Dezful	April	-
Isfahan	May	Dec.
Kerman	June	Nov.
Rasht	May	-
Shiraz	May	Dec.
Uromieh	Apr.	Nov.
Yazd	May	Dec.
Zahedan	Apr.	Dec.

Table 2. Climatic conditions of Kahnooj

Month	T_{max} (^{0}C)	T_{min} (^{0}C)	Relative Humidity (%)
Jan.	21.1	8.7	70.1
Feb.	21.0	11.7	72.0
Mar.	27.3	14.5	60.3
Apr.	32.2	18.7	60.1
May	40.5	24.8	40.0
June	44.4	29.8	38.9
July	45.4	30.0	42.0
Aug.	44.0	30.0	45.9
Sep.	40.7	30.3	46.0
Oct.	38.7	23.5	53.0
Nov.	30.5	17.0	66.0
Dec.	24.0	11.4	64.0

Table 3.Comparison among sugarcane, sugar beet and sweet sorghum [6]

	Sugar cane	Sugar beet	Sweet sorghum
Crop duration	About 7 months	About 5-6 months	About 4 months
Growing season	Only one season	Only one season	One season in temperate and two or three seasons in tropical areas
Soil requirement	Grows well in drain soil	Grows well in sandy loam; also tolerates alkalinity	All types of drained soil
Water management	36000 m^3/ha	18000 m^3/ha	12000 m^3/ha
Crop management	Requires good management	Greater fertilizer requirement; requires moderate management	Little fertilizer required; less pest disease complex; easy management
Yield per ha	70-80 tons	30-40 tons	54-69 tons
Sugar content on weight basis	10-12%	15-18%	7-12%
Sugar yield	7-8 tons/ha	5-6 tons/ha	6-8 ton/ha
Ethanol production directly from juice	3000-5000 L/ha	5000-6000 L/ha	3000 L/ha
Harvesting	Mechanical harvest	Very simple; normally manual	Very simple; both manual and mechanical

3.3. Energy balance

Among feedstock that currently are used in different countries for bio- ethanol production reported sweet sorghum has the highest energy output/input (Table 4). Wheat in Canada has the lowest energy input/output (1.2) while sweet sorghum in temperate areas has the highest output/input (12-16) [7]. Most parts of Iran have high day and low night temperature. During the day because of high temperature through photosynthesis more carbohydrates will be accumulated. Cool nights cause respiration to be decreased. As a result, higher sweet sorghum biomass and sugar will be produced.

Table 4. Energy output/input for different feedstock

Feed stock	Energy output/input
Sugarcane (Brazil)	8.3
Sugar beet (European Union)	1.9
Corn (United States)	1.3-1.8
Wheat (Canada)	1.2
Fossil- fuels	0.8
Sweet sorghum	8(12-16 in temperate ares)

3.4. Comparison among 29 sweet sorghum cultivars and lines for stem yield, brix and sucrose content.

Mean comparisons are presented in Table 5. Since both stem yield and brix has more important role in ethanol production from sweet sorghum, therefore cultivars and lines have that more than 60t/ha stalk yield and brix more than 20% were selected. These cultivars are Vespa, MN1500, Soave, Sofra, SSV108, SSV94, SSV96, Foralco and Rio. A further selection among these cultivars indicated that Rio had the highest stalk yield (95 t/ha) and highest brix (22.36). Although the stem yield of M81-E, Theis and Wray was more than 100 t/ha but their brix was lower than Rio. None of the sweet sorghum lines due to their low stem yield and brix were suitable for ethanol production.[8].

Table 5. Mean comparisons among 29 sweet sorghum cultivars and lines regarding stem yield, ^{o}Brix, Sucrose and purity at university of Isfahan, Iran [8].

Genotypes	Stem yield (t/ha)	Brix (%)	Sucrose (%)	Purity (%)
Cultivars				
Roce	39.14	21.96	14.39	66.71
Vespa	84.53	20.99	13.05	74.59
Brandes	77.14	18.72	8.92	46.39
MN1500	83.71	20.71	12.00	57.59
E36-1	48.00	18.26	13.41	76.02
Soave	61.57	20.73	13.46	65.00
M81-E	103.57	16.01	10.26	65.10
Somac	44.43	21.12	12.85	60.10
Sofrah	85.57	19.63	12.61	64.05
SSV-108	62.85	22.25	13.97	62.26
SSV-94	70.14	20.64	11.75	57.12
SSV-96	62.00	22.54	13.71	60.10
Theis	100.14	19.10	7.26	37.59
Foralco	97.71	20.40	12.64	60.83
Rio	95.00	22.36	16.06	71.31
S-35	58.43	19.78	11.58	58.75
Turno	39.86	11.16	6.00	35.86
Satiro	27.86	17.16	10.33	60.02
Wray	126.42	15.84	7.85	49.40
Lines				
IS 686	61.43	16.54	9.00	54.39
IS 16054	51.85	21.07	11.73	55.83
IS 18154	42.14	19.04	12.71	66.71
IS 6962	43.00	23.01	13.61	58.85
IS 9639	54.00	21.77	14.31	65.23
IS 2325	59.57	20.70	14.28	60.18
IS 6973	33.43	22.85	14.21	61.88
IS 4546	56.43	22.03	13.05	60.12
IS 19273	46.28	20.29	15.04	73.69
IS 4354	33.86	17.66	9.80	55.28
W[1]	**2.53**	**6.18**	**5.05**	**23.981**

[1].Tukey's value for 5% level

4. Conclusions

It is clear that fuel ethanol from sweet sorghum is the best choice to be implement under hot and dry climatic conditions regarding both economic and environmental considerations. Because, sweet sorghum has higher tolerance to drought [9], water logging and salt [10, 11], alkali and aluminum soils; It may be harvested 3 - 4 months after planting (Table 1) and planted 1 - 2 times a year (in tropical areas); Its energy output / fossil energy input is higher than sugarcane, sugar beet, corn, wheat and etc… specially in temperate areas; It is more water use efficient (1/3 of water used by sugarcane at equal sugar production); Its production can be completely mechanized and its bagasse has higher nutritional value than the bagasse from sugarcane, when used for animal feeding. Also, by implementing agricultural practices such as adequate water and fertilizers, suitable cultivars or hybrids, crop rotation, pest management and etc… can increase productivity with focus on bio-fuel production [12].

In addition, sweet sorghum has high amount of sucrose [8] and invert sugar [13] which are easily converted to ethanol [14, 15]. Therefore, it seems that sweet sorghum is the most suitable crop for bio-fuel production in arid regions of the world. This awareness should push government of the countries with such climatic conditions to promote the development of projects for fuel ethanol production from sweet sorghum. However, social aspects (including environmental concerns) should play a more significant role in the selection of the most suitable feed-stocks for the alcohol industry. In this way, financial indicators would not be necessarily the decisive factors when new large-impact projects for bio-fuels production are studied and implemented in developing countries.

References

[1] L.H. Chum, R.P. Overend. Biomass and renewable fuels, Fuel Bioprocess Technology 17, 2001, 187-195.

[2] W.L., Bryan, Solid state fermentation of sugars in sweet sorghum. Enzyme Microb. Technol., 12, 1990, 437-442.

[3] E. Billa, D.P. Koullas, B. Monties and E.G. Koukios, Structure and composition of sweet sorghum stalk components. Ind. Crops Prod., 6, 1997, 297-302.

[4] N. Kosaric, Vardar-Sukan, Potential Source of Energy and Chemical Products. In: The Biotechnology of Ethanol: Classical and Future Applications, Roehr, M. (Ed.). Wiley-VCH, Weinheim, 2001.

[5] N.C. Varma, System of technical control for cane sugar factories in India. The sugar Technologist's Associations. India, 1988.

[6] A. Almodares, M.R. Hadi. Production of bioethanol from sweet sorghum: A revies. Afr.J. Agric.Res. 4, 2009, 772-780.

[7] H.Shapouri, M. Salassi and J.N. Fairbank. The economic feasibility of ethanol production from sugar in the United State. Washington, office of Energy Policy and new uses, office of the chief economist, United State Department of Agriculture, Baton Roughe, Louisiana State University. 2006.

[8] A. Almodares,A. Sepahi, Comparison among sweet sorghum cultivars, lines and hybrids for sugar production. Ann. Plant Physiol. 10, 1996, 50-55.

[9] T.T. Tesso, L.E.Claflin, M.R. Tuinstra, Analysis of Stalk Rot Resistance and Genetic Diversity among Drought TolerantSorghum Genotypes. Crop Sci. 45, 2005, 645-652.

[10] A, Almodares, M,R. Hadi, H. Ahmadpour, Sorghum stem yield and soluble carbohydrates under phonological stages and salinity levels Afr. J. Biotech. 7, 2008, 4051-4055.

[11] A, Almodares, M,R. Hadi, B.Dosti, The effects of salt stress on growth parameters and carbohydrates contents in sweet sorghum. Res. J. Environ. Sci. 2, 2008a, 298-304.

[12] B.V.S. Reddy, S,Ramesh, P.S. Reddy, B. Ramaiah, P.M. Salimath, R. Kachapur, Sweet Sorghum–A Potential Alternate Raw Material for Bio-ethanol and Bio-energy. Int. Sorghum Millets Newslett. 46, 2005, 79–86.

[13] A. Almodares, R.Taheri, S. Adeli, Stalk yield and carbohydrate composition of sweet sorghum [Sorghum bicolor (L.)Moench] cultivars and lines at different growth stages. J. Malesian Appl. Biol. 37, 2008b, 31-36.

[14] K. Jacques, T.P. Lyons, D.R.Kelsall, The Alcohol Textbook. 3rd Eds. Nottingham Univesity Press.1999, P. 388.

[15] S. Prasad, A. Singh,N. Jain, H.C. Joshi, Ethanol production from sweet sorghum syrup for utilization as automotive fuel in India. Energy Fuels 21, 2007, 2415-2420.

Evaluation of greenhouse gas emission by ethanol production from sugarcane (case study of Minas Gerais, Brazil)

Juan C.C.Garcia[1], Eduardo v. Sperling[2*]

[1] *PhD Student, Federal University of Minas Gerais , Belo Horizonte, Brazil*
[2] *Lecturer, Department of Sanitary and Environmental Engineering, Federal University of Minas Gerais, Brazil*
** Corresponding author. Tel: +55 31 34091019, Fax: +55 31 34091879, E-mail: eduardo@desa.ufmg.br*

Abstract: The paper presents an evaluation of greenhouse gas emission during the industrial process of ethanol production from sugarcane crops. The production of biofuels is experiencing an increasing trend in most regions of the world, following the need of the optimization of renewable energy from biomass. In Brazil sugarcane is one of the main raw materials for the production of ethanol. The research summarized in this paper was carried out in the period 2008-10 in the State of Minas Gerais, Brazil. The tool *Ecoinvent* has been used for the estimation of the environmental magnitude of the components of bioethanol production. Moreover a field survey has been carried out, which involved the visit to 11 selected distilleries, together with the application of questionnaires related to the whole ethanol production process and to the utilization of chemical components and by-products. The total emission of CO_2eq (representing the whole amount of greenhouse gases: CO_2, CH_4 and N_2O) could be estimated in 1540 kg/ha.year. The key sources of greenhouse gas emissions in the bioethanol production are sugarcane burning and use of fuels, which account for more than 50 % of total emissions. This shows a clear environmental limitation in the process of sugarcane utilization.

Keywords: *Ethanol, Greenhouse Gases Sugarcane*

1. Introduction

The environmental constraints related to the explotation of fossile fuels, together with the current concerns regarding the massive production of hydropower lead to the convenience of searching alternative energy sources. In this sense the production of biofuels is experiencing an increasing trend under a global perspective. Countries like Brazil, which present large agricultural areas, are intensively researching the optimization of renewable energy from biomass. In Brazil sugarcane is one of the main raw materials for the production of ethanol. The fermentation of sugar into ethanol is one of the earliest organic reactions employed by humanity. Sugarcane is a semiperennial grass of the genus *Saccharum*, which is native to warm temperate to tropical regions of Asia. They present stout, jointed, fibrous stalks that are rich in sugar. Two countries (Brazil and India) are together responsible for around 50 % of the world sugarcane production. Sugarcane products include table sugar, molasses, alcoholic beverages (e.g. rum) and ethanol. World's ethanol production forecast for 2012 will pass 20 billion gallons and Brazil will be responsible for one third of this amount [1]. The largest single use of ethanol is as motor fuel and fuel additive. Gasoline sold in Brazil contains at least 20 % anhydrous ethanol, which is blended since 1933. In 2003 the country started a massive production of vehicles flex-fuel, which function with gasoline as well as with ethanol. The cane delivered to the processing plant is called *burned and cropped* and represents 77 % of the mass of the raw cane. The reason for this reduction is that the stalks are separated from the leaves (which are burned and whose ashes are left in the field as fertilizer) and from the roots that remain in the ground to sprout for the next crop. The basic steps for large scale production of ethanol are: microbial fermentation of sugars, distillation and dehydration. Some crops require previous saccharification or hydrolysis of the carbohydrates such as cellulose and starch into sugars. Currently only the sugar (from sugarcane) and starch (from corn) portions can be economically converted to sugars. However there is much activity in the area of cellulosic ethanol, where the cellulose part of a plant is broken down to sugars and subsequently converted to ethanol. Greenhouse gases (CO_2, CH_4 and N_2O) are generated

during the agricultural process together with the corresponding inputs manufacturing emissions.

Fig. 1 presents the main steps in conventional ethanol production in Brazil [2].

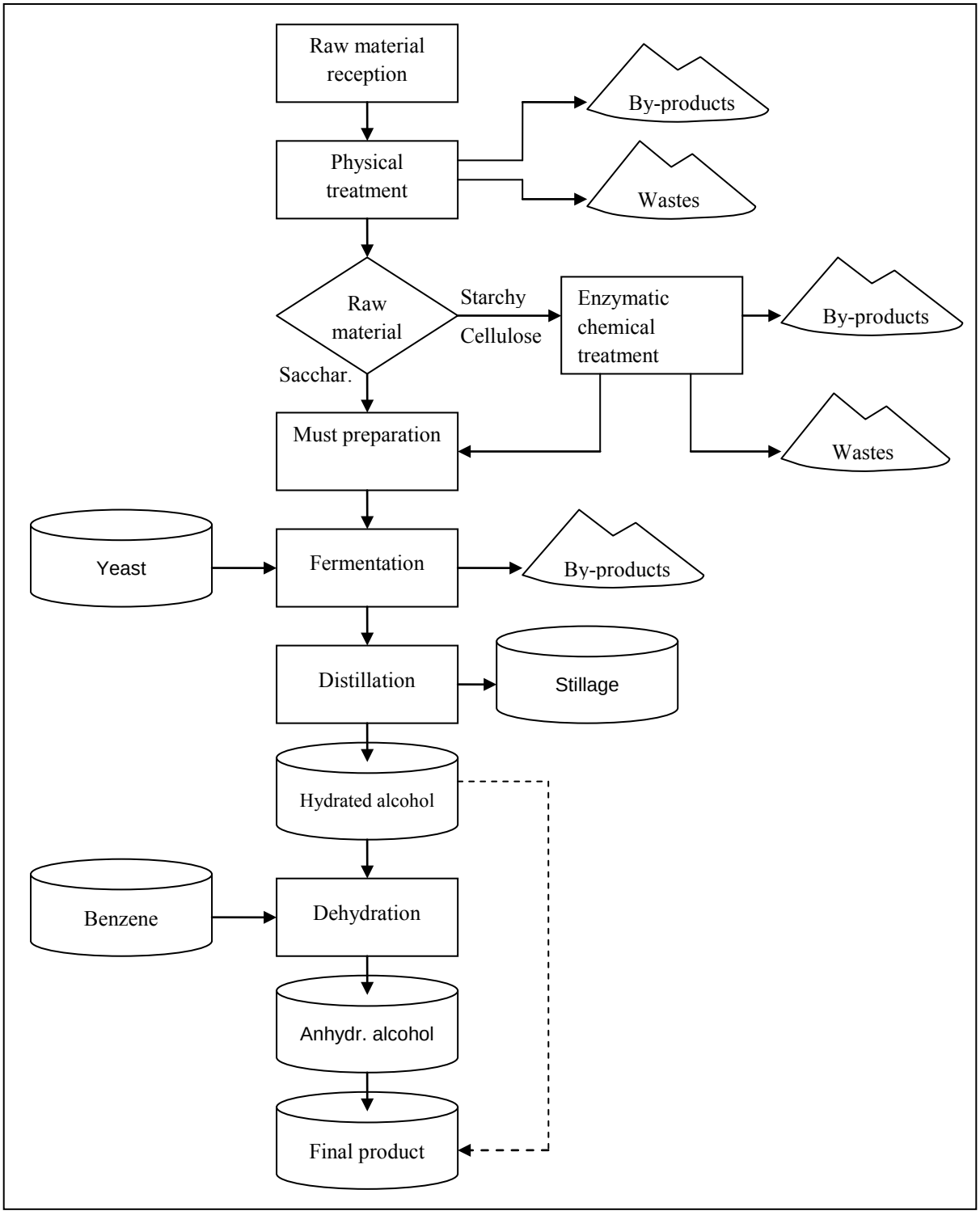

Fig. 1: Technological routes for ethanol production in Brazil

Some international studies [3, 4, 5] have been dedicated to the evaluation of energetic efficiency and the corresponding mitigation of the emission of greenhouse gases. However

there is no broad consensus about energetic gains due to ethanol utilization and its impact on generation of greenhouse gases. Major inconsistencies are related to assumptions adopted by the quantification of inputs and outputs in ethanol life cycle [6]. Also technological differences in the local ethanol production process affect the accuracy of the results [7]. Consequently further studies are demanded in order to solve these limitations.

2. Methodology

The research presented in this paper was carried out in the period 2008-10 in the state of Minas Gerais, one of the 27 states which forms the Federative Republic of Brazil. Minas Gerais is currently the second largest sugarcane and ethanol producer state in Brazil, being placed after the state of São Paulo. In order to estimate the environmental magnitude of the components of bioethanol production the tool *Ecoinvent* has been used, which provides data for inputs and outputs of lifecycle of thousands of materials. The field survey involved the visit to 11 selected distilleries in the State of Minas Gerais, together with the application of questionnaires related to the whole ethanol production process and to the utilization of chemical components and by-products.

The first step for the evaluation of greenhouse emission gases in ethanol production was the correct identification of all relevant stages in the agricultural phase and in the sugarcane industrialization. Technological variations in both phases may result in quite different numbers for the emission values. Principles of Life Cycle Evaluation [8] together with IPCC recommendations [9] have been used in this phase. Only the most important greenhouse gases have been considered (CO_2, CH_4 and N_2O) and total emissions are expressed in (kg CO_2eq) as follows: 1 kg CH_4 = 21 kg CO_{2eq} and 1 kg N_2O = 310 kg CO_{2eq} [10]. Emissions estimation assumed 1 ha of cultivated soil as the functional unity. Adopted time span was 6 years, which encompasses seedling application, sugarcane cycle and 4 cycles of agricultural plant resprout. Emissions were calculated using Eq. 1:

$$Ei = \frac{Ij \times nc \times FEj}{6} \quad (1)$$

Where: *Ei* = greenhouse gas emission corresponding to activity (*i*) *i* = fuel consumption in agricultural operations, fuel consumption in seedling transport, fuel consumption in filtercake, ashes and sediments transport, fuel consumption in lime and fertilizers transport, fuel consumption in irrigation, fuel consumption in mechanical harvest, fuel consumption in loading and sugarcane transport, crop burning, N_2O emission from soil, seedling production, consumption of chemical products in the industrial phase; *Ij* = consumed quantity of raw materials in each category; *nc* = number of cycles; *FEj* = emission factor corresponding to raw material *Ij*; *j* = fuel, lime, fertilizers, pesticides, burnt sugarcane during crop and chemical products used in industrial stage.

Emission factors were obtained from *Ecoinvent* [11] and, when available, from [9]. *Ecoinvent* is a broad data base which shows environmental loads, including here gaseous emissions associated with lifecycle of agricultural and industrial products. Data about fuel consumption in vehicles and agricultural machines, eventually not available in visited industries, have been extracted from [12].

3. Results and Discussion

The calculated emissions have been obtained by multiplying *activity data* (e.g. liters of diesel in a selected agricultural operation) and *emission factor* (average values found in the Brazilian technical literature).

All researched distilleries send the whole amount of generated filtercake, ashes and sediments to further utilization in sugarcane farming. Average waste generation rates are respectively 2051.63 kg/ha·a, 659.60 kg/ha·a and 1430.02 kg/ha·ano (total = 4141.25 kg/ha·a. Average distance between processing plant and agricultural area is 13 km.

For the calculation of gas emission in transport of lime and fertilizers it was assumed the utilization of a 12 t truck, with fuel consumption of 2,5 km/L and an average distance of 25 km between supplier and farming. In a period of 6 years around 3640 kg load would be transported [12]. All researched farms use wastewater for sugarcane culture irrigation (24 cycles in 6 years). With respect to fertilizers, the emissions have been calculated considering the most frequent chemical inputs used in the country: N in the ammonium form, P_2O_5 and K_2O [13]. Pesticides have been classified according to their active components and the emissions have been calculated based on literature values [9] (Table 1).

Table 1. Emission of greenhouse gases in lime and fertilizers consumption

Inputs	**Consumption (kg/ha)**	**Gas emission (kg CO_2eq/ha)**
Lime	1520	228
Fertilizers		
N	84	254
P_2O_5	123	328
K_2O	163	85
Total		895

The gaseous emissions from burning activity in sugarcane plantations have been estimated by the corresponding factors for agricultural wastes recommended by IPCC [9]: 2.7 g CH_4/kg and 0.07 g N_2O/kg of dry mass, which is equivalent to 82.82 g CO_2eq/kg considering a combustion factor of 0.80. CO_2 emissions are here not taken into account since the emitted carbon will be reassimilated in the next crop. Nitrogen addition to the soil through the use of fertilizers intensifies nitrification and denitrification processes and liberates N_2O as a by-product to the atmosphere. N_2O emissions are around 20 g per kg of N used in the soil [9].

In the present case all energy consumed in the researched factories is generated by burning bagasse (crushed sugarcane), therefore no gas emission from fossile fuels are registered. Direct CO_2 emissions, which are associated with bagasse burning and molasse (sugarcane syrup) fermentation, are not considered in these calculations since, as pointed before, carbon will be reassimilated by the vegetation. Consequently only emissions coupled with the use of chemical products take part in the general account for the indudtrial phase of ethanol production.

Productivity variations in irrigated and non irrigated areas have been also taken into account in loading, transport and sugarcane industrialization. Field research showed that average distances were 18 km for trucks of 28 and 45 t and 40 km in the case of heavier trucks (58 t).

Moreover inputs transport from suppliers to the industries are carried out by 15 t trucks which cover an average distance of 400 km.

After computing the emission of greenhouse gases in all the necessary steps for ethanol production, following number could be estimated: 1539 kg/ha.year of CO_2eq (representing the whole amount of greenhouse gases: CO_2, CH_4 and N_2O). Table 1 summarizes the corresponding emissions and percent values in each of the most relevant categories in ethanol production from sugarcane.

Table 2. Emission of greenhouse gases in agriculture and industrialization of sugarcane for ethanol production

Category	**Gas emission ($kgCO_2$.eq/ha.a)**	**% contribution in total emission**
Fuel consumption	337.18	21.9
Fertilizers consumption	298.38	19.38
Biocides consumption	30.39	1.97
Crop burning	434.31	28.21
N_2O from soil	331.52	21.54
Seedling production	72.81	4.73
Chemical products	35.01	2.27
Total	**1539.6**	**100**

4. Conclusions

It can be seen that the key sources of greenhouse gas emissions in the bioethanol production are sugarcane burning, fuel consumption, N_2O liberation from soil and fertilizers consumption, which account for more than 90 % of total emissions. One of the learning points of this research is that the consideration of other technological scenarios can lead to significant differences in the quantification of greenhouse gases emissions. Moreover, in spite of favourable points in the utilization of ethanol, there are clearly environmental limitations in the process of sugarcane utilization, which are represented by the possibility of the generation of greenhouse gases during the lifecycle of biofuels production.

References

[1] Sites of OECD (www.oecd.org) and FAO (www.fao.org), 2010

[2] Esteves, O. Exergetic analysis of ethanol production from sugarcane (in Portuguese), Federal University of Minas Gerais, School of Engineering, Brazil, Master Course in Nuclear Sciences and Techniques, 1996. 120 p.

[3] Kaltschmitt, M., Reinhardt, G., Stelzer, T., Life cycle analysis of biofuels under different environmental aspects, Biomass and Bioenergy 12, 1997, pp. 21-34

[4] Kadam, K. L., Environmental benefits on a life cycle basis of using bagasse-derived ethanol as a gasoline oxygenate in India, Energy Policy, 2002, pp. 371-384

[5] Luo, L., Voet, E., Huppes, G., Life cycle assessment and life cycle costing of bioethanol from sugarcane in Brazil, Renewable and Sustainable Energy Reviews, 2008

[6] Liska, A. J., Cassman, K. G., Towards standardization of life-cycle metrics for biofuels: greenhouse gas emissions mitigation and net energy yield, Journal of biobased materials and bioenergy, 2008. pp. 187-203

[7] Soares, L. H. de B.. Mitigation of greehouse gas emissions by the use of ethanol from sugarcane (in Portuguese). Technical Paper 27, Ministry of Agriculture, 2009

[8] United States Environmental Protection Agency, Life Cycle Assessment: principles and practice. Cincinnati, USEPA, 2006. 88 p.

[9] Intergovernamental Panel on Climate Change (IPCC), Guidelines for National Greenhouse Gas Inventories, National Greenhouse Gas Inventories Programme, 2006

[10] Intergovernamental Panel on Climate Change (IPCC), Climate Change 2007: The Physical Science Basis, Cambridge, Cambridge University Press, 2007

[11] Institut für Umweltinformatik, Institut für Energie & Umweltforschung. Ecoinvent v2.01a for Umberto 5.5. Hamburg, 2006. 1 CD-ROM.

[12] Macedo, I. C.; Leal, M.; Silva, J. Balance of the emission of greenhouse gases in production and utilization of ethanol in Brazil (in Portuguese), Environmental Agency of the State of São Paulo, 2004. 32 p.

[13] Oliveira, M. W., Mineral nutrition and fertilization of sugarcane (in Portuguese), Agricultural News, Belo Horizonte, Brazil. 239, 2007, p. 30-43

An environmental optimization model for bioenergy plant sizes and locations for the case of wood-derived SNG in Switzerland

Bernhard Steubing[1,2*], Isabel Ballmer[3], Oliver Thees[4], Léda Gerber[2], François Maréchal[2], Rainer Zah[1], Christian Ludwig[5]

[1] *Swiss Federal Laboratories for Materials Science and Technology (Empa), 8600 Dübendorf, Switzerland*
[2] *Swiss Federal Institute of Technology (EPFL), 1015 Lausanne, Switzerland*
[3] *Swiss Federal Institute of Technology (ETHZ), 8092 Zurich, Switzerland*
[4] *Swiss Federal Institute for Forest, Snow and Landscape Research (WSL), 8903 Birmensdorf, Switzerland*
[5] *Paul Scherrer Institute (PSI), 5232 Villingen, Switzerland*
** Corresponding author. Tel: +41 44 823 4219, E-mail: bernhard.steubing@empa.ch*

Abstract: Bioenergy from woodfuel has a considerable potential to substitute fossil fuels and alleviate global warming. One issue so far not systematically addressed is the question of the optimal size of bioenergy plants with regards to environmental and economic performance. The aim of this work is to fill this gap by modeling the entire production chain of wood and its conversion to bioenergy in a synthetic natural gas plant both with respect to economic and environmental performance. Several spatially explicit submodels for the availability, harvest, transportation and conversion of wood were built and joined in a multi-objective optimization model to determine optimal plant sizes for any desired weighting of environmental impacts and profits.
We find a trade-off between environmental and economic optimal plant sizes. While the economic optima range between 75 – 200 MW, the environmental optima are with 10 – 40 MW significantly smaller. Moreover, the economic optima are highly location specific and tend to be smaller if the biomass resource in the geographic region of the plant is scarcer. The results are similar with regards to the effect on global warming as well as with respect to the aggregated environmental impact assessment methods Ecoindicator '99 and Ecological Scarcity 2006.

Keywords: *Biofuels, Wood energy, SNG, Life cycle assessment, Environmental optimization*

1. Introduction

Bioenergy from woodfuel has a large potential to substitute fossil fuels and alleviate global warming. At the same time, it is a limited resource, which should be used optimally from the environmental perspective. An important variable determining the sustainability of wood energy production chains, which has not yet been systematically addressed, is the influence of the size of bioenergy plants on the environmental impacts generated along the bioenergy production chain.

The size of a bioenergy plant affects several variables at the plant and production chain levels. At the plant level the size of a bioenergy plant influences the technology choice and configuration and therefore the efficiency of the biomass conversion, the generated environmental impacts as well as production costs. At the production chain level, the size of a bioenergy plant influences mainly the geographical area needed for the biomass supply, which affects the average transport distance and therefore again environmental impacts and costs. If the biomass is more or less equally distributed on a regional scale, the average transport distance could be estimated by a simple radius-surface relationship. However, in countries with large regional differences in biomass availability – either due to geographic factors such as mountains or deserts, or due to variations of regional demand – this relationship may be different.

The aim of our model is to show how these variables affect the environmental and cost performance of bioenergy plants at different plant sizes and locations. We choose the case of

the production of synthetic natural gas (SNG) from forest wood (mainly residues from the roundwood production and thinning operations) in Switzerland.

2. Material and Methods

2.1. Overall approach

In order to model the entire production chain of SNG from wood four submodels were designed to model (A) the spatial wood availability, (B) harvest, (C) transport and (D) the conversion to SNG at the bioenergy plant (Fig. 1). Each submodel models the costs as well as environmental impacts based on life cycle assessment (LCA) resulting for its part of the production chain. Data from the submodels is then processed in the optimization model. The latter first chooses optimal technology configurations for the bioenergy plant from a set of potential technologies for each plant size based on a weighting of environmental impacts and profits. Second the environmental and economic performance is calculated for plant sizes from 5 – 200 MW. Third the optimal plant size is determined and the procedure is repeated for plants in different geographic contexts of Switzerland.

Environmental impacts are assessed with the methods global warming potential (GWP) [1], the Ecoindicator ’99 (H/A) (EI’99) [2] and the Ecological Scarcity 2006 (ES’06) [3]. Life cycle inventory has been taken from the ecoinvent database [4].

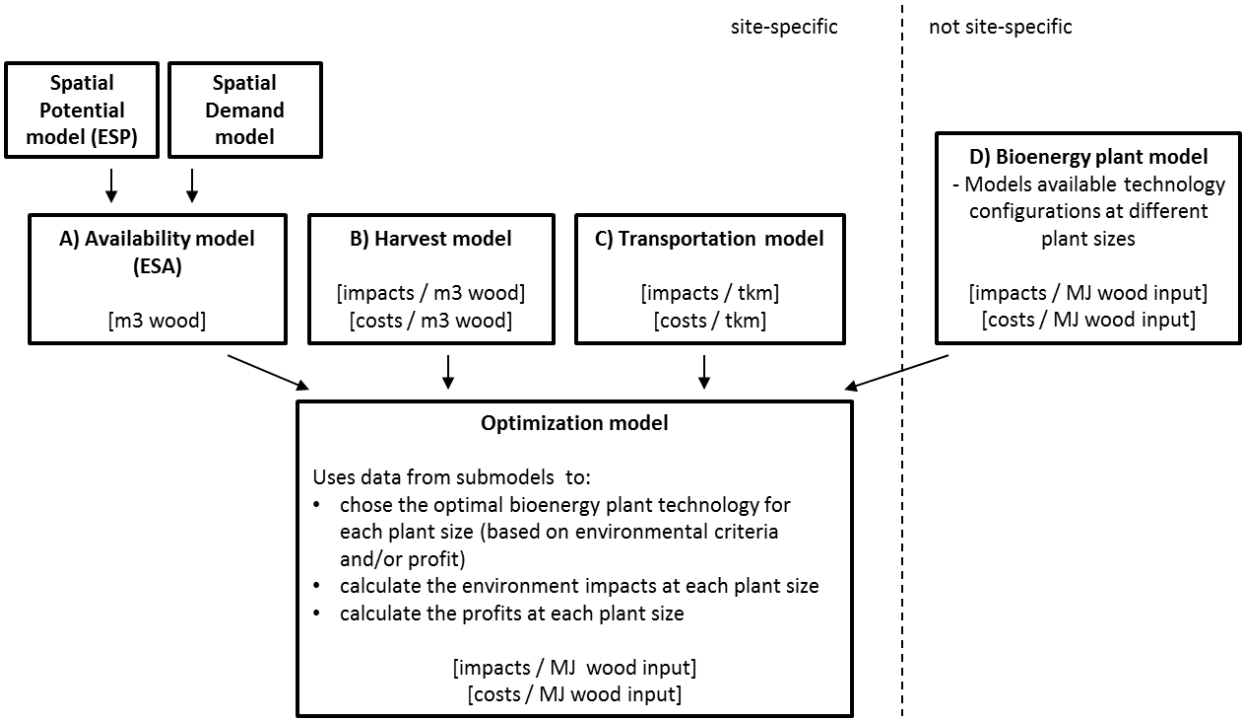

Fig. 1. Methodological approach used

2.2. Submodels

2.2.1. Availability model

The spatial wood availability model consists of two separate models. The first is the *spatial potential model.* It derives the effective spatial potential (ESP) of forest fuel based on data from the Swiss national forest inventory (NFI) as well as sustainability criteria such as biological, societal and economic restrictions [5]. The ESP was calculated for two different harvest scenarios, reflecting on the one hand the current situation where approximately 7 million m^3 are harvested in total and on the other hand a maximum scenario where 12 million

m^3 are harvested. The maximum scenario involves a reduction of the stock which has been built up during recent decades as the growth of approximately 9.5 million m^3 has been higher than the harvested quantities [6]. The maximum scenario could be sustained for about 30 years.

The *spatial wood demand model* [5] is based on the one hand on a database containing spatially explicit information for automated wood energy installations in Switzerland [7] and on the other hand on the overall demand from households [8], which was spatially distributed according to population density.

The *effective spatial availability* (ESA) is yielded by subtracting the spatial wood demand from the spatial wood potential.

2.2.2. Harvest model

The calculation of the environmental impacts of the harvest is based on ecoinvent data, which includes stand development and forest maintenance as well as the felling and chipping of the wood. The price for forest fuel at the SNG plant site is assumed to be 37 CHF / b-m^3 (bulk cubic meters) [9], excluding transport costs.

2.2.3. Transportation model

The transportation model calculates the costs and environmental impacts resulting from the transport of wood chips from the forest to the SNG plant by lorry. Transportation distances from NFI sample points to all plant locations have been calculated along the forest road network and the adjacent street network from Vector25 [10]. The environmental impacts are based on ecoinvent data for a 20-28t lorry. We assume average transportation costs of 6.50 CHF per driven vehicle kilometer[1].

2.2.4. Bioenergy plant model

The conversion of wood to SNG has been comprehensively modeled using different technologies and configurations including directly and indirectly heated fluidized bed gasification systems as well as several alternatives for gas separation [11-13]. Our bioenergy plant model contains the results for these technology configurations with respect to economic and environmental performance. In addition we defined the restriction that more sophisticated technologies, e.g. directly heated oxygen-blown gasification or pressurized indirect gasification may only be chosen for plant sizes greater than 25 MW. The bioenergy plant model therefore represents a set of potential technology options for each plant size from which the optimization model can choose the optimal one given the environmental and economic weighting.

2.3. Optimization model

An optimization model was implemented in Matlab. It first chooses optimal technology configurations from the bioenergy model for each plant size. The choice is based upon weighted environmental and economic performances. To be able to calculate the economic performance (profit), we must also include the revenues from the sale of SNG as well as the co-products electricity and heat. For the revenues we assume the following prices per MWh:

[1] Own calculation based on data from the ASTAG (Swiss Association for Road Transportation: www.astag.ch)

90 CHF for SNG, 135 CHF for electricity[2] and 60 CHF for heat. To calculate the environmental impacts we assume a substitution of fossil energy. We expect that SNG is used in natural gas cars (Euro 5 emission standard[3]) to replaces petrol driven cars (Euro 5), electricity is used to replace the marginal future Swiss electricity mix which consists of nuclear power (90%) and power from natural gas combined cycle plants (10%), and the excess heat from the SNG production is fed into a district heating network to substitute heat otherwise provided by natural gas boilers. Profit and environmental impacts are calculated according to equations (1) and (2):

$$\text{Profit} = \text{Revenues}_{\text{bioenergy}} - \text{Production Costs}_{\text{bioenergy}} \quad (1)$$

$$\text{Env.Imp.}_{\text{net}} = \text{Env.Imp.}_{\text{bioenergy}} - \text{Env.Imp.}_{\text{fossil energy}} \quad (2)$$

Profit and environmental impacts are calculated for each technology option from the bioenergy plant model. Then a weighted score is calculated for each technology choice based on normalized profits and environmental impacts as well as weighting criteria, as in Eq. 3. The technology with the highest score is then chosen for the specific plant size and location.

$$\text{Score}_{\text{technology choice}} = \text{Env.Imp.}_{\text{normalized}} * \text{weight}_{\text{env}} + \text{Profit}_{\text{normalized}} * \text{weight}_{\text{eco}} \quad (3)$$

Next, the environmental and economic performance is calculated for plant sizes from 5 – 200 MW for different locations in Switzerland. We choose these locations to be close to populated areas to allow for a potential heat use of the plant as well as with the aim to represent the different regions of Switzerland. Sensitivity analysis is performed with regards to weighting criteria as well as wood availability scenarios.

3. Results

Fig. 2 shows the average transport distances that are covered to supply SNG plants with wood for different locations and sizes from 5-200 MW for the maximum effective spatial potential (ESP) and the maximum effective spatial availability (ESA) scenarios. It can be observed that the variation of the transport difference at a given plant size is considerable for different locations, especially for larger plant sizes. This effect becomes even more important in the ESA scenario due to the increased scarcity of wood. It should also be noticed that for some locations a simple radius-surface relationship would not be correct to assume (e.g. St. Gallen).

[2] Not in all cases electricity is produced. If it is not produced then the same price is paid for the electricity consumption of the plant.

[3] http://europa.eu/legislation_summaries/environment/air_pollution/l28186_en.htm

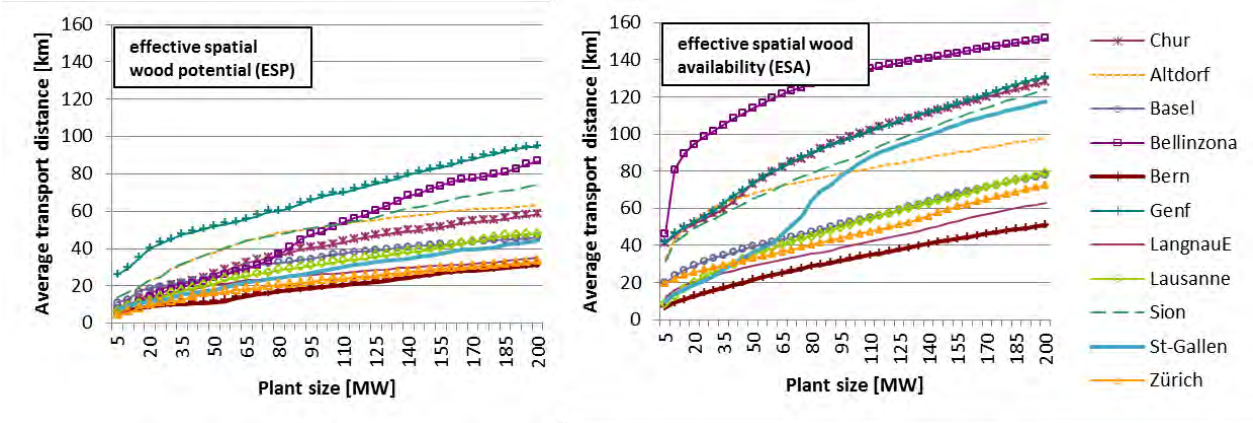

Fig. 2. Average wood transport distances for plant sizes from 5-200 MW for different locations in Switzerland (right: without demand consideration (ESP), left: with demand consideration, both maximum scenario)

Fig. 3 (left and middle) show the economic and environmental performance for a specific SNG plant (Chur) for an equal weighting of profits and environmental performance. First of all, it can be observed that the environmental performance of the system is dominated by the effect of the substitution of fossil fuels through the plant's products SNG and heat. In other words, what really matters is a high wood-to-fuel conversion efficiency, whereas the impacts of the production of the biofuel are rather small. Nevertheless, the impacts of transportation are responsible for the general slope of the environmental performance. Concerning the profits, however, the increased transport distance is more relevant and responsible for the overall decline of profits at large plant sizes. The most important factor for the profits are economies of scale that can be achieved at higher plant sizes due to decreasing production costs. The drastic change at 50 MW is due to a shift in technology with lower production costs as well as a higher SNG efficiency and a lower heat production. As a result of this technology change, profits increase, whereas the environmental performance decreases, which is also due to the fact that the new technology is more sophisticated and more environmental impacts arise during the SNG production. Note that if the wood price (harvest) would increase (or decrease), it would lead to lower (or higher) overall profits and thus influence the plant size at which SNG plants become profitable.

Fig. 3 (right) shows the normalized and weighted performance[4] over the entire range of 5-200 MW. It can be observed that for an equal weighting of environmental performance and profits, the highest weighted performance is achieved between 20-50 MW for this location. For smaller plant sizes it decreases significantly due to considerably lower profits whereas for larger plant sizes it decreases only slightly.

[4] The environmental curve has the opposite shape as in Fig. 3 (left) since negative environmental impacts are avoided impacts and need therefore to be valued positively

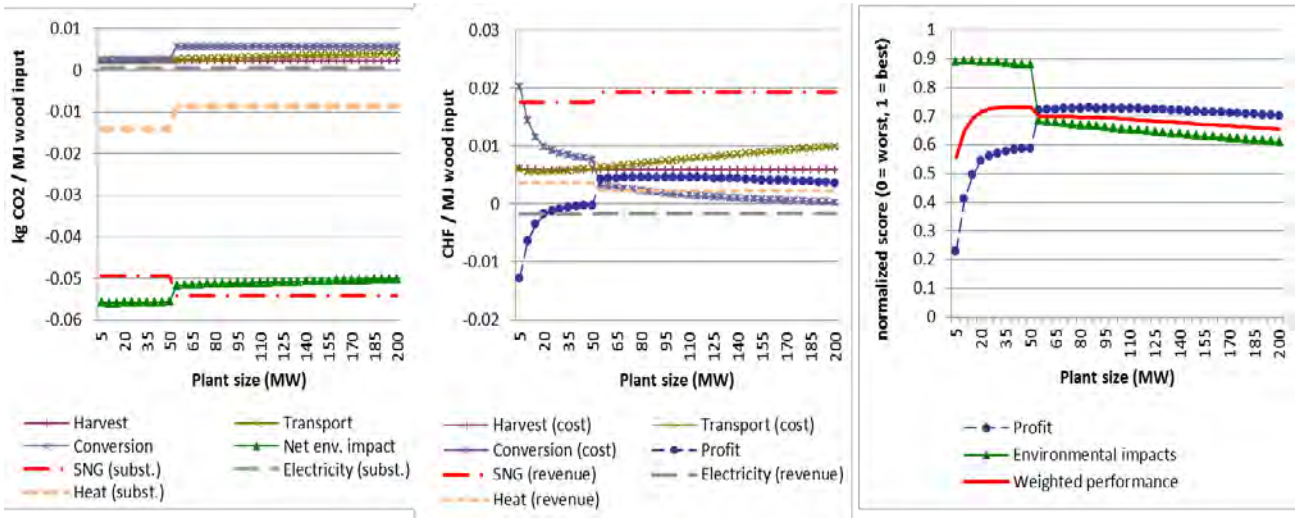

Fig. 3. Environmental impacts, costs and weighted performance for the location of Chur (ESA, equal weighting for profits and environmental performance)[5]

Since weighting between decision parameters is generally a subjective choice, it is important to understand how the weighting parameters influence the results. In our case, weighting strongly affects the optimal sizes for SNG-plants (Fig. 4). This is due to the fact that environmental performance generally decreases for larger plant sizes (economies of scale are too small or outweighed by increased transport distances), whereas profits generally increase with increasing plant sizes (or have a least a maximum at a higher plant size). This holds also true for a change in wood prices (harvest) since the latter only vertically shifts the profits curve but does not change its shape. Fig. 4 also shows that for a pure environmental weighting (GWP) the optimal plant size converges towards 10 MW, while at pure economic weighting the range of optimal plant sizes is large, from 75 – 200 MW, depending strongly on the spatial wood availability. The same results are obtained for an aggregated impact assessment with Ecoindicator'99 and Ecological Scarcity 2006 except that for at a pure environmental weighting plant sizes converge between 20 – 40 MW.

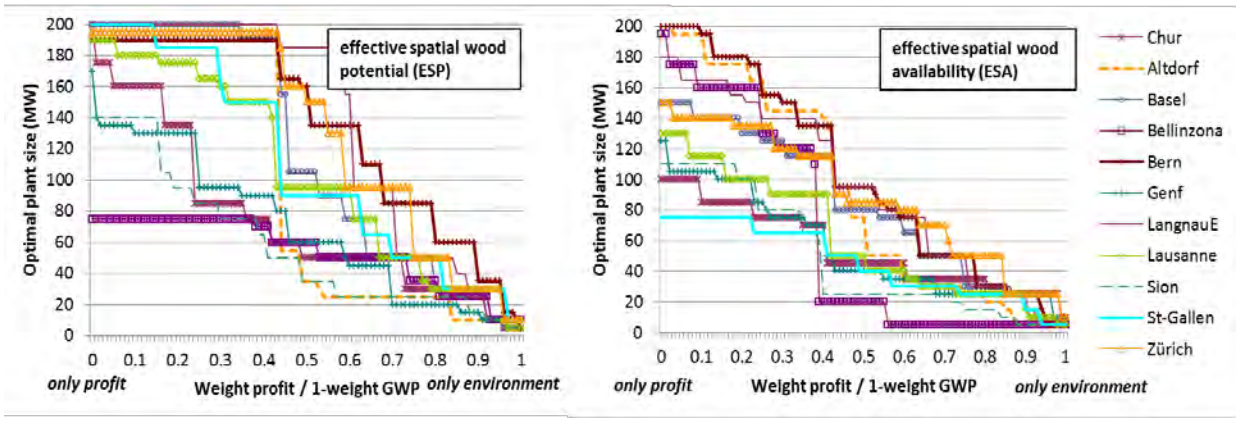

Fig. 4. Relationship of optimal SNG plant scales and weighting of environmental performance (GWP) and profits for different locations

[5] At the state of writing 1 CHF was worth 0.78 Euro or 1.04 USD

4. Discussion

The sensitivity analysis for the weighting parameters suggests that the final decision must be based on a subjective choice since environmental and economic criteria lead to different optima regarding the plant size (trade-off situation). Even though this conclusion seems to be robust at least for three different environmental evaluation methods, more sensitivity analysis needs to be performed for other model parameters. These include the wood price, sale prices of SNG, electricity and heat (revenues), transport costs, substitution choices (which fossil energy SNG, electricity and heat replace), the heat utilization ratio throughout the year and wood availability. This analysis would also help to understand which factors are the most relevant and need therefore be considered when building SNG plants.

More research is also needed concerning the question whether the results presented here can be generalized for other types of bioenergy plants, e.g. conventional wood district heating systems or combined heat and power plants. An important step missing so far to proceed into this direction is a quantification of the relationships between environmental impacts and plant size for these applications. A recent study however produces empirical evidence that power-law relationships could be used for the scaling of environmental impacts at different plant sizes [14].

5. Conclusions

We conclude that there seems to be a trade-off between environmental performance and profits regarding optimal plant sizes. While the environmentally optimal plant sizes were found to be between 10 – 40 MW, the economically optimal plant sizes range between 75 – 200 MW. The economic optima are highly location-specific and locations with a lower wood availability also lead to smaller plant sizes from the economic perspective. The results are similar with regards to the impact on global warming as well as two aggregated impact assessment methods. The most important drivers for the economic performance are production and wood transportation costs. The most important drivers for the environmental performance are the effect of the substitution of fossil energy as well as the impacts generated during wood transportation and conversion.

6. Acknowledgements

The study is based on results from the master thesis of Isabel Ballmer. We thank the Swiss National Forest Inventory (NFI) and swisstopo for providing the road and forest road network data that have been used within the scope of the thesis. We also like to thank Fritz Frutig (harvesting and transportation model) and Kalin Müller (technical support on GIS) from the Swiss Federal Institute for Forest, Snow and Landscape Research (WSL) for their advices.

References

[1] IPCC Climate Change 2007: Synthesis Report; IPCC, Intergovernmental Panel on Climate Change: 2007.

[2] Goedkoop, M.; Spriensma, R. The Eco-indicator 99: A damage oriented method for Life Cycle Impact Assessment; PRé Consultants B.V.: Amersfoort, NL, 22. June 2001, 2001; p 132.

[3] Frischknecht, R.; Steiner, R.; Niels, J. Methode der ökologischen Knappheit - Oekofaktoren 2006; 28/2008; Bundesamt für Umwelt (BAFU), ÖBU Schweizerische Vereinigung für ökologisch bewusste Unternehmensführung: Zürich und Bern, 2008; p 4.

[4] Ecoinvent, Ecoinvent, database version 2.2. In Swiss Center for Life Cycle Inventories: Empa, Dübendorf, Switzerland, 2010.

[5] Pampuri, L. A model of the Spatial Potential and Demand of Energy Wood in Switzerland. Master thesis, Swiss Federal Institute of Technology (ETHZ), Zürich, 2010.

[6] Brändli, U.-B., Schweizerisches Landesforstinventar. Ergebnisse der dritten Erhebung 2004-2006. Eidgenössische Forschungsanstalt für Wald, Schnee und Landschaft (WSL) and Bundesamt für Umwelt (BAFU): Birmensdorf, 2010; p 312.

[7] HES Holzenergie Schweiz. www.holzenergie.ch (14.12.2010),

[8] Primas, A.; Müller-Platz, C.; Kessler, F. M. Schweizerische Holzenergiestatistik 2008; Bundesamt für Energie BFE: 2009; p 78.

[9] WVS Zur Holzmarktkampagne 2010/2011: Richtpreise für Energieholz in Energieholz-Hackschnitzel zu Beginn der Holzmarktkampagne; Waldwirtschaft Schweiz 2010; p 3.

[10] LFI Schweizerisches Landesforstinventar LFI, Datenbankauszug vom Oktober 2010; Eidg. Forschungsanstalt WSL, Birmensdorf / Digitale Daten aus der Landeskarte der Schweiz, Bundesamt für Landestopographie (DV043730): 2010.

[11] Gassner, M.; Maréchal, F., Thermo-economic process model for thermochemical production of Synthetic Natural Gas (SNG) from lignocellulosic biomass. Biomass and Bioenergy 2009, 33, (11), 1587-1604.

[12] Gassner, M.; Maréchal, F., Thermodynamic comparison of the FICFB and Viking gasification concepts. Energy 2009, 34, (10), 1744-1753.

[13] Gassner, M.; Maréchal, F., Methodology for the optimal thermo-economic, multi-objective design of thermochemical fuel production from biomass. Computers and Chemical Engineering 2009, 33, (3), 769-781.

[14] Caduff, M.; Huijbregts, M. A. J.; Althaus, H. J.; Hendriks, A. J., Power-Law Relationships for Estimating Mass, Fuel Consumption and Costs of Energy Conversion Equipments. Environmental Science and Technology 2011, accepted for publication.

Synergy effects on combining hydrogen and gasification for synthetic biogas

Farzad Mohseni[1,*], Martin Görling[1], Per Alvfors[1]

[1] *Royal Institute of Technology – KTH*
School of Chemical Science and Engineering, Chemical Engineering and Technology, Division of Energy Processes, Stockholm, Sweden
** Corresponding author. Tel: +46 8 790 9480, Fax: +46 8 7230858, E-mail:fmt@kth.se*

Abstract: This paper focuses on biogas and suggests methods for strongly increasing its production potential by combining gasification with hydrogen addition. By utilizing hydrogen produced from non-fossil energy sources, synthetic biogas can be obtained. The suggested methods are gasification combined with the Sabatier reaction, and hydrogasification. Both processes utilize hydrogen as a co-feedstock which can be produced via electrolysis from renewable electricity. Hydrogen addition to the gasification enhances the conversion efficiency and this synergy effect leads to higher fuel output compared to separate use of biomass and hydrogen.

The exploitation of renewable sources such as wind- and solar power is rapidly increasing since many countries have introduced incentives for these alternatives to expand. Since these are intermittent sources it would be highly beneficial to use electrolysis for balancing excess power in the grid during e.g. high loads or off-peak periods. Additionally, there would be an economical benefit as well since the price of electricity during these periods often is reduced.

The suggested methods could increase the biogas output by 130 – 150 % from the same amount of biomass as in conventional gasification. Contrary to upcoming fuels and solutions in the transport sector, biogas can be considered as conventional since a developed distribution system and storage capacity exists. It would also be a first step of introducing renewable electricity to the transport sector.

Keywords: *Synthetic biogas, Gasification, Transport sector, Hydrogen, Renewable fuels Introduction*

1. Introduction

The transport sector today poses one of the largest emitting sources of carbon dioxide. In a global perspective CO_2 from transport is responsible for approximately 23 % of the total green-house gas (GHG) emissions [1]. Moreover, the share of fossil energy used in the transport sector amounts to almost 95 %, most of it originating from oil [1]. With such a high share of fossil energy, the global transport sector is highly vulnerable and dependent on the fossil fuel market. Therefore, many regional and intergovernmental goals have been set, aiming for heavy reductions of fossil energy usage in the future as an act of CO_2 mitigation as well as an increased security of supply for their region. However, it is still highly uncertain how these goals could be reached. Many proposed solutions, e.g. the hydrogen economy, electric vehicles; CCS etc. are concepts and technologies still under development which probably cannot be used in any significant magnitude in a near future.

The most noticeable reaction from society towards a more climate neutral transport sector has been an increased usage of biofuels (mainly ethanol) and hybridized vehicles. The use of biofuels has increased quite rapidly during the past decade. However, the potential of biofuels from biomass is quite limited. The topic has been studied by many research groups such as [2, 3, 4] using Sweden (or local regions in Sweden) as an example, which is a particularly rich country in terms of forest (lignocellulosic biomass). Their studies have shown that even a forest rich country like Sweden will only be able to support parts of the total energy needs in the transport sector. Moreover it is shown that it will be necessary to combine different

solutions, both for the supply-side and the demand-side in order to reach highly reduced levels of fossil energy in the transport sector [2].

Another renewable fuel that lately has received more and more attention is biogas. Today biogas constitutes only a minor part of the energy usage in transport. Biogas consists mainly of methane and is usually produced through digestion of organic materials. The amount of biogas that could be obtained from each alternative depends on available raw material (waste water sludge, manure and to some extent crops). Among others, [5,6] have studied the biogas potential from waste water sludge and solid municipal waste depending on the amount of inhabitants in a region and have estimated that it is possible to obtain a total of about 0.8 GJ biogas/person/year [5,6].

This paper suggests methods and technologies for strongly increasing the biogas potential by producing synthetic biogas from renewable energy sources. Synthetic biogas is a good alternative in the transport sector, which could contribute to large reductions of fossil fuel related CO_2 emissions. Biogas is in this paper defined as a biofuel containing mostly methane, independent of the route used to produce it.

1.1. Aim and Scope

The aim of the paper is to present possibilities for utilising biomass, mainly lignocellulosic, more efficiently than via conventional gasification. With the suggested methods it is possible to convert larger fractions of the tree into a propellant (in this case methane). It would result in an almost 100 % increase in fuel potential from forest biomass compared to when conventional methods are used. Such increase would have a substantial effect on the total biomass potential as raw material for propellant production. Accordingly, the transport sector would take a leap towards the possibility of achieving a transport sector with no net emissions of greenhouse gases.

The paper suggests implementing:
- Gasification combined with the Sabatier reaction
- Hydrogasification

These methods use the same fundamental principle i.e. thermal degradation of a given material. However, there are some key differences that are presented, discussed and evaluated in this paper. Comparisons are made and suggestions given for where each process should be implemented to make the greatest contribution.

2. The processes

Both suggested processes use biomass and hydrogen as raw materials for producing methane (synthetic biogas). They reach almost the same yield, however the main difference is that the hydrogen is introduced into the process at different stages. To keep the product (i.e synthetic biogas) CO_2 lean the suggested processes are will use hydrogen produced from renewable sources. In such case water electrolysis would be an excellent alternative. Electrolysis could be driven by renewable electricity (which often is intermittent) which gives the possibility of obtaining pure hydrogen at relatively low cost if run at e.g. off-peak periods when electricity is in excess. The two processes are illustrated and more thoroughly described in the following sections.

2.1. Gasification combined with the Sabatier reaction

Gasification is a known application and is commonly used to produce syngas, a mixture of mainly hydrogen and carbon monoxide. CO and H_2 in combination are suitable for production of hydrocarbons e.g. synthetic methane, methanol and Fischer-Tropsch fuels.
Generally, there is a shortage of hydrogen in syngas if the aim is to produce synthetic biogas. Therefore, WGS is used to increase the share of hydrogen before the methane synthesis. However, when applying WGS, carbon dioxide is formed as a by-product which must be separated. It is a target for removal in the upgrading step after the fuel synthesis and vented to the air. The biomass to biogas efficiency in terms of energy is approximately 60 % [7] even though most of the carbon feed (about 65 %) is removed as CO_2 [8]. Table 1 displays the general chemical reaction for methane production via gasification where oxygen is used as the gasification agent.

Table 1. Reaction and energy balance for oxygen gasification based on 1 mole produced methane.

Oxygen gasification					
Reaction	2.7 $CH_{1.5}O_{0.6}$	+ 1.4 O_2	$\rightarrow CH_4$ +	reaction heat	$+1.7CO_2$
Energy	1127	0	676 (60 %)	450	[kJ/mol CH_4]

To increase the methane yield from biomass it would be possible to use the separated CO_2 for additional methane production. This could be done by implementing the Sabatier reaction which is showed in Eq. (1). Due to a very beneficial equilibrium in the Sabatier reaction it would be possible to convert most of the CO_2 to additional methane [9,10]. Hence, in this report it is assumed that 90 % of the input CO_2 is converted and such process would increase the total amount of methane produced, significantly.

$$CO_2 + 4H_2 \rightarrow CH_4 + 2H_2O \qquad \Delta H = -165 \text{ kJ/mol} \qquad (1)$$

As can be seen in Eq. (1), there is need for four hydrogen molecules per carbon dioxide molecule for the reduction of the carbon dioxide to methane according to the Sabatier reaction. As a by-product, two water molecules are produced for every molecule of methane; additionally the reaction is exothermal according to the equation. In Fig. 1 it is illustrated how the Sabatier process could be used to retrofit a gasification process.

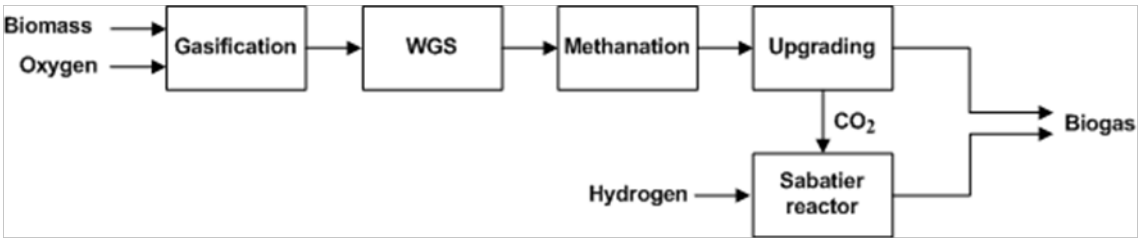

Fig. 1. Oxygen gasification combined with the Sabatier reaction.

After separation from the methane, the CO_2 stream could be directed to an external reactor where the Sabatier reaction takes place. The reaction could be run at atmospheric pressure but needs temperatures between 250 - 400°C. If running close to equilibrium it would be possible to increase the methane yield significantly, hence about 85 – 90 % of the carbon dioxide would be converted to additional methane [9,10]. To keep the "new" methane CO_2-clean the hydrogen is supposed to originate from electrolysis driven by a renewable source e.g wind power or photovoltaics (PV).

2.2. Hydrogasification

As stated in the previous section, the limiting factor for methane formation in the fuel synthesis is the low proportion of hydrogen in syngas. If WGS is used to obtain hydrogen, carbon dioxide is produced simultaneously and must be removed. By adding hydrogen in an earlier stage, i.e. in the gasifier, WGS can be avoided, moreover less or even no CO_2 removal is necessary. Adding hydrogen to the gasifier also has the positive effect of eliminating the need for oxygen as a gasification agent. Since the produced biogas has a low CO_2 content, the only upgrading that is needed is to remove the water by condensation. The process is illustrated in Fig. 2.

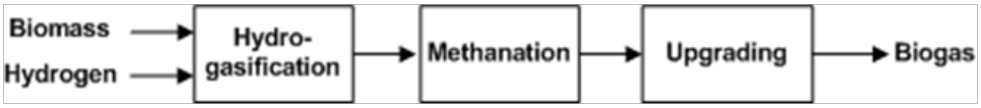

Fig. 2. Hydrogasification process

Table 2 shows the theoretical reaction and energy balance for hydrogasification which may be compared to oxygen gasification in Table 1. As can be seen, less reaction heat is produced and there are no CO_2 in the product (assuming total reaction).

Table 2. Reaction and energy balance for hydrogasification

Hydrogasification						
Reaction	$CH_{1.5}\ O_{0.6}$	+	1.85 H_2	$\rightarrow CH_4$ +	reaction heat	+ 0.6H_2O
Energy	420		448	676 (78 %)	192	[kJ/mol CH_4]

3. Potential for enhanced methane production

The mentioned processes are suggested as alternatives which significantly can enhance the yield of fuel obtained from biomass compared e.g. with biological processes. One must keep in mind though, that hydrogen is needed for both processes. The needed hydrogen is suggested to be produced through water electrolysis using a renewable energy source e.g. wind power or PV. It has been suggested by many researchers that electricity could be stored as hydrogen (which in turn can be used to produce propellants) through electrolysis [11-13]. This is especially beneficial when considering intermittent power i.e. wind- and solar power. Accordingly, electrolysis could act as stabilizer when electricity production is high and the grid load is low. In the Nordic countries the electricity price varies continuously and depends on supply and demand [14]. When high amounts of electricity are produced with few end users, the price will naturally decrease. Therefore, if running the electrolysis during these periods, the produced hydrogen will be as cheap as possible. It could also be stored for later use which could create possibilities for producing methane in a cost efficient manner.

In Table 3 and Table 4 examples for both processes are presented. The calculations are based on input biomass containing 100 moles of carbon (C). As stated earlier a 90 % conversion rate of the CO_2 is used in the calculations with the Sabatier reaction. It must be noted that in Table 3 the system boundaries for the gasification also includes the WGS reaction i.e. the flow is led in to the gasification and out from the upgrading process.

Table 3. Potential for increased biogas production by using the Sabatier reaction (input data for gasification from [7])

Gasification	Biomass	H_2	CO_2	CH_4
In (mol)	100 (mol C)	-		
Out (mol)		0.7	54	36
Sabatier				
In (mol)		217	54	
Out (mol)		22	5.4	49
Total CH_4 out				85

By using the removed carbon dioxide from the biogas, production can be increased by 136 %. In addition to the produced methane some un-reacted hydrogen is added to the biogas.

Table 4. Potential for increased biogas production by hydrogasification [7]

Hydrogasification	Biomass	H_2	CO_2	CH_4
In (mol)	100 (mol C)	178	12	
Out (mol)		8	8	83
Total CH_4 out				83

The input of CO_2 in the hydrogasifier is used as inert gas in the feeding process to avoid nitrogen in the system. The increase in biogas production can be calculated by comparing with the case of oxygen blown gasifier. In the case of hydrogasification the yield of methane will increase 130% compared to oxygen gasification (without Sabatier).

It is important to consider not only the yield of methane since biogas contains other combustible gases e.g. hydrogen which will increase the total energy output. In Table 5 it is possible to see the total energy balance. There are some facts to consider when reading Table 5 regarding the carbon input and the hydrogen content in the biogas. There is a higher carbon input in the hydrogasification process since carbon dioxide is used as feed, and it will also take part in the reaction and forms methane. Carbon dioxide is also used for feeding the oxygen-blown gasifier, but in that case a part of the produced carbon dioxide is re-circulated, thus no additional carbon source is added. The higher biogas output from the Sabatier reactor, despite the lower carbon input, can be traced to the higher hydrogen content in the produced biogas (20 mol-% from Sabatier and 8 mol-% from hydrogasification).

Table 5. Example of the efficiency of SNG production [7]

SNG production		**Hydrogasification**	**Gasification + Sabatier**	**Oxygen gasification**
Input	Biomass [MW]	100	100	100
	Hydrogen [MW]	94.8	117.7	
Output	Biogas [MW]	154	165.9	66.3
Efficiency		79 %	76.2 %	66.3 %
Hydrogen efficiency[1]		92.5 %	84.6 %	

[1]*Hydrogen efficiency refers to the increase in fuel production compared with amount added hydrogen. In the hydrogasification case, 94.8 MW hydrogen is added which increases the output by 87.7 MW compared to the oxygen blown gasifier. The efficiency is obtained by dividing the increase (87.7MW) with added hydrogen (94.8 MW), 87.7/94.8 = 0.925*

Adding hydrogen increases the efficiency which gives a high yield based on the LHV of hydrogen, 92 % for the hydrogasification case and 85 % when the Sabatier reactor is used. Table 5 also shows that the suggested methods could increase the biogas output with 130 – 150 % from the same amount of green carbon. Furthermore, the hydrogasification has a positive power balance with the possibility to export 4.5 MW; meanwhile oxygen gasification requires an import of 2.7 MW. If the oxygen is taken from the electrolysis in the case of oxygen gasification, the plant would lower the electric demand by 4 MW resulting in a 1.3 MW power export[7].

4. Discussion

Biogas' corresponding fossil fuel is CNG (compressed natural gas). The main difference between biogas and CNG is that biogas, when upgraded for vehicle usage, contains about 98 % pure methane and the remaining carbon dioxide. Natural gas however, contains mainly methane (about 80-90 %), higher hydrocarbons and carbon dioxide. Today many vehicles are driven by CNG, e.g. private cars, buses, trucks, taxicabs etc. In many urban areas (and to some extent in rural areas), there is a grid for CNG distribution. Hence, existing grids would be suitable for introducing biogas since both gases can be used in the same applications due to similar combustion qualities and energy content.

In both suggested processes small amounts of hydrogen are present in the product flow. Technically, the hydrogen does not need to be separated. According to test runs from 2006 in Malmö, Sweden, natural gas buses have tried driving on hydrogen blended CNG (HCNG) with promising results. The buses used up to 25 vol-% hydrogen with no, or only minor changes, in the system depending on blend [15].

Acquiring the essential hydrogen is one of the key issues for the processes. In this paper, electrolysis has been suggested for hydrogen production. However, electrolysis is energy demanding with an efficiency of about 70 % from electricity to hydrogen (LHV) [16]. Additionally, energy is lost when the actual reaction takes place. On the other hand, using electrolysis opens for possibilities of storing electricity in a manner the does not exist today; especially intermittent power which is growing rapidly. Moreover it is possible to produce a variety of different valuable products from hydrogen. Battery electric vehicles or plug-in hybrids have been suggested as possible electricity depots, however the technology and infrastructure for this kind of usage is still not commercially available.

An important matter regarding synthetic biogas is that it depends on renewable electricity for hydrogen production. Wind power and PV are renewable energy sources that have shown promising future potential. However, these sources produce intermittent power which is entirely controlled by current weather conditions. Hydrogen production through electrolysis would therefore be an effective method to regulate the fluctuations when excess power is produced.

Transporting and storing hydrogen for use as a vehicle fuel are issues that have not been solved yet. In such terms, it would be more favorable to use the hydrogen as a component for further conversion, in this case to produce synthetic biogas. One of the main problems when storing hydrogen is that a significant compression work is needed if stored as compressed gas. Biogas contains over 3 times more energy per volume than hydrogen which makes compression of biogas much more beneficial compared to hydrogen. Additionally, storage and infrastructure for biogas is more developed and the vehicles are available today, both as private cars and buses for public transportation.

As can be seen in the results, both processes show a significant increase in biogas production with the highest hydrogen efficiency when using hydrogen in the gasifier. An advantage of the Sabatier reaction however, is that it is not limited to gasification processes; basically any process with CO_2 emissions would be possible to retrofit. The fact that energy is lost as heat when adding hydrogen to the processes, could be solved (to some extent) by recovering the heat for power production in a steam cycle. Excess heat from the electrolysis could also be integrated in the steam cycle as preheating energy or used in e.g biomass drying.

5. Conclusions

Based on the presented information in this paper, it would be feasible to implement the suggested methods for fuel production. These would increase the capacity of biogas production greatly in areas where sufficient sustainable electricity is available.

It would be an excellent synergy opportunity to use intermittent electricity from renewable power production, to run the electrolysis when loads are high on the grid or during off-peak periods.

In a short time scale, the methods would be feasible options, since gasification and the Sabatier reaction are known technologies and furthermore biogas is used as vehicle fuel commercially.

Acknowledgments

The research has been supported by Agrivind AB, Formas and the Swedish Energy Agency, Siemens Industrial Turbomachinery AB, Volvo Aero Corporation, and the Royal Institute of Technology through the Swedish research program TURBOPOWER, the support of which is gratefully acknowledged.

References

[1] IPCC (Intergovernmental Panel on Climate Change). Climate Change 2007: Mitigation of Climate Change. Chapter 5: Transport and its Infrastructure. Contribution of Working Group III to the Fourth Assessment Report of the Intergovernmental Panel on Climate Change, 2007. Cambridge, United Kingdom and New York, USA; 2007. http://www.ipcc.ch/publications_and_data/ar4/wg3/en/ch5.html (Retrieved May 2010).

[2] Lindfeldt E.G, Saxe M, Magnusson M, Mohseni F. Strategies for a road transport system based on renewable resources – The case of an import-independent Sweden in 2025. Applied Energy 2010;87(6):1836-45.

[3] Robèrt M, Hultén P, Frostell B. Biofuels in the energy transition beyond peak oil. A macroscopic study of energy demand in the Stockholm transport system 2030. Energy 2007;32:2089-98.

[4] Åkerman J, Höijer M. How much transport can climate stand? –Sweden on a sustainable path in 2050. Energy Policy 2006;34:1944-57.

[5] Murphy J.D, McCarthy K. The optimal production of biogas for use as transport fuel in Ireland. Renewable Energy, 2005;2111-2127.

[6] Van herle J, Membrez Y, Bucheli O. Biogas as a fuel source for SOFC co-generators. Journal of Power Sources, 2004;:300-312.

[7] Mozaffarian, M., Zwart, R. & Boerrigter, H., 2003. Biomass and waste-related SNG production technologies; technical, economic and ecological feasibility, EP Deurwaarder Energy research Centre of the Netherlands (ECN).

[8] Duret, A., Friedli, C. & Maréchal, F., 2005. Process design of Synthetic Natural Gas (SNG) production using wood gasification. Journal of Cleaner Production, 13(15), 1434-1446.

[9] Brooks K.P, Hua J, Zhub H, K eeb R.J. Methanation of carbon dioxide by hydrogen reduction using the Sabatier process in microchannel reactors. Chemical Engineering Science 2007;62:1161-70.

[10] Lunde P.J, Kester F.L. Carbon dioxide methanation on a ruthenium catalyst. Industrial and Engineering Chemistry Process Design and Development 1974;13(1):27-33.

[11] Magnusson M, Mohseni F, Görling M, Alvfors P. Introducing renewable electricity to increase biogas production potential. International Conference on A pplied Energy 2010 (ICAE 2010), April 2010.

[12] Olah G.A, Goeppert A. and Prakash G.K.S. Beyond Oil and Gas The Methanol Economy. WILEY-VCH Verlag GmbH, Weinheim, Germany 2006]

[13] Takeuchi M, Sakamoto Y, Niwa S. Study on CO2 global recycling system. The Science of the Total Environment 2001;277:15-19

[14] Nordic electricity market where prices are set on a continuous basis. http://www.nordpoolspot.com/

[15] Swedish Gas Centre Development and demonstration of usage of methane/hydrogen mixtures as fuel in existing methane driven buses, Report SGC 170 1102-7371 (Utveckling och demonstration av användning av metan/vätgasblandningar som bränsle i befintliga metangasdrivna bussar). Malmö, Sweden (in Swedish) 2006.

[16] StatoilHydro (information handout) Hydrogen Technologies – World leader in electrolysis for hydrogen solutions. Norway, 2008.

Economic feasibility of biomass gasification for small-scale electricity generation in Brazil

Guilherme P. M. Fracaro[1,*], S. N. M. Souza[1], M. Medeiros[1], D. F. Formentini[1], C. A. Marques[1]

[1] *UNIOESTE (Universidade Estadual do Oeste do Paraná), Cascavel, Brazil*
[*] *Corresponding author. Tel: +55 4532248233, E-mail:guifracaro@yahoo.com.,br*

Abstract: Although Brazil has a clean energy matrix, factors such as increased electricity consumption forecast for the next 25 years and the peculiarities of the isolated systems of electricity generation in the north of the country could require the inclusion of alternative energy sources that can show competitive production costs. This study aimed to evaluate the feasibility of a 100 kW_e gasification system including an engine generator set, examining the major costs in using this technology and the sensitivity of different factors on the variation of the electricity cost. With a capital cost of 1,100.50 €.kW_e^{-1}, the levelized unit cost of electricity delivered (LUCE) found was 459,83 €.MWh^{-1}, which would make this technology uncompetitive even in places where the generation is done using diesel oil. The parameters that showed to have a greater impact on LUCE were, in decreasing order, the load factor, the gasifier capital cost, the electric conversion efficiency, the capacity utilization factor and the gasifier useful lifetime, but even with variations of 30% within the range considered no parameter alone would allow reducing the LUCE to a competitive level.

Keywords: *Alternative energy sources, Biomass-based power plant, Levelized unit cost of electricity*

Nomenclature

E_O	*annual delivered electricity output*. $kWh.y^{-1}$	R	*capital recovery factor*.....*fraction*
P	*rated power output*..... kWh	c_d	*diesel price* ..... $€.L^{-1}$
CUF	*capacity utilization factor*.....*fraction*	c_b	*biomass price*..... $€.kg^{-1}$
α	*generated power consumed by the auxiliaries*.....*fraction*	sc_d	*diesel specific consumption*..... $L.kWh^{-1}$
		sc_b	*biomass specific consumption*..... $kg.kWh^{-1}$
l	*electricity losses in the local distribution network*.....*fraction*	m_l	*manpower wage*..... $€.h^{-1}.man^{-1}$
		d	*discount rate*.....*fraction*.y^{-1}
AC	*annual cost of BGPP* ..... $€.y^{-1}$		*LUCE levelized unit cost of electricity*.. $€.kWh^{-1}$

1. Introduction

Biomass used in a sustainable way has a very important role to reduce the climate changes because it presents a carbon neutral balance, is relatively abundant and also because its forms of energy conversion have been already studied for a long time. Sustainable use of biomass can be defined as an infinite and continuous use which won't pollute and will maintain the natural resources and its benefits to humanity [1].

The energy conversion of biomass can be made by biological processes such as fermentation and digestion, by thermochemical processes such as combustion, pyrolysis and gasification, and also by mechanical extraction processes. Gasification can be defined as the conversion of biomass, or any solid fuel, into a gas fuel by partial oxidation at elevated temperatures [2]. The most common classification of types of gasifiers refers to the bed type, in the fixed bed gasifiers the biomass movement only occurs by gravity and in the fluidized bed gasifiers the fuel is kept in suspension by an intense oxidant medium flow, which can be air, oxygen or steam.

The produced gas has a combination of CO, CO_2, CH_4, H_2, N_2, tar, particulates and water, but its composition is extremely variable depending on the type and characteristics (texture,

moisture, ash content and volatile compounds) of fuel used and the type and operating conditions (oxidant medium, temperature, pressure, etc.) of the gasifier [3]. For small-scale electricity generation, fixed bed downdraft gasifiers are generally more suitable due to lower tar levels in the produced gases [4].

Renewable sources, with the exception of hydropower, still have higher costs of electricity conversion [5], however, for small rural communities, their low levels of energy demand and high costs of transmission lines usually restrict the energy supply to these communities by connecting them to the conventional power grid, which can make the use of renewable sources in decentralized systems to become economically viable.

This paper aims to present an economic assessment of small-scale electricity generation from biomass gasification in Brazil. The technology considered for biomass energy conversion was a 100 kW_e downdraft fixed bed gasifier coupled to a diesel engine operation on dual-fuel mode.

2. Characteristics of the Brazilian electrical system

The Brazilian energy matrix can be considered "clean", renewable sources are responsible for 48.7% of its primary energy [6], it has an installed capacity of 111 GW and nearly 80% of electricity produced in the country comes from a renewable source, 7% from biomass and 72% from hydropower [7], which makes the country's third biggest consumer of hydropower in the world, consuming 391 TWh in 2009 [8]. The country is currently experiencing a good economic period and it is expected an annual growth of 4.53% in electricity consumption for the next 25 years [9].

The Brazilian electrical system is formed by both the National Interconnected System (NIS) and the Isolated Systems (IS). NIS has a transmission network that sum 89,200 km and is responsible for 96.6% of the full capacity of electricity production in the country. The high costs of the national grid expansion in northern region of the country, due to its geographical characteristics and its low population density, makes the IS the major supplier of energy in this region. These systems cover an area equivalent to 45% of the national territory but they supply energy for only 3% of the population, with 8.7 TWh of electricity generated from fossil fuels in 2009. Despite the large subsidies FROM the government (about 1.05 billion Euros in 2007) [11], the average price of electricity paid by the customers in the Northern region is the country´s most expensive, 105 €.MWh^{-1} [7], currently, some isolated communities in the Amazon region use diesel generators at an average generating cost ranging between 143 and 205 €.MWh^{-1}, whereas in the interconnected system the generating cost is around 22 €.MWh^{-1} [12].

3. BGPP-based decentralized electricity generation

Decentralized systems are designed to meet the demands and needs of a small local population [13], often in areas previously without access to electricity. The use of biomass gasification for energy supply in this kind of community is a reality as demonstrated in countries such as India and China [14,15]. The most suitable technology for small-scale electricity generation (lower than $1MW_e$) through gasification processes is a downdraft fixed bed gasifier coupled to an internal combustion engine [17], because the gas produced into reactor is forced to pass through a high temperature throat, which produces a low tar content gas. Despite the fact that an ideal downdraft gasifier produces very low tar content gases, in practice the tar and particulates levels are still higher than the recommended levels, < 50

mg.Nm^{-3} and < 100 mg.Nm^{-3}, respectively [17]. consequently, it is necessary to use a gas cleaning system before feeding to an internal combustion engine.

the capacity utilization and the load factors of a rural village, where the demand for electricity is primarily for lighting, are commonly low and this lead to high electricity generation costs [21,24]. a low capacity utilization factor results in a underutilization of the biomass gasification power plant (BGPP) capacity. Furthermore, a low load factor has negative impacts on specific fuel consumption, and consequently in its conversion efficiency, and also in NOx and SOx emissions [19].

4. Economic feasibility

The economic feasibility of a BGPP is dependent on several factors, mainly the capital costs of the equipments (i.e. gasifier, engine-generator set, civil works and local distribution network), the specific fuel consumption, the capacity utilization factor (CUF) the useful lifetime of the equipments and fuel's prices. To assess the economic feasibility there are also several indicators, the most used are the levelized unit cost of electricity (LUCE) and the breakeven analysis values (e.g. the diesel price estimative or the distance of transmission lines under which the electricity generated by a BGPP becomes feasible), but also the Internal Rate of Return (IRR) and the Net Present Value (NPV) [17,20].

5. Methodology

Aiming to compare the financial results found in this study with other studies that considered different currencies, the values were converted to a common currency (Euro), considering the average of the quotations made in 2009 [23]. The conversion values are: 0.3608 (Brazilian Real), 0.7178 (American Dollar), 0.0148 (Indian Rupees) and 0.1046 (Chinese Yuan).

The non-monetary data that were needed to estimate the cost of electricity produced by the BGPP, as well as the methodology to calculate the LUCE were adopted based on the work of Nouni et al [21], this methodology is described below:

5.1. Levelized unit cost of electricity delivered output

The levelized unit cost of electricity (*LUCE*) delivered by BGPP, can be calculated as a function of the annualized cost of the BGPP and its amount of annual electricity delivered, as follows:

$$LUC = \frac{AC}{E_O} \quad (1)$$

Where AC is the annualized cost and E_O is the annual delivered electricity output of the BGPP with a rated power output (P) can be calculated by the following expression:

$$E_O = (P * L) * (8760 * CUF) * (1 - \alpha) * (1 - l) \quad (2)$$

Where LF represents the load factor of the BGPP, CUF is the capacity utilization factor, α is the fraction of generated power consumed by the auxiliaries of the BGPP and l is the losses in the local distribution network.

The annualized cost of the BGPP (AC) has been calculated as follows:

$$A\ C = F\ C + V\ C \quad (3)$$

Where *FC* and *VC* represent the fixed and variable costs of the BGPP, respectively.
The *FC* are the costs that doesn't vary with the BGPP productivity, they can be estimated using Eq. (04):

$$F\ = A C_{g} + A_{e} + A_{c} + A_{l a} \quad (4)$$

Where *AC* represents the annualized capital cost of each item of the power plant, they are the gasifier (*g*), engine-generator set (*eg*), civil works (*cw*) and the local distribution network (*ldn*), they can be calculated according to their capital costs (C) and capital recovery factors (*R*), which is a function of the discount rate (*d*) established. The equation to obtain *R* is described below:

$$R = \frac{d(1+d)^{T}}{(1+d)^{T} - 1} \quad (5)$$

Where *T* is the useful life time of each item of the power plant. The *AC's* were obtained according to Eq. (06), described below:

$$A\ C_{x} = C_{x} * R_{x} \quad (6)$$

The *VC* represent the costs that vary according to BGPP productivity, as follows:

$$V\ = A\ C_{O\&M} + A\ C_{F} \quad (7)$$

Where $AC_{O\&M}$ are the annual operation and maintenance costs of each item of the BGPP, and AC_F are the annual costs with fuel, calculated as follows:

$$A\ C_{O\&M} = C_{g} * m_{g} + C_{e} * m_{eg} + C_{cw} * m_{cw} + 8_{w} * C\ 7 * m_{l} * n \quad (8)$$

Where m_g, m_{eg} and m_{cw} represent the fraction of the capital cost of each item of the BGPP that is necessary to its operation and maintenance, m_l is the Brazilian manpower wage rate and *n* is the manpower required.

$$A\ C_{F} = 8C * C\ * 8 * 7 * (c_{d} * s_{d} + c_{b} * s_{b}) \quad (9)$$

Where c_d and c_b are respectively the local prices of diesel and biomass, sc_d and sc_b are the specific consumption of diesel and biomass in the power plant.

5.2. Simplifications and assumptions explanation

Table 1 shows all the values that were utilized to estimate the electricity generated cost of the BGPP:

5.2.1. Capital costs

The capital costs of equipments (i.e. the gasifier and the engine-generator set) were established with the intention of reflecting the reality of the Brazilian market. For this, it was made quotes from some of the industries that produce these equipments in a commercial scale, however, currently Brazil has only one company producing gasifiers in a commercial

scale and the capital cost of the gasifier was obtained from this company. It refers to a 500 kW_{th} fixed bed downdraft gasifier including the additional costs with auxiliary systems (e.g. an automatic feeding system, two cyclones, a fabric filter and a gas cooling system) and transportation, resulting in a capital cost of € 70,350.00. The established capital cost for a 100 kW_e diesel engine-generator set adapted to operate on dual fuel mode represents an average cost of € 32,500.00. The civil works cost were estimated at € 7,200.00, the amount is related to a facility with 50 m² at a average specific cost of 144 €.m^{-2}. the capital cost of the local distribution network was estimated based on an average value obtained from a local energy company, called COPEL.

Table 1. Parameters values to LUCE calculation.

Parameter	Unity	Value
Power rated capacity of BGPP	kW_e	100
Capital cost of gasifier	€	70,350.00
Capital cost of engine-generator	€	32,500.00
Capital cost of civil works	€	7,200.00
Specific capital cost of local distribution network	$€.km^{-1}$	5,000.00
Size of local distribution network	*km*	3
Price of biomass	$€.kg^{-1}$	0.0180
Price of diesel	$€.L^{-1}$	0.7190
Specific consumption of biomass (referred to the electric output)	$kg.kWh^{-1}$	1.21
Specific consumption of diesel (referred to the electric output)	$L.kWh^{-1}$	0.10
Capacity utilization factor	%	25
Load factor (function of BGPP's rated capacity)	%	75
Generated power consumed by BGPP	%	10
Electrical losses in local distribution network	%	10
Discount rate	%	10
Useful lifetime of gasifier	*h*	10,000
Useful lifetime of engine-generator	*h*	20,000
Useful lifetime of civil works	*y*	20
Useful lifetime of local distribution network	*y*	20
Manpower required by BGPP	-	2
Brazilian's manpower wage	$€.man^{-1}.h^{-1}$	2.35
Maintenance cost of gasifier (function of its capital cost)	%	5
Maintenance cost of engine-generator (function of its capital cost)	%	10
Maintenance cost of civil works (function of its capital cost)	%	2
Northern Brazil's reference tariff	$€.MWh^{-1}$	105
Isolated systems reference tariff	$€.MWh^{-1}$	174

5.2.2. Brazilian's manpower wage

The forecast labor cost was calculated based on the Brazilian minimum wage, equal to about € 186 a month, with an additional of 104% related to the charges applied.

5.2.3. Specific fuel consumptions

Based on current market price, it was stipulated the value of 18 €.t^{-1} for prepared wood. The value of 0.7190 €.L^{-1} for diesel based on the average prices paid in 2008 by the Isolated Systems power plants [22].

6. Results

6.1. BGPP's capital cost

The BGPP's capital costs found in this study were 703.5 €.kW_e^{-1} to gasifier, 325 €.kW_e^{-1} to engine-generator set and 1100.50 €.kW_e^{-1} to the power plant. These values don't differ much

from the values presented by Nogueira and Lora [24] WHO stipulated 861.36 €.kW_e^{-1} as a reference to power plants using gasifiers coupled to internal combustion engines. Liu et al [25] quoted a value around 1046 €.kW_e^{-1} as the capital cost of a BGPP in China. Due to several factors involved in setting the capital cost of a BGPP (mainly the scale of the project and the technologies considered) can also be found values with greater discrepancy [26,27].

6.2. BGPP's annualized costs

Figure 1 shows the extent of the impact of the studied costs on the LUCE. The annualized capital cost proved to be the main factor impacting the BGPP annualized cost (approximately 47% of the total) out of which 33% are due to the gasifier capital cost. Expenditures with labor and diesel proved to be almost equivalent, around 17% and 19% respectively. Although several authors cite that the diesel can be responsible for less than 30% of the energy produced by an engine-generator set operating on dual fuel mode [15,19,27,28] the spending with this fuel has represented more than 3 times the spending with biomass, this occurs due to much higher diesel specific cost compared to the cost of biomass.

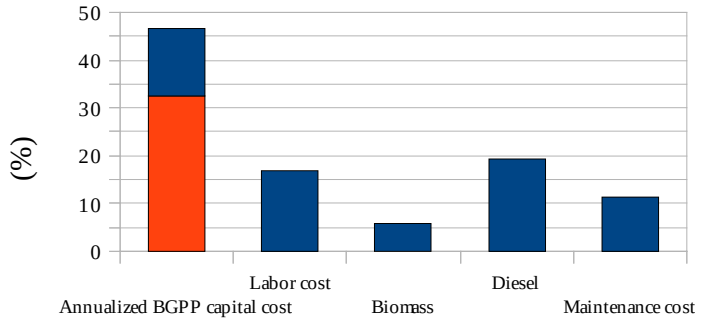

Fig. 1. Different costs responsibilities in BGPP annualized cost.

6.3. Delivered electricity cost

The estimated cost of electricity delivered by the BGPP under the established conditions was 459.83 €.MWh^{-1}, which represents approximately 4.38 times the price of the electricity paid by the customers in the Northern region of the country. Even when the comparison is based on the average price of electricity produced by diesel engine-generator sets in the Isolated Systems, the established luce showed no economic feasibility to an investment in a BGPP with these characteristics (264% of the isolated systems reference tariff).

6.4. Sensitivity analysis

As shown in Figure 2, the load factor is the parameter whose variation has greatest impact on the LUCE, if the BGPP operates at its rated capacity, the LUCE would be reduced to 380.41 €.MWh^{-1}, kept constant all the other factors. This reduction has even greater potential because the performance of both gasifier and engine-generator set tend to increase at higher load factors [19,21]. Also factor with important impact on LUCE were the electric conversion efficiency, the CUF and the gasifier useful lifetime, which with a 30% increase in their values could have respectively 7.5, 6 and 6% in LUCE reduction. Furthermore, a 30% reduction in gasifier capital cost could represent a 11.5% reduction in LUCE.

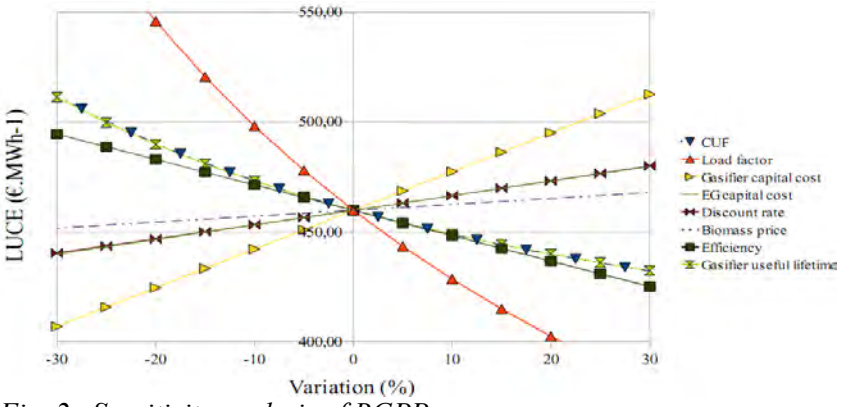

Fig. 2. Sensitivity analysis of BGPP.

7. Conclusions

It IS concluded that, under the studied conditions, the biomass gasification technology is still economically unfeasible to small-scale electricity generation in Brazil.

The main costs involved in BGPP electricity production, in descending order, were: the annualized capital costs (mainly the gasifier annualized capital cost), diesel, labor, maintenance and biomass costs.

In an attempt to reduce the LUCE of this BGPP, the load factor was the parameter that showed a higher sensitivity to reach this goal, followed by the gasifier capital cost, the electric conversion efficiency, the capacity utilization factor and the gasifier useful lifetime. however, with a variation of ±30% in the values previously established none of these factors would have a sufficient impact in LUCE to make this BGPP economically competitive in the Brazilian energy market. Even with a 30% variation of all factors at the same time (a 30% increase to the cuf, load factor, efficiency and gasifier useful lifetime and a 30% reduction of the gasifier and eg capital costs, discount rate and biomass price) the LUCE would be equal to 232.95 Euros. This value is still higher than the isolated systems reference tariff.

References

[1] L.Reijnders, Conditions for the sustainability of biomass based fuel use, Energy Policy 34, 2006, pp. 863–876

[2] P.Mckendry, Energy production from biomass (part 2): conversion technologies, Bioresource Technology 83, 2002, pp. 47-54

[3] P.Mckendry, Energy production from biomass (part 3): gasification technologies, Bioresource Technology 83, 2002, pp. 55-63

[4] A.F. Kirkels, G.P.J. Verbong, Biomass gasification: Still promising? A 30-year global overview, Renewable and Sustainable Energy Reviews 15, 2011, pp. 471-481

[5] D.Popp, I.Hascic, N.Medhi, Technology and the diffusion of renewable energy, Energy Economics, In Press, Corrected Proof, Available online 7 September 2010

[6] MME – Ministry of Mines and Energy/EPE – Energy Research Company, National Energy Balance, 2008

[7] ANEEL – National Electric Energy Agency website: www.aneel.gov.br

[8] BP Statistical Review of World Energy, June 2010

[9] MME – Ministry of Mines and Energy/EPE – Energy Research Company, National Energy Matrix 2030, 2007

[10] A.C.A. Costa, N.P. Junior, D.A.G. Aranda, The situation of biofuels in Brazil: New generation technologies, Renewable and Sustainable Energy Reviews 14, 2010, pp. 3041-3049

[11] ANEEL – National Electric Energy Agency, Atlas of electricity power in Brazil, 3rd Edition, 2008

[12] E.S. Lora, R.V. Andrade, Biomass as energy source in Brazil, Renewable and Sustainable Energy Reviews 13, 2009, pp. 777-788

[13] D.P. Kaundinya, P. Balachandra, N.H. Ravindranath, Grid-connected versus stand-alone energy systems for decentralized power – A review of literature, Renewable and Sustainable Energy Reviews 13, 2009, pp. 2041-2050

[14] C.Z. Wu, H. Huang, S.P. Zheng, X.L. Yin, An economic analysis of biomass gasification and power generation in China, Bioresource Technology 83, 2002, pp. 65-70

[15] B. Buragohain, P. Mahanta, V.S. Moholkar, Biomass gasification for decentralized power generation: The Indian perspective, Renewable and Sustainable Energy Reviews 14, 2010, pp. 73-92

[16] E. Alakangas, M. Flyktman, Biomass CHP technologies, VTT Energy Reports 7, 2001

[17] P. Hasler, T. Nussbaumer, Gas cleaning for IC engine applications from fixed bed biomass gasification, Biomass and Bioenergy 16, 1999, pp. 385-395

[18] M.R. Nouni, S.C. Mullick, T.C. Kandpal, Providing electricity access to remote areas in India: An approach towards identifying potential areas for decentralized electricity supply, Renewable and Sustainable Energy Reviews 12, 2008, pp. 1187-1220

[19] R. Uma, T.C. Kandpal, V.V.N. Kishore, Emission characteristics of an electricity generation system in diesel alone and dual fuel modes, Biomass and Bioenergy 27, 2004, pp. 195-203

[20] F. Goor, J.-M. Jossart, J.F. Ledent, ECOP: and economic model to assess the willow short rotation coppice global profitability in a case of small scale gasification pathway in Belgium, Environmental Modelling & Software 15, 2000, pp. 279-292

[21] M.R. Nouni, S.C. Mullick, T.C. Kandpal, Biomass gasifier projects for decentralized power supply in India: A financial evaluation, Energy Policy 35, 2007, pp. 1373-1385

[22] ELETROBRÁS, Anual plan for fuels – Isolated sytems, 2009

[23] Central Bank of Brazil website: www.bcb.gov.br

[24] L.A.H. Nogueira, E.E.S. Lora, Dendroenergia: fundamentos e aplicações, Interciência, 2nd edition, 2003

[25] T. Liu, G. Xu, P. Cai, L. Tian, Q. Huang, Development forecast of renewable energy power generation in China and its influence on the GHG control strategy of the country, Renewable Energy 36, 2011, pp. 1284-1292

[26] T. Buchholz, I. Da Silva, Potential of distributed wood-based biopower systems serving basic electricity needs in rural Uganda, Energy for Sustainable Development 14, 2010, pp. 56-61

[27] D. Brown, M. Gassner, T. Fuchino, F. Maréchal, Thermo-economic analysis for the optimal conceptual design of biomass gasification energy conversion systems, Applied Thermal Engineering 29, 2009, pp. 2137-2152

[28] N. Tippayawong, A. Promwungkwa, P. Rerkkriangkrai, Durability of a small agricultural engine on biogas/diesel dual fuel operation, Iranian Journal of Science & Technology 34, 2010, pp. 167-177

Evaluation of biodiesel production from babassu oil and ethanol applying alkaline transesterification under ultrasonic technology

Paiva, E. J. M., Silva, M. L. C. P., Castro, H. F., Barboza, J. C. S., Giordani, D. S.*

School of Engineering of Lorena – University of São Paulo, Lorena, Brazil
** Corresponding author. Tel: +55 12 31595142, Fax: +55 12 31533224, E-mail: giordani@dequi.eel.usp.br*

Abstract: Babassu oil is a clear light yellow vegetable oil extracted from the seeds of the babassu palm (Attalea speciosa), which grows in most areas of South America. It is about 70% lipids, with 50% of lauric composition. Brazil is the world's second largest producer of ethanol and the world's largest exporter; the advantages of ethanol are concerned to its renewable origin and low toxicity. In this work ethyl esters of babassu oil were synthesized by alkaline catalysis in homogeneous medium. The experimental design was used as a tool for optimization of the transesterification reaction and also in identifying key factors influencing the conversion into ethyl esters. The transesterification reactions were performed using two methods - the traditional mechanical agitation and agitation promoted by ultrasound waves. The nuclear magnetic resonance spectroscopy was used to quantify the conversion of all reactions of transesterification. According to the model obtained by the experimental design for mechanical agitation, conversions above 99% are obtained when the stoichiometric ratio is set at 6:1, with 1.0% KOH, under stirring at 400 rpm, in 60 min. Alkaline transesterification assisted by ultrasound waves produced the best results with respect to time of reaction and phase separation of glycerin and ethyl esters. The experimental model showed that conversions above 99% can be obtained in 10 min after adjusting the other independent variables.

Keywords: *Biodiesel, Babassu oil, Transesterification, Ethanol, Ultrasound.*

1. Introduction

The vegetable oil transesterification yields biodiesel as the main product. However, the final mixture is composed of free glycerol, alcohol, catalyst and unreacted mono-, di- and triglycerides [1]. These contaminants can lead to environmental and operational problems. Achieving high conversions in mono-alkyl esters, to ensure the removal of free glycerin, catalyst, alcohol and fatty acids in biodiesel are critical issues to the quality control and is one of the main challenges to be overcome to make feasible the industrial production of these fuels. In another approach, the fatty acid composition of vegetable oils is a significant factor influencing the performance of biofuels, carbon chains with a high number of unsaturations are more susceptible to oxidation as well as they have better performance with low temperatures, in contrast, saturated chains are desirable [2,3], especially due to the higher oxidation resistance and improved cetane number, but its use in cold climates is conditioned to its cloud point.

Among all feasible vegetable oil to cultivation and to oil extraction , this study employed the babassu, a generic name given to palm oil belonging to the *Palmae* family and members of the genera *Orbignya* and *Attalea*. The babassu oil constitutes 66% of kernel weight, and its composition is mainly saturated (83% of the grease composition) which makes it an excellent alternative for biodiesel production. In fact, in Brazil there is a range of oilseed crops that can be used in biodiesel production; currently almost all manufacturing process uses soybean oil as the main raw material. However, some oilseeds, especially soybean oil, run directly into the food industry market, besides extensive area must be used to afford good production. In this sense, non edible crops, as the babassu oil which presents annual productivity and a good yield per hectare, became an excellent alternative [4].

This work proposed ethanolysis of babassu oil employing the alkaline hydroxides most commercially used, the sodium and potassium hydroxides, which were evaluated independently. The aim was to study the process performance aided by statistical methodology proposed by Genichi Taguchi [5] to obtain robust processes, i.e., processes with low variation due to uncontrolled variables. So, the homogeneous alkaline transesterification reaction was evaluated in the presence of side reactions – the saponification and hydrolysis, which are inherent to the use of these hydroxides to generate the effective catalysts [6].

2. Methodology

The Taguchi designs with orthogonal arrays were performed according to the factors and levels presented in Table 1 to the conventional agitation and in Table 2 to the ultrasound method .

Table 1. Levels and controllable factors used in babassu oil ethanolysis reaction with conventional agitation.

Factor	Units	Levels	
		1	2
Turbulence	rpm	200	400
Temperature	ºC	30	60
Molar ratio ethanol/oil	Mol	4:1	6:1
Hydroxide/oil ratio	% by weight	0.5	1.0
Reaction time	min	30	60
Hydroxide type		NaOH	KOH

Table 2. Levels and controllable factors used to babassu oil ethanolysis reaction with ultrasound agitation.

Factor	Units	Levels	
		1	2
Molar ratio ethanol/oil	Mol	3:1	6:1
Hydroxide/oil ratio	% by weight	0.5	1.0
Reaction time	min	10	20
Hydroxide type		NaOH	KOH

2.1. Materials

Refined babassu oil was kindly provided by the company COGNIS Brazil Ltda.; NaOH (99%), KOH (85%), Na_2SO_4, anhydrous ethanol (99.8%) and hexane were obtained in analytical grade and used as received. The properties of the babassu oil in terms of fat acid composition was not determined and it was used the values available in the literature [7].

2.2. Procedure to the conventional transesterification reaction

Catalyst and anhydrous ethanol were premixed at 40 °C under magnetic stirring for 20 min or until complete dissolution. Then, the solution of the corresponding ethoxide was added to 70 g of refined babassu oil, previously heated at the same temperature. The reactions were performed in a jacketed glass reactor of 300 mL with reflux condenser; the temperature control was performed by a thermostatic bath. Mechanical stirring was performed with a mechanical stirrer and glass double curved blades; rotation control was done by mixer brand IKA RW20-digital model. After the predetermined time for each reaction, the reaction mixture was transferred to a vessel to ensure phase separation between ethyl esters and glycerin.

2.3. Procedure to the transesterification reaction with ultrasound

In a 125 mL Erlenmeyer flask, it was added 22 g of refined babassu oil. In parallel, appropriate amounts of anhydrous ethyl alcohol and sodium or potassium hydroxides were mixed until complete dissolution in a glass flask equipped with reflux condenser, under moderate magnetic stirring for 20 min at 40 °C. In the sequence, the solution containing the corresponding ethoxide catalyst was added to the flask containing the oil preheated to 30 °C. The tub of ultrasonic bath was filled with 300 mL of distilled water and then the flask containing the reactants was placed inside. The temperature was maintained in 30 ºC and the flask was not sealed, considering that at this temperature the evaporation of ethanol is negligible. The position inside the tub and height of the flask were standardized with markers, in order to use always the same tridimensional position. The equipment was set to operate at 600 W and 20 kHz.

2.4. Purification process and conversion evaluation

After phase separation and removal of glycerin produced (lower phase), 200 mL of hexane were added to the upper phase containing the non reacted intermediates and ethyl esters. This promotes new glycerin phase separation. After collecting this new phase, a new step involving several washings with 0.1 $mol.L^{-1}$ solution of HCl were done, in order to reach neutral pH. After rinsing, this phase was dried with approximately 0.5 g of anhydrous Na_2SO_4 to remove remaining water, followed by vacuum filtration and, finally, residual alcohol and hexane were evaporated by a rotary evaporator at 72 °C during 20 min under atmospheric pressure.

The conversion into ethyl esters was evaluated by NMR in a Mercury 300 MHz – Varian spectrometer, with 5 mm glass tubes, using $CDCl_3$ as solvent and 0.3% TMS as internal standard. The calculations involving the conversion of esters were determined using the formula proposed by Garcia [8]. This methodology basically consisted in the identification, by ^1H NMR, of molecules that present peaks in the region of 4.05 to 4.35 ppm during a transesterification reaction.

3. Results

3.1. Evaluation of controllable variables as a function of the process noises

According to the methodology proposed by Taguchi [5], the signal to noise ratio (S/N) can, in this case, be interpreted as conversion into ethyl esters in the presence of noise (uncontrollable) factors. Figure 1 shows the effects of controllable factors in the signal to noise ratio, measured independently, i.e. without considering interactions between these factors, this figure was produced by the software Minitab®, that was used to perform the statistical analysis.

3.2. Molar ratio ethanol / babassu oil in the conventional procedure

The data showed that among all the factors, taken individually, the ethanol / oil ratio was the most important factor in conversions into ethyl esters. Due to the existence of a dynamic equilibrium between reactants and products, it is expected that excess alcohol increases the conversion to esters. In this sense, the results show that ethanolysis of babassu oil behaves similarly to the results already reported to other vegetable oils.

One of the advantages of applying statistical designs on the experiments is the evaluation of interactions between the factors; sometimes these interactions may be more important than the controlled variables. As stated, this factor presents a significant interaction with the reaction time, as it could be demonstrated by the interactions analysis, showing that regardless of the

time adopted (30 or 60 min), the conversions are higher when used the molar ratio 6:1 of ethanol / oil.

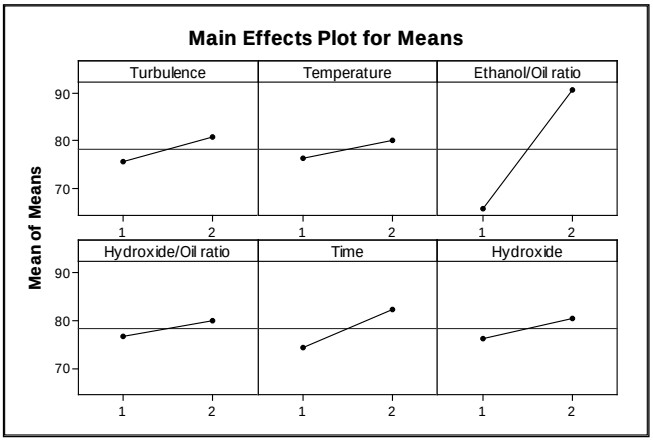

*1 and 2 correspond to low and high levels respectively

Fig. 1. Effects of controllable factors in the average conversion to ethyl esters as a function of noise in the conventional procedure

3.3. Effect of temperature

When temperature is evaluated individually its effect is modest, as it can be observed in Figure 1. However, considering the interactions, best conversions are obtained with temperatures set at low level, i.e., 30 °C (Figure 2a). Likewise, the turbulence generated by mechanical agitation at 400 rpm promotes best conversion into ethyl esters with temperature of 30 ºC (Figure 2b). This peculiar behavior can be explained by hydrolysis and saponification reactions, enhanced by higher temperatures, which promote the consumption of the catalyst reducing the yield of conversions [6].

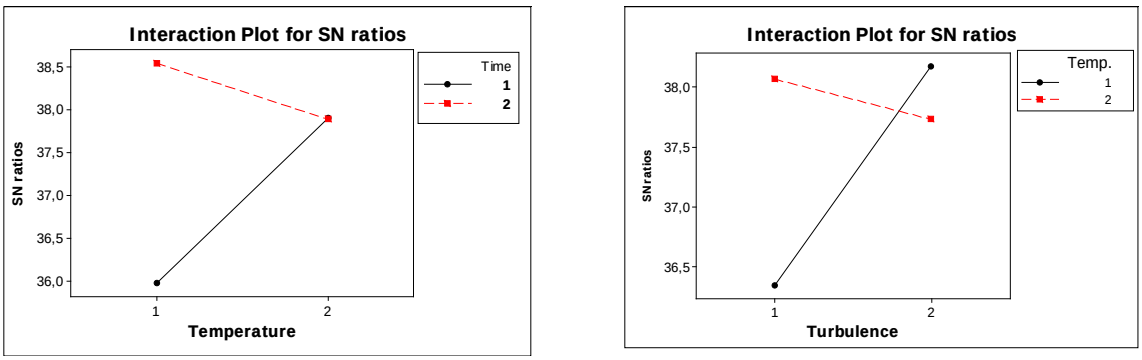

(a) (b)

Fig. 2. Interaction of (a) temperature/time and (b) temperature/turbulence on the signal to noise ratio in the conventional procedure

3.4. Effect of amount and type of hydroxide

In most industrial processes the catalyst is expensive when compared to reagents and adds additional costs for its removal from the final product. The effective catalyst in a homogeneous transesterification reaction is the anion formed from the reaction between basic hydroxide and the alcohol. However, for practical and industrial purposes, the percentage ratio by weight of the hydroxide to vegetable oil is commonly used to describe the effect of the catalyst involved.

It was used 1 % (wt) of both hydroxides, what is equivalent to 0.0125 mol of KOH and 0.0175 mol of NaOH. So, regarding the type of hydroxide, the data show that the use of KOH

is desirable, since lower molar quantities promoted better conversion into ethyl esters. Furthermore, the purification procedures were significantly facilitated when using potassium hydroxide, this experimental finding supports the conclusion that the generation of soap with KOH is lower.

Regarding the amount of hydroxide, this study showed that the use of 1 % by weight of it in relation to the mass of babassu oil leads to better results.

3.5. Effect of turbulence

The literature highlights the importance of agitation during the early stages of alkaline transesterification reactions, because during the initial stages, the mass transfer is limited [9,10]. The results suggested that the turbulence levels adopted in this study are sufficient for good conversions into ethyl esters, i.e., higher values of mechanical agitation than 400 rpm do not improve the yield of conversion.

Besides interaction with the temperature, this factor also had another significant interaction with the amount of hydroxide used, showing that the best conversions are obtained when these factors are set at higher level, i.e., mechanical agitation of 400 rpm and 1 % hydroxide (Figure 3). The behavior exhibited by this interaction can be explained by an improvement in the conditions of mass transfer with more turbulence and also due to increase on availability of catalysts for the reaction with the use of 1 % hydroxide in relation to initial mass of oil babassu.

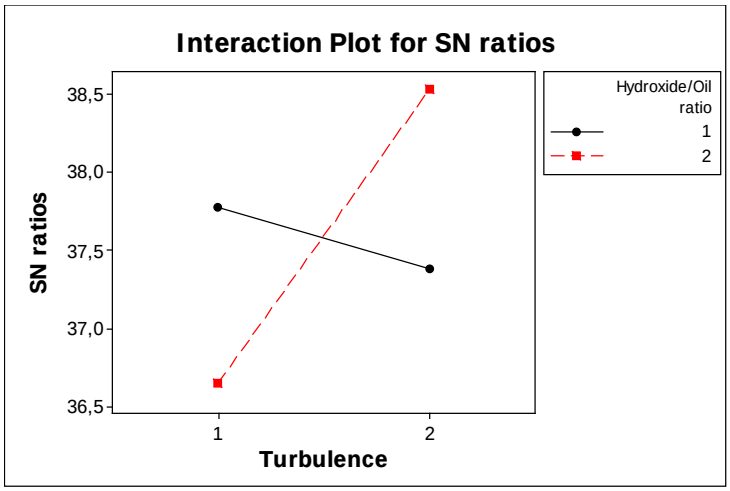

Fig. 3. Interaction plot between turbulence and % by weight ratio hydroxide / babassu oil in the conventional procedure

3.6. Effect of Time

The reaction time showed to be a dependent controllable factor, and with optimization of no other factors, the data showed that satisfactory conversions were reached within 60 min of reaction.

Thus the technological model obtained with this methodology was adjusted to the temperature at 30 °C, 400 rpm of mechanical agitation, using 1 % potassium hydroxide during 60 min of reaction. The conversion into ethyl esters obtained were above 99 %, determined by ^{1}H NMR, and the weight of esters recovered after the purification procedures was 94.59 % compared to the initial mass of this product.

3.7. Mathematical model

The evaluation of controllable factors to babassu oil ethanolysis reaction as a function of the noises was useful in determining the influence of the main variables in the conversion to ethyl esters, as can be seen in the Figure 1 and in the discussion about the effect of the temperature. After that, new experimental design was employed with the two main variables and the response surface methodology (RSM) was applied, with the development of new 2^2 complete factorial design with axial points, in order to identify the optimum conditions of babassu oil ethanolysis.

The mathematical model proposed to describe babassu oil ethanolysis is shown in Equation (1). The quadratic coefficients of correlation show that the model can explain 96.21 % of the variability in the response and further simulations with this equation are able to predict 80.47 % of the results.

$$\%CEE=54.37 - 1.836\theta + 3.020r + 0.021\theta^2 - 0.025r^2 - 0.007(\theta \times r) \quad (1)$$

Where %CEE is the ethyl esters conversion percentage, θ is the temperature and r the ethanol/Oil ratio

Figure 4 was generated with the software Minitab® from Eq. (1) and show the best fit to a babassu oil ethanolysis. As can be seen, with temperatures below 40 °C there is a narrow range in which the conversion into ethyl esters is higher, reaching the highest value in temperature around 30 °C and ethanol/oil ratio around 6:1 (60 in the figure).

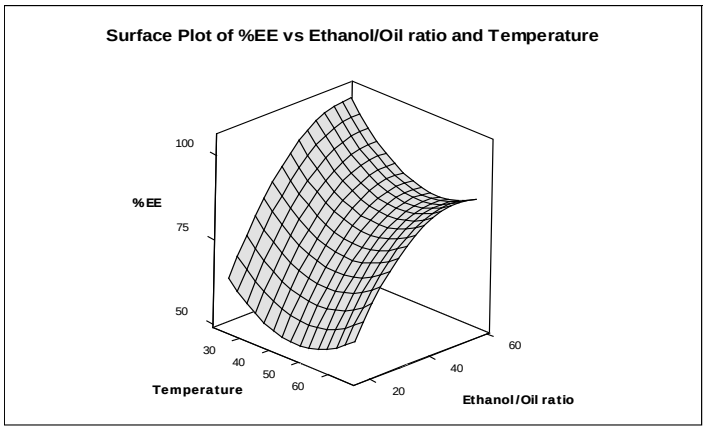

Fig. 4. Response surface to ethyl esters conversions as a function of the ethanol/oil ratio and temperature in the conventional procedure

3.8. The effect of the use of ultrasound

As it can be seen in de Figure 5, since there are no crossings between the effect lines of the variables, does not exist interactions of relevance to this system, thus the interpretation of controllable factors can be made directly.

In the Figure 6 it can be observed that the ratio ethanol/oil was also the most important factor involved in ethanolysis under ultrasound, showing that both processes, traditional agitation and sonication, are primarily dependent on this factor; no matter how intense are the physical conditions to which the medium is submitted. Similar results were reported in literature to the ethanolysis coconut oil [11].

Figure 6 also shows that the ratio hydroxide/oil was relevant to the sonolysis of babassu oil, the degree of conversion significantly responded to the variation of levels. The best conversions are obtained when employing the mass ratio of 1.0 % (wt) of catalyst of babassu oil. This result was expected because the greater availability of catalyst greater the generation of the active component of the reaction, in this case, the ethoxide catalyst and, due to the phenomena of sonoluminescence and cavitation noise, which are responsible for creating unique conditions for transfer mass, the greater amount of this active component had its effect enhanced [12].

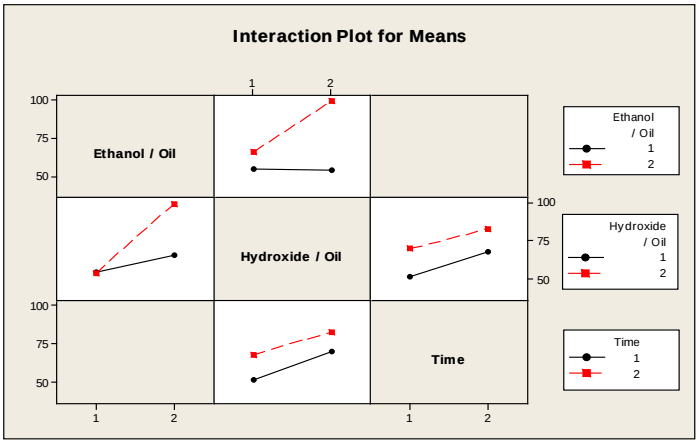

Fig. 5. Interaction plot on the signal to noise ratio for studied variables in the sonication procedure

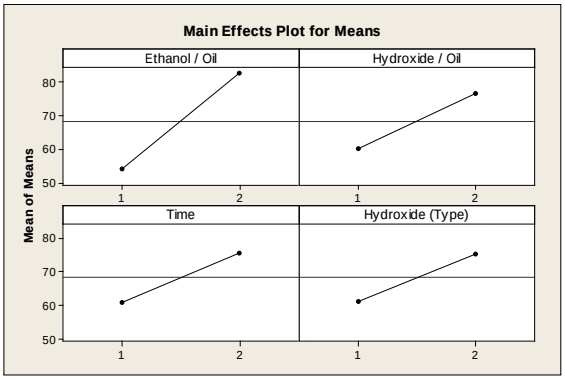

Fig. 6. Effects of controllable factors in the average conversion to ethyl esters as a function of noise in the sonication method

When compared to the traditional method, the time factor of sonication was considerably reduced and conversions above 99 % were obtained in 10 min, meaning that despite the significance showed for this variable in Figure 6, there is no practical reason to use the upper level of time. The important reduction in time compared to traditional methodology, can be explained by the intense mass transfer promoted by cavitation noise, implying a reduction of time intervals spent on the diffusion of reagents.

4. Conclusions

The refined babassu oil has shown excellent qualities as a raw material. Even in ethanolysis reaction this oil presented a similar behavior to reactions that used methanol showed in the literature [4,13]. The experiments showed that the correct tuning in the process variables is able to promote higher conversions into ethyl esters.

Among all the controllable factors evaluated, the ratio ethanol/oil decisively influenced the conversions into ethyl esters; highest conversions are achieved at the stoichiometric ratio of 6:1. The temperature showed a peculiar behavior, pointing out that the best conversions are obtained at 30 ºC. Other important conclusion is about the amount of hydroxide employed that suggests that a rate around 1.0 % is sufficient to obtain good conversions. KOH proved to be preferable if compared to NaOH, since better conversions were obtained and purification steps were easier.

The sonolysis of babassu oil showed considerable gain in time with respect to classical transesterification, principally during the stages of phase separation, which were substantially facilitated. Similar results were obtained for the preparation of biodiesel by the transesterification of coconut oil [11]. The remarkable results obtained with the reaction time can be explained by intense mass transfer afforded by the unique conditions generated by cavitation noise. In addition, possible reductions in the concentrations of mono- and di-glycerides during the reaction may explain the reduction in the time for phase separation. Thus, the method presents itself as a potential technological route of production of biodiesel, capable of meeting high demands in short periods of time. Adjustments related to the type of ultrasonic reactor (or transducer) and in the process of vegetable oils sonolysis can lead to an excellent alternative for biodiesel production, with energy costs that may be less than the expenses involved with the traditional method of mechanical agitation.

References

[1] Pinto, A. C., Guarieiro, L. L. N., Rezende, M. J. C., Ribeiro, N. M., Torres, E. A., Lopes, W. A., Pereira, P. A. P.; de Andrade; J. Braz. Chem. Soc 2005, v. 16, p. 1313.

[2] Knothe, G., Dunn, R. O., Biofuels Derived from Vegetable Oils and Fats. In Oleochemical Manufacture and Applications. Academic Press: Sheffield, U.K., 2001.

[3] Dorado, M. P., Ballesteros, E., Almeida, J. A.; Schellet, C., Lohrlein, H. P., Krause, R., Trans ASAE 2005, v. 45, p. 525.

[4] Lima, J. R.; Silva, R. B.; Silva, C. C. M.; Santos, L. S. S.; Santos JR., J. R.; Moura, E. M.; de Moura, C. V. R., Química Nova, 2007, v.30, n.3, pp. 600-603.

[5] Taguchi, G. Introduction to Quality Engineering: Designing Quality into Products and Processes, White Plains, NY. Kraus International Publications, 1986.

[6] Schuchardt, U.; Sercheli, R.; Vargas, R. M. Transesterification of vegetable oils: a review. J. Braz. Chem. Soc., 1998, v.9, pp. 199-210.

[7] Gunstone, F. D.; Harwood, J. L.; Padley, P. The Lipid Handbook 2. ed. London: Chapman and Hall, 1994.

[8] Garcia, C. M., Master Dissertation - State Univ. of Campinas, UNICAMP, Brazil, 2006.

[9] Noureddini, H.; Zhu, D. J. Am. Oil Chem. Soc., 1997, v.74.

[10] Freedman, B.; Butterfield, R. O.; Pryde, E. H. Transesterification kinetics of soybean oil, J. Am. Oil Chem. Soc., 1986, v. 63.

[11] Kumar, D., Kumar, G., Singh, P. C. P., Ultrasonics Sonochemistry, 2010, v.17, pp. 555-559.

[12] Stavarache, C.; Vinatoru, M.; Maeda, Y. Ultrasonic versus silent methylation of vegetable oils, Ultrasonics Sonochemistry, 2006, v.13, pp. 401–407.

[13] Nogueira, Jr., C. A. F.; Filipe, X.; Fernandes, F. A. N., Santiago, R. S. and Sant'Ana, H. B., J. Chem. Eng. Data 2010, v. 55, pp. 5305–5310.

A Comparative Study of Immobilized-Whole Cell and Commercial Lipase as a Biocatalyst for Biodiesel Production from Soybean Oil

S.N. Hashemizadeh[1,2], O. Tavakoli[1]*, F. Tabandeh[2], A.A. Karkhane[2], Z. Forghanipour[1,2]

[1]*School of Chemical Engineering, College of Engineering, University of Tehran, 16 Azar Street, Tehran, Iran*
[2]*Industrial and Environmental Biotechnology Department, National Institute of Genetic Engineering and Biotechnology (NIGEB), Tehran, Iran*
** Corresponding author. Tel: +98 21 61112187 Fax: +98 21 66498984, E-mail: otavakoli@ut.ac.ir*

Abstract: Recently, there has been considerable attention in the direct use of intracellular lipase as a whole-cell biocatalyst (indirect immobilization of the enzyme) for biodiesel production since immobilization can be carried out spontaneously during the process of cell cultivation. In this research the ability of *Rhizopus oryzae* (ATCC 9374) whole-cell biocatalyst that was immobilized within biomass support particles (BSPs) was investigated and compared with Novozym 435 (most effective extracellular immobilized lipase) for methanolysis of soybean oil in solvent free system. The maximum methyl esters content in the reaction mixture reaches 84 wt% using *R.oryzae* whole-cell biocatalyst in optimum condition (6mm×6mm×3mm BSPs size, olive oil as carbon sources in basel medium, emulsification using ultrasonicated of reaction mixtures, 15 wt% water content and 7 wt% immobilized BSPs, addition of methanol at 0, 4 and 18 h) and at reaction time of 48 h which is remarkably comparable with yield of biodiesel at 90 wt% obtained with Novozym 435. Both the lipases can be used for repeated batches cycles. These findings indicate that, given the simplicity of the lipase production process and the long-term stability of lipase activity, the use of whole-cell biocatalysts immobilized within BSPs and treated with glutaraldehyde solution suggest a favorable means of biodiesel fuel production for industrial application.

Keywords: *Biodiesel, Whole-Cell Biocatalyst, Rhizopus oryzae, Novozym 435.*

1. Introduction

The consideration depletion of fossil resources and increasing social environmental awareness has led to a search for fuels that can be produced from renewable sources such as plant biomass [1]. A number of studies have examined the methods that are promising use of triglycerides (vegetable oils or animal fats) as an alternative fuel for diesel engines. However, the direct use of vegetable oils or oil blends is generally considered impractical because of high viscosity, acid composition and free fatty acid content. Facing these issues, transesterification; also called alcoholysis, were used to reduce viscosity and improve the physical properties of such fuels. Transesterification which has been recently developed to replace oils and fats as renewable energy resources is similar to hydrolysis reaction in which water is substituted with alcohol [2]. Biodiesel is explained as the non-petroleum-based diesel fuel be made up of short chain alkyl (methyl or ethyl) esters, typically made by transesterification of vegetable oils or animal fats, which can be used (alone, or blended with routine petrodiesel) in unchanged diesel-engine vehicles. It is biodegradable and nontoxic, has low discharge profile and so is environmentally advantageous [3]. Transesterification of triacylglycerides can be carried out by different catalytic processes. Alkali catalysis is widely applied for the commercial production of biodiesel fuel. However, enzymatic transesterification using lipase enzymes offers considerable advantages, including reducing process operations in biodiesel fuel production and an easy separation of the glycerol byproduct [4]. There are two major classification of enzymatic biocatalyst: (1) extracellular lipases (i.e. the enzyme has previously been recovered from the live-producing microorganism broth and then purified) which the major producer microorganisms are *Mucor miehei*, *Rhizopus oryzae*, *Candida Antarctica*, *Pseudomonas cepacia*; and (2) intracellular lipase which remains either inside or in the cell-producing walls which in both cases the

enzyme is immobilized. The advantage of immobilization in this system is frequent utilization due to its easy recovery from the reaction mixture [5].

Several researchers have reported that the commercially available Candida antarctica lipase immobilized on acrylic resin (Novozym 435) was the most effective lipase between any of the extracellular lipases tested for transesterification reaction of vegetable oils where methanol is used as acyl acceptor [6-8]. Although immobilization of extracellular enzyme seemed to be a common method for enzymatic alcoholysis, it needs complicated methods for separation, purification and stabilization of lipases which in turn increase the process cost in industrial scale [9]. In recent years, there has been considerable interest in the direct use of intracellular lipase as a whole-cell biocatalyst (indirect immobilization of the enzyme) for biodiesel production. Utilizing whole cell overproducing intracellular lipase in which the purification and stabilization of the enzyme are not necessary instead of conventional immobilized lipase for biodiesel production is a potential way to reduce the biocatalyst cost, because immobilization can be carried out spontaneously during the process of cell cultivation [10]
In this research the ability of *Rhizopus oryzae* (ATCC 9374) whole-cell biocatalyst that was immobilized within biomass support particles (BSPs) made of reticulated polyurethane foam was investigated and compared with that of commercially available most effective lipase (Novozym 435) for methanolysis of soybean oil in solvent free system.

2. Materials and methods

2.1. Materials

Refined soybean oil was purchased from Behshahr Industrial Co. (Tehran, Iran). Commercial immobilized lipase from Candida antarctica, namely Novozym 435 was provided as a gift from Novo Nordisk (A.S., Denmark-Tehran Office).

Rhizopus oryzae ATCC 9374 purchased from PTCC (Persian Type Culture Collection, Tehran, Iran). Palmitic acid methyl ester, stearic acid methyl ester, oleic acid methyl ester, linoleic acid methyl ester, linolenic acid methyl ester were purchased from Sigma and were chromatographically pure. All other chemicals were obtained commercially and were of analytical grade.

2.2. R. oryzae whole cell biocatalyst preparation

Whole cell biocatalyst experiments were carried out using R. oryzae ATCC 9374, which has a 1,3-positional specify lipase. The culture medium contains in 1l tap water (its pH was initially adjusted to 5.6) were 70 g polypeptone (50 wt% pepton, 50 wt% trypton), 1 g NaNO3, 1 g KH2PO4, 0.5 g MgSO4.7H2O, and 30 g oil (refined olive, soybean and canola oil).

At first stage, R.oryzae grown on potato dextrose agar (PDA) slant. Erlen flask (500 ml) containing 100 ml of the basel medium were inoculated by aseptically transferring spores (about 106 spores) from slant, and incubated for 60–72 h at 35°C on a reciprocal shaker (150 oscillations/min) with 0.33 g BSPs subjected to prior sterilization. Reticulated Poly Urethane Foam (PUF) with a particle voidage of more than 97% and a pore size of 50 pores per linear inch used as BSPs. To examine the effect of BSPs size, these were cut into 6mm×6mm×3mm cuboids and 6mm cubes and added to basel medium. The R.oryzae cells became well immobilized within the BSPs as a natural result of their growth during shake-flask cultivation. After cultivation, the BSP-immobilized cells were separated from the culture broth by filtration, washed with tap water for few minutes, dried at 25°C temperature for 1 day, and for increase stability of lipase activity crosslinked with glutaraldehyde according to

Ban et al method [12]. In this way the dried cells were treated with a 0.1% (v/v) glutaraldehyde (GA) solution at 25°C for 1h then were shaken in phosphate buffer at 4°C for 5 min, washed with tap water for few minutes, and dried for 24 h at room temperature. Finally the GA-treated cells were used as a methanolysis catalyst.

2.3. Lipase-catalyzed transesterification

2.3.1. R.oryzae whole-cell biocatalyst

The methanolysis reactions have taken place at 35°C in a 50-ml erlen flask with incubation on a reciprocal shaker (150 oscillations/min). The reaction mixture contained: 9.65 g soybean oil, 0.1M phosphate buffer (pH 6.8) in range of 0–2.5 ml (0–25 wt.% water content by substrate weight), 0.1–1.0 g BSPs (1 – 10 wt%), 0.35 g methanol (One molar equivalent of methanol was 0.35 g against 9.65 g soybean oil) was added stepwise to the reaction mixtures three times at 0 and different hours after start of reaction. For full convert of oil to Fatty acid methyl esters, at least three molar equivalents of methanol are necessary.

2.3.2. Novozym 435 as a biocatalyst

The methanolysis reaction has taken place with the immobilized lipase from Candida antarctica (Novozym 435) in the solvent-free system in a 50-ml erlen flask at 35°C with incubation on a reciprocal shaker (150 oscillations/min). The reaction mixture contained 9.65 g soybean oil, 0.4 g immobilized lipase and 0.35 g methanol (without any distilled water) was added stepwise to the reaction mixtures three times at 0 and different hours after start of reaction.

2.4. Analytical procedure

The methyl esters contained in the reaction mixture was analyzed using a GC-3800CP gas chromatography (Varian Crop. Netherland) connected to a cpsil-5CB Capillary column (0.32mm×30 m, Varian, Netherland). Samples (200µl) were taken from the reaction mixture at specified time and centrifuged at 13,000 rpm for 5 min to obtain the upper layer. The methanolysis products were analyzed by capillary gas chromatography (cGC) as described below. The upper layer (80µl) and tricaprylin (20µl) which is served as the internal standard were precisely measured and mixed thoroughly in bottle with 2 ml hexane as solvent to which a small amount of anhydrous sodium sulfate as dehydrating agent were added. A 1.0 µl aliquot of the treated sample was injected into cGC. The column temperature was held at 150 °C for 1 min, raised to 200°C at rate of 20°C/min then raised to 207°C at rate of 1°C/min, finally raised to 300°C at rate of 30°C/min and maintained at this temperature for 24 min. The temperature for injector and flame ionization detector (FID) were set at 270 and 300°C, respectively.

3. Results and Discussion

3.1. Effect of BSPs size

To examine the effect of BSPs size on methanolysis of soybean oil, PUFs cut into 6mm×6mm×3mm cuboids and 6mm cubes and added to basel medium in different erlen flasks. After preparation as mention above, these cuboids and cubes use as BSPs and 50 BSPs added to reaction mixture in present of 15 wt% water. Table 1 presents data on the methanolytic activity of the different size of BSP-immobilized cells after adding methanol in start of reaction. Results indicated that in case of using 6mm×6mm×3mm immobilized BSPs methyl esters production is greater than 6mm cubes BSPs because of the specific surface area

in 6mm×6mm×3mm BSPs is larger than other one. Therefore 6mm×6mm×3mm immobilized BSPs was used for this research study.

Table 1. Methyl esters production (Wt%) in different size of BSPs

Time(h)	6mm×6mm×3mm BSPs	6mm×6mm×6mm BSPs
4	29	21
8	30	27
12	32	31

3.2. Effect of carbon sources in basel medium

To elucidate the effect of carbon source on cell growth and methyl esters production, various refined oils were used as carbon sources in basel medium. Figure 1 shows the time course of methanolysis catalyzed by cells grown with different carbon sources. As shown in figure 1, we can see that during whole cell catalyzed methanolysis of soybean oil for biodiesel production, the cells cultured with refined olive oil have highest activity than cells cultivated with refined soybean and canola oils. So the experiments continued using olive oil as carbon source in basel medium.

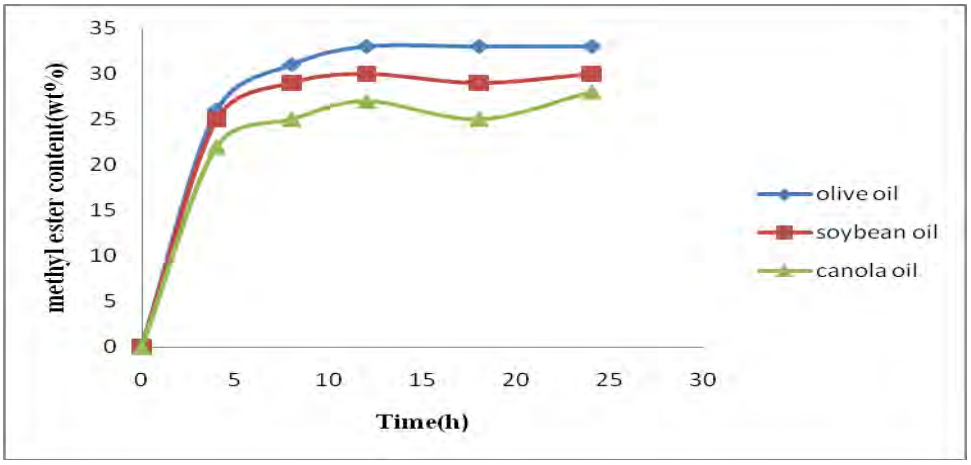

Fig. 1. Methyl ester content in methanolysis of soybean oil at different carbon source in cell cultivates (50 BSPs as a catalyst and reaction temperature at 35°C).

3.3. Effect of Emulsification of reaction mixture

To examine the effect of emulsifying of reaction mixture over producing methyl esters, ultrasonicated and non-ultrasonicated reaction mixtures were used for methanolysis of soybean oil. Figure 2 shows the time course of methyl esters content in reaction mixture with ultrasonicated and non-ultrasonicated feed. When the reaction mixture was emulsified before methanolysis, higher lipase activity was achieved. Because the lipase catalysis occurs in the interfacial layer between the hydrophobic and hydrophilic phases, the much larger surface area of the water/oil interface seems to result in increased accessibility of the substrates to the lipase [14]. This finding suggested that emulsification of the reaction mixture has an advantageous effect on biodiesel production using whole-cell biocatalyst. Further experiments were therefore made use of emulsified substrates.

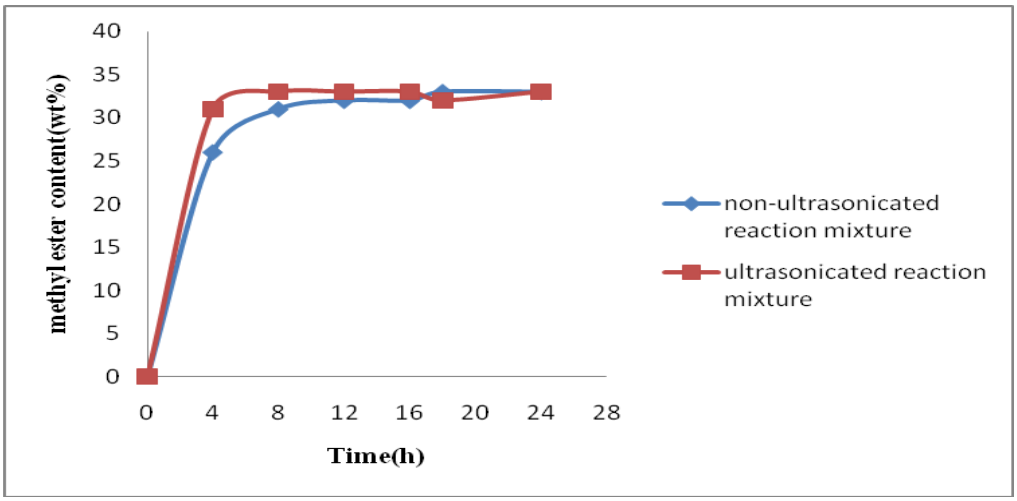

Fig. 2. Methyl ester content in methanolysis of soybean oil using ultrasonicated and non-ultrasonicated reaction mixtures (50 BSPs as a catalyst and reaction temperature at 35°C).

3.4. Effect of water content and weight of biocatalyst in reaction mixture

Figure 3 shows the activities of whole-cell biocatalyst at different water content and weight of biocatalyst. As shown in Figure 3 biodiesel achieved in the reaction mixture (after 96 h) increasing with increase in water content ratio up to 15 wt% and decreasing after that ratio. Therefore the optimum water content for Rhizopus oryzae whole cell was obtained as 15% that confirm results indicated by ban et al [12] whereas this parameter is limited the activity of Novozym 435 for methanolysis reaction since needs closely anhydrous reaction mixture [13]. Shimada et al [14] reported that water content (>500 ppm) in soybean oil decreased the rate of methyl ester production using Novozym 435 as biocatalyst. An insufficient amount of water in whole-cell biocatalyst methanolysis probably results in irreversible inactivation of lipase, which may be due to denaturation of the enzyme by methanol [15]. Moreover, figure 3 shows that by increasing weight of BSPs up to 7 wt%, methyl esters production increased and remained approximately constant up to BSPs amount of 10 wt%.

The highest methyl ester content (after 96 h); 84 wt%, was attained when the reaction mixture contained 1.5 ml buffer solution (15 wt% water by substrate to weight) and 0.7 g BSPs (7 wt.% BSPs by substrate to weight) which is remarkably comparable with methyl esters production using Novozym 435 as a biocatalyst. Since alkyl migration happens with intracellular lipase of immobilized cell and water can enhance cell permeability, the rate of methanolysis catalyzed by *R.oryzae* whole-cell biocatalyst increases in the presence of additional water. However, the excess water reduces methyl esters production due to its acts as a competitive inhibitor for lipase-catalyzed transesterification [16]. Subsequent experiments were therefore carried out using a 15 wt% water content and 7 wt% BSPs in reaction mixture.

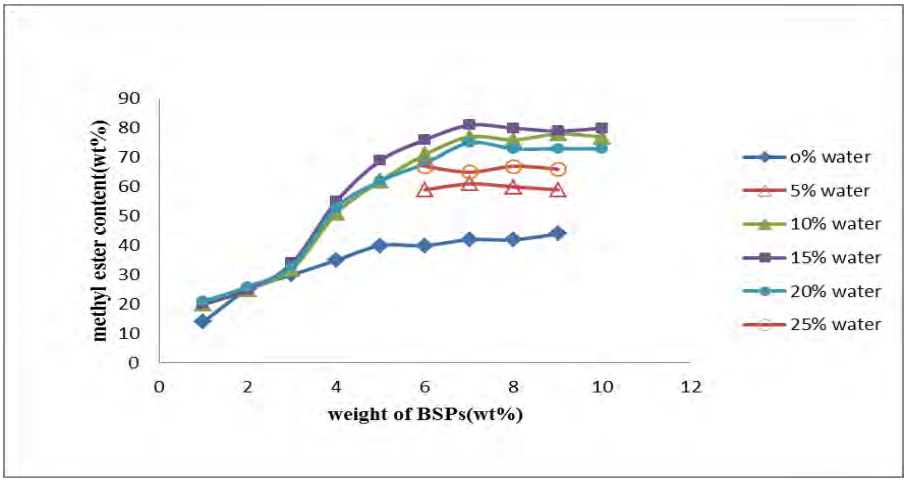

Fig. 3. Methyl ester content in methanolysis of soybean oil at different water content and weight of BSPs after 96 h (addition of methanol 0, 24, 48 h and reaction temperature at 35°C).

3.5. Time course methanolysis of soybean oil and optimization of methanol addition strategy

In this part the authors investigated the time course methanolysis of soybean oil with stepwise additions of methanol in 0, 24 and 48 h. Figure 4 shows the time courses of methyl esters production in different time after reaction started. As shown in figure 4, reaction continues up to 96 hours that is relatively long time while at the time such as 4 to 24 h and 36 to 48 h the methyl esters production had not much progress. The highest methyl ester content, 84 wt.%, was attained after 96 h. In order to reduce time of reaction progress, we tried to optimize the addition strategy of methanol. So the methanol was added in different strategy as stepwise additions of methanol in 0, 4 and 18 h after reaction. Figure 5 shows the time courses of methyl esters production using this new strategy of methanol addition. As shown in figure 5, 84 wt.% methyl esters production was attained after 48 h reaction.

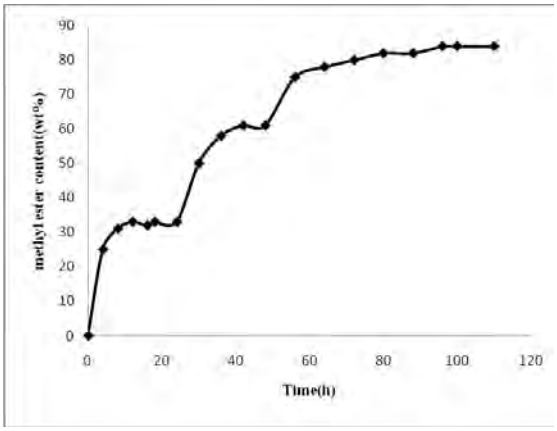

Fig. 4. Methyl ester content in methanolysis of soybean oil (addition of methanol at 0, 24 and 48 h).

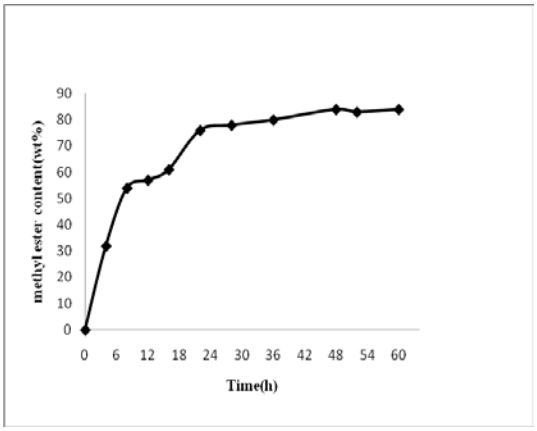

Fig. 5. Methyl ester content in methanolysis of soybean oil with new strategy (addition of methanol at 0, 4 and 18 h).

3.5. Enzymatic methanolysis reaction using Novozym 435 as a biocatalyst

For the methanolysis reaction using immobilized lipase from *Candida antarctica* (Novozym 435) in the solvent-free system, 0.35 g methanol was added stepwise to the reaction mixtures at the start of the reaction (0), 4 and 18 h. The reaction has been carried out for 48 h. The

methyl ester content in the reaction mixture reached 90 wt% after 48 h that was slightly more than *R.oryzae* whole-cell biocatalyst.

3.6. Stability study of BSP-immobilized cells with GA treatment and Novozym 435 for methanolysis of soybean oil

In order to test the stability of Novozym 435 (stepwise addition of 1 molar equivalent methanol at 0, 4, and 18 h respectively) and GA treated *R.oryzae* whole-cell as biocatalyst with new methanol addition strategy (stepwise addition of 1 molar equivalent at 0, 4, and 18 h respectively), both the biocatalysts were separated from the reaction mixture by filtration and directly used for the next cycle. The time of methanolysis using *R.oryzae* whole-cell and Novozym 435 are kept constant at 48 h for each reaction cycle (as shown in figure 6). It was found that there was almost no significant decrease in methyl esters production even after 5 batches cycle in both lipases and both can be used for repeated batches cycles.

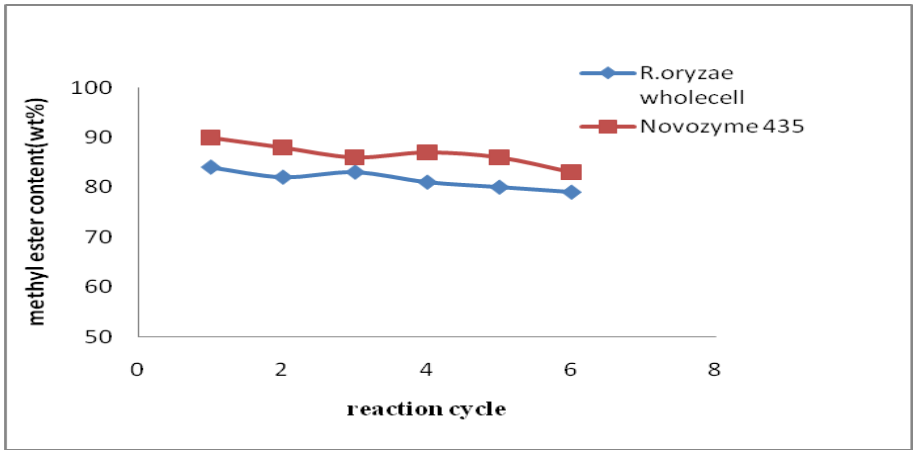

Fig. 6. Methyl ester content in methanolysis of soybean oil using GA treated R.oryzae whole-cell and Novozym 435 as biocatalyst for repeated reaction cycles (addition of methanol in 0, 4 and 18 h).

4. Conclusions

This work deals with the enzymatic transesterification of refined soybean oil using *Rhizopus Oryzae* (ATCC 9374) whole-cell biocatalyst and Novozym 435 (Commercial immobilized lipase from *Candida antarctica*) as biocatalyst. In the case of using whole-cell biocatalyst effect of BSPs size, carbon sources in basel medium, emulsification of reaction mixture, water content and weight of biocatalyst in reaction mixture on yield of biodiesel production were investigated. The maximum methyl esters content in the reaction mixture reaches 84 wt% using *Rhizopus oryzae* whole-cell biocatalyst in optimum condition of reaction after 48 h which is remarkably comparable with biodiesel yield 90 wt% of Novozym 435. The optimum water content for *Rhizopus oryzae* was obtained as 15% whereas this parameter is limited the activity of Novozym 435 for methanolysis. Both the lipases can be used for repeated batches cycles. These findings indicate that, given the simplicity of the lipase production process and the long-term stability of lipase activity, the use of whole-cell biocatalysts immobilized within BSPs and treated with GA solution suggest a favorable means of biodiesel fuel production for industrial application.

References

[1] M. S. Antczak, A. Kubiak, T. Antczak, S. Bielecki, Enzymatic biodiesel synthesis – Key factors affecting efficiency of the process, Renewable Energy 34, 2009, 1185–1194.

[2] H. Fukuda, A. Kondo, H. Noda, Biodiesel fuel production by transesterification of oils, J. Biosci. Bioeng. 92, 5, 2001, 405–416.

[3] P. S. Bisen, B. S. Sanodiya, G. S. Thakur, R. K. Baghel, G. B. K. S. Prasad, Biodiesel production with special emphasis on lipase-catalyzed transesterification, Biotechnology Letters 32, 2010, 8, 1019-1030.

[4] H. Fukuda, S. Hama, S. Tamalampudi and H. Noda, Whole-cell biocatalysts for biodiesel fuel production, Trend in biotechnology 26, 2008, 12, 668-673.

[5] A. Robles-Medina, P.A. González-Moreno, L. Esteban-Cerdán, E. Molina-Grima, Biocatalysis: Towards ever greener biodiesel production, Biotechnology Advances 27, 2009, 398–408.

[6] Y. Shimada, Y.Watanabe, T. Samukawa, A. Sugihara, H. Noda, H. Fukuda, Y. Tominaga, Conversion of vegetable oil to biodiesel using immobilized Candida antarctica lipase, J. Am. Oil Chem. Soc. 76, 1999, 789–793.

[7] Y. Xu, W. Du, D. Liu, J. Zeng, A novel enzymatic route for biodiesel production from renewable oils in a solvent-free medium, Biotechnology Letters 25, 2003, 1239–1241.

[8] W. Du, Y. Xu, D. Liu, J. Zeng, Comparative study on lipase-catalyzed transformation of soybean oil for biodiesel production with different acyl acceptors, J. Mol. Catal. B: Enzym. 30, 2004, 125–129.

[9] S. V. Ranganathan, S. L. Narasimhan, K. Muthukumar, An overview of enzymatic production of biodiesel", Bioresource Technology 99, 2008, 3975–3981.

[10] Ting Sun, Wei Du and Dehua Liu, Prospective and impacts of whole cell mediated alcoholysis of renewable oils for biodiesel production, Biofuels, Bioprod. Bioref. 3, 2009, 633–639.

[11] K. Ban, S. Hama, K. Nishizuka, M. Kaieda, T. Matsumoto, A. Kondo , H. Noda, H. Fukuda, Repeated use of whole-cell biocatalysts immobilized within biomass support particles for biodiesel fuel production, Journal of Molecular Catalysis B: Enzymatic 17, 2002, 157–165.

[12] K. Ban, M. Kaieda, T. Matsumoto, A. Kondo, H. Fukudac, Whole cell biocatalyst for biodiesel fuel production utilizing Rhizopus oryzae cells immobilized within biomass support particles, Biochemical Engineering Journal 8, 2001, 39–43.

[13] S. Tamalampudi, M. R. Talukder, S. Hama, T. Numata, A. Kondo, H. Fukuda, Enzymatic production of biodiesel from Jatropha oil: A comparative study of immobilized-whole cell and commercial lipases as a biocatalyst, Biochemical Engineering Journal 39, 2008, 185–189.

[14] Y. Shimada, Y. Watanabe, A. Sugihara, Y. Tominaga, Enzymatic alcoholysis for biodiesel fuel production and application of the reaction to oil processing, J. Mol. Catal. B: Enzym. 76, 2002, 133–142.

[15] S. Hama, H. Yamaji, T. Fukumizu, T. Numata, S. Tamalampudi , A. Kondo, H. Noda, H. Fukuda, Biodiesel-fuel production in a packed-bed reactor using lipase-producing Rhizopus oryzae cells immobilized within biomass support particles, Biochemical Engineering Journal 34, 2007, 273–278.

[16] R.H. Valivety, G.A. Johnston, C.J. Suckling, P.J. Halling, Solvent effects on biocatalysis in organic systems: equilibrium position and rates of lipase-catalysed esterification, Biotechnol. Bioeng. 38, 1991, 1137–1143.

Methyl ester production from chicken fat with high FFA

Ertan Alptekin [1, 2], Mustafa Canakci [1, 2, *], Huseyin Sanli [2, 3]

[1] *Department of Automotive Engineering Technology, Kocaeli University, 41380 Izmit, Turkey*
[2] *Alternative Fuels R&D Center, Kocaeli University, 41275 Izmit, Turkey*
[3] *Golcuk Vocational High School, Kocaeli University, 41650 Golcuk, Turkey*
**Corresponding author; Tel: +90 262 303 22 85, Fax: +90 262 303 22 03, E-mail: mustafacanakci@hotmail.com*

Abstract: In biodiesel production, to use low cost feedstock such as rendered animal fats may reduce the biodiesel cost. One of the low cost feedstock is the chicken fat for biodiesel production. However, chicken fats often contain significant amounts of free fatty acid (FFA) which cannot be converted to biodiesel using an alkaline catalyst due to the formation of soap. Therefore, the FFA level should be reduced to desired level (below 1%) by using an acid catalyst before transesterification. For this aim, sulfuric, hydrochloric and sulfamic (amidosulphonic) acids were used for pretreatment reactions and the variables affecting the FFA level were investigated by using the chicken fat with 13.45% FFA. After reducing the free fatty acid level of the chicken fat to less than 1%, the transesterification reaction was completed with an alkaline catalyst. Potassium hydroxide, sodium hydroxide, potassium methoxide and sodium methoxide were used as catalyst and methanol was used as alcohol for transesterification reactions. The effects of catalyst type, reaction temperature and reaction time on the fuel properties of methyl esters were investigated. In terms of high ester yield, the measured fuel properties of the chicken fat methyl ester met EN 14214 and ASTM D6751 biodiesel specifications.

Keywords: *Biodiesel, Low cost feedstock, Chicken fat, Transesterification*

1. Introduction

Biodiesel which can be produced from vegetable oils and animal fats is an alternative fuel for diesel engines. Biodiesel is nontoxic, biodegradable and environmentally friendly fuel. Biodiesel contains almost no sulfur and does not contribute to greenhouse gases due to its closed carbon cycle [1]. The major component of oils and fats is triglycerides which compose about 90-98% of total mass [2]. Transesterification is a chemical process of reacting triglycerides with alcohol in the presence of a catalyst. If the reaction is not completed, then there will be mono-, di- and triglycerides left in the reaction mixture [3-5]. Alcohols such as methanol, ethanol or butanol can be used in the transesterification [5, 6]. The most preferred alcohol used in biodiesel production. The most commonly preferred catalysts are sulfuric, sulphonic, and hydrochloric acids as acid catalysts, and sodium hydroxide (NaOH), sodium methoxide (NaOMe), potassium hydroxide (KOH) and potassium methoxide (KOMe) as alkaline catalyst [7]. Water is formed when KOH and NaOH are used to produce the methoxide. Water limits the completion of transesterification reaction. Therefore, industrial biodiesel processes run on alkoxides such as NaOMe and KOMe which can be bought as liquid form. They do not contain water and are usually commercially available as ready-to-use methanol solution [8]. NaOMe is offered as a 30% or 25% methanol solution and KOMe as a 32% methanol solution whereas NaOH and KOH are offered as solids and not premixed in methanol [9].

The most common feedstock of biodiesel is rapeseed oil in Europe and soybean oil in the United States of America [10]. The major handicap is the high cost of biodiesel for its commercialization. Chicken fat is a low cost feedstock for biodiesel production compared to high-grade vegetable oils. It is extracted from feather meal which is prepared from chicken wastes such as chicken feathers, blood, offal and trims after rendering process. Feather meal contains significant amount of chicken fat. The fat content of the feather meal varies from 2 to

12% depends on the kind of used feathers [11, 12]. However, they often contain significant amounts of free fatty acid (FFA). The fats with high FFA cannot be converted to biodiesel using alkaline catalysts. FFAs react with an alkaline catalyst and thus soaps are produced by this reaction. Soaps prevent the separation of the ester, glycerin, and wash water [13]. Acid catalysts are too slow to be suitable for converting triglycerides to biodiesel. However, they appear to be quite effective at converting FFAs to esters [14]. For these reasons, an acid catalyst can be used to esterify the FFAs to esters. The acid-catalyzed process is called as pretreatment. FFAs are converted to monoesters through the pretreatment of the feedstock with high FFA and thereby the FFA level reduces. The major handicap for the acid-catalyzed esterification of FFAs is the water formation. The water formation is the primary mechanism limiting the completion of the acid catalyzed esterification reaction with FFAs [13]. After pretreatment, the pretreated feedstock can be transesterified with an alkali catalyst to convert the triglycerides to esters [15-17]. Some researchers [18, 19] stated that the feedstock should not contain more than 1% FFA for alkaline catalyzed transesterification reactions, whereas some researches [1] stated that an alkaline catalyst can be used in the transesterification up to the FFA level of 5%, but it reduces the biodiesel yield.

Many researchers have investigated the availability of animal fats and waste oils for biodiesel production. However, few researchers have studied on the chicken fat especially with high FFA. Mattingly [20] produced biodiesel from chicken fat with 2.3% FFA. He concluded that it was needed to perform a pretreatment reaction to get high biodiesel yield. Bhatti et al. [21] obtained high ester yields up-to 99% from chicken fat after 24 h in the presence of sulfuric acid. Kondamudi et al. [11] chosed the chicken fat for biodiesel production. They used potassium hydroxide to remove FFA in the form of soap. After separating the soap, the optimization of transesterification parameters was researched. They obtained good results and managed to produce biodiesel whose fuel properties were suitable for American Society of Testing and Materials (ASTM) biodiesel standards. Schulte [22] investigated optimum reaction parameters for biodiesel production from chicken fat. He obtained high biodiesel yields up-to 91% by using supercritical methanol. The purpose of the present study was to produce biodiesel from chicken fat with high FFA. Therefore, the optimization of pretreatment reaction was investigated with different acid catalysts to reduce FFA level (below 1%) of chicken fat. The effects of catalyst type, catalyst amount, alcohol molar ratio and reaction time on the FFA level were also analyzed. After the optimum pretreatment parameters were determined, the transesterification reaction was carried out with an alkaline catalyst to produce biodiesel. The optimization of biodiesel production from the chicken fat was investigated with different alkaline catalysts, reaction temperatures and reaction times. The obtained esters were characterized by determining its fuel properties according to the standard test methods. The obtained products were named as chicken fat methyl ester (CFME) because all fuel properties in the standards were not measured.

2. Materials and method

In this study, chicken fat was obtained from Şenpiliç Chicken Slaughterhouse in Sakarya, TURKEY. The chicken fat was subjected to a heating at 110°C for one hour to remove water and then filtered to remove the insoluble materials. The FFA level of the rendering plant feedstock is generally between 5% and 25% [14]. The researchers have suggested that the FFA level of the feedstock should be reduced to less than 1% before using an alkaline catalyst [18, 19]. This was the initial target for the pretreatment. The chicken fat used in this study had an acid value of 26.89 mg KOH/g which corresponds to FFA level of about 13.45%. Because the acid value of the chicken fat was greater than 2 mg KOH/g, it was needed to perform a

pretreatment to the feedstock. Some properties and fatty acid composition of the chicken fat are shown in Tables 1 and 2, respectively.

Table 1. Some properties of chicken fat

Properties	Unit	Chicken Fat
Density (at 15°C)	$kg.m^{-3}$	932
Viscosity (at 40°C)	$mm^2.s^{-1}$	59.2
Acid Number	mg $KOH.g^{-1}$	26.89
Heat of Combustion	$kJ.kg^{-1}$	39407
Water Content	% mass	0.3

Table 2. Fatty acid composition of chicken fat

Fat	Fatty acid composition (%)						
	C16:0	C16:1	C18:0	C18:1	C18:2	C18:3	C20:4
Chicken	19.82	3.06	6.09	37.62	31.59	1.45	0.37

2.1. Pretreatment Process

Sulfuric acid (Merck), hydrochloric acid (Merck) and sulfamic acid (Merck) were used as catalyst and methanol was used as alcohol for the pretreatment of chicken fat. The esterification process of FFAs was repeated for different alcohol molar ratios, amounts of acid catalysts based on the weight of FFAs and reaction times at 60°C. In the calculations, the molecular weight of FFA was obtained from the reference [22]. The experiments were performed in a laboratory scale apparatus. The chicken fat was added into the reaction flask equipped with reflux condenser, magnetic stirrer and thermometer, and then it was heated. When the temperature reached to 60°C, the alcohol/catalyst mixture was added into the fat. The final mixture was stirred for the desired reaction time at 60°C. The mixture was settled overnight and two phases were formed after the pretreatment. The upper phase consists of a mixture of methanol, sulfuric acid and water whereas the lower phase mainly consists of chicken fat and esterified FFAs. The upper phase was removed. After this step, the lower phase was subjected to a heating at 110°C for one hour to remove any remaining alcohol and water. And then, the acid value of the fat-ester mixture was measured and recorded.

2.2. Transesterification Process

In this study, potassium methoxide solution (32% in methanol) and sodium methoxide solution (30% in methanol) were supplied from Evonik Industries in Germany. These alkoxides, potassium hydroxide (Carlo Erba) and sodium hydroxide (Merck) were used as the catalysts for transesterification reactions to investigate the effect of catalyst type on the fuel properties of biodiesel. Molar ratio between alcohol and fat-ester mixture was 6:1 for the transesterification reaction. The catalyst amount was selected as 1% of the weight of the initial amount of fat in the chicken fat and the neutralization amount which was calculated from the reference [3] for KOH and NaOH catalyst whereas the catalyst amounts were (FFA% x 0.64) + 1.7% and (FFA% x 0.78) + 2.0% for NaOMe and KOMe catalysts, respectively. The catalyst amounts for NaOMe and KOMe were calculated according to the manufacturer recommendation. In the calculations for transesterification, the molecular weight of chicken fat was obtained from the reference [22]. The transesterification process and laboratory apparatus were the same as those of pretreatment experiments except for catalyst. The reaction temperature was selected as 25°C and 60°C, and reaction time was selected as one, two and four hours. After the transesterification reaction, the glycerin layer was separated in a separating funnel and the ester layer was washed with warm water. After

washing, the methyl ester was subjected to a heating at 110°C to remove excess alcohol and water, and then filtered. The obtained methyl esters were characterized in the Fuel Laboratory of the Department of Automotive Engineering Technologies and Alternative Fuels R&D Center in Kocaeli University.

3. Results and discussion

Some researchers [14, 16] tried to reduce high FFA level of the feedstock by two step pretreatment process. After the first treatment, the reaction mixture is allowed to settle. Since the water formation when the FFAs are converted to esters inhibits the reaction, the methanol-water mixture is separated from the oil phase. Then, additional methanol and acid catalyst can be added and the reaction continued for the second step. Increasing the number of pretreatment steps reduces the ester yield due to the solubility of the fat and ester in methanol [15]. Therefore, in this study, it was tried to reduce the FFA level by one step pretreatment to get high ester yield and save time for producing biodiesel.

3.1. Pretreatment of the Chicken Fat with Sulfuric Acid

Sulfuric acid was selected as reference catalyst. The esterification process was repeated for different alcohol molar ratios (10:1, 15:1, 20:1, 25:1, 30:1) and amounts of sulfuric acid (3%, 6%, 15%, 20%, 35%) based on the FFA level of the chicken fat for one hour reaction at 60°C. The initial experiments were performed with 3% and 6% catalyst at different methanol molar ratios. Good results were not obtained when using 3% and 6% sulfuric acid, and methanol molar ratios from 10:1 to 30:1 for one hour reaction at 60°C. The FFA level was only reduced to 11.25% when using 6% sulfuric acid and methanol molar ratio of 30:1. Therefore, greater amount of sulfuric acid and methanol molar ratio were used. The reaction conditions of the next pretreatments were two different methanol molar ratios of 20:1 and 30:1, and three different sulfuric acid amounts of 15%, 20% and 35% for one hour reaction at 60°C. The FFA level of the chicken fat decreased with rising of sulfuric acid amount and methanol ratio in the pretreatment reaction. The FFA level was reduced to 6.26%, 2.27% and 1.20% for 15%, 20% and 35% sulfuric acid with methanol molar ratio of 20:1, respectively. The aim of the pretreatment reaction was to decrease the FFA level from 13.45% to less than 1%. Therefore, the methanol ratio was raised to 30:1. In this case, the FFA level decreased to 4.92%, 1.40% and 1.04% for 15%, 20% and 35% sulfuric acid, respectively.

3.2. Pretreatment of the Chicken Fat with Hydrochloric Acid

The pretreatments were repeated with 6%, 15% and 20% hydrochloric acid and methanol molar ratio of 20:1 and 30:1 for one hour reaction at 60°C. Six percent of hydrochloric acid was not effective in decreasing the FFA level of the chicken fat with methanol molar ratios 20:1 and 30:1 for one hour reaction at 60°C such as in sulfuric acid experiments. The FFA level was only reduced to 12.99% and 12.46% with using 6% hydrochloric acid for methanol molar ratio of 20:1 and 30:1, respectively. Consequently, the catalyst amount was raised to 15% and 20%. The FFA level of the chicken fat was reduced to 5.26% and 2.83% for 15% and 20% hydrochloric acid at methanol molar ratio of 20:1, respectively. The FFA level of the chicken fat was strongly affected by the molar ratio of methanol. With using methanol molar ratio of 30:1, the FFA level was reduced to 3.89% and 1.67% for 15% and 20% hydrochloric acid, respectively. The FFA level of the chicken fat was decreased to about 1% when using 20% hydrochloric acid and methanol molar ratio of 30:1. The pretreatment results with sulfuric and hydrochloric acids were very close to each other. The differences of FFA level were only 0.56% and 0.27% for 20% acid catalyst with methanol molar ratio of 20:1 and 30:1, respectively.

3.3. Pretreatment of the Chicken Fat with Sulfamic Acid

The third acid catalyst which was used for esterification of FFAs was sulfamic acid in this study. Sulfamic acid is slightly soluble in methanol. For this reason, it needs to be heated to prepare a mixture of alcohol-acid catalyst. The esterification process was repeated for 6% sulfamic acid and alcohol molar ratios of 20:1 and 30:1. Six percent of sulfamic acid did not affect the FFA level of the chicken fat significantly with methanol molar ratios of 20:1 and 30:1 for one hour reaction at 60°C. The FFA level was only reduced to 12.78% and 12.32% when using 6% sulfamic acid for methanol molar ratio of 20:1 and 30:1, respectively. Therefore, the catalyst amount was raised to 15% with methanol molar ratio of 30:1 for one hour reaction at 60°C. But, satisfactory results were not reached with 15% sulfamic acid. The FFA level was only reduced to 11.97%. For this reason, the pretreatment was not continued with sulfamic acid.

3.4. Effect of Reaction Time on the FFA Level of Chicken Fat with Sulfuric Acid

According to the results, sulfuric acid gave the best results among the three acid catalysts used in this study. The initial target was to reduce the FFA level of the chicken fat less than 1%. Thirty-five percent of sulfuric acid was better than 20% for converting FFAs to monoesters. However, the loss of feedstock after the pretreatment was the highest for 35% sulfuric acid. Lower feedstock amount means lower biodiesel yield after transesterification. For this reason, 20% sulfuric acid was selected as acid catalyst amount. Beside, methanol molar ratio was raised to 40:1 to decrease the FFA level below 1%. The effect of reaction time on the FFA level of the chicken fat was investigated. Reaction time was chosen as 60, 70 and 80 minutes at 60°C in these pretreatments. The FFA levels of the chicken fat were 0.93%, 0.80% and 0.67% for 60, 70 and 80 minutes with 20% sulfuric acid and methanol molar ratio of 40:1, respectively. The FFA level decreased below 1% for these three experiments. The pretreatment with 20% sulfuric acid and methanol molar ratio of 40:1 for 80 minutes at 60°C was thought to be sufficient for reducing FFA level less than 1% to get high ester yield after transesterification. Thus, these reaction parameters were selected for pretreatment.

3.5. Characterization of Fuel Properties after Transesterification

After pretreatment reaction, the FFA level of the chicken fat was 0.67% which is sufficient to complete the reaction with alkaline catalysts. The effects of variables such as catalyst type, reaction temperature and reaction time on the fuel properties of the CFMEs were investigated. The gathered ester yield results are shown in Table 3. The ester yield increased with the increasing reaction temperature from 25°C to 60°C for all esters. But the ester yield did not change significantly with the increasing reaction time. In this study, the minimum and maximum ester yields were 71.3% (at four-hour, 25°C and NaOH catalyzed reaction) and 88.5% (at one-hour, 60°C and KOMe catalyzed reaction), respectively. The total-free glycerin, mono-, di- and triglyceride results are illustrated in Table 3. Standard total glycerin results were obtained only when using KOH and NaOH in the transesterification. Better total glycerin results were determined for NaOH catalyzed reactions compared to KOH. However, the ester yield was significantly lower for NaOH catalyzed reactions. Free glycerin results show that it is not directly affected by reaction parameters. Mono-, di and triglyceride values generally reduced with increasing reaction time at 25°C. But, these values show different changes at 60°C because of reversible reaction.

*Table 3. Fuel properties of produced CFMEs **

1	2	3	4	5	6	7	8	9	10	11	12	13	14	15	16	17
a	25	1	886	1	170	0.04	4	40.1	0.49	0.03	0.71	0.82	1.50	0.30	5.4	80.2
a	25	2	885	1	171	0.11	3	40.3	0.35	0.03	0.56	0.54	0.90	0.29	5.2	82.1
a	25	4	884	1	172	0.13	3	40.3	0.16	0.03	0.40	0.03	0.20	0.25	5.1	84.8
a	60	1	885	1	171	0.01	2	40.2	0.20	0.03	0.55	0.03	0.27	0.25	5.1	88.1
a	60	2	884	1	171	0.01	2	40.2	0.19	0.04	0.45	0.11	0.14	0.24	5.0	87.6
a	60	4	883	1	172	0.01	2	40.2	0.19	0.02	0.56	0.09	0.12	0.22	4.9	87.4
b	25	1	885	1	170	0.12	3	40.1	0.05	0.02	0.01	0.13	0.06	0.30	5.4	72.8
b	25	2	885	1	172	0.06	2	40.1	0.08	0.03	0.16	0.01	0.04	0.29	5.3	71.7
b	25	4	884	1	172	0.03	2	40.2	0.07	0.02	0.16	0.01	0.03	0.24	5.2	71.3
b	60	1	885	1	171	0.20	2	40.1	0.10	0.02	0.31	0.01	0.02	0.28	5.2	79.1
b	60	2	884	1	172	0.08	2	40.2	0.12	0.01	0.41	0.01	0.01	0.24	5.1	78.4
b	60	4	883	1	172	0.09	2	40.3	0.15	0.01	0.55	0.01	0.02	0.23	4.9	77.3
c	25	1	891	1	170	0.02	4	40.0	NT	NT	NT	NT	NT	0.30	6.7	84.6
c	25	2	890	1	172	0.01	3	40.1	1.10	0.02	1.99	2.81	1.57	0.27	6.3	82.7
c	25	4	888	1	172	0.01	3	40.1	0.68	0.01	1.30	1.08	1.74	0.25	5.8	81.9
c	60	1	887	1	171	0.01	3	40.1	0.55	0.01	0.90	0.84	1.81	0.29	5.6	88.5
c	60	2	886	1	172	0.01	3	40.1	0.49	0.01	0.99	0.15	2.04	0.26	5.6	85.2
c	60	4	886	1	172	0.01	3	40.1	0.72	0.01	1.02	1.25	2.56	0.24	5.6	86.2
d	25	1	891	1	171	0.03	4	39.9	NT	NT	NT	NT	NT	0.30	6.8	75.8
d	25	2	890	1	171	0.12	3	40.1	1.07	0.02	1.50	2.23	3.31	0.28	6.2	79.1
d	25	4	888	1	172	0.05	3	40.1	0.71	0.04	1.23	1.58	1.18	0.25	5.9	80.3
d	60	1	886	1	171	0.20	2	40.2	0.50	0.02	0.96	0.70	1.32	0.26	5.4	85.9
d	60	2	886	1	173	0.12	2	40.2	0.58	0.01	0.94	0.91	1.94	0.25	5.5	85.3
d	60	4	885	1	173	0.15	2	40.1	0.44	0.01	1.52	0.04	0.34	0.22	5.5	88.3

*1: catalyst (a: KOH, b: NaOH, c: KOMe, d:NaOMe), 2: reaction temperature (°C), 3: reaction time (hour), 4: density (15°C, $kg.m^{-3}$), 5: copper strip corrosion (degree of corrosion), 6: flash point (°C), 7: methanol content (%), 8: pour point (°C), 9: heat of combustion ($MJ.kg^{-1}$), 10: total glycerin (%), 11: free glycerin (%) 12: monoglyceride (%), 13: diglyceride (%); 14: triglyceride (%), 15: acid number (mg $KOH.g^{-1}$), 16: viscosity (40°C, $mm^2.s^{-1}$), 17: ester yield (%)., NT: not tested.

Generally, the density of CFME decreases with increasing of reaction time and reaction temperature. There is no significant difference among the densities for transesterification reactions catalyzed with KOMe and NaOMe compared to KOH and NaOH. In general, the viscosity of CFME decreases with the increasing reaction time and reaction temperature. However, there is a significant difference among the viscosities when using KOMe and NaOMe catalysts compared to KOH and NaOH. The viscosities of CFMEs are higher for transesterification reactions catalyzed with KOMe and NaOMe. This situation can be explained with incomplete transesterification reaction. The methanol contents of CFMEs vary from 0.01% to 0.20% as seen in Table 3. It clearly shows that the methanol content values of biodiesel do not directly depend on transesterification reaction parameters. The flash points of CFMEs do not change mostly and range from 170°C to 173°C. The CFMEs produced in this study have high pour point. The minimum and maximum pour point is 2°C and 4°C, respectively. The acid value of pretreated chicken fat was 1.34 mg $KOH.g^{-1}$ and this value was reduced to 0.22 mg $KOH.g^{-1}$ after transesterification reaction. The maximum acid value was measured to be 0.30 mg $KOH.g^{-1}$ which is much below the required biodiesel standards.

The heat of combustion results are around 40 $MJ.kg^{-1}$ and they are slightly lower than those of petroleum diesel fuels. According to the results, there is no significant difference among the heat of combustion results depending on transesterification reaction parameters. The copper strip corrosion results gathered with each of CFME are the lowest level of corrosiveness (No 1a). This means that corrosion would not be a problem for CFMEs.

4. Conclusion

The objective of this study was to produce biodiesel from low-cost chicken fat with high FFA. The FFA level of the feedstock should be reduced to less than 1% before using the alkaline catalysis. For this aim, three acid catalysts were used in the pretreatment reactions and the variables affecting the acid value including alcohol molar ratio, acid catalyst amount and reaction time were investigated. After determining the optimum pretreatment conditions to reduce the FFA level of the chicken fat below 1%, the process was completed by using the alkaline catalysts. The effects of the variables on the fuel properties such as catalyst type, reaction temperature and reaction time were investigated. According to the results, the following conclusions can be drawn:

- The acid catalyst type and amount have effect to reduce the FFA level of the chicken fat in the pretreatment reaction. Sulfuric acid is the best catalyst for reducing FFA level among the acid catalysts used in this study. Low amount of acid catalyst (3% and 6%) is not effective for reducing FFA level of the feedstock for all acid catalysts.
- The FFA level of the chicken fat is strongly affected by the molar ratio of methanol, acid catalyst amount and reaction time. Sulfuric and hydrochloric acids give similar pretreatment results.
- Sulfamic acid does not have significant effect on the reduction of acid value of the chicken fat. The FFA level of the chicken fat with about 15% FFA may be reduced to below 1% when using 20% sulfuric acid and methanol molar ratio of 40:1 for 60, 70 and 80 minutes at 60°C. The ester yield increased with increasing reaction temperature.
- The viscosity and glyceride values of CFME decreased with increasing reaction temperature. The catalyst type especially affects viscosity and glyceride values.
- The fuel properties such as density, flash point, methanol content, pour point, heat of combustion, acid value and copper strip corrosion values did not change significantly with the reaction parameters.
- The required viscosity for EN 14214 standards was only obtained using KOH and NaOH at 60°C. KOH and NaOH are superior to KOMe and NaOMe with the catalyst amounts used in this study. But, the effect of catalyst amounts for KOMe and NaOMe on the fuel properties should be investigated for further studies.
- The measured fuel properties of the CFME met both the ASTM D6751 and EN 14214 biodiesel standards when using KOH and NaOH at 60°C for a four-hour reaction.

References

[1] Van Gerpen JH. Biodiesel processing and production. Fuel Processing Technology 2005;86:1097-1107.

[2] Srivastava A, Prasad R. Triglycerides-based diesel fuels. Renewable Sustain. Energy Rev. 2000;4:111-33.

[3] Van Gerpen JH, Shanks B, Pruszko R, Clements D, Knothe G. Biodiesel production technology. National Renewable Energy Laboratory Report, NREL/SR-510-36244, 2004.

[4] Darnoko D, Cheryan M. Kinetics of palm oil transesterification in a batch reactor. JAOCS 2000;77(12):1263-67.

[5] Canakci M. The potential of restaurant waste lipids as biodiesel feedstocks. Bioresource Technology 2007;98:183-90.

[6] Sanli H, Canakci M. Effects of different alcohol and catalyst usage on biodiesel production from different vegetable oils. Energy and Fuels 2008;22:2713-19.

[7] Sridharan R, Mathai MI. Transesterification reactions. 1974;33(4):178-87.

[8] Van Gerpen JH, Peterson CL, Goering CE. Biodiesel: An alternative fuel for compression ignition engines. American Society of Agricultural and Biological Engineers Distinguished Lecture Series 2007;31:1-22.

[9] Ruwwe, J. Metal alkoxides as catalysts for the biodiesel production. Chemistry Today 2008:26(1);26-28.

[10] Canakci M. Combustion characteristics of a turbocharged DI compression ignition engine fueled with petroleum diesel fuels and biodiesel. Bioresource Technology 2007;98:1167-75.

[11] Kondamudi N, Strull J, Misra M, Mohapatra SK. A green process for producing biodiesel from feather meal. J. Agric. Food Chem. 2009;57:6163-66.

[12] Dale N. True metabolizable energy of feather meal. J. Appl. Poult. Res. 1992;1:331-34.

[13] Canakci M, Van Gerpen JH. Biodiesel production via acid catalysis. Trans. of ASAE 1999;42(5):1203-10.

[14] Canakci M, Van Gerpen JH. Biodiesel production from oils and fats with high free fatty acids. Trans. of ASAE 2001;44(6):1429-36

[15] Canakci M. Production of biodiesel from feedstocks with high free fatty acids and its effect on diesel engine performance and emissions. Ph.D. Dissertation, Iowa State University (2001).

[16] Ghadge SV, Raheman H. Biodiesel production from mahua (madhuca indica) oil having high free fatty acids. Biomass and Bioenergy 2005;28:601-5.

[17] Tiwari AK, Kumar A, Raheman H. Biodiesel production from jatropha oil (jatropha curcas) with high free fatty acids: an optimized process. Biomass and Bioenergy 2007;31:569-75.

[18] Freedman B, Pryde EH, Mounts TL. Variables affecting the yields of fatty ester from transesterified vegetable oils. JAOCS 1984;61(10):1638-43.

[19] Liu K. Preparation of fatty acid methyl esters for gas-chromatographic analysis of lipids in biological materials. JAOCS 1994;71(11):1179-87.

[20] Mattingly BG. Production of biodiesel from chicken fat containing free fatty acids. Master of Science Thesis, University of Arkansas (2006).

[21] Bhatti HN, Hanif MA, Qasim M, Rehman A. Biodiesel production from waste tallow. Fuel 2008;87:2961-66.

[22] Schulte WB. Biodiesel production from tall oil and chicken fat via supercritical methanol treatment. Master of Science Thesis, University of Arkansas (2007).

Optimization on the use of crude glycerol from the biodiesel production to obtain poly-3-hydroxybutyrate

John A. Posada[1], Juan C. Higuita[1,*], Carlos A. Cardona[1]

[1] *Universidad Nacional de Colombia sede Manizales. Colombia-S.A.*
** Corresponding author, Tel: +57-6-8879300 ext: 55880, Email: jchiguitav@unal.edu.co.*

Abstract: The biotechnological production of poly-3-hydroxybutyrate (PHB) from crude glycerol obtained during the biodiesel production was techno-economically assessed. For the fermentation process, two different strains, *Cupreavidus necator* and *Bacillus megaterium* were considered. Moreover, three downstream processes for PHB separation and purification were analyzed. Thus, in total six biotechnological schemes to transform the crude glycerol obtained in the biodiesel industry were compared. Each biotechnological scheme considered five main process stages namely: (*i*) glycerol purification, (*ii*) glycerol fermentation to PHB, (*iii*) mass cell pretreatment, (*iv*) PHB isolation, and (*v*) PHB purification. Aspen Plus and Aspen Icarus were used for the processes simulation and for the economic assessment, respectively. During the processes simulation the crude glycerol stream was purified from 60 to 98 wt %, and the fermentation process was considered in two continuous stages where mass cell growth and PHB accumulation occurred, respectively. Also, the three downstream processes were based on: (*i*) heat pretreatment and chemical-enzymatic digestion, (*ii*) high pressure homogenizer and solvent extraction, and (*iii*) alkaline pretreatment and chemical-enzymatic digestion. Economic results showed that the best technological scheme uses *C. necator* for the fermentation stage, with a heat pretreatment and enzymatic-alkaline digestion for the downstream process.

Keywords: *Glycerol fermentation, PHB production, Process simulation, Process assessment.*

1. Introduction

Glycerol as a by-product on biodiesel production is obtained at high concentration in a weight ratio of 1/10 (glycerol/biodiesel) [1]. Moreover, the growing market of biodiesel has generated a glycerol oversupply, where its production increased 400% in a two-year period and consequently the commercial price of glycerol fell down about 10 times. As a result of the low prices of glycerol, traditional producers such as Dow Chemical and Procter and Gamble Chemicals, stopped the glycerol production [2].

Since glycerol sales have represented an important profitability for the biodiesel industry, it is reasonable to think that low prices of glycerol could affect negatively the economy of biodiesel producers. For this reason, the correct exploitation of glycerol as raw material should be focused on its transformation to added-value products [3]. Thus, the use of glycerol is a high-priority topic for managers and researchers related to the production of biodiesel. In this sense, the establishment of glycerol's biorefineries capable to co-generate added-value products is an excellent opportunity not only to increase the biodiesel profitability, but also to produce high-demanded chemicals from a biobased raw material [4].

Glycerol as the structural component of many lipids is abundant in nature. It is produced by yeasts during osmoregulation to decrease extracellular water activity due to its compatible solubility [5]. Wide glycerol occurrence in nature allows different kinds of microorganisms to metabolize it as a sole carbon and energy source. Thus, in some industrial fermentation processes, glycerol can substitute traditional carbohydrates, such as sucrose, glucose, and starch [5]. In this way, one of many promising applications to take advantage of the glycerol surplus is its bioconversion to high value compounds through microbial fermentation. An interesting application is to transform glycerol to poly-3-hydoroxybutyrate (PHB), which has similar properties to conventional plastics such as polypropylene or polyethylene. Also, PHB

can be extruded, molded, spun into fibers, made into films, and used to make heteropolymers with other synthetic polymers [6].

Here, the biotechnological production of PHB from crude glycerol obtained during the biodiesel production was techno-economically assessed. For the fermentation process, two different strains, *Cupreavidus necator* and *Bacillus megaterium* were considered. Moreover, three downstream processes for PHB separation and purification were analyzed. Thus, six biotechnological schemes to transform the crude glycerol obtained in the biodiesel industry were compared.

2. Methodology

The approach used for the processes design was a knowledge-based strategy that considers both heuristic rules and researcher's experience. Process simulation and economic assessment were carried out utilizing the Aspen Plus software and the Aspen Icarus package, respectively. Material and energy balances were obtained as simulation results for each technological scheme. As a result, requirements of raw materials, services, and energy were obtained. Also, estimation of energy consumption and related costs were calculated based on the simulation results for thermal units such as heat exchangers, reboilers, and evaporators. This methodology has been previously presented by Cardona et al. [5-10].

2.1. Process description

The PHB production process from crude glycerol requires five main stages [11], namely: glycerol purification, glycerol fermentation (cell growth and PHB accumulation), mass cell pretreatment, PHB isolation, and PHB purification. *Cupreavidus necator* and *Bacillus megaterium* were considered as the bacterial strains in order to compare the fermentation process. Glycerol purified at 98 wt % was considered as substrate in all cases and the three different downstream processes were analyzed with each strain, as shown in Fig. 1.

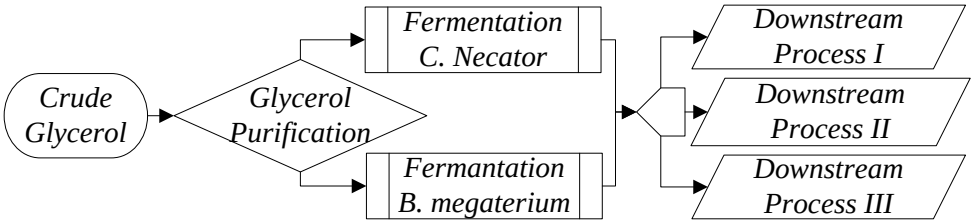

Fig. 1. Schematic representation of the PHB production from crude glycerol by C. necator and B. megaterium.

2.1.1. Glycerol purification

A typical composition for a crude glycerol stream obtained from the biodiesel production process is as follows: 32.59 wt % methanol, 60.05 wt % glycerol, 2.62 wt % $NaOCH_3$, 1.94 wt % fats, and 2.8 wt % ash [3].

Fig. 2 shows the flowsheet for crude glycerol purification up to 98 wt % [4]. The crude glycerol is initially evaporated and 90 % of the methanol is recovered at 99 wt %. Also, this obtained stream meets the necessary conditions to be reused in the transesterification process. The resulting bottom stream from the evaporation stage is neutralized using an acid solution where both the salts produced during the neutralization and the remaining ashes are removed by centrifugation. The fluid stream is washed with water using a weight ratio of 2.4 (water/glycerol stream), and thus an aqueous glycerol free of salts and solids, with a low

concentration of methanol and triglycerides is obtained. More than 90 % of water and the remaining methanol are then removed by evaporation. At this point the purity of the obtained glycerol is 80 wt %, and the glycerol stream is finally purified through a distillation column up to 98 wt %.

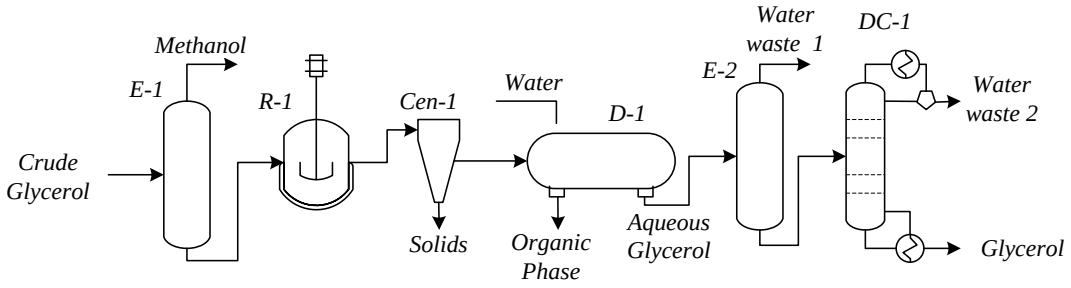

Fig. 2. Simplified flowsheet of the glycerol purification process up to 98 wt%.E-1: Evaporator I, R-1, Neutralizing Reactor I, Cen-1: Centrifuge I, D-1: Decanter I, E-2: Evaporator II, DC-1: Distillation Column I.

2.1.2. Fermentation process

Biotechnological production of PHB from glycerol requires a limitation of an essential nutrient such as: N, P, Mg, K, O or S, and an excess of a carbon source. Some of the bacterial strains capable of doing this transformation are *Bacillus megaterium*, *Cupriavidus necator*, *Alcaligenes eutrophus*, *Pseudomonas extorquens, and Pseudomonas oleovoran,* among others. Also, during the fermentation process the PHB accumulation could reach values between 40 to 70 wt %, with productivities up to 1.5 g/(L h) [6].

For the fermentation process two strains were compared, *C. necator* and *B. megaterium*, using a two stages fermentation process. In the first stage the cell growth occurs, while in the second stage the PHB accumulation takes place. Since the dissolved oxygen in the cell growth media must be between 15 and 20 %, air and oxygen should be fed in the first fermentation stage. Prior to the fermentation process, the diluted glycerol should be sterilized at 25 atm and 139 °C, as shown in Fig. 3.

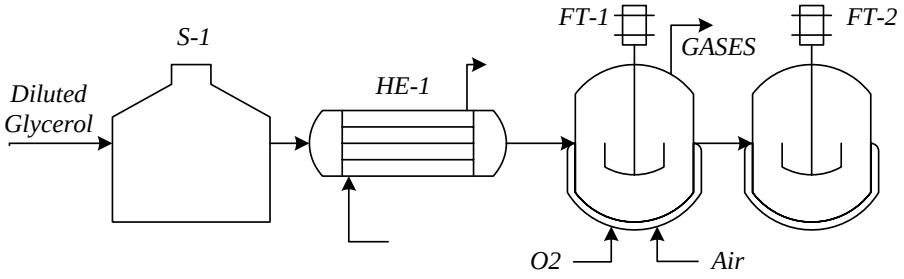

Fig. 3. Simplified flowsheet for the glycerol fermentation to PHB. S-1: Sterilizator I, HE-1: Heat Exchanger I, FT-1: Fermentation Tank I, FT-2: Fermentation Tank II

When the fermentation is carried out by *C. necator* the glycerol stream is diluted at 249 g/L [12], and the residence time for both fermentation stages are 21 and 22.5 h. In the case of *B. megaterium*, the glycerol stream is diluted at 50 g/L [13] with the respective residence times of 75 and 21 h.

2.1.3. Downstream processes

The downstream process for PHB purification from a fermentation broth can be divided in three parts: pretreatment, extraction, and purification. In the pretreatment step, cell disruption can be carried out by the action of heat, alkaline media, salty media, or freezing. In the case of extraction, some alternatives such as: solvent extraction, chemical digestion, enzymatic digestion, mechanical cell disruption, supercritical fluid extraction, cell fragility, and spontaneous liberation can be used. Finally, the purification methods involve a hydrogen peroxide treatment combined with the action of enzymes or chelating agents. [11].

The first considered downstream process starts with a heat pretreatment stage at 85 °C, followed by a simultaneous chemical-enzymatic digestion with both NaOCl (30 wt %) and the enzyme *Burkholdeira sp. PTU9* (2 wt %), at 50 °C and pH 9. Then the disrupted mass cell is discarded by a centrifugation process. The suspended PHB stream is washed with a H_2O_2 diluted stream (1.2 v/v %). Finally, the PHB is purified up to 99.9 wt % by evaporation and spray drying, as shown in Fig. 4.

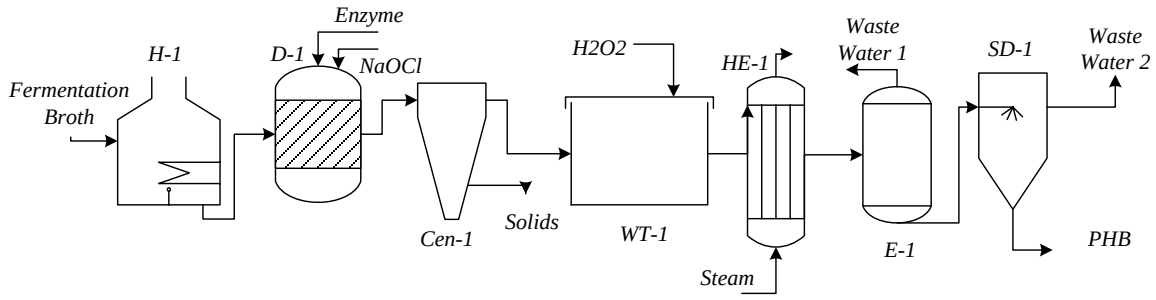

Fig. 4. Simplified flowsheet for the first downstream process. H-1: Heater I, D-1: Digestor I, Cen-1: Centrifuge I, WT-1: Washer Tank I, HE-1: Heat Exchanger I, E-1: Evaporator I, SD-1: Spray Drier I.

The second downstream process starts with a high pressure homogenizer at 70 MPa and 110 °C, where the cell mass is disrupted. Then, the centrifugation is carried out prior to the solvent extraction. In this extraction diethyl-succinate (DES) at 110 °C in a mass ratio of 1/20 (PHB/solvent) is used. A second centrifugation stage is employed in order to withdraw the residual cell mass. Thus, a mixture of PHB-water is gelled by cooling and the DES is recovered. Finally, the PHB at 99.9 wt % is obtained by spray drying, as shown in Fig. 5.

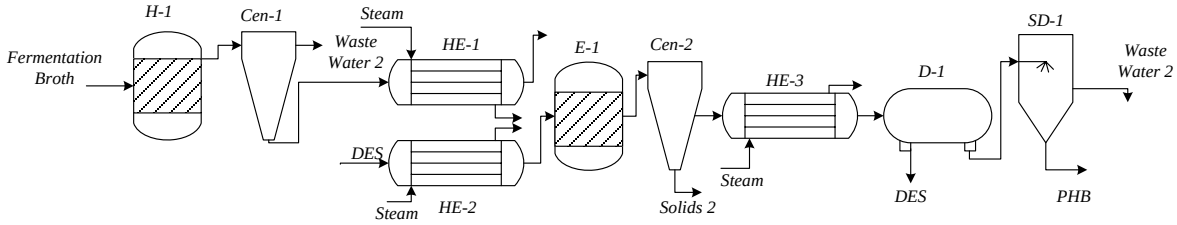

Fig. 5. Simplified flowsheet for the second downstream process. H-1: Homogenizer I, Cen-1: Centrifuge I, HE-1: Heat Exchanger I, HE-2: Heat Exchanger II, E-1: Extractor I, Cen-2: Centrifuge II, HE-3: Heat Exchanger III, D-1: Decanter I, SD-1: Spray Drier I.

In the third downstream process, the fermentation broth is pretreated with an alkaline solution of NaOH at 70 MPa and 110 °C. Then, a digestion process is carried out using NaOCl and sodium dodecylsulfate (SDS) at 55 °C. The disrupted cells are centrifuged and the PHB is washed with H_2O_2 (1.2 v/v %). The obtained mixture is subjected to an evaporation process

and most of the water content is discarded. Finally, PHB at 99.9 wt % is obtained by spray drying, as shown in Fig. 6.

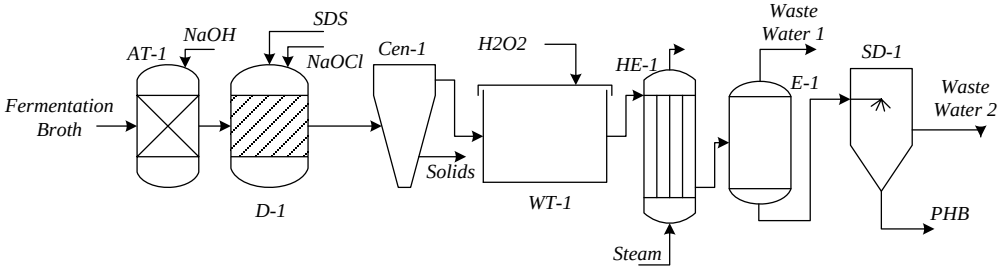

Fig. 6. Simplified flowsheet for the third downstream process. AT-1: Alkaline Tank I, D-1: Digester I, Cen-1: Centrifuge I; WT-1: Washer Tank I, HE-I: Heat Exchanger I, E-1: Evaporator I, SD-1: Spray Drier I.

2.2. Simulation procedure

The PHB production processes were simulated using Aspen Plus (Aspen Technologies Inc., USA). Thus, the design of the distillation columns in all cases required the definition of the preliminary specifications using the DSTWU shortcut method included in Aspen Plus. This method uses the Winn–Underwood–Gilliland procedure providing an initial estimate of the minimum number of theoretical stages, the minimum reflux ratio, the localization of the feed stage, and the products split. To perform the rigorous calculation of the distillation columns, the Rad-Frac module (based on the MESH equations) was used. Also, in order to study the effect of the main operation variables (e.g., reflux ratio, feed temperature, number of stages, etc.) on the glycerol composition, a sequential design procedure including a sensitivity analysis was performed.

On the other hand, *C. necator* and *B. megaterium* were simulated as solid compounds while the enzymes were simulated as non-conventional compounds. For the thermodynamic analysis, the UNIFAC model was used. The fermentation process was simulated based on a yielding approach where glycerol is completely consumed in two continuous fermentation stages. The first fermentation stage is governed by mass cell growth and the second fermentation stage is governed by PHB accumulation. The enzymatic digestion was simulated based on a stoichiometric approach. Calculation of energy consumption was based on the thermal energy required by heat exchangers, reboilers, flash drier units and the power supply required by the pumps.

The economic analysis was performed using the Aspen Icarus (Aspen Technology, Inc., USA) package. This software estimates the capital costs of process units as well as the operating costs, among other valuable data, utilizing the design information provided by Aspen Plus and the data introduced by the user for specific conditions such as project location among others. This analysis was estimated in US dollars for a 10-year period at an annual interest rate of 16 %, considering the straight-line depreciation method and a 33 % income tax. The cost of crude glycerol was USD$ 0.0554/L [3]. The labor cost used for operatives and supervisors was USD$ 2.14/h and USD$ 4.29/h, respectively. Also, the prices used for electricity, water and low pressure vapor were USD$ 0.03044/kWh, USD$ 1.252/m^3 and USD$ 8.18/ton, respectively [5]. All of these values are based on Colombian conditions.

3. Results and Discussions

The PHB production processes from crude glycerol require the glycerol purification up to 98 wt %. During this purification process, methanol at 99 wt % is recovered and thus for the economic assessment, two scenarios can be analyzed. In the first scenario, the obtained methanol is considered as a process waste. In the second scenario the methanol is considered as a co-product which could be recycled to the transesterification process and an economic value is given to this stream. The lowest cost for glycerol purification was obtained under the second scenario conditions (0.149 USD$/kg). This value was used as the raw material cost in all cases, thus only the purification cost was considered since the purification process was assumed to be adjacent to the biodiesel production process.

Glycerol fermentation was analyzed using two different strains and two glycerol concentrations in the fermentation media were considered (249g/L and 50 g/L). The cell mass values were 81.6 and 15.8 g/L and the PHB concentrations were and 57.1 and 8.8 g/L when *C. necator* and *B. megaterium* were used respectively. Thus, the reached yields to biomass and PHB were 5.16 and 6.49 fold higher when *C. necator* was used. These differences may be due to the fact that the first strain is a well adapted bacterium meanwhile the second one is still under adaptation to the fermenting conditions used in this work.

The fermentation broth is mainly a mixture of incorporated PHB in the cell mass and water. In order to recover the PHB from this broth, three different downstream processes were compared. The total production costs of PHB at 99.9 wt % from crude glycerol using *C. necator* and *B. megaterium* are shown in Table 1, where the costs were discriminated by raw material, services, operatives, maintenance, administration, and depreciation.

Table 1. Total PHB production cost from crude glycerol using C. necator and B. megaterium.

Item	***Cost (US$/kg) and Share (%)***	***Downstream Process I***		***Downstream Process II***		***Downstream Process III***	
		B. megat.	*C. necator*	*B. megat.*	*C. necator*	*B. megat*	*C. necator*
Raw material	***Cost***	*0.149*	*0.149*	*0.149*	*0.149*	*0.149*	*0.149*
	Share	*3.80*	*7.71*	*3.15*	*6.27*	*3.60*	*7.07*
Utilities	***Cost***	*1.358*	*0.658*	*1.908*	*0.953*	*1.691*	*0.841*
	Share	*34.64*	*33.96*	*40.36*	*39.97*	*40.88*	*39.77*
Operating labor	***Cost***	*0.151*	*0.066*	*0.156*	*0.068*	*0.146*	*0.064*
	Share	*3.85*	*3.41*	*3.30*	*2.85*	*3.53*	*3.03*
Maintenance and opera. charges	***Cost***	*0.479*	*0.210*	*0.492*	*0.236*	*0.485*	*0.223*
	Share	*12.22*	*10.84*	*10.41*	*9.90*	*11.73*	*10.55*
Plant overhead and admin. costs	***Cost***	*0.407*	*0.186*	*0.427*	*0.218*	*0.414*	*0.191*
	Share	*10.38*	*9.6*	*9.03*	*9.14*	*10.01*	*9.03*
Depreciation of capital	***Cost***	*1.376*	*0.668*	*1.595*	*0.76*	*1.251*	*0.646*
	Share	*35.10*	*34.48*	*33.74*	*31.87*	*30.25*	*30.55*
Total	***Cost***	***3.920***	***1.937***	***4.727***	***2.384***	***4.136***	***2.114***
	Share	***100***	***100***	***100***	***100***	***100***	***100***

The glycerol purification process represents only between 3.1 and 3.8 % of the total PHB production cost when *B. megaterium* is used. These values are higher, between 6.3 and 7.7%, when *C. necator* is used. In all cases, the raw material cost is lower than the obtained value

for traditional chemical processes considering that for most industrial processes the cost of raw material represents near 50% of the total production cost. In this way, the use of crude glycerol represents a significant decrease in the cost for raw material.

In general terms, due to the higher PHB yield, substrate tolerance, and lower energy requirements in the downstream processes, the lower production costs are obtained when *C. necator* is used for the fermentation process. Also, for both strains, the higher value for the total production cost was obtained in the second downstream process, which uses a solvent extraction stage. This extraction requires heating the expensive solvent DES up to 110 °C which increases the utility costs.

The total PHB production costs were between 3.92 and 4.73 US$/kg when *B. megaterium* was considered in the fermentation process, and between 1.94 and 2.38 US$/kg when *C. necator* was considered. These production costs were close to the sale prices of PHB reported in the literature for other substrates (i.e., 2.75-6.27 USD/Kg) [6].

Economically wise, the first downstream process was the most appropriate since the total production costs were the lowest obtained for both strains. This process was based on the BIOPOL flowsheet [14]. Moreover, the total production cost was almost twice as higher when *B. megaterium* was used for the fermentation stage compared to *C. necator*.

Generally, it has been suggested that the higher share of the total PHB production cost from other raw materials is the substrate cost [6]. Meanwhile, if crude glycerol is used as feedstock this share is lower than 8 %. These results indicate that using crude glycerol as feedstock to produce PHB could be a profitable alternative to develop biorefineries in the biodiesel industry.

4. Conclusions

Three downstream processes and two strains, *C. necator* and *B. megaterium,* were techno-economically compared to produce PHB from crude glycerol. Although in all the simultaed cases it was possible to obtain PHB at 99.9 wt %, the total production costs were twice as higher when *B. megaterium* was used compared to *C. necator*. This result is explained by the fact that *C. necator* is capable to consume glycerol at a higher concentration and yield than *B. megaterium*. The comparison showed here is important for the industrial production of PHB using crude glycerol since not only a profitable alternative was designed but also the fermentation conditions that take to a profitable process were clarified.

5. Acknowledgements

The authors express their acknowledgements to the National University of Colombia at Manizales for funding this research and to Dr. M.A. Villar and his group at PLAPIQUI (UNS-CONICET) in Argentina for the *B. megaterium* strain.

References

[1] J.A. Posada, C.A. Cardona., D.M. Cetina, C.E. Orrego, Bioglycerol as raw material to obtain added value products. In: Cardona, C.A., (Ed.), Reasearching advances for biofuels production. Artes Gráficas Tizán, Manizales, 2009, pp. 103-127 (In Spanish).

[2] C.A. Cardona, J.A. Posada, J.A. Quintero. Use of agroindustrial wastes and by-products: Glycerin and Lignocellulosics. Manizales: Artes Graficas Tizan, 2010, pp. 218 (In Spanish).

[3] J.A. Posada, C.A. Cardona, Validation of glycerin refining obtained as a by-Product of biodiesel production, Ingeniería y Universidad, 14, 2010, pp. 2-27 (In Spanish).

[4] J.A. Posada, C.E. Orrego, C.A. Cardona, Biodiesel production: Biotechnological approach. International Review of Chemical Engineering 1, 2009, pp. 571-580.

[5] J.A. Posada, C.A. Cardona, Design and analysis of fuel bioethanol production from raw glycerol, Energy, Article in Press. doi:10.1016/j. energy.2010.07.036.

[6] J.A. Posada, J.M. Naranjo, J.A. López, J.C. Higuita, C.A. Cardona, Design and analysis of phb production processes from crude glycerol, Process Biochemistry, Article in Press. doi:10.1016/j.procbio.2010.09.003.

[7] C.A. Cardona, O.J. Sánchez, Energy consumption analysis of integrated flowsheets for production of fuel ethanol from lignocellulosic biomass, Energy 31, 2006, pp. 2447-2459.

[8] J.A. Quintero, M.I. Montoya, O.J. Sánchez, OH Giraldo, CA Cardona, Fuel ethanol production from sugarcane and corn: comparative analysis for a Colombian case, Energy 33, 2008, pp. 385-399.

[9] L.F. Gutiérrez, O.J. Sánchez, C.A. Cardona, Process integration possibilities for biodiesel production from palm oil using ethanol obtained from lignocellulosic residues of oil palm industry, Bioresour. Technol., 100, 2009, pp. 1227-1237.

[10] C.A. Cardona, O.J. Sánchez, LF Gutiérrez, Process synthesis for fuel ethanol production, Francis Group: CRC Press Taylor, 2010. pp. 390.

[11] N. Jacquel, C.W. Lo, Y.H. Wei, H.S. Wu, S.S. Wang, Isolation and purification of bacterial poly(3-hydroxyalkanoates), Biochem. Eng. J., 39, 2008, pp. 15–27.

[12] G. Mothes, C. Schnorpfeil, C.J.U. Ackermann, Production of PHB from crude glycerol, Eng. Life. Sci. 7, 2007, pp. 475–479.

[13] J.M. Naranjo, Production of PHB from agroindustrial wastes. Master Thesis. National University of Colombia, 2010, pp. 151.

[14] K.G. Harding, J.S. Dennis, H. von Blottnitz, S.T.L. Harrison, Environmental analysis of plastic production processes: Comparing petroleum-based polypropylene and polyethylene with biologically-based polyhydroxybutyric acid using life cycle analysis, J. Biotechnol., 130, 2007, pp. 57–66.

Theoretical Bioenergy Potential in Cambodia and Laos

Orkide Akgün[1,*], Mika Korkeakoski[1], Suvisanna Mustonen[2], Jyrki Luukkanen[1]

[1] *University of Turku, Turku, Finland*
[2] *Tampere University of Technology, Tampere, Finland*
** Corresponding author. Tel: +90536 238 0265, Fax: +35832238363, E-mail: orkideakgun@yahoo.com.tr*

Abstract: This paper investigates theoretically potential energy of residues of some biomass sources in Cambodia and Laos by considering agricultural residues and forestry residues for the year 2006 since both country have limited access to grid-quality electricity. The theoretical potential biomass energy of rice husk, straw, corn cob, cassava stalk, bagasse and sugarcane trash and logging residues, sawnwood and plywood residues are calculated by using their lower heating values (LHV). The potential biomass energy obtained from these residues in Cambodia can contribute approximately 1.4 Mtoe to the total final energy consumption of Cambodia. On the other hand, 0.6 Mtoe biomass energy can be obtained potentially from the biomass residues in Laos, 2006. Furthermore, the paper presents the theoretical bioethanol production from some biomass residues such as rice straw, corn stover, bagasse, and cassava pulp in Cambodia and Laos. The potential bioethanol production in Cambodia is about 0,648 Gl for the year 2006 whereas 0,355 Gl of bioethanol can be produced in Laos from 2006 biomass residues. The potential results are investigated in whole country level and they do not consider the collecting and transportation cost of the biomass residues, their possible other usage purposes, exports and imports.

Keywords: *Biomass, Energy Potential, Crop Residue, Cambodia, Laos.*

1. Introduction

Due to the increase in energy demand and environmental concerns over fossil fuel consumption, biomass has been of interest in recent years in terms of renewable energy source [1]. Biomass energy can be converted into useful energy for both traditional and modern uses. Firing for cooking and heating is a simple example of traditional uses. In modern uses allow to conversion of biomass in the form of electricity, steam and liquid biofuels next to the heating use [2].

Ethanol, as a modern form of biomass energy, can be converted from any kind of starchy biomass source which is rich in sugar content. Agricultural crops, forestry products and their residues are potential sources for ethanol production. Ethanol has a great energy potential in terms of transportation fuel. It can be blended with gasoline and used in the commercial forms of E5, E10 and E85 [2, 3].

This study estimated the biomass energy potential of Cambodia and Laos in terms of agricultural and forestry biomass residues as solid fuel and their ethanol production capacity considering production quantities in 2006. In order not to cause any conflict between food and energy production and considering the high poverty rates of Cambodia and Laos, this study only focused on the biomass energy obtained from agricultural residues and forestry wastes. Mainly, the potential of biomass energy of rice husk, rice straw, corn cob, cassava stalk, bagasse, and trash of sugarcane were estimated. Furthermore, the residues of coconut-husk, shell, and frond- and groundnut-shell- were considered as potential biomass energy sources for Cambodia. Moreover, the study found that some residues such as rice straw, corn stover, bagasse and cassava pulp have a potential to contribute a considerable amount of bioethanol in both countries. Finally, the amount of potential energy obtained from biomass residue resources examined for Cambodia and Laos was compared to the total final energy consumptions of the countries in the same year.

2. Methodology

The production data of each biomass resource was obtained from FAO statistics (FAOSTAT) [4]. The production quantities in 2006 for related biomass sources were used in order to compare the available energy consumption in 2006 for Cambodia and Laos. The production data statistics of Laos taken from FAO were also compared with the statistics presented in National Statistics Centre of Lao PDR [5]. Both production data statistics were found to be consistent. However, Cambodian production data statistics presented in FAOSTAT was used without any modifications as only data source in this study. Also, in order to estimate the amount of agricultural biomass residues RPR (residue-product ratio) values were used. The RPR values of rice husk are specific for Cambodia and Laos. However, the RPR value of rice straw, which is specific for Laos, was also used for Cambodia. These values were taken from previous studies carried out in these countries [6, 7]. However, other biomass residues were calculated in this study by taking the RPR values which have been used in similar studies conducted for Thailand [8]. On the other hand, recovery rates (RR) of forestry biomass residues were used in this study to estimate the available amount of logging residues, mill residues and plywood residues. The recovery rates of mill residues and plywood residues were taken from FAO [9]. On the other hand, recovery rate of logging residues were based on the study of A. Koopmans and J. Koppejan for Cambodia and Laos [10].
Lower Heating Values (LHV) of agricultural residues were taken from the study conducted for Thailand biomass energy estimations [8]. LHV of forestry wastes, however, were based on values studied by Suzuki and Yoshida (2009) [11].

Bioethanol production calculations in Cambodia and Laos for the year 2006 were carried out in the light of the ethanol yield according to a study by Kim and Dale (2003) [2]. That study was conducted by first calculating theoretical ethanol yields of each biomass residue and converting this theoretical yield to possible yield by assuming that ethanol production efficiency from other crop residues is equal to approximately 67%, which is the ethanol production efficiency of corn stover [2]. The same procedure was followed to estimate the potential bioethanol production in Cambodia and Laos.

This study did not consider the imports and exports of any biomass sources. All the potential residues of biomass sources in Cambodia and Laos were calculated in the study without considering their other possible usage purposes and the losses due to the transportation.

3. Results

3.1. Agricultural Residues

3.1.1. Rice

Rice is the main agricultural crop and staple food in both Cambodia and Laos. 84.4% of cultivated area in Cambodia is used for rice cultivation and it constituted 25% of Cambodian agricultural GDP in 2006 [12]. In Laos 80% of area under cultivation has been devoted to rice. Rice accounted for 38% of agricultural GDP, which is higher than Cambodia (1999) [13, 14]. High amount of rice production in both countries contributes to high availability of rice residues such as rice husk and rice straw. These residues could be an option for any biomass energy systems. Rice husk is the outer cover of rice which comes from rice milling process as by-product. The unutilized rice husk mainly causes waste disposal problems and breathing problems because of its low density. The usage of rice husk as solid fuel can be a promising way to avoid these problems and provide considerable amount of useful energy [15]. Rice straw, on the other hand, is another by-product of rice and great bio-resource since it is one of the richest material in terms of its lignocelluloses [16]. However, it has to be taken into

account that rice straw is an import fodder for animals in Cambodia. RPR and LHV of rice husk and rice straw are shown in the Table 1 with their calculated potential energy values.

Table 1. 2006,rice residues biomass energy

	Rice (Mt)	Rice Residue	RPR	Residue (Mt)	LHV (MJ/kg)	Potential Energy (10^6GJ)
Cambodia	6.26 [4]	Husk	0.27 [8]	1.69	12.85 [8]	21.73
		Straw	0.33 [7]	2.07	14 [17]	28.92
Laos	2.66 [4]	Husk	0.25[7]	0.67	12.85 [8]	8.56
		Straw	0.25 [7]	0.88	14 [17]	12.31

3.1.2. Maize

Since maize is the second most produced crop after rice for both Cambodia and Laos, it can supply a considerable amount of corn cob as biomass energy source. Moreover, the chemical and physical properties of corn cob enable it to be suitable feedstock for several energy generation methods [14]. Table 2 below shows potential energy obtained from corn cob.

Table 2. 2006, corn cob biomass energy

	Maize (Mt)	RPR	Corn cob (Mt)	LHV (MJ/kg)	Potential Energy (10^6GJ)
Cambodia	0.38 [4]	0.25 [8]	0.09	16.63 [8]	1.57
Laos	0.45 [4]	0.25 [8]	0.11	16.63 [8]	1.87

3.1.3. Cassava

Cassava is another important agricultural crop in Cambodia and Laos as staple food and animal feed in similar way as in many subtropical regions [18]. Cassava stalk, the residue of cassava, is an agricultural biomass feedstock which can be used for biomass energy purposes. Its primary energy was tabulated in Table 3 for Cambodia and Laos.

Table 3. 2006, cassava stalk biomass energy

	Cassava (Mt)	RPR	Cassava stalk (Mt)	LHV (MJ/kg)	Potential Energy (10^6GJ)
Cambodia	2.18 [4]	0.088[8]	0.192	16.99 [8]	3.26
Laos	0.17 [4]	0.088[8]	0.015	16.99 [8]	0.26

3.1.4. Sugarcane

Bagasse and top and trash of sugarcane are the main residues of sugarcane. While bagasse is dry, fibrous residue remaining after sugarcane stalk after extraction of juice, trash of sugarcane is the remaining of the plant in the field after the harvest [19]. The primary biomass energy of bagasse and trash of sugarcane was tabulated by assuming their RPR and LHV as same in Table 4.

Table 4. 2006, sugarcane residues biomass energy

	Sugarcane (Mt)	Sugarcane Residue	RPR	Residue (Mt)	LHV (MJ/kg)	Potential Energy (10^6GJ)
Cambodia	0.14 [4]	Bagasse	0.250 [8]	0.035	6.43[8]	0.228
		Trash	0.302 [8]	0.043	6.82[8]	0.292
Laos	0.217[4]	Bagasse	0.250 [8]	0.054	6.43[8]	0.349
		Trash	0.302 [8]	0.066	6.82[8]	0.447

3.1.5. Groundnut Shell and Coconut

Groundnut shell and coconut husk - rough exterior shells of the coconut -, shell, and empty bunches and frond can be counted as considerable biomass energy sources in Cambodia. Table 5 was prepared to show the potential biomass energy value of these residues.

Table 5. Cambodia, 2006, groundnut shell and coconut residues biomass energy

	Production (Mt)	Residue	RPR	Residue (Mt)	LHV (MJ/kg)	Potential Energy (10^6GJ)
Groundnut	0.024 [4]	Shell	0.323[8]	0.0077	11.23 [8]	0.086
Coconut	0.07 [4]	Husk	0.362 [8]	0.025	14.71 [8]	0.373
		Shell	0.160[8]	0.011	16.43 [8]	0.184
		Frond	0.225[8]	0.016	14.55 [8]	0.229

3.2. Forestry Residues

3.2.1. Logging Residues

Logging residues constitute woody residues that remain after cutting in the forest area, such as tops and branches. Logging residue calculations require the amount of industrial round wood production and an average recovery rate (RR) which is generally estimated since logging can be done in many innumerable and unsystematic ways [9]. Logging recovery rate can be estimated with the idea that "6 cubic meters of logs extracted from the forest leave 4 cubic meters of waste remaining in the forests" [10]. Cambodia's and Laos' forestry biomass energy estimations were carried out and tabulated in the Table 6.

Table 6. 2006, logging residue biomass energy

	Industrial round wood (10^6CUM)	RR	Logging Residue (10^6CUM)	LHV (GJ/m^3)	Potential Energy (10^6GJ)
Cambodia	0.113 [4]	0.60 [10]	0.075	7.4 [11]	0.557
Laos	0.194 [4]	0.60 [10]	0.129	7.4 [11]	0.955

3.2.2. Mill Residues from Sawnwood Production Residues

The residues from wood-processing factories are called mill residues [11]. Therefore, the calculations are based on the amount of sawnwood production volume. Table 7 shows the primary biomass energy content of mill residues.

Table 7. 2006, mill residue biomass energy

	Sawnwood (10^6CUM)	RR	Mill Residue (10^6CUM)	LHV (GJ/m^3)	Potential Energy (10^6GJ)
Cambodia	0.002 [4]	0.43 [9]	0.0029	8.4 [11]	0.024
Laos	0.13 [4]	0.60 [9]	0.087	8.4 [11]	0.728

3.2.3. Plywood Residues

Plywood residues comprise of the which are log ends and trims, bark, log cores, green veneer waste, dry veneer waste, trimmings and rejected plywood [9]. Calculations of primary energy of plywood residues in this study are shown in the Table 8 for both countries.

Table 8. 2006, plywood residue biomass energy

	Plywood (10^6CUM)	RR	Plywood Residue (10^6CUM)	LHV (GJ/m^3)	Potential Energy (10^6GJ)
Cambodia	0.0045 [4]	0.47 [9]	0.0051	8.4 [11]	0.043
Laos	0.027 [4]	0.47 [9]	0.031	8.4 [11]	0.256

3.3. Bioethanol Production

This part of the study estimated how much bioethanol can potentially be produced from rice straw, corn stover, bagasse, cassava pulp. Bioethanol calculations were carried out on dry-based biomass residues and are shown in Table 9 in Cambodia and Laos.

Table 9.Cambodia and Laos, 2006,bioethanol production from agricultural residues

	RPR	Residue,Mt Cambodia	Residue,Mt Laos	Ethanol yield(l/t)	Ethanol,10^6l Cambodia	Ethanol,10^6l Laos
Rice Straw	0.33[7]	807	0.77	280 [2]	506	214.9
Corn Stover	1 [2]	0.38	0.45	290 [2]	109.3	130.5
Bagasse	0.25 [8]	0.018	0.03	280 [2]	4.96	7.6
Cassava pulp	0.15[21]	0.327	0.03	83.3 [21]	27.28	2.18

3.4. Final Energy Potential of Biomass

In this study the total potential biomass energy from biomass residues in Cambodia and Laos was found to be about 1.4 Mtoe ($57*10^6$ GJ) and 0.6 Mtoe ($26*10^6$ GJ) respectively. The total final energy consumption (TFEC) in Cambodia was about 4.5 Mtoe in 2005 [22]. This means that the biomass residue energy potential is about one third of the total energy consumption in Cambodia. The total final energy consumption (TFEC) in 2006 in Laos was about 2.0 Mtoe [22]. This indicates that the biomass residue energy potential estimated for Laos could contribute about 30% of the total energy consumption.

Figure 1.a, 1.b and 2.a, 2.b show the total final energy consumption and theoretically calculated potential biomass energy from residues and the contributions of different sources to energy potentials in ktoe in Cambodia and Laos, 2006.

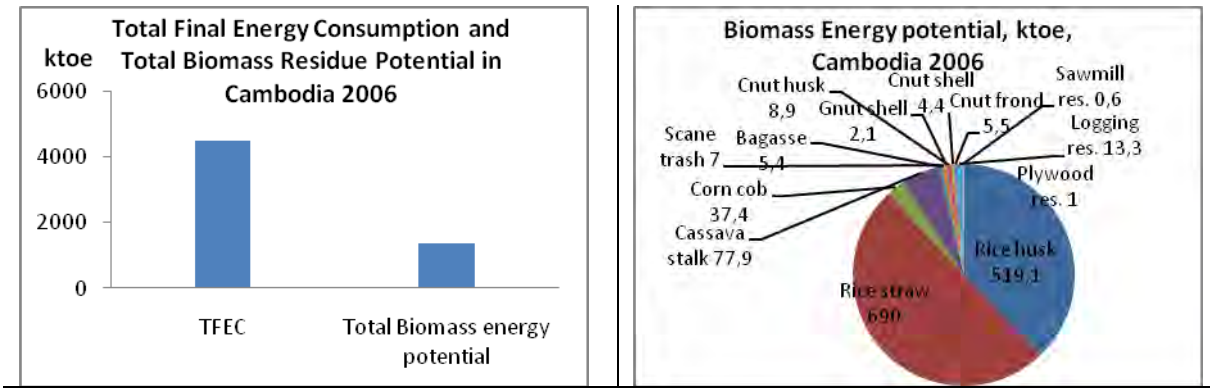

Figure 1.a. Total final energy consumption and calculated potential biomass residue energy content 1.b. Different sources of biomass residue energy potentials in Cambodia, 2006

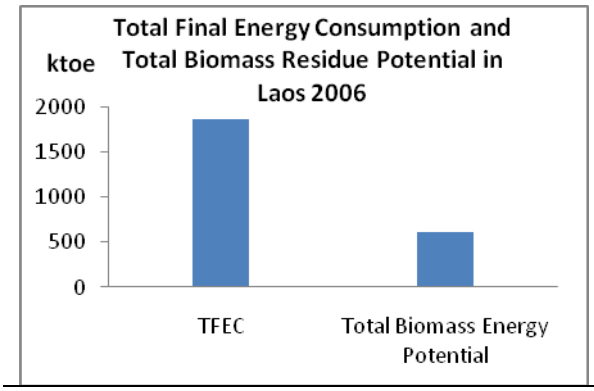

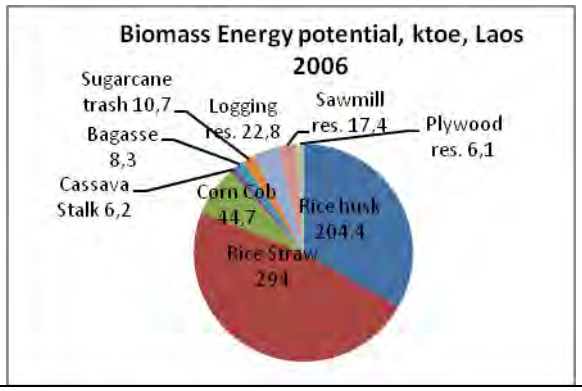

Figure 2.a. Total final energy consumption and calculated potential biomass residue energy content 2.b. Different sources of biomass residue energy potentials in Laos, 2006

3.5. Bioethanol Potential

The study found that some agricultural residues in Cambodia such as rice straw, corn stover, bagasse and cassava pulp have a potential to produce approximately 648*10^6 l ethanol production for the country. However, the potential of ethanol production from same residues in Laos was estimated about 355*10^6 l. The amounts of potential bioethanol for both countries were found to be enough to correspond to the amount gasoline consumed in road transport in Cambodia and Laos. Figure 3.a, 3.d and Figure 4.a and 4.b s ummarize the gasoline consumption in 2006 and the potential gasoline production from biomass residues and the contributions of different biomass residues for gasoline productions in Cambodia and Laos, 2006 [21, 22].

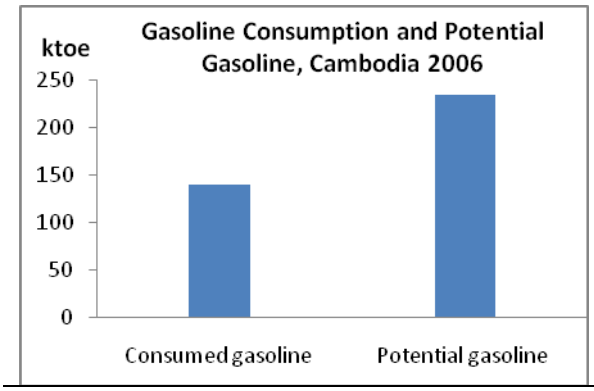

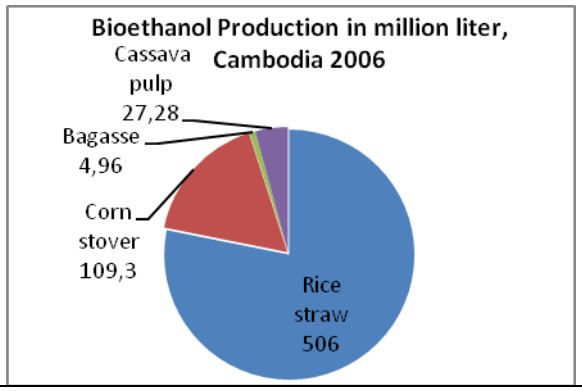

Figure 3.a. Gasoline consumption and potential biomass residue based gasoline production 3.b. Different sources of biomass residue potential for ethanol production in Cambodia, 2006

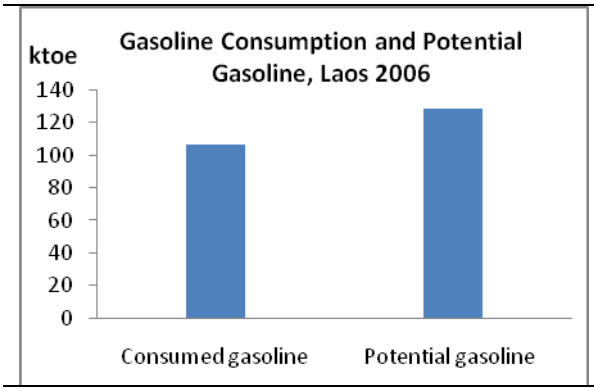

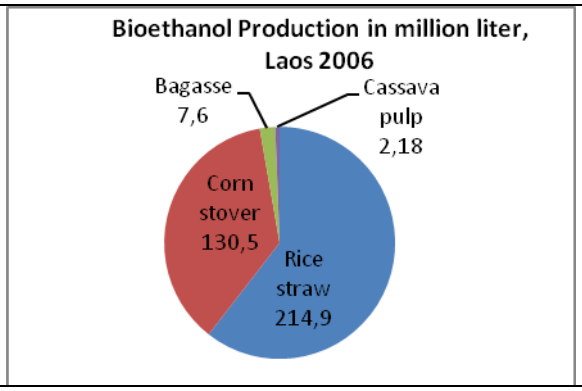

Figure 4.a. Gasoline consumption and potential biomass residue based gasoline production 4.b. Different sources of biomass residue potential for ethanol production in Laos, 2006

4. Conclusions

The results indicate that the biomass residue potential could contribute such energy production that can reach up to 30% of energy consumed in 2006 for both Cambodia and Laos. There are, however, some practical limitations and restrictions in the use of the residues such as collection and transportation of them, marketing systems and other usage possibilities. Furthermore, the results show that rice straw and rice husk in Cambodia and Laos seem to be potentially the most favorable biomass sources in terms of the quantity of biomass production availability and comparably higher contribution to biomass energy production. Totally, all biomass residues including both agricultural residues and forestry residues have a potential to provide 1.4 Mtoe and 0.6 Mtoe energy productions in Cambodia and Laos respectively.

Moreover, the study covers the bioethanol production from some residues such as rice straw, corn stover, bagasse and cassava pulp in Cambodia and Laos. Theoretically, potential bioethanol production in Cambodia has and Laos could provide approximately the same amount of energy as the present gasoline consumption is in both countries.

The results clearly show that biomass residues provide a promising potential for distributed renewable energy production in Cambodia and Laos.

References

[1] J. Wannapeera, N. Worasuwannarak, S. Pipatmanomai, Product yields and characteristics of rice, rice straw and corn cob during fast pyrolysis in a drop-tube/fixed-bed reactor, Songklanakarin Journal of Science and Technology , 2008, pp. 393 – 404.

[2] S. Kim, B.E. Dale, Global potential bioethanol production from wasted crops and crop residues, Elsevier Ltd., 2003, pp. 361- 375

[3] IEA Energy Technology Essentials, Biofuel production, 2007, Available at http://www.iea.org/techno/essentials2.pdf .

[4] Food and Agricultural Organization (FAO). FAOSTAT. Available at http://apps.fao.org.

[5] National Statistics Centre of Lao PDR. NSC-LAO PDR. Available at http://nsc.gov.la.

[6] Enabling Activities for the Preparation of the Kingdom of Cambodia's second National Communication to the UNFCCC (Project ID: 00044653), Greenhouse Gas Mitigation Analyses for the Energy and Transport Sector, 2010.

[7] Asia Pro Eco project TH/Asia Pro Eco/05 (101302), Study on Solar and Biomass Energy Potential and Feasibility in Lao PDR, 2006.

[8] B. Sajjakulnukit, R. Yingyuad, V. Maneekhao, V. Pongnarintasut, S.C. Bhattacharya, P. A. Salam, Assessment of sustainable energy potential of non-plantation biomass resources in Thailand, Elsevier Ltd., 2005.

[9] Fao Corporate Document Repository, Trash or Treasure? Available at http://www.fao.org/docrep/003/x6966e/X6966E02.htm .

[10] A. Koopmans, J. Koppejan, Agricultural and forests residues-generation, utilization and availability, the Regional Consultation on Modern Applications of Biomass Energy, 1997.

[11] H. Suzuki, T. Yoshida, Current Situation and concerns with woody biomass use in ASEAN countries, 2009.

[12] B. Yu, S. Fan, Rice production response in Cambodia, presented at the International Association of Agricultural Economists Conference, Beijing, China, 2009.

[13] D.T. Tu, K. Geheb, U. Susumu, Vitoon, Rice is the life and culture of the people of the Lower Mekong Basin Region, presented Mekong Rice Conference, 2004.

[14] L. Douangsavanh, B. Bouahom, K. Pouyavong, Enhancing sustainable development of diverse agriculture in Lao's People Democratic Republic, Working paper 89, UNESCAP-CAPSA

[15] T. Chungsanguit, S.H. Gheewala, S. Patumsawad, Emission Assessment of Rice Husk Combustion for Power Production, World Academy of Science, Engineering Technology Civil and Environmental Engineering, 2010

[16] N. Yoswathana, P. Phuriphipat, P. Treyawatthiwat, M.N. Eshtiaghi, Bioethanol production from rice straw, 2010.

[17] B. Gadde, C. Menke, R.Wassmann, 2009, Rice straw as a renewable energy source in India, Thailand, and the Philippines: Overall potential and limitations for energy contributions and greenhouse gas mitigation.

[18] Cropgenebank Knowledge Base, Cassava Genetic Resource. Available at http://cropgenebank.sgrp.cgiar.org/index.php?option=com_content&view=article&id=132&Itemid=232.

[19] Janghathaikul D., Gheewala S. H.,2004, Bagasse-A Sustainable Energy Resource from Sugar Mills, The Joint international Conference on "Sustainable Energy and Environment (SEE)" Hua HİN, Thailand.

[20] K. Siriroth, Outlook of Biomass Utilization as Biofuel in Thailand

[21] IEA (International Energy Agency) 2009. Energy Balances for Non-OECD Countries, 2009 edition. CD-ROM. Paris: OECD/IEA.

[22] Trading Economics. Available at http://www.tradingeconomics.com/cambodia/road-sector-gasoline-fuel-consumption-kt-of-oil-equivalent-wb-data.html

Growing Biomass Fuel Industry, Declining Local Forage Demands, and Changing Greenhouse Gas Emissions from US Agriculture: A Case Study

Paul W. Gallagher[1,*], Jeremiah Richey[2]

[1] *Iowa State University,Ames, Iowa/USA*
[2] *Iowa State University, Ames,Iowa/USA*
** Corresponding author. Tel:010-515 294 6181, Fax: 010-515-294-0221, E-mail:paulg@iastate.edu*

Abstract: This paper investigates the effect of a biomass crop introduction in a local market where field crops, cattle forage and biomass crops compete for the agricultural resources and determine land use. A simulation study for a State in the US (Minnesota) with extensive and diverse agricultural resources that could also support a biomass industry is reported. Local market impact on prices and land use is summarized. A local biofuel industry with 1.0 billion gallon capacity can transform declining local land values to stable or moderately increasing land values, partly because secular declines in cattle forage can be replaced with biofuel demands. The effects of greenhouse gas emissions and sinks are also estimated. The local agriculture sectors' net greenhouse gas changes are converted from a net emission to a net sink position with a biofuels industry-we calculate an annual net improvement of 55 bil. Lbs CO_2 –equivalent, due, in part, declining cattle emissions and favorable land use effects from expanding hay production.

Keywords: *Land rent, Land Use, livestock emissions, Switchgrass, Greenhouse gas(GHG).*

In the US, Biomass fuel technology broadens the potential agricultural resource base to include marginal land that is not suitable for corn production. There are some concerns about increasing greenhouse gas emissions when a land conversion process accompanies a biomass processing expansion [1]. However, existing analyses do not account for the market environment and dynamic adjustments already occurring in local agricultural resource markets. This paper accounts for the local competition between biomass feedstock and cattle forage, the land conversion that would accompany an unrestricted biomass fuel expansion, and the cattle industry decline that is already occurring in potential biomass supply areas of the United States. Since the relevant markets are local, we report a case study of a *representative* State (Minnesota) in the United States that has extensive and diverse agricultural resources that could adapt to biomass crops.

The first section reports an econometric estimation of the profit and dynamic factors influencing cattle population. The second section summarizes a model of the local forage market that presently defines the use of low grade agricultural land. The third section reviews CO_2 accounting procedures, specifically explaining how market changes influence emissions from crops, livestock, and pasture land. Estimates of changes in equilibrium soil carbon levels are also provided. The fourth section presents some 10 year projections of economic variables and global warming indicators. A well-known baseline for US agriculture is the reference for the global commodity markets that define resource market outcomes, and global warming indicators. Then local market outcomes and global warming indicators are given for the case where an expanding biomass fuel industry uses some of the local resources in the given market environment.

1. Market Environment

This section is an overview of the simulation model. There are three main elements in the market model. First, a land use model defines the amount of land used for crops, pasture, and left idle. Second, new estimates of the factors determining local cattle populations are presented. Third a model that incorporates the competition among supply of the three main forage types(hay, pasture and stover) is discussed. *Additional documentation, such as the*

land use model, Worksheets for greenhouse gas emissions and sinks, and the local forage baseline are available at www2.econ.iastate.edu/faculty/gallagher

1.1. Land Use.

Land demand is determined in local agricultural land rental markets. We use an updated version of a recent land use model [2]. Revised estimates land use data from the 2007 census of agriculture, and include land demands for each major crop (corn, soybeans, wheat, cotton, and hay).

1.2. Cattle Population Adjustment

Minnesota's cattle population adjustment is typical of the states in the eastern half of the US. That is, there has been a steady decline mixed with episodes of cyclical adjustment. The decline is likely due to contracting US beef consumption and squeezing marginal producers. Cyclical adjustments likely occur in response to changing market conditions. Beef and Dairy cattle response estimations for Minnesota suggests population slowly adjusts to past profits, populations and also exhibits a secular decline. Our results were estimated using data from the 1969 to 2009 period:

$$Nb_t = 0.741 + 0.118\pi b_t + 0.952Nb_{t-1} - 0.191Nb_{t-2} + 0.118\ln(T) \quad (1)$$
$$(2.3) \quad (1.8) \quad (6.0) \quad (1.1) \quad (1.8)$$
$$adj - R^2 = 0.96 \qquad DW = 1.9 \qquad s = 0.103$$

$$Nm_t = 0.105 + 0.710\pi b_t + 0.710Nb_{t-1}\,0.021\ln(T) \quad (2)$$
$$(1.5) \quad (2.2) \quad (2.2) \quad (2.2)$$
$$adj - R^2 = 0.97 \qquad DW = 2.5 \qquad s = 0.037$$

where k=b for beef, d for dairy

Nk_t is the cattle population in year t, in million head;

πk_t is the profit margin, in \$/lb output

T=1 before 1976, 2 in 1976,3 in 1977,…,

1.3. Forage Substitution Model

We assumed that forage demand is a fixed proportion of the cattle population. Then substitution among the three main forage inputs (hay, pasture, and corn stover) is described with a constant elasticity of substitution demand function. The demand equation satisfies baseline market shares of hay, pasture, and stover. It also has an elasticity of substitution of 3.0.

A 2009 baseline for forage consumption and market shares of hay, pasture, and stover was deduced available information. Total forage demands were developed from recommended rations and averages were constructed across a typical age and sex distribution. Pasture consumption of forage was approximated from baseline cattle populations, grazing season length and daily forage requirements. Hay consumption is approximated by hay production. Finally, stover demand is the difference between total forage demand versus hay and pasture demand.

2. Measuring Global Warming Sinks and Emissions

Existing procedures for measuring CO_2 equivalent emissions were restated as functions of appropriate economic variable instead of numbers calculated on baseline levels, in order to

account for the effect of changes in economic variables. G enerally, emissions functions depend on production, area, and livestock populations. All relationships are proportional. All measurements are expressed in a common CO_2-equivalent basis.

The GREET model of agricultural emissions is used for corn and soybeans. But revisions for recent fertilizer and energy use data were included [3]. Similarly, GREET fertilizer and fuel emissions coefficients were combined with appropriate fertilizer and fuel data for wheat, hay and switch grass.

IPCC Tier I procedures for beef and dairy cattle were used to estimate livestock based emissions [4]. Enteric and Manure emission of dairy and beef cattle in North America are included. Also, the N2O equivalent emissions from spreading livestock manure on land are included with livestock instead of land, because this activity is economically linked to the livestock population.

Estimates of the equilibrium soil carbon stock are also provided. Here we use the IPCC teir I procedure, which identifies a reference level for soil carbon in undisturbed soil, and a set of multipliers for several different categories of land use [5]. The reference carbon level and multipliers for the land use categories in our model are shown below:.

Table 1.multipliers for soil carbon, by land type

IPCC Classification (Table #)	Native-C multiplier (0/1)	Model's land use variable (symbol)
Native (5-11)	1.00	Other farmland (Lg-Gs)
Unimproved Grassland (5-10)	0.77	Pasture Supply (Gs)
Idle cropland (5-12)	0.70	Cropland in pasture (Cdg)
Set Aside<20 yr (5-12)	0.80	CRP land (Cdz)
Cropland in Crops (5-12)	0.70	Corn, Soybeans, Wheat (Cdc,Cds,Cdw)
Improved pasture, Hay (5-10)	1.10	Hay (Cdh)
Improved pasture, Hay (5-10)	1.0	Switchgrass (Cdsg), conservative

Native C-stock: 80 mt / ha (130.87 ton CO_2 / acre)

It is important that minimal carbon release is possible when converting land from pasture to hay or biomass crops. Indeed, switch grass is already used as forage in managed pasture [6]. Further, no-till planting methods for switch grass on pasture appear to have a minimal environmental effect [7].

Three main aspects of Carbon are summarized in simulations. First, the CO_2 sink associated with the switch grass crop is an initial approximation for the fossil fuel replacing benefit of biofuel. Second, the change in livestock emissions, a decline, represents a potential offset for adverse lanc-conversion emissions associated with starting a bio fuel industry. Third, the change in soil carbon stocks (expressed as CO_2-equivalent) is calculated as the difference between annual estimates of equilibrium soil carbon stocks. Also, the net sink of other crops (corn, soybeans, wheat, and hay) is also calculated, even though much of this sink likely belongs to an out-of-state carbon budget for corn-ethanol, consumption in other states, or use in a foreign country. It is helpful to see how field crop CO_2 sinks change with changes in switchgrass sinks, livestock emissions, or soil carbon capture/release.

3. Baseline

The most recent USDA 10 year baseline defines reference levels for the main commodity prices that drive (are exogenous to) the local biomass supply/forage demand model [8]. However, the reference prices for corn, soybeans, wheat, beef, and milk are adjusted to reflect a distortion-free policy environment that would put a new biomass industry on equal footing with other established industries.

First, the corn-ethanol industry has over-expanded as a result of a mandate for minimum ethanol use, called the Renewable Fuel Standard (RFS). About 4.0 billion gallons per year (BGY) of the RFS extends beyond supply increases that can be gathered from corn yield growth on land that is presently used. The price-effects of one-half of the overexpansion, or 2.0 BGY, is subtracted from the baseline corn and soybean prices using multipliers developed elsewhere [9]. Hence some overexpansion effects, which result in artificially high prices for substitute commodities and land rent, are removed from the baseline.

Second, a 30% import duty on US Beef imports [10] artificially holds US beef prices above market levels, encourages overproduction, and inflates local forage demands and prices for marginal land. For a first approximation, USDA baseline prices for beef are reduced by 30%. Milk prices are also reduced by 30%, because domestic milk prices are supported by an elaborate quota system.

Other exogenous assumptions for the projection period also fit today's apparent circumstances. For instance, cropland declines at 0.7 million acres (3.1%) per decade, as defined by the most recent census of agriculture. But other(non-cropland)farmland remains constant at about 5.0 million acres. Hay yields remain constant at at the average of recent values- the experience of the last two decades. Corn yields increase 20% over the first few years of the projections, and then remain level. Finally, a zero inflation rate for the CPI reflects today's depressed macro-economy.

The hypothetical baseline defines a scenario of declining commodity prices, cattle populations (figure 1), and local land prices (figure 2). Consequently, the demands for local resources are also declining. The prices of grains that are internationally traded would also gradually decline. Thus, the demand for local land resources and land rental rates are also declining.

Figure 1. The catle pouplation will continue declining in the future and decline somwhat faster with switchgrass

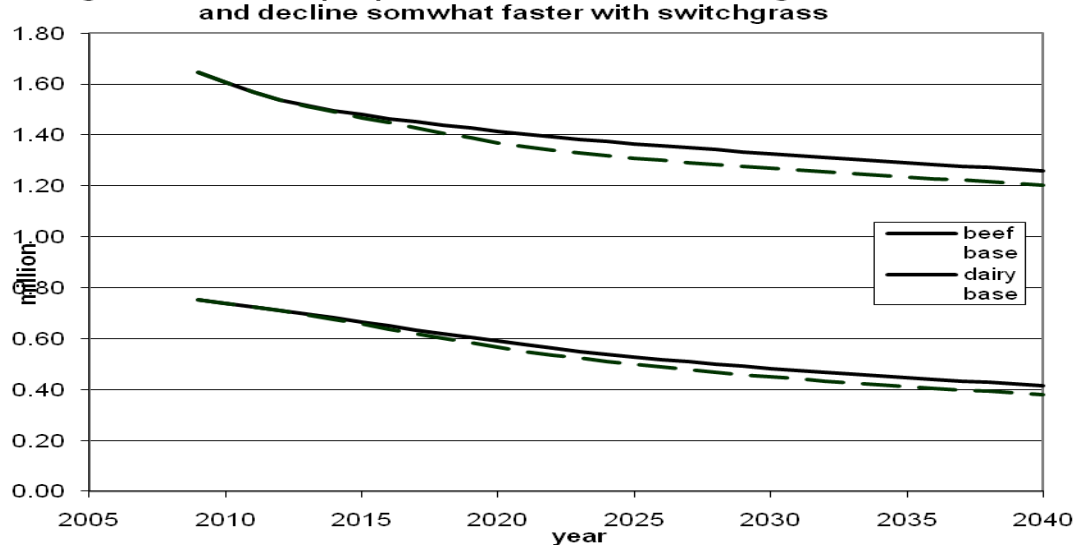

Figure 2. Land rental values decline until the switchgrass expansion stablizes pastureland values and induces risingcropland values

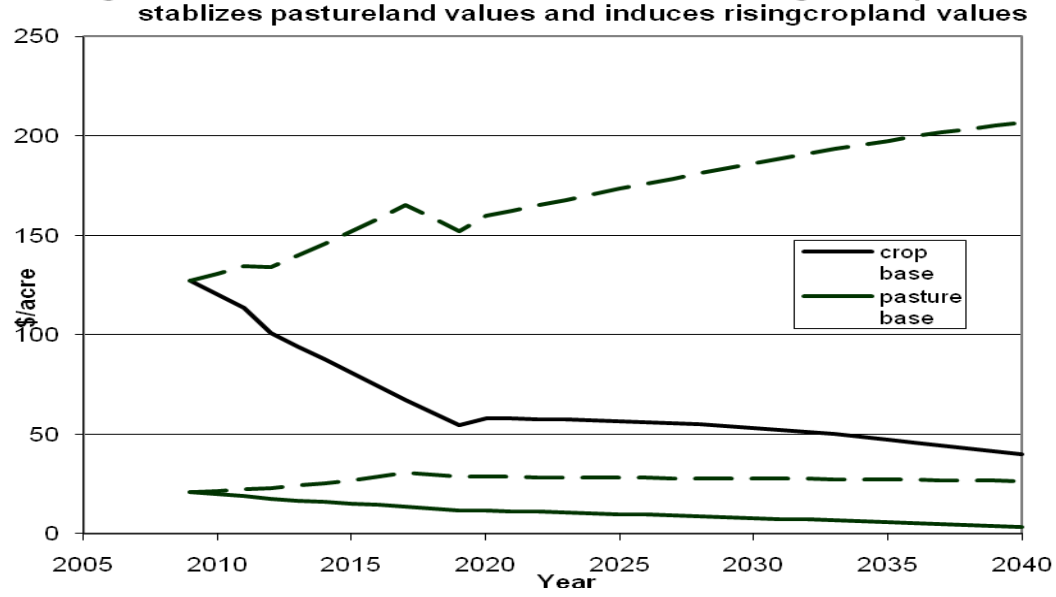

Emissions for two of our three main activities are reinforcing, and produce net CO_2 emissions under baseline conditions. Cattle emissions are substantial, but declining. In 2009, emissions are 22.6 bil. lbs CO_2-equivalent, but decline to 15.2 bil. lbs at the end of the simulation period. Equilibrium Carbon stocks decrease steadily at a rate of about 12.0 bil. lbs CO_2, annually, throughout the 30 year simulation period (figure 3b).

Figure 3b. local land change and cattle emissions contribute to global warming without switchgrass although emissions improve with cattle

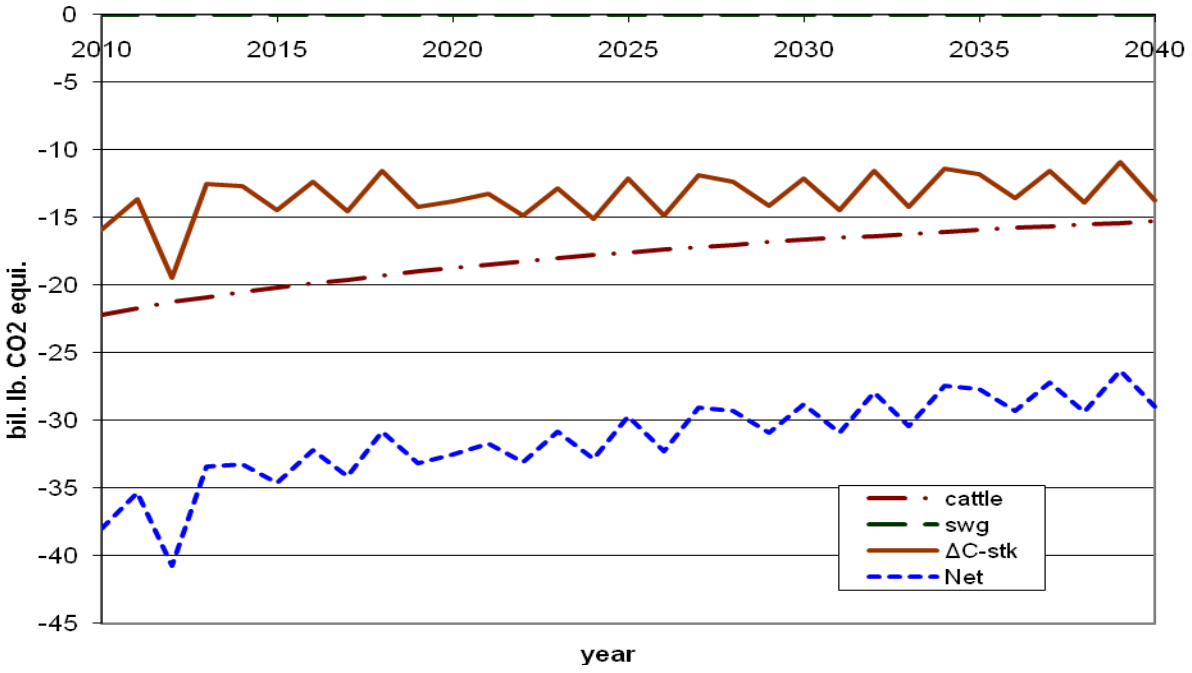

4. Biomass Fuel expansion

Here, an exogenous land demand expansion for a biomass crop (switchgrass) gradually increases the total area used for biomass to 4.0 million acres over a 5 year period that begins in 2010 (the first year of the simulation). The 4.0 million acre area is split equally between

cropland and pastureland. Switchgrass is only one of several potential biomass crops, but still has a representative crop yield and carbon sink/emission profile.

The gradually expanding land demands restore increasing land prices (figure 2). But the increases are moderate; cropland rentals take three decades to double; pasture rental rates increase by about 20% over the first ten years, and remain stable thereafter.

The Greenhouse gas profile would also improve (figure 3s). First, increasing switchgrass production implies a substantial net carbon sink, most of which replace fossil fuels. Second, livestock emissions continue to improve through cattle reductions, accounting for about 20% of switchgrass emissions. Third, the equilibrium carbon stock would increase substantially during the biomass crop expansion phase, mainly because of the carbon storage profile of switchgrass. But the annual increment to the equilibrium carbon stockreverts to an emission thereafter. Nonetheless, three main activities combine for a net carbon sink (figure 3s).

Figure 3s. GHG sink from growing biomass fuel adds to a beneficial land use sink and offsets cattle emissions.

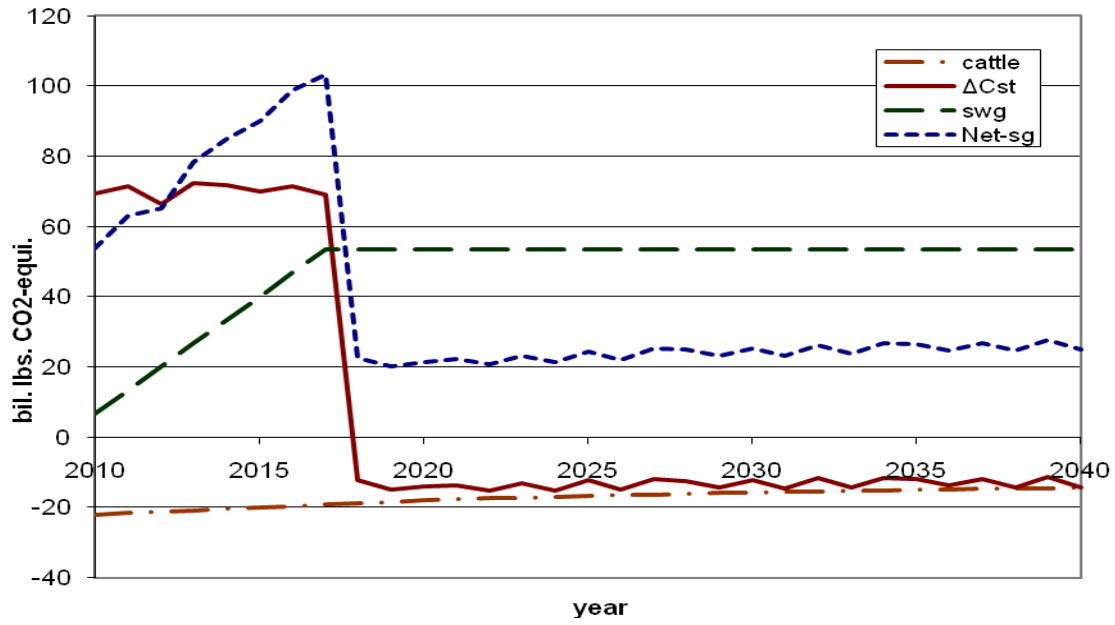

5. Conclusions

This study looks at the introduction of biomass fuel in local agricultural markets where land use and forage demand are defined. The hypothetical biomass expansion was split between cropland and pastureland, even though land costs per unit of biomass appear lower using marginal land.

The reference point is a distortion-free baseline created by removing recent over-expansion in corn ethanol and protection for livestock products. The baseline is characterized by declining land use values for cropland and pasture land.

The substantial biomass expansion is enough to support a 1.0 billion gallon ethanol industry. And the expansion merely restores stable or moderately increasing land values. Hence, The local agricultural resource is large enough to accommodate biomass ethanol production at a large scale.

The expansion on marginal land has mainly a local market impact. About 40% of the marginal land comes from the secular decline in cattle population and overall forage needs.

Otherwise, cattle rations shift away from pasture and towards hay and corn stover. In fact, hay demand grows despite declining cattle populations in the biofuel scenario. Compared to the baseline, the switch grass expansion restores stability to pasture rental rates.

The CO2 accounting focuses on changes in local agriculture as well. First, the direct benefit for switchgrass used as biofuel is included. Second, declining cattle emissions are also included. Third, the land use change effects on equilibrium soil carbon storage are included. Results suggest an increase in soil carbon storage, especially during the switchgrass expansion phase. Increasing hay production likely contributed to improving carbon storage as well. The change in net greenhouse gas sinks from the three local sources is 60 bill lbs CO2 equivalent, annually, after switchgrass production is established. The change in net sinks exceeds 100 bill. Lbs during the switchgrass expansion phase.

Two tasks remain for a comprehensive CO2 accounting. First, several other states with similar agricultural resources that are potential biomass supply areas should be incorporated into the analysis. Second, the totality of local changes must be considered in national and international markets. It seems plausible that the cattle decline would be absorbed into a declining demand for beef. However, the corn land expansion induced by the cropland expansion for switchgrass already appears large relative to the corn ethanol shift used to produce a distortion-free baseline. Accordingly, further simulations might usefully focus exclusively on expansions on marginal land.

The moderate price impact, beneficial lifecycle analysis, and potentially local impact for the marginal land expansion merits further attention. EPA regulations that restrict changes in use of permanent pasture may also deserve further scrutiny.

Figure 4. moderate net GHG sink with biomass replaces a net GHG emission without biomass for a large improvement.

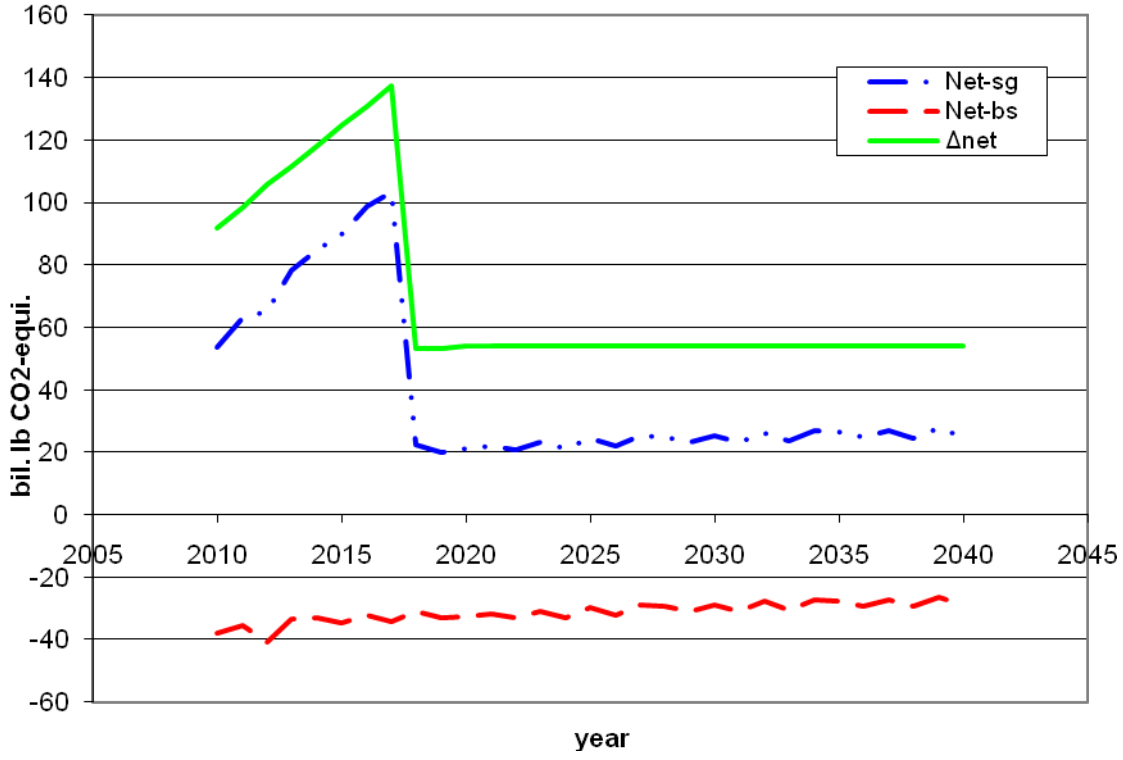

References

[1] J. Fargione, J. Hill, D. Tilman, S. Polasky, P. Hawthorne, Land Clearing and the Biofuel Carbon Debt, Science, Vol 319, 29 February 2008, p.1235-1238.

[2] P. Gallagher, P. and H. Shapouri, Biomass Crop and Ethanol Supply from Agricultural Lands in the United States, AER No. 844, U.S.. Dept. of Agriculture, Nov. 2008.

[3] M. Wang, Y.Wu, and A. Elgowainy, The Greenhouse Gases, Regulated Emissions, and Energy Use in Transportation Model,' Operating Manual for GREET: Version 1.7, Center for Transportation Research, Argonne National Laboratory, http://www.transportation.anl.gov/software/ Greet/index.html, February 2007.

[4] Intergovernmental Panel on Climate Change. Revised 1996 IPCC Guidelines for National Greenhouse Gas Inventories, Reference Manual (Volume 3) Agriculture, 1997. http://www.ipcc-nggip.iges.or.jp/public/gl/invs6c.html

[5] Intergovernmental Panel on Climate Change. Revised 1996 IPCC Guidelines for National Greenhouse Gas Inventories, Reference Manual (Volume 3) Land Use Change and Forestry,1997.

[6] J C Henning, Big Bluestem, Indiangrass and Switchgrass, University of Missouri Extension G4673 October 1993,

[7] KJ Goddard and JWalton, Switchgrass for Biofuels University of Tennessee Biofuels Initiative, October 10, 2007.

[8] Interagency Agricultural Projections Committee, USDA Agricultural Projections to 2019, Long-term porojections report OCE-2010-1, February 2010.

[9] PW Gallagher, Corn Ethanol Growth in the US without Adverse Foreign Land Use Change: Defining Limits and Devising Policies, Biofuels, Bioproducts, and Biorefining, May/June 2010.

[10] PW Gallagher, A look at US-Brazil ethanol trade and policy, Biofuels, Bioproducts, and Biorefining, September 2007.

Enhanced Renewable Energy Adoption for Sustainable Development in India: Interpretive Structural Modeling Approach

Vimal Kumar Eswarlal [1*], Prasanta Kumar Dey [1], Ravi Shankar [2]

[1] *Aston University, Birmingham, United Kingdom*
[2] *Indian Institute of Technology Delhi, New Delhi, India*
[*] *Corresponding author. Tel: +44 7843946797, E-mail: vimaleswarlal@yahoo.com / eswarlvk@aston.ac.uk*

Abstract: Poverty alleviation and social upliftment of rural India is closely linked with the availability and use of energy for development. At the same time, sustainable supply of clean and affordable renewable energy sources is required if development is to be sustainable, so that it does not cause any environmental problems. The purpose of this paper is to determine the key variables of renewable energy implementation for sustainable development, on which the top management should focus. In this paper, an interpretive structural modeling (ISM) - based approach has been employed to model the implementation variables of renewable energy for sustainable development. These variables have been categorized under 'enablers' that help to increase the implementation of renewable energy for sustainable development. A major finding of this research is that public awareness regarding renewable energy for sustainable development is a very significant enabler. In this paper, an interpretation of variables of renewable energy for sustainable development in terms of their driving and dependence powers has been examined. For better results, top management should focus on improving the high-driving power enablers such as leadership, strategic planning, public awareness, top management support, availability of finance, government support, and support from interest groups.

Keywords: *Sustainable development, Renewable energy, Performance measures, Interpretive structural model, India*

1. General structure of the paper

The world energy forum has pointed out that coal and gas reserves will become depleted in less than the next 10 decades. Ashwani Kumar et al, [1] observed that fossil fuels account for around 79% of the energy consumption in the world, and 57.7% is consumed by the transport sector and is being depleted very speedily. Apart from this, various environmental problems are also related with the increasing use of fossil based oils, coal and gas. So there is an urgent need to develop the alternative energy resources in order to overcome the future energy shortage. Also, the depletion of natural resources and increasing demand of energy nowadays has forced policymakers to consider alternative energy sources for sustainable development. 'Sustainable development' means development which is capable of being sustained for the future stability. Where, renewable energy sources are regenerative and do not get exhausted. Renewable energy helps the world in reducing their carbon emission and cleans up the air and helps in achieving sustainable development. The most important feature of renewable energy sources is their environmental suitability but sustainable development does not only revolve around the environmental stability but it a lso deals with social and economical stability. Hence, nowadays investigation of energy strategies for renewable energy has become crucial, particularly for the stability of future energy.

India's population has been increasing very rapidly and it is also the fastest growing economy in world (with GDP of $ 1 trillion measured in 2008) after china, which further leads to a hike in energy demand and its impact on the environment in India. Mohit Goyal et al, [2] pointed out that India's power sector has shown tremendous increase from 30,000 M W in 1981 to 143,000 MW by March 2008. As the fossil fuels are depleting fast, India will face the energy shortages in future which need to be addressed by developing alternative energy resources the country can rely on. India is left with no option but to concentrate towards the maximum use

of renewable energy. Fortunately India has plenty of renewable resources such as wind energy, biomass energy, small hydro power and solar energy to exploit for sustainable development. India is set to reach the aim of producing 10% of total power supplied through renewable energy by 2012 [1]. The government of India has promoted the use of renewable energy for sustainable development through several policy and provision interventions. Since 2007 power generation from renewable wind energy has increased by 3,857 MW; small hydro has increased by 619.53; biomass has increased by 322 MW; solar energy has increased by 8.10 MW and industrial and urban waste to energy has increased by 20.10 MW. Investment of around 3.9 billion Indian rupees ($86 million) has been made for different renewable energy projects and programs. Meanwhile, the World Bank has also allotted $4 billion in loans for India's renewable energy projects.

The purpose of this paper is to search the variables affecting the progress of the renewable energy for the sustainable development in India. Policy makers would face many difficulties in implementing renewable energy for sustainable development due to various variables affecting its performance. These variables not only affect the performance of renewable energy development but also act upon each other. Hence, the methodology of Interpretive Structural Modeling (ISM) has been applied in this paper to establish the conceptual relationship amongst various variables which are hindering the path of renewable energy for the sustainable development.

2. Literature review

A lot of research has been done before to find out the variables which affect the implementation of the renewable energy for the sustainable development. Fred Beck et al, [3] have observed the main barriers to renewable energy development in 2004. McCormic et al, [4] observed the major barriers that affect the implementation of energy for the sustainable development on the basis of research conducted by Bioenergy network of excellence. Himri et al, [5] has worked on formulating barriers which are hindering the full potential and advantages of the renewable. Lidula et al, [6] has formulated the barriers for clean and sustainable energy in the ASEAN member countries. Mayfield et al, [7] has developed a new methodology to deal with the barriers affecting the performance of Biomass operations. Sharma et al, [8] has studied the parameters of waste management in India. New York State Energy Research and Development Authority and Oak Ridge National Laboratory (ORNL) have identified some of the barriers to energy through research [9].

An important barrier for renewable energy development is lack of leadership qualities in managers. A good strategic plan identifies the renewable energy goals and then formulates policies to achieve these goals. Sustainable energy development strategies should deal with energy saving, improvement in the efficiency of energy production and replacement of the fossils based oils, coal and gas reserves [10]. There are two major factors which have affected the energy pattern most; the technological changes and the availability of energy resources [11]. Renewable sources are present in abundance but still cannot be harnessed for sustainable development due to lack of technology and public awareness. Continuing innovation in technology is necessary to harness each form of renewable energy [12]. The major challenge for the renewable energy industry is the timely availability of resources [10]. Himri et al, [5] has pointed out that lack of information dissemination would lead to lack of support from different stake holders. So, the availability of data and information acts as an enabler for the renewable energy for the sustainable development. The shortage of skilled professionals which includes designers, installers, service and sales representatives, policy analysts, scientists, engineers, teachers and researchers can also affect the quality of the system [13].

Government has put lots of effort towards enhancing the use of renewable energy for the sustainable development through subsidies, fiscal incentives and has encouraged investors to invest in renewable energy through various relevant supportive policies. Moreover, huge amount of investment is needed in developing the advanced technology required to fully exploit some renewable resources. Due to longer investment periods the risk of return on investment is high [14]. Hence it is necessary to incorporate the relevant policies in order to attract the interest groups to invest in it. The market for renewable energy has increased significantly and manufacturers are investing huge amount of money in R&D (research and development) of RET (renewable energy technology) which will further lead to economically sustainable growth. Table 1 below shows the 14 variables chosen based on the previous research.

Table 1. Variables affecting the performance of renewable energy for sustainable development

S. No.	Variables
1.	Leadership
2.	Strategic planning
3.	Availability of technology
4.	Public awareness
5.	Top management support
6.	Sustainable growth
7.	Return on investment
8.	Availability of finance
9.	Skilled man power
10.	Government support
11.	Availability of data and information
12.	Availability of energy resources
13.	Support from interested groups (stake holders)
14.	Efficiency of process and execution

3. Methodology

Interpretive structural modeling is a tool which here is applied for the analysis of the interaction amongst variables of the renewable energy for sustainable development. This approach has been used in many fields by scholars to investigate the inter-relationship amongst many variables. Warfield, [15] is the one who has introduced interpretive structural modeling (ISM) and Malone, [16] is the second one who conducted brief review of the ISM. It provides us means by which order can be imposed on the complexity of such elements [17, 18]. This method is known as 'interpretive structural modeling' because all the variables and their interrelationships are decided by group judgment. The ISM methodology is an interactive learning process in which a set of different and directly or indirectly related elements affecting the system under consideration is structured into a comprehensive systemic model [9]. Finally the graphical representation of the relationships among the variables is demonstrated. This methodology (ISM) has attracted a great deal of interest recently due to its high flexibility. Following are the steps involved in the formulation of ISM:

1.The variables affecting the performance of the system are listed with the help of literature review and expert opinion.

2.A conceptual relationship amongst the variables is made by the help of opinion of the experts.

3.Then a structural self-interaction matrix (SSIM) is formulated which entails the pair wise relation of the variables.

4.Now, the reach ability matrix is derived from the structural self interaction matrix (SSIM) by putting '1' and '0' which shows pair wise relationship accordingly.
5.Then the transitivity is removed from the reach ability matrix and transitivity rule says that if variable 'A' leads to variable 'B' and 'B' leads to variable 'C' then 'A' will also lead to variable 'C'.
6. The reachability matrix is divided into different partition levels.
7.The directed graph is drawn on the basis of the relationship between the variables discussed in the above reachability matrix and all the transitive links are removed.
8. The digraph is converted into ISM by converting variables nodes in to statements.
9. Finally a review of the ISM model is done and any necessary modifications are carried out.

After the final ISM structure MICMAC analysis of the variables is done on the basis of their driving and dependence power. MICMAC was first proposed by Duperrin and Godet in 1973 [19]. MICMAC analysis can be used to categorize variables in a complicated system [20]. The prime function of MICMAC analysis is to examine the driving and dependence power of the variables [17, 18]. Here the barriers are divided into four classifications according to their driving and dependence power known as autonomous, linkage, dependent and independent barriers [18]. The first cluster is known as 'autonomous barriers' which have very weak driving power and simultaneously have weak dependence power. These variables mostly have no connection with the system or with other variables; they only share few links which can be strong. The second cluster is known as 'dependent barriers' which consist of variables having weak driving power and strong dependence power. These variables mostly depend on other variables so; any action on other variables will affect the dependent variables. The third cluster consists of the 'linkage variables' which have strong driving and strong dependence power. These variables are highly unstable so, any action on these variables will affect other variables and also have a feedback effect on the linkage variable. Lastly the fourth cluster is basically the 'independent barriers', consists of variables which have strong driving power and weak dependence power.

4. Results

The ranking of all variables is known through level partitions so they have been put at their respective levels in the ISM hierarchy. Interpretive structural model is finally formulated with the help of final reach ability matrix and level partitions, which is shown in Fig. 1. It is observed from the ISM based model that public awareness about renewable energy is a very important variable as it has highest driving power and zero dependence power. This means this variable is very significant and drives all other variables. So, the policy maker has to keep more focus on public awareness in order to implement renewable energy for the sustainable development successfully. Awareness about renewable energy among the public will lead to top management support (variable 5). Conversely leadership qualities of a manager (variable 1) can act as a tool only if there is a top management support. Good strategic planning (variable 2) needs manager leadership quality and incentive support from top management. Support from interested groups (variable 13) cannot exist if there are no top management support withinpolicy makers. Availability of finance (variable 8) is ensured by support from the interested groups (stakeholders). Skilled man power (variable 9) and availability of information is very necessary for the successful implementation of renewable energy projects for sustainable development. Availability of finance actually helps in achieving the skilled man power as skilled man power is highly costly. Information management (variable 11) ensures the effective utilization of the resources.

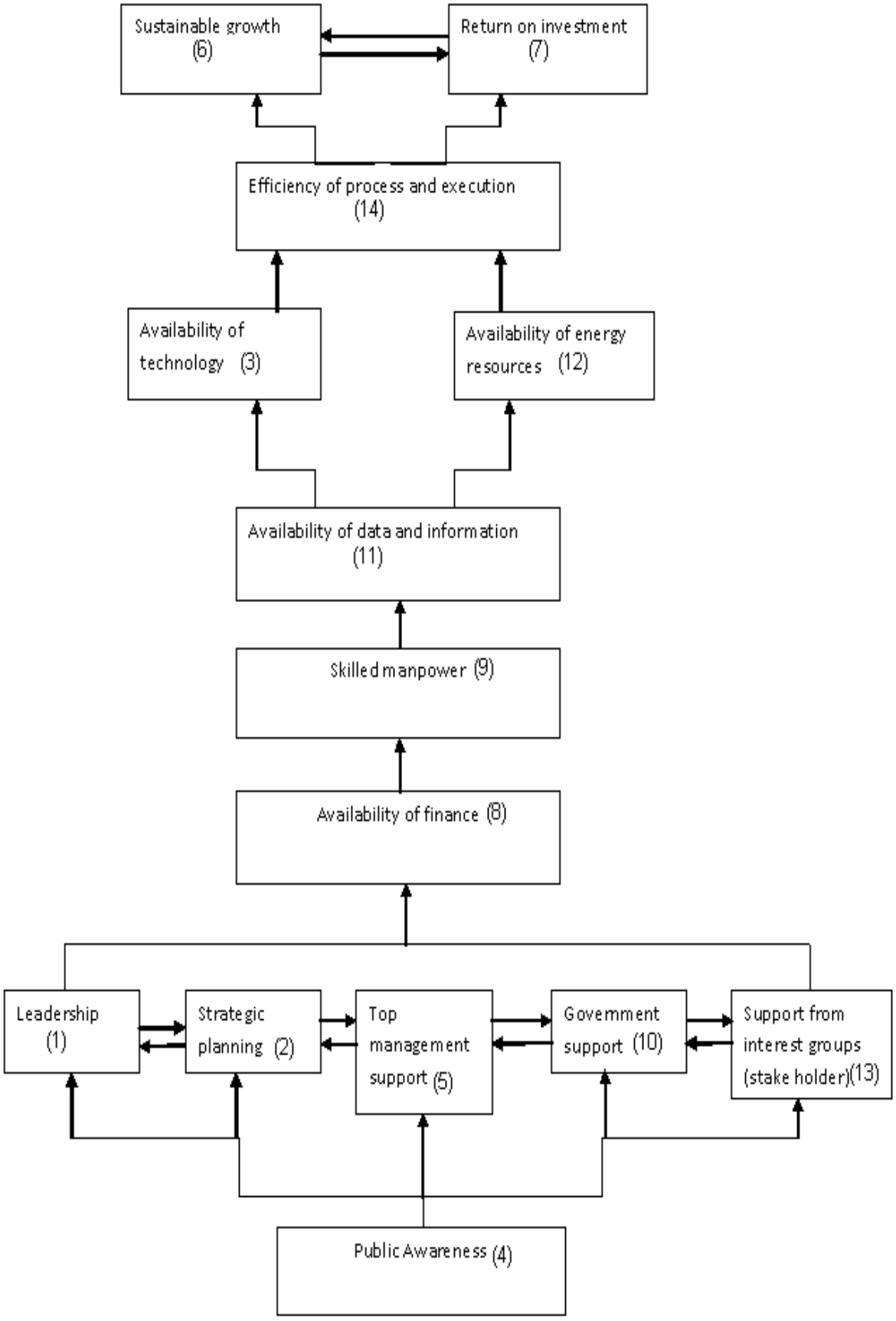

Fig. 1. ISM Based Model

Lack of appropriate data and information will lead to lack of interest from public and management, which further leads to lack of energy resources (variable 12) and lack of renewable energy technology (variable 3). Outdated technology has a direct impact on the efficiency of the process and its execution (variable 14). So, more and more money should be invested in the development of new technologies for the successful implementation of the renewable energy projects. High efficiency of the process will lead to sustainable growth (variable 6), which further leads to return on investment (variable 7) or vice versa. Good return on investment is a symbol of an economically sustainable system. This study shows that all the above discussed variables are enablers which enable the successful implementation of the project. According to ISM hierarchy there is a great need to work upon these variables for the sustainable development through renewable energy sources.

The MICMAC analysis has been drawn as shown in Fig. 2 below, the driving and dependence power has been shown in final reachability matrix. In the MICMAC diagram below the column and rows represent the driving and dependence power respectively. All the variables have been placed in the diagram according to their driving and dependence power. As an example variable 4 (public awareness) has driving power of 14 and dependence power of 1 and therefore has been placed accordingly in the MICMAC diagram at the extreme top left of the diagram.

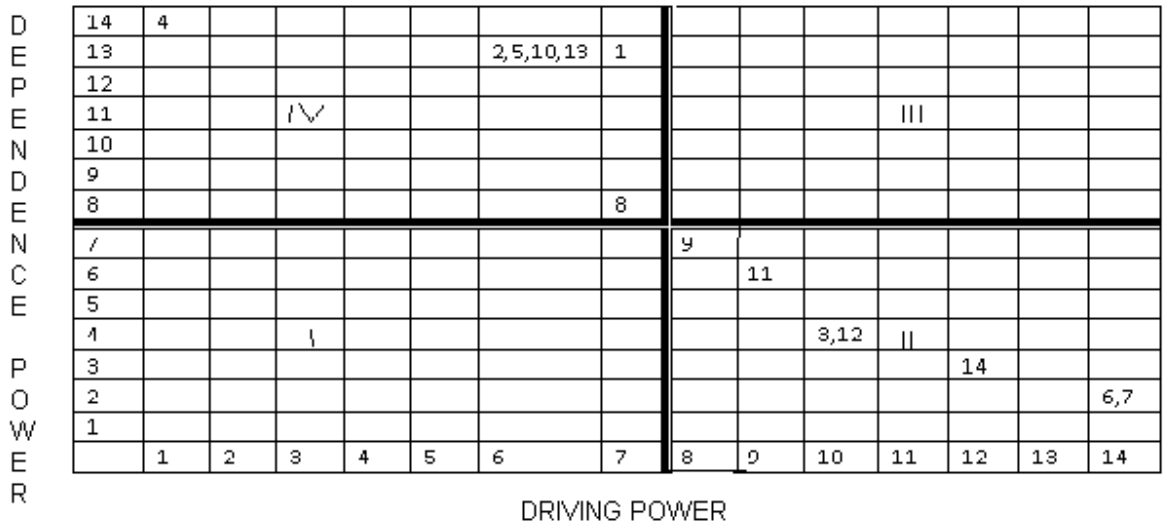

Fig. 2. MICMAC Diagram

5. Discussion and Conclusion

India is growing very fast approximately at a rate of 9% and the situation of energy shortage gets darker with the increase in the economic growth of the country. India has to exploit all sources of renewable energy in order to tackle the energy shortage problem [2]. The only solution remaining to the policy makers is using renewable energy as fossil based oils, coal and gas reserves are at the verge of depletion. But there are lots of variables which affect the implementation of renewable energy for sustainable development. Policy makers therefore face lots of challenges in identifying these variables and then working upon them to improve the performance of the system. Some variables termed as 'enablers' have been identified in this paper and interrelationships among these variables have been formulated using ISM methodology. This provides the hierarchy of action which has to be performed by the policy makers in order to improve the efficiency of the system.

From ISM based model (drawn above) it can be concluded that variable 4 (public awareness) is of top most priority as it has highest driving power of 14 and lowest dependence power of 1. This also states that policy makers have to create public awareness about the use of renewable energy for the sustainable development. In MICMAC analysis this has been concluded that there are no autonomous variables which prove that all variables stated above influence the implementation of the renewable energy for the sustainable development. Similarly from the MICMAC analysis it has also been concluded that there are no variables in the third cluster which is linkage barriers. This shows that all the variables stated above are stable. From the diagram it has been observed that variables such as leadership, strategic planning, public awareness, top management support, availability of finance, government support, and support from interest groups (stakeholders) fall under the fourth cluster which is 'independent barriers'. All these variables have high driving power and policy makers should focus more on these variables as they affect or influence other enabling variables. Availability of technology, availability of data and information, sustainable growth, return on investment, skilled manpower, availability of energy resources and efficiency of processes are those variables which fall under second cluster (dependent barrier) and have high dependence power.

Basically ISM based model in Fig.1, represents an overall picture of the problems in implementing renewable energy for the sustainable development in front of the policy makers. This research has most importantly identified the variable affecting the performance of the process and interrelationship among them. This model works for the better managerial decisions in order to have more efficient and effective renewable energy project for sustainable development. Also this work identifies leadership, strategic planning, public awareness, top management support, availability of finance, government support, and support from interest groups (stake holders) as very important factors, which needs immediate and high attention from the policy makers.

In this research work, interrelationship among the variables of implementation of renewable energy for sustainable development has been formulated, but it has to be mentioned that this model is not statistically validated. SEM (Structural equation modeling) sometimes also referred as linear structural relationship approach acts as a tool in order to test the validity of such hypothetical models [18]. The scope for future work following this research is to test the validity of this hypothetical model i.e. ISM using SEM.

References

[1] A. Kumar, K. Kumar, N. Kaushik, S. Sharma and S. Mishra, Renewable energy in India: current status and future potentials, Renewable and Sustainable Energy Reviews 14, 2010, pp. 2434 - 2442

[2] M. Goyal and R. Jha, Introduction of Renewable Energy Certificate in the Indian scenario, Renewable and Sustainable Energy Reviews 13, 2009, pp. 1395 - 1405

[3] F. Beck and E.Martinot, Renewable Energy Policies and Barriers, Chapter of the Book: C. J. Cleveland, and R.U. Ayres (Ed.), Encyclopedia of Energy, Elsevier Academic Press, 2004.

[4] K. McCormick and T. Ka berger, Key barriers for bioenergy in Europe: economic conditions, know-how and institutional capacity, and supply chain co-ordination, Biomass and Bioenergy 31, 2007, pp. 443 - 452.

[5] Y. Himri, A. S. Malik, A. B. Stambouli, S. Himri and B. Draoui, Review and use of the Algerian renewable energy for sustainable development, Renewable and Sustainable Energy Reviews 13, 2009, pp. 1584 - 1591.

[6] N.W.A. Lidula, N. Mithulananthan, W. Ongsakul, C. Widjaya and R. Henson, ASEAN towards clean and sustainable energy: potentials, utilization and barriers, Renewable Energy 32 (9), 2007, pp. 1441 - 1452.

[7] C. Mayfield, C.D. Foster, C.T. Smith, J. Gan, and S. Fox, Opportunities, barriers, and strategies for forest bioenergy and bio-based product development in the Southern United States, Biomass and Bioenergy 31, 2007, pp. 631 - 637.

[8] H.D. Sharma, A.D. Gupta, and A. Sushil, The objectives of waste management in India: a futures inquiry, Technological Forecasting and Social Changes 48, 1995, pp. 285 - 309.

[9] B. Tonn, and J.H. Peretz, State-level benefits of energy efficiency, Energy Policy 35, 2007, pp. 3665 – 3674.

[10] H. Lund, Renewable energy strategies for sustainable development, Energy 32, 2007, pp. 912 - 919.

[11] N.H. Afgan, D.A. Gobaisi, M.G. Carvalho and M. Cumo, Sustainable energy development, Renewable and Sustainable Energy Reviews 2, 1998, pp. 235 – 286.

[12] B.S.K. Naidu, Indian scenario of renewable energy for sustainable development, Energy policy 24 (6), 1996, pp. 575 - 581.

[13] P. Jennings, New directions in renewable energy education, Renewable Energy 34, 2009, pp. 435 – 439.

[14] G.H. Wanga, Y. X. Wangb, and T. Zhaoa, Analysis of interactions among the barriers to energy saving in China, Energy Policy 36, 2008, pp. 1879 – 1889.

[15] J.W. Warfield, Developing interconnected matrices in structural modeling, IEEE Transactions on Systems, Man and Cybernetics 4 (1), pp. 51 - 81.

[16] D.W. Malone, An introduction to the application of interpretive structural modeling, IEEE 63 (3), 1975, pp. 397–404.

[17] A. Mandal and S.G. Deshmukh, Vendor selection using interpretive structural modeling (ISM), International Journal Operations and Production Management 14 (6), 1994, pp. 52 - 59.

[18] S. Jharkharia and R. Shankar, IT-enablement of supply chains: understanding the barriers, The Journal of Enterprise Information Management 18 (1), 2005, pp. 11 - 27.

[19] J.C. Duperrin and M. Godet, Methode De Hierar Chization Des Elements D'um System, Proceedings of Rapport Economique De CEA, Paris, 1973, pp. 45 - 51.

[20] J.W. Warfield, A science of generic design: managing complexity through systems design: volume 1, Intersystems Publications, Salinas, CA, 1990.

Promoting Biofuels Adoption in Nigeria: A Review of Socio-economic Drivers and Incentives

Nelson Abila

Department of Industrial Management, University of Vaasa
P.O. Box 700, 65101 Vaasa, Finland
Tel: +358 44 3177440, E-mail: nelson.abila@uwasa.fi

Abstract: The adoption of biofuels holds a diversity of opportunities and potentials for the Nigerian economy. Some of these opportunities are key socio-economic drivers and incentives promoting the increasing adoption of biofuels. From the upstream to the downstream sub-sectors, there is an increasing entry of players and participants (private and public investors). This paper explores the underlining socio-economic drivers and incentives promoting and encouraging more investments in the biofuels subsectors of the Nigerian economy. The research sourced data from basically secondary sources and through desk-reviews. The papers identifies essential socio-economic indices which include the default dependence of biomass fuels, poverty and unemployment, declining agricultural productivity, underutilization of arable lands, potential demand for biofuels and government policy and incentives. As the global trend shows increasing adoption of biofuels, this paper reveals and discusses the socio-economic drivers peculiar to Nigeria. These key factors identified are issues to put into consideration for sustainably managing biofuels investments in Nigeria. Some of these factors present prospects and problems requiring medium and long term policy interventions from government to ensure an efficient transition into a bioenergy driven economy. The socio-economic factors identified also presents key variables for further socio-economic and bio-economic modelling studies focusing on Nigeria.

Keywords: *Biofuels, Drivers, Incentives, Policy, Bioenergy, Economy.*

1. Introduction

This paper explores the underlining socio-economic drivers and incentives promoting and encouraging the investments and participations in biofuels adoption, development and utilization in Nigeria. Nigeria joined other nations in the quest for adopting biofuels as the continuous reliance on the fossil fuels continues to receive criticism and fire from scientists, activists, and a wide range of peoples and interests promoting and implementing a shift in energy sources to more clean and environmentally friendly options. The global cries for renewable alternatives energy sources combine with default potentials for large scale production of biofuels created the platform for Nigeria's gradual incursion into the biofuel era. Though Nigeria is a major petroleum exporting country (1, 2), the drivers and incentives for promoting biofuels adoption are deeply connected with the roots of the many problems impeding the growth and development of the nation's economy. There is a preponderance of rural communities and populations with a default energy reliance sourced mainly from renewable sources and primary biofuels such as fuelwood, charcoal, palm kernel shells, palm-oil wastes (shaft and slurry), sawmill waste, cow dung among others. Though there is also a rapid growth of urban centers across Nigeria, majority of the population in urban areas also still depend on these renewable sources such as charcoal because of the very low rate of access to electricity, natural gas or other improved energy sources.

This paper identifies and explores the underlining socio-economic drivers, relative incentives as well as exogenous and endogenous inducements for promoting and encouraging more investments in the biofuels subsectors of the Nigerian economy. From the analysis, the paper presents a multilevel, multifactor and multi-actors framework that constitute the drivers for biofuels adoption in Nigeria.

2. Methodology

This research is a review of the socio-economic and related factors that explain the default renewable energy dependence and stimulating the trend in the investments in the broader biofuels subsector ranging from feedstock production to biofuels refining and biofuels distributions networks across Nigeria. The research sourced data from basically secondary sources and through desk-reviews. This review work is limited by the inability to conduct primary survey and the attendant gaps in information. Secondary data are sourced from the Nigeria Bureau of Statistics reports and other available secondary sources including previous publications and report from the International Energy Agency. Data sourced were analysed using descriptive statistics. The paper also presents a preliminary framework for driver of biofuels.

3. Biofuel Development in Nigeria

3.1 Biofuels in Nigeria

Though the traditional energy sources in Nigeria are predominantly combustible renewable fuels (3), there is an increasing shift and adoption of the first and second generation biofuels. The first generation biofuels which include biodiesel, bioethanol and biogas (4) are sourced mainly from edibles sources or current food material such as maize, soyabean, sugarcane, cassava for ethanol or oil production which can also be used as energy sources after further processing. The second generation biofuels which are fuels sourced from mainly non-edible sources such as jatropha, algae (4). A range of first generation biofuels are already being produce at small scales in Nigeria. Ethanol production is part of the traditional livelihood systems in the Niger Delta area and extending to some part of the south western States. Various individual and public investment projects in first generation biofuels are taking up in various part of Nigeria. These investment projects are at various stages of implementation ranging from feasibility studies to refinery plant installation. Progress have been reported in the designing of biogas plants at the Usman Danfodiyo University where a biogas digester with 425 litres capacity adequate for household cooking energy need has been developed (5). Other experimental efforts are also ongoing at the University of Nigeria, Nsukka and at the Global Network for Environment and Economic Development Research (GNEEDER) in Ibadan. Nigeria import about 4.5 tonnes of motor gasoline in 2008 (6) from refineries in countries which are already blending the fuels according to their blending regimes. There is no information on the blending rate of fuel used in Nigeria sourced from imports or refined locally.

3.2 Nigerian Biofuel Policy and Incentives

In promoting biofuels, the government in 2005 gave the Automotive Biomass Program for Nigeria directive to the Nigerian National Petroleum Corporation (NNPC) to facilitate the adoption on biofuels and promote investment in the sector. This led to the birth of the Nigerian biofuel policy and incentives (7), a government whitepaper for promoting biofuels in Nigeria. The white papers provide a broad policy platform for promoting the adoption of biofuels and for fast tracking the investment in biofuels value chain from feedstock production to biofuel refining and distribution. It set a target of 10 years for attaining full E-10 blending of gasoline and by implication B-10 for diesel. Though the whitepaper identified very few source of biofuels feedstock in Nigeria particularly for producing first generation biofuels, Nigeria has the potential for producing feedstocks for second generation biofuels including jatropha, algae and Shea nut. The underlining objectives for government interest in a national biofuel promotion are among other revenue diversification, job creation, improving agricultural productivity, meeting energy needs as well as deriving environmental benefits.

4. Drivers of Biofuels Adoption

4.1 Default dependence on renewable biomass fuels

International Energy Agency (3) estimates put the total energy consumption for Nigeria at 4 Quadrillion Btu or 107,000 kilotons of oil equivalent. This IEA estimate shows that combustible renewable fuels providing 80.2 percent of the total energy need. According to the IEA report, the highest contribution for renewable biomass fuels serves the energy requirements for heating, and cooking needs particularly in the rural areas where access to the national grid is currently not available or still a dream in the pipeline. A previous national survey of the National Bureau of Statistics - NBS in 2005 which profiled the poverty level in Nigeria provided national estimate of the sources fuel for cooking as shown in Figure 1. Firewood contributed nearly 70 percent based on this estimate (8). In 2007, an economic survey by the NBS shows there has a gradually climb in the proportion of the population of Nigeria who depend on fuelwood for cooking. NBS estimates put the proportion at 74.1 percent. Previous study (5) had also reported a 1991 energy source survey in which fuelwood contributes about 66 percent. The electricity supply and sources survey for the same year 2007 also indicated that only about 47 percent of the population access electricity from the main national grid while considerable proportion (41 percent) do not have access to any form electricity supply. IEA data for 2008 indicated that electrification rate for Nigeria was 47 percent for the entire country. In urban areas, 69 percent of the population had access to electricity compared to rural areas where electrification rates were 26 percent. Approximately 81 million people do not have access to electricity in Nigeria.

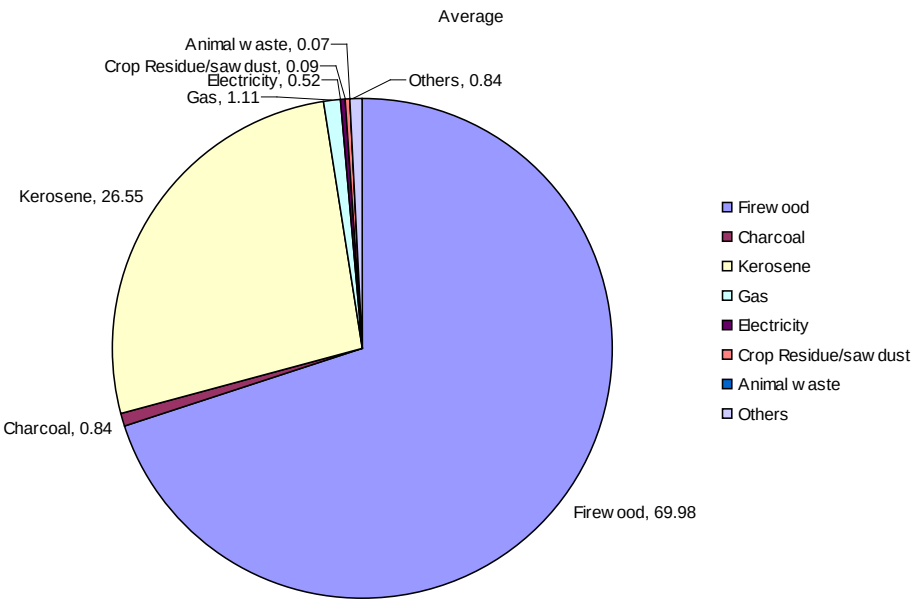

Fig. 1. Energy consumption by source in Nigeria (Source: NBS, 2007)

4.2 Poverty and Unemployment

The poverty level and unemployment rate in Nigeria and the declining capacity for electricity generation has deeply entrenched the dependence on renewable biomass fuels. The current level of poverty and the default reliance of energy from renewable source provide opportunity for a transition to improved technologies and techniques of using the traditional biofuels. The use of improved wood stoves and small family biogas initiatives, briquetting of sawdust and

other agricultural waste in yet another option in promoting biofuels. Though the use of traditionally produced fuels of kernel oil or other oil as lighting reduced over the years, there is an opportunity to stimulate the local production of biodiesel for off-grid electricity for powering homes and appliances that are far from the national electricity grid infrastructure. Table 1 below shows the increasing poverty rate and incidence in Nigeria between 1980 and 2004. The increasing poverty level is an indicator of the lack of access to improved energy sources, an existing need and potential demand for alternatives such as biofuels.

Table 1. Trends in Poverty Levels between 1980 and 2004

Year	Population Estimate (million)	Poverty Incidence (%)	Rate of Poverty Increase	Rate of Population Growth
1980	65	28.1	0	0
1985	75	46.3	64.8	15.4
1992	91.5	42.7	-7.8	22.0
1996	102.3	65.6	53.6	11.8
2004	126.3	54.4	-17.1	23.5

4.3 Potential Demand for biofuels

The Nigerian Biofuel Policy and Incentive gave an estimate of fuel ethanol requirement at 10-percent blending rate to be about 1.3 billion litres per annum with projected increase to 2 billion litres by 2020. This estimate gives the worth of the bio-ethanol market at a 30 percent less the price of gasoline to be $391 million annually. Table 2 below shows the various substitution capacity for biofuels based on the 2008 average consumption of the petrol, household kerosene and diesel. A combined capacity for the major fuels consumption at the blending rate 10-percent proposed by the Nigerian biofuels policy gives a demand of 2.8mt of biofuels.

Table 2. Nigeria's Biofuel substitution capacity on 5, 10, 20, 30 percent fuels blending rates ('000 mt)

Fuel Types	Yearly Average Consumption ('000 mt)	Biofuels substitution capacity for blending rates			
		5	**10**	**20**	**30**
PMS	20,822.45	1041.12	2082.25	4164.49	6246.74
HHK	3,766.13	188.31	376.61	753.23	1129.84
AGO	5,524.94	276.25	552.49	1104.99	1657.48

PMS – Premium Motor Spirit (Petrol), HHK – Household Kerosene, AGO – Automotive Gas Oil (Diesel)

4.4 Feedstocks production and productivity improvement

Nigeria falls with the region of the world rated to have high potential for biofuel production based on the three-criterion of the level water availability, level of available arable land and the state of food insecurity (10). This high potential is further buttressed by the current production capacity for the basic feedstocks for first generation biofuels. The argument for improving the level of productivity of crops with very high potentials and currently command a high demand for biofuel production was made in previous study (2). Table 3 shows the key crops for which Nigeria ranked between first and twentieth position in terms of nominal

production globally. The ranking of productivity per hectare cultivated for this crops shows Nigeria has much room for improving on productivity of these crops. The data shows even for cassava for which Nigeria leads in the production globally, the country ranks 13th globally in terms of productivity per hectare cultivated. This underpins one of the underlining objectives for promoting crops based biofuels investment in Nigeria. The Nigerian biofuels policy classified investments with the biofuels value chain as an agro-allied sector to benefit from various incentives such as government guaranteed insurance, long term loans, value added tax waiver and custom duties waiver in attempt to stimulate biofuels production for achieving multi-objectives.

Table 3. Nigeria's production, productivity and cultivated area ranking for edible feedstocks

Crop	2008 Average Yield (MT)	Nigeria's Nominal Production Rank (Global)	Nigeria's Yield (land productivity) Rank (Global)	*Nigeria's Cultivated Area (Ha) Rank*
Sesame	110000	7th	13th	*6th*
Palm fruits	8500000	4th	20th	*3rd*
Ground Nut	3900000	3rd	6th	*3rd*
Soybean	591000	13th	20th	*10th*
Coconut	234000	19th	10th	*17th*
Cotton Seed	492000	12th	18th	*9th*
Cassava	44582000	1st	13th	*1st*
Maize	7525000	14th	17th	*7th*
Maize Green	*5709000*	*3rd*	*17th*	*2nd*

Source: Adapted from Food and Agriculture (FAO) Statistics 2008

5. Framework for Biofuels Adoption in Nigeria

The review of available literatures, the adopted National policy on biofuels and incentives brought to the fore key drivers promoting biofuels adoption in Nigeria. Figure 2 shows a multilevel, multifactor and multi-actors framework that constitute the drivers for biofuels adoption in Nigeria. On the government side are exogenous and endogenous inducements which brought about the development of biofuel policies and laws, incentives and investment funds for driving the national Automotive Biomass Programme for Nigeria. The government whitepaper target the private sectors and other players including State governments, cooperative groups and associations for the economic, environmental, socio-cultural and technical and infrastructural benefits which the increase in the biofuels investments will bring to the country.

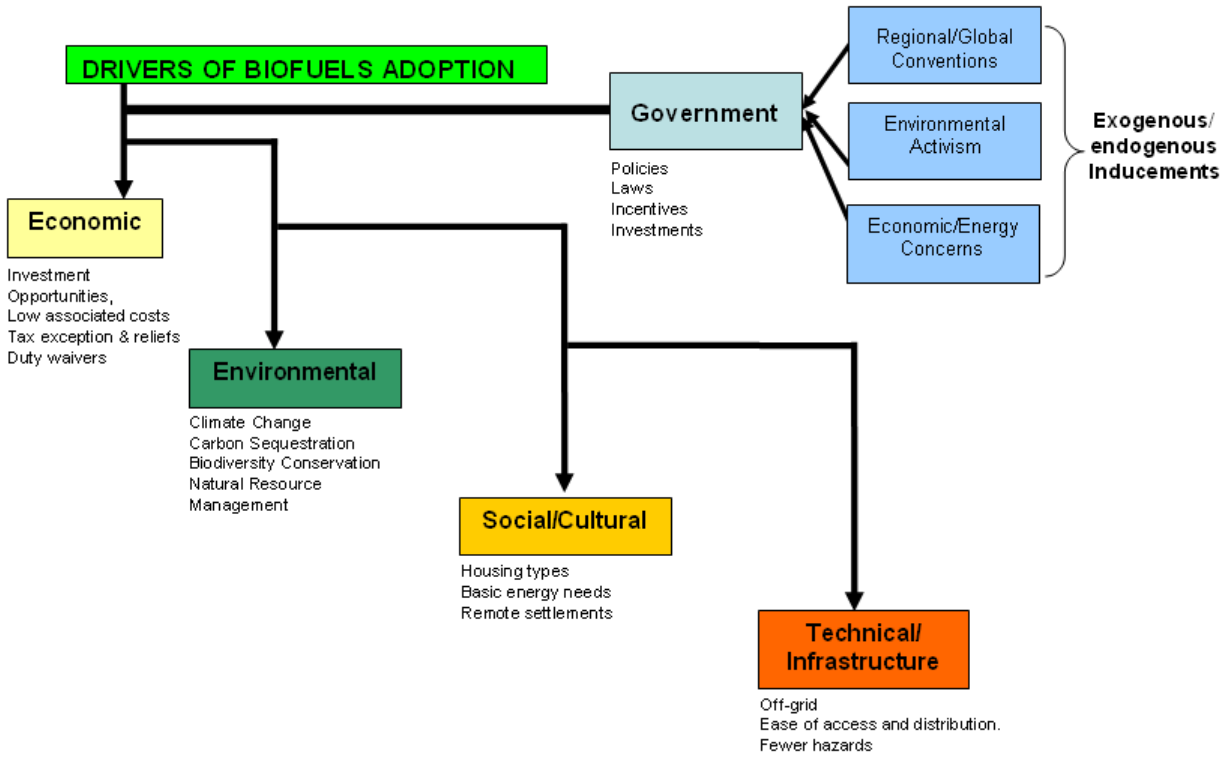

Fig. 2: Framework of biofuels adoption in Nigeria

6. Conclusion

This paper attempted to highlight some of the key drivers of biofuels adoption in Nigeria. The current dependence on renewable biomass fuels, poverty level, unemployment and the existing lack of access to improve energy sources are evidences of the existing gap in energy supply. This gap provides a strong incentives for attracting investment in biofuel production value chain considering the enabling environment and incentives created by the government. The multilevel framework on biofuels adoption identified the key drivers and the underlining motivations. The drivers which are peculiar to the Nigerian socio-economic condition hold the key to the nation's capability to be a major player in the increasing global biofuels market. These key factors identified are issues to put into consideration for sustainably managing biofuels investments in Nigeria. Some of these factors present prospects and problems requiring medium and long term policy interventions from government to ensure an efficient transition into a bioenergy driven economy. The socio-economic factors identified also presents key variables for further socio-economic and bio-economic modelling studies focusing on Nigeria. The framework provides a pillar for further analysis of the relationship between actors, the drivers and motivations for biofuels adoption in Nigeria.

Acknowledgement

This article is part of an ongoing doctoral research on bio-economic and environmental modeling of biofuels adoption in the energy sector in Nigeria and Finland. The funding for the research comes from the FORTUM Foundation and the Evald and Hilda Nissi Foundation.

References

[1] A.S. Sambo, Strategic Developments in renewable energy in Nigeria, Newsletter of the International Association for Energy Economics, Third Quarter 2009, pp. 15-19 available at www.iaee.org/en/publications/newsletterdl.aspx?id=75 sited 12 October 2010.

[2] N. Abila, Biofuels adoption in Nigeria: a preliminary review of feedstock and fuel production potentials, Management of Environmental Quality: An International Journal Vol. 21, No 6, 2010. pp. 785-795.

[3] International Energy Agency (IEA), 2007 Energy Statistics available at http://www.iea.org/statist/index.htm sited 14 October 2010.

[4] S.N. Naik, Vaibhav V. Goud, Prasant K. Rout, Ajay K. Dalai, Production of first and second generation biofuels: a comprehensive review, Renewable and Sustainable Energy Reviews, Volume 14, Issue 2, February 2010, pp. 578-597

[5] J. F. K. Akinbami, M.O. Ilori and I.O. Oyebisi, Biogas enegy use in Nigeria: current status, future prospects and policy implications. Renewable and Sustainable Energy Reviews Vol 5, 2001, pp. 97-112.

[6] International Energy Agency (IEA). 2008 IEA Energy Statistics available at http://www.iea.org/statist/index.htm sited 20 October 2010.

[7] Nigerian National Petroleum Corporation (NNPC), Nigerian Biofuel Policy and Incentives.

[8] National Bureau of Statistics (NBS) 2005. Poverty Profile for Nigeria. Federal Republic of Nigeria

[9] National Bureau of Statistics (NBS) 2007. Social Statistics in Nigeria. Federal Republic of Nigeria

[10] J. von Braun, "When food makes fuel: the promises and challenges of biofuels", keynote speech at the Crawford Fund Annual Conference, 2007, Melbourne.

The bioenergy potential for the centre Region of Portugal: the use of biomass as a fuel source

Tanya C.J. Esteves[1*], António J.D. Ferreira[1], José C. Teixeira[2], Pedro Cabral[3]

[1] *Escola Superior Agrária de Coimbra, Coimbra, Portugal*
[2] *Universidade do Minho, Guimarães, Portugal*
[3] *Instituto Superior de Estatística e Gestão de Informação, Lisboa, Portugal*
** Corresponding author. Tel: +351 239 802940, Fax: +351 239 802979, E-mail: tanya@esac.pt*

Abstract: Renewable energy is one of the most effective ways to achieve the sustainability essential for our future. The consumption of fossil fuels is rapidly depleting resources deemed essential for Man's survival.
This work's main focus is to increase bioenergy use in the centre region of Portugal by allying R&D to facilitate bioenergy availability and distribution throughout the study area.
Accordingly, the available bioenergy potential was important to determine once this knowledge is very limited in the Centre Region of Portugal. Biomass residues for forest stands, burned areas, shrublands and agriculture land uses, municipal solid waste, animal husbandry waste, used vegetable oils, agricultural and food industry and energy crops were the considered material, once they represent great part of the regional available biomass. Additionally, the ideal location for the implementation of the Bioenergy Competency Centre (BCC) was determined, using a GIS approach that considered four scenarios.
Results show the most favorable for the yield of each of the bioenergy sources for bioenergy and that there are minor variations for the BCC best location for the 4 considered scenarios.

Keywords: *Geographical Information Systems, Bioenergy potential, Land use, Bioenergy resources, Kyoto protocol.*

1. Introduction

Fossil fuels are extremely attractive as energy sources, once they are relatively easy to distribute, especially oil and gas which are fluids [1]. It is still unknown when cheap fossil fuels will end, but it is estimated that it may happen in just one generation, or even sooner. We currently live what may be considered an oil crisis. Just recently, the price of the barrel of crude oil was above of 135 dollars, whereas in 2004, the price was located at around 35 dollars per barrel [2]. The substantial fluctuation of the oil price may cause serious worldwide economic disruption and lead to protests, as seen recently all around the world [1].

Oil exhaustion is a recurrent subject, with specialists indicating the year that production will reach its peak and when the major oil reserves will finally be depleted [3]. Knowing that fossil fuels will become a rare commodity in the near future, and knowing that humanity is utterly dependant on energy, a new path needs to be traced as to support our energy consuming way of life. Otherwise, serious consequences will outcome from this fact. Sustainability is a key point in today's society, once it involves environmental, social and operational management strategies, an equilibrium that is not easy to control due to their interdependency. According to Boyle [3], a sustainable energy source is ideally one that is not substantially depleted by continued use, does not entail significant pollutant emissions or other environmental problems, and also does not involve the perpetuation of substantial health hazards and/or social injustices. But only a few energy sources come close to this ideal: they are essentially inexhaustible and their use usually entails much lower emissions of GHG or other pollutants, and fewer health hazards [3]. With the use of natural and renewable resources as an alternative to fossil fuels for the production of energy, a higher level of sustainability may be achieved by modern society [4]. The renewables are based on energy flows that are replenished by natural processes, not becoming depleted with use. The environmental impacts

of renewable energy sources vary, but they are generally much lower than those of conventional fuels [1].

Countries with low or inexistent access to fossil fuels such as Portugal have an elevated price to pay for oil importation: in 2007 the consumption of primary energy from oil represented approximately 54% of the total [5]. However, Portugal has a final energy consumption per inhabitant that is still low when compared with other EU countries – 1,7 toe/inhabitant against an EU-25 mean of 2,5 toe/inhabitant [6]. Nevertheless, the price raise of fossil fuels represents an exit of a substantial amount of currency to foreign countries, consequently weakening the economy. All together, oil, natural gas and coal represent over 80% of the Portuguese national energetic balance [5].

Bioenergy is the general term for energy derived from biomass material, such as trees, plants, manure, and sometimes wastes. Such materials can be processed through transformation processes, where the biomass is transformed into biofuels, bioheat or bioelectricity and used for energetic purposes [5, 7]. The renewable energy directive [8] defines biomass as being "the biodegradable fraction of products, wastes and residues from biological origin from agriculture (including vegetable and animal substances), forestry and related industries including fisheries and aquaculture, as well as the biodegradable fraction of industrial and municipal waste" [7].

1.1. Aim

Therefore, the first and utmost goal is to analyze the potential of bioenergy for the Centre Region of Portugal for several bioenergy sources, namely from forest stands, burned areas, shrublands and agriculture land uses, municipal solid waste, animal husbandry waste, used vegetable oils, agricultural and food industry and energy crops. To achieve this goal, spatial and non-spatial data is collected, transformed into a comparable energy unit (tonne of oil equivalent - toe) and analyzed in order to evaluate the availability of biomass for energy production throughout the study area.

Having the previously stated information, an analysis of the optimal location for the Bioenergy Competency Centre (BCC) is made. This is an entity that includes a large range of services before and after bioenergy production, such as technical assistance during the production process, research, personnel training and product certification. The adequate implementation of this infra-structure in the terrain is essential for a flourishing development of the use of bioenergy in the study area.

The two overall outcomes of the developed work will be a map of the bioenergy potential for the Centre region of Portugal and a map with recommendations for the optimum location of the implementation of the BCC.

1.2. Characterization of the study area: the Centre Region of Portugal

Portugal is geographically located on the European west coast, in the Iberian Peninsula. Is has Spain as boundaries to the North and West and to its West and South, it encounters the Atlantic Ocean. The Centre Region of Portugal is divided into 12 NUTS III areas: Baixo Vouga; Baixo Mondego; Pinhal Litoral; Pinhal Interior Norte; Dão-Lafões; Pinhal Interior Sul; Serra da Estrela; Beira Interior Norte; Beira Interior Sul; Cova da Beira; Oeste and Médio Tejo (Fig. 1). It occupies a total area of 28.200 km^2, 30,6% of the country. All these areas comprise a total of 100 municipalities (25,2% of the countries' total) [9]. According to the

2001 Census, this region has a population of 2.371.700 inhabitants, 22,6% of the Portuguese total, with a population density of 83,5 inhab/km^2 [9].

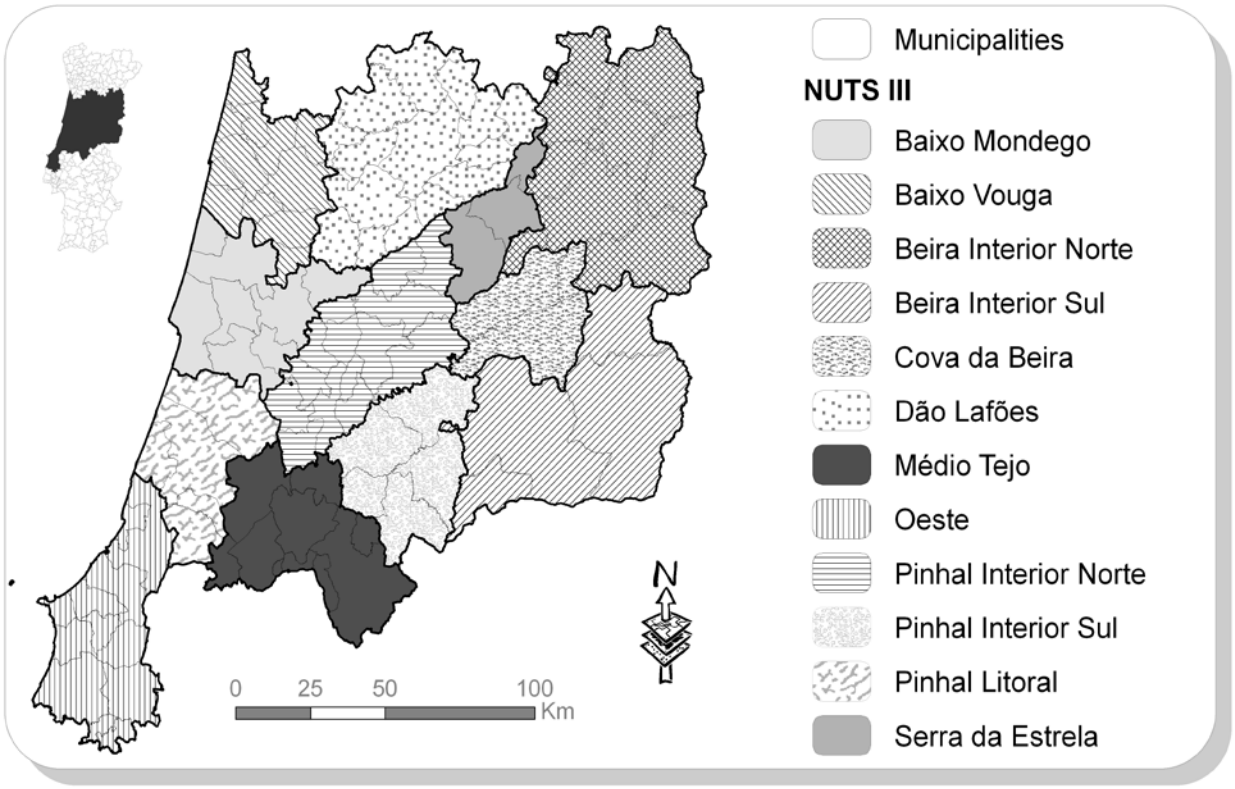

Fig. 1. Study area, the Centre Region of Portugal.

2. Methodology

2.1. The Bioenergy Potential Map for the Centre Region of Portugal

A primordial step was to join all pertinent information to calculate the amount of the various residues that are passable to be transformed into bioenergy. This extensive research work consisted in using freely available information from several Portuguese organizations that aim to produce both numerical and statistical data for the general public. In what respects to the date of the available information, the most recent data was preferable in opposed to more dated records; nevertheless, some of the gathered information is rather old (e.g., 1999 agricultural census). Regarding to the geographical data, only the Official Administrative Map of Portugal (CAOP) was used [10]. This information uses the European Terrestrial Reference System 89 (ETRS89) coordinate system with a Transverse Mercator projection.

Multiple information was collected and treated for a variety of sources, namely: Forest residue biomass; Agricultural residues biomass; Energetic cultures; Animal husbandry residues; Municipal solid waste; Used vegetable oils; Agricultural and food industries. The collected information was treated as to obtain bioenergy production values in toe. Note that each bioenergy transformation process has a determinate yield for each of the presented residues. However, in this stage of the study, 100% of the transformation yield was considered.

Afterwards, GIS software was used in order to process all the collected and treated information. For that effect, a model was created which allowed uniting all the information, presenting an output as a final result for the determination of the bioenergy potential of the Centre Region of Portugal.

2.2. Location of the Bioenergy Competency Centre

The BCC will not produce energy itself. Rather, it will have several critical functions for the further development of the bioenergy production area. This Centre will encompass a logical integrated network with the main stakeholders in the Centre Region of Portugal, as to maximize the profitability of the various laboratorial, management and economical infra-structures and available knowledge. Information flow will be crucial in this organism's work processes. Acknowledging the significance of its activities, it should be in a location that is of easy access to all the stakeholders.

For its implementation, several suppositions have to be taken into consideration, some of common sense and others of environmental and legal restraints. As before, all the used information is freely available to the general public. Both alphanumerical and geographical information is used as to achieve the best possible results. This information is collected from several national and international institutes [10, 11, 12, 13, 14]. GIS software was once again used as a valued resource to build this tool.

All the input information is classified into five different classes, being 1 the least preferable condition and 5 the most preferable condition. Four different scenarios are considered in order to verify the applicability of the tool and compare results, where each one varies an input parameter weighting in order to understand its influence on the final result.

3. Results and Discussion

3.1. The Bioenergy Potential Map for the Centre Region of Portugal

Intermediate results for each of the biomass types have different expressions throughout the territory. Where in some cases, biomass was more prominent in the inland area (e.g., forest biomass), in other cases bioenergy production was more expressive in the littoral area (e.g., animal biomass).

The final result's most influencing component is forest waste biomass. The amount of bioenergy that this source is capable to produce actually overshadows the remaining sources, mainly due to the contribution that forest shrublands make. As an overall result, we verify that the most promising area in terms of bioenergy production is the northern inland area, Beira Interior Norte. This may be due to the combination of climatic factors (e.g., high water availability) with the high amount of rural agricultural and forest areas, leading to a higher biomass yield. The littoral part of the Centre Region of Portugal has significantly lower potential for the production of bioenergy, whereas the middle and Oeste regions of the study area is not at all optimal for production of biomass for bioenergy (Fig. 2).

Shrubland residues aren't correctly handled in most areas, remaining unmanaged in the terrain, hampering greatly the amount of biomass passable to be used. In order to use this material, proper management has to be made in order to guarantee that the full potential can be used for bioenergy, without damaging forest ecosystem equilibrium. Other than yielding bioenergy, another very important consequence would take place, which is the prevention of wildfires, helping to drastically reduce the risk. These ravage the country on a yearly basis leading to important environmental, social and economical losses.

Another consideration may be the analysis of the actual production of bioenergy from some sources. In some cases, using an energy source may be more expensive than not using it (in an

energetic perspective). In this particular study, it is thought that energy crops are a source of this type, once the amount of produced bioenergy by the different crops is very low, being that their use would be simply impermissible.

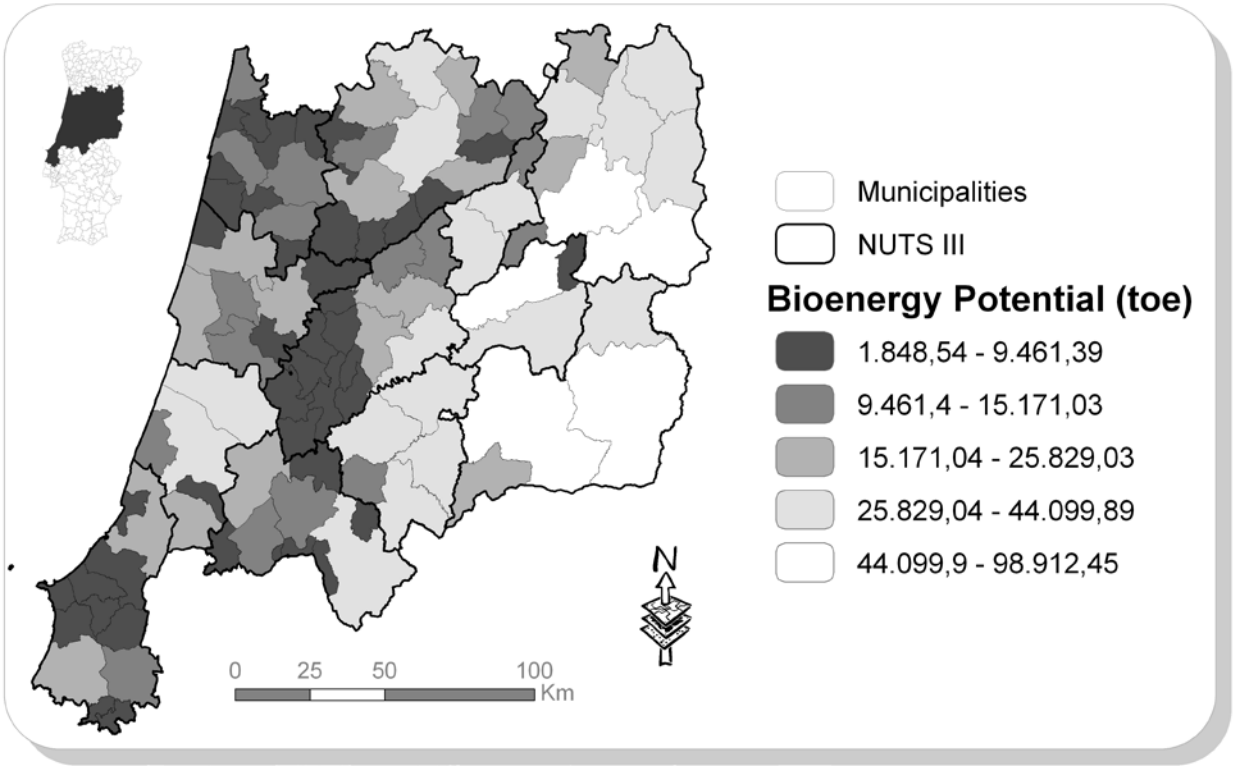

Fig. 2. Bioenergy potential for the Centre Region of Portugal.

3.2. Location of the Bioenergy Competency Centre

Properly locating the BCC is of great importance, once it will allow easier access to all stakeholders to the services to be provided by this institution. All inputs are considered key to the location of this institution, once they take into account different aspects that represent reality constraints and allowances. For this study, these are: road types, road distance, travel time, bioenergy potential and slope.

Four different scenarios are traced as to evaluate how different weightings can affect the location of the BCC. For the final map, only values of 4 and 5 are selected. It is also considered that the inputs slope and restrictions have the same weight in each scenario. A delicate balance is used to consider the inputs, and overall, it is thought that the achieved weighting is quite satisfying to construct viable outputs (Fig. 3).

When analyzing the results, at first glance we can verify that they are very similar between them. Most of the locations suggested in the different scenarios are coincident, although with visible changes in the area for every scenario. Another clearly visible result is that there are more areas to implement the BCC with a classification of 4 than with a classification of 5.

By making a global analysis of all scenarios, we can say that Scenario 2 is the most limitative one, once a lower area with classification 5 is usable. Scenario 3 is the broadest of them, where a higher area is available, although the one with classification 5 is higher in Scenario 1.

If it were preferable to use only locations with classification 5, the solution would be almost the same in all scenarios. In general, preferable locations would be situated in the main inland urban municipalities. For the majority of the remaining cases, values vary from scenario to scenario. In most cases, Scenario 3 has the most amount of area for almost all municipalities.

It should be noted that after a final selection of the location for the BCC, it should be confronted with the Municipal Master Plans of the respective municipality. This is a matter of extreme importance, once this legal document will determine the ability or inability to locate the BCC at a given location.

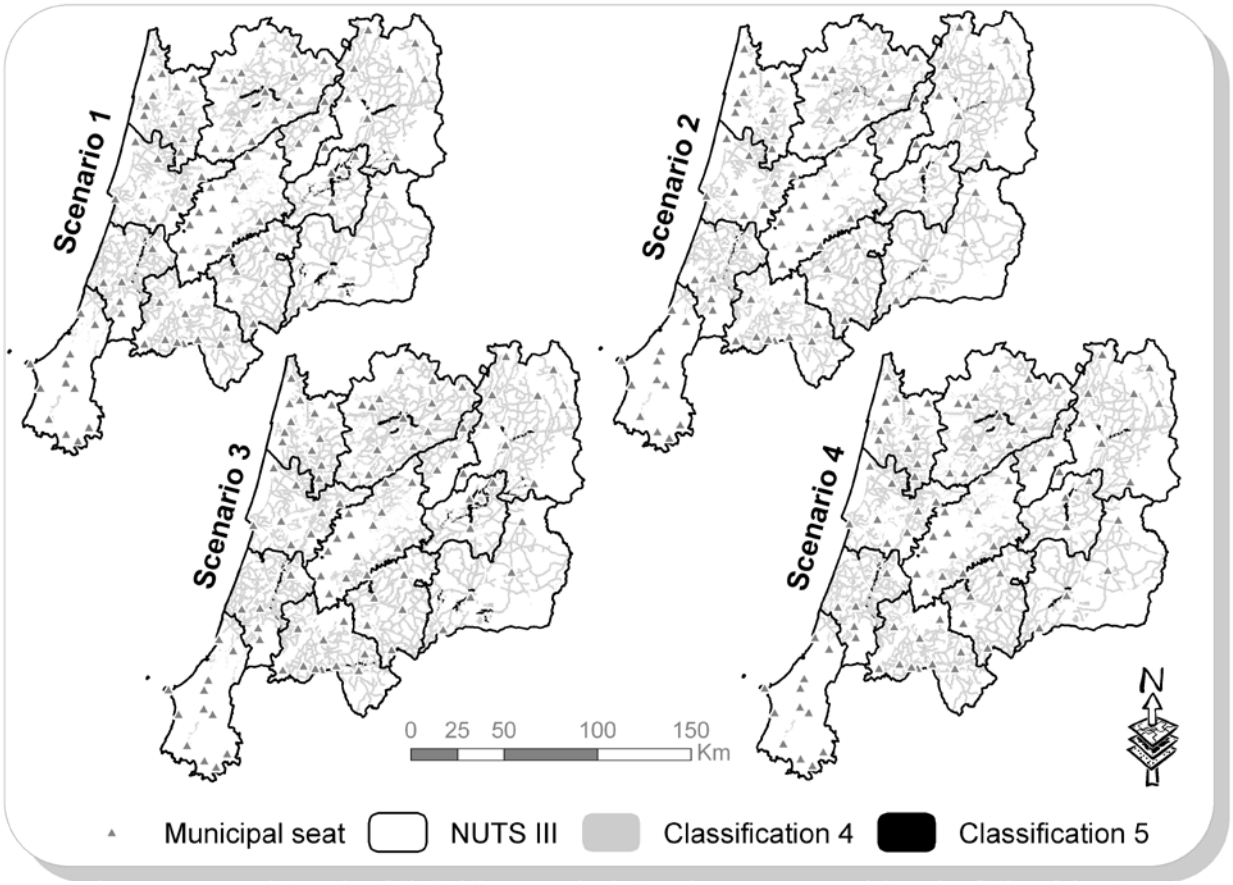

Fig. 3. Scenario results for the location of the Bioenergy Competency Centre.

Picking a specific location for the BCC depends widely on what the directors and main stakeholders are looking for. Do they want more options? Do they want a lesser amount of optimum locations to pick from? Do they only want locations with classification 5? Is there no difference in using classification 4 or 5? Are they interested in a certain municipality? As like other technologies, GIS and its results are socially constructed via negotiations between various social groups such as developers, practitioners, planners, decision-makers, special interest groups, citizens, and others who may have interest in the planning and policy making process [15]. All these questions have to be weighted by these key actors, mainly by the directors of the future BCC.

An interesting option for the location of the BCC could be the inland area of the country, giving dynamism to this area, once that this population is increasingly fleeing to the littoral, looking for better life conditions. This leads to the abandonment of the land, turning rich soils into inaccessible and unusable terrains for agriculture, forestry, or whichever activity over

time. This location could very well mean local creation of more jobs, as well as the possibility of awakening the surrounding population to the possibility of this new business and delay (or even mitigate) the abandonment of land.

4. Conclusions

The world will soon face an energy problem with the potential to destroy civilizations. It is urgent to seek new energy sources and new management strategies in order to prevail, ones that are optimized and sustainable. So why not use available disposable material and make it work for mankind?

Resources with great promise exist in the Centre Region of Portugal, but one stands out. Forest wastes are a main contributor for the augmentation of the amount of bioenergy that the study area can produce. Another advantage of the use of this material is that it is homogeneously distributed throughout the whole study area, in high amount. The use of this type of material in particular has a double function: the production of bioenergy and the aid in the prevention of forest fires, a yearly affliction for Portugal. As for the other biomass sources presented in this work, they also assume an interesting role in bioenergy production, although not as an important one as forest biomass.

The Centre Region of Portugal has, in general, great potential for the use of biomass for the production of bioenergy. As can be seen in the final results, the interior region of the study area is the one with higher bioenergy potential yield. This fact may bring several consequences to these areas, in which local richness may be enhanced. Reactivating these rural areas and giving them a sustainable way to earn money would greatly help the overall conditions of this population and local environment.

The location of the BCC is the second result from the present study, where the main results point to more adequate areas in the inland area, a highly desirable result. Varying the weights of the input information has little influence regarding the location of the BCC. Favorable results were generally very similar for all the four scenarios. What varied greatly between these scenarios was the amount of available area in each classification.

By having a rather large study area, several particularities of each and every municipality had to be overlooked. This study only presents an initial evaluation of the bioenergy potential, and not an in depth analysis for a given municipality. Regrettably, these small particularities may come to influence the final result of the potential for the municipality. That is why further analyses have to be done as to verify in detail the actual potential for a given municipality.

A strong point of this study is the adaptability of the resulting models. In a fairly easy way, one can open the created tool and alter whatever needed parameters as to meet emerging requirements. This is an extremely important aspect of these tools, once flexible tools accompany the necessary changes in reality throughout time

As to enhance the present study results, some alterations/improvements are necessary in the future, such as introduction of recent information in the modeled tools; consideration of transformation yields of the several bioenergy sources; introduction of other sources of bioenergy present in the study area (e.g., biogas from wastewater treatment plants and industrial sources); and results validation through, e.g., SWOT analysis.

References

[1] G. Boyle, B. Everett, and J. Ramage, Energy Systems and Sustainability. Power for a sustainable future. United Kingdom: Oxford University Press, 2004.

[2] U.S. Department of Energy. 2009. Department of Energy. [Online] 2009. http://tonto.eia.doe.gov/oog/info/twip/twipcrvwall.xls#'Data 2'!A1.

[3] G. Boyle, Renewable energy: power for a sustainable future. 2nd edition. United Kingdom: Oxford University Press, 2004.

[4] J. Richardson, and T.Verwijst, Sustainable bioenergy production systems: environmental, operational and social implications. Biomass and Bioenergy. 2005, Vol. 28, Preface, pp. 95–96.

[5] Direcção Geral de Energia e Geologia. 2005. Direcção Geral de Energia e Geologia Homepage. [Online] 2005. http://www.dgge.pt/.

[6] Agência Portuguesa do Ambiente. 2008. Dossier de Prevenção (redução) de Resíduos - Nível mais básico. Amadora: Agência Portuguesa do Ambiente, 2008.

[7] AEBIOM. 2010. European Biomass Association. [Online] 2010. [Cited: 6 May 2010.] http://www.aebiom.org.

[8] European Parliament and of the Council. 2009. Directive 2009/28/CE. Promotion of the use of energy from renewable sources and amending and subsequently repealing Directives 2001/77/EC and 2003/30/EC. s.l., Brussels: Official Journal of the European Communities, 23 April 2009.

[9] AICEP Portugal Global. 2008. Portugal - Perfil país. Lisboa: AICEP Portugal Global, 2008.

[10] Instituto Geográfico Português. 2009. Instituto Geográfico Português. [Online] Grupo de Detecção Remota, 2009. [Cited: 12 September 2009.] http://www.igeo.pt/gdr/.

[11] Instituto da Conservação da Natureza e da Biodiversidade. 2005. Instituto da Conservação da Natureza e da Biodiversidade. [Online] Instituto da Conservação da Natureza e da Biodiversidade, 2005. [Cited: 23 August 2010.] http://portal.icnb.pt/ICNPortal/vPT2007/Valores+Naturais/Informação+Geográfica/.

[12] Instituto Geográfico do Exército. 2010. Instituto Geográfico do Exército. [Online] Instituto Geográfico do Exército, 7 October 2010. [Cited: 7 October 2010.] http://www.igeoe.pt/.

[13] CGIAR - Consortium for Spatial Information. 2008. CGIAR - Consortium for Spatial Information. [Online] CGIAR - Consortium for Spatial Information, 19 August 2008. [Cited: 26 July 2010.] http://srtm.csi.cgiar.org/.

[14] REN. 2010. REN. [Online] REN, 17 August 2010. [Cited: 14 September 2010.] http://www.ren.pt/vPT/Gas/Transporte/tiap/Documents/Rede%20Nacional%20de%20Transporte%20de%20Gás%20Natural%202010%20(mapa).jpg.

[15] Malczewski, J. 2004. GIS-based land-use suitability analysis: a critical overview. Progress in Planning. 62, 2004, pp. 3-65.

Improvement of sweet sorghum bagasse hydrolysis by alkali and acidic pretreatments

Amir Goshadrou[1,*], Keikhosro Karimi[1,2], Mohammad J. Taherzadeh[2]

[1] *Department of Chemical Engineering, Isfahan University of Technology, Isfahan, 84156-83111, Iran*
[2] *School of Engineering, University of Borås, SE-501 90 Borås, Sweden*
** Corresponding author. Tel: +98 3113915623, Fax: +98 3113912677, E-mail:goshadrou@ce.iut.ac.ir*

Abstract: The present work deals with enzymatic hydrolysis of sweet sorghum bagasse to fermentable sugars. The bagasse was treated with phosphoric acid and sodium hydroxide prior to enzymatic hydrolysis by commercial cellulase and β-glucosidase. The phosphoric acid pretreatment was performed at 50°C for 30 min, while 12% NaOH was used for the alkali treatment at 0°C for 3 h. The phosphoric acid pretreatment resulted in improving the subsequent enzymatic hydrolysis up to 79% of the theoretical yield. However, the best results of enzymatic hydrolysis were obtained in the hydrolysis of pretreated bagasse by NaOH solution, where more than 92% of the theoretical sugar yield was obtained.

Keywords: *Lignocellulosic material, Sweet sorghum, Enzymatic hydrolysis, Pretreatment*

1. Introduction

Fossil fuel limitations and constraints on carbon dioxide emissions have a high impact in the market of bioethanol, which is the most commonly used biofuel for petrol substitution in the world [1]. Fermentative ethanol can be produced from a variety of feed stocks such as saccharine materials, starchy materials and many types of lignocellulosic waste and harvestings, whichever has the best well-to-wheel assessment [2]. Lignocellulosic biomass is considered a future alternative for the agricultural products that are currently used as raw material for bioethanol production, because it is more abundant and less expensive than food crops, especially when waste streams are used. Furthermore, the use of lignocellulosic biomass is more attractive in terms of energy balances and emissions [3]. Sweet sorghum is an interesting annual plant that can be cultivated in widespread areas from tropical to temperate climates with the potential to produce more ethanol per acre than corn [4]. In addition, it has a high yield of green biomass and different part of this plant, such as bagasse, can be hydrolyzed to fermentable sugar before further bioconversion to ethanol. Similar to all lignocellulosic biomass, the main components of SSB are cellulose, hemicellulose and lignin [4, 5]. Hydrolysis of cellulose part can be carried out by dilute acid, concentrated acid or enzymatically, whereas the latter can be performed under mild condition with higher yield of glucose [6, 7]. However, the main purpose of this article was to enzymatic hydrolysis of the sweet sorghum bagasse (SSB) to fermentable sugars. In any case, access of cellulase to cellulose and lignin strongly limits the efficiency of enzymatic hydrolysis because Lignin, which is a complex polymer, provides structural integrity in plants. Therefore, the pretreatment is an important process before hydrolysis in order to remove or alter lignin and increase the accessibility of enzyme to cellulose [3]. Among all methods available for the pretreatment of lignocelluloses, acidic and alkaline treatments have been proven to have practical advantages. Concentrated phosphoric acid can dissolve cellulose in the presence of water without inhibitory effect, while it is non-corrosive, safe to be used and inexpensive chemical [8]. Similarly, sodium hydroxide can remove the lignin barrier and reduce cellulose crystallinity and therefore, increase the accessibility of enzyme cellulose part [9]. In addition, both processes

utilize lower temperatures and pressures compared to other pretreatment technologies and even may be carried out at ambient conditions.

The current study deals with the effect of sodium hydroxide (12%) and phosphoric acid (85%) pretreatments on improvement of sugar yield in enzymatic hydrolysis of sweet sorghum bagasse.

2. Materials and Methods

2.1. Raw materials

The sweet sorghum bagasse (Sofra, Italy) used in all experiments was kindly provided by Dr. A. Almodares (Department of Biology, University of Isfahan, Iran). The bagasse was initially dried at room temperature and then was hammer milled and screened to achieve a particle size in the range of 20-80 mesh.

2.2. Sodium hydroxide pretreatment

The sweet sorghum bagasse was treated with 12% (W/V) NaOH solution. A 5% bagasse suspension (based on the dry weight) was thoroughly mixed for 10 min at 0°C, then placed in a laboratory ice-water bath for 3 h and mixed every 15 min. The pretreated materials were then washed with distilled water until pH 7 was detected. The solids were then dried at 40±1°C until constant weight and kept in a refrigerator until use.

2.3. Phosphoric acid pretreatment

The bagasse was thoroughly mixed with phosphoric acid (85%) in a 50 mL plastic centrifuge tube at 12.5% solid loading. The mixture shacked at 90 rpm and the temperature was controlled at 50±1°C for 30 min. The treated slurry was then washed with 20 mL cold acetone and centrifuged at 4000 rpm for 20 min. The washing process was repeated three times with 40 mL acetone, followed by three times with 40 mL distilled water. The residual acetone from washing stages was removed from supernatant after simple evaporation in a fume hood. The treated bagasse was finally washed by hot distilled water to neutralize the pH to 7.

2.4. Enzymatic hydrolysis

Commercial cellulase (Celluclast 1.5L, Novozyme, Denmark) and β-glucosidase (Novozyme 188, Novozyme, Denmark) were used for all enzymatic hydrolysis. Celluclast 1.5-L showed 87 FPU/ml activity, measured according to the procedure presented by Adney and Baker [10], while β-glucosidase activity was 240 IU/ml according to Ximenes et al. method [11]. The hydrolysis process was performed at 45±0.5°C in 50 mL sodium citrate buffer (0.05 M) using 115 mL glass bottles. The initial pH was adjusted to 4.8±0.1, and substrate concentration was 20 g/L dry weight for untreated and pretreated materials. The suspension was then autoclaved at 121°C and pre-incubated for 20 min prior to addition of enzymes. The enzymes loadings for hydrolysis were 20 FPU cellulase and 50 IU β-glucosidase per grams of dry substrates. The reaction mixture hydrolysis performed at 120 rpm for 72 h and the samples were periodically taken for sugar analysis. The yield of enzymatic hydrolysis was calculated as a ratio of theoretical glucose production yield using the following equation:

$$\text{Yield of enzymatic hydrolysis}(\%) = \frac{\text{Produced glucose } (g/L) \times 100}{1.111 \times \text{Substrate concentration}(g/L) \times F} \quad (1)$$

where F in denominator is the biomass glucan fraction, which is presented in Table 1 for untreated and different pretreated bagasse. The conversion factor of 1.111 was applied to consider the conversion of glucan to glucose.

2.5. Analytical methods

The untreated and pretreated sweet sorghum bagasse were analyzed for carbohydrate and lignin (acid-soluble and insoluble) according to the method presented by Sluiter et al. [12]. The method was based on de gradation of carbohydrates to monomeric sugars by two-stage acid hydrolysis and quantification of the sugars by HPLC. Furthermore, the acid-soluble was determined by UV/vis spectroscopy at 320 nm, and acid-insoluble lignin contents was determined by drying of the acid treated samples at 575°C.

The structural properties of the bagasse, before and after pretreatment by sodium hydroxide were analyzed by Fourier transform infrared (FTIR) spectrometer (Impact 410, Nicolet Instrument Corp., Madison, WI). The spectra were obtained using 60 scans of the samples with resolution of 4 cm-1 in the range of 600 to 4,000 cm-1. Nicolet OMNIC 4.1 analyzing software was used for correcting baseline and smoothing of the spectra.

Scanning electron microscopy (SEM) was used for study of the effect of pretreatments on physical property changes in the biomass. The freeze-dried samples were placed on carbon taps and subjected to the high performance scanning electron microscope (Quanta 200 ESEM FEG, FEI, ORA) and the micrographs were taken using an Everhart Thornley Scanning Electron Detector (ETD) at 20 Kv and a high vacuum mode.
The detection of sugars including glucose, xylose, mannose, galactose, and arabinose in the hydrolyzates and carbohydrate analyses were performed by High performance liquid chromatography using an anion-exchange column (Aminex HPX-87P, Bio-Rad) at 85ºC with 0.6 ml/min eluent of ultra-pure water.

All the experiments were performed in duplicates and all data reported in this paper are the average of the two replications.

3. Results

3.1. Pretreatment and materials characterization

The sweet sorghum bagasse used in this study mainly contained glucan (41.3%), xylan (17.9%), and lignin (18.2%) (Table 1). The native bagasse was pretreated with NaOH solution at 0°C for 3 h and concentrated phosphoric acid for 30 min at 50°C. The composition of the bagasse after the pretreatments was analyzed and results are presented in Table 1.

Table 1. Composition of the bagasse before and after pretreatments.

Pretreatment method	Glucan (%)	Xylan (%)	Mannan (%)	Galactan (%)	Arabinan (%)	Acid soluble lignin (%)	Acid insoluble lignin (%)
Untreated	41.33	17.96	0.85	1.26	1.94	1.78	16.47
Sodium hydroxide	58.66	12.72	0.69	0.66	1.10	1.01	11.50
Phosphoric acid	52.25	11.88	0.34	0.39	0.46	1.15	23.02

Glucan was the dominant component in all materials in the range of 41.3% to 58.6% and xylan was in the second place in the range of 11.8-17.9%. Other carbohydrates were mannan, galactan, and arabinan with 0.34-0.85%, 0.39-1.26%, and 0.46-1.94% depending on the pretreatment method. There was a remarkable increase in glucan fraction after the pretreatments. The glucan fraction increased by 41.9% and 26.4% after the pretreatment by sodium hydroxide and phosphoric acid, respectively. On the contrary, to glucan, other sugars decreased after the pretreatments. In addition, all pretreatments reduced the acid-soluble lignin and the minimum change, from 1.78% to 1.15%, was observed in phosphoric acid pretreatment. The highest loss in acid soluble and insoluble lignin was observed in sodium hydroxide pretreatment where the total lignin content decreased from 18.2% to 12.5%. However, an increase in acid-insoluble lignin content in phosphoric acid pretreated bagasse was detected.

The structural change in the bagasse was followed by FTIR analysis. As an example, the spectra of untreated and sodium hydroxide pretreated bagasse are presented in Fig. 1. Comparing the FTIR spectra of untreated and pretreated bagasse shows that the absorbance at 898 cm-1, which is assigned to cellulose I, increased after pretreatment by sodium hydroxide. The total crystallinity indexes (TCI) that was defined as the absorbance ratio of A_{1430} to A_{898} were 0.83 and 0.73 for untreated and NaOH treated, respectively. In addition, the absorbance at about 3,350 cm-1, which is related to O-H stretching band of hydroxyl group, was increased after pretreatment by sodium hydroxide. Moreover, sodium hydroxide resulted in broadening at this wave number. This indicated the weaker intra- and intermolecular hydrogen bonding and lower crystallinity. Lignin characteristic can be followed by the peaks at 1218 cm-1 (C-O of guaiacyl ring). The band intensity at this wavelength for pretreated materials was significantly lower than that of the untreated bagasse, indicating the delignification effect of the corresponding pretreatment.

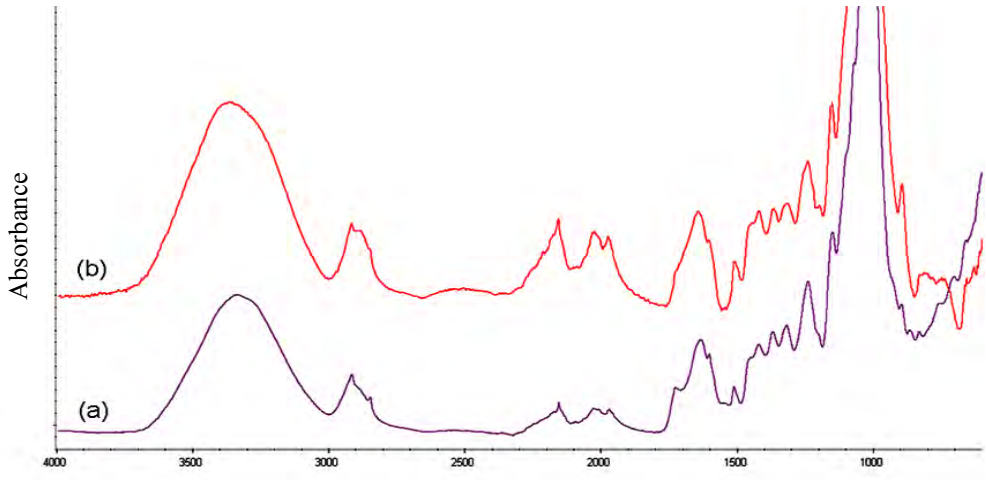

Fig. 1. FTIR spectra of (a) untreated bagasse and (b) NaOH pretreated bagasse.

SEM was used to study the morphological features and surface characteristics of materials after the pretreatment compared with the untreated bagasse. The pretreatment resulted in significant physical changes (Fig. 2). Both sodium hydroxide and concentrated phosphoric acid disrupt the structure of the fibers. Furthermore, the structure of the lignocellulosic biomass was opened up

and more sponge-like structures were observed after the pretreatment that can provide higher surface area for subsequent enzymatic reactions.

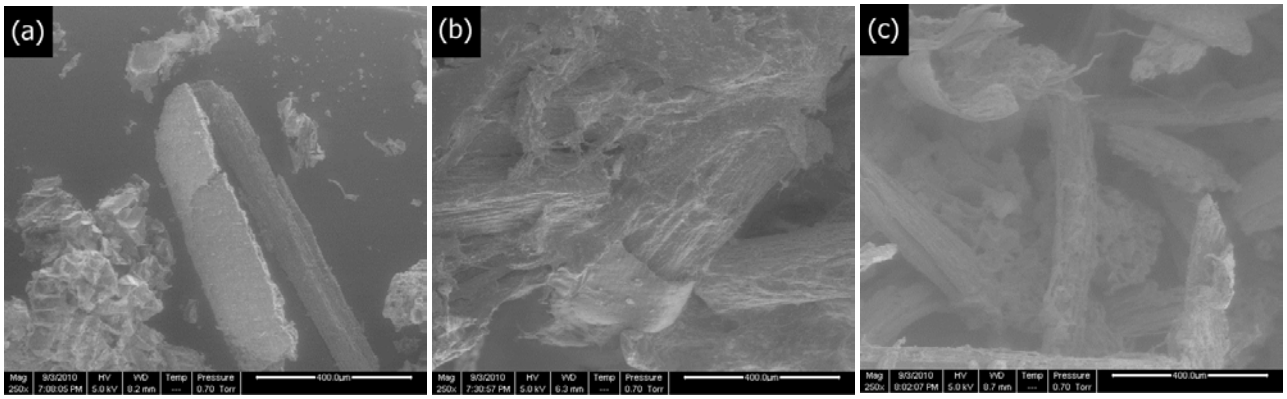

Fig. 2. SEM images of (a) untreated, (b) NaOH pretreated and (c) phosphoric acid pretreated bagasse.

3.2. Enzymatic hydrolysis

Different preparations of sweet sorghum bagasse were subjected to 72 h enzymatic hydrolysis by addition of cellulase and β-glucosidase. Pure cellulose was used as a reference in the hydrolysis experiments. The most important hydrolysis results are presented as percentages of theoretical sugar yield in Table 2. The yield of hydrolysis of native bagasse was effectively improved after sodium hydroxide and concentrated phosphoric acid pretreatments. The sugar content in the hydrolyzates increased sharply in the first 12 h and gradually continued until 72 h. Hydrolysis of the untreated bagasse resulted in 42% and 65% conversion after 12 h and 72 h, respectively. The hydrolysis yield increased from 65% to 79% after 30 m in pretreatment by concentrated phosphoric acid. The best results of enzymatic hydrolysis were obtained in the hydrolysis of pretreated bagasse by NaOH solution, where more than 92% of the theoretical glucose yield was obtained.

Table 2. Yield of enzymatic hydrolysis for the bagasse before and after the pretreatments.

	Yield of enzymatic hydrolysis (% theoretical sugar yield)		
Pretreatment method\Hydrolysis time	12h	24h	72h
Untreated	42%	43%	65%
Avicell	46%	60%	70%
NaOH	79%	80%	92%
Phosphoric acid	70%	79%	79%

3.3. Discussion

Sweet sorghum considered as a potential energy crop in nearly all temperate, subtropical, and tropical climates. It produces sugars juice, grains with high starch content, and bagasse. The bagasse is usually used for energy production by incineration. The native sweet sorghum bagasse which was used in the current work contains over 63% carbohydrate mainly in the form of glucan

and xylan, respectively, and about 18% lignin, which is comparable with the typical composition of other agricultural residues. The present work dealt with the pretreatment of sweet sorghum bagasse by sodium hydroxide and phosphoric acid followed by enzymatic hydrolysis to fermentable sugars.

As expected, a pretreatment was necessary in order to efficiently convert the cellulose in the bagasse to fermentable sugars by hydrolytic enzymes. Besides, the pretreatment could increase the glucan fractions. The bagasse was partially delignified by sodium hydroxide pretreatment.
The FTIR technique can be applied to examine the structural changes in the biomass during pretreatments [13]. The analysis showed increasing the band intensity at 898 cm^{-1} and decreasing the band at 1,427 cm^{-1} which indicated the lower crystallinity and increasing the amorphous form of cellulose as a result of alkali pretreatment.

Also, the SEM images showed the rigid structure of untreated bagasse. The fibers of pretreated materials appear to be distorted and separated from the initial connected structure, thus increasing the external surface area and the porosity. Such improved morphological properties generated by pretreatments appeared to be the primary reason for the enhancement of enzymatic hydrolysis yield.

3.4. Conclusion

It can be concluded that the sweet sorghum bagasse is a r emarkable feedstock for ethanol production regarding to its easy cultivation and favor properties as well as high glucan fraction. The comparison between the hydrolysis results of pretreated and untreated bagasse proved that enzymatic hydrolysis of sweet sorghum bagasse could be significantly improved after pretreatment by sodium hydroxide and phosphoric acid. However, it seems that the sodium hydroxide is a more efficient pretreatment method before production of fermentable sugars from sweet sorghum bagasse for further processing to, e.g. ethanol.

References

[1] M. J. Taherzadeh and K. Karimi, Bioethanol: Market and Production Processes, in Biofuels refining and performance, A. Nag (Ed.), McGraw-Hill, 2008, pp. 69-106.

[2] Ó. J. Sánchez and C. A. Cardona, Trends in biotechnological production of fuel ethanol from different feedstocks, Bioresource Technology 99, 2008, pp. 5270-5295.

[3] M. J. Taherzadeh and K. Karimi, Pretreatment of lignocellulosic wastes to improve ethanol and biogas production: a review, International Journal of Molecular Sciences 9, 2008, pp. 1621-1651.

[4] X. R. Wu, et al., Features of sweet sorghum juice and their performance in ethanol fermentation, Industrial Crops and Products 31, 2010, pp. 164-170.

[5] S. Balint, et al., Sweet Sorghum as Feedstock for Ethanol Production: Enzymatic Hydrolysis of Steam-Pretreated Bagasse, Applied Biochemistry and Biotechnology 153, 2009, pp. 151-162.

[6] M. J. Taherzadeh and K. Karimi, Enzyme-Based Hydrolysis Processes for Ethanol from Lignocellulosic Materials: A Review, Bioresources 2, 2007, pp. 707-738.

[7] M. J. Taherzadeh and K. Karimi, Acid-Based Hydrolysis Processes for Ethanol from Lignocellulosic Materials: A Review, Bioresources 2, 2007, pp. 472-499.

[8] Y. H. P. Zhang, et al., Fractionating recalcitrant lignocellulose at modest reaction conditions, Biotechnology and Bioengineering 97, 2007, pp. 214-223.

[9] J. Xu, et al., Sodium Hydroxide Pretreatment of Switchgrass for Ethanol Production, Energy Fuels 24, 2010, pp. 2113-2119.

[10] B. Adeny and J. Baker, Measurement of Cellulase Activities, Laboratory Analytical Procedure (LAP), National Renewable Energy Laboratory, 2008.

[11] E. A. Ximenes, et al., Production of cellulases by Aspergillus fumigatus and characterization of one β-glucosidase, Current Microbiology 32, 1996, pp. 119–123.

[12] A. Sluiter, et al., Determination of Structural Carbohydrates and Lignin in Biomass, in Laboratory Analytical Procedure (LAP), National Renewable Energy Laboratory, 2008.

[13] S. Y. Oh, et al., FTIR analysis of cellulose treated with sodium hydroxide and carbon dioxide, Carbohydrate Research 340, 2005, pp. 417-428.

Intensification of Bioethanol Production by Simultaneous Saccharification and Fermentation (SSF) in an Oscillatory Baffled Reactor (OBR)

Joseph Ikwebe[1*] and Adam P Harvey[1]

[1]*Newcastle University, Newcastle upon Tyne, United Kingdom*
**Corresponding author. Tel. +441912227169, Email: joseph.ikwebe@ncl.ac.uk*

Abstract: Bioethanol is an alternative transport fuel produced mainly by the biochemical conversion of biomasses. This can be carried out efficiently and economically by simultaneous saccharification and fermentation (SSF): a process which integrates the enzymatic saccharification of the cellulose to glucose with the fermentative synthesis of ethanol. However, the SSF unit operation still contributes nearly 50% to the cost of ethanol production. For cellulosic ethanol to be cost competitive, there is the need to intensify the production process in smaller, more efficient and more economical bioreactors. In this work, SSF was performed in an intensified form of plug flow reactor, called the Oscillatory Baffled Reactor (OBR). The OBR is a continuous tubular reactor fitted with equally-spaced orifice plate baffles. An oscillatory component, provided by moving bellows in this design, is superimposed on the net flow through the reactor, generating short-lived vortices due to the interaction of the oscillating fluid with the baffles. This results in uniform mixing in each of the inter-baffle regions, with each behaving as a stirred tank reactor (STR), producing a plug flow residence time distribution (RTD) for the reactor as a whole, in which the mixing effects are largely decoupled from the mean flow (unlike conventional PFRs). The process was evaluated using 2.5% SigmaCell cellulose, 40 FPU cellulase loading/g of cellulose and 10% cellobiase. *Saccharomyces cerevisiae* was employed as the fermenting organism at 38 ^{o}C and pH 4.8. In the first part of this work the use of the OBR resulted in a 7% increase in glucose yield compared to a shake flask, after 48 h of saccharification and 8.0 g/L ethanol in the OBR. This represented 89.8 % of the theoretical yield, as compared to 7.7 g/L in the shake flask representing 81.29%, a difference of 9 percentage point. This increased glucose yield is attributable to better mixing in the OBR.

Keywords: *Cellulose, Cellulase, Saccharification, Fermentation, OBR.*

1. Introduction

The need to meet the ever-increasing demand for energy is probably one of the greatest challenges that society has to grapple with in this new millennium. Virtually every aspect of life on planet earth (heating, transportation, etc.,) requires energy input in one form or another. Hitherto, this energy need has been met principally by the use of fossil fuel resources [1]. However, it has been recognised that global crude oil reserves are finite, and their depletion is occurring much faster than previously predicted [2, 3]. In 2008, just at the onset of the global economic meltdown, crude oil price rose steeply up to a record USD 145. Also, the combustion of fossil fuels inevitably contributes significantly to elevated levels of greenhouse gases (GHG) and the attendant global warming [4]. Therefore, the need for more environmentally sustainable energy sources and the increased concern for the security of oil supply has put pressure on society to find renewable fuel alternatives [5].

Currently bioethanol is the dominant global renewable transport fuel and offers GHG savings of up to 80% over conventional fossil fuels [6]. It is produced primarily by the fermentative action of microorganisms (principally yeasts) on simple sugars [7]. Simultaneous saccharification and fermentation (SSF) can be used to convert the cellulosic part of biomass efficiently and commercially [8]. SSF combines the enzymatic saccharification of polymeric cellulose to simple monomeric forms such as glucose and its eventual fermentation by yeast to ethanol in the same vessel [9, 10]. The enzymatic hydrolysis of cellulose is a complex reaction that depends on the synergistic action of several cellulases, which include endoglucanases that attack β-1,4 bonds randomly within the cellulase chains, β-1,4

cellobiohydrolases that remove successive cellobiose units from free chain ends, and β-glucosidase that break cellobiose up into glucose units[11, 12].

Most bioethanol companies that employ SSF technology use traditional stirred tank reactors in batch or continuous modes. Technology drawbacks associated with these conventional bioreactors are well-documented. These include inadequate mixing resulting in inconsistent product qualities. Ni et al.[13] have demonstrated that consistent product quality results from and is inherently associated with consistent fluid mechanics in OBRs. Also, Mackley and Ni [14] have shown that product uniformity is determined by efficient fluid mixing which also is dependent on efficient heat and mass transfer. Other drawbacks include huge inventories[15], the prohibitive costs of large reactors, and associated downtimes which impact negatively on profitability. In spite of the advantages the SSF brings to bioethanol fermentation, its unit operation still contributes nearly 50% to the cost of ethanol production [16]. For cellulosic ethanol to be cost competitive, there is the need to intensify the production process in smaller, more efficient and more economical bioreactor. The oscillatory baffled reactor (OBR) is one such bioreactor.

1.1 The Oscillatory Baffled Reactor

The OBR is a continuous tubular reactor fitted with equally-spaced orifice plate baffles[15]. An oscillatory component, provided by moving bellows in this design, is superimposed on the net flow through the reactor, generating short-lived vortices due to the interaction of the oscillating fluid with the baffles. This results in uniform mixing in each of the inter-baffle regions, with each behaving as a stirred tank reactor (STR)[13], producing a plug flow residence time distribution (RTD), in which the mixing effects are largely decoupled from the mean flow (unlike conventional PFRs)[17]. It has been demonstrated by Mackley and Ni[18], Ni et al.[19], and Ni et al.[20] that excellent mixing conditions in a tubular reactor can be achieved when vigorous eddies are generated between periodically-spaced baffles as a result of the introduction of oscillations. A typical OBR configuration is revealed in Figures 1 while Figure 2 shows a typical flow pattern in a cell.

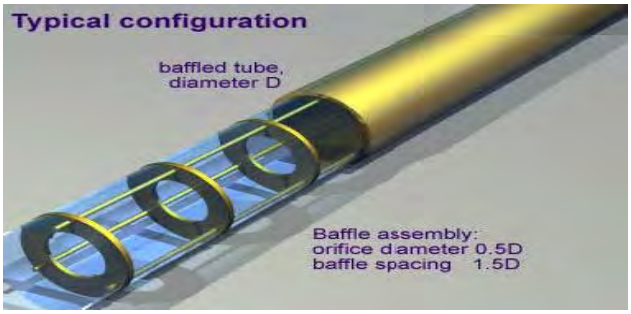

Figure 1. Layout of the OBR[21]

The intensity of the mixing under oscillatory flow is characterised by the oscillatory Reynolds number, Re_0 defined as:

Oscillatory Reynolds number: $\mathrm{Re}_o = \dfrac{\rho 2\pi f x_o d}{\mu}$

where d is the internal tube diameter (m), f is the fluid oscillation frequency (s^{-1}), x_o is the fluid oscillation amplitude (m) measured from centre-to-peak, and μ and ρ are the fluid viscosity (kg m^{-1} s^{-1}) and density (kg m^{-3}), respectively.

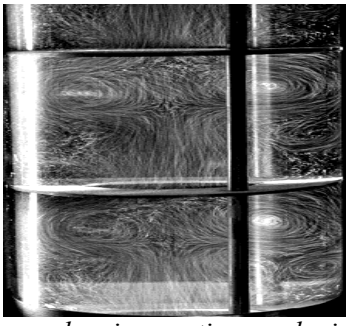

Figure 2 Flow patterns showing vortices and mixing in individual OBR cells[13].

The OBR has already been touted [22] to have the potential to lower costs by 50% and process times by 90% in the manufacture of commodities including chemicals, drugs and biofuels. Reis et al.[23] have demonstrated the potential of the OBR for bioreactions by achieving a 50% decrease in process time of the production of γ-decalactone compared to the stirred tank bioreactor and shake flasks. Gaidhani et al.[24] demonstrated the adaptability of the OBR in the cultivation of microorganisms for the synthesis of pullulan when then they also achieved a 50% reduction in process time in comparison with a parallel STR. They argued that the process time reduction is as a result of a more uniform mixing environment for cell growth and excellent mass transfer characteristics.

In this study the OBR is used in the simultaneous saccharification and fermentation of cellulose to produce ethanol.

2 Methodology

2.1 Enzymatic saccharification

The enzymatic saccharification was carried out using SigmaCell cellulose, Type 50 from Sigma-Aldrich following the NREL LAP, "Enzymatic saccharification of lignocellulosic biomass"[25]. This method measures the rate of conversion of cellulose by the synergistic action of cellulases. 250 mL conical flasks were used in the shake flask experiments and a total saccharification volume of 50 mL containing 2.5% w/v cellulose loadings. Cellulolytic enzymes, cellulose and β-glucosidase (both kind gifts from Novozymes, Denmark) with activity of 100 Filter Paper Unit (FPU)/g and 250 Cellobiose Units (CBU)/g respectively were employed. 10, 20, 40 70 and 100 FPU/g cellulose loadings each containing 10% β-glucosidase were evaluated. The shake flasks were incubated at 50 ^{o}C, the optimum temperature of the enzymes, and a pH of 4.8 and 200 RPM agitation. The saccharification was also carried out at 38 ^{o}C the optimum fermentation temperature of the yeast ascertain the glucose available to the yeast during the fermentation. However, the saccharification medium contained 1% yeast extract and 2% peptone on this occasion. The experiments were run for 168 h and replicate samples collected periodically over time.

In the OBR saccharification 2.5, 5 and 10% w/v cellulose loadings were also evaluated but with 40 FPU/g and 10% β-glucosidase at the same temperatures and pH as the shake flasks. The oscillation frequency was 3 Hz, centre-to-peak amplitude 0.03m and a Reynolds number Re_o of 1760. The OBR experimental set up is as shown in Figure 3 below.

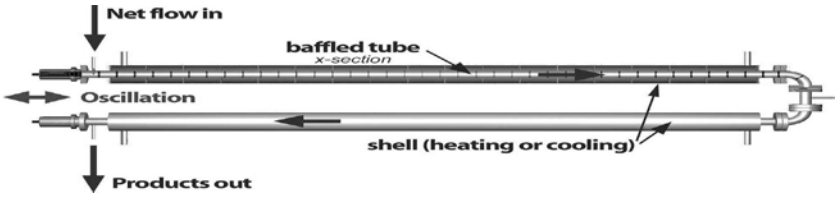

Figure 3 Typical OBR experimental set up[26].

2.2 Simultaneous Saccharification and Fermentation (SSF)

The SSF experiments were performed using 2.5% w/v cellulose and 40 FPU/g in both the shake flasks and OBR. YP medium (10 g/L yeast extract and 20 g/L peptone) was used. The pHs was 4.8 and temperature 38 ^{o}C in both systems and were also all equipped with carbon dioxide traps to simulate anaerobic conditions. The same agitation conditions were maintained in both systems as in the saccharification experiments. The inocula were prepared from a pure culture of baker's yeast *Saccharomyces cerevisiae* and cultivated on YPD medium (10 g/L yeast extract, 20 g/L peptone and 50 g/L glucose-filter-sterilised). The NREL LAP "SSF Experimental Protocols- Lignocellulosic Biomass Hydrolysis and Fermentation"[27] was followed completely in the SSF experiments in both cases. A 10% inoculum was used to initiate the SSF and replicate samples collected periodically.

2.3 Analyses

In both the saccharification and fermentation experiments, samples were collected periodically, spun in a microcentrifuge (Sanyo) at 13000 RPM. The supernatants were analysed for glucose using the dinitrosalicylic acid (DNS) method [28] and absorbance measured with a Jenway 6105 UV/VIS spectrophotometer. Ethanol was analysed using gas chromatograph (Hewlett-Packard 5890 Series II) with column packed with porapak 50/80 mesh as instructed in the NREL LAP[29].

3 Results

Enzymatic saccharification experiments in both the shake flasks and OBR were carried out under identical conditions and the degree of cellulose conversion- representing the concentration of glucose produced were monitored (Figure 4). 78.3% saccharification of cellulose was observed in the shake flasks at 100 FPU/g cellulose and 71% at 40 FPU/g cellulose after 144 h of hydrolysis at 50 ^{o}C. Hence 40 FPU/g cellulose was used in the OBR experiment which represented a trade-off between cellulase efficiency and enzyme cost. 78% saccharification was recorded in the OBR at the end of 144 h of hydrolysis at 50 ^{o}C.

The 5 and 10% cellulose loadings exhibited various degrees of reduced saccharification (data not shown). Figure 5 represents the results of the saccharification experiment at 38 ^{o}C, the fermentation temperature of the yeast. The OBR also showed at least 10 percentage point more conversion than the shake flask at 40 FPU/g of cellulose.

Samples were taken periodically during the SSF and analysed for glucose and ethanol as described above. Figure 6 shows the time-course of the ethanol production and glucose production/utilisation during the SSF of 2.5% cellulose at 40 FPU/g cellulose in both shake flasks and OBR. Whereas ethanol fermentation peaked at 45 h in the OBR it was at 70 h in the shake flasks. Glucose production peaked at 20 h and then began to drop steeply until it was almost completely used up by the yeast by the end of the fermentation. Ethanol yield

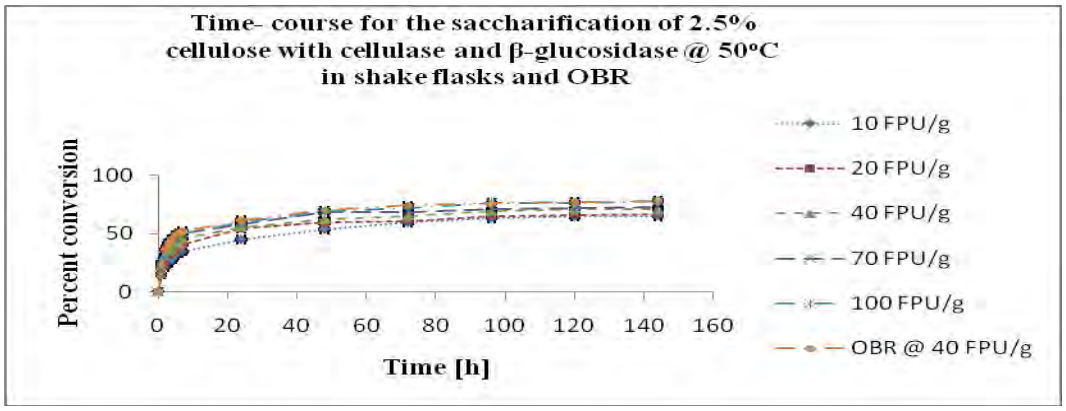

Figure 4. Time-course for the saccharification of 2.5% cellulose with cellulase and β-glucosidase @ 50 °C in shake flasks and OBR.

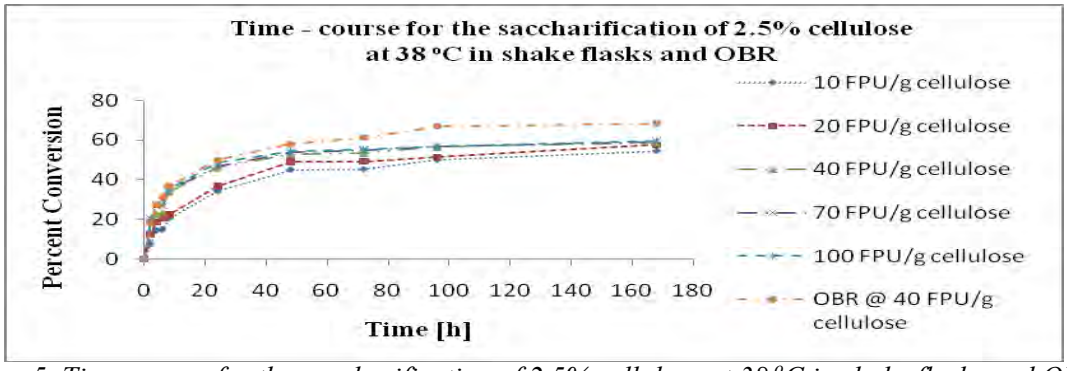

Figure 5. Time-course for the saccharification of 2.5% cellulose at 38 °C in shake flasks and OBR.

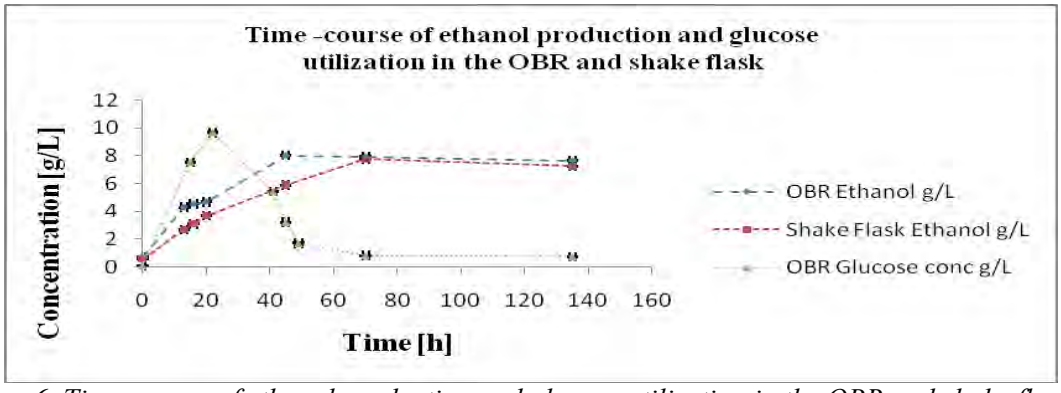

Figure 6. Time-course of ethanol production and glucose utilization in the OBR and shake flask.

increased steadily in both systems but in the OBR it peaked at 8 g/L (89.8% of theoretical yield) after 45 h fermentation and then began to decline. However, in the shake flasks it peaked at 7.7 g/L (81.29% theoretical yield) after 70 h fermentation and began to decline.

4 Discussion and conclusion

The saccharification experiments exhibited classical cellulosic hydrolysis characteristics: an initial rapid saccharification phase within the first 24 h and a much slower later phase (Figure 4 and 5) [30, 31]. The initial rapid phase may be as a result of the easily digestible amorphous part of the cellulose which is more readily available to the cellulases [32]. The later slower phase may be as a result of the crystalline, more recalcitrant part of the cellulose which limits accessibility to the enzymes [9]. The OBR and shake flask experiments exhibited a similar

SSF pattern. 2.5% cellulose loading was chosen for the SSF as it registered the highest percent saccharification as compared to the 5 and 10% (data not shown). The probable reason may be mixing problems and substrate inhibition as the substrate concentration increases [30, 31]. However using the OBR resulted in 7% more saccharification over the shake flask at the end of 168 h of saccharification is possibly as a result of a better mixed hydrolysis environment.

During the first phase of the SSF glucose accumulated within the first 22 h of the process (Figure 6) indicating the yeast cells could not cope with the rate of glucose generation by the enzymes[9]. But as cell mass continued to increase there was also a corresponding uptake of glucose which resulted in a steady rise in ethanol concentration up to the 45 h in the OBR and 70 h in the shake flasks. However, as the generated glucose was used up, the cells began to use ethanol as a carbon source corresponding to the gradual decline in the concentration of ethanol. This probably happened during sampling as air entered the systems to enable a switch of carbon source to ethanol by the cells. A similar phenomenon was also observed by Philippidis and Smith[9].

Although the concentration of ethanol from the two systems were similar (8 g/L OBR vs. 7.7 g/L shake flask), the OBR attained this concentration 25 h earlier than the shake flask. This would lead to a ~30% higher productivity for the same size of reactor. Furthermore it should be noted that OBRs are scaleable: what can be achieved at this scale, can probably also be achieved at industrial scale [33]. The same cannot be said of conventional stirred vessels, in which reaction times increase with scale, as good mixing becomes increasingly difficult to achieve. This also is possibly due to a better mixed SSF environment in the OBR which promoted better mass transfer characteristics. It agrees with the findings of Gaidhani et al.[34] who showed that it took 52 h for the cells to reach the stationary phase in the OBR compared to128 h in the STR.

These results provide a platform for further investigation into the applicability of the OBR in continuous SSF.

Acknowledgement
This study was funded by the Petroleum Technology Development Fund (PTDF) and the Nigeria government.

References

[1]. B. Palmarola-Adrados, T. Juhász, M. Galbe, and G. Zacchi, *Hydrolysis of nonstarch carbohydrates of wheat-starch effluent for ethanol production.* Biotechnology Progress. **20**(2), 2004, p. 474-479.

[2]. F.W. Bai, W.A. Anderson, and M. Moo-Young, *Ethanol fermentation technologies from sugar and starch feedstocks.* Biotechnology Advances. **26**(1), 2008, p. 89-105.

[3]. R. Möller (2006) *Cell Wall Saccharification: Outputs from the EPOBIO projects*. Cell Wall Saccharification **Volume**, 1-69

[4]. T.M.L. Wigley, *The climate change commitment.* Science. **307**(5716), 2005, p. 1766-1769.

[5]. B. Hahn-Hägerdal, M. Galbe, M.F. Gorwa-Grauslund, G. Lidén, and G. Zacchi, *Bio-ethanol- the fuel of tomorrow from the residues of today.* TRENDS in Biotechnology. **24**(12), 2006, p. 8.

[6]. P. Billins, J. Woods, and R. Tipper, *Developing carbon and greenhouse gas assurance for bioethanol production in the UK*. 2005, Home Grown Cereals Authority (HGCA). p. 1-64.

[7]. A. Demirbas, *Bioethanol from cellulosic materials: A renewable motor fuel from biomass.* Energy Sources. **27**(4), 2005, p. 327-337.

[8]. J.D. Wright, C.E. Wyman, and K. Grohmann, *Simultaneous Saccharification and Fermentation of Lignocellulose: Process Evaluation.* Applied Biochemistry and Biotechnology. **18**, 1988, p. 75-90.

[9]. G.P. Philippidis and T.K. Smith, *Limiting factors in the simultaneous saccharification and fermentation process for the conversion of cellulosic biomass to fuel ethanol.* Applied Biochemistry and Biotechnology. **51/52**, 1995.

[10]. M. Ballesteros, J.M. Olivia, M.J. Negro, P. Manzanares, and I. Ballesteros, *Ethanol from lignocellulosic materials by a simultaneous saccharification and fermentation process (SFS) with Kluyveromyces marxianus CECT 10875.*Process Biochemistry. **39**, 2004, p. 6.

[11]. Z. Xiao, R. Storms, and A. Tsang, *Microplate-based filter paper assay to measure total cellulase activity.* Biotechnology and Bioengineering. **88**(7), 2004, p. 832-837.

[12]. C. Breuil and J.N. Saddler, *Comparison of the 3,5-dinitrosalicylic acid and Nelson-Somogyi methods of assaying fo reducing sugars and determining cellulase activity.* Enzyme and Microbial Technology. **7**, 1985, p. 327-332.

[13]. X. Ni, M.R. Mackley, A.P. Harvey, P. Stonestreet, M.H.I. Baird, and N.V. Rama Rao, *Mixing through oscillations and pulsations -A guide to achieving process enhancements in the chemical and process industries.* Chemical Engineering Research and Design. **81**(3), 2003, p. 373-383.

[14]. M.R. Mackley and X. Ni, *Experimental fluid dispersion measurements in periodic baffled tube arrays.* Chemical Engineering Science. **48**(18), 1993, p. 3293-3305.

[15]. A. Harvey and P. Stonestreet, *Oscillatory flow: A technology ready to deliver.* Chemical Engineer. (720), 2001, p. 41.

[16]. NREL, *Research Advances- Cellulosic Ethanol.* National Renewable Energy Laboratory. A National Laboratory of the U.S. Department of Energy, Office of Energy Efficiency & Renewable Energy. 2008.

[17]. A.P. Harvey, M.R. Mackley, and T. Seliger, *Process intensification of biodiesel production using a continuous oscillatory flow reactor.* Journal of Chemical Technology and Biotechnology. **78**, 2003, p. 338-341.

[18]. M.R. Mackley and X. Ni, *Mixing and dispersion in a baffled tube for steady laminar and pulsatile flow.* Chemical Engineering Science. **46**(12), 1991, p. 3139-3151.

[19]. X. Ni, J.A. Cosgrove, A.D. Arnott, C.A. Greated, and R.H. Cumming, *On the measurement of strain rate in an oscillatory baffled column using particle image velocimetry.* Chemical Engineering Science. **55**(16), 2000, p. 3195-3208.

[20]. X. Ni, H. Jian, and A.W. Fitch, *Computational fluid dynamic modelling of flow patterns in an oscillatory baffled column.* Chemical Engineering Science. **57**(14), 2002, p. 2849-2862.

[21]. X.-W. Ni, A. Fitch, and P. Webster (2003) *From a Maximum to Most Efficient Production Using a Continuous Oscillatory Baffled Reactor*. Centre for Oscillatory

Baffled Reactor Applications (COBRA), Chemical Engineering, School of Engineering and Physical Sciences, Heriot-Watt University, Edinburgh, EH14 4AS **Volume**,

[22]. The Scotsman, *Scottish Business Briefing: Tuesday, 2nd October, 2007.* Scotsman.com http://business.scotsman.com/scottishbusinessbriefing/Scottish-Business-Briefing--Tuesday.3465134.jp. 2007.

[23]. N. Reis, C.N. Goncalves, M. Aguedo, N. Gomes, J.A. Teixeira, and A.A. Vicente, *Application of a novel oscillatory flow micro-bioreactor to the production of γ-decalactone in a two immiscible liquid phase medium.* Biotechnology Letters. **28**(7), 2006, p. 485-490.

[24]. H.K. Gaidhani, B. McNeil, and X.W. Ni, *Production of pullulan using an oscillatory baffled bioreactor.* Journal of Chemical Technology and Biotechnology. **78**(2-3), 2003, p. 260-264.

[25]. N. Selig, N. Weiss, and Y. Ji, *Enzymatic Sacharification of Lignocellulosic Biomass.* Laboratory Analytical Procedure (LAP) National Renewable Energy Laboratory (NREL) 2008, p. 1-5.

[26]. A. Harvey and P. Stonestreet, *A mixing-based design methodology for continuous oscillatory flow reactors.* Trans IChemE, Part A, Chemical Engineering Research and Design. **80**, 2002, p. 31-44.

[27]. N. Dowe and J. McMillan, *SSF Experimental Protocols- Lignocellulosic Biomass Hydrolysis and Fermentation.* National Renewable Energy Laboratory Analytical Procedure. **LAP**, 2001, p. 1-16.

[28]. G.L. Miller, *Use of Dinitrosalicylic Acid Reagent for Determination of Reducing Sugar.* Analytical Chemistry. **31**(3), 1959, p. 426-428.

[29]. D.W. Templeton, *Determination of Ethanol Concentration in Biomass to Ethanol Fermentation Supernatants by Gas Chromatography.* National Renewable Energy Laboratory Analytical Procedure. **LAP-011**, 1994, p. 1-10.

[30]. J. Szczodrak, *The enzymatic hydrolysis and fermentation of pretreated wheat straw to ethanol.* Biotechnology and Bioengineering. **32**, 1988, p. 771-776.

[31]. S. Hari Krishna, K. Prasanthi, G.V. Chowdary, and C. Ayyanna, *Simultaneous saccharification and fermentation of pretreated sugar cane leaves to ethanol.* Process Biochemistry. **33**(8), 1998, p. 825-830.

[32]. M.R. Ladisch, C.M. Ladisch, and G.T. Tsao, *Cellulose to sugars: New path gives quantitative yield.* Science. **201**(4357), 1978, p. 743-745.

[33]. K.B. Smith and M.R. Mackley, *An experimental investigation into the scale-up of oscillatory flow mixing in baffled tubes.* Chemical Engineering Research and Design. **84**(11 A), 2006, p. 1001-1011.

[34]. H.K. Gaidhani, B. McNeil, and X. Ni, *Fermentation of pullulan using an oscillatory baffled fermenter.* Chemical Engineering Research and Design. **83**(6 A), 2005, p. 640-645.

Chemical and Microbial Hydrolysis of Sweet Sorghum Bagasse for Ethanol Production

Anusith Thanapimmetha[1,2], Korsuk Vuttibunchon[1], Maythee Saisriyoot[1,2], Penjit Srinophakun[1,2]*

[1]*Bioprocess Laboratory, Department of Chemical Engineering, Faculty of Engineering, Kasetsart University, 50 Ngamwongwan Road, Jatujak, Bangkok 10900, Thailand*
[2]*Thailand and The Center of Excellence for Petroleum, Petrochemicals and Advanced Materials, S&T Postgraduate Education and Research Development Office (PERDO), Thailand.*
** Corresponding author. Tel: +662942-8555 ext. 1234 or 1203, Fax: +662561-4621, E-mail: fengpjs@ku.ac*

Abstract: Sweet sorghum (*Sorghum bicolor L.* Moench) is the potential raw material of ethanol production. As a lignocellulosic material, hydrolysis is needed to transform it to sugar. Usually, this sugar was used as substrate for ethanol production by fermentation. In this study, the composition of sweet sorghum bagasse was analyzed. The compositions of the sweet sorghum bagasse before hydrolysis are 58.23% cellulose, 25.42% hemicellulose and 14.95% lignin. It was then cut, dried and pretreated at 121 ^{o}C, 25 min by sodium hydroxide. Then the experimental design is performed to design the experimental runs. Box-Behnken was used to design the experiment of chemical hydrolysis. The factors of sulfuric acid concentration (15-55 %w/w), solid to liquid ratio (1:10-1:30 w:w) and reaction time (40-120 minutes) affecting reducing sugar production were optimized for the chemical hydrolysis. At the optimum condition, the maximum reducing sugar was equal to 33.49% (g/g dry substrate). On the other hand, microbial hydrolysis with *Trichoderma harzianum* gave the maximum reducing sugar of 10.34 % (g/g dry substrate) at optimum condition. Then type of reducing sugar was analyzed using High Performance Liquid Chromatography (HPLC). It is obvious that glucose is the dominated reducing sugar. Finally, the reducing sugar (glucose, xylose and arabinose) from chemical and microbial hydrolysis is usually fermented with *Saccharomyces cerevisiae* to produce ethanol.

Keywords: *Hydrolysis, Sweet Sorghum Bagasse, Ethanol, Trichoderma harzianum*

1. Introduction

Sweet sorghum (*Sorghum bicolor L.* Moench) is a renewable, cheap, widely available resource. It is used as an alternative material for ethanol production since it is high biomass and sugar yielding crop. It contains soluble (glucose and sucrose) and insoluble carbohydrates (cellulose and hemicellulose) [1]. The juice extracting from the fresh stem is easily converted to ethanol. The remaining solid residue (bagasse) is a byproduct representing about 30% of the whole plant fresh weight. Bagasse, an important residue from sweet sorghum processing, could become an important biomass source for saccharification and fermentation for bioethanol production in the near future.

Sweet sorghum bagasse which is lignocellulosic biomass is mainly composed of cellulose, hemicellulose and lignin. Cellulose is a linear polymer that is composed of glucose subunits linked by β-1, 4 glycosidic bonds. These long chains linked together by hydrogen bonds and van der Waals forces. Cellulose is usually present as a crystalline form while a small amount of nonorganized cellulose chains forms amorphous cellulose. Hemicellulose is a polysaccharide with a lower molecular weight than cellulose. Hemicellulose contains xylose, mannose, galactose, glucose, arabinose and glucuronic acids, and are linked together by β-1,4- and sometimes by β-1,3-glycosidic bonds. Lignin is physical seal of hemicellulose and cellulose, which is an impenetrable barrier in the plant cell wall [2]. In order to obtain sugar, it is necessary to degrade the polymers to monomer, which can be done by physical, chemical or biological methods.

Generally, the chemical used in the hydrolysis is sulfuric acid. Acids can breakdown the heterocyclic bonds between sugar monomers in polymeric chain, which are formed by hemicellulose and cellulose [3].

For microbial hydrolysis, numerous bacterial and filamentous fungi can produce cellulolytic enzyme such as cellulase and hemicellulase. One of the most extensively studied of cellulolytic microorganism is *Trichoderma spp.,* which is also industrially used for enzyme production.

The aim of this work was to determine the optimum conditions for reducing sugar production from sweet sorghum bagasse by acid hydrolysis comparing with *Trichoderma harzianum* hydrolysis. In this experiment, three factors were optimized namely acid concentration, solid to liquid ratio and reaction time. Response Surface Methodology (RSM) using Box-Behnken Design (BBD) was applied for optimizing these independent variables.

2. Methodology

2.1. Microorganisms

The fungal strain *Trichoderma harzianum*, was obtained from Uniseeds Co., LTD. The inoculum of *T. harzianum* was in powder form and contained 10^8 spores per gram.

2.2. Substrate preparation and compositional analysis

Sweet sorghum bagasse was obtained from Suwan Farm, Kasetsart University. This material was thoroughly washed and dried at 65 ^oC until constant weight was obtained. The air-dried bagasse was then milled and subsequently sieved to a size of 2-4 mm. The composition of material was then analyzed by the methods of Goering and Van in 1970 [4] to analyse cellulose, hemicellulose, lignin and ash content in the material.

2.3. Alkali pretreatment

The sweet sorghum bagasse was soaked with 1, 5, 10 and 15% (w/w) NaOH solution at a solid to liquid weight ratio of 1:10 and consequently autoclaved at 121 ^oC for 25 min. The mixture was filtered to separate the solid residues and the filtrate fraction. At the end of the reaction, the solid residues were thoroughly washed with water to remove the residual alkaline until neutral pH was obtained, then dried at 65 ^oC, and analyzed the compositions of the solid residues.

2.4. Optimization of reducing sugar production by acid hydrolysis

One gram of pretreated material was soaked with 10-30 gram of 5-55% (w/w) sulfuric acid solution in the 250 ml Erlenmeyer flask and then autoclaved at 121^oC for 40-120 minutes. After hydrolysis, the suspended material was separated using filter paper. The total reducing sugars in the filtrate were determined by the 3,5-dinitrosalicylic acid (DNS) method described by Miller in 1959 [5].

RSM was applied for the optimization of the reducing sugars production. Three parameters namely concentration of sulfuric acid (X_1), solid to liquid ratio (X_2) and reaction time (X_3) with the ranges of minimum (-1), maximum (+1) and central point (0) were assigned to investigated experimental conditions of reducing sugar production. The levels of parameters for the experimental design are shown in Table 1.

Table 1. Experimental range and coded levels of factors for reducing sugars production

Factors	Symbol	Range and levels		
		-1	0	1
concentration (%v/v)	X_1	15	35	55
solid:liquid ratio (w:w)	X_2	1:10	1:20	1:30
reaction time (min)	X_3	40	80	120

The total of 15 experimental runs with three variables was designed according to a BBD using the statistical software MINITAB release 14. The detailed experimental designs with coded of three parameters are shown in Table 3. The behavior of the system was explained by the following quadratic model equation which includes the effects of linear, quadratic and interaction was used to determine the predicted response as follows:

$$Y = \beta_0 + \beta_1 X_1 + \beta_2 X_2 + \beta_3 X_3 + \beta_{11} X_1^2 + \beta_{22} X_2^2 + \beta_{33} X_3^2 + \beta_{12} X_1 X_2 + \beta_{13} X_1 X_3 + \beta_{23} X_2 X_3 \quad (1)$$

Where Y is the predicted response, β_0 is the intercept; β_1, β_2 and β_3 linear coefficient; β_{11}, β_{22} and β_{33} square coefficient; and β_{12}, β_{13} and β_{23} interaction coefficients with X_1, X_2 and X_3 corresponding to the principal factors of sulfuric acid concentration, solid to liquid ratio and reaction time, respectively

2.5. Reducing sugar production by microbial hydrolysis

Reducing sugar production under Solid-State Fermentation (SSF) was conducted in the 250 ml flask covered with cotton at optimum conditions previously optimized for maximum reducing sugar from pretreated sweet sorghum bagasse by *T. harzianum* [6]. Each flask containing 5 g dried pretreated sweet sorghum bagasse, which was used as the carbon source. Standard Mandel medium in 50 mM sodium citrate buffer (pH 4.8) that contained of 0.3 g/l urea, 1.4 g/l $(NH_4)_2SO_4$, 2.0 g/l KH_2PO_4, 0.4 g/l $CaCl_2 \cdot 2H_2O$, 0.3 g/l $MgSO_4 \cdot 4H_2O$, 0.75 g/l peptone, 0.25 g /l yeast extract, 5 m g/l $FeSO_4 \cdot 7H_2O$, 1.6 m g/l $MnSO_4 \cdot 4H_2O$, 1.4 mg/l $ZnSO_4 \cdot 7H_2O$ and 20 m g/l $CoCl_2 \cdot 6H_2O$, was added into the substrate for adjusting initial moisture content (77.5% w/w) before autoclaving at 121 ^oC for 20 min. Each flask was inoculated with 10% (w/w) fungal spore of *T. harzianum* and incubated at 25^oC for 88 hours. After suitable periods of time, reducing sugar was extracted from the fermented medium by adding 100 ml distilled water to each flask. The flasks were then shaken at 200 rpm for 2 hr at 60 ^oC. Suspended solid were separated and the reducing sugars (filtrate) were determined by the DNS method [5]. The composition of reducing sugars (glucose, xylose and arabinose) in hydrolysates was determined by HPLC.

3. Results and discussion

3.1. Chemical composition of substrates

The main compositions as cellulose, hemicelluloses, lignin and ashes content of sweet sorghum bagasse before and after pretreatment with 1, 5, 10 and 15% (w/v) of sodium hydroxide are shown in Table 2.

The alkali pretreatment was conducted by pretreating sweet sorghum bagasse at high temperature. When the concentration of sodium hydroxide increased, lignin content was decreased. As a result, the cellulose fraction increased more than 90% (w/w) when 10 and 15% (w/v) of sodium hydroxide were used. This is typical of alkaline pretreatment, which

generally has a stronger effect on lignin than cellulose [7]. It was observed that pretreated biomass was swollen, which leaded to the decrease in the degree of polymerization and crystallinity, disruption of the lignin structure, and separation of structural linkages between lignin and carbohydrates [8]. However, the compositions of sweet sorghum bagasse when using 10 and 15% (w/v) of sodium hydroxide were not different, so that 10% (w/v) of sodium hydroxide was chosen for the pretreatment as the suitable concentration.

Table 2. Main compositions of sweet sorghum bagasse in untreated bagasse and after alkaline pretreatments

Composition (%dry weight)	NaOH concentration (%w/v)				
	Untreated bagasse	1	5	10	15
Cellulose	58.23	68.66	86.18	90.37	91.10
Hemicellulose	25.42	19.28	9.70	5.97	5.82
Lignin	14.95	12.02	3.97	3.56	2.97
Ash	1.40	0.04	0.15	0.10	0.11

3.2. Optimization of reducing sugar production by acid hydrolysis

In the present study, BBD was used to investigate the optimal conditions of the reducing sugar production from pretreated bagasse. There were three factors namely concentration of sulfuric acid, solid to liquid ratio and reaction time and three levels of each parameter were varied as shown in Table 3.

Table 3. Reducing sugar from pretreated bagasse in experiments obtained by Box-Behnken design

Run number	Level of experimental factors			Reducing sugar (%g/g dry weight)
	Concentration (X_1)	Solid to liquid ratio (X_2)	Reaction time (X_3)	
1	-1	-1	0	28.46
2	1	-1	0	16.90
3	-1	1	0	24.99
4	1	1	0	6.53
5	-1	0	-1	23.06
6	1	0	-1	13.01
7	-1	0	1	27.35
8	1	0	1	7.75
9	0	-1	-1	25.81
10	0	1	-1	18.09
11	0	-1	1	20.36
12	0	1	1	12.24
13	0	0	0	31.11
14	0	0	0	29.81
15	0	0	0	29.92

The fifteen experiments were designed as shown in Table 3 and the maximum reducing sugar is 31.11% (g/g dry substrate), which was observed at the experimental run number 13. The statistical software MINITAB release 14 was used to design of experiments, to determine the

coefficients of linear, quadratic and interaction terms, and to build the quadratic model and response surface plots.

The BBD was used to investigate the effects of the assigned parameters on the reducing sugar production. The experimental results were analyzed by regression analysis consisting of the effect of linear, quadratic and interaction which gave the following regression equation with reducing sugar production as a function of concentration of sulfuric acid (X_1), solid to liquid ratio (X_2) and reaction time (X_3). Reducing sugar (Y) at specific combination of three variables can be predicted by substituting the corresponding values of each variable in Eq. (2).

$$Y = -24.5581+1.1226X_1+1.1375X_2+0.7000X_3-0.0155X_1^2-0.0175X_2^2 -0.0039X_3^2-0.0030X_1X_3 \quad (2)$$

The probability value (p-value) is a tool for evaluating the significance and contribution of each parameter and the statistical polynomial model equation. The smaller p-value is an indication of high significance of corresponding coefficient [9]. The regression coefficient in the response surface model for the linear, quadratic and interaction effects of the variables are shown along with p-value in Table 4. The p-value suggested that the coefficient for the linear effect of sulfuric acid concentration ($p < 0.01$), solid to liquid ratio ($p < 0.01$) and reaction time ($p < 0.01$) were statistically significant for reducing sugar production.

Table 4. Estimated regression coefficient and corresponding p-value for reducing sugar production

Term	Coefficient	p-value
Constant	-24.5581	0.027*
X_1	1.1226	0.003**
X_2	1.1375	0.007**
X_3	0.7000	0.001**
X_1^2	-0.0155	0.001**
X_2^2	-0.0175	0.003**
X_3^2	-0.0039	0.001**
X_1X_2	-0.0052	0.102
X_1X_3	-0.0030	0.039*
X_2X_3	-0.0001	0.913

* $p < 0.05$, ** $p < 0.01$

Analysis of variance (ANOVA) for proposed model is shown in Table 5. The p-value of the regression model ($p<0.001$) implies that the model is significant. In addition, the coefficient of variation ($R^2= 0.986$) indicates a high correlation between the observed and predicted values from model Eq. (2). Therefore, this equation can be used for predicting the amount of reducing sugar production under parameter ranges of assigned three variables.

Table 5. Analysis of variance (ANOVA) for reducing sugar production

Source	Degree of Freedom (DF)	Sum of square (SS)	Mean square (MS)	F	*p*-value
Regression model	9	2024.63	224.959	38.49	0.000
Residual Error	5	29.22	5.844		
Total	14	2053.85			

R^2= 98.6% R^2 (adj) = 96.0%

The two-dimensional (2D) contour plots and three-dimensional (3D) response surface of the interactions are presented in Figure 1, 2 and 3. These observations also identified the optimal conditions with the maximum response for the levels of the factors in the design of experiments. The maximum response is referred to the surface confined in smallest ellipse in the contour plot. The perfect interaction between the independent variables can be shown when elliptical contours are obtained [9].

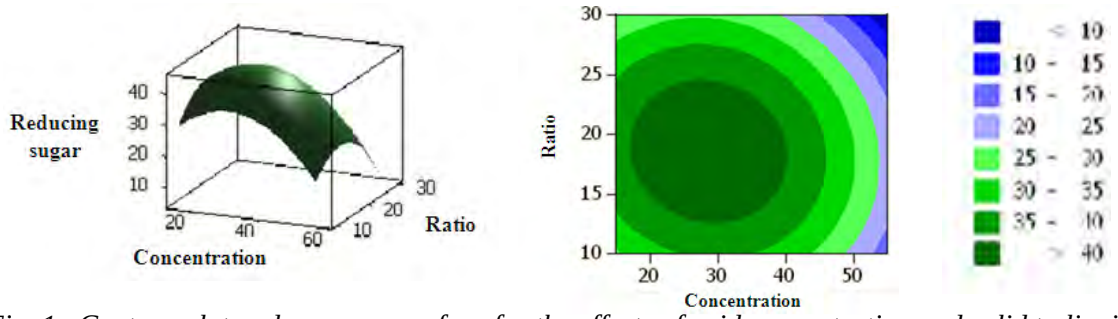

Fig. 1. Contour plot and response surface for the effects of acid concentration and solid to liquid ratio at a constant reaction time (80 minutes).

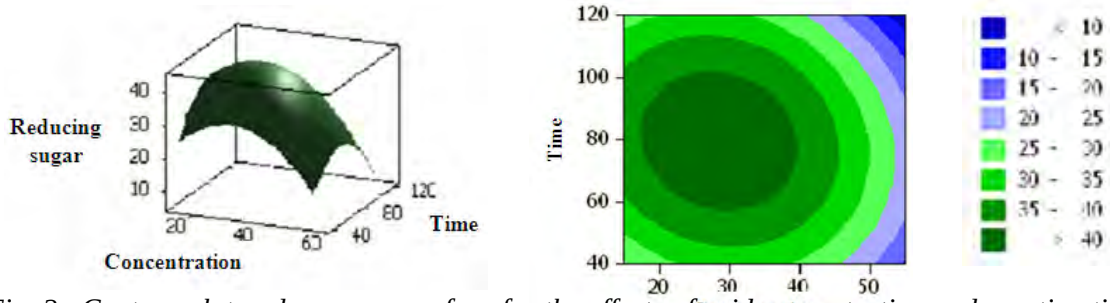

Fig. 2. Contour plot and response surface for the effects of acid concentration and reaction time at a constant solid to liquid ratio (1:20).

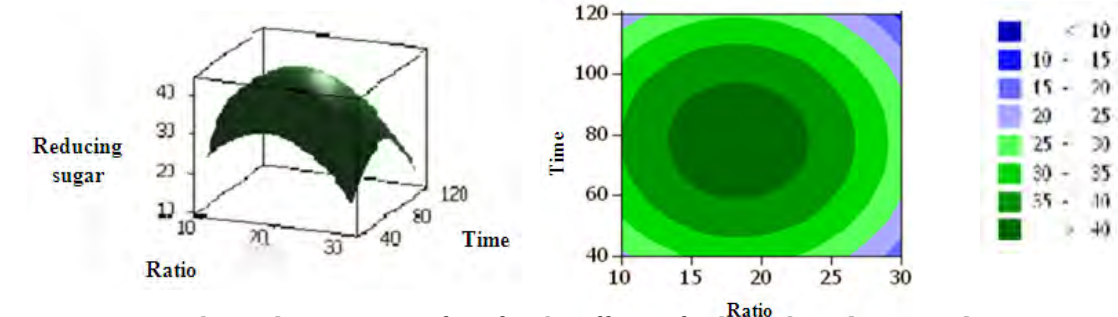

Fig. 3. Contour plot and response surface for the effects of solid to liquid ratio and reaction time at a constant acid concentration (35% v/v).

Application of RSM with BBD predicted that the maximum reducing sugar production must occur at decoded values of condition parameters at sulfuric acid of 21.44% (v/v), solid to liquid ratio of 1:12.5 and reaction time of 73.24 minutes. At this maximum condition, the reducing sugar should reach 34.97% (g/g dry substrate). A repeat acid hydrolysis for reducing sugar production under optimal conditions is carried out to confirm the prediction. After performing the hydrolysis under optimal condition, the obtained reducing sugar is 33.49% (g/g dry substrate). Since the difference between predicted and actual confirmed result was only about 4.23%, it should be regarded as acceptable.

3.3. Reducing sugar production by microbial hydrolysis

In this respect, preatreated sweet sorghum bagasse was conducted for the production of reducing sugar by *T. harzianum* under SSF. An inoculum (10%w/w) was added to a medium of 77.5% (w/w) moisture content and incubated at 25°C for 84 hours. Reducing sugar was expressed based on weight of dry substrate and carried out in triplicates and standard deviation was less than 6%. As shown in Figure 4, the highest reducing sugar, 10.34 % (w/w), was obtained at 56 hours of fermentation time. The conditions used in the experiment were the optimum conditions previously studied [6].

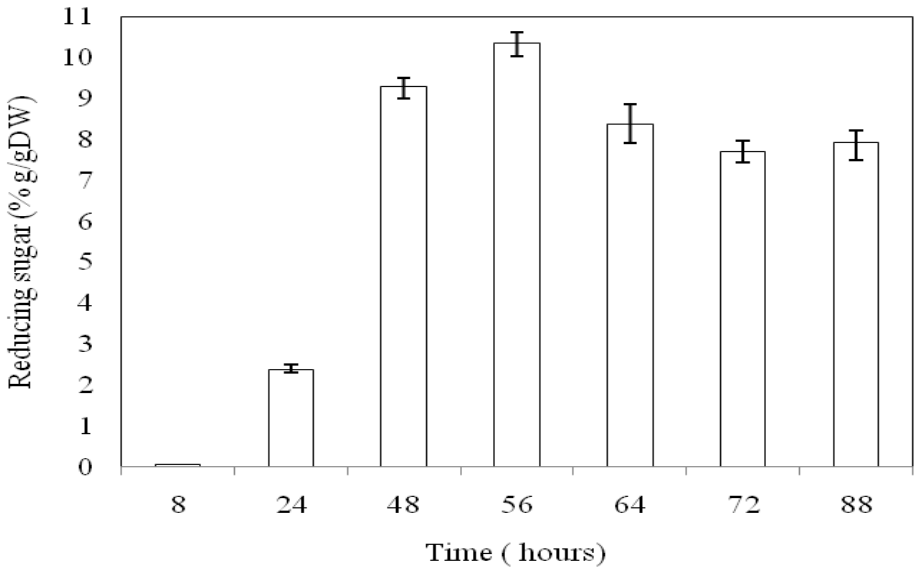

Fig. 4. Reducing sugar production by T. harzianum under SSF using pretreated sweet sorghum bagasse as the substrate (inoculum of 10% w/w and moisture content of 77.5% w/w)

The reducing sugar obtained from acid hydrolysis (33.49%) was higher than from microbial hydrolysis **(**10.34%) because the conditions of chemical hydrolysis are stronger than microbial hydrolysis. However, acid hydrolysis has several disadvantages over microbial hydrolysis due to formation of toxic compounds, such as furfural, hydroxylmethylfurfural, acetic acid, formic acid, levulinic acid etc. These toxic compounds can inhibit the yeast fermentation in next step of ethanol production. Removal of these compounds increases the additional costs for ethanol production [10].

The advantages of microbial hydrolysis include low energy requirement, mild conditions and the ready sugar for further fermentation. However, the rate of hydrolysis in most microbial hydrolysis processes is very low.

4. Conclusions

The optimal conditions obtained through a statistical Box-Behnken Design are successfully determined to maximize the reducing sugar production from acid hydrolysis. The result from the second order polynomial model developed indicated that the optimal conditions for reducing sugar production from pretreated sweet sorghum bagasse by sulfuric acid hydrolysis are 21.44 %(v/v) of sulfuric acid, solid to liquid ratio of 1:12.5 and reaction time of 73.24 minutes which give the maximum reducing sugar of 33.49% (g/g dry substrate) higher than the maximum reducing sugar of microbial hydrolysis (10.34% g/g dry substrate).

Acknowledgements

This study was supported by Kasetsart University Reseach and Development Institute (KURDI), Department of Chemical Engineering, Faculty of Engineering, Kasetsart University, Thailand and The Center of Excellence for Petroleum, Petrochemicals and Advanced Materials, S&T Postgraduate Education and Research Development Office (PERDO).

References

[1] D. Mamma, P. Christakopoulos, D. Koullas, D. Kekos, B.J. Macris and E. Koukios, An alternative approach to the bioconversion of sweet sorghum carbohydrates to ethanol, Biomass and Bioenergy 8, 1995, pp. 99-103.

[2] S. Carmen, Lignocellulosic residue: Biodegradation and bioconversion by fungi, Biot. Adv 27, 2009, pp. 185-194.

[3] R. Aguilar, J.A. Ramirez, G. Garrote, and M. Vazquez, Kinetic study of acid hydrolysis of sugarcane bagasse, J. Food Eng 55, 2002, pp. 309-318.

[4] H.K. Goering and P.J. Van, Forage fibre analysis Agriculture handbook, Agricultural Research Services, 1970, pp. 20.

[5] G.L. Miller, Analytical Chemistry 31, 1959, pp. 426-428.

[6] K. Vuttibunchon, Box-Behnken experimental design of reducing sugar production from sweet sorghum bagasse by *Trichoderma harzianum*, M.S.Thesis (Thai), Kasetsart University, 2010.

[7] J.M. Gould, Studies on the mechanism of alkaline peroxide delignification of agricultural residues, Biotechnol. Bioeng 27, 1985, pp. 225-231.

[8] L.T. Fan, M.M. Gharpuray, and Y.H. Lee, In: Cellulose hydrolysis Biotechnology Monograph, Springer Berlin 57, 1987, pp. 211.

[9] A. Md. Zahangir, A. M. Suleyman and W. Rosmaziah, Statistical optimization of process conditions for cellulase production by liquid state bioconversion of domestic wastewater sludge, Bioresource Technology 99, 2008, pp. 4709-4716.

[10] E. Palmqvist and B. Hahn-Hagerdal. Fermentation of lignocellulosic hydrolysates. I: inhibition and detoxification, Bioresource Technology 74, 2002, pp. 17-24.

Ethanolysis of Soybean Oil Using Mesoporous Molecular Sieves

Solange A. Quintella[1], Davi C. Salmin[1], Antonio S. Araújo[2], Monica C.G. Albuquerque[1], Célio L. Cavalcante Jr. [1,*]

[1] *Universidade Federal do Ceará, Fortaleza, Brazil*
[2] *Universidade Federal do Rio Grande do Norte, Natal, Brazil*
** Corresponding author. Tel: +55 85 3366-9611, Fax: +55 85 3366-9611, E-mail: celio@ufc.br*

Abstract: This study evaluates the use of nanostructured materials as catalyst in biodiesel production from soybean oil using ethanol as transesterificant agent. Ethanol can be environmentally advantageous over methanol (more frequently used as reagent in biodiesel production) because it can be obtained from renewable sources whilst methanol is usually derived from mineral sources. The catalyst (La_{50}SBA-15) has lanthanum oxide as active phase which was inserted by isomorphous substitution into the SBA-15 network. The LaSBA-15 mesoporous molecular sieves were synthesized using pluronic (P123) dissolved in aqueous HCl solution with tetraethyl orthosilicate and a given amount of hydrated lanthanum chloride (Si:La = 50) at 333K. The reaction was performed using the molar ratio soybean oil:ethanol of 1:20 at inert atmosphere (N_2) at 343K with 1wt% of catalyst mass relative to total oil mass added to the reaction mixture. The reaction was evaluated for ethyl ester conversion after 3h and 6h. The ethyl esters content was measured using low frequency ^{1}HNMR spectroscopy (200MHz). A conversion of soybean oil in ethyl esters (biodiesel) of 80% after reaction time of 6h was obtained. The La_{50}SBA-15 heterogeneous catalyst showed good performance in the ethanolysis of soybean oil, comparing well with previous reports for methanolysis of soybean oil.

Keywords: *Biodiesel, ethanolysis, heterogeneous catalysis, La_{50}SBA-15.*

1. Introduction

Biodiesel can be defined as a fuel composed of mono-alkyl esters of long chain fatty acids derived from vegetable oils or animal fats. The most common process for biodiesel production consists in a transesterification reaction in which a triglycerides source (vegetable oil or animal fat) reacts to a short chain alcohol (usually methanol) in catalyst presence [1-3]. Since ethanol is largely obtained in Brazil from renewable sources (mostly sugarcane) it might be advantageous to replace methanol in the transesterification reaction for biodiesel production [4].

The transesterification reaction may be catalyzed by acids, bases or enzymes [5]. Industrially, basic homogeneous catalysts such as potassium hydroxide and sodium hydroxide are often used in biodiesel production, because they display high reactivity, low cost and mild reaction conditions. However, as usually observed in homogeneous catalyst systems, they require downstream separation of the catalyst and byproducts, thus increasing the process complexity and cost [6-9]. Therefore process development for biodiesel production from heterogeneous catalysts has been largely studied in recent years [5,6,10-12]. Albuquerque et al. [11] studied calcium oxide catalytic proprieties supported on s everal mesoporous SBA-15 silica in transesterification of castor and sunflower oil with methanol. Yan et al. [6] studied the use of calcium oxide modified with lanthanum in the transesterification reaction with methanol. The mixture CaO-La_2O_3 showed higher catalytic activity than when using pure calcium oxide or pure lanthanum oxide. Yan et al. [7] also studied the use of ZnO-La_2O_3 as heterogeneous catalyst in the transesterification of unrefined or waste oil with methanol with noticeable strong interaction between zinc and lanthanum species. The catalyst sample with a 3:1 zinc lanthanum molar ratio displayed higher activity compared to pure metal oxides. Sun et al. [13] studied the properties of ZrO_2 impregnated with La_2O_3 as a cat alyst in sunflower oil transesterification with methanol . The best methyl ester conversion was found when using a catalyst concentration of 21wt.% La_2O_3 on ZrO_2.

This study intends to investigate the use of La_{50}SBA-15 in soybean oil transesterification using ethanol. The La_{50}SBA-15 has lanthanum oxide as active phase inserted into SBA-15 framework by isomorphous substitution.

2. Materials and Methods

2.1. Catalyst Preparation and Characterization

The SBA-15 modified with lanthanum was synthesized by hydrothermal method using 4.0 g of Pluronic P123 (BASF Co.) as template, dissolved in 10.3 mL of aqueous HCl solution (VETEC, Brazil). Thereafter 10.3 mL of tetraethyl orthosilicate (Sigma-Aldrich) and a given amount of previously dissolved hydrated lanthanum chloride (VETEC, Brazil) were added (Si/La = 50), and the mixture stirred for 22 h at a temperature of 333 K. The resulting gel was placed into a Teflon container and submitted to hydrothermal treatment at a temperature of 373 K for 48 h. The solid was then filtered at room temperature, washed with a solution of HCl in ethanol 2 wt%, dried at 333 K for 1 h, and finally the solid was calcined at 823 K (heating rate=1 K/min). The samples, designated as La_{50}SBA-15 (where 50 refers to the Si/La molar ratio) were characterized through X-ray diffraction (DRX), N_2 adsorption and desorption isotherms at 77 K, and scanning electron microscopy (SEM). Further details may be found in Quintella [14].

2.2. Reaction

The reaction experimental set-up consisted of a 100 mL round-bottomed flask with four outlets. A thermometer was attached to the first outlet for temperature control. The reflux condenser was inserted into the second one to minimize the ethanol loss through evaporation and the third received nitrogen flow providing inert atmosphere. The fourth outlet was used to introduce the catalyst and remove aliquots in order to monitor the reaction.

Initially the catalyst was activated at 1073 K, under inert atmosphere, during 1 hour in order to convert carbonates eventually formed by atmosphere contact into oxides since carbonates do not show catalytic activity [10]. In the transesterification reactor, 30.3 g of commercial soybean oil (Liza, Sao Paulo, Brazil) were added to 99.6% ethanol (J.T.Baker, Mexico). The molar ratio of soybean oil and ethanol used was 1:20. The reaction was carried out at inert atmosphere using 1000 rpm agitation. When the oil and alcohol mixture reached the desired temperature, 343 K, the catalyst was inserted to the reaction mixture using a catalyst/oil mass ratio of 0.01. Samples of 5 mL were taken after 3h and 6h, filtered under vacuum to extract the catalyst from the reaction mixture. To improve the phase separation in the reaction mixture, 99.5% dichloromethane (Cromolina, Diadema, Brazil) was added, and subsequently vaporized from the ester phase at 373 K.

The ethyl ester conversion was evaluated through hydrogen nuclear magnetic resonance spectroscopy (^{1}H NMR) with 60 MHz frequency using Varian EM-360 equipment and $CDCl_3$ as solvent [15,16]. The ^{1}H NMR technique for ethyl esters determination is based on the analysis of three sets of signals: (A_1) the hydrogen from the ester ethoxy carbons; (A_2) the four methylene hydrogens from glycerol; (A_3) the α-methylene carbonyl hydrogen present in all mono, di and triglycerides from both oil and fatty acid ethyl esters [17]. The conversion of soybean oil (EE) into biodiesel (ethyl esteres) was obtained from the ^{1}H NMR technique using Eq. (1).

$$EE(\%) = \frac{(A_1 - A_3)}{A_2} \times 100 \qquad (1)$$

3. Results and Discussions

3.1. Catalyst Characterization

The diffractograms of SBA-15 and La_{50}SBA-15 are shown in Fig. 1. T hree major peaks, referring to Miller index crystalline plans (100), (110) e (200), are characteristic of hexagonal symmetry p6mm (punctual planar group two-dimensional 6mm), common in mesoporous materials similar to SBA-15 [18-20]. It may be observed that the incorporation of lanthanum did not affect the hexagonal structure typical of SBA-15.

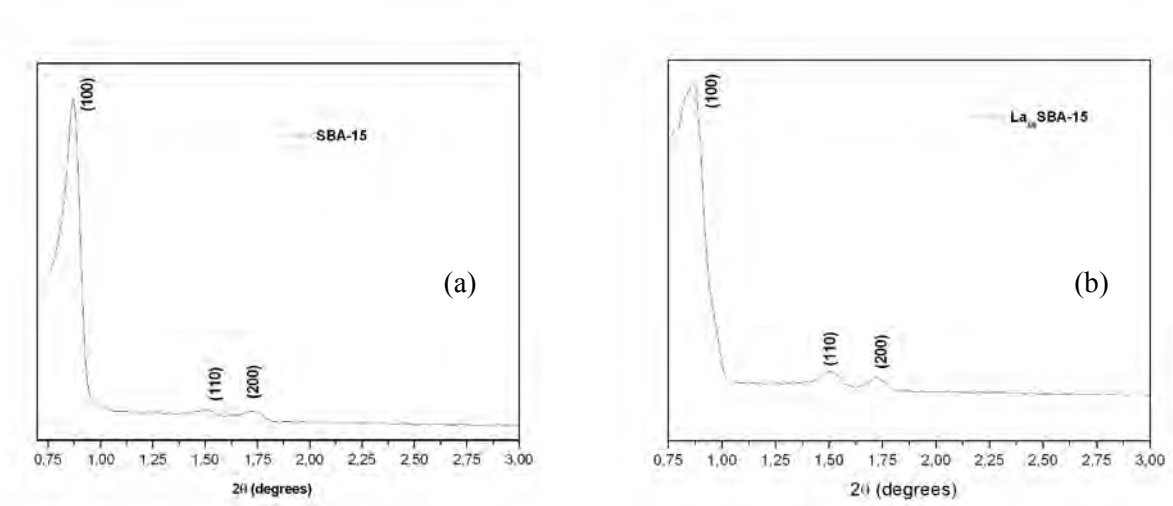

Fig. 1. X-Ray Diffractograms (a) SBA-15 ; (b) La_{50}SBA-15.

The nitrogen adsorption and desorption isotherms for samples show a t ype IV shape (Brunauer classification) as characteristic for nanoporous materials (see Fig. 2). Table 1 summarizes the textural properties of both samples (SBA-15 and La_{50}SBA-15).

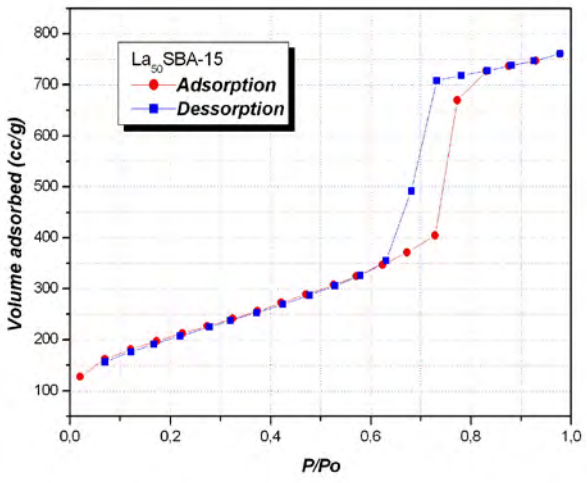

Fig. 2. N_2 adsorptior

Table 1. Textural characteristics synthesized materials samples

Sample	a_0(nm)	D_p(nm)	V_p(cm^3g^{-1})	S_{BET}(m^2g^{-1})
SBA-15	11.88	4.33	0.95	931.3
La_{50}SBA-15	11.88	7.29	1.09	735.2

The SEM micrographs for both samples are shown in Fig. 3. It may be observed that SBA-15 displays a non uni form morphology showing irregular spheres (Fig. 3a). For La_{50}SBA-15 (Fig. 3b), it may be noted some regions with clearer areas than others, indicating the presence of another material, probably lanthanum, which had not been observed in Fig. 3a. The lanthanum addition to the support framework caused morphological changes indicated by the noticeable stick shapes.

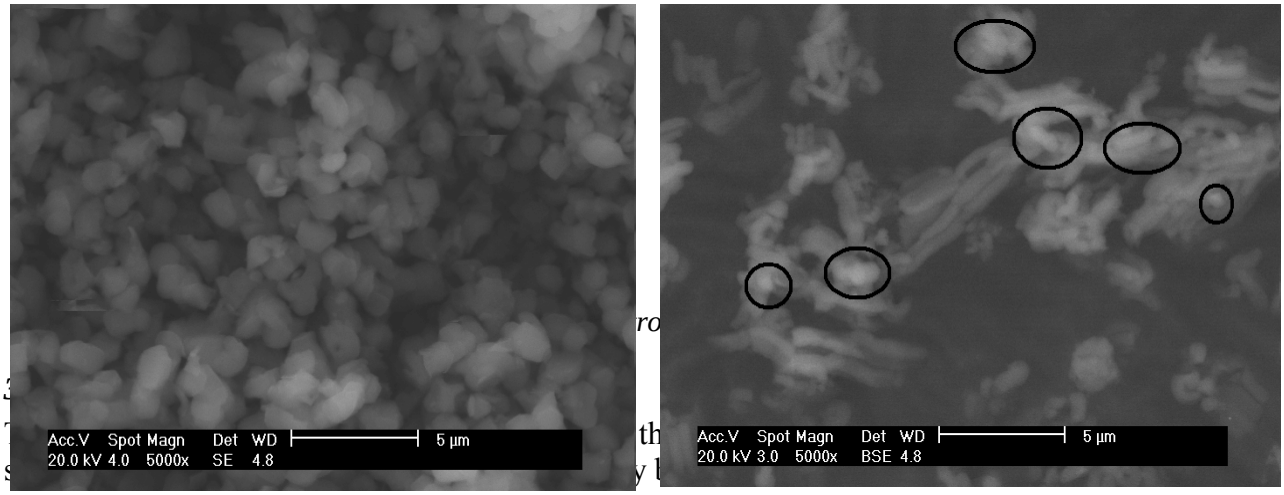

glycerol methylenic hydrogen; four glycerol hydrogens; dimethylenic hydrogens; three CH_2 α-carboxílic groups; CH_2 carbon groups neighboring the unsaturated carbons; CH_2 carbons neighboring the saturated carbons; CH_2 carbons bonded to 2 s aturated carbons atoms; and three terminal methyl groups.

The ^{1}H RMN spectrum of the ethyl ester product is shown in Fig. 5. The quartet signal relative to the OCH_2- group hydrogen, which appears exclusively at the spectrum of the ethyl esters molecule, may be observed in the region of 3.8-4.2 ppm. Also, the triplet signal relative to α-CH2- groups, which may be found in both oil and ethyl esters, is seen in the region of 2.2-2.5 ppm.

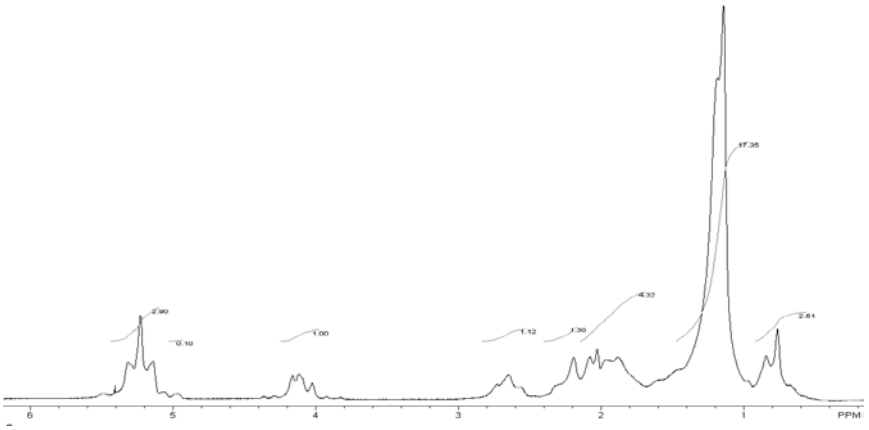

Fig. 4. ^{1}H NMR spectrum of pure soybean oil.

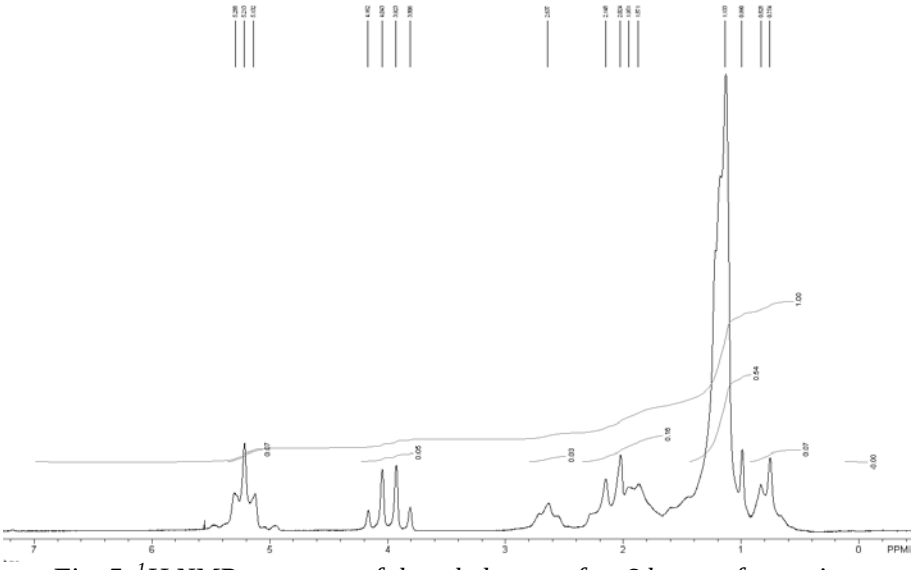

Fig. 5. ^{1}H NMR spectrum of the ethyl ester after 6 hours of reaction.

The ^{1}H RMN spectrum of the product after reaction time of 3 hs showed no conversion to ethyl ester. After 6 hs (Fig. 5), the calculated value of the conversion of soybean oil with ethanol using as catalyst in the transesterification reaction was 80% v/v, which is comparable to previously reported values (see Table 2). The classical homogenous process catalyzed by KOH is reported using ethanol as transesterificant agent with conversions as high as 96%v/v, however the downstream separation of the products (ester/glycerin phases) is rather difficult if compared to heterogeneous systems.

Other studies using heterogeneous catalysts with methanol, instead of ethanol, have been reported (also seen in Table 2). Those studies present somewhat higher values for conversion (as high as 98%v/v of methyl ester), however at more extreme operation conditions (temperature and time) and higher ratios of alcohol/oil and catalyst/oil.

Table 2. Comparison of conversion to biodiesel with previously reported values.

Oil/Alcohol	Alcohol/Oil molar ratio	Catalyst	Catalyst/oil mass ratio	Temp. (K)	Time (h)	Conv. (%vv)	Ref.
Soybean/EtOH	20	LaSBA15	0.01	343	6	80.0	This study
Soybean/EtOH	18.8	homogeneous (KOH)	0.01	n.a.	4	96.0	22
Soybean/MeOH	21	Ca_3La_1	0.05	331	3	94.3	6
Waste/MeOH	36	$ZnO\text{-}La_2O_3$	0.023	473	2	95.0	7
Sunflower/MeOH	30	La_2O_3/ZrO_2	0.05	473	5	98.1	13

4. Conclusions

The results of the transesterification reaction of soybean oil using La_{50}SBA-15 as heterogeneous catalyst confirm the possibility of its use in the ethanolysis of soybean oil at milder operation conditions than previously reported studies with methanol. A conversion of 80.0%v/v could be obtained using oil/ethanol molar ratio of 1:20; catalyst/oil mass ratio of 0.01; temperature 343 K; inert atmosphere; and 6 hours of reaction.

Acknowledgments

The authors wish to acknowledge the financial support provided by Conselho Nacional de Desenvolvimento Científico e Tecnológico (CNPq).

References

[1] L.C. Meher, V. Sagar, S.N. Naik, Technical aspects of biodiesel production by transesterification – a review. Renewable & Sustainable Energy Reviews 10, 2006, pp. 248-268.

[2] F. Ma, M.A. Hanna, Biodiesel production: a review. Bioresource Technology 70, 1999, pp.1-15.

[3] S.A. Basha, K.R. Gopal, S. Jebaraj. A review on bi odiesel production, combustion, emissions and performance. Renewable and Sustainable Energy Reviews 13, 2009, pp . 1628-1634.

[4] J.M. Encinar, J.F. González, A.R. Reinares. Ethanolysis of used frying oil. Biodiesel preparation and characterization. Fuel Processing Technology 88, 2007, pp. 513-522.

[5] B. Hamad, R.O.L. Souza, G. Sapaly, M.G.C. Rocha, P.G.P. Oliveira, W.A. Gonzalez, E.A. Sales, N. Essayem. Transesterification of rapeseed oil with ethanol over heterogeneous heteropolyacids. Catalysis Communications 10, 2008, pp. 92-97.

[6] S. Yan, M. Kim, S.O. Salley, NG, K.Y. Simon. Oil transesterification over calcium oxides modified with lanthanum. Applied Catalysis A: General 360, 2009, pp. 163-170.

[7] S. Yan, M. Kim, S.O. Salley, NG, K.Y. Simon. Simultaneous transesterification and esterification of unrefined or waste oils over ZnO-La_2O_3 catalysts. Applied Catalysis A: General 353, 2009, pp. 203-212.

[8] B. Freedman, E.H. Pryde, T.L. Mounts. Variables affecting the yields of fatty esters from transesterified vegetables oils. Journal of the American Oil Chemists Society 61, 1984, pp. 1638-1643.

[9] M. Di Serio, R. Tesser, M. Dimicccoli, F. Cammarotaa, M. Nastasi, E. Santacesaria, Synthesis of biodiesel via homogeneous lewis acid catalyst,Journal of Molecular Catalysis A: Chemical, 239, 2005, pp. 111-115, 2005.

[10] H. Hattori, Heterogeneous basic catalysis Chemical Reviews 95, 1995, pp. 537-558.

[11] Albuquerque, M.C.G., I. Jiménez-Urbistondo, J. Santamría-González, J.M. Mérdia-Robles, R. Moreno-Tost, E. Rodriguez-Castellón, A. Jimenéz-Lopez, D.C.S. Azevedo, C.L. Cavalcante JR., CaO support on m esoporous silicas as basic catalysts for transesterification reactions. Applied Catalysis A: General 334, 2008, pp. 35-43.

[12] M. Zabeti, W.M.A.W. Daud, M.K. Aroua, Activity of solid catalysts for biodiesel production:A review. Fuel Processing Technology 90, 2009, pp. 770-777.

[13] H. Sun, Y. Ding, J. Duan, Q. Zhang, Z. Wang, H. Lou, X. Zheng, Transesterification of sunflower oil to biodiesel on ZrO_2 supported La_2O_3 catalyst. Bioresource Technology 101, 2010, pp. 953-958.

[14] S.A. Quintella, Synthesis, characterization and catalytic properties of molecular sieve SBA-15modified with nanostructured lanthanum. PhD dissertation, Universidade Federal do Rio Grande do Norte, Brazil, Natal, 2009.

[15] G. Knothe, Monitoring a progressing transesterification reaction by fiber-0opic near infrared spectroscopy with correlation to ^{1}H nuclear magnetic resonance spectroscopy. Journal of the American Oil Chemists Society 77, 2000, pp. 489-493.

[16] P.R. Costa Neto, M.S.B. Caro, L.M. Mazzuco, M.G. Nascimento, Quantification of soybean oil ethanolysis with ^{1}H NMR. Journal of the American Oil Chemists Society 81, 2004, pp. 1111-1114.

[17] C.L.M. Silva, Obtenção de ésteres etílicos a p artir da transesterificação do óleo de andiroba com etanol. Master thesis, Universidade Estadual de Campinas, Brazil, Campinas, 2005.

[18] G.M. Dhar, G.M. Kumaran, M. Kumar, K.S. Rawat, L.D. Sharma, B.D. Raju, K.S.R. Rao, Physico-chemical characterization and catalysis on SBA-15 supported molybdenum hydrotreating catalysts. Catalysis Today 99, 2005, pp.309-314.

[19] G.M. Kumaran, S. Garg, K. Soni, M. Kumar, L.D. Sharma, G. M. Dhar, K.S.R. Rao, Effect of Al-SBA-15 support on c atalytic functionalities of hydrotreating catalysts I. Effect of variation of Si/Al ratio on catalytic functionalities. Applied Catalysis A:General 305, 2006, pp.123-129.

[20] D. Zhao, Q. Hou, J. Feng, B. F. Chmelka, G. D. Stucky, Nonionic triblock and star diblock copolymer and oligomeric surfactant syntheses of highly ordered, hydrothermally stable, mesoporous silica structures. Journal of the American Chemical Society 120, 1998, pp.6024-6036.

[21] Y. Miyake, K. Yokomizo, N. Matsuzaki, Determination of unsaturated fatty acid composition by high-resolution nuclear magnetic resonance spectroscopy. Journal of the American Oil Chemists Society 75, 1998, pp. 1091-1094.

[22] D.C. Barbosa, T.M. Serra, S.M.P. Meneghetti, M.R. Meneghetti, Biodiesel production by ethanolysis of mixed castor and soybean oils. Fuel 89, 2010, pp. 3791-3794.

Parametric study of portable floating type biogas plant

Ravi P. Agrahari[1,*], G. N. Tiwari[1]

[1] *Centre for Energy Studies, Indian Institute of Technology, Delhi, Hauz khas, New Delhi, India-110016*
** Corresponding author. Tel: +91 9911 809 808, E-mail: ravipagrahari2010@yahoo.com, ravipagrahari_iitd24@yahoo.com*

Abstract: In this paper, an attempt has been made to design and test the performance of a portable floating type biogas plant of volume capacity 0.018 m3 for outdoor climatic condition of New Delhi, India. The field study has been carried under the monsoonal season of New Delhi, India. In this experiment, we have taken an aluminium made digester of 30 Kg slurry capacity for batch system. In the batch system, the slurry has been added once to the digester for whole duration of the process. The rate of biogas production with slurry temperature has been observed.
It has been observed that (i) the biogas production depends strongly on slurry temperature and (ii) the retention period is nearly 85 days. The range of slurry and ambient temperature of atmosphere recorded during the observed period have been found as 26 to 42 ºC and 30 to 40 ºC respectively. Physical and chemical analysis of biogas and slurry have also been carried out. Further, the CO2 mitigation and carbon credit has also been evaluated for the present system.

Keywords: *Biogas, Batch system, Carbon credit, Digester.*

1. Introduction

Biogas technology provides an alternate source of energy in rural India, and is an appropriate technology that meets the basic need for cooking fuel in rural areas by using local resources, viz. cattle waste and other organic wastes. Realization of this potential and fact that India supports the largest cattle wealth led to the promotion of National Biogas Programme in major way in the late 1970s as an answer to the growing fuel crisis. In India alone, there are an estimated over 250 million cattle and if one third of the dung produced annually from these is available for production of biogas, more than 12 million biogas plants can be installed which have the estimated biogas potential capacity of 17,000 MW.

Biogas is produced from organic wastes by concerned action of various group of anaerobic bacteria through anaerobic decomposition. Anaerobic decomposition is a two-stage process as specific bacteria feed on certain organic materials. In the first stage, acidic bacteria dismantle the complex organic molecules into peptides, glycerol, alcohol and the simpler sugars. When these compounds have been produced in sufficient quantities, a second type of bacteria starts to convert these simpler compounds into methane. These methane producing bacteria are particularly influenced by the ambient conditions, which can slow or halt the process completely. Globally, the reduction of green house gas emissions particularly of CO_2 has become more important. Currently much of the carbon dioxide emitted to the atmosphere is a result of anthropogenic activities from the use of the fossil fuel in the transportation and energy sectors. Significant emission reductions may be achieved in the energy sector by improving efficiency through the use of alternative fuels. Through the use of biogas plant we can save the CO_2 emission in the atmosphere which has been measured in the term of carbon credit.

Carbon credit is a key component of national and international attempts to mitigate the growth in concentrations of green house gases (GHGs). One Carbon Credit is equal to one ton of carbon, which is the chief element of carbon dioxide. Carbon trading is an application of an emission trading approach through carbon credit. Greenhouse gas emissions are capped and

then markets are used to allocate the emissions among the group of regulated sources. The idea is to allow market mechanisms to drive industrial and commercial processes in the direction of low emissions than are used when there is no cost to emitting carbon dioxide and other GHGs into the atmosphere. Since GHG mitigation projects generate credits, this approach can be used to finance carbon reduction schemes between trading partners and around the world.

Usmani et al (1996) have analysed the performance of a greenhouse integrated biogas plant. In this paper their basic aim was to reduce thermal loss to ambient in harsh cold climates. According to Lau et al. (1987) due to the lower temperature, biogas production decreases drastically and may stop. Thus, for enhancing biogas production, a higher digester temperature than ambient temperature is required. The green house concept should be integrated for larger capacity biogas plant. Tiwari et al. (1988) and Tiwari and Chandra (1986) have suggested that the rate of biogas production and the period to achieve the optimum temperature are function of the temperature of the slurry. Also, for a required production rate of biogas, the period to achieve the optimum temperature should be reduced. Tiwari et al. (1992) have suggested heating of the slurry by a heat exanger connected to a flat plate collector. Gupta et al. (1998), Sodha et al. (1987, 1989), Tiwari et al. (1997) have suggested installation of PVC greenhouse type structure over a biogas plant. This allowed solar heating of the substrate from 18 °C to about 37 °C. Kumar et al. (2008) have done experiments with solar greenhouse assisted biogas plant in hilly region and have come to conclusion that biogas- green house hybrid system may be successful in hilly regions where average temperature remains below 37 °C throughout the year. Prabhakant et al. (2009) evaluate the carbon credits earned by energy security in India and also analyses the return on capital for biogas plants with and without embodied energy.

The 70% of livestock in India is owned by 67% of small and marginal farmers and by the land less farmers. The 60% of livestock farming labor is provided by women and more than 90% of work related to care of animals is rendered by womenfolk of the family. India ranks fifth after Australia, China, Iran, and New Zealand. The fabrication of biogas plant is tried with different materials based on which the cost of installation is highly dependent. The few data of biogas production and its composition (CH_4 fraction) with the operating temperature of slurry is available in the literature. In this paper an attempt has been made to study the biogas production with its composition with the temperature throughout retention period w.e.f. July 12, 2010 to September 29, 2010.

2. Experimental setup and instrumentation

An aluminium made biogas chamber of 30 kg slurry capacity has been used under the outdoor simulation above the ground, so that the digester and dome both can direct receive the solar radiation. The diameter and height of digester have been taken as 0.34 and 0.38 m respectively. Similarly the diameter, depth and weight of dome have been taken as 0.30 m, 0.35 m and 0.18 kg, respectively.
Aluminium metal is more efficient to increase the sufficient temperature inside the digester which increases the production rate of biogas. Four calibrated thermocouples have been used to measure ambient, slurry, gas and dome temperature by using digital temperature indicator of resolution 0.1 °C. A thermocouple is a junction between two different metals that produces a voltage related to temperature difference. Thermocouples are a widely used type of temperature sensor for measurement and control and can also be used to convert heat into electric power. They are inexpensive and interchangeable, are supplied fitted with standard connectors, and can measure a wide range of temperatures. The main limitation is accuracy

system errors of less than one degree Celsius can be difficult to achieve. These thermocouples are calibrated by constant temperature controlled calibration baths. A calibration bath is a uniform temperature enclosure with a constant temperature setting that can be adjusted manually or with automation. This field study has been done at the Solar Energy Park, IIT Delhi, New Delhi, under the monsoonal season, which is highly under the fluctuating environmental condition.

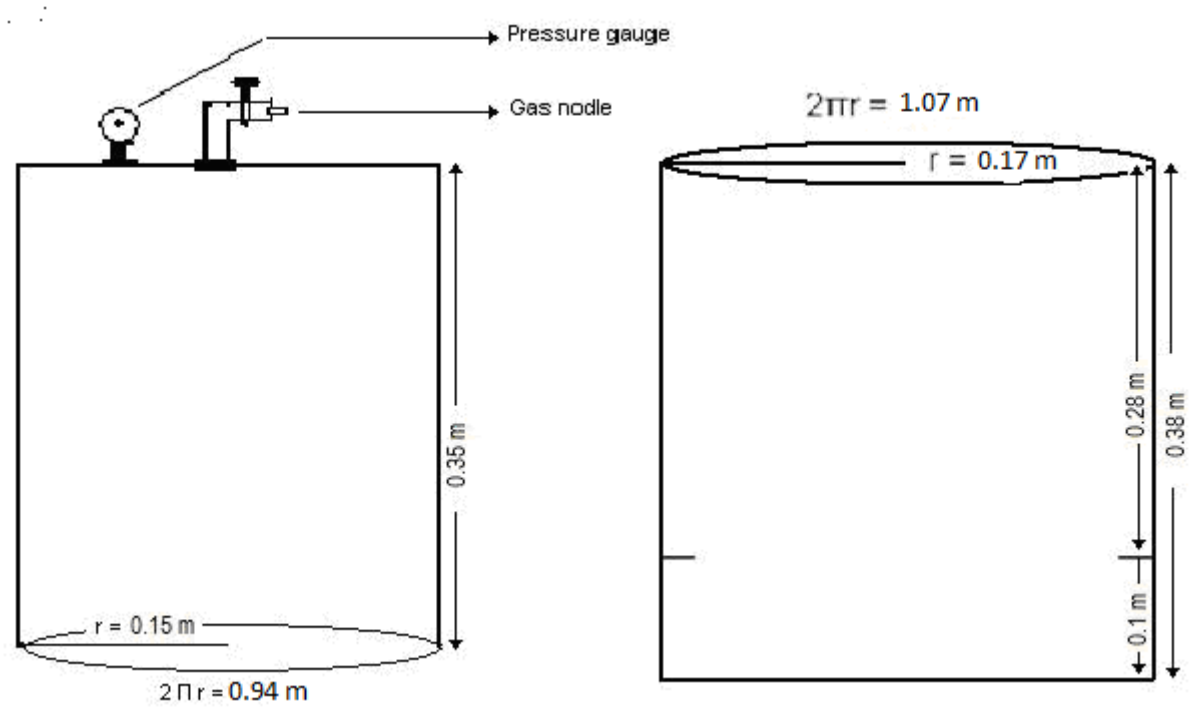

(a) (b)

Figure 1. Schematic view (a) Dome (b) Digester

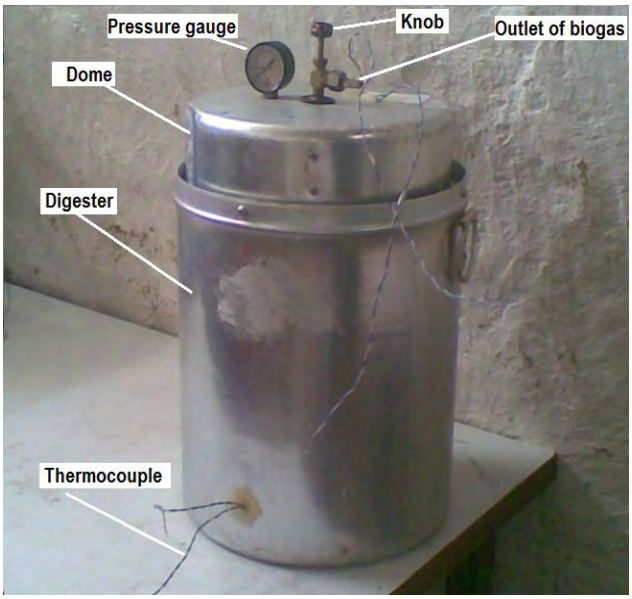

Figure 2. : Photograph of experimental setup

These observation has been taken during day time due to presence of sunlight at 9:00 am, 1:00 pm and 5:00 pm during the month of July to September 2010 (monsoon season) in Delhi, India. Ambient temperature, relative humidity, average precipitation and solar intensity have been measured during this experiment. Gas production have been recorded on daily basis by the observation of upliftment of dome and volume production. This biogas sample have been taken out by the help of toddler bags, which is safe to carry biogas without any leakage and entry of atmospheric air, which has been tested through gas chromatography.

3. Methodology and experimental observations

Different parameters like solar intensity, ambient temperature, slurry temperature, average humidity and average precipitation are measured on daily basis. These data have been taken at the interval of 4:00 hours between 9:00 am to 5:00 pm due to presence of solar radiation. Three readings have been taken in every day at 9:00 am, 1:00 pm and 5:00 pm. Under the analysis we have calculated the average of solar intensity and relative humidity at these three different times in a day upto every two weeks, until the biogas production inside the biogas chamber stop. In this manner we have also calculated the average ambient temperature and average slurry temperature to find the different result and observation, which shown in figure 3 and figure 4. We have also tried to measure the pressure inside the dome through the help of pressure gauge in kg/cm^2 but it did not provide any data due to generation of very less pressure inside the dome. The production rate and methane fraction has also been observed under the influence of various temperature range during the monsoonal season in New Delhi, India.

4. Results and discussions

In this study, it has been observed that the production of biogas is dependent upon the temperature and the solar intensity of the atmosphere. The methane fraction has found to increase up to first six weeks and then it become constant. The synthesis of biogas have been started from the third day of the slurry feeding inside the biogas chamber. There has no role of humidity and precipitation under biogas production. Initially solar intensity increased upto two weeks but after this it decreases due to cloudy weather condition, because the monsoonal season is very fluctuating. Where as the slurry temperature was always more than ambient temperature during the whole experimentation period. These all parameters are shown in figure 3. In this continuation, initially in first two week, the rate of biogas production was very fast but after it gradually decreases. During experimentation, the minimum and maximum fraction range of methane and the rate of biogas production has also been observed in every week which shown in figure 4.
The total biogas volume produced during the experimentation has been recorded 0.378 m^3 under three month of observation. So the total volume of biogas produced in a year (4 × 0.378 m^3) 1.512 m^3 . Therefore the total carbon credits which has been earned in a year 0.019 units/year or € 0.285 / year. Carbon dioxide mitigation and carbon credit are calculated below:

Carbon credit earned by biogas plant

Total volume of biogas produced during experiment (July to September) = 0.378 m^3

Total volume of biogas produced in a year = 4 × 0.378 m^3 = 1.512 m^3

(Taking calorific value of biogas = 6 kWh/ m^3)
So total energy produced in a year = 6 × 1.512 = 9.072 kWh

(Taking 1kWh = 2 kg CO_2 under mitigation)
Total CO_2 mitigated = 9.072 × 2 = 18.144 kg/ year

It is known that in one meter cube of biogas there is an average 62.5% natural gas by volume and the weight of natural gas is 0.68 kg/ m^3

The weight of natural gas present in the given volume of biogas = 0.68 × 1.512 = 1.028 kg/ year

Methane is 18.25 times more potent than carbon dioxide. Taking this ratio the equivalent carbon dioxide can be computed as = 18.25 × 1.028 = 18.761 kg/ year = 0.019 ton/year
(1 ton CO_2 = 1 credit)

Therefore total carbon credits earned in a year = 0.019 units/year = € 0.285 / year.
(Assuming 1 carbon credit = € 15/ unit)

Table 1. Different parameters (solar intensity, relative humidity, ambient temperature, slurry temperature and average precipitation) and their effect with biogas production and methane fraction.

	Observation	2 week	4 week	6 week	8 week	10 week	12 week
Avg. solar intensity (W/m2)	9:00 am	230	248	226.5	215	218	209.5
	1:00 pm	491.5	504	613	511	474.5	557.5
	5:00 pm	121.5	124.5	145	134.5	131.5	166.5
(AVG.) (W/m2)	(9:00 am to 5:00 pm)	**281**	**292.2**	**328.2**	**286.8**	**274.7**	**311.2**
Avg. humidity (%)	9:00 am	67.1	73	76.5	80.2	64.2	64.9
	1:00 pm	52.6	63	69.9	67.3	56.9	60.3
	5:00 pm	61.6	70	79.3	80.3	58.9	67.7
(AVG.) (%)	(9:00 am to 5:00 pm)	60.4	68.7	75.2	75.9	60.0	64.3
Avg. Ambient temperature (°C)	Whole day (24 hours)	31	30.5	30.3	30.0	29.5	29
Avg. Slurry temperature (°C)	(9:00 am to 5:00 pm)	**32.4**	**32.5**	**35.1**	**36.5**	**35.7**	**35.1**
Volume of biogas (m3)	Whole day (24 hours)	**0.033**	**0.133**	**0.102**	**0.040**	**0.054**	**0.016**
Methane fraction(min.) (%)	Whole day (24 hours)	**5**	**35**	**40**	**40**	**40**	**30**
Methane fraction(max.) (%)	Whole day (24 hours)	**40**	**55**	**55**	**55**	**55**	**40**

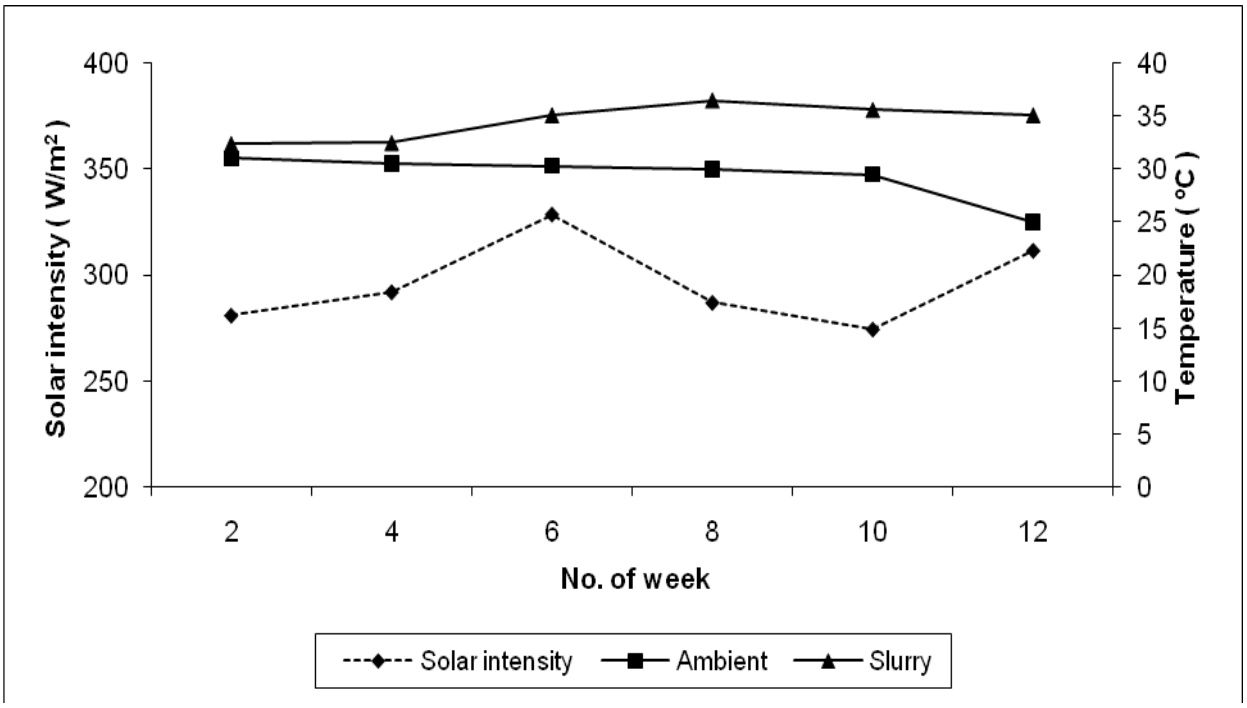

Figure 3. The weekly variation of solar intensity, ambient temperature and slurry temperature

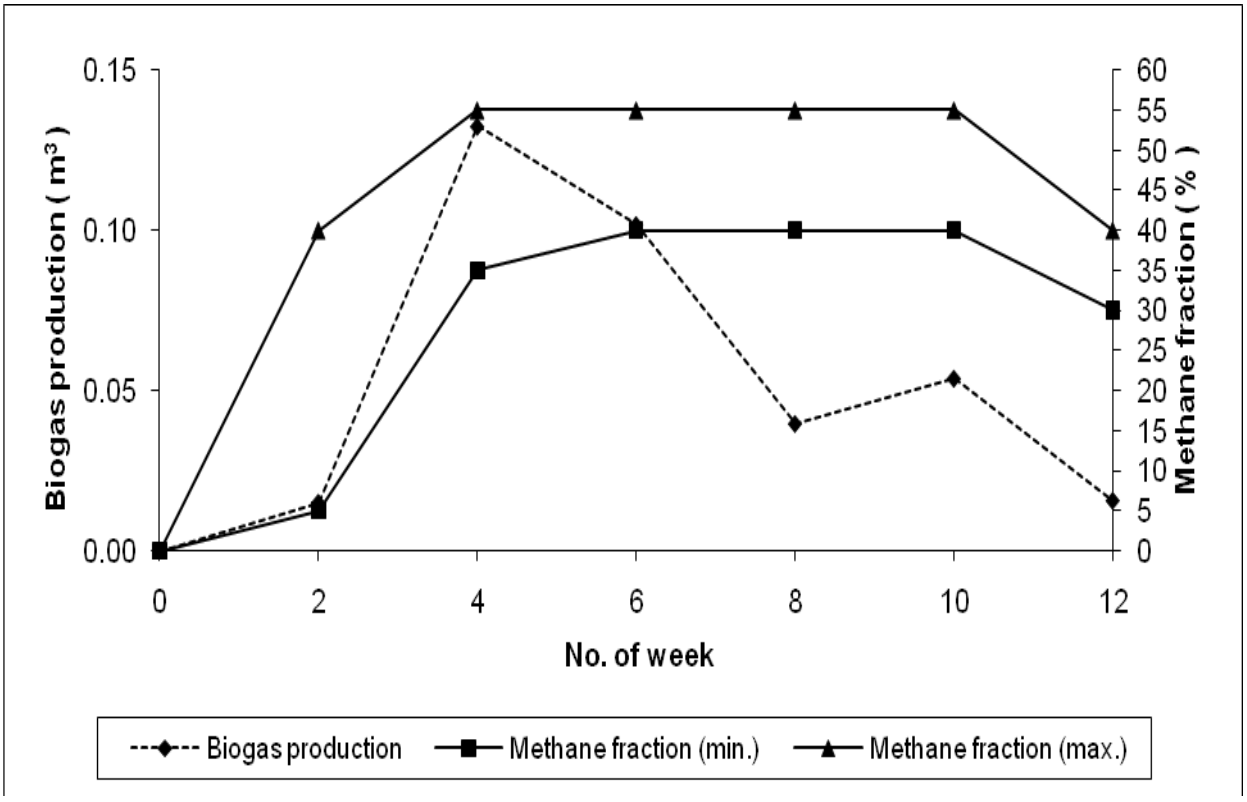

Figure 4. Rate of biogas production and methane fraction shown on weekly basis

5. Conclusions and recommendations

In this experiment it has been observed that the biogas plant is successful during the monsoon season because here the temperature varies between 26 to 39°C. Aluminium made biogas plant is other alternative which we can use for biogas production because it is more durable, less prone to corrosion, light in weight and more heat absorbing capacity comparative to iron made biogas plant, so it maintains sufficient temperature inside the digester which increases the rate of production of biogas. These are also economically feasible for developing country specially for India. We can also increase the slurry temperature inside the digester if we coat a black paint on the surface of aluminium made biogas chamber. Because it will increase the absorbtion capacity of sunlight on its surface. In next experiment we will also analyse the rate of production of biogas and its methane fraction under greenhouse chamber.

Acknowledgement

We are thankful to the Centre for Rural Development and Technology (CRDT), IIT Delhi, for their help to measure the biogas fraction and analysis of spent sample.

References

[1] Usmani J.A., Tiwari G.N. and Chandra A., 1996. Performance Characteristic of greenhouse integrated biogas system. Energy Conservation and Management. 37(9): 1423-1433

[2] Lau A.K., Staley L.M., 1987. A design procedure for an air-type solar heating system for green houses. Energy in Agriculture. 6(2): 95-119

[3] Tiwari G.N., Sharma S.B. and Gupta S.P., 1988. Transient performance of a horizontal floating gas holder type biogas plant. Energy Conservation and Management. 28(3): 235-239

[4] Tiwari G.N., Chandra A., 1986. Solar assisted biogas system: a new approach. Energy Conversion and Management. 26(2): 147-150

[5] Tiwari G.N., Singh S.K. and Thakur K., 1992. Design criteria for an active biogas plant. Energy. 17(10): 955-958

[6] Gupta R.A., Rai S.N. and Tiwari G.N., 1988. An improved solar assisted biogas plant (fixed dome type): a transient analysis. Energy Conservation and Management. 28(1): 53-57

[7] Sodha M.S., Ram S., Bansal N.K. and Bansal P.K., 1987. Effect of PVC greenhouse in increasing the biogas production in temperature cold climate conditions. Energy Conversion and Management. 27(1): 83-90

[8] Sodha M.S., Goyal I. C., Kishor J., Jayashankar B.C. and Dayal M., 1989. Solar assisted biogas plants IV A: Experimental validation of a numerical model for slurry temperature in a glazed fixed-dome biogas plant. International Journal Energy Research. 13: 621-625

[9] Tiwari G.N., Dubey A.K. and Goyal R.K., 1997. Analytical study of an active winter greenhouse. Energy.; 22(4): 389-392

[10] Kumar K. Vinoth, Bai R. Kasturi, 2008. Solar greenhouse assisted biogas plant in hilly region – A field study. Solar Energy. 82: 911-917

[11] Prabhakant and G.N.Tiwari, 2009. Evolution of carbon credits earned by energy security in India. International Journal of Low Carbon Technologies. Vol 4: 42-51

Effect of organic loading rates (OLR) on production of methane from anaerobic digestion of vegetables waste

Azadeh Babaee[1], Jalal Shayegan[2,*]

[1] *School of Chemical and Petroleum Engineering, Sharif University of Technology, Tehran, Iran*
[2] *School of Chemical and Petroleum Engineering, Sharif University of Technology, Tehran, Iran*
** Corresponding author. Tel: +98 2166165420, Fax: +98 2166022853, E-mail: shayegan@sharif.edu*

Abstract: In this study, experiments were conducted to investigate the production of biogas from vegetable wastes by using anaerobic digestion process. The complete-mix, pilot-scale digester with working volume of 70 l was used. The experimental protocol was defined to examine the effect of the change in the organic loading rate on the efficiency of the production of biogas and to report on its steady-state performance. The digester was operated at different organic feeding rates of 1.4, 2 and 2.75 kg VS/ (m^3.d). The biogas produced had methane composition of 49.7- 64% and biogas production rates of 0.12-0.4 m^3 biogas/(kg VS input). The reactor showed stable performance with highest methane and yield (0.25 m^3CH4/kg VS) with VS reduction of around 88% during loading rate of 1.4 kg VS/(m^3.d). As the organic loading rate was increased, the VS degradation and biogas yield decreased. Based on data from this study, OLR of 1.4 kg VS/(m^3.d) is suggested as design criteria with methane production rate of 0.25 m^3CH_4/kg VS input and successful implementation of anaerobic digestion as the method of waste treatment leads to the regional utilization of renewable energy resources, energy requirements and costs.

Keywords: *Anaerobic Digestion, Biogas, Methane, Vegetable Wastes*

1. Introduction

Municipal solid waste (MSW), when landfilled, causes several environmental problems such as the biogas production, volatile organic compounds emission, leachate, public health hazard and plants toxicity [1]. In light of rapidly rising costs associated with energy supply and waste disposal and increasing public concerns with environmental quality degradation, conversion of food wastes to energy is becoming a more economically viable practice. Anaerobic digestion has become an established and proven technology as a means of managing solid organic waste [2]. Besides generating biogas for energy use, the process also destroys pathogens and produces stabilized material to be used as fertilizer in land applications. Anaerobic digestion may lead to environmental benefits with regard to waste treatment, pollution reduction, energy production and improvements in agricultural practices [3]. The amount of MSW generated in Iran is around 60000 ton/day and contains more than 70% of organic wastes. The easy biodegradable organic matter content of vegetables waste with high moisture facilitates their biological treatment and shows the trend of these wastes for anaerobic digestion [4]. Many factors affect the performance of anaerobic digestion processes. Some of them are related to feedstock characteristics, reactor design and operational conditions [5]. The organic loading rate (OLR) is an important parameter because it indicates the amount of volatile solids to be fed into the digester each day [6]. Volatile solids represent that portion of the organic-material solids that can be digested, while the remainder of the solids is fixed. The 'fixed' solids and a portion of the volatile solids are non-biodegradable. The actual loading rate depends on the types of wastes fed into the digester [6], because the types of waste determine the level of biochemical activity that will occur in the digester. The aims of this study were to investigate the influence of OLR on performance and treatment efficiency (based on volatile solids removal) of vegetable wastes digestion.

2. Materials and methods

2.1. Experimental setup

The digester experiments were carried out in a semi-continuously pilot-scale with a total volume of 70 L. Fig.1 illustrates the experimental set-up. The reactor was fitted with a top plate, which supported the mixer, mixer motor, gas sampler. Sampling valves were located at positions corresponding to the top, middle and bottom layer of digester contents. The reactor had one outlet at the bottom for effluent removal. The contents of the reactor were mixed as controlled by a timer, which was activated for 15min every 45 minutes. Reactor temperature was maintained at 34 ºC.

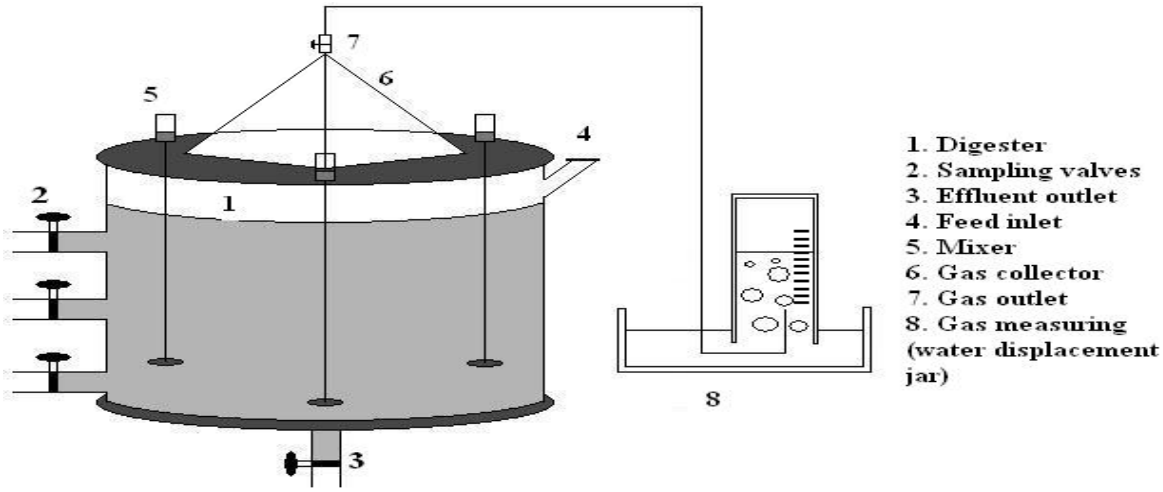

Fig. 1. The experimental set-up

2.2. Wastes sources and characteristics

The vegetable wastes used in this study were collected from the group market of Iran. The vegetable wastes consisted of potatoes, lettuce, tomatoes, eggplant, cucumber, and carrot to give 8-9% TS with VS content of 95-97%. The COD/N ratio of vegetables waste is balanced, being around 30 and therefore, no nitrogen was added to the reactor. In fact the optimum C:N ratio for microbial activity involved in bioconversion of vegetable biomasses to methane is 25-30 [7]. The anaerobically sludge from Ekbatan wastewater treatment plant was added as seed.

2.3. Anaerobic digester operation

Experiments were operated in semi-continuous mode with daily feeding. Dry semi-continuous anaerobic digestion of vegetable waste was investigated in mesophilic condition with three different organic loading rates (OLR) of 1.4, 2 and 2.75 kg VS/(m^3.d) for constant retention time of 25 days. Retention time of 25 days was maintained by feeding 2.4 l of substrate and removing 2.4 l of effluent daily. Table 1 shows the characteristics of each feeding rate.

Table 1: Characteristics of each feeding rate

	Organic loading rate (kg VS/m^3.d)	%TS	%VS	Wet waste (kg/d)	Inlet COD (mg/l)
Loading rate 1	1.4	8.9	95	1	2150
Loading rate 2	2	8.7	95	1.5	3300
Loading rate 3	2.75	8.6	96	2	4100

2.4. Analytical methods

The biogas produced was measured daily by water displacement method and its composition was measured by gas chromatograph. Total solids (TS), volatile solids (VS), pH, alkalinity were determined according to the APHA Standard Methods [8]. Total nitrogen (TN) was estimated by the Kjeldahl method [9].

3. Results and discussion

3.1. Biogas and methane production

One of the main objectives of this research was to determine the performance of the anaerobic digestion process when operated at different loading rates. For this reason, it was highly important to evaluate process performance in term of biogas composition and production to various loading rates. Production of biogas during anaerobic process at different organic loading rates is shown in Fig. 2. The daily biogas production obtained during run 2 and 3 were approximately 27.6 l/d and 21.3 l/d respectively whereas the daily biogas production in run 1 was found approximately 33.3 l/d. Further increase of the organic loading rate as 1.4kgVS/(m^3.d) results in decreased biogas production rates.

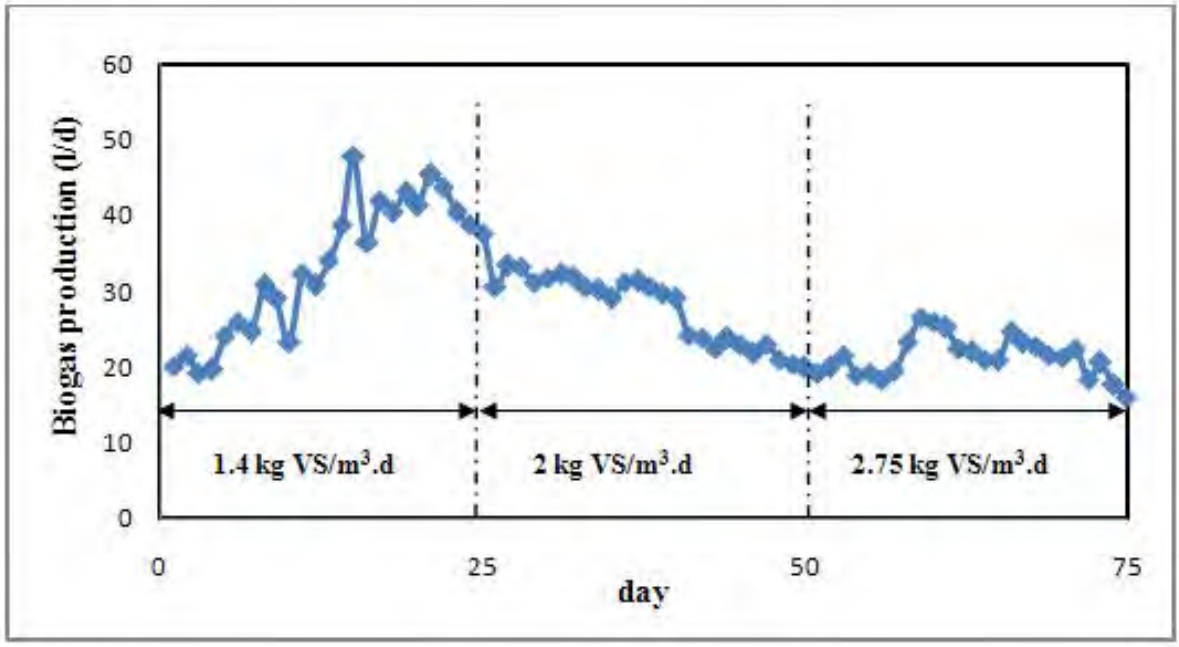

Fig. 2. The amount of biogas production for various loading rates

The reactor showed stable performance with highest methane (64%) during loading rate of 1.4kgVS/(m^3.d). Fig.3 illustrates the biogas composition. Methane concentration in biogas was observed around 60% in run 2 whereas it was found less than 49.7% in run 3. The measurement of the quantity and composition of the biogas produced in terms of methane and carbon dioxide content is of fundamental importance to evaluate the performance of the process. The increase of carbon dioxide in biogas means that the acidifying microorganisms are prevailing on the methanogens which may lead to volatile fatty acids accumulation.

3.2. Leachate characteristics

The stability of the reactor performance was investigated through leachate characteristics analysis besides biogas production and composition. In the anaerobic digestion process,

methanogenic bacteria are more sensitive to environmental conditions than hydrolytic and acidogenic bacteria.

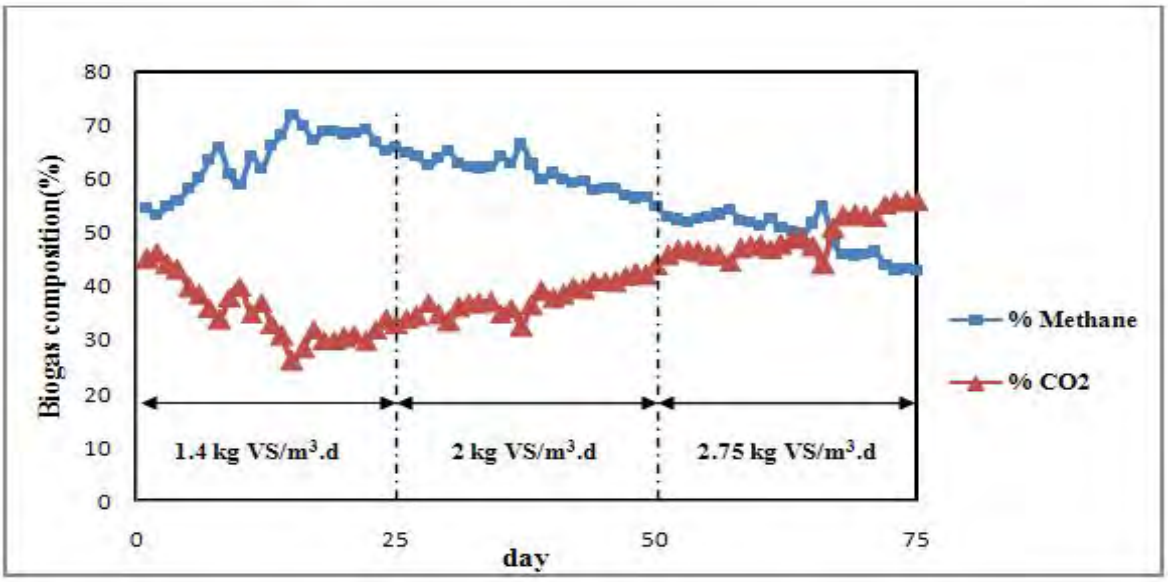

Fig. 3. Biogas composition for various loading rates

Among the environmental conditions, the pH is the most sensitive parameters. For example, the pH of digester liquid effluent indicates the stability of the system and its variation also depends on the buffering capacity of the system [10]. The pH of effluent leachate from the continuous digester remained steady state to the range of 7.75 - 8.0 during the loading rate of 1.4 kg VS/m^3.d. This shows that the system was well buffered. When the loading rate was increased to 2 kg VS/(m^3.d), the pH value dropped from 7.75 and reached to lower value of 7.3 but it was still above 7 which were in the methanogenic range. The methane content in the biogas also dropped and the system showed signs of overloading. As the pH was in the methanogenic range, the methane content in the biogas was above 60%. Fig.4 illustrates that the pH in loading rate of 2.75 kg VS/m^3.d was dropped from 7.3 to 6.8. Since the pH is controlled by the volatile organic acids concentration, the alkalinity showed similar trends. This was resolved by immediately stopping the feeding and adding alkaline solution. But the condition could not be recovered during run 3.

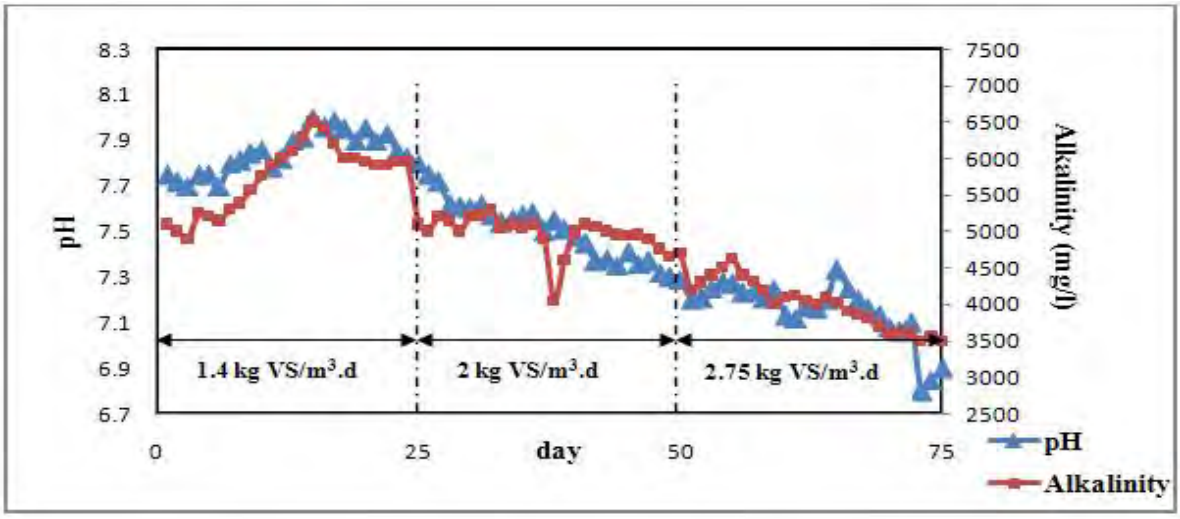

Fig. 4. Values of pH and alkalinity for various loading rates

In loading rate of 1.4 kg VS/(m^3.d), the COD concentration was decreased significantly after the completion of the retention time. While in run 2 and 3 higher concentrations of COD were observed. This can be explained that there was higher hydrolysis but less methanogenesis activities. In general hydrolytic bacteria are more robust to environmental condition.

3.3. Process efficiency

For the purpose of evaluating the effect of loading rate on the process efficiency, VS reduction and biogas yield were both taken into account as the indicators to assess the reactor performance and efficiency of each loading rate. VS degradation value of 88 % was achieved while operating loading rate 1.4 kg VS/(m^3.d). This VS reduction is higher compared with the result of 77.1% reported by Castillo [11]. By increasing the loading rate in run 2 and 3, VS removals were decreased to 80 % and 76 % respectively as illustrated in Fig. 5. The COD degradation was also decreased while organic loadings were increased. In run 1, the reactor stabilized and the COD was reduced to 65%, which corresponds to high efficiency of COD removal.

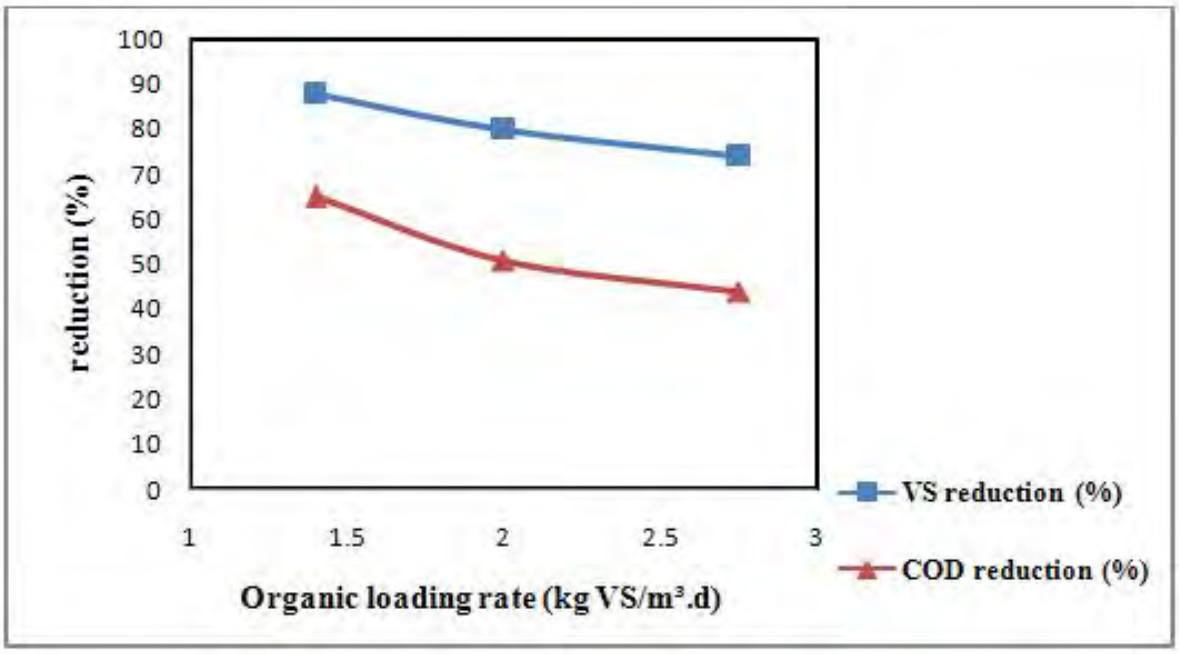

Fig. 5. VS and COD degradation for various organic loading rates

For further illustration, biogas and methane yield for various loading rates are presented in Fig.6. The highest biogas and methane yield observed was 0.4 m^3biogas/kg VS and 0.25m^3CH_4/kg VS in run 1 (1.4 kg VS/m^3.d). As the loading rate was increased, a gradual decrease in the biogas production (0.22 and 0.12 m^3biogas/kg VS in run 2 and 3 respectively) were observed. The overloading was marked by the fall in pH and gas yield and increase of carbon dioxide content in the biogas. In this study, the best results were obtained with an organic loading rate of 1.4 kg VS/(m^3.d). The biogas and methane yield of 0.4m^3biogas/kg VS obtained in this optimum loading rate was found to be satisfactorily successful when compared to literature data which were obtained using fruit and vegetable wastes (Table 2). It should be cautioned here that the optimum loading rate of 1.4 kg VS/(m^3 .d) observed here is not universal as the optimal rate depends upon the reactor configuration and other operating conditions.

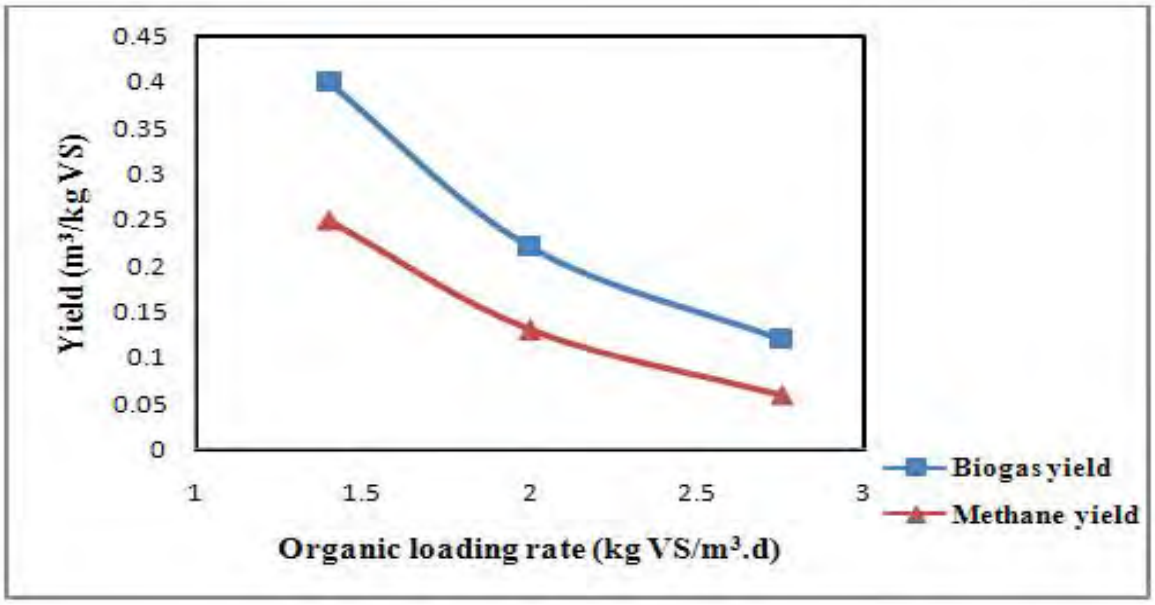

Fig. 6. Biogas and methane yield for various organic loading rates

Table 2. Performance data of different anaerobic process

Substrate	Organic loading rates (kg VS/m^3.d)	Biogas yield (m^3/kg VS)	Methane (%)	Degradation (% of VS)	References
Vegetable wastes	1.4	0.4	64	88	Current study
Organic fraction of municipal solid wastes	0.8	0.26	60	61	[12]
Municipal solid wastes	2.5	0.38	61	70	[13]
Fruit and vegetable wastes	0.3-1.3	0.3	54-56	67	[14]
Fruit and vegetable wastes	1.6	0.47	65	88	[15]

4. Conclusion

Anaerobic digestion is promising process for reducing the amounts of biodegradable waste in MSW stream and is also an energy producer from renewable resources. Considering the characteristics of the high-moisture solid waste, anaerobic digestion represents a feasible and effective method to convert the waste to biogas fuel. The reactor showed stable performance with highest methane (64%) with VS reduction of around 88% during loading rate of 1.4 kg VS/(m^3.d). Based on data from this study, OLR of 1.4 kg VS/(m^3.d) is suggested as design criteria with methane production rate of 0.25 m^3CH_4/kg VS input. Successful implementation

of anaerobic digestion as the method of waste treatment leads to the regional utilization of renewable energy resources, as well as the disposal of high moistening content of MSW.

References

[1] Thorneloe, S.A., Pacey, J.G., Landfill Gas Utilization-Database of North American Projects. Proc. 17th Annual Landfill Gas Symposium, Solid Waste Association of North America, Silver Spring, Maryland, 1994, pp.197-208.

[2] De Baere L. Anaerobic digestion of solid waste: state-of the art. In: Proceedings of the Second International Symposium on Anaerobic Digestion of Solid Waste, Barcelona, Spain, 1999.

[3] Chynoweth DP, Owens JM, Legrand R., Renewable methane from anaerobic digestion of biomass, Renewable Energy, 2001, 22:1–8.

[4] Bouallagui H., Ben Cheikh R., Marouani L., Hamdi M., Mesopholic biogas production from fruit and vegetable waste in a tubular digester, Bioresource Technology, 2003, 86, 85–89.

[5] Hawkes, D.L., Factors affecting net energy production from mesophilic anaerobic digestion. In: Stafford, D.A., Wheatley, B.I., Hughes, D.E. (Eds.), Anaerobic Digestion. Applied Science Publishers Ltd., London, UK, 1980.

[6] Mattocks R., Understanding biogas generation, Technical Paper No. 4.Volunteers in Technical Assistance, Virginia, USA, 1984. p. 13.

[7] Kivaisi AK., Mtila M., Production of biogas from water hyacinth in a two-stage bioreactor, World J Microbiol Biotechnology, 1998, 14, 125–31.

[8] APHA, Standard methods for the examination of water and wastewater, 20th ed. American Public Health Assoc., Washington, DC, 1998.

[9] Greenberg A.E., Clesceri L.S., Eaton A.D., Standard Methods for the examination of water and wastewater, 18th ed. APHA, AWWA, WPCF, Washington, DC, 1992.

[10] Mata-Alvarez, J., Mace, S., and Llabres, P., Anaerobic digestion of organic solid wastes. An overview of research achievement and perspectives, Bioresource Technology, 2000, 74, 3-16.

[11] Castillo M.E.F., Cristancho D.E., Arellano V.A., Study the operational condition for anaerobic digestion of urban solid waste, Waste management, 2006, 26, 546-556.

[12] Nguyen, P.H.L., Kuruparan, P., and Visvanathan, C., 2007. Anaerobic digestion of municipal solid waste as a treatment prior to landfill. Bioresource Technology, 98, 380-387.

[13] Fruteau de Laclos, H., Desbois, S., Saint-Joly, C., 1997. Anaerobic digestion of municipal solid organic waste: Valorga full-scale plant in Tilburg, the Netherlands. Water Science and Technology 36 (6-7), 457-462.

[14] Rene Alvarez, Gunnar Liden, 2008. Semi-continuous co-digestion of solid slaughterhouse waste, manure, and fruit and vegetable waste, Renewable Energy, 33, 726-734.

[15] Mata-Alvarez J, Cecchi F, Llabrés P, Pavan P. Anaerobic digestion of the Barcelona central food market organic wastes: experimental study. Bioresour Technol 1992; 39:39–48.

Potential for the production of biogas in alcohol and sugar cane plants for use in urban buses in the Brazil

Samuel N. M. de Souza[1,*], Reginaldo F. Santos[1], Guilherme P. M. Fracaro[1]

[1] *State University of the West Paraná (UNIOESTE), Department of Agricultural Engineering, Cascavel, Brazil*
** Corresponding author. Tel: +554532203155, Fax: +554532203153, E-mail:samuel.nelson@pq.cnpq.br*

Abstract: Brazil is one of the major alcohol and sugar producers in the world. The plants of alcohol and sugar cane have as waste the vinasse, which is used as organic fertilizer in the cane plantations and it cause contamination of the soil and water. The anaerobic digestion treatment can be used to reduce the pollution with vinasse, and at the same time increase the production of biogas. In this study, is proposed to find the potential of biogas production from anaerobic digestion of vinasse in Brazil and the availability of its use in urban buses as gas fuel. Biogas can be important to reduce the dependence of diesel, a non renewable fuel, in Brazil. Theoretical data of vinasse and biogas production, 14,6 m^3 of biogas per 1 m^3 of vinasse, were used to estimate the biogas potential. Using an estimated consumption of biogas in buses, 295,5 m^3 per bus with 400 km of autonomy per day, the total of buses supplied with biogas was estimated. The potential of biogas production estimated in Brazil by vinasse (2008/2009) is 4016892452 $m^3.crop^{-1}$ or approximately 20 million per day, which could replace 64,7% of the urban buses fleet in Brazil. A big plant of alcohol production has autonomy to supply 1018 buses per day. It has been assumed in this study the plant will produce biogas only during 200 days per year, in the others 165 days the buses could running with compressed natural gas (CNG) or the digesters can be fed on of bagasse's sugar cane as wet feedstock.

Keywords: *Bioenergy, fuel, vinasse, waste*

1. Introduction

Biomass is an important renewable source of energy in the world and its increasing has been useful to replace the fossil fuels. There are some kinds of agricultural feedstocks those can be converted in biofuels, as alcohol, biodiesel and others. The wastes of the process in food industries could be utilized for anaerobic digestion for biogas and biofertilizer production. The biofuels are expected to be one of the most important in the near future, because they will contribute to the decreasing of the global warming in the world.

The commercial sugar cane produced in Brazil is destined for alcohol and sugar production. The alcohol is utilized for domestic supply and exportation; it is available in Brazil since year 1973 as fuel in vehicles, mixed in the gasoline and in the bi-fuels vehicles. The alcohol is one renewable fuel and its combustion produces less pollution than fossil fuel. The wastes produced in the processing of alcohol and sugar is the bagasse and the vinasse.

The sugar cane industrialized in Brazil, increased 47% in five years, reaching 569063 million of tonnes in 2008/09 crop, where the central south of Brazil is responsible for 89% of the production. [1]. An increasing of the exportation of sugar and the high consumption of alcohol in Brazil have been the mainly factors of expansion the sugar cane production and its processing.

Sugar cane after the harvest gets to the mill and the juice is extracted and leavened, then the results are the alcohol and a raw material called vinasse, which is produced at high temperature and has a high chemical oxygen demand (COD), organic matter and high polluting power. In Brazil the plants of alcohol use the vinasse as a fertilizer directly applied in the soil, because it is rich in potassium. On the other hand, there is a limit of application by the environmental agencies [2,3]. The major problem of the vinasse application is the

possibility of its flowage to rivers and lakes, specially during rainy days. Moreover there is the risk of contamination the superficial water, which is response to the supply of water in some cities and rural community. In some regions of Brazil the locals environmental agencies has not powerful and the owners of sugar and alcohol plants does not respect the law.

Vinasse before disposed in the soil, should be treated in anaerobic reactors as a thermophilic UASB [2]. This kind of treatment will produce the biofertilizer and biogas. The table 1 shows the physical chemical parameters of the São Martinho Industry of Sugar and Alcohol before and after the biodigestion [4,5].

Table 1. Physical and chemical parameters – São Martinho Industry of Sugar and Alcohol.

Parameter	Vinasse before the digestion	Vinasse after the digestion
pH	4,0	4,9
Chemical oxygen demand, COD ($mg.L^{-1}$)	29.000	9.000
Nitrogen total, N ($mg.L^{-1}$)	550	600
Phosphor, P2O5 ($mg.L^{-1}$)	17	32
Sulfate, SO2 ($mg.L^{-1}$)	450	32
Potassium, K2O ($mg.L^{-1}$)	1.400	1.400

According to table 1, the anaerobic digestion of the vinasse will reduce the organic charge, but the power as fertilizer will remain the same. On the other hand the plant of sugar and alcohol will produce biogas.

According to [3] biogas is composed of methane (40-75%), dioxide of carbon (25-40%) and other compounds. The biogas can be used as biofuel in engines of internal combustion. In this study is proposed estimate the supply of urban buses with biogas produced in the big plants of sugar and alcohol in Brazil.

2. Methodology

The production of biogas of vinasse and the bus supply capacity were estimated using data from literature. The most of plants of cane processing are placed in central south region of Brazil, where the cities of São Paulo, Rio de Janeiro, Belo Horizonte, Brasília, Goiania, Curitiba and Porto Alegre are situated. The biggest plant of sugar and alcohol in Brazil is São Martinho, which process about 40.000 $ton.day^{-1}$ of sugar cane, during approximately 200 days per year [1] and is close to São Paulo.

According to [4,6], the production of 1 liter of alcohol discharges 10 liters of vinasse and with the digestion of 1 m^3 of vinasse approximately 14,6 m^3 of biogas are produced. These values were used to estimate the production of biogas and vinasse in the plants of sugar cane studied and the total estimation of biogas production in Brazil.By using data of alcohol production in Brazil and in the plants of production obtained of UNICA [1], was possible estimate the production of vinasse and biogas.

According to literature [7,8,9] the biogas (55% methane) has an energy value of 20,8 $MJ.m^{-3}$ and the diesel has 36,4 $MJ.L^{-1}$. In the composition of biogas, there are approximately 55% of methane (CH4), which has a specific mass of 0,714 $kg.m^{-3}$, then 1 m^3 of biogas is equivalent 0,393 kg of methane [8]. The currently specific consumption of diesel in one bus is 0,40

$L.km^{-1}$ [10,11]. Once upon time the bus autonomy assumed is 400 km per day, the diesel daily consumption of one bus is 160 liters, which has an equivalent energy of 5824 MJ.

Volvo's bus has an autonomy of 400 km running with compressed natural gas cylinders (200 bar) of 1055 m^3 and weigh 136,20 kg [10]. If compressed natural gas has an energy value of 47,5 $MJ.kg^{-1}$ [9], then a volvo's bus consumes a daily energy equivalent of 6469,5 MJ. Analysing the data above, was estimated a daily medium biogas consumption of approximately 6147 MJ per bus or 295,5 m^3 of biogas per bus. These data were utilized in the estimation of the number of bus supplied with biogas.

The data of the bus fleet in Brazil were obtained from CNT and ANTT [12,13], and the estimation of carbon emission by bus was made using the index 74.100 kg $CO_2.TJ^{-1}$ of diesel found in the guidelines of IPCC [14], this index is 2,61 kg $CO_2.L^{-1}$ or 0,71 kg $C.L^{-1}$ of diesel, and was useful to estimate the decreasing of carbon emission with the replacement of diesel for biogas.

3. Results

Table 2 below shows the production of alcohol in Brazil and the estimated production of vinasse. The alcohol production were obtained from UNICA [1]. The amount of vinasse disposal in the environment in 2008/09 crop was 275 million of m^3, certainly it caused a high environmental impact in Brazil polluting the water and soil. The production of vinasse increases a rate of 12,7% per year since 2000/01 to 2008/09 crop. Brazil has between 12 and 20% of the potable water in the world and the increasing of the sugar cane industries could be a threat because of the directly disposal of the vinasse on the soil. If the vinasse would have been treated in anaerobic reactor the impact would be less.

Table 2. Production of alcohol and estimated vinasse production in Brazil .

Crop	Alcohol production in Central South (m^3)	Alcohol production in North Northeast (m^3)	Total alcohol production in Brazil (m^3)	Total Vinasse estimated in Brazil (m^3)
00/01	9064364	1528671	10593035	105930350
01/02	10176290	1359744	11536034	115360340
02/03	11152084	1471141	12623225	126232250
03/04	13068637	1740068	14808705	148087050
04/05	13591355	1825313	15416668	154166680
05/06	14352542	1594452	15946994	159469940
06/07	16006345	1712864	17719209	177192090
07/08	20333466	2193358	22526824	225268242
08/09	25101963	2410999	27512962	275129620

With the vinasse disposed in 2008/09 crop could produce 4016892452 m^3 or 20 million m^3 per day of biogas, enough to supply 67968 buses, or better, 64,7% of the Brazilian fleet of urban bus, which have been estimated on 105000 buses in 2008 [12].

The biogas that could be produced in Brazil, only with vinasse (4 billion m^3, 2008/09), correspond to 40% of the biogas produced in Europe, 10 billion m^3, in 2005, which is derived essencialy from landfills (64%), degradation of urbans and industrial waste (18,8%), and agriculture and energy crops (17,2%) [15]. According a study aimed in Brazil [3], the

potential of biogas from vinasse estimated was 2,74 billion m^3 (2003/04). Both studies show that Brazil has an enormous potential of biogas production by vinasse.

Table 3 presents some plants of sugar and alcohol localized in the central south region and the respective capacity of biogas and biomethane production.

Table 3. Production of alcohol and estimated vinasse in central south region of Brazil(2008/2009) .

Industry of alcohol	Alcohol m^3/crop 08/09	Vinasse m^3/crop 08/09	Biogas m^3/day	Buses (400 km of autonomy per day)
São Martinho	411991	4119910	300753	1018
Equivap	347298	3472980	253528	858
Da Barra	315804	3158040	230537	780
Santa Elisa	246591	2465910	180011	609
Colombo	200093	2000930	146068	494
Santa Candida	142436	1424360	103978	352
Santo Antônio	111615	1116150	81479	276

Figure 1 and table 3 presents the number of buses that could be supplied for the industries of alcohol above. The biggest industry (São Martinho) could supply 1018 buses per day, which represents 2,7 % of replacement the diesel fleet running in the city of São Paulo.

A big plant milling of 40.000 $ton.day^{-1}$ could supply 1018 buses and a smaller plant milling 12.500 $ton.day^{-1}$ 276 buses. In São Paulo state there are 145 plants with milling between 40.000 and 4.000 $ton.day^{-1}$, those would supply all buses of São Paulo city with biogas. The advantage is that they are not placed far from São Paulo city.

According to literature [10], in 1996 the bus fleet that could be fuelled with biogas from landfills of São Paulo city were estimated in 3005 buses which could supply 8% of the São Paulo's fleet currently. In comparison, three big plants of sugar and alcohol (milling 40.000 ton.day-1) could produce the same amount of biogas.

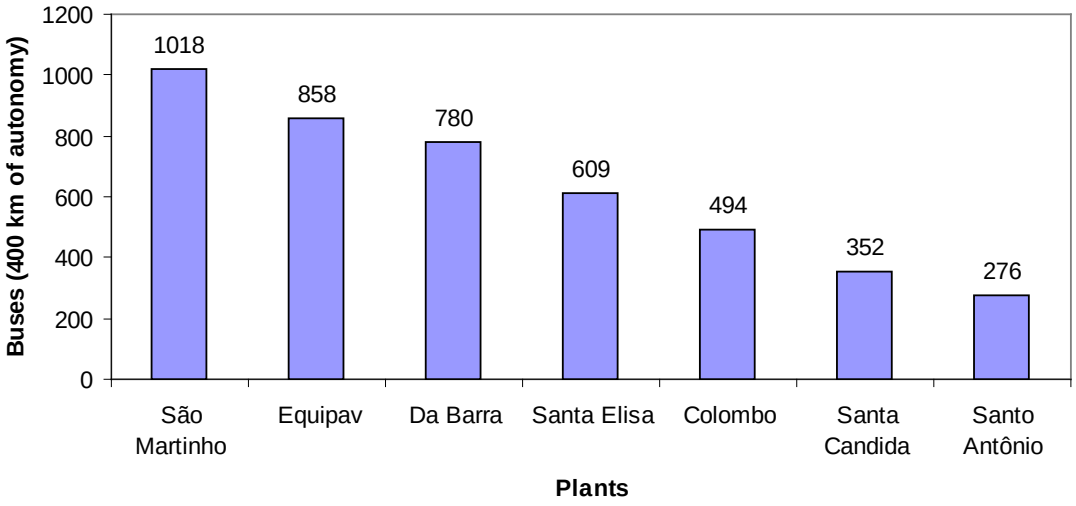

Fig. 1. Number of buses possibly supplied by industry of alcohol.

The total replacement of the bus fleet of São Paulo city for biogas could avoid the emission of 4,3 $ton.day^{-1}$ of carbon from fossil fuel (diesel) into atmosphere.

One limitation in this study is that the plant will produce biogas only during 200 days per year, in the others 165 days the buses could running with compressed natural gas (CNG) or the digesters can be use the bagasse's sugar cane as wet feedstock.

Figure 2 presents the bus fleet running in the big cities in Brazil in the year 2007 [13].

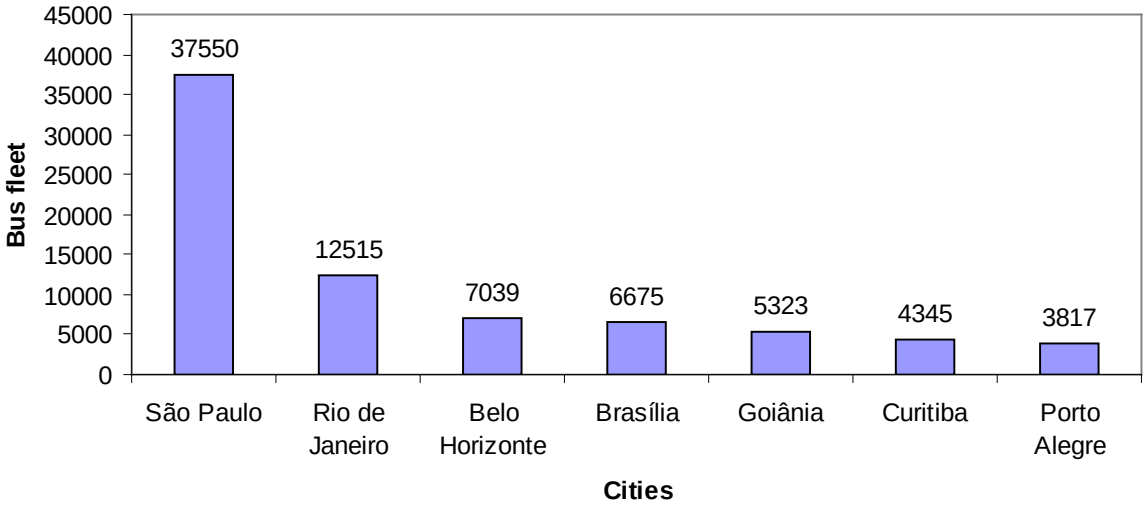

Fig. 2. Bus fleet in the mainly cities of central south region from Brazil (2007).

The possibility of replacement the buses to run with biogas could became the big cities in Brazil more sustainable, by other hand there are technical and market limitations. The gaseous form of biogas at normal temperature and pressure require its compression in cilynders to be used and, the cost will increase.

There is a lack in technology innovation to convert the vinasse to biogas in Brazil. Surely , the use of diesel is aconomically better than biogas to the owner's buses and the utilization of biogas feasibility depends of financial and policy incentives by the government.

In Brazil there is other forms of feedstocks to biogas production which could be explored togheter with vinasse and, the biogas in set with liquid biofuels (alcohol and biodiesel) could help the big cities of the country became more sustainable. By other hand the urban transport system need to be organized before this. The major of the big cities in Brazil need create BRT's as Curitiba city, an international reference.

The economy of Brazil is growing quickly and there is yet a lack of development in technological innovation in diverse sectors of economy, specilly in the development of the new forms of renewable energy, wich could help it increase with an economy sustainable.

4. Conclusions

With the increase rate (12,7% per year) of the vinasse disposal in Brazil, the better option is to promote the anaerobic digestion of the vinasse and produce biofertilizer and biogas. Brazil has a great number of buses, running mainly in the central south region cities, that could use the biogas as fuel replacing the diesel.

The biogas that could be produced with digestion of vinasse in Brazil had been estimated in 20 million m^3 per day, enough to supply 67968 buses, or better, 64,7% the Brazilian fleet. The use of the biogas to supply this fleet could reduce the emission of carbon from fossil fuel diesel in 21 $ton.day^{-1}$.

Acknowledgments

This research has received financial support of CNPq (Brazilian Council of Research), CAPES, SETI-FUNDAÇÃO ARAUCÁRIA and FPTI C&T (Itaipu Binacional).

References

[1] UNICA (União da Indústria de cana-de-açúcar). Produção do centro-sul de cana-de-açúcar das safras 2001/02 a 2008/09, 2010. Disponível em: http://www.portalunica.com.br>Acesso em:18 novembro 2010.

[2] H. Harada, S. Uemura, A. C. Chen, J. Jayadevan, Anaerobic treatment of a recalcitrant distillery wastewater by a thermophilic UASB reactor, Bioresource Technology 55, 1996, pp. 215- 221

[3] K. R. Salomon, E. E. S. Lora, Estimate of the electric energy generating potential for different sources of biogas in Brazil, Biomass and Bioenergy 33, 2009, pp. 1101-1107

[4] K. R. Salomon, E. E. S. Lora, Monroy, E. F. C., Custo do biogás proveniente da biodigestão da vinhaça e sua utilização, Proceedings of the 8º Congresso Ibero Americano de Engenharia Mecânica, Cusco/Peru, 2007.

[5] L. A. B. Cortez, W. J. Freire, F. Rosillo-Calle, Biodigestion of vinasse in Brazil, International Sugar Journal, 100, 1998, pp 403-413.

[6] C. P. Pinto, Tecnologia da digestão anaeróbia da vinhaça e desenvolvimento sustentável, dissertação de mestrado, UNICAMP, Campinas, Brasil, 1999.

[7] J. D. Murphy, N. M. Power, An argument for using biomethane generated from grass as a biofuel in Ireland, Biomass and Bioenergy 33, 2009, pp. 504-512.

[8] N. M. Power, J. D. Murphy, Wich is the preferable transport fuel on a greenhouse gas basis; biomethane or ethanol?, Biomass and Bioenergy 33, 2009, pp. 1403-1412.

[9] R. Fearghal, B. Caulfield, Examining the benefits of using bio-CNG in urban bus operation, Transportation Research Part D 15, 2010, pp. 362-365.

[10] N. Kuwahara, M. D. Berni, S. V. Bajay, Energy supply from municipal wastes: the potential of biogas – fuelled buses in Brazil, Renewable Energy 16, 1999, pp. 100-1003

[11] D. Lobkov, Análise econômica para substituição do uso de combustível diesel por GNC no transporte público de passageiros, dissertação de mestrado, UNICAMP, Campinas, Brasil, 2005.

[12] CNT (Confederação Nacional do Transporte), Boletin estatístico, 2009, disponível em http://www. cnt.org.br, acesso em 20 de novembro 2010.

[13] ANTT (Agência Nacional de Transportes Terrestres), Anuário estatístico dos transportes terrestres – AETT, 2008, disponível em http://www.transportes.gov.br, acesso em 22 de novembro 2010.

[14] IPCC Guidelines for national Greenhouse Gás Inventaries, 2006, Energy, v.2, Chapter 3: Mobile Combustion, revised of June 2010.

[15] C. Tricase, M. Lombardi, State of the art and prospects of Italian biogas production from animal sewage: Technical-economic considerations, Renewable Energy 34, 2009, pp. 477-485.

Brazil's potential for generating electricity from biogas from stillage

Reginaldo Ferreira Santos[1*], Augustinho Borsoi[1], Deonir Secco[1], Samuel Nelson Melegari de Souza[1], Ricardo Nagamine Constanzi[1]

[1] *State University of western Paraná, Cascavel, Brazil*
** Corresponding author. Tel: +55 33213155, E-mail: rfsantos@unioeste.br*

Abstract: The aim of this study was to evaluate potential of vinasse as an alternative source of electricity generation through the burning of biogas produced by anaerobic digestion process. The stillage residue is a process of producing ethanol, used as fertilizer on farming's, but with environmental problems of its application. This study was conducted on the basis of theoretical data to calculate the potential for methane generate and energy. Our purpose is to use an up flow anaerobic-UASB to accomplish the digestion of stillage and engines to burn the gas and electric power generation. The paper presents a case study of a distillery with a production of 580 m^3 day^{-1} ethanol. In Brazil in the harvest 2009/10 would have produced the stillage potential to produce 1.81 billion m^3 of methane and 4.070 GWh of energy. Whereas the case study of sugarcane in the interior of Parana, are produced 5,800 m^3 day^{-1} stillage, with the potential to generate 2.75 MWh of electricity $month^{-1}$, which results in a income of US$ 218,586,32 a month. The use of vinasse as a source of energy has great potential energy for Brazil.

Keywords: *Cane Sugar, Anaerobic Digestion, UASB, Renewable Energy.*

1. Introduction

Sugar cane is as one of the most promising crops of the country to generate energy through biomass. To produce 1 m^3 of alcohol are needed 13 tons of cane sugar, which should generate 10 m^3 of slop, this figure varies from 10 to 15 m^3. Due to nutrient content, stillage is used of fertigation, as far as not even there an alternative more practical and economical use of this waste, and in this case, there is an effective cost reduction with fertilization [1].

Despite the significant amount of fertilizer, this residue has a huge potential for generating energy by converting organic matter into methane, while minimizing any risk of accidents during handling of this waste, facilitating its application in agriculture due to increased pH neutralization of the effluent [1], [2].

The use of vinasse as fertilizer causes concern because of their high degree of impact when distributed in the environment, while there are technological mastery of the chain of sugar cane, today there is real need for studies to would define the best rate application in the extrinsic characteristics of soil and vinasse [2].

Due to the chemical oxygen demand (COD) is the a wastewater stillage with high pollution potential. The reason for this striking power is due to the high content of colloidal organic matter, which leads to oxidation of virtually all the available oxygen in the water. The use of stillage for biogas production is an alternative that may become viable economically and environmentally by three points: treatment of the waste, producing biogas for electricity generation and still has treated fertilizer of application in farming's [2].

With the increase of ethanol production in recent years, there was increased production of vinasse, increasing the environmental risks of its application in nature. Seeking an alternative for the treatment of stillage and also produce renewable energy, the objective this study was to evaluate the potential use of vinasse as an alternative biomass in the Brazilian energy as a source of generating electricity by burning biogas generated by anaerobic digestion process.

2. Methodology

This paper is an exploratory literature research and a case study, based on published data in literature. The sources consulted for the preparation of this work were government agencies and the productive sector of sugar cane from Brazil, using historical data from the past 20 years, compared to growth of the ethanol market in Brazil during this period.

Data regarding the production of sugar cane and ethanol were obtained from the Union of Industries of Cane Sugar (UNICA) [3], the representative organization of the sugar and ethanol from Brazil. The paper presents the process of biogas production in an up flow anaerobic reactor (UASB reactor), demonstrating feasibility aspects of the project.

The feasibility of anaerobic treatment of vinasse in Brazil was confirmed with the use of UASB reactors (reactors and up flow anaerobic sludge blanket) under conditions mesophilic and thermophilic and reactor fluidized, both with suspended biomass [2]. The UASB reactor enables the movement of stillage through a region with high concentration of microorganisms. This reactor allows the separation of solid phases, liquid and gas, with the gas being driven to the top and solids and liquids directed.

Following suggestion from Rego and Hernandez [1], the biogas collected should be sent to a pressurized gas tank in which pressure is maintained at 1.15 bar for a diaphragm. For safety and to prevent leaks, any possible unused of gas will be automatically sent to burn. The treated effluent will be sent through channels to ponds or storage tanks for later be used as liquid biofertilizer.

Table 3 shows the parameters used in the work to convert the theoretical potential for electric energy production of vinasse into electrical energy by burning biogas produced by its anaerobic digestion in UASB.

Table 1. Parameters used for the elaboration of the potential for energy production

Parameter	Indicator	Unit	Reference
Vinasse production	10	m^3 m^{-3} of ethanol	[3]
Ethanol production	90	L t^{-1} cane	[3]
COD typical of vinasse	20	kg m^{-3}	[4]
Concentration methane in biogas	60	% Methane	[5]
Typical production of methane	0.35	Nm^3 kg^{-1}CODremoved	[6]
Net calorific value of methane	35.558	kJ Nm^{-3}	[7]
Overall efficiency of motor-generator	26	% to IBW	[8]
Energy	9.88	kWh m^{-3} methane	Calculated from the PCI methane
Amount received from sale of energy	79.41	US$ MWh^{-1}	[9]
Dollar exchange rate (US$ 1.00)	1.70	R$	Commodities- BMF

Nm^3=normal m^3

For the calculations were accounted directly the amount of methane produced, discounting the other gases present in the biogas, using the theoretical stoichiometric value of 0.35 m^3 CH4 $kgDQO^{-1}$removed [6].

Contributing to the analysis, presents a case study from a plant producing 580 m^3 day^{-1} of ethanol, located within the State of Parana. With data from ethanol production proceeded to the calculations of potential generation vinasse quantity and biogas produced, and how much electricity could be generated using internal combustion engines to gas burning. The production of vinasse this plant is 5,800 m^3 day^{-1}, since for each m^3 of ethanol is produced approximately 10 m^3 of vinasse.

The selling price of electricity was calculated based on power purchase auctions conducted by ANEEL (National Electric Energy Agency), federal government agency that regulates power sector. The available data were processed in a spreadsheet, for construction generation of graphs and figures of the potential production described [9].

3. Results

Brazil is the world's largest producer of sugar cane, Brazilian mills in the harvest 2009/10 sued 604.514 million tons (Figure 1), with estimates for the harvest 2010/11 season to process 651.514 million tones [3].

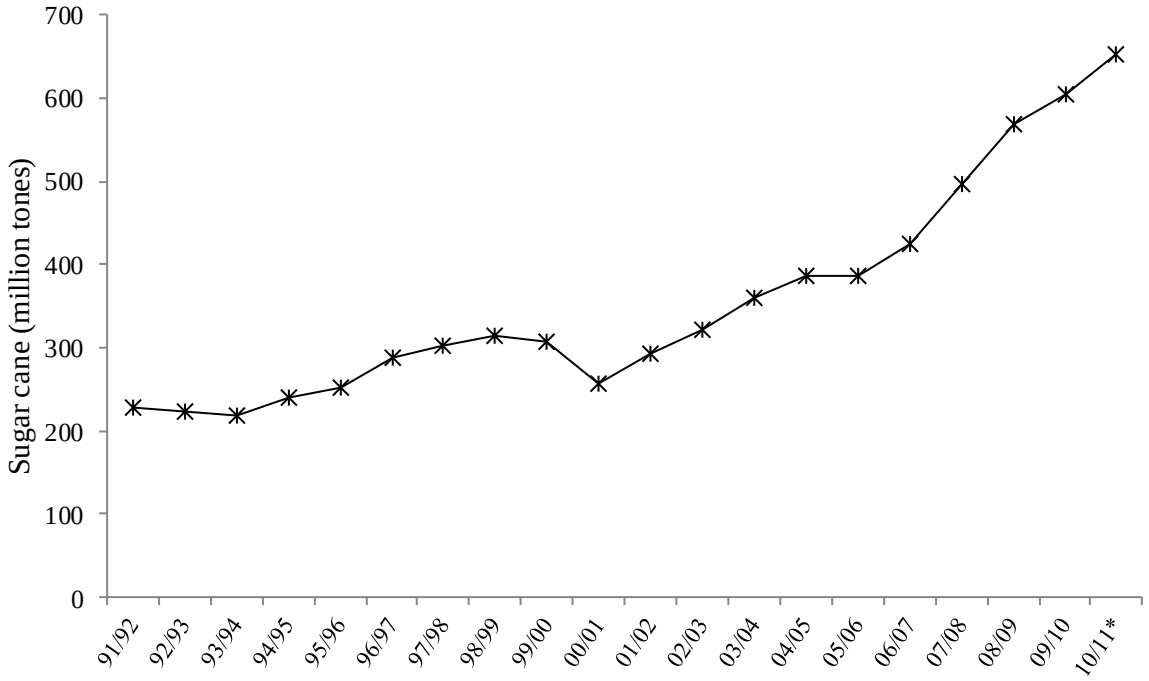

** Projection for the harvest 2010/11*
Fig. 1. Sugar cane processed by mills in Brazil for sugar and ethanol.

Recent years have seen average growth of 14.6% per annum on the amount of sugar cane processed in Brazil, from 229.22 million tons in the harvest 1991/92 to 604.51 million tons in 2009/10, with growth forecast to 1 billion tons by 2015, up almost 50% over the 2009/10 crop, increasing production of ethanol and sugar and generating more effluent.

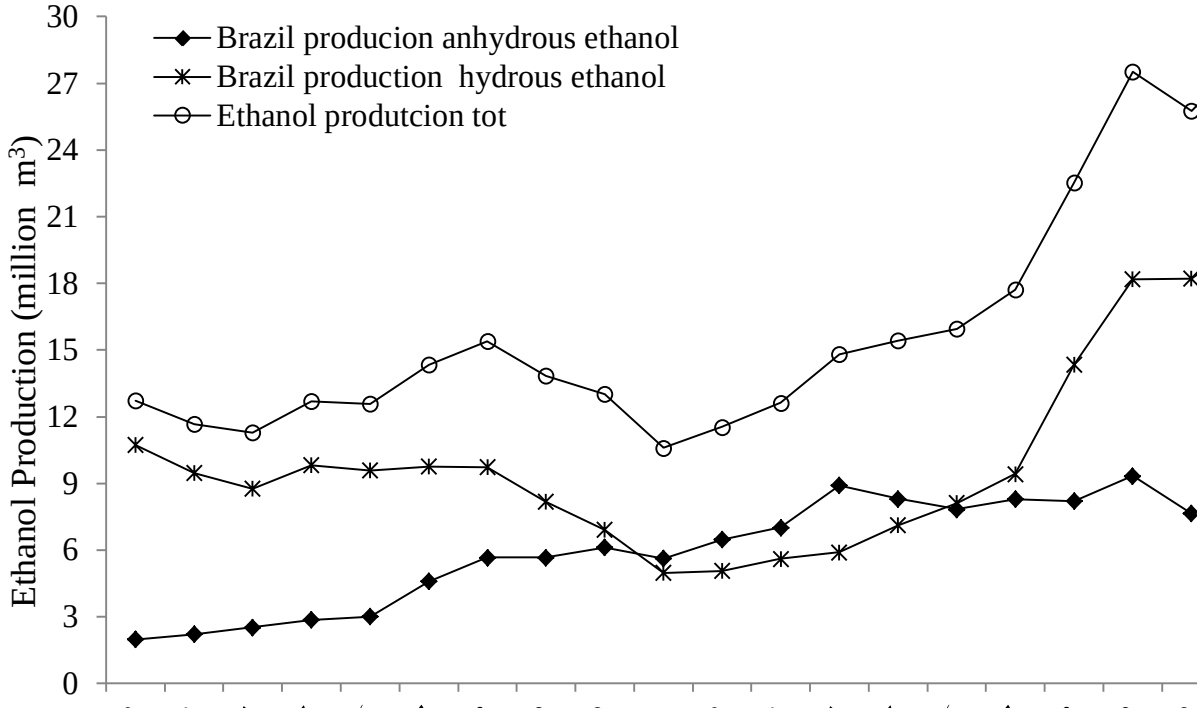

** Projection for the harvest 2010/11*

Fig. 2. Comparative history of Brazilian ethanol anhydrous, hydrated and total production

Looking at Figure 2, it appears that, in the harvest 2009/10 ethanol production was 25.8 million m^3, being 70.7% (18.2 million m^3) with ethanol and 29.3% (7.6 m^3) of anhydrous ethanol. Recent years was seen huge increase in ethanol production, mainly hydrated for use as fuel in car engines that run on ethanol or flex fuel. Also according to the data the average productivity of ethanol was 90 L t^{-1} of sugar cane, a little above the average that is 85 L t^{-1} [3].

In Figure 3, can be observed the potential production historic of vinasse in Brazil from the production of ethanol, whereas to produce one liter of ethanol are produced on average 10 liters of vinasse.

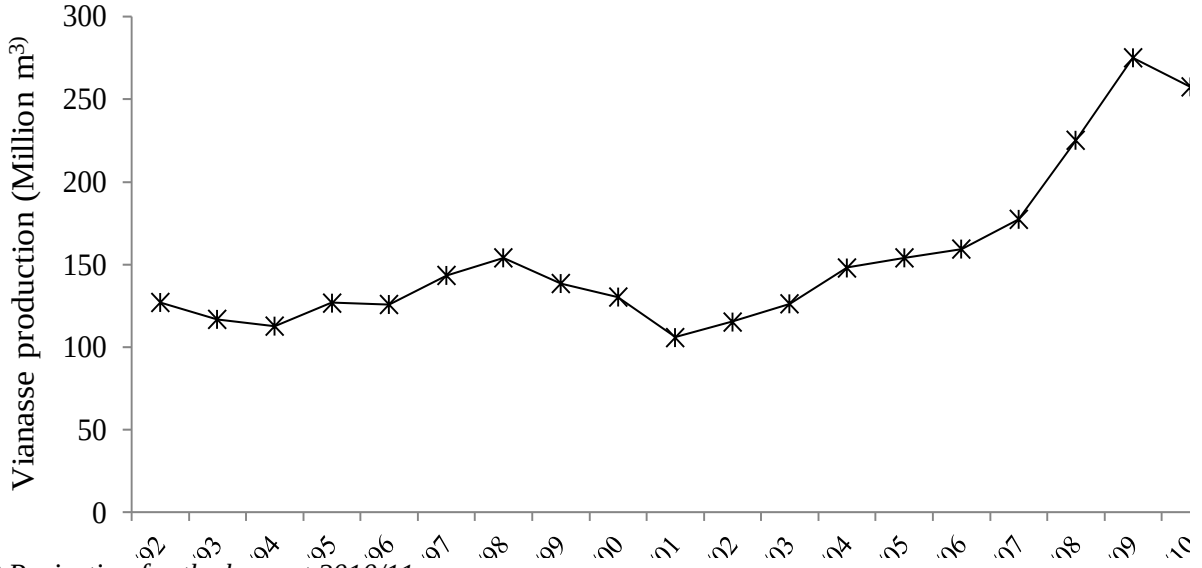

** Projection for the harvest 2010/11*

Fig. 3. History of the Brazilian production of vinasse.

According to literature data, it was found that for every liter of ethanol production, results in an average of 10 liters of vinasse. The potential for production of vinasse in Brazil in the harvest 2009/10 was 257.63 million of m^3 (Figure 3), for the harvest 2010/11 the forecast is a production of 284.17 million m^3, an increase of 26 million m^3 compared the previous harvest.

Figure 4 presents the potential for methane production from vinasse in Brazil, considering that the whole stillage was treated by anaerobic digestion in UASB reactor type.

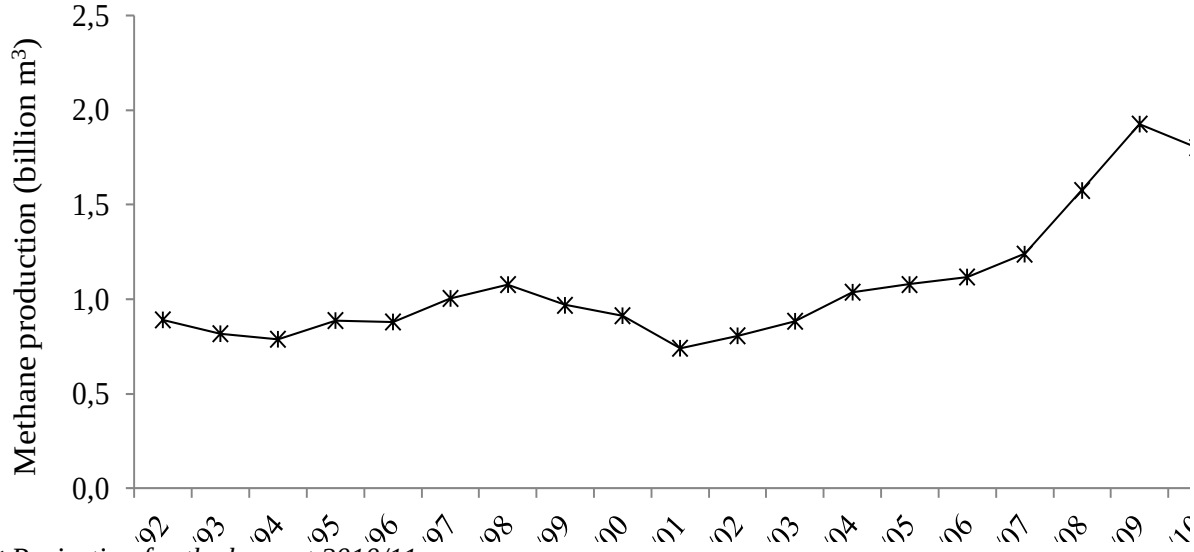

** Projection for the harvest 2010/11*

Fig. 4. History of the potential production of methane from the digestion of vinasse

The potential for methane production in the harvest 2009/10 would be 1.81 billion m^3 (Figure 4) for 2010/11 forecast of 1.98 billion m^3, considering that the whole stillage produced by plants was transforming into methane gas, which could be burned in engines to generate mechanical energy or thermal energy, and transformed into electrical energy.

Figure 5 shows the historical potential of generating electricity from the burning of biogas from the digestion of vinasse in UASB reactors, using internal combustion engines.

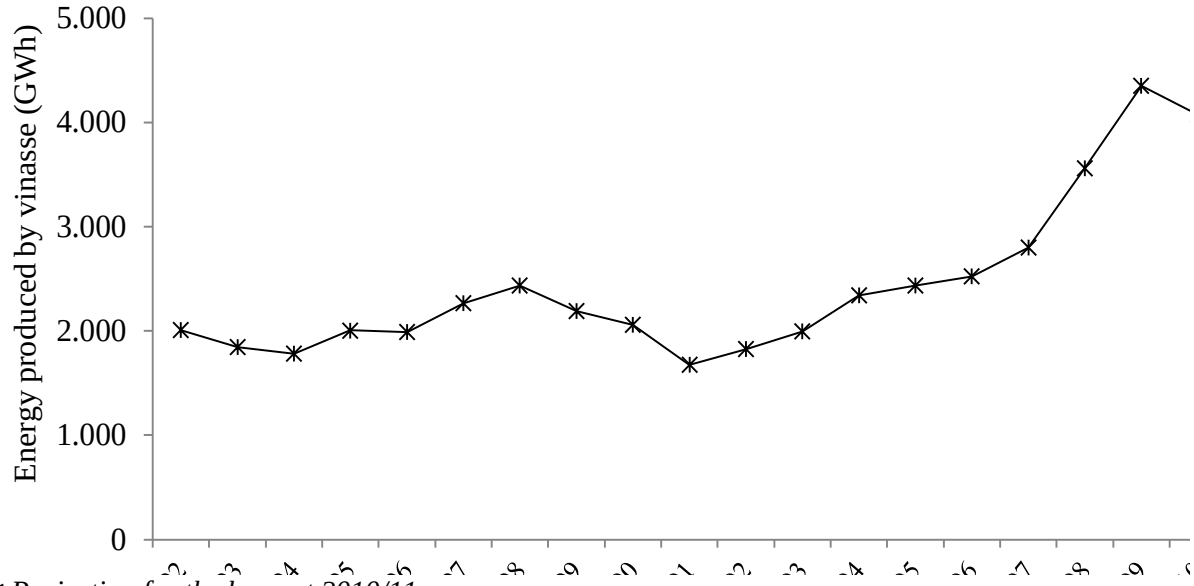

** Projection for the harvest 2010/11*

Fig. 5. History of the potential for electric energy production by vinasse.

The historical potential for generating electric power from the stillage (Figure 5), if it was all treated in digesters and the biogas gotten burned for power generation. If added all the production of the last 20 years, we would have a potential to generate 50,700 GWh of electricity.

For a production of 605 million tons of processed cane sugar in Brazil in the harvest 2009/10, using the anaerobic digestion process, we obtain a potential to produce approximately 1.4 billion m^3 of methane, would amount to 4.075 thousand GWh of electricity, equivalent to about 5% of the generation of the Itaipu plant, the world's largest hydroelectric dam, which generated during the year 2009 produced 91 thousand GWh, almost 20% of Brazilian electricity , which totaled to 466.16 thousand GWh in 2009.

3.1 Commercialization of energy produced

In the 2009/10 cane crop, the potential value received by throughout the production of energy, sold at a price of US$ 79.41 MWh (MWh price paid by system auctions conducted by ANEEL), generating revenues of US$ 323.6 million for the plants, by the production of 4.075 GWh of electrical energy.

3.2 Case study

The following table (Table 2) presents a case study of a sugar and ethanol located in the State of Parana, Brazil. The facility has an area of approximately 6,000 ha of planted area, between owned and leased areas and a producing 580 m^3 of alcohol/day.

Outcome of case study of an ethanol plant

Parameter	Indicator	Unit
Vinasse production	5,800	$m^3\ day^{-1}$ (241.67 $Nm^3\ h^{-1)}$
Methane gas production	40,600	$Nm^3\ d^{-1}$ (1691.6 $Nm^3\ h^{-1)}$
Power generation	91,752.28	kWh day^{-1} (91.75 MWh day^{-1})
Produced energy monthly	2,752.57	MWh $month^{-1}$
Monthly price from the sale of energy	218,586.32	US$ $month^{-1}$

The plant produces 5,800 m^3 daily stillage, which is used in fertigation of planting areas of the plant. Itself this stillage was used to produce methane gas ode through the process of anaerobic digestion in UASB reactor, would have a potential to generate 91.75 MWh day^{-1}, or 2.75 thousand MWh $month^{-1}$. If this energy was marketed at prices current (US$ 79.41 MWh) would generate revenues of US$ 218,586.32 month for the plant, beyond diversify their revenues.

4. Discussion and Conclusions

For this study, was used a potential of producing 10 liters of vinasse per liter of ethanol, the literature speak that to each liter of ethanol are produced 10 to 15 liters of vinasse [11], other authors argue that in producing 1 liter of ethanol produces a quantity minim than 10 liters of vinasse [12].

With respect to COD from stillage, the literature says that every m^3 of ethanol generates 200 to 500 kg of COD, in study was considered a minimum quantity of 200 kgCOD m^{-3} ethanol. From the amount of COD was estimated production potential of methane [13], [2].

The calorific value of biogas is variable and is in the range from 22.500 to 25.000 kJ m^{-3}, admitting the methane with about 35,580 kJ m^{-3}. This means a recovery from 6.25 to 10 kWh m^{-3} [14]. Due to the high concentration of methane in the biogas and consequently your potentially flammable, the main applications are in generating heat, cold and power [11].

Studies show that for the harvest 2004/05, the potential for producing electricity using the biogas produced by digestion of vinasse in motor-generators, internal combustion was 9.292 TJ $year^{-1}$ (2.6 TWh $year^{-1}$), representing 0.75% of national consumption of electricity in the year 2003 [5], data similar to those found in this work, where for the harvest 04/05 identified a potential to generate 2,43 GWh.

Lamo has built a prototype plant for the demonstration, consisting of a production unit (reactor of 120 m^3), purification, compression and use of biogas. This plant produced gas fuel at levels up to 0.35 m^3CH4 $kgCOD^{-1}$removed [15], agreeing with data of Cabello [16], that working with Ralf (fluidized bed reactor) also reached this relation.

Granato and Silva [2] performed a case study in a distillery with capacity to produce 600 m^3 day^{-1} of ethanol, as a result of digestion of stillage generated, they obtained a production of 75,600 Nm^3biogas day^{-1}. Considering a gas turbine efficiency of 35%, production would be 6,540 kWh of electrical energy alternative.

The stillage represents an important potential for renewable energy generation in Brazil, being a residue of ethanol production, which can generate energy and still be used as an important source of fertilizer for crops, in addition, your treatment will reduce environmental risks their application in nature.

Acknowledgements

The authors acknowledge Fundação Araucária, Coordenadoria de Aperfeiçoamento Profissional (CAPES) and Conselho de Desenvolvimento Tecnológico (CNPQ) for support in expenditure for registration and participation in the Congress.

References

[1]. E. E. Rego, F. Del M. Hernandez, Eletricidade por digestão anaeróbia da vinhaça de cana-de-açúcar: contornos técnicos, econômicos e ambientais de uma opção. In: Encontro De Energia No Meio Rural, 6., 2006. Anais... Campinas, Unicamp, 2006.

[2]. E. F. Granato, C. L. Silva, Geração de energia elétrica a partir do resíduo vinhaça. In: Encontro de Energia no Meio Rural, 4., 2002, Campinas. Anais eletrônicos... Campinas: Unicamp, 2002. Disponível em: <http://www.feagri.unicamp.br/energia/agre2002/pdf/002-7.pdf> Acesso em: 22 ago. 2010.

[3]. União Da Indústria De Cana-De-Açúcar – UNICA, Dados e Cotações. 2010. Disponível em: <http://www.unica.com.br/default.asp> Acesso em: 20 set. 2010.

[4]. W. J. Freire, L. A. B. Cortez, Vinhaça de cana-de-açúcar. Ed. Agropecuária, Guaíba. 2000. 203p.

[5]. H. M. Lamonica, Potencial de geração de excedentes de energia elétrica a partir da biodigestão da vinhaça, Campinas, 06 jun. 2006. Palestra proferida no AGRENER 2006.

[6]. M. Perez, R. Rodriguez-Cano, L. I. Romero, D. Sales, Anaerobic thermophilic digestion of cutting oil wastewater: Effect of co-substrate. Biochemical Engineering Journal, v. 29, 250–257, Apr. 2006.

[7]. N. J. B. Castañón, Biogás, originado a partir dos rejeitos rurais. São Paulo, 2002.

[8]. C. Chevalier, F. Meunier, Environmental assessment of biogas co- or tri-generation units by life cycle analysis methodology. Applied Thermal Engineering, vol. 25, p. 3025-3041, dec. 2005.

[9]. Empresa De Pesquisa Energética – EPE, Os Leilões de Fontes Alternativas de Energia Elétrica de 2010. São Paulo: EPE, 2010.

[10]. L. A. B. Cortez, E. E. S. J. A. C. Lora, Biomassa no Brasil e no mundo. In: L. A. B. Cortez, E. E. S. Lora, E. O. Gomez (org), "Biomassa para energia". Campinas: Editora UNICAMP, 2008.

[11]. T. Szmrecsányi, Tecnologia e degradação ambiental: o caso da agroindústria canavieira no Estado de São Paulo. Revista Informações Econômicas, São Paulo, Vol. 24, n.10, out. 1994.

[12]. M. T. Ludovice, Estudo do efeito poluente da vinhaça infiltrada em canal condutor de terra sobre o lençol freático. Campinas, FEC-UNICAMP. Dissertação de Mestrado, 1996.

[13]. V. Hanndel, Valorização de subprodutos gerados nas destilarias de etanol. São Paulo: 2003.

[14]. E. P. Jordão, C. A. Pessoa, Tratamento de esgotos domésticos. 3. ed. Rio de Janeiro: ABES – Associação Brasileira de Engenharia Sanitária e Ambiental, 1995. 720 p.

[15]. P. de Lamo, Sistema produtor de Gás Metano Através de Tratamento de Efluentes Industriais – METHAX/BIOPAQ – CODISTIL – Piracicaba, 1991.

[16]. P. E. Cabello, F. P. Terán, F. J. C. Scognamiglio, Tratamento de vinhaça em reator anaeróbio de leito Fluidizado. Engenharia Ambiental, v. 6, n. 1, p. 321-338, jan./abr. 2009.

Electricity generation from biogas of poultry slaughterhouse biomass in Matelandia – Brazil

Diana Fatima Formentini[1,*], Guilherme de Paula Mmoreira Fracaro[1], Ricardo Nagamine Costanzi[1], Samuel Nelson. Melegari de Souza[1], Cleber Aimone Marques[1]

[1] UNIOESTE/CASCAVEL/CCET/PPGEA - Universidade Estadual do Oeste do Paraná – Programa de Pós Graduação em Energia na Agricultura – Rua Universitária 2069 - Jardim Universitário- Cascavel/Paraná- Brasil- 85819-110

** Corresponding author: Tel.: +55 45 32203151; E-mail: mpbambiental@yahoo.com.br*

Abstract: Brazil has great potential for biomass production. There are several processes to convert biomass into energy, among these is the biological conversion of organic carbon into methane. This work aimed to estimate the production of biogas in a poultry slaughterhouse in Matelandia state of Paraná, Brazil, by the IPCC methodology. The poultry slaughterhouse slaughter 140,000 poultries a day and generates a wastewater FLOW OF 3,360 $m^3.d^{-1}$. Electricity consumption by the industry plant is about 3,600 $MWh.month^{-1}$. The treatment system used in industry is the physical and biological process, and the pre-treatment consists of a static sieve and a flotation equipment, followed by stabilization ponds. Two anaerobic ponds were covered with a geomembrane of High Density Polyethylene and was installed a gas meter to measure the flow rate of biogas production. The biogas generation potential estimated can reduce 3.89% of the electricity consumed.

Keywords: *Bioenergy, Anaerobic digestion, Wastewater, IPCC.*

1. Introduction

In the past decades, the consumption of meat chicken in many countries has been on the increase. As a result of the growing poultry industry, poultry slaughterhouses are producing increasing amounts of by-products and wastes[1].

The production and export of chicken meat perform an important role in the Brazilian economy. According to the ABEF - Brazilian Association of Chicken Producers and Exporters, in 2009, Brazil was among the international reach first place in the export sector and third in world production of chicken meat, behind the United States and China. The southern region of Brazil has an important role in the achievement of these data, because it focuses on the major poultry production and consequently the processing industries of chicken meat, accounting for approximately 75% of national production. The State of Paraná is the largest producer of chicken meat from Brazil, exporting in the year 2009 a total of 954,653 5 tonnes of chicken meat[2].

The interest in recovering the biogas generated by stations for sewage treatment, urban solid waste landfills, residue of sugar cane, by the biodigestion of the vinasse, livestock manure anaerobic digestion and poultry slaughterhouse wastewater associated with its energetic use and managing these residues, have been discussed in Brazil[3].

Anaerobic digestion is a biological process that occurs in the absence of oxygen, where organic matter is degraded and transformed in gaseous mixture called biogas. The biogas composition is highly variable depending on various aspects like the characteristics of biomass and environmental conditions offered. The average composition of biogas has the following values: CH_4 (50-75%), CO_2 (25-50%), N_2 (0-10%), H_2 (0-1%), H_2S (0-3) and O_2 (0-2)[4].

Wastewater as well as its sludge components can produce CH_4 if it degrades anaerobically. The extent of CH_4 production depends primarily on the quantity of degradable organic material in the wastewater, the temperature, and the type of treatment system. With increases in temperature, the rate of CH_4 production increases. Below 15°C, significant CH_4 production is unlikely because methanogens are not active and the lagoon will serve principally as a sedimentation tank. However, when the temperature rises above 15°C, CH_4 production is likely to resume[5].

This paper objectives to evaluate the potential for methane production in a poultry slaughterhouse by the IPCC methodology, and the potential for generating electricity from the energy use of the methane produced in anaerobic digestion process.

2. Methodology

2.1. *Water consumption and wastewater characteristics in poultry slaughterhouses*

The according to the sanitary requirements related to processing and industrialization of meat, the demand for water in this activity is high, it can be considered an average consumption of 25 a 50 L[6], 25 L[7,8] ou 17 L a 20 L by poultry slaughtered[9].

It is recognized that minimising water consumption and contamination has wide reaching environmental benefits. Increasing the volume of water used automatically affects the volume of waste water which has to be treated at either an on-site or a municipal waste water treatment plant. Water makes contact with a carcass or any animal by-product, whether during production or cleaning, contaminants such as fats or blood are entrained and these increase the burden on the waste water treatment plant. In many cases the water used is hot, so energy will have been used to heat it. Also the fats can melt in hot water and then become more difficult to separate from the water[5].

The references of wastewater characteristics available in the literature described in Table 1, have several values due different water consumption by poultry slaughtered, operational practices, size of the industry, collecting the effluent at different points, among others.

Table 1: Characteristics of wastewater poultry slaughterhouse

References	COD ($mgO_2.L^{-1}$)	BOD ($mgO_2.L^{-1}$)
AGUILAR, et al., 2005[10]	5,400	2,760
CHAVEZ, et al., 2005[11]	7,333	5,500
DORS, 2006[12]	6,720	4,434
MARQUES, 2007[13]	4,325	3,346
DE NARDI, et al., 2008[14]	6,880	-
AMORIM, et al., 2008[15]	3,102	-
MATSUMURA & MIERZWA, 2008[16]	9,115	4,593

2.2. *Characterization of the case study*

The industrial plant slaughter 140,000 poultry.d^{-1}, generating a flow of wastewater from 3.360 $m^3.d^{-1}$, resulting in 24 L.poultry slaughtered^{-1}.

The wastewater treatment system use in the industry is compound by categories pre-treatment, primary and secondary through the physical and biological processes. Pre-treatment consists of a static sieve to remove solids, the primary treatment in flotation

equipment for the physical process for removal of oils and greases and secondary treatment is the arrangement of two biodigesters in parallel, an aerated pond with aeration sub- surface endowed with aerators and 6 also air vents and a facultative pond.

The main physical and chemical characteristics of wastewater are COD average Biodigester influent: 3,390 ± 1,275 mg L^{-1} and COD average Biodigester effluent: 1,205 ± 300 mg L^{-1}.

Measurements of water consumption were made by water meters installed at seven points of the production process, which resulted in consumption values by sector.

The industry in question has a demand of 3,360 $m^3.d^{-1}$ accounting for water consumption in all productive sectors, from receipt of the birds, washing trucks, bleeding, scalding, evisceration, cooling room, cuts, water sanitation cleaning equipment and industrial plant, boiler until the dispatch of meat.

Electricity consumption from the poultry slaughterhouse is 3,600 $MWh.month^{-1}$, resulting in approximately 1.07 $kWh.poultry\ slaughtered^{-1}$.

2.3. *Estimate of the methane potential production*

The principal factor in determining the CH_4 generation potential of wastewater is the amount of degradable organic material in the wastewater. Common parameters used to measure the organic component of the wastewater are the Biochemical Oxygen Demand (BOD) and Chemical Oxygen Demand (COD). Under the same conditions, wastewater with higher COD, or BOD concentrations will generally yield more CH_4 than wastewater with lower COD (or BOD) concentrations[5].

Considering the IPCC Guidelines for National Greenhouse Gas Inventories – Chapter 6: Wastewater Treatment and Discharge, was used following the methodology to account the methane production potential in poultry slaughterhouse in Matelandia, Paraná, Brazil.

Emissions are a function of the amount of organic waste generated and an emission factor that characterises the extent to which this waste generates CH_4.

Three tier methods for CH_4 from this category are summarised below:

The Tier 1 method applies default values for the emission factor and activity parameters. This method is considered good practice for countries with limited data.

The Tier 2 method follows the same method as Tier 1 but allows for incorporation of a country specific emission factor and country specific activity data. For example, a specific emission factor for a prominent treatment system based on field measurements could be incorporated under this method. The amount of sludge removed for incineration, landfills, and agricultural land should be taken into consideration.
For a country with good data and advanced methodologies, a country specific method could be applied as a Tier 3 method. A more advanced country-specific method could be based on plant-specific data from large wastewater treatment facilities.

This paper follow the Tier 2 method.

Step 1: Estimate total organically degradable carbon in wastewater (TOW) for industrial

sector i.

$$TOWi = Pi \bullet Wi \bullet CODi \quad (1)$$

Where:
TOWi = total organically degradable material in wastewater for industry *i*, kg COD/yr
i = industrial sector
Pi = total industrial product for industrial sector *i*, t/yr
Wi = wastewater generated, m^3/t product
CODi = chemical oxygen demand (industrial degradable organic component in wastewater) $kg.COD.m^{-3}$

Step 2: Select the pathway and systems according to country activity data. Use Equation 2 to obtain emission factor. For each industrial sector estimate the emission factor using maximum methane producing capacity and the average industry-specific methane correction factor.

$$EFj = Bo \bullet MCFj \quad (2)$$

Where:
EFj = emission factor for each treatment/discharge pathway or system, $kgCH_4$ /kg.COD
j = each treatment/discharge pathway or system
Bo = maximum CH_4 producing capacity, $kg.CH_4$/kg.COD
MCFj = methane correction factor

Good practice is to use country and industry sector specific data that may be available from government authorities, industrial organizations, or industrial experts. However, most inventory compilers will find detailed industry sector-specific data unavailable or incomplete. If no country-specific data are available, it is good practice to use the IPCC COD-default factor for Bo (0.25 kg CH_4/kg.COD).

2.4. *Electricity Generation Potential*

The estimate electricity generation potential by the biogas produced was calculated following this equation:

$$P_{el} = \frac{PCI_{CH4} * MJ * P_{CH4} * \eta_{el}}{kWh * 1000 * 100}$$

Onde:
P_{el}: Electricity generation potential $MWh.year^{-1}$;
PCI_{CH4}: Methane Calorific value: 50 $MJ.kg^{-1}$ [17];
$\frac{MJ}{kWh}$: Unit conversion factor: 0,2778;
η_{el} : Electricity Generation System Efficiency: %.

3. Results

The methane generation potential is 515,963 $kgCH_4.year^{-1}$, equivalent 1.414 $kgCH_4.d^{-1}$. Considering a electric generation efficiency of 30% for the motor, the methane generation can produce 1,681 $MWh.year^{-1}$, or 4.61 $MWh.d^{-1}$.

4. Conclusion

The biogas produced by the anaerobic digestion process can reduce 3.89% of the electric energy consumption at poultry slaughterhouse.

5. Acknowledgments

The authors acknowledge ITAI – Instituto de Tecnologia Aplicada e Inovação, FPTI – Fundação Parque Tecnológico de Itaipu and FINEP – Financiadora de Estudos e Projetos for the operacional and financial support.

References

[1] Salminen, E.; Rintala, J.; Anaerobic digestion of organic solid poultry slaughterhouse waste – a review; Bioresource Technology; 83; pp. 13-26; 2002.

[2] ABEF – Associação Brasileira dos Produtores e Exportadores de Frango – Relatório Anual, 2009/2010.

[3] Salomon K. R., Lora, E. E. S. Estimate of the electric energy generating potential for different sources of biogas in Brazil. Biomass and Bioenergy, 33, p. 1101 – 1107. 2009.

[4] Speight, J.G.; Synthetic fuels handbook; 1ª Edição; Editora McGraw-Hill; pg 351; 2008.

[5] IPCC; Guidelines for National Greenhouse Gas Inventories; Chapter 6; 2006.

[6] CETESB - Companhia de Tecnologia e Saneamento Ambiental & SMA-SP – Secretaria do Meio Ambiente do Estado de São Paulo; Relatório técnico n. 2 do convênio SMA/MCT n. 01.0053.00/2001 – Efluentes; 2003. Disponível em www.mct.gov.br/CLIMA/brasil/pdf/Efluente_preliminar.pdf. Acesso em: 20/07/2010.

[7] SUDERHSA – Superintendência De Desenvolvimento De Recursos Hídricos E Sanemanento Ambiental. Manual Técnico de Outorgas; Novembro de 2006.

[8] Mierzwa, J. C.; Hespanhol, I. Água na Indústria – Uso – Uso Racional e Reúso; São Paulo. Ed. Oficina de Textos;143 pg; 2005.

[9] Philippi Jr, Arlindo., Bruna, Gilda Collet., Romero, Marcelo De Andrade; Curso de Gestão Ambiental; 1045 p. 1ª Ed. São Paulo; 2004.

[10] Aguilar, M. I., Saéz, J., Llórens, M., Soler, A., Ortunõ, J. F., Meseguer, V., Fuentes, A.; Improvement of coagulation-flocclation process usinganionic polyacrylamide as coagulation aid; Chemosphere; 58 47-56; 2005.

[11] Chavez, C. P., Castillo, R. L., Dendooven, L., Escamilla-Silva, E. M., Poultry slaughter wastewater treatment with an up-flow anaerobic sludge blanket (UASB) reactor; Bioresource Technology; 96; 1730-1736; 2005.

[12] Dors, Gisenara. Hidrólise Enzimática e Biodigestão de Efluentes da Indústria de Produtos Avícolas; Dissertação de Mestrado - Programa de Pós-Graduação em Engenharia Química. Universidade Federal de Santa Catarina – UFSC; 2006.

[13] Marques, Valmir; Kato, Mario T., Florencio, Lurdinha. Caracterização e Avaliação da Eficiência do Tratamento de Efluentes de Abatedouro Avícola na Região do Semi-Árido. 24º Congresso Brasileiro de Engenharia Sanitária e Ambiental. Belo Horizonte – MG, 2007.

[14] De Nardi, I.R., T.P. Fuzi A, V. Del Nery; Performance evaluation and operating strategies of dissolved-air flotation system treating poultry slaughterhouse wastewater; Resources, Conservation and Recycling; 52; 533–544; 2008.

[15] Amorim, A.K.B., De Nardi, I.R., Del Nery, V. Water conservation and effluent minimization: Case study of a poultry slaughterhouse. Resources, Conservation and Recycling; 51; 93–100; 2007.

[16] Matsumura, E.M., Mierzwa, J. C. Review - Water conservation and reuse in poultry processing plant— A case study; Resources, Conservation and Recycling 52; 835–842; 2008.

[17] Heywood, J.B.; Internal combustion engine Fundamentals; Editora McGraw-Hill; pg 915; Nova Iorque; 1988.

[18] UNFCCC; Report of the subsidiary body for scientific and technological advise on its eighteenth session; Junho; 2003.

Economic evaluation of an industrial biogas system for production of gas, electricity and liquid compost

S. Ghazi[1*], M. Abbaspour[2]

[1] *Islamic Azad University, Parand Branch, Parand , Iran*
[2] *School of Mechanical Engineering, Sharif University of Technology , Tehran, Iran*
** Corresponding author. Tel: +982144004586, Fax: +982144865002*
E-mail: sanaz_ghazi2001@yahoo.com / ghazy.iau.ir@gmail.com

Abstract: Iran is on the verge of elimination of energy subsidies. This means a sudden increase in prices such as gas, electricity, etc.... On the other hand, the different means of the different means of energy production is a great concern for human being. Amongst all different methods of energy production, renewable energy is paid more and more attention due to the least consequences concerning the diverse climate change effects. However, the economic factors are also important in order to bring a project into reality. In this paper, the potential of biomass energy in an industrial scale is investigated under this great change on national policies. Then the economic analysis of an industrial biogas system in a rural area near the province of Tehran, the capital of I.R.I., as a case study is illustrated .In this process several products will be produced such as organic compost by anaerobic fermentation of agricultural and organic wastes, liquid fertilizer, Methane and Carbonic gases, electricity and heating. The results of economical evaluation shows that the use of methane-fired generators for the production of electricity is economical because of the high amount of biogas production. So, the revenue gained from produced electricity is more than produced compost. Also, in the process of biogas production, the huge amount of Carbonic gas will be produced which can be used after purification in industry. The result show a promising future for the use of bio gas, specially under new policies of zero energy subsidies for households , commercial, and public use.

Keywords: *Biogas, Economical evaluation, Renewable energy.*

1 Introduction:

Biogas is a renewable energy source which is produced on the basis of organic waste from the agriculture, food trade industry and households. Furthermore, biogas can be extracted from sludge in the wastewater treatment plants and from landfill sites [1].

Biogas is produced in the process of anaerobic digestion. Anaerobic Digestion is process whereby organic waste is broken down in a controlled, oxygen free environment at certain temperature by using bacteria naturally occurring in the waste material [1,2]. Biogas can be extracted from landfill sites by using collection pipes and wells, which uses vacuum to collect the gas. For the gas production from organic waste, sewage sludge and manure, a hermetical digestion tank is needed. Biogas is composed of approximately 50 to 70 % methane (CH4), 30 to 40 % carbon dioxide (CO2), as well as water vapor and a small quantity of nitrogen (N2), sulfur (S) and other trace compounds. Biogas has the same characteristics as the natural gas, which allows using it in the same appliances [2,3]. But its calorific value can be up to two times lower than natural gas. The collection of biogas actually removes pollution from the atmosphere. If the gas is emitted to the air, it would contribute to the global warming as methane is one of greenhouse gases. The impact of methane emissions on global warming is 21 times bigger than that of CO2 emitted during the burning of biogas [2]. There are many biogas plants all over the world, mainly in USA, India, Mexico, Africa, but as well in Denmark, Sweden, Germany and Austria. It is used for heat production and cogeneration of heat and power, alternatively as well as vehicle fuel in the public transportation [3].

2 Potential of Biomass energy in Iran

Considering, the availability of all types of Biomass resources in Iran, Power Ministry did a research to evaluate the potential to use biomass for renewable energy. This research was conducted in 1976 and conclusions are as follow [4]:
1- Quantity of accessible Animal Waste in Iran is 74.95 million tons(MT); Biogas could be produced by this amount is 8668 Million cubic meter(MCM) and energy equivalent this biogas is 193299TJ. (TJ=10^{12} J)
2- Quantity of accessible Urban Waste in Iran is 10.6 MT: Biogas could be produced by this amount is 1645.7 MCM.
3- Quantity of accessible Biogas from Urban Waste Water in Iran is 98.85 MCM/day. (Waste Water specifications are: 160 Litter per capita per day and BOD per capita is 33-40 gr/d.c)
4- Quantity of accessible Methane from Industrial Waste Water in Iran is 167.67 MCM/year. Energy equivalent this quantity is 6153TJ per year. (This Waste Water is from Big Food Industry in Iran.)
5-Total gross energy potential from Agricultural and Wood Waste is 411.9 PJ from 3285.5 MCM Methane and 33.95 MCM Ethanol which could be produced [4].

3 Availability of industrial biogas plants in Iran:

In Iran, presently two main industrial biogas plants are exist which include Mashhad Landfill Power Plant and Saveh Biogas Plant [5,6].

3.1 Summary of Mashhad Landfill Power Plant:

The first Landfill-Gas (LFG) power generation project was initiated in Mashhad, the second largest city in Iran, located on the north east part of Iran, through a memorandum of understanding between "Renewable energy Organization of Iran (SUNA)" and "Waste Recycling and Processing Organization of Mashhad Municipality (WRPO)". Based on the mentioned memorandum, SUNA took the responsibility of preparing technical investigations and tender documents and follow-up the electricity purchase contract between Mashhad LFG power plant and Ministry of Energy. Investment for power plant and commissioning was accepted by WRPO. Feasibility studies, conceptual design and tender documents preparation were consequently allocated to Renewable Energy Department of NRI [5].

The first phase of this project, included design criteria for engineering landfills and gas extraction systems and transmission lines, introduction to energy conversion and power generation technologies for LFG, field investigations and measurement methods and monitoring of LFG. The next phase was feasibility study for installation of power generation unit in Mashhad Landfill, in which, estimation of landfill gas theoretical yield for Mashhad municipal solid wastes, LFG generation modeling and gas flow prediction for long term periods, evaluation of confident power capacity for Mashhad Landfill, technical assessment of power generation equipment for LFG and introduction of more appropriate commercial generating sets for utilization of LFG in Mashhad Landfill, were performed. In the third phase, economical studies, three alternatives were selected on the base of feasibility study results. These alternatives were assessed as economical aspects and finally, installation of generating sets near the guard room of Mashhad Landfill, which is located near to irrigation station and a 20kV line, was selected as the most useful option for utilization of the whole gas which can be collected through the existing gas extraction systems. The generated electricity in this unit will be sold to power network at an average price of 0.61 dollars per kWh [4,6].

The phase of conceptual design included: pipeline design for LFG transmission to central gas station, gas blower station, gas treatment process, foundation and structure of generating house, power generation unit arrangement and grid interconnection system plus protection and confidential instruments. Technical characteristics and tender documents were consequently prepared on conclusions [6]. The contract for construction and start-up of Mashhad Landfill power generation unit will be as an Engineering Procurement Construction (EPC) contract. The results of this project shows:

- Pipeline and collection systems were designed on the basis of 13 years useful operation period of a biogas fueled generating set, and LFG generation modeling results, for average gas flow rate of 550 Nm3/h and maximum gas flow rate equal to 660 Nm3/h. A minimum power capacity of 435 kW is expected to be achievable until the end of 2018 by existing gas extraction systems [6].
- The power capacity can be increased to at least 715 kW if Mashhad municipality develop the gas extraction systems to recent buried layers of solid wastes which are dumped in period of 2004-2006.
- Generating sets with LFG fueled internal combustion engines are the best option for Mashhad Landfill, furthermore, a list of qualified manufacturers of these equipment, has been presented in the project documents.
- Economical assessment results showed the best alternative is the installation of power generating unit in near of Landfill irrigation station.

A case study with capacity of 400 kW (due to capacity of commercial models) will have the generation cost of electricity relevant to discount rates of 8%, 12% , 16% and 20% equal to: 293, 320, 350 and 0.39 dollars per kWh, respectively [5,6].(It should be noted for the exchange of Rls rate to dollar, one dollar was considered as 10000Rls.)

- LFG power plant interconnection with regional power grid is feasible through the existing 20kV line in Mashhad Landfill. Electrical circuit drawing and single-line diagram for connection to 20kV network were obtained and presented in project documents [8,9].

3.2 Summary of Saveh Power Plant:

The city of Saveh is in the central province, 150 km from Tehran with a population of 120,000. It has a Semi-arid climate and the temperature during different seasons of the year fluctuates within the range of –10°C to 40°C. In order to establish the Bio-gas power plant in this city, the usable pollutants in Saveh were studied and they were divided into four groups: Household garbage, sludge of sewage treatment, slaughter house waste water and sludge of leaching pit [3]. Through statistical studies, separation operation, sampling and executing physical, and chemical tests, quantity and quality specifications of each of the four types of pollutants were determined. The results are shown in the following tables[6]:

Table 1: MSW Specification[4]

Parameters	**Quantifies**
Average garbage / day	78.3 tons
Household garbage/ day	58.7 tons
Organic material of garbage /day	38.2 tons
Total solids (15%)/ day	5.73 tons

Table 2. Specification of sewage treatment sludge[4]

Parameters	Quantifies
Annual average of sludge	10000 tons
Daily average of sludge	27.4 tons/day
Total solids (1.002%)/ day	274.54 kg/day
Volatile solids/ day	5.73 tons

Table 3: Specifications of the Slaughterhouse sludge[4]

Parameters	Quantifies
Annual average of slaughterhouse waste water	4380 m^3
Daily average of slaughterhouse waste water	12 m^3
Total solids (0.508%)/day	60.96 kg
Volatile solids/day	51.39 kg

Table 4: Specification of leaching pit sludge[4]

Parameters	Quantifies
Annual average of discharged sludge from household wells	5000 tons
Daily average of discharged sludge of household wells	13.7 tons
Total solids (1%)/ day	137 kg
Volatile solids/day	83.57 kg

After determining the quantity and quality of each pollutant separately, anaerobic digestion situation, and the production of Bio-gas from combination feed including above mentioned pollutants, considering the existing real relations in the city in anaerobic reactor at 35 degree centigrade was investigated in a semi-industrial anaerobic reactor.
This reactor is metallic and has a volume equal to 10 cubic meters. In order to control the heat, it is completely isolated and in order to heat up the contents and create suitable heating conditions, the reactor is equipped with an internal coil and a sludge evacuation pump is also installed to mix the content. The reactor has been designed in a way that is the capable of operating both continually and dis- continually (batch). (Fig.1)

In order to study the anaerobic digestion of these feeds on a continuous basis, determining the stoppage time of the material in reactor becomes necessary. Thus, at first, the situation for producing gas in the related reactor on dis- continuous basis was studied. By investigating the volume of daily gas production and the speed of production during the dis-continuous period and the related curve, the stoppage time was determined to be 20 days and for continuous studies the 20 days stoppage was also agreed[8].

Fig.1. Anaerobic metallic digestion reactor with 10m^3 volume

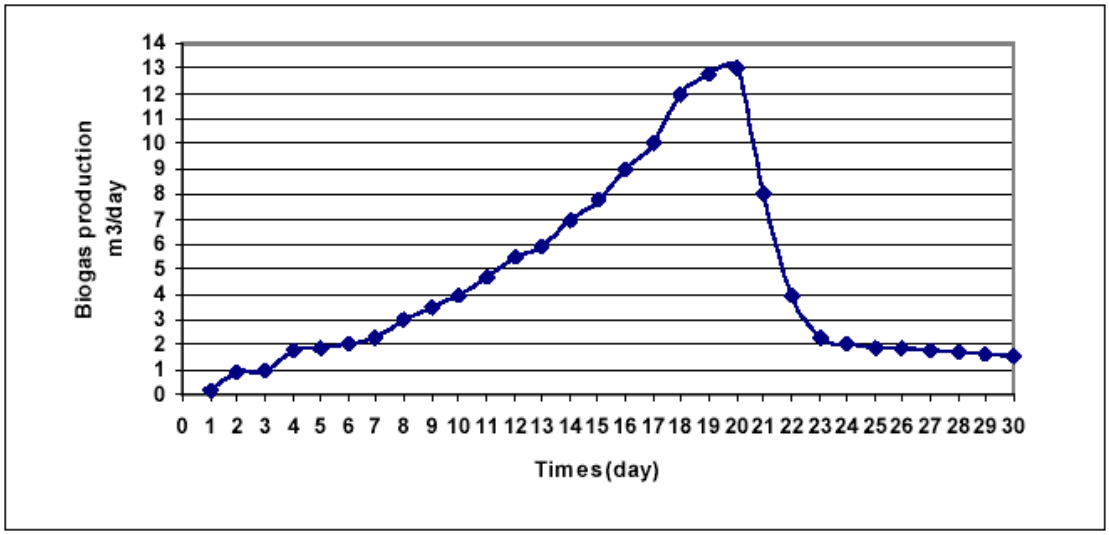

Fig.2. Bio-gas production curve in dis-continuous loading at 35°C[3].

Studies during the continuous loading of combination feed including the four groups of urban pollutants with actual existing recording in the city of Saveh shows that for each kilogram of total solid as input, 500 liters of Bio-gas is produced in anaerobic digestion process. Thus on the basis of scientific studies carried out in Saveh Bio-gas power plant, the operation can be summarized as follows:

Table 5. Summary of operation and technical specifications of Saveh power plant[4]

1	Amount of bio-gas produced for every kilogram of dried input/ day	500 liter/kg of total Solid
2	Percentage of T.S in combination feed entering reactor, including four types of pollutants	6.794%
3	Amount of daily input to the power plant	91.3 ton/day
4	Amount of Total Solids as input/day	6202.5 kg/day
5	The most suitable stoppage time in 35°C	20 Days
6	Total volume of Bio-gas produced/day	3101 m^3/day
7	Amount of Fertilizer produced / day	2500 kg/day
8	Extracted water suitable for agricultural irrigation	31025 m^3/year

4 Methodology:

This paper provides a case study for an industrial biogas system to be built on Eshtehard industrial city near the province of Tehran. Since, more than 40% of husbandries and also an accountable number of settled livestock farming are located in this region, therefore it is possible to collect a total volume of five thousand cubic meters of feedstock per day to feed the system for production of gas, electricity and liquid compost. For feasibility study of this plan, the economical evaluation is considered based on the cost benefit analysis of this project. To calculate the capacity of the system the following assumptions were made:

- The amount of biogas production is equal to 100-160 cubic meter from each ton of organic wastes which can be produced about 170 kwh of electricity and 340 kwh of heating energy.

- Each 10 cubic meters of biogas can be produced about 15 kw of AC electricity and 35000 kcal of heating water
- Each unit of biogas can produced about 25-30 cubic meter of organic fertilizer per day in 55-60˚C during 15 to 20 days.
- Each cubic meter of organic compost weights 0.7 ton and the weight of 25-30 cubic meters of produced compost is equal to 17.5 or 21 ton.

5 Results:

Whereas a lot of husbandries and settled livestock farming are located at Eshtehard region, the amount of substrates for feeding the biogas system could be very high. The estimated amount of substrates at this region is presented at table 6.

Table 6.The estimated amount of substrates at Eshtehard region

Type of substrate	Existing amount	Unit
Cattle dung	219000	tons
Chicken dung	87600	tons

For design and installation of this project, different parameters such as the total capital cost, number of persons who can be involved in this project, total area for project installations, the amount of electricity, water and energy consumption were calculated for the implementation of this project.

- The required area for biogas unit installation is equal to 136,000 square meter at Eshtehard industrial region which is located near to the more than 40% of husbandries and also an accountable number of settled livestock farming of the country
- Total capital cost is assumed as 22.8 million dollars
- The total number of persons for this project include 103 persons as a producer and 43 persons as a supporter
- The power of consumed electricity is equal to 259 kwh of total 5950 kwh of electricity which is produced by the biogas unit. Total production capacity of products is presented in table7.

Table7. Total production capacity of products

Type of product	Amount of production(per hour)	Amount of production (per year)	Unit
Electricity	5950	52,122,000	kwh
Carbonic gas	2.36	20,673.6	ton
Heating	11900	104,244,000	kwh
Cattle dry compost	7.98	69,934	ton
Chicken dry compost	3.193	27,959	ton
Liquid compost	58.8	515,288	Cubic meter

It should be mentioned, from the total amount of produced electricity, 250 kwh consumes for the biogas system and the rest can be delivered to grid electrical network. Also, the produced dry compost which contain 35% humidity can be packed for domestic consumption.

- The annual amount of consumed water is equal to 342144 cubic meter which can be used for agricultural land after an anaerobic fermentation process.

- The annual amount of consumed energy is equal to 1,569,000 litres of gasoil for combustion of electrical generator and 21,900 litres of gas for the vehicles during the installation of plant

Based on the mentioned characteristics, the following economical parameters were calculated for the presentation of economic analysis of this project. The calculate amount of these parameters were shown in table8.

Table8.Economical evaluation of this project based on financial calculations

Financial parameter	Estimated cost (Dollars)
The amount of fixed investment	22 million Dollars
The amount of investing turnover	0.85 million Dollars
Total amount of investment	22.9 million Dollars
Actual cost of products in final capacity	0.36 Dollars per kwh of electricity 87.5 Dollars per ton of Carbonic gas 26 Dollars per ton of Cattle dry compost 65 Dollars per ton of chicken dry compost 3.5 Dollars per cubic meter of liquid compost
The amount of total sale in final capacity	13 million Dollars
Annual return of investment in final capacity	3.4 million Dollars
Return investment time	3.3 years
Rate of return	0.22 %
Per capita investment	0.17 million Dollars

It should be noted for the exchange of Rls rate to dollar, one dollar was considered as 10000Rls.

As the above table illustrates, the time for capital cost return is equal to 3.3 years and the amount of earnings after this time is about 3.9 million dollars.

6 Conclusions:

The aim of this project is the conversion of low-value organic wastes to organic compost with high value at industrial scale based on anaerobic fermentation. The anaerobic digestion has numerous advantages rather than aerobic digestion. The most advantages include:

- The value of the produced compost is so high rather than traditional fertilizer. For example by the use of this compost the production of agricultural crops such as corn and tomato can be increased respectively up to 49% and 35%.
- Elimination of pathogenic bacteria, viruses, agents and odour in anaerobic digestion
- The huge amount production of methane and carbon dioxide gases. Methane gas can be used to produce electricity with the use of methane burner.

Calculation indicates that it is possible to produce 5950 kw electricity which 250 kw should be consumed for the process itself. This system can produce 2.36 tons of gas, 58.8 cubic meters of liquid compost, 11 tons of dry compost and equivalent of 11900 kwh of heat per hour. The results of economic analysis shows that this project can be beneficial and economical in a short time period. Finally, with consideration of economical, environmental and social issues, the promotion of this types of industrial biogas system can be an attractive project at regional and national level.

For accelerating the execution of this kind of projects in Iran and similar developing country, the following recommendations are suggested:

- As discussed, the elimination of energy subsides help the rapid development of this kind of renewable energy systems. The government can encourage the use of these systems by setting the purchase policy for the electricity production from these systems. To do so, some technical steps should be carried out to make this action possible.
- It is necessary to implement some policies to encourage the private sector participation in this issue.
- It is necessary to imply some policies to increase the awareness of decision makers, especially managers, authorities and experts about the benefits and advantages of this kind of energy.
- The CDM mechanism was not brought into account in this study. However, the implementation of CDM mechanism can help to have even a better outlook using this type of energy system.

References

[1] The renewable energy organization of Iran, "biogas and development", 4th national conference on renewable energies, 2001,pp. 80-88

[2] GH. A.Omrani, "The principal of biogas production from urban and rural waste", 2000, pp. 125-142

[3] The renewable energy organization of Iran, "The practical use of biogas unit in Kish island"2006, pp. 54-67

[4] I, Nahvi , Z. Sahbaee, “Biogas production and its role in the control of the environmental pollution”, Proceeding of 4th seminar of bigas in Iran, 2008, pp. 145-152.

[5] http://www.iranenergy.org.ir

[6] http://www.suna.org.ir

[7] J.Wiley, "Biogas from waste & renewable resources"2008, pp 167-173

[8] D.House, "Biogas handbook",2006

[9] J.Barrie, "Everything biogas", 2009

Development of an anaerobic hydrogen and methane fermentation system for kitchen waste biomass utilization

Noriko Osaka[1], Kohki Nagai[2], Shiho Mizuno[2], Makiko Sakka[3], and Kazuo Sakka[3]

[1]*Fundamental Technology Department, Technology Research Institute, Tokyo Gas Co., LTD, 1-7-7, Suehiro-cho, Tsurumi-ku, Yokohama-City, Kanagawa 230-0045, Japan*
[2]*Fundamental Research Department, Technical Research Institute, Toho Gas Co., LTD, 507-2 Shinpo-Machi, Tokai-City, Aichi 476-8501, Japan*
[3]*Applied Microbiology Laboratory, Graduate School of Bioresources, Mie University, 1577 Kurima-Machiyacho, Tsu-City, Mie 514-8507, Japan*
** Corresponding author. Tel: +81 45 500 8769, Fax: +45 500 8790, E-mail: nosaka@tokyo-gas.co.jp*

Abstract: Utilization of kitchen waste as biomass resources has been of growing importance in urban areas of Japan. Present-day standards have set much sterner target recycling rates especially for kitchen waste from food industry, e.g. restaurants and food retail dealers. Aiming at high-efficiency energy recovery from kitchen waste, we have developed a two-step anaerobic fermentation system for generating hydrogen and methane. Bio-hydrogen is produced in the initial fermentation step by thermophilic microbiota mainly consisting of *Clostridium* species. Then, residues such as organic acids are converted into bio-methane in the second methane fermentation step. By proficiently combining these two fermentation steps, high system efficiency can be achieved. Optimum operating conditions have been found in the laboratory test of hydrogen fermentation operated over 300 days using artificial kitchen waste.

Keywords: *Biomass, Methane fermentation, Hydrogen fermentation*

Nomenclature

TS Total solid ..... %
VFA Volatile fatty acid ..... mg/L
COD Chemical oxygen demand ..... mg/L
HRT Hydraulic retention time ..... days

1. Introduction

Energy from biomass is the promising renewable energy. In Japan, “Biomass Japan broad strategic view" was determined in December 2002. The concrete target value of greenhouse gas discharge reduction was set to develop the recycling society. We are demanded to plan maximum profit utilization of biomass. In particular of them, it needs great amount of energy as oil and gas to incinerate sewage sludge and kitchen wastes which content much water. Great amount of energy as oil and gas is particularly required to incinerate sewage sludge and kitchen wastes, which contain much water. The realization of fermentation technology recovering energy from biomass reduces CO_2 emission from the garbage disposal. H_2 produced from biomass (Bio-H_2) is especially expected as one of the important energy sources in the future plan of hydro-energy. We know bacteria fermenting carbohydrates as glucose and cellulose. The bacteria make organic acids in their metabolic process. H_2-CH_4 fermentation is known as an efficient energy recovery system because organic acids can be used for substrate of fermented methane. Methane fermentation is available for many carbonic wastes, however, HRT is long. Therefore, pre–treatment to oxidize carbonic wastes in the fermentation process is needed to shorten HRT. Some trial tests have been conducted to apply H_2 fermentation as pre-treatment for acceleration of energy generation.

2. Materials and methods

2.1. Materials

Our research is aimed for the realization of efficient recycle and disposal system. We used artificial kitchen wastes as the substrate in our lab. In the pilot plant, the kitchen waste discharged from our canteen and dog foods are made use of raw materials. The composition and contents of substrates in the laboratory test are as follows. (Table1, 2, 3) The ratio of carbon and nitrogen is about 15. It is slightly lower than ideal condition for CH_4 fermentation. Table4 shows materials in the pilot plant. These materials are diluted and regulated the ratio of total solid. (Table5)

Table 1 *Composition of the material as artificial kitchen waste in the laboratory test*

	Shredded vegetable	Minced meat	Boiled fish	Cooked Rice
Weight ratio (wt %)	86.7	3.3	3.3	6.7

Table 2 *Contents of the material as artificial kitchen waste in the laboratory test*

Content	Water	Protein	Oil	Carbohydrates	Ash
Weight ratio (wt %)	77.8	4.4	2	15	0.8

Table 3 *Ratio of elements of the material as artificial kitchen waste in the laboratory test*

Element	C	H	N	S	O	Ash
(%)	45.5	7.3	3.2	0.1	41.2	2.7

Table 4 *Composition of the material for the plant test*

	Kitchen waste	Dog food
Weight (kg)	20	12

Table 5 *TS in the diluted materials*

	Laboratory	Pilot plant
TS (%)	7.5	6.5

2.2. Methodology

2.2.1. H_2–CH_4 fermentation

The metabolism of H_2–CH_4 fermentation is as follows. Bacteria generate H_2 on two pathways concerning glucose as carbohydrate in kitchen waste. Much hydrogen can be generated from glucose in the pathway (1). The generation rate of hydrogen is 4mol / 1mol-glucose, and that of acetic acid is 2mol / 1mol-glucose.

$$C_6H_{12}O_6 + 2H_2O \rightarrow 4H_2 + 2CO_2 + 2CH_3COOH \quad (1)$$

$$C_6H_{12}O_6 \rightarrow 2H_2 + 2CO_2 + CH_3CH_2CH_2COOH \quad (2)$$

In the case of CH4 fermentation, acetic acid and H2 are the substrate for generating CH4. There are 3 main pathways as follows. 70% of Bio-CH4 is generated as the deconstruction of acetic acid in the pathway (3), and about 30% of Bio-CH4 is generated in the pathway (4). The pathway (5) is a rare case.

$$CH_3COOH \rightarrow CH_4 + CO_2 \quad (3)$$

$$4H_2 + CO_2 + H_2O \rightarrow 4H_2 + HCO_3^- + H^+ \rightarrow CH_4 + 3H_2O \quad (4)$$

$4HCOOH \rightarrow CH_4 + 3CO_2 + 2H_2O$ (5)

When we develop high-efficient H_2-CH_4 fermentation system, the pathway (1) and (3) should be activated.

A pre-treatment process is generally adopted in commercial plants to promote the methane fermentation.

In the process, carbohydrate is converted to organic acetic acids in the following pathway (6). The acetic acids are equivalent to 3mol methane / 1mol-glucose.

$C_6H_{12}O_6 \rightarrow 3CH_3COOH$ (6)

Table 6 shows estimated calorific values of generated bio-H_2 and bio-CH_4. H_2-CH_4 fermentation is more efficient than Acidizing-CH_4 fermentation to recover energy.

Table 6 *Calorific values of generated biogas on two pathways*

	Calorie [kJ/ mol-glucose]
Acidizing – CH_4 fermen.	2405
H_2 fermen. - CH_4 fermen.	2570

Representative bacteria of H_2 fermentation include the Clostridium genus of the obligate anaerobe, and Escherichia coli of the facultative anaerobic bacterium. These bacteria have a weak property in concentration of organic acids, especially lactic acid. Acid generation bacteria are cultured in medium temperature and prefer neutrality to acidity not in thermal and aciditic environment. Therefore, it is most important to look for H_2 generation bacteria with thermal and high acidity tolerance. The microbiota named OF-1 we use in this research was collected from soil samples. In addition, it can be cultured in high temperature as 60°C and acid atmosphere as pH 5.5. OF-1 includes the bacteria saccharifying cellulose and thermophilic bacteria generating H_2.

2.2.2. Test equipment

The outline of test equipments in the laboratory is indicated in Fig.1. The volume of H_2 fermenter (ABLE & Biott Co.,Ltd., Japan) is 1L and the effective volume is 600cc. Dilution materials adjusted to TS 7.5% are crushed by a food processor. The crushed dilution materials and additional minerals, e.g. Ni and Co, were thrown into the fermenter. The additional minerals have a role to promote the methane fermentation. NaOH is used as pH control chemical. The residue of H_2 fermentation is used as materials for CH_4 fermentation. CH_4 fermener (PRECI Co.,Ltd., Japan) has a carrier which is pumice stone. An operation of feeding materials and pulling up fermentation liquid is in the atmosphere.

The pilot plant flow is shown in Fig. 2. Kitchen wastes from our canteen are classified and crushed. They are mixed with crushed dog food and water. The materials are diluted to TS 6.5%. The lower TS than laboratory test depends on a feeding ability of a pump. pH was adjusted to be 5.5 by $Ca(OH)_2$. A feeding and pulling up is anaerobic operation. Other experimental conditions are written in Table7.

The devices for analyzing the materials, biogas and fermentation liquid are as follows. Calorific values of materials are measured by a calorie meter EA6320 (Parr Instrument

Company, U.S.). Elements are analyzed by an elemental analyzer Vario EL Ⅲ（Elementar Americas, Inc. U.S.）. An absorption meter DR2800 (Hach Company, U.S.) measures COD. Biogas analysis is used by a gas chromatography GC-8A (Shimazu Corporation, Japan). Fermentation liquids are analyzed by a liquid chromatograph HPLC-20AD (Shimazu Corporation, Japan).

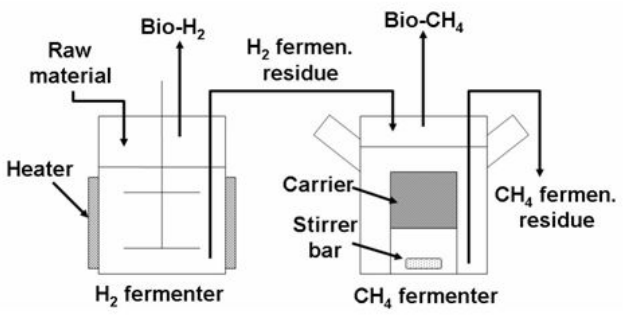

Fig. 1 Schematic diagram in the laboratory

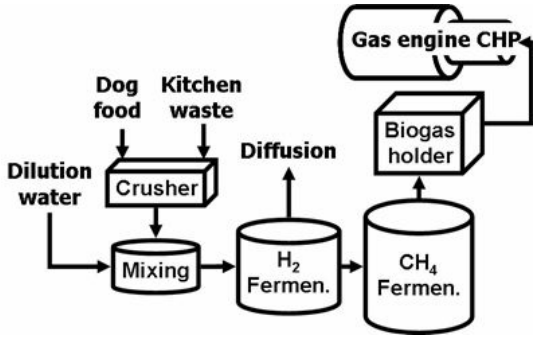

Fig. 2 Plant flow

Table 7 Experimental conditions

Equipment	Laboratory		Pilot plant	
Fermentation	H_2	CH_4	H_2	CH_4
Material	Artificial kitchen waste	Residue of H_2-fermen.	Kitchen waste Dog food	Residue of H_2-fermen.
Feed	1 feed / day（5days / week）			
HRT (days)	4.2, 2.8	14	4.2, 2.8	14
Volume	600cc	800cc	0.4Nm^3	4Nm^3
Temp. (˚C)	60	55	60	55
pH	5.5(Controlled)	7(Uncontrolled)	5.5(Controlled)	7(Uncontrolled)
Carrier	×	○	×	○
Stirring	Stirrer	Magnetic stirrer	Stirrer	Stirrer Circulation pump
Varied sludge	OF-1 (Microbiota from soil)	Sludge of high temp. CH_4 fermen.	OF-1 (Microbiota from soil)	Sludge of high temp. CH_4 fermen.

3. Results

3.1. Laboratory test

Figure 5 shows the time variation of bio-H_2 volume. The stable and successive operation over 300 days was achieved. On the 350th day, the amount of feedstock was changed. Though HRT was shortened from 4.2 to 2.8 days, the condition of H_2 fermentation was well maintained and the stable running could be continued. But it is too difficult to realize shorter HRT. Because the feeding was once a weekday, in the perspective of only weekday, HRT is calculated as only 2 days. In the short HRT, H_2 fermentation became unstable. The determined feeding on weekday made the fluctuations of bio-H_2 in the all run time. In beginning of the week, bio-H_2 reduced and increased in weekend. The bands of fluctuation in the amount of bio-H_2 became smaller as HRT shortening.

Though the materials and reactors were not sterilized, the density of lactic acid was under 2000 mg/L almost all the run time. A contamination was almost avoided since the operation

temperature is high. H_2 generation bacteria OF-1 has heat resistance, however, concentrated metabolites harm it. Figure 4 shows the relation between the density of lactic acid and the generated bio-hydrogen. The decrease in H_2 was caused by the increase in the lactic acid. In this case we fed materials including large amount of lactic acid. The density control of lactic acid under 10000mg/L is needed for efficient H_2 fermentation.

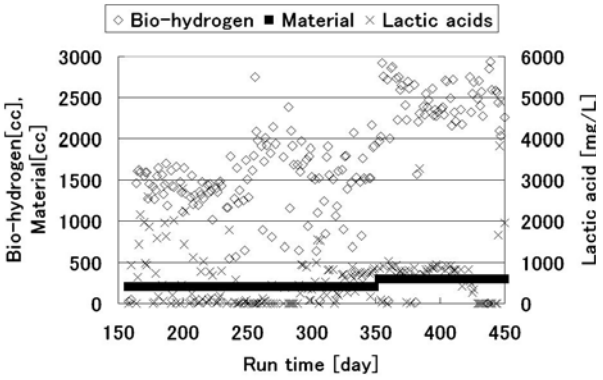

Fig.3 Generated bio-hydrogen

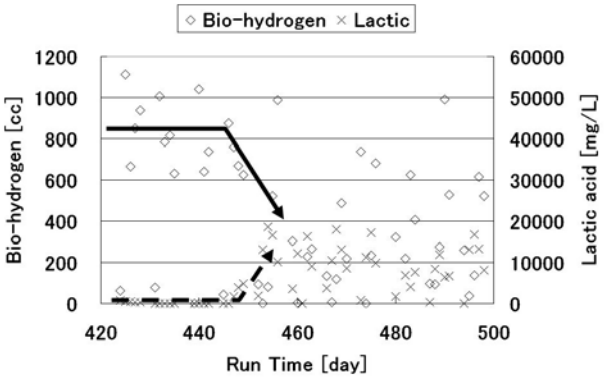

Fig.4 Increased lactic acid

Figure 7 shows the time variations of COD and VFA in the residue of H_2 fermentation. The residue of H_2 fermentation was a good substrate for methane fermentation since the residue contained much organic acids and the density of COD is suitable. The residue feeded into CH_4 fermenter generated biogas including CH_4 of 60%. The energy recovery efficiency from biomass to bio-H_2 and bio-CH_4 is shown in Fig.6. The efficiency is the average value in one month. The efficiency was nearly 80 %, which was almost all derived from the generation of bio-methane. In this experimental condition, feeding and pulling up was operated in the atmosphere, therefore it is severe circumstances for anaerobic bacteria.

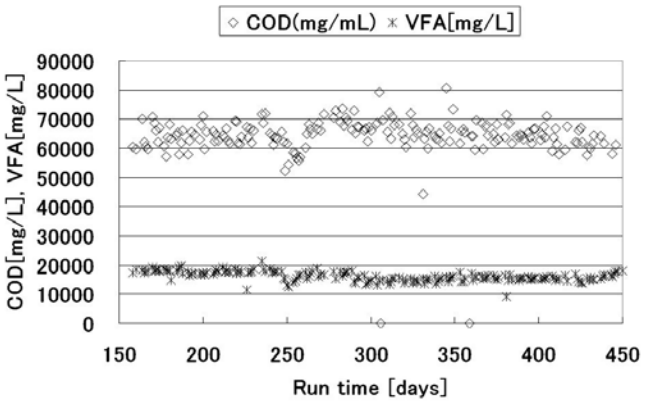

Fig. 5 COD-VFA in the residue of H_2 fermen.

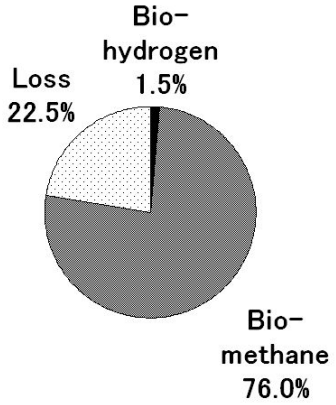

Fig. 6 Energy recovery in the laboratory

3.2. Pilot plant test

H_2-CH_4 fermentation was carried out in the pilot plant. Figure 7 shows the time variation of the generated bio-hydrogen. Stable operation continued over 150 days though the material injection was sometimes stopped. Kitchen wastes from the canteen were used in the pilot plant. Therefore feedstock was involved large amount of organic acids. Measured Lactic acid was about 1000 - 5000 mg/L in materials and 2000 – 8000 mg/L in the residue of H_2 fermentation. The lactic acid density in the pilot plant test was higher than that in the

laboratory test. The increased lactic acid affected H_2 fermentation in the pilot plant compared with the results of the laboratory test. The concentration of lactic acid over 10000 m g/L prevents the generation of bio-H_2. In the pilot plant, the density of lactic acid was scarcely kept under 10000 mg/L.

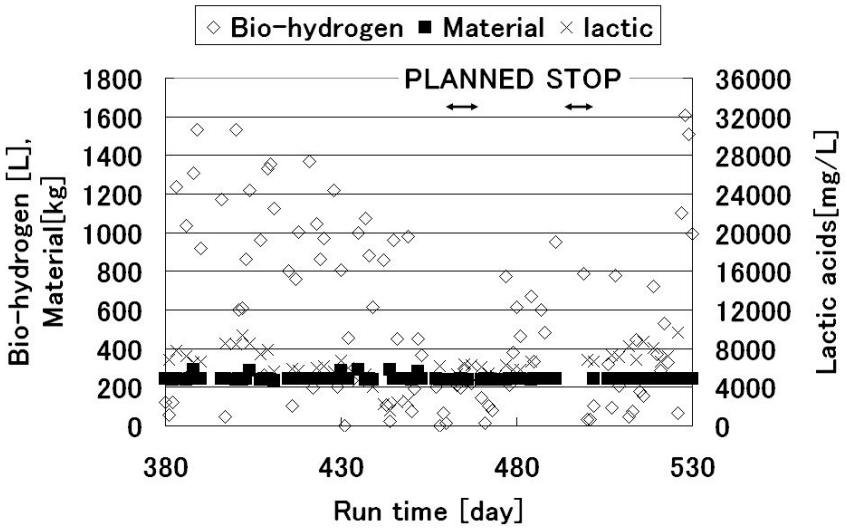

Fig. 7 Bio-hydrogen in the pilot plant

The residue of H_2 fermentation was sent into the CH_4 fermenter. The amount of bio-methane is indicated in Fig.8. Bio-CH_4 was stably produced during the operation period.

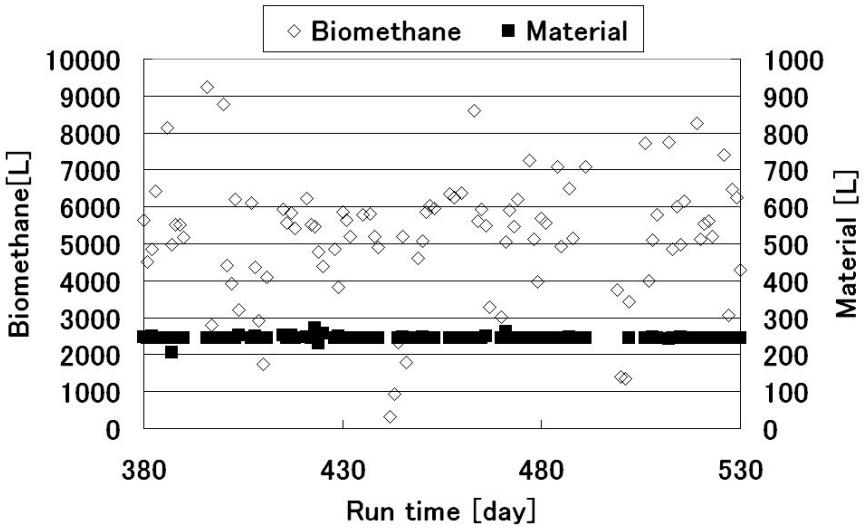

Fig. 8 Bio-methane in the pilot plant

Figure 9 shows the progress of energy recovery from materials in this pilot plant test. Almost all converted energy was the bio-methane as well as the laboratory test. The energy recovery efficiency was kept about 80 % during the operated period. I In the same plant, another test was carried out, in which the oxidization was pretreated instead of the H_2 fermentation. Figure 10 compares the recovery efficiency when the different pretreatment was conducted. Though the real kitchen wastes included lactic acid concentration and had contamination, the equal energy recovery was achieved.

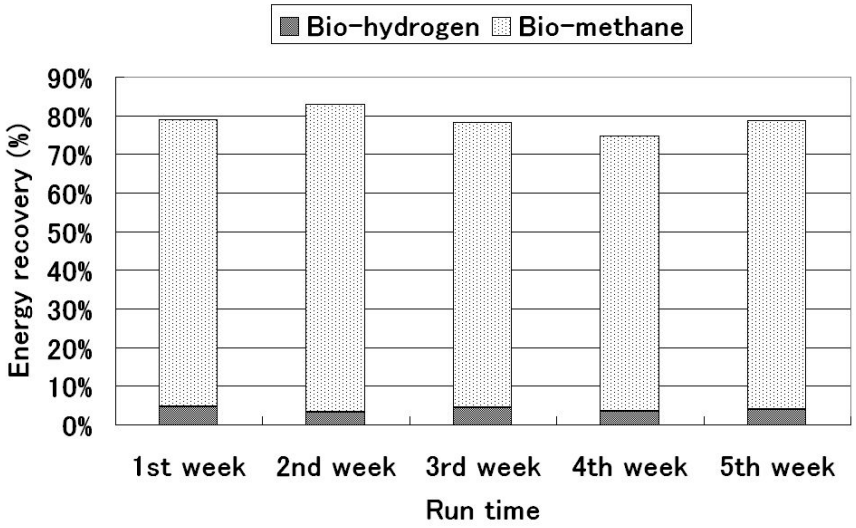

Fig. 9 Energy recovery

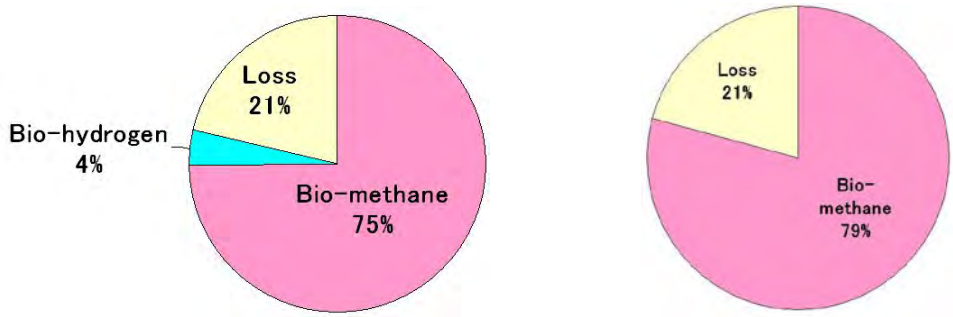

Fig. 10 Comparison of recovery efficiency
(Left: H2-CH4 fermentation, Right: Acidizing – CH4 fermentation)

4. Conclusions

OF-1 is determined to generate H_2 in the environment which is high temperature and acidic. The stable operation in the H_2 – CH_4 fermentation system was developed. Though metabolites generated by H_2 fermentation harm the H_2 generation bacteria itself, the running was stably kept due to high temperature operation and shortened HRT. The operation was stably conducted in 300 days in the laboratory and 150 days in the pilot plant. The residue of H_2 fermentation was found to be good substrates for CH4 fermentation. The energy recovery efficiency in H_2 – CH_4 fermentation was about 80 %. The efficiency value was equivalent to that of the acidizing – CH_4 fermentation.
Future plan is aimed for increasing bio-H_2 from the biomass consisted of cellulose. OF-1 includes cellulose decomposition bacteria. We will consider the possibility of disposing kitchen wastes with the biomass consisted of cellulose.

Acknowledgement

This research depends on the collaborative investigation with Toho Gas Co., LTD, and Mie University. I thank the concerned members.

References

[1] F.R.Hawkes, et al., "Continuous Fermentation Hydrogen Production from a Wheat Starch Co-Product by Mixed Microflora", B iotechnology and Bioengineering vol.84 No.6 (2003)619-626

[2] Y.J.Lee, et al., "Effect of Iron Concentration on Hydrogen Fermentation", Bioresource Technology 80 (2001) 227-231

[3] Van Niel et al.,"Distinctive properties of Hugh producing extreme thermophiles Caldicellulosiruptor Saccharolyticus and Thermotoga elfii", International Journal of Hydrogen Energy 27(11-12) (2002) 1391-1398

[4] Van Niel et al., "Substrate and product inhabitation of hydrogen production by the thermophile, Caldicellulosiruptor *sacharolyticus*"in; Biotechnology and Bioengineering 81(3) (2003) 255-262

An environmental assessment of the production of biodiesel from waste oil : two case studies

Marcelle C McManus[1,*]

[1] *University of Bath, UK.*
** Corresponding author. Tel: +44 1225 383877, E-mail:M.McManus@bath.ac.uk*

Abstract: The UK transport sector is currently responsible for 30% of UK CO_2 emissions. Therefore, the use of biofuels is explored. As the CO_2 released when energy is generated from biomass is generally balanced by that absorbed during the fuel's production it is often regarded as a 'carbon neutral' process. However, there are impacts associated with bioenergy production, including, for example, the growth and transportation of feedstock. One way to overcome these is to use a waste oil feedstock. Whilst there will not be enough waste oil to meet all our fuel demands, some firms in the UK have started to use their waste catering oil for transport. Collection and conversion is often done on a small scale and a number of methods are used for the processes. Therefore, the associated environmental impacts are variable. The environmental impact of the production and use of biodiesel from waste oil based on two case studies has been assessed. The impacts associated with the use of fossil fuels and climate change gas production is lower than that of the production of conventional fossil fuel diesel. The biggest impact within the process is associated with the use of methanol and the waste oil collection.

Keywords: *Biofuels, environmental life cycle assessment, waste oil.*

1. Introduction

Climate change and energy security have become major concerns in recent times and many countries have agreed, under the Kyoto Protocol, to reduce emissions of greenhouse gases. One of the ways in which this is being done is through the pursuit of bio-energy. As the carbon dioxide (CO2) released when energy is generated from biomass is generally balanced by that absorbed during the fuel's production it is often regarded as a 'carbon neutral' process [1]. However, there are impacts associated with various stages of bio-energy production, including, for example, the boiler production and transportation of feedstock.

Bio-energy is unique amongst renewable energy in that it is not immediately dependant on the weather (unlike, for example, wind and solar). However, it is also unusual in that it requires a feedstock of often bulky materials which can limit its capacity and the geographical extent of its supply chain [2]. The production of this feedstock can also be associated with environmental consequences, with some citing rising food prices and land use conflict as an unwelcome side effect of its use. This is due to the land required to grow specialist biomass crops such as miscanthus or oilseed crops. One way to overcome the issues associated with "land squeeze" is to use waste oil to produce bio-fuels. This study examines two such systems. Both use waste oil to produce bio-diesel. One system works on a fairly small scale, and the other on a larger scale. Life Cycle Assessments (LCA) of the systems have been undertaken in order to examine their environmental costs and benefits.

LCA is an environmental management tool which examines the environmental burden of a product or system over its entire life, from production, through use and on to disposal or recycling. The energy and materials used, pollutants or wastes released into the environment as a consequence of a product or activity are quantified over the whole-life cycle from "cradle-to-grave". Two case studies were selected and a truncated LCA was undertaken. Data for the collection of the waste oil and its conversion into biodiesel were determined and analysed. Impacts associated with the previous life of the oil were not considered; nor were impacts associated with the biodiesel's use in vehicles after conversion. These data are then

examined with regard to a number of environmental impacts. The embodied energy and greenhouse gas emissions are calculated for both systems and are compared with the production of biodiesel from virgin rapeseed oil and the energy output when used.

2. Methodology

The methodology of LCA has been standardised via Society of Environmental Toxicology and Chemistry (SETAC) guidelines subsequently codified in ISO Standards [3&4]. There are four main stages in the LCA process: Goal Definition, Inventory, Impact Assessment and Improvement Assessment and Interpretation. These are described below;

- **Goal definition** is the stage in which the scope of the project is outlined. Here the study boundaries are established and the environmental issues that will be considered are identified.
- The **inventory** is where the bulk of the data collection is performed. This can be done via literature searches, practical data gathering or through the use of software. Most commonly, a combination of the three is adopted.
- **Impact assessment** is where the actual effects on the chosen environmental issues are assessed. This stage is further subdivided into three (or four) elements: classification, characterisation, (normalisation) and valuation.
    - **Classification** is where the data in the inventory are assigned to the environmental impact categories. In each class there will be several different emission types, all of which will have differing effects in terms of the impact category in question.
    - A **characterisation** step is therefore undertaken to enable these emissions to be directly compared and added together. This step yields a list of environmental impact categories to which a single number can be allocated.
    - These impact categories are very difficult to compare in terms of relative impact and so the **valuation** step is employed so that their relative contributions can be weighted. This is subjective and difficult to undertake and many studies omit this step from their assessment. The LCA ISO standards state that it should not be used in any comparative or decision making study.
        - Instead of, or as well as, **valuation** many people employ **normalisation** as an intermediate step. Normalisation allows a degree of comparison between data types by determining the relative contribution of the calculated damage to the total damage caused by a reference system. Within this research the LCA impact assessment method, EI99 was used. It is a damage-oriented method, which considers, by means of damage factors, the effects of the emitted or used substances in three damage categories: human health, ecosystem quality, and resources (both fossil and mineral). Within this report the data have been normalised with respect to the average emissions or damage within Europe. In order to give a more comprehendible number this is then divided by the amount of people within Europe. Because the normalisation step compares the emissions or damage generated by a particular system with those generated at a European or global level the result of a normalisation step are dimensionless. Within this paper the normalisation method proposed and used in the methodology Eco-Indicator 99 has been followed [5]
- **Improvement assessment** is the final phase of an LCA in which areas for potential improvement are identified and implemented.

LCA requires all the energy inputs, raw materials inputs, emissions to air, soil and water, and waste to be examined at every stage of the life of the product or system. It is a simple, elegant idea, but it can become convoluted in practice [6].

3. The Case Studies

Two case studies have been examined and produced; these have both followed on from previously funded research [7&8]. Details about the composition, use and performance of the systems, together with information about feedstock sourcing, were obtained from the case study companies. This was done through a combination of visits, emails, phone conversations and augmentation of the data gathered from the previous case studies [8].

Data for the production of the materials used to produce the systems were calculated using generic life cycle inventory data. Where possible the EcoInvent database [9] was used. Where data required some geographical amendments (for example, changing to the UK electricity mix) this was done. Some estimation was made in the material composition of the systems, but generally there was detailed information about their size, weights, and composition. In general it was assumed that virgin materials, for example steel and rubber, were used in the production of the systems. However, where specific alternative information was available, for example the large tanks in the case studies had been reclaimed and were being reused, this was modelled accordingly and not all of the environmental impacts associated with the production of these units were allocated to this life cycle.

The first case study is based on a small company based in the south west of England, UK. Used cooking oil is collected from pubs, hotels, restaurants and schools in the local area; some is also delivered by customers who purchase their biodiesel. Where collected, a flat bed truck which runs on their own product is used. They make 220,000 litres per year, using a system that they have built and designed themselves. The company sells the biodiesel on site.

The second case study is a larger business with the capacity to produce 1,000 litres per hour, utilising automated control systems as far as possible. The processing site is also in the south west of England, UK, and the system was purchased from a UK manufacturer. The company purchases their oil from national oil collectors. The oil is delivered in 30,000 litre loads and is brought in by the company's own oil tanker which collects the oil from the collectors. After the biodiesel has been produced, the tanker is used to haul the biodiesel out of the plant, which means that the tanker avoids empty journeys. The tanker runs on 100% biodiesel. Much of the biodiesel is sold to haulage companies; some is sold on site to local customers. The company produces approximately 3 million litres a year. The processes followed for both case studies are shown in Figure 1.

4. Results

4.1. System Production

Within both case studies, much of the equipment has been hand made or assembled and so, whilst these case studies are a good example of local businesses, the results from this may not be indicative as an average of the whole industry. Some parts of the equipment have been re-used, for example the large holding tank was originally an old printers' ink tank. It is possible that this is due to cost, but also that those involved with making a product such as biodiesel are interested in the re-use of products for their environmental benefits. Therefore, whilst the re-use of materials does in some way make each system unique; it is possible that many companies will use re-cycled and re-used materials.

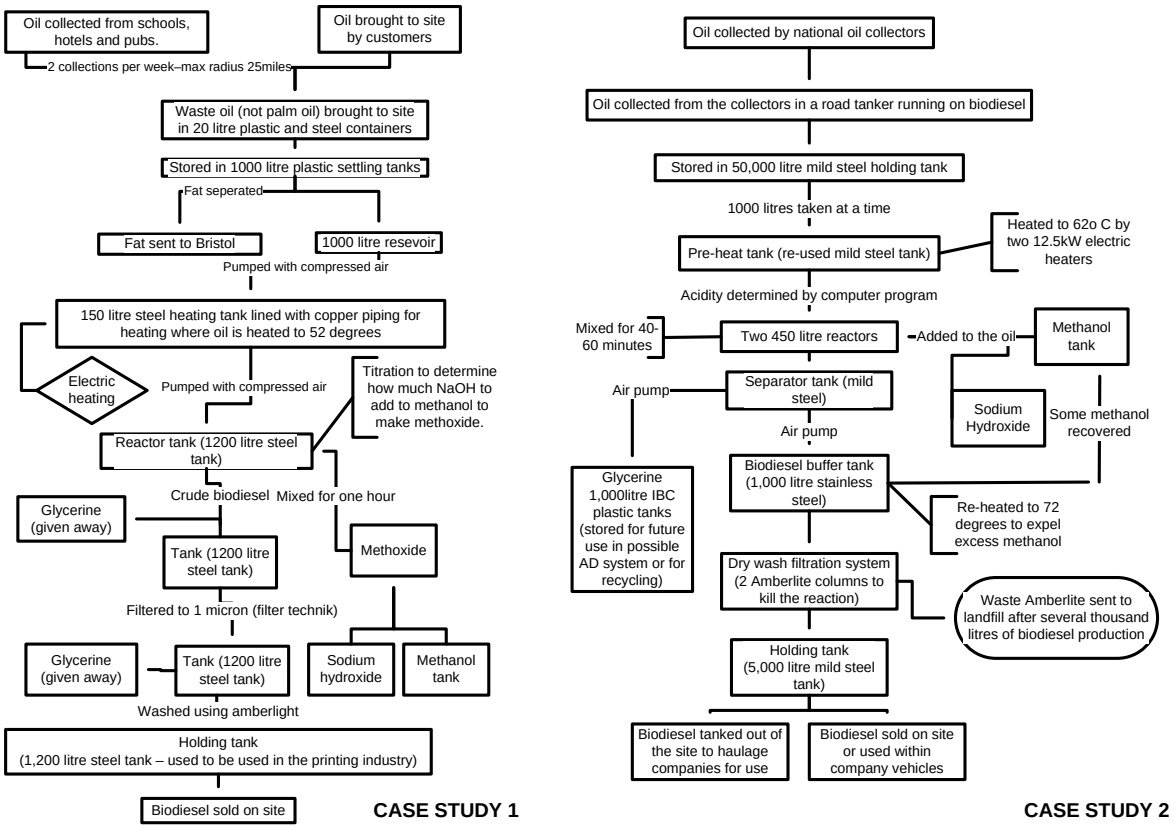

Figure 1. Waste oil collection and biodiesel production processes.

A fair way to determine the allocation of environmental burden to a re-used product is difficult. If a product is used once then all of the burdens must be attributed to that one use. If it is certain that the product will be recycled then any benefit associated with the recycling, eg any reduction in the amount of virgin material used, can be attributed to the product during the recycling stage. However, where there is no knowledge of the full life cycle of a product, for example, how many times it will be used and for what period of time, it is more difficult to attribute environmental burdens to its different life cycle stages. However, it is known that many of the tanks used have been bought second hand and so have therefore had a previous life. This previous life should be allocated some of the burdens. It is not acceptable to attach none of the environmental burdens to the second use of the system, as there is clearly a good second hand market for these tanks. Therefore, it is proposed that half of the environmental impacts associated with the production of these re-used tanks are attributed to this system.

Figure 2 shows the normalised data for the production of both systems. This includes all the components within the system. In case study 1 there are in total six 1000 litre plastic tanks, one 150 litre steel tank, four 1,200 litre steel tanks, one 25,000 litre steel tank and one 100 litre plastic tank. The production of the larger tanks (unsurprisingly) has the biggest impact. Within the second case study the predominant impacts are shown to be attributed to fossil fuel use, mineral depletion and the production of respiratory inorganics (Figure 2). Similarly to the first case study these are due to the production of steel, which is one of the largest material components of the system. Note the differing scales on the y axis – whilst case study two system production has a larger production impact it is a larger system that can produce more fuel, therefore at this stage the figures should not be compared against each other in terms of scale, but they do show where differences in production impact occur.

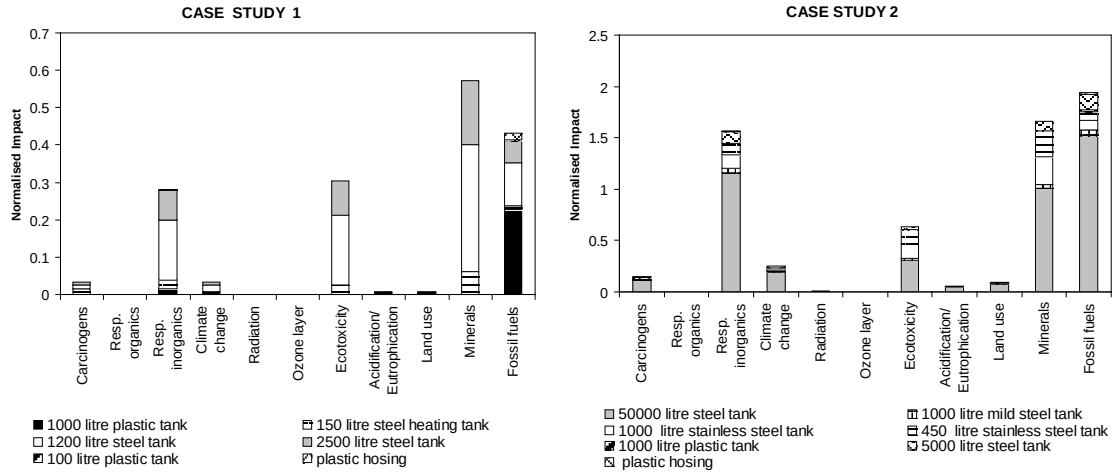

Figure 2. Normalised data for the production of the two systems; this shows the entire production systems and is not a comparison based on the final functional unit.

4.2. Production of the biodiesel

In order to determine the impact of the production of the fuel the production of the system, the use of electricity and any other consumables – such as the washing and filtering system and the collection of the oil etc, must also be examined. Specific data for the trade marked washing and filtering system used in case study 1 were not available and so this has been estimated using a generic ionic resin (of which the trade marked system is one). With used oil, there is a variation in the conversion rate from approximately 98% - 60% if the oil supplied is bad.

For the first case study, once the oil has been collected or delivered it is stored in an Intermediate Bulk Container (IBC) in the yard. From there it is pumped to a 150 litre heating tank in the building, where the oil is heated to 52ºC by electricity. It is then pumped to a reactor tank where a titration test determines the necessary quantities of methanol and sodium hydroxide needed to create a complete reaction process. The chemicals are mixed in a small methoxide tank and passed into the reactor tank. The reaction takes about one hour after which the liquid is pumped to a holding tank, which used to be a printers' ink tank. The glycerine settles to the bottom overnight and is then pumped to 150 litre tanks outside. The biodiesel then passes through a 1 micron filter to a further holding tank during which most of the particulates are removed. Further filtration then takes place via a resin filter system. The biodiesel is then stored in a final tank from which it is dispensed to customers through a metered pump. The glycerine made as a by-product of the process is given away (Figure 1).

In the second case study the oil delivered by the tanker is pumped into a 50,000 litre holding tank. From this, 1000 litres at a time are pumped into a pre-heat tank. This heats the oil to 62^{o}C using two 12.5kW electric heaters. To this is added methanol and methalate (the control systems automatically add the specified amounts) and the oil is then mixed for between forty and sixty minutes (Figure 1).

From the reactor tanks, the liquid is pumped into a separator tank where most of the glycerine falls to the bottom as the liquid flows continuously over flow plates. This means that there are no filters that need to be changed periodically in this stage of the process. The glycerine is pumped out of the bottom of the tank and currently is stored for possible future use in anaerobic digestion systems or other forms of recycling. This potential use has not been modeled here, as it held no commercial value to the companies. The biodiesel still contains

some methanol and glycerine, and the next stage involves heating the liquid to 72°C in a buffer tank. The methanol evaporates at 68°C and by then re-condensing the vapour in the exhaust pipe, some of the methanol is captured and then re-cycled.

Glycerine causes problems if it is found within biodiesel and the reaction can continue after this stage, so in order to stop the reaction the liquid is then pumped through a washing and filtration process. The filters are the same as in the first case study and contain a polymeric resin that absorbs sodium and fats and attracts glycerol to the outside of the polymer beads. The system can filter 14 litres per minute and the columns can process 300,000 litres of biodiesel before they need to be emptied. The waste is inert and is sent to landfill.

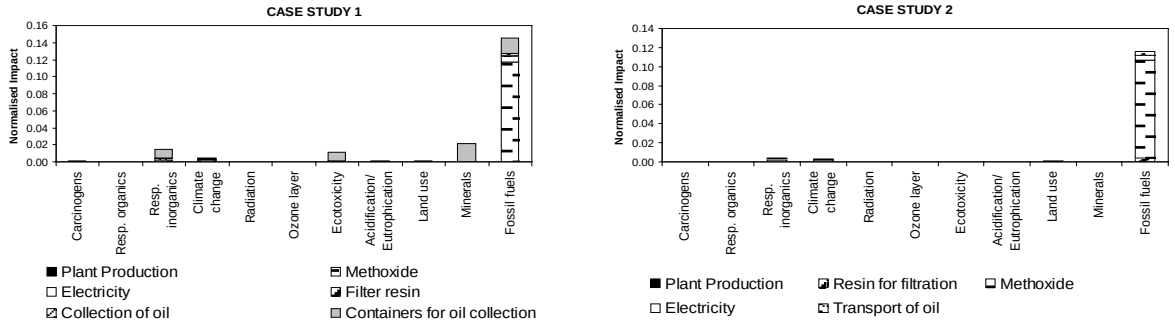

Figure 3. Normalised data for the production of 1000 litres of biodiesel using the two systems

Figure 3 shows the normalised data for the production of 1000 litres of biodiesel. Both plants are assumed to have a working life of ten years. In both cases the use of fossil fuels is the largest impact; predominantly associated with the production of methoxide, this finding is consistent with other publications in this area, for example Morais et al [10]. This is because methanol is made from either natural or coal gas. Methanol can be produced from a number of sources, and so it might be possible to reduce the impact of the methoxide by purchasing methanol that has not been made from fossil fuels. Another option would be to recover some of the methanol. This is done in case study 2; resulting in a slightly lower impact (see again the differing values on the y axis). Within case study 1 the use of the small steel and plastic collection containers also has a visible impact. These containers have been re-used, and so only half of their production impact has been allocated to them. The remaining impact is considered to be attributable to their first life.

4.3. Disposal of the Systems

No disposal options have been modelled for the plants as it is not possible to determine how they will be disposed of at this time. If the plant were to be recycled and any benefits were associated with this at the end of its life, the impact of the plant production would be reduced. However, as the plant production has a relatively small impact in the life cycle impacts, this would not have as significant effect as any change in the production methods of the methanol or a change in the collection system.

4.4. Energy and Green House Gas Emissions Analysis

There is little point producing biodiesel if it uses more energy in its production that it can produce when it is in use. Therefore the embodied energy of the biodiesel has been calculated. This has been calculated using the same processes and boundaries shown in the previous parts of the paper and includes the energy required to produce the systems, collect the waste oil and process it into biodiesel. In order to produce one litre of biodiesel with the first case study process approximately 11 MJ of energy are required, and for the second case study the figure is slightly lower at 8MJ. The difference between the two systems is predominantly due to the

different scales of the systems and the way in which the oil is collected. By comparison, the energy content of diesel is approximately 38MJ/litre and the energy content of biodiesel is approximately 37MJ/litre [1]. Published ranges of embodied energy of bio-diesel from rapeseed varies; but is approximately 15MJ/L [11] to 30MJ/L [1&6]. Therefore, the production of the biodiesel from waste oil requires significantly less energy than that from rapeseed, and also provides much more energy than it requires in its production.

The total greenhouse gas emissions (GHG) have been calculated for both systems using IPCC 100 year time horizon data. The production of one litre of biodiesel generates 343g and 228g CO_{2eq} from case studies one and two respectively. Much of the GHG result from the use of the methanol and also from the collection of waste oil process. Compared to published literature these results are high. Alternatives suggest values from 87g/litre [12] to 343g/litre [11]. The differences primarily occur due to differing boundaries and allocation procedures. For example, in many cases the glycerine is used, therefore some of the burden can be and is attributed to that. As the glycerine was not used in either of these cases no burden was allocated to it. Also, the boundaries selected here do not attribute any impact to the initial production of the oil before it becomes waste. However, there are also differences that can be attributed to the producers examined; larger, more commercial producers may produce biodiesel more efficiently.

5. Discussion and Concluding Remarks

A significant impact in both of the biodiesel production systems is the use of methanol. This is due to the methanol production process which uses natural gas or coal gas. An alternative method for its production is through the gasification of a range of renewable biomass materials, such as wood and black liquor from pulp and paper mills. However, this is not as common as its production from fossil fuels. One way in which both companies could reduce their impact would be to source methanol produced from these more renewable sources.

Both systems use materials and parts that have been used before. This brings some interesting issues associated with how the burdens should be divided between the product's current use and any previous or future uses. Within any life cycle system, if an individual component is to be used two or three times then each use would be allocated half or a third of its environmental burden. However, these products have been used in completely different situations and how the burden is allocated for this is more difficult. It is unrealistic to say that the second use should have all of the burdens, as it has already fulfilled one function elsewhere. However, the second use cannot be ignored and be said to have no burden as the product clearly has a market value and therefore has been sold. It is not known whether the product has had one or two previous lives, or if it will be further used after being used in these systems. Therefore, the burden has been divided by two in order to simulate two lives for these products. As the impact of these products is small during the life time of the system, this is not a significant issue.

However, this does raise inconsistencies with the way in which the oil has been treated and modeled. Within this system the oil used has been treated as a waste. That means that no environmental burdens have been allocated to it for its production or transport to the place of its original use. Within this study the boundaries have been set at the point where the oil becomes no longer useful to its owner and is collected by the waste carrier. Often this oil is free of monetary cost to the collector, who then adds value to it by collecting it and delivering it in bulk to a second user. Previously much of this oil would have found itself as waste. Sometimes energy might have been recovered from it, sometimes not. As a waste product, it is acceptable to decide that all the production impacts are associated with the first use.

However, if this becomes a commercial product, is this method still acceptable? At this point within an LCA these issues become more philosophical than scientific. The impacts still happen, so one is only then deciding to whom or what the impact is attributed. The allocation of such burdens is an area of ongoing research within the life cycle community.

In order to improve the two systems in question less methanol use, or methanol produced from renewable sources, would improve the environmental performance of the biodiesel. In addition, a more efficient collection system would improve the process. For any further studies using the data produced, the issues associated with the system boundaries and environmental burden allocation must be noted.

Acknowledgements
This research was funded by Knowledge West and is an extension of the KW project report. Great Western Research funded the author during this research period, and her current bioenergy research is funded through the UK BBSRC Sustainable Bioenergy Centre [Grant Ref: BB/G01616X/1]. The author would specifically like to thank the Royal Agricultural College for their help and time during this research and the collaborating companies.

References

[1] G.P Hammond, S. Kallu, & M.C. McManus. Development of biofuels for the UK automotive market, Applied Energy. 2008 Vol 85, Issue 6, pp 506-515.

[2] P Upham, & D Speakman,. Stakeholder opinion on constrained 2030 bioenergy - scenarios for North West England. Energy Policy. 2007. Vol 35, Issue 11, pp 5549-5561

[3] International Organisation for Standardisation [a]. Environmental Management – life cycle assessment – principles and framework, 2nd edn, ISO, Geneva, 2006. ISO 14040.

[4] International Organisation for Standardisation [b]. Environmental Management – life cycle assessment – requirements and guidelines, 2nd edn, ISO, Geneva, 2006. ISO 14044.

[5] M Goedkoop & R SpriensmaThe EcoIndicator 99. A Damage Orientated Method for Life Cycle Impact Assessment. Methodology Report.. 2001 Available from http://www.pre.nl/download/EI99_methodology_v3.pdf

[6] M.C M^{c}Manus, G.P. Hammond and C.R Burrows. Life-Cycle Assessment of Mineral and Rapeseed Oil in Mobile Hydraulic Systems. 2004 Journal of Industrial Ecology. Vol 7. 3-4. pp 163-177.

[7] M.C. McManus. LCA of Biofuels – Two South West Case Studies. 2009. Accessed from: http://www.knowledgewest.org.uk/news/?id=96 (December 9th 2010)

[8] D Lewis. South West Region Biomass and Biofuels Review. 2007. Accessed from: http://www.knowledgewest.org.uk/news/index.asp?id=43 (December 9th 2010)

[9] EcoInvent Life Cycle Inventory Database. http://www.ecoinvent.ch/

[10] S Morais, T.M Mata, A.A Martins, G.A Pinto. & C.A.V Costa. Simulation and life cycle assessement of process design alternatives for biodiesel production from waste vegetable oils. Journal of Cleaner Production. 2010 Vol 18. pp 1251 – 1259.

[11] MA Elsayed, R Matthews, N Mortimer, Carbon and energy balances for a range of biofuels options. 2003 Study for DTI URN 03/836

[12] S Pleanjai, H.G Shabbir & S Garivait Greenhouse gas emissions from production and use of used cooking oil methyl ester as transport fuel in Thailand. Journal of Cleaner Production. 2009. Vol 17 pp 873- 876.

Feasibility of Jatropha oil for biodiesel: Economic Analysis

Ofori-Boateng Cynthia*, Lee Keat Teong

School of Chemical Engineering, Universiti Sains Malaysia, 14300 Nibong Tebal, Pulau Pinang, Malaysia
**Corresponding Author: Tel: +60164302025, E-mail:* cyndykote@yahoo.com

Abstract: *Jatropha curcas L.* (also called the physic nut) is found to be a potential alternative source of renewable energy since its cultivation and oil extraction contribute to sustainable development, poverty alleviation, combating of desertification and women empowerment in developing countries. The jatropha seeds after three years of cultivation have an oil yield between 1-4 tonnes and 2.5-12 tonnes per hectare when rain fed and irrigated respectively. The Operational and maintenance costs for the oil extraction are minimal, and can be estimated at approximately 10 – 15% of the capital cost per year. In Ghana, for instance, in 2010, whilst the cost of jatropha oil and kerosene were estimated to be US$0.085/liter and US$1.23/liter respectively, the cost of biodiesel from jatropha oil and petroleum diesel were also estimated at US$0.99/liter and US$1.21/liter respectively. This indication gives jatropha oil the best 'candidate' for 'green kerosene' and biodiesel in diesel engines and particularly in multi-functional platforms (MFPs) used agro-processing/industrial applications in rural areas of Ghana. This paper presents a comparative technical feasibility of jatropha oil as fuel and biodiesel in MFPs. It also presents the findings from a study carried out in Ghana with respect to the promotion of jatropha oil as a fuel in rural areas of Ghana.

Keywords*: Jatropha, Crude oil, Renewable energy, Biodiesel*

1. Introduction

Jatropha curcas L. has various socio-economic benefits which makes it more economical when cultivated on commercial scale. A hectare of jatropha plantation is reported to yield 2.5-3.5tonnes of seeds in the third year and increases sharply to 5000-12,000 tonnes per hectare from the sixth year onwards [1]. Like other vegetable oils, jatropha oil can be used directly in modified diesel engines for automobile applications in Europe, North America and some other parts of the world. It is however found from researches that the neat jatropha oil can be used to run the engines in mini-vans for rural transportation, haulage trucks, farm tractors and other agricultural machinery, but may require little modification [10]. According to Achten et al., 2008, at full output, hydrocarbon emission level using neat jatropha oil was observed to be 532ppm against 798ppm for fossil diesel, NO level was 1163ppm against 1760ppm and smoke was reduced to 2.0 Btu against 2.7 Btu [2]. In the northern part of Ghana, women engaged in shea butter production, use jatropha oil in place of diesel the MFPs comprising shea butter press, dehuller and the mill. Since it's quite cheaper to use jatropha oil in these MFPs, commercial cultivation of jatropha and subsequent extraction of the oil for such purposes are done in the rural northern Ghana to empower women in the area of job creation. To enhance and improve the viscosity of jatropha oil, this study assesses the feasibility of the oil for biodiesel instead based on the Ghanaian production conditions. In the rural areas where jatropha plantation and extraction are done, the drying of the seeds are done by spreading the fruit on the ground or a dark-coloured mesh net to dry in the sun. Solar and forced air dryers offer faster drying capabilities. According to research performed at the Kwame Nkrumah University of Science and Technology (KNUST) in Ghana, a fabricated 500 kg tent dryer suitable for small scale applications [3] was about US$2000 but may be costly for rural folks. This research work considered drying in the sun to minimize cost. From the roots to the seeds of the plant are numerous uses which solve some of the socio-economic problems of most people in the rural sectors of the world. The oil extracted from jatropha can be used as a substitute for kerosene without any further processing. This is more economical compared to kerosene from crude oil, which are used for rural electrification. Moreover, the raw oil is used

by most rural folks for soap making which ease them of most economic problems. Jatropha farming is labour intensive thus providing job for many people in the rural areas. This paper assesses the potential of local production of biodiesel in remote areas of Ghana where jatropha plantation is done in commercial scales and used for other purposes other than biodiesel production. Since every economy is driven by the quantum of energy produced, utilized and destroyed in a particular section of the economy, the sustainability of energy systems needs to be analysed critically to allow room for improvements, process and material optimization.

Sustainability of any industrial process design comprises three main parts namely social, economic and environmental aspects. The economic indicator is based on the costs of purchasing material and energy, employing labourers, and other product prices [4] [12]. This paper focuses on the economic feasibility of biodiesel production from *Jatropha curcas L.* considering the processes from jatropha farming, through oil extraction to biodiesel production. Each unit process contains different inputs and outputs of which some have more than one alternative. Each alternative carry different values in terms of costs and to make a more proper renewability analysis in terms of economy, each production unit needs to be quantified accordingly. The economic analysis is done to compare the various alternatives for getting the final product, biodiesel. This paper assesses the cost benefits of biodiesel produced from *Jatropha curcas* considering all the processes from jatropha farming to biodiesel purification, and present the results in monetary units. Data in this research were obtained from literature [5] [9] and situations in Ghana as well as some parts of the world where jatropha is grown on commercial scale. The economic analysis of any project can only be done based on the estimates from the investments required and the cash flows. The actual cash flows achieved in any year will be affected by any changes in raw material costs and other operating costs, which may also dependent on the sales volume and price of the products [6] [13].

2. Methodology

The traditional method of producing jatropha biodiesel in the northern parts of Ghana were analysed and compared to those employed in modern technologies worldwide. In this work, the criteria used to determine the economic viability of jatropha oil for biodiesel production include the total capital cost, the total production cost, profitability and sensitivity assessments. There are currently no tax credits or subsidies for renewable energy production in Ghana and so no consideration of it in this work.

2.1 Total capital investment

This is the amount of money that must be supplied or required to finance the purchasing of equipments as well as its auxiliary parts, spare parts, construction of the plant and the acquisition of items necessary for plant operation. The total capital investment comprises the fixed capital, i.e. investment needed to supply all production facilities as well as supply of construction overheads and plant components that are directly or indirectly related the biodiesel process from jatropha; and the working capital, i.e. the amount of money needed to start the project. This is normally estimated as 0.15times the Fixed Capital Investment [6]. Total capital cost may include costs of land, equipment and installations, building and construction costs.

2.1 Total production Investment

The total production investment involves the cost needed to run the project including marketing of the product. This generally consists of the variable cost, fixed costs and general expenses. Variable cost consists of direct and indirect costs. Generally, variable cost may include costs of raw materials, utilities, miscellaneous materials, shipping and packaging which are negligible in this work because the biodiesel processor is fabricated locally in Ghana. Fixed costs also include the cost of maintenance, operating labour, supervision, plant overheads, capital charges, Insurance rates and Royalties [6]. General expenses are made up of administrative costs, engineering and legal costs, office maintenance and communications, distribution and selling cost [7].

2.3 Profitability analysis

The methods used in estimating the profitability of the project are Rate of Return on Investment (ROR), pay back period, break even point, discounted Cash Flow Rate of Return (DCCFRR) and the net present/future value [5].

2.4 Sensitivity Assessment

Sensitivity analysis is a way of examining the effects of uncertainties in the forecast on the viability of a project. This is achieved by the most probable values for various factors which establish the base case for the analysis. The cash flows and criteria of performance used are calculated assuming a range of error for each of the factors in turn [6].

2.5 Process Description and Assumptions

Fig. 1 shows the system boundary for the jatropha cultivation, oil extraction and biodiesel production.

2.5.1 Jatropha curcas farming

A case study of Jatropha curcas cultivation in Gbimsi, a village located in the northern part of Ghana was used. Organic fertilizer used for the cultivation is assumed to be produced from the seed cake through composting [8], in which the energy input is considered negligible. Labour work was assumed to replace diesel fuel consumed by the machines used in cultivation, i.e. one labour hour is approximately equivalent to 0.8 liters diesel [6]. Many researchers have argued that jatropha plant can succeed without irrigation and therefore does not compete for water or displace food production from prime agricultural land [14]. However, Ariza-Montobbio et al. reports that irrigation makes a big difference to yields, and even with irrigation the yields are so much lower than those reported from experimental plots [11]. For this study, on the other hand, irrigation of the jatropha plant was considered as done in Ghana. Harvesting of fruits starts from the 2nd year of plantation, where seed yield would have increased.

2.1.2 Jatropha oil extraction

Solvent (hexane) extraction, mechanical screw press and manual ram press are the most used methods but this work employed the mechanical screw press. The oil cake generated after oil extraction can be used as organic fertilizer for jatropha cultivation. For mechanical screw press extraction 77% oil content is obtained after extraction [6]. The screw press is locally fabricated.

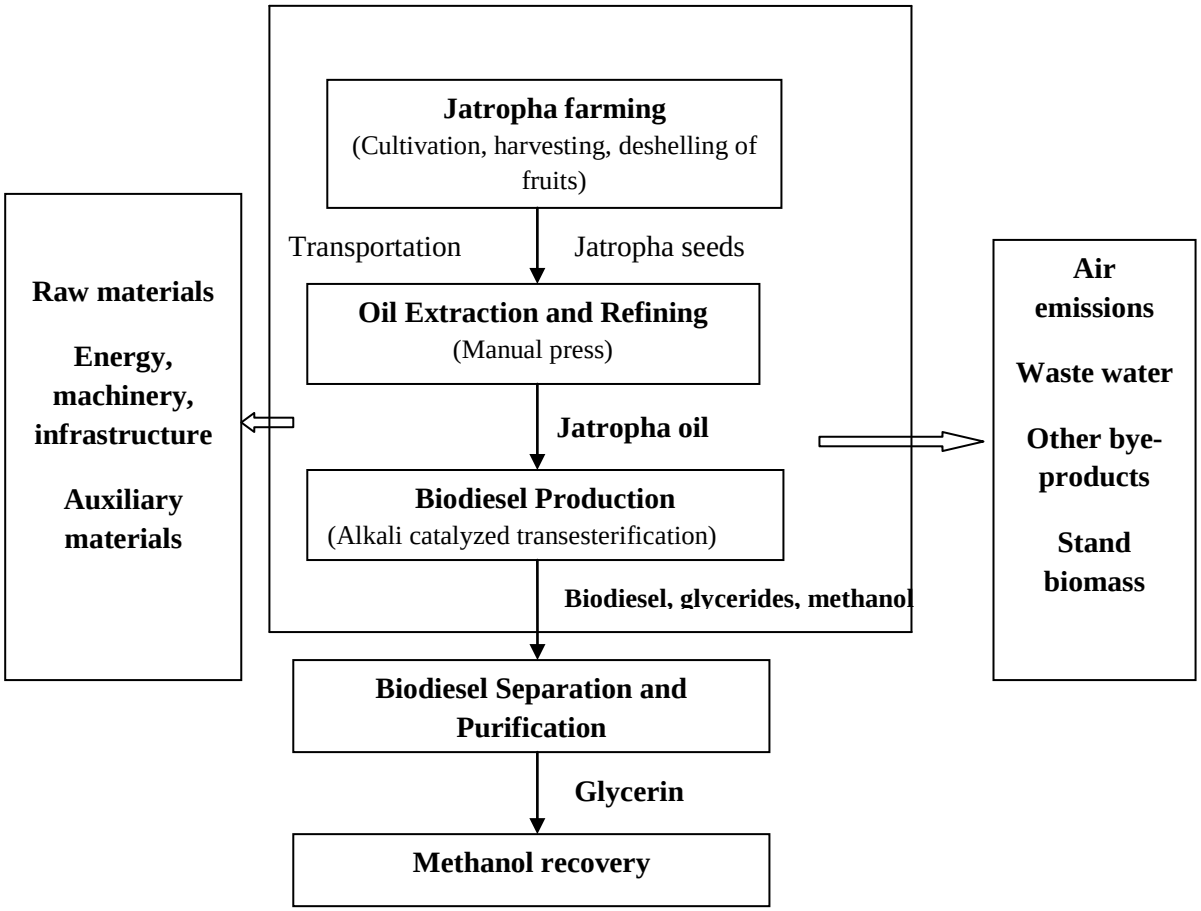

Fig. 1 Process flow diagram of biodiesel production from jatropha curcas L.

2.1.3 Jatropha biodiesel production

1 tonne of biodiesel output (apprx. 1136l) was chosen for the material balance. Alkali-catalyzed transesterification is used. All results were estimated under conditions in Ghana, and some data obtained from literature [9].

Three scenarios (Cases 1-3) were considered for jatropha oil cost at various economic conditions of Ghana, to obtain and estimated cost of the biodiesel as well as profit.

Case 1 shows present economic conditions of Ghana but estimated high cost of jatropha oil

Case 2 shows present economic conditions of Ghana but reduced cost of jatropha oil

Case 3 shows slightly reduced present economic state of Ghana yet reduced jatropha oil cost.

These three cases were chosen based on present and future cost of living in Ghana.

3. Results and Discussion

Assuming holidays and days for maintenance, the plant will work for 230 days/year

Table 1. Estimation of Fixed Capital Investment (FCI)

Item	Quantity	Estimated cost, US dollar
Land	0.67ha	496.7
Irrigation Pump	1 Hp	168
Mechanical Screw Press	1.5 tonne capacity	1000
Biodiesel Reactor	1.5 tonne capacity	11,944.41
Other land area for work	0.405ha	299
TOTAL		**13908.11**

Total Capital Investment (TCI) = FCI + Working Capital (WC) = **16362.48USD**
WC = 0.15TC

Table 2. Estimation of Total Production Cost (TPC)- Variable costs

Item	Quantity	Estimated cost, US dollar
Organic fertilizer	30kg	0
Pesticides	0	0
Cultivation Total Cost		**0**
Irrigation water	147680 l	147.68
Jatropha seeds	3.5 tonne	1750
Diesel	10.91 l	12.2
Extraction Total Cost		**1909.88**
Process water	3408 l	3.408
Methanol	227.5 l	49.98
Electricity	120kWh	14.4
Catalyst	0.082 tonne	82
Biodiesel production Total		**149.79**
TOTAL		**2059.67**

Table 3. Estimation of Total Production Cost (Fixed cost and General Expenses)

Item	Factor	Estimated cost, US dollar
Maintenance cost	0.05FCI	695.41
Operation labour	-	705.14
Administration	0.02TPC	41.19
Miscellaneous	0.1Maintenance	13.9
TOTAL		**1455.64**

Source: (Sinnot et al, 1985)

3.1 Profitability analysis

Based on the following assumptions and the estimates made in Tables 1 to 3, Table 4 was developed with the help of software for modeling the cost of an industrial plant.
Production capacity is 1136 litre for 8hour shift
The number of 8 hour shifts per day is 1
Yield of biodiesel is assumed to be 0.93

Table 4. Profitability Assessment Results of a Biodiesel Production Plant from Jatropha oil

Item	Unit	Estimated cost, US dollar excluding VAT		
		Case 1	**Case 2**	**Case 3**
Jatropha oil	per litre	2.5	0.18	0.18
Methanol	per litre	0.22	0.22	0.25
Labour cost	per week	76	76	350
Rent	per month	50	50	50
Insurance	per year	2500	2500	2500
Interest rate	percent	12	12	12
Biodiesel plant	per tonne	13849	13849	13849
Catalyst	per litre	0.006	0.006	0.006
Duty on biodiesel	per litre	0	0	0
VAT rate	percent	14	14	14
Water	per litre	0.001	0.001	0.002
Electricity	per kWh	0.120	0.120	0.120
Overheads costs	per year	4,762	4,762	4,762
Overheads costs	per litre biodiesel	0.018	0.018	0.018
Labour costs	per litre biodiesel	0.013	0.011	0.062
Water cost	per litre biodiesel	0.002	0.002	0.015
Electricity cost	per litre biodiesel	0.015	0.015	0.004
Estimated Biodiesel cost	per litre	2.779	0.383	0.339
PROFIT		**-89.42**	**803.03**	**409.91**

Source: Cash flow calculations from data collected for this work **[6] [15]**

Case 1 which also shows the conditions for maximum profits (almost at breakeven) resulted in a loss after the cash flow analysis. The loss per day is minimal recorded as -89.42 US Dollar. In this case, we assumed higher cost for jatropha oil at the present Ghana's economic status, and a higher biodiesel cost was estimated after cash flow calculations. For the second case where the cost of jatropha oil was similar compared to cost on the international market, maintaining minimal conditions, profit was observed at 803.03 US dollar per day. For case 3, profit was observed on extreme conditions i.e. the prices of jatropha oil maintained as that of the international market whilst biodiesel cost was kept low, yet there was a marginal profit of 409.91 US dollar per day. No scenario was created for harsh economic conditions because the three cases showed profitable and feasible results.

These results therefore show that the project which produces 1tonne of biodiesel per day is viable economically (except in case 1 where there was a loss) and if the plant's capacity is increased profit per day will also increase even when biodiesel price is kept as low as US$0.339. Jatropha plantation for biodiesel is worth a project considering the economic analysis with conditions and assumptions made in this report. In the northern part of Ghana where jatropha is grown on large scale, the oil after extraction is used mainly on multifunctional platforms where the oil is used purposes for fueling engines of machines which otherwise may be used manually. For instance in the northern part of Ghana, the oil is used to power the mechanical screw press instead of using diesel which is environmentally unfriendly when burnt.

Multifunctional platforms have been introduced in Ghana for such purposes to empower women especially. From the analysis, the cost of jatropha oil is much cheaper at

0.18USD/litre compared to that of biodiesel at 0.3-2.7USD/litre. It therefore presents a much more economical sense currently to use biodiesel oil from jatropha in diesel engines instead of using for producing biodiesel. However, it is still viable to go into biodiesel production using jatropha oil as detailed in the results of this work. Table 5 shows the comparison of prices between petroleum diesel, jatropha oil, gasoline and biodiesel from jatropha oil in Ghana from the year 2000 to 2010.

Table 5. Comparative prices of jatropha oil, kerosene and biodiesel in Ghana

Product	Estimated cost, US dollar/litre		
	2005	2008	2010
Jatropha oil	0.154	0.191	0.085
Kerosene ex-refinery	0.92	0.85	0.87
Kerosene ex-pump	0.83	0.77	1.23
Jatropha Biodiesel	1.54	1.02	0.99
Diesel ex-refinery	0.56	0.90	1.12
Diesel ex-pump	0.78	1.01	1.21

Source: Energy Commission, Ghana and TradingEconomics.com [16]

4. Conclusion and Recommendation

Biodiesel produced from jatropha oil is assessed to be feasible economically when the seeds are cultivated on large scale. In Ghana where jatropha plantation is done on commercial basis for multifunctional platforms in rural areas, jatropha oil is more economical to use compared to jatropha biodiesel. It is however viable to produce jatropha oil and further processing it when the oil is in large quantities. As reported by other studies in India, Mali etc, jatropha oil produced on commercial basis is less costly hence biodiesel production from this oil is feasible especially in MFPs which can keep the engines for a long time. Therefore, if 1tonne of biodiesel can be produced from jatropha at quite a minimal cost, then on commercial basis, when this quantity is normalized to a desired capacity, marginal profit will be reported after payback time of not more than three years. For better efficiency of diesel engines, biodiesel from jatropha is however preferred to raw jatropha oil especially in MFPs.

References

[1] R. K. Henning, Combating Desertification: The Jatropha project of Mali, West Africa, Arid Lands Newsletter, Fall/Winter 1996, Issue No. 40, pp. 1-5.

[2] W.M.J. Achten, L. Verchot, Y.J. Franken, E. Mathijs, V.P. Singh, R. Aerts, B. Muys, Jatropha Biodiesel Production and Use, Biomass and Bioenergy, Volume 32, Issue 12, 2008, pp. 1063-1084

[3] F.K. Forson, M.A.A. Nazha, F.O. Akuffo, H. Rajakaruna, Design of Mixed-mode Natural Convection Solar Crop Dryers: Application of Principles and Rules of Thumb, Renewable Energy, Volume 32, Issue 14, 2007, pp. 2306-2319

[4] L. Stephenson, J. S. Dennis and S. A. Scott, Improving the Sustainability of the Production of Biodiesel from oilseed rape in the UK, Process Safety and Environmental Protection 86, 2008, 427-440.

[5] W. M. J. Achten**,** L. Verchot, Y. J. Franken, E. Mathijs, V. P. Singh, Jatropha Bio-diesel Production and Use, Biomass & Bioenergy 32, 2008, pp. 1063-1084.

[6] R. K. Sinnot, An Introduction to Chemical Engineering Design, The Chemical Engineering Journal, Volume 33, Issue 2, 1986, pp. 116-117.

[7] M. S. Peters and K. D. Timmerhaus, Plant Design and Economics for Chemical Engineers, McGraw-Hill Book Company, 3rd Edition, 1981, pp. 143

[8] S. Ucar, and A. R. Ozkan, Characterization of products from the pyrolysis of rapeseed oil cake, Bioresource Technology 99, 2008, pp. 8771-8776

[9] G. Reinhardt, P. Ghosh, K. Becker, Basic data for Jatropha production and Use, Report 1, Hohenheim, 2008, pp. 8-9

[10] J. Sheehan**,** V. Camobreco, J. Duffield, M. Graboski, H. Shapouri, Life Cycle Inventory of Biodiesel and Petroleum Diesel for Use in an Urban Bus, Report, Midwest Research Institute, 1998, pp. 98 - 107

[11] P. Ariza-Montobbio, S. Lele, Jatropha Plantations for Biodiesel in Tamil Nadu, India: Viability, livelihood trade-offs and latent conflict, Ecological Economics, Volume 70, Issue 2, 2010, pp. 189-195

[12] M. Hasheminejad, M. Tabatabaei, Y. Mansourpanah, M. Khatami, A. Javani, Upstream and Downstream Strategies to Economize Biodiesel Production, Bioresource Technology, Volume 102, Issue 2, 2011, pp. 461-468

[13] K. Prueksakorn, S. H. Gheewala, P. Malakul, S. Bonnet, Energy Analysis of Jatropha Plantation Systems for Biodiesel Production in Thailand, Energy for Sustainable Development, Volume 14, Issue 1, 2010, pp. 1-5

[14] Y. Tomomatsu, B. Swallow, Jatropha curcas Biodiesel Production in Kenya: Economics and Potential Value Chain Development for Smallholder Farmers, Working Paper 54, World Agro forestry Centre, 2007, pp. 33

[15] http://www.vegetableoildiesel.co.uk/

[16] Strategic National Energy Plan 2005-2020, Integrated Resource Planning, Energy Commission, Ghana.

Novel Production Of Biofuels From Neem Oil

K.V.Radha[1,*], G.Manikandan[1]

[1] *Department of chemical Engineering, Anna University, Chennai, India*
** Corresponding author. Tel: +91 044 22359124, E-mail: radha@annauniv.edu*

Abstract: Biodiesel production is a valuable process which needs a continued study and optimization process because of its environmentally advantageous attributes and its renewable nature. In India Neem tree is a widely grown crop, termed as Divine Tree due to its wide relevance in many areas of study. The present study is intended to consider aspects related to the feasibility of the production of biodiesel from neem oil. This report deals with biodiesel obtained from neem oil which are mono esters produced using transesterification process. The optimum conditions to achieve maximum yield of biodiesel were investigated at different temperatures and with different molar ratio of neem oil and methanol. The temperature increases yield of methyl ester at 55 ^{0}C and a molar ratio of 1:12 were found to be beneficial. From the obtained results it was apparent that the produced biodiesel fuel was within the recommended standards of biodiesel fuel. The fuel properties of biodiesel including kinematic viscosity and acid value were examined. The engine power and pollutant emissions characteristics under different biodiesel percentages were also studied. Experiments demonstrated that the biodiesel produced using neem oil could reduce smoke and Carbon monoxide emissions, significantly while the Nitrogen oxide emission changed slightly. Thus, the ester of this oil can be used as environment friendly alternative fuel for diesel engine.

Keywords: *Biodiesel, Transesterification, Methyl ester of neem oil, Emissions*

1. Introduction

Vegetable oils have become more attractive in the recent past owing to its environmental benefits and the fact that it is made from renewable resources. Vegetable oils are a renewable and potentially inexhaustible source of energy with an energetic content close to diesel fuel. Oils derived from vegetable and microbial sources may in course of time become as important as petroleum and the coal tar products of present time [1]. Recent increases in petroleum prices and due to uncertainties concerning petroleum availability, there is renewed interest in vegetable oil fuels for diesel engines [2].

Neem (*Azadirachta indica*) is a tree in the mahogany family Meliaceae which is abundantly grown in varied parts of India. The Neem grows on almost all types of soils including clayey, saline and alkaline conditions. Neem seed obtained from this tree are collected, de-pulped, sun dried and crushed for oil extraction. The seeds have 45% oil which has high potential for the production of biodiesel [3]. Neem oil is generally light to dark brown, bitter and has a rather strong odour that is said to combine the odours of peanut and garlic. It comprises mainly of triglycerides and large amounts of triterpenoid compounds, which are responsible for the bitter taste. It is hydrophobic in nature and in order to emulsify it in water for application purposes, it has to be formulated with appropriate surfactants.

Neem oil also contains steroids (campesterol, beta-sitosterol, stigma sterol) and a plethora of triterpenoids of which Azadirachtin is the most widely studied [4].This study is intended to consider aspects related to the feasibility of the production of biodiesel from neem oil in an attempt to produce biodiesel using the abundantly grown tree naturally as the use of vegetable oils for engine fuels seems insignificant at present day scenario. Neem oil will become a potential supplier of Biodiesel in future. Biodiesel is a mono alkyl ester (methyl or ethyl ester) of long chain fatty acids derived from renewable lipid of neem oil. Biodiesel thus obtained can be used in any compression ignition (diesel) engines without the need of modification and is therefore a good substitute for diesel fuel. The first documented commercial production of

rapeseed oil methyl esters is reported to be in 1988 [5]. It possesses several distinct advantages over petro-diesel in following safety, biodegradability and environmental aspects [6].

This present study is intended to consider aspects related to the feasibility of the production of biodiesel from neem oil. The variables affecting the yield and characteristics of the biodiesel made were studied. The obtained results were analyzed and compared with conventional diesel fuels.

2. Methodology

Neem oil was obtained commercially. Chemicals such as Sodium hydroxide, Methanol, Sulphuric acid, Phosphoric acid were purchased from Merck. All the chemicals used were of analytical reagent grade.

2.1. Experimental Setup of Transesterification Process

Biodiesel fuel blend can be conventionally prepared by using alkali or acid as catalyst.100gm of refined neem oil is mixed with 12gm of alcohol and 1gm of sodium hydroxide (NaOH) which acts as catalyst. The experiments were conducted in a m anner similar to Soxhlet extraction apparatus [7].This mixture is taken in a 500ml round bottomed flask .The amount of catalyst that should be added to the reactor varies from 0.5% to 1% w/w. Using magnetic stirrer and heater equipment the above mixture is thoroughly mixed and maintained at a temperature of 50-55 ^{0}C for two hours. The mixture is now allowed to settle for 24 hours at which two separate layers are obtained. The top layer will be methyl ester of neem oil (fatty acid methyl ester (FAME) i.e, .biodiesel) and the bottom one glycerin. Using a conical separating funnel the glycerin is separated at the bottom. To separate the FAME (fatty acid methyl ester) from glycerol, catalyst (NaOH) and methanol, washing was carried out with warm water. Further water and methanol will be removed by distillation. Then the NaOH, Glycerol, methanol and water was treated with phosphoric acid for neutralizing the catalyst. Finally glycerin is obtained as a byproduct in case of alkali transesterification process. Fig.1. shows the experimental set up of the process.

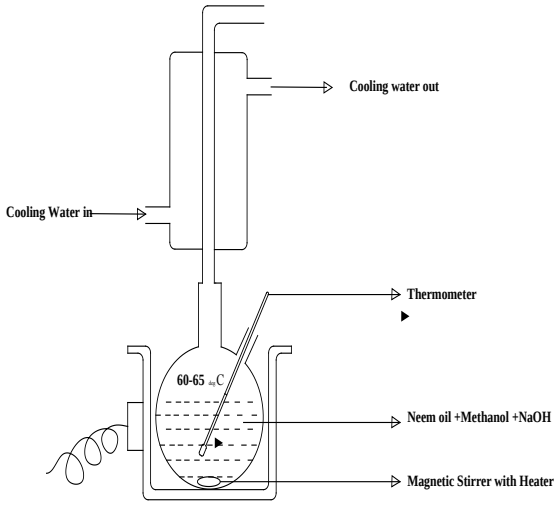

Fig.1. Experimental set-up

Acid catalyst production is the second conventional way of making the biodiesel. The most commonly used acid is sulfuric acid. This type of catalyst gives very high yield in esters but the reaction is very slow, requiring almost always more than one day obtaining the final product [8].

2.2. Distillation of Crude Biodiesel

The crude biodiesel was composed of FAME and methanol. FAME was purified by a distillation system. It was provided with an evaporator and an internal condenser. Feed (0.2 L/h) was let in using a jacketed glass vessel equipped with a flow regulation valve, where the temperature was maintained at 40^0C.The discharge of distillate and residue was done in glass flasks. The vacuum system was composed of a mechanical pump and a diffusion pump. The heating of the evaporator was provided by a j acket. The yield of the purified biodiesel (FAME) was calculated by from the ratio of the mass of the purified biodiesel to that of the crude biodiesel. Biodiesel was distilled from the crude biodiesel at evaporator temperatures of 40, 50, 60, and 70 °C. Other conditions for distillation were maintained at evaporator vacuum to be 1.0 Pa, the condenser temperature at 40 °C.

3. Results and Discussion

The raw neem oil has high moisture content and contains other impurities. In order to remove the moisture and impurities from the neem oil it has to be refined. The purification process can be accelerated tremendously by boiling the oil with about 20 % of water. The boiling should continue until the water has completely evaporated (no bubbles of water vapor anymore). After few hours the oil then becomes clear**.** This refined neem oil is taken as raw material for transesterification process. If the neem oil is having 6% free fatty acid content alkali transesterification process seems to be better option otherwise acid transesterification process is carried out. Since the free fatty acid content was observed to be 5.7 i n weight percentage alkali transesterification process was carried out. The refined neem oil was checked before doing transesterification process and properties are tabulated in Table 1.

Table 1. Properties of Neem oil

Properties	Quantity	Fatty Acid	Weight %
Moisture content (wt %)	0.4	Oleic acid	51.3
Free Fatty Acid Content (wt %)	5.7	Palmitic acid	17.8
Refractive Index	1.47	Linoleic acid	14.7
Gum Content (wt %)	0	Steric acid	14.4
Iodine Value	80	Arachidic acid	1.6
Density(kg/m3)	1024	Myristic acid	0.03

3.1. Transesterification process at different molar ratios of methanol and neem oil-alkali catalyst

Different molar ratios of methanol and neem oil were taken for studying the yield percentage. The mole ratio of 1:12 was found to be efficient compared to lower or higher molar ratios where the conversion was around 83%. On further increase in the methanol it leads to a

saturation curve as shown in Fig.1 , 1: 12 molar ratio were taken for further studies. Temperature effects were conducted on transesterification process (Fig.2). As the temperatures increases, the yield of methyl ester also increases to a maximum of 92% which was at 55^{0}C.If the temperature reached a value beyond 60^{0}C the yield started decreasing drastically.

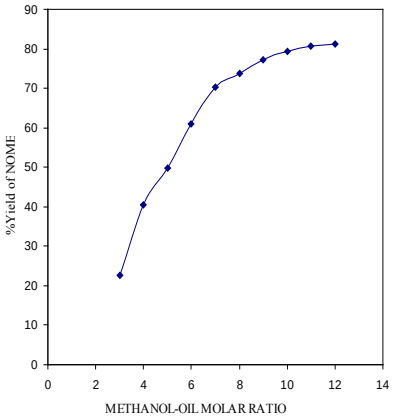

Fig.2. Different molar ratio of methanol and oil

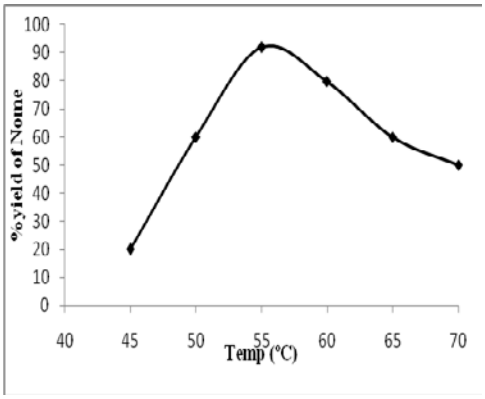

Fig. 3. Effect of temperature

Table 2. Comparison of Biodiesel obtained from acid, alkali catalysts and Commercial Diesel

PROPERTIES	**NOME (ACID CATALYST)**	**NOME (ALKALI CATALYST)**	**DIESEL FUEL**
Viscosity at 40 ^{0}C (cP)	5.3	4.9	6.8
Density at 15 ^{0}C (g/cc)	0.78	0.81	0.8
Heating value(Mj/kg)	39.1	39.4	44.5
Cetane number	46.0	46.0	51.0
Carbon mass (wt %)	76.7	76.7	86.8
Hydrogen (wt %)	12.1	12.1	13.1
Oxygen (wt %)	11.15	11.15	0.00
C/H ratio	6.33	6.33	6.63
Sulphur (wt %)	≤ 0.004	≤ 0.004	0.042
Total glycerin (%)	0.027	0.03	-
Free glycerin	0	0.00	-

3.2. Properties of NOME

The comparison of properties between neem oil and diesel are tabulated in Table 2.Testing was done to study the properties of the neem oil after undergoing transesterification process and properties of neem oil methyl ester is tabulated in Table 2. The cetane number was found to be 46 which are in par with commercially available diesel. Sandun Fernando et al., stated that the cetane number for biodiesel should be a minimum of 47[9]; as high cetane number could lead to engine performance problems. Glycerin result measures the amounts of unconverted and partially converted fats and oils which are in comparison in both the catalysts. The neem oil properties were compared with the normal diesel fuel. The sulphur content of NOME was found to be less than 0.004. Compared to diesel it is very less. So neem oil is found to be nontoxic.

3.3. FTIR results of nonesterified and esterified neem oil

The FTIR test of nonesterified and esterified neem oil is carried out using MATSEN equipment. The IR spectra of neat esterified and nonesterified neem oil show (Fig.4 & Fig.5) the pronounced functional groups which indicate the presence of alkanes and lesser extent of aromatics and polyaromatics groups, with a clear absence of phosphorous and sulfur. The IR

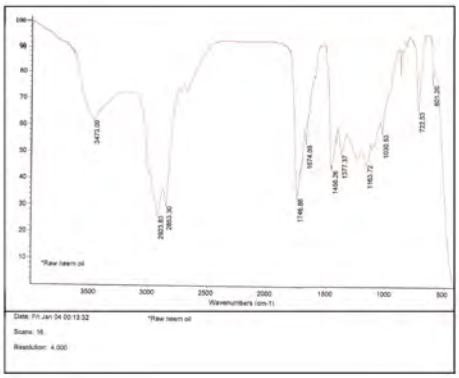

Fig.4. IR Spectra of Esterified neem oil

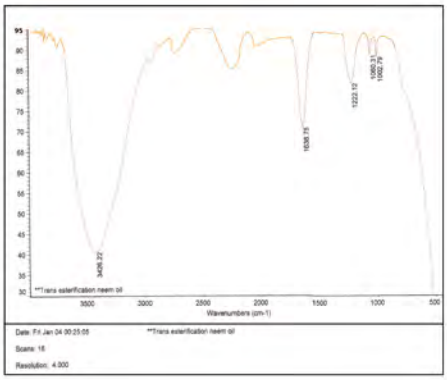

Fig. 5. IR Spectra of non Esterified neem oil

spectra of the esterified neem oil also show that they contain significant amount of esters. The esterified neem oil contains little amount of water and this water was removed by heating the oil before using in the engine. The comparative frequency ranges of IR-spectra, their corresponding functional groups and indicated compounds were performed by Nurun Nabi et al. [10].

3.4. Distillation of Crude Biodiesel

The yield of purified biodiesel increased as the evaporator temperature increased from 40 to 70 °C, the yield increased from 55.45% ± 0.5% to 63.67% ± 0.25%. However, the color of the final products changed from being colorless to light yellow when the evaporator temperature increased. Distillation was introduced as an alternative practice for biodiesel production via two ways. One method was to remove the FFAs from the feedstock with a high acid value to a very low extent, so the base-catalyzed transesterification was easy to perform. The other method was to purify FAME at 50−80 °C from the crude biodiesel from low-quality feedstock to meet a high biodiesel standard. Distillation was also employed to remove FFAs from acidic neem seed oil at 60°C for the production of biodiesel.

3.5. Analysis Of Exhaust Emissions With Neat Diesel Fuel And Diesel Neem Oil Blends

3.5.1. Effect of engine speed on brake thermal efficiency

In order to study the effect of Brake thermal efficiency, the speed of engine was operated at various levels ranging from 500-1500rpm. In this study, four cylinders IDI diesel engine was used as a test engine. The test engine specifications as reported by them were injection time 20^{o} CA BTDC and pressure of 120 bar.

An increase in the engine speed of upto 1050 rpm the Brake thermal efficiency increased as also the fuel consumption. Beyond 1050rpm there was a s light decrease in Brake thermal efficiency even with higher fuel consumption. This is an indication of low calorific value with an increase in fuel consumption. At 1050rpm, there was high Brake thermal efficiency indicating complete combustion of fuel hence further studies were carried out at this rpm.

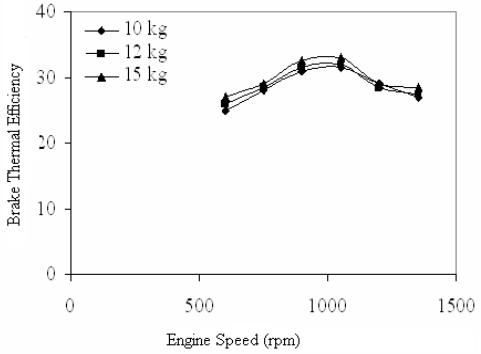

Fig.6. Brake Thermal efficiency

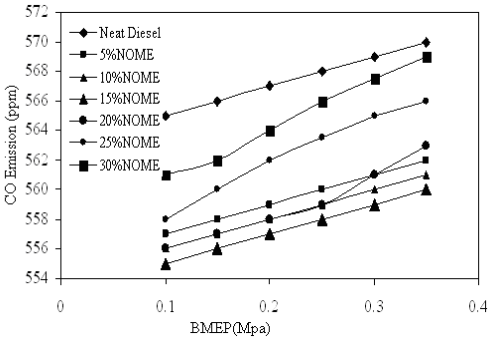

Fig. 7. Carbon monoxide emission

3.5.2. Carbon monoxide emission

The carbon monoxide emissions of the Neem oil methyl ester and various other blends of biodiesel were found at the rated engine speed of 1050 rpm for different Brake Mean Effective Pressure (BMEP). The result shows (Fig.7) carbon monoxide emissions are found to be increasing with increasing BMEP. This is typical with all internal combustion engines, since air fuel ratio decreases with increase in load. The engine emits more CO using diesel as compared to that of biodiesel blends under all BMEP conditions. With increasing biodiesel percentage CO emission level decreases up to 15%blend, increasing the percentage of NOME in diesel more than 15% CO emission is increases. Biodiesel itself has about 11.15 % oxygen content in it. This helps for the complete combustion. Reports show that the carbon monoxide emissions emerging from the biodiesel will lower the overall load and speed ranges up to 51.6% [10].

3.5.3. NO_X emission

The NO_X emission characteristics with respect to various BMEP's at various blends of Neem oil was found. The result shows (Fig.8) the diesel fuel is having lower NO_X emission and blended Neem oil is having higher NO_X emission. Compared to conventional fuel the NO_X emission is increased by 5% with the blend of Neem oil. The presence of oxygen in NOME helps to produce more amount of NO_X The impact of fuel injection also play a role in the higher NO_X emissions in the NOME. The NOx variations were less than 8%, which is consistent with most published results [11].

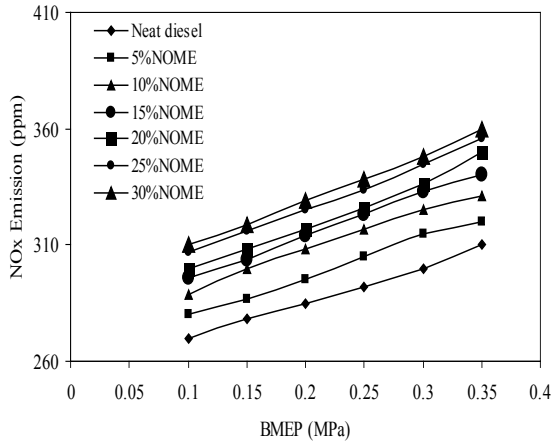

Fig.8. No_x Emission

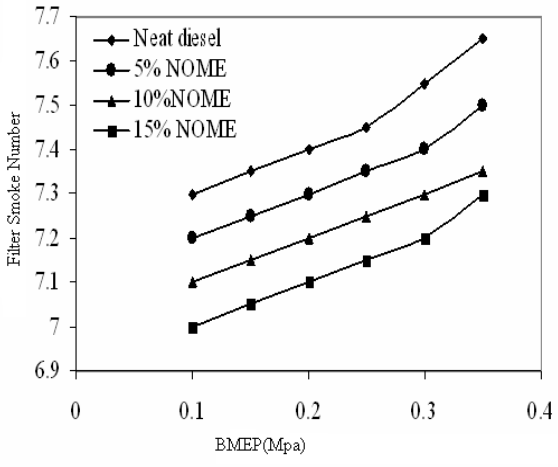

Fig. 9. Smoke emission

3.5.4. Smoke emission

Fig.9 represents filter smoke number with respect to different BMEP. The filter smoke number with respect to different BMEP was analyzed for various blends of fuel. The results confirm that filter smoke number for biodiesel blend to be lower for NOME than that of the diesel fuel. 15% blend show low smoke number contributing to the factor that lesser amount of unburnt hydrocarbons is present in the engine exhaust emission**.** Previous researchers *showed* the visible smoke emerging from the biodiesel over all load and speed ranges are lower by 13.5% to 60.3% [12].

4. Conclusion

Studies have been made using neem oil, a novel feedstock of obtaining biodiesel which is renewable in nature. The effect of methanol to oil molar ratio and acid & alkali catalyst transesterification were analyzed. The exhaust emissions of neem oil blended biodiesel are studied. Compared with conventional diesel fuel, diesel exhaust emissions including smoke and CO were reduced, while NO_X emission was increased with the diesel-NOME blends. The reductions in CO and smoke emissions and the increase in NO_X emission with Diesel – NOME blends may be associated with the oxygen content in the fuel. More than 15% NOME-diesel blends created poor atomization tendency and incomplete combustion in engine. So the engine exhaust emission level is increased. The ester of this oil can be used as environment friendly alternative fuel for diesel engine creating a greener environment in the future.

References

[1] Ganguli, S. (2002) 'Neem: A therapeutic for all seasons', Current Science, Vol. 82, pp.1304.

[2] Mishra, A.K., Singh, N. and Sharma, V.P. (1995) 'Use of neem oil as a mosquito repellent in tribal villages of mandla district', Indian J Malariol, Vol.3, pp.99-103.

[3] M.A. Fazal, A.S.M.A. Haseeb and H.H. Masjuki .(2011) 'Biodiesel feasibility study: An evaluation of material compatibility; performance; emission and engine durability',Renew. sustain.Engy Reviews, Vol.15,2, 1314-1324.

[4] Foglia, T.A., Jones, K.C., Haas, M.J. and Scott, K.M. (2000) 'Technologies supporting the adoption of biodiesel as an alternative fuel. The cotton gin and oil mill presses.

[5] Fukuda, H., Kondo, A. and Noda, H. (2001) 'Biodiesel fuel production by transesterification of oils', J Biosci Bioeng, Vol.5, pp. 405–416.

[6] Barnwal, B.K. and Sharma, M.P. (2005) 'Prospects of Biodiesel production from vegetable oils in India', Renew Sust Energy Rev 9, Vol.4, pp. 363–378.

[7] Mittelbach, M. and Tratnigg, **B.** (1990) 'Kinetics of alkaline catalyzed methanolysis of sunflower oil', Fat Sci Technol, Vol.4, pp.145–148.

[8] Sandun Fernando., Prashanth Karra., Rafael Hernandez and Saroj kumar jha. (2007) 'Effect of incompletely converted soyabean oil on bi odiesel quality'Energy, Vol.32, pp.844-851.

[9] Nurun nabi, Md.,Shamim Akhter.,Mhia Md and Zaglul Shahadat. (2006) 'Improvement of engine emissions with conventional diesel fuel and diesel-biodiesel blends', Bioresource technology, Vol.97, pp.372-378.

[10]. Anjana Srivastava and Ram Prasad. (2004) 'Triglycerides based diesel fuels', Renewable and sustainable energy reviews, Vol.4, pp.111-133.

[11] Sahoo, P.K.,Das, L.M,Babu., M.K.G. and Naik, S.N. (2007) 'Biodiesel development from high acid value polanga seed oil and performance evaluation in a CI engine', Bioresorce Technology,Vol.86,pp.448-454.

[12] Gvidonas Labeckas and Stasys Slavinskas. (2006) 'The effect of rapeseed methyl ester in direct injection diesel engine performance and exhaust emissions',Energy conversion and Management,Vol.47,pp.1954-1967.

[13] Carmen María Fernández, María Jesús Ramos, Ángel Pérez and Juan Francisco Rodríguez, (2010)‘Production of biodiesel from winery waste: Extraction, refining and transesterificationofgrapeseedoil,Biores.Technol.Vol.101,18, pp.7019-7024

Characterization of Waste Frying Oils Obtained from Different Facilities

Huseyin Sanli[1, 3], Mustafa Canakci [2, 3, *], Ertan Alptekin [2, 3]

[1] *Golcuk Vocational High School, Kocaeli University, 41650 Golcuk, Turkey*
[2] *Department of Automotive Engineering Technology, Kocaeli University, 41380, Izmit, Turkey*
[3] *Alternative Fuels R&D Center, Kocaeli University, 41275, Izmit, Turkey*
** Corresponding author: Tel: +90 262 303 22 85, Fax: +90 262 303 22 03,Email:mustafacanakci@hotmail.com*

Abstract: Biodiesel cannot economically compete with petroleum-based diesel fuel because of its high cost problem. This problem may be solved with the use of low cost feedstocks in biodiesel production. Waste frying oils are one of the low cost feedstocks. However, the feedstocks' properties to be processed must be controlled in detail prior to transesterification reaction, since the physical and chemical properties of the feedstock significantly influence biodiesel production reaction as well as fuel properties. Frying oils which are used in various facilities in different conditions (such as frying temperature, time, and kind of food) have significantly different physico-chemical properties. Therefore, in this study, 30 different waste frying oil samples (14 from fish restaurants, 5 from fast-foods, 5 from hospitals, 4 from pastry shops, and 2 from restaurants) were collected and their density, viscosity, total polar material, water content, acid value, iodine value, peroxide value, and heating content were determined and compared to each others. The correlations between the total polar material content (which has to be legally determined to monitor frying oil's degradation level) and density, viscosity, acid value and water content were remarkable. The usage of peroxide value to decide the quality of an oil was misleading.

Keywords: *Biodiesel, Low cost feedstock, Waste frying oil, Characterization.*

1. Introduction

One of the most important and critical parameters which are effective in social and economical development of a country is energy. Energy consumption is steadily increasing each passing day as a result of rising world population, technological developments and living standards. At the present day, about 90% of the world's total energy needs are met by fossil fuels and 45% of these fossil fuels is petroleum (petroleum's share is supposed to rise to 58% in 2030) [1, 2]. Although petroleum is the most of energy sources used in the world, its reserves originate from some regions. Thus, the world's many countries such as the USA and European Union (EU) countries have to import their energy requirements. In Table 1, daily petroleum production and consumption amounts of some countries are seen.

Table 1. The petroleum production and consumption amounts of some countries [3]

Country	Petroleum Consumption (barrel/day)	Petroleum Production (barrel/day)
USA	18,690	9,056
EU	13,680	2,383
China	8,200	3991
India	2,980	879
Russia	2,850	9,932
Germany	2,437	157
France	1875	71
Turkey	580	53
Greece	414	7

As seen in Table 1, the USA which has the largest industry in the world can produce only the half amount of its petroleum consumption. Situation of EN countries which are poor in terms

of fossil fuels is worse. These 27 countries can only produce about 17% of the consumed amount with their own resources. As the result of increased dieselization, diesel fuel (D-2) is the most consumed oil-based engine fuels, and this share is rising progressively each passing year. For example, in Turkey, about 7.4 million tons of D-2 was consumed, while gasoline consumption was only 2 million tons in the year of 2009 [4].

When we consider the pessimistic situation explained above, the importance of alternative diesel fuel which is renewable, sustainable, green (not causing global warming and acid rains) and producible with domestic sources is evidently understood.

Biodiesel which is defined as fatty acid alkyl monoesters derived from feedstocks such as vegetable oils and animal fats is one of the most important renewable energy sources. It has many superior properties over D-2 including renewability, lubricity, biodegrability, exhaust emission etc. Increasing environmental concerns and the need for energy independence have led to the biodiesel market. The global biodiesel market is expected to grow from $8.6 billion in 2009 to $12.6 billion in 2014 [5]. The EU is the biggest biodiesel producer in the world. As seen in Table 2, annual production of 27 EU countries increased from 3.20 million tons in 2005 to 9.04 million tons in 2009 which means the increase is about 3 times.

Table 2. EU biodiesel production and capacity amounts [6]

Year	Annual Production (million tons)	Annual Growth (%)	Annual Production Capacity (million tons)	Annual Growth (%)
2005	3.20	65.0	4.23	88
2006	4.90	54.0	6.07	43.50
2007	5.74	16.8	10.29	69.55
2008	7.70	35.7	16.00	54.49
2009	9.04	16.6	20.91	30.69

However, this must be remembered that these figures have been essentially attained through governments' economic stimulations and subsidies which were enforced in accordance with EU directive (2003/30/EC) and this has led to serious tax losses. Biodiesel cannot economically compete with D-2 because of its high cost. As biodiesel is usually obtained from high quality food-grade vegetable oils, the biggest reason of the high cost problem is feedstock cost which approximately accounts for 70 – 90% of the total cost of biodiesel production [7, 8]. This problem may be solved with the use of low cost feedstocks in biodiesel production. Waste frying oils are one of these low cost feedstocks. Compared to neat vegetable oils, the cost of waste frying oils is anywhere from 60% less to free, depending on the source and availability [9]. With this decrease in the feedstock cost, the great difference between the prices of biodiesel and D-2 can be lowered to an acceptable value.

2. Waste Frying Oils as Biodiesel Feedstock

In Europe, a total of about 17 million tons vegetable oils are annually consumed and this amount raises approximately 2% each passing year [10]. It is clearly understood from this figure that there are very big amounts of waste frying oil resources. However, there is no comprehensive study carried out on the waste frying oil potential of the EU countries and very little portion of this waste oil can be collected. When waste frying oils are poured into kitchen sink; they block drains in the course of time, and cause the sewerage not to be used by catching other waste materials in the sewerage system. Thus, they damage waste water

treatment plants and raise processing costs. According to a study performed in USA, 40% of the sewerage system blockages are caused by the waste frying oils poured into kitchen sink [10]. Moreover, waste frying oils have eco-toxic properties. If they are spilled onto ground, they will contaminate the soil and so damage plants.

Waste vegetable oils usage in the production of animal feed has been forbidden by European Commission since 2001 because of bovine spongiform encephalopathy (mad cow disease). In addition, these waste oils and fats have not been used in soap production since they may cause health problems. Thus, waste oils and fats can only be used as feedstock in the production of biodiesel. Furthermore, by using waste frying oils as feedstock in biodiesel production, in addition to their positive influence in reducing the final cost of biodiesel, serious environmental pollution problems causing from these waste oils can be eliminated. However, the physical and chemical properties of the feedstock significantly influence biodiesel production reaction as well as fuel properties. Because of this, in order to obtain fuel quality biodiesel, the feedstocks' properties to be processed must be controlled in detail prior to transesterification reaction.

3. Chemistry of Frying Process

During frying process, oil is continuously or repeatedly subjected to high temperatures in the presence of air and moisture. Three essential degradation reactions occurs under these conditions are:

- Hydrolysis causing from the moisture content of fried food. This reaction produces free fatty acids (FFA), mono- and diglycerides.

- Oxidation causing from the contact with oxygen. Reaction products are oxidized momomeric, dimeric and oligomeric triglycerides and volatile materials such as aldehydes and ketones.

- Polymerization causing from these two reactions, and high temperatures. This reaction produces dimeric and polymeric triglycerides with ring structure [11-13].

Because of these degradation reactions mentioned above, a number of physical and chemical changes occur in frying oils including increase in viscosity, density, FFA content, total polar material (TPM), polymerized triglycerides, and decrease in smoke point, the number of double bonds, etc. If the frying process is continued, these materials will undergo further degradation and finally the oil will not be appropriate for frying. The frying oil has to be discarded.

Since all degradation products are of polar character, TPM content of frying oil is a good indicator of its degradation level. Thus, in many countries, TPM content of frying oil has been legally accepted as the limit value to decide discard it or not. For example, in Turkey, TPM content of frying oil must not exceed the top level of 25%. In addition to TPM, as the oil deteriorates, some changes in its physical and chemical properties occur. For instance, during frying, oil's double bonds are ruptured and so its fatty acid composition changes, FFA level and saturation degree increase [14, 15]. The change in the fatty acid composition influences some oil properties such as iodine value, viscosity, density, heating content. Thus, these properties can also be used to monitor the quality of the frying oil.

4. Methodology

Waste frying oils which are used in different conditions (such as frying temperature, duration, the type and shape of the fryer, kind of food etc.) have significantly different physico-chemical properties. In this study, in order to decrease this difference, after classifying the facilities producing waste frying oils into categories, 30 different waste frying oil samples (14 from fish restaurants, 5 from fast-foods, 5 from hospitals, 4 from pastry shops, and 2 from restaurants) were collected and their density, kinematic viscosity, TPM, water content, acid value (AV), iodine value (IV), peroxide value (PV), and heating content were determined and compared to each other. It must be pointed out that, at the end of the project which is carried out with the collaboration of Izmit Municipality, totally, 150 waste frying oil samples will be collected from 7 different sectors and also, in addition to the physico-chemical properties mentioned in this article, saponification value, cetane index and smoke points of all samples will be determined.

The procedures used in the determination of AV, PV, and IV are AOCS Cd 3a-63, AOCS Cd 8-53, and TS EN 14111, respectively.

Samples were coded according to their origins. Namely, FR means waste frying oil sample obtained from fish restaurants, FF means waste frying oil sample from fast-foods, H means from hospitals, PS means from pastry shops, and R means from restaurants.

5. Results and discussion

All results determined are shown in Table 3. When the waste frying oil samples obtained from fast-foods are examined and compared to each other, it is seen that FF1 has the TPM content of 30% and exceeded the top limit of 25%. Moreover, in addition to TPM, water content, PV and AV of this waste frying oil was the highest. Its AV (17.85 mg KOH/g) was more than twice of that of FF5 which was the second highest. FF4's TPM content (24.5%) was close to the top limit value. In addition, density and viscosity values of this sample were the highest. Its viscosity was 6.95 mm^2/s higher than that of the second highest viscosity. It was a reasonable result that the peroxides values of FF1 and FF4 which had the highest TPM contents were almost same (50.61 and 50.42 meq/kg). However, among the samples obtained from fast-foods, FF4's AV (1.78 mg KOH/g) was the lowest and its IV (95.38 $gI_2/100g$) which is the indicator of unsaturation level was the highest. Whereas its iodine value was expected to be low as the result of destruction of double bonds, the result was not in this expectation. As the heating content increases with saturation, the highest heating content (39741 kJ/kg) belonged to FF5 which was the most saturated sample having an IV of 52.17 $gI_2/100g$.

Among the samples collected from hospitals, TPM content of H1 (29%) was the highest and higher than the top limit. Again, the result of the same sample had the highest density, viscosity, water content and lowest iodine value. However, high TPM level which is the indicator of massive deterioration made us think that its peroxide value would be the highest, but it was in the third order among the waste frying oils from hospitals with the value of 20.82 meq/kg. This may be explained by splitting of hydro peroxides which form during the first stage of the oxidation, in the course of time. AVs of the samples were closer to each other and all of them were lower than 1 mg KOH/g.

*Table 3. Data obtained from waste frying oil samples**

1	2	3	4	5	6	7	8	9
FF1	0.9237	42.28	1657.00	17.85	85.53	50.61	30.0	39223
FF2	0.9194	39.81	1310.30	3.74	82.29	33.78	16.0	39259
FF3	0.9183	42.37	441.76	2.64	66.48	36.84	15.5	39090
FF4	0.9273	51.44	1059.30	1.78	95.38	50.42	24.5	39007
FF5	0.9207	44.47	1181.90	8.62	52.17	19.05	19.5	39741
H1	0.9311	47.24	1208.7	0.52	97.30	20.82	29.0	38925
H2	0.9231	34.80	956.78	0.93	119.81	7.75	13.5	39650
H3	0.9273	39.91	1050.70	0.50	124.28	26.65	23.0	39322
H4	0.9242	34.81	1021.30	0.65	126.90	10.74	15.5	39498
H5	0.9231	35.18	785.31	0.25	121.13	28.41	14.0	39689
PS1	0.9238	39.89	710.03	0.56	141.26	55.92	16.0	39632
PS2	0.9237	34.28	533.75	0.39	124.09	93.94	12.0	40336
PS3	0.9232	32.85	568.52	0.22	126.54	74.22	16.0	39466
PS4	0.9223	33.79	566.53	0.17	120.86	200.38	11.5	39276
R1	0.9219	34.34	530.05	0.37	109.19	85.17	18.0	39270
R2	0.9216	34.64	556.44	0.63	108.26	20.69	13.0	39399
FR1	0.9264	40.52	1200.10	5.25	112.57	43.42	20.0	39344
FR2	0.9269	39.86	1089.50	0.36	128.84	42.51	22.0	39404
FR3	0.9248	36.94	753.37	0.49	122.29	49.05	16.5	39492
FR4	0.9252	37.12	714.90	0.41	122.99	52.05	20.0	39449
FR5	0.9238	35.99	817.73	0.28	121.71	44.46	17.0	39519
FR6	0.9236	35.61	966.50	0.29	127.07	46.64	16.0	39556
FR7	0.9241	34.89	915.33	0.75	118.83	53.77	15.5	39367
FR8	0.9243	37.74	669.46	0.32	120.70	31.43	16.0	39518
FR9	0.9238	35.58	1024.10	0.34	108.58	25.39	17.0	39449
FR10	0.9238	36.37	732.64	0.43	124.37	21.72	16.5	39652
FR11	0.9233	33.74	670.11	0.29	120.70	39.74	17.0	39624
FR12	0.9239	34.85	713.93	0.41	124.48	34.24	15.5	39562
FR13	0.9249	38.14	827.15	0.41	124.33	40.49	16.5	39465
FR14	0.9262	41.60	1017.80	0.48	119.72	48.31	19.5	39474

*1;Company Code, 2;Density (g/cm^3 @ 15 °C), 3;Viscosity(mm^2/s @ 40 °C), 4;Water Content (ppm), 5;Acid Value (mgKOH/g), 6;Iodine Value (gI_2/100g), 7;Peroxide Value (meq/kg), 8;Total Polar Material (%), 9;Heating Content (kJ/kg)

Within the waste frying oils from pastry shops, the one which had the highest density, viscosity, water content, AV, and TPM was PS1. However, this sample had the lowest PV (55.92 meq/kg) and the highest IV (141.26 gI_2/100 g). Normally, low PV and high IV are attributed to slight oxidative degradation. However, this oil was one of two samples which had the highest TPM content. This situation made us think that the degradation reactions which had increased the TPM content of the oil caused from hydrolysis and polymerization rather than thermal oxidation. High water content and AV can be interpreted as the result of hydrolysis. PS4 which was the first waste frying oil in terms of PV (106.44 meq/kg higher than the second one) had the lowest TPM content (11.5%) and it was amazing.

In this study, 2 samples were collected from restaurants. When we examine the results of these samples, it was seen that their density and viscosity values were almost the same. R1 had higher values than R2 in terms of PV (the difference is 64.48 meq/kg) and TPM content (the difference is 5%). This showed us that this frying oil was subjected to more degradation

reaction. However, IVs of these two oils were almost same. Whereas, it was expected that R1 had the lower IV due to higher oxidation reaction leading to splitting of double bonds.

Among the waste frying oil samples obtained from fish restaurants, FR1's AV of 5.25 mg KOH/g was 7 times higher than that of second oil. The AVs of other 13 samples were less than 1 mg KOH/g. The density, viscosity, water content and TPM amounts of this oil were within the highest ones.

FR2 which had the highest TPM content (22%) was within the first three samples in terms of density, viscosity and water content. One of the most remarkable results among waste frying oils obtained from fish restaurants was that all the heating contents were almost the same. The difference between the highest heating value (39624 kJ/kg) and the lowest heating value (39344 kJ/kg) is only 0.7%.

6. Conclusions

According to the results, at first, it must be strongly emphasized that waste frying oils are very heterogeneous feedstock for biodiesel production in terms of physico-chemical properties and must be characterize in detail prior to biodiesel production.

When waste frying oils were compared to each other, it was seen that, in general, fast-food origin waste frying oils' viscosities, water contents and AVs were higher and iodine values were lower than those from other sectors. The most suitable feedstocks were from pastry shops in terms of TPM, AV, and water content. The densities of all the samples were generally close to each other.

The correlation between TPM, density, viscosity, AV, and water content were remarkable. Heating contents of the samples were almost the same. In addition, the measurement of PV as an indicator of oil quality was misleading.

References

[1] http://www.turksam.org/tr/a1343.html, (accessed on 25.04.2010)

[2] Knecht W, Diesel Engine Development in view of Reduced Emission Standards, Energy 33, 2008, pp.264-271

[3] http://www.cia.gov/library/publications/the-world-factbook/goes/br.html, (accessed on 09.11.2010)

[4] http://www.tupras.com.tr, (accessed on 25.04.2010)

[5] http://www.researchandmarkets.com/research/16d117/global_biodiesel_m, (accessed on 08.03.2010)

[6] http://www.ebb-eu.org/stats.php, (accessed on 07.12.2010)

[7] Predojevic Z, The Production of Biodiesel from Waste Frying Oils: A Comparison of Different Purification Steps, Fuel 17, 2008, pp.3522-3528

[8] Canakci M, Sanli H, Biodiesel Production from Various Feedstocks and Their Effects on the Fuel Properties, Journal of Industrial Microbiology and Biotechnology 35, 2008, pp. 431-441

[9] Canakci M, The Potential of Restaurants Waste Lipids as Biodiesel Feedstocks, Bioresource Techn 98, 2007, 183-190

[10] Agriculture and Food Development Authority, Waste Oils and Fats as Biodiesel Feedstocks: An Assessment of Their Potential in the EU, ALTENER Program NTB-NETT Phase IV, Task 4, Final Report, March 2000

[11] Gertz C. Chemical and Physical Parameters as Quality Indicators of Used Frying Fats, Euro Lipid Science Technology 102, 2000, pp. 566-572

[12] Stevenson SG, Vaisey-Genser M, Eskin NAM, Quality Control in the Use of Deep Frying Oils, JAOCS 61, 1984, pp. 1102-1108

[13] Choe E, Min DB, Chemistry of Deep-Fat Frying Oil, Journal of Food Science 72, 2007, pp. 78-86

[14] Aladedunye FA, Przybylski R, Protecting Oil During Frying: A Comparative Study, Eur J Lipid Sci Tech 111, 2009, pp. 893-901

[15] Knothe G, Steidly KR, A Comparison of Used Cooking Oils: A Very Heterogeneous Feedstock for Biodiesel, Bioresource Technology 100 (23), 2009, pp. 5796-5801

Ethanol production by *Mucor indicus* using the fungal autolysate as a nutrient supplement

Reihaneh Asachi [1,*], Keikhosro Karimi[1], Mohammad J. Taherzadeh[2]

[1] *Department of Chemical Engineering, Isfahan University of Technology, Isfahan, 84156-83111, Iran*
[2] *School of Engineering, University of Borås, SE-501 90 Borås, Sweden*
** Corresponding author. Tel: +983113915623, Fax: +983113912677, E-mail: asachi@iut.ac.ir*

Abstract: To develop a cost-effective fermentation medium, fungal extract (FE) of *Mucor indicus* biomass, which is a by-product of fermentation processes, was evaluated as a nutrient source for ethanol production by the fungus. Autolysis as a natural process of self-digestion of fungal cells was used to release the nutrients in surrounding medium leading to the production of the FE. Glucose consumption and ethanol production were followed using several media made with different concentrations of FE as nutrient supplementation replacing either yeast extract (YE) or whole nutrient. According to the results, 5 g/L YE could be successfully replaced with 5 g/L FE, resulting in higher ethanol yield (0.46 g/g) and productivity (0.69 g/L.h). Yield of glycerol production, the major byproduct of fermentation, was also increased by supplementation of the FE.

Keywords: *Bioethanol; Fungal extract; Autolysis; Mucor indicus.*

1. Introduction

Amongst all liquid biofuels, bioethanol is widely recognized these days as a promising renewable and environmentally friendly source of energy. It is an alternative fuel with the recognition that the global crude oil reserve is finite, and its depletion is occurring much faster than previously predicted [1]. Recently, saprophytic zygomycetes strain *Mucor indicus* (formerly *M. rouxii*) has been identified as an ethanol-producing organism, capable to grow aerobically or anaerobically on a number of different carbon sources including hexoses and pentoses with yield and productivity in the same order as *Saccharomyces cerevisiae* [2]. Furthermore, the interest in the potential utilization of fungal biomass zygomycetes as a valuable product is increasing due to the structural composition of cell walls [3]. Ethanol production by fermentation of natural feedstocks usually requires the use of complex growth supplements, such as yeast extract (YE) [2, 4]. The high cost of YE and other commercial nutrients is a limitation to its application in industrial processes, including the fermentation of biomass to ethanol. Thus, it is desirable to develop media that are likely to perform well in conditions that are representative in microbial fermentation. Several studies have concentrated on the use of yeast autolysate as effective nutrients in wheat fermentations and ethanol production [5, 6]. Fungal biomass as a by-product of fungal fermentations can be used as a source of nutrients for microbial fermentations. This can be achieved by disintegration and releasing materials hydrolyzed in-to assimilable monomers to produce a fungal autolysate as a nutrient-rich solution containing such as amino-acids, peptides, phosphorus and carbohydrates. Cell autolysis as an economical method is the natural degradation process, which starts after the exhaustion of major nutrients and reserves [7]. The objective of the present study was to develop a low-cost and suitable fermentation medium based on the utilization of filamentous fungus biomass, *M. indicus*, as a nutrient source for production of ethanol with the same fungal strain.

2. Materials and Methods

2.1. Microorganism strain and media

The fungus *M. indicus* 22424 CCUG (Culture Collection University of Göteborg, Sweden) was used in all experiments. The fungus was cultivated on agar slants containing (g/L):

glucose monohydrate, 40; peptone, 10; and agar 20 at pH 5.5±0.1 and 32±0.5°C for 5 days, where the fungus grew to form a cotton-like mycelium and spores. The agar slants were stored at 4°C until use.

2.2. Fungal spore germination

The batch cultivations were carried out in 500-ml cotton-plugged conical flasks with 300 ml working volume containing glucose monohydrate (40 g/L), supplemented with (per liter): 5 g YE, 7.5 g $(NH_4)_2SO_4$, 3.5 g K_2HPO_4, 1 g $CaCl_2$.$2H_2O$, 0.75 g $MgSO_4.7H_2O$ at pH 5.5±0.1. The flasks were incubated at 32±0.5°C and 180 rpm for 30 h, which provided initial biomass for further fungal autolysis.

2.3. Fungal autolysis

The produced biomass (fungal cells) from the fungal germination were recovered and separated from the liquid broth by filtration under aseptic conditions and washed at least three times with sterile distilled water to remove any residual nutrients. The clean solids were then re-suspended in sterile distilled water to achieve a concentration of 50 g/L fungal biomass. The fungal suspensions were then placed in 250 ml glass vessels immersed in a temperature-controlled shaking water bath. The initial pH was adjusted to 5.2±0.1 using either 10% sulfuric acid or 1 N sodium hydroxide. The autolysis was carried out at 55±1°C and 120 rpm for 72 h. After autolysis, the suspension was centrifuged for 15 min at 4°C and 4500 rpm, and the supernatant was designated as autolysate of fungal cells. The solubilized cell constituents in autolysate of fungal cells resulting from the autolysis were referred to as "FE".

2.4. Ethanol production

The fermentation experiments were carried out anaerobically in 120 ml glass bottles with 50 ml working volume, containing 40 g/L glucose monohydrate and different media supplementation (Table 1) in 50 mM sodium citrate buffer with pH 5.5±0.1. The media were sterilized by autoclaving at 121°C for 20 min, and then inoculated with 1.0 ml of a suspension containing 4.5(±0.5) $\times 10^5$ spores of *M. indicus*. The fully nutrient medium containing YE (5 g/L) supplemented with mineral salts (g/L): $(NH_4)_2SO_4$, 7.5, K_2HPO_4, 3.5, $CaCl_2.2H_2O$, 1, $MgSO_4.7H_2O$, 0.75. Table 1 shows the type of supplementation corresponding to the various media assayed. All fermentations were performed in a shaking incubator at 32±0.5°C with the agitation speed of 180 rpm for 72 h. The fermentation samples were stored at -20°C before metabolite analysis.

2.5. Analytical methods

For determination of the amount of materials released from the cells into the surrounding liquid phase during autolysis (FE), 10 ml of autolysate of fungal cells after autolysis process was separated and dried in an oven at 55±1 °C until constant weight was achieved. The liquid samples from fermentations were analyzed by high performance liquid chromatography (HPLC), which was equipped with UV/vis and RI detectors (Jasco International Co., Tokyo, Japan). Glucose, ethanol, glycerol were analyzed on an Aminex HPX-87H column (Bio-Rad, Richmond, CA, USA) at 60ºC with 0.6 ml/min eluent of 5mM sulfuric acid. All components were detected on RI chromatograms. All experiments in this work were duplicated and the averages of two replications are presented.

3. Results

3.1. Effect of the supplementation of fungal extract on ethanol production

M. indicus was produced in the fully supplemented medium containing 40 g/L glucose monohydrate and other nutrient components, and the produced fugal cells were recovered by filtration and were subjected to fungal autolysis process. To verify the potential of FE as an alternative nutrient supplementation replacing YE, a series of experimental fermentations were performed at two concentrations (2.5 and 5 g/L) of FE (Table 1).

Table 1. Results of ethanol production by M. indicus in different media.

Nutrient Supplementation	Maximum ethanol volumetric productivity (g/L h)	$Y_{E/S}$[b] (g/g)	$Y_{Gly/S}$[c] (mg/g)	Terminal time (h)[d]
YE (5 g/L), mineral salts[a]	0.67	0.45	47.3	24
YE (5 g/L)	0.37	0.43	46.4	48
FE (2.5 g/L)	0.34	0.39	43.3	72
FE (2.5 g/L), mineral salts	0.53	0.40	42.0	36
FE (5 g/L)	0.54	0.43	45.1	36
FE (5 g/L), mineral salts	0.69	0.46	49.0	24

[a] Mineral salts supplementation (g/L): $(NH_4)_2SO_4$ (7.5), K_2HPO_4 (3.5), $MgSO_4.7H_2O$ (0.75), $CaCl_2.2H_2O$ (1)
[b] Maximum ethanol yield on consumed glucose.
[c] Maximum glycerol yield on consumed glucose.
[d] Time needed for total consumption was defined as the period between addition of glucose and its exhaustion to concentration below 0.5 g/L.

To establish a basis for comparison, a fermentation run was carried out in a fully supplemented medium (YE (5 g/L) and mineral salts). The results showed that, glucose was rapidly consumed and mainly converted to ethanol (Fig. 1a and b), reaching a maximum yield of 0.45 g/(g glucose) and a volumetric productivity of 0.67 g/L h in less than 24 h cultivation under anaerobic conditions. Glycerol was the most important byproduct of the fermentation with maximum yield of 47.3 mg/g glucose (Table 1). As can be seen from Table 1, *M. indicus* gave the ethanol yield of 0.43 g/g and low productivity with the supplementation of only 5 g/L YE (Table 1). A preliminary experiment was carried out using 2.5 g/L of FE as unique supplementation (Table 1). As a result, the low glucose consumption indicated the existence of nutrient limitation in the medium and the maximum ethanol concentration was reached after a relatively long reaction time (about 72 h). However, the experiment with supplementation of 2.5 g/L FE gave a poor performance in ethanol production because of nutrient limitation in fermentation media relative to YE or whole nutrient supplementations.

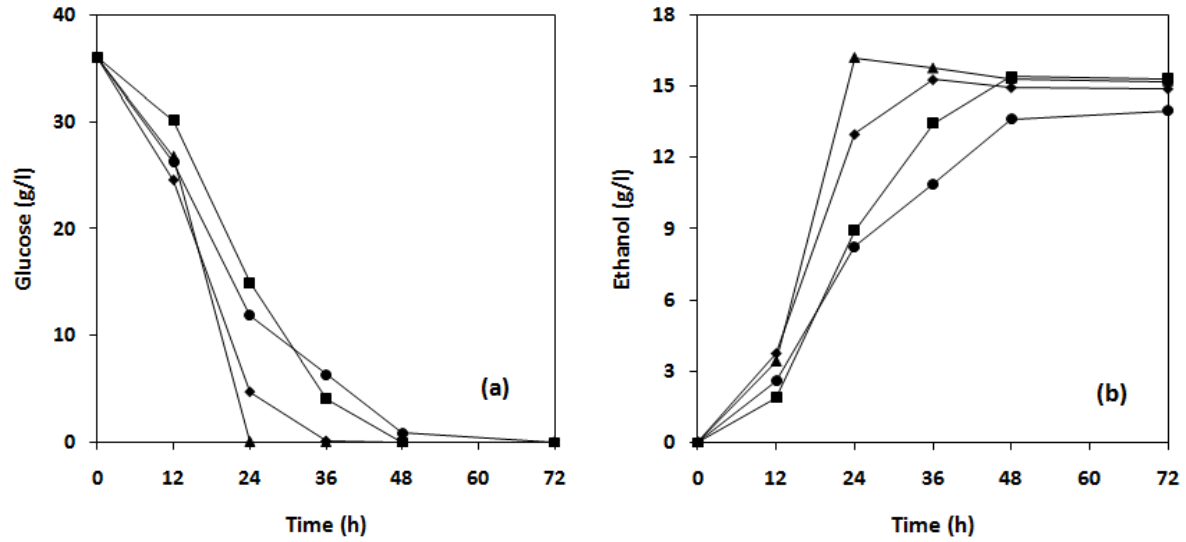

Fig.1. Effect of the supplementation of fungal extract on glucose assimilation (a) and e thanol production (b). The symbols represent of supplementation of YE (5 g/L) (■); YE (5 g/L) with mineral salts (▲); FE (2.5 g/L) (●) and FE (5 g/L) (♦).

In this direction, an additional experiment performed in order to increase the nutrient concentration with 5 g/L FE of *M. indicus* as unique supplementation (Table 1). Compared with 5 g/L YE, 5 g/L FE resulted in a higher ethanol yield with a maximum of 0.43 g/g. However, the low glucose consumption indicated the existence of nutrient limitation in the medium. As a result, the maximum yield and productivity of ethanol in this medium was still lower than the fully supplemented medium (Table 1).

3.2. Evaluation of fungal extract for media supplementation replacing yeast extract

The possibility of supplementing of FE (2.5 g/L) in the fermentation media with combination of mineral salts (Table 1) was assessed in an additional experiment to overcome nutrient limitation. According to Table 1, addition of the mineral salts provided a gradual increase in ethanol yield and volumetric productivity in comparison with addition of only 2.5 g/L FE. However, it was comparatively low due to result obtained in a fully supplemented medium. Considering that a deficit in mineral salts with 5 g/L FE supplementation could be partially responsible for the prolonged fermentation time, additional experiment was prepared by adding the mineral salts presented in the full nutrient medium. As a result of this modification, the bioconversion to ethanol was further improved and showed results closely related to the ones observed for the fully supplemented medium (Fig. 2a and b), with a maximum ethanol yield and productivity of 0.46 g/g and 0.69 g/L h in less than 24 h, respectively. The maximum glycerol yield of 0.49 mg/g was achieved at this condition. It came, therefore, to the conclusion that autolysis of *M. indicus* biomass as a valuable by product from ethanol fermentation could be used as a microbial nutrient source for further fermentation with supplementation of 5 g/L FE replacing 5 g/L YE.

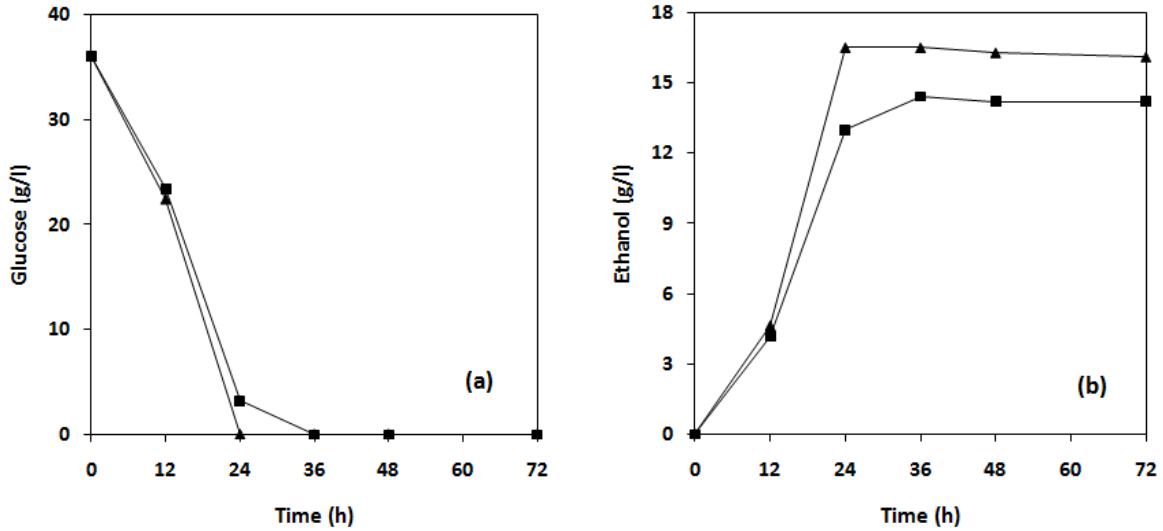

Fig.2. Effect of the supplementation of fungal extract with combination of mineral salts on glucose assimilation (a) and ethanol production (b). The symbols represent of supplementation of FE (2.5 g/L) with mineral salts (■); FE (5 g/L) with mineral salts (▲).

4. Discussion

The main purpose of the current work was the fermentative production of ethanol by the filamentous fungus, *M. indicus*, using a fungal autolysate as a low-cost complex nutrient solution. *M. indicus* is a fungus that has recently been identified as a candidate for industrial production of ethanol [2, 4]. Considering the similarity of chemical components between *M. indicus* and yeasts, it might be assumed that the fungal extract might be a feasible alternative to yeast extract as a nutrient source for fermentation media. Thus, the fungal cells of *M. indicus*, as a by-product of fermentation processes, were then subjected to autolysis to produce nutrient supplements for the following fermentations by similar fungus *M. indicus.* Therefore, the autolysis of the fungal cells biomass produced during fermentation may be considered as a suitable replacement for YE. Thus, the natural enzymatic process of fungal autolysis under oxygen starvation conditions was used in order to disrupt *M. indicus* cells and release various nutrients into the surrounding liquid. On the other hand, this process could be applied as an effective approach to nutrient regeneration/ production due to its simplicity [7]. In this study, autolysate of fungal cells, referred to as FE resulted in high performance in ethanol production. Media containing FE (5 g/L) replacing YE as nutrient source led to high-yield and high-volumetric productivity of ethanol. In addition high-yield of glycerol was obtained in FE concentration (5 g/L) relative to fully supplemented medium. This demonstrates clearly that the FE of *M. indicus* contains sufficient essential nutrients for the ethanol fermentation.

5. Conclusion

The biomass of *M. indicus* can be used as a nutrient source for ethanol production by this fungus. Autolysate of the fungal cells could successfully replace the major nutrients which are necessary for the fermentation.

References

[1] A. Demirbas, Progress and recent trends in biofuels, Progress in energy and combustion science 33, 2007, pp. 1-18.

[2] A. Sues, et al., Ethanol production from hexoses, pentoses, and dilute-acid hydrolyzate by Mucor indicus, Fems Yeast Research 5, 2005, pp. 669-676.

[3] S. Chatterjee, et al., Chitosan from Mucor rouxii: production and physico-chemical characterization, Process Biochemistry 40, 2005, pp. 395-400.

[4] K. Karimi, et al., Mucor indicus as a biofilter and fermenting organism in continuous ethanol production from lignocellulosic hydrolyzate, Biochemical Engineering Journal 39, 2008, pp. 383-388.

[5] S. W. York and L. O. Ingram, Ethanol production by recombinant Escherichia coli KO11 using crude yeast autolysate as a nutrient supplement, Biotechnology Letters 18, 1996, pp. 683-688.

[6] A. Jones and W. Ingledew, Fuel alcohol production: appraisal of nitrogenous yeast foods for very high gravity wheat mash fermentation, Process Biochemistry 29, 1994, pp. 483-488,.

[7] A. A. Koutinas, et al., Development of a process for the production of nutrient supplements for fermentations based on fungal autolysis, Enzyme and Microbial Technology 36, 2005, pp. 629-638.

Yeast adaptation on the substrate straw

Heike Kahr[1*], Sara Helmberger[1], Alexander G. Jäger[1]

[1] *Upper Austria University of Applied Sciences Research and Development Ltd, Campus Wels*
Stelzhamerstrasse 23, A-4600 Wels, Austria
** Tel: +43 7242 728114170, Fax: +43 7242 7281194170 E-mail: heike.kahr@fh-wels.at*

Abstract: Bioethanol production of lignocellulosics is technologically analyzed, but requires further investigations concerning yield optimization and economic efficiency. One important aspect is to obtain an ideal yeast strain for the fermentation process, which should possess the ability of a stable conversion of C5- and C6-sugars, resistance/tolerance against inhibitory compounds, temperature, ethanol, sugar and industrial stability. The use of genetically-modified microorganisms is reported. Problems with the stability of the microorganisms and public concerns with regard to/about the use of genetically-modified organisms led us to seek other strategies. For this purpose, several yeast strains were adapted to the mentioned characteristics using specific natural adaptation and systematic selection.
For improved utilization of xylose, several yeast strains have been cultivated on xylose-minimal agar for various generations. Yeast strains have been adapted to grow in ascending concentrations of wheat straw hydrolysate medium. Furthermore, several yeast strains have been bred at increased temperatures, with enhanced ethanol and sugar concentrations.
Some xylose- as well as hydrolysate-adapted yeast strains show an increased fermentative competence. A few of the thermally adapted yeast strains represent an enhanced fermentative capacity at higher temperature (42°C). Various yeast strains are tolerant concerning 8-12 % of ethanol and 400-450 g/l of glucose. Some significant improvements concerning ideal yeast strain could have been reached. These improvements offer new possibilities for further optimization.

Keywords: *Lignocellulosic remnant straw, Ideal yeast strain, Natural adaptation, Systematic selection, Bioethanol*

1. Introduction

Economic production of bioethanol using lignocellulosic biomass involves quantitative fermentation of cellulosic as well as hemicellulosic fraction, which contains xylose as major sugar component in agricultural remnant materials [1]. By use of the yeast strain *Saccharomyces* only C6-sugars can be converted to ethanol, but not C5-sugars [2]. If the pentoses were also converted, ethanol yield could be increased significantly.

In the literature, numerous approaches are described where due to genetic engineering the pentose phosphate pathway in yeast cells (especially in *Saccharomyces cerevisiae*) is modified, so that the yeasts are able to convert xylose into ethanol, reviewed in [3]. Anyway, during longer application in the laboratory, the stability of recombinant yeast strains is not guaranteed, moreover, global acceptance concerning GM-organisms is another serious problem [4]. Therefore, development of non-GM yeast strains, capable of utilizing and converting xylose efficiently for production of bioethanol, using natural selection and breeding would be advantageous. When lignocellulosic biomass (e.g. straw) is pretreated (with Steam Explosion), substances, such as phenols, hydroxymethylfurfural (HMF), furfural and organic acids are generated. Those substances inhibit yeast cells, resulting in a highly constrained growth and ethanol production.

The majority of fermenting yeasts generally have limited osmotolerance and thermotolerance, with an optimum temperature ranging from 30 to 37°C [5]. Therefore, the development and use of osmotolerant and thermotolerant yeast strains, capable of growing and fermenting with good yields at temperatures above 40°C would be advantageous, especially with regard to

simultaneous saccharification and fermentation (SSF) [6]. Yeast growth and fermentation at high initial sugar concentrations and high temperature not only minimizes contamination chances, reduces cooling costs, has faster fermentation rates, but also facilitates the attainability of high ethanol concentrations, therefore reducing subsequent distillation costs.
Ethanol is known to act as an inhibitor to yeast cells, inducing loss of cell viability and inhibition of both yeast growth and different transport systems [7]. Thus, ethanol tolerant yeast strains are beneficial, in order to achieve high fermentation efficiency and finally a high yield of ethanol.

Summing up, the ideal yeast strain for bioethanol production of lignocellulosic biomass (e.g. straw) should possess the following characteristics: stable conversion of C5 and C6-sugars, resistance against inhibitory compounds, tolerance concerning temperature, ethanol as well as sugar and industrial stability. In this paper, we demonstrate that various yeast strains could have been adapted to the mentioned characteristics using specific natural adaptation and systematic selection.

2. Methodology

2.1. Microorganisms

The following microorganisms have been used: *Kluyveromyces marxianus (DSM 5418), Kluyveromyces marxianus (DSM 5420), Kluyveromyces thermotolerans (DSM 3434), S.C.BUT8, S.C.BUT4, Candida utilis, S.C.BUT3, Rhodotorula, Kluyveromyces lactis (DSM 4909), osmophilic yeast strain, Saccharomyces cerevisiae, Malaga, white wine yeast strain, Pichia stipitis, Pachysolen tannophilus (DSM 70352)* and *industrial baker´s yeast (S.C.BUT2).*

All yeast strains, used for adaptation, were grown in YGC medium at 30°C and maintained at 4°C on YGC agar plates. *Pichia stipitis* and *Pachysolen tannophilus (DSM 70352)* are maintained on Xylose agar plates.

2.2. Media

YGC medium (yeast extract 5 g/L, glucose 20 g/L, chloramphenicol 0.1 g/L) was routinely used as growth and testing medium. Agar plates have been prepared by adding agar 15 g/L. Xylose medium (urea 6.4 g/L, KH_2PO_4 1.2 g/L, Na_2HPO_4 0.18 g/L, yeast extract 10 g/L, xylose 50 g/L, chloramphenicol 0,1 g/L) was used as xylose-growth medium. Xylose agar plates have been prepared using yeast extract 10 g/L, peptone 20 g/L, xylose 20 g/L, agar 20 g/L, chloramphenicol 0.1 g/L. Xylose minimal-medium (DIFCO® yeast nitrogen base without amino acids 6.7 g/L, xylose, 50 g/L, chloramphenicol 0.1 g/L) was used as xylose-adaptation minimal medium [8].

Agar plates have been prepared by adding agar 18 g/L. Hydrolysate adaptation medium was prepared, similar to [9], by adding xylose 15 g, glucose 30 g, yeast extract 1.5 g, peptone 3 g, KH_2PO_4 2 g, $(NH_4)_2SO_4$ 1 g and $MgSO_4$-$7H_2O$ 0.5 g in 1 L of 10 – 30 % (dry substance) pre-fabricated straw hydrolysate (described in chapter 2.3), the pH was adjusted to 5.0 ± 0.1. In normal straw hydrolysate (10 % dry substance), the average xylose yield accounts for about 15 g/L and average glucose yield accounts for about 30 g/L. With increasing hydrolysate concentrations (dry substances of up to 30 %), glucose and xylose input amounts were reduced in adaptation media. Adaptation media have been finished by sterilely filtrating.

2.3. Preparation of wheat straw hydrolysate

With pretreated, dried and grinded straw, a 10 to 30 % suspension has been produced, using citrate-buffer solution (acetic acid 9.6 g/L, pH 5.0 ± 0.1). Suspension has been enzymatically solubilised at a temperature of 50 °C for 96 hours. After hydrolysis, suspension has been filtered and further used in hydrolysate adaptation media.

2.4. Determination of sugars, ethanol, organic acids, furans, xylitol

For precise sugar and ethanol analytics, as well as for determination of HMF, furfural and xylitol, HPLC from Jasco and BioRad AMINEX® HPX 87H with ultra-pure water as eluent, RI detection has been used. For precise organic acids analytics, as well as for lateral validation of sugar-, HMF-, furfural- and xylitol-concentrations, HPLC from Agilent Technologies, Varian Metacarb 87 H with 5 mM H_2SO_4 as eluent, UV 210 nm and RI detection has been used.

2.5. Xylose-solution for fermentation

Xylose solution was produced using xylose, 125 g/L, filled up with citrate buffer solution. After sterilely filtrating, a fermentation nutrient solution has been added. pH-value has been adjusted to 6.3.

2.5.1. Fermentation nutrient solution

Fermentation nutrient solution has been prepared using DIFCO® yeast nitrogen base without amino acids 85 g/L, urea 113.5 g/L, peptone 328 g/L.

2.6. Glucose-solution for fermentation

Glucose-solution was produced using glucose 140 g/L, filled up with citrate buffer solution. After autoclaving, $(NH_4)_2HPO_4$, $CaCl_2$-$2H_2O$, KH_2PO_4 and $MgSO_4$-$7H_2O$ have been added, pH-value has been adjusted to 4.6.

2.7. Adaptation of yeast strains on xylose as sole carbon source

Selected, analyzed yeast strains have been streaked constantly on xylose-containing agar plates (rich medium) for several generations (approx. 15 passages). Those yeast strains have been adapted to grow on Xylose-minimal agar. Yeast strains have been streaked again constantly on that minimal agar for several generations (currently passage 50).

2.8. Fermentation analyses with xylose-adapted yeast strains

Fermentation analyses with xylose-adapted yeast strains have been conducted, using xylose liquid medium as yeast growth medium and xylose solution for fermentation, including the fermentation nutrient solution, pH 6.3. Fermentation has been practised aerobically and anaerobically at 30 °C for 168 hours. As positive control, not adapted yeast strains have been cultivated in YGC-medium and used in fermentation process with identical parameters.

2.9. Adaptation of yeast strains on wheat straw hydrolysate

Selected yeast strains have been cultivated in ascending concentrated hydrolysate adaptation media. Adaptation of yeast strains has been conducted at 30°C. Simultaneously, several yeast strains were cultivated additionally at higher temperatures (up to 41°C). Therefore, increased inhibitor-resistant yeast strains with a higher temperature tolerance could be achieved.

2.10. Fermentation analyses with wheat straw hydrolysate-adapted yeast strains

Fermentation analyses with hydrolysate-adapted yeast strains have been conducted, using hydrolysate adaptation medium as yeast growth medium. Fermentation has been conducted using pre-fabricated and concentrated straw hydrolysate (60 % of straw dry substance) at 30°C for 168 h. As positive control, not adapted yeast strains have been cultivated in YGC-medium and used in fermentation process with identical parameters.

2.11. Adaptation of yeast strains on increased temperatures

Several yeast strains have been streaked on YGC agar plates and incubated at increasing temperatures up to 42 °C. *Kluyveromyces marxianus* has been bred at temperatures up to 45°C. Thermotolerant yeast strains have been tested additionally in a fermentation approach at higher temperatures.

2.12. Determination of alcohol and sugar tolerance

Yeast strains have been grown in YGC medium at 30°C for 24 hours and inoculated into YGC medium plus different ethanol concentrations (ranging from 0-13 %). Yeast cell concentrations have been determined using spectrophotometer (OD 600 nm) after incubation at 30°C. Sugar tolerance of yeast strains have been tested after growth in YGC medium, including different concentrations of glucose (up to 450 g/L). Yeast cell concentration was determined using spectrophotometer (OD 600 nm) after incubation at 30°C. Sugar tolerant yeast strains have been tested additionally in a fermentation approach using glucose solution with different glucose concentrations (up to 450 g/L) at 30°C for 168 hours.

3. Results

3.1. Fermentation analyses with xylose-adapted yeast strains

Several xylose-adapted yeast strains (about 50 passages) produced slightly increased ethanol yields, especially during aerobic fermentation process. Using xylose-adapted *Pichia stipitis* (passage 48) in the aerobic fermentation process, a significant increase in ethanol production with 4.6 %vol. could be observed (table 1 and 2).

Table 1. Ethanol yields after aerobic and anaerobic fermentation of xylose-solution, including fermentation nutrient solution, with non-adapted control yeast Pichia stipitis.

Control yeast *Pichia stipitis*	Fermentation condition	EtOH [% vol.]	remaining xylose [g/L]	xylitol [g/L]
	aerob	3,4	34,5	2,5
	anaerob	2,1	73,4	2,4

Table 2. Ethanol yields after aerobic and anaerobic fermentation of xylose-solution, including fermentation nutrient solution, with Pichia stipitis, adapted on xylose as sole carbon source.

Xylose-adapted *Pichia stipitis*	Fermentation condition	EtOH [% vol.]	remaining xylose [g/L]	xylitol [g/L]
	aerob	4,6	19,7	14,4
	anaerob	4	19,1	16,2

3.2. Adaptation of yeast strains on wheat straw hydrolysate medium

Yeast strains have been adapted successfully to ascending concentrations of wheat straw hydrolysate medium. Both, at 30 °C and also at increased temperatures (up to 41°C), yeast growth in straw hydrolysate medium is successful.

3.3. Fermentation analyses with wheat straw hydrolysate-adapted yeast strains

Fermentation approaches with hydrolysate-adapted yeast strains have been conducted using concentrated wheat straw hydrolysate (with 60 % of dry substance) (table 3). Fermentation approaches have shown that some adapted yeast strains have increased resistance concerning existent inhibitory compounds (table 4).

Table 3. List of sugars, organic acids and furans, contained in concentrated wheat straw hydrolysate (with 60 % of dry substance).

Components of concentrated hydrolysate	[g/L]
Glucose	140.3
Xylose	55.8
Acetic acid	9.9
Formic acid	1.2
Propanoic acid	1.1
Hydroxymethylfurfural	0.3
Furfural	0.2

Table 4. EtOH-yields [%vol.] after fermentation of concentrated wheat straw hydrolysate, using adapted yeast strains and non-adapted control yeast strains.

Adapted yeasts	EtOH [%vol.]	Control yeasts	EtOH [%vol.]
S.C.BUT3	4,8	*S.C.BUT3*	0,7
S.C.BUT8	4,2	*S.C.BUT8*	2,9
S.C.BUT4	4,6	*S.C.BUT4*	0,7

3.4. Adaptation of yeast strains on increased temperatures

Several yeast strains show very good growth on YGC-agar plates at temperatures up to 42°C, except *Saccharomyces cerevisiae*, which is only able to grow well at 30°C. Exclusively, *Kluyveromyces marxianus* can grow at a temperature up to 45°C.

3.5. Analysis of fermentative capacity of different yeast strains at increased temperatures

Several yeast strains have been tested in a fermentation process, using glucose-solution for fermentation at 40°C. As positive approach, several yeast strains have also been tested in a fermentation process at 30°C. Most of the yeast strains produced similar ethanol yields during fermentation at 30°C (between 5.3 and 7.2 %vol.) and 40°C (between 4.7 and 6.1 %vol.). Only a few yeast strains show a significant collapse concerning fermentative capacity at 40°C.

3.6. Determination of alcohol tolerance

Several yeast strains have been tested concerning growth in YGC medium, including ascending concentrations of ethanol (0-13 %). Yeast cell density has been examined using spectrophotometer (OD 600 nm) after incubation at 30°C. Using 11 % of EtOH in the growth medium, several yeast strains still have good cell density (60 %, 74 %, 58 %, 61 %, 60 % and 75 %, respectively). With 13 % of EtOH, only one yeast strain has 61 % cell density. Only 3 used yeast strains have low ethanol tolerance (2-4 % EtOH).

3.7. Determination of sugar tolerance and fermentative competence

After analysis of yeast cell growth in YGC medium with ascending glucose-concentrations, several yeast strains have been tested additionally in a fermentation process, using glucose solution with different concentrations of glucose at 30°C for 168 hours. Almost all yeast strains have produced high ethanol yields after fermentation with increased glucose-concentrations (up to 450 g/L glucose). Best results have been reached using two special types of yeast.

4. Discussion

Lignocellulosic raw materials contain 5-20 % of the pentose sugars xylose and arabinose [10]. Microorganisms, able to ferment xylose are found among bacteria, yeast and filamentous fungi [11]. However, natural xylose-fermenting yeast strains, such as *Pichia stipitis*, *Candida shehatae* and *Pachysolen tannophilus* [12] are known to produce low ethanol yields and to re-assimilate the produced ethanol [13]. However, *Pichia stipitis* is known as one of the better yeast strains, able to ferment xylose. During anaerobic fermentation conditions a large portion of xylose is converted to xylitol therefore ethanol yield is accordingly low. Low levels of oxygen are important in the conversion of xylose into ethanol, so that cell viability and NADH balance are maintained.

Agbogbo et al. [14] have tested *Pichia stipitis* in fermentation approaches on various glucose and xylose mixtures. Maximum ethanol concentration with 100 % of xylose (60 g/L) was 24.3 ± 0.34 g/L, which corresponds to about 3.03 %vol. We have successfully adapted many yeast strains to grow on xylose-minimal medium, according to Attfield and Bell [8], who have demonstrated the development of non-GM yeast strains (*Saccharomyces cerevisiae*), capable of efficiently growing on xylose.

In our study, xylose-adapted yeast strains, regularly bred on xylose-minimal agar for several generations, produced slightly increased ethanol yields, especially during aerobic fermentation process. Using xylose-adapted *Pichia stipitis*, a significant increase in ethanol production after aerobic fermentation process of about 35 % can be observed (ethanol yield of 4.6 %vol., see table 1 and 2). Also within anaerobic fermentation process, using xylose-adapted *Pichia stipitis*, an increase in ethanol production of 90 % can be observed (ethanol yield of 4 %vol., see table 1 and 2). All xylose-adapted yeast strains show good tendency of getting adaped to convert xylose to ethanol, but also with a high production of xylitol as by-product. However, yeast strains will be further cultivated on xylose-minimal agar, as well as in xylose-liquid medium and fermentative capacity concerning increased xylose conversion will be regularly analyzed.

The most widely studied yeast strains for ethanol fermentation using wheat straw hydrolysate as feedstock are *Pichia stipitis* [9], *Kluyveromyces marxianus* [15], native as well as recombinant strains of *S.cerevisiae*. Best ethanol yields have been obtained with the native non-adapted *S.cerevisiae* with 31.2 g/L, which corresponds to about 3.9 %vol. [16]. However, those yeast strains are hindered during fermentation process by inhibitory compounds, generated during pretreatment and hydrolysis of lignocellulosic biomass [17]. Bjorling and Lindman [18] reported, that *Pichia stipitis* is completely inhibited during fermentation by using a medium, containing 3.9 g/L acetic acid, known as an inhibitory component in hydrolysates. In his study, Nigam [9] has improved fermentation performance by adapting xylose-fermenting yeast *Pichia stipitis* on higher concentrations of acetic acid. The addition of 5 g/L acetic acid in hydrolysate medium significantly inhibited sugar utilization and ethanol production. Maximal ethanol yield with inhibitor-adapted yeast culture was 14.5 g/L, which

corresponds to about 1.8 %vol. In order to adapt yeast strains to inhibitory compounds in the hydrolysat, several yeast strains, used in our study, have been successfully bred in ascending concentrations of wheat straw hydrolysate medium at 30 °C and also at increased temperatures (up to 41 °C). Fermentation approaches have shown that some hydrolysate-adapted yeast strains have increased resistance concerning existent inhibitory compounds. Fermentation has been conducted in pre-fabricated wheat straw hydrolysate, containing among glucose and xylose, 9.9 g/L acetic acid, 1.2 g/L formic acid, 1.1 g/L propanoic acid, 0.3 g/L hydroxymethylfurfural and 0.2 g/L furfural.

The adapted yeast strain *S.C.BUT3* produced an ethanol yield of 4.8 %vol., whereas the not adapted control yeast only 0.7 %vol. Also the adapted yeast *S.C.BUT8* yielded an increased ethanol concentration of 4.2 %vol. (not adapted control yeast only 2.9 %vol.). By use of adapted *S.C.BUT4*, an ethanol yield of 4.6 %vol. could be reached, the not adapted control yeast only produced 0.7 % vol. (see table 4).

A serious problem concerning simultaneous saccharification and fermentation (SSF), which appears as a promising alternative among all processes for bioethanol production from lignocellulosic biomass is the different optimum temperatures for saccharification (45 - 50 °C) and fermentation (25 - 30°C) [6]. The majority of fermenting yeasts generally have limited osmotolerance and thermotolerance, with an optimum temperature ranging from 30 to 37°C [5]. In our study, we could thermally adapt several yeast strains to grow at temperatures up to 42°C, *Kluyveromyces marxianus* is able to grow at a temperature of 45°C. Fermentation approaches at 40°C provided good ethanol yields (up to 6.1 %vol).

Ethanol is known to be an inhibitor to yeast cells, inducing amongst others loss of cell viability which results in less efficient fermentation process and thus to reduced ethanol yield. The receipt of highly ethanol tolerant yeast mutants is very difficult, isolation requires long-term selection techniques in continuous culture [19]. In our study, numerous yeast strains have been tested concerning growth in YGC medium, including ascending concentrations of ethanol (0-13 %). Using 11 % of EtOH, several yeast strains have good cell viability. With 13 % of EtOH, one yeast strain has still 61 % cell density. Fermentation at high initial sugar concentrations provides high ethanol concentrations, which reduces subsequent distillation costs. After analysis of yeast cell growth in YGC medium with ascending glucose-concentrations, used yeast strains have been tested additionally in a fermentation process, using glucose solution with different concentrations of glucose at 30°C for 168 hours. Several yeast strains have produced high ethanol yields after fermentation with increased glucose-concentrations (up to 450 g/L glucose).

5. Conclusion

The ideal yeast strain for bioethanol production of lignocellulosic biomass has not been produced yet, because the mentioned requirements could not have been combined completely into one ideal yeast strain. However, some significant improvements with regard to the ideal yeast strain could have been reached. These improvements offer new possibilities for further optimization.

References

[1] B. C. Saha, Hemicellulose bioconversion, J. Ind. Microbiol. Biotechnol. 30, 2003, pp. 279-291.

[2] B. C. H. Chu and H. Lee, Genetic improvement of *Saccharomyces cerevisiae* for xylose fermentation, Biotechnology Advances 25, 2007, pp. 425–441.

[3] B. Hahn-Hägerdal et al., Towards industrial pentose-fermenting yeast strains, Appl. Microbiol. Biotechnol. 74, 2007, pp. 937–953.

[4] I. S. Pretorius, Tailoring wine yeast for the new millennium: novel approaches to the ancient art of winemaking, Yeast 16, 2000, pp. 937-953.

[5] J. B. Kristensen et al., Use of surface active additives in enzymatic hydrolysis of wheat straw, Enzyme Microb. Technol. 40, 2007, pp. 888-95.

[6] H. Jorgensen, J.B. Kristensen, C. Felby, Enzymatic conversion of lignocellulose into fermentable sugars: challenges and opportunities, Biofuels Bioprod. Bioref. 1, 2007, pp. 119-34.

[7] H. Alexandre and C. Charpentier, Biochemical aspects of stuck and sluggish fermentation in grape must, J. Ind. Microbiol. Biotechnol. 20, 1998, pp. 20–27.

[8] P. V. Attfield and P. J. L. Bell, Use of population genetics to derive non-recombinant *Saccharomyces cerevisiae* strains that grow using xylose as a sole carbon source, FEMS Yeast Res. 6, 2006, pp. 862-868.

[9] J. N. Nigam, Development of xylose-fermenting yeast *Pichia stipitis* for ethanol production through adaptation on hardwood hemicellulose acid prehydrolysate, Journal of applied microbiology 90, 2001, pp. 208-215.

[10] B. Hahn-Hägerdal et al., Bioethanol – the fuel of tomorrow from the residues of today, Trends in Biotechnology 24, 2006, pp. 549-556.

[11] L. Skoog and B. Hahn-Hägerdal., Xylose fermentation, Enzyme Microb. Technol. 10, 1988, pp. 66-80.

[12] A. K. Chandel et al., Economics and environmental impact of bioethanol production technologies: an appraisal, Biotechnology and Molecular Biology Review 2, 2007, pp. 014-032.

[13] D. Karakashev et al., Anaerobic biotechnological approaches for production of liquid energy carriers from biomass, Biotechnology Letters 29, 2007, pp. 1005-1012.

[14] F. K. Agbogbo et al., Fermentation of glucose/xylose mixtures using *Pichia stipitis*, Process Biochemistry 41, 2006, pp. 2333-2336.

[15] E. Tomás-Pejó et al., Bioethanol production from wheat straw by the thermotolerant yeast *Kluyveromyces marxianus CECT 10875* in a simultaneous saccharification and fermentation fed-batch process, Fuel 88, 2009, pp. 2142-2147.

[16] H. Jorgensen, Effect of nutrients on fermentation of pretreated wheat straw at very high dry matter content by *Saccharomyces cerevisiae,* Applied biochemistry and Biotechnology 153, 2009, pp. 44-57.

[17] B. Hahn-Hägerdal et al., An interlaboratory comparison of the performance of ethanol-producing microorganisms in a xylose-rich acid hydrolysate, Appl. Microbiol. Biotechnol. 41, 1994, pp. 62-72.

[18] T. Bjorling and B. Lindman, Evaluation of xylose-fermenting yeasts for ethanol production from spent sulfite liquor, Enzyme and Microbial. Technology 11, 1989, pp. 240-246

[19] S. W. Brown and S. G. Oliver, Isolation of ethanoltolerant mutants of yeast by continuous selection, Eur. J. Appl. Microbiol. Biotechnol. 16, 1983, pp. 116-122

Thermodynamic analysis and potential efficiency improvements of a biochemical process for lignocellulosic biofuel production

M. Imroz Sohel,* and Michael W. Jack

Scion, Te Papa Tipu Innovation Park, 49 Sala Street, Rotorua, New Zealand
** Corresponding author. Tel: +64 7 3435730; fax: +64 7 3435375; E-mail address: mohammed.sohel@scionresearch.com*

Abstract: This paper presents a thermodynamic analysis of a biochemical process for the production of bioethanol from a lignocellulosic feedstock. The major inefficiencies in the process are identified as: i) the combustion of lignin for process heat and power production and ii) the simultaneous saccharification and fermentation process. As lignin is not converted to ethanol and lignin has a high value of chemical exergy, the overall efficiency of the biochemical process largely depends on how the lignin is utilized. We therefore consider integrating a source of low temperature heat, such as waste heat or low-enthalpy geothermal heat, into a biochemical lignocellulosic biorefinery to provide process heat. This enables the lignin-enriched residue to be used either as a feedstock for chemicals and materials or for on-site electricity generation. Our analysis shows that integrating low temperature heat source into a biorefinery in this way represents an improvement in overall resource utilization efficiency.

Keywords: *Bioenergy; biorefinery; geothermal energy; process heat; integrated approach.*

Nomenclature

Ex exergy ..... $MJ \cdot s^{-1}$
P electric power ..... $MJ \cdot s^{-1}$
η efficiency ..... *[-]*
δ exergy loss for heat transfer ..... *[-]*
subscript
bio ..... *biomass*
ch ..... *chemical*
geo ..... *geothermal*
HT ..... *heat transfer*
ph ..... *physical*
proc ..... *process*
prd ..... *product*
wstprd ..... *waste product*
SN ..... *sink*
SR ..... *source*
0 ..... *dead state*

1. Introduction

Increasing the percentage of liquid transport fuel from renewable biomass sources is an important opportunity in the move towards a more sustainable energy system. Recent political and research and development trends show a clear move towards lignocellulosic feedstocks for these biofuels [1]. Lignocellulosic feedstocks mitigate competition for land and water used for food production, increase biomass production per unit of land and reduce the inputs needed to grow the biomass [2-4].

A key challenge for biofuel production systems is to develop efficient conversion technologies which are able to compete economically with fossil fuels. The biorefinery concept [5, 6], where a range of high-value co-products are produced in addition to commodity fuel products, attempts to achieve increased efficiency by making full use of biomass feedstocks [5, 7-9]. Due to the potential cost reductions from this strategy, biorefineries are seen as a key step towards the commercial implementation of biofuels [5].

A large percentage of the lignocellulosic biorefinery concepts that have so far been proposed are based on a biochemical conversion platform where the polysaccharides in lignocellulosic material are converted to liquid fuel using enzymes [10, 11]. In these systems it has been proposed that the lignin by-product and other extractives can be used for higher value uses

such as the production of high-value chemicals and materials [5, 7] or on-site electricity production [12].

One of the major impediments to the lignocellulosic biorefinery concept is that the liquid fuel production from lignocellulosic biomass is a very energy intensive process [5, 11, 13, 14]. Current integrated biorefinery concepts use the lignin-enriched residue as a fuel to meet process energy demands, reducing the possibility of higher-value uses of lignin. A potential option to overcome this is to introduce an external source of low-enthalpy heat, such as geothermal or waste heat, to meet the process heat demand and thereby leave the lignin-enriched residue available for higher-value uses.

As with other energy technologies, thermodynamic analysis provides a powerful tool to guide technology selection and research efforts towards more efficient biofuel production systems. Conventional energy analysis based only on the first-law of thermodynamics cannot be used reliably for these purposes as it does not embody second law constraints on energy conversion and erroneously treats all energy types as equal [15].

Exergy analysis is a convenient method of carrying out thermodynamic analysis of complex systems and has been applied to a wide range of different processes, including; energy technology, chemical engineering, transportation and agriculture [16]. A number of authors have recently applied exergy analysis to biofuel production process [17-26]. While a number of exergy analyses of thermochemical pathways exist [18, 19, 22, 23] applications of exergy analysis to biochemical pathways are limited [20, 24, 25].

In paper we present an updated synthesis of our previous work [25, 26] on applying exergy analysis to identifying the inefficiencies in a biochemical process for producing biofuel and evaluating the potential efficiency gains from integrating low-enthalpy heat into the process. The analysis is based on the National Renewable Energy Laboratory (NREL) process [11] for producing ethanol from a lignocellulosic feedstock.

2. Methodology

2.1. Exergy analysis

Unlike energy, exergy is exempt from the law of conservation. Every irreversible phenomenon causes exergy losses leading to the reduction of the useful effects of the process or to an increased consumption of the original energy source. The main aim of exergy analysis is to identify and quantify the causes of this thermodynamic imperfection in the process under consideration. The methodology of exergy analysis is presented by Szargut et al. [15] and the general approach to applying exergy analysis to biofuel production processes are given in Lu et al. [19] and Prins et al. [21]. One of the major difficulties in applying exergy analysis to biochemical process for biofuel production is that a number of components are not present in standard exergy tables [15]. In our previous work [25], a table of exergy values for these components and the methods used to calculate them are presented.

2.2. The biochemical production process

Several process models for the production of ethanol from biomass have been reported in the literature [11, 13, 14]. In particular, in a NREL publication Wooley et al. [11] have described in detail the overall process for ethanol production from wood chips via a process of simultaneous scarification and co-fermentation (SSCF). They considered a process that on average converts about 44.44 kg/s of biomass to 5.52 kg/s of ethanol. The process utilizes lignin enriched by-products to meet process heat demand. The model showed that such a plant

can produce more energy than required for process demands. The model includes an integrated power plant capable of producing 44 MW of electricity (33 MW for internal use and 11 MW for export). Piccalo and Bezzo[14] have developed an optimized system by applying pinch analysis to the original system described by Wooley et al. [11]. The analysis presented here is based on this optimized system. An overview of the process is shown in Fig 1.

Following Piccalo and Bezzo [13], the base case considered here processes 160 metric Ton of wet chip per hour, where the composition of the wood chip is cellulose: 22.2%, xylan: 9.9%, arabinan: 0.4%, mannan: 2%, galactan: 0.1%, acetate: 2.4%, lignin: 14.4%, ash: 0.5%, and moisture: 47.9%.

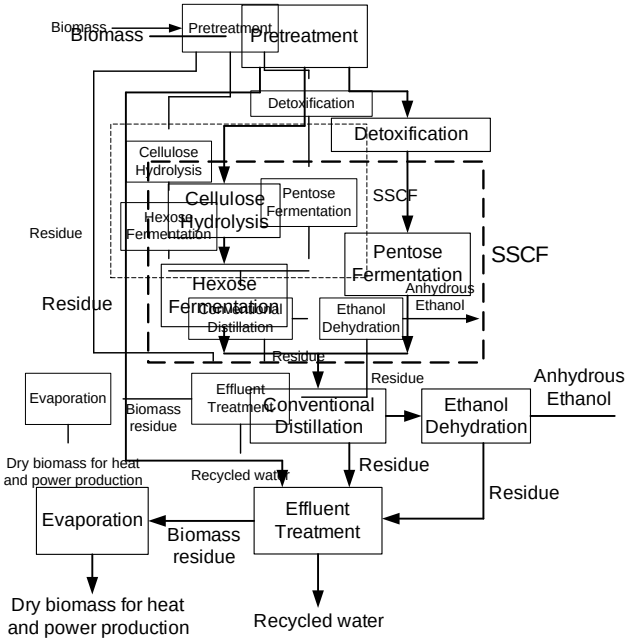

Fig. 1. Process diagram of ethanol production from lignocellulosic biomass

2.3. The efficiency of biochemical production process

One of the key parameters that can be evaluated in an exergy analysis is the overall thermodynamic efficiency. The thermodynamic efficiency of a system is defined as [15]:

$$\eta = \frac{Exergy\ of\ useful\ products}{Input\ Exergy} \tag{1}$$

In the current case, the overall efficiency of ethanol production via the biochemical process described in section 2.2 can be written as

$$\eta = \frac{E_{X,Fuel} + P_{net} + E_{X,lignin\ residue}}{E_{X,Biomass} + \sum E_{X,ch} + E_{X,low\ temp}} \tag{2}$$

Here, $E_{X,Biomass}$ is the input chemical exergy of biomass, $\sum E_{X,ch}$ is the sum of the chemical exergies of all input chemicals to the process, $E_{X,low\ temp}$ is the exergy of a potential low temperature heat source supplied to the system, $E_{X,Fuel}$ is the chemical exergy of the fuel,

$E_{X,lignin\ residue}$ is the exergy of the lignin-enriched residue and P_{net} is the net electricity produced by the system. To evaluate the efficiency of the NREL process described in section 2.2 we put $E_{X,low\ temp} = 0$ and $E_{X,lignin\ residue} = 0$.

Exergy analysis can also be used to evaluate thermodynamic losses in each unit process of the system. The exergy balance [27] applied to the system boundary of a unit operation of a process gives

$$\sum_{in} E_X = \sum_{out} E_{X,prd} + \sum_{out} E_{X,wstprd} + I \qquad (3)$$

where $\sum_{in} E_X$ is the total input exergy flow, $\sum_{out} E_{X,prd}$ is the total output exergy flow in the products, $\sum_{out} E_{X,wstprd}$ is the total output exergy flow in the waste products from the unit process and *I* is the exergy destruction due to internal irreversibility. The last two terms in the exergy balance represent the total exergy loss associated with the unit process. For an irreversible process $I \neq 0$ and Eq. (3) expresses the fundamental property that, unlike energy, exergy is not conserved.

2.4. Efficiency improvements by integrating a low temperature heat source

One possibility for improving the efficiency of biofuel production is to integrate a low temperature heat source to meet process heat demands. We consider three discrete cases and calculate the corresponding efficiencies. Here we assume that the internal electricity demand is met from the combustion of lignin-enriched residue. The rejected heat from lignin combustion can also be used to meet all the low temperature heat demand (150 ºC or less).

The highest quality steam required for the biorefinery process is 192ºC (saturated at 13 bar). This steam demand can be met from any suitable low temperature heat source. The energy required for the highest quality steam is about 46 MW (or 17.6 MW of exergy). We could meet this heat demand by using an external 210ºC heat source in the biofuel production system, thus integrating heat and biomass resources in a single process. An alternative use for this steam is in an independent power plant. Assuming a typical binary cycle power plant first law efficiency of 15% [28] we can get about 6.9 MW of electricity from this same heat source. In this work we would like to compare the overall resource efficiency of the integrated vs. independent use of the two resources. We consider 3 cases:

Case 1

This represents the base case, here we operate the biorefinery and the low temperature heat source independently, with the low-temperature heat being used in an independent power plant. The overall efficiency can be calculated from Eq. (2) where, $E_{X,Biomass}$ = 454.8 MW, $\sum E_{X,ch}$ = 12.3 MW, $E_{X,low\ temp}$ = 17.6 MW, $E_{X,Fuel}$ = 147.1 MW, P_{net} = 17.9 MW and $E_{X,lignin\ residue}$ = 0 MW. For the biorefinery we use the system described in Section 2.2.

Case 2

Here we integrate the heat source into the biorefinery to meet the high-temperature heat demands (in the biochemical process) and combust the available lignin-enriched residue to produce additional power. The overall efficiency is calculated from Eq. (2) with $E_{X,Biomass}$ =

454.8 MW, $\sum E_{X,ch}$ = 12.3 MW, $E_{X,low\ temp}$ = 17.6 MW, $E_{X,Fuel}$ = 147.1 MW, P_{net} = 22 MW and $E_{X,lignin\ residue}$ = 0 MW.

Case 3
In this case we meet internal electricity demand from lignin combustion and leave any additional lignin for some higher value use. The overall efficiency is calculated from Eq. (2) with $E_{X,Biomass}$ = 454.8 MW, $\sum E_{X,ch}$ = 12.3 MW, $E_{X,low\ temp}$ = 17.6 MW, $E_{X,Fuel}$ = 147.1 MW, P_{net} = 0 MW and $E_{X,lignin\ residue}$ = 45.8 MW.

3. Results

3.1. Exergy analysis of the biofuel production process

The efficiency of the standard NREL process [11] is calculated to be 34% using Eq. (2). Fig. 2 (b) provides a breakdown of the exergy losses in various unit operations of the production process. For comparison we have also provided a breakdown of the energy losses in Figure 2 (a). It is clear from the figures that heat and power production is the major contributor to both energy and exergy losses. The second, third and fourth largest contributors to energy loss are evaporation, distillation and dehydration and the pre-treatment & detox processes, respectively. Unlike the energy losses, the second, third and fourth largest contributors to exergy losses are SSCF, SSCF seed and pre-treatment processes, respectively. Feed handling and lignin separation have similar levels of contribution to energy and exergy losses (less than 1%).

3.2. Efficiency improvements by integrating a low temperature heat source

The calculated overall efficiency for case 1 is 34.0% which is considered as the base case here. If we integrate the low temperature heat source to the biorefinery (case 2) efficiency becomes 35%. Although, the overall improvement is only 1%, there is a significant improvement in low temperature heat utilization. In particular, an additional 4.1 MW of electricity is generated which represents a 40% gain in electricity generation from the same low temperature heat source. The overall efficiency for case 3 is 40%. Fig. 3 presents a Grassman diagram of case 3, showing the exergy flow through the various stages of the system.

4. Discussion and conclusion

The difference in the breakdown of energy and exergy losses in the system presented in Fig. 2 emphasises the importance of exergy analysis. While both the energy and exergy analysis show that heat and power production is the major loss, there is a significant difference for most of the other unit processes. This difference arises from the fact that first law analysis (energy) treats all forms of energy to be the same, whereas exergy analysis takes into account the available work in different forms of energy. For example, although evaporation, distillation and dehydration are associated with large energy demands, this demand can be met with low temperature heat sources (low exergy sources). In contrast, the SSCF and SSCF seed processes consume very little heat (low exergy) but require a significant amount of electricity (high exergy). A thermochemical process involving gasification and Fisher-Tropsch synthesis was found to have a similar overall efficiency of biochemical process [22]. A more detailed comparison is presented in [25].

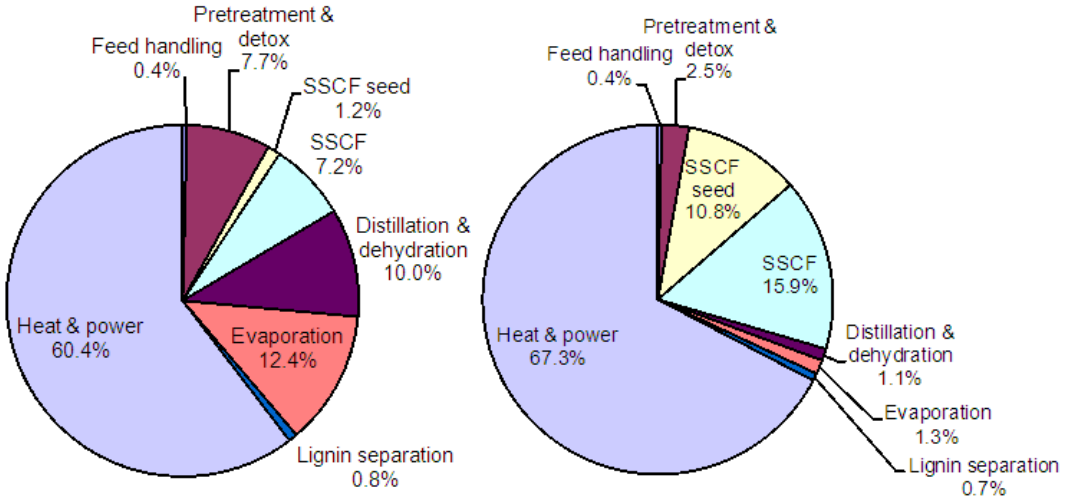

Fig. 2. Breakdown of energy (a) and exergy (b) losses for a biochemical process of biofuel production from lignocellulosic feed stock.

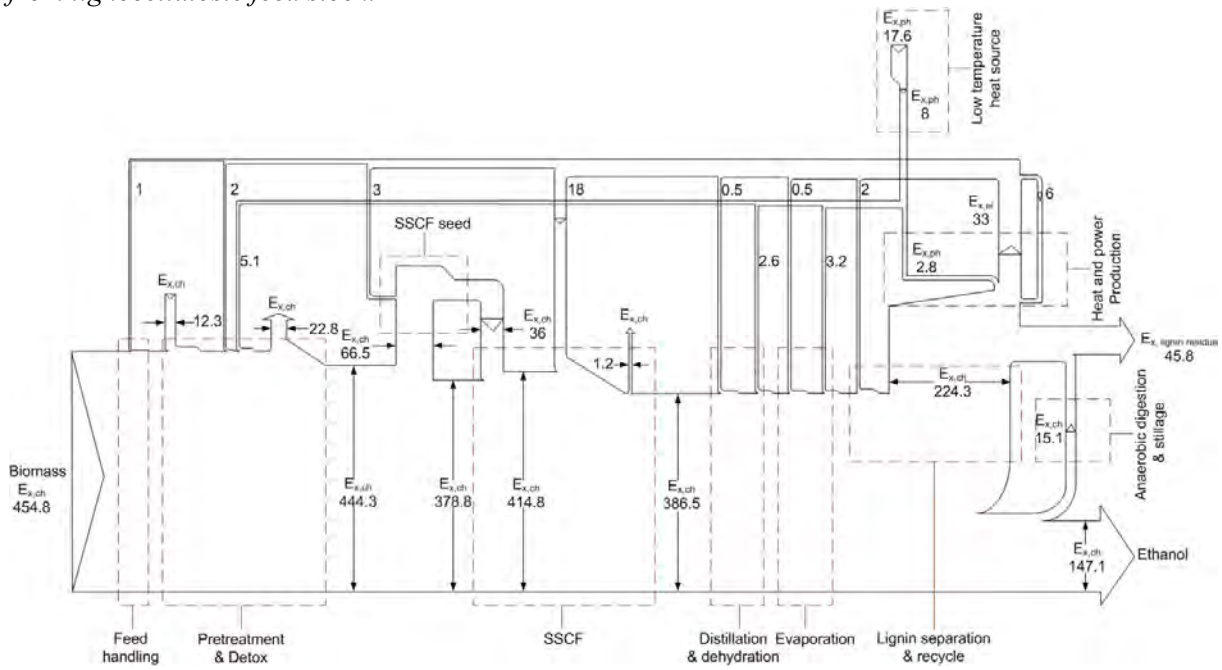

Fig. 3. Grassman diagram for an ethanol and lignin-enriched residue production process where the 192ºC heat demand is met from low temperature heat source and the remaining internal electricity demand is met from lignin combustion

There are two main reasons that heat and power generation is the largest area of exergy loss in the process. Firstly, due to the inherent inefficiency of combustion, much of the chemical exergy in the lignin is lost. The Carnot efficiency places limits on the ability of future technologies to improve this efficiency. Secondly, the direct reduction in temperature from the combustion temperature (815 ºC for lignin) to that of the process heat (200 ºC) leads to a further loss of exergy. The exergy loss due to entropy generation associated with heat transfer to a cooler medium can be easily deduced from the Carnot efficiency [15]

$$\delta_{HT} = \frac{T_0}{T_{SN}}\left(\frac{T_{SR} - T_{SN}}{T_{SR} - T_0}\right) \qquad (7)$$

where all temperatures are in Kelvin. From Eq. (7) the exergy loss due to entropy generation associated with heat transfer from 815ºC to 200ºC with ambient temperature of 25ºC is

calculated to be 49% of the original exergy, whereas if we meet the heat demand from low temperature heat source of 210ºC, the exergy loss due entropy generation associated with heat transfer becomes only 3% of original exergy. This explains the improvement in efficiency by integrating a low-enthalpy heat source to meet the process heat demand.

Producing co-products or usable by-product can also change the efficiency of the system significantly. For instance, gypsum and ammonium acetate (4.8 MW, 16.8 MW equivalent of exergy, respectively) are produced in the detox process. If we can recover and utilize even 50% of these two wastes/by products, the overall efficiencies for case 1, case 2 and case 3 increase to 35%, 37% and 42%, respectively.

In summary, this analysis shows that, in essence, the lignin enriched residue is too valuable from a thermodynamic perspective to be combusted for process heat. This is therefore a thermodynamic justification for the biorefinery concept which proposes making the most out of the biomass by using the lignin-enriched residue as a feedstock for higher value products. For current technologies, to support this concept requires a source of low-temperature heat to meet process heat demands. Using a heat source with a temperature very close to that of process heat demand reduces the losses incurred by this approach. Potential sources of this heat are waste heat and geothermal. Overall, this process of integrating low-enthalpy heat and thus leaving the lignin enriched residue available for higher value uses can lead to significant improvements in overall efficiency of a biochemical biofuel process. This analysis also showed that if we can recover and utilize some of the key wastes and by-products, the overall efficiency increases due to the large exergy content in these chemicals.

References

[1] IEA, From 1st to 2nd Generation Generation Biofuel Technologies. 2008.

[2] Metzger, J.O. and A. Huttermann, Sustainable global energy supply based on lignocellulosic biomass from afforestation of degraded areas. Naturwissenschaften, 2008. 96: p. 279-288.

[3] Schmer, M.R., et al., Net energy of cellulosic ethanol from switchgrass. Proc. Natl. Acad. Sci. USA, 2008. 105: p. 464-469.

[4] Tilman, D., et al., Beneficial Biofuels-The Food, Energy, and Environment Trilemma. Science, 2009. 325: p. 270.

[5] Ragauskas, A.J., et al., The path forward for biofuels and biomaterials. Science, 2006. 311: p. 484-489.

[6] Demirbas, A., Biorefineries: Current activities and future developments. Energy Conversion and Management, 2009. 50(11): p. 2782-2801.

[7] Dodds, D.R. and R.A. Gross, Chemicals from Biomass. Science, 2007. 318: p. 1250-1251.

[8] Elnashaie, S.S.E.H., et al., Integrated system approach to sustainability bio-fuels and bio-refineries. Bulletin of Science, Technology and Society, 2008. 28(6): p. 510-520.

[9] Zhang, Y.H.P., Reviving the carbohydrate economy via multi-product lignocellulose biorefinaries. J Ind Microbiol Biotechnol: BioEnergy- Special Issue, 2008. 35(5): p. 367-75.

[10] Huber, G.W., S. Iborra, and A. Corma, Synthesis of Transportiation Fuels from Biomass: Chemistry, Catalysis, and Engineering. Chem. Rev., 2006. 106: p. 4044-4098.

[11] Wooley, R., et al., Lignocellulosic Biomass toEthanol Process Design and Economics Utilizing Co-Current Dilute Acid Prehydrolysis and Enzymatic Hydrolysis Current and Futuristic Scenarios. 1999, National Reneable Energy Laboratory.

[12] Larsen, J., et al., The IBUS Process – Lignocellulosic Bioethanol Close to a Commercial Reality. Chem. Eng. Technol, 2008. 31(5): p. 765–772.

[13] Cardona Alzate, C.A. and O.J. Sánchez Toro, Energy consumption analysis of integrated flowsheets for production of fuel ethanol from lignocellulosic biomass. Energy, 2006. 31(13): p. 2447-2459.

[14] 14. Piccolo, C. and F. Bezzo, A techno-economic comparison between two technologies for bioethanol production from lignocellulose. Biomass and Bioenergy, 2009. 33(3): p. 478-491.

[15] Szargut, J., D.R. Morris, and F.R. Steward, Exergy analysis of thermal, chemical, and metallurgical processes. 1988: Hemisphere publishing corporation.

[16] Dincer, I. and M.A. Rosen, Thermodynamic aspects of renewables and sustainable development. Renewable and Sustainable Energy Reviews, 2005. 9(2): p. 169-189.

[17] de Koeijer, G. and R. Rivero, Entropy production and exergy loss in experimental distillation columns. Chemical Engineering Science, 2003. 58(8): p. 1587-1597.

[18] Jarungthammachote, S. and A. Dutta, Thermodynamic equilibrium model and second law analysis of a downdraft waste gasifier. Energy, 2007. 32(9): p. 1660-1669.

[19] Lu, Y., et al., Thermodynamic modeling and analysis of biomass gasification for hydrogen production in supercritical water. Chemical Engineering Journal, 2007. 131(1-3): p. 233-244.

[20] Ojeda, K. and V. Kafarov, Exergy analysis of enzymatic hydrolysis reactors for transformation of lignocellulosic biomass to bioethanol. Chemical Engineering Journal, 2009. 154 (1–3), 390–395.

[21] Røsjorde, A. and S. Kjelstrup, The second law optimal state of a diabatic binary tray distillation column. Chemical Engineering Science, 2005. 60(5): p. 1199-1210.

[22] Prins, M.J., K.J. Ptasinski, and F.J.J.G. Janssen, Exergetic optimisation of a production process of Fischer-Tropsch fuels from biomass. Fuel Processing Technology, 2005. 86(4): p. 375-389.

[23] Talens, L., G. Villalba, and X. Gabarrell, Exergy analysis applied to biodiesel production. Resources, Conservation and Recycling, 2007. 51(2): p. 397-407.

[24] Tan, H.T., K.T. Lee, and A.R. Mohamed, Second-generation bio-ethanol (SGB) from Malaysian palm empty fruit bunch: Energy and exergy analyses. Bioresource Technology, 2010. 101 p. 5719–5727.

[25] Sohel, M.I. and M.W. Jack, Thermodynamic analysis of lignocellulosic biofuel production via a biochemical process: guiding technology selection and research focus. Bioresource Technology. DOI:10.1016/j.biortech.2010.10.032.

[26] Sohel, M.I. and M. Jack, Efficiency improvements by geothermal heat integration in a lignocellulosic biorefinery. Bioresource Technology 2010. 101 p. 9342-9347.

[27] Dincer, I. and M.A. Rosen, Exergy: energy, environment and sustainable development. 2007: Elsevier.

[28] DiPippo, R., Second Law assessment of binary plants generating power from low-temperature geothermal fluids. Geothermics, 2004. 33(5): p. 565-586.

Co-production of electricity, heat and biocoal pellets from biomass: a techno-economic comparison with wood pelletizing

Berit Erlach*, Benjamin Wirth, George Tsatsaronis

Technische Universität Berlin, Institute for Energy Engineering, Berlin, Germany
** Corresponding author. Tel: +49 30 31428449, Fax: +49 30 31428613, E-mail: erlach@iet.tu-berlin.de*

Abstract: Hydrothermal carbonization (HTC) is an artificial coalification process which converts raw biomass into a coal-like product, biocoal. Biocoal has a higher energy density than the original biomass and is easier to transport, store and process. Hence, HTC is recently promoted as an upgrading technology, especially for wet biomass. For HTC to become a commercial technology, it is essential to identify applications which offer technical or economic advantages over conventional biomass processes. This paper presents a process design where HTC is integrated with wood-fired combined heat and power production (*HTC-CHP*), and compares it to standalone HTC (*HTC-sep*) and to wood pelletizing integrated with CHP (*WP-CHP*). The respective plant designs are modeled with Aspen Plus and an economic analysis is performed using investment costs from literature. The overall efficiency of electricity, heat and wood or biocoal pellet production is very close in all considered cases. When biodegradable waste is available at zero cost, the production costs of biocoal pellets are similar to those of wood pellets. If wood chips are used as an HTC feedstock, the production costs are 32–38% higher. The average cost of CO_2 avoidance is highest for the standalone HTC plant, due to the auxiliary consumption of natural gas and electricity.

Keywords: *hydrothermal carbonization, biocoal, biomass, wood pellets*

1. Introduction

Co-firing with coal has been identified as one of the least expensive and most efficient technologies for converting biomass to electricity [1]. This gives rise to a demand for biofuels with a uniform quality and high energy density, which can be processed in the fuel handling and combustion equipment of existing coal-fired power plants. Since most raw biomass falls short of these requirements, upgrading technologies, which improve the properties of biomass for transport, storage, combustion and gasification, have become of interest. The most established upgrading technology today is wood pelletizing, whereby wood is dried, milled and pressed into pellets of a defined form and size. Several technologies which convert biomass into a more coal-like product through chemical processing are currently being developed, but not yet commercialized. While torrefaction and fast pyrolysis have been mainly applied to dry wood and straw, hydrothermal carbonization (HTC) does not require prior drying and has been successfully tested with a wide range of biomass including wood, straw, cut grass, municipal waste, digestate, and bark mulch in laboratory scale experiments [2,3].

To achieve a high overall energetic efficiency of 80 to 90% (HHV basis), efficient heat recovery within an HTC plant is required [4]. However, complex heat recovery might not be attractive due to operability issues and cost. This paper presents a process design in which the need for a complex heat recovery design within the HTC process is eliminated by integrating the HTC process with wood-fired combined heat and power production (CHP). Steam for the HTC reactor is bled from a steam turbine extraction, while low temperature heat from the cooling of the HTC reaction products is used for district heating and for combustion air and water preheating for the CHP process. This integrated design is compared to a stand-alone HTC plant and to wood pelletizing, also integrated with CHP, in relation to energetic efficiency and production costs. Poplar wood chips from short rotation coppice and biodegradable waste are considered as feedstocks for the HTC process.

2. Hydrothermal carbonization as an upgrading technology for biomass

HTC is an artificial coalification process which takes place in pressurized water at 200 to 250°C at or above saturation pressure and is slightly exothermic. Oxygen is removed from the feedstock through the formation of water and CO_2, thereby increasing the carbon content and higher heating value (HHV). HTC renders gaseous and dissolved byproducts containing CO_2, carbon monoxide, organic acids, phenol, furfural and hydroxymethylfurfural [5,6]. Minerals contained in the biomass are partly dissolved in the aqueous phase [7]. By destroying the cell structure of the biomass and removing oxygen-containing functional groups, HTC makes the product hydrophobic [8] and facilitates mechanical dewatering, which is much less energy intensive than thermal drying. Previous simulation studies show that for fresh wood with 50 to 60% moisture (wet basis), pre-treatment with HTC before combustion could increase the overall energetic efficiency compared to the combustion of the untreated wood by 5 to 12 percentage points, given that dissolved organics losses are limited to 5% (by weight) and that mechanical dewatering yields 70% dry matter content [4]. In laboratory scale dewatering experiments, a dry matter content of 57 to 68% was achieved for biocoal from biodegradable waste [9].

Fig. 1 presents a flow diagram for a continuous HTC plant. The heat recovery scheme is adopted from a pilot plant for the hydrothermal treatment of peat [10]. The biomass is mixed with recycled process water to create a pumpable slurry, and then preheated in several stages by mixing with steam recovered at different temperature levels from the product de-pressurizing. Only direct heat exchange is employed at temperatures greater than 100°C because (carbonized) peat slurry was found to cause fouling and clogging problems within heat exchangers [11]. The additional steam required to reach the reaction temperature is produced by a natural gas boiler. The product is mechanically dewatered, dried to a moisture content of 10% (w.b.) and pelletized. Low temperature drying uses steam at 100°C to heat up the drying air. The gaseous byproducts from the HTC reactor are co-combusted in the natural gas boiler. We described a similar plant design in detail in [4].

The need for a complex heat recovery scheme within the HTC process can be eliminated by integrating the HTC process with a CHP plant using wood chips as a fuel, as shown in Fig. 2. Steam for the HTC reactor is taken from the steam turbine. The biocoal slurry is de-pressurized in two steps. Some of the recovered steam is used to preheat the biomass slurry to 90°C and to supply the biocoal dryer. The remainder of the steam, plus heat from the waste water, gaseous byproducts and biocoal slurry cooling are used to generate steam at 0.2 MPa for the deaerator, for the combustion air and make-up water preheating, and for district heat production.

3. Methodology

The standalone HTC plant (*HTC-sep*) and the integrated plant design (*HTC-CHP*) described above are modeled with *Aspen Plus V7.1*, a simulation package which calculates material and energy balances for a given flowsheet of a steady-state chemical process. A stand-alone CHP plant (*CHP-sep*) and a CHP plant integrated with wood pelletizing (*WP-CHP*) are also modeled for comparison. The design of *CHP-sep* and *WP-CHP* corresponds to the integrated CHP process (marked by grey underlay in Fig. 2), without flow streams A, B, G, F, and H. In *WP-CHP,* additional steam is extracted at 0.12 MPa for drying the wood to a water content of 10% before milling and pelletizing. Based on the simulation results, raw material and auxiliary energy demand are obtained, and plant equipment is sized. Investment costs for the plant equipment are estimated, and the annual levelized product costs are calculated for each

simulation case. Poplar chips from short rotation coppice with a water content of 50% (w.b.) are used as a fuel for the CHP plant and as the raw material for the HTC and wood pelletizing. For the *HTC-CHP*, a second case is analyzed, with biodegradable waste as the HTC feedstock. All HTC simulation cases have an input of 11.15 MW_{HHV}, requiring either 4 t/h wood or 8.6 t/h biodegradable waste.

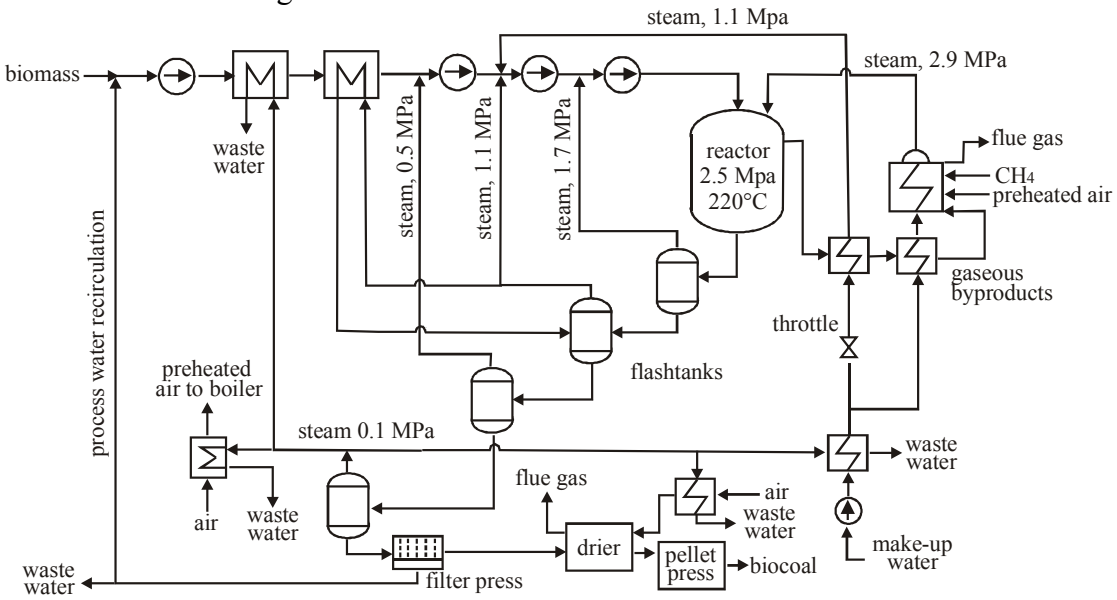

Fig. 1. Flow diagram of a stand-alone HTC plant (HTC-sep) with staged heat recovery.

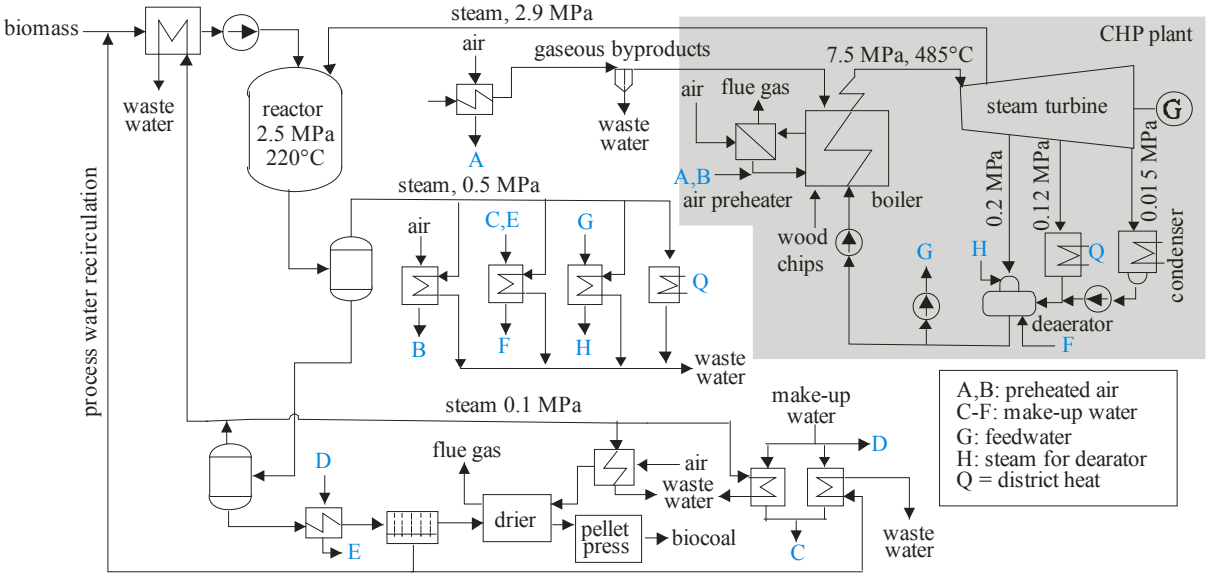

Fig. 2. Flow diagram of an integrated HTC and CHP plant (HTC-CHP).

3.1. Modelling assumptions

The operation of each plant is simulated for an average day within and outside the heating season, a cold winter day of -10°C with maximum heat load and frozen biomass, and a hot summer day of 30°C. The district heat load is taken to be 1.0 MW outside the heating season, 15.7 MW on the average winter day and 20.7 MW at capacity. Outside the heating season, the boiler runs at approximately 40% capacity, and the steam not used for district heating (7.0 MW) is discharged to the condenser. For the biomass upgrading processes, an availability of 80% is assumed, due to maintenance requirements and fluctuation in biomass supply.

The HTC reactor is modeled as a black box, with yields and composition of the biocoal and byproducts based on experimental data using poplar wood and straw at 220°C with a residency time of 4 hours [12] and on published data [13]. The composition (wt%, d.b.) of biomass and biocoal is given in Table 1. Mass yields (d.b.) are 70.3% to 70.9% for the biocoal from wood and 71.9% for the biocoal from waste. Dissolved organic byproducts account for 10.1% of the feedstock dry mass. The solid matter content is assumed to be 15% at the slurry pump inlet and 60% after mechanical dewatering with a filter press. Since biocoal is brittle, it is assumed that it can be fed directly to the pellet press without prior milling.

Table 1. Characteristics of wood, biodegradable waste, biocoal and dissolved organics.

	wood	waste	biocoal (wood)	biocoal (waste)	dissolved organics
Carbon	49.75%	38.60%	63.68%	48.54%	40.52%
Hydrogen	6.08%	5.30%	5.65%	4.27%	5.36%
Oxygen	42.85%	36.10%	29.47%	21.96%	54.12%
Ash	1.32%	20.00%	1.21%	25.23%	—
HHV (d.b.) (MJ/kg)	20.07	15.58	25.81	19.18	—
Water content (w.b.)	50%	70%	10%	10%	—

3.2. Economic analysis

Module costs for the plant equipment are estimated based on vendors data (for the wood pelletizing equipment) and literature. For the biomass upgrading processes, overdesign (safety) factors of 10-20% are applied. All components in contact with the biomass or biocoal slurry are stainless steel. Costs are converted to 2009 €. The total capital investment (TCI) comprises the total module costs plus fees and contingencies (15% of module costs), offsite costs (land, ancillary buildings, site development, utilities), working capital and start-up costs. The investment annuity is calculated with an economic plant life of 15 years and an interest rate of 7.0% p.a. Constant money values are used with real escalation rates of 0.5% p.a. for natural gas and purchased electricity, and 0.3% p.a. for wood chips and bituminous coal. Annual levelized costs for auxiliary energy, raw materials, and operation and maintenance are calculated with the constant escalation levelization factor (CELF).

The costs for the wood chips from short rotation coppice are calculated including cultivation and harvest, transportation and seasonal storage. It is assumed that the standalone HTC-plant is located in the centre of the cultivation area and that wood chips are stored onsite. The transport distance is calculated relative to the biomass demand under the assumption that 10% of the surrounding area is used to grow short rotation coppice. The location for the CHP plant would be selected based on district heat demand rather than biomass supply, and the seasonal storage of biomass has to be off-site. Therefore, an additional truck reload and transport of 100 km are assumed in this case. Biodegradable waste is assumed to be available at zero cost, including delivery to the HTC plant.

The total annual levelized revenue requirement (TRR) in €/a of the *HTC-CHP* plant equals the production costs of the three products, namely electricity, district heat and biocoal pellets. Assuming that specific revenues for district heat and electricity are the same for all plant designs, the specific cost of the biocoal pellets ($c_{pellets}$) in €/GJ can be calculated according to Eq. (1), where W is the net annual electricity production in GJ/a, c_w the renumeration for electricity feed-in from the CHP plant in €/GJ, and $Q_{pellets}$ is the annual pellet production in GJ/a. The specific costs of wood pellets in *WP-CHP* are calculated in the same way.

$$c_{pellets} Q_{pellets} = (TRR_{HTC-CHP} - TRR_{CHP-sep}) - c_w (W_{HTC-CHP} - W_{CHP-sep}) \quad (1)$$

The cost of CO_2 avoidance is calculated with Eq. (2), assuming that the upgraded biofuel substitutes bituminous coal, that no additional investment at the power plant is required and that efficiency is not affected. $c_{pellets,LHV}$ and $c_{bit.coal,LHV}$ are the specific costs in €/GJ_{LHV}, and $e_{pellets}$ and $e_{bit.coal}$ the specific emissions in t CO_2 per GJ_{LHV} for the respective fuels.

$$c_{CO2} = \frac{c_{pellets,LHV} - c_{bit.coal,LHV}}{e_{bit.coal} - e_{pellets}} \quad (2)$$

4. Results

In the following, the standalone HTC and CHP plants, *HTC-sep* and *CHP-sep*, are treated as one system with two separately located plants for the purpose of the economic analysis, in order to better identify the effects of the integration.

4.1. Technical performance

Low ambient temperatures lead to a higher energy demand for preheating the drier air and the biomass. At 5°C, the natural gas demand in *HTC-sep* is 13% higher than at 15°C, at -10°C with frozen biomass it is 50% higher. At +30°C, a surplus of heat (191 kW) has to be discharged to the environment, for which coolers are required. Annual energy balances for the analyzed cases are given in Table 2. The overall efficiency on an HHV (LHV) basis of *HTC-sep* is 81.1% (92.9%). The electrical efficiency of *CHP-sep* is 16.3% (20.1%), and the energetic efficiency 53.4% (65.8%). The overall energetic efficiency, where the sum of biofuel energy (HHV), net electricity and district heat is the product and the raw biomass is the fuel, is very close in all considered cases — it ranges from 60.8% when biocoal is produced from wood to 59.7% when biocoal is produced from waste.

Table 2. Annual energy balances (on HHV basis).

		HTC-sep	CHP-sep	HTC-CHP wood	HTC-CHP waste	WP-CHP
Inputs						
Biomass (upgrading)	(GWh/a)	75.14	—	75.14	75.14	75.14
Biomass (combustion)	(GWh/a)	—	224.65	232.60	233.88	255.17
Natural gas	(GWh/a)	7.68	—	—	—	—
Net electricity consumption	(GWh/a)	1.16	—	—	—	—
Products						
Net electricity Production	(GWh/a)	—	36.69	35.47	34.60	39.51
District heat	(GWh/a)	—	83.33	83.33	83.33	83.33
Upgraded biofuel	(GWh/a)	67.72	—	68.24	66.54	75.14

The HTC process receives 21.7 GWh/a from the CHP plant, of which 75% is returned at a lower temperature level, resulting in a net import of 5.4 GWh/a. This leads to an increased demand for boiler fuel wood chips for *HTC-CHP* compared to *CHP-sep*. Using biodegradable waste instead of wood for the HTC increases the steam flow by 14%. The wood pelletizing requires 15.7 GWh/a of steam, resulting in a 10% higher consumption of boiler fuel wood chips compared to *HTC-CHP*. Since the turbine extraction in *WP-CHP* is at a lower pressure,

additional electricity is produced in co-generation. The yield of upgraded biofuel is higher for *WP-CHP*, since in the HTC reaction, part of the biomass is converted to heat and byproducts.

4.2. Economic analysis

Wood chip costs including transport and storage result in 3.86 €/GJ for *HTC-sep*, with a land requirement of 1710 ha of short rotation coppice and an average transport distance of 9 km. For *CHP-sep*, *HTC-CHP* and *WP-CHP*, wood chips costs are 4.48 to 4.50 €/GJ, due to the larger catchment area, and additional transport from the seasonal storage site to the plant.

Table 3. Economic results.

		HTC-sep, CHP-sep	HTC-CHP wood	HTC-CHP Waste	WP-CHP
Investment costs					
HTC reactor	(k€)	1206	1133	1176	0
Slurry pumps, flash tanks, screw feeder	(k€)	754	460	491	0
Filter press	(k€)	846	799	951	0
Drying, milling, pelletizing	(k€)	1496	1495	1728	2595
Heat exchangers, product coolers	(k€)	740	735	825	0
Auxiliary boiler	(k€)	141	0	0	0
Waste water treatment	(k€)	245	288	419	0
Biomass sizing, metal/plastic screening	(k€)	0	0	218	0
Upgrading plant, total module costs	(k€)	5427	4910	5807	2595
CHP plant module costs	(k€)	17313	17717	17674	18633
Total capital requirement (TCI)	(k€)	30819	30600	31586	28733
Levelized costs					
Carrying charges [1)]	(k€/a)	3698	3672	3789	3448
Operation & maintenance [2)]	(k€/a)	1733	1517	1720	1145
Wood chips	(k€/a)	4763	5077	3858	5449
Electricity and natural gas [3)]	(k€/a)	276	0	0	0
Total revenue requirement	(k€/a)	10470	10265	9367	10041
Revenues electricity [3)]	(k€/a)	2936	2837	2768	3161
Revenues district heat [4)]	(k€/a)	4248	4249	4248	4248
Production cost upgraded biomass	(k€/a)	3286	3178	2351	2632
Specific cost upgraded biomass	(€/GJ_{HHV})	13.48	12.94	9.81	9.73
Specific cost upgraded biomass	(€/GJ_{LHV})	14.32	13.74	10.47	10.57
CO_2 avoidance cost [5)]	(€/tCO_2)	135.14	115.75	81.28	82.36

[1)] Annuity plus tax and insurances (1% of TCI)

[2)] Operating labour requirement estimated based on plant equipment. Plant operators: 27.63 €/h, biomass yard workers: 20.75 €/h. Material costs: 10% of module costs for high wear components, 2% for other components.

[3)] Energy prices: natural gas: 6.31 €/GJ_{HHV}, purchased electricity: 22.22 €/GJ, electricity revenues: 22.22 €/GJ

[4)] Calculated from *CHP-sep*

[5)] Coal price: 2.69 €/GJ_{LHV}, emission factor for purchased electricity in *HTC-sep*: 641.3 kg CO_2/MWh_{el}

The results of the economic analysis are shown in Table 3. The equipment costs for HTC are about twice than that for wood pelletizing. The higher complexity of the HTC plant compared to wood pelletizing also leads to a higher labour requirement and operation and maintenance costs. The integrated plant design saves 10% on the equipment cost for HTC, mostly related to biomass pressurizing, flash tanks, heat exchangers and the omission of the auxiliary boiler. However, this is offset by higher investment in the CHP plant, which needs a higher capacity due to the additional steam production. The investment for HTC utilizing biodegradable waste

is 18% higher than that for the plant using wood, due to higher biomass and biocoal mass flows and additional metal and plastic contaminant screening equipment.

Product costs of the upgraded biomass range from 9.73 €/GJ (175.7 €/t) for wood pellets to 13.48 €/GJ for biocoal produced in the standalone HTC plant. Despite the higher cost of wood chips due to transportation logistics, integration with the CHP plant leads to a slight decrease in biocoal cost. Biocoal pellets produced from biodegradable waste are comparable to wood pellets, assuming zero cost for the biodegradable waste. The cost for CO_2 avoidance when the biofuel is used to substitute bituminous coal is lowest for the biocoal from waste. For *HTC-sep*, only 90% of the CO_2 is avoided due to consumption of natural gas and electricity from the grid, while in the integrated cases, the HTC energy requirements are completely covered by biomass, resulting in zero direct emissions (supply chain emissions aside). The product costs are strongly dependent on the cost of the biomass, which contributes 32% of the annual cost in *HTC-sep*, and around 50% for the integrated plants.

5. Further technical considerations

While wood pelletizing is an established technology, there remains significant uncertainty about some technical aspects and the economics of the HTC plant, because there are no commercial-scale HTC plants yet in operation. Data for the HTC reaction is currently based on laboratory-scale batch experiments. Optimization of the design and operating parameters of the HTC plant might yield higher efficiencies. Key technical issues include biomass pressurizing and the dissolved organics. The dissolved organics result in a substantial energy loss and require waste water treatment. However, the quantity and composition of dissolved organics from laboratory scale experiments may not be representative for a continuous HTC process with process water reflux. In the analyzed plant designs, 21 600 to 68 400 m^3 per year of waste water are generated. That said, experiments on aerobic and anaerobic degradation are reported to indicate good degradability [9]. Low-boiling organics might evaporate in the drier and necessitate remedial treatment of the drier exhaust for VOC emissions.

Regarding product quality, biocoal pellets from wood have a higher calorific value than wood pellets. Biocoal pellets from biodegradable waste are likely to have a higher ash content, resulting in a lower calorific value. The quantity and composition of mineral matter in the biocoal is a consideration for combustion applications. In particular, ash melting temperature, flue gas cleaning requirements and corrosion need to be examined in greater detail. If biocoal is co-fired with coal, sulfur in the biocoal should not be an issue, since coal-fired power plants are equipped with desulfurization. However, the gaseous phase from the HTC of biodegradable waste was found to contain significant amounts of H_2S [13], which could prove more problematic. For biocoal to become a commodity fuel, quality standards regarding ash, sulfur and heavy metal content need to be developed and implemented to avoid damage to combustion equipment and the environment.

6. Conclusions

Hydrothermal carbonization (HTC) is an artificial coalification process which is being promoted as an upgrading technology for high moisture biomass. Under the economic assumptions made in this paper, biocoal pellets from biodegradable waste can be produced at a cost of 9.8 €/GJ_{HHV} when the waste is available at zero cost. This is comparable to the cost of wood pellets. The economics of HTC from biodegradable waste would be further improved if the HTC operator is paid for the disposal of the waste. When wood chips are used as a feedstock for HTC, the pellet costs are 30% higher. This raises the question whether the

application of HTC can be justified for biomass that can be easily pelletized without further pretreatment. Since the biocoal pellets produced by HTC are closer to coal, they might be better suited than wood pellets for co-firing in existing coal-fired power plants. Regarding plant design, integrating HTC with a CHP-plant eliminates the need for a complex heat recovery scheme within the HTC-plant and thereby aids operability. The modeling in this paper relied on laboratory scale data and simulation. Operational data from HTC pilot plants is needed to reduce uncertainty regarding conversion efficiency, availability and investment costs.

Acknowledgements: This work has been funded by the German Federal Ministry of Education and Research as part of the joint research project 01LS0806B.

References

[1] L. Baxter, Biomass-coal co-combustion: opportunity for affordable renewable energy. Fuel 84, 2005, pp. 1295-1302.

[2] C. Grimm, Fördervorhaben der DBU zur Hydrothermalen Karbonisierung – Ziele und Stand. Gülzower Fachgespräche 33, F achagentur Nachwachsende Rohstoffe (FNR), 2010, pp. 33-41.

[3] A. Funke, F. Ziegler, Hydrothermal Carbonization of Biomass: A Literature Survey Focussing on i ts Technical Application and Prospects, Proc. 17th European Biomass Conference & Exhibition, 2009, Florence, Italy, and Munich, Germany, pp. 1037−1050.

[4] B. Erlach, G. Tsatsaronis, Upgrading of biomass by hydrothermal carbonisation: Analysis of an industrial-scale plant design. Proc. ECOS – 23rd International Conference. Jun 14-17, 2010, Lausanne, Switzerland.

[5] F. Bergius, Beiträge zur Theorie der Kohleentstehung, Die Naturwissenschaften, 16 (1), 1928, pp. 1−10.

[6] M. Gerhardt, M. Berg, B. Kamm, Hydrothermal carbonization of lignocellulosic biomass and its precursors. Proc. International Conference on Polygeneration Strategies with special Focus on Integrated Biorefineries, Sep 07-09, 2010, Leipzig, Germany.

[7] J. Pels, P. Bergman, TORWASH. Proof of Principle. Phase 1, Technical Report, ECN-E-06-021, Energy research Centre of the Netherlands (ECN), 2006, Petten.

[8] W. Yan, et al., Thermal Pretreatment of Lignocellullosic Biomass, Environmental Progress & Sustainable Energy 28 (3), 2009, pp. 435−440.

[9] H. Ramke, Hydrothermale Carbonisierung organischer Siedlungsabfälle, 22. Abfallwirtschaftsforum, Gießen, 2010.

[10] M. Mensinger, Wet Carbonization of Peat: State-of-the-Art Review, Symposium Proceedings: Peat as an Energy Alternative. IGT, 1980, Chicago, Ill., pp. 249−280.

[11] S. Hägglund, (ed.), Vatkolning av Torv AB. Svensk Torvförädling, Lund, Sweden, 1960.

[12] M. Gerhardt, S. Kieseler, pers. comm. [experiments conducted at Technische Universität Berlin and Forschungsinstitut Bioaktive Polymersysteme, Berlin], Jun-Nov 2010.

[13] K. Serfass, Hydrothermale Carbonisierung. Eignung und Verarbeitung unterschiedlicher Biomassen zu Biokohle. Presentation at C.A.R.M.E.N Statusseminar Hydrothermale Karbonisierung (HTC), Aschaffenburg, Okt 5, 2010.

Effect of atmosphere on torrefaction of oil palm wastes

Yoshimitsu Uemura[1*], Wissam N. Omar[1], Noor Aziah Bt Othman[1], Suzana Bt Yusup[1] and Toshio Tsutsui[2]

[1] *Chemical Engineering Department, Universiti Teknologi PETRONAS, Tronoh, 31750 Perak, Malaysia*
[2] *Chemical Engineering Department, Kagoshima University, 1-21-40 Korimoto, Kagoshima 890-0056, Japan*
** Corresponding author. Tel: 05-378-7644, Fax: 05-365-6176, E-mail:yoshimitsu_uemura@petronas.com.my*

Abstract: Torrefaction is a low temperature treatment for lignocellulosic biomass at lower temperatures between 473 K and 573 K under an inert atmosphere, which has been found to be effective not only for improving the quality of lignocellulosic solid fuels, such as their energy density and shelf life, but also to make them useful as a feedstock for further decomposition such as gasification and liquefaction. Although more than ten papers on this subject have been published in the last several years, in all of these studies, the atmosphere has been inert (nitrogen). When we try to utilize waste thermal sources, such as flue gas from boilers for torrefaction, the gas contains some components other than nitrogen such as oxygen, carbon dioxide and water vapor. The most serious problem is thought to be the existence of oxygen in the gas. In this study, torrefaction of Malaysian oil palm wastes was carried out in a fixed bed tubular reactor under oxygen/nitrogen flow at a temperature range of 494 to 573 K, in order to clarify the effect of oxygen on torrefaction of lignocellulose. The effects of torrefaction conditions such as atmosphere, temperature and time, on the torrefaction behavior were investigated. The lignocellulosic biomass wastes utilized were mesocarp fiber and kernel shell of oil palm, which are typical agricultural wastes in Malaysia.

Keywords: *Torrefaction, Oil palm waste, Lignocellulose, Oxygen*

1. Introduction

One of the promising renewable energy sources is biomass, which can be utilized as solid, liquid or gas fuels. Specifically, lignocellulosic biomass residues are attracting interest worldwide because they are non-edible. Due to their availability in Malaysia, oil palm wastes are considered as the best among all biomass wastes [1]. In 2008, Malaysia was the second largest producer of palm oil with 17.7 million tonnes, or 41% of the total world supply, while Indonesia was the world's largest producer of palm oil with 19.3 million tonnes of oil, or 45% of the total world supply [2]. In 2008, productive oil palm plantations in Malaysia covered 4.5 million hectares, a 4.3% increase from the figures in 2007, which stood at 4.3 million hectares [3]. The types of biomass produced by the oil palm industry include empty fruit bunches (EFB), mesocarp fiber, kernel shells, fronds and trunks. EFB, mesocarp fiber and kernel shells are either utilized or discarded at palm oil mills. Similarly, the rest, fronds and trunks are either utilized or discarded at plantations. The amount of each type of biomass is summarized in Table 1. Since the current primary energy supply in Malaysia is about 70 Mtoe (million tons of oil equivalent), the total oil palm biomass energy potential of 17 Mtoe may be able to contribute considerably to the decrease in consumption of fossil fuels (natural gas, coal and oil). In order to utilize biomass wastes efficiently, the following drawbacks about biomass compared to fossil fuels must be properly solved:
(1) Higher energy consumption during collection
(2) Heterogeneous and uneven composition
(3) Lower calorific value.
(4) Quality decay by biodegradation.

There are a few options to solve some of those problems; the major ones are pelletization, liquefaction and gasification of biomass. Pelletization includes the following processes: drying, chipping, grinding and pelletizing of lignocellulosic biomass. Though pelletization is

the least expensive option, there are some problems associated with it; lower heat value and quality deterioration by moisture (pellet disintegration, moss growth and bioorganic decomposition). In recent investigations, a low temperature treatment at 473 to 573 K under an inert atmosphere was found to be effective for improving the energy density and shelf life of the biomass. The treatment is called 'torrefaction,' and has been reported for wood and grass biomass over the past few years [4-16]. Arias et al. torrefied woody biomass (eucalyptus) at 513 to 553 K, and found that the grindability of the biomass was improved [5]. Prins et al. proposed a kinetic model of torrefaction [9], and reported the details of torrefaction mass balance [10]. Some papers have focused on the fuel quality [6] and the feedstock quality for gasification [4,7] of the torrefied lignocellulosic biomass. Uslu et al. focused on a comparison of torrefaction, fast pyrolysis and pelletization from the viewpoint of international bioenergy logistics [8]. Currently, experimental torrefaction studies are mostly conducted on woody and grass biomass; wood dusts [8], beech [4, 9, 10], eucalyptus [5], willow [6, 7, 9, 10], larch [9, 10], and canary grass [6]. Few academic papers have been found for torrefaction of agricultural lignocellulosic wastes, such as wheat straw [6, 9, 10], although they are among the most promising renewable resources, especially in Southern Asia. The authors have already reported on the torrefaction behaviour of three types of oil palm residue; empty fruit bunches (EFB), mesocarp fiber and kernel shell [17].

Table 1. Oil palm biomass wastes and their potential.

Site	Waste type	Generation rate		Plantation area or FFB processed		Annual gene-ration	Mois-ture	CV (LHV, dry base)	Annual energy (dry base)	
						million t-wet/y	wt%	GJ/t	PJ	Mtoe
Palm plan-tation	Trunk	40	t-dry/ha-replantation/y	0.08	million ha-replantation	11	71	16.4	52	1.2
	Fronds	15				4.1	71	14.4	17	0.4
	Fronds	6	t-dry/ha-plantation/y	4.488	million ha-plantation in 2008	92.9	71	14.4	388	9.2
Palm oil mill	EFB	0.2	t-wet/t-FFB	85.71	million t-FFB processed in 2009	17.1	65	15.8	95	2.3
	Fiber	0.12				10.3	42	18.3	109	2.6
	Shell	0.05				4.3	17	18.5	66	1.6
	POME	0.6				51.4	-	-	28	0.66
Total									727	17.3

At palm oil mills in Malaysia, we may be able to utilize flue gas from the boilers as a thermal energy source for torrefying unutilized residues. Currently, in most of the palm oil mills, all the mesocarp fiber and part of the kernel shell generated at the mills are utilized as fuel for the boilers. EFB and most of the shell are not utilized. Specifically, EFB is simply incinerated without any thermal recovery due to its high moisture content. If it is possible to utilize the flue gas from the boilers for torrefying EFB, (1) a considerable quantity of energy can be saved in the process; and (2), EFB could be sold as a solid fuel. This makes the oil mill more economically viable. In this case, the problem is that no data are available to demonstrate if torrefaction can be carried out properly in the presence of oxygen, because flue gas from the boilers at palm oil mills contains oxygen. According to our survey, the oxygen concentration in the flue gas is around 13%. Based on this point of view, the authors have already studied and reported the effect of oxygen on torrefaction behavior of EFB [18]. In addition, recent developments in boiler technology have improved their efficiency considerably. If such

updated technology is applied, boilers at oil mills will only consume part of the fiber generated at the mills. In the very near future, kernel shell and part of the mesocarp fiber, therefore, could be the source for torrefaction to produce solid fuel.

In this paper, torrefaction of mesocarp fiber and kernel shell residue was carried out in a fixed bed tubular reactor in the presence of oxygen in the range of 3 to 15 %, in order to answer the question above. The effects of torrefaction conditions, oxygen concentration, temperature and biomass size, on the mass and energy yields were investigated.

2. Experimental

2.1. Biomass samples

Mesocarp fiber and kernel shell were collected from an oil palm plantation at Bota in Perak, Malaysia in July, 2010. After drying at 378 K for 24 h, they were ground by a mechanical grinder. The ground powders were sieved into four fractions as shown in Table 2.

Table 2. Biomass size used in this study.

Range of sieve opening [mm]	Nominal average diameter [mm]
0.25-0.50	0.375
1.0-2.0	1.5
2.0-4.0	3.0
4.0-8.0	6.0

2.2. Torrefaction

Torrefaction of the biomass samples was carried out using a horizontal tubular type reactor made of stainless steel, with a 46 mm internal diameter. The entire set-up is illustrated in Fig. 1.

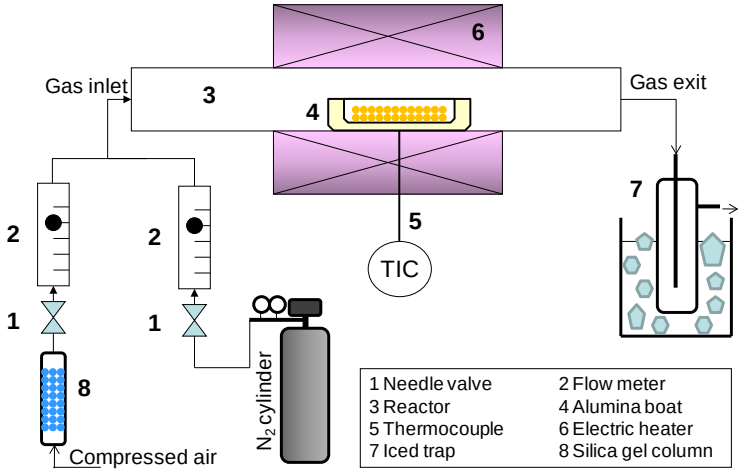

Fig. 1. Experimental apparatus used in this study.

A prescribed amount of biomass waste (1.6 g) was weighed, and put in a ceramic boat. The boat was placed at the center of the reactor. After flushing the reactor with torrefaction gas for 15 min, the temperature of the reactor was raised to different desired levels, *i.e.* 493, 523 or 573 K at a constant rate of 10 deg/min by an electric furnace surrounding the reactor. The temperature range (493 to 573 K) was chosen because selective decomposition of hemicelluloses occurs between 473 and 573 K. The reason for selecting the minimum

temperature as 493 K is that we may not have a substantial torrefaction rate at less than 493 K. After 30 min of torrefaction, the heater was turned off and the reactor was left to cool down to an ambient temperature. The torrefied sample was then recovered, weighed and kept in an air-tight vessel till the characterization. Throughout the procedure described above, 0.1 L/min of torrefaction gas was flowed through the reactor. The concentration of oxygen in the gas was adjusted to 3, 9 or 15 %, in order to investigate the effect of oxygen concentration on torrefaction. During each torrefaction experiment, collection of volatile substances generated from the reactor was attempted by an iced trap as shown in Fig. 1. After all, no condensation was observed in the trap for all the runs.

2.3. Measurements

For all the eight samples used in this study, the mass and the calorific value were measured before and after torrefaction. The calorific value was measured using a bomb calorimeter, model C2000 series manufactured by IKA Werke. The calorific value from a bomb calorimeter is the high heat value (HHV), which includes the latent heat of the vapor emitted from the specimen. From the experimental results described above, the three parameters were calculated by the following three equations:

$$y_M = \frac{Mass\ of\ \ solid\ \ after\ torrefaction}{Mass\ of\ \ EFB\ used} \quad (1)$$

$$CV\ \ ratio = \frac{CV\ \ of\ \ solid\ \ after\ torrefaction}{CV\ \ of\ \ EFB\ used} \quad (2)$$

$$y_E = y_M \times CV\ \ ratio \quad (3)$$

Where y_M means the mass yield, CV means the calorific value, and y_E means the energy yield.

3. Results and Discussion

The biomass samples after torrefaction and their physical properties are listed in Tables 3 and 4. In this study, the calorific values of the untorrefied mesocarp fiber and the untorrefied kernel shell were 18.6 and 19.9 MJ/kg, respectively. Wahid reported 18.8 and 20.1 MJ/kg as the calorific values of mesocarp fiber and kernel shell [19]. The difference between this and other studies is surprisingly small, although the physical properties of biomass frequently depend on soil conditions and the harvesting season [20].

Table 3. Torrefaction results for fiber of 0.375mm.

Temp [K]	O_2 conc [%]	Calorific value [MJ/kg]	CV ratio [%]	Mass yield [%]	Energy yield [%]
493	3	21.2	114.2	94.0	107.4
523	3	21.3	114.6	92.8	106.3
573	3	22.1	118.8	90.3	107.3
493	9	21.0	113.2	93.7	106.1
523	9	21.4	114.8	92.4	106.1
573	9	22.1	119.0	89.8	106.9
493	15	21.1	113.4	93.1	105.5
523	15	21.6	116.1	91.2	105.9
573	15	22.1	118.8	89.5	106.3

Table 4. Torrefaction results for shell of 0.375mm.

Temp [K]	O_2 conc [%]	Calorific value [MJ/kg]	CV ratio [%]	Mass yield [%]	Energy yield [%]
493	3	22.0	110.4	95.8	105.8
523	3	21.7	109.0	94.3	102.8
573	3	22.8	114.5	93.1	106.6
493	9	21.9	110.2	95.4	105.2
523	9	21.6	108.8	93.8	102.0
573	9	22.7	114.3	92.5	105.7
493	15	21.8	109.8	94.9	104.2
523	15	21.6	108.7	93.6	101.7
573	15	22.7	114.3	91.9	105.0

3.1. Effect of biomass size on mass yield

Figures 2 and 3 show the results of mass yield for mesocarp fiber and kernel shell, respectively. It is obvious that mass yield shows no significant dependency on particle size under the conditions of this study. Hereafter, the effects of temperature and oxygen concentration on the torrefaction results will be discussed. Also, the results are for 0.375 mm biomass unless otherwise noted in the text.

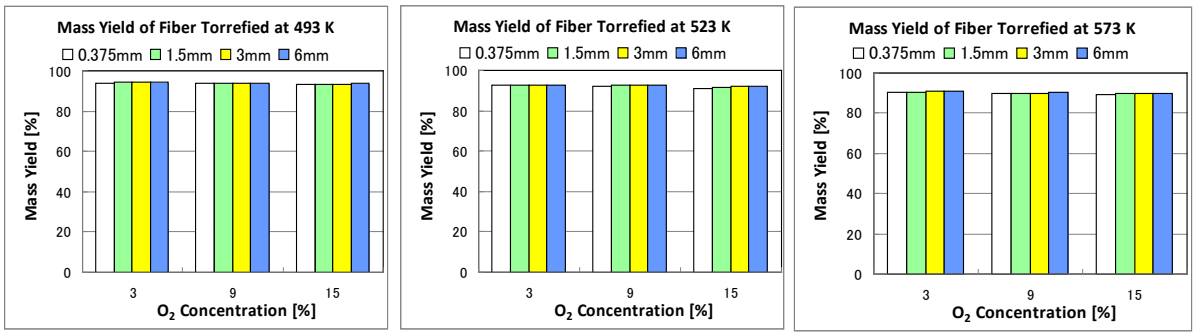

(a) (b) (c)

Fig. 2. Mass yield for mesocarp fiber.

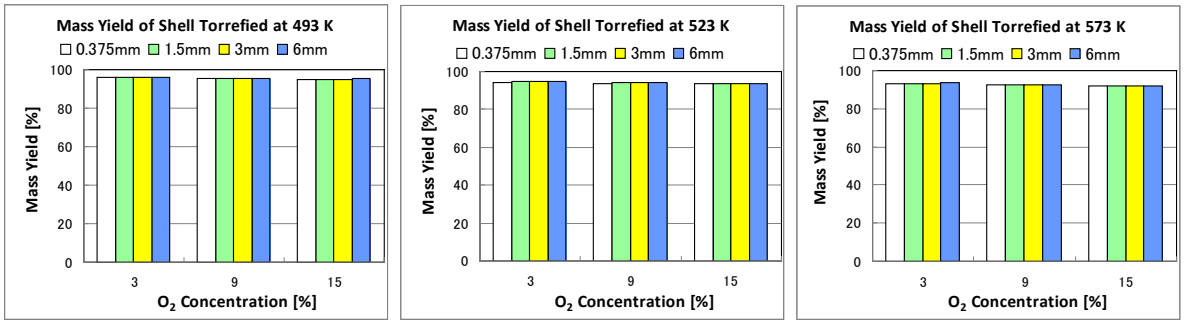

(a) (b) (c)

Fig. 3. Mass yield for kernel shell.

3.2. Effects of temperature and oxygen concentration on mass yield

Figures 4 and 5 show the relationship between mass yield and temperature at oxygen concentrations of 3, 9 and 15 % for mesocarp fiber and kernel shell, respectively. The mass yield decreases with an increase in temperature. A similar tendency was reported in previous torrefaction studies [6, 11] as well as in our study on EFB torrefaction [18]. This tendency reflects the positive effect of temperature on the torrefaction rate. On the other hand, the mass yield slightly decreases with an increase in oxygen concentration as shown in Figs. 4 and 5. As we have reported already, for torrefaction of EFB, the mass yield decreased with an increase in oxygen concentration. EFB is found to be not as resistant to oxygen in the atmosphere as mesocarp fiber or kernel shell. When the mass yield of fiber is compared with that of shell, shell always shows a larger mass yield than fiber at any temperature.

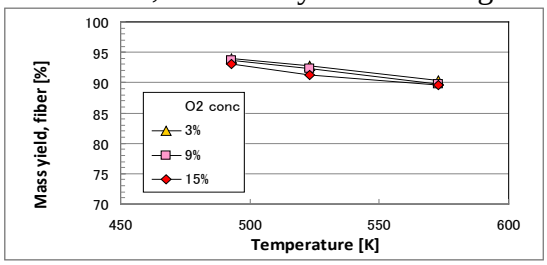

Fig. 4. Effects of temperature and O_2 conc. on mass yield for mesocarp fiber.

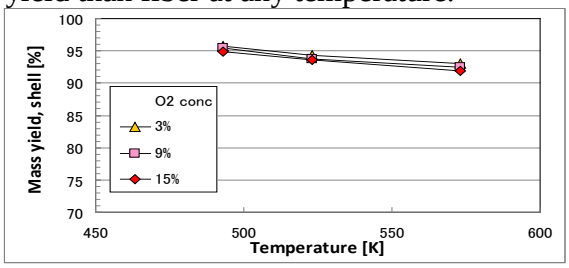

Fig. 5. Effects of temperature and O_2 conc. on mass yield for kernel shell.

This tendency may be attributed to the fact that shell contains 22.7 % hemicellulose, which is less than that of fiber, which contains 38.8 % hemicellulose [21].

3.3. Effects of temperature and oxygen concentration on calorific value

Figures 6 and 7 show the relationship between calorific value and temperature at oxygen concentrations of 3, 9 and 15 % for mesocarp fiber and kernel shell, respectively. The calorific value increases with an increase in temperature. This tendency has been reported in previous papers, in which wood and grass-type lignocellulosic biomass samples were used. It can be explained by the fact that the main gaseous products during torrefaction are water and carbon dioxide [4,10]. Surprisingly, the calorific value has little dependency on oxygen concentration in the range of 3 to 15%. This is the same tendency as what the authors already reported in a previous paper [18]. In that report, the authors proposed that EFB may undergo torrefaction and oxidation in parallel during torrefaction in the presence of oxygen, and these two reactions do not interact with each other. From the results as shown in Figs. 6 and 7, it is likely that the torrefaction mechanism of mesocarp fiber and kernel shell is similar to that of EFB.

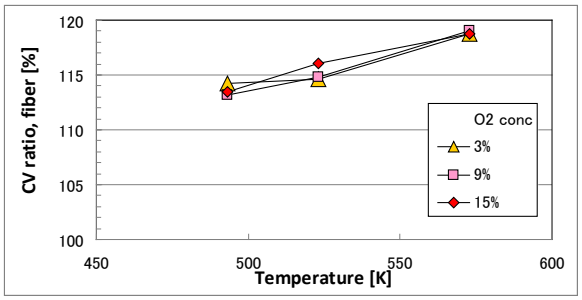

Fig. 6. Effects of temperature and O_2 conc. on CV ratio for mesocarp fiber.

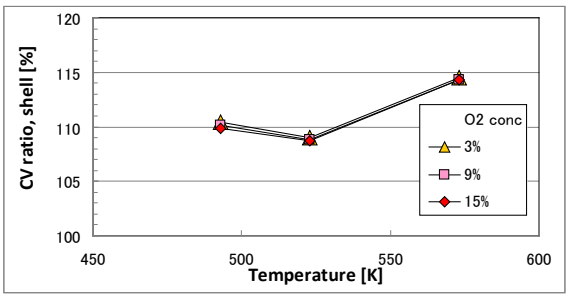

Fig. 7. Effects of temperature and O_2 conc. on CV ratio for kernel shell.

3.4. Effects of temperature and oxygen concentration on energy yield

Figures 8 and 9 show the relationship between energy yield and temperature at oxygen concentrations of 3, 9 and 15 % for mesocarp fiber and kernel shell, respectively. The energy yield is the key parameter to understand how much energy has been reserved after torrefaction. For both types of biomass, the energy yield slightly decreases with an increase in oxygen concentration. For mesocarp fiber, the energy yield has little dependency on temperature. From this result, when we focus only on the energy yield, it is recommended that mesocarp fiber be torrefied at 493 K. Sometimes, however, the calorific value itself does matter. In that case, the torrefaction temperature should be 573 K. For kernel shell, the energy yield shows a concave profile against temperature. This tendency is attributed to the fact that the energy yield is a product of the mass yield and the CV ratio; the former decreases with an increase in temperature, and the latter increases with an increase in temperature. Kernel shell shows a smaller energy yield value than that of fiber under the same conditions. From this fact,

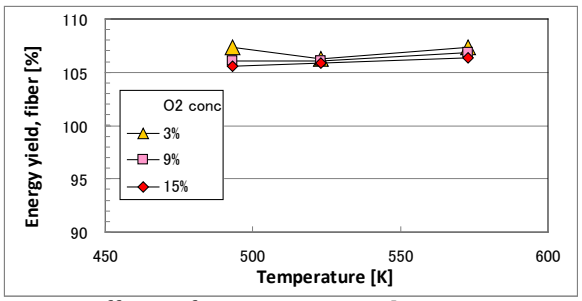

Fig. 8. Effects of temperature and O_2 conc

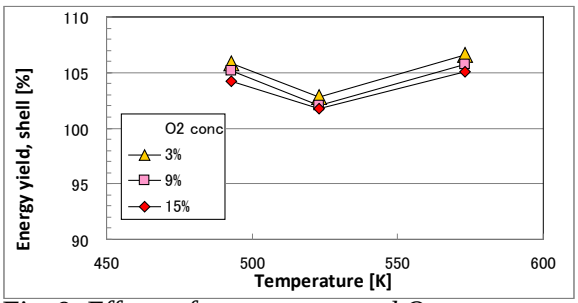

Fig. 9. Effects of temperature and O_2 conc

on energy yield for mesocarp fiber. *on energy yield for kernel shell.*
mesocarp fiber is more suitable than kernel shell as a feedstock for torrefaction.

4. Conclusion

Torrefaction of mesocarp fiber and kernel shell was carried out in the presence of oxygen in order to investigate the effects of various torrefaction conditions, *i.e.*, oxygen concentration (3, 9 and 15 %), temperature (493, 523 and 573 K) and biomass size (0.375, 1.5, 3 and 6 mm), on the mass and energy yields. The mass yield decreased considerably with an increase in temperature, and decreased slightly with an increase in oxygen concentration, but showed very little dependency on biomass size. In other words, the torrefaction reaction rate was affected only by temperature. The other two factors, oxygen concentration and biomass size, had no significant effects on the rate. The energy yield against temperature showed either a slight and steady increase profile or a concave profile. This rather complex behavior is due to the fact that energy yield is a product of the mass yield and the CV ratio; the former decreases with an increase in temperature, and the latter increases with an increase in temperature. The energy yield slightly decreased with an increase in oxygen concentration, but all the values fell between 105 and 108 % for mesocarp fiber and between 102 and 107 % for kernel shell. It is worthwhile pointing out that torrefaction in the presence of oxygen can be carried out without any significant problem, while the mass and energy yields slightly decrease with an increase in oxygen concentration from 3 to 15%. Since the flue gas from a palm oil boiler contains around 13% oxygen based on our survey described in the introduction, direct use of boiler flue gas to torrefaction will not deteriorate the quality of the torrefied biomass.

Acknowledgments

The authors acknowledge that this work was supported financially by the Mitsubishi Foundation.

References

[1] Suzana Yusup, Mohamad Taufiq Arpin, Yoshimitsu Uemura, Anita Ramli, Lukman Ismail, Siew Hoong Shuit, Kok Tat Tan, Keat Teong Lee, Review on agricultural biomass utilization as energy source in Malaysia, Proceedings for the 16th ASEAN Regional Symposium on Chemical Engineering, Manila, 2009, pp.86-89.

[2] MPOB (Malaysian Palm Oil Board), 2008, "6.8 World Major ProducersOf Palm Oil: 1999 – 2008." Retrieved Jan 28, 2010 from http://econ.mpob.gov.my/economy/annual/stat2008/ei_world08.htm.

[3] MPOB (Malaysian Palm Oil Board), 2008, "1.2 Area Under Oil Palm [Mature And Immature]: 1975 - 2008." Retrieved Jan 28, 2010 from http://econ.mpob.gov.my/economy/annual/stat2008/ei_area08.htm

[4] C. Couhert, S. Salvador, J-M. Commandré, Impact of torrefaction on syngas production from wood, Fuel, 88, 2009, pp. 2286-2290.

[5] B. Arias, C. Pevida, J. Fermoso, M.G. Plaza, F. Rubiera, J.J. Pis, Influence of torrefaction on the grindability and reactivity of woody biomass, Fuel Processing Technology, 89, 2008, pp. 169-175.

[6] T.G. Bridgeman, J. M. Jones, I. Shield, P.T. Williams, Torrefaction of reed canary grass, wheat straw and willow to enhance solid fuel qualities and combustion properties, Fuel, 87, 2008, pp. 844-856.

[7] Mark J. Prins, Krzysztof J. Ptasinski, Frans J.J.G. Janssen, More efficient biomass gasification via torrefaction, Energy, 31, 2006, pp. 3458-3470.

[8] Ayla Uslu, André P.C. Faaij, P.C.A. Bergman, Pre-treatment technologies, and their effect on international bioenergy supply chain logistics. Techno-economic evaluation of torrefaction, fast pyrolysis and pelletisation, Energy, 33, 2008, pp. 1206-1223.

[9] Mark J. Prins, Krzysztof J. Ptasinski, Frans J.J.G. Janssen, Torrefaction of wood Part 1. Weight loss kinetics, J. Anal. Appl. Pyrolysis, 77, 2006, pp. 28-34.

[10] Mark J. Prins, Krzysztof J. Ptasinski, Frans J.J.G. Janssen, Torrefaction of wood Part 2. Analysis of products, J. Anal. Appl. Pyrolysis, 77, 2006, pp. 34-40.

[11] G. Almeida, J.O. Brito, P. Perré, Alterations in energy properties of eucalyptus wood and bark subjected to torrefaction: The potential of mass loss as a synthetic indicator, Bioresource Technology, 101, 2010, pp. 9778-9784.

[12] M. Phanphanich, S. Mani, Impact of torrefaction on the grindability and fuel characteristics of forest biomass, Bioresource Technology, 2010, in press.

[13] Wei-Hsin Chen, Po-Chih Kuo, A study on torrefaction of various biomass materials and its impact on lignocellulosic structure simulated by a thermogravimetry, Energy, 35, 2010, pp. 2580-2586.

[14] V. Repellin, A. Govin, M. Rolland, R. Guyonnet, Modelling anhydrous weight loss of wood chips during torrefaction in a pilot kiln, Biomass and Bioenergy, 34, 2010, pp. 602-609.

[15] Jian Deng, Gui-jun Wang, Jiang-hong Kuang, Yun-liang Zhang, Yong-hao Luo, Pretreatment of agricultural residues for co-gasification via torrefaction, Journal of Analytical and Applied Pyrolysis, 86, 2009, pp. 331-337.

[16] Felix Fonseca Felfli, Carlos Alberto Luengo, Jose Antonio Suárez, Pedro Anibal Beatón, Wood briquette torrefaction, Energy for Sustainable Development, 9, 2005, pp. 19-22.

[17] Y. Uemura, Wissam N. Omar, T. Tsutsui, D. Subbarao, Suzana Yusup, Relationship between calorific value and elementary composition of torrefied lignocellulosic biomass, Journal of Applied Sciences, 10, 2010, in press.

[18] Y. Uemura, Wissam N. Omar, Noor Aziah Othman, Suzana Yusup, T. Tsutsui, Torrefaction of Oil Palm EFB in the Presence of Oxygen, Proceedings for The Second International Symposium on Gasification and Its Application (ISGA2010), Fukuoka, 2010, B43.

[19] M. B. Wahid, Renewable resources from oil palm for the production of biofuels, Proceedings for the International Conference on Biofuels, Kuala Lumpur, 2007, pp.163-169.

[20] Lisardo Núñez-Regueira, Jose A. Rodríguez-Añon, Jorge Proupín-Castiñeiras, A. Vilanova-Diz, N. Montero-Santoveña, Determination of calorific values of forest waste biomass by static bomb calorimetry, Thermochemica Acta, 371, 2001, pp.23-31.

[21] Chun Sheng Goh, Kok Tat Tan, Keat Teong Lee, Subhash Bhatia, Bio-ethanol from lignocellulose: Status, perspectives and challenges in Malaysia," Bioresource Technology, 101, 2010, pp. 4834–4841.

Biofuels Production Process and the Net Effect of Biomass Energy Production on the Environment

M.R. Heydariazad [1,*], R. Khatibi nasab[2], S. Givtaj [2], S.J. Amadi Chatabi [2]

[1] *No.7 east Shirzad Street, Valiasr crossroads, Tehran, Iran*
[2]*Department of Mechanical & Aerospace Engineering, Science and Research Branch, Islamic Azad University, Tehran, Iran*
** Corresponding author. Tel: +98 21 66720338, Fax: +98 21 66720519, E-mail: azad138887@yahoo.com*

Abstract: Biomass is based on carbon. It is also the admixture of organic molecules that include hydrogen, oxygen, often nitrogen and small amounts of other atoms like alkali metals, alkaline earth metals and heavy metals. Better method of producing biomass for more energy production has the potential to replace fossil fuels.
Converting biomass to liquid, gaseous or solid fuel depends on four main characteristics:
1) Platforms 2) processes 3) feedstock 4) products
Platforms are the most important feature in this classification; they are the key intermediate between raw materials and final products.
There are two main methods to convert biomass to liquid, gaseous or solid fuel: Biochemical and thermo chemical. Biochemical method is known as the sugar platform that is based on enzymatic hydrolysis and fermentation. Thermo chemical method depends on thermo chemical process. Methods that are in this category contain Direct Combustion Gasification and Pyrolysis.
Utilizing biofuels instead of fossil fuels due to a lot of reasons are preferred. They produce less CO_2 than fossils, they produce a little bit of brimstone and they do n ot produce pure C. Moreover, they can help to reduce greenhouse gasses and can save the environment from destruction. On the other hand, using such fuels help not only the nature to be more stable, but also to gain stable increment in future.
This article is seriously focused bio fuels production process and the net effect of biomass energy production on the environment, tools and combining methods to produce components that cover the mechanism of biomass energy production process and the unique performance of these parts. In this paper the development of biorefinery technologies and using renewable resources in national and international level is studied.
Of course it would be considered that producing more biomass for energy has the potential to pollute water resources and decrease food security.

Keywords: *Biomass energy production process, Bio fuels production process, Renewable energy resources.*

1. Introduction

Changes in utilization of the Earth and combustion of fossil fuels are the worst mankind's effects on the Earth which have changed the cycle of carbon in the planet.
Combustion of fossil fuels enters huge amounts of carbon dioxide (CO_2) into the atmosphere. Biofuel is a kind of energy which is very important according to the following reasons:

1. Environmental concerns
2. for security reasons
3. Currency saving (frugality in foreign currency savings), social and economical issues related to rural sector and so on.

Biomass is a renewable energy resource which is produced from bio materials. Bio materials contain herbaceous reliquiae which are used for producing electricity and heat. Biomass is one of the most important factors in the economy of the world. If we use biofuels, cost of production will be reduced because of dramatic improvement in efficiency, paying attention to the environmental systems and development of rural places.

Biofuels are vegetable oil, Biodiesel, Bioethanol, bio methanol, Biogas, etc. Most of the biofuels, like ethanol are produced from corn, wheat or sugar beets. Biodiesels are usually

produced from oil seeds. For example the amount of energy that can be gained from each m^3 of wood with moisture content of 60% is7GJ or the amount of energy that can be gained from each m^3 of new harvested herbaceous is 3GJ. Bio-ethanol is a s uitable replacement for gasoline or it can also be used as its supplement. By using bio-syngas, Bio ethanol can be gained from the steam of biomass which is obtained from the reformed biomass process. Bio-methanol recovers easier from biomass than bio-ethanol. Biodiesel is an environmental friendly fuel and is a good replace for liquid fuels in diesel engines that can be used without change. Using herbaceous oils to make biodiesels has been significantly developed due to these reasons:

1. They produce fewer amounts of CO_2 and pollutant in comparison of fossil fuels in the time of combustion.

2. Ability of being renewable for bio diesel in comparison of conventional diesel fuel oil.

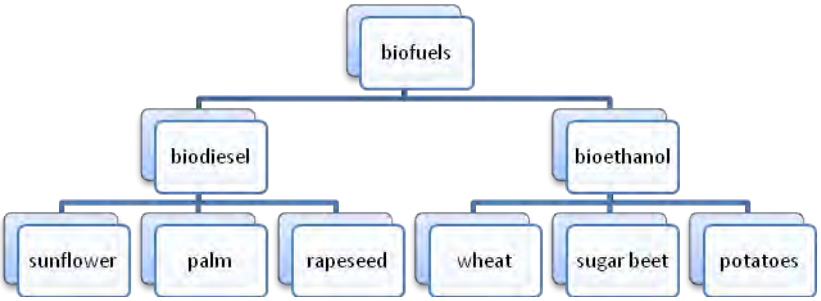

Fig.1. Resources of bioethanol and biodiesel

Technology of producing biomass energy in use of waste or plant matter to produce energy with lower level should be in a way that prevents production of greenhouse gases. [1]
In developed countries there are some modern and efficient technologies for converting bio-energy or at least such kinds of technologies are growing. Hence biofuels in industrialized countries compete with fossil fuels. [2]
Using of bio energy as a fuel of vehicles is getting more and more popular and it can get some portions of fuel market in future decades. In below, some advantages of using it are listed:

1. It helps to the structure of nature and stability of environment which is at risk.
2. Biofuel resources are accessible easily.
3. An economic frugality for consumers. [3]

1.1. How to get energy from biomass

So as to get energy from crude oil it must be refined in order to gain energy, processes must be done on biomass so that energy can be gained from it. Generally, the methods, processes and equipments that can be used to produce energy from Biomass are called Biorefinery. In fact Biorefinery is placed in front of refinery in oil and gas industry.

1.2. Biorefinery energy production methods

1. Sugar platform: This method is based on biochemical reactions and processes
2. Thermo chemical Platform: This method is based on thermo chemical processes

1.3. Sugar platform

In general in this method biomass converts into sugar or other fermented food. In the next steps the result of the material will be fermented by bacteria, yeasts and other microorganisms. Finally, because of processes which occur on the material, products like alcohol or other products that energy can be obtained from them is produced.

1.4. Thermochemical Platform

Methods that are in this category are:

1. Direct Combustion
2. Gasification
3. Pyrolysis

1.5. Direct Combustion

In fact the first people who produced biomass energy through the burning were early humans. This method is not very useful in terms of efficiency and productivity. In other ways through the biomass heating in the absence of oxygen or gas into liquid fuels, you can have high energy efficiency. Besides in comparison of Direct Combustion they have less pollution and higher economic efficiency.

1.6. Gasification

In this method biomass is heated in the absence of oxygen. The product is mixed with carbon monoxide and hydrogen, which is called Syngas. The outcome product will be synthesized with oxygen easily and can be used in turbines, boilers, etc. as a fuel.

As it was mentioned, using such kinds of fuels make not only high efficiency but also lower pollution.

1.7. Pyrolysis

Solid biomasses can be turned into liquid using chemical and catalysis methods. In method Pyrolysis like the method Direct Combustion, biomasses are heated in the absence of oxygen. These products, which are normally liquid, can be used as a fuel.

Now, this method is under research and study for a better environment.

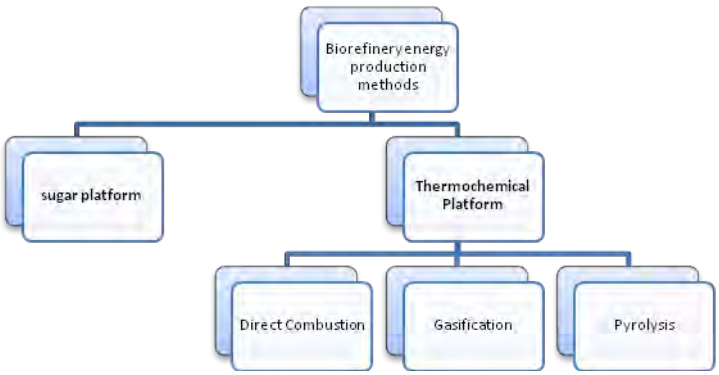

Fig.2. Flow Chart of Biorefinery energy production methods

2. Biofuels

2.1. Bioalcohols

Biofuels which are in forms of gas and liquid are mostly used in a 100% pure as a fuel for vehicles. They are also used, in some cases, with mixture of other fuels, For example, ethanol can be mixed with gasoline as15-20% alcohol by volume without any problem. [4]
Alcohol can be used as vehicles fuel according to the following:

1. Methanol (CH_3OH)
2. Propanol (C_3H_7OH)
3. Butanol (C_4H_9OH)
4. Ethanol (C2H5OH)

They are known as BIOALCOHOLS when they are obtained from land resources. Bio-ethanol contains about5% water. This compound can be purified by simple distillation and becomes as azeotropic mixture. Mixture of gasoline and ethanol is known as gasohol. Gasohol can even be as follow: 97% gasoline, 3% ethanol

However, this gasohol has higher percent octane compared with the previous. In general, this mixture can cause to reduce emissions of greenhouse gasses and some other pollutants. Of course, it should not been forgotten that ethanol evaporates easily and we know that its evaporation in hot weather causes pollution and produces greenhouse gas. Ethanol can be combined with gasoline easily without water. Hydrated ethanol includes not entire 2% of water volume. Mixture of gasoline- hydrated ethanol cannot be combined with diesel.

But we can use emulsion, to form diesohol. Bio ethanol is a petrol additive/substitute. It is possible that wood, straw and even household wastes may be economically converted to bioethanol.fig. 3. Shows ethanol production in different continents.

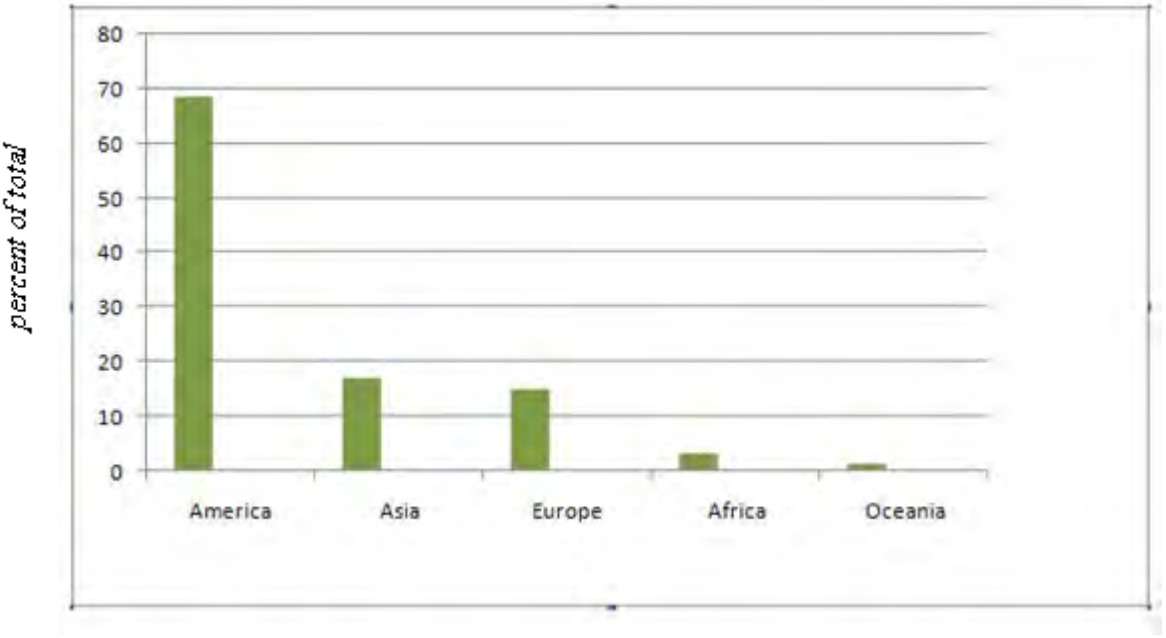

Fig.3. Ethanol in different continents

2.2. Biodiesel and Vegetable oils

Triglyceride chemical molecules with three molecules of fatty acid esters are joint to a glycerol molecule of herbaceous oils.

Herbaceous oils can be used as fuels for diesel engines; but they are more viscose than normal diesel fuels so they need to be reformed before they enter an engine.
There are different ways to reduce the viscosity of the herbaceous oils:
1-pyrolysis
2-Dilution
3-microemul-sifications
4-catalytic cracking
5-transesterifications

Process Pyrolysis has more benefits than Transesterifications. The components of the liquid fuels which produced in process Pyrolysis are resembled to the chemical components of the normal diesel petroleum fuel. Herbaceous oils can be turned into the maximum liquid and gas hydrocarbons using the processes pyrolysis، catalytic cracking, decarboxylation and deoxygenating. [5, 6]

Using herbaceous oils for making biodiesels, which is a renewable energy, introduces a new profitable way of using herbaceous oils. It means that this fuel produces lower pollutant in comparison of usual diesel which causes potential exhaustion. [7]

3. Conclusion

Biofuel, a pure fuel and a renewable energy, is obtained from biomaterials like herbal residue (corn, wheat, sugar beet and wood, straw, oilseeds, etc.). Biofuel is a good replacement for fossil fuels (non renewable) and with mentioning economical, safety and environmental reasons it is so crucial. Besides, it has more advantages than fossil fuels due to these reasons:

1- Frugality for users; Utilizing herbal residue and other agricultural products which have not been able to use by now.
2- Biofuels are renewable in comparison of normal diesel petroleum fuels.
3- They produce less amount of CO_2 in comparison of fossil fuels in the time of combustion.
4- They produce less pollutant which is a good help to the structure of nature and stability of environment which is at risk.
5- The resources of biofuels are available and their row materials are varied for producing biofuels.

A biofuel is produced in this way:

1- Thermochemical Platform (1.Direct Combustion 2.Gasification 3. Pyrolysis)
2 - Sugar platform

Biofuels which are in forms of gas and liquid are mostly used in a 100% pure as a fuel for vehicles. It is also used, in some cases, with mixture of other fuels.

References

[1] Sheehan J,Cambreco V,Duf .eld J,Garboski M,Shapouri H.An overview of biodiesel and petroleum diesel life cycles.A report by US Department of Agriculture and Energy;1998. p.1 –35.

[2] Puhan S,Vedaraman N,Rambrahaman BV,Nagarajan G.Mahua (Madhuca indica)seed oil:a source of renewable energy in India.J Sci Ind Res 2005;64:890 –6.

[3] Puppan D.Environmental evaluation of biofuels.Periodica Polytechnica Ser Soc Man Sci 2002;10:95 –116.

[4] IEA (International Energy Agency).Renewables in global energy supply.An IEA FactSheet.Paris,November 2002.

[5] Cadenas A,Cabezudo S.Biofuels as sustainable technologies:Perspectives for less developed countries.Technol Forecasting Soc Change 1998;58:83 –103.

[6] Di .glio C.Using advanced technologies to reduce motor vehicle greenhouse gas emissions.Energy Policy 1997;25:1173 –8.

[7] Reijnders L.Conditions for the sustainability of biomass based fuel use.Energy Policy 2006;34:863 –76.

Simple extraction method of green crude from natural blue-green microalgae by dimethyl ether: Extraction efficiency on several species compared to the Bligh-Dyer's method

Hideki Kanda[1,*], Peng Li[1]

[1] *Energy Engineering Research Laboratory, Central Research Institute of Electric Power Industry, Yokosuka, 240-0196 Japan*
** Corresponding author. Tel: +81-46-856-2121, Fax: +81-46-856-3346, E-mail: kanda@criepi.denken.or.jp*

Abstract: We proposed a simple, energy-efficient and environmental friendly method to extract green crude oil from microalgae by using dimethyl ether (DME). In this study, this method was tested on several species of natural blue-green microalgae. Consequently, the green crude was successfully directly extracted from high-moisture microalgae (78.2–93.4 % water content) with an extraction rate ranging from 9.9 to 40.1 % of the dry weight of the microalgae. The extraction yield of total green crude on these species by liquefied DME was compared to the widely-used Bligh-Dyer's method. The DME method almost achieved an extraction capacity approximately equivalent to the Bligh-Dyer's method. Furthermore, the dewatering properties of the proposed method on several species of wet microalgae, and the extraction efficiency were also investigated.

Keywords: *Biofuel, Blue-green microalgae, Extraction, Dimethyl ether.*

1. Introduction

Fossil fuel depletion and global warming issues have strongly motivated research on fuel production from biomass such as corps, animal fat, and micro algae [1]. Among these options, microalgae have attracted significant attention as a new generation biofuel resource [2]. Compared with terrestrial plants, microalgae have a high oil content and growth rate; mass algal cultivation can be performed on unexploited lands using systems supplied with nutrients, thus avoiding competition for limited arable lands [3].

In general, all type of microalgae biosynthesize oleic compositions. The oleic contents of many natural microalgae were approximately 20–50% of dry weight [3, 4]. The overall process related to microalgae biofuel include: species selection, microalgae cultivation, recovery of biofuel (the so-called green crude), and biofuel refining. Methods of microalgae cultivation have been widely studied [5, 6]. Green crude is basically recovered from microalgae by solvent extraction.

In the conventional process, the recovery of green crude from microalgae generally requires multiple solid-liquid separation steps. These processes involve drying, cell wall disruption, and solvent extraction; on a laboratory scale [7]. The extraction of green crude is usually performed with toxic organic solvents such as hexane, chloroform, and methanol, meaning these processes are highly energy-intensive and environmentally damaging [7]. In the lab-scale, green crude extraction with hexane normally carried out by soxhlet at 70 °C for 18 hours [4]. This long time of extraction and heating is drawback in the hexane extraction method. The most rapid and effective conventional extraction method for green crude is the Bligh-Dyer's method [8], which uses drying, cell disruption, solvent (chloroform-methanol) extraction, and evaporation of the solvent. This method has been indispensable and standard, not only for green crude extraction from micro algae but also the quantification of the crude oil from biological materials [9–11].
In the previous study, we proposed a simpler green crude recovery method, which combined drying, cell wall disruption, solvent extraction, and solvent evaporation in a single step [12].

By using liquefied dimethyl ether (DME) as an extractant, green crude was extracted directly from high-moisture natural microalgae without drying and cell wall disruption. This method was conceptualized from our previously established low-energy dewatering [13–16] and deoiling method [17–19], based on the following DME characteristics, namely (i) high affinity with oil and partial miscibility in water (ii) lower boiling point and stable pressure at normal temperature (iii) harmless and naturally decomposable [20, 21].

In the conventional method, the latent heat, sensible heat of water is lost since water should be evaporated in the pretreatment. The calorific value required for heating 1 g of water from 20°C to 100°C and for evaporating water at 100°C is 2,590 Jg^{-1}. Here, the initial moisture content of the micloalgae slurry is assumed to be 90.0% [12]. Therefore, the weight of water was 9 times of the dry weight of the micloalgae. Green crude content in micloalgae is also assumed to be 20% as we will describe later. In the green crude weight basis, theoretical heat loss is 2,590 × 9 / 0.2 = 116,550 Jg^{-1}. Moreover, the calorific value required for heating 1 g of chloroform-methanol mixture from 20°C to its boiling point (approximate 63°C) and for evaporating extraction solvent at 63°C is around 700 Jg^{-1}. This is assumed from average latent heat of chloroform (247 Jg^{-1}) and methanol (1,155 Jg^{-1}). Here, the final green crude oil concentration in the chloroform-methanol mixture is 3.3% which estimated from current study in the case of green crude content was 20%. Therefore, the weight of chloroform-methanol mixture was 29.3 times of the green crude weight. Therefore, the theoretical heat loss for evaporating the chloroform-methanol mixture is 700×29.3 = 20,510 Jg^{-1}. In addition, the energy consumed for cell disruption is unidentified and must be large. Therefore, the total required energy is roughly 137,060 Jg^{-1} and plus the unidentified part for cell disruption.

In contrast, in the proposed method, the energy required to remove 1 g of water is 1,109 J [13, 16]. As we will discuss later, extraction rate of green crude is faster than that of water. This implies that DME amount for extraction of green crude is less than that for removing of water. In other words, the required energy for extraction of green crude is less than water. Thus, the available calorific value for extraction of green crude oil from microalgae is less than 1,109 ×9 = 9,981 Jg^{-1}. Therefore, the proposed method is more energy efficient than the conventional method from the perspective of energy balance.

Considering both the need for sustainable energy and environmental concerns, this method was initially tested on a natural blue-green microalga (a species usually causing harmful algal blooms in human ecosystems) collected at Hirosawa Mere in Kyoto City, Japan [12]. By using dimethyl ether (293 K, 0.51 MPa) as an extractant, the green crude was successfully extracted from natural blue-green microalgae (91.0% water content) with a high extraction capacity of 40.1% of the dry weight of the microalgae. The extraction yield by liquefied DME was 99.7 %. The resulting green crude was further analyzed by GC-MS, and the result showed that the lipid substance was predominant chemical composition in the extracted green crude. The calorific value of the green crude was 45,790 J g^{-1}.

The practical application of this method will require fundamental research to evaluate its effectiveness for different types of algae. In this study, we investigate the extraction yield of green crude by liquefied DME on several natural blue-green microalgae and the results were compared to the Bligh-Dyer's method.

2. Methodology

2.1. Materials

The samples were five selected species of microalgae and two mixed-species of microalgae as follows. (i, ii) *Oscillatoria agardhii* NIES-595 and NIES-1263, collected in Northern Ireland, and Germany, respectively. The water contents of both microalgae were 85.0 %. (iii, iv) *Microcystis aeruginosa* ONC and GSK, collected in the main Okinawa island, Japan. The water contents were 93.4 and 91.1 %, respectively. (v) *Monoraphidium chlorophyta* GK 12. The water content was 78.2 %. (vi) Mixed-species (mainly *Cymbela*) collected at Lake Kanogawa in Ozu City, Japan. The water content was 93.0 %. (vii) The same sample used in the previous study [12]. Mixed-species (mainly *Microcystis*) collected at Hirosawa Mere in Kyoto City, Japan. The water content was 91.0 %.

2.2. Experimental apparatus and methods

The experimental apparatus was the same as that described in the previous study [12]. Briefly, a vessel used for storing liquefied DME (volume: 100 cm^3; TVS-1-100, Taiatsu Techno Corp., Saitama, Japan), a vessel as an extraction column (diameter, 11.6 mm; length, 190 mm; HPG-10-5, Taiatsu Techno Corp.) and a storage vessel for a mixture of DME, water and extracted crude oil (HPG-96-3, Taiatsu Techno Corp.) were connected in series. The microalgae sample was loaded into the lower half of the extraction column and the upper half was loaded with glass beads (of diameter between 0.71 and 0.99 mm; BZ-08, Asone Co., Inc., Osaka, Japan). Nitrogen gas (0.51 MPa) was supplied to flow through the extraction system. The DME flow rate was 10cm^3 min^{-1}, and the temperature was 293 K. The experiments were all performed three times independently and the data reported in this paper are the mean values with ± deviation.

2.3. Total crude oil content

The total crude oil content was determined using a widely-used gravimetric analysis based on Bligh-Dyer's method [8]. Briefly, 1g of the dried microalgae was mixed and homogenized with chloroform-methanol (1:1 vol/vol). An equivalent volume of distilled water was added to the microalgae and chloroform-methanol mixtures. Subsequently, the mixtures were transferred into a separatory funnel and agitated for 5 minutes. The mixtures separated into double layers of water-methanol and chloroform phases. The green crude dissolved easily in the low-polar chloroform phase. The green crude in the chloroform layer was separated from the separatory funnel and the separated chloroform was evaporated under reduced pressure.

3. Results and Discussion

3.1. Extraction of green crude from several microalgae

The extraction rate and yield of green crude on the blue-green microalgae by liquefied DME was examined. We would emphasize that the microalgae had high moisture and unbroken cell walls, in the extraction with sufficient liquefied DME. The extraction volumes achieved by liquefied DME and the Bligh-Dyer's method were respectively shown in Fig. 1. White expresses the green crude extraction rate by liquefied DME on the dry weight of the microalgae. Black expresses the results of the Bligh-Dyer's method. The superscript "^{a}" represents the extraction yield of the DME extraction method relative to the Bligh-Dyer's method.

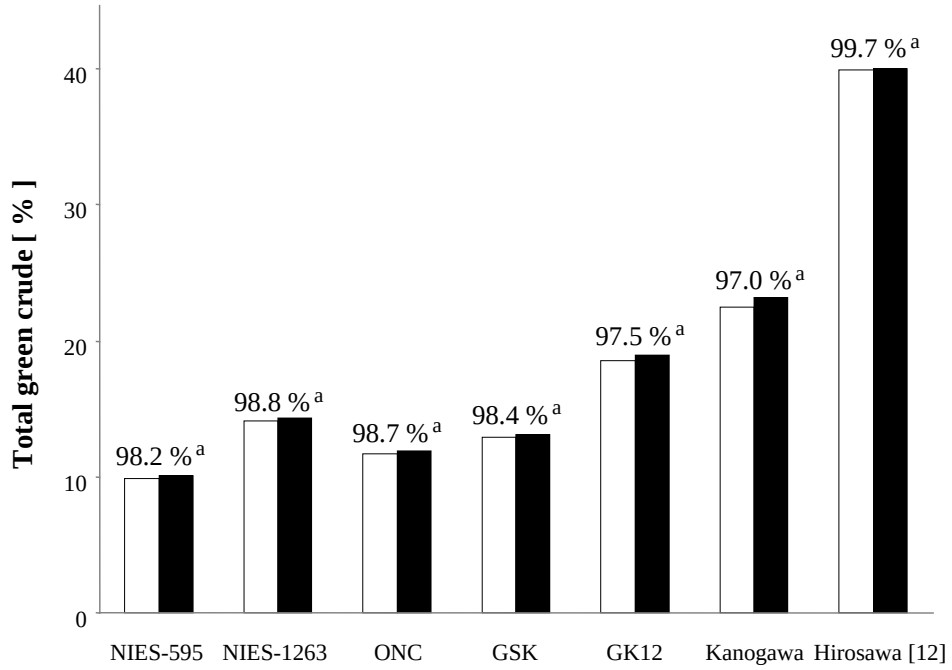

Fig. 1. Green crude extraction rate and yields on several microalgae.

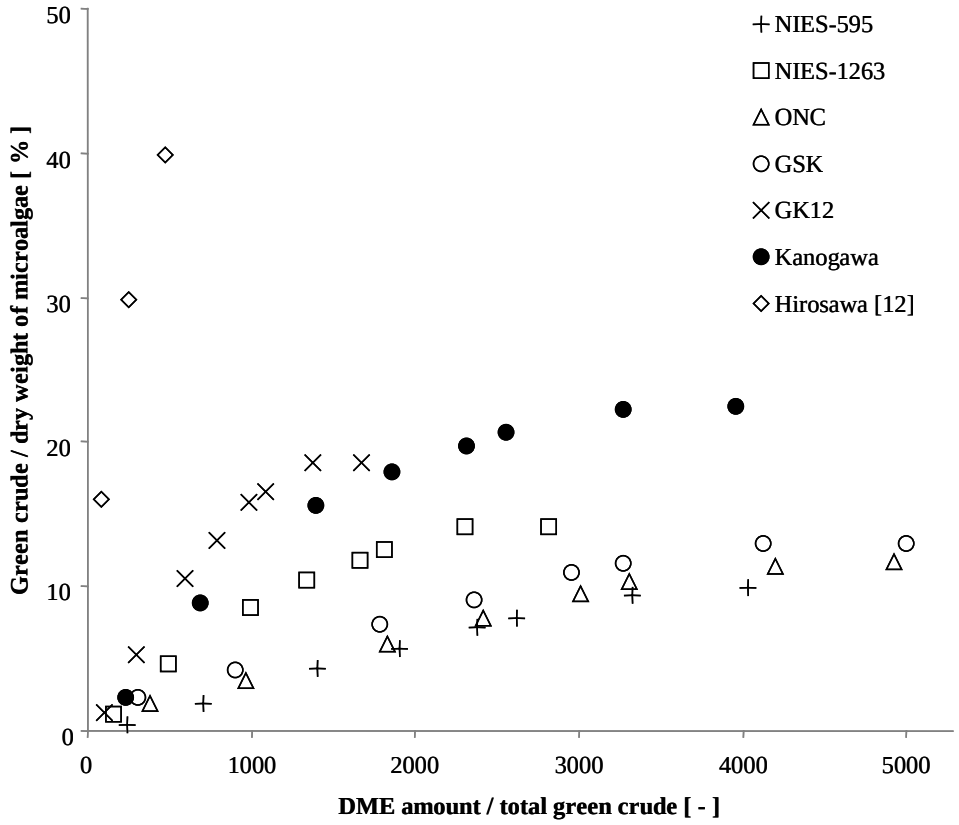

Fig. 2. Extraction of green crude from several microalgae by liquefied DME.

Both NIES-595 and NIES-1263 belong to *Oscillatoria agardhii*, but their extraction rates differ as 9.9 ± 1% and 14.0 ± 1%, respectively. Conversely, the extraction rates of ONC 11.0 ± 2% and GSK 12.0 ± 1.5 % are similar. The extraction rate of GK12 was 18.5 ± 2%. The extraction rate of the mixed-species of microalgae collected at Lake Kanogawa was 22.5 ± 1 %. The extraction rate of Hirosawa Mere showed the highest extraction rate of 40.1 ± 2 %.

The extraction yield of all species achieved more than 97.0 % of total crude oil as determined by the Bligh-Dyer's method. This implies that the DME extraction method provides comparable results to the Bligh-Dyer's method.

The extraction efficiency of green crude by liquefied DME on these microalgae was shown in Fig. 2. For each of the samples, the liquefied DME amount was converted into a ratio of the DME amount relative to total green crude, since the total green crude amount differed. In general, solvent is reused until the green crude concentration in the solvent increases sufficiently, whereupon the usual solvent ratio may apparently be much smaller. On the other hand, in this study, the liquefied DME was not reused after extraction, hence the liquefied DME ratio must be large.

The DME amounts required to reach equilibrium in the extraction of green crude in increasing order were Hirosawa < GK12 < NIES-1263 < Kanogawa < NIES-595 < ONC < GSK. This sequence almost corresponds with the total green crude amount.

3.2. Dewatering from several microalgae

The dewatering by liquefied DME on these microalgae was shown in Fig. 3. Since the water content also differed for each of the samples, the liquefied DME was converted into the ratio

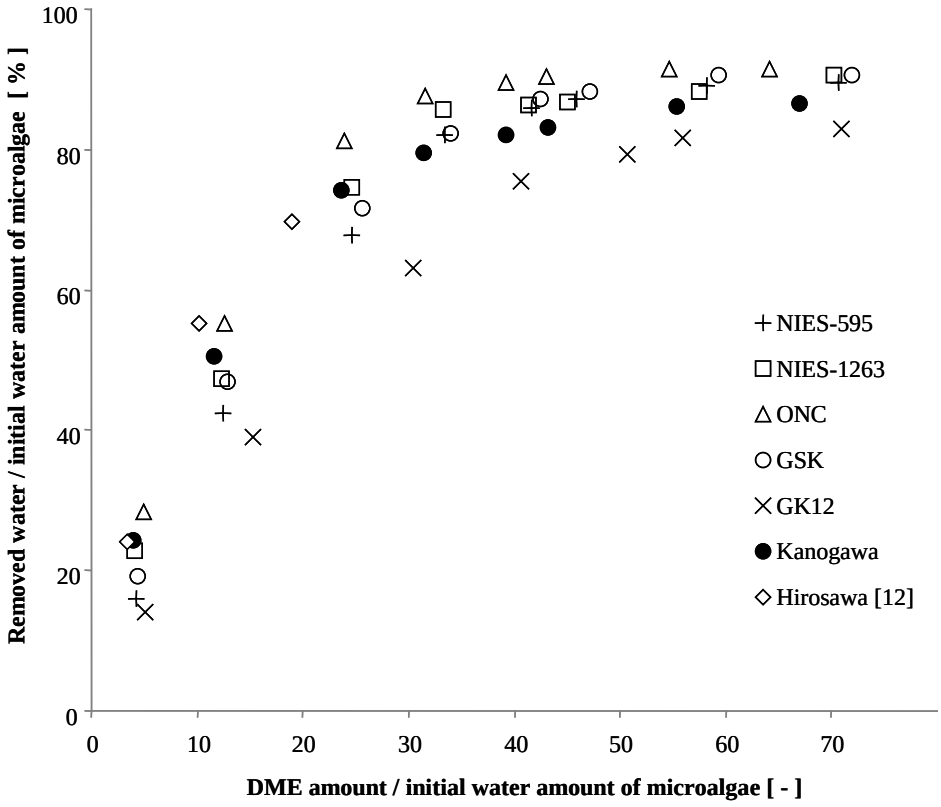

Fig. 3. Dewatering of several microalgae by liquefied DME.

of the DME amount relative to initial water content. By increasing the amount of liquefied DME, the water was extracted from the high-moisture microalgae together with green crude. Moreover, no obvious difference was observed in the dewatering for all samples. While green crude is confined in the microalgae cell wall, most of water exist outside the microalgae cell wall. This make a difference between the green crude extraction and the dewatering.

4. Conclusions

This study confirmed the direct extraction of green crude from several high-moisture natural microalgae by using liquefied DME. Moreover, the extracted amount was almost equal to the Bligh-Dyer's method. Here it is notable that conventional methods are unable to directly extract green crude from high-moisture microalgae, and the cell disruption must be carried out before solvent extraction. The other advantage of this method is the dewatering effect. This method has the potential to reuse the removed water as microalgae broth. The materials in the removed water will be examined from the perspective of the water shortage crisis.

Acknowledgements

This research was supported by a grant from the Industrial Technology Research Program (Project ID: 09B40009c) of the New Energy and Industrial Technology Development Organization (NEDO). We are deeply grateful to Drs. Tadaaki Tokashiki, Tsuyoshi Ikehara, Mina Yasumoto-Hirose and Atsushi Yoshino at the Tropical Technology Center, Associate Professor Katsuhiko Fujii at Yamaguchi University, and Mr. Tomoyuki Akasaka at the Ozu City government for providing the microalgae.

References

[1] M. Xin, Y. Jianming, X. Xin, Z. Lei, N. Qingjuan, X. Mo, Biodiesel production from oleaginous microorganisms. Renewable Energy 34, 2009, pp.1-5.

[2] B.J. Gallagher, The economics of producing biodiesel from algae. Renewable Energy 36, 2011, pp. 158-162.

[3] B. Liam, O. Philip, Biofuels from microalgae- A review of technologies for production processing, and extraction of biofuels and co-products. Renewable and Sustainable Energy Reviews 14, 2010, pp. 557-577.

[4] A. Demirbas, S. Science, T. Turkey, Production of biodiesel from algae oils. Energy Sources, Part A, 31, 2009, pp. 163-168.

[5] X. Miao, Q. Wu, Biodiesel production from heterotrophic microalgal oil. Bioresource Technology 97, 2006, pp. 841-846.

[6] C. Posten, G. Schaub, Microalgae and terrestrial biomass as source of fuels- A process view. Journal of Biotechnology 14, 2009, pp. 64-69.

[7] E. Molina Grima, E. Belarbi, F. Fernandez, A. Medina, Y. Chisti, Recovery of microalgal biomass and metabolites: process options and economics. Biotechnology Advances 20, 2003, pp. 491-515.

[8] E.G. Bligh, W.J. Dyer, A rapid method of lipid extraction and purification. Canadian Journal of Biochemistry and Physiology 37, 1959, pp. 911-917.

[9] L. Jae-Yon, Y. Chan, J. So-Young, A. Chi-Yong, O. Hee-Mock, Comparison of several methods for effective lipid extraction from microalgae. Bioresource Technology 101, 2010, pp. 75-77.

[10] C. Samori, C. Torri, G. Samori, D. Fabbri, P. Galletti, F. Guerrini, R. Pistocchi, E. Tagliavini, Extraction of hydrocarbons from microalga *Botryococcus braunii* with switchable solvents. Bioresource Technology 101, 2010, pp. 3274-3279.

[11] M. Zhu, P.P. Zhou, L.J.Yu, Extraction of lipids from *Mortierella* alpine and enrichment of arachidonic acid from the fungal lipids. Bioresource Technology 84, 2002, pp. 93-93.

[12] H. Kanda, P. Li, Simple extraction method of green crude from natural blue-green microalgae by dimethyl ether. Fuel 2010, doi:10.1016/j.fuel.2010.10.057.

[13] H. Kanda, H. Shirai, Method for removing water contained in solid using liquefied material. 2002, Patent number – JP 4 291 772 B2 WO2003/101579.

[14] H. Kanda, Y. Urakawa, Method for dehydrating water-containing substance using liquefied matter. 2006, Patent number – US 7 803 253 B2.

[15] H. Kanda, H. Makino, M. Miyahara, Energy-saving drying technology for porous media using liquefied DME gas. Adsorption 14, 2008, pp. 467-473.

[16] H. Kanda, H. Makino, Energy-efficient coal dewatering using liquefied dimethyl ether. Fuel 89, 2010, pp. 2104-2109.

[17] H. Kanda, Method for deoiling oil-containing substance using liquefied material. 2006, Patent number – JP 4 542 517 B2.

[18] H. Kanda, H. Makino, Clean up process for oil-polluted materials by using liquefied DME. Journal of Environment and Engineering 4, 2009, pp. 356-361.

[19] K. Oshita, M. Takaoka, S. Kitade, N. Takeda, H. Kanda, H. Makino, T. Matsumoto, S. Morisawa, Extraction of PCBs and water from river sediment using liquefied dimethyl ether as an extractant. Chemosphere 78, 2010, pp. 1148-1154.

[20] H. Holldorff, H. Knapp, Binary vapor–liquid–liquid equilibrium of dimethyl ether–water and mutual solubilities of methyl chloride and water: experimental results and data reduction. Fluid Phase Equilibria 44, 1988, pp. 195-209.

[21] TA. Semelsberger, RL. Borup, HL. Greene, Dimethyl ether (DME) as an alternative fuel. Journal of Power Sources 156, 2006, pp. 497-511.

Production of synthetic alcohol from syngas using MoS_2/γ-Al_2O_3

S. W. Chiang, C. C. Chang, H. Y. Chang, C. Y. Chang*

Graduate Institute of Environmental Engineering, Nation Taiwan University, Taipei 106, Taiwan
** Corresponding Author. Tel: (886) 223638994, Fax: (886) 223638994, E-mail: cychang3@ntu.edu.tw*

Abstract: This study examined the transformation of the biomass gasification synthesis gas (syngas, CO and H_2) to liquid fuels and chemicals via the high pressure fixed packed bed (HPFPB). The MoS_2/γ-Al_2O_3 catalyst was packed in the packed bed (PB) to enhance the selectivity (S) and yield (Y) products. The effect of reaction temperature (T), pressure (P_{ST}), gas flow rate (Q_G) and H_2/CO (vol./vol.) ratio oon the system performance were investigated. Typical reaction conditions unless otherwise specified were as follows: T = 423, 473, 523 and 573 K, P_{ST} = 3 MPa, Q_G = 300 cm^3 min^{-1}, and mass of catalyst (m_S) = 30 g.

The main products include CH_4, C_2H_6 and C_2H_5OH (EtOH) that EtOH being the target product. The results indicate that with packing MoS_2/γ-Al_2O_3 catalyst in PB, the conversion of CO (X_{CO}) and alcohol production rate (R) are highly depended on T. At T = 573 K, X_{CO} = 8.19%, R of CH_4 (R_{CH4}) = 194.1 mg h^{-1} and selectivity of CH_4 (S_{CH4}) = 34.57%. For the production rate of C_2H_5OH (R_{EtOH}), the maximum R_{EtOH} of 134.25 mg h^{-1} takes place at T = 523 K while X_{CO} = 8.10% and S_{EtOH} = 51.98%. As T increase to 573 K, the EtOH is further decomposed into simple hydrocarbons (HCs) such as C1-C3 alkanes. Thus, for producing more alcohols and less alkanes, the optimal temperature condition is 523 K. For the case of varying H_2/CO ratio, the values of X_{CO} are about 7.55 to 8.32%) at 523 K with H_2/CO ratios of 1 to 4, indicating no significant variation. However, the optimal ratio of H_2 and CO to produce EtOH is 2 with maximum R_{EtOH} = 134.25 mg h^{-1} and S_{EtOH} = 51.98% while X_{CO} = 8.10%, R_{CH4} = 56.05 mg h^{-1} and S_{CH4} = 10.85%. Hence, increasing the H_2/CO ratio to 3 to 4 is not beneficial for the formation of EtOH. The results also show that a higher PST of HPFPB yields more products. For the EtOH production, the maximum R_{EtOH} (= 156.65 mg h^{-1}) occurs at P_{ST} = 3.6 MPa with corresponding S_{EtOH} = 51.16%, X_{CO} = 9.57%, R_{CH4} = 70.31 mg h^{-1} and S_{CH4} = 12.46%. Among various Q_G of 300, 450, 600 to 900 mL min^{-1} of HPFPB tested, the best X_{CO} is at Q_G = 300 mL min^{-1} with X_{CO} = 8.10%, R_{CH4} = 56.05 mg h^{-1} and S_{CH4} = 10.85%. Also, the maximum Y_{EtOH} take place at Q_G = 300 mL min^{-1} with corresponding S_{EtOH} = 51.98%. It shows that a low flow rate gives a longer residence time for reaction of the syngas and thus enhances the yield of products. However, there's no advance for S_{EtOH}.

For the production of EtOH from syngas, the Y_{EtOH}, S_{EtOH} and R_{EtOH} are key factors for the success of process. The results of this study shows that MoS_2/γ-Al_2O_3 catalyst can give satisfactory S_{EtOH} and R_{EtOH}, especially the Y_{EtOH} high selectivity.

Keywords: *Reforming of syngas; Synthesis of alcohol; MoS_2/Al_2O_3; catalytic synthesis; alcohol; alkane*

1. Introduction

Energy crisis has been a great concerned issue in recent years. With the continued climbing of crude oil price, studies on alternative energy become more and more essential. The use of biomass, such as agriculture residues and woody waste, to provide energy and chemicals is receiving increasing interest because these resources can supplement the existing supplies of raw materials while have less net environmental impact [1]. The biomass of agriculture and the biomass fibers of municipal solid waste (MSW) are among the suitable bio-energy sources that can be used for generation energy [1-2].

Gasification technologies have been developed for the possible replacement of traditional combustion technologies because of their higher power generation efficiency while lower environmental pollution [2]. Gasification is a thermochemical process yielding major product of synthesis gas (syngas) consisting of CO and H_2. Syngas can be used to produce hydrocarbons such as ethanol (EtOH) via Mo-based catalytic reaction and other high-value-added fuels via the Fischer-Tropsch process. Although the syngas has been also used as fuel gas, however, its storage, stabilization and transportation exhibit some problems. On the other

hand, alcohols converted form syngas have high heating value with small volume and are stable as liquid phase. Moreover, the use of EtOH as a part of the automobile fuel offers the same chemical energy as that of gasoline. Besides, ethanol is a good additive for improving gasoline octane value and burning efficiency [3].

In this study, a high pressure fixed packed bed (HPFPB) with continuous flow was used to synthesize the syngas yielding alcohols. A $MoS_2/\gamma\text{-}Al_2O_3$ catalyst was packed in the bed to enhance the production. The MoS_2 based catalysts, such as K_2CO_3/MoS_2 and Ni-K_2CO_3/MoS_2, have been already verified as effective catalysts in the synthesis of mixed alcohols [4-7]. The distinct points of this study were the use of HPFPB and preparation method of MoS_2 on the $\gamma\text{-}Al_2O_3$ support with high surface of catalyst. The production rates (R), yield (Y) and selectivity (S) of alcohols and conversion of CO (X_{CO}) were examined and elucidated.

2 Materials and Methods

2.1 Preparation of $MoS_2/\gamma\text{-}Al_2O_3$

The MoS_2 was loaded on $\gamma\text{-}Al_2O_3$ pellet ($MoS_2/\gamma\text{-}Al_2O_3$). In preparation, about 30 g $\gamma\text{-}Al_2O_3$ (φ = 3 m m) were soaked in 200 mL solution containing 5% ammonium heptamolybdate ($(NH_4)_6Mo_7O_{24}$) with the adjustment of pH < 2 us ing nitric acid for adsorbing ionic Mo on the alumina surface for 12 h. It was then sintered at 773 K with N_2 for 3 h to form $Mo_XO_Y/\gamma\text{-}Al_2O_3$. The resulted $Mo_XO_Y/\gamma\text{-}Al_2O_3$ was further reduced and sulfurized in the mixed gas stream of H_2S/H_2 with volume ratio of 5/95 at 673 K for 2 h to produce $MoS_2/\gamma\text{-}Al_2O_3$ catalyst [8]. The $\gamma\text{-}Al_2O_3$, MoS_2 and $(NH_4)_6Mo_7O_{24}$ were supplied by First Chemical (Taipei, Taiwan), ProChem (Miaoli, Taiwan) and J.T. Baker (Phillipsburg, New Jersey, USA), respectively.

2.2 HPFPB system

The HPFPB system (Fig. 1) was carried out via continuous flow type operation. The synthesis reaction proceeded in a high pressure. Two packing materials of $MoS_2/\gamma\text{-}Al_2O_3$ and spherical glass beads were used and tested in the packed bed. The polar organic products such as alcohols and acids were collected by DI water (4 ˚C) in a condenser. The syngas was simulated with H_2/CO mole ratio of 2. The HPFPB system was operated under the conditions with mass flow rates of H_2 and CO (dmH_2/dt and dmCO/dt) of 1070.4 and 7492.8 mg h^{-1}, gas flow rate of syngas (Q_G) = 300 mL min^{-1}, temperature (T) = 423-573 K, mass of catalyst (m_S) = 30 g, flow rate (Q_G) = 300-900 mL min^{-1}, gas hourly space velocity (GHSV) = 600-1800 cm^3 $gcat^{-1}$ h^{-1}, and pressure (P_{ST}) = 1.5-3.6 Mpa (reading at 298 K).

2.3 Products analysis

The analyses of gaseous organic compounds were performed using the gas chromatography/flame ionization detector (GC/FID, 6890 GC, Agilent Technologies, Santa Clara, CA, USA) with AB-5 column (30m × 0.53mm × 5.00 μm, Abel Industries, Pitt Meadows, BC, Canada) to separate the organic products. A p urge-and-trap sample concentrator (Model 4560, OI Analytical, College Station, TX, USA) was used to purify and inject liquid samples into GC/FID for analyses.

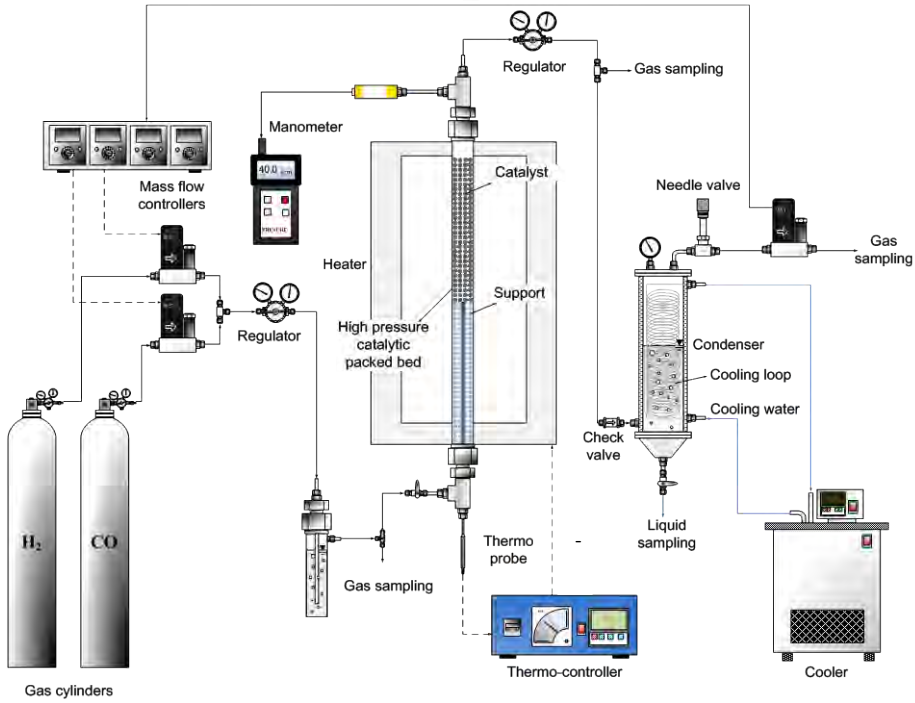

Fig. 1. Schematic diagram of HPFPB system.

3 Results and discussion

3.1 Properties of catalyst and support

The MoS_2/Al_2O_3 catalyst used is spherical with 3 mm diameter and bulk density of 3.2055 g cm^{-3}. The MoS_2 was loaded on the surface of porous Al_2O_3 pellet. The BJH (Barrett-Joyner-Halenda) average pore sizes obtained by adsorption and desorption are 70.404 and 57.841 Å, respectively, indicating mesoporous nature of catalyst. The corresponding BET surface area is 210.345 m^2 g^{-1}. The XRD (X-ray diffraction) spectrum of catalyst surface is shown in Fig. 2, exhibiting significant specific characteristics of MoS_2 at $2\theta = 14.5^{\circ}$, 39.6° and 60.18°.

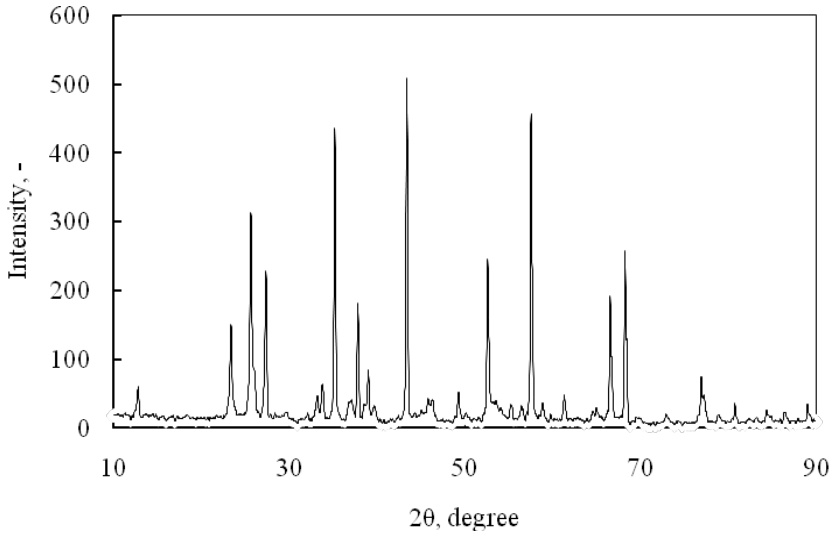

Fig. 2. XRD spectrum of MoS_2/Al_2O_3.

3.2 Effect of temperature

As shown in Fig. 3a, the production rate R of alkane via MoS_2/γ-Al_2O_3 synthesis increases with increasing reaction temperature, especially when T reaches 573 K. For the (b) alcohol products, the productions were not effected as the regular pattern as the increase T for the alkane products.

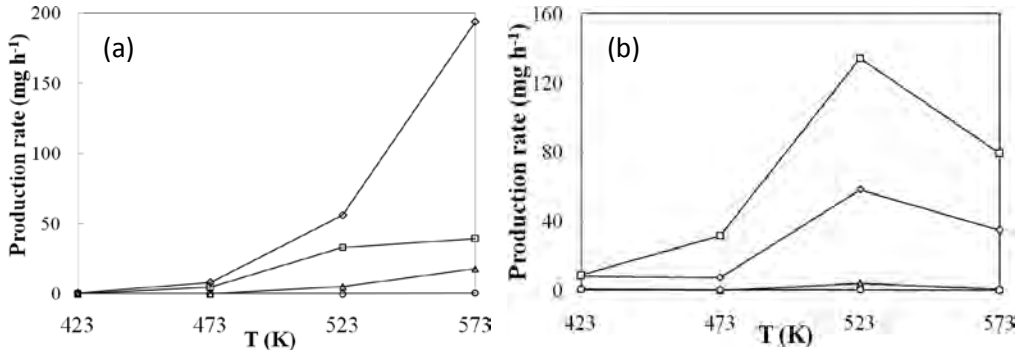

Fig. 3. Production rates of (a) alkane and (b) alcohol products at various temperatures via HPCPB-MoS_2 process. ◇, □, △, ○: C1, C2, C3, C4.

Table 1 illustrates the conversion of CO (X_{CO}) and selectivies (S) of synthesis products at the four different temperature conditions. Setting the reaction at the conditions of T = 473 K, P_{ST} = 3 MPa, H_2/CO = 2, Q_G = 300 cm^3 min^{-1}, and GHSV = 600 cm^3 $gcat^{-1}$ h^{-1}, the selectivties of synthesis products shows the highest forming favourable S_{EtOH} = 54.02% within four different temperatures and accompanies with lower forming S_{CH4} = 2.09%. S ince X_{CO} is also a meaningful efficiency index, the best X_{CO} is 8.19% while the condition at T = 573 K.

Table 1. Conversion of CO and selectivities of products at various temperatures.

T	Conversion	Selectivity (%)								
(K)	(%)	CH_4	C_2H_6	C_3H_8	C_4H_{10}	CH_3CHO	MeOH	EtOH	PrOH	BuOH
423	0.59	1.19	0.74	-	-	31.12	16.69	36.43	6.53	7.30
473	2.09	6.88	8.06	-	-	22.50	6.38	54.02	0.30	1.86
523	8.10	10.85	12.84	3.00	-	7.48	11.29	51.98	2.27	0.29
573	8.19	34.57	14.06	9.58	0.48	6.28	6.21	28.28	0.39	0.16

MeOH: methanol; EtOH: ethanol; PrOH: propanol; BuOH: butanol.

At first appearance, the highest S_{EtOH} and the best X_{CO} seem to be well performances. In fact, they still could not represent the optimal condition because of theirs uncompleted well-performances which comparing these with the condition at T = 523 K. Setting the reaction T at 523 K is the optimal set point which not only yields more alcohol products, especially for higher S_{EtOH}, but also restrains the amount of alkanes formed.

3.3 Effect of H_2/CO ratio

Besides the temperature factor, the H_2/CO feed ratio is also a key adjustable variable affecting the conversion of syngas to ethanol or higher alcohols. The H_2/CO could be adjust to maximize S_{EtOH} and restrain methane forming that because methane is the most thermodynamically favored product, however, its economical value is less than alcohols [9]. The reactions of ethanol and methane are as the showing in following equations:

$$2CO + 4H_2 \rightarrow C_2H_5OH + H_2O \qquad (1)$$

$$\Delta H_r = -61.20 \text{ kcal/mol}; \Delta G_r = -29.32 \text{ Kcal/mol}$$

$$CO + 3H_2 \rightarrow CH_4 + H_2O \qquad (2)$$

$$\Delta H_r = -49.27 \text{ kcal/mol}; \Delta G_r = -33.97 \text{ Kcal/mol}$$

According the ratio of H_2/CO from the above equations, it is obvious to understand that higher ratio (eq. 2) is more favourable to produce methane than producing ethanol (eq. 1). As the shown in fig. 4, the productions present desired results which are higher production of alcohols accompany with lower production of alkanes when setting H_2/CO ratio as 2.

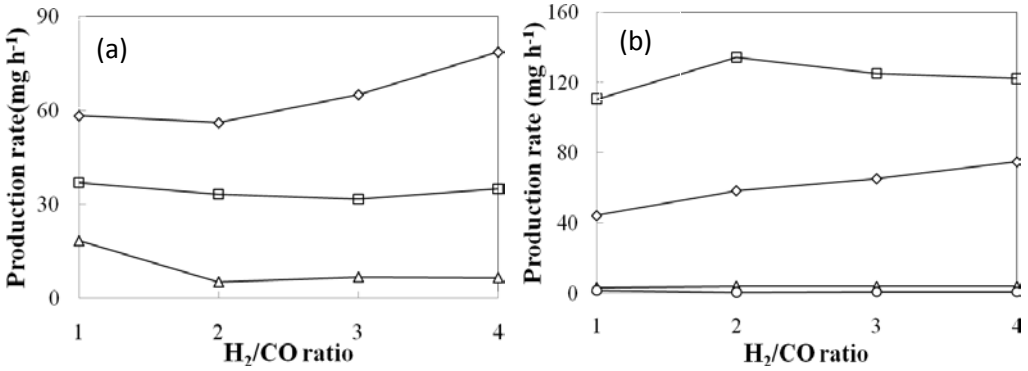

Fig. 4. Production rates of (a) alkane and (b) alcohol products at various H_2/CO ratios via HPCPB-MoS_2 process. ◇, □, △, ○: C1, C2, C3, C4.

Table 2. Conversion of CO and selectivities of products at various H_2/CO ratios.

H_2/CO	Conversion	Selectivity (%)								
	(%)	CH_4	C_2H_6	C_3H_8	C_4H_{10}	CH_3CHO	MeOH	EtOH	PrOH	BuOH
1	7.55	11.84	15.01	11.21	-	5.09	8.97	44.9	1.82	1.16
2	8.10	10.85	12.84	3.00	-	7.48	11.29	51.98	2.27	0.29
3	8.01	12.67	12.34	3.94	-	6.97	12.69	48.73	2.13	0.53

4	8.32	14.67	13.05	3.67	-	6.52	13.94	45.57	2.05	0.53

MeOH: methanol; EtOH: ethanol; PrOH: propanol; BuOH: butanol.

Table 2 illustrates X_{CO} and S of synthesis products at the four different H_2/CO ratios. Setting the reaction at the conditions of T = 523 K, P_{ST} = 3 MPa, Q_G = 300 cm^3 min^{-1}, and GHSV = 600 cm^3 $gcat^{-1}$ h^{-1}, X_{CO} is 8.10% and S_{EtOH} and S_{CH4} are 51.89% and 10.85%, respectively. In these conditions, MoS_2 catalyst shows obvious favour for EtOH and slight restraint for CH_4. For this reason, the results of the shown at $H_2/CO = 2$ are desired and acceptable even if the conversion of CO is not the highest performance.

3.4 Effects of pressure

Increasing pressure is equal to increase the providing raw materials and the equilibrium concentration of products from the hydrogenation of CO [1]. As the shown in fig. 5, both of the productions of alkane and alcohol products increase as the increasing reaction pressure. Therefore, the effects of reaction pressure appear as though Le Chatelier's Principle.

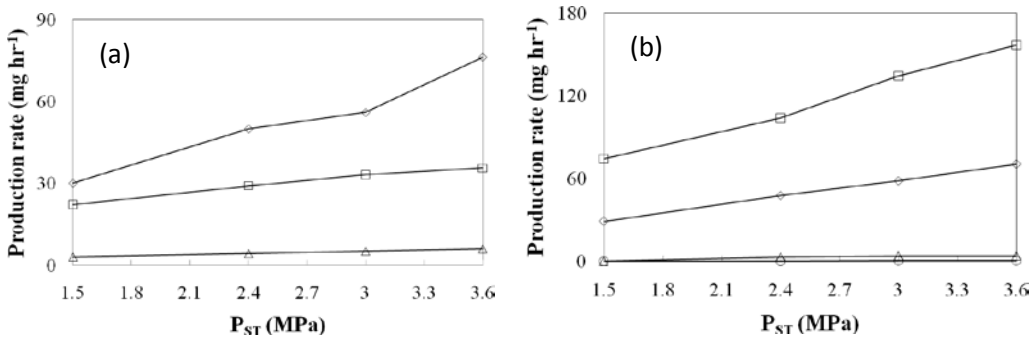

Fig. 5. Production rates of (a) alkane and (b) alcohol products at various pressures via HPCPB-MoS_2 process. ◇, □, △, ○: C1, C2, C3, C4.

Table 3. Conversion of CO and selectivities of products at various pressures.

P_{ST}	Conversion	Selectivity (%)								
(MPa)	(%)	CH_4	C_2H_6	C_3H_8	C_4H_{10}	CH_3CHO	MeOH	EtOH	PrOH	BuOH
1.5	4.6	11.84	15.01	11.21	-	-	9.93	50.92	2.47	-
2.4	6.48	12.05	14.04	3.08	-	7.27	11.29	50.00	2.27	-
3.0	8.10	10.85	12.84	3.00	-	7.48	11.29	51.98	2.27	0.29
3.6	9.57	12.46	12.63	2.96	-	3.71	13.94	51.16	2.86	0.28

MeOH: methanol; EtOH: ethanol; PrOH: propanol; BuOH: butanol.

Table 3 illustrates X_{CO} and S of synthesis products at the four different reaction pressures (reading at 298 K). Setting the reaction at the conditions of T = 523 K, $H_2/CO = 2$, $Q_G = 300$ cm^3 min^{-1}, and GHSV = 600 cm^3 $gcat^{-1}$ h^{-1}. As the increased pressure in this study, there are only increasing effects for X_{CO} as the shown in table 3, however, the selectivities of both alkane and alcohol products are not affected by changing the reaction pressures.

3.5 Effects of flow rate

A high flow rate into the reactor gives a higher space velocity through the fixed catalytic bed, which is equivalent to change the volume of catalyst in the reactor. As the shown in fig. 6, increasing the flow rate also means more reactants input, enhancing the production rates for both of alkanes and alcohols.

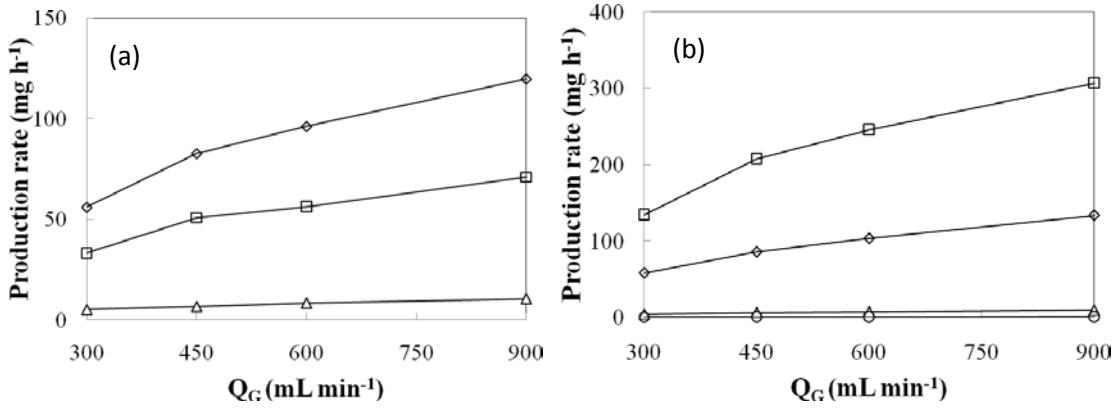

Fig. 6. Production rates of (a) alkane and (b) alcohol products at various flow rates via HPCPB-MoS_2 process. ◇, □, △, ○: C1, C2, C3, C4.

Table 4 illustrates the conversion of CO and selectivies of synthesis products at the four different flow rates. Setting the reaction at the conditions of T = 523 K, $H_2/CO = 2$, $P_{ST} = 3$ MPa, and GHSV = 300 cm^3 min^{-1}. As the shown in table 4, increasing the flow rate obviously decrease X_{CO} because the retention time is too small to finish more number of completed reactions. The increase of space velocity results in a slight decrease in selectivity of alkanes while an insignificant increase of alcohols in the reaction products. Besides, the effects of changing flow rate are similar with those of the changing of reaction pressures.

Table 4. Conversion of CO and selectivities of products at various flow rates.

Q_G	Conversion	Selectivity (%)								
(mL min^{-1})	(%)	CH_4	C_2H_6	C_3H_8	C_4H_{10}	CH_3CHO	MeOH	EtOH	PrOH	BuOH
300	8.10	10.85	12.84	3.00	-	7.48	11.29	51.98	2.27	0.29
450	5.44	10.54	12.95	2.52	-	7.54	10.91	52.91	2.37	0.26
600	4.83	10.41	12.18	2.70	-	7.82	11.16	53.14	2.34	0.25
900	4.12	10.25	12.14	2.68	-	8.38	11.39	52.50	2.40	0.26

MeOH: methanol; EtOH: ethanol; PrOH: propanol; BuOH: butanol.

4. Conclusions

In HPFPB system, the main organic products of alkane and alcohols of $MoS_2/\gamma\text{-}Al_2O_3$ catalytic synthesis are ethanol and methane, respectively. From the previous results shown, ethanol selectivity decreases at all temperatures when methane is the major product. For this reason, setting the reaction temperature at T = 523 K is the optimal set point which not only yields more alcohol products, especially for higher S_{EtOH}, but also restrains the amount of alkanes formed. Furthermore, it could increase S_{EtOH} versus CH_4 while setting the H_2/CO feed ratio as 2. C onsidering the effects of P_{ST} and Q_G, there are similar trends for both of alkane and alcohol products besides of the trend for the conversion of CO. Increasing the flow rate would decrease X_{CO} because the retention time is too small to finish more number of completed reactions.

Taken together, these observations suggest that setting the parameter as T = 523 K, H_2/CO = 2, higher pressure, and lower flow rate to reach the purpose of obtaining higher X_{CO} and outstanding S_{EtOH}.

References

[1] Spivey, J.J. and A. Egbebi, *Heterogeneous catalytic synthesis of ethanol from biomass-derived syngas.* Chemical Society Reviews, 2007. **36**(9): p. 1514-1528.

[2] Ragauskas, A.J., et al., *The path forward for biofuels and biomaterials.* Science, 2006. **311**(5760): p. 484-489.

[3] Subramani, V. and S.K. Gangwal, *A review of recent literature to search for an efficient catalytic process for the conversion of syngas to ethanol.* Energy & Fuels, 2008. **22**(2): p. 814-839.

[4] Haider, M.A., M.R. Gogate, and R.J. Davis, *Fe-promotion of supported Rh catalysts for direct conversion of syngas to ethanol.* Journal of Catalysis, 2009. **261**(1): p. 9-16.

[5] Li, D., et al., *The performances of higher alcohol synthesis over nickel modified K2CO3/MoS2 catalyst.* Fuel Processing Technology, 2007. **88**(2): p. 125-127.

[6] Li, D.B., et al., *Higher alcohol synthesis over a La promoted $Ni/K_2CO_3/MoS_2$ catalyst.* Catalysis Communications, 2004. **5**(10): p. 605-609.

[7] Woo, H.C., et al., *Alkali-promoted MoS2 catalysts for alcohol synthesis- the effect of alkali promotion and preparation condition on activity and selectivity.* New Frontiers in Catalysis, Pt C, 1993. **75**: p. 2749-2752.

[8] Sakashita, Y., Y. Araki, and H. Shimada, *Effects of surface orientation of alumina supports on the catalytic functionality of molybdenum sulfide catalysts.* Applied Catalysis a-General, 2001. **215**(1-2): p. 101-110.

[9] Egbebi, A. and J.J. Spivey, *Effect of H2/CO ratio and temperature on methane selectivity in the synthesis of ethanol on Rh-based catalysts.* Catalysis Communications, 2008. **9**(14): p. 2308-2311.

Thermal treatment of Rapeseed oil

Shanmugam Palanisamy, Börje S. Gevert

Chalmers University of Technology, Göteborg, Sweden
Corresponding author. Tel: +46 31 7722812, E-mail: shapal@chalmers.se

Abstract: The thermal decomposition of rapeseed oil lowered cetane value of the product through decarboxylation and decarbonylation. In this study the thermal decomposition in rapeseed oil was estimated with different temperatures (300 to 410^{o}C) with or without hydrogen at 1 bar partial pressure. Initially, the reactor is loaded with glass pellets and then the rapeseed oil was fed into the reactor. At hydrothermal condition of 300 to 410^{o}C, the formation of oxygenate groups (i.e. esters, acids and aldehydes) were 15 to 30%, while the rest contained thermally cracked hydrocarbons with excluded un-reacted feed. In residue oil, cyclic group formation was observed. The formation of acidic and aldehyde resulted in carbon dioxide and carbon monoxide in outlet gases. The hydroprocess of higher temperatures leaded higher cracking and cyclic groups with more dense and viscous residue oil.

Keywords: *Hydrodeoxygenation, Decarboxylation, Thermal conversion, Vegetable oil, Bio-fuels.*

1. Introduction

Recently, traditional oil refineries have started to hydroprocessing vegetable oil and fatty acids. Traditional renewable fuels were (1) fuel production based on a super critical process, (2) bio-ethanol technology and (3) production of FAME. All three fuel sources have received considerable attention over the past decade in order to achieve bio-refinery status. Apart from this research development, hydroprocessing was a friendly and suitable process for existing oil refinery concepts to include biomass as a co-feed. One big advantage is the factor of scale in oil refinery. The cost for processing is low per unit and the biomass can ride on this low cost of production and distribution of the products [1, 2]. During hydroprocessing, water is removed from the carboxylic group from tri-glycerol to give C_{18} hydrocarbon and propane, is known hydro-deoxygenation. The product had a high cetane value, low density and poor cold flow properties [3].

Thermal decomposition is unfavorable at deoxygenation mechanism. Usually, excess hydrogen partial pressure is needed for deoxygenation because of certain diffusion limitations over films. These limitations favored for thermal effect on carboxylic group to form CO_2 and CO. Thermal decomposition of the carboxylic group reduced to C_{17} and expelled CO and CO_2 in the gas phase, is known as decarboxylation/decarbonylation. Indeed, loss of one carbon at each hydrocarbon chain in decarboxylation resulted in a difference in the cetane value. Also, methylation and water-gas shift reaction (WGS) were evident as part of the catalytic thermal conversion [2- 4]. Eventually, the temperature around 300 to 360^{o}C proved feasible for deoxygenation, and some researcher indicate it increases the decomposition [5, 6].

Much research on hydroprocessing could explain deoxygenation, thermal conversion, hydration and WGS reaction, but had trouble predicting the exact evaluation of the reaction path due to change in properties of vegetable oil during pre-heating [5-8]. Pre-heating in reactor is common technique for catalytic process. As a part on thermal effect of preheating, we focused only on the thermal effect to identify the modification in vegetable oil with hydrogen as co-feeding at ambient pressure and reinstate the result for future work on our catalytic process. During hydro deoxygenation, the vegetable oil has been subjected with hydrogen into reactor on concurrent flow. This assignment was to characterize the feed before introduce into Hydro deoxygenation catalytic process.

2. Experiment

The experimental setup consisted of a continuous reactor, a feed and product tank, a gas flow meter, pump, a gas chromatography and controllers. The major reaction conditions parameters were liquid hourly space velocity (LHSV = ml of liquid/g.cat*hr), gas hourly space velocity (GHSV= ml of gas/g.cat*hr), reaction pressure (bar) and reaction temperature (^{o}C). However, in our experiment, overall reaction conditions were adjusted with constant feed flow on the continuous reactor on a weight basis. The sample and gas outlet were collected under ambient atmospheric conditions. The reaction condition was stabilized through proportional–integral–derivative (PID) controllers. The samples were withdrawn subject to a manual time control and all samples were taken under a stabilized system.

2.1. Reactor

The experimental setup consisted of a feed tank, fixed-bed reactor, product tank, gas collector and dossier pump. The fixed-bed reactor was fixed with an electric furnace, connected with an instrumental controller to regulate thermal and pressure conditions. The vertical height of the reactor was 619.4 mm, excluding an external clump with bolt; the reactor was filled with 2 mm diameter glass pellets. The maximum temperature, taken at the middle of the reactor, was the indicated temperature point. There are another two more thermocouple connected at inlet and outlet on reactor to monitor the reaction temperature.

2.2. Analytical work

The gas outlet and liquid products from the reactor were analyzed with different gas chromatography equipment. The liquid analysis was performed according to ASTM D2887 using a gas chromatograph (GC) (Varian 3400) equipped with a packed column (OV101) and flame ionization detector (FID) with nitrogen as carrier gas. The outlet gas from the reactor was analyzed by the Clarus 500 GC online, which was connected with 600 link switch controllers; the signal was integrated to receive analytical data. Gas analysis consisted of the use of a thermal conductivity detector (TCD) to analyze CO, CO_2, CH_4 and H_2, as well as FID for hydrocarbons.

Elemental analysis of C, H and O was analyzed by Karlshamn Kraft AB. The ASTM D 5291 standard test method for instrumental determination of carbon, hydrogen and nitrogen in petroleum products and lubricants was used in our samples. Further, traces of nitrogen, sulphur and other metals in the sample were neglected and oxygen content was estimated from carbon and hydrogen content. The accuracy of the elemental analysis was ± 0.4 wt%.

The samples were analyzed with the Perkin–Elmer Spectrum One Fourier Transform Infrared Spectroscopy (FTIR) to identify the internal change in processed vegetable oil. The liquid samples were placed between two plates in pure sodium chloride salt without any bubbles. The mid-infrared was used between wavelengths 400 and 4000 cm^{-1} to study the fundamental structure of the sample.

3. Results

The continuous reactor was heated to 350^{o}C temperature, after which vegetable oil was fed into the system. Initially, the feed was supplied for 48 h without any interruption to make sure the system was clean and to achieve a steady state. After this phase, the reactor conditions were changed systematically to obtain the samples for the appropriate conditions. The

samples were collected on a weight basis at ambient pressure from a fixed feed rate of 200 ml/min over 19 h for each condition.

The rapeseed oil contains 7% stearic (18:0), 61.1% oleic acid (18:1), 20.9% linoleic acid (18:2) and the rest consisted of omega-3. At 300^{o}C, 5.12 wt% of free C_{17}-COOH and 1 wt% of other hydrocarbons appeared in the products. In addition to C_{17}, there were traces of lighter hydrocarbon with less than 2 mol% and 10 mol% of CO in the gas phase (Figure 1). At 330^{o}C, the carboxylic group increased to 8 wt% and 2 wt% of other products. Over 330^{o}C, there was a steady increase of both - (COO) - and – (CO) – groups can be seen in Table 1, as well as some lighter hydrocarbons. The results of the thermal effect on (C=O)-O-C bond detachment had observed uniform distribution in gas chromatography.

Table 1. Rapeseed oil hydro-treatment at LHSV = 20 mln/min, 1 bar and H_2/oil = 10. R-(C=O)O refers to BP from 340 to 360^{o}C while R-(C=O) refers to BP about 330^{o}C.

Temp. (°C)	**R-(C=O)O** (wt%)	**R-(C=O)** (wt%)
300	5.12	0
330	7.95	1.9
350	6.55	2.65
370	8.43	3.99
390	11,56	3,64

High concentration of methane and ethane/ethane in the gas outlet were observed for lower temperatures. The dispersed gas in the liquid sample was not recoverable, so it was difficult to make mass balance for in and out of gas flow. Thus, we avoided dealing with the mass balance and instead just showed the concentration in the gas phases. The changes in flow of liquid in and liquid out were almost the same (variation of 0.01 to 0.05 wt%).

4. Discussion

In our study the carboxylic groups were mostly converted to free fatty acid and some traces of alcohol and aldehyde between 330^{o}C and 350^{o}C. This finding implies that the carboxyl groups were influenced by temperature and induced both decarbonylation and decarboxylation. However, there was less evidence of glycerol or glycol groups under these conditions. The gas phase contained CO as the main substitute (Figure 2). The CO outlet shows that the bonding of the carboxyl group was weaker than the C-C bond.

The carboxyl groups tended to detach above 350^{o}C in high yield as acids, aldehyde, esters and paraffin. The concentration of carboxylic acid was doubled and paraffin concentration increased one- to three-fold for every 20^{o}C rise in temperature. The product was distilled in simple distillation at a cut-off of 235^{o}C, which removes water and lighter naphtha named distillate. The distillate had greenish appearance, with gasoline density and viscosity [9]. It had acidic compound. In figure 2 shows the FTIR result of distillate without water in it. Here, C=O groups identified in FTIR mainly of acids while the bottom product consisted of aldehyde and esters. The information in the figure proves that distillate had lighter hydrocarbon with acid group; these conclude that distillate mostly formed from C-C cracking. However, the esters and aldehyde groups had C-O-C- bond breaking, as was evident from the thermal impact.

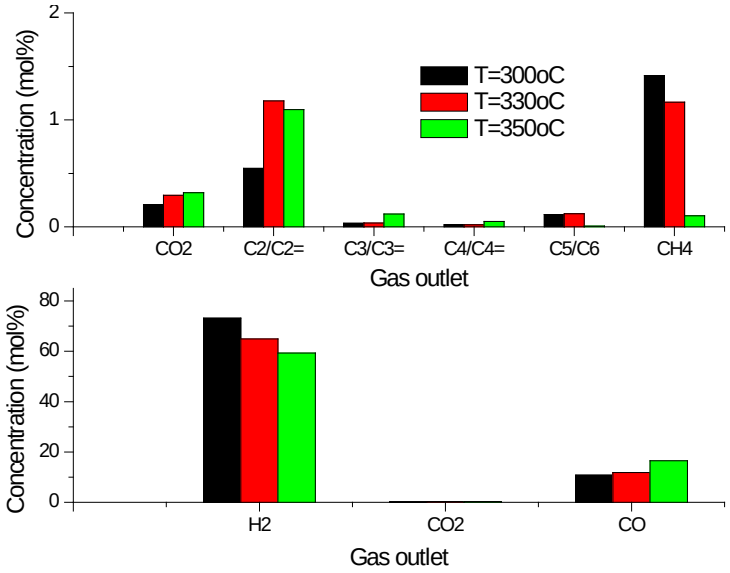

Figure. 1. Rapeseed oil hydro-treatment: gas outlet at LHSV = 20 mln/min, 1 bar and H_2/oil = 10.

At higher temperature (above 350°C) the oxygen content reduced between 10 and 12% into water, CO and CO_2. The distilled sample contained water from 0.04 to 0.1 wt%. The presences of water indicate that the hydroprocess was part in thermal reaction [10].

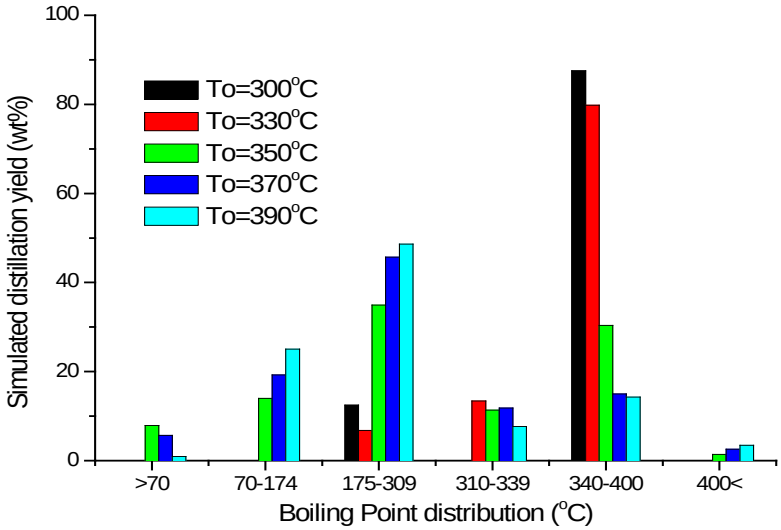

Figure 2. Rapeseed oil hydro-treatment at LHSV = 20 mln/min, 1 bar and H_2/oil = 10 excluding untreated rapeseed oil.

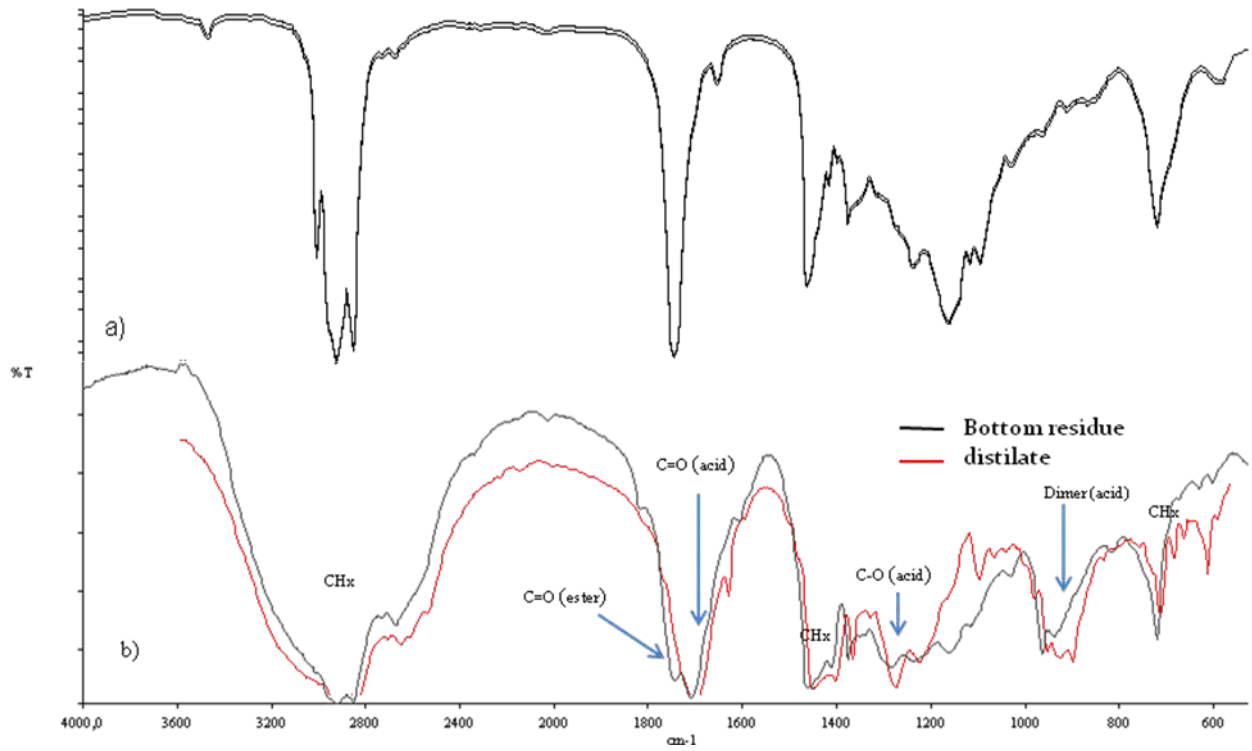

Figure 3. FTIR analysis for distilled product (LHSV = 20 mln/min, 1 bar, H_2/oil = 10 & T = 350 ^oC). (a) Rapeseed oil and (b) Simple distillation at a cut-off point of 235^oC.

5. Conclusion

The hydroxyl groups in triglycerides were found to be sensitive to temperature. The product variant in different temperatures was dependent on only CO and water outlet. Of the major gas outlets, CO dominated the composition at higher temperatures. Thermal cracking of C=C bonds between 300 and 350^{o}C, was minimal in this study. The condition between 330 to 360^{o}C indicates that CO formation has more dominant during thermal decomposition.

References

[1] S.N. Naik, Vaibhav V. Goud, Prasant K. Rout and Ajay K. Dalai, Production of first and second generation bio-fuels: A comprehensive review, Renewable and Sustainable Energy Reviews 14, Issue 2, February 2010, Pages 578-597.

[2] Ayhan Demirbas, Progress and recent trends in bio-fuels, Progress in Energy and Combustion Science 33 (2007) 1–18.

[3] David Kubic.ka, Lude.k Kaluz´, Deoxygenation of vegetable oils over sulfided Ni, Mo and NiMo catalysts, Applied Catalysis A: General 372 (2010) 199–208.

[4] Jeong-Geol Na, Bo Eun Yi, Ju Nam Kim, Kwang Bok Yi, Sung-Youl Park, Jong-Ho Park, Jong-Nam Kim, Chang Hyun Ko, Hydrocarbon production from decarboxylation of fatty acid without hydrogen, Catalysis Today 156 (2010) 44–48.

[5] Bjorn Donnis, Rasmus Gottschalck Egeberg, Peder Blom and Kim Gron Knudsen, Hydro-processing of Bio-oils and Oxygenates to Hydrocarbons. Understanding the Reaction Routes, Top Catalyst 52, 2009, pp. 229 – 240.

[6] Thiam Leng Chew and Subhash Bhatia, Catalytic processes towards the production of bio-fuels in a palm oil and oil palm biomass-based bio-refinery, Bio-resource Technology 99, Issue 17, November 2008, Pages 7911-7922.

[7] Serdar Yaman, Pyrolysis of biomass to produce fuels and chemical feedstock's, Energy Conversion and Management 45, Issue 5, March 2004, Pages 651-671.

[8] Pavel Šimác.ek, David Kubic.k, Gustav Šebor, Milan Pospíšil, Hydroprocessed rapeseed oil as a source of hydrocarbon-based biodiesel, Fuel 88 (2009) 456–460.

[9] Pavel Šimác.eka, David Kubic.kab, Gustav Šebor, Milan Pospíšil, Fuel properties of hydroprocessed rapeseed oil, Fuel 89 (2010) 611–615.

[10] Marton Krar, Sandor Kovacs, Denes Kallo, Jenö Hancsok, Fuel purpose hydro treating of Sunflower oil on Co/Al_2O_3 catalyst, Bioresource Technology 101 (2010), 9287-9293.

Catalytic cracking characteristics of bio-oil molecular distillation fraction

Zuogang Guo[1,2], Shurong Wang[1,*], Qianqian Yin[1], Guohui Xu[1],
Zhongyang Luo[1], Kefa Cen[1], Torsten H. Fransson[2]

[1] *State Key Laboratory of Clean Energy Utilization, Zhejiang University, Hangzhou, China*
[2] *Department of Energy Technology, Royal Institute of Technology (KTH), Stockholm, Sweden*
* *Corresponding author. Tel: +86 571 87952801, Fax: +86 571 87951616, E-mail: srwang@zju.edu.cn*

Abstract: The catalytic cracking characteristics of a bio-oil molecular distillation fraction using HZSM-5 were investigated. Properties of upgraded products and formation mechanism for gasoline components were discussed. The cracking products included 56.00wt.% upgraded liquid oil, 1.27wt.% coke and 42.73wt.% gas products. The conversion yield for components in bio-oil fraction was influenced by their cracking reactivity and their concentration. The cracking reactivity of phenols was strongly affected by the connected functional groups. Alkyl groups had a positive influence on phenols reactivity, while methoxy groups had a negative influence. Reactivity of typical phenols in bio-oil fraction followed the order: Phenol, 4-methyl-> Phenol, 4-ethyl-2-methoxy->Phenol> Phenol, 2-methoxy-. Expected gasoline components including ethylbenzene, p-xylene and benzene, 1-ethyl-3-methyl were detected in the upgraded liquid oil, which indicates liquid hydrocarbon fuels can be produced from bio-oil. A two-step reaction mechanism was proposed which successfully explains the formation routes for gasoline components. In the first step, dehydration and decarbonylation reactions generate H_2O, CO and CO_2. The cracking reaction produces free radicals including $-CH_3$, $-CH_2-$ and -H. In the second step, these free radicals form gaseous and liquid hydrocarbons.

Keywords: *Bio-oil, Molecular Distillation Technology, Cracking, HZSM-5, Gasoline Components*

1. Introduction

Supply security and price concerns for fossil oil have led to renewed interests in renewable energy resources as alternative feedstocks for the production of transport fuels. Biomass resources are among the most promising feedstocks because of their abundant reserves and carbon-neutral property. Fast pyrolysis technology is a key thermochemical process that can convert solid biomass waste into liquid bio-oil under atmospheric pressure[1-3]. Bio-oil has better fuel properties in terms of transportation suitability and energy density than solid biomass waste. However, it is only used as fuel in boiler[4, 5] but can not be directly substituted for fossil fuels because of its high viscosity and corrosiveness[6, 7]. Bio-oil refinement has become a key issue for its utilization as a high-grade transport fuel.

Catalytic esterification has been used to decrease corrosiveness of bio-oil by converting carboxylic acids into neutral esters. Carboxylic acid conversion of approximately 90% was achieved and the corrosiveness of bio-oil obviously decreased[8, 9]. Emulsification can be used to refine bio-oil by mixing diesel and bio-oil to produce a homogeneous fuel. Zhang et al. [10] studied the emulsification behavior of diesel and bio-oil using nonionic surfactants. The effects of HLB value, emulsifying temperature and time on emulsion stability were investigated. Wang et al. [11] compared the emulsification properties of different bio-oils and diesel combined at the same ratio(diesel/emulsifier/bio-oil was 92wt.% /3wt.% /5wt.%). Emulsion made from diesel and straw bio-oil showed the best stability. The corrosion properties of emulsions on four metals were measured at different temperatures by Lu[12]. Ikura et al. [13] determined the relationship between process conditions, emulsion stability and processing costs using bio-oil and No.2 diesel. Catalytic esterification and emulsification can improve bio-oil fuel properties to a certain extent, but they can not convert oxygenated bio-oil into pure liquid hydrocarbon fuels.

Among the technologies available for bio-oil upgrading, catalytic hydrogenation and catalytic cracking have been used to produce hydrocarbon fuels from oxygenated bio-oil. Oxygen in bio-oil was removed in the form of CO_2 and H_2O during catalytic hydrogenation[14, 15]. Hydrogenation process can only occur under high temperature and high hydrogen pressure, which limit its economic efficiency. By contrast, catalytic cracking technology is more economically efficient. It can produce liquid hydrocarbon fuels from bio-oil without consuming hydrogen. Adjaye et al. [16] investigated upgrading research of a fast pyrolysis bio-oil using different catalysts. Aromatic and aliphatic hydrocarbons were obtained. Gayubo et al. [17] produced olefins by catalytic transformation of crude bio-oil using HZSM-5. Besides, other researchers studied the cracking behavior of bio-oil using its model components[18, 19]. The key problem in catalytic cracking is the high coke yield, which leads to catalyst deactivation. Catalytic cracking research has mainly focused on crude bio-oil in recent years. The complex composition of crude bio-oil means that qualitative and quantitative analysis of its components is difficult. What more, the strong interaction between different components enhances the probability of coke formation. In the present study, the cracking behavior on HZSM-5 zeolite was investigated for a unique bio-oil fraction produced by molecular distillation technology.

2. Methodology

2.1. Experimental methods

HZSM-5(Si/Al=25) was used as the catalyst for cracking of a Bio-oil Middle Fraction (BMF) , which was obtained by molecular distillation using KDL5 equipment as described in our earlier papers[20, 21]. Cracking experiment was performed upon a fixed-bed reactor at 330 °C. The liquid hourly space velocity (LHSV) was 2 h^{-1} with a HZSM-5 volume of 2 ml. BMF was first vaporized in the pre-heater and then carried to the catalytic bed by a stream of nitrogen. After each run, catalytic bed was subjected to stripping with nitrogen for 40 minutes, with the aim of eliminating the reaction medium components that may remain adsorbed on the catalyst.

2.2. Catalyst characterization

Textural properties were determined by N_2 adsorption–desorption isotherms measured at 196°C below zero on a Quantachrom-Autosorb-1-C apparatus. HZSM-5 had a BET surface area of 283.97m^2/g, a pore volume of 0.07cm^3/g and an average pore size of 5.65nm. Coke deposition on the catalyst was measured during temperature-programmed combustion on a Mettler-Toledo TGA/SDTA851e thermogravimetric balance. Sample of approximately 15 mg was burnt at 30–650°C with an oxygen flow rate of 60 ml/min. The total coke weight was calculated according to the coke content and the total catalyst weight.

2.3. Analysis of liquid products

Liquid products were identified on a Trace DSQII system using a 30m×0.25mm×0.25μm Agilent DB-WAX capillary column. The oven was heated at 40°C for 1 min and then the temperature was increased to 240°C at 8 °C/min and held at this temperature. Data were acquired using Xcalibur software according to the NIST mass spectra library data base.

3. Results and discussion

3.1. Distribution of cracking products

Upgraded Liquid Oil (ULO), coke and gas products were obtained from catalytic cracking of BMF. ULO yield (Y_{ULO}) and coke yield (Y_{coke}) were calculated from Eq. (1) and (2). Yield of gas products (Y_{gas}) was calculated by difference.

$$Y_{ULO} = 100wt\% \times Weight_{ULO} \div Weight_{BMF} \quad (1)$$

$$Y_{Coke} = 100wt\% \times Weight_{Coke} \div Weight_{BMF} \quad (2)$$

Values for Y_{ULO}, Y_{coke} and Y_{gas} were 56.00 wt.%, 1.27 wt.% and 42.73 wt.%, respectively. Gas products accounted for large proportion. The coke yield was low, which means that cracking of bio-oil fractions is a feasible method for decreasing catalyst coking. Graca et al. [22] obtained a coke yield of 16 wt.% for cracking of a mixture of bio-oil and gasoil over ZSM-5. Adjaye et al. [23] obtained a coke yield about 22.5 wt.% for cracking of maple pyrolysis oil over HZSM-5 and silica-alumina catalysts. Thus, cracking of bio-oil fractions has obvious superiority over crude bio-oil in decreasing the coke yield.

3.2. Analysis of liquid products

Compounds in BMF and ULO were identified by GC-MS and quantified using peak area normalization method. The conversion yield was determined as a measure of reactivity during cracking, which was calculated by Eq. (3).

$$\eta_i = 100\% \times (C_{1i} - Y_{ULO} \times C_{2i}) \div C_{1i} \quad (3)$$

Where η_i represents the conversion yield of compound *i*. C_{1i} is its content in BMF and C_{2i} is its content in ULO. Y_{ULO} is the yield of ULO with a value of 56.00 wt.% in this experiment.

3.2.1. Cracking behavior of different compounds

Reactivity of different compounds is indicated by conversion yields. Typical compounds in BMF are listed from Table 1 to Table 3. The conversion yield of a compound during the cracking is determined by two main factors. The first is its cracking reactivity. Compounds with higher reactivity may have a higher conversion yield. The second is its concentration in BMF. Compounds with higher concentration may have a lower conversion yield because of catalyst deactivation. In Table 1, compounds with content below 1% had conversion yield of 100%. For example, 4-methyl-5H-furan-2-one and 2-furanmethanol were absolutely cracked. Three compounds had high content but were completely cracked. It indicated that they were very active during the cracking process. Combining with their concentration in BMF and conversion yields, the reactivity of these three compounds followed the order：Furan, 2,5-diethoxytetrahydro- > 2-Cyclopenten-1-one, 3-methyl- > 2-Cyclopenten-1-one, 2-hydroxy-.

Table 1 Compounds in BMF with the highest conversion yields

Compounds	Content (%)		η_i (%)
	C_1	C_2	
Heptane, 1,1-diethoxy-	3.41	0.44	92.77
Eugenol	1.24	0.07	96.84
4-Methyl-5H-furan-2-one	0.36	0.00	100.00
2-Furanmethanol	0.50	0.00	100.00
1,2-Ethanediol, monoacetate	0.72	0.00	100.00
2-Cyclopenten-1-one, 2-hydroxy-	1.28	0.00	100.00
2-Cyclopenten-1-one, 3-methyl-	1.52	0.00	100.00
Furan, 2,5-diethoxytetrahydro-	13.11	0.00	100.00

The conversion yields for compounds listed in Table 2 varied from 60% to 90%. Phenol derivates were the predominant chemicals in Table 2 and showed a clear cracking principle. Cracking activity of phenols was strongly affected by connected functional groups. Methoxy groups had a negative influence while alkyl groups had a positive influence on the phenols reactivity. Phenol had a conversion yield of 75.63%. This decreased to 59.87% when a methoxy group was attached, such as Phenol, 2-methoxy-. The conversion yield increased to 89.20% when a methyl group was attached, such as Phenol, 4-methyl-. When phenol derivates had alkyl and methoxy groups at the same time, their conversion yields were intermediate between phenol and Phenol, 4-methyl-. The cracking activity of different phenol derivates followed an order as: Phenol, 4-methyl-> Phenol, 4-ethyl-2-methoxy->Phenol> Phenol, 2-methoxy-.

Table 2 Compounds in BMF with moderate conversion yields

Compounds	Content (%)		η_i (%)
	C_1	C_2	
Phenol, 2-methoxy-	5.04	3.61	59.87
Ethanol, 2,2-diethoxy-	16.43	8.18	72.10
Phenol	1.45	0.63	75.63
Phenol, 2-methoxy-4-methyl-	4.98	2.02	77.29
2(5H)-Furanone	1.13	0.42	79.16
Phenol, 4-ethyl-2-methoxy-	1.14	0.36	82.31
2-Cyclopenten-1-one, 2-hydroxy-3-methyl-	2.56	0.57	87.55
Phenol, 2-methyl-	1.87	0.40	88.02
Phenol, 4-methyl-	1.61	0.31	89.20
2-Pentanone, 5,5-diethoxy-	3.02	0.54	89.99

Compounds in Table 3 had lower conversion yields than those in Table 1 and Table 2. Acetic acid, 2-Propanone, 1-hydroxy- and furfural were the most abundant compounds in Table 3. Subsequent to the cracking process, their contents in ULO increased. Content of acetic acid increased from 15.70% to 28.00%. This phenomenon can be well explained as follows. Compounds with high activity were cracked firstly, which generated gaseous hydrocarbons and micro-coke. The active surface of HZSM-5 catalyst was clogged by the micro-coke and deactivated. The cracking of the less reactive compounds, like acetic acid, was interrupted. Thus, the relative concentration of less reactive compounds in the upgraded liquid oil increased. The conversion yields of these compounds can be calculated by Eq. (3). The conversion yield of acetic acid was as low as 0.1%, followed by furfural (15.24%) and 2-Propanone, 1-hydroxy (26.85%).

Table 3 Compounds in BMF with the lowest conversion yields

Compounds	Content (%)		η_i (%)
	C_1	C_2	
Acetic acid	15.70	28.00	0.10
2-Cyclopenten-1-one	1.01	1.66	8.37
Furfural	3.11	4.71	15.24
2-Propanone, 1-hydroxy-	9.50	12.40	26.85
Butanoic acid, 2-methyl-	1.13	1.23	38.96
1-Hydroxy-2-butanone	0.97	1.03	40.47
2(5H)-Furanone, 5-methyl-	0.92	0.68	58.76

3.2.2. Identification of the gasoline components

Bio-oil is considered as one of the most promising substitute for fossil fuels. The most important issue involves the removal of bio-oil oxygen and its conversion to pure liquid hydrocarbons. Some liquid hydrocarbons and other new products were detected in ULO by GC-MS technology. Liquid hydrocarbons were listed in Table 4. The new products in ULO accounted for a total content of 29.74%, including liquid hydrocarbons, liquid ethers and esters. Besides liquid hydrocarbons, ethers and esters can be used as transport fuels or to produce emulsification fuels with gasoline and diesel. Aromatic hydrocarbons, such as toluene, ethylbenzene and benzene, 1-ethyl-3-methyl-, were produced during this cracking experiment. Elucidation the mechanism for formation of these aromatic hydrocarbons is very important for hydrocarbon fuels production from oxygenated bio-oil.

Table 4 Gasoline compounds in the ULO

Compounds	Content (%)	Compounds	Content (%)
Toluene	0.31	Benzene, 1,3-diethyl-	0.49
Ethylbenzene	0.55	Benzene, 1,2,3-trimethyl-	0.44
p-Xylene	1.69	Naphthalene, 1,4,6-trimethyl-	0.42
Benzene, 1-ethyl-3-methyl-	2.76	Naphthalene, 1,7-dimethyl-	0.50

3.3. Mechanism of aromatic hydrocarbons production

Transport fuel is the ultimate aim of bio-oil refinement. Liquid hydrocarbons were detected after cracking of BMF. Exploring the formation mechanism of liquid hydrocarbons was very important for selective enhancement of expected products. In earlier literatures[18, 19], researchers suggested reaction pathways for chemical groups such as acids, phenols and alcohols. But the exact formation mechanism of the liquid hydrocarbons was not proposed. Here, we proposed a two-step mechanism model to explain how the liquid hydrocarbons were produced from oxygenated bio-oil.

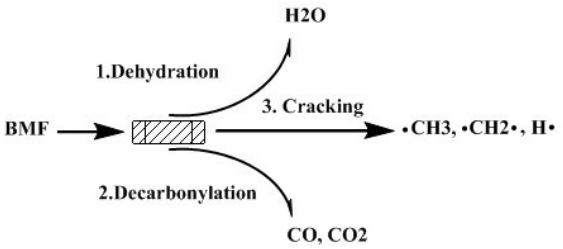

Fig. 1 The first step of the cracking mechanism

The first step is shown in Fig. 1 and it consists of three main reactions, dehydration, decarbonylation and a cracking reaction. Dehydration reaction produces a H_2O molecule, while decarbonylation reaction generates CO and CO_2 molecules. The cracking reaction results in free radicals including -CH_3, -CH_2- and -H. All these free radicals participate in the second step to form liquid hydrocarbons.

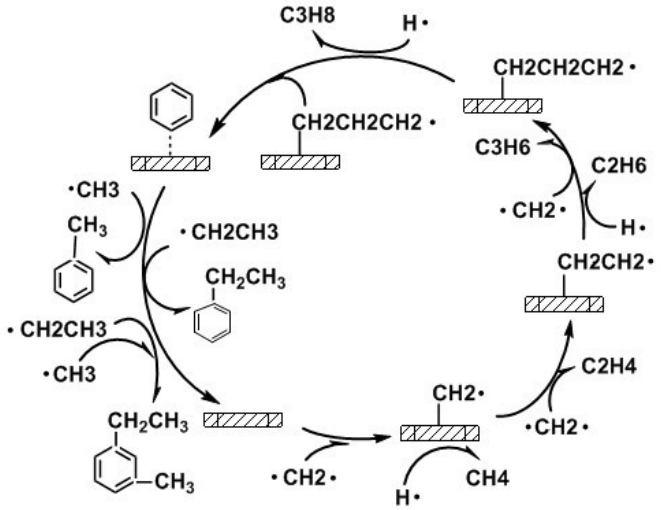

Fig. 2 The second step of the cracking mechanism

Fig. 2 gives a clear overview of the formation process for gaseous hydrocarbons (CH_4, C_2H_4, C_2H_6, C_3H_6 and C_3H_8) and liquid hydrocarbons (toluene, ethylbenzene and benzene,1-ethyl-3-methyl-). The reaction starts with adsorption of -CH_2- on HZSM-5 catalyst surface. When another -CH_2- group is adsorbed to the catalyst surface, the carbon chain becomes longer to form -CH_2CH_2- group. Some of the -CH_2CH_2- groups desorb to form ethylene (C_2H_4). Some of the -CH_2CH_2- groups further adsorb on the catalyst surface to continue the cycle. Ethane (C_2H_6) is released when the adsorbed -CH_2CH_2- groups are attacked by -H groups. The carbon chain increases to form -$CH_2CH_2CH_2$- when an adsorbed -CH_2CH_2- group is attacked by another -CH_2- group. Propylene (C_3H_6) and propane (C_3H_8) are formed via the same mechanism as for ethylene and ethane. Adsorbed -CH_2CH_2-CH_2- groups undergo an aromatization reaction to produce active benzene, which is further attacked by -CH_3 and -CH_2CH_3 groups to form liquid aromatic hydrocarbons. Another cycle is started by -CH_2- group attacking the blank HZSM-5 catalyst surface.

4. Conclusion

A bio-oil fraction separated by molecular distillation technology was subjected to catalytic cracking for gasoline production using HZSM-5 catalyst. Gasoline components were detected in the upgraded liquid oil. A two-step mechanism model for gasoline components production was proposed.

The coke yield for cracking of the bio-oil fraction was only 1.27 wt.%, which was much lower than that for crude bio-oil. Compounds in bio-oil fraction were classified into three groups according to their conversion yields. Furan, 2,5-diethoxytetrahydro- was one of the most abundant components in bio-oil fraction, but was completely cracked. Reactivity of phenol derivatives was strongly affected by the connected functional groups. Methoxy groups had a negative influence on their cracking reactivity, while alkyl groups had a positive influence. The cracking activity of typical phenol derivates in bio-oil middle fraction followed an order

as: phenol, 4-methyl-> phenol, 4-ethyl-2-methoxy->phenol> phenol, 2-methoxy-. Acetic acid and 2-propanone, 1-hydroxy- showed much lower cracking reactivity.

A two-step mechanism model was proposed according to the gasoline components detected in the upgraded liquid oil. Oxygenated compounds in bio-oil were subjected to dehydration, decarbonylation and cracking reactions in the first step. Free radicals including $-CH_3$, $-CH_2-$, and -H were involved in the second step to form gaseous hydrocarbons and liquid gasoline components (toluene, ethylbenzene and benzene, 1-ethyl-3-methyl- and etc.).

Acknowledgement

The authors appreciate financial support granted from the International Science and Technology Cooperation Program (2009DFA61050), the National High Technology Research and Development Program (2009AA05Z407), the National Natural Science Foundation (90610035), the Program of Introducing Talents of Discipline to University (B08026) and the National Basic Research Program of China (2007CB210204).

References

[1] Q. Wang, Z.Y. Luo, S.R. Wang, K.F. Cen, Products of high-grade liquid fuels by biomass fast pyrolysis, Journal of Zhejiang University(Engineering Science), 2010, pp. 988-990.

[2] Q. Lu, X.F. Zhu, Q.X. Li, Q.X. Guo, Q.S. Zhu, Biomass Fast Pyrolysis for Liquid Fuels, Progress in Chemistry, 2007, pp. 1064-1071.

[3] A.V. Bridgwater, G.V.C. Peacocke, Fast pyrolysis processes for biomass, Renewable & Sustainable Energy Reviews, 2000, pp. 1-73.

[4] D. Chiaramonti, A. Oasmaa, Y. Solantausta, Power generation using fast pyrolysis liquids from biomass, Renewable & Sustainable Energy Reviews, 2007, pp. 1056-1086.

[5] S. Czernik, A.V. Bridgwater, Overview of applications of biomass fast pyrolysis oil, Energy & Fuels, 2004, pp. 590-598.

[6] N. Ozbay, A.E. Putun, B.B. Uzun, E. Putun, Biocrude from biomass: pyrolysis of cottonseed cake, Renewable Energy, 2001, pp. 615-625.

[7] M. Garcia-Perez, A. Chaala, H. Pakdel, D. Kretschmer, D. Rodrigue, C. Roy, Evaluation of the influence of stainless steel and copper on the aging process of bio-oil, Energy & Fuels, 2006, pp. 786-795.

[8] Y.L. Gu, Z.G. Guo, L.J. Zhu, G.H. Xu, S.R. Wang, Experimental research on catalytic esterification of bio-oil volatile fraction, 2010 Asia-Pacific Power and Energy Engineering Conference, 2010, DOI: 10.1109/APPEEC.2010.5448436.

[9] Y. Tang, W.J. Yu, L.Y. Mo, H. Lou, X.M. Zheng, One-step hydrogenation-esterification of aldehyde and acid to ester over bifunctional Pt catalysts: A model reaction as novel route for catalytic upgrading of fast pyrolysis bio-oil, Energy & Fuels, 2008, pp. 3484-3488.

[10] Z. Jian, L. Wenzhi, L. Qiang, Z. Xifeng, Emulsification Technology of Bio-oil in Diesel with Combined Surfactants, Transactions of the Chinese Society of Agricultural Machinery, 2009, pp. 102-106.

[11] W. Qi, L. Xinbao, W. Shurong, L. Zhongyang, C. Kefa, Experimtnal research on emulsions from biomass pyrolysis liquid and diesel, Acta Energiae Solaris Sinica, 2010, pp. 380-384.

[12] Q. Lu, J. Zhang, X.F. Zhu, Corrosion properties of bio-oil and its emulsions with diesel, Chinese Science Bulletin, 2008, pp. 3726-3734.

[13] M. Ikura, M. Stanciulescu, E. Hogan, Emulsification of pyrolysis derived bio-oil in diesel fuel, Biomass & Bioenergy, 2003, pp. 221-232.

[14] D.C. Elliott, Historical developments in hydroprocessing bio-oils, Energy & Fuels, 21 2007, pp. 1792-1815.

[15] J. Wildschut, J. Arentz, C.B. Rasrendra, R.H. Venderbosch, H.J. Heeres, Catalytic Hydrotreatment of Fast Pyrolysis Oil: Model Studies on R eaction Pathways for the Carbohydrate Fraction, Environmental Progress & Sustainable Energy, 2009, pp. 450-460.

[16] J.D. Adjaye, N.N. Bakhshi, Production of hydrocarbons by catalytic upgrading of a fast pyrolysis bio-oil: 1. conversion over various catalysts, Fuel Processing Technology, 1995, pp. 161-183.

[17] A.G. Gayubo, B. Valle, A.T. Aguayo, M. Olazar, J. Bilbao, Olefin Production by Catalytic Transformation of Crude Bio-Oil in a Two-Step Process, Industrial & Engineering Chemistry Research, 2010, pp. 123-131.

[18] A.G. Gayubo, A.T. Aguayo, A. Atutxa, R. Aguado, J. Bilbao, Transformation of oxygenate components of biomass pyrolysis oil on a HZSM-5 zeolite. I. Alcohols and phenols, Industrial & Engineering Chemistry Research, 2004, pp. 2610-2618.

[19] J.D. Adjaye, N.N. Bakhshi, Catalytic conversion of a biomass-derived oil to fuels and chemicals.1. model-compound studies and reaction pathways, Biomass & Bioenergy, 1995, pp. 131-149.

[20] S.R. Wang, Y.L. Gu, Q. Liu, Y. Yao, Z.G. Guo, Z.Y. Luo, K.F. Cen, Separation of bio-oil by molecular distillation, Fuel Processing Technology, 2009, pp. 738-745.

[21] Z.G. Guo, S.R. Wang, Y.L. Gu, G.H. Xu, X. Li, Z.Y. Luo, Separation characteristics of biomass pyrolysis oil in molecular distillation, Separation and Purification Technology, 2010, pp. 52-57.

[22] I. Graca, F.R. Ribeiro, H.S. Cerqueira, Y.L. Lam, M.B.B. de Almeida, Catalytic cracking of mixtures of model bio-oil compounds and gasoil, Appl. Catal. B-Environ., 2009, pp. 556-563.

[23] J.D. Adjaye, S.P.R. Katikaneni, N.N. Bakhshi, Catalytic conversion of a biofuel to hydrocarbons: Effect of mixtures of HZSM-5 and silica-alumina catalysts on pr oduct distribution, Fuel Processing Technology, 1996, pp. 115-143.

Improvements in Bioethanol Production Process from Straw

Heike Kahr[1,*], Alexander G. Jäger[1]

[1] *Upper Austria University of Applied Sciences Research and Development Ltd, Campus Wels*
Stelzhamerstrasse 23, A-4600 Wels, Austria
** Tel: +43 7242 728114463, Fax: ++43 7242 7281194463, E-mail: Heike.Kahr@fh-wels.at*

Abstract: An efficient production of sustainable, carbon-neutral, renewable fuels like bioethanol and biogas from straw and other agricultural by-products has to be developed to guarantee mobility. The scientific focus is the improvement of the bioethanol production using straw as an alternative energy source.
The ethanol production process is already established on a laboratory scale. The process involves the following steps - the pretreatment of straw with steam explosion and enzymatic hydrolysis. Subsequently, yeast ferments the obtained glucose to ethanol. Unfortunately, inhibitors such as weak acids, furans and phenolic compounds are generated during the pretreatment and hydrolysis process, thereby reducing the glucose concentration and ethanol yield.
Glucose concentration was raised up to 140 g/l and ethanol content up to 7% by means of optimization of the process (washing steps and recirculation). Diverse substances inhibit the fermentation and reduce the ethanol content. One washing step prior to hydrolysis clearly reduced the inhibitory substances.
The ethanol and glucose yield was improved due to optimization of the bioethanol production. Now an efficient procedure to reduce the inhibitors has to be established to plan a pilot plant.

Keywords: *bioethanol, lignocellulose, straw*

1. Introduction

Due to climate change, dramatic fluctuations of the oil price, decline of oil and increased prices for foodstuffs it becomes more and more important to find alternatives like bioethanol produced from renewable lignocellulosic residues without competition to foodstuff.

The bioethanol production process of the 2nd generation involves the following steps: the pretreatment to open the three-dimensional structure from lignocellulose, alternatively chemical hydrolysis or enzymatic hydrolysis to obtain sugars and subsequently, yeast ferments the obtained sugars to ethanol.

However, the essential requirement in bioethanol fermentation is a highly concentrated sugar solution which leads to an increased product concentration and furthermore reduced purification costs. Unfortunately the agricultural lignocellulosic by-products solubilize at relatively low concentrations. Increasing the dry matter and fed-batch process overcome this problem. The final solids content could be raised up to 21 % during the hydrolysis process [1-3]. Using fed-batch process, where fresh substrate is successively fed into the hydrolysis reaction, final solids loading can reach amounts of up to 17 % [2, 3].

Thirty percent solid loading and a final sugar concentration of 20 % were reached with corn stover based on combined pretreatments and fed-batch process [4]. Pretreatment and hydrolysis of straw cause the formation of compounds (organic acids, phenols, furanes) inhibiting the fermentation through yeast [reviewed in 5].

In this study the bioethanol production from staw was investigated and improved. Several improvements, particularly one washing step before hydrolysis and recirculation strategy, were made. These improvements increase both sugar concentration and bioethanol yield up to 7 %.

2. Methodology

2.1. Pretreatment, hydrolysis, recirculation

For pretreatment the milled wheat straw was heated in steam explosion process at various temperature and conditions (120-200 °C, 5-60 minutes). The pressure was suddenly released and made the material accessible to subsequent enzymatic hydrolysis. The removal of potential inhibitors was conducted by a washing step prior to enzymatic hydrolysis. After washing, wheat straw has been dried and milled. The enzyme mixture Accellerase TM1000 from Genencor® has been used with enzyme activities of 775 IU cellulase (CMC)/g solids and 138 IU beta-glucosidase/g solids.

Suspensions with various dry substances (10-20%) have been produced with the pretreated straw in citrate buffer (50 mM, pH 5.0). The suspensions have been enzymatically solubilised (aerobically) at a temperature of 50 °C for 96 hours in a shaking incubator. The hydrolysis of pretreated straw (10 to 20 % solid) has been repeated three times in a recirculation process. After the first hydrolysis step (96 hours), suspension has been centrifuged and the hydrolysate has been used for the next hydrolysis step with fresh substrate (10 to 20 % solid). Then, the hydrolysate has been recirculated in a third step.

2.2. Determination of sugars, ethanol, organic acids, furans

For precise sugar and ethanol analytics, as well as for determination of HMF, furfural and xylitol, HPLC from Jasco and BioRad AMINEX® HPX 87H with ultra-pure water as eluent and RI detection has been used. The bioethanol yield has additionally been determined using a Anton Paar Alcolyzer Beer from DMA. For precise organic acids analytic as well as for HMF-, furfural-concentrations, HPLC from Agilent Technologies, the ion exclusion column Varian Metacarb 87 H with H_2SO_4 (5 mM) as eluent, UV-detection at 210 nm and a RI detector (Jasco) has been used.

2.3. Determination of phenols

Phenols have been determined as gallic acid equivalent, using folin-ciocalteu reagent [6].

2.4. Fermentation

Diverse salts were added to the wheat straw hydrolysate for the fermentation (di-ammonium hydrogen phosphat, 4.4 g/l, calciumchlorid 3 g/l, potassiumhydrogenphosphat 2.86 g/l, magnesiumsulfat 1.5 g/l. The pH-value has been adjusted to 4.6. Exclusively, a wild-type strain of *Saccharomyces cerevisiae* has been used. Fermentation process has been conducted at a temperature of 30 °C in a shaking incubator for one week.

3. Results

3.1. Straw pretreatment

Pretreatment of lignocellulose offer a rapid and efficient hydrolysis of cellulose [7]. Steam explosion is one possibility for removing lignin and hemicellulose as well as making cellulose accessible to subsequent conversion into monomers with enzyme [reviewed in 8-13].

3.2. Enzymatic batch and fed-batch hydrolysis

The glucose and xylose concentrations reached amounts of 64 g/L and 16 g/L after enzymatic hydrolysis with 20 % solids using unwashed straw, respectively. Due to a washing step prior to hydrolysis, glucose concentration could have been increased to 80 g/L. Xylose

concentration has reduced from 16 g/L to 5 g/L after washing. Final glucose and xylose amounts after hydrolysis using unwashed and washed straw are shown in table 1 and 2.

Table 1: Sugar yield after the first hydrolysis with unwashed straw (10, 15 and 20 % solids).

	10 % solid	15 % solid	20 % solid
Glucose [g/L]	20	39	64
Xylose [g/L]	5	10	16

Table 2: Sugar concentrations after the first hydrolysis of washed straw (10, 15 and 20 % solids).

	10 % solid	15 % solid	20 % solid
Glucose [g/L]	31	52	80
Xylose [g/L]	2	3	5

3.3. Recirculation strategies and fermentation

Recirculation strategies have been developed, where the sugar solution of a first hydrolysis reaction is recycled to fresh straw and subsequent hydrolysis reaction.
For this approach, wheat straw has been pretreated with steam explosion. After the first recirculation step to fresh unwashed solids and subsequent hydrolysis (20 % solids, 2nd hydrolysis), glucose and xylose concentrations have reached 108 g/L and 28 g/L, respectively. Due to a washing step prior to hydrolysis, a glucose concentration of more than 116 g/L could have been reached. Xylose was removed to some extent during this washing step.
However, glucose concentration has been further increased by a second recirculation step to fresh washed solids and subsequent hydrolysis (20 % solids, third hydrolysis) to an amount of 143 g/L. After fermentation with *Saccharomyces cerevisiae*, an ethanol yield of 7.5 %vol. could have been produced.

In figure 1 a, b the final glucose concentrations after hydrolysis (10, 15 % and 20 %) and recirculation processes with unwashed and washed straw, as well as produced bioethanol yields after fermentation were demonstrated.

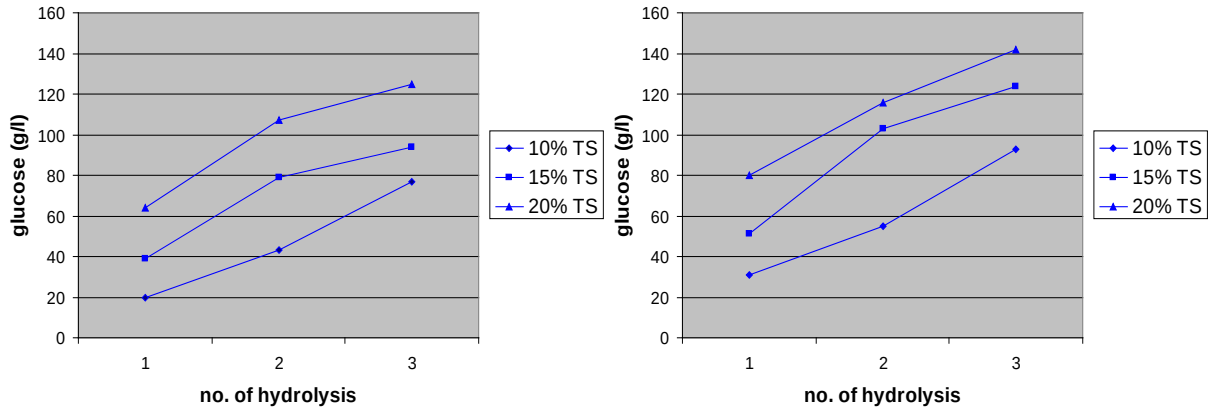

Fig. 1a: Final glucose concentrations after recirculation process (1st, 2nd, 3rd hydrolysis) with 10, 15 and 20 % solids loading of unwashed (left) and washed straw (right).

The hydrolyses from unwashed straw operated definitely superior to the hydrolyses from washed straw. Obviously the washing step reduced inhibitory compounds released during

pretreatment and hydrolysis. However, even the sugar concentration from 2nd and 3rd hydrolysis with washed straw didn´t increase linear possible due end product inhibition.

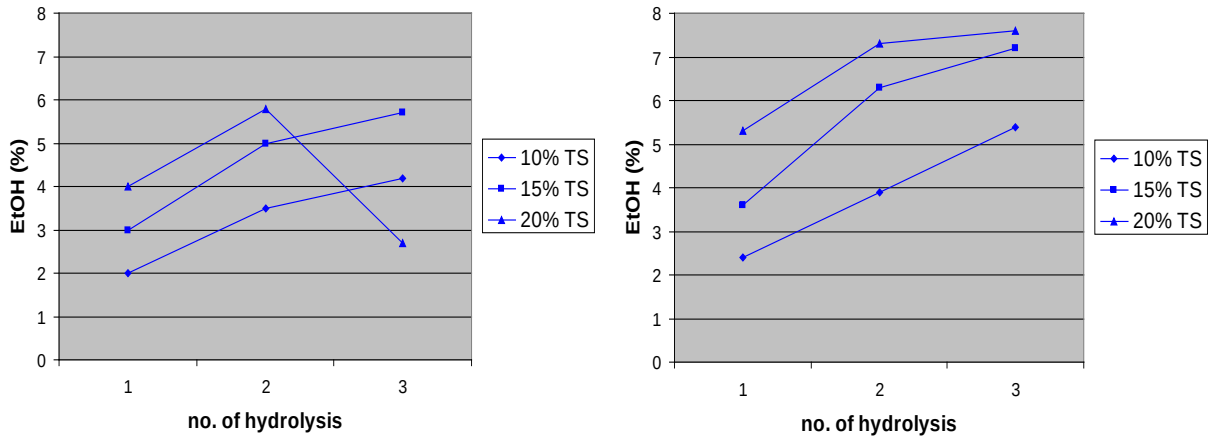

Fig. 1b: Produced bioethanol yields after fermentation of unwashed (left) and washed straw (right).

However, during pretreatment and hydrolysis of straw, groups of inhibitory compounds (phenols, organic acids, furanes) were generated, which had a negative influence on the ethanol-producing yeast. During recirculation procedures, the inhibitory compounds accumulate, resulting in a dramatic decrease of fermentative efficiency. The washing step before hydrolysis removed presumably the inhibitory compounds.

The concentration of diverse potential inhibitors was determined with HPLC analysis and phenol using folin-ciocalteu reagent (figure 2 and 3).

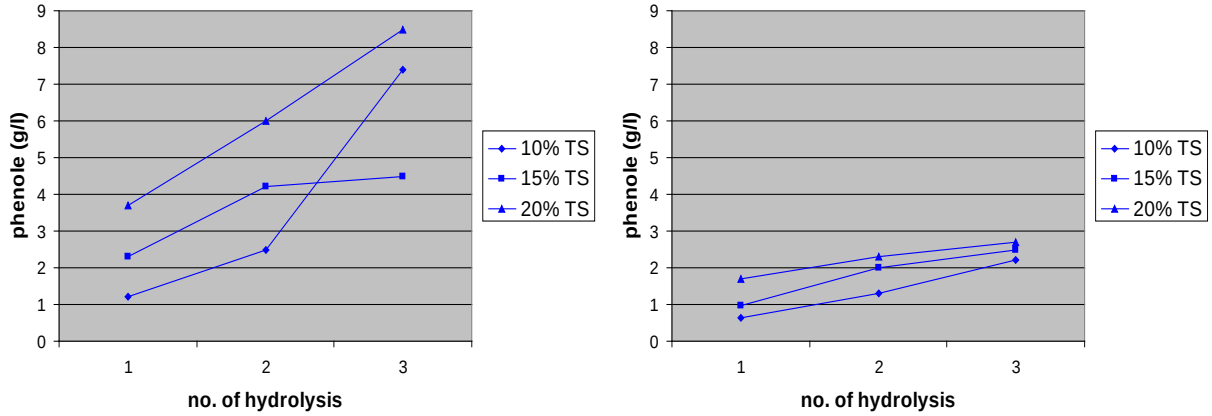

Fig. 2: Phenole concentrations after recirculation process (1st, 2nd, 3rd hydrolysis) with 10, 15 and 20 % solids loading of unwashed straw (left) and washed straw (right).

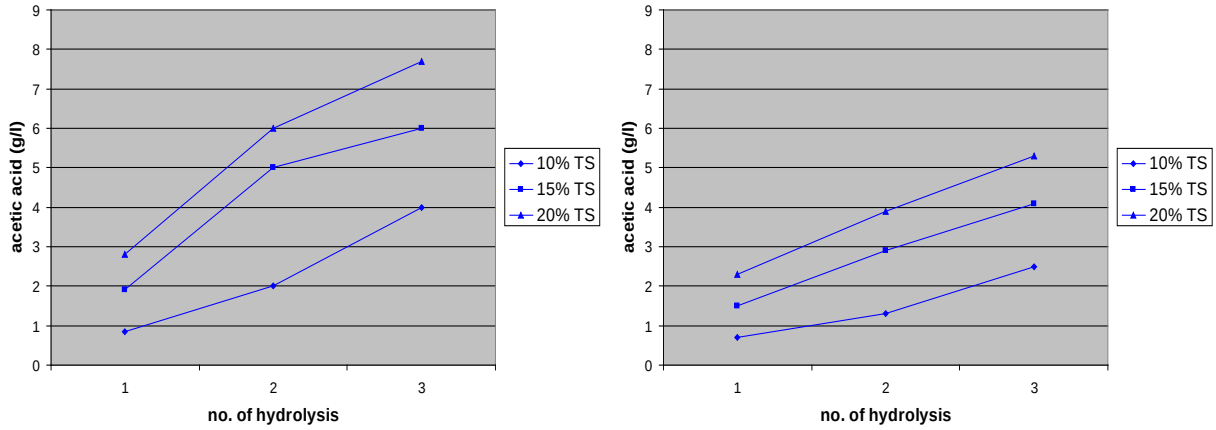

Fig. 3: Acetic acid concentrations after recirculation process (1st, 2nd, 3rd hydrolysis) with 10, 15 and 20 % solids loading of unwashed straw (left) and washed straw (right).

A clearly reduction of potential fermentation inhibitors like phenol (figure 2), acetic formic acid (figure 3), propionic acid, HMF and furfural were detected between unwashed and washed straw (data not shown).

4. Discussion and Conclusions

An efficient bioethanol production requires an effective pretreatment, hydrolysis and fermentation resulting high sugar concentration and subsequent high ethanol yield without inhibitory compounds.

In this study one new strategy – recirculation – was chosen to raise the sugar and ethanol yield. Therefore steam exploded straw was washed, hydrolyzed and fermented reaching sugar concentration of 140 g/l and EtOH yield of about 7.5 %. A comparison with unwashed straw revealed that obviously the inhibitory compounds formed during pretreatment were removed through the washing step.

This washing step must be considered critically - a high water consumption and pollution – could be a tender point in the bioethanol production from straw. In the future the washing water can maybe purified through membrane technology and reused and/or fed in a biogas plant.

Unfortunately also xylose was removed through this washing step. At present xylose can not efficient ferment to bioethanol but maybe xylose could be used in another way for example as biopolymer. Therefore the recovery of xylose has to established to get more products from a bioethanol plant.

Furthermore the recirculation strategy must be improved – the actual sugar and bioethanol yield is two times lower than the theoretical value and is at the moment to inefficient for an industrial application. The cellulase activity during the hydrolyses was obviously reduced through end production inhibition and/or inhibitors. New enzyme and/or enzyme mixture can enhance the sugar yield.

In the future diverse improvements have to be done:

- particularly the inhibitory compound(s) or the combination of the inhibitory compounds have to be determined and
- an efficient reduction method of the relevant inhibitors has to be established
- and/or adapted yeast to the inhibitors has to be developed
- creation of product(s) from xylose.

In addition the cycle of materials must made to enable a cost-effective bioethanol production from straw. The energy for steam explosion step should be provided from a biogas plant and the fermentation remains fed in a biogas plant. The biogas remains should be manure the agricultural area.

References

[1] Pristavka et al., High-solids enzymatic hydrolysis of steam-exploded willow without prior washing, Applied Biochemistry and Microbiology 36, 2000, pp. 101-108

[2] Varga et al., High solid simultaneous saccharification and fermentation of wet oxidized corn stover to ethanol, Biotechnology and Bioengineering 88, 2004, pp. 567-574

[3] Rudolf et al., A comparison between batch and fed-batch simultaneous saccharification and fermentation of steam pretreated spruce, Enzyme Microbial Technology 37, 2005, pp. 195-204

[4] Yang et al., High-concentration sugars production from corn stover based on combined pretreatments and fed-batch process, Biorescource Technology 101, pp. 4884-4888

[5] Demirbas, Products from lignocellulosic materials via degradation processes, Energy Source 30, 2008, pp. 27-37

[6] Waterhouse, Determination of total phenolics. In: Wrolstad, Editor, Current protocols in food analytical chemistry, Wiley, New York, 2002, pp. I1.1.1–I1.1.8

[7] Chang and Holtzapple, Fundamental factors affecting biomass enzymatic reactivity, Applied Biochemistry and Microbiology, 84/86, 2000, pp. 5-37

[8] Taherzadeh and Karimi,, Pretreatment of Lignocellulosic Wastes to Improve Ethanol and Biogas Production: A Review, International Journal of Molecular Sciences 9, 2008, pp.1621-1651

[9] Tablenia et al., Production of bioethanol from wheat straw: An overview on pretreatment, hydrolysis and fermentation, Bioresource Technology 101, 2009, pp. 4744-4753

[10] Alvira et al., Pretreatment technologies for en efficient bioethanol production process based on enzymatic hydrolysis: a Review, Bioresource Technology 101, 2009, pp. 4851-4861

[11] Da Costa Sousa et al., ´Cradle-to-grave´ assessment of existing lignocellulose pretreatment technologies, Current Opinion in Biotechnology 20, 2009, pp. 339-347

[12] Hendriks and Zeeman, Pretreatments to enhance the digestibility of lignocellulosic biomass, Bioresource Technology 100, 2009, pp. 10-18

[13] Balat, Production of bioethanol from lignocellulosic materials via the biochemical pathway: A review, Energy Conversion and Management 52, 2011, pp. 858-875

Improvement of enzymatic hydrolysis of rice straw by N-methylmorpholine-N-oxide (NMMO) pretreatment

Nafiseh Poornejad[1], S.M. Amin Salehi[1,*], Keikhosro Karimi[1], M.J. Taherzadeh[2], Tayebeh Behzad[1]

[1] *Department of Chemical Engineering, Isfahan University of Technology, Isfahan, Iran*
[2] *School of Engineering, University of Borås, Borås, Sweden*
* *Corresponding author. E-mail: a.salehi@ce.iut.ac.ir*

Abstract: "Food versus energy" analysis resulted in demanding raw materials which don't have conflict with food industries. The lignocellulosic materials are the most interested option, since not only these materials don't have conflict with food industries, but also there several economical and environmental advantages in those substrates for bioethanol production.
However, the lignocellulosic materials are recalcitrant to both acid and enzymatic hydrolysis. As a result, some pretreatment steps must be taken before hydrolysis. One of the most effective pretreatment methods is treatment with cellulosic solvent.
In this work rice straw, an agricultural residue which is mainly unused was pretreated with an industrial solvent, N-methylmorpholine-N-oxide (NMMO). The pretreatments were performed at 120°C for 1, 3,5 hours with 85% NMMO solution. The treated materials were then subjected to enzymatic hydrolysis by a mixture of commercial cellulase and glucosidase.
The results showed significant improvement on the enzymatic hydrolysis. Almost complete hydrolysis of the cellulose in the straw was observed after 5 h treatment with NMMO at ambient pressure and 120°C.

***Keywords**: pretreatment, NMMO, rice straw, enzymatic hydrolysis*

1. Introduction

Nowadays different resources are applied for ethanol production in all over the world. The dominant of these resources are agricultural residue such as corn, sugar, starch, and lignocellulosic materials. Increasing growth of industrial ethanol production cause debates on "food & fuel" and afflicted the food industries [1]. Therefore, researchers are trying to find renewable resources that don't have conflict with food resources. Cellulosic wastes are the most possible option. The largest source for this purpose is lignocellulosic materials such as agricultural residue (bagasse, sugar cane stalk etc), forestry wastes (hard and soft wood), and municipal materials.

For a long time, researchers are aspiring to enhance digestibility of lignocellulosic biomass to convert cellulose to ethanol [2]. These materials are reluctant to enzymatic hydrolysis, as a result, conversion of them to ethanol consists of five main steps as shown Fig. 1:

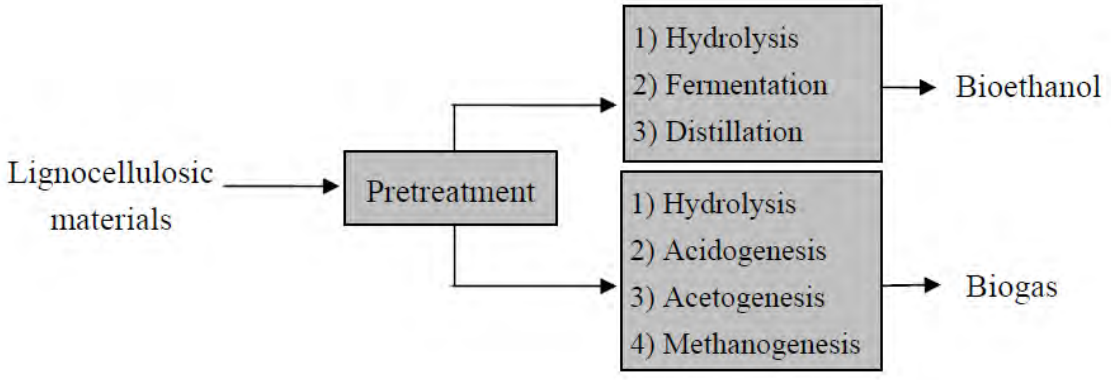

Fig. 1. Pretreatment of lignocellulosic materials prior to bioethanol prodyction [3]

Lignocellulosic materials consist of mainly three different types of polymers, namely cellulose, hemicelluloses, and lignin which are associated with each other [2].

Rice straw is one of the lignocellulosic waste materials could be found in the world. The estimation of annual production of rice by FAO is about 600 million tons per year in 2004. On the other hand, every kilogram of grain harvested is associated with production of 1-1.5 kg of the straw. It gives an estimation of global production of 600-900 million tons per year of straw. The ways of the disposition of rice straw are limited by the great bulk of material, slow degradation in the soil, harboring of rice stem diseases, and high mineral content. Field burning is the major practice for getting rid rice straw, but it increases air pollution and consequently affects the public health. Many counties in Western Europe have already banned open field burning and some other countries have considered it seriously [4].

Depend on the structure of lignicellulosic materials (the portion of these three polymers), the most effective pretreatment method could be selected. There are different kinds of pretreatment. The main categories are: physical pretreatment, chemical and physicochemical pretreatment, and biological pretreatment [3].

One of the chemical pretreatment methods is using solvent for solving the substrate and then regenerating the cellulose part by adding an anti solvent. N-methylmorpholine-N-oxide (NMMO) is among the nonderivatizing solvents which can dissolve cellulose by breaking the intermolecular forces. NMMO is one of the direct solvent for cellulose, which is nowadays applied in the industrial Layocell process. This process is one of the modern and environmentally friendly industrial fiber-making technologies with direct dissolution of cellulose without chemical derivatization. T he solvent does not produce toxic waste pollutants, and can be recycled with over 98% recovery. After dissolution in NMMO, cellulose can be regenerated by rapid precipitation with and anti solvent, which is usually water. The dissolution in NMMO can change the crystal structure of cellulose.

The treatment with NMMO has several advantages in comparison with other pretreatment methods such as conventional acid, alkali, and thermal pretreatments. Most of the other pretreatment methods change the composition of the substrates by e.g., removing hemicelluloses by dilute-acid or lignin by sodium hydroxide. However, NMMO keep the same composition as is reported in many researches. The NMMO process is performed in milder conditions, such as atmospheric pressure and lower temperature (<130°C) than for e.g., in dilute-acid, which results in less energy consumption of the entire process. In addition, no need for chemical neutralization and the possibility of more than 98% recovery of the solvent in industrial processes are other significant property of using NMMO. These properties in addition to the high amount of conversion of cellulose to ethanol which is presented here make the pretreatment with NMMO a good alternative for lignocellulosic ethanol production [5].

Different researchers have been working on the effect of NMMO on enzymatic hydrolysis of various substrates. As reported by Chai-Hung et al, the amount of reducing sugar released from sugar cane bagasse after 7 hr pretreatment in 100°C by NMMO was at least two times more than untreated sugar cane bagasse [6]. In another study, Shafiei et al have reported an increase about 75% and 50% in the yield of enzymatic hydrolysis of spruce and oak respectively after 3 hr NMMO pretreatment in 130°C in comparison with untreated substrates [5].

Because of all the mentioned reasons, the current study aimed at pretreatment of rice straw with NMMO.

2. Methodology

2.1. Raw materials and their analysis

The rice straw used in these experiments was obtained from Lenjan field (Isfahan, Iran). The original length was between 2 and 50 mm. It was partly screened to achieve a size of less than 0.8mm prior to the pretreatment. Its dry weight content was measured at 105°C for 24 h. The rice straw structure is reported by Karimi *et al* [4].

2.2. Pretreatment

The 85% NMMO solution was used for the pretreatment. The pretreatment performed in 200 ml Erlenmeyer flasks, where 1 g of rice straw (dry weight) was added to 19 g of the NMMO solvent and mixed every 15 min. Treatment was done in an oil bath at 120°C and for three different durations (1, 3, and 5 h). The pretreated rice straw was then regenerated by addition of 30 ml boiling deionized water, followed by vacuum filtration and washing until a clear filtrate appeared.

2.3. Enzymatic hydrolysis

NMMO-treated and untreated rice straw was subjected to 72 h enzymatic hydrolysis using 20 FPU cellulase and 30 IU β-glucosidase per gram cellulose [7]. Then the reminder solid was separated by centrifuge from the supernatant. The yield of enzymatic hydrolysis is defined as (grams of glucose released + grams of xylose released)/(grams of initial solid used for hydrolysis × 1.111). The dehydration factor (1.111) is used to convert cellulose chains to glucose monomers.

2.4. Analytical method

All the samples were analyzed by high-performance liquid chromatography (HPLC), equipped with UV/VIS and RI detectors (Jasco International Co., Tokyo, Japan). Glucose and xylose were determined by an Aminex HPX-87P column (Bio-Rad, Richmond , CA, USA) at 80°C. Deionized water was used as efluent at a flow rate of 0.6 ml/min.

3. Result and discussion

As shown in Fig.2, 3 h NMMO-treated substrate shows significant improvement in hydrolysis than 1 h NMMO-treated substrate and there is no significant change in the performance of NMMO after 5 h pretreatment in comparison with 3 h pretreatment. The glucose concentration in hydrolysate (liquid phase) after 24 h increase significantly by pretreatment, as a result, the rate of hydrolysis improve radically. The rate of hydrolysis (concentration after 24 h) increases about 100% after even 1 h treated straw in comparison with untreated straw and the concentration of glucose increases about 400%. All of these show significant improvement in enzymatic digestibility of rice straw after being treated with NMMO. That's because of destruction of intermolecular interactions.

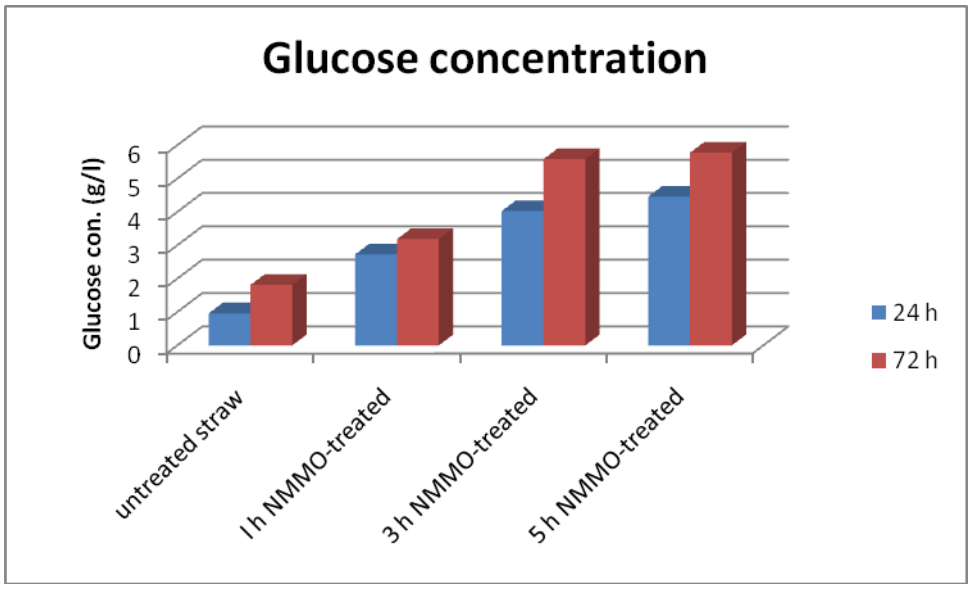

Fig. 2. Glucose concentration in hydrolysate during enzymatic hydrolysis

As shown in Fig. 3, x ylose concentration increases, too. The xylose concentration by 5 h treatment increases about 500% after 72 h h ydrolysis, moreover, the rate of hydrolysis increases by 300%. These results show undeniable superiority of NMMO over other solvents.

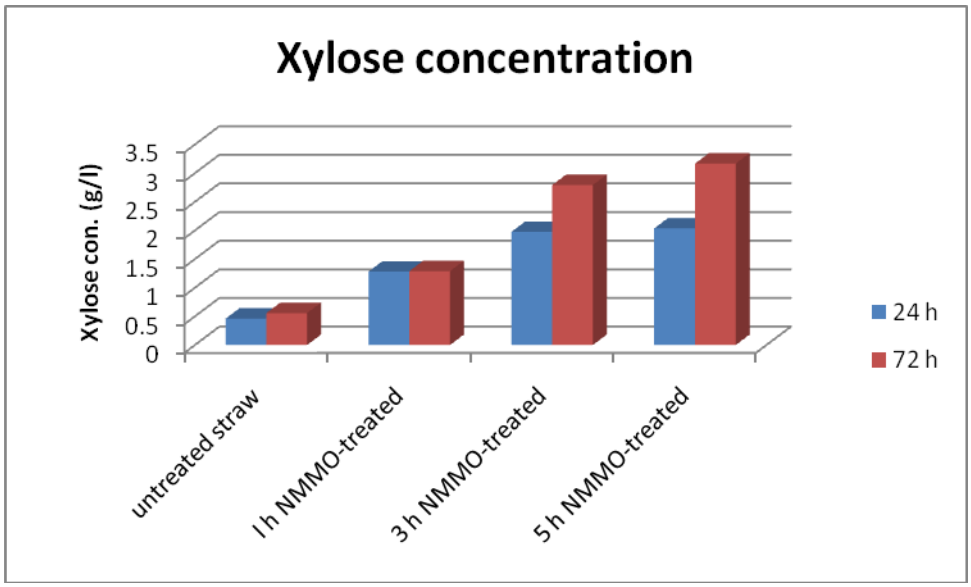

Fig. 3. Xylose concentration in hydrolysate during enzymatic hydrolysis

As shown in the last figure (Fig. 4.), the total sugar yield increases from 23.69% (untreated straw) to 84.42% (5 h NMMO-treated straw). This means an outstanding improvement in terms of industrial process.

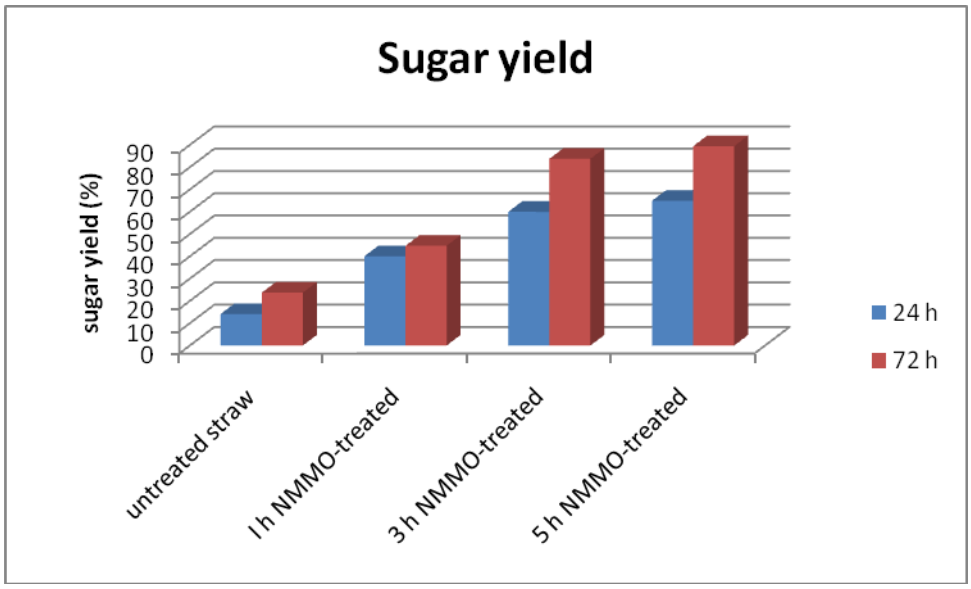

Fig. 4. Total yield of sugar during hydrolysis

4. Conclusion

Treatment with NMMO would be one of the promising ways for preparing rice straw for ethanol production. Having the capacity of being recovered and then reused, NMMO is a good alternative solvent for cellulose. As discussed above in atmospheric pressure and 120°C after 5 hr pretreatment the yield of about 90% could be achieved after 72 hr enzymatic hydrolysis of rice straw.

References

[1] G.J. Hayes, An examination of biorefining processes, catalysts and challenges, Catal. Today (2008), doi:10.1016/j.cattod.2008.04.017.

[2] A.T.W.M. Hendriks, G. Zeema, pretreatment to enhance the digestibility of lignocellulosic biomass, Bioresource Technology 100 (2009) 10–18.

[3] M.J. Taherzadeh, K. Karimi, pretreatment of lignocellulosic wastes to improve Ethanol and Biogas production: A review, *Int. J. Mol. Sci.* 2008, *9*, 1621-1651; DOI: 10.3390/ijms9091621.

[4] K. Karimi, Sh. Kheradmandinia, M.J. Taherzadeh, Conversion of rice straw to sugars by dilute acid hydrolysis, Biomass and Bioenergy 30(2006)247-253.

[5] M. Shafiei, K. Karimi, M.J. Taherzadeh, Pretreatment of spruce and oak by N-methylmorpholine-N-oxide (NMMO) for efficient conversion of their cellulose to ethanol, Bioresource Technology 101 (2010) 4914–4918.

[6] Ch-H. Kuo, Ch-K. Lee, Enhanced enzymatic hydrolysis of sugar cane bagasse by N-methylmorpholine-N-oxide pretreatment, Bioresource Technology 100(2009) 866-871.

[7] A. Jeihanipour, M.J. Taherzadeh, Ethanol production from cotton based waste textiles, Bioresource Technol 100(2):1007-1010.

Volume 2

Climate Change Issues

Risk based adaptation to climate change

Kjell Eriksson[1,*], Peter Friis-Hansen[1]

[1] *DNV Research & Innovation, Veritasveien 1, 1363 Høvik, Norway*
** Corresponding author. Tel: +47 95468338, E-mail: Kjell.Eriksson@DNV.COM*

Abstract: Climate change is real and owners and operators of critical infrastructures need to adapt to a different environment. Decisions will have to be made under large degree of uncertainty. There are today no specific methods that combine global climate models with infrastructure design methods. Hence the uncertainty in the decisions becomes even larger.

The paper presents a method for combining state-of-the-art climate modelling, meteorological approaches, with state-of-the-art structural design methods in a decision theoretic frame. This has, to our knowledge, not been done before. The decision framework will help authorities to make complicated and critical decisions with respect to how to prepare for future changes in the environment. The work is based on the climate models used in the current and updated IPCC Reports, regional and local meteorological and oceanographic models, and the DNV Recommended Practice on environmental loads, DNV-RP-C205.

The decision theoretic frame is risk-based where expected loss will be expressed in monetary terms. The approach is applicable to critical infrastructures, power generation and transmission, and offshore oil and gas installations.

The paper will address key design parameters, likely climate change scenarios, time horizon of the infrastructure or installation in question, limitations of existing climate models, combination of global and regional climate models, how to downscale results and, ultimately, how to convert the results into a design basis.
The methodology presented in the paper is based on ongoing research partly financed by the Norwegian Research Council and partly by DNV.

Keywords: *Climate change, Adaptation, Risk management, Infrastructures*

1. Introduction

"*Every year, climate change claims lives and seriously affects much of our planet. The scale and breadth of the challenge as identified by the Climate Vulnerability Monitor is already immense. So is the explosive growth of its negative effects on human society. Everyone should be aware of the risks we are running by not tackling the climate crisis, and how simple it is in many cases to avoid damage now and tomorrow. Still, only truly urgent action will prevent increasingly irreversible harm to the earth and the life it sustains. Equally urgent support is currently needed to help populations in places most vulnerable to the worst effects of climate change. They are on today's frontlines of our common struggle with a now rapidly changing planet.*" This citation is taken from the DARA [1] homepage, where their recently published report "Climate Vulnerability Monitor 2010" is published. The *Climate Vulnerability Monitor 2010* report draws attention to approximately 350,000 lives already lost each year as a result of global warming and changes to our climate. The annual number of lives lost is forecasted to increase to nearly 1 million by year 2030. The report further estimates that US$ 150 billion is lost in today's economy as a result of climate changes. These losses will increase in the future. More than half of the total economic losses will occur in industrialized countries. Moreover, DARA estimates that around 170 countries (i.e. most of the world) have high vulnerability to climate change in at least one key impact area already today.

The evidence in the DARA report highlights that decision-makers worldwide will face huge challenges in selecting effective means for adapting costly infrastructures to the changing climate. If decision makers fail to properly adapt infrastructures in time, the potential losses

may well exceed far beyond the cost of the infrastructure itself. Lost infrastructures such as part of e.g. a transport system, energy system, or vital public facilities (for instance hospitals), may paralyse society for a long time and therefore create a setback for the economy and a whole community.

What aggravates the decision making is the overwhelming amount of uncertainties that the decision maker is facing. The decision maker must not only consider uncertainties in relation to future climatic changes (temperature, storms, precipitation, waves, subsidence, etc.) and how these correlate, but also the health state of the degrading infrastructure prior to the occurrence of the events, as well as estimate direct and indirect consequences that follow. However, uncertainties are not limited to this. Mathematical models that use semi-empirical models of vegetation, soils, ice-sheets, etc., are invoked to forecast future climate change effects. These models are imprecise and will add further uncertainty into the decision problem.

The forecasting of the climate is based on four representative CO2 emission scenarios; however, we do not know which scenario that best will describe the future. Finally, it is the extreme events that govern failure of the structures, and these extremes are by nature hard to predict. Therefore, also statistical uncertainty enters the decision problem.

Although most decision-makers are increasingly concerned with the adverse impacts of climate variability and change, decision-makers rarely possess the composite knowledge needed to understand the complexity, interconnectivity, and limitations of uncertainty modelling, to make effective decisions to manage current and future climate risks. The challenge in establishing this technical understanding requires that risk-based adaptation to climate change assume a new level of integration and coordination.

DNV is currently developing a Recommended Practice (RP) for risk-based adaptation to climate change. The objective of the RP is to assist decision makers, such as public authorities, to exercise critical and sound decision-making on how to prepare and adapt to future changes in the environment. This is sought achieved through the formulation of a structured method that combines state-of-the-art climate modelling, meteorological approaches, with state-of-the-art structural design methods. The method is based on the climate models used in the current and updated IPCC Reports, regional and local meteorological and oceanographic models; and finally, it is risk-based where all uncertainties are accounted for. Such a recommended practice has, to our knowledge, never been developed before.

Since the majority of the uncertainties to a large extent are rooted in expert judgement in combination with mathematical modelling, the recommended practice will also include methods for identification of what uncertainties affect the decision making the most, and provide guidance for reducing these uncertainties. This is central since decisions made on adapting infrastructures to climate change are very costly in general; wherefore it is of paramount importance for decision-makers to identify means to effectively reduce the probability of making a wrong decision.

DNV is aware of the work undertaken by the World Meteorological Organization under the Global Framework for Climate Services (GFCS) [2]. GFCS was established by the Heads of State and Government, Ministers and Heads of Delegations present at the UN World Climate Conference-3 (WCC-3) in September 2009 with the mandate to: "*Enable better management of the risks of climate variability and change and adaptation to climate change at all levels, through development and incorporation of science-based climate information and prediction into planning, policy and practice.*" As such, the GFCS activity may seem identical to the

work that DNV is undertaking to establish an RP. However, the work of GFCS appears (at present) to have focus on strengthening the global observing capability of the members by optimising the density and spatial distribution of observing networks, ensuring data compatibility and increasing the quality of observations. Such work is very important to arrive at better and more reliable predictions in climate modelling, which will also be undertaken by GFCS. However, in our work on the RP, focus is on formulating a structured method that effectively will allow decision makers to effectively control and handle all uncertainties involved in the decision-making and as such to arrive at better decision. Hence, the RP and the GFCS work complement each other. At present our RP is not based on the GFCS work, but this may change in future.

In this paper we describe the general background and applied principles behind the recommended practice. The paper is compiled as follows: In section 2 the applied terminology for risk related elements are defined. Here it is argued why risk is defined as expected monetary loss. In section 3, we discuss climate modelling and how to arrive at a description of the outmost important assessment of extreme events of the climate impacts as well as the correlation among different climate impacts. Section 4 discusses the existing design principles for infrastructures. It is highlighted that extreme events for such structures have a completely different meaning than that applied in the IPCC reports. Section 5 shortly presents the risk modelling and describes how the dominating uncertainties in the model can be identified. For this set of dominating uncertainties effective uncertainty reductions can be made. In section 6, we present a graphical overview of the overall method, and finally in section 7, we summarise and conclude the expected benefits from establishing and applying the recommended practice to costly decisions on adaptation of important infrastructures to a chancing climate.

2. Risk related terminology

2.1. Risk

Intuitively a measure of risk should be some increasing function of both the probability of occurrence of the adverse event and the consequence of the adverse event represented on some numerical (monetary) scale. If an adverse event A occurs once within a year with probability p, and two or more occurrences of A within a year have negligible probability as compared to p and, moreover, the consequence of the occurrence of A can be represented by a loss L equal to a known monetary cost c, then the expected value of the yearly cost is $pc+(1-p)0=pc$, because there is no cost from A if A does not occur. There is a decision theoretical reason[i] to take this *expected cost* as the definition of the yearly risk $r(A)$ associated with the event A, i.e. $r(A)=pc$. This definition may easily be relaxed to apply for events that occur in time with frequency λ, to become $r(A)=\lambda c$.

Typically, risk analysis is performed without a clear definition of how to measure risk, and only displayed by a simple, crude colour coding. Such an approach is not sufficient to be applied for decision making of complex costly structures. In the RP we advocate for detailed modelling of both frequencies and consequences.

[i] The decision theoretical argument is, of course, that decisions on risk reduction initiatives are measured on monetary scale, and that risk as such directly is in agreement with the fundament of decision theory.

2.2. Vulnerability

There exist several definitions for "vulnerability" that all depend upon the type of system they relate to (e.g. technical, computer, networks, organisational and societal systems). The set of definitions all refer to *weaknesses* or *flaws* embedded within the system caused by some event combined with the capability of the environment (or external circumstances) to *exploit such weaknesses* to impair the functioning of the system [3,4,5].

The provided definitions of vulnerability are imprecise, and are not operable within the quantitative framework of the RP being established. Therefore, we define *vulnerability* as the *conditional expected loss*; that is, the risk calculated conditional on the occurrence of the unwanted event. This implies that vulnerability will be decreasing when the failure probability of any implemented barrier decreases or when the consequences decreases. This definition is operable and is in agreement with common use of the word *vulnerability*.

2.3. Resilience

There exist several definitions of resilience in literature. Within the resilience engineers there seem to be consensus along the line that is well defined by Wreathall [6]: "*Resilience is the ability of an organization (system) to keep, or recover quickly to, a stable state, allowing it to continue operation during and after a major mishap, or in the presence of continuous significant stresses*".

Unfortunately, this definition makes it difficult to measure resilience. We therefore propose the definition: "Resilience is the *ability to control* the risk that follows after a major mishap. The risk includes operational loss, emergency recovery, etc., of the continuously stressed system." This implies that resilience also can be defined as controlling the vulnerability that follows after the occurrence of the direct losses, i.e. controlling the follow consequences.

3. Climate models

The assessment of statistics on extreme events in weather variables influenced by a changing climate is of outmost importance to adaptation decisions for future infrastructures. This is a complex task. Firstly, it is difficult to estimate the extreme value statistics, since it by nature is hard to get reliable statistics of rare events from available observations. Secondly, for a changing climate, statistics based on past observations cannot directly be extrapolated, and we must rely on theories, models and past analogies. Research shows that some of the largest impacts of climate change will be through more extreme climate events [7].

The primary tool for assessing climate changes is emission scenario simulations using General Circulation Models (GCM), which in a rather coarse resolution solve the flow and energy equations for the atmosphere and oceans. Furthermore, these models are combined with semi-empirical models of vegetation, soils, ice-sheets etc, to form Earth System Models. The models are extremely costly to run at a level with reliable predictive power, which creates two types of limitations. Firstly, while they provide reasonable predictions at the large scales, they generally underestimate extremes. This is both due to the fact that the coarse resolution makes the meteorological fields unrealistically smooth and the fact that the models are too costly to run for reliable simulation of the extreme tails of the probability distributions of the meteorological fields. Secondly, the global models do not provide the probabilistic information of extreme local climate events needed for risk analysis. For the task of assessing the statistics of a specific climatologic variable, relevant for a specific location (say 10m wind over the North Sea), there are some main techniques:

Dynamical downscaling is based on Regional Climate Models (RCM) that uses GCMs as boundary conditions to simulate the state of the atmosphere in a region with a smaller grid resolution than used in the GCM. RCM models are usually defined at a grid size of 10-50 km and are able to better represent topography and land use than GCM models. However, these models inherit some of the biases of the GCM, and in most cases further statistical downscaling and adjustment is required.

Statistical downscaling techniques are needed to obtain bias-corrected, high-resolution local projections from GCM and RCM simulations. The basic idea behind statistical downscaling is to define a relationship between large scale and local scale climate variables. Presently little emphasis has been put towards downscaling of extremes.

Stochastic weather generators have been applied for downscaling precipitation and derivation of extreme value statistics. These models are typically empirical Markov chain models for generating surrogate climate variables based on parameters estimations from observations and models. Downscaling using stochastic weather generator may change the GCM results considerable. Semenov and Barrow [8] reports an increase in monthly average precipitation by up to a factor of three in some areas.

Climate statistics derives distributions based on past observations. These are based on the assumption of stationarity where past observations are used to estimate the extreme value distributions and associated risks. IPPC operates with approximately 25 GCM models, among which around 8 differ in the underlying semi-empirical models. This implies that that these models do have different competences in capturing different climate change effects in different regions. Similarly there exist of the order of 15 different RCM models that again each have their own competences and weaknesses in different areas.

One of the objectives of the RP that we are developing is to identify what climate change effects are important (for offshore structures in the first version) at different locations around the world. This is used to highlight the relevant weather features that the chosen GCMs and RCMs must be able to capture to arrive at trustworthy climate change predictions. For instance, for the Barents Sea it is important that the models capture polar lows, synoptic lows, and sea ice extent, otherwise extreme winds and waves may be grossly underestimated.

Meehl et al. [9] discussed that though the climate models can simulate many aspects of climate variability and extremes, they still are characterized by systematic simulation errors and limitations in accurately simulating regional climate such that appropriate caveats must accompany any discussion of future changes in weather and climate extremes. However, as computers become more powerful this allow for taking into account more climatological effects and at the same time increasing the grid size. However, when errors are systematic, then the increase in computer power may be of limited use.

Depending on the structures that are evaluated the climate predictions shall be evaluated for the following time periods: present, 20, 50 and 100 years forecasting. Infrastructures are typically designed for 100 year lifetime, whereas offshore structures generally have an expected lifetime of 50 years. The need for all periods for infrastructures is due to dominating uncertainties may change at the different time scales and result in a different mixture of extremes. This may initiate new failure modes to the infrastructures.

Today the climate models are evaluated only for the extreme emission scenarios (currently the A1B-scenario). This may result in too conservative adaptive measures are implemented. This

may result in unjustified large investments being allocated at the expense of other initiatives not being implemented. For this reason it is desirable to have climate model runs for all emission scenarios and to assign a probability distribution over the set of analysed scenarios.

4. Design principles for infrastructures

The structural dimensioning of civil infrastructures is made according to requirements formulated in a structural design code. The code requirements are interpreted and formulated within a mathematical model for the geometric and mechanical properties of the structure and for the actions on the structure. For a carefully selected set of the (random) variables that independently contribute to that part of the mathematical model that concerns geometry, strength properties and actions, the code committee calibrates the set of (random) variables such that the design code can control the safety level of a broad class of structures for which the code is meant to cover. The variables are called *design variables*. Control over the safety level is achieved by selecting a *characteristic value* for all design variables (this is typically the 98% or 2-5% fractile value of the random variable) and calibrating *partial safety factors* that amplify the design variables such that the desired safety level is obtained.

For example, consider a simple steel rod with load that pulls at the end of the rod. Let the random strength of the rod be R and the random load be S. The critical situation is clearly when the strength is small and the load is high. Therefore the characteristic value, r_c, of the strength is defined as the 5% fractile value of R and the characteristic value, s_c, of the load takes the 98% fractile of S. The partial safety factor on r_c is γ_r and γ_s on s_c. The design equation in this example becomes:

$$g = \frac{r_c}{\gamma_r} - s_c \gamma_s \geq 0 .$$

The magnitude of the partial safety factors depend on how critical the required safety level of the structure is. Table 1 presents the required reliability (safety) index requirements for building structures.

Table 1. Example of reliability index requirements. From NKB [10].Values in parenthesis is the failure probability.

		Type of failure		
(Reference period 1 year)		Ductile with reserves	Ductile without reserves	Brittle
Safety class	Low	3.1 ($1.0 \cdot 10^{-3}$)	3.7 ($1.1 \cdot 10^{-4}$)	4.2 ($1.3 \cdot 10^{-5}$)
	Normal	3.7 ($1.1 \cdot 10^{-4}$)	4.2 ($1.3 \cdot 10^{-5}$)	4.7 ($1.3 \cdot 10^{-6}$)
	High	4.2 ($1.3 \cdot 10^{-5}$)	4.7 ($1.3 \cdot 10^{-6}$)	5.2 ($1.0 \cdot 10^{-7}$)

The table shows that the required reliability (safety) level depends both on safety class and type of failure. Both the safety class and type of failure refer to consequences of failure. The levels have been identified and validated through cost-benefit analysis of a large suite of structures. Low safety level refers to warehouses whereas the high safety class refers to grandstands and critical infrastructures. The work by NKB forms the basis for all structural codes in Scandinavia, and the principle is now also applied in the Eurocode [2] for structural design.

The table provide valuable information about the fractile level of the extreme value distribution that is of real interest. Critical infrastructures will typically be designed to reliability level of 4.2 to 4.7. It can be shown that this level corresponds to annual exceedance probabilities of the order of $1.3 \cdot 10^{-3}$ to $1.3 \cdot 10^{-5}$.

In the document IPPC [11] rare events are defined as: "*An event that is rare at a particular place and time of year. Definitions of 'rare' vary, but an extreme weather event would normally be as rare as or rarer than the 10th or 90th percentile of the observed probability density function. By definition, the characteristics of what is called extreme weather may vary from place to place in an absolute sense.*" It is seen that what IPPC consider as rare events significantly differs from the extreme values that is required in structural design, which is a factor of 100 to 10.000 less than the IPPC definition of rare events. The need to extend extremes far beyond what is normally classed as rare within the climatological terminology is very important and a very challenging task.

5. Risk modelling and identification of the dominating uncertainties

The risk modelling contains two interconnected parts: one is to estimate the annual probability of the structure failing and the second is to identify the spectrum of consequences that may materialise following the occurrence of unwanted events. The considered consequence spectrum shall cover both direct and indirect losses, and loss types will not only address loss of life and material losses, but shall also account for production losses and environmental losses. When estimating the indirect losses it is important to consider how the evaluated infrastructure relates and impinge on the surrounding society.

We consider three means for running the risk analysis: The first approach is to establish a Bayesian network (BN) construct for the entire problem. This approach requires a descretisation of the random variables and losses. The second is to apply a full structural reliability approach that use continuous distribution. The third approach is to apply Monte Carlo simulation to estimate the risk. This approach may be combined with the two former through discrete event simulations.

The two first approaches almost directly facilitate identification of the most dominating uncertainties as this can be extracted almost as a bi-product of the analysis. For the BN approach we use so-called *max-propagation* to identify dominating uncertainties, and for the second approach the importance factors directly provide the information. The third approach is somewhat more involved as it requires multiple runs to evaluate the 'value of information' for each random variable. Means will be identified for reducing the uncertainties for the set of variables that dominate the risk modelling, since it will be those variables influences the probability of making a wrong decision the most. Hence, this information gathering may represent a significant cost savings at limited cost.

6. Overview of the risk based method

Figure 1 presents a graphical overview of the overall method. The procedure has 6 steps. The first step is to identify a probability distribution over the emission scenarios thereafter to identify relevant GCMs and RCMs to predict the distributions of future climate. The risk analysis completed by first completing a vulnerability analysis. This facilitates future updates due to changes in emission scenarios, GCM/RCM choices, implementation of adaptation measures.

7. Summary and conclusion

Climate change is real and owners and operators of critical infrastructures need to adapt to a different environment. Climate change is analysed by different global climate models. One fundamental difference between global climate models and design codes for infrastructure is that the climate models operate with average values, whereas one needs extreme values for design codes. It should be noted that the definition of a rare event used by IPCC is fundamentally different from the definition of an extreme event in a design code. There is a significant

difference in designing a roof for total of 10% more snowfall if the additional snowfall is evenly distributed throughout the winter versus if the additional snowfall is concentrated for a few days. Designing infrastructure for future climate conditions will involve handling a large number of factors with significant uncertainties. We propose to use a risk based method to handle these uncertainties, and as a means to building a bridge between the climate models and design methods used for infrastructure. More work is needed to clearly describe and quantify the characteristics of the different climate models, better understand the limitations different downscaling methods and to identify the dominating uncertainties.

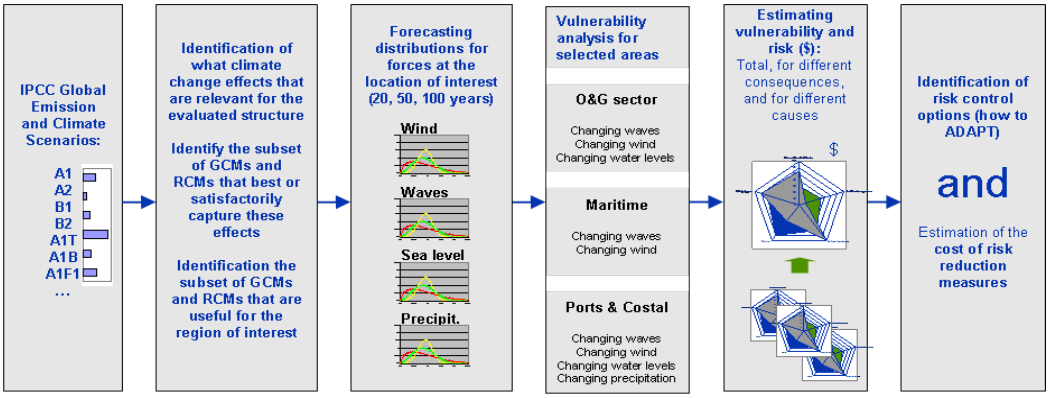

Fig. 1. Overall methodology.

References

[1] DARA, Climate Vulnerability Monitor 2010, http://daraint.org/climate-vulnerability-monitor/climate-vulnerability-monitor-2010/download-the-report/, 2010.

[2] GFCS, Position Paper on Global Framework for Climate Services. Submitted by the World Meteorological Organization. 2010. http://www.wmo.int/pages/gfcs/documents/GFCS_Position_Paper_DRAFT_REV_1_en_1.pdf

[3] ISO 27005, ISO 27000 Directory, http://www.27000.org/iso-27005.htm 2008.

[4] European Network and Information Security Agency (ENISA). www.enisa.europa.eu

[5] The Open Group (an industry consortium to set vendor- and technology-neutral open standards for computing infrastructure)

[6] Wreathall, J. Properties of Resilient Organisations. An Initial View. In Resilience Engineering Concepts and Precepts". pp. 275-285. Eds. E. Hollnagel, D.D. Woods, and N. Leveson,. Ashgate, 2008.

[7] IPCC, 2007, http://www.ipcc.ch/publications_and_data/publications_and_data.htm

[8] M.A. Semenov and E. M. Barrow, Use of Stochastic Weather Generators in the Development of Climate Change Scenarios. Climatic Change 35: 397–414, 1997.

[9] G.A. Meehl, F. Zwiers, J. Evans, T. Knutson. L. Mearns, and P. Whetton, Trends in Extreme Weather and Climate Events: Issues Related to Modeling Extremes in Projections of Future Climate Change. Bulletin of the American Meteorological Society, Vol. 81, No. 3. 2000. Pp. 427-436

[10] Nordic Committee for building structures (NKB), Recommendations for Loading and Safety Regulations for Structural Design. NKB Report No. 36, 1978.

[11] IPCC report … On extreme events and definition of rare, 2007

How much energy can we consume?

Oleg P.Dimitriev*

V.Lashkaryov Institute of Semiconductor Physics, Kiev, Ukraine
** Corresponding author. Tel: +38 044 5259706, Fax: +38 044 5255530, E-mail: dimitr@isp.kiev.ua*

Abstract: This report considers the global energy consumption from the viewpoint of thermodynamic balance between the Earth and the cosmic environment. To follow such a balance is postulated to be necessary to maintain proper functioning of the biosphere and stable climate conditions on the Earth. This viewpoint implies the following principles of energy consumption: (i) the energy should be consumed from the renewable sources only and (ii) the amount of the consumed energy should not exceed the amount of energy that incomes to the Earth. Three major sources of the renewable energy are considered, i.e., a direct incoming solar irradiation, a chemical energy through products of photosynthesis and, finally, an outgoing radiation from the Earth as a heated body. It is shown that the first and the third sources are potentially the most effective ways of the energy consumption. The last one, however, is not properly developed now. With the first two sources, the energy consumption rate cannot exceed a limit of 10^{17} W, but practically due to technical restrictions it can be set as 10^{14} W, which is approximately an order higher of the contemporary rate of energy consumption by the mankind. Development of the third source of energy is shown to allow us to increase the above limit up to one order of magnitude more. However, one should take great care of using this source of energy since it can affect climate changes also.

Keywords: *Thermodynamic balance, Renewable energy, Consumption limit*

Nomenclature

P_{sun} *energy power incoming from the sun to the earth-atmosphere system* ..... *W*
P_{earth} *energy power incoming to/outgoing from the earth surface* ..... *W*
$P^{\downarrow}_{org}$ *energy power stored via photosynthesis* .. *W*
P_{sc} *energy power produced by solar cells* ..... *W*
P_{O2} *energy power to produce oxygen through photosynthesis* ..... *W*
η_{org} *power conversion efficiency of photosynthesis* ..... *%*
η_{indir} *power conversion efficiency of solar energy used via produ*
η_{sc} *power conversion efficiency of solar cells %*
N_A *Avogadro's constant*..... mol^{-1}

1. Introduction

The global strategy of energy consumption has not ever been developed or widely accepted yet. However, there are several signals indicating in favor of such a strategy to be assumed in the near future. One signal comes from the fact that the organic fuel supplies (oil and gas) are exhausted and will come to the end in a few tens of years, and even the coal reserves will run out faster than many believe [1]. The second signal comes from the fact that the global climate is now sensitive to the increasing level of energy consumption and carbon dioxide production as a result of such kind of activity, respectively.

This report considers the principles of the global energy consumption from the viewpoint of thermodynamic balance between the Earth and the cosmic environment, which is necessary to maintain stable and unchanged conditions for proper functioning of the biosphere on the Earth. This viewpoint implies the following principles: (i) The energy should be consumed from the renewable sources only; (ii) The amount of the consumed energy should not exceed the natural production of energy through formation of organic fuel, income of solar energy, etc.

Solar energy is considered as a global supplier of the renewable energy on the Earth, which gives rise to formation of all sources of the organic fuel through photosynthesis, as well as

energy of wind, hydro-energy through local heating of the earth surface, melting of ice, etc. Nuclear energy is not included in this balance since nuclear materials are not renewable and, moreover, nuclear waste still represents a very dangerous factor for the biosphere.

We consider three possible ways of using a solar energy, namely, the use of a direct incoming solar irradiation, the use of an indirect solar energy through products of photosynthesis and, finally, the use of a reemitted energy from the Earth after the heating of the planet and its irradiation as a black body at the heated temperature. It is considered for the first way that although the power of incoming solar irradiation to the Earth is of the order of 10^{17} W, only a small part of that, approximately 10^{14} W, can be utilized by solar cells due to limitations in their power conversion efficiency, as well as limitation in surface area on the Earth suitable for their displacement. The second way of using the energy through products of photosynthesis can also yield a maximum consumption of 10^{14} W which is equivalent to the energy power production by the biosphere. The total power of human energy consumption is of the order of 10^{13} W at the moment [2]. With the modern 4% annual increase of the energy consumption on the Earth it will take about 60 years to reach the maximal possible limit of 10^{14} W. Finally, there is a large domain of the renewable energy resource in the form of the outgoing terrestrial radiation which could yield additional income and shift the above limit of consumption to higher values. The methods to develop this domain will be discussed below. However, such a shift in energy consumption can be accompanied with unpredictable changes in temperature regimes on the Earth surface. Therefore, the energy consumption limit should be postulated anyway as soon as possible in the near future.

2. Methodology: the energy balance on the Earth

The law of energy conservation states that any energy can be spent for performing some work and/or heating. The main source of the incoming energy on the Earth is the Sun. The solar radiation reaching the earth surface has an average power per square meter of about 230 W/m^2 and its spectrum extends from the UV to the IR, with the major part of energy lying in the visible range which has the maximum at the wavelength of about 0.5 μm (Fig.1). Eventually, an equal amount of energy must be lost from the Earth-atmosphere system if the internal energy of this system remains constant and the climate is stable. Therefore, the Earth emits the terrestrial radiation as a heated body. However, the spectral range of this outgoing radiation is shifted to the IR since the average temperature of the radiative body, i.e., the Earth, is 288^0 K (Fig.1). Although the peak amount of the outgoing terrestrial radiation (which is at the wavelength of 10 μm) is much smaller as compared to the corresponding peak of the incoming solar radiation at 0.5 μm, namely, *ca.* $7\text{x}10^{-3}$ (calculated using the data from ref. [3]) versus $1.5\text{x}10^3$ W/(m^{2}μm), respectively, the outgoing radiation has a much wider spectral range, so that the total amounts of the both radiations are equal in accordance with the thermodynamic balance of the planet.

On the other hand, the amount of photons incoming to and outgoing from the Earth is rather different according to the balance of the incoming and outgoing energy, i.e.,

$$E(\nu)=\int h n d\nu = (\sum h\nu_i n_i)_{sun} = (\sum h\nu_k n_k)_{earth},$$

where n_i is the amount of photons with the frequency ν_i, h the Planck constant. It can be roughly evaluated this relationship as $N_{earth}/N_{sun}=20$, where N_{earth} is the average number of photons with the wavelength 10 μm emitted by the earth-atmosphere system and N_{sun} is the average number of photons with the wavelength 0.5 μm from the Sun.

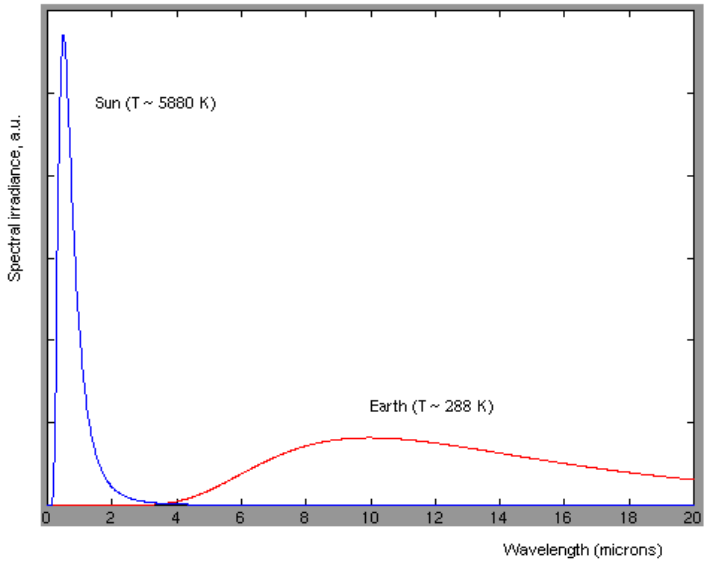

Fig.1. Relationship between incoming solar (blue curve) and outgoing terrestrial (red curve) radiation. The magnitude of the terrestrial radiation is magnified by a factor of 500,000.

However, a small part of photons from the Sun is stored in the form of chemical energy due to photosynthesis. This part of photons can be evaluated taking into account the energy conversion efficiency of photosynthesis to be of the order of 0.1% (see section 3 for details) that results in only a single stored photon of the thousand ones that are coming from the Sun. As a result, the relationship of the incoming, stored and outgoing energies can be presented schematically in Fig.2. Since only one incoming photon of one thousand gives rise to formation of all organic minerals and fuel, such as coal, natural gas, and petroleum as the products of photosynthesis, it can be easy to understand that only a small part of the incoming energy is mainly consumed now by the mankind.

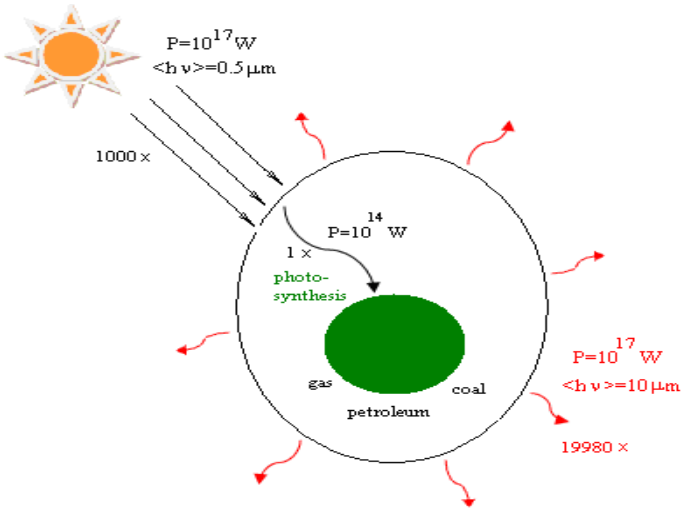

Fig.2. Relationship between incoming, stored, and outgoing energy rates per each 1000 incoming photons from the Sun.

3. Use of renewable sources of energy

3.1. Indirect consumption of solar energy through products of photosynthesis

The energy flux utilized by photosynthesis is $P^{\downarrow}_{org} \sim 10^{14}$ W. This value can be calculated from the photosynthesis equation, i.e.

$$CO_2 + H_2O \Rightarrow CHOH + O_2 \qquad (1).$$

The process described by Eq. (1) involves 4 electrons to be transferred; each of them requires the energy of 1.2 eV per electron. Therefore, formation of an O_2 molecule requires consumption of 4.8 eV. However, quantum efficiency of the system requires 8 to 12 quanta of light to be adsorbed which results in synthesis of one molecule of oxygen. Therefore, the total energy consumed by the photosynthetic system to produce one molecule of O_2 will be approximately $E_{O2} \sim 10$ quanta x 2 eV = 20 eV. Green plants produce totally 10^{14} kg of O_2 per year on the Earth, or $m_{O2} = 3x10^9$ g per second. The energy power necessary to produce O_2, therefore, will be

$$P_{O2} = E_{O2}(m_{O2}/M)N_A = 1.8 \cdot 10^{14}\ W \qquad (2),$$

where M=32 is the molar mass of O_2. Using this result and the power of solar energy reaching the Earth surface which is

$$P_{sun} - albedo\ (\sim 28\%) = P_{earth} \sim 1.2 \cdot 10^{17} W,$$

one can evaluate the average efficiency of photosynthesis as

$$\eta_{org} = P_{O2}/P_{earth} \sim 1.5 \cdot 10^{-3} = 0.15\ \% \qquad (3).$$

The same value for η_{org} can be also obtained via expression $P^{\downarrow}_{org} = \eta_{org}\ S_{earth} \cdot 230\ W/m^2$, where an assumption is made that the plants cover the overall earth surface S_{earth}. In fact, this assumption is rather crude, because there are large deserts, ice or mountain areas free of plants, but which can be overcompensated, however, by plant diversity in forests which occupy a few levels of space from the earth surface.

The efficiency value (3) can also vary depending on l ocal conditions of grow of plant organisms, for example, reaching up to 2% for water-plants grown in special pools [4].

It is natural to assume that the rate of energy consumption based on products of photosynthesis (gas, oil, coal, etc.), if the concept of energy consumption sets these resources as the basic sources of energy, cannot exceed the rate of formation of the organic products through photosynthesis calculated above. Thus, the energy consumption rate should be limited to $P_{org} < 10^{14}$ W which is only one order of magnitude exceeds the total power of all industrial energy producers currently on the Earth of about 10^{13} W [5]. The contemporary rate of energy consumption by the mankind can be calculated also by using the data on total mass of burning of dry fuel equivalent to $5 \cdot 10^{12}$ kg of carbon per year. The energy of reaction $C+O_2 \Rightarrow CO_2$ is $3.3 \cdot 10^7$ J/kg which gives the energy power of $5 \cdot 10^{12}$ W, which is consistent also with the year energy consumption data of the order of 10^{17} W·h [2]. It is easy to calculate, assuming the annual increase of the contemporary energy consumption of about 4% [5] that the above limit will be reached in the next 60 years ($(1.04)^N = 10$, from where N=59).

Finally, the efficiency of conversion of the solar energy by indirect way through burning of the organic products of photosynthesis, assuming that power conversion efficiency of the burning process is about 40%, will be only

$$\eta_{indir} = 6 \cdot 10^{-2}\% \qquad (4).$$

3.2. Direct consumption of incoming solar radiation

The power of solar energy irradiated the Earth is of the order of 10^{17} W. That means that the theoretical maximum of the solar energy consumption can be of the same order, i.e., $P_{sc} \sim 10^{17}$ W, if the power conversion efficiency of the corresponding devices approaches 100%. There are limitations, however, because power conversion efficiency of the conventional solar cells is far lower, of the order of η_{sc} ~10%, and because these cells cannot be set over the whole surface of the Earth. For example, in order to produce energy comparable with that stored by photosynthesis, the area of the solar cells S_{sc} should be as much as 1% of the Earth surface S_{earth}, which can be calculated from the following expressions with account of power conversion efficiency for photosynthesis (Eq.(3)),

$$P_{sc} = P^{\downarrow}_{org} \Rightarrow \eta_{sc} S_{sc} \cdot 230\ W/m^2 = \eta_{org} S_{earth} \cdot 230\ W/m^2 \Rightarrow S_{sc}/S_{earth} = \eta_{org}/\eta_{sc} \qquad (5)$$

1% of the earth surface is rather big, but reasonable value which seems to not significantly affect the biosphere and cropland areas. For comparison, the total urban area on the Earth is now approximately $3.4 \cdot 10^2$ km^2 [6] which cover approximately 0.07 % of the Earth surface. To cover an approximately one order of magnitude higher surface seems to be a challenging, but achievable task. However, additional studies are needed to confirm that this value is acceptable and compatible with the living areas on the Earth.

Thus, the energy production through a direct consumption of the solar irradiation energy can reach theoretically one order of magnitude higher value as compared with the contemporary production of energy through burning of organic fuel (see previous section). In addition, power conversion efficiency of the direct conversion of solar energy (η_{sc} ~10%) is three orders of magnitude higher as compared with that of the indirect production of energy (see Eq.(4)). Thus, a direct consumption of the solar energy is more efficient than the apparent efficiency of burning of the carbon-containing products.

3.3. Consumption of outgoing terrestrial radiation

There is a large part of IR energy, $P^{\uparrow}_{earth}$, which is reemitted from the earth surface in the form of the terrestrial radiation the Earth emits as the black body with the temperature of $T_{earth} = 255^0$ K. The amount of this energy is huge and comparable with that coming from the sun to the earth surface, due to the thermodynamic balance of the planet (see Fig.1),

$$P^{\uparrow}_{earth} \sim P_{sun} \sim 10^{17}\ W$$

There are several candidates that can serve as converters of this IR energy to electricity, such as pyroelectric and thermoelectric materials, gapless semiconductors, thermocouples, etc.; however, their application in respect to the terrestrial energy has not been developed yet. The advantages of the consumption of the terrestrial radiation is, first, that this radiation is highly scattered and therefore there is no need for orientation of the corresponding IR receivers or this orientation is not so critical as compared with the solar cells converting direct solar irradiation, so that the IR receivers can occupy several levels upward and, second, they do not

compete for the solar light with green plants. Below we consider three classes of materials which can be potentially used for the above energy domain.

It is well known that some organic compounds, such as metal complexes, ionic dyes, extended π-conjugated chromophores, and donor–acceptor charge transfer chromophores can absorbs near-IR (NIR) light with the wavelengths up to 1 μm [7]. Recent effort of chemists, however, resulted in development of a new series of donor-acceptor and donor-acceptor-donor D-π-A-π-D NIR compounds whose absorption can be tuned within the wavelength region of 0.6–1.4 μm [7]. Even more exciting examples include donor-acceptor covalently linked compounds of tetrathiafulvalene-tetracyanoquinodimethane (TTF-σ-TCNQ), fused porphyrin ribbons and TTF-dithiolato metal complexes, which demonstrate the absorption spectra extended to the middle-IR with the absorption maxima at 1.6, 2.9, and 4.6 μm, respectively, where the thermo-excited electron transfer has been observed experimentally [8]. Great opportunity can be expected also from the carbon materials and particularly graphene [9] which has a zero band gap and, therefore, can absorb photons from the whole IR range. Thus, design of energy converters based on organic molecules which combine high stability and electronic absorption extended to the middle and far IR is an exciting and challenging problem.

The second class of materials to be used for IR absorption is gapless or narrow-gap semiconductors whose band gap is smaller than 1 eV (equivalent to ~0.8 μm). Many of semiconductors, such as InSb (0.17 eV), InAs (0.36 eV), PbSe (0.82 eV), PbTe (0.31 eV) have the band gap values (shown in parenthesis) that allow them to absorb in the near-IR range. However, there are few candidates, i.e., HgSe, HgTe, which can collect energy from the middle IR range also. These last compounds, however, are toxic, and their application, therefore, are to be restricted. Nevertheless, development of these materials in the form of colloidal particles [10] packed in the inert matrix might overcome this problem. The advantages of the nanoparticle application also will give the opportunity to tune the range of absorption by simple change of the particle size.

The above types of the IR receivers produce an electron-hole pair upon absorption of an IR quantum. Their advantage as compared with the solar cells operating in the visible spectrum is that the amount of IR quanta is much larger as compared with the quanta of visible light (see Fig.2); therefore, the IR devices can potentially collect more quanta and produce a larger amount of electron-hole pairs as compared with the conventional solar cells. On the other hand, the devices which can respond in the middle and far IR still should be developed to collect quanta from a more extended spectral range.

The third class of materials perspective for harvesting IR radiation is thermoelectric materials. The thermoelectric energy conversion unit normally consists of two different (n- and p-type) semiconducting materials connected together in the form of a thermocouple; these materials are now actively developed [11], although some skepticism concerning their perspective in the energy solution domain exists [12]. It should be noted that the advantage of thermoelectric devices is that these can consume IR energy of practically all wavelengths and they do not have a quantum threshold restriction from which the device becomes active. However, a sufficiently large thermal gradient is needed for their effective work.

It is a question which part of the IR spectrum is most suitable to consume. If, for example, the corresponding devices will collect IR energy which normally leaves the Earth through the transparency window of the atmosphere (i.e., within the wavelength range of 8-13 μm) their work can promote the increase in the temperature regime at the earth surface. On the other

hand, if the IR converters will collect energy in the region of absorption of greenhouse gases and scatter it in the transparency window, their work can weaken the green-house effect and decrease the temperature, respectively. Therefore, the use of the above converters could help in controlling the climate regimes. However, such effects, if any, can be expected only if the converters of IR energy are applied on the large scale.

4. Conclusions

The energy consumption rate limit should be set as a necessary concept in the near future to conserve thermodynamic balance on the Earth. Such a limit, if based on the major production of energy through burning of organic fuel, has been shown to exceed the contemporary rate of energy consumption by approximately one order of magnitude and can be reached in the next 60 years. Consumption of direct solar energy and reemitted IR radiation from the Earth-atmosphere system on the large scale can somewhat extend the above limit. Optimistic estimates above show that use of the direct solar energy can double this limit. There is no estimate at the moment how much terrestrial radiation can be consumed, since the respective energy converters are at the beginning of their development. It is known, however, that power conversion efficiency of thermoelectric devices is of the order of few percents [12]. The same order of magnitude is typical for the best photovoltaic cells based on organic materials, therefore, it can be expected the same value for power conversion efficiency of the best organic IR converters also. Taking into account some advantages of the IR energy converters discussed above we can suppose very tentatively that their use on the large scale might yield another portion of energy of the order of 10^{14} W. Thus, the overall increase of the total limit of the renewable energy production rate can be very modest, being within 10^{14}-10^{15} W range. Therefore, the necessary political and economical steps should be undertaken towards the necessity of the energy consumption constraint to keep the living conditions on the Earth constant.

References

[1] R. Heinberg, D. Fridley, The end of cheap coal, Nature 468, 2010, pp. 367-369.

[2] S.K. Aggarwal, A.K. Gupta, D.G. Lilley, Terrestrial energy, Aerospace America, Dec. 2006, p.70.

[3] C.G. Abbot, Terrestrial temperature and atmospheric absorption, Proc. Natl. Acad. Sci. USA 4, 1918, pp. 104-106.

[4] V.V.Alexeev, K.V.Chekarev, Solar energetics, Nauka, 1991, 60 p.

[5] K.Ya. Kondratyev, I. Galindo, Contemporary stage of civilization development and its perspectives, Univ. of Colima Press, 2002, 139 p.; K. Ya. Kondratyev, I. Galindo, Global change situation: today and tomorrow, Univ. of Colima Press, 2002, 164 p; K.Ya.Kondratyev, Key aspects of global climate change, Energy and Environment 15, 2004, pp. 467-501.

[6] Demographia world urban areas & population projections: Edition 6.1, July 2010, pp.1-128 (www.demographia.com/db-worldua.pdf).

[7] G. Qian, Z. Y. Wang, Near-infrared organic compounds and emerging applications, Chem. Asian J. 5, 2010, pp. 1006–1029.

[8] D. F. Perepichka, M. R. Bryce, Molecules with exceptionally small HOMO–LUMO gaps, Angew. Chem. Int. Ed. 44, 2005, pp. 5370–5373.

[9] J.M. Dawlaty, S. Shivaraman, J. Strait, P. George, M. Chandrashekhar, F. Rana, M.G. Spencer, D. Veksler, Y. Chen, Measurement of the optical absorption spectra of epitaxial graphene, Appl. Phys. Lett. 93, 2008, 13195.

[10] M. T. Harrison, S. V. Kershaw, M. G. Burt, A. L. Rogach, A. Kornowski, A. Eychmüller, and H. Weller, Colloidal nanocrystals for telecommunications. Complete coverage of the low-loss fiber windows by mercury telluride quantum dots, Pure Appl. Chem. 72, 2000, pp. 295-307.

[11] J.F. Li, W.S. Liu, L.D. Zhao, M.Zhou, High-performance nanostructured thermoelectric materials, NPG Asia Mater. 2, 2010, pp. 152-158.

[12] C.B.Vining, An inconvenient truth about thermoelectrics, Nature Mater., 8, 2009, pp. 83-85.

Effective Urban Energy Planning and Governance: A New Conceptual Framework

Yosef R. Jabareen[1*]

[11] *Technion – Israel Institute of Technology, Haifa, Israel*
** Corresponding author. Tel: +922 52865336, Fax: +972 48294617, E-mail:jabareen@technion.ac.il*

Abstract: Beyond any doubt *climate change* and its resulting uncertainties challenge the concepts, procedures, and scope of conventional approaches to the planning of our cities. Thus, demanding from us to situate the energy issue in the central when planning urban spaces. Yet, the literature is vague in the context of urban energy, and there is a lack of a theoretical framework that conceptualizes urban energy planning. Therefore, the aim of this paper is to propose a new multifaceted conceptual framework for theorizing urban energy planning based on multidisciplinary literature. Eventually, this study elaborates a conceptual framework that consists of eight concepts that were identified through a conceptual analysis of interdisciplinary literature on sustainability, climate change, ecology, economics, and urban planning. These concepts, which together constitute the theoretical framework of urban energy planning for climate change, are: *Utopian Vision*, *Equity*, *Uncertainty*, *Natural Capital*, *Eco-Form*, *Integrative Approach*, *Ecological Energy*, and *Ecological Economics*.

Keywords: *Urban Planning, Energy, Theory, Conceptual Framework*

1. Introduction

Climate change poses new risks and uncertainties that often lie outside our range of experience (IPCC, 2007: 719) and that have the potential to affect the social, economic, ecological, and physical systems of any given city. In this way, climate change and its resulting uncertainties challenge the concepts, procedures, and scope of conventional approaches to city planning, creating a need to rethink and revise current approaches. Decisively, it demands from us to situate the energy issue in the central when planning urban spaces. Yet, a striking weakness of the scholarship on the subject is its lack of multifaceted theorizing and the fact that it typically overlooks the multidisciplinary and complex nature of urban energy planning. Moreover, the literature is vague in the context of urban energy, and there is a lack of a theoretical framework that conceptualizes urban energy planning. Therefore, the aim of this paper is to propose a new multifaceted conceptual framework for theorizing urban energy planning based on multidisciplinary literature.

2. Methodology

A *conceptual analysis method* was used to build the conceptual framework (Jabareen 2009). This method is a grounded theory technique that aims "to generate, identify, and trace a phenomenon's major concepts, which together constitute its theoretical framework" (Jabareen 2009). Each concept possesses its own attributes, characteristics, assumptions, limitations, distinct perspectives, and specific function within the conceptual framework. The methodology delineates the following stages in conceptual framework building: a) mapping selected data sources; b) reviewing the literature and categorizing the selected data; c) identifying and naming the concepts; d) deconstructing and categorizing the concepts; e) integrating the concepts; f) synthesis, resynthesis, and making it all make sense; g) validating the conceptual framework; and h) rethinking the conceptual framework (Jabareen 2009).

3. Results

The Concepts of the Conceptual Framework

The conceptual framework is composed of eight concepts (see Jabareen, 2006), as Fig1 shows. These concepts are:

a. Utopian Vision: This concept is concerned with a plan's future vision. Usually, urban planning seeks to bring about a different and more desirable future. Theoretically, the power of visionary or utopian thinking lies in its inherent ability to envision the future in terms of radically new forms and values (de Geus, 1999). An urban vision incorporating climate change as a central theme is of the utmost importance to practitioners, decision makers, and the public. Visionary frames are important in climate change, as they serve to identify problematic conditions and the need for change, to propose future alternatives, and to urge all stakeholders to act in concert to affect change. Climate change planning visions must provide people with an interpretive framework that enables them to understand how the issue is related to their own lives in the present and future, and to the world at large (Taylor, 2000; Benford and Snow, 2000: 614). This concept addresses the visionary and utopian aspects regarding future urban life, the city's potential role in climate change mitigation, and the city vision regarding energy production and consumption as well.

b. Equity: Equity is a key concept in evaluating climate change policies (IPCC, 2001). The impacts of climate change and climate change mitigation policies are "socially differentiated," and are therefore matters of local and international distributional equity and justice (Adger, 2001: 929; O'Brien et. al., 2004; Paavola et al., 2006). Some argue that inequality leads to greater environmental degradation and that a more equitable distribution of power and resources would result in improved environmental quality (Boyce et al. 1999; Agyeman et al., 2002; Solow 1991, Stymne and Jackson, 2000). Moreover, there are individuals and groups within all societies who are more vulnerable than others and lack the capacity to adapt to climate change (IPCC, 2007: 719). A society's vulnerability is influenced by its development path, physical exposure, resource distribution, social networks, government institutions, and technological development (, 2007: 719-720). The concept of equity addresses social aspects, including: environmental justice; public participation; and methods of addressing each community's vulnerability to climate change (urban vulnerability matrix).

c. Uncertainty Management: Uncertainty "is a perceived lack of knowledge, by an individual or group, which is relevant to the purpose or action being undertaken and its outcomes" (Abbot, 2009: 503). The new urban uncertainties posed by climate change challenge the concepts, procedures, and scope of planning. In order to cope with the new challenges, planners must develop a greater awareness and place mitigation and policies for "adaptation," or actual adjustments that might eventually enhance resilience and reduce vulnerability to expected climate changes, at the center of the planning process (Adger et. Al., 2007: 720). Planners must also develop a better understanding of the risks climate change poses for infrastructure, households, and communities. To address these risks, planners have two types of uncertainty or adaptation management at their disposal: 1) Ex-ante management, or actions taken to reduce and/or prevent risky events; and 2) Ex-post management, or actions taken to recover losses after a risky event (Heltberg et al., 2009).

d. Natural Capital: Natural capital refers to "the stock of all environmental and natural resource assets, from oil in the ground to the quality of soil and groundwater, from the stock of fish in the ocean to the capacity of the globe to recycle and absorb carbon" (Pearce et. al., 1990: 1). Maintaining constant natural capital is an important criterion for sustainability

(Pearce and Turner, 1990: 44; Geldrop and Withagen, 2000). The stock of natural capital should not decrease, as this could endanger the ecological system and threaten the ability of future generations to generate wealth and maintain their well-being. This concept addresses the consumption and - equally as important - the renewal of natural assets that are used for development, such as land, water, air, and open spaces.

***e. Integrative Approach*:** Planning for climate change is more complex than the conventional approach to planning as it is undertaken in a context of great uncertainty. This context poses new challenges for collaboration among public, private, and civil institutions and organizations on all levels. Integrating the many different stakeholders and agents into planning is essential for achieving climate change objectives. The "ability of a governance system to adapt to uncertain and unpredicted conditions is a new notion" (Mirfenderesk and Corkill, 2009: 152). Therefore, adaptive management requires new planning strategies and procedures that transcend conventional planning approaches by integrating uncertainties into the planning process and prioritizing stakeholders' expectations in an uncertain environment. Plans should also be "flexible enough to quickly adapt to our rapidly changing environment" (Mirfenderesk and Corkill, 2009).

***f. Ecological Energy*:** The clean, renewable, and efficient use of energy is a central theme in planning for the achievement of climate change objectives. This concept evaluates how a plan addresses the energy sector and whether it proposes strategies to reduce energy consumption and to use new, alternative, and clean energy sources.

***g. Ecological Economics*:** This concept is based on the assumption that environmentally sound economics can play a decisive role in achieving climate change objectives in a capitalist world. Cities that are committed to climate change mitigation and sustainability should stimulate markets for 'green' products and services, promote environmentally friendly consumption, and contribute to urban economic development by creating a cleaner environment (Hsu, 2006: 11; Mercer Human Resources Consulting, 2005). In this spirit, the American Recovery and Reinvestment Plan, proposed by President Barack Obama, calls for spurring "job creation while making long-term investments in energy, and infrastructure," and increasing "production of alternative energy" (White House, 2009).

h. Eco-Form: The physical form of a city affects its habitats and ecosystems, the everyday activities and spatial practices of its inhabitants, and, eventually, climate change. This concept evaluates spatial planning, architecture, design, and the ecologically-desired form of the city and its components (such as buildings and neighborhoods). Jabareen (2006) suggests the following set of nine planning typologies, or criteria of evaluation, which are helpful in evaluating plans from the perspective of eco-form as follows:

Compactness refers to urban contiguity and connectivity and suggests that future urban development should take place adjacent to existing urban structures (Wheeler, 2002). Compact urban space can minimize the need to transport energy, materials, products, and people (Elkin et. al., 1991). Intensification, a major strategy for achieving compactness, uses urban land more efficiently by increasing the density of development and activity, and involves: developing previously undeveloped urban land; redeveloping existing buildings or previously developed sites; subdivisions and conversions; and additions and extensions (Jenks, 2000: 243).

Sustainable Transport suggests that planning should promote sustainable modes of transportation through traffic reduction; trip reduction; the encouragement of non-motorized travel (such as walking and cycling); transit-oriented development; safety; equitable access for all; and renewable energy sources, (Cervero, 2003; Clercq and Bertolini, 2003).

Density is the ratio of people or dwelling units to land area. Density affects climate change through differences in the consumption of energy, materials, and land for housing, transportation, and urban infrastructure. High density planning can save significant amounts of energy (Carl, 2000; Walker and Rees, 1997; Newman and Kenworthy, 1989).

Mixed Land Uses indicates the diversity of functional land uses, such as residential, commercial, industrial, institutional, and transportation. It allows planners to locate compatible land uses in close proximity to one another in order to decrease the travel distance to between activities. This encourages walking and cycling and reduces the need for car travel, as jobs, shops, and leisure facilities are located in close proximity of one another (Parker, 1994; Alberti, 2000; Van and Senior, 2000; Thorne and Filmer-Sankey, 2003).

Diversity is "a multidimensional phenomenon" that promotes other desirable urban features, including a larger variety of housing types, building densities, household sizes, ages, cultures, and incomes (Turner and Murray, 2001: 320). Diversity is vital for cities. Without it, the urban system declines as a living place (Jacobs 1961) and the resulting homogeneity of built forms, which often produces unattractive monotonous urban landscapes, leads to increased segregation, car travel, congestion, and air pollution (Wheeler, 2002).

Passive Solar Design aims to reduce energy demands and to provide the best use of passive energy through specific planning and design measures, such as orientation, layout, landscaping, building design, urban materials, surface finish, vegetation, and bodies of water. This facilitates optimum use of solar gain and microclimatic conditions and reduces the need for the heating and cooling of buildings by means of conventional energy sources (Owens, 1992; Thomas, 2003; Yannis, 1998: 43).

Greening, or bringing "nature into the city," makes positive contributions to many aspects of the urban environment, including: biodiversity; the lived-in urban environment; urban climate; economic attractiveness; community pride; and health and education (Beatley 2000; Swanwick et al., 2003; Forman, 2002; Dumreicher et al., 2000; Beer et. al.,, 2003; Ulrich, 1999).

Renewal and Utilization refers to the process of reclaiming the many sites that are no longer appropriate for their original intended use and can be reclaimed for a new purpose, such as brownfields. Cleaning, rezoning, and developing contaminated sites are key aspects of revitalizing cities and neighbourhoods and contribute to their sustainability and to a healthier urban environment.

Planning Scale influences and is influenced by climate change. For this reason, desirable planning scale should be considered and integrated in plans for regional, municipal, district, neighbourhood, street, site, and building levels. Planning that moves from macro to micro levels has a more holistic and positive impact on climate change.

4. Discussion and/or Conclusions

The *conceptual framework* is not a mere collection of concepts. Rather, all concepts are interrelated and interwoven with one another; each plays an important role in the framework as a whole. The conceptual framework consists of eight concepts of assessment that were identified through conceptual analyses of interdisciplinary literature on sustainability and climate change. Together, these concepts – each of which represents a distinctive aspect of urban energy planning - form the conceptual framework. Importantly, each concept contributes to the planning of urban energy in its domain. The positive contribution o all concepts together will lead to effective urban energy governance. The overlooking of one concept or more will cause various negative externalities to climate change.

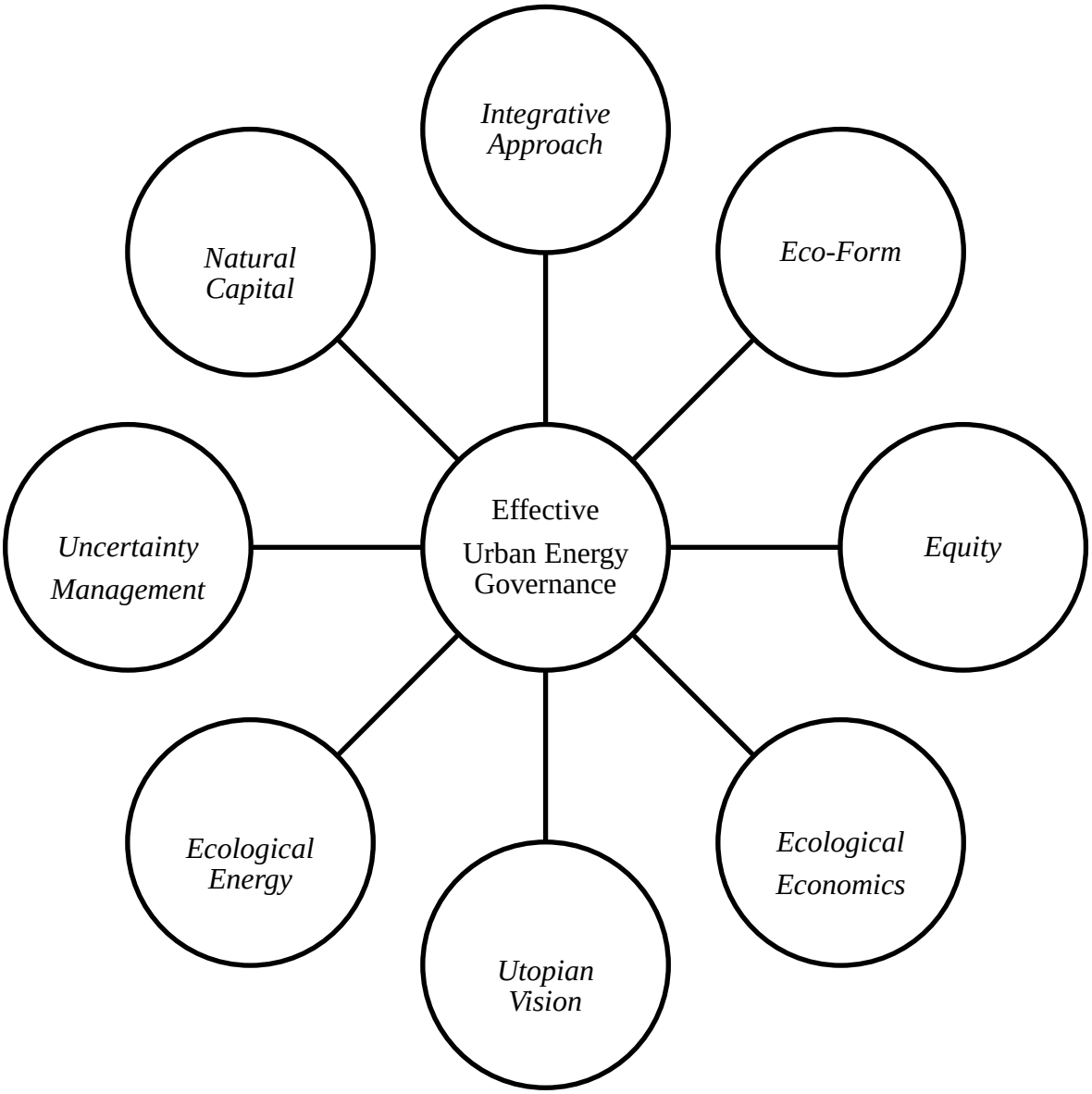

Fig. 1 Conceptual framework for urban energy.

References

[1] IPCC - S.H. Schneider, S. Semenov, A. Patwardhan, I. Burton, C.H.D. Magadza, M. Oppenheimer, A.B. Pittock, A. Rahman, J.B. Smith, A. Suarez and F. Yamin, Assessing key vulnerabilities and the risk from climate change. Climate Change 2007: Impacts,

Adaptation and Vulnerability. Contribution of Working Group II to the Fourth Assessment Report of the Intergovernmental Panel on Climate Change, M.L. Parry, O.F. Canziani, J.P. Palutikof, P.J. van der Linden and C.E. Hanson, Eds., Cambridge University Press, Cambridge, UK, 2007, pp. 779-810.

[2] Y. Jabareen, Building Conceptual Framework: Philosophy, Definitions and Procedure, International Journal of Qualitative Methods, Vol 8(4), 2009, pp. 49-62.

[3] Y. Jabareen, Sustainable Urban Forms: Their Typologies, Models, and Concepts, Journal of Planning Education and Research, Vol. 26 (1), 2006, pp. 38-52.

[4] M. de. Geus, Ecological Utopias: Envisioning the Sustainable Society. Utrecht: International Books, 1999.

[5] D. E. Taylor, The Rise of the Environmental Justice Paradigm: Injustice Framing and the Social Construction of Environmental Discourses American Behavioral Scientist 43, 2000, pp. 508-580.

[6] Benford Robert D. and Snow David A. 2000. Framing Processes and Social Movements: An Overview and Assessment. *Annual Review of Sociology*, Vol. 26: 611-639

[7] IPCC.Third Assessment Report: Climate Change 2001 (TAR).

[8] W.N Adger,. S. Agrawala, M.M.Q. Mirza, C. Conde, K. O'Brien, J. Pulhin, R. Pulwarty, B. Smit and K. Takahashi, Assessment of adaptation practices, options, constraints and capacity. Climate Change 2007: Impacts, Adaptation and Vulnerability. Contribution of Working Group II to the Fourth Assessment Report of the Intergovernmental Panel on Climate Change, M.L. Parry, O.F. Canziani, J.P. Palutikof, P.J. van der Linden and C.E. Hanson, Eds., Cambridge University Press, Cambridge, UK, 2007, pp. 717-743.

[9] R. O'Brien, Leichenko, U. Kelkar, H. Venema, G. Aandahl, H. Tompkins, A. Javed, S. Bhadwal, A. Barg, L.P. Nygaard and J. West, Mapping vulnerability to multiple stressors: climate change and globalization in India, Global Environmental Change 14, 2004, pp. 303–313.

[10] J. Paavola, and Adger W. Neil, Fair adaptation to climate change. Ecological Economics. Volume 56, Issue 4, 2006, pp. 594-609.

[11] J.K. Boyce, Klemer, A.R., Templet, P.H. and Willis, C.E, Power distribution, the environment, and public health: a state-level analysis. Ecological Economics. 29, 1, 1999, pp. 127–140.

[12] J. Agyeman, Bullard, R. D., & Evans, B. Exploring the nexus: Bringing together sustainability, environmental justice and equity. Space & Polity, Vol 6(1), 2002, pp. 77-90.

[13] R. Solow, Sustainability: An Economist's Perspective. The Eighteenth J. Seward Johnson Lecture. Woods Hole, MA: Woods Hole Oceanographic Institution, 1999.

[14] J. Abbott. Planning for complex metropolitan regions: A better future or a more certain one? Journal of Planning Education and Research, vol.28, 2009, 503-517.

[15] W.N. Adger, Scales of governance and environmental justice for adaptation and mitigation of climate change. Journal of International Development, Vol. 13(7), 2001, pp. 921-931.

[16] R. Heltberg, Paul Bennett Siegel, Steen Lau Jorgensen. 2009. Addressing human vulnerability to climate change: Toward a 'no-regrets' approach. Global Environmental Change, 19, 2009, pp. 89–99.

[17] D. Pearce, Edward, Barbier., and Anil Markandya. Sustainable development: Economics and environment in the Third World. London: Earthscan Publications, 1990.

[18] Geldrop, J. and C. Withagen, Natural capital and sustainability. *Ecological Economics*, Vol. 32 (3), 2000, pp. 445-455.

[19] H. Mirfenderesk and Corkill David, Sustainable management of risks associated with climate change. *International Journal of Climate Change Strategies and Management*, Vol. 1(2), 2009, pp.146-159.

[20] D. Hsu David, *Sustainable New York City.* New York City: Design Trust for Public Space and the New York City Office of Environmental Coordination, 2006.

[21] Mercer Human Resources Consulting, Quality of Living Survey: New York City. Private communication, 2004.

[22] White House http://www.whitehouse.gov/issues/Economy; see also http://www.recovery.gov/Pages/home.aspx, 2009.

[23] S. Wheeler, Stephen. M. Constructing sustainable development/safeguarding our common future: Rethinnking sustainable development. *Journal of the American Planning Association* 68:1, 2002, pp. 110-111.

[24] T. Elkin, McLaren, Duncan, and Hillman, Mayer, *Reviving the city: Towards sustainable urban development*, Friends of the Earth, London, 1991.

[25] M. Jenks, The acceptability of urban intensification. In *Achieving sustainable urban form*, edited by Williams K., Burton E., and Jenks M., London: E & FN SPON, 2000.

[26] S. Owens, Energy, environmental sustainability and land-use planning. In *Sustainable development and urban form*, edited by Michael, Breheny. London: Pion, 1992, pp. 79-105,

[27] R. Cervero, RobertCoping with Complexity in America's Urban Transport Sector. *The 2nd International Conference on the Future of Urban Transport*, Göteborg, Sweden, 2003.

[28] F. Clercq, and L. Bertolini, Achieving sustainable accessibility: An evaluation of policy measures in the Amsterdam area. *Built Environment* 29:1, 2003, pp. 36-47.

[29] P. Carl, Urban density and block metabolism. In *Architecture, city, environment. Proceedings of PLEA 2000*, edited by Steemers Koen and Simos Yannas, London: James & James, 2000, pp. 343-347.

[30] L. Walker, and Rees William. Urban density and ecological footprints – An analysis of Canadian households. In *Eco-city dimensions: Healthy communities, healthy planet*, edited by Roseland Mark, New Society Publishers, 1997.

[31] P. Newman, and Kenworthy, J. Gasoline consumption and cities: a comparison of US cities with a global survey. *Journal of the American Planning Association* 55, 1989, pp. 23-37.

[32] T. Parker, *The land use—air quality linkage: How land use and transportation affect air quality*. Sacramento: California Air Resources Board. 1994.

[33] Alberti, M. (2000) Urban form and ecosystem dynamics: Empirical evidence and practical implications. In *Achieving sustainable urban form*, edited by Williams K., Burton E., and Jenks M., London: E & FN Spon. 2000, pp. 84-96.

[34] Van Uyen-Phan and Martyn Senior. The contribution of mixed land uses to sustainable travel in cities. In *Achieving sustainable urban form*, edited by Williams K., Burton E., and Jenks M., London: E & FN Spon, 2000, pp. 139-148.

[35] R. Thorne, and William, Filmer-Sankey, Transportation. In *Sustainable urban design*, edited by Thomas Randall, 25-32, London: Spon Press, 2003.

[36] S. R. Turner S. and Margaret. S. Murray, Managing growth in a climate of urban diversity: South Florida's Eastward ho! Initiative. Journal of Planning Education and Research 20, 2001, 308-328

[37] J. Jacobs, Jane, The death and life of great American cities, New York: Random House, 1961.

[38] R. Thomas, Building design. Sustainable urban design: An environmental approach, edited by In Thomas R. and Fordham M., 46-88, London: Spon Press, 2003.

[39] S. Yanns, Living with the city: Urban design and environmental sustainability. In Environmantly friendly cities, edited by Maldonado Eduardo and Simon Yannas, 41-48, London: James & James, 1998.

[40] T. Beatley, Green urbanism: Learning from European cities. Washington, D.C.: Island Press, 2000.

[41] C. Swanwick, , Nigel Dunnett., and Helen Woolley, Nature, role and value of green space in towns and cities: An overview, Built Environment 29:2, 2003, pp. 94-106.

[42] R. T. Forman, Richard, The missing catalyst: Design and planning with ecology. In Ecology and design: Frameworks for learning, edited by Johnson Bart T. and Hill Kristina, Washington, DC: Island Press, 2000.

[43] H. Dumreicher, Heidi, L. Richard S., and Yanarella, Ernest J, The appropriate scale for "low energy": Theory and practice at the Westbahnhof. In Architecture, city, environment. Proceedings of PLEA 2000, edited by Steemers Koen and Simos Yannas, London: James & James. 2000, pp. 359-363.

[44] A. Beer, T. Delshammar, and P. Schildwacht, A changing understanding of the role of greenspace in high-density housing: A European perspective. Built Environment, 29:2, 2003, pp. 132-143.

[45] R. S. Ulrich, Roger, Effects of gardens on health outcomes: theory and research, in Healing gardens: Therapeutic benefits and design recommendations, edited by Marcus, Clare Cooper. and Marni Barnes., New York: Whiley, 1999.

Simple Statistical Model for Complex Probabilistic Climate Projections: Overheating Risk and Extreme Events

Sandhya Patidar[1,*], David Jenkins[2], Phil Banfill[2], Gavin Gibson[1]

[1] *Maxwell Institute for Mathematical Sciences , School of Mathematical and Computer Sciences, Heriot-Watt University, Edinburgh, UK*
[2] *Urban Energy Research Group, School of Built Environment (address as above)*
* *Corresponding author. Tel: +44 1314514365, E-mail: S.Patidar@hw.ac.uk*

Abstract: Climate change could substantially impact the performance of the buildings in providing thermal comfort to occupants. Recently launched UK climate projections (UKCP09), clearly indicate that all areas of the UK will get warmer in future with the possibility of more frequent and severe extreme events, such as heat waves. This study, as part of the Low Carbon Futures (LCF) Project, explores the consequent risk of overheating and the vulnerability of a building to extreme events. A simple statistical model proposed by the LCF project elsewhere has been employed to emulate the outputs of the dynamic building simulator (ESP-r) which cannot feasibly be used itself with thousands of available probabilistic climate database. Impact of climate change on the daily external and internal temperature profiles has been illustrated by means of 3D plots over the entire overheating period (May - October) and over 3000 equally probable future climates. Frequency of extreme heat events in changing climate and its impact on overheating issues for a virtual case study domestic house has been analyzed. Results are presented relative to a baseline climate (1961-1990) for three future timelines (2030s, 2050s, and 2080s) and three emission scenarios (Low, Medium, and High).

Keywords: *Probabilistic climate projections, Building and Adaptation, Overheating*

1. Introduction

Experiments based on an advanced scientific methodology and general circulation models (GCM), commonly known as global climate models, reveal that there is an exponential increase in the global concentration of greenhouse gases [1]. According to a UK Climate Projections (UKCP09) [2] briefing report, central England's temperature has already increased by 1 ^{o}C since the 1970s and this increase is most likely due to anthropogenic emission of greenhouse gases [3]. This excessive addition of the greenhouse gasses in the atmosphere is warming up the Earth's surface causing climate change and thus altering the weather pattern. Climate change could hasten species extinction, cause coastal flooding, and lead to more frequent and severe storms and extreme temperature events such as heat waves. Such extreme temperature events could cause catastrophic losses to both human and natural systems and thereby have dramatic ecological, economic and sociological impact [3-8].

For the UK, projections for future changes to climate are provided by the UK Climate Projections (UKCP09) and are available in probabilistic format to address the uncertainty associated with future climate change. To include a measure for the uncertainty, these climate projections are generated by multiple simulations of global climate models (in particular HadCM3 [9]) combined with a new methodology designed by the Met Office. The projections also include the results of other IPCC [1] climate models, and are constrained by observations of past climate. Thus to describe just any single future climate scenario a range (in fact thousands) of possible climates are available where each climate has a certain probability of occurring.

Extreme events, by definition, are in the tails of such probability distributions. Interestingly, events in the tail of the distribution are the ones that change most in frequency of occurrence as the distribution shifts due to global warming [10-11]. The work presented in this paper will

focus on the potential impact of future climate changes on the frequency of the extreme temperature regimes (heat wave) and how this could influence the overheating issues in the UK's domestic house sectors.

The suite of probabilistic climates projection available from UKCP09 for a London location at three future timelines, namely 2030's, 2050s, and 2080s, including a baseline [1960-1990] has been carefully analyzed to quantify the future change in the frequency of extreme heat events. The impact of extreme heat events on indoor comfort temperatures of a domestic building case study has been assessed by means of a simple statistical model proposed by the Low Carbon Futures (LCF) project [12] elsewhere [13-14]. This simple statistical tool is mainly based on multiple regression techniques and could efficiently emulate the outputs of traditional dynamics building simulation software ESP-r [15], which cannot be practically used with thousands of potential climates available for each future scenario.

This project is sponsored by the Adaptation and Resilience in a Changing Climate (ARCC) Programme [16], looking at possible methods, i.e. adaptations, for coping with a future climate.

2. Methodology

To analyze complex probabilistic climate information and to generate corresponding indoor temperature profiles for a case study dwelling, an elegant regression tool has been developed by the LCF project which is described in detail elsewhere [14]. The simple regression tool which is based on data reduction methods such as Principal Component Analysis (PCA) and multiple regressions is validated at an hourly scale to provide a close match (within a range of 1 °C) for the outputs of dynamic building simulation software (ESP-r). More details on the development procedure of the regression tool are found elsewhere [13].

This section should present a brief description of probabilistic climatic information available from UKCP09, profiles of the domestic building case study simulated with ESP-r, and a short note on the regression tool which has been employed to emulate outputs of ESP-r for quantifying extreme heat events and its impact on overheating issues in the case-study building. A short review on the possible definitions of the heat wave is also included.

2.1. Probabilistic Climate Projections and Regression Tool

The UKCP09 provides climate change information focused on the UK. The projections are presented for seven 30 years time periods ("2020s" denoting as 2010 – 2039, "2030s" denoting 2020 – 2049, … , up to "2080s" denoting 2070 - 2099), and at three different future greenhouse gas emissions scenarios represented as "High", "Medium" and "Low". These projections are based on change relative to a baseline time period (1961–1990) and, by means of a *Weather Generator* (WG) [17] tool, are available at an hourly temporal resolution with a 5×5 km^2 spatial resolution for any user defined UK location.

For the work presented in this article, climatic information has been downloaded from UKCP09's WG tool for a London location corresponding to all three greenhouse gas emissions scenarios and at three future time periods, namely 2030s, 2050s and 2080s, including baseline. Notably for any user specified future scenario, the WG tool could provide at least 3000 equally probable hourly climate files (each climate file represents a prototype climate year for that scenario) in the form of 100 statistically equivalent time series, where each of the time series is equally probable and of 30 years in length. For each of the future scenarios under investigation a representative sample of 100 climate years is formed by means

of a random sampling algorithm, which selects one year randomly from each of the 100 time series.

To formulate the regression tool, a 3-bedroom cavity-wall house with a total floor area of 144 m^2 has been simulated with ESP-r for one randomly chosen climate file from the 100 available climate years (additional information on the virtual case study building can be found elsewhere [18]). The regression tool is based on the concept of underpinning the existing relationship between available climate variants and the indoor temperatures, where each climate variant first need to be carefully analyzed and simplified by means of PCA. The model has been formulated to capture indoor temperature profiles during the period of May to October only. To allow time-based sensitivity analysis, the idea of segmented modelling has been applied and data fitted in parts, namely a) May – June; b) July-August; and c) September – October, to cover the entire period (May-October) [13].

A regression tool which could be formulated from the one climate file had been validated across all the available 100 climates files and corresponding to all different future scenarios as described above. Moreover, the proposed statistical regression tool has been demonstrated to efficiently estimate the outputs of ESP-r at an hourly scale within a single degree centigrade for up to 90% of the entire data set [13-14]. Thus, it is reasonable to consider an application of the proposed simple and efficient regression tool for quantifying frequency of heat waves and analyzing overheating issues in that context.

2.2. Heat waves and Overheating

Research conducted by Met Office clearly shows that even in the UK heat waves could be lethal, when hotter summers are predicted in foreseeable future [19]. There is no universal definition of a heat wave, however a heat wave could be considered as a prolonged period of excessively hot weather accompanied by high humidity, where temperatures are outside the normal climate pattern for that period [20]. For the UK, the Met Office defines summer heat wave duration as "***the sum of days with daily maximum temperature more than 3 °C above 1961–90 daily normal for ≥5 consecutive days (May–October)***" [21].

As stated previously, extreme events formulate tails of the probability distribution and therefore for the present study of heat waves and overheating analysis, it is essential to consider all 3000 climates corresponding to each available future scenario. An initial analysis of 3000 baseline climate files identified 15.6 ^{o}C as the daily normal temperature for 1961 – 1990. For each climate file daily normal temperature has been averaged over the overheating period and then again averaged over all equally probable 3000 climate years.

Thus, **summer heat wave duration** could be defined as – "*sum of days with daily maximum temperature more than 18.6 ^{o}C for 5 or more days during May to October*". In this context, to examine the impact of heat waves on indoor temperatures, two overheating criterion had been designed and compared with corresponding heat wave durations:
Overheating Criterion 1 - "*Sum of the days with average of night time (11pm – 7am) bedroom temperature more than 24 ^{o}C for 5 or more days during May to October*".
Overheating Criterion 2 - "*Sum of the days with average of night time (11pm – 7am) bedroom temperature more than 28 ^{o}C for 5 or more days during May to October*".

Notably, overheating Criteria 1 and 2 are designed by the author and are mainly motivated from the Met Office definition of summer heat wave in order to compare the influence of external climates on the indoor comfort temperatures.

3. Result

Following the above definition of a heat wave and overheating criteria, some key results has been presented in this section for a London location.

3.1. External and Internal Temperatures

An analysis of external and internal temperatures are performed at an hourly scale and presented at daily scale corresponding to 3000 climate years (during summer period, May - October) by means of 3D color coded plots in Figs. 1 and 2. Climatic files have been analyzed to measure change in daily maximum external temperature and corresponding average night time (11pm – 7am) bedroom temperatures in three future time periods: 2030s, 2050s and 2080s, in relation to a baseline period for the medium emission scenario.

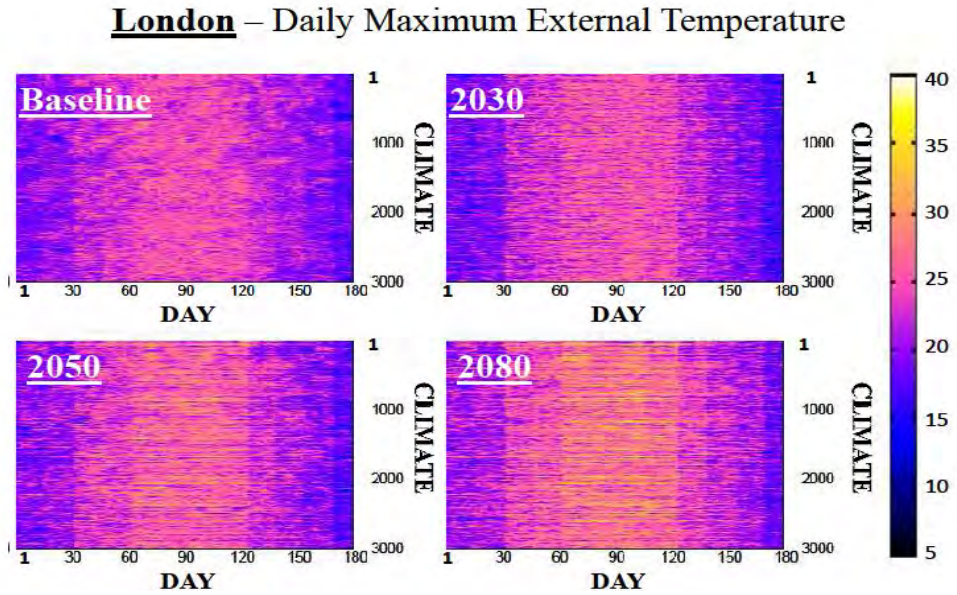

Fig. 1. Daily maximum of external temperature measured over 3000 climates for London - Medium Emission Scenario.

A visual inspection of Fig. 1 suggests that, for the baseline period daily maximum external temperature varies between 10 - 20 ^{o}C. Notably, temperatures around 10 ^{o}C could be observed as a less probable event on a distribution curve of the entire dataset, however it can be easily confirmed from the 3D plots that 10 ^{o}C is the most probable temperature for the start and end of the period i.e. May and October. During the 2030s, a temperature range of 15 - 20 ^{o}C appears to predominate, whereas during the 2050s, maximum external temperature could reach 30 ^{o}C, though less often and mainly during peak summer time (July – August). Events of maximum external temperature reaching 30 ^{o}C during peak summer period (July-August) could become more frequent in 2080s.

A simple statistical tool (as described in Section 2) has been used to reflect the changes in the averaged night time bedroom temperatures over the corresponding three future time periods: 2030s, 2050s and 2080s, in relation to the baseline period Fig. 2. Visual inspection of Fig. 2 suggests that for the baseline period the most probable average night time bedroom temperature ranges is 15 - 20 ^{o}C (May and October), 20 - 25 ^{o}C (June and September), and 25 - 27 °C (July and August). However, for the 2030s the most probable temperature range appears to be 20 - 25 ^{o}C, whereas 25 - 30 ^{o}C appear to be dominating during peak summer period (July - August). In the 2050s, the most probable temperature range still appears to be

20 - 25 °C with more probabilities, in comparison to 2030s, shifted to the temperature range 25 - 30 °C during peak summer period (July - August). The impact of climate change could further raise the probability attached to temperature ranges 25 - 30 °C in 2080s with the peak summer period (July and August) mainly dominated by the temperatures above 30 °C.

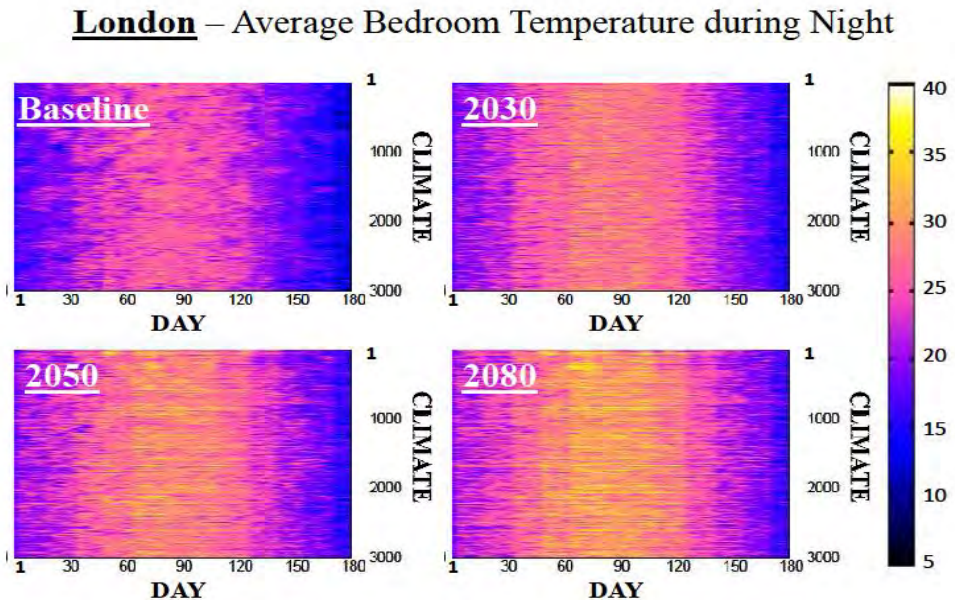

Fig. 2. Daily average of bedroom temperature during night (11pm – 7am) measured over 3000 climates for London - Medium Emission Scenario.

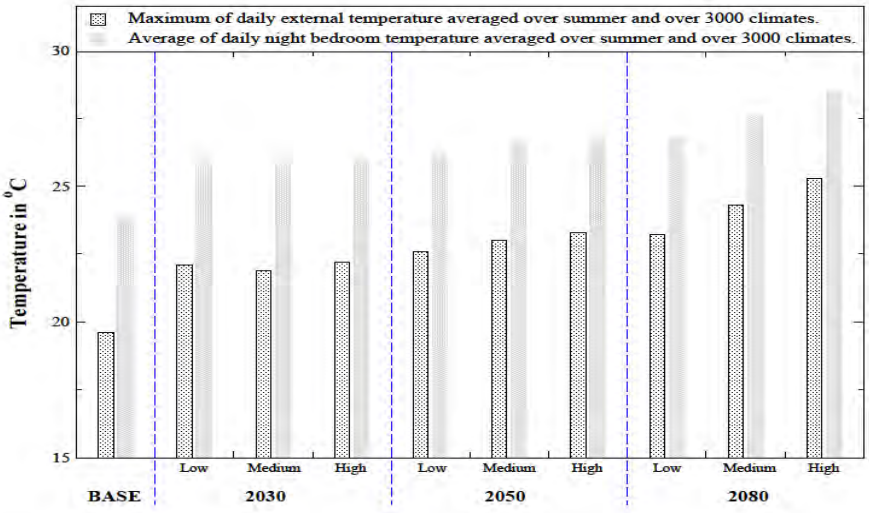

Fig. 3. Averaged daily maximum external temperature and average night bedroom temperature. Averaged over summer period and over 3000 climate years for three future time periods (2030s, 2050s, 2080s), three emission scenarios (Low, Medium, High) and baseline(1960-1990). Location: London

Finally, Fig. 3 shows the average maximum daily external temperature and corresponding average night bedroom temperature across three future time periods considered in the paper, alongside three carbon emission scenarios and the baseline period. For each scenario the average daily measurements for internal and external temperature parameters are firstly calculated over the May to October period and then over all 3000 climate years. The average of maximum daily external temperature in medium emission scenario rises to approximately 22 °C (2030s), 23 °C (2050s), and 24 °C (2080s) from 19 °C (baseline period). Average night

bedroom temperature in medium emission scenario approximately rises to 26 ^{o}C (2030s), 27 ^{o}C (2050s), and 28 ^{o}C (2080s) from 24 ^{o}C (baseline period).

3.2. Heat wave and Overheating Analysis

This subsection presents a complete analysis of summer heat wave duration and its impact on consequent overheating duration defined in criterion 1 and 2. The result has been presented across three future time periods (2030s, 2050s, and 2080s), three emission scenarios (upper panel), and the baseline period.

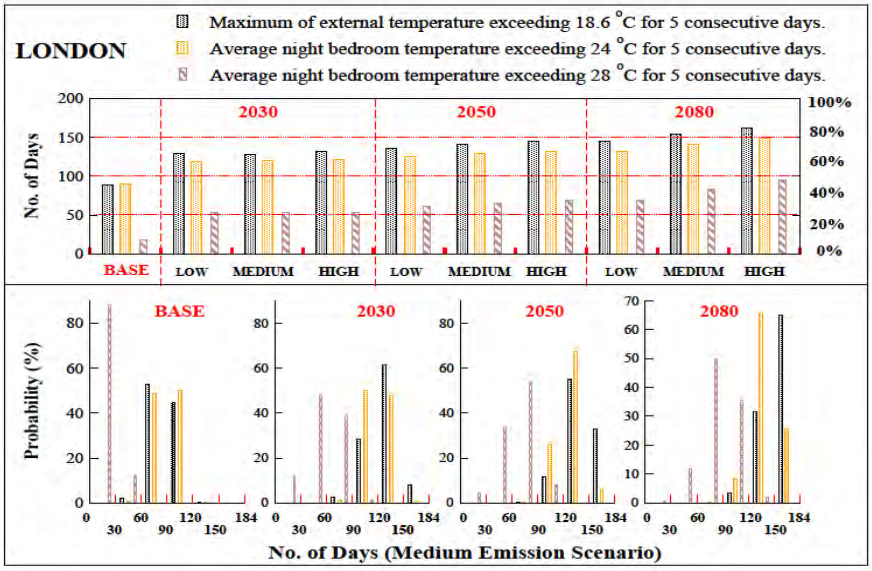

Fig. 4. Summer heat wave duration and overheating criterion 1 and 2 measured and compared. Dotted black bar: summer heat wave duration, gray (yellow online) dotted bars: overheating criterion 1, and gray (brown online) filled with slanted lines: overheating criterion 2.

In Fig. 4 the upper panel quantifies averaged (taken over 3000 climates) summer heat wave duration, overheating duration (defined in criterion 1 and 2) across all scenarios, in terms of total number of days during the identified period (May to October) along the left hand side of the *x* - axis, and in % of the May - October period along the right hand side of the *x* - axis. Dot filled black bars measure the averaged summer heat wave duration, while gray (yellow online) dotted bars measure the average duration of overheating defined under criterion 1 and gray (brown online) bars filled with slanted lines represents the average duration of overheating defined under criterion 2. Heat-wave duration and overheating duration defined in criterion 1 show similar trends in different future scenarios and, in particular, for medium emission scenario appears to rise by approximately 20 % (2030s), 30 % (2050s), and 40% (2080s) of total period in relation to baseline period. Overheating duration defined in criterion 2 increased by 15 % (2030s), 20 % (2050s), and 30 % (2080s) of total period in relation to baseline period.

Fig. 4 lower panel displays variation in summer heat wave duration, overheating duration (defined in criterion 1 and 2) across medium scenario for baseline, 2030s, 2050s and 2080s, distributed along total number of days during the period (May to October) for London - medium emission scenario. For a total of more than 90 % central probability over 3000 climates, summer heat wave duration and overheating duration defined in criterion 1 could shift from 60 - 120 days in the baseline period to 90 - 120 days in 2030s, to 90 - 184 days in 2050s, and to 120 - 184 days in 2080s. Overheating duration defined in criterion 2 could shift

from 30 - 60 days in baseline period to 30 - 90 days in 2030s, to 60 - 90 days in 2050s, and to 90 - 120 days in 2080s.

4. Discussion and Conclusions

This study presents an application of the simple statistical model which forms part of a methodology proposed by the Low Carbon Futures project to integrate future climate projections into building design and simulation. The statistical model presented in the form of a simple linear predictor has been used to describe the influence of climate change on the pattern of extreme heat events and its impact on the indoor comfort temperatures for a simple domestic building case study. Heat-wave duration and overheating duration defined under two distinct temperature based criteria in section 2.2 have been used as appropriate measures.

The results presented in Section 3.1 clearly illustrate the impact of climate change on the daily external and internal temperature profiles by means of 3D (color online) plots for given probabilistic climate projections. The average of maximum daily external temperature in the medium emission scenario appears to increases to 22 ^{o}C - 24 ^{o}C (2030s to 2080s) from 19 ^{o}C (baseline period), whereas average night bedroom temperature could reach 26 ^{o}C - 28 ^{o}C (2030s to 2080s) from 24 ^{o}C (baseline period).

In section 3.2 the summer heat-wave duration and overheating duration defined in criterion 1 appears to display a similar trend and up to a 20 % - 40% rise in total overheating period (2030s to 2080s) in relation to baseline period has been observed, whereas for the overheating duration defined in criterion 2 a 15% - 30% rise has been noticed. Outputs displayed in probabilistic format clearly show an increase in the total number of heat-wave duration days and overheating duration days defined in criteria 1 and 2.

Notably, the statistical model employed for overheating analyses has been demonstrated to replicate the outputs of ESP-r at an hourly scale within a single degree centigrade. The work presented in this paper could be used to develop methodologies for sustainable building design which could achieve a more acceptable level of thermal comfort in extreme climates. The effects of various adaptation techniques could be assessed to offset the predicted risk of overheating and in combating the influence of extreme events. Moreover, a range of possible climates, location and building variants could be investigated following the proposed methodology.

References

[1] IPCC, IPCC Fourth Assessment Report: Climate Change, 2007. Online at: http://www.ipcc.ch/publications and data/publications and data reports.htm

[2] J. Murphy et al., UK Climate Change Projections science report: Climate Change Projections., Technical report, Meteorological Office Hadley Centre, Exeter, UK, 2009.

[3] G. J. Jenkins, J. M. Murphy, D. M. H. Sexton, J. A. Lowe, P. Jones, and C. G. Kilsby, UK Climate Projections: Briefing report, Met Office Hadley Centre, Exeter, UK (2009). Online at: http://ukclimateprojections.defra.gov.uk/images/stories/briefing_pdfs/UKCP09_Briefing.pdf

[4] D. R. Easterling, G. A. Meehl, C. Parmesan, S. A. Changnon, T. R. Karl, and L. O. Mearns, Science 289, 2000, pp. 2068 – 2074.

[5] L. S. Kalkstein, and J. S. Greene, Environ. Health Perspect. 105, 1997, pp. 84 – 93.

[6] G. R. Walther, E. Post, P. Convey, A. Menzel, C. Parmesan, T. J. C. Beebee, J. M. Fromentin, O. Hoegh-Guldberg, and F. Bairlein, Nature 416, 2002, pp. 389 – 395.

[7] A. T. DeGaetano, Int. J. Biometeorol. 49, 2005, pp. 345 – 353.

[8] P. P. Marra, S. Griffing, C. Caffrey, A. M. Kilpatrick, R. McLean, C. Brand, E. Saito, A. P. Dupuis, L. Kramer, and R. Novak, Bioscience 54, 2004, pp. 393 – 402.

[9] Hadley centre coupled ocean atmosphere global climate model is known as HadCM3.

[10] 2010 — How Warm Was This Summer? NASA Goddard Institute for Space Studies (GISS), 28 September 2010. See also How Warm Was Summer 2010?, Research News (30 Sep 2010) from NASA GISS. Online at: http://data.giss.nasa.gov/gistemp/

[11] J. Hansen, R. Ruedy, M. Sato, and K. Lo, Global Surface temperature Change, NASA Goddard Institute for Space Studies, New York, New York, USA. Online at: http://data.giss.nasa.gov/gistemp/paper/gistemp2010_draft0803.pdf

[12] LCF, Low Carbon Future Project, 2009. Online: http://www.ukcip-arcc.org.uk/index.php?option=com contenttask=viewid=589Itemid=542

[13] S. Patidar, D. P. Jenkins, G. J. Gibson, P. F. G. Banfill, Statistical techniques to emulate dynamic building simulations for overheating analyses in future probabilistic climates, Journal of Building Performance Simulation, 1-14, iFirst article, 2011.

[14] D. P. Jenkins, S. Patidar, G. J. Gibson, P. F. G. Banfill, Incorporating future probabilistic climate projections into dynamic building simulation, Energy and Buildings, in correspondence.

[15] J. Clarke, N. Kelly, and D. Tang, A review of ESP-rs exible Solution Approach and its Application to Prospective Technical Domain Developments V1, In: Advances in Building Energy Research. UK: Earthscan, 2007, chap. 11.

[16] ARCC, Adaptation and Resilience in a Changing Climate, 2009. Homepage: http://www.ukcip-arcc.org.uk/

[17] P. D. Jones et al., UK Climate Projections science report: Projections of future daily climate for the UK from the Weather Generator, 2009. Homepage: http://ukclimateprojections.defra.gov.uk

[18] A. Peacock, D. Jenkins, and D. Kane, Investigating the potential of overheating in UK dwellings as a consequence of extant climate change. Energy Policy, 38 (7), 2010, pp. 3277 - 3288.

[19] http://www.metoffice.gov.uk/weather/uk/heathealth/

[20] P. J. Robinson, On the Definition of a Heat Wave, Journal of Applied Meteorology (American Meteorological Society) 40 (4), April 2001, pp. 762–775.

[21] M. Perry, A spatial analysis of trends in the UK climate since 1914 using gridded datasets. Climate Memorandum No. 21, Met Office, Exeter, 2006, pp. 29.

Incorporating Climate Change Projections into Building design: A Qualitative Study

Mehreen Gul*, Gill Menzies, Phil Banfill

Urban Energy Research Group, School of Built Environment, Heriot-Watt University, Edinburgh, UK
** Corresponding author. Tel: +44 1314514637, E-mail: M.Gul@hw.ac.uk*

Abstract: The UK climate of the future cannot be predicted with certainty and this is reflected in the current UK Climate Projections (UKCP09), which are probabilistic in nature. It is anticipated that the conventional approaches to building design will not adequately represent the effects of future warming and therefore guidance is required to overcome future overheating of a building by making it thermally more comfortable. The study presented here relates to a qualitative investigation and aims to draw out the needs and preferences of building design professionals to develop an easy to use formulation for adequately sizing Heating, Ventilation and Air-Conditioning (HVAC) plants. It will serve as an interface between professional building services engineers and the research team working on probabilistic weather data and a building simulation package. This investigation deploys a qualitative research approach of *Methodological triangulation*, which refers to the use of more than one method for gathering data. Herein, the three strands of research that will be used are the questionnaire, semi structured interviews and focus groups. This work is ongoing and the analysis is due for completion in 2012. This paper focuses mainly on some of the initial findings of the qualitative approaches mentioned above for domestic buildings only.

Keywords: *Qualitative investigation, Future climates, Focus groups*

1. Introduction

In the absence of formalised design requirements that take account of climate change, there is a need for pragmatic guidance on pro active design measures to ensure that the construction of new, and the refurbishment of older buildings avoids unacceptable problems or failures in the future. There has been growing concern that the trend towards hotter drier summers will lead to a reduction in the quality of the internal environment within buildings. Potentially this could lead to a wide range of health problems for occupants, and a significant deterioration in comfort conditions. In particular there is a concern that the overheating of buildings during the summer months could become an issue within the UK. [1]

The UK climate of the future cannot be predicted with certainty and this is reflected in the current UK Climate Projections (UKCP09) [2], which are probabilistic in nature. It is anticipated that the conventional approaches to building design will not adequately represent the effects of future warming and therefore guidance is required to inform adaptation decisions i.e. the adjustments required to overcome future overheating of a building by making it thermally more comfortable.

The Low Carbon Futures Project, as part of the Adaptation and Resilience to Climate Change (ARCC) programme in the UK, integrates UKCP09 into dynamic building simulation calculations [3]. The study presented here relates to a qualitative investigation and aims to draw out the needs and preferences of building design professionals to develop an easy to use formulation for adequately sizing Heating, Ventilation and Air-Conditioning (HVAC) plants. It will serve as an interface between professional building services engineers and the research team working on probabilistic weather data and a building simulation package [4]. Interaction with building professionals will ensure that the approach taken leads to a practitioner-focused rather than an academic outcome.

This work is ongoing and the analysis is due for completion in 2012. This research output enables the project team to tailor a design tool module that might potentially be integrated with existing building simulation packages to assess the overheating risk for future climates. The project is looking at domestic and non-domestic buildings but this paper is focusing only on domestic buildings and will present the results of initial qualitative investigation.

2. Methodology

A holistic overview of the HVAC building design process was undertaken. The initial questions were constructed after reviewing steps in the design process from statement of need to the final solution. The questions are based on issues of current and future overheating assessment, climate change impact, building performance metrics, adaptation techniques and probabilistic climatic data for the future. The aim was to get feedback and advice from the user community to understand the current practice of building design process and the measures required to combat changes that may occur due to changes in the future climate.

Since the project is reliant on feed-back from user groups to tailor the outcome of this project, this investigation deploys a qualitative research approach of *Methodological triangulation*, which refers to the use of more than one method for gathering data. The use of more than one approach to the investigation of a research question enhances confidence in the ensuing findings. Since much social research is founded on the use of a single research method and as such may suffer from limitations associated with that method or from the specific application of it, triangulation offers the prospect of enhanced confidence. By and large, researchers viewed the main message of the idea of triangulation as entailing a need to employ more than one method of investigation and hence more than one type of data. Social scientists are likely to exhibit greater confidence in their findings when these are derived from more than one method of investigation. Of course, the prospect is raised that the two sets of findings may be inconsistent, but such an occurrence underlines the problem of relying on just one measure or method [5].

Herein, the three strands of research that will be used are the questionnaire, semi structured interviews and focus groups. The results of each will be 'triangulated' to provide additional confidence in the conclusions – ideally, findings in each strand will help to support findings in the others.

Questionnaires are used in a wide range of settings to gather information about the opinions and behaviour of individuals. Questionnaires are objective and gathered in a standardised way thus providing an initial indication of the trends behind the current building services design process.

Semi-structured Interviews This type of research is valuable for an in-depth examination of people's attitudes and beliefs, and will provide insight into some of the reasons behind the decisions made. These interviews confirm what is already known and can provide reliable and comparable qualitative data.

Focus Groups can provide a dimension that is simply unavailable with a traditional survey as the interaction between participants can lead to new issues being identified. The combined effort of the group will produce a wider range of information, insight, and ideas than the responses of a number of individuals when these replies are secured privately. A bandwagon effect often operates in a group interview situation, in that a comment by one individual often triggers a chain of responses from the other participants. A signature aspect of a focus group

is the objective to better understand the group dynamics that affect individuals' perceptions, information processing, and decision making. [6]

3. Results and Discussion

3.1. Questionnaire

A questionnaire was designed with the main focus on highlighting the current process of building design, importance of different design variables, factors affecting thermal comfort, overheating and adaptation methods to mitigate the climate change for future years. The questions were orientated to gauge the differences between the typical practice and the best practice for HVAC design.

Normally, to limit the population surveyed, a sample is drawn to reflect the characteristics of the total population. By using a carefully drawn sample, there is an assurance that potential respondents have been selected in a standard, scientific manner. In this research the survey population was the Building Industry. The questionnaire was distributed via the fortnightly electronic newsletter of a building services professional body to all of its members. The resulting drawn sample therefore attempts to reflect the characteristics of the total population involved in the designing, structuring and engineering of buildings.

In this instance a total number of 42 people actually responded to the survey but as expected it was a diversity of professionals consisting of Architects, Electrical/Mechanical Engineers, Technical Directors, Energy Consultants and Sustainability Engineers. Although the responses were self selected and few in number, they still appear to suggest some trends within the Building Industry. The distorting effect of differential response rates has long been recognised as a limitation on inferences drawn from questionnaires in social research. Bias may arise even where the response is 100% and it is commonly understood that even where questionnaire response is poor, correlational studies are affected only by loss of degrees of freedom or precision [7]. In instances where the response rate is low or non neutral with regard to the topic of investigation, it is held that the conclusions suffer only from an increased sample variability, rather than from a substantial problem of bias. Increasing the response rate does not necessarily improve the precision of survey results [8]

Fig. 1 shows the hypothesis that emerged from the 31 responses to one of the questions of the questionnaire. It can be seen that the most important drivers in HVAC design are those of Building Characteristics, Available Budget, Comfort Criteria and CO_2 Emissions. Weighted scoring of these responses provides a method for evaluating the priority level of an individual at a glance. Weightings with values of 4, 3, 2 and 1, corresponding to very important, important, least important and not considered, respectively, were assigned to the columns. It can be seen that the Building Characteristics and Available Budget are the top rated parameters, followed by Comfort Criteria, Life Cycle Costs and CO_2 emissions. Plant Space and Ease of Installation are the least voted parameters.

Thermal comfort in a room is determined mostly on the basis of room air temperature, followed by external temperature and occupant activity. When asked about the incorporation of summer conditions of future climates into the design process, 77% of the professionals admitted including it, but only 33% implemented any measures to overcome future summer overheating. It emerged that adaptation is not always a part of the designing process but in some instances where it is, window opening, moveable internal blinds, air-conditioning and occupant control are highly regarded. It is also seen that beyond meeting Building Regulations and the requirement of Energy Performance Certificates, Good Practice Guides

and Building Research Establishment Environmental Assessment Method (BREEAM) are gaining priority.

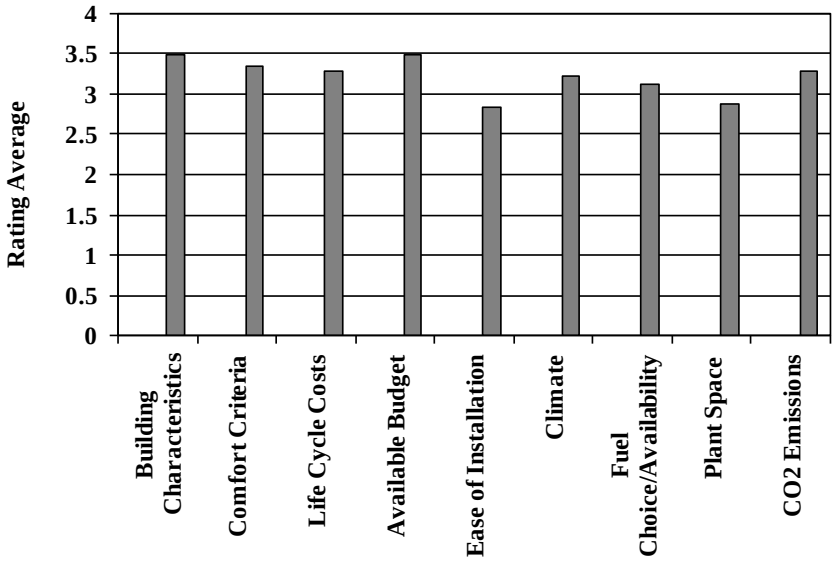

Fig. 1. Most important drivers in HVAC design

3.2. Semi-structured Conversation

The project team plans to hold at least 18 semi structured interviews, 6 of which will be undertaken for domestic and 12 for the non domestic sector (6 for offices and 6 for schools). The first round of these interviews will take place in early 2011.

There have been 2 Focus Groups held so far (see Section 3.3) where opportunities to speak to participants were fully utilized. Each Focus Group had 6 participants comprising of architects, building surveyors, building services engineers, property managers, environmmental consultants and sustainability officers. Prior to commencing the actual Focus Group sessions, a semi structured discussion ensued when an initial task was set where the participants were provided with a list of 9 factors (same as shown in Fig. 1) from which to choose, in their opinion, the 3 most important drivers for HVAC design. On selection, the participants were asked to provide the reasoning behind their choices based on their experiences.

The results of these semi structured conversations are included in this section. The generic message was that there are obvious design features that could and should be optimised to ensure efficient HVAC systems. These include Building Characteristics such as location and the orientation of buildings on a site, thermal insulation levels, glazing type, the use of shading and the use of exposed thermal mass in the structure to moderate temperature extremes. Some of the comments are quoted below.

> *''The main one that stands out probably is the Building Characteristics - absolutely getting the fabric of the building right whether that's working on an existing building or a brand new building''*

> *''HVAC design- design it out as far as possible so Building Characteristics''* (is the most important factor)''

The design process seems to rely heavily on the Available Budget as some respondents agree

that money is usually the driving force behind the decisions made and other issues are only secondary.

> *''If we have all the money in the world we could do everything but we can't - so Available Budget restricts it all''*

> *''Available Budget, I spend all of my day discussing designs with different developers to minimise spend on budget''*

> *''Available budget because there is precious little of it''*

Most of the professionals agree on CO_2 emissions to be the most important driver as it is seen as a significant problem currently and in the future. Different councils have different CO_2 emissions criteria and designers have to follow it by choosing fuels source that will produce minimal emissions. Some people are of the view that buildings are for people and whichever way the buildings are designed, comfort should be the main priority.

> *''CO_2 emissions because it seems to be a significant problem we are going to have in the future''*

> *''As the designers we have responsibility towards a cut in carbon emissions because the way we use buildings accounts for nearly half of all are national emission."*

> *''Comfort Criteria - we are designers and we are designing to know the person and always take that into account whether it's an office building or an individual's requirement''*

> *''Comfort is becoming very important in the long term especially with questions over what the future climate is doing''*

3.3. Focus Groups

There will be 6 focus groups throughout the UK, 2 for the domestic and 4 for the non domestic sector (schools and offices). To date, 2 Focus Groups on overheating in the domestic sector have been held as explained in section 3.2. Focus Groups were conducted in Edinburgh and in London to ascertain the differences in regional and climatic variations that would have an impact on the attitudes and experience of the participants. There is no magic number and more is not necessarily better, although holding 2 focus groups with similar group characteristics may place the results on firmer ground in relation to the patterning of the data. This is because it would suggest that the differences observed are not just a feature of a one-off group, but are likely to be related to the different characteristics of participants reflected in the selection [9]. A total of 6 research questions were explored in detail in these sessions but only some of the main themes that emerged are included in this paper and are as follows:

There is general agreement that the UK is in a comparatively good position as far as overheating in dwellings due to climate change is concerned. From the quotes given below one can observe the difference in trends due to regional variation. It is clear that there is little or no concern of overheating in Edinburgh (Scotland) whereas, although not regarded as an important issue in London (South England) it is nevertheless borne in mind that with suitable measures, this problem can be prevented.

"Currently, Overheating is not necessarily seen as a problem as we do not tend to install air conditioning in to domestic buildings as a norm'' (Edinburgh Focus Group)

''The UK is really in a privileged position as far as Overheating is concerned, with suitable interventions one can get both cooling in the summer and heating in the winter''(London Focus Group)

No significant attention is being paid to future overheating in the domestic sector. Strategic decisions from the outset are essential. Getting the fabric of the building absolutely right for both existing buildings and brand new buildings is imperative thus dealing with what you can within the building characteristics/fabric and then looking at what you need to add in to the building to overcome any overheating problems. Typical comments are:

''Building Characteristics top of my list because we are trying to make (these) strategic decisions from the outset''

''Building Characteristics obviously dictate whether you need HVAC for the start, whether you have to work from where you are or where you want to be"

"You have to get more mass into buildings to try and soak it up and redistribute it at times of the day when it's more beneficial''

''Some house builders have kind of set parameters for a fabric designed solution for reducing carbon and energy output"

''Building Characteristics - that's the most important - it's about reducing mechanical ventilation in the building - to maximise the way that natural ventilation can work well and also simply without being overly complex''

For normal domestic developments the envelope design is deemed critical and construction elements seem more of a concern to future climate than overheating. Improvements in windows are required as double glazed windows still let in and let out substantial heat. By moving to a proper standard triple glazed passive house window, conditions can be maintained where no matter the external temperature, internal conditions can remain stable. Experience dictates that the main driver in people to overcome overheating will be legislation. A full impact will only be achieved if stipulated in Building Regulations.

''Until we have to do it we won't do it, the money is not there and nobody is going to spend over the top"

***''**We are driven by legislation in terms of what criteria we have to actually meet and our question is whether legislation is actually accurate where it's driving us to''*

''If there is no legislation saying that you have got to do it at the moment you just have to use the latest national calculation methodology software and that's got a bit of overheating and that's all people will do''
''Every time we build one of these buildings we are almost building a little experiment based on legislation''

There is a fundamental need to inform the user. Building Regulations can change and

buildings can become more and more efficient but it is imperative to also educate in order to change user habits. Habit means that thermostats are set at the same level even though a reduction of a couple of degrees would also be perfectly acceptable.

> *''Our behaviours have got to change- The barrier is actually the values of our society and the literacy of our society to the changing climate as much as it is about regulations''*

> *''We can change the Building Regulations and buildings can become more and more efficient but people don't change their habits so how much of this energy is going into the building fabric needlessly?''*

> *''We are technical people, we come up with technical solutions and we are forgetting that there are people living in these places who may not understand''*

All participants agree that the weather will get warmer in the future, which although alarming is ignored, as it is not considered an issue at the moment. Some participants said that they preferred to keep their 'heads in the sand' in the hope that it can be avoided until it is no longer their problem. The prevalent feeling is that probability is the only way forward to deal with future predictions otherwise people will want proof. If a tool is to be provided, that specifies the overheating risk of a building, as part of an overheating analysis based on probabilistic climate projections, it needs to be really simple and understandable.

> *''There is no intrinsic value to creating a better building or a more energy efficient building at this moment in time''*

> *"Yes it's going to get warmer but not in my lifetime so I don't need to bother about it - it's my children's problem they can deal with it"*

> *''Climate Change and Overheating is actually quite difficult at the moment to calculate anything on but the construction element is even worse - how can we design better buildings and better details''*

> *''The Probability aspect is probably the only way that you can model it - you have to have those variables and perhaps some kind of benchmarks.*

> *''The Tool needs to be a form where you can add it to the way you model the building as it stands''*

4. Conclusions

The Low Carbon Futures project relies on feedback from the Building Design Community to design a tool that can predict the risk of future overheating in buildings. This paper presented the initial findings of a qualitative investigation performed to gain insights into some of the decision making process. An important aspect of this study was to get the feedback of the Building Industry, surrounding aspects of HVAC design. As with any other branch of science, the validity and reliability of the measurement tools, needs to be rigorously tested to ensure that the data collected is meaningful. Depth of qualitative information may be difficult to analyse for example, deciding what is relevant and what is not. This investigation has therefore adopted the triangulation approach to analyse the resulting data from 3 modes: A questionnaire, semi- structured conversations and focus groups.

The Questionnaire results have suggested that the Building Characteristics and Available Budget are the top rated parameters, followed by Comfort Criteria, Life Cycle Costs and CO_2 emissions. Semi-structured Conversation with 12 experienced professionals indicated that the reduction of CO_2 emissions is the lead factor as it is a regulatory requirement. The majority agreed that many problems could be solved if a building is designed properly taking into account Building Characteristics. Available Budget and Comfort Criteria also play a key role in this aspect. Analysis of the Focus Group discussions revealed that the initial decision needs to be made on the building characteristics and then what is to be added in to the building to design the HVAC system needs to be addressed. There is a need to get the fabric of the building absolutely right whether that is working on an existing building or a brand new one.

The Triangulation methodology adopted herein seemed successful in validating the suggested hypothesis from the questionnaire by confirming it with the findings of the focus groups and the semi structured conversation. Since this is an initial analysis, these issues will be fully explored and on a larger scale with the semi- structured interviews taking place in early 2011 and with more focus groups.

After the initial questionnaire and focus groups there is a strong suggestion that currently overheating is not considered as a critical element when designing or refurbishing new and existing domestic buildings. However, the use of probabilistic climate information has been heard with interest inferring that a probabilistic approach may be the way forward to tackle the unpredictable nature of the weather in the coming years. The unanimous belief was that until the building industry is forced to consider climate change they will not do it. It is also accepted that a tool, based on probabilistic predictions, that is a simple add on to existing techniques will be well-received.

References

[1] Good Building Guide 63 (GBG 63), Climate change: Impact on building design and construction. BRE press 2004, pp. 1-6

[2] P.D. Jones et al., UK Climate Projections science report: Projections of future daily climate for the UK from the Weather Generator, available from http://ukclimateprojections.defra.gov.uk

[3] Adaptation and Resilience in a Changing Climate Network (ACN), Programme website http://www.ukcip-arcc.org.uk/content/view/605/519/

[4] S. Patidar, D.P. Jenkins, G. Gibson, and P.F.G. Banfill, Statistical techniques to emulate dynamic building simulations for overheating analyses in future probabilistic climates, Journal of Building Performance Simulation, In Press, 2010

[5] A. Bryman, Quantity and Quality in Social Research. Routledge, 1988, pp. 131-134

[6] D. W.Stewart, P.N. Shamdasani and D.W.Rook, Focus groups Theory and Practice, 2nd Edition, Sage, 2007, pp. 1-16

[7] R. J. Bowden, Self-Selection Biases in Correlational Studies Based on Questionnaires, Psychometrika 51, 2, 2010, 1986, pp. 313-325

[8] W. Jones and J. Lang, Sample composition bias and response bias in a mail survey: A comparison of inducement methods. *Journal of Marketing Research* 17, 1980 pp. 69-76

[9] R.Barbour, Doing Focus groups, First Edition, Sage, 2007, pp. 57-60

Towards a unifying visualization modelling platform for supporting climate change conscious urban neighbourhood design

Amr Elwan[1,2], Chengzhi Peng[1], Mohammad Fahmy [2]

[1] *School of Architecture, University of Sheffield, Sheffield, UK*
[2] *Department of Architecture, Military Technical College, Cairo, Egypt*
** Corresponding author. Tel: +447578409402, Fax: +441142220315, E-mail: a.elwan@sheffield.ac.uk*

Abstract: Urban physical environments will face up to the challenges posed by global climate change. Various software packages for urban environmental simulation have been created to aid predictions of design performance under climate change conditions as understood today. However, the outputs from these simulation packages present great difficulties for planners, architects and urban designers working in urban neighbourhood projects. Furthermore, designers lack proper tools to bring the outdoor and indoor simulation results together to form an integrated picture at the urban neighbourhood level. It is vital that designers are enabled to achieve such a holistic understanding of their design consequences simply because those indoor and outdoor environments are constantly interconnected with each other. This paper presents this pilot study on setting up an environmental visualization methodology of global climate change at a local scale and how it can be applied to a real urban neighbourhood development project proposed for a site in the City of Cairo, Egypt. The result shows an initial step of addressing the urgent need for a practical visualization modelling platform accessible to urban designers, architects, and decision makers towards sustainable urban forms.

Keywords: *Urban neighbourhood, Outdoor-indoor climate coupling, Sustainable urban neighborhood developments.*

1. Introduction

Urban climatology is an interdisciplinary field related to urban form design. Its complexities have prevented applying climate knowledge within the urban planning process and practice (Oke 1984; Eliasson 2000; Ali-Toudert, Djenane et al. 2005; Oke 2006; Ali-Toudert and Mayer 2007b; Fahmy and Sharples 2008b; Fahmy 2010a).Recently the challenges posed by global climate change have attracted intense research attention world-wide (McEVOY 2007; Levermore 2008; Fahmy 2010a). Due to the long shelf-life of carbon dioxide in the atmosphere, much of the climate change over the coming decades has already been determined by historic emissions (Hulme, Lu et al. 2002). Additionally statistics show that urban environments caused 75% of pollution and 20 percent of carbon dioxide emissions is caused by transport which constitutes 50% of global warming (Barton 1995 and Levermore 2008). Scientists believe that greenhouse gas concentration is increasing global warming(Radhi 2009).Climate change, and increasing urbanisation will mean that, for the rest of this century, urban thermal comfort will become an increasingly important issue for many city residents. The increased use of air conditioning is not available as a long term solution as it will, not only discharge more waste heat into the urban environment, but will also add to CO2 emissions (Fahmy and Sharples 2010b).

Oke (1999) highlighted the meteorological locations and their importance on urban microclimate, this means a weather data files (WDF) of typical meteorological years is measured at weather stations. WDF is used for indoor and outdoor thermal performance simulations by many models either in their EPW, WEA, EPS-r formats to provide hourly data of the whole year or a STAT format to provide an averaged hourly data of the months (DOE, 2009; Radhi, 2009 and Fahmy et al., 2009). This hourly WDF contains the different measured hourly meteorology for a specific location extracted from 30 years ago. WDF represents meteorological parameters e.g. dry bulb temperature, wet bulb temperature, relative humidity,

Specific humidity, direct normal radiation, diffuse horizontal radiation, and global horizontal radiation illuminance.

The intergovernmental panel for climate change (IPCC) has recently drawn attention to the significant warming of capital cities across the world. Understanding the influence of the emissions on air quality motivates the planners to use near-term scenarios. *"Near-term adaptation and mitigation analyses can be matched to conventional planning time scales, can explore opportunities and constraints given institutional and technological inertia, and can play an important role in integrating climate change considerations into other areas of management and policy."(IPCC 2007).* There are several methods capable of creating near-term scenarios of climate change. One of these methods is weather data morphing methodology which manipulates historical weather data for climate scenarios. This will be provided by Climate Change World Weather File Generator, which generates future WDF for 2050(IPCC 2010).

In this research, ENVI-met 3.1 simulation software is used to relocate the measured EnergyPlus Weather (EPW), and generate an accurate WDF. Furthermore, ENVI-met 3.1 takes into consideration the influence of urban neighbourhood elements e.g. buildings, soil, vegetation, and trees. Finally, the generated WDF is used in CC World Weather Gen Tool and ECOTECT 2011. Simulation method is important to visualize the effect of outdoor thermal environment on indoor environment(He, Hoyano et al. 2009). Therefore this paper aims to assess the potential of this methodology in a pilot study, which supports climate change conscious urban neighbourhood design.

1.1. Methodology

The outdoor assessment of urban form is carried out by using the numerical model ENVI-met, which simulates the microclimatic changes within urban environments. The relationship between buildings and urban climate can be understood through the connection between indoor and outdoor thermal, comfort which have shared issues (coupling methodology)(Ali-Toudert and Mayer 2006). The relationship between buildings and urban climate can be understood through the numerical coupling methodology. that connects between indoor and outdoor thermal performances (Fahmy et al., 2009).

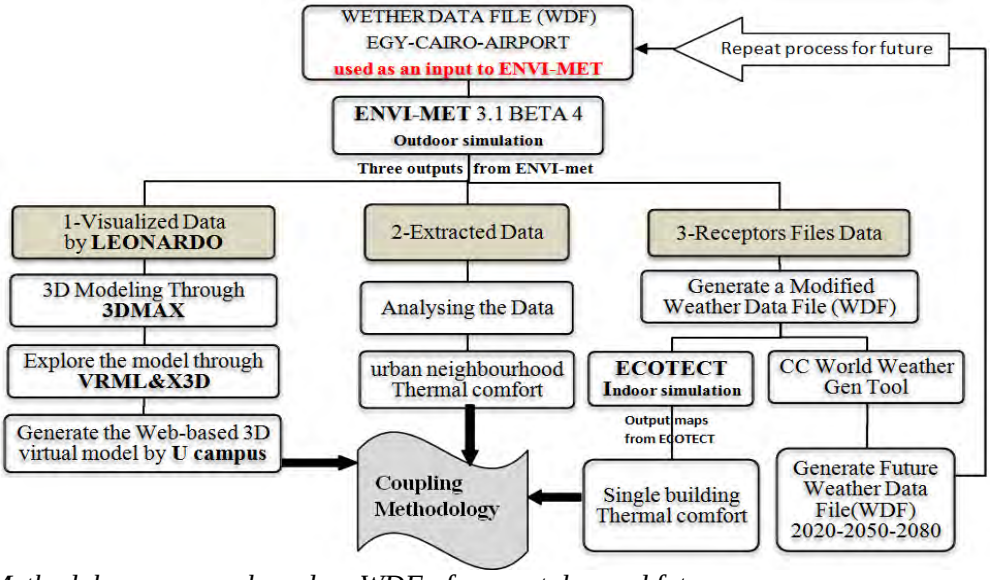

Fig.1. Methodology process based on WDF of present day and future.

The methodology has been carried out in four stages (Fig.1): Firstly, the outdoor simulation of an urban neighbourhood by numerical modeling to obtain present day outdoor meteorological

data which in turn affects the neighbourhood indoor conditions. ENVI-met 3.1 BETA4 is used to generate fine-tuned meteorological parameters at different heights of a building unit by placing snapshot receptors around the unit to obtain the near walls present day climate conditions for the building. Secondly, for the indoor simulation and thermal analyses of the prototypes residential clusters, ECOTECT 2011 is used for its computability with the various used software packages. ECOTECT uses EnergyPlus as a core for the calculation of thermal interactions in a specific location using EnergyPlus Weather data file, EPW. Cairo's EPW file is compiled from about 30 years of meteorological measurements in Cairo International Airport weather station, which ENVI-met results were added to the urban settings effects and represented in a new EPW file, fig.1.Thirdly, given the outdoor-indoor coupled simulations performed on a common set of meteorological parameters. We can plot (a) outdoor ground contoured maps for thermal comfort extracted from ENVI-met, and (b) multiple indoor thermal profiles along the building unit compartments using ECOTECT. Finally, a Web-based 3D virtual model of the entire urban neighbourhood is built to insert both the ENVI-met outdoor mapping and ECOTECT indoor profiling results. Viewers are thus able to perceive the combined results from (a) and (b) via interactive navigation through the 3D virtual urban neighbourhood. These simulations software can be used to calculate and assess comparative environmental impacts by 3D master planning of urban form. This can be applied to present and future weather by generating morphed data to be used with building performance simulation. Eventually, for an executable regeneration policy, such 3D illustrations can be accessed over the Web to support both policy and decision makers for further investigations to avoid the negative impact due to the future global warming by upgrading and regenerating urban forms. For the preparation of a morphed weather data files in the Energy Plus format, CCWorldWeatherGen1.4 will be used and the previous steps for the new future weather data file will be repeated. (CCWorldWeatherGen 2010).

2. Case study description

Due to the expected large area of a selected case study, field work including measurements is not a suitable method of assessment for the existing situation. Particularly, the simulation process will be repeated many times with different conditions. The selected Case study is in a new compound development at the east of the existing old city in Cairo. The new development is an ongoing project held by DAMAK Company, fig.2. The master plan contains repeated prototypes which consist of 3 floors. Four single semidetached building units in different locations in the neighbourhood were chosen, *Table1.*

Table1. Detailed model description of the case study.

Parameter	Detailed model(1,2)	Detailed model (3,4)
Total area	540 m2	500 m2
No. of floor	3 floors	3 floors
Ext. walls	0.25m brick 20 mm plaster inside	0.25m brick 20 mm plaster inside
Int.walls	0.25m brick 20 mm plaster inside	0.25m brick 20 mm plaster inside
Floor height	3.2m	3.2m
Orientation	North to south	East to west
Roof	20 tiles 20 mortar 50 sand 150 mm concert	20 tiles 20 mortar 50 sand 150 mm concert
Glazing	6 mm single glass	6 mm single glass
Thermal zones	Multi zones	Multi zones

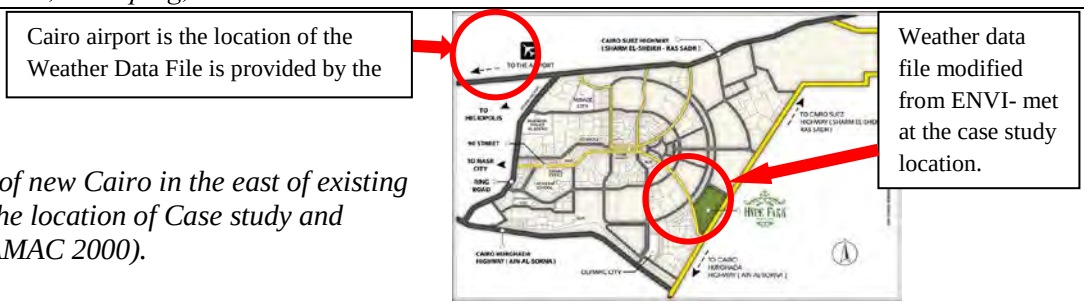

Fig.2.map of new Cairo in the east of existing old town, the location of Case study and airport(DAMAC 2000).

3. Results and analyses

Scenarios use simple models to measure the existing climate projections. This gives comparable results to the full three dimensional climate models. There are limitations of these scenarios; Firstly, the scenarios should not be considered forecasts or predictions, but representative scenarios. Secondly, these scenarios support scientific research to test their implication for adaptation and mitigation. Thirdly, there are uncertainties about using future scenarios particularly for emissions profiles. There are new techniques are developed for translating emissions and uncertainty analyses.(IPCC 2007)In this respect the morphing methodology used in CC World Weather Gen, which might include uncertainties due to wind information unchanged, but other modified meteorological parameter in the new WDF provide an acceptable level of knowledge (McEvoy 2007). Another sort of uncertainties can be expected through the applied software cycle by feeding the tool output to another with a converted file extension between them. However, there was no other way to check such methodology, because all models in literature visualize separately both outdoor and indoor simulation. In addition, architects, and planners need to communicate this software process for climate knowledge. This might height the gap between outdoor and indoor invironmental simulation software.

3.1. Outdoor simulation

The three dimensional model ENVI-met 3.1 BETA4 was chosen to simulate comfort quantities and the meteorological factors within an urban microclimate model. Our three dimensional model ENVI-met requires a few input parameters which are entered to a configuration file. Whenever the simulation starts to calculate the meteorological factors e.g.

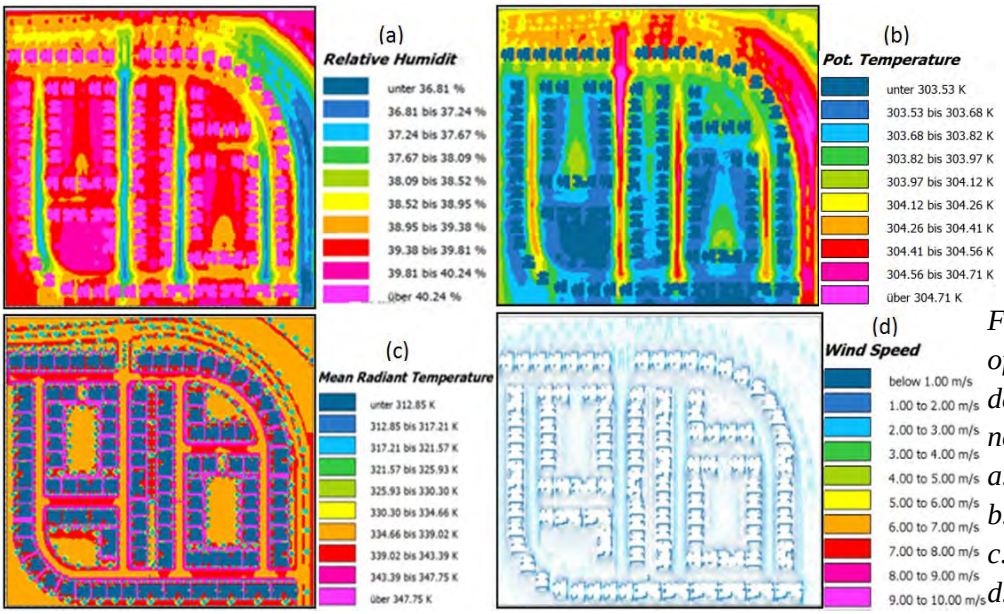

Fig.3.Visualization of metrological data of urban neighborhood: a. Relative humid. b. air temperature c. Tmrt d. wind speed.

wind speed and direction, air and surface temperature, air humidity, short- wave and long-wave radiation fluxes, in addition to the mean radiant temperature which is needed for comfort analyses. The Simulation date was on 1st of June, because it is the typical summer day and started at peak time from10:00 to 1600. After the simulation finished by 3D numerical model ENVI-met 3.1 Beta 4, we had three outputs: firstly, the maps which illustrate the different metrological factors by colors; secondly, receptors file which are used to generate an accurate WDF instead of the one provided by the USDOE, which was measured at the Cairo Airport, about 30 km away from the study site; and finally, extracted data for every hour of the simulation, fig.3.

As can see in Fig.3, there is a higher temperature at outer and inner roads. Wind speed at the outer roads is higher than the inner roads because wind direction is blocked by the buildings. Additionally, specific and relative humidity are lower inside the neighbourhood. This will lead to a lower mean radiant temperature. Eventually all the previous conditions will affect pedestrians' thermal comfort. The comparison among the meteorological data influences the thermal comfort of the urban neighbourhood, therefore air temperature, specific humidity, wind speed, relative humidity and mean radiant temperature are the parameters which control the urban neighbourhood thermal comfort.

3.2. Indoor simulation

Four housing units in different locations of the neighbourhood were selected and the closed thermal zones of every model inside ECOTECT 2011 built. The provided weather data file by ENVI-met used into the simulation. Eventually, the detailed model built by 3D MAX in separated floors and the resulted thermal maps by ECOTECT attached into the model, fig.4.

3.3. Coupling outdoor and indoor

Outdoor and indoor simulations are held and followed by 3DMAX to collect the different results in a rendered thematic model with a detailed terrain and elements of microclimate, (Fig.4). Then the models were grouped into different categories. E.g. group 1 contains the urban terrain and separated floors of the detailed modes, group 2 for the ENVI-met outdoor simulations and group 3 for ECOTECT indoor simulations. Finally, a Web-based 3D virtual model of the entire urban neighbourhood was built through VRML, X3D and made available on the web via the uCampus platform (Peng and Blundell Jones 2004).

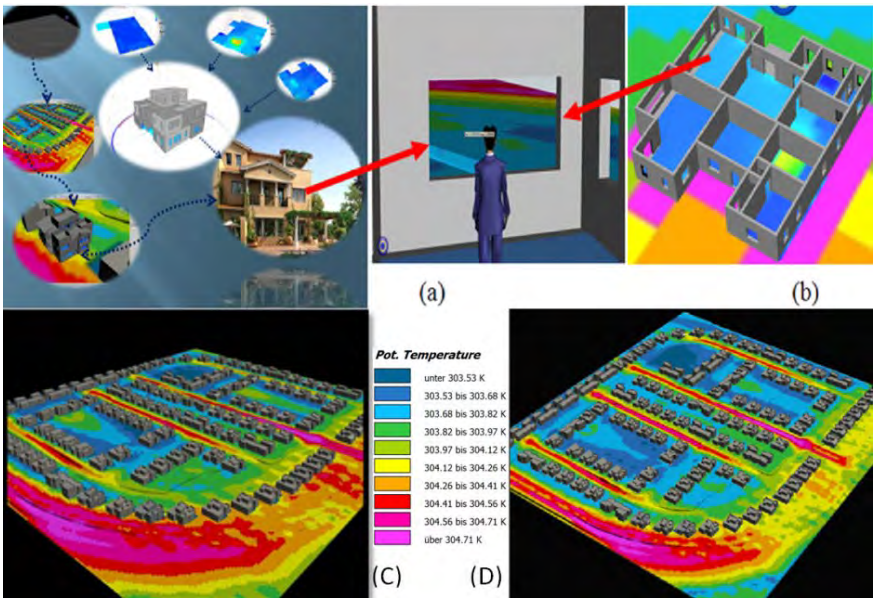

Fig.4 Bring outdoor and indoor simulation together (a) & (b) illustrate the 3D virtual model.(c)Air temperature predicted by the morphed 2050 scenario and (d) Air Temperature of present day.(c) and (d) illustrate the difference in temperature, not only at inner roads, but also at all spatial urban canyons, due to the increase in air temperature in the 2050.

Following the work of Fahmy et al., (Fahmy, Trabolsi et al. 2009), as ENVI-met does not have the capability to simulate indoor climate (it just deals with it as a heat sink through steady state conduction), ECOTECT 2011(AUTODESK 2010) was used to investigate the means of indoor climate conditions for the case study. ECOTECT has built a comprehensive 3D interface over EnergyPlus v3.1 (USDOE 2009), as an architectural dynamic modelling platform has simulated indoor thermal interactions. The meteorological factors (air temperature, wet bulb temperature, relative humidity, global radiation, short-wave direct and diffuse radiations and wind speed) for all site outdoor grids were added in their cells in a comma separated Value (CSV) file extension. This allows easy editing of the climate hourly data in an Egyptian Typical Meteorological Year (ETMY2) weather data format which can be used for Egypt, (USDOE 2009). In this study, WDF was used basically as an energy plus format, EPW, and EnergyPlus converter tool, which was used for conversion after writing new hourly data in the (CSV) file.

4. Generating Future Weather Data File (WDF)

A numerically air Temperature map (T_a) was plotted as an example of the 3D thematic maps, which was based on the morphed WDF for 2050 scenario and present day, fig.4. Climate conditions scenarios was through the weather data morphing methodology that was provided by CC World Weather Gen Tool which WDF 2020-2050-2080 e.g. WDF Of 2050, fig.5.

18	Date	HH:MM	Datasour	DryBulb {	DewPoin	RelHum {	Atmos Pr	ExtHorz
3653	01/06/2050	10:00	'?'?'?'?'	24.2	15	56	101502	1117
3654	01/06/2050	11:00	'?'?'?'?'	26.2	13.8	46	101491	1248
3655	01/06/2050	12:00	'?'?'?'?'	28.4	13.2	39	101470	1311
3656	01/06/2050	13:00	'?'?'?'?'	29.2	11.4	33	101429	1301
3657	01/06/2050	14:00	'?'?'?'?'	31.2	11.7	30	101378	1220
3658	01/06/2050	15:00	'?'?'?'?'	32	11.3	28	101337	1073
3659	01/06/2050	16:00	'?'?'?'?'	31.1	12.1	31	101317	869
3660	01/06/2050	17:00	'?'?'?'?'	32.2	12.5	30	101306	624

Fig.5. part of the weather data morphing (01/06/2050) contained meteorological factors e.g. dry bulb temperature, Dew point, Relative humidity, Atmospheric pressure

5. Implications for present and future urban developments

In a hot climate country like Egypt many planning projects have been produced and executed to cope only with population growth (Ali 2003). Particularly in Cairo, the overwhelming population growth rate did not allow the chance for full environmental studies for both the built and the natural environment, whereas buildings and open spaces have to be adequately climate responsive. Through the methodology, which visualizes the coupled outdoor-indoor climate condition, the construction market stockholders can have an idea about the whole thermal performance and energy consumption, Fig.6.

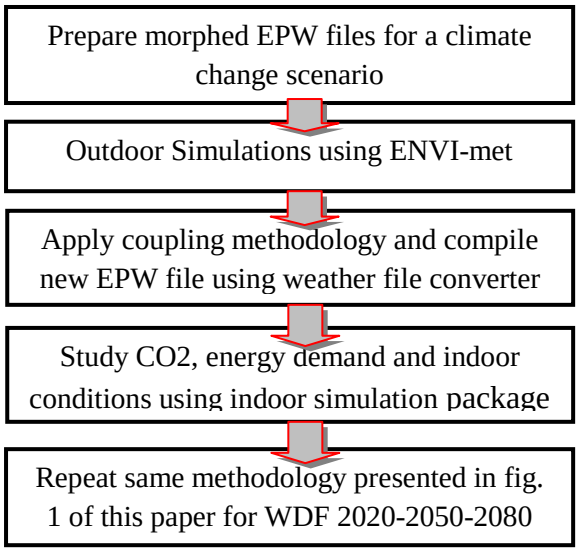

Fig.6: Climate change based outdoor-indoor coupled 3-D visualization methodology modified after Fahmy (Fahmy 2010), p-175.

6. Conclusion and future studies

This study has not developed a tool, but has carried out the process manually. This paper could lead to new software which enables architects and planners to realize the relationship between outdoor and indoor conditions. This methodology identifies the gaps between simulation software, and how a new system can be developed to connect these results. Therefore, comparison between different design alternatives would become possible, as will measuring thermal comfort efficiency of the urban neighbourhood.

This paper has investigated an approach of the combination between micro climate scale using ENVI-met and building scale using ECOTECT, and illustrated the importance of the interaction between outdoor – indoor thermal comfort. 3D virtual modeling supported planners, companies and civil society. Firstly, for visualizing the numerical calculation results; secondly, for developing outdoor – indoor coupling methodology, and understanding the comparison between present and future meteorological data; and thirdly, realizing the climate change conscious urban neighbourhood design.

Further research should draw attention to the prevailing wind due to the simulation for the typical summer day of the hot arid conditions in Cairo, which is noticed that the wind direction is blocked by some buildings, and consequently the canopies' air temperature increased and affected pedestrians' thermal comfort. Therefore future studies should focus on improving the spatial distribution of wind velocity by changing building shapes & tree lines and using green roads techniques.

References

[1] Ali-Toudert, F., M. Djenane, et al. (2005). "Outdoor thermal comfort in the old desert city of Beni-Isguen, Algeria." Climate Research 28(3): 243-256.

[2] Ali-Toudert , F. and H. Mayer (2006). "Numerical study on the effects of aspect ratio and orientation of an urban street canyon on outdoor thermal comfort in hot and dry climate." Building and Environment 41(2): 94-108.

[3] Ali-Toudert, F. and H. Mayer (2007b). "Effects of asymmetry, galleries, overhanging fac¸ades and vegetation on thermal comfort in urban street canyons." Solar Energy 81(6): 742–754.

[4] Ali, E. (2003). "Evaluation of the Egyptian Experiment in Establishment the new Towns in the Desert Areas." Journal of Engineering Sciences, Assiut University of Egypt 31(1).

[5] AUTODESK. (2010). "ECOTECT2011 [Available Online] http://www.autodesk.co.uk/adsk/servlet/mform?validate=no&siteID=452932&id=14205163 " Retrieved 19/4/2010.

[6] Barton, H. (1995). "(1995) Sustainable Settlements: A Guide for Planners, Designers and Developers, Government Management Board, University of West of England, Bristol."

[7] CCWorldWeatherGen. (2010). "Climate Change World Weather File Generator." V1.4. Retrieved 25-5, 2010.

[8] DAMAC (2000). Hyde Park. Adobe reader. H. e. Brochure. New Cairo.

[9] Eliasson, I. (2000). "The use of climate knowledge in urban planning." Landscape and urban planning 48(1-2): 31-44.

[10] Fahmy, M. (2010a). Interactive urban form design of local climate scale in hot semi-arid zone. School of Architecture. Sheffield, University of Sheffield. PhD.

[11] Fahmy, M. and S. Sharples (2008b). "The need for an urban climatology applied design model, [Online]. Available at: http://www.urban-climate.org/IAUC028.pdf." The online newsletter of the International Assocciation for Urban Climatology 2008(28): 15-16.

[12] Fahmy, M. and S. Sharples (2010b). "Urban form adaptation towards minimizing climate change effects in Cairo, Egypt. Accepted Manuscript." Building Services Engineering Research and Technology.

[13] Fahmy, M., A. Trabolsi, et al. (2009). Dual stage simulations to study microclimate thermal effect on comfort levels in a multi family residential building. 11th International Building Performance Simulation Association Conference University of Strathclyde in Glasgow, 27-30 July.

[14] He, J., A. Hoyano, et al. (2009). "A numerical simulation tool for predicting the impact of outdoor thermal environment on building energy performance." Applied Energy 86(9): 1596-1605.

[15] Hulme, M., X. Lu, et al. (2002). Climate change scenarios for the United Kingdom; The UKCIP02 scientific report. UK Climate Impacts Programme (UKCIP), Oxford (United Kingdom); Funded by the Department for Environment, Food and Rural Affairs. See m02/35481 for the briefing report.

[16] IPCC. (2007). "TOWARDS NEW SCENARIOS FOR ANALYSIS OF EMISSIONS, CLIMATE CHANGE, IMPACTS, AND RESPONSE STRATEGIES http://www.ipcc-data.org/docs/ar5scenarios/IPCC_Final_Draft_Meeting_Report_3May08.pdf."

[17] IPCC. (2010). "HadCM3 climate scenario data download page, www.ipcc-data.org/sres/hadcm3_download.html." Retrieved 25-5, 2010.

[18] Levermore, G. J. (2008). "A review of the IPCC Assessment Report Four, Part 2: Mitigation options for residential and commercial buildings." Building Service Engineering 29(4): 363-374.

[19] McEVOY, D. (2007). "Climate Change and Cities." Built Environment 33(1): 5-9.

[20] Oke, T. R. (1984). "Towards a prescription for the greater use of climatic principles in settlement planning." Energy and Buildings 7(1): 1-10.

[21] Oke, T. R. (2006). "Towards better scientific communication in urban climate." Theoretical and Applied Climatology 84(1-3): 179-190.

[22] Peng, C. and P. Blundell Jones (2004). "Reconstructing urban contexts online for interactive urban designs." Design Studies 25(2): 175-192.

[23] Radhi, H. (2009). "Evaluating the potential impact of global warming on the UAE residential buildings - A contribution to reduce the CO2 emissions." Building and Environment 44(12): 2451-2462.

[24] USDOE. (2009). "Egypt weather data [Available Online], http://apps1.eere.energy.gov/buildings/energyplus/cfm/weather_data3.cfm." Retrieved 18/7/2009.

[25] USDOE. (2009). "EnergyPlus Energy Simulation Software, [Available Online], www.apps1.eere.energy.gov/buildings/energyplus/cfm/reg_form.cfm." Retrieved 15/1/2009.

Influence of Indirect Land Use Change on the GHG Balance of Biofuels – A Review of Methods and Impacts

Elisa Dunkelberg[1,*], Matthias Finkbeiner[2], Bernd Hirschl[1]

[1] *Institute for Ecological Economy Research, Berlin, Germany*
[2] *Technische Universitaet Berlin, Berlin, Germany*
** Corresponding author. Tel: +49 30 88459436, Fax: +49 308825439, E-mail: elisa.dunkelberg@ioew.de*

Abstract: The greenhouse gas (GHG) balance or carbon footprint of biofuels, generally calculated by life cycle assessments (LCA), is heavily influenced by the modeling of land use changes (LUC). This includes direct land use changes (DLUC) and indirect land use changes (ILUC). Various methodical approaches for the integration of ILUC in LCA have recently evolved. In this study several approaches for calculating ILUC and the effects on GHG balance are compared. These are economic modeling, deterministic modeling and regional modeling. Papers published on this topic since 2007, when the ILUC debate began, are reviewed considering the following main criteria: methodological approach, uncertainties of assumptions, and the level of the GHG emissions due to ILUC. The results show that the existing approaches lead to strongly divergent results. This is due to uncertainties about relevant assumptions, e.g. the methods of linking commodity prices to ILUC, assumptions about yields, soil carbon contents, and the effect of by-products. These uncertainties and other methodological inconsistencies, e.g. the allocation issue with respect to displacing vs. displaced crops, imply that further research is needed and that current methods are not robust enough for adoption in regulation.

Keywords: *Biofuels, Greenhouse-gas balance, Life cycle assessment, Indirect land use change, EU policy*

1. Introduction

The worldwide expansion of biofuel production is being driven by several forces; these include, first and foremost, rising oil prices, promotion of a secure energy supply, and rural development [1]. In the European Union (EU), the reduction of GHG emissions in the mobility sector has been another important factor, leading to national policy objectives designed to increase the biofuels share ([1, 2]). To ensure that biofuels achieve a significant reduction in GHG emissions, the Renewable Energy Directive (RED) indicates that a life cycle GHG emissions reduction of roughly 35% as compared to fossil fuels is necessary; otherwise, biofuels will not be counted towards attainment of the quota. By 2017, this increases to a 50% reduction vs. fossil fuels [3]. Other regulations, e.g. the US Energy Independence and Security Act (EISA) of 2007, include similar reduction targets [4]. These objectives are met by most of the biofuels if LUC are not considered [5]. In 2007, however, in the context of increasing food prices, LUC linked to biofuel expansion became a topic of public discussion; the same year, EISA directed the US government to develop a LCA for biofuels that includes DLUC and ILUC [6]. The 2009 RED similarly directs the European Commission (EC) to investigate "the inclusion of a factor for indirect land-use changes in the calculation of greenhouse gas emissions" [3]. As a consequence of such political pressures, but also a growing interest in research into LUC issues, a number of ILUC studies have recently been published (e.g. [5, 7-16]).

Biofuel production-related DLUC occur when a previous land use especially a natural habitat is converted to bioenergy crop production. The conversion of grassland, tropical rain forest or peat bogs into agricultural land will generally lead to a release of additional carbon dioxide over several years or even decades [17]; these GHG emissions are often referred to as the "carbon debt" of biofuels. Depending on the previous land use, the time needed to repay this carbon debt through annual savings in GHG emissions vs. fossil fuels can range between zero and 423 yr [17]. Feedstock cultivation on degraded lands with low carbon contents, on the

other hand, can lead to a sequestration of carbon dioxide (e.g. [5, 18]). According to the IPCC [19], emissions due to LUC are generally allocated across the yields of 20 yr when calculating the emission factor for DLUC; however, since carbon contents depend not only on land use but also on tillage methods (e.g. [7,20,21]), soil texture, and hydrological and climatic conditions [22], the use of default emission factors, such as those provided by the EC, is quite imprecise − there is a lack, in particular, of reliable data on GHG balances for biofuels cultivated on degraded land [23].

ILUC occur when biofuel feedstock cultivation replaces other crops and, consequently, natural habitats are then converted to arable land to meet the demand for the displaced commodities [8]. Inclusion of ILUC in GHG balances is more difficult than with DLUC because of the high system complexity: ILUC are tied to global market dynamics. Some scientists assume that if a crop is displaced, the prices for this crop will increase and farmers will react by creating new arable land [24]; however, because of increasing global market prices, ILUC can occur anywhere in the world – not only in the country where biofuels are being produced ([8, 9]); in such situations, measuring these effects at the regional level is not sufficient. Likewise, national regulations, e.g. customs, subsidies or trade restrictions, also influence prices and trade flows and thus ILUC [25]; hence, a consideration of global prices alone is also not sufficient. Moreover, biofuel production is a multi-product system: by-products, such as dried distillers' grains with solubles, also accrue; these can substitute for fodder crops and thus reduce total land demand ([26-28]). Furthermore, forces other than agricultural expansion, such as timber harvest and infrastructure development (e.g. road building), also drive LUC [7]. ILUC-specific methodologies are thus needed. Currently three basic approaches to quantify ILUC exist: economic models, i.e. partial or general equilibrium models, that provide for calculation of ILUC (e.g. [10,11]); deterministic or descriptive-causal models, which attempt to estimate ILUC based on a set of simplified assumptions (e.g. [5]); regional models that try to take into account regional influences on ILUC [25].

Purpose of this work is to present a systematic overview of the body of literature in the area of ILUC research and to assess its influence on the GHG balance of biofuels. Therefore in the present article, these different approaches for calculating ILUC and the effects on GHG balance are described and compared.

2. Methodology

For this purpose the relevant literature (since 2007) relating to this topic was identified and evaluated; some grey literature was also considered when appropriate. The following three main criteria for evaluation were considered: methodological approach, uncertainties of assumptions, and the level of the GHG emissions due to ILUC. For the purpose of comparing the various approaches, some conversions were necessary; in these cases, conversion values (e.g. carbon contents) were taken from the original literature. The study further addresses the question and extent of ILUC integration into EU policy and poses questions for further research and development. A clear response to the question of the extent to which ILUC influence the GHG balance is not offered, but the study does address their relevance; the advantages and disadvantages of the various methodological approaches are also indicated.

3. Results

3.1. Economic modeling of ILUC

Both partial-equilibrium models (e.g. FAPRI, AGLINK, IMPACT, CAPRI) and general-equilibrium models (e.g. GTAP, LEITAP) are used to project ILUC [12]. Partial-equilibrium

models are based on linear relationships between prices, demand, and production in the agricultural market, whereas general-equilibrium models model the whole world economy (e.g. interactions of the agricultural sector with chemical industries) [12]. In general, economic modeling of ILUC follows three main steps. First, the economic model is given a so-called biofuel shock or policy shock, i.e. biofuel production is increased; the model projects the effects of nationally increased biofuel production on global commodity markets and on additional land requirements. In this step, the model also provides indications as to the countries in which additional land will need to be converted. In the second step, LUC are then mapped to specific land-cover types (e.g. grassland, forest), based on historical patterns of LUC. Finally, biophysical models are used to project the GHG emissions from land use conversion. The size of the shock allows GHG emissions to be attributed to a specific quantity of biofuels. Nearly all studies calculating ILUC by means of economic modeling found that ILUC significantly influence the GHG balance of, at a minimum, first-generation biofuels ([10-13]). Current investigations indicate that second-generation biofuels could lead to a negative ILUC effect [29]. Since the various models used different shocks respectively, it has not been possible to compare results for recent years; therefore, at the direction of the EC, modelers calculated the crop area changes for specific biofuels scenarios [12]. The results show that the range of crop area changes is quite high: for the EU biodiesel scenario, for example, the values range between 242 and 1928 kha $Mtoe^{-1}$ (see Table 1) [12] .

Table 1. Minimum and maximum values of LUC calculated with different economic models (source: authors, based on [12])

Scenario	Minimum		Maximum	
	(kha $Mtoe^{-1}$)	Model	(kha $Mtoe^{-1}$)	Model
EU biodiesel scenario	242	AGLINK	1928	LEITAP
EU ethanol scenario	223	IMPACT	743	LEITAP
US ethanol scenario	107	IMPACT	863	LEITAP
Palm oil scenario	103	GTAP	425	LEITAP

These deviations are caused by assumptions about input data made at each stage of the modeling. Many assumptions are uncertain and therefore differ among the models [9]. First, the extent to which farmers will react to rising prices by increasing yields through irrigation or fertilization is uncertain [24]; whether extra emissions due to the use of additional fertilizers are accounted for is also uncertain [12]; moreover, feedstock yields vary among the models, particularly in expansion areas [12]; the extent to which reductions in food consumption will take place as a consequence of increasing food or fodder prices is also unknown. Likewise, the share of additional crops saved by by-products differs among the models; one reason for this are differences in the methods of calculation: in GTAP and LEITAP, by-products are accounted for by substitution on the basis of relative prices; other models, such as CAPRI, account for them through physical replacement ratios [12]. Additionally, controversy exists about the extent to which production is shifted from countries with high yields to relatively less developed countries with lower yields [12] and about the share of forest and grassland conversions [9]; and, finally, as mentioned previously, emission factors related to LUC are also uncertain. To characterize ranges for the GHG emissions of different scenarios, we multiplied the ILUC values in kha $Mtoe^{-1}$ taken from Edwards. et al. [12] (see table 1) and carbon dioxide emission factors using three different values for soil C emissions: 40 tC ha^{-1} as an average value and 10 and 95 tC ha^{-1} as lower and upper values (cf. [11, 12]). Fig. 1 shows that the range for the EU biodiesel scenario, in particular, is quite large, whereas those of the EU and US ethanol scenarios as well as that for palm oil are narrower. Results for the EU ethanol scenario range between 14 and 309 g CO_2 MJ^{-1} due to

LUC. Since the default carbon footprint of fossil fuels is set at 83.8 g CO_{2e} MJ^{-1} in RED, it can be assumed that this scenario and likewise the EU biodiesel scenario will not lead to a 35% GHG reduction in comparison to fossil fuels.

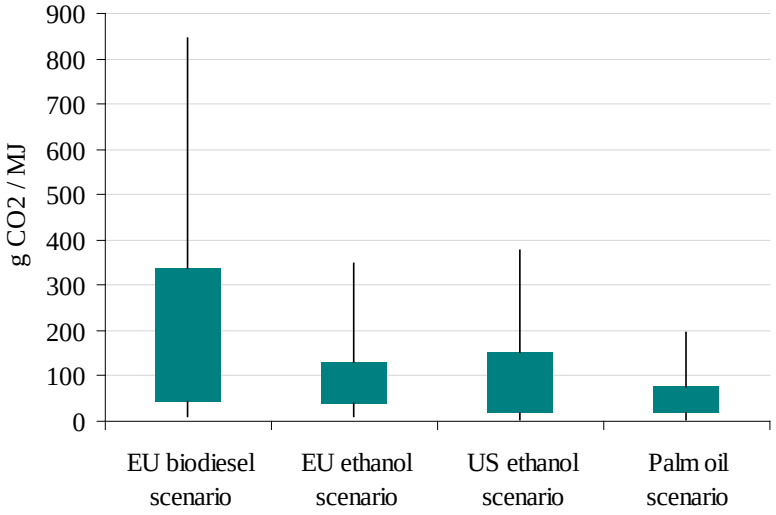

Fig. 1. Range of CO_2 emissions due to LUC calculated on basis of results of various economic models Maximum and minimum LUC values resulting from economic models in ha $Mtoe^{-1}$ [see Table 1] were multiplied with typical C emission factors 40 tC ha^{-1}[error bars: 10 tC ha^{-1}, 95 tC ha^{-1}] – authors' calculations, based on Edwards et al. [12].

3.2. Deterministic modeling of ILUC

The second main approach is called deterministic or descriptive-causal modeling. These models are simplified calculations based on explicit assumptions and are usually realized with a spreadsheet calculator. In general, these models use cause-and-effect logic to describe system behavior. One example of this approach is the ILUC factor developed by the Institute for Applied Energy, in Germany [5]. A crucial assumption in this model is that ILUC can be estimated by looking at the exported products relevant for the bioenergy sector, e.g. soy, corn (maize) and palm oil. Calculations are based on 2005 product exports, but for the purpose of simplification, only key regions, such as Argentina, Brazil, the EU, Indonesia, Malaysia, and the USA, are considered; these countries are responsible for more than 80% by mass of the global trade in the respective commodities [5]. Using the mass of commodities traded divided by the respective country-specific yields, the area needed to produce these products was calculated. From the sum of all land use for agricultural exports, each country's proportionate share could be derived – the "world mix." Next, additionally needed areas were combined with country-specific assumptions about the specific DLUC associated with the production of the export commodities. Following the application of conversion factors from IPCC, the interim results were then weighted according to each country's share of the "world mix," resulting in an ILUC factor of 13.5 t CO_2 $ha^{-1}a^{-1}$ [5]. This means that 1 ha of bioenergy feedstock production displaces 1 ha of previous production. The authors suggest three different levels of ILUC (25%, 50%, and 75% of the theoretical ILUC factor), as they anticipate yield increases and assume that a share of the expansion occurs on degraded lands [5]. Fig. 2 breaks down the level of CO_2 emissions by type of biofuel, country of production, and prior land use. The high level of GHG emissions when ILUC are included means that most biofuels will not achieve the GHG reductions called for in the RED [5]. Compared to the results of economic modeling (see Fig. 1), the results for CO_2 emissions due to DLUC, plus

the differing ILUC factors calculated with this approach, are low for biodiesel but in the same range for ethanol if calculated with 40 tC ha^{-1}.

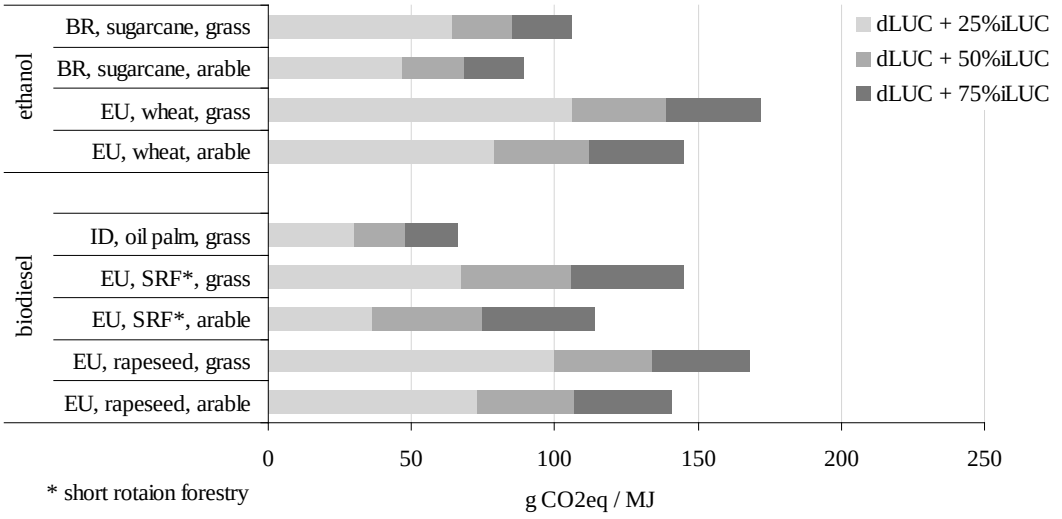

Fig. 2. CO_2 emissions calculated on basis of a deterministic model (figures from Fritsche et al. [5]).

Another deterministic model, developed by Plevin et al. [9], attempts to characterize a robust range of ILUC. For this purpose, the authors include four main parameters in a reduced-form model: net displacement factor (NDF) (ha converted land / ha biofuels), average emission factor (Mg CO_{2e} ha^{-1}), production period (yr) and fuel yield (MJ $ha^{-1}yr^{-1}$). Setting an upper and lower value for these parameters, based on the literature, the ILUC emission factor for US corn ethanol ranges between 10 and 340 g CO_{2e} MJ^{-1}, which is similar to the range as calculated according to Edwards et al. [12] (see Fig. 1). The results suggest that the NDF accounts for the major part of the variance in the ILUC factor; it includes the effects mentioned above, e.g. price-induced yield increases, relative productivity of land converted to cropping, price-induced reductions in food consumption, and by-product substitutions [9].

3.3. Regional modeling of ILUC

In Germany, another method has been discussed: regional modeling. This approach was developed, first, in response to criticism that other models do not properly consider the effects of state regulation on the global agricultural market; these can take the form of subsidies, customs duties, and trade restrictions (bans on import/export, etc.). Second, the deterministic model of Fritsche et al. [5] is limited to LUC due to product exports ([5,25]) and thus does not consider ILUC effects due to domestic trade, which, according to Lahl [25], must be included as internal trade is quantitatively more important than global trade. Lahl [25] suggests the following method for regional modeling: first, all LUC in a country and for a specific period must be ascertained. Country-specific CO_2 emissions (E^RLUC) are then calculated for the respective carbon stocks in vegetation and soil, before and after conversion. In order to calculate the share of the various biofuels in total emissions, the change in biofuel production is divided by the change in agricultural production in total and multiplied by E^RLUC. Next, the portion of total emissions due to DLUC is subtracted, and finally, the remaining emissions are allocated to the "originator," which can be separate farms or regions. In some cases a correction factor for by-products or transnational effects must be included. To determine whether transnational effects are relevant for a specific country, one should look for a drop in agricultural import levels for recent years and an absolute value of the reduction in agricultural imports higher than the absolute value of the increase of agricultural exports [25].

An application of this model is not yet known. A method of economic modeling that combines regional aspects with economic modeling was applied to the biofuels sector in Brazil [10]. Methodologically, a land-use change model was linked with a partial equilibrium model of the agricultural sector economy and a dynamic global vegetation model. Using these models, it was determined that in Brazil ILUC influence the GHG balance of biofuels much more than DLUC [10].

4. Discussion and Conclusions

LUC are of central importance for the GHG balance of biofuels. For the purpose of GHG mitigation, the EC is directed to consider inclusion of an ILUC factor in the calculation of GHG emissions of biofuels. Currently, three main approaches, economic modeling, deterministic modeling and regional modeling, exist for calculating ILUC. The results of these methods vary greatly – by a factor of more then ten, but nearly all methods indicate that ILUC increase GHG emissions significantly. With respect to the relevance of ILUC, they are thus unambiguous and call into question the viability of biofuels as a climate protection instrument. Many of the results suggest that most of the currently available biofuels will not reach the GHG reduction targets of the RED after inclusion of ILUC. The effect of biofuel specific ILUC factors may be critical with respect to their attainment of the mandated 35% reduction in GHG emissions vs. fossil fuels; this in turn is decisive for whether a specific biofuel is to be included in the intended biofuels share of total fuel consumption; thus care needs to be taken with the development of such a factor.

The deterministic model from Fritsche et al. [5] indicates that oil palm biodiesel and sugarcane ethanol are accompanied by lower ILUC effects than biodiesel produced from rapeseed and ethanol from wheat and corn. Results from economic models exist for only a few biofuel scenarios; thus it is not yet known whether deterministic and economic models will lead to corresponding results for specific biofuels. Characteristic of all ILUC modeling is that input data and assumptions are often uncertain. Some uncertainties are present in all of the methodologies, in particular, assumptions about CO_2 emission factors for various LUC; feedstock yields, particularly in expansion areas; extra emissions due to fertilizing to increase yields; and the share of extra crops replaced by by-products. In some models, by-products are accounted for by substitution on the basis of relative prices; other models account for them through physical replacement ratios [12]. It is possible to set default values, e.g. CO_2 emission factors, or calculation types, e.g. for the consideration of by-products as in RED [3]; this would lessen the deviation between the outcomes of the different models but also limit possible results. Additional uncertainties exist specific to the type of model. For economic and deterministic models, this includes assumptions about the extent to which production is shifted from countries with high yields to relatively less developed countries with lower yields, the share of forest, grassland and wetland that will be converted, and the levels of reductions in food consumption that occur as a consequence of increasing food or fodder prices. Furthermore, economic models do not take into account market distortions due to national policy [25]. Missing or dubious land-use rights in specific countries may also affect ILUC. This is not taken into account in economic and deterministic modeling. For the deterministic model from Fritsche et al. [5], the main question is whether it is sufficient to calculate ILUC on the basis of exported products or whether internal trade should also be included. Regional modeling can probably provide more precise information about real ILUC effects in specific countries; it can also be a suitable method if countries or farms that allow ILUC are to be sanctioned. However, availability of regional data is a precondition for this method and applications of the regional methods remain largely unknown. Each of the current models thus has its pros and cons.

Before establishing a specific method for calculating ILUC or setting default ILUC factors via regulatory policy, these methods should first be improved and applied to various scenarios and regions. Information and data about ILUC effects in specific regions, especially, are still lacking and need to be further explored. Some theoretical considerations are also necessary before ILUC should be accounted for in policy regulation: From the point of view of LCA, a precondition for the comparison of two products, e.g. biofuels and fossil fuels, are consistent boundaries for both systems; therefore, when calculating GHG balances including ILUC, other indirect effects arising from the production and use of biofuels and fossil fuels, e.g. price-induced increases or decreases in fuel consumption (cf. [30]), should be analyzed and similarly included. Furthermore, in most of the current methods the product previously cultivated does not receive any of the GHG emissions due to DLUC if it is displaced; once again, from the point of view of LCA, this is questionable because all environmental impacts should be allocated on all accruing products in the systems being analyzed.

References

[1] E. van Thuijl and E. Deurwaarder, European biofuel policies in retrospect, Energy Research Centre of the Netherlands, 2006.

[2] CRS, EU biofuels policy and agriculture: an overview - CRS Report for Congress, 2006.

[3] 2009/28/EC, Directive 2009/28/EC of the European Parliament and of the Council of 23 April 2009 on the promotion of the use of energy from renewable sources and amending and subsequently repealing Directives 2001/77/EC and 2003/30/EC, 2009.

[4] USEPA, Renewable Fuel Standard Program (RFS2) Regulatory Impact Analysis. US Environmental Protection Agency, 2010.

[5] U. Fritsche, K. Hennenberg, and K. Huenecke, The “iLUC factor” as a means to hedge risks of GHG emissions from indirect land use change, Darmstadt: Oeko-Institut, 2010.

[6] D. Morris, Ethanol and Land Use Changes. Policy Brief, 2008.

[7] H. Kim, S. Kim, and B. Dale, Biofuels, land use change, and greenhouse gas emissions: some unexplored variables, Environmental Science & Technology 43, 2009, pp. 961-967.

[8] E. Gnansounou, L. Panichelli, A. Dauriat, and J. Villegas, Accounting for indirect land-use changes in GHG balances of biofuels: Review of current approaches, 2008.

[9] R. Plevin, M. O’Hare, A. Jones, M. Torn, and H. Ginss, Greenhouse gas emissions from biofuels indirect land use change are uncertain but may be much greater than previously estimated, Environmental Science and Technology 44, 2010, pp. 8015-8021.

[10] D. Lapola, R. Schaldach, J. Alcamo, A. Bondeau, J. Koch, C. Koelking, and J. Priess, Indirect land-use changes can overcome carbon savings from biofuels in Brazil, Proceedings of the National Academy of Sciences 107, 2010, pp. 3388-3393.

[11] R. Searchinger, R. Heimlich, R. Houghton, F. Dong, A. Elobeid, J. Fabiosa, S. Tokgoz, D. Hayes, and T. Yu, Use of U.S. Croplands for biofuels increased greenhouse gases through land-use change, Science 319, 2008, pp. 1238-1240.

[12] R. Edwards, D. Mulligan, and L. Marelli, Indirect land use change from increased biofuels demand, European Commission, Joint Research Institute, 2010.

[13] J. Melillo, J. Reilly, D. Kicklighter, A. Gurgel, T. Cronin, S. Paltsev, B. Felzer, X. Wang, A. Sokolov, and C. Schlosser, Indirect emissions from biofuels: how important?, Science 326, 2009, pp. 1397-1399.

[14] W. Lywood, Indirect effects of biofuels, Renewable Fuels Agency, 2008.

[15] A. Liska and R. Perrin, Indirect land use emissions in the life cycle of biofuels: regulations vs. science, Biofuels, Bioproducts and Biorefining 3, 2009, pp. 318-328.

[16] J. Kløverpris, K. Baltzer, and P. Nielsen, Life cycle inventory modeling of land use induced by crop consumption. Part 2: Example of wheat consumption in Brazil, China, Denmark and the USA, Int. Journal of Life Cycle Assessment 15, 2010, pp. 90-103.

[17] L. Fargione, J. Hill, S. Polasky, and P. Hawthorne, Land clearing and the biofuel dept, Science 319, 2008, pp. 1235-1238.

[18] B. Wicke, V. Dornburg, M. Junginger, and A. Faaij, Wicke B, Dornburg V, Junginger M, Faaij A. Different palm oil production systems for energy purposes and their greenhouse gas implications, Biomass and Bioenergy 32, 2008, pp. 1322-37.

[19] IPCC, Good Practice Guidance for LULUCF, 2003.

[20] N. La Scala, A. Lopes, K. Spokas, D. Bolonhezi, D. Archer, and D. Reicosky, Short-term temporal changes of soil carbon losses after tillage described by a first-order decay model, Soil and Tillage Research 99, 2008, pp. 108-118.

[21] D. Reicosky, W. Dugasb, and H. Torbert, Tillage-induced soil carbon dioxide loss from different cropping systems, Soil and Tillage Research 41, 1997, pp. 105-118.

[22] F. Scheffer and P. Schachtschabel, eds., Lehrbuch der Bodenkunde, Heidelberg, Germany: Spektrum Akademischer Verlag, 2002.

[23] E. Menichetti and M. Otto, Energy balance and greenhouse gas emissions of biofuels from a life-cycle perspective, Biofuels: Environmental Consequences and Interactions with Changing Land Use, R. Howarth and S. Bringezu, eds., International Biofuels Project Rapid Assessment, 2009, pp. 81-109.

[24] RFA, Indirect effects of biofuels. Study by the Renewable Fuels Agency, 2008.

[25] U. Lahl, iLUC und Biokraftstoffe in der Analyse - Regionale Quantifizierung klimaschädlicher Landnutzungsänderungen und Optionen zu deren Bekämpfung, Oyten.

[26] J. Fabiosa, Land-use credits to corn ethanol: accounting for distillers dried grains with solubles as a feed substitute in swine rations. Working Paper 09-WP 489, Center for Agricultural and Rural Development. IOWA State University, 2009.

[27] W. Lywood, J. Pinkney, and S. Cockerill, Impact of protein concentrate coproducts on net land requirement for European biofuel production, GCB Bioenergy 1, 2009, pp. 346-359.

[28] E. Özdemir, M. Härdtlein, and L. Eltrop, Land substitution effects of biofuel side products and implications on the land area requirement for EU 2020 biofuel targets, Energy Policy 37, 2009, pp. 2986-2996.

[29] P. Havlik, U. Schneider, E. Schmid, H. Böttcher, S. Fritz, R. Skalsky, K. Aoki, S. De Cara, G. Kindermann, F. Kraxner, S. Leduc, I. Mc Callum, A. Mosnier, T. Sauer, and M. Obersteiner, Global land-use implications of first and second generation biofuel targets, Energy Policy. Article in press, 2010.

[30] D. Rajagopal, G. Hochman, and D. Zilberman, Indirect fuel use change (IFUC) and the lifecycle environmental impact of biofuel policies, Energy Policy 39, 2011, pp. 228-233.

Climate change mitigation through increased biomass production and substitution: A case study in north-central Sweden

Bishnu Chandra Poudel[1,*], Roger Sathre[1], Leif Gustavsson[1,2], Johan Bergh[1,3]

[1] *Ecotechnology, Mid Sweden University, Östersund, Sweden*
[2] *Linnaeus University, Växjö, Sweden*
[3] *Southern Swedish Forest Research Centre, Swedish University of Agricultural Sciences, Alnarp, Sweden*
** Corresponding author. Tel: +4663165535, E-mail: bishnu.poudel@miun.se*

Abstract: In this study, we perform an integrated analysis to calculate the potential increases in forest biomass production and substitution as an effect of climate change and intensive management. We use the BIOMASS model to simulate change in Net Primary Production due to climate change. Then we estimate the development of forest biomass growth and harvest by using the HUGIN model, the change in soil carbon stock by the use of the Q-model, and the biomass substitution benefits by the use of an energy and material substitution model. Our results show that an average regional temperature rise of 4 °C could increase annual whole tree forest biomass production by 32% and harvest by 29% over the next 100 years. Intensive forest management including climate effect could increase whole tree biomass production by 58% and harvest by 47%. A total net reduction in carbon emissions of up to 89 Tg C and 182 Tg C over 100 years is possible due to climate change effect only and due to climate change plus intensive forestry, respectively. The carbon stock in standing biomass, forest soils and wood products all increase, but the carbon stock changes are less significant than the substitution benefits.

Keywords: *Forest biomass, Carbon, Bioenergy, Construction material, Intensive forestry*

1. Introduction

Increasing atmospheric concentration of greenhouse gases (GHGs) increase earth's surface temperature [1]. The Intergovernmental Panel on Climate Change (IPCC) [2] affirms that the temperature increase will be greater in the higher latitudes. The regional climate model by the Swedish Meteorological and Hydrological Institute (SMHI) [3] based on IPCC B2 scenario projects a 4 °C average temperature increase in north-central Sweden in the next 100 years.

The increasing temperature has significant impact on physical systems. It provides a longer growing season for the trees and favorable conditions for photosynthesis that stimulates Net Primary Production (NPP) [4]. Thus, an increased temperature is expected to produce more biomass in the boreal forests [5]. Although the boreal forest is considered as less productive due to low soil temperature and low nitrogen availability [6], production can further be increased by adding nutrients, by species change, and by changes in management practices [7, 8]. As a result, there will likely be larger harvest levels available in future.

The increased forest biomass can be used as a substitute for fossil fuels and carbon intensive materials to reduce carbon emissions through several mechanisms [9]. Using biomass to substitute for fossil fuels directly avoids fossil carbon emissions, except to the extent that fossil fuels are used to operate the biomass system [10]. Using biomass to substitute for carbon-intensive materials may reduce carbon emissions by lowering fossil energy use during the manufacture of products, by avoiding industrial processes emissions, by increasing carbon stocks in wood materials, by using biomass residues to replace fossil fuels, and possibly by carbon sequestration or emissions from wood products deposited in landfills [11, 12].

This paper describes an integrated assessment of the potential forest biomass increase as an effect of climate change and intensive forestry practices in north-central Sweden, and

potential climate change mitigation with increased biomass use. Using five scenarios for forest production and two scenarios for biomass utilization, we estimate the increased biomass production, its harvest level, and carbon benefits from the substitution of non-wood materials and fossil fuels. We also estimate the carbon stock changes in standing biomass, soil, and wood products, and finally quantify the overall carbon balance for each scenario.

2. Methodology

2.1. Study area

This study considers Jämtland and Västernorrland, two counties in north-central Sweden. The area lies from 61° 33' to 65° 07' N latitude and from 12° 09' to 19° 18' E longitude. The forest land area is about 3.5 and 1.9 million ha, respectively. Of this area, productive forests[1] excluding protected areas cover about 2.6 million ha and 1.7 million ha, respectively [13].

2.2. Climate change

IPCC Special Report on Emission Scenarios (SRES) [14] describes potential GHG emissions pathways during the 21st century based on the main driving forces of GHG emissions, considering their underlying uncertainties. Our regional climate scenarios are based on the IPCC B2 global scenario, corresponding to moderate emissions of GHGs leading to an atmospheric CO_2 concentration of 572 ppm by the year 2085, with model RCA3 (The Rossby Centre's regional Atmospheric model) that uses a grid of approximately 50 km x 50 km. The RCA3 model uses global driving variables from the general circulation model ECHAM4/OPYC3 [15] covering the period of 1961-2100. Climate projections for north-central Sweden are for an increase in average annual temperature of 4 °C by 2100 [16].

2.3. Scenarios

We compare forest biomass production in a *Reference* scenario that assumes the current forest management practices without any climate change effect, and four scenarios that include climate change effect: *Current*, *Environment*, *Production*, and *Maximum*, (Table 1).

Table 1. Overview of scenarios analyzed in this study.

Scenario	Climate	Forest management goals	Biomass use
Reference	No change	Reference (current management)	Stem wood or whole tree
Current	Change	Current management	Stem wood or whole tree
Environment	Change	Fulfill environmental goals	Stem wood or whole tree
Production	Change	Increase biomass production	Stem wood or whole tree
Maximum	Change	Maximize biomass production	Stem wood or whole tree

The Current scenario assumes a continuation of current forest management practices. The Environment scenario assumes the fulfillment of additional environmental goals, e.g. 8% of total forest land is set aside for reserves, and 14% of total forest land is given special environmental care. The Production scenario uses additional silvicultural practices, e.g. improved genetic material plantation, soil scarification, selection of tree species, increased traditional fertilization and a balanced nutrient supply [8]. The Maximum scenario uses silvicultural practices to maximize the production by replacing of Scots pine with lodge-pole

[1] Non-productive forests are defined as forests with production capacity less than 1 m^3 per ha and year.

pine (*Pinus contorta*) and by adding balanced nutrient supply in young stands of lodge-pole pine and Norway spruce. The effect of a lower and higher precipitation is considered in the scenarios and had no significant effect on production in northern Sweden [4]. The scenarios are described in more detail in [17].

2.4. Forest production modeling

The process-based growth model BIOMASS describes the processes of radiation absorption, canopy photosynthesis, phenology, allocation of photosynthates among plant organs, litter-fall, and stand water balance in a tree [18]. BIOMASS uses Swedish National Forest Inventory (NFI) database and current temperature for *Reference* scenario and increased temperature based on RCA3 climate model (see Section 2.2) for the estimation of NPP. Values of daily precipitation are used in NPP simulations. The parameterization is valid for mesic soils, and the effects of water deficits would be more pronounced on drier sites [7]. Water deficits seem to be at a low level in simulations, since extremely dry summers didn't occur in the data set, which could lead to substantial losses in production. Output data on NPP from the BIOMASS are used to determine the growth functions in the HUGIN model [5, 17] an empirical model for long-term forecasts of timber yield and harvest level [19]. It uses sample plots from NFI, defining initial conditions for the model in order to describe the forest conditions during the development of young stands, their establishment, and the sivicultural treatments. The growth simulators in HUGIN are valid for all forest land in Sweden, for all types of stands, with a wide range of management alternatives [19].

2.5. Soil carbon modeling

The Q-model describes changes in soil carbon stock based on litter inputs, soil temperature, and the decomposition of litter fractions [20]. It uses old carbon in the soil, litter inputs from standing trees, thinnings and harvests, and soil carbon from fine roots. The decomposition in response to temperature is calculated as in Ågren et al. [21] and Bosatta and Ågren [20]. For more details see [5].

2.6. Biomass use modeling

The harvested biomass in thinnings and final fellings is assumed to substitute non-wood materials and fossil fuels. In the "stem wood" option we assume that 95% of coniferous stem wood (>20 cm diameter) is harvested and used as construction material to replace reinforced concrete [5, 11, 17]. The small stems and processing residues of coniferous trees, and all deciduous stem wood, is used as biofuel. In the "whole tree" option, in addition to stem wood use, 75% of branches and tops, 25% of needles, and 50% of stumps are harvested and used as biofuel [5, 11, 17]. Biofuel is assumed to replace coal in stationary plants.

2.7. Forest operations and fertilization

We account for emissions from fossil fuels used for forest management activities including stand establishment, thinnings, final harvest of round wood, and forwarding and transport of round wood to mills [22]. GHG emissions associated with production and use of fertilizers include CO_2, N_2O and CH_4 and are converted to CO_2 equivalent using global warming potentials (GWP) over a 100-year time horizon [1]. Primary energy use and GHG emissions for the production of Skog-CAN fertilizer (27-0-0) and Opti-Crop fertilizer (24-4-5) are based on Davis and Haglund [23]. The amount of fossil fuel used for fertilizer application by helicopter is based on Mead and Pimentel [24].

3. Results and discussions

3.1. Forest biomass production and harvest

Figure 1 shows the annual forest biomass production and harvest in all scenarios at the end of the study period. The annual whole tree biomass production in the *Reference* scenario is 12.8 Tg year^{-1} at the end of the study period compared to 11.0 Tg year^{-1} in the beginning of the study, a 17% increase during the 100-year period. The corresponding increases for the *Current, Environment, Production and Maximum* scenarios are 49%, 40%, 53%, and 75%, respectively. Thus biomass production increases in the *Current, Environment, Production and Maximum* scenarios are respectively 32%, 23%, 36% and 58% greater compared to the *Reference* scenario increase. The whole tree harvest in the *Current* scenario increases by 31% more and in the *Maximum* scenario by 50% more than the *Reference* scenario. The increase in stem wood biomass production for the *Maximum* scenario is 57% greater and the harvest is 54% greater compared to the *Reference* scenario.

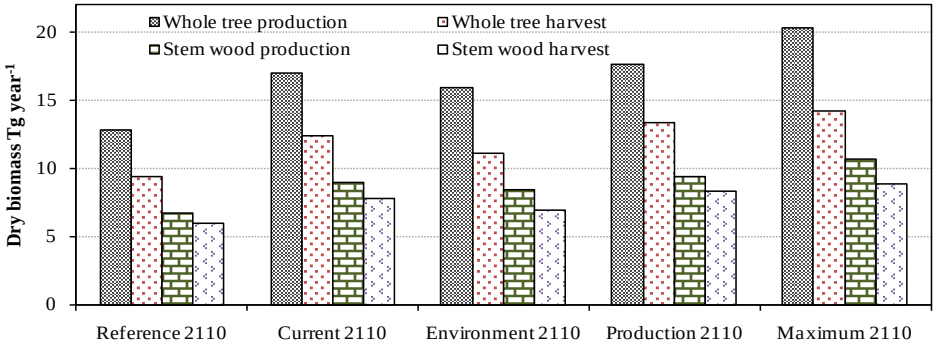

Fig. 1. Annual forest biomass production and harvest (Tg year^{-1}) in all scenarios at the end of the study period in Jämtland and Västernorrland.

Figure 2 shows the cumulative biomass harvest for all products in different scenarios during the 100 year. Stem wood is the largest fraction, while stumps are the second largest. The stump values might be slightly overestimated because of the Marklund's revised function [25] that estimates stump biomass based on spruce stumps which likely overestimates the deciduous tree stumps [5].

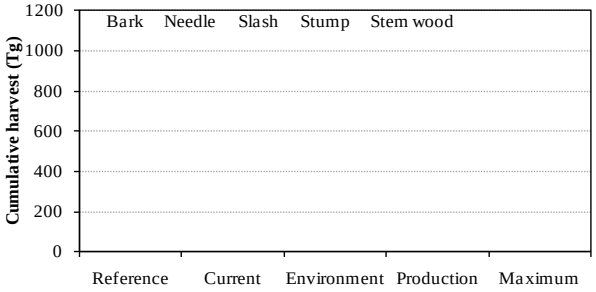

Fig. 2. Cumulative biomass harvest (Tg dry matter) for all products in the different scenarios during 100-years in Jämtland and Västersorrland.

The increased production in the *Current* scenario is caused by climate change, while in the other scenarios are the results of climate change plus intensive forestry practices such as species change, fertilization, and intensive silvicultural action [5].

3.2. Carbon stock in standing biomass, forest soils, and wood products

Annual carbon stocks in living tree biomass, soil and harvested wood products with whole tree harvest increase in all scenarios (Fig. 3). *Maximum* scenario has the largest carbon stock in forest biomass, followed in descending order by *Environment*, *Production*, *Current* and *Reference* scenarios. *Maximum* scenario has the largest soil carbon stock, followed by the *Reference* and *Production* scenarios. Caron stock increases slowly in the *Environment* and *Current* scenario after 30 years compared to the other scenarios (Fig. 3). Wood product carbon stock is also largest in *Maximum* scenario, followed by the *Production* and *Current* scenarios, while *Environment* and *Reference* have smaller. The larger carbon stock is due to larger volume of stem wood harvested and used as building materials, however, after the life span of buildings, the carbon stock may stabilize due to the demolition of old buildings [17].

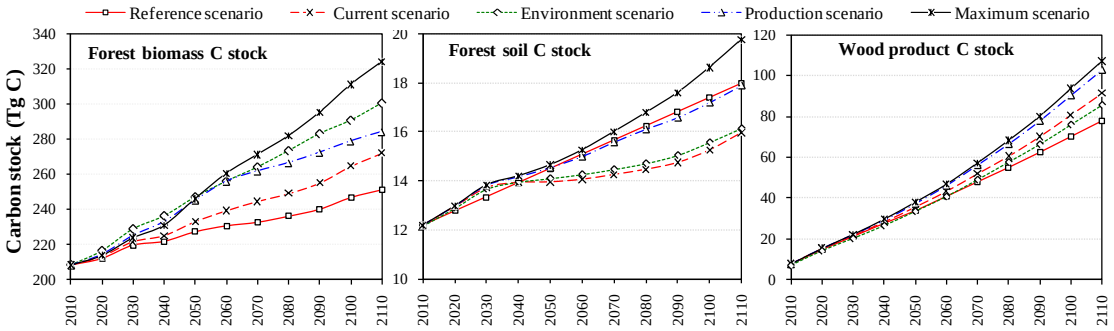

Fig. 3. Annual carbon stocks (Tg C) in living forest biomass, forest soil, and wood products in the different scenarios during 100-years in Jämtland and Västernorrland. Note differences in scale.

Table 2. Average annual avoided carbon emissions due to forest biomass use (Tg C y^{-1}) during each 10-year period for Jämtland and Västernorrland.

	2010-2019	2020-2029	2030-2039	2040-2049	2050-2059	2060-2069	2070-2079	2080-2089	2090-2099	2100-2109
Reference Scenario										
Stem wood	3.8	3.7	3.6	3.7	3.9	3.9	3.9	4.0	4.0	4.2
Whole tree	4.9	4.7	4.8	4.8	5.1	5.1	5.0	5.1	5.1	5.4
Current Scenario										
Stem wood	3.9	3.8	3.8	3.9	4.3	4.4	4.7	4.7	5.1	5.6
Whole tree	5.0	4.9	5.0	5.1	5.6	5.7	6.1	6.1	6.5	7.1
Environment Scenario										
Stem wood	3.6	3.6	3.6	3.7	4.0	4.1	4.3	4.5	4.8	5.0
Whole tree	4.6	4.6	4.7	4.9	5.2	5.3	5.5	5.7	6.1	6.4
Production Scenario										
Stem wood	3.9	3.8	4.0	4.2	4.6	5.0	5.3	5.4	5.8	6.2
Whole tree	4.9	5.0	5.2	5.5	6.0	6.4	6.7	6.8	7.3	7.8
Maximum Scenario										
Stem wood	3.9	3.9	4.1	4.3	4.7	5.0	5.5	5.7	6.0	6.6
Whole tree	5.0	5.0	5.4	5.6	6.0	6.4	7.0	7.2	7.6	8.4

3.3. Biomass substitution

Biomass substitution is largest in Maximum scenario (Table 2). The cumulative avoided carbon emission due to use of stem wood and whole tree biomass for Maximum scenario is 497 and 635 Tg C, respectively. As Maximum and Production scenarios have larger harvests,

they will give larger substitution benefits. When compared to the Reference scenario, Maximum and Production scenarios give 136 Tg C and 116 Tg C greater benefits, while Environment and Current scenario have comparatively smaller substitution benefits.

3.4. Carbon balance

Cumulative avoided carbon emission over 100 years for all scenarios with the use of whole tree biomass is shown in Figure 4. Biomass substitution is the largest contributor to the carbon balance. The avoided carbon emission due to biomass substitution with recovered harvest slash and stumps is greater than the reduced increase in soil carbon stock in the forest due to harvest of whole tree biomass. The total avoided emissions in the Maximum and Production scenarios are 182 Tg C and 117 Tg C greater than in the Reference scenario over the 100-year period for whole tree biomass use. The corresponding numbers for the Environment and Current scenarios are 31 and 48 Tg C, respectively.

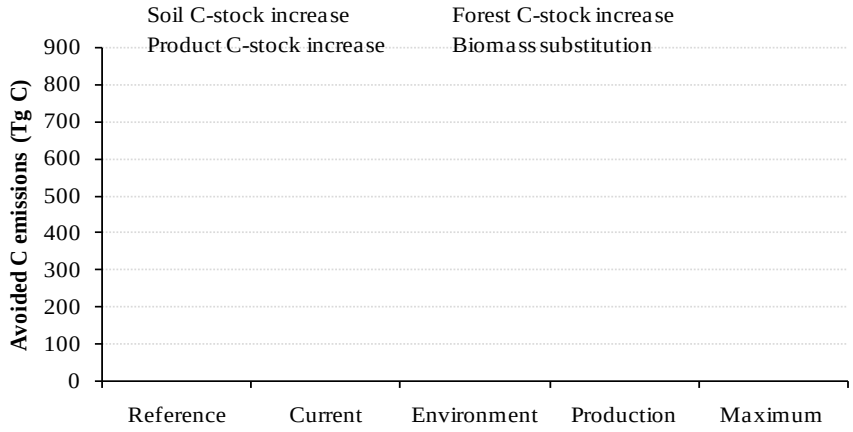

Fig. 4.Cumulative avoided carbon emissions (Tg C) over 100- years for all scenarios with whole tree biomass use for Jämtland and Västernorrland.

4. Conclusions

Climate change may substantially increase the production of biomass in boreal forests. The production can be further increased by intensive forestry practices. The increased forest biomass, if used to substitute for fossil fuels and carbon intensive materials, can avoid carbon emissions, thus contributing to climate change mitigation. This is a negative feedback on climate change. The substitution potential depends on the amount and type of forest biomass harvest. Thus, larger biomass harvests create greater substitution potential.

In this study, significant uncertainties can be observed. Net increase of greenhouse gases, driving the temperature change, depends on several factors as the development of the global population, economic growth, and on mitigation actions to be taken. The results may vary somewhat with differences in the temperature and other corresponding variables. Regional temperature increases may differ from our assumptions. Fire risk, pathogens and insect damage which may cause tree mortalities are not accounted in our study. The HUGIN model overestimates biomass in deciduous living mature trees and stumps. HUGIN does not have a function to calculate self thinning in living deciduous trees, which may lead to an overestimation of biomass in *Environment* scenario. Nevertheless, although these uncertainties may alter the exact values that we have calculated, it appears that our general conclusions are robust.

Acknowledgement
We gratefully acknowledge the support of European Union, County Administrative Board of Jämtland, Sveaskog AB, SCA Forest Products, Norrskog/SÅTAB, Jämtkraft AB. We also thank two anonymous reviewers for their comments.

References

[1] IPCC, Climate Change: The Physical Science Basis. Contribution of Working Group I to the Fourth Assessment Report of the Intergovernmental Panel on Climate Change, ed. S. Solomon, et al. 2007: Cambridge University Press, United Kingdom and New York, USA.

[2] IPCC, The Scientific Basis: Contribution of Working Group I to the Third Assessment Report of the Intergovernmental Panel on Climate Change. 2001, New York , USA: Cambridge University Press.

[3] SMHI. Climatic data, Swedish Meteorological and Hydrological Institute. 2009 [cited 2009 2, August]; Available from: http://www.smhi.se/cmp/jsp/polopoly.jsp?d=8785&l=sv.

[4] Bergh, J., U. Nilsson, B. Kjartansson, and M. Karlsson, Impact of climate change on the productivity of Silver birch, Norway spruce and Scots pine stands in Sweden with economic implications for timber production., Eco.Bulletins, 53(15), 2010: pp. 185-195.

[5] Poudel, B.C., R. Sathre, L. Gustavsson, J. Bergh, A. Lundström, and R. Hyvönen, Effects of climate change on biomass production and substitution in north-central Sweden, Manuscript, 2010.

[6] Tamm, C.O., Nitrogen in terrestrial ecosystems, Ecological Studies, (81) 1991: pp. 1-115.

[7] Bergh, J., U. Nilsson, B. Kjartansson, and M. Karlsson, Impact of climate change on the productivity of Silver birch, Norway spruce and Scots pine stands in Sweden with economic implications for timber production., Ecological Bulletins, 53(15), 2010: pp. 185-195.

[8] Skogsstyrelsen, Skogliga konsekvensanalyser – SKA-VB 08 in Swedish Forest Agency Rapport. 2008, Skogsstyrelsen, Sweden.

[9] Schlamadinger, B., M. Apps, F. Bohlin, L. Gustavsson, G. Jungmeier, G. Marland, K. Pingoud, and I. Savolainen, Towards a standard methodology for greenhouse gas balances of bioenergy systems in comparison with fossil energy systems, Biomass and Bioenergy, 13(6), 1997: pp. 359-375.

[10] Hall, D.O. and J.I. House, Trees and biomass energy: Carbon storage and/or fossil fuel substitution?, Biomass and Bioenergy, 6(1-2), 1994: pp. 11-30.

[11] Gustavsson, L., K. Pingoud, and R. Sathre, Carbon dioxide balance of wood substitution: comparing concrete- and wood-framed buildings, Mitigation and Adaptation Strategies for Global Change, 11(3), 2006: pp. 667-691.

[12] IPCC, Climate Change: Mitigation of Climate Change. Contribution of Working Group III to the Fourth Assessment Report of the Intergovernmental Panel on Climate Change. 2007: Cambridge University Press, United Kingdom and New York, USA.

[13] Skogsstyrelsen. Forestry Statistics, Swedish Forest Agency. 2009 [cited 2009 2, August]; Available from: http://www.svo.se/episerver4/default.aspx?id=38515

[14] IPCC, Special Report on Emissions Scenarios, in Emission Scenarios. Special Report of Working Group III of the Intergovernmental Panel on Climate Change. 2000, Cambridge University Press, UK.

[15] Kjellström, E., L. Bärring, S. Gollvik, U. Hansson, C. Jones, P. Samuelsson, M. Rummukainen, A. Ullerstig, Willén, and K. Wyser, A 140-year simulation of European climate with the new version of the Rossby Centre regional atmospheric climate model (RCA3), in SMHI Reports in Meteorology and Climatology, No. 108. 2006, SMHI: Norrköping, Sverige. pp. 54.

[16] SMHI. Climatic data, Swedish Meteorological and Hydrological Institute. 2009 [cited 2009, August, 2]; Available from: http://www.smhi.se/cmp/jsp/polopoly.jsp?d=8785&l=sv.

[17] Poudel, B.C., R. Sathre, L. Gustavsson, J. Bergh, A. Lundström, and R. Hyvönen, Potential effects of intensive forestry on biomass production and substitution in north-central Sweden, Manuscript, 2010.

[18] McMurtrie, R.E., D.A. Rook, and F.M. Kelliher, Modelling the yield of Pinus radiata on a site limited by water and nitrogen, Forest Ecology and Management, 30(1-4), 1990: pp. 381-413.

[19] Lundström, A. and U. Söderberg. Outline of the Hugin system for longterm forecasts of timber yields and possible cut. In Large-Scale Forestry Scenario Models: experiences and requirements. 1996: EFI proceeding.pp. 63-77

[20] Bosatta, E. and G.I. Ågren, Theoretical analyses of carbon and nutrient dynamics in soil profiles, Soil Biology and Biochemistry, 28(10-11), 1996: pp. 1523-1531.

[21] Ågren, G., R. Hyvönen, and T. Nilsson, Are Swedish forest soils sinks or sources for CO_2—model analyses based on forest inventory data, Biogeochemistry, 82(3), 2007: pp. 217-227.

[22] Berg, S. and E.-L. Lindholm, Energy use and environmental impacts of forest operations in Sweden, Journal of Cleaner Production, 13(1), 2005: pp. 33-42.

[23] Davis, J. and C. Haglund, Life cycle inventory (LCI) of fertiliser production - Fertiliser products used in Sweden and Western Europe, in SIK Report No. 654, SIK. 1999, The Swedish Institute for Food and Biotechnology Göteborg, Sweden.

[24] Mead, D.J. and D. Pimentel, Use of energy analyses in silvicultural decision-making, Biomass and Bioenergy, 30(4), 2006: pp. 357-362.

[25] Pettersson, H. and G. Ståhl, Functions for belowground biomass of Pinus sylvestris, Picea abies, Betula pendula and Betula pubescens in Sweden, Scandinavian Journal of Forest Research, (21) 2006: pp. 84-93.

Influence of biofuels production on the climate change

Carlos A. Cardona[1,*], Monica J. Valencia[1], Julian A. Quintero[1]

[1] *Universidad Nacional de Colombia, Manizales, Colombia*
** Corresponding author. Tel: +0578879300, Ext50199, Fax:+0578879300, Ext 501199, E-mail: ccardonaal@unal.edu.co*

Abstract: This work technically analyzes the biodiesel production from palm, bioethanol production from sugar cane and biotechnological hydrogen productions as well as the GHG emissions associated with the feedstocks production and processing. For this purpose modeling and simulation was used in combination with ASPEN PLUS software and Ecoinvent database for GHG calculations derived from material and energy balances obtained by process simulation. Different critical stages were simulated and analyzed: fertilizers production and use, biofuel production and pesticide production. Results indicated the importance of considering different stages and how these inclusions or exclusions affect GHG balances. For instance, fossil fuel used for industrial stage in bioethanol production increase GHG emissions eighteen-fold. According to this work, bioethanol from sugar cane was the system with largest emissions while biodiesel from palm oil had lowest emissions.

Keywords: *Green House Gas emissions, Climate change, Biodiesel, Bioethanol, Biohydrogen.*

1. Introduction

Current energy situation has reached a critical point according to different points of view: economical, social and environmental aspects [1]. It is necessary to find substitutes for conventional fuels in order to avoid environmental and social adverse effects derived from its non-renewability [2-6]. Usually, the best alternative to conventional fuels should be a substance with high calorific value, availability, easy production, transport and use. However, last is also limited by several social and environmental policies which can frustrate the possibilities to find quick and satisfactory solutions [6-7].

In the last decades it has been found as possible solution the development of biofuels as replacement for fossil fuels [8,9]. The biofuels are produced from different types of biomass and they are subject of exhaust investigations [5,8]. Today, biofuels are considered to be bioethanol, biobutanol, biodiesel, biogas and biohydrogen [9].

Bioethanol and biodiesel have been thoroughly investigated worldwide and a proof of this is the industrial plants available in America, Asia and Europe [7]. Bioethanol is produced by fermentation of sugars, starch crops or lignocellulosic materials [10]. Biodiesel is produced by extraction and methyl or ethyl- transesterification of oils contained in oleagineous plants or waste oils [4,8]. Regardless development level reached for these fuels it is suggested, but not unequivocally proven, the connection to global warming because GHG emissions with their production and use, specifically in agricultural stage [1-3,5,8,11,12]. Scientists hold unprecedented debate relating to assessment of environmental aspects in biofuels production. Many studies have been made, but their results have not helped to provide strong response and quantitative information about relationship between biofuels production and use and climate change using global warming potential [2,5,8].

Hydrogen is an energy source of recent consideration although it is a very important industrial material and its heating value and clean combustion are already well known [13-15]. Extensive investigation for this fuel use is a relatively new issue [16,17]. Different researchers focus new goals in finding biological pathways for competitive hydrogen production [16,18]. Currently, there is no a known biohydrogen production technology competitive compared to

other fuels[19-22]. The present work analyses for biohydrogen case the environmental assessment for dark fermentation technology.

2. Methodology

Biofuel assessment was carried out through quantification of GHG emissions associated with biofuel production. Input information is listed in table 1. Figure 1 shows generic process flowsheet for biofuels analysis. Analysis was separated in two parts:

- Agricultural stage: This phase contains all GHG emissions associated with biomass growth. It was assumed that the respiration process during the growth of biomass absorbs CO_2 emissions from biofuel combustion. Considered N-fertilizer was ammonium nitrate, P-fertilizer was triple superphosphate and K-fertilizer was potassium chloride. The used pesticide was carbofuran. During the mechanical harvest, the fuel used was diesel. 1.325% N-fertilizer was emitted as N_2O to the atmosphere [5].
- Industrial stage: Where biomass is converted to biofuel. GHG emissions were calculated from mass and energy balances of the biofuel production from biomass using Aspen Plus ® and Matlab® Softwares following rigorous models and synthesis procedures as described in [31,32]. Production rates were based mostly on Colombian biofuels production.

The functional unit was megajoule of energy per biofuel produced. Comparisons between studies are made using the work with lowest GHG emissions for each biofuel. Below are described the systems studied.

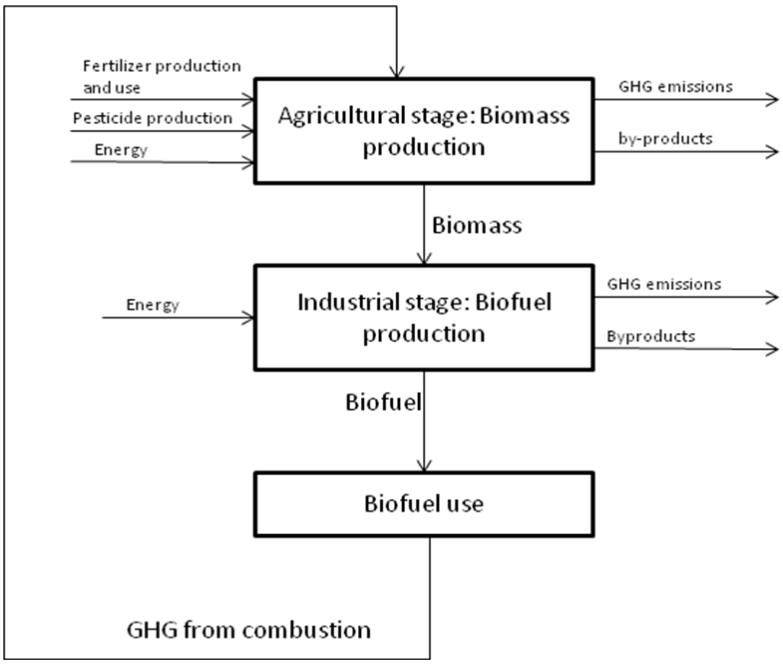

Fig 1. Process included in this work for all biofuels studied

2.1. Bioethanol from sugarcane

Information for agricultural stage was obtained from Ecoinvent database [33], which includes emissions from: fertilizer production, fertilizer use, pesticide uses, harvesting, 20% mechanical harvest. Industrial stage phase was simulated using Aspen Plus® software. Conversion technologies were fermentation, distillation and dehydration with molecular sieves.

Table 2. Values used in this study

Parameter	*Value*	*Reference*
Production rate (L/yr). Bioethanol from sugarcane	*52,800,000*	
Production rate (L/yr). Biodiesel from palm	*33,400,000*	
Production rate (L/yr). Biohydrogen from molasses	*9,504,000*	
N-P-K fertilizer. Palm. (kg/Ha)	*41.2-147.8-804*	*[23]*
Pesticide. Palm. (kg/Ha)	*1.2*	*[23]*
Factor emissions for N-fertilizer ($KgCO_2e/KgN$)	*8.66*	*[24]*
Factor emissions for P-fertilizer ($KgCO_2e/KgP_2O_5$)	*2.1*	*[24]*
Factor emissions for K-fertilizer ($KgCO_2e/KgK_2O$)	*0.90*	*[24]*
Factor emissions for pesticide ($KgCO_2e/Kg$)	*12.98*	*[24]*
Factor emissions for agricultural stage. Sugarcane. ($KgCO_2e/Kgsugarcane$)	*0.028*	*[24]*
Factor emissions for electricity ($KgCO_2e/Kwh$)	*0.306*	*[25]*
Isothermal compression efficiency (biohydrogen) (%)	*65*	*[20]*
Recuperation percentage of biofuel (%)	*99*	
Compression pressure (biohydrogen) (atm)	*200*	
Maximum hydrogen production rate (ml H_2/h)	*13.7*	*[26]*
Lag-time (h)	*4.04*	*[26]*

2.2. Biodiesel from palm

GHG emissions in agricultural stage were considered for: fertilizer production and use, pesticide production and manual harvest. Location of the production plant was considered close to the field. Industrial phase was simulated using Aspen Plus ® S oftware and the conversion technology included oil extraction followed by transesterification with methanol, neutralization and distillation.

2.3. Biohydrogen from molasses

Agricultural phase was considered to be the same as sugarcane case. Molasses were obtained as co-product from sugar industry. Information required was taken from Ecoinvent database. Biohydrogen was produced by dark-fermentation using mixed culture for their production. Data for industrial phase was calculated using Matlab® software and the emissions corresponded to fermentation, separation and compression steps.

3. Results and Discussion

Figure 2 summarizes GHG emissions associated to biofuel production for each feedstock. According to the Figure 2, biodiesel from palm was the system with the lowest GHG emissions for all stages, while bioethanol from sugar cane showed the biggest GHG emissions in its industrial phase. The total GHG emissions for bioethanol were eight-fold related to biodiesel and total GHG emissions for biohydrogen is twice bigger that biodiesel.

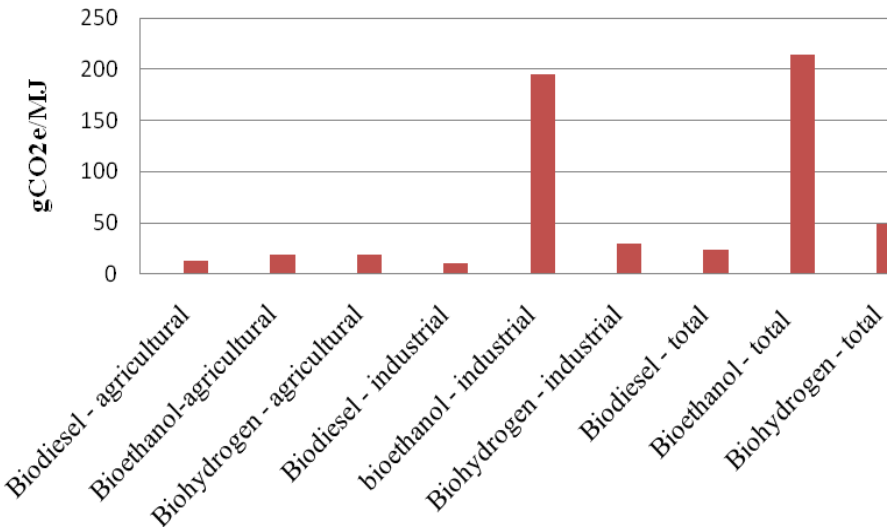

Fig. 2. GHG emissions for each system studied

Figure 3 shows emissions from different works. Macedo et al [27] and Smeets et al. [28] calculated emissions for bioethanol from sugarcane in Brazil; Yee et al [29] calculated emissions for biodiesel from palm in Malaysia and de Souza et al [23] studied biodiesel from palm oil in Brazil; Manish and Banerjee [30] estimated emissions for biohydrogen from sugarcane juice in India. In figure 3 differences between all studies are observed, even in works considering the same biofuel production. Taking as basis work for the bioethanol comparisons the one of Smeets et al. [28], GHG emissions obtained by Macedo et al [27] were almost twice bigger while for this work were eighteen-fold bigger. Based on de Souza et al [23] work for the Biodiesel comparisons, GHG emissions obtained by Yee et al [29] were more than twice bigger while for this work was one-third bigger. GHG emissions for biohydrogen in this work were eleven-fold bigger than that obtained by Manish and Banerjee [30]. Below, the obtained results are discussed in detail for each biofuel.

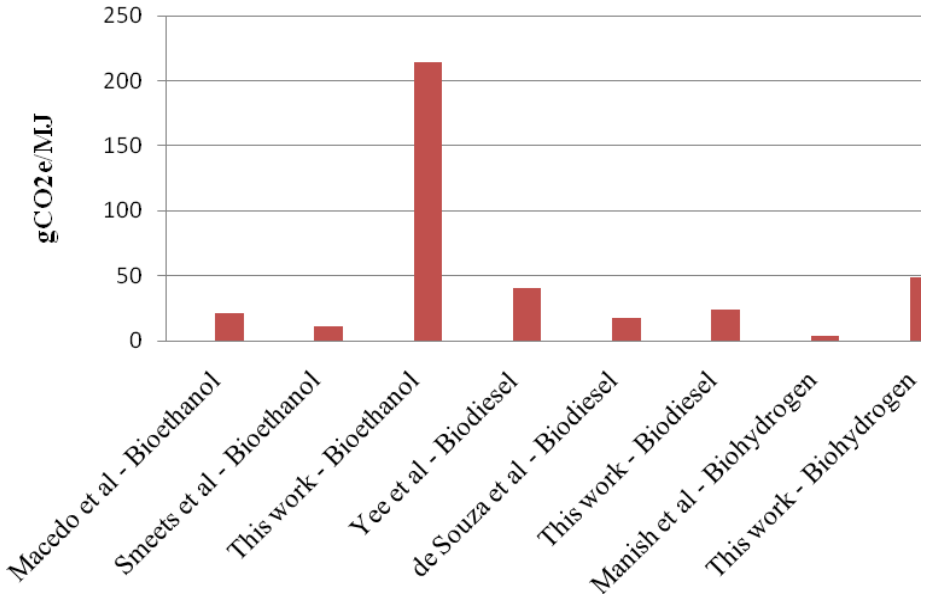

Fig. 3. GHG emissions for different studies

3.1. Bioethanol

Smeets et al. [28] study, Macedo et al. [27] study and this work differ in GHG emissions values. Smeets et al. [28] study reported lowest GHG emissions but in this paper were obtained the highest emissions. Macedo et al. [27] is considered a rigorous analysis for agricultural stage and took into account sugarcane burning. However, these authors assumed a self-sustainable plant, which implied zero GHG emissions for industrial stage. This assumption led to obtain low values in this stage.

In the case of Smeets et al. [28] study, it was similar to the Macedo et al [27] study. They assumed a global approach for bioethanol impact and their results were similar to that of Macedo et al [27]. In this work, emissions of industrial phase are bigger because alcoholic fermentation generates large amount of CO_2. Comparison of these works is significant because were made in Brazil and Colombia, countries with similar conditions. Macedo et al. [27] study reported twice GHG emissions and this work report eighteen fold GHG emissions compared to Smeets et al. study. Industrial stage proves to be very significant because of CO_2 emissions from fermentation. The CO_2 release is a problem to be stated seriously specially when land use change applied (and biomass per hectare is reduced).

3.2. Biodiesel

Yee et al. [29] study is very complete. They considered for agricultural stage: planning, nursery establishment, site preparation, field establishing, field maintenance, harvesting, and collection and replanting; milling stage: Fresh Fruit Bunches extraction, stripping and oil extraction. For industrial phase: oil conversion with methanol.

De Souza et al. [23] considered for agricultural stage: Fertilizer, pesticides, transport and manual harvest. For industrial phase: electricity and diesel use, methanol and catalyst; co-products are used for energy cogeneration.

De Souza et al. [23] study showed the lowest emissions while Yee et al. [29] reported the biggest. In this work were obtained intermediate values for emissions. Yee et al. [29] study, considered the largest secondary processes and, therefore, highest GHG emissions were obtained. Nevertheless, Yee et al [29] study was made for Malaysia while de Souza et al. [23] study was performed for Brazil. Using Colombian conditions then is more significant to compare de Souza work with the developed in this work. Taking as reference de Souza et al [23] study, Yee et al. [29] obtained 132% larger GHG emissions and this work reports 35% larger GHG emissions. Differences between De Souza et al. [23] study and these works are due to cogeneration and waste uses. Last, because these aspects change energy balance, and therefore, emissions values and rates.

3.3. Biohydrogen

GHG emissions for this work were around tenfold bigger than that obtained by Manish and Banarjee [30] because they considered exclusively industrial aspects and the input was sugarcane without any reflection of agricultural phase.

3.4. Final analysis

Agricultural stage generates significant GHG emissions because nitrous oxide and methane are emitted into the atmosphere and these gases have a Global Warming Potential (GWP) of 300 and 15 times more than carbon dioxide, respectively. Methane and nitrous oxide come from fertilizers and pesticides application, explaining the importance of their application rate

in biofuels environmental assessment. Moreover, fertilizer production methods are essential for environmental evaluation. This fact explains high emissions factors (table 1) for fertilizer production using conventional technologies.

GHG emissions for biodiesel production were greater for agricultural stage while industrial stage emissions were greater for hydrogen and bioethanol production. This is due to fermentation emissions that strongly influenced the obtained values. Carbon substrate is inadequate, almost from environmental point of view, and traditional biochemical pathways promote high emission levels.

4. Conclusions

Results indicate that the most efficient system, in terms of GHG emission balances, was biodiesel production from palm oil while the system with highest emissions was the bioethanol production. Alcoholic and acetic fermentation proved to be of great influence on emissions balances and demonstrating a number of restrictions if compared to other studies. According to results presented in this paper, bioethanol from sugarcane contribute more to climate change that biohydrogen from sugarcane and biodiesel from palm oil.

References

[1] A. Demirbas, Political, economic and environmental impacts of biofuel: A Review, Applied Energy 86, 2009; pp. S108-117.

[2] D. Larson, A review of life-cycle analysis studies on l iquid biofuel systems for the transport sector, Energy Sustainable Development, X, 2006, pp. 109-126.

[3] S.C Davis, K.J. Andenson-Texeira, E.H. De Lucia, Life cycle analysis and the ecology of biofuel, Trends in Plant Science 14, 2009, pp. 140-146.

[4] R. Hoefnagels, E. Smeets, A Faaij, Greenhouse gas footprints of different biofuel production systems, Renewable and Sustainable Energy Reviews 14, 2010, pp. 1661 - 1694.

[5] F. Cherubini, N.D Bird, A Crowie, G. Jungmeier, B Schlamandinger, S. Woess-Gallasch, Energy and Greenhouse gas-based LCA of biofuel and bioenergy systems: Key issues, ranges and recommendations, Resources, Conservation and Recycling 53, 2009, pp. 197-208.

[6] A. Zidanšek, R. Blinc, A Jeglič, S Kabashi, S. Bekteshi, I. Šlaus, Climate change, biofuel and sustainable future, International Journal of Hydrogen Energy 34, 2009, pp. 6980 - 6983.

[7] E.A. Kaditi, Bioenergy policies in a global context, Journal of Clean Production 17, 2009, pp. 4-8.

[8] P. Borjeson, L.M Tufvesson, Agricultural crop-based biofuel – resource efficiency and environmental performance including direct land use change, Journal of Clean Production, 2010, submitted for publication.

[9] A. Demirbas, Biofuels sources, biofuel policy, biofuel economy and global projections, Energy Conversion and Management 49, 2008, pp. 2106-2116.

[10] M.I. Montoya, J.A Quintero, O.J Sánchez, C.A. Cardona, Evaluación del impacto ambiental del proceso de obtención de alcohol carburante utilizando el algoritmo de

reducción de residuos, Revista Facultad de Ingeniería de la Universidad de Antioquia 36, 2006, pp. 85-95.

[11] H.V. Blottnitz, M.A. Curran, A review of assessment conducted on bioethanol as a transportation fuel from a net energy, greenhouse gas, and environmental life cycle perspective, Journal of Clean Production 15, 2007, pp. 607-619.

[12] S Kim, B.E Dale, Life cycle assessment of various cropping systems utilized for production biofuels: Bioethanol and biodiesel, Biomass and Bioenergy 29, 2005, pp. 426-439.

[13] R. Kothari, D. Buddhi, R.L. Sawhnet, Comparison of environmental and economic aspects of various hydrogen production methods, Renewable and Sustainable Energy Reviews 12, 2008, pp. 2008.

[14] X. Deng, H. Wang, H. Huang, M. Ouyang, Hydrogen flow chart in China, International Journal of Hydrogen Energy 35, 2010, pp. 6475-6481.

[15] M. Balat, M. Balat, Political, economic and environmental impacts of biomass-based hydrogen, International Journal of Hydrogen Energy 34, 2009, pp. 3589-3606.

[16] S.M Kotay, D. Das, Biohydrogen as a renewable energy source – Prospects and potentials, International Journal of Hydrogen Energy 33, 2008, pp. 258-263.

[17] C.J. Winter, Hydrogen energy – Abundant, efficient, clean: A debate over the energy-system-of-change, International Journal of Hydrogen Energy 34, 2009, pp. S1-S52.

[18] D. Das, T.N. Veziroglu, Advances in biological hydrogen production process, International Journal of Hydrogen Energy 33, 2008, pp. 6046-6057.

[19] L.B. Bentner, J. Peccia, J.B. Zimmerman, Challenges in developing biohydrogen as a sustainable energy source: Implications for a research agenda, Environmental Science & Technology 44, 2010, pp. 2243-2254.

[20] M. Granovskii, I. Dincer, M.A. Rosen, Environmental and economic aspects of hydrogen production and utilization in fuel cell vehicles, Journal of Power Sources 157, 2006, pp. 411-421.

[21] D.B. Levin, R. Chahine. Challenges for renewable hydrogen production from biomass. International Journal of Hydrogen Energy 35, 2010, pp. 2243-2254.

[22] M. Ball. M. Wietschel, The future of hydrogen – Opportunities and challenges, International journal of Hydrogen Energy 34, 2009, 615-627.

[23] S.P. de Souza, S. Pacca, M.T. de Ávila, J.L.B. Borges, Greenhouse gas emissions and energy balance of palm oil biofuel. Renewable Energy 35, 2010, pp. 2552-2561.

[24] Ecoinvent, 2006, Swiss Center for Life Cycle Interventories. Switzerland.

[25] Misterio de Minas y energía, Cálculo del factor de emisión de CO_2 del sistema eléctrico interconectado colombiano. 2008.

[26] W.H. Chen, S.Y. Chen, S.K. Khanal, S. Sung, Kinetic study of biological hydrogen production by anaerobic fermentation, International Journal of Hydrogen Production 31, 2006, pp. 2170-2178.

[27] I.C. Macedo, M.R. Lima, J.E. Ramos, Assessment of greenhouse gas emissions in the production and use of fuel ethanol in Brazil, Government of the State of São Paulo, Brazil, 2004.

[28] E. Smeets, M. Junginger, A. Faaij, A. Walter, P. Dolzan, W, Turkenburg., The sustainability of Brazilian ethanol – An assessment of the possibilities of certified production, Biomass and Bioenergy 32, 2008, pp. 781-813.

[29] K.F. Yee, K.T. Tan, A.Z. Abhullah, K.T. Lee, Life cycle assessment of palm biodiesel: Revealing facts and benefits for sustainability, Applied Energy 86, 2009, pp. S189-S196.

[30] S. Manish, R. Banerjee, Comparison of biohydrogen production processes, International Journal of Hydrogen Energy 33, 2008, pp. 279-286.

[31] C.A. Cardona Alzate, Oscar Julian Sanchez Toro, Luis Fernando Gutierrez Mosquera, "Process synthesis for fuel ethanol production" United States of America, 2009. ed: CRC Press Taylor & Francis Group, ISBN: 978-1-4398-1597-7, v. 1, p. 390.

[32] L.F. Gutierrez Mosquera, O.J. Sanchez Toro, C.A Cardona Alzate, "Process integration possibilities for biodiesel production from palm oil using ethanol obtained from lignocellulosic residues of oil palm industry". England, Bioresource Technology ISSN: 0960-8524 ed: Elsevier. v.100 2009p.1227 – 1237.

[33] Frischknecht R., Jungbluth N., Althaus H.-J., Doka G., Dones R., Hischier R., Hellweg S., Nemecek T., Rebitzer G. and Spielmann M. Overview and Methodology. Final report Ecoinvent data v2.0, No. 1. 2007. S wiss Centre for Life Cycle Inventories, Dübendorf, CH.

Impact of Climate Change on Wheat Production for Ethanol in Southern Saskatchewan, Canada

Hong Wang[1,*], Yong He[1,2], Budong Qian[3], Brian McConkey[1], Herb Cutforth[1], Tom McCaig[1], Grant McLeod[1], Robert Zentner[1], Con Campbell[3], Ron DePauw[1], Reynald Lemke[4], Kelsey Brandt[1], Tingting Liu[1,5], Xiaobo Qin[1,6], Gerrit Hoogenboom[7], Jeffrey White[8], Tony Hunt[9]

[1]*Semiarid Prairie Agricultural Research Centre, Agriculture and Agri-Food Canada, Box 1030, Swift Current, Saskatchewan, S9H 3X2, Canada*
[2]*Department of Soil and Water Sciences, Resources and Environmental Sciences College, China Agricultural University, Beijing, 100094, China*
[3]*Eastern Cereal and Oilseed Research Centre, Agriculture and Agri-Food Canada, Ottawa, Ontario, Canada*
[4]*Saskatoon Research Centre, Agriculture and Agri-Food Canada, Saskatoon, Saskatchewan, Canada*
[5]*Renmin University of China, Beijing, 100872, China*
[6]*Institute of Agro-Environment and Sustainable Development, Chinese Academy of Agriculture Sciences/The Key Laboratory for Agro-Environment and Climate Change, Ministry of Agriculture, Beijing, 100081, China*
[7]*Washington State University, 24106 North Bunn Road, Prosser, Washington 99350-8694, USA*
[8]*USDA ARS, ALARC, 21881 N Cardon Lane, Maricopa, AZ 85138, USA*
[9]*University of Guelph, Canada*
** Corresponding author. Tel: +1 3067787288, Fax: +1 3067783188, E-mail: hong.wang@agr.gc.ca*

Abstract: This study assessed the impact of climate change on wheat production for ethanol in southern Saskatchewan, Canada. The DSSAT-CSM model was used to simulate biomass and grain yield under three climate change scenarios (IPCC SRES A1B, A2 and B1) in the 2050s. Synthetic 300-yr weather data were generated by the AAFC stochastic weather generator for the baseline period (1961-1990) and scenarios. Compared to the baseline, all three scenarios increase precipitation every month except July and August and June (A2 only), when less rains are projected. Annual air temperature is increased by 3.2, 3.6 and 2.7 ^{o}C for A1B, A2 and B1, respectively. The model predicted increases in biomass by 28, 12 and 16% without the direct effect of CO_2 and 74, 55 and 41% with combined effect (climate and CO_2) for A1B, A2 and B1, respectively. Similar increases were found for yield. However, the occurrence of heat shock (>32^{o}C) will increase during grain filling under climate change conditions and could cause severe yield reduction, which is not simulated by DSSAT-CSM; therefore, the yield could be overestimated. Several measures such as early seeding must be taken to avoid heat damage and take the advantage of projected increase in precipitation.

Keywords: *Climate change, Wheat, Bioenergy crop, Heat shock, Seeding date*

1. Introduction

Because of the shortage of fossil fuels and the negative impact of fossil fuel consumption on global climate and environment, the production of bioenergy crops as an alternative to traditional fossil fuels has become much more attractive to the world. Approximately 44% of Canada's agricultural land is located in the province of Saskatchewan and the major (close to 40%) crop is wheat (*Triticum aestivum* L.), which is a potential bioenergy crop. No matter what measures are taken, global climate change will continue. Since the process of substituting energy crops for fossil fuels would occur gradually over several decades, climate change will affect its production. The objective of this study was to use the DSSAT-CSM model to assess the impact of climate change on the production of wheat as a bioenergy crop grown in southern Saskatchewan.

2. Methodology

2.1. Site Condition

The site selected for this study was located on a gently sloping Swinton silt loam (Typic Haploboroll) at the Semiarid Prairie Agricultural Research Centre, Swift Current, in southern Saskatchewan. Daily maximum and minimum air temperatures and precipitation were obtained from the weather station located on the research site. Daily solar radiation was calculated using the Mountain Climate Simulator [1]. Soil property inputs for DSSAT-CSM (organic carbon, total nitrogen, clay and silt in percent, cation exchange capacity, pH, soil lower, drained upper and saturated points, saturated hydraulic conductivity, and bulk density) were observed on the site. The management used for simulation was a continuous wheat rotation under no-till with a seeding depth of 5 cm. Nitrogen fertilizer was assumed to be applied at a rate of 100 kg ha^{-1} at planting time. Seeding dates were predicted with the model developed by Bootsma and De Jong [2], and subsequently modified by McGinn et al. [3].

2.2. The DSSAT-CSM Model

The Decision Support System for Agrotechnology Transfer-Cropping System Model (DSSAT-CSM), a widely used process-based modeling package [4], was selected for simulating the wheat production system. This model simulated wheat yield and biomass generally well in western Canada [5-7]. The wheat module of DSSAT-CSM (v4.0) was modified to improve the prediction of seedling emergence rate [8-9] and leaf appearance rate [10]. The spring wheat cultivar Biggar (Canada Prairie Spring Wheat class) was used for modeling because this wheat class has higher starch content and lower protein concentration in comparison to bread wheat class and is recognized as a viable feedstock for ethanol [11]. Genetic coefficients of Biggar were calibrated with the data collected by Jame and Cutforth [12] and tested using data from the New Rotation experiment at Swift Current [13]. In order to predict the long-term effect we used the Sequence Analysis of DSSAT to run the model.

2.3. Climate Change Baseline and Scenarios

Weather data during the period of 1961-1990 were treated as baseline climate. Climate change scenarios in 2050s (2040-2069) were projected by the third generation global climate model developed at Canadian Centre for Climate Modelling and Analysis (CGCM3) with the forcing of three greenhouse gas (GHG) emission scenarios (i.e., IPCC SRES A1B, A2 and B1) [14]. Synthetic 300-yr weather data were generated by the AAFC Stochastic Weather Generator (AAFC-WG) for the baseline period and each scenario [15]. These generated data were used to predict the climate effect on wheat production with the DSSAT model. Qian et al. [16] found that simulations of crop models with 30-yr observed and the 300-yr synthetic weather data generated by AAFC-WG with parameters calibrated from the same 30-yr observed data, in general, do not show significant differences, with regard to timing of biomass accumulation, crop maturity date, as well as final biomass and grain yield at maturity. The simulations were run with and without direct effects of increased atmospheric CO_2 levels. The CO_2 levels were 550 ppm for A1B and A2 and 450 ppm for B1 [14]. The hourly air temperature was calculated using the subroutine HTEMP of DSSAT-CSM [17].

2.4. Data Analysis

Statistical analyses were done by SAS [18]. Means, lower and upper limits of the 95% confidence interval and standard deviation of synthetic air temperature and precipitation were calculated and compared among baseline and climate change scenarios by PROC MEANS. Predicted and calculated variables were compared between scenarios with PROC MIXED [19].

3. Results

3.1. Climate Change Baseline and Scenarios

3.1.1. Precipitation

All the climate change scenarios increased annual precipitation compared to the baseline period (331 mm, Fig. 1). The most significant increase is scenario A1B (55 mm), followed by A2 (39 mm) and B1 (37 mm). All three scenarios increase precipitation every month except July and August and June (A2 only), when less rains are projected. Scenario A2 was similar to A1B in terms of precipitation distribution except that it was markedly (10 mm) less than A1B in June. Precipitation for scenario B1 was generally slightly less than that of A1B, except in July and August when B1 had more rain than A1B.

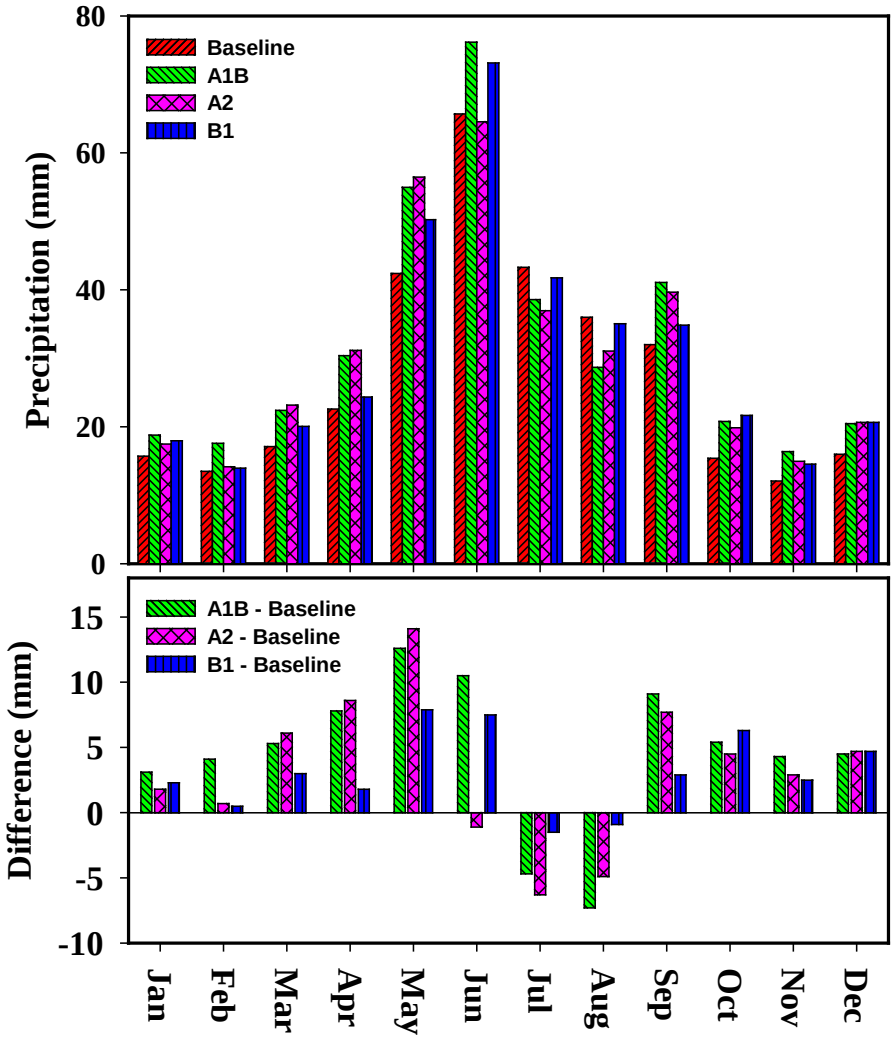

Fig. 1. Monthly precipitation under baseline and three scenarios and difference between baseline and scenarios.

3.1.2. Air temperature

Air temperature in all climate scenarios was increased compared to the baseline climate (Fig. 2). Scenarios A1B, A2 and B1 had 3.2, 3.6 and 2.7 ^{0}C higher annual mean air temperatures than the baseline, respectively. The highest differences in temperature occurred in the winter, followed by summer, and relatively small differences occurred in the spring and fall. Scenario

A2 had the highest temperature in most of the days of the year. The change in pattern and difference between scenarios in daily maximum and minimum air temperatures were similar to that in daily mean temperature (data not shown).

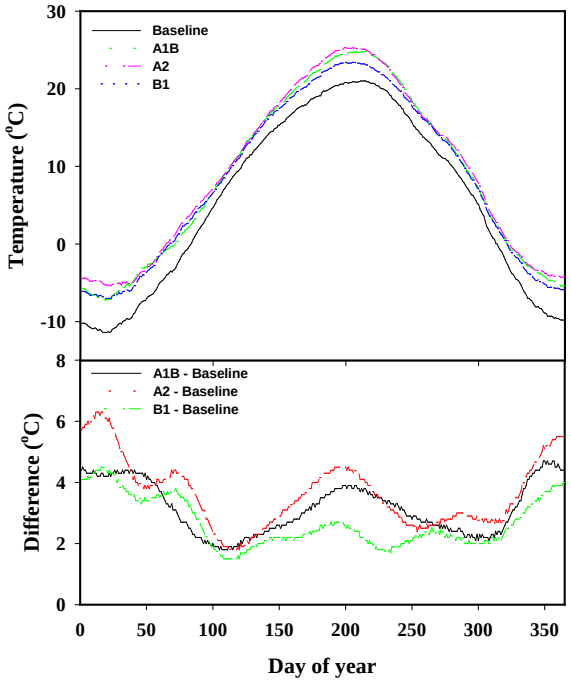

Fig. 2. Daily mean air temperature under baseline and three scenarios and difference between baseline and scenarios.

3.2. Phasic Development

The predicted seeding dates under all climate change scenarios are six days earlier than the prediction under the baseline climate (Day 124, May 10) (Table 1). Because of the earlier seeding and higher temperatures, predicted dates of anthesis and maturity averaged nine and 13 d earlier than simulations based on the baseline climate, respectively. The vegetative (from emergence to anthesis) and grain filling stages were shortened by 2-3 and 3-5d, respectively. The total time to maturity was shortened by 6-9 d. Among the three climate scenarios, the scenario that reduced days to plant maturity the most was scenario A2, which is associated with its higher temperature.

Table 1. Effects of climate change on phasic development of wheat

	Day of year			Duration (days)			
Scenario	Seeding	Anthesis	Maturity	Seeding to emergence	Emergence to anthesis	Grain filling	Seeding to Maturity
Baseline	123.5a[z]	185.2a	218.4a	11.3a	50.4a	33.1a	94.8a
A1B	118.0b	176.7bc	205.5c	10.9ab	47.9c	28.7c	87.5c
A2	117.8b	175.7c	203.8d	10.7b	47.1d	28.1d	86.0d
B1	118.1b	177.5b	207.5b	10.9ab	48.6b	30.0b	89.4b

[z] Within columns and depth, values followed by the same letter are not significantly different at the 0.05 level of probability.

3.3. Biomass and Grain Yield

Without the direct effect of CO_2, the model predicted that all three climate change scenarios significantly increases biomass production compared to the baseline (Table 2), with A1B

increasing the most (28%) followed by B1 (16%) and A2 (12%). The combined effect (climate and CO_2) increased biomass production much more, with A1B increasing the most (74%) and A2 (55%) and B1 (41%) being similar. Increased CO_2 concentrations of 220 and 120 ppm resulted in increased biomass production of 43-45% and 25%, respectively. The effect of the climate change scenarios on grain yield shows the same trend as biomass with a slightly higher increase rate.

Table 2. Effects of climate change on biomass and grain production of wheat.

Scenario	CO2 ppm	Biomass kg ha-1	Grain Yield kg ha-1
Baseline	330	5039f[z]	2467f
A1B	330	6463d	3167d
A1B	550	8753a	4349a
A2	330	5651e	2834e
A2	550	7813b	3978b
B1	330	5856e	2880e
B1	450	7104c	3520c

[z] Within columns and depth, values followed by the same letter are not significantly different at the 0.05 level of probability.

4. Discussion and Conclusions

The estimated increase in yield under climate change is consistent with the study by Arthur [20] who predicted an increase in wheat yield under four climate change scenarios in Saskatchewan. However, caution must be exercised when interpreting the model-simulated results as the effect of heat stress on wheat growth is not well described by the model. Heat stress occurs often in wheat on the Canadian Prairies especially during reproductive growth, which has markedly negative impacts on yield [21]. At the grain growth stage (anthesis to maturity), heat stress is divided into two types according to Wardlaw et al. [22]: chronic stress (20–32°C) and heat shock (>32°C). Chronic stress involves a progressive decrease in kernel weight with increasing temperature because the increase of grain filling rate associated with the increase of temperature does not compensate enough for the reduction of grain filling duration [23]. In southern Saskatchewan, McCaig [21] found that the cumulative maximum daily air temperature >20°C during and after anthesis was negatively correlated with the yield of wheat. Heat shock can inhibit pollen growth, cause sterility and abortive grain, trigger premature senescence, inhibit kernel development and cause significant reduction in yield [24-25].

The occurrence of chronic stress increased for all the climate change scenarios compared to baseline (data not shown). Significant and more obvious increase of heat shock incidence was found for all scenarios (Table 3). Under the baseline climate, heat shock (>32 ^{o}C) occurred for only 30 hours during the first 20 days of grain filling. Heat shock occurred for 73, 87 and 56 hours during this same period under climate change scenarios A1B, A2 and B1, respectively, which are 1.8-2.9 times of that under the baseline climate. Note that if daily temperature is used, increases of heat shock are significant, but not as tremendous as calculated by using hourly results. This means that under climate change conditions heat shock will occur longer in a day than under the baseline climate. It is obvious that heat shock will damage the kernel development and reduce grain yield if the future cultivars are not improved in heat shock resistance. This is not predicted by the model because the DSSAT-CSM model, like many other models, does not simulate the yield loss caused by heat shock [26]. Therefore, grain yield, and probably biomass, is likely overestimated.

Table 3. Effects of climate change on duration of air temperature surpassing 32 ^{o}C during the first 20 days of grain filling.

Scenario	Day	Hour
Baseline	5.0d[z]	30.1d
A1B	9.3b	72.8b
A2	10.9a	87.3a
B1	7.6c	55.5c

[z] Within columns and depth, values followed by the same letter are not significantly different at the 0.05 level of probability.

Adaptation measures must be taken in regards to the high temperature under climate change. One possible strategy is early seeding. This would allow wheat to mature earlier, avoiding heat shock which will mostly occur in July. The prediction of seeding dates in this paper (Table 1) was calculated by an empirical model [3] which is based on observations from 1956 to 1984 [2]. In recent years, the adoption of no-till and stubble mulch tillage systems allows seeding even earlier. Therefore, if this technique is used in the 2050's the seeding dates could be significantly earlier than the predicted dates. Early seeding of wheat on the Canadian Prairies may have other advantages, such as reducing the application of herbicides for weed control [27], and could possibly reduce the incidence of some insects and diseases and improve the timeliness of planting operations in the spring. Dormant-seeding in the fall or winter is another method to be considered. This is already practiced by some farmers and some research has been conducted [28].

Two other strategies to cope with the heat stress are breeding heat resistant cultivars [29] and adopting improved tillage methods. The surface residue and standing stubble in a no-till and stubble mulch system act as insulation and impede the exchange rate of thermal energy between the soil and atmosphere. The slightly higher soil moisture under this system can also help buffer the extremes in daily soil temperatures and reduce near-surface root heat stress. Merrill et al. [30] and Wang et al [25] observed that no-till mitigated heat stress of wheat and improved growth and yield.

Although the projected increase of air temperature, especially the increase of heat shock, may cause yield loss, all three climate change scenarios projected an increase in precipitation. Proper management methods are needed to capitalize on this advantage. Fortunately, one of the strategies is also to seed wheat early which allows wheat to take advantage of the wetter spring while avoiding the drier period in July [31-32].

References

[1] P.E. Thornton, H. Hasenauer, M.A. White, Simultaneous estimation of daily solar radiation and humidity from observed temperature and precipitation: an application over complex terrain in Austria, Agricultural and Forest Meteorology 104, 2000, pp. 255–271.

[2] A. Bootsma, R. De Jong, Estimates of seeding dates of spring wheat on the Canadian Prairies from climate data, Canadian Journal of Plant Science 68, 1988, pp. 513–517.

[3] S.M. McGinn, A. Touré, O.O. Akinremi, D.J. Major, A.G. Barr, Agroclimate and crop response to climate change in Alberta, Canada, Outlook On Agriculture 28(1), 1999, pp. 19–28.

[4] J.W. Jones, G. Hoogenboom, C.H. Porter, K.J. Boote, W.D. Batchelor, L.A. Hunt, P.W. Wilkens, U. Singh, A.J. Gijsman, J.L. Ritchie, The DSSAT cropping system model, European Journal of Agronomy 18, 2003, pp. 235–265.

[5] A.P. Moulin, H.J. Beckie, Evaluation of the CERES and EPIC models for predicting spring wheat grain yield, Canadian Journal of Plant Science 73, 1993, pp. 713–719.

[6] A.C. Chipanshi, E.A. Ripley, R.G. Lawford, Large–scale simulation of wheat yields in a semi–arid environment using a crop–growth model, Agricultural Systems 59, 1999, pp. 57–66.

[7] H. Wang, G.N. Flerchinger, R. Lemke, K. Brandt, T. Goddard, C. Sprout, Improving SHAW long–term soil moisture prediction for continuous wheat rotations, Alberta, Canada, Canadian Journal of Plant Science 90, 2010, pp. 37–53.

[8] H. Wang, H. Cutforth, T. McCaig, G. McLeod, K. Brandt, R. Lemke, T. Goddard, C. Sprout, Predicting the time to 50% seedling emergence in wheat using a Beta model, NJAS – Wageningen Journal of Life Sciences 57, 2009, pp. 65–71.

[9] H. Wang, H. Cutforth, P.R. Bullock, R.M. DePauw, T. McCaig, G. McLeod, K. Brandt, G.J. Finlay, Testing a nonlinear model for simulating the time of seedling emergence of wheat, Canadian Biosystems Engineering 51, 2009, pp. 4.1–4.6.

[10] H. Wang, H.W. Cutforth, R. DePauw, T. McCaig, G. McLeod, K. Brandt, X. Qin, Modeling leaf appearance rate for Canada Western Red Spring wheat cultivars, Canadian Journal of Plant Science 90, 2010, pp. 399–402.

[11] K. Sosulski, F. Sosulski, Wheat as a feedstock for fuel ethanol, Applied Biochemistry and Biotechnology 45(6), 1994, pp. 169–180.

[12] Y.W. Jame, H.W. Cutforth, Simulating the effects of temperature and seeding depth on germination and emergence of spring wheat, Agricultural and Forest Meteorology 124, 2004, pp. 207–218.

[13] R.P. Zentner, C.A. Campbell, F. Selles, B.G. McConkey, P.G. Jefferson, R. Lemke, Cropping frequency, wheat classes and flexible rotations: Effects on production, nitrogen economy, and water use in a Brown Chernozem, Canadian Journal of Plant Science 83, 2003. pp. 667–680.

[14] N. Nakicenovic, R. Swart, Emissions Scenarios IPCC Special Report, 2000. Nebojsa Nakicenovic and Rob Swart (Eds.) – Cambridge University Press, UK, 2000, pp. 570.

[15] B.D. Qian, S. Gameda, H. Hayhoe, R. De Jong, A. Bootsma, Comparison of LARS–WG and AAFC–WG stochastic weather generators for diverse Canadian climates, Climate Research 26, 2004, pp. 175–191.

[16] B.D. Qian, R. De Jong, J.Y. Yang, H. Wang, S. Gameda, Comparing the simulation of climate impacts on crop yields with observed and synthetic weather data, 2010. 2010 AGU Fall Meeting. 13–17 December, San Francisco, California, USA.

[17] W.J. Parton, J.A. Logan, A model for diurnal variation in soil and air temperature, Agricultural Meteorology 23, 1981, 205-216.

[18] SAS Institute, Inc., SAS procedures guide. Version 8. SAS Institute, Inc., Cary, NC, USA, 1999.

[19] I.P. Little, The relationship between soil pH measurements in calcium chloride and water suspensions, Australian Journal of Soil Research 30, 1992, pp. 587–92.

[20] L.M. Arthur, The implication of climate change for agriculture in the prairie provinces, Climate Change Digest 88-01. 1988, Downsview, ON. Atmospheric Environment Service.

[21] T.N. McCaig, Temperature and precipitation effects on durum wheat grown in southern Saskatchewan for fifty years, Canadian Journal of Plant Science 77, 1997, pp. 215–223.

[22] I.F. Wardlaw, C. Blumenthal, O. Larroque, C.W. Wrigley, Contrasting effects of chronic heat stress and heat shock on kernel weight and flour quality in wheat,Functional Plant Biology 29, 2002, pp. 25–34.

[23] I.F. Wardlaw, C.W. Wrigley, Heat tolerance in temperate cereals: An overview, Australian Journal of Plant Physiology 21, 1994, pp. 695–703.

[24] P.J. Stone, M.E. Nicolas, The effect of duration of heat stress during grain filling on two wheat varieties differing in heat tolerance: grain growth and fractional protein accumulation, Australian Journal of Plant Physiology 25, 1998, pp. 13–20.

[25] H. Wang, R. Lemke, T. Goddard, C. Sprout. Tillage and root heat stress in wheat in Central Alberta, Canadian Journal of Soil Science 87, 2007, pp. 3–10.

[26] T.R. Wheeler, P.Q. Craufurd, R.H. Ellis, J.R. Porter, P.V. Vara Prasad, Temperature variability and the yield of annual crops, Agriculture, Ecosystems & Environment 82, 2000, pp. 159–167.

[27] K.N. Harker, G.W. Clayton, R.E. Blackshaw, J.T. O'Donovan, E.N. Johnson, Y. Gan, F.A. Holm, K.L. Sapsford, R.B. Irvine, R.C. Van Acker, Glyphosate–resistant wheat persistence in western Canadian cropping systems, Weed Science: November 2005, Vol. 53, No. 6, 2005, pp. 846–859.

[28] R.O. Ashley, D. Barondeau, H. Peterson, J. Larson, B. Rettinger, A survey of dormant–seeded Hard Red Spring Wheat fields in Southwest North Dakota, 2001. Annual Report. Dickinson Research Extension Center, http://www.ag.ndsu.nodak.edu/dickinso/

[29] M.A. Semenov, N.G. Halford, Identifying target traits and molecular mechanisms for wheat breeding under a changing climate, Journal of Experimental Botany 60(10), 2009, pp. 2791–2804.

[30] S.D. Merrill, A.L. Black, A. Bauer, Conservation tillage effects root growth of dryland spring wheat under drought, Soil Science Society of America Journal 60, 1996, pp. 575–583.

[31] H.W. Cutforth, B.G. McConkey, R.J. Woodvine, D.G. Smith, P.G. Jefferson, O.O. Akinremi, Climate change in the semiarid prairie of southwestern Saskatchewan: Late winter–early spring, Canadian Journal of Plant Science 79: 1999, 343–350.

[32] H. Harricharan and J. McKinlay, Frost Seeding - A Cheaper Alternative. 2010. Ministry of Agriculture, Food and Rural Affairs. Government of Ontario, Canada. http://www.omafra.gov.on.ca/english/crops/facts/98-071.htm.

Thermodynamic and dynamic investigation for CO_2 storage in deep saline aquifers

Xiaoyan Ji[1,*], Yuanhui Ji[1], Chongwei Xiao[2]

[1] *Division of Energy Engineering, Luleå University of Technology, Luleå, Sweden*
[2] *Petroleum Recovery Research Center, New Mexico Institute of Mining and Technology, New Mexico, USA*
** Corresponding author. Tel: +46 920492837, Fax: +46 920491074, E-mail: xiaoyan.ji@ltu.se*

Abstract: Thermodynamic and dynamic investigations are needed to study the sequestration capacity, CO_2 leakage, and environmental impacts. The results of the phase equilibrium and densities for CO_2-sequestration related subsystems obtained from the proposed thermodynamic model on the basis of statistical associating fluid theory equation of state were summarized. Based on the equilibrium thermodynamics, preliminary kinetics results were also illustrated with chemical potential gradient as the driving force. The proposed thermodynamic model is promising to represent phase equilibrium and thermodynamic properties for CO_2-sequestration related systems, i.e. CO_2-(H_2S)-H_2O-ions (such as Na^+, K^+, Ca^{2+}, Mg^{2+}, Cl^-, CO_3^{2-}), and the implementation of thermodynamic model into kinetics model to adjust the non-ideality of species is vital because of the high pressure for the investigation of the sequestration process.

Keywords: *Carbon sequestration, CO_2 storage, Thermodynamics, Dynamics, CO_2 diffusion*

1. Introduction

Storage of CO_2 in deep saline aquifers is one way to limit the buildup of greenhouse gases in the atmosphere. Large-scale injection of CO_2 into saline aquifers will induce a variety of coupled physical and chemical processes including multiphase fluid flow, solute transport, and chemical reactions between fluids and formation minerals. Thermodynamic and dynamic investigations are needed to study the sequestration capacity, CO_2 leakage, and environmental impacts. Co-injection of CO_2 and H_2S (from flue gases and natural gas fields) may substantially reduce the capture and sequestration costs, and the effect of H_2S on bot h thermodynamic and dynamic models is also needed.

In thermodynamics, experimental solubility data for the CO_2 in water and aqueous NaCl solution and for the H_2S in water and aqueous NaCl solutions have been determined in a wide temperature and pressure range[1, 2]. However, only few experiments are for CO_2 solubility in brines[3]. For more complicated system, there is no available experimental data. Density is also essential to reservoir/aquifer simulation applications. The dissolution of CO_2 in aqueous solutions under most reservoir, aquifer, or deep-ocean conditions results in an increase in the density of the solution, which can induce a natural convection[3-5]. Meanwhile, the properties of the H_2O-rich phase are also strongly dependent on de nsity, which varies greatly with temperature, pressure, CO_2 concentration and salinity[6]. However, the experimental data of density for the related system are much less than those of the solubility data[7, 8].

Meanwhile, thermodynamic models have been proposed to represent the CO_2 or H_2S solubility in H_2O or aqueous NaCl solutions. The models proposed by Spycher et al.[9] and Duan et al.[2] for CO_2+H_2O and CO_2+H_2O+salt are examples of a γ-ϕ approach, where an equation of state (EOS) is used to describe the non-ideality in the CO_2-rich phase and Henry's law or an activity model is used to describe the non-ideality in the H_2O-rich phase. The inherent disadvantage of this approach is that it does not allow for estimating the density of the H_2O-rich phase. This is not an issue in a ϕ-ϕ approach, where an EOS is used for both phases. The ϕ-ϕ approach has been applied to the CO_2+H_2O+NaCl[1], H_2S+H_2O[10-14]

systems. However, to the best of our knowledge, the ϕ-ϕ approach has never been used to describe the phase equilibrium and density for other or more complicated systems.

Dynamic models were investigated on the basis of the available thermodynamic models, and sometimes the effect of ions on the CO_2 solubility is neglected[15]. Moreover, the empirical models with the concentration difference as the driving force were used to represent the dynamic process[3], such as gas dissolution, diffusion, mineral dissolution and precipitation. All these assumptions will bring uncertainty of the simulation results. It is crucial to develop a both reliable thermodynamic model and theory-based dynamic (kinetics) model in order to provide a reliable prediction for CO_2 storage in deep saline aquifers.

We have been working on the related studies for several years and obtained promising results[8, 16-21]. Thermodynamic study is on the basis of statistical associating fluid theory (SAFT) EOS, and preliminary kinetics investigation is based on the non-equilibrium thermodynamics with chemical potential gradient as driving force. In this work, our work on the thermodynamic and dynamic models is summarized, and then perspective is given.

2. Modeling

The thermodynamic properties are represented using SAFT EOS in which the dimensionless residual Helmholtz energy is defined as:

$$\tilde{a}^{res} = \tilde{a}^{seg} + \tilde{a}^{assoc} + \tilde{a}^{chain} + \tilde{a}^{ion} \qquad (1)$$

where the superscripts refer to terms accounting for the residual, segment, association, chain, and ionic interactions, respectively. The model was proposed as SAFT1-RPM first, and then improved to SAFT2. The detailed description for both SAFT1-RPM and SAFT2 was in references[8, 16-20].

In model, each component is modeled as one kind of segments with parameters, i.e. segment number m, segment volume v^{oo}, segment energy u/K, and the reduced range of the potential well λ. For molecule with association interactions, there are two additional parameters, i.e. the well depth of the association site-site potential ε, and the parameter related to the volume available for bonding κ. For ions, there is one additional parameter, effective diameter d. The mixing rules are followed those in our previous work[8, 16-19, 20].

To describe the CO_2 diffusion in water or brine, non-equilibrium thermodynamic model was used in which the chemical potential gradient was used as the driving force with the following equation:

$$\frac{\partial f_i(x,t)}{\partial t} = D_{eff} \frac{\partial^2 f_i(x,t)}{\partial x^2} \qquad (2)$$

where x is the position in m, t is the time in s, f is the fugacity of a component that is calculated with SAFT EOS, and D_{eff} is the effective diffusion constant that is a combination of a molecule diffusion and natural convection. The detail description was in reference[21].

3. Results and perspective

To represent properties of CO_2-(H_2S)-H_2O-ions (such as Na^+, K^+, Ca^{2+}, Mg^{2+}, Cl^-, CO_3^{2-}) up to high pressures, research has been carried out for several years for different subsystems.

3.1. Phase equilibrium and properties for CO_2-H_2O-NaCl system

Phase equilibrium and thermodynamic properties of CO_2-H_2O and CO_2-H_2O-NaCl system are very important for the CO_2 sequestration, and then they were investigated firstly with the SAFT1-PRM model[8] in which CO_2 was modeled as a molecule with three association sites, two sites of type O and one site of type C. H_2O was modeled as a molecule with four association sites, two sites of type O and two sites of type H. The salt was modeled as a molecule composed of two charged, but non-associating, spherical segments, of which one represents the cation and one represents the anion. For the CO_2-H_2O system, only one type of cross association was assigned, i.e., between site of type O in CO_2 and site of type H in H_2O. Using temperature-dependent parameters, SAFT1-RPM is found to represent the density and equilibrium data for the CO_2-H_2O system, including the minimum H_2O concentration in the CO_2-rich phase in the composition (y)- pressure (P) diagram, as shown in Fig. 1 (a) at 308.15 K. For CO_2-H_2O-NaCl system, an additional binary interaction constant was used, the same for both CO_2-Na^+ and CO_2-Cl^- pairs, which was needed to correct the short-range interactions. SAFT1-RPM is also found to represent the equilibrium and density data for the CO_2-H_2O-NaCl system. As shown in Fig. 1 (b), the CO_2 solubility decreases with increasing salt concentration (molality, m, mol/kgH_2O), salt-out effect, and the model captures not only the pressure effect on the CO_2 solubility but also the salting-out effect.

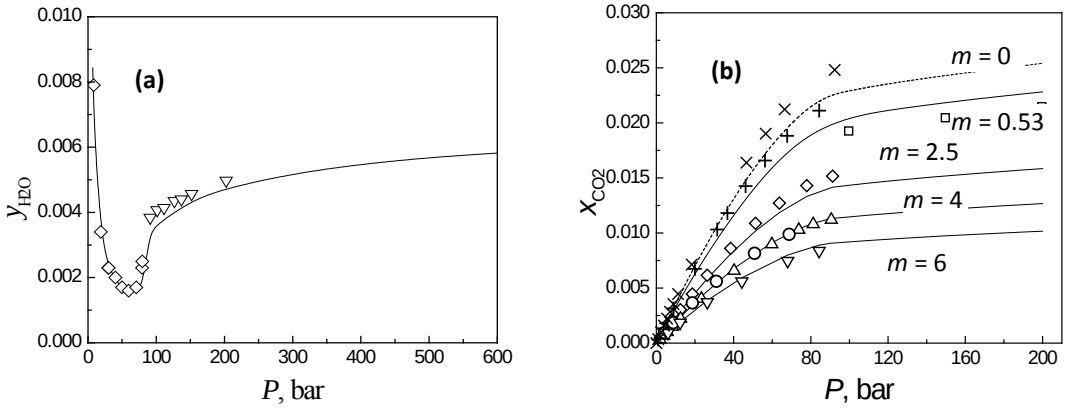

Fig. 1. (a) Mole fractions of H_2O in CO_2-rich phase (y_{H2O}) for CO_2-H_2O at 308.15 K at different pressures (P). Experimental data[22-24]; —, calculated. (b) Mole fractions of CO_2 in H_2O-rich phase (x_{CO2}) for CO_2-H_2O-NaCl at 313.15 K, different pressures (P), and salt concentration (molality, m). Experimental data[23, 25-27] : —, calculated (m = 0.5292, 2.5, 4.0 and 5.999). ···; calculated (m = 0).

3.2. CO_2 diffusion in brines

Numerous investigations on the mass transfer of CO_2 in high-pressure water or brines have been pursued to simulate the CO_2 geological and ocean disposal processes. It has been showed that the dissolution of CO_2 in brines increases the density, and then induces the density-driven natural convection, which then significantly accelerates the diffusion of CO_2 in the brine. Yang and Gu[3] investigated experimentally the CO_2 dissolution in brine at elevated pressures and described the mass transfer of CO_2 in brine using a modified diffusion equation with an effective diffusion coefficient. The effective diffusion coefficients are two orders of magnitude larger than the molecular diffusivity of CO_2 in water, which implies that the density-driven natural convection greatly accelerates the mass transfer of CO_2 in brines.

Since the salinity of brines is low for the experimental data of Yang and Gu[3], the main components are Na^+ and Cl^-, it is reasonable to assume that the brine is the aqueous solution of NaCl[21]. Based on this assumption, the CO_2 equilibrium concentration was calculated with SAFT1-RPM and compared with those measured experimentally with good agreement, as shown in Fig. 2 (a). Moreover, the mass transfer of CO_2 in brines was investigated further by chemical potential gradient model based on non-equilibrium thermodynamics[21]. Fig. 2 (b) illustrates the CO_2 concentration distribution at 300.15 K calculated with the non-equilibrium thermodynamics and those obtained from the modified Fick's second law. The difference in the concentration distribution reveals the importance to combine the thermodynamic model with kinetics model.

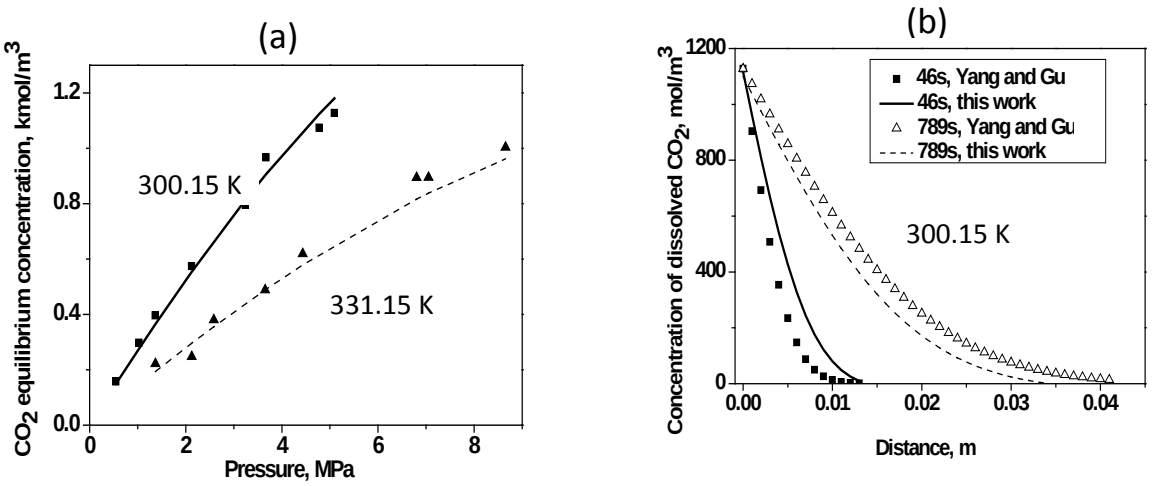

Fig. 2. (a): Equilibrium concentration of CO_2 in brine, symbols: experimental data[3], curves: prediction. (b): CO_2 concentration distribution. Curves: calculation with chemical potential gradient as driving force. Symbols: calculation with concentration difference as driving force[3].

3.3. Properties for aqueous electrolyte solutions

Properties of brines are different from different sources, and it is not always reasonable to assume it be aqueous NaCl solution when the effect of other ions is considerable. Generally, the components in brines include Na^+, K^+, Ca^{2+}, Mg^{2+}, Cl^-, CO_3^{2-}. Meanwhile, ions of Li^+, Br^-, I^-, NO_3^-, HCO_3^-, and SO_4^{2-} play important roles in other industries. Thus, the properties of such aqueous electrolyte solutions were studied. In SAFT1-RPM, except the diameter, the parameters for electrolytes are ion-based. Later, the ion-based SAFT EOS was proposed and called ion-based SAFT2[19, 20].

To represent the properties of aqueous single-salt solutions in the temperature, pressure, and concentration ranges of 298.15 to 473.15 K, 1.013 to 1000 bar, and 0 to 6 mol/kgH_2O in ionic strength, respectively, the short-range interaction between cation and anion was needed to capture the effect of pressure on the properties of electrolyte solutions. A set of parameters at 298.15 K for 5 cations (Li^+, Na^+, K^+, Ca^{2+}, Mg^{2+}) and 7 anions (Cl^-, Br^-, I^-, NO_3^-, HCO_3^-, SO_4^{2-}, CO_3^{2-}) was obtained from the fitting of the experimental mean ionic activity coefficients and liquid densities of 26 aqueous single-salt solutions. An additional set of ion-specific coefficients used in the temperature-dependent parameter expressions for 5 cations (Li^+, Na^+, K^+, Ca^{2+}, Mg^{2+}) and 5 anions (Cl^-, Br^-, HCO_3^-, SO_4^{2-}, CO_3^{2-}) was obtained from the fitting of the experimental mean ionic activity coefficients and liquid densities of 15 aqueous single-salt solutions at low pressures and temperatures up to 473.15 K.

For the properties of aqueous multiple-salt solutions at ambient and elevated temperatures and pressures, the short-range interactions between two different cations were allowed to obtain better representations of the solution properties. The adjustable parameter used in the mixing rule for the segment energy was fitted to the experimental osmotic coefficients of two-salt solutions containing one common anion at various temperatures and low pressures. The predictions of the osmotic coefficients, densities, and activity coefficients of multiple-salt solutions including brine/seawater are found to agree with experimental data. Fig. 3 illustrates the comparison of the density calculated with model and reference data[28] for aqueous NaCl solutions and experimental data for brines[29].

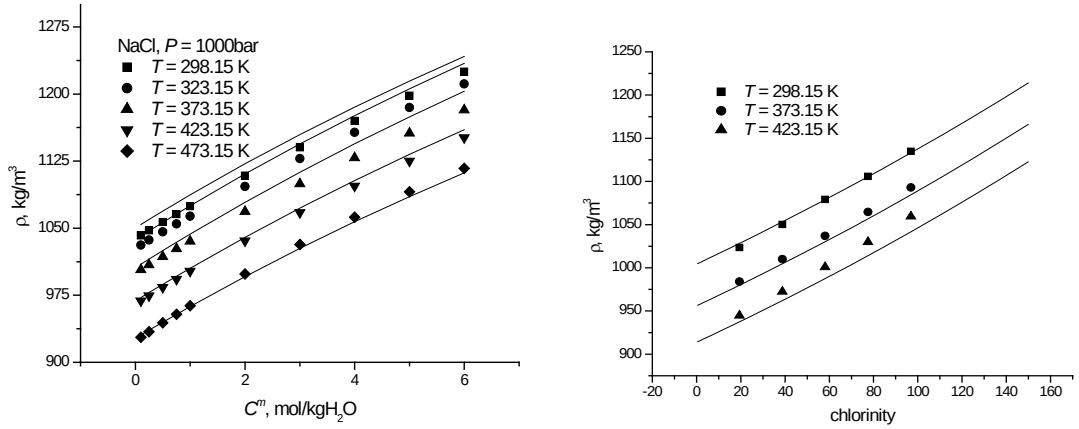

Fig. 3. Density (ρ) for aqueous NaCl solutions and brines. Symbols: experimental data[28, 29]; —, calculation.

3.4. Phase equilibrium for H_2S-H_2O system

CO_2 capture is a former step of CO_2 sequestration. Research reveals that the cost for CO_2 capture is two thirds of the totally cost for CO_2 capture and storage. How to cut the cost for CO_2 capture is one of the main barriers. Generally, H_2S is another main component in flue gases and natural gas fields, the co-injection of H_2S and CO_2 will substantially reduce the capture and sequestration costs, while it will also affect the sequestration capacity and the sequestration process (from solubility to transfer to reaction with rocks). This leads to the significance of the study of the thermodynamics and kinetics for H_2S-CO_2 related sequestration systems.

Thus, the phase equilibrium of the binary system of H_2S-H_2O was represented using ion-based SAFT2[14] in which H_2S was modelled as a molecule with four association sites, i.e., two sites of type S and one site of type H, and sites of the same type did not associate with each other. The parameters of H_2S were fitted to its vapor pressure and saturated liquid density. Cross association between the association site H in H_2S and the site O in H_2O was allowed, and two temperature-dependent parameters were used to describe this cross association. A temperature-dependent binary interaction parameter was used to correct the cross dispersive energy for this binary system. Cross parameters were fitted to mole fractions both in H_2S-rich/vapor and H_2O rich phases[30]. The model is found to represent the phase equilibria from 273 to 630 K and at pressure up to 200 bar[14]. Fig. 4 shows the equilibrium compositions. At 310.93 and 366.48 K, the vapor phase changes to H_2S-rich liquid phase when the pressure increases up to a certain value, while at higher temperatures of 422.04K and 477.49K, no H_2S-rich liquid phase exists in the investigated pressure range. This observation is represented with the model.

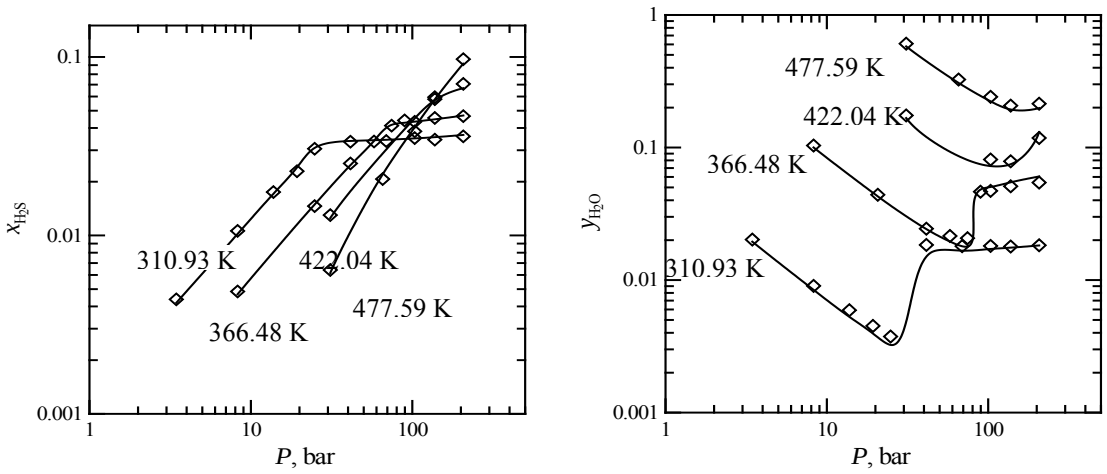

Fig. 4. Mole fractions of H_2S in H_2O-rich phase (x_{H2S}) and mole fractions of H_2O in H_2S-rich/vapor phase (y_{H2O}) for H_2S-H_2O system. ◇: experimental data[14]; —, calculation.

3.5. Perspectives

To represent properties of CO_2-(H_2S)-H_2O-ions (such as Na^+, K^+, Ca^{2+}, Mg^{2+}, Cl^-, CO_3^{2-}), the phase equilibrium and thermodynamic properties for CO_2-H_2S, H_2S-H_2O-NaCl, H_2S-brines, CO_2-brines system are needed to investigated further. In kinetics, the preliminary result reveals the importance of the combination of thermodynamic model with mass transfer model. While the improvement itself relates both the thermodynamic model and the description of the CO_2 sequestration process of solubility, dissolution, transfer, and reaction with rocks. The implementation of the thermodynamic model into the process model to provide reliable long-term prediction pertaining to geochemical carbon sequestration, such as sequestration capacity, CO_2 leakage, and environmental impacts, is another main part of the further work.

4. Conclusions

Storage of CO_2 in deep saline aquifers is one way to limit the buildup of greenhouse gases in the atmosphere, and the co-injection of CO_2 and H_2S may substantially reduce the capture and sequestration costs, and the effect of H_2S on both thermodynamic and dynamic models is also needed to study the sequestration capacity, CO_2 leakage, and environmental impacts. Based on SAFT EOS, the phase equilibrium and densities for H_2S-CO_2-sequestration related subsystems have been investigated and summarized. Meanwhile, using non-equilibrium thermodynamics in which the chemical potential difference as the driving force, preliminary kinetics results were illustrated. The proposed thermodynamic model is promising to represent phase equilibrium and thermodynamic properties for CO_2-sequestration related systems, i.e. CO_2-(H_2S)-H_2O-ions (such as Na^+, K^+, Ca^{2+}, Mg^{2+}, Cl^-, CO_3^{2-}), and it is necessary to implement the reliable thermodynamic model into kinetics model to adjust the non-ideality of species because of the high pressure to investigate the sequestration process.

Acknowledgment

X. Ji and Y. Ji thank the Swedish Research Council for the financial support.

References

[1] Y. H. Ji, X. Y. Ji, X. Feng, C. Liu, L. H. Lu, X. H. Lu, Progress in the study on the phase equilibria of the CO_2-H_2O and CO_2-H_2O-NaCl systems. Chinese Journal of Chemical Engineering 15(3), 2007, pp. 439-448

[2] Z. H. Duan, R. Sun, R. Liu, C. Zhu, Accurate thermodynamic model for the calculation of H_2S solubility in pure water and brines. Energy & Fuels 21(4), 2007, pp. 2056-2065

[3] C. D. Yang, Y. G. Gu, Accelerated mass transfer of CO_2 in reservoir brine due to density-driven natural convection at high pressures and elevated temperatures. Industrial & Engineering Chemistry Research 45(8), 2006, pp. 2430-2436

[4] J. J. Adams, S. Bachu, Equations of state for basin geofluids: algorithm review and intercomparison for brines. Geofluids, 2, 2002, pp. 257–271

[5] A. Riaz, M. A. Hesse, H. Tchelepi, F. M. Orr Jr., Onset of convection in a gravitationally unstable, diffusive boundary layer in porous media. J. Fluid Mech., 548, 2006, pp. 87 – 111

[6] V. Vilarrasa, D. Bolster, M. Dentz, S. Olivella, J. Carrera, Effects of CO_2 compressibility on CO_2 storage in deep saline aquifers. Transp. Porous Media, 85, 2010, pp. 619-639

[7] J. J. Adams, S. Bachu, Equations of state for basin geofluids: algorithm review and intercomparison for brines. Geofluids, 2, 2002, pp. 257–271

[8] X. Y. Ji, S. P. Tan, H. Adidharma, M. Radosz, SAFT1-RPM approximation extended to phase equilibria and densities of CO_2-H_2O and CO_2-H_2O-NaCl systems. Industrial & Engineering Chemistry Research 44(22), 2005, pp. 8419-8427

[9] N. Spycher, K. Pruess, J. Ennis-King, CO_2-H_2O mixtures in the geological sequestration of CO_2. I. Assessment and calculation of mutual solubilities from 12 to 100 degrees C and up to 600 bar. Geochimica et Cosmochimica Acta 67(16), 2003, pp. 3015-3031

[10] Z. D. Li, A. Firoozabadi, Cubic-Plus-Association Equation of State for Water-Containing Mixtures: Is "Cross Association" Necessary? AIChE Journal 55(7), 2009, pp. 1803-1813

[11] E. Perfetti, R. Thiery, J. Dubessy, Equation of state taking into account dipolar interactions and association by hydrogen bonding: II - Modelling liquid-vapour equilibria in the H_2O-H_2S, H_2O-CH_4 and H_2O-CO_2 systems. Chemical Geology 251(1-4), 2008, pp. 50-57

[12] M. C. dos Ramos, C. McCabe, Modeling the phase behavior, excess enthalpies and Henry's constants of the H_2O + H_2S binary mixture using the SAFT-VR plus D approach. Fluid Phase Equilibria 290(1-2), 2010, pp. 137-147

[13] X. H. Tang, J. Gross, Modeling the phase equilibria of hydrogen sulfide and carbon dioxide in mixture with hydrocarbons and water using the PCP-SAFT equation of state. Fluid Phase Equilibria 293(1), 2010, pp. 11-21

[14] X. Y. Ji, C. Zhu, Modelling of phase equilibria in the H_2S-H_2O system with statistical associating fluid theory. Energy & Fuels 24, 2010, pp. 6208-6213

[15] B. McPherson, W. S. Han, B. S. Cole, Two equations of state assembled for basic analysis of multiphase CO_2 flow and in deep sedimentary basin conditions. Computers & Geosciences 34(5), 2008, pp. 427-444

[16] S. P. Tan, X. Y. Ji, H. Adidharma, M. Radosz, Statistical associating fluid theory coupled with restrictive primitive model extended to bivalent ions. SAFT2: 1. Single salt plus water solutions. J. Phys. Chem. B 110(33), 2006, pp. 16694-16699

[17] X. Y. Ji, S. P. Tan, H. Adidharma, M. Radosz, Statistical associating fluid theory coupled with restrictive primitive model extended to bivalent ions. SAFT2: 2. Brine/seawater properties predicted. J. Phys. Chem. B 110(33), 2006, pp. 16700-16706

[18] X. Y. Ji, H. Adidharma, Ion-based SAFT2 to represent aqueous single- and multiple-salt solutions at 298.15 K. Ind. Eng. Chem. Res. 45(22), 2006, pp. 7719-7728

[19] X. Y. Ji, H. Adidharma, Ion-based statistical associating fluid theory (SAFT2) to represent aqueous single-salt solutions at temperatures and pressures up to 473.15 K and 1000 bar. Ind. Eng. Chem. Res. 46(13), 2007, pp. 4667-4677

[20] X. Y. Ji, H. Adidharma, Ion-based SAFT2 to represent aqueous multiple-salt solutions at ambient and elevated temperatures and pressures. Chemical Engineering Science 63(1), 2008, pp. 131-140

[21] Y. H. Ji, X. Y. Ji, X. H. Lu, Modeling Mass Transfer of CO_2 in Brine at High Pressures by Chemical Potential Gradient. Fluid Phase Equilibria, submitted 2010

[22] A. Valtz, A. Chapoy, C. Coquelet, P. Paricaud, D. Richon, Vapour-liquid equilibria in the carbon dioxide-water system, measurement and modelling from 278.2 to 318.2K. Fluid Phase Equilibria 226, 2004, pp. 333-344

[23] R. Wiebe, V. L. Gaddy, The solubility of carbon dioxide in water at various temperatures from 12° to 40° and at pressures to 500 atmospheres. Critical phenomena. J. Am. Chem. Soc. 62, 1940, pp. 815-817

[24] M. B. King, A. Mubarak, J. D. Kim, T. R. Bott, The mutual solubilities of water with supercritical and liquid carbon dioxide. Journal of Supercritical Fluids 5(4), 1992, pp. 296-302

[25] J. Kiepe, S. Horstmann, K. Fischer, J. Gmehling, Experimental Determination and Prediction of Gas Solubility Data for CO_2 + H_2O Mixtures Containing NaCl or KCl at Temperatures between 313 and 393 K and Pressures up to 10 MPa. Industrial & Engineering Chemistry Research 41(17), 2002, pp. 4393-4398.

[26] S. Bando, F. Takemura, M. Nishio, E. Hihara, M. Akai, Solubility of CO_2 in Aqueous Solutions of NaCl at (30 to 60) °C and (10 to 20) MPa. Journal of Chemical and Engineering Data 48(3), 2003, pp. 576-579

[27] B. Rumpf, H. Nicolaisen, C. Ocal, G. Maurer, Solubility of carbon dioxide in aqueous solutions of sodium chloride: experimental results and correlation. Journal of Solution Chemistry 23(3), 1994, pp. 431-48

[28] K. S. Pitzer, J. C. Peiper, R. H. Busey, Thermodynamic properties of aqueous sodium chloride solutions. J. Phys. Chem. Ref. Data 13, 1984, pp. 1-102

[29] B. M. Fabuss, A. Korosi, A. Huq, Densities of binary and ternary aqueous solutions of NaCl, Na_2SO_4, and $MgSO_4$, of sea waters, and sea water concentrates. J. Chem. Eng. Data 11, 1966, pp. 325-31

[30] P. C. Gillespie, G. M. Wilson, Vapor-Liquid and Liquid-Liquid Equilibria: Water-Methane, Water-Carbon Dioxide, Water-Hydrogen Sulfide, Water-nPentane, Water-Methane-nPenatne, RR-48; Utah, 1982

Mineral sequestration for CCS in Finland and abroad

Ron Zevenhoven[1,*], Johan Fagerlund[1]

[1] *Åbo Akademi University, Thermal and Flow Engineering Laboratory, Åbo/Turku, Finland*
** Corresponding author. Tel: +358 2 2153323, Fax: +358 2 2154792 E-mail: ron.zevenhoven@abo.fi*

Abstract: The long-term storage of CO_2 using mineral sequestration is becoming increasingly interesting in many regions, especially where CO_2 underground sequestration is considered impossible or unfeasible. Despite the recognised and documented advantages of CO_2 mineral sequestration, twenty years of R&D work did not yet result in mature, economically viable technology that can be applied on a large scale. Lacking other CCS options while having access to large resources of suitable rock material, a route for carbonation of magnesium silicate mineral is currently being optimised in Finland. It involves the production of magnesium hydroxide, $Mg(OH)_2$ from the mineral followed by carbonation of this in a pressurised fluidised bed reactor. Although the $Mg(OH)_2$ production requires energy the consequent carbonation step is exothermic and the overall process could still be rendered energy neutral. Significant amounts of iron oxides are obtained as by-products. Carbonation levels of ~50% of several 100 μm diameter $Mg(OH)_2$ particles were obtained within 10 minutes at pressures > 20 bar and temperatures up to 500ºC. This paper reports on the latest developments of the work, addressing also process energy efficiency. Also, the large-scale application of this in Finland and at the locations of project partners abroad is briefly addressed.

Keywords: *Carbon dioxide sequestration, Mineral carbonation*

1. Introduction

The long-term storage of CO_2 using mineral sequestration is becoming of increased interest in many regions, especially where CO_2 underground sequestration is not possible or considered unfeasible. At many locations worldwide very large deposits of suitable mineral, usually magnesium silicates (serpentine, olivine) but sometime also calcium silicates (wollastonite) are available. Examples for this are Finland, East-coast Australia, Portugal and regions at the west coast of the USA and Canada. Despite the recognised and documented advantages of CO_2 mineral sequestration (very large capacity, no post-storage monitoring needed, exothermic overall process chemistry) the development work is still in the laboratory demonstration scale: twenty years of R&D work did not yet result in mature technology that can be applied on a large scale in an economically viable way [1,2,3]. Motivated by the slow deployment of large scale underground storage of CO_2 or simply the availability of large amounts of suitable mineral, progress on mineral sequestration is being steadily made and reported from an increasing number of research teams and projects worldwide. Also, increasingly realistic understanding of usable storage capacity for underground sequestration is changing the relative positioning of different CCS methods [4]. As a result, CO_2 mineral sequestration shows a clear trend towards scale-up and commercialisation, as is further illustrated by a significant number of patents awarded quite recently [5,6]. In addition, the issue of what to do with the solid product material has resulted in developments in CO_2 mineral sequestration towards both low value (land reclamation) and high value (pharmaceutics) applications.

Development work in Finland, where the exothermic carbonation chemistry is the reason for focussing on high temperature, gas/solid carbonation at elevated pressures involves cooperation with a growing list of international partners, such as in the Baltic states Estonia and Lithuania but also in the Netherlands, Portugal, UK and more recently also Canada and Singapore. The route for carbonation of magnesium silicate mineral as currently being optimised at Åbo Akademi University (ÅA) in Finland involves the production of magnesium

hydroxide, $Mg(OH)_2$ from the mineral followed by carbonation of this in a pressurised fluidised bed (PFB) reactor. Although the $Mg(OH)_2$ production step requires energy the consequent carbonation step is exothermic and the overall process could still be rendered energy neutral (or even negative). This energy recovery distinguishes the method from other routes for CO_2 mineralisation. In addition, significant amounts of iron oxides are obtained as by-products [7]. Carbonation levels of ~50% of several 100 µm diameter $Mg(OH)_2$ particles where obtained within 10 minutes at pressures > 20 bar and temperatures up to 500 ºC [8-11]. The production of $Mg(OH)_2$ currently requires more heat than is generated by its carbonation, but nonetheless this route shows similar or better energy economics (0.9 - 1.2 vs. 1.0 - 2.3 kWh/kg CO_2 fixed) than the more straightforward route that is widely considered as "state of the art", i.e., direct mineral carbonation of superheated aqueous suspensions under high CO_2 pressure [12, 1 (p. 326)]. The route via $Mg(OH)_2$ also shows (much) faster carbonation kinetics than the conventional process, especially for larger particles – see below for more detail and results. One important benefit of the stepwise approach is that oxides of iron and calcium are obtained as separate by-products, such that magnesite ($MgCO_3$) is the unique carbonation product. The main mineral contaminant (iron oxide) thus extracted is sufficiently abundant to be of interest to the iron- and steelmaking industry [13].

This paper reports on the latest results of the development work where the carbonation of several rock types are compared, addressing the production of $Mg(OH)_2$ and the rate and final level of $Mg(OH)_2$ carbonation, and process energy efficiency. Also, the application of this for large-scale CO_2 mineral sequestration in Finland and at the locations of our project partners abroad will be addressed. This includes the use of the (by-) products of the process which can be used for land reclamation (as is an objective in Singapore), heat storage, or iron- and steelmaking. Finding such uses or markets for the solid products and by-products is essential.

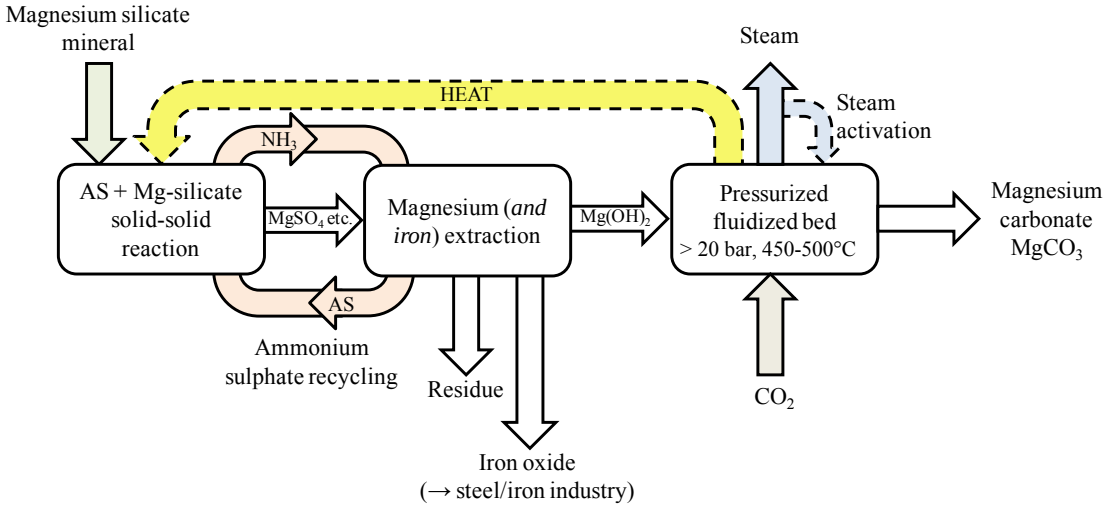

Fig. 1. A schematic illustration of the mineral carbonation process under development at ÅA

2. Process description: serpentinite carbonation via $MgSO_4$ and $Mg(OH)_2$

The staged process under development at ÅA is schematically given in Fig. 1. As raw material, serpentinite rock rich in serpentine ($Mg_3Si_2O_5(OH)_4$) is considered (being abundant in Finland), although most carbonation tests have been made using a commercial $Mg(OH)_2$ sample. Besides this, tests were made with magnesium silicate-based rock material from Lithuania, Portugal, Australia and other locations [14,15]. Table 1 lists selected composition data for some of the materials studied.

Table 1. Composition of some of the magnesium silicate rock samples being studied

Rock	MgO (% wt)	CaO (% wt)	Fe_2O_3 * (% wt)	SiO_2 (% wt)	Al_2O_3 (% wt)	Others (% wt)
Hitura, FI	38.1	0.5	14.8	47.6	10.0	6.2
Vammala, FI	14.5	5.6	12.5	49.5	8.8	9.1
Varena, LT	31.4	1.2	17.6	34.0	0.5	15.3
Braganca, PT	35.8	< 0.1	8.2	41.9	1.2	12.9
Great Serpentine Belt, AU	49.0	< 0.1	6.9	41.9	1.8	0.4

* Calculated, presumably a mixture of FeO and Fe_2O_3, i.e. Fe_3O_4.

2.1. $Mg(OH)_2$ production

In the first process step, (preheated) serpentinite rock is thermally treated with ammonium sulphate (AS) at 400 – 500 °C and atmospheric pressure for 10 – 60 minutes. A significant amount of the magnesium, Mg, in the rock is thus converted to sulphate, $MgSO_4$, which is highly soluble in water. Unfortunately, $MgSO_4$ cannot be directly converted with CO_2 to $MgCO_3$, but in an aqueous solution it can be converted to $Mg(OH)_2$. After cooling, the solid from the reaction with AS is slurried in water, leaving behind unreacted mineral and insoluble reaction products, e.g., silica. The pH of the filtrate solution is raised to 8 – 9, precipitating iron and calcium (from the mineral, see Table 1) as FeOOH and $Ca(OH)_2$, respectively, while increasing the pH further to 10 – 11 precipitates $Mg(OH)_2$. For the Finnish Hitura mineral, the preferable conditions for extraction of Mg (and Fe) to $MgSO_4$ (and $FeSO_4$) are temperatures 400 – 440 °C, for 30 – 60 minutes at S/AS = 0.5 – 0.7 kg/kg, with 60 – 66 % extraction of Mg. Lower temperatures and longer reaction times give a higher (relative) extraction of iron. Ammonia vapour, NH_3, released during the thermal step is collected and used to give the necessary pH increases for precipitation. It is thereafter recovered for regeneration of the AS salt downstream, using heat from another process step. Nonetheless, the recovery of solid ammonium sulphate from the aqueous form incurs a not insubstantial energy penalty.

2.2. $Mg(OH)_2$ carbonation

The $Mg(OH)_2$ produced as described above is converted into $MgCO_3$ in a pressurised fluidised bed (PFB) reactor at pressures > 20 bar and temperatures 450 – 600 °C. Results on conversion levels obtained under varying conditions (temperature, pressure, water content of the gas, time, fluidisation velocity) are reported elsewhere [9-11] for both the synthetic, commercial $Mg(OH)_2$ material and $Mg(OH)_2$ produced from Finnish or Lithuanian serpentinites. A few tests were made under supercritical CO_2 conditions (pressure > 74 bar) which showed significantly lower conversion levels and rates, suggesting that little benefit should be expected from operating at such pressure levels. It was found that the $Mg(OH)_2$ materials produced from the serpentinites are much more reactive (as a result of a ~10× larger specific surface of ~45 m^2/g vs. ~5 m^2/g), giving conversion levels of 50 % within 15 minutes for ~300 μm particles. The product gas from the carbonator is a hot, pressurised mixture of CO_2 and H_2O, the solids obtained will be partly recycled for further carbonation conversion. Unfortunately, although the carbonation reaction is rapid it levels off at a carbonation level of 50-55 % for the synthetic, commercial $Mg(OH)_2$ which may be the result of calcination of $Mg(OH)_2$ to MgO. However, it is noted that in order for $Mg(OH)_2$ to carbonate, dehydroxylation (i.e. calcination) has to occur. Apparently, carbonation takes place at a slower rate than dehydroxylation, resulting in a partially calcined and carbonated product. The amount of $Mg(OH)_2$, MgO and $MgCO_3$ in samples after test is plotted in Fig. 2 as a function of temperature for ~ twenty experiments (CO_2 pressure range 20 – 58 bar) with varying experiment time, fluidisation velocity, particle size, etc.

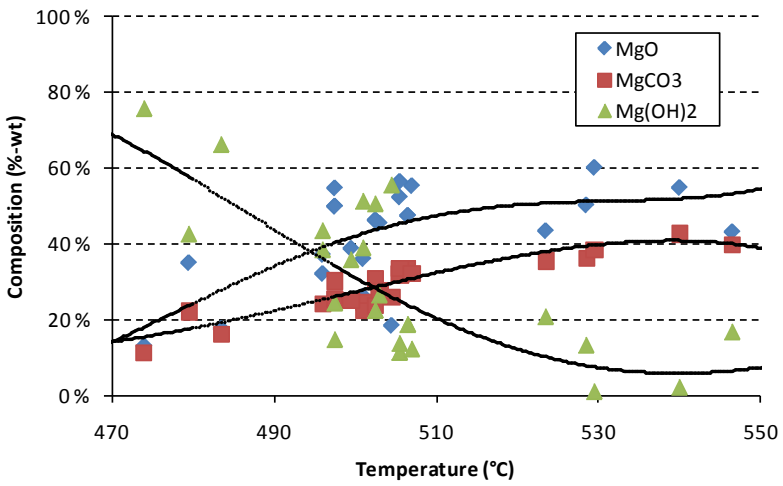

Fig. 2. Composition of Mg-species as a function of temperature for various experimental conditions using a PFB reactor [11].

2.3. Process (energy) efficiency

One of the features of CO_2 mineralisation using magnesium silicates is that the overall chemical reaction is exothermic. However, the direct carbonation of magnesium silicates is too slow, too energy demanding, or otherwise economically unviable, although work on improving the rate of processes based on pressurised aqueous solutions is still ongoing at several locations [3,6]. For the process route presented above an analysis was made of the heat requirement of the thermal treatment of Finnish Hitura (nickel mine tailing) serpentinite (see Table 1) with ammonium sulphate and the heat generated by carbonation of the resulting $Mg(OH)_2$. This showed that producing $Mg(OH)_2$, at 400 – 500 °C will require 4× more heat than what is obtained, at 450 – 550 °C, from carbonating it. Although ~1.2 MJ/kg CO_2 can be recovered as reaction heat the overall heat input requirements add up to 4 – 5 MJ/kg CO_2, consuming 3 – 4 ton rock per ton CO_2 [16]. An improved design using pinch analysis to optimise the heat exchanger network of the process, followed by process simulation with Aspen Plus® and exergy analysis (of the process heat input and outputs) reduces this to ~3 MJ/kg CO_2 heat input requirements while consuming ~3.1 ton rock per ton CO_2. The regeneration of ammonium sulphate (AS), which is obtained as aqueous solution after $Mg(OH)_2$ precipitation (while powdered, dry AS is used in the thermal treatment of serpentinite) puts a high energy penalty on the process [16].

It has been reported [17] that AS crystallisation from an aqueous solution can be accomplished at ~90 °C against a moderate heat input of ~120 kW/m^3 (residence time 95 minutes in a 0.97 m^3 DTB crystalliser). Nonetheless, a less energy consuming alternative for the AS recovery must be found and the solid/solid extraction must be improved, not only for energetic reasons, but also to recover more by-products thereby reducing the amount of solid residue. The rather high solubility of magnesium sulphate and ammonium sulphate in water should allow the use of minimal amounts of water in the precipitation steps towards $Mg(OH)_2$. Further improvement is obtained by optimising the different temperatures in the three aqueous precipitation steps. A variety of process refinements that lead to better energy efficiency, extraction from serpentinite, and AS recovery, was recently reported by Romão et al. [14] A recent study by Björklöf [18] applies mechanical vapour recompression (MVR) for the recovery of AS salt, making use of pinch analysis combined with chemical exergy analysis (in a spreadsheet calculation). The outcome of the study gives an energy penalty of 5.54 MJ/kg CO_2 fixed, expressed as exergy (using conservative data for the magnesium

sulphate solubility in water). Fig. 3 gives a so-called Grassmann diagram that clearly points out the exergy destruction in the various stages. Similar to Romão et al. [14,16] the energy penalty of the process (as exergy losses) was identified to arise primarily from 1) the AS recovery from dilute aqueous solutions, 2) the magnesium extraction using AS, and 3) the cooling of hot extraction products to aqueous solution temperature.

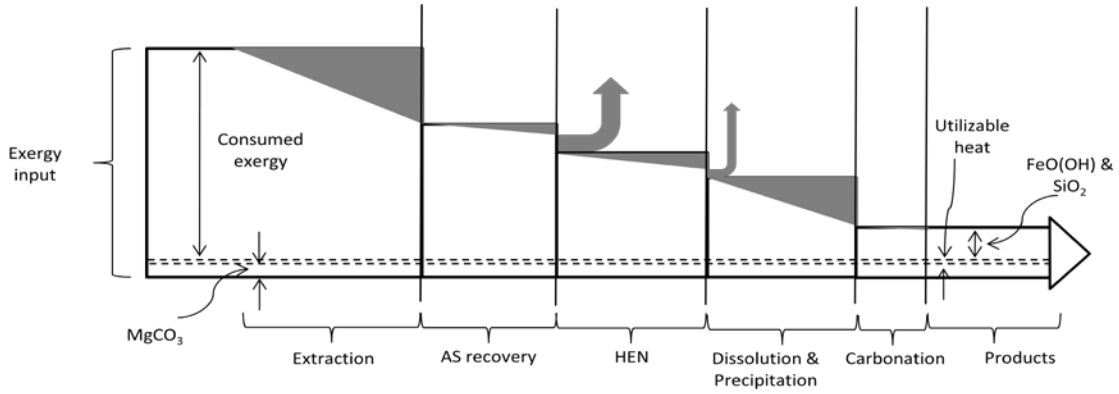

Fig. 3. A Grassmann diagram of the staged ÅA process. The gray triangles represent exergy destruction in the various process steps and the arrows represent exergy losses. At the far right, the products consist of the chemical exergies of the products and the recoverable heat from the carbonation step. [18]

2.4. Magnesium extraction and carbonation efficiency, ammonium sulphate recovery

Besides carbonation efficiencies for $Mg(OH)_2$ in the PFB levelling off at 50-55 % (for a synthetic, commercial sample) also the extraction of magnesium from serpentinite needs improvement, with extraction efficiencies obtained so far seldom exceeding 60% of the Mg content of the rock. For this, development work commences at ÅA, aiming at using a rotary kiln for the magnesium extraction, instead of using a fixed bed ("heap") for the conversion because this requires higher temperatures than necessary to compensate for heat and mass transfer limitations. The excess temperature leads to irreversible loss of the AS salt as SO_2 and N_2O. Detailed chemical reaction and solid product analysis suggest that temperatures should not exceed 400 °C. The possibility of losses of AS, e.g., occluded within the solid residue of unreacted serpentinite, silica etc., or in the $Mg(OH)_2$ fed to the carbonator (probably as NH_4^+ & SO_4^{2-} ions) was addressed by Björklöf [18]. Analysis showed that the solid residue contained < 0.1 %-wt nitrogen and < 0.9 %-wt sulphur which corresponds to ~ 0.15 % and ~ 1.5 %, respectively, of the incoming AS. For the $Mg(OH)_2$ the nitrogen – and sulphur contents were 0.1 %-wt and 0.8 %-wt, respectively.

3. Implementation of the results in Finland and abroad

Finland, like many countries in the EU, has commitments with respect to greenhouse gas emissions under the Kyoto Protocol and a continuation of the use of fossil fuels may be difficult without also implementing a CCS method. In Finland, the following schemes can be considered – see also Fig. 4 for industry sector integration:

- CO_2 from large-scale producers in Central / Northern Finland can be fixed using the vast resources of serpentinite-containing rock (estimated CCS capacity 2.5 – 3.5 Gt CO_2 [19]). One example is Ruukki's iron- and steelmaking plant at Raahe, which is ~110 km from the nickel mine at Hitura where large amounts of mine tailings are deposited. At the same time, large amounts of iron oxide by-products will be obtained from the rock, ready for use at the iron- and steelmaking plant. And, the slag by-products, most importantly steel

converter slag, may be carbonated to yield valuable calcium carbonates of PCC (precipitated calcium carbonate) quality [20].

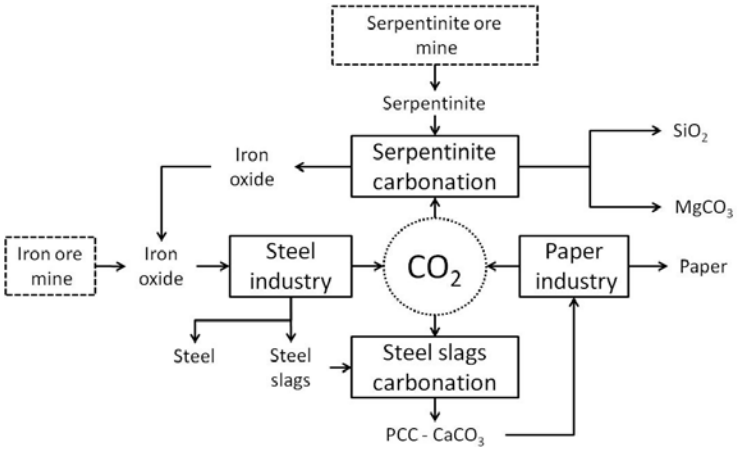

Fig. 4. Integrated processing for magnesium silicate carbonation, iron- and steelmaking and steel slag carbonation [13]

- With most CO_2 produced in Southern Finland, lower-grade minerals than found in Central/Northern Finland must be made use of. At several locations in South / South-west Finland rock with an MgO content of 10-15 %-wt were found, offering potential for source-sink combinations such as
  * Vammala serpentinite for use at the coal-fired plant at Meri-Pori (distance ~ 90 km)
  * Suomusjärvi serpentinite for use at a lime kiln in Parainen (distance ~ 90 km) or at a power plant in Naantali (distance ~ 95 km)

Also abroad the technology can be made use of, for example our cooperation with:

- Lithuania, where significant and suitable (although maybe located somewhat deep) serpentinite were found in the Varena region in the South-east of the country [15]
- In Portugal, suitable rock was located at several locations within the country [14], offering good opportunities for CO_2 mineralisation while also the option of (on-shore) underground sequestration is being investigated [21]
- Singapore, where CCS is combined with land reclamation during the next decade, using rock material that is imported from the region, for example from Australia [22]

In most of the cases, except the last mentioned obviously, CO_2 would be transported to the mineral site. On the other hand, like fossil fuels, metal ores or other raw material also rock transport can be feasible, with the advantage that the carbonation process can operate directly on the CO_2-containing gases. This removes the CO_2 capture step from the CCS chain.

4. Conclusions

The performance and efficiency (with respect to energy and chemicals recovery) of a staged process for serpentinite carbonation as under development at ÅA was described and assessed. It involves the production of magnesium hydroxide, $Mg(OH)_2$ from the mineral using ammonium sulphate, AS (which is later recovered) followed by carbonation of this in a pressurised fluidised bed (PFB) reactor. The process can be considered to be a variety of a process route patented by Pundsack in 1967 [23], which is based on extraction of magnesium from serpentine using an aqueous solution of ammonium bisulphate (ABS). The ÅA route for serpentinite carbonation, instead, uses AS in a high temperature step for magnesium

extraction that proceeds much faster than that with ABS in an aqueous solution (<< 1 h vs. >> 1 h) whilst also the reaction heat release from the carbonation is taken advantage of in the gas/solid reactor. However, recovery of solid ammonium sulphate from the aqueous form incurs a not insubstantial energy penalty. Thus, there seems to be a need to develop an alternative route to $Mg(OH)_2$ that bypasses the aqueous stage, and/or a route in which $MgSO_4$ is carbonated directly, e.g., using ammonium (bi)carbonate produced from CO_2 absorption in (aqueous) ammonia in an upstream scrubbing stage. Ammonium sulphate is a cheap and abundant reagent for extracting magnesium from serpentinite, but its performance must be evaluated under milder conditions as predicted by thermodynamics. The other technical issue linked with its use is the containment of NH_3 in the system.

Ammonium salts, i.e., (bi-)carbonate and (bi-) sulphate, could play an important role for extracting magnesium from rock material and as reactants produced from scrubbing CO_2 from process gases with chilled aqueous ammonia solutions – see for example [24]. An important benefit of the CO_2 mineral sequestration routes that look most promising for scale-up and large-scale application is that the expensive and potentially problematic CO_2 capture stage can be removed from the CCS chain. This is one of the drivers of current interest for CO_2 mineral sequestration. It is also considered for the ÅA process route, although the gas/solid carbonation will require CO_2 partial pressures > 20 ba r. On the other hand, scrubbing CO_2 from a power plant flue gas will introduce water and other species (and potential contaminants) into the process loop, eventually contaminating the sorbent.

Acknowledgements

This work was supported by the Academy of Finland program “Sustainable Energy” (2008 – 2011), with further support from KH Renlund Foundation (2007 - 2009). Thomas Björklöf, Experience Nduagu and Joel Songok of ÅA, Inês Romão of the University of Coimbra, Portugal and Dr. James Highfield of ICES/A*Star, Singapore are acknowledged for valuable comments and contributions.

References

[1] IPCC. Special Report on Carbon Dioxide Capture and Storage. Metz, B., Davidson, O., de Coninck, H.C., Loos, M., Meyer, L.A. (Eds.) Cambridge University Press, 2005.

[2] Lackner, K S. A guide to CO_2 sequestration. Science 300, 2003, pp. 677-1678.

[3] Zevenhoven, R., Fagerlund, J. Mineralisation of CO_2 Chapter 16 in: Developments and innovation in CCS technology M. Maroto-Valer (Ed.), Woodhead Publishing Ltd., Cambridge (UK), 2010, pp 433-462

[4] IEA. Carbon capture and storage – Progress and next steps. IEA/CSLF Report to the Muskoka 2010 G8 Summit. IEA, Paris, 2010, 39 pp.

[5] Delgado Torróntegui, M. Assessing the mineral carbonation science and technology M.Sc. Thesis ETH Zürich, Switzerland, 2010

[6] Zevenhoven, R., Fagerlund, J., Songok, J.K. CO_2 mineral sequestration – developments towards large-scale application. Greenhouse Gases: Science and Technology, 2011, *accepted / in press* doi: 10.1002/ghg3.007

[7] Nduagu, E. Mineral carbonation: preparation of magnesium hydroxide [$Mg(OH)_2$] from serpentinite rock, M.Sc. Thesis, Åbo Akademi University, Finland, 2008

[8] Fagerlund, J. Teir, S. Nduagu, E., Zevenhoven, R. Carbonation of magnesium silicate mineral using a pressurized gas/solid process. Energia Procedia 1, 2009, pp. 4907-4914.

[9] Fagerlund, J., Nduagu, E., Romão, I., Zevenhoven, R. A stepwise process for carbon dioxide sequestration using magnesium silicates. Front. Chem. Eng. China 4(2), 2010, pp. 133-141.

[10] Fagerlund, J., Nduagu, E. Zevenhoven, R. Recent developments on the carbonation of serpentinite- derived $Mg(OH)_2$ using a pressurised fluidised bed. Presented at GHGT-10, Amsterdam (the Netherlands) September 19-23, 2010. (Energia Procedia 2011)

[11] Fagerlund, J., Nduagu, E., Romão, I. & Zevenhoven, R. CO_2 fixation using magnesium silicate minerals. Part 1: Process description and performance. Energy – the Int. J. (special edition ECOS2010), *submitted (October 2010)*

[12] Gerdemann, S.J., O'Connor, W.K., Dahlin, D.C., Penner, L.R., Rush, H. Ex Situ Aqueous Mineral Carbonation Environ. Sci. Technol. 41, 2007, pp. 2587-2593

[13] Zevenhoven, R., Fagerlund, J., Nduagu, E., Romão. I. Mineralisation of CO_2 and recovery of iron using serpentinite rock. Proceedings of R´09, Davos (Switzerland), Sept. 14-16, 2009 (paper 149)

[14] Romão, I., Gando Ferreira, L. M., Fagerlund, J., Zevenhoven, R. CO_2 sequestration with Portuguese serpentinite. in: Proceedings of ACEME10, Turku (Finland) Nov. 29 - Dec.1, 2010, p. 77-87

[15] Stasiulaitiene I., Fagerlund J., Nduagu E., Denafas G., Zevenhoven R. Carbonation of serpentinite rock from Lithuania and Finland. Presented at GHGT-10, Amsterdam (the Netherlands) September 19-23, 2010. (Energia Procedia 2011)

[16] Romão, I., Nduagu, E., Fagerlund, J., Gando-Ferreira, L. M. & Zevenhoven, R. CO_2 Fixation Using Magnesium Silicate Minerals. Part 2: Energy Efficiency and Integration with iron-and steelmaking. Energy – the Int. J. (special edition ECOS2010), *submitted (October 2010)*

[17] O'Meadhra, R., and van Rosmalen, G.M. Scale-up of ammonium sulphate crystallization in a DTB Crystallizer. Chem. Eng. Sci. 51(16), 1996, pp. 3943-3950

[18] Björklöf, T. An energy efficiency study of carbon dioxide mineralization. M.Sc. Thesis, Åbo Akademi University, Finland, 2010

[19] Teir, S. Fixation of carbon dioxide by producing carbonations from minerals and steelmaking slags. PhD (Eng) thesis, Helsinki Univ, of Technol., Espoo Finland, 2008

[20] IEA, Carbon capture and storage: a key carbon abatement option. IEA, Paris, France, 2008. pp. 189-190

[21] Eloneva, S. Reduction of CO_2 emissions by mineral carbonation: steelmaking slags as raw material with a pure calcium carbonate end product. PhD (Eng) thesis, Aalto Univ. School of Sci and Technol., Espoo Finland, 2010

[22] Khoo, H.H., Sharatt, P.N., Bu, J., Borgna, A., Yeo, T.Y., Khor, T.Y., Björklöf, T.G., Zevenhoven, R. Carbon capture and mineralization in Singapore: preliminary environmental impacts and costs via LCA. Sci. Total Environ., *submitted (July 2010)*

[23] Pundsack, F.L., Recovery of silica, iron oxide and magnesium carbonate from the treatment of serpentine with ammonium bisulphate. U.S. Patent 3,338,667, 1967

[24] Hunwick, R.J., System, apparatus and method for carbon dioxide. World patent WO2008101293(A1), Australian patent AU2008000232, 2008

CO_2 capture in oil refineries – an evaluation of different heat integration possibilities for heat supply to the post-combustion process

Daniella Johansson[1,*], Per-Åke Franck [2], Thore Berntsson[1]

[1] *Heat and Power Technology, Chalmers University of Technology, Gothenburg, Sweden*
[2] *CIT Industriell Energi AB, Gothenburg, Sweden*
** Corresponding author. Tel: +46 317723008 Fax: +46 317721152, E-mail:Daniella.johansson@chalmers.se*

Abstract: This paper estimates the costs of CO_2 post-combustion capture for two refineries by comparing different alternatives for supplying the heat needed for the regeneration of the absorbent. The cost of capture ranges from 30 to 472 €/ tCO_2 avoided, depending on technology choice for heat supply and energy penalty for the CO_2 separation. In this study, it is concluded that process integration leads to a reduction in avoidance costs. However, the avoidance cost depends greatly on which system perspective is considered, i.e. whether CO_2 emission changes outside the refinery are included or not.

Keywords: *Carbon capture and storage, Post combustion, Oil refinery, Process integration*

1. Introduction

The oil refining industry generates large amounts of CO_2 emissions. Today and in the future, harder regulations (e.g. the EU ETS system and the Renewable Energy Directive) both on CO_2 emissions from the refinery process and on the refinery products will give new incentives for the oil refining industry to act towards CO_2 mitigation measures. However, the process structure of a refinery implies that even a perfect, energy-efficient refinery will continue to emit significant amounts of CO_2. Carbon Capture and Storage (CCS) is an alternative that can further reduce CO_2 emissions from the oil refining process. The interest in CCS has grown over the past years, among researchers as well as companies. Different capture technologies are possible: post-combustion, oxy-fuel combustion, chemical looping and pre-combustion. However, post-combustion is the most studied technology and is chosen in this paper as a promising technology since it does not require any extensive rebuilding of the existing refinery. Several previous studies have evaluated the costs for CCS at refineries [1-3], but none has been found that has investigated the costs with different heat supply options in combination with future energy market scenarios. Therefore, the aim of this paper is to examine how the avoidance costs for CO_2 in refineries are affected by different heat integration possibilities and future energy market scenarios.

In this paper, the CO_2 avoidance cost for post-combustion carbon capture, with mono-ethanolamine (MEA), is evaluated at two case refineries in the Skagerrak region. The oil refining industry is rather complex and therefore often offers opportunities for process integration which can facilitate substantial cost reductions for the heat supply. In this paper, possibilities to use excess heat from the main process to supply heat to the desorption unit, with or without the need of a heat pump, are evaluated as well as integration of a Natural Gas Combined Cycle (NGCC), a natural gas boiler and a biomass boiler. Also combinations of these alternatives are evaluated which is described in Section 2.1.

2. Studied systems and alternatives with related assumptions

The first case refinery is a hydroskimming refinery (Refinery no. 1) with a crude oil capacity of 6 Mt/y and ca. 0.5 Mt CO_2. The second is a complex refinery (Refinery no.2) with a crude oil capacity of 11.4 Mt/y and ca. 1.9 Mt CO_2. CO_2 emissions from the oil refining process originate from several sources. Only the largest CO_2 emission sources (89% of the total CO_2

emissions) have been selected for capture, resulting in 2 sources (totally 0.45 Mt CO_2/y) for Refinery no.1, and 4 sources (totally 1.7 Mt CO_2/y) for Refinery no. 2.

In this analysis the desorption column in the CO_2 capture unit has a working temperature of 120°C. After capture, the CO_2 is compressed to a pressure of ca. 75 bar with an absorber efficiency of 0.85. In order to generate the absorbent (MEA), large quantities of energy are needed. There are uncertainties regarding the heat demand needed per CO_2 emission captured, and therefore, to handle this discrepancy, two levels of desorption heat demand in the desorption are used, 2800 kJ/kg CO_2 and 4700 kJ/kg CO_2. The heat demand needed for desorption can be satisfied in different ways, and the alternatives used in this paper are described in more detail below. Key figures for the different alternatives are found in Table 1.

2.1. Process integration, utilization of excess heat (EH)

In this alternative the excess heat available above 129°C (EH) has been investigated in order to produce steam for the desorption unit. Two cases are used in Refinery no. 1. First, all excess heat is assumed to be available, presented as EH[1]&HP in Table 1. In the alternative with low heating demand (2800kJ/kgCO_2) enough heat above 129°C is available. However, in the alternative with high heating demand (4700kJ/kg CO_2) a heat pump must be used for supplying the additional heat needed. Second, due to contract regulations the amount of excess heat delivered to the current district heating network is assumed to be reserved. In this case only remaining excess heat is available for heat supply, and additional heat is supplied by a NGCC (EH[2]&NGCC), Biomass boiler (EH[2]&BB) or a Natural gas boiler (EH[2]&NB). Hence, the latter alternatives are a combination of excess heat above 129° (heat left after district heat delivery) and NGCC, BB and NB.

The prerequisites for Refinery no. 2 are different. The current district heat delivery is only a few percent of the excess heat, compared to over 50 percent for the first refinery. According to this fact, the alternative where the current level of district heat is reserved is not examined in Refinery no.2. On the other hand Refinery no.2 has the opportunity to increase the capacity of the current boilers. When evaluating Refinery no.2, the excess heat above 129°C is not enough to cover the whole heating demand for any of the levels of heating demands. Here, several alternatives to supply the additional energy needed are explored. First, a heat pump is used to supply the extra energy, presented as EH[1]&HP. Second, the capacity of the current steam boiler is increased (SP) and a biomass boiler, a natural gas boiler or a NGCC is used to supply the rest of the steam needed, presented as EH[3]&BB, EH[3]&NB and EH[3]&NGCC respectively. In both alternatives the available excess heat above 129°C has been used.

2.2. Heat pump (HP)

The heat pump uses heat available above 90°C at the refinery to produce LP steam (2.3 bar). The configuration is shown in Fig. 1. It is assumed that the temperature drop of available heat, related to the collection of heat from process streams, is 5°C. The heat pump is a semi-open cycle Mechanical Vapour Recompressor (MVR) using water vapour as working fluid [4].

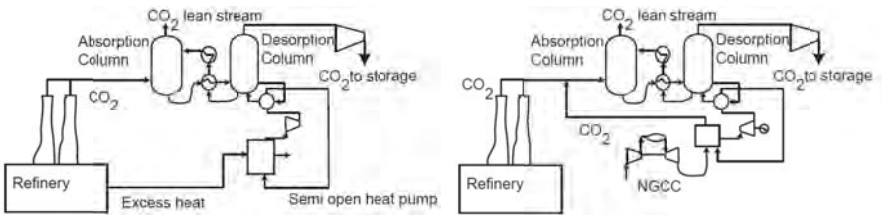

Figs. 1 & 2. The design of the capture unit using a HP (Fig. 1) or a NGCC (Fig. 2) for heat supply.

2.3. Natural gas combined cycle (NGCC)

The NGCC alternative is designed so that the heat recovery steam generator (HRSG) produces enough HP steam (80 bar) to cover the demand of LP steam (2.3 bar) needed for capturing CO_2 generated from both the refinery process and the NGCC; see Fig. 2.

2.4. Biomass and natural gas boilers (BB and NB)

In the biomass boiler alternative, a boiler (with efficiency 0.9) is installed. The boiler produces HP steam (80 bar) that is expanded in a back-pressure steam turbine to produce LP steam (2.3 bar). The boiler capacity is adjusted to produce enough LP steam to cover the heat demand for CO_2 capture from both the current process and the biomass boiler; see Fig 3. The natural gas boiler follows the design of the biomass boiler, except from the efficiency (0.94).

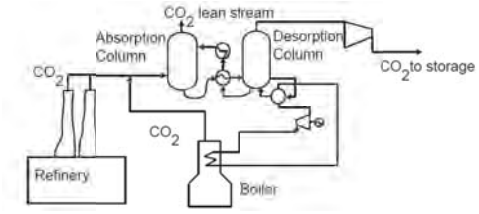

Fig. 3. The design of the capture unit using a biomass boiler or a natural gas boiler for heat supply.

Table .1 Key figures for the case refineries and the studied alternatives. Numbers within parentheses indicate figures for the high desorption heating demand (4700 kJ/kg CO_2). Ref. indicates the current figures for the refinery. In the current refinery (ref.) excess heat used refers to district heat delivery.

Refinery no.1	**Ref.**	**EH[1] &HP**	**NGCC**	**BB**	**NB**	**EH[2]& NGCC**	**EH[2] & BB**	**EH[2] NB**
Natural gas (MW)	19	19 (19)	178 (458)	19 (19)	86 (153)	142 (397)	19 (19)	70 (134)
Biomass (MW)	-	-	-	86 (195)	-	-	58 (195)	-
Excess heat used (MW)	120	37 (62)	-	-	-	129	129	129
CO_2 captured (t/h)	48	48	75 (123)	73 (114)	59 (71)	84 (113)	65 (105)	56 (67)
Electricity import (MW)	21	29 (30)	-39 (-157)	15 (-8)	16 (3)	-21 (-132)	19(-3)	19 (6)
Refinery no.2	**Ref.**	**EH[1] & HP**	**EH[3]& NGCC**	**EH[3] &BB**	**EH[3] &NB**	**NGCC**	**BB**	**NB**
Natural gas (MW)	-	-	118(843)	67 (67)	88 (304)	470(1420)	67(67)	236 (480)
Biomass (MW)	-	-	-	28 (400)	-	-	218 (697)	-
ΔSP[1] (t/h)	-	-	80	80	80	80	80	80
Excess heat used (MW)	27	136 (227)	82	82	82	-	-	-
CO_2 captured (tone/h)	174	174 (174)	195(319)	194 (303)	189 (226)	255 (418)	250 (391)	215 (257)
Electricity import (MW)	654	683 (704)	650(331)	668 (596)	668 (623)	637 (586)	631 (539)	638 (587)

[1,] Increased capacity of the current boiler

3. Methodology

The main methodology in this work is to combine knowledge from process integration in the refinery industry with knowledge about the CCS technology (similar methodology is used in [5]). The methodology and data collection are described by the following steps:

- The potential for steam savings and usage of excess heat from the refinery process are investigated using Pinch analysis. A thorough description of the methodology can be found in several editions; one of the most recently updated is [6]. Heat exchanger cost calculations for collection of excess heat are taken from [7], and used also for calculations for collection of excess heat streams for heat pumping.
  The data regarding the CO_2 capture unit are taken from previous studies of the MEA absorption process [3, 5, 8, 9]. The cost for the capture plant (excluding costs for the energy plant) has originally been taken from studies by Tel-tek [8] and adjusted to fit the refineries studied by using cost information in [9].
- The SGT-800 is assumed to be representative for gas turbines and data are taken from [10]. The size of the gas turbine is scaled to fit the applications studied in this paper, and economic scaling is based on price levels for different NGCC sizes in [11].
- The heat pump is designed using the software IEA Annex 21[4]. Using the chemical engineering plant cost index from 2010, updated investment cost is provided by the software.
- Economic data for the biomass boiler case are taken from [12], including installation and engineering costs, and data for the natural gas boiler are taken from [5].
- To include costs for installation and engineering, the budget prices for all equipment are scaled using a factor 2 (in cases when this is not already included), which is a mean value from [11] and [13]. For the heat exchangers, however, a factor of 3.5 is used [7]. Data for economic calculations for the steam turbines are taken from [14].
- Finally, to evaluate the costs for the different cases, future energy market scenarios are used. The scenarios are based on an energy market model adapted for evaluation of long-term investments in the process industry; a thorough description is found in [15].

3.1. Pinch analysis at the refineries

The pinch analysis only includes streams that are not already integrated (i.e. streams that are heated and cooled with utility, e.g. air). It shows that a significant amount of excess heat is available at Refinery no.1. Theoretical, 54 MW is available above 129°C, and 53 between 90° & 129°C. In the case when the current excess heat used for district heating delivery is inaccessible (EH[2]) the available excess heat is less: 9 MW above 129°C, and 15 MW between 90°C & 129°C. In Refinery no.2 the result shows a theoretically potential of 82 MW available excess heat above 129°C and 145 MW between 90°C & 129°C.

3.2. Economic calculations

In order to evaluate the above-described alternatives, the cost of each avoided tonne of CO_2 emitted is calculated from both a company and a society point of view, in Eqs. (1-5).

$$C_{avoided,company} = \frac{C_{annual}}{CO_{2\_avoided,company}} \quad \textbf{or} \quad C_{avoided,society} = \frac{C_{annual}}{CO_{2,\_avoided,society}} \quad [€/\text{tonne } CO_2] \quad (1,2)$$

$$CO_{2\ \text{avoided, company}} = CO_{2\ \text{before capture}} - CO_{2\ \text{after capture}} \quad (3)$$

$$CO_{2\ \text{avoided, society}} = CO_{2\ \text{before capture}} - CO_{2\ \text{after capture}} + CO_{2\ \text{reduced by replacing electricity production}} \quad (4)$$

$$\text{Where: } C_{annual} = \Delta C_{inv} + \Delta C_{running\ costs} + \Delta E * p_e + \Delta F * p_f - \Delta n_{biomass} * p_{Co2}\ [€/year] \quad (5)$$

ΔC_{inv} = Annualised investment costs (including installation costs)

$\Delta C_{running\ costs}$ = Annual change in running costs except for energy (e.g.MEA costs)

ΔE= Annual change in electricity

ΔF= Annual change in fuel use

$\Delta n_{biomass}$ = Annual captured CO_2 from biomass (from BB)

p_{Co2} = Price of CO_2 permits

p_f = Fuel price

p_e= Electricity price

The avoided amount from a society point of view also includes the CO_2 emissions saved from replacing marginal electricity production, as shown in Fig. 4. In all calculations an annuity factor of 0.1 and operation time of 8000h are used. All costs are calculated in 2010 prices levels. In this paper, CO_2 emissions generated from biomass are evaluated as not included in the EU ETS system. However, since capturing CO_2 emissions from the biomass boiler leads to a reduction of CO_2, and since alternative use of biomass – for example combustion for heat and power production – would otherwise release this CO_2, revenues related to the price of the CO_2 emissions (p_{CO2}) are allocated to the captured CO_2 emissions from the biomass.

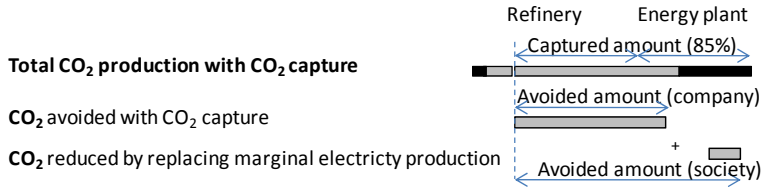

Fig. 4. Description of the avoided amount of CO_2.

3.3. Future energy market scenario

The performance of the CO_2 capture investments is evaluated by using consistent energy market scenarios based on the tool ENPAC [15]. The scenario data are shown in Table 2.

Table 2. Energy market parameters for the different scenario

Scenario	1	2	3	4	5	6	7	8
Fossil fuel price	Low	Low	Low	Low	High	High	High	High
CO_2-price [€/tCO2]	15	27	45	85	15	27	45	85
RES-E support[1] [€/MWh_{el}]	20	20	20	20	20	20	20	20
El price [€/MWh-el]]	56	66	81	87	62	72	87	95
CO_2 from el [kg/MWh_{el}]	679	679	679	129	679	679	679	129
Marginal technology for electricity production	Coal	Coal	Coal CCS	Coal CCS	Coal	Coal	Coal	Coal, CCS
Price of biomass [€/MWh_{fuel}]	26	31	39	56	29	34	42	60
Natural gas price [€/MWh_{fuel}]	33	33	33	33	51	51	51	51

[1]Premium paid to producers of renewable electricity from combustible renewable

By using a number of different scenarios that outline possible cornerstones of the future energy market, robust investments can be identified and the climate benefit can be evaluated. Since CO_2 capture is a technology under development and will most likely not be implemented before 2030, scenarios for 2030 are used. This case consists of eight scenarios which are a result of combining two levels of fossil fuel and four levels of CO_2 prices.

4. Results

The results of the calculated avoidance costs are presented in Figs. 5 and 6, together with the price of the CO_2 emission certificates. The CO_2 price can be viewed as an estimate of the possible income from performing these measures at the refinery.

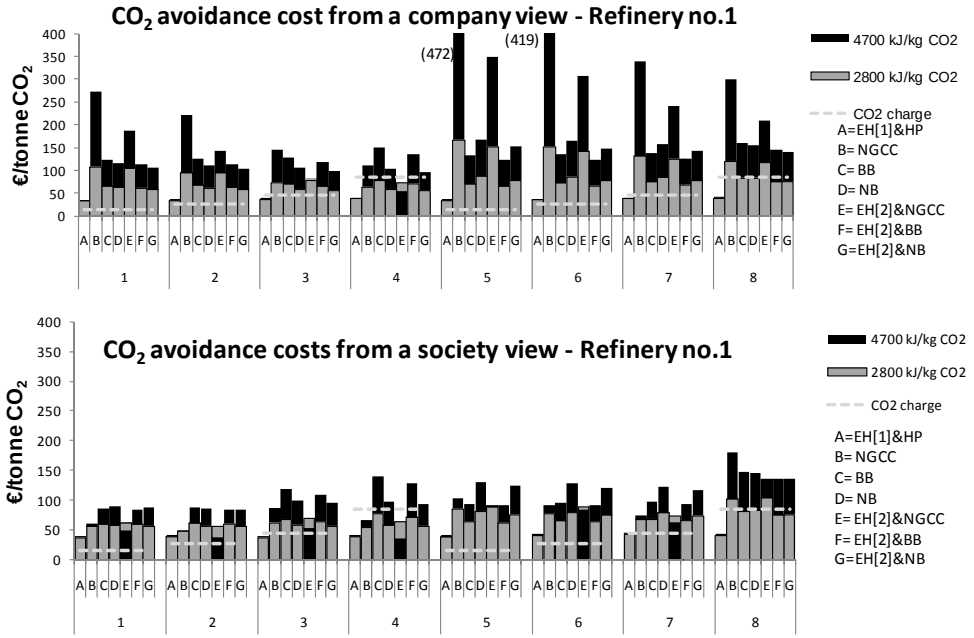

Fig. 5. The avoidance costs (from a company and a society view) for the different alternatives in Refinery no.1. Black bars lower than grey bars indicate that the high heating demand causes lower avoidance costs. Only one bar indicates that the avoidance costs for the two energy levels are similar.

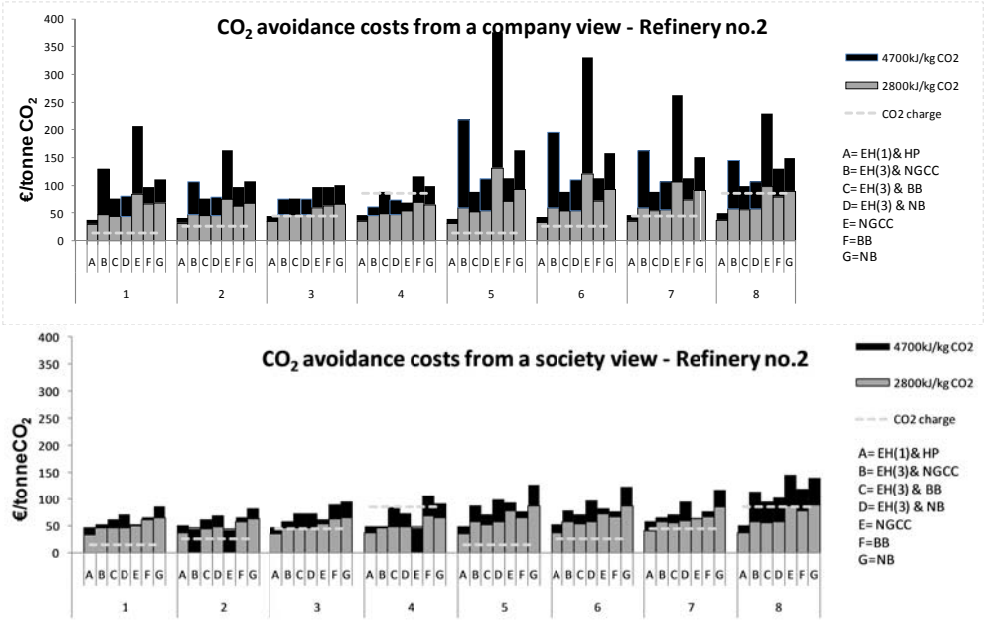

Fig. 6. The avoidance costs (from a company and a society view) for the different alternatives in Refinery no.2. Black bars lower than grey bars indicate that the high heating demand causes lower avoidance costs. Only one bar indicates that the avoidance costs for the two energy levels are similar.

The avoidance costs from a company view are for both refineries, in most scenarios, lowest for the alternatives using excess heat and heat pump. The avoidance costs for these

alternatives are also robust with respect to changes in scenario data, which is due to the relatively small amount of electricity used and the fact that no additional fuel is necessary. Figs. 5 and 6 show that only if the price of CO_2 emissions will become high (85 €/tCO_2), and if excess heat is used to supply the heat demand, could investing in a capture unit be a robust and promising alternative. If the fossil fuel price is low at this level of CO_2 price, several more alternatives could be promising. Moreover, the results from Refinery no. 2 show lower avoidance costs for almost all alternatives compared to Refinery no.1. This can be explained by cheaper investment costs (in relative terms) and the fact that Refinery no. 2 has the opportunity to increase the capacity of current boiler.

When evaluating the costs from a society view, meaning that CO_2 changes outside the refinery are considered, most alternatives will have much lower avoidance costs compared to the results from a company view; see Figs. 5 and 6. The largest impact can be seen for the NGCC alternative. The large generation of electricity from the NGCC implies large CO_2 savings from marginal production of electricity, especially in Scenarios 1, 2, 5, 6 and 7 when marginal electricity producers are coal power plants without CCS. The benefits from including the reduction of CO_2 emissions from electricity production result in a lower avoidance cost for the high heating demand in almost all cases for the NGCC alternatives. The NGCC alternatives (in both refineries) with high heating demand (4700kJ/kg CO_2) have the lowest avoidance costs.

5. Conclusions and discussion

The main conclusion from this study is that process integration of the capture process at the refinery, i.e. use of excess heat and heat pumping, can significantly reduce the avoidance costs for CO_2 capture at a refinery and be a robust and promising alternative at high CO_2 price levels. However, the avoidance cost depends greatly on which system perspective is considered, i.e. including CO_2 changes in marginal electricity production or not. The alternatives with NGCC could be competitive if high heating demand is needed in combination with a high CO_2 price and low fossil fuel prices (an unlikely combination).

Previous research by [1], [2] and [3] examining CO_2 capture at refineries reported capture costs in the range 50-120 €/tCO_2. This study's estimates range between 30 and 472 €/ tCO_2 avoided. However, the previous studies have all used natural gas CHP to supply the extra energy needed, and in this study that alternative ranges from 45 to 168 € /tCO_2 avoided. It should be noted that the estimated costs in other studies arise from different assumptions and the costs can be calculated per CO_2 captured or CO_2 avoided (as in this study and in [1] and [3]). First, different values for the desorption heat are used in the different studies: 2800 kJ/kg CO_2 in [3] , 4700 kJ/kg CO_2 [2] and undefined in [1]. Second, the values for the different costs (e.g. investments and fuel) also arise from different assumptions. In this study, for example, fuel and electricity costs are calculated from future energy market scenarios. Moreover, in this study the transport costs are not included: however, studies by [16] indicate that the costs for transport and storage are around 15-25 €/t CO_2.

Before CCS becomes a commercial technology, a lot can occur with the available excess heat levels and demands at a refinery. This is to be investigated in more detail in other studies. Finally, to improve the cost estimations of the post-combustion capture process, future work would also include a comparison of the avoidance costs for other absorbents, e.g. ammonia.

Acknowledgement

This work has been carried out within the Energy Systems Programme, which is primarily financed by the Swedish Energy Agency, and within the project *CCS in the Skagerrak/ Kattegat region*, which is an intraregional CCS project partly funded by the EU. The work has also been co-financed by Preem AB. Finally, the authors would also like to thank Preem AB for valuable inputs.

References

[1] MT. HO, GW. Allison, DE. Wiley, Comparison of MEA capture cost for low CO2 emissions sources in Australia, International Journal of Green Gas Control.2011;5(1), pp. 49-60

[2] Tel-Tek, CO_2 capture from industrial facilities, Tel-Tek, 2009, Tel-Tek Porsgrunn, Norway, 2009

[3] J. Van Straelen, F. Geuzebroke, N. Goodchild, L. Mahony, CO2 capture for refineries, a practical approach. Energy Procedia. 2009, pp.179-185

[4] IEA Annex 21, Industrial heat pump screening program, IEA Heat Pump Centre c/o SP Technical Research Institute of Sweden, 1997

[5] E. Hektor, Post-Combustion CO_2 Capture in Kraft Pulp and Paper Mills – Technical, Economic and System Aspects, PhD thesis, Chalmers University of Technology, Sweden, 2008

[6] Kemp I, Pinch Analysis & Process Integration – A user guide on process integration for the efficient use of energy, 2nd ed., Butterworth-Heinemann, Oxford, UK, 2007

[7] R. Sinnot, G. Towler, Chemical engineering design, 5th ed., Elsevier Ltd, 2009

[8] Personal communication with Stefan Nyström and Christina Simonsson, Refinery Development, Preem AB, 2010-12-08

[9] Sherif A, Integration of a Carbon Capture process in a chemical industry – Case study of a steam cracking plant, Master Thesis, Chalmers University of Technology, Gothenburg, Sweden, 2010

[10] Siemens SGT-800 brochure, available online 2010-12-3:http://www.energy.siemens.com

[11] Gas Turbine World Handbook, Performance Spec, 2007

[12] E. Pihl, Integrating biomass in existing natural gas-fired power plants – a techno-economic assessment, Lic. Thesis, Chalmers University of Technology, Sweden, 2010

[13] J. Strömberg, P.Å Franck, T. Berntsson, Learning from experiences with Gas-Turbine-Based CHP in Industry, CADDET Analyses Series No.9, 1993

[14] E. Axelsson, Energy Export Opportunities from Kraft Pulp and Paper Mills and Resulting Reductions in Global CO2 Emissions, PhD thesis, Chalmers University of Technology, Sweden, 2008

[15] E. Axelsson, S. Harvey, Scenario assessing profitability and carbon balances of energy investments in industry, The AGS report: 2010: EU1, 2010

[16] McKinsey & Company, Carbon Capture & Storage: Assessing the Economics, 2008

BECCS in South Korea – An Analysis of Negative Emissions Potential for Bioenergy as a Mitigation Tool

Florian Kraxner[1,*], Kentaro Aoki[1], Sylvain Leduc[1], Georg Kindermann[1], Jue Yang[2], Yoshiki Yamagata[2], Kwang Il Tak[3], Michael Obersteiner[1]

[1] *Forestry Program, International Institute for Applied Systems Analysis (IIASA), Laxenburg, Austria*
[2] *Center for Global Environmental Research (CGER), National Institute for Environmental Studies (NIES), Tsukuba, Japan*
[3] *Forestry Department, Kookmin University, Seoul, Republic of Korea*

** Corresponding author. Tel: +43 2236 807 233, Fax: +43 2236 807 299, E-mail: kraxner@iiasa.ac.at*

Abstract: The objective of this study is to analyze the in-situ BECCS capacity for green field bioenergy plants in South Korea. A technical assessment is used to support a policy discussion on the suitability of this mitigation tool. We first examined the technical potential of bioenergy production from domestic forest biomass. For this exercise, in a first step, the biophysical Global Forestry Model G4M was applied in order to estimate the biomass availability. In a second step, the biomass results from the forestry model were used as input data for an engineering model (BeWhere) for optimized scaling and locating of coupled heat and power plants (CHP). The obtained geographically explicit locations and capacities for forest-based bioenergy plants were then overlaid with a geological suitability map for carbon storage. From this, a theoretical potential for in-situ BECCS was derived. Results indicated that, given the abundant forest cover in South Korea, there is a substantial potential for bioenergy production which could contribute to substituting emissions from fossil fuels and to meeting the targets of the country's commitments under any climate change mitigation agreement. However, there seems to be only limited potential for direct in-situ carbon storage in South Korea.

Keywords: *BECCS, Bioenergy, Carbon Capture and Storage, Biomass modeling, Energy policy*

1. Introduction

An active debate in the scientific community is revolving around the possibility of using bioenergy in combination with carbon capture and storage (BECCS), which could remove CO_2 from the atmosphere in order to contribute substantially to achieving low levels of concentration. In the Fourth Assessment Report of the Intergovernmental Panel on Climate Change (IPCC), BECCS is considered "a potential rapid-response prevention strategy for abrupt climate change" and is consequently considered as one of the options to comply with the targets agreed in the Kyoto Protocol [1]. During the last decade it was demonstrated by e.g. [2-4] that terrestrial ecosystems when combined with the use of biomass energy can offer a permanent carbon sink by capturing carbon from biomass conversion facilities and permanently storing carbon in geological formations. However, compared to CCS (Carbon Capture and Storage) combined with conventional fossil fuel systems, very little information can be found in scientific literature so far for both the technical and potential application of BECCS. Moreover, apart from engineering papers presented at e.g. special BECCS conferences such as [5] on Europe, there is - according to our knowledge - to date no literature available that features geographic explicit BECCS applications, especially not for non-European countries.

Although the land base of Korea is small, as much as 64% of the country is forested. Due to a highly efficient and rapid national reforestation program in the 1970s, a majority of the forests in Korea has now reached age classes of 30 and 40 years, which require intensive care in terms of thinning and pruning. By-products from these silvicultural activities can generate a significant amount of raw material to produce e.g. wood pellets and wood chips. Korea

appears further to be an interesting study area for bioenergy, since the country's forestry regained importance both from an ecological as well as from an economical point of view only recently. While trying to build up a bioenergy sector for both energy security and contributing to reduce CO_2 emissions in order to comply with climate change mitigations efforts, sustainable forest management is seen as a key for mobilizing forest biomass for energetic use or direct carbon sequestration. Consequently, ambitious policies and plans for bioenergy production were introduced by the country's government (e.g. "Low Carbon – Green Growth" initiative by the National Energy Plan [6]). However, the lack of forestry infrastructure such as adequate forest roads - for important management activities like harvesting or replanting - causes still too high costs for biomass and related energy production [e.g. 7]. Moreover, this alternative energy sector is facing strong competition from e.g. lower cost fossil and nuclear energy sectors. Hence, being able to better quantify the sustainable bioenergy potential in these countries by identifying economically and biophysically optimized locations for new bioenergy plants and adding value to this information by selecting those locations with promising in-situ combination with CCS technology, policy makers in Korea would be able to develop and support improved and better targeted policies in the area of energy, climate and environment while being supportive to various co-benefits such as rural development, (re-) activation of sustainable forest management etc. The aim of the technical part of our manuscript was threefold. First, to help identifying - in a geographically explicit manner - the available biomass from forest for bioenergy production under sustainable management conditions in South Korea; second, to indicate the optimal size and location of green-field forest biomass-based bioenergy CHP (Coupled Heat and Power technology) plants; and third, to identify the amount and capacity of in-situ BECCS units in South Korea.

2. Method

There are various systems for CCS, such as underground geological storage, ocean storage, mineral carbonation, or industrial use. In this study, we considered the CCS System (with post combustion capture technology) for the underground geological storage into a certain geological formation in the on-shore earth's subsurface. Additionally, we were especially aiming at direct "in-situ" storage. The storage happens in direct vicinity to the combustion units (CHP plants) in order to minimize transport costs and complications. Further we assumed that the total amount of CO_2 - emissions generated at a BECCS unit will be captured and stored in-situ. A technical assessment was used to support a policy discussion on the suitability of this mitigation tool. We first examined the technical potential of bioenergy production from domestic forest biomass. For this exercise, in a first step, the biophysical global forestry model G4M [8] was applied in order to estimate the biomass availability. In a second step, the biomass results from the forestry model were used as input data for the engineering model BeWhere [9] for optimized scaling and locating of CHP plants. The obtained geographically explicit locations and capacities for forest-based bioenergy plants were consequently overlaid with a geological suitability map for carbon storage. From this, a theoretical potential for "in-situ" BECCS was derived.

2.1. The Global Forest Model (G4M)

The Global Forest Model (G4M) from IIASA was used to calculate the growing stock and the sustainable biomass extraction rate. G4M, as described by [8], has been developed in order to predict wood increment and stocking biomass in forests. As input parameter it uses yield power which is achieved through the net primary productivity (NPP) for a specific region. This NPP can be supplied by existing NPP-maps [e.g. 10] or – for higher accuracy – estimated with the help of driver information of soil, temperature and precipitation. The

model can be used like common yield tables to estimate the increment for a specific rotation time. It can further be used to estimate the increment– related optimal rotation time and to provide information on how much biomass can be harvested under a certain rotation time and how much biomass is stocking in the forest. G4M also supplies information on the harvesting losses like needles, leaves and branches which typically remain in the forests under sustainable management. Further, other economic parameters such as harvesting costs - depending on tree size and slope - can be calculated.

2.2. The BeWhere Model

The BeWhere Model - a spatially explicit optimization model, depicting the supply chain of bioenergy industries - was used for the in-situ BECCS assessment [9]. The model, developed at IIASA, considers industries competing for wood resources. On the supply side, forest wood harvests, sawmill co-products (SCP) and wood imports serve as biomass resources for possible new bioenergy plants. Wood demand of pulp-and-paper mills, of existing bioenergy plants and of private households is considered on the demand side The model assumes that the existing wood demand has to be fulfilled, allowing new plants to be built only if there is enough surplus of wood available. The model is spatially explicit and the transportation of wood from biomass supply to demand spots is considered either by truck, train or boat. The model selects optimal locations of green-field bioenergy plants by minimizing the costs of biomass supply, biomass transport and energy distribution. Full costs and emissions at the optimal locations were calculated such that we were able to indicate the BECCS potential for the country under investigation. Spatial distribution of forestry yields was estimated and provided by the G4M, as well as the harvesting costs (as a function of tree size depending on site quality and rotation time) and the slope steepness were provided by the same model.

3. Results

There were 3 complementary main sets of results derived from this study and indicated at country level: 1) the sustainably available biomass potential for harvest together with the national heat demand as a main prerequisite for the installation of green-field CHP plants; 2) the geological suitability for CS (Carbon Storage); and 3) the identified locations for BECCS units together with their individual bioenergy production capacity as well as their carbon capture and storage capacity. All presented geographically explicit data sets were compiled at a 0.25-deg (degree grid cell) resolution (25 x 25 km). We used a conversion factor of 0.5 to estimate dry matter biomass (ton dry matter, tdm) from stem volume irrespective to the tree species. The defined forest harvesting scenarios were based on the amount of extracted biomass, while the baseline for harvesting was considered under a sustainable forest management regime, assuming that the average annual harvesting rate is substantially lower than the annual allowable cut. We further assumed that only stem biomass was extracted from the forest stands and that 100% of the extracted biomass was used for energy production. Following conversion factor for the national currency was applied for economic calculations of harvesting, transport and energy (heat) costs: 1 Korean Won = 0.000908987 USD (2008).

3.1. Biomass availability and energy demand

For our analysis, we assigned a managed forest area of 4,852,330 ha (about 78 % of total South Korean forest area) for biomass extraction dedicated to energy production. This forest area was modeled as an aggregated forest cover map based on GLC 2000 [11], the Relative Human Influence concept for each terrestrial biome [12], a classification of pristine and non-pristine forest [13] and protected area [14]. We excluded the forest area where the Relative Human Influence was less than 50 % and where protected areas designated by IUCN

Categories I – VI were located. For the geographical distribution of the actual growing stock we calculated 555,363,300 m^3 (protected area excluded), which was achieved with the help of the global biomass map [15] which was harmonized with FAO statistics of 2005 [13], while the official national statistics of South Korea reported a total growing stock of 506,376,806 m3 for 2005 [16]. Derived from Korean forest statistics in 2008, we limited the biomass extracted annually for energy production to 0.36 % of the total growing stock (sustainable forest management criteria), amounting 999,653 tdm/year (on average 1.62 tdm/ha-year) - see Fig. 1 for the spatial distribution. Further information for our economic optimization process with respect to costs (wood chip and stumpage price, harvesting and extraction costs) were derived from various Korean resources and adapted to local slope conditions for harvesting operations with different technologies.

In South Korea, the total heat energy consumption was 625,915 GJ/year in 2008 [6]. As input for the energy demand calculations, we geographically weighted the heat demand with the population for 2005 at 0.25 degree resolution and assumed that the average heat demand per person was 0.0127 GJ/person (Fig. 1). The average energy prices for Korea in 2008 were adapted from the national statistics.

The demand-supply optimization routines of the BeWhere model also consider transportation costs (truck, train, ship - derived from [17]), as well as the existing road and railway networks for South Korea which were taken from vmap0 [18], also considering different travel speeds.

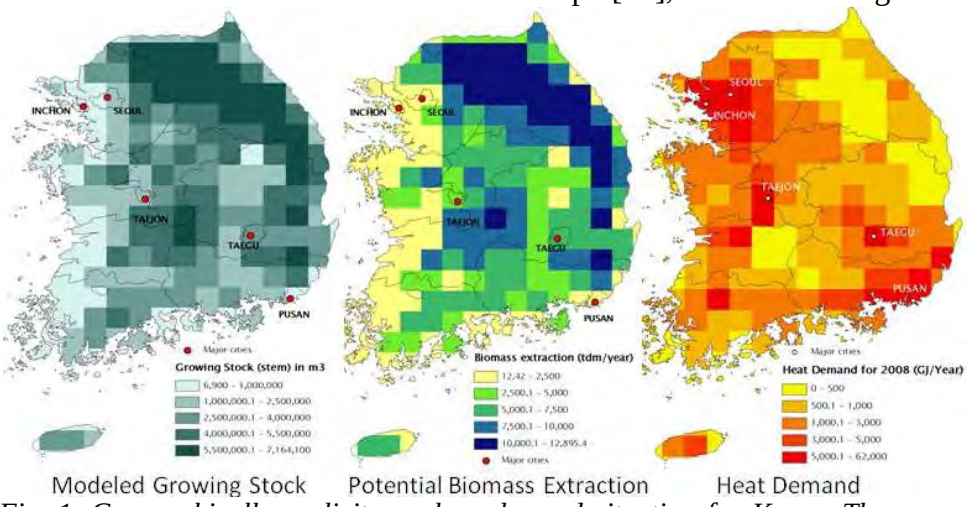

Fig. 1. Geographically explicit supply – demand situation for Korea. The map on the left hand side indicates the modeled spatial distribution of the growing Stock (m^3) in Korean forests (biomass supply). The highest growing stock could be identified in the north-east and the center of Korea (dark pixels). The map in the center indicates the modeled potential biomass extraction rate (tdm/year) - under sustainable conditions - from Korean forests (biomass supply). Highest biomass extraction rates could be achieved also in the north-east and center of the country. The map on the right hand side indicates the modeled spatial distribution of the heat demand (GJ/year). Highest demand was identified around the large urbanized areas (e.g. Seoul) in the western and south-eastern part of the country.

3.2. Identification of geological suitability for C - storage

The geological CS facility can be installed only under specific conditions such as geological characteristics (e.g. tectonic activity, sediment type, geothermal and hydrodynamic regimes) and maturity of infrastructure to build CCS units. In general, sedimentary basins are the sites with the highest potential for geological CS. Suitable sites for geological CO_2 storage can be found on: 1) basins formed in mid-continent locations, 2) basins formed near the edge of stable continental plates, 3) basins behind mountains formed by plate collision such as European

basins immediately north of the Alps and Carpathians, 4) fold belts, and 5) some of the highs [e.g. 1]. Other geological formations such as shield areas (e.g. Scandinavia) or tectonically active areas (e.g. Japan) are less suitable for geological CO_2 storage. However, the suitability for geological CS depends to a great extent on their local conditions. We identified mostly basins as potentially suitable locations for geological in-situ CS in South Korea. The geological map shown in Fig. 2 was mainly based on the studies by [19] and [20]. The location for CO_2 injection can be different from the site of the bioenergy plants where CO_2 emissions occur. In the case of South Korea mainly the geological Gyeongsang Basin located in the south-east of the country could be identified to be potentially suitable for in-situ CS.

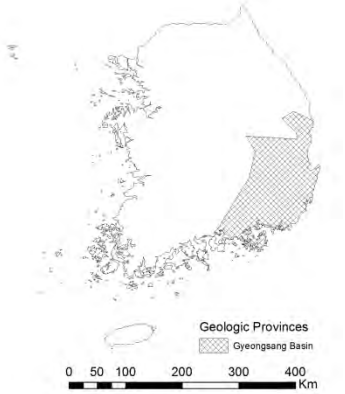

Fig. 2 Potential locations (Geologic Province) suitable for geological CO2 storage in South Korea (on-shore only). Source: modified after [19] and [20].

3.3. Potential in-situ BECCS units identified for South Korea

To identify the optimal locations for green-field bioenergy plants, three different sizes of CHP plants are considered (5, 20, and 70 MW). We assumed that diversification with respect to plant size would on the one hand result in a better distribution of plants within the country, which increases usually also the co-benefits of bioenergy plants. On the other hand we expected to identify more bioenergy plants suitable for in-situ CS. Within each scenario (plant capacity) the aim was to meet the target for the maximum sustainable biomass extraction (about 1 M tdm/year).

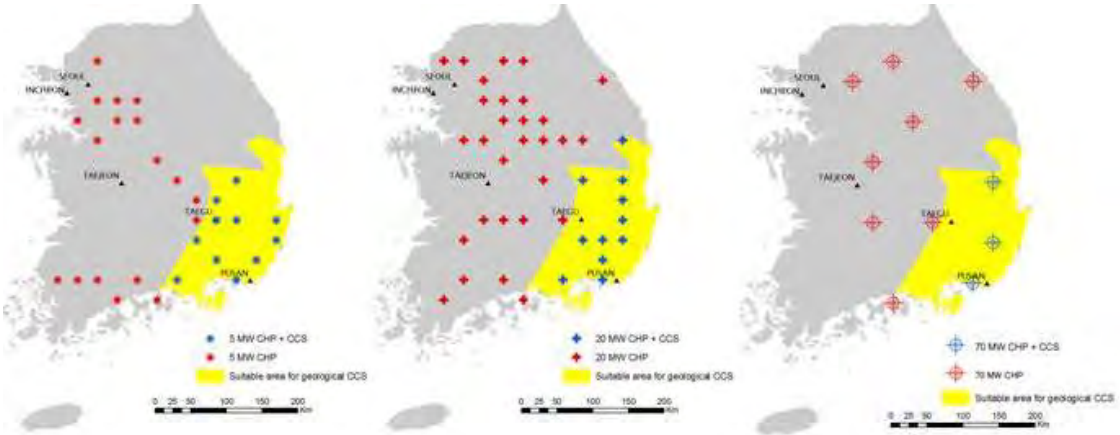

Fig. 3. Three different scenarios (from left to right 5; 20; 70 MW) for optimized green-field biomass plant locations in South Korea. The geographic explicit location of bioenergy plants without CCS is indicated in red color and the BECCS unit locations are indicated in blue color on light yellow background (geologically suitable formation for CS).

For this study we defined in-situ CS suitability such that the bioenergy plant needs to be located within a 0.5 degree grid cell (about 55 x 55 km) of the suitable geologic province in

order to directly inject CO2 underneath a plant or at any place up to a maximum of 25 km radius distance (e.g. with the help of a short pipeline).

Based on these assumptions, Fig. 3 shows the optimized location in a geographically explicit manner by plant size. Table 1 indicates the optimized amount of green field bioenergy plants for Korea, listed by plants with and without in-situ CS suitability, divided into the different plant capacity categories.

Table 1. Energy produced, emissions substituted and CCS Capacity by forest biomass CHP plants with/without BECCS system under a sustainable forest biomass production regime.

Plant size Technology	5 MW **NO** CCS	20 MW **NO** CCS	70 MW **NO** CCS	5 MW CCS	20 MW CCS	70 MW CCS
Plant #	18	29	8	11	11	3
Biomass used (tdm/year)	117,000	716,300	712,400	71,500	271,700	267,150
Heat produced (GJ/year)	1,190,475	7,288,353	7,248,670	727,513	2,764,548	2,718,251
El. produced (GJ/year)	757,575	4,638,043	4,612,790	462,963	1,759,258	1,729,796
Subst. emissions (tCO_2/year)	215,516	627,050	625,036	131,704	237,847	234,389
CCS Capacity (tCO2/year)	***0***	***0***	***0***	***131,704***	***237,847***	***234,389***

We could identify a maximum of 40 green-field bioenergy plants under the 20 MW-scenario of which 11 plants were located on geologically suitable ground in order to meet the criteria for BECCS units. Under the 5 MW scenario, 29 bioenergy plants were optimally distributed over the country, among which also 11 plants qualified as BECCS plants. Under the 70 MW scenario a total of 11 bioenergy plants were computed of which 3 met the criteria for BECCS units. In the best case (20 MW scenario), the "BECCS-effect" (emissions accounted as negative) could reach a potential capacity of some 238,000 tons of CO_2 to be directly stored permanently belowground per year and to be accounted as negative emissions.

4. Discussion and Conclusions

Our BECCS exercise offers several new insights to the bioenergy sector in South Korea and provides crucial information for policy support and design. First of all, it is important to note that even under our rather conservative assumptions – especially with respect to sustainable biomass extraction - we still could theoretically produce some 10% of the present heat demand (being equivalent to a 20 times increment of the present bioenergy share for heat production in Korea [21]), and 1.3% of the total electricity produced in South Korea (15 times the present bioenergy share for electricity production [21]). These results indicate a substantial potential of bioenergy growth in South Korea – especially given the present policies and targets of the National Energy Plan to e.g. increase the bioenergy share in total energy production from 0.2% (2007) to 3.4% by 2030 [6].

Among the 3 different scenarios (plant capacities), the 20 MW scenario turned out to offer the best country-wide coverage with its 40 green-field bioenergy facilities, which consequently could provide direct and indirect co-benefits such as driving the green economy, i.e. providing job opportunities both at the facility and in the biomass production. Another major benefit of growth in the bioenergy sector would be the resulting investments in forest and forest management primarily by small-scale forest owners, e.g. in forest infrastructure. These benefits are based on the assumption that forest biomass would see a price increase, which justifies investments into forest infrastructure (to harvest the biomass more easily) which lowers harvesting costs and increases competitiveness.

Although the suitable geological formations for in-situ CS in South Korea are limited to about 1/5 of the country area (the Gyeongsang Basin), with the help of this study we could show that there is a theoretical potential for 3 (70 MW plants) to 11 (5 / 20 MW plants) green-field BECCS plants with in-situ CS. Based on our assumptions, the BECCS-effect might amount to 130,000 – 240,000 tons CO_2 per year in addition to a similar amount of substituted fossil fuel emissions. This means that about 3-4% of the total demand for heat energy in South Korea could be produced in BECCS plants with in-situ CS. As a consequence, 3-4% of the fossil fuel emissions could be substituted and additionally accounted as negative because they would be actively removed from the atmosphere by BECCS plants. This BECCS effect comes additionally to the biomass co-benefits discussed earlier and could be used as a key issue for future policy design and decision makers.

However, the BECCS effect - and with it a crucial lever for climate, environment and rural development policies - could certainly be substantially increased and strengthened. An important caveat to bear in mind is that with our study we only could point out the theoretical potential without considering the costs of the actual CCS process. If bioenergy plants with higher capacities would be applied, costs could be substantially decreased (scale effect or poly-production). Further, although the suitable geological formations for geological CCS appearing in South Korea are limited (e.g. earthquake and volcanic activity), there are wide off-shore prospective areas in this region (e.g. East Sea). Using further capacity for CS (non in-situ), basically all substituted emission from bioenergy production could additionally be stored and accounted as negative. The use of a (trans-national) CO_2-pipeline could actually boost the BECCS effect and lower the costs, but further research needs to be done in this field. Also the joint use of off-shore CS together with e.g. Japan would substantially increase BECCS capacity, which requires similar research to be extended to South East Asia, potentially using a higher data resolution than 0.25-deg.

We conclude that policy targeted bioenergy-based re-activation of forest management in South Korea would evoke a real win-win-situation. First, bioenergy production and BECCS would directly contribute to meet ambitious climate change mitigation targets. Second, the forest ecosystem would benefit from sustainable management (including thinning etc.) e.g. in terms of improved forest health, stand stability and lower exposure to threatening hazards like wind throw or pests. Third, the forest owners - and with them the forest sector industry - would benefit from an increased value of the forest property, from better prized forest products, as well as from a higher quality of the grown timber and competitive harvesting conditions as a consequence of investment into forest infrastructure. And last not least, society would benefit through e.g. an improved protective function (from e.g. flooding, landslides, avalanches etc.) and an increased recreational value of the forest.

References

[1] IPCC, Special Report on Carbon Dioxide Capture and Storage. ISBN-13 978-0-521-86643-9. Cambridge University Press, 2005.

[2] M. Obersteiner, C. Azar, P. Kauppi, K. Möllersten, J. Moreira, S. Nilsson, P. Read, K. Riahi, B. Schlamadinger, Y. Yamagata, J. Yan, J-P. van Ypersele, Managing climate risk, Science 294(5543), 2001, pp. 786–787.

[3] F. Kraxner, S. Nilsson, M. Obersteiner, Negative emissions from BioEnergy use, carbon capture and sequestration (BECS)—the case of biomass production by sustainable forest management from semi-natural temperate forests, Biomass and Bioenergy 24, 2003, pp. 285–296.

[4] C. Azar, K. Lindgren, M. Obersteiner, K. Riahi, D.P. van Vuuren,· K.M.G.J. den Elzen, K. Möllersten,·E.D. Larson, The feasibility of low CO_2 concentration targets and the role of bio-energy with carbon capture and storage (BECCS). Climatic Change 100, 2010, pp. 195–202.

[5] F. Kraxner, G. Kindermann, S. Leduc, K. Aoki, M. Obersteiner, Bioenergy Use for Negative Emissions – Potentials for Carbon Capture and Storage (BECCS) from a Global Forest Model Combined with Optimized Siting and Scaling of Bioenergy Plants in Europe. Paper presented at the First International Workshop on Biomass & Carbon Capture and Storage October 2010, University of Orléans, France, 2010.

[6] Korea Energy Management Corporation, 2010, available at: http://www.kemco.or.kr/new_eng/main/main.asp

[7] F. Kraxner, J. Yang, Y. Yamagata, Attitudes towards forest, biomass and certification – A case study approach to integrate public opinion in Japan. Bioresource Technology, 100(17), 2009, pp. 4058–4061.

[8] G. Kindermann, M. Obersteiner, B. Sohngen, J. Sathaye, K. Andrasko, E. Rametsteiner, B. Schlamadinger, S. Wunder, R. Beach, Global cost estimates of reducing carbon emissions through avoided deforestation, PNAS 105(30), 2008, pp. 10302-10307.

[9] S. Leduc, E. Schmid, M. Obersteiner, K. Riahi, Methanol production by gasification using a geographically explicit model. Biomass and Bioenergy, 33(5), 2009, pp. 745-751.

[10] S.W. Running, Terrestrial remote sensing science and algorithms planned for EOS/MODIS. International Journal of Remote Sensing 15, 1994, pp. 3587-3620.

[11] JRC Global Land Cover 2000 version 1. Database. Joint Research Centre, European Commission, 2000, http://bioval.jrc.ec.europa.eu/products/glc2000/products.php

[12] WCS-CIESIN, Last of the Wild Data Version 2, 2005 (LWP-2): Global Human Footprint data set (HF), 2005, http://sedac.ciesin.columbia.edu/wildareas/downloads.jsp#infl

[13] FAO Global Forest Resources Assessment 2005. FAO Forestry Paper 147. Food and Agriculture Organization of the United Nations, Rome, 2005.

[14] UNEP-WCMC, World Database on Protected Areas (WDPA), United Nations Environment Programme World Conservation Monitoring Centre, 2009.

[15] G. Kindermann, I. McCallum, S. Fritz, M. Obersteiner, A global forest growing stock, biomass and carbon map based on FAO statistics. Silva Fennica 42(3), 2008, pp. 387-396.

[16] Korea Forest Service, Statistical Yearbook of Forestry 2009. Korea Forest Service, Daejeon, 2009.

[17] P. Börjesson, L. Gustavsson, Regional Production and Utilization of Biomass in Sweden. Energy 21, 1996, pp. 747-764.

[18] National Imagery and Mapping Agency, World roads (VMAP0) Fairfax, VA: National Imagery and Mapping Agency, 1997

[19] J.B. Bradshaw, T. Dance, Mapping geological storage prospectivity of CO_2 for the world sedimentary basins and regional source to sink matching, GHGT-7, September 5–9, 2004, Vancouver, Canada, v.I, pp. 583-592.

[20] USGS, U.S. Geological Survey World Petroleum Assessment 2000 - Description and Results, DDS-60. United States Geological Survey, 2001.

[21] IEA, International Energy Agency, Country Statistics, 2008, available at: http://www.iea.org

What are the rules for biofuel carbon accounting?

Eric P Johnson[1,*]

[1] *Atlantic Consulting, Gattikon, Switzerland*
** Corresponding author. Tel: +41 44 772 1079, E-mail: ejohnson@ecosite.co.uk*

Abstract: Most quantitative assessments of biomass fuels or biofuels assume that bioenergy is inherently carbon neutral, that biogenic emissions of carbon dioxide should be excluded from a carbon footprint. This 'carbon neutral' assumption makes an enormous difference in carbon accounts and in the policies that those accounts would suggest. For instance, if harvested logs burnt as fuel are considered carbon neutral, their carbon footprint is far lower than that of natural gas. However, if the logs' biogenic carbon emissions are counted, then their carbon footprint is much higher than gas's. Moreover, this can lead to absurd conclusions. If carbon neutrality is presumed, it makes no difference to a carbon footprint if a forest is standing or if it has been chopped down for fuel wood. Since the mid-1990s, some researchers have contradicted the 'carbon neutral' assumption, and their view that biogenic emissions should be counted has begun to attract significant attention of policy makers. This paper reviews the history and current state of biogenic-carbon accounting rules, including the ISO/CEN rules being developed under the EU Renewable Energy Directive. Without taking sides, it will define the debate for researchers and policy-makers, reflect on its significance and suggest possible means of resolution.

Keywords: *biofuels, carbon accounting, carbon neutral*

1. Introduction: The premise of carbon neutral

In the fields of life-cycle assessment and carbon footprinting, biofuels traditionally have been considered as inherently carbon neutral: biogenic emissions of carbon dioxide are excluded from the inventory or footprint. Two landmark studies in the field, (Argonne Labs GREET) and (Joint Research Centre of the EU Commission, EUCAR et al. 2008) take this position as given, and many other studies follow their leads.

More recently, however, some researchers have begun to question this approach. Probably the best-known are (Searchinger, Hamburg et al. 2009), but the issue had already been raised by others, namely (Rabl, Benoist et al. 2007) and (Johnson 2009). More recently (Manomet Center for Conservation Sciences 2010) published a large report that questioned the 'carbon-neutral-assumption'. The International Energy Agency's (IEA) Bioenergy Task 38 group, 'Greenhouse Gas Balances of Biomass and Bioenergy Systems', has also raised questions[1], particularly from (Berntsen and Peters 2010) and (Cowie 2010).

Some regulators appear to be taking these questions seriously. The (Manomet Center for Conservation Sciences 2010) report was commissioned by and adopted by the US Commonwealth of Massachusetts with respect to its regulation of biomass-fueled power plants. Presumably Task 38 is being taken seriously by IEA member governments, and at the United Nations level, the idea of that REDD (Reducing Emissions from Deforestation and Forest Degradation) is generally desirable seems to be undisputed.

Furthermore, the issue has come into the domain of standards organizations. Technical Committee 383 at CEN is working on norms in this area, as is ISO Project Committee 248 (of which the author is a member).

[1] See a March 2010 conference record at http://ieabioenergy-task38.org/workshops/brussels2010/

And what is the question? Primarily it is this: should biofuels be considered inherently carbon neutral? The first-generation position was yes (although it was more an assumption than an answer to a question); the emerging position is at minimum not an automatic yes, but a definitive second-generation answer is yet to be determined fully.

The importance of this question, in environmental terms, is very high. Biofuels are clearly the main solution proposed by governments to the twin problems of climate change and energy security. Non-bio, non-fossil energies – such as solar, tidal and wind – are and will for the medium term be marginal contributors, whereas biofuels are aimed at taking, for instance, a 20% share of the EU energy mix by 2020. If these biofuels turn out to be, relative to conventional fossil fuels, carbon negative rather than positive, then their subsidies will not only have cost billions[2], they will also have worsened rather than mitigated global warming!

This paper is meant to elaborate the issue from the perspective of carbon footprinting. After a brief statement of method, it presents results, i.e. characterization of the 'carbon neutral' question from six different methodological perspectives. It concludes with findings and suggestions for further study.

2. Method

The author has reviewed the literature as well as the political and the standards documentation, and then refracted these in the light of carbon-footprint methods.

3. Results: how the 'carbon neutral' question can be categorised

Using the method of carbon footprinting or life-cycle assessment, the question of biofuel carbon neutrality can be characterized in six ways, which are described in the following six subsections.

3.1. Boundary of the system

In impact analyses such as life-cycle assessment or carbon footprinting, for a full life-cycle the ideal boundary is 'cradle-to-grave', i.e. from the environment to the environment. As the ISO standard for life cycle assessment (ISO 2006, section 5.2.3) expresses it: "Ideally, the product system should be modelled in such a manner that inputs and outputs at its boundary are elementary flows." In other words, the life-cycle boundary begins and ends with human intervention. Purely natural processes – biogenic as opposed to anthropogenic – are not included.

Growing of crops, say as feedstock for fuel, is of course an anthropogenic activity. Fields of rapeseed, soybeans or wheat do not spring up on their own. The carbon released in creating and maintaining such fields (so-called 'land-use change' emissions), as well as the carbon emitting in cropping them, is included in current assessments; however, the carbon taken in during a growing season is netted out against the carbon emitted in combustion. And this seems consistent with the boundary definition above.

But what about a natural forest? If human activity was not needed to create it, why should its carbon emitted in combustion – clearly a human activity – be netted against carbon taken from the atmosphere to create the trees? This seems inconsistent with the human/nature

[2] OECD countries' annual subsidy of biofuels in 2007 was estimated at about $15 billion.

boundary applied to other assessments. To be consistent, human harvesting of natural forests should not be netted against their biogenic creation. (Plantations are a different matter; they are created by humans.) This would be consistent with how harvest of other natural resources – say, oil or limestone – is treated in LCA and footprints. Harvest of these is not netted against their creation.

3.2. Temporal definition of the system

In common usage, the terms biofuels and renewables are actually misnomers. Surely conventional oil and gas, which are derived from long-dead plants and animals – are biofuels? And solar power, as astrophysicists tell us, is not renewable. The sun is does not recycle its hydrogen, and in some millions of years will burn itself out. These observations are more than just amusing. They point out the temporal boundaries placed implicitly on LCAs and carbon footprints. To be careful in carbon accounting, analyses should recognize such temporal boundaries explicitly.

Also, researchers should consider the theoretical basis for granting carbon credits to biofuels, yet not doing so to fossil-biofuels. At present this appears to be done out of intuition – not out of thought-through reasoning. The reasoning should be developed, or the practice should be ended.

People often justify 'carbon neutrality' of biofuels by saying: 'the tree will grow back'. If it grows back in 10 minutes, fine. But what if if grows back in 10 years, or 100 years? Surely there is an inflection point (and it could be calculated) as to when the grow-back timing changes from favourable to unfavourable.

3.3. Shadow/alternative/counterfactual scenarios

If we had not grown a crop to be used as fuel, what would have happened to the carbon balance then?

This idea of a 'shadow' or alternative scenario, sometimes called 'the counterfactual', is not present in most studies of biofuels. In a 2008 survey of over 100 publications by 56 researchers about solid biomass fuels (Johnson 2009), not one of them postulated a shadow scenario. After extensive work on liquid biofuels over the past eight years, the author is aware of only two researchers who have applied it in this area: (Joint Research Centre of the EU Commission, EUCAR et al. 2006) and (Heinen and Johnson 2008).

Broader research by (Manomet Center for Conservation Sciences 2010) and IEA Task 38 suggest that shadow scenarios should be standard, not the exception. Moreover, the idea of REDD (Reducing Emissions from Deforestation and Forest Degradation) in the UNFCCC and the idea of 'additionality' in the Clean Development Mechanism (CDM) and elsewhere, both suggest that counterfactuals should be customary.

3.4. Allocation

There are two open issues here. One is allocating carbon burden to crop components by weight. This has led to the dubious practice of assigning the majority of a grain footprint to the straw that is grown along with the grain. Dubious yes, but it has been applied in numerous studies for the German government, only a few years ago, that the government then promoted.

The other is the allocation of CO_2 capture, i.e. the removal of carbon dioxide from the atmosphere by photosynthesis. Why is the captured CO_2 always allocated to a biofuel? Why

cannot a fossil fuel take that carbon credit? Or should the credit be shared proportionately between the two? The answers here are not immediately obvious, but even more obvious is that the questions appear not to be asked in most studies – and yet they should be.

3.5. Marginal/consequential modelling

Simply put, current practice presumes that every additional unit of biogenic CO_2 emitted is recycled to the biosphere via photosynthesis – from the earth to the earth. By contrast, every additional unit of fossil CO_2 emitted stays in the atmosphere, creating more heat.

Yet as pointed out in the allocation discussion, this cannot make sense: carbon dioxide is carbon dioxide. Also, the ability of the biosphere to capture carbon can and does change, depending particularly on forest conditions and water-saturation levels. Once again, the answers here are not immediately obvious, but the questions should be addressed.

3.6. Additionality and subtractionality

The idea of additionality may be useful in creating accurate accounts of forest carbon. If a forest is planted on previously non-forested land, with the express intent of using the harvested trees as biofuel, then this might properly be considered as carbon neutral. Indeed, it probably is carbon negative: although carbon is being harvested, on a net basis, more carbon might be returned to the soil and the vegetation above.

Likewise, what about 'subtractionality'? If trees are being harvested for fuel that otherwise would have remained standing, their carbon surely should be removed from the forest's carbon stock, and debited against the footprint. The case for this has been made by (Rabl, Benoist et al. 2007), (Johnson 2009) and (Searchinger, Hamburg et al. 2009), but the term subtractionality – you first heard it here.

4. Discussion and conclusions

This paper has raised more questions than it has answered – and that is its intent. Without addressing these questions, carbon accounting will continue to be wildly inaccurate. And 'wildly' is no overstatement: the current discussion in CEN and ISO[3] of biofuel standards demonstrates how divergent current opinion is on these issues.

Getting more convergent opinion is important, and not just for the reputation of LCA and carbon footprint analysts, who often are cursed with the epithet of 'you can get any answer you want'. More convergence will be critical to investors, policy makers and the general public. If we really believe that reducing carbon emissions is critical to our future, the questions raised in this paper are worth serious exploration.

To conclude, there might be a simple principle to guide further research: *efficiency is the key*. The source of carbon is surely less important than the efficiency by which it is used. Moreover, efficiency also drives economics; efficient fuels generate the most consumer demand. Efficiency can and should guide the evaluation of future fuels, and the rules of carbon accounting should be constructed to promote this.

Put another way, the key to reducing atmospheric concentrations of carbon is to put less carbon up there in the first place and to keep more of it down here on the ground. We should

[3] The author is a delegate and part of the ongoing discussions.

be more worried about how much net carbon is being emitted, and less worried about which kind of carbon, i.e. biogenic or fossil, is being emitted. If we use this simple concept as our guide, I think we will make much greater progress toward solving this great problem.

References

[1] Argonne Labs GREET, Greenhouse Gases, Regulated Emissions, and Energy Use in Transportation, Version 1.8c.

[2] Joint Research Centre of the EU Commission, EUCAR, et al. (2008). Well-to-Wheels analysis of future automotive fuels and powertrains in the European context.

[3] Searchinger, T. D., S. P. Hamburg, et al. (2009). "Fixing a critical climate accounting error." Science 326 (23 October 2009): 527-528.

[4] Rabl, A., A. Benoist, et al. (2007). "How to Account for CO_2 Emissions from Biomass in an LCA." International Journal of LCA 12(5): 281.

[5] Johnson, E. (2009). "Goodbye to carbon neutral: getting biomass footprints right. ." Environmental Impact Assessment Review.

[6] Manomet Center for Conservation Sciences (2010). Massachusetts Biomass Sustainability and Carbon Policy Study: Report to the Commonwealth of Massachusetts Department of Energy Resources. Brunswick, Maine.

[7] Berntsen, T. and G. P. Peters (2010). CO_2 perturbation and associated global warming potentials following emissions from biofuel based on wood. Greenhouse gas emissions from bioenergy systems: impacts of timing, issues of responsibility Brussels.

[8] Cowie, A. (2010). Is bioenergy really carbon neutral? Greenhouse gas emissions from bioenergy systems: impacts of timing, issues of responsibility Brussels.

[9] ISO (2006). ISO 14040: Environmental management — Life cycle assessment — Principles and framework.

[10] Heinen, R. and E. Johnson (2008). "Carbon footprints of biofuels & petrofuels." Industrial Biotechnology 4(3): 257-261.

Coupling mass transfer with mineral reactions to investigate CO_2 sequestration in saline aquifers with non-equilibrium thermodynamics

Yuanhui Ji[1,*], Xiaoyan Ji[1], Xiaohua Lu[2], Yongming Tu[3,4]

[1] *Division of Energy Engineering, Luleå University of Technology, 971 87 Luleå, Sweden*
[2] *State Key Laboratory of Materials-Oriented Chemical Engineering, Nanjing University of Technology, 210009, Nanjing, P. R. China*
[3] *Key Laboratory of Concrete and Prestressed Concrete Structures of Ministry of Education, Southeast University, 210096, Nanjing, P. R. China*
[4] *Division of Structural Design and Bridges,Royal Institute of Technology (KTH),10044 Stockholm, Sweden*
** Corresponding author. Tel: +46 920491271, Fax: +46 920491074, E-mail: yuanhui.ji@ltu.se*

Abstract: The coupling behaviors of mass transfer of aqueous CO_2 with mineral reactions of aqueous CO_2 with rock anorthite are investigated by chemical potential gradient and concentration gradient models, respectively. SAFT1-RPM is used to calculate the fugacity of CO_2 in brine. The effective diffusion coefficients of CO_2 are obtained based on the experimental kinetic data reported in literature. The calculation results by the two models and for two cases (mass transfer only and coupling mass transfer with mineral reaction) are compared. The results show that there are considerable discrepancies for the concentration distribution with distance by the concentration gradient and chemical potential gradient models, which implies the importance of consideration of the non-ideality. And the concentrations of aqueous CO_2 at different distances by the concentration gradient model are higher and further than that by the chemical potential gradient model. The mineral reaction plays a considerable role for the CO_2 geological sequestration when the time scale reaches 10 years for the anorthite case.

Keywords: *CO_2 geological sequestration, Non-equilibrium thermodynamics, Chemical potential gradient, Mass transfer, Geochemical reaction*

1. Introduction

Geological sequestration of anthropogenic CO_2 is a promising carbon mitigation strategy[1, 2], which includes the injection of CO_2 into deep saline aquifers, depleted oil and gas reservoirs, and deep coal seams[2, 3], and the storage in deep saline aquifers seems to have the largest potential capacity[3, 4, 5]. The four main CO_2 sequestration mechanisms in deep saline aquifers proposed are solubility trapping; capillary trapping; hydrodynamic trapping and mineral trapping[1, 2]. In order to study the long-term behaviors of CO_2 in formations, and to estimate the possible CO_2 leakage risk, it is necessary to investigate the dissolution of CO_2 in brine, the mass transfer of dissolved CO_2 and the coupling behaviors of mass transfer with the mineral reactions of aqueous CO_2 with rocks over a wide range of spatial and temporal scales[1, 3, 6-8].

Phase equilibria of CO_2 in water and brines have been widely studied[9-12]. The molecular-based statistical associating fluid theory (SAFT) equation of state (EOS) is a promising model for systems up to high pressures, which represents the density and phase equilibrium for CO_2-H_2O from 285 to 473 K and up to 600 bar, and for CO_2-H_2O-NaCl from 298 to 373 K and up to 200 bar[10, 13]. For the kinetics research, numerous investigations on the mass transfer of CO_2 in high-pressure water or brines have been conducted to simulate CO_2 geological or ocean disposal processes[5, 14-16]. Yang and Gu[5] studied CO_2 dissolution in brine at elevated pressures experimentally and described the mass transfer of CO_2 in brine using Fick's Second Law with an effective diffusion coefficient considering the effect of convection, which are two orders of magnitude larger than the molecular diffusivity of CO_2 in water[5], and it implies that the density-driven natural convection greatly accelerates the mass transfer of CO_2 in brines. Generally, mass transfer flux is described with concentration gradient as the driving

force. However, in real systems, Fick's law must be amended to account for nonideal behavior. So the driving force for solute fluxes is not the concentration gradient, but the chemical potential gradient[17, 18]. Our previous work[19, 20] also reveals that it is necessary to consider the non-ideality of the complicated systems. Therefore, on the basis of the work by Yang and Gu[5], the mass transfer of CO_2 in brines is investigated by chemical potential gradient model[21] based on derivation of $\partial a_i/\partial t$ (a_i is the activity of species i). The calculated results show the importance of the consideration of the non-ideality. Moreover, path-of-reaction and kinetic modeling of CO_2-brine-mineral reactions in deep saline aquifers have been conducted[9, 22-25]. The nonisothermal reactive transport code TOUGHREACT[26, 27] were developed which introduced reactive chemistry into the multi-phase fluid and heat flow code TOUGH2[28].

In this paper, the coupling behaviors of the mass transfer of aqueous CO_2 with the typical mineral reactions of aqueous CO_2 with rocks will be investigated and analyzed by chemical potential gradient and concentration gradient models, respectively.

2. Thermodynamic model

The fugacities of the aqueous CO_2 are calculated using SAFT1-RPM EOS[13] and the details are described in literature[13].

3. Kinetics modeling

3.1. Model description

3.1.1. Mass transfer

Concentration gradient model

The flux generalized to three dimensions is described as[18, 29]

$$J_i = -D_C \nabla C_i \tag{1}$$

where, J_i is molar flux of species i; D_C is the effective diffusion coefficients in concentration gradient model; C_i is the molar concentration of species i.

Chemical potential gradient model

As described in above text, in real systems, chemical potential gradient is the driving force for solute fluxes[17, 18], and the flux generalized to three dimensions is described as[18, 29]

$$J_i = -(D_\mu C_i / RT) \nabla \mu_i \tag{2}$$

where, J_i is molar flux of species i; D_μ is the effective diffusion coefficients in chemical potential gradient model; μ_i is the chemical potential of species i and described by Eq. (3)[30].

$$\mu_i = \mu_i^0 + RT\ln(f_i / f_i^0) = \mu_i^0 + RT\ln a_i \tag{3}$$

where, μ_i^0, a_i, f_i and f_i^0 are the standard chemical potential, activity, fugacity and standard fugacity of component i, respectively. At a certain T and P, both μ_i^0 and f_i^0 are constants. In this paper, one-dimensional case is studied, and the convective molar flux by the bulk motion of the fluid is not added in Eqs. (1) and (2), but an effective diffusion coefficient considering the effect of convection is used. Combining Eq. (2) with Eq. (3), Eq. (4) can be obtained.

$$\boldsymbol{J_i = -\frac{D_\mu C_i}{RT}\nabla(RT \ln f_i) = -D_\mu C_i \nabla \ln f_i} \tag{4}$$

Diffusion coefficient determination

The effective diffusion coefficient is obtained based on the experimental kinetic data in Test 4 reported by Yang and Gu[5]. At the temperature and different pressures of Test 4, the quantitative relations of fugacities of aqueous CO_2 with their concentrations are determined from fitting according to the calculation results by SAFT1-RPM EOS[13] with a function form as $f_{CO2(aq)}=a+b\cdot C_{CO2(aq)}$ in which a and b are parameters at a certain temperature and pressure. The aqueous CO_2 concentrations at the interface are calculated with SAFT1-RPM[13] by assuming instantaneous saturation of CO_2[21]. In the work of Ref. [5], the CO_2 dissolution was performed in a PvT cell with a cross-sectional area A (7.9273×10^{-4} m^2) and brine phase height H (0.0442 m), the CO_2 pressures P_t at different time t were recorded. The number of moles of dissolved CO_2 (n_t) are determined from the gaseous pressure at different time t and the initial experimental conditions. Based on the mass balance, Eq. (5) can be obtained.

$$\int_0^x C_{CO_2(aq)} A dx = n_t \tag{5}$$

where $C_{CO2(aq)}$ ($mol\cdot m^{-3}$) is the concentration of aqueous CO_2 in brines, and A (m^2) is the contact area of gaseous CO_2 with brine and is assumed to be the cross-sectional area of the cell, and x (m) is the mass transfer distance. In the work of Yang and Gu[5], only the experimental kinetics data after 180s were used to analyze the mass-transfer process of CO_2 in the brine. In this paper, we also take the flux J and n_t after 180s.

According to the flux J and n_t at different pressures in Test 4[5] and combining Eqs. (1) with (5), the effective diffusion coefficient at respective pressures in the one-dimensional concentration gradient model can be determined directly. While for the effective diffusion coefficient in the chemical potential gradient model, a simple but effective method, direct search method, can be used, in which the initial value and step length of the effective diffusion coefficient are assumed as 1.0×10^{-9} $m^2\cdot s^{-1}$, while the maximum value is 1.0×10^{-6} $m^2\cdot s^{-1}$. The minimum, maximum values and step length of the distance x are assumed as 1.00×10^{-6}, H and 5.00×10^{-4} m. Then according to the flux J and n_t at different pressures in Test 4[5] and combining Eqs. (4) and (5), the effective diffusion coefficient at respective pressures can be determined by the numerical simulation calculation.

3.1.2. Mineral reaction rate

Mineral reaction

Mineral trapping is the fixing of CO_2 in carbonate minerals due to a series of geochemical reactions[9, 31]. It is reported that the most promising reactions for mineral trapping involve the minerals which provide divalent cations (Ca^{2+}, Mg^{2+}, Fe^{2+}) for precipitation of carbonate[9, 31]. One of the most common sedimentary-mineral sources of divalent cations is anorthite and is studied as a case in this paper. The mineral trapping takes place due to the following reactions as demonstrated by the example of anorthite dissolution:

Dissolution of CO_2 acidifies formation water through the following reaction[31].

$$CO_2(aq)+H_2O \rightleftharpoons H_2CO_3 \rightleftharpoons HCO_3^- + H^+ \rightleftharpoons CO_3^{2-} + 2H^+ \tag{6}$$

Aqueous CO_2 dissociates in water and produces carbonic acid, bicarbonate and carbonate ions, the acid attacks anorthite, leaching Ca^{2+} and neutralizing the acid through Reaction (7)[9, 31].

$$CaAl_2Si_2O_8 + 2H^+ + H_2O \rightleftharpoons Ca^{2+} + Al_2Si_2O_5(OH)_4 \tag{7}$$

The divalent cations precipitates as calcium carbonate through Reactions (8) and (9)[9, 31].

$$Ca^{2+} + HCO_3^- \rightarrow CaCO_3 + H^+ \quad (8)$$

$$Ca^{2+} + CO_3^{2-} \rightarrow CaCO_3 \quad (9)$$

In this work, Eq. (7) and the following net reaction are considered to study the mineral reaction rate.

$$Ca^{2+} + CO_2(aq) + H_2O \rightarrow CaCO_3 + 2H^+ \quad (10)$$

Mineral reaction rate

According to nonequilibrium thermodynamics, the chemical reaction rate of a single reaction is described as Eq. (11)[32],

$$\text{Rate} = R_f (1 - e^{-A/RT}) \quad (11)$$

where, R_f is the forward rate of the reaction, A is the affinity and is described as the negative of the molar Gibbs free energy change of reaction, R is the gas constant, T is the temperature. Based on Eq. (11), the general rate equation for geochemical reaction kinetics is[22, 24]:

$$\mathbf{Rate} = (1/V) \cdot \mathrm{d}n_i / \mathrm{d}t = (1/V) \cdot K \cdot A_{\min} \cdot \exp(-E_a / RT) \cdot [1 - \frac{Q}{K_{eq}}] \quad (12)$$

where, V is the volume of brines, K is the rate constant, $A_{\min}$ is the reactive surface area, E_a is the activation energy, Q is the activity product and is described through Eq. (13), and K_{eq} is the equilibrium constant.

$$Q = \frac{[H^+]}{[Ca^{2+}] \cdot f_{CO_2(aq)}} \quad (13)$$

In Eq. (13), $[H^+]$ and $[Ca^{2+}]$ are the molar concentrations of H^+ and Ca^{2+} ions, respectively.

Mineral reaction rate parameters

Anorthite is chosen for a case study. The volume of brines is assumed as 1 m^3 (approximately equals to 1 kg). The rate constant, activation energy and specific reactive surface area of the rocks used are taken from literature[23] and shown in Table 1. The water:rock ratio is fixed at 1 kg water per 15 kg of rock[24]. The gas constant is taken as 8.3145 $J \cdot mol^{-1} \cdot K^{-1}$. The effect of temperature on the mineral reaction rate is neglected and the temperature is taken as 298.15K. In the calculation of Q, $[H^+]$ and $[Ca^{2+}]$ are taken from the pH value and composition of Rose Run brines[22]. The fugacities of aqueous CO_2 are determined by SAFT1-RPM EOS[13]. According to the equilibrium constants of the following Eqs. (14) and (15), the equilibrium constant of Eq. (10) can be obtained as shown in Eq. (16).

$$CO_2(aq) + H_2O \rightarrow HCO_3^- + H^+ \quad \log K(298.15K) = -6.37 \quad (14)$$

$$CaCO_3(calcite) + H^+ \rightarrow Ca^{2+} + HCO_3^- \quad \log K(298.15K) = 1.71 \quad (15)$$

$$Ca^{2+} + CO_2(aq) + H_2O \rightarrow CaCO_3 + 2H^+ \quad \log K(298.15K) = -8.08 \quad (16)$$

Table 1. The mineral considered and its reaction rate constant (K), activation energy (Ea) and specific reactive surface area[23].

Mineral	K ($mol \cdot m^{-2} \cdot s^{-1}$)	Ea ($J \cdot mol^{-1}$)	Specific reactive surface area ($m^2 \cdot g^{-1}$)
Anorthite	7.6×10^{-10}	1.78×10^{4}	1.00×10^{-3}

3.1.3. Model of coupling mass transfer with mineral reaction

The model of coupling mass transfer with mineral reaction can be derived from the equation of continuity for species *i* in a multicomponent reacting mixture as shown in Eq. (17)[29].

$$\frac{\partial C_i}{\partial t} = -(\nabla \cdot J_i) - r_i \tag{17}$$

where, r_i is the consumption rate of *i* by reaction. According to the different flux forms of Eqs. (1) and (4) and the reaction rate form of Eq. (12), the concentration gradient and chemical potential gradient models of coupling mass transfer with mineral reaction can be obtained.

3.2. Initial and boundary conditions

The initial condition is given by Eq. (18)

$$C_i(x,t)\big|_{t=0} = \begin{cases} C_{i0} & (x=0) \\ 0 & (x>0) \end{cases} \tag{18}$$

where, C_{i0} is the aqueous CO_2 saturated concentration. The left boundary conditions are the interface concentrations of aqueous CO_2 calculated with SAFT1-RPM[13] by assuming instantaneous saturation of CO_2[21]. The right boundary condition is

$$\frac{\partial C_i(x,t)}{\partial x}\Big|_{x=x_R} = 0 \quad (t>0) \tag{19}$$

where, x_R represents the distance between the right boundary and the interface.

3.3. Numerical solution

The partial differential equations are solved numerically using the built-in "pdepe" in the MATLAB program, which solves initial-boundary value problems for systems of parabolic and elliptic partial differential equations. The diffusion coefficient is taken the value calculated in this paper at 7.5322 MPa and the other experimental conditions of Test 4[5].

4. Results and Discussions

4.1. Effective diffusion coefficient

The effective diffusion coefficients at different pressures and other experimental conditions of Test 4[5] are calculated and shown in Fig. 1. Fig. 1 shows that the effective diffusion coefficients by both concentration gradient and chemical potential gradient models are close to each other and decrease with increasing pressure. Moreover, the effective diffusion coefficients calculated in this paper are close to that in our previous work by the chemical potential gradient model based on the derivation of $\partial a_i/\partial t$[21].

4.2. Concentration distribution by concentration and chemical potential gradient models

The concentration distribution of aqueous CO_2 with distance at 10 and 20 years through the concentration gradient and chemical potential gradient models coupling mass transfer with mineral reaction is shown in Fig. 2. From Fig. 2, there are considerable discrepancies for the concentration distribution with distance by the two models, which implies the importance of the consideration of non-ideality. The concentrations of aqueous CO_2 by the concentration gradient model are higher and further than that by the chemical potential gradient.

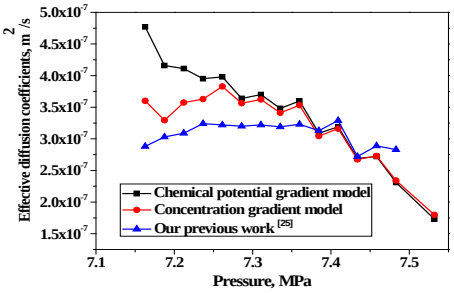

Fig. 1. Calculated effective diffusion coefficients at different pressures

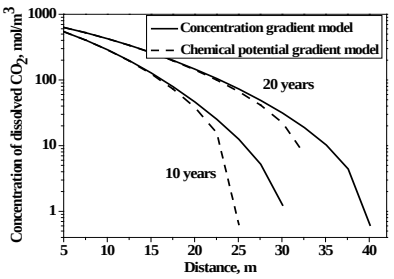

Fig. 2. Concentration distribution with distance for coupling mass transfer with mineral reaction.

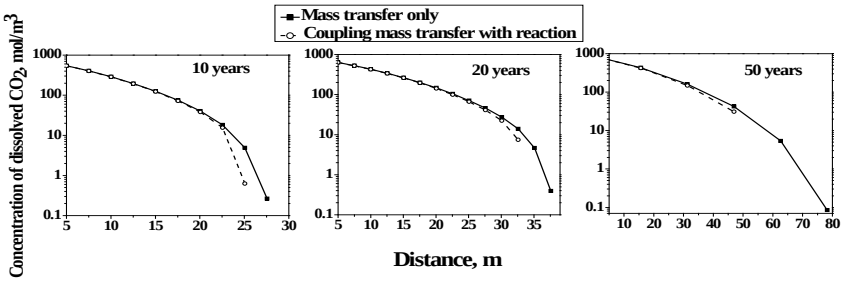

Fig. 3. C alculated concentration distribution with distance at different time scales in which two different cases are considered (1) mass transfer only; (2) coupling mass transfer with mineral reaction.

4.3. Concentration distribution by chemical potential gradient model for two cases: mass transfer only and coupling mass transfer with mineral reaction.

The concentration distribution of aqueous CO_2 with distance at 10, 20, 50 years by the chemical potential gradient model for two cases (mass transfer only and coupling mass transfer with mineral reaction) is shown in Fig. 3. From Fig. 3, for the anorthite case, it is observed that the mineral reaction plays a considerable role for the geological sequestration when the time scale reaches 10 years. Moreover, our results show that the mineral reaction does not bring obvious effect on the concentration distribution of aqueous CO_2 for time scale less than 10 years, and when the time scale is 1000 years, the aqueous CO_2 by the mass transfer can be completely reacted by the model rock anorthite due to the neglection of the effects of hydrodynamics and gravity. In future work, more types of rocks and the effects of hydrodynamics and gravity should be considered.

5. Conclusions

In this paper, the coupling behaviors of the mass transfer of aqueous CO_2 with the mineral reactions of aqueous CO_2 with model rock anorthite are investigated by chemical potential gradient and concentration gradient models, respectively. The effective diffusion coefficients of CO_2 are obtained based on the experimental kinetic data reported in literature. The results

show that there are considerable discrepancies for the concentration distribution with distance by the concentration gradient and chemical potential gradient models, which implies the importance of the consideration of the non-ideality. And the concentrations of aqueous CO_2 at different distances by the concentration gradient model are higher and further than that by the chemical potential gradient. The mineral reaction plays a considerable role for the geological sequestration when the time scale reaches 10 years for the anorthite case.

Acknowledgment

The authors thank Luleå University of Technology, the Swedish Research Council, the National Basic Research Program of China (2009CB226103), the National Natural Science Foundation of China (50808039) and the Natural Science Foundation of Jiangsu Province, China (BK2009138) for the financial supports.

References

[1] D. P. Schrag, Preparing to capture carbon, Science 315, 2007, pp. 812-813.

[2] A. Firoozabadi, P. Cheng, Prospects for subsurface CO_2 sequestration, AIChE J. 56, 2010, pp. 1398-1405.

[3] R. G. Jr. Bruant, A. J. Guswa, et al. Safe storage of CO_2 in deep saline aquifers, Environ. Sci. Technol. 36(11), 2002, pp. 240A-245A.

[4] S. Bachu, J. J. Adams, Sequestration of CO_2 in geological media in response to climate change: capacity of deep saline aquifers to sequester CO_2 in solution, Energy Convers. Manage. 44, 2003, pp. 3151-3175.

[5] C. Yang, Y. Gu, Accelerated mass transfer of CO_2 in reservoir brine due to density-driven natural convection at high pressures and elevated temperatures, Ind. Eng. Chem. Res. 45, 2006, pp. 2430-2436.

[6] S. M. V. Gilfillan, B. S. Lollar, et al. Solubility trapping in formation water as dominant CO_2 sink in natural gas fields, Nature 458, 2009, pp. 614 -618.

[7] D. W. Keith, J. A. Giardina, et al. Regulating the underground injection of CO_2, Environ. Sci. Technol. 39, 2005, pp. 499A-505A.

[8] C. M. Oldenburg, Transport in geologic CO_2 storage systems, Transp. Porous Med. 82, 2010, pp. 1-2.

[9] B. Zerai, CO_2 sequestration in saline aquifer: geochemical modeling, reactive transport simulation and single-phase flow experiment. Doctoral Dissertation, January, 2006.

[10] Y. H. Ji, X. Y. Ji, et al. Progress in the study on the phase equilibria of the CO_2-H_2O and CO_2-H_2O-NaCl systems. Chin. J. Chem. Eng., 15(3), 2007, pp. 439-448.

[11] N. A. Darwish, N. Hilal, A simple model for the prediction of CO_2 solubility in H_2O-NaCl system at geological sequestration conditions, Desalination 260, 2010, pp. 114-118.

[12] N. N. Akinfiev, L. W. Diamond, Thermodynamic model of aqueous CO_2-H_2O-NaCl solutions from 22 to 100 degrees C and from 0.1 to 100 MPa, Fluid Phase Equilibria 295, 2010, pp. 104-124.

[13] X. Y. Ji, S. P. Tan, et al. SAFT1-RPM approximation extended to phase equilibria and densities of CO_2-H_2O and CO_2-H_2O-NaCl systems. Ind. Eng. Chem. Res. 44, 2005, pp. 8419-8427.

[14] B. Arendt, D. Dittmar, R. Eggers, Interaction of interfacial convection and mass transfer effects in the system CO_2-water, Int. J. Heat Mass Transfer 47, 2004, pp. 3649-3657.

[15] R. Farajzadeh, H. Salimi, et al. Numerical simulation of density-driven natural convection in porous media with application for CO_2 injection projects, Int. J. Heat Mass Transfer 50, 2007, pp. 5054-5064.

[16] R. Farajzadeh, P. L. J. Zitha, J. Bruining, Enhanced mass transfer of CO_2 into water: experiment and modeling, Ind. Eng. Chem. Res. 48, 2009, pp. 6423-6431.

[17] N. Kocherginsky, Y. K. Zhang, Role of standard chemical potential in transport through anisotropic media and asymmetrical membranes, J. Phys. Chem. B 107, 2003, pp. 7830-7837.

[18] G. A. Truskey, F. Yuan, D. F. Katz., Transport phenomena in biological systems. Prentice Hall, 2009.

[19] C. Liu, Y. Ji, et al. Thermodynamic analysis for synthesis of advanced materials. Molecular Thermodynamics of Complex Systems, Struct Bond 131, 2009, pp. 193-270.

[20] Y. H. Ji, X. Y. Ji, et al. Modelling of mass transfer coupling with crystallization kinetics in microscale, Chem. Eng. Sci. 65(9), 2010, pp. 2649-2655.

[21] Y. H. Ji, X. Y. Ji, X. H. Lu, Modeling mass transfer of CO_2 in brine at high pressures by chemical potential gradient, Fluid Phase Equilibria 2010 submitted.

[22] B. Zerai, B. Z. Saylor, G. Matisoff, Computer simulation of CO_2 trapped through mineral precipitation in the Rose Run Sandstone, Ohio, Applied Geochemistry 21, 2006, pp. 223-240.

[23] F. Gherardi, T. Xu, K. Pruess, Numerical modeling of self-limiting and self-enhancing caprock alteration induced by CO_2 storage in a depleted gas reservoir, Chemical Geology 244, 2007, pp. 103-129.

[24] R. T. Wilkin, D. C. Digiulio, Geochemical impacts to groundwater from geologic carbon sequestration: controls on pH and inorganic carbon concentrations from reaction path and kinetic modeling, Environ. Sci. Technol. 44, 2010, pp. 4821-4827.

[25] T. Xu, Y. K. Kharaka, et al. Reactive transport modeling to study changes in water chemistry induced by CO_2 injection at the Frio-I Brine Pilot, Chemical Geology 271, 2010, pp. 153-164.

[26] T. Xu, K. Pruess, Modeling multiphase non-isothermal fluid flow and reactive geochemical transport in variably saturated fractured rocks: 1. Methodology. Am. J. Sci. 301, 2001, pp. 16-33.

[27] T. Xu, E. L. Sonnenthal, et al. TOURGHREACT: a simulation program for non-isothermal multiphase reactive geochemical transport in variably saturated geologic media. Comp. Geosci. 32, 2006, pp. 145-165.

[28] T. Xu, J. A. Apps, K. Pruess, Numerical simulation to study mineral trapping for CO2 disposal in deep aquifers. Appl. Geochem. 19, 2004, pp. 917 – 936.

[29] R. B. Bird, W. E. Stewart, et al. Transport Phenomena, John Wiley & Sons, Inc., 2006.

[30] J.M. Prausnitz, R.N. Lichtenthaler, E.G. de Azevedo, Molecular Thermodynamics of Fluid-phase Equilibria. Third edition, NJ, Prentice Hall PTR, 1999.

[31] J. M. Matter, P. B. Kelemen, Permanent storage of carbon dioxide in geological reservoirs by mineral carbonation, Nature Geoscience 2, 2009, pp. 837 – 841.

[32] D. Kondepudi, I. Prigogine, Modern Thermodynamics: From Heat Engines to Dissipative Structures. John Wiley & Sons, Chichester, 1998.

Clean Coal Utilization Based on Underground Coal Gasification Integrated Solid Oxide Fuel Cells and Carbon dioxide Sequestration

Prabu V*, Jayanti S

Indian Institute of Technology Madras, Chennai, India
** Corresponding author. Tel: +4422575152 E-mail: vprabu1979@yahoo.co.in*

Abstract: Underground coal gasification (UCG) is a clean coal technology which converts coal into a combustible gas *in situ* without mining and without bringing up the ash contained in the coal. Thus, the attendant problems of coal washing, ash handling and disposal can be avoided. The combustible gas mixture, consisting primarily of hydrogen, methane, carbon monoxide--all of which are fuels for an solid oxide fuel cell (SOFC) system-- and carbon dioxide, can be fed to a battery of SOFC after gas cleaning to remove hydrogen sulphide and other impurities. A large portion, typically 50%, of the chemical energy contained in the product gas can be converted into electrical energy by the SOFC. The exhaust gases from the SOFC are typically at a temperature of the order of 600 to 800 deg C. Heat energy from these will be extracted to produce steam, part of which will be used for UCG and the rest will be sent for SOFC internal reforming and shifting reactions. The exhaust gases, consisting primarily of carbon dioxide and steam, will be finally fed through a condenser and will then be sent for compression and sequestration. Thus, the overall system envisaged makes use of oxygen-fed UCG and SOFC to generate electrical energy and an exhaust gas consisting primarily of carbon dioxide and the easily condensable steam which enables CO_2 sequestration. The overall integrated system can be divided into five units namely underground coal gasification, UCG product gas purification, electrical power generation from SOFC, heat recovery system and carbon sequestration unit. An energy analysis with heat integration of all the systems for a nominal 500 MWt will be discussed.

Keywords: *Underground coal gasification, Solid oxide fuel cell, Carbon sequestration, Heat integration.*

Nomenclature

W_{ele}	electrical work ..... kJ	η	efficiency.....
F	Faraday's constant C	f	flow rate ..... $mol \cdot s^{-1}$
K	equilibrium reaction constant.....	c_p	specific heat..... kJ/kg K
p	partial pressure..... bar	E	Nernst potential V
T	mean temperature ..... K	E_o	Ideal potential at standard condition V
R	universal gas constant ..... kJ/kmol K	j	electron number.....
H	enthalpy ..... kJ	U_f	fuel utilization factor……
N_{H_2}	moles of hydrogen converted……..mol	HV	Heating value……..kJ/mol
ΔH_R	Heat of reaction……..kJ/mol	Q	excess heat……..kW

1. Introduction

Coal is the major fossil fuel in the world and 70% of electricity produced in India comes from coal. Coal is expected to be the mainstay of electricity generation in India for the next several decades. However, coal utilization is fraught with environmental problems. Given that Indian coal typically has large ash content, its mining, washing, and final utilization in pulverized coal boilers leads to significant land, water and air pollution. The ash collected from the stacks also poses a disposal problem. On top of these, there is increased awareness of the need to reduce CO_2 emissions into the atmosphere. Hence it is necessary to develop suitable technologies for coal conversion efficiently without environmental pollution.

Underground coal gasification (UCG) is a clean coal technology with *in situ* gasification having no mining problem, no ash disposal, offering economical exploitation of low grade coal. It is a clean coal technology which enables exploitation of coal reserves in an

environmental friendly manner. A large amount of work has been reported in the 1970s and 80s on UCG [1-5] and there has been renewed interest in UCG as showed by a number of publications in the last decade [6-10]. These studies have focused on coal gasification per se and not much on CO_2 sequestration. In the present paper, we describe a process by which UCG can be coupled to a solid oxide fuel cell (SOFC) system to develop an integrated power plant which makes use of the fuel gas from the UCG, generates electricity from it and leaves an exhaust gas consisting of 85% CO_2 which can therefore be readily sequestered. The layout of the proposed plant is described in Section 2 and a thermodynamic analysis of the system is discussed in Section 3.

2. Description of the coupled UCG-SOFC system

A schematic diagram of the integrated UCG-SOFC system is shown in Figure 1. The product gas from the UCG system typically has some particulate matter and impurities in the form of tar, sulphur and its compounds. These are removed as the gas passes through a cyclone separator, a gas filter unit and a tar removal unit. The hot gas from the cyclone separator exchanges heat with the clean gas coming from the tar removal system in a gas-to-gas heat exchanger. The clean fuel gas is further heated (by the hot anode side exhaust of the solid oxide fuel cell (SOFC) unit) and is mixed with steam and is fed to the anode side of the SOFC unit. The unused portion of hydrogen and carbon mono oxide (85% fuel utilization efficiency is assumed in the SOFC) is then fed to a combustor to completely convert the remaining fuel into CO_2 and steam. These gases are fed to a condenser in which most of the steam is removed and the remaining gas, consisting mostly of CO_2 is sent to the CO_2 sequestration unit. The thermal energy in the exhaust gas of the combustor is used to generate steam in the condenser unit which is used for fuel reforming in the SOFC as well as for coal gasification in the UCG gasifier. Further, the thermal energy of the hot air from the cathode code is also used to preheat the air that is supplied to the cathode so as to maintain the SOFC temperature at the design condition. In order to eliminate nitrogen from the system (so as to facilitate CO_2 sequestration), an air separation unit is used to supply oxygen in required quantity to the combustor (this is especially needed to maintain stable combustion as the anode gas from the SOFC contains only a small percentage of fuel, namely, H_2 and CO, the rest being CO_2 and steam) as well as that required for gasification in the UCG gasifier unit. The flow paths of the various streams are shown in Figure 1.

The above coupling of the UCG with an SOFC enables proper thermal integration of the various units to produce electrical energy directly from the product gas of the UCG. Moreover, the combination of UCG and SOFC is such that the integration can be done in such a way that all the CO_2 that is produced in the fuel utilization can be captured in a relatively straightforward manner without the need for an external CO_2 absorption unit as is required in normal combustion of the UCG gas. One disadvantage however is the need to clean the UCG gas to remove tar and sulphur products so that it can be used in an SOFC. The technology for the required gas cleaning already exists; the calculations described in the next section show that the gas cleaning can also be done without a significant energy penalty resulting in a combined system with a significantly higher overall thermal efficiency and little environmental pollution.

3. Thermodynamic model and analysis

The overall integrated plant consist of five units, namely, underground coal gasification, UCG product gas purification, electrical power generation from SOFC, heat recovery systems and carbon sequestration unit. An energy balance on these units has been carried out to determine

the overall utilization of energy. The UCG system is considered to be operating at atmospheric pressure and the bituminous grade coal in underground undergoes partial oxidation and gasification in presence of pure oxygen to produce calorific value synthesis gas. The electrical efficiency of SOFC fuel cell is found out based on the shifting, reforming and electrochemical reaction with reaction kinetics.

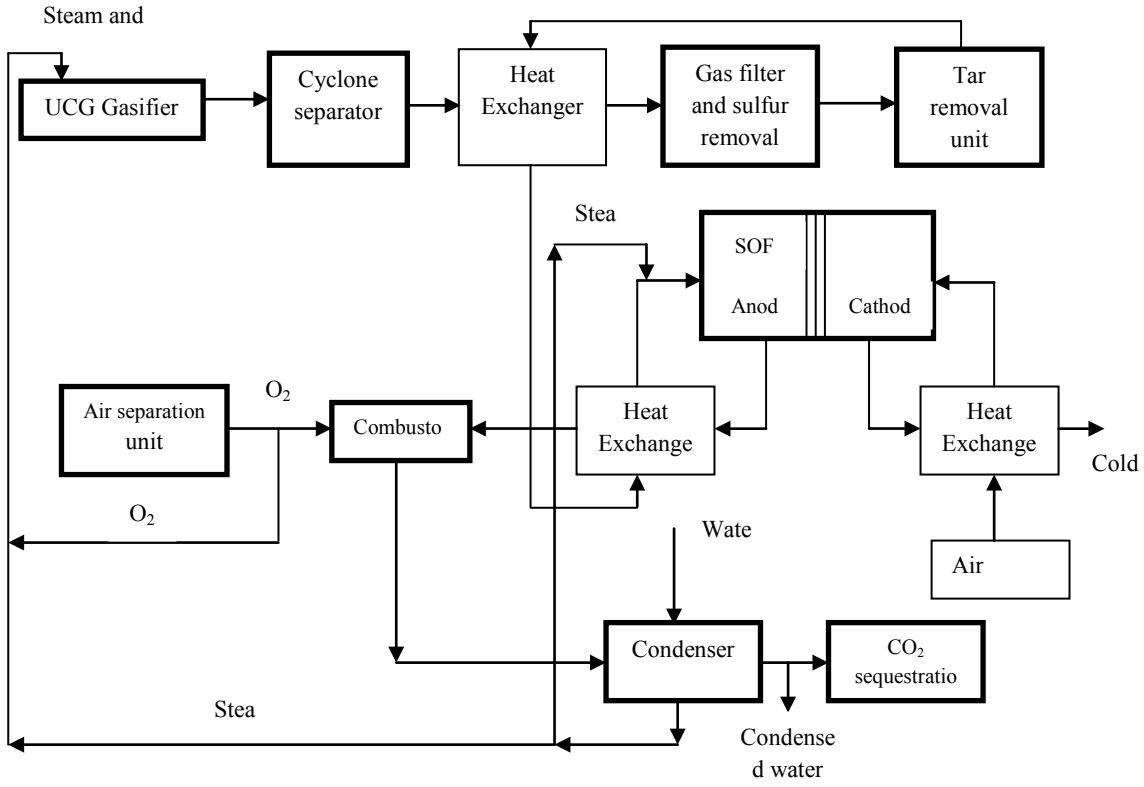

Fig.1. Schematic of the integrated underground coal gasification with solid oxide fuel cell

3.1. UCG Plant

A 500 MW of product gas generated from UCG and the flow rate of input and output stream of gases and its molar composition has taken from Lawrence Livermore national laboratory (LLNL) literature [11] and used for the basis of theoretical calculation. Table 1 represents the product gas molar composition and total product gas flow rate from UCG of 2600 mol/s.

Table 1. Product gas composition from UCG plant

Species	Mole fraction	Product gas flow rate[mol/s]
N_2	0.018	47.36
CO	0.11	289.47
CO_2	0.44	1157.89
H_2	0.37	973.68
CH_4	0.05	131.58

Heat of combustion of product gas (HV) = 190 kJ/mol
Product gas flow rate from UCG to SOFC (f_p) = 2631.58 mol/s
Total injection flow rate of steam and oxygen = 2255.63 mol/s
Injection mole fraction of oxygen = 0.47
The UCG gasifier operating temperature is assumed to about 800°C in oxyfuel mode. Pure oxygen from air separation unit and steam generated from condenser unit are injected into

injection hole and the gasified products at 650°C are collected from the production hole of UCG.

3.2. UCG product gas purification system

In UCG system, volatile matter liberated during combustion, gasification and pyrolysis zone will move along the cavity and make contact with the fresh coal. This would results in product gas enriched with tar content since there is no further thermal cracking [12]. The issue of removal of mercury, arsenic and other trace metals is not addressed here as not much is known about their formation and presence in the UCG gas. In order to utilize these product gases in SOFC for power generation, it is necessary to remove the tar and sulfur content impurities. Cyclone separator and ceramic filters are used to remove the particulate matter and alkali compounds from product gases before the tar removal. A wet electrostatic precipitator is used for tar condensation and removal. The purified gas stream is cooled to about 50° C and the enthalpy is again gained from the inlet gas stream of purification system and fed into the SOFC.

3.3. SOFC fuel cell system

The purified hot gas stream from with steam is introduced at the anode side of the SOFC. To avoid the carbon deposition in SOFC, a steam to carbon ratio of 2:1 is assumed [13]. Excess oxygen of 400% in air is supplied at the cathode side to recover the generated heat energy. The operating temperature of SOFC is assumed to be 700°C. The temperature of exit stream from anode and cathode side is same as the operating temperature of SOFC. In IRSOFC (Internal reforming SOFC), only hydrogen is assumed to undergo oxidation for electric power generation. Carbon monoxide, methane undergoes reforming and water gas shifting reactions [Eq. (1)] with steam and produces hydrogen. High operating temperature of SOFC is suitable for reforming and shifting reaction which converts the CO and other hydrocarbons to hydrogen. A fuel utilization factor of 0.85 is assumed for the fuel cell.

Reforming reaction: $CH_4 + H_2O \overset{K_{ref}}{\longleftrightarrow} CO + 3H_2$ (1)

Water gas shifting reaction: $CO + H_2O \overset{K_{shf}}{\longleftrightarrow} CO_2 + H_2$

$$K_{ref} = [CO][H_2]^3/[CH_4][H_2O] \quad (2)$$

$$K_{shf} = [H_2][CO_2]/[CO][H_2O] \quad (3)$$

where K_{ref} and K_{shf} are the equilibrium constants for reforming and shifting reaction respectively. The equilibrium constants are calculated using the temperature dependent polynomial expressions [14]. The equilibrium gas composition can be determined using Eq. (2 & 3).

3.4. Estimation of Overall Thermal Energy Conversion Efficiency

The overall thermal energy conversion efficiency (η) of the coupled UCG-SOFC process can be estimated from the thermal energy content in the UCG gas and the electrical power output from the SOFC system. The latter is estimated as follows. The cell e.m.f, E, of the SOFC is calculated for the particular concentrations of hydrogen, oxygen and steam produced (p_{H_2}, p_{O2}, p_{H_2O}) used in the cell using the Nernst equation [15]:

$$E = Eo + (RT/jF) \ln[(p_{H_2}.p_{O_2}^{1/2})/p_{H_2O}] \quad (4)$$

where Eo is the ideal potential at standard condition, j is the electron number.

The electrical power output from the SOFC is then calculated as

$$W_{ele} = EN_{H_2} jF \quad (5)$$

where N_{H2} is the number of moles of hydrogen, and F is the Faraday's constant.
The overall thermal energy conversion efficiency can now be calculated by dividing the electrical power output by the thermal energy flow rate in the UCG gas:

$$\eta = W_{ele} / (f_p \times HV) \quad (6)$$

where f_p is product gas flow rate from UCG in mol/s and HV is the heating value of the product gas from UCG.

3.5. Estimation of the air inlet temperature for the SOFC

Energy balance can be made over the SOFC fuel cell system to calculate the air inlet temperature to the cathode side [Fig.2]. Eq. (7) gives the excess energy generated in the fuel cell is taken up by the incoming air and gas stream to maintain a constant operating temperature in the cell.

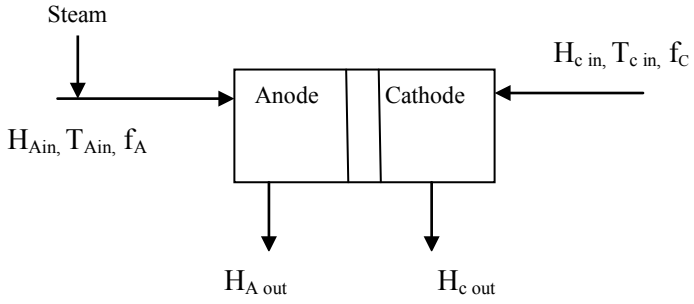

Fig.2. Schematic diagram of SOFC Model

$$\Delta H_R = W_{ele} + Q \quad (7)$$

where ΔH_R is the heat of reaction (kJ/mol), Q is the excess energy generated in the fuel cell.

$$Q = f_A \int_{T_{Ain}}^{T_{sofc}} Cp\, dT + f_C (H_{SOFC} - H_{C\ in}) \quad (8)$$

where f_A and f_c are the input flow rates of anode side gas stream and cathode side air stream respectively.
From Eq. (8), the air inlet temperature to cathode side of the fuel cell is calculated.

3.6. Heat recovery system

The outlet gas from anode and cathode of SOFC at high temperature of 700°C are utilized for the heat recovery system. The inlet gas streams of cathode and anode are heated using heat exchangers by their respective outlet gas streams. The trace quantity of unconverted gas from SOFC can be burnt in a combustor with oxygen and the hot gas from combustor has sent to the condenser. A fresh steam is generated from condenser which is then supplied to the SOFC

cathode inlet and UCG injection hole. The two heat exchangers at the inlet of SOFC system of cathode and anode and the combustor and the condenser for fresh steam generation will constitutes the heat recovery system of the integrated system.

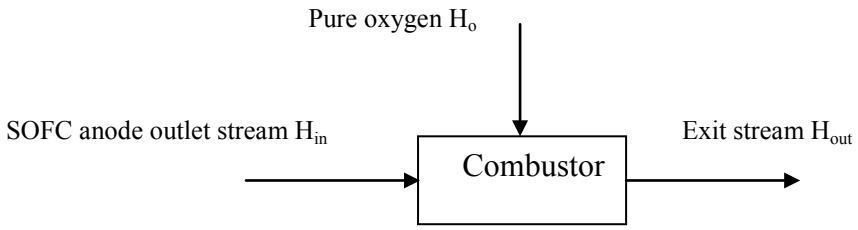

Fig.3. Schematic diagram of combustor model.

Complete combustion of remaining hydrogen, carbon monoxide and trace amount of methane are assumed in the combustor. Pure oxygen of 150% in excess of stoichiometric requirement for complete combustion is supplied to the combustor. The temperature of the exit stream from combustor (Fig.3) can be calculated from the enthalpy balance [Eq. (9)] over combustor.

$$H_{in} + H_o = H_{out} \tag{9}$$

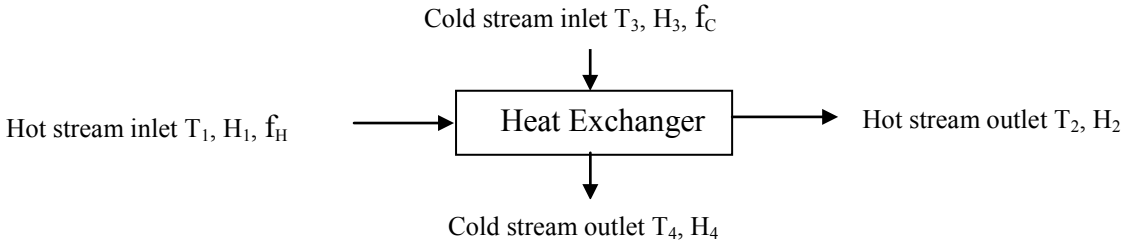

Fig.4. Schematic diagram of Heat Exchanger model

Fig.4 represents the schematic diagram of heat exchanger model. The cold stream outlet temperature can be calculated from the enthalpy balance equation [Eq. (10)].

$$f_H (H_1 - H_2) = fc \int_{T_3}^{T_4} Cp \, dT \tag{10}$$

where f_H and f_C are the flow rates of hot and cold streams respectively.

4. Results and Discussion

An overall energy balance is made for the entire thermodynamic model for the integrated system of UCG and SOFC. The steam generated from condenser at 600°C is sent to the UCG and SOFC with approximately equal proportion.

The hot product gas from the UCG plant enters the purification system at 650°C and cooled in a heat exchanger to 200°C and then it enters into the filter. Small particulate matters and condensed alkali compounds are filtered through the gas filter. Particulate free gases are then entered into the wet electrostatic precipitator to remove the tar which is enriched in the product gases. The tar free product gas are coming out from the wet ESP at about 50°C are heated to about 525°C using the exit gas stream of UCG. In order to raise the temperature of

the product gas at about 650°C to meet the SOFC operating temperature, the purified gas is heated again with the outlet gas stream of SOFC at anode side.

Table 2. SOFC inlet and outlet gas stream composition.

Species	Inlet stream mole percent	Outlet stream mole percent
N_2	1.28	1.19
CO_2	31.25	38.15
CO	7.81	1.64
CH_4	3.55	0.000044
H_2	26.28	6.52
H_2O	29.83	52.5

Table 2 represents the SOFC inlet and outlet gas composition of cathode side. In outlet gas stream, only a trace amount of methane is present and constitutes 50 mole % of steam. The electrochemical work done by the SOFC can be calculated using the Nernst equation as 312.53MW. Electrical efficiency of the SOFC cell is found as 62.5%.

The unconsumed fuel from SOFC is burnt in the combustor with pure oxygen to extract more energy and the outlet gas is purely a composition of steam and carbon dioxide. The combustion of unconsumed fuel from SOFC in the combustor can be carried out using excess oxygen.

Table 3. Combustor inlet and outlet gas stream composition

Species	Inlet stream mole percent	Outlet stream mole percent
N_2	1.08	1.125
CO_2	34.62	37.49
CO	1.49	0
CH_4	0.00004	0
H_2	5.91	0
H_2O	47.64	55.62
O_2	9.25	5.77

Table 3 shows the combustor outlet gas composition. Combustor outlet stream contains 37% of CO_2 and 55% of steam which is then sent to the condenser to extract the heat energy. All the steam can be condensed and the pure CO_2 is separated and sent to sequestration unit.

5. Conclusion

A fully integrated UCG-SOFC system is proposed to provide clean electrical energy from underground coal. The combination of UCG and SOFC is such that thermal as well as system integration of the two units can be carried out readily. A first-cut energy analysis, without including the cost of the air separation unit and the cost of compression of the CO_2 for the purposes of, say, underground sequestration, gives an overall thermal efficiency of above 60%. The combined system also utilizes fossil fuel in a clean manner without any particulate or gaseous emissions, thus providing a clean source of energy from conventional sources.

References

[1] W.R.Aiman, W.T.Fisher, Lawrence Livermore National Laboratory Insitu coal gasification Program Quarterly Progress Report. January through March 1978, UCRL 50026-78-1

[2] C.B.Thorsness, J R Creighton. Review of underground coal gasification field experiments at HOE creek. Report No.UCRL-87662-Rev.1. U.S.DOE. Livermore, CA: Lawrence Livermore National Laboratory; 1983

[3] P.N.Thompson, Gasifying coal underground. Endeavour 1978;2: 93 -97

[4] A.M.Winslow, Numerical Model of coal gasification in a packed bed. S ymbosium on combustion (international) 1977:16:503 – 513.

[5] C B Thorsness, E A Grens, A Sherwood, A one dimensional Model for Insitu coal gasification. Report No.UCRL-52523, U.S.DOE.Livermore, CA: Lawrence Livermore National Laboratory; 1978.

[6] M.S.Blinderman, D.N.Saulov, A.Y.Klimenko. Forward and reverse combustion linking in underground coal Gasification. Energy 2008; 33: 446-454.

[7] L Yang, J Liang, L Yu, Clean coal technology – Study on the pilot project experiment of underground coal gasification. Energy 2003;28:1445 – 1460

[8] L Yang, X Zhang, S Liu, W. Zhang, Field test of large-scale hydrogen manufacturing from underground coal gasification. International journal of Hydrogen Energy 2008; 33:1275 – 1285.

[9] G.Perkins, V.Sahajwalla. A Mathematical Model for the chemical reaction of a s emi-infinite block of coal in underground coal Gasification. Energy and fuels 2005;19:1679 – 1692

[10] S.Daggupati, N.Ramesh. R.N.Manadapati, S.M.Mahajani, A.Ganesh, D.K Mathur, R.K Sharma, P.Aghalayam, Laboratory studies on c ombustion cavity growth in lignite coal blocks in the context of underground coal Gasification. Energy 2010;35: 2374-2386.

[11] W.R.Aiman, M L Donohue, LLL insitu coal gasification project, Quarterly progress Report, Lawrence Livermore laboratory, Report No. UCRL 50026 -79 -3, 1979.

[12] T.Kivisaari, P Bjornbom, C Sylwan, B Jacquinot, D Jansen, A Groot, The feasibility of a coal gasifier combined with a high temperature fuel cell, Chemical Engineering Journal 100, 2004, pp 167 -180.

[13]A.O.Omosun, A.Bauen, N.P.Brandon, C.S.Adijman, D.Hart, Modelling system efficiencies and costs of two biomass-fuelled SOFC systems, Journal of power sources 131, 2004, pp 96 – 106.

[14] S.Ghosh, S.De, Thermodynamic performance study of an integrated fuel cell combined Cycle- an energy analysis, Journal of Power and Energy 217, 2002, pp 137 -147.

[15] S.Ghosh, S.De, Energy analysis of a cogeneration using coal gasification and solid oxide fuel cell, Energy 31, 2006, pp 345 – 363.

Climate Change and Water Resources for Energy Generation in Tanzania

Z. J .U. Malley[1*]

[1]*Agricultural Research Institute-Uyole P.O. Box 400, Mbeya, Tanzania*
**Corresponding author's Tel: +255252510363, Fax: +255252510065, Email: zjmalley@yahoo.co.uk*

Abstract: Tanzania is one of the low income countries, which heavily depends on hydro-power for electric energy supply to the national grid. Impacts of climate change patterns on water resources supply to dams for hydro-energy generation is now evident. In turn, this has impacted national socio-economic development in numerous ways. The objective of this work was to analyze the link of climate change to water shortages for hydro-power generation in the Mtera reservoir, which supply 50% of the hydro-power to the national grid. Literature survey, records collection and analyses and observations were research tools used. The study revealed that, 64% of increasing variability in rainfall over years in the watersheds described declining water levels in Mtera dam. This strong relationship means that climate change is main driver of water shortages for hydro-power generation. This suggests a need for national adaptation strategies to water supply shortages. Improvements in the present hydro-power sources for water recycling and/or development of micro-dams for storage of excess water need exploration. Rain-water harvesting and recycling seems important adaptation strategies to changing hydrological patterns for water supply to the hydro-energy plants in Tanzania.

K***eywords:*** *Electric energy supply, Hydro-energy plants, Increasing rainfall variability, National grid, Water supply*

1. Introduction

Climate change and variability are now becoming one of the significant development challenges due to shift in the average patterns of weather. Environmental change, manifested by climate change and variability, is no longer a mythical discourse; the scientific consensus is not only that, human activities have contributed to it significantly, but that the change is far more rapid and dangerous than thought earlier (IPCC, 2007). While climate change results from activities all over the globe, with rather unevenly spread contributions to it, it may lead to very different impacts in different countries, depending on local, regional environmental conditions and on differences in vulnerability to climate change (UNEP/Earthscan, 2002). The Millennium Ecosystem Assessment (2005) shows that, in all ecosystems of the world, the climate changes impacts are rapidly increasing, such as, on water resources, environmental services and other livelihoods capital assets for sustainable human development. In the World Summit on Sustainable Development (WSSD) held from August 26-4 September 2002 in Johannesburg, South Africa, the UN Secretary General outlined priority areas for sustainable development as water and sanitation, energy, health, agriculture and biodiversity protection and ecosystems management (WSSD, 2002).

Climate change impact on water resource supply significantly affects all aspects of sustainable socio-economic development of a country or a society, where energy sector is heavily dependent on hydropower. Current contribution of hydro-power in Tanzania to national grid is 52% and the rest is from thermal sources (Karekezi et al. 2009). There has been a concern over water supply for energy generation in Mtera reservoir. This concern is manifested at national level a decade ago by the government declaration in March 2001 that, the Great Ruaha River should return to its year-round flow characteristics by 2010. The concern comes from power shortages in early-

1990s, attributed to low water flows into the Mtera/Kidatu hydropower system from the Great Ruaha River (Lankford *et al*, 2004; Yawson, *et al*, 2003). The hydrological change in the Usangu-Mtera ecosystem has attracted number of investigations into causes of this problem, which include: Sustainable Management of the Usangu Wetlands and its Catchments (SMUWC) from 1998-2002 (Lankford *et al*, 2004); investigation into cause of the failure of the Mtera-Kidatu Reservoir system (Yawson *et al*, 2003); a study of the effects of land degradation in the uplands on land use changes in the plains (Mwalukasa, 2002); a study of the socio-economic root cause of the loss of biodiversity in the Ruaha Catchment Area (Sosovele and Ngwale, 2002). These studies agree that, there is hydrological flow change in Mtera reservoir, but there is no consistent consensus on cause of hydrological change. These studies did not attempted to directly link change in rainfall variability with water supply from Mtera reservoir. This work focuses on the hydrological flow change and how it links to changes in rainfall variability. Therefore, this paper explores the trends in variability of the Mtera reservoir mean water levels and watershed rainfall amounts and discusses linkages to energy generation for the national grid and socio-economic development. Furthermore, it recommends opportunities for harnessing in the national adaptations strategies to climate influenced hydrological flows changes.

2. Methodology

The study area is Usangu-Mtera ecosystem, which covers, south-western Tanzania's highlands watershed catchments to the Mtera reservoir, which is used to conserve water for hydro-electricity generation in Kidatu, downstream. Data collection tools from the area were survey of literature, key informants interviews, informal appraisals, questionnaire interviews and biophysical records collections and analysis.

The literature was searched from the Internet, published and grey materials of the relevant regional, national and area studies. Then a critical analysis of information gathered through literature surveys was undertaken. Key informants interviews were held with Rufiji Basin Water Office (RBWO) and the Tanzania Electricity Company (TANESCO). Informal village appraisals were conducted in six villages, which were Ikoga and Sololwambo in lower part, Yala and Matebete middle part, and Mhwela and Mabadaga in upper part of the Usangu central plain. Informal interviews were supplemented with participatory village resources mapping and on the ground observations through transect walks.

Household questionnaire interviews were held in April to December 2004, involving 266 households in six above villages. Interviews assessed climate change perceptions and its link to water problems at local level. Verification of this perceptions, were done through collection and analysis of biophysical records on rainfall and water levels in the Mtera reservoir over 22-years (1982-2003). A 22-years measurements data of Mtera reservoir water levels collected from TANESCO and rainfall data from the Agricultural Research Institute meteorological station located in the Uyole-Uporoto uplands watershed, typical of the south-western watersheds.

Analysis of the total annual rainfall amounts were summation of monthly precipitations. Monthly sum of each rainfall year starts in October of the preceding year and ends in September of the following year. The relationship was tested and linkage established between rainfall variability and water supply shortage experienced by analyses of the collected information. Quantitative data were analysed using the Statistical Package for Social Science (SPSS).

3. Results

3.1 Climate change Indicators

Local people experience strongly attested links of climate changes with respect to water resources, rainfall amount and duration, temperature, land resources degradation and land use change in the Usangu-Mtera ecosystem (SMUWC, 2002; Malley *et al*, 2007). Interview of 266 household, in area of study, about 82.6% of respondents, reiterated that rainfall amount has decreased, and a similar number (83%), reported shortened duration of rainfall in Usangu-Mtera ecosystem. These perceptions are supported by analysis of rainfall trends (Table 1).

Analysis revealed that annual rainfall amounts in the south-western watershed, is declining, though not statistically significant (p= 0.05). However, a high variability pattern of rainfall amount from year to year is evident. More frequencies of below average annual rainfall amounts were conspicuously notable, from late 1980s to 2003, which indicate increased frequency of drier-years than normal in about last 22 years.

3.2 Water supply for energy generation in Mtera

The Mtera reservoir mean annual water levels trend, over 22-years, depicts closely similar pattern to the annual rainfall amounts trend in the south-western highlands watersheds (Table 1). More frequencies of low mean annual water levels were observed from the late 1980s to 2003. This similarity in the pattern, attest a possible linkage between the annual hydrological droughts in the reservoir to the rainfall amount and pattern change in the south-western highlands watersheds.

Table 1 Trends in rainfall, water levels and their relationships in Usangu-Mtera ecosystem

Environmental variable	Direction	Method of analysis	Extent (%)	Sign.
Trends				
Rainfall quantity	Declining	PRA	-	
		Respondents perception	82.6	***
		Regression over years	6.8	Ns
Rainfall variability	Increasing	PRA	-	
		Respondents perception	83	***
Patterns of mean annual water levels in Mtera reservoir	Declining	Regression over years	5.8	Ns
Mean annual water level variability	Increasing	Regressions over years	10.2	Ns
Rainfall variability vs water levels	Positive and strong	Regression	64.2	***

Ns = not significant, * significant at P ≤0.05; ** significant at P ≤ 0.01, *** Significant at P ≤ 0.001
Source: Own analyses of field data (2004)

3.3 Climate change indicators and Mtera reservoir water supply

Regression analysis of variations in the amounts of rainfall, significantly ($p<0.001$) accounted for 64.2% of the variations in mean annual water levels in Mtera reservoir (Table1). This suggests that, the lower the annual rainfall amount in the upper catchments the lower the mean annual

water supply from the Mtera reservoir. It implies that, increasing variability in the annual rainfall amounts is a cause of increasing variability in the mean annual water supply in the Mtera reservoir for electricity generation. These direct close relationship, gives new evidence, that there is a strong causal relationship between the perceived changes in climate indicators with the changes in the hydrology of the Usangu-Mtera eco-system.

4. Discussions

Lankford *et al*, (2004), showed that SMUWC investigation found that hydrological change in the Great Ruaha River is linked to dry season abstraction for irrigation activities and environmental losses, but not to climate change. Mwalukasa (2002) showed that, there is significant degradation of the land cover in the plain and upland of the Chimala River catchments, and there is increase in land use for irrigated agriculture in the plain. According to Yawson *et al*, (2003), the failure of the Mtera/Kidatu system is due to unaccounted spillage from Mtera reservoir, caused by inefficient management of the system. These investigations did not attempt to analyse linkage of climate indicators with water supply from Mtera reservoir. Sosovele and Ngwale, (2002) and Malley *et al*., (2007) analysed rainfall trends from different stations which indicated that climate change might have played a significant role in the experienced water supply shortages. These studies supported the anecdotal evidence that, climate change plays a greater role in the observed hydrological flow change. The results of present findings, which established direct relationships between water supply change and rainfall variability further supports findings of Sosovele and Ngwale (2002) and Malley *et al* (2007) and the anecdotal evidence.

According to Karl *et al*., (1995), increase in frequency of drought or rainfall variability is linked to climate change, which is also characterised with events of short severe storms. According to U.S. National Drought Monitor (2006), hydrological drought is manifested by shortfalls in surface and sub-surface water supply, which can be detected through decline in water levels in rivers, reservoirs, lakes and aquifers. Frequency and severity of hydrological drought is discernible at a watershed or river basin scale (Wilhite and Glantz, 1985). Mbwambo (2010) reported decline in number of flowing rivers from 79 to 39 now in Kilombero basin in Morogoro, Tanzania, due to climate change. In the Usangu-Mtera ecosystem, work of Sosovele and Ngwale (2002) reported that, rivers from upper watersheds of Uporoto and Mbeya mountains, which flow into the Usangu plain, and then to the Great Ruaha River only Chimala and Mbarali still have flows, however, amount of flowing water has declined substantially. These observations are supported by SMUWC (2002) measurements of flows in the rivers, which show that dry season flows of rivers have declined. Dried and silted up perennial rivers and streams were encountered during the course of this study, in the middle and lower villages of the Usangu plain. The SMUWC (2002), indicated that the western wetlands area (about 900 km^2), experienced reduced seasonal flooding in recent years, and it seem it no longer qualifies as a wetland, only remaining indicators of its past wetlands status is vegetation and soils. Kashaigili (2005) results show that, the eastern wetland perennial swamp size has shrunk by almost 70% between 1984 and 2000. According to Yawson *et al* (2003), in 1991 and 1992, water levels in the Mtera-Kidatu reservoir system, went very low to its dead levels. This is attested by the increasing frequency of below average mean annual water levels in Mtera reservoir. Presence of these indicators in the watersheds, fans and wetlands ecosystems in Usangu, and in the Mtera reservoir, explain the link of climate change-to-water supply problem from Mtera reservoirs for hydropower generation.

4.1 Impact of climate change on energy generation and socio-economic development

According to Libiszewski (1992), socio-economic impacts of environmental change may include: (1) decrease economic production, (2) general economic decline, (3) population displacements, and (4) disruption of institutions and the social relations. In the Usangu-Mtera ecosystem, similar socio-economic impacts, linked to hydrological change are evident. To abate, water shortage problem for energy generation, pastoral communities were forcefully displaced from their livelihood resources, water sources and dry season grazing land (Edwin, *The East African,* April 9-15, 2007). This forceful displacement of pastoral people has resulted into disruptions of their social institutions and soured their relations with the state, which mean a disruption of social capital, important in development process.

Climate change impact on water supply, results into reduced hydro-power production, which causes increase in outages and load shedding. In Tanzania, in dry year of 1997, the Mtera dam water went down, due to drought causing 17% drop in hydropower generation (Karekezi *et al*, 2009). In the period, 1990-2008, the water supply problem from the Mtera reservoir led to electric power shortage, which in turn affected the national grid, because the Mtera-Kidatu system generates about 50% of the power to national grid (WWF, 2002). The electric generation failures caused the nation wide power rationing, which impacted the industrial economic production, either, through increased costs of production of goods, or through reduced level of production, due to unavailability of power during certain periods of operations. Energy shortage affected economic production, raises the costs of electricity and thus goods and socio-economic service provisions from trade, health, education and domestic sectors, which in turn affect the welfare and livelihoods of the people in different ways. The emergency response, to reduce the impacts of the national power crisis, by hiring and/or investing into expensive alternative power sources, greatly constrained the government budget for the socio-economic development activities, and has forced the nation to a debt burden (Simbeye, *The East African*, July 12-18, 2004). Furthermore, in 2006, according to analysis of Kerekezi *et al* (2009), Tanzania incurred a loss of about 1% of its GDP earnings due to drought related load shedding exercise.

4.2 Conclusion and Recommendations

4.2.1 Conclusion

Climate change and variability is evident from increasing frequency of annual rainfall amounts variability in the upper catchments of south-western highlands of the Usangu-Mtera ecosystem. Increasing frequency of hydrological drought as manifested by mean annual water supply from Mtera reservoir for energy generation has strong relationship with increasing rainfall amount variability.

4.2.2 Recommendations

- Micro-dams for rainwater harvesting to adapt to years of extreme rainfall variability would help conserve water to support the main dam if constructed on the upper side of the Mtera reservoir along the Great Ruaha River to harvest excess water and store it, when the reservoir capacity approaches its maximum (698.5m.a.s.l). The stored water would be the source for recharge of the reservoir, when its water level approaches the critical minimum level (690m.a.s.l). The restriction at Nyaluhanga is another opportunity need to be explored for storage

of water in the western wetlands, and then slowly released over time to recharge eastern wetlands and hence the Great Ruaha River.

- An investment into alternative energy sources is a commendable strategy. The use of coal in electricity generation appears available and potentially cheap alternative in Tanzania. However, in the long term, the coal burning is one of the highest emitters of a greenhouse gas, the carbon dioxide, which significantly contribute to the environmental changes, which would be environmentally un-friendly investment. This means heavy investment to this source, would seem to compromise the environmental sustainability efforts in a long-term, therefore a modest investment in coal energy plants as an emergency backups during the hydropower shortage is recommended.

- The hydro-power remains the known clean and cheapest sources of electric energy for sustainable economic development. This implies that, more careful considerations should be on improvement and maintenance of the present hydro-power sources and new ones identified and developed. The design should incorporate multiple and efficient re-use of water through recycling system as an important aspect of water management, which should be considered in planning and designs of new development in hydro-power generation plants.

Acknowledgements

The data was collected by the financial support of the International Foundation for Science (IFS) in Sweden and the United Nations University Institute of Advanced Studies (UNU/IAS) in Japan. The Ministry of Agriculture and Food Security in Tanzania made its research facilities available for the work and administered the funds at the Agricultural Research Institute-Uyole (ARI-Uyole). I wish to thank and appreciate the assistance of the Mbarali District council, the TANESCO, Regional Water Engineer-Mbeya and the Directorate of Meteorological services, Tanzania for availing the information needed to undertake the reported analysis in this work.

References

[1] IPCC, Climate Change 2007: The Physical Science Basis: Summary for Policy Makers, Paris: IPCC, WMO, 2007.

[2] UNEP/Earthscan, United Nations Environmental Program/ Earths can. Global Environmental Outlook 3. London: Earthscan, 2002.

[3] Millennium Ecosystem Assessment (MA), International scientific assessment: ecosystem changes and human well-being. www.millenniumassessment.org, 2005.

[4] World Summit on Sustainable Development (WSSD), A framework for Action on Agriculture. Johannesburg: WEHAB Working Group, 2002

[5] S. Karekezi, J. Kimani, O. Onguru, Climate Change and Energy Security in East Africa. Energy Environment and Development Network for Africa (AFREPREN/FWD), 2009 46 pp.

[6] B. Lankford, B. Koppen, T. Franks, and H. Mahoo, Entrenched views or insufficient science? Contested causes and solutions of water allocation, insights from the Great Ruaha River Basin, Tanzania. Agricultural Water Management 2004, pp 135-153.

[7] D.K. Yawson, J.J. Kashaigili, J. Kachroo, and F.W. Mtalo, Modelling the Mtera-Kidatu reservoir system to improve integrated water resources management. International Conference on Hydropower. (Arusha: Hydro Africa), 2003.

[8] SMUWC, Baseline 2001. http://www.usangu.org/baseline2001/part1-5.shtml, 2001.

[9] E.H. Mwalukasa, Effects of Land Degradations in the Uplands on Land Use Changes in the Plains: The Case Study of Chimala River Catchment in the Usangu Plains. MSc. Dissertation. Sokoine University of Agriculture, 2002.

[10] H. Sosovele, and J.J. Ngwale, Socio-economic Root Cause of the Loss of Biodiversity in the Ruaha Catchment Area. (Dar-es-salaam: WWF-Tanzania), 2002.

[11] Z.J.U. Malley, M. Taeb, T. Matsumoto, T. and H. Takeya, Environmental change and vulnerability in Usangu plain, South-western Tanzania: Implications for Sustainable Development. The International Journal of Sustainable Development and World Ecology, 2007, pp 145-159.

[12] T.R. Karl, R.W. Knight, and N. Plummer, Trends in High Frequency of Climatic Variability in the Twentieth Century. Nature, 1995, pp 217-220.

[13] U.S. National Drought Monitor, http://www.drought.unl.edu/dm/monitor.html, 2006.

[14] D.A. Wilhite, and M.H. Glantz, Understanding the drought phenomenon: the role of definitions. Water International 1985, pp 111-120.

[15] J. Mbwambo, Kilombero: Kutoka mito 79 hadi 39 ya sasa, kulikoni? (Kilombero: From 79 rivers to 39 now, what need be done?), Raia Mwema Issue No 161, November 24-30, 2010, pp 12-13.

[16] J. J. Kashaigili, Integrated Hydrological Modelling of Wetlands for Environmental Management: The Case of the Usangu Wetlands in the Great Ruaha Catchment. RIPARWIN Seminar Presentation, Mbeya Peak Hotel: Mbeya, 2005.

[17] S. Libiszewski, What is an environmental conflict? (ENCOP Occasional papers: Center for Security Studies, ETH Zurich/Swiss Peace Foundation Zurich/ Berne 1992-1995), 1992.

[18] W. Edwin, Thousands of cattle dying as Dar relocates herders from the Wetlands, The East African, 2007, April 9-15.

[20] F. Simbeye, Songas to Replace Imported Furnace Oil. The East African, July 12-18, 2004.

[21]World Wide Fund (WWF), African Rivers Initiative: Concept Paper. Living Water Programme. Iringa, WWF, 2002.

Optimal hydraulic structures profiles under uncertain seepage head

Raj Mohan Singh[1,*]

1 Motilal Nehru National Institute of Technology, Allahabad-211004, India
** Corresponding author. Tel: +91-532-2271322(O); Fax: +91-532-2545341 E-mail: rajm@mnnit.ac.in; rajm.mnnit@gmail.com*

Abstract: Most of the hydraulic structures are founded on permeable foundation. There is, however, no procedure to fix the basic barrage parameters, which are depth of sheet piles/cutoffs and the length and thickness of floor, in a cost-effective manner. Changes in hydrological and climatic factors may alter the design seepage head of the hydraulic structures. The variation in seepage head affects the downstream sheet pile depth, overall length of impervious floor, and thickness of impervious floor. The exit gradient, which is considered the most appropriate criterion to ensure safety against piping on permeable foundations, exhibits non linear variation in floor length with variation in depth of downstream sheet pile. These facts complicate the problem and increase the non linearity of the problem. However, an optimization problem may be formulated to obtain the optimum structural dimensions that minimize the cost as well as satisfy the exit gradient criteria. The optimization problem for determining an optimal section for the weirs or barrages normally consists of minimizing the construction cost, earth work, cost of sheet piling, length of impervious floor etc. The subsurface seepage flow is embedded as constraint in the optimization formulation. Uncertainty in design, and hence cost from uncertain seepage head are quantified using fuzzy numbers. Results show that an uncertainty of 15 percent in seepage will result in 22 percent of uncertainty in design represented by overall design cost. The limited evaluation show potential applicability of the proposed method.

Keywords: *Nonlinear Optimization Formulation, Genetic Algorithm, Hydraulic Structures, Barrage Design, Fuzzy Numbers, Uncertainty Characterization.*

1. Introduction

Hydraulic structures such as weirs and barrages are costly water resources projects. A safe and optimal design of hydraulic structures is always being a challenge to water resource researchers. The hydraulic structure such as barrages on alluvial soils is subjected to subsurface seepage. The seepage head causing the seepage vary with variation in flows. Design of hydraulic structures should also insure safety against seepage induced failure of the hydraulic structures.

The variation in seepage head affects the downstream sheet pile depth, overall length of impervious floor, and thickness of impervious floor. The exit gradient, which is considered the most appropriate criterion to ensure safety against seepage induced piping (Khosla, et al., 1936; Asawa, 2005) on permeable foundations, exhibits non linear variation in floor length with variation in depth of down stream sheet pile. These facts complicate the problem and increase the non linearity of the problem. However, an optimization problem may be formulated to obtain the optimum structural dimensions that minimize the cost as well as satisfy the safe exit gradient criteria.

The optimization problem for determining an optimal section for the weirs or barrages consists of minimizing the construction cost, earth work, cost of sheet piling, and length of impervious floor (Garg et al., 2002; Singh, 2007). Earlier work (Garg et al., 2002) discussed the optimal design of barrage profile for single deterministic value of seepage head. This study first solve the of nonlinear optimization formulation problem (NLOP) using genetic algorithm (GA) which gives optimal dimensions of the barrage profile that minimizes unit cost of concrete work, and earthwork and searches the barrage dimension satisfying the exit gradient criteria. The work is then extended to characterize uncertainty in design due to

uncertainty in measured value of seepage head, an important hydrogeologic parameter. Uncertainty in design, and hence cost from uncertain head value are quantified using fuzzy numbers

2. Subsurface flow

The general seepage equation under a barrage profile may be written as:

$$\frac{\partial^2 h}{\partial x^2}+\frac{\partial^2 h}{\partial y^2}+\frac{\partial^2 h}{\partial z^2}=0 \qquad (1)$$

This is well known Laplace equation for seepage of water through porous media. This equation implicitly assumes that (i) the soil is homogeneous and isotropic; (ii) the voids are completely filled with water; (iii) no consolidation or expansion of soil takes place; and (iv) flow is steady and obeys Darcy's law.

For 2-dimensional flow, the seepage equation (1) may be written as:

$$\frac{\partial^2 h}{\partial x^2}+\frac{\partial^2 h}{\partial y^2}=0 \qquad (2)$$

The need to provide adequate resistance to seepage flow represented by equation (1) both under and around a hydraulic structure may be an important determinant of its geometry (Skutch, 1997).The boundary between hydraulic structural surface and foundation soil represents a potential plane of failure.

Stability under a given hydraulic head could in theory be achieved by an almost limitless combination of vertical and horizontal contact surfaces below the structure provided that the total length of the resultant seepage path were adequately long for that head (Skutch, 1997; Leliavsky, 1979). In practical terms, the designer must decide on an appropriate balance between the length of the horizontal and vertical elements. Present work utilized Khosla's Method of independent variables (Asawa, 2005) to simulate the subsurface behavior in the optimization formulation. Method of independent variables is based on Schwarz-Christoffel transformation to solve the Laplace equation (1) which represents seepage through the subsurface media under a hydraulic structure. A composite structure is split up into a number of simple standard forms each of which has a known solution. The uplift pressures at key points corresponding to each elementary form are calculated on the assumption that each form exists independently. Finally, corrections are to be applied for thickness of floor, and interference effects of piles on each others.

3. Optimal design methodology

Minimize $C(L, d_1, d_d) = c_1(f_1) + c_2(f_2) + c_3(f_3) + c_4(f_4) + c_5(f_5)$ (4)

Subject to $$SEG \geq \frac{H}{d_d \pi \sqrt{\lambda}} \qquad (5)$$

$$L^l \leq L \leq {}^u \qquad (6)$$

$$d_1{}^l \leq d_1 \leq d_1{}^u \qquad (7)$$

$$d_d^{\,l} \le d_d \le d_d^{\,u} \quad (8)$$

$$L, d_1, d_d \ge 0 \quad (9)$$

where C (L, d_1, d_d) is objective function represents total cost of barrage per unit width (Rs/m), and is function of floor length (L), upstream sheet pile depth (d_1) and downstream sheet pile depth (d_d); f_1 is total volume of concrete in the floor per unit width for a given barrage profile and c_1 is cost of concrete floor (Rs/m^3); f_2 is the depth of upstream sheet pile below the concrete floor and c_2 is the cost of upstream sheet pile including driving (Rs/m^2); f_3 is the depth of downstream sheet pile below the concrete floor and c_3 is the cost of downstream sheet pile including driving (Rs/m^2); f_4 is the volume of soil excavated per unit width for laying concrete floor and c_4 is cost of excavation including dewatering (Rs/m^3); f_5 is the volume of soil required in filling per unit width and c_5 is cost of earth filling (Rs/m^3); SEG is safe exit gradient for a given soil formation on which the hydraulic structure is constructed and is function of downstream depth and the length of the floor; $\lambda = \frac{1}{2}[1+\sqrt{1+\alpha^2}]$; $\alpha = \frac{L}{d_d}$; L is total length of the floor; H is the seepage head ; d_1 is the upstream sheet pile depth; d_2 is downstream sheet pile depth; L^l, $d_1^{\,l}$, and $d_d^{\,l}$ is lower bound on L, d_1 and d_d respectively**;** L^u, $d_1^{\,u}$, $d_d^{\,u}$ are upper bound on L, d_1 and d_d respectively. The constraint equation (5) may be written as follows after substituting the value of λ :

$$L - d_d\left(\{2(\frac{H}{d_2\pi(SGE)})^2 - 1\}^2 - 1\right)^{1/2} \ge 0 \quad (10)$$

In the optimization formulation, for a give barrage profile and seepage head H, f_1 is computed by estimating thickness at different key locations of the floor using Khosla's method of independent variables and hence nonlinear function of length of floor (L), upstream sheet pile depth (d_1) and downstream sheet pile depth (d_2). Similarly f_4, and f_5 is nonlinear. The constraint represented by equation (10) is also nonlinear function of length of the floor and downstream sheet pile depth (d_2). Thus both objective function and constraint are nonlinear; make the problem in the category of nonlinear optimization program (NLOP) formulation, which are inherently complex. Characterization of functional parameters is available in literature (Singh, 2007; Garg et al., 2002).

3.1. Characterizing model functional parameters

For a given geometry of a barrage and seepage head H, the optimization model functional parameters f_1, f_2, f_3, f_4 and f_5 are characterized for the barrage profile shown in Fig. 1.

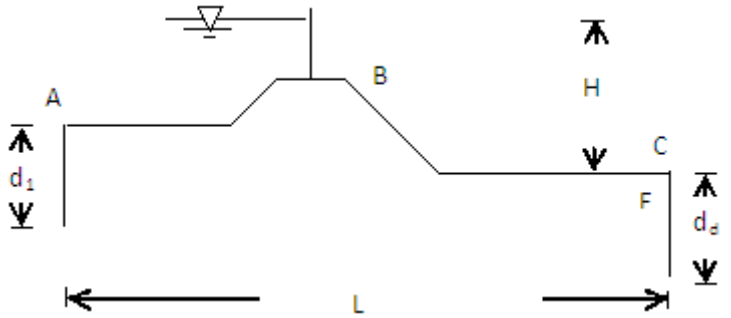

Fig. 1. Schematic of barrage parameters utilized in performance evaluation

Intermediate sheet-piles are not effective in reducing the uplift pressures and only add to the cost of in reducing the uplift pressures and only add to the cost of the barrage (Garg et al., 2002). In present work, no intermediate sheet piles are considered.

3.2. Optimization procedure using genetic algorithm

GA was originally proposed by Holland (Holland, 1975) and further developed by Goldberg (Goldberg, 1989). It is based on the principles of genetics and natural selection.GA's are applicable to a variety of optimization problems that are not well suited for standard optimization algorithms, including problems in which the objective function is discontinuous, non-differentiable, stochastic, or highly nonlinear (Haestad 2003). The GA search starts from a population of many points, rather than starting from just one point. This parallelism means that the search will not become trapped on local optima (Singh and Datta, 2006).

The optimization model represented by equations (4)-(10) and the functional parameters embedded in the optimization model are solved using Genetic Algorithm on M ATLAB platform. The basic steps employed in solution are available in Singh, 2007. Table 1 shows physical parameters obtained by conventional methods for Fig. 2.

Table 1. Physical parameters values of barrage profile

Physical parameters	Values (meters)
*L	105.37
H	7.12
*d_1	5.45
*d_2	5.9

* Decision variables to be optimized

4. Uncertainty characterization in the optimization model

Real-world problems, especially those that involve natural systems, such as soil and water, are complex and composed of many non-deterministic components having non-linear coupling. In dealing with such systems, one has to face a high degree of uncertainty and tolerate imprecision. There is a high degree of local soil variability, and imprecision in the determination of soil parameters and hydrological parameters like seepage head. Statistical techniques have been traditionally used to deal with parametric variation in model inputs, but these require substantial hydrogeologic explorations data for estimates of probability distributions. In the presence of limited, inaccurate or imprecise information, simulation with fuzzy numbers represents an alternative tool to handle parametric uncertainty. Fuzzy sets offer an alternate and simple way to address uncertainties even for limited exploration data sets. In the present work, the optimal design is first obtained assuming a deterministic value of hydrogelogic parameter, safe exit gradient, in optimization model. Uncertainty in safe exit gradient is then characterized using fuzzy numbers. The fuzzified NLOF is then solved using GA.

Uncertainty in general comes in two forms: aleatory (stochastic, random natural variability or noncognitive) and epistemic (cognitive or subjective) (Hofer et al., 2002). Recently, Srinivasan et al. (2007) identified these uncertainties in hydrogeological applications. Aleatory uncertainty refers to uncertainty that cannot be reduced by more exhaustive

measurements or by a better model. Epistemic uncertainty, on the other hand, refers to uncertainty that can be reduced (Ross et al., 2009).

One of the milestones in the evolution of these new uncertainty theories is the seminal paper by Lofti A. Zadeh (1965). He proposed a new mathematical tool in his paper and called this new mathematical tool "fuzzy sets." He proposed the concept of fuzzy algorithms in 1968 (Zadeh, 1968), and together with Bellman, proposed a new approach for decision-making in fuzzy environments in 1970 (Bellman & Zadeh, 1970). Fuzzy set theory has been recently applied in various fields for uncertainty quantification (Cho et al., 2002; Hanss, 2002; Kentel & Aral, 2004; Mauris et al., 2001).

The transformation method presented by Hanss, (2002) uses a fuzzy alpha-cut (FAC) approach based on interval arithmetic. The uncertain response reconstructed from a set of deterministic responses, combining the extrema of each interval in every possible way unlike the FAC technique where only a particular level of membership (α-level) values (Hanss & Willner, 1999) for uncertain parameters are used for simulation.

Fuzzy modeling of uncertainty for hydrogeologic parameters such as exit gradient and seepage head is based on Zadeh's extension principle (Zadeh, 1968) and transformation method (TM) (Hanss, 2002). In present study only seepage head is considered to be imprecise. Input seepage head as imprecise parameter, is represented by fuzzy numbers. The resulting output i.e. minimum cost obtained by the optimization model is also fuzzy numbers characterized by their membership functions. The reduced TM (Hanss, 2002) is used in the present study. The measure of uncertainty used is the ratio of the 0.1-level support to the value of which the membership function is equal to 1 (Abebe et al., 2000).

5. Results and discussion

Earlier (mid 19th century), weirs and barrages have been designed and constructed in India on the basis of experience using the technology available at that period of time. Some of them were based on Bligh's creep theory, which proved to be unsafe and uneconomical. Comparison of the parameters of these structures with the proposed approach is, thus, not justified. Therefore, a typical barrage profile, a spillway portion of a barrage, is chosen for illustrating the proposed approach as shown in Fig. 2. The barrage profile shown in Fig. 2 and parameters values given Table 1 is solved employing the methodology presented in this work. The optimized values of parameters for a deterministic seepage head value of 7.12m are shown in Table 2. During the process of optimization, the process of going into new generation continues until the fitness of the population converged i.e. average fitness of population almost matches with the best fitness. This criterion proves the solution to be optimized. The optimized values of parameters for a deterministic seepage head value of 7.12m are shown in Table 2.

Table 2. Optimized parameters for safe exit gradient equal to 1/8 and minimum thickness of floor as 1m

Physical parameters	Values
L	61
d_1	3.1
d_2	9.2

It also resulted in a smaller floor length and overall lower cost. It has shown a savings in the barrage cost ranging from 16.73 percent.

For characterization of uncertainty, seepage head is assumed to vary from 6.0m to 8.19m with central value of 7.12m i.e. almost 15 percent in triangular fuzzy numbers representation. The result of variation in cost is corresponding different degree of membership for seepage head shown in Fig.2. The measure of uncertainty is found to be 22 percent. Since, left and right spread from central value of exit gradient is almost 15 percent, it can be concluded that uncertainty in seepage head reflects comparatively more uncertainty) more than 15 percent) in cost.

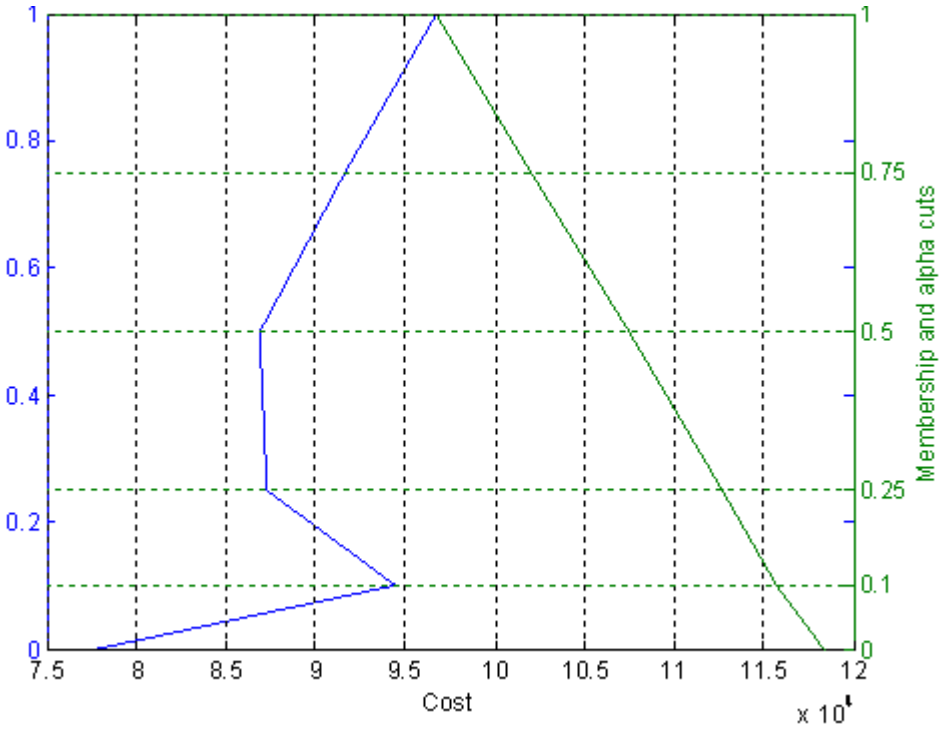

Fig.2. Costs variations corresponding to different α-cuts of seepage head

6. Conclusions

The present work also demonstrates the fuzzy based framework for uncertainty characterization in optimal cost for imprecise hydrologic parameter such as seepage head. The uncertainty in cost is found not to be directly proportional to uncertainty in seepage head. The GA based optimization approach is equally valid for optimal design of other major hydraulic structures.

References

[1] Khosla, A. N., Bose, N. K., and Taylor, E. M., Design of weirs on permeable foundations. *CBIP Publication No. 12*, Central Board of Irrigation and Power, New Delhi, 1936, Reprint 1981.

[2] Asawa, G.L. Irrigation and water resources engineering, New Age International (P) Limited Publishers, New Delhi. 2005.

[3] Garg, N.K., Bhagat, S.K., and Asthana, B.N., Optimal barrage design based on subsurface flow considerations. *Journal of Irrigation and Drainage Engineering*, Vol. 128, No. 4, 2002, 253-263.

[4] Singh. R.M., Optimal design of barrages using genetic algorithm. Proceedings of National Conference on Hydraulics & Water Resources (Hydro-2007) at SVNIT, Surat, 2007, 623-631.

[5] Skutch, J., Minor irrigation design DROP - Design manual hydraulic analysis and design of energy-dissipating structures. *TDR Project R 5830,* Report OD/TN 86, 1997.

[6] Leliavsky, S., Irrigation engineering: canals and barrages. Oxford and IBH, New Delhi, 1979.

[7] Holland, J. H., Adaptation in natural and artificial systems. University of Michigan Press, Ann Arbor, MI,1975.

[8] Goldberg, D. E., *Genetic algorithms in search, optimization and machine learning*. Kluwer Academic Publishers, Boston, MA, 1989.

[9] Haestad, M., Walski ,T. M., Chase, D. V., Savic, D. A., Grayman, W., Beckwith, S., and Koelle, E., *Advanced water distribution modeling and management.* Haestad Press, Waterbury, CT, 2003, 673-67.

[10] Singh, R. M., and Datta, B. 2006. Identification of unknown groundwater pollution sources using genetic algorithm based linked simulation optimization approach. *Journal of Hydrologic Engineering,* ASCE, Vol. 11, No.2, 101-109.

[11] Hofer, E., Kloos, M., Krzykacz-Hausmann, B., Peschke, J. and Woltereck, M., An approximate epistemic uncertainty analysis approach in the presence of epistemic and aleatory uncertainties. *Reliab. Eng. Syst. Safety*, 77(3), 2002, 229– 238.

[12] Srinivasan, G., Tartakovsky, D. M., Robinson, B. A., and Aceves, A. B., Quantification of uncertainty in geochemical reactions. Water Resour. Res. 43, 2007, W12415.

[13] Ross, J.L., Ozbek, M.M. and Pinder, G.F., Aleatoric and epistemic uncertainty in groundwater flow and transport simulation. Water Resour. Res., 45, 2009, W00B15.

[14] Zadeh, L., Fuzzy sets. *Information and Control*, 8, 1965, 338– 353.

[15] Zadeh, L. A., Fuzzy algorithms. Information and Control 12, 1968, 94-102.

[16] Bellman, R.E., Zadeh, L.A., Decision-making in a fuzzy environment. *Management Science,* 17, 1970, 141-164.

[17] Cho, H.N., Choi, H.-H., Kim, Y.B., A risk assessment methodology for incorporating uncertainties using fuzzy concepts. Reliability Engineering and System Safety 78, 2002, 173-183.

[18] Kentel, E., Aral, M.M., Probabilistic-fuzzy health risk modeling. Stochastic Environmental Research and Risk Assessment (SERRA) 18, 2004, 324-338.

[19] Mauris, G., Lasserre, V., Foulloy, L., A fuzzy approach for the expression of uncertainty in measurement. Measurement, 29, 2001, 165-177.

[20] Hanss, M., Willner, K., On using fuzzy arithmetic to solve problems with uncertain model parameters. In Proc. of the Euromech 405 Colloquium, Valenciennes, France, 1999, 85-92.

[21] Abebe, A.J., Guinot, V., Solomatine, D.P., Fuzzy alpha-cut vs. Monte Carlo techniques in assessing uncertainty in model parameters. 4th Int. Conf. Hydroinformatics, Iowa, USA, 2000.

The impact of the March 10, 2009 dust storm on meteorological parameters in central Saudi Arabia

Abdullrahman H. Maghrabi

National Centre For Mathematics and Physics, King Abdulaziz City For Science and Technology, Riyadh , Saudi Arabia
** Corresponding author. Tel: +966-501051884, Fax: +966-14813521, E-mail. amaghrabi@kacst.edu.sa*

Abstract: Dust particles play an important role in air quality and environmental health. They affect both solar and terrestrial radiation by scattering and absorption and are therefore considered to be a significant climate-forcing factor. Dust storms are natural hazards that affect daily life for an interval ranging from a few hours to a few days, and they are a very frequent phenomenon in Saudi Arabia, especially in the pre-monsoon season.
On 10th March 2009 a widespread and severe dust storm event that lasted several hours struck Riyadh (24.9 1° N, 46.41° E, 764 m) and represented one of the most intense dust storms experienced in Saudi Arabia in the last two decades. In this study, the effect of this dust storm on meteorological parameters was investigated. These parameters are relative humidity, air temperature, visibility and atmospheric pressure. Around noon local time on the event day, with the arrival of the dust plume, there were dramatic changes in weather conditions. Air temperature dropped by about 6 ^{o}C, relative humidity increased dramatically reaching a value of 33 %. The visibility deteriorated dramatically to a value of 1 m. These results also, show that the effect of this storm was associated with an increase in both atmospheric pressure and relative humidity as well as a r eduction in temperature and visibility for the two days following the storm in comparison with conditions before the storm. The impact of several other dust storms on meteorological parameters during the year of 2009 were investigated and compared to the March 10th storm. It was found that this storm had a greater effect on the meteorological variables than the other storms.

Keywords: *Dust Storm, Riyadh, Temperature, Solar Radiation*

1. Introduction

Atmospheric aerosols are linked to the climate system and to the hydrologic cycle. Depending on their composition, atmospheric aerosols can absorb solar radiation in the atmosphere, producing further cooling of the surface and warming the atmosphere. Dust particles affect both solar and terrestrial radiation and are thus considered a significant climate-forcing factor and an important parameter in radiation budget studies [1]. The net effect of atmospheric aerosols is to cool the planet by reflecting incoming solar radiation. One of the major problems associated with dust storms is the considerable reduction of visibility that limits various activities, increases traffic accidents, and may increase the occurrence of vertigo in aircraft pilots [2]. Other environmental impacts include reduced soil fertility at the source area, damage to crops, a reduction of solar radiation, and, consequently, a reduction in the efficiency of solar devices, damage to telecommunications and mechanical systems, dirt, and air pollution. In addition, aerosols have a significant impact on hum an health. Goudie[3] recently provided an up-to-date and comprehensive review on dus t storms and their significance for many fields.

The frequency of dust-storm occurrence in Saudi Arabia is at a maximum during the pre-monsoon (March–May) season, when dust aerosols are transported by south-westerly winds from the arid and semi-arid regions around the Arabian Sea.

In Saudi Arabia, dust storms are considered among the most severe environmental problems. Several investigators have studied desert dust in Saudi Arabia [4]. Most of the previous studies have used either surface or satellite observations to characterise the large-scale dust loading of the atmosphere over the Arabian Peninsula. H owever, almost nothing has been

done to study the effect of these dust storms on meteorological parameters and solar and infrared radiation in this region.

On the 10th of March 2009, a dramatic windstorm moved over Riyadh that was accompanied by a strong dust storm. This short-lived but intense dust storm caused a widespread, heavy dust load, greatly affected visibility and air quality, and caused a total airport shutdown as well as damage to buildings, vehicles, power poles and trees throughout the city of Riyadh. This storm was massive enough to be seen clearly from outer space and is considered to be one of the heaviest recorded dust storms in the last two decades. The outbreak of the dust storm was associated with a cold frontal passage that coincided with the propagation of a pre-existing synoptic-scale upper tropospheric jet stream over the northern and central parts of Saudi Arabia.

An investigation of the impact of this storm on solar and infrared radiation will be presented in another paper. This paper studies the impact of this severe storm on meteorological parameters and shows the variability of these parameters due to the storm.

2. Experimental Site and data:

The study area of Riyadh lies in the central region of the Arabian Peninsula at 24° 43 ′N; 46° 40′E, 764 m a.s.l. Riyadh is the capital of Saudi Arabia and its largest city; its population is 4500000 according to the 2005 census. It is a purely urbanised area and is one of the most polluted areas in the Kingdom because it is surrounded by industrial areas and traffic arterials, with the natural environment of the Empty-Quarter Desert lying beyond. The arid conditions prevailing at this site are responsible for large seasonal temperature differences, providing cool winters and very hot summers. The area experiences extremely low humidity, particularly in the summer. The climate of the region exhibits four dominant seasons each year: winter (December–February), pre-monsoon (March–May), monsoon (June–August), and post-monsoon (September–November). The pre-monsoon season, during which the present case study was conducted, is characterised by frequent dust storms and long dry spells.

Standard meteorological observations such as air temperature, relative humidity, and cloud information were used in the current study. These data were obtained using Riyadh Airport records provided by the Presidency of Meteorology and Environment.

3. Results and Discussion

3.1. Event Description

For the purpose of clarification the discussion of results will include the behaviour of the considered variables two days before and two days after the storm along with the event day. These will be referred as pre-event, post-event and the event day respectively.

The hourly values of four meteorological variables; relative humidity (RH), temperature (T), visibility (vis), and atmospheric pressure (P) for March 8-12, 2009, are plotted in Figure 1. As shown in Figure 1a, both T and RH reveal a diurnal cycle throughout, displaying a trend opposite to what one would expect. Visibility was in the 8-10 km range on the 8th and 9th of March and on the morning of the 10th, which is the normal maximum visibility found in Riyadh at this time of the year. The atmospheric pressure shown in Figure 1b shows a less clear diurnal cycle with some variability from one hour to the next on each day. Through most of the period from the morning of the 8th of March until the morning on the 10th, wind

directions were consistently southerly. Wind speeds increased during this period from ~10 m/s on the 8th to ~20 m/s on the 9th.

On the day of the event, before the arrival of the storm, the weather was stable; T was ~28 °C, P was 939.8 hPa, RH was 10%, and the local wind was relatively light towards the south. Around noon local time, with the arrival of the dust plume, there were dramatic changes in weather conditions. The wind swung to a northerly direction and wind speed rapidly increased to a maximum of 30 ms^{-1}.

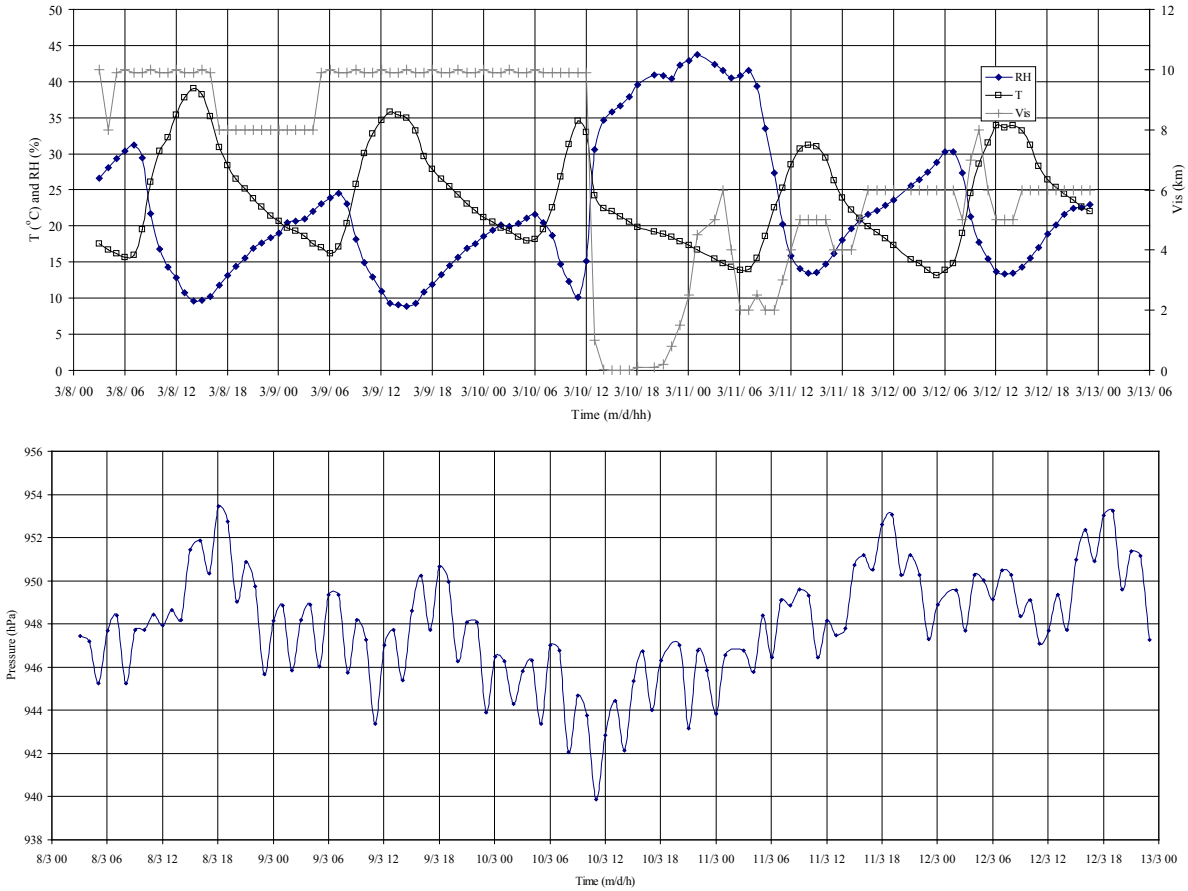

Fig. 1. Day-to-day variations of meteorological parameters (a) relative humidity ,air temperature, and visibility ;and(b) atmospheric pressure for the period from March 8th to March 12th 2009.

Because of the wind change and dust storm, T dropped by about 6 °C within an hour to reach 22 °C. The temperature continued to decrease until it reached the daily minimum of about 14 °C at 07:00 a.m. on the 11th. The air temperature then resumed its normal daily cycle, although temperatures remained cool on the 11th with a maximum of only 23 °C. It is likely that this reduction in the daytime temperature was caused by the reduced heating near the surface resulting from shortwave energy extinction by the additional aerosol loads arriving with the storm on the 10th. Relative humidity, on the other hand, increased dramatically with the arrival of the dust storm, reaching a maximum of 44 % at 01:00 on the 11th. The change in relative humidity is partly due to the cooler air temperatures but is also likely due to the moisture brought to the region by the storm. The visibility deteriorated dramatically with the arrival of the dust storm and then remained around 1 m for the 3 hours following the event. It then increased to 6 km by 03:00 on the 11th. After another decrease to ~ 2 km in the early

hours of the morning, it rose to between 5 km and 6 km and stayed around this mark for the rest of the period considered.
Several investigations on the dust storms in the Arabian Gulf and adjacent Gulf countries [5] and other places around the world [6] have reported similar variations and characteristic changes in meteorology.

3.2. Comparisons with other events

Table 1 shows a list of seven storm events during 2009. It summarises the change of the four meteorological parameters during these events. These changes represent the difference between the measured value immediately before the event and the maximum and minimum values reached immediately due to the event. In the last column, the time of maximum change occurs after the arrival of the storm is provided. Three of these events occurred in the pre-monsoon season, two in spring, one in summer and one in winter. In the last row of the table, the changes in the meteorological parameters for the 10th of March are summarised. Apart from the 18/9 event, the ranges of the changes in both atmospheric pressure and air temperature are confined between 2-4 hPa and 2-3 ^{o}C, respectively. The drop in the visibility varies between a minimum of 4 to a maximum of 8 km. The maximum changes in the relative humidity occurred on 4/6 and 18/9, followed by that on 20/5. For the events on 19/3 and 6/10, the RH dropped by -7 and -5 respectively. This drop may be due to the characteristics of the dry air mass that brought the storm to the study region. The 4/6 event is considered the strongest of the seven events. For this event, two hours after the storm, RH and atmospheric pressured increased by 10% and 3 hPa; temperature and visibility dropped by 3^{o}C and 8 km, respectively. Comparisons between the 10th of March event and the seven other storm events showed, with the exception of the atmospheric pressure, that the changes in the meteorological variables are higher for the 10th March. In addition, although the two hours after the event on the 10th are considered to be relatively short, dramatic changes occurred during this time.

Table 1 shows the difference between the meteorological variables before the storm and after the storm for the storm event in 2009. The last column is the time when maximum change occurred after the arrival of the storm

DAY/MONTH	Δ VIS (KM)	Δ T (^{O}C)	Δ P (HPA)	ΔRH (%)	TIME OF MAX. (HOURS)
20/5	4	2	3	9	2
28/5	7	3	2	7	3
4/6	8	3	3	10	2
19/3	8	3	2	-7	2
6/10	5	2	4	-5	2
28/2	6	2	3	9	3
18/9	5	4	5	10	2
10/3	**9.9**	**6**	**4**	**25**	**2**

The effect of different aerosol loads on both the spectral and broadband solar radiation components have been investigated extensively both experimentally and theoretically by several researchers. It has been found that the aerosols may reduce the solar radiation by as much as 50% [7]. Additionally, it was found that dust storms severely affect meteorological variables. Their impact on these variables is different and becomes severe in some cases,

such as the one presented in this paper. Moreover, because several models have been developed to predict the solar radiation components (e.g., global and diffuse), it is important to consider the impact of such transient and severe events and study their effects to produce the appropriate predictability.

4. Conclusion

On 10 March 2009, a severe and extensive dust storm event struck Riyadh and lasted for several hours. The impact of this event on ground–based measurements of meteorological parameters was investigated. These parameters are relative humidity, air temperature, visibility and atmospheric pressure. The analysis for the behaviour of the considered variables two days before and two days after the storm along with the event day were conducted and presented.

The investigations show significant changes in all of the measured parameters as a result of this event. Around noon local time on the event day, with the arrival of the dust plume, there were dramatic changes in weather conditions. Air temperature dropped by about 6 ^{o}C, relative humidity increased dramatically reaching a value of 33 %. The visibility deteriorated dramatically to a value of 1 m. These results also, show that the effect of this storm was associated with an increase in both atmospheric pressure and relative humidity as well as a reduction in temperature and visibility for the two days following the storm in comparison with conditions before the storm. Comparisons between this storm event and seven other reported events that occurred in the same year showed that this event was the most extreme and the most severe.

References

[1] A. Jayaraman, Lubin, D., Ramachndran, S., Ramanathan, V., Woodbridge, E., Collins W. and Zalupuri, K. S.. Direct observation of aerosol radiative forcing over the tropical Indian Ocean during the Jan.- Feb. 1996 pre-INDOEX cruise. J. Geophys. Res. 1998, 103,13827–13836.

[2] H. Kutiel, and Furman, H.,. Dust storms in the Middle East: Sources of origin and their temporal characteristics. Indoor and Built Environment, 2003, 12(6),419-426

[3] A.S., Goudie, Dust storms: Recent developments. Journal of Environmental Management, 2009,90,89-94.

[4] B. H. Alharbi, and Moied, K. 2005. Riyadh air quality report (1999-2004), King Abdulaziz City for Science and Technology, No. 279-25-ER.

[5] D. L. McNaughton, Possible connection between anomalous anticyclones and sandstorms. Weather, 1987, 42 (1),8-13.

[6] P. M., Pauley, Baker, N. L. and Barker, E. H., An Observational Study of the "Interstate 5" Dust Storm Case; Bulletin of the American Meteorological Society, 1996, 77 (4), 693-720.

[7] K.V.S., Badarinath, Kharol, S.K, , Kaskaoutis, D.G., and Kambezidis , H.D. 2007. Case study of a dust storm over Hyderabad area, India: Its impact on solar radiation using satellite data and ground measurements; Science of the Total Environment 384 :316–332.

The medium to long-term role of renewable energy sources in climate change mitigation in Portugal

Sofia Simões[1,*], Júlia Seixas [1], Patrícia Fortes[1], Luís Dias[1], João Gouveia[1], Bárbara Maurício[1]

[1] *CENSE, Departamento de Ciências e Engenharia do Ambiente, Faculdade de Ciências e Tecnologia, Universidade Nova de Lisboa, Caparica, Portugal*
** Corresponding author. Tel: +351 212948354, Fax: +351 212948354, E-mail: sgcs@fct.unl.pt*

Abstract: Portuguese policy-makers have adopted ambitious targets for RES promotion until 2020, but there are no national targets for the medium to long -term (2050) and it is not clear to what extent which RES can contribute to CC mitigation. This paper aims to assess the contribution of RES for the CC mitigation in Portugal until 2050, under cost-effectiveness criteria. The TIMES_PT linear optimization bottom-up technology model was used to generate six scenarios to 2050 combining GHG emission caps, levels of socio-economic growth and share of RES electricity. In order to meet the 2050 energy demand, the share of RES in primary energy consumption increases 4 to 6 times from 2005 and in final energy grows from 15% in 2005 to 56-59% in 2050. RES were found to be cost-effective even without a GHG cap. Regarding CC mitigation the high RES shares in final energy correspond to less 49-74% GHG emissions in 2050 compared to a baseline without cap. The role of renewable electricity is determinant to mitigate CC especially due to hydro and onshore wind. Other important deployments of RES technologies are solar water heating and heat pumps in buildings, biomass use for process heat in industry and biodiesel in transport.

Keywords: *Climate change mitigation, Renewable energy, Energy modeling, Portugal.*

1. Introduction

Renewable energy sources (RES) play a key-role in climate change (CC) mitigation. Moreover, RES have added benefits of reducing external energy dependency and fostering economic development. Acknowledging this, Portugal has been pointed worldwide as a success case for RES deployment (IEA, 2009, NYT, 2010). National CC & energy policy-makers have adopted ambitious targets for RES promotion until 2020. The National Energy Strategy for 2020 (Cabinet Resolution n. º 29/2010 of April 15) defines the following main objectives: i) reduce the external energy dependency to 74% (it was 87% in 2008); ii) ensure compliance of commitments within EU climate change policies, allowing that in 2020 60% of generated electricity is renewable based (RES-E) and 31% of final energy consumption is from RES (respectively 50% RES-E in September 2010 and 20% in 2005), and iii) achieving a reduction of 20% final energy consumption in the terms of the Energy-Climate policy package. The Portuguese National Action Plan (PNAER) within the Directive 2009/28/EC sets even more ambitious policies & measures (P&M) that will allow reaching 70% RES-E in 2020 and 10% biofuels in transport (update on PNAER by the Decree-Law nº 117/2010 of October 25). Other P&M are in place to promote RES heating and cooling and end-use energy efficiency, namely through the National Energy Efficiency Action Plan (RCM 80/2008).

Although there is high policy focus on medium-term RES promotion (2020) there are no national targets for the medium to long-term (2050). Likewise there are no quantitative estimates on avoided GHG emissions due to RES promotion, both in medium and long-term. Furthermore, there is no information on which RES (e.g. solar or waves) and which RES technologies (e.g. PV panels or biomass boilers) are the most cost-effective for Portugal. This is highly relevant to support national policy making, particularly regarding the design of incentives to promote the most cost-effective RES. This paper aims to assess the contribution of RES for the reduction of GHG emissions in Portugal until 2050 looking into detail into which technologies are most cost-effective.

2. Methodology

To assess the role of RES in CC mitigation in Portugal up to 2050, we used the TIMES_PT model to generate six scenarios combining different assumptions as presented in Table 1.

Table 1. GHG and RES scenarios for Portugal up to 2050

Scenario	GHG cap	Economic Growth[a)]	Minimum fossil electricity
C	None	Conservative	30% of total electricity
F	None	Fenix	30% of total electricity
-50C	-50% in 2050 / 1990	Conservative	30% of total electricity
-50F	-50% in 2050 / 1990	Fenix	30% of total electricity
Cefre	None	Conservative	None
Fefre	None	Fenix	None

[a)] Two socio-economic scenarios were developed for Portugal as briefly outlined below.

To assess RES contribution to CC mitigation, we consider a **GHG[1] emission cap** in the -50C and -50F scenarios starting from 2015 with +27% of the 1990 (the Kyoto target for 2010-2012 extended to 2015) and linearly more stringent until -50% of 1990 for combustion and productive processes GHG emissions in 2050. (A trend line was then generated from the 2015 to the 2050 cap to obtain intermediate emission caps for every 5 years. The -50% cap is quite severe as it roughly leads to per capita emissions of 2.04 t CO2e in 2050 whereas in 2008 Portugal had 7.4 t CO2e. The per capita EU 15 average in 2008 was 10.1 tCO2e according to EEA data.

Regarding **economic growth and demand for energy services**, two contrasting socio-economic scenarios were used: Conservative and Fenix. The Conservative scenario follows the current economic and demographic trends (1% GDP annual growth rate and population decrease); whereas the Fenix scenario has more optimistic economic and population evolution forecasts (2 to 2.26% GDP annual growth rates and more 12% inhabitants in 2050 compared to 2005). These scenarios were used to generate two demand projections for materials and energy services such as residential lighting or cement which are inputs of the TIMES_PT model. More information on the demand projections and can be found on Seixas *et al.* (2009).

Finally, in four of the six studied scenarios (C, F, -50C and -50F) we assumed a conservative requirement to assure the reliability of the power system translated as a **minimum of 30% of total generated electricity is produced by centralized fossil plants** from 2015 to 2050. In the Cefre and Fefre scenarios we removed this constraint and the system is free to adopt as much RES-E as needed according to cost-effectiveness criteria. Such approach could be associated with ensuring security of supply via expanded transmission capacity and increased electricity trade. In this paper however, we do not deal with electricity trade. We assumed that the net electricity imports are nil from 2025 onwards following the Portuguese transmission system operator expectations. If assumed otherwise the entire configuration of the electricity system would alter depending on how much electricity could be exported. However, at the moment there are absolutely no expectations on amounts of electricity traded after 2025 and any scenarios would by highly uncertain and out of the scope of this paper. Thus we have focused instead on the cost-effective assessment of maximum potential of national renewable

[1] This paper solely refers to energy related GHG emissions, i.e. from fuel combustion activities, fugitive emissions from oil, natural gas and other sources and from major industrial processes. These were approximately 81% of 2005 national emissions.

resources for the national CC mitigation considering nil electricity imports after 2025.

All these assumptions were inputted into the linear optimization bottom-up technology TIMES_PT[2] model which represents the Portuguese energy system from 2005 to 2050. The TIMES_PT is an implementation of the TIMES family of models developed by ETSAP of IEA which has been implemented at global, regional or national level (ETSAP, 2008), namely for the whole of UE (Pan European Times model from the NEEDS project) or for the countries Spain (Labriet, *et al.*, 2010), Belgium (Proost, *et al.*, 2009) or Germany (Blesl, *et al.*, 2007), among other EU countries. It considers both the supply and demand sides and disaggregates the energy demand sectors. The model is supported by a detailed database, which includes the technical and economical characteristics of the existing and future energy technologies and present and future sources of primary energy supply and their maximum technical and economic potentials (e.g. maximum available biomass or area for solar panels). TIMES_PT finds the optimum combination of energy supply and demand technologies to satisfy the demand with the lowest possible total costs. More information on the details of the model can be found in Simões *et al.* (2008) and more details on the technology and primary energy assumptions in Seixas *et al.* (2009). The learning curves for RES-E solar and wave technologies are from the IEA (IEA, 2010, IEA, 2008) which were validated by national stakeholders. Wind RES-E technologies learning curves were supplied by national experts of the National Energy and Geology Research Institute (LNEG, 2010).

Other exogenous assumptions are very briefly outlined: 1) 8% discount rate for centralized electricity generation, buses and trains; 12% for commercial, industry, decentralized electricity generation, CHP and freight transport; and 17.5% for residential, cars and motorcycles. 2) maximum of 5000 Gg CO2 carbon capture and storage potential were assumed as available since there is no data at the moment available for Portugal. More information on CCS cost data can be found at Simões *et al.* (2008); 3) no nuclear due to current policies and the purpose of this work focusing the role of RES; 4) new coal power plants without CCS not allowed due to climate policy; 5) RES targets, subsidies or feed-in tariffs not considered; 6) cost of oil barrel of 100 USD$_{2008}$ for the year 2020, 115 in 2030 and 145 in 2050.

3. Results

3.1. RES in primary energy consumption

In order to meet the 2050 energy demand, the share of RES in primary energy consumption can increase to two to three times the 2005 values in the scenarios without GHG emission cap (Figure 1) which shows the cost-effectiveness of RES. To meet the CO2 caps (-50C and -50F) RES can further increase to 4 to 6 times the 2005 values. The most competitive RES in all scenarios are wind and hydro which achieve its maximum potential in 2050. Solar, national biomass and, to a lesser scale, geothermal are also competitive but only if a GHG cap is in place. Removing the 30% fossil electricity requirement does not lead to significant changes in RES in 2020. However, in 2050 the higher RES-E share leads to higher consumption of solar especially in the Fefre scenario, where it achieves its maximum potential.
The increase in RES allows decreasing the external energy dependency from 87% in 2008 to 70-77% in 2020 and to 58-72% in 2050. The lowest values are not obtained due to the GHG

[2] The Portuguese model development was undertaken within the EU FP7 research project NEEDS (www.needs-project.org). The NEEDS RS2a research team is responsible for the model structure. The authors are responsible for some structural changes, the base-year and new technologies information and for calibration and validation of the national model.

cap but instead due to 100% RES-E. If a backup of 30% fossil electricity is removed imports of natural gas for centralized CCGT plants can be reduced already in 2020. In any case, in 2050 a new energy import paradigm appears; instead of being dependent on imported fossil fuels the energy system will import biomass, particularly biofuels for transports.

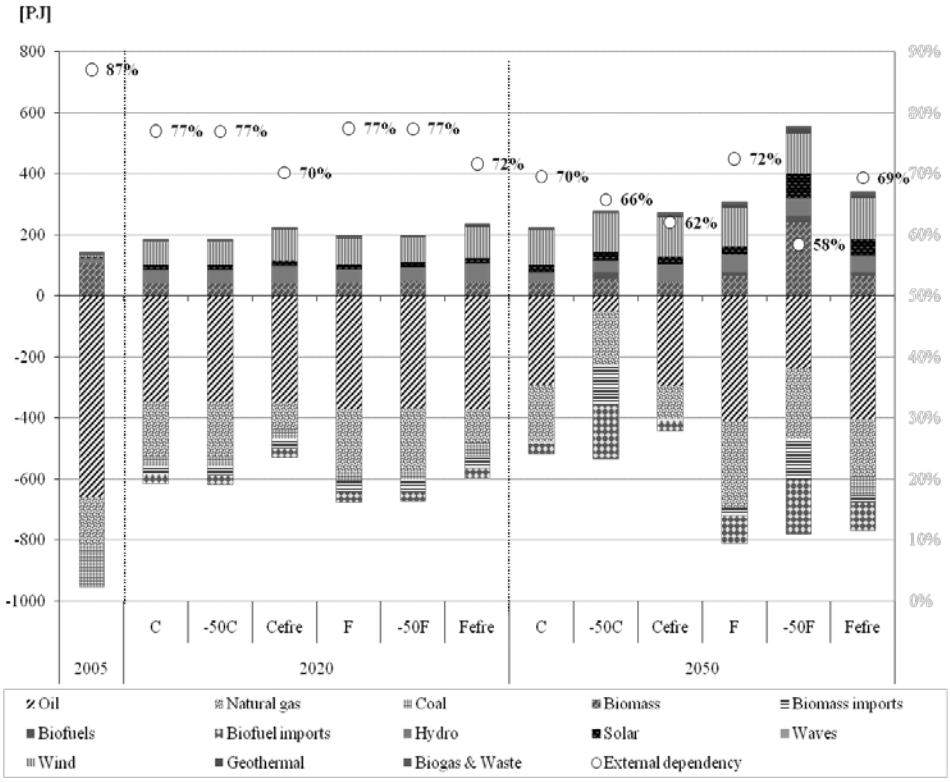

Fig. 1. Primary energy consumption in the studied scenarios, % of external energy dependency and % of RES (in the top rectangle). The lower values for 2020 are due to increase of refinery exports, decommissioning of a major coal power plant and slow recovery from 2010-2015 economic crisis.

3.2. RES in electricity generation

Until 2020 the electricity sector profile will be similar to 2009 since it will rely in recent investments both on RES (wind and hydro) and on new gas CCGT. Globally, approximately 58% of total electricity in 2020 is RES-E, in all scenarios with minimum 30% fossil electricity. In 2050 the GHG cap has a significant effect in RES-E technologies profile only in the -50F scenario since there is a higher overall demand for electricity (107.16 TWh, in comparison with 84.03 TWh in F). In -50C wind and hydro are sufficient to meet the demand. The system will firstly use all available hydro and onshore wind resources and in -50F this is followed by centralised PV, biomass and biogas CHP, and both geothermal steam turbines and hot dry rock systems. These technologies are practically negligible in 2050 in C, F, and -50C as the demand for RES-E is not high enough also due to the requirement for minimum 30% electricity from centralised fossil fuel. Without this requirement, in Cefre and Fefre, already in 2020 at least 78% of electricity will be RES-E and hydro and wind potentials will be achieved (9.7 and 6.5 GW, respectively). In 2050 74-89% electricity is RES and in Fefre large PV plants achieve the maximum potential (9.33 GW) and appears 0.50 GW of wind offshore. Both in 2020 and 2050 the gas CCGT plants will not work due to higher fuel and O&M costs.

In Cefre and Fefre there is a lower demand for electricity than in the other scenarios due to the higher contribution of efficient equipments and appliances in buildings, district heating in

commercial and biomass and insulation in the residential. This means that the 30% fossil electricity requirement hampers energy efficiency and RES use in final energy.

3.3. RES in final energy consumption

Concerning final energy consumption (FEC) in 2020, no significant changes in the energy profile are expected, even with the cap, although RES share increases from15% of total FEC in 2005 to 30-35%. In the long term (2050) it is clear that the increase in electricity is a major strategy to mitigate CC as there are endogenous energy resources used to generate RES-E, especially wind and hydro, as mentioned before. In 2050, the FEC in the F scenario is almost 70% higher than in the C leading to new technologies to meet the cap, such as H2 for transports. The share of RES in FEC in 2050 varies from 31-36% in scenarios without the GHG cap to 56-59% with the cap (Table 2). The RES share grows more due to the GHG cap in the transports (both in C and F) and industry (only in the -50F scenario) sectors.

Table 2. RES contribution in final energy consumption for the six scenarios

Sector/Scenario [PJ]	2005	2050					
		C	-50C	Cefre	F	-50F	Fefre
RES Electricity	32	159	188	203	221	300	252
RES Heath & cold	96	69	68	69	91	206	93
Residential	50	34	32	34	39	38	39
Commercial	0	11	8	10	14	13	13
Industry	45	25	27	25	39	155	41
RES in Transport	0	36	245	36	98	200	98
Final Renewable Energy (a)	128	263	501	307	410	707	442
Total Final Energy (b)	826	863	846	860	1225	1253	1224
% Renewables (a/b)	**15**	**31**	**59**	**36**	**33**	**56**	**36**

Other relevant uses of RES are solar for water and space heating in buildings, which in all scenarios, regardless of GHG cap and RES-E restrictions; achieve its maximum potential already in 2020. In 2050 with the GHG cap, solar panels are also cost-effective to generate heat for industry and the potential is also achieved. The role of biomass is reduced in buildings as electricity, solar thermal and heat pumps become more appealing. On the other hand, biomass will become more cost-effective in CHP to generate heat for industry. In transports the share of biofuels is expected to increase above 10% in 2020 in all scenarios and in 2050 up to 60-40% due to the GHG cap. Other impacts of the GHG cap in 2050 in the transport sector are to create room and need for electric vehicles and for H2 freight trucks.

4. Discussion

We found that RES technologies are highly cost–effective in the Portuguese energy system even without any CO2 cap (36-38% of PEC and 31-33% of FEC in 2050). If an ambitious CC mitigation cap is in place, the contribution of RES is even higher to 65-72% of PEC and 59-56% of FEC in 2050. If the layout of the power sector does not require centralised fossil plants, for example by ensuring security of supply via expanded transmission capacity, RES contribute with 41-44% of PEC and 36% of FEC in 2050. So, a cap on GHG emissions has a larger impact in RES contribution than a reconfiguration of the power system. Although RES play a fundamental role in CC mitigation in Portugal it should be noted that it is not possible to reduce external energy dependency below 77% in 2020 and below 50% in 2050. Further reductions are only possible with stronger efforts on energy efficiency, which were not in the

scope of this paper.

Regarding RES technologies, hydro and wind power can achieve the maximum technical and economic potential in Portugal in the medium run (2020) and contribute significantly to generated electricity. To some extent, this already occurs as in 2009 wind and hydro ensured 34% of total generated electricity. Until 2050 they can generate 60-80% of total electricity, respectively if a GHG cap is in place or if no fossil electricity backups are required. On the other hand, electricity generation technologies from solar are still in an early-phase and need extra incentives to become competitive before 2050. Nonetheless, policy support to solar technologies should be considered from a R&D perspective anticipating future technology costs reductions since Portugal already has know-how in this area and some national companies manufacture components. Electricity generation from waves and offshore wind technologies are competitive from 2035 onwards only if Portugal adopts an aggressive GHG cap or no centralised fossil backup is needed. In these conditions and considering the existing national R&D capacities and wind parts supply chain, these two technology groups should be considered by policy makers as a priority.

Besides RES electricity, solar (both for water and space heating) is highly competitive already in the medium term (2020) even without any GHG emission cap. Heat pumps are also extremely competitive but only if a cap is in place. On the other hand electric vehicles are only cost-effective in 2050 if a cap is in place and the technology evolves to supply long-distance mobility as existing cars do. Otherwise, biofuels are a cheaper alternative.

Finally, the results presented have the following main caveats: 1) learning curve for energy technologies with high uncertainty, especially for the least mature technologies; 2) high uncertainty of profile of electricity trade within the Iberian electricity market; 3) high uncertainty on the availability of endogenous and imported biomass and biofuels. Moreover, the TIMES_PT is a partial equilibrium model and thus does not model economic interactions outside the energy sector and does not consider in detail demand curves and non-rational aspects that condition investment in new technologies. All of these caveats reflect real life uncertainties which policy makers have to deal with especially when thinking of long-term policies. An approach to try to handle uncertainty is to perform sensitivity analysis which the authors did for the RES electricity technologies learning curve (solar, wind offshore and waves) and for available biofuels and biomass. For electricity trade this was no done due to lack of any indication of plausible scenarios and involved amount of work considering the scope of the paper, as mentioned in section 2. It was found that assumptions on the technology learning rate affect the share of the different RES-E technologies in the energy system but the total share of RES-E is not altered. Variations on the amounts and prices of available biomass significantly affect RES potential for CC mitigation in Portugal, as biomass and biofuels are preferable to RES-E in the industry and transport sectors, since they are more cost-effective. However, it is not in the scope of this paper to discuss and assess uncertainty in detail and thus it is not possible here to present and discuss in detail the performed sensitivity analysis, but only to draw attention to the limitations of the results, which serve to illustrate that in Portugal RES are very effective for CC mitigation goals.

5. Conclusions

This paper's objective is to assess the contribution of RES for CC mitigation in Portugal until 2050 looking into detail into which technologies are most cost-effective. We have found that the RES share in final energy consumption can increase from 15% in 2005 to 31-33% in 2050 in a baseline scenario without an emission cap. This illustrates that RES are cost-effective

regardless of the goal of CC mitigation, especially in the electricity generation sector (mostly hydropower and wind onshore technologies). To meet the GHG cap of-50% in 2050 this share can further increase to 56-59% of total final energy consumption. This represents a growth of more than 200% of 2005 values. Although the increase of energy efficiency is an alternative cost-effective strategy to CC mitigation, the GDP energy intensity in 2050 is only less 32-40% of 2005 values. This seems to suggest that RES can contribute more significantly to the emission targets than energy efficiency improvements.

Regarding GHG emission reduction, a49-74% emission reduction is achieved in 2050 for the -50% cap compared to the baseline. Electricity generation is the most relevant sector for abatement. This sector can be responsible for up to 98% of all abatement in 2050 if the constraint of a minimum of 30% total generated electricity is produced by centralized fossil plants is not present. In this situation all electricity will be renewable. In the scenarios where this minimum fossil electricity is required the electricity sector is not completely renewable and the transport sector is the most important sector for total GHG abatement (up to 57% of total GHG emission reduction in 2050 compared to baseline). In both sectors RES are the main reason for emission abatement, both hydropower and onshore wind technologies, followed to a lesser extent by solar PV and geothermal electricity generation technologies, and biofuels for individual cars and freight trucks.

References

[1] IEA. Energy Policies of IEA Countries – Portugal 2009 Review. OECD / International Energy Agency. Paris, France, 2010, pp. 131-146.

[2] J. Seixas, S. Simões, P. Fortes, L. Dias, J. Gouveia, B. Alves, B. Maurício, [New Energy Technologies: Road Map Portugal 2050, D3: Competitiveness Assessment of New Energy Technologies], Novas Tecnologias Energéticas: Road Map Portugal 2050, D3: Análise da Competitividade das Novas Tecnologias Energéticas, Portuguese Innovation Fund for Renewable Energy of the Ministry of Economy, 2010, pp. 1-88.

[3] NYT. Portugal Gives Itself a Clean-Energy Makeover, The New York Times, August 10th, 2010.pp. A1. Available at: [http://www.nytimes.com/2010/08/10/science/earth/10portugal.html?_r=2&ref=global-home]

[4] ETSAP – International Energy Agency Implementing Agreement for a Programme of Energy Technology Systems Analysis, Global Energy Systems and Common Analysis Final Report of Annex X (2005-2008), Ed. G. Goldstein, G. Tosato, ETSAP, 2008, pp. 21 - 77.

[5] S. Simões, J. Cleto, P. Fortes, J. Seixas, G. Huppes, Cost of energy and environmental policy in Portuguese CO_2 abatement - scenario analysis to 2020. Energy Policy, 2008, Vol. 36, Issue 9, pp. 3598 - 3611.

[6] M. Labriet, H. Cabal, Y. Lechon, G. Giannakidis, A. Kanudia, The implementation of the EU renewable directive in Spain. Strategies and challenges. Energy Policy, 2010, Vol. 38, Issue 5, pp. 2272 - 2281.

[7] S. Proost, E. Delhaye, W. Nijs, D. van Regemorter, Will a radical transport pricing reform jeopardize the ambitious EU climate change objectives? Energy Policy, 2009, Vol. 37, Issue 10, pp. 3863 - 3871.

[8] M. Blesl, A. Das, U. Fahl, U. Remme, Role of energy efficiency standards in reducing CO2 emissions in Germany: An assessment with TIMES. Energy Policy, 2007, Vol. 35,

Issue 2, pp. 772 - 785.

[9] IEA, Technology Roadmap – Solar Photovoltaic Energy, OECD/International Energy Agency. Paris, France, 2010, pp. 7 – 9.

[10] IEA, Technology Roadmap – Concentrating Solar Power, OECD/International Energy Agency. Paris, France, 2010, pp. 27 - 28.

[11] IEA, Energy Technology Perspectives, OECD/International Energy Agency. Paris, France, 2008, pp. 400.

[12] LNEG, 2010. Personnel communication from Eng. Ana Estanqueiro from LNEG Unit of Solar, Wind and Ocean Energy. June 16, 2010.

Diversified analysis of renewable energy contribution for energy supply in Asian regions

Genku Kayo[1,*], Takashi Ikegami[2], Tomoki Ehara[3], Kazuyo Oyamada[3], Shuichi Ashina[1], Junichi Fujino[1]

[1] *National Institute for Environmental Studies (NIES), Ibaraki, Japan*
[2] *Institute of Industrial Science (IIS), Tokyo, Japan*
[3] *Mizuho Information and Research Institute (MHIR), Tokyo, Japan*
** Corresponding author. Tel: +81-29-850-2019, Fax: +81-29-850-2422, E-mail:kayo.genku@nies.go.jp*

Abstract: Renewable energy is one of the key drivers for reducing CO_2 emissions in the future. In order to support effective policy-making relating to renewable energy, estimation of available potentials mixed with all energy resources including fossil fuels is needed. However, previous research has sometimes focused on only one particular approach. Therefore, a diversified analysis of potential renewable energy contributions to energy supply in Asian regions was carried out in this paper. In order to estimate physical potential, a grid cell approach using geographical information system (GIS) data was adopted. Once the physical and technical potential had been estimated, the economic potential was then calculated. Socio-economic potential was analyzed using energy outlook data collected and reviewed from various publications in order to assess trends in energy demand and supply. The results indicate that almost all Asian countries will continue to develop and that the demand for energy will grow. With the aspect from potential amount, renewable energy supply is effective even though fossil fuels will continue to dominate totally energy mixes for the foreseeable future. In renewable energy supply, potential of solar is dominated and bears on wide implication compared with that of wind and biomass. To ensure the best possible results, further research should be carried out on the optimal schedule for the multi-phased introduction of renewable energy in long-term policy.

Keywords: *Solar energy potential, Wind energy potential, Biomass energy potential, Asian region*

1. Introduction

Renewable energy is one of the key drivers for reducing CO_2 emissions in the future. The third annual report (TAR) compiled by the IPCC expresses the relative potential of several phases of renewable energy in terms of physical, technological, socio-economic, economic and market potentials. In order to support effective policy-making relating to renewable energy, estimation of available potentials mixed with all energy resources including fossil fuels is needed. However, previous researches have sometimes focused on only one particular resource, for instance, solar energy (Hofman et al., 2002), wind energy (Grubb and Meyer, 1993) and biomass energy (Berndes et al., 2003). In this paper, diversified analysis of renewable energy contributions was carried out considering energy mix with fossil fuels and trends of energy demand. Renewable energy potentials were estimated in ten Asian regions. These regions included Japan (JPN), China (CHN), India (IND), Indonesia (IDN), Korea (KOR), Thailand (THA), Malaysia (MYS), Viet Nam (VNM), the Philippines (PHL) and Singapore (SGP).

1.1. Renewable energies

In this paper, three renewable energy sources were selected for investigation: solar, wind and biomass energy. It is expected that technologies to make use of these energy sources will be introduced into Asian countries in order to create a decentralized energy generation and supply system. Solar energy is included in this paper only in terms of the electricity generation provided by photovoltaic (PV) cells.

1.2. Definition

According to TAR (IPCC, 2001a), renewable energy can be described in terms of the following "potentials". The physical potential of a renewable energy source is the amount of that resource theoretically available in the area in question, and which can be considered suitable for production. This includes any constraints imposed by land use considerations or local site characteristics such as elevation and slope. The technical potential of a renewable energy source is the part of physical potential remaining after all losses due to conversion from the extractable primary energy source to secondary energy carriers or other forms of energy (electricity, fuel etc.) are taken into account. The socio-economic potential of a renewable energy source is the actual capacity for renewable energy use, taking into consideration the distribution of energy mixes and the growth of primary energy demand. The economic potential of a renewable energy source is the technical potential, based on the estimated production cost of a secondary form of energy which is competitive with a specified, locally relevant alternative. A flexible way to represent the economic potential is, therefore, in the form of energy production potential, expressed as a function of the production cost.

2. Methodology

2.1. Estimation of physical and technological potential

2.1.1. Data collection

In order to estimate physical potential, a grid cell approach using geographical information system (GIS) data was adopted. The physical potentials were estimated on a global basis using previously collected data such as insolation and wind speed measurements, land cover, elevation and wilderness area data. After calculation of the optimal inclination angle for solar PV cells in each grid cell, the total amounts of generation were estimated per cell and aggregated on a country-by-country basis. Table 1 shows the GIS data list that was used in this estimation process. (All the data used has been published on websites and made available for simulation purposes [5, 6, 7, 8, 9, 10, 11]).

Table 1. Data sources

Category	Data source	Original data provider
Land cover	MODIS/Terra Land Cover Type Yearly L3 Global 1km, Land Cover Type 1 (IGBP), 2005	NASA Land Processes Distributed Active Archive Center
Elevation	The Global Land One-km Base Elevation (GLOBE) Data, 1999	National Geophysical Data Center
Bathymetry	GEBCO One Minute Grid Version 2.00, 2006	General Bathymetric Chart of the Oceans
Wilderness	World Wilderness Areas, 1993	UNEP/GRID
Insolation	Surface Meteorology and Solar Energy Release 6.0 Data Set; Monthly averaged insolation incident on a horizontal surface, 2008	NASA Langley Research Center, Atmospheric Science Data Center
Wind Speed	Surface Meteorology and Solar Energy Release 5.0 Data Set; Monthly averaged wind speed at 50m above the surface, 2005	

2.1.2. Solar energy potential

Monthly and hourly solar energy potential in 3-by-3 arc-minute grid cells was calculated from averaged insolation data, averaged wind speed data, land cover type data, and so on. Compared with the previous method used (Bert. J. M. de Vries, 2007), extra parameters were included in the form of solar elevation angle, solar azimuth angle, land surface slope and elevation angle. In addition, the optimum inclination angle of each solar PV cell was calculated per grid cell and this information was also taken into account. The inclusion of these factors allowed a more accurate estimation to be made of the solar energy potential. The available area was determined using a suitability fraction, as shown in Table 2. For technical reasons, the area studied was limited to less than 5000m elevation and less than 60% slope. Solar energy potential, *EPS* [kWh/yr], was calculated using Eq. (1).

$$EPS_g = \sum_{M,T} I_{g,M,T} \cdot A_g \cdot \frac{e}{100} \qquad (1)$$

where *I* is the insolation intensity at the optimum inclination angle of solar PV [kW/m^2], *A* is the PV cell area [m^2], and *e* is the PV module efficiency (=13%). The subscripts *g*, *M* and *T* stand for the grid cell, month and time, respectively.

2.1.3. Wind energy potential

The wind turbine was assumed to be 80m high with a capacity of 2MW and rotors 90m in diameter. The available area was determined using a suitability fraction, as shown in Table 2, and restricted to less than 2000m elevation and less than 60% slope. Since the reference wind measurements provided by the surface meteorology dataset (NASA, 2005) were for a height of 50m, averaged wind speed was adjusted to a height of 80m, equal to that of the wind turbine. When the wind energy potential, *EPW* [kWh/yr], was calculated the probability distribution of wind speed *v* [m/s], the wind power correction factor *k,* and the availability rate j [%] were also taken into account, as shown in Eq. (2).

$$EPW_g = \sum_{v,LC} P(v) \cdot R(v) \cdot 8760 \cdot j \cdot k_{LC} \cdot (1-l) \cdot Nw_{g \cdot LC} \qquad (2)$$

where l is the loss rate, *LC* is the land cover, *P(v)* [kW] is the output of the wind turbine when the wind speed is *v* [m/s], and *R(v)* refers to the appearance probability distribution of the wind speed *v* [m/s]. Table 2 shows the parameter values for each type of land cover. Seventeen land cover categories were consolidated into four land use patterns. The suitability fraction values were one of the effective factors used in this estimation method. Therefore, in future, adequate suitability fractions should be estimated and modified by comparison with other, more precise calculations.

Table 2. Parameter values for each type of land cover

Land cover	Suitability Fraction [%]		Power Correction Factor [%]
	Solar	Wind	
All Forest, Closed Shrublands, Woody Savannas, Permanent Wetlands, Snow and Ice, Water Bodies	0	0	90
Urban and Built-Up Areas	1	0	90
Croplands, Natural Vegetation Mosaic	0	30	90
Open Shrublands, Savannas, Grasslands, Barren or Sparsely Vegetated Areas	1	50	95

2.1.4. Biomass energy potential

In the biomass energy potential calculation, twelve different resources (provided by the FAO statistical report, FAOSTAT, FAO, 2001) were taken into account. These resources included industrial round wood residues, pulp used for paper, sawn wood, mill residues, paper scrap, timber scrap, crop residues, sugarcane residues, bagasse, dung, kitchen refuse, and human feces. Each resource was assigned a different residual rate - defined as the fraction of the total amount available in production and able to be used for production purposes. Statistical data were, therefore, prepared in terms of volume or weight. The residual volumes were then converted to calorific values for calculation purposes.

2.1.5. Renewable energy potential grades

Renewable energy potentials were calculated and classified into three grades. When physical potentials were calculated, each grid cell was classified in terms of its renewable resource advantage. Grade I had some specific advantage in terms of its use as a renewable energy source, while grade III had some specific disadvantage associated with its use, due to location or climatic conditions. In the case of solar energy, the grade was determined by the insolation intensity received by each solar PV module [kWh/m^2/yr]. In the case of wind energy, the grade was determined by the utility operation rate, *UC* [%], defined by the percentage of annual electricity [TWh/yr] generated by full load operation throughout the year. The classified grades are shown in Table3 and 4.

2.2. Socio-economic potential estimation

Many institutes have published reports presenting statistical data or perspectives concerning the future of the Asian region, and this information is essential in order to estimate the contribution of renewable energies. However, because the Asian region is growing so rapidly and so dramatically, it is difficult to accurately construct future scenarios. Some reports published by international institutes (IPCC, 2001; IEA, 2009; EUROPEAN COMMISION, 2006; ADB, 2009; Greenpeace, 2008; Shell, 2008; Energy Research Institute, 2009; OECD, 2008 and so on) present various possible energy outlooks for future scenarios. Consequently, in this study, data relating to energy outlook were collected and reviewed in order to estimate expected trends in energy demand, supply and energy share in each country. After collecting data on the relevant parameters, maximum and minimum values were selected and a range of growth rates were established.

2.3. Economic potential estimation

After the calculations for physical and technical potential were completed, the production cost in each grid cell, *g*, was determined for each energy generation system. The production costs of solar energy, *CS* [USD/kWh], and wind energy, *CW* [USD/kWh], were calculated using Eq. (3) and Eq. (4).

$$CS_g = \frac{r}{1-(1+r)^{-LS}} \cdot \frac{(1+OM)\cdot INVS \cdot A_g}{EPS_g} \quad (3)$$

$$CW_g = \frac{r}{1-(1+r)^{-LW}} \cdot \frac{(1+OM)\cdot INVW \cdot A_g}{EPW_g} \quad (4)$$

where *OM* is the operation and maintenance cost expressed as a fraction of the investment cost, *r* is the discount rate, and *LS* or *LW* is the durable period. *EPS* and *EPW* are the energy potentials calculated using Eq. (1) or Eq. (2). *INVS* and *INVW* represent the cost of the system. In the case of solar energy, *INVS* was set at 780 [USD/m^2], which assumes 6 [USD/Wp]

included per PV module and BOS. *A* represents the area of the PV cell [m^2]. On the other hand, in the case of wind power, *INVW* was set at 760 [USD/kW], and *A* represents the construction area in each grid cell.

3. Results

3.1. Physical and technical potentials

3.1.1. Potential grades

Table 3 and 4 show the calculated results for physical and technical potential, broken down by grade. Comparing the three renewable energies studied shows that the solar energy potential is the largest, especially in grade II. China, India and Indonesia have some potential in grade I, reflecting good insolation conditions. However, regions such as Japan, China, Indonesia, Korea and Malaysia have more potential in grade III, overall, than in grade II. Wind energy potential is not as large as that of solar energy. Only China possesses significant potential in grade I. However, in the case of biomass energy, both China and India possess large potentials because of their large population and large plantation area. This physical potential analysis confirms that some countries have suitable renewable energy resources.

Table 3. Physical and technical potential, by grade (Solar Energy and Wind Energy)

Country code	Solar Energy Potential [TWh/yr]				Wind Energy Potential [TWh/yr]			
	Grade I 2200-2600 [kWh/m^2/y]	Grade II 1800-2200 [kWh/m^2/y]	Grade III 0-1800 [kWh/m^2/y]	Total	Grade I 40-100 [%]	Grade II 30-40 [%]	Grade III 0-30 [%]	Total
JPN	0	465	39,692	40,157	0	38	26	64
CHN	434	32,845	45,610	78,889	337	1,925	3,318	5,580
IND	4,255	46,136	169	50,560	0	177	721	898
IDN	5	1,625	3,699	5,329	0	0	45	45
KOR	0	3,759	6,604	10,363	0	0	17	17
THA	0	10,322	881	11,203	0	0	38	38
MYS	0	1,243	2,361	3,604	0	0	5	5
VNM	0	1,278	535	1,813	0	3	60	63
PHL	0	1,304	9	1,313	0	0	42	42
SGP	0	1,180	776	1,956	0	4	88	92

Table 4. Physical and technical potential, by grade (Biomass Energy)

Country code	Biomass Energy Potential [TWh/yr]			
	Grade I	Grade II	Grade III	Total
JPN	109	15	15	139
CHN	735	51	51	837
IND	577	8	8	593
IDN	121	7	7	135
KOR	25	3	3	31
THA	79	1	1	80
MYS	47	1	1	48
VNM	19	5	5	29
PHL	39	1	1	40
SGP	1	0	0	1

3.2. Socio-economic potentials

3.2.1. Review of expected energy demand in Asia

Fig. 1 shows expected total primary energy demand throughout Asia, as reported by IPCC (SRES2001, IPCC, 2001b). The curved lines indicate the forecasts simulated by several different models. The predicted maximum value in 2050 is approximately 3.84 times larger than the minimum value in 2050. The calculated results for physical and technical potentials are represented by the horizontal dashed lines in Fig. 1. The solar energy potentials, alone, can be seen to be large enough to meet the primary energy demand in all future scenarios. Wind energy potentials can also be seen to constitute an effective energy source. On the other hand, the biomass energy calculation shows that it is not large enough to constitute a major energy supply resource.

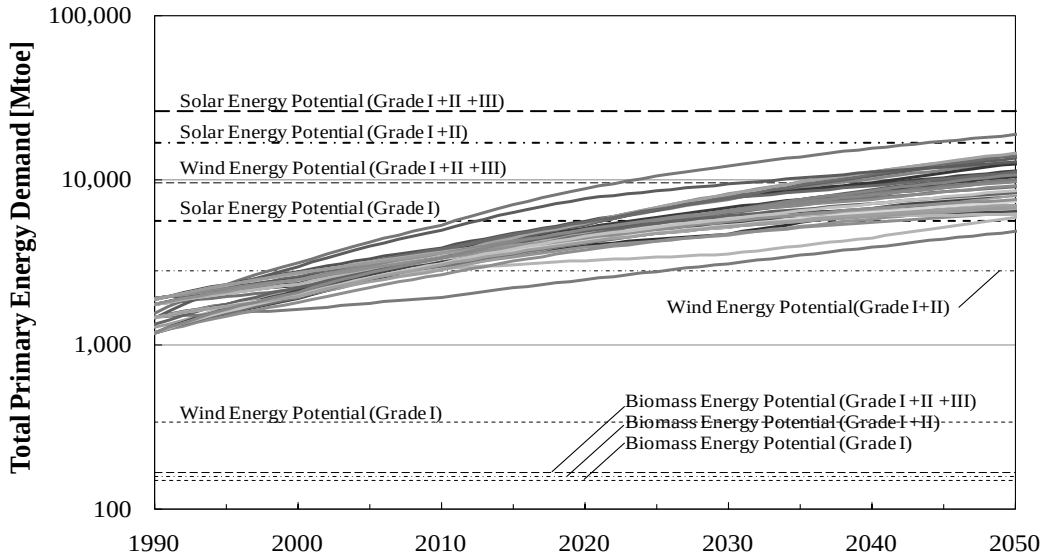

Fig. 1. Total primary energy forecast in published reports, and renewable energy potential

3.2.2. Renewable energy contributions in each region

Fig. 2 shows the outlook for primary energy supplies, fossil fuel supplies and renewable energies in three Asian regions: Japan, China and India. Each graph includes the maximum and minimum trends derived from the various reports collected and reviewed as part of this study. It can be seen that the renewable energy share is extremely small, overall. Fig. 2 also shows the calculation results obtained for physical and technical potentials (bold dashed lines). In the case of Japan and India, the solar energy potential (alone) exceeds the maximum predicted primary energy demand. On the other hand, China's energy growth is more rapid and larger than that of other Asian countries. Therefore, the renewable energy potential of China is not large enough to meet all of China's expected primary energy demand in the predicted maximum growth scenario. Renewable energy supply is effective even though fossil fuels will continue to dominate totally energy mixes for the foreseeable future.

3.3. Economic potentials

Fig. 3 shows the potential cost curve for three Asian regions: Japan, China and India. The horizontal axis (logarithmic scale) indicates the market potential. In the case of Japan, grade III solar energy shows most potential but has a high introduction cost. In contrast, the introduction cost of biomass energy is very low but the expected potential is small. In order to increase its share of renewable energy, Japan should, therefore, focus mainly on the installation of solar energy generation systems. In the case of China, the most potential is for grade II solar energy. The cost of grade III wind energy is more than 0.9USD/kWh higher

than other renewable resources. In India, grade I solar energy shows the most potential. Grade III wind energy also has a high cost, even in China and India. Consequently, solar energy should receive first priority for introduction and wind energy should be second. The potential for biomass energy is not as large, but its cost intensity is lower than either wind or solar power. Therefore, the immediate introduction of biomass energy systems could be an effective strategy in some Asian regions.

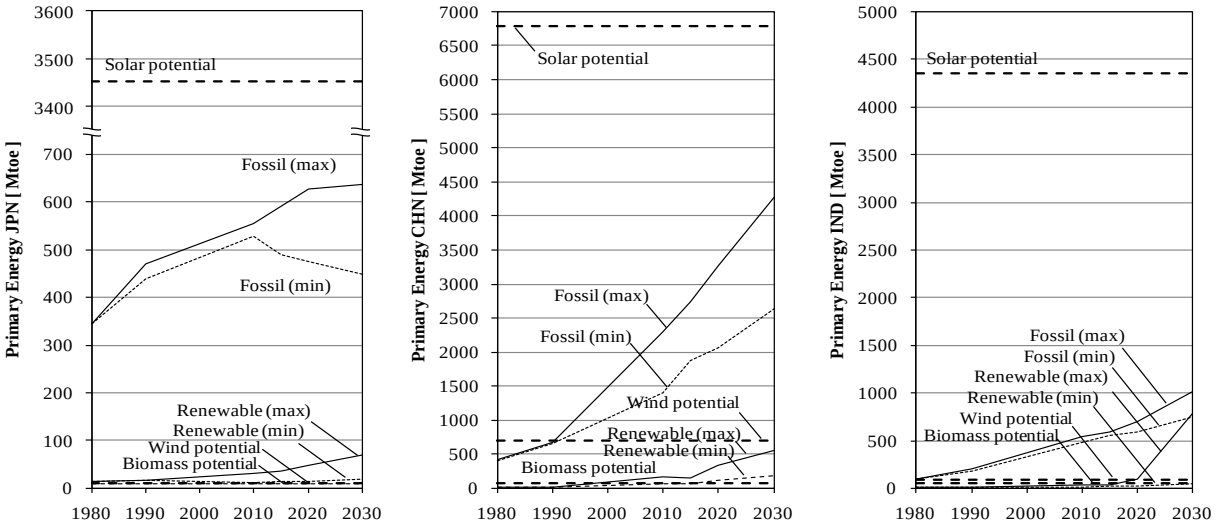

Fig. 2. Primary energy trends and renewable energy potentials in Japan (left), China (center), and India (right)

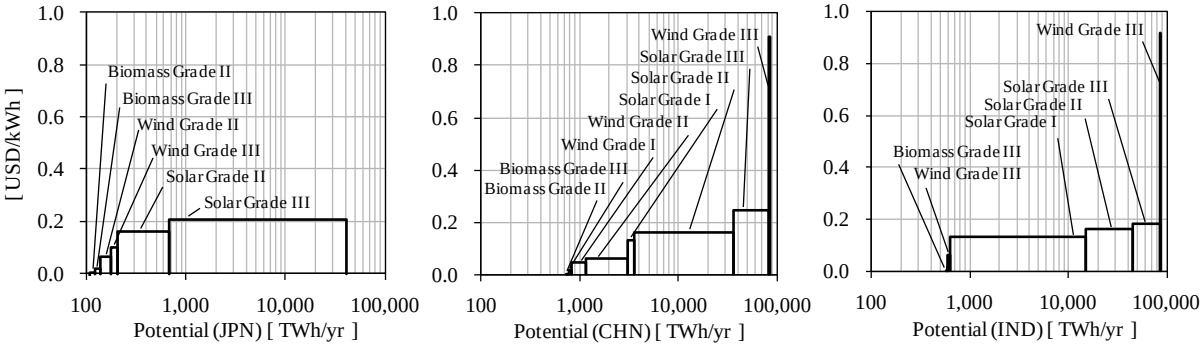

Fig. 3. Potential cost curves in Japan (left), China (center), and India (right)

4. Conclusions

Diversified analysis of potential renewable energy contributions to energy supply in Asian regions was carried out. As a result, estimates of renewable energy potential were refined, the socio-economic mechanisms associated with the introduction of renewable energy were calculated, and the relevant characteristics of each Asian country were analyzed. The results suggest that almost all Asian countries will continue to develop and that the demand for energy will grow drastically and rapidly. The results indicate that almost all Asian countries will continue to develop and that the demand for energy will grow. With the aspect from potential amount, renewable energy supply is effective even though fossil fuels will continue to dominate totally energy mixes fora the foreseeable future. In renewable energy supply, potential of solar is dominated and bears on wide implication compared with that of wind and biomass. To ensure the best possible results, further research should be carried out on the optimal schedule for the multi-phased introduction of renewable energy in long-term policy.

References

[1] IPCC 2001a, Climate Change 2001 – IPCC Third Assessment Report, Working Group III: Mitigation, 2001

[2] Hofman, Y., de Jager, D., Molenbroek, E., Schilig, F., Voogt, M., 2002. The Potential of Solar Electricity to Reduce CO2 Emissions. Ecofys, Utrecht.

[3] Grubb, M.J., Meyer, N.I., 1993. Wind energy: resources, systems, and regional strategies. In: Johansson, T.B., Kelly, H., Reddy, A.K.N., Williams, R.H. (Eds.), Renewable Energy: Sources for Fuels and Electricity. Island Press, Washington, DC.

[4] Berndes, G., Hoogwijk, M., van den Broek, R., 2003. The contribution of biomass in the future global energy supply: a review of 17 studies. Biomass and Bioenergy 25 (1), 1–27.

[5] MODIS/Terra Land Cover Type Yearly L3 Global 1km SIN Grid, 2005: Land Processes Distributed Active Archive Center (LPDAAC), U.S. Geological Survey (USGS).

[6] GLOBE: The Global Land One-km Base Elevation 30-sec. DEM, National Geophysical Data Center (NGDC), NESDIS, NOAA, U.S. Department of Commerce.

[7] Hastings, D. A. and Dunbar, P. K., 1999: Global Land One-km Base Elevation (GLOBE) Digital Elevation Model Documentation, Boulder, Colorado, NOAA National Geophysical Data Center, Publication KGRD 34.

[8] GEBCO One Minute Grid - Version 1.02, 2006: General Bathymetric Chart of Oceans.

[9] World Wilderness Areas, 1993: the Sierra Club and World Bank, as integrated by UNEP/GRID.

[10] Insolation Incident On A Horizontal Surface (22-year Monthly & Annual Average for July 1983 - June 2005), 2008: Surface meteorology and Solar Energy (SSE) Release 6.0 Data Set, Atmospheric Science Data Center, NASA Langley Research Center (LaRC).

[11] Wind Speed At 50m Above The Surface Of The Earth (10-year Monthly & Annual Average for July 1983 - June 1993), 2005: Surface meteorology and Solar Energy (SSE) Release 5 Data Set, Atmospheric Science Data Center, NASA Langley Research Center.

[12] Bert J.M. de Vries, Detlef P. van Vuuren, and Monique M. Hoogwijk, Renewable energy sources: Their global potential for the first-half of the 21st century at a global level: An integrated approach, Energy Policy, 35, 2007, 2590-2610

[13] FAO, FAOSTAT 2001 CD-ROM, Rome, 2001

[14] IPCC 2001b, Special Report on Emissions Scenarios, 2001

[15] IEA, World Energy Outlook, 2008

[16] EUROPEAN COMMISION, World Energy Technology Outlook 2050, 2006

[17] ADB, Energy Outlook for Asia and the Pacific, 2009

[18] Greenpeace, Energy Revolution Sustainable Energy Global Energy Outlook, 2008

[19] Shell, Shell Energy Scenarios to 2050, 2008

[20] OECD, OECD Environmental Outlook to 2030, 2008

Scenario analysis of the potential for CO_2 emission reduction in the Iranian cement industry

Farideh Atabi [1,*], Mohammad Sadegh Ahadi [2], Kiandokht Bahramian [3]

[1*] *Assistant Prof., Graduate School of Energy and the Environment, Science & Research Branch, Islamic Azad University, Tehran, Iran, P.O.Box: 14155/4933*
[2] *National Climate Change Office, Department of Environment, Tehran, Iran*
[3] *Environmental Engineer, Graduate School of Energy and the Environment, Science & Research Branch, Islamic Azad University, Tehran, Iran*
** Corresponding author. Tel: +989121341702, E-mail: far-atabi@jamejam.net*

Abstract: This article investigates the impact of various policies on the reduction of CO2 emissions from Iranian cement industry using a long range energy alternative planning (LEAP) model. A Business-as-Usual (BAU) scenario for the existing Iranian cement industry was applied. Moreover, the current and future demands for the cement industry were defined for 2005-2020. The current and future productivity of the cement industry was predicted in the BAU scenario. Then, three alternative scenarios were considered: replacement of heavy oil with natural gas, implementation of energy efficiency policies and integrated emission reduction, which includes all of the options over a 15-year period. The results indicated that in 2020, CO2 equivalent emissions would reach 61 million tons in the baseline scenario and 53 million tons in the integrated emission reduction scenario. If fuel switching were employed, the emissions would reach 58 million tons (4.9 % reduction) and in the energy efficiency scenario, the emissions would reach 55 million tons (9.8% reduction) in 2020. Therefore, the integrated scenario reduces the total CO2 equivalent emissions by 8 million tons (13% emission reduction).

Keywords: *CO_2 emission, cement industry, scenario analysis, energy model*

1. Introduction

Even though many countries have started to develop climate policies, scenario studies indicate that greenhouse gas emissions are likely to increase in the future in most regions around the world [1]. After the energy crisis of the 1970s, many researchers developed models to generate accurate predictions. Various models for prediction and the development of policies for mitigation can be divided into two groups: those used for mitigation in the energy sector, and those used to survey mitigation methods in the agriculture, forest and land use sectors [2]. One of the most important energy carriers in the industrial sector is natural gas, which plays a significant role in the reduction in the emission of environmental pollutants [3]. A study in Iran, evaluated the impacts of price reform and energy efficiency programs on the consumption of energy carriers and on GHG mitigation in the Iranian residential buildings sector using the LEAP model [4]. Research on substituting biomass with other energy carriers in Vietnam using the LEAP model, has shown that this fuel substitution leads to a 10.83 million-ton reduction in GHG emissions [5].

Another analysis of the environmental and economic impact of landfill gases (LFG) electricity generation in Korea using the LEAP model showed that LFG electricity generation would be an effective solution for CO_2 displacement over the medium term with additional energy profits and will reduce the global warming potential by a maximum of 75% when compared to spontaneous emissions of CH_4 [6]. Another study in Korea evaluated the environmental and economic aspects of chemical CO_2 absorption in power plants using this model; That study demonstrated that by applying various policies, the rate of CO_2 emissions will decrease by approximately 15% by 2014 [7]. Another study was also conducted to show the potential reduction in CO_2 emissions from oil refineries in Korea. Production analysis using the energy planning model showed that a 48% reduction in CO_2 emissions is feasible [8]. In this study, the energy demand of the Iranian cement industry is analysed with an

energy planning LEAP model. The effects of various policies on the baseline scenario and GHG mitigation scenario are also analysed and surveyed in the cement industry.

2. Methodology

Greenhouse gas emissions in the Iranian cement industry was surveyed in the format of a BAU scenario using the LEAP energy planning model. The results of employing different policies of energy efficiency and fuel switching on GHG mitigation in the format of mitigation scenario were then observed. Finally, the effectiveness of each policy applied in the cement industry over a 15-year period, from 2005 to 2020, was surveyed. In each scenario, the level of technological activity and energy intensity were specified, and in the activity data section, data relevant to consumption in the cement industry and the number of factories that use a specific resource, were defined in each scenario. Additionally, data describing the energy intensity of each type of fuel in each Factory were determined [9].

2.1. LEAP model

LEAP is an energy planning model that consists of an end-use structural model. Based on procedural analysis of the supply and demand network, the considered model describes technological energy carrier utilisation based on energy demand on one hand, and technological changes and therefore structural changes and efficiency of energy conversion systems as well as the rate and type of available primary energy resources on the other hand. This model consists of a hierarchical structure in which energy flows from the last point of usage (equipment and technology) toward higher levels. In fact, total energy demand is computed from each subcategory and category in a tree structure. In this model, the rate of total energy demand is computed according to Eq. 1.

$$\sum E_t = T_i \times I_i \tag{1}$$

where, E_t is the total energy demand (J), T_i is the data (i) activity level (ton), and I_i is energy intensity ($^{j}\!/\!_{ton}$) [6].

2.2. BAU scenario

In the (BAU) scenario, it is assumed that the current status of the Iranian cement industry will be maintained in the future, and that greenhouse gas emission in Iran's cement industry will be predicted by the main variables of BAU, such as the growth rate of cement production from 2005 to 2020, the type and rate of fuel consumption, the rate of technological changes and energy intensity.

In this scenario, 2005 was selected as the base year and all relevant information was gathered from this year [10]. Then, a BAU scenario was developed according to current plans as well as future policies, changes in cement production capacity, energy intensity, the fuel contribution that supplies the energy demand and other factors in the cement industry from 2005 to 2020. The GHG emission rate was assessed, and analysed. It was predicted that in the BAU scenario, the natural gas share of the total energy carriers, will increase from 63.11% in 2005 to 80% in the 2020 in the cement industry [11]. The amount of energy intensity of the whole cement industry in the country can be calculated using Eq. 2:

$$I_t = \sum c_i I_i \quad (2)$$

where, I_t is total energy intensity (j), I_i is energy intensity of respected technology (J/ton), and c_i is the technology (i) share in the total cement production in the country (%).

Energy demand as shown in Eq. 3 is calculated by multiplying cement production (activity data) by energy intensity:

$$E = \sum_{i=1}^{n} A_i \times I_i \quad (3)$$

where, E is energy demand (million GJ), A_i is cement production (million tons), and I_i is energy consumption for each activity (million GJ/ton).

The LEAP model is used to calculate the equivalent emission of CO_2 in the cement industry in three forms: (1) emission from direct consumption of energy carriers in cement industry, (2) emission from consumption of energy carriers in oil and gas refineries and power plants in order to supply the cement industry with both fuel and electricity (indirect), and (3) emissions from consumption of energy carriers in the industry, refineries and power plants to supply the energy demand to the cement industry (total emission).

2.3. Mitigation scenario

In the mitigation scenario, different policies to mitigate the energy demand are considered as input data for the LEAP model. Then, the model is compared with the BAU scenario by predicting the demands of energy carriers and the calculated mitigation in emissions. The policies surveyed here are fuel switching and more energy efficient technologies. In this scenario, it is assumed that all cement production units older than 20 years are replaced with new and efficient technologies and that energy efficient improvement plans are implemented on units that are 10 to 20 years old [12]. It is also assumed that the natural gas and biomass share in the mitigation scenario is 5% more than that in the BAU scenario in 2020. Energy carrier demand will increase 139% in this period.

3. Results and discussion

In Table 1, the average energy intensity for Iran's cement industry was calculated and presented separately based on the type of process. In the calculations, the average energy intensity weight was compared to the capacity of the entire cement industry in the country.

Table1. Energy intensity rate in the various cement industry technologies in Iran in 2005 [13]

Technology	Proportion of Total Production (percent)	Production (ton/yr)	Capacity (ton/day)	Fuel Consumption Intensity (kcal/kg.clinker)	Electricity Consumption Intensity (kWh/ton)
Dry high heater	5.14	1,600,500	4,850	1125	111
Dry pre heater	40.51	12,606,000	38,200	950	108
Dry pre heater & precalcinors	51.70	16,087,500	48,750	890	114
Mid dry pre calciners	0.64	198,000	600	1020	110
Wet process	2.01	627,000	1,900	2000	150
Total / Weighted average	100	31,119,000	94,300	949.6	112.1

To evaluate the changes in energy intensity, in addition to recognizing current infrastructures in each of the subsectors of the industry, the theoretical potential for increasing the efficiency of equipment and energy intensity of industrial products in developed countries is also needed. In the BAU scenario, the annual increase in energy demand reaches 11.51% and the demand for all energy carriers shows an annual increase of 10.7%.

It is predicted that the share of natural gas in the BAU scenario among all energy carriers in this industry will increase from 63.11% in 2005 to 80% in 2020. Meanwhile, the mitigation scenario shows a 5% increase in 2020 compared to the BAU scenario in the same year. Results from LEAP in Fig. 1 show that in the BAU scenario, emissions of CH_4, CO_2 and NO_x have also increased during this period; CO_2 has the highest increase.

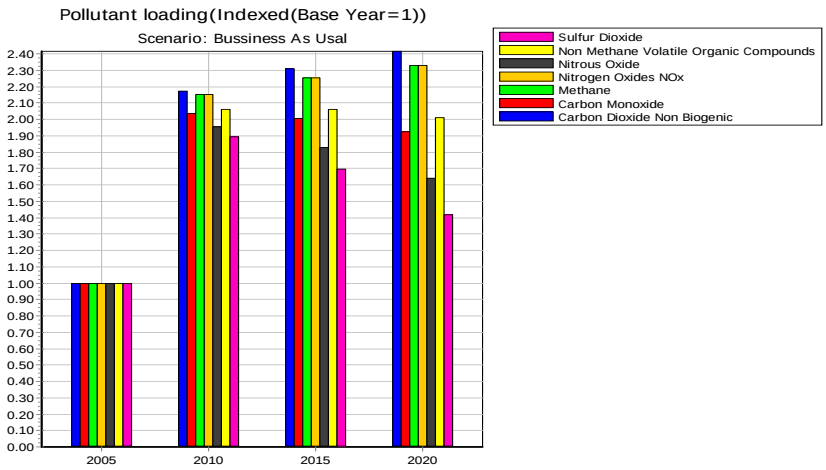

Fig.1. Prediction of the trends of the emission of pollutants and GHG (dimensionless) in the Iranian cement industry in the baseline scenario.

Meanwhile, the thermal energy demand in the mitigation scenario in 2020 shows a 33% reduction in the thermal energy demand compared to that of the BAU scenario. The emissions of all pollutants increase until 2010 and then decline because of the replacement of units that are older than 20 years with new and more efficient technologies. It should be noted that the emission of SO_2 and NO_x in 2020 are 40% and 10% less than the emission of these pollutants in the first year (2005) respectively, whereas, the emission of NO_x and SO_2 in the baseline scenario has increased by 40% and 65% , respectively. Therefore, after applying the

emission reduction policies (mitigation scenario), the emissions of SO_2 and NO_x show 80% and 75% reduction in 2020 respectively, compare to those of the BAU scenario.Table 2. shows the energy carriers in the BAU scenario and the mitigation scenarios.

Table 2. Comparison among the different energy carriers, that are needed in the Iranian cement industry in the year 2020 in the BAU and mitigation scenarios

Fuel	Share of the total demand (%) 2005	Share of the total demand (%) 2020	
		Mitigation scenario	BAU Scenario
Fuel oil	36.1	9.21	19.3
Natural gas	63.11	85	80
Diesel fuel	0.79	0.79	0.79
Biomass	0	5	0

As shown in Fig. 2, by implementing the policy of changing the process on one hand and the energy efficiency on the other hand, the amount of required energy carriers decreased from 340 million GJ in 2020 to 310 million GJ, and consequently, energy demand decreased by 11.5 percent.

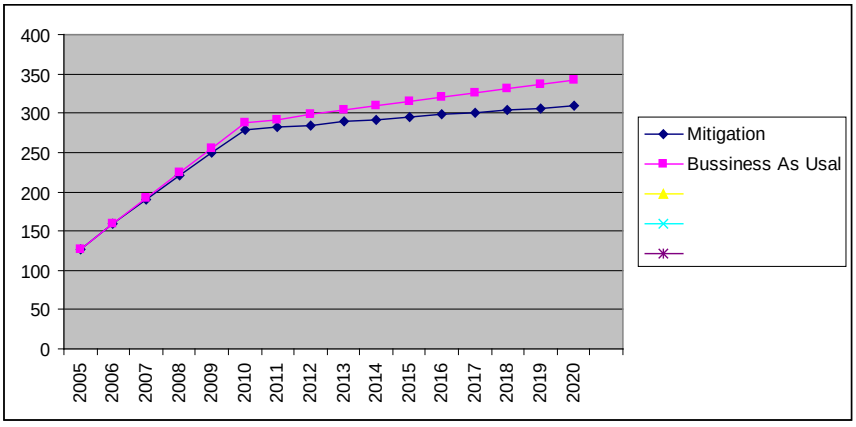

Fig. 2. Comparison of energy carriers demand in the baseline and mitigation scenarios in the Iranian cement industry (million GJ)

Results show that employing different policies regarding CO_2 emissions reduces these emissions from 16 million tons to 11 million tons in 2020. Fig. 3 shows a comparison of the CO_2 emissions in the BAU and mitigation scenarios in the Iranian cement industry.

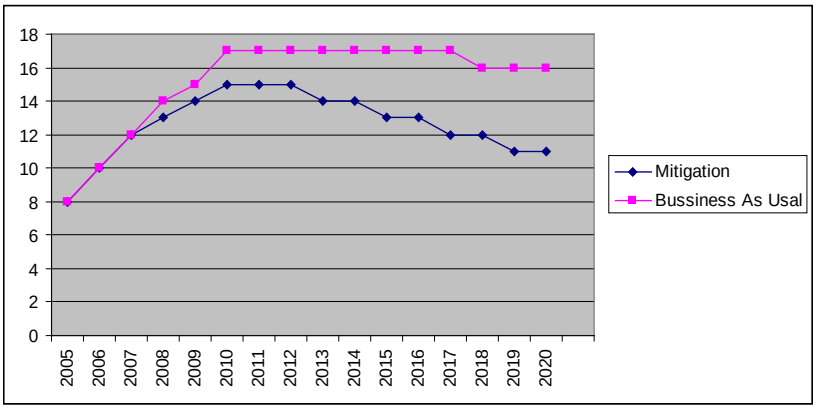

Fig.3. A comparison of CO2 emission in the BAU and mitigation scenarios in the Iranian cement industry (million tons).

As shown in Fig. 4, GHG emission (CO_2 equivalent) is reduced as a result of the efficiency policy and the fuel switching policy by 9.8% and 4.9%, respectively. However, emission reduction will be up to 13% by employing both policies**.**

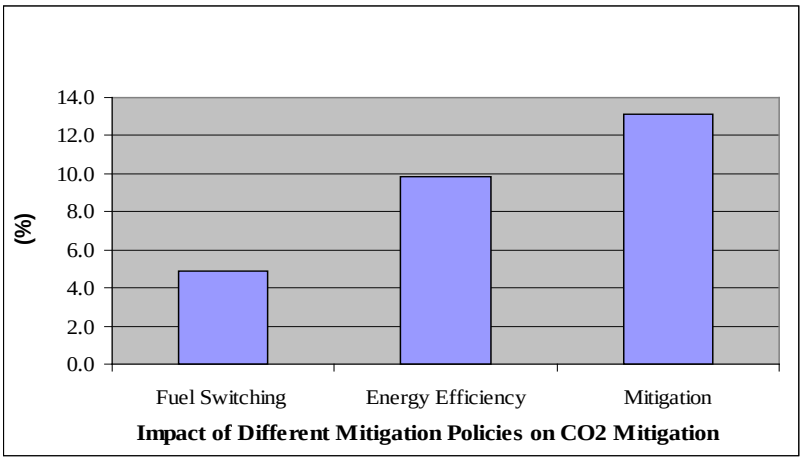

Fig. 4. Comparison of exerting different policies for GHGs (CO2 equivalent) reduction and integration of different scenarios in the Iranian cement industry

4. Conclusion

In this study, the process of technological changes that have improved the energy intensity in the Iranian cement industry specifically are used to predict the energy intensity in the BAU scenario and the mitigation scenario using LEAP software. To predict the greenhouse gas emissions rate in the different scenarios, the effects of the application of these actions on energy demand and fuel make-up are specified. A comparison of the effectiveness of different policies shows that the energy efficiency is more important than fuel switching in reducing CO_2 emissions.

Acknowledgement

The authors are especially grateful to Iran Fuel Conservation Company (IFCO) for its financial support.

References

[1] IPCC, 2000, Special Report on Emission Scenarios, A special report of working group III of Intergovernmental Panel on Climate Change, Cambridge University Press, Cambridge, UK

[2] IPCC, 1997, Technical Paper 2 , Second assessment report

[3] Ministry of energy, 2007, Energy balance, Energy Department, I.R.I

[4] Ahadi, M.S. et al., 2005, Policy making of energy resources in industry, National Climate Change Office, Department of Environment, Tehran, Iran

[5] Kumar Amit, et al., 2003, Greenhouse gas mitigation potential of biomass energy technologies in Vietnam using the long range energy alternative planning system model, Energy Policy Journal, No. 28, pp. 627-654

[6] Shin, H.C., Park J.W., Kim, H.S., Shin, E.S., Environmental and economic assessment of landfill in Korea using LEAP model, Energy Policy Journal, No. 33, 2005 , pp.1261-1270

[7] Song, HO-JUN, et al., 2007, Environmental and economic assessment of the chemical absorption, Energy Policy Journal, No. 35, pp. 5109-5116

[8] Sangwon Park, et al., 2007, Assessment of CO_2 and reduction potential in Korea petroleum using energy models, Energy Journal, No. 35,pp. 2419-2420

[9] Ministry of Industry, 2006, Cement production in 2020, Energy department, I.R.I

[10] Energy Efficiency Office, 2005, Report on energy efficiency in the cement industry, Ministry of Energy, I.R.I

[11] Institute for International Studies, 2004, Prediction of energy demand for in various energy sectors, Ministry of Oil, I.R.I

[12] Hoseini, S.A., 2009, Assessment of energy efficiency potential in cement industry, Cement Research Center, I.R.I

[13] Ministry of Energy, 2005, Report on energy intensity in the cement industry, Energy Department, I.R.I

Volume 3

Energy End-Use Efficiency Issues

Review on graphite foam as thermal material for heat exchangers

Wamei Lin, Jinliang Yuan, Bengt Sundén*

Department of Energy Sciences, Lund University, P.O.Box 118, SE-22100, Lund, Sweden
** Corresponding author. Tel: +46 46 2228605, Fax: +46 46 2224717, E-mail: bengt.sunden@energy.lth.se*

Abstract: Due to the increased power consumptions in equipment, the demand of effective cooling methods becomes crucial. Because of the small scale spherical pores, graphite foam has huge specific surface area. Furthermore, the thermal conductivity of graphite foam is four times that of copper. The density of graphite foam is only 20 % of that of aluminum. Thus, the graphite foam is considered as a novel highly - conductive porous material for high power equipment cooling applications. However, in the commercial market, aluminum and copper are still the preferred materials for thermal management nowadays. In order to promote the graphite foam as a thermal material for heat exchangers, an overall understanding of the graphite foam is needed. This paper describes the structure of the graphite foam. Based on the special structure, the thermal properties and the flowing characteristics of graphite foam are outlined and discussed. Furthermore, the application of graphite foam as a thermal material for heat exchangers is highlighted for electronic packages and vehicle cooling systems. The physical problems and other aspects, which might block the development of graphite foam heat exchangers, are pointed out. Finally, several useful conclusions and suggestions are given to promote the development of graphite foam heat exchangers.

Keywords: *Graphite foam, heat exchanger, thermal management*

1. Introduction

Nowadays the power of equipment is increased. For instance, the power of computer chips is increased, and the power of vehicle engines is also increased. This increased power leads to a requirement of an effective cooling method. Currently the thermal management has focused on aluminum and copper heat exchangers, because of high thermal conductivity (180 W/(m.K) for aluminum 6061 and 400 W/(m.K) for copper). However, when the density is considered, the specific thermal conductivity of aluminum or copper (thermal conductivity divided by specific gravity) is only 54 and 45 W/(m.K), respectively. Thus, when the weight is a significant factor, it is necessary to introduce a thermal material with low density, high thermal conductivity and large specific surface area.

An efficient thermal management method is the utilization of microcellular foam materials such as metal or graphite foams, based on the enhancement of heat transfer by huge fluid-solid contact surface area and the fluid mixing. An example of graphite foam application was developed at Oak Ridge National Laboratory (ORNL) in 1997. Klett et al. [1] found that the thermal conductivity of the solid component of graphite was as high as 1700 W/(m.K), which was around four times that of copper. The effective thermal conductivity of graphite foam was more than 150 W/(m.K), which was higher than the value of aluminum foam (2 - 26 W/(m.K)). On the other hand, the density of graphite foam was 0.2 - 0.6 g/cm^3, which was only 1/5 of that of aluminum. The specific surface area was between 5000 and 50000 m^2/m^3.

Because of the high thermal conductivity, low density and large specific surface area, the graphite foam is recognized as an appropriate material for the thermal management. It is primarily focused on the electronic power heat sinks. A large number of studies have been carried out to analyze graphite foam heat exchangers. However, in the commercial market of heat exchangers, aluminum and copper are still the preferred thermal material. Thus, there are several problems blocking the development of graphite foam heat exchangers. Otherwise the graphite foam heat exchangers would be easily found in the market.

In order to promote the development of graphite foam as a thermal material for heat exchangers, this paper will present an overall view or conception about graphite foam heat exchangers. Firstly, the structure of graphite foam is introduced in Section 2. Based on the structure of graphite foam, the thermal properties and flow characteristics of graphite foam are explained in Section 2 as well. After that, the application of graphite foam heat exchangers is outlined in Section 3. In Section 4, potential problems blocking the development of graphite foam heat exchangers are pointed out. Based on the review and analysis, several useful conclusions and suggestions are highlighted in Section 5.

2. Structures and properties of graphite foam

2.1. Structures

Carbon foams were first developed in the late 1960s as reticulated vitreous (glassy) foam [2]. The initial carbon foams were made by pyrolysis of a thermosetting polymer foam to obtain a carbonaceous skeleton or reticulated vitreous carbon (RVC) foam. A blowing technique or pressure release is utilized to produce foam of the pitch precursor. Then the pitch foam is stabilized by heating in air or oxygen for many hours to cross-link the structure, and 'set' the pitch. In this case, the foam does not melt during the further heat treatment. However, stabilization can be a very time consuming and expensive process depending on the pore size. So ORNL [3] developed a new, little time consuming process to fabricate pitch - based graphitic foams without the traditional blowing and stabilization steps. This new foam is believed to be less expensive and easier to fabricate than the traditional foams.

Klett et al. [1] gave an overall view of the structure of the new graphite foam. The average pore diameter is from 275 to 350 μm in the ARA24 - derived foams. The scanning electron micrographs of fracture surfaces, which reveals the pore structure of the ARA24 - derived foams heat - treated at 1000 ℃, are shown in Fig. 1. Inside the foam, there are many spherical pores with small openings. These pores are three - dimensionally interconnected.

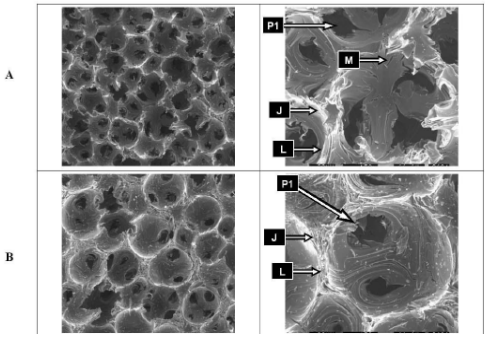

Fig. 1. Photomicrographs of the foams produced from Mitsubishi ARA 24 pitch at different densities A < B (P1: opening pore; M: microcrack; J: junction; L: ligament)[1].

2.2. Thermal properties of graphite foam

Because of the special structure of graphite foam, there are several prominent thermal properties in the graphite foam. The graphite foam made by the ORNL process exhibits high effective thermal conductivity (up to 182 W/(m.K)) and low density (0.2 -0.6 g/cm^3). The data in Table 1 show that the thermal conductivity in the z – plane is much larger than the one in the x – y plane. It implies that the high thermal conductivity of the graphite foam only exists in a certain direction. This is a disadvantage of the graphite foam. Klett et al. [4] found out that the heat inside the graphite lattice was transferred down the graphite lattice fast, because of the very stiff nature of the covalent bonds (as shown in Fig. 2). Moreover, the position and

vibration of atoms in the neighboring planes may impede the vibration of atoms in the plane of interest. The crystal perfection controls the thermal performance. In order to achieve high thermal conductivity in the graphite crystal, the structure must be comprised of aligned, straight grapheme planes, and so on.

Table 1. Properties of various graphite foams made by the ORNL method compared to Poco Foam[4].

	Graphitiza -tion rate (℃/min)	Average bulk density (g/cm^3)	z -Plane thermal conductivity k_z (W/(m.K))	x-y Plane thermal conductivity k_{xy} (W/(m.K))
ORNL graphite foam (A)	10	0.45	125	41
ORNL graphite foam (B)	1	0.59	181	60
PocoFoam™	-	0.61	182	65

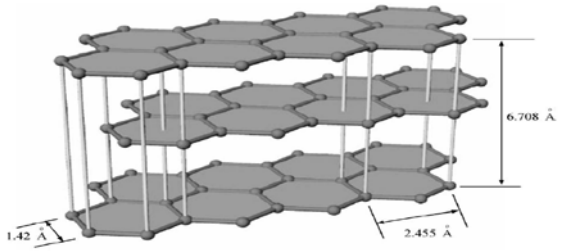

Fig. 2. Planar structure of hexagonal graphite [4].

On the other hand, Yu et al. [5] presented a model which was based on sphere - centered and interconnected unit cubes. The effective thermal conductivity was proved to be a function of the porosity of the graphite foam. Tee et al. [6] used a tapered, anisotropic strut model to predict the overall thermal conductivity of the porous graphite foam. When the size of the foam pores was increased, the convective heat transfer coefficient of the foam was reduced. By using graphite foams as the heat sinks, the enhancement of the convective heat transfer was not only because of its open and inter-connected pores, but also due to its high thermal conductivity and the extremely large surface areas. Furthermore, Straatman et al. [7] validated that the optimal thickness of graphite foam was 3 mm based on the thermal performance. Meanwhile the heat transfer increase was 28 % at low Reynolds numbers (150000). However, at high Reynolds number, the increase of the heat transfer was only 10 %.

2.3. Pressure drop of graphite foam

Graphite foam has a very high thermal conductivity, but it also has very high pressure drop, due to the large hydrodynamic loss associated with the open pores in the graphite foam [8]. Leong et al. [9] investigated pressure drop of four different configurations of graphite foams (as shown in Fig. 3). The pressure drops of these four configurations of graphite heat sinks are shown in Fig. 4. For the same inlet flow velocity, the block and baffle foams present the highest and the lowest pressure drop, respectively. On the other hand, Lin et al. [10] approved that the pressure drop through the corrugated passages could be reduced significantly while maintaining a high heat transfer coefficient. As shown in Fig. 5, for forced convection, the air is forced to go through a thin porous wall of graphite foam. Due to the short flow length inside the graphite foam, the pressure drop could be reduced greatly.

2.4. Advantages and disadvantages

Based on the special microscopic structures in graphite foams, the advantages of these materials can be summarized:

(1) High thermal conductivity (thermal conductivity of solid graphite is 1700 W/(m.K), and the effective thermal conductivity of graphite foam is more than 150 W/(m.K));
(2) Low density (0.2 to 0.6 g/cm^3);
(3) High specific surface area (5000 to 50000 m^2/m^3);

On the other hand, there are some disadvantages for the graphite foam materials:
(1) High thermal conductivity only exists in a certain direction;
(2) Due to the small scale pores and complex structures of the foam, the pressure drop through graphite foam is very high.

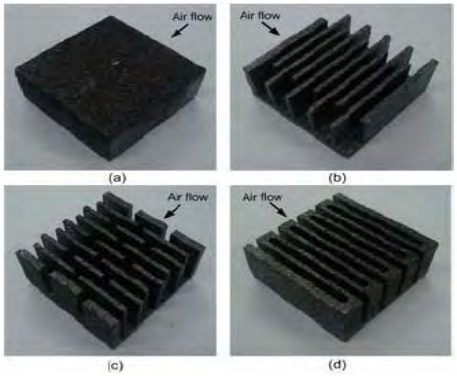

Fig. 3. Tested graphite foam heat sinks of (a) block, (b) staggered, (c) baffle and (d) corrugated configurations [9].

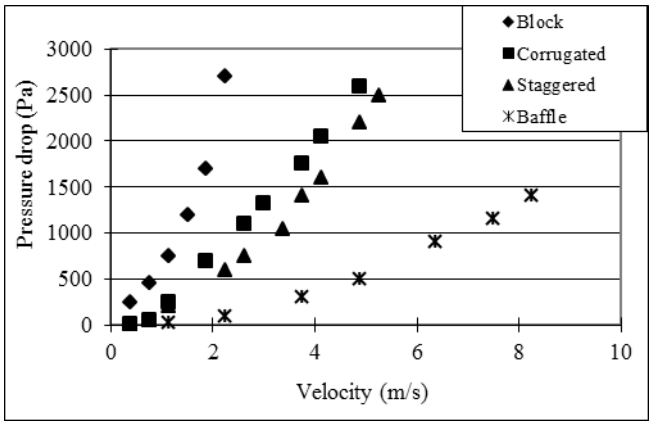

Fig. 4. Pressure drop versus inlet flow velocity of air flow through tested configuration [9].

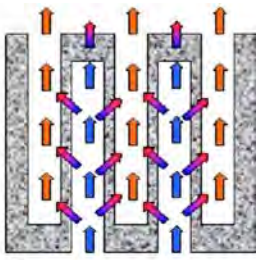

Fig. 5. Flow path inside the corrugated foam [10].

3. Applications of graphite foams

Due to the high thermal conductivity, low density and large specific surface area, the graphite foam is a good thermal material for heat exchangers or heat sinks. The major applications of graphite foam as materials for heat exchangers are: electronic package cooling, vehicle cooling systems, energy storage systems, and others.

3.1. Electronic package cooling

Because of the large internal interfaces and the high thermal conductivity, the usage of graphite foam is considered as an effective cooling method to dissipate the high heat flux in electronic equipment. Furthermore, the coolant of electronic equipment can be air instead of water, due to the high thermal conductivity of graphite foam. The removal of water can avoid shorting the circuitry of electronic equipment by water leakage.

Gallego et al. [11] demonstrated that the foam-based heat sink can be used to reduce the volume of the required cooling fluid or eliminate the water cooling system altogether. In terms of thermal performance, the graphite foam is much better than the aluminum. Meanwhile, the graphite foam heat sinks respond to transient loads faster than the traditional aluminum heat sinks. This response time may be crucial for the power electronics. Williams et al. [12] investigated several different channel - insert configurations as mini - heat exchangers by using both copper fins and graphite foams. The graphite foam was proved to have strong potential as a mini - heat exchanger.

On the other hand, the usage of thermosyphons in the thermal management of electronics is established and the methods for evaporator enhancement are of interest. Gandikota et al. [13] investigated the cooling performance of graphite foams for evaporator enhancement in thermosyphons and in pool boiling with FC-72 as the operating fluid. The exhibited thermal resistance was very low, averaging at about 0.024 K/W at low heat flux. The thermal resistance rose with increasing heat flux, but still remained very low. Lu et al. [14] used the graphite foam as a wick in a vapor chamber. With ethanol as the coolant, the vapor chamber (25 mm x 25 mm x 6 mm) had been demonstrated at a heat flux of 80 W/cm^2. The results showed that the performance of a vapor chamber using graphite foam was about twice that of one using a copper wick structure. Furthermore, Coursey et al. [15] found that 149 W heat load could be dissipated from a 1 cm^2 heated base at the operating temperature of 52 ℃, by usage of a graphite foam thermosyphon evaporator.

3.2. Vehicle cooling systems

Another important utilization of the graphite foam heat exchangers is in vehicle cooling systems. Because of the low density and large specific surface area, it might lead to a light and compact heat exchanger in vehicles. Meanwhile, graphite foam is considered as a potential material to solve critical heat rejection problems that must be solved before fuel cell and advanced power electronics technologies are introduced into automobiles.

The graphite foam could be utilized to produce a light and compact radiator in vehicles. In this case, the radiator might be placed away from the front of vehicles. If the size of the front of vehicles can be reduced, the vehicle does not push so much air in its forward motion. This implies less aerodynamic drag and increase of the fuel efficiency in vehicles. Kett et al. [16] designed a radiator (as shown in Fig. 6) with the carbon foam. Due to the increase of heat transfer coefficients, the number of coolant tubes in the radiator was reduced significantly. A typical automotive radiator with cross section of 48 cm x 69 cm might be reduced to 20 cm x 20 cm at the same heat removal rate. The reduced size will cut down the overall weight, cost, and volume of the cooling system. Thereby the fuel efficiency can be improved. Moreover, Yu et al. [17] compared a carbon foam fin - tube radiator with a conventional aluminum fin - tube radiator. The thermal performance of the carbon foam radiator was increased around 15 % without changing the frontal area or the air flow rate and pressure drop.

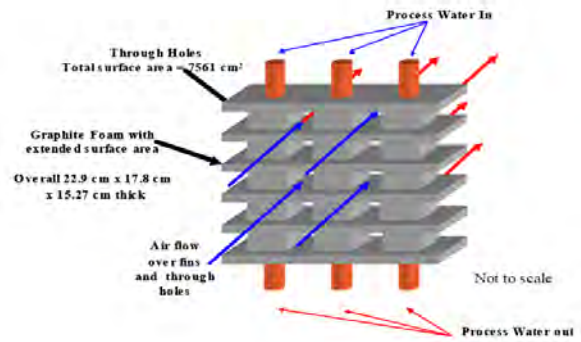

Fig. 6. Configuration of graphite foam radiator [16].

3.3. Energy storage system

Because of the high thermal conductivities in the graphite foam, the time used for heat transfer inside the material will be very short. This is a big advantage for energy storage applications. Lafdi et al. [18] investigated the thermal performance of graphite foams infiltrated with phase change materials for space and terrestrial energy storage systems. Because of the high thermal conductivity of graphite foams, the thermal performance of phase change material and foam system was improved significantly. In the phase change material related energy storage process, the higher thermal conductivity leads to a shorter time to charge or discharge, which implies better system performance.

4. Problems

Even though the graphite foam is an excellent thermal material, it is still very hard to find graphite foam heat exchangers in the commercial market. Thus, there are some problems blocking the development of graphite foam heat exchangers.

The most important problem facing the graphite foam heat exchanger is the high pressure drop. Because of the complex internal structure of the foam, the flow resistance inside the graphite foam is very high. This causes a high pressure drop through the graphite foam. Due to the high flow resistance, it is difficult for the cooling air to reach all the inter - faces and transfer the heat. Thus, the effective area of heat transfer is reduced greatly, which will result in a low thermal performance. Furthermore, the high pressure drop requires large input of pumping power to push the air through the graphite foam heat exchangers, which will cause a low coefficiency of performance (COP, the ratio of the removed heat to the input pumping power). Garrity et al. [19] proved that the graphite foam heat exchanger had lower COP than the aluminum multilouvered fin. In order to reduce the high pressure drop, it is important to adopt an appropriate configuration of the graphite foams, as discussed in [9-10].

The second problem is that the mechanical properties of the graphite foam are not as good as those of the metal foam. The tensile strength of graphite foam with porosity of 75 % is only 0.69 MPa [20]. However, the tensile strength of nickel foam with the same porosity is 18.44 MPa, which is much higher than the one of graphite foam [21]. In order to reinforce the mechanical properties of graphite foam, it might be useful to introduce some other material to the graphite foam. For instance, the compressive strength can increase ten times after the graphite foam has been mixed with epoxy resin. However, by changing the fabrication process to improve the foam's mechanical properties, the high thermal conductivity might sacrifice [22].

The third problem is the dust block. Most research of the graphite foam focus on the electronic equipment heat sinks. Little attention was put to the vehicle radiator applications. The major reason is the dust blocking problem. When the open pores in graphite foams are blocked by dust, the cold air can not reach all inter - faces and bring away the heat. Thus, the effective heat transfer area is reduced greatly and the thermal performance will decrease too. Due to the operating conditions, the dust block problem is more serious in vehicle radiators than in the electronic equipment heat sinks.

Due to these problems, the development of graphite foams is relatively slow and difficult. Much work has to be done before a mature graphite foam heat exchanger appears in the commercial market.

5. Conclusions and suggestions

The graphite foam has very high thermal conductivity, low density and large specific surface area. Because of these properties, the graphite foam is considered as a potential thermal material for heat exchangers. The graphite foam can be used as heat sinks to cool electronic packages. Also the graphite foam can be used as a radiator to cool the vehicle engines. Sometimes, the graphite foam can be used in energy storage applications.

However, due to the complex internal structure of the graphite foam, there is a very high pressure drop when the air flows through the graphite foams. There are also some other problems blocking the development of graphite foam, such as the low tensile strength, and the dust block. In order to promote the development of graphite foams as thermal material for heat exchangers, adopting an appropriate configuration might be useful to reduce the pressure drop through the graphite foam. On the other hand, mixing some other material with graphite foam might be helpful to reinforce the mechanical properties of graphite foam. Thus, much work has to be conducted before the graphite foam is accepted as a thermal material of heat exchangers.

Acknowledgments

The authors acknowledge the financial support from the Swedish Energy Agency and industries.

References

[1] J. Klett, R. Hardy, E. Romine, C. Walls, and T. Burchell, High-thermal-conductivity, mesophase-pitch-derived carbon foams: effect of precursor on structure and properties, Carbon 38, 2000, pp. 953-973.

[2] W. Ford, Method of making cellular refractory thermal insulating material, 1964, US Patent 3121050.

[3] J. W. Klett, Process for making carbon foam, 2000, US Patent 6033506.

[4] J. W. Klett, A. D. Mcmillan, N. C. Gallego, and C. A. Walls, The role of structure on the thermal properties of graphite foams, Journal of Materials Science 39, 2004, pp. 3659-3676.

[5] Q. Yu, B. E. Thompson, A. G. Straatman, A unit cube-based model for heat transfer and fluid flow in porous carbon foam, Journal of Heat Transfer 128, 2006, pp. 354-360.

[6] C. C. Tee, N. Yu, and H. Li, Modeling the overall heat conductive and convective properties of open-cell graphite foam, Modelling Simulation Material Science Engineering 16, 2008, 075006.

[7] A. G. Straatman, N. C. Gallego, B. E. Thompson, H. Hangan, Thermal characterization of porous carbon foam - convection in parallel flow, International Journal of Heat and Mass Transfer 49, 2006, pp. 1991-1998.

[8] A. G. Straatman, N. G. Gallego, Q. Yu, and B. E. Thompson, Characterization of porous carbon foam as a material for compact recuperators, Journal of Engineering for Gas Turbines and Power 129, 2007, pp. 326-330.

[9] K. C. Leong, L. W. Jin, H. Y. Li, and J. C. Chai, Forced convection air cooling in porous graphite foam for thermal management application, 11th Intersociety Conference on Thermal and Thermomechanical Phenomena in Electronic Systems, 2008, pp. 57-64.

[10] Y. R. Lin, J. H. Du, W. Wu, L. C. Chow, W. Notardonato, Experimental study on heat transfer and pressure drop of recuperative heat exchangers using carbon foam, Journal of Heat Transfer 132, 2010, 091902-1.

[11] N. C. Gallego, and J. W. Klett, Carbon foams for thermal management, Carbon 41, 2003, pp. 1461-1466.

[12] Z. A. Williams, and J. A. Roux, Graphite foam thermal management of a high packing density array of power amplifiers, Journal of Electronic Packaging 128, 2006, pp. 456-465.

[13] V. Gandikota, and A. S. Fleischer, Experimental investigation of the thermal performance of graphite foam for evaporator enhancement in both boiling and an FC-72 thermosyphon, Heat Transfer Engineering 30(8), 2009, pp. 643-648.

[14] M. H. Lu, L. Mok, and R. J. Bezama, A graphite foams based vapor chamber for chip heat spreading, Journal of Electronic Packaging 128, 2006, pp. 427-431.

[15] J. S. Coursey, J. Kim, and P. J. Boudreaux, Performance of graphite foam evaporator for use in thermal management, Journal of Electronic Packaging 127, 2005, pp. 127-134.

[16] J. Klett, R. Ott, and A. McMillan, Heat exchangers for heavy vehicles utilizing high thermal conductivity graphite foams, SAE Technical Paper 2000-01-2207, 2000.

[17] Q. Yu, A. G. Straatman, B. E. Thompson, Carbon - foam finned tubes in air - water heat exchangers, Applied Thermal Engineering 26, 2006, pp. 131-143.

[18] K. Lafdi, O. Mesalhy, and A. Elgafy, Graphite foams infiltrated with phase change materials as alternative materials for space and terrestrial thermal energy storage applications, Carbon 46, 2008, pp. 15-168.

[19] P. T. Garrity, J. F. Klausner, R. Mei, Performance of aluminum and carbon foams for air side heat transfer augmentation, Journal of Heat Transfer 132, 2010, 121901-1.

[20] M. D. Haskell, Thermal resistance comparison of graphite foam, aluminum, and copper heat sinks, http://www.electronics-cooling.com/2006/02/thermal-resistance-comparison-of-graphite-foam-aluminum-and-copper-heat-sinks/.

[21] S. B. Zhao, Thought about the exponential item in formulas calculating tensile strength for high - porosity materials, Materials and Design 23, 2002, pp. 497-499.

[22] ORNL's graphite foam may aid transportation, http://www.ornl.gov/info/ornlreview/v33_3_00/foam.htm.

The thermal response of heat storage system with paraffin and paraffin/expanded graphite composite for hot water supply

P. Zhang*, L. Xia, R.Z. Wang

Institute of Refrigeration and Cryogenics, Shanghai Jiao Tong University, Shanghai 200240, China
** Corresponding author. Tel.: +86-21-34205505; fax: +86-21-34206814 E-mail: zhangp@sjtu.edu.cn (P. Zhang)*

Abstract: The low thermal conductivity of phase change material (PCM) leads to low heat storage/retrieval rates. The expanded graphite (EG) was used to enhance the thermal conductivity. EG/paraffin composite with the 7% mass fraction of EG was prepared as a good candidate for the latent thermal energy storage (LTES) system. A shell and tube LTES system built for room heating and hot water supply in a family was experimentally investigated. The paraffin and paraffin/EG composite were used as the heat storage material, respectively. The experimental results indicated: The utilization of EG/paraffin composite PCM greatly improved the heat storage/retrieval rates of the LTES system. The LTES system with paraffin/EG composite showed a 44% reduction in heat storage duration and a nearly 69% reduction in the retrieval duration, respectively, compared to those for the system using pure paraffin. The most outstanding advantage, for the LTES system filled with paraffin/EG composite, was that the outlet temperature of water can be maintained at a higher level for a longer term than that with paraffin. However, the LTES system filled with EG/paraffin composite did not show an obvious advantage in the step-by-step heat retrieval mode, compared with paraffin.

Keywords: *Latent thermal energy storage, Paraffin/expanded graphite composite, Heat storage/retrieval rate*

1. Introduction

In a latent thermal energy storage (LTES) system by solid-liquid phase change, energy is stored during melting while it is retrieved during solidification of a phase change material (PCM), thus a LTES system with a good performance requires that the PCM possesses the appropriate phase change temperature, high heat storage density and high thermal conductivity. Besides, a good LTES system also lies on a rational structure design of the system which will decide the filling capacity of PCM and the heat exchange surface.

Based on an extensive study by Lane et al. [1] there are about 20,000 substances with the melting point in the range 10-90 oC. Majority of them was abandoned for application due to improper melting point, melting with decomposition or lack of essential reference data [2]. Among these PCMs, normal paraffin of type C_nH_{2n+2} has shown outstanding performance for application in LTES systems for solar heating and cooling [3-4]. This is because of its appropriate melting point, large latent heat, low cost, high stability and compatibility, and a low negative environmental impact. Despite the many desirable properties of paraffin, its low thermal conductivity, generally below 0.4 W/(m·K), is one of the major drawback.

The PCM containers with different geometries have their own advantages and disadvantages. Various LTES techniques have been developed and various encapsulations have been used in LTES systems. Two geometries commonly employed as PCM containers are the rectangular and cylindrical containers [5]. In particular, cylindrical containers accounts for more than 70% in all the used LTES system which commonly involves the three modes. The first is the heat storage unit in which the PCM fills the shell and the heat transfer fluid (HTF) flows through the central tube [6-8]. In the second mode, the PCM fills the tube and the HTF flows parallel to the tube [9]. The third cylinder mode is the shell and tube system [10, 11].

In the present work, expanded graphite (EG), with high thermal conductivity, was added into PCM to form a kind of composite phase change material and to enhance the heat transfer of the inner PCM. EG/paraffin composite PCM with 7% mass fraction of EG was prepared. This ratio was considered as the balance by compromising the heat transfer enhancement and latent heat storage capacity [12]. The EG/paraffin composite PCM was filled in the stainless steel tubes, and then these LTES tubes were compactly arranged in a tank. As a comparison, the paraffin was also used in this system as the heat storage material. The heat storage and retrieval performance of this LTES system, filled with EG/paraffin composite and paraffin, were experimentally tested, respectively. The influence of the HTF flow rate on the performance of the LTES system was also investigated. Moreover, two heat retrieval modes viz.: continuous and step-by-step heat retrieval, which were commonly used in the utilization of LTES system, were executed respectively for testing the heat retrieval performance of the LTES system with two PCMs.

2. Experimental setup and procedure

The PCM used in this study was technical grade paraffin with the purity of 99% and a melting temperature of 62 ^{o}C. The EG was prepared by making the raw expandable graphite (mesh 80, type KP80, from Qingdao Tianhe Graphite Co. Ltd, China) subjected to heat treatment in a furnace at 700 ^{o}C for a duration of 15 minutes. These paraffin and EG were used to prepare EG/paraffin composite. The paraffin was heated to a temperature of 85 ^{o}C, in order to be liquefied, after which the liquid paraffin was impregnated into EG and was stirred using a roll mixer. Then, the EG/paraffin composite with 7% mass fraction of EG was obtained.

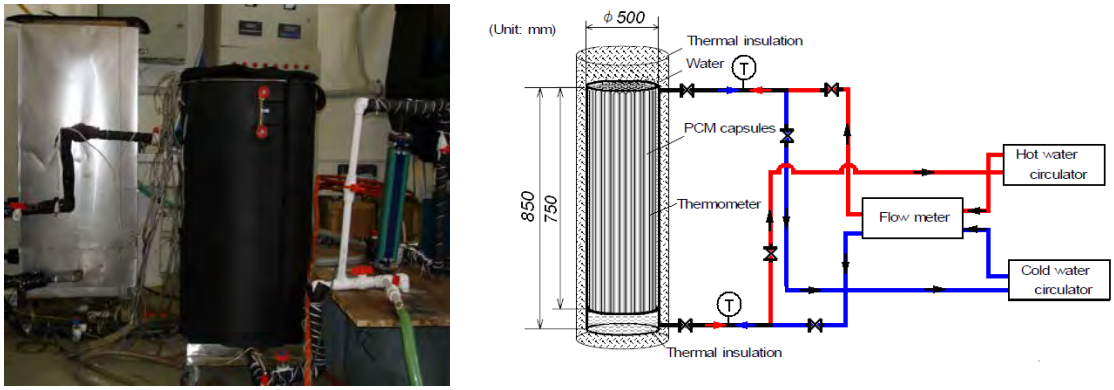

(a) (b)

Fig. 1 Experimental setup (a) Photographic view (b) Schematic of LTES system

The schematic diagram of the experimental apparatus is shown in Fig. 1. The stainless-steel LTES tank, insulated with thermal insulation material of 50 mm in thickness, had a capacity of 166 L (500 mm diameter and 850 mm height), in which 27 heat storage tubes with the 76 mm in inner diameter and 750 mm in height were uniformly packed and supported by a wire mesh. The paraffin and EG/paraffin composite PCM were used as PCMs and water was used as the HTF. A hot water tank was used for heating during the heat storage and cold water from a cold water tank was used for cooling during the heat retrieval. During heat storage, the hot water was supplied from the top of LTES tank and was drained from the bottom, whereas, during heat retrieval, the flowing direct for the cooling water was just reversed. The temperatures of HTF at the inlet and the outlet were measured by two PT1000 platinum resistance temperature sensors.

The schematic of the cylindrical heat storage unit, as shown in Fig. 2, was a vertical tube (stainless steel, outer diameter of 78 mm and wall thickness of 1 mm) in which the PCM was impregnated. Four thermocouples (K-type) were used to measure the temperature of the PCM and were fixed near the centre axis of the tube, as shown in Fig. 2 (b). The heat storage unit which was equipped with thermocouples was set at the center of the LTES tank. The temperature variations of PCM during heat storage and retrieval were monitored and collected using a data logger.

Initially, 80% of the tube volume was filled with the solid PCM at a room temperature of 28 oC. The remaining 20% of the volume was left to accommodate the volume increase of the PCM during melting. Water was used as HTF, whose temperature at the inlet of the heat storage unit was kept at 85 ^{o}C during heat storage and was kept at 28 ^{o}C during heat retrieval. There were three different flow rates of the hot water (100, 150, 200 L/h) during heat storage and three different flow rates of the cooling water (150, 200, 250 L/h) during heat retrieval.

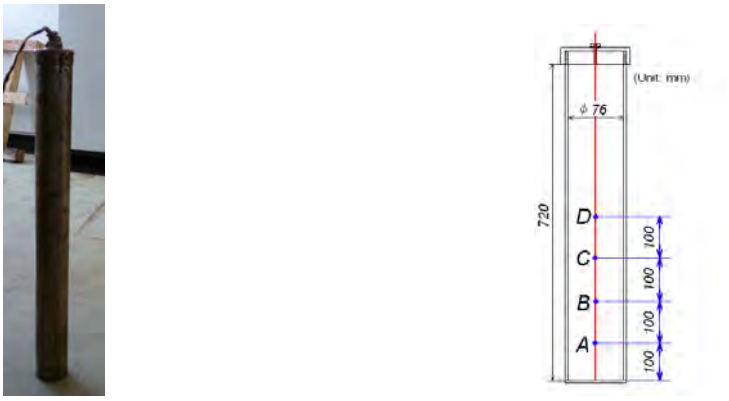

(a) (b)

Fig. 2. LTES unit (a) and locations of the thermocouples (b)

After heat storage of the LTES tank, the heat retrieval experiments were carried out in both continuous and step-by-step heat retrieval modes. In the continuous mode, the cold water of 28 ^{o}C continuously flew through the storage tank until the temperature of the water at the outlet reached 28 ^{o}C; while in the step-by-step heat retrieval mode, the cold water at 28 ^{o}C was impregnated in the LTES tank and had been kept there for one hour. Then, the heated HTF was withdrawn and at the same time the temperature was recorded. The above process was repeated until the temperature of the withdrawn HTF is below 35 ^{o}C. Nearly five batches of hot water could be withdrawn from the LTES tank in the step-by-step heat retrieval mode.

3. Results and discussion

3.1. Heat storage and retrieval performance

In the experiment for investigating the heat storage and retrieval performance of the LTES system, flow rate of the water was kept constantly at 150 L/h and the inlet HTF temperature during the heat storage and retrieval was 85 oC and 28 oC, respectively. The heat retrieval is in the continuous mode.

Figure 3 shows the temperature evolutions at the tested point C (as shown in Fig. 2) of pure paraffin and EG/paraffin composite during heat storage and retrieval circle. It can be found in

Fig. 3 that the tested point in both pure paraffin and EG/paraffin composite experienced three steps during melting, viz.: the sensible heat storage where the temperature rose rapidly, the latent heat storage (phase change) with the isothermal behavior and the following sensible heat storage where the temperature rose rapidly again until it reached the thermal equilibrium. The similar analysis was also effective during freezing. However, a discrepancy between the measured results of pure paraffin and those of the EG/paraffin composite was observed. The heat storage and retrieval durations of the LTES tank with EG/paraffin composite was much shorter than those with pure paraffin, i.e., the addition of EG drastically enhanced the heat transfer of inner PCM.

It took about 8000 s for pure paraffin to finish the heat storage, whereas, it took only 4500 s for EG/paraffin composite to reach the temperature equilibrium with the heating source, showing a 44% time reduction compared with that for pure paraffin. It was obvious that the heat storage rate of the composite PCM was higher than that of pure paraffin. It can also be seen from Fig. 3 that it took about 18000 s for the temperature of pure paraffin to drop from 85 ^{o}C to 30 ^{o}C, whereas, it took only 5500 s for EG/paraffin composite to complete the heat retrieval, indicating a 69% reduction in the heat retrieval duration.

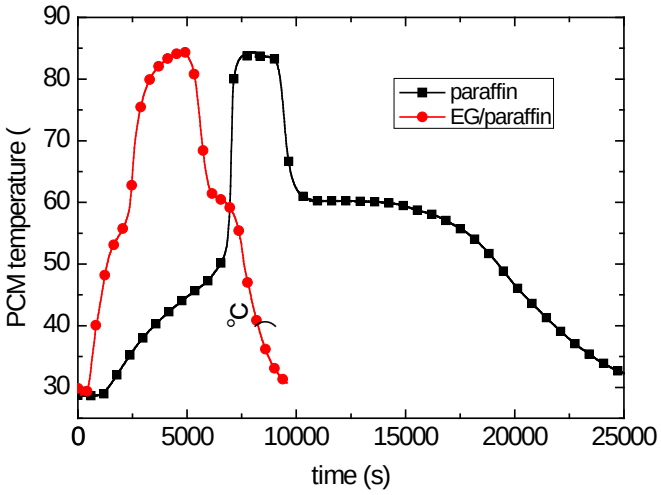

Fig. 3. Temperature evolutions of the LTES unit with pure paraffin and EG/paraffin composite during heat storage and retrieval circle

The heat storage and retrieval durations were both considerably reduced for EG/paraffin composite which was attributed to the addition of EG. However, it can also be seen that the effect of EG was more significant in heat retrieval than in heat storage. These phenomena can be attributed to the melting/freezing characteristic of each PCM: the melting of pure paraffin was accelerated during heat storage (melting) because of the intensive natural convection in the melted paraffin, whereas the natural convection did not play significant role in the heat transfer during heat retrieval (freezing); as for EG/paraffin composite, the natural convection could be neglected during both melting and freezing because of the existence of EG.

The outlet temperature evolutions of HTF during heat storage and retrieval are shown in Fig. 4(a) and (b), respectively. During heat storage, the outlet temperature of the HTF in the LTES system filled with EG/paraffin composite was more rapidly raised to the inlet temperature (85 ^{o}C) than in the system filled with paraffin, as shown in Fig. 4(a),. Moreover, in the earlier stage of the heat storage the outlet temperature of the HTF for the LTES system filled with EG/paraffin composite was higher than that with paraffin. These phenomena both indicated

the system filled with EG/paraffin composite had a better heat transfer performance than the system with paraffin.

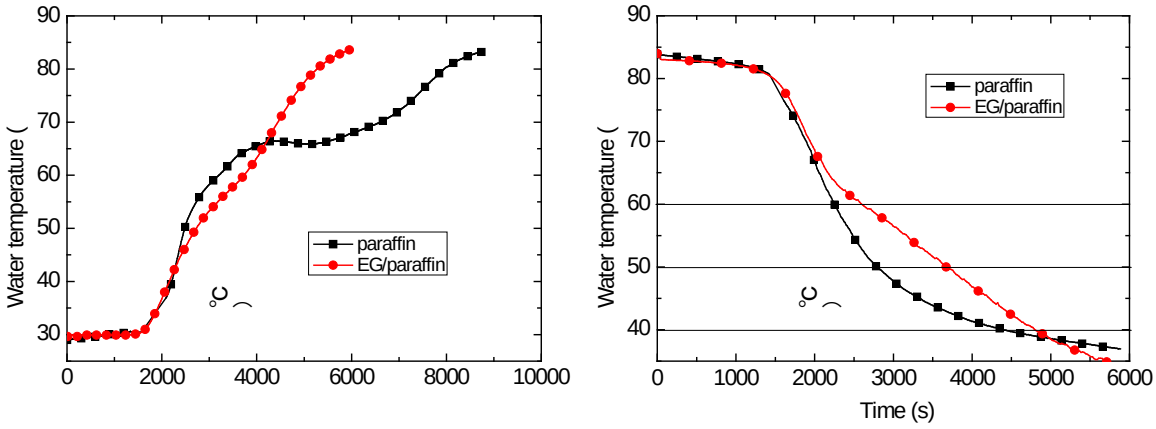

(a) (b)

Fig. 4. Outlet temperature evolutions of the HTF during (a) heat storage and (b) heat retrieval

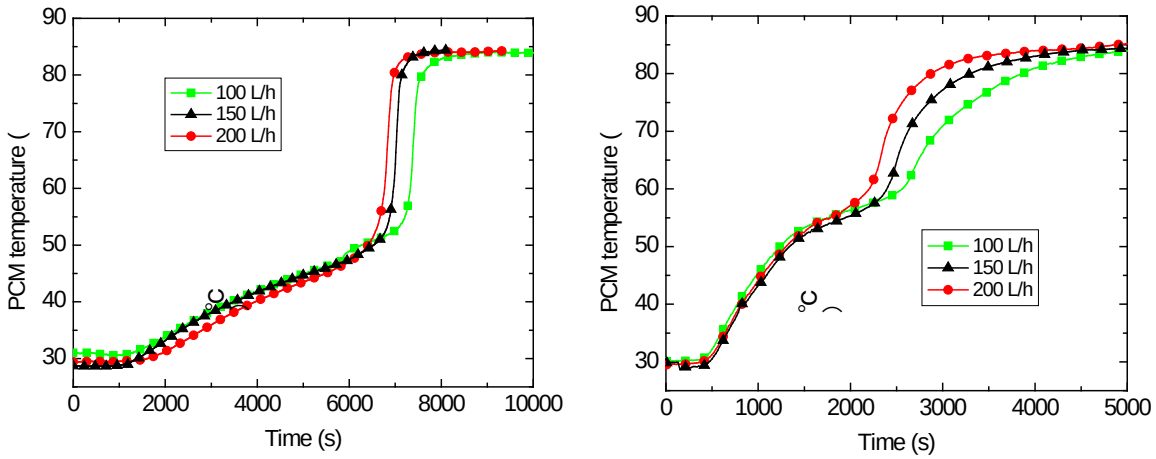

(a) (b)

Fig. 5. Temperature evolutions of the pure paraffin (a) and EG/paraffin composite (b) with the varying flow rate of the HTF during heat storage

As well known, for a LTES system, it is important to have a large heat storage capacity; however, the most important performance is whether it can supply a high heat retrieval power. In an excellent LTES system, the HTF should be heated up rapidly and the temperature of the HTF can be raised to a higher value so as to meet the requirement of the user as the HTF flows through it during heat retrieval. As can be seen from Fig. 4 (b) for the LTES system filled with paraffin/EG composite, the outlet temperature of the HTF could maintain a high level in a longer term than that with paraffin, such as the outlet temperature of HTF of the LTES system filled with paraffin/EG composite could be maintained above 50 ^{o}C for another more 1000 s than that with paraffin. Thus, it is indicated the stored thermal energy can be rapidly and intensively released in the system filled with paraffin/EG composite, which was significant for the utilization of the LTES system.

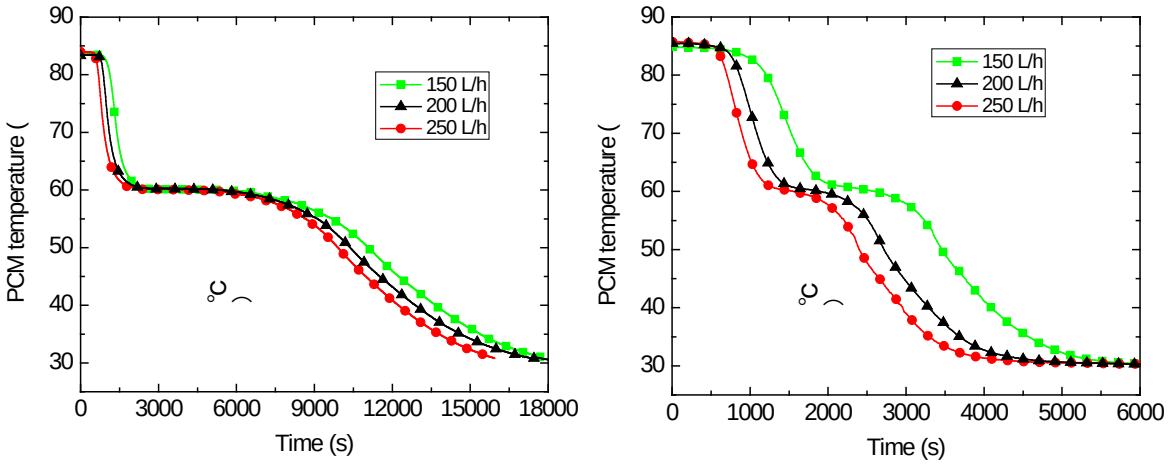

Fig. 6. Temperature evolutions of the pure paraffin (a) and EG/paraffin composite (b) with the varying flow rate of the HTF during heat retrieval

3.2. Influence of the flow rate of the HTF on the heat storage and retrieval performance

Figure 5 shows the temperature evolutions of PCM when varying flow rate of the HTF during heat storage, where Fig. 5(a) is temperature evolutions of the paraffin and Fig. 5(b) is temperature evolutions of the paraffin/EG composite. Figure 6 shows the temperature evolutions of PCM when varying flow rate of the HTF during heat retrieval.

From Fig. 5 and 6, it can be obviously seen that a higher flow rate of the HTF led to a better heat transfer performance and consequently a more rapid heat storage and retrieval. To increase the flow rate is always an effective and positive means during heat storage, whereas higher flow rate of the HTF may cause lower outlet temperature of the HTF during heat retrieval though it can enhance the heat retrieval power.

3.3. Test for the step-by-step heat retrieval mode

For the utilizations of the LTES system, the heat retrieval mode is not only continuous but also discontinuous, for example, the requirement of the hot water is intermittent in the domestic hot water system. Thus, the information about the step-by-step heat retrieval mode of the LTES system was also necessary and the retrieval performance of the LTES system was investigated in such case. Figure 7(a) shows the temperature evolutions of PCM and Fig. 7(b) shows the temperature evolutions of the outlet HTF during step-by-step heat retrieval. In each figure, the performance of the LTES system with paraffin was compared with that with EG/paraffin composite. The experimental result indicated: 1. There is a large difference between the temperature evolutions of the pure paraffin and EG/paraffin composite. This is because the EG/paraffin composite with high thermal conductivity is more sensitive to the varying of the HTF temperature and can quickly response this varying; 2. The temperature evolutions of the outlet HTF in the two LTES systems are almost the same with each other. This is because the waiting duration of one hour in each step is an enough time period to allow new temperature equilibrium is reached and maintained between PCM and HTF for both two LTES systems.

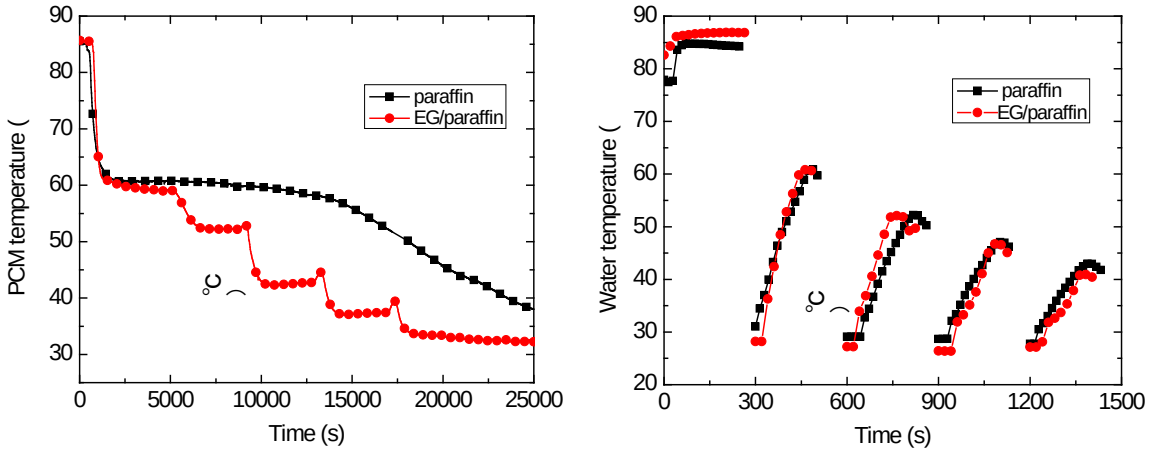

(a) (b)

Fig. 7. Temperature evolutions of PCM (a) and the outlet HTF (b) during step-by-step heat retrieval

4. Conclusions

Paraffin/EG composite PCM with 7% mass fraction of EG was prepared for enhancing the heat transfer of paraffin. The paraffin/EG composite PCM and the paraffin were used in a shell and tube heat storage system and the performance of the LTES system was experimentally investigated. The following conclusions were drawn:

1. The utilization of paraffin/EG composite PCM greatly enhanced the heat storage/retrieval rates of the LTES system. The LTES system with paraffin/EG composite PCM, under the operation condition (flow rates: 150 L/h during both heat storage and heat retrieval; the inlet temperature of HTF: 28 ^{o}C during heat retrieval and 85 ^{o}C during heat storage), showed a 44% reduction in heat storage duration and a nearly 69% reduction in the retrieval duration, respectively, compared to those for pure paraffin.

2. The most outstanding advantage, for the LTES system filled with paraffin/EG composite, was that the outlet temperature of HTF can be maintained at a higher level in a longer term than that with paraffin, which was significant for the utilization of the LTES system.

3. A higher flow rate of the HTF led to a better heat transfer performance and consequently more rapid heat storage and retrieval. It is positive for heat storage, whereas higher flow rate of the HTF may cause lower outlet temperature of the HTF during heat retrieval though it can enhance the heat retrieval power.

4. There was a large difference between the temperature evolutions of the pure paraffin and paraffin/EG composite PCM in the step-by-step heat retrieval mode, whereas the temperature evolutions of the outlet HTF in the two LTES systems were almost the same with each other.

References

[1] G.A. Lane, Solar heat storage: latent heat materials, background and scientific principles vol. I. Florida: CRC Press Inc, 1983.

[2] A. Felix Regin, S.C. Solanki, J.S. Saini, Heat transfer characteristics of thermal energy storage system using PCM capsules: A review, Renewable and Sustainable Energy Reviews12, 2008, pp. 2438–2458.

[3] C. Arkar, B. Vidrihb, S. Medveda, Efficiency of free cooling using latent heat storage integrated into the ventilation system of a low energy building, International Journal of Refrigeration 30, 2007, pp. 134–143.

[4] A. Benmansour, M.A. Hamdan, A. Bengeuddach, Experimental and numerical investigation of solid particles thermal energy storage unit, Applied Thermal Energy 26, 2006, pp. 513–518.

[5] F. Agyenim, N. Hewitt, P. Eames, M. Smyth, A review of materials, heat transfer and phase change problem formulation for latent heat thermal energy storage systems (LHTESS), Renewable and Sustainable Energy Reviews 14, 2010, pp. 615–628.

[6] A. Trp, An experimental and numerical investigation of heat transfer during technical grade paraffin melting and solidification in a shell-and-tube latent thermal energy storage unit, Solar Energy 79, 2005, pp. 648–660.

[7] H.A. Adine, H.E. Qarnia, Numerical analysis of the thermal behaviour of a shell-and-tube heat storage unit using phase change materials, Applied Mathematical Modelling 33, 2009, pp. 2132–2144

[8] F. Agyenim, P. Eames, M. Smyth, A comparison of heat transfer enhancement in a medium temperature thermal energy storage heat exchanger using fins, Solar Energy 83, 2009, pp. 1509–1520.

[9] M. Esen, A. Durmus, Geometric design of solar-aided latent heat store depending on various parameters and phase change materials. Solar Energy 62, 1998, pp. 19–28.

[10] F. Agyenim, P. Eames, M. Smyth, Heat transfer enhancement in medium temperature thermal energy storage system using a multitube heat transfer array. Renewable Energy 35, 2010, pp. 198–207.

[11] A.A. Ghoneim, Comparison of theoretical models of phase-change and sensible heat storage for air and water-based solar heating systems, Solar Energy 42, 1989, pp. 209–220.

[12] L. Xia, P. Zhang, R.Z. Wang, Preparation and thermal characterization of expanded graphite/paraffin composite phase change material, Carbon 48, 2010, pp. 2538-2548

Effect of different working fluids on shell and tube heat exchanger to recover heat from exhaust of an automotive diesel engine

S. N. Hossain*, S Bari

Sustainable Energy Centre, School of Advanced Manufacturing and Mechanical Engineering, University of South Australia, SA 5095, Australia
** Corresponding author. Tel: +61430854206, Fax: +61 8302 3380, E-mail: shekh.rubaiyat@unisa.edu.au*

Abstract: In this research, experiments were conducted to measure the exhaust waste heat available from a 60 kW automobile engine. The performance of an available shell and tube heat exchanger using water as the working fluid was conducted. With the available data, computer simulation was carried out to improve the design of the heat exchanger. Two heat exchangers were used: one to generate saturated and the other to generate super heated vapours. These two heat exchangers can be arranged in parallel or series. In series arrangement, the exhaust gas was first passed through superheated heat exchanger and then through the saturated heat exchanger. Whereas, in parallel arrangement, the exhaust gas was divided to pass through saturated and superheated heat exchangers. In both cases, working fluid was passed first through saturated heat exchanger and then through superheated heat exchanger. Computer simulation was carried out to investigate the effectiveness of the proposed heat exchanger for different working fluid like water, ammonia, and HFC-134a. It is found that with the exhaust heat available from the diesel engine additional 15%, 13% and 8% power can be achieved by using water, HFC-134a and ammonia as working fluid respectively.

Keywords: *Waste heat recovery, Organic Rankine Cycle, Diesel engine*

1. Introduction

Diesel engines represent a major kind of Internal Combustion Engine (ICE). These diesel engines have a wide field of applications and as energy converters they are characterized by their high efficiency. Trucks and road engines usually use high speed diesel engines with 220 kW output or more. Earth moving machineries use engines with an output of up to 520 kW or even higher up to 740 kW. Diesel engines are also used in small electrical generating units or as standby units for medium capacity power stations. However, Small air-cooled diesel engines of up to 35 kW output are used for irrigational purposes, small agricultural tractors and construction machines whereas large farms employ tractors of up to 150 kW output.

In general, diesel engines have an efficiency of about 35% and thus the rest of the input energy is wasted. Despite recent improvements of diesel engine efficiency, a considerable amount of energy is still expelled to the ambient with the exhaust gas. In a water-cooled engine about 35 and 30-40% [1] of the input energy is wasted in the coolant and exhaust gases respectively. The amount of such loss, recoverable at least partly, greatly depends on the engine load. Johnson [2] found that for a typical 3.0 l engine with a maximum output power of 115 kW, the total waste heat dissipated can vary from 20 kW to as much as 40 kW across the range of usual engine operation. It is suggested that for a typical and representative driving cycle, the average heating power available from waste heat is about 23 kW.

Since the wasted energy represents about two-thirds of the input energy and for the sake of a better fuel economy, exhaust gas from diesel engines can provide an important heat source that may be used in a number of ways to provide additional power and improve overall engine efficiency. These technical possibilities are currently under investigation by research institutes and engine manufacturers. For the heavy duty automotive diesel engines, one of the most promising technical solutions for exhaust gas waste heat utilization appears to be the use of a ‘‘Bottoming Rankine Cycle”. A Rankine cycle using water as working fluid is not enough

efficient to recover waste heat below 640 K [3]. The Organic Rankine Cycle (ORC) is a promising process to recover the heat from the exhaust of an engine and generate electricity from it [4, 5]. The ORC works like a simple Rankine steam power cycle but uses an organic working fluid instead of water. A certain challenge is to choose a suitable organic working fluid for the ORC. The working fluid should fulfil safety criteria; it should be environmentally friendly, and inexpensive. Another important aspect for the choice of the working fluid is the temperature of the available heat source. A question, which also has to be considered for using ORC, is whether an organic substance is really better than water as working fluid for a given task.

A systematic approach towards using an installation based on the Rankine Cycle in truck applications dates back to the early 1970s where a research program funded by the US Department of Energy (DOE) was conducted by Mack Trucks and Thermo Electron Corporation [6-8]. Under this program, an ORC system was installed on a Mack Truck diesel engine and the lab test results revealed an improvement of bsfc of 10–12%, which was verified by highway tests. During the following years similar research programs were performed by other research institutes and vehicle manufacturers. Aly [9] was able to produce 16% additional power from the exhaust of a Mercedes-Benz OM422A diesel engine by using R-12 as working fluid for the ORC. ORC systems with capacities from 750 to 1500 kWe were examined by Koebbman [10]. Recently, the solution of Rankine Cycle Systems has increased its potential competitiveness in the market even more [11, 12]. This is a result of technical advancements in a series of critical components for the operation of such an installation (heat exchanger, condenser and expander) but also stems from the highly increased fuel prices. Nowadays, the installation of a Rankine Cycle is not only considered as a feasible solution for efficiency improvement in heavy duty diesel engines for trucks [13, 14] but also for smaller application such as passenger cars [15].

In this project, experiments were conducted to measure the exhaust heat available from a 60 kW automobile engine at different speeds and loads. A shell and tube heat exchanger was purchased and installed into the engine. The performance of the heat exchanger using water as the working fluid was then conducted. With the available data, computer simulation was carried out to improve the design of the heat exchanger. The optimized model of the heat exchanger was then simulated to generate super heated vapour. Ammonia and HFC-134a is used as working fluids. Water is used as reference for comparison. The thermo physical properties of working fluids are compared and presented in Table 1. It is apparent that dry and isentropic organic fluids generally have much lower relative enthalpy drops during expansion than the water-steam mixture. Unlike water, most organic fluids suffer chemical decomposition and deterioration at high temperature and pressure. Therefore, an ORC system must be operated well below the temperature and pressure at which the fluids are chemically unstable. Most organic fluids have relatively low critical pressures and are therefore usually operated under low pressures and with much smaller heat capacities than water-vapour cycles. A suitable organic fluid must have a relatively high boiling point. Based on these features ammonia and HFC-134a are selected for the current study. Finally, power output from the turbine is calculated considering isentropic efficiency of real turbine[16, 17].

Table 1. Thermophysical properties of working fluids.

Parameter	H_2O	NH_3	HFC-134a
Molecular weight	18	17	102
Slope of the saturation vapour line	Negative	Negative	Isentropic
Enthalpy drop across the turbine (kJ/kg)	1570~900	725~70	55~22
Max. Stability Temperature (K)	None	750	450
Critical point (K)	647	405.3	374.15
Boiling point at 1 atm (K)	373	239.7	248
Latent heat at 1 atm (kJ/kg)	2256.6	1347	215.52

2. Experimental setup

The engine used in the current study is a four cylinder Toyota 13B diesel engine which is coupled with a water dynamometer. The specification of the engine is given in the Table 2. The schematic of the experimental setup is shown in Fig. 1. The engine run at different loads with variable speeds and exhaust temperatures were recorded to calculate available heat energy from the exhaust. Then the exhaust of the engine was connected to a shell and tube heat exchanger to study the performance of the heat exchanger and those data were used to improve the design of the heat exchanger by computer simulation.

Table 2. Engine specification.

Engine model	13B
Make	Toyota
Type of engine	4 cylinder charged water cooled diesel engine
Bore	102 mm
Stroke	105 mm
Compression ratio	17.6:1
Torque	217 N.m @ 2200 rpm

3. Heat Exchanger design

The data found from the experiment are used to optimize the design of shell and tube heat exchanger by computer simulation. Effect of important parameter of heat exchanger like radius of the shell, no of tubes, length of the heat exchanger, pressure drop is investigated and final model of the heat exchanger is proposed. The specification of the model of the proposed shell and tube heat exchanger is shown in the Table 3. Two heat exchangers are used: one heat exchanger is used to generate saturated vapor from the liquid working fluid and the second heat exchanger is used to generate super heated vapor from that saturated vapor. These two heat exchangers can be arranged into two configurations, parallel and series as shown in the Fig. 2.

Table 3. Heat exchanger specification.

Heat exchanger type	Shell and tube counter flow, hot fluid in tubes and cold fluid in the shell
Shell inside radius	35.4 mm
No of tube	18
Tube inside diameter	10 mm
Length of the heat exchanger	2 m

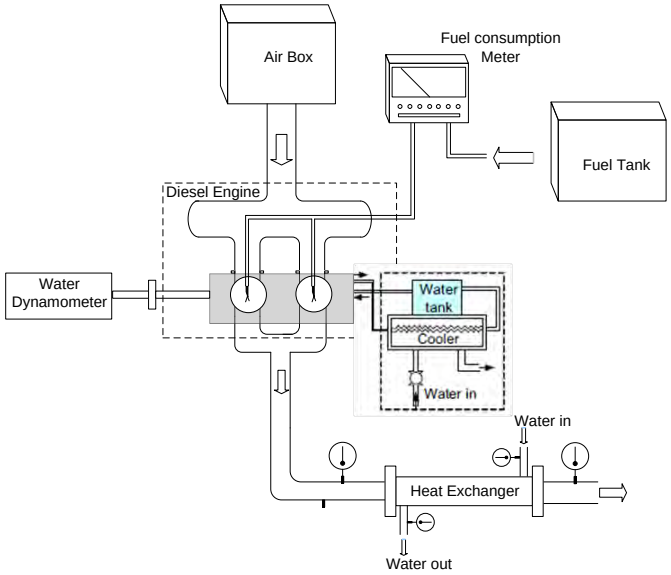

Fig. 1: Schematic diagram of experimental setup.

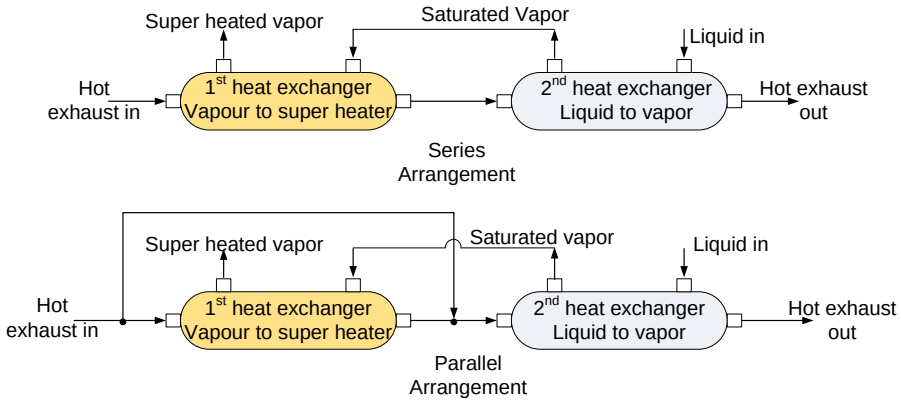

Fig. 2: Heat exchanger arrangement.

4. CFD Model

The optimized design of the shell and tube heat exchanger is modeled for heat transfer between hot and cold fluid in Flow Simulation which is CFD simulation module of Solidworks 2009. The computational mesh used to solve the model heat exchanger contained 109,992 cells. The cold fluid was considered to be liquid phase at 323K with corresponding saturation pressure for the second heat exchanger (Fig. 2) and saturated vapor at working pressure for the first heat exchanger (Fig. 2). The hot fluid considered as air with mass flow rate of 0.10215 kgs^{-1} and temperature of 938 K. The operating pressure of hot fluid is set to101.325 kPa and the cold fluid supply pressure and mass flow rate are varied. Steady and incompressible flow was assumed in all models. The Standard *k*- ε , a two-equation Reynolds-Averaged Navier-Stokes (RANS) model that is currently the most widely used for calculating flow problems has been used in this model.

5. Results

To design an effective heat exchanger for heat recovery from the exhaust of an engine, it is required to know how much energy is available in the exhaust. So some base line tests are performed. The exhaust gas temperature at various speed and engine power is presented in the Fig. 3. It is found from the figure that engine power and the temperature of the exhaust gases

for all three engine speeds show an approximately linear relationship. Exhaust gas temperature increases with increase of power output and speed of the engine. This indicates that heat recovery will be more viable for higher powers.

In the relationship between power and temperature there is a definite relationship between engine power and the amount of recoverable energy present in the exhaust gases. The relationship this time is not linear but there is still a general upward trend, revealing that, as the engine power increases, so does the amount of recoverable energy. This is clearly seen in Fig. 4. This finding is highly significant section in terms of the focus of this research project.

In particular, the potential applications which formed the original thinking behind this project are given credibility, in that the amount of energy which may be tapped is of an order that

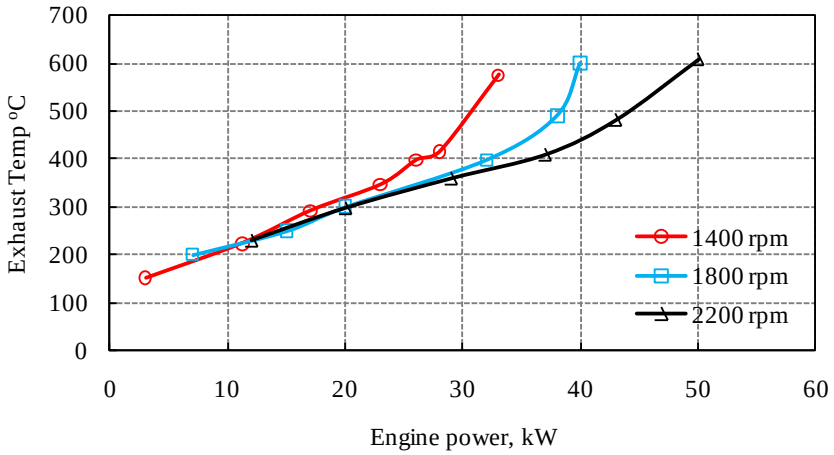

Fig. 3: Exhaust gas temperature variation with engine power from experiment.

justifies the attempt to capture and exploit it. For example, even if the results of just the lowest speed (1400 rpm) are considered, the potential to capture and use what is currently wasted energy, is extremely significant - the maximum recoverable energy for this speed is approximately 17 kW from the exhaust gas with the engine running at 33 kW (which is half the engine's power). Similarly, at 1800 rpm, a maximum value of approximately 21 kW was obtained from the exhaust gases, with the engine running at approximately 39 kW. At 2200 rpm the results show a maximum recoverable potential of approximately 23 kW when running at 45 kW. These results indicate that some 50% of the engine's running load is currently wasted but could be recoverable and converted to a usable form. All the above calculations were based on the abilities of a heat exchanger to be able to reduce the initial exhaust temperature at any particular speed and load to 50°C.

Based on the available data from the experiment, the heat exchanger design was optimized by computer simulation. Fig. 5 shows that the effectiveness of the heat exchanger decreases with the larger shell diameter for all three working fluids. Rubaiyat and Bari [18] found that there is no significant effect of working pressure on heat exchanger effectiveness. They also found that average pressure drop for different parameter of heat exchanger was about 250 Pa[18]. Effectiveness is higher for smaller diameter of the shell because of turbulent flow which facilitates the heat transfer. Heat exchanger effectiveness increases with the length of the heat exchanger as presented in the Fig. 6. It is found from the figure that after 1.6 m length the effectiveness increase is not very significant.

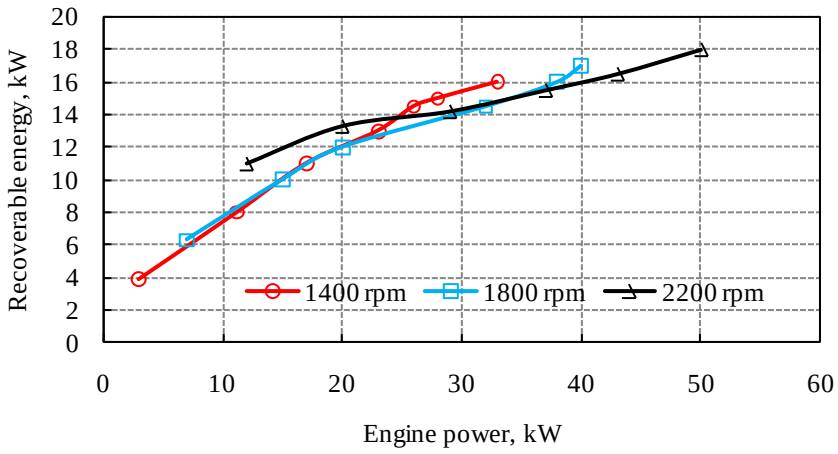

Fig. 4: Recoverable energy variation with engine power from experiment.

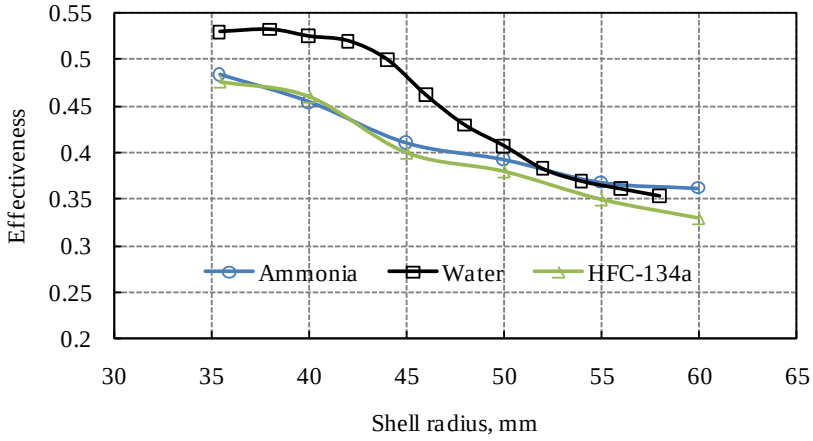

Fig. 5: Heat exchanger effectiveness vs. shell radius from CFD simulation.

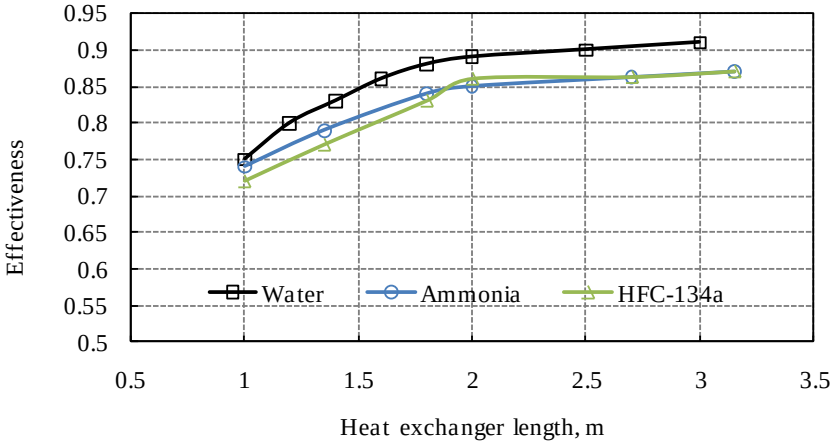

Fig. 6: Heat exchanger effectiveness vs. heat exchanger length from CFD simulation.

Extra power that can be recovered from the exhaust of the diesel engine with the proposed shell and tube heat exchanger model is presented in the Fig. 7. It is found that additional output power increases as the working pressure increases for both the parallel and series

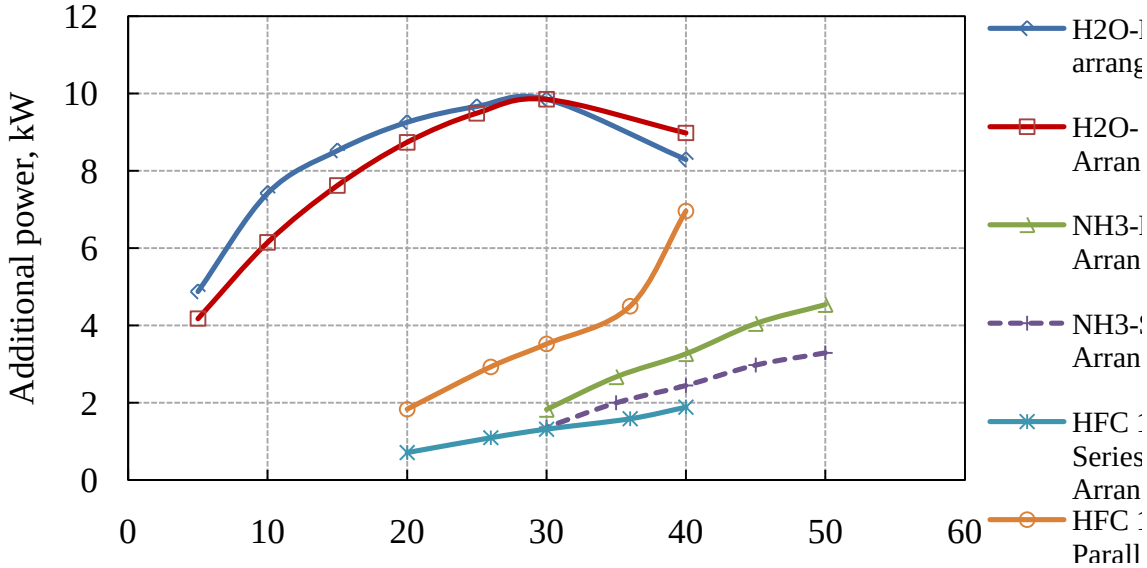

Fig. 7: Additional power output variation for different working fluids with working pressure from CFD simulation.

arrangement (Fig.2) of the heat exchangers for all three working fluids. This is because the condensing pressure was kept constant and as the working pressure increases the enthalpy drop across the turbine also increases. From the figure it is clear that water can recover heat most efficiently from the exhaust of the engine than the other organic fluids. This is because water has very high enthalpy drop across the turbine (Table 1) compared to other two organic fluids. Interestingly, it is found for water that higher power output can be achieved for parallel arrangement below 30 bar working pressure than the series arrangement whereas series arrangement can achieve higher power output above 30 bar working pressure than parallel arrangement. Maximum power output also achieved at the 30 bar working pressure. But other working fluids, ammonia and HFC-134a do not show any trend like that. For both ammonia and HFC-134a working fluid, parallel arrangement of the heat exchangers gives more additional power output. The proposed shell and tube heat exchanger can recover maximum 15%, 13% and 8% additional power from the exhaust of the diesel engine using water, HFC-134a and ammonia as working fluid respectively considering 70% isentropic efficiency of the turbine [16, 17].

6. Conclusion

The experimental and simulation results of the current project proved the concept of heat recovery from waste heat from the exhaust of diesel engines by using different working fluids. This research work shows that ORC can be a good option for waste recovery from diesel engines. This technique can increase the overall efficiency of diesel engine. Hence, this technology will reduce the fuel consumption and thereby will also reduce Green House Gases (GHG) and toxic emissions per kW of power produced. Additional 15%, 13% and 8% more power can be achieved with the proposed shell and tube heat exchanger by using water, HFC-134a and ammonia respectively.

References

[1] M. Hatazawa, H., Sugita, T.,Ogawa, Y.,Seo, "Performance of a thermoacoustic sound wave generator driven with waste heat of automobile gasoline engine," Transactions of the Japan Society of Mechanical Engineers (Part B, vol. 70, pp. 292–299, 2004.

[2] V. Johnson, "Heat-generated cooling opportunities in vehicles," SAE Technical Papers 2002.

[3] T. C. Hung, et al., "A review of organic rankine cycles (ORCs) for the recovery of low-grade waste heat," Energy, vol. 22, pp. 661-667, 1997.

[4] J. E. Boretz, in 5th Proceedings of the International Offshore Mechanics and Arctic Engineering Symposium (4th ed.), 1986, p. 279.

[5] P. De Marchi Desenzani and M. Gaia, Performance analysis of innovative collector fields for solar-electric plants, using air as heat transfer medium, 1984.

[6] F. DiBella, et al., "Laboratory and on-highway testing of diesel organic Rankine compound long-haul vehicle engine," SAE Technical Papers 1983.

[7] E. Doyle, DiNanno, L, Kramer, S, "Installation of a Diesel-Organic Rankine Compound Engine in a Class 8 Truck for a Single-Vehicle Test," SAE Technical Papers 1979.

[8] P. Patel, Doyle, EF, "Compounding the Truck Diesel Engine With An Organic Rankine-Cycle System," SAE Technical Papers 1976.

[9] S. E. Aly, "Diesel engine waste-heat power cycle," Applied Energy, vol. 29, pp. 179-189, 1988.

[10] W. Koebbeman, "Geothermal wellhead application of a 1-MW industrial ORC power system," 1985, pp. 2712-2717.

[11] S. Hounsham, Stobart, R, Cooke, A, Childs, P, "2008-01-0309 Energy Recovery Systems for Engines," SAE SP, vol. 2153, p. 79, 2008.

[12] M. Kadota and K. Yamamoto, "Advanced transient simulation on hybrid vehicle using Rankine cycle system," SAE International Journal of Engines, vol. 1, p. 240, 2009.

[13] C. Nelson, "Exhaust Energy Recovery," presented at the Diesel Engine-Efficiency and Emissions Research (DEER) Conference, Dearborn, Michigan, 2008.

[14] R. W. Kruiswyk, "An Engine System Approach to Exhaust Waste Heat Recovery," presented at the Diesel Engine-Efficiency and Emissions Research (DEER) Conference, Dearborn, Michigan, 2008.

[15] J. Ringler, et al., "Rankine cycle for waste heat recovery of IC engines," SAE International Journal of Engines, vol. 2, p. 67, 2009.

[16] M. J. Moran and H. N. Shapiro, Fundamentals of Engineeering Thermodynamics, USA: John Wiley & Sons, 4th ed., 2000, pp. 281-283.

[17] Y. A. Cengel, et al., Fundamentals of Thermal-Fluid Sciences, McGrawHill, 3rd ed., 2008, pp. 337-339.

[18] S. N. H. Rubaiyat and S. Bari, "Waste heat recovery using shell and tube heat exchanger from the exhaust of an automotive engine," in 13th Asian Congress of Fluid Mechanics, Gazipu, Bangladesh 2010.

Working fluid selection for Organic Rankine Cycle applied to heat recovery systems

D. C. Bândean [1], S. Smolen [2*], J. T. Cieslinski [3],

[1] *Technical University of Cluj-Napoca, Cluj-Napoca, Romania*
[2] *University of Applied Sciences, Bremen, Germany*
[3] *Gdansk University of Technology, Gdansk, Poland*
** Corresponding author. Tel: 0049-(0)421-5905-3579, Fax: 0049-(0)421-5905-3505, E-mail: smolen@fbm.hs-bremen.de*

Abstract: The selection of suitable organic fluids for use in Organic Rankine Cycle (ORC) for waste energy recovery from many potential sources of low-medium temperature (up to 350 ºC) is a crucial step to achieve high thermal efficiency. In order to identify the most suitable organic fluids, several general criteria have to be taken into consideration, from the thermophysical properties of the fluids leading to the environmental impact and cost related issues. The aim of the study is to elaborate a tool for the comparison of the influence of different working fluids on performance of an ORC heat recovery power plant installation. A database of a number of organic fluids as well as a s oftware (code) which allows the user to select the proper organic fluid for particular application have been developed. Calculations have been conducted for the same heat source and installation component parameters. The elaborated tool should create a support by choosing an optimal working fluid for special applications and become a part of a bigger optimization procedure by different frame conditions.

Keywords: *Organic Rankine Cycle, Database, Heat Recovery*

Nomenclature

$\dot{Q}_{in}$ *heat flux input* ..... *.kW*
$\dot{m}$ *mass flow rate*.....*kg·s*$^{-1}$
π *pressure ratio*
h_i *specific enthalpy for process point i*...*kJ·kg*$^{-1}$
T_{high} *high system temperature*..... *°C*
T_{low} *low system temperature* ..... *°C*
p_{high} *high system pressure*.....*MPa*
p_{low} *low system pressure*.....*MPa*
$\eta_{turbine}$ *internal efficiency of the turbine*..... *%*
η_{pump} *internal efficiency of the pump*..... *%*
η_{system} *system efficiency* ..... *%*
P_{pump} *power used by the pump*..... *kW*
$P_{turbine}$ *output power of the turbine* ..... *kW*
$\dot{Q}_{out}$ *heat flux output in the condenser* ..... *.kW*

1. Introduction

Nowadays, with energy demand rising at an ever increasing rate, efficient use of energy has become a m ajor issue. One candidate suitable for improving efficiencies of existing applications and allowing the extraction of energy from previously unsuitable sources is the Organic Rankine Cycle. Applications based on t his cycle allow the use of low temperature energy sources such as waste heat from industrial applications, geothermal sources, biomass fired power plants and micro combined heat and power systems.

Waste heat represents the heat produced by machines, electrical equipment and industrial processes which has no practical use. Usually it's generated by fuel combustion or by chemical reaction. The difficulty of capturing, distribution or transformation into other forms of energy comes from the characteristics of the heat source and the high costs connected to the equipment needed to transform the heat into useful energy. Statistical investigations indicate that low-grade waste heat accounts for 50% or more of the total heat generated in industry [1]. There are several types of industrial waste heat sources, some of which are presented in Table 1.

Table 1. Waste heat sources and their quality. [2]

Waste heat source	Quality of waste heat and possible use
Heat in flue gases	The higher the temperature, the greater the potential value for heat recovery
Heat in vapor streams	As for heat in flue gases, but when condensed, latent heat is also recoverable
Convective and radiant heat loss from the exterior of equipment	Low grade – if collected, may be used for space heating or air preheating
Heat losses in cooling water	Low grade – useful gains if heat is exchanged with incoming fresh water
Heat losses in providing chilled water or in the disposal of chilled water	1. High grade if it can be utilized to reduce demand for refrigeration 2. Low grade if refrigeration unit used as a form of heat pump
Heat stored in products leaving the process	Quality depends upon temperature
Heat in gaseous and liquid effluents leaving process	Poor, if heavily contaminated & thus require alloy heat exchanger

Organic Rankine cycle is a Clausius – Rankine cycle which uses an organic fluid instead of water. The replacement of water with organic fluids brings a number of advantages over the classical steam process. Due to their thermophysical characteristics, such as low critical point, low boiling temperature and high molecular mass, the transformation of low temperature heat into useful electrical energy is possible and can be effective (higher efficiency than other possibilities).

Because of the low critical point relative to water and because the temperature level of the heat input is much lower than in the case of steam processes, the working pressures are lower and thus, they lead to a small-scale, low-cost installation which in most cases does not require permanent supervision [6].

Fluid selection for any type of ORC application is a very important step in designing an efficient working system. There are many important aspects that need to be taken into consideration before choosing an organic fluid. In this context a special fluid database with an implemented selection algorithm has been created with the possibility of continuous development.

2. Database

The database has been assembled in MS Excel due to the wide spread of the program and the fact that it facilitates the structuring and organization of data sets in an easy and intuitive way. Another major advantage of MS Excel is the relative ease with which one can import data either from other databases or from experimental data. The characteristics of the fluids have been sorted in two major groups, each containing multiple parameters: thermophysical characteristics and environmental characteristics.

2.1. Themophysical characteristics

One of the thermophysical characteristics of the organic fluids is the slope of the saturation curve in the temperature-entropy diagram. It can be negative, isentropic or positive, as shown in Fig. 1.

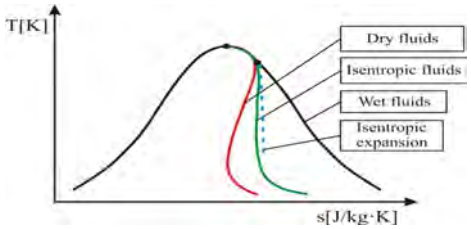

Fig. 1. Typical T-s diagram for dry, isentropic and wet fluids

In the case of dry and isentropic fluids there is no need for overheating. Because of the theoretical isentropic expansion in the turbine, in the case of wet fluids, overheating must be applied in order to avoid the creation of liquid droplets during the expansion in the turbine which would damage the turbine blades. Due to this characteristic the database contains information about the type of saturation curve for each contained fluid.

For practical reasons the low pressure value has been set to just above the atmospheric pressure (0.15 MPa). This limit must be imposed in order to avoid infiltration of air in the installation which would lead to the damaging of components. Also, for the moment, the low temperature value has been set to the value of normal ambient temperature (20 °C). Of course the real frame conditions of a real process, especially the temperature of the cooling medium, determine these values, which can be varied.

Another important characteristic is the boiling temperature at the low pressure value of the fluid. If it's lower than the ambient temperature then the minimal pressure value at which the fluid is in a liquid state at room temperature must be identified and set as the new low pressure value. This has to be done in order to maintain the highest possible value for the pressure ratio π of the expander, as a higher pressure drop yields a higher efficiency and it has been done for each fluid in the database.

There are other thermophysical parameters that must be taken into consideration when choosing a working fluid. Some of these are:
- low freezing point, so that the fluid will not solidify when it's in the low-temperature area of the process;
- the critical pressure and temperature should be above the highest values of these parameters in the process;
- the vaporization heat and the density of the fluid should be high, as a fluid with these characteristics will absorb more energy from the source in the evaporator and thus reduce the required flow rate, the size of the facility, and the pump consumption.

2.2. Environmental characteristics

Although high system efficiency is the main goal when designing heat recovery systems, one has to take into account the environmental characteristics for safety and practical considerations. For example, as the HCFCs still contain chlorine and have an associated Ozone Depletion Potential, they will be phased out in the EU Community from the 1st of January 2010 [3]. So, the availability of HCFCs for equipment servicing following the phase-out may not allow for predictable economical use.

Two main environmental characteristics are the ODP (Ozone Depletion Potential) and the GWP (Global Warming Potential). ODP represents the relative amount of degradation that a fluid can cause to the ozone layer. The standard of reference has been set for trichlorofluoromethane (R11). It has the value of 1 and the maximum potential of ozone depletion among chlorocarbons because of the three chlorine atoms in its composition. [4]

GWP represents a parameter that quantifies the contribution of a given mass of greenhouse gas to global warming. The standard of reference in this case is set for carbon dioxide with a given value of 1. Another important characteristic is the safety classification. After a careful analysis the ASHRAE (American Society of Heating, Refrigerating and Air-Conditioning Engineers) classification has been chosen because of the high number of organic fluids covered and the relative simplicity of the annotations of the safety classes. These are as follows in Table 2:

Table 2. ASHRAE safety classification. [5]

Flammability	Low toxicity	High toxicity
High	A3	B3
Low	A2	B2
Non-flammable	A1	B1

2.2.1. Toxicity classification [5]

Refrigerants are divided into two groups according to toxicity:
• Class A signifies refrigerants for which toxicity has not been identified at concentrations less than or equal to 400 ppm;
• Class B signifies refrigerants for which there is evidence of toxicity at concentrations below 400 ppm.

2.2.2. Flammability classification [5]

Refrigerants are divided into three groups according to flammability:
• Class 1 indicates refrigerants that do not show flame propagation when tested in air at 21°C and 101 kPa;
• Class 2 indicates refrigerants having a lower flammability limit of more than 0.10 kg/m^3 at 21°C and 101 kPa and a heat of combustion of less than 19 kJ/kg;
• Class 3 indicates refrigerants that are highly flammable as defined by a lower flammability limit of less than or equal to 0.10 kg/m^3 at 21°C and 101 kPa or a heat of combustion greater than or equal to 19 kJ/kg.
The database interface allows the user to select the type of installation for which the fluid data will be analyzed. Momentarily the installation layouts that are available are:

- Undercritical single stage;
- Undercritical single stage with recovery;
- Undercritical two-stage;
- Supercritical single stage.

The major fluid parameters are introduced for each existing fluid in the database, with the possibility of adding either other fluids and/or other parameters of interest. The general layout of the existing list with some of the parameters present in the developed program can be seen in Fig. 2:

		Critical point					
Working fluid	Boiling point at p=0.1 MPa [°C]	Temperature [K]	Pressure [MPa]	Molar mass [g/mol]	Slope	Toxicity group	ODP
R11 (Trichlorofluoromethane)	23,77	471	4,41	137,37	Isentropic	A1	1
R113 (Trichlorotrifluoroethane)	47,6	487,26	3,39	187,37	Positive	A1	0,9
R114 (Dichlorotetrafluoroethane)	3,5	419,1	3,25	170,9	Positive	A1	0,85
R115 (Chloropentafluoroethane)	-39,1	353,1	3,15	154,5	.	A1	0,4
R116 (Chloropentafluoroethane)	-78,2	293,1	3,04	138	.	A1	0
R12 (Dichlorodifluoromethane)	-29,8	385	4,41	120,91	Negative	A1	0,82
R123 (Dichlorotrifluoroethane)	27,8	456,9	3,7	152,93	Positive	B1	0,02
R124 (Chlorotetrafluoroethane)	-11	395,5	3,62	136,5	Isentropic	A1	0,022
R125 (Pentafluoroethane)	-48,5	339,4	3,63	120	Isentropic	A1	0
R13 (Chlorotrifluoromethane)	-81,3	302	3,97	104,5	Negative	A1	1
R1381 (Bromotrifluoromethane)	-57,75	340,08	3,95	148,91	.	A1	13
R134a (Tetrafluoroethane)	-26,1	374,2	4,06	102	Isentropic	A1	0
R14 (Tetrafluoromethane)	-127,8	227,5	3,75	88	Negative	A1	0
R141b (dichlorofluoroethane)	32,05	477,6	4,25	117	.	.	0,1
R142b (chlorodifluoroethane)	-9,8	410,4	4,12	100,5	.	A2	0,07
R143a (Trifluoroethane)	-47,6	346,1	3,78	84	.	A2	0
R152a (Difluoroethane)	-25	386,5	4,52	66,1	Negative	A2	0
R21 (Dichlorofluoromethane)	8,92	451,7	5,71	102,9	Negative	.	0,04
R218 (Octafluoropropane)	-36,7	345,1	2,68	188	.	A1	0
R22 (Chlorodifluoromethane)	-40,8	363,3	4,99	86,5	Negative	A1	0,05

Fig. 2. Fluid list with selected available fluids and parameters

Each fluid has a series of static parameters, such as ODP, GWP, molar mass, boiling point at atmospheric pressure and others, which are introduced when the fluid is added to the database and which never change. The dynamic parameters such as the cycle efficiency, the mass flow rate and the pressure ratio are calculated and are modified with the alteration of the input parameters which will be described in the following section.

Because the program is developed in MS Excel the interface and the fluid data are stored in the same document on different worksheets. Fig. 3 presents captions from both the interface and the database and the flow of data through them:

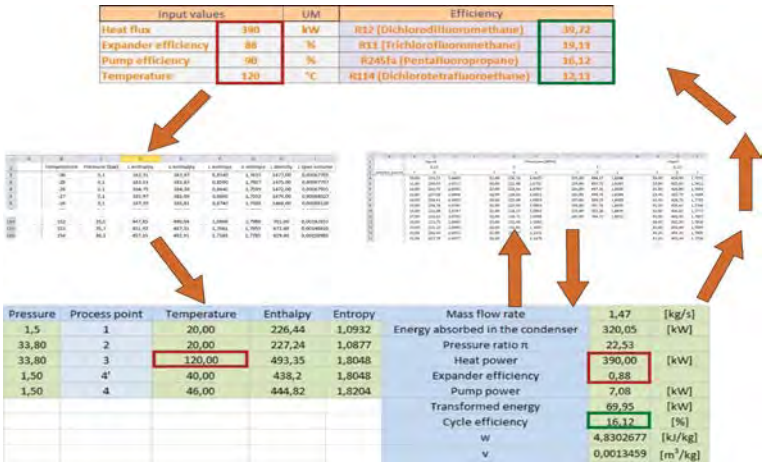

Fig. 3. Flow of data through the program

For each fluid from the database there are three worksheets. One contains the liquid and vapor enthalpy and entropy and other parameter values for the fluid along the saturation curve, one contains temperature, enthalpy and entropy values for the different process points and the third worksheet contains the calculation interface for the fluid and all the functions needed to implement the calculation procedure in the program.The user introduces the values for the input parameters, marked by the red rectangles, and the program returns the output parameters, marked with the green rectangles. For example, the program reads the temperature value introduced by the user and, by using the ”MATCH” function from Excel, it extracts the values for the enthalpy, entropy and pressure from the first data worksheet (saturation property curve) for each fluid. With these values, the program calculates and extracts values for the parameters for each process point and, finally, it returns the cycle efficiency. This value is introduced in the fluid list and it is updated whenever the input parameters are modified. From here the program returns a list of the fluids which yield the highest efficiencies (the top 4 in example from Fig. 3) for this set of input parameters.

3. Calculation procedure

As mentioned above, beside the general and environmental properties, the program returns the cycle efficiency for each fluid. This is done by employing a set of functions embedded in Excel which interrogate, search, match and return the desired data.

For the moment, the program executes calculations for a standard single stage cycle without recovery. The general layout of the installation, the process points and the T-s diagram (in this case for R114) can be seen in Fig. 4.

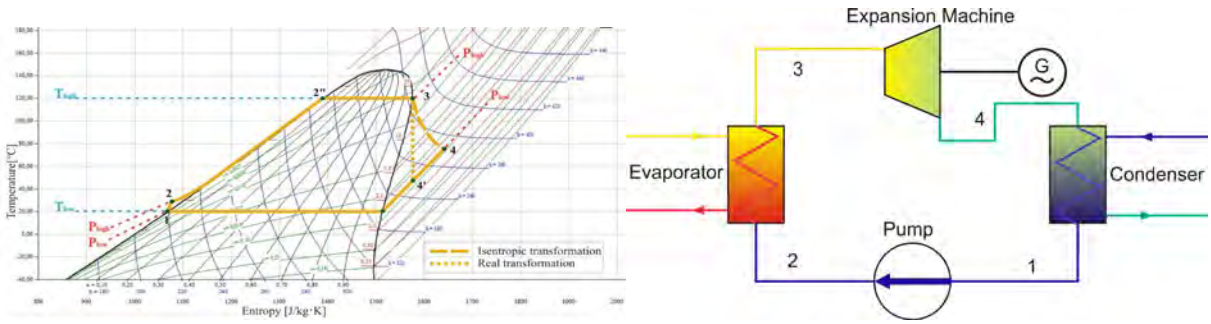

Fig. 4. T-s diagram and installation layout for a simple one-stage process

At the current state, the major input parameters for the program are the heat flux transferred to the system and the temperature at the inlet of the turbine (process point 3 in this case). The program calculates the efficiency of the cycle without overheating. So after introducing the heat flux and the turbine inlet temperature, the program chooses the corresponding pressure from the saturation curve for each fluid. The low pressure value is set to just above the atmospheric pressure (at 0.15 MPa) and the low temperature is set to the standard ambient temperature (20 °C).

With the value of the heat flux, the program calculates the mass flow rate:

$$\dot{m} = \frac{\dot{Q}_{in}}{h_3 - h_2} \tag{1}$$

where h_2 *and* h_3 represent the enthalpy values for process points 2 and 3.
By obtaining the high pressure value from the saturation curve, the program calculates the pressure ratio which is a good indicator for the system efficiency.

$$\pi = \frac{p_{high}}{p_{low}} \tag{2}$$

The internal efficiencies of the turbine and the pump are also input values. They can be selected from a drop-down list within the range of 0% to 100%, leading to a number of four input parameters. The expansion in the turbine is theoretically isentropic. The values for the irreversible process are obtained from the internal efficiency of the turbine.

$$\eta_{turbine} = \frac{h_3 - h_4}{h_3 - h_4'} \tag{3}$$

where the enthalpy values are obtained from the database for each fluid by matching the temperature and entropy values. By obtaining the value for the enthalpy in process point 4 the other parameters are extracted from the database. The power required for the pump is calculated with the following formula:

$$P_{pump} = \frac{v \cdot (p_{high} - p_{low})}{\eta_{pump}} \cdot \dot{m} \tag{4}$$

The output power of the turbine is calculated with the help of the internal efficiency of the turbine and by extracting the enthalpy values for process points 3 and 4 from the database:

$$P_{turbine} = \dot{m} \cdot \eta_{turbine} \cdot (h_3 - h_4) \tag{5}$$

The heat flux extracted in the condenser is calculated with the following formula:

$$\dot{Q}_{out} = \dot{m} \cdot (h_4 - h_1) \qquad (6)$$

After obtaining the values for each of these parameters, the program calculates the system efficiency as follows:

$$\eta_{system} = \frac{P_{turbine} - P_{pump}}{\dot{Q}_{in}} \cdot 100 \ [\%] \qquad (7)$$

The program returns the value for the system efficiency for each fluid in the database. If the input parameters lead to data that is outside the set conditions it will return "N/A" which signifies that the fluid is not suitable for the given input parameters.

In the current version the program returns a list of fluids which allow the highest system efficiencies for the input data set. In the following months more data and calculation procedures will be introduced so the program can calculate efficiencies of other types of installations, as shown in Figures 5, 6 and 7.

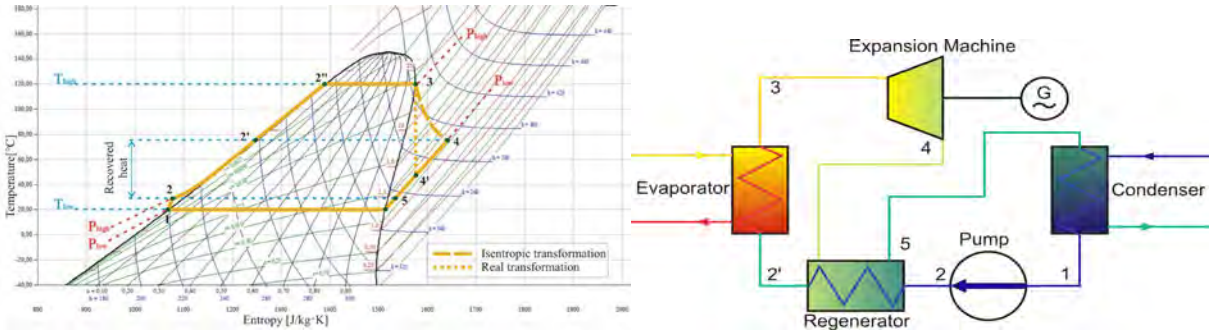

Fig. 5. T-s diagram and installation layout for a one-stage with recovery process

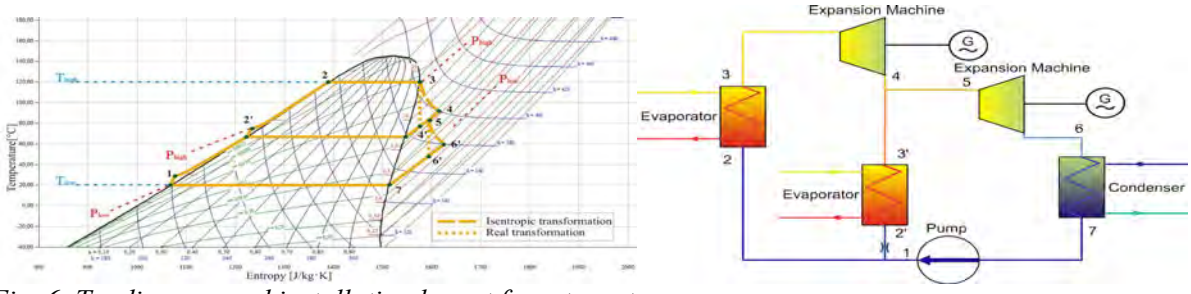

Fig. 6. T-s diagram and installation layout for a two-stage process

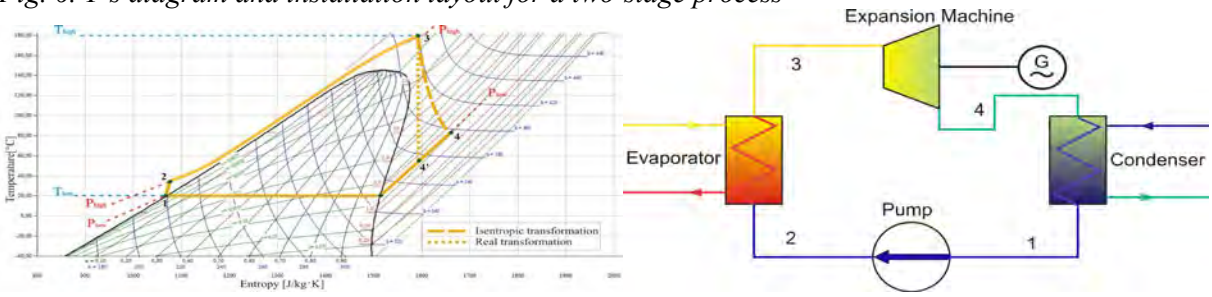

Fig. 7. T-s diagram and installation layout for a supercritical one-stage process

Further steps will consist of introducing the possibility of overheating and thus moving away from the saturation curve, the possibility of modifying the set values for the low pressure and

temperature as well as different sorting criteria such as cost, environmental aspects, availability and others.

4. Conclusions

Fluid selection is a major step in designing heat recovery systems based on the organic Rankine cycle. Although at this moment the sorting criterion for the fluids is the system efficiency, further development of the proposed program will create the possibility for different sorting criteria.

Developing this application has revealed that a program dedicated to fluid selection for heat recovery systems has a high degree of complexity. Although this application can give an idea to the user about the performance of different fluids applied to the same type of installation, one has to remember that the data still has to be compared to experimental data.

While the program is a good indicator for the influence on the system performance of different organic fluids, returning other fluid parameters in the process, the final decision of selection of an organic fluid for a given set of frame conditions remains to be made by the engineer designing the system. Costs related to fluid purchase, lifetime costs, taxes and availability may lead the designer to choose a lower efficiency yielding fluid.

To increases the level of complexity of the program and to bring the results, from theoretical, closer to real, measurable values, the interface from the heat source and the system will be investigated.

Another task that needs to be considered within the next steps is the investigation of energy and exergy losses in the expansion machine and exergy losses in the heat exchangers.

References

[1] T. C. Hung, T. Y. Shai, S. K. Wang, A review of organic Rankine cycles (ORCs) for the recovery pf low-grade waste heat, Energy, Vol. 22, No. 7, 1997, pp. 661 – 667.

[2] United Nations Environment Programme, 2006, www.energyefficiencyasia.org.

[3] Europa, Summaries of EU legislation, <http://europa.eu/legislation_summaries/environment/air_pollution/ev0021_en.htm>.

[4] Ozone Depletion and Chlorine Loading Potential of Chlorofluorocarbon Alternatives, CIESIN Thematic Guides, < http://www.ciesin.org/TG/OZ/odp.html>.

[5] Classification of refrigerants, International Institute of Refrigeration, <http://www.iifiir.org/en/doc/1034.pdf>.

[6] A. Pîslă, D.C. Bândean, Investigations on a Two Stage ORC Installation, 2010 IEEE International Conference on Automation, Quality and Testing, Robotics, AQTR 2010 - THETA , Cluj-Napoca, Romania.

Examining the effect of heat storage in a cogeneration system

G.R. Salehi [1*], E. Taghdiri [2], D. Deldadeh[2]

[1]*Islamic Azad University Noshahr Branch,Noshahr,Iran*
[2] *KNToosi University of Technology,Tehran,Iran*
** Corresponding author. Tel: +989122031671, E-mail: rezasalehi20@gmail.com*

Abstract: Small power plants of cogeneration of power, heat and cooling are good solutions of increasing the efficiency of energy consumption for fossil fuels in order to protect natural resources and the environment. However, at moments when heat demand is lower than the heat production of the CHP module, the excess heat has to be rejected to the environment and this fact results in waste of energy. Also, since CHP modules are basically heat driven, when heat demand is lower than a certain value, the module will be switched off just to be switched on later when heat demand increases. This cycle of switching on and off is harmful for the CHP module if it happens repeatedly. A solution is to use heat storage and an alternative control method. In this paper, a CHP system is chosen for an educational building and the design is carried out in two forms, with and without heat storage and the results are compared and judgment is made about the optimal system.

Keywords: *CHP, optimization, environment, heat storage*

1. Introduction

When power is produced traditionally, a large portion of original energy of the fuel is wasted as heat and hardly more than 40 pe rcent of this energy is transformed into electricity. Moreover, usually consumers are located far away from the power plant and this distance causes more waste of energy in distribution of electricity. One way to tackle these problems is using local cogeneration. In this modern method of power generation, power is produced at the location of consumption and the majority of lost heat is recovered to supply heat demands of the user. This results in a considerable improvement in efficiency. Furthermore, since power is generated at the same location where it is consumed, distribution losses will be avoided. The total efficiency of cogeneration power plants amounts up to 90%, while the electrical efficiency of a traditional power plant hardly reaches 40%.

Among different options of power generation in the form of cogeneration, reciprocating engines seem to be the most suitable for buildings which essentially have small demands. They have high power to heat ratios compared to gas turbines and due to advances made in automotive industry, enjoy a higher degree of modernization [9]. Although stationary reciprocating engines have traditionally been diesel engines but some issues like environmental issues and good access, have been promoting the users in recent years to use natural gas as the fuel instead. In Iran, a Persian gulf country with the second largest resource of natural gas in the world, even automobiles are increasingly using gas burning and dual fuel engines.

X Q Kong et al (2004) optimized a trigeneration system (cogeneration of heat, power and cooling) based on gas turbine. In their research a trigeneration system was modeled and then, after specifying constraints and an objective function, the solution was optimized using a linear modeling program [2]. In another work, they examined a co generation system and presented the results as graphs and tables [3]. In 2005 P. Arcuri et al designed optimally a trigeneration system using a mixed integer model. They optimized a trigeneration system for a hospital employing a reciprocal engine as its prime mover [4]. In 2006 E. Cardona and A. Piacentino designed and optimized a trigeneration system for a hospital application from the thermoeconomic point of view [5]. The same researchers carried out another analysis for an apartment building using the thermoeconomic method [6]. In 2008, Behbahani Nia et al. [7]

optimized a cogeneration system based on gas turbine with the aim of minimizing the capital cost in which they considered electricity, heat and cooling demands for each month.

In this paper, a cogeneration system is designed and optimized for the building of mechanical engineering faculty of K.N. Toosi University of technology in Tehran, Iran, using two different strategies, with heat storage and without heat storage. First, energy simulation is carried out using the software Carrier HAP 4.2 resulting in values of electricity and heating demands in all 8760 hours of the year. Later, based on these demands, the main components of the CHP system are designed based on products of the Austrian manufacturer, Jenbacher®. Products of this company are cogeneration modules including the reciprocating engine, heat recovery system and electrical generator all in one, covering a range of capacities from 400kWth to 3MWth.

2. A description of the building

The building of mechanical engineering faculty of K.N. Toosi University of technology is a ten-floor building, including 3 underground floors and covering about 20 thousand square meters of area. The second and third floors contain classes, fourth and fifth floors contain administrative rooms, almost all of which benefit from natural light during daytime. The sixth floor is dedicated to professors' rooms about half of which have access to natural light. The library and some laboratories are placed on the first floor. Ground floor primarily contains public places like the big lobby, the pray place, computer services hall and so forth. The floor -1 contains laboratories, cafeteria, the big restaurant and the amphitheatre. The floors -2 and -3 are for workshops and labs and also sport activity salons. Table 1 shows a list of areas of these floors.

Table 1. Area of each floor of the building

Floor	Area (m^2)	Floor	Area (m^2)
Ground floor	2561.6	Fifth	1005
First	2500	Sixth	1007
Second	1006.9	-1	3100
Third	1005.99	-2	3100
Fourth	1004.36	-3	3100

3. Calculation of loads

Thermal and electrical loads have been calculated using the energy simulation function of the software Carrier HAP 4.2. All parts of the building were modeled and wattages of lights, electrical equipments, geometrical and heat transfer features of rooms were entered in the software. A total of 270 spaces were defined in the process. Another important issue in determining loads is the presence of people in different spaces. Schedules were defined for presence of people in different types of spaces including classes, amphitheatre, computer services salon, corridors, administrative rooms, pray place, restaurant and security compartments, and also for lighting for each of these types of places, based on percentages of full presence or full lighting in different hours of the day and different days of the year. National holidays and weekends were considered based on the year 2009 which covers portions of Persian years 1387 and 1388. The difference of intensity of natural light in summer and winter days and different levels of presence of students and employees in different months of the year and different hours of the day were all considered based on personal observation of the second author who has been a studying in the same building for two years. The monthly distribution of heating and cooling loads resulting from this energy simulation is as shown in figure 1.

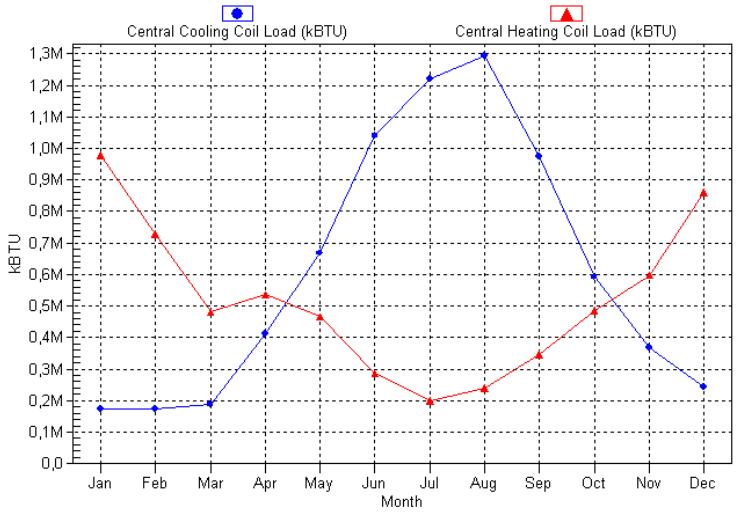

Fig. 1. Heating and cooling loads throughout the year.

The weather conditions were defined based on simulation information of www.Carrier.com of Tehran including hot and cold bulb temperatures and sunlight situation throughout the year.

4. Selection of cogeneration modules

Selection was carried out based on products of Jenbacher, including 13 models of CHP modules. The manufacturer did not reply requests of price quotation and purchase equipment costs and O&M charges were estimated using the information in [9] and by curve fitting. The cost of natural gas and electricity were taken 690 Rials per m3 and 773 Rials per kWh, equal to Iranian unsubsidized rates.

Another issue which was considered in this optimization was the environmental issue. According to [9], emission of pollutants imposes costs which are in fact costs of reduced performance of human beings caused by these pollutants. This fact is considered as costs assigned to pollutants CO, CO2 and NOx. According to catalogs of the manufacturer, using the lean combustion system and SCR catalysts, emissions of CO and NOx caused by their products are limited to 100 mg/Nm3 for Nox and 300 mg/Nm3 for CO. CO2 emission from natural gas combustion is equal to 1.15m3/1m3 Natural Gas according to [11] which by considering the density of carbon dioxide in normal conditions equals to 20420mg/Nm3. Values of emissions of CO and NOx for small boilers are 641mg/Nm3 and 1506 mg/Nm3 respectively, according to [12]. As calculated in [9], the social cost associated with these emissions is 81750 Rials/kg for carbon monoxide, 240 Rials/kg for carbon dioxide and 64240 Rials/kg for Nitrogen oxides. Therefore, the social costs for burning of each cubic meter of natural gas for Jenbacher® reciprocating engines and the boiler are as shown in tables 2 and 3.

Table 2 Emissions and their costs for natural gas-burning boiler

	(mg/m^3)	kg/kWh	Unit cost($/kg)	Unit cost ($/kWh)
NOx	1506	0.014843136	6.424	0.095352306
CO	641	0.006317696	8.175	0.051647165
CO_2	20420	0.20125952	0.024	0.004830228
		Total emission cost($/kWh)		0.151829699

Table 3 Emissions and their costs for natural gas-burning engine

	(mg/m^3)	kg/ kWh	Unit cost($/kg)	Unit cost($/kWh)
Nox	100	0.0009856	6.424	0.006331494
CO	300	0.0029568	8.175	0.02417184
CO_2	20420	0.20125952	0.024	0.004830228
		Total emission cost($/kWh)		0.035333563

5. Choosing capacities of components and optimization

5.1. The case without heat storage

In this section, sizing is carried out in two different strategies, one is the absence of heat storage and the other is its presence. In both strategies, modules of cogeneration and their annual working durations are determined so that the total annual cost is minimized.

For the case where there is no heat storage system, the CHP system is designed based on load-duration curves. These curves are constructed using the hourly load data taken from energy simulation, i.e. first values of heating and electrical loads for all 8760 hours of the year are taken from outputs of Carrier HAP and then, those numbers are put in descending order and plotted against duration, from 1 hour to 8760 hours. According to [13], the largest rectangle which can be circumscribed in that curve represents the optimal choice of the CHP system, in terms of capacity (on the vertical axis) and number of total working hours throughout the year, on the horizontal axis. Here, the basic idea is quiet similar. However, this curve is used here to determine the capacity of the supplementary boiler which is the difference of maximum load with the heat production of the CHP module and its total heat production throughout the year being equal to all heat demand not satisfied by the module.

Electricity is considered as a bi-product of the system that can be used locally or sold to the network. The rates of buying and selling power to the network are very close to each other in Iran [20] and both are assumed to be 773 Rials. If a CHP system is independent from the grid, it can employ batteries to store excess electricity to be used later but when selling power to the grid is possible, using storage of electrical energy is not economical [9].

The control strategy used for the case where there is no heat storage system is as follows: When the number of working hours of the CHP module determined from optimization is plot with load-duration curve, the point where it intersects that curve shows the value of minimum load for operation of the module, i.e. when the thermal load is lower than that value, the module will be switched off and when the load exceeds that value, the module will be switched back on.

In manufacturer's catalogs, two heuristics are suggested:

- The thermal power of the cogeneration power should be between 30 to 50 percent of the peak value of thermal power demand.
- The module of cogeneration should work at least 4000 hours during a year.

Figure 2 shows an example of load-duration curve.

Figure 2. Load duration curve for heating load

Naturally there will be times when the heat demand is higher than the production of modules and at these times this heat shortage is covered by the auxiliary boiler.

Load-duration curves for heating, and electrical loads of our building are shown in figures 3 and 4.

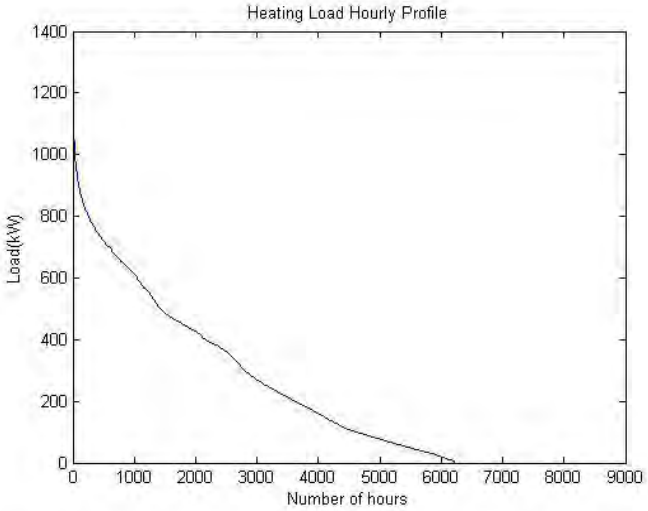

Figure 3. Load-duration curve for heating load

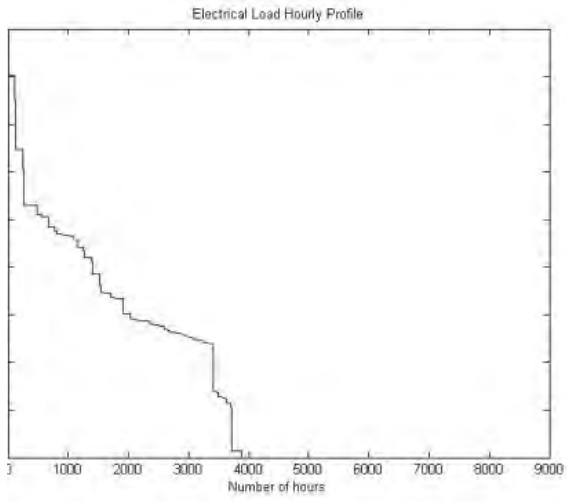

Figure 4. Load-duration curves for electrical load

Now, the objective function for the optimization is defined as the total annual cost of the system. To calculate the total annual cost, first we should annualize capital investments using the capital recovery factor (CRF) .

Where i_r , the interest rate, according to [14] is taken 12 percent, and *n* is the number of years of life time of the system, here taken 20 years. Thus, the objective function is:

$$C_{Ann} = CRF \times (C_{TCM} + C_{TCAB} + C_{TCST}) + C_{O\&M\,Module} + C_{O\&MAB} + C_{Emi} - C_{el} \quad (1)$$

Where C_{Ann} is the total annual cost, C_{TCM} is the total capital investment for the CHP module, C_{TCAB} is the total capital cost for the auxiliary boiler, C_{TCST} Is the total capital cost for the storage tank (if included), $C_{O\&M\ Module}$ is yearly O&M plus fuel costs for the cogeneration modules, $C_{O\&MAB}$ is the yearly O&M plus fuel costs for the auxiliary boiler, C_{Emi} is the yearly emission cost and C_{el} is yearly cost of electricity production which is the profit of the system and therefore appears with a negative sign in the total annual cost. The optimization is carried out using the direct search method. For this optimization, decision variables are taken to be capacities of CHP modules and their durations of operation throughout the year. Constraints are defined based on heuristics provided by the manufacturer, namely each module should not operate less than 4000 hours in the year, and the values of capacities of modules and the boiler, naturally may not be negative and the values of working hours of each of modules cannot be more than 8760 hours. Results are as presented in the next section.

5.2. The case with heat storage

If we decide to employ heat storage in our system for more smooth operation and less waste of energy, a different design and operation strategy has to be used. Heat is stored as hot water (90^oC) in a well insulated storage tank. Its cost data is taken from [14] and (1) is also used for cost estimation, using two different values of the exponent α (0.3 and 0.65) based on the calculated volume. The cost data is available in terms of volume of the storage tank while in the optimization, the capacity in terms of energy storage is considered. As mentioned in [15], the CHP module receives cooling water at 40^oC and sends it out at 90^oC. Thus, in order to determine the volume of the storage tank conservatively, we take the unit volume energy of the water stored in this tank as the difference of enthalpy of water in those input and output states.

Thus, by storing each cubic meter of water in the storage tank, we have stored 58.167kWh thermal energy.

After calculating the Purchased Equipment Cost (PEC) in terms of energy storage capacity, we calculate the Total Capital Investment (TCI) based on the Fixed Capital Investment (FCI) and the PEC using the factors listed in table 4. The data in this table are based on results reported in [14]. For costs having upper and lower bounds of the range of value, in absence of other data, the average of the two bounds mentioned in table 4 is used in calculations.

Table 4. Components of total capital investment

I - Fixed Capital Investment (FCI)
A- Direct costs 1- Costs associated with the site
• Purchased Equipment Cost (15-40% FCI) • Installation cost (20-90% PEC) • Piping (10-70% PEC) • Instrumentation and control equipments (6-40% PEC) • Electrical Equipments (10-15% PEC)
2- Off-site costs • Land (0-10% PEC) • Civil, architectural and structural costs (15-90% PEC) • Service facilities (30-100% PEC)
B- Indirect costs
1- Engineering and supervision (25-70% PEC) 2- Construction cost including the profit of the contractor (15% of direct cost) 3- Contingencies (8-25 % the sum of the above costs)
II- Other costs
A- Start up cost (5-12% FCI) B- Working capital (10-20% TCI) C- Research and development (not considered in this paper)

When designing the cogeneration system with heat storage, we need to use load-time curves instead of load-duration curves. These curves show the value of thermal/electrical load at every hour for all 8760 hours of the year. Load-time curves for thermal and electrical loads are shown in figures 5 and 6.

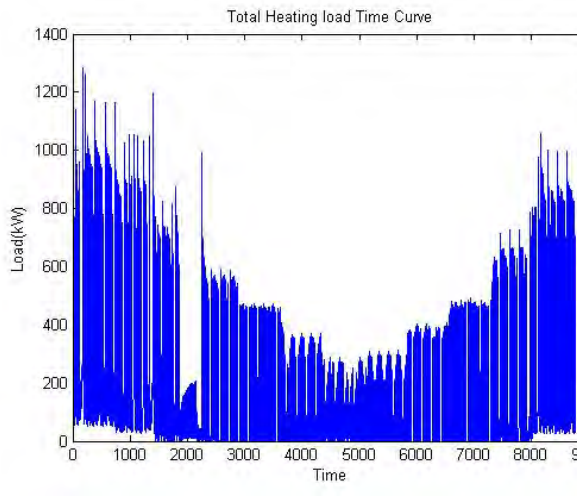

Figure 5. Load-time curve for heating load

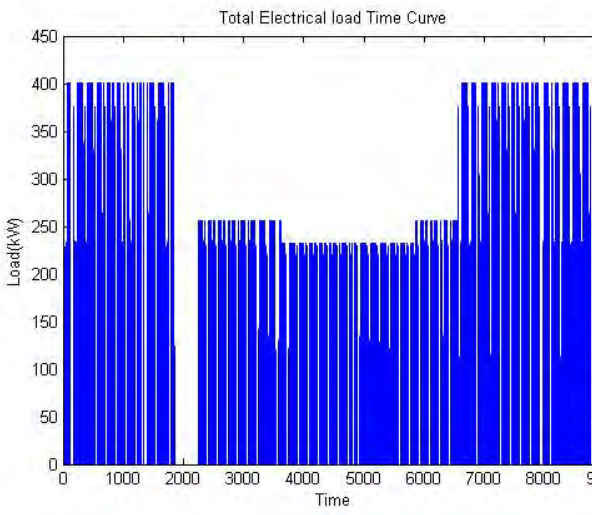

Figure 6. Load-time curve for electrical load

As a result of the above mentioned strategy, there will be fewer start-stop cycles and probably, less heat rejection to the surroundings. When optimizing the system in this case, working duration of the module will no longer be a decision variable but instead, the volume of the storage tank will be searched for its optimal value and working duration of the module will be determined from the volume of the storage tank and load-time curve. The other decision variable will be the size of the CHP module, as before. The results of optimization of this case are presented in the following section.

6. Results

Table 5. Optimization results for a CHP module without heat storage

	Capacity	Duration/amount of yearly operation	Capital investment cost (Rials)	O and M +Fuel costs (Rials per year)	Emission cost (Rials per year)
CHP Module	497kWth (J 312L)	4011h	8.63E+09	5.79E+08	1.55E+09
Boiler	786.6kW	439843kWh	3.44E+09	4.25E+07	9.21E+08
Value of yearly electricity production of the CHP module (Rials)				1.35E+09	
Maximum load (kW)				1284	
Total annual cost (Rials)				3.36E+09	
Yearly heat dissipation to surroundings(thermal energy waste)(kWh)				450306	

Table 6. Optimization results for a CHP module with heat storage

	Capacity	Duration/amount of yearly operation	Capital investment cost (Rials)	O and M +Fuel costs (Rials per year)	Emission cost (Rials per year)
CHP Module	497kW(312L)	8550h	8.63E+09	1.24E+09	3.31E+09
Boiler	994.1kW	292966 kWh	3.44E+09	2.83E+07	6.14E+08
Storage Tank	3.474m^3	202.1kWh (Max storage)	3.36E+08	-	-
Value of yearly electricity production of the CHP module (Rials)				2.88E+09	
Maximum load (kW)				1284	
Total annual cost (Rials)				4.06E+09	
Yearly heat dissipation to surroundings(thermal energy waste) (kWh)				1.95E+06	

As it is evident from tables 5 and 6, heat dissipation to surroundings and total annual cost are both higher for the case with heat storage than the simple case. Moreover, as illustrated in results, curves of electrical and thermal loads have more consistency with curves of energy production of the module in the simple case. However, in the case with the possibility of heat storage, more electricity is produced and the module works for a longer total duration, representing a smaller number of switching off and on cycles which is better for durability of the reciprocal engine and the whole module.

7. Conclusion

Heating and electrical loads were calculated for a 10-floor educational building using energy simulation of Carrier HAP®, and based on those loads, cogeneration systems were designed

to provide electricity and heating needs of the building. The CHP module was selected among 13 models of a globally renowned manufacturer.

Firstly, a simple CHP system was designed containing a CHP module and an auxiliary boiler. Secondly, the possibility of heat storage was taken into account using a storage tank as heat accumulator. Two different control strategies were considered for these two cases and consequently, design and optimization were also carried out differently.
Comparison of results showed that the simple system excluding heat storage had a lower total annual cost and heat dissipation to surroundings. On the other hand, it had a lower work duration for the CHP module and consequently, a larger number of switching on and off cycles representing its disadvantage to the system with heat storage.

References

[1] X. Q. Kong، R. Z. Wong، X. H. Huang، Energy optimization model for a CCHP system with available gas turbines، Applied Thermal Engineering 25 (2005) 377–391.

[2] D. W. Wu، R. Z. Wang، Combined cooling، heating and power: A review، Progress in Energy and Combustion Science 32 (2006) 459–495.

[3] P. Arcuri، G. Florio، P. Fragiacomo، 2007، A mixed integer programming model for optimal design of trigeneration in a hospital complex، Energy 32، 1430–1447.

[4] E. Cardona، A. Piacentino، A new approach to exergoeconomic analysis and design of variable demand energy systems، Energy 31 (2006) 490–515.

[5] E. Cardona، A. Piacentino، Optimal design of CHCP plants in the civil sector by thermoeconomics، Applied Energy 84 (2007) 729–748.

[6] Karimi Alavijeh, Saeed. Behbahaninia, Ali. Amidpour, Majid, Modeling and optimization of energy in a CHCP system with gas turbine prime mover, International Conference of Nonlinear Problems (ICNPAA 2008), 24-26 June 2008, Italy.

[7] Feasibility study of private sector's investment in development of local cogeneration systems in Iran, The department of power and energy of Iranian ministry of power, 2008, Tehran, Iran,24-26

[8] Technology characterization, reciprocating engines, Energy and Environmental analysis, Arlington,Virginia, December 2008, 12-16

[9] Mahdi Ali Ahyayi, Sharif University of technology, Tehran, Iran, Design and optimization of cogeneration of power, heating and cooling in different climate conditions of Iran, 2007, 41-45

[10] S.K. Sadr Nezhad, A. Kermanpour, Fuel and Energy, 2001, Tehran, Iran

[11] www.epa.gov/ttnchie1/ap42/ch01/final/c01s04.pdf

[12] S.S Bernow, D.B.Marron "Valuation of Environmental Externalities for Energy planning and Operations", May 1990, Tellus Institute, Boston, Mass., 1990

[13] Dries Haeseldonckx, Leen Peeters, Lieve Helsen, William D'haeseleer, The impact of thermal storage on the operational behaviour of residential CHP facilities and the overall CO2 emissions, 26 September 2005

[14] Adrian Bejan et al, Thermal design and optimization, 1996

[15] A.D. Hawkes a, P. Aguiar b, B. Croxford c, M.A. Leach a, C.S. Adjiman b,d, N.P. Brandon Solid oxide fuel cell micro combined heat and power system operating strategy: Options for provision of residential space and water heating, 28 November 2006

Low exergy heat recovery for sustainable indoor agriculture

Anthony Goncalves[1], Daniel Rousse[1,*], Julien Milot[2]

[1] *t3e Industrial research chair, École de technologie supérieure, Montréal, Canada*
[2] *Energy Solutions Associates, Lévis, Canada*
** Corresponding author. Tel: +1 (418) 833-2110, Fax: +1 (418) 396-8950, E-mail: daniel@t3e.info*

Abstract: With improved greenhouses, farmers have to ventilate. An air-to-air multi-tube counter flow heat exchanger unit was installed in a greenhouse used for the experimental cultivation of hydroponic tomatoes and cucumbers. This 24m long unit involves a 12" O.D. external shell used to exhaust moist air and five inner tubes to bring fresh air inside. The tests, carried out between March and May in a 576 m^3 enclosure, demonstrated that average efficiencies of η=84% and η=78% were obtainable with air volumetric exchanges rates of 0.5 and 0.9 change per hour, respectively. Latent heat was found to play a major role in the overall heat transfer, contributing about 40% of the total energy exchanged in some situations. The exchanger could be buried underneath the ground or suspended above the crops. The unit made of plastic is durable, rot and rust resistant, affordable, and is ice and frost compliant. A pre commercial implementation with an improved design is now considered in collaboration with Gaz Metro. This paper presents the original prototype that help in reducing the consumption of natural gas, fuel, bunker, or propane.

Keywords: *Heat exchanger, Latent heat recover, Sensible heat recovery, Plastic.*

Nomenclature

A	*Surface area*	m^2	
cp	*specific heat*	$J.kg^{-1}$	
f	*friction factor*	m^2	
D	*diameter of the tubes*	*m*	
h	*heat transfer coefficient*	$W.m^{-2}$	
k	*thermal conductivity*	$Wm^{-1}K^{-1}$	
L	*contribution of latent heat*	*%*	
l	*length of the tubes*	*m*	
$\dot{m}$	*mass flow rate*	$kg.s^{-1}$	
Nu	*Nusselt number, hD/k*	-	
Re	*Reynolds number*	-	
T	*temperature*	*K*	
i	*specific enthalpy*	$J.kg^{-1}$	

1. Introduction

1.1. Context

In recent years, passive infiltration of air into greenhouses has been reduced from three or more air changes per hour to less than one half [1]. The reduction of air infiltration into greenhouses leads to significant reductions in heating costs. However, this may be achieved to the detriment of the crops being grown. Very low air exchange rates can lead to abnormally high levels of humidity both during the daytime and at night.

The characterization of the influences of humidity on plant response has not yet been thoroughly investigated unlike those of light, temperature, and carbon dioxide [2]. This may be, in part, due to the difficulty in measuring and controlling humidity in large enclosures and to relate the humidity measurements to the transpiration rates of the crops [3]. Nevertheless, an afternoon above 95% RH may kill or damage a whole harvest. Furthermore, even when the crops are producing at high levels of humidity without any damage, their production rate is much lower than in a controlled environment.

To avoid excessively high humidity levels, venting and heating often remains the only solution to the farmer and this may annihilate the gains achieved by the reduction of infiltration. Traditional heating and ventilation systems result in an inefficient and expensive use of energy, especially during winter in cold regions of the world. To keep sustainable

development strategies, this exchanger should be low cost, user friendly, rot and corrosion resistance, efficient even when ice and frost are present, and, obviously, save energy. The purpose of this study is to design, build, and test such an exchanger to be used in greenhouses located in Northern countries.

1.2. Economics in cold regions

The *Syndicat des Producteurs en Serres du Québec* (SPSQ) [4] lists the problem of humidity control in greenhouses as a top priority for this industry. Table 1 [5] indicates the average annual energy requirement per unit area and its corresponding unit cost of operation, for a greenhouse located in Quebec (Canada), as a function of its dehumidification strategy. The data for unit costs are updated for 2011.

Table 1. Energy requirements and costs as a function of the ventilation strategy in greenhouses.

Dehumidification Strategy	Energy Requirement (MJ/m^2)	Cost* ($/m^2$)			Difference with/without ($/m^2$)		
		Gas	Oil	Electricity	Gas	Oil	Electricity
None	1672	29,14	44,13	35,76	-	-	-
1 vol/h	1883	32,81	49,70	40,28	3,68	5,57	4,51
Proportional	1980	34,50	52,26	42,35	5,37	8,13	6,59

Cost estimates based on: 37.3MJ/m^3@0.48$/$m^3$ and 80% efficiency for natural gas
38.9MJ/L@0.54$/L and 75% efficiency for oil no.2
3.6MJ/kW-h@0.077$/kW-h for electricity

In Table 1, the first row corresponds to unit heating costs when dehumidification is due to exfiltration of moist air only (balanced by infiltration of cold air), while most of the vapour condenses on the roof and the walls of the greenhouse. This situation is mostly found in old installations where passive infiltration is important. The second row shows figures for a situation where a whole change of air is made in the greenhouse in an hour. The last results presented in the third row of Table 1 pertain to the situation where the farmer ventilates to maintain an adequate level of humidity all the time. Table 1 shows that in cold climates: (1) about 13% to 18% of the heating costs of a standard greenhouse are due to humidity management; (2) proportional ventilation is about 5.4 (for natural gas) to 8.1 CDN$/$m^2$ (for Oil, indeed electricity is cheaper than oil in Québec) per year more expensive than no ventilation. This is twice as much as in the 1990s for which this cost varied from about 2.5 (for natural gas) to 4.7 CDN$/$m^2$ (for electricity). This represents a minimum extra cost of about 800$/y for a small 144 m^2 unit which results in millions of dollars for the 110 hectares of crops and 134 hectares of ornamental plants being grown in Quebec only. Hence, one of the objectives of the work is to provide an equipment with a low payback period to be used by most farmers. At last, it should be stated that the critical periods for ventilation are fall and spring for which crops are growing and a fast rate and condensation on the walls is not as important as in winter.

2. Methodology

2.1. Description of the prototype

After a feasibility study, it was decided to build a multi-tube counter-flow heat exchanger. In view of the restrictions formulated in the introduction, corrugated and flexible thermoplastic drainage tubing [6] was selected to serve as the core of the multi-tube exchanger, four thermoplastic tubes 76 mm I.D. wrapped around a central 101 mm I.D. tube were used. The external kernel or shell of the exchanger that carries the warm and moist air was a tube 305

mm I.D. with a corrugated outer surface (361 mm O.D.) and a smooth inside surface to permit ease of assembly [7], see Fig. 1.

Due to the unlimited amount of space available within greenhouses and because the major part of the exchanger could be buried or suspended, compactness [8] was not a critical parameter here. As a result the heat transfer area density of the first prototype was about 27 m^2/m^3. The first exchanger prototype was 24.3 m long and involved about 66.9 m^2 of direct exchange area. In the calculation of the exchange area, the effects of the corrugations have been taken into account. This yields about 100% increase over smooth tubes. The surface increase for the 76 mm tube is the same. Fig. 2(a) shows the warm end of the unit: the four gray tubes are carrying the warm moist air which is injected in the external shell. Fig. 2(b) shows the cold end of the prototype.

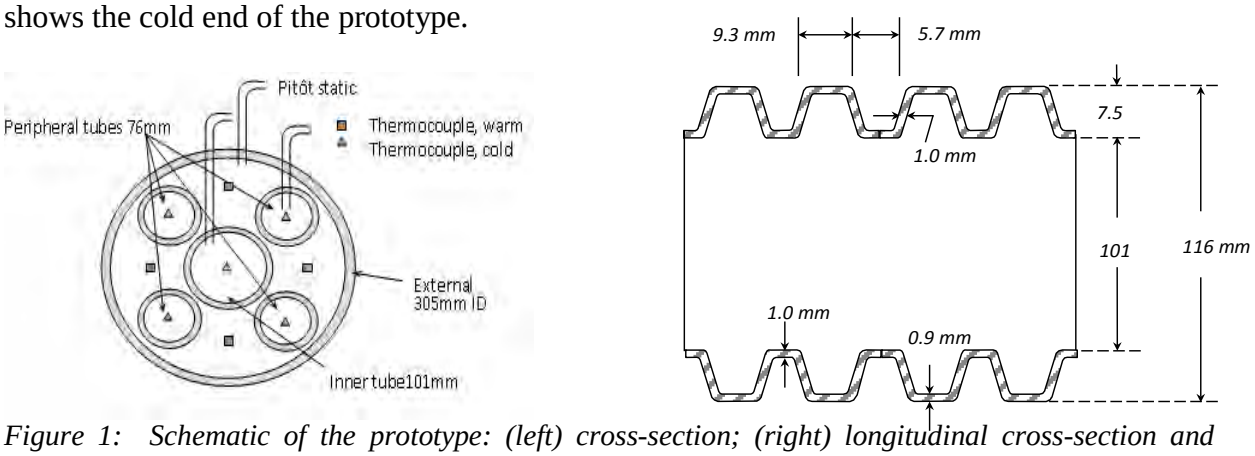

Figure 1: Schematic of the prototype: (left) cross-section; (right) longitudinal cross-section and geometrical details of the 101mm I.D. tube

It can be seen in Fig. 2b that the ventilator is built into the plenum and that the tubes are isolated to prevent condensation in the greenhouse. The overall cost of this prototype, excluding the fans, is much below 2000 CDN$.

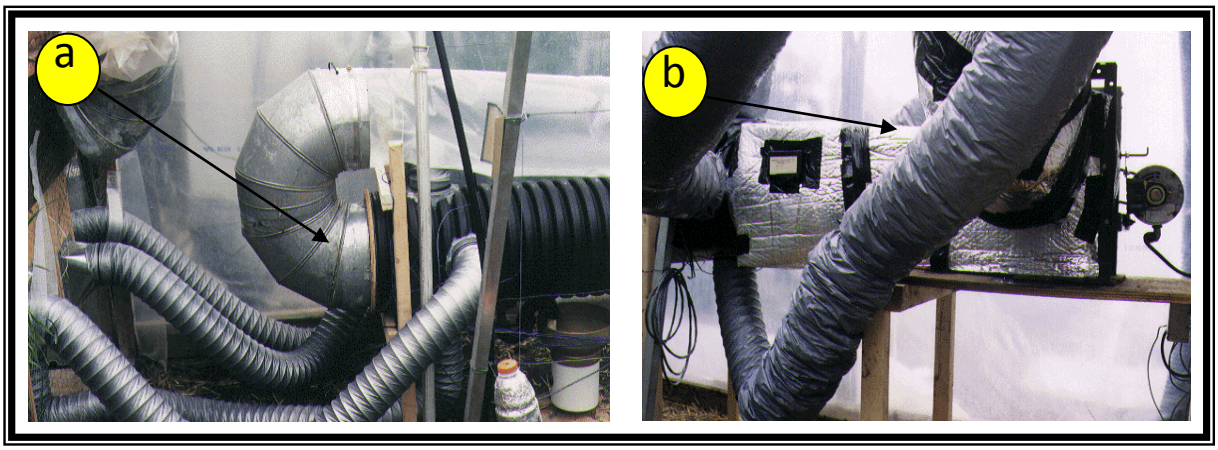

Figure 2: (a) The warm end of the unit; (b) The cold end of the unit

The size of the prototype is justified by the requirement to operate at subzero temperatures for which accumulation of ice should not significantly increase the pressure drop and decrease the overall efficiency. In addition to having a low area density, the original unit has been designed to permit a maximum volumetric exchange rate of one volume per hour in a 576 m^3 greenhouse located at the *Institut des Technologies Agro-alimentaires de St-Hyacinthe,*

Québec. The greenhouse is part of a larger complex involving several units. It is entirely covered by polyethylene films on the top and on its sides.

2.2. Numerical design tool

Brundrett et al. [1] proposed a simple model to design heat exchangers to be used as dehumidifiers in greenhouses. In [1], the authors proposed to carry out energy balances along the axis of the exchanger from one volume to the next. In dry and wet zones, the overall heat transfer coefficient is calculated differently while the external kernel is assumed to be adiabatic. These researchers validated their model with respect to results obtained from two prototypes. The prototypes involved two air streams separated by a polyethylene film on which condensation occurred as the warm and moist stream reached its dew point. In [1], the comparison between experimental and predicted performance is reported to be excellent. In that study [1], the discrepancies are believed to be due to heat transfer to the outer shell of the exchanger which is neglected in the model. Nevertheless, based on the model of Brundrett *et al*. [1], a one-dimensional basic numerical design tool was developed and implemented to allow for the design of the above-described prototype. The correlation that was used for the internal and external surfaces of the five tubes that constitute the core of the unit is the acknowledged relation proposed by Gnielinski [9,10] with the entrance correction factor derived by Hausen [11,12]. For the internal Nusselt number this yields:

$$Nu_i = \frac{(f/8)\left(\mathrm{Re}_{D_i} - 1000\right)\mathrm{Pr}}{1 + 12.7\sqrt{f/8}\left(\mathrm{Pr}^{2/3} - 1\right)}\left[1 + \left(\frac{D_i}{l}\right)^{2/3}\right] \quad (1)$$

where Re_{Di} is the Reynolds number, based upon the tube diameter D_i, Pr is the Prandtl number, and f is the friction factor [8]. For corrugated drainage tubes, there are no data available to quantify the relative roughness, ε/D. Hence, after a series of pressure drop measurements, ε was approximated to an average of 0.001m.

The outer shell was assumed to be adiabatic. The predictions then have to include the specifications of the psychometric properties of the hot air, with wet and dry bulb air temperatures and absolute pressure being required. The prediction model thus determines where the warm fluid will experience condensation of moisture by dropping below its dew point temperature. The calculation of the overall exchanger is then divided into two sections: the first where heat transfer occurs exclusively by sensible transfer and the second where heat transfer involves latent as well as sensible heat. The overall heat transfer between the hot and cold fluids is given by:

$$q = \dot{m}_o\left(i_{o,inlet} - i_{o,outlet}\right) = \dot{m}_i\left(i_{i,outlet} - i_{i,inlet}\right) \quad (2)$$

An iterative procedure is employed in the two sections until a balance is obtained in the calculation of the heat transfer with Eq.(2) and that with UA LMTD [8]. The contribution of latent heat to the total heat transfer was estimated with:

$$L = \left[1 - \frac{c_p\left(T_{o,inlet} - T_{o,outlet}\right)}{i_{o,inlet} - i_{i,inlet}}\right] * 100 \quad (3)$$

where subscript *i* refers to the stream inside the tubes and subscript *o* refers to that outside the tubes or into the kernel. The efficiency is defined as:

$$\eta = \frac{T_{o,inlet} - T_{i,inlet}}{T_{i,outlet} - T_{i,inlet}}$$

3. Results

3.1. Global results

In this section overall results are provided for the period extending from March 21st to May 21st. Spring is selected as it corresponds to a critical period as the plants are active and condensation rates on the walls very low due to higher temperatures than those found in the winter. At a rate of $\dot{Q}$=0.5 air change per hour, the average efficiency based on temperature for the whole period of investigation was about : η=84% with a 5% standard deviation. For the results obtained with $\dot{Q}$=0.9 air change per hour, the average efficiency decreased to η=78% with a 3.5% standard deviation.

The experimental results carried out over the two months period indicate that for $T_{i,inlet}$ varying between 1 and 3°C with RH varying between 63% and 70%, the contribution of the latent heat to the overall heat transfer fell within a 39 to 43% range. To obtain such results, the amount of condensation recovered is measured (to estimate latent heat recovery) as well as the overall temperature differences.

The amount of water that condenses on the walls is calculated based on the variation of the absolute water content of the warm moist fluid along the exchanger. A typical rate of condensation is about 1680 mL/h. The maximum condensation rate was found to reach 3200 mL/h when the external temperature was –10°C and the internal temperature 20°C with 85% RH. The maximum power used by the Delhi fans was 637 W, and the rate of heat gained by the cold fluid varied from 874 W at $T_{i,inlet}$ = 14°C to 3 089 W at $T_{i,inlet}$ = -10°C. This indicates a variation in the COP such that: 1.4 < COP < 4.8.

The first day was March 26th, when the volumetric flow rate of warm fluid, $\dot{v}_h$, was 0.099 m3/s and that of the cold fluid, $\dot{v}_c$, was 0.079 m3/s. The profile presented in Fig. 3 (a) is typical of what was observed when the prototype operated at 0.5 air change per hour.

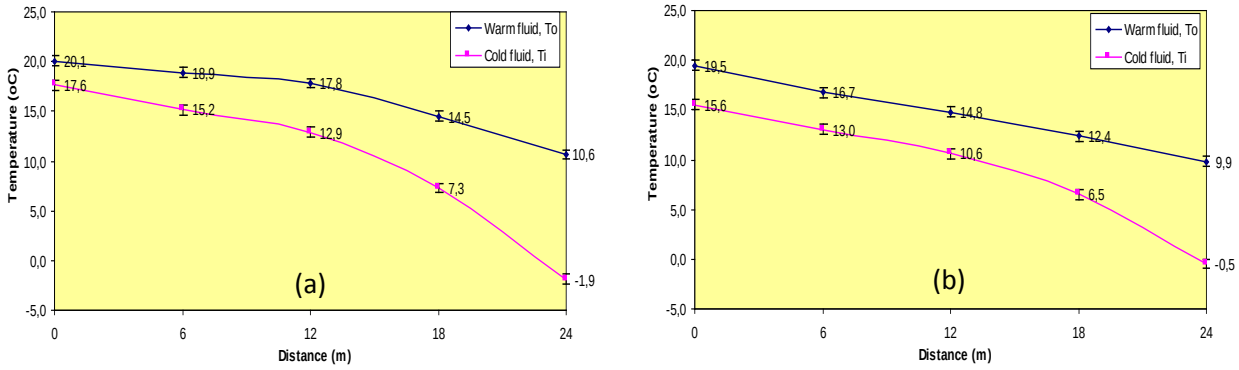

Fig. 3: Temperature distribution. (a) March 26th: 8h10, 0.5 air chg / h; (b) April 5th: 4h50, 0.9 air chg / h

For this case, the relative humidity at the warm exit of the cold stream was 15.7% while it was almost completely saturated at 93.5% at the cold exit of the warm stream. The efficiency was 89%. The heat recovery was excellent: 1948W. And at that time of the day, provided that the fans needed 355W, the COP was 5.51.

Fig. 3(b) shows results for April 5th, when $\dot{v}_h$ was 0.148 m^3/s and $\dot{v}_c$ was 0.141 m^3/s. Similar trends can be observed. For this second case, the relative humidity at the warm exit of the cold stream was 18.9% and the efficiency was 81%. 2856W were recovered while 637W were used: the COP was 4.48.

3.2. Psychometrics results

The relative humidity was also monitored to assess the ability of the unit to fulfil the needs of the plants. It is worth noting that 0.9 air chg/h is not enough to maintain an adequate level of humidity in the complex all year long: it should be adequate about 80% of the time. But for this design, only general characteristics were to be obtained. The test was carried out in the critical period of growth for a greenhouse in Québec. As a result, it was expected that the humidity level would be very high in this period even under operation: traditional ventilation had to be used as a complement. Fig. 4 shows the relative humidity distribution for March 26th.

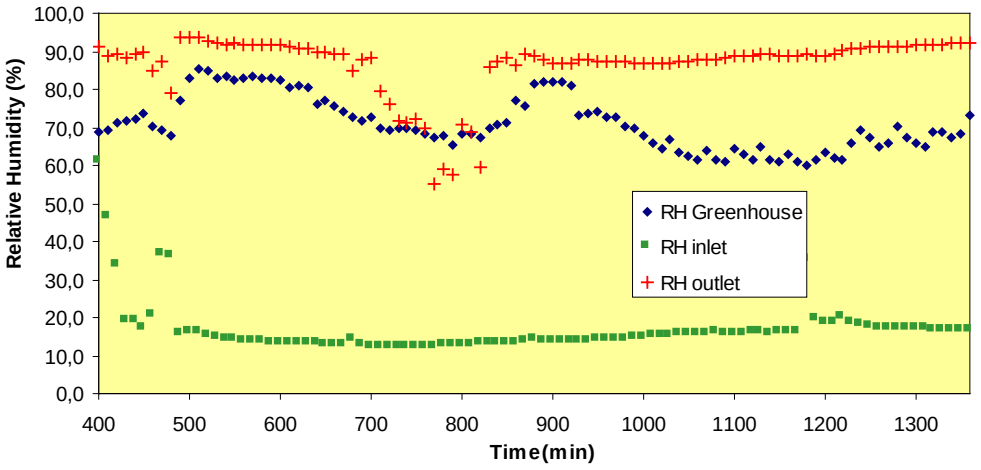

Fig. 4: Relative humidity distribution in the greenhouse on March 26th

The results for the humidity in the greenhouse (diamonds) show a first peak early in the morning: March 26th was sunny and the plants were active early. The humidity had to be lowered with standard ventilation as the unit was not able to deliver a sufficient flow rate to evacuate a sufficient amount of moisture. A second peak appears at about t = 900 min, that is when the sun sets. At that time, the greenhouse had to be closed as the external temperature became too low to maintain an adequate temperature level inside. The interesting part of the curve is that the unit was able to lower the humidity level rapidly after sunset. In brief, a bigger unit would have been needed only in the morning for that day. The inlet stream humidity results (squares) show the period in the day when it stopped: the unit operated almost continuously. The last results (crosses) show that air was saturated in the warm stream except when additional ventilation was used. In these conditions, the humidity level in the greenhouse was below 75%.

Fig. 5 presents typical results obtained for a period ranging from April 5th to April 9th. This sequence demonstrates the performance of the prototype as a dehumidifier over an extended period. At that time, about 300 mature plants of tomato and cucumber were growing. During this period, the exchanger was operated continuously with a RH threshold of 75%. The transpiration cycle of the plants can be interpreted as follows. The photosynthesis activities diminish after sunset. As shown in the figure, the relative humidity then reaches peak lows of

about 79 to 82%. The high peaks occur at about noon with maximum relative humidity of about 90 to 91%. On an average, the relative humidity was about 85% in the greenhouse.

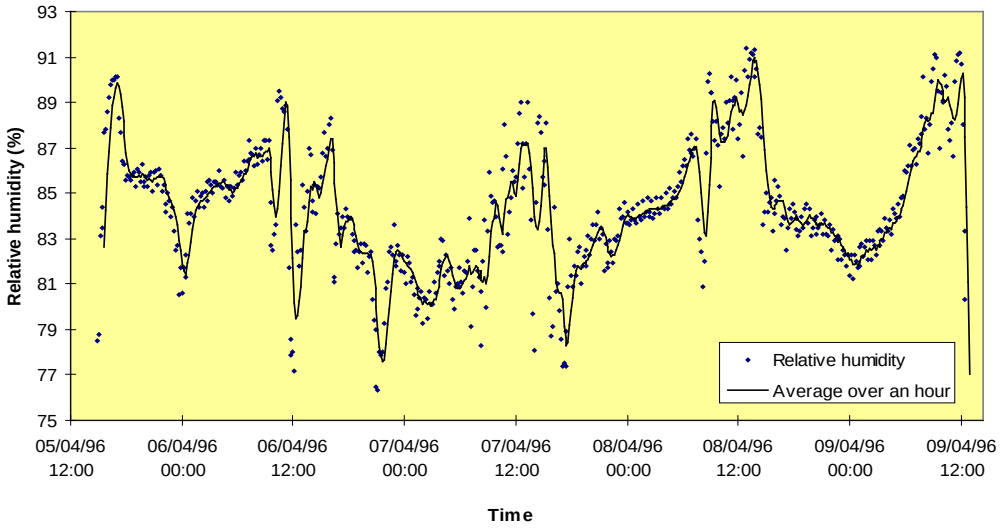

Figure 5: Relative humidity distribution in the greenhouse between April 5th and 9th

Again, it is shown in Fig.5 that the prototype is too small to permit a total compensation for the needs of the plants: the threshold of 75%RH is never reached. This was predicted as the capacity of the exchanger is about 5 times lower than the maximum greenhouse requirement. However, these results are interesting as they permit one to compare the humidity management using the undersized unit with traditional ventilation techniques. Here, the cycles never reach 100% relative humidity which would sometimes be nearly the case with manual ventilation. This indicates that although two to five air changes/h may be needed in critical periods, the smaller unit of about one air change/h can nevertheless permit preventing relative humidity to shoot above 91%. Results from Fig.4 and 5 were used in the design of a second generation of pre-commercial units that are now undergoing a more thorough experimental testing procedure. Knowing both incoming and outgoing volumetric flow rates in conjunction with their relative humidities and temperatures, a mass balance can be performed for water vapor in the greenhouse.

3.3. Payback period

Here the payback period is estimated with no account for the improvement of the crops growth with adequate level of humidity: the "real" performance of the exchanger should be better. The integrated heat recovery is used to estimate the payback with no account of the fan power as if they were used anyway to extract the moisture from the greenhouse. It has been found that the units were able to recover 9840 kW-h over the whole year which corresponds to a cost of 617$ for gas heating and 935$ for oil heating. As the experimental unit costs 1140$ (calculations carried out for a production and installation of 100 per year), the simple payback period is about 1,5 year (from 1,2 to 1,9 years, without subsidy).

4. Conclusion

A prototype air-air counter-flow multi-tube heat exchanger has been designed and built to meet the specific greenhouse requirements of operating in a cold climate. The uncompact design involving plastic components was retained so as to meet the following requirements: (1) low cost, CDN$ < 2000 (1,5 year pay-back period); (2) ease of assembly, maintenance,

repair, and operation; (3) corrosion and rottenness resistance; (4) satisfactory operating efficiency when frost present.

The prototype was designed using a basic numerical tool. Drainages tubing were retained as they readily permitted one to meet the design requirements. One of the goals was to convince producers that such a simple design could spare them a substantial part of their yearly heating costs. The unit was assembled and calibrated in a greenhouse used for the experimental cultivation of hydroponic tomatoes and cucumbers during winter. The first series of tests, carried out between March to May, demonstrated that average efficiencies of η=84% and η=78% were obtainable with air volumetric exchanges rates of 0.5 and 0.9 change per hour, respectively, in a 576m^3 greenhouse. Latent heat was found to play a major role in the overall heat transfer, contributing about 40% of the total energy exchanged in some situations.

In conclusion, with sufficient exchange area, simple heat exchangers can be economically used as dehumidifiers in several applications. The encouraging results presented and mentioned here demonstrate that yet other applications could be found for heat exchangers in sustainable development strategies.

References

[1] E. Brundrett, T.J. Jewett, and R. Quist, Evaluation of polytube heat exchangers for greenhouse ventilation". *Acta-horticultarae,* 148, 1984, pp.49-55.

[2] J.N. Walker and D.J. Cotter, Condensation and resultant humidity in greenhouses durng cold weather, Trans. ASEA, 11(2), 1968, pp.263-266.

[3] D.J.Cotter and R.T. Seay, The effect of circulating air on the environment and tomato growth response in a plastic greehouse, Roc. ASHS, 77, 1961, pp.345-342.

[4] SPSQ., Ékiloserre; Projet d'amélioration de la situation énergétique de l'industrie serricole québécoise, Rapport Final, Syndicat des Producteurs en Serre du Québec, St-Hyacinthe, 1995.

[5] D. DeHalleux, and L. Gauthier, Consommation énergétique due à la déshumidification des serres au Québec, Université Laval, Québec, 1995.

[6] BNQ., Norme 3624-115 (91-08-01); Tubes annelés flexibles et raccords en thermoplastique pour le drainage des sols, Bureau de Normalisation du Québec, Québec, 1991.

[7] BNQ., Norme 3624-120 (90-02-20); Tuyaux annelés à l'intérieur lisse et raccords en plastiques Pe ou PP pour l'évacuation des eaux pluviales, Bureau de Normalisation du Québec, Québec, 1990.

[8] A. Bejan, Convection Heat Transfer, 2nd ed., Wiley, New-York, 1993

[9] V. Gnielinski, New Equations for Heat and Mass Transfer in Turbulent Pipe and Channel Flow, Int. Chem. Eng., vol.16, 1976, pp.359-368.

[10] V. Gnielinski, Forced Convection in Ducts, in G.F.Hewitt (ed.), Handbook of Heat Exchanger Design, Begell House, NY, 1952, section 2.5.1-5.

[11] H. Hausen, Darstellung des Wärmeüberganges in Rohren durch verallgemeinerte Potenzbezeihungen, Z. Ver. Dtsch. Ing. Beiheft Verfahrenstech., vol.4, 1943, pp.91-134.

[12] H. Hausen, Heat Transfer in Counterflow, Parallel Flow and Cross Flow, McGraw-Hill, USA, 1983.

Environmental analysis of various systems for the cogeneration of biogas produced by an urban wastewater treatment plant (UWTP). (III).

J.J. Coble[1] and A. Contreras[2*]

[1] *Department of Industrial Engineering. Nebrija Universidad. Madrid , Spain*
[2] *Department of Chemistry. ETSII. UNED. Madrid. Spain.*
** Corresponding author. Tel: 34 91 3986496, Fax: 34 91 3986043. Email: acontreras@ind.uned.es*

Abstract: To complete the study on harnessing the biogas produced by a UWTP as an energy source, using cogeneration with motor-generators and phosphoric acid fuel cells, in this paper we present the results of the environmental study. This completes the study made of both systems, enabling us to conclude which of the two methods is best in terms of obtaining the largest amount of energy, at the lowest cost, and with minimum impact on the environment.

For the environmental analysis we compared, amongst other parameters, the contaminating gas emissions produced by each cogeneration device, and assessed the financial cost of the environmental damage caused by these emissions. We also bore in mind the emission levels created by the emissions from each system, both immediately around the plant and in the surrounding areas affected by prevailing wind directions. Finally, we compared the noise levels of the two devices and determined the financial cost of applying corrective acoustic insulation where necessary.

The overall study of both systems has made it clear that to evaluate them correctly, it is necessary to internalize all the costs that are currently externalized. This is the only way to find the true cost of each system.

Keywords: *Cogeneration, UWTP, Motor-generators, Phosphoric acid fuel cell, Environmental analysis, Emissions.*

1. Introduction

In the first part of this study [1], it was found that both systems showed substantial differences in terms of their energetic, exergetic and thermo-economic performance. The irreversible factors of both systems are shared out among their components in different ways but, overall, there are fewer of these factors in the phosphoric acid fuel cell system. However, if we take the energy analysis alone into account, the total year-on-year costs are lower for the motor-generation system, and this is the option that would normally be chosen.

In this second part of the study it becomes apparent that if we add up the costs of both thermo-economic analysis and environmental analysis, i.e.: by internalizing all the costs of both systems, cogeneration with phosphoric acid fuel cells is an investment that can be eventually be recovered. However, this is not the case with cogeneration using motor-generators.

2. Methodology

The environmental analysis compares the two cogeneration systems on the basis of the following features:

Emission levels of atmospheric pollutants and greenhouse gases, along with their financial cost.
Emission levels in surrounding and sensitive areas, and their environmental impact.
Noise levels and their financial cost.
Once the environmental impacts have been assessed, they must be assigned a financial cost and this must be internalized with the rest of the system's costs. The cost of externalities has

been evaluated by various international organizations. Two studies are fundamental if we wish to make an assessment of the costs of the externalities of the systems studied in this paper: one is European [2], and was subsequently developed in [4, 5], and the other is American [3]. The American model basically uses resolution algorithms, which are in turn based on the same concept: the cost of environmental damage attributable to each unit of mass or volume of pollutant.

However, we decided to use the European model [2, 4, 5], because its conclusions are better suited to the environment in which this study took place, but mainly because it is a more conservative model insofar as the numeric values that are obtained are always higher than the real ones. This provides us with a safety margin that is always appreciated by technicians.

In order to assign costs to the externalities, it is first necessary to decide which of these should be taken into account. In this study, we considered those that are due to the emission and noise levels produced by the systems.

We also calculated the levels of emission of chemical pollutants (gaseous compounds and particles), depending on the location's various climatic conditions, so as to compare the final environmental impact of the emissions from each system. No cost was assigned to them, however, because taking into account the costs of the irreversible energy factors and the emissions alone was sufficient proof of the financial difference between the two systems.

From the results obtained in the studies mentioned [2, 4, 5], the emission costs for various scenarios can be inferred, as shown in Table 1. These differ depending on the financial valuation of the emissions.

Table 1. Costs of the emissions of pollutants in various scenarios (euros/ton)

ATMOSPHERIC POLLUTANT	LOW LEVEL (€/t)	MEDIUM LEVEL (€/t)	HIGH LEVEL (€/t)
CO_2	9.90	26.40	41.60
CO	506.23	1,055.87	2,494.26
SO_2	1,635.98	1,869.77	4,933.99
NO_X	1,049.27	7,919.03	10,030.77
PM	3,128.55	4,839.41	13,616.33
VOC	1,113.06	5,265.79	6,489.20

In this study, we have chosen the medium-level costs of emissions shown in Table 1, as we consider them to be the most representative. The nomenclature used for the financial costs that have been developed and used in this study (set-up and operation, energy inefficiency, emissons) is as follows:

C_1 (€/year): Set-up and operating costs during the first year. In subsequent years only operating costs will be taken into account.
C_2 (€/year): Costs of energy inefficiency derived from the thermo-economic analysis.
C_3 (€/year): Costs of noise emissions and atmospheric pollutants.

3. Results

The results of the emission and noise levels for each of the two cogeneration systems studied are shown below.

3.1. Level of emissions from the cogeneration system using motor-generators

The combustion reactions of the motor-generators were modelled on the basis of the excess of air n = 1.5 that was considered. Using the formula created with the EES programme [10], we obtained the motor-generator emission results shown in Table 2, and these were compared with those of the phosphoric acid fuel cells.

Table 2. Comparison of gases emitted by biogas cogeneration by motor-generators and in fuel cells, in grams per second.

NOx EMISSIONS(g/s)		SO_2 EMISSIONS (g/s)		CO_2 EMISSIONS(g/s)		CO EMISSIONS(g/s)	
Motor-generator	PAFC	Motor-generator	PAFC	Motor-generator	PAFC	Motor-generator	PAFC
4.51364	0.00214	0.03482	0	731.13516	244.66268	24.48778	0.00497

3.2. Level of emissions from the cogeneration system using phosphoric acid fuel cells.

Using the available data [7, 8], the emissions from fuel cells were modelled on the basis of the level of working power. With the formula created by the EES programme [6], we obtained the emission results that are also shown in Table 2, above.

The SO_2 emissions for fuel cells are negligeable and have not been taken into account. To make a financial assessment of the emissions, we used the average value of emission costs shown in Table 1. Using these values as a reference, we were able to determine the emission costs of all the compounds mentioned in the study.

Table 3 shows the costs resulting from the emissions from each cogeneration system and compound, whereas Table 4 shows the sum of all the costs for each case.

Table 3. Financial comparison of emission costs for NOx, SO2, CO2 and CO emissions, from both cogeneration systems (€/year).

COST OF NOx EMISSIONS (€/year)		COST OF SO_2 EMISSIONS (€/year)		COST OF CO_2 EMISSIONS (€/year)		COST OF CO EMISSIONS (€/year)	
Motor-generator	PAFC	Motor-generator	PAFC	Motor-generator	PAFC	Motor-generator	PAFC
539,285.94	256.02	981.63	0.00	291,219.64	97,452.22	390,071.85	79.25

Table 4. Financial comparison of total costs (C_3) from emissions of NO_x, SO_2, CO_2 and CO, from both cogeneration systems (€/year).

TOTAL COST OF C_3 EMISSIONS (€/year)	
Motor-generator	PAFC
1,221,559.06	97,787.49

As can be seen from Table 4, the total costs of atmospheric emissions from the motor-generators are 5.64 times higher than those of fuel cells.
As shown by the figures in Table 1, the financial cost of emissions is considered to be included in the cost of emissions shown in the previous section. However, in this study, we took into account the dispersion of pollutants according to the atmospheric conditions of the location, and emission maps were subsequently made. This was because the way in which emissions are financially assessed - which currently includes the effects of immissions - needs to be improved. It should be requisite for a device's emission levels to be used simultaneously with emission maps calculated for the device's various weather scenarios. This study will make it possible to achieve a more accurate financial assessment of the environmental impact.

Level of emissions from the cogeneration system using motor-generators.
We show below a summary of the results of the emission level calculations for each pollutant and each cogeneration system. We used the DISPER 3.0 programme [9] and an Excel spreadsheet [10], introducing the emission data calculated in Table 2 into the programme's user interface (except for the CO_2 figures). By also introducing the weather and other relevant location data, we obtained the CO results shown below, in Figure 1, as well as each kind of atmospheric stability for the profile on the XZ plane of the central line of the plume (X axis).

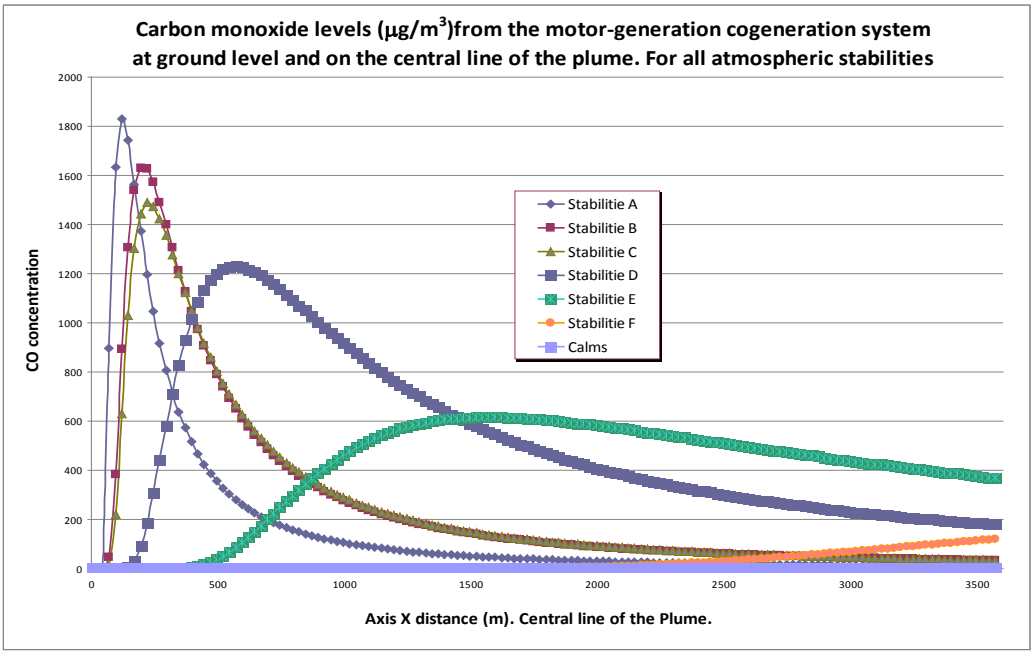

Figure 1. Carbon monoxide levels from the motor-generation cogeneration system at ground level and on the central line of the plume. For all atmospheric stabilities.

As can be seen in Figure 1, the maximum concentration of carbon monoxide immission for the most unfavourable atmospheric stability is:

1800 $\mu g/m^3$ = 1,8 mg/m^3 < 6 mg/m^3 (legal limit).

This in no case exceeds the legal limits in force since January 1, 2005 [11].

Level of emissions from the cogeneration system using phosphoric acid fuel cells.

Carbon monoxide is mainly produced in the fuel cell during the process of reforming the biogas vapour to obtain hydrogen. This carbon monoxide has to be removed from the fuel flow into the cell to avoid poisoning the catalyst.

This CO has to be removed from the reformed gas flowing into the fuel cell, because carbon monoxide concentrations as low as 1% in the input flow of these cells can poison the platinum catalyst. Although the operating temperature of the cells is between 150-200ºC, the effects of catalyst poisoning can be detected at concentrations of 10,000ppm of CO in the input flow. The main effect of such poisoning is either an increase in the input flow required to produce the same power, or a drop in the power output [12].

The results of the levels of carbon monoxide emission calculated in this case provide a maximum concentration figure for the most unfavourable atmospheric stability of:

2.5 $\mu g/m^3$ = 0.0025 mg/m^3 <<< 6 mg/m^3 (legal limit)

If the above figure is compared to the concentration level of CO emissions from motor-generator emissions for the least favourable atmospheric stability, it can be seen that emissions from the motor-generators are around 720 times higher than those of the set of fuel cells.

Similar results were obtained for the rest of the polluting gases considered in this paper. As for emission and emission levels, the motor-generator cogeneration system is at a clear disadvantage when compared to the phosphoric acid fuel cell system.

The noise level of the motor-generator cogeneration system.

For the calculations in this section, we used the data provided by the manufacturers – which, in both cases, dealt with emissions into the indoor (rather than outdoor) atmosphere of 95 dBA for motor-generators, and 60 dBA for fuel cells [13, 14], as well as current regulations.

To check that the noise level limits set by the current legislation were not exceeded, we used the CUSTIC 1.0 application, by Canarina Software Ambiental [15], to calculate the noise emission levels. These were viewed on isophonic layout maps, for both the installation using motor-generators and the one using phosphoric acid fuel cells.

In the case of the motor-generators, the noise levels calculated in the simulation would exceed the 60dBA day-time limit, beyond the walls of the motor-generation building, unless appropriate corrective measures were put in place. In order to comply with the law, it would be necessary to take corrective measures amounting to 43,500 Euros. With fuel cells, no corrective measures are required

4. Conclusions

By considering environmental effects in our analysis of the two cogeneration systems, we were able to reach the following conclusions.

The most important aspect of this second part of the study is that the environmental cost of the phosphoric acid fuel cell cogeneration system has been valued at 97,787.487 €/year, whereas that of the motor-generator cogeneration system was 1,221,559.061 €/year. As you can see, the latter is far higher than the phosphoric acid fuel cell system.

Furthermore, in the case of motor-generators, acoustic insulation would need to be provided for the building in which they are installed, so as to comply with current legislation on noise emission levels. In the case of the fuel cell cogeneration system, however, no corrective measures are needed to comply with these regulations.

References

[1] J.J. Coble, and A. Contreras. Energetic, Exergetic, Thermoeconomic and Environmental Analysis of Various Systems for the Cogeneration of Biogas Produced by an UWTP (1). 18 World Hydrogen Energy Conference, 16-21 May 2010, Essen, Germany.

[2] Scheleisner and Nielsen, (1997). ExternE National Implementation Project (CEC, 1995)

[3] R. D. Rowe et al.,. The New York Electricity Externality Study. Oceana Publications, New York. 1995.

[4] Carlson Annelie, Energy system analysis of the inclusion of monetary values of environmental damage, Biomass and Bioenergy (2002), 22,3,177-177

[5] European Commission ExternE- Externalities of Energy, EUR 16520 EN-EUR 16525 EN, Directorate-General XII, Office for Official Publications of the European Communities, Luxembourg, 1995.

[6] EES (Engineering Equation Solver). F-Chart Software. www.fchart.com.

[7] Greenhouse Gas Technology Center Southern Research Institute. EPA & New York State Energy Research and Development Authority (2004). "Environmental Technology Verification Report: Electric Power and Heat Generation Using UTC Fuel Cells´ PC25C Power Plant and Anaerobic Digester Gas".

[8] Ott G. Sanger D. Tooze D. Hydrogen Fuel Cells: A Solution for Utilizing Waste Methane at Columbia Boulevard Wastewater Treatment Plant. Final Technical Report. Climate Change Fuel Cell Program (2000). City of Portland. Oregon

[9] Canarina environmental software, program DISPER 3.0 advanced version. www.canarina.com

[10] Microsoft Excel software. http://office.microsoft.com

[11] BOE num. 260, 30/10/2002. Ministry of the Presidency. Royal Decree 1073/2002, of 18 October, on the evaluation and management of air quality in relation to sulphur dioxide, nitrogen dioxide, nitrogen oxide, particles, lead, benzene and carbon monoxide.

[12] Song Rak-Hyung, Shin D. R., Influence of CO concentration and reactant gas pressure on cell performance in PAFC, International Journal of Hydrogen Energy 26 (2001) 1259-1262.

[13] PureCellTM Model 200 power solution. www.utcpower.com.

[14] J. Larminie and A. Dicks. Fuel Cell Systems Explained (Second Edition). J. Wiley and Sons.

[15] Canarina environmental software, program CUSTIC 1.0 advanced version. www.canarina.com.

Research on energy-saving and exhaust gas emissions compared between catalytic combustion and gas-phase combustion of natural gas

Shihong Zhang[1,*], Zhihua Wang [1]

[1] *Beijing University of Civil Engineering and Arch, Beijing, China*
** Corresponding author. Tel: +86 168322124, Fax: +86 168322124, E-mail:shihongzhang @bucea.edu.cn*

Abstract: In this paper, exhaust gas emissions were compared between conventional gas-phase combustion in both forced exhaust gas concentration of hot-water burner & premixed natural gas/air burner with heater and the catalytic combustion in catalytic honeycomb monolith burner. Test proved that the pollutant emissions of gas-phase combustion **were** higher than that of catalytic combustion. It is shown that the conversion of conventional gas-phase combustion **was** lower than that of catalytic combustion by measured experimental data. It indicated the advantages of energy-saving and environmental protection for the catalytic combustion.

Keywords: *catalytic combustion, exhaust gas analysis, near zero pollutant emissions, energy-saving*

1. Introduction

Catalytic combustion of natural gas has received considerable attention in the last decades due to its practical applications in both power generation and pollutant abatement[1-4]. This reaction has been shown to be effective in producing energy in gas turbine combustors. Compared to the conventional thermal combustion process, using a heterogeneous catalyst can remarkably decrease the reaction temperature, thereby reducing the noxious emissions of nitrogen oxides[5-6]. By enabling the combustion of extraordinarily lean fuel/air mixtures, the catalytic combustion of natural gas provides a low-emission alternative to gas-phase flames[7-9].

In this paper, exhaust gas emissions were compared between conventional gas-phase combustion and the catalytic combustion in catalytic honeycomb monolith burner VI. In order to study the exhaust gas of both forced exhaust gas concentration of hot-water burner & premixed natural gas/air burner with heater and catalytic combustion burner VI, their composition and content were measured, respectively. Meanwhile their combustion efficiency were calculated.

2. Experimental set-up and steps

Figure 1 illustrates the exhaust gas analysis system of catalytic combustion burner VI, The square honeycomb monoliths were 150mm in side of the square and 20mm long, with square-shaped cells which sectional area was 1mm×1mm. The support for all the monoliths tested here was cordierite. The four square catalytic honeycomb monoliths were installed in the burner VI each time. The lengths of catalytic honeycomb monoliths were 20mm for the catalytic combustion burner. In order to decrease the temperature of mixtures in chamber connected with the monolith's entrance, the 20mm long blank monoliths were inserted between the chamber and the Pd based catalytic monolith's entrance as assembly of monolith. In the experiment, the reactant gas feeds of natural gas and air were regulated via GMS0050BSRN200000 natural gas meter and CMG400A080100000 air meter with 0~50 L/min and 0~80m3/h of full-scale range , respectively. The two meters were provided electric current through manostat.

In the process of ignition, we need to swept the inside of burner VI by air for five minutes to ensure that there was no residual natural gas. In order to warm the honeycomb monoliths, the

burner VI must be ignited by gas phase combustion with the excessive air coefficient at 1.3. When the catalytic surface came to be red, the excessive air coefficient should be adjusted to 2.0. Until it came into the steady state of catalytic combustion, the exhaust gas could be measured by the analyser. At the same time we observed and recorded the data.

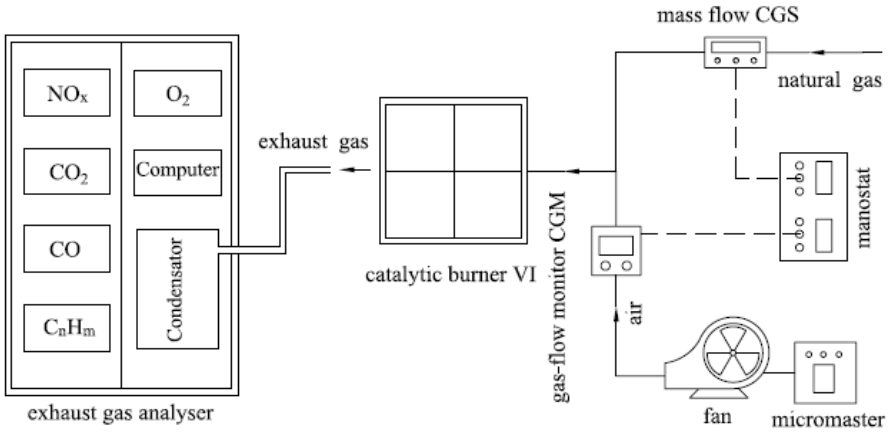

Fig. 1. Exhaust gas analysis system of catalytic combustion burner VI.

Figure 2(a) illustrates the exhaust gas analysis system of premixed natural gas/air burner with heater. This burner was ignited by gas phase combustion with the excessive air coefficient at 1.1 and 1.3. When the water heater came into the steady state of gas phase combustion, we observed and recorded the experiment data from its chimney. Also the Figure 2(b) illustrates forced exhaust gas concentration of hot-water burner with the excessive air coefficient at 1.3. and the exhaust gas concentrations were measured above the burner.

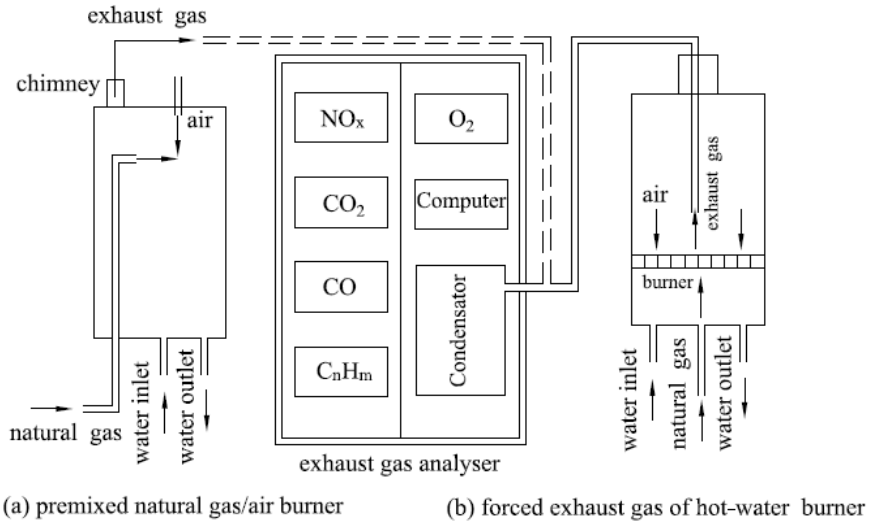

Fig. 2. Exhaust gas analysis system of premixed natural gas/air burner with heater and forced exhaust gas concentration of hot-water burner .

3. Results and Discussion

3.1. Emission characteristics of catalytic combustion and conventional gas-phase combustion

Form figure 3(a) plots the content of NOx was very low , because the temperature(T around 1000℃) of catalytic combustion and gas-phase combustion did not reach the degree which

could generate a large number of heat-type NOx. But the emission of NOx in gas-phase combustion ascended gradually with the increase of natural gas flow rate.

The content of CO in catalytic combustion was very small **(closed to 0)**. From the data of CO **[figure 3(b)]** we got that the combustion efficiency of catalytic combustion burner VI is very high and its heat had been released fully. However, the content of CO of gas-phase combustion was higher than that of catalytic combustion. The maximum of CO emission reached about 150 ppm. It was shown that natural gas of gas-phase combustion did not oxidized completely.

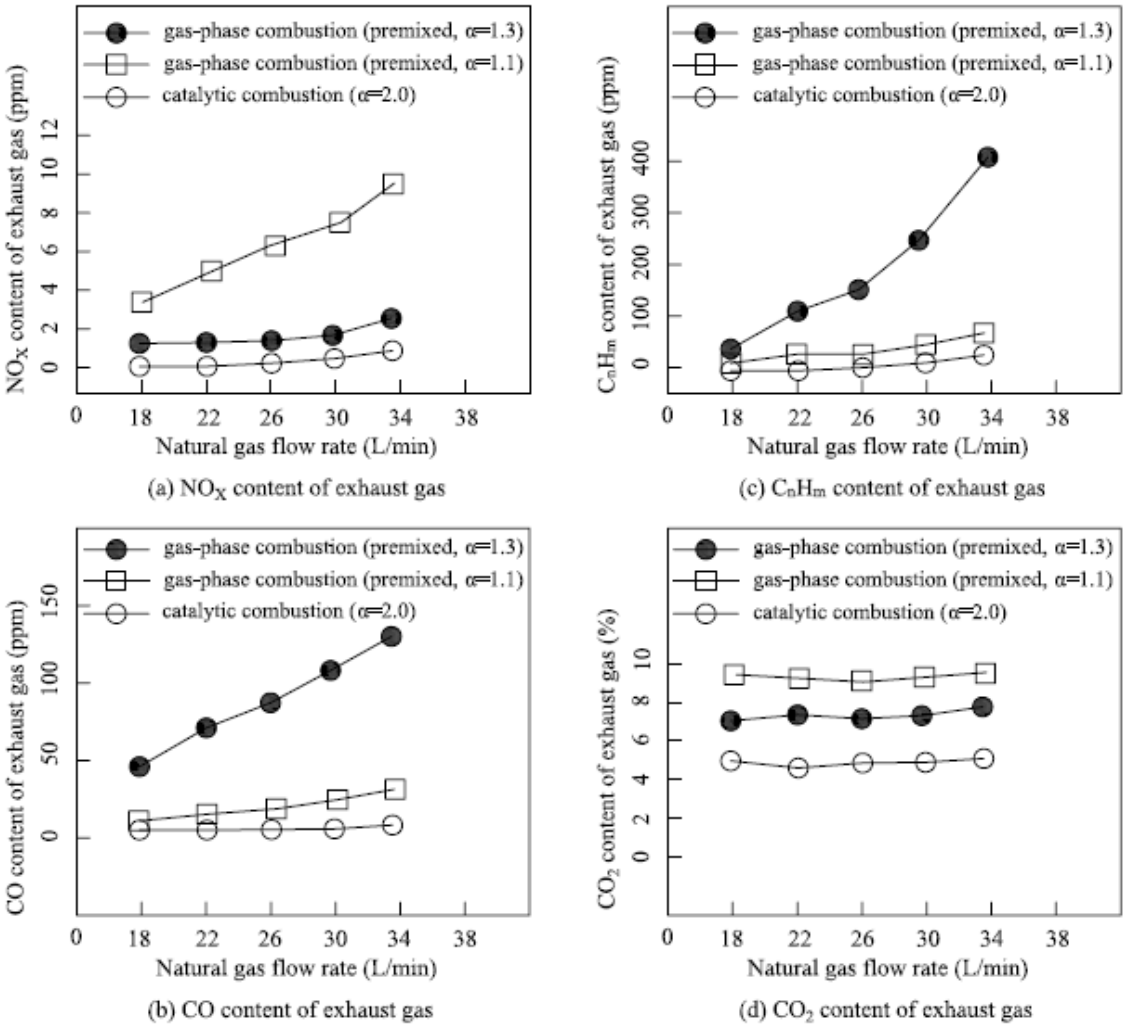

Fig. 3. The exhaust gas content of catalytic combustion and conventional gas-phase combustion （premixed, α=1.3 and 1.1） under the condition of different natural gas flow rate (α is the excessive air coefficient).

The figure 3(c) also shows that there was no C_nH_m from the exhaust gas of catalytic combustion. It was evidenced that the catalytic combustion efficiency was almost closed to 100%. It was seen that the content of C_nH_m in gas-phase combustion was 39.3 ppm～428 ppm. At the same time, C_nH_m was increased quickly with the increasing natural gas flow rate. It proved that the conversion of gas-phase combustion was lower than that of catalytic combustion.

When the excessive air coefficient decreased from 1.3 to 1.1 in premixed natural gas/air burner with heater the conversion of gas-phase combustion increased dramatically, saturating at near 100%, the CO decreased with very lower value (about 8 ppm) in the cases of the high temperature chamber of furnace under certain conditions. But the exhaust gas temperature and heat loss increased from its chimney **with the same water flow rate.** The emission of NOx was increased quickly with the increase of natural gas flow rate. Simultaneously, the nosie happened during the combustion of premixed natural gas/air burner and the blue flame changed gradually into dark red **one.**

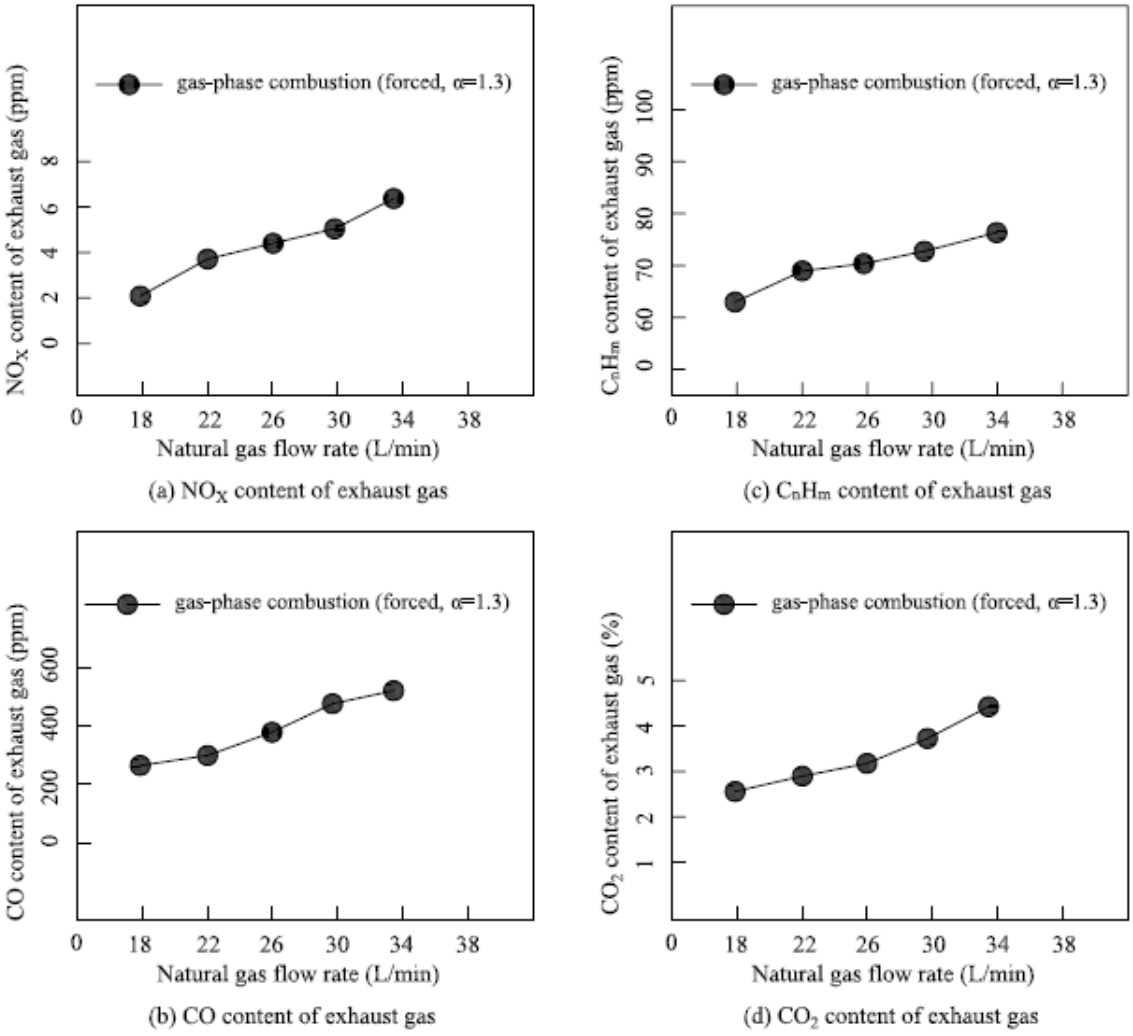

Fig. 4. The exhaust gas content of conventional gas-phase combustion（forced, a=1.3）under the condition of different natural gas flow rate.

The NOx、CO and un-burnt CH_4 concentrations in forced exhaust gas concentration of hot-water burner existed more with the excessive air coefficient 1.3. Its exhaust gas concentrations have been significantly diluted in large space by measured CO_2 data as shown in figure 4. Otherwise, the percentage of CO_2 should remain about 7-8% without vapor by CO_2 analyser.

For all tested of the catalytic combustion, only extremely small amount of CO, unburned fuel and NOx were detected inside the monolith channels and over the open

end of the burner VI. A catalytic combustion process can achieve 'near-zero' pollutant emissions.

3.2. Calculation of combustion efficiency in gas-phase combustion

It was evidenced that the catalytic combustion efficiency was almost closed to 100%. But there were a lot of C_nH_m and CO from the exhaust gas in gas-phase combustion. It proved that gas-phase combustion had not oxidized completely and its combustion efficiency should be calculated. As the main composition of natural gas was methane, so the chemical reaction equation is (1) in the following:

$$CH_4 + 2O_2 = CO_2 + 2H_2O \qquad (1)$$

CO was a kind of intermediate which was generated during combustion of hydrocarbons. The number of C atom remained unchanged in the reaction process. The total volume of CO and CO_2 were the same as that of CH_4 via the reaction equations (1) ($V_{CO} + V_{CO_2} = V_{CH_4}$). Given the volume of methane was 1 Nm^3 (V_{CH4}=1). According to equations (2), the volume of CO was calculated as:

$$\begin{cases} V_{CO} + V_{CO_2} = 1Nm^3 \\ \dfrac{V_{CO}}{V_f^d} = \gamma_{CO} \\ \dfrac{V_{CO_2}}{V_f^d} = \gamma_{CO_2} \\ \dfrac{V_{CH_4}^1}{V_f^d} = \gamma_{CH_4}^1 \end{cases} \qquad (2)$$

Where V_{CO} and V_{CO_2} are the volume of CO and CO_2 in exhaust gas(m^3), respectively. V_f^d is the total volume of exhaust gas. γ_{CO} and γ_{CO_2} are ratio of CO volume and CO_2 volume to that of exhaust gas, respectively. $V_{CH_4}^1$ is the volume of unburnt CH_4 in exhaust gas(m^3). $\gamma_{CH_4}^1$ is ratio of CH_4 volume to that of exhaust gas. $\gamma_{CO}, \gamma_{CO2}, \gamma_{CH_4}^1$ are measured by the analyser.

According to equation (3): For 1m^3 CO oxidized completely to CO_2 could generate 12644 kJ heat (H_2=12644 kJ). It proved that the content of CO had an important influence for utilization of thermal energy of the fuel.

$$CO + 0.5O_2 = CO_2 + \Delta T \qquad (3)$$

So, the heat released of unburnt CH_4 and CO were calculated as:

$$Q_{CH_4} = V_{CH_4}^1 \times H_1 \qquad (4)$$

$$Q_{CO} = V_{CO} \times H_2 \qquad (5)$$

Where H_1 is net calorific value of methane under standard conditions which is 33.70MJ/Nm^3. H_2 is calorific value of CO which is 12644kJ/m^3.

The following equations(6) for heat released percent of unburnt CH_4 and CO to reactant (natural gas) was derived:

$$K = \frac{Q_{CH_4} + Q_{CO}}{V_{CH_4} \times H_1} \qquad (6)$$

The combustion efficiency of gas-phase was calculated by equation (7):

$$\eta = 1 - \frac{V^1_{CH_4} + V^2_{CH_4}}{V_{CH_4}} \qquad (7)$$

Where $V^2_{CH_4}$ is the volume of CH_4 which has been used in generating CO, which was $V^2_{CH_4} = \mathrm{V_{CO}}$.

According to above equations and experimental data, table 1 shows ratio of heat released of unburnt CH_4 and CO and combustion efficiency under the condition of different natural gas flow rate. It was seen that part of the energy were wasted in gas combustion which did not oxidized completely.

Table 1. Ratio of heat released of unburnt CH_4 and CO and combustion efficiency

Natural gas flow rate		L/min	18	22	26	30	34
forced, a=1.3	k_1	%	0.58	0.63	0.65	0.66	0.67
	η_1	%	98.82	98.7	98.63	98.55	98.51
premixed, a=1.3	k_2	%	0.078	0.17	0.27	0.41	0.62
	η_2	%	99.88	99.76	99.66	99.49	99.27
premixed, a=1.1	k_3	10^{-2} %	0.94	1.00	1.05	1.10	1.20
	η_3	%	99.987	99.986	99.984	99.983	99.981

4. Conclusions

Exhaust gas emissions were compared between gas-phase combustion and catalytic combustion in catalytic honeycomb monolith burner VI. It proved that the concentration of pollutant emissions of gas-phase combustion were morehigher than that of catalytic combustion. It was shown that the conversion of gas-phase combustion was lower than that of catalytic combustion by calculated data. It can be concluded that catalytic combustion was completed oxidation combustion of the heterogeneous reaction. The emissions of NOx, unburnt C_nH_m, CO was very small, so the catalytic combustion would not cause serious environmental pollution. Therefore, High combustion efficiency and near zero pollution emissions of catalytic honeycomb monolith burner VI were its advantages which should be applied for industry.

Acknowledgments

The project sponsored by the Beijing Municipality Key Lab of Heating, Gas Supply, Ventilating and Air Conditioning Engineering (KF201002)and Funding Project for Academic

Human Resources Development in Institutions of Higher Learning of Beijing Municipality in 2010（PHR201007127）.

References

[1] E.Tzimpilis, N.Moschoudis, M.Stoukides,P.Bekiaroglou, Ageing and SO_2 resistance of Pd containing perovskite-type oxides, Appl.Catal.B84, 2008, pp. 607–615.

[2] T.V. Choudhary, S. Banerjee, V.R. Choudhary, Catalysts for combusion of methane and lower alkanes, Appl. Catal. A 234, 2002, pp. 1–23.

[3] Q. Liu, A.Q. Wang, X.H. Wang, P. Gao, X.D. Wang, T. Zhang, Micropor. Mesopor. Mater.111 ,2008, pp. 323–333.

[4] O.R. Inderwildi, S.J. Jenkins, D.A. King, Dynamic interplay between diffusion and reaction: Nitrogen recombination on Rh{211} in car exhaust catalysis, Angew. Chem.Int.Ed.47, 2008, pp. 5253–5255.

[5] J.G. McCarty, Perovskite catalysts for methane combustion, Nature 403, 2000, pp. 35–36.

[6] V. Dupont, S.H. Zhang, R. Bentley, A. Williams, Experimental and modeling studies of the catalytic combustion of meth-ane, Fuel 81, 2002, pp. 799–810.

[7] L.D. Pfefferle, and W. C. Pfefferle, Catalysis in combustion, Catal. Rev—Sci.Eng.29, 1987, pp. 219–267.

[8] R. Dalla Betta, Catalytic combustion gas turbine sys-tems: The preferred technology for low emissions elec-tric power production and co-generation, A. Catal. Today 35, 1997, pp. 129–135.

[9] D. B. Fant, G. S. Jackson, H. Karim, D. M. Newburry, P. Dutta, K. O. Smith, and R. W. Dibble, Gas Turbines Power122, J.Eng, 2000, pp. 293–300.

Experimental and theoretical evaluation of the performance of a Whispergen Mk Vb micro CHP unit in typical UK house conditions

A. Alexakis, G. Gkounis, K. Mahkamov*, J. Davis

*School of Computing, Engineering and Information Sciences, Northumbria University, Newcastle upon Tyne, NE1 8ST, UK**
**Corresponding author, Tel:+44 191 2274739, Fax: +44 191 2437630,*
Email: khamid.mahkamov@northumbria.ac.uk

Abstract: A Whispergen Mk Vb 1KW$_e$ Stirling Engine mCHP unit was integrated into a test rig simulating a typical UK domestic hydronic heating system and tested implementing derived heat demand profiles in the house over the yearly period. The obtained experimental performance was used as input data for static simulations in CANMET Energy RETScreen software to calculate economical and environmental benefits from deployment of the mCHP instead of a condensing boiler. Simulation results show that a 16% annual monetary savings can be achieved due to the introduction of new UK feed–in tariffs. The payback period when using the mCHP system instead of a condensing boiler is about 8 years. These results can be used for determination of strategy for further improvement of the performance of the unit.

Keywords: *Domestic mCHP, Fuel combustion, Energy conversion efficiency*

1. Introduction

mCHP is a promising on-site generation technology which, under particular conditions, can provide energy, carbon and cost savings. The installation of large scale CHP systems (hospitals, airports etc.) has been already proven beneficial due to the high combined efficiency. Those have made the installation of CHP for much smaller applications (domestic) an attractive option and have led to the development of a number of mCHP systems with some being already commercially available.

For small scale domestic applications the Stirling Engine based mCHP systems are considered more suitable due to their quiet operation and high heat/power ratio. The aforementioned, combined with the newly introduced UK feed-in tariff, can have a significant impact on domestic sector carbon emissions and energy consumption.

The scope of this research is to obtain a thorough understanding of the parameters that affect the performance of domestic Stirling Engine mCHP systems and engineer solutions for their feasible deployment. The evaluated deployment scenarios differ mainly in the house size, age and occupancy pattern. These are very important factors which affect the magnitude of the energy demand [1].

2. Methodology

2.1. *Experimental Apparatus*

All experiments were carried out with a 1 kW$_e$ Whispergen Mk Vb Stirling Engine gas fired unit integrated with a test rig which simulates a conventional hydronic space heating system with four panel radiators. The mCHP unit is equipped with two gas burners; the main burner has a heat generation capacity of 6 kW$_{th}$ with no part load operation capability and provides the heat to run the Stirling engine. The auxiliary burner generates an additional 5 kW$_{th}$ and its operation is controlled by the system's electronics. A 150 l tank has been retrofitted to the test rig to allow simulation of Domestic Hot Water (DHW) heating-up and consumption. A three-way valve has been installed to split the water circulation to the two water circuits. The

auxiliary burner is controlled by a Honeywell Outside Temperature Compensator (OTC) sensor. A number of meters are used for data acquisition. These include a gas meter, two ultrasonic heat meters and a data logging system for obtaining the mCHP operating parameters during experimentation via a computer interface. The operation of the mCHP unit is controlled by a programmable thermostat-controller device. Unlike pre-commercial prototype Whispergen Mk III system Mark Vb mCHP system does not have a modulation capability, e.g. it can operate only at a full load or is switched off when the heat demand is satisfied.

2.2. *Experimental Procedure*

The procedure followed for the performance evaluation of the Whispergen Mk Vb mCHP includes dynamic and steady state performance analysis and efficiency calculations and carbon emissions analysis, similar to [2, 3]. Heat demand is modeled by determining an occupancy pattern and programming the thermostat-controller to signal it. For the analysis, data is logged every minute [4]. The most important information is provided by the flow and return temperatures, the power generated and the exhaust temperature. The heat meters installed on the water pipes provide information about the water flow rate and the heat generated by the unit. This is sufficient for steady state efficiency calculations. However, since their output cannot be logged to the computer, the temperatures are taken from the engine log for transient state calculations. Then, the generated thermal energy (in $kWh_{thermal}$) is calculated as

$$Q_{gen} = \frac{\sum_{i=0}^{n} Cp_{water}(T_{flow} - T_{return})(\dot{m}_{CH} + \dot{m}_{DHW})}{60} \quad (1.1)$$

where n is the cycle duration in minutes, T_{flow} and T_{return} are the cooling water outlet and inlet temperatures respectively and $\dot{m}_{CH}$ and $\dot{m}_{DHW}$ are the mass flow rates of the heating and the hot water circuits, respectively.

The heat input to the engine is calculated by recording the fuel consumption and using its Low Heating Value. Then efficiencies are calculated as

$$n_{thermal} = \frac{Q_{gen}}{Q_{fuel}} \quad (1.2)$$

and

$$n_{electrical} = \frac{E_{gen}}{Q_{fuel}} \quad (1.3)$$

where Q_{gen} is the heat generated from the mCHP, E_{gen} is the electricity generation and Q_{fuel} is the energy content of the fuel.

The total fuel utilization efficiency is the sum of the thermal and electrical efficiencies.

Another area of interest is the engine's time response to heat demand signals. Therefore, once heat and power generation values have been obtained, they are plotted against time.

2.3. *Domestic Operation Modeling*

For modeling procedures CANMET RETScreen [5] and EnergyPlus [6] software packages are used in this work. These packages use algorithms based on application of energy balance equations. For example, EnergyPlus uses energy balance equations for a number of zones in the simulated dwelling. Software contains library with a set of material properties used in the structure of the building, data on the climatic conditions and experimental and theoretical correlations to calculate heat losses and the temperature rise inside the house.

Data collected from experiments are used as input to CANMET RETScreen software. This software is a useful tool for comparing a proposed energy plant (mCHP) to a conventional one (grid electricity and gas fired condensing boiler). The user can provide parameters such as the house size and location, the fuel and electricity prices and the operating characteristics of the systems such as their efficiency. Software estimates the annual energy demand and performance of the systems in terms of carbon emissions and economics. There are, however, indications that this software cannot take into account the transient character of the energy demand and of plant operation. Such coarse temporal analyses are likely to lead in over-prediction of the systems' performance [7, 8]. Therefore, the results from RETScreen are used for initial estimations. Then, more detailed models are built in EnergyPlus, which is capable of modeling energy performance on a more detailed basis by considering the transient operational states of the systems under investigation. The results from EnergyPlus are validated by comparing theoretical data obtained with information derived from gas and electricity bills for real houses. The modeled houses are of the semi-detached or detached type which represent a large farction of the UK housing stock [9]. The chosen location was London, UK. Electricity demand data and appliance wattage ratings are found in [10]. Finally, the mCHP unit is programmed to run to meet the demand profile generated by the domestic energy modeling process. For example, *table 1 presents* a mCHP running schedule for a design day during a winter. The operation strategy was based on heat-led mode and focused on minimizing heat generation surplus.

Table 1. mCHP running operation schedule for a typical winter day.

Type of Day	Weekday	Weekend
Morning	2–hours run	6-hours run
Evening	6-hours run	6-hours run

3. Results and Discussion

The performance of the conventional heating system throughout the year was modeled in EnergyPlus software. The results for a design day during the cold season are presented in *Fig. 1*.

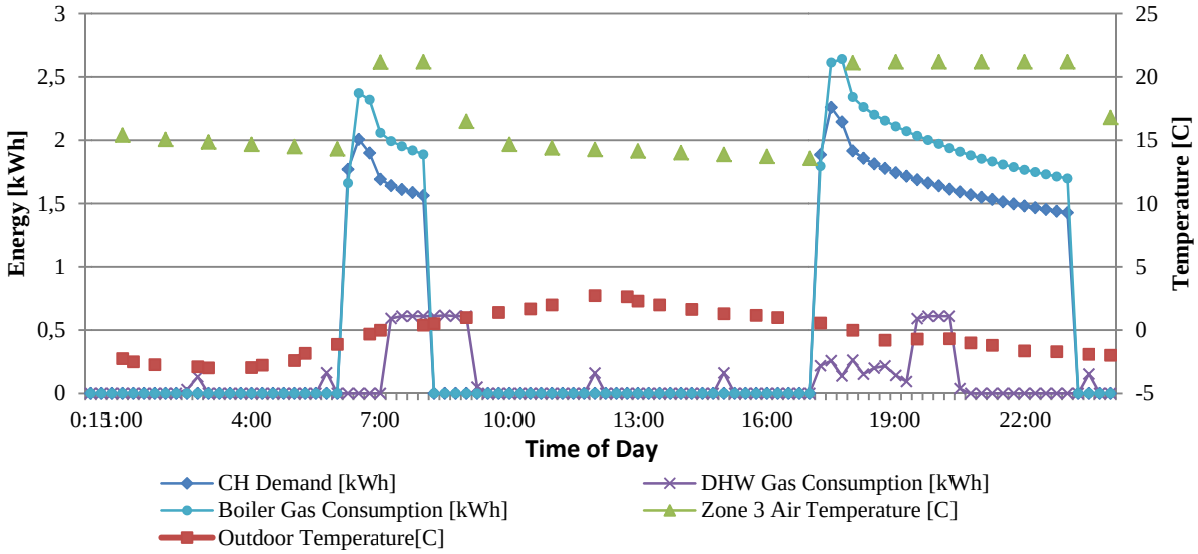

Fig. 1. Demand and temperature profiles on a design day during heating season

It can be seen from *fig. 1* that the gas consumption of the heating system decreases as the ambient temperature raises towards midday. The inner temperature increases once the heating system is fired.

The calculated monthly energy demand profiles are presented in *fig. 2.*

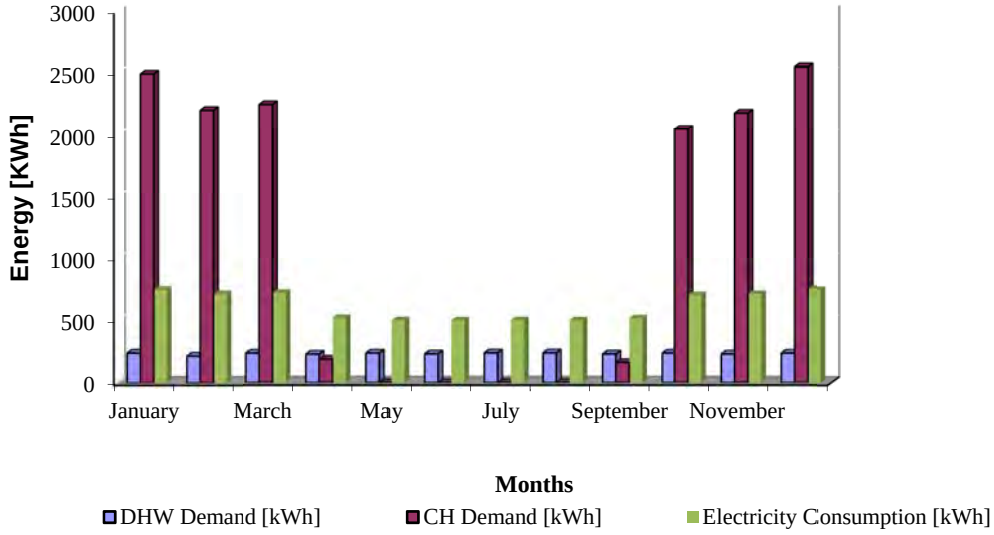

Fig. 2. Calculated monthly energy demand profiles

It can be seen from *fig. 2*, that simulations reflect that the heating and electricity demands are higher during the heating season. The electricity consumption of the heating system has been included in the monthly electricity demand.

The steady state and cycle electrical and thermal efficiencies of the Whispergen mCHP system have been calculated and are presented in *fig. 3.*

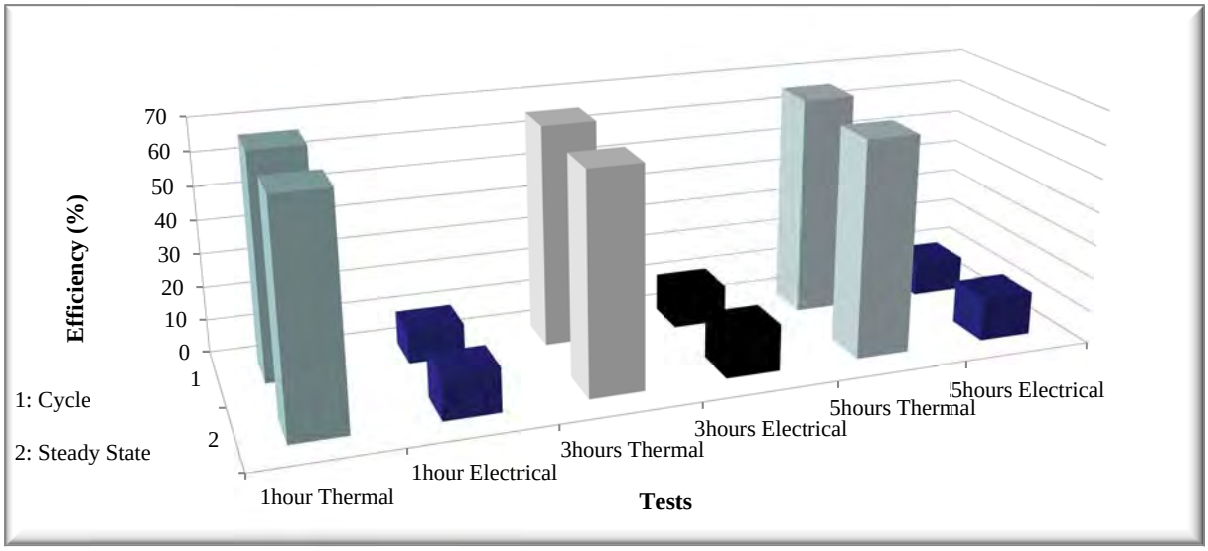

Fig. 3. Steady state and cycle efficiency measurements for different test durations.

It can be observed in *fig. 3* that the thermal efficiency is about 66% for all tests during the steady state operation and for the whole cycle monitoring. The electrical efficiency was found to be about 10% for the whole cycle measurements and 12% for the steady state measurements. These values were consistent for all tests. The thermal efficiency of the mCHP has been found to be considerably lower than that of a condensing boiler. This finding is consistent with [11]. In cycle and steady state measurements, the thermal efficiency remained at approximately the same level. This is due to the water circulator pumping water throughout the system after the combustion process has ended to allow more effective cooling of the engine (*fig. 5*). The cycle electrical efficiency is affected by the dynamic performance during start-up (*fig. 4*) and is lower than the steady state efficiency. It is believed that this low performance is caused by the lower gas pressure of the working gas inside the Stirling engine. This was a design trade-off to avoid wear of moving parts.

The start-up and rundown characteristics of the Whispergen Mk Vb mCHP are presented in *fig. 4* and *5*, respectively.

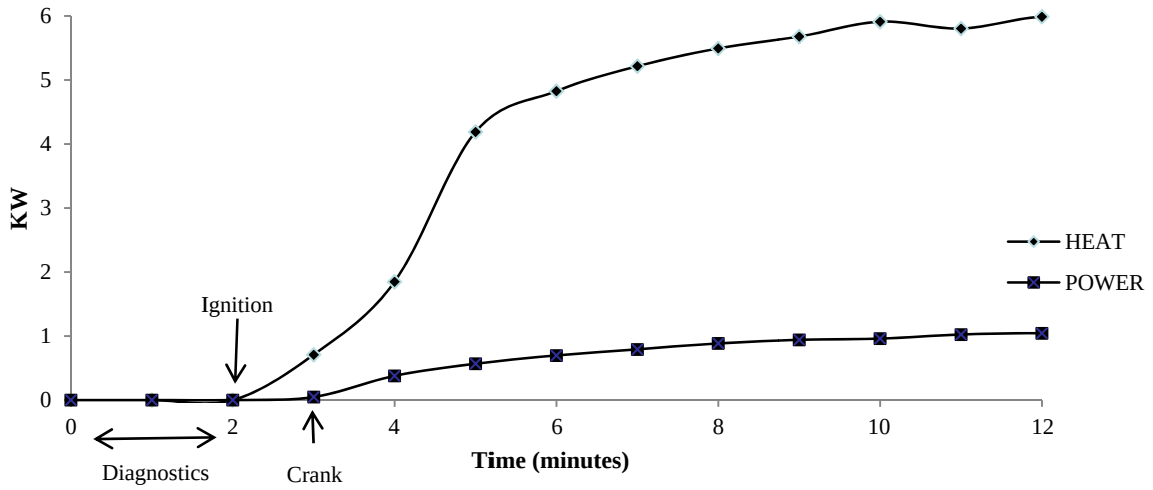

Fig.4. Breakdown of Whispergen Mk Vb start-up characteristic.

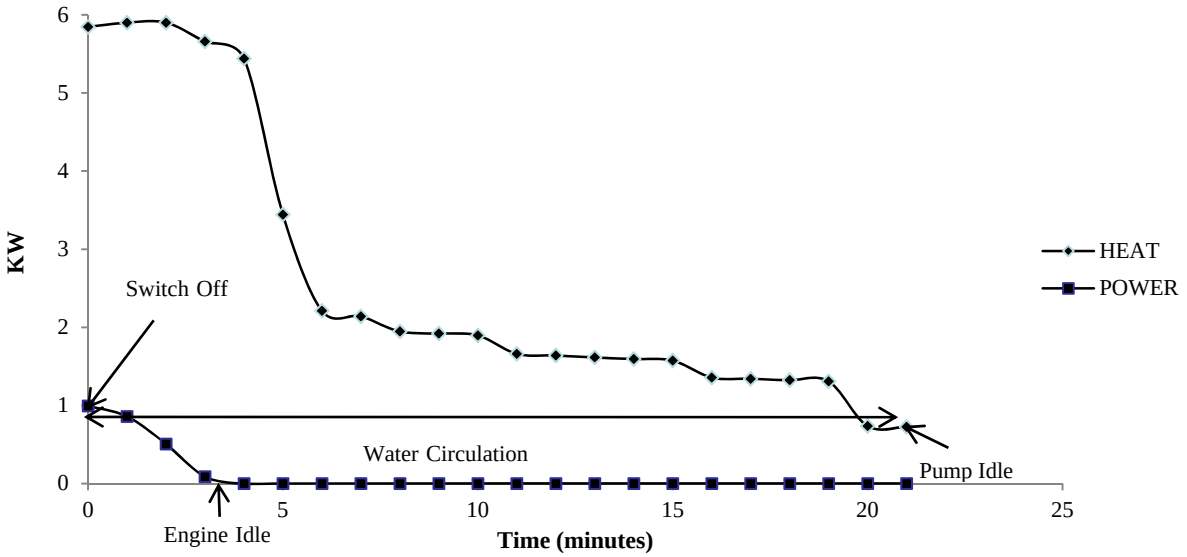

Fig. 5 Breakdown of Whispergen Mk Vb run-down characteristic.

The results presented above were used as input data for RETScreen software and a comparison between the mCHP system and a conventional energy scenario including a condensing boiler and grid electricity was carried out. The results are presented in *table 2* for two houses with different heat demands.

Table 2. Annual performance of mCHP compared to a conventional system for 2 houses.

House Type	5 kWth semi -detached	9.5 kWth detached
Annual Benefits	£-54	£87
Annual carbon savings	-500 Kg	300 Kg

Results obtained using RETScreen indicated that the particular mCHP system would be unfeasible for a relatively new semi-detached house with a low heat demand. The feasibility of the system was considerably improved for a larger house with a higher heat demand. Similar results can be found in literature [12]; however, different methods and models were used. It is believed that the particular software neglects the transient performance of both the mCHP unit and the heating boiler, as well as the dynamics of domestic energy demand and energy pricing. Furthermore, the estimated electricity demand does not include the electricity consumption of the heating boiler which may add up to the electrical about 10% of the boiler rated output [11]. Additionally, the software sizes the conventional heating boiler based on solely heat demand (5 kW_{th}). In reality, this demand would be met by a 15 kW_{th} boiler. This over sizing limits the efficiency of the boiler. The software prediction is more encouraging for the detached type house as the mCHP displaces more grid electricity by operating for longer periods to meet the higher heat demand. The economic savings are attributed to the recently introduced feed-in tariff (10 pence per every kWh of electricity) [13] and the carbon savings are associated to the carbon intensity of the displaced grid electricity.

The mCHP was tested using the programmer controller to set conditions for typical days during the annual period. The transient characteristics of its performance including the hot water consumption and reheating were included in all calculations and the yearly performance was modeled. The heat generated from the mCHP is plotted in *fig. 6*. The temperature line illustrates the increase of the heat load when the hot water consumption occurs. This

additional heat load is met by the auxiliary burner. It can be seen from *fig. 6* that the total heat generation for approximately two hour period is equal to 11.5 kW_{th}.

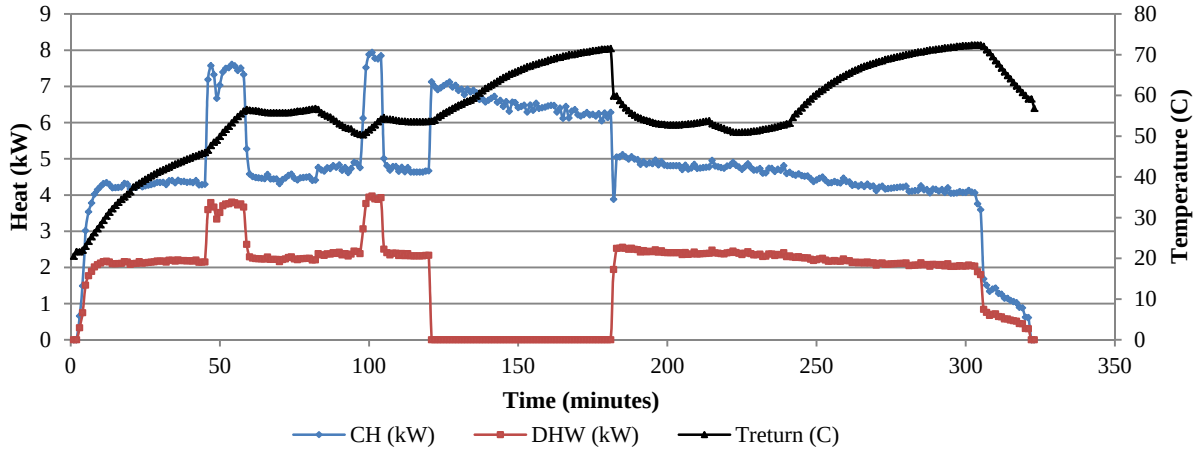

Fig. 6. Heat generation during the evening of a winter weekday

The annual performance of the mCHP compared to the dynamic simulation results of the conventional heating system is presented in *table 3*. The price of the mCHP unit and condensing boiler installed is about £3500 and £750, respectively. The simple payback period is calculated taking into account the difference in the capital cost, fuel consumption and the feed-in tariff.

Table 3. Annual performance of MCHP compared to a dynamically modeled conventional system.

Heating Plant	mCHP
Annual monetary savings	16%
Annual carbon savings	0.17%
Simple Payback Period	8 years

4. Conclusions

The feasibility study demonstrates that the mCHP compared to a condensing boiler in conventional domestic energy scenario can provide annual monetary benefits of up to 16% (taking into account new feed-in tariff, difference in the fuel consumption and assuming the same level of maintenance costs).

The performance of the mCHP is enhanced by a hot water consumption. This additional heat load caused the cooling water temperature to drop at around 50 ^{o}C where condensation is believed to take effect. This improved the mCHP thermal efficiency from 66% to 73%. This improvement however was associated with marginal carbon savings (0.17%) compared to a conventional energy scenario. This is believed to be caused by the low electrical and thermal efficiencies of the particular unit along with the electricity generated during the pre-heating period which is not consumed and therefore does not displace any grid electricity. To support this conclusion, research on the previous Whispergen Mk III mCHP unit [9] with 10% higher overall efficiency indicated higher carbon saving potential. The difference between the current results and those obtained by RETScreen is believed to be due the the deficiencies in electricity demand modeling, energy pricing variations and the thermal efficiency of the mCHP varying with the heat demand.

References

[1] Reacock, A., Newborough, M. (2008) Effect of Heat Saving Measures on the CO_2 Savings Attributable to micro- Combined heat and Power (μCHP) Systems in UK Dwellings. *Energy*, 33 p. 601-612

[2] Thomas, B. (2008) Benchmark Testing of Micro-CHP Units. *Applied Thermal Engineering*, 28 p. 2049-2054

[3] Dorer, V., Weber, A. (2009) Energy and CO_2 Emissions Performance Assessment of Residential micro-cogeneration Systems with Dynamic Whole-Building Simulation Programs. *Energy Conversion and Management*, 50 p. 648-657

[4] Hawkes, A., Leach, M. (2004). Impacts of Temporal Precision IN Optimisation Modelling of micro-Combined Heat and Power. *Energy*, 30 p. 1759-1779

[5] Combined Heat & Power (Cogeneration) Project analysis. Available at: http://www.retscreen.net/ang/tools_and_other_algorithms.php#a3. Date accessed: 24 January 2011

[6] Design Builder EnergyPlus Simulation Documentation. Available at: http://www.designbuilder.co.uk/component/option,com_docman/task,cat_view/gid,20/Itemid,30/. Date accessed: 24 January 2011

[7] Voorspools, K. R., D'haeseleer, W.D. (2003). The Impact of the Implementation of Cogeneration in a Given Energetic Context. IEEE Transactions on Energy Conversion, 18(1) p.135-141

[8] Oda, T., Akisawa, A. and Kashiwagi T. (2004). A Theoretical Evaluation of a Cogeneration System's Total Energy Efficiency Considering Fluctuation in Heat and Power Demands. *World Renewable Energy Congress VIII (WREC 2004)*

[9] Veitch, D. C. G., Mahkamov, K. (2009). Assessment of Economical and Ecological Benefits from Deployment of a Domestic CHP Unit Based on its Experimental Performance. In: *Proceedings of Institute of Mechanical Engineers, 223, Part A: Journal of Power and Energy*

[10] Newborough, M., Augood, P. (1999). Demand-Side Management Opportunities for the UK Domestic Sector. *IEE Proceedings: Generation Transmission and Distribution*, 146(3) P. 283-293

[11] Carbon Trust. *Micro CHP Accelerator*. Interim report

[12] Reacock, A., Newborough, M. (2005). Impact of micro-CHP on Domestic Sector CO_2 Emissions. *Applied Thermal Engineering*, 25 p. 2653-2676

[13] Introducing the Feed-in Tariff Scheme. Available at: http://www.ofgem.gov.uk/Media/FactSheets/Documents1/fitfs_energy%20prices%20update%20FS.pdf. Date accessed: 24 January 2011

Performance analysis of integrated wind, photovoltaic and biomass energy systems

Anis Afzal

Faculty of Engineering & Technology, Aligarh Muslim University, Aligarh, India
**Corresponding author: Tel: +919412593840, Fax: +915712721136, E-mail:anis_afzal@hotmail.com*

Abstract: In this paper performances of different combinations of integrated RE systems are analyzed and compared for various suitable locations in India for a load demand of 1.5 MW. These combinations of integration of REs are wind energy system (WES) and photovoltaic (PV) system; PV system and biomass energy system (BES); and BES and WES. Maximum annual electricity generated by integrated PV system and BES 8,672 MWh while maximum annual income from electricity export is $ 561,078 from integrated BES and WES system. Reduction in net annual greenhouse gas (GHG) emission is found highest of 8,850 tonnes of CO_2 in the case of integrated BES and WES with income from the GHG reduction of $ 177,013 and total annual saving/income of $ 738,091. Equity payback period of integrated BES and WES is estimated as minimum of 2.7 years when cash flow becomes positive.

Performance analyses and cash flows of the integrated RE systems are carried out using RETScreen software tool. It is concluded from the results that integration of BES with another RE is more feasible than without BES in terms of electricity generation, electricity export income, GHG emission reduction, income from carbon trading and equity payback period.

Keywords: *Emission, Renewable Energy Integration, World Renewable Energy Congress 2011*

1. Introduction

Integration, which is also referred as hybridization, of renewable energy (RE) sources involves combining two or more systems of energy resource that naturally over a period of time. This time scale is derived directly from sun (such as for thermal, photochemical, and photoelectric), indirectly from the sun (such as for wind, hydropower, photosynthesis, energy stored in biomass), from other natural movements and mechanisms of the environment (such as for geothermal and tidal energy). The depletion of fossil fuels reserves, the increasing demand for electricity and the harmful effect of CO_2 output on the climate force nations - especially developed countries and their governments - to find new ways of generating the sufficient amount of energy in demand. The integration of alternative energies to reduce emissions and to conserve available fossil sources is a well known fact.

Like other developing countries, India faces a formidable challenge in meeting its energy needs and providing adequate and affordable energy to all sections of society in a sustainable manner. The country today faces an energy demand-supply gap of 8% with peak shortages to an order of 11%-12%. The hospitality industry is one of the major energy and water intensive sectors and to deal with the situation, the utilization of RE sources has to maximize for meeting energy demands [1].

An evaluation of integrated system of PV and wind energy sources of those systems has been done to study reliability of the systems [2]. The supply pattern of different RE sources can be intermittent with different patterns of intermittency. It is often possible to achieve a better overall supply pattern by integrating two or more sources, sometimes also including a form of energy storage system. In this way the energy supply can effectively be made more secure, less intermittent, or more firm. [3]. A comparative study has been made for energy security of the two locations for the same load demand by simulating hybrid renewable energy systems (HRESs) [4].

Some of the reasons of using integrated/HRES are outlined as under:

- Reduction of greenhouse gas (GHG) emissions through increased use of RE and other clean distributed generation
- Increase in use of integrated distributed systems and customer loads to reduce peak load and thus price volatility
- Enhancement in RE system (RES) and energy efficiency
- Increase in reliability, security, and resiliency from microgrid applications in RES to improve system

In this analysis integration of wind energy system (WES), photovoltaic (PV) system and biomass energy system (BES) are carried out for the purpose of analysis to achieve the objectives.

2. Methodology and Objectives

The following objectives of the paper are achieved by using Renewable Energy Technology Screen (RETScreen) Version 4 software simulation tool. The RETScreen International Clean Energy Project Analysis Software is a unique decision support tool designed with the contribution of numerous experts from government, industry, and academia. The software can be used worldwide to evaluate the energy production and savings, costs, emission reductions, financial viability and risk for various types of Renewable-energy and Energy-efficient Technologies (RETs). The software also includes product, project, hydrology and climate databases, a detailed online user manual, and a case study. RETScreen International is getting financial support from Natural Resources Canada's (NRCan) CANMET Energy Technology Centre - Varennes. The software is developed in collaboration with a number of other government and multilateral organisations, and with technical support from a large network of experts from industry, government and academia [5].

For this purpose of simulation, weather data of various places is taken from drop down list and used for analysis purpose so that suitability of integrated RE system may be judged. The software provides simulation by Method 1 and Method 2. Second method is an extension of Method 1 providing more detail analysis. The main inputs used in the analysis are multiple technologies options from drop down list, power capacity required, initial cost, type of fuel, selection of RE system from drop down list, rate of energy export, transmission and distribution loss, rate of inflation, project life, rate of interest and debt term etc. Energy models are prepared using above mentioned input data to obtain the following outputs:

- Calculation of energy exported to grid from RE sources
- Income from energy export
- Gross and net GHG emission reduction
- GHG reduction income
- Total annual cost
- Total annual saving and income
- Financial viability including simple and equity payback
- Cumulative cash flow

3. Integration of RE systems

A large-scale integration of optimal combinations of PV, wind and wave power into the electricity supply has been carried out by Lund (2006) using computer software namely EnergyPLAN [6]. In another paper a load balance model has been suggested to evaluate economic and environmental effects of integrating wind power into three typical generation

mixtures. The results have been indicated that the system operating cost increased by 83%–280% (depending on generation mixture) at a wind penetration of 100% of peak demand and system emissions decreased by 13%–32% (depending on the generation mixture) [7]. In the present paper RE integration of WES, PV system and BES are carried out. Costs of RES per kW are taken as $ 1,900, $ 9,100 and $ 467 for WES, PV system and BES respectively. Cost of energy to be exported from the microgrid of the proposed system is taken as $ 70/MWh [5, 8]. The following combinations of integration are chosen:

- WES and PV system
- PV system and BES
- BES and WES

3.1. Integration of Wind and Photovoltaic Energy Systems

Weather data of Jaisalmer found suitable for integration of wind and PV energy systems which is used to develop energy model and cash flow curve of the integrated RES. The place is situated in the western state of Rajasthan, India at latitude of 26.9° N, longitude 70.9° E and elevation of 130 m. The daily average radiation of the place is 5.16 kWh/m^2/d and average wind speed of 3.9 m/s, maximum 4.9 m/s in June and minimum 3.4 m/s in Oct. Government of India has an elaborate program to install 1000 MW PV system at a nearby place in the desert of Rajasthan Thar desert in the coming decade. The area is selected for a proposed distributed generation from integrated WES and PV system to study the feasibility of integrated system. A load demand of an area Manak Chowk of Jaisalmer is chosen, having a load of 1.47 MW, say 1.5 MW to install an integrated system of WES and PV system [9].

Before building a system with several intermittent energy sources and variable consumption, guidance on selecting the dimensions of the individual components should be obtained by simulating the system operation under the local conditions like weather, insolation, wind speed etc. In general, a key objective of such a system is to use the maximum proportion of RE as mentioned above, but other factors including the financial investment, social aspects, local infrastructure, durability etc. must also be considered.

3.1.1. Results of Performance and Emission Analysis of Integrated 750 kW Wind and 750 kW Photovoltaic Energy System at Jaisalmer

Although the behaviour of wind and PV energy systems are different, equal power capacity of 750 kW each considered shown in Figure 1. Simulation results are obtained indicating total energy export to the grid 3,285 MWh giving an income $ 229,950. The results are shown in the energy model in Table 1 achieving net GHG emission reduction 3,730 tCO_2 (tonnes of CO_2), GHG reduction income $ 74,607 giving a total annual saving and income of $ 304,557. Complete GHG emission analysis, total annual cost, and financial viability are also shown in Table 1. The detail specification, manufacture and models are suggested by the tool itself. Wind turbine 15 units of Atlantic Orienet make with Model No. AOC 15/50-23m and PV system 3000 units of Uni-Solar make with Model No. a-Si-SSR-256W are chosen from the drop down list of the software tool. Other options of wind turbines and PV systems are also available in the list which may be selected depending upon requirement of the site and load demand. Cumulative cash flow graph is illustrated in Figure 2, showing equity pay back starts after 6.9 yr when cash flow becomes positive [9, 10].

Table 1. Results of Energy Model of 1.5 MW integrated energy project of WES 750 kW and PV energy system 750 kW indicating detail of proposed case power system, GHG emission analysis and financial analysis

Proposed power case system		**Financial parameters**	
Technology 1	Wind turbine	**Inflation rate**	2.0 %
Power capacity	750 kW	**Project life**	20 yr
Capacity factor	30%	**Debt ratio**	70%
Manufacturer	Atlantic Orienet	**Debt interest rate**	5.00%
Model	AOC 15/50 -23m – 15 units	**Debt term**	14 yr
Electricity exported to grid	1,971 MWh	**Annual savings and income**	
Total initial costs	$ 1,384,666	**Fuel cost - base case**	$ 0
Technology 2	PV	**Electricity export income**	$ 229,950
Power capacity	750 kW	**GHG reduction income -14 yr**	$ 74,607
Manufacturer	Uni-Solar	**Total annual saving & income**	$ 304,557
Model	a-Si-SSR-		
Capacity factor	20%	**Emission analysis**	
Electricity export rate	$ 70		
Electricity exported to grid	1,314 MWh	**GHG emission propose case**	0
Country-Region	India	**GHG credits transaction fees**	2.0%
Fuel type	Coal	**Net annual GHG emission reduction**	3,730 tCO_2
GHG emission factor Excl. T&D losses	0.927 tCO_2/MWh	**Acres of forest absorbing carbon**	1,283
T&D losses	20%	**GHG reduction credit rate**	**2**0 $/ tCO_2
GHG emission factor Incl. T&D losses	1.159 tCO_2/MWh	**GHG reduction credit duration**	14 yr
GHG emission base case	3,806 tCO_2	**GHG reduction credit escalation duration**	2.0 %
Annual costs and debt payments		**Financial viability**	
O&M (savings) costs	$ 0	**Pre-tax IRR – equity**	16.3 %
Fuel cost - base case	$ 0	**Pre-tax IRR – assets**	2.8%
Debt payments - 10 yrs	$ 203,994	**Simple payback**	9.5 yr
Total annual costs	$ 203,994	**Equity payback**	6.9 yr

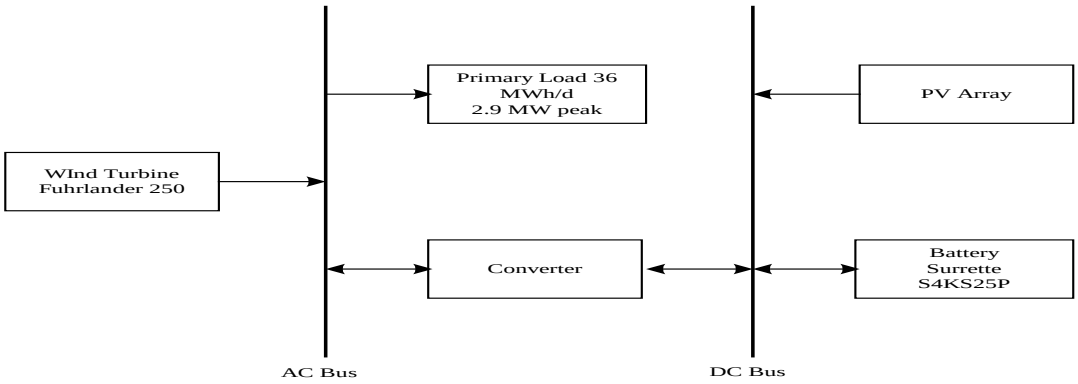

Fig. 1. Basic block diagram of integrated wind and PV energy systems

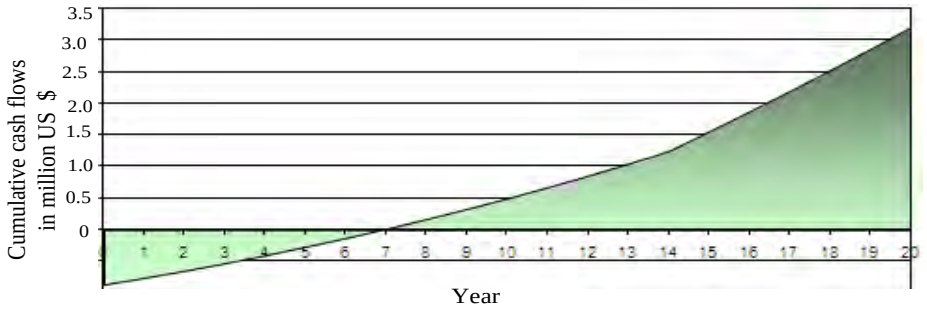

Fig. 2. Cumulative cash flows graph of integrated WES 750 kW and PV energy system 75

3.2. Integration of other RE Systems

Minambakkam, a suburb of Chennai, India is selected for a project of integrated of PV energy system and BES suitable for a comparable load demand of 1.5 MW as in the case of section 3.1. Rice is one of the main agricultural products in this area; hence availability of rice husk is sufficient to supply any biomass gasifier generating electricity. Simulation by RETScreen software is based on specific fuel consumption of rice husk 2.096 kg/kWh with heat rate of 22,200 kJ/kWh [11, 12]. Sufficient amount of solar insolation is also available at the site. The place is located at a latitude 13.0° N, longitude 80.2° E and elevation 16.0 m. The daily average solar radiation is 5.49 kWh/m^2/d with maximum 6.78 kWh/m^2/d in April and minimum 4.17 kWh/m^2/d in December and average temperature 28.8° C [13]. All these weather and agricultural data are used to develop energy model, the results of which shown in Table 2 and cash flow curve as shown in Figure 3.

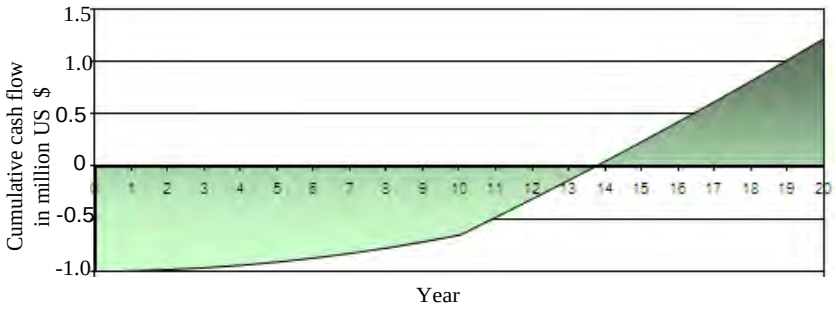

Fig. 3. Cumulative cash flows graph of integrated PV energy system 750 kW and BES 750 kW

Integration of BES and WES suitable for the same load demand of 1.5 MW is proposed to carry out at a coastal area Veraval in western Indian state of Gujrat, located at latitude 20.9° N, longitude 70.4° E at an elevation of 8 m. Mean temperature of the area is 26.6° C, average daily radiation 5.94 kWh/m^2/d and average wind speed 4.3 m/s, maximum wind speed 7.1 m/s in July and minimum 2.7 m/s in Nov. Rice is the main foodstuff of the people of Veraval; hence rice husk is available in abundance around the vicinity of the place suitable to supply rice husk based gasifier for the proposed BES. Uninterrupted flow of wind is available in the coastline area, making WES option feasible particularly during summer days, when the wind speed is high [13]. Energy model of the system prepared, the results of which are shown in Table 2 and cash flow of the project shown in Figure 4.

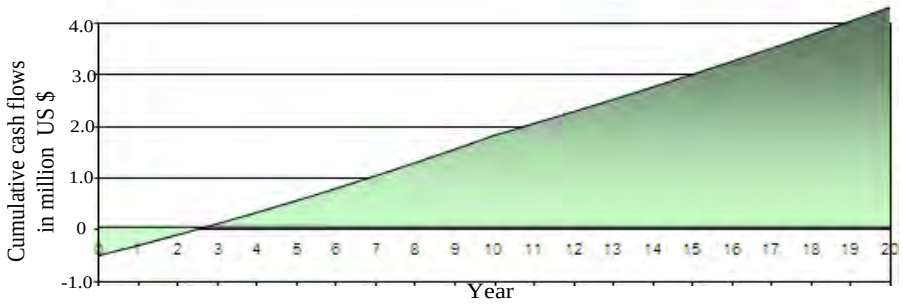

Fig. 4. Cumulative cash flows graph of integrated BES 750 kW and WES 750 kW

4. Comparative results obtained from energy models

Comparative results of analysis of integrated systems on annual basis are tabulated from the energy models data of the various integrated systems, i.e. WES 750 kW with PV energy system 750 kW, PV system 750 kW with BES 750 kW and BES 750 kW with WES 750 kW shown in Table 2.

Table 2. Comparative results of Energy Models of 1.5 MW integrated energy project of WES, PV system and BES each of 750 kW indicating detail energy generated, GHG emission analysis and financial analysis

Integration systems	WES+PV system	PV system +BES	BES+WES
Electricity generated MWh	3,285	**8,672**	8,015
Income from electricity export $	229,950	515,088	**561,078**
Total annual cost $	203,994	**677,523**	546,779
GHG emission reduction tCO_2	3,730	8,105	**8,850**
Income from GHG emission reduction $	74,607	162,092	**177,013**
Total annul saving /income $	304,557	677,180	**738,091**
Equity payback period yr	6.9	13.7	**2.7**
Feasibility/remarks	Not so feasible	Not so feasible	Most feasible

5. Conclusions and recommendations

- Maximum energy 8,672 MWh generated and exported annually from integrated PV system and BES whereas nearly half energy 3,285 MWh is generated in the case of integrated WES and PV system. Therefore, the integrated system of PV system and BES is recommended for energy generation rather than using other integrated RES of similar power rating.

- Annual energy export income $ 561,078 is highest in the case of integrated BES and WES and less than half $ 229,950 from integrated WES and PV system. The integrated system of BES and WES is economically most feasible. Hence, this system is recommended for a windy place where biomass is cheaply available.

- Total annual cost $ 677,523 is highest in integrated PV system and BES and lowest of $ 203,994 (nearly less than one third) in integrated WES and PV system. The high total annual cost is due to consumption of biomass (rice husk) used with the BES gasifier. Hence, integrated system of PV and BES not feasible to opt for generation purpose if low annual cost is the preference. Integration of WES and PV system is suggested where lesser annual cost is desirable for a windy place.

- Annual reduction in GHG emission is least of 3,730 tCO_2 in case of integrated WES and PV energy system whereas highest of 8,850 tCO_2 (nearly 2.5 times) in case of integrated BES and WES. Annual GHG emission of 8,105 tCO_2 is found in case of integrated PV system and BES. In the present scenario of the world growing air pollution, GHG emission reduction is the prime factor while considering electricity generation options. Therefore, integrated system containing BES should be given preference over other integration of RE systems without BES.

- Annual income from GHG emission reduction $ 177,013 is highest in integrated BES and WES and lowest of $ 74,607 (nearly less than half) in integrated WES and PV system. Whereas the annual income is $ 162,092 in integrated PV system and BES. The analysis results show that income from integrated systems containing BES with other RES is more than any other RE integration running without BES because of higher reduction in GHG emission. Therefore, integrated system BES with WES should to be preferred over other integrated systems to get more annual income from carbon trading.

- Total annual saving /income $ 738,091 is also maximum from integrated BES and WES and nearly less than half $ 304,557 from integrated WES and PV system. Total annual saving/income is estimated as $ 677,180 in case of integrated PV system and BES. It is found that results are in favour of integration of BES with other RES. Hence, integration of BES with WES and PV system with BES is suggested to use in any part of the world wherever biomass available.

- Equity payback period is shortest of 2.7 years in case integrated BES and WES and longest of 13.7 years (nearly more than 5 times) in case of integrated PV system and BES. A major portion of cash flow curve of integrated of PV system and BES lies in the negative side and positive cash flow starts after 13.7 years indicating non-feasibility of the system; hence this system of RE integration is not suggested to opt. Integrated BES and WES is estimated to be the best option since a major portion of cash flow curve lies in positive side and system starts giving return just after 2.7 years.

Therefore to get quickest positive cash flow, integrated system of BES and WES is recommended.

- Comparing all positive and negative aspects of combinations of integration, best system for integration is BES with WES. Moreover, this integration of RE has minimum environmental impact while generating electricity. That also provides huge income from carbon trading.

- The not-so-feasible combination of integration is PV system with BES due to high total initial annual cost. But it may be also suggested for use because of more generation, high GHG emission reduction and total annual saving. WES and PV system may be opted where less total annual cost required.

References

[1] MNES, Ministry of Non-conventional Energy Sources, Government of India, Ministry Reports 2008.

[2] R. Billinto, and R. Karki, Maintaining supply reliability of small isolated power systems using renewable energy, IEE Proc.-Gener. Transm. Distrib., DOI: 10.1049/ip-gtd:20010562, Vol. 148, No. 6, Nov. 2001, pp. 530-534.

[3] http://www.doe.energy.gov /renewable

[4] A. Afzal, Mohibullah and V. K. Sharma, Optimal hybrid renewable energy systems for energy security: a comparative study, International Journal of Sustainable Energy, Taylor and Francis, 2009, 29:1, 48-58.

[5] http://www.retscreen.net, 8 Sep. 2010.

[6] H. Lund, Large-scale integration of optimal combinations of PV, wind and wave power into the electricity supply, Renewable Energy, 2006, Vol. 31, pp. 503–515.

[7] J. D. Maddaloni, A. M. Rowe and G. C. V. Kooten, Wind integration into various generation mixtures, Renewable Energy, 2009, Vol. 34, pp. 807–814.

[8] UPPCL, Uttar Pradesh Power Corporation Limited, Government of Uttar Pradesh, India, 2010.

[9] Afzal, A., Sharma, V.K., and Mohibulalh, 2007. Performance evaluation of wind energy conversion system as an alternative energy source in Indian condition, International J. of Mathematical Sci. & Engg. Appls. (IJMSEA), Vol. 1, No. 1, pp. 155-171.

[10] Afzal, Anis, Sharma, V. K., and Mohibullah "Energy Analysis of Solar Photovoltaic System for an Academic Institution in Northern India," International J. of Engg. Research & Indu. Appls. (IJERIA), ISSN 0974-1518, Vol. 1, No. VII (2008), pp 99-112.

[11] Afzal, A., Sharma, V.K., and Mohibullah, 2010. Performance analysis of rice husk power generating system: a case study. International Journal of Sustainable Energy, Taylor & Fancis, DOI: 10.1080/14786461003802100.

[12] Ahiduzzaman, M., 2007. Rice husk energy technologies in Bangladesh. Agricultural Engineering International: The CIGR Ejournal, Invited Overview, No. 1, vol. IX, 1-10

[13] http://www.mnes.in/, 23 Oct. 2010

Feasibility Study of Solar-Wind Based Standalone Hybrid System for Application in Ethiopia

Getachew Bekele Beyene*

Addis Ababa Institute of Technology, Addis Ababa University Addis Ababa, Ethiopia
**Getachew Bekele. Tel : +251(0)911 24 50 88 ; Fax:+251(0)111 239480, e-mail:*
getachew@ece.aau.edu.et; getachewbk@yahoo.com

Abstract: Shortage of electric power is a serious problem in Ethiopia. As recently as the year 2009 electric power supply in the country including the capital Addis Ababa, was at best every other day for several months. Until recently, the sole power producer in the country, Ethiopian Electric Power Corporation (EEPCo) produces a total of 800 to 900 MW of power for a country with a population of about 80 million. This clearly shows as to what the shortage would look like.

In this regard, this study investigates the possibility of providing electricity from solar/wind based hybrid standalone system for remotely located people detached off the main grid line. Within the hybrid system setup PV panels, wind turbines, a bank of batteries and for a backup diesel generator is included.
The wind potential of the area has been assessed in a previously published article. The solar potential has also been investigated in another article awaiting publication. It is based on the findings of the solar and the wind energy potential that this study is carried out.

A model community of 200 families, comprising of approximately 1000 to 1200 people in total is considered for the study. A community school together with a health post is also included. The electric load comprises of lighting, water pumps and other small appliances.

For the techno-economic analysis in the feasibility study of the hybrid system the National Renewable Energy Laboratory's (NREL) HOMER software is used. Given all the necessary inputs to the software, the results showed a list of feasible electric supply systems, sorted according to their total net present cost (NPC). Cost of energy (COE in $/kW), penetration level into the renewable resources (renewable fraction), the number of liters of diesel oil used by the generator and also the generator working hours is also given out in the results table. The greenhouse gas emission level of the system is also incorporated within the results.

Furthermore, a sensitivity analysis is carried out for the major sensitive components of the hybrid system. The major sensitive components of the system recognized are the changing price of PV panels and the ever hiking price of diesel oil. From the results it is concluded that the solar energy potential is the most promising resource that can be utilized.

Keywords: *Wind Energy potential; Solar Radiation potential; Primary Load; Deferrable Load; Net Present Cost (NPC)*

1. Introduction

Power generation in Ethiopia started at the end of the 19th century, during the then king Minilik time. The first generator was used in the palace around 1906 and in 1912 the first hydropower plant at a place called Akaki, very close to the capital, Addis Ababa. Ever since, the country could produce only 814 MW (until recently) in its over 100 years long history.
Currently shortage of electric power is a serious problem in Ethiopia. As recently as the year 2009 electric power supply within Addis Ababa, the capital of the country, was at best every other day for several months. Even in the same year we are electricity supply with in the capital is intermittent.

As mentioned in previous articles [1] [2][3], the Ethiopian Electric Power Corporation (EEPCo), the only proprietor of the electric power production corporation with total

management control (issue license, set tariff, supervise the generation, transmission, and distribution, sales, import export, etc.), currently produces between just over one MW of power. It is only this amount which is available for a country with a population well over 75 million. Over 95% of the resource for electricity generated is Hydropower. Although the country is endowed with enormous resource of solar energy there is no solar or wind energy contribution in the EEPCo's system.

The total countrywide coverage of the generated electricity is estimated to be some 15%. With only so small coverage, electricity supply in the deeper rural regions is unthinkable. This clearly indicates that something has to be done and the responsibility should all lie on the shoulders of the engineers within the country. The depletion of fossil fuel and the climbing up of the oil price with its involved politics, the pollution associated with the use of fossil fuel is are all left for the reader of this piece of work to consider as additional motivation.

"That the human race must finally utilize direct sun power or revert to barbarism because eventually all coal and oil will be used up. I would recommend all far-sighted engineers and inventors to work in this direction to their own profit, and the eternal welfare of the human race" Frank Shuman -1914

2. Methodology

The location under investigation is Debrezeit, 08″44′N, 39″ 02′E 1850 m. Wind and solar energy potential of the location is studied and have been given in previously published articles and a book [1][2][3]. As it is clearly shown in the references the wind energy potential is not so promising. However, the solar energy potential is absolutely usable. Figure 1 shows the monthly average wind speed at a height of 10 m. At a certain height, Z, the wind speed increases according to equation (1). It has been shown in [1] that average annual wind speeds of 3 to 4 m/s may be adequate for non-grid-connected electrical and mechanical applications such as battery charging and water pumping.

$$v(z)\cdot \ln\left(\frac{z_r}{z_0}\right) = v(z_r)\cdot \ln\left(\frac{z}{z_0}\right) \qquad (1)$$

Where: Z_r is the reference height (10 m); z_0, is the roughness length.

The solar energy potential of the location is given in figure 2. As can be seen from the figure the solar energy potential is more than 6 kWh /m^2 for almost the whole time of the year. It is only in the rainy season, July and August the potential falls to between 5 and 6 kWh/m^2. This is indeed excellent situation for working on this resource.

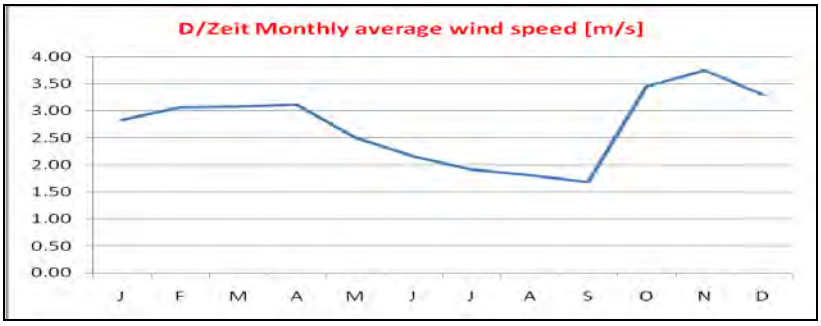

Figure 1: Monthly average wind speed

Having determined the solar and the wind energy potential energy of the location under investigation, a model community of two hundred families is considered for which the necessary basic load of electric lighting and water pumping system is suggested.

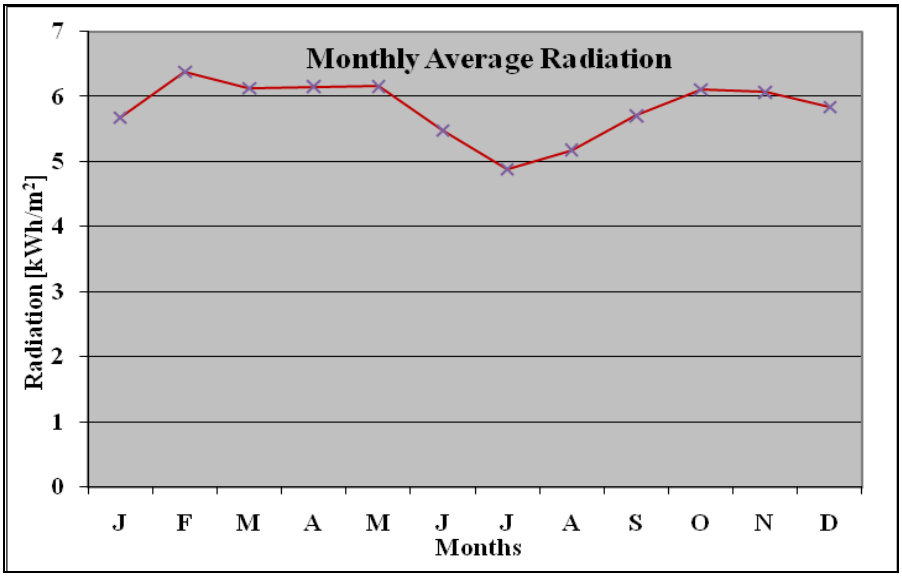

Figure 2 Monthly average daily solar radiations

HOMER software is used for the analysis. HOMER is a micropower design tool developed in 1992 to simulate and optimize stand-alone and grid-connected power systems with any combination of wind turbines, PV arrays, run-of-river hydro power, biomass power, internal combustion engine generators, micro-turbines, fuel cells, batteries, and hydrogen storage, serving both electric and thermal loads (by individual or district-heating systems) [4]. HOMER can perform a 'what-if' analysis to investigate uncertainties or changes in the input variables such as price variation of: fuel, PV panels, turbines or others in the one hand and wind speed, solar radiation, etc. on the other. The simulation results are economically and technically optimal and feasible solutions of hybrid setups listed according to their net present cost (NPC).

The net present cost (or life-cycle cost) of a component is the present value of all the costs of installing and operating that component over the project lifetime, minus the present value of all the revenues that it earns over the project lifetime. HOMER calculates the net present cost of each component of the system, and of the system as a whole.[5]

3. Electric Load

As mentioned earlier, the assumed 200 family community is nothing but a model community. It is to be noted that this number can shrink or expand if need be. Five to six family members are considered in each family. Two load types are suggested: primary load, load that must be met immediately, and deferrable load, load that must be met within a certain time (exact timing is not important).

A community school and a health post are also included within the community. Electric load suggested are lighting, water pumping, radio receiver, and some clinical equipment. It is to be noted that the load suggested here is estimated by considering the poorest people in the remotest corners of the country with no access to any of the modern energy supply types, not even a kerosene lamp or a candle light. A typical daily load pattern is presented in table 1.

The primary load consists of 2 to 3 light bulbs and a radio receiver per household and also some more light bulbs for the for the community school and the health post. Limited clinical equipment such as vaccine refrigerators, communication VHF radio, microscope, and AM/FM stereo are also considered.

Table 1 Monthly average daily electrical load [kWh]

Months	Jan	Feb-May	June	July	Aug	Sep	Oct-Dec
Deferrable Load	6	6	5	4	4	5	6
primary load	139	141	141	139	139	141	141
Total Load	145	147	146	143	143	146	147

The deferrable load is mainly water pumping. Four to five family members per house hold and about 100 liters of water per day is suggested. Water Pumps of a 150 W power rating and pumping capacity of 10 liters per minute is chosen. Six pumps at six convenient locations are to be installed. Additional pump for the School and the clinic is also to be installed. A four day storage system is considered. The resulting total load is as given in Table 1.

4. The Hybrid Setup and the Findings

The hybrid system studied is one combining solar and wind energy conversion system, with diesel generator(s) and a bank of batteries included for backup purposes. Power conditioning units, such as converters, are also a part of the system. The operational concept of the hybrid system is that renewable resources are the first choice for supplying load and any excess energy produced is stored in the battery. The diesel generator is a secondary source of energy. Electronic controller circuitry is used to manage energy supply and load demand. A schematic diagram of the standalone hybrid power supply system sought is shown in figure 3.

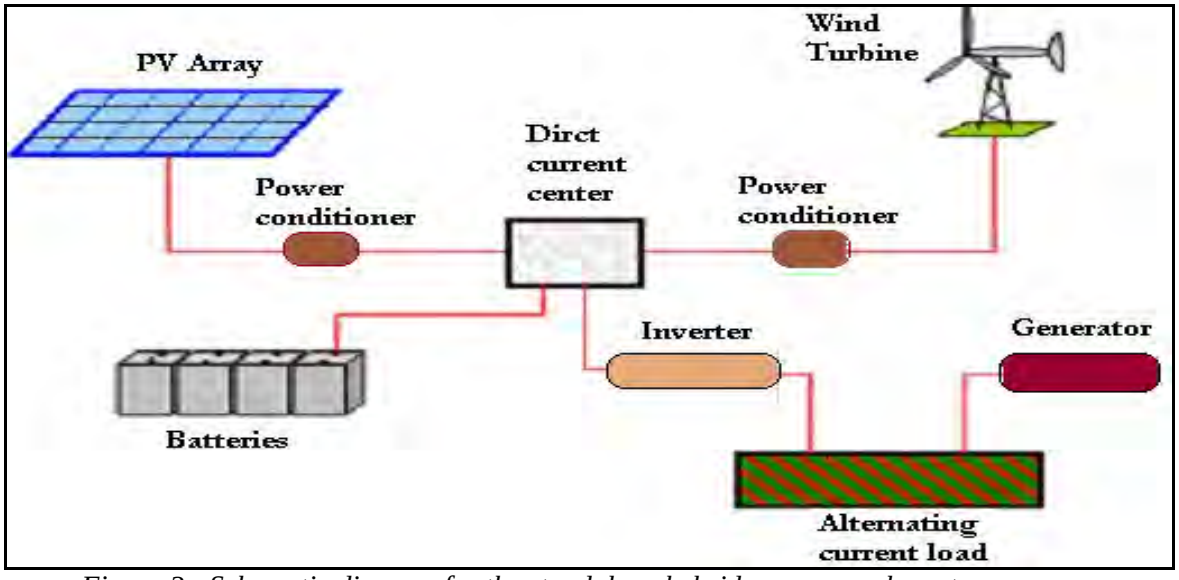

Figure 3: Schematic diagram for the standalone hybrid power supply system

HOMER requires input information in order to analyze the system and to give the feasible solutions. The main input to the software is the load. After carefully determining the hourly community electric load for both the primary and the deferrable load types the monthly average of the daily load is supplied to the software. The load profiles are shown in figure 4 and figure 5.

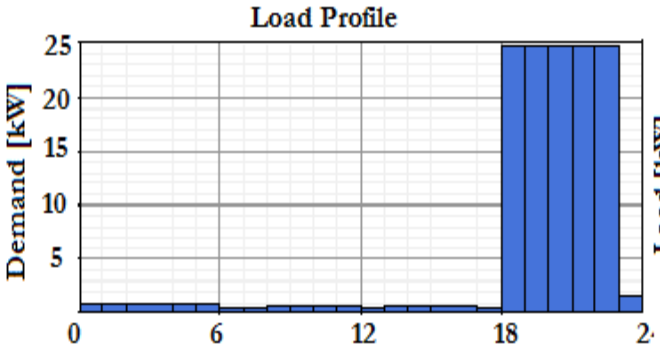

Figure 4 Primary load profile

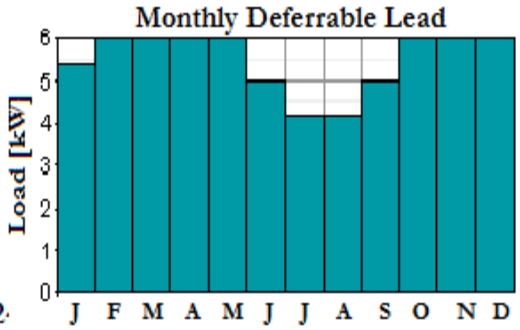

Figure 5 Deferrable load profile

Additional data supplied to the software is summarized in table 2.

Table 2 Input data to HOMER

	PV	Wind Turbine G20	Diesel Generator	Battery (Surrette 6CS25P)	Convertor
Size (kW)	1	20	44	1156 Ah	1
Capital ($)	1200-6000	45,000	11,000	833	700
Replacement cost ($)	1200-6000	30,000	7,000	555	700
O & M cost ($/yr)	0	900	0.4 ($/hr)	15	0
Sizes considered (kW)	0, 5, 10, 15, 20, 30, 50, 70, 100		0, 44, 88		0, 20, 40, 60, 80, 100
Quantities considered		0, 1, 2, 3		0, 40, 60, 80, 100, 200	
Life time	25 yrs	25 yrs	40,000 hrs	9,645 kWh	15 yrs

5. Results

Having fed the necessary input data given in the earlier section to the software the software is run. The resulting list of optimal combinations of realizable setups obtained is given in both overall and categorized forms. Table3 shows extracted part of the long list from the complete overall table. The extraction is based on the contribution made by renewable resources in the realizable set-ups.

As can be seen in the table the first row contains a system with no contribution (0 %) from the renewable resources. The next row contains a PV-Gen-battery-Converter set-up. For just a 16.7 % increase in total NPC over the first set-up ($201,609 to $235,177), the percentage contribution made by renewables increased from 0 to 58 %. This can be an attractive solution for implementation. Of course, there is no wind turbine involved in the system; the wind energy potential at this location is quite low, as can be seen from figure 4-19 and also from previous investigation [1].

Table 3 Extracts from the overall optimization results list

PV(kW)	Wind Turbine G20	Diesel Generator (kW)	Battery	Converter (kW)	Dispatch strategy	Initial capital	Total NPC	COE ($/kWh)	Renewable fraction	Diesel (L)	Generator (hrs)
		44	40	20	CC	$ 58,320	$ 201,609	0.322	0	18623	1785
20		44	40	20	LF	$ 130,320	$ 235,177	0.376	0.58	12078	1909
15	1	44	40	20	LF	$ 157,320	$ 276,081	0.441	0.53	12550	1947
20		44	80	20	LF	$ 163,640	$ 276,560	0.442	0.62	10617	1729
30		44	40	20	CC	$ 166,320	$ 278,443	0.445	0.66	13037	2127
30		44	60	40	LF	$ 196,980	$ 279,851	0.448	0.77	7048	1062
20	1	44	40	20	LF	$ 175,320	$ 285,862	0.457	0.62	11339	1811
30		44	80	40	LF	$ 213,640	$ 290,597	0.465	0.83	4883	716
20	1	44	60	20	LF	$ 191,980	$ 305,266	0.488	0.64	10417	1701
30		44	100	40	LF	$ 230,300	$310,604	0.497	0.85	4053	590

Figure 6 shows the monthly average electrical production and table 4 the overall system report.

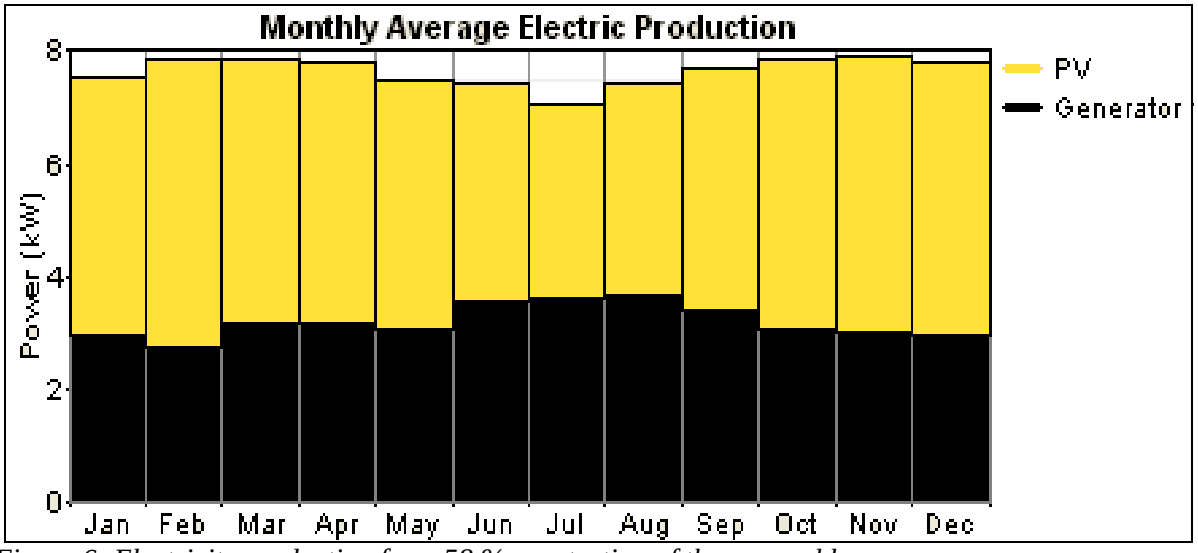

Figure 6: Electricity production for a 58 % penetration of the renewable

The maximum contribution by renewables, 85 %, is achieved by the set-up given in the last row of the table. For this set-up the NPC is $310,604, which is a 32 % increase in the total NPC over the setup with a renewable contribution of 58 %. This setup can also be seen as an alternative for implementation despite the higher cost. It is understood that a system is considered as renewable system if the renewable contribution is about 27% or above. Hence, if the renewable future is to be given its merits then this system will be the option. It should be noted that this set-up once again does not include a wind turbine as the wind potential of the location is minimal.

Table 4 System report for the 58 % renewable penetration

System architecture		Sensitivity case	
PV Array	20 kW	Solar Data	5. 81 kWh/m^2/d
Wind turbine		Wind Data	2.51 m/s
Gen.	44 kW	Diesel Price	0.5 $/L
Battery	40 Surrette 6CS25P	PV Capital Cost Multiplier	0.6
Inverter	20 kW	PV Replacement Cost Multiplier	0.6
Rectifier	20 kW		

Annual electric production (kWh/yr)			Annual electric energy consumption (kWh/yr)			Emissions (kg/yr)	
PV array	38,823	58%	AC primary load	50,772	97%	CO2	31,806
Wind turbine			Defferable load	1,306	3%	CO	78.5
Generator	28,152	42%	Total	52,077	100%	Unburned HC	8.7
Excess electricity	5,591					Particulate matter	5.92
			Cost summary				
Unmet load	0		Total NPC	$ 235,177		SO2	63.9
Capacity shortage	0		Cost of energy	0. 376 $/kWh		NOx	701

The cost breakdown for the set-up of 58% penetration of the renewable supported by a pie-chart, is also given in figure 7.

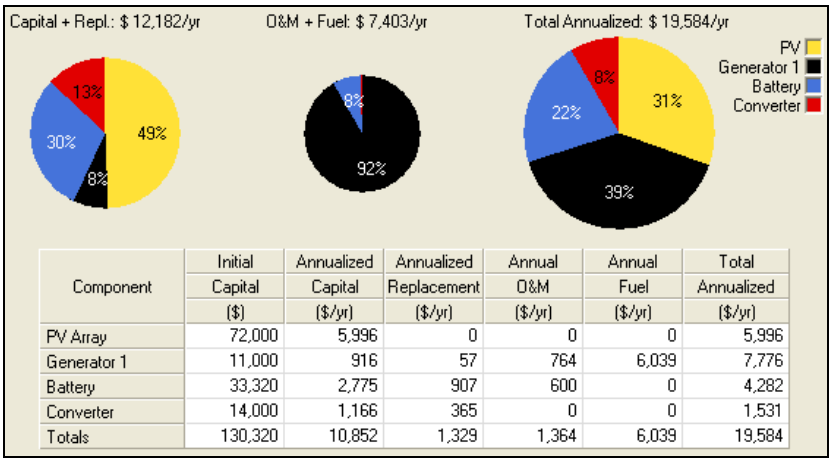

Component	Initial Capital ($)	Annualized Capital ($/yr)	Annualized Replacement ($/yr)	Annual O&M ($/yr)	Annual Fuel ($/yr)	Total Annualized ($/yr)
PV Array	72,000	5,996	0	0	0	5,996
Generator 1	11,000	916	57	764	6,039	7,776
Battery	33,320	2,775	907	600	0	4,282
Converter	14,000	1,166	365	0	0	1,531
Totals	130,320	10,852	1,329	1,364	6,039	19,584

Figure 7 Cost summary for the 58 % renewable resource contribution

The sensitivity analysis given in figure 8 shows the PV capital cost multiplier against diesel price. The net present cost of the most cost effective set-ups for a particular set of diesel and PV price is shown.

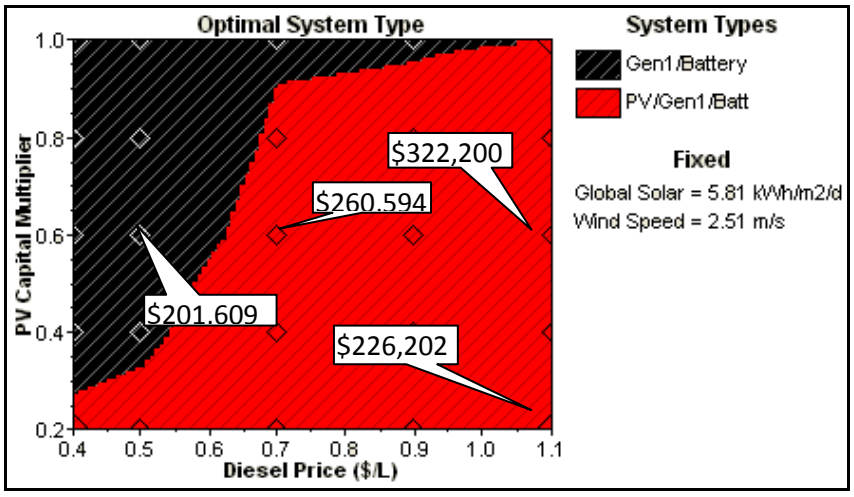

Figure 8 Sensitivity of PV cost to diesel price

6. Discussion and/or Conclusion

The feasibility study for the hybrid system is based on the findings of the wind and solar energy potentials at the particular locations. From the results, the wind energy potential of this site, Debrezeit, is not attractive enough for independent wind farm applications. However, it can be concluded that the potential in some cases could be a viable option if integrated into other energy conversion systems such as PV, diesel generator and battery. The results of this study can be considered as applicable to a significant size of the regions in the country having similar climatic conditions.

Regarding the solar energy it is definitively conclusive that there is abundant resource. The feasibility study, which is based on the findings of the two potential showed a list of possible feasible set-ups according to their Net Present Cost (NPC). The level of the renewable resource penetration can be said is closely tied with the net present cost. The choice as to which feasible system to pick from the list is linked to the choice of whether to consider the renewable resource or the net present cost. This decision is left to the policy makers of the country. However, as in the quotation given in the Introduction part Engineers shoed persistently press the policy makers to consider the utilization of the renewable resource.

References

[1] G. Bekele, B. Palm, Wind energy potential assessment at four typical locations in Ethiopia, Applied Energy. 86, 2009, PP. 388–396

[2] G. Bekele, B. Palm, Feasibility study for a standalone solar–wind-based hybrid energy system for application in Ethiopia, Applied Energy, 87, 2010, PP. 487-495

[3] G. Bekele, Study of a Standalone Solar-Wind Hybrid Electric Energy Supply System: For Rural Electrification in Ethiopia, VDM Verlag, 1st ed., 2010, PP. 20-24

[4] D. Connolly, et.al, A review of computer tools for analysing the integration of renewable energy into various energy systems, Applied Energy, 87, 2010, PP. 1059–1082

[5] HOMER, The micropower optimization model, WWW.homerenergy.com, Jan. 2011

Analysis of the training metrics of ANNs and linear MCP models used for wind power density estimation at a candidate site

Sergio Velázquez [a]*, José A. Carta [a], José Mª Matías [b]

[a] *University of Las Palmas de Gran Canaria, Las Palmas, Canary Islands, Spain.*
[b] *University of Vigo, Vigo, Spain.*
**Corresponding author. tel.: +34 928 45 96 71, Fax: +34 928 457319, E-mail: svelazquez@diea.ulpgc.es.*

Abstract: In order to estimate the amount of electricity that can be produced by a potential wind farm it is important to know how the wind resource performs at the site where it is to be installed. Of fundamental importance in an analysis of the wind resource is the wind speed parameter. Understanding how this parameter behaves over periods of time that cover ten or more years (long-term) is vital for an accurate estimation that will span the working life of the wind installation. However, in most cases there is insufficient data available about the candidate site to enable a long-term study.

In this work, the long-term wind power density at a candidate site is estimated through the use of a Measure-Correlate-Predict (MCP) algorithm and an Artificial Neural Network model (ANN). To evaluate the accuracy of the estimations different metrics are used, with a comparison of the results obtained for each of them .

The mean hourly wind speeds and directions obtained from twenty-two weather stations located on different islands in the Canary Archipelago (Spain) are used for this study.

Among the conclusions that are reached is that the use of one or another metric (or combination of metrics) in the wind power density estimation process can lead to differing interpretations and/or conclusions. For this reason, it is important that the most appropriate metric (or set of metrics) is chosen at each moment for the study that is being carried out.

Keywords: *Wind Power Density, Short-Term estimation, Long-Term estimation, Artificial Neural Networks, Measure Correlate Predict*

1. Introduction

The wind speed at any given site varies from one year to another [1]. For this reason, the long-term performance of the wind resource (10 years or more) needs to be known as accurately as possible to enable precise estimation of the power output of a wind farm over its working life [2-4]. In most cases there is insufficient data available about the candidate site to carry out long-term analyses. As a general rule, the information available about the wind resource at a candidate site only covers short periods of time (not more than one year).

In order to estimate the long-term wind speed at a candidate site, a number of authors have used long-term wind data obtained from reference stations in combination with estimation models. The traditional Measure Correlate Predict (MCP) algorithms [5-7] and methods which use Machine Learning [8-12] are the most commonly used techniques to generate the models in the estimation processes. The former generally use a single reference station to generate the model. With some exceptions, most of the MCP methods use linear regression algorithms to characterise the relationship between the wind speeds at the candidate and reference sites. Two different methods will be used in this paper. One employs the theory of Artificial Neural Networks (ANNs), and the other a traditional MCP linear regression algorithm.

The ANNs used in this paper were comprised of three layer networks with feedforward connections. More specifically, multilayer perceptron topologies (MLPs) were used [13]. A

single hidden layer with 15 neurons was employed so as not to increase the training time. This architecture has demonstrated its ability to satisfactorily approximate any continuous transformation [13].

The models used to carry out the aforementioned estimations are trained, validated and tested using the available short-term (one year) wind data from reference and candidate weather stations. Using the model thereby obtained and the observed long-term reference station wind data, the candidate station long-term wind data can be estimated. In order to evaluate the performance of the models generated during the test stage of the study, different authors use a wide variety of metrics. Some of these metrics use the ratios between the mean observed and estimated values for different parameters of the wind resource [6,10], Eq. (1), while others [9,11,12] use point-to-point metrics such as, for example, the coefficient of correlation (CC) between the estimated and observed wind speeds, Eq. (2), and the Mean Absolute Percentage Error (MAPE), Eq. (3).

$$Ratio = \frac{\frac{1}{n}\sum_{i=1}^{n} E_i}{\frac{1}{n}\sum_{i=1}^{n} O_i} \tag{1}$$

$$CC = \frac{\sum_{i=1}^{n}\left(O_i - \overline{O}\right)\left(E_i - \overline{E}\right)}{\sqrt{\left[\sum_{i=1}^{n}\left(O_i - \overline{O}\right)^2\right] \times \left[\sum_{i=1}^{n}\left(E_i - \overline{E}\right)^2\right]}} \tag{2}$$

$$MAPE = \frac{100}{n}\sum_{i=1}^{n}\frac{\left|O_i - E_i\right|}{O_i} \tag{3}$$

where E_i are the estimated data; O_i, are the observed or measured data and *n* is the number of data.

2. Meteorological data used

The meteorological data used in this paper correspond to the mean hourly wind speed and directions of twenty-two weather stations located in six of the seven islands that make up the Canary Archipelago (Spain).
The data series used were provided by the State Meteorological Agency (Spanish initials: AEMET) of the Ministry of the Environment and Rural and Marine Environs of the Spanish Government and by the Canary Islands Technological Institute (Spanish initials: ITC).
The available wind data are as follows:

- Six (6) weather stations with 10 years of available wind data (1999-2008)
- Five (5) weather stations with data available for the year 2002.
- Eleven (11) weather stations with data available for the year 2006.

3. Methodology

The methodology employed in the analysis undertaken in this paper consisted of: the generation of models for short-term (one year) estimation and the generation of models for

long-term (ten years or more) estimation. The first type of model generation used data from all twenty-two weather stations, while the second (long-term) type used only those stations for which meteorological data was available for a ten year period (six weather stations).

As many models (cases) were generated for the short-term study as possible combinations, taking as the starting point one station as reference station and another as candidate station. In this way, 55 combinations were generated for the year 2002 and 136 for 2006, making a total of 191 different cases. On the same basis, and using the six weather stations for which ten years worth of data were available, a total number of 15 cases were generated for the long-term study.

Following is an explanation of the different baseline scenarios used in the study.

Scenario A): Estimation of the short-term wind data using ANNs.

The models are generated from the known wind data for the reference and candidate stations (one year). The data available for the reference and candidate stations is randomly divided for use in the training, validation and test stages in respective proportions of 60%, 20% and 20%.

Different networks or estimation models are generated using the data from the training and validation stages. Using these models and the test data for the reference station (which is not used in the generation of the model), data estimation is performed for the candidate station. The estimated data is then compared with the observed data to generate the different metrics used in the analysis.

The wind speed and direction of the reference station (input weather station) are used as input parameters of the neural network. The candidate station (target weather station) wind speed is used as the output parameter (Fig. 1).

Scenario B): Short-term estimation using an MCP method

A simple linear regression between the wind speed of the reference and candidate stations is used for the MCP method. Wind direction is considered in the generation of the models, with the parameters of the model calculated for twelve direction bins of 30º. A simple validation is carried out to evaluate the quality of the models. That is, 20% of the data is reserved as a test subset, which is not used in the construction of the model. The remaining 80% is used for training. The data is randomly allocated to these two groups.

Scenario C): Long-term estimation using ANNs

Only the six weather stations for which data is available for a ten year period are used in the generation of the different networks or models in the long-term estimation study. One of the available years (in this case 2008) is used for generation of the network. All the data for the year is randomly allocated to two sub-groups (80% to training and 20% to validation). As in the case of Scenario A), the different models or networks are generated using this information. The candidate station long-term data is estimated using these models and the data corresponding to the other years of the reference station. By comparing the estimated data and the observed long-term data at the candidate station, the different metrics to be used in the analysis of the results are calculated.

Scenario D): Long-term estimation using an MCP method

The same stations are used as in Scenario C), as well as the same reference year. The models are generated in the same way as in Scenario B), except that in this case 100% of the year's data is used in the construction of the models. Once the parameters of the model have been calculated, the long-term candidate station data is estimated using the data from the remaining years of the reference station.

Matlab software (the MathWorks, Inc) was used to implement the different scenarios.

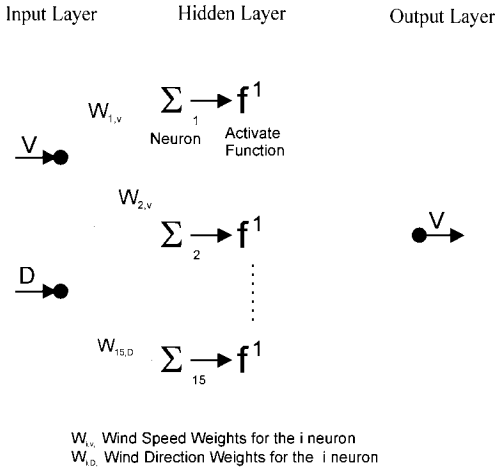

Fig. 1. ANN Schematic diagram with wind speed (V) and wind direction (D) of a reference weather station as input signals, and wind speed (V) of a candidate (target) station as output signal.

4. Analysis of Results.

Figure 2 shows the results obtained for the mean wind speed ratio in the case of Scenarios A) and B). This comparison is performed by representing on the x-axis the existing coefficients of correlation R, Eq. (4), between the wind speeds measured at the reference and candidate stations.

$$R = \frac{\sum_{i=1}^{n}\left(Vr_i - \overline{Vr}\right)\left(Vc_i - \overline{Vc}\right)}{\sqrt{\left[\sum_{i=1}^{n}\left(Vr_i - \overline{Vr}\right)^2\right] \times \left[\sum_{i=1}^{n}\left(Vc_i - \overline{Vc}\right)^2\right]}} \qquad (4)$$

where Vr_i and Vc_i are the measured wind speeds at the reference and candidate weather stations, respectively. $\overline{Vr}$ and $\overline{Vc}$ are the mean wind speeds at the reference and candidate weather stations.

Based on Figure 2, and for the cases studied, the following conclusions were reached: a) the ratio between the estimated and observed mean wind speed is independent of the existing coefficient of correlation, R, between the mean wind speeds at the reference and candidate stations. This becomes more noticeable for coefficients of correlation greater than 0.4. b) for cases where the coefficient of correlation is less than 0.4, the dispersion in the results obtained for the different cases analysed is relatively high (in the range between 0.82 and 0.99). For coefficients of correlation higher than 0.4, the results are concentrated principally between the values 0.95 and 1.01.

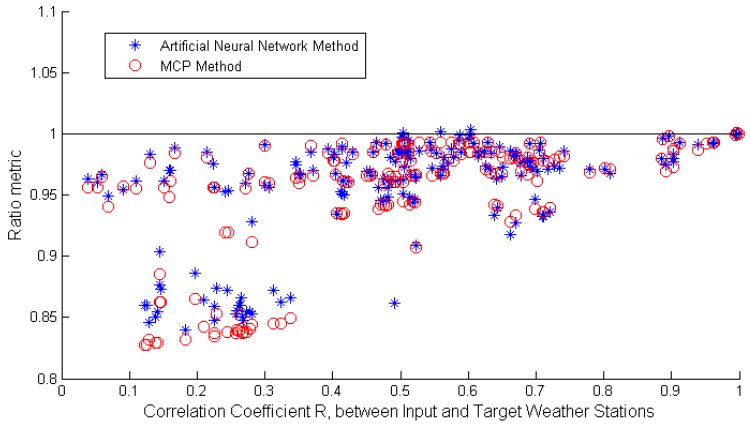

Fig. 2. Variability of the ratio of the mean wind speed with the correlation coefficient between reference (input) and candidate (target) weather station wind speed. Scenarios A) and B).

In the same analysis, but using the Mean Absolute Relative Error (MARE) point-to-point calculation metric for the wind speed, S. Velázquez et al. [11] found that this was dependent on the coefficient of correlation, R, between the wind speeds at the reference and candidate stations.

Figure 3 shows the results for the wind power density ratio, for the different cases studied in Scenarios A) and B). Unlike the previous results, obtained for the mean wind speed ratio, the mean wind power density ratio does depend on R, Eq. (4).

The wind power density P_i, or power per unit of area perpendicular to the direction from which the wind is blowing, is given by Eq. (5). Where ρ_i is expressed in kg m^{-3} and V_i is expressed in m s^{-1}, P_i is obtained in W m^{-2}. P_i, which depends on the air density ρ_i and on the wind speed v_i, is the basic unit for measuring the power contained in the wind.

$$P_i = \frac{1}{2}\rho_i V_i^3 \qquad (5)$$

If the results obtained in Fig. 2 and Fig. 3 are compared it can be observed in many cases that, though a good result is obtained for the mean wind speed ratio (values close to 1), the same cannot be said for the mean wind power density ratio. This can be seen, for example, in the results in the range of coefficients of correlation between 0.4 and 0.8. In the case of the mean wind speed ratio, these values are generally between 0.95 and 1.01, while for the mean wind power density ratio the results are between 0.5 and 0.8. It can be deduced from this analysis that a good result in the mean wind speed ratio is not always equivalent to a good result in the estimation of the wind power density.

The coefficient of correlation, CC, between the estimated and observed wind speeds at the candidate site, Eq. (2), depends on the existing coefficient of correlation, R, between the wind speeds at the reference and candidate stations, Eq. (4) [11]. So, the higher CC is, the closer to 1 will be the mean wind power density ratio.

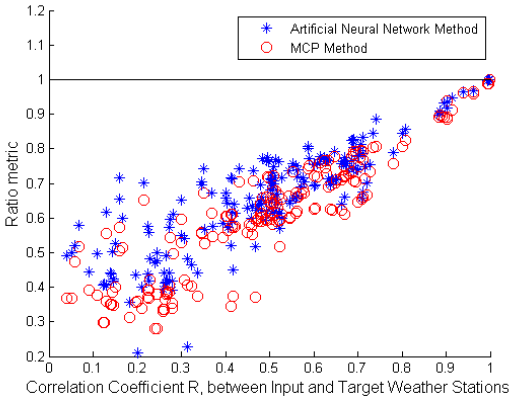

Fig. 3. Variability of the ratio of the mean wind power density with the correlation coefficient, R, between reference (input) and candidate (target) weather station wind speed. Scenarios A) and B).

Figure 4 show the results obtained in the 15 cases analysed in Scenario C) for the mean wind speed ratio metric and the mean wind power density ratio metric. Also shown, for each case, is the coefficient of correlation, R.

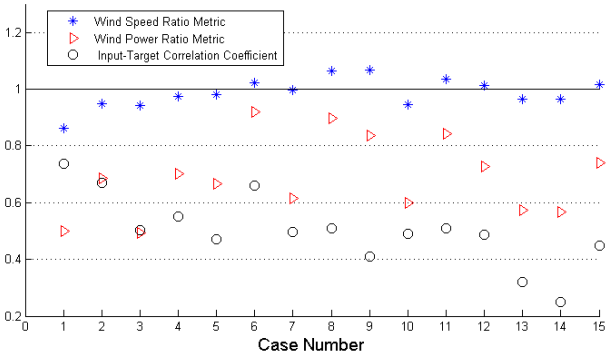

Fig. 4. Results for the ratio of the mean wind speed and ratio of the mean wind power density (long-term). Scenario C).

The basic conclusions obtained from the results for Scenario C) are the same as for Scenarios A) and B). The values, for example, in cases 7, 12 and 15, of 0.9959, 1.0132, and 1.0165, respectively, for the mean wind speed ratio are close to the target value of 1. However, the results in the same cases for the mean wind power density ratio are, respectively, 0.6141, 0.7272 and 0.7392, some way off the target value of 1.

If a point-to-point calculation metric like the Mean Absolute Percentage Error (MAPE) is used for the same Scenarios C) and D), then the results shown in Figures 5 and 6 are obtained.

If Figures 4 and 5 are compared, cases such as case 1 are observed which, while displaying the worst result for the mean wind speed ratio, has the third best result for the MAPE-based analysis. Meanwhile, case 7 gives a mean wind speed ratio of 0.9959 (the best of the results for this metric), which is practically equal to the target value, but has one of the worst results for the MAPE metric of wind speed, with values of 55.90% and 56.41% with respect to the

observed value depending on whether the estimation is conducted using ANNs or MCP methods, respectively. Identical conclusions are obtained if the ratio of the mean wind power density, Fig. 4, is compared with the MAPE metric of wind power density, Fig. 6.

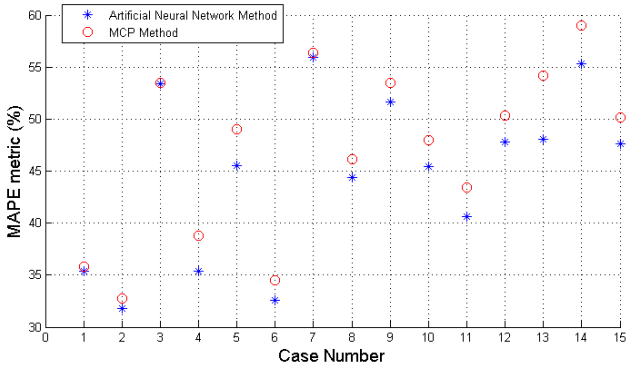

Fig. 5. Results for the MAPE metric of the wind speed. Scenarios C) and D).

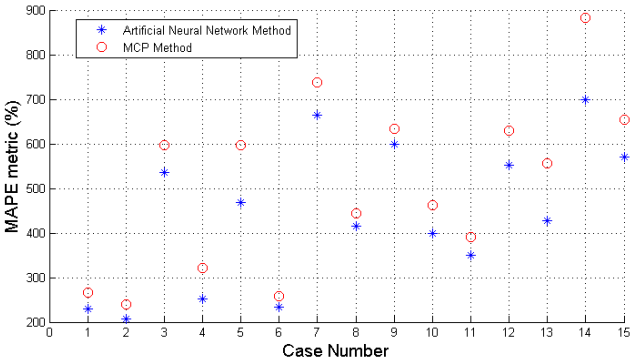

Fig. 6. Results for the MAPE metric of wind power density. Scenarios C) and D).

It can also be concluded from Figures 4 to 6 that the errors calculated when using point-to-point calculation metrics are much higher than when using metrics such as the ratios between the mean values of the entire data series.

5. Conclusions

The most important conclusions that have been reached in this paper are as follows:

a) The results of the metric of the ratio between mean estimated and observed wind speeds are independent of the coefficient of correlation between the reference and candidate wind speeds, Eq. (4). This is not the case with the metric of the ratio of the mean wind power density which is dependent on this coefficient of correlation.

b) In the estimation of short and/or long-term wind power density, the ratios between the mean values of the observed and estimated parameters, Eq. (1) are, on their own, not good indicators for decision-taking in analyses of the estimation of the wind resource, since values close to the target value of 1 in the ratio of the mean wind speed are not always equivalent to good results in the estimation of the wind power density, Figs. 4-6.

If the above metrics are considered for use in analysis of the performance of the estimation models, additional metrics should also be used such as the coefficient of correlation, CC, between the estimated and observed values of the wind speed. This metric takes into account the combined performance over time of the estimated and observed values.

c) The interpretations that can be made when using metrics such as the ratio between the mean values of parameters and point-to-point calculation metrics such as the MAPE, are very different. Case 7, for example (Fig. 4), with a mean wind speed ratio close to 1, gives a relative error (MAPE), with respect to the wind speed, higher than 55%, Fig. 5.

d) When the objective is the estimation of the wind power density for a subsequent point-to-point calculation (as is, for example, an hourly calculation), metrics like the MAPE and the CC are considered to be better indicators when it comes to analysing the accuracy of the models.

References

[1] TR. Hiester, WT. Pennell, The siting handbook for large wind energy systems. 1st ed. New York: WindBook; 1981.

[2] GW. Koeppl, Putnam's power from the wind. Second ed. New York: Van Nostrand Reinhold Company; 1982.

[3] CG. Justus, K. Mani, AS. Mikhail, Interannual and month-to-month variations of wind speed. Journal of Applied Meteorology 18, 1979, 913–932.

[4] CI. Aspliden, DL. Elliott, LL. Wendell, Resources assessment method, siting, and performance evaluation. In: Guzzi R, Justus CG. Physical climatology for solar and wind energy, New Jersey: World Scientific; 1988, pp 321-76.

[5] R. García-Rojo, Algorithm for the estimation of the long-term wind climate at a meteorological mast using a joint probabilistic approach, Wind Engineering 28, 2004; pp 213-236.

[6] AL. Rogers, JW. Rogers, JF. Manwell, Comparison of the performance of four Measure-Correlate-Predict algorithms. Journal of Wind Engineering and Industrial Aerodynamics 93, 2005, pp 243-264.

[7] JC. Woods, SJ. Watson, A new matrix method of predicting long-term wind roses with MCP, Journal of Wind Engineering and Industrial Aerodynamics 66, 1997, pp 85-94.

[8] JA. Carta, S. Velázquez, JM. Matías, Use of Bayesian Networks classifiers for long-term mean wind turbine energy output estimation at a potential wind energy conversion site, Energy Conversion and Management 52, 2011, pp 1137-1149.

[9] A. Oztopal, Artificial Neural Network approach to spatial estimation of wind velocity, Energy Conversion and Management 47, 2006, 395-406.

[10] P. Lopez , R. Velo, F. Maseda, Effect of direction on wind speed estimation in complex terrain using neural networks, Renewable Energy 33, 2008;33, pp 2266-2272.

[11] S. Velázquez, JA. Carta, JM. Matías, Influence of the input layer signals of ANNs on wind power estimation for a target site: A case study, Renewable and Sustainable Energy Reviews, 15, 2011, pp 1556-1566

[12] DA. Fadare, The application of artificial neural networks to mapping of wind speed profile for energy application in Nigeria, Applied Energy, 87, 2010, pp 934-942.

[13] JC. Principe, NR. Euliano, WC. Lefebvre, Neural and Adaptive Systems. Fundamentals Through Simulations, first ed. New York: John Wiley & Sons, Inc.; 2000.

Using Electric Water Heaters (EWHs) for Power Balancing and Frequency Control in PV-Diesel Hybrid Mini-Grids

K. Elamari[1,*], L.A.C. Lopes[1], R. Tonkoski[1]

[1] *Department of Electrical and Computer Engineering, Concordia University, Montreal, Canada*
** Tel: +15146389155, E-mail: k_elama@encs.concordia.ca*

Abstract: Electricity is usually supplied by diesel generators in remote communities at costs that can reach up to $1.50 per kWh in northern Canada. At these costs, several renewable energy sources (RESs) such as wind and photovoltaic (PV) can be cost effective to meet part of the energy needs. Their main drawback, being fluctuating and intermittent, can be compensated with either storage units, which are costly, and/or by adapting the electrical power consumption (load) to the availability of RESs. Electric water heaters (EWHs) are good candidates for demand side management (DMS) because of their relatively high power ratings and intrinsic thermal energy storage capabilities. The average power consumed by an EWH is strongly related to the set point temperature (*Td*) and to the hot water draw (*Wd*). A 5.5 kW, 50 gallon EWH is modeled in MATLAB-Simulink and a typical 24-hour water draw profile is used to estimate the potential range of power variation offered by an EWH for power balancing purposes. Besides, a strategy for controlling the power consumed by the EWH, by means of *Td*, using a grid frequency versus temperature/power droop characteristic is proposed. In this way, the EWH can be used for power balancing and for assisting with the mini-grid frequency control.

***Keywords**: Diesel hybrid system, electric water heater, power balancing, frequency regulation*

Nomenclature

t_{on} *time period that EWH is ON* ..... *h*
t_{off} *time period that EWH is OFF* *h*
T total operation cycle of EWH ..... *h*
Tin incoming water temperature ..... *°F*
Ta ambient air temperature outside tank ..... *°F*
Td reference temperature for the EWH ..... *°F*
T_H *temperature of water in tank* *°F*
ρ *density of water* ..... *lb/gal*
C thermal capacity of water the tank .. *BTU/°F*
B thermal capacity of water usage ..... *BTU/°F*
Q energy input rate ..... *Btu/h*
Wd average water draws per hour ..... *gal/h*
Cp specific heat of water ..... *BTU/lb. °F*
SA surface area of tank ..... ft^2
U stand-by heat loss coefficient ..... $Btu/°F.\ h.\ ft^2$
$P_{EWH\ average}$ *power consumed by EWH* ..... *kW*

1. Introduction

Diesel generators sets (gensets) are a relatively expensive way to produce electricity in remote areas when connection the main grid is not feasible. Renewable energy sources (RESs) such as wind and photovoltaic (PV) are an attractive solution to reduce cost of electricity in these systems. They are environmentally friendly and their incorporation into diesel based mini-grids is relatively simple [1] for low penetration levels. They are usually controlled as passive units, injecting as much of intermittent and fluctuating power as possible, while the grid forming unit(s), usually gensets, have to match the power generated and consumed in the system [2]. This is not an easy task considering that remote communities are characterized by highly variable loads with the peak load as high as 5 to 10 times the average load. What is more, gensets should not operate at low load conditions (~0.3-0.4 pu), due to maintenance problems in the diesel engine, and should provide spinning reserve for cases of sudden load surges or renewable generation reduction [3]. It should be noted that diesel gensets are usually Operated in parallel with frequency x power droop characteristics what facilitates active power dispatch. Besides, operation with variable frequency conveys the message of surplus

(higher frequencies) or shortage (lower frequencies) of active power in systems with non-dispatchable renewable sources.
Power balance issues can be overcome with energy storage units but this is a relatively costly solution [4]. Alternatively one can use controllable loads to help with the power balancing and frequency regulation in a diesel hybrid mini-grid. Due to their relatively large time constants, thermal loads such as electric water heaters (EWH) present an energy storage characteristic and are good candidates for power balancing and frequency control [5].
The use of EWHs in load side demand control was introduced in 1934 by Detroit Edison. Timers were employed to cut off energy flow to EWHs during peak periods for four hours [6]. Later, many other control strategies were developed.

This paper discusses the use of EWHs to help balance the active power and assist with the frequency regulation in diesel hybrid mini-grids. A model of 5.5kW-50gal EWH is implemented in Matlab/SIMULIINK in order to observe the impact of varying the set point temperature (*Td*) on the power consumed by the EWH supplying a typical residential water draw (*Wd*) profile. Analytical equations are derived and used for estimating how much power an EWH can take or drop during each hour of the day, by varying *Td*, while keeping the hot water temperature (T_H) within acceptable values.

2. Methodology

2.1. Electric water heater (EWH) model:

The following first-order differential equation, which represents the energy flow in an electric water heater [7], was used to implement a simple model of an EWH.

$$C\frac{dT_H}{dt} = U\,SA(Ta - T_H) + Wd\,\rho C(Tin - T_H) + Q \tag{1}$$

The first part at the right side represents the heat losses to the ambient, the second the heat needed to heat the inlet cold water, and the last one is the input heat energy from the resistive element of the EWH.
By integrating both sides one gets

$$T_H = \frac{1}{\tau}\int (R'GTa + R'BTin - T_H + R'Q)dt \tag{2}$$

Where $G = U\,SA$, $B = Wd\,\rho C$, $R' = 1/(G+B)$ and $\tau = R'C$

By implementing (2) in Matlab/SIMULINK one can see the variation of the temperature of the hot water in the tank (T_H) for various conditions. The heating element of the EWH is turned ON and OFF so as to keep T_H within a tolerance band (+/- Δ) of *Td*. When the heating element of the EWH is ON, T_H rises until it reaches (*Td*+Δ). Then the heating element is turned OFF and T_H decreases until it reaches (Td-Δ), when the heating element is turned ON again. In this study, the rated power of the EWH (P_{rated}) is assumed to be 5.5 kW and *Td* for the base case (Td_b) is set at 120 °F with Δ equal to 2.5 °F. The 24-hour hot water draw (*Wd*) profile used in this paper refers to the hourly profile proposed by the American Society of Heating, Refrigerating and Air-Conditioning Engineers (ASHRAE) [8]. The other main parameters used in the simulations are shown in Table 1.

In this study, the following assumptions are made:

- The hot water temperature in the entire tank is the same.
- The ambient and the inlet water temperature (*Ta* and *Tin*) are constant during the day.
- The variation of *Td* does not affect *Wd*.

The variation of T_H for one day is shown in Fig. 1(a) using the ASHRAE *Wd* schedule shown in Fig. 1(b). The instantaneous power consumed by the EWH is shown in Fig. 1(c). A simulation (time) step of 0.0001 h was considered.

Table 1. Main EWH parameters

Q(Btu/h)	*ρ*(Ib./gal)	*V*(gal)	*C*(BTU/°F)	*Ta*(°F)	*Tin*(°F)	*G*(Btu/ °F.h)
18771.5	8.34	50	417	67.5	60	3.6

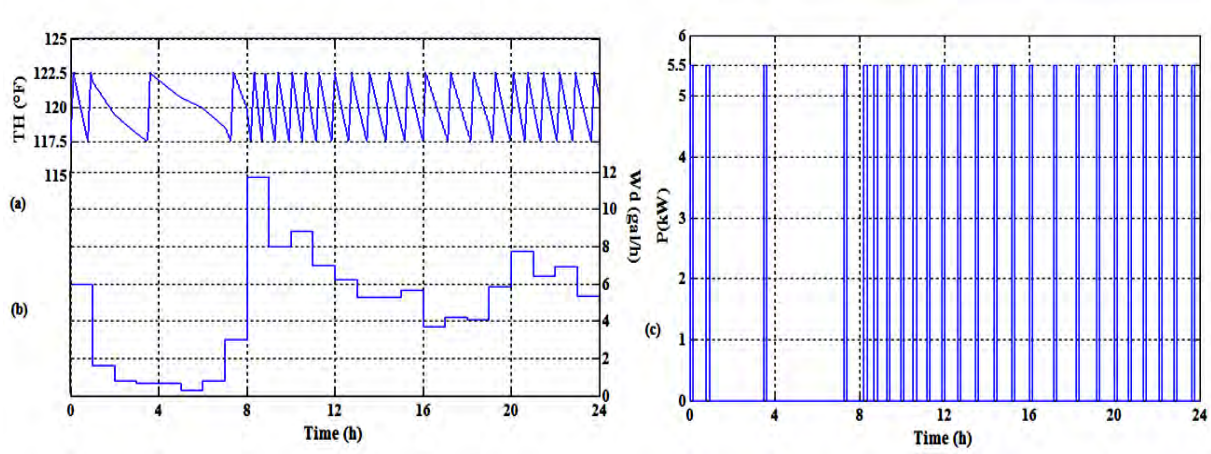

Fig. 1: (a) Variation of T_H (°F). (b)Wd schedule (gal/h). (c) EWH power consumption (kW).

One can see from Fig. 1(c) that t_{on} and t_{off} and the operation period ($T = t_{on} + t_{off}$) of the EWH during the day are not constant. t_{off}, in particular, varies significantly with *Wd*. Table 2 shows the maximum and minimum values of t_{on}, t_{off} and T during the one day period considered.

Table 2. Maximum and minimum on, off and operation period of the EWH.

$t_{on-\max}$ (h)	$t_{on-\min}$ (h)	$t_{off-\max}$ (h)	$t_{off-\min}$ (h)	$T_{\max}$ (h)	$T_{\min}$ (h)
0.1639	0.1143	3.6571	0.3453	3.7714	0.5092

2.2. Mathematical analysis:

An equation that describes how T_H varies in time can be obtained by solving Eq. (1) as

$$T_H(t) = T_H(t_0)\,e^{-(1/\tau)(t-t_0)} + \left(R'\,G\,Ta + R'\,B\,Tin + R'\,Q\right)[1 - e^{-(1/\tau)(t-t_0)}] \qquad (3)$$

With the appropriate modifications, it can be used for obtaining expressions to calculate t_{on} and t_{off}. However, exponential equations are not very convenient to use. Alternatively, one can derive linear expressions for t_{on} and t_{off}. This can be done by replacing dT_H by T_{high}-T_{low} (T_{low} - T_{high}) in Eq. (1) when the EWH is ON (OFF) and dt by t_{on} (t_{off}). Besides, T_H is

assumed equal to *Td* in order to calculate the average heat losses to the ambient and due to inlet cold water replacing the water drawn from the tank. In this case

$$t_{on} = \frac{C\,(T_{high} - T_{low})}{G\,(Ta - Td) + \rho\, Cp\, Wd\,(Tin - Td) + Q} \tag{4}$$

$$t_{off} = \frac{C\,(T_{high} - T_{low})}{G\,(Td - Ta) + \rho\, Cp\, Wd\,(Td - Tin)} \tag{5}$$

With Eq. (4) and (5) one can calculate the operation period of the EWH ($T = t_{on} + t_{off}$) and the average power consumed by the EWH in that operation period ($P_{EWH} = D\, P_{rated}$), where

$$D = \frac{t_{on}}{T} = \frac{G\,(Td - Ta) + Wd\,(Td - Tin)\,\rho\, Cp}{Q} \tag{6}$$

The value of *Wd* for the above equations should be the average water draw for the period under consideration (*T*). As shown in Table 2, for T_{high}-T_{low}=2Δ and with Δ = 2.5 °F, t_{on} is always smaller than 1h what allows the use of the hourly ASHRAE *Wd* schedule for validating Eq. (4). By comparing the values of t_{on} obtained with eq. (4) with those of the simulations one sees that the error were smaller than 0.01%. On the other hand, t_{off} varies more with *Wd* and can be larger than 1 h, usually for low values of *Wd*. In this case, an average value for *Wd* valid for that duration needs to be considered.

The values of *D* obtained from (6), which are equivalent to P_{EWH} in pu, are shown in Table 3 for different values of *Wd* and *Td*. There one sees that P_{EWH} at *Td* = 140 °F is around twice that at *Td* = 100 °F for all values of *Wd*. Besides, operation at low values of *Wd*, limits significantly the variation of P_{EWH} one can get by varying *Td*. Thus, in these cases, the EWH will be less effective as a means for balancing active power in the electric system.

Table 3. Variation of P_{EWH} (pu) with Wd and Td.

Wd(gal/h) / *Td*(°F)	0.25	0.75	1.5	3	6	9	12
100	0.0107	0.0196	0.0329	0.0595	0.1129	0.1662	0.2195
108	0.0131	0.0238	0.0398	0.0717	0.1357	0.1997	0.2637
116	0.0155	0.028	0.0466	0.0839	0.1586	0.2332	0.3079
124	0.0179	0.0322	0.0535	0.0961	0.1814	0.2667	0.3521
132	0.0204	0.0364	0.0604	0.1083	0.2043	0.3003	0.3962
140	0.0228	0.0406	0.0672	0.1205	0.2272	0.3338	0.4404

One important aspect when designing the control scheme of a given system is to identify the sensitivity of a quantity of interest to variations in some of its key parameters. This can be done by means of partial derivatives. For *D*, and consequently P_{EWH}, these key parameters are *Td*, taken here as the control parameter, and *Wd*, assumed as a disturbance in the system. From Eq. (6) one can get

$$\Delta P_{EWH}\,(pu) = \Delta D = \frac{\partial D}{\partial Td}\Delta Td + \frac{\partial D}{\partial Wd}\Delta Wd = \frac{G + Wd\,\rho\, Cp}{Q}\Delta Td + \frac{(Td - Tin)\,\rho\, Cp}{Q}\Delta Wd \tag{7}$$

For the case under consideration assuming that *Wd* is constant

$$\Delta P_{EWH}(pu) = \Delta D = \frac{3.6 + 8.34 Wd}{18771.5} \Delta Td \tag{8}$$

This equation is very useful when one wishes to compute by how much one should change *Td*, for the EWH operating with a given value of *Wd*, in order to change P_{EWH} by a certain value in steady-state. The limit values for P_{EWH} and *Td* are those shown in Table 3.

Another important aspect of the operation of an EWH for active power balancing is the amount of power it can drop or take under transient conditions. Since the EWH operates in an ON/OFF mode, its instantaneous power consumption is either rated or zero. This cannot be changed. However, one can during transient condition values for t_{on} and t_{off} significantly larger than those obtained for steady-state conditions.

Let's consider first the case where the EWH should take additional load. From Fig. 1(a) one sees that T_H increases almost linearly when the EWH is ON and t_{on} is the time required for T_H to increase by 2Δ, 5 °F in this study, when *Td* remains constant. As shown in (4), t_{on} increases as *Wd* increases but it does not vary significantly with *Wd* since *Q* is the dominant element in the denominator of (4). If *Td* is suddenly increased by a value larger than the tolerance band ($\Delta Td > 2\Delta$), the EWH will be turned ON immediately and remain ON until the value of T_H increases by at least ΔTd. Based on this, one can estimate that the increase in t_{on} during transient conditions, with respect to the previous value in steady state, for a given ΔTd on average, for $T_H = Td$, as

$$\Delta t_{on}(\%) = \frac{\Delta Td + \Delta}{2\Delta} \tag{9}$$

Table 4 shows the maximum values of t_{on} that one can have during each time of the day, assuming the ASHRAE *Wd* schedule, as one changes *Td* from an initial value, either 120 °F or 100 °F, to 140 °F. Td_b = 120 °F is the base case, when one does not expect the need to take or drop power during the next few hours. However, if one knows that there will be a need to take as much load as possible, due to a typical surge in production of wind power or due to a decrease in the regular electric load in the system, then one could operate with *Td* = 100 °F.

Table 4. t_{on_max} for different values of initial Td using the ASHRAE Wd schedule. Case #1 (Td=120°F, *ΔTd*=20°F, *Δt_{on}=4.5.) Case#2 (Td*=100°F, *ΔTd*=40°F, *Δt_{on}=8.5).*

Time (h)	0	1	2	3	4	5	6	7	8	9	10	11
Wd(gal/h)	6.0	1.6	0.8	0.7	0.7	0.3	0.8	3.0	11.7	8.0	8.8	7.0
ton(h), Case1	0.646	0.537	0.522	0.519	0.519	0.512	0.522	0.568	0.876	0.712	0.743	0.677
ton(h), Case2	1.221	1.016	0.986	0.981	0.981	0.966	0.986	1.074	1.656	1.346	1.403	1.280
Time(h)	12	13	14	15	16	17	18	19	20	21	22	23
Wd(gal/h)	6.25	5.30	5.30	5.65	3.70	4.20	4.10	5.85	7.73	6.38	6.90	5.30
ton(h), Case1	0.654	0.626	0.626	0.636	0.585	0.597	0.595	0.642	0.702	0.658	0.674	0.627
ton(h), Case2	1.236	1.183	1.183	1.202	1.105	1.128	1.124	1.213	1.327	1.244	1.274	1.185

An useful expression for Δt_{off} cannot be obtained in a similar way because the curve for T_H decreasing does not resemble a straight line. Nonetheless, one knows that t_{off} is usually long

enough for power balancing operation. Therefore, in this case, one can define a worst case conditions (Wd =11.7 gal/h) for which t_{off_min} = 2.3337 (4.4081) h when Td = 120(140) °F.

2.3. Temperature Control Using Frequency Droop

Droop control is a well-known technique used for operation and power sharing of power generators connected in parallel. The relationship between frequency and power can be described by

$$P_g = s_p(f_{nl} - f) \tag{9}$$

Where P_g is the output power of the generator (kW) s_P is the slope of the curve (kW/Hz), f_{nl} is the no-load frequency of the generator (Hz) and f is the operating frequency of the system (Hz) [3].

As the actual loading of the genset is proportional to the frequency, it is proposed that the power consumed by the EWH to be controlled by means of the Td, using the frequency versus temperature droop function

$$Td = Td_b + m(f - f_c) \tag{10}$$

Where m is a slope factor equivalent to s_p and f_c is the center frequency (Hz). Td is equal to half its total excursion. Fig. 2 (a) shows the frequency x temperature droop function with m = 20 °F/Hz, Td_b=120°F, and f_c = 61 Hz. The value of T_H will vary within Td ±Δ as shown with the dotted lines. The action of droop is limited to when Td is within acceptable limits of temperature; in this case it was limited between 100 °F and 140 °F. From Eq. (9), when the load increases, the frequency of the generator decreases. This frequency reduction will cause Td in the EWH to decrease, while when the generator load decrease the frequency will increase making Td increase. Varying Td during steady and transient condition will affect the average power consumption, as can be seen on Fig 2 (b) for different values of Wd, for the EWH described on Section 2.1. Varying Td between 140° F and 100 °F would result in a 1.13 kW variation in the average power consumed. However for periods of lower water draw (Wd ~ 1 gal/h) this variation is limited to 0.15 kW, which makes this control strategy sensitive to the water draw condition. It is important to note that have been reported in the literature that the electricity consumption is directly related to water consumption [9], what makes the effect on peak load shaving improved with this strategy.

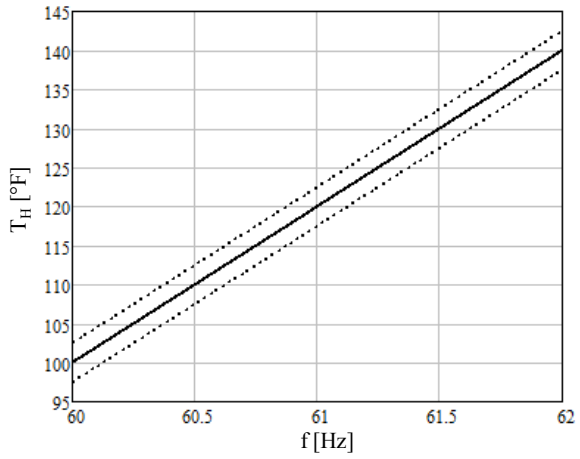

(a)

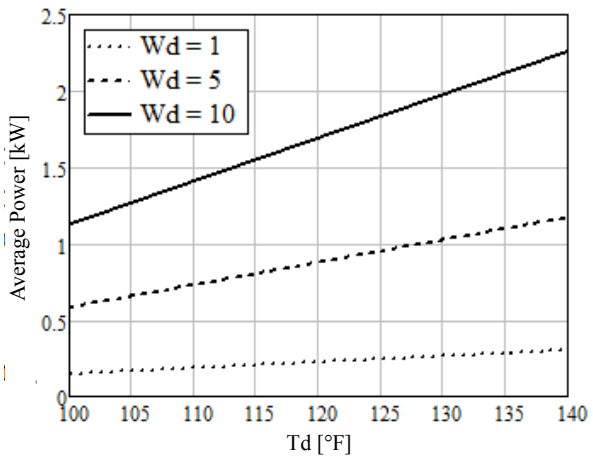

(b)

Fig. 2: (a) Frequency x temperature droop variation (b) Average power consumption variation with Td for different average water draw.

3. Results

A mini-grid with a genset feeding a network with 20 houses in a single phase connection where only two of the three outputs of the genset are used is presented in [3] and is used in this paper to evaluate the impact of the frequency x temperature droop control in the loading of the generator and grid frequency. The genset is rated at 95kW on a three phase basis, however in practice it means that only about 2/3 of the generator power is available. The droop parameter of the genset are s_p = 29.4 kW/Hz and f_{nl} = 62.3 Hz.

A residential load profile for a house without EWH based on [10] was scaled to have a daily energy consumption of 20 kWh and used as reference for all 20 houses to determine the 24 h load profile of the mini-grid. Fig. 3 (a) presents the single house load profile used and the power consumption profile of the EWH with *Td* = 120 °F. The *Wd* schedule considered was the one presented in Fig. 1 (b). Two cases are considered, first the EWH operates with constant *Td*, base case, and the second one using the frequency x temperature droop strategy (Tdroop) with *m* = 20 °F/Hz and f_c = 61 Hz. Fig. 3 (b) presents the genset load for each hour of the day. The load variation is reduced with the droop approach. The peak load from this day decreases from 56 kW to 52 kW, while in the lower load region, the load increases from 8.3 kW to 9.5 kW. This small difference in the low load region is due to the fact that varying *Td* for controlling the power is sensitive to the water profile that during that period was low. Fig. 4 presents the frequency variation regarding the change in the genset load (a) and the variation on *Td* due to the frequency droop implemented.

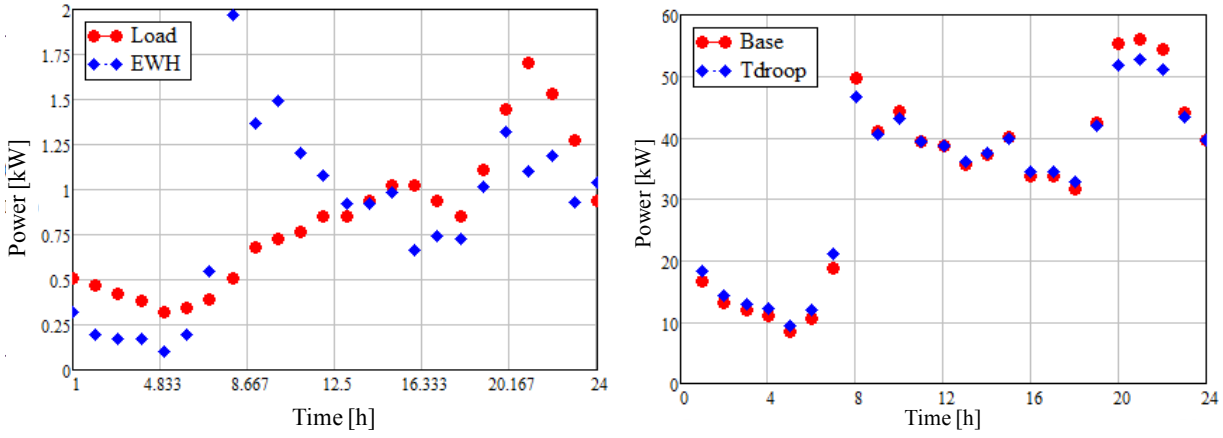

(a) (b)

Fig. 3. (a)Load Profile and EWH Power Profile for Td = 120° F and (b) Genset power.

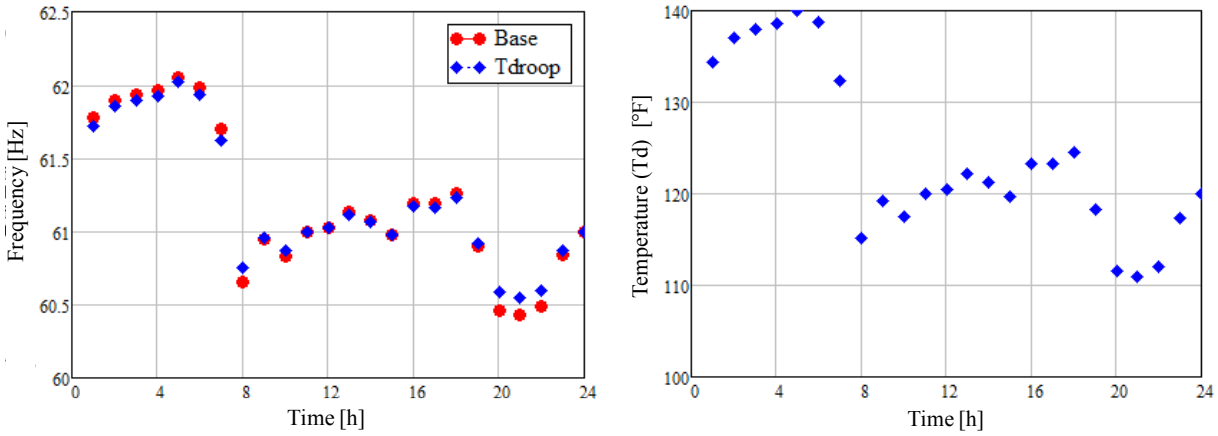

(a) (b)

Fig. 4. (a) Minigrid frequency and (b) individual EWH Td during the 24 h case study.

4. Conclusions

This paper presented EWHs as candidates for DMS due to the fact that the average power consumed is strongly related to the set point temperature (*Td*) and to the hot water draw (*Wd*). A mathematical model was obtained for the EWH. It was proposed a strategy for controlling the power consumed by the EWH, by means of *Td*, using a frequency versus temperature droop characteristic. A 5.5 kW, 50 gallon EWH was modeled in MATLAB-Simulink and a typical 24-hour water draw profile was used to estimate the steady state performance in a 95 kW diesel based mini-grid. Results showed that with the proposed control strategy power variations in the mini-grid can be reduced; however it is strongly dependent on the values of water draw from the houses.

References

[1] J.A.P. Lopes, C.L. Moreira, and A.G. Madureira, "Defining Control Strategies for Microgrids Islanded Operation," IEEE Transactions on Power Systems, vol. 21, no. 2, May 2006, pp. 916-924.

[2] M. Tokudome, K. Tanaka, T. Senjyu, A. Yona, T. Funabashi, and Kim Chul-Hwan, "Frequency and Voltage Control of Small Power Systems by Decentralized Controllable Loads", Power Electronics and Drive Systems, 2009, International Conference on, 2-5 Nov. 2009,pp. 666 – 671.

[3] R. Tonkoski, L. A. C. Lopes, and D. Turcotte, "Active Power Curtailment of PV Inverters in Diesel Hybrid Mini-grids". In: IEEE EPEC 2009 - Electrical Power and Energy Conference Montreal, QC, 2009

[4] J. P. Barton and D. G. Infield, "Energy Storage and Its Use with Intermittent Renewable Energy," IEEE Transactions on Energy Conversion, vol. 19, no. 2, J un. 2004, pp. 441 - 448.

[5] J.C. Van Tonder and I.E. Lane, "A load model to support demand management decisions on domestic storage water heater control strategy". IEEE Transactions on Power Systems vol.11,no 4, 1996, pp.1844–1849.

[6] C. H. K. Goh and J. Apt, "Consumer Strategies for Controlling Electric Water Heaters Under Dynamic Pricing", Carnegie Mellon Electricity Industry Center working paper CEIC-04-02, 2004.

[7] Kar AK, Kar U. Optimum design and selection of residential storage-type electric water heaters for energy conservation. Energy Conversion and Management 1996; 37(9):1445–52.

[8] American Society of Heating, Refrigerating and Air-Conditioning Engineers, Inc. (ASHRAE) Handbook–Heating, Ventilating, and Air-Conditioning (HVAC) Applications (2007). Typical Residential Family's Hourly Hot Water Use. Fig. 12. Page 49.12.

[9] M.H. Nehrir, R. Jia, D.A. Pierre, and D.J. Hammer strom, "Power management of aggregate electric water heater loads by voltage control," 2007 IEEE Power Engineering Society General Meeting, p. 4275790, 2007.

[10] S. Papathanassiou, N. Hatziargyriou, and K. Strunz, "A Benchmark Low Voltage Microgrid Network.," presented at the Proceedings of the CIGRE Symposium: Power Systems with Dispersed Generation, Athens, Greece, 2005.

Impacts of large-scale solar and wind power production on the balance of the Swedish power system

Joakim Widén[1,*], Magnus Åberg[1], Dag Henning[2]

[1] *Department of Engineering Sciences, Uppsala University, Uppsala, Sweden*
[2] *Optensys Energianalys AB, Linköping, Sweden*
** Corresponding author. Tel: +46 (0) 18 471 37 82, E-mail: joakim.widen@angstrom.uu.se*

Abstract: Higher targets for renewable energy and current trends in wind power and photovoltaics (PV) suggest that future power systems will include large amounts of renewable and variable power generation. Integration of large-scale variable power generation changes the balance and operation of power systems, including scheduling of conventional generation units, transmission and use of balancing power. In this paper the Swedish power system is studied with the energy system optimisation model MODEST in a number of scenarios involving different combinations of large-scale solar and wind power. The model includes a representation of the Swedish district-heating systems to determine the effects on combined heat and power (CHP) operation. It is found that when renewable power generation is added to the present system, utilisation of investments in CHP plants is reduced due to an increased electricity surplus that favours use of heat pumps for district heating. At high penetration levels of both solar and wind power, water is spilled from hydropower reserves.

Keywords: *Solar power, Wind power, Power system, Optimisation*

1. Introduction

According to the EU directive on renewable energy, 20 % of the energy use within the union is to be covered by renewable energy sources by 2020 [1]. An important part of this goal is to transform the power system to include more renewable electricity generation. The power source most likely to reach substantial integration levels within this time frame is wind power. Although wind power currently covers 4.8 % of the total electricity demand within the EU, penetration levels in some individual countries are higher, for example Denmark (19 %), Portugal (15 %), Spain (14 %) and Ireland (11 %) [2]. Solar power generation, mainly from grid-connected photovoltaics (PV), is also increasing worldwide, although the contribution is smaller than for wind power. In Germany, the country with the highest solar power penetration, PV electricity covers 1-2 % of the national electricity demand [3]. However, if current developments continue, combined with decreasing costs for solar cells, a future expansion of solar power does not seem unlikely. The EU directive on energy efficiency in buildings, which states that all new buildings must be nearly zero energy buildings by 2020, also suggests a future widespread integration of on-site solar technologies [4].

Solar and wind power are both *variable* power sources, which means that the output varies both systematically and randomly on different time scales. The power generation can be forecast to some extent, but not controlled. In the case of wind power, the variation is due to moving weather fronts. Solar power has a more predictable seasonal and diurnal pattern, although the output during daytime can be heavily fluctuating due to variations in cloudiness. Variable power sources have a number of impacts on the balance, operation and reliability of power systems. The hour-to-hour varying production pattern alters scheduling of other generation units in the system and affects transmission between geographic areas. Furthermore, power generation that deviates from the forecast must be handled by system reserves. Depending on the power system, an increase in the penetration level of variable power sources has to be met by some increase in reserve requirements. For large-scale wind power it has been estimated that an increased penetration that corresponds to 10 % of the total annual demand increases the reserve requirements by 2-8 % of rated wind power capacity [5].

An important aspect is how addition of volumes generated by wind and solar power affects scheduling of other generation units and the total system balance. In this paper, the impacts of a large-scale integration of solar and wind power on the balance of the Swedish power system, a high-latitude and hydro-dominated system, is investigated. For example, how is scheduling of other generation units affected and how do electricity exports and imports and CO_2 emissions change?

A model of the Swedish power system was built in the MODEST optimisation model [6]. The model encompasses and optimises the whole chain of energy flows from sources to end-uses. An aggregated but detailed representation of the total Swedish generation capacity, including nuclear power, hydropower, combined heat and power plants, *etc.*, is included and the time resolution captures important fluctuations in demands and renewable power generation. The Swedish district heating systems are also explicitly represented to capture the effects on CHP operation. Solar and wind power are integrated in different scenarios as additions to the existing system. In these scenarios, it is recognised that wind power will most likely be integrated on a large scale before solar power.

The rest of the paper is structured as follows. Section 2 presents an overview of the applied methodology, including the optimisation model and the parameters and data used. Section 3 presents the results from the different studied scenarios. These results are discussed in Section 4 and some conclusions are drawn in Section 5.

2. Methodology

Energy system modelling enables important properties of a real system to be varied in a controlled environment. Using a validated model with a realistic performance, the impact of future changes to the system can be estimated. With an optimisation model, the best performance of a system under certain conditions is found. This section describes the applied optimisation model of the Swedish power and district heating systems. It also presents the studied scenarios for solar and wind power integration.

2.1. The MODEST power system and district-heating model

MODEST (Model for Optimisation of Dynamic Energy Systems with Time-dependent components and boundary conditions) uses linear programming to optimise the energy flows of a system to supply demands while minimising the total cost. In MODEST, an energy system is modelled as a set of nodes interconnected by energy flows. For each node and flow, a set of characteristics can be defined to relate, direct and constrain the flows. Typical such characteristics in a MODEST model are energy balances, dimensioning of maximum outputs for energy conversion and limitations of supplies. A cost can be associated with each flow and node, reflecting for example fuel costs.

Using MODEST, an energy system model of the Swedish power system was created. In the model, energy flows from resources (water and fuels) via generation units to distribution systems and finally to demand nodes representing the national electricity and district heating loads. For electricity, there is also an exchange with Nordic and continental European electricity markets. A flowchart showing the energy flows and nodes of the model is provided in Fig. 1. In the model, time is represented by a ‘quasi-dynamical’ time division, with a variable resolution that is more fine-grained for peak-load or peak-production periods. The time division is adapted to capture the relevant variability in solar and wind power generation.

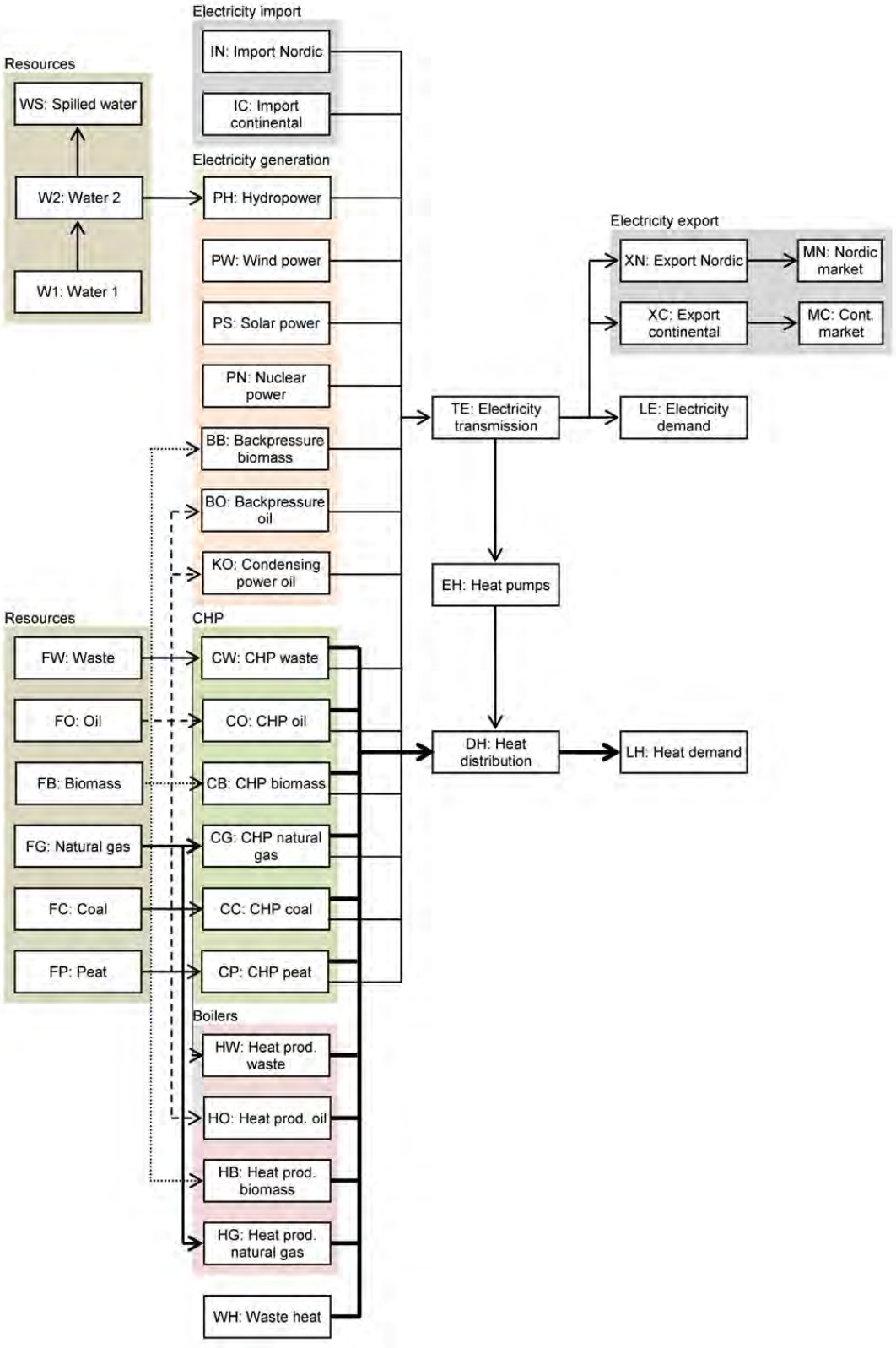

Fig. 1. Flowchart showing the nodes and energy flows in the MODEST model of the Swedish power and district-heating systems.

2.2. Studied scenarios

Two scenarios are studied. Scenario A represents today's system while Scenario B involves large-scale solar and wind power integration. In the latter scenario it is assumed that 30 TWh of wind power generation annually has been added to the existing system, which increases the total generation capacity of the system and turns the Swedish power system into a net producer of electricity. In three cases (B2-B4) besides the base case of today's solar power (B1), solar power is added to the system in 10 TWh steps, up to 30 TWh. In the most extreme scenario (B4), 60 TWh of renewable power generation are added, which is almost equal to the total current nuclear power generation. The main questions are how large volumes of electricity from plants with practically no running costs entering the system alter the scheduling of other power plants within the country, if the mix for heat production changes, how net exports and imports change and how CO_2 emissions are affected.

2.3. Input data

Model parameter values were chosen to make the model correspond to today's power system, with the year 2008 chosen as a representative year. All data were collected with the aim of reproducing the system performance of this year. Data for system parameters such as capacities, conversion efficiencies, resource limitations, prices, emission factors, *etc.*, were collected from a variety of sources, including different statistics sources, authorities' reports and business reports. Some data, which were still considered sufficiently up-to-date were collected from a previous national-level MODEST study. Data for estimating the variable components in the system were obtained from empirical time series with an hourly resolution. Some variable components are electricity and heat loads, solar and wind power generation and electricity market prices. Electricity prices were collected from NordPool and EEX spot market data, solar power data from a previous study of large-scale solar power variability in Sweden, wind power data from a database with modelled wind power data based on a scenario for widespread wind power in Sweden, electricity demand from NordPool's power system data and heat demand data scaled up from heat load data for a local district-heating system. All data series are from 2008 except the wind power and solar power data, which are from 1999, a representative year in terms of annual availability of solar irradiation and wind energy. All of these data are reported in detail in [7].

3. Results

The results of the energy system optimisations for the studied scenarios are shown in Fig. 2 and Fig. 3. Fig. 2 shows the energy balances for scenarios A and B. The impacts on the electricity and district heating production and the fuel use are visualised, as well as occasionally spilled energy, electricity imports and exports and CO_2 emissions. Fig. 3 shows duration graphs for district heating in scenario A and in the extreme case B4. The bold lines in the latter figure represent the district heating demand and show the different demand levels sorted in decreasing order. The step length corresponds to the length of each individual time period in the model. The other curves show plant outputs in the time periods.

As can be seen in Fig. 2 for the electricity production, the total production increases gradually in scenario B due to integration of wind and solar (B2-B4) power. This has no significant effect on the other parts of the electricity mix, apart from in case B4, where there is a small decrease in hydropower production. This is because some water has to be spilled as the capacity for electricity export is reached. This can also be seen in the graph for spilled energy. In the heat production mix, there is an incrementally larger contribution from heat pumps. This is because it is occasionally feasible to use excess electricity in the system for heating,

compared to other more costly alternatives. This is generally on the expense of heat-only production, but in B4 also of CHP. As seen in the graph for fuel use, the total use of fuels decreases accordingly, mainly biofuel but in all cases also oil as compared to scenario A. From the heat duration curve in Fig. 3 (case B4) it can be seen that the heat pumps, which in scenario A are exclusively used at high loads, are now feasible to use even at lower loads.

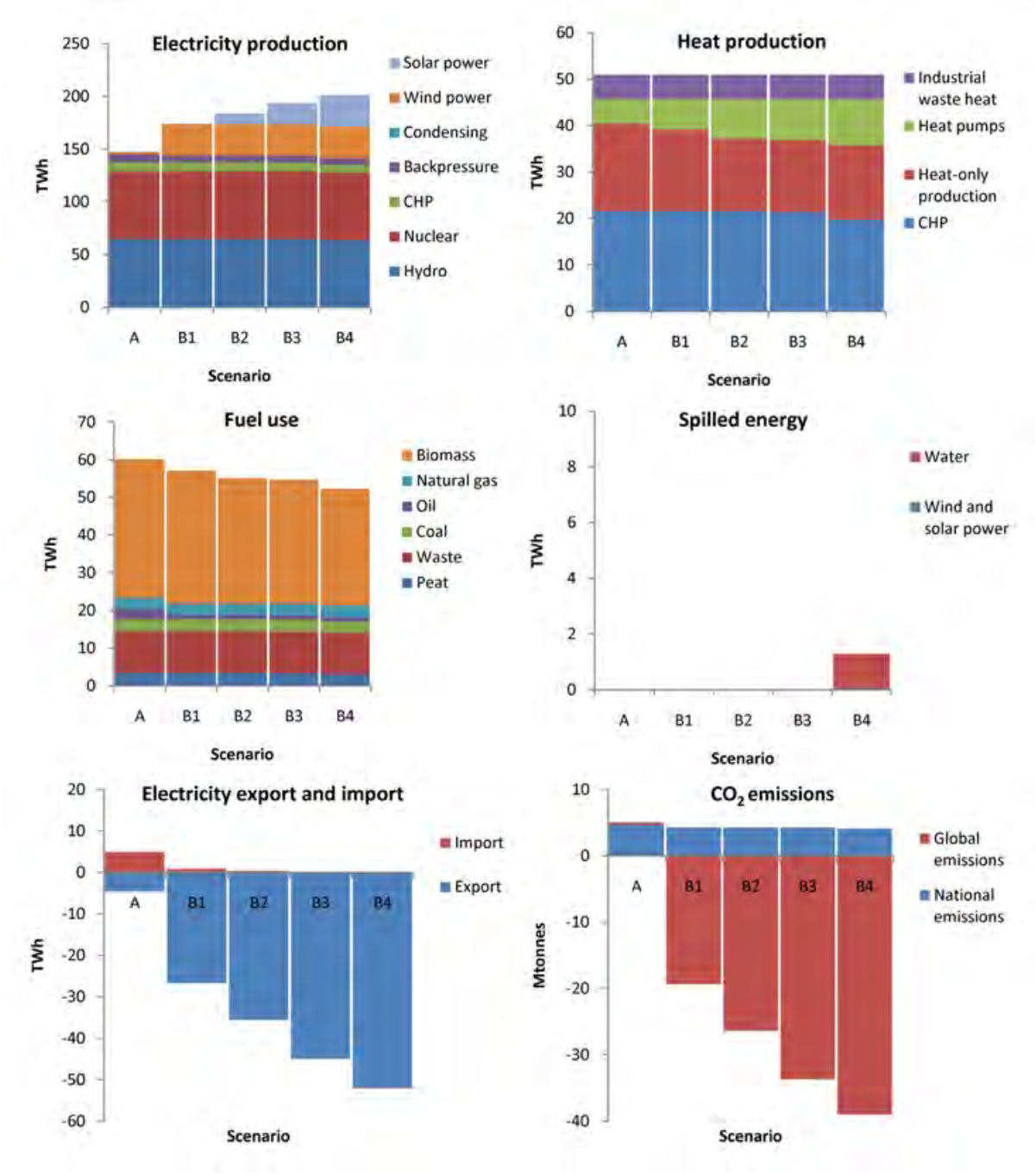

Fig. 2. Energy system characteristics in Scenarios A (base scenario) and B (addition of wind power) with cases 1-4 (different solar power integration levels).

Electricity exports increase due to the excess generation (Fig. 2), while imports decrease due to wind and solar electricity replacing imported electricity. This is reflected in the CO_2 emissions: emissions are reduced in power systems abroad due to export of electricity, which

is assumed to replace coal-fired marginal electricity production. National emissions, resulting from fuel combustion in the studied system, and global emissions, being emissions caused or replaced by electricity exchange with continental Europe, are shown separately in Fig. 2. The reduction of global emissions vastly exceeds the local emissions.

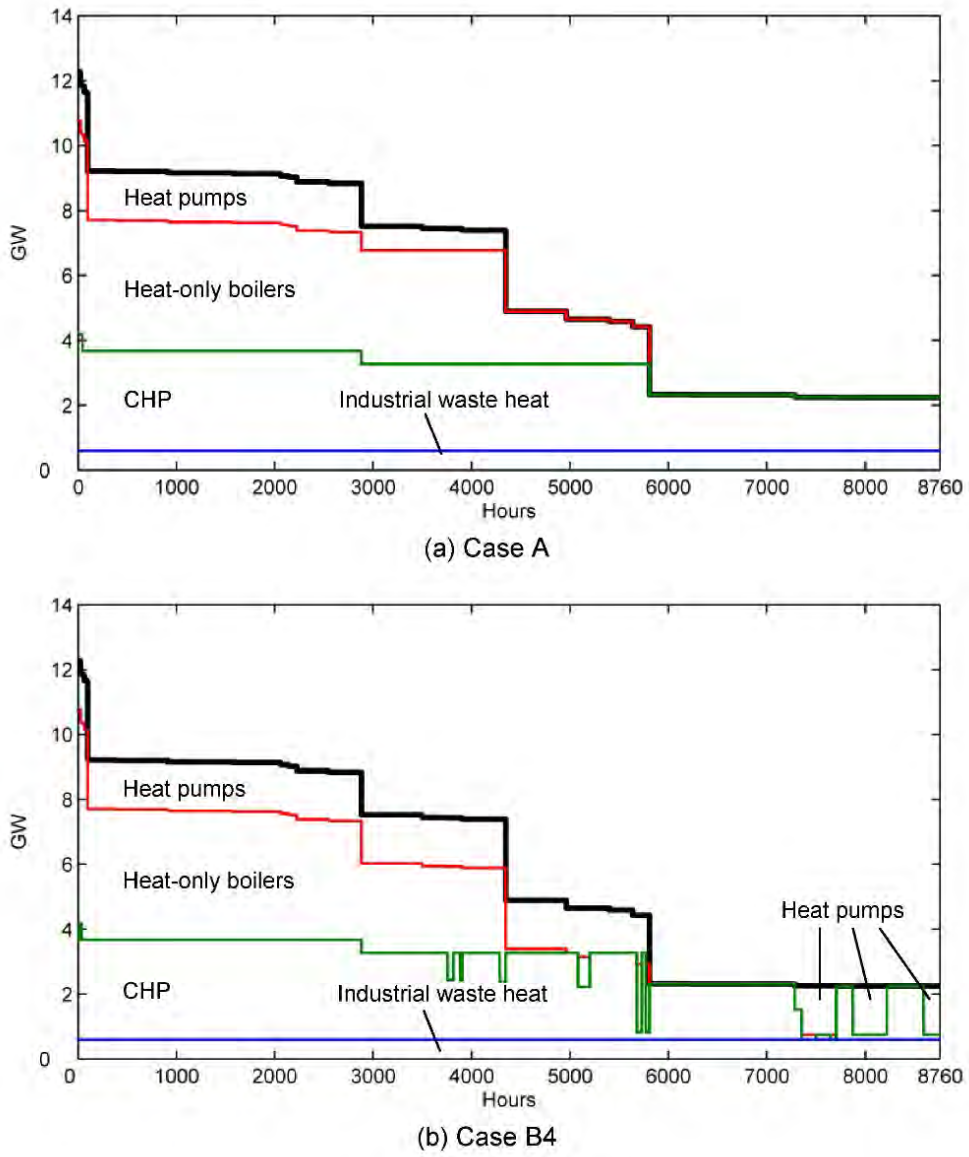

Fig. 3. Duration curves for the district heating demand (solid bold staircase line) and contribution of different types of heat production meeting this demand.

4. Discussion

The major impact on the district heating system in scenario B is biomass-fuelled CHP being replaced by heat pumps. This is perhaps a questionable system solution because investments in CHP plants are utilised to a lesser degree. From an overall systems perspective it may seem more reasonable to use CHP in Sweden where the heat can be utilised in district heating systems and to install solar cells in countries with less district heating and a higher and less seasonally fluctuating insolation. However, on a liberalised electricity market, if solar cells become cost-effective, a large-scale integration is possible and would be something that district heating utilities would have to adapt to. With a large surplus generation from

renewables, the electricity prices would occasionally be very low, which would make it reasonable to decrease CHP production because of the low revenues from sold electricity. At the same time the low electricity prices would make electric heating, at least with heat pumps, cost-effective. It is important to note that neither competition with CHP, nor other impacts such as water spillage, pose any definitive limits to the integration of solar and wind power. In general, integration of variable power generation is not primarily restricted by any fundamental technological limits but is rather determined by economic trade-offs, depending on the balance between demand and generation locally and in neighbouring areas, transmission capacities, hydropower control and spillage [8].

Some limitations of the studied scenarios, which are based on today's power and district heating systems, have impacts on the results. For example, the increased use of heat pumps occurs when transmission capacities restrict the possibilities for electricity export. Therefore, increased transmission capacity to neighbouring countries would make it possible to export the electricity instead of using it for electric heating. An increased transmission capacity would probably accompany an extensive integration of renewable power generation. However, if solar and wind power penetration levels increase in other countries, its variability will to some extent be correlated to the variability of the Swedish plants. A production surplus in neighbouring countries would therefore reduce the possibilities for exports, despite a higher transmission capacity. Additional scenarios that take this into account would be needed for further studies.

Another possibility that should be included in future scenarios is load management, which could help absorbing solar and wind power variability. Increased use of heat pumps could be seen as one type of load management, as it occasionally increases the electricity demand. Other types of demand response should be included as well. Another possible feature of the future power system is a changed electricity demand due to a large-scale introduction of electric vehicles. These could also introduce additional storage capacity to the system. A large-scale change to the district heating load is also possible, following energy efficiency measures in the built environment, which could possibly change the basis for the CHP production. But district heating may, on the other hand, also serve new purposes, such as industrial heat demand, absorption cooling and washing machines, which reduce seasonal demand variations and improve conditions for CHP production. Global warming and its effects on the climate could also be taken into account. For example, precipitation will probably increase in Sweden [9], which improves the hydropower ability to balance variable power generation. All of these possibilities should be included in further research.

Some more fundamental limitations of the applied model should also be mentioned. The variability of combined solar and wind power is described in detail, but not the short time-scale fluctuations that determine the instantaneous utilisation of reserve capacity. Moreover, hydropower control is modelled in an aggregated form and does not consider individual rivers where the flows between hydropower plants may be coupled. Another simplification is that bottlenecks in transmission capacity within the Swedish power system are not included. Combined, these simplifications may overestimate the flexibility of the power system. In reality, it would be possible e.g. for water spillage to occur for lower penetration levels of renewable power generation than the ones in case B4.

5. Conclusions

The energy system optimisation model MODEST has been used to study the Swedish power and district-heating systems with large-scale renewable power integration. It was found that

incremental amounts of solar and wind power added to the existing system do not cause any spilled energy until they reach the levels in the most extreme case where solar and wind power each produce 30 TWh annually. However, the large-scale renewable power integration reduces utilisation of investments in CHP plants due to an increased use of heat pumps and, as a consequence, leads to reduced use of biofuels for district heating. A major proportion of the added generation capacity produces a surplus that is exported. Further research should include scenarios for the major influential system components and parameters, such as domestic and foreign transmission capacity.

References

[1] European Parliament, Directive 2009/28/EC, Apr. 23 2009.

[2] IEA Wind, IEA Wind Energy Annual Report 2009, 2010. Available online at: http://www.ieawind.org/AnnualReports_PDF/2009.html.

[3] German Solar Industry Association (BSW-Solar), Statistic data on the German photovoltaic industry, Jun. 2010. Available online at: http://www.solarwirtschaft.de/fileadmin/content_files/factsheet_pv_engl.pdf.

[4] European Parliament, Directive 2010/31/EU, May 19 2010.

[5] H. Holttinen, R. Hirvonen, Power system requirements for wind power, in Wind Power in Power Systems, T. Ackermann (ed.), John Wiley & Sons Ltd., 2005, pp. 144-167.

[6] D. Henning, Optimisation of Local and National Energy Systems: Development and Use of the MODEST Model, PhD Thesis, Department of Mechanical Engineering, Linköping University, Sweden, 1999.

[7] J. Widén, System Studies and Simulations of Distributed Photovoltaics in Sweden, PhD Thesis, Department of Engineering Sciences, Uppsala University, Sweden, 2010.

[8] L. Söder, On limits for wind power generation, International Journal of Global Energy Issues 21, 2004, pp. 243-254.

[9] J. Fenger (ed.), Impacts of Climate Change on Renewable Energy Sources: Their Role in the Nordic Energy System, Nord 2007:003, Nordic Council of Ministers, 2007.

Sustainable working media selection for renewable energy technologies

Victor A. Mazur[1,*], Dmytro Nikitin[1]

[1] *Academy of Refrigeration, Odessa, Ukraine*
** Corresponding author. Tel: +38 0487209169, Fax: +38 0487231145, E-mail: mazur@paco.net*

Abstract: The sustainable working media selection is one of the most important stages in renewable energy technologies. The compromise among such properties as contribution to greenhouse effect, flammability, toxicity, thermodynamic behaviour, performance specifications, and the others defines a sustainable decision. The aim of present work is to apply a fuzzy set methodology providing sustainability among thermodynamic, economic, and environmental requirements. The organic Rankine cycle (ORC) for the class of working fluids based on the hydrofluoroethers (HFE) is considered to demonstrate a proposed approach. To select new working fluids, which have no information on thermodynamic behavior, artificial neural networks (ANN) approach is offered to forecast the ORC energy efficiency. The ANN correlations for coefficient of performance (COP) and pressure ratio (output) as functions of critical temperature, critical pressure and normal boiling temperature (input) are built via REFPROP database. The validation set has been used to estimate the ORC energy efficiency without of thermodynamic property calculations. The accuracy of ANN prediction for the cycle performances does not exceed 4% relative to the training set values. The Bellman – Zadeh model as the intersection of membership functions (fuzzy criteria mappings) is applied to sustainable selection of working media.

Keywords: *Working Fluids, Organic Rankine Cycle, Coefficient of Performance, Artificial Neural Networks*

Nomenclature

COP	*coefficient of performance*	Z	*compressibility factor*
$\boldsymbol{K}$	*generalized criterion*	μ	*membership function*
K_i	*local criterion*	ρ	*density* $kg \cdot m^{-3}$
M	*molar mass* $g \cdot mole^{-1}$	Ψ	*flammability index*
n_i	*number of atomic species (i)*		*Subscripts*
p	*pressure* MPa	C	*critical*
RD	*relative deviation* %	B	*boiling*
T	*temperature* K	*opt*	*optimum*
		th	*thermodynamic*

The paradigm of sustainable development considers an integrated solution of the ecological, economic, social and cultural problems arising from the design of technical systems. The transformation of renewable energy sources into mechanical work mainly is based on the application of the Rankine cycle. The Rankine cycle working on organic substances, the Organic Rankine Cycle, has found wide application as renewable energy technologies (RET). There are many criteria of efficiency of RET and the extreme values are desirable to reach for each ones taken separately. Usually, three main goals are involved in the design process: thermodynamic, economic and environmental. The problem of prospective working media selection is closely connected with modern technologies based on the concept of sustainable development. To utilize low potential heat source, the ORC working fluids should possess normal boiling temperature below 350 K, practically vertical right boundary curve in the temperature – entropy diagram, high heat of evaporation, high density and comprehensible operational qualities. The selection of working fluids with desirable combination of such properties as contribution to greenhouse effect, flammability, toxicity, thermodynamic behavior, performance specifications, and the others is one of the most important stages in RET simulation and design. Working fluid selection problem has been tackled using achievements of molecular theory, engineering experience and experimental studies [1] - [4]. Clearly, a working fluid that combines all the desirable properties and has no undesirable properties does not exist.

1. Sustainable ORC working fluids selection

The aim of present work is to include a fuzzy set methodology in order to meet thermodynamic, economic, and environmental goals for working fluid selection in the ORC. To solve this problem, achievements of information technologies and the molecular theory, technical experience and experimental data are used. There is a multitude of efficiency criteria and the attainment of the extreme for each of them is the ultimate goal of the design. Usually a compromise among three basic criteria – energy, economic and ecological is considered. The generalized criterion of efficiency for all system as a whole is represented by a vector $\boldsymbol{K}$, which includes local criteria $\boldsymbol{K_i}$ that reflect the set of requirements to ORC working fluids by the consumer.

1.1. Tailored working fluid concept

We consider here only such criteria, which are linked by certain relations R to the properties of working fluids P, i.e. the system defined by a three-tuple { K, R, P }. The relation R is a kind of technological operator and its structure can be determined via the equations of mass, momentum and energy balance, supplemented with the characteristic equation of state. It is usually impossible to estimate the performance attributes of refrigeration system from target properties (physical, chemical, ecological, and etc) correlated with molecular structure following to fundamental principles only. So, we need to enlist restricted experimental information to define real properties P via their model properties M (X). The set of model parameters X, as a mapping of the experimental data containing the observed properties P, gains in importance as information characteristics of substance by which its property behavior can be restored. A physical meaning is no less important for the vector X and should map the working fluid characteristics on the molecular level to select a proper molecular configuration. This is very convenient when one needs to be able to predict the properties of any molecular structure. The working fluid selection problem can be mathematically formulated as the multi-criteria optimization problem: to find

$$\boldsymbol{Opt\ K}\ [K_1\ \boldsymbol{(X)}, K_2\boldsymbol{(X)}, \ldots, K\boldsymbol{n(X)}],\ \boldsymbol{X} \in \boldsymbol{X_P} \qquad (1)$$

We assume that $K_j(X) = \| \boldsymbol{P_j}, \boldsymbol{M_j(X)} \|$ is a "distance" between the desired (ideal) efficiency of system $\boldsymbol{P_j}$ and its real model $\boldsymbol{M_j}$. For thermodynamic criterion, K_{th} the value $\boldsymbol{P_j}$ corresponds to the theoretical maximum of the efficiency objective function, e.g. efficiency of the Carnot cycle. Solution of multi-criteria problem is a finding of compromise among all criteria and constraints and can be formulated as follows: to construct the function

$$\boldsymbol{K} = K_1 \cap K_2 \cap \ldots \cap K_n\,. \qquad (2)$$

The formal solution of problem is added up to determination of the optimum vector $\boldsymbol{X_{opt}}$ of such kind that $|\boldsymbol{K}\ (\boldsymbol{X_{opt}})| \succ |\boldsymbol{K}\ (\boldsymbol{X})|$ for any $\boldsymbol{X} \neq \boldsymbol{X_{opt}}$ where $\succ$ is preference sign. The model parameters $\boldsymbol{X_{opt}}$ identify a trade-off decision possessing to desired efficiency criteria. In our case the model parameters ***Xopt*** identify an optimum working medium having the desired complex of properties ("*tailored" working fluid*). Critical or/and fixed parameters of working fluids are typical examples of the information characteristics of substance linked with its molecular structure.

Attainment of the optimum decision corresponds to the compromise among various criteria and displays the quality of engineering decisions. Criteria of sustainable development cannot be formulated on a strict mathematical basis and always have subjective character. The several approaches for finding the compromise between local criteria and constructions of generalized criterion function were offered. For example, in traditional thermodynamics

analysis, the concept exergy or exergy-ecological costs is introduced for monetary and power values. Additive convolution of power (*COP*) and ecological (Global Warming Potential – *GWP*) parameters of efficiency has been offered for the analysis of refrigerating systems in TEWI criterion [4]. A weak point of such approaches is the implicit assumption about conformity of the economic (ecological) and energy efficiency objectives that contradicts a real situation. Finding the compromise actually is a non-trivial decision-making problem and cannot be formalized. There are some ways of transformation of vector criterion in scalar which were discussed earlier [5], [6].

1.2. Multicriteria making decision

Design objectives usually contradict with each other, so that is difficult to provide sustainable solution, which simultaneously satisfies both of them. Meaningful analysis of this ill-structured situation should include uncertainty conception. For the multicriteria problems the local criteria usually have a different physical meaning, and consequently, incomparable dimensions. It complicates the solution of a multicriteria problem and makes it necessary to introduce the procedure of normalizing criteria or making these criteria dimensionless. There is no unique method for the criteria normalizing and a choice of method depends on statement of problem having subjective nature. In the present study, a next sequence of decision-making steps is applied [6].

- Determination of the Pareto optimum (or compromise, or trade off) set $\boldsymbol{X_P}$ as the formal solution of multicriteria problem to minimize uncertainty sources;
- Fuzzification of goals as well as constraints to represent an ill-structured situation;
- Informal selection of convolution scheme to transform a vector criterion into scalar combination of vector components.

Sustainable decision is defined by the Bellman and Zadeh model [7] as the intersection of all local fuzzy criteria and is represented by its membership function μi(X) as follows:

$$\boldsymbol{\mu_C(X) = \mu_1(X) \cap \mu_2(X) \ldots \cap \mu_n(X)}, \; i = 1,2,\ldots, \; \boldsymbol{n}; \quad \boldsymbol{X \in X_P} \tag{3}$$

The membership function of the objectives and constraints can be chosen linear or nonlinear depending on the context of problem. One of possible fuzzy convolution schemes is presented below.

– Initial approximation ***X***-vector is chosen. Maximum (minimum) values for each criterion K_i are established via scalar maximization (minimization). Results are denoted as "ideal" points $\{ X_j^0 , j = 1 \ldots m \}$.

– Maximum and minimum boundaries for criteria are defined:

$$K_i^{min} = \min_j K_j(X_j^0) = K_i(X_i^0), \; i = 1 \ldots n; \; K_i^{max} = \max_j K_j(X_j^0), \; i = 1 \ldots n. \tag{4}$$

– The membership functions are assumed for all fuzzy goals as follows

$$\mu_{Ki}(X) = \begin{cases} 0, & if \;\; K_i(X) > K_i^{max} \\ \dfrac{K_i^{max} - K_i}{K_i^{max} - K_i^{min}} & if \;\; K_i^{min} < K_i \le K_i^{max}, \\ 1, & if \;\; K_i(X) \le K_i^{min} \end{cases} \tag{5}$$

A final decision is determined as the intersection of all fuzzy criteria represented by its membership functions. This problem is reduced to the standard nonlinear programming problem.

1.3. Cycle configurations

Three main configurations of ORC are considered (Fig. 1) for typical working fluids R717, R123, and cyclohexane. The modeling of characteristics of the ORC is based on the First and Second Laws of thermodynamics and described elsewhere [8].

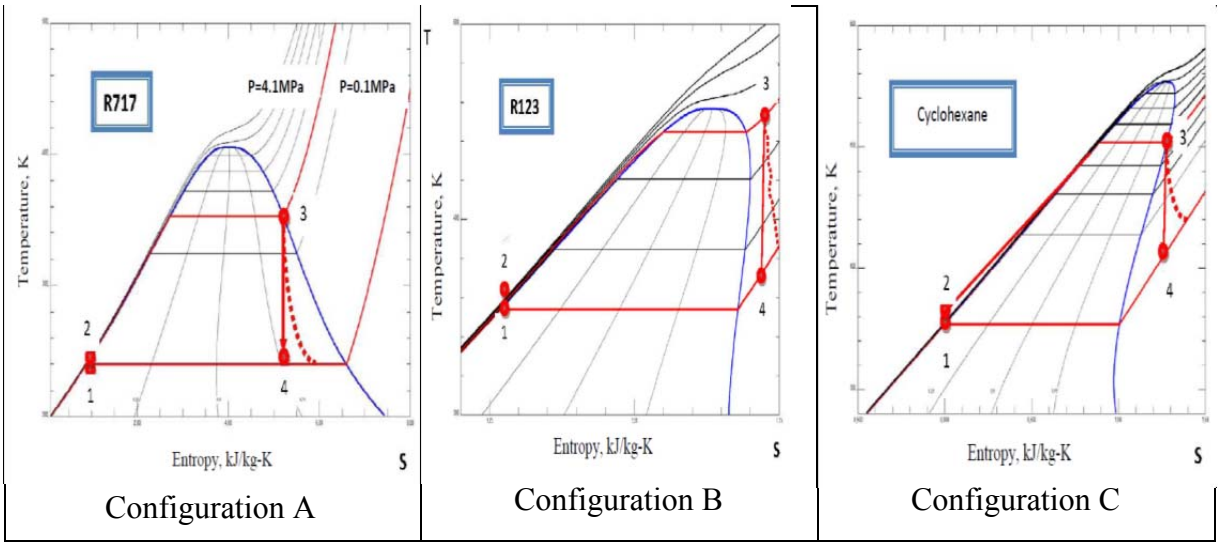

Configuration A | Configuration B | Configuration C

Fig. 1. ORC cycle configurations for different working fluids

2. ORC energy efficiency appraisal via artificial neural networks

Thermodynamic behavior of one-component substances in gas and liquid phases has identical topological structure similar to the cubic equations of state. The reliable quantitative description of a thermodynamic surface can be achieved via similarity theory. From this point of view, critical temperature – T_C and pressure – P_C together with normal boiling temperature – T_B are the most rational parameters which provide correct description of thermodynamic surfaces near the saturation curve.

2.1. Construction of ANN correlations. Results and discussion

To select the ORC working fluid with better properties we need preliminary estimating thermodynamic properties and assessment of different efficiency criteria. To evaluate the cycle performance data the artificial neural networks capable to recognize complex input – output relationships is applied. At first step the training set was used to calculate the main cycle characteristics. In Table 1 temperature boundaries (T_3, T_4) and a range of admissible pressures (*Pmin, Pmax*) which characterize the operating conditions for ORC configurations are given.

ANN represents the mathematical tool which during training allows establishing dependences between input data and target characteristics of any complexity. The purpose of training is to find factors of communications between neurons, which define abilities of a neural network to allocation of the latent relationships between input and output values. After training, the network becomes capable to forecast new data on the basis of the limited sample of known interrelations between input and output values. In this case, we aspire on the basis of the known information on the input T_C, P_C and T_B for restricted set of known substances which are connected by complex relationships with output value – *COP*, to predict energy efficiency

of the Rankine cycle for little-studied working fluids only from critical parameters and normal boiling temperature. The ANN correlations for COP (output) as function of critical temperature, critical pressure and normal boiling temperature (input) are built on the REFPROP 8.0 database [9]. The training set consists of 15 components (R134a, R123, R1270, R717, R600a, R290, R245fa, R245ca, R236fa, R227ea, R142b, R125, R113, R22, R32).

Table 1. COP comparison for the organic Rankine cycle with ANN calculations

Working fluid	*Cycle Type*	T_C, ^0C	P_C, *MPa*	T_B, ^0C	T_3, ^0C	T_4, ^0C	P_{min}, *MPa*	P_{max}, *MPa*	*COP, %,[8]*	*COP, %, ANN*	*RD, %*
R32	A	78.11	57.8	-51.7	31.3	30.0	19.3	20.0	0.36	0.38	-4.5
R32	B	78.11	57.8	-51.7	100.0	97.7	19.3	20.0	0.42	0.44	-4.3
R125	A	66.18	36.3	-48.1	40.1	30.0	15.6	20.0	2.32	2.38	-2.3
R125	B	66.18	36.3	-48.1	100.0	91.9	15.6	20.0	2.36	2.36	0.1
RE125	A	81.34	33.5	-35	100.0	79.0	10.1	20.0	5.77	6.02	-4.3
R134a	A	101.0	40.6	-26.1	67.7	30.0	7.7	20.0	7.74	7.73	0.1
RE134	C	147.1	42.3	5.5	100.0	41.0	2.5	16.6	12.56	12.48	0.7
R143a	A	72.73	37.6	-47.2	43.6	30.0	14.4	20.0	3.14	3.08	1.9
R143a	B	72.73	37.6	-47.2	100.0	87.3	14.4	20.0	3.31	2.98	10.0
R152a	A	113.5	44.9	-24	72.6	30.0	6.8	20.0	8.82	8.78	0.4
R152a	B	113.5	44.9	-24	100.0	53.8	6.9	20.0	9.22	9.27	-0.5
RE170	A	126.8	52.4	-24.8	75.1	30.0	6.7	20.0	9.38	9.29	0.9
RE170	B	126.8	52.4	-24.8	100.0	53.0	6.7	20.0	9.68	9.84	-1.6
R218	C	71.89	26.8	-36.8	58.9	33.6	10.0	20.0	5.22	5.22	0.0
R227ea	C	101.7	29.3	-16.4	83.8	44.2	5.3	20.0	9.20	9.22	-0.2
R236ea	C	139.2	34.1	6.19	100.0	53.9	2.4	15.7	12.02	12.16	-1.1
R245ca	C	174.4	39.2	25.1	100.0	53.7	1.2	9.3	12.79	12.96	-1.3
R236fa	C	125.5	32.0	-1.4	100.0	48.6	3.2	19.3	11.63	11.55	0.6
R245fa	C	154.0	36.4	15.1	100.0	50.7	1.8	12.7	12.52	12.51	0.1
RE245mc	C	133.6	28.9	5.59	100.0	54.5	2.4	14.9	11.84	11.82	0.2
RC270	A	124.6	54.9	-31.5	100.0	41.6	8.2	20.0	8.86	8.62	2.7
R290	A	96.65	42.5	-42.1	57.1	30.0	10.7	20.0	5.91	5.91	-0.1
R290	B	96.65	42.5	-42.1	100.0	76.0	10.7	20.0	6.11	6.18	-1.2
RC318	C	115.2	27.8	-6	98.9	54.7	3.6	20.0	10.97	10.69	2.6
RE347mc	C	164.5	24.8	34.23	100.0	56.4	3.6	20.0	11.72	11.22	4.3
R600	C	152.0	38.0	-0.5	100.0	48.4	2.8	15.3	12.58	12.53	0.4
R600a	C	135.0	36.5	-11.7	100.0	45.3	4.0	20.0	12.12	12.11	0.1
R601	C	196.5	33.7	27.8	100.0	57.7	0.8	5.9	12.91	12.87	0.3
R601a	C	187.7	33.9	36.1	100.0	58.4	1.1	7.2	12.75	12.75	-0.0
R1270	A	92.42	46.7	-47.7	48.5	30.0	13.1	20.0	4.28	4.28	-0.1
R1270	B	92.42	46.7	-47.7	100.0	81.2	13.1	20.0	4.53	4.16	8.2
C5F12	C	148.8	20.4	29	100.0	72.7	1.04	7.6	10.49	10.49	0.0
CF3I	A	123.3	39.5	-21.9	85.2	30.0	5.6	20.0	10.63	10.68	-0.5
CF3I	B	123.3	39.5	-21.9	100.0	39.6	5.6	20.0	10.93	10.93	-0.0
n-hexane	C	234.7	30.1	341.8	100.0	61.9	0.2	2.5	13.00	13.00	0.0

The construction of ANN includes the following sequence of actions: a choice of initial data for training; a choice of architecture of a network; dialogue selection of ANN parameters; process of training; check of adequacy of training (validation); and forecasting. Calculations were performed in Matlab Neural Network Toolbox environment (**http://**www.mathworks.com). The back propagation algorithm has been used for ANN training. Output values in the initial

sample were calculated for various configurations of cycles based on thermodynamic properties as reported in [8]. As input values the given T_C, P_C and T_B are used. The various architectures of neural networks with different neuron numbers and activation functions in the first and second layers were considered. The third layer of a network always contains one neuron with linear active function.

For configuration A two hidden layers were used. The first contained two neurons and the second – one. As activation function the hyperbolic tangent was used. The training sample data for working fluids R125, R143a, R32 and R1270 were chosen. Testing was done for R152a, CF3I, and RE170. Check of adequacy was done for R290 and R134a. Results are listed in Table 1.

For configuration B two hidden layers were used. The first contained five neurons and the second – one. As activation function the hyperbolic tangent was used. As training sample data for working fluids R125, R143a, R152a, and RC270 were used. Testing was performed for RE125, R1270 CF3I and RE170. Check for adequacy was considered for R32 and R290. Results are listed in Table 1.

Construction of an artificial neural network for a configuration C coincides with architecture of a network for a configuration B. Training sample included the following working fluids: R218, R236fa, RE245mc, C_5F_{12}, R600, R601a, and n-hexane. Testing was done on the set of substances: R227ea, R236ea, RE134, R245fa RE347mcc, R601, and final verification accordingly for RC318, R600a, and R245ca.

Results of COP calculation for different ORC configurations are given in Table 1. Deviations of "experimental" values of COP [8] from calculated by means of the trained artificial neural network are within the error of calculations via the multi-constant equations of state [10] – [12]. Appreciable deviations of a relative error (more than 5 %) are observed for low COP values that have no principal meaning because we are interested by the working fluids with the maximal power efficiency.

The organic Rankine cycle for the class of working fluids based on the hydrofluoroethers (HFE) is considered to demonstrate a proposed approach. Critical properties of HFEs were taken from Ambrose *et al* [13]. Flammability indices correlated to atomic species by simple ratio of fluoride (n_F) and hydrogen (n_H) atoms $\Psi = n_F/(n_F+n_H)$ are given in Table 2. The normal boiling points for HFEs were restored from Murata *et al*. correlations [14]. Temperature boundaries were taken for configuration A in range 300…315K.

To select the trade-off working fluid the membership functions (5) for energy efficiency (μ_{COP}) and ecological safety (μ_{GWP}) as function of critical parameters were calculated at following assumptions: $COP^{max} = COP^{Carnot}$; $COP^{min} = 3.64$ and $GWP^{max} = 500$; $GWP^{min} = 0$. Flammability index ($\Psi > 0.7$) was considered as constraint. Intersection of membership functions defines the compromise solution for each HFEs under consideration. Final decision is chosen after comparison of compromise solutions with flammability index.

The *COP* comparison among the ORC with HFE working fluids (Table 2) shows the maximum value 4.1% for $C_5H_2F_6O_2$ and minimum *COP* – 3.6% for C_2HF_5O. The energy efficiency of HFE – $C_5H_2F_6O_2$ looks more attractive among widespread industrial HFEs: HFE-125 (CF_3OCF_2H), HFE-134 (CHF_2OCHF_2) HFE-143a (CF_3OCH_3), HFE-227me ($CF_3OCFHCF_3$), HFE-245mf ($CF_3CH_2OCF_2H$), HFE-245mc($CF_3CF_2OCH_3$),HFE-254pc ($CHF_2CF_2OCH_3$), HFE-356mec ($CF_3CHFCF_2OCH_3$), HFE-356mff ($CF_3CH_2OCH_2CF_3$), HFE-7000 (HFE-347mcc) (n- $C_3F_7OCH_3$), HFE-7100 (HFE-449mccc) ($C_4F_9OCH_3$), (HFE-

449mccc) ($C_4F_9OCH_3$), and HFE-7200 (HFE-569mccc) ($C_4F_9OC_2H_5$). The $C_5H_2F_6O_2$ flammability index is also appropriate ($\Psi = 0.75$) but near limiting value 0.7.

Table 2. Critical parameters, COP, and flammability index for hydrofluoroethers

Working fluids	*M, gmole^{-1}*	*T_c, K*	*p_c, MPa*	*ρ_c, g cm^{-3}*	*Z_C*	*Ψ*	*COP,%*
C_2HF_5O	136.021	354.49	3.35	0.579	0.267	0.83	3.64
$C_2H_2F_4O$	118.030	420.25	4.23	0.529	0.270	0.67	3.94
$C_2H_3F_3O$	100.040	498.50	4.82	0.485	0.240	0.50	3.94
C_3F_6O	166.022	361.90	3.06	0.610	0.277	1.00	3.64
$C_3F_8O_2$	220.018	372.40	2.33	0.610	0.271	1.00	3.65
C_3HF_7O	186.028	387.80	2.62	0.550	0.275	0.88	3.75
$C_3H_2F_6O$	168.038	428.90	3.04	0.553	0.269	0.75	3.94
$C_3H_3F_5O$	150.047	462.03	3.54	0.553	0.259	0.63	3.94
$C_3H_3F_5O$	150.047	406.82	2.89	0.500	0.256	0.63	3.92
$C_3H_5F_3O$	114.066	449.05	3.51	0.412	0.260	0.38	3.94
C_4F_8O	216.029	400.00	2.69	0.680	0.257	1.00	3.89
$C_4F_{10}O$	254.026	391.70	1.87	0.630	0.232	1.00	3.75
$C_4HF_7O_2$	214.038	452.88	2.87	0.597	0.273	0.88	3.94
$C_4HF_7O_2$	214.038	435.06	2.65	0.569	0.275	0.88	3.94
C_4HF_9O	236.036	412.63	2.26	0.499	0.311	0.90	3.93
$C_4H_2F_8O$	218.045	421.60	2.33	0.533	0.272	0.80	3.94
$C_4H_2F_8O$	218.045	444.63	2.57	0.581	0.261	0.80	3.94
$C_4H_2F_8O_2$	234.045	449.81	2.41	0.571	0.265	0.80	3.94
$C_4H_3F_5O$	162.058	455.03	2.91	0.486	0.258	0.63	3.94
$C_4H_3F_7O$	200.055	455.10	2.77	0.576	0.255	0.70	3.94
$C_4H_3F_7O$	200.055	437.60	2.48	0.530	0.257	0.70	3.94
$C_4H_3F_7O$	200.055	433.21	2.55	0.542	0.261	0.70	3.94
$C_4H_3F_7O$	200.055	463.89	2.71	0.541	0.260	0.70	3.96
$C_4H_4F_6O$	182.064	459.60	2.70	0.481	0.267	0.60	3.95
$C_4H_4F_6O$	182.064	476.31	2.78	0.500	0.256	0.60	4.03
$C_4H_5F_5O$	164.074	431.13	2.53	0.448	0.258	0.50	3.94
$C_5F_{10}O$	266.037	427.00	1.90	0.600	0.237	1.00	3.82
$C_5H_2F_6O_2$	208.059	485.10	2.77	0.720	0.198	0.75	4.11
$C_5H_2F_{10}O$	268.053	447.40	2.14	0.582	0.265	0.83	3.84
$C_5H_3F_7O$	212.066	476.55	2.58	0.538	0.256	0.70	4.03
$C_5H_3F_7O$	212.066	467.64	2.52	0.518	0.266	0.70	4.00
$C_5H_3F_9O$	250.062	475.74	2.23	0.563	0.251	0.75	3.90
$C_5H_3F_9O$	250.062	462.72	2.37	0.558	0.276	0.75	3.93
$C_5H_3F_9O$	250.062	473.01	2.24	0.550	0.259	0.75	3.90
$C_5H_5F_5O$	176.085	475.54	2.64	0.494	0.238	0.50	4.05
$C_5H_5F_7O$	214.081	481.54	2.38	0.497	0.256	0.58	3.92
$C_6H_3F_9O$	262.073	498.97	2.20	0.520	0.267	0.75	3.82
$C_6H_3F_{11}O$	300.070	486.48	1.95	0.567	0.255	0.79	3.89
$C_6H_5F_9O$	264.089	482.02	1.98	0.518	0.251	0.64	3.90

2.1. Conclusions

Fuzzy set approach is powerful tool to finding of compromise among energy efficiency, environmental constraints and economic indices of working media in conceptual RET design. In this work, criteria of sustainable development for renewable energy technologies of transformation low potential sources of heat into work on the basis of the ORC were

developed. For search of new working fluids, which have no information on thermodynamic behavior, ANN approach is proposed to forecast energy efficiency of the Rankine cycle. On the basis of the limited data about critical parameters and normal boiling temperature of substances for various configurations of cycles, the values of COP are determined without the calculation of thermodynamic properties.

This study is one of first attempts to apply methodology of tailored substances to selecting optimum working fluid for ORC. Construction of ANN correlations between information characteristics of working fluids and criteria of efficiency of Rankine cycle narrows the area of compromise search in the space of competitive economic, environmental and technological criteria.

References

[1] S. Quoilin, V. Lemort, Technological and Economical Survey of Organic Rankine Cycle Systems, The 5th European Conference on Economics and Management of Energy in Industry, 2009, Algarve, Portugal.

[2] K. Joback, G. Stephanopoulos, Designing Molecules Possessing Desired Physical Property Values, Proceedings of the Foundations of Computer-Aided Process Design (FOCAPD), Snowmass, CO, July 12-14, 1989, pp. 363 – 387.

[3] A. Duvedi, E. Achenie, Designing Environmentally Safe Working fluids Using Mathematical Programming, Chem. Eng.Science, 51, No.15, 1996, pp. 3727 - 3739.

[4] The refrigeration sector's commitment to sustainable development and mitigation of climate change, www.iifiir.org

[5] V. Mazur, Optimum Working fluid Selection, Low Temperature and Cryogenic Refrigeration, Kluwer Academic Publishers, 2003, pp.101–118.

[6] S. Artemenko, V. Mazur, The choice of working fluids in energy transforming systems on the basis of fuzzy multicriteria analysis, East-European Journal of Modern Technologies, 4/11(40), 2009, pp. 41-47.

[7] R. Bellman, L. Zadeh, Decision-making in a fuzzy environment, Management Science, 17, 1970, pp. 141–164.

[8] B. Saleh, G. Koglbauer, M. Wendland, Working fluids for low temperature Organic Rankine cycles, Energy, 32, 2007, pp.1210–1221.

[9] E. Lemmon, M. Huber, M. McLinden, 2007, NIST Reference Fluid Thermodynamic and Transport Properties – REFPROP. Version 8.0. National Institute of Standards and Technology, Boulder, USA.

[10] B. Saleh, U. Weinger, M. Wendland, Description of the thermodynamic properties of natural working fluids with BACKONE equations, In Proceedings of the IIR conference on thermophysical properties and transfer processes of new working fluids, October 3–5; Paderborn, Germany, 2001, pp. 31–38.

[11] M. Wendland, B. Saleh, J. Fischer, Accurate thermodynamic properties from the BACKONE equation of natural gas, Energy Fuels, 18, 2004, pp. 938–951.

[12] B. Saleh, M. Wendland, Screening of pure fluids as alternative working fluids, International Journal of Refrigeration, 29, 2006, pp. 260–269.

[13] D. Ambrose, C. Tsonopoulos, E. Nikitin , Vapor-Liquid Critical Properties of Elements and Compounds. 11. Organic Compounds Containing B + O; Halogens + N, + O, + O + S, + S, + Si; N + O; and O + S, + Si , J. Chem. Eng. Data, 54, 2009, pp. 669–689.

[14] J. Murata, S. Yamashita, M. Akiyama, S. Katayama, T. Hiaki, F. Sekiya, Vapor Pressures of Hydrofluoroethers, J. Chem. Eng. Data, 47 (4), 2002, pp. 911-915.

Interactions between selected energy use and production characteristics of German manufacturing plants

Sebastian Petrick[1,*], Katrin Rehdanz[1,2], Ulrich Wagner[3]

[1] *Kiel Institute for the World Economy, Kiel, Germany*
[2] *Christian-Albrechts-University of Kiel, Germany*
[3] *Universidad Carlos III de Madrid, Spain*
** Corresponding author. Tel: +49 431.8814263, Fax: +49 431.8814500, E-mail: sebastian.petrick@ifw-kiel.de*

Abstract: This paper analyzes the interactions between a number of key energy characteristics of German industrial plants in 2006, using an exceptionally rich dataset comprising more than 44 000 plants. Already by using basic descriptive statistical techniques we find that larger energy users tend to use energy less efficiently. This correlation is particularly prevalent in sectors with high energy intensity. We identify an energy mix effect as the main driver of this interrelation, since larger energy consumers tend to use less electricity in relation to other fuels, and electricity can be deployed more efficiently. The energy mix effect is also one of the reasons behind a negative correlation between energy intensity and the emission factor. From the correlation between plant-level energy intensity and gross output, we infer on the existence of increasing and decreasing returns to energy. We identify increasing returns to energy in most sectors, but decreasing returns to energy in some of the particularly energy intensive sectors.

Keywords: *Energy intensity, Emission factor, Manufacturing, Microdata*

1. Introduction

The industry sector[1] is a major energy consumer and it is receiving growing attention from researchers and politicians, who see it as a prominent battle ground in the fight against climate change, resource scarcity and energy insecurity. According to IEA data for 2006 [1][2], the German industrial sector Germany is responsible for 22 % of total final energy use and 15 % of CO_2 emissions. As the industry sector is fundamental for economic growth and employment in most countries, politicians are reluctant to cut industrial energy use by limiting the overall size of the industry sector. Consequently, policy initiatives mostly aim at boosting industrial energy efficiency and reducing the average carbon factor of energy inputs. Recent examples of policies in Germany include, amongst others, the "Heat-Power Cogeneration Act", the Ecological Tax Reform and the "Large Combustion Plant Directive". The effectiveness of such measures, however, is limited by economic and technological restrictions inherent to the industry sector, and a thorough understanding of these restrictions is vital for policy design. In particular, energy intensity[2] and total energy use are not independent of each other. Several effects link a plant's level of energy use and energy intensity.[3] Conceptually, these effects can result in either a positive or a negative correlation between the two measures.

For example, if the amount of energy needed to produce the last unit of output decreases with rising energy use, larger energy users would on average use energy more efficiently. Such *increasing returns to energy* would imply a negative correlation between energy intensity and energy use. Conversely, in the case of *decreasing returns to energy*, the amount of energy

[1] We define the industry sector as the mining, quarrying and manufacturing sectors with ISIC codes C and D.
[2] We use energy intensity as an inverse measure of energy efficiency and calculate it as the ratio between total energy use (in kWh) of a plant and gross output (in 1000 EUR) of a plant. The use of gross output instead of value added which accounts for inputs is dictated by data availability. See Petrick et al. [3] for further discussion of this issue.
[3] The existing literature on the interaction between energy use and energy intensity as well as their determinants is widely ramified. Since a comprehensive review of the existing literature is beyond the scope of this paper, the reader is referred to the excellent review by Gillingham et al. [4] and the references given therein.

needed for the last unit of output increases with rising output, and energy intensity and total energy use would be positively correlated. Note that in both cases a correlation between energy intensity and output is also implied. In the first case, a (ceteris paribus) concave demand function for energy implies a negative correlation between energy intensity and output, while in the second case the demand function is convex and energy intensity and output are positively correlated.[4] In either case the effect of returns to energy can be distorted by an *energy mix effect*. We hypothesize that with rising overall energy use, the composition of plants' energy mixes changes and, in particular, the share of primary fuels, such as natural gas or coal, rises at the cost of the share of electricity and other processed fuels. Since electricity can be used more efficiently than primary fuels (with regards to output per used kilowatt hour), overall energy intensity is (ceteris paribus) expected to decrease with a rising electricity share and thus to increase with a rising fuel use due to the energy mix effect.

Apart from the interaction between total energy use and energy intensity, we analyze the link between energy use, energy intensity and the plant-specific emission factor, i.e. the ratio between CO_2 emissions (in t) and energy used (in kWh). At first glance it appears that exceptionally efficient energy users also try to minimize their carbon footprint (in part in response to policy) since plants with advanced technology are more likely to be both efficient and clean. At second glance, however, the energy mix effect might distort this picture; because the carbon factor of electricity is high due to conversion losses. The energy mix effect could thus lower the emission factor with increasing energy use and increasing energy intensity. To combine the interactions between efficiency of energy use and the carbon factor, we complement this part of the analysis with findings about a plant's carbon intensity, defined as the ratio of CO_2 emissions per gross output (in g/1000 EUR).[5]

In this paper we analyze the impact of returns to energy and energy mix effects on the link between energy use and energy intensity by measuring the net correlation between energy use and energy intensity. We also analyze the link between energy and carbon intensities as well as the plant specific emission factor in order to answer the question whether more efficient

[4] To understand why increasing returns to energy imply a negative interrelation between output and energy, consider a production function that abstracts from all other production factors. Such a production function *y=f(e)*, where *y* is the output und and *e* is the production factor energy, exhibits increasing returns to energy if it is convex. The implied factor demand function *e=g(y)* is the inverse of the production function and concave, i.e. the second derivative is negative. From the factor demand function, energy intensity (denoted *eint*) can be derived as a function of output:

$$\text{eint} = \frac{g(y)}{y} \tag{1}$$

The sign of the derivative of *eint* with respect to *y* depends on the sign of the difference between marginal productivity and average productivity:

$$\frac{d\,\text{eint}}{d\,y} > 0 \quad \square \quad g'(y) - \frac{g(y)}{y} > 0 \tag{2}$$

Since the second derivative of the factor demand function is negative, average factor demand will always be larger than marginal factor demand – which is exactly the intuition of increasing returns to energy (we assume that the Inada conditions hold). Thus, in the case of increasing returns to energy, the interrelation between energy intensity and output should be negative. In the case of decreasing returns to energy, the implied factor demand function would be convex, and the same argument (with exchanged sign) would hold – in the case of decreasing returns to energy, the interrelation between energy intensity and output should be positive.

[5] The same caveat as in the case of energy intensity applies, cf. footnote 2.

plants are also cleaner. To get a better picture of the differences between sectors, we present results not only at the aggregate level, but also for selected sectors of particular interest.

2. Data and Methodology

This paper is part of a research project that uses an exceptionally rich dataset, parts of which have only recently been made available by a research data centre of the German Official Statistics. The "AFiD panels"[6] are a collection of microdatasets comprising observations at the plant and enterprise level for various sectors, including industry. For this paper we use the panel "Industrial Plants" [5] in combination with an energy use module [6]. The combined dataset contains annual observations for up to 68 000 industrial plants per year from 1995 to 2006. In this paper we concentrate on the most recent cross section and use 2006 data, comprising 44 080 plants. An important feature of the data at hand is that it is based on a mandatory survey that each plant with more than 20 employees is required to answer. Thus, the degree of representativeness of our dataset is exceptionally high.[7] A more detailed description including a list of all variables included in the datasets as well as information on the underlying statistics can be found in Petrick et al. [3].[8]

To analyze the interrelation between the energy and production characteristics, we use basic correlation analysis. We calculate Spearman's rank correlation coefficients for all plants in the dataset as well as for selected sectors that are particularly interesting with regards to their energy use patterns. We use Spearman's correlation coefficient instead of Pearson's in order to minimize sensitivity to outliers. However, results based on Pearson's correlation coefficient can be obtained from the authors on request.

3. Results

To study the link between total energy use and energy intensity as well as the underlying mechanisms, we begin with the aggregate effect. For the German industry as a whole we find a strong and significant positive correlation between energy use and energy intensity (Table 1). This implies a negative correlation between energy use and energy efficiency which could be explained either by decreasing returns to energy for energy or by a fuel mix effect.

At the aggregate level, it is not clear whether this correlation is driven mainly by differences between plants or between sectors. Since energy intensive sectors like the cement, glass and ceramics, paper or metal manufacturing industries are responsible for the lion's share of overall energy consumption, plants in these sectors are also large energy users. This is confirmed by Petrick et al. [3], who isolated the heterogeneity between different sectors by calculating the correlation between the sector medians of total energy use and energy intensity.[9] To control for cross-sectoral heterogeneity in this paper, we compute correlation measures within sectors (see Figure 1). We find that energy intensity and total energy use of plants are positively correlated also within sectors. The correlation is particularly strong in sectors that are highly energy intensive, like the paper and pulp, glass and ceramics, mineral

[6] AFiD: "Amtliche Firmendaten für Deutschland", English: Official Firm Data for Germany.
[7] In the process of data cleansing we drop plants with an annual turnover below 10 000 EUR and those that reported an electricity consumption of zero. In 2006, 3 586 out of 47 666 plants were dropped.
[8] Presentation of results is limited by the legal requirement to preserve the confidentiality of data on individual plants. For this reason, all research output has to be approved by staff at the research data centre before publication.
[9] Aiming to get results that are robust towards large differences between different plants of different sectors is one reason why we use Spearman's rank correlation coefficient instead of Pearson's correlation coefficient.

processing (incl. cement) or iron and steel sectors. Since energy use and carbon emissions (and also energy intensity and carbon intensity) are highly correlated, we also find a positive correlation between carbon emissions and energy intensity, as well as between carbon intensity and energy use (Table 1).

Table 1. Spearman's rank correlation coefficients for selected variables at the plant level (2006 data).

	Energy use (kWh)	Energy intensity (kWh/1 000 EUR)	CO_2 emissions (t)	Carbon intensity (g/1 000 EUR)	Emission factor (g CO_2/kWh)	Share of electricity in total energy use (%)
Energy intensity (kWh/1 000 EUR)	0.60					
CO_2 emissions (t)	> 0.9	0.58				
Carbon intensity (g/1 000 EUR)	0.59	> 0.9	0.61			
Emission factor (g CO_2/kWh)	-0.15	-0.20	-0.02	-0.01		
Share of electricity in total energy use (%)	-0.14	-0.21	(-0.01)	-0.03	> 0.9	
Gross Output (1 000 EUR)	0.68	-0.09	0.69	-0.08	(-0.01)	-0.01

Own calculations. In cases of ">0.9" the exact value is not available to ensure confidentiality of the data. Coefficients in brackets are not significant at the 1 % level.

While increasing returns to energy should allow larger plants to use energy more efficiently, this is obviously not the case in the data, either because there are no increasing returns to energy or because increasing returns to energy are outweighed by a counteracting fuel mix effect, as described in section 1. To shed more light on this issue, we study the correlation between energy intensity and gross output. Aggregated across all sectors, we find a statistically significant but very weak positive correlation. This picture becomes more diverse as we look at the correlation in specific sectors (Figure 1). In energy intensive sectors, namely in the paper and pulp, glass and ceramics, mineral processing as well as iron and steel sectors, correlation between energy intensity and gross output is positive, indicating decreasing returns to energy. Notable exceptions among the energy intensive sectors are the mining, quarrying, chemicals as well as the non-ferrous metals and foundries sectors. In most other sectors energy intensity and gross output are negatively correlated, indicating increasing returns to energy. Nevertheless, since the correlation coefficient does not usually exceed 0.25 in absolute value and the correlation between energy intensity and gross output is only a rough indicator, the impact of increasing or decreasing returns to energy seems to be limited.

Apart from increasing and decreasing returns to energy, we earlier identified an energy mix effect as another potential driver linking energy use and energy intensity. As the negative correlation between the share of electricity in the energy mix and total energy use of a plant illustrates, excessive energy users tend to use relatively little electricity but rely more on other fuels (Table 1 and Figure 1). Natural gas is especially important as an alternative; in certain

cases also coal (e.g. in the iron and steel sector, the mineral products sectors or the mining and quarrying sectors) or renewables like biomass (the pulp and paper sectors are one example; cf. Petrick et al. [3]). Since electricity is already a highly processed fuel, it can be employed very efficiently – energy intensity and the electricity share in a plant's fuel mix are negatively correlated, both at an aggregated and mostly also at the sectoral level (Figure 1). Note that the correlation coefficients for electricity share and energy intensity as well as for the electricity share and total energy use are much larger than the correlation coefficient for energy intensity and gross output, in most sectors and at the aggregate level. From this we infer that the strong positive correlation between energy use and energy intensity found at the sectoral and aggregate level is mainly driven by the energy mix effect: with rising overall energy use the share of electricity in a plant's fuel mix decreases. Since electricity can be used rather efficiently, overall energy intensity is expected to rise accordingly.

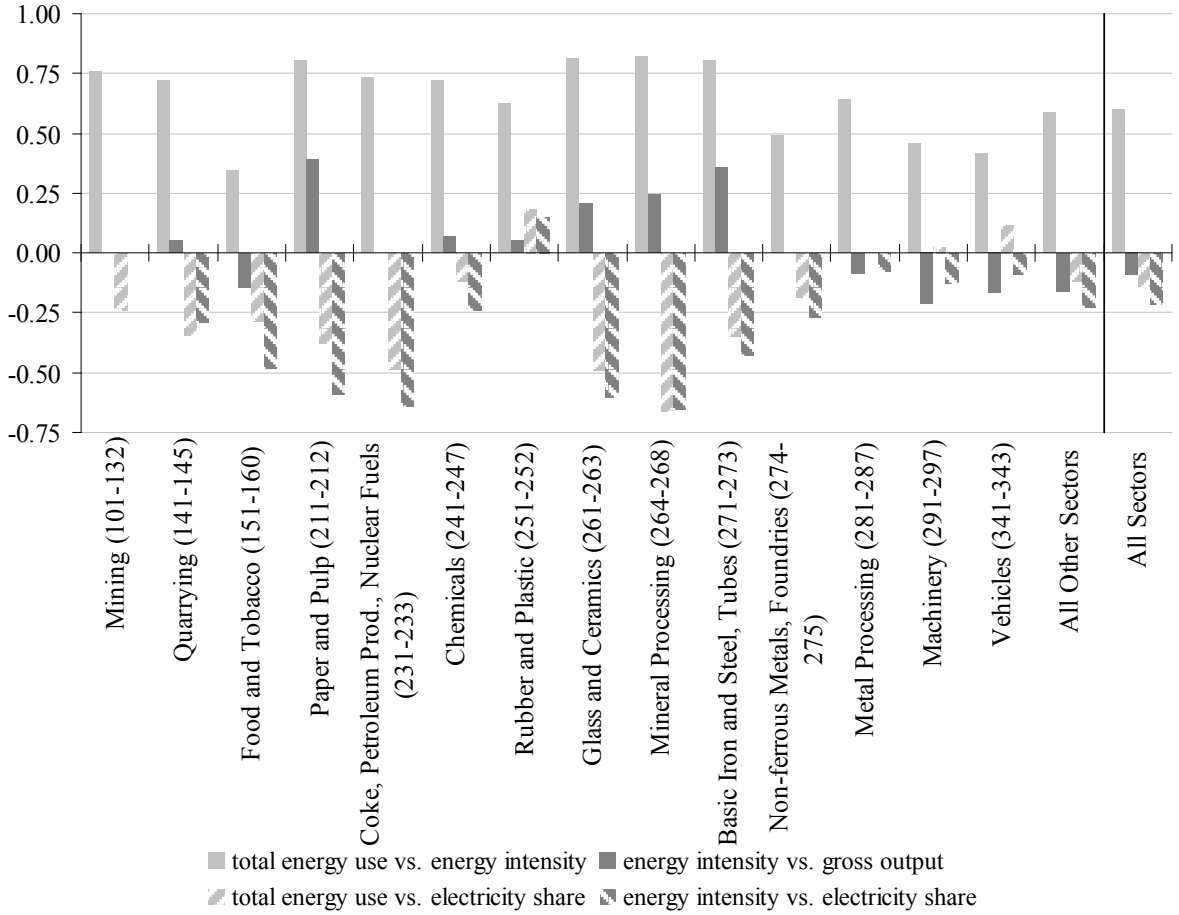

Figure 1. Spearman's rank correlation coefficients between selected variables within sectors (2006). Only coefficients that are significant at the 1 %-level are shown. The three-digit sector identifiers refer to the corresponding ISIC codes.

Apart from the link between total energy use and energy intensity, we also analyze the mechanisms linking energy use – and thus energy intensity – and the emission factor. The emission factor (or carbon factor) is the ratio of emitted CO_2 from fuel combustion per unit of energy (in g CO_2/kWh). We find a statistically significant negative correlation between emission factor and energy use as well as energy intensity (Table 1). The link between energy intensity and emission factor stands out in particular. Contrary to intuition, more energy efficient plants actually use a dirtier fuel mix in the sense of a higher carbon factor. This result

not only holds for all sectors in general, but also for most individual sectors, especially for the energy intensive ones, with the exception of the rubber and plastics sector (Figure 2).

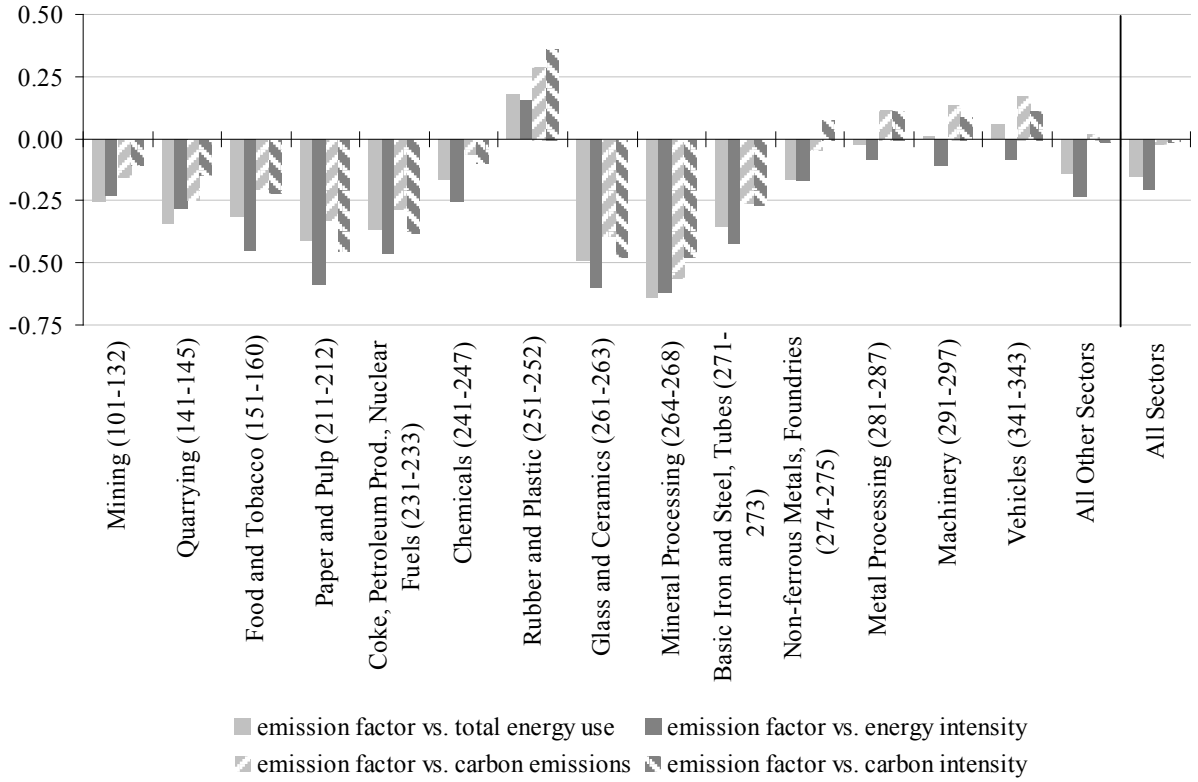

Figure 2: Spearman's rank correlation coefficients between emission factor and selected variables within sectors (2006). Only coefficients that are significant at the 1 %-level are shown. The three-digit sector identifiers refer to the corresponding ISIC codes.

To understand this paradox, it is vital to understand the role of electricity. As mentioned before, electricity can be used very efficiently, but at the same time its emission factor is high due to conversion losses in the energy conversion sector. In fact, the 2006 carbon factor for electricity was 2.9 times the carbon factor of natural gas and still 1.7 times the carbon factor of hard coal.[10] Consequently, a production technology that uses a lot of electricity may be very energy efficient, but since the carbon factor of electricity is very high, the carbon efficiency advantage of that technology may be smaller than the energy efficiency advantage relative to a technology less intensive in electricity. These two opposing effects also account for a low correlation between the emission factor and carbon intensity for some sectors and for the aggregate of all sectors (Figure 2). Some particularly energy intensive sectors, like the glass and ceramics sector, the mineral processing sector or the paper and pulp sector, are exceptional here. In these cases energy intensity and emission factor are especially highly correlated, implying that the energy efficiency advantage of using electricity is particularly large (cf. also the correlation between energy intensity and electricity share for these sectors from Figure 1). In fact, it is large enough to outweigh the carbon factor disadvantage, leading to the paradoxical situation of a high emission factor together with low carbon intensity.

[10] The carbon factor of electricity in 2006 was 585 g per kWh. It is calculated for the average German electricity mix as the ratio of all direct CO_2 emissions from fossil fuel combustion divided by the available electricity supply. Thus, different emission factors for the primary fuels used by the power plants are accounted for, but indirect emissions through production and transport of the primary fuels are not accounted for (own calculations on the basis of AGEB [7] and Umweltbundesamt [8]).

The same argument explains why larger energy consumers have lower emission factors, both across and within sectors. Since plants that use more energy tend to rely less on electricity, they do not have to shoulder the burden of conversion losses in their specific emission factor. At the same time, their energy intensity tends to be higher. The two effects partly offset each other and the effect of the emissions factor on total CO_2 emissions is small, although still negative, with the same aforementioned exceptions (Figure 2).

4. Discussion and Conclusions

In this paper we use new microdata on 44 000 industrial plants to analyze the use of energy in industrial production in Germany. Our dataset allows for the analysis of plant-level energy use and emission patterns with extraordinary detail, accuracy and representativeness. Since the dataset also includes information on the plants' monetary gross output, we are able to draw conclusions not only about the level, but also about the productivity of industrial energy use in Europe's largest economy.

We find that energy use and energy intensity are positively correlated, both at the aggregate level and within specific sectors, i.e. larger energy users tend to use energy less efficiently. This correlation is especially high for sectors with high energy intensity. We identify an energy mix effect as the main driver of this interrelation, since larger energy consumers tend to use less electricity in relation to other fuels, and electricity can be deployed more efficiently. Increasing and decreasing returns to energy are of less importance and not uniform across sectors. By means of the correlation between energy intensity and gross output, we identify increasing returns to energy in most sectors, but decreasing returns to energy in some of the particularly energy intensive sectors. The energy mix effect is also one reason for a negative correlation between energy intensity and the emission factor, since energy efficient plants tend to use more electricity, which has a comparably high emission factor. The efficiency advantage of electricity is outweighed by a carbon factor disadvantage, at least for industry as a whole.[11]

Our paper sheds light on the crucial role of electricity. Despite the fact that electricity is often seen as a climate friendly alternative in industrial production in the public discussion, we find that the carbon burden from conversion inefficiency in the power producing sector usually leads to higher emissions in end use. Nonetheless, it would be hasty to discard the emission saving potential of electricity in industrial final energy use in future policies because the emission factor of electricity is decreasing over time (Figure 3). In 1995, the emission factor of electricity was 694 g CO_2/kWh, i.e. 110 g more than in 2006. Once the share of low-carbon fuels and renewables in electricity generation is sufficiently high, their emission-reducing effect might outweigh the detrimental effect of conversion losses. Technological progress is also working in favor of electricity, enhancing not only end use efficiency but also conversion efficiency in the power sector. This adds to the many other arguments for using electricity in the industrial sector, such as the high flexibility of use, resilience towards supply insecurities because of substitutability of primary fuels and ease of handling.

On balance, this paper has shown that the plant-level energy mix, energy intensity and level of energy use are not independent of each other. Hence, it is important to take into account the energy mix when designing policy measures targeted at reducing energy intensity.

[11] A note of caution is advised with regard to the methodology. We focus on absolute correlations that should not be interpreted as causal relationships. Analysis of partial correlations, e.g. via regression analysis, is left as a task for future research.

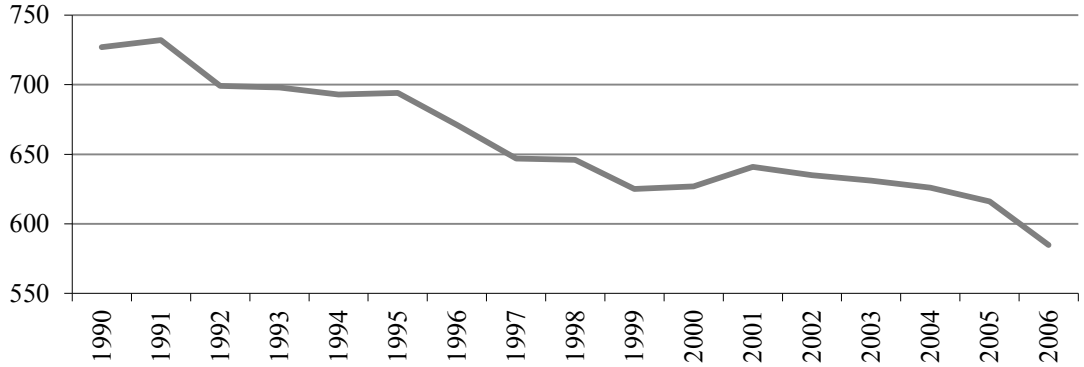

Figure 3: Development of average emission factor of electricity in the German public grid (in g CO_2/ kWh). Source: 1995-2005:Umweltbundesamt [9], 2006: own calculations based on the same source.

Acknowledgements

We would like to thank Alexander Vogel of the research data centre in Kiel for running the estimation code and performing the confidentiality checks. The staff of the research data center of the Statistical Offices of the Länder made the data provision possible. Ulrich Wagner gratefully acknowledges financial support from the Spanish Ministry for Science and Innovation under grant SEJ2007-62908.

References

[1] IEA (International Energy Agency), World Energy Balances, 2008.

[2] IEA (International Energy Agency), CO_2 emissions from fuel combustion, 2009.

[3] S. Petrick, K. Rehdanz and U. J. Wagner, Energy Use Patterns in German Industry: Evidence from Plant-level Data, Journal of Economics and Statistics, forthcoming.

[4] K. Gillingham, R. G. Newell and K. Palmer, Energy Efficiency Economics and Policy, Annual Review of Resource Economics 1, 2009, pp. 597-619.

[5] FDZ (Forschungsdatenzentrum der Statistischen Ämter der Länder), AFiD-Panel Industriebetriebe der Jahre 2003-2006, own calculations.

[6] FDZ (Forschungsdatenzentrum der Statistischen Ämter der Länder), AFiD-Modul Energieverwendung der Jahre 2003-2006, own calculations.

[7] AGEB (Arbeitsgemeinschaft Energiebilanzen), Energy Balances for the Federal Republic of Germany, 2009, http://www.ag-energiebilanzen.de/viewpage.php?idpage=63, accessed September 4, 2010.

[8] Umweltbundesamt, Tables with the derived CO2 Emission Factors for the German Athmospheric Emission Reporting 1990-2008 (Version: EU-Submission 15.01.2010).

[9] Umweltbundesamt, Entwicklung der spezifischen Kohlendioxid-Emissionen des deutschen Strommix, 2007.

Robin Hood and Donkey Principles: renewable energy proposals for Ghana

Emmanuel Ndzibah[1]

[1] *Industrial Management Unit,University of Vaasa,Finland*
P.O. Box 700, 65101. Vaasa – Finland.
Tel: +358 44 5321752, E-mail: endzi@uwasa.fi

Abstract: This study proposes a reliable way of distribution and transfer of electricity cost to both the urban and rural consumers in Ghana. While the Robin Hood principles borrows the essence of the strategy used in this model by a British folklore character by the same name, in providing resources for the deprived and in this context an equitable demand and supply of electricity. The Donkey principle highlights the strategic billing policy used in Ghana, which suggests that urban communities should carry some of the cost burden of energy used by rural communities. The study aims at promoting strategies and educating the public on realistic solutions to the energy crisis. In Ghana, people in the rural communities lacks credit to afford almost any form of renewable energy system due to irregular source of income, although the bulk of consumables (agro based) are produced by them. Infrastructure in some rural communities is inadequate. In contrast, majority of the urban dwellers have access to credit and spend a reasonable amount of their earnings on electricity primarily focused on business and leisure. The study also addresses cost, motive, frequency and reasons for acquiring and using a secondary source of energy (SSE). The results of the study suggest a more just and equal system of distribution and billing of electricity cost.

Keywords: *Robin Hood, Donkey, Secondary Source of Energy (SSE), Distribution, Ghana*

1. Introduction

Rapid increase in population and increased material consumption always has its toll on the general resources of any given economy. Energy seen as the bedrock of every society is vital for a growing economy to flourish. In Ghana, many rural sectors do not have access to electricity[1, 4, and 8]. The government often spread out the hope of embarking on an extensive electrification project. However, lack of capacity, quality planning and sound framework always turns up to become the "Achilles´ heel" in economic development and environmental sustainability. For those rural areas that are accessible to the national electricity grid, lack of technical and economic capacity undermines the efficiency and reliability of systems; these are plagued with unauthorized excessive power failures making it impossible for the citizens in these communities to be able to utilize the full potential of the energy to increase productivity.

Over the years, there have been advocacy for a solar home solution (SHS) for the rural communities of developing countries. As thoughtful as some of these arguments and proposed models might sound, they most often than not miss the point in their generalization of systematically unproven panacea for the entire energy situation in all rural communities in developing countries. These experts end up re-grouping at the *theory-formulation* table to either revise their theories or come up with newer perceived solutions convinced that it would work the next time round.

For instance, Srinivasan[7] proposed pre-payment system as a way to curb SHS acquisition defaults as well as enhance the degree of acquisition in the rural communities. As laudable as the proposal is, it seems to ignore or did not anticipate some factors that have direct or indirect influence in such systems. To date, many energy service providers in developing countries have battled the complex nature of the process of prepayment and its collection system, thus meriting a careful scrutiny. It is noteworthy to examine some of the impacting

factors, which include but not limited to a country´s infrastructure (*accessibility to internet and related mobile service that are essential support systems for pre-payment mode as well as reliable banking and financial institutions willing to provide credit for the needy*), economic and social configuration, per-capita income with special emphasis on individual/household income, the reliability of such income and its purchasing power as well as levels and classifications of such income and its determinants in developing countries. Moreover, administrative logistics and its bottlenecks which includes cost of personnel to inaccessible rural communities' makes pre-payment difficult and inaccessible for many people.

2. Definitions and Limitations

The social background of the principle: In most developing countries, the urban communities enjoy a relatively large percentage of the national cake in the forms of basic amenities and infrastructures like roads, access to good drinking water, affordable housing, and a reasonable access to modern health care unlike their rural counterparts. The situation compounds with an ongoing problem in that most of the rural communities have to contend and be content with an under-developed agro-based industry. This agro-based industry lacks proper incentives to help them add value to their produce. Inadequate infrastructure in the context of storage facilities as well as good transport network exposes these rural dwellers to opportunist intermediaries who offer to take their produce at less than the realistic market price. Consequently, rural economic development often stalls since they lack enough compensation for their hard work resulting in their inability to save some of their earnings – thus the typical cyclical nature of poverty.

The Robin Hood principle: This principle denotes taking from the rich and giving to the poor thus becoming a proposed model recommended by this study to help policy makers to resolve energy distribution for both urban and rural sectors of the Ghanaian economy[2, 3]. The concept of 'taking' in the principle denotes 1) weaning the urban dwellers off the main grid to help allocate the excess capacity to the rural areas. The urban dwellers are then encouraged to 2) adapt to renewable energy systems. Since there are few industrial activities in the rural areas and the need of the energy are simple, the benefits of this proposal become sound because the rural communities get the needed opportunity to develop the agro-base sector, creating jobs and mitigating the rural – urban migration influx. The Robin Hood principle also presumably suggests that most urban dwellers are in better position to afford renewable energy arguably due to access to credits and loans from financial institutions[6].

The Donkey principle: Donkeys have the potential of easily carrying 20 to 30 percent of their own body weight and thus suitable as beast of burden; other use of donkeys includes farming and transportation. Donkeys have the tendency to resist any form of force or intimidation if for whatever reason they consider submitting to such demand to be dangerous to them[9]. The Donkey principle is an allegory used in promoting the practicality and transparency required to ensure a fair billing system of electricity usage. The Donkey principle is coined from a billing policy in Ghana, where a government directive through levies makes it possible for corporate firms and urban communities to carry some of the cost burden of the electricity used by the poor rural communities. The same policy suggests that the extra cost paid by the urban citizens covers rural electrification projects as well as setting up streetlights at strategic locations across the country. Since the core idea is to promote social fairness, the noble assumption will be for the administrative aspects including methods for collecting, managing, monitoring and executing that the required projects are made public. On the contrary, everything concerning rural electrification and other related projects are usually activities initiated under cloak and dagger. Giving power to the people in essence should include some

measure of openness and this usually aims at building trust. The people paying these monies often feels cheated since there is no formal accountability from the authorities that are supposed to be in charge of providing this vital service for the nation. Thus, the donkey theorem recommend a clear-cut system, where an institution is set up to monitor and report all the monies accumulated from this strategic billing as well as give a clear framework and timeline as to how the monies are disbursed for the projects that they are collected for.

Social responsibility: The adoption of a photovoltaic system often reduces pollution. Thus photovoltaic system promises clean sources of energy especially the reduction of carbon emission. The conventional energy systems on the other hand, use other types of fuel (*gas, diesel, petroleum products and wood*) in generating energy, thus depleting the natural resources and causing environmental harm. For these reasons, adapting green energy sources promotes social responsibility.

For this study, the term ***energy*** refers to both conventional and renewable systems for generating or providing electricity.

Secondary source of energy from this point cited as SSE; is the sum total of all sources of energy and light generating systems readily available to end user both in the urban and rural communities. The list includes but not limited to candles, kerosene lamps, torch and flash lights, generators.

Distribution of photovoltaic energy identifies all the efforts made to deploy the technology to the end user. The processes involved in the distribution details down to where and how to make the photovoltaic technology available to the end user. These include profiling of end users energy needs, packaging, transportation and installation among others.[6]

Ghana is a West African country with a population of about 24 million with an approximately 1.9 percent population growth rate. Ghana´s electricity production and consumption and exports as at the year 2007 were 6.7 billion kWh (kilowatt hours), 5.7 billion kWh and 2.49 billion kWh respectively. Since the demand of energy outweighs it supply, availability and accessibility to alternative sources of energy would be preferred by the over 9.2 million citizens in Ghana without electricity[6].

This research does not take into consideration issues like the per-capita income of the rural-urban population. Nevertheless, it mentions the minimum income of the people in Ghana and figures out the percent of such income that goes to energy consumption. Furthermore, there were practically no individual volunteers ready to divulge their actual income as well as the percentage they spend on SSE. In addition, there proved to be virtually no relevant secondary sources of reference in relation to this parameter. Information gathered and used to develop the principles, is primarily based on covert questions asked under friendly atmosphere and mainly through acquaintance, which involves among others some speculative responds and pure approximations. Furthermore, omitted in this research, justifiably for future study, is the mechanism to map up a profitability ratio of how much savings is actually attainable from the use of renewable energy systems.

The study does not include any discussion on the potential of a feed in tariff system, since Ghana, as a developing country, has not yet implemented a full-scale de-regulated energy system. Feed in tariff would have required an economic system to have a pure privatization of its energy industry as well as market-regulated prices of energy. This study is designed to

serve as part of a series of proposals (1. *diffusion of photovoltaic technology for developing countries and 2. financing alternatives for renewable energy systems for renewable energy systems*) intended to act as a ´wakeup call´ and support for the energy regulatory bodies in Ghana (Ministry for Energy, Ghana Energy Commission, etc).

This paper attempts to answer the following questions:

How can the Robin Hood (RH) theorem be applied to disseminate energy to rural and urban communities and what benefits can be derived from it?

How can policy makers adopt and adapt the Donkey theorem; in helping reduce cost burden of especially low-income earners in the rural communities?

The primary objective of this study is to develop and justify a proposal on an efficient energy distribution protocol as well as flexible billing system, with the aim of helping especially the energy administrators of Ghana to re-structure the current energy policies and justify the proposed principles. Although the principles proposed would have their own specific set of limitations, the findings of this study could serve as a preliminary framework for further studies in addition to its potential for future replication in other developing economies faced with similar energy crisis.

3. Methodology

To help promote and justify the adoption of the Robin Hood and Donkey principles, this paper discusses types of SSE available and in use. Knowledge about the cost, purpose, frequency and reasons for purchasing and using a particular SSE by both rural and urban communities would help address a realistic payment plan for renewable energy systems such as photovoltaic or SHS. It is noteworthy that, the idea of availability, affordability and reliability of the renewable energy systems was part of the focus group discussion that helped generate simple questions for the interview[6]. For each of the SSE under consideration, a random sample size of 5 - 10 retail outlets at different towns in different regions (*Accra municipalities and Tema all in the Greater Accra region, Cape Coast, Apam, Winneba all in the Central region, Takoradi in the Western region and Kumasi in the Ashanti region*) responded favorably to the interview. The questions used to derive at the objective were simple and given in the local language - Akan, similar questions were used for the different form of secondary energy source. The questions were as follows:

1. What type of SSE do you prefer and why?
2. What triggers the purchase of a SSE?
3. How often is the purchase of an SSE made?
4. What are the main uses of any specific SSE?

4. Results

Table 1 below, represents a summary result of the study. When the question on an individual or household preference of a SSE was asked, the answers varied greatly. Two main reasons were identified - *the household income* and *the purpose for which the secondary energy is needed*. In Ghana, the current minimum income effective February 2010 is 3.11 Ghana cedis, a 17 percent increment from the previous level of 2.65 Ghana cedis[5]. The assumption is that, a household had to carefully consider their net income and consider as to how much of such income could be set aside for such emergencies related to power outages very prominent in the life of a Ghanaian. Although the purpose was clear and easy to understand, the issue of

household income proved to be very difficult to ascertain. This is due to the fact that, most Ghanaians are reluctant to reveal how much they actually earn for two main reasons: reluctance to expose themselves to rigorous scrutiny if found to be hiding some other source of household income as well as fear of being over taxed. Furthermore, Ghana´s gross domestic product (GDP) as at January, 2011 is estimated at $ 38.24 billion with an average per capita income of $ 1,600. It is important to mention that, GDP is not the only viable index to adeptly measure the collective household's decision on energy consumption[6,10]. The household income of the urban dwellers in Ghana varied heavily based on academic qualification and the nature of work under consideration. Meanwhile, an extrapolation of the lowest to the highest income levels based on the minimum wage is considered. The monthly income level within the urban dwellers ranged from as low as 50 euro to about 2,000 euro per month (approx. 100 - 4000 GHc). Upon this finding, one can easily assume the type of SSE affordable to the people. Based on this premise the conclusion is that, the higher the income the more expensive the type of SSE considered.

Nevertheless, the frequency of power outages per location would also easily affect the type of SSE adopted despite the price factor. A typical situation in the urban communities of Ghana is found in numerous high and low capacity generators and rechargeable lamps in contrast with those living in the poorer communities using candles, kerosene lamps, flash light, low priced rechargeable lamps as well as low capacity car batteries. Future field studies aims at unraveling aspects of the aforementioned points to help present a model for calculating the percentage of household income used on any specific secondary source of energy.

As to the reasons for the need of a SSE, the findings revealed yet two more underlining motives: *what triggered the purchase and why the particular purchase*. The finding concludes that *regular power outage, brownout and inaccessibility to grid* were the main triggers. Power outage affects both rural and urban dwellers that have access to the national grid. For this reason, lack of electricity supply appears to be the major cause for the need of a SSE. Moreover, there are situations whereby there is power, yet with insufficient voltage (brownout) to power basic devices like TV and refrigerators among others. For the aforementioned reasons, the need of a reliable SSE increases at such times. At the extreme end of the situation are sections of both the urban and rural dwellers that do not have power at all due to inaccessibility to the national grid. The situation leads such citizens without any other choice than a SSE, thus the need of these sources becomes a daily concern. There are so many people who are into petty trading especially at night selling almost anything from a home cooked meal to simple household items like toilet tissues.

Apparently, these household and petty traders' resort to the purchase of specific types of secondary energy source most suitable for varied needs. Popular among such purchase includes candles, portable flashlights and generator to take care of immediate household needs or to power such facilities used for petty trading, thus answering the underlining motive on why a particular secondary source of energy is purchased. The positive aspect of this is that the energy is sometimes acquired and used for productive activities that generates income other than merely using it for relaxation or recreational activities like watching television or listening to the radio. Nonetheless, these two underlining reasons are applicable to both urban and rural people.

A probe into the uses of a SSE also varies greatly based on the type of SSE available to the user. Candles are primary needed for lighting, batteries for powering radios and lamps, whereas car batteries are used to power TV sets and other smaller appliances. Generators are

on the other hand really used for various needs based on their capacities. Therefore, the issue of usage type and rate enormously triggers the purchase of any of these SSE.

The situation in the rural communities is relatively different compared to the urban dwellers. Within the rural communities, the main source of income comes from peasant farming generated from seasonal sales of crops. The study established that some rural citizens' livelihood is highly dependent on their farming activities with virtually no source of extra or other income to save. It therefore leads to yet a more positive conclusion that, their need of a SSE highly varies. The basis for the usage of both primary (conventional) and SSE is for powering lights, radios, TV sets and in some circumstances refrigerators. In view of the fact that most food stuffs come from the rural areas the implications was obvious: Most rural communities are instrumental in serving one of the basic necessities in life: sustenance. It is thus socially justifiable if some of their energy needs are met and supplementary financed by people in the urban communities. Nevertheless, the donkey principle tries to emphasize the need for transparency in all the activities for which such extra levies are collected, thus justifying the extra load they have to carry on behalf of the rural communities.

Table 1. Secondary sources of energy production in Ghana

Source of energy	Fuel	Capacity	Usage	Price Range (GHC*)	Consumer Category
Candle	Paraffin	Unknown	Light	.20 - .50	The product is available to both rural and urban communities.
Lamps/Torch/ Flash Lights	Kerosene and Dry cell batteries	1 – 9 Volts	Light	.50 - 3	The product is available to both rural and urban communities.
Car Battery		12 – 24 Volts	Light, Radio, Television	50 – 200 depending on brand and ampere	Higher percentage by some rural communities
Generator	Petrol / Diesel	2-7.5 Kva[1]	General household appliances including fridge and other portable equipments	590	Urban households and small and medium sized enterprise (SMEs)

*c. 1 dollar = 1.5 GHC as at 1st March 2010, *GHC – Ghana Cedis, [1]Kva – kilovolt-ampere*

5. Conclusions

Considering these parameters and the configuration of energy usage give a glimpse into reasons why political decisions and state-based activities are needed for a reasonable distribution and billing of energy systems in the country. It is noteworthy to mention that people often adopt and adapt different forms of energy systems due to desperation and the unreliability of the national grid. Although the purpose for using these SSE might not often be seen or directed to productive activities, it was observed that the bottom line of the quest for acquiring such systems is for the end user to have their peace of mind.

Interestingly, the research discovered a different sense of sharing. During an earlier focus group discussion leading to this supplementary research, one of the participants explained an interesting scenario involving how generators are used in the country; this was confirmed by others present. Apparently, households who own generators developed their own distributed energy solution, in that they share excess capacity of their system with their neighbor for a small fee. Although the original objective was to avoid being a nuisance to one's neighbor due to the noise made by generators, the individual/household have found a mutual way to share both the pain and gain from this specific energy system.

Evidently, the study helps in identifying certain shortcomings of the SSE discussed and it was applicable to both the urban and rural dwellers. The disadvantages were as follows:

1. Variable cost factors (*regularity of refueling and recharging car batteries etc*)
2. Environmental pollution and unfriendliness (*noise from generators, burning of fuels, disposal of batteries etc*)
3. The unreliability of supply

From the aforementioned points, it is apparent that following the Robin Hood principle in electricity distribution has the inherent possibility in bringing an end or reducing immensely the purchase of SSE like candles, generators, batteries etc. This is possible since the diverted energy weaned from the urban to the rural communities will help improve the agro-base industry by helping them to add value to its production and distribution cycle. Furthermore, these SSE that is erratic at best, with seemingly shorter life span cannot be compared to a lasting solution (photovoltaic or any renewable energy systems) which in itself could promote tremendous amount of savings on energy over a realistic period. Since patronizing tendencies are rampant in developing countries whose government, NGO, and other advocates tend to propose, build and launch laudable but limited energy programs to the few only to repeat the phenomenon at their political whims, makes consideration to the Robin Hood theorem a paramount issue. It is obvious that giving power to the people promotes individual and social responsibility as well as fosters a conscious effort to building a viable platform for economic development and growth.

Furthermore, the Donkey principle suggests that urban dwellers should carry some of the burden of energy costs of the rural communities. Moreover, policy makers should promote transparency and to implement policies that uphold trust among the people. Since taxpayers' money is involved, accountability goes a long way to foster mutual understanding of the direction and developmental objective of the authorities. The principle also suggests an educational platform where all parties involved (policy makers, service providers, households and individuals) gain access to relevant information by any medium available to not only be aware but also be concern about the needs of the people and how to serve them better.

References

[1] G. C. Abavana, Ghana: Energy and Poverty Reduction Strategy, Facilitation Workshop and Policy Dialogue, Ouagadougou, Burkina Faso, 26-29 October 2004.

[2] D. Blamires, Robin Hood: A Hero for All Times, J. Rylands Univ. Lib. of Manchester,1998, ISBN 0-86373-136-8.

[3] S.T. Knight, Robin Hood: A Complete Study of the English Outlaw, Blackwell Publishers, *1994*, ISBN 0-631-19486-X.

[4] P.S. Leite, A. Pellechio, L. Zanforlin, G. Begashaw, S. Fabrizio, and J. Harnack, Ghana: Economic Development in a Democratic Environment, 2000, IMF, Washington D.C.

[5] GNA, New National Daily Minimum wage is 3.11 Cedis, 2010, [online] available at:http://www.ghanaweb.com/GhanaHomePage/NewsArchive/artikel.php?ID=175749

[6] E. Ndzibah, Diffusion of solar technology in developing countries – focus group study in Ghana. Management of Environmental Quality: An International Journal, Vol 21:6, 2010, pp. 773 – 784.

[7] S. Srinivasan, Solar Home Systems: Offering Credit and Ensuring Recovery, Refocus, Jan-Feb, 2005 Vol. 6, No. 1, pp. 38 - 41.

[8] H. White, The welfare impact of rural electrification: a reassessment of the costs and benefits, 2008, An IEG impact evaluation - The World Bank, Washington D.C.

[9] Wikipedia, Donkey, [online] available at: http://en.wikipedia.org/wiki/Donkey.

[10] CIA-The World Fact Book, Ghana, [online] available at: https://www.cia.gov/library/publications/the-world-factbook/geos/gh.html

Energy efficiency optimization algorithm for roadway illumination using ARM7TDMI architecture

Rafael B. de Oliveira[1,*], Fausto B. Líbano[1,**]

[1] *Faculdade de Tecnologia Senai Porto Alegre, LEEQEE (Energy Efficiency and Quality Energy Laboratory), Porto Alegre, Brazil*
** Rafael Oliveira. Tel: +55 51 98898610, E-mail: rafael.oliveira@senairs.org.br*
*** Fausto Bastos Libano. Tel: +55 51 91867363, E-mail: fausto.libano@senairs.org.br*

Abstract: This paper presents an algorithm developed in C language that aims to help roadway illumination designers to create an illumination system that meets the standard's limits with minimum electrical energy consuming. As a secondary function, the program allows the user to get approximate luminance and illuminance values for a specific system without field measuring. The algorithm was created to fit into a hardware prototype based in ARM7TDMI architecture, with no need for complicated and heavy software running in PC machines. The main system variables regarded by the optimization function are pole height (H) and pole spacing (S), putting the luminaries as far from each other as possible, in order to use the minimum power per km. Through calculation of the system's luminance, the algorithm starts with S and H in their maximum values, decreasing every loop, subtracting the results from the standard limit (NBR5101-Brazil, CIE 118, EN 13201 or other standard loaded into the program) seeking for zero. Once the zero is found, the H and S values are put on a LCD or USB port, as algorithm results.

Keywords: *Roadway illumination algorithm, ARM application, Illumination energy efficiency*

Nomenclature

L	*roadway average luminance*..... cd/m^2	β	*Horizontal observer angle*..... °
E	*roadway average illuminance*..... *lux*	P_a	*active power* ..... *W*
H	*pole height* ..... *m*	W	*roadway wideness* .....*m*
S	*pole spacing*..... *m*	U_o	*overall uniformity*.....
I	*luminous intensity*..... *cd*	n	*lanes number* .....
Ir	*relative luminous intensity*.....*cd/klm*	P_r	*distance relative power* .....*kW/km*
φ	*luminary luminous flux*..... *lm*		
ψ	*Luminary azimuth angle*..... °		
θ	*Vertical luminary angle*..... °		

1. Introduction

One of the main problems in developing countries regarding electrical energy waste is the roadway illumination design, as the majority is over or under dimensioned, using old technology luminaries and with pole height and spacing in such values that the standard's limits are rarely achieve, which increase car accidents and criminality rate and decreasing the system's efficiency [1,2].

In order to develop a new roadway illumination system or evaluate an existing one, simulation software (Dialux, Lumisoft, Calculux) are used to calculate the main parameters required by standards such as NBR 5101, CIE 115, CIE 180, EN 13201 and others, running in PC platforms.

Another way to evaluate an existing illumination system is by field measuring, which implies in marking the grid on the ground level and taking an illuminance or luminance measure for each grid point, demanding time and a roadway free of traffic [2-4].

Therefore, facing these problems, the hypotheses of a small, low cost, device which could run an algorithm to simulated the main parameters needed to evaluate a roadway illumination system (in case of an existing system) or calculate how far away the poles could be spaced in order to consume less power (in case of a new system), was tested. It is important for the algorithm to be autonomous, that is, no computer aid.

2. Methodology

The main result variable for the algorithm implemented is P_r which is directly connected with energy consuming, therefore, it has to be as low as possible and still allows lighting parameters to meet the chosen standard's limits. For that to happen, the space between poles (S) is loaded with 50m and decreased gradually until the required value is reached. The same is done to the luminary height (H), as presented in Fig. 1.

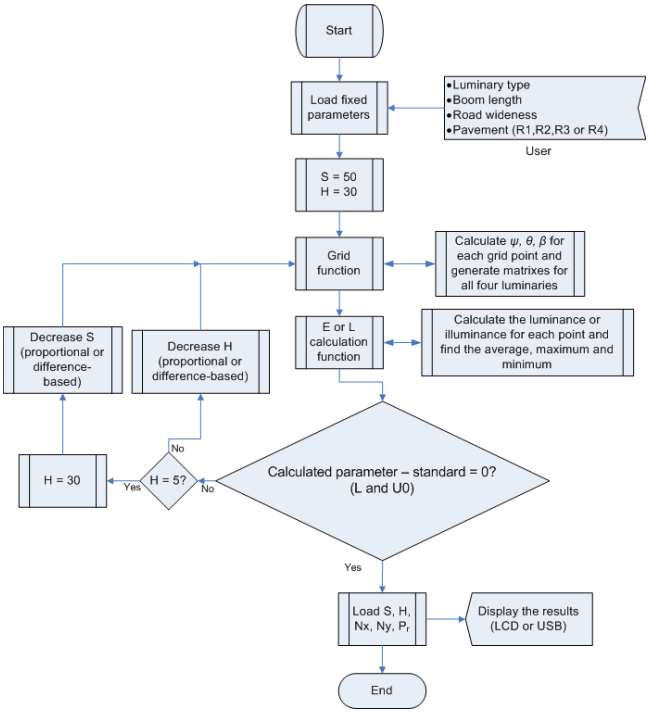

Fig.1 Block diagram of the optimization algorithm.

2.1. Hardware

The first thing to choose in the hardware design is the microcontroller where the algorithm will be running. The ARM7TDMI architecture, more precisely the Analog Device's microcontroller ADUC7026, was chosen by its processing capability of 32bits, low clock frequency (32.768kHz) with high internal speed (41MHz), the I/O pin quantity (ADCs, DACs, GPIOs) and the flash memory space of 62kB and the long multiplication and thumb mode support, allowing the process to run much faster than 16bits architecture or even standard ARM7 devices.

The hardware must have a display capable of reporting to the user of the algorithm variable results, such as: E, L, Emin, Emax, Lmin, Lmax, U_o, H, S, number of grid columns, number of grid rows and the active power consumed by kilometer (P_r).

2.2. Virtual grid creation

To calculate the system main parameters, a grid must be created on the roadway, between two luminaries with interference of, at least, one luminary after and one later, with rows spacing 1m maximum from each other and columns spacing 5m maximum [2,3], as shown in Fig. 2, where S_x is the space between grid points on a line parallel to the curb line and S_y is the space between grid points on a line orthogonal to the curb line. It was stated the symbol N_x for the total number of rows (x axis) and N_y for the total number of columns (y axis).

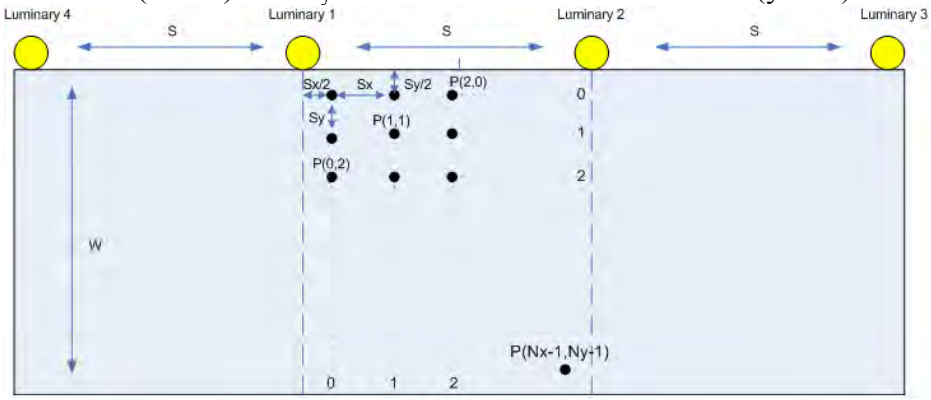

Fig.2 Creation of the calculation grid.

In order to keep the grid centralized on the space between two luminaries, the first point must be located at $S_x/2$ from the x axis and $S_y/2$ from the y axis. S_x and S_y are set by the user from the beginning and N_x and N_y are calculated dividing space between luminaries (S) by S_x and road wideness (W) by S_y.

After finding the rounded values of N_x and N_y, S_x and S_y have to be recalculated.

Each calculation point has two coordinates (x,y) that correspond with its place in relation to the grid. The real distance for each point in relation to the system's origin (Luminary 1) is calculated by Eq. °(1).

$$P(x,y) = P_0\left(\frac{S_X}{2} + x * S_X, \frac{S_Y}{2} + y * S_Y\right) \quad (1)$$

where P_0 is the coordinates of P in relation to the system's origin.

E.g. a point located at P(2,3) with a S of 35m and a W of 9m has an N_x equal to 8 and a N_y equal to 9 (using initial $S_x = 5$ and $S_y = 1$), therefore the real values of S_x and Sy are 4.375m (S/N_x) and 1m (W/N_y), respectively, and its coordinates in relation to origin, calculating from Eq. °1, are represented by P_0(10.938m,3.5m). These coordinates are used to calculate the system's main angles.

On this first part, the algorithm creates eight 10x10 matrixes based always on the same grid: one matrix for azimuth angle (ψ) and one matrix for inclination angle (θ) for each luminary in relation to every grid point. Later, the observer matrixes will be created as well, for the observer angle (β). All angles used to execute the main calculations (L and U_o) are presented in Fig. 3.

The γ is the angle between the roadway horizontal plane and the observer's eye, used to find the reduced luminance coefficient in the r-tables [2,4-6].

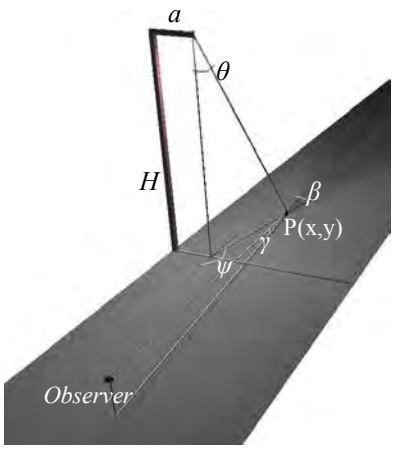

Fig.3 Main angles used to calculate E and L.

The angles represented in Fig. 3 can be calculated using straight trigonometry or algebra and are very important for the calculus, as the luminous intensity tables and r-tables are based on them. For study sake, both methods were used on this work, as the following description.

2.2.1. Azimuth angle (ψ)

The azimuth is the angle between the luminary plane and the calculation point on a horizontal plane (road plane) and is used together with the vertical luminary angle (θ) to find the luminous intensity module in the calculation point direction [2,6].

In this work, ψ was calculated based on the triangle formed by the luminary position and the calculation point position on the road plane, as presented in Fig. 4, where *a* is the boom length, X_0 is the real coordinate (in relation to the origin) of the calculation point on the X axis and Y_0 is the real coordinate of the calculation point on the Y axis.

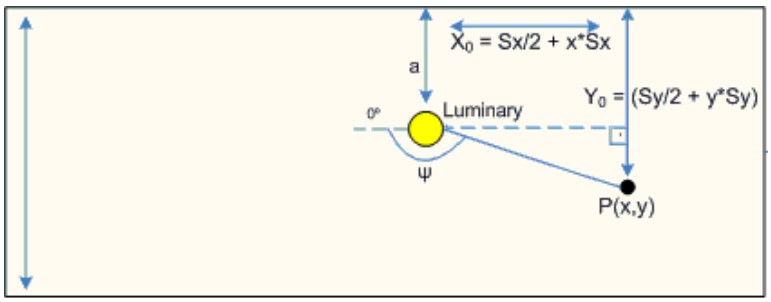

Fig.4 Triangle formed by the luminary position and the calculation point position.

The angle must be calculated in relation to each luminary (four luminaries, as previously stated) in two cases: for $Y_0 < a$ and for $Y_0 \geq a$.

For the first case, ψ can be calculated for the four luminaries using Eq. °(2-5).

$$\Psi_{L1} = 180 + \tan^{-1}\left(\frac{|Y_0 - a|}{X_0}\right) \quad (2)$$

$$\Psi_{L2} = 360 - \tan^{-1}\left(\frac{|Y_0 - a|}{S - X_0}\right) \quad (3)$$

$$\Psi_{L3} = 360 - \tan^{-1}\left(\frac{|Y_0 - a|}{(S - X_0) + S}\right) \quad (4)$$

$$\Psi_{L4} = 180 + \tan^{-1}\left(\frac{|Y_0 - a|}{X_0 + S}\right) \quad (5)$$

In the second case, ψ can be calculated for the four luminaries using Eq. °(6-9).

$$\Psi_{L1} = 180 - \tan^{-1}\left(\frac{|Y_0 - a|}{X_0}\right) \quad (6)$$

$$\Psi_{L2} = \tan^{-1}\left(\frac{|Y_0 - a|}{S - X_0}\right) \quad (7)$$

$$\Psi_{L3} = \tan^{-1}\left(\frac{|Y_0 - a|}{(S - X_0) + S}\right) \quad (8)$$

$$\Psi_{L4} = 180 - \tan^{-1}\left(\frac{|Y_0 - a|}{X_0 + S}\right) \quad (9)$$

The azimuth matrixes are generated using Eq. °(2-9) for each grid point.

2.2.2. Vertical luminary angle (θ)

The vertical luminary angle is the angle between the luminary and the calculation point on the vertical plane, as it is shown in Fig. 3, forming another rectangle whose base is the hypotenuse of the triangle presented in Fig. 4. The angle can be calculated using Eq. °(10).

$$\theta = \tan^{-1}\left(\frac{\sqrt{X_0^{\,2} + (Y_0 - a)^2}}{H}\right) \quad (10)$$

where H is the pole height.

2.2.3. Observer angle (β)

The observer has two angles, as it can be seen in Fig. 3: the angle in relation of the road plane (γ) and the angle in relation to the luminary-point vector (β).

The first is fixed in 1° to 1.5° interval [1-6] and the second is calculated using algebra, assuming two vectors $\vec{AP}$ *and* $\vec{LP}$, as presented in Fig. 5:

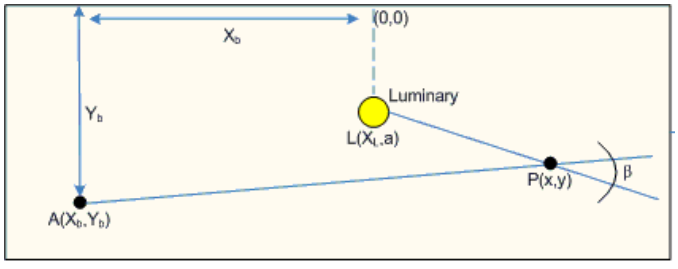

Fig.5 Angle β formed by vector $\vec{AP}$ *and* $\vec{LP}$.

Both vectors are defined by two points and the angle between them is β, which is calculated by the arccosine of the vectors scalar product over the multiplication of their modules [7], as represented in Eq. °(11).

$$\beta = \cos^{-1}\left(\frac{\vec{AP}\cdot\vec{LP}}{\left|\vec{AP}\right| * \left|\vec{LP}\right|}\right) \tag{11}$$

After this part, all angle matrixes are ready and stored in the microcontroller's memory and the parameters calculation can now start.

2.3. Illuminance calculation (E)

The illuminance is calculated using the traditional cosine equation published in several studies [2,6,8,9] represented by Eq. °(12).

$$E = \frac{I_r(\psi,\theta) * \frac{\varphi}{1000} * \cos^3\theta}{H^2} \tag{12}$$

where $I_r(\psi,\theta)$ is the relative luminous intensity taken from the luminary *I table* and φ is the luminary luminous flux.

2.4. Luminance calculation (L)

For the luminance calculation, the *r_tables* where used to find the approximate result. The equation used is represented in Eq. °(13) [2,6].

$$L = \frac{\frac{r(\beta,\theta)}{10000} * I_r(\psi,\theta) * \frac{\varphi}{1000}}{H^2} \tag{13}$$

where $r(\beta,\theta)$ is the reduced luminance coefficient taken from the *r_table*.

2.5. Optimization function

The calculation functions were designed to calculate E, L and U_o starting from six variables: *a*, W, luminary type, pavement type (R1, R2, R3 or R4), S and H. The first four variables are defined by the user, leaving only two variables to be calculated through optimization: H and S. With S been the most important as it is directly connected to energy consuming.

The optimization algorithm start placing the luminaries 50m (S) away from each other and 30m (H) high and begin to decrease S and H, calculating L (E was not used in the optimization function) and U_o every iteration, subtracting the result from the standard value (loaded into the memory) until it reaches zero, when the optimum values of S and H, together with other secondary results, are displayed on a LCD or sent through USB to a computer.

The optimization function was implemented in two ways: proportional and difference-based.

2.5.1. Proportional form

In the proportional form, both S and H are decremented in one unit each iteration making the process very simple but taking a long time to converge, as the decrement doesn't depend on the difference from the parameter being calculated (L and U_o).

Process is done using two loops: an outer loop for S decrementing and an inner loop for H decrementing. Then, for each meter taken from S, all H range is tested.

2.5.2. Difference-based form

This form was called this way for the variable decrease is based on the difference between the last parameter (k-1) calculated and the standard's limit, following Eq. °(14) and Eq. °(15). Therefore, the farther the parameter is from the standard, the bigger the decrease will be, resulting on a faster algorithm conversion.

$$H_k = H_{k-1} - [K_1 * (L_{k-1} - L_{st})] \quad (14)$$

$$S_k = S_{k-1} - [K_2 * (L_{k-1} - L_{st})] \quad (15)$$

3. Results

All algorithm results were compared with simulations on Dialux software which was taken as reliable CAD lighting software, used in several international projects.

The graphic of the algorithm conversion are presented in Fig. 6 and Fig. 7, using a = 1m, W = 8m, n = 2 lanes, SRC 612 Philips sodium-vapor luminary with P_a = 443W and road pavement R3.

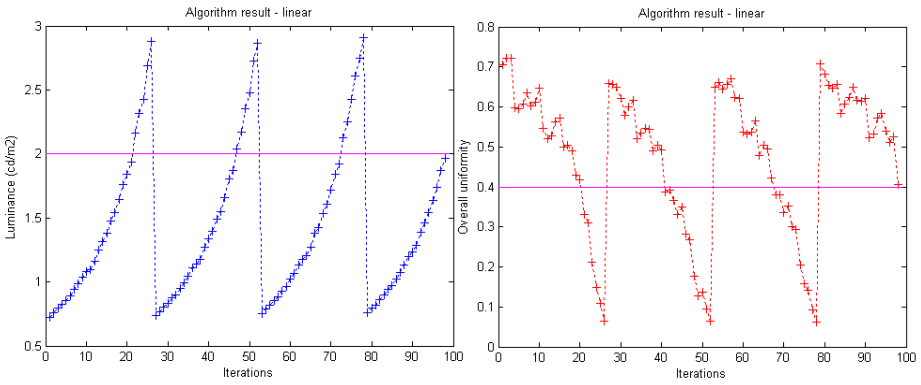

Fig.6 Algorithm graphic conversion for proportional optimization.

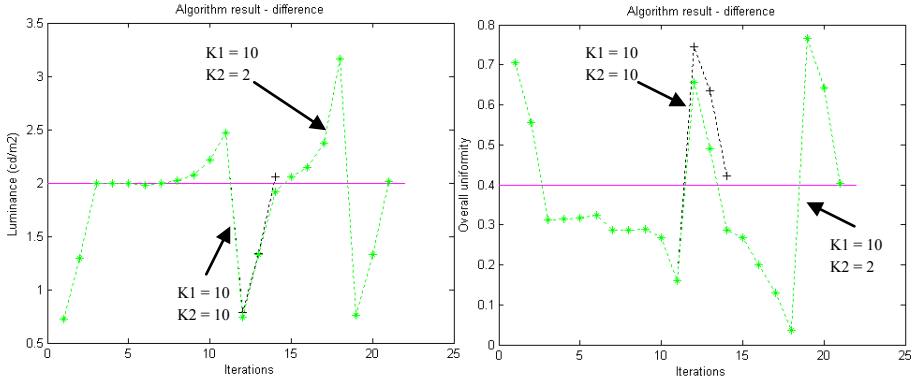

Fig.7 Algorithm graphic conversion for difference-based optimization.

On Fig. 6, the graph shows that the algorithm takes about 96 iterations to convert to the desired pattern, using proportional optimization and on Fig. 7 it takes about 22 iterations using difference-based optimization with K1 = 10 and K2 = 2 (green) and 12 iterations with K1 = 10 and K2 = 10 (black). The continuous lines indicate the EN 13201-1 standard recommendation (L = 2 cd/m^2 and U_o = 0.4) for ME1 class.

The final results, comparing with Dialux, are presented on Table 1.

Table 1. Final algorithm results.

Parameters	Proportional optimization	Difference-based optimization K1 = 2, K2 = 10	Difference-based optimization K1 = 10, K2 = 10	Dialux (validation)
L (cd/m^2)	1.969	2.009	2.058	2.0
U_o	0.406	0.404	0.422	0.4
S (m)	47	46.72	45.28	47
H (m)	11	10.9	11.25	11
P_r (W/km)	9.4k	9.5k	9.8k	9.4k

4. Conclusions

The final results confirmed that the optimization algorithm is able to calculate a distance between luminaries which meets the standard limit with minimum power consuming and a pole height to guarantee the uniformity, being sufficiently light to be run on a simple hardware (formed by the microcontroller ARM7TDMI ADUC7026, some keys to enter data and a LCD) with no need for an external memory or any other device, becoming an easy-to-use tool to new or existing roadway lighting designs, even though the algorithm secondary function, simulation, was not presented in this work due to space restrictions.

References

[1] CIE Pub. Nº 180, Road Transport Lighting for Developing Countries, 2007, pp. 2 – 31.

[2] IESNA, The IESNA Lighting Handbook Reference and Application, IES, 9th edition, 2000, pp. 757 – 790.

[3] ABNT, NBR 5101 Iluminação Pública, 1992, pp.5 – 9.

[4] W. J. Frith, M. J. Jacket, Road Lighting for Safety – a forward-looking, safe system-based review, Procedings of Australasian Road Safety Research, Policing and Education Conference, 2009, pp. 408-418.

[5] Ö. Güler, S. Onaygil, Evaluation of Visibility Level Formula in Road Lighting with Field Measurements, Istanbul Technical University, 2002.

[6] Luce e Illuminazione, EN 13201 – 3: Road Lighting Calculation for Performance, UNI, 2004, pp. 5-39.

[7] A. Steinbruch, P. Winterle, Algebra Linear, Pearson-Makron Books, 2nd edition, 2005, pp. 8-12.

[8] G. J. C. da Costa, Iluminação Econômica, EDIPUCRS, 1st edition, 1998, pp. 299-326.

[9] Luce e Illuminazione, EN 13201 – 2: Road Lighting Performance Requirements, UNI, 2004, pp. 7-14.

Experimental Evaluation of a Gas Engine Driven Heat Pump Incorporated with Heat Recovery Subsystems for Water Heating Applications

E. Elgendy [1,*], G. Boye[1], J. Schmidt[1], A. Khalil[2], M. Fatouh[3]

[1]*Institute of Fluid Dynamics and Thermodynamics, Faculty of Process and System Engineering, Otto-von-Guericke University, Universitätsplatz 2 D-39106 Magdeburg, Germany*
[2]Mechanical *Power* Engineering Department, Faculty of Engineering, *Cairo University, Giza 12316, Egypt*
[3]*Mechanical Power Engineering Department, Faculty of Engineering at El-Mattaria, Helwan University, Masaken El-Helmia P.O., Cairo 11718, Egypt*
** Corresponding author. Tel: +493916712558, Fax: +493916712762, E-mail: essam.elgendy@st.ovgu.de*

Abstract: Engine waste heat recovery represents one of the main advantages of a gas engine heat pump (GEHP) as compared to conventional heat pump system. Engine waste heat can be recovered to heat the supply water (at high ambient air temperature) or to evaporate the refrigerant in the refrigerant circuit (at low air ambient temperature). At the middle range of ambient air temperature (10:15°C), the two possibilities are valid but the GEHP performance is different. The present work is aimed at comparing the performance characteristics of the gas engine heat pump with waste heat recovery subsystems for supplying the hot water demands. In order to achieve this objective, a test facility was developed and then experiments were performed over a wide range of condenser water inlet temperature (34°C to 48°C) and at ambient temperature of 13°C. Performance of the gas engine heat pump was characterized by the supply water outlet temperature, heating capacity, gas engine energy consumption and primary energy ratio. The results showed that a water outlet temperature up to 70°C is obtained when the recovered engine heat is transferred to the supply water circuit. On the contrary, a higher condenser heating capacity (13%) and higher gas engine energy consumption (12.8%) are obtained when the recovered engine heat is transferred to the refrigerant circuit. Furthermore, primary energy ratio of the gas engine heat pump is increased by 17.5% when recovered engine heat is transferred to the supply water circuit. Also, GEHP incorporated with heat recovery subsystems can be used for utilizing the waste heat to provide efficient supply of hot water.

Keywords: *Gas engine heat pump, Heating mode, Water heating, Primary energy ratio, Engine waste heat recovery.*

1. Introduction

In Europe, more than 50% of the total final energy consumption depends on fossil fuel [1]. However, environmental pollution problems increase with consumption of fossil fuels. In order to solve these problems, a development for alternative energy sources and improvement of energy utilization efficiency are required. Heat pumps (HPs) play an important role in solving energy and environment problems as they can improve the overall energy utilization efficiency and can work with environmentally friendly refrigerants [2-4].

Heat pumps can be divided into many categories according to energy sources, namely electric driven heat pumps (EHPs), ground-source heat pumps (GSHPs), solar-assisted heat pumps and gas engine driven heat pumps (GEHPs). A GEHP usually consists of a reversible vapor compression heat pump with an open compressor driven by an engine. In recent years, the GEHP has been paid more attention due to its advantage of reducing the energy consumption, especially in the heating process. Another two advantages of the GEHP are (1) the ability to recover the waste heat released by the engine cylinder jacket and exhaust gas and (2) the easy modulation of compressor speed by adjusting the gas supply. Therefore, the GEHP has a better performance than that of the electric driven heat pump (EHP), especially in the heating mode [5].

Performance characteristics of the GEHP during heating mode were evaluated by many investigators using theoretical modeling [5-7] and experimental approach [8]. Regarding to theoretical modeling of the GEHP, Zhang et al. [5] analyzed the effect of both ambient temperature and engine speed on the heating performance of air to water GEHP based on steady state model. Their results proved that the engine speed had a remarkable effect on both the engine and the heat pump, but ambient air temperature had a little influence on the engine performance. Yang et al. [6] reported an intelligent control simulation model for the GEHP system in heating mode to study the dynamic characteristics of the system. The results showed that the model was very effective in analyzing the effects of the control system. The steady state accuracy of the intelligent control scheme was higher than that of the fuzzy controller. Sanaye and Chahartaghi [7] predicted the performance of the GEHP under cooling and heating operating modes and then compared the simulation and experimental results for various amounts of suction and discharge pressures, fuel consumption and coefficient of performance. They noted that error percentages of suction and discharge pressures, fuel consumption and coefficient of performance are 3.4%, 4%, 6.7% and 7.2% for cooling mode, respectively, and 3.7%, 5.4%, 8.1% and 7.8% for heating mode, respectively.

Regarding to the experimental studies of the GEHP, Lazzarin and Noro [8] evaluated the performance of 'S. Nicola' plant in Vicenza during three years of operation. Plant heating loads are supplied using the GEHP and two condensing boilers. Recovered engine heat is used in water heating. The economic analysis was taken into account while the energy efficiencies were not taken into considerations.

The above review revealed that various investigations on modeling of the GEHPs are available in the literature while there is a lack of experimental data on the GEHPs working with R22 alternatives such as R410A. Thus, the present work is carried out with the aim of evaluating the performance characteristics of the GEHP used in water heating incorporated with different heat recovery sub-systems. In order to achieve this aim, a test facility of the GEHP is constructed and equipped with the necessary instrumentation. This paper is organized as follows. The experimental apparatus to predict the performance of characteristics of the GEHP is described in Section 2 while the data reduction manipulation is given in Section 3. This is followed by the experimental results and discussion in Section 4. Finally, conclusions based on the present work results are reported in Section 6.

2. Experimental apparatus

Fig. 1 shows a schematic diagram of the experimental apparatus, which includes three circuits; namely primary working fluid circuit, engine coolant circuit and secondary working fluid circuit. R410A is used as a primary working fluid while both air and water are used as secondary heat transfer fluids at the heat source (evaporator) and the heat sink (condenser). In the engine coolant circuit, both ethylene-water mixture (65% by volume) and propylene-water mixture (45% by volume) are used as cooling mediums. Pre-calibrated PT100 sensors are used to measure operating temperatures while digital pressure gauges are used to determine the operating pressures at four locations in the refrigerant circuit of the heat pump. The mass flow rate of refrigerant is measured using KROHNE Optimass 7000-T10 while engine coolant and water flow rates are measured using Ultego-II flow sensors. The measurement locations are shown in Fig. 1. All the measuring instruments have been installed and connected to 64 channels in the data acquisition cards (FP-1000). The control system has been established using PRIVA software which provides several possibilities for indoor unit selection and consequently system operation. All the measured data are recorded using DIAdem software and analyzed using an EES program [9] to evaluate the system performance. Performance

characteristics of the system in both cooling, heating and combined modes were published by Elgendy et al. [10-12].

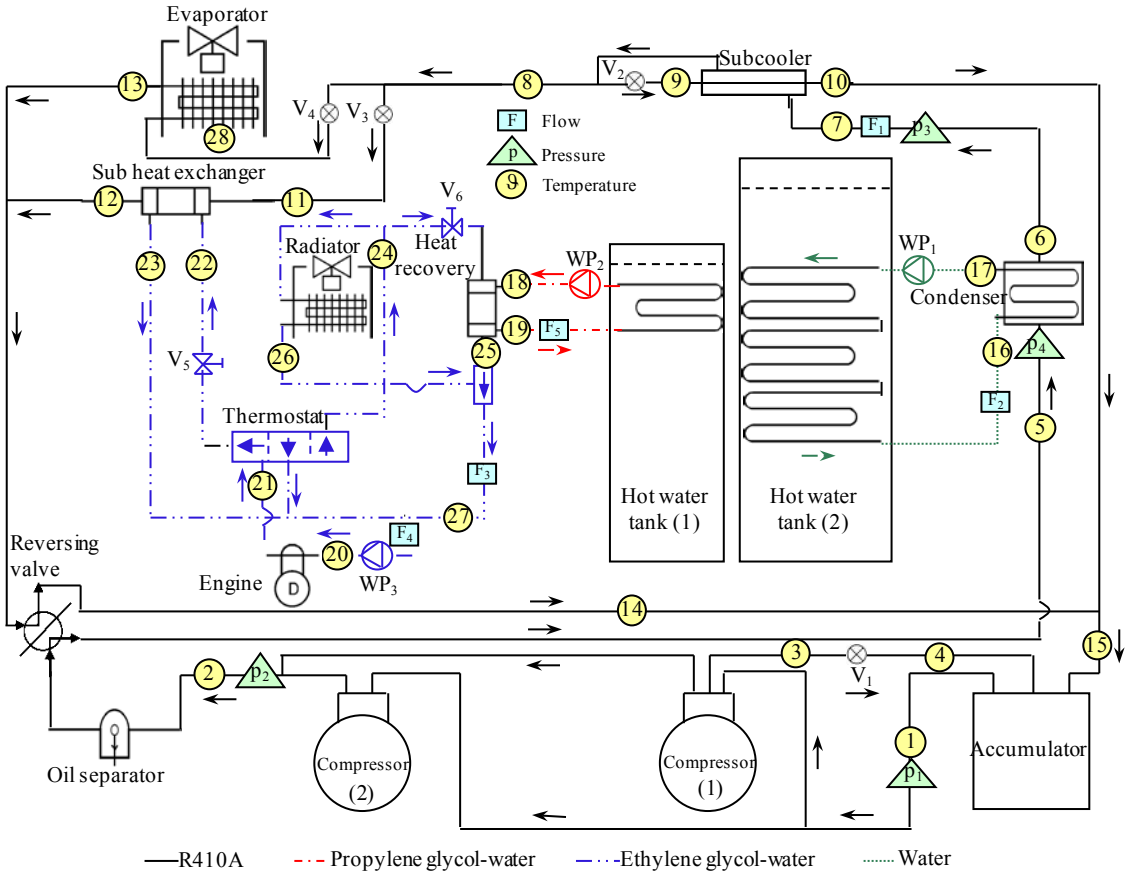

Fig. 1. Schematic diagram of the experimental apparatus with measuring point locations.

2.1. Primary working fluid circuit

The primary working fluid circuit is a vapor compression heat pump. It comprises an expansion device, an evaporator, an open compressor and a condenser followed by a sub-cooler. The expansion device is an electronic expansion valve whereas the compressor is a scroll open type with swept volume of 104cm^3/rev. The type of condenser is a plate heat exchanger with a heat transfer area of 4.6m^2. Two pressure-stats, one on the suction side and the other on the discharged side, are used to protect the compressor from under and over operating pressures. If the pressure exceeds its limits, the compressor would be automatically disconnected. In order to reduce the heat transfer to and from the surroundings, the primary fluid circuit is thermally insulated.

As the refrigerant flows to the compressors (state point 1), the compressors raise the pressure of the refrigerant and deliver superheated vapor (state point 2) to the condenser (state point 5) through an oil separator and a reversing valve. The condensation heat of refrigerant vapor is released to the water flowing through the condenser. Thus, R410A vapor gets condensed (state point 6) and its mass flow rate is measured using flow-meter F_1 before it flows to the sub-cooler. The liquid refrigerant in the sub-cooler is sub-cooled (state point 8) by transfer its heat to the throttled refrigerant flowing through valve V_2. Then, the refrigerant is throttled using expansion devices V_3 and V_4 and evaporated inside either the evaporator or the sub heat exchanger using the heat transferred from either ambient air or the recovered heat from the engine, respectively. Superheated refrigerant coming out of sub-cooler (state point 10),

sub heat exchanger (state point 12) and outdoor unit (state point 13) are mixed (state point 15) before entering the accumulator and then returning back to the compressors (state point 1).

2.2. Secondary fluid circuit

The experimental apparatus has two secondary heat transfer fluid circuits; namely hot water circuit and outdoor air circuit. The hot water circuit contains a hot water tank of $1m^3$ capacity, a hot water pump, a condenser and control valves. The water pump (single phase, variable speed) is used to suck and pump the hot water through the condenser and hot water pipeline. The hot water flow rate is adjusted via pump speed. The hot water circuit is thermally insulated to minimize heat loss. The outdoor air circuit consists of an air filter, a fan and an evaporator. The hot water coming out of the condenser (state point 17) is pumped to a storage tank (1) using variable speed water pump WP_1. Storage tank (1) is used for hot water coming from the engine heat recovery while storage tank (2) is used for the hot water coming out of the condenser. The volume flow rates of hot waters are measured using ultrasonic flow meters F_2 and F_5, respectively.

2.3. Engine coolant circuit

The engine coolant circuit includes a gas engine, a coolant tank, a coolant pump, valves and coolant pipeline. Coolant discharged from the coolant pump (state point 20) is heated by the heat released from the engine block and exhaust gas (state point 21). The heated coolant returns to the coolant pump by making a shortcut via a thermostat valve when the coolant temperature is low (lower than 53°C) at engine start-up. When the coolant temperature is high (higher than 53°C) the coolant flows into sub heat exchanger while it flows through all of sub heat exchanger, radiator and heat recovery heat exchangers when the coolant temperature is very high (higher than 67°C). The outlet coolant from both heat recovery heat exchanger (state point 25) and radiator (state point 26) is mixed (state point 27) and its volume flow rate is measured using ultrasonic flow meter (F_3) before returning back to the coolant pump. Heat gained in the heat recovery heat exchanger is supplied to the water in the tank (1) using propylene-water mixture as a working medium (state points 18 and 19). According to engine heat recovered utilization (from the engine block and exhaust gas), the system can be worked in two sub modes:

Mode-I: in which the recovered engine heat is transferred to the secondary water circuit in order to reach higher hot water supply (using the heat recovery heat exchanger). So, valves V_3 and V_5 are closed while V_6 is open.
Mode-II: in which the recovered engine heat is transferred to the primary refrigerant circuit to evaporate the working fluid, especially at low ambient air temperature (using the sub heat exchanger). Hence, valves V_3 and V_5 are open while V_6 is closed.

3. Data reduction

Using the measured data of operating pressures and temperatures of R410A, ethylene glycol-water mixture, propylene glycol-water mixture and water, the specific enthalpy values at the inlet and outlet of each component ($h_1 \rightarrow h_{27}$) are estimated. Then, energy and mass balances are carried out for the main components of the gas engine heat pump to compute their loads in addition to the overall system performance. Condenser heat load ($\dot{Q}_{con}$) can be written based on either primary working fluid (Eq. 1.a) or secondary working fluid (Eq. 1.b) as follows;

$$\dot{Q}_{con} = \dot{M}_{ref,p}(h_5 - h_6) \quad (1.a)$$

$$\dot{Q}_{con} = \dot{V}_{con,w}\rho_w(h_{17} - h_{16}) \quad (1.b)$$

Applying energy balance around sub-cooler, the secondary refrigerant mass flow rate ($\dot{M}_{ref,s}$) flowing through sub-cooler can be calculated as follows;

$$\dot{M}_{ref,s} = \frac{\dot{Q}_{sub}}{(h_{10} - h_9)} \quad (2.a)$$

where,

$$\dot{Q}_{sub} = \dot{M}_{ref,p}(h_7 - h_8) \quad (2.b)$$

$\dot{M}_{ref,p}$ is the primary refrigerant mass flow rate, which is measured using flow meter F_1. Gas engine heat recovery ($\dot{Q}_{HR}$) can be calculated using Eq. (3);

$$\dot{Q}_{HR} = \dot{V}_{hw}\rho_w(h_{19} - h_{18}). \quad (3)$$

Ultrasonic flow meters F_2 and F_5 are used to measure condenser water ($\dot{V}_{con,w}$) and hot water ($\dot{V}_{hw}$) volume flow rates through the condenser and heat recovery heat exchanger, respectively. Primary energy ratio (PER), gas engine heat consumption ($\dot{Q}_{gas}$) and total heating capacity ($\dot{Q}_{tot}$) are the main parameters to be considered in the performance evaluation of the GEHP [13]. PER and $\dot{Q}_{gas}$ can be expressed as follows;

$$PER = \frac{\dot{Q}_{tot}}{\dot{Q}_{gas}}, \quad (4)$$

$$\dot{Q}_{tot} = \dot{Q}_{con} + \dot{Q}_{HR}, \quad (5)$$

$$\dot{Q}_{gas} = \dot{V}_{gas}LHV, \quad (6)$$

where LHV is the gas lower heating value and $\dot{V}_{gas}$ is the measured gas volume flow rate using diaphragm gas meter.

4. Results and discussions

Fig. 2 shows comparison of performance characteristics of the GEHP for the prescribed mode-I and mode-II and at ambient temperature of 13°C. In mode-I, recovered engine heat is transferred to the water supply while recovered engine heat is transferred to the refrigerant in mode-II. The system hot water outlet temperature was adjusted between 35°C and 70°C to

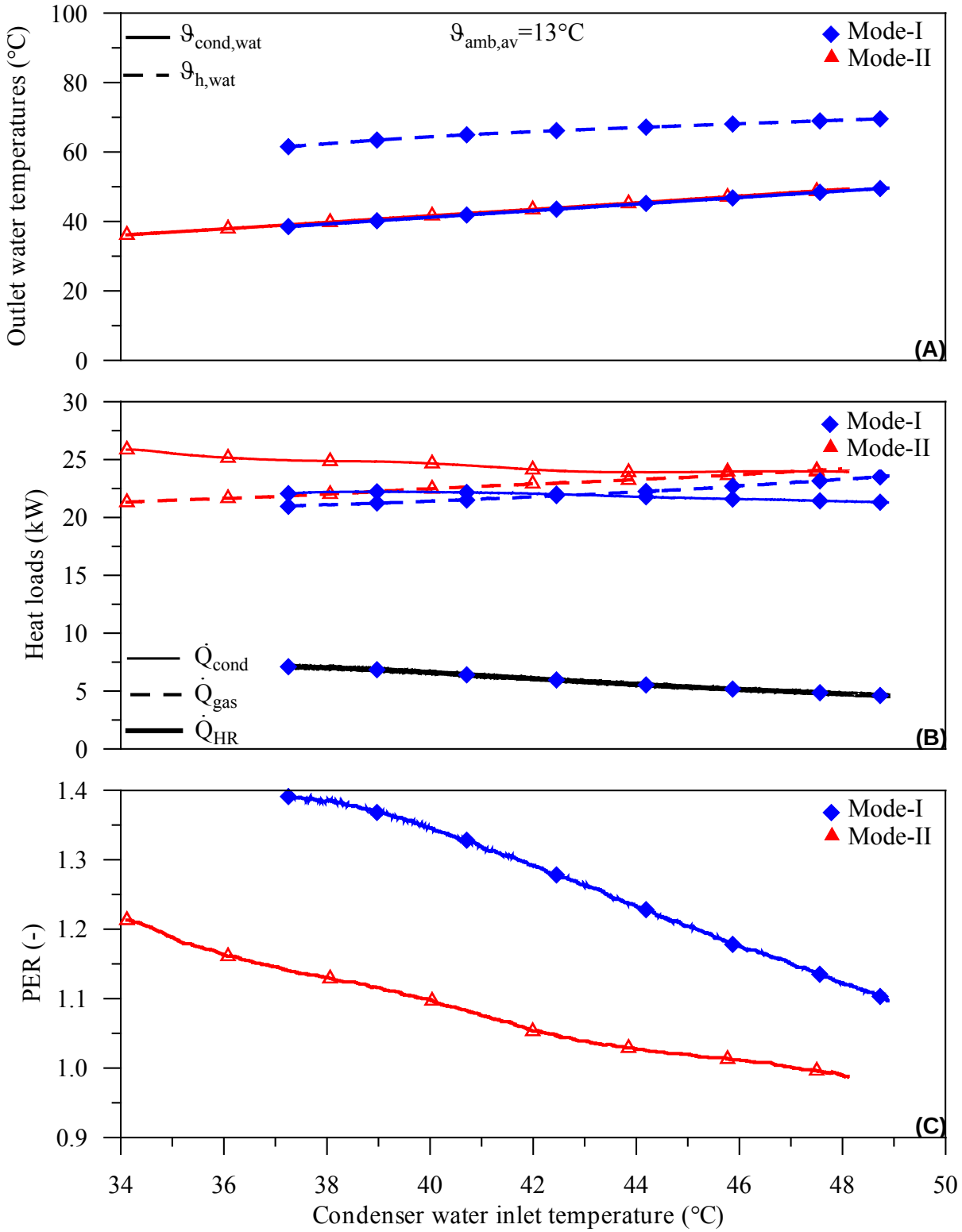

Fig. 2. Effect of condenser water inlet temperature on the performance characteristics of the GEHP for Mode-I and Mode-II. (A) outlet water temperatures, (B) heat loads and (C) PER.

provide heating requirements for several applications like shaving, residential dish washing and laundry [14].

4.1. Effect of condenser water inlet temperature

Measured condenser and heat recovery water outlet temperatures against the condenser water inlet temperature are presented in Fig. 2.A, which indicates that condenser and heat recovery water outlet temperatures increase when condenser water inlet temperature increases. Variations of actual heat loads with condenser water inlet temperature are shown in Fig. 2.B. It is evident from this figure that total heating capacity and gas engine heat recovery decrease while gas engine energy consumption $\dot{Q}_{gas}$ increases as condenser water inlet temperature increases. It is observed that both of the condenser and heat recovery water temperature differences decrease causing the decrease of total heating capacity. In general, as the condenser water inlet temperature changes from 37°C to 48°C, total heating capacity decreases by 8.3% and 4.7% while gas engine energy consumption increases by 14.1% and 11.9% for mode-I and mode-II, respectively. The effect of condenser water inlet temperature on PER can be predicted from Fig. 2.C. A higher condenser water inlet temperature yields a lower PER. This trend is mainly due to both decrease in total heating capacity and increase in the gas engine energy consumption as shown in Fig. 2.C. Clearly, primary energy ratio of the GEHP decreases by 27.2% and 17.3% as the condenser water inlet temperature varies from 37°C to 48°C for mode-I and mode-II, respectively.

4.2. Comparison between mode-I and mode-II

Comparison of the measured condenser and heat recovery water outlet temperatures for mode-I and mode-II are presented in Fig. 2.A. In the two modes, the condenser water outlet temperature lies between 35°C and 50°C. For mode-I, a higher hot water temperature (up to 70°C) can be achieved as a result of recovered engine heat transfer. Variations of actual heat loads for the modes are shown in Fig. 2.B. It is evident from this figure that condenser heating capacity and gas engine energy consumption are high when recovered engine heat is transferred to refrigerant. In general, both condenser heating capacity and gas engine energy consumption increase by 13% and 12.4% as an average values, respectively. So, it is better to transfer recovered engine heat to the refrigerant when one needs a large amount of heat at lower range of temperature (35°C:50°C) while it is better to transfer engine heat to water when a higher water temperature (up to 70°C) is required. The effect of the condenser water inlet temperature on the PER for the two modes can be predicted from Fig. 2.C. A higher PER can be reached when the recovered engine heat is transferred to the water. This can be attributed mainly to the higher gas engine heat recovery. Clearly, primary energy ratio of the GEHP increases by 17.5% as an average value over the entire range of the condenser water inlet temperature (from 37.2°C to 48°C).

5. Conclusion

In the present work, performance characteristics of R410A gas engine heat pump have been experimentally compared under two different modes of heat recovery utilization. In mode-I, recovered engine heat is transferred to the water supply while recovered engine heat is transferred to the refrigerant in mode-II. Based on t he reported results, the following conclusions are drawn:

- Hot water outlet temperatures between 35°C and 50°C are obtained during the considered modes.
- Water outlet temperatures up to 70°C can be reached in a separate tank when recovered engine heat is transferred to water.

- As the condenser water inlet temperature varies from 37°C to 48°C, total heating capacity decreases by 8.3% and 4.7% while gas engine energy consumption increases by 14.1% and 11.9% for mode-I and mode-II, respectively.
- Primary energy ratio of the GEHP increases by 17.5%, when recovered engine heat is transferred to water.

Acknowledgment

The Authors are grateful for the installation of the testing plant and the financial support provided by Wärmetechnik Quedlinburg (WTQ) GmbH. The financial support of the Egyptian government for the Ph.D. of Mr. Elgendy is gratefully acknowledged.

References

[1] H. Laue, Heat Pumps, Heinloth K. Renewable Energy, Germany, Springer Berlin Heidelberg, 2006.

[2] J. P. Meyer, G. P. Greyvenstein, Hot water for homes in South Africa with heat pumps, Energy 1991, 16(7), pp.1039–44.

[3] G. P. Greyvenstein, J. P. Meyer, The viability of heat pumps for the heating of swimming pools in South Africa, Energy 1991, 16(7), pp.1031–1037.

[4] S. Garimella, Innovations in energy efficient and environmentally friendly space-conditioning systems, Energy 2003, 28(15), pp.1593–1614.

[5] R. R. Zhang, X. S. Lu, S. Z. Li, W. S. Lin, A. Z. Gu, Analysis on the heating performance of a gas engine driven air to water heat pump based on a steady state model, Energy Conversion and Management 2005, 46, pp.1714–1730.

[6] Z. Yang, Z. Haibo, F. Zheng, Modeling and dynamic control simulation of unitary gas engine heat pump, Energy Conversion and Management 2007, 48(12), pp.3146–3153.

[7] S. Sanaye, M. Chahartaghi, Thermal modelling and operating tests for the gas engine-driven heat pump systems, Energy 2010, 35(1), pp.351-363.

[8] R. Lazzarin, M. Noro, District heating and gas engine heat pump: economic analysis based on a case study, Applied Thermal Engineering 2006, 26, pp.193–199.

[9] S. A. Klein, EES-Engineering Equation Solver, Professional Version, Middleton, WI, F-Chart Software, 2009.

[10] E. Elgendy, J. Schmidt, Experimental study of gas engine driven air to water heat pump in cooling mode, Energy 2010, 35(4), pp.2461-2467.

[11] E. Elgendy, J. Schmidt, A. Khalil, M. Fatouh, Performance of a Gas Engine Driven Heat Pump for Hot Water Supply Systems, Energy 2011, In press.

[12] E. Elgendy, J. Schmidt, A. Khalil, M. Fatouh, Performance of a Gas Engine Heat Pump using R410A for Heating and Cooling Applications, Energy 2010, 35(12), pp.4941-4948.

[13] K. Taira, Development of a 2.5-RT multiple-indoor-unit gas engine heat pump, ASHRAE Trans 1998, 24, pp.982-988.

[14] ASHRAE, ASHRAE handbook, application, Atlanta, American Society of Heating Refrigerating and Air-conditioning Engineers, 2007.

Building performance based on measured data

S. Andersson[1,*], J-U Sjögren[2], R. Östin[1] and T.Olofsson[1]

1. Department of applied physics and electronics, Umeå, Sweden
2. NCC Ltd, Stockholm, Sweden
** Corresponding Author Tel: +46-9078679 45; E-mail staffan.andersson@tfe.umu.se*

Abstract: With increasing liability for builders, the need for evaluation methods that focuses on the building's performance and thus excludes the impact from residents' behavior increases. This is not only of interest for new buildings but also when retrofitting existing buildings in order to reduce energy end-use.

The investigation in this paper is based on extensive measurements on two fairly representative type of buildings, a single family building in Ekerö, Stockholm built 2000 and two apartment buildings in Umeå (1964) in order to extract key energy performance parameters such as the building's heat loss coefficient, heat transfer via the ground and heat gained from the sun and used electricity.

With access to pre-processed daily data from a 2-month periods, located close to the winter solstice, a robust estimate of the heat loss coefficient was obtained based on a regression analysis. For the single family building the variation was within 1% and for the two heavier apartment buildings an average variation of 2%, with a maximum of 4%, between different analyzed periods close to the winter solstice.

The gained heating from the used electricity in terms of a gain factor could not be unambiguously extracted and therefore could only a range for the heat transfer via ground be estimated. The estimated range for the transfer via ground for the two apartment buildings were in very good agreement with those calculated according to EN ISO 13 370 and corresponded to almost 10% of the heating demand at the design temperature. For the single family building with an insulated slab and parts of the walls below ground level, the calculations gave slightly higher transfer than what was obtained from the regression analysis. For the estimated gained solar radiation no comparison has been possible to make, but the estimated gain exhibited an expected correlation with the global solar radiation data that was available for the two apartment buildings.

Keywords: *Regression analysis, Heat loss coefficient, Heat transfer via ground, Gained heat*

Nomenclature

C	*thermal mass* ..... $J/^{\circ}C$	g	*ground*
F	*heat loss coefficient* ..... $W/^{\circ}C$	h	*heating system*
G_L	*heat transfer via ground* ..... W	i	*indoor*
P	*power* ..... W	o	*outdoor*
T	*temperture* ..... $^{\circ}C$	p	*heat from persons*
α	*gain factor* ..... *(-)*	s	*sun*
		t	*total purchased energy*
	Indices	v	*ventilation*
d	*dynamic heat storage*	w	*water*
el	*electricity*		

1. Introduction

Energy performance assessment [1] is normally done by energy consumption calculations, estimations based on energy bills, extensive measurements [2-4] or a combination of these methods. Assessments that are based on extensive measurements are often done by identifying the parameters of the used model The used models may basically be divided in two groups, dynamic or static, and where the overall heat loss coefficient is a commonly used performance parameter.

With increased demands, that new or renovated building meet promised performance, the demands on validation but also on the used energy consumption calculations in the design stage increases. Today, in Sweden, a buildings energy performance usually is expressed in terms of energy use per square meter heated area. The problem with this performance measure is that only a part of the supplied energy is considered, i.e energy directly used for space heating and domestic hot water preparation together with electricity used for the buildings technical systems and common areas. Contributions related to user behaviors such as household electricity, indoor temperature and personal heating are not included together with the contribution from solar radiation.

The objective behind this work is to investigate the possibility to, based on extensive measurements, extract the thermal performance parameters that describes the building itself and where the contributions from the users and the sun are filtered out. This has great significance for a buyer or seller/manufacturer from liability point of view, since the behavior of the building itself is the only thing a seller/manufacturer can guarantee.

2. Methodology

Measurements have been carried out during a year (March 2009-March 2010) in two types of buildings, a single family building outside, Stockholm (built 2000) and two apartment buildings in northern Sweden, Umeå. The apartment buildings (#1 and #2), were built 1962 with 12 and 9 apartments, respectively. Common for all studied objects, are an exhaust ventilation system with a fan operating at a constant speed and no heat recovery and that they are connected to district heating.

Extensive measurements of indoor and outdoor temperatures, used district heating for domestic hot water and heating as well as the total electricity use (households and electricity for the technical systems). In addition, the global solar irradiation has been measured in the near vicinity of the two apartment buildings located in Umeå.

To analyze the energy use, we have used average daily values together with a simplified power balance of a building. In the results presented here, the indoor temperature was taken to be the exhaust air temperature. The main simplification lies in the fact that the effects of wind are not considered together with any impact from humidity and that the heat loss coefficient between indoor and external temperature has been taken to be constant. The latter assumption is based on a constant operation of the exhaust fan in each building. Based on these simplifications the power balance of a building could be described by

$$P_h + \alpha P_{el} + P_p + P_s + P_w = F(T_i - T_o) + G_L + P_d \quad (1)$$

with $P_d = C\frac{T_d}{dt}$ and where T_d is the temperature of the thermal mass.

The contributions to heating from the sun, P_s, gained heat or heat loss due to domestic hot and cold water usage P_w, contribution from body heat, P_p, together with the dynamic heat storage, P_d, is very difficult to measure. These parameters of Eq. 1 have been treated in the following way.

P_s: Experimental data from periods around the winter solstice has been used, in order to minimize contribution from solar radiation when determining the heat loss coefficient, F

P_w: Assumed that the heat transfer from the domestic hot water circulation equals the heating of domestic cold water.
P_p: Based on data from a survey, the contribution to heating was assessed from the number family members and their presence at home.
P_d: Two different approaches A and B for pre-processing measured data have been used to minimize this contribution.

A) Averaging over a time period longer than the estimated time constant of each building.
B) Averaging over two days, that has an estimated equal change of T_d in magnitude but in opposite direction. For an ideal building that has a constant indoor room temperature and is not exposed to solar radiation, the dynamic heat storage could be eliminated by taking the average over two days for which the change in outdoor temperature are equal but opposite, for instance +5 and -5 ˚C. Based on this approach, an estimate of the change in the temperature of the buildings thermal mass, ΔT_d, was taken to be represented by the change in $\frac{Ti+To}{2} + \omega T_i$ between two consecutive days. The weight factor, ω, between the two terms should be used in relation to the thermal mass the two terms represent.

The advantage with B) is that the number of data is only reduced by approximately half, whereas an averaging over a time period longer than the time constant of a heavy building may reduce available data to a degree that a regression analysis becomes hazardous.

Thermal performance measures, such as the heat loss factor, ground transfer and contribution from solar radiation and gained heating from electricity has been estimated by a linear regression analysis but also the sensitivity of these parameters to the choice of indoor temperature, length of analyzed period, variation in ambient temperature etc. For a full description, see [5].

3. Results

A basic approach in this work is to use the period of the year when the contribution from the solar radiation is smallest, in order to simplify Eq. (1). In Figure 1 below, the measured global solar radiation is shown. The measurements are made at Umeå University which is in the close vicinity of the two apartment buildings, less than one kilometer.

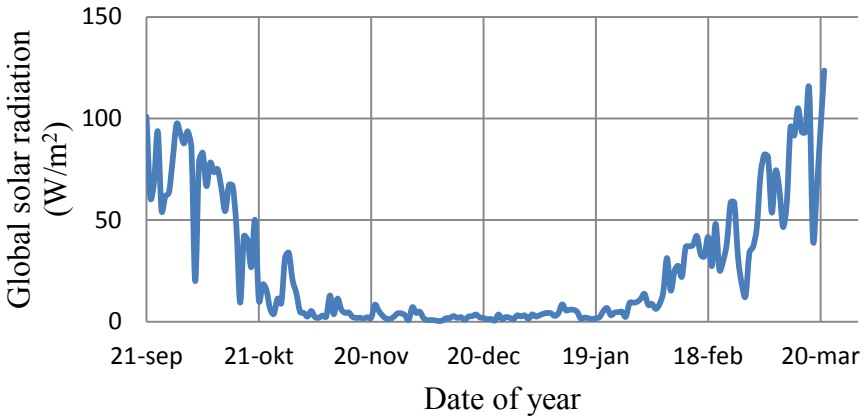

Fig.1. Global solar radiation, measured at Umeå University

When analyzing data from periods around the winter solstice (December 21: st), the contribution P_s is negligible according to Figure 1. Together with P_w = 0 and using pre-

processed data to minimize the dynamic heat storage, Eq. (1) simplifies to

$$P_h + \alpha P_{el} + P_p = F(T_i - T_o) + G_L \quad (2)$$

With access to measured data of P_h and P_{el} together with P_p based on a survey, Eq. (2) becomes

$$P_t = F(T_i - T_o) + (1 - \alpha)P_{el} + G_L \quad (3)$$

Where $P_t = P_{el} + P_h + P_p$.

The total electricity use, P_{el}, is a parameter of Eq. (3) and in Figure 2 below, data from the period 1 November to February 6 is presented versus $(T_i - T_o)$. The data have been pre-processed according to B).

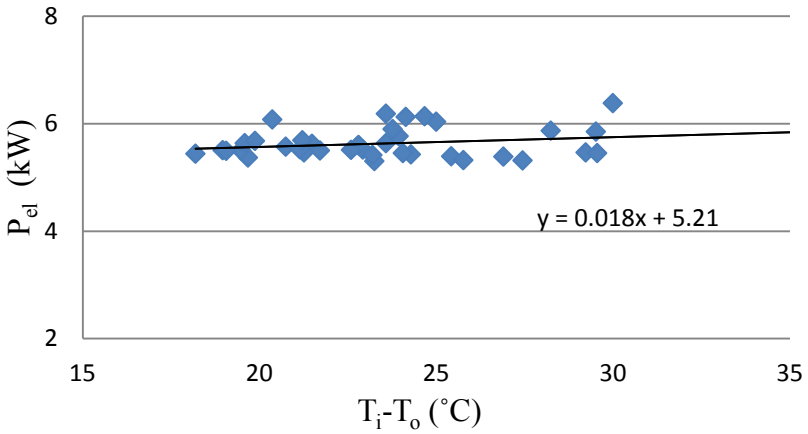

Fig.2. P_{el} versus $(T_i$-$T_o)$ for building #1 together with a linear regression

As seen from Figure 2 the measured total use of electricity is fairly constant and may, with a fairly good accuracy be represented by a linear function of $(T_i - T_o)$. The pre-processing of data (according to B) reduces strongly the daily variation of P_{el} and yields similar results as pre-processing by averaging daily data over a period longer than the time constant. This behavior is found for both apartment buildings as well as the single family building.

If P_{el} may be described as

$$P_{el} = P_{el,0} + k(T_i - T_o) \quad (4)$$

a linear regression according to

$$P_t = F_t(T_i - T_o) + P_{t,0} \quad (5)$$

would, based on Eq. (3) yield the following relation between F and F_t according to

$$F = F_t - (1 - \alpha)k \quad (6)$$

based on the assumption that the heat transfer via ground is constant during the analyzed period and that gain factor, α, also is fairly constant. Since k in Eq. (4) is small (Figure 2), the

impact on the value of F_t, determined by a linear regression according to Eq. 5 is very small. This means that α may be treated as constant, but also that $F \cong F_t$ since k is small and α is expected to be closer to unity than zero.

The following alternatives for pre-processing data according to A) and B) were investigated.

A*n*: Average over *n* consecutive days, where n is between four days (A4) for the single family building and six days (A6) for the apartment buildings.

B1: Apartment buildings: Since the estimated thermal mass is fairly equal for the climate shell and the internal walls, ω was taken to be equal to 1 and thus was ΔT_d taken as the change of $(T_i + T_o)/2 + T_i$ between two consecutive days.

B2: Single family building. Since the internal walls were light, ω was taken to zero, and thus ΔT_d was calculated as the change of $(T_i + T_o)/2$ between two consecutive days.

A linear regression according to Eq. (5) (Building #1 for the period 1 November to February 6) are presented in Figure 3. Data has been pre-processed according to B6.

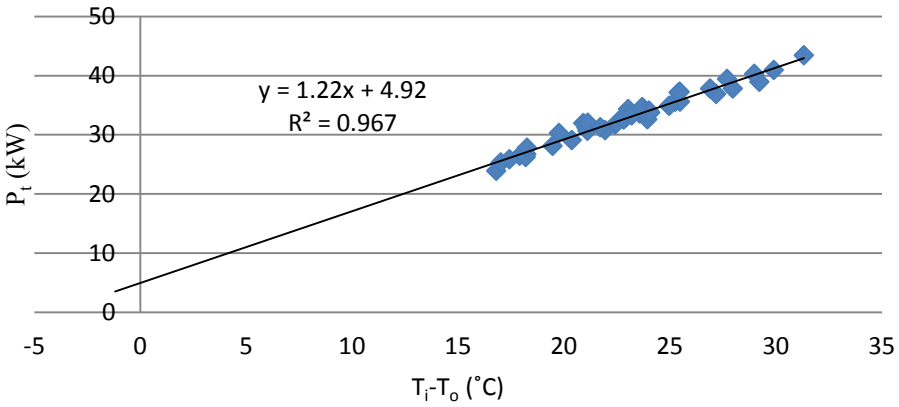

Fig. 3. P_t versus (T_i-T_o) for building #1. The data are from the period, 1 November to 6 February 6, and the data has been preprocessed according to B6.

The results in Figure 3 support the assumption of a constant heat loss coefficient. In table 1, the results based on a regression analysis (Eq. 5) for all investigated buildings are compiled for time periods of two month around the winter solstice using different pre-processing techniques.

For the two apartment buildings, as seen in table 1, the variation in the estimate of F_t is reduced when using pre-processing of data according to B1 than compared to A6, with an average variation of 2%, and a maximum of 4%, between different analyzed periods close to the winter solstice. For the single family building the variation is within 1% for both methods of pre-processing data.

Besides F_t, the regression analysis also gives the intercept, see Figure 3, which could correspond to the heat transfer via ground during that period. But P_t includes the total electricity use, P_{el}, and the contribution to heating is only αP_{el}, where $0 \leq \alpha \leq 1$. This means that the for the case shown in fig. 4, the intercept $P_{t,0} = 4.9$ kW should be reduced with $(1-\alpha)\cdot P_{el,0}$ to obtain an estimate of the heat loss via ground, G_L.

Besides F_t, the regression analysis also gives the intercept, see Figure 3, which could correspond to the heat transfer via ground during that period. But P_t includes the total electricity use, P_{el}, and the contribution to heating is only αP_{el}, where $0 \leq \alpha \leq 1$. This means

that the for the case shown in fig. 4, the intercept $P_{t,0}$ = 4.9 kW should be reduced with (1-α)·$P_{el,0}$ to obtain an estimate of the heat loss via ground, G_L.

Table 1. Compilation of the results based on a two month period, with different schemes for preprocessing experimental data. The relative deviation from the average value is given within brackets. For the apartment buildings the results are also given for the longest period when the measured global radiation was less than 20 W/m^2.

		F_t [kW/°C]			
		Building #1		**Building #2**	
Pre-processing		A6	B1	A6	B1
2-month	21/11-21/1	1.34 (6%)	1.23 (1%)	1.04 (4%)	1.01 (1%)
	1/11-31/12	1.22 (-3%)	1.24 (2%)	1.01 (1%)	1.02 (2%)
	1/12-31/1	1.22 (-3%)	1.19 (-3%)	0.95 (-5%)	0.96 (-4%)
$\bar{F}_t$ 2-month		*1.26*	*1.22*	*1.00*	*1.00*
	1/11-6/2	*1.26*	*1.22*	*1.00*	*0.98*

		Single family building	
Pre-processing		A4	B2
2-month	21/11-21/1	0.150 (1%)	0.148 (-1%)
	1/11-31/12	0.146 (-1%)	0.150 (1%)
	1/12-31/1	0.149 (0%)	0.149 (0%)
$\bar{F}_t$2-month		*0.148*	*0.149*

The value of α, is difficult to determine from available data. Method by using multivariate regression (PLS) [6,7] have been examined, but due to the fact that P_{el} behave very "nice" and is correlated to $(T_i - T_o)$, the uncertainty in the determination of α becomes very large and no clear estimates could be obtained. Of the actual electricity use in building #1, hous ehold electricity constitutes about 70% and the remaining 30% for lighting outdoors and for common areas and for the exhaust fan that is situated under the roof and thus out-side the climate shell. An approximate estimates of α, yield a value between 0.6 and 0.8. Based on this, the heat transfer via ground is estimated to be in the range of 2.9 and 3.9 kW. With access to measurements of the basement temperature of building #1, t he design of the building and the fact that the building is situated on a former sea bottom, calculation of the heat transfer via ground was performed according to EN-ISO-13370, se Figure 5.

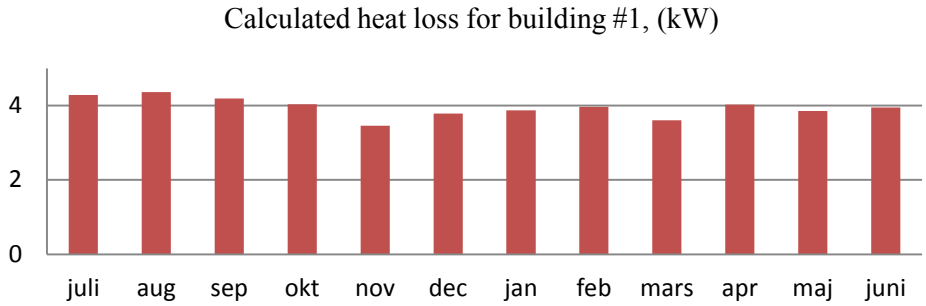

Fig.4. Calculated monthly heat loss via ground according to EN-ISO-13370, clay soil.

Figure 4 shows that the calculated heat transfer via ground both on an annual basis and for the periods analyzed are relatively constant and in good agreement with the estimated transfer of 2.9-3.9 kW for the time period closed to the winter solstice.

If the heat transfer via ground are constant over the year, the utilized solar radiation for heating, P_s, may be estimated, based on a constant heat loss coefficient, F. The results for building #1, are displayed in Figure 6 for the entire measured period assuming a constant level of the heat transfer via ground. The data presented in Figure 5 consists of daily data from 1 January to 31 March of 2010 and 1 April to 31 December 2009 and hence the step in the graph.

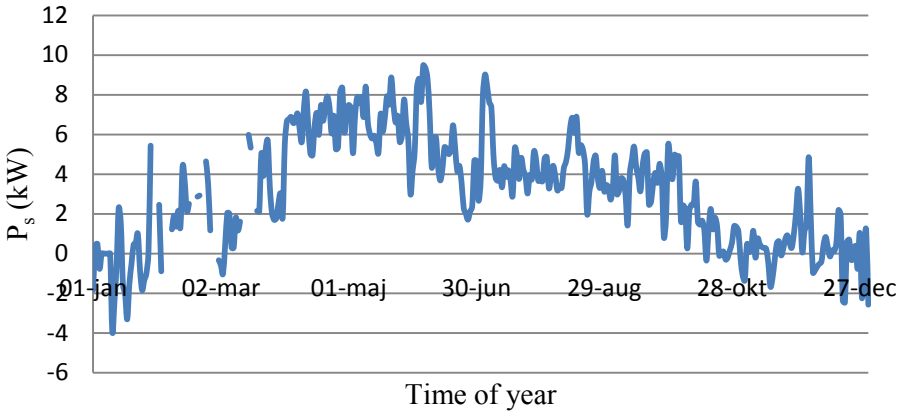

Fig. 5. Estimated gained heat from solar radiation, building #1.

At the beginning and end of the year, P_s fluctuates around zero. The main reason behind this is the use of daily data, and the variation thus reflects dynamic heat storage. If data were pre-processing according to B6, these fluctuations would be reduced, but at the same time, data could not be present in this way since time loses its meaning. The fact that P_s is lower than expected around the summer solstice is probably explained by the Swedish tradition to have open doors and windows during our short but cherished summer.

Since the theoretical calculations of the monthly heat transfer via ground, for the single family building indicated a fairly large variation over the year, a similar analysis is not possible. But based on an estimate of $0.6 \leq \alpha \leq 0.8$], an estimated range for the heat transfer via ground, during the 2-month period of 0.22 t o 0.39 kW was obtained, to be compared with the calculated 0.5 kW for this split level building. Since the heat transfer via ground has a strong variation over the year, could only the difference between gained solar radiation and heat transfer via ground be estimated, (P_s - L_G), if α is known and constant. With $\alpha = 0.7$, the results shown in Figure 6 was obtained. For the single family building, only incomplete data was available for the summer period and are thus missing in Figure 6.

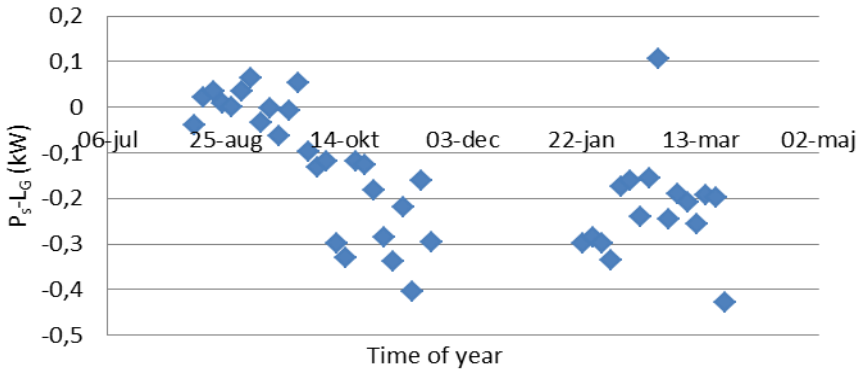

Fig. 6. Estimated $P_{sol} - L_G$ over the period where measured data was available.

Figure 6, indicates that the contribution to heating from solar radiation exceeds the heat transfer via ground until the beginning of October and this situation is reversed in the end of March.

4. Discussion

In this work we have used experimental data from time periods close to the winter solstice and data has been pre-processed to reduce dynamic heat storage effects. Based on this and with access to extensive measurements, the heat loss factor has been determined with a high precision for the investigated buildings. Unfortunately, a fundamental problem remains; no correct answer is available for the heat loss coefficient as reference.

However, based on the high precision and the fact that the obtained estimate of the heat transfer via ground are in good agreement with calculations based on ISO-EN-13370 indicates that the used approach gives consistent results. In addition, the estimated gained solar radiation, of Figure 4, increases in a basically linear way when plotted versus the global solar radiation. This means that the obtained results could be used as feedback to energy calculations.

The buildings investigated in this study have a simple HVAC-system and the next step is therefor to extend this work to more energy efficient buildings with complex systems and also to focus on methods to obtain an estimate of the gain factor α for the electricity use. This could be achieved by a close survey of where and for what the electricity has been used or using multivariate methods or artificial neural networks [8,9].

References

[1] ASHRAE Handbook Fundamentals 2005, Atlanta, USA

[2] F.W. Yu and K.T. Chan, Energy signatures for assessing the energy performance of chillers, Energy and Buildings, 2005 Vol. 37 (7), pp. 739-746.

[3] C. Ghiaus, Experimental estimation of building energy performance by robust regression, Energy and Buildings, 2006 Vol. 38(6), pp. 582-587

[4] A Rabl and R Rialhe, Energy signature models for commercial buildings: test with measured data and interpretation, Energy and buildings, 1992 Vol. 10, pp.143-154.

[5] S. Andersson, J-U. Sjögren, T Olofsson and R Östin, Prestanda- och beteendeuppföljning av byggnaders energianvändning. 2010, Internal report. Dept. of Applied Physics and Electronics, Umeå University

[6] S Wold, M Sjöström and L Erikson, PLS-regression: A basic tool of chemometrics, Chemometrics and intelligent laboratory systems, 2001 Vol. 58, pp 109-130

[7] T Olofsson, S Andersson and J-U Sjögren, Building energy parameter investigations based on multivariate analysis, Energy and Buildings, 2009 Vol. 41(1), pp. 71-80

[8] M Lundin, S Andersson, R Östin A.R. Further validation of a method aimed to estimate building performance parameters, Energy and Buildings, 2005 Vol.37 (8), pp. 867-871

[9] P.A. Gonza´lez, J.M. Zamarren˜o, Prediction of hourly energy consumption in buildings based on a feedback artificial neural network, Energy and Buildings 2005 Vol. 37(6) pp. 595–601.

Sustainable use of electrical energy at the University of Sonora, Mexico

N. Munguía, [1*] A. Zavala [1], L. Velázquez [12]

1. *Industrial Engineering Department, University of Sonora, México*
2. *Work Environment Department, University of Massachusetts Lowell*

** Corresponding author. Tel/Fax +52 662 2516574, email nmunguia@industrial.uson.mx*

Abstract: The University of Sonora as a sustainable higher education institution has been committed for almost two decades to continuously increase its involvement with society by helping in their transition to more sustainable lifestyle and recently by implementing and maintaining a Sustainability Management System (SMS) on Campus which it is actually certified under the ISO 14001:2004 international standard. One of the sustainability programs within the SMS is the Sustainable Management of Electrical Energy (SMEE) that comprises not only energy efficiency initiatives but also energy conservation initiatives. This paper is aimed at describing the experience of the University of Sonora in fostering changes on attitudes and behaviors that result in energy conservation. Before the implementation of the SMEE was common to find lack of interest among students, professor, and employees for energy conservation behaviors such as shutting down air conditioners or turning off lights when they were not necessary given as a result a repeatedly energy wastage and consequently, the generation of CO2 emissions that increase climate change. Findings presented in this paper indicate that changes on attitudes and behaviors can generate good practices for conserving energy and reduce the environmental burden of universities. Sustainability indicators have proven the efficacy and efficient of the SMEE; at the financial dimension, the SMEE has reached savings of over 5, 840 USD in three years; from the environmental dimension, the SMEE has avoided the emissions of 33,287 kg of CO2, but the most important indicator come from the social dimension where wasting behaviors have been modified by increasing community awareness. Positive trends on the SMEE indicators suggest the increasing of awareness of the impact of energy wastage among the university community who act in consequence of this in favor of the environment. Additionally, an awareness survey was conducted to 650 members of the university community such as faculty, students, administrative staff and service personnel to reveal which energy conservation initiatives would be willing to follow, such as: turn off the lights at the term class, turn off the air conditioned when the classroom is not in use, close doors and windows to avoid that the air-conditioning air leakage, etc. Findings show that most of participants are becoming aware of the impact of the energy wastage and they are willing to participate in the SMEE in order to reduce those environmental impacts. Findings also show that willingness of the university community for participating or supporting more than one energy conservation initiatives on campus; the behavior of turn off lights and air conditioners when finishing the class is the preferred option.

Keywords: *Energy conservation, Sustainable management system, Climate change*

1. Introduction

The dependence of petroleum and coal has had terrible consequences for the planet, such as global warming, pollution, and the dependency of some countries over other countries [1]. On global scale, climate change has raised lots of concerns; international initiatives such as the UN Framework Convention on Climate Change have raised alertness about the role of energy in human's impacts reflecting on the environment and the same manner effecting for sustainable development [2]. There is no doubt that human activities alter the climate mainly where CO2 is emitted to the atmosphere producing the greenhouse effect [3]. Clearly, this situation has forced individuals and organizations to put into practice efforts to reduce energy consumption and in particular energy wastage. According to EPA, opportunities for energy conservation are increasingly available in almost every application in any setting such as homes, schools, offices, and industrial environments [4].

The University of Sonora in its intent to become a more sustainable higher education institution has been committed for almost two decades to energy conservation by implementing and maintaining a Sustainability Management System (SMS) on Campus [5].

After more than 5 years of its implementation, the SMS succeed, in July 2008, an ISO 14001:2004 external audit and as a consequence it got the ISO certification; two years later, the SMS was challenged again by two follow-up audits that were conducted and approved with success. So far, this accomplishment has not been mirrored by any other public university in Latin-America.

The goal of the SMS is the protection of natural resources and the prevention, reduction and/or elimination of environmental and occupational risks generated by the members of the university community when using resources in order to carry out its substantive functions of teaching, research, outreach & partnership, and stewardship.

One of the sustainability programs within the SGS is the Sustainable Management of Electrical Energy (SMEE) that comprises not only energy efficiency initiatives but also energy conservation initiatives with the purpose of reducing energy consumption and in particular, energy wastage. For the University of Sonora, energy conservation is related to human behavior; therefore, the SMEE strives to changes negative lifestyles of its community.

Before the implementation of the SMEE was common to find lack of interest to energy conservation initiatives among students, professor, and employees; hence, electrical bills and CO2 emissions were out of control; however, this situation has gradually changed.

Under this context, this paper is going to be aimed at describing the experience of the University of Sonora in fostering changes on attitudes and behaviors that result in energy conservation.

2. Methodology

The Sustainable Management of Electrical Energy (SMEE) Program has several steps that work integrated to reach the strategic objective of changing of attitudes and behaviors and energy efficiency initiatives. These steps can be summarized as follows:

2.1. SMS Scope

The scope of the SMS is the engineering college; this means that energy conservation efforts are focused on facilities within this college. The engineering college is located at block five of the campus which includes eleven typical buildings of a higher education institution such as classrooms, laboratories, and administrative offices.

2.2 Inventory of electrical equipment and accessories

Commonly, energy is used in lighting, computers and peripherals; science equipment and office devices. The inventory of electrical equipment and accessories is conducted annually and involves not only the accounting but also the physical shapes of equipment and installations within the scope of the Sustainability Management System (SMS). The minimum information required by equipment and / or accessory is their power consumption on watt, or its equivalent, as well as their physical condition at the time of conducting the inventory.

2.3 Monitoring procedure.

The monitoring procedure is intended to verify if the electricity is being used efficiently and rationally by the university community. This procedure is done each day, but reporting is on a weekly basis; this consists on certain number of visits made by the reviewers assigned to specific areas in buildings to record if there is a waste of energy. Each wasteful behavior is considering a failure and, if it is possible, interventions on situ must be conducted to timely eliminate and / or reduce energy wastage.

2.4 Indicators

Sustainable indicators are calculated based on weekly records. There are several factors to consider for measuring performance. Wastages are expressed in financial, environmental, and power metrics. Indicators from 2008 to 2010 are shown in tables 2 to table 4.

2.5 Dissemination of information

Increasing energy conservation awareness among the university member is imperative in order to reduce energy wastage behaviors. A key requirement of the SMS is the divulgation of indicators on a quarterly basis. This is done throughout flyers, brochures, and emails.

2.3 *Sustainability Management System (SMS) Survey*

A survey was conducted to faculty members, students, administrative staff and service personnel to indicate which energy conservation initiatives would be willing to follow, such as: turn off the lights at the term class, turn off the air conditioned when the classroom is not in use, close doors and windows to avoid that the air-conditioning air leakage, etc. The surveys were applied to 650 members of the university community. The selection of individuals was selected by a simple random sampling method. The sampling Eq. (1) is following showed:

$$n = \frac{Z^2 \; p \; q \; N}{\mathrm{N\,E^2 + Z^2\,pq}} \qquad (1)$$

Where n is the sampling size, Z is confidence level, p is positive variation, q is negative variation and N is population size.

3. Results

3.1 Awareness Survey

The results of the SMS survey are presented in Table 1. In general, most of participants are becoming aware of the impact of the energy wastage and they are willing to participate in the SMEE in order to reduce those environmental impacts. Findings also show that willingness of the university community for participating or supporting more than one energy conservation initiatives; the behavior of turn off lights and air conditioners when finishing the class is the preferred option.

Table 1 Awareness survey

Item	Yes	No
Support the SMS	75	25
Energy Wastage Awareness	70	30
Willingness to participate in the SMEE	90	10
Participation on more than one initiative	95	5
Turn off the lights/ classrooms/room	38	62
Turn off the AC	35	65
Closing door or window/ AC	18	82
Turn off the PC Monitor	9	91

3.2 Calculations of electrical energy metrics

Table 2 shows the monitoring records for 2008, there were recorded 1759 energy wastage events, denominated failures; however; it was possible to intervene an avoid the impacts associated with in 882 out of those 1759. Thank to these interventions, there were avoided the wastage of 10,188 kw; and consequently, the emissions of 9271 kg of CO2. In monetary terms, savings were 1,626 USD.

Table 2. 2008 Sustainability Indicators

Indicator	Units	Amount
Failures	events	1759
Interventions	events	882
Avoided Energy Wastage	kw	10,188
Avoided CO2 emissions	kg	9271
*Savings	USD	1,626

* Exchange rate: US$ 1.00 = MX$ 12.53 at December 14, 2010.
Source: Banco Nacional de México, S.A.

Records for the entire 2009 are shown in Table 3. During this year, there were 446 interventions that avoided the wastage of 11,579 kw and the emissions of 1265.63 kg of CO2. This represented a saving of 1,848 dollars for the institution.

Table 3. 2009 Sustainability Indicators

Indicator	Units	Amount
Failures	events	2,322
Interventions	events	756
Avoided Energy Wastage	kw	11,579
Avoided CO2 emissions	kg	10,536
*Savings	USD	1,848

* Exchange rate: US$ 1.00 = MX$ 12.53 at December 14, 2010.
Source: Banco Nacional de México, S.A.

Table 4 shows records for 2010; the energy wastage avoided was 14,812 kw that represents 13,479 kg of CO2. Figure 1 illustrates the 2008-2010 trend of each indicator; it is possible observe on it the improvements per year of each indicator which suggest that SMEE is fulfilling its goal.

Table 4. 2010 Sustainability Indicators

Indicator	Units	Amount
Failures	events	3,467
Interventions	events	936
Avoided Energy Wastage	kw	14,812
Avoided CO2 emissions	kg	13,479
*Savings	USD	2,364

* Exchange rate: US$ 1.00 = MX$ 12.53 at December 14, 2010.
Source: Banco Nacional de México, S.A.

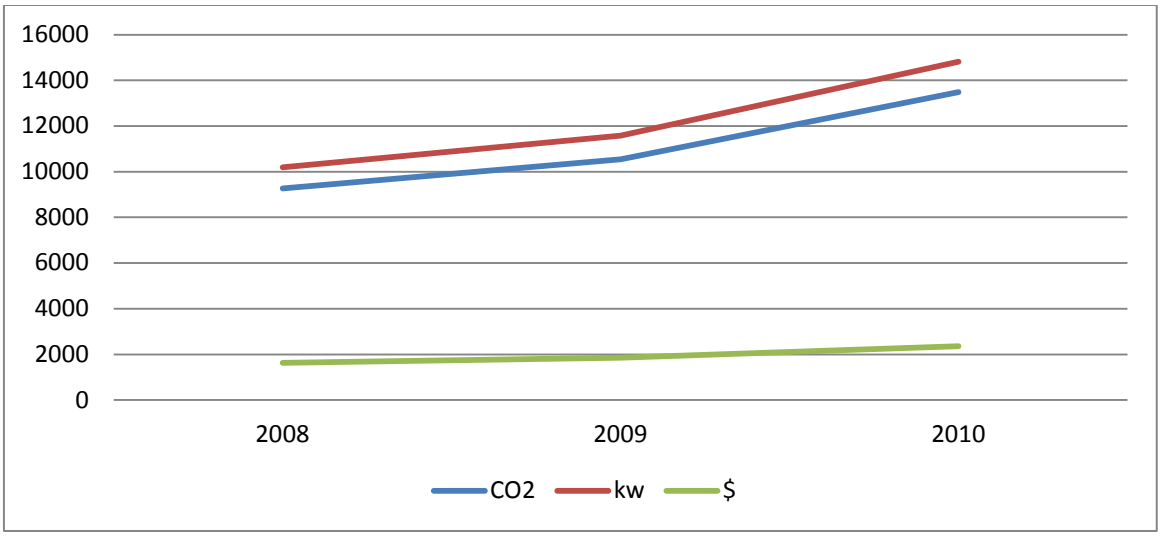

Fig 1. Sustainability Indicators Trend

4. Conclusion

The University of Sonora, through initiatives like the Sustainable Management of Electrical Energy (SMEE) Program, shows that it is possible for universities to reach important economic, social and environmental outcomes.

Findings presented in this paper indicate that changes on attitudes and behaviors can generate good practices for conserving energy and reduce the environmental burden of universities.

Sustainability indicators have proven the efficacy and efficient of the SMEE; at the financial dimension, the SMEE has reached savings of over 5, 840 USD in three years; from the environmental dimension, the SMEE has avoided the emissions of 33,287 kg of CO2, but the most important indicator come from the social dimension where wasting behaviors have been modified by increasing community awareness. Positive trends on the SMEE indicators suggest the increasing of awareness of the impact of energy wastage among the university community who act in consequence of this in favor of the environment.

Result from the 2010 survey indicated the willingness of the community to support and fully commitment to the SMS and in particular with the SMEE.

Become a more sustainable university is a hard task that cannot achieve without the participation of the community, mainly students; they need to get a better understanding of human health exposures and environmental impacts generated because energy wastage.

Turning off lights when the classrooms are not being used or by closing doors when the air conditioned equipment is in use, it can be very helpful for sustainability on campus; yet, before the operation of the SMEE, these events were very common in university lifestyle. Although today those practices still are present, they are not the common denominator. It is clear that the path to sustainability is full of obstacles; yet, there is no other way.

References

[1] D. Aerts, B. True, Energy Conservation and Renewable Energy in Homes, Journal of Chemical Education Vol. 83, No. 10, 2006, pp 1440-1443

[2] B. Gallachoir, M. Keane, E. Morrissey, E. O´Donnell, Energy and Buildings 39, 2007, pp. 913-922

[3] W. Burroughs, Climate Change: A multidisciplinary Approach, Second Edition, 2007, Cambridge University Press, ISBN 978-0-521-87015-3.

[4] Environmental Protection Agency 2010. On line: January 25, 2011 Available at:

(http://www.epa.gov/greenkit/q5_energ.htm).

[5] L.Velazquez, N. Munguia, J. Esquer, et. al., Sustainability leadership by implementing the ISO 14001 framework on a Latin-American Campus, in book Sustainability at Universities-opportunities, challenges and trends, Peter Lang , 2009, vol. 31, pp. 207-224

[6] Banco Nacional de México (2010). Online: December 12, 2010. http://www.banamex.com/

Energy and Environmental Aspects of Data Centers

Sabrina Spatari[1,*], Nagarajan Kandasamy[2], Dara Kusic[3], Eugenia V. Ellis[4], Jin Wen[1]

[1]*Dept. of Civil, Architectural, and Environmental Engineering, Drexel University, Philadelphia, USA*
[2]*Dept. of Electrical and Computer Engineering, Drexel University, Philadelphia, USA*
[3]*Coriell Institute, Camden, USA*
[4]*Dept. of Architecture & Interiors, Drexel University, Philadelphia, USA*
** Corresponding author. Tel: +215-571-3557, Fax: +215 895-1363, E-mail: spatari@drexel.edu*

Abstract: Data centers have become an essential operational component of nearly every sector of the economy, and as a result growing consumers of energy and emitters of greenhouse gases (GHGs). Developing strategies for optimizing power usage and reducing the associated life cycle GHG emissions are critical priorities for meeting climate policy objectives. We investigate data center power management through virtualization, a technique that consolidates data center workloads onto fewer computing resources within a data center and deploys computing resources only as needed. Based on an experimentally validated dynamic resource provisioning framework applied to a small scale computing cluster at Drexel University that employed lookahead control, a control scheme using virtualization demonstrated a 25% reduction in power consumption over a 24-hour period. Using the power savings results from the virtualization experiments, and extrapolating those savings to a medium-sized data center that hosts 500 servers, we estimate the avoided life cycle GHG emissions for implementing a virtualization strategy in hourly time-steps for marginal and average electricity units over a 24-hour day during the month of August, when electricity loads are typically highest for the year. Results from this work show virtualization could avoid the emission of approximately 0.8 to 1.2 metric tons CO_2e/day.

Keywords: *Energy, Power management, Buildings, Information technology, Life cycle assessment*

1. Introduction

Data centers have become an essential operational component of nearly every sector of the economy, and are additionally growing consumers of energy, and as a result, a burgeoning source of greenhouse gas (GHG) emissions. In 2008, data centers worldwide emitted 170 million tons of CO_2, an output on parallel with the total GHG inventory of countries such as Argentina and the Netherlands. Moreover, data center GHG emissions are expected to grow four-fold by 2020 and surpass those of the airline industry [1]. Therefore, developing strategies for optimizing power usage and reducing the associated life cycle GHG emissions are critical priorities for meeting climate policy objectives.

This paper investigates use of new techniques for server power management and validates them using a small-scale computing testbed. The validation experiments are integrated with environmental life cycle models that evaluate the consequential reduction in life cycle GHG emissions of computing equipment and data centers as a whole as a result of the power management strategy in combination with expected input sources of electricity and regional electricity mixes. We accomplish this by coupling the data center power optimization strategy with a life cycle model of electricity supply that examines the average electricity mix and marginal units of power supply over a 24-hour period. The power management strategy we examine is known as virtualization, a technique that consolidates multiple online services onto fewer computing resources within a data center and deploys computing resources only as needed.

1.1. Background

Energy management in data centers involves three main components of computer hardware, building, electricity infrastructure: power load distribution of the data operations; cooling

systems employed to control ambient conditions in the buildings that house the computers (the HVAC systems); and the electric power supply system (the electricity grid) and sources that make up each composite unit of electricity (measured in kWh) delivered to the data center, consisting of hydro-electric, nuclear, coal, natural gas, oil, and renewable sources (e.g., wind power, biomass, geothermal, etc). In addition to the in-use consumption of energy and emission of GHGs, the three components of a data center (building, hardware, electric utility infrastructure) carry "upstream" energy and GHG emissions owing to the processes and resource inputs and capital equipment used to produce (mine, manufacture, transport, and construct) a data center.

A typical data center serves a variety of companies and users, and the computing resources needed to support such a wide range of online services leaves server rooms in a state of "sprawl" with under-utilized resources. Moreover, each new service to be supported often results in the acquisition of new hardware, leading to server utilization levels, by some estimates, at less than 20%. With energy costs rising and society's need to reduce energy consumption, it is imprudent to continue server sprawl at its current pace.

Virtualization provides a promising approach to consolidating multiple online services onto fewer computing resources within a data center. This technology allows a single server to be shared among multiple performance-isolated platforms known as virtual machines (VMs), where each virtual machine can, in turn, host multiple enterprise applications. Virtualization also enables on-demand or utility computing, a dynamic resource provisioning model in which computing resources such as the central processing unit (CPU) and memory are made available to applications only as needed and not allocated statically based on the peak workload. By dynamically provisioning virtual machines, consolidating the workload, and turning servers on and off as needed, data center operators can maintain service-level agreements (SLAs) with clients while achieving higher server utilization and energy efficiency.

In this research paper, we apply an experimentally validated dynamic resource provisioning framework for integrated power and performance management in virtualized computing environments developed by Kusic and Kandasamy [2,3,4]. Prior research by the authors demonstrated the novelty of the application of advanced control, optimization, and mathematical programming concepts to provide the necessary theoretical basis for this framework. The authors posed the power/performance management problem as one of sequential optimization under uncertainty and solve this problem using limited lookahead control (LLC), an adaptation of the well-known model-predictive control approach [2]. The framework solves an online optimization problem that maximizes the performance objective over a given prediction horizon, and then periodically rolls this horizon forward. The LLC approach allows for multiple objectives (such as power and performance) to be represented as optimization problems under explicit operating constraints and solved for every control step. It is also applicable to computing systems with complex non-linear behavior where tuning options must be chosen from a finite set at any given time (such as the number of physical machines and/or VMs to power up/down). Experimental results obtained using a small-scale cluster show significant promise that LLC can systematically address performance/power problems within the highly dynamic operating environment of a data center. Table 1 summarizes results from prior research that demonstrated that the server cluster, which hosted six heterogeneous servers that host multiple online services, when managed using LLC saved, on average, 26% in power consumption costs over a 24-hour period, when compared to the uncontrolled case when no servers are ever switched off.

Table 1 Control performance, measured as average energy savings and SLA violations, for different workloads[a]

Workload	Total Energy Savings (%)	% SLA Violations (Silver)	% SLA Violations (Gold)
Workload 1	18	3.2	2.3
Workload 2	17	1.2	0.5
Workload 3	17	1.4	0.4
Workload 4	45	1.1	0.2
Workload 5	32	3.5	1.8

[a] Notes: The cluster hosts two services, termed "Gold" and "Silver" enabled by the Trade6 and DVDStore applications. The services generate revenue as per a non-linear pricing scheme that relates the achieved response time-300 ms for each Gold request and 200 ms for each Silver request-to a dollar value. Response times below the threshold result in a reward paid to the service provider, while response times violating the SLA result in the provider paying a penalty to the client.

2. Methodology

We apply life cycle assessment (LCA) methods following ISO 2006 [5] procedures to examine the potential for reducing life cycle greenhouse gas (GHG) emissions when employing power management via virtualization. We examine avoided electricity consumption and GHG emissions based on hourly marginal units of electricity in the Pennsylvania-New Jersey-Maryland (PJM) power mix, and in this way use a consequential LCA approach to the problem [6]. The system boundary investigated consists of the data center work load management on 500 central processing units (CPU), overhead building HVAC needs, and the power grid mix that comprises power supply to the data center (Figure 1). A complete LCA model of the system performance outlined in Figure 1 would normally account for the "upstream" energy and associated GHG emissions of the building, computer hardware, and electric utility infrastructure) in addition to their contributions during operation. However, in this paper we limit our scope to operation related energy and environmental performance to isolate the performance of the virtualization strategy independent of system attributes, but we evaluate the changes in life cycle performance induced on the system by the virtualization strategy.

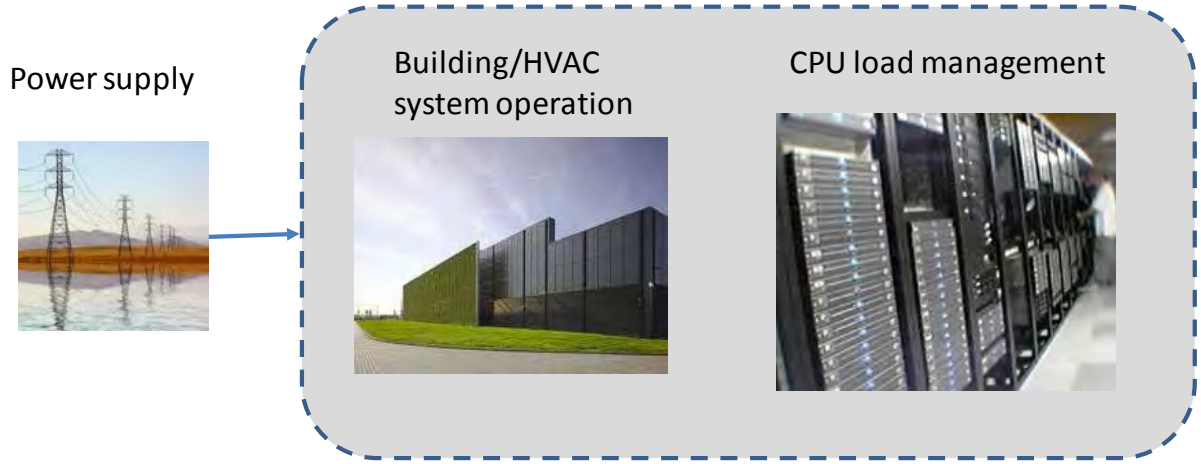

Figure 1: Systems boundary comprising data center and power supply

2.1. Power Management by Virtualization

As noted above, experiments conducted on a cluster of Dell PowerEdge servers indicate that the controller achieves a 25% to 46% reduction in power consumption costs for six different

workloads over a 24-hour period when compared to an uncontrolled system while achieving the desired QoS goals.

Figure 2 shows the LLC scheme where we obtain the control actions governing system operation by optimizing the forecast system behavior for the performance metric over a limited prediction horizon [3]. The controller obtains the sequence of control actions that results in the best system behavior over this horizon and applies the first action within this sequence as input during the current time instant. It then discards the rest and repeats this process at each time step. Thus, in a predictive-control design, the controller optimizes the performance metric at each sampling-time instance, taking into account future variations in the environment inputs and their effects on system behavior.

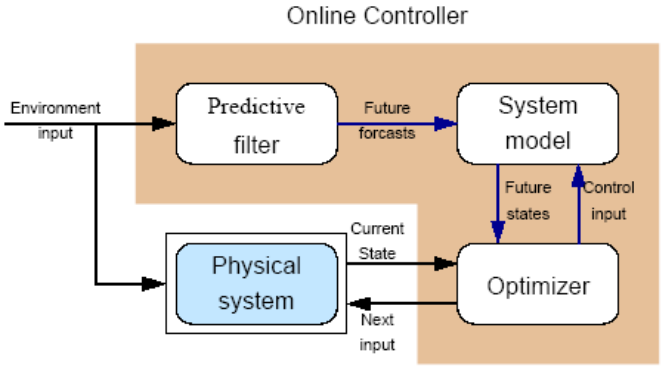

Fig. 2: Structure of the limited lookahead controller

The computer testbed cluster, when managed using LLC saves, on average, 26% in power consumption costs over a 24-hour period, when compared to the uncontrolled case when no servers are ever switched off. Also, when the incoming workload is noisy, the risk-aware controller provides superior performance compared to a risk-neutral one by reducing both SLA violations and host switching activity.

2.2. Life Cycle Inventory Analysis

We constructed a life cycle assessment (LCA) model focused on the consequential GHG emissions avoided through implementation of the virtualization experiments scaled to a small-medium sized data center hosting 500 CPUs. We applied tests from workload simulations that achieved a 41% energy savings relative to the uncontrolled case noted in section 2.2 and assume that power savings scale linearly from the testbed cluster experiments to the 500-CPU data center. For the LCA model that we construct here, we consider the reduced demand for power to the data center resulting from consolidating workloads onto fewer machines. Therefore with respect to unit processes considered in the LCA model, we take into account only the power supply needed for the CPUs in the data center, and do not take into account optimizing the HVAC system shown in Fig. 1. However, we note that a control scheme that seeks to minimize overall energy consumption can include inputs from the building cooling systems and environmental ambient conditions.

3. Results

A systematic analysis of energy savings allowed through optimization of power management in a data center requires consideration of the electricity supplying the data center and the upstream fuel/resource extraction and transport of energy sources to individual power plants (e.g., coal, nuclear, natural gas, and fuel oil). Typically LCA models employ life cycle

inventory (LCI) data that describe electricity grid mixes averaged over time. Over a year, the national U.S. electricity grid tends to average out to approximately 51% coal, 21% nuclear, 16% natural gas, 7% hydro-electric, 3% petroleum, and 3% other, including renewable sources [7]. However, around the different regions of the U.S., regional averages are known and can be used to estimate net life cycle emissions related to power consumption.

LCA attempts to quantify the resource intensity and damages associated directly with the flow of resources and wastes associated with products, processes, and activities, or more generally, "systems". Analysts have tried for some time to track inputs and outputs across different economic sectors in order to capture actual energy and materials consumed for those systems. The structure of electric power distribution within a regional grid does not make it possible to trace individual electrons from source to sink, which is why analysts use average electricity mixes. In the case of data centers, a better approach for understanding power consumption by source, is to track electricity consumption by time of day, as this would show how the data center consumes electricity during peak and off-peak times, and thus the implications for using coal, the highest carbon emitting power sources, versus natural gas, the more efficient of the carbon-emitting sources.

Another debate in LCA literature regarding the trace of electricity usage is the question of whether to count the marginal or the average unit of electricity output. Some argue that each additional unit of demand placed into an electricity grid should correspond to the marginal unit consumed. For example, if a new data center is constructed and it sources its power from the Northeast electricity grid, the marginal unit approach would assume that electricity consumed came from the last kWh of output, the marginal source, since the overall mix at any given time is already meeting existing demand. Analyzing the problem this way, we would expect that a new data center built into a region and relying on electricity supply, would therefore use the marginal unit at each time step during the day. Put another way, any savings in energy from the data center would save GHGs from the marginal unit of output. For the majority of the peak hours, of the day, this could reduce coal-sourced power. At mid-peak hours this may reduce lower-GHG emitting natural gas sources, and in off-peak hours it may save coal-GHG emissions. Approaching the problem this way, we took data from a typical power supply curve on a peak August month, approximated the electricity mix based on peak load distribution curves (Figure 3), and then approximated the mix and GHG savings or avoided coal power based on a data center optimization strategy.

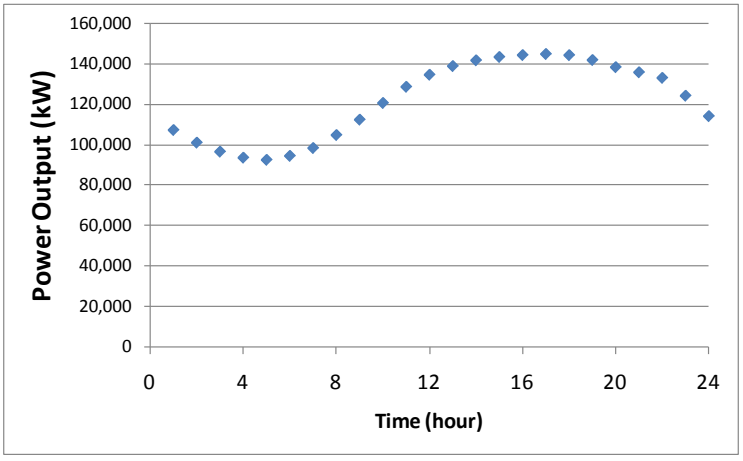

Figure 3: Peak load distribution in August 2006 (source: PJM)

The energy savings over the 24 hour day allow up to 61% power savings during late hours and early afternoon, when marginal sources shift between coal and natural gas. Figure 4 shows the energy savings over the 24-hour period resulting from optimizing workloads in the data center (see References [3] and [4] for further detail on the workload trace and optimization scheme applied). The largest energy savings occur during hours 3 to 15 of the day, corresponding largely with peak power demand times. Accordingly, there could be significant savings in net life cycle GHG emissions from fossil energy sources.

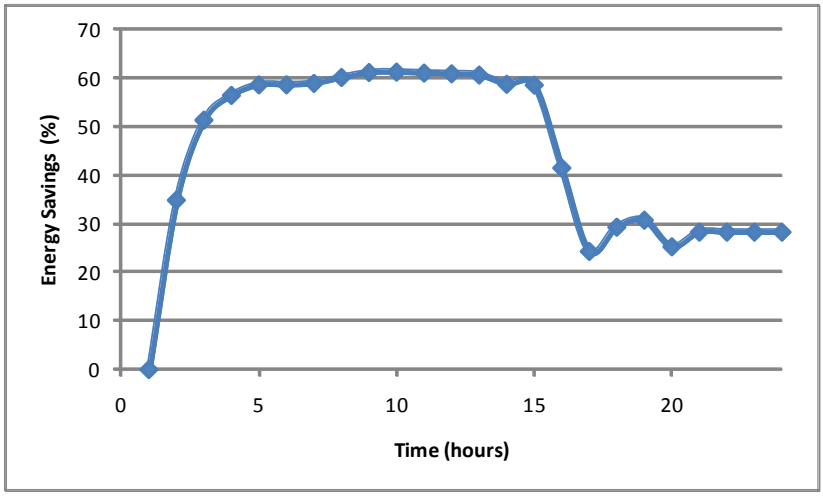

Figure 4: Energy Savings over a 24-hour period estimated in 2-minute intervals

We combined the hour-by-hour energy savings estimates with the life cycle electricity supply measured in average and marginal units based on the PJM electricity grid. Figure 5 shows the avoided GHG emissions from deploying the virtualization strategy. We see that counting the marginal unit of electricity results in a larger estimate of avoided GHG emissions. This is especially evident between hours 4 through 11, and is the result of an expected reduction in GHG emissions from coal-based electricity, the marginal unit used during that time interval.

When we sum up the avoided GHG emissions over the day by integrating over the two curves shown in Figure 5, we find that a medium sized data center can avoid 0.8 metric tons CO_2e day^{-1} and 1.2 metric tons CO_2e day^{-1} when counting the average and marginal units of electricity avoided, respectively.

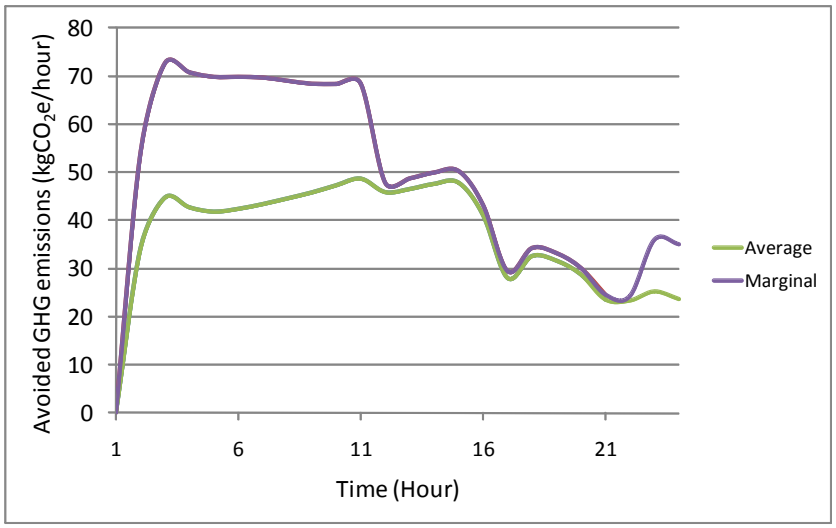

Figure 5: Estimated avoided greenhouse gas emissions resulting from Energy Savings over a 24-hour period estimated in 2-minute intervals

4. Discussion

This research demonstrates the usefulness of LCA models to estimate the full set of resources saved and environmental damages avoided by power management in data centers. We focused on energy savings enabled through power management. During runtime, the data center is typically managed to reduce resource consumption from the computing, power and cooling infrastructures, and SLAs are used to define the operational requirements of the infrastructure based on the desired performance. The life cycle approach builds in the upstream resources that supply the data center, and time-of-day analysis further delineates specific resources consumed coupled with typical demand patterns of internet resources.

The model tested herein describes performance of one data center located in a particular climate zone during summer peak power demand times, with electricity supply from that zone. This may not be the case in practice since data centers are located throughout the world and different data centers may be deployed as coupled systems when needed in order to optimize performance constraints other than energy/environmental. Knowing this, there may be opportunities to migrate workloads to data centers around the globe to take advantage of latitudes and climates that have the ability to employ passive cooling, and thereby reduce further the need for energy demand on data center HVAC. Design and control of the data centers may also create synergies with renewable power such as wind that tend to go online at night or potentially other day-time renewable energy sources such as photovoltaic for electricity supply. Through scenario analysis that uses LCA, novel building and locating strategies can be identified to further reduce the energy and carbon intensity of this sector. Understanding the interaction between data center location and real time power consumption is critical to optimizing computer cluster usage, since demand during peak hours tends to source marginal sources of power (coal), which tend to be the highest CO_2 emitting sources, rather than low-emission alternative sources of energy. These aspects will be investigated in relation to data center design, resource planning, and operation in future work.

There is much opportunity to improve data center performance as part of building design for specific climate zones and in selecting power aware computing hardware. Addressing building design, cooling strategies may include locating the data center on the ground floor or in underground spaces. Certain design approaches for passive cooling of the data center include use of underfloor air distribution systems with natural convection to create zoned

ecosystems around equipment, localized air-handling units to redirect warm air from equipment rooms to other building zones, and outside air for cooling. Much additional energy savings can be achieved through coupling building/architectural design components into the power management and control strategy. Temperature sensors, embedded in the physical infrastructure, can be used to guide resource-provisioning decisions that consider the data center as a whole rather than at the level of an individual cluster(s). Workload can be dynamically managed taking into account the impact of provisioning decisions on the overall operating cost of the data center (for example, cooling costs). Automated migration of a virtualized workload from one set of servers located in a hot zone to a cooler zone in the data center (or one that costs less to cool) has potential to significantly reduce cooling costs and overall energy and GHG emissions.

Building on the preliminary results discussed here, our future work will aim to develop a control framework wherein power/performance criteria can be applied to all aspects of data center operation. Such a framework would aim to analyze the three critical components, hardware, building, and electric utility infrastructure (Figure 1) for designing “green” data centers on a life cycle basis, along with operational control and location choice.

Acknowledgements

This research was supported by the Drexel Engineering Cities Initiative (DECI) at Drexel University. Spatari thanks A.E. Huemmler of the University of Pennsylvania for comments and discussion on this manuscript.

References

[1] McKinsey & Co., Report: Revolutionizing Data Center Efficiency, 2008.

[2] D. Kusic and N. Kandasamy, "Risk-Aware Limited Lookahead Control for Dynamic Resource Provisioning in Enterprise Computing Systems," Cluster Computing: Special Issue on Autonomic Computing, v. 10, n. 7, Kluwer Academic Publishers, Dec. 2007, pp. 395-408.

[3] Kusic, D., J. O. Kephart, J. E. Hanson, N. Kandasamy, and G. Jiang, “Power and Performance Management of Virtualized Computing Environments via Lookahead Control," Cluster Computing, vol. 12, no. 1, pp. 1-15, Springer Netherlands, March 2009.

[4] D. Kusic, J. Kephart, J. Hanson, N. Kandasamy and G. Jiang, "Power and Performance Management of Virtualized Computing Environments via Lookahead Control," Proc. IEEE Conf. on Autonomic Computing (ICAC'08), Chicago, IL, Jun. 2008, pp 3-12.

[5] ISO, 2006. ISO 14044: Environmental management — Life cycle assessment — Requirements and guidelines. International Standards Organization, Geneva.

[6] Ekvall, T., Weidema, B.P., 2004. System boundaries and input data in consequential life cycle inventory analysis. International Journal of Life Cycle Assessment 9, 161-171.

[7] Kim, S.; Dale, B., “Life Cycle Inventory Information of the United States Electricity System,” (11/17 pp). The International Journal of Life Cycle Assessment 2005, 10, (4), 294-304.

An Intelligent Knowledge Representation of Smart Home Energy Parameters

Mario J. Kofler*, Christian Reinisch, Wolfgang Kastner[1]

Vienna University of Technology, Automation Systems Group, Vienna, Austria
** Corresponding author. E-mail: mjk@auto.tuwien.ac.at*

Abstract: Homes in today's world tend to include more and more electrically powered devices. Much effort is put on improving these facilities, but their integration towards a smart home often remains unconsidered. While there are some promising approaches to integrate devices with the help of knowledge bases, they are still not fully convincing. In all cases they fail to cover the energy behavior of installed devices which is a severe shortcoming with respect to the increasing energy demand of a home. As most residents are still unaware where the energy is consumed and which actions eventually lead to a lower demand, an energy related knowledge representation is of importance. This paper proposes such an energy knowledge base modeled as ontology. This artifact comprises a comprehensive collection of miscellaneous energy related information and allows home automation systems to make intelligent decisions upon this knowledge. Using the ontology, energy consumption in the home itself can now be optimized by executing intelligent control strategies that incorporate and exploit the additional knowledge in their algorithms. Likewise, also renewable energy suppliers are represented and may be considered by a smart home system in order to reduce the overall ecological footprint of the residents and provide additional services for home control.

Keywords: *Energy Parameters, Smart Homes, Ontologies*

1. Introduction

The deployment of automation technology in the home offers several attractive benefits, among them most prominently increased energy (or even resource) efficiency, improved residential comfort and peace of mind for the home owner. As private households are undoubtedly one of the main energy consumers today, also a positive effect for the environment can be expected if energy consumption is reduced. In the last decade, **smart homes** have emerged as the keyword for such automated dwellings. The vision is a house populated by a multitude of devices (actuators and sensors) that cooperate in an intelligent way to control different domains of the home such as lighting/shading, heating/ventilation/air-conditioning but also home appliances and consumer electronics. While in building automation well established solutions have already existed for a longer time, additional challenges arise for systems that need to be tailored to the needs of private households: In this domain, integration of diverse appliances into a homogeneous system is far from trivial due to different interfaces, usage paradigms and operation modes. Additionally, the intelligence promised by smart homes requires tailored use cases and scenarios to be developed and offered by the future systems. Consider, for example, a smart home system automatically scheduling a dishwasher to start when energy from renewable energy sources becomes available, e.g., when the sun is shining on a photovoltaic installation or once some energy provider offers cheap energy. Such a system could also be the central point to integrate demand side management [1] applications into the house, e.g., by shifting energy intensive operations to a more convenient point in time. These use cases require not only all devices to be interoperable but also demand some understanding of the current state of the affected environment. Information about the building, its embedded devices, its tenants and their

[1] This work was funded by the HdZ+ fund of the Austrian Research Promotion Agency FFG under the project 822170.

behavior as well as of the inside and outside conditions must be available and represented in some way for the smooth and successful operation of the smart home system.

2. Motivation

More and more energy facilities in modern buildings become interlinked in order to allow advanced control over various parts of the house. Up to now, however, only basic services are featured: lights and shutters can be linked via pre-configured scenes, or, for example, a central "OFF" function can be provided. More intelligent functions like ensuring comfort in a residential home while at the same time behaving energy efficiently are not feasible yet. The reasons for this are manifold, but one of the most important issues is the interoperability of devices. This integration is often not guaranteed due to the heterogeneity of underlying technologies. An orchestration of their services can often just be achieved through interconnection using gateways which are difficult to configure and may still limit inter-device services [2]. Once integrated, all devices may be controlled and operated through a central home control system. However, this does not automatically imply that also all data of the devices becomes available throughout the integrated system. Based on these current shortcomings of smart homes, two main challenges can be identified: the need for an integrated system where all devices can equally participate, and some storage facility that provides pervasive access to all kinds of data originating from devices, the smart home or other sources. Thus, an abstract view on the underlying technologies is desirable to facilitate the integration of different building automation devices and also home applications. Further, often it is not known to a resident how much energy certain devices in the household consume. Many devices also waste energy when they are currently not in use e.g., during their stand-by times. To reduce these idle times it would help a smart home to know about the occupancy of rooms and during which times facilities in the home are mainly used. Especially in the case of consumer electronics like TVs it makes sense to unlink them from the power grid during times when the residential home is not occupied and just turn them back into stand-by mode when usage is expected. For household appliances like dishwashers or washing machines it would be beneficial to know how to schedule tasks with respect to the energy supply side. This way, peak loads on the power grid can be reduced and at the same time the environmentally friendliest energy provider can be chosen. The definition of energy tariffs and providers in the knowledge base of the smart home therefore allows yet unconsidered improvements with respect to energy consumption. The representation of such facts needs to be sophisticated and open to changes, because it is not only likely that new and probably unknown devices are added to the smart home, but also information about energy providers and their tariff schemes are changing frequently. These difficulties are addressed by the realization of a knowledge base for smart homes that is proposed in the following chapter.

3. Methodology: An Ontology for Smart Homes

The intelligent information representation in smart homes is necessary, not least because of the vast amount of influences to be considered for an energy efficient operation of the building. To model the data dependencies in an expressive way, the representation as OWL ontology is proposed. OWL is a recommendation of the World Wide Web Consortium (W3C) [3] and its Semantic Web Initiative. The Web Ontology Language bases its form and representation on a formal logic called Description Logic (DL) [4]. With this formal grounding, relationships and concepts existent in DL as well as the possible logical implications can be used in OWL for modeling the represented domain in a sophisticated manner. This way, more complex structures can be expressed than in alternative possibilities like relational database systems. Opposed to classical database schemes, the well-defined

logics of DL further allow reasoning over explicitly modeled facts in the knowledge base. This way, the inference of new information out of existing data becomes possible, and queries can be already stated in the knowledge base itself (cf. Sect. 4.2). Also the consistency of the knowledge representation can be assured automatically by the reasoning mechanism, when considering for example the addition of new concepts and relationships. In the case of smart homes, all knowledge can therefore be well organized and brought into an intelligent structure that subsequently can be accessed by the smart home system.

3.1. Ontology Overview

The proposed knowledge base consists of several modules which contain different kinds of parameters important for an energy efficient operation of smart homes (Fig.1).

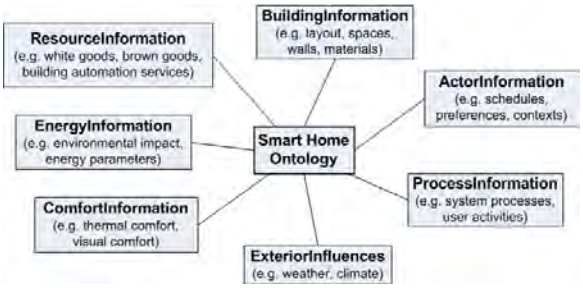

Fig. 1. Smart Home Ontology Main Modules

These different parts are, for example, a building representation including information about architecture and building physics, a user part with preferences as well as an exterior influences module holding for example weather data. In this work, focus is put on the resources and energy parts of the knowledge base: The **resource representation** describes the available facilities and their characteristics. The entire home environment and equipment has to be modeled in the knowledge base for a control system to have a complete view of the operable world, i.e., the building and its devices. The **energy representation** is an important source of information about energy demand and energy supply of the smart home. One of its purposes is to allow a software system to base its operational decisions on the status of the connected facilities in the smart home. Further, a representation of energy providers and energy tariffs enables an ecological and economical use of different energy forms such as electricity or district heating, with respect to renewability and energy costs. The next section describes these two parts in detail and explains the benefits of expressing facility and energy parameters as a linked knowledge store.

3.2. Facilities and Home Automation Systems

In home and building automation (HBA), the interaction of numerous kinds of devices is desirable. In most cases integration is not directly possible because of the heterogeneity of different home automation network standards. With DomoML [5] and DogOnt [6], there already exist two approaches that propose the use of ontologies in this context. DomoML is one of the first proposals structurally modeling household appliances with the help of ontologies. While DogOnt reuses certain ideas of this taxonomy, it tries to overcome limitations of DomoML. As ontology reuse [7] is highly recommended in ontology design, the DogOnt ontology was chosen as a starting point for the resource module of the proposed knowledge base. While not perfectly suitable for reuse, the DogOnt implementation provides an extensive and sophisticated representation of building facilities, functions and possible modes of operation. The authors of DogOnt put the focus of their knowledge base on the

intelligent integration of home facilities and automation components and aim at building automation service interoperability [6]. However, energy related issues like energy supply or demand of mapped home automation systems and home appliances have not been considered. Also, building information has only been rudimentarily treated. These facts make the DogOnt ontology a good candidate for integration into the proposed smart home ontology. Referring to Fig.1, the DogOnt ontology can represent the resource part, while interfacing with the more detailed building information branch as described in [8] and the newly developed energy representation module presented in Chapter 4. However, the ontology of the DogOnt project contains several severe design flaws, especially with respect to ontology normalization. Among others, important ontology normalization steps like avoiding asserted polyhierarchies and instead using hierarchical tree structures have been ignored by the creators of DogOnt. Nevertheless, as stated in [9], a normalized ontological representation significantly raises the reusability and is therefore considered as key requirement for large ontologies. As a consequence, the DogOnt representation is first adapted into a semi-normalized form by reformulation of comparatively weak parts of the ontology while making a tradeoff between fully normalized form and practicability. The key design focus of this reformulation is to keep the original hierarchy as far as possible, but, for example, to only allow polyhierarchies to be automatically asserted by a DL reasoner (e.g., Pellet [10]). This normalized version of DogOnt is subsequently integrated into the proposed knowledge base.

4. Results: Energy Information Representation

In order to describe information from the energy domain for a smart home system, some important concepts need to be modeled. These so-called top-level concepts contain the following necessary classifications:

- *Energy providers*: This concept comprises all external energy suppliers providing some form of energy for the residential home.
- *Energy tariffs*: The tariffs that are charged by an energy provider to supply a certain energy type.
- *Energy types*: The different energy types that are available and are either supplied by energy providers, or used as source of energy to produce some secondary energy.
- *Energy facilities*: All energy consuming or energy producing applications that are installed in a smart home.
- *Energy properties*: This concept contains information needed to model energy demand and supply as well as energy costs.

Energy representation, as module of the proposed smart home knowledge base (cf. Fig.1), therefore keeps a wide variety of different parameters useful for the energy efficient operation of a home. To provide the system with a general notion of energy, a classification of **energy types** is needed. This classification has to be tailored to the needs of a smart home with respect to modeled energy types. Therefore, a distinction between final energy, energy sources and useful energy was taken (Fig. 2). This distinction reflects the varied usage of energy types viewed from the providing side as well as from the consuming side.

The concept EnergySource is used to classify different energy providers as explained in Section 4.1 and follows the general definition of sources of energy. Two distinctions are made: The first distinction is into primary and secondary sources of energy. Electricity, for example, is a secondary energy source because it has to be gained through some primary energy source. The second distinction into renewable and non-renewable sources is especially

important for resource-efficient energy consumption in a smart home. These two concepts are finally super-concepts of the actual energy sources. Some design decisions are made in order to classify sources of energy: For example, nuclear power is assigned to the non-renewable branch as concept Nuclear, because also nuclear waste is taken into account as some type of environmental pollution.

The other two main concepts are FinalEnergy, and UsefulEnergy which both represent energy that is available for consumption in the smart home. A distinction between these two concepts is realized such that final energy contains energy types that can still be transformed to other energy forms inside the smart home while useful energy types are inconvertible. For example, gas as final energy can be used directly by a gas oven or, with the help of a gas heater, can be transformed to heat, which can subsequently be seen as useful energy.

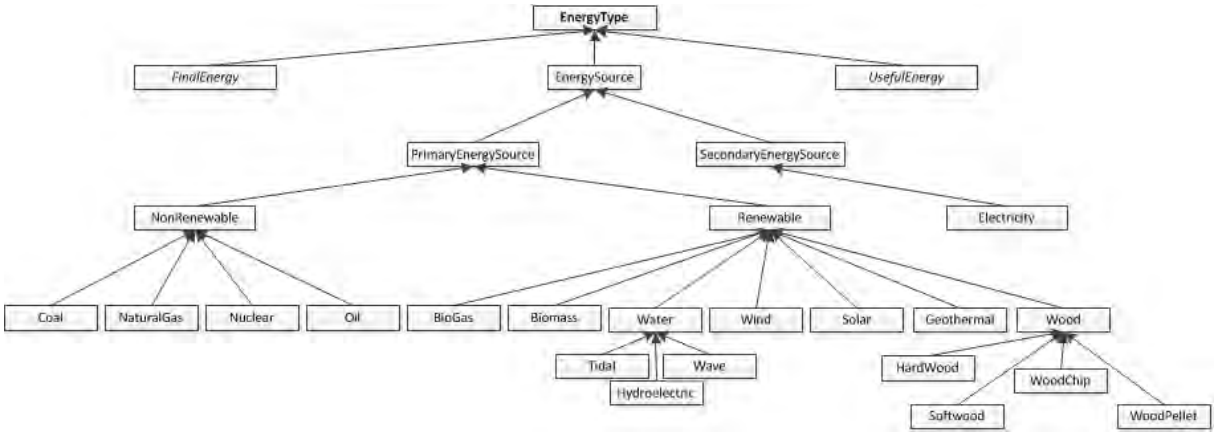

Fig. 2. Types of Energy

These two classifications of energy types do not have subclasses like the energy source branch, but merely contain concrete values which correspond to different forms of energy. This modeling technique is chosen, because for the appliance it does not make a difference if a green or non-green provider supplies the energy, however for the ecological footprint of the smart home user it does (cf. Sect. 4.2). The concrete members of the concept FinalEnergy are for example *Coal*, *ElectricEnergy*, *Gas* and *Wood*, while the concept UsefulEnergy has the members *Heat*, *Cold*, *Light* and *Water*. These groups can always be enlarged or narrowed, according to which end energies should be covered by the smart home system. As can be seen, some energy types occur twice in the knowledge base: once as energy sources and secondly as members of one of these two concepts (cf. Fig.2). The reason for this is that basically two viewpoints are being represented in the energy ontology: The **demand side** and the **supply side**. These two sides need to have a different idea of energy, because there exist energy sources that can be used by an energy provider to generate secondary energy but can also be directly used for consumption in the smart home as final energy. Also for the UsefulEnergy concept such a special case can be found: the specific resource *Water* on one hand acts as a source of energy to generate hydroelectricity, on the other hand it can be directly seen as useful energy in the smart home with different water providers and tariffs. Therefore, the classification shown in Figure 2 is considered as the one with least redundancies and most practical use. The benefits of the realization of final energy and useful energy types as individual values instead of concepts are further discussed in Section 4.2.

On one side it is important to model the demand and supply facilities which are available in the smart home itself. Certainly, it is a better choice to use energy produced by home facilities from solar radiation and geothermal heat than having to rely on the supply of energy from

energy providers. On the other side it is also necessary to keep knowledge about different energy providers and their conditions in case energy demand exceeds homemade supply. Therefore, energy information representation is divided in two main axes which contain facilities in the smart home itself, i.e., the demand side and energy producing facilities, and the supply side like energy providers and tariffs, respectively. The following two sections go into detail and describe the certain constructs that have to be modeled for these two main parts. Although a description of the whole energy knowledge representation would go beyond the scope of this paper, important constructs and design paradigms are discussed in order to demonstrate the representation of energy demand and supply in the proposed knowledge base.

4.1. Energy Providers and Supply Side

With the ongoing liberalization of energy markets, knowledge about different energy providers and their tariffs are a valuable addition to the smart home ontology. It is assumed that like in the electric energy market also other markets will be liberalized in the future and therefore a variety of energy suppliers is classified in the proposed knowledge base (Fig.3).

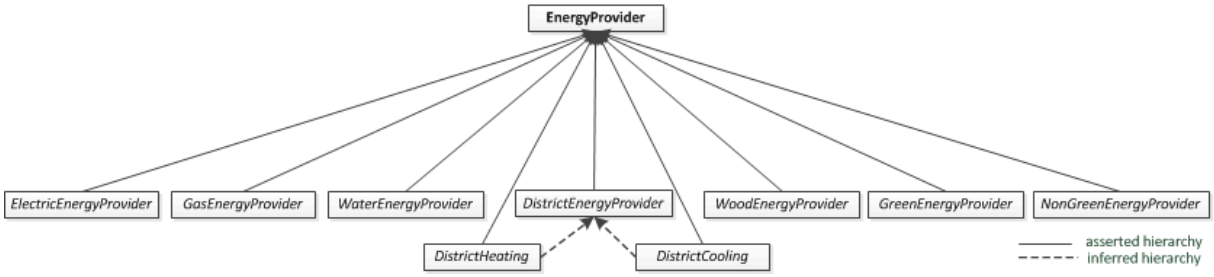

Fig. 3. Classification of Energy Providers

This conceptualization of energy providers comprises different energy forms as well as the distinction between green and non-green suppliers. Reasoning on this hierarchy with a DL-reasoner, makes inferred hierarchies possible as shown in Figure 3 for district energy providers. Furthermore, reasoning can classify newly added individual energy providers and associate them with the respective subclass. This quality of an ontological representation can aid the characterization of green and non-green energy providers with respect to the way they supply energy. For example, some electricity provider which provides electric energy only through hydropower will become a member of the classes ElectricEnergyProvider and GreenEnergyProvider. In case this energy provider adds some non-green way to provide energy (e.g., nuclear power), the classification will be automatically corrected by the reasoning mechanism and the company will further be listed as NonGreenEnergyProvider. In addition to the way how suppliers generate energy, it is needful to know the different kinds of **energy tariffs**. Of course not every company has the same rates for energy supply and also different tariff switching times can exist which have to be considered in the knowledge base too. Therefore, a general notion of time is required which is achieved by integrating the OWL-Time ontology for time representation [11]. With the reuse of this time ontology, characterization of tariffs according to their active times becomes possible. Together, energy provider and energy tariff form the main concepts of the supply side. They can further be used by a smart home control system to choose the environmentally friendliest and monetarily optimal energy supply at a specific point in time.

4.2. Energy Facilities and Demand Side

Energy facilities with respect to the smart home are all appliances which either consume or produce energy. For the facilities represented in the ontology, the actual energy consumption

as well as the maximum energy consumption per defined state of operation is stored. Further, it is important for an autonomous system to know if a certain facility needs permanent power supply. With this information, an intelligent system can for example unlink appliances from the power grid when they are not immediately needed.

The connection between energy demand side and energy supply side is made via an ontology design pattern called **class-individual mirror** described in [12]. For this design pattern, the final energy types already explained at the beginning of this chapter act as pivotal elements. The example in Fig. 4 shows the application of the pattern for these two parts of the ontology.

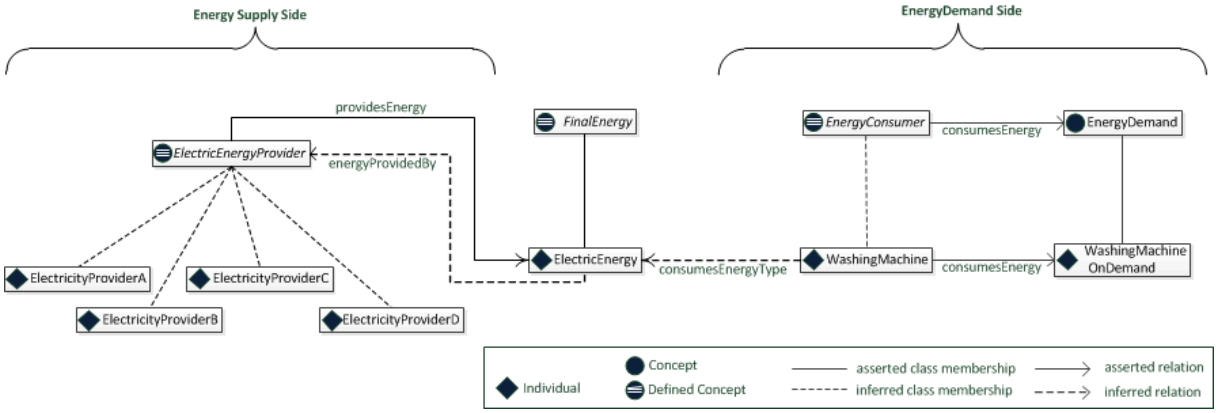

Fig. 4. Connection between Energy Providers and Energy Facilities

The benefit of using this pattern is that the pivotal *ElectricEnergy* element holds information from the energy supply side. This can be used for choosing the electricity provider on an appliance level: If the depicted washing machine is scheduled to start at a certain point in time, the home automation system just needs to know which energy type it consumes. The *ElectricEnergy* element already holds information about which energy providers supply the energy by the energyProvidedBy relation that has been inferred by the DL-reasoner. Energy tariffs and other properties of the energy providers like if they are green or non-green suppliers can subsequently be retrieved from the ontology by the properties that have been defined for each electricity company. This way, important queries have already been modeled in the knowledge base, which represents a clear advantage over classical database systems. Among other things, this leads to a higher independency between the data representation and the software system.

5. Conclusion and Outlook

This paper proposed a central knowledge base which is mandatory to enforce novel energy efficiency control strategies in smart homes. It was shown that ontologies are a well suited technology to use as smart home knowledge representation. The ontology constructs as well as the formal grounding in Description Logics allow the depiction of more detailed and interconnected information than known from classical information representation systems. Additionally, because of the foundation in logics, reasoning on stored facts becomes possible which allows inference of new information and guarantees the knowledge model's consistency. As a proof of concept, the part of energy related data was modeled as OWL ontology. Special focus was given to the domains demand side and supply side, where in particular the interrelations between the parts were discussed extensively.

A practical example of the application of the energy knowledge base is the energy efficient operation of household appliances and consumer electronics. Information about scheduled programs and desired finishing times can, for example, be used by a software system to derive which renewable energy provider offers the optimal tariff for the planned task. Furthermore, time slots for the execution of tasks give the system the ability to wait until off-peak electricity is offered, thus on one hand saving money for the customer, while on the other hand behaving environmentally friendly by consuming excess energy.

Next steps regarding the presented resource and energy ontologies will concern their integration into a software framework as well as the definition of an interface that allows autonomous smart home control systems to easily access the knowledge store. Finally, other important parts of the comprehensive knowledge base for smart homes will be defined, modeled and constantly refined.

References

[1] P. Jazayeri, A. Schellenberg, W.D. Rosenhart, J. Doudna, S. Widergren D. Lawrence, J. Mickey, S. Jones, A Survey of Load Control Programs for Price and System Stability, IEEE Transactions on Power Systems, Vol. 20, No. 3, 2005, pp 1504 – 1509.

[2] W. Kastner, G. Neugschwandtner, S. Soucek, H. M. Newman, Communication Systems for Building Automation and Control, Proc. of the IEEE 93(6), 2005, pp 1178 – 1203.

[3] W3C Recommendation, OWL 2 Web Ontology Language Document Overview, http://www.w3.org/TR/owl2-overview/, 2009, (online).

[4] F. Baader, D. Calvanese, D. L. McGuinness, D. Nardi, and P. F. Patel-Schneider (Eds.), The Description Logic Handbook: Theory, Implementation, and Applications, Cambridge University Press, 2003.

[5] L. Sommaruga, A. Perri, F. Furfari, DomoML-env: An ontology for Human Home Interaction, Proc. of the 2nd Italian Semantic Web Workshop, 2005.

[6] D. Bonino, F. Corno, DogOnt – Ontology Modeling for Intelligent Domotic Environments, Proc. of the 7th International Conference on The Semantic Web, 2008.

[7] E. Paslaru Bontas, M. Mochol, R. Tolksdorf, Case Studies on Ontology Reuse, Proc. of the 5th International Conference on Knowledge Management , 2005.

[8] M. J. Kofler, W. Kastner, A Knowledge Base for Energy-Efficient Smart Homes, Proc. of the International Energy Conference ENERGYCON, 2010.

[9] A. L. Rector, Modularisation of Domain Ontologies Implemented in Description Logics and related formalisms including OWL. Proc. of the International Conference on Knowledge Capture, 2003, pp. 121-128.

[10] E. Sirin, B. Parsia, B. Cuenca Grau, A. Kalyanpur, Y. Katz, Pellet: A practical OWL-DL reasoner, Journal of Web Semantics, Volume 5, Issue 2, 2007, pp 51 – 53.

[11] F. Pan, A Temporal Aggregates Ontology in OWL for the Semantic Web, Proc. of the AAAI Fall Symposium on Agents and the Semantic Web, 2005.

[12] D. Allemang, J. Hendler, Semantic Web for the Working Ontologist, Morgan Kaufmann Publishing/Elsevier, 2008, pp. 251 – 253.

Modeling phase change materials behaviour in building applications: selected comments

Yvan Dutil[1],*, Daniel Rousse[1], Stéphane Lassue[2], Laurent Zalewski[2], Annabelle Joulin[2], Joseph Virgone[3,5], Frédéric Kuznik[4,5], Kevyn Johannes[3,5], Jean-Pierre Dumas[6], Jean-Pierre Bédécarrats[6], Albert Castell[7], Luisa F. Cabeza[7]

1 t3e Industrial research chair, École de technologie supérieure, Montréal, Canada
2 Univ. Lille Nord de France, F-59000 Lille, France ; Univ. Artois, LGCgE, F-62400 Béthune, France
3 Université de Lyon, CNRS, UMR5008, F-69622 Villeurbanne, France
4 INSA-Lyon, CETHIL, F-69621 Villeurbanne, France
5Université Lyon 1, CETHIL, F-69622 Villeurbanne, France
6 LATEP, Université de Pau et des Pays de l'Adour, Pau, France
7 GREA Innovació Concurrent,Universitat de Lleida, Lleida, Spain
** Corresponding author. Tel: +1 (418) 653-2910, Fax: +1 (514) 396-8950, E-mail: yvan@t3e.info*

Abstract: In a recent meeting of IEA's Annex 23, several members presented their conclusions on the modeling of phase change materials behavior in the context of building applications. These conclusions were in agreement with those of a vast review, involving the survey of more than 250 journal papers, undertaken earlier by the group of École de technologie supérieure. In brief, it can be stated that, at this point, the confidence in reviewed models is too low to use them to predict the future behavior of a building with confidence. Moreover, it was found that overall thermal behaviors of PCM are poorly known, which by itself creates an intrinsic unknown in any model. Models themselves are most of time suspicious as they are often not tested in a very stringent or exhaustive way. In addition, it also appears that modeling parameters are somewhat too simplified to realistically describe the complete physics needed to predict the real life performance of PCMs added to a building. As a result, steps are now taken to create standard model benchmarks that will improve the confidence of the users. Hopefully, following these efforts, confidence will increase and usage of PCM in buildings should be eased.

Keywords: *Phase change material, PCM characterization, Mathematical model, Model validation*

1. Context

The ever increasing level of greenhouse gas emissions combined with the overall rise in fuel prices (although fluctuations occur) are today's main reasons behind efforts devoted to improve the use of various sources of energy. Economists, scientists, and engineers throughout the world are nowadays in search of: 1) strategies to reduce the demand; 2) methods to ensure the security of the supplies; 3) technologies to increase the energy efficiency of power systems; and 4) new and renewable sources of energy to replace the limited and harmful fossil fuels.

One of the options to improve energy efficiency is to develop energy storage devices and systems in order to reduce the mismatch between supply and demand. In this context, latent heat storage could be considered. Indeed, it is particularly attractive since it provides a high-energy storage density and has the capacity to store energy at a constant temperature – or over a limited range of temperature variation – which is the temperature that corresponds to the phase transition temperature of the material. For instance, it takes 80 times as much energy to melt a given mass of water (ice) than to raise the same amount of water by 1°C. For the interested reader, excellent global reviews that pertain to phase change materials and their various applications were proposed by Zalba et al. [1], Farid et al. [2], Zhang at al. [3], Tyagi and Buddhi [4], Regin et al. [5], Mondal [6], Mehling & Cabeza [7], Sethi & Sharma [8], Verma et al. [9], Sharma et al. [10], Dutil et al. [11] and Cabeza et al. [12].

2. Modeling in building applications

A better management of the fluctuations of the external temperatures, wind, solar load, and heating or cooling needs is possible by the use of phase change materials. In building applications, these materials undergo a phase change close to the desired room temperature, which allow storing a large amount of heat in a relatively small volume compared to liquid water, brick or concrete. This results in direct energy savings as the solar gains can be used when needed, thus reducing the energy consumption for heating in the winter and cooling in the summer. Moreover, in many countries, these materials could also be used to reduce the peak consumption leading to money savings in this particular case.

Nevertheless, high fidelity models are needed to guide the decisions of the architects and/or HVAC engineers in choosing optimum designs. Unfortunately, to formulate, implement, and validate such models is a rather difficult task mainly due to the non-linear nature of the problem. In addition, other technical issues add complexity to this problem. Here, we will discuss two of the most significant problems that should be addressed by the scientific community: phase change material characterization and model validation [11].

2.1. PCM characterization

The first problem faced even before beginning the modeling process is the characterization of the phase change materials (PCMs) themselves. In building applications, composite PCMs are the favored packaging method for inner walls applications. In this form, PCMs can be integrated into a building using the same techniques used for gypsum panel, which would provide a seamless integration. However, this type of material is rather difficult to characterize.

The key problem comes from the interaction with the substrate and the PCM in confined pores. This interaction affects both the melting and freezing temperatures as their respective enthalpy. To our knowledge, this phenomenon was first observed in building application by Hawes et al. [13], when they noted a drift in thermal properties of a PCM laced concrete over time. They attributed this effect to a migration of PCM in smaller pores. Their interpretation was supported by a previous work of Harnik et al. [14] on icing behavior of concrete.

Many physical models have been proposed to explain this behavior [15-25]. The thermodynamic properties of PCM composites are related in complex way to the size of the pores and to the chemical properties of the matrix and of the PCM. Mechanical confinement shifts the phase transition to higher temperatures due to increased pressure. Chemical interaction including dissolution between the compounds can shift up or down the melting/freezing temperature. The stochastic nature of the nucleation process means that supercooling is favored in small volumes. In consequence, melting and freezing phase change occurs at different temperatures. The phase change range is also broadened. This has the practical consequence that it is necessary to measure both melting and freezing curves and this over a wide range of temperature.

Even then, adequate characterization of PCM is a difficult task. For example, we have observed that reported enthalpy of melting and freezing can differ by more than as 15% in composite PCMs (ex: construction material [26-28] and polymer [29-31]). This is obviously unphysical since conservation of energy imposes that both values should be equal if the energy is stored in the PCM. Still, there is a possibility that some energy might be stored mechanically by the deformation of the matrix as a consequence of the PCM dilatation. To

our knowledge, this hypothesis has never been tested. While, if proven true, this phenomenon might provide new approaches to fine tune composite PCM thermal behavior.

In practice, the broad width of the composite PCM freezing/melting curve impairs the separation between latent and sensible heat. In addition, in some cases, there is an indication in many published measurements that at least a part of the PCM stays in supercooling state during the whole thermal cycle. In addition, heat capacity value and conductivity are different between liquid and solid phases. All these problems make very difficult to define a meaningful baseline to extract the latent heat curve.

In addition, hysteresis in the cooling/heating curve has been observed [32-36]. This behavior is not fully explained but is likely to be related to a complex interaction between the stochastic nature of the nucleation process (heterogeneous or homogeneous), progressive dissolution, glass transition or metastable crystalline phases. This has for consequence that each DSC curve is dependent on the history of temperature and its rate of change. Measurement procedures for this effect are still in development.

In general, thermophysical properties measurements are done on a small sample. However, due to the non classical behavior of composite PCM, it is unclear whether these measurements are representative of the macroscopic thermal properties of the material. A more detailed study is under investigation, which consists on the consideration of the heat transfers within the calorimeter cells. The goal is to determine the true value of specific enthalpy regardless of experimental conditions (sample mass, heating and cooling rates) [38]. This method also allows the determination of thermal properties by inverse methods [39]. In addition, potential drift in the thermophysical properties overtime are not always taken into account in the experimental protocol. Through a literature review, we have observed that tests of the stability of PCM composite extend from a few cycles to 5000 thermal cycles! Since, for building applications, lifetime of components are decades long the latter value is certainly more suitable.

In conclusion, improved thermal characterisation procedures are needed and will be certainly welcomed by modellers.

2.2. Model validation

The validation of modelling algorithms is also troublesome. While not restricted to building applications [11], it is more critical in this case due to the relatively small temperature changes involved in a typical building application. In surveyed papers on modeling, all older models for PCMs behavior had experimental counterparts to validate the modeling of the problem. This was done to adequately validate the appropriateness of the set of equations and that of the subsequent formulation of a numerical method to solve the relevant sets of discretized equations. Many of these early studies also involved analytical solutions used to validate the model for selected problems that admit closed form solutions [11].

However, as time went by, the authors relied more and more on other studies, mostly numerical ones, to validate their own numerical results. Many of the recent studies discuss their results qualitatively only, as the comparison with a graph taken from a publication may be somehow hazardous. And, interestingly, among the numerous – more than 250 – references and studies reported in [11], in only one the authors stated that the results were not "in good agreement with those found in the references". In recent studies, the proportion of

analyses which rely on commercial codes increases and the discussions that pertain to stability, convergence, grid independence and other related numerical issues decrease.

Statements are almost never made on the agreement or disagreement with previous results. This may be explained partly by the engineering scientific culture, where challenging or trying to duplicate previous works is not a common practice. As an illustration of this observation, we noticed that the work of Heim and Clark [40-41] predicts accumulation of heat on a seasonal basis. This is certainly an extraordinary claim that would open door to new applications. Nevertheless, up to now, nobody has either duplicated or refutated it.

However, engineering sociology merely reflects the practical constraint of doing such cross-validations. Materials, geometries, testing conditions and models are almost always different from one study to another. In such conditions, even for the most dedicated researcher, it is very hard to validate previous work. In our mind, this is a serious issue. Without a common ruler, it is impossible to formulate a meaningful recommendation about a technology.

Finally, we found that there is little comparison between various models and experiments. Every research group seems to have its own numerical model. To our knowledge, all these models were claimed to work well. Nevertheless, recent works [32-37] indicate that the presence of hysteresis creates some problem in the modeling itself since the thermal behavior of the PCM will depend on the history of heat loading. At this moment, solution to this problem is an open question. While this is a very new concern and might not be that important, this raises some doubts on previous results.

2.3. Further steps

To address some of these problems, the IEA annex 23 has prepared two standard cases to test numerical models [29-30]. The first of these tests was a simple unidirectional wall, with inclusion of a classical phase change material within the wall. Three teams developed a model for this case. While two of those models were closely predicting the same results, a third model presented a significant discrepancy with the other two. At this moment, not enough models are available to find the root cause of the observed difference. The main suspect is a small variation in the numerical description of the latent energy curve.

The existence of such divergence with a simple situation is by itself a strong warning about the models reliability. A second benchmark is now proposed. This benchmark is based on a small cubicle using PCM in its walls. In that case, high quality experimental data are used as a reference. To populate a database of benchmark, members of the annex 23 are invited to submit there own experimental data.

These initiatives are certainly a step in the right direction. Their use as a validation tool should be considered by any researchers working into application of PCM in building. Nevertheless, results are too fragmentary at this point to produce general guideline for researchers.

3. Conclusion

While the applications of PCM in building are promising as a tool to reduce energy consumption, there are still many roadblocks on the widespread utilization. To optimize their utilization in buildings, reliable models are needed. At this point, the confidence in models is too low to be use to predict the future behavior of a building. However, thermal behavior of PCM themselves are poorly known, which by itself create a huge unknown in model. Models themselves are suspicious as they are rarely tested in a very stringent way.

In addition, it also appears to us that modeling parameters are somewhat too simplified to realistically describe the real life performance of PCM addition into buildings. For example, seldom complete meteorological information (solar irradiation, external temperature and wind) are used as inputs. However, correlation and anti-correlation between these factors could strongly affect the results. In addition, in most systems modeled, thermal loads are restricted to solar heating. Additional heat from appliances will certainly affect the results. Also most of the time modeling is done on individual rooms or few rooms aligned in a perfect east-west alignment and empty. In real life, most houses are not perfectly oriented, have additional room with little solar heating, are equipped with furniture, and are occupied by people. This will both modify the thermal loading and the effective storage mass of the building. From our analysis of the literature, typical gain in energy efficiency by the utilization of PCM is expected to be roughly about 10-15%. In consequence, the factors not included in models could easily change the overall conclusion about the pertinence of PCM in building application.

The steps taken now by the IEA ECES IA Annex 23 to create standard model benchmark will improve the confidence of the users. Phase change material characterization is still an unresolved issue, but many research teams work on it. Hopefully, following these efforts, confidence will increase and usage of PCM in building will be more straightforward.

Acknowledgements

This work was supported by the t3e industrial research chair and its financial partners. The authors would like to acknowledge their invaluable contributions. The work was partially funded by the European Union (COST Action COST TU0802) and the Spanish Government (project ENE2008-06687-C02-01/CON). The authors would like to thank the Catalan Government for the quality accreditation given to their research group (2009 SGR 534).

References

[1] B. Zalba, J.M. Marín, L.F. Cabeza, H. Mehling, Review on thermal energy storage with phase change: materials, heat transfer analysis and applications, Applied Thermal Engineering 23, 2003, pp. 251-283.

[2] M. M. Farid, A. M. Khudhair, S. A. K. Razack, and S. Al-Hallaj, A review on phase change energy storage: materials and applications, Energy Conversion and Management, vol. 45 (9-10), 2004, pp.1597-1615

[3] Y. Zhang, G. Zhou, K. Lin, Q. Zhang, and H. Di , Application of latent heat thermal energy storage in buildings: State-of-the-art and outlook, Building and Environment, vol. 42(6), 2007, pp. 2197-2209

[4] V. V. Tyagi, and D. Buddhi, PCM thermal storage in buildings: A state of art, Renewable and Sustainable Energy Reviews, vol. 11(6), 2007, pp. 1146-1166

[5] A. F. Regin, S.C. Solanki, and J.S. Saini, Heat transfer characteristics of thermal energy storage system using PCM capsules: A review, Renewable and Sustainable Energy Reviews, vol. 12(9), 2008, pp. 2438-2458

[6] S. Mondal, Phase change materials for smart textiles – An overview, Applied Thermal Engineering, vol. 28(11-12), 2008, pp. 1536-1550

[7] H. Mehling, L.F. Cabeza. Heat and cold storage with PCM. An up to date introduction into basics and applications. Berlin, Springer, 2008. ISBN: 978-3-540-68557-9

[8] V.P. Sethi, and S.K. Sharma, Survey and evaluation of heating technologies for worldwide agricultural greenhouse applications, Solar Energy, vol. 82(9), 2008, pp. 832-8598

[9] P. Verma, Varun, and S.K. Singal, Review of mathematical modeling on l atent heat thermal energy storage systems using phase-change material, Renewable and Sustainable Energy Reviews, vol. 12(4), 2008, pp.999-1031

[10] A. Sharma et al., Review on thermal energy storage with phase change materials and applications, Renewable and Sustainable Energy Review, Volume 13 (2) , Issue 2, 2009, pp. 318-345

[11] Y. Dutil, D. R. Rousse, N. Ben Salah, S. Lassue, L. Zalewski A review on phase-change materials: Mathematical modeling and simulations, Renewable and Sustainable Energy Reviews 15, Issue 1, 2011, pp. 112-130

[12] L.F. Cabeza, A. Castell, C. Barreneche, A. de Gracia, A. I. Fernández, Materials used as PCM in thermal energy storage in buildings: A review, Renewable and Sustainable Energy Reviews, 2011, doi: 10.1016/j.rser.2010.11.018.

[13] D.W. Hawes, D. Banu, D. Feldman, The stability of phase change materials in concrete, Solar Energy Materials and Solar Cells 27, 1992, pp. 103-118

[14] A.B. Harnik, V. Meier and A. Rosli, in: Combined Influence of Freezing and Deicing Salt on Concrete - Physical Aspects, Durability of Building Materials and Components, ASTM STP 691, Eds. P.J. Sereda and G.G. Litvan, ASTM, 1980, pp. 476-483.

[15] J. P. Bédécarrats, F. Strub, B. Falcon and J. P. Dumas, Phase-change thermal energy storage using spherical capsules: performance of a test plant, Int J. Refrig. Vol. 19, No. 3, 1996, pp. 187-196

[16] R. Radhakrishnan, K.E. Gubbins, Free energy studies of freezing in slit pores: an order-parameter approach using Monte Carlo simulation, Mol. Phys. 96, 1999, pp. 1249–1267

[17] R. Radhakrishnan, K.E Gubbins, K.,Watanabe, K., Kaneko, Freezing of simple fluids in microporous activated carbon fibers: comparison of simulation and experiment. Journal of Chemical Physics 111, 1999, pp. 9058–9067

[18] G. H. Findenegg, A. Schreiber, Freezing and melting of water in ordered nanoporous silica materials. In: Setzer, M.J., Auberg, R., Keck, H.J. (Eds.), Proceedings of the International RILEM Workshop on Frost Resistance of Concrete, Cachan Cedex, France, 2002, pp. 105–116

[19] Y. Cai et al, Preparation and characterizations of HDPE–EVA alloy/OMT nanocomposites/paraffin compounds as a shape stabilized phase change thermal energy storage material, Thermochimica Acta 451, 2006, pp. 44–51

[20] Q. Cao, P. Liu, Hyperbranched polyurethane as novel solid–solid phase change material for thermal energy storage, European Polymer Journal 42, 2006, pp. 2931–2939

[21] Q. Cao, P. Liu, Crystalline-amorphous phase transition of hyperbranched polyurethane phase change materials for energy storage, J Mater Sci 42, 2007, pp. 5661–5665

[22] D. Zhang, K. Wu, Z., Li, Tuning effect of porous media's structure on the phase change behaviour of organic phase change matters. Journal of Tongji University 32, 2004, pp . 1163–1167

[23] D. Zhang, J. Zhou, K. Wu, Z. Li, Granular phase changing composites for thermal energy storage, Solar Energy 78, 2005, pp. 471–480

[24] D. Zhang, S. Tian, D. Xiao, Experimental study on the phase change behavior of phase change material confined in pores, Sol. Energy 81, 2007, pp. 653–660

[25] Y. Yamagishi, T. Sugeno, T. H. Takeuci-II, A. T. Pyatenko, An evaluation of microencapsulated PCM for use in cold energy transportation medium, Energy Conversion Engineering Conference, 1996, pp. 2077 - 2083

[26] A. Karaipekli, A. Sarı, Capric–myristic acid/vermiculite composite as form-stable phase change material for thermal energy storage, Solar Energy 83, 2009, pp. 323–332

[27] W. Wang, X.Yang, Y. Fang, J. Ding, J. Yan, Enhanced thermal conductivity and thermal performance of form-stable composite phase change materials by using b-Aluminum nitride, Applied Energy 86, 2009, pp. 1196–1200

[28] G. Fang,H. Li, X. Liu, Preparation and properties of lauric acid/silicon dioxide composites as form-stable phase change materials for thermal energy storage, Materials Chemistry and Physics 122 , 2010, pp. 533–536

[29] I. Krupa, A.S. Luyt, Thermal properties of uncross-linked and cross-linked LLDPE/wax blends, Polymer Degradation and Stability 70, 2000, pp. 111-117

[30] H.S. Mpanza, A.S. Luyt, Comparison of different waxes as processing agents for low-density polyethylene, Polymer Testing 25, 2006, pp. 436–442

[31] M. You, X. Wang, X. Zhang & W. Li, Effects of Microencapsulated Phase Change Materials Granularity and Heat Treat Treatment Condition on the Structure and Performance of Polyurethane Foams, Modern Applied Science, vol2, number 4, 2008

[32] Kuznik, F., Virgone, J. Experimental investigation of wallboard containing phase change material: Data for validation of numerical modeling, Energy and Buildings 41, 2009, pp. 561–570

[33] Kuznik, F., Virgone, J., Experimental assessment of a phase change material for wall building use, Applied Energy 86, 2009, pp. 2038–2046

[34] Diaconu, B. M., Cruceru, M., Novel concept of composite phase change material wall system for year-round thermal energy savings, Energy and Buildings 42, 2010, pp. 1759–1772

[35] B. M. Diaconu, S. Varga, A. C. Oliveira, Experimental assessment of heat storage properties and heat transfer characteristics of a phase change material slurry for air conditioning applications, Applied Energy 87, Issue 2, 2010, pp. 620-628

[36] Z. Younsi, L. Zalewski, S. Lassue, D. R. Rousse, A. Joulin, A Novel Technique for Experimental Thermophysical Characterization of Phase-Change Materials, International Journal of Thermophysics, Online First™, 28 December 2010

[37] A. Joulin, Z. Younsi, L. Zalewski, D. Rousse, S. Lassue, A numerical study of the melting of phase change material heated from a vertical wall of a rectangular enclosure, Int. Journal of Computational Fluid Dynamics, Vol. 23, No. 7, 2009, pp. 553–566

[38] T. Kousksou, A. Jamil, Y. Zeraouli, J.P. Dumas, Experimental and Modeling Study of Ice Melting, Journal of Thermal Analysis and Calorimetry 89, 1, 2007, pp. 31-36<

[39] Program MICMCP of the French National Research Agency (Stock-E) [laboratories: LaTEP, LGCgE, CETHIL]

[40] D. Heim, J.A. Clarke, Numerical modelling and thermal simulation of PCM– gypsum composites with ESP-r. Energy and Buildings, 36, 8, 2004, pp. 795–805

[41] D. Heim, Isothermal storage of solar energy in building construction, Renewable Energy 35, 2010, pp. 788–796

[42] K. Johannes, J. Virgone, F. Kuznik, X. Wang, T. Haavi, One dimensional Benchmark based on PCM, IEA, Annex 23, Applying Energy Storage in Buildings of the Future, 2010

Energy efficiency learning and practice in housing for youths

Wiktoria Glad[1*], Josefin Thoresson[2]

[1] *Department of Thematic Studies, Linköping University, Linköping, Sweden*
[2] *Department of Thematic Studies, Linköping University, Linköping, Sweden*
** Corresponding author. Tel: +46 13282259, E-mail: wiktoria.glad@liu.se*

Abstract: This paper explores the energy efficiency learning and practices of youths aged 18–25 years. The studied youths are involved in a project, initiated by a municipally owned housing company, to educate residents and change everyday behaviour, making it more sustainable and energy efficient. This project, which forms our case study, covers socio–technical features such as energy systems and the individual metering and billing of heating, electricity, and hot and cold water. How did the youths perceive and use the systems? Have their attitudes and behaviours concerning energy-related practices changed during the project? The results indicate that a combination of technology (e.g. metering and visualized energy use) and social activities (e.g. educational activities and meeting neighbours and housing company staff) changed some practices involving what was perceived as energy wasting behaviour (e.g. using stand-by modes and taking long hot showers), while other practices (e.g. travelling and heating) were harder to change due to socio–technical barriers. The youths displayed knowledge gaps in relation to the energy system and their basic understanding of energy (the difference between heating and electricity).

Keywords: *Everyday life, youths, housing, socio–technical systems*

1. Introduction

A common notion is that children and youths represent our future hope in terms of changing unsustainable behaviour. Sustainability is now integrated into Swedish pre-school and primary school curricula and covered in secondary school and university courses. Environmental awareness might also be important in working life, for example, if an employer is involved in an environmental certification scheme. However, for most people, learning about sustainability and, for example, energy conservation and low-energy lifestyles is not included in their everyday activities. As an adult, education is voluntary, and it can be assumed that few people intentionally seek a deeper understanding of environmental issues. Many are exposed to information from various sources, such as their energy supply company or local municipal energy advisors. However, mere information provision is considered a soft and perhaps weak policy means, and research finds that it has little or no effect on behaviour [1], while learning can reach deeper into people's values and might even change behaviour [2–4]. One key difference between learning and information provision is that learners receive feedback on their thoughts and actions, as learning often involves communicating with other people (possibly using various information and communication technology tools) [1]. Information provision is one-way and, by definition, is not communication at all. Published research into intervention and energy conservation behaviour is mostly found in the areas of psychology and social psychology [1,5–7], while the present research focuses on another level of behaviour, namely, socio–cultural and socio–technical behaviour; consequently, we chose *learning* and *practice* as our central areas of research [8–13].

The starting point of this research was to explore the learning of youths and young adults in an after-school setting outside conventional formal learning facilities. Specifically, we examine learning about sustainable energy-use behaviour and energy conservation in the homes of 18–25-year-olds. We use a qualitative case study methodology, the overarching aim of which is to understand energy learning among youths and young adults in a project targeting energy conservation attitudes and behaviour. The main objectives are to explore

stated energy-use behaviour from the end-user perspective and to assess the success or failure of a project aiming to change behaviour through learning. We would also like to suggest ideas for improving the learning approach that may be useful to stakeholders and policy-makers.

2. Theory and methodology

The analyses presented here will be based on our understanding of social learning; this concept stems from research into the learning in action approach [14] and practice theory [15]. Under certain circumstances, knowledge can be assimilated by an individual and put into action, possibly leading to change [16]. Liedman [17] stresses that knowledge must be *put in a wider context* and be *put to the test*. This is also the basis of Säljö's situated learning approach [14], according to which learning is not a harmonious occurrence but the result of individual struggle and commitment, hence, a *process*. Practice theory takes a similar approach to understanding human action, which is seen as resulting from a combination of structural prerequisites and individual and social processes. Instead of making situations the centre of analysis, Gram-Hanssen [8] emphasizes people's practices and activities when performing everyday tasks. We take this approach here, starting our analysis with *how* the studied youths and young adults *do things*. Practices are complex phenomena and can extend outwards from the home or the places where they usually occur. Gram-Hansen quotes Schatzki when defining practices as our "doings and sayings" [15]. Gram-Hansen has developed Schatzki's theories by introducing physical features and technology, making the approach more socio–technical.

Given the qualitative approach of this research and our aim of understanding a socio–technical phenomenon, case study methodology is suitable. Case study research focuses on real-life phenomena, and the inclusion of various contexts is encouraged when relevant [18]. Qualitative research aims at making detailed descriptions and creating in-depth understanding of phenomena. The boundaries of a case study can either be well defined in advance [19] or gradually be defined during the research [20]. The present research is a small case study based in a well-defined geographical area, the Ringdansen development, but the boundaries of the examined social learning extend beyond the neighbourhood.

The case study focuses on the "Youth Housing" project in the Ringdansen development in the town of Norrköping, Sweden. Since 2008, Linköping University has collaborated with the owner of this development, Hyresbostäder i Norrköping AB (HNAB), a housing company owned by Norrköping municipality. In 2009, HNAB initiated a project to attract a "new group" of tenants to the Ringdansen neighbourhood and enhance its green profile. The concept and organization of the project were not created in collaboration with Linköping University but were HNAB's own initiative and design; the collaboration merely gave Linköping University researchers easy access to the neighbourhood. HNAB has recently been promoting Ringdansen using the Climate-Clever Living programme, and a new logo has been launched. The programme offered a 50% rent discount to people aged 18–25 years, who could earn two-year leases for two- or three-bedroom flats in one of the residential buildings. To earn a lease (20 in total), one had to commit to involvement in a programme including various activities, for example, meetings and practical outdoor actions such as picking up litter in a recreational area near the neighbourhood. The meetings the housing company organized for the youths typically included a presentation on an environmental issue, such as global warming or global food consumption, supported by a movie or guest lecturer, followed by discussion of practical actions for reducing one's environmental impact, as related to the issue presented. The meetings were independent of each other and entailed no homework or reflections between the meetings. It was our initiative to ask permission to evaluate the project after one year.

Various data collection techniques can be used with case study methodology [18]; for our objectives, however, we chose to conduct focus group interviews. Focus group interviews produce primary data on the thoughts and understandings of people talking with each other in the same situation [21,22]. In the focus groups for the present research, we concentrated on issues related to energy and the environment. The analyses of interviews are our own; the results of the analyses were presented to housing company representatives, who gave us feedback on them. Since only 20 households participated in the Youth Housing project, yielding a small number of possible respondents, we invited all members of these households to attend the focus groups. Fifteen household members participated, representing almost 50% of the total, comprising nine women and six men. Four focus groups were organized by two researchers, one responsible for recording the interviews and taking notes and the other for keeping the conversation going and introducing new topics when the current topic seemed to be exhausted. The topics were presented using six pictures depicting the neighbourhood, energy, and the housing company. The youths responded to and understood what the pictures visualized in quite similar ways, even though divergent practices were related to the pictures during discussion; these results will be presented in the next section. The interviews were digitally recorded and transcribed, resulting in 50 pages of text. The relatively small amount of text made it possible to manually organize the primary data into various themes in accordance with the energy and environmental focus of the research project. The analyses were inspired by the hermeneutic research tradition and the hermeneutic circle [23]. There is always a risk of "going native" relative to the object of study and when interpreting the results. However, the researchers did not participate in conceiving or organizing the "Youth Housing" project and had no vested interests in whether or not the results of the project could be considered fulfilled.

3. Results

The results of the focus group interviews can be organized into three themes: stated behaviour in relation to heating, stated behaviour in relation to electricity and stated behaviour in relation to the individual metering and billing system (IMB) of the Ringdansen neighbourhood.

3.1. Stated behavior in relation to heating

Chilliness and technical issues were central when the youths talked about their behaviour in relation to heating. All apartments are equipped with a thermostat for temperature control device which should allow occupants to set indoor temperatures of 18-22° C and each flat pays individually for its use of heath. However, most youths found the indoor temperature too cold, with the thermostat set at its highest level, compared with earlier living experiences and with what they were used to in earlier homes (this was the youths' own impressions and does not reflect measured values). A common observation was that the insulation performance was inadequate due to a design flaw concerning the windows. One interviewee thought that the sealing around the windows was not good enough, and many youths experienced air ingress around windows and draughty flats. All flats are equipped with a ventilation outlet under the windows and many youths created their own solutions to prevent cold air coming into the flats through these outlets, for example, by using towels to block the ventilation outlet to raise the indoor temperature. Another practice was to put on slippers and more clothes if the indoor temperature was perceived as too cold. One interviewee claimed that it was unnecessary always to turn up the thermostat and said "If it is cold indoors, I put on my slippers and a cardigan". That was a common practice for many youths, said that the fear of higher energy bills was their main motivation. For some people, environmental factors such as melting polar icecaps and dying polar bears were important reasons for not using more energy than

needed. One youth claimed that these issues could be difficult to understand, but said: "I think that we here (i.e. in the Youth Housing project) can learn from each other".

Many youths struggled to learn how to use the thermostat as a temperature control device and it was described both as a tool for heating control and as a tool that simply did not work.

> Respondent 1: I thought that it (i.e. the thermostat) would be better than it was. I thought that it was pretty cool to have a thermostat indoors, only because I've seen them on TV but later I was …
> Respondent 2: Always in American movies.
> Respondent 1: Yes, everybody has a thermostat as a temperature-control device, and they can lower their thermostat because it is often very warm inside. But we have more like …
> Respondent 2: Raise the thermostat because it is so cold.
> Respondent 1: Yes it is like that here.

Some perceived the thermostat, as a temperature control device, as difficult to understand and as a barrier to controlling the indoor temperature. One youth said that it was strange that you could not simply set the thermostat to the temperature you wanted indoors (the thermostat was not marked with numbers). Some thought that the thermostats should function differently, and others did not like the thermostats at all because they were difficult to understand ("I do not like it at all"). Some youths described the thermostats as a tool for deciding how much heat to use in the flat, saying that it was a useful innovation since everybody had to pay for their own energy use. A common practice among many youths was to lower the thermostat in daytime and then raise it in the evenings. It was also common to turn off the heating system in summer, since it was usually not needed then. Youths with small children said it was a difficult decision to turn off the heat, since the children needed a warmer indoor temperature.

3.2. Stated behaviour in relation to electricity

The difference between heat and electricity was not obvious to all the youths. During discussions about the thermostat, it turned out that many had a knowledge gap regarding how their flats were heated, and one youth did not distinguish between electricity and heating consumption, even though the flats were heated with district heating and not with electricity. The thermostat technology was a barrier to a few who equated the thermostat with both temperature control and electricity, assuming that if the thermostat was turned off, the electricity to the flat would be cut, which was not the case. One also assumed that the level on the thermostat would affect the electricity bill, and was afraid of receiving higher electricity bills if the thermostat was set too high. All youths, however, said it was important to save electricity because this affects the global environment and can reduce the greenhouse effect.

Trying to reduce the amount of electricity used was an ongoing process in many households. A common energy-saving practice that many were using was turning off electrical appliances when not in use and not simply leaving them in stand-by mode. As one youth put it:

> We always unplug all the cords for our electrical appliances, like all lamps, the TV, the microwave, for everything. The cords have to be unplugged.

Interviewees said that it was easy to forget to unplug cords and turn off appliances when unused, although many said that they tried remember. One respondent said that, before the household had moved to the neighbourhood they seldom turned off the TV when they went to bed, now, however, they always turned it off. Another respondent claimed that the computer was always left on before, even though no one was using it. The move to the youth living project had changed that, and nowadays the household always turns off the computer when not in use. Most respondents found that it easy to remember to save electricity when they first

moved into the neighbourhood, though many remarked that it was easy to forget about electricity use in everyday life. Similar studies have noted the same phenomenon (24).

> Respondent 7: You forget. It is so easy to forget.
> Respondent 8: I thought about it a lot at the beginning, but I can say that now I am a bit careless about it.

During the focus group interviews, energy were also connected to travelling and small-scale energy production, which some youths wished was installed in the neighbourhood. Many youths used cars for transportation but not all households had access to a car, so many used the bus or bicycle for everyday transportation. The bus was said to be slow, and it was sometimes faster to ride a bicycle instead of taking the bus to the city centre. Many youths had great hopes that the housing company would embark on small-scale energy production, and expected leading-edge energy-production innovations and energy-efficient technology to be implemented in the neighbourhood. The youths described the housing company in mostly positive terms. They appreciated its accessibility and the meetings it organised in the Youth Housing project, though some wanted more concrete action from the housing company.

> Respondent 3: It is the next step. For now they try to engage people. The next step is …
> Respondent 4: Action.

3.3. Stated behaviour in relation to individual metering and visualization

The system for individual metering and billing was appreciated by most youths. The ability to influence the costs by paying for the rent and energy use separately was regarded as an advantage of the Youth Housing project, since it is seldom the case in Sweden. One youth said individual metering and billing was the best thing about the Youth Housing project. Many thought that this system was environmentally friendly, since it makes individuals start thinking about the energy they use, as they have to pay for it themselves. By making it obvious that energy has a cost, the system almost challenges individuals to save energy:

> It is good, especially from an environment perspective, and I think that you should not use more than you need. That is important.

When the bill came every month the system visualized the energy used in numbers and kilowatts, although many were vague as to what a kilowatt really represented or how it was measured. Understanding the energy consumption data on the bill or how the system worked was not considered that important. Feedback systems have been used in earlier studies with varying results, frequent feedback being found most effective [1]. In the present case, the energy bill functioned almost like a feedback system, giving feedback every month on energy used in terms of how much money the youths had to pay. Saving energy was often equated to saving money, since lower electricity use results in a lower electricity bill. Households would even compete against themselves, by trying to get lower electricity bills every month. They would think back over their energy behaviour in the current month versus in earlier months, and try to learn what to do or not to do the next month. The incentive to save money was a frequently citied reason, since many households were low-income or student households.

Trust in system's features and functions was high among the youths. No one doubted that their bill accurately recorded their energy use, but assumed that the technological system was working as it was supposed to, although it is always possible for technical systems to have flaws. The youths could not really determine by themselves whether the metering system was working as intended, and it was not usual to compare one's energy used with one's neighbours'. Social activities initiated by the housing company helped influence resident

attitudes and were appreciated. One youth said that before he did not think his use could make a difference. After he moved to the neighbourhood, however, he changed his mind:

> I think that involvement with the other youths in the block affects my consciousness and has made me more aware of the importance of everybody doing something when it comes to energy saving.

4. Discussion

Results indicate that a combination of technology (i.e. metering and visualized energy use) and social activities initiated by the housing company (e.g. educational activities and meeting neighbours and housing company staff) changed some of the practices involved in what were perceived as energy-wasting behaviour (e.g. using stand-by modes and taking long hot showers), though other practices (e.g. transportation and heating) were more difficult to change due to socio–technical barriers. Learning related to the home and various household activities might, according to the theories of situated learning [14] and practices [15], be the right approach to altering unsustainable behaviour, shifting it in the direction of low-energy living. The housing company is on the right track in choosing a learning approach for their Climate-Clever Living project. However, regarding the Youth Housing project, few respondents referred to specific things they had learnt in the first year of the project. Instead, reference was made to the fellowship between young residents of the neighbourhood. Most respondents, however, approved of the housing company's ability to inform them of energy and climate issues. Over the course of the year the project had run, the housing company had earned the youths' trust when it came to environmental matters [25].

Learning as a struggle [14] to become more knowledgeable was not acknowledged to any great extent by either the housing company or its tenants. The struggle mostly involved learning how to use devices, such as a thermostat, in the meetings, not learning and retaining changed behaviour, for which information provision alone has been demonstrated to be insufficient [1]. No pressure was put on the youths to reflect on or analyse their behaviour. Formal learning usually involves homework and studying for tests; in this project, however, learning was supposed to take place in the homes of the tenants and in the interaction with other tenants and the housing company. As a result, changing basic practices at home was never discussed in depth, and some youths went back to their former and less-energy-efficient modes of behaviour – as exemplified when they talked about saving electricity. Instead, the youths emphasized new, more innovative initiatives and a desire for the housing company to take action, rather than emphasizing how to do one's laundry in an energy-efficient way or manage the temperature of one's flat. The more innovative ideas included bicycle pools, second-hand clothing businesses, and solar panel and PV installation. Ongoing reflection on current practices and struggle to change one's behaviour may not be fun, but are necessary in order to change behaviour.

Putting new knowledge in a wider context is also crucial in efforts to create change [17]. It might be difficult to recognize the relationship between individual energy consumption and environmental problems [26] – although this was not a problem here – so context is always important. The contexts made available in the project were either the neighbourhood of Ringdansen or the other extreme, the globe. The neighbourhood might be too narrow a context in which to fully understand a new behaviour, while the globe might be too overwhelmingly large to relate to. Here, learners need help navigating through various contexts and must be shown how a behavioural change might influence contexts at various scales, i.e. the household, building, neighbourhood, precinct, town, region, country, continent, and globe. It was possible for the youths to compare their energy use with their neighbours',

but they said they seldom did that. We suggest that the data collected through the IMB system be used to set household behaviour in a wider context and make it possible to compare individual efforts with those of the entire neighbourhood and at other geographical levels.

5. Conclusions

An overall conclusion is that the project was successful in terms of changing some attitudes and energy-related behaviour. However, the youths displayed knowledge gaps in relation to the energy system and their basic understanding of the installed energy systems (e.g. the difference between the heating and electricity systems). Learning as a process must be acknowledged and the difference between providing and obtaining *information*, and learning and assimilating *knowledge* must be recognized when designing change-creation projects and schemes. Learning is an ongoing process that differs between individuals. Consequently, changing behaviour is better approached as a *scheme* than a project.

Learning includes *socio–technical features*. To facilitate learning and change, it is essential to provide infrastructure so that learning can take place in a wide range of places and not be restricted to certain, special places. In this case, HNAB has provided some state-of-the-art technical infrastructure, such as individual metering and billing. However, the infrastructure might also be social networks and include, as in this case, neighbours or even professionals from the housing company. These networks can give rise to more formal support groups than those existing between some youths, either in person or via the Internet. Technology has great potential as a tool for change, but that potential is underused in Ringdansen. We should not be afraid to approach learning about low-energy living in a fun way, making use of residents' creative ideas, like those of the studied youths.

For HNAB and perhaps other housing companies in Sweden, our results suggest that the present model of education for youths might be made more accurate and more flexible. It might be too challenging to target all groups of tenants at the same time, but starting with "easy" groups that are already somewhat interested in environmental issues is definitely the right way to proceed. The next group to target might be senior tenants, for example. According to a survey conducted in Ringdansen, the housing company is perceived as trustworthy by youths and young adults, so HNAB representatives should be the ones presenting data and discussing environmental issues with tenants. However, it is crucial to focus more on facts and data about a range of environmental issues and then provide opportunities to reflect on and discuss the information given. We would like to see *a more comprehensive model* of how the housing company will work on change creation in the future.

References

[1] W. Abrahamse, L. Steg, C. Vlek, & T. Rothengatter, A review of intervention studies aimed at household energy conservation, Journal of Environmental Psychology 25, 2005, pp. 273–291.

[2] L. S. Vygotskij, Mind in society: the development of higher psychological processes, Harvard University Press, 1978.

[3] A. Bandura, Social learning theory, Prentice Hall, 1977.

[4] M. S. Reed, A. C. Evely, G. Cundill, I. Fazey, J. Glass, A. Laing, J. Newig, B. Parrish, C. Prell, C. Raymond, & L. C. Stringer, What is social learning? Ecology and Society 15, 2010, online.

[5] W. O'Dwyer, F. Leeming, M. Cober, B. Porter, & J. M. Jackson, Critical review of behavioural intervention to preserve the environment: research since the 1980s, Environment and Behaviour 25, 1993, pp. 275–321.

[6] T. Jackson, Motivating sustainable consumption: a review of evidence on consumer behaviour and behavioural change, Energy Environment 15, 2005, pp. 1027–1051.

[7] L. Steg & C. Vlek, Encouraging pro-environmental behaviour: an integrative review and research agenda, Journal of Environmental Psychology 29, 2009, pp. 309–317.

[8] L. Lutzenhiser, Social and behavioural aspects of energy use, Annual Review of Energy and Environment 18, 1993, pp. 247–289.

[9] H. Wilhite, H. Nakagami, T. Masuda, Y. Yamaga, & H. Haneda, A cross-cultural analysis of household energy use behaviour, Energy Policy 24, 1996, pp. 795–803.

[10] H. Wilhite, E. Shove, L. Lutzenhiser, & W. Kempton, Twenty years of energy demand management: we know more about individual behaviour, but how much do we really know about demand, Proceedings of the ACEEE, 2000, pp. 8435–8453.

[11] A. Kollmuss & J. Agyeman, Mind the gap: why do people act environmentally and what are the barriers? Environmental Education Research 8, 2002, pp. 239–260.

[12] E. Shove, Comfort, cleanliness and convenience, Berg Publishers, 2003.

[13] S. Moloney, R. E. Horne, & J. Fien, Transitioning to low carbon communities – from behaviour change to systemic change, Energy Policy 38, 2010, pp. 7614–7623.

[14] R. Säljö, Lärande i praktiken: ett sociokulturellt perspektiv, Norstedts, First edition, 2005.

[15] K. Gram-Hanssen, Introducing and developing practice theory – towards a better understanding, in: K. Karlson & K. Ellegård, eds., Proceedings of the sustaining everyday life conference, Linköping University Electronic Press, 2010, pp. 45–57.

[16] P. Wickenberg, Information, kunskap och lärande, Att handla rätt från början, Naturvårdsverket, 2001, pp. 159–171.

[17] S. Liedman , Ett oändligt äventyr: om människans kunskaper, Bonnier, 2001.

[18] R. K. Yin, Case study research: design and methods, SAGE, Second edition, 1994.

[19] S. B. Merriam, Qualitative research and case study applications, Jossey-Bass, 1998.

[20] C. C. Ragin & H. S. Becker, What is a case? Exploring the foundation of social inquiry, Cambridge University Press, 1992.

[21] R. S. Barbour & J. Kitzinger, Developing focus group research: politics, theory and practice, SAGE, 1999.

[22] D. L. Morgan, Focus group kit. Vol. 1, The focus group guidebook, SAGE, 1999.

[23] J. Willis, Foundations of qualitative research: Interpretive and critical approaches, SAGE, 2007.

[24] E. S. Geller, Evaluating energy conservation programs: Is verbal report enough? Journal of Consumer Research 5, 1981, pp. 331–335.

[25] W. Glad & J. Thoresson, Values, knowledge and behaviour – results of a survey, forthcoming.

[26] G. Brandon & A. Lewis, Reducing household energy consumption: a qualitative and quantitative field study, Journal of Environmental Psychology 19, 1999, pp. 75–85.

Reducing Households' Energy Use: A Segmentation of Flanders on Adoption Intention of Smart Metering Technology

Jeroen Stragier[1,]*, Laurence Hauttekeete[1], Lieven De Marez[1]

[1]*IBBT-MICT-Ghent University, Ghent, Belgium*
** Corresponding author. Tel: +3292649745, Fax: + 3292646992, E-mail: Jeroen.Stragier@Ugent.be*

Abstract: Research has shown that feedback on energy use can aid households to reduce it significantly. In this context, smart metering technologies, and more specifically technology components interacting with data gathered and provided by a smart meter, allowing to provide the consumer with personalized feedback, consumption visualization, automated control,… could play an important role. After all, by means of this technology, households can be made more aware of their energy use and encouraged to reduce it. This paper applies a user centered approach towards the estimation of the adoption potential for smart metering technologies in Flanders, Belgium. We conducted a representative quantitative survey with 1314 respondents living in Flanders. A segmentation on ownership of, attitude towards and adoption intention of smart metering devices was performed on the data. Traditional approaches of intention surveying often result in an overestimation of the innovation adoption potential. To overcome this problem, the Product Specific Adoption Potential scale (or PSAP-scale) was used and 6 segments were found. These segments were labeled "Current Owners", "Innovators", "Early Adopters", "Early Majority", "Later Adopters" and "Out of Potentials. The verification of the adoption potential of smart metering devices for different pricing scenarios revealed a rather high price sensitivity.

Keywords: *Consumer behaviour, smart metering, adoption potential, willingness to pay*

1. Introduction

Most residential energy users are not aware of their usage pattern. On a global level, the amount paid every month is the only indicator of energy use for the majority of the households. On appliance level, households have little or no knowledge on the amount of energy that their appliances consume, or its share in the total household energy use. Mansouri-Azar et al. [1] proved that a majority of their respondents did not know which of their electric appliances consumed most energy. At the time the research was carried out, lighting, freezer and dishwasher were the most consuming appliances in the UK households. Nonetheless, most of the respondents mentioned the washing machine in their top three.

The positive effect of feedback on energy use has been examined and confirmed in many studies [2-6]. It is generally recognized that households can be motivated to reduce their energy use when receiving correct feedback. Several forms of feedback can be distinguished ranging from more detailed billing over comparative and historic feedback to direct feedback at the time of use. According to Raaij and Verhallen [7] feedback has three functions:

(1) learning: the provided feedback gives the consumer information on the results of certain actions;
(2) habit formation: the feedback helps in forming certain new habits with regard to energy conservation. These habits should remain when the feedback is removed;
(3) internalization of behaviour: feedback helps to create new attitudes and habits that become embedded in a person's behaviour. These habits and attitudes will influence energy-related actions in situations where the feedback will not be present.

Smart meters can play an important role in providing this feedback to consumers and many applications are possible. Smart meters connected to in-home displays, internet applications,

smart phone and tablet apps can provide residential consumers with basic insight into their energy use at a given time during the day, but the possibilities go far beyond this. Smart appliances connected to smart meters can stimulate an efficient appliance use supported by time-of-use pricing mechanisms and availability of renewable energy sources. The question however remains to what extent the consumer is interested in adopting these smart metering applications and, from a business perspective, what is their willingness to pay for these applications? These two questions will be addressed in this paper.

2. Methodology

We conducted a quantitative survey with a representative sample of the population of Flanders, Belgium. The questionnaire was designed to make a segmentation based on attitude towards smart metering technologies and distributed through both online and offline channels in June, 2010. A total number of 1314 respondents completed the survey.

Two parameters were taken into account for creating the segmentation: the ownership of smart metering devices (such as power meters) and the interest and purchase intention of smart metering devices.

The first parameter could easily be measured using one question asking for the ownership of these smart metering devices.

The second parameter concerns the interest and purchase intention of devices for smart metering in terms of adopter segments as formulated in diffusion theory [8]. According to this diffusion theory, the adoption of an innovation depends largely on a person's innovativeness determined by the moment upon which a person decides to start using an innovation. The diffusion of an innovation in a social system follows a clockwise pattern. Rogers [8] distinguishes between five adopter segments. The Innovators (2.5% of the population) are the most innovative group of adopters. They will be among the first to adopt an innovation, followed by those categorised as Early Adopters (13.5%), Early Majority (34%), Late Majority (34%) and Laggards (16%). In order to assign the respondents to one of the adopter segments for smart metering devices, the Product Specific Adoption Potential scale (PSAP) [9-11] was used. The scale was developed as a valid alternative to traditional single-intent questions used in traditional market research, which systematically lead to over- or underestimation of the adoption potential of innovations. The model has been validated for several innovations (e.g. [11, 12]). Instead of a single intent question asking for the adoption likelihood of an innovation, three questions are asked. The adoption intention is measured for optimal and suboptimal product offerings. A calibration heuristic based on the answers on all 3 intention questions assigns the respondent to the appropriate adoption segment [9].

First, the respondents received an introductory text about smart metering devices and their possibilities. Smart metering was described as the use of a new type of electricity meter, which offers households the ability of closely monitoring their energy consumption. After reading this text, **the first (traditional) intention question was asked (PSAP question 1):**
"If you would have the opportunity tomorrow to buy a smart metering device, to what extent do you think that you would buy this device"? The answering scale provided 5 possible answers:

- I would immediately buy this device;
- There is a large probability that I would buy this device;
- I think I would wait, maybe later;
- I don't think I would buy this device;

- I definitely won't buy this device.

Second, the respondents were asked to rate 10 possible use cases of smart metering on a 5-point scale ranging from "not interested at all" to "very interested". The use cases were:

- Receiving personalized tips to save energy based on your energy usage data;
- Insight in your energy use in real time at every moment of the day;
- Receiving graphs and reports with an overview of the total energy use in a certain period;
- Postulate goals to save energy in the future;
- Making an estimation of the future energy use during a certain period;
- Comparing your energy use with other (comparable) households or houses (e.g. in your neighbourhood);
- Receiving feedback when the energy use exceeds that of a previous comparable period;
- Entering in competition with other households to keep the energy use low;
- Graphs and reports with detailed energy use data per appliance;
- Automatic switch-on/–off of appliances, based on time of the day (e.g. day/night).

Furthermore, the respondents were asked to specify an "acceptable price limit" they are willing to pay for a smart metering device that is capable of providing the 10 use cases that we provided in the previous question. No limitations were imposed. The respondents were free to give any price they thought was acceptable.

After these questions, **a second more personalized intention question was asked (PSAP question 2).** This time, an ideal product was composed using those use cases from the aforementioned list of 10 that the respondent was either "interested" or "very interested" in. This ideal product was then presented as a "smart metering offer" at a price that was acceptable for the respondent, according to the price limit (s)he had indicated, and containing all the applications/use cases (s)he was interested in. Hence, every respondent had to give their adoption intention for this ideal product at their ideal price (which was different for every respondent).

Finally, **a third intention question was asked (PSAP question 3)**. This time, the adoption intention for a "suboptimal product" was measured. Again their ideal product was provided, but at a higher price than the limit they indicated (the ideal price was raised with 20%).

Based on a calibration heuristic, checking for the consistency in intention statements over the different answers on the 3 PSAP questions, each of the respondents was assigned to one of the adopter segments: Innovators, Early Adopters, Early Majority, Late Majority and Laggards.
Furthermore, 2 more segments were added to the segmentation: "Current Owners" and "Out of Potentials". Current Owners are those who indicated that they already possess certain smart metering devices. Although they don't possess a smart meter yet, they have already invested in devices with similar possibilities. Out of Potentials are respondents that showed no interest in any of the use cases that were provided. Late Majority and Laggards were merged into one single segment labeled "Later Adopters" due to small socio-demographic and attitudinal differences.

3. Results

3.1. Segmentation on attitude towards smart metering

Figure 1 indicates that a market potential exists for smart metering in Flanders, as the high proportion of Current Owners, Innovators and Early Adopters and Early Majority indicates. Still, there is also a high proportion of Out of Potentials, which indicates that for certain consumers, using smart metering is already out of the question, no matter the cost of the investment.

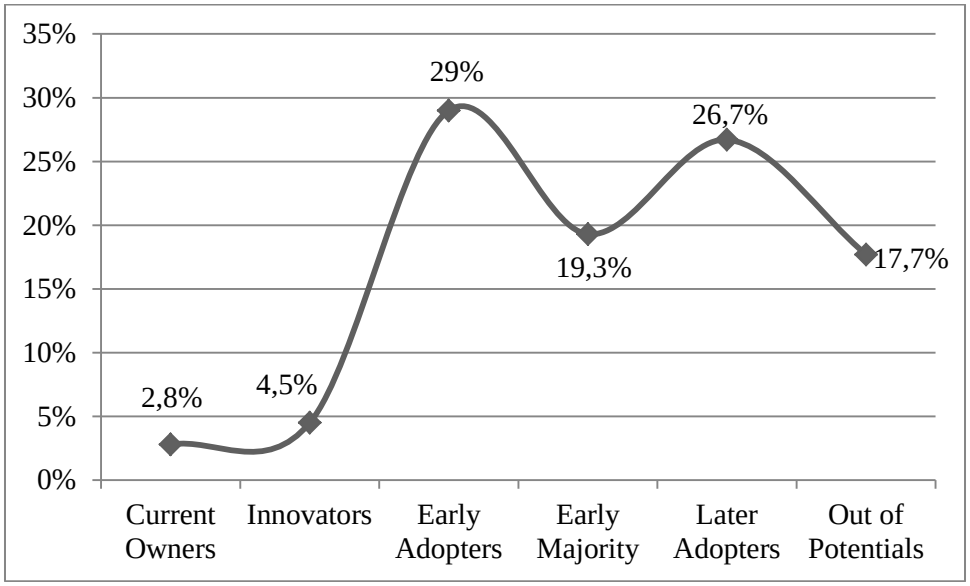

Fig. 1. Segmentation of Flanders on attitude towards smart metering.

Current Owners are the segment that already made some (minor) investments in equipment with smart metering capabilities. These Current Owners were identified by asking for the ownership of appliances that have smart metering capabilities (after being given an introductory text to the possibilities of smart metering). 40 respondents indicated to have such an appliance. When asked for the capabilities of their appliance, … 75% of them appear to have one that displays the energy use per appliance, 20% has a device that displays the total energy use and 5% has a tool that allows monitoring the energy use per circuit. The Current Owners are among the "younger" respondents (average age = 44.3 years). They mainly live in younger households with children.

Innovators are the first segment that did not yet invest in appliances for energy use monitoring. They are very interested in using smart metering devices and exploiting the possibilities. The average age within this segment is 44.8 which makes them on average as old as the Current Owners. The majority of them is married and/or has children. Early Adopters are also interested in using smart metering devices, but to a lesser extent than the Innovators. They are somewhat more reserved. The average age within this segment is 46.3 years. The Early Majority can still be situated within the same age category as the Early Adopters and Innovators (average age: 46.5 years), but they are the less interested group. Their interest in and buying intention of smart metering devices is again lower than that of the previous segments. The difference between the Later Adopters and the previously mentioned segments is larger. Their interest and buying intention of smart metering devices is quite low. The average age in this segment is 50.5 which makes it significantly older than the other segments. Out of potentials are completely uninterested in smart metering devices. They are the oldest

segment (with an average age within the segment of 54.6 years). More than a third of them are retired.

3.2. Willigness to pay

Of course, an important factor is the willingness to pay for a smart metering device. The adoption potential forecast for smart metering devices presented in figure 1 is not only based on interest, but also on an assessment of their willingness to pay. However, it is important to keep in mind that this first forecast is based on a scenario without pricing restrictions. The respondents had to indicate which price they are willing to pay for a smart metering device, without any control mechanisms or checks whether the indicated price is also a feasible price for the supply side. Therefore, a next step must be a comparison of the adoption potential for different pricing levels.

The PSAP-scale allows checking the possible influence of pricing. Five scenarios were created in which a cut-off (€50, €100, €150, €200, €300) was made at a given price. Figure 2 presents these five scenarios.

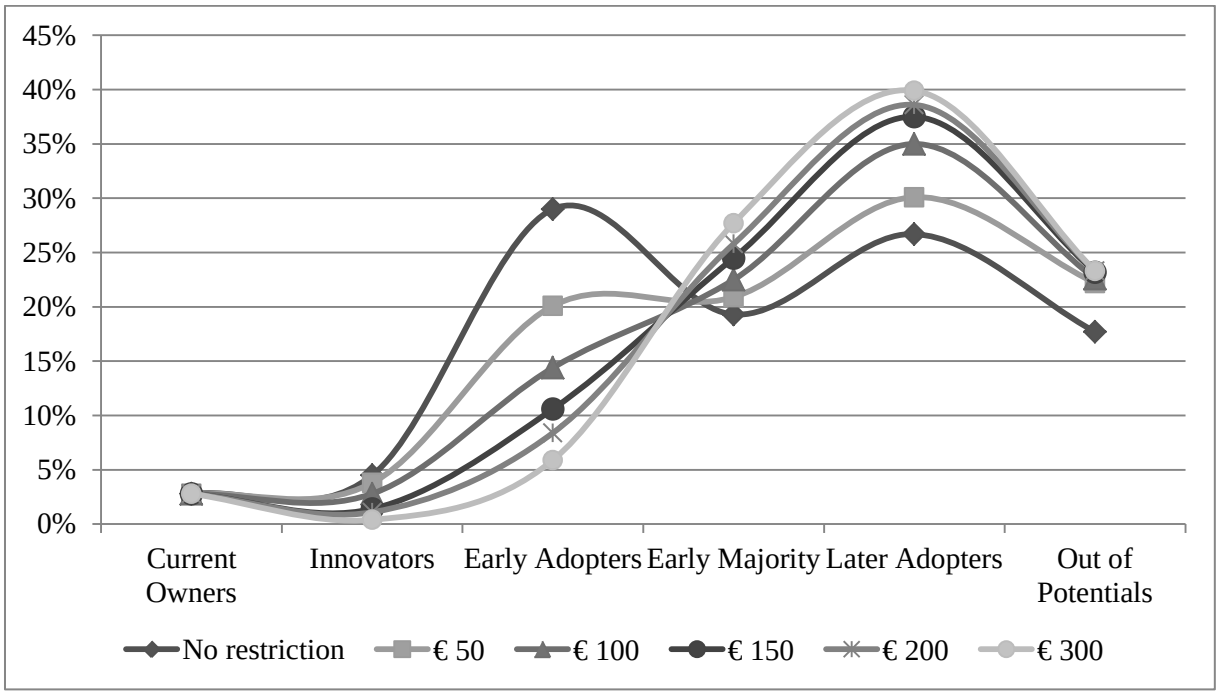

Fig. 2. Adoption potential curves for different pricing scenario.

Evidently, it can be assumed that enthusiasm will decrease as the pricing of the smart metering device increases. The question however is *how much* potential will be lost with each price increase? In the context of delineation of target markets and business cases it will be important to determine a kind of "tipping point" where a certain price increase holds the risk for a too big loss of potential. The "No restriction" scenario provides the original segmentation, in which the respondents could freely indicate how much they are willing to pay for their "ideal" smart metering device. Each of the succeeding scenarios (€50, €100, €150, €200, €300) gives the cut-off that was set. If the price that a respondent was willing to pay is lower than the cut-off that was set, the respondent shifts back one segment in the segmentation. In other words, respondents that combine a high enthusiasm for smart metering with a less realistic willingness to pay (according to the cut-off), slide to the rear of the segmentation. In the scenario in which the smart meter is offered at €100 for example, an

initial innovator will not remain an innovator if (s)he indicated his/her willingness to pay to be e.g. €60 or €80.

As can be seen in figure 2, it is clear that the enthusiasm for smart metering is accompanied by a rather high price sensitivity. Where the forecasted size of the innovator segment in Flanders (originally 4.5%) remains almost 4% and 3% in the €50 and €100 scenario, it shrinks to 1% or less if the price threshold of €150 is surpassed. The Early Adopters segment shows a significant drop in size (from 29% to 20%) when a pricing restriction of €50 is imposed. In spite of their high interest in smart metering devices, a considerable proportion of Early Adopters shows a rather low willingness to pay. The drop in size of the segment continues over the following pricing scenarios with a tipping point around €100-€150. After this point, the divergence in the curves remains rather low.

4. Discussion

Providing insights and feedback about energy use is an essential means to create awareness and encourage an efficient energy conservation behaviour. Smart metering can be an excellent means to provide this feedback in real time. However, the question is who's interested in adopting this technology and what is their willingness to pay? In this paper, a segmentation on the adoption potential of smart metering devices was presented. Only a small proportion already own devices with some smart metering capabilities. This segment was called "Current Owners". The rest of the sample was classified in adopter segments. The large proportion of Early Adopters indicates a substantial base of interest in the possibilities of smart metering with regard to energy conservation for households. However, when different pricing scenarios for a smart metering device were applied to the data, a significant drop in the Innovator and Early adopter segments was noticed. In this research, the respondents were asked to indicate the price they are willing to pay for a smart metering device, without any checks whether their indicated price is also a realistic one. The results indicate that households want to invest in energy efficiency, as could be seen from the interest in smart metering devices, but the return must be worth the investment. Therefore, the yearly household electricity use is important to keep in mind. The average consumption of a household in Flanders is about 3500-4000 kWh per year, which corresponds with about €550-€650 per year. If e.g. a saving of 10% can be realized using smart metering devices, this leads to reduction of around €60 on the yearly electricity bill. For households with a significantly higher electricity use, high investments will be more relevant and therefore, their willingness to pay will be higher than that of households with an average electricity use.

Acknowledgement
This article is based on results from the SmartE project which is funded by IWT and various partners: IBBT, IBBT-iLab.o UGent-MICT, UGent-IBCN, KULeuven-CUO, KULeuven-ESAT-Electa, VITO, VUB-SMIT, Telenet, SPE-Luminus, Alcatel-Lucent Bell, Niko, Ferranti and Xemex.

References

[1] I. Mansouri-Azar, M. Newborough, and D. Probert, "Energy-consumption in UK domestic households: impact of domestic electrical appliances," *Applied Energy*, vol. 54, pp. 211-285, 1996.

[2] C. Fischer, "Feedback on household electricity consumption: a tool for saving energy?," *Energy Efficiency*, vol. 1, pp. 79-104, 2008.

[3] A. Faruqui, S. Sergici, and A. Sharif, "The impact of informational feedback on energy consumption--A survey of the experimental evidence," *Energy*, 2009.

[4] R. M. J. Benders, R. Kok, H. C. Moll, G. Wiersma, and K. J. Noorman, "New approaches for household energy conservation--In search of personal household energy budgets and energy reduction options," *Energy Policy*, vol. 34, pp. 3612-3622, 2006.

[5] L. T. McCalley and C. J. H. Midden, "Energy conservation through product-integrated feedback: The roles of goal-setting and social orientation," *Journal of Economic Psychology*, vol. 23, pp. 589-603, 2002.

[6] S. Darby, "Making it obvious: designing feedback into energy consumption," 2001.

[7] W. F. Van Raaij and T. M. M. Verhallen, "A behavioral model of residential energy use," *Journal of Economic Psychology*, vol. 3, pp. 39-63, 1983.

[8] E. M. Rogers, *Diffusion of innovations*, 4th ed. New York (N.Y.): Free press, 1995.

[9] L. De Marez, "Diffusie van ICT-Innovaties: Accurater Gebruikersinzicht Voor Betere Introductiestrategieën," Gent: Universiteit Gent, 2006.

[10] L. De Marez and G. Verleye, "ICT-innovations today: making traditional diffusion patterns obsolete, and preliminary insight of increased importance," *Telematics and Informatics*, vol. 21, pp. 235-260, 2004.

[11] L. De Marez, P. Vyncke, K. Berte, D. Schuurman, and K. De Moor, "Adopter segments, adoption determinants and mobile marketing," *Journal of Targeting, Measurement and Analysis for Marketing*, vol. 16, pp. 78-95, 2007.

[12] T. Evens, D. Schuurman, L. De Marez, and G. Verleye, "Forecasting broadband Internet adoption on trains in Belgium," *Telematics and Informatics*, vol. 27, pp. 10-20, 2010.

A simple estimation method to find the proper capacity of a combined heat and power unit

Woojin Cho[1], Janghyun Kim[1], Kwan-Soo Lee[1,*], Seung-Kil Son[2], Kwon Woo Lee[2]

[1] *School of mechanical engineering, Hanyang University, Seoul, Republic of Korea*
[2] *R&D center, KD Navien co., ltd., 459-2 Gasan-dong, Geumcheon-gu, Seoul 153-803, Republic of Korea*
** Corresponding author. Tel: +82-2-2220-0426, Fax: +82-2-2295-9021, E-mail: ksleehy@hanyang.ac.kr*

Abstract: Selecting a proper capacity of the CHP unit is a complicated problem where energy usage pattern of end users and energy price structures must be considered. Thus, advanced computer simulations are used to predict the proper capacity of the unit, however, certain methods require expensive information such as part load performance of the unit and load profiles of end users. This paper suggests a simple method of predicting proper capacity by presenting analytical equations which calculate annual savings with different capacity of the CHP unit. These equations have merit which can be applied to various conditions by covering the energy usage patterns and energy price structures.

Keywords: *Combined heat and power, Capacity*

Nomenclature

c_e	*price of electricity*	*cents/kWh*	p	*power*	*kW*
c_f	*price of fuel*	*cents/kWh*	q	*heat*	*kW*
c_t	*price of heat*	*cents/kWh*	T	*time*	*hr*
hpr	*heat to power ratio*	*kW/kW*	η	*efficiency*	*dimensionless*

1. Introduction

Although a combined heat and power (CHP) unit produces both heat and electricity, it cannot control the ratio of output heat to power (heat-to-power ratio). Thus there is a potential discrepancy between the heat/electricity production of a CHP unit and the heat/electricity consumption on the demand side. This issue can be resolved by using a power grid and supplementary water heating system in conjunction with the CHP unit. However, the varying prices of energy consumed by the CHP unit, power grid, and supplementary heating system complicate the proper choice of CHP unit size. This problem is significantly different from selecting a boiler size solely on the basis of the consumption of heat by the end user.

Contrary to expectation, there are only few existing studies on selecting the optimum capacity of a CHP unit. It is certain that appropriate criteria for selecting the proper capacity of a CHP unit cannot be derived from a case study based on parameters that are limited, or classified only into 3 or 4 levels. Procedures such as modeling techniques, mathematical optimization, or simulation programs obtained from other researchers could help to provide relevant standards. However, these methods are actually difficult to adopt, and the use of other people's results requires expensive information, such as long-term accumulated minute-by-minute load profiles. The performance of a CHP unit varies according to the manufacturer, and energy usage patterns vary from one household to the next. Moreover, energy prices related to the use of a CHP system vary in different regions. Thus, although a solution to the problem of selecting the proper capacity of a CHP unit should account for parameters such as system performance, pattern of energy usage, and energy price structure, the required methodology is not easily found in the literature.

This study uses information that is easily obtained (annual average heat load, base/peak power load), and presents a simple and intuitive method for predicting proper CHP unit capacity for

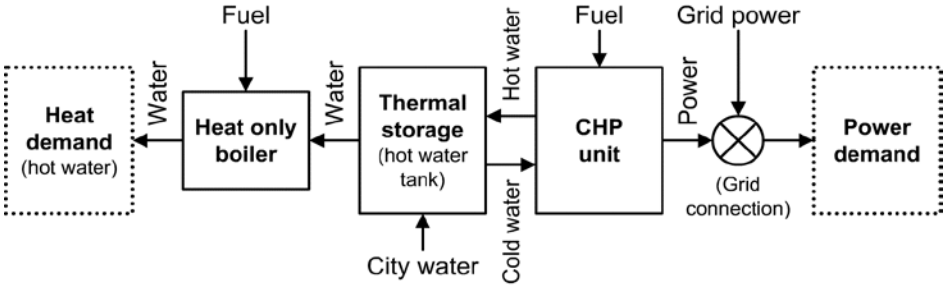

Figure 1. Schematic of the CHP system

end users. The final result is a set of equations for calculating the proper capacity for three classifications (three types of energy usage patterns), and is verified via computer simulation.

2. CHP system

This research is based on a CHP system that includes a CHP unit, thermal storage unit, and HOB (heat only boiler), as shown in Figure 1. The CHP unit operates when there is a heat demand, and the power output of the unit follows the power load on the demand side. This operating strategy is called the "following heat demand and chasing power load" (FHD-CPL) strategy, and is usually preferred where selling electricity back to the grid is impossible, or offers no economic advantage.

3. Problem formulation

In this paper, the objective function for determining the proper capacity is defined as the annual economic savings from using the CHP system. The problem is formulated as follows. The cost of energy consumption per unit time step by a CHP system is denoted by ec_{CHP}, and the cost of energy consumption per unit time step by a separated heat and power (SHP) system is denoted by ec_{SHP}. Equation (1) presents the formulation procedure and its result. When an arbitrary time T is divided into N intervals of length h, the cost saving in the nth interval is calculated as follows:

$$ECR_n = h\left(ec_{CHP,n} - ec_{SHP,n}\right) = h \cdot c_t \cdot q_{TS,n} + h \cdot \delta_n \cdot f_n \tag{1}$$

$$f_n = \left(c_e - c_e \max\left(1 - r_n, 0\right) - \left(c_f / \eta_{e,n}\right) r_n\right) p_{load,n} \tag{2}$$

where r_n is the power share of the CHP unit against the power load, η_e is the electrical efficiency of the unit, and c_t is the equivalent price of the energy. The above equations are also represented in Figure 2.

$$r_n = p_{CHP,n} / p_{load,n}, \quad \eta_{e,n} = p_{CHP,n} / f_{CHP,n}, \quad c_t = c_t^* / \eta_{t,HOB} \tag{3}$$

Also, δ_n is a parameter which value is 0 or 1 depending on the CHP units operation status in nth interval.

$$\delta_n = \begin{cases} 1 & \text{if CHP unit runs at } n \\ 0 & \text{if CHP unit halts at } n \end{cases} \tag{4}$$

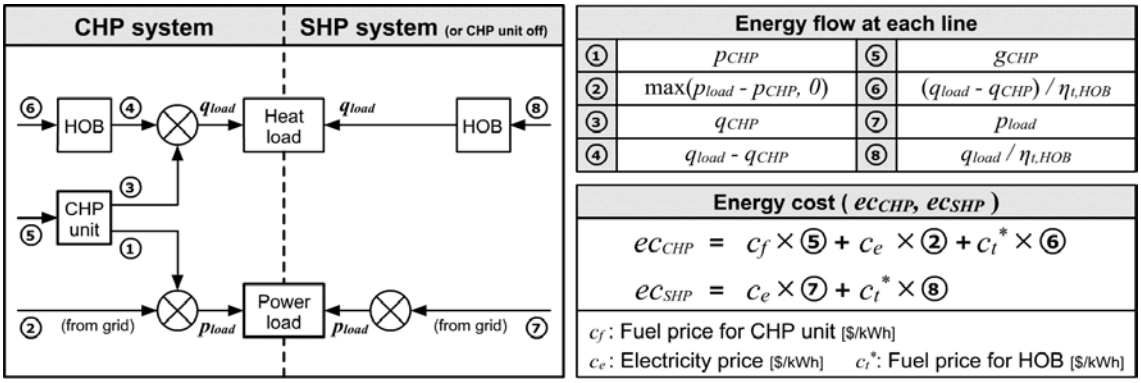

Fig. 2. Problem formulation

The total *ECR* (economic cost reduction) over an arbitrary period *T* is the sum of the ECR_n of the individual intervals.

$$ECR = \sum_{n=1}^{N} ECR_n = h\sum_{n=1}^{N}\left(c_t \cdot q_{TS,n}\right) + h\sum_{n=1}^{N} f_n \tag{5}$$

The first term on the right-hand side of Equation (5) represents the total amount of heat supplied to the end user over period *T*. Since only heat from the CHP unit is supplied to the thermal storage unit, this amount is the same as the total thermal output of the CHP unit over the period.

$$Q_{TS} = h\sum_{n=1}^{N}\left(\delta_n \cdot q_{CHP,n}\right) = h\sum_{n=1}^{N}\left(\delta_n \cdot hpr_n \cdot r_n \cdot p_{load,n}\right) \tag{6}$$

In the above equation, hpr_n denotes the ratio of the electrical output to the thermal output.

$$hpr_n = q_{CHP,n} / p_{CHP,n} \tag{7}$$

Equations (5), (6) and (7) can be rearranged as follows:

$$ECR = h\sum_{n=1}^{N}\left(\delta_n \cdot ecr_n \cdot p_{load,n}\right) \tag{8}$$

$$ecr_n = c_t \cdot hpr_n + c_e \min\left(r_n, 1\right) - \left(c_f / \eta_{e,n}\right) r_n \tag{9}$$

The maximum power load during period *T* is denoted by p_{peak}, and the range from 0 to p_{peak} is divided into a uniform number of classes *M*. The m[th] class frequency, corresponding to the class mark $p_{load,m}$, can be expressed as a function $n(p_{load,m})$, and the mathematical relationship between the period *T*, the number of intervals *N*, the number of classes *M*, and the frequency of each class $n(p_{load,m})$ is given by

$$T = h \cdot N = h\sum_{m=1}^{M} n(p_{load,m}) \tag{10}$$

$$\sum_{n=1}^{N} p_{load,n} = \sum_{m=1}^{M}\left\{p_{load,m} \cdot n(p_{load,m})\right\} \tag{11}$$

The following equation for ECR can be obtained by rearranging Equations (8), (10) and (11):

$$ECR = T\sum_{m=1}^{M}\left\{or_m \cdot ecr_m \cdot p_{load,m} \cdot \mathrm{n}\left(p_{load,m}\right)\Big/N\right\} \tag{12}$$

where or_m is the availability factor of the CHP unit in the mth class. Over period T, or_m is assumed to have a constant value or, which is unrelated to any of the classes.

$$or_m = \left(\sum \delta_n \middle| p_{load,n} \in p_{load,m}\right)\Big/\mathrm{n}\left(p_{load,m}\right) \approx or \tag{13}$$

For an infinitely large number of intervals N and number of classes M, Equation (12) can be expressed as follows:

$$ECR = T \cdot or \cdot \overline{ecr} \tag{14}$$

$$\overline{ecr} = \int_0^{p_{peak}} \mathrm{ecr}\left(p_{load,m}, p_{CHP,nom}\right) \cdot p_{load,m} \cdot \mathrm{pdf}\left(p_{load}\right) dp_{load} \tag{15}$$

Here PDF(p_{load}) is the probability density function of the continuous random variable p_{load}.

To satisfy Equation (6), the heat and power load over period T should be periodic. Also, the thermal storage unit should compensate for any discrepancies between thermal output and heat load over period T. Thus it is appropriate to define period T to be a day. The annual energy cost savings are then calculated as follows:

$$AECR = \sum_{\mathrm{day}=1}^{365} ECR_{\mathrm{day}} = \sum_{\mathrm{day}=1}^{365}\left\{T_{day} \cdot or_{\mathrm{day}} \cdot \overline{ecr_{day}}\right\} \tag{16}$$

Also, for the demand side (which has a similar annual power load distribution pattern), Equation (16) can be simplified as follows:

$$AECR = T_{year} \cdot \overline{or_{year}} \cdot \overline{ecr_{year}} \tag{17}$$

$$\overline{or_{year}} = \sum_{day=1}^{365} or_{day} \Big/ 365 \tag{18}$$

4. Simple estimation via linearization

In this paper, a simple estimation method for predicting the proper capacity of a CHP unit is proposed, based on linearization of the non-linear functions in Equation (17).

4.1. Partial load performance of the CHP unit and CDF of the power load

Equation (9) includes η_e and hpr, which are related to the performance of the CHP unit. In this study, the partial load performance is assumed to be as shown in Figure 3 (a). Applying this to Equation (9), and substituting into Equation (15) yields

$$\overline{ecr} = \left\{\alpha + \beta \cdot \mathrm{cdf}\left(p_{CHP,nom}\right)\right\} p_{CHP,nom} \tag{19}$$

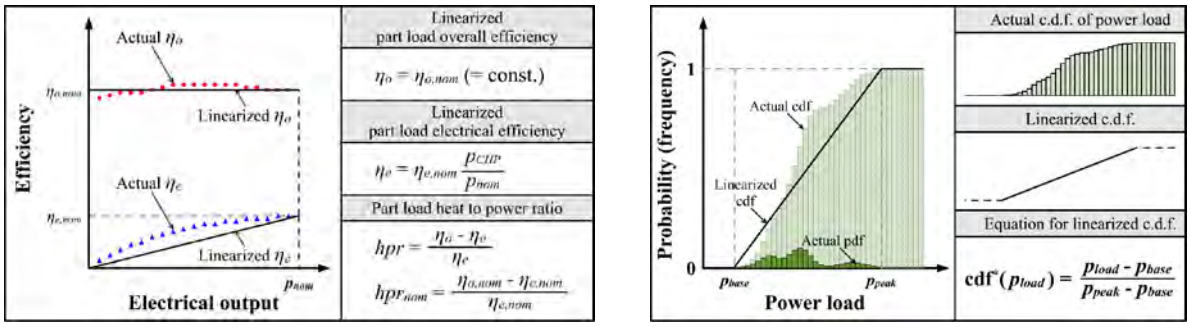

(a) Partial load linearization (b) CDF of power load

Figure 3. Part load performance and cumulative distribution function

Here,

$$\alpha = c_t \cdot hpr_{nom} + c_e - c_f / \eta_{e,nom}, \quad \beta = c_t - c_e, \quad \text{cdf}\left(p_{load}\right) = \int_0^{P_{load}} \text{pdf}\left(p\right) dp \tag{20}$$

The PDF and cumulative distribution function (CDF) of the demand-side power load follow the pattern shown in Figure 3 (b). The CDF in Equations (20) is assumed to be a first-order function, as shown in Figure 3 (b). The assumed CDF for each interval, based on division in terms of the base power load and peak power load of the demand side, is as follows:

$$\text{cdf}^*\left(p\right) = \begin{cases} 0 & \left(p < p_{base}\right) \\ \left(p - p_{base}\right) / \left(p_{peak} - p_{base}\right) & \left(p_{base} \le p < p_{peak}\right) \\ 1 & \left(p \ge p_{peak}\right) \end{cases} \tag{21}$$

4.2. Distribution of the daily average heat load

The maximum daily average heat load of the demand side is denoted by $\overline{q_{max}}$, and the minimum daily average heat load of the demand side is denoted by $\overline{q_{min}}$. If the daily average heat load for the k[th] day is assumed to be a first-order function, as shown in Figure 4 (a), or_{year} in Equation (18) can be obtained as shown in Figure 4 (b). Based on the procedure illustrated in Figure 4 (b), or_{year} can be expressed as a function of p_{nom} as follows:

$$\overline{or_{year}} \begin{cases} 1 & \text{for} \quad p_{nom} < \overline{q_{load}} / \left\{hpr + \text{cdf}\left(p_{nom}\right)\right\} \\ \overline{q_{load}} / \left[\left\{hpr + \text{cdf}\left(p_{nom}\right)\right\} \cdot p_{nom}\right] & \text{for} \quad p_{nom} \ge \overline{q_{load}} / \left\{hpr + \text{cdf}\left(p_{nom}\right)\right\} \end{cases} \tag{22}$$

Here,

$$\overline{q_{laod}} = \left(\overline{q_{\max}} + \overline{q_{\min}}\right) / 2 \tag{23}$$

Thus *or* can be calculated solely on the basis of the CDF of the average annual heat (q_{load}) and the power load on the demand side.

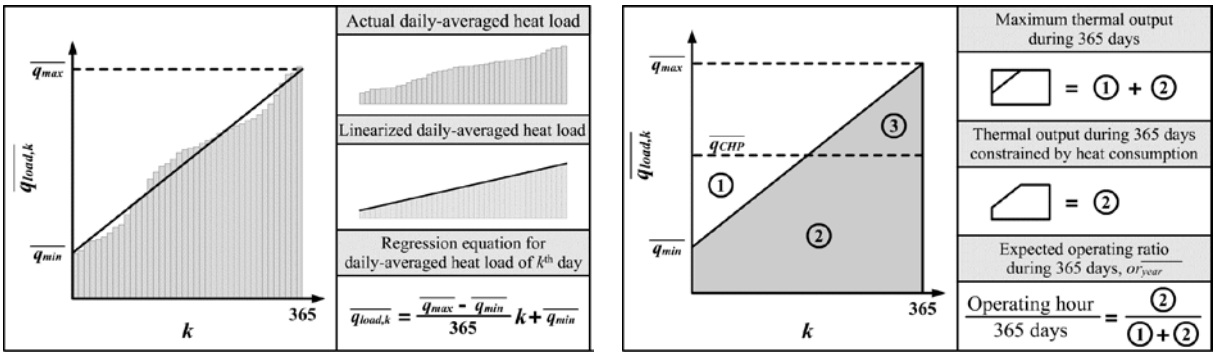

(a) Linearization of heat load (b) Calculation of operating ratio

Figure 4. Distribution of daily-averaged heat load

5. Simple estimation method

Equation (17) can be written as follows:

$$AECR = T_{year} \underbrace{\left(\overline{or_{year}} \cdot p_{nom}\right)}_{U} \underbrace{\left(\overline{ecr_{year}} \Big/ p_{nom}\right)}_{V} \tag{24}$$

In Figure 5, p_{nom} is divided into intervals according to energy usage patterns (Type 1, Type 2, Type 3), and the forms of U and V in Equation (24) are graphically expressed for each interval. The proper capacity $p_{nom,pr}$ can be obtained by finding the maximum value of this simple polynomial (the order of UV is less than 2 over the entire range). The proper capacities for each type are shown in Table 1, based on the simple estimation method. However, one should be aware that this method does not provide the optimal capacities when α is negative or β is positive. In these circumstances, a CHP system cannot guarantee an economic advantage.

6. Validation

We verified the performance of our technique with a previously validated simulation program. This program was developed in earlier research, and the results (such as the amount of electricity generated and the thermal output) were obtained from a simulation based on the end user's load profiles. The details of this program are not included in the present paper, but can be found in the article "Optimum generation capacities of micro combined heat and

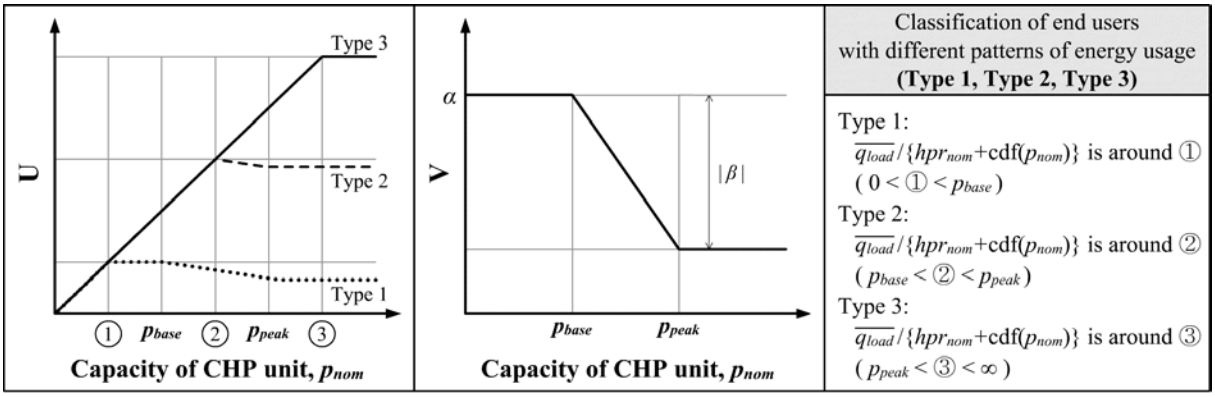

Figure 5. Simple estimation method

Table 1. Proper capacities for each type

Pattern of energy usage	**Proper capacity**
Type 1	$p_{nom,pr} = \overline{q_{load}} \big/ hpr_{nom}$
Type 2	$\alpha/\beta \geq -p_{base} \big/ \left(p_{peak} - p_{base} \right) \rightarrow p_{nom,pr} = p_{base}$ $\alpha/\beta < \left(p_{base} - 2\overline{q_{load}} \big/ \overline{hpr} \right) \big/ \left(p_{peak} - p_{base} \right) \rightarrow p_{nom,pr} = \overline{q_{load}} \big/ \overline{hpr}$ otherwise $\rightarrow p_{nom,pr} = \left\{ \left(1-\alpha/\beta\right) p_{base} + \left(\alpha/\beta\right) p_{base} \right\} \big/ 2$
Type 3	$\alpha/\beta \geq -p_{base} \big/ \left(p_{peak} - p_{base} \right) \rightarrow p_{nom,pr} = p_{base}$ $\alpha/\beta < \left(p_{base} - 2p_{peak} \right) \big/ \left(p_{peak} - p_{base} \right) \rightarrow p_{nom,pr} = \overline{q_{load}} \big/ \overline{hpr}$ otherwise $\rightarrow p_{nom,pr} = \left\{ \left(1-\alpha/\beta\right) p_{base} + \left(\alpha/\beta\right) p_{base} \right\} \big/ 2$
Parameters	$\alpha = c_t \cdot hpr_{nom} + c_e - \frac{c_f}{\eta_{e,nom}}, \quad \beta = c_t - c_e, \quad \overline{hpr} = hpr_{nom} + X$ $X = -A + \left\{ A^2 + \frac{\overline{q_{load}} - hpr_{nom} \cdot p_{base}}{p_{peak} - p_{base}} \right\}^{1/2}, \quad A = \frac{1}{2} \left\{ hpr_{nom} + \frac{p_{base}}{p_{peak} - p_{base}} \right\}$

power systems in apartment complexes with varying numbers of apartment units.”[1]

The AECR (annual economic cost reduction) result derived from Equation (24) was compared with that obtained from the simulation (numerical experiment). The partial load performance, demand-side energy usage pattern, and other information used in each method are listed in Table 2. We point out that the predictions obtained by the simple estimation method were based solely on the boldface entries in Table 2.

Table 2. Information used in each method

	Simulation program	Simple estimation
$\eta_{e,nom}$, hpr_{nom}	0.32, 1.78 [1]	**0.32**, **1.78**
η_e (*lf*) / $\eta_{e,nom}$	$1.03 - 0.98 \cdot 0.0315^{lf}$ [1]	*lf*
hpr (*lf*) / hpr_{nom}	$\left(0.96 + 0.76 \cdot 0.0454^{lf}\right) \big/ \left(1.03 - 0.98 \cdot 0.0315^{lf}\right)$ [1]	1
Distribution of p_{load} (PDF and CDF)	(Simulation uses load profiles [1])	Using equation (21) (p_{base} = **10 kW**, p_{peak} = **280 kW**)
Annual-averaged heat load	(Simulation uses load profile [1])	**242 kW**
c_t, c_e, c_f	6 cents/kWh, 12 cents/kWh, 6 cents/kWh (both)	

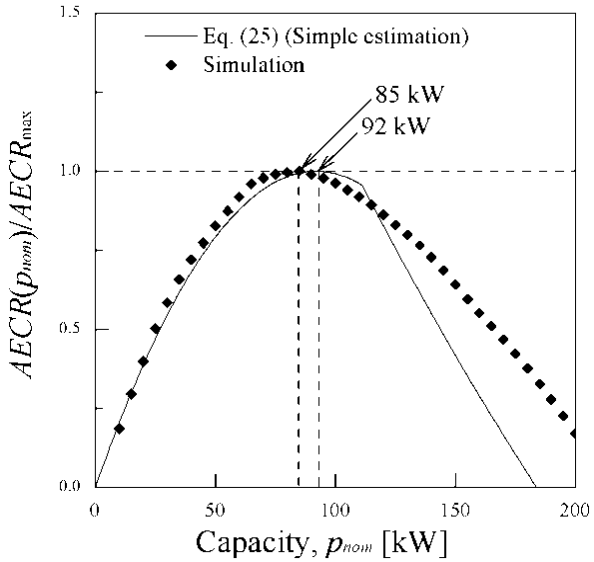

Figure 6. Comparison of the simple estimation method and a previous study

Figure 6 compares the standardized AECRs of each method (*AECRs* of different capacities, $AECR(p_{nom})$ divided by the maximum AECR, $AECR_{\max}$). The AECR calculated via Equation (24) attained a maximum at p_{nom} = 92 kW, while the AECR calculated via the simulation program reached a maximum at p_{nom} = 85 kW. Hence the results were in good agreement. In this manner, we can calculate the maximum (proper capacity) of a CHP unit by using the simple estimation method shown in Table 1.

7. Conclusions

In this paper, a simple estimation method was proposed to predict the proper capacity of a CHP unit. The advantages of this technique are described below.

First, if the relevant information (such as electrical and thermal load profiles and nominal efficiencies of the CHP system) are opened to the public, the technique proposed in this paper provides useful method to estimate the proper capacity of the micro-CHP system without using complicated (and expensive) simulation programs suggested from others.

Second, the method that has been suggested in this paper could handle different kinds of conditions by employing various energy prices and system's performances. For example, it could be applied into different situations in various countries (having different energy price policies and different CHP prime movers such as stirling or turbine engine).

Third, the most important aspect in this paper is that we suggested the simplest model among the others which can be cost-effective and easy to apply.

Reference

[1] J. Kim, W. Cho, K.-S. Lee, Optimum generation capacities of micro combined heat and power systems in apartment complexes with varying numbers of apartment units, Energy, 2010, Vol.35, Issue 12, pp. 5121-5131.

Electricity intensities of the OECD and South Africa: A comparison

Roula Inglesi[1,*], James N. Blignaut[2]

[1] *Department of Economics, University of Pretoria, Pretoria, South Africa*
[2] *Department of Economics, University of Pretoria, Pretoria, South Africa*
** Corresponding author. Tel: +27 12 4204504, Fax: +27 865 695811, E-mail: roula.inglesi@up.ac.za*

Abstract: Improving a country's electricity efficiency is considered one of the important ways to reduce a country's greenhouse gas emissions. This paper's main purpose is to compare the South African total electricity intensity with these of the OECD members, in order to establish a sense of South Africa's relative performance. These results will assist in ascertaining possible scope for improvement, and if such exits, determining in which of the industrial sectors. To calculate the electricity intensities, we defined them as the ratio of electricity consumption to total output and then compare the South African with their OECD counterparts in total and disaggregated levels. For some of the countries the data were not sufficient for analysis over a long time period. Our results indicate that South Africa not only suffers from higher total and sectoral intensity levels but also the gap between them is increasing at an alarming rate. We conclude that for South Africa to improve its industrial competitiveness and achieve its stated commitments to the reduction of greenhouse gas emissions, it will have to improve its efficiency. This is likely to be achieved only through a concerted sector-specific approach.

Keywords: *Electricity, Intensity, South Africa, OECD, Comparative Analysis*

1. Introduction

Improving the electricity efficiency of a country is an important step towards decreasing greenhouse gas emissions originating from fossil fuel based electricity generation and consumption. From a policy-making perspective, the studying of efficiency is significant since it is a measure that combines the electricity consumption with the economic output [1] and the comprehension of the behavior of electricity demand under economic structural changes is imperative [2]. In the past a large number of studies were conducted to identify the dynamics, determinants and characteristics of electricity intensity in developed and developing economies [3, 4, 5, 6], resulting in showing the electricity intensity increases, as a consequence of economic growth and decreases as the economy progresses, shifting to services-based sectors [7]. This trend can be compared to the famous environmental Kuznets-curve [8, 9], but applied to the electricity intensity.

Here we seek to answer the question whether South Africa follows the international trends regarding electricity intensity. We do this by conducting a comparison between South Africa's national and sectoral electricity intensities and the equivalents thereof of the member countries of Organisation for Economic Co-operation and Development (OECD).

The main reason for focusing on the electricity intensity and not on energy in general lies with the fact that the energy sector is too diverse for comparative analysis. For instance, the intensity trends in the use of petrol are dependent on whether the country is an oil-producer or not. On contrary, the OECD members and South African electricity sectors present similar characteristics, especially regarding their generation, which is regulated and controlled by a monopolist. Hence, we argue that energy intensities would not be a comparable indicator between the selected groups of countries.

On a national level, the exercise will indicate whether there is scope for improvement. Furthermore, the analysis on a sectoral level will be beneficial because, firstly, it is imperative

to understand the differences in economic and energy characteristics of each sector [10]; and secondly, not all the economies produce the same goods and service in the same proportion [11].

The next section of this paper will introduce the meaning of electricity efficiency and intensity as well as the current situation of electricity efficiency in South Africa. This is followed by the description of the data used and an international electricity intensity comparison on both a national and a disaggregated level. Finally, we conclude with a discussion on the findings.

2. Background

Following the political transition in 1994, the new democratically elected South African government considered energy issues as of great importance for the economic development of the country. In the first White Paper on Energy Policy [12] energy efficiency was mentioned among the cross-cutting issues. More specifically for the industrial and commercial sectors, the government committed itself to the following:

- Promotion of energy efficiency awareness
- Encouragement of the use of energy efficiency practices
- Establishment of energy efficiency standards for commercial buildings
- Monitoring the progress

While progress on these was slow due to pressing socio-economic and development considerations, the South African Department of Minerals and Energy released its first Energy Efficiency Strategy in 2005 [13]. The purpose of the Strategy was to provide a policy framework toward affordable energy for all and diminish the negative consequences of the extensive energy use in the country. Its national target was to improve electricity efficiency by 12% by 2015. The document, however, had limited impact to date and is currently being revised.

Fig. 1 shows the economy-wide electricity intensity and its growth for the period 1994–2006. Total electricity intensity showed a sharp upward trend until 2004. The period 2005-2006 was characterised by a notable decrease in the electricity intensity of 8.4% Firstly, the electricity prices increased by 182% in 2003 and it was highly impossible for the electricity consumers to react and change their behaviour in the short-run. Hence, the drop in electricity intensity (caused by a decrease in electricity consumption) might be considered the lagged impact of the high increase in electricity prices. Also, from a policy perspective, the first Energy Efficiency Strategy in 2005 [13] might also be the cause of a decrease in 2005/06.

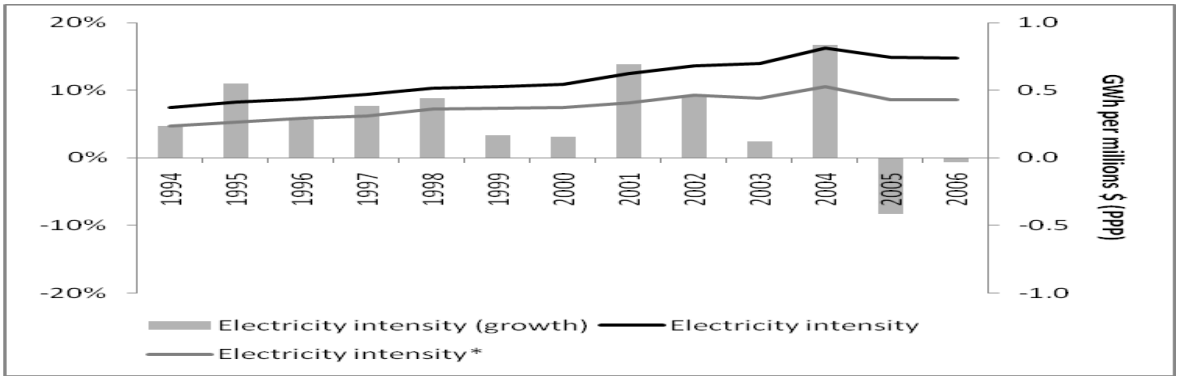

Fig. 1: Electricity intensity and its growth in South Africa: 1994 to 2006
**excluding residential, commercial and non-classified electricity consumption*

Sources: Authors' calculations based on IMF [14] and OECD [15]
However, if the industrial, transport, and agriculture sectors' electricity consumption is included only in the calculation, a lower intensity is observed with the growth not being as steep as before. Large inter-sectoral variations, however, exist[1].

Given this general information, how does South Africa compare, both on a national as well as sectoral level, with the OECD countries? We turn to this next.

3. Methodology and data

Several studies concerned with inter-country comparison of electricity intensities have been conducted [16, 17, 18, and 19]. These studies have, however, encountered certain difficulties, such as the heterogeneous definition of the variables as well as the diverse interpretations of the ratios calculated. We tried to avoid these problems by estimating the electricity intensities for each country using the same definition (i.e. electricity consumption/gross domestic product (GDP)) and the same dataset. We selected the OECD members because this group provides us with a wide spectrum of developed and developing countries with different economic and energy-related characteristics, but with its data and definitions being consolidated under one umbrella organisation. This limits the risk of data inconsistencies.

The data for electricity consumption (total and sectoral) were obtained from the OECD's Energy balances for OECD countries [20] and for South Africa from Energy balances for non-OECD countries [15]. The national GDP data (in current prices), the consumer price index (base year 2000) and the Power Purchasing Parity (PPP) adjusted real exchange rate values for all the countries were derived from the World Economic Outlook April 2010 of the International Monetary Fund (IMF). The disaggregated data for output for OECD members were derived from the STAN Database for Structural Analysis of OECD.

4. Results of comparative analysis

In 1980 South Africa's electricity intensity was substantially lower than that of OECD countries (see Fig. 2). This is to be expected to some extent given the high level of welfare enjoyed by a minority of people based on an industrial sector that services only a few with limited focus on exports at that point in time. Given the country's skew income distribution, a skew electricity usage was also presented: the higher income sectors were the most electricity intensive, too.

The country's electricity use rose sharply since the early 1990s with the abolishment of sanctions, the internationalisation of the markets to international trade, and the more stable economic and political situation after its first democratic elections in 1994. Hence, after 1994, the country's exports of electricity have been increased as well as the growth of the economy. These facts led to a strong impact on electricity use and since the 1990s, however, the electricity intensity in South Africa kept rising at an alarming rate (0.329 GWh/ mil $ adj PPP in 1990 to 0.713 GWh/ mil $ adj PPP in 2007) and currently far exceeds that of the OECD countries (0.318 GWh/ mil $ adj PPP in 1990 to 0.3422 GWh/ mil $ adj PPP in 2007) with no sign of any change.

[1] Data available upon request

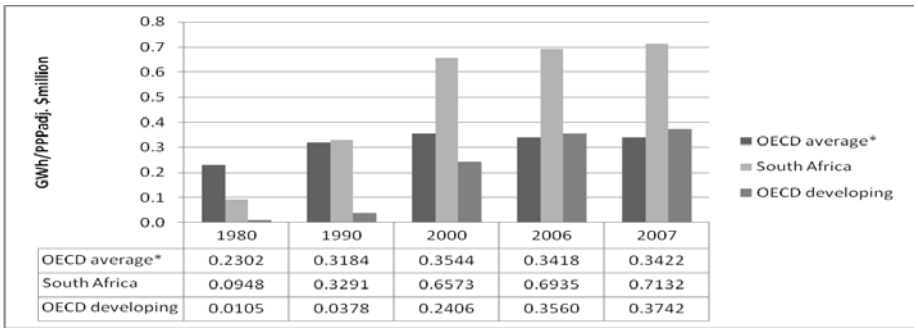

	1980	1990	2000	2006	2007
OECD average*	0.2302	0.3184	0.3544	0.3418	0.3422
South Africa	0.0948	0.3291	0.6573	0.6935	0.7132
OECD developing	0.0105	0.0378	0.2406	0.3560	0.3742

Fig. 2: Evolution of electricity intensity: Average OECD and South Africa
** It excludes Czech Republic, Slovak Republic and Turkey due to lack of data of 1980 and 1990.*
Source: Authors' calculations based on IMF [24] and OECD [25, 28]

In the same figure, we extracted the developing economies of the OECD group (Hungary, Poland, Mexico and Turkey) and weight their average against South. Its electricity intensity was higher than that of the average of the OECD developing economies, throughout the years. Following this analysis, we disaggregate the OECD average to examine how South Africa compares with the OECD countries individually over the study period. The economy-wide percentage change of electricity intensity for the period 1990 to 2007 as well as the electricity intensity of 2007 for the OECD members and South Africa is presented in Fig. 3.

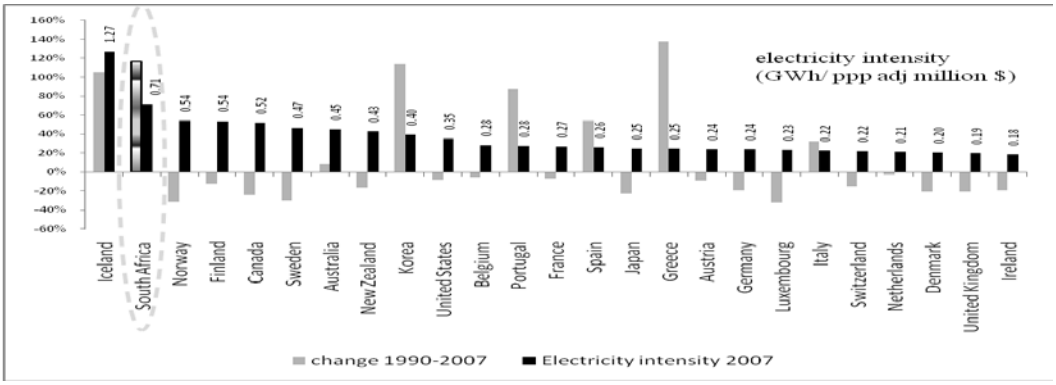

*Fig. 3*a*: Electricity intensity in 2007 and its growth (1990 to 2007) for South Africa and OECD members* [2]
Source: Authors' calculations based on IMF [14] and OECD [15, 20].

From Fig. 3a it is clear that South Africa has shown an increase in electricity intensity of 117% over the study period. This is in sharp contrast to the average of the OECD members which was only 10.09%. Only the Mediterranean countries (Spain, Greece, Portugal and Italy) as well as Korea and Iceland experienced an increase in their electricity intensities. Both their output and electricity consumption increased substantially, but the increase in consumption was higher than the growth in output and therefore their intensities experienced such sharp increases.

A further remarkable trend can be observed from Fig. 3a. There is a statistically significant negative, or inverse, relationship between the level of electricity intensity in 1990 and its

[2] It should be noted that Poland, Hungary, Mexico and Turkey were outliers (hence, excluded from the figure) with changes in electricity intensity for the examined period of 382%, 401%, 493% and more than 1,000% (from 0.0006 in 1990 to 0.723 in 2007) respectively. Also, the Czech and Slovak Republics were excluded due to lack of data points for 1990

growth over the study period[3]. This implies and that the higher the electricity intensity of a country in 1990 was, generally speaking, the more negative its growth was from 1990 to 2007. Countries such as Norway, Canada and Sweden, who were the most electricity intensive in 1990, were the ones that managed to decrease their intensity of electricity usage meaningfully, namely by 32%, 24% and 30% respectively. On the contrary, Italy, Portugal and Greece with the lowest intensities in 1990, raised them by 33%, 88% and 138% respectively. South Africa, however, does not fit this trend well. It had an average electricity intensity in 1990 and yet it had the second highest increase (after Greece) of its intensity (117%). The country, therefore, does not follow international trends in this regard.

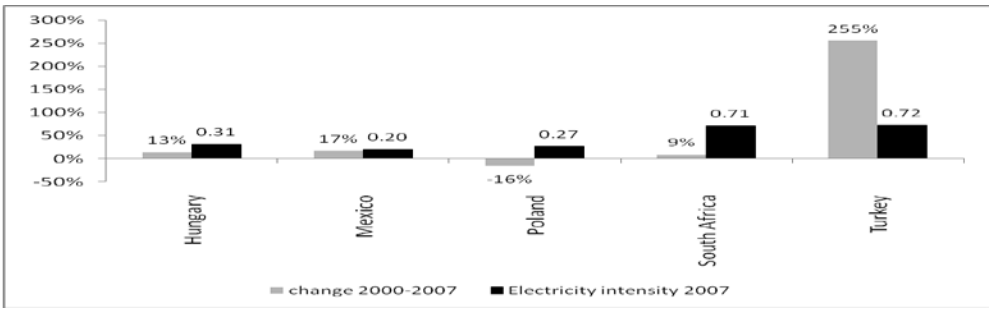

Fig. 3b Electricity intensity in 2007 (in GWh. $million (PPP adj)) and its growth: 2000-2007 for South Africa and OECD developing countries.
Source: Authors' calculations based on IMF [14] and OECD [15, 20].

Figure 3b presents a rather dismal picture for South Africa's electricity intensity in comparison with developing countries of the OECD. Its intensity was more than three times higher than this of Hungary, Mexico and Poland and at the same levels as Turkey. However, its growth for the period 2000 to 2007 was significantly less than this of Turkey (255%) and less than Hungary's and Mexico's (13% and 17%). However Poland managed to reduce its electricity intensity by 16% for the same period.

The results from Fig. 3 clearly indicate that South Africa's electricity intensity was not only higher than the majority of OECD countries in absolute terms (for 2007), but also showed excessive increase for the period 1990 to 2007 compared to the rest of the countries in the studied group. The next question that arises is whether this trend holds for all the economic sectors of South Africa.

To investigate the differences among industrial sectors, Table 1 presents the sectoral electricity intensities for South Africa and OECD average in 2006 and their differences. The majority of the South African sectors are more electricity intensive than the OECD average. Only four out of thirteen were more efficient than OECD and they are 'construction', 'food and tobacco', 'machinery' and 'transport equipment'. The order of magnitude in which they outperformed their OECD counterparts is on average 150.5%. This is in stark contrast to the degree in which the sectors whose intensity levels are worse than their OECD counterparts, namely 980.7% - a 6.5-fold difference.

[3] The results of the chi-square test and the Bartlett chi-square test are statistically significant confirming the existence of such relationship (chi-square= 3.63 (p-value=0.057) and Bartlett chi-square=3.41 (p-value=0.065)

Table 1: Sectoral electricity intensities in 2006 and output share: South Africa and OECD (Intensity: GWh/millions $ adj PPP; output: percentage)

	South Africa		OECD		Differences	
Sectors	**Intensity**	**Output**	**Intensity**	**Output**	**Intensity**	**Output**
Agriculture and forestry	0.316	6.00%	0.016	4.00%	1875.0%	50.00%
Basic metals*	1.095	7.10%	0.111	5.10%	886.5%	39.22%
Chemical and petrochemical	0.203	16.30%	0.034	15.20%	497.1%	7.24%
Construction	0.002	10.50%	0.087	16.60%	-97.7%	-36.75%
Food and tobacco	0.021	12.00%	0.023	8.30%	-8.7%	44.58%
Machinery	0.005	2.90%	0.028	15.00%	-82.1%	-80.67%
Mining and quarrying	0.634	14.60%	0.026	3.00%	2338.5%	386.67 %
Non-metallic minerals	0.524	1.60%	0.02	2.00%	2520.0%	-20.00%
Paper, pulp and printing	0.207	2.80%	0.021	5.50%	885.7%	-49.09%
Textile and leather	0.067	2.50%	0.01	1.90%	570.0%	31.58%
Transport equipment	0.003	9.80%	0.004	10.50%	-25.0%	-6.67%
Transport sector	0.089	12.50%	0.013	11.20%	584.6%	11.61%
Wood and wood products	0.069	1.40%	0.027	1.50%	155.6%	-6.67%

* Includes ‘iron and steel’ and ‘non-ferrous metals’

‘Basic metals’ have the highest electricity intensity in both South Africa and the OECD countries. Comparatively speaking, however, South Africa’s ‘basic metals’ sector was significantly more intensive (886%) than the OECD average before adjusting it to its respective size (or contribution to output) and 644% thereafter. The most efficient sector was ‘construction’, mainly due its high labour intensity and lower use of electricity-demanding technologies. On top of that the South African ‘construction’ sector was significantly more efficient than the OECD average. Why the ‘construction’ sector is more efficient compared to the rest can only be speculated about. This is due to a number of inter-linked factors; one of them being the labour intensity of the sector. This is since all the South African sectors are more labour intensive in comparison with the OECD countries, especially “construction”, which is 600% higher than its OECD equivalents. The difference of the rest of the South African sectors to the OECD ones is in the range of 100-300%. The weighted difference shows that the South African intensity was 156% lower than the OECD average.

While most electricity intensive South African sectors, i.e. ‘basic metals’ and ‘non-metallic minerals’ present high differences with the OECD average (644% and 2517%), ‘Mining and quarrying’ does not follow suit. The South African electricity intensity was 2305% higher than the OECD average, however, considering that the South African mining sector is a dominant one for the economy (14.6%) while a very small proportion of the OECD production (3%), the difference albeit is still very meaningful.

5. Conclusions

The study of electricity efficiency has recently become an important topic for two main reasons. Firstly, it is highly linked to negative consequences of greenhouse gas emissions and secondly it is a measure that combines electricity use with economic output [1]. Our analysis shows that South Africa's electricity intensity was at a level much higher than that of the OECD countries and the gap between South Africa and OECD is also increasing at an alarming rate. While alarming, it points towards scope for improvement necessary if South Africa is to remain competitive in trade regimes including carbon trading considerations with its OECD counterparts [21, 22].

South Africa has shown an increase in electricity intensity over the study period of 117% – more than doubling its electricity intensity from 0.32 GWh/ millions $ adj PPP to 0.71 GWh/millions $ (PPP). This is in sharp contrast to the average of the OECD members, which was only 10.09%. From our results, nine out of thirteen South African sectors are more intensive than their OECD equivalents, and by a considerable margin. Although 'basic metals', 'mining and quarrying' and 'non-metallic minerals' were the most electricity intensive sectors, these sectors presented the greatest gap with those of OECD being more efficient.

In summary, it became apparent that for South Africa to reduce its electricity intensity it has to either reduce its electricity usage or increase its production while keeping its electricity consumption stable. The lack of appropriate policies and the low and stable prices of electricity in the country for the studied period might be the main reasons for the results. South African producers were not concerned for electricity efficiency given the relatively low price levels of electricity over the period. Progress can be made by a concerted industrial policy to enhance the use and development of electricity efficient appliances. Electricity price reform, such as what has been recently announced, whereby the electricity price level is significantly increased in conjunction with block rate tariffs that charges a higher rate to those that consume more, is also vital. A nation-wide demand-side management program is also essential in the wake of these results in order to improve efficiencies.

References

[1] B. Liddle, Electricity intensity convergence in IEA/OECD countries: Aggregate and sectoral analysis, Energy Policy 37, 2009, pp. 1470-1478.

[2] A. Markandya, S. Pedroso-Galinato, & D. Streimikiene, Energy intensity in transition economies: Is there convergence towards the EU average?, Energy Economics 28, 2006, pp. 121-145.

[3] X. Zhao, C. Ma, & D. Hong, Why did China's energy intensity increase during 1998–2006: Decomposition and policy analysis, Energy Policy 38, 2010, pp. 1379-1388.

[4] M. Mendiluce, I. Pérez-Arriaga, & C. Ocaña, Comparison of the evolution of energy intensity in Spain and in the EU15. Why is Spain different?, Energy Policy 38, 2010, pp. 639-645.

[5] F.I. Andrade Silva & S.M.G. Guerra, Analysis of the energy intensity evolution in the Brazilian industrial sector—1995 to 2005, Renewable and Sustainable Energy Reviews 13, 2009, pp. 2589-2596.

[6] P. Tiwari, An analysis of sectoral energy intensity in India, Energy Policy 28, 2000, pp. 771-778.

[7] K. Medlock III, & R. Soligo, Economic Development and End-Use Energy Demand, The Energy Journal 22, 2001, pp. 77-106.

[8] S.E. Gergel, E.M. Bennett, B.K. Greenfield, S. King, C.A. Overdevest, & B. Stumborg, A Test of the Environmental Kuznets Curve Using Long-Term Watershed Inputs, Ecological Applications14, 2004, pp. 555-570.

[9] D. Baker, The Environmental Kuznets Curve, The Journal of Economic Perspectives 17, 2003, pp. 226-227.

[10] R. Inglesi, & J.N. Blignaut, Estimating the demand elasticity for electricity by sector in South Africa", Putting a price on carbon: Economic instruments to mitigate climate change in South Africa and other developing countries. Energy Research Center, University of Cape Town, 2010, pp. 65.

[11] C.L. Weber, Measuring structural change and energy use: Decomposition of the US economy from 1997 to 2002, Energy Policy 37, 2009, pp. 1561-1570.

[12] Department of Minerals and Energy (DME). 1998, White Paper on the Energy Policy of the Republic of South Africa, Department of Minerals and Energy, Pretoria.

[13] Department of Minerals and Energy (DME). 2005, Energy Efficiency Strategy of the Republic of South Africa, Department of Minerals and Energy, Pretoria.

[14] International Monetary Fund (IMF). 2010, World Economic Outlook April 2010, International Monetary Fund (IMF), Washington D.C., USA.

[15] Organisation for Economic Co-operation and Development (OECD). 2009, Energy balances for non-OECD countries, OECD , Paris, France.

[16] L. Schipper, M. Ting, M. Khrushch, & W. Golove. The evolution of carbon dioxide emissions from energy use in industrialized countries: an end-use analysis, Energy Policy. 25, 1997, pp. 651-672.

[17] Economic Commission for Europe (ECE). 1996, Worldwide Energy Conservation Handbook, Energy Conservation Center, Tokyo.

[18] Energy Information Administration (EIA). 1999, Energy Efficiency page: Defining Energy efficiency and its measurement. Available at: http://www.eia.doe.gov/emeu/efficiency/ee_ch2.htm

[19] D. Bosseboeuf, B.Chateau, & B. Lapillonne, B. Cross-country comparison on energy efficiency indicators: the on-going European effort towards a common methodology, Energy Policy. 25, 1997, pp. 673-682.

[20] Organisation for Economic Co-operation and Development (OECD). 2009, Energy balances for OECD countries, OECD , Paris, France.

[21] J.N. Blignaut, R.M. Mabugu, & M.R. Chitiga-Mabugu, Constructing a greenhouse gas emissions inventory using energy balances: the case of South Africa: 1998, Journal of energy in Southern Africa16, 2005, pp.105-116.

[22] J. Van Heerden, R. Gerlagh, J.N. Blignaut, M. Horridge, S. Hess, R. Mabugu, & M. Mabugu, Searching for triple dividends in South Africa: Fighting CO_2 pollution and poverty while promoting growth, The Energy Journal 27, 2006, pp.113-142.

Direct energy use in the livestock-breeding sector of Cyprus

Nicoletta Kythreotou[1,*], Georgios Florides[2], Savvas A. Tassou[1]

[1] *School of Engineering and design, Brunel University, Uxbridge, Middlesex, UK*
[2] *Department of Mechanical Engineering and Materials Science and Engineering, Cyprus University of Technology, Limassol, Cyprus*
** Corresponding author. Tel: +357 22 408947, Fax: +357 22 344556, E-mail: nikoletta.kythreotou@brunel.ac.uk*

Abstract: Energy consumption for most sectors in Cyprus is not well monitored and therefore their impact on greenhouse gases emissions has never been estimated. Thus, the aim of this study was to estimate the energy consumption in livestock breeding activities in Cyprus, and estimate the respective emissions of greenhouse gases. The energy consumption considered is related to all direct energy uses on a farm except transport. All data available from national sources have been taken into account and the consumption of energy per animal was estimated to be 401 k Wh/cow, 624 k Wh/sow and 0.618 kWh/chicken. The direct energy consumption in livestock breeding was estimated to be 53 G Wh for 2008. The greenhouse gas emissions from this were estimated to be 15.6 kt CO_2 equivalent of which 91% is CO_2. The contribution of livestock breeding to the total agricultural energy consumption has been found to be 10-15%. Comparing the energy consumption per animal to other countries in a sample for which data was available, the consumption for Cyprus has been found for all animal species to be lower, mainly due to the warmer climatic conditions.

Keywords: *Direct energy consumption, Livestock breeding, Cyprus, Greenhouse gases emissions*

1. Introduction

Sustainability, energy and climate change during the recent years are increasingly gaining political attention. The European Union has already set legally regulated targets on climate and energy in June 2009 [1] and has just recently agreed to the new sustainability and financial strategy of the Union, the EU2020 [2] which also includes climate and energy targets. Currently, there are several legal obligations in the European Union at country level and installation level that require baseline data on sectoral energy consumption to be available. Decision 406/2009/EC [3] is among those obligations that requires Member States of the European Union to reduce greenhouse gases emissions from sectors not included in the European emissions trading system, i.e. waste, agriculture, transport, energy use in household and services and agriculture. Cyprus is facing a large deficiency in statistics for several sectors, among which the energy sector. One source of greenhouse gases emissions for which a target has been set by Decision 406/2009/EC [3] is energy use by livestock breeding.

The uses of energy in a farm can be classified into direct and indirect [4]. Direct energy use is associated with the consumption of energy (fuels and electricity) in a farm. Indirect energy use is the energy consumed for the production and transport of materials used in a farm (e.g. feed and machinery). 70% of total energy use on dairy cattle and pig farms is for indirect uses [5].

Traditionally, animal farming in Cyprus was characterized by small; family ran units, spread throughout the island, but the increasing demand in meat and other products, the production of genetic material and the automation introduced in the production, have caused an increase in animal farming, which have caused certain areas of the island to have high animal density. A typical animal farm in Cyprus, as in the rest of the world, consists of one or more buildings distinguished in three types: animal breeding areas, support buildings and waste treatment and storage areas. In most areas in Cyprus, electricity is supplied by the central network of the

solely electricity provider, the Electricity Authority of Cyprus (EAC). Electricity in Cyprus is produced predominately by heavy fuel oil (HFO), with only a small amount produced by diesel [6]. It is expected that by 2014, natural gas will also be available for use. The most commonly used fuel in farms in Cyprus is diesel, which is mainly used for heating of the housing areas. During the last years the consumption of Liquid Petroleum Gas (LPG) for heating is rapidly increasing.

Not much data is readily available on energy consumption for livestock breeding in Cyprus. This paper brings together all the available data for stationary uses of energy for cattle, pig and poultry farming in Cyprus. Based on this data, the total energy consumption is estimated for the total population of the three animal species in Cyprus for 2005-2008. For 2008 the greenhouse gases emissions are also estimated and compared to other sources of emissions. Finally, results for both energy consumption and greenhouse gases emissions are compared to international literature.

2. Methodology

The main stages of the methodology applied are presented in Figure 1: (a) estimation of total energy consumption, (b) estimation of energy consumption according to source of energy and (c) estimation of the greenhouse gases emissions.

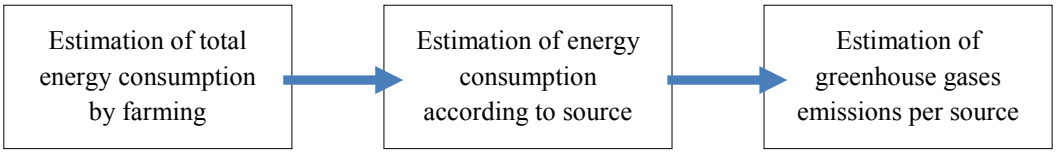

Fig. 1. Methodology implemented for the estimation of greenhouse gases emissions from energy consumption in livestock breeding in Cyprus.

2.1. Estimation of direct energy use from livestock breeding of Cyprus

The main sources of available data in Cyprus is limited to environmental impact assessment reports for animal farms submitted to the Department of Environment according to the Cyprus Law No. 140(I)/2005 on the assessment of environmental impacts from works [7] and annual reports submitted by installations that are above the benchmarks of the Integrated Pollution Prevention (IPPC) Directive [8]. Table 1 summarises the weighted energy consumption per animal in Cyprus as these were reported by the sources presented above; i.e. total amount of energy divided by total number of animals.

Table 1. Annual energy consumption per animal in Cyprus.

	Dairy cattle farms (kWh/cow)	Pig farms (kWh/sow)		Chicken farms (kWh/chicken)	
	178*	763+	1015+	0.741+	0.500+
	908*	1282+	244+	0.498+	0.292+
	610*	918+	1742*	0.578+	0.344+
		892+	64*	0.592+	0.760*
		181+	328*	layer chicken	0.864 [10,11]
		1087+	111*	broiler chicken	0.644 [10,11]
		225+	227*		
Weighted Average	401	624		0.618	

+ data submitted by installations that are above the IPPC levels for 2008 [9]
* data submitted for new installations according to the Environmental Impact Assessment report prepared [10]

Using the average annual energy consumption per animal in Cyprus of 401 kWh/cow, 624 kWh/sow and 0.618 kWh/chicken and using the animal population for 2005 - 2008, the total energy consumption for animal breeding of cattle, pigs and chicken in Cyprus for the same period was estimated by multiplying the animal population by the per animal consumption (Table 2). The animal population data used was according to the latest published annual animal population census of the Department of Agriculture [12]. The results of Table 2 were also based on the following assumptions:

(a) Layer chicken and broiler chicken have the same, average energy consumption because not sufficient data was available for the population of each type.
(b) Dairy cows and other cattle were assumed to have the same energy consumption per animal because in Cyprus the animals are in the same farms.
(c) Goats and sheep are not taken into account for the estimation of the total energy consumption by livestock breeding in Cyprus because no data is available yet.
(d) No distinction is made into breeding methods and waste management technologies used.
(e) Energy consumption of waste management technologies is also included in the energy consumption of the farm.
(f) Both gestating and farrowing sows have been considered for the population of sows because the difference in energy consumption is small to be taken into consideration.

Table 2. Animal population and total energy consumption from livestock breeding in Cyprus for 2005 - 2008.

	Animal population (x1000)				Annual energy consumption (GWh)			
	2005	2006	2007	2008	2005	2006	2007	2008
Cattle	57.6	56.1	54.9	55.9	23.1	22.5	22.0	22.4
Sows	61.4	64.7	64.3	46.6	38.3	40.4	40.2	29.1
Chicken	3007	2763	2800	2820	1.9	1.7	1.7	1.7
Total					63.3	64.6	63.9	53.3

2.2. Estimation of greenhouse gas emissions from direct energy use in livestock breeding of Cyprus

The distribution of energy consumption according to source (Table 3) was estimated using the average energy breakdown according to the IPPC annual reports for pig and chicken farming [9].

Table 3. Average energy breakdown of energy consumption in Cyprus for chicken and pig farms according to IPPC annual reports [9]

	Electricity	Diesel	LPG
Cattle*	28.5%	44.8%	26.7%
Pigs	28.7%	48.3%	23.0%
Chicken	28.3%	41.3%	30.4%

* cattle farms energy consumption = average of pigs and chicken due to lack of data

Using the emission factors of the greenhouse gases and the fuel densities proposed as default by the IPCC 2006 guidelines [13], the CO_2 emission factors from electricity production based on the weighted average specific emissions of the electricity producing units of Cyprus [6], and the global warming potentials proposed by the 1996 IPCC guidelines [14], the emissions of a specific greenhouse gas by an animal species (GHG_{animal}) were estimated by equation 1 in t CO_2 equiv.

$$GHG_{animal} = (EF_{GHG})_{fuel} \times EC_{fuel} \times GWP_{GHG} \quad (1)$$

where $(EF_{GHG})_{fuel}$= emission factor for a specific gas for a specific energy source (or fuel), t/TJ and GWP_{GHG}= is the global warming potential of a specific gas. The energy consumption of a specific energy source (or fuel), in (EC_{fuel}) was estimated by Eq.2:

$$EC_{fuel} = (\%_{fuel})_{animal} \text{ x } EC_{animal} \quad (2)$$

where $(\%_{fuel})_{animal}$ = percent contribution of a specific energy source (or fuel) to the total energy (or fuel) consumption of an animal species, % and EC_{animal} is the total energy (or fuel) consumption of an animal species, TJ. All the data used is presented in Table 4.

Table 4. Parameters used for the estimation of GHG emissions

Parameter in Eq.1	Description	Value
$(EF_{CO2})_{electricity}$	Electricity CO_2 EF*	78.94 t/ TJ [6]
$(EF_{CH4})_{electricity}$	Electricity CH_4 EF	3 kg/ TJ [13]
$(EF_{N2O})_{electricity}$	Electricity N_2O EF	0.6 kg/TJ [13]
$(EF_{CO2})_{diesel}$	Diesel CO_2 EF	74.1 t/ TJ [13]
$(EF_{CH4})_{diesel}$	Diesel CH_4 EF	10 kg/ TJ [13]
$(EF_{N2O})_{diesel}$	Diesel N_2O EF	0.6 kg/TJ [13]
$(EF_{CO2})_{LPG}$	LPG** CO_2 EF	63.1 t/ TJ [13]
$(EF_{CH4})_{LPG}$	LPG CH_4 EF	5 kg/ TJ [13]
$(EF_{N2O})_{LPG}$	LPG N_2O EF	0.1 kg/TJ [13]
GWP_{CO2}	GWP*** of CO_2	1 [14]
GWP_{CH4}	GWP of CH_4	1 t CH_4 = 21 t CO_2 eq. [14]
GWP_{N2O}	GWP of N_2O	1 t N_2O = 296 t CO_2 eq. [14]
	Energy conversion	3600 kJ/kWh [13]
	Diesel Energy content	43 TJ/ Gg [13]
	Diesel Density	0.85 kg/l [13]
	LPG Energy content	47.3 TJ/ Gg [13]
	Butane liquid density	0.57-0.58 kg/l [13]
	Propane liquid density	0.50-0.51 kg/l [13]

* EF = emission factor, ** LPG = liquid petroleum gas, *** GWP = global warming potential

3. Results and Discussion

Data collected from the available studies and reports in Cyprus, have shown that energy consumption per animal varies considerably among farms. The available data has a very large range for all animal species, i.e. 178 - 908 kWh/cow, 64 - 1742 kWh/sow, 0.292 – 0.760 kWh/chicken. Nevertheless, the average of the results are reasonable when compared to other countries and the total contribution of the sector to energy consumption by agriculture.

3.1. Contribution of livestock breeding to agricultural energy uses

Comparing the results obtained for livestock breeding energy consumption (Table 2) to the total energy consumption by agriculture [15], the contribution of direct energy use in livestock breeding to the total energy consumption by agriculture has been found to decrease from 14% in 2005 to 11% in 2008. The energy consumption by livestock breeding has reduced considerably from 63 GWh in 2005 to 53 GWh in 2008, due to a decrease in the animal population, which is probably due to the increase in imports of meat. The total energy consumption of the sector has increased from 439 GWh in 2005 to 504 GWh in 2008, probably due to the change in climate conditions. The years of 2006 to 2008 were years with extensive droughts in Cyprus. This has caused the cultivations to require more artificial irrigation since natural precipitation was very limited. Consequently, the energy demand for

the irrigation systems was larger. Additionally, the number of small desalination plants installed for agricultural use in coastal areas where saline intrusion takes place has been increasing during the last few years. This has been again caused by the reduction in precipitation and the need for farmers to use their already exhausted water extracting boreholes.

3.2. Comparison of direct energy consumption in livestock breeding in Cyprus to other countries

Cattle in most farms throughout the world are field-grazing most of the time of the year. When the cows are collected indoors due to weather conditions, the housing areas are closed. Therefore energy for ventilation and lighting is needed. In the case of Cyprus cattle is kept in the open but restricted areas instead of fields. With no lighting and ventilation used, energy per animal is considerably less. The comparison is presented in Fig. 2(a).

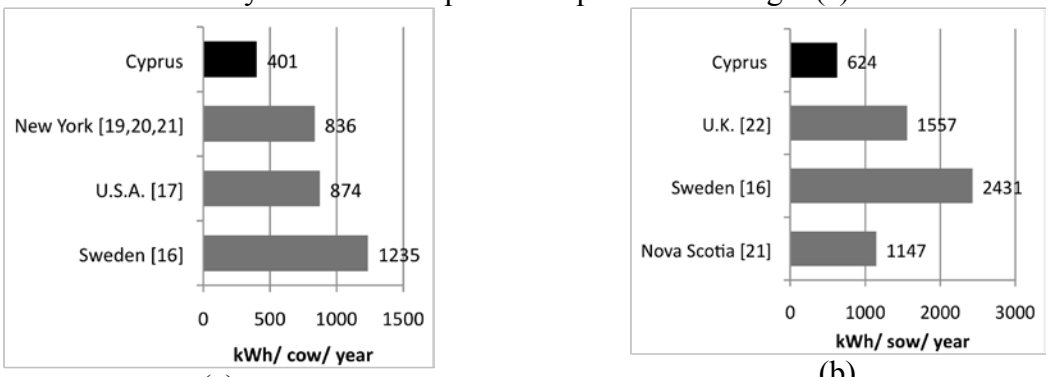

Fig. 2. Annual energy consumption for various countries compared to energy consumption in Cyprus (a) per dairy cow found and (b) per sow for farrow to finish.

Figure 2(b) presents the Nova Scotia [18], U.K. [19] and Sweden [16] consumption per sow compared to Cyprus. Cyprus has the smallest consumption among the four areas. This is due to the reason that in pig farming most of the energy demands is for heating. Therefore, in Cyprus, where heating days are significantly less than Nova Scotia [18], U.K. [19] and Sweden [16], the energy demand is also significantly less compared to the same countries.

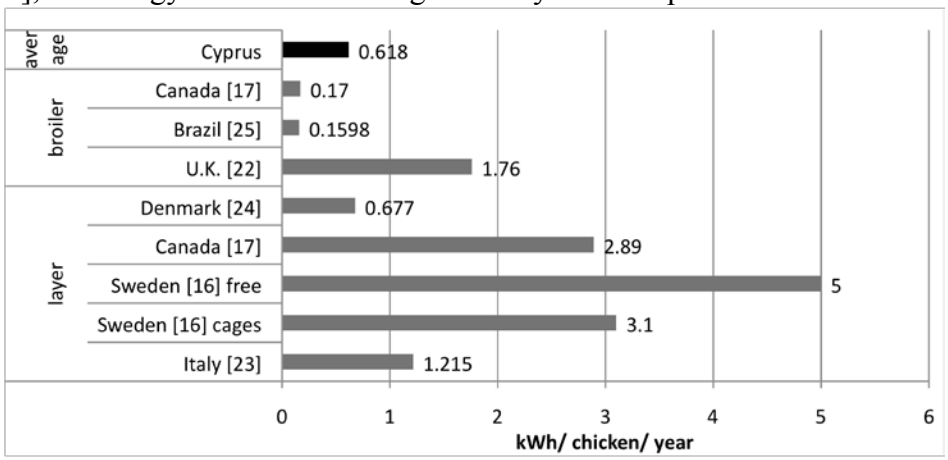

Fig. 3. Annual energy consumption per chicken for various countries compared to energy consumption in Cyprus for layer and broiler chicken.

The energy consumption estimated for chicken farming (Fig. 3) appears not very dissimilar to other countries. Most of the energy consumption is expected to be during summer for ventilation purposes as in Italy [20]. The per-chicken consumption of Denmark [21], Brazil

[22] and Canada [17] is smaller than Cyprus. A probable reason for this is that Denmark has well-developed technologies and therefore higher efficiency in energy consumption than Cyprus. For Brazil and Canada the smaller energy consumption could be due to differences in the methods of breeding.

3.3. Greenhouse gas emissions from energy consumption in livestock breeding

The total GHG emissions from energy consumption in livestock breeding have been estimated to be 15.26 kt CO_2e for 2008 of which 91% is CO_2. For the same year other agricultural greenhouse gas emissions according to the Greenhouse Gas Inventory of the country were 348 kt CO_2e [24]. The emissions according to gas and energy sources are presented in Table 5. The larger emissions are CO_2 emissions from diesel consumption in cattle and pig farming, which correspond to 21% and 29% of the total emissions respectively. Energy related emissions contribute approximately 3% to the total for cattle, 2% for pigs and 1.4% for poultry. Comparing the results to emissions from total agricultural use of energy, energy use in livestock breeding contributes 4% to the total agricultural emissions and 13% to the total agricultural energy emissions. This result is supported by the estimations of "Compassion in world farming" [23] where energy contributes 2% to the total livestock emissions.

Table 5. GHG emissions from direct energy consumption in livestock breeding in Cyprus according to gas and energy source, 2008.

	Cattle	Pigs	Poultry	TOTAL
CO_2 from Electricity, t	1,816	2,375	140	4,331
CO_2 from Diesel, t	2,679	3,752	192	6,624
CO_2 from LPG, t	1,360	1,521	120	3,002
Total CO2, t	5,855	7,649	453	13,956
CH_4 from Electricity, kg	69	90	5	165
CH_4 from Diesel, kg	362	506	26	894
CH_4 from LPG, kg	108	121	10	238
Total CH_4, kg	538	717	41	1,296
N_2O from Electricity, kg	14	18	1	33
N_2O from Diesel, kg	1,608	2,251	115	3,974
N_2O from LPG, kg	136	152	12	300
Total N_2O, kg	1,757	2,421	128	4,307
Total GHG from Electricity, kt CO_2 equiv.	1.82	2.38	0.14	4.34
Total GHG from Diesel, kt CO_2 equiv.	3.16	4.43	0.23	7.82
Total GHG from LPG, kt CO_2 equiv.	1.40	1.57	0.12	3.10
TOTAL GHG, kt CO_2 equiv.	6.39	8.38	0.49	15.26

4. Conclusions

In Cyprus, the annual consumption per animal was estimated to be 401 kWh/cow, 624 kWh/sow and 0.618 kWh/chicken. The estimates were based on available data for Cyprus. According to these figure, the direct energy consumption in livestock breeding of cattle, pigs and poultry is estimated at 53 GWh for 2008, which corresponds to 10-15% of the total agricultural energy consumption. Comparing the energy consumption per animal to other countries in the sample used in the study it was found that energy consumption per animal for Cyprus was, on average, lower. Energy consumption for cows was much lower than the countries for which data was available (Canada, Nova Scotia, U.K., Sweden) mainly because the majority of energy consumption in these countries is for heating which is not needed in Cyprus due to the relatively warm weather conditions. For chicken farming, the results are

comparable to Italy, since a large portion of the country has similar climatic conditions to Cyprus (hot and dry).

Using the emission factor of each greenhouse gas according to fuel type proposed by the IPCC 2006 guidelines [13] and for electricity as proposed by national specific data by the Electricity Authority of Cyprus [6], the greenhouse gas emissions for each animal species and energy source were estimated. Comparing these to emissions from total agricultural use of energy, the results show that the emissions from energy use in livestock breeding contribute approximately 4% to the total agricultural emissions and 13% to the total agricultural energy emissions.

These results can be used by relevant Cyprus authorities for the assessment of the impact of measures for the reduction of energy consumption and greenhouse gases emissions.

References

[1] Council of the European Union, Climate and energy package, Official Journal of the European Union. L140 Volume 52 5 June 2009, ISSN 1725-25555

[2] Council of the European Union, Conclusions of the Summer European Council, 17 June 2010, EUCO 13/10, CO EUR 9, CONCL 2, General Secretariat of the Council

[3] Council of the European Union, Decision No 406/2009/EC of the European Parliament and of the Council of 23 April 2009 on the effort of Member States to reduce their greenhouse gas emissions to meet the Community's greenhouse gas emission reduction commitments up to 2020, Official Journal of the European Union L 140, 5.6.2009, p. 136 – 148

[4] K.J. Hulsbergen, B. Feil, S. Biermann, G.W. Rathke, W.D. Kalk, W.A. Diepenbrock, Method of energy balancing in crop production and its application in a long-term fertilizer trial. Agric Ecosyst Environ, 2001 86(3): 303–21.

[5] M. Meul, F. Nevens, D. Reheul, G. Hofman, Energy use efficiency of specialized dairy, arable and pig farms in Flanders. Agric Ecosyst Environ 2007 119(1–2): 135–44.

[6] Department of Environment, Ministry of Agriculture, Natural Resources and Environment. 2009. Annual report on Emissions Trading System of Electricity Authority of Cyprus for 2005 - 2008. Personal communication

[7] Cyprus Laws of 2005 to 2007 on the Assessment of the Environmental Impacts of certain Projects, basic Law No. 140(I)/2005, latest amendment Law No. 42(I)/2007 in Cyprus Gazette no. 4120, Publication date: 05/04/2007, Page: 00501-00507.

[8] Council of the European Union, Council Directive 96/61/EC of 24 September 1996 concerning integrated pollution prevention and control. Official Journal of the European Union L 257, 10/10/1996 P. 0026 – 0040

[9] Department of Environment; Ministry of Agriculture, Natural Resources and Environment, 2010 Annual report of Integrated Pollution Prevention Control poultry farms and piggeries 2007, Personal communication.

[10] Environmental Impact Assessments (EIA) submitted for examination to the Department of Environment for the purposes of Laws of 2005 to 2007 on the Assessment of the Environmental Impacts of certain Projects, Personal data collection, 2010.

[11] NPRO Engineering Ltd., A study on law enforcement for integrated pollution prevention control in poultry farming in Cyprus, Prepared for the Department of Environment of Ministry of Agriculture, Natural Resources and Environment (in greek), 2006, Nicosia, Cyprus (in greek).

[12] Department of Agriculture; Ministry of Agriculture, Natural Resources and Environment, Pig farming review for the year 2008. 2009, Nicosia, Cyprus (in greek).

[13] IPCC, 2006 IPCC Guidelines for National Greenhouse Gas Inventories, Prepared by the National Greenhouse Gas Inventories Programme, Eggleston H.S., Buendia L., Miwa K., Ngara T. and Tanabe K. (eds). Published: IGES, 2006, Japan.

[14] IPCC, Revised 1996 IPCC Guidelines for National Greenhouse Gas Inventories, Prepared by the National Greenhouse Gas Inventories Programme, Published: IGES, 1998, Japan.

[15] Energy Service, Ministry of Commence, Industry and Tourism, Energy balance 1990-2008, Personal communication, Nicosia, Cyprus.

[16] T. Hörndahl, Energy Use in Farm Buildings. Swedish University of Agricultural Sciences, Faculty of Landscape Planning, Horticulture and Agricultural Science, Report 2008:8, ISSN 1654-5427, ISBN 978-91-85911-76-9, Alnarp 2008

[17] J.A. Dyer, R.L. Desjardins, An Integrated Index of Electrical Energy Use in Canadian Agriculture with Implications for Greenhouse Gas Emissions, Biosystems Engineering, 2006 95 (3), 449–460.

[18] Business Development and Economics, Swine farrow to finish results individual report prepared for: all farm average, Farm Management Analysis Project (FMAP).,Truro, NS: Nova Scotia Department of Agriculture, 2004.

[19] H.R.I. Warwick, AC0401: Direct energy use in agriculture: opportunities for reducing fossil fuel inputs, Final report to Defra, 2007, U.K.

[20] European Commission, Integrated Pollution Prevention and Control - Reference Document on Best Available Techniques for Intensive Rearing of Chicken and Pigs, 2003.

[21] A. Annuk, H. Nurste, S. Skau Damskier, Energy Efficiency in intensive livestock, Estonia, Energy saving measures on poultry farms, Carl Bro Intelligent solutions, 2004.

[22] Turco, J.E.P., Ferreira, L.F.S.A., Furlan, R.L., 2002. Consumption and electricity costs in a commercial broiler house. Rev. bras. eng. agrvc. ambient. [online]. vol.6, n.3, pp. 519-522. ISSN 1415-4366. doi: 10.1590/S1415-43662002000300023.

[23] Compassion in World Farming, Global Warning: Climate Change and Farm Animal Welfare. Revised 2009, UK.

[24] Department of Environment, Cyprus national greenhouse gas inventory 1990 – 2008, Ministry of Agriculture, Natural Resources and Environment, Cyprus, 2010.

Active demand response strategies to improve energy efficiency in the meat industry

Manuel Alcázar-Ortega [1,*], Guillermo Escrivá-Escrivá [1], Carlos Álvarez-Bel[1], Alexander Domijan [2],

[1] *I Universidad Politécnica de Valencia, Institute for Energy Engineering, Valencia, Spain*
[2] *University of South Florida, Dept. of Engineering, Tampa, USA*
** Corresponding author. Tel: +34 963 879 240, Fax: +34 963 877 272, E-mail: malcazar@iie.upv.es*

Abstract: This paper is focused on the evaluation and assessment of different energy efficiency strategies applied to electrical appliances related to cool production and ventilation in industrial facilities which manufacture different types of meat products. Two strategies have been analyzed. Firstly, speed variation of fans in drying chambers, which implies modification of the on-off sequences in a way that the fans work for a longer time at a lower speed. A reduction of 1.65% in the total consumption of electricity is achieved. Lastly, use of flexibility in drying rooms based on the interruption of the electricity supply for the cooling production. Using this strategy saves of 5% in the total cost of electricity are achieved. Such results are very promising and demonstrate the effectiveness of these techniques, opening the gate to an innovative point of view about the management of this type of infrastructures to get significant energetic, economic and environmental savings with reduced and acceptable impact in the production process.

Keywords: *Full Food Industry, Power Demand, Energy Conservation, Electric Variables Control, Load Modeling*

1. Introduction

The meat industry is one of the most energy consumption intensive industrial sectors [1] and it is an industrial segment with one of the highest potentials for demand response (DR) implementation [2, 3]. It is the largest segment in U.S. agriculture [4], where poultry and pig meat segment represents the 16% in total World production [5]. The share for the European Union is similar, with the 18% in total World production. In the case of Spain, where techniques exposed in this paper have been tested, the elaboration of different pig meat products, as cured ham or deli products, is worldwide known. Spain produces the 3% of total pig meat in the world.

Regarding the type of energy sources used by such type of consumers, heating processes generally use fossil fuels, as natural gas or diesel, while electricity is mainly used for cooling. Refrigeration constitutes between 45% and 90% of the total final electricity consumption in working days [6], so that efficiency and saving actions must be focused on this energy source.

Different works have been presented in the past [7, 8] in order to evaluate customer demand response in different sectors (mainly for commercial and industrial segments). Nevertheless, they were not commonly applied to the meat industry processes since they are directly related to the final quality of the product, so customers were not willing to change any element or parameter of those processes.

In spite of that fact, these rigid industrial practices are being questioned because of the gradual increase in prices of energy, the higher concern in environmental issues as well as the evolution in technology solutions, so new actions, like the ones proposed in this paper, oriented to improve the energy consumption, start to be taken into account.

This paper presents such type of efficiency and saving actions as the effect of reducing the rotation speed of fans in drying chambers or the use of flexibility that customers may have under a novel approach focused on the identification of packages of energy [8] that could be reduced or eliminated for a period of time without impacting in production processes.

2. The drying process in a cured ham factory

The process of drying in a cured ham factory takes place in especially designed chambers and requires an accurate control of temperature, relative humidity and speed of air [9]. Historically, the process of drying was carried out in specific zones with Continental Mediterranean climate. The process started in December, where temperature and humidity are low, and it used to be completed in summer. Currently, artificial drying chambers reproduce such conditions permanently, so that a continuous production could be achieved.

2.1. The whole process: stages

The traditional Spanish dry-cured ham production is initiated with a salting process and storing of fresh ham at a low temperature before drying in order to stabilize the meat [10]. The temperature of the drying air is gradually increased during the drying process in order to accelerate the reduction of water in meat and the development of the typical aged flavor. According to available bibliography [9, 11] and after studying in detail the process of drying in different factories devoted to the production of Spanish cured ham, four drying stages can be identified for a typical plant, as shown in Fig. 1.

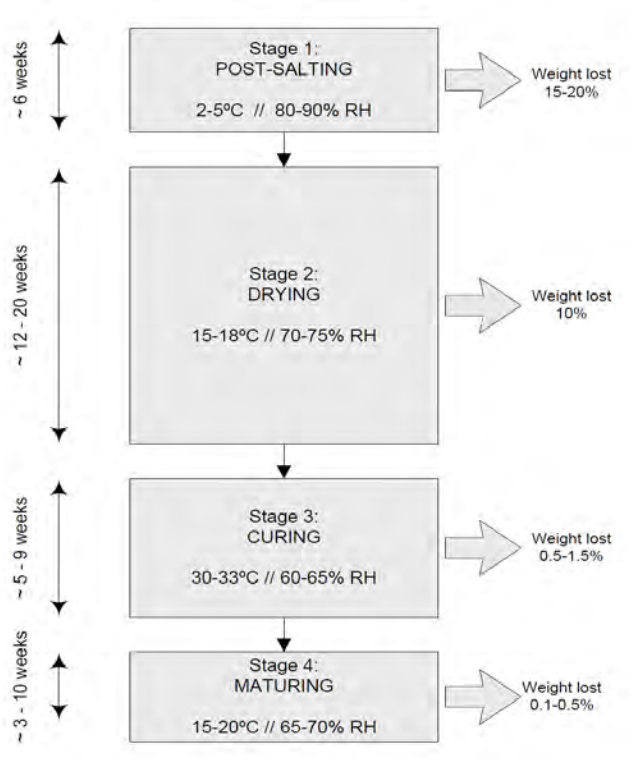

Fig.1. Drying processes in a typical cured ham factory.

- Post-salting stage. Temperature inside the chamber is set between 2 and 5ºC while humidity remains controlled between 80% and 90%. The average duration of this stage is about six weeks, depending on the type of product. The amount of water contained in the

meat is deeply reduced during this stage, reaching values between 15% and 20% in the total weigh of the product.

- Drying stage. The meat loses about 10% of weigh during this phase of the process. Temperature is maintained in 15-18ºC range and humidity take values of 70-75%. It usually takes between 3 and 5 months.
- Curing stage. Temperature is higher (30-33ºC) and humidity decreases up to 65% in this stage, with a typical duration of 5 to 9 weeks. Ham loses between 0,5 and 1,5% of weight in this phase.
- Maturing stage. The ham is introduced then in a maturing chamber until the experts consider that the product is finished. Therefore, the duration of this stage strongly depends on the particular situation of each product, as well as the type of final product to be obtained. Accordingly this stage could take from 20 to 70 days, depending on the type of final product and the amount of water it has already lost. Humidity is maintained below 70% and temperature reaches values of 15-20ºC.

A piece of ham loses during the whole drying process about 35% of the initial weigh that it had at the beginning of the process.

2.2. Psychrometric analysis of a drying chamber

Drying chambers are equipped with different air drying units, which are distributed on the ceiling of each room. Each device consists on a heat exchanger and a fan which forces the air to go through the unit. At the entrance of the unit, there is a first group of pipes containing cold water to cool the moist air and produce the condensation. At the exit, there is another group of pipes containing in that case hot water, which allow the dry air to recover the initial temperature.

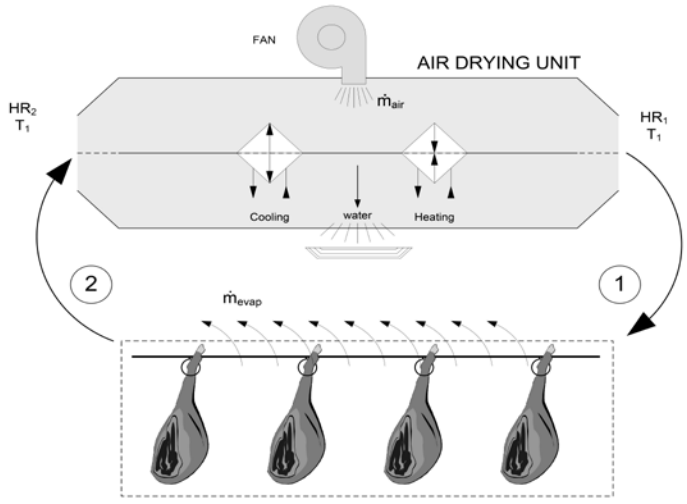

Fig.2. Meat drying process scheme.

The processes involved in a drying chamber facility, regarding the air parameters and flow, are schematically shown in Fig. 2. Dry air starts contacting with the surface of meat inside the drying chamber in point 1. Dry air absorbs the humidity from the surface of meat from point 1 to point 2 so that the humidity ratio ω grows adiabatically [11] from ω_1 to ω_2, as shown in Fig. 3, that depicts the psychrometric chart during the process.

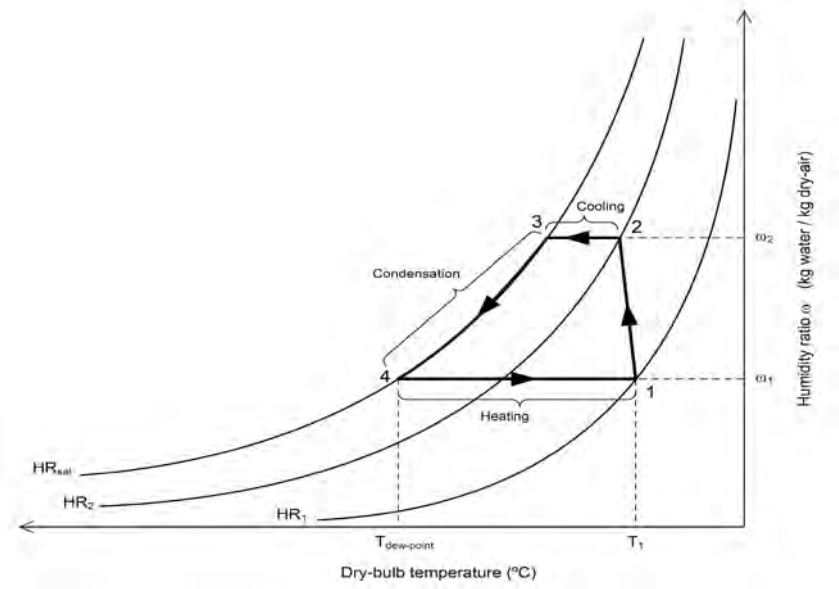

Fig.3. Psychrometric chart for a drying room.

When moist air gets in the air drying unit, the temperature decreases from point 2 to point 3, where the dew-point is reached. Moisture condensation occurs when moist air is cooled to a temperature below its initial dew-point [12]. From point 3 to point 4 temperature decreases while the air drives the water out since the humidity ratio is lower, as the capacity of the air to keep the water is reduced. Dry air is heated again from point 4 to point 1 in order to maintain the temperature inside the drying room, so initial conditions for the air are achieved to start the drying process again.

3. Proposed saving strategies

Two different strategies have been evaluated and assessed in order to achieve significant reductions in the electricity bill in factories devoted to the elaboration of meat products. In particular, speed variation of fans and flexibility strategies have been tested in different factories that produce Spanish cured ham, as it is exposed below.

3.1. Strategy 1: Speed variation of fans in drying chambers

Fans forcing the air to go through the drying units, located on the ceiling of the drying chambers, work intermittently according to the drying plan established by experts for the proper development of the process. The first action proposed is based on the modification of the on-off sequences in a way that the fans work for a longer time at a lower speed, so that the total amount of water extracted from the drying chamber remains constant.

The computation of boundary limits on possible savings with different operation conditions can be done according to the fan performance equations, and it can be summarized according to the following simple relationships linking fan capacity, speed and power:

- The airflow volume is directly proportional to the fan speed.
- The power required by fans is proportional to the cube of the fan speed [13]

In case the speed of fans were to be reduced, the duration of the ventilation cycle needs to be increased in order not to reduce the total amount of air required to remove all the water transferred by the ham, so the speed reduction would be achieved if fans were working at reduced regime for a longer time.

3.1.1. Obtained results

Results presented in this section have been obtained in a real factory which produces cured ham in Spain.

Four different drying chambers were studied in detail according to the design conditions of the considered factory. Table 1 shows the set point parameters for each one of these chambers:

Table 1. Set point parameters for the different drying chambers in a cured-ham factory.

Drying chamber / stage	**Set point temp.**	**Set point humidity**	**Duration**	**Reduction of water**
	ºC	*%*	*weeks*	*%*
Post-salting	*3.0*	*82.0*	*6.4*	*12.0*
Drying (I)	*8.0*	*77.0*	*7.1*	*9.0*
Drying (II)	*18.0*	*74.0*	*7.1*	*3.0*
Curing	*30.0*	*70.0*	*3.6*	*3.0*

A psychrometric analysis of each chamber, based on a methodology proposed by authors in [14], was performed in order to get the different values for points from 1 to 4, as described in section 1.2. Table 2 includes the humidity ratio, dry-bulb and humid-bulb temperatures, specific enthalpy and relative humidity for each drying chamber at a pressure of 760 mmHg.

Table 2. Set Characteristic points in the psychrometric chart for the different chambers.

Chamber	**Point**	**Humidity Ratio ω**	**Dry-bulb temperature**	**Humid-bulb temperature**	**Enthalpy**	**Relative humidity**
		kg-w/kg-da	*ºC*	*ºC*	*kJ/kg-da*	*%*
Post-salting	*1*	*0.00376*	*3.00*	*1.66*	*12.29*	*80*
	2	*0.00389*	*2.65*	*1.66*	*12.68*	*84*
	3	*0.00389*	*0.51*	*0.51*	*10.62*	*100*
	4	*0.00376*	*0.09*	*0.09*	*9.85*	*100*
Drying (I)	*1*	*0.00520*	*8.00*	*6.22*	*20.72*	*78*
	2	*0.00542*	*7.45*	*6.22*	*21.3*	*84*
	3	*0.00542*	*5.18*	*5.18*	*19.12*	*100*
	4	*0.00520*	*4.56*	*4.56*	*17.94*	*100*
Drying (II)	*1*	*0.00970*	*18.00*	*15.28*	*41.69*	*75*
	2	*0.01018*	*16.85*	*15.28*	*42.95*	*84*
	3	*0.01018*	*14.40*	*14.40*	*40.68*	*100*
	4	*0.00970*	*13.61*	*13.61*	*38.65*	*100*
Curing	*1*	*0.02019*	*30.00*	*26.23*	*79.58*	*75*
	2	*0.02140*	*27.20*	*26.23*	*82.85*	*93*
	3	*0.02140*	*26.08*	*26.08*	*82.13*	*100*
	4	*0.02019*	*25.23*	*25.23*	*78.06*	*100*

The next step was to calculate the value of reduced speed at which fans need to be adjusted. The rated power of motors is 1 HP at 1500 rpm. The initial time during that fans are switched on is equal to 50% of the stage for post-salting and drying (I), 40% for drying (II) and 35% for curing. The evaluation has been performed by considering that fans will be switched on for the 80% of the duration of each drying stage. Table 3 shows below the variations that affect to speed, power a duration of the different drying stages after implementing the speed reduction of fans.

Table 3. Ratios of speed, power and time after applying the proposed actions.

Drying chamber / stage	**Reduced speed** *rpm*	**Speed ratio**	**Δ power** *%*	**Δ time** *%*
Post-salting stage	*938.0*	*1.6*	*-37.5*	*60.0*
Drying stage (I)	*750.0*	*2.0*	*-80.8*	*100.0*
Drying stage (II)	*656.0*	*2.3*	*-92.5*	*128.6*
Curing stage (I)	*563.0*	*2.7*	*-91.8*	*166.7*

The application of these actions would allow the customer to save 172458 kWh every year, which supposes the 1.65% in the total consumption of electricity. Such savings imply reductions of 13642 € in the annual electricity bill, as well as 67.2 tCO2 are avoided to be emitted into the atmosphere a year.

As shown in this section, significant energy savings can be obtained. However, it is important to take into account that too high reductions of speed, as obtained for the curing stage, could result in the stratification of the air in the chamber and the inappropriate development of the drying process. For that reason, additional ventilation or a lower reduction of power must be assessed in order to apply this type of actions.

3.2. Strategy 2: Use of flexibility in drying rooms

This strategy is based on the interruption of the electricity supply for the cooling production so that the thermal inertia of the system could be used to keep both temperature and humidity inside under limits. Temperature and consequently the humidity ratio for point 4 increases when the cool production is interrupted. Therefore, the duration of this action will depend on the ability of the product not to be affected by that action. Interruptions of about 1 hour do not have negative effects on this type of products. Similarly, the cooling activity will be more intensive during the subsequent minutes after the interruption (payback period), so point 4 will decrease until the set-point is achieved again.

3.2.1. Obtained results

After a period of pre-evaluation which proved the effectiveness of proposed actions [1], the implementation of an intensive campaign of interruptions was carried out in order to reduce the monthly electricity bill. During the whole month of February 2010, two interruptions a day of two ours each interruption were performed in working days. Fig. 4 shows different daily load profiles when interruptions were performed, as well as an average profile and the standard deviation, represented below.

Interruptions were carried out on peak periods, which are established in the contract from 10:00 AM to 1:00 PM and from 6:00 PM to 9:00 PM in January, February and December. As daily interruptions of 6 hours were considered unacceptable, only the last two hours of each peak period were used for flexibility purposes. Consequently, the reconnection of cooling

devices took place on shoulder period where prices are lower. As can be checked in fig. 4 the energy saved during each interruption is much higher than the one consumed during the recovery period.

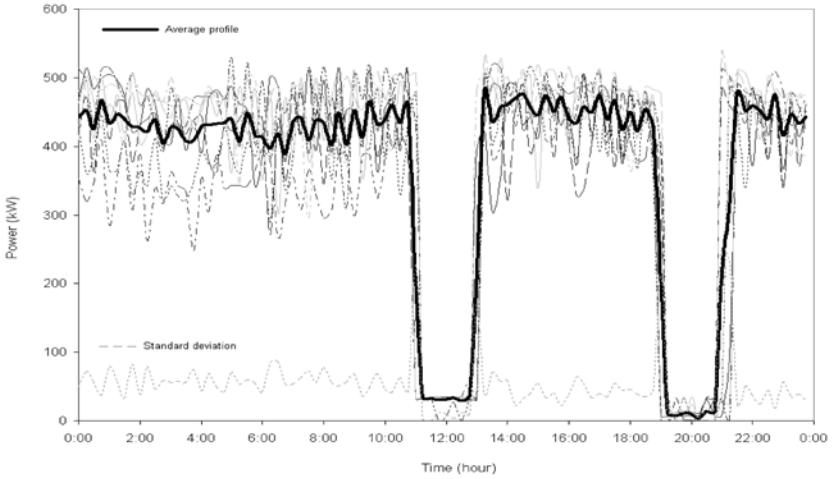

Fig.4. Daily electricity profiles during the campaign of interruptions in February 2010.

The application of such actions allowed the customer to save 1555 kWh every working day in February, equivalent to savings of 207.3 € and 1.52 tCO2 a day. The customer saved 4147 € during February, equivalent to a reduction of 6.21% in the monthly electricity bill. This percentage would be reduced to about 5% if these results are extrapolated for the whole year because the periods defined in the contract are different in other seasons and the difference between peak and shoulder prices is not as high in warmer months as in winter.

4. Conclusions

The use of electricity for intensive cooling processed in the meat industry has been analyzed in this paper, as well as different actions aimed to the improvement of energy efficiency in this sector have been proposed.
This paper provides empirical evidence about the importance that the use of flexibility in such a promising sector as the meat industry could represent in order to reduce the consumption of primary energy and emissions into the atmosphere, at the same time that attractive reductions in the electricity bill are achieved by customers.
Two strategies have been analyzed. Firstly, speed variation of fans in drying chambers, which implies modification of the on-off sequences in a way that the fans work for a longer time at a lower speed. Using this strategy, a reduction of 1.65% in the total consumption of electricity is achieved. Secondly, use of flexibility in drying rooms based on the interruption of the electricity supply for the cooling production obtaining saves of 5% in the total cost of electricity.

Such results are very promising and demonstrate the effectiveness of these techniques, highlighting that a different management of this type of infrastructures can be performed to get significant energetic, economic and environmental savings with reduced and acceptable impact in the production process.

Acknowledgment

The authors gratefully acknowledge the contributions of Campofrío Food Group, S.A.
This work was supported by the Spanish Government (Ministerio Ciencia e Innovación, MICINN) under Research Project ENE2007-67771-C02-01&02/CON

References

[1] Alcázar-Ortega, M., Escrivá-Escrivá, G., Álvarez-Bel, C., Domijan, A. "Evaulation and assessment of flexibility potential in the meat industry: application to intensive cooling processes", submitted to IEEE Trans. on Power Systems in April 2010.

[2] The birth of a EUropean Distributed EnErgy Energy Partnership that will help the large-scale implementation of distributed energy resources in Europe (EU-DEEP), the European Project supported by the Sixth Framework programme for Research and Technological Development. http://www.eu-deep.com

[3] Afonso, D., Pérez-Navarro, A., Encina, N., Álvarez, C., Rodríguez, J. and Alcázar, M. "Methodology for ranking of customer segments by their suitability for distributed energy resources applications", Elsevier Energy Conversion and Management, 48, pp. 1615-1623, January 2007

[4] The United States Meat Industry. American Meat Institute AMI. March 2009 Report. Available on http://www.meatami.com

[5] FAOSTAT. Food and Agriculture Organization of the United Nations. Annual Statistical Report, 2005. http://faostat.fao.org, accessed on February 2009.

[6] Ramírez, C.A., Patel, M., Blok, K. "How much energy to process one pound of meat? A comparison of energy use and specific energy consumption in the meat industry for European countries". Elsevier Energy, 31, pp. 2047-2063, September 2006

[7] Álvarez, C., Alcázar, M., Escrivá., G, Gabaldón, A. "Technical and economical tools to assess customer demand response in the commercial sector". Elsevier Energy Conversion and Management, 50, pp. 2605-2612, July 2009

[8] Álvarez, C., Gabaldón, A., and Molina, A.: "Assessment and simulation of the responsive demand potential in end-user facilities: Application to a university customer", IEEE Trans. Power Syst., vol. 19, no. 2, pp. 1223-1231, May 2004

[9] Comaposada, J. "The Sorption Isotherms and Water Diffusitivity in Muscles of Pork Ham at Different NaCl Contents". Ph.D. Dissertation, Dept. of Thermal Engines and Machines. Univ. Polit. Cataluña. 1999

[10] 1Arnau J., Gou P., Comaposada J. "Effect of the relative humidity of drying air during the resting period on the composition and appearance of dry-cured ham surface". Elsevier Meat Science, 65 (4), pp. 1275-1280. January, 2003.

[11] Ventanas, J. "Tecnología del jamón ibérico". Ed. Mundi-Prensa, Madrid, 2001. ISBN 8471149443

[12] ASHRAE. "Psychrometrics - SI Units Edition" in Fundamentals Handbook Ed. American Society of Heating, Refrigerating and Air-Conditioning Engineers, 2005. Chapter 6, pp. 6.1-6.17.

[13] Naughton, P., Wang, R.D., Filipovic, A., Hundt, A. and Cooper, D.W. "High efficiency particulate air (HEPA) filter velocity reduction study". International SEMATECH manufacturing Initiative (ISMI). August, 2006. Available in www.ismi.sematech.org

[14] Alcázar-Ortega, M., Escrivá-Escrivá, G., Álvarez-Bel, C., Domijan, A. "A case of improvement of efficiency in the meat industry: Speed variation of fans in drying chambers", submitted to ELSEVIER, Energy Conversion and Management in May 2010

The importance of end-use technologies for long-term energy use in Sweden

M. Bladh

Department of Thematic Studies—Technology and social change
Linköping University, SE-581 83 Linköping, Sweden
+46 13 284453; mats.bladh@liu.se

Abstract: Energy consumption has stagnated in Sweden since the 1970s. It is not known how this was accomplished, but increasing efficiency in consumption has played an important role. In order to understand this a Change-of-stock approach is presented. Basically this approach says that stocks of energy converting artefacts on the consumption side comprise mature technologies with advantages of a path dependent character. These advantages create obstacles for radical technological changes and pushes in favour of incremental changes within dominating technologies. For the sake of testing the relevance of this approach five cases are highlighted. Data over stocks and replacement rates are estimated in three cases. Both factual and counterfactual estimations are presented. What is tested is the fruitfulness of the Change-of-stock approach as a tool for analysis of long-term changes in energy efficiency.

Results from the cases show considerable gains of efficiency in fuel consumption in private cars, and heating efficiency in multi-dwelling houses. Thus incremental changes are important, but are partially offset by changes in characteristics of the artefacts. Radical changes, as the factual change from air to rail, and a counterfactual double switch from gasoline to electric cars and from electric heating to district heating, and probable gains from the phase-out of incandescent lamps, show even bigger gains. Both incremental and radical changes are subject of counteracting tendencies, of a broader nature than that associated with rebound effects, such as more cars per inhabitant and fewer people in each dwelling.

The approach seem to promise a way to analyse energy efficiency that captures both promoting and counteracting factors, and at both the micro and macro level.

***Keywords**: Stock, Replacement, Characteristic, Energy efficiency.*

1. Introduction

In several countries energy consumption has been decoupled from economic growth since the 1970s, one of which is Sweden [11]. Since the 1970s total energy consumption has stagnated despite a growth trend in GDP, and since the mid 1980s consumption of electricity has stagnated despite the role of electricity as a factor increasing overall energy efficiency. The oil price shocks initiated a switch of focus from supply to efficiency. Decoupling was a drawn-out affair as there is inertia due to past investments. Path dependence theory explains non-change basically with reference to cost advantages of existing technologies both on production and consumption side (for an introduction to path dependence see [2]). Today it is common to use an analogy to pedagogy, so that "learning curves" represents cost reductions in production of energy converters (in a broad sense) and in the familiarity in use of these converters. Due to cost advantages of widely used technologies the most likely path will be incremental change: Raising efficiency in gasoline cars instead of switching to electric cars, improving insulation in existing buildings instead of erecting passive houses, etc. When it comes to lighting the purchase price is much lower but the number of lamps make a radical break quite costly, and here we have the problem of the norm the warm glow of the incandescent as associated with.

Because sunk costs in stocks are important not only for the large number of units but also for the inertia it represents. IN THE FOLLOWING A CHANGE-OF-STOCK MODEL WILL BE TRIED OUT AS A STARTING POINT FOR THE ANALYSES. A point of departure for the model is the fact that energy is never used directly but always by way of some artefact—a paper machine, a car, a

dwelling, a dishwasher, etc. [4]. There is a stock of machines, vehicles, buildings and appliances that demand energy. Every type of such energy converters comes in different models, and they are not only energy converters, they also have other qualities that are important for the buyer and user. A car, for instance, has several "characteristics" [6] of which fuel consumption is just one of many. THUS THE WORD "ARTEFACT" USED HERE STANDS FOR A COMPOSITE, OR COMPLEX UNIT. The stock is renewed through scrapping of old units, and through adding of new units. Additions can be of two kinds basically: Incremental improvements on technologies dominating the stock, or radically different technologies surviving at the margin of the stock.

A challenge for the efficiency strategy is the "rebound effect". It has been debated several times, beginning with Brookes' and Khazzoom's articles 1979 and 1980 (for an introduction see [7]). From an historical, or rather dynamic, point of view, the neoclassical formulation of the theory is limiting. As it stands it says basically that the acting factor (improvements in energy efficiency) causes a counteracting factor (increased use of the service in question or other services requiring energy) to operate. This narrow definition is too limited, for two reasons: First, counteracting tendencies can also work in parallel without direct link to prices and costs of particular type energy use. Increasing population, the decreasing number of people in the average household and new areas of consumption can increase the aggregate consumption of energy. Second, radical changes are associated with such drastic improvements in efficiency that it is impossible to outdo the gain through increased consumption.

WHAT IS TESTED HERE IS THE FRUITFULNESS OF THIS 'CHANGE-OF-STOCK' APPROACH.

2. Method

Three types of artefacts were chosen, all associated with private consumption (households)—cars, dwellings and lamps. Data of aggregate stocks over the long-run were collected from different sources. For cars and multi-dwelling houses the rate of renewal was estimated, and fuel and heating consumption of the average car and dwelling respectively. Counterfactual developments were estimated where certain variables were held constant, such as car-intensity, mileage per car, longer use-life of cars, and no energy-demanding changes in cars. Basically the same thing was done on heating of dwellings in multi-family houses. Due to lack of historical data the development of the residential lighting stock could not be disclosed. Instead data from a monitoring study performed by the Swedish Energy Agency was used for an estimation of the future of the Swedish residential lighting stock during the phase-out of incandescent lamps.

These incremental changes were contrasted with radical changes. In one it was estimated how much had been gained by the factual switch in long-distance domestic travel from air to rail, and in the other the aggregate effects of a counterfactual double-switch from gasoline to electric cars plus a switch from electric heating to district heating. The rationale for these cases is that in the first a radically different transport technology actually had been chosen, and in the other preferred choices of technologies from a sustainability point of view were estimated.

As society is an open system, one factor cannot be isolated as is possible in a laboratory experiment. Thus, whatever method used, the result cannot be unequivocal, and therefore can, and must, be the object of several possible interpretations. Counterfactual studies in social sciences can better be looked at as thought-experiments, in this study closely related to issues

of trade-offs and choices of path in energy policy. When such problems and choices are discussed the relative magnitudes of gains in energy efficiency are of interest.

3. Results

3.1. Cars

The stock of private cars has been increasing in the long run, from 250,000 in 1950, to 2.5 million in 1973, and to 4.3 million in 2009. This rate of growth has exceeded the growth of population by far: In 1956 there were 10 inhabitants per car, in 2009 there were 2.2. Growth of the stock stagnated in the late 1970s and in the early 1990s. The age of the average car in 2009 is 9.3 years. [1].

The car is a complex durable commodity with several characteristics. The composition of characteristics of the average car changes through scrapping of old and adding of new cars. Energy efficiency is dependent not only of the energy conversion efficiency of the engine, but of several other characteristics, such as rate of acceleration, engine power, weight, air drag, the quality of tyres, etc. These characteristics, in turn, are connected to usefulness in terms of safety of driving, passenger and luggage space, low noise level and many others.

Sprei et al [16] investigated the conflicting tendencies in the composition of characteristics of new cars in Sweden: Better performance on one hand and lower fuel consumption on the other. New cars in 1975, 1985, 1995 and 2002 were studied in regard to passenger space, luggage space, top speed, time for acceleration, frontal surface area, weight, maximum power, cylinder volume, and fuel consumption. They found that increased space, acceleration and weight had reduced the gains from technical improvements of the engine, air drag and rolling resistance of tyres. About 65 per cent of the possible gains had been eliminated by comfort and acceleration only 35 per cent came out as better fuel economy.

Table 1. Descriptive and counterfactual data on the stock of private cars in Sweden and their fuel consumption 1950–2009.

	1950-59	**1970-79**	**2000-09**
A. No of cars in stock, millions	0.62	2.65	4.14
B. Inhabitant per car	11.5	2.9	2.0
C. New cars as share of stock, %	17.9	8.9	6.5
D. Scrapped cars as share of stock, %	4.3	6.7	5.7
E. Mileage, passenger km, billions	16.6	63.8	96.4
F. Mileage per car, km	26774	24075	22419
G. Fuel consumption per car, l/100 km		10.15	8.32
H, a. Total fuel consumption, index		100	115
b. Index when B and F constant		100	96
c. Slower renewal of stock		100	119
d. Only energy-saving features new cars		100	112

The average car consumed 8.32 litres per 100 kilometres when the factual development was estimated, and 8.08 when a possible development of smaller, slower and lighter cars was calculated (index value 112 in the last row). The slower renewal of the stock is estimated as the equivalent to the average fuel consumption of the stock in the period 1990-99. The average car of such a stock would have been very old, about 20 years (index value 119 next to last row). When car intensity and mileage per car is held constant at the 1970-79 level, total fuel consumption in 2000-09 is not only lower than it actually was, but also lower than in the 1970s, despite the fact that mileage was higher in the 1970s [14]. Note that in this

counterfactual case the number of cars has been allowed to increase in parallel to the size of the population. The rate of replacement is in the long run slowing down, additions more so than scrappings (row C and D).

3.2. An imagined double switch to and from electricity

What would a double conversion—replacing electric heating with district heating, and replacing petrol cars with electric cars—mean for total energy consumption in Sweden? Assumptions used were 20% efficiency for combustion engine and 70% for electric motor [15], and 95% for electric heating and 84% for district heating [5]. The phase-out of electric heating and phase-in of electric cars were distributed equally for each year over a 30 year-period, 1975-2006. Input data on petrol ("bensin", excluding diesel) refers to total use of petrol in the transport sector, not only for private cars, and is thus exaggerated. It is assumed that electric heating will be replaced by combined heat and power production in district heating systems, but the additional electric energy produced has not been added to the total amount of electricity (which is a measure of consumption, not production). The fuel used in this counterfactual increase in CHP is left unspecified.

Table 2. Estimated changes in energy consumption when gasoline cars are replaced by electric cars, and electric heating with district heating.

	TWh 1975	TWh 2006	Index 2006
Gasoline cars, factual	38.2	45.2	100
Electric cars, counterfactual	10.9	12.9	29
Electric heating, factual	9.3	22.1	100
District heating, counterf.	10.5	25.0	113

Replacing gasoline cars with electric cars would reduce energy consumption with 32.3 TWh, while replacing electric heating with district heating would increase consumption with 2.9 TWh. The net gain would thus be 29.4 TWh.

3.3. Dwellings

The housing stock changes through a combination of building new and scrapping or rebuilding old houses. During a long post-war period, from 1959 to 1975, new build dominated restructuration with more than 60,000 dwellings per year (a peak occurred also around 1991). Since 1993 renovation of existing dwellings has dominated, at least in regard to multi-dwelling houses where reliable statistics is at hand.

Table 3. Descriptive and counterfactual data on the stock of dwellings in multi-family houses 1980, 1990 and 2008.

	1980	**1990**	**2008**
A. No of dwellings in stock, thousands	2043	2171	2440
B. Persons per dwelling	1.70	1.51	1.53
C. Change of stock, %	1.3	2.6	1.9
D. Square meter per dwelling	65	78	*80
E. Heating per square meter, kWh	295	190	145
F, a. Total heating, TWh	39.2	21.1	28.3
F, b. Total heating, index	100	82	72
F, c. Index when B and D constant	100	66	55
F, d. Index when E is constant	100	127	147
F, e. Index when B, D and E constant	100	103	111

Source: [9] [10] [12]. * = guess.

The last census, including housing conditions, was made in 1990. After that date data on housing has not been renewed at the same level of quality. This is the reason why a guess had to be made concerning the size of the average dwelling in 2008. Change of stock (row C) includes demolished, refurbished as well as new built houses. The rate of replacement (2%) is much lower than for the car stock (12-13%). Efficiency of heating has improved considerably since 1980, especially during the 1980s (and probably during the 1970s too, if the trend for multi-dwelling houses followed that of the small houses). Total heating has thus been reduced despite a growing number of dwellings.

When household formation and size of the average dwelling is held constant, total heating is reduced even more (see row F, c). If improvements in heating efficiency would stop at the 1980 level, 47 per cent more energy would have been consumed (row F, d). If changes in household formation and changes in the stock would have been neutral in regard to dwelling size and heating efficiency, then total heating would have been higher than it was in 1980.

3.4. A real switch from air to rail

According to statistics domestic air travel (from and to destinations within Sweden) increased from 1970 to 1990 [14]. After this year domestic air stagnated—in 2008 it was still lower than it was in 1990. Travel by railroad stagnated 1980-1992 but increased quite fast after this period. It seems that a change has occurred in the choice between train and aviation in long-distance domestic travel, in favour of train and thereby a switch from aviation fuel to electricity. If this interpretation is correct the change has lowered energy consumption for this purpose. A CALCULATION HAS BEEN MADE OF THE ENERGY CONSUMPTION IN TWO CASES: One the factual case, and a counterfactual case where rail had followed a stagnating trend while air had increased. In the factual case 13 TWh were used for domestic travel, in the counterfactual case 20 TWh—quite big a difference.

3.5. Lamps

We do not know so much about the lighting stock. The most comprehensive study made so far, is that by the SEA 2005-2008. Data from this source is shown in Table 4.The studies made so far are not representative of the whole household population. The number of households covered is small, from a statistical reliability point of view, due to the fact that data collection is cumbersome as the hours-of-use is essential information to collect.

Table 4. Unweighted averages on Swedish household's use of electric lighting 2005-2008.

	Small houses	**Multi-dwelling houses**
Number of lamps	55.2	31.2
Wattage per lamp (W)	29.3	26.6
Hours-of-use per day and lamp	1.60	1.94
Number of households (000)	1,978	2,238
Electricity for lighting (TWh)	1.87	1.31
Lighting/all electricity (%)	22.7	19.0

Sources: [17], [18], [8]. "Small houses" include detached houses and houses with two dwellings. "Multi-dwellings houses" often contain shops, offices and other non-residential spaces, but the main purpose is residential.

The sample is small in relation to the population of households, and the geographical distribution of the sample is quite narrow. On the other hand data covers several types of

households in regard to housing, age, number of people, etc., and it is very detailed comprising observations on each appliance. With this in mind, we can let data give us a hint of what the national consumption of electricity for lighting would look like. From data in Table 4 it can be calculated that there are 179 million lamps in total.

Table 5. The distribution on lamp types in Swedish households, and assumed lifetime and price level for each type. Per cent, hours, Euro.

Lamp type	Share, %	Life time, h	Price level, €
Incandescent	60.5	1000	1
Halogen	16.2	3000	4
CFL	13.1	7000	6
Fluorescent tubes	10.2	10000	6

Sources: [17], [13]. Currency rate assumed: 10 SEK=1€. 1 USD ≈ 0.75€ in May 2010.

The effects of the phase-out [3] can be described as a comparison of the residential lighting stock before and after the transition period. It is assumed that all incandescent lamps will disappear and be replaced by CFL and halogen lamps. Then the replacement rate will decrease from 43 to 14 per cent per year (or from 2.3 years to 7.1 years for the whole stock to be replaced). Average power will be lower and thus electricity consumption for lighting (assuming constant hours-of-use).

Table 6. Economics of the phase-out.

	2010	2013
Replacement rate, %	43	14
Power per lamp, W	28	18
Electricity for residential lighting, TWh	3.2	2.1
Lamp sales, m€	113	119
Electricity sales, m€	483	308

"m€" = millions of Euro.

4. Concluding discussion

The change of stock approach says that the stock consists of mature energy converting technologies with cost advantages in production and advantages of familiarity among consumers and users. Because of these advantages an incremental path of improvements in energy efficiency is often chosen, the path of improvements of dominating technologies. For example higher fuel efficiency of the combustion engine, and additional insulation of existing houses.

Radical changes through the introduction of basically different technologies meet barriers of entry and must overcome the obstacles associated with path dependence. They are implemented only at the margin of the stock and meet increasingly higher barriers as dominating technologies are improved upon. This explains why the electric car has difficulties to gain wide diffusion.

Incremental changes in energy efficiency can be displaced by changes in other characteristics counteracting the efficiency gain. A heavier car, for instance, requires a more powerful engine, which can partially or completely outdo improvements of the engine. The compound effects of all relevant changes are what matters. Nevertheless, estimations of energy efficiency improvements shown in this paper have been quite substantial, more so in heating than for cars. Still, radical changes, such as a double switch from gasoline to electric cars and

from electric heating to district heating would not only include a higher gain in efficiency but also a change of path.

The phase-out of incandescent lamps is a special case as it relies on a long period of preparation. The CFL has been around since the 1980s and is now more competitive in terms of purchase cost and familiarity among the public. The phase-out pushes consumers over the last threshold of a somewhat higher purchase price and forcing the user to forget the warm glow of the incandescent.

In the 1990s in Sweden there occurred a switch from air to rail in long-distance travel within the country. Many passengers changed their mode of transportation in favour of the train. This switch was a switch from the use of one existing stock to another, rather than a change of one stock. Energy saved from this switch was considerable.

There are, however, counteracting tendencies of a more purely social nature that partially outdo the gains efficiency in the more purely technological sense. Increasing population, a higher number of cars per head, and fewer people in the average household, are examples of such tendencies. They play a significant role for the total consumption of energy.

The strength of the change-of-stock approach is that it enables us to capture both promoting and offsetting factors, and both details and aggregate effects of changes related to energy efficiency in consumption. Taking the stock into consideration has implications for the future: The stock will be there in the future, it represents decisions of yesterday and today. Old innovations, both conservative and radical, may result in improvements in energy efficiency but are dependent on what is added to and scrapped from the stock and shifts between stocks.

5. References

[1] Bil Sweden, Statistik, 2010, http://www.bilsweden.se/web/Ny_statistik.aspx

[2] M. Bladh, Spårbundenhet. Från fysik till historia, Historisk tidskrift, 128, 2008:4, pp. 671–692.

[3] EC, European Commission, Commission Regulation (EC) No 244/2009 of 18 March 2009 implementing Directive 2005/32/EC of the European Parliament and of the Council with regard to ecodesign requirements for non-directional household lamps. 2009. http://eurlex.europa.eu/smartapi/cgi/sga_doc?smartapi!celexplus!prod!DocNumber&lg=en&type_doc=Regulation&an_doc=2009&nu_doc=0244 (downloaded 2009-10-06).

[4] R. B. Howarth, Energy efficiency and economic growth, Contemporary Economic Policy, XV, 1997, pp. 1–9.

[5] T. B. Johansson & P. Steen, Perspektiv på energi. Om möjligheter och osäkerheter inför energiomställningen. Stockholm: Liber, Energiforskningsnämnden, 1985, pp. 319, 321.

[6] K. J. Lancaster, A new approach to consumer theory, Journal of Political Economy, April 1966, 74, 1966:2, pp. 132-157.

[7] R. Madlener & B. Alcott, Energy rebound and economic growth: A review of the main issues and research needs, Energy, 34, 2009, pp. 370-376.

[8] SCB, Antal hushåll (HEK) efter hushållstyp, boendeform och tid, referring to 2006. Extract from database, Statistics Sweden, 2008, http://www.scb.se, downloaded 2008-11-04.

[9] SCB, Yearbook of Housing and Building Statistics 2010. Stockholm: Statistiska centralbyrån, 2010.

[10] SEA, Effektiv energianvändning – en analys av utvecklingen 1970-1998. ER 22:2000. Swedish Energy Agency, 2000.

[11] SEA, Energy in Sweden. Facts and figures 2009. Swedish Energy Agency, 2009. Downloaded from http://www.energimyndigheten.se, January 2010.

[12] SEA, Energy statistics for dwellings and non-residential premises (several publications 2000-2008 from the same series). Swedish Energy Agency. Downloaded from http://www.energimyndigheten.se, June 2010.

[13] SEA, Hushållen tycker att energieffektiv belysning är bra, press release from the Swedish Energy Agency, 2010-04-28.

[14] SIKA, SIKA Basfakta, 2010. http://www.sika-institute.se/Templates/Page____1785.aspx

[15] V. Smil, Energy in Nature and Society. General Energetics of Complex Systems. Cambridge: MIT, 2008, p. 395.

[16] F. Sprei, S. Karlsson & J. Holmberg, Better performance or lower fuel consumption: Technological development in the Swedish new car fleet 1975–2002, Transportation Research Part D, 13, 2008, pp. 75–85.

[17] J. P. Zimmerman, End-use metering campaign in 400 households in Sweden. Assessment of the potential electricity savings. Enertech & Energimyndigheten, 2009.

[18] E. Öfverholm, sheet with data from the monitoring study performed by the Swedish Energy Agency, 2009.

Households' energy use – which is the more important: efficient technologies or user practices?

Kirsten Gram-Hanssen

Danish Building Research Institute, Aalborg University, Denmark
**Corresponding author:Tel: (+45) 23605653, E-mail:kgh@sbi.dk*

Abstract: Much policy effort focuses on energy efficiency of technology, though not only efficiency but also user practices is an important factor influencing the amount of consumed energy. This paper will explore to what extent energy efficiency of appliances and houses or user practices are the more important, both for understanding why some households consume much more energy than others, and when looking for relevant approaches to a future low carbon society. The paper uses several sources to explore this question, including results from the researcher's own projects, review of other studies and national statistics. Through the presentation of these different projects and examples it is shown how user practices are at least as important as the efficiency of technology when explaining households' energy consumption. The paper concludes that more research in this field is necessary. In relation to energy policy it is argued that it is not a question of efficiency *or* practices, as both have to be included in future policy if energy demand is actually to be reduced.

Keywords: *Households, Consumption, User practices, Energy efficiency.*

1. Introduction

In Western societies households stand for approx. one third of the energy consumption, and throughout the last thirty years efforts to reduce this has included research on and development of more efficient technologies and buildings, as well as policy activities directed at households encouraging them to purchase these more efficient technologies. To a much lesser extent focus and interest have been directed at how the actual use of technologies and houses influence the final energy consumption. However, recently an emerging interest is seen in research documenting the importance of user practices.

A Dutch study documents that building characteristics determine 42% of the variation in energy use for heating (water and space), leaving more than 50% of the explanation for user practices, though only 4.2% extra explanation of the variation in energy consumption can be explained by occupant characteristics [1]. This indicates that user practices are important, though only to a limited degree determined by objective occupant characteristics. A study based on US data concluded in line with this that besides weather characteristics, building characteristics are the main determinant of energy for space heating and cooling purpose followed by behavioral aspects, though in this study they further include the relation between occupant characteristics (like age and income) and building characteristics (like size and type of dwelling) making the indirect effect of the occupants much more important [2]. Besides building characteristics, some studies also include information on type of heat control system, like programmable thermostats, manual thermostats or manual valves and contrary to many assumptions, these studies conclude that those with programmable thermostats have the radiators turned on for more hours than others [3], and do not keep lower temperatures [4], and furthermore they conclude that the type of heating system has an influence on occupant behavior.

In this paper focus will be on presenting and analyzing different types of data which can further enlighten the question of how important user behavior is compared to efficient technology. The final energy consumption in households is a result of the number/size of the technology, the energy efficiency of the technology and the user practice in relation to the

technology. In the following a distinction will be made between electricity (for appliances and lighting) and energy for heating (space and water) when exploring the relation between these four elements.

2. Analysis and results

2.1 Danish national statistics on electricity consumption

From the Danish national statistics [5] we have obtained data on the development of energy efficiency of appliances during the last thirty years and the development in the numbers of appliances in Danish households in the same period (see Figure 1). Data in this figure are based on analysis from a bottom-up computer model (ELMODEL-bolig), where input comes from surveys of some thousand households every third year on ownership and use of appliances, combined with information on numbers and types of sold appliances from industry and trade organizations. By combining the left and the right part of this figure, we learn that the growing energy efficiency gained over the last thirty years in the appliances in Danish households is counterbalanced by the growing amount of appliances in use.

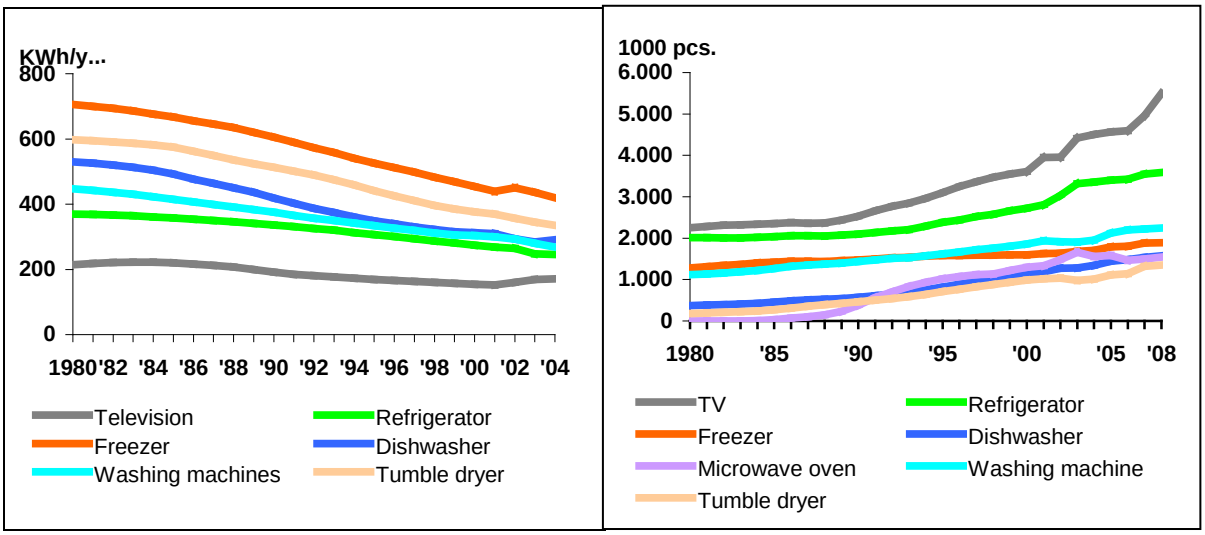

Figure1: Energy efficiency of Danish household appliances 1980-2004, left (KWh/year) and number of appliances in Danish households 1980-2008, right, (1000 pcs). Source [5].

2.2 Different energy consumption in similar houses

The explanatory power of energy efficiency, user practices and the number of appliances to explain energy consumption has been investigated in a study of 1000 quite similar houses, which in spite of similarity show huge variation in energy consumption. Comparing identical houses for heating (space and water) show that those using the least, use less than a third of those using the most, and for electricity (appliances and lighting) those using the most use five times as much as those using the least. The study included among others a survey with a response rate of 50%, combined with heat, electricity and water consumption as delivered by utilities and technical calculations and measurements of temperature and air exchange. The study has previously been reported in Danish [6], and different aspects have been published in English as well [7], [8].

For heat consumption the simple fact that technically completely identical houses can have heat consumption varying with a factor 3, show that user behavior related to heat consumption plays an important role. In this case the size and the energy efficiency of the technology (the

house) are identical and variations in energy consumption thus have to relate solely to user practices related to space heating and hot water use.

In relation to electricity the analysis is more complicated as appliances and lighting is bought individually and we have to rely on self-reported data from the survey on number, efficiency and use of appliances. Statistical analysis of data divided households into three equal groups consisting of a third of the households with the highest level of consumption, a third with the lowest and a third with the middle level. Statistical analysis between this grouping and questions of (self-reported) use of appliances, number of appliances and energy efficiency of appliances has been conducted for different types of appliances. As self-reported information on energy efficiency cannot be completely reliable, people are only given the possibility of indicating whether their cold appliances are low-energy or not, or whether they do not know. For light bulbs, they have been asked, whether the share of low-energy bulbs is less than 25%, 25-50%, or more than 50%. In Table 1 it is seen that there is no correlation between people having indicated that their refrigerator is low-energy and the household being among the high, middle or low energy consumers. Correspondingly analysis shows that there is no correlation between the share of low-energy bulbs and which consumer group the household belongs to (not shown in table). On the contrary, there are other factors which do correlate with the energy consumer groups. The question of how many appliances people have show strong correlation as seen in Table 2, where the number of cold appliances per households is shown, and correspondingly analysis for how many televisions and videos the household have also correlates strongly with the energy consumer groups (not shown here). Furthermore the use of appliances also shows strong correlation to the energy consumer group: in Table 3 the correlation between use of tumble dryer is shown, and similar correlation can be found e.g. for the use of washing machine (not shown here).

Table 1. The share of households indicating whether their refrigerator is energy efficient or not is divided into three different energy consumer groups of households. The table should be read vertically. Analysis shows that there is no correlation (n=214, gamma=-0.055, not significant p=0.628).

	Consumer group Low	Consumer group Middle	Consumer group High	Total
Inefficient refrigerator	38%	26%	37%	100%
Efficient refrigerator	26%	35%	29%	100%

Table 2. Households' information on their number of refrigerator-freezer units, compared with the energy consumer group of the household. The table should be read vertically. Analysis shows a strong positive relation (n=286, gamma=0.306, significant with p=0.000).

	Consumer group Low	Consumer group Middle	Consumer group High	Total
1 Refrigerator-freezer unit	41%	31%	28%	100%
2 Refrigerator-freezer unit	21%	37%	42%	100%
3 Refrigerator-freezer unit	17%	35%	48%	100%

Table 3. Households' information on their weekly use of tumble dryer, compared with the energy consumer group of the household. The table should be read vertically. Analysis show a strong positive relation (n=199, gamma=0.334, significant with p=0.000).

Use of tumble dryer	Consumer group Low	Consumer group Middle	Consumer group High	total
1 time a week	28%	33%	38%	100%
2 times a week	13%	39%	48%	100%
3 times a week	14%	28%	58%	100%
4 times a week	8%	28%	64%	100%
5 or more times a week	9%	21%	70%	100%

In general the energy efficiency of household appliances does thus not contribute to the explanation of the huge differences that can be found between the electricity consumption in these households. What does contribute to the explanation is the number and the use of the appliances. However, the number and the use of appliances also correlate to the number of people living in the house. Analysis confirms that number of persons in the household is a strong determinant for the size of the electricity consumption, however, it also shows that it is more energy efficient to live more people together. This will be further explored in the following section.

2.3. Socio-economics in the understanding of user practices

A database with registered data of approx. 50,000 households including socio-economic information on their inhabitants, building information (building type, year, size, installations etc.) and meter readings from utilities on heat (space and water) and electricity consumption (lighting and appliances) show some correlations between users, buildings and energy consumption [9]. Even this type of data does not include any direct information on user practices or energy efficiency, the data can throw light on some of the questions raised in this article. For electricity consumption, regression analysis for 8,500 detached houses is shown in Table 4. The number of inhabitants in the home is the strongest explanation of electricity consumption; income is the second most important and the size of the home the third. Similar relations between socio-economics and electricity consumption have been found in a study using detailed measurements of electricity consumption in Northern Ireland homes [10]. Furthermore Table 4 shows that other variables like age and education of the inhabitants only contribute with little extra explanatory power. Households' electricity consumption is strongly dependent on the number of members of the household. If, however, we compare electricity consumption per person with the number of members of the household, it becomes clear that it is more energy efficient to live more people together (see Figure 2). This is an important result related to user practices as still more people in most Western societies live alone. Today this applies to almost 40% of the population in Denmark, which thus can be seen as a main driver towards still higher energy consumption. From Table 4 it can furthermore be learned that even if we compare households in detached houses of the same size and with the same income, they can have huge variations in the electricity consumption as income and household size together only explain approx. one third of the variation in electricity consumption. The variation in households' electricity consumption can only to a very limited degree be explained by the age of the inhabitants or the level of education of the inhabitants; the greater part of the understanding of this user practice thus has to be understood by applying more qualitative approaches to the understanding of the everyday life of households.
When analysing heat consumption, the database includes type, size and year of construction. The year of construction can to some extent be equated with energy efficiency, especially for

more recent buildings. As the building type is an important factor in the technical description of the houses, analyses has been separated for different types. As an example of the analysis, detached houses will be used. Regression analysis on heat consumption of 22,000 detached single family homes show that the size can explain 28.3% (R^2) of the variation in heat consumption, and the year of construction can explain an added 10.5 % (R^2) of the variation in heat consumption (not shown in tables). When these two factors have been accounted for, other characteristics of the household members such as age, number of persons living in the house and income only contribute all together with approx. 4% (R^2) explanation of the variation.

Table 4. Regression analysis, detached houses: Background variables effect on electricity use, n=8.573

Background Variables	Effect on Electricity Use (kWh/year)	Explanatory Power, Change in R2 (%)
Per person in the household	541	27.6
Per 100,000 DKK in gross income	90	5.8
Per 10 m^2floor area	95	2.5
Per age square of oldest person	-0.35	1.3
Per 0-6 years old children	-158	
Per 13-19 years old children	179	0.5
Long education - primary school	-278	0.02

Figure 2. Average electricity consumption per household and per person compared with the number of inhabitants in the household, including households in detached housing, sem- detached housing and in apartments. 9+ refers to 9 or more inhabitants, n=53,804

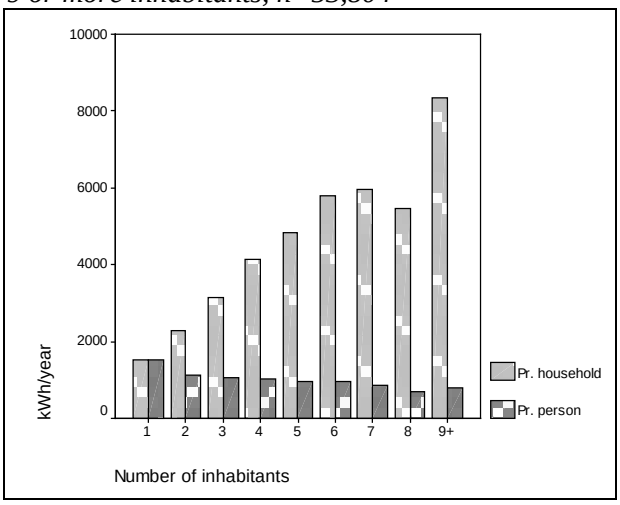

In relation to the question of this article it is obvious that heat consumption is much more dependent on building characteristics than electricity consumption is, even though heat consumption also includes water heating which must be considered quite dependent on the number of inhabitants. Related to both heat and electricity consumption it is furthermore apparent that there is a huge variation in energy consumption which must be explained by differences in user practices. Furthermore it can be concluded that these differences in user practices only to a very limited degree can be explained by socio-economic descriptions of the inhabitants.

2.4. Low-energy buildings and user practices

As it seems that heat consumption is more dependent on building physics than electricity consumption is on energy efficiency of appliances and lighting, it is thus relevant to focus explicitly on new low-energy buildings and user practices. In Sweden a comprehensive study of 20 low-energy row houses have been conducted and measurements of total energy consumption (heat and electricity) show that user practices account for a variation of factor 2 as those using the least uses 49.2 kWh/m^2, and those using the most use 101.7 kWh/m^2 [11]. In UK similar studies of 26 low energy houses with post occupancy evaluation show that those using the least uses 46 kWh/m^2 and those using the most use 144.9 kWh/m^2 for space and water heating, equivalent to a factor 3 in variations in heat consumption depending on user practices [12]. The average in these UK low energy houses was 92.9 kWh/m^2 and the corresponding average for the local area is 172 kWh/m^2. In this study there is thus a factor 2 between the average for heat consumption for "normal housing" and the average for low energy housing, which could be interpreted as a factor 2 related to the energy efficiency of the house, whereas the user practices correspond to a factor 3.

3. Discussion

Above the different approaches to answering the question whether energy efficiency or user practices are the most important has been presented. In the following two different discussions will be introduced. First a discussion of the rebound effect, and second a discussion of the future developments in the composition of households' energy consumption.

3.1. Rebound effect and how it relates to discussions on user practices vs. efficiency

There is a huge international amount of literature on the rebound effect indicating that improvements in energy efficiency make energy services cheaper and thereby encourage to an increased consumption within the same services. In a recent review of empirical estimates of the rebound effect within the household sector, it is concluded that the rebound effect of household energy consumption for heating is approx. 20% [13]. This means that 20% of the efficiency gained through technical improvements of building and appliances are turned into increased consumption (higher comfort) following from direct change in user behavior. This understanding of the rebound effect builds on an economic understanding of household behavior i.e. that people consume more because they can afford it, which follows from the reduced energy consumption gained by energy efficiency. It should not be denied that economy can partly explain household behavior related to energy consumption. However, it should be emphasised that there are other relevant explanations than economy, including psychological and social understandings. If people feel they have done something to save energy, like buying an energy efficient appliance, then they might feel that they do not have to think so much about how they use it. Growing consumption however does not necessarily relate to energy efficiency. The growing number of appliances and inhabited floor area must also be understood as a consequence of other societal processes, which have been described as drivers behind consumption, including changing social norms and expectations following from new technical possibilities [14].

3.2. Future development in the composition of household energy consumption

As shown previously, heating consumption seems to be more dependent on the energy efficiency of buildings, whereas electricity consumption is more dependent on user practices including the number and size of appliances. There are, however, good reasons to believe that this relation varies with the different types of appliances. In Figure 1 (left) it is shown that energy consumption of freezers, dishwashers and tumble dryers has been reduced by approx.

one third the last thirty years, whereas no substantial energy reduction has been seen related to televisions. In general it must be expected that households' energy consumption to a still higher degree will be caused by information and communication technology (ICT) in the future. A Danish study showed that ICT from 2000 to 2007 rose from approx. 10% to 20% of a household's total energy consumption and that it can be expected to rise up till 50% of a household's total energy consumption within the coming 5-10 years [15]. These scenarios include assumptions of a continued efficiency of ICTs; however, they also assume that the size and number of ICTs will continue to grow. As it must be assumed that energy consumption related to refrigerators and freezers are more dependent on appliance efficiency than on user practices, compared with the use of ICT, these assumptions point towards a future where it must be expected that user practices as compared with energy efficiency will be even more important for the final electricity consumption in households.

4. Conclusions

This paper has dealt with the question whether user practices or energy efficiency is the most important for the size of a household's energy consumption. The answer to that question is slightly different if it is asked for heating (space and water) or for electricity (lighting and appliances). For heating it is shown that building characteristics, including size and year of construction, can explain approx. 40-50% of the variation in energy consumption, whereas inhabitant characteristics can only explain very little of the variation when the building characteristics has been accounted for. Furthermore studies confirm that completely identical houses can have heating consumption that vary with a factor 2-3 depending on user practices. This means that user practices are at least as important as building physics when it comes to energy consumption related to heating, though the user practices can only to a very limited degree be explained by objective characteristics.

Data analysis on electricity consumption for lighting and appliances suggest that this is more dependent on user practices than on energy efficiency, especially if the number of appliances are counted as part of the user practice. On a national level, a 30-40% increase in efficiency has been gained during the last thirty years. However, in the same period the number of appliances in households has risen more than the energy efficiency. When comparing households living in similar houses, electricity consumption can vary with a factor 5, thus indicating that electricity consumption is less linked with building size and type than with heating consumption. Analysis of data on type, use and number of appliances shows that the number and the use of appliances have a strong correlation to household electricity consumption, whereas information on energy efficiency does not show any correlation. Regression analysis on large databases shows that the number of inhabitants in households is the most important factor for describing electricity consumption; the more inhabitants in a household the higher the consumption. Electricity consumption per person shows the opposite correlation, meaning that it is more energy efficient to live more people together. Data also show that economy correlates with electricity consumption, which corresponds to the fact that the more affluent households can afford to have more appliances.

Even this article raised the question whether efficiency or user practice is the more important, it is relevant to establish that both efficiency and practices are important when seeking to reduce energy consumption. To realise substantial energy reductions, which is an important part of a future renewable energy system, we need consumers who choose efficient technologies, reduce the number of appliances and think about how they use them.

References

[1] O. G Santin, L. Itard, H. Visscher, The effect of occupancy and building characteristics on energy use for space and water heating in Dutch residential stock, Energy and buildings 41, 2009, pp 1223-1232

[2] K. Steemers, G. Y. Yun, Household energy consumption: a study of the role of occupants, Building Research and Information, 37:5, 2009, pp 625-637.

[3] O. G Santin, L Itard, Occupants' behaviour: determinants and effect on residential heating consumption, Building Research and Information, 38 (3), 2010, pp 318-338.

[4] M. Shipworth, S. K Firth, M. I. Gentry, A. J. Wright, D. T. Shipworth, K. Lomas, Central heating thermostats settings and timing: building demographics. Building Research and Information, 38 (1), 2010, pp 50-69.

[5] Danish Energy Authorities. Energy statistics 2009.

[6] K. Gram-Hanssen, Boligers energiforbrug - sociale og tekniske forklaringer på forskelle. By og byg resultater 029. Statens Byggeforskningsinstitut, 2003.

[7] K. Gram-Hanssen, Residential heat comfort practices: Understanding users. Building Research and Information, 38(2), 2010, pp 175-186.

[8] K. Gram-Hanssen, Domestic electricity consumption - Consumers and appliances. In: L. Reisch and I. Røpke (Eds.): The ecological economics of consumption. Edward Elgar publishing, 2004.

[9] K. Gram-Hanssen, C. Kofod, K. N Petersen, Different Everyday Lives - Different Patterns of Electricity Use. Proceedings of the 2004 American Council for an Energy Efficient Economy Summerstudy in Buildings. Washington, D. C.: ACEEE

[10] Y.G. Yohanis J.D Mondol, A. Wright, B Norton, Real-life energy use in the UK: How occupancy and dwelling characteristics affect domestic electricity use, Energy and Buildings 40, 2008, pp1053–1059

[11] J.F Karlsson, B Moshfegh, A Comprehensive investigation of a low-energy building in Sweden, Renewable energy 32, 2007, pp. 1830-1841.

[12] Z. M. Gill, M. J. Tierney, I. M. Pegg, N. Allan, Measured energy and water performance of an aspiring low energy/carbon affordable housing site in the UK. Energy and Buildings 43, 2010,117–125.

[13] S.Sorrel, J Dimitropoulos, M. Sommerville, Empirical estimates of the direct rebound effect: A review, Energy Policy 37, 2009, pp 1356-1371.

[14] I. Røpke. The dynamics of willingness to consume. Ecological Economics 28, 1999, pp 399–420

[15] J.O. Jensen, K. Gram-Hanssen, I. Røpke, I., & T. H. Christensen, Household's use of information and communication technologies - a future challenge for energy savings? I: Conference proceedings: ECEEE Summer Studies 2009. Ile Saint-Denis: ECEEE.

Energy variations in apartment buildings due to different shape factors and relative size of common areas

I. Danielski*

Mid Sweden University, Östersund, Sweden
** Corresponding author. Tel: +46 (0)63 5416, Fax: +46 (0)63 165500, E-mail: itai.danielski@miun.se*

Abstract: A multi-storey residential building includes different sub areas, for example: apartment areas and common areas (corridors, basements, attic etc.). Each sub area may have different specific final energy use. Areas with lower specific final energy use will have a relatively lower contribution to total final energy use of a building. Examples of areas with low specific final energy use are corridors, basement and attics. All these areas are included in the calculation of a building's total final energy use. As a result, there is a risk that buildings designers may fulfill stricter end-use energy requirements simply by constructing buildings with larger areas containing a lower specific final energy use. In addition, the envelope area of the building may vary for a given floor area depending on the shape factor of the building. The heat losses of a building depend on the envelope area, the area that is in direct contact outdoor environment. Thus, buildings with a lower shape factor will have lower heat losses and hence a lower specific final energy use.

In this paper, we study the impact of those two factors on the specific final energy use of similar constructed apartment buildings in Stockholm. We consider 22 multi-storey residential buildings in ten locations that were built in accordance with the Stockholm program for environmental adapted buildings. They were chosen since they have different ratio of common area to total heated area and large variation in specific final energy use. Other characteristics such as energy systems, construction properties and population density were similar.
The analyses showed a high correlation between the shape factor of the buildings and their specific final energy use. An increased shape factor of a building by 0.1 increased the specific final energy use by 5.3 kWh/m^2. The specific final energy use of the studied buildings could vary up to 30 kWh/m^2 only because of the shape factor. Therefore it is recommended that the shape factor is considered in building codes for new buildings especially in cold climates. The energy simulations showed that the specific final energy use in the common areas was about 75% lower than in apartment areas. Hence, including larger common areas in the design of new apartment buildings reduce the specific final energy use significantly while the final energy use per resident will increase. This needs to be considered in energy requirements of buildings. Normalizing the final energy use by the apartment area should be considered as alternative method as it reduces variations in specific final energy use due to the relative size of common areas and increases the quality of using the SFEU for energy requirements.

Keywords: *Specific final energy use, Shape factor, Surface area to volume ratio, Energy variation.*

Nomenclature

SF *Shape factor*……..m^{-1} *VHR* *Ventilation Heat Recovery*
SFEU *Specific final energy use*...kWh/m^2,a

1. Introduction

Several programs have been launched in Sweden with the aim of improving the energy efficiency of new buildings. One example is the Stockholm program for environmental adapted buildings [1], which aims to stimulate the construction of buildings with final energy use lower than required by the Swedish building code. The Stockholm program covers apartment buildings constructed between 1997 and 2005, and requires certain limits for the final energy use as listed in Table 1

Table 1. Final energy requirements for the SFEU and final electricity use in kWh/m2,a.

Type of heating system	Total final energy use	Maximum final electricity use
District heating	140	50
District heating with ventilation heat recovery (VHR)	125	60
Electric resistance heaters	90	90

Since the lunch of the Stockholm program, new apartment buildings were built in 77 different locations within the Stockholm municipality. All of these buildings were built in accordance with the program's specifications, yet only 35% of the locations fulfil the final energy use requirements. In addition, the SFEU vary widely between different locations (Fig. 1). In this study, we analyzed the variations in SFEU due to the surface-area-to-volume ratio of apartment buildings (henceforth shape factor) and the relative size of the common area.

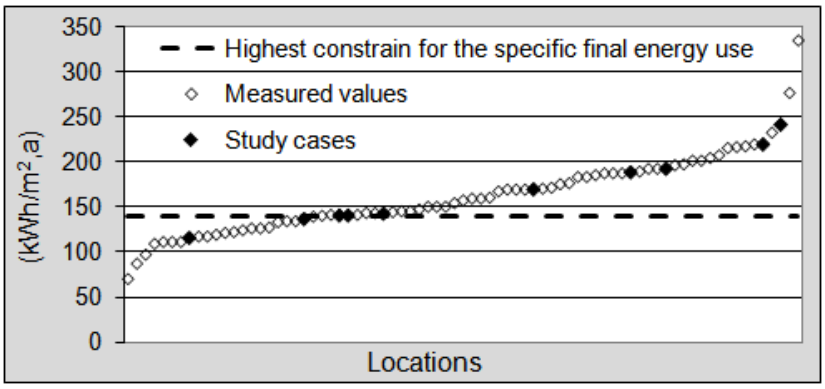

Fig. 1. The SFEU of new apartment buildings built in 77 locations that participated in the Stockholm program. The black points represent the study cases in this study.

1.1. The shape factor (SF)

The shape factor (SF) of a building is its surface-area-to-volume ratio and is a measure of a building's compactness. Buildings with a higher SF are less compact and therefore have a larger surface area for a given building's volume. The surface area of a building is the boundary between heated spaces and unheated spaces, and accounted for large percentage of the heat losses in buildings. Depecker et al. [2] showed that in colder climates the correlation between the final energy use and the SF is strong. Buildings with a higher value of SF have a higher final energy use. China has integrated the SF of buildings into its design standard for energy efficiency of public buildings, which applies stricter values for new buildings in colder climates [3]. Sweden is located in cold climate and the impact of the SF on the final energy use is expected to be significant.

1.2. The specific final energy use

The SFEU, i.e. the final energy use per unit of floor area, is used to compare final energy use in buildings with different sizes, and it is affected by how the floor area size is calculated. According to CEN [4], the floor area of a building can vary by 20% depending on the measurement method. In Sweden, the area that is used for calculating the specific final energy use in buildings is defined by the National Board of Housing, Building and Planning [5] and is measured according to standard SS 021053 [6]. The area definition is equivalent to the European "overall internal dimension" [4] with a few differences: it excludes unheated areas and adjacent garages. An unheated area is defined as an area with temperature lower then 10°C during the heating season. This is due to the low energy contribution of unheated areas

or adjacent garages relative to the relative increase in floor area. Including these areas will result in lower SFEU values [7] without increasing the building's energy efficiency.

The heated floor area in apartment buildings that agrees with the above Swedish definition is not homogeneous and includes different sub-areas including apartments, corridors and basements. The SFEU of apartment building is an average of the SFEU of its different sub areas. Each of these sub-areas has its own functionality and energy characteristics that determine its contribution to the average SFEU of the building. Designing new buildings with relative large sub-areas with low SFEU, for example due to lower temperatures, can reduce the value of the average SFEU of the building.

In this study, we distinguish between apartment areas and common areas. The common areas including: corridors, basements, attics and all other heated areas that are not part of the apartments. We do not consider buildings with integrated areas for commercial purposes, e.g. offices and small shops. Our hypothesis is that the SFEU in the common areas is lower than that in the apartment areas. Thus, the relative size of the common area (common-area-to-total-floor-area ratio) will affect the average SFEU of the building. The reasons for the low SFEU in the common areas are discussed below in the Swedish context.

In Sweden, the indoor temperature in the apartment areas should satisfy the minimum thermal comfort conditions. According to ASHRAE, the comfort zone for the operative temperature is between 20°C and 25°C [8]. In common areas 18°C, can be used to reduce heating costs [5]. Hence the temperature in common areas can be a few degrees lower than in apartment areas.

The energy used for domestic water heating is also higher in the apartment areas. Households in Sweden use 1200 kWh/person,a on average [9]. In common areas, the use of hot water and energy for water heating is negligible. Here we argue that the energy use by central laundry machine located in the common areas should be allocated to the apartment areas. The amount of energy used can be related to the number of residents and therefore to the total size of the apartments' area. Increasing the common area size will not increase the energy use for laundry. It does not matter if the laundry is made in each apartment or in a central laundry room. This argument can be apply to other apparatus that use energy in the common areas for example elevators.

Common areas have a lower windows-area-to-floor-area ratio than the apartment areas because of the natural light requirements in areas that residents visit often. Basements and attics may not have windows at all, whereas corridors that are surrounded by apartments have fewer windows per façade area in comparison with apartment's façade. Due to the higher U-values of windows in comparison with walls, the average U-value of the façade that is in contact with the common area is lower.

The minimum requirement for the ventilation flow-rate in apartment areas is 0.35 litter/sec,m^2 [5]. In common areas it is possible to reduce the ventilation flow-rate to 0.1 litter/sec,m^2 because of the low occupancy, which reduces ventilation heat losses.

2. Methodology

Twenty-two buildings built in 10 locations out of the 77 locations that participated in the Stockholm program were chosen for an in-depth analysis. These buildings have no commercial areas, i.e. offices and small shops, but large variations in SFEU (Fig. 1) despite similar constructions and energy supply systems. Each location consisted of one or several

apartment buildings with at least three floors. All of the buildings have concrete foundations and use forced ventilation with fresh air entering through special openings in the façade, located under the windows and behind the radiators. In one location, ventilation heat recovery (VHR) using a heat pump was installed. All of the buildings were connected to the district heating network. The final energy use was measured during 2006 by Fortum-Värme, which is the energy supplier company in Stockholm. The areas in each building were measured manually using the architectural drawings of the buildings. For energy simulations we used the VIP Energy, which is a commercial dynamic energy balance simulation program that calculates the energy performance of buildings using real climate data. It was validated by IEA-BESTEST, ASHRAE-BESTEST and CEN-15265 [10].

2.1. The shape factor (SF)

The final energy use of the case-study buildings was compared to a final energy use of hypothetical reference buildings with similar sizes for volume, floor area sizes, ground floor, roof and windows-to-façade-area ratio but with SF of 1. To meet the lower SF the reference buildings need to be more compact with lower façade area size as illustrated in Fig. 2. The differences in final energy use assume to be related only to the smaller façade area of the reference buildings. Heat losses due to resident behaviour and ventilation heat losses assume to remain constant because of the similar volume and floor area size.

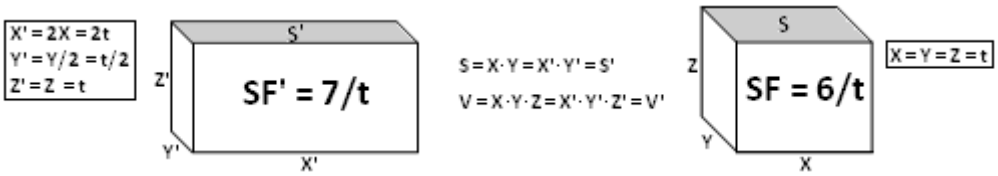

Fig. 2. Two buildings with similar volume, floor area, ground floor area, roof area and different SF.

The difference in final energy use between each case-study building and its reference buildings (ΔE) was calculated according to Eq. (1). Where ΔA_{Wall} and ΔA_{Win} are the area differences of wall and windows respectively between the case-study building and its reference buildings. E_{Wall} and E_{Win} are the difference in heat losses through 1 m^2 of walls and windows respectively between the case-study building and its reference buildings. ΔA_{Wall} and ΔA_{Win} were calculated from the difference in SF and assuming constant windows-to-façade-area ratio. E_{Wall} and E_{Win} were calculated by the VIP Energy simulation program [10] assuming similar values for all the buildings. The volume of the building is equivalent to the floor area multiplied with the floor height, which is 2.7 meters for all the case-study buildings. Therefore we defined the SF as the surface-area-to-floor-area ratio instead of volume.

$$\Delta E = \Delta A_{Wall} \times E_{Wall} + \Delta A_{Win} \times E_{Win} \quad (1)$$

2.2. The relative size of the common area

To determine how the relative size of the common area affects the SFEU of the buildings, five energy simulations were conducted. The following parameters were kept constant to reduce the influence of other factors: 1) the total floor area of the building; 2) the ratio of the glazed area to the floor area: 13% for the common areas and 22% for the apartment areas; and 3) the ratio of the apartment floor-area to the apartment façade-area. In each additional simulation, 75 m^2 of floor-area and 66.8 m^2 of façade area were allocated from the apartment area to the common area, which increased the relative size of the common area by 5% as listed in Table 2. The allocated areas were taken from the first floor in all simulations until the entire first

floor was used as a common area. Parameters with values that differ between the apartment areas and common areas are listed in Table 3.

Table 2. Area sizes for each energy simulation. The first value relates to the apartment area and the second to the common area.

	Common area/ Total floor area	Floor area (m2)	Wall area (m2)	Glazed area (m2)	Roof (m2)	Ground floor area (m2)
1	0.1	1475 / 163	805 / 7	472 / 21	404 / 24	376 / 52
2	0.15	1392 / 246	771 / 57	450 / 28	404 / 24	266 / 162
3	0.2	1310 / 328	733 / 116	428 / 29	404 / 24	147 / 281
4	0.25	1229 / 409	710 / 153	405 / 38	404 / 24	73 / 355

Table 3. Parameters related to energy use used in all energy simulations.

Parameter		Apartment area	Common area
Indoor temperature	(°C)	22	18
Ventilation air flow	(litre/sec-m2)	0.35	0.1
Electricity use	(W/m2)	5.4	2
Energy use for domestic water heating	(W/m2)	5.8	0
Body heat from tenants	(W/m2)	1	0

The energy simulations were performed using the Stockholm's climate data and were done by the VIP Energy simulation program [10] for one of the study cases, with a total floor area of 1500 m^2. The roof consists of two layers of asphalt-impregnated felt, on 25 mm polywood board, 300 mm mineral wool between wooden roof trusses, and 150 mm concrete, giving an overall U-value of 0.129 W/m^2,K. The external walls have a U-value of 0.249 W/m^2,K and consist of 8 mm of plaster, 150 mm of mineral wool between wooden studs and 150 mm of bricks. 25% of the façade made up of triple glazed windows and doors and has overall U-value of 1.2 W/m^2,K. The ground floor consists of 20 mm oak boarding on 180 mm concrete slab laid on 150 mm expanded polystyrene and 100 mm macadam, resulting in a U-value of 0.236 W/m^2,K°.

The final energy use from each simulation was normalized by two different area definitions: 1) the total heated floor area of the building (the current used method) and 2) the total apartments' area. The two area definitions provide two sets of calculated SFEU values for each energy simulation. The energy simulation results were compared to the SFEU of the reference buildings (SF=1).

3. Results

3.1. The shape factor (SF)

A high correlation was found between the SF and the SFEU as illustrated by the trend line in Fig. 3. Buildings with the VHR system were excluded but should follow the trend line as well because they have similar construction properties as the buildings without VHR system. The specific final energy use of buildings with VHR system is clearly noticeable in and is roughly the vertical distance to the trend-line (arrow in Fig. 3).

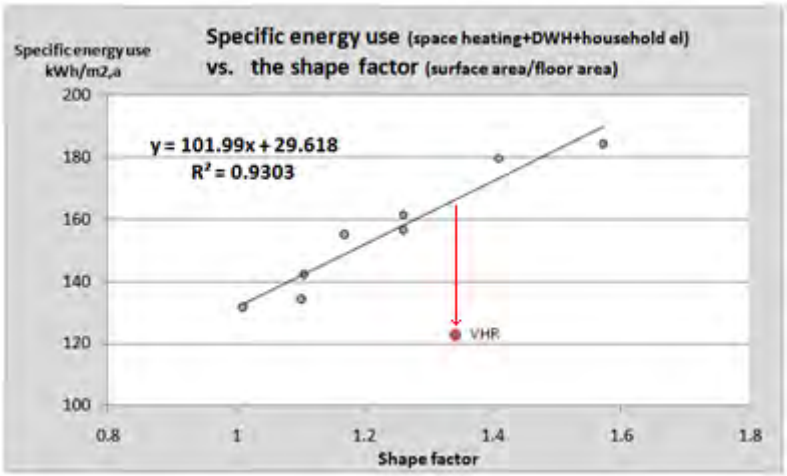

Fig. 3: A correlation between the SFEU and the shape factor of the building.

Fig.3 illustrates the difference in final energy use between each case-study building and its corresponding hypothetical case (SF=1). The SFEU is increasing by about ~5.3 kWh/m^2,a for each increase of 0.1 in the SF up to of 30 kWh/m^2,a.

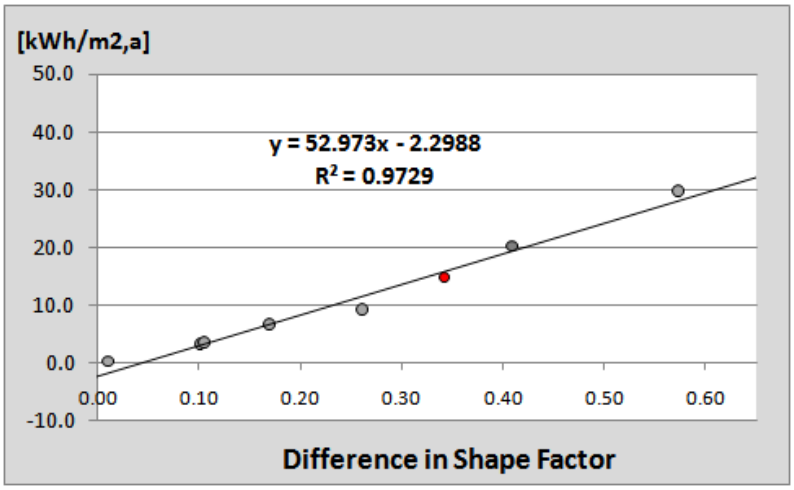

Fig. 4. SFEU losses (Y-Axis) in each study case due to difference in SF (X-axis).

3.2. The relative size of the common area

The SFEU of the buildings and the results from the energy simulations were calculated based on the total floor area (current used method) and the apartment area and plotted vs. the relative size of their common areas in Fig. 5. According to the energy simulation results, the SFEU in the common areas is about a quarter of the SFEU in the apartment areas. Increasing the relative size of the common area reduces the average SFEU of the building calculated by the current used method, although the SFEU in the apartment areas is nearly constant. When normalizing by the apartment area (new method) the average SFEU of the building slightly increases with increased common-area-to-floor-area ratio because the common area contributes more to the final energy (due to its increasing size), which is divided by smaller size of apartment area.

The trend of the specific final use of the study cases, calculated by the two methods, agrees with the simulation results (Fig. 5). Therefore, it is possible to conclude that the constant SFEU in the apartment areas calculated by the energy simulations valid for the study cases as well, and the variations in SFEU in Fig.4 (~30 kWh/m^2,a) are only due to the differences in

the relative size of areas with low SFEU (i.e. common areas). The variations reduced by half if applying the new method.

The savings in *SFEU* associated with the VHR system are clear, and are the vertical distance to the trend of the *SFEU* (arrows in Fig. 5 in both methods). However, the savings are questionable if comparing by the current method because the value of the *SFEU* use of the location with the VHR system is only slightly lower than values of other study cases.

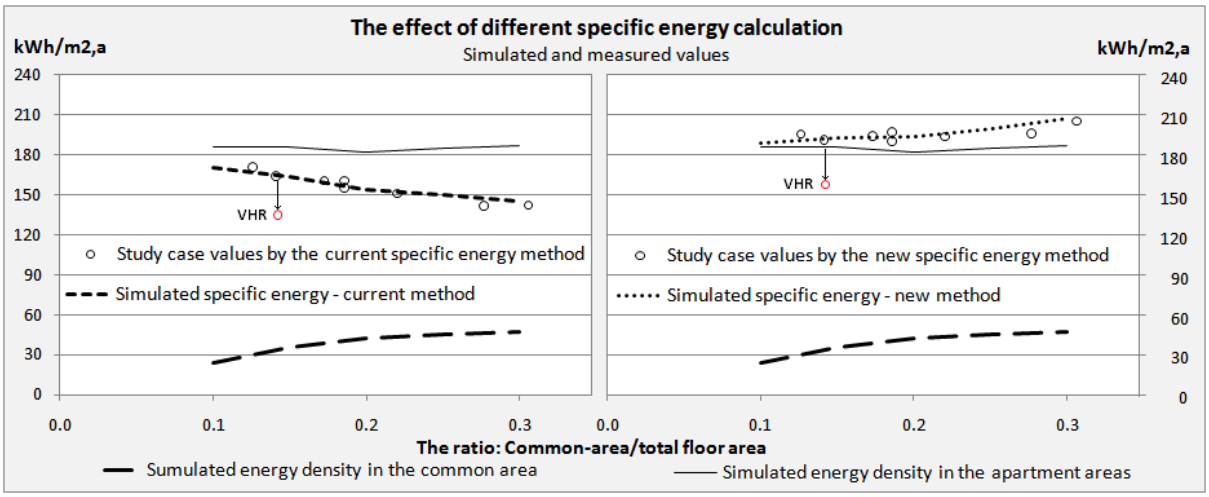

Fig. 5. The energy simulation results (lines) compared to the SFEU (circles) of the different study cases based on the total floor area (left diagram) and on the apartment area (right diagram).

4. Discussion

In this study we analysed the influence the shape factor (SF) of the building and the relative size of the common area, i.e. common-area-to-total-floor-area ratio, on the SFEU. Both parameters are together responsible for a variation in calculated SFEU of more than 50 kWh/m^2,a for the different case-study buildings. As a result reduction in SFEU use due to efficiency measures, as ventilation heat recovery, were not noticeable.

The SF has large effect on the building's final energy use. Buildings designed with large value of SF have larger surface area per floor and larger heat losses. As a result, larger heat losses exists and larger amount of energy is needed during the construction period. Therefore it is recommended that the shape factor is considered in building codes for new buildings especially in cold climates.

When calculating the SFEU based on the total floor area of the building (current used method) the SFEU of the building decrease as the relative size of the common area increases (i.e. corridors, basement, attics etc.) because the SFEU in the common areas is significantly lower than the SFEU in the apartment areas. In addition increasing the relative size of the common areas for a given total apartment's area will increase the final energy of the building because more common area needs to be heated. The final energy used in the common areas is used by the building's residents and the number of residence does not increase with increasing size of the common areas therefore the final energy use per residence will increase. Furthermore, increasing the relative size of the common area increases the building size per apartment area. Consequently, the energy use required to construct the building will increase per apartment area or alternatively per resident. As a result, designing buildings with larger relative size of common areas will reduce the average SFEU of the building, and stricter energy requirements could be achieved without implementing energy efficiency measures. However the final energy use per

residence will increase. This needs to be considered in energy requirements of buildings. Normalizing the final energy use by the apartment area should be considered as alternative method because it reduces variations in SFEU due to the relative size of common areas and increases the quality of using the SFEU for energy requirements.

References

[1] The Stockholm municipality (2004) Program för Miljöanpassat byggande vid nybyggnad.

[2] Depecker, P., et al., Design of buildings shape and energetic consumption. Building and Environment, 2001. **36**(5): p. 627-635.

[3] Yu, Z., S. Wang, and Y. Xie. Energy policy in public buildings -Challenges for China. 2007.

[4] CEN, Energy performance of buildings - Methods for expressing energy performance and for energy certification of buildings, in CEN/TC89, 2006.

[5] The Swedish Board of Housing Building and Planning, Building Regulations (BBR) in BFS 2006:22, Boverket, Editor. 2008, Boverket.

[6] SS 21054:2009, Area och volym för husbyggnader – Terminologi och mätregler. 2009, SIS.

[7] SOU 2005:67, Energideklarationer Metoder, utformning, register och expertkompetens. 2005, Statens Offentliga Utredningar: Stockholm.

[8] ASHRAE 55-2004, Thermal Environmental Conditions for Human Occupancy 2004.

[9] The Swedish Energy Agency. Vatten och varmvattenberedare. cited 2010; Available from: http://www.energimyndigheten.se

[10] Strusoft. VIP-Energy. Available from: www.strusoft.com.

Energy Consumption In Non-Domestic Buildings: A Review of Schools

Richard A.R. Kilpatrick[*], Phillip FG. Banfill[1]

[1] *Heriot-Watt University, Edinburgh, Scotland*
** Corresponding author. Tel: +44 131 451 4637, E-mail: rark4@hw.ac.uk*

Abstract: The energy consumption associated with non-domestic buildings represents 11% of the UK's total energy consumption, 11% of Europe and 18% of the USA's. Annual non-domestic building energy consumption is often presented in the form of average benchmarks, such as 450kWh/m²/year for a large air-conditioned building and 200kWh/m²/year for a small naturally ventilated office. Benchmark values give very little insight into how and where a building consumes energy. While some benchmarks provide a breakdown of energy use by energy category (lights, IT, cooling, heating), these data still fails to demonstrate how the energy associated with each category varies throughout the year. To further understand building energy use, a more detailed data breakdown and analysis is required. The electricity demand data for a variety of school buildings (secondary, primary, specialised) in Scotland has been made available for analysis. This consists of half hourly resolution data spanning several years for 50 schools, allowing key trends and patterns in energy use to be identified. These trends can include differences between annual profiles, differences between winter and summer months, and differences in weekday and weekend energy use. Additionally, the effect of other variables such as climate, user behaviour and general building data on the buildings energy consumption can be investigated. A database of half-hourly school energy demand data, with corresponding building details has been set up and a preliminary analysis preformed. Alternative method of pattern recognition in non-domestic energy usage are discussed, and the variables necessary to calibrate this information. This demonstrates the possibility of creating generic energy profiles and hence new benchmarks.

Keywords: *Non-Domestic Energy, Electricity Demand, School Energy*

1. Introduction

Energy consumption is continually increasing throughout the world and a large proportion of this can be associated with non-domestic buildings. In 2007 the UK consumed 157.8 million tons of oil equivalent (Mtoe) or alternatively 1,835TWh of energy [1]. To better understand how energy is used in the UK, it is necessary to breakdown the energy consumption into the different sectors. The total energy distribution of the UK is as follows; domestic consumption: 29.4%, transport consumption: 37.1%, industry consumption: 20.8% and "other" consumptions: 12.7% of total UK energy consumption [2]. The percentage of energy consumption associated with buildings in relation to total energy consumption was 42.3% [2]. The assumption is that the "buildings" mentioned in, [2], consists of both domestic and non-domestic properties.

Non-domestic buildings in 2003 were reported to account for 11% of total energy consumption in the UK, 11% in the EU and 18% in the USA [3]. The similarity between UK and EU consumption is probably due to their similar work habits, daylight hours and climate, while the USA's higher proportion may be due to the higher presence of air conditioning, or due to a different proportion of offices to other types of buildings.

Only by collecting and analysing building energy consumption data can an idea into how and when a building uses energy be gained. Introducing other factors such as seasonal demand profiles, both for weekdays and weekends, average daily consumption for each month, and determining any trends in standby/peak power over one year for each school, can ideally identify trends in energy use. With the help of this information, 'generic' profiles can be constructed allowing quick power reference and the creation of newer benchmarks for non-domestic energy use in this particular environment.

2. Current Benchmarks

A key area in the non-domestic sector is education. There have been numerous studies ([1], [4 -11]) into the energy consumption of schools and school energy performance benchmarks, and benchmark data us readily available for schools in the UK (as well as other counties) for the last few decades. Primary schools in the UK typically consume 119kWh/m²/year of energy [4], with the UK one of the few countries that have set energy benchmarks for schools. A target of 110kWh/m²/year is considered as an ideal or "good practice" target [5]. Other school benchmarks are detailed in the "Good Practice Guide 343, or more commonly known as GPG343 [6]. For a primary school, the 'typical' annual consumption target is 191kWh/m²/year where as the 'good practice' value is 135kWh/m²/year. For a secondary school without a pool, the 'typical' benchmark is 196kWh/m²/year and for a secondary school with a swimming pool, the benchmark is 223kWh/m²/year. This guide also divides the benchmarks into either electricity or fossil fuels, and provides a generalised breakdown of energy use in schools represented in a pie-chart.

In comparison French primary schools average 197kWh/m²/year, Greek schools consume 57kWh/m² and Irish primary schools consume 119kWh/m²/year [5]. Hermandez, [5], used 'GPG343' to establish that the typical value for UK primary schools is 157kWh/m²/year whereas the best practice value is 110kWh/m²/year. They used EnergyPlus software for the energy consumption calculations and a grading system based on a methodology outlined in "Energy Performance of Buildings"[12]. This method involved using the schools energy consumption (kWh/m²), a stock regulation value, and a stock reference value (based on either a sample mean or the building stock mean). A table of different conditions involving the three values determined the energy rating and benchmark.

A problem with previous studies and results is that they do not provide sufficient information to give a full understanding of how energy is used in a building. Energy performance benchmarks only provide the total annual energy consumption of a generalised school per floor area. Details such as weekly, monthly and seasonal trends are omitted. However, benchmarks can be used as a quick indication of energy efficiency or a simple tool for quick school comparison but are limited due to this additional detail. This paper discusses the analysis of a sample of schools and the key outputs of the analysis, aimed at providing more detail of school energy consumption than the standard benchmarks. In addition, average electricity demand profiles are analysed and their potential use in explaining energy usage are discussed.

3. Methodology

The interpretation of energy usage in schools is completely dependent on the availability of accurate energy data from a wide range of schools. The first stage therefore is identifying a reliable source or organisation that is willing to provide the data. Several local authorities in Scotland were contacted to allow monitoring of schools in their area to take place. Initially it was decided to select various school buildings and install several non-intrusive load monitoring (NILM) equipment in the schools. There are several advantages of using NILM systems, opposed to introducing equipment into the electricity network. A key advantage is that the buildings electricity supply is not interrupted, minimising disruption to the building. Another advantage is that the equipment can be set up without the need of an electrician or power engineer.

There are several disadvantages to using NILM electricity equipment. The first is that NILM equipment (for a 3-phase electricity monitor) is expensive, (about £4000 per unit). The

second problem is the equipment is limited in monitoring the meter side of the buildings electricity supply. Further equipment is needed to monitor each distribution board, to fully understand how the building uses energy. To create a large database of different types of schools, several sets of equipment would be needed, increasing the project costs. Lastly, the data collection phase of the project was relatively short. Ideally several years of data would be needed to ensure it is representative.

An economical alternative was available because several of the authorities, who agreed to participate in the energy data collection, had access to electricity consumption data from their power suppliers. This was in half hourly time resolution that represents the meter side of the building. Having access to this data overcame the possible limitations of using expensive NILM equipment and the short assessment/data gathering period.

Table 1 highlights the studied schools and the associated details, such as year of construction, number of pupils, school type, total energy consumption and whether the school has a swimming pool. This table is used as a reference in determining any trends in energy use. The data presented in table 1 was collected by contacting the schools directly and by referencing the school's website.

4. Normalisation of Data

An important part of analysing the data is comparing the schools energy consumption against other schools. A basic idea of energy consumption can be gained by just comparing kW in terms of load profiles, or kWh in terms of total energy consumption. One hypothesis is that a large school will consume more energy than a small school. By normalising by floor area, this size factor is removed. By introducing pupil numbers, further normalisation can occur. Normalising by pupil number, however, is not as straightforward as normalising by floor area as it is influenced by how the building is used. Floor area and number of occupants are not entirely independent from each other. A school is built to accommodate a maximum number of students. Even with varying number of students, the assumption is that the same number of classrooms, sports halls and even IT facilities will be continually used. This results in similar total energy consumption for the school, regardless of pupil numbers. In contrast, normalising energy consumption of office buildings by occupant numbers appears to be more appropriate, due to the differences in how both schools and offices are used. Office workers generally use their own PC, or their own IT equipment, hence the energy usage associated with IT will vary with the number of occupants. This an important factor to consider when normalising by pupil number. For this reason, the presented results and charts are given in kW/m² or W/m²

5. Categorisation

Table 1- Key School details

School	Year	Floor Area (m^2)	Total Energy use(kWh)	School	Year	Floor Area (m^2)	Total Energy (kWh)
A	1983	8042	667,233	**L**	1960	9561	888,443
B	1960	2535	195,221	**M**	1930*	14909	687,511
C	1980	9835	342,507	**N**	1940*	13559	607,708
D	1989	11430	512,819	**O**	1940*	11052	730,518
E	1991	12349	863,421	**P**	1950	14265	602,720
F	1954	13145	441,056	**Q**	1960	11852	605,890
G	1960	15368	695,154	**R**	1979	10156	492,587
H	1970	11535	643,994	**S**	1975	11927	945,627
I	1893*	11742	565,302	**T**	1960	1225	235,543
J	1978	11436	1,433,075	**U**	1980	7871	354,727
K	1965	11918	584,281	**-**	**-**	**-**	**-**

*School built at this date, but renovated post 2000

The complete database consists of 48 schools, including 32 Secondary schools, 11 primary schools and 5 specialised schools. Within the secondary school category, 21 schools were built before 2000, and 11 were built after 2000.

To analyse energy usage in schools, it is important to compare schools with similar properties. A large modern secondary school and a old small primary school will have different building characteristics, and differing electricity demands. In order to determine key trends in energy usage, the schools were initially categorised into two key groups: Primary and Secondary schools.

Secondary schools, or High schools, can be defined as premises that educate children from the ages of 11 to 17. High schools have a total floor area from 1,225m² to 15,368m² and total electricity usage between 1,433,075kWh to 195,221 (Table 1). It should be noted that the smallest school (by floor area), school 'T', does not have the smallest energy use (instead school 'B' has) emphasises the importance in normalising the data if comparisons are to be made. This result highlights the need for normalisation of energy use. Within the High/Secondary school category, two additional sub categories can be defined. The new categories are based on age of construction of the school; pre-2000 and post-2000.

The primary schools are defined as the first stages of education, catering for children aged from 5-11. Primary schools tend to be considerably smaller than secondary schools, as well as having smaller pupil numbers and represents 23% of the schools within the database.

Specialised schools are smaller, more focused schools, aimed at helping students with learning difficulties. These schools represent 10% of the studied secondary schools, but because of their small floor area and small pupil number, it is necessary to analyse these buildings separately from the other secondary schools.

6. Results

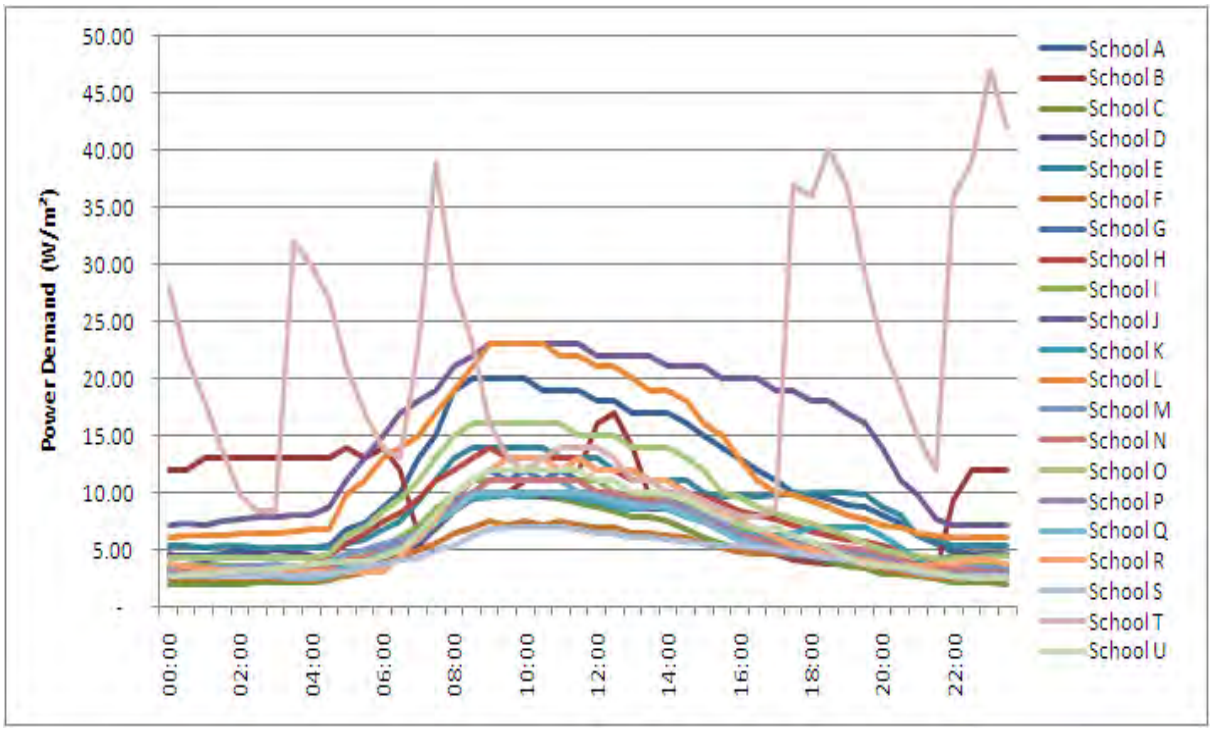

Figure 1- Average Power Demand Profiles

The collected school data was processed automatically by a FORTRAN based analysis program and several output files and profiles were produced. The designed analysis program outputs both a yearly average profile and four seasonal average profiles for each of the studied schools. For this paper, only Secondary schools built before 2000 will be discussed. Figure 1 demonstrates the average daily demand profiles for 21 secondary schools in Scotland, built before 2000. The daily power demand profiles represent the average working day power requirement over the entire year. This eliminates any possible seasonal variation.

School L's power demand profile can be used as an example to describe how a school consumes energy. School 'L' has a standby demand of 6.1W/m² and remains at baseload until 05:00 where it begins to rise. The rise continues until 0600, where the gradient reduces, then increases again. This step in energy use is most likely the result of heating systems (though heating pumps) being turned on. From 06:00 onwards the power demand increases until 09:00 where it reaches a plateau of 23W/m². This second rise is the lighting and IT equipment being switched on, as students and staff start interacting with the school. After 12:00 the power demand starts descending gradually, and at 14:00, the power demand falls from 19W/m² to 10W/m² by 17:00. From 17:00, the power demand steadily falls back to the baseload value by 22:00.

Figure 1 also demonstrates several profiles that have very atypical shapes. Schools 'B','J' and 'T' have power demand profiles that do not appear to resemble other schools. School 'J' has a fixed baseload of 12W/m², and rises slightly to 13W/m² until 07:00. At this point, it then reduces to 6W/m² and proceeds to rise and peak at 12:30 with a peak value of 17W/m². The power demand then falls to 3.1W/m² and sharply rises back to the original value of 12W/m². Although during the time period of 09:00 to 17:30 this profile demonstrates similar characteristics to the other schools in this study (excluding schools 'B','J' and 'T'), the large and constant power demand in the morning and in the evening are atypical. Further

investigation has not yet determined why this school has such a profile. Establishing if the demand profile varied from season to season could indicate if the morning/evening demand is heating or lighting related.

The second atypical profile belonged to School 'B'. The profile initially follows the other schools, in that it rises to a plateau at 08:30. The main difference in profile shape occurs after this plateau. While other schools tend to drop in demand, and return close to the standby value between 1600 and 1800. The profile for school 'B' slowly dropped from 22W/m² to 16W/m² from 12:00 to 19:30. After 19:30, the profile returned to the base load value of 7.7W/m² at 21:30hrs. The initial assumption was that this extended power demand outside the normal school hours is due to the school being used for evening classes or for sports activities. However when the profile was compared to other schools that are opened in the evening, School 'B' appeared to have a very high power demand that fell only slowly, and did not present the same 'hill' of power demand seen between 17:00 and 21:00 (as shown in school 'L' for example). On further investigation it was found that the school is part of a larger complex, which includes a large public pool, library and gym. These additional components of the school are open until 22:00 and are used by the local community.

Lastly the atypical profile of School 'T' consists of five peaks occurring at 00:00, 03:30, 07:30, 18:30 and 23:30, with peak power demands of 28, 32, 39, 40 and 47W/m² respectively. An interesting observation was that between 12:00 and 15:00hrs, the profile matches the same shape as the other schools. Upon further investigation, it was discovered that school 'T' has electric space heating, and not gas heating. The large peaks that occur are the result of the heating being switched on during the morning and evening. The spikes occurring early in the morning and late in the night could be a poorly set-up energy management system or the result of a heating system with a basic thermostat. The full explanation of this profile remains to be established.

7. Discussion and Conclusion

The research discussed in this paper aimed at determining if analysing an energy database can provide information on how buildings use energy, and in turn overcome the current limitations with existing benchmarks. The analysis of the school data to produce average power demand profiles, as shown in Figure 1, helped determine when power is used in a wide range of schools and how much power is required (peaks, and standby loads). The results demonstrate that there is a common shape within the profiles especially within the time period between 07:00 to 16:00. The results also demonstrated that it is possible to group the schools into 'good', 'average' and 'poor' energy/power rating, similar to the system used in the Good Practice Guides [6,13].

Several profiles were identified that did not share a similar shape to schools in the data base. Schools 'B', 'J' and 'T' had atypical profiles that could not be grouped with the other schools. This is an important finding as it highlighted one problem with using 'generic; profiles and the 'reliability' of their widespread application.

This preliminary report of continuing work suggests that it is possible to analyse the different seasonal demand profiles, both for weekdays and weekends, average daily consumption for each month, and determine any trends in standby/peak power over one year for each school. Future analysis will help determine: a) if there are any seasonal trends between the schools, b) how energy consumption varies between each month, c) how the peak values vary throughout the year (highlighting school holidays) and lastly d) if the schools are used during the

weekends, and if energy is being wasted. In addition, analysis will be extended on the different categories of schools (primary/secondary). As well as normalising by total floor area and by pupil number (although as already discussed, there may be no additional benefit normalising by pupil number), the data will need to be corrected for local climate. The schools analysed in this study were spread throughout Scotland and variations in local temperature is likely. Analysing local temperature as an independent variable will allow its impact on energy usage profiles to be established. Lastly, user behaviour or interaction will be introduced into the analysis, to help determine when and where energy is being used in the schools. Currently only basic information on pupil numbers for each schools is available. It is unknown how this study will measure, record and normalise pupil behaviour for each studied school.

Generic profiles are of use provided their limitations are recognised. Key information such as peak demands, school type, opening hours, after school use, standby load and construction date can be used to generate generic profiles. A possible approach is to average the school profile data for each school category and produce one profile. A difficulty with this is that atypical profiles, such as for schools B', 'J' and 'T', would be averaged as well, resulting in averaging problems. Additionally, one approach would be taking an average of an average (due to the analysed profiles being constructed using average values). This could lead to errors forming, or incorrect profile shapes. Another possible approach could be creating probability distribution, using every data value in each of the schools. This results in 17,250 data points being analysed, hence 840,960 data points in total for the entire database. The original data analysis program could be altered to include this possible approach. Generic profiles do have several beneficial uses. Energy managers could use a data input screen and enter key building details such as opening times, total area, etc and output a profile that could match their building. Additionally a level of good, average and poor profiles could be outputted as well as new benchmarks. The profiles could be used for determining the impact of renewable energy generation on a buildings daily demand, and could be used by power companies to guide on investment decisions or determining if power upgrades are needed.

The work discussed in this paper is continuing and key outputs, trends and conclusions are being established as the data analysis stage nears completion. This paper has discussed key stages of the methodology, data collection and normalisation. It has also discussed the results of initial analysis of one category of school and one average profile output from a designed analysis program. Lastly this paper introduced the concept of 'generic' profiles, and a possible methodology to gain these profiles. With further research and analysis of the data base, a better understanding of non-domestic energy use can be gained, and new benchmarks created.

References

[1] 'UK Energy in Brief', A National Statistics Publication, (2006), available from www.berr.gov.uk

[2] Steemers, K., Energy and the City; density, buildings and transport, Energy and Buildings, (2003), 35(1), p3,

[3] Pe´rez-Lombard L, Ortiz J , Pout C. A review on building energy consumption information, Energy and Buildings, 40 (2008) 394–398, available from www.sciencedirect.com

[4] Dimoudi A, Kostarela P, Energy monitoring and conservation potential in school buildings in the C' climatic zone of Greece, Renewable Energy, 34 (2009) 289–296, available from www.sciencedirect.com

[5] Hernandez P, Burke K, Lewis J, Development of energy performance benchmarks and building energy ratings for non-domestic buildings: An example for Irish primary schools, Energy and Buildings 40, (2008) 249–254, available from www.sciencedirect.com

[6] Good Practice Guide - 343 (GPG343), Saving Energy – A whole school approach, Carbon Trust publication, (2008), available from www.carbontrust.co.uk.

[7] Desideri U, Proietti S, Analysis of energy consumption in the High schools of a province in Italy, Energy and Buildings 34 (2002) 1003-1016

[8] C. Filippin, Benchmarking the energy efficiency and greenhouse gas emissions of school buildings in central Argentina, Building and Environment 35 (2000) 407-414

[9] Energy and Water Benchmarks for Maintained Schools in England 2002-03, Department For Education, 2004, available from www.education.gov.uk

[10] Stuart G, Fleming P, Ferreria V, Harris P, Rapid analysis of time series data to identify changes in electricity consumption patterns in UK secondary schools, Building and Environment 42 (2007) 1568–1580

[11] Energy Saving Case Study (CTS092),Windygoul Primary: A low carbon school by east Lothian Council, Carbon Trust publication, (2009), available from www.carbontrust.co.uk

[12] Energy performance of buildings—Methods for expressing energy performance and for energy certification of buildings (prEN 15217:2005), The European Committee for Standardization (CEN), (2005)

[13] Energy Consumption Guide - 19 (ECG-19), Energy Use in Offices, Carbon T rust publication, (2008), available from www.carbontrust.co.uk

Modeling Building Semantics: Providing Feedback and Sustainability

Hubert Grzybek[1], Hussnan H. Shah[2,*], Isaac Wiafe[1], Stephen R. Gulliver[1], Keiichi Nakata[1]

[1] *Informatics Research Centre (IRC), University of Reading, Reading, UK*
[2] *TSBE Centre, University of Reading, Reading, UK*
** H. H. Shah. Tel: +44(0)7931 300695, E-mail: h.h.shah@student.reading.ac.uk*

Abstract: Even minor changes in user activity can bring about significant energy savings within built space. Many building performance assessment methods have been developed, however these often disregard the impact of user behavior (i.e. the social, cultural and organizational aspects of the building). Building users currently have limited means of determining how sustainable they are, in context of the specific building structure and/or when compared to other users performing similar activities, it is therefore easy for users to dismiss their energy use. To support sustainability, buildings must be able to monitor energy use, identify areas of potential change in the context of user activity and provide contextually relevant information to facilitate persuasion management. If the building is able to provide users with detailed information about how specific user activity that is wasteful, this should provide considerable motivation to implement positive change. This paper proposes using a dynamic and temporal semantic model, to populate information within a model of persuasion, to manage user change. By semantically mapping a building, and linking this to persuasion management we suggest that: i) building energy use can be monitored and analyzed over time; ii) persuasive management can be facilitated to move user activity towards sustainability.

Keywords: *Semantic Modeling, Energy Use, User Behavior, Building Performance, Persuasive modeling*

1. Introduction

The cost and environmental impact of inefficient energy use in buildings, in combination with increased focus on legislation, has increased pressure on users to assess and adjust their behavior in order to lower energy consumption. Whilst users are aware of these issues, and often have a positive attitude towards a change in behavior, they are not provided with sufficient information to manage change towards sustainability. Whilst several standards exist for analyzing building energy efficiency (i.e. BREEAM, LEED, HK-BEAM and GB Tool), they largely focus on building structure and components without taking into account contextual information dynamic building usage, i.e. occupant behavior, organizational culture, etc.

To facilitate positive change, information concerning the building, user energy use and attitude, has to be monitored in order to provide contextually relevant feedback to persuade the user to change behavior towards target behavior (i.e. sustainable energy use). Since existing standards provide insufficient information structures to inform users of their energy usage, in context of building and environmental variation, we must find and use alternative means of informing persuasion techniques. In this paper we propose the use of a semantically rich building model. By storing information relating to building usage (occupant numbers, activities, organizational culture, location etc.) we are able to group and compare energy consumption and energy efficiency of building with similar factors, and/or as a result of user activity. This information can be used to facilitate and inform persuasion management techniques, and therefore supports change in activity toward target behavior.

2. Problems with Building Performance Assessment

Building performance assessment methods and tools have been developed worldwide, to assess the energy efficiency of physical building structures. Current building performance assessment methods can be crudely split into two categories: i) those based on criteria and

weighting systems - e.g. BREEAM (UK); or ii) those that use a checklist of building performance aspects - e.g. LEED (US). If such assessment performance is properly applied, they can provide a useful set of tools to identify Key Performance Indicators (KPI) and monitor improvements in the environmental performance of the building structure [1], however such performance assessment often fail to consider energy sustainability in context of building type, location and/or use.

Current building assessment techniques are applied on a voluntary basis, fail to support the full life-cycle of the building, and make it hard to understand the impact of user behavior (i.e. the social, cultural and organizational aspects of the building). Research conducted by Foresight [2] shows that building usage is significant to an individuals overall energy usage. Mackay [3] also argues that minor changes in the way we live and work within buildings, such as personalized heating / lighting settings, can bring variation in energy savings. Users currently have limited means of determining how sustainable they are, especially when energy capture via meter feedback ignores contextual information relating to building type and/or business activity. To facilitate long-term sustainability, buildings assessment must be able to monitor energy use over time in order to determine areas of potential change in context of building type, building structure and user activity. Only by providing feedback in light of live semantic context can appropriate persuasion be provided to users to encourage manageable change.

3. Semantic Building Information Modeling

In order to place building energy assessment in context of building use and user activity, we need to be able to create associations between the data and the specific characteristics (intrinsic) and context (extrinsic) properties of the building. This is important since it allows us to more precisely define acceptable and unacceptable energy usage for buildings based on numerous contextual factors. Buildings in colder climates, for instance, are likely to spend more resources on heating, which will in turn affect their energy efficiency. Publically comparing otherwise identical buildings in different climates will result in a range of energy usage levels.

The more specific we can be regarding the characteristics and use of buildings, the more detailed we can be when considering energy analytics, the better we can support a move towards sustainability that considers both building fabric and building use. By applying MEASUR methods, as proposed in [4], we suggest that the following factors should be considered as KPI when adding contextual information to building space:

- Physical building structure: including building size, floor space, number of floors and size of rooms.
- Building material: old/new building, presence of double glazed windows, energy efficient technologies etc.
- Building Occupants: number, average time spent in the building, average start/end times, occupancy variance.
- Building Usage: common occupant activities, presence and usage of building systems and electrical appliances.
- Social/Organisational: Building occupant usage policies, organisational culture.
- Geographical Context: location, climate, weather, temperature sun-light level variance, seasonal changes.

Assessment of buildings, in relation to their intrinsic and extrinsic properties, allows us to compare and identify buildings with similar properties. This enables us to quantifiably determine energy waste and therefore key areas of change that could improve sustainability. In contrast simple monitoring of energy usage readings, which provide only basic information with no reference to context, we can separate energy consumption and efficiency as being a result of either building structure and/or building use. Energy readings alone are unable to define whether a building is being used in an efficient or inefficient manner, yet the comparison between buildings with similar key properties allows direct comparison of energy performance, indicating whether a particular building is being used well or not. Such information can only be determined by semantically populating a live model of the building with temporal information about energy use.

Semantic building models can be developed through the specification of building property types and activity use definitions. When activity information is linked to as-built CAD drawings, existing building assessment methods, BMS (Building Management System) data streams, energy usage policies etc., a considerably flexible and semantically rich energy model can be developed.

4. Model Data Storage and Temporal Issues

We advocate that semantic building data models, using records to represent buildings along with their properties, should be represented using a historical relational database. The relational functionality supports arbitrary data structures, powerful data manipulation and querying capabilities. Use of a historical database supports temporal analysis of building use.

Most database systems are referred to as ‘snapshot’ databases, since they record the state of their domain at a single point in time. This means that any updates made to a record, results in the previous value being permanently lost. Likewise, any entities that are deleted imply that those entities never existed. In contrast, historical databases never delete records and only update and insert new records in order to maintain an object‘s historical audit trail. This supports data mining and the recognition of trends as a result of object states. Moreover analytics can effectively consider changes to building use over time. Such temporal databases manage time values in one of two ways: i) valid time and ii) transaction time. Valid time denotes the time period during which a fact is true with respect to the real world. Transaction time is the time period during which a fact is stored in the database [5].

The application of a temporal database to the problem of recording semantic building models is appropriate since user attitude and occupant behavior patterns (and therefore energy usage) are likely to change over time; and we need to be able to represent the impact of change or behavior in context of the specific time scale and/or season during which it was deemed accurate.

Whilst the use of a temporal database adds significant complexity to the semantic model, such systems allow increasingly powerful queries of stored information, which supports the provision of contextually persuasive feedback and management of user change towards sustainable energy use. In order to manage positive user change, towards target behavior, we must first understand how persuasion management is facilitated via information provision.

5. Persuasive Management

The issue of user persuasion is becoming increasingly incorporated into systems design, and is used in areas including social networking, online videos, and mobile devices, etc. [6].

Research in this area shows that there are multiple means of changing user behavior and this has a strong relationship with user current activity and attitudes. Fogg [6] stipulates that a change in behavior occurs at the moment at which the user has sufficient motivation, i.e. feels able to make the change; which often occurs as a result of external triggers acting on the individual. By understanding the user's current behavior towards energy use, and by managing triggers by providing relevant stakeholders with appropriate feedback / information, persuasive management can be used to enthuse users towards target behavior. In this work we used the 3D-RAB persuasive model [7] to support persuasive feedback management. To understand this model, and how it relates to energy sustainability and persuasion management, the following sections introduce information concerning: assessment of current behavior, attitude toward target behavior, attitude towards change, and behavior state change.

5.1. Assessment of Current Behavior (CB)

Current behavior is defined as the existing actions of a person in relation to the environment. Such actions may be conscious or subconscious, overt or covert, voluntary or involuntary. In order to measure behavior, and support a positive movement towards target behavior, current behavior must be assessed. This is to say that appropriate user behavioral change, and therefore information feedback, must be personalized. For simplicity, behavior is measured as being either positive or negative, when considered in context of energy sustainability. A user, either a person or organization, is considered to have a positive behavior if current behavior is the same as the target behavior, i.e. actions that make efficient use of energy. CB can be defined as being positive or negative by analyzing BMS energy streams in the semantic model. By looking at specific energy use, i.e. that identified as being related to a specific activity, over the defined time scale of the activity, and by placing this information in context of the building type and fabric we are able to assess energy use against personalized targets.

5.2. Attitude towards Target Behavior (ATTB)

User attitude towards target behavior is defined as the like or dislike of target behavior; and is, for the purpose of simplicity, defined as being either positive or negative in this research. If someone's attitude supports energy sustainability then they are deemed as having a positive attitude towards the target behavior. Interestingly, user's attitude towards behavior is not always consistent with current behavior. ATTB is captured via experimentation, normally involving decision making results and / or questionnaire feedback.

5.3. Attitude towards Changing/Maintaining Current Behavior (ATCMB)

Attitude towards change is a measure of whether, in a particular case, a person is positive, negative or neutral towards change. This measure is considered to be positive when a user agrees to change to the target behavior, or when they are willing to maintain positive current behavior. Aronson [8] argues that changing a user's behaviour can result in attitude change, since new attitudes are formed to justify behavior. He explained that people adjust their attitudes to fit new behaviours in order to reduce or eliminate the "tension of dissonance". The theory of cognitive dissonance proposes that two cognitions are considered to be in dissonance if one opposes the other creating an unpleasant psychological tension [9]. The foundation of this theory is based on the fact that in order to eliminate dissonance, a user changes their belief, action, or perception of the action. ATCMB is captured via experimentation, normally involving decision making results and / or questionnaire feedback.

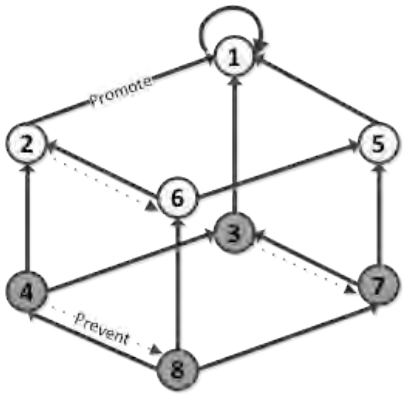

Fig. 1: Transitions in 3D – RAB

5.4. 3D- RAB Model

The 3D-RAB model [7] enables the persuader (i.e. the stakeholder interested in obtaining sustainability) to categorize users into groups depending on CB, ATTB and ATCMB being positive or negative. In total, eight categories of user were identified (see figure 1). The various states are analyzed, in context of energy use, in order to ascertain possible transitions for persuasion. Combining Figure 1 and Table 1, we can see how states are either stable or unstable, and explains how users in unstable states can transfer states as a result of persuasive feedback. The relationship of, and transition route of users, is based on the theory of cognitive dissonance, which is defined as being: i) strong, ii) moderate, iii) weak or iv) absent.

Table 1: Definition of current behavior, attitude and its impact of dissonance

State	Current Behavior	Attitude towards target behavior	Attitude towards changing/ maintaining current behavior	Cognitive Dissonance	Stability of state	Natural State tendency	Targeted state for Persuasion
1	+	+	+	No	Stable (+)	1	1
2	+	+	-	weak	Unstable (+)	1	1
3	+	-	+	moderate	Unstable (-)	7	1
4	+	-	-	Strong	Unstable (-)	8	2 or 3
5	-	+	+	Strong	Unstable (+)	1	1
6	-	+	-	moderate	Unstable (-)	8	2 or 5
7	-	-	+	weak	Unstable (-)	8	3 or 5
8	-	-	-	No	Stable (-)	8	4 or 6 or 7

Strong cognitive dissonance is formed when there is a very strong disagreement between one's attitude and current energy use and it results in a strong unpleasant psychological tension and produces a greater probability that one may change his/her attitude or behavior in order to eliminate the dissonance. At such a state the user experiences a very uncomfortable cognition state that he/she recognizes the need for a change in attitude or behavior. For example, if a user wishes to save energy and/or cost, providing his/her with information about energy waste of equipment being left on overnight, may result in the user turning off the devices at the end of the day. When there is a weak or moderate dissonance the disagreement between one's attitude and behavior is not enough to motivate change. In the case of no

cognitive dissonance, user attitude agrees with his/her energy use and there is no psychological tension. Variation in dissonance therefore creates stable and unstable states that can be positive or negatively towards the target behavior.

In states 1-4 (see Figure 1) the user is already performing the target behaviour (i.e. positive and/or sustainable use of energy). Accordingly feedback information should be given to move the user towards, or keep in the state 1 (positive action and attitude, low dissonance). If current behaviour is in states 5-8, then a change is required toward positive activity. This change can be facilitated by providing energy feedback information, either directly to users or, depending on the user state and level of dissonance, to related stakeholders (i.e. user / activity / building managers). Such feedback is likely to increase stakeholder level of dissonance, due to financial and/or energy targets. To remove this dissonance, alternative external triggers can be placed on the user (e.g. loss of bonus, or enforced process change). By changing user incentive (e.g. bonus), which ideally leads to a change in user or user attitude, or by enforcing change in current behavior, a transition in user state occurs towards a more positive stable state. Information provision and regular use assessment, supported by analysis of the semantic temporal model, can be used over time to facilitate positive change, whilst identifying and highlighting existence of negative state transitions.

6. Conclusions

Currently building assessment methods largely ignore building context and / or activity. We are therefore unable to define whether a building is being truly used in an efficient or inefficient manner. In this paper we have discussed how using a dynamic and temporal semantic model, to populate information within a model of persuasion, can be used to manage users towards lasting behavioral change.

If Building Management System, building structure, and activity information can be captured and integrated within a temporal semantic building model, then personalized feedback concerning user energy usage can be used to prompt positive change in either, occupant and / or related stakeholder attitudes or current behavior to minimize cognitive dissonance. By combing physiological principles with information from live semantic temporal building models, we can identify energy waste in context of building, context and activity type. Such modeling approaches, although still largely unsupported by mainstream building modeling and database technologies, would provide huge potential when integrating energy information about building structure, systems, context, and users.

References

[1] Clements-Croome, D.J et al., Creating the Productive Workplace. London: Taylor & Francis. 2006.

[2] Foresight's Sustainable Energy Management and the Built Environment (SEMBE) Project. Presentation 24 April 2009. www.foresight.gov.uk accessed 5th June 2010.

[3] MacKay D. J. C. Sustainable Energy - Without the Hot Air. Chapter 22: Efficient electricity use. UIT Ltd., 2008.

[4] Shah, H. H., Ma, Y., Gulliver, S. R., "Selecting Key Performance Indicators for Sustainable Intelligent buildings", ACM SIGDOC 2010, San Paulo, Brazil.

[5] Grzybek, H, Gulliver, S. R., Huang Z. "Inclusion of Temporal Databases with Industry Foundation Classes – A Basis for Adaptable Intelligent Buildings", 12th International

Conference on Informatics and Semiotics in Organisations, ICISO 2010, pp. 24-31, 2010

[6] Fogg B., "A Behavior Model for Persuasive Design" in 4th International Conference on Persuasive Technology, Claremont, California, 2009.

[7] Wiafe I, Nakata K., Gulliver S. R. “Designing Persuasive Third party Applications for Social Networks: The 3D-Bar Model”, International Workshop on SocialCo mputing, Network, and Services (SocialComNet 2011), Crete, 2011 (submitted)

[8] Aronson E. "Back to the Future: Retrospective Review of Leon Festinger's" A Theory of Cognitive Dissonance"," *The American Journal of Psychology,* vol. 110, pp. 127-137, 1997.5

[9] Brehm J. and Cohen A. *Explorations in cognitive dissonance*: Wiley New York, 1962.

[10] Griffin E. and McClish G. *A first look at communication theory*: McGraw-Hill New York, 1991.

Energy Cultures - a framework for interdisciplinary research

Janet Stephenson[1,*], Rob Lawson[2], Gerry Carrington[3], Barry Barton[4], Paul Thorsnes[5]

[1]*Centre for the Study of Agriculture, Food and Environment, University of Otago, Dunedin, New Zealand*
[2]*Marketing Department, University of Otago, Dunedin, New Zealand*
[3]*Physics Department, University of Otago, Dunedin, New Zealand*
[4]*School of Law, University of Waikato, Hamilton, New Zealand*
[5]*Economics Department, University of Otago, Dunedin, New Zealand*
** Corresponding author. Tel: +64 3 479 8779, Fax: +64 3 479 5266, E-mail:janet.stephenson@otago.ac.nz*

Abstract: The Energy Cultures framework aims to assist in understanding the factors that influence energy consumption behaviour, and to help identify opportunities for behaviour change. Building on a history of attempts to offer multi-disciplinary integrating models of energy behaviour, we take a culture-based approach to behaviour, while drawing also from cultural theories, actor-network theory, socio-technical systems, and lifestyles literature. The framework provides a structure for addressing the problem of multiple interpretations of 'behaviour' by suggesting that it is influenced by the interactions between cognitive norms, energy practices and material culture. By conceptualising the research arena, the framework creates a common point of reference for the multi-disciplinary research team. The Energy Cultures framework has proven to be unexpectedly fruitful. It has assisted in the design of the 3-year research programme, which includes a number of different qualitative and quantitative methodologies. In application to a given example, it helps to position the complex drivers of behaviour change. Although the framework has not yet been fully tested as to its ability to help integrate findings from our various research methods, we believe the Energy Cultures framework has promise in furthering interdisciplinary studies of energy behaviours in a wide variety of situations, being relevant to different contexts and different scales.

Keywords: *Household energy behaviour, Theoretical framework, Multi-disciplinary, Research design*

1. Introduction

There is huge potential for greater efficiencies in consumer energy behaviour, but achieving the necessary behaviour changes is proving exceedingly difficult. The International Energy Agency (IEA) advises that energy efficiency improvements across the end-use sector have the potential to achieve 52% of the CO_2 emissions reduction required by 2030 to contain atmospheric CO_2 concentrations at 450 ppm. This is more than the combined contributions of renewable energy systems, biofuels and carbon-capture-and-sequestration. The IEA calls this transition the 'energy environmental revolution', and notes that many nations face challenges in achieving behavior change in the demand-side area [1]. It is well accepted that interdisciplinary studies are likely to offer enhanced insights into the vexed question of energy behaviours [2], but interdisciplinary research itself can be highly challenging especially in the absence of common conceptual agreements.

Our 3-year research programme, 'Energy Cultures' [3], is attempting to achieve an integrated understanding of household energy behaviours, and to identify promising opportunities for behavior-change interventions, by bringing together an interdisciplinary team. The core members are five university-based researchers with backgrounds in consumer psychology, economics, sociology, law and engineering. We share an interest in the behaviour of energy consumers, but approach the concept of behaviour through very different disciplinary lenses. In order to bring some coherence to our interactions and to the research programme as a whole, we developed a theoretical model - the 'Energy Cultures framework'. Here we describe the framework, and how, while it was initially developed to depict the nature of the problem, it has proven to be unexpectedly fruitful in supporting collaboration, designing the research programme, and characterising the complexity of household behaviour.

2. Designing the Framework

Since the 1970s there have been numerous studies of energy consumption behaviours from a wide range of disciplinary perspectives, including microeconomics; behavioural economics; technology adoption models; social and environmental psychology; and sociological theories. No single analytical approach provides a framework for analysing more than a small portion of behaviour, or for providing reliably successful interventions [4-6].

There is clearly value in developing a framework to support more integration across disciplines, but despite a number of attempts to establish unifying models [5-12] they are little used, and in practice single-discipline studies dominate the literature [5]. Wilson and Dowlatabadi [6] suggest that a successful integrating model would need to be relevant across three characteristics of energy behaviour—context, scale, and heterogeneity. In other words the model would need to be applicable to a wide range of determinants of behavior; to different scales (for example from a single household to an industry sector); and would need to be able to account for the wide variability in energy behaviours and responses to interventions.

In developing the Energy Cultures Framework, the initial purpose was to create a model that incorporated all of the potential drivers of household energy behavior as perceived by the Energy Cultures team members, so that we had a commonly agreed notion of the problem and its potential influences. This was crucial because different disciplines have quite different notions of what 'behaviour' actually is, as well as what its drivers are. Behaviour is sometimes characterised in terms of the energy technologies acquired or adopted by the consumer (e.g. is the house well-insulated? does it have a heat pump?); sometimes in terms of the consumer's *use* of energy-related technologies (do they drive or walk to work? do they use a dishwasher?); sometimes in terms of the consumer's aspirations (e.g. cleanliness, a healthier environment), and also as various interrelationships between these factors [5, 6, 13]. From our inter-disciplinary perspective, we felt it was important to include all of these notions of behaviour – technologies, activities and aspirations, and their interrelationships. We also wanted to be able to take into account the very broad range of factors that have been identified as affecting or driving behaviour, including the values, beliefs and knowledge of the consumer, the wider social and cultural values that impact on the consumer, the availability of technologies, the pricing and market conditions, the regulatory and policy environment, incentives and disincentives, and many other influences.

We were influenced by several theoretical streams. Socio-Technical Systems (STS) theories consider the role technologies play in influencing behaviours and expectations, and suggest that ''social practices and technological artefacts shape and are shaped by one another'' [14, p. 351]. We also draw from Bourdieu, who theorises that the practices that make up a social life are largely generated and regulated by 'habitus' – persistent patterns of thought, perceptions and action – which themselves are a response to the objective conditions within which the individual exists. Habitus is self-generative and can constrain an individual's aspirations so that practices that lie outside their habitus may be excluded from consideration as unthinkable. This is not to say that we believe cultures are fixed and immutable (nor does Bourdieu, who discusses the possibilities of strategic action to alter habitus). On the contrary, as is evident everywhere in society, cultural groups change their characteristics and membership, cultural traits are mutable, and they can be rapidly adopted by new groups in conducive conditions. For our purposes, it is how individuals and groups shift from the self-replicating stasis of habitus into the adoption of new practices, new beliefs and aspirations, and new technologies, that are the core of our interest. Our approach is also strongly

influenced by 'soft systems' thinking—ways of understanding a particular context in a holistic way through considering interactivities between its attributes. Systems thinking attempts to address the shortcomings of reductionist approaches, recognising the complexity of the real world. We use 'system' not in the sense of a real-world entity, but as a construct to aid understanding [16, 17].

'Culture' is another core concept, and here we are not using the term to refer to any particular pre-defined ethnic or social group, but in recognition of the diversity of values, beliefs, knowledge, practices, technologies, and other cultural determinants that exist within any given society. Our hypothesis is that distinctive clusters of cultural norms, energy practices and material culture will be able to be identified within a given society, and that identifying and studying the characteristics of these 'energy cultures' will give insights into the heterogeneity of energy behaviours. The term 'energy cultures' brings the norm-practice-material culture dynamic to the fore, rather than the more decentred influences that are the focus of much STS literature (although still recognizing the influence of external agents.

Within the energy literature, the concept of culture has generally been more implied than overt. The key exception is in the work of Loren Lutzenhiser [12] who suggests that energy consumption is embedded in cultural processes. Material culture (buildings, furnishings, technologies, etc.) interweaves with "roles, relationships, conventional understandings, rules and beliefs into the cultural practices of groups" (12, p. 54). Our 'energy cultures' framework builds on Lutzenhiser's insights.

3. The Energy Cultures Framework

The Energy Cultures framework (Fig 1) proposes that consumer energy behaviour can be understood at its most fundamental level by examining the interactions between cognitive norms (e.g. beliefs, understandings, motivations etc), material culture (e.g. heating technologies, building form, etc) and energy practices (e.g. activities, processes). These are all aspects of 'behaviour', and using a household as an example, cognitive norms might include social aspirations, expected comfort levels, environmental values and respect for tradition; material culture might include heating devices, house structure, and insulation; and energy practices might include temperature settings, hours of heating, and maintenance of technologies. Each of these three components (cognitive norms, material culture and energy practices) individually affects energy use, yet they are also strongly interactive. For example, the existence of a heat pump (material culture) will result in very different practices from a household with an open fire; or a frugal upbringing (cultural norms) will impact on energy practices and possibly on the choice of technologies (material culture).

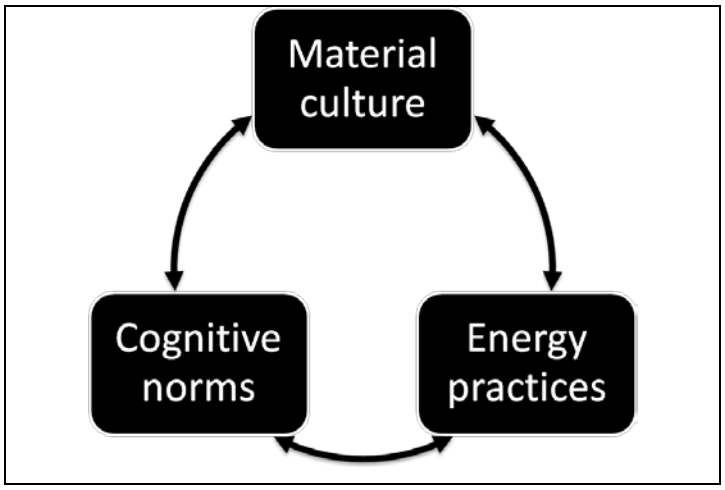

Fig. 1. The core concept of the Energy Cultures framework: cognitive norms, material culture and energy practices and the interactivity between them.

The three components and their interactions form the core of the Energy Cultures framework, but there are also wider systemic influences on behavior (Figure 2). Each aspect of material culture, energy practice or cognitive norm is impacted in some way by these wider influences—for example, cognitive norms around home heating will be affected by such things as upbringing, age and education; choice of home heating technologies may be impacted by such things as income level, availability of technologies, law and regulations and efficiency rating schemes; and heating control settings (if any) may be influenced by such things as the energy price structure and social marketing campaigns.

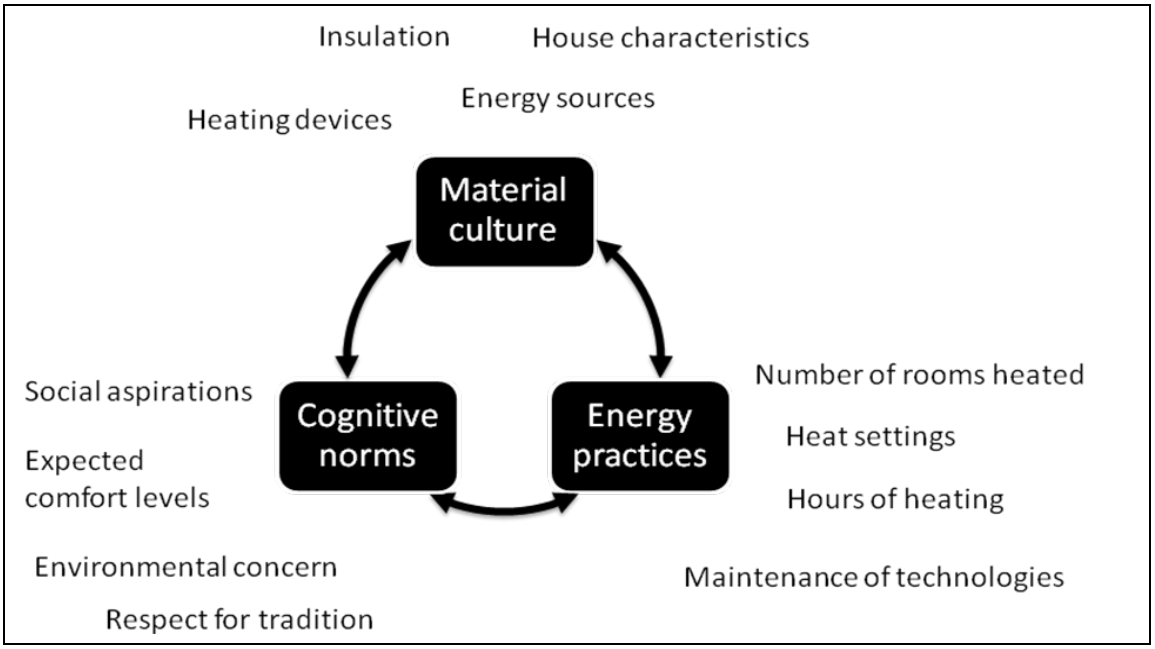

Fig. 2. Using the Energy Cultures framework to depict some of the wider systemic influences on behaviour.

4. Application of the Energy Cultures Framework

Having initially developed the Energy Cultures framework as a commonly agreed depiction of the problem we were seeking to address, we found it had other uses. Firstly, it aided in constructing hypotheses for our research into household energy behavior. For example, we hypothesise that clusters of similar norms, material cultures and/or practices will be

observable in a given population, enabling segmentation of the population in terms of reasonably distinctive 'energy cultures'. Characterising these different 'cultures' will assist in both understanding the range and nature of consumer behaviour, and in identifying what sorts of interventions may be effective in achieving a move towards greater energy efficiencies for any given 'culture'.

Secondly, the framework has provided a conceptual structure for the design of the research programme. Each of the disciplines has particular methodologies which can help inform different components of the energy cultures framework, and the interactions between them. To date (at the end of our first year), we have studied cultural norms (and in particular the influence of values on practices and material culture) using 'values laddering', a method from consumer psychology involving in-depth interviews. Households have been surveyed to identify their material culture, practices and cognitive norms, as well as some of the external influences recognized by householders such as information sources and social networks. Choice modelling, an economics method, has been used to identify the tradeoffs that people make in their preferences for household heating and hot water systems, which in terms of the models informs the interactivity of cognitive norms with both material culture and energy practices. The data is being collected at three scales – some households are being subject to all three data collection methods; the latter two methods being applied both within our three case study areas and nationally.

A third use of the framework is as an integrating tool. We use the framework as the basis for staging the streams of the multi-method research project so that one informs the other—for example, findings from values research (cognitive norms) was used to design the choice modelling. By using common case studies (where relevant) for all of the research, data from different research streams can be contrasted across households or groups of households, building up a rich picture of household behaviours. Integrated analysis of this data will start to identify clusters of 'energy cultures', which will then be studied in greater depth in segmented focus groups of householders using soft systems methodology. The wider legal and policy context affecting behavior will be examined through legal desktop investigations. Opportunities for effective interventions will be sought both from the reported experiences of energy culture group members, and from the policy review. In year 3 some interventions will be trialled within culture groups.

A fourth application of the framework has been to understand behavior change in retrospect. The Transition Town movement is a 'vibrant international grassroots movement that brings people together to explore how we – as communities – can respond to the environmental, economic and social challenges arising from climate change' [18]. We have examined the behavioural shifts occurring in a New Zealand transition town, Waitati, using the Energy Cultures framework.

Possibly, the most prominent and far-reaching transition activity that community members are engaged in is known as the Waitati Energy Project (WEP). This is a multifaceted set of proposals to move the community to more sustainable patterns of energy consumption and supply. The Waitati Energy Project had its beginnings when a small group of enthusiasts invited a prominent Green politician to speak to the community on sustainability issues. Building on interest aroused by this meeting, they organised over the next year a series of well-attended events to help develop 'energy literacy' in the community, including a day-long fair with speakers, stalls and hands-on activities like a cycle-powered television.

In terms of the Energy Cultures framework, these activities helped shift the cognitive norms of the community towards an improved awareness of global and local imperatives for greater energy efficiency and more renewable energy supplies, a better self-awareness of the community's own characteristics, and improved energy literacy. This shift paved the way for changes in practices and material culture.

To date, the most significant change in material culture is in home insulation. Most of Waitati's homes are poorly insulated because they were built before mandatory insulation standards were introduced in the 1970s, so there are ready opportunities for improvements energy efficiency. The WEP organisers secured government subsidies for a mass home insulation project in 2009 and facilitated the project. As a result, 53 of the 200 houses in Waitati received subsidised insulation upgrades. WEP's success in gaining the funding, and the significant level of uptake, would have been unlikely if the community had not been cognitively 'primed' (for example a far lower level of uptake was achieved in other areas). Other changes in material culture have been enabled through genuinely cooperative activities such as the exchange of technical advice, the organisation of bulk purchasing to secure discounts and the establishment of partnerships with local suppliers and builders.

On the energy supply side, WEP proposes to build a community owned wind turbine to provide power for the district while feeding surplus electricity into the distribution grid. While community owned turbines are not uncommon in other countries, this would be a first in New Zealand. It represents a significant change in thinking at the local community level that requires changes also to the cultural infrastructure and practice at a national level. Current industry norms are not supportive of locally distributed generation, and the legal and financial structures for ownership and operation of such a venture are untested. Based on the Energy Cultures framework, we anticipate that progress in this area will require harmonisation of community members' cognitive norms and practices, prior to being able to achieve a shift in material culture and an overall transition to a new energy system 'habitus'. Steps have been taken to develop the turbine project with a community planning exercise, the identification of sites, initial evaluation of the generation potential, discussions with the lines company and a turbine manufacturer, as well as gaining Government funding to develop a financial model and business plan take the proposal to the next stage. The fact that the community is prepared to take on such a challenging proposal represents a significant shift in the 'energy culture' of the individuals directly involved and of the community as a whole.

These are all examples that illustrate the ways in which energy behaviours are influenced by the interactions between cognitive norms, material culture and energy practices,
and that these interacting components can be examined at both a personal and community/social level. We consider that visualising, and analysing, the system as an interconnecting set of attributes helps to reveal the need, the options and the staging for change strategies. Understanding how Waitati has achieved a significant shift in the direction of household energy efficiency and supply can offer clues as to how change might be initiated in other contexts.

Finally, a further intention with the Energy Cultures research programme is to identify suitable interventions for behavior change. It was clear from the literature [6] and from our own observations that there is surprising variability in energy-related behaviour, even across households or firms with apparently similar characteristics. We suspect that the lack of success with interventions might be related, in part, to their being designed to influence an imaginary typical consumer, rather than selected as 'best fit' for definable behavioural

clusters. The research programme aims to describe and characterise this heterogeneity, so as to be in a better position to match interventions to specific energy cultures. This will undertaken and tested in Year 3 of the programme.

5. Conclusions

The Energy Cultures model is fundamentally a conceptual framework to help articulate a particular class of problems relating to why individuals and groups use energy in the way they do. Nevertheless we have found it to have a number of other potential applications, some of which we are only beginning to explore. At an applied level, the Energy Cultures framework has already provided a basis for crossdisciplinary collaboration, and for multi-disciplinary research design. It enables identification of the relative roles of different disciplines in contributing to exploring the research problem, and the linkages between findings, and thus facilitates cross-disciplinary interactions. We are using it as a common point of reference and a tool for integration of research findings from our multi-stream research project.

The adaptability of the Energy Cultures framework is such that it displays Wilson and Dowlatabadi's three requirements for a successful integrating model [6]. It accounts for different *contexts*—the wide range of drivers of behaviour, through its modelling of the interactivities between the three core components of behaviour, and between these and wider societal and structural influences. It works at different *scales*, being applicable to understanding a single household, a group of households, a community (such as Waitati), an industrial sector, or conceivably at a national level (as in potentially considering the difference in 'energy cultures' between one nation and another). And it is particularly designed to characterise *heterogeneity* – the wide variability in behaviours – through the identification of different energy cultures.

The Energy Cultures framework has been developed in part to assist in policy development, regulation and market design to achieve greater energy efficiency through improved understanding of the interactions between context and behaviour. In particular, by identifying clusters of people or households with similar behavioural patterns, it may assist in the crafting of more effective interventions and incentives targeted to specific energy cultures. We also note its potential to help energy supply companies understand different behavioural clusters ('energy cultures') among their customers, so as to better tailor their tariff schemes and products. However, only further application of the approach will show whether it has real utility in helping to understand energy behaviours in a holistic way, and in guiding the development of projects and programmes to achieve greater adoption of energy-efficient behaviours.

References

[1] World Energy Outlook, International Energy Agency, Paris, 2009, p. 211.

[2] DEFRA, A Framework for Pro-environmental Behaviours. Department for Environment, Food and Rural Affairs, British Government, London, 2008, p. 76.

[3] J. Stephenson, B. Barton, G. Carrington, D. Gnoth, R. Lawson, P. Thorsnes , Energy Cultures: A framework for understanding energy behaviours, Energy Policy 38, 2010, pp. 6120–6129

[4] N.W. Biggart, L. Lutzenhiser, Economic sociology and the social problem of energy inefficiency. American Behavioral Scientist 50, 2007, pp.1070–1087.

[5] J. Keirstead, Evaluating the applicability of integrated domestic energy consumption frameworks in the UK, Energy Policy 34, 2006, pp. 3065–3077.

[6] C. Wilson, H. Dowlatabadi, Models of decision making and residential energy use, Annual Review of Environment and Resources 32, 2007, pp.169–203.

[7] R.R. Dholakia, N. Dholakia, A.F. Firat, From social psychology to political economy: a model of energy use behavior. Journal of Economic Psychology 3, 1983, pp. 231–247.

[8] W.F. Van Raaij, T.M.M. Verhallen, A behavioral model of residential energy use, Journal of Economic Psychology 3, 1983, pp. 39–63.

[9] R. Wilk, Consumption, human needs, and global environmental change. Global Environmental Change 12, 2002, pp. 5–13.

[10] S. Barr, A.W. Gilg, A conceptual framework for understanding and analyzing attitudes towards environmental behavior, Geografiska Annaler 89B(4), 2007, pp. 361–379.

[11] G. Hitchcock, An integrated framework for energy use and behaviour in the domestic sector. Energy and Buildings 20, 1993, pp. 151–157.

[12] L. Lutzenhiser, A cultural model of household energy consumption. Energy 17, 1992, pp. 47–60.

[13] E. Shove, Comfort, Cleanliness and Convenience. Oxford International Publishers, Oxford, 2003.

[14] A. Smith, A. Stirling, Moving outside or inside? Objectification and reflexivity in the governance of socio-technical systems. Journal of Environmental Policy & Planning 9, 2007, pp. 351–373.

[15] P. Bourdieu, The Logic of Practice (transl. R. Nice). Polity Press, Cambridge, 1992.

[16] P. Checkland, Soft systems methodology: a thirty year retrospective. Systems Research and Behavioural Science 17, 2000, pp. S11–S58.

[17] G. Midgely, Systems Thinking. Sage publications, London, 2003.

[18] Transition Towns New Zealand Aotearoa, n.d. What are transition towns? /http://www.transitiontowns.org.nz/node/1667S. (accessed 15.12.2010).

Appliances facilitating everyday life – electricity use derived from daily activities

Kajsa Ellegård[1,*], Joakim Widén[2], Katerina Vrotsou[3]

[1]*Dept of Thematic Studies, Linköping University, Sweden*
[2]*Dept of Engineering Sciences, Uppsala University, Sweden*
[3]*Dept of Science and Technology, Linköping University, Sweden*
**Corresponding author. Tel +4613285836; Fax +4613284461; e-mail: kajsa.ellegard@liu.se*

Abstract: The purpose of this paper is to present how, using a visualization method, electricity use can be derived from the everyday activity patterns of household members. Target groups are, on the one hand, professionals in the energy sector and energy advisors who need more knowledge about household energy use, and, on the other hand, household members wanting to reduce the energy use by revealing their own habits and thereby finding out how changed activity performance may influence electricity use. The focus is on the relation between utilizing electric appliances to perform everyday life activities and the use of electricity. The visualization method is based on the time-geographic approach developed by Hägerstrand and includes a model that estimates appliance electricity use from household members' activities. Focus, in this paper, is put on some basic activities performed to satisfy daily life needs: cooking and use of information, communication and entertainment devices. These activities appear frequently in the everyday life of households, even though not all household members perform them all. The method is applied on a data material comprising time-diaries written by 463 individuals (aged 10 to 85+) in 179 households in different parts of Sweden. The visualization method reveals when and for how long activities that claim electric appliances are performed by which individual(s). It also shows electricity load curves generated from the use of appliances at different levels, such as individual, household and group or population levels. At household level the method can reveal which household members are the main users of electricity, i.e. the division of labour between household members. Thereby it also informs about whom could be approached by energy companies and energy advisors in information campaigns. The main result of the study is that systematic differences in activity patterns in subgroups of a population can be identified (e.g. men and women) but that directed information based on these patterns has to be made with care and with the risk of making too broad generalizations.

Keywords: *Electricity use, Everyday activity sequence, Visualization, Activity pattern, Load curve.*

1. Introduction

Information is a relatively cheap way to make efforts to influence people to change their everyday life activities in order to better comply with the policies aiming at mitigating climate change from overuse of resources, among them electricity [1,2]. Information as a means to influence people's daily routines is not effective unless the individuals judge the information to be relevant to them. Therefore information must be targeted carefully. Who is to be targeted with information about energy saving and energy efficiency activities? This question has to do with the correspondence between which household members are in the energy company's billing register and which household member(s) utilize the electricity demanding appliances in the home. The aim of this paper is to present how the visualization method *VISUAL-TimePAcTS/energy use*[1] can be used to study energy use in households and can facilitate the identification of the actual users of electric appliances within these households. Thereby relevant information for various target groups can be developed. The method has been developed in an interdisciplinary research group in which scientists from social science, visualization science and physics cooperate on a long term basis [3,4,5,6,7]. The method aids

[1] VISUAL-TimePAcTS: VISUAL = visualization, P = place, Ac = activity, T = technology, S = social companionship; time is, of course, time.

in increasing our knowledge about human daily activities and the use of electric appliances for performing them.

Gram-Hanssen showed that even if households are similar in many respects, their energy use may differ a lot [8]. This has to be handled. A basic assumption is that in order to influence people to change their everyday life habits and routines, the information presented to them must address problems that are relevant to them. This means that they should be able to recognize their own daily situation in the material presented and thereby find substance in the arguments.

2. Method and the models for accounting electricity use

VISUAL-TimePAcTS/energy use is developed in the tradition of time geography [9,10,11,12] and its point of departure is the individual and her daily activities as they are seen in a sequence over the day. If data allows (i.e. if there are diaries from more than one person in a multi person household), the individual is seen in the context of her household. Even when individuals are aggregated to group or population levels the important information distinguishing one individual from another is still visible, figure 1.

The data used for developing the method is collected by Statistics Sweden in a pilot study in 1996. An important and valuable characteristic of this dataset is that it contains individuals in households, i.e. individuals of 10 years and older in the 179 households have written time-diaries. The age span of the total dataset is 10 to 97 years and the household sizes vary from 1 person upwards. The households included in the study are situated in different parts of Sweden and their income, education and accommodation forms vary.

The individuals (N=463) have written time-diaries during one weekday and one weekend day. Their weekday activity sequences forming an activity pattern of the population is shown in figure 1 (right). Members of the same household have written diaries on the same date, which means that it is possible to couple and compare the individuals' activities to each other. For example, which person cooks and which person buys the ingredients for cooking within the same household can be revealed.

The diary data considered in this paper are categorized into 7 main activity categories and each of these categories is broken up into more detailed descriptions of a performed activity. Apart from activity type, information about companionship while performing each activity is also available, meaning together with whom or what appliance an individual is. This makes possible the extraction of information concerning energy use of individuals, households and whole populations.

A model for computing load profiles for household electricity and hot water use based on activities has been presented by Widén [13,14]. In the developed model, activity diary data are converted to energy load profiles by considering an energy-use category and a corresponding energy-use pattern for each activity. Each energy-use category is described by a number of parameter values corresponding to standard powers and runtime of appliances used for performing activities within it (fig. 2, right). There are two main schemes describing how energy is consumed while performing activities (fig. 2, left). The first one includes activities that consume energy while they are being performed, like cooking, watching TV or using the radio. The second scheme refers to activities that start consuming energy for a period of time after the activity has been completed, like starting the washing machine or dishwasher. Based on these energy use schemes and the energy type parameter values for

power consumption, power demanding activities can be highlighted within VISUAL-TimePAcTS/energy use and load curves can be computed and drawn.

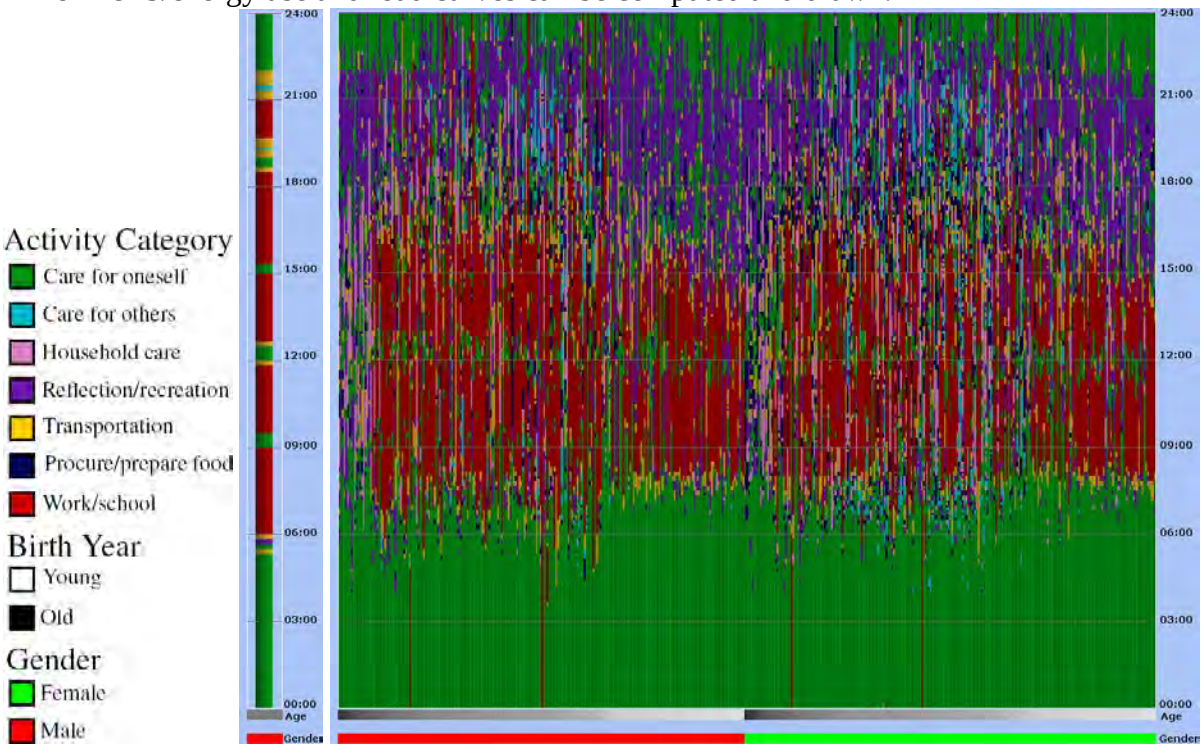

Figure 1. The time geographical representation principle used for visualizing activity diaries. The colour legend to the left shows the colour correspondence of the activities and the sorting variables, a single individual's diary is shown in the middle, and a population of 463 individuals' diaries is shown to the right. Each individual is represented by a stacked bar composed of the sequence of activities she performs during the day (middle). The activities are coloured according to the colour legend (left). Time is represented on the y-axis going upward, and individuals are drawn along the x-axis sorted by gender and age (see legends in the bottom of the figure and colour legend in the left). In the population representation (right) the dominance of sleep during night-time hours (green, care for oneself) and work/school activities (red) during daytime hours is prominent. Travel to work/school in the morning and back in the afternoon is indicated by the yellow parts of the bars representing the individuals. In the evening, reflection/recreation activities (dark lilac) dominate, the most significant of them being watching TV. Dark blue indicates activities to procure and prepare food.

3. Electricity use derived from daily activities

VISUAL-TimePAcTS/energy use makes it possible to reveal the following aspects of electricity use in everyday life of individuals:

- which activities relate to electricity use
- the time of the day when these activities that demand electricity use are performed
- the distribution in the population of these activities (age and gender)
- power load curves displaying the mean electricity use per person in the population

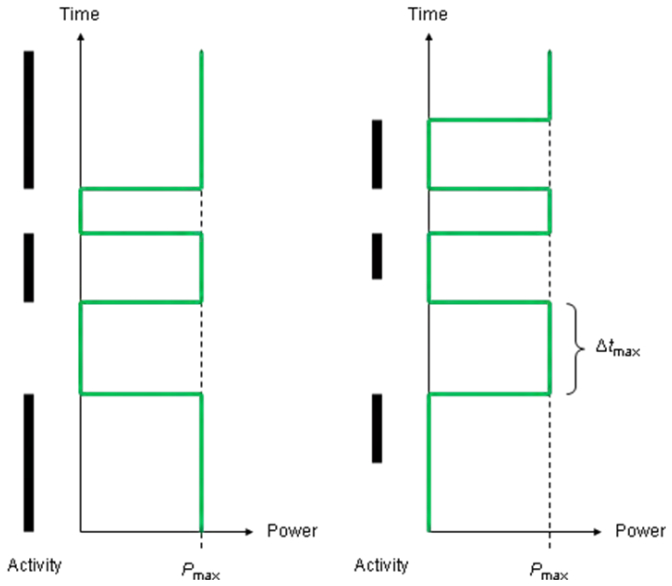

	Power	Runtime	Color
Audio	100	--	
Cleaning	1000	--	
Computer	100	--	
Cooking	1500	--	
TV	200	--	
Ironing	1000	--	
Washing	490	130	
Dishwashing	430	160	
Drying	1650	90	

Figure 2. Left: The left scheme in the left part of the figure shows that a constant power Pmax is demanded during use, while the scheme to the right in the left figure shows that the power demand starts after the activity is finished and goes on until a limiting time Δtmax has elapsed. (Widén 2009). Right: Parameters used for electricity demand and runtime of appliances according to the two schemes, and the colour legend for load curves.

In this paper we investigate the energy use patterns of activities related to "cooking" and "information and communication" using representations created through VISUAL-TimePAcTS/energy use.

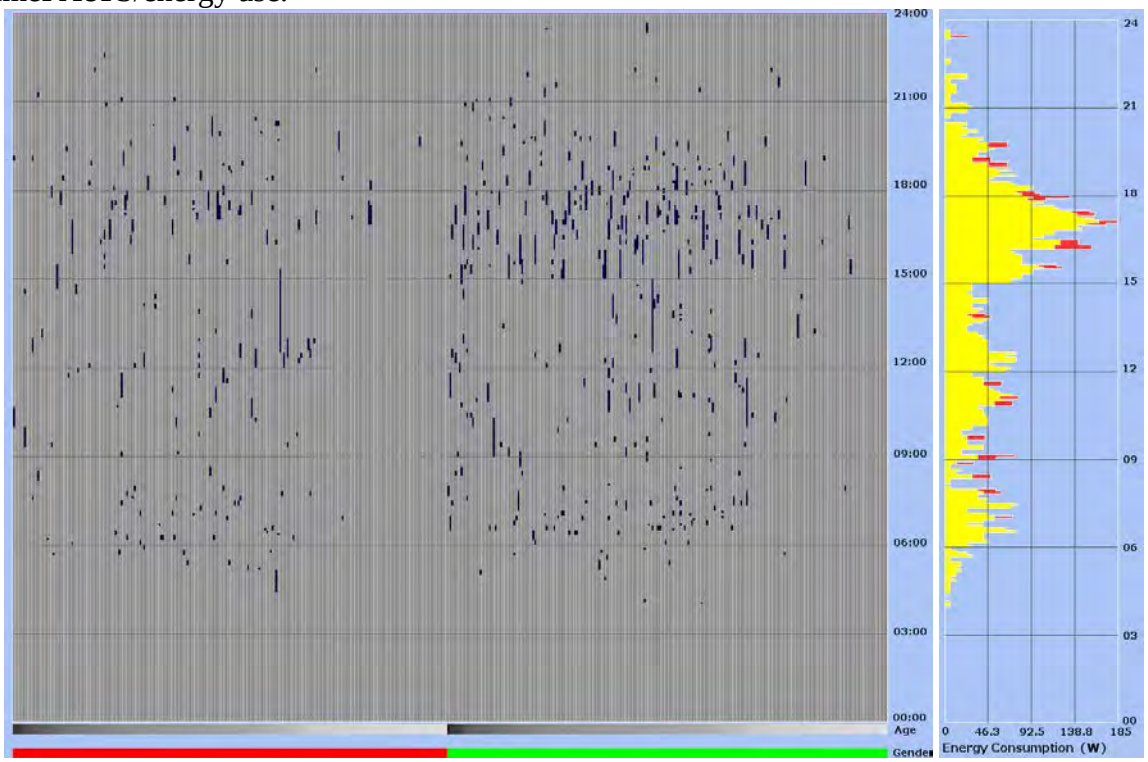

Figure 3. Left: Distribution pattern of cooking and dishwashing activities. Right: Corresponding power load curve showing electricity use in Watt per person in 5 minute intervals (yellow for cooking, red for dishwashing, max ~185 W/person).

Figure 3 shows the distribution of cooking and dishwashing activities (left) and the corresponding load curve (right) of these activities. There is a peak in the late afternoon, smaller peaks in the morning and at lunchtime. These activities are predominantly performed by women, very few children and older men are doing them.

In figures 4 and 5 the activity pattern related to individuals' use of information and communication technologies (TV, computer and radio) is shown. Figure 4 reveals computer use (computer play), which is predominantly performed by younger persons, and especially boys (doing this activity as a main activity). Among women there are some turquoise activity indicators showing that they play with their children who play with the computer (the main category of these activities is "Care for others").

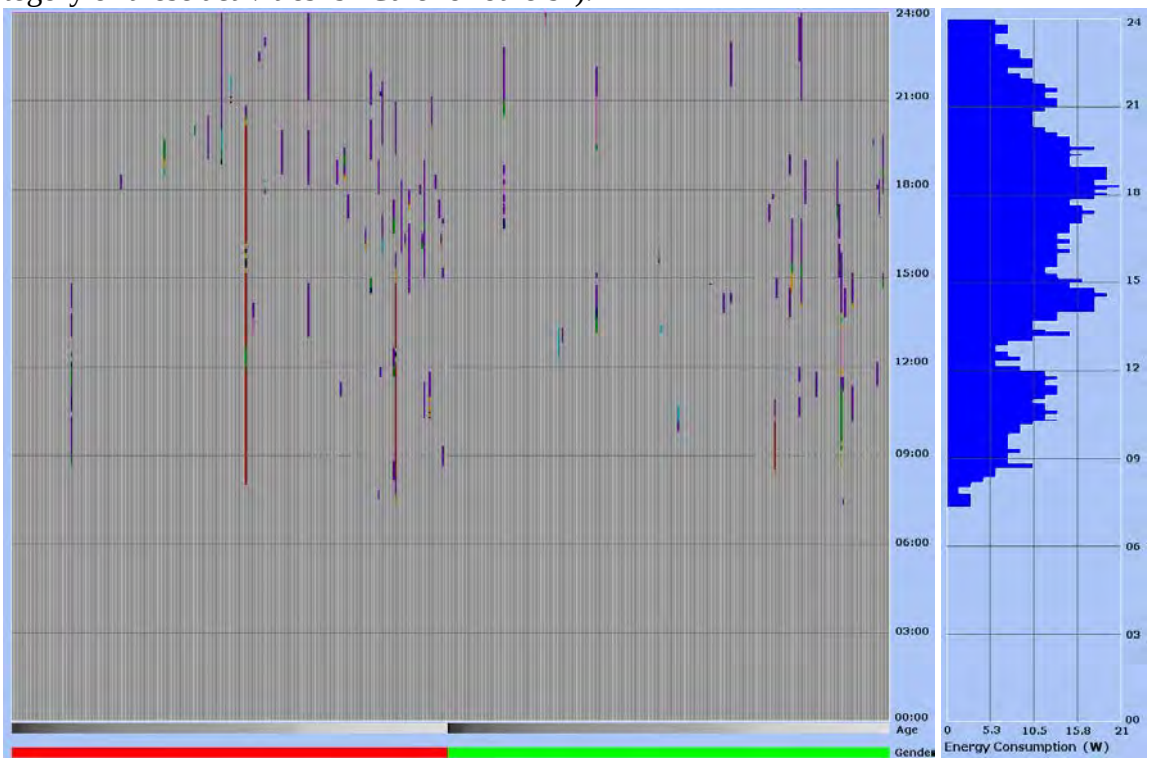

Figure 4. Left: Distribution pattern of activities claiming computer use. Right: Corresponding power load curve for computer use showing electricity use in Watt per person in 5-minutes intervals (max ~21 W/person).

Figure 5 shows the difference between electricity use generated by the activity watch TV and listen to radio (TV and radio as main activity) and electricity use generated by having the TV-set or the radio turned on while doing something else (TV and radio as secondary activities). Most people watch TV as a main activity in the evenings (fig. 5 bottom left), in the afternoon it is mostly girls, boys and old men who watch TV. Among older women and children the TV is also on while they do other things. The frequency curves for TV and radio activities show the total number of people performing them as main activities during the course of the day (fig. 5 left, in dark lilac), while the load curves for these activities show the mean power consumed per person (fig. 5 right, in pinkish for TV and red for radio) and consider also them performed as secondary activities. For this reason the two curves are different. Figure 5 right, also shows what main activity people perform when they listen to radio, which reveals that the radio is, to a great extent, on while working (red) and at breakfast time (green in the morning) – and this goes for people of all ages and both men and women. There is a big difference between TV and radio in this respect: radio is turned on much more than the TV when people do something else.

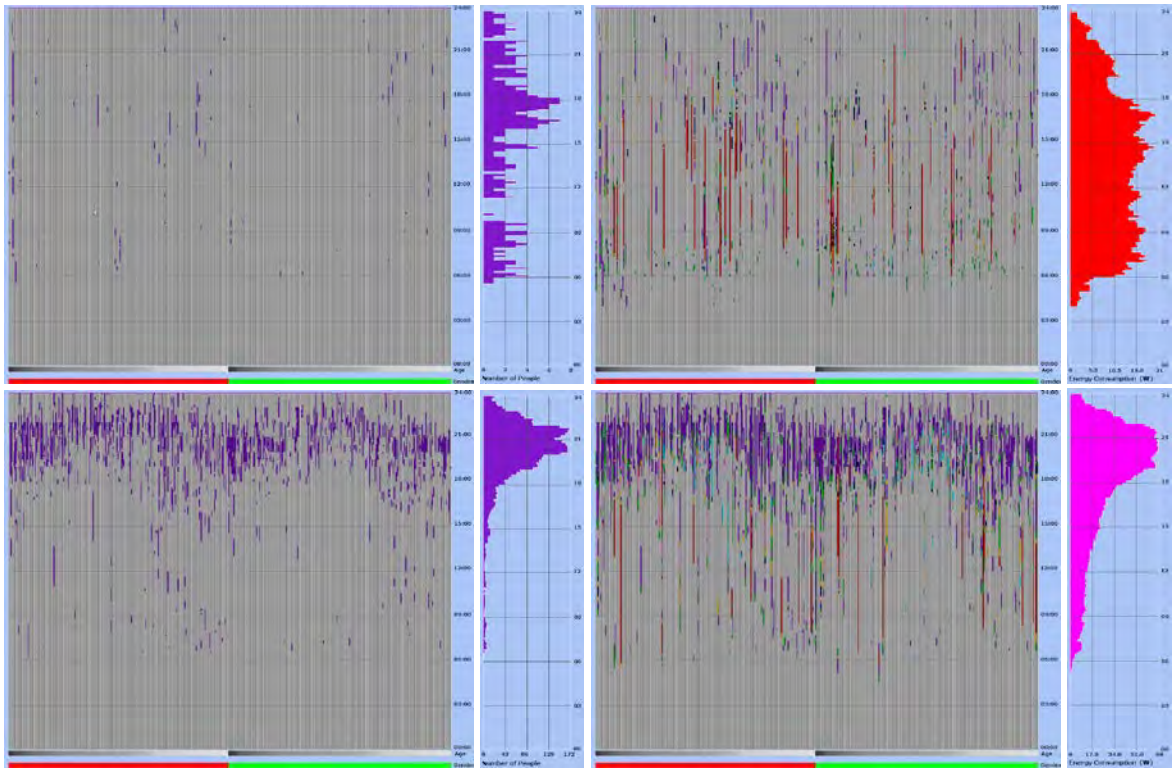

Figure 5. ***Top:*** *Left: Activity pattern and frequency graph for listening to radio as a main activity (max 7 persons at a time). Right: Activity pattern and power load curve for radio use (main and secondary activity) in Watt per person in 5 minute intervals (max ~ 70 W/person).* ***Bottom****: Left: Activity pattern and frequency graph for watching TV as a main activity (max 170 persons at a time). Right: Activity pattern and power load curve for TV use (main and secondary activity) in Watt per person in 5 minute intervals (max ~ 70 W/person).*

In figure 6 the total electricity use generated by using appliances for satisfying the need of information and communication (radio, computer and TV) and for food preparation (cooking and dishwashing) is visualized. The max load is about 250 W/person and it appears in the late afternoon, when cooking, TV, computer use and listening to radio appear at the same time. This figure makes it clear that it is cooking activities (the yellow load curve) that demand most electricity. Also clearly shown is that cooking and watch TV have distinct peak hours; especially in the afternoon of weekdays. Due to its mass performance, also watching TV generates a substantial energy demand in the evening hours.

4. Results

The VISUAL-TimePAcTS/energy use method helps reveal collective activity patterns at aggregate level, while at the same time it can help identify differences within groups (here men and women of different ages). In this paper we have demonstrated the potential of the method by investigating the energy consumption patterns generated by activities related to cooking, information and communication.

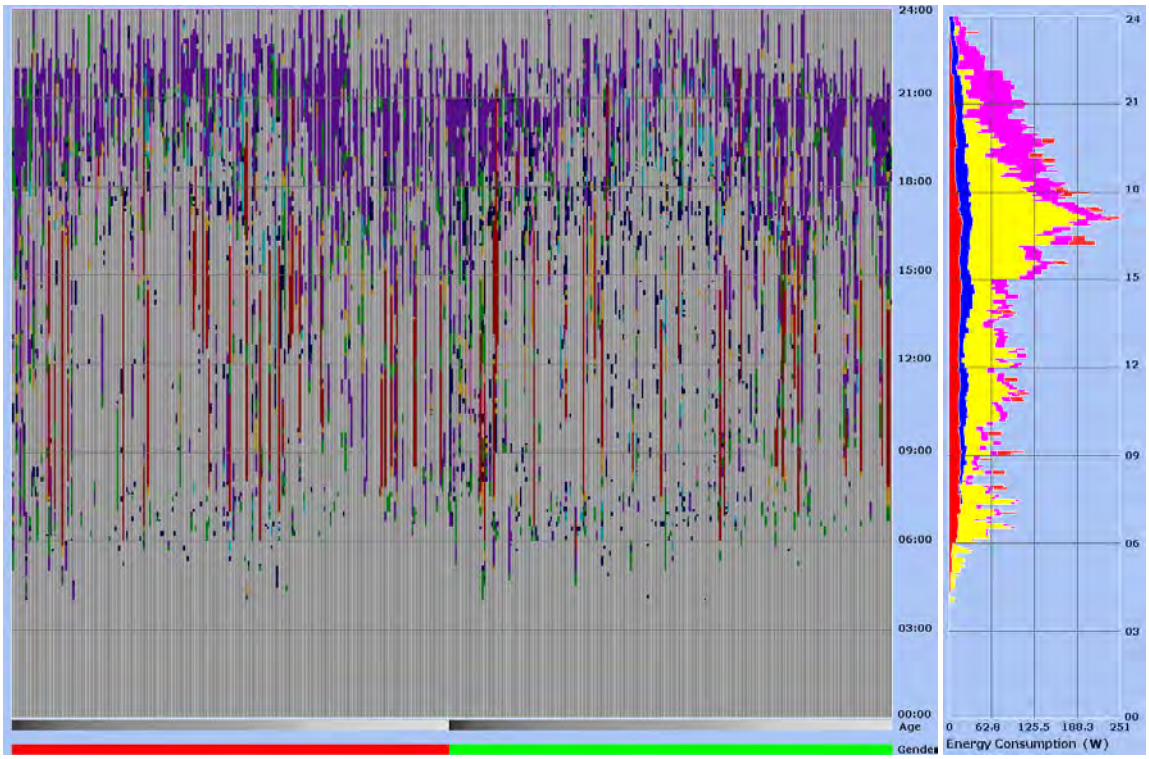

Figure 6. Left: Distribution pattern of all activities claiming the use of the considered electric appliances; TV, radio, computer, kitchen appliances. Right: Corresponding power load curve showing electricity use in Watt per person in 5 minute intervals (max ~250 W/person).

Through this example it becomes obvious that cooking is a daily activity that is to a large extent female gendered. Also shown is that children do not cook. The use of the TV-set is more equally divided between genders and is primarily performed in the evenings, but it differs with respect to age –younger people watch TV also in the afternoon after school. There were big differences between ages when it comes to computer use which was dominated by boys. Listening to radio was more evenly spread over the day, and between ages and gender. Finally, watching TV and especially listening to radio are activities that allow people to do other things and are often performed as secondary activities. This is especially true for listening to radio, an activity that seldom appear in its own right.

5. Conclusions and recommendation

The knowledge that can be acquired from representations created through VISUAL-TimePAcTS/energy use can be useful when policy makers and energy companies try to target information in order to reduce energy use and make it more efficient. For example, in a household with a man and a woman where the man receives the electricity bill, the man might not be the ideal receiver of attached information about energy-efficient cooking because, as we have seen, women cook more often. Information directed to women would perhaps be more effective. However, such directed information faces the risk of being too generalized and not reflecting the diversity between households in terms of both habits and family constellations. This particular analysis is also limited because of the relatively old data.

In general, the visualizations can be used to improve knowledge about what purpose people utilize electric appliances for. At individual and household levels the method can be utilized for communicating energy efficiency advice since it is easy for the individuals to recognize

their own daily life in the visualizations of their time-diaries. In order to improve its general applicability, the method will be extended with a module for heating, hot water use and energy use for daily transportation. The method can serve as complement, and maybe also as substitute, to expensive metering studies.

References

[1] Lindén, Anna-Lisa, Carlsson-Kanyama, Annika & Eriksson, B (2006), Efficient and inefficient aspects of residential energy behavior. What are the policy instruments of change", *Energy Policy*, 34, 1918-1927.

[2] Lindén, Anna-Lisa (2007) *Hushållens energianvändning och styrmedelsstrategier*, Report ER 2007:41, Swedish Energy Agency, Eskilstuna, Sweden.

[3] Ellegård, Kajsa & Cooper, Matthew (2004) Complexity in daily life: A 3D visualisation showing activity patterns in their contexts. *eIJTUR*, 37, 37–59.

[4] Ellegård, Kajsa & Vrotsou, Katerina (2006) Capturing patterns of everyday life – presentation of the visualization method VISUAL-TimePAcTS, Paper presented at the IATUR Annual Conference 2006. Copenhagen.

[5] Vrotsou, Katerina, Ellegård, Kajsa & Cooper, Matthew (2009) Exploring time diaries using semi-automated activity pattern extraction. *Electronic International Journal of Time Use Research 2009, Vol. 6, No. 1, 1-25.*

[6] Ellegård, Kajsa, Vrotsou, Katerina & Widén, Joakim (2010) VISUAL-TimePAcTS/energy use – a software application for visualizing energy use from activities performed. Paper presented at the Scientific session, Energitinget, Stockholm Älvsjö Fairs. March 2010 (http://works.bepress.com/dr_erik_dahlquist/6/)

[7] Vrotsou, Katerina (2010) *Everyday mining. Exploring sequences in event-based data*. Linköping studies in Science and technology. Dissertations no 1331. Linköping University, Sweden

[8] Gram-Hanssen, Kirsten (2004) Different Everyday Lives – Different Patterns of Electricity Use. In: *Proceedings of the 2004 American Council for an Energy Efficient Economy. Summer study in Buildings*. Washington DC: ACEEE.

[9] Hägerstrand, Torsten (1974) Tidsgeografisk beskrivning - syfte och postulat. *Svensk Geografisk Årsbok* 50, 86-94.

[10] Hägerstrand, Torsten (1985) Time-Geography. Focus on the Corporeality of Man, Society and Environment. *The Science and Praxis of Complexity.* The United Nations University, Tokyo, pp 193-216. French translation in *Science et pratique de la complexité La Documentation Francaise*, Paris 1986, pp 225-250

[11] Hägerstrand, Torsten & Lenntorp, Bo (1993) Region och miljö - sammanfattning av ett projekt om ekologiska perspektiv på den rumsliga närings- och bosättningsstrukturen, *NordREFO* 1993:5. pp 229-237.

[12] Hägerstrand, Torsten (2009) *Tillvarovären*. (K Ellegård & U Svedin Eds). Forskningsrådet Formas, Stockholm.

[13] Widén, Joakim (2009) Distributed Photovoltaics in the Swedish Energy System. Model Development and Simulations. Licentiate Thesis, Uppsala University, Sweden.

[14] Widén, Joakim (2010) System Studies and Simulations of Distributed Photovoltaics in Sweden. PhD Thesis, Uppsala University, Sweden.

Providing a Heating Degree Days (HDDs) Atlas across Iran Entire Zones

M. Mehrabi[1,*], A. Kaabi-Nejadian [1,2], M. Khalaji Asadi[1]

[1]*Department of Environment and Energy, Science and Research Branch, Islamic Azad University, Tehran, Iran*
[2]*Renewable Energy Organization of Iran, Ministry of Energy, Tehran, Iran*
** Corresponding author. Tel: +98912 6431993, Fax: +9821 44696541, E-mail: meh_mehrabi@yahoo.com*

Abstract: Considering fossil fuels depletion and increasing of energy demand in Iran, a special attention is required toward the energy conservation. Energy demand of building section in Iran is very high, which is as a result of many factors such as governmental huge subsidies for energy, lack of energy conservation culture in building inhabitants, poor insulation of buildings and poor heating or cooling control systems.
Most of buildings heating control systems in Iran do not respond properly to weather temperature changes during winters, therefore most of the time the interior temperature of these buildings exceed the comfort temperature, thus these buildings are not energy efficient and consume excessive amount of energy. The most important index to identify these buildings across the country is to know HDDs for each point of the country.
Unfortunately, up to now no comprehensive research has been conducted in Iran about HDDs, and thus no HDDs atlas has been provided, therefore it is essential for energy managers, engineers and in particular for the government to be supplied with HDDs for each point of Iran. By taking this fact into account, we decided to prepare a comprehensive HDDs atlas for Iran entire zones.
In this paper authorized temperature databases of 255 meteorological stations in 30 provinces of Iran have been collected from Iran meteorological organization, thereafter HDDs for each station were calculated, then a mathematical modeling (multiple regression analysis technique) was employed in order to simulate the HDDs of other places in Iran. Consequently, a HDDs Atlas across Iran entire zones was provided.
These results can widely be used in energy consumption planning and prediction of the heating energy demand in buildings and enhances the government abilities to manage the rate of energy consumption in buildings.

Keywords: *Iran heating HDDs atlas, Energy management.*

Nomenclature

HDDs	*Heating Degree Days ..... °C·day*	*Lat*	*latitude ..... °N*
T_b	*base temperature ..... °C*	*Long*	*longitude ..... °E*
T_{mean} *.....*	*daily mean temperature*	*Alt °C*	*Altitude ..... m*

1. Introduction

Unfortunately, until now no comprehensive research about HDDs has been conducted in Iran. In this paper authorized daily temperature databases of 255 meteorological stations in 30 provinces of Iran have been collected, thereafter the annually HDDs for each station were calculated. Then a mathematical modeling (multiple regression analysis technique) was employed to simulate the HDDs of other places. Consequently, a HDDs Atlas across Iran was provided.

2. Methodology

Fundamentally HDDs are a summation of the differences between the outdoor temperature and base temperature over a specified time period. HDDs are a useful tool that can be used in the assessment of weather related energy consumption in buildings, according to Eq. (1).

Heating energy demand (kWh) =
Overall heat loss coefficient ($kW \cdot °C^{-1}$) × HDDs ($°C \cdot day$) × 24 ($h \cdot day^{-1}$)
(The 24 is included to convert from days to hours.) (1)

In current study accessible authorized daily temperature databases have been collected from 255 meteorological stations (Fig. 1) during last 5 years.

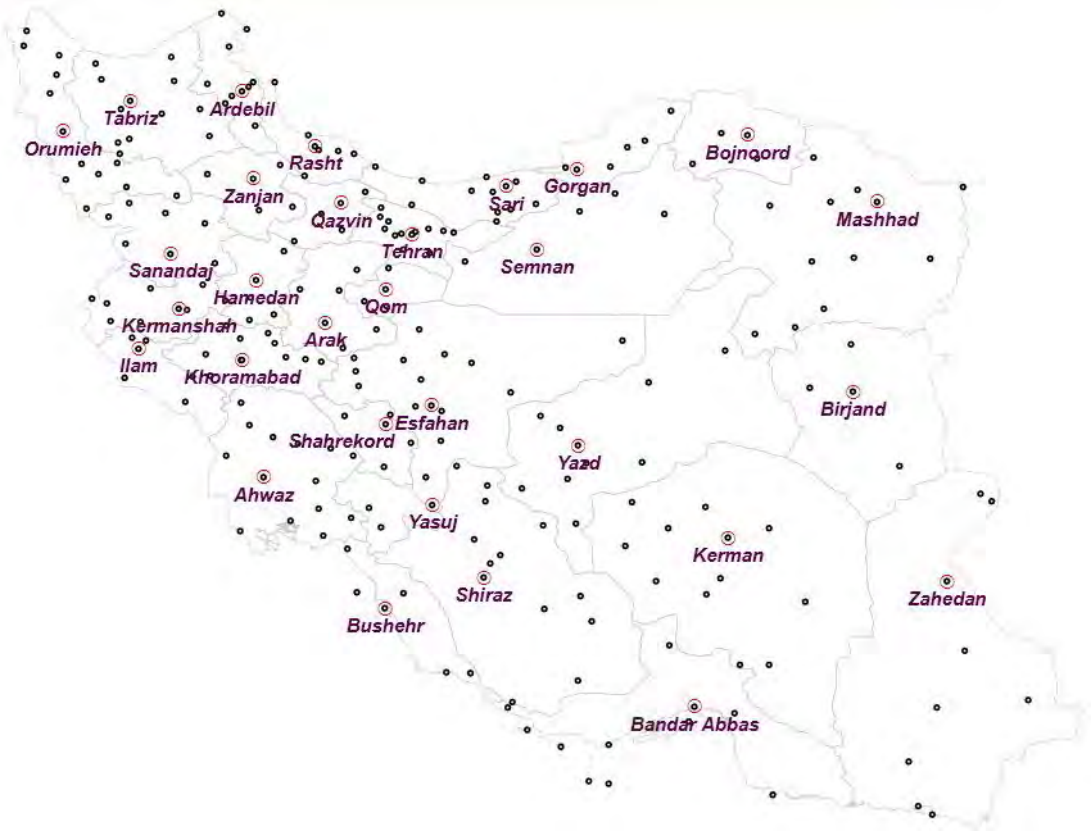

Fig. 1. Location of 255 Iran official meteorological stations in 30 provinces.

In this paper mean daily temperature method has been employed that is generally used in countries, such as USA [1] and Germany [2], where HDDs are calculated from the mean daily temperature. This makes the definition and calculation of HDDs simpler, and makes the reasonable assumption that efficient heating systems do not operate on days where outdoor temperature averages exceed the base temperature [3]. In this method we have applied Eq. (2).

$$\begin{cases} HDDs = T_b - T_{mean} & \text{if} \quad T_b > T_{mean} \\ HDDs = 0 & \text{if} \quad T_b \leq T_{mean} \end{cases}$$

(Based on local conditions, we assume $T_b = 18°C$) (2)

To calculate HDDs, at first the mean temperature was calculated for each day of the year, Thereafter, by applying Eq. (2) HDDs were calculated. Then by summation of HDDs during each year, we obtained annually HDDs during 5 years, subsequently annually HDDs average during this period attained (Table.1.).

Afterwards by computerizing the calculated HDDS, spline multiple regression analysis technique was employed in order to simulate the annual HDDs over each other point of country. In this method, a two dimensional function (surface) has been constructed closely fits range of a discrete set of known data points (HDDS in 255 stations), so we could estimate HDDs values in other points of country. Spline surfaces are very popular in computerized regression because of the simplicity of their construction, their ease and accuracy of evaluation, and their capacity to approximate complex shapes through surface fitting and interactive design [4]. In this paper by constructing spline surface from calculated HDDs, the comprehensive HDDs Atlases were provided (Fig.2. and Fig.3.).

3. Results

In Table 1, for each 255 meteorological stations longitude, latitude, elevation and calculated annual HDDs average have been determined. These results show various kinds of climate zones in Iran.

Table 1. Calculated annual HDDs in Iran meteorological stations.

Station Name	Lat	Long	Alt	HDDs	Station Name	Lat	Long	Alt	HDD
Abadan	30.37	48.25	7	428	Boinzahra	35.77	50.07	1282	2098
Abadeh	31.18	52.67	2030	2076	Bojnoord	37.47	57.32	1091	2319
Abali	35.75	51.88	2465	3544	Bonab	37.33	46.07	1290	2549
Abarkuh	31.13	53.28	1524	1387	Bookan	36.53	46.22	1386	2600
Abbor	36.93	48.97	703	1503	Borazjan	29.25	51.17	90	263
Abumusa island	25.83	54.83	7	5	Borujen	31.95	51.30	2197	2937
Aghda	32.43	53.62	1150	1173	Borujerd	33.92	48.75	1629	2184
Ahar	38.43	47.07	1391	2869	Bostan	31.72	48.00	8	550
Ahwaz	31.33	48.67	23	406	Bostan Abad	37.85	46.85	1750	3533
Alasht	36.08	52.85	190	2820	Bushehr	28.98	50.83	20	253
Aleshtar	33.82	48.25	1567	2476	Chahbahar	25.28	60.62	8	12
Aliabad	36.90	54.87	140	1414	Chalderan	39.07	44.38	1788	3811
Aligudarz	33.40	49.70	2022	2649	Chitgar	35.70	51.13	1215	1737
Amol	36.47	52.38	24	1333	Damavand	35.72	52.07	1960	2928
Anar	30.88	55.25	1409	1337	Damqan	36.10	54.32	1155	1801
Anzali	37.47	49.47	-26	1408	Darab	28.75	54.53	1140	777
Aqdasieh	35.78	51.62	1548	1911	Daran	32.97	50.37	2290	3042
Arak	34.10	49.77	1708	2363	Darehshahr	33.13	47.40	670	1065
Ardebil1	38.33	48.40	1314	3414	Dashtenaz	36.63	53.18	20	1318
Ardebil2	38.25	48.28	1332	3049	Dayyer	27.83	51.93	4	100
Ardestan	33.38	52.38	1252	1466	Dehdasht	30.78	50.55	820	889
Astara	38.42	48.87	-18	1676	Dehdoz	31.72	50.27	1457	1448
Avaj	35.57	49.22	2035	3087	Dehloran	32.68	47.27	232	473
Azna	33.45	49.42	1872	2801	Delijan	33.98	50.68	1524	1964
Babolsar	36.72	52.65	-21	1196	Deylaman	30.05	50.17	4	359
Badrabad	33.43	48.27	1155	1619	Dezful	32.27		83	523
Bafq	31.60	55.43	991	950	Dogonbadan	30.43	50.77	700	711
Baft	29.23	56.58	2280	1837	Dorud	33.48	49.07	1527	1953
Bam	29.10	58.35	1067	628	Doshantappeh	35.70	51.33	1209	1433
Bandar Abbas	27.22	56.37	10	86	Eivane Qarb	33.83	46.32	1170	1675
Bandar Torkaman	36.88	54.07	-20	1314	Eqlid	30.90	52.63	2300	2371
Baneh	36.00	45.90	1600	2459	Esfahan	32.62	51.67	1550	1952
Bavanat	30.47	53.67	2231	2148	Esfarayen	37.05	57.48	1216	2172
Behbahan	30.60	50.23	313	537	Eslam abad	34.12	46.47	1349	2276
Beshruyeh	33.90	57.45	885	1450	Fasa	28.97	53.68	1288	1142
Biarjmand	36.05	55.83	1106	1905	Ferdos	34.02	58.17	1293	1587
Bijar	35.88	47.62	1883	3014	Firuzkuh	35.92	52.83	1976	3479
Bileh Savar	39.37	48.37	90	1937	Gariz	31.30	54.10	2100	2194
Birjand	32.87	59.20	1491	1651	Garmsar	35.20	52.27	825	1444

Table 1 (continued). Calculated annual HDDs in Iran meteorological stations.

Station	Lat	Long	Alt	HDDs	Station	Lat	Long	Alt	HDDs
Geophysics	35.73	51.38	1419	1725	Kish island	26.50	53.98	30	17
Germi	39.05	48.05	749	2222	Komijan	34.70	49.32	1741	2734
Gilaneqarb	34.13	45.93	816	1167	Kuhdasht	33.53	47.63	1200	1818
Golmakan	36.48	59.28	1176	2259	Kuhrang	32.43	50.12	2285	3398
Golpayegan	33.47	50.28	1870	2318	Kushk Nosrat	35.08	50.90	948	1292
Gonabad	34.35	58.68	1056	1646	Lahijan	37.18	50.00	86	1445
Gonbade Kavous	37.25	55.17	37	1252	Lalehzar	29.52	56.83	2775	3127
Gorgan	36.85	54.27	13	1338	Lamerd	27.30	53.12	411	353
Haji Abad	28.32	55.92	931	638	Lar	27.68	54.28	792	561
Hamedan	34.87	48.53	1742	2805	Lavan	26.80	53.38	22	26
Hashtgerd	36.00	50.75	1613	2314	Lengeh	26.53	54.83	23	40
Hendijan	30.28	49.73	3	440	Lordegan	31.52	50.82	1580	1865
Hoseinieh	32.67	48.27	354	494	Mahabad	36.77	45.72	1385	2435
Ilam	33.63	46.43	1337	1776	Mahneshan	36.77	47.67	1282	2305
Imam Airport	35.42	51.17	990	1675	Mahshahr	30.55	49.15	6	409
Iranshahr	27.20	60.70	591	248	Makoo	39.33	44.43	1411	3126
Izadkhast	31.53	52.12	2188	2299	Malayer	34.25	48.85	1778	2459
Izeh	31.85	49.87	767	913	Malekan	37.13	46.10	1300	2501
Jajerm	36.95	56.33	984	1966	Maneh	37.50	56.85	890	1962
Jam-Tohid	27.82	52.37	655	534	Manjil	36.73	49.40	333	1343
Jask	25.63	57.77	5	10	Marand	38.47	45.77	1550	2891
Jolfa	38.75	45.67	736	2363	Maraqeh	37.40	46.27	1478	2445
Kabutar Abad	32.52	51.85	1545	1885	Maravetappeh	37.90	55.95	460	1409
Kahak	34.40	50.87	1403	1884	Marivan	35.52	46.20	1287	2463
Kahnooj	27.97	57.70	470	304	Marvast	30.50	54.25	1547	1415
Kalaleh	37.37	55.48	150	1324	Mashhad	36.27	59.63	999	1904
Kaleibar	38.87	47.02	1180	2540	Masjed	31.93	49.28	321	535
Kangavar	34.50	47.98	1468	2518	Mehran	33.12	46.18	150	711
Karaj	35.92	50.90	1313	2003	Mehriz	31.58	54.43	1520	1319
Kashan	33.98	51.45	982	1498	Meshkin	38.38	47.67	1569	2951
Kashmar	35.20	58.47	1110	1588	Meybod	32.22	53.97	1108	1411
Kenarak	25.43	60.37	12	41	Meymeh	33.43	51.17	1980	2742
Kerman	30.25	56.97	1754	1538	Miandoab	36.97	46.05	1300	2586
Kermanshah	34.35	47.15	1319	2012	Mianeh	37.45	47.70	1110	2359
Khalkhal	37.63	48.52	1796	3566	Minab	27.10	57.08	30	62
Khansar	33.23	50.32	2300	2752	Moallemkelay	36.45	50.48	1629	2325
Khark	29.27	50.33	4	205	Murche Khort	33.08	51.48	1669	1927
Khash	28.22	61.20	1394	914	Nahavand	34.15	48.42	1681	2398
Khodabandeh	36.12	48.58	1887	3037	Nahbandan	31.53	60.03	1211	1179
Khomein	33.65	50.08	1835	2346	Najafabad	32.60	51.38	1641	1798
Khor Birjand	32.93	58.43	1117	1316	Namin	38.42	48.48	1450	3055
Khoramabad	33.43	48.28	1148	1625	Naqdeh	36.95	45.42	1338	2598
Khoramdarreh	36.18	49.18	1575	2584	Natanz	33.53	51.90	1685	1993
Khorbiabanak	33.78	55.08	845	1186	Nayin	32.85	53.08	1549	1692
Khoy	38.55	44.97	1103	2660	Nayyer	38.03	47.98	1600	2932
Kiasar	36.23	53.53	1294	2263	Neyriz	29.20	54.33	1632	1149

Table 1 (continued). Calculated annual HDDs in Iran meteorological stations.

Station Name	Lat	Long	Alt	HDDs	Station Name	Lat	Long	Alt	HDDs
Neyshabur	36.27	58.80	1213	2129	Saravan	27.33	62.33	1195	655
Nikshahr	26.23	60.20	510	91	Sardasht	36.15	45.50	1670	2429
Noshahr	36.65	51.50	-21	1415	Sare Ein	38.17	48.10	1632	3303
Nourabad	34.05	48.00	1859	2798	Sari	36.55	53.00	23	1225
Omidieh	30.77	49.65	35	437	Sarpolezahab	34.45	45.87	545	1075
Orumieh	37.53	45.08	1316	2694	Saveh	35.05	50.33	1108	1600
Parsabad	39.65	47.92	32	1922	Semirom	31.33	51.57	2274	2568
Parsian	27.20	53.03	70	84	Semnan	35.42	53.55	1131	1610
Payam Karaj	35.78	50.83	1261	2153	Shahdad	30.42	57.70	400	447
Piranshahr	36.67	45.13	1455	2513	Shahrebabak	30.10	55.13	1834	1870
Poldokhtar	33.15	47.72	714	899	Shahrekord	32.28	50.85	2049	3020
Polesefid	36.13	53.08	610	1703	Shahreza	31.98	51.83	1845	2067
Qaen	33.72	59.17	1432	2001	Shahriar	35.67	51.02	2986	1817
Qarakhil	36.45	52.77	15	1348	Shahrud	36.42	54.95	1345	1956
Qare Ziaeddin	38.90	45.02	1108	2724	Shiraz	29.53	52.60	1484	1331
Qasre Shirin	34.53	45.60	376	860	Shushtar	32.05	48.83	67	390
Qazvin	36.25	50.05	1279	2168	Siahbisheh	36.22	51.32	2165	2881
Qeshm island	26.95	56.27	13	64	Silakhor	33.73	48.87	1497	2186
Qom	34.70	50.85	877	1553	Siri island	25.88	54.48	4	12
Qorveh	35.17	47.80	1906	2887	Sirjan	29.47	55.68	1739	1419
Quchan	37.07	58.50	1287	2509	Sonqor	34.78	47.58	1700	2568
Rafsanjan	30.42	55.90	1581	1270	Tabas	33.60	56.92	711	929
Ramhormoz	31.27	49.60	151	406	Tabriz	38.08	46.28	1361	2555
Ramsar	36.90	50.67	-20	1376	Tafresh	34.68	50.02	1979	2582
Rasht1	37.27	49.58	-10	1507	Takab	36.38	47.12	1765	3353
Rasht2	37.20	49.65	37	1457	Takestan	36.05	49.70	1283	2199
Ravansar	34.72	46.65	1380	2159	Takhtjamshid	29.93	52.90	1605	1487
Razan	35.38	49.03	1840	2902	Taleqan	36.17	50.77	1857	2920
Robat	33.03	55.55	1188	1378	Tehran	35.68	51.32	1191	1495
Rudan	27.97	57.18	220	84	Torbate Hey.	35.27	59.22	1451	2230
Rudsar	37.13	50.28	-19	1463	Torbate Jam	35.25	60.58	950	1969
Sabzevar	36.20	57.72	978	1669	Tuyserkan	34.55	48.43	1783	2471
Sad Dorudzan	30.22	52.43	1620	1482	Varamin	35.35	51.63	927	1603
Sahand	37.93	46.12	1641	2783	Yasuj	30.83	51.68	1832	1927
Salafchegan	34.48	50.47	1381	1799	Yazd	31.90	54.28	1237	1185
Salmas	38.22	44.85	1337	2955	Zabol	31.03	61.48	489	883
Saman	32.45	50.93	2057	2541	Zahak	30.90	61.68	495	838
Sanandaj	35.33	47.00	1373	2244	Zahedan	29.47	60.88	1370	1093
Saqez	36.25	46.27	1523	3015	Zanjan	36.68	48.48	1663	2884
Sarab	37.93	47.53	1682	3517	Zarand	30.80	56.57	1670	1422
Sarableh	33.78	46.57	1045	1513	Zarineh Obato	36.07	46.92	2143	3814
Sarakhs	36.53	61.17	235	1516	Zarqan	29.78	52.72	1596	1574
Sararud	34.33	47.30	1362	2118					

Then spline method was applied to construct interpolated surface from above discrete set of results, to provide below Atlases (Fig.2. and Fig.3.).

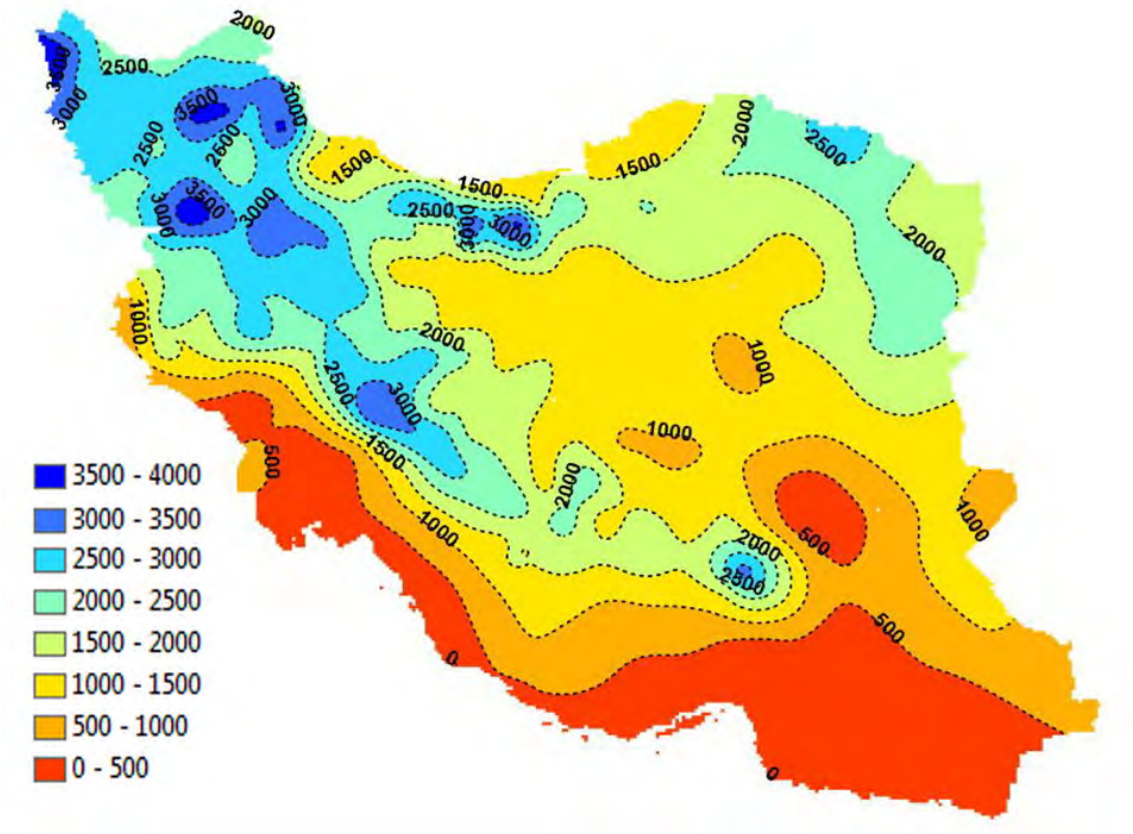

Fig. 2. Annual HDDs contours atlas over Iran entire zones, using spline interpolation

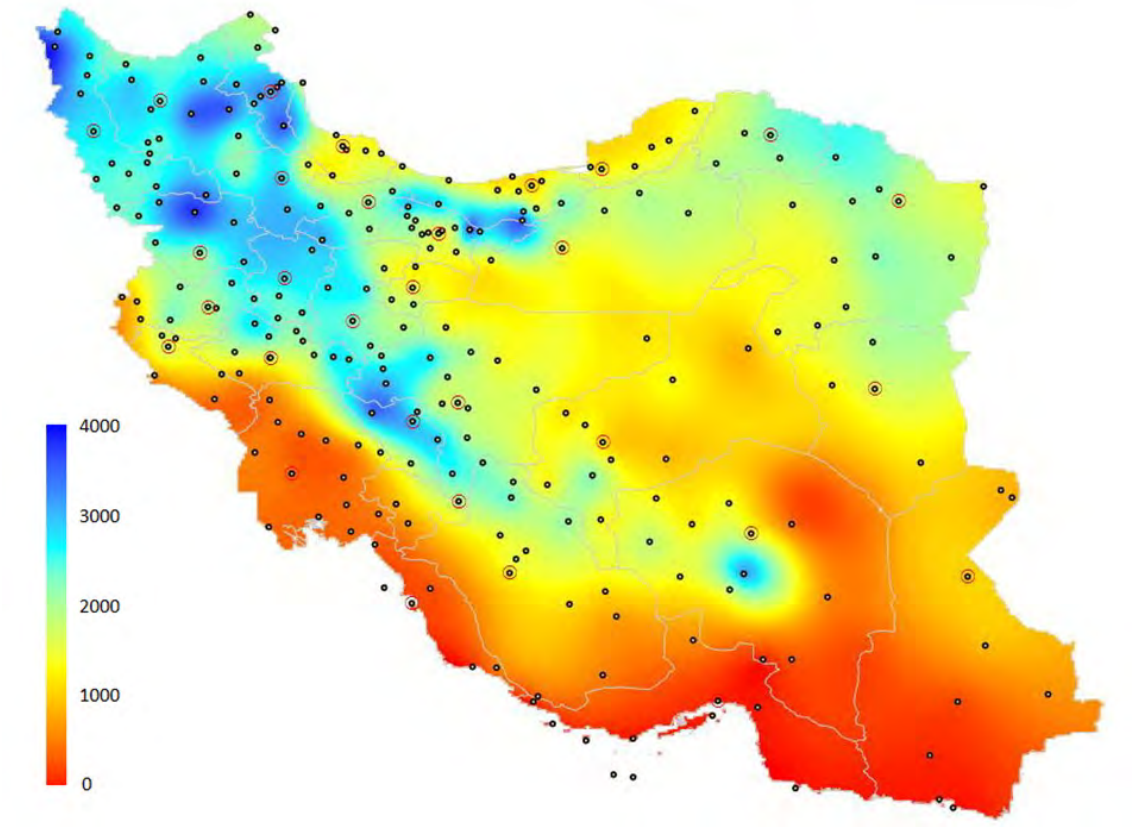

Fig. 3. Annual HDDs spectral atlas over Iran entire zones, using spline interpolation

The highest value of HDDs is in Zarineh Obato mountainous city (3814°C.day), in western region of Iran, and the lowest value of HDDs is in Abumusa island (5°C.day), in the southern region. This large difference in HDDs shows the intense contrast in the climatic characteristics between these two extreme geographic points (The gheographical specifications of each point have been indicated in Table.1).

High values of HDDs can be observed in blue zones, mainly in northwestern regions of country, such as Chalderan (3811°C.day), Khalkhal (3566°C.day), and Ardebil1 (3414°C.day), and some western regions such as Zarineh Obato (3814 °C.day) as mentioned before. All of these points are located beside Zagros mountain range. In addition they also can be observed in northern regions such as Firuzkuh (3479°C.day) because of locating beside Alborz mountain range.

Low values of HDDs can be observed in red zones, mainly in southern regions of country such as Jask Island (10°C.day) and Chahbahar (12°C.day) because of Persian Gulf and Oman Sea climatic effects. They also can be observed in eastern regions of country such as Kahnuj (304°C.day) because of locating beside Lut desert.

Fig.3 shows high contrast values of HDDs in Iran that introduces the exceptional climates over Iran. The uniqueness of these climates originates from several variables such as mountains and deserts especially Zagros and Alborz mountain ranges, Persian Gulf and Oman Sea, in addition unique deserts like Markazi and Lut. In country with these variations of climates, proposing appropriate HDDs can prevent higher escalation in energy consumption.

In Iran with governmental huge subsidies on n atural gas as a predominant heating energy carrier, government can set appropriate subsidies related on HDDs for each point of country.

4. Conclusions

HDDS over Iran entire zones, based on databases of 255 meteorological stations have been calculated and presented in a comprehensive table. Furthermore, contours and spectral atlas using spline interpolation have been demonstrated.

High contrast values of HDDs show the exceptional climates over Iran. In country with these variations of climates, proposing appropriate HDDs can prevent higher escalation in energy consumption.

References

[1] American Society of Heating, Refrigerating and Air-Conditioning Engineers, ASHRAE Handbook ,Fundamentals, Energy estimating and modeling methods, 2001, Ch.31 : Energy estimating and modeling methods.
[2] VDI, Economic efficiency of building installations, VDI 2067, Verein Deutscher Ingenieure.
[3] The chartered institution of building Services Engineers, Energy theory and applications, TM41-2006.
[4] Helmuth Späth, Two dimensional spline interpolation algorithms, A K Peters, Ltd., 1995.

Covariates of fuel saving technologies in urban Ethiopia

Abebe Damte[1]* and Steven F Koch[1]

University of Pretoria, Pretoria, South Africa
**Corresponding author: Email: abebed2002@yahoo.co.uk*

Abstract: The current government of Ethiopia has devised supply augmented and demand management strategies in order to reduce pressure on forests and the adverse impact of indoor air pollution. This paper tries to examine and understand the determinants of the speed of adoption of one of the demand side strategies, fuel saving technologies (Mirt and Lakech), in urban Ethiopia. The result of the duration analysis shows that income level is a significant factor in the adoption decision of the technologies. This indicates that households will not shift to other better sources of energy as their income increases, as postulated by the energy ladder hypothesis. Education is positively and significantly related to the speed of adoption of Mirt biomass cook stoves but its effect on adoption of Lakech charcoal stove is insignificant. Electric Mitad (substitute for Mirt *injera* stove) does not have any effect on the adoption of Mirt biomass cook stoves. However, ownership of Metal charcoal stove is negatively correlated with the adoption of Lakech charcoal stoves. This may suggest that there is a need to reconsider the promotion strategy given the better performance of Lakech charcoal stove over Metal charcoal stove. The implications of other covariates have also been discussed.

Keywords: *Improved stoves, Duration, Adoption, Ethiopia*

1. Introduction

The heavy dependence and inefficient utilization of biomass resources for energy have resulted in high depletion of the forest resources in Ethiopia (EPA, 2004). In order to reduce pressure on forests and plantations and the adverse impact of indoor air pollution, the government has devised supply augmented and demand management strategies. The supply side management deals with increasing the availability of fuel wood through distribution of free seedlings, plantations, supply restrictions, and enforcement of property rights. The demand side management deals with reducing the demand for biomass energy sources by promoting alternative modern fuels, promoting income growth and increasing the availability of fuel saving technologies such as improved biomass cooking stoves (Cook et al., 2008). Large scale distribution of improved stoves will help reduce pressure on biomass resources, increase land productivity by reducing crop residue and dung usage for fuel, and improve family health. The intervention benefits women and children in particular, minimizing their high workloads to collect and supply fuel wood, and their exposure to flame hazard, high smoke emission and harmful pollutants (EPA, 2004).[1] It is assumed that if all rural and urban households (estimated to be about 14.44 million) in Ethiopia shift to the improved *Lakech* and *Mirt* stoves[2], a saving of about 7,778,800 tones of fuel wood which requires clear cutting of 137,192.24 ha of forest will be achieved on an annual basis (EPA, 2004). This implies that

[1]The World Health Organization estimates that, each year, 1.6 million women and children in developing countries are killed by the fumes from indoor biomass stoves (IEA, 2004).

We are very grateful to Ato Melesaw Shanko, managing director of MEGEN Power Ltd, and W/t Hiwote Teshome from GTZ for making available the data analyzed in this paper. We also gratefully acknowledge their kind explanation for questions related to improved biomass cook stoves in Ethiopia. Thanks also go to Dr. Alemu Mekonnen who helped us in facilitating the process of getting the data used for this paper.

[2]Lakech and Mirt are local words which mean 'excellent' and 'best', respectively.

sufficient distribution of these improved stoves will have significant contribution to save the biomass resources of the country in general and forest resource in particular and to combat land degradation and mitigate the effects of drought (EPA, 2004).

By recognizing the benefits of improved stoves, a number of governmental and non-governmental institutions have been involved in the development and dissemination of different types of biomass stove technologies since early 1970s in the history of Ethiopia (EPA, 2004). However, the efforts by these institutions to disseminate various types of fuel saving technologies have faced different problems at different times. Some introduced improved biomass cook stoves were not successful due to problems related to the stove itself (technical problems), lack of understanding of consumer's taste, lack of appropriate promotion strategy, etc. Most of these inferences are based on qualitative assessments by various stakeholders and scholars working on the area of natural resource conservation and energy. Moreover, the available limited studies on technology adoption in general and improved biomass cook stoves technologies in particular in most developing countries have generally focused on applying the limited dependent variable models such as probit or logit models. Although informative, these types of specifications are static and ignore the dynamic nature of the adoption process. That means, the binary dependent variable (adoption or non-adoption), which is commonly applied in empirical works, does not pick up adoption over time, as it does not allow for household's different waiting times. In general, the available studies failed to examine and understand why some households take some time to adopt the technology while others are quick to adopt and exploit the benefits of using the technology. Therefore, this paper has tried to address this gap and employs a duration analysis. To our knowledge, this technique is applied for the first time in fuel saving technology adoption studies. The next section deals with explaining the methods of analysis. Section three presents the data and some descriptive statistics. The results of the empirical analysis are presented in section four. The last section is the conclusion.

2. Duration analysis

Analysis of duration data is often referred to as survival analysis. This term is mostly used in the medical research, analysis of child mortality, and unemployment. It has also been applied in the area of technology adoption (i.e. Hannan and MacDowell, 1984; Dadi et al., 2004 and Burton et al., 2003). The purpose of Duration Analysis is to statistically identify those factors which have a significant effect (both positive and negative) on the length of a spell. A spell starts at the time of entry into a specific state and ends at a point when a new state is entered. For details on duration analysis see Kiefer (1988) and Green (2003).

The presence of unobserved heterogeneity leads to bias in the estimates of duration dependence. Following Gutierrez (2002), we fit a Weibull regression model with gamma-distributed heterogeneity using the frailty (gamma) option to streg. One can estimate frailty models and test whether unobserved heterogeneity is relevant using likelihood ratio tests based on the results from a likelihood ratio test that STATA reports.

3. Data and descriptive statistics

3.1. The nature and source of data

The data for the empirical analysis come from the survey on 'Mirt Biomass Injera Stoves Market Penetration and Sustainability' study conducted by Megen Power Limited in 2009. The survey was conducted in Amahra, Oromiya and Tigray Regions. Three towns from each

region were selected for the survey. The sample size for each region and town was determined proportionately based on the total number of households. Finally, based on sampling frames (lists of households) obtained from the respective Kebeles[3], households were selected using a simple random sampling technique. Accordingly, Oromiya region was allocated 667 households (42.3%) followed by Amhara with 580 households (36.8%) and Tigray with 330 (20.9%). Therefore, the total number of sample households was 1577.

3.2. Description of covariates and descriptive statistics

Table 1: The descriptive statistics of covariates of fuel saving technologies and their expected signs (N=1557)

Variable[4]	Mean	S.D.	Min	Max
GENDER(Gender of household head) (-)	0.68	0.47	0	1
AGEHH (age of household head at the time of the survey)(+)	44.88	13.50	18	102
EDUCATION				
EDilliterate (if the household head is illiterate)(-)	0.21	0.41	0	1
EDreadelm (if the head can read and write or grade (1-8)(+)	0.42	0.49	0	1
EDsecond (if the head is between grade 9 & 12)(+)	0.20	0.40	0	1
EDhigher (if the head has a certificate or above)(+)	0.17	0.37	0	1
CHILD15(No. of children and youths whose age ≤ 15 (+)	1.75	1.54	0	14
ADULTS15(number of adult members of the family)(+/-)	3.38	1.87	1	15
HOWNERSHIP(Ownership status of the house, 1 if privately owned and 0 otherwise)(+)	0.72	0.45	0	1
COOKINGPLACE (1 if the HH has a separate kitchen, 0 otherwise)(+)	0.75	0.44	0	1
INCOME (+)				
MONINCOME1(if monthly income is less than 500 Birr*)	0.57	0.49	0	1
MONINCOME2 (if Monthly income is between 501 & 1499)	0.30	0.46	0	1
MONINCOME3 (if monthly income is between 1500 & 2499)	0.09	0.29	0	1
MONINCOME4 (if monthly income is above 2500)	0.04	0.20	0	1
DELEMITAD (dummy for electric Mitad) (-)	0.08	0.27	0	1
DMETALSTOV (dummy for Metal stove)(-)	0.48	0.50	0	1

NOTE: The signs on the second parenthesis show the expected sign. Birr is the national currency of Ethiopia and the exchange rate was 1 USD ≈ Birr 12.615 during the survey period

The majority of households are highly dependent on biomass energy sources for baking *injera* which is the main staple food in most parts of the country. The descriptive statistics in table 1 above show that only 7.8% of the sampled households use electricity for baking *injera*. More than 85 % of the household heads who are using electric *Mitad*[5] have secondary education or above. This may suggest that education is important for households to move up the energy ladder.

[3]Kebele is the lowest administrative unit in Ethiopia.
[4]Except for the variables AGEHH, CHILD15 and ADULT15, the rest are dummy variables. This is because of the nature of the data. For example, since the data do not have information on income as a continuous variable, we considered it as a categorical variable.
[5]The preparation of the traditional pan-cake like Ethiopian food, *injera*, requires an appliance known as Mitad. 'Mitad' is a clay-made circular pan used for baking '*injera*'

The dependent variable used in the analysis was the time (in years) households waited before adopting Mirt and Lakech improved stoves, measured by the number of years elapsed since their introduction, which was taken to be in the year 1991 and 1994 for Lakech and Mirt biomass cook stoves, respectively. For those households who had not yet adopted, the duration was right-censored at the year of data collection.[6] That is, we know the period of introduction of the technology (the beginning of the duration), but we do not know the end for some observations. The start date is the time when the improved biomass cook stoves were first introduced and the exit date, or the end of a spell, is the time a household adopts the fuel saving technology (Mirt improved biomass cook stove or Lakech Charcoal stove).

4. Results of duration analysis

4.1. Non parametric results

When the data is censored the density and cumulative distributions are not appropriate. An alternative non parametric approach called Kaplan Meier-Estimator has been developed for non-parametrical estimation of survival functions and the related distributions. This is a non-parametric approach, making no assumptions regarding the underlying distribution of survival times. The figure below shows the survival functions for the Mirt biomass *injera* stoves by income level. The survival function for income category 1 is higher than category 2, which in turn is higher than category 3. The survival function for income category 1 suggests that households in the lower income groups have higher probability of survival than those households from the relatively high income groups. We used both the logrank and Wilcoxon test to test whether the above graphs are statistically different or not. Both tests for equality of survivor functions show that we reject the null hypothesis of equality at 1% level of significance. In other words, we can reject the null hypothesis that the four groups face the same hazard of failure. The results of both tests are also the same for Lakech charcoal stove.

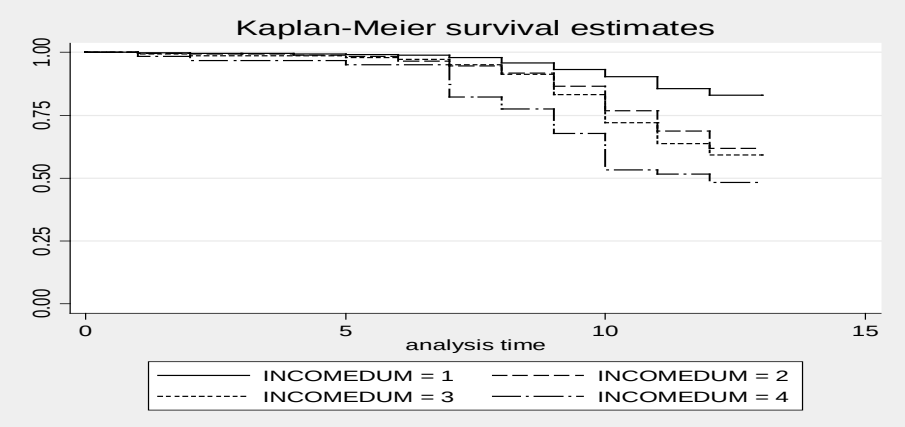

Figure 1. Survival function for MIRT improved biomass cook stoves

When we see the nature of the graphs it seems constant for the first 6 or 7 years. The Kaplan-Meier survivor function does not change indicating that there are no adoptions of the stove at the beginning, irrespective of the level of income. Then the values of the function fall quickly

[6]Lack of consistency in the various reports was our main problem in setting the period of introduction of the fuel saving technologies. Moreover, there is no information on the specific year for the introduction of each technology in each region. So we take the same year for all surveyed households.

from year to year. That means there are adopters of Mirt biomass cook stove every year. We did not report the survival function for Lakech charcoal stove since it is more or less similar with Mirt *injera* stove. That of Lakech charcoal stove falls quickly at a later stage (after 10 years) compared with Mirt.

4.2. Results of parametric regression

The results of the Akaike's Information Criterion (AIC) and Bayesian Information Criterion (BIC) model selection criteria show that the Weibull model is preferred to the exponential model for both kinds of stoves. Hence we report the results of the Weibull model only. Another issue in duration analysis is the issue of unobserved heterogeneity. The 'theta' value reported in table shows that the frailty model is preferred to the reference non-frailty model according to the likelihood ratio test (for Mirt). For lakech charcoal stove, we estimated without taking the issue of hetrogenity since convergence was not achieved. Table 2 presents the results of the Weibull estimation for Mirt and Lakech stoves.

Table 2: Determinants of covariates of Mirt injera and Lakech charcoal biomass cook stove

	MIRT			Lakech		
Variables	Coef.	S. E.	*p*>z	Coef.	S.E.	*p*>z
GENDER	-0.321	0.151	0.034	0.114	0.111	0.307
AGEHH	0.006	0.006	0.296	-0.036	0.005	0.000
EDreadelm	0.636	0.220	0.004	-0.039	0.138	0.777
EDsecond	1.240	0.253	0.000	-0.015	0.164	0.927
EDhigher	1.085	0.267	0.000	0.156	0.172	0.365
CHILD15	-0.042	0.040	0.292	-0.043	0.031	0.165
ADULTS15	0.088	0.033	0.008	0.069	0.024	0.005
HOWNERSHIP	0.296	0.153	0.053	0.117	0.109	0.286
DELEMITAD	0.206	0.198	0.297			
DMETALSTOV				-0.906	0.107	0.000
COOKINGPLACE	0.486	0.170	0.004	-0.053	0.111	0.634
MONINCOME2	0.695	0.152	0.000	0.378	0.111	0.001
MONINCOME3	0.692	0.219	0.002	0.351	0.165	0.033
MONINCOME4	1.303	0.297	0.000	0.541	0.215	0.012
DTigray	-1.184	0.216	0.000	-0.045	0.165	0.786
DAmhara	-0.447	0.137	0.001	0.044	0.102	0.668
_cons	-11.995	0.765	0.000	-11.391	0.523	0.000
/ln_P	1.287	0.071	0.000	1.481	0.039	0.000
/ln_the	-0.343	0.610	0.574			
P	3.620	0.257		4.398	0.173	
1/P	0.276	0.020		0.227	0.009	
Theta	0.710	0.433				

Likelihood-ratio test of theta=0: chibar2(01) = 3.05, Prob>=chibar2 = 0.040

In the Weibull model, P >1 means that the hazard is monotonically increasing. That is the observations are failing at a faster rate as time goes on. The value of P for Lakech charcoal stove is also greater than one, showing that the hazard, like in the case of Mirt, is monotonically increasing. Stata also estimates the log of P (for computational reasons) and

provides a test of the hypothesis that the log of p is equal to zero (which is equivalent to testing for P=1), which is rejected as indicated in the table above. That means the test also rejects the null hypothesis of no duration dependence; i.e log of P is equal to zero.

Note that a negative value of a coefficient β implies that the variable increases the time until adoption whereas a positive coefficient means that the times taken to adopt the fuel saving technology were shorter. Our result shows that education will speed up the adoption of the Mirt biomass *injera* stove compared with illiterate households. Surprisingly, education has no effect on the adoption decision of Lakech charcoal stove. For Lakech charcoal stove income is more important than education. Compared with households earning monthly income of Birr 500 or less, the probability of adopting Lakech charcoal stove increases for those households whose monthly income is 501 and above. The effect of income on the speed of adoption of Mirt biomass *injera* stove is not different from Lakech charcoal stove. The result implies that the design and price of new improved biomass stoves should take into consideration the capacity of households to pay for it. This is very important given the nature of households who are highly biomass dependent. Poor households are usually dependent on biomass sources for cooking. In general, the higher the income, the higher the probability of adopting improved stoves in urban Ethiopia. According to Jones (1989), cited in Barnes et al. (1994), middle-income families have adopted improved stoves far more quickly than poor families in most African countries. In our case, even high income households are using the improved biomass stove. This also shows that households may not necessarily shift to other better sources of energy as their income increase, as postulated by the energy ladder hypothesis. This is because the process depends on many other factors such as affordability, availability, and cultural preferences.

The estimated coefficient for the variables 'ownership of private house' and 'separate kitchen' suggests that households who possess these basic facilities are more likely to adopt Mirt Biomass *injera* stove. Mirt is a domestic appliance which requires some space and larger in size than many modern and improved-biomass cook stoves. Hence, its installation and proper utilization requires access to basic facilities (Shanko et al., 2009). However, these variables do not have any significant effect in the case of Lakech charcoal stove. This is for the simple reason that the stove is simple and easily mobile. Similarly, Lakech does not require separate kitchen. It is usually used in the main house since it is small, light and convenient for cooking. As a result, the ownership of house and possession of separate kitchen may not be significant factors in adopting Lakech charcoal stove.

The negative sign of the variable 'Gender' suggests that the conditional probability of adoption of Mirt Biomass stove declines if the household head is male. The result is expected because female headed households can appreciate the importance of the stove more than male headed households. This variable is, however, not significant in the case of adoption of Lakech charcoal stove. Age of the household head is negatively related to the speed of adoption of Lakech charcoal stove suggesting that younger households are more likely to adopt the technology compared with households with older heads. The number of adults is positively and significantly correlated with the speed of adoption of both types of stoves. The number of children and youths with age less than 15 does not affect the speed of adoption of both types of stoves. This result may not be reliable as the variable includes household members whose ages are less than 15 years old. The data do not have separate information for children and youths. It is known that availability of children (less than 5 years) usually increase the probability of adoption of the improved biomass stove technologies.

The impacts of substitute technologies were also examined. Electric Mitad is considered as a substitute for Mirt *injera* stove. Metal charcoal stove is a substitute for Lakech charcoal stove. The coefficient for electric Mitad is not significant suggesting that households are not using electric Mitad for baking *injera*. The reason might be the relative cost of using electric Mitad is so expensive compared with Mirt *injera* biomass cook stove. The availability of metal charcoal stove, however, negatively and significantly affects the probability of adopting Lakech charcoal stove. Given the better performance of Lakech charcoal stove over that of Metal charcoal stove, we need to understand why households with metal charcoal stove take longer time to adopt the Lakech charcoal stove than those without metal charcoal stove. The role of marketing and promotion strategies may be significant here. We need to design marketing strategies that attracts households who already possess other kind of stoves, serving the same purpose.

Location variable shows that the speed of adoption of Mirt *injera* stove decreases for a household in Amhara and Tigray region compared with households residing in Oromiya region. We would have expected a different sign as the level of biomass in these areas is usually low (relatively degraded compared with Oromiya region). The result may be justified by the fact that households in Oromiya region are better exposed to the technology than households in Amhara and Tigray regions. Moreover, differences in other factors such as price and level of involvement of NGOs could result in differences in the adoption decision of households between the regions.

5. Conclusions and policy implications

This paper deals with one of the demand side strategies, distribution of improved biomass cook stoves, which will help reduce pressure on biomass resources, save fuel, reduce time for cooking, and reduce the risk of fire hazards. The paper tried to find out the determinants of adoption of two different types of fuel saving technologies (Mirt and Lakech) in Ethiopia by using data collected from selected towns in three regions of the country. We applied a duration analysis to examine the impacts of different socioeconomic variables on the speed of adoption of both types of stove technologies.

The result of the analysis shows that income level is a significant factor in the adoption decision of the improved biomass cook stoves in urban Ethiopia. This may suggest that households will not shift to other better sources of energy as their income increase, as postulated by the energy ladder hypothesis. Moreover, since poor households are highly dependent on biomass sources for cooking, the design and price of new technologies should take into consideration the interest of the lower income groups.

Education (increasing awareness of the people) might increase the probability of adopting the Mirt biomass *injera* stove. We also found possession of Electric Mitad (a technological substitute for Mirt *injera* stove) does not have any effect on the adoption decision of Mirt biomass cook stoves. This may be due to the better performance of Mirt in reducing the energy cost of preparing the staple food, *injera*. Therefore, ownership of electric Mitad does not necessarily mean that households will substitute it for Mirt. This requires the attention of policy makers or energy planners to further assess the potential impact of electric Mitad on household's overall welfare and biomass use (forest pressure). However, ownership of Metal charcoal stove is negatively correlated with the adoption of Lakech charcoal stoves. This may suggest that there is a need to reconsider the promotion strategy given the better performance

of Lakech charcoal stove over Metal charcoal stove. The findings further show that access to basic facilities such as private house and separate kitchen for cooking increases the probability of adopting Mirt biomass improved stove. Given the importance of the improved biomass stoves in saving biomass, money, reducing indoor air pollution, etc. future study should give more attention to collecting more information such as prices and subsidies (if any) and examine their impact on the adoption decision. Second, this study examined the adoption of improved stoves technologies, but not the efficient use. We need to see how much fuel wood and charcoal were saved due to these improved biomass cook stoves. Some studies (for ex, Muneer and Mohamed, 2003) also shows that convenience of new stoves over the traditional stoves has increased consumption of fuel wood or charcoal (rebound effect). Future study on this area should also address this issue.

References

[1] EPA (Environmental Protection Authority), The third national report on the implementation of the UNCCD/NAP in Ethiopia, 2004.

[2] Cooke, P, St. Clair, William F. Hyde, and Gunnar Köhlin, Fuelwood, forests and community management–evidence from household studies. Environment and Development Economics 13, 2008, pp. 103–135.

[3] IEA (International Energy Agency), World Energy Outlook. Paris: OECD, 2004.

[4] Hannan, T.H. and MacDowell, J.M., The determinants of technology adoption: The case of the banking firm, Rand Journal of Economics, 15, 1984, pp. 328–335.

[5] Dadi, L., Burton, M. and Ozanne, A, Duration Analysis of Technological Adoption in Ethiopian Agriculture, Journal of Agricultural Economics 55(3), 2004, pp. 613-631.

[6] Burton, M., Dan Rigby and Trevor Young, Modelling the adoption of organic horticultural technology in the UK using Duration Analysis. The Australian Journal of Agricultural and Resource Economics, 47:1, 2003, pp. 29–54.

[7] Kiefer, N. M, Economic duration data and hazard functions, Journal of Economic Literature. 1988, pp. 646-679.

[8] Green, W, Econometric Analysis, 5rd ed, New York, Macmillan, 2003.

[9] Barnes, D.F., Openshaw K, Smith KR, and van der Plas R, What Makes People Cook with Improved Biomass Stoves? A Comparative International Review of Stove Programs, World Bank Technical number 242, 1994.

[10] Shanko, M, Abebe, T and Lakew, H, A report on Mirt biomass Injera Stoves Market Penetration and Sustainability Study in Amhara, Oromiya and Tigray National Regional States: GTZ Sun Energy, 2009.

[11] Muneer, S.E.T. and M.E.W. Mokhtar, Adoption of biomass improved cook stoves in a patriarchal society: an example from Sudan: The Science of the Total Environment 307, 2003,pp. 259–266.

Energy performance of Portuguese and Danish wood-burning stoves

Ricardo L. T. Carvalho[1,*], Ole M. Jensen[1], Luís A. C. Tarelho[2], Alireza Afshari[1], Niels C. Bergsøe[1], Jes S. Andersen[3]

[1] *Danish Building Research Institute, Aalborg University, Hørsholm, Denmark*
[2] *Department of Environment and Planning, University of Aveiro, Aveiro, Portugal*
[3] *Centre for Renewable Energy and Transportation, Technological Institute, Aarhus, Denmark*
**Corresponding author. Tel: +45 99402373, Fax: +45 45867535, E-mail: rlc@sbi.dk*

Abstract: In Europe, considerable amounts of renewable energy resources are used for residential heating with wood-burning stoves, which can cause considerable energy losses and environmental impacts. A better understanding of its operating characteristics will permit to improve the buildings energy efficiency and indoor climate, and to reduce the emission of air pollutants to the environment.
This study aimed to analyze the operating conditions of a Portuguese made stove and compare it with the most efficient Danish made stoves tested at the Technological Institute.
The combustion experiments were carried out through the measurement of the main operating parameters: flue gas temperature and composition, combustion air flow rate, and fuel consumption rate. The results showed that the appliances emitted energy intermittently, with a mean heat flow rate into the indoors of 5 kW_{th}, representing mean thermal energy efficiencies of 70% and 76%, respectively for the Portuguese and Danish stoves. The Carbon Monoxide concentration in the flue gas was lower than 0.4 % (v/v; 13% O_2) for all stoves.
There is still a need for more accurate knowledge the relationship between the energy and the environmental performance of the appliances. A dynamic analysis of the problem will permit to increase the households energy savings.

Keywords: *Wood-burning stoves, thermal energy efficiency, heat flow rate, flue gas composition.*

Nomenclature

η	*energy efficiency* ... %	c_{pi}	*mean calorific capacity* ... $kJ\ mol^{-1}K^{-1}$
h_a	*ambient air specific enthalpy* ... $kJ\ kg^{-1}$	h_{fg}	*latent heat of H2O* ... $kJ\ kg^{-1}$
m_b	*fuel consumption rate* ... $kg\ h^{-1}$	m_{ca}	*combustion air flow rate* ... $kg\ h^{-1}$
n_i	*molar flow rate* ... $mol\ s^{-1}$	PCI	*lower heating value* ... $kJ\ kg^{-1}$
Q_g	*thermal energy gains* ... kW	Q_l	*thermal energy losses* ... kW
T_{EG}	*flue gas temperature* ... K	T^0	*reference temperature* ... K
w_{wF}	*fuel moisture* ... $kg_{H2O}\ kg^{-1}$		

1. Introduction

Nowadays, a great amount of energy is used for residential heating and even in the European modern houses is possible to save considerable amounts of thermal renewable energy. Among the existing sustainable energy systems are the wood-burning stoves that are still commonly used for space and sanitary water heating.

In Portugal, it is estimated that 32% of the houses are using either wood-burning stoves or open fireplaces for space heating, whereas in Denmark 26% of the households are using wood-burning stoves being estimated that wood share is estimated to 18% of the total amount of fuel used for heating in single family houses, and amounts to 60 % of renewable energy contribution in this category of houses [1;2].

However, these equipments can reveal low thermal energy efficiency when operated under deficient conditions also causing considerable impacts in the environment. During the last few

years there was an effort to improve both the energy and environmental performance of such equipments, through the establishment of national and international guidelines and standards.

The international standard EN 13240 for "room heaters" and EN 13229 for "insert appliances and open fire places" establish requirements concerning the thermal energy efficiency and operating conditions of the equipments [3;4]. The standards determine the laboratory test procedures and required emission factors concerning the appliances certification. At the same time the new version of the Energy Performance Building Directive (EPBD 2010) is asking the member states to implement an integrated building certification system and that means the energy analysis must consider both the thermal efficiency of the households and its elements, through the establishment of labeling systems for the building equipments. Moreover, the certification of energy systems should take into account its impacts on thermal comfort and indoor air quality [5].

Some countries have been developing national standards for wood-burning stoves, namely the Swan Labeling created in the Nordic countries that present tighter requirements concerning for example the emission factors of total particle matter (PME). In Denmark, most stove manufactures are applying this labeling system through tests in certified laboratories such as the testing laboratory of the Technological Institute [6]. During the last decades, these regulations have been adopted by European stove manufacturers and sellers and this has contributed to the improvement of the energy performance of the marketed wood-burning stoves. The problem and hypothesis is that the increase of the equipments thermal efficiency can in certain extend be related to a decrease in the environmental performance of the biomass stoves, namely concerning its impacts in both the ambient and indoor air quality [7;8].

There is still a lack of knowledge about the relation between the wood-burning efficiency, the heat transfer processes from the combustion chamber to the indoors and the emission of pollutants to the environment. In this context, the aim of this study was to analyze and compare the operating conditions of wood-burning stoves made in two different European countries with distinct energy demands but where the use of wood-burning stoves are still a solution for residential heating. The objective is to contribute to the increase of knowledge about processes involving wood-burning stoves in order to identify practices that can promote higher energy savings in buildings and a cleaner wood-burning process, as well as the creation of guidelines for manufactures, sales men and stove users.

2. Methodology

The present study was carried out in a laboratory test installation at the University of Aveiro (Portugal) projected and implemented for monitoring several operating parameters of the typical Portuguese made wood-burning stove. The project carried out at the Portuguese university aims to increase the knowledge about the test methods used to evaluate the energy and environmental performance of such appliances. The experimental results obtained were compared with the data acquired during similar tests carried out for a Danish made stove - tested at the testing laboratories at the Technological Institute (Denmark), following the European standard EN13240. In both cases, it was considered that the studied equipments are representative of the commonly used wood-burning stoves in Portugal and in Denmark, respectively. The biomass used in this comparative study was wood commonly collected in the Portuguese forest (used for residential wood-burning), for example the ash tree (*Fraxinus Angustifolia*) and for the Danish stove birch wood following the requirements of the EN

13240. The general information about the experimental conditions used are presented in the Table 1.

2.1. Experimental installation and test conditions

In Portugal, the experimental installation integrated a wood-stove (insert appliance) with a mechanical ventilation system used for forced convection, a set of on-line gas analyzers, temperature sensors, a combustion air flow meter, a weight sensor and an automatic control and data acquisition system operated by a computer. During the experiments the following parameters were monitored continuously: the temperature in the combustion chamber and on the stove walls, the flue gas temperature at several locations along the reactive system (at the chimney entrance and exit), the flue gas composition, the combustion air flow rate and the rate of biomass combustion.

The temperature in the different points along the experimental installation was measured with K-type thermocouples while the flue gas composition was determined applying the following continuous measurement methods: a paramagnetic analyzer (ADC model O_2-700 with a Servomex Module) for O_2, and a non-dispersive infrared analyzer (Environnement, MIR 9000) CO and CO_2. The composition of the combustion gas was measured in the chimney at 2.8 meters above the combustion chamber exit. The combustion air flow rate was determined using a mass flow rate meter (Kurz, series 155) while the biomass consumption was monitored through a weight sensor (DS Europe 535 QD – A5) [9].

In Denmark, the stove was tested under the operating conditions established by the European standard, through the determination of the CO and CO_2 concentrations by means of IR spectroscopy using an ABB AO 2020 gas-analyzer. The flue gas temperature and other temperatures were measured with K-type thermocouples. The test laboratory is accredited by the European standard EN 17025 by DANAK (with accreditation number 300 and notified body with notification number 1235). The measurements in the flue gas of both the CO and CO_2 concentrations were carried out at 1.43 meters above the combustion chamber using the test section specified by the EN 13240 Fig. A.9.

Table 1. Operating conditions during the wood-burning stoves monitoring (mean values for the 60 minutes period).

Appliance (country)	Type of appliance	Fuel consumption (kg h^{-1})	Combustion air flow rate (Nm^3 h^{-1})	Forced convection rate (Nm^3 h^{-1})
Portuguese	Insert	1.7	29.97	40.00
Danish	room heater	1.6	27.30	N.A.

The laboratory experiments were carried during the heating season of 2010 using typical operating conditions for the studied wood-burning stoves. The duration of each laboratory experiment (wood-burning cycle) was 60 minutes, according to the European standards EN 13240 and EN 13229, respectively for the Danish (wood stove) and Portuguese (wood stove, insert appliance) equipments.

The experimental results obtained were considered in both the mass and energy balance to the wood-burning stoves in order to calculate the thermal energy efficiency of the appliances during a typical wood combustion cycle.

3. Results

The behavior of the monitored operating variables (flue gas temperature in the combustion chamber, both the CO and CO_2 concentrations in flue gases, and mass of fuel in the grate of the stove) during the combustion of biomass is shown in the Figures 1 and 2, respectively for the Portuguese stove and Danish stoves.

The combustion of wood in both equipments shows some major differences. For example, in the Danish stove both the flue gas CO_2 concentration and temperature increased in the initial stages of the combustion cycle, whereas in the Portuguese stove those variables achieve maximum values only after 20 minutes after to the fire lightning (Figures 1 and 2).

An increase in the flue gas CO concentration at the initial stages of combustion was observed for both stoves, although in the case of the Portuguese insert appliance the CO concentration value is higher than for the Danish stove, and lasts for a longer time period. For both cases it is possible to observe an increase in the concentration of CO in combustion gases during the final stages of wood combustion (Figures 1 and 2).

The temperature in the combustion chamber varied between 200 and 600 ^{o}C in the Portuguese wood stove – similar to the temperatures expected for the Danish stove based on thermal calculations.

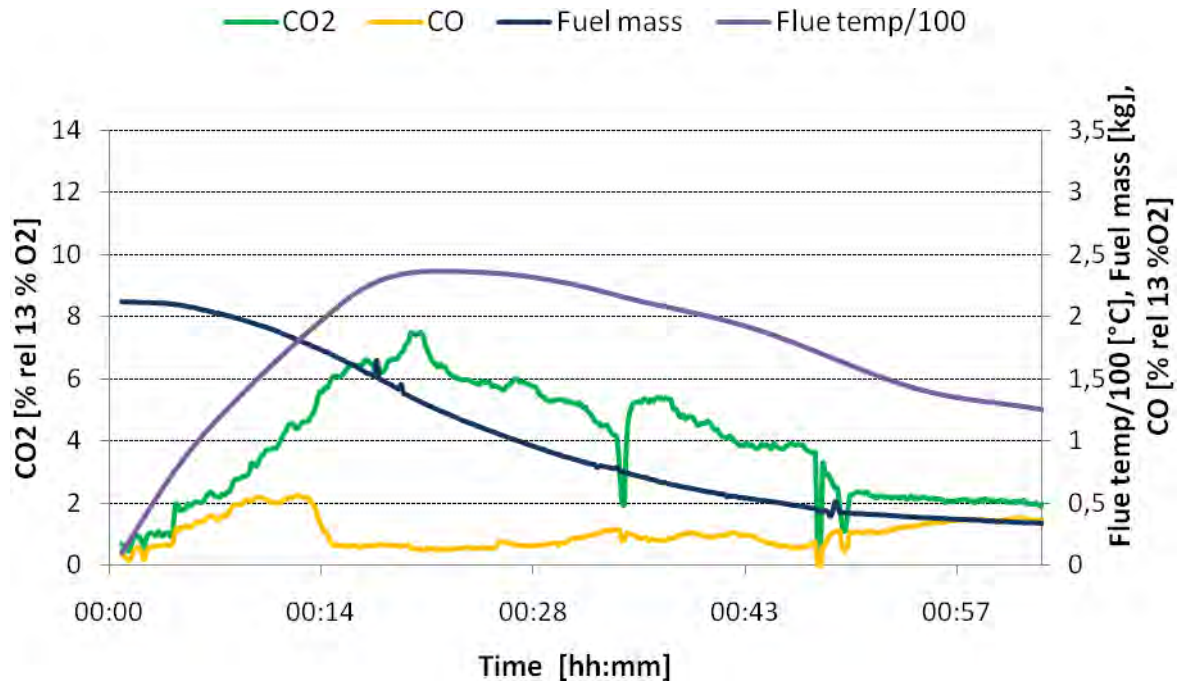

Figure 1. *Fuel consumption, CO and CO_2 concentration (13% O_2, dry gases) in the exit flue gas, and temperature of the flue gas over the test period in the Portuguese stove.*

The Figure 1 shows that there was a rapid decrease in both the flue gas CO concentration and temperature, respectively 35 and 48 minutes after to light the fire in the stove. The first case is

associated to the door opening after 35 minutes of sampling, due the verified problems with the combustion bed. The second situation is related to the automatism of the software sampling systems, since it was programmed for a certain period of measurements and as a consequence it was not registering any values at the 48 minutes time instant.

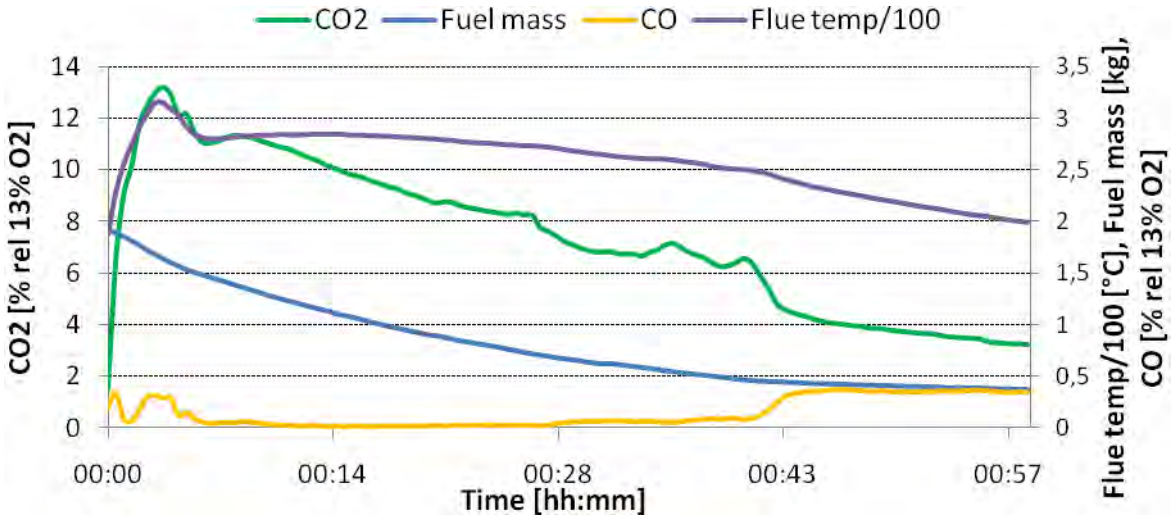

Figure 2. Fuel consumption, CO and CO_2 concentration (13% O_2, dry gases*) in the flue gas and temperature of the flue gas over the test period in the Danish stove.*

For the Portuguese stove, the mean CO concentration in the combustion flue gas over the test period was 0.27% (v/v, dry gases), while the mean CO_2 concentration was 3.6% (v/v, dry gases), and the mean flue gas temperature was 173 ºC. The biomass combustion rate was around 1.7 kg/h. Important is to point out that during the wood combustion experiment it was necessary to handle one of the wood logs in the stove grate in order to maintain the combustion process under satisfactory conditions; this handling interventions are reflected in Figure 1 by the decrease in both the flue gas CO_2 concentration and temperature around 35 minutes after the beginning of the wood combustion cycle.

For the Danish stove, the mean CO concentration in the flue gas was 0.10 % (v/v, dry gases) while the mean CO_2 concentration was 7.3 % (v/v, dry gases), and the mean flue gas temperature was 250 ºC. The biomass combustion rate was around 1.6 kg/h.
Important is to point out that, the gas flow rate throughout both of the stoves is varying in same range (25 to 30 $m^3 h^{-1}$).

The mean thermal efficiency of both wood-burning stoves was determined for each testing period (60 minutes) in order to compare the energy performance of the studied equipments.

The thermal efficiency was calculated considering two European standards, namely the EN 13240 (insert appliances) and EN 13299 (room heaters) that establish a minimum testing period of 45 minutes [3;4]. The calculation of the energy efficiency of each stove was carried out through an energy balance to the equipments. The system boundary considered for the calculation of the energy loss from the stove to the outdoors was the top of the chimney in both equipments.

The amount of energy losses was exclusively associated to the sensible and latent heat of combustion gases leaving the chimney.

The Equations 1 to 3 were used for the calculation of the thermal efficiency of the two stoves. The obtained results are presented in Table 2.

$$\eta = \frac{\dot{Q}_g - \dot{Q}_l}{\dot{Q}_g} \cdot 100 \quad (1)$$

$$\dot{Q}_g = \dot{m}_b \cdot PCI_b + \dot{m}_{ca} \cdot h_a \quad (2)$$

$$\dot{Q}_l = \sum_{i=1}^{i=n} \dot{n}_i \cdot \bar{c}_{p_i} \cdot \left(T_{EG} - T^0\right) + m_b \cdot w_{wF} \cdot h_{fg} \quad (3)$$

Table 2. Nominal heat output and energy efficiency of the Danish and Portuguese tested wood stoves.

	Danish *	Portuguese **
Nominal heat output (kW)	5.2	5,2
Nominal burn time (min.)	60	60
Efficiency (%)	76	70
Mean flue gas temperature (ºC at 20ºC ambient temp.)	250	180

**) Claimed values from the CE-dataplate – Tecnological Institute.*
***) Experimental values obtained at the University of Aveiro laboratory.*

4. Discussion and conclusions

The knowledge about the energy and environmental performance of wood-burning stoves is still insufficient and there is a need to improve them concerning the sustainability of the integration of such a kind of energy conversion systems in the modern energy efficient households.

The development and implementation of testing methods and laboratories is a step stone towards a better knowledge about the operating conditions of such equipments, and the consequent improvements on both its energy efficiency and environmental performance all over Europe.

During the last few years, there was an effort to improve the thermal efficiency of the wood combustion appliances from 50% to more than 80%, however, it is well known that the use of such energy systems continue to cause considerable impacts on the environment.
The presented work revealed that the thermal efficiency of the studied stoves varied between 70% and 76%, respectively for both the Portuguese insert appliance and Danish stove; the nominal thermal heat output considered was around 5 kW_{th}. Regarding the energy efficiency, it can be concluded that the two equipments have efficiencies in the same range, even though the combustion characteristics are pretty uneven, as indicated by the behavior of the operating variables along the time and its mean values. The background is that the energy efficiency is

derived from the ratio CO_2 concentration / Flue gas temperature. So offsetting the two parameters in parallel upwards or downwards will return no change in the actual efficiency.

Normally, one cannot avoid a CO peak in the beginning of the burn cycle (devolatilization), and neither a moderate increase of CO concentration at the end of the burn cycle, due to incomplete combustion (associated to low temperatures) once the flame did extinguish.

However, the presence of CO concentrations varying from 0.2 to 0.4 % (Portuguese insert appliance) in between the peaks at the beginning and at the end of the combustion cycle indicates incomplete combustion conditions, also indicated by the relatively low CO_2 concentration (inserts having an air excess rate of approximately 250% indicates that theoretical mean CO_2 concentrations of up to 8.3 % are achievable).

Thus it ought to be possible to improve the combustion conditions, leading to higher CO_2 concentrations, higher flue gas temperature (and consequently more or less unaffected thermal efficiency), and lower CO concentrations, for benefit of the external environment, as the stove would emit less organic carbon residuals in the flue gas.

However, in comparing the two appliances one should bear in mind that the Danish stove was tested at ideal test conditions and settings during a type test, whereas the Portuguese insert appliance was tested in a university environment (testing conditions similar to that established by the European standard), and considering normal user operating conditions.

As a consequence, there is still a demand for improving the test methods and developed a mathematical tools (numerical models) that will integrate and describe both the combustion and heat transfer processes involved. The use of numerical models will permit to identify solutions to save considerable amounts of energy in households, for example through both a more efficient energy utilization and storage.

The develpment of a new energy simulation computerized tool will help the manufactures and technical consultants to design more efficient wood-burning stoves adapted to different types of building constructions and wood fuels all over the world.

Aknowlegements

The experimental work developed in Portugal was funded by the Portuguese Science and Technology Foundation (FCT) through the project with reference PTDC/AGR-CFL/64500/2006.

References

[1] P. Fernandes, Emissão de PM2.5 e gases em sistemas domésticos de queima de biomassa, Tese de Mestrado de Engenharia do Ambiente, Universidade de Aveiro, 2009.

[2] L. Keiding, L. Gunnarsen, N.R.M. Machon, R. Moller, et al, Environmental factors of everyday life in Denmark – with special focus on housing environment, Edited by Lis Keiding, National institute of Public Health, Copenhagen, 2003.

[3] Danish Standard, Room heaters fired by solid fuels – Requirements and test methods, EN 13240:2003, Denmark, 2007.

[4] Danish Standard, Inset appliances including open fires fired by solid fuels, EN 13229:2001, Denmark, 2001.

[5] The European Parliament and of the Council, Energy Performance Building Directive, Official Journal of the European Union, pp. 153/13-153/34, 2010.

[6] Nordic Labeling, Nordic Eco-labeling Closed Fireplaces, version 2.2, 2006.

[7] Personal communication of Jes Sig Andersen, Technological Institute, 2010.

[8] A. Afshari, O. J. Michael, N. C. Bergsøe, R. L. Carvalho, Impact of operating wood-burning stoves on indoor air quality, Danish Building Research Institute, International Society of Indoor Air Quality and Climate, The 12th Conference of Indoor Air 2011, 2010.

[9] R. L. Carvalho, Energy performance of wood-burning stoves and its impact on indoor air quality, Danish Building Research Institute, Master thesis in Sustainable Energy Systems, University of Aveiro, Portugal, 2010.

Field study of energy performance of wood-burning stoves

Ole M. Jensen[1*], Alireza Afshari[1], Niels C. Bergsøe[1], Ricardo L. Carvalho[1]

[1] *Danish Building Research Institute, Aalborg University, Hoersholm, Denmark*
** Corresponding author. Tel: +45 99402373, Fax: +45 45867535, E-mail: omj@sbi.dk*

Abstract: In Europe, large amounts of renewable energy are lost when residential buildings are heated by means of wood-burning stoves. Still, too many wood-burning stoves are energy inefficient, the knowledge of their operation is insufficient and the interaction between the stove and the house to be heated is not adequate. This applies in particular to old wood-burning stoves in old houses. However, this field study, the first ever dealing with new stoves in new houses, revealed that even in new houses with new wood-burning stoves of today the interplay between stove and house can still be improved as well as the modern wood-burning stoves could be designed to perform even better. However, calculation of heat balances and measurement of temperature in a series of single family houses showed that wood-burning stoves actually contribute considerably to the heating of new houses, although their intermittent working led to overheating and conflicts with the primary heating system. Moreover, measurements of particles showed that emission of fine and ultrafine particles to the indoor climate can easily occur.
The study made it clear that information and guidelines to be disseminated among stove manufactures, salesmen, and home owners are needed regarding dimensioning, installation of wood-burning stoves and their lighting and operation as well.

Keywords: *Residential heating, wood-burning stoves, energy performance, particle emission, ultrafine particles*

Although wood-burning stoves are mostly used as a supplementary heating source, they represent a notable part of the carbon-free heating. In Denmark, which has a well-developed gas and district-heating net, the share of wood is estimated to be 18 % of the total amount of fuel used for heating in single-family houses, and amounts to 60 % of the renewable energy contribution in these houses [1]. The large share of wood, mainly consumed in wood-burning stoves, can be ascribed to the fact that firewood is cheaper than other fuels and that Danish wood-burning stoves are popular due to their high efficiency, their certificates of low particle emission [2] and their design - not to forget their ability to create a cosy atmosphere. Therefore, when developing new models, the manufacturers have in turn focused on efficiency, environment and design. The focus on these elements has made it possible to meet the demands of a wide customer segment, including owners of new single-family houses with low energy demand.

So far, new single-family houses continue to have a decreasing demand of energy for heating. This is encouraged by the European Directive on the Energy Performance of Buildings (EPBD), which led to national legislation on better energy performance, i.e. better insulation and airtight building envelopes combined with ventilation systems with heat exchanger [3]. On this background, the aim of the field study was to:

- Investigate the energy performance of stoves in operation, the overall efficiency and utilisation of firewood.
- Determine the impact of wood-burning stoves used on the indoor environment in terms of particle pollution and thermal comfort.
- Give recommendations, guidance to manufacturers and users of wood-burning stoves.

1. Study design

A study design was chosen where seven residential buildings were selected for case studies. The criteria for selecting the houses were that they were built after 1995, i.e. within the period

covered by the last two editions of the Danish Building Regulations and that they were equipped with a certified wood-burning stove. However, one house built in 1977 was included the study, because it was equipped with a masonry stove and because one elderly house would probably clarify the study.

A total of seven families with single-family houses hosted the surveys. The specifications concerning the selected houses are shown in Table 1. The experimental hosts were identified by addressing stove manufacturers and suppliers. This resulted in five cast-iron stoves, certified according to Danish Standard, four of which were certified according to the Nordic Swan standard [4]. Two masonry stoves built on location were not certified. Instead similar masonry stoves were known for their quality and tested for their high energy efficiency.

Table 1. Hosts for the field study with type of house and type of stove listed with certification of house and stove included. Building energy class A refers to the most energy efficient buildings. DS (Danish Standard) + Swan (Nordic eco-label) refers to certified clean and energy efficient wood-burning stoves.

Hosts	Type of house	Building year	Energy class	Type of stove	Certification
Espergaerde	detached	1977	D	masonry	(Solbyg)
Ringsted	detached	2006	B	masonry	(Helbro)
Hilleroed	detached	2001	C	cast iron	DS + Swan
Virum	detached	2007	B	cast iron	DS Plus
Værloese	row house	2008	B	cast iron	DS + Swan
Esrum I	detached	2009	A2	cast iron	DS + Swan
Esrum II	detached	2009	A2	cast iron	DS + Swan

2. Measurements

The experimental hosts were visited in the heating seasons 2008/2009 and 2009/2010 respectively. The houses in Ringsted and Virum were not included in the first series of measurements. In turn, Esrum II was not included in the second series of the field study. In the first series, particles, gases and air-change rates were measured, before, during and after lighting. In these cases, the host lighted the fire in the stoves. In the second series also particles, gases and air-change rates were measured. This time also the temperature close to and at some distance from the stoves were measured. To ensure uniform lighting, a stoking expert was engaged to perform the lighting in the second series. In addition, programmable data loggers (TinyTags) recorded temperature and humidity continuously for the following months.

Each of the hosts was interviewed and questionnaires were distributed. The interview was conducted in order to clarify the occupants' habits concerning their use of the stove, the family's experience with using the stove, techniques for lighting etc. The survey was aimed at quantifying technical issues, including consumption of firewood, the type of any primary heating, preferred room temperature and bathing habits, etc.

3. Energy performance

Energy performance has become the mantra of energy supply. Focus has been directed at electric appliances, cars and buildings, but also at the way we produce energy. This demand has reached the energy performance of wood-burning stoves as well. Their energy performance has bee increased and as a consequence the new wood-burning stoves have reached an

efficiency rate of 75-80 %. At this level, however, the energy performance of wood-burning stoves cannot be seen in isolation from the building that is supplied. Therefore, the first move was to chart the heat balance of the system. The second move was to detect instances of over-heating

3.1. Heat balances

For each of the houses involved in the field study, a heat balance was drawn up. One side of this balance gave the total of all inputs of fuel converted to a net heat production (excluding conversion loss). The other side of the balance gave the annual heat loss adjusted for the actual indoor temperatures, and the domestic hot water consumption. The total was termed gross heat consumption (including hot water etc.)

On the production side of the balance, the conversion of wood was rather uncertain. First the volume of firewood, the type of stack and the type of wood, included moisture content, must be known to estimate the dry firewood mass. Next, the heating value of the wood and the efficiency of the stove were needed for the calculation. Finally the extra heat loss caused by the additional air change of the wood burning must be taken into consideration, see Table 2.

Table 2. Firewood converted to heat production. The efficiency of the stoves is determined from test results field studies [5]. The calculation of the ventilation heat loss is based on the need of 11 m^3 air to convert 1 kg of dry wood.

Host	Firewood (kg)	Calorific value (kWh/kg)	Efficiency (%)	Ventilation loss (MWh)	Net heat contribution (MWh)
Espergaerde	2520	4.,1	80	0.16	8.1
Ringsted	980	4.1	85	0.06	3.4
Hilleroed	1750	4.1	75	0.11	5.5
Virum	350	4.1	70	0.02	1.1
Værloese	350	4.1	75	0.02	1.1
Esrum I	875	4.1	75	0.06	2.7
Esrum II	1400	4.1	75	0.09	4.4

Altogether the different fuels contributed to the net heat production of the houses as seen in Table 3.

Table 3. Merging the heat production of firewood with the heat production of other energy sources.

Host	Firewood (MWh)	District heating (MWh)	Natural gas (MWh)	Heat pump (MWh)	Net heat production (MWh)
Espergaerde	8.1		31.7		39.8
Ringsted	3.4	7.8			11.2
Hilleroed	5.5		9.9		15.2
Virum	1.1		15.3		16.3
Værloese	1.1		12.0		13.1
Esrum I	2.7			8.5	11.2
Esrum II	4.4			12.0	16.3

On the consumption side of the balance, the gross heat consumption was determined by the energy class of the house, as stated in the energy performance (EP) certificate. The net heat consumption is defined as the maximum of heat per square meter per year that is allowed to pass through the building envelope set off against heat gained from solar radiation and internal loads such as people and appliances. Applied to the area of the house this loss must be added to the hot water consumption and adjusted for a possible indoor temperature other than 20°C, see Table 4. The supplement for higher indoor temperature is 7-10 % per degree, lower for old houses and higher for new houses. The domestic hot water consumption was measured or stated to be 1 MWh per person.

Table 4. The gross heat consumption as a total of the standard loss for the building adjusted for indoor temperature and hot water consumption.

Host	Energy class	Maximum heat loss (kWh/ m^2)	Building area (m^2)	Net heat consumption (MWh)	Gross heat consumption (MWh)
Espergaerde	D	134	226	30.3	43.5
Ringsted	B	76	170	12.8	17.7
Hilleroed	C	76	188	14.1	18.8
Virum	B	65	175	11.4	15.7
Værloese	B	65	126	8.2	14.0
Esrum I	A2	65	132	8.6	13.3
Esrum II	A2	65	120	7.8	11.7

The resulting heat balance showed that in most cases the net heat production (excluded transformation loss) was lower than the expected gross heat consumption (included hot water consumption). This could be ascribed to low estimates of the amount of firewood consumed. However, in two cases the net heat production was higher than the expected heat consumption. In Esrum II this was presumably related to an inefficient heat pump, so that the yearly coefficient of performance was even lower that stated.

The energy balances also showed the share of heating resulting from wood burning as a total of the yearly energy production and as at total of the yearly consumption (see Figure 1). In these balances it was found that the share of heat production from wood burning was rather small. So far, an old house, like Espergaerde, with a masonry stove only had a wood-burning share of 20 %. Nevertheless, two new houses, Hilleroed and Esrum II reached a rather high share of 35 % and 26 % of the total energy consumption respectively. Still, the amount of wood used in Espergaerde was 2500 kg and by far the largest amount of wood used by any of the hosts. This showed that it was less demanding to cover the need for heating by use of a wood-burning stove in a modern house than in an elder house. By consuming a smaller amount of wood, a larger amount of fossil energy could be replaced and at larger amount of carbon circulation could be sustained. In that perspective it seemed promising to use firewood in new houses.

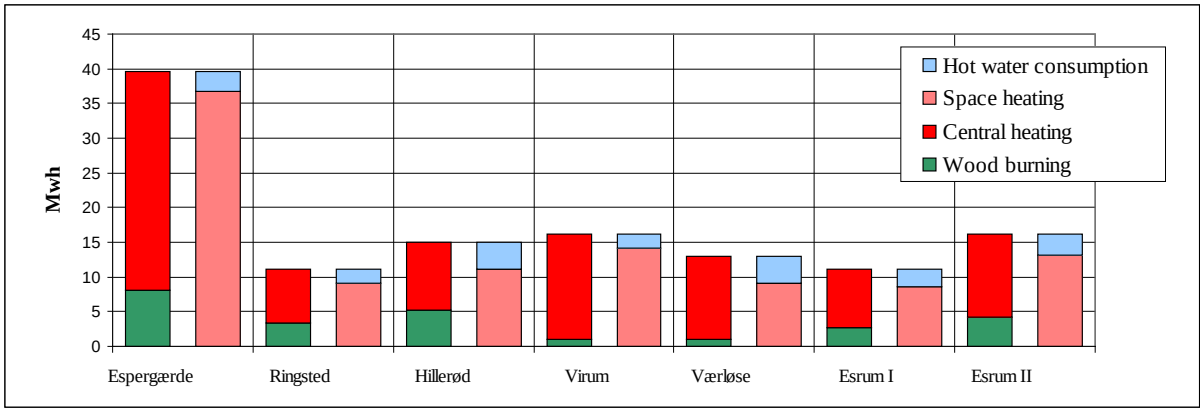

Figure 1. The heat balance based on the figures of net heat production, on one side divided into wood burning and central heating and on the other side into space heating and hot water production.

3.2. Over heating

An adjustment was made in the calculation of the gross energy to compensate for a possible indoor temperature other than 20°C. In any case an average higher than 20°C was found, and as a consequence an adjustment of 3 MWh per house on average was made (see above). This indicated that periods with high comfort temperature or even excessive temperatures might take place in houses heated by means of wood-burning stoves. To investigate the character of possible excessive temperatures, in the second period of measurement, the indoor temperature was logged every hour during the field measurements. In a few cases, temperature loggings were made in steps of two minutes. In short, the loggings showed that excessive temperatures, i.e. temperatures higher than 22°C often occurred. Usually the excessive temperatures happened once or twice a day during the heating season solely in houses with cast iron stoves. In contrast to houses with masonry stoves, the indoor the temperature in houses with cast-iron stoves often oscillated up and down once or twice a day, and sometimes more than 5 degrees in the heating season, see Figure 2.

The biggest adjustment for a high comfort temperature was made in the Espergaerde house. Here an average indoor temperature of 24.8°C was measured. However, in this house heated by masonry stove the temperature around the clock was rather constant.

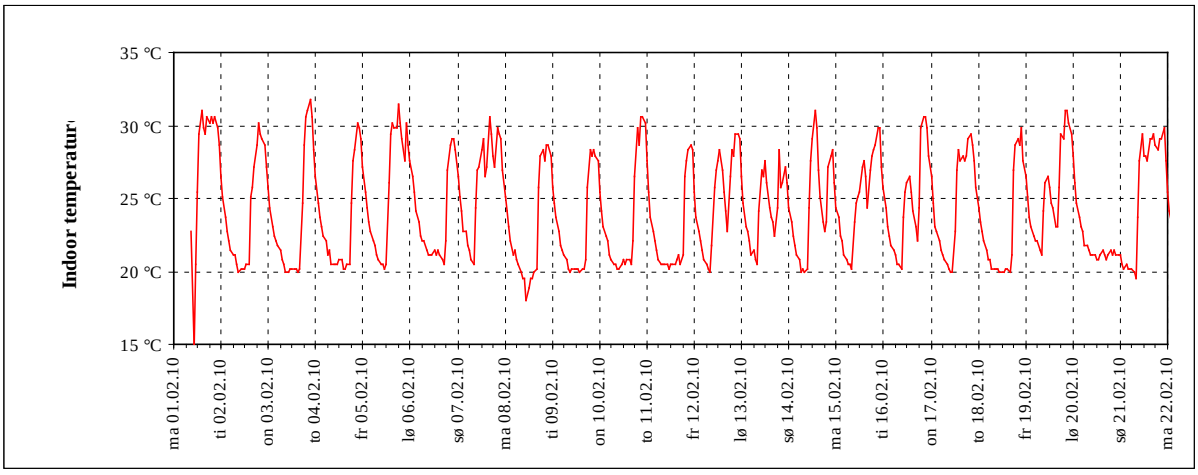

Figure 2. An example of temperature logging in an energy-efficient house carried out over 3 weeks in February 2010. The outdoor temperature in the period was just below 0°C. (Energy Class A).

3.3. Energy performance discussion

Comparing data from the measurements, the interviews and the questionnaires, it became evident that modern wood-burning stoves do function and to a large extent contribute to the heating, also in brand new houses. The advantage of masonry stoves is that they can distribute heat over a long period this way counteracting overheating. Surprisingly, the masonry stoves did not cover the biggest share of the heating, neither in the old house from 1977 (Espergaerde) nor in the new one from 2006 (Ringsted). In the first case the house had large energy consumption and in the second case, the house was equipped with floor heating. Combining stove heating and floor heating was usually less efficient.

4. Indoor emission of particles

Much research has been carried out to detect particle emission rates to the ambient environment. Through laboratory tests, and through measurement on the field is has been possible to set standards of particle emission from wood-burning stoves and to determine the environmental impact to neighbourhoods [6]. A topic neglected is that stoves emit particles to the indoor climate when being operated. Furthermore, among these particles are numerous of ultrafine particles, i.e. particles smaller than 0.1µm. Particles of that scale are suspected of being even more harmful to health than particles smaller than 2.5µm, which are the particles usually being measured. Therefore, the field study set out to look at how operation of a wood-burning stove could cause emission of ultrafine particles and release of gases.

4.1. Particle measurements

Measurements were carried out in two periods, the heating seasons 2009/10 and 2009/10. The measurements started by monitoring the background concentration of particles indoors and outdoors. Then the wood-burning stove was lighted to operate for 1 or 2 hours. [7; 8]. The concentrations of ultrafine particles were monitored by means of two condensation particle counters; one was placed close to the stove, while the second one was used for sampling the outdoor concentration. The two instruments facilitated real-time measurement of particle number concentration. The detection ranges of the instruments ranged between 0.02 and about 1.0 µm. Carbon dioxide, temperature and relative humidity were recorded as well. Finally a passive, multiple tracer gas technique, the so-called PFT technique (PFT: PerFluorocarbon Tracer) was used to measure air-change rates [9]. The duration of the PFT measurements in each house was one week.

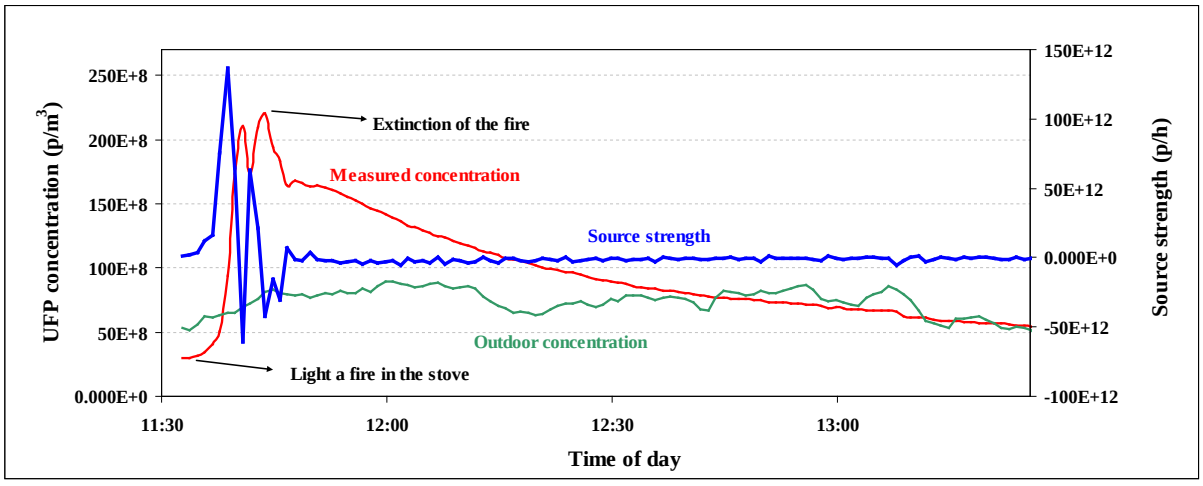

Figure 3. Typical picture of the development of ultrafine particles (UFP). In this case a large emission took place immediately after lighting a fire.

Figure 3 shows that the concentration of ultrafine particles fluctuated for the first 15 minutes after the stove was lighted. A mass balance model, previously applied to analysis of gaseous contaminant concentration, was used. The calculated maximum source strengths and maximum concentration for al measurements of ultrafine particles is shown in Table 5. The concentration of measured ultrafine was fist published in [7; 8].

Table 5. Calculated maximum source strength ($\dot{M}_{max}$), and maximum concentration (C_{max}) for the ultrafine particles studied.

Measured and calculated parameters	C_{max} (p/m^3)		$\dot{M}_{max}$ (p/h)	
	Series 1	Series 2	Series 1	Series 2
Espergaerde	$0.03 \cdot 10^{11}$	$0.24 \cdot 10^{11}$	-	$0.20 \cdot 10^{15}$
Ringsted	-	$1.55 \cdot 10^{11}$	-	$1.96 \cdot 10^{15}$
Hilleroed	$0.05 \cdot 10^{11}$	$0.11 \cdot 10^{11}$	0.00	$9.19 \cdot 10^{7}$
Virum	-	$0.99 \cdot 10^{11}$	-	$1.60 \cdot 10^{15}$
Værloese	$0.22 \cdot 10^{11}$	$0.80 \cdot 10^{11}$	$0.14 \cdot 10^{15}$	$0.44 \cdot 10^{15}$
Esrum I	$2.23 \cdot 10^{11}$	$2.16 \cdot 10^{11}$	$2.14 \cdot 10^{15}$	$1.46 \cdot 10^{15}$
Esrum II	$2.36 \cdot 10^{11}$	-	$0.03 \cdot 10^{15}$	-
Espergaerde	$0.02 - 0.05 \cdot 10^{11}$	$0.02 - 0.05 \cdot 10^{11}$	0.00	-

4.2. Particle emission discussion

During the field study it became clear that in both series, with and without an expert lighting the fire, considerable emission of ultrafine particles to the indoor air might happen, in particular at lighting the fire and adding more wood. But other causes were identified as possibilities for particle pollution, like use of fabric gloves, touching the air valve and suddenly indoor draught. Peak concentration of particles was measured during lighting of a new stove installed in a brand new house (Esrum I and II). One possible explanation for the emission of particulate matter could be a negative indoor-outdoor pressure difference due to the mechanical ventilation system. Moreover, both of the houses mentioned were new, presumably rather airtight and the stoves had chimneys with a height of about 5 meters indoors.

The house in Hilleroed formed an exception in the series of measurements. In this house no elevated concentrations of ultrafine particles were measured except from a slight increase when the side lining of the furnace was dismounted in order to demonstrate the convection principle. The increase was recorded to be a maximum concentration of $0.11 \cdot 10^{11}$, i.e. double background concentration.

5. Conclusion and recommendations

It still seems promising to use a wood-burning stove in new houses. By using small amounts of wood up till one third of the heating demand could be met by this renewable energy resource. However, the field study confirmed that it is still a challenge for the manufactures of wood-burning stoves to meet the decreasing demand of wattage. Still more efficient buildings call for scaling down of the wattage, if overheating is to be prevented in future design. In this perspective masonry stoves were found to be the most adequate to new houses (e.g. the Ringsted house). The challenge to manufacturers of cast-iron stoves is to develop stoves with smaller combustion chambers and a better capability for distributing the heat. Use of heavy

materials, like masonry stoves, phase change materials or connection to water reservoirs, if not to floor heating system it self may be a way of meeting the challenge. Scaling down the stoves means scaling down the size of the combustion chamber. This however makes it even more difficult to obtain a clean and efficient combustion process. Furthermore, possible pollution with particles and hazardous substances is more likely to happen. The tendency will be strengthened by the fact that highly developed wood-burning stoves are already today sensitive to airtight building envelopes and mechanical ventilation. In this field study it was found that modern stoves were actually extremely difficult to light and add more wood without causing particle emissions.

To conclude, there is a call for innovation of new smaller, more efficient and more particle-safe wood-burning stoves. Today already there is a need for guidance for salesmen and users of wood-burning stoves explaining not only the right size of the stove and the correct way of lighting it, but also the importance of an optimal interaction between stove and building.

References

[1] Danish Energy Agency, Energy Statistics, 2009.

[2] Danish Ministry of the Environment, Bekendtgørelse om regulering af luftforurening fra brændeovne m.v. (Executive order on regulation of air pollution from wood-burning etc), BEK nr 1432 af 11/12/2007.

[3] The European Parliament and of the Council of 16 December 2002 and of 19 May 2010 (recast) Directive 2002/91/EC and 2010/31/EU on the energy performance of buildings (EPBD).

[4] Nordic Labeling, Nordic Eco-labeling Closed Fireplaces, version 2.2, 2006.

[5] J. S. Andersen, Dimensionering af brændeovne (dimensioning of Wood-burning stoves), Danish Energy Agency (http://www2.mst.dk/WebApps/aspnetApps/_ex/Braendeovne/)

[6] M. Glasius, M. Ketzel, P. Wåhlin, R. Bossi, J. Stubkjær, O. Hertel, F. Palmgren, Characterization of particles from residential wood combustion and modelling of spatial variation in a low-strength emission area, Journal of Atmospheric Environment 42, 2008, pp 8686–8697, Elsevier.

[7] A. Afshari, O. J. Michael, N. C. Bergsøe, R. L. Carvalho, Impact of operating wood-burning stoves on indoor air quality, Danish Building Research Institute, International Society of Indoor Air Quality and Climate, The 12th Conference of Indoor Air 2011, 2010.

[8] R. L. Carvalho, Energy performance of wood-burning stoves and its impact on indoor air quality, Danish Building Research Institute, Master thesis in Sustainable Energy Systems, University of Aveiro, Portugal, 2010.

[9] N. C. Bergsøe, Passiv sporgasmetode til ventilationsundersøgelser (Passive tracer gas method for ventilation investigations). Danish Building Research Institute, SBi-rapport 227, 1992.

Energy Led Refurbishment of Non-Domestic Buildings – Who Leads?

Megan E. Strachan* and Phil Banfill

Heriot Watt University, Edinburgh, Scotland
**Megan E. Strachan. Tel: +44 1314514664, E-mail:mes8@hw.ac.uk*

Abstract: Innovative and efficient refurbishment offers significant carbon savings and is a growing activity, driven by Government imposing energy or carbon related standards and policies upon building owners. Many businesses are becoming aware of the wider benefits of these improvements and therefore, their requirements as construction industry clients are changing. Built environment professionals need to recognize this change to remain competitive. This paper considers the question of whether there is a need for a re-alignment of disciplines within the industry to fulfill this growing role. A desk study, supported by structured interviews with users of large, non-domestic buildings and with industry professionals concluded that there is a role within the construction industry for a new built environment professional. A competence specification for this professional was defined and this paper outlines the skill set and knowledge base that this individual would require in order to deliver a truly innovative, comprehensive and compatible intervention set within an energy led refurbishment.

Keywords: *Energy, Refurbishment, Client requirements*

1. Introduction

The pressure placed on the built environment to reduce its CO_2 emissions affects how clients treat their property portfolios. They expect construction professionals to take the lead in energy led refurbishment. The purpose of this paper is to explore the effectiveness of construction professionals, who already deal with a range of design-related issues, in leading such energy-led refurbishment. The main objective of this paper is to identify the competences required of built environment professionals able to lead this work, informed by both a desk study of their governing bodies' requirements and interviews with a small but representative group of professionals.

2. Methodology

A desk study surveyed the competency sets required by professional institutions. Structured interviews with 4 experienced professionals from building surveying, facilities management, project management and quantity surveying, and 3 clients (2 facilities managers and one energy manager) used open-ended questions to encourage discussion. The individuals were very experienced and the interviews were held in their offices, recorded and transcribed afterwards. This process allowed for reflection of the results and key points. .

3. Interview Results

Due to the number of interview questions - twenty-three questions for the construction industry professionals and sixteen for the industry clients – and the limitation on page numbers, the questions will not be presented. However, the questions and corresponding responses have been grouped into themes and it is these themes that are presented within 3.1 and 3.2 of this paper.

3.1. Construction Industry Professionals

3.1.1. Refurbishment Context

The interviewees generally agreed that the refurbishment process can vary widely, with works ranging from cosmetic to changing the function of an entire building.

3.1.2. Education and Training

All the interviewees felt that their original education and training equipped them for their work, but their, possibly over ten years old, qualifications lack emphasis towards energy performance in buildings. Participant 1 stated that sustainability was addressed by their assessment of professional competence with the Royal Institute of Chartered Surveyors (RICS) but at insufficient depth for their day to day work. Those interviewees responsible for building design felt that they were under pressure to be aware of new technologies and materials as well as sustainability policies. Whereas those responsible for managing the design felt under less pressure, but need sufficient awareness to participate in design team discussions. The main pressure was coming from their clients' need for advice on sustainability issues. All were keen to undertake some re-training in the area of low carbon building design and operation, and stated that it would be beneficial if there were more Continuous Professional Development (CPD) events in this subject. The main barrier to undertaking re-training is finding the time to attend due to the pressures of their current role.

3.1.3. Professional Governing Body's Attitude

The participants felt that their professional bodies had recently increased the focus on sustainability and its related issues, evidenced by an increased number of seminars and events on the subject. Participant 2 (engineering background) felt the Chartered Institution of Building Services Engineers (CIBSE) was pushing the 'Low Carbon Consultant' qualification forward, and he wished to pursue this as a credible path to specialising in low carbon design and operation of buildings. The others felt that their professional governing bodies were providing more guidance and seminars in the area but envisaged no change to their core competencies, from what they currently perceive, as an outline overview of sustainability.

3.1.4. Companies' Attitudes

All interviewees were aware of their companies' environmental policies and mission statements. Participant 3 remarked that information on the company's intranet brought the issues to their attention. Participant 4 described his company as forward thinking recognising the great commercial opportunity offered by becoming leaders in the field of sustainability, but did not apply the same practices to their own property portfolio. He believed that true leaders should improve their own properties as well as their clients'. Those needing to advise clients on technical aspects remarked that the message they got from their company was to present improving energy performance as a cost saving for the client, whereas those in a management role felt the company would never tell their clients what to do but rather base everything upon the client's requirements. Participant 4, involved in a range of project types within existing buildings, highlighted that within his company, there are several experts in the low carbon area because they have a keen interest in it or because they are part of the small teams the company creates to work on such projects, but their expertise was not transferred across all disciplines. Although, they felt they could always go to them to discuss issues or ask for advice. Overall the main conclusion drawn from the interviews was that the professionals are supported by their company if they choose to become more interested in sustainability, but are neither incentivised nor penalised if they do not.

3.1.5. Clients' Attitudes

Over the last five years many clients have run projects looking at lighting, cooling, controls etc, but this had slowed down with the recession. Conversely, since the Carbon Reduction Commitment Energy Efficiency Scheme (CRC) – a UK based mandatory emissions trading scheme for large energy users - was launched, clients are being forced to consider energy

performance, and so far the professionals have found some clients to be wary of the scheme and try to avoid financial penalties, while others see it as an opportunity to show how energy conscious they are. Participant 3's comment "got to link it to cost to force change" referred to the need to link energy performance initiatives to financial incentives or penalties. They explained how many public sector clients have to achieve certain environmental performance standards, such as a BREEAM excellent rating, as a minimum in order to gain funding for their project. Other public sector bodies are appointing internal sustainability managers that the client must answer to and this pressure is then being passed onto the design team.

3.1.6. Importance of Energy in Buildings

All of the professionals concurred that energy performance of the building comes third behind health and safety and operational performance. However participant 1 did consider energy performance to form a major part of the operational considerations. In terms of the importance of energy performance of a building within a refurbishment scheme, the participants all agreed that capital cost comes first, although participant 4 stated that they try to communicate the benefits of lower operational costs due to energy saving interventions in the design and it was a matter of convincing clients to look beyond capital cost.

3.1.7. Decision Making in Refurbishment

The level of client involvement on projects depends upon the client type; the professionals explained that some clients are happy to provide basic requirements, e.g. function and seating capacities, while others want to be aware of all decisions made. They found that larger companies with internal design teams already have design guides in place to aid selection of interventions and it depends upon the client how closely the external consultants must follow these guides. The main point made by the professionals was that there is no standard process to refurbishment; the decisions are made based upon the design team's experience.

3.1.8. Who Leads?

All of the professionals stated that the mechanical and/or electrical engineer could be suited to taking the lead as they have an in depth understanding of the building's energy consumption but debated whether they would have the leadership competencies to do so, since experience suggests they are very focused upon their area and reluctant to comment more widely. Other professionals identified the building surveyor as a potential candidate due to their broader technical knowledge of buildings combined with their project management competence.

3.2. Construction Industry Clients Interview Results

3.2.1. Company's Attitude

All participants take a proactive approach to works on their property portfolio. Participant 5's internal team of designers creates design guides with energy performance requirements which external consultants follow. Some admitted that their buildings weren't at the leading edge of energy efficiency but they took responsibility for what they consumed and wanted to reduce that as far as possible. All had witnessed a change in their companies' attitudes, since the late nineties, driven by their clients wanting to see evidence of effective and efficient working practices. Participant 5's organisation has seen three pressures to become more focused upon sustainability and energy in buildings: firstly, their corporate responsibility reporting, a key driver, secondly, cost reduction to allow money saved on energy to be spent elsewhere, and thirdly, the CRC scheme (see 3.1.5), the introduction of which has driven their organisation to make changes such as accreditation of their building to the Carbon Trust standards. Initially their organisation's concerns were with the reputational aspect of the CRC Scheme and they

were determined to be in the upper quartile of the public CRC league table alongside their industry competitors. However, this puts them at risk of future changes to the scheme.

3.2.2. Company Strategy towards its Stock

Participant 5's company has a proactive strategy towards improvement of their stock, with a continuous upgrade investment programme. Participant 6's company has guidelines for improvement of their portfolio with an energy performance charter, supported by an internal, Europe-wide forum to learn and share best practice. All participants have internal energy performance targets that work in line with their businesses. Participant 5's sustainability framework includes scrutiny of energy performance and puts the highest responsibility on a non-executive director at board level. All agreed that energy performance is high on their agenda. Participant 7's organisation's main driver for building selection is location quality. Energy efficiency comes third and if necessary they will include energy interventions such as fabric upgrades and controls within the fit out, but no major changes to key plant items.

3.2.3. Whom do you consult?

All explained that their organisations use both internal and external construction consultants, depending on the complexity and scale of the project at hand. Participant 5's company use an internal, technical compliance team to prepare and ensure compliance with their own design guides and the energy standards. They have a framework of external consultants who carry out and manage the design in accordance with these internally set standards. All of the participants stated that they have contractual relationships with external consultants and those contracts include energy performance related clauses. The most specific are with the repair and maintenance engineers, and participant 5 explained that the engineer must deliver year on year energy consumption reductions, the progress of which are discussed at monthly contract framework meetings. Participant 7 explained that they need to see evidence of the experience of these external professionals in energy performance improvements and how they have been innovative in past, similar projects. Participant 5 explained that clients are frustrated by the same initiatives and ideas/approaches to improvements in their properties coming from different consultants who are afraid to take risks with newer technologies/ideas. They look for openness and an ability to provide non-standard solutions, achieving the same conditions in their properties but without being restricted to standard, constant volume systems. They expect innovation from the industry experts.

3.2.4. Your Optimum Professional

The majority of the participants agreed that a mechanical and electrical consultant or engineer who has the competencies required to run or lead a project would be the ideal candidate because electricity is their largest outgoing. However they emphasised that they want someone who doesn't cover old ground, who can bring innovative ideas to the table and who can also build strong relationships with similarly innovative contractors and consultants. Participant 5's ideal professional is a controls engineer because focusing on controls does not require replacement of key plant and takes the control of the building to some extent out of the occupier's hands so they can be comfortable but not wasteful. However, they did state that they have not yet worked with a controls engineer who can work with and be intimately knowledgeable of the building, communicate their findings or ideas successfully and then be able to lead a project as well.

4. Discussion

4.1. Potential for a New Professional

Both professionals and clients agreed that a mechanical or electrical engineer is associated most with energy usage in buildings and has the required detailed technical knowledge, and that they would have an in depth understanding of how the building consumes energy and the standards that must be met in non-domestic properties. However, they had never worked on a project where the mechanical or electrical engineer was the lead except where the building required an unusually high level of plant. One professional explained that, in their experience as a project manager, mechanical or electrical engineers tend to focus entirely upon their area of expertise. So the project manager felt that the response to any questions outside that area of expertise was "can't answer that question, we've done our bit". In contrast, the clients wanted a leader to invoke innovative solutions across the property, that were not restricted to the plant room, and they hadn't so far found these leadership qualities in the mechanical or electrical engineers. Half of the professionals stated that the building surveyor may be suited to running an energy-led project due to their broad knowledge of building fabric and mechanical and electrical services as well as their ability to manage projects, and the building surveyor agreed that he would be wish to become more specialised in sustainability and energy in buildings. To lead such a project they would need training to become more familiar with both the legislative and policy side, alongside the technical interventions available. In summary both the professionals and clients interviewed saw the potential for a new service, potentially provided through existing professional routes. The professionals agreed that they all need to learn more in the area but a new or existing discipline needs to branch out into energy in buildings, existing disciplines expanding upon their original technical and management skills.

4.2. Barriers to a New Professional

Developing a new professional would alter the structure of the design team and require a client to accommodate an additional set of fees on projects where an entire design team is required. Participant 3 provided an example of where many of their clients are required, by their organisation, to achieve a minimum BREEAM rating [1], thus forcing them to consult a BREEAM advisor. However, due to the low fees available for this advisor, that individual is not used to their full potential, and is brought in for an initial workshop which often turns into a checkbox exercise, when they could be assessing and contributing to the design. In order to get the client to pay an additional set of fees on larger projects, they would need to be forced to employ that professional to ensure delivery of a particular credit or rating level. Participant 3 also remarked that the new professional would have to be accredited in some form to prove to the client that they are worth employing due to the new nature of the role.

4.3. Drivers behind Energy-Led Refurbishment

One of the major drivers behind energy improvements to client properties is government policies that force them to review and improve their energy performance through reputational and financial penalties. An interesting point to arise from the interviews was the need for careful design of these policies to ensure the desired results are achieved. For example one professional described how a public sector client was forced to meet the local council's renewable energy policy, by ensuring that their properties included a minimum level of energy supply through renewable technologies. There was debate over which heating system to implement and due to such a heavy focus on renewables, the decision was taken to install a cheaper (capital cost) electric heating system instead of a more energy efficient alternative and an air source heat pump was installed to meet the renewables requirement. As a result the building only achieved a C/D rating in its Energy Performance Certificate [2]. If the focus had

been on the energy performance of the building as a whole then perhaps a B rating could have been achieved instead, resulting in a more energy efficient property. Following the interviews with owners of large, non-domestic portfolios, it was clear that the drive for refurbishment will also come from their own business needs. Some of those interviewed explained that in the current financial climate they are trying to reduce their property portfolio whilst ensuring growth in the core services they provide. This has resulted in less new build procurement and potentially decreasing the number of properties already in use by moving staff into the same buildings. This adaptation of existing buildings can only provide increased opportunity for energy efficient improvements.

4.4. Construction Industry Views on Energy-Led Refurbishment

One professional pointed out that some other professionals believe that the clients must ask for specific energy requirements during the project briefing and that it is not their job to tell the client what their requirements are. Other professionals disagree and see it as their job as the industry expert to inform the client of opportunities available to them if they consider the energy performance of their property. Some of the professionals explained that they feel it is inappropriate to put forward energy performance requirements to the client as they may not have the budget or may be running a separate energy related project. These barriers to pushing the focus onto energy performance need to be overcome if energy performance is to be taken seriously. In recent years, a sustainable building that does not waste energy is now being seen as a higher quality building. The United Kingdom's Green Building Council's Chairman states that "...good sustainability practice is good business practice – it's about producing better quality products, materials and buildings." [3]. The triangle of cost, time and quality is still prominent in the industry and some professionals do not see efficient energy usage in buildings fitting into that shape. However the clients interviewed have shown that they are eager for the construction industry to take the lead and to show them true innovation.

5. Optimum Built Environment Professional Competency Set

Consideration of the competency sets laid down by the governing bodies of the construction industry professionals, combined with the outcome of the interviews held with built environment professionals and clients, leads to the following set of optimum competencies. This optimum competency set aims to define the core skills that a construction professional must fulfil in order to successfully promote and lead an energy-led refurbishment of a non-domestic property, one that will deliver a truly innovative, comprehensive and compatible intervention set. Table 1 presents the established built environment professions against the optimum competency set and shows which competencies each professional currently fulfils in accordance with their governing bodies' guidance. This is not the first time that the competency sets offered by built environment professionals have been critically examined in response to externally imposed changes. For example the development of project management into a clearly defined, accredited profession within the construction industry, codified a role that was previously considered as an additional competency of other construction professions. Accreditation of architects in building conservation is now established, and offers an alternative route to competence. It is evident that clients want to make their buildings more energy efficient but they are not getting what they need from the industry. They want innovative bespoke solutions that work for their buildings but to offer these the professional needs to be knowledgeable about new technologies and materials and to be able to present their benefits clearly. Current professionals admit that they do not know enough about energy in buildings so either a new profession is needed or the competences of existing professions must be overhauled.

Table 1 Optimum Built Environment Professional Competency Set for Energy-led Refurbishment

Quantity Surveyor	Project Manager	Facilities Manager Consultant	Building Surveyor	Building Services Consultant	Architect	ESTABLISHED BUILT ENVIRONMENT PROFESSIONS		
✓	✓		✓		✓	Contract Practice [Awareness of construction contract types and contract law & how to incorporate energy performance criteria into contract clauses]	MANGEMENT	OPTIMUM COMPETENCY SET
		✓				Energy-Led Project Appraisal [Analysis of client requirements to establish a project brief. Gain thorough understanding of the client's organisation, how they obtain project funding, their sustainability policies/targets/managers]		
	✓	✓			✓	Leadership [Core to the role, aware of leadership/motivation techniques, and encourage innovative working environments]		
✓	✓	✓				Programme and Planning [Key competency of any project leader]		
	✓					Project Administration [Key competency of any project leader]		
		✓		✓	✓	Relationships with Suppliers and Specialists [Appoint innovative, experienced design teams & have strong networking capabilities]		
✓	✓	✓	✓			Risk Management [Manage risk especially where new technologies are employed]		
✓	✓	✓	✓		✓	Sustainability Knowledge [Full understanding of sustainability in construction be able to communicate and make it relevant to a client]		
✓			✓		✓	Design Economics and Cost Planning [Aware of how interventions impact capital cost & operational cost using whole life costing techniques to communicate this]	FINANCIAL	
✓	✓				✓	Procurement and Tendering [Sound knowledge of different procurement routes]		
			✓			Building Pathology [Thorough knowledge of building fabric, must understand typical defects that may arise due to particular interventions and how they can be addressed. Aware of how the building fabric affects building air movement, moisture movement and temperature variations]	TECHNICAL	
			✓			Conservation and Restoration [Aware of conservation principles as this professional will be specialising in the existing built environment]		
✓	✓	✓	✓	✓	✓	Construction Technology [Understanding of common & emerging technologies]		
			✓			Energy Performance Policies/Initiatives [Aware of and communicate the significance of energy performance related policies/initiatives and how they can be met within a refurbishment project]		
✓		✓	✓	✓	✓	General Understanding of Building Services [Understanding of building services & how they can be made more efficient, be able to communicate with M&E specialists]		
						Holistic Approach [Must have a holistic view of the property and understand what interventions are compatible with one another and the building. Consider energy demand before energy supply solutions to reduce energy wastage]		
		✓	✓	✓		Inspection [Able to lead a thorough pre-refurbishment inspection & be able to guide the focus towards energy performance improvements]		
		✓	✓	✓	✓	Legal and Regulatory Compliance [Specific knowledge of energy requirements]		

.

6. Conclusion

For the growing field of energy-led refurbishment, industry and clients desire competencies that are not currently offered by any existing professional group practising in the UK. This deficiency can be remedied either by developing a new profession, for which the desired competencies have been presented in this paper, in the same way as Construction Project Management was developed, or by establishing a recognizable specialized branch of an existing profession, in the same way as with architects or building surveyors who specialize in building conservation/preservation. Even though the study was carried out in the UK, the professions of those interviewed are internationally recognized. It would be interesting in a future study to compare the views expressed in other countries.

References

[1] BREEAM (2009) BREEAM Bespoke Single and Multiple Building Criteria [online]. Available from: http://www.breeam.org/page.jsp?id=181 (Accessed 21 November 2010)

[2] Directgov (2010) Energy Performance Certificates - What they are [online]. Available from: www.directgov.uk/en/HomeAndCommunity/BuyingAnd Selling Your Home /Energy performancecertificates/DG_177026 (Accessed 21 November 2010)

[3] King, P (2010) Good Sustainability Practice is Good Business Practice [online]. Available from: www.british-gypsum.com/literature/brochuresleaflets/csr report 2010 pdf.aspx (Accessed 21 November 2010)

[4] Royal Institute Of British Architects (2010) It's Useful to Know... [online]. Available from: www.arc-in-form.com/free/ItsUsefultoKnow.pdf (Accessed 21 November 2010)

[5] Royal Institute of Chartered Surveyors (2006a)Your Pathway to Qualifying in Building Surveying [online]. Available from: www.rics.org/site/scripts/documents_info.aspx?documentID=390&pageNumber=3 (Accessed 21 November 2010)

[6] Royal Institute of Chartered Surveyors (2006b)Your Pathway to Qualifying in Project Management [online]. Available from: www.rics.org/site/scripts/documents_info.aspx?documentID=390&pageNumber=3 (Accessed 21 November 2010)

[7] Royal Institute of Chartered Surveyors (2006b)Your Pathway to Qualifying in Quantity Surveying [online]. Available from: www.rics.org/site/scripts/documents_info.aspx?documentID=390&pageNumber=3 (Accessed 21 November 2010)

[8] Chartered Institution of Building Services Engineers (2009) Competence Criteria for MCIBSE [online]. Available from: www.cibse.org/pdfs/M2.pdf (Accessed 21 November 2010)

[9] British Institute of Facilities Management (2010) The BIFM Revised Competencies [online]. Available from: www.bifm.org.uk/bifm/membership/individualmembership/FMcompetences (Accessed 21 November 2010)

[10] Mansfield, J. (2001) 'What's in a name? Complexities in the definition of "refurbishment"', Property Management, vol.20, no.1, pp.22-30

Influence of external actors in Swedish homeowners' adoption of energy efficient windows

Gireesh Nair[1*], Krushna Mahapatra[1], Leif Gustavsson[1, 2]

[1]*Mid Sweden University, Östersund, Sweden*
[2] *Linnaeus University, Växjö, Sweden*
[*] *Corresponding author. Tel: 46 63165428, Fax: +46 63165500, E-mail: gireesh.nair@miun.se*

Abstract: A questionnaire survey of 1010 homeowners (response rate of 59%) in two counties in central Sweden viz., Jämtland and Västernorrland was conducted to understand the influence of external actors on homeowners' decision to install energy efficient windows. We complemented this survey with interview of 12 window sellers/installers in the Jämtland county. Majority of homeowners (74%) contacted more than one external actor for information when they plan to replace their windows. Window sellers/installers have a strong influence on homeowners' window selection as 97% of homeowners bought the windows that were recommended to them. The sellers/installers recommended windows with a U-value in the range of 1.1 to 1.8 W/m^{2}K and cited that condensation and high cost are the major drawbacks of windows with a U-value < 1.2 W/m^{2}K.

Keywords: *Energy efficient windows, homeowners, sellers, installers, Sweden*

1. Introduction

Diffusion of energy efficient windows in Swedish building sector may reduce fossil fuel dependency and mitigate climate change. The thermal performance of windows in Sweden has improved over the years and the energy efficiency standard is higher than that of many other countries. For example, in Sweden a window is considered energy efficient if its U-value is ≤ 1.2 W/m^{2}K [1], while in Denmark the U-value for such windows is ≤ 1.8 W/m^{2}K [2].

About 85% of detached houses in Sweden are more than 30 years old [3], and windows in many of these buildings may be in poor condition. Moreover as these buildings were built before energy efficiency was emphasized in the building codes in 1977, a large market is available for energy efficient windows. A survey of owners of detached houses in Sweden revealed that homeowners are more likely to replace/change windows than other building envelope components [4]. Due to their long life span the type of windows installed will influence the energy use of the buildings for a long time. From primary energy saving perspective, it is important that homeowners adopt the most energy efficient windows available in the market.

Homeowners may not adopt energy efficiency measures because of lack of adequate and reliable information, lack of awareness [5, 6], or the inability to interpret the available information. Furthermore, potential adopters may have difficulties in perceiving the performance and advantages of energy efficiency measures if the gains are not directly visible [7], are insignificant or are delayed. In such situations homeowners' final choice of a particular measure is influenced by actors whom they consider as experts in the field. Homeowners' adoption of a particular type of window may depend on the recommendation of the sources important to homeowners. Window sellers/installers are the closest link to customers in the demand chain, and could exert a strong influence on consumer's choice. To the best of our knowledge, no e mpirical studies about influence of external actors on homeowners' adoption of energy efficient windows have been conducted in Sweden. In this paper, we analyse the role of external actors especially window sellers/installers in homeowners' adoption of energy efficient windows.

2. Role of external actors

Homeowners may seek information or advice because of uncertainties regarding information alternatives or due to uncertainties on which alternative to choose. For high investments, customers may search for information from various sources [8]. The degree to which customers' search for information depends on their perception of the costs associated with the search [8], or their ability and motivation [9]. Sources of information include mass media, interpersonal sources, sellers/installers and neutral sources like municipal energy advisers. Though mass media could improve consumers' awareness about various products their ability to influence consumers' adoption decision is limited to a small group of innovators and early adopters [10]. To reduce the burden of interpreting vast amount of information and to obtain appropriate information homeowners' may seek advice from expert(s) whom they think are credible. The external advice may help the potential consumer to clear their thoughts about the decision and improve their decision confidence [11]. Individuals give more weightage to advice while performing a difficult task compared to an easy one [12]. Hence the relevance of advice may be more pronounced in the adoption of investment intensive measures like windows.

Trustworthiness of a organization working without profit motive (e.g. state agents or non-governmental organizations) is higher than one working for profit motive (e.g. marketing agents) [10]. However, store sales personnel were found to influence customers' choice [13, 14]. Store visits and salespeople are very important source of information for buyers of durables [15, 16, 17], and individuals who are susceptible to interpersonal influence are more influenced by salespersons [18]. Studies in Sweden have shown that homeowners consider sellers/installers as an important source of information when adopting heating system [19], energy efficient building envelope components [4]. This may be because of homeowners' perception that the sellers/installers are experts in their respective field and/or they usually make house visits to make on the spot assessment of the requirements of their prospective clients. Moreover homeowners may consider the window sellers/installers in their locality similar to themselves, and the influence of an *expert* salesperson is high in such circumstances [20].

3. Methodology

The research methodology includes both quantitative and qualitative analysis.
Homeowners' perception of external actor's influence in the adoption decision is based on a mail-in questionnaire survey of homeowners who availed investment subsidy to replace their windows with energy efficient windows (U-value $\leq$ 1.2 W/m^{2}K). Questionnaire were sent to 1010 homeowners in the two neighbouring counties in central Sweden (315 in Jämtland and 695 in Västernorrland) whose addresses were collected from Boverket (Swedish National Board of Housing, Building and Planning) which administrated the programme during 2007-2008. On an average, the homeowners in our survey received 14% of their investment cost as subsidy. The survey was conducted during November – December 2009. 25 questionnaires were returned either due to incorrect address or non residence of the addressee. The response rate for the survey after one reminder was 59%. The questionnaire consisted of mainly three parts. Section A included questions about the reasons for replacement of windows, factors influencing respondents choice of windows, influence of external actors, perception towards energy efficiency measures. Questions regarding the influence of policy instruments in respondents' adoption of energy efficiency measures were covered in Section B. Section C included questions related to socio-economic variables.

To understand the supply side actors' perspective on energy efficient windows, we conducted interview of window sellers/installers in Jämtland county. A list of window sellers/installers in the Jämtland county was prepared based on a search on the yellow pages. All the 29 listed window sellers/installers/repairers were contacted for a semi structured interview. However some of them did not participate because they had discontinued their business or merged with other companies or did not have time or were just into window cleaning business, while three sellers/installers were not interested to participate. Accordingly, we interviewed 12 sellers/installers. The interviews were conducted during November 2009 – March 2010. We asked the interviewees mostly open ended questions about their influence on homeowners' choice of windows and their perception towards energy efficient windows.

The interviewed personnel were highly experienced in window business as nine persons had more than 25 years of experience, while two had more than 10 years of experience. Ten of the interviewees were owner or partner of their firm, while two were sales personnel of their organization.

4. Results

4.1. Respondents who availed investment subsidy to install energy efficient windows

79% and 19% of the sample (1010 homeowners) installed windows with U-value 1.2 W/m^{2}K and 1.1 W/m^{2}K, respectively, while the rest 2% installed windows with U-value less than 1.1 W/m^{2}K. The composition of the respondents according to age, education, household income, building age and duration of occupancy in their house is provided in Table 1. Respondents who were old, university educated and who lived in old houses were more likely to replace their windows with energy efficient windows.

Table 1: Composition of the respondents

Age group in years (N=574)	Education (N= 573)	Annual household income ('K SEK) (N= 563)	Building age in years (N=566)	Occupancy period (N=562)
≤ 35 - 9%	Primary - 28%	≤ 150 - 2%	≤ 20 - 1%	≤ 3 year - 15%
36-45 - 18%	Upper - 33% secondary	150 – 300 - 23%	21-30 - 3%	4-10 years - 21%
46-55 - 20%	University - 39%	300 – 450 - 24%	31-40 - 35%	11-20 years - 17%
56-65 - 23%		450 – 600 - 24%	41-50 - 21%	21-30 years - 15%
>65 - 30%		> 600 - 27%	>50 - 40%	31- 40 yeas - 20%
				>40 years - 12%

Note: Percentages are rounded to the nearest unit.

4.2. Information search and role of external actors

For most respondents' window sellers/installers (which include glass working companies) was the most influential actor in their window choice (Table 2). Interpersonal sources such as friends/peers/relatives were reported to be the second most influential external actors. Other external actors were important for only fewer respondents.

Table 2: Importance of external actors' advice in homeowners' choice of windows

Influence of external actor	% of respondents				
	N	Important	Neither nor	Not important	Mean
Window sellers/installers	489	56	22	22	3.51 (0.064)
Friends, relatives and peers	396	33	17	50	2.56 (0.079)
Window manufacturers	388	27	11	62	2.23 (0.080)
Internet forums	373	21	13	66	2.03 (0.075)
Carpenters	377	21	8	71	1.97 (0.077)
Building companies	378	18	8	74	1.83 (0.077)
Municipal energy advisers	363	14	6	80	1.63 (0.066)
Energy companies	345	1	4	95	1.15 (0.029)

N = Number of respondents in respective category. Mean values are based on homeowners' response on a Likert scale of 1 to 5 (1 = not at all important, 5 = very important). Values in parentheses are standard errors.

There was no significant relationship among respondents preference for information sources on windows and their demographic characteristics. However, there was a trend that suggests that respondents with different demographic characteristics accorded varying level of importance to the external actors (Table 3). For example, university educated or aged up to 45 years or female respondents gave higher importance to interpersonal sources.

Table 3: Respondents in different demographic groups who attributed greater importance to an information source compared to other groups of respondents

External actor	Respondents' socio-demographic characteristics			
	Gender	Education	Age	Annual household income (1000 SEK)
Window sellers/installers	Female	Basic	>45 years	
Friends, relatives and peers	Female	University	Upto 45 years	150-300
Window manufacturers			>65 years	
Internet forums		University	Upto 35 years	450-600
Carpenters			46-55 years	150-450
Building companies		Basic	>65 years	
Municipal energy advisers		Basic		

Majority of homeowners (74%) contacted more than one external actor for information when they plan to replace their windows. About 60% of homeowners contacted two or more different type of external actors for information. Majority of homeowners contacted window sellers/installers for information on windows, while energy advisers and energy companies were contacted by least number of homeowners (Table 4).

Table 4: Homeowners' frequency of contact to external actors for information about windows

External actor contacted by homeowners	N	% of respondents contacting a specific external actor		
		Contacted many	Contacted only one	Did not contact any
Window sellers/installers	519	47	37	16
Friends, relatives and peers	431	24	24	52
Window manufacturers	430	17	17	66
Building companies	438	10	18	72
Carpenters	427	5	23	72
Municipal energy advisers	418	2	14	84
Energy companies	410		1	99

N – Number of respondents; 5% of the respondents did not contact any of the above external actors.

26% of respondents bought and installed windows themselves, 21% bought windows themselves and installed it through professionals, and 53% replaced windows on *turnkey* basis wherein a professional did the entire window replacement. The homeowners who bought and installed windows themselves may be more knowledgeable in windows as they were more likely to be aware of better energy efficient windows in the Swedish market ($p \leq 0.01$ as per chi-square test) than those who replaced their windows through professionals. 69%, 18% and 11% of respondents entrusted the *turnkey* job to window sellers/installers, construction companies and carpenters, respectively. The various reasons homeowners' entrust the window replacement task to the professionals is given in Table 5.

Table 5: Reasons for entrusting the window replacement task on a turnkey basis

Reasons for entrusting the work on a *turnkey* basis	N	% of respondents		
		Agree	Neither nor	Disagree
The quality of the work would be high	274	85	4	11
It was time consuming to do it myself	251	84	5	11
It was complex to do it	263	75	9	16
Did not have the skill to install windows myself	281	67	10	23
Did not have the knowledge to select right window	272	43	14	43
It was the cheapest option	253	31	19	50
Friends, relative and peers recommended	241	20	10	70

The most important factors for selecting a particular vendor for window replacement was easiness to contact them and the company's reputation to undertake good quality work and service (Table 6).

Table 6: Reasons for selecting a particular vendor for turnkey replacement of windows

Reason for selecting a particular vendor	N	% of respondents		
		Agree	Neither nor	Disagree
It was easier to contact the company	242	69	16	15
Has the reputation of undertaking good quality work	239	65	23	12
Has the reputation of good service	240	63	25	12
Offered the best price	241	49	24	27
Have good experience of their past work	229	28	12	60
Friends, relative and peers recommended	223	22	13	65
Only one who could offer the manufacturer I wanted	220	18	14	68
Only company available locally	214	8	5	87

53% of the total respondents and 64% of those who entrusted the window replacement task on *turnkey* basis reported that the company from which they bought windows had recommended a specific window. About 97% of respondents had installed the windows that were recommended to them.

4.3. Window sellers/installers perspective

The window sellers/installers believed that they exert a very strong influence on their customer's choice of windows. Some of them stated that their suggestions/information had a very strong impact as often the customers were not aware about the choices.

"Normally they [homeowners] decide about the type of windows when I visit them".

"They [homeowners] have many questions, …generally the advice we give weighs heavily".

Window sellers/installers recommend/prefer windows with U-value from 1.1 to 1.8 W/m^2K (Table 7).

Table 7: U-value window sellers/installers prefer/recommend

U- value (W/m^2K)	Number of interviewees
1.1 -1.2	2
1.2	6
1.3	2
1.5	1
< 1.8	1

Majority of the sellers/installers do not recommend U-value less than 1.2 W/m^2K mostly due to condensation problem and high cost of such windows. Some of the interviewees on condensation stated:

" Below 1.2 [U-value] you can get problems with condensation…. There is a wild chase to reduce U-values…. But in reality it does'nt work…"

"Customers think it is too damn that they bought new windows and it gets condensation in the outside"

"…if you get down to 1.2,…, the risk of condensation is large and I think the requirement is too hard"

"If you get highly annoyed if you see a white window when you come down to eat breakfast in the kitchen, it was not nice of you to bought a low U-value window"

According to a couple of sellers/installers, it is difficult to *sell* the window manufacture's argument that the external condensation in windows indicates its high energy efficiency. As per four sellers/installers, condensation in external surface of energy efficient windows occurs only during a very few occasion in Jämtland. As per many sellers/installers if the homeowners were informed about the potential condensation problem then the homeowners will not be "surprised" by condensation and thereby would not be dissatisfied by it. Window sellers/installers usually inform their customers about condensation issue associated with energy efficient windows.

The price of windows with U-value < 1.2 W/m^2K was a concern for many of the interviewees. Eight sellers/installers reported that it was expensive to buy windows with U-value 1.0 W/m^2K, and energy efficiency benefits of such windows compared to windows with U-value of 1.2 W/m^2K was only marginal. Hence, according to window sellers/installers it is not worth to buy such windows.

5. Discussion and conclusion

Prior to window purchases, majority of homeowners approached multiple external actors for information. Hence, Swedish homeowners may undertake active pre-purchase information search before buying windows. This study shows that majority of homeowners' considered window sellers/installers as the most influential actor in their window choice. We found that the influence of window sellers/installers on homeowners was so strong that if window sellers/installers recommended a particular window, homeowners' usually would install it. Other external actors were not that influential. This indicates that window sellers/installers have a determinant role in the diffusion of energy efficient windows in Swedish detached houses Majority of homeowners in our sample (79%) who availed the investment subsidy for window replacement had installed windows that had a U-value of 1.2 W/m^2K. Their choice of

windows with U-value of 1.2 W/m^{2}K may be due to the favourable advice they received from window sellers/installers on such windows and that a U-value of 1.2 was required to receive the subsidy.

Window sellers/installers preferred a window that was "reasonably" energy efficient, and majority did not recommend windows with U-value <1.2 W/m^{2}K. They believed that the investment required for windows of U-value <1.2 W/m^{2}K is not economically justifiable and also such windows cause condensation problem. To convince homeowners about the cost benefits and condensation issues, the sources they rely most (viz., window sellers/installers) need to be confident on those issues. The adoption rate of higher energy efficient windows could be increased by addressing the concerns of window sellers/installers towards condensation issues and higher prices of such windows.

For a significant percentage of homeowners professionals did the entire window replacement. This is mainly because of respondents' perception that the quality of the work would be good or due to time constraints to install windows themselves. Window sellers/installers were the most preferred actor for installing windows on *turnkey* basis. The most common reasons reported for selecting a particular vendor was easiness to contact them and reputation to undertake good quality work and service. The price offered was reported by relatively less number of homeowners in selecting the vendor. This may be because owing to the competition there could be only small price difference similar windows sold by vendors.

Only 14% of respondents considered energy advisers as an important source of information on windows, and only 16% contacted an energy adviser. Our result is similar to earlier findings on homeowners contact with energy advisers [21]. The reasons could include low awareness about the energy advice service and a perception that energy advisers may not be experts in windows.

Our discussions on ho meowners' adoption decision are based on a mail-in questionnaire survey, and this has some disadvantages. For example, about 41% of the homeowners did not respond, and therefore, non-response bias might be a concern which we did not investigate. Furthermore, the respondents may not have entirely understood the questions, as in all questionnaire surveys, and we were not able to clarify the questions, which in turn might have influenced the responses. Similarly, as local climate may influence external condensation on windows, the perception of window sellers/installers on c ondensation in energy efficient windows and their subsequent recommendations may vary across Sweden.

Acknowledgments

The authors gratefully acknowledge the financial support from Swedish Energy Agency and from the European Union. We like to thank Kerstin Hemström for conducting the interviews.

References

[1] B. Kiss, Energy efficient window development – Historical overview of the development of energy efficient windows in Sweden, Energitinget, 11- 12 March, 2009, Stockholm.

[2] D. Avasoo, Energy transparency for energy efficiency. A Future buildings forum event - Cooling buildings in a warming climate, 21-22 June, 2004, Sophia Antipolis, France.

[3] SCB, Yearbook of Housing and Building Statistics 2009 (Bostads- och byggnadsstatistisk årsbok 2009), 2009, Statistics Sweden, Örebro, Sweden, ISSN 1654-0921

[4] G. Nair, L. Gustavsson, K. Mahapatra, Owners perception on adoption of building envelope energy efficiency measures in Swedish detached houses, Applied Energy, Applied Energy 87, 2010, pp 2411-2419.

[5] S. Birner, E. Martinot, Promoting energy-efficient products: GEF experience and lessons for market transformation in developing countries, Energy Policy 33, 2005, pp 1765–1779.

[6] S. Owens, L. Driffill, How to change attitudes and behaviours in the context of energy, Energy Policy 36, 2008, pp 4412–4418.

[7] M. Levine, D. Ürge-Vorsatz, K. Blok, L. Geng, D. Harvey, S. Lang, G. Levermore, M.A. Mehlwana, S. Mirasgedis, A. Novikova, J. Rilling, H. Yoshino, Residential and commercial buildings. In Climate Change: Mitigation. Contribution of Working Group III to the 4th Assessment Report of the IPCC, Cambridge University Press. NY, 2007.

[8] D.I. Hawkins, D.L. Mothersbaugh, R.J Best, Consumer Behavior: Building Marketing Strategy. McGraw Hill/Irwin, New York, 2007.

[9] J.R. Bettman, C.W. Park, Effects of prior knowledge and expereince and phase of the choice process on c onsumer decision processes: A protocol analysis, Journal of Consumer Research 7, 1980, pp 234-248.

[10] E.M. Rogers, Diffusion of Innovations. The Free Press, New York, 2003.

[11] F. Gino, D.A. Moore, Effects of task difficulty on use of advice, Journal of Behavioral Decision Making 20, 2007, pp 21–25.

[12] C. Heath, r. Gonzalez, Interaction with others increases decision confidence but not decision quality: evidence against information collection views of interactive decision making. Organizational Behavior and Human Decision Process 61, 1995, pp 305–326.

[13] R.W. Olshavsky, Consumer-Salesperson interaction in appliance retailing, Journal of Marketing Research 10, 1973, pp 208-212.

[14] B.G. Goff, J.S Boles, D.N Bellenger, C. Stojack, The influence of salesperson selling behaviors on customer satisfaction with products, Journal of Retailing 73, 1997, pp 171 - 183.

[15] A.L. Pennington, Customer-Salesman bargaining behavior in retail transactions, Journal of Marketing Research 5, 1968 pp 255-262.

[16] J.T. Rothe, L.M. Lamont, Purchase behavior and brand choice determinants for national and private brand major appliances, Journal of Retailing 49, 1973, pp 19-33.

[17] A.G. Woodside, J.T. Sims, Retail sales transactions and customer 'Purchase Pal' effects on buying behavior, Journal of Retailing 52, 1976, pp 57-64.

[18] T.Sun, Z.Tai, K-C, Tsai, The role of interdependent self-construal in consumers' susceptibility to retail salespersons' influence: A hierarchical approach, Journal of Retailing and Consumer Services 16, 2009, pp 360-366.

[19] K. Mahapatra, L. Gustavsson, An adopter-centric approach to analyze the diffusion patterns of innovative residential heating systems in Sweden, Energy Policy 36, 2008, pp 577–590.

[20] A.G. Woodside, J.W.Jr. Davenport, The effects of salesman similarity and expertise on consumer purchasing behavior, Journal of Marketing Research 11, 1974, pp 198-202.

[21] K. Mahapatra, G. Nair, L. Gustavsson, Energy advice service as perceived by Swedish homeowners, International Journal of Consumer Studies 35, 2011 pp 104-111.

The 'time' dimension of electricity, options for the householder, and implications for policy

Sarah J. Darby

Environmental Change Institute, University of Oxford, UK
Tel: +44 1865 285163, E-mail: sarah.darby@ouce.ox.ac.uk

Abstract: Electricity has always had a 'time' dimension for suppliers, and the advent of variable renewable generation may make this dimension more obvious to consumers than it has been in the past. Variable generation increases the need for an 'active demand-side', in order to balance load and achieve security of supply, and various forms of smart grid are under consideration and trial, possible prototypes for the grids of the future. However, it is often not clear what the implications of an active demand side are for small-scale end-users, although their participation (or cooperation, at a minimum) is seen as essential. As utilities increasingly require the cooperation of their customers in managing distribution networks, so they need to persuade them to adopt new tariffs, technologies and customer-utility relationships. Four options are outlined and discussed, with the aim of developing a better understanding of the social and behavioural dimensions of distributed generation. The options are based on work carried out as part of the SUPERGEN HiDEF (Highly Distributed Energy Future) project in the UK. The focus is on householders, who have been used to a passive relationship with their energy retailers, along with simple tariffs. Policy questions revolve around how to encourage the cooperation of end-users – an 'active demand side' - and questions of control, equity and data privacy are significant factors in the embryonic public debate over smart grids.

Keywords: *household, electricity, dynamic demand, tariffs*

1. Introduction

Electricity has always had a 'time' dimension from the viewpoint of suppliers: it must be generated, transmitted and distributed in order to meet demand with as little wastage as possible. This has entailed careful planning so that generating plant is available when needed and, increasingly, a degree of planning so that demand from larger consumers is predictable and manageable. However, most residential and small business customers in most parts of the world have been used to a flow of electricity at any time, and at constant prices per unit.

With growing demand, especially growing peak demand, the time dimension has become more and more important to planners – hence the attention paid to demand-side management over the past few decades in parts of the world with sharp peaks, most commonly associated with high demand for air-conditioning on hot afternoons. In regions with a high proportion of nuclear generation, too, there have been adaptations to shift electricity demand in order to use the baseload available at night, such as storage heaters. Now, an increasing proportion of renewable generation increases the need to move from the old 'predict and provide' utility paradigm to one with a more 'active' demand side – where demand can be decreased *or* increased in order to match supply with demand.

Various forms of 'smart grid' are proposed in order to make this accurate matching possible. The term is used to mean many things, just as the term 'smart meter' has meant many things to many people [1]. In essence, though, a smart grid involves the merging of communication networks (fast-evolving technologies) with electricity grids and networks (not much changed in their basic structure since the time of Edison). The European Technology Platform defines the Smart Grid as:

– *an electricity network that can intelligently integrate the actions of all users connected to it -generators, consumers and those that do both –in order to efficiently deliver sustainable, economic and secure electricity supplies.* [2]

The intention is that smart grids will enable and/or require customer 'participation' , allowing for better control of generation, distribution and usage at all levels. But early pilot grids (such as those in Boulder, Colorado, and Amsterdam) are raising as many questions as they are answering. There are still fundamental questions to be asked about approaches to the smart grid. For example, should it be incremental and carefully costed and tested at each stage, or implemented comprehensively through massive infrastructure investments, in confidence that enough applications will emerge to justify those investments? If the latter, how are customers to be persuaded to fund the SG through their taxes and electricity charges? If the former, how much will consumer priorities influence SG development, and how much will the SG influence consumer practices?

While much attention has been paid to technical specifications for these grids, it not always clear what the implications are for small-scale end-users. While the grid itself is seen as an intelligent agent, it is often not clear how electricity customers may also be agents. They tend to be seen as passive elements in the system, communicating only through the billing system and the complaints system. The UK government has probably gone as far as any in its stated ambition for consumer/prosumer participation, in setting out a specification for smart meters that includes provision for microgeneration, customer feedback displays, ability to change supplier and tariff readily, and ability to control devices in the home; and in its statements on the nature of a smart grid. For example:

> A focus on the consumer's perspective must be at the heart of decision making at each stage under the programme; as well as the views of industry participants who will take on responsibility for delivery following changes to the regulatory framework [3].
>
> Consumers will need to be involved in the process of developing the electricity system… plans need to be developed in consultation with consumer interests… Clear rules and arrangements for the protection of consumer privacy will need to be a priority. First step: building increased smartness into homes, giving a clearer picture of energy use, greater choice and control [4].

If there is a sufficiently powerful combination of factors in implementing an active demand side, then the distribution of activity could change significantly. These factors would need to include:

(a) suppliers' and distributors' strong need to cultivate an 'active demand side' in order to manage the system;

(b) the ability and willingness of consumers to become prosumers, contributing to supply and storage as well as using it;

(c) regulatory support for distributed generation and equitable participation; and

(d) reliable and trusted technology.

It may be useful to break down the idea of 'activity' into aspects of control, investment decisions (e.g. network operators investing in substation equipment, or customers investing in efficient freezers or frequency-response-enabled appliances). It is unrealistic to imagine that

all consumers will change from their relatively passive positions in the system to active , interested engagement, but there is potential for some change in most consumers [5].

As utilities increasingly need some cooperation from their customers in managing distribution networks, so they may need to 'teach' customers about the time dimension of electricity flows, in order to persuade them to adopt new tariffs and technologies more readily. An early example of this sort of practical education, conducted in the course of a trial of real-time pricing, is given in [6]. Technological and commercial drivers are moving in the direction of more sophisticated control and pricing arrangements, including real-time pricing, remote control of appliances by the utility, demand aggregation, and 'dynamic demand' through smart appliances. The purpose of this paper is to examine some of these options in order to move towards a better understanding of the social and behavioural dimensions of both 'active demand' and distributed generation.

2. Method

The material for this paper comes mostly from a literature review carried out as part of the SUPERGEN HiDEF (Highly Distributed Energy Future) project in the UK. The project is developing approaches, technologies and policies for an electricity system that provides sustainability, security and low carbon emissions through widespread deployment of distributed energy resources. It analyses possibilities for decentralising five features of electricity systems: resources, control, network infrastructure, participation (markets and commercial arrangements), and policy.

A number of possible types of customer-utility relationship arise from these possibilities. In this paper, four are selected and discussed with an eye to their policy implications. This of course means that other options are ignored – for example, demand aggregation and community energy services companies – but the aim is to open up the debate on active demand, not to give an exhaustive account of all that it might involve.

3. Themes in the active demand literature

The research literature on demand management does not always acknowledge or reflect the variety in electricity systems. This variety can be assessed on a number of scales, but three immediately come to mind: composition and timing of demand, type and scale of generation, and degree of regulation. For example, what are the current patterns of demand, and how much are they likely to alter in future, in what directions? Does the system have large-scale biddable centralized generation, a high proportion of nuclear (inflexible) generation, or a significant proportion of distributed and variable generation? How heavily regulated is the market?

The answers to these questions will affect what is seen as possible and desirable for the future. So will the technologies that are available, and the extent to which they are marketed around the world. Grid management that is suitable for a summer-peaking region with highly regulated utilities may not be applicable to a temperate region with liberalized markets, yet there will be an inevitable push to increase the market for technologies that have been designed for one set of circumstances into areas with other conditions. But as yet, there is not a great deal of experience in implementing demand response in parts of the world other than North America. A recent review of experience in the EU concludes that progress has been slow because of limited knowledge of demand response-related energy-saving capacities. The high estimated cost of necessary technologies and infrastructure, and the policy focus on

market liberalisation [7]. Nor is there much on the relationship between demand response and demand reduction, in spite of its clear importance in terms of reducing the environmental impact of electricity more generally [8, 9]. And neither is there a great deal of research on what demand response means to consumers. Most of what there is comes from research carried out with customers who have opted into a programme, typically a very small proportion of the population to which they belong.

Therefore it is still useful to do some basic thinking about how we might best research demand response as seen from the standpoint of the end-user. As an exercise in this, four possible ways of encouraging an active demand side have been selected, to take an initial look at what they might mean to small-scale consumers or prosumers. They are outlined below.

3.1. Demand reduction via efficiency, rethinking energy services and lowering discretionary demand

Demand reduction is not always included in discussions of active demand, but I would argue that it is a central consideration. Managing a high-demand system is very different (and, mostly, more problematic) than managing a low-demand system. Climate change and energy security considerations mean that demand reduction is still normally a governmental policy objective, even if not necessarily a central objective for de-regulated utilities.

For demand reduction, the supplier-consumer relationship is normally voluntary/persuasive, sometimes assisted by technology. Although improved customer feedback from the supplier is useful, highly detailed data are not essential [10]. Some benefits are realised through changes in daily routines and practices, some through investment in improved technology, retrofits or efficiency measures, and some through rethinking the customer's approach to energy services – for example, car-sharing, turning down heating in unoccupied rooms, or line-drying laundry rather than using a mechanical tumble drier.

This would seem to be the simplest form of active demand, one that affects overall *and* peak demand. Truly 'active' customers minimise demand as a conscious exercise, often becoming more energy literate in the process. At the extremes, they may live in passive-standard homes and go off-grid. Much of this is likely to be beyond the control of suppliers, although there are structured and monitored forms of demand reduction in which suppliers are incentivised to invest in efficiency. An example is the Carbon Emissions Reduction Target in the UK, one of a number of initiatives introduced in the EU in response to concerns that market liberalisation would lead to increased consumption through lower prices. Under schemes such as this, although suppliers have no obvious reason to minimise demand in a competitive market, they do have an obligation to act in concert with their customers by funding efficiency measures and feedback/advice programmes (and, for CERT, some microgeneration), in order to be able to continue their business. Reference [11] gives an account of lessons learned in three EU countries from demand reduction obligations.

In demand reduction initiatives, control of usage normally rests with the customer. There may be equity considerations: who benefits most from subsidies, grants or demand reduction incentivizing tariffs? CERT has rules which address equity issues by defining priority groups and requiring suppliers to give minimum levels of assistance to them. Data privacy is rarely a problem, as benefits are likely to be estimated rather than measured, but even if they are measured, there is no need for high-resolution data. Evaluation of this type of active demand initiative can be a problem, though, when benefits are estimated.

3.2. 'Static' time-of-use pricing to minimise peak demand, through reduced discretionary demand and load-shifting

Static time-of-use (TOU) tariffs – static in that they stay the same over relatively long time periods of time, are often cited as the main reason for introducing smart metering. The customer-supplier relationship here is normally voluntary, with customers choosing to opt into TOU pricing, although there are moves in some parts of the world (e.g. Ontario) towards making it the default mode, especially for business customers. The tariffs rely on interval metering and an upgraded billing system, each of which is expensive and time-consuming to implement.

From the customer standpoint, adopting TOU tariffs need not mean any change in activity at all. Some will benefit in any case if they move away from a flat rate, depending on how the TOU tariff is structured and what their normal daily routines are. The TOU prices are dependable, and provided the customer has accurate information about when it is best to avoid high consumption, new habits of demand reduction and load-shifting can be formed.

The supplier continues to carry any risk associated with volatile electricity prices in the short term, even if that is likely to be passed to the customer in the longer term. There is a degree of supplier-customer engagement, and TOU pricing could be seen as a means of educating customers about the 'time' dimension of electricity, opening their eyes to the concepts of peak and trough demand. There is also scope for some automation, with a simple example being the programmable thermostat or washing machine, so that customers can cut down or cut out consumption at certain times of day; and scope for direct load control by the utility, to use consumer heat stores at certain times of day and reduce load at others.

Most of the control of consumption (and generation) still normally rests with the customer, although a range of options exist. Still, the customer can normally choose how much control to hand over to a supplier or network operator, and whether to adopt any form of 'enabling technology'. Typically, customer participation in TOU programmes is very low, around 1%, if they are expected to opt into the programme. There is resistance to *compulsory* smart metering in several regions at the time of writing, on grounds of cost, invasion of privacy, and even the claimed damaging impact of radio waves from smart meters on health. Data privacy may be an issue for some customers, as individual load curves are being recorded and used for billing, and direct load control is certainly an extension of supplier power into the home, likely to be seen as a loss of privacy. Equity issues become more complex than they are for demand reduction: for example, why should a low consumer subsidise the installation of load-control technologies in the homes of high consumers? And the system can be somewhat inflexible, not offering any incentives for extra demand reduction at the times of greatest stress [12]. Evaluation of TOU pricing, though, can be fairly straightforward: what was the peak demand reduction in different weather conditions? Did consumer response persist? How many people participated? And who were the main gainers and losers from the new tariffs? (More difficult, this, but still possible to establish).

3.3. Dynamic (real time) pricing

One of the main features of real time pricing is the way in which it transfers some of the risk of price volatility to customers, by charging them the current spot price for electricity. It is mediated by smart metering and billing systems, and is likely to be of particular interest for microgenerators and/or for anyone interested in energy storage. There are few examples of real-time pricing (RTP) for small-scale end-users, beyond the trial stage. To date, the

relationship between supplier and consumer/producer is normally voluntary, though contractual.

RTP requires a constant flow of information between supplier, consumer (and microgeneration technologies), so is heavily reliant on functioning ICT. Because of the unpredictable nature of local load balance at any point, response is best not left to the voluntary choice of the customer, but requires some automation. For example, the customer could set the upper boundary beyond which s/he will not pay for any more supply and the system must cap supply to the home; or the lower boundary beyond which s/he will not export any own-generation to the grid.

There is little experience with RTP for residential customers, and there is a great deal to be discovered about their response in terms of price elasticity and wider impacts on behavior patterns. A couple of early trials show some encouraging results when a relatively simple, robust scheme is put in place with well-informed customers [13, 14]. But we still know very little about how RTP might fit with microgeneration, storage generally, and new technologies such as heat pumps and electric vehicles. There are clearly both equity and data protection considerations, considering the potential complexity of RTP systems.

3.4. Dynamic demand – automated network balancing

Dynamic demand comes at the least 'active' end of the active demand spectrum. The relationship between network operator and customer is essentially one in which they co-manage the load in a locality through frequency response in smart appliances. The appliance responds to minute changes in frequency by cycling on or off according to the load on the network at any instant. Customers make the investment; it is not yet clear whether or how this type of arrangement might be formalised through contracts in which the customer payments are reduced in recognition for their contribution of ancillary services to the network operator. There is no householder intervention, other than choosing to buy the appliance, and even that may become a non-choice in time.

The four options are summarised in Table 1 overleaf.

4. Conclusions

The purpose of this paper was to examine some 'active demand' options for householders, in order to move towards a better understanding of social and behavioural dimensions of both 'active demand' and distributed generation. Involvement in active demand involves recognition of a dimension in electricity supply and usage – time – that is new to many consumers. However, 'active' can have many meanings, and an active demand side does not always mean that the people making the demand are consciously thinking about it. Indeed, they typically think about it very little and, for the more fine-tuned types of active demand, thinking is unnecessary: the function has to be automated.

Overall demand reduction – where conscious activity counts for most – tends to be relegated to the fringes of the debate on active demand. The debates on demand reduction and better load management are sometimes confused: achieving the latter does not necessarily mean that any progress is made on the former, although the former is, in the long term, the most important issue. Questions of control, equity and data privacy emerge as significant factors in the debates that are already taking place in California, Ontario, Victoria, and the Netherlands (to give a few examples) – debates that will spread to other regions before long.

Table 1: Summary of four 'active demand' options, from the end-user standpoint

Options for householders in a 'new dimension' world	**Main objectives**	**Householder activity**	**Comments**
Demand reduction	Better-informed energy management; retrofits and investment in energy efficiency.	Question routines and practices, change practices, invest in efficiency measures, develop energy literacy.	The most conscious and obviously 'active' option. Enabling technology or measures can be very simple or non-existent.
Static time-of-use tariffs	System management to reduce peak load and need for expensive 'peaking plant'	Choice of tariff and possible direct load control by utility; possible changes in routines / investment in enabling technology.	Must have interval metering. Raises some equity and data management issues. May have application for microgenerators, to optimise generation in home over time.
Real-time pricing	Load management to reduce peaks *and* utilize variable generation efficiently	Choice of tariff/ contract, and technologies.	More complexity and risk than TOUP, but more flexibility – necessary for less predictable supply. Relatively untried, but central to the idea of the smart grid.
Dynamic demand, smart appliances	Network management to maintain grid frequency	Choice of appliances and possible contract with network operator.	Least problematic of all options, and compatible with any of them. But requires highly reliable, robust technology.

There are likely to be tensions between approaches that aim to inform and involve householders (leaving them with considerable control), and those that encourage them to adopt technologies that will lessen their control and/or transfer it to the utility. Consumers and prosumers vary in their willingness to pay attention to their energy use, let alone to manage it. There is scope for a suite of approaches, in order to involve as many of the population as necessary in system management; however, there is a strong case for incentivising active consumer involvement in the first instance.

Acknowledgements

The author was funded for this work by the Engineering and Physical Sciences Research Council, under the SUPERGEN Highly Distributed Energy Future research programme. The author is also grateful to the reviewers of the paper.

References

[1] Darby, S. (2008) Why, what, when, how, where and who? Developing UK policy on metering, billing and energy display devices. Proceedings of ACEEE Summer Study on Energy Efficiency in Buildings, Asilomar, CA. August 17-22, 2008.

[2] European Technology Platform, http://www.smartgrids.eu/?q=node/163

[3] DECC (2009) *Towards a smarter future: government responses to the consultation on electricity and gas smart metering.* Department of Energy and Climate Change, London. http://www.decc.gov.uk/assets/decc/Consultations/Smart%20Metering%20for%20Electricity%20and%20Gas/1_20091202094543_e_@@_ResponseElectricityGasConsultation.pdf

[4] DECC (2009) *Smarter Grids: the opportunity.* Department of Energy and Climate Change, London. http://www.decc.gov.uk/assets/decc/what%20we%20do/uk%20energy%20supply/futureelectricitynetworks/1_20091203163757_e_@@_smartergridsopportunity.pdf

[5] Valocchi M, Schurr A, Juliano J and Nelson E (2009) *Plugging in the consumer: innovating utility business models for the future.* IBM report, http://www-05.ibm.com/de/energy/pdf/plugging-in-the-consumer.pdf

[6] Isaacson M, Kotewa L, Star A and Ozog M (2006) *Changing how people think about energy*. Proceedings, ACEEE, 7-124 - 7-139

[7] Torriti J, Hassan MG and Leach M (2010) Demand response experience in Europe: policies, programmes and implementation. *Energy* **35**, 1575-1583

[8] York D and Kushler M (2005) Exploring the relationship between demand response and energy efficiency: a review of experience and discussion of key issues. American Council for an Energy-Efficient Economy research report, http://www.aceee.org/research-report/u052

[9] Shaw R, Attree M, Jackson T and Kay M (2009) The value of reducing distribution losses by domestic load-shifting; a network perspective. *Energy Policy* **37**, 3159-3167

[10] Ehrhardt-Martinez K, Donelly KA and Laitner JA (2010) Advanced metering inititatives and residential feedback programs: a meta-review for household electicity-saving opportunities. American Council for an Energy-Efficient Economy research report, http://www.aceee.org/research-report/e105

[11] Eyre N, Pavan M and Bodineau L (2009) *Energy company obligations to save energy in Italy, the UK and France: what have we learnt?* Proceedings, ECEEE 2009 Summer Study.

[12] Herter K (2007) Residential implementation of critical-peak pricing of electricity. *Energy Policy* **35**, 2121-2130

[13] PNNL (2007) *Pacific Northwest GridWise Testbed demonstration projects. Part 1. Olympic Peninsula project.* Pacific Northwest National Laboratory. http://gridwise.pnl.gov/docs/op_project_final_report_pnnl17167.pdf

[14] Star A, Evans A, Isaacson M and Kotewa L (2008) *Making waves in the heartland: how Illinois' experience with residential real-time pricing can be a national model.* Proceedings, American Council for an Energy-Efficient Economy summer study, 2,281-2,291. ACEEE

Impacts of end-use energy efficiency measures on life cycle primary energy use in an existing Swedish multi-story apartment building

Ambrose Dodoo[1,*], Leif Gustavsson[1,2], Roger Sathre[1]

[1] *Mid Sweden University, 83125 Östersund, Sweden*
[2] *Linnaeus University, 35195 Växjö, Sweden*
** Corresponding author. Tel: +46 63165383, Fax: +46 63165500, E-mail: ambrose.dodoo@miun.se*

Abstract: In this study we analyze the effects of energy efficiency measures on the life cycle primary energy use of a case-study (reference) 4-story wood-frame apartment building using electric resistance heating, bedrock heat pump, or cogeneration-based district heating. The reference building has an annual final heat energy demand of 110 kWh/m^2. The energy efficiency measures analyzed are improved windows and doors, increased insulation in attic and exterior walls, installation of improved water taps, and installation of a heat recovery unit in the ventilation system. We follow the buildings' life cycles and calculate the primary energy use during the production, retrofitting, operation and end-of-life phases, and the energy reduction achieved by the measures. The results show that the measures give significantly greater life cycle primary energy savings when using resistance heating than when using district heating. However, a resistance heated building with the efficiency measures still has greater life cycle primary energy use than a district heated building without the measures. Ventilation heat recovery is the most effective measure when using resistance heating while improved windows and doors is the most effective when using district heating. This study shows the importance of considering the interactions between individual measures and the type of heat supply system when selecting energy efficiency measures.

Keywords: *Life cycle, Primary energy, End-use energy efficiency measures, Retrofitting, Low energy buildings*

1. Introduction

The building sector offers significant potential to reduce primary energy use and thereby reduce CO_2 emission [1]. Several strategies can be used to realize this potential, e.g. reduced heating demands and increased efficiency in energy supply chains. The construction of new low energy buildings is important in the long term, but has small effect on the building sector's overall energy use in the short term, as the rate of addition of new buildings to the building stock is low [2]. Large potential exists to reduce primary energy use in existing buildings in the short term, through energy efficiency measures. Energy efficiency measures may be implemented at any time in a building's service life, but some measures are more cost-effective during major renovation works [3].

The life cycle of a building encompasses production, retrofitting, operation and end-of-life phases, which all are interlinked. The final operation energy use in existing buildings can be reduced considerably by implementing energy efficiency measures, e.g. improved insulation, efficient windows, heat recovery from exhaust ventilation air and efficient appliances. These building retrofitting measures also increase material use and the production energy use. Together that reduce the dominance of the operating phase and other life cycle phases becomes relatively more important [4]. The primary energy use depends on the energy supply systems. The energy supply of a building can be provided by different types of supply systems resulting in a large variation in primary energy use for a given final energy use [5]. Hence, the primary energy savings of energy efficiency measures depend on the energy supply systems. Commonly, the difference in final operation energy use before and after implementing energy efficiency measures is used to estimate the savings from such measures. This is inadequate because the energy implications of implementing energy efficiency measures extend beyond the operation phase. Instead, a comprehensive approach to analyze the savings of energy efficiency measures requires a system-wide perspective, including all life cycle phases of a

building and the entire energy chains, from natural resources to final energy services.

In this study we analyze the potential final energy savings in an existing Swedish apartment building by energy efficiency measures, and explore the life cycle primary energy implications of implementing the measures. We consider space heating systems using electric resistance heating, heat pump or district heating.

2. Method

We calculate the primary energy use for all life cycle phases of a reference building before and after implementing the energy efficiency measures, taking into account the production, retrofitting, operation and end-of-life phases.

2.1. Case-study building

The case-study building is a 4-storey wood frame apartment building constructed around 1995 in Växjö, Sweden. It has 4 floors and 16 apartments, and a total heated floor area of 1190 m^2. The roof consists of two layers of asphalt-impregnated felt, wood panels, 40 cm mineral wool between wooden roof trusses, polythene foils and gypsum boards, giving an overall U-value of 0.13 W/m^2 K. The windows are double glazed and have a U-value of 1.9 W/m^2 K. The external doors have a U-value of 1.19 W/m^2 K and consist of framing with double glazed window panels. The external walls have a U-value of 0.20 W/m^2 K and consist of three layers: 5 cm plaster-compatible mineral wool panels, 12 cm thick timber studs with mineral wool between the studs, and a wiring and plumbing installation layer consisting of 7 cm thick timber studs and mineral wool. Two-thirds of the facade is plastered with stucco, while the facades of the stairwells and the window surrounds consist of wood paneling. The ground floor consists of 1.5 cm oak boarding on 16 cm concrete slab laid on 7 cm expanded polystyrene and 15 cm macadam, resulting in a U-value of 0.23 W/m^2 K. The construction and thermal characteristics of the building, including the U-values of the components are given by Persson [6].

2.2. Energy efficiency measures considered

We model energy efficiency measures to the case-study building to achieve a passive house standard. The energy efficiency measures are shows in Table 1. We calculate the U-values resulting from implementing these measures using the method recommended by Swedisol [7].

Table 1. End-use energy efficiency measures applied

Description	*Effect of improvement*
Improved taps	Reduced hot water used
15 cm additional mineral wool insulation to the roof	U-value from 0.13 to 0.08
Windows replaced by triple glazed units (krypton filled)	U-value from 1.9 to 0.90
Doors replaced by triple glazed units (krypton filled)	U-value from 1.19 to 0.90
25 cm additional mineral wool insulation to external walls	U-value from 0.20 to 0.10
Incorporation of heat recovery unit in the ventilation system	Reduced ventilation heat loss

We use simplified assumptions when modeling the measures for the building. For the exterior walls, we assume that the additional 25 cm mineral wool insulation is added to the exterior façade of the building, and covered by new stucco and plasterboard cladding supported by wooden studs spaced at 0.6 m apart. We assume that the original roof overhang is sufficient to cover the wider walls. For the roof, we assume that the additional 15 cm mineral wool insulation can be installed in the existing attic space. We assume that the ventilation heat

recovery unit with 85% efficiency is installed and that the ventilation ducts for incoming air can be fitted in the buildings [8]. Based on data from the Swedish Energy Agency [9], we assume that final energy for tap water heating is reduced by 40% by changing from conventional to efficient water taps.

2.3. Production and retrofitting phases

During the production and retrofitting phases we account for all the materials used in the building, including the initial construction and the energy efficient retrofitting. We calculate the primary energy used to extract, process, transport and assemble the materials, and also the available bioenergy recovered from biomass residues in the wood product chain [10]. The specific end-use energy for building material production is based on two Swedish studies [11, 12]. The on-site construction energy used to assemble the building material is estimated using data from Adalberth [13]. We assume that the on-site energy used for the retrofitting work is proportionally equal to the on-site energy used for the initial building construction, weighted by the relative amounts of energy used to produce the building materials used in the reference building and in the improved building. For calculations of biofuel recoverable from biomass residues we use data from Lehtonen et al. [14] and Sathre [10]. To convert end-use energy for material production to primary energy, we use fuel cycle loss values of 10% for coal, 5% for oil and 5% for natural gas, and we assume electricity comes from coal-fired plants [15].

2.4. Operation phase

During the operation phase, we consider the primary energy used for space heating, ventilation, domestic hot water, and household electricity. We model the operating energy of the building before and after applying each of the energy efficiency measures, to determine the final energy savings from the measures. The reference building was built in 1995, and we model the pre-retrofitting operating energy use for 15 years. We assume the retrofitting takes place in 2010, and we assume a building lifespan of 50 year after retrofitting. The final energy for space heating, ventilation, domestic hot water and household electricity are modeled using ENORM software [16]. We assume an indoor temperature of 22^{o}C and use climate data for Växjo, in southern Sweden. The average annual maximum and minimum temperatures of Växjo are 28 and -18 ^{o}C, respectively.

To quantify the primary energy required to meet the final operation energy use we use the ENSYST software [17], which calculates primary energy use considering the entire energy chains from natural resource extraction to final energy supply. We analyze cases where heat is delivered by electric resistance heating, heat pump or district heating. For the electric resistance heating and heat pump, 95% of the electricity is assumed to be supplied from stand-alone biomass steam turbine (BST) plants and the remaining from light-oil gas turbine plants. For district heating, 90% of the district heat production is assumed to be supplied from combined heat and power (CHP) BST plant, with oil boilers accounting for the remainder. We credit the cogenerated electricity to the district heat plant assuming that it replaces electricity produced from a stand-alone plant with similar technology and fuel [18].

2.5. End-of-life phase

We assume that the building is demolished after its service life, with the concrete, steel and wood materials recovered. We calculate the net end-of-life primary energy use as the primary energy used to disassemble and transport the building materials, minus the primary energy benefits from the recovered concrete, steel and wood. We follow the methodology developed by Dodoo et al. [4], and use data from Adalberth [13] and Björklund and Tillman [12].

3. Results

Table 2 shows the final and primary energy use for heating and ventilating of the reference building and after applying each of the energy efficiency measures to the building. The measures cumulatively decrease the primary energy use by 61%, 52% and 39% for the resistance heating, heat pump and district heating scenarios, respectively. Heat recovery of ventilation air gives the biggest single decrease in primary energy use when using resistance heaters and heat pump, while efficient windows and doors give the highest primary energy savings when using district heating. The use of heat recovery ventilation system also increases the electricity use, reducing the primary energy savings of ventilation heat recovery. For district heating system mainly based on CHP production, a reduced heat use also reduces the potential production of electricity.

Table 2. Annual final and primary energy use (kWh/m^2) for operation after implementation of different measures. Each successive measure includes the effects of all previous measures.

Applied end-use energy efficiency measures	*Final energy use for different energy services*				*Total Primary energy use for space and tap water heating, and ventilation*		
	Space heating	Tap water heating	Venti-lation electricity	Total	Resistance heating	Heat pump	District heating
Reference	70	40	4	114	340	109	72
+Improved taps	70	24	4	98	293	95	63
+ Additional roof insulation	69	24	4	97	290	94	63
+ Improved windows/doors	51	24	4	79	236	78	53
+ Additional external walls insulation	43	24	4	71	212	71	49
+ Ventilation heat recovery	13	24	8	45	134	57	44

Table 3 shows the net primary energy used for the production of the building in the reference and the improved cases. The primary energy balance for the improved building comprises the initial construction primary energy plus the additional primary energy due to the energy efficient retrofitting. Material production primary energy use increases by about 17% when the measures are cumulatively applied.

Table 3. Production primary energy balances for the reference building and the improved building with all the energy efficiency measures applied.

Description	*Primary energy used (kWh/m^2)*	
	Reference	Improved
Production of building materials	579	680
On-site construction work	50	59
Recovered biomass residues	-345	-355
Total	**284**	**384**

Fig. 1 shows the primary energy use during 50 years of operation of the reference building and the improved building with all the measures implemented when using BST supply technology. In the improved building the primary energy for space and water heating decreases, but that for ventilation increases, as additional electricity is used to run the heat recovery ventilation system. The cumulatively applied measures results in greater decrease in

operation primary energy in the cases where the building is heated with electricity. However, the reference building with district heating has lower operating primary energy than the improved building with resistance heating. Thus, the type of heat supply has greater impact on primary energy use than do the energy efficiency measures.

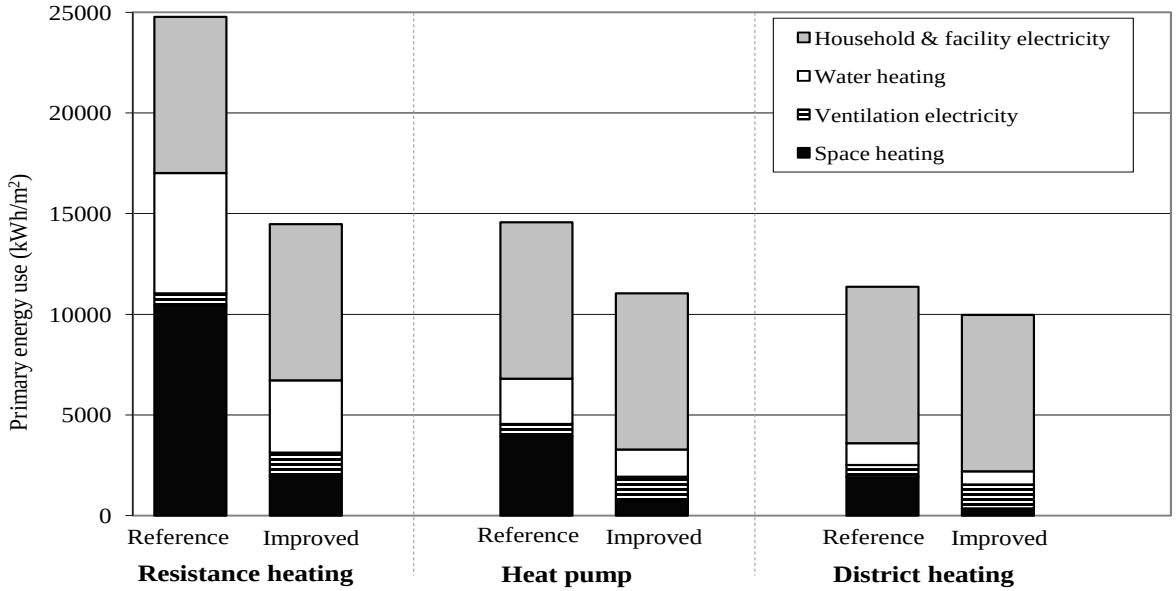

Fig 1. Primary energy use for building operation for 50 years, for the reference building and the improved building with all the measures cumulatively applied.

Table 4 shows the primary energy balances of the end-of-life phase of the buildings. Recovery of wood for use as biofuel gives the greatest end-of-life primary energy benefit, followed by recycling steels to replace ore-based steel. Recycling of concrete as crushed aggregate gives a minor end-of-life primary energy benefit.

Table 4. End-of-life primary energy balances for the reference building and the improved building with all the energy efficiency measures applied.

Description	*Primary energy used (kWh/m²)*	
	Reference	Improved
Disassembly	5	5
Concrete recovery for crushed aggregate	-3	-3
Steel recovery for feedstock	-60	-60
Wood recovery for fuel	-305	-311
Total	**363**	**369**

Fig. 2 shows the development over time of the primary energy use of the building with and without the energy efficient retrofitting for space and tap water heating and ventilation. The construction of the building in 1995 uses 579 kWh/m^2 of primary energy, while 345 kWh/m^2 of bioenergy can be recovered from biomass residues. From 1995 to 2010, energy is used for space and tap water heating and ventilation of the reference building, and is greater for the resistance heated building than for the building with district heating or heat pump. In 2010, additional energy is used to retrofit the buildings. The primary operation energy from 2010 to 2060 is significantly lower if the building is improved. The energy "pay-back period" for the energy used for retrofitting is short. The net life cycle energy benefit of the improvement is the difference between the unmarked and the corresponding marked lines at the year 2060. The benefit is positive in all cases and is greatest when the building uses electric resistance heating.

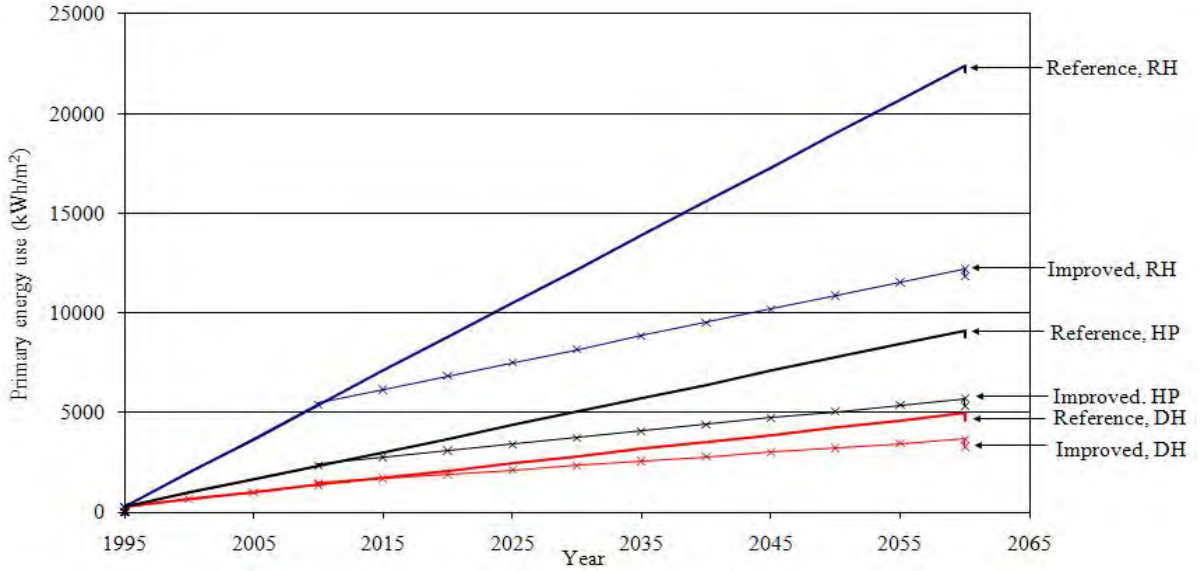

Fig 2. Cumulative primary energy use for space and tap water heating, and ventilation for the buildings with (marked lines) and without (unmarked lines) improvement, with resistance heating (RH), heat pump (HP) or district heating (DH).

Fig. 3 shows the total cumulative primary energy use of the building with and without the energy efficiency measures but including the primary energy for household electricity. The energy benefits of improvements to the building are still apparent, but are proportionally less significant as the total primary energy use is considered.

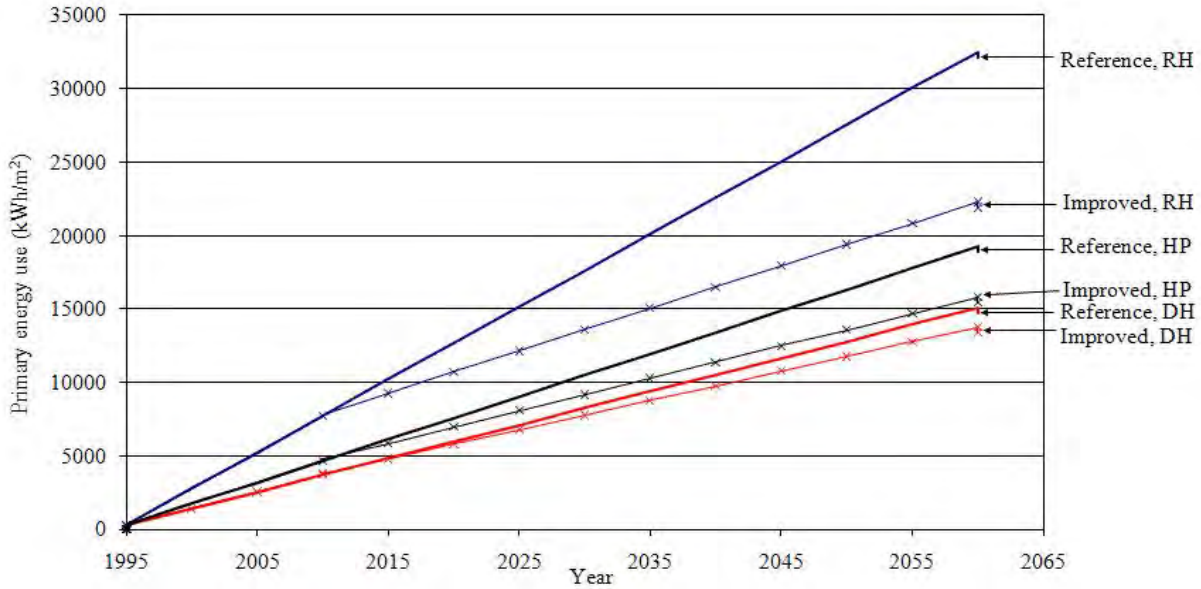

Fig 3. Cumulative primary energy use, for the buildings with and without improvement, including space heating and ventilation as well as energy for household electricity.

Table 5 shows the primary energy use during the life cycle phases of the buildings. The primary energy use during the operation phase dominates, but the relative importance of other life cycle phases increase when the energy efficiency measures are implemented. The primary energy balance during the production phase is relatively small because the primary energy used for material production is largely offset by energy gained from the biomass residues.

Table 5. Net primary energy use of the life cycle phases of the reference and improved buildings, including the production, operation and end-of-life phases.

Life cycle phases	*Primary energy use* *(kWh/m^2)*					
	Resistance heating		Heat pump		District heating	
	Reference	Improved	Reference	Improved	Reference	Improved
Production/retrofitting	284	384	284	384	284	384
Operation (50 years)	24781	14481	14569	11046	11365	9968
End-of-life	-363	-369	-363	-369	-363	-369
Total	**24702**	**14496**	**14490**	**11061**	**11286**	**9983**

4. Discussion and conclusions

The primary energy savings of different energy efficiency measures depend in part on used heat supply system. Heat recovery from ventilation air is most effective where heat supply is from electricity-based systems. The increase in ventilation electricity, however, erodes part of the primary energy reduction. For heat supply from cogeneration-based district heating, efficient windows and doors are the most effective.

The production primary energy becomes increasingly important as buildings become more energy efficient. Primary energy used for production increases significantly by retrofitting a building, but the resulting reduction in space heating primary energy is much higher, resulting in an overall life cycle primary energy reduction.

The results show that the choice of heat supply system has greater impact on primary energy use than the end-use energy efficiency measures, confirming the results of Gustavsson and Joelsson [5]. Hence, to further minimize primary energy use when buildings are refurbished, priority should be given to energy efficient supply systems such as district heating where possible. When selecting energy efficiency measures, attention should be given to the interaction between individual measures and the type of heat supply system, in particular the electricity use for ventilation heat recovery together with cogeneration-based district heating.

References

[1] IPCC (Intergovernmental Panel on Climate Change), Climate Change 2007: Mitigation. Contribution of Working Group III to the Fourth Assessment Report, Cambridge University Press, UK, 2007.

[2] M. Bell, Energy efficiency in existing buildings: the role of building regulations, Proceedings of the RICS Foundation Construction and Building Research Conference, 2004.

[3] IEA (International Energy Agency), Energy efficiency requirements in buildings codes, energy efficiency policies for new buildings, 2008. Web accessed at www.iea.org on Nov. 26, 2008.

[4] A. Dodoo, L. Gustavsson, and R. Sathre, Life cycle primary energy implication of retrofitting a Swedish apartment building to passive house standard, Resources, Conservation and Recycling, 54 (12), 2010, pp. 1152-1160.

[5] L. Gustavsson, and A. Joelsson, Life cycle primary energy analysis of residential buildings, Energy and Buildings, 42(2), 2010, pp. 210-220.

[6] S. Persson, Wälludden trähus i fem våningar: Erfarenheter och lärdomar, Report TVBK-

3032, Department of Structural Engineering, Lund Institute of Technology, Sweden, 1998.

[7] SWEDISOL, Isolerguiden bygg 06, 2006.Web accessed at http://www.stenull.paroc.se on July 7, 2009.

[8] Å. Wahlström, Å. Blomsterberg, and D. Olsson, Värmeåtervinningssystem för befintliga flerbostadshus, Förstudie inför teknikupphandling, 2009.

[9] Swedish Energy Agency, Effektiva kranar sparar energi, 2006. Web accessed at http://www.swedishenergyagency.se on June 17, 2009.

[10] R. Sathre, Life-cycle energy and carbon implications of wood-based products and construction, PhD dissertation, Department of Engineering, Physics and Mathematics, Mid Sweden University, Östersund, Sweden, 2007.

[11] T. Björklund, and A-M. Tillman, LCA of building frame structures: environmental impact over the life cycle of wooden and concrete frames, Technical Environmental Planning Report 2, Chalmers University of Technology, Gothenburg, Sweden, 1997.

[12] T. Björklund, Å. Jönsson, and A-M. Tillman, LCA of building frame structures: environmental impact of the life cycle of concrete and steel frames, Technical Environmental Planning Report 8, Chalmers University of Technology, Gothenburg, Sweden, 1996.

[13] K. Adalberth, Energy Use and Environmental Impact of New Residential Buildings, Ph.D. Dissertation, Department of Building Physics, Lund University, Sweden, 2000.

[14] A. Lehtonen, R. Mäkipää, J. Heikkinen, R. Sievänen, and J. Liski, Biomass expansion factors (BEFs) for Scots pine, Norway spruce and birch according to stand age for boreal forests, Forest Ecology and Management; 188(1-3) , 2004, pp. 211-224.

[15] L. Gustavsson, and R. Sathre, Variability in energy and CO_2 balances of wood and concrete building materials, Building and Environment, 41(7), 2006, pp. 940-951.

[16] EQUA (Simulation AB), ENORM, Version 1000, Stockholm, Sweden, 2004.

[17] Å. Karlsson, ENSYST, Version 1.2, Lund University, Sweden, 2003.

[18] L. Gustavsson, and Å. Karlsson, CO2 mitigation: on methods and parameters for comparison of fossil-fuel and biofuel systems, Mitigation and Adaptation Strategies for Global Change, 11(5-6), 2006, pp. 935-959.

Mechanical ventilation and heat recovery for low carbon retrofitting in dwellings

Phil F. G. Banfill[1*], Sophie A. Simpson[1], Mark C. Gillott[2], Jennifer White[2]

[1] *Heriot-Watt University, Edinburgh, UK*
[2] *The University of Nottingham, Nottingham, UK*
* *Corresponding author. Tel: +44 (0)131 451 4648, E-mail: P.F.G.Banfill@hw.ac.uk*

Abstract: The ventilation heat loss in a typical unimproved UK dwelling is approximately equal to the conduction loss; therefore draught-proofing measures should form part of any energy refurbishment package. This will improve the building's air permeability but risks incurring additional energy costs associated with the need to provide controlled ventilation to maintain indoor air quality. This paper aims to determine the point at which the air permeability of the building improves the energy performance by enough to justify the increase in energy associated with the installation of mechanical ventilation with heat recovery (MVHR). A 1930's style semi-detached house, representative of a large proportion of solid wall dwellings in the UK, has been improved by a package of measures including MVHR. The building air tightness plays a critical role in reducing the building energy consumption and CO_2 emissions.

Keywords: *Retrofitting, Building Simulation, Mechanical Ventilation, Heat Recovery*

1. Introduction

The UK has the oldest housing stock in the developed world with over 8.5 million properties over 60 years old1. The consequence of this is that building energy performance was not a concern at time of construction, therefore space heating dominates as a result of poor heat transfer characteristics associated with the building envelope and high infiltration rates. Of the 25 million dwellings in the UK, 34% are solid-wall dwellings and responsible for 50% of the total UK domestic sector CO_2 emissions[2]. CALEBRE (**C**onsumer-**A**ppealing **L**ow **E**nergy technologies for **B**uilding **Re**trofitting) is a £2 million research project, funded jointly by Research Councils UK Energy Programme and E.On. The project aims to establish a validated, comprehensive refurbishment package for reducing UK domestic CO_2 emissions, whilst being acceptable and appealing to householders. As part of this project, a newly-constructed occupied test house (the E.On house), specially built to 1930s standards and located on the campus of the University of Nottingham, is being used to evaluate retrofit solutions specifically targeted at solid-wall properties (classified as 'hard-to-treat'). Currently a number of improvements to the thermal properties of the construction and glazing fittings have been applied, in addition to a series of draught-proofing measures to improve the building air-tightness. An air permeability test is carried out after the application of each measure, and the ongoing energy performance of the building is recorded using a comprehensive monitoring system.

As the air tightness of the building improves it will become necessary to introduce a controlled ventilation system to maintain the indoor air quality (IAQ). As part of this research project a mechanical ventilation system with heat recovery (MVHR) has been installed and the impact on the building performance with regards to energy performance and IAQ is being monitored. The combined effects of improving the air tightness and installing MVHR reduces the building's space heating demand by decreasing infiltration and recovering thermal energy from the exhaust air to preheat the supply air. These savings come at the expense of the energy associated with the system's continuous operation; therefore there is a delicate balance between energy conservation and energy consumption associated with the system.

This paper reports a preliminary study to understand the relationship between energy savings attributable to the MVHR system and whole house air tightness, and to determine the critical value of air permeability above which MVHR is ineffective as a means of energy saving in the dwelling.

2. Building Air Tightness

Findings generally support the notion that dwellings in more severe climates, such as Sweden, Norway and Canada are built more airtight, where the primary aim is to conserve energy and improve thermal comfort[3]. This level of air tightness necessitates a method of controlled ventilation and MVHR is generally installed as standard. The UK experiences a milder climate and dwellings are predominantly less airtight[4], relying on infiltration combined with natural ventilation to provide the necessary air change rate to maintain indoor air quality. Boost extract is employed to remove high levels of pollutants at the point of production, but this strategy cannot guarantee a sufficient level of ventilation throughout the year. The consequences of this could be a build-up of pollutants, and conditions which permit the development of allergens[5], whereas the installation of a mechanical ventilation system can help to mitigate this risk.

In modern society, people spend up to 90% of their time in an artificial environment[6], whether it is a dwelling, workplace or transport vehicle. The ventilation of these spaces plays a critical role in maintaining indoor air quality and ensuring the well being and comfort of the occupant. An insufficient supply of fresh air can be a contributor to 'sick building syndrome', where occupants may be susceptible to a range of symptoms such as lethargy, headaches and respiratory problems. Improvements to building air tightness over the last two decades are thought to have contributed to a degradation in indoor air quality where ventilation has been reduced or poorly addressed. An effective ventilation strategy plays an essential role in introducing outdoor air, to dilute contaminants, and promote air movement within the occupied space.

Moisture, although in itself innocuous, is considered a pollutant within the built environment as it is continuously emitted by occupants and the processes they carry out in their day to day activities. As the moisture levels increase, so too does the risk of condensation forming on areas with cool surface temperatures, which can lead to the degradation of the building fabric, as well as other problems such as spores of mould and fungi. This can pose a health hazard causing allergies and illness such as asthma, rhinitis and conjunctivitis[5]. A ventilation strategy plays a key role in controlling humidity levels which can be the driving force behind the specified flow rate.

3. Methodology

A model of the E.On house was built using dynamic thermal modelling software IES Virtual Environment. The Test Reference Year (TRY) weather data for Nottingham was applied and used to predict the annual building energy consumption. Templates were created for each room type, specifying values for internal gains and corresponding diversity profiles. This was based on information detailed for domestic buildings in the NCM database[7], which also provided room heating set-points and domestic hot water consumption. This information was consistent for all analyses.

A series of studies were carried out to determine the critical performance parameters of the MVHR system and whole house air tightness to ensure a net reduction in building energy:

- An initial study considers the energy performance of the E.On house in its original state, and the performance associated with the application of each retrofit measure
- Subsequent studies consider the energy performance associated with an MVHR unit specified to minimum building standards at varying levels of air tightness, and compares this with system components specified to best practice performance standards.

The 'leakiness' of the building is determined by carrying out an air permeability test, or 'fan-blower door test'[8] which creates a differential pressure between the indoor and external environment. Numerous researchers have tried to link this empirically tested value to a background infiltration rate. Kronvall[9] developed a rule of thumb method, dividing the tested air change rate by 20, whereas Dubrul[10] increased the divisor range to between 10 and 30, depending on the exposure of the site. Sherman[11] produced a complex model which incorporated a number of influencing parameters including climate zone, wind shielding, height of the house and size of cracks, whereas Jukisalo[12] further developed this to include leakage distribution and balance of ventilation strategy.

Energy modelling is a detailed and time consuming process if the set-up is to accurately represent the building design and operation, therefore a degree of simplification has been applied to the modelling to provide an initial indication of the impact the variables have on the building performance and energy savings achieved. After assessing the site exposure, Kronvall's rule of thumb has been applied to the analyses to determine the background infiltration rate based on the measured air permeability values. This information will be used to select a number of investigations to consider in more detail, based on information obtained from the extensive measuring and monitoring which is continuing on the house. This preliminary report focuses on modeled output and measured data will be reported later.

4. Results and Discussion

4.1. Application of retrofit measures to the E.On House

The following investigation considers the annual building performance of the E.On House. Table 1 summarises the series of improvements, and the air permeability values tested at 50Pa. These are detailed in units of $m^3/m^2.h$, and corresponding values in ach^{-1}. Notice the poor workmanship which resulted in only a small change in air permeability between stage 1 and 2, and the extensive detailed interventions necessary to achieve low air permeability in this house.

Figure 1 shows the heat losses occurring when the peak space heating load occurs in the E.On house. The improved thermal properties applied in stage 1 halve the external conduction losses, but there is little change in the infiltration losses due to only a marginal improvement in the building air tightness. Infiltration now forms a greater proportion of the overall heat loss, and the introduction of the MVHR system has increased the building air change rate, adding to the load placed on the space heating system. As more draught proofing measures are applied for stage 2, the tested air permeability is significantly reduced contributing to a considerable decrease in infiltration losses. The stage 3 draught-proofing measures provide yet further reductions.

Table 1. E.On House Series of retrofit measures

Stage	Description of work carried out	Air Permeability ($m^3/m^2.h$)	Air Permeability (ach^{-1})
Base Case	Single glazed windows, uninsulated walls, floor and roof space, no draught-proofing	15.57	14.85
1	Double Glazing, wall and loft insulation, draught proofing applied to most windows and doors. Installation of MVHR system	14.31	13.65
2	Draught proofing throughout house re-done as inadequate installation previously, and extended to remaining windows and vents.	9.84	9.39
3	Service risers sealed. Covers fitted to door locks, pipe work envelope penetrations sealed (radiators, water pipes etc), Kitchen fan removed and bricked-up. Sealing around boiler flue.	8.6	8.21

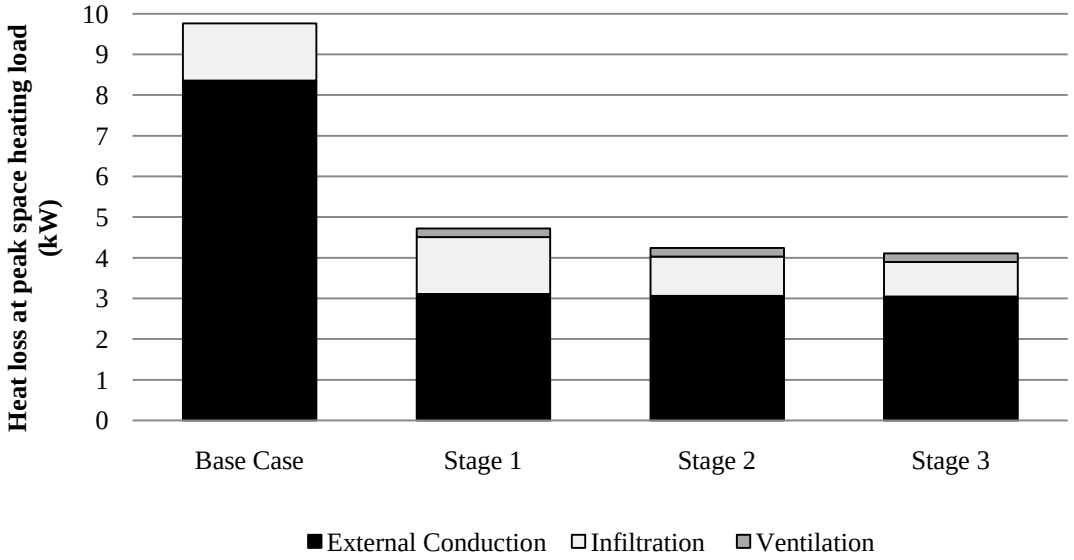

Fig. 1. E.On house heat loss at peak space heating load

Figure 2 details the distribution of the annual building's energy consumption, and the percentage reduction achieved after applying the series of retrofit measures. The MVHR system installed in stage 1 contributes to an increase in auxiliary energy, but the impact is minimal in this instance because of the considerable reduction in space heating due to the thermal upgrades. Stage 2 and stage 3 improvements demonstrate further reductions in annual energy performance, totalling 64% as a result of the improvements to the building air tightness and heat recovery efficiency.

Although stage 3 displays lower building energy consumption compared to the previous analyses, the comparison is not a fair one as there is debate about the point at which a controlled ventilation strategy becomes necessary. BRE Digest 398[12] advises that a whole house ventilation strategy should maintain an air change rate of $0.5ach^{-1}$, less the background infiltration rate. Applying Kronvall's rule, a tested air change rate of $13.65ach^{-1}$ corresponds to a background infiltration rate of $0.68ach^{-1}$ for the E.On house, indicating that a forced ventilation system is unnecessary. If the MVHR system was not included in stage 1 and stage

2 analyses, the building energy consumption would be lower as the auxiliary energy would decrease, and the lack of ventilation losses would mean less demand on the space heating. Stage 3 therefore does not necessarily demonstrate an improved energy performance compared to less airtight buildings when they are considered without a forced ventilation strategy.

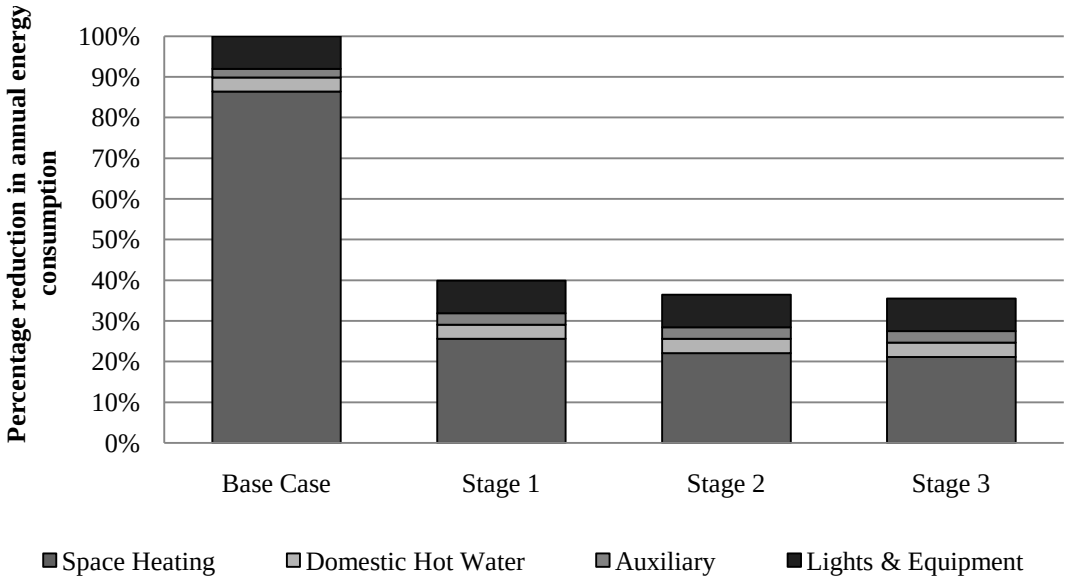

Fig. 2. E.On house percentage reduction in annual building energy consumption

4.2. Impact of building air permeability on the thermally improved E.On House

The second investigation assesses the impact on the performance of the E.On house if future draught-proofing measures were able to achieve lower air permeability values. A ventilation strategy was applied based on the guidance outlined in Approved Document F[13], detailed in table 2. The results are compared against a naturally ventilated E.On house, at an air permeability of $10m^3/m^2.h$ at 50Pa.

Table 2. Building Regulation Criteria

Standard	Criterion	Infiltration Reduction	E.On House Ventilation Flow Rate (l/s)
Approved Document F (Air permeability > 5 $m^3/m^2.h$)	0.3 $l/s/m^2$*	0.04 x gross internal volume	21 l/s
Approved Document F (Air permeability < 5 $m^3/m^2.h$)	0.3 $l/s/m^2$*	n/a	30 l/s

* 21 l/s flow rate is stated for a three bedroom house, but the ventilation should not be less than 0.3 $l/s.m^2$, therefore the greater of the two values should be applied.

The introduction of the ventilation flow rate initially increases the E.On house heat losses at the time of the peak space heating load (Figure 3), however the combined effects of the MVHR system and improvements to the building air tightness to achieve $7m^3/m^2.h$ at 50Pa decrease the infiltration by enough to reduce the overall heat loss to less than the naturally ventilated case.

The ventilation losses are greater for the last two analyses, but it should be noted that the peak space heating load occurs at a different time for these from the first three analyses. The

ventilation losses are dependent on the temperature difference between the supply air and the room temperature, which vary over the course of the day depending on the room use. This means the peak ventilation loss does not necessarily coincide with the peak space heating load. As a result, figure 3 shows that improving the building air permeability to $5m^3/m^2.h$ or less reduces the infiltration losses by enough to move the peak space heating load to a different time, when the ventilation losses form a greater proportion of the total heat loss.

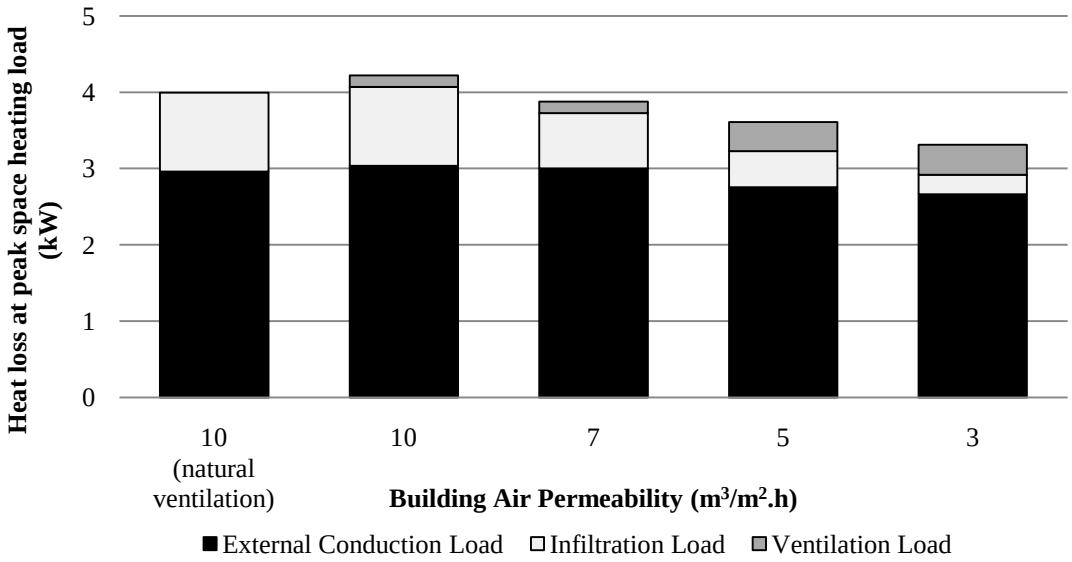

Fig. 3. Heat loss at peak space heating load for improving building air permeability

The annual energy consumption associated with the operation of the building is attributable to the space heating, auxiliary energy (e.g. pumps and fans), domestic hot water, lighting and equipment. The last three parameters are related to occupancy behavior, and predefined by the room templates. Based on the assumption that there is no change in occupancy behavior, table 4 reports the annual energy consumption associated with the space heating and auxiliary systems for the E.On house at different air permeability values. Table 4 details values associated with the E.On house for a natural ventilation strategy with an air permeability of $10m^3/m^2.h$ at 50Pa, an MVHR system specified to minimum building standards and an MVHR system specified to best practice standards. Table 3 gives the performance parameters of system components associated with these strategies.

Table 3. Performance parameters of system components

Component	Minimum Building Standards[14]	Best Practice[15]
Specific Fan Power (Exhaust Only)	0.5 W/l/s	n/a
Specific Fan Power (Whole House Ventilation)	1.5 W/l/s	1 W/l/s
Heat Recovery Effectiveness	70%	85%

The introduction of the MVHR system increases auxiliary energy consumption, and initially increases the space heating energy as a result of forcing an increased building air change rate which places an additional load on the boiler. The combined effects of improved building air tightness and effective heat recovery need to reduce the space heating energy by enough to negate the increase in auxiliary energy.

For an MVHR system specified to minimum building standards, a reduction in annual energy is achieved when the building air permeability has been improved to $3m^3/m^2.h$ at 50Pa, compared to the naturally ventilated case.

In contrast, an MVHR system operating at best practice standards achieves the break-even point at an air permeability of $7m^3/m^2.h$ at 50Pa. Further improvements contribute to overall energy savings, with an air permeability of $3m^3/m^2.h$ at 50Pa achieving a 10% reduction in the combined annual space heating and auxiliary energy from the naturally ventilated case.

However, an energy reduction does not directly equate to a CO_2 reduction because of the higher carbon intensities associated with electricity compared to gas. The combined effects of reduced air permeability and MVHR must reduce the space heating energy by nearly three times the increase in auxiliary energy to ensure a net reduction in CO_2 emissions. Improving the building air permeability to $3m^3/m^2.h$ at 50 Pa successfully realises a total reduction in CO_2 emissions for the E.On house when the MVHR equipment is specified to both minimum and best practice standards, though the saving is more significant for the latter.

Table 4. Annual space heating and auxiliary energy consumption for improving air permeability

Building Air Permeability at 50Pa ($m^3/m^2.h$)		**10**	**7**	**5**	**3**
Naturally Ventilated Building	Space Heating (kWh/m^2)	85.19	-	-	-
	Auxiliary (kWh/m^2)	9.55	-	-	-
	Combined (kWh/m^2)	**94.74**	**-**	**-**	**-**
Minimum Building Standards MVHR equipment	Space Heating (kWh/m^2)	96.67	85.83	83.42	76.32
	Auxiliary (kWh/m^2)	11.83	11.83	12.72	12.72
	Combined (kWh/m^2)	**108.50**	**97.66**	**96.13**	**89.04**
Best Practice Standards MVHR equipment	Space Heating (kWh/m^2)	94.67	83.92	80.72	73.73
	Auxiliary (kWh/m^2)	10.81	10.81	11.40	11.40
	Combined (kWh/m^2)	**105.48**	**94.73**	**92.12**	**85.13**

5. Conclusion

The modelling indicates that the application of all the retrofit measures detailed in table 1 have successfully reduced the energy consumption associated with the E.On house by 64% compared to the initial 1930's base case scenario.

An MVHR system operating at minimum building standards achieves an overall reduction in building energy consumption compared to the naturally ventilated case only when the air permeability has been reduced to $3m^3/m^2.h$ at 50 Pa, based on the E.On house which has been thermally upgraded.

On the other hand, an MVHR system operating at best practice standards can equal the energy performance of the naturally ventilated case when an air permeability of $7m^3/m^2.h$ at 50 Pa is

achieved. Further improvements to the building air tightness to achieve $5m^3/m^2.h$ at 50 Pa or less will contribute to net energy savings.

The results from the modelling show that the building airtightness plays a critical role in achieving a reduction in building energy consumption, and more significantly CO_2 emissions. The difficulties experienced by the E.On house in improving the building air tightness suggest that the challenge of achieving the necessary air permeability should not be under-estimated, and the practicalities should be carefully considered when addressing existing dwellings in the UK.

References

[1] Energy Saving Trust, Energy-efficient refurbishment of existing housing (CE83), EST, 2003.

[2] www.calebre.org.uk (accessed 28/1/11).

[3] M. Sherman et al, Building airtightness: research and practice, Lawrence Berkeley National Laboratory, LBNL-53356, 2003.

[4] R.K. Stephen, Airtightness in UK Dwellings: BRE's Test Results and Their Significance, Report 359, Building Research Establishment, 1998.

[5] P. Carrer et al, Allergens in indoor air: environmental assessment and health effects, The Science of the Total Environment, 2001, 270(1-3): 33-42.

[6] H.B. Awbi, Ventilation of buildings, Spon, Second Edition, 2003, pp. 37- 45.

[7] www.2010ncm.bre.co.uk (accessed 28/1/11)

[8] Chartered Institute of Building Services Engineers, Testing buildings for air leakage, CIBSE, 2000.

[9] J. Kronvall, Testing of houses for air leakage using a pressure method, ASHRAE Transactions, 1978, 84(1): 72-9

[10] C. Dubrul, Inhabitants behavior with respect to ventilation, UK: Air Infiltration Centre, Technical Note 23, 1988.

[11] M. Sherman, Estimation of infiltration from leakage and climate indicators, Energy and Buildings, 1987, 10(1): 81-6.

[12] J. Jokisalo et al, Building leakage, infiltration and energy performance analyses for Finnish detached houses, Building and Environment, 2009, 44(2): 377-387.

[13] Building Research Establishment, Continuous mechanical ventilation in dwellings, BRE, Digest 398, 1994.

[14] Department for Communities and Local Government, Approved Document F: Means of Ventilation, NBS, 2010.

[15] Department for Communities and Local Government, Domestic Building Services Compliance Guide, NBS, 2010.

[16] Energy Saving Trust, Energy efficient ventilation in dwellings – a guide for specifiers, EST, 2006.

Barriers to implement energy efficiency investment measures in Swedish co-operative apartment buildings

Gireesh Nair[1*], Leif Gustavsson[1,2], Krushna Mahapatra[1]

[1]*Mid Sweden University, Östersund, Sweden*
[2] *Linnaeus University, Växjö, Sweden*
[*]*Corresponding author. Tel: +46 63165428, Fax: +46 63165500, E-mail: gireesh.nair@miun.se*

Abstract: We sent a questionnaire to chairmen of 3000 co-operative hosing association across Sweden to analyse their perception about energy efficiency aspects during June-October 2010, and 24% responded. About 80-95% of the respondents had no intention to retrofit their building envelope components during the next ten years measures. A greater proportion of respondents perceived that energy efficient windows were more advantageous than improved attic, basement and external wall insulation. Respondents gave high priority to economic factors in deciding on an energy efficiency investment measure. For 54% of the respondents, lack of expertise of the executive board to assess the benefits of energy efficiency measures was a barrier to energy efficiency investments. Majority of respondents considered economic policy instruments, like investment subsidies and tax deductions, as the most effective method to improve energy efficiency.

Keywords: *Co-operative apartment buildings, energy efficiency, Sweden*

1. Introduction

In Sweden, the residential and service sector's final energy use in 2008 was about 141 TWh, or 36% of the national final energy use [1]. Building envelope components offer a large potential to reduce energy use in existing buildings as they are important source of heat loss. For example, approximately 15 TWh of heat is lost annually through windows of Swedish residential buildings [2], and this loss could be reduced significantly by upgrading the window stock [3]. Sweden has around 2.44 million dwellings in multi-storey buildings [4], which constitute about 55% of the total dwelling units. These buildings provide considerable opportunities for energy efficiency measures and many of them were built in the *million house* programme[1], and require renovation.

The ownership pattern of multi-storey apartment buildings can be categorised into municipal, private and tenant-ownership (henceforth co-operative). Approximately 40% of apartments in multi-storey buildings belong to municipal housing companies, while the rest is equally shared by private companies and co-operative housing associations. The municipal housing and private companies give their apartments for rent, while the co-operative sector resembles a condominium sector [5]. In this paper we discuss co-operative housing associations plan to replace/change their building envelope components, and the barriers to implement investment intensive energy efficiency measures.

There are about 26500 co-operative housing associations in Sweden. These housing associations usually do not have individual measurements for heating and hot water consumption. Typically, the billing for heating and hot water use is included in a monthly rent and is based on the apartment size. The household electricity bill is usually metered separately, and charged to individual apartment owners. The decisions pertaining to the buildings are usually made by the executive board which is headed by a chairman. The executive board members and the chairman are elected by the members of the association and

[1] The decision to built one million dwelling was made in 1965 to address the housing shortage and to stimulate the construction industry.

they occupy the post for a specific time period. The chairmen are in a good position to share information about the implementation of energy efficiency measures in their association's buildings. The paper is based on the response of the chairmen of co-operative housing associations to our questionnaire.

2. Theoretical Background

Potential adopters consider adopting an innovation if they feel a *need* for it [6]. Need is a state of dissatisfaction or frustration that occurs when there is a difference between the desire and perceived actual state [7], i.e., when a problem is recognised [8]. Potential adopters may gather information on various alternatives and process the information to make the decision that best fulfil their prioritised need [8]. In doing so, they usually compare various alternatives based on their perception of the alternatives' attributes, e.g. investment cost, environmental performance, ease of installation. A measure that has greater *perceived* advantages compared to others is likely to be adopted.

In building envelope component replacement decisions, need may arise because of the condition of the existing component(s). The conditions generally depend on the age of installation. In addition, the perceived high cost of energy or a positive attitude to reduce energy use may induce the implementation of such measures. Furthermore, the awareness level [7] of such measures influence the adoption.

However, there may be barriers to implement energy efficiency measures. Building owners or housing associations may not adopt such measures due to lack of awareness or lack of adequate and reliable information [9, 10], or the inability to interpret the available information. Furthermore, potential adopters may have difficulties in perceiving the performance and advantages of energy efficiency measures if the gains are not directly visible [11], insignificant, or delayed. Financial constraints such as difficulty to access capital also hinder investments in energy efficiency [12]. Even if owner/organizations have access to capital, still they may not invest in energy efficiency measures due to the perceived risk of such investment. The perceived risk may be due to their inability to understand the performance and benefits of the installation or due to the uncertainty in future energy price. For example, the return on investment for an energy efficiency measure will be less attractive if the energy price falls [12]. In such situation a risk-averse investor may avoid, or postpone or expect higher returns from energy efficiency investments [12]. A potential adopter may be able to collect information about energy efficiency measures from various sources. But, time, money or both is needed to acquire relevant information [13]. Such hidden costs could act as a barrier to invest in energy efficiency. Moreover, organizations might consider other matters for example cleaning and maintenance of the buildings more important than spending resources in energy efficiency.

3. Methodology

To investigate the adoption of energy efficiency measures in co-operative apartment buildings we sent a questionnaire to the chairman of about 3000 co-operative housing associations across Sweden. Major building management-decisions in co-operative housing associations are made by an executive board, which is headed by a chairman. The chairmen are in a good position to share information about the implementation of energy efficiency measures in their association's buildings. As the number of such association varies significantly across different regions in Sweden, we sent the questionnaire to about 10-11% of associations in each of the 21 counties in Sweden to avoid regional bias. The addresses of the associations were collected from Bolagsverket which drew the address randomly. The questionnaires were sent during

June-October 2010. Some of the associations replied that they could not respond to the questionnaire for various reasons, including their association is very small or their apartments were not currently occupied. Some questionnaires were returned unanswered due to a change in the recipients' addresses. In total, we received approximately 675 completed questionnaires, which corresponded to a response rate of 24%.

4. Results

Approximately 50%, 19% and 14% of the respondents reported that their associations' apartments were heated by district heating, combination with a heat pump and electrical heating, respectively. Approximately 15% of the respondents thought that their annual heating cost was high, while only 6% respondents considered their annual electricity cost as high. Still, for 55% and 38% of respondents, it was important to reduce heating and electricity use, respectively.

About 80-95% of the respondents had no intention to retrofit their building envelope components during the next ten years (Table 1). One of the reasons was that they were satisfied with the condition of the existing installations. The majority of the respondents felt that their windows (76%), attic insulation (59%), basement insulation (64%) and insulation of external walls (80%) were in good condition (Table 2).

Table 1: Plan to improve/change the majority of the building envelope components

Building envelope components	% of respondents			
	No	Yes, with in 3 years	Yes, 3-10 years	
Windows (N=578)	79	8	13	
Attic insulation (N=555)	84	8	8	
Basement insulation (N=534)	94	2	4	
External wall insulation (N=548)	94	3	3	

"Do not know" responses were considered as missing value

Table 2: Perceived condition of the building envelope components

Building envelope components	% of respondents			
	Good	Medium	Bad	Do not know
Windows (N=662)	76	19	4	1
Attic insulation (N=654)	59	25	10	6
Basement insulation (N=636)	64	19	5	12
Facade (N=658)	80	16	3	1

Potential adopters typically compare various energy efficiency measures based on a number of factors. The factors that are given high priority guide the decisions. A ranking of the priority of various factors is presented in Table 3. The results showed that annual energy cost saving and investment cost were the most important factors. Environmental factors were given low priority. 41% of the respondents reported that their associations consider life cycle cost while making investment intensive measures, while 26% and 32% of respondents reported that will not consider life cycle cost and sometime consider such cost, respectively (not shown in the table).

Table 3: Importance of various factors in respondents' energy efficiency investment decisions

Factors		% of respondents		
	N	Important	Medium	Less important
Reduce annual energy cost	597	88	10	2
Investment cost	593	88	9	3
Functional reliability	532	70	25	5
Improve indoor environment	540	60	35	5
Payback period	547	59	30	11
Environmental benefit	523	42	45	13
Improve market value	525	43	34	23
Technical limitation of buildings (for example no space to add more insulation)	510	37	41	22
Reduce greenhouse gas emission	514	32	47	21
Small/no disturbance to residents	523	33	43	24

N = Number of respondents

We compared the respondents' preference of various energy efficiency measures in building envelope to the ten factors mentioned in Table 3. Table 4 shows that significant percentage of respondents did not know about which building envelope components fares better among the various factors. However, those respondents who were aware about performance of building envelope components preferred energy efficient windows followed by improved attic insulation. More respondents were found to be aware or very much aware about energy efficient windows (59%) than about attic (53%) or basement (42%) or external wall insulation (50%) improvements (not shown in the table).

Table 4: Preferred building envelope measure against the various factors

	% of respondents (N=673)				
	Energy efficient window	Attic insulation improvement	Basement insulation improvement	External wall insulation improvement	Do not know
Annual energy cost reduction	26	24	7	12	27
Investment cost	27	21	6	10	25
Functional reliability	14	9	3	5	43
Improve indoor environment	19	7	4	7	37
Payback period	9	8	3	6	48
Environmental benefit	11	9	5	6	47
Improve market value of the property	17	7	3	6	44
Technical limitation of the buildings	4	6	4	4	54
Reduce GHG emission	7	7	3	5	50
Small/no problem for residents	8	9	3	5	45

Respondents' views on issues that may influence implementation of investment intensive energy efficiency measures (like building envelope components, improvement in ventilation system) are presented in Table 5. For 54% of the respondents, lack of expertise of the executive board to assess the benefits of energy efficiency measures was a barrier to such investments. About 35-40% of respondents thought lack of appropriate and easily available information was a barrier, while economic constraints were reported to be a barrier by 34% of the respondents. Approximately 77% of respondents considered the financial position of their association as good and 61% considered it would be easy to finance renovation of their buildings. Similarly, about 40% of the respondents reported that their associations were interested to invest in energy efficiency measures if they receive attractive financing (not shown in the table). Respondents' did not think that residents would oppose energy efficiency investment measures. However, in response to another question, a large number of respondents (45%) believed that if the investment in energy efficiency measure will increase the monthly payment then the residents will resist investments in such measures.

Table 5: Issues regarding investment intensive energy efficiency measures in apartment buildings

Statements	% of respondents		
	Agree	Neither nor	Disagree
The board does not have own expertise to assess the benefits of energy efficiency measures (N=629)	54	22	24
Uncertainty about future energy prices makes it difficult to invest in energy efficiency measures (N=608)	40	31	29
It is difficult to obtain reliable information about costs and benefits of energy efficiency measures (N=611)	37	33	30
Time and effort required to collect necessary information is too high (N=612)	35	31	34
Financial constraints makes it difficult to invest in energy efficiency measures (N=611)	34	29	37
If the association reduce heat energy, district heating companies will increase energy price, thus making the effort worthless (N=550)	26	26	48
Changing behaviour like switching off lights is more beneficial than investments in energy efficiency measures	22	40	38
Investments in energy efficiency measures are low priority compared to other measures (N=622)	21	38	41
Members of association does not support investments in energy efficiency measures (N=609)	8	34	58
Association has a complex chain of decision making process which makes it difficult to invest in energy efficiency	7	15	78

N = Number of respondents

Sweden uses an array of policy instruments to promote energy efficiency in building sector. However, the effectiveness of policy instruments may vary. Majority of respondents considered economic policy instruments, like investment subsidies and tax deductions, as the most effective method to improve energy efficiency (Table 6). More frequent meter reading and energy billing was favoured by less number of respondents.

Table 6: Chairmen's responses to the question, "Irrespective of how much you know about the following measures – How effective do you think the following measures are to encourage you to implement measures to reduce energy use in your apartment buildings"

	% of respondents		
	Effective	Moderately effective	Less effective
Investment subsidy (N=568)	73	18	9
Tax deduction (N=563)	64	20	16
Individual metering of tap water (N=555)	41	27	32
Individual metering of space heating (N=555)	41	27	32
Building regulations (N=546)	34	38	28
Energy tax (N=574)	39	32	29
Energy declaration (N=564)	29	31	40
Energy labelling (N=531)	22	41	37
Carbon dioxide tax (N=561)	27	33	40
More frequent reading of energy (N=550)	28	29	43
Electricity certificate (N= 551)	20	38	42
Voluntary program (N=528)	14	40	46
More frequent billing of energy (N=549)	22	26	52

N = Number of respondents

5. Discussion and Conclusions

Approximately 55% of the chairmen of co-operative housing associations' have a positive attitude to reduce heat use. The lower concern towards electricity use by the respondents could be because the household electricity bill is usually metered separately and the collective burden of electricity cost is less. However, majority of co-operative housing association did not intend to replace/change majority of their building envelope components during the next ten years. One of the reasons is that the associations were satisfied with the condition of existing building envelop components. In this situation, it is important to increase the awareness of energy efficient alternatives. A large percentage of respondents were not aware about the various energy efficient possibilities in building envelope. Moreover, about 35-40% of respondents thought lack of appropriate and easily available information was a barrier to implement energy efficiency investment measures. Information stressing the cost benefits of the energy efficient alternatives should be effectively communicated. The source of information is also very important in the adoption of investment measures. Hence, it is necessary to use the sources such associations consider important in adoption of energy efficiency measures.

As annual energy cost reduction is a very important guiding factor in associations' adoption of energy efficiency measures, information campaigns announcing the cost advantages of energy efficiency measures may be helpful in adoption decisions. However, majority (54%) of respondents reported that they did not have the expertise to assess the benefits of energy efficiency measures, while 34% of respondents reported financial constraints as the barrier. Innovative energy efficiency renovation package which include consulting, financing, contract work and follow up may be able to tap this segment.

Since respondents gave higher priority to reduce the annual cost of energy than to environmental benefits, increasing energy prices using economic instruments to internalise the environmental costs could encourage people to implement energy efficiency measures. In Sweden, external cost of energy use is internalized through taxes on emission of CO_2, sulphur and NO_x. However the price elasticity of energy demand in Sweden is low [14], and in such situations imposition of taxes to reduce energy use may be less effective [15].

Respondents gave high priority to investment cost in their energy efficiency decisions. Respondents also favour economic policy instruments compared to other policy instruments as the most effective method to improve energy efficiency. Subsidies may encourage the adoption of investment intensive energy efficiency measures by reducing the investment cost. The cost effectiveness of the subsidies could be improved by restricting its beneficiaries, for example subsidies may be granted based on the age of the components/buildings.

More respondents were unsatisfied with their attic insulation compared to other building envelope components. However, the respondents were more likely to replace windows than attic insulation. This could be because windows have a higher degree of *observability* as compared to attic insulation. If we encounter a problem frequently, we give priority to that problem more so than to others that are less observable [16]. Also more respondents had a favourable attitude towards energy efficient windows compared to other building envelope measures on various factors that influence the adoption decision.

A large percentage of respondents were unaware about various aspects of different energy efficient building envelope measures. The situation calls for measures to improve awareness about such measures among co-operative housing associations. As many respondents were not satisfied by the attic insulation of their buildings, it may be relatively easier to influence them to implement energy efficiency improvements in the attic insulation.

Acknowledgments

The authors gratefully acknowledge the financial support from the Swedish Energy Agency and from the European Union.

References

[1] STEM. Energy in Sweden 2009, Swedish Energy Agency, Eskilstuna, Sweden.

[2] A, Werner, External Water Condensation and Angular Solar Absorptance: Theoretical Analysis and Practical Experience of Modern Windows. PhD Thesis. Uppsala University, Sweden, 2007, ISSN 1651-6214.

[3] D, Avasoo, The European window energy labelling challenge. In: Proceedings of the European council for an energy efficient economy (ECEEE) summer study, Côte d'Azur, Paris, France; 4 -9 June, 2007.

[4] SCB, Yearbook of Housing and Building Statistics 2009 [Bostads- och byggnadsstatistisk årsbok 2009], Statistics Sweden, Örebro, Sweden, ISSN 1654-0921.

[5] B. Turner, Housing cooperatives in Sweden: The effects of financial deregulation, Journal of Real Estate Finance and Economics 15, 1997, pp 193- 217.

[6] E. Hassinger, Stages in the adoption process. Rural Sociology 24, 1959, pp 52–3.

[7] E.M. Rogers, Diffusion of Innovations, The Free Press, New York, 2003.

[8] D.I. Hawkins, D.L. Mothersbaugh, R.J Best, Consumer Behavior: Building Marketing Strategy. McGraw Hill/Irwin, New York, 2007.

[9] S. Birner, E. Martinot, Promoting energy-efficient products: GEF experience and lessons for market transformation in developing countries, Energy Policy 33, 2005, pp 1765–1779.

[10] S. Owens, L. Driffill, How to change attitudes and behaviours in the context of energy, Energy Policy 36, 2008, pp 4412–4418.

[11] M. Levine, D. Ürge-Vorsatz, K. Blok, L. Geng, D. Harvey, S. Lang, G. Levermore, M.A. Mehlwana, S. Mirasgedis, A. Novikova, J. Rilling, H. Yoshino, Residential and commercial buildings. In Climate Change 2007: Mitigation. Contribution of Working Group III to the 4th Assessment Report of the IPCC, Cambridge University Press. NY, 2007.

[12] J. Schleich, E. Gruber, Beyond case studies: Barriers to energy efficiency in commerce and service sector, Energy Economics 30, 2008, pp 449-464.

[13] W.H. Golove, J.H. Eto, Market barriers to energy efficiency: A critical reappraisal of the rationale for public policies to promote energy efficiency. Lawrence Berkeley National Laboratory, University of California, Berkeley, California, 1996.

[14] J. Nässén, F. Sprei, J. Holmberg, Stagnating energy efficiency in the Swedish building sector —Economic and organisational explanations, Energy Policy 36, 2008, pp 3814-3822.

[15] D. Ürge-Vorsatz, S. Koeppel, S. Mirasgedis, Appraisal of policy instruments for reducing buildings' CO2 emissions, Building Research & Information 35, 2007, pp 458 — 477.

[16] E. Milbourne. Perception and individual decision making; 2001. <http:// home.ubalt.edu/ntsbmilb/ob/ob3/tsld001.htm> [accessed 02.12.10].

Performance of a cold storage air-conditioning system using tetrabutylammonium bromide clathrate hydrate slurry

Z.W. Ma, P. Zhang*, R.Z. Wang

Institute of Refrigeration and Cryogenics, Shanghai Jiao Tong University, Shanghai 200240, China
** Corresponding author. Tel: +86 021 34205505, Fax: +86 021 34206814, E-mail: zhangp@sjtu.edu.cn*

Abstract: A cold storage air-conditioning system was built to investigate the energy saving effect of using tetrabutylammonium bromide (TBAB) clathrate hydrate slurry (CHS) as cold storage medium, the corresponding *COP* during TBAB CHS generation and the pumping power during the cold release were measured. As the increase of the TBAB CHS mass fraction during the generation, the system *COP* generally decreased from about 1.92−2.95 to about 1.05−1.49, depending on TBAB CHS flow rate. To clarify the performance of this system, several cold storage strategy cases are studied, the corresponding electric power consumption and the cost saving, compared with water as the cold transportation medium, are shown in this work as well.

Keywords: *Clathrate hydrate slurry, Secondary loop air-conditioning system, evaluation.*

1. Introduction

As a n ew kind of phase change slurry material, tetrabutylammonium bromide ($[CH_3(CH_2)_3]_4NBr$, TBAB in abbreviate) clathrate hydrate slurry (CHS) was studied by many researchers in recent years. Due to the adjustable phase change temperature over the range of 5−12 ^oC, the good cold-carry capacity which is about 2−4 times of that of chilled water and the good fluidity, TBAB CHS is considered promising in an air-conditioning system, where this slurry can be used both as cold storage and transportation medium.

Researchers in Japan firstly reported this new material for air-conditioning using, and measured the basic thermo-physical properties, including the phase diagram, latent heat, density, heat capacity, thermal conductivity etc. [1, 2], and they also applied it to a real application [3]. Hayashi et al. [1], Darbouret et al. [4], Xiao et al. [5] and Ma et al. [6] all investigated the flow characteristics of TBAB CHS in straight tubes, nevertheless, the results reported were divergent. Moreover, Ma et al. [6] reported the forced convective heat transfer characteristics. However, the application of TBAB CHS is still limited by the deficient studies, and the performance in an air-conditioning system is rarely reported.

In the present study, a cold storage air-conditioning system using TBAB CHS was built and the corresponding performance was presented. System *COP* during TBAB CHS generation and the pumping power during cold release were both measured, based on which the system energy consumption was numerically estimated in different cases. In addition, the cost saving of using TBAB CHS compared with that of using chilled water as the cold transportation medium was evaluated.

2. Methodology

2.1. Basic thermo-physical properties of TBAB CHS

The TBAB CHS is a kind of solid-liquid suspension with white color, as shown in Fig. 1, which can be easily generated at atmosphere condition by cooling down the TBAB aqueous solution to supercooling state. The melting temperature, mass fraction, latent heat and other properties (such as density, heat capacity and thermal conductivity) of TBAB CHS are introduced in this section.

Fig. 1. Photo of the TBAB CHS.

The melting temperature could be determined with the aid of the phase diagram, which describes the relation between it and the corresponding solution concentration. Differential Scanning Calorimeter (DSC, TA, Q2000) was applied to record the heating processes of TBAB CHS at a heating rate of 0.5 ^{o}C/min, and then the phase diagram could be plotted based on the test results, which is shown in Fig. 2 as well as the comparison with that obtained by other researchers.

The volume and mass fraction of CHS can be determined by Eq. (1) and (2), with several requisite parameters provided by the phase diagram.

$$\omega_{\mathrm{p}} = \frac{\omega_0 - \omega_{\mathrm{liq}}}{\omega_{\mathrm{H}} - \omega_{\mathrm{liq}}} \tag{1}$$

$$\varphi = \frac{\omega_{\mathrm{p}} / \rho_{\mathrm{p}}}{\omega_{\mathrm{p}} / \rho_{\mathrm{p}} + (1-\omega_{\mathrm{p}}) / \rho_{\mathrm{liq}}} \tag{2}$$

where ω_{p} is the crystal mass fraction of TBAB CHS, ω_0 is the initial solution concentration, ω_{H} is the TBAB mass fraction in the hydrate crystal, ω_{liq} is the concentration of the liquid phase in the slurry, φ is the TBAB CHS volume fraction, ρ_{p} and ρ_{liq} are densities of the crystal and the liquid phase, respectively. Two different hydrates with different hydration numbers were observed, and the corresponding thermo-physical properties have been summarized by Ma et al. [6], as shown in Table 1, the two values of some properties in the table were the result of different researches referenced.

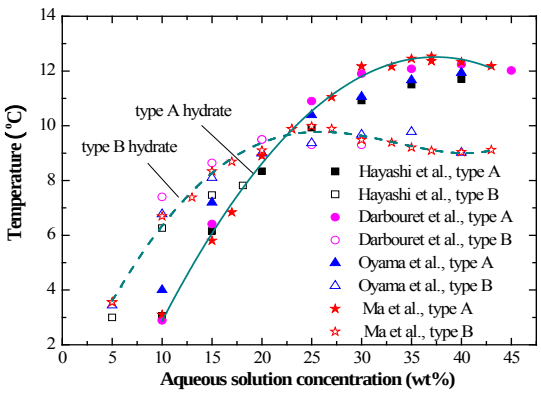

Fig. 2. Phase diagram of TBAB CHS. [6]

Table 1. Thermo-physical properties of TBAB hydrate crystals [6].

	Hydration number -	Melting temperature (ºC)	Density (kg/m^3)	Latent heat (kJ/kg)	Heat capacity (kJ/(kg·K))	Thermal conductivity (W/(m·K))
type A	26	11.8/12.0	1080	193.18±8.52	2.22/1.86–2.61	0.42
type B	36/38	9.90	1030	199.59±5.28	2.00–2.54	–

Density of TBAB aqueous solution was measured using a balance (FS: 2200g, accuracy: 0.01 g) and a graduated flask (FS: 50 mL, accuracy: 1 mL), while the heat capacity was measured based on the heat balance with water in a plate heat exchanger. Thereafter, these properties of TBAB CHS can be calculated by the corresponding values of TBAB solution we measured and that of TBAB hydrate crystal given in Table 1. M eanwhile, thermal conductivity of TBAB aqueous solution as well as TBAB CHS was measured by a transient hot-wire unit (the measuring error was less than ±3% while water was applied). All the properties of TBAB CHS (type B hydrate, original 15 wt% solution) are presented in Table 2.

Table 2. Thermo-physical properties of TBAB CHS (type B hydrate crystal, original 15 wt% solution).

Mass fraction (wt%)	Density (kg/m^3)	Heat capacity (kJ/(kg·K))	Thermal conductivity (W/(m·K))
5	1015.690	4.001	0.469
10	1015.656	3.933	0.473
15	1015.635	3.865	0.476
20	1015.608	3.798	0.480
25	1015.585	3.732	0.483
30	1015.560	3.667	0.485

The enthalpy change (Q) of TBAB CHS in a certain temperature range, 5–12 ^{o}C for example, is an important parameter which indicates how much cold energy is stored or released. Basically, there are two methods to calculate the enthalpy change of this slurry. One is introducing the slurry fraction change ($\Delta\omega$), the latent heat (ΔH) and the sensible heat ($Cp\Delta T$) into Eq. (3):

$$Q = \Delta\omega\Delta H / 100 + Cp\Delta T \quad (3)$$

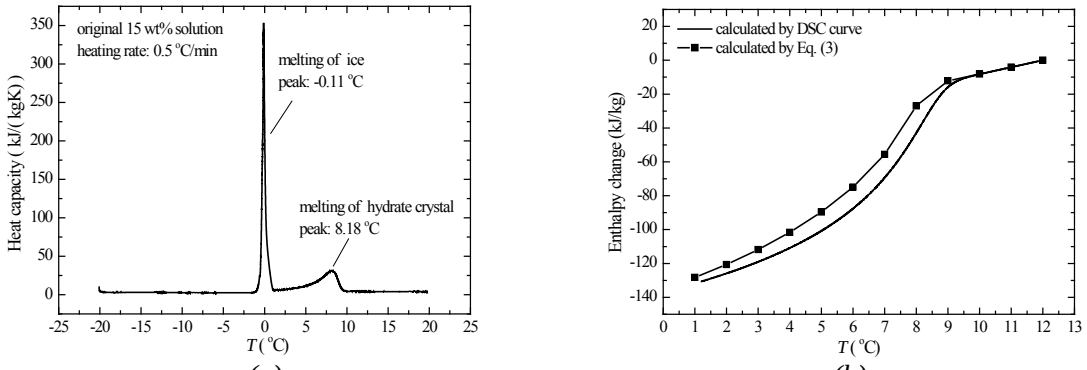

(a) *(b)*

Fig. 3. (a) DSC curve; (b) enthalpy change of TBAB CHS.

The other method is integrating the DSC heating curve against temperature shown in Fig. 3(a). The comparison between these two methods is shown in Fig. 3(b). The enthalpy change within the temperature range of 5 to 12 ^{o}C calculated by Eq. (3) is about 10.9% smaller than that calculated by DSC curve, and the latter method was applied in the present work.

2.2. Experimental set-up and CHS generation method

Fig. 4 shows the schematic diagram of the constructed cold storage air-conditioning system using TBAB CHS. Two thermal insulated tanks (1.2 m^3) were used for solution and slurry, respectively. Three Pt100 sensors (accuracy: ±0.15 ^{o}C) were employed to record the temperature variations at the bottom, middle and top of the each tank. A double-tube heat exchanger (ShenShi, GT-U0480) with corrugated flow passage was applied to undertake the heat exchange between solution and the evaporating refrigerant. The refrigerator used was an outdoor unit of a commercial air-conditioner, which can switch from cooling to heating by a four-way valve. The used slurry pump was a speed adjustable rotational pump and a stabilizing tank located at the downstream of the pump was used to stabilize the flow. A simple agitator was mounted on the slurry tank, which was operated to avoid the deposition of crystals. A plate heat exchanger (Swep, B8×30) was selected as the load side heat exchanger since its high heat transfer rate, and hot water acted as the cooling load. The hot water was stored at an insulated water tank before experiment and was drained after used. Moreover, pressure sensors (accuracy: 0.1%) were located at different positions of the fluid flow to measure the pressure drop, and the electric power consumed by the refrigerator and the pump were measured as well.

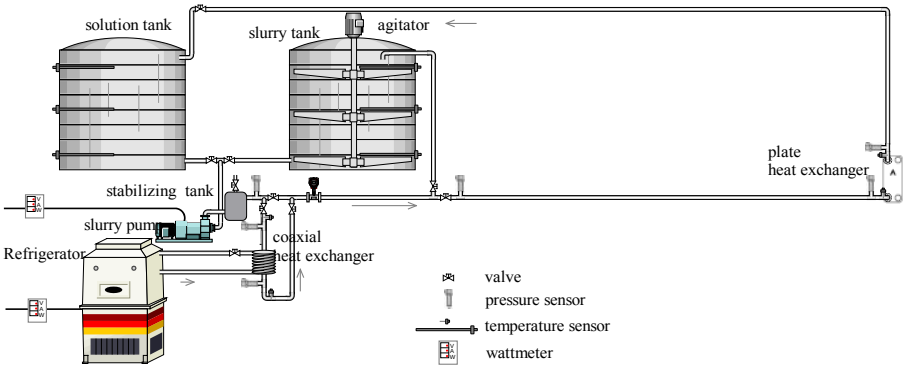

Fig. 4. Schematic diagram of the experimental set-up.

The test was divided into three steps based on the state of the TBAB CHS: (1) The aqueous solution was cooled to supercooling state. However, the supercooling state cannot be achieved by only one cycle from the solution tank to the slurry tank due to the limited cooling power of the refrigerator. As a consequence, the solution must be continuously pumped through the double-tube heat exchanger from and back to the slurry tank. (2) Hydrate crystals appeared. Accompanied with mechanical shocks between the returned fluid and the stored fluid, TBAB hydrate crystals can be generated in the supercooled solution, and the fluid temperature increased because of the released latent heat. Moreover, sometimes the agitator should be operated to accelerate the hydrate crystal generation. (3) TBAB CHS was kept cooled to reach the desired crystal fraction. (4) TBAB CHS was pumped to the load side to release the stored cold energy, and afterwards became aqueous solution again and flowed back to the solution tank.

The crucial disadvantage during the entire test occurred in step 3. Before the desired hydrate fraction was achieved, TBAB CHS was continuously cooled and hydrate crystals grown

inside the heat exchanger. The generated crystals would adhere to the heat transfer surface where the temperature was extraordinary low. The adhered crystals layer deteriorated the heat transfer between refrigerant and TBAB CHS. The worse thing was that the refrigerant temperature dropped a lot to maintain the heat exchange, which resulted in forming more hydrate crystals and creating thicker crystal layer on the heat transfer surface. A malignant cycle occurred, the hydrate crystals were difficult to be continuously produced and the system efficiency became low.

Three methods are mainly proposed to solve the aforementioned low-efficiency problem: (1) Maintaining the refrigerant temperature at a certain temperature range by adjusting the refrigerant flow rate. (2) Increasing the flow velocity of the TBAB CHS to be high enough to flush and break off the crystal formed on the flow passage wall so that to ensure a good heat transfer. (3) Operate the refrigerator reversely from cooling to heating for a while to melt the adhered hydrate crystals. In this work, a manual needle throttle valve was applied to implement the first method, and it was found that more accurate control of the throttle valve was needed. Thus, the method (2) and (3) were applied to ensure the continuous generation of hydrate crystals and high system efficiency, as shown in Fig. 5. With high flow rate (about 16–18 kg/min in Fig. 5) and reverse operation, we obtained 31 wt% TBAB CHS successfully.

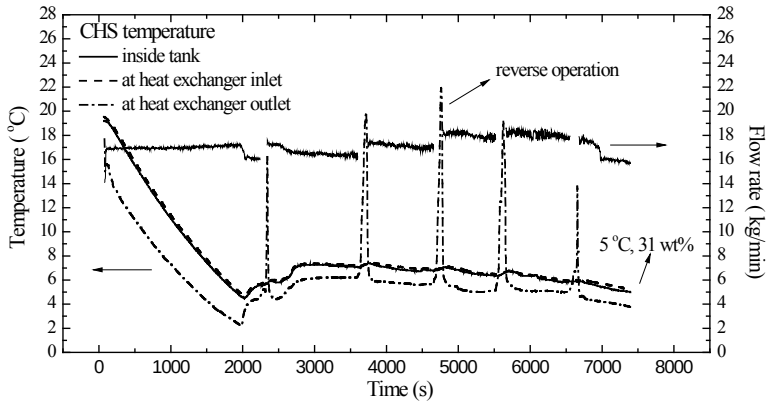

Fig. 5. Typical generation process of TBAB CHS.

3. Results and discussions

The system *COP* during the CHS generation was calculated by Eq. (4):

$$COP = \frac{\text{cold energy stored by TBAB CHS}}{\text{refrigerator power} + \text{pumping power}} \tag{4}$$

It should be claimed that the stored cold energy was all calculated from 15 °C solution to the stored TBAB CHS. Fig. 6 shows *COP* as function of the mass fraction as well as the flow rate. The *COP* of 0 wt% TBAB CHS shown in the figure was the average system *COP* before the hydrate appearance. The hydrate crystals were generated instantaneously, thereafter about 14–16 wt% mass fraction was soon reached, hence *COP* from the beginning to this moment was higher than that before the generation. However, as increase of the mass fraction, *COP* reduced from about 1.92–2.95 to about 1.05–1.49 due to the aforementioned crystals adherence to the heat transfer surface. Meanwhile, the reverse operation of refrigerator consumed additional energy, which was another attributor to the *COP* reduction. As mentioned, high flow velocity was beneficial to the heat transfer between TBAB CHS and refrigerant, since the adhered crystals would be flushed down by the strong shear force, which

was validated by *COP* profile shown in the figure—higher flow rate generally led to a higher *COP*. However, this phenomenon depended on the performance of the pump.

The pumping power during the cold release will be reduced if TBAB CHS is applied as the secondary refrigerant instead of chilled water due to its higher cold-carry capacity and thus the flow rate is lower. Fig. 7 presents the pumping power of water, 20 wt% CHS, 25 wt% CHS and 30 wt% CHS as the function of the cooling load during the cold release. As seen in the figure, more energy saving on pumping power was achieved by using TBAB CHS with higher mass fraction.

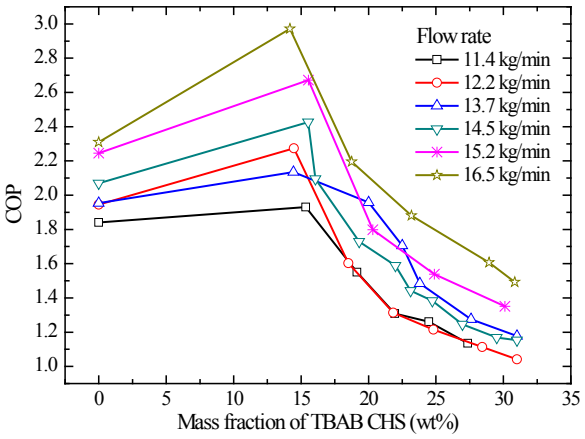

Fig. 6. System COP during the CHS generation.

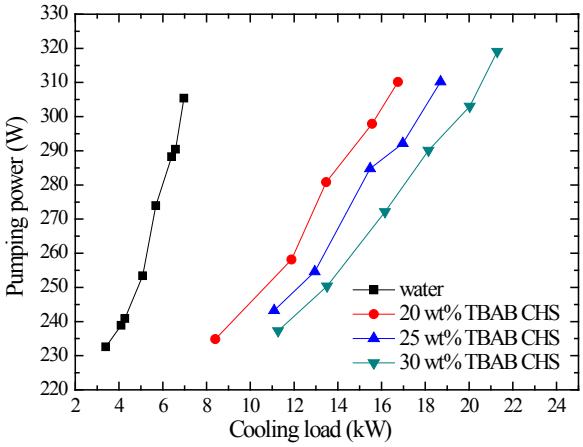

Fig. 7. Pumping power during the cold release.

A study case is assumed for better exhibiting the performance of TBAB CHS. The assumed cooling load is in eight hours in daytime, during which the average cooling load is 21 kW and the maximum value is 33 kW, therefore the totally cooling duty is 604800 kJ. Fig. 8 shows four types of system operation strategies. For each case, 20 wt%, 25 wt% and 30 wt% CHS are applied, the system *COP* during the TBAB CHS generation is about 2.10, 1.79 and 1.54, respectively based on the results in Fig.6 (flow rate: 16.5 kg/min). The storage ratio (which is the ratio of the storage cold energy to the total required cold energy) of case 1 and case 2 is 40% while that of case 3 and case 4 is 60%, the other cooling load is satisfied by the refrigerator (average system *COP* is about 2.32) while considering water as the secondary refrigerant. Moreover, assume the application of water as case 5 for the comparison, and consider water as the secondary refrigerant for all the cold release and no cold storage is conducted.

Fig. 9(a) shows the electric power consumption with all the study cases based on the present system. It can be seen from the figures, the power consumption increases as the increase of the mass fraction, which is obviously caused by the lower system *COP*. All the power consumptions in cases 1-4 are higher than that of case 5, which means there is no energy saving of the application of TBAB CHS compared with water. However, the operation cost does decrease as the increase of TBAB CHS mass fraction and the cost saving is shown in Fig. 9(b) (the price of the electricity is taken as 0.3 RMB/kWh during night time while 0.6 during daytime), about 8–27% cost saving can be achieved. However, since the the present system is limited by the room space, the piping from the storage tank to the load side is very short and thus the pumping power shown in Fig.7 is not coincident to the practical system with the assumed cooling load. Therefore, we re-calculate all the cases with amplifying the pumping power to 3 times as large as the present measured values during the cold release, the original case 1–5 become to case 1'–5'. Fig. 10(a) and (b) show the corresponding electric power

consumption and the cost saving. It is noticed that about 1.4–3.5% energy saving is achieved, calculated by 20 wt% TBAB CHS with all the operation strategies, while the cost saving increases to about 10–29%.

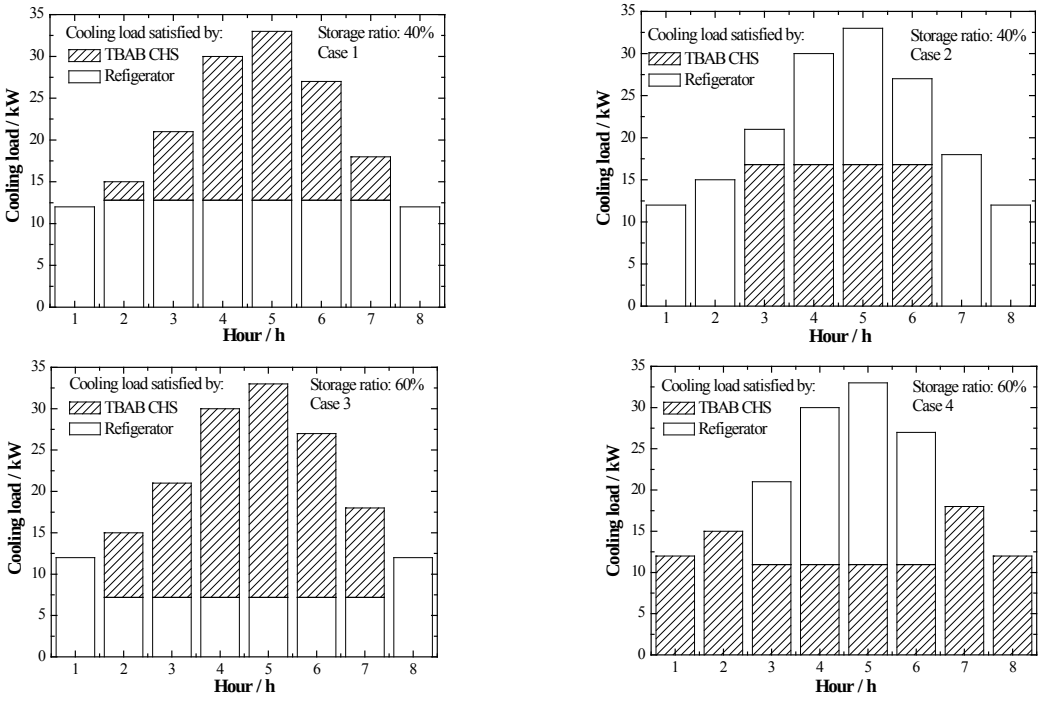

Fig. 8. System operation strategies.

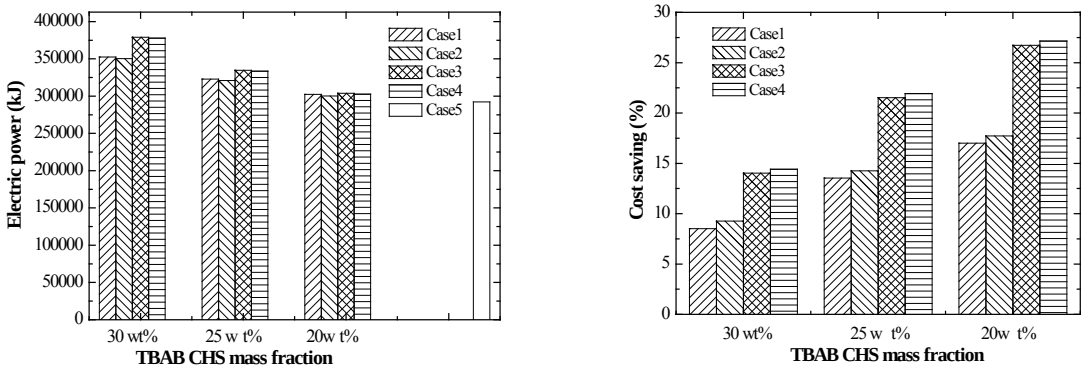

(a) *(b)*

Fig. 9. Electric power consumption and cost saving.

4. Conclusion

The present work mainly constructed and tested a cold storage air-conditioning system using TBAB CHS and estimates the energy consumption. The system *COP* decreased from about 1.92–2.95 to about 1.05–1.49 during CHS generation. The energy saving by using TBAB CHS instead of water was not achieved as expected since the piping was short and the pumping power was low in the present system, while 8–27% cost saving was achieved. However, about 1.4–3.5% energy saving could be achieved if the pumping power was amplified to 3 times as large as the original values, meanwhile the cost saving was about 10–29%.

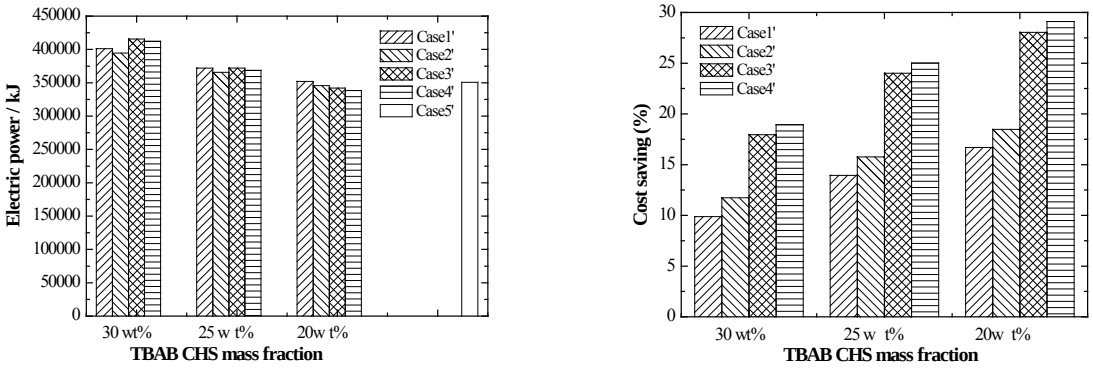

(a) *(b)*

Fig. 10. Electric power consumption and cost saving with amplified pumping power.

Acknowledgements

The authors are grateful to the "Shu Guang" project supported by Shanghai Municipal Education Commission and Shanghai Education Development Foundation under the Contract No. 09SG11 and the Science and Technology Commission of Shanghai Municipality under the Contract No. 10160710700. This research is also partially supported by the Specialized Research Fund for the Doctoral Program of Higher Education under the Contract No. 20100073110039.

References

[1] K. Hayashi, S. Takao, H. Ogoshi and S. Matsumoto, Research and development on high-density cold latent-heat medium transportation technology, IEA Annex-10-PCMs and Chemical Reactions for Thermal Energy Storage 4th Workshop, Japan, 2000.

[2] H. Oyama, W. Shimada, T. Ebinuma, Y. Kamata, S. Takeya, T. Uchida, J. Nagao and H. Narita, Phase diagram, latent heat, and specific heat of TBAB semiclathrate hydrate crystals, Fluid Phase Equilibria 234, 2005, pp. 131–135.

[3] S. Takao, H. Ogoshi, S. Matsumoto, K. Takashi, M. Sugiyama, T. Akiyama, S. Fukushima, New air conditioning systems using hydrate slurry, NKK Technical Report 174, 2001, pp. 6–11. [in Japanese]

[4] M. Darbouret, M. Cournil, and J.M. Herri, Rheological study of TBAB hydrate slurries as secondary two-phase refrigerants, International Journal of Refrigeration 28, 2005, pp. 663–671.

[5] R. Xiao, S.S. Wu, L.G. Tang, C. Huang, and Z.P. Feng, Experimental investigation of the pressure-drop of clathrate hydrate slurry (CHS) flow of tetra butyl ammonium bromide (TBAB) in straight pipe, Proceedings of 10th International Conference on T hermal Energy Storage, Stockton, USA, 2006.

[6] Z.W. Ma, P. Zhang, R.Z. Wang, S. Furui, and G.N. Xi, Forced flow and convective melting heat transfer of clathrate hydrate slurry in tubes, International Journal of Heat and Mass Transfer 53, 2010, pp. 3745–3757.

Understanding occupant heating practices in UK dwellings

T. Kane[a*], S. K. Firth[1], D. Allinson[1], K. N. Irvine[2], K. J. Lomas[1]

[1] *Department of Civil and Building Engineering, Loughborough University, Loughborough, Leicestershire, UK*
[2] *The Institute of Energy and Sustainable Development, De Montfort University, Leicester, UK*
** Corresponding author. Tel: +44 (0) 1509 223780, E-mail: t.kane@lboro.ac.uk*

Abstract: The 2008 Climate Change Act has committed the UK government to reduce CO_2 emissions by 80% of 1990 levels by 2050. To meet this target a significant reduction in energy consumption will be required from domestic dwellings and in particular space heating which accounts for more than 50% of the energy used in the UK housing stock. The UK government has initiated a number of policies to reduce energy use from UK dwellings. Energy savings that result from energy efficiency improvements to dwellings have sometime been lower than expected as a result for the rebound effect. Discussion of the rebound effect has questioned whether these polices will result in the CO_2 reductions required to meet the national targets. Large-scale survey research has shown that energy use is related to climate, built form of properties, efficiency of heating systems, socio-economic indicators and occupant behaviour. Temperature monitoring studies have been undertaken to gain insight into how occupants heat their homes. If the variation in indoor temperatures can be explained by; (1) social determinants such as age, income and the number of household occupants and; (2) technical determinants such as house type, house age and level of insulation then this would enable energy efficiency initiatives (e.g. cavity wall installation or education programmes) to be targeted where they will be most effective. This paper presents preliminary results from a large-scale city-wide survey of over 500 homes in the city of Leicester, UK. temperature measurements were recorded at hourly intervals over a nine month period for the living room and main bedroom spaces in over 300 homes. Household data, including socio-demographic information, was collected for each household. This dataset is used to investigate indoor temperatures across house types. The results confirm that house type is related to differences in indoor temperatures. Flats have the highest average temperatures while detached homes have the lowest. To gain insight into heated periods households with average evening temperatures were identified. It was found 45% of mid terrace properties had evening temperatures below 18°C and more than a third of detached and semi detached home also had cold evening temperatures. There are a number of reasons for low indoor temperatures in dwellings during occupied periods including inefficiency of buildings and heating systems, the inability of occupants to afford heating and personal choice. It is concluded that to meet Government CO_2 reduction targets the rebound effect should be taken into account when calculating the energy savings expected from energy efficiency programmes. Further analysis is ongoing to identify how other social and technical factors relate to indoor temperatures. Multiple regression analysis will be used to identify how internal temperatures are correlated against a number of determinants including building characteristics (built form type, age, heating system type, heating controls) and household characteristics (age of occupants, income).

Keywords: *Indoor temperature, Heating practices, Household behaviour, Space heating, Energy efficiency.*

1. Introduction

The 2008 Climate Change Act committed the UK government to reduce CO_2 emissions by 80% of 1990 levels by 2050 [1]. To meet this target a significant reduction in emissions will be required from all energy sectors. In 2008 energy use from domestic buildings accounted for 27.5% of total UK energy consumption [2]. CO_2 emissions associated with domestic buildings are predominantly related to electricity generation and energy used for space and water heating. Space heating accounts for 57% of all energy used in UK domestic buildings [3]. Reducing the energy used for space heating is a challenge as it is related to the technical performance of the building and its heating systems, as well as the behaviour of occupants [4, 5]. The UK government has introduced a number of policies that are designed to reduce the energy use related to space heating. One of these is the 'Green Deal' which was announced by the UK government in 2010. Householders will be given a loan to make energy efficiency improvements to their properties and are expected to make repayments using money saved due to lower energy bills [6]. Technical improvements to dwellings such as cavity wall or loft

insulation or the installation of energy efficient boilers do not always result in the expected energy savings [7]. This was evidenced by the Warm Front study, energy use was measured before and after energy efficiency improvements and theoretical energy use compared to actual energy use. It was found that actual energy improvements were approximately 30% less than expected [7]. This phenomenon is called the 'rebound effect' and brings into question the ability of households to make payments based on energy savings [8]. Literature on the 'Green Deal' does not discuss how payments will be made if energy efficiency improvements do not result in financial savings. The rebound effect has been used to argue against making efficiency improvements in the existing housing stock [9]. As a consequence, Government emissions targets based on expected energy savings are unlikely to be met. This criticism, however, does not account for the improvements in health and wellbeing of occupants that are related to the increase in indoor temperatures that can be the result of energy efficiency measures [10]. The challenge for policy makers is to address energy and CO_2 reduction while accounting for the 'rebound' effect. One example of this is the households in fuel poverty. A household is said to be in fuel poverty if they require more than 10% of their income to heat their home to a comfortable temperature [11]. In 2007 3.5 million households in the UK were in fuel poverty [11], if energy efficiency improvements were made in these dwellings it is assumed that energy savings would be minimal, as indoor temperatures would increase in many of the households.

The health and wellbeing of the occupants has been addressed for new builds since the publication of the Code for Sustainable Homes in April 2007 [12]. Health and wellbeing have, however, not been addressed in discussions about energy efficiency improvements in older properties which make up the majority of the housing stock or in the energy saving advice that is provided by local and national government. Generic energy saving advice such as 'turn your thermostat down 1°C will save you 10% of your heating bills' may be appropriate for some households but not occupants that are already living in cold homes [13]. These issues raise two concerns; (1) how can energy efficiency policies ensure both energy savings and improved health and comfort of occupants and; (2) what energy savings should be expected as a result of energy policies after the indoor temperatures in some households have increased. The mitigation of the effects of climate change is a strong driver for energy reduction but should not be addressed outside of the context of other health and comfort issues. For energy policy to effectively reduce CO_2 emissions and improve the health and comfort of building occupants more information about the housing stock and the drivers of indoor temperatures is required. The accidental benefits of energy improvements such as improved health of occupants should not be ignored. Joined up solutions designed to reduce energy consumption in the housing stock while improving the thermal comfort of vulnerable household occupants are required to address a fully sustainable approach to emissions reduction programmes. The benefits of the rebound effect should, therefore, be recognised despite the reduction in CO_2 emissions savings that may result in a portion of the housing stock. For policy makers to accurately predict the result of energy efficiency improvements at the national scale the proportion of dwellings where reduced savings are expected should be considered.

To promote the health and wellbeing of building occupants the World Health Organisation (WHO) has suggested dwellings are heated to indoor temperatures of 21°C in the living room and 18°C in bedroom spaces [14]. Previous temperature monitoring studies provide insight into the temperatures to which UK dwellings are heated. To understand whether dwellings are heated to the recommended temperatures it is important to ascertain what the indoor temperatures are in living spaces during occupied periods. Shipworth et al. (2010) measured temperature in a large sample across the UK [15]. Daily peak temperature was estimated to be

21.1°C. This finding, however, can be easily influenced by periods of high internal or solar heat gain. Other studies have reported temperatures averaged over the whole day. Oreszczyn et al. (2006) monitored temperature in over 1600 low income dwellings. Average living room temperature, adjusted for outdoor temperature, was reported to be 19.1°C [10]. Summerfield et al. (2006) monitored indoor temperatures in 14 UK dwellings built to high thermal standards and found that the average living room temperature was 19.1°C [16]. Yohanis and Mondol (2010) reported an average living room temperature of 19.4°C measured in 25 dwellings in Northern Ireland [17]. All of the average temperatures reported in the UK studies are lower than the recommended temperature of 21°C.

The temperatures reported in these papers have not been analysed to ascertain which dwellings have low indoor temperatures. In order to inform how policy can be targeted a sample which includes all house types and people groups is required. These studies have gained valuable insights into indoor temperatures in UK dwellings but have not reported indoor temperatures during occupied periods. Isaacs et al. (2010) monitored temperature in New Zealand homes and calculated average temperatures for different parts of the day [18]. Average temperatures suggested that many dwellings were not heated to the 21°C recommended by the WHO [18]. Dwellings heated by solid fuel were found to have warmer living room temperatures on average than those heated in other ways. This finding led to a policy change by the New Zealand government to subsidise the installation of wood burners as well as gas and electric fires. Empirical evidence is required to see if any changes to UK CO_2 reduction policy are necessary.

This paper presents initial analysis of temperature data collected in over 300 houses across Leicester, UK between July 2009 and March 2010. This data set is novel as it is the first large scale study to focus on a single UK city. This work seeks to identify where energy efficiency initiatives should be targeted. This information is key for the accurate prediction of CO_2 savings so that Government can ensure that targets are met. Dwellings with low indoor temperatures during heated periods will be identified as it is assumed that these dwellings would benefit from efficiency improvements without the expectation of energy savings. Findings will be valuable for policy makers to ensure that energy efficiency policy will deliver estimated CO_2 emissions reductions and additional benefits for the health and comfort of vulnerable portions of society.

2. Methodology

Data were collected during a large-scale city-wide housing survey carried out in Leicester, UK in 2009-2010 [19]. The Living in Leicester (LIL) Survey was designed by the 4M project - Measurement, Modelling, Mapping and Management (4M): An Evidence-Based Methodology for Understanding and Shrinking the Urban Carbon Footprint - a collaboration between four Universities funded through the Engineering and Physical Sciences Research Council (ESPRC). 4M is studying CO_2 emission sources and sinks in urban areas and has collected data from households within Leicester including indoor air temperatures in domestic buildings. Households were randomly selected after stratifying by percentage of detached homes and percentage of households with no dependent children in each of the 36 middle layer super output areas. 575 households were involved in face to face interviews which were conducted by the National Centre for Social Research (NatCen).

Hobo data loggers (Figure 1) were used to monitor air temperature every hour between July 2009 and March 2010 in a subset of these households. The sensors were calibrated by Tempcon Ltd and were found to be accurate to ±0.4°C [20]. NatCen interviewers asked the occupants to place the Hobos in the living room and main bedroom. Guidance on the placement of sensors was provided and stated that the Hobos should be placed away from heat sources and not in direct sunlight. A distinct advantage of this data set compared to previous national studies is that outdoor temperature and climate can be assumed to be the same across the whole sample. At the end of the monitoring period the Hobos were returned in pre-paid envelopes. 620 Hobos were returned from 321 households. Only households with temperature data for living room spaces were suitable for this analysis. 31 households were excluded from the analysis for a number of reasons including; loggers failing to download; data not being available for the whole monitoring period; and average temperatures being below 10°C (when it was assumed that sensors were in unheated spaces, misplaced or faulty).

Figure. 1 Hobo data logger used to measure indoor air temperature in 290 dwellings in Leicester City.

Temperature data for the month of February 2010 were analysed to provide understanding of heating patterns during a typical winter heating period. The average daily temperature profile was calculated for each house. Although average temperatures were calculated for both living room and bedroom spaces only living room temperature considers the ability for households to heat their living spaces to adequate temperatures. Consequently, this analysis concentrates on living room temperatures. Average temperatures for morning (7:00-9:00), day (9:00-17:00), evening (17:00-23:00) and night (23:00-7:00) were calculated to aid understanding heated and unheated periods. Temperature data were combined with data on the built form of the properties for analysis.

3. Results

3.1. Analysis of indoor temperature data

Average temperatures were compared to those measured in New Zealand homes, which is a comparable study reporting average evening temperatures [18] (Table 1).

Table 1. Average temperatures reported. Temperatures in Leicester for the 4M project are reported for February 2010. New Zealand (HEEP) temperatures are for the whole winter.

Room		Average evening temperature (°C)			
		Morning (7:00-9:00)	Day (9:00-7:00)	Evening (17:00-23:00)	Night (23:00-7:00)
Living room	4M (n=290)	17.4	17.8	18.7	18.9
	HEEP (n=348)	13.5	15.8	17.8	14.8
Outdoor	Leicester	1.5	3.6	2.6	1.6
	New Zealand	7.8	12.0	9.4	7.6

Indoor temperatures measured in Leicester were found to be higher than those measured in New Zealand; average evening temperatures were 18.7°C and 17.8°C respectively. Temperatures in UK dwellings are also more uniform throughout the day; New Zealand morning temperatures were 13.5°C compared to 17.4°C in Leicester. There are numerous

reasons why this might be that case, these include that homes in Leicester may have longer heating periods, better thermal insulation, more efficient heating systems or occupants that prefer warmer indoor temperatures. Average temperature profiles were used to identify the variation of indoor temperatures relating to different house types (Figure 2). None of the property types had average temperatures that reached the temperatures recommended by the WHO. It was observed that flats were warmer for the majority of the day, on average, compared with other house types. It is hypothesised that this is due to flats being more thermally efficient than other property types as they have less exposed surface area. Detached dwellings reach the lowest temperatures. Although mid terrace properties have less exposed wall area than end terraces and are assumed be more thermally efficient, lower temperatures on average were observed. Further data analysis is required to comment on the reasons or validity of this observation.

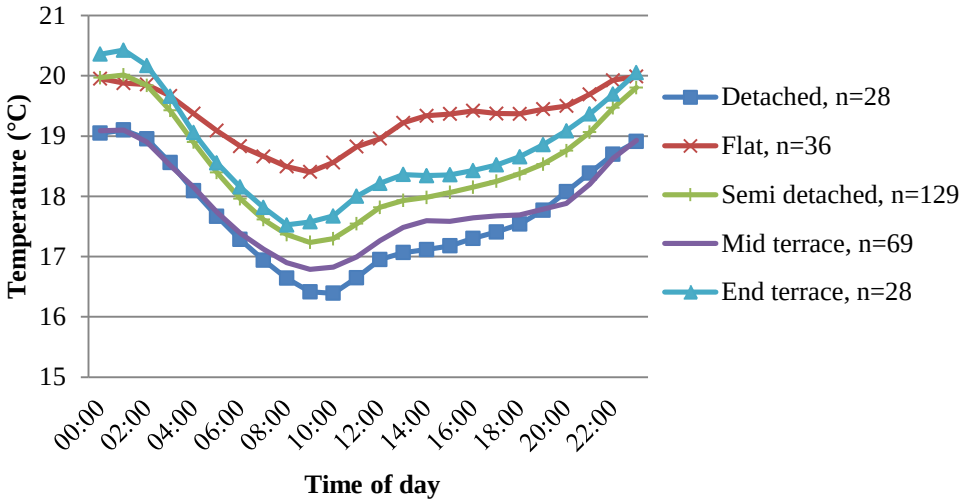

Figure 2. Daily living room temperature profile averaged for each hour in February 2010 for indoor temperatures measured in 290 homes in Leicester.

3.1 Recognising rebound in UK policy making

Analysis was carried out to identify the proportion dwellings where energy efficiency improvement may not result in the expected energy savings. To do this it was assumed that the heating was operational in all dwellings during evening periods. A histogram of average evening (17:00 – 23:00) temperatures illustrates the variation in indoor temperatures during heated periods (Figure 3). Mean evening indoor temperature was 19.9°C with a standard deviation of 2.1°C. 7% of dwellings can be observed to have evening temperatures over 22°C (Table 2). In these homes it is assumed that energy efficiency improvements are expected to result in energy savings as higher indoor temperatures are unlikely to be desired. 36% of dwellings had evening temperatures below 18°C and therefore it is assumed that energy efficiency improvements may not deliver energy savings but contribute to increased indoor

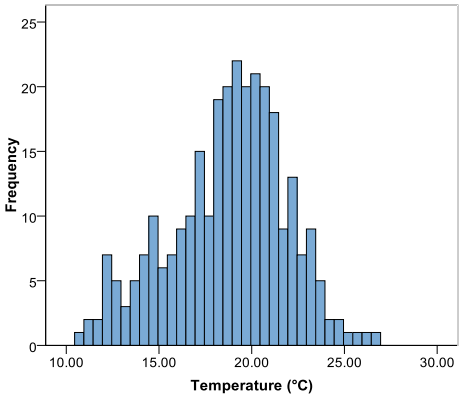

Figure 3. Histogram of average evening living room temperature measured in 290 households in Leicester during February 2010.

temperatures. These data were divided into house types to see whether certain house types could be targeted by policy makers. 45% of mid terrace properties were found to have low evening temperatures and more than a third of detached and semi detached homes also had low evening temperatures. Further analysis of these data is required to identify which other social and technical variables also relate to indoor temperatures and to test the statistical significance of these results.

Table 2. Average evening temperatures under18°C measured in dwellings in Leicester in February 2010

	% with average evening temperature under 18°C	% with average evening temperature above 22°C
All dwellings (n=290)	36	7
Detached (n=28)	39	4
End terrace (n=28)	29	7
Flat (n=36)	25	14
Mid terrace (n=69)	45	6
Semi detached (n=129)	35	6

3.2 Discussion

A challenge in this analysis is the number of influences on indoor temperatures. Thermal comfort is defined as a product of indoor temperature, mean radiant temperature, air speed and occupant activity. Indoor temperature is related to the outdoor climate, the efficiency of the built form and heating systems in dwellings as well as occupant behaviour. Gathering and analysis of data to inform policy makers is therefore complex and it is important not to make assumptions. For example, if improvements were made to a buildings' air tightness this would reduce the energy lost via infiltration and reduce drafts (air speed). This could increase occupant thermal comfort while indoor temperatures could remain the same or even be lowered. This measure would reduce energy use from the dwelling but this could not be observed by using only indoor temperature data. It should also be noted that although it is assumed here that there is a portion of the housing stock where occupants are unable to maintain their preferred temperature due to the inefficiency of building fabric or heating systems or the inability to afford heating, there are some occupants that prefer lower indoor temperatures. Further analysis and data collection are therefore required to continue to develop the understanding of the drivers of indoor temperatures in domestic dwellings and how these can be analysed to inform policy makers. This will include using analysis of covariance to identify the variables which influence households to have high or low temperatures during occupied periods. This analysis will address whether other social and technical factors can explain more of the variation in indoor temperatures. This dataset will be used to explore relationships between indoor temperature and income, house price, built form, controllability of heating systems, age of property and number of occupants. Outdoor air temperature, average temperatures during heated periods and estimations of daily heating period and demand temperature based upon analysis of daily temperature profiles will also be considered.

4. Conclusion

This paper presents initial analysis of indoor temperature data measured during February 2010 in 290 households in Leicester, UK. Average temperatures were calculated to identify variations in indoor temperature in dwellings. The data were used to address how house type relates to indoor temperatures. Temperature profiles showed that on average flats had higher

indoor temperatures than other house types. It is suggested that this was due to flats being more thermally efficiency due to their limited exposed wall. Average temperatures for evening periods were calculated to identify the proportion of Leicester properties which have high and low evening temperatures. It was found that 36% of the households had average evening temperatures below 18°C which is below the 21°C recommended by the WHO. Nearly half of all mid terrace properties and over a third of detached and semi detached properties were found to have evening temperatures below 18°C. Further analysis is required of this data set to fully address the reasons why these properties have low temperatures during occupied periods. There are many drivers of indoor temperatures in domestic dwellings which require understanding if energy reduction policy is to be fully effective. It is concluded that to meet Government CO_2 reduction targets the rebound effect should be taken into account when calculating the savings expected as a result of energy efficiency programmes.

Acknowledgements

4M is a consortium of four UK universities, funded by the Engineering and Physical Sciences Research Council under the Sustainable Urban Environments programme (grant reference EP/F007604/1). The university partners are assisted by an advisory panel drawn from UK central and local government, and UK and overseas industry and academia. For further information please see www.4Mfootprint.org. The Living in Leicester survey was carried out by the National Centre for Social Research. We are grateful for the participating households without whom this work would not be possible.

References

[1] DEFRA, UK - Adaptation in the Climate Change Act - Adapting to climate change, London, 2008.

[2] Office for National Statistics (ONS). Digest of UK Energy Statistics 2009, London, TSO, 2009.

[3] BERR. UK Energy in Brief, National Statistics. 2008 http://webarchive.nationalarchives.gov.uk/+/http://www.berr.gov.uk/energy/statistics/publications/inbrief/page17222.html - Accessed 22nd November 2010

[4] R. Yao, K. Steemers. A method of formulating energy load profile for domestic buildings in the UK, Energy & Buildings. 37, 2005, pp. 663-671.

[5] H. Meier, K. Rehdanz. Determinants of residential space heating expenditures in Great Britain, Energy Econ. 32 (5), 2010, pp. 949-959.

[6] Department of Energy and Climate Change (DECC). The Green Deal, 2010. http://www.decc.gov.uk/en/content/cms/what_we_do/consumers/green_deal/green_deal.aspx accessed 22nd November 2010 - Accessed 22nd November 2010

[7] S. H. Hong, T. Oreszczyn, I. Ridley. The impact of energy efficient refurbishment on the space heating fuel consumption in English dwellings, Energy & Buildings. 38, 2006, pp. 1171-1181.

[8] R. Lowe. Technical options and strategies for decarbonizing UK housing, Building Research & Information. 35, 2007, pp. 412-425.

[9] H. Herring. National building stocks: addressing energy consumption or decarbonization? Building Research and Information. 37, 2009, pp. 192-195.

[10] T. Oreszczyn, S. H. Hong, I. Ridley, P. Wilkinson. Determinants of winter indoor temperatures in low income households in England, Energy & Buildings. 38, 2006, pp. 245-252.

[11] Department of Energy and Climate Change (DECC). Annual report on fuel poverty statistics 2009. London, 2009.

[12] Communities and local government (CLG) Code for sustainable homes: A step-change in sustainable home building practice. London, 2006.

[13] Directgov. Top Tips on Saving Energy, Directgov, London, 2010. http://www.direct.gov.uk/en/Environmentandgreenerliving/Energyandwatersaving/Energyandwaterefficiencyinyourhome/DG_064371 - Accessed 28th September 2010.

[14] World Health Organisation (WHO) Extreme Weather Events: Health Effects and Public Health Measures. Fact Sheet No. EURO/04/03, Copenhagen, Rome, 29 September, WHO, Geneva, 2003.

[15] M. Shipworth, S. K. Firth, M. I. Gentry, A. J. Wright, D. T. Shipworth, K. J. Lomas. Central heating thermostat settings and timing: building demographics, Building Research & Information. 38, 2010, pp. 50-69.

[16] A. J. Summerfield, R. J. Lowe, H. R. Bruhns, J. A. Caeiro, J. P. Steadman, T. Oreszczyn. Milton Keynes Energy Park revisited: Changes in indoor temperatures and energy usage, Energy & Buildings. 39, 2007, pp. 783-791.

[17] Y. G. Yohanis, J. D. Mondol. Annual variations of temperature in a sample of UK dwellings, Applied Energy. 87, 2010, pp. 681-690.

[18] N. Isaacs, K. Saville-Smith, M. Camilleri, L. Burrough. Energy in New Zealand houses: comfort, physics and consumption, Building Research & Information. 38, 2010, pp. 470-480.

[19] K. J. Lomas, M. C. Bell, S. K. Firth, K. J. Gaston, P. Goodman, J. R. Leake, A. Namdeo, M, Rylatt, D. Allinson, Z. G. Davies, J. L. Edmondson, F. Galatioto, J. A. Brake, L. Guo, G. Hill, K. N. Irvine, S. C. Taylor and A. Tiwary. 4M: Measurement, modelling, mapping and management the carbon footprint of UK cities. ISOCARP Review 06, 2010.

[20] Tempcon Instrumentation Ltd 2010 http://www.tempcon.co.uk/index.html Accessed 23rd December 2010

Volume 4

Fuel Cells

Beyond the simplicity: optimizing the hydrogen production process

Miguel A. Bernal Pampín, Laura Cristóbal Andrade, Pastora M. Bello Bugallo*

Department of Chemical Engineering and Seminar of Renewable Energy (Aula de Energías Renovables), University of Santiago de Compostela, Spain
** Corresponding author. Tel: +34 881816757, Fax: +34981528050 , E-mail: pastora.bello.bugallo@usc.es*

Abstract: This paper presents the optimization of the consumption and production rates of a steam reforming plant using natural gas as raw material for generating hydrogen as principal product. Different strategies are applied to select the most adequate techniques and to obtain different configurations or alternatives for the process. The methodology used in this work includes both quantitative and qualitative analyses. The aim of this work is to apply various possible alternatives to control emissions and reduce energy inputs, according to the recommendations of the European IPPC Bureau and the United Nations Framework Convention on Climate Change. The actions are oriented towards reducing the consumption of the plant by improving process heat recovery and improving energy integration. The results will be focused on the energy consumption analysis for the different alternatives, showing the best option to design the plant, maximizing production and optimizing energy use. This approach produces large amounts of hydrogen, decreases environmental impacts and increases economical profits.

Keywords: *Hydrogen production, Natural gas, Energy efficiency, Best Available Techniques*

1. Introduction

The synthesis of hydrogen has been largely used to obtain ammonia and related derivates. As a result of the growth of the industry during the last century, new processes and methods using hydrogen as raw material appeared. Some examples are Fischer-Tropsch processes, hydrogenation processes for the petrochemical industry, direct use of hydrogen as an energy vector, and others [1-6]. Nowadays this continuous improvement not only responds to compliance with the normative, but also to the demands and expectations of consumers. To get quality products at the lowest possible cost, it is necessary to implement optimization techniques that reduce material and energy use, taking advantage of the recent revolutionary technological changes related with energy optimization patterns. These technology advances can lead to more efficient processes that reduce energy use and pollutants emissions.

Environmental problems, such as global warming, may lead to restrictions on the use of energy in the near future. CO_2 emissions reduction goals can be achieved by introducing energy efficiency improvements in the production processes [7].

Hydrogen plants are major energy-demanding processes and important CO_2 releasers [1, 2, 8]. According to the latest surveys, the greenhouse gas emissions from the hydrogen industry were calculated to be around one hundred million tonnes CO_2 equivalent per year. In spite of that, this industry has already come a long way towards reducing energy use and related emissions by improving its performance.

An industrial sustainable system is characterized by minimal environmental exchanges, with a more rational use of the available resources. This implies the integrated reduction of the environmental impacts, acting over the effects derived from the activities (waste generation, air pollution, etc) and implementing measures related to resources exploitation and pollution prevention.

In this context the EU published in 1996 the IPPC Directive [9] (meaning Integrated Pollution Prevention and Control) that introduced, among others, the Best Available Techniques (BAT) and the Emission Limit Values (ELV) for the affected industrial potentially polluting sources.

On the other hand the United Nations created in 1988 the Intergovernmental Panel on Climate Change (IPCC). They published in 1996 the Kyoto Protocol fixing the objective of greenhouse gases reduction for the signatory countries. It includes the Clean Development Mechanisms, which enables developed countries to accredit units or credit emissions reduction when projects are financed in developing countries [10].

The world H_2 production is estimated to be around 45 million tonnes (500 million m^3) per year. Around 96% of it is derived from fossil fuels. In 2000 crude oil was the dominant fossil fuel to produce H_2 (55%), followed by natural gas and coal. At present, 49% of the hydrogen is produced by reforming natural gas, 29% (Fig. 1).

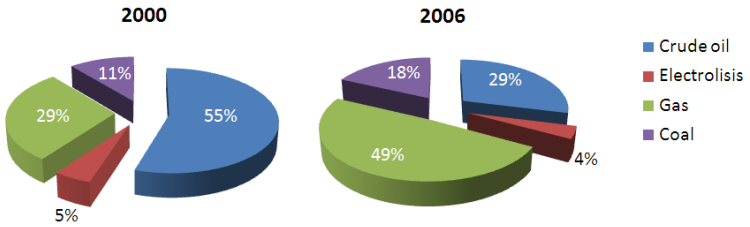

Fig. 1. Current worldwide H_2 production [11].

Natural gas has been selected as raw material in the steam reforming process as it is the least polluting alternative within the group of hydrocarbon feedstock. Comparatively, other processes consuming different raw materials have not been completely developed, so they imply high energy costs and show some technological limitations [6-8, 11, 12].

This paper presents the optimised design of a steam reforming plant using natural gas as raw material for producing hydrogen as principal product. Various possible alternatives are proposed to prevent and control emissions and reduce energy inputs. This work follows the recommendations of the European IPPC Bureau [13] and the United Nations Framework Convention on Climate Change [10].

2. Methodology

The methodology includes both quantitative and qualitative analyses that were developed and applied to meet the objectives of this work, which was oriented to prevent and control emissions and reduce energy demand in the case study. The qualitative analyses begins with a detailed description of the process, followed by the study of the main environmental impacts that leads to an inventory of the BAT, the evaluation of these techniques and finally the assessment of the possible improvements of the environmental performance of the plant achieved after the application of the selected techniques. On the other hand, quantitative analysis includes process modelling and simulation, solving material and energy balances for each configuration by using a process simulation tool, Aspen Plus HYSYS®.

The qualitative and quantitative analyses carried out during this work were developed according to the sections included below.

2.1. Qualitative analysis

2.1.1. Detailed description of the process

In order to provide proper results, the process is divided into stages, including inputs and outputs of materials and energy (Fig. 2).

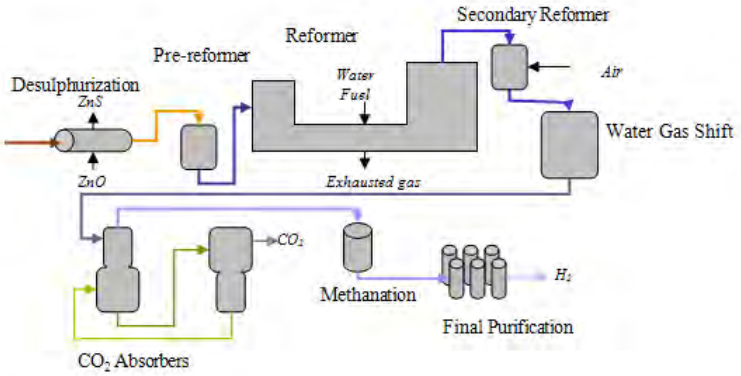

Fig. 2. Flow-sheet of the hydrogen production process.

2.1.2. Study of the main environmental impacts to be addressed by the process which can cause negative effects (atmospheric emissions, liquid effluents and solid wastes)

The reforming reaction is strongly endothermic so it is required a large input of heat, around 70%. Pumps and refrigeration from the CO_2 removal section account for 10% of the total energy needed [14]. Linked to the high-energy requirements, relevant greenhouse emissions are produced. For instance, within the hydrogen production field, the CO_2 generation from NH_3 production ranges from 1.52 to 3.06 t CO_2/t NH_3 produced [15]. On average, one-third of CO_2 emissions result from burning fuel and two-thirds from the use of hydrocarbon feedstock. Fig. 3 shows that energy consumption decreases with time in NH_3 plants.

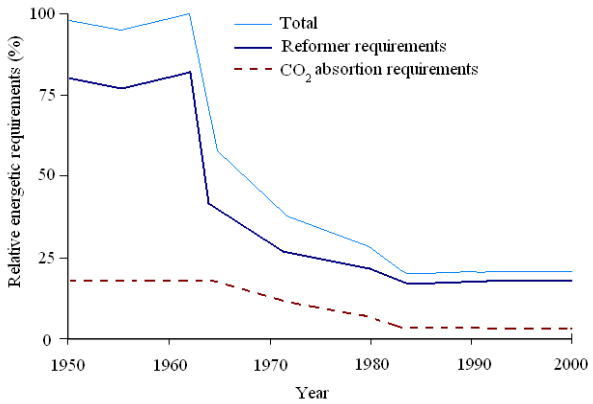

Fig. 3. Relative energy requirements as a function of time (adapted from [17]).

Due to the high temperatures of the combustion process, large amounts of NO_x are generated in the reformer and in the auxiliary boilers. The kind of burning fuel and the usage of hydrocarbon feedstock determine the quantity of SO_x emissions. Pollution problems related to water are associated to the formation of condensates or to the scrubbing of waste gases. Spent catalysts and molecular sieves are solid waste sources [16].

2.1.3. Inventory of BAT using different sources of background information available

The proposed techniques [18-23], which are candidate to be BAT for the analysed processes, are summarized in Fig. 4.

Stage	Techniques
Reformer section	Selective Non-Catalytic Reduction (SNCR) at the primary reformer
	Low NOx burners
	Pre-reforming
	Extended preheating of the hydrocarbon/steam feed
	Reduce steam-carbon ratio to 3.0
	Pre-heating of the combustion air with waste heat from the flue-gases going to the stack
	ATR system
Converters	Pressure drop optimization of HTS and LTS converters
CO_2 removal system	Using MDEA technology
	PSA system

Stage	Techniques
Combustion	Burner regulation and control by monitoring and controlling fuel flow, air flow, oxygen levels and heat demand
	Proper furnace insulation to reduce wall heat losses (mid-term implementation)
	Clean heat transfer surfaces (short-term implementation)
Steam system	Pre-heat feed-water by using economisers
	Reducing the amount of total dissolved solids in the boiler water to reduce blow down and energy loss (short-term implementation)
	Optimise deareator vent rate (mid-term implementation)
Heat recovery and cooling	Monitoring and maintenance of heat exchangers
Pumping system	Control and maintenance

Fig. 4. Inventory of the best available techniques.

2.1.4. Analysis of the previously reported measures

All the techniques are analysed in order to select those that are already implemented and those that are not, bearing in mind the improvement of global energy efficiency. To facilitate this task, a technical data sheet for each technique is done taking into account some of the items established by the EIPPCB [13]: technical description of the measure, benefits or environmental data, secondary effects, implementation, applicability and characterization.

2.1.5. Assessment of the possible environmental performance improvement of the plant by selected techniques.

After a careful evaluation of the understudy hydrogen plant, a retrofit was decided. According to the current methodology, a combination of the proposed measures is selected to assess the energy savings of the new flow-sheet. Thereby, in this paper the potentiality of the highlighted measures (Fig. 5.) is tested.

Stage	Techniques		Environmental achievements
Reformer section	**T2.1**	Extended pre-heating of the feed Reduction of steam/carbon ratio in the reformer feed Reduction of outlet temperature of the exhaust gases	Global energy savings Reduced NOx emissions <200 mg/Nm^3
	T2.2	Pre-reforming	Energy reduction rates of 5-10% and energy savings
	T2.3	Pre-heating of combustion air	Energy savings
	T.ATR	Substitution to ATR system	Total integration of the consumption
CO_2 removal system	**T.PSA**	Substitution to PSA system	Total saving of the energy consumed in absorption

Fig.5. Techniques selected for the reformer section.

2.2. Quantitative analysis

Aspen HYSYS 7.1 has been used to model the process in order to compare different possible configurations. The improvement of the process has been done progressively (Fig. 6). Once the model is ready (the base case and the retrofit), several simulations are carried out to obtain the main parameters of the equipment and flows.

BASE CASE

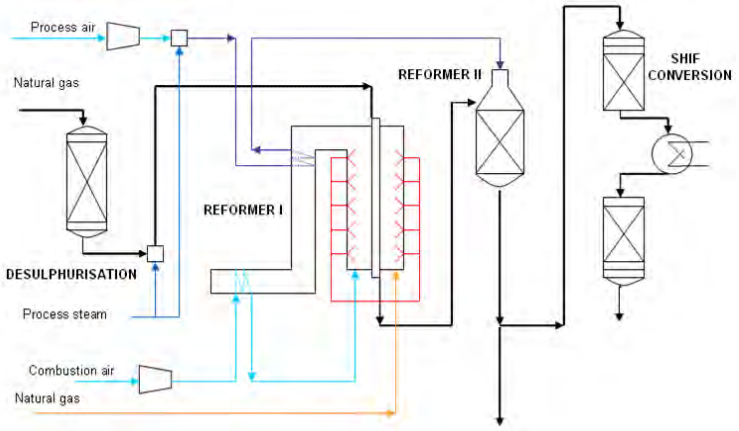

IMPROVED CASE

Improvement 1

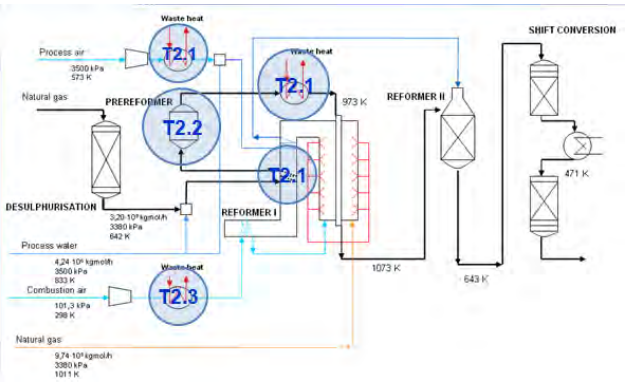

Improvement 2

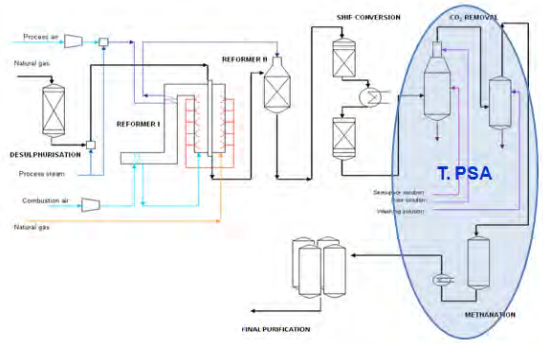

Improvement 3

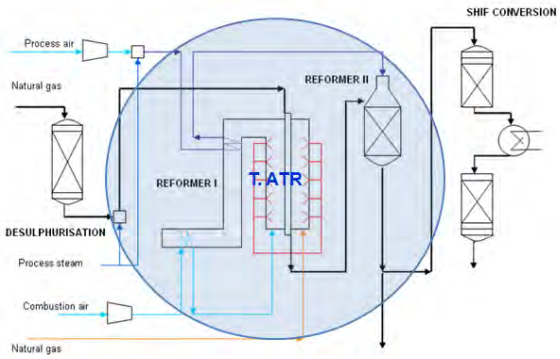

Fig. 6. Comparison of the base case with the improved case.

3. Results

Simulation results show that energy can be saved by implementing the selected techniques. The implementation of a pre-reforming reduces more than 10% the required energy input. Moreover, energy consumption is reduced 21.5%, regarding the base case, by implementing preheating of combustion air (Table 1). The final substitution of the purification stage by the PSA eliminates de energy requirements of the absorption stage (Table 2).

Table 1. Energy savings in the reforming section

Technique	*Energy required in the reforming section*	
	Before implementation	*After implementation*
T 2.2. Pre-reforming	107.2 MW	95.8 MW
T 2.3. Pre-heating of combustion air	95.8 MW	84.2 MW

Table 2. Energy savings in the purification section

Technique	*Energy required in the purification section*
T PSA. Substitution to PSA tech	5,000 MJ/t CO_2 saved by eliminating absorption stage

Besides these data, Fig. 7 shows how energy consumption in the plant decreases by the progressive implementation of the selected techniques in the corresponding sections. The base case is not energetically integrated at all. The proposed techniques achieve the maximum energetic integration for this process, reducing 85.9% energy consumption (Fig. 8).

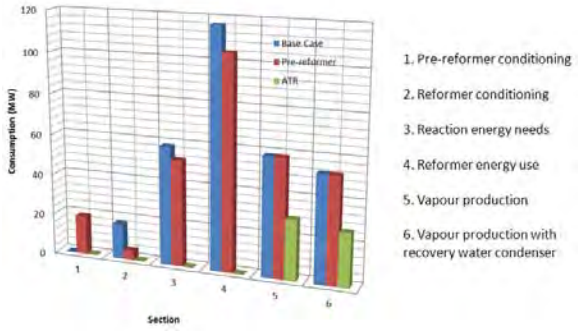

Fig. 7. Energy consumption evolution

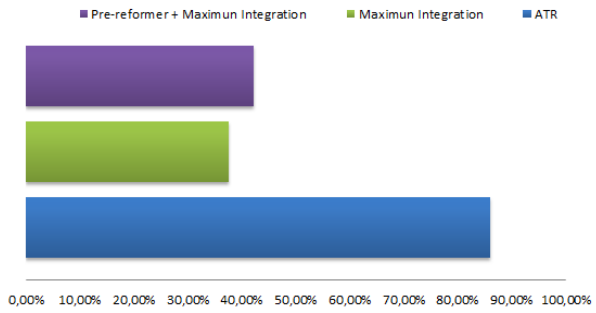

Fig. 8. Energy consumption reduction

4. Conclusions

This work shows an assessment of the potential measures to reduce and control emissions and energy use in a hydrogen plant. Consequently, a methodology was introduced including both quantitative and qualitative analysis. From the qualitative analysis, a list of specific measures was proposed. The achieved results showed that, despite being a mature technology, important energy efficiency improvements and CO_2 emissions reduction could be achieved. Therefore, the proposed methodology has turned out to be satisfactory.

The highlights are:

- The consumption in the primary reformer is reduced. Nevertheless, this option can cause problems if an integrated energy balance is not done properly.
- A pre-reforming installed prior to the first reformer reduces energy consumption.
- The substitution to ATR technique provides a significant reduction of the energy needs and improves the yield (steam needs are reduced to ratio V/C = 1).
- The substitution to PSA technique provides a reduction of energy needs, but it is necessary more adsorbent.

References

[1] Ullmann's Encyclopedia of industrial chemistry, Gas production, G**,** 2007, pp.91-259.

[2] Ullmann's Encyclopedia of industrial chemistry, Hydrogen, H**,** 2007, pp. 827-959.

[3] A.C. Vosloo, Fischer–Tropsch: a futuristic view, Fuel Processing Technology 71, 2001, pp.149–155.

[4] D.J. Wilhelm; D.R. Simbeck; A.D. Karp; R.L. Dickenson, Syngas production for gas-to-liquids applications: technologies, issues and outlook, Fuel Processing Technology 71, 2001, pp.139-148.

[5] T. Rostrup-Nielsen, Manufacture of hydrogen, Catalysis Today 106, 2005, pp. 293–296.

[6] J.I. Linares Hurtado; B.Y. Moratilla Soria, Hydrogen as an energetic vector (I/II) (in Spanish), 2007, available at https://www.icai.es/.

[7] I. Rafiqul; C. Weber; B. Lehmann; A. Voss, Energy efficiency improvements in ammonia production perspectives and uncertainties, Energy 30, 2005, pp. 2487-2504.

[8] C. Koroneos; A. Dompros; G. Roumbas; N. Moussiopoulos, Life cycle assessment of hydrogen fuel production processes, International Journal of Hydrogen Energy 29, 2004, pp. 1443-1450.

[9] European Commission, Council Directive 96/61/EC concerning integrated pollution prevention and control, Official Journal of the European Communities L 257, 1995, pp. 26-40.

[10] United Nations Framework Convention on Climate Change, Reports of Clean Development Mechanism (CDM) project activities, available at http://cdm.unfccc.int/.

[11] A. A. Evers FAIR-PR, http://www.hydrogenambassadors.com/, (accessed 10/12/2010).

[12] Florida Solar Energy Center, Hydrogen basics, www.fsec.ucf.edu/, (accessed 10/12/2010).

[13] European Commision, European IPPC Bureau (EIPPCB), http://eippcb.jrc.es/.

[14] J. Ruddock; T.D. Short; K. Brudenell, Energy integration in ammonia production. Sustainable World 7, 2003, pp. 267-276.

[15] The International Fertilizer Industry Association IFA, Fertilizer supply statistics, available from http://www.fertilizer.org/ifa.

[16] The International Fertilizer Industry Association. IFA, Fertilizers and Climate Change, available from http://www.fertilizer.org/ifa.

[17] R. Mendivil; U. Fischer; M. Hirao; K. Hungerbühler, A New LCA Methodology of Technology Evolution (TE-LCA) and its application to the production of ammonia (1950-2000), International Journal of Life Cycle Assessment 11 (2), 2006, pp. 98-105.

[18] E. Worrell; K. Blok, Energy savings in the nitrogen fertilizer industry in the Netherlands. Energy 19 (2), 1994, pp. 195-202.

[19] European Commission, Reference Document on Best Available Techniques for the Manufacture of Large Volume Inorganic Chemicals-Ammonia, Acids and Fertilisers, Institute for Prospective Technological Studies (IPTS), 2007, pp 35-94.

[20] European Commission, Reference Document on Best Available Techniques for Energy Efficiency, Institute for Prospective Technological Studies (IPTS), 2008.

[21] European Fertilizer Manufacturers Association EFMA, Best Available Techniques for Pollution Prevention and Control in the European Fertilizer Industry, Production of ammonia, Booklet 1, 2000.

[22] U.S. EPA. (U.S. Environmental Protection Agency), Department of Energy, A Consumer`s Guide to Energy Efficiency and Renewable Energy, Industry Plant Managers and Engineers, 2008, available at http://www.epa.gov/.

[23] U.S. Department of Energy-Energy Efficiency and Renewable Energy, Industry plant Managers and Engineers: 20 Ways to Save Energy Now, 2008, available at http://www.eere.energy.gov/.

The effect of a boron oxide layer on hydrogen production by boron hydrolysis

Tareq Abu Hamed[1,2*], Bara Wahbeh[3], Roni Kasher[3]

[1]*The Dead Sea and Arava Science Center, Tamar Regional Council, Israel*
[2]*Arava Institute for Environmental Studies, Hevel Eilot, Israel*
[3,] *Ben-Gurion University of the Negev, Sde-Boqer, Israel*
**Corresponding author. Tel: +97286356694, Fax: +97286356634, E-mail: tareq@arava.org*

Abstract: Hydrolysis of boron is investigated as a part of a boron/boron oxide solar, water-splitting, thermochemical cycle. Boron was hydrolysed and boron oxide was gasified with steam in a tubular reactor. The influence of the reactor temperature and time on hydrogen conversion was measured at furnace set point temperatures of 873, 973 and 1073 K. The hydrogen production rate was measured by inline gas chromatography. The products were analyzed by X-ray diffraction. The average hydrogen production efficiency of 92% was obtained for both 973 and 1073 K. The formation of a boric acid layer on the reactor walls was attributed to the gasification of the boron oxide. The X-ray analysis shows 100% conversion of the boron to boron oxide and boric acid.

Keywords: *hydrogen, thermochemical cycle, boron, oxide layer removal*

1. Introduction

Hydrogen is an abundant and clean fuel with high energy density, making it a leading candidate in the search for an alternative to fossil fuels. However, the storage and transportation of hydrogen fuel for practical applications (e.g. internal combustion engine or fuel cells) remain among the most difficult problems to overcome before hydrogen can serve as a real alternative to fossil fuels [1]. Numerous methods for storage of hydrogen on-board vehicles have been considered, including compressed gas, liquid hydrogen and hydride compounds. Each method has significant and unresolved technical, safety and economic issues. Finding a feasible, on-board hydrogen storage solution is one of the major challenges in achieving a hydrogen economy. One such solution may be to produce the hydrogen on-board the vehicle at a rate that matches the rate of demand of the car engine. One method of on-board hydrogen production is to react a light metal with water. Boron is one of the most promising metal candidates for this purpose [2]. It is a light element with a molecular weight of 10.8g/mol. The reaction of boron with water yields a high hydrogen-to-metal ratio compared to other metals (see Table 1) [3]. Moreover, boron is very safe to store and to transport because its ignition temperature is high in dry or moist air and even in water.

Table 1. Theoretical H_2 produced by the hydrolysis of metals

Reaction	mole H_2/g-Fuel	STP L H_2/g-Fuel
$2B + 3H_2O \rightarrow 3H_2 + B_2O_3$	0.139	3.00
$2Al + 3H_2O \rightarrow 3H_2 + Al_2O_3$	0.056	1.25
$Mg + H_2O \rightarrow H_2 + MgO$	0.041	0.92
$Fe + H_2O \rightarrow H_2 + FeO$	0.018	0.40
$Zn + H_2O \rightarrow H_2 + ZnO$	0.015	0.34

The ignition and combustion processes of boron have been of great interest to many researchers because of its high heating value. Considerable experimental [4-5] and theoretical research [4-9] has been conducted with the objective of understanding the ignition and combustion of boron particles in oxygen. The data show the ignition of boron particles is

significantly delayed because of the formation of a layer of boron oxide (B_2O_3) on the surface of the boron.

Several studies prove that adding water to the oxygen environment can increase the oxidation rate. This finding is of particular significance to the proposed study. It is suggested that the increased oxidation rate is due to gasification of the protective B_2O_3 layer to boric acid (HBO_2). Smolanoff et al. [10] showed that the addition of water to the boron/oxygen reaction yields a higher reaction rate than when HF(g), CO_2(g), and BF_3(g) are added. Data obtained by Krier et al. [11] show that the addition of water reduces the ignition delay time and reduces the ignition temperature for combustion of boron when compared to combustion in pure oxygen. Vovchuk et al. [12] measured B_2O_3 gasification rates in pure water and dry air atmospheres for temperatures as high as 1303 K. They found that the gasification rates for B_2O_3 in water vapor were significantly greater than those in air. Sontgen et al. [13] found that the addition of 3 to 8% water vapor to air significantly increased the oxidation rate at 803 K.

Data on the hydrolysis of boron in the absence of oxygen are limited. Experiments in steam by Rosenband et al. [14] were the first to demonstrate that the production of hydrogen by this method is feasible. Vishnevetsky et al. [15] considered the hydrolysis of boron in the absence of oxygen at moderate reactor temperatures (below 873 K). The hydrogen yield was 47 to 62% of the theoretical equilibrium value. It was confirmed that the reaction occurs only at temperatures above the melting point of boron oxide (723 K). Removal or thinning of the liquid oxide layer is attributed to a gasification reaction with steam that produces volatile metaboric acid. Limitations of the test apparatus excluded experiments above 873 K, where the gasification rate of boron oxide increases and higher hydrogen production yields are expected.

The objective of this paper is to investigate the effect of temperature on boron hydrolysis ($2B + 3H_2O \rightarrow 3H_2 + B_2O_3$) and to study the effect of boron oxide gasification reaction ($B_2O_3(l) + 3H_2O(g) \rightarrow 2H_3BO_3(g)$) on the hydrolysis process.

2. Methodology

The experimental setup is shown in Figure 1. A 100 cm long and 2.3 cm i.d. tubular, quartz reactor is placed inside a tubular furnace (40 cm long, concentric, cylindrical, electric ceramic heater). Steam was generated upstream in an electrical heater. The amount of steam generated was controlled by controlling the water flow via a peristaltic pump. Prior to each experiment, a crucible was loaded with weighed boron particles of 0.1 grams (amorphous, 97% pure) and placed in the reactor. Each time, the reactor was closed, evacuated and purged with N_2. The nitrogen flow rate was 0.3 l/min during the whole experiment. When the desired temperature (873 K, 973 K, 1073 K) in the furnace was reached, the steam flow was directed into the reactor (0.54 mL/min, equivalent to 1 rpm in the peristaltic pump). During the experiment, the excess of steam was condensed into a water vapor trap. The outlet gas was analyzed continuously using an inline gas chromatograph (Varain 430 GC). The GC was fixed in automatic sampling mode and started to record data as soon as the steam valve was opened. Each run lasted 2 minutes.

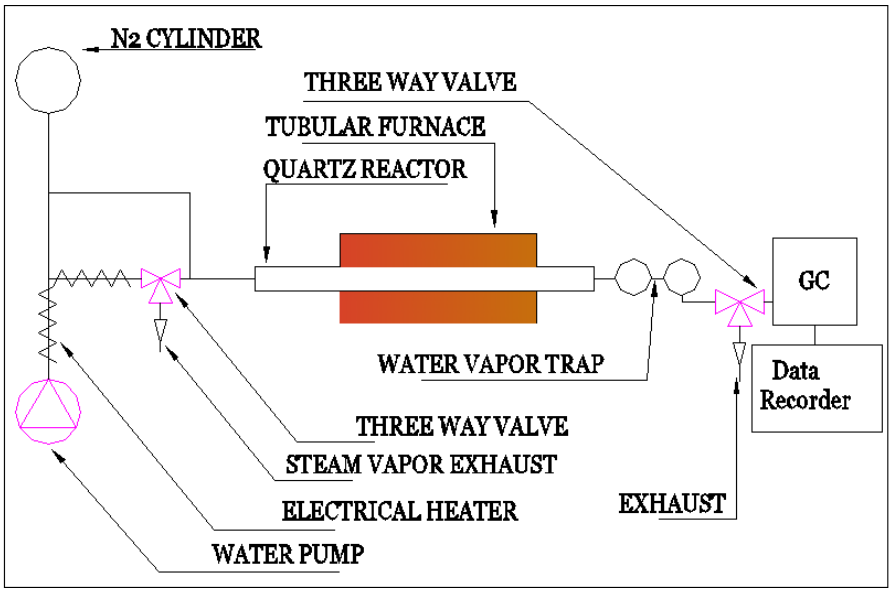

Fig. 1. Boron hydrolysis experimental setup

To examine the gasification of the oxide layer produced, small changes have been made to the experimental setup. A shorter quartz reactor (60 cm length, 2.3 cm i.d.) was placed in the tube furnace. The outlet of the quartz tube was open. Prior to each experiment, 4 crucibles were inserted into the reactor with the same amount of boron powder (0.1g) and placed in the reactor (dry and purged with N_2). During the experiment, boron crucibles were pushed out from the reactor into 500 mL flasks that contain nitrogen gas in order to prevent any further oxidation with air. This process was conducted on a regular time interval: 3 minutes between each crucible. Then the mass of the crucible was recorded.

3. Results and Discussion

Figures 2a and 2b show the hydrogen production at 973 and 1073 K. The hydrogen production efficiency at 973 K was 86 and 98% for run 1 and 2, respectively. At 1073 K, the efficiency was 93 and 90% for run 1 and 2 respectively. These values are much higher than the efficiency values obtained by Vishnevetsky at. al., [15]. In both of the runs at both of the temperatures, the hydrogen production followed the same trend. The hydrogen production reached the maximum at t = 8 and 10 minutes for 973 and 1073 K, respectively.

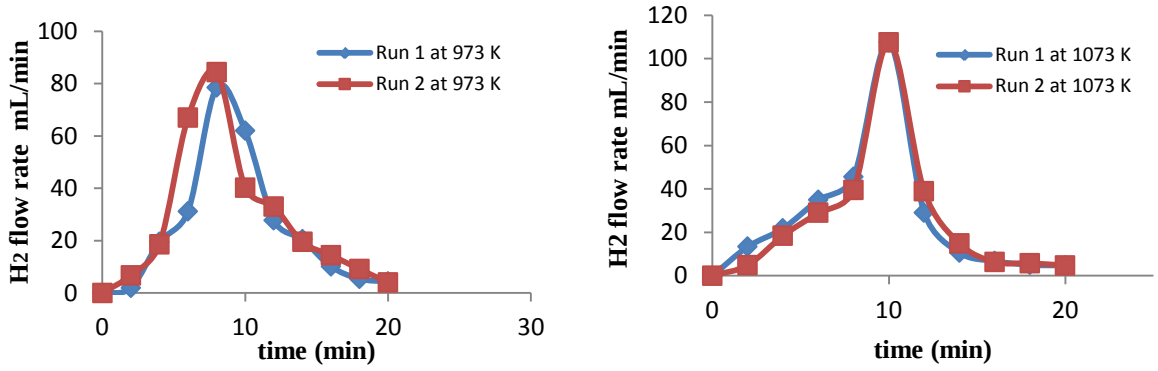

(a) *(b)*

Fig. 2. Hydrogen production at a: 973 K and b: 1073 K

Figure 3 shows a comparison of the hydrogen production at 873, 973 and 1073 K. As seen from this figure, at 873 K, there was very low hydrogen production (efficiency only 5%) for

the period of the experiment. At 973 and 1073 K, the first detected hydrogen production was after 2 minutes. At 1073 K, the hydrogen production was higher than at 973K, but the efficiency was lower. Here, it is important to mention that the hydrogen analysis was performed every 2 minutes and that, most likely, there was more hydrogen produced than the values measured. The X-ray analysis shows that all the boron was converted to boron oxide and boric acid in the first 3 minutes.

In all runs, the hydrogen production started immediately after switching the steam valve on. This is confirmed by the visual observation of the condensation of boric acid and the gas chromatography analysis.

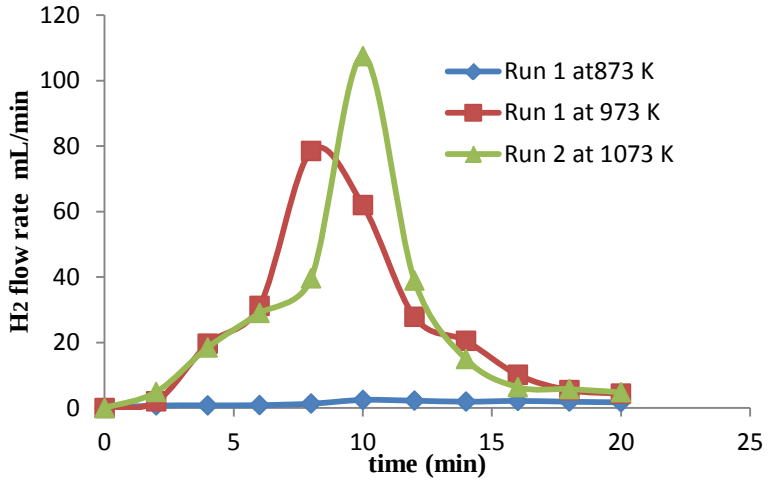

Fig. 3. H_2 production comparison for different temperatures

From the first minutes of the reaction, a formation of white, glittery particles was observed on the inner wall of the quartz tube outside the furnace where the temperature is 376 K. These particles start to condense on the tube directly after the steam valve is switched on (Figure 4a and 4b). These condensed particles continued to accumulate during the experiment and were very easy to remove. The X-ray analysis of these particles indicates that they are orthoboric acid (Figure 5). The formation of this layer is evidence of the gasification of boron oxide ($B_2O_3(l) + 3H_2O(g) = 2H_3BO_3(g)$) in parallel with the hydrolysis reaction.

(a) *(b)*

Fig 4. The condensation of boric acid on the inner wall of the reactor during the hydrolysis experiment. a: at the beginning and b: at the end of the experiment.

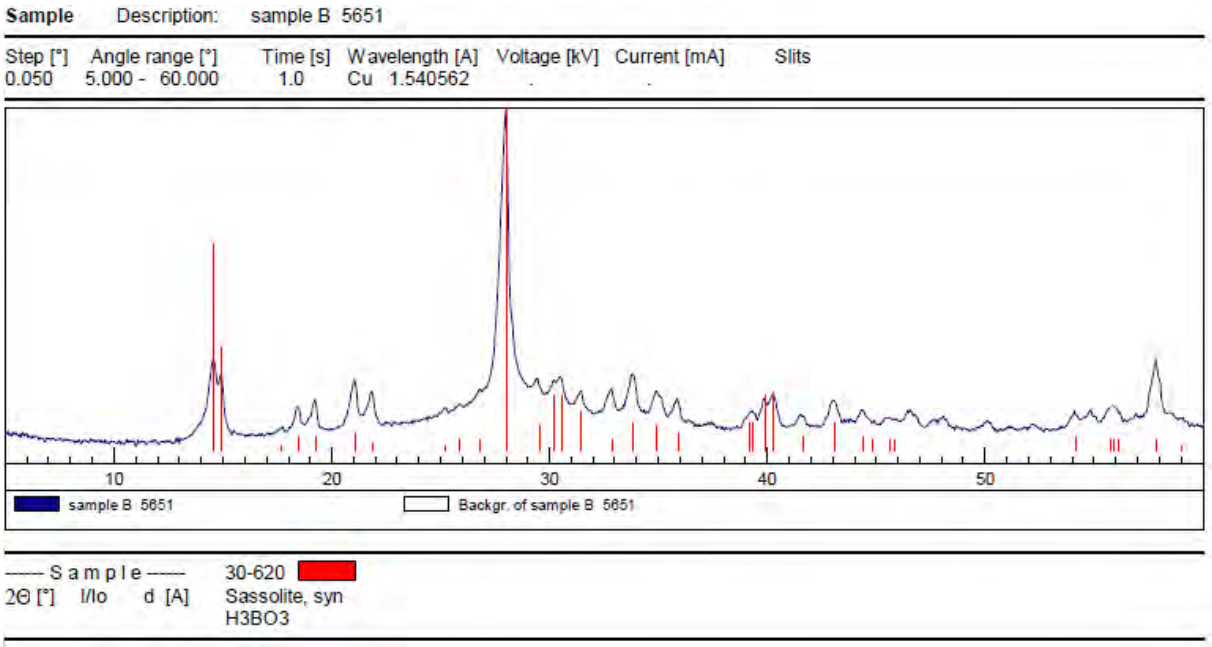

Fig 5. X-Ray analysis of condensed powder layer outside the furnace

Figure 6 shows the mass change during the hydrolysis of the boron powder at 973 K. Theoretically the hydrolysis of 0.1 grams of boron will generate 0.638 g of boron oxide; but the maximum weight recorded during the experiment was 0.229 g after 6 minutes of the reaction. This is due to the immediate gasification of the boron oxide layer. This gasification process was observed during the hydrolysis experiments: a white color deposition of boric acid was observed at t = 1 min of the hydrolysis experiment. After the sixth minute of the reaction, the weight of the particles in the crucible started to decrease. The X-ray analysis of the particles that remained in the crucibles shows 100% boron oxide after 3 minutes (Figure 7).

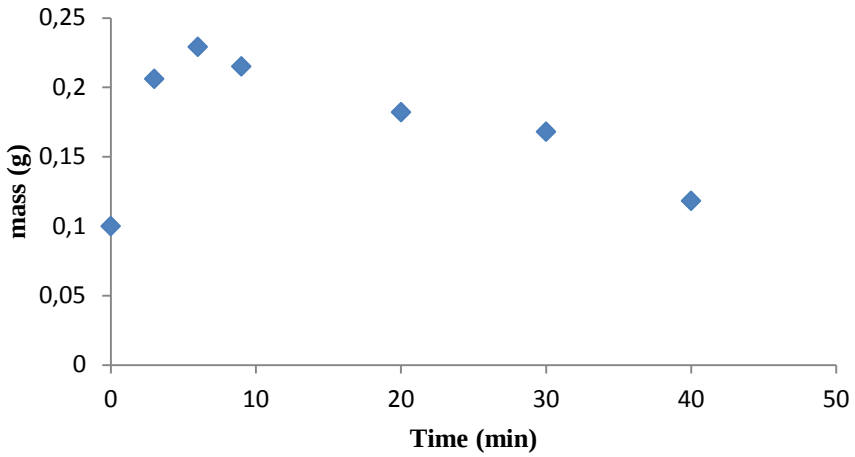

Fig. 6. Mass change in the boron sample during the hydrolysis process

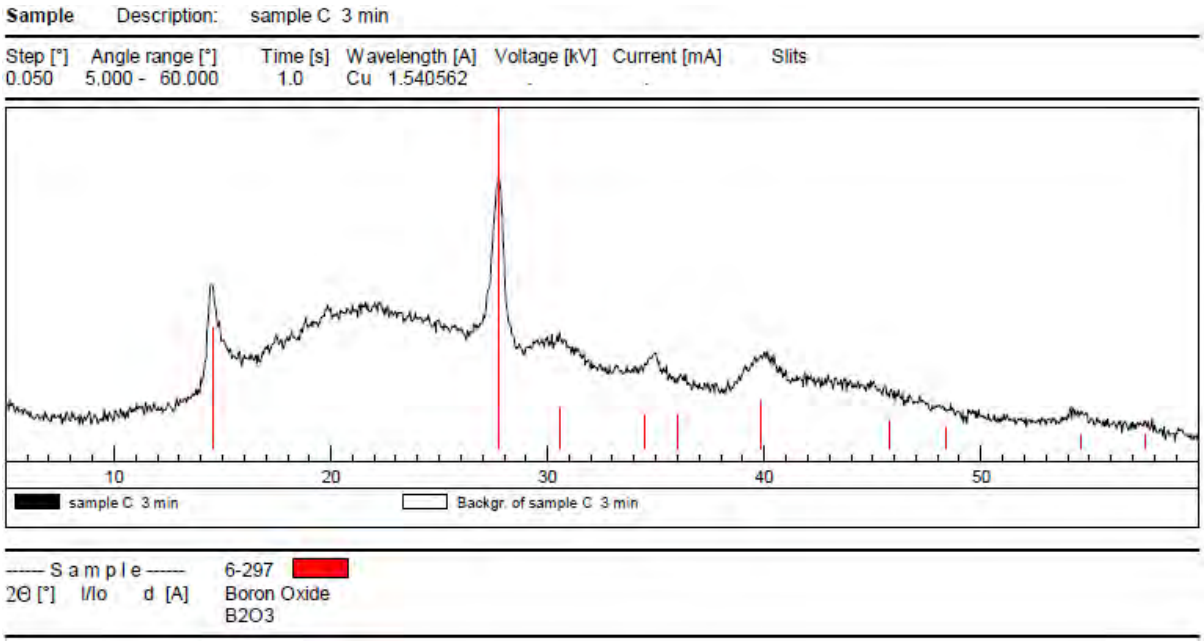

Fig 7. X-Ray analysis of particles remaining after the boron hydrolysis process (t = 3 min)

4. Conclusion

In this study, a tubular reactor was built and operated for the hydrolysis of boron and the gasification of boron oxide in nitrogen carrier gas. Hydrogen production was measured at furnace set point temperatures of 873, 973 and 1072 K. The primary objective of these initial experiments was to understand the boron hydrolysis process.

Hydrogen conversion was 92% for both 973 K and 1073 K. Very slow hydrogen production was observed at the temperature of 873K. Extensive deposition of boric acid was observed on the wall of the reactor outside the furnace where the temperature was 376 K.

The hydrolysis experiments show parallel processes of boron hydrolysis and boron oxide gasification. X-ray analysis of the particles remaining in the crucible shows 100% boron oxide. Thus, we conclude that the boron hydrolysis reaction is faster than the boron oxide layer gasification. In other words, the chemical reaction between the boron and the steam is much faster than the chemical reaction between the boron oxide and the steam. The use of the boron/boron oxide thermochemical cycle for hydrogen production shows an advantage over other cycles, due to the ease of removal of the oxide layer. By comparison, in the zinc/zinc oxide (ZnO) cycle, once a ZnO layer is formed, the hydrolysis reaction becomes limited by the diffusion of the reactants through the layer, which is harder to remove than the boron oxide layer [16].

References

[1] G. Karim, Hydrogen as a spark ignition engine fuel, International Journal of Hydrogen Energy 28, 2003, pp. 569-577.

[2] M. Epstein, Solar induced solid fuels for transportation, Proceedings of the 12th International Symposium on Solar Power and Chemical Energy System, 2004, Oaxaca, Mexico, paper No. 302.

[3] T. Abu Hamed, J. Karni, M. Epstein, The use of boron for thermochemical storage and distribution of solar energy, Solar Energy 81, 2007, pp. 93-101.

[4] C. L. Yeh, K. K. Kio, Ignition and combustion of boron particles, Progress in Energy and Combustion Science 22, 1996, pp. 511-541.

[5] C. C. Li, F. A. Williams, Ignition and combustion of boron particles in Combustion of boron-based solid propellants and solid fuels, Kuo, K. K., and Pein, R., Eds., Begell House Publishing Co. and CRC Press, Inc., 1993, pp. 248–271.

[6] S. C. Li, F. A. Williams, Ignition and combustion of boron in wet and dry atmospheres, Proceeding of the 23rd Symposium on Combustion, 1990, pp. 1147–1154.

[7] M. K. King, Boron ignition and combustion in air-augmented rocket afterburners, Combustion Science and Technology, 1972, pp. 155–164.

[8] W. Zhou, R. A. Yetter, F. L. Dryer,H. Rabitz, R. C. Brown, C. E. Kolb. Comprehensive physical and numerical model of boron particle ignition. Proceeding of the 26th International Symposium on Combustion, 1996 pp. 1909–1917.

[9] R. C. Brown, C. E. Kolb, S. Y. Cho, R. A. Yetter, H. Rabitz, F. L. Dryer, Kinetic model for hydrocarbon-assisted particulate boron combustion, International Journal of Chemical Kinetics 26, 1994, pp. 319–332.

[10] J. Smolanoff, M. Sowa–Resat, A. Lapicki, L. Hanley, S. Ruatta, P. Hintz, S. L. Anderson, Kinetic parameters for heterogeneous boron combustion reactions via the cluster beam approach, Combustion and Flame 105, 1996, pp. 68–79.

[11] H. Krier, R. L. Burton, S. R. Pirman, M. J. Spalding, Shock initiation of crystalline boron in oxygen and fluorine compounds. Proceeding of the 30th American Institute of Aereonautics and Astronautics Thermophysics Conference, 1995, paper No. 2095-2120.

[12] Y. A. Vovchuk, A. N. Zolotko, L. A. Klyachko, D. I. Polishchuk, V. G. Shevchuk, Gasification of boron oxide, Fizika Goreniya i Vzryva 10, 1972, pp. 615-618.

[13] R. Sontgen, A. Freidrich, A simple model of the oxidation kinetics of boron in a medium containing water vapor, in Combustion of Boron Based Propellant and Solid Fuels, K. K. Kuo and R. Pein, Eds., Begell House Publishing Co. and CRC Press, Inc., 1993, pp. 211-217.

[14] V. Rosenband, A. Gany, Y.M. Timnat, Magnesium and boron combustion in hot steam atmosphere, Defense Science Journal 48, 1998, pp. 309-315.

[15] I. Vishnevetsky, M. Epstein, T. Abu-Hamed, J. Karni, Boron hydrolysis at moderate temperatures – First step to solar fuel cycle for transportation, Journal of Solar Energy Engineering 130, 2008, pp. 14506-14511.

[16] R. J. Weiss, H. C. Ly, K. Wegner, S. E. Pratsinis, A. Steinfeld, H_2 production by Zn hydrolysis in a hot-wall aerosol reactor, AIChE Journal 51, 2005, pp. 1966–1970.

Case study: Technical assessment of the efficiency optimization in direct connected PV-Electrolysis system at Taleghan-Iran

Abolfazl Shiroudi[1], Seyed Reza Hosseini Taklimi[2,*], Nilofar Jafari[1]

[1]*Ministry of Energy-Renewable Energy organization of Iran (SUNA), Tehran, Iran*
[2] *Linkoping University of Technology, Linkoping, Sweden*
** Corresponding author. Tel: +46 760830785, E-mail: seyho130@student.liu.se*

Abstract: The use of PV array energy in supplying the electrolyzer systems is very suitable. During the daylight hours, the sunlight converts by PV array into electrical energy which will be used for electrolyzing process. Then hydrogen produced by the electrolyzer is compressed and stored in hydrogen vessel. This provides energy for the fuel cell to meet the load when the solar energy is insufficient. Solar hydrogen technology is relatively simple and the only raw material for the production of solar hydrogen is water. In this study technical results obtained from direct connection of 10 kW PV array with 5 kW electrolyzer systems for hydrogen production and storage at Taleghan site. Variations of the solar radiation intensity, hydrogen production rate, solar hydrogen efficiency and overall efficiency of solar hydrogen energy were considered as base of analyses. It is found that the minimum and maximum overall energy efficiency values of the system are 0.93 % and 5.01 %, respectively. The result shows a great potential in direct solar radiation for absorbing and converting it to other types of energy in Iran. Using solar energy required high initial investment, so converting solar energy to other types of energy with high efficiency systems is vital.

Keywords: *Photovoltaic, Water Electrolysis, Hydrogen Production, System Efficiency, Taleghan*

Nomenclature

E	*calorific value of hydrogen*	T_r	*PV cell reference temperature*
Q	*hydrogen production rate*	v	*hydrogen production*
S	*solar radiation intensity*	β	*Temperature coefficient of a solar cell in STC*
A	*PV array surface*		
I_e	*current*		
T_c	*the PV cell temperature*		

E *calorific value of hydrogen* ..... $J.ml^{-1}$
Q *hydrogen production rate* ..... $ml.sec^{-1}$
S *solar radiation intensity* ..... $W.m^{-2}$
A *PV array surface* ..... m^2
I_e *current* ..... A
T_c *the PV cell temperature* ..... ^oC
T_r *PV cell reference temperature* ..... ^oC
v *hydrogen production* ..... $m^3.hr^{-1}$
β *Temperature coefficient of a solar cell in STC* ..... $°C^{-1}$

1. Introduction

As conventional fossil fuel energy sources diminish and the world's environmental concern about acid deposition and global warming increasing, renewable energy (RE) resources are attracting more attention as alternative energy sources [1]. The use of RE resources, which do not endanger the environmental balance, is a way to solve many of the environmental problems caused principally by the excessive use of fossil fuels. RE resources are free of pollution during their development and operation for power generation [2]. RE systems based on intermittent sources exhibit strong short term and seasonal variations in their energy outputs. Therefore, the need for storage of energy arises; storing the energy produced in periods of low demand to utilize it when the demand is high, ensuring full utilization of intermittent sources available [3]. Solar photovoltaic energy has been widely utilized in small size application and is the most promising candidate for research and development for large-scale use, as the fabrication of less costly photovoltaic devices becomes reality [1]. Hydrogen holds a preeminent position among the solar fuel candidates because of its high energy content, low environmental effect, storage compatibility and distribution [4-6]. Solar hydrogen is described as a potential energy storage medium to offset the variability of solar energy [7]. The seasonal storage of solar energy in the form of hydrogen can provide the basis for a completely renewable energy system [8]. Hydrogen can be generated by using different

technologies, but only some of them are environmentally friendly. It is argued that hydrogen generated from electrolyzing water is a leading candidate for a r enewable and environmentally safe energy carrier due to the following reasons [9]:

- Solar hydrogen technology is relatively simple and, therefore, the cost of such a fuel is expected to be substantially less than the present price of gasoline.
- The only raw material for production of hydrogen is water, which is a renewable resource.
- Large areas of the globe have access to solar energy which is the only required energy source for solar hydrogen generation.

Country of Iran with more than 4.5 kWh/m^2.day radiations has a great potential for converting solar radiation to electricity. One of the efforts done in the field of constructing and utilization solar hydrogen plant is constructing stand-alone energy system PV-electrolyzer-fuel cell in Taleghan-Iran. The purpose is to demonstrate the technical feasibility of using hydrogen as solar energy storage medium. This small scale demonstrative energy system uses PV as the primary energy conversion technology, hydrogen as the storage medium and a fuel cell as the regenerative technology [10].

2. Methodology

In this study, we will evaluate overall efficiency from connection of 10 kW PV array with 5 kW alkaline electrolyzer systems for hydrogen production and storage at Taleghan renewable energies site. We assumed that water electrolysis operated during a sample day in summer season during 150 minutes (10:30 until 12:50). Variations of the solar radiation intensity, hydrogen production rate, solar hydrogen efficiency and overall efficiency of solar hydrogen energy in operating conditions were gathered and considered as base of analyses.

3. Results

3.1. Description of the solar hydrogen energy system

This energy system is located in a mountainous area with latitude N 36^o, 8', longitude E 50^o, 34' and altitude 1700 m. The system consists of a 10 kW photovoltaic (PV) array coupled to a 5 kW bipolar, alkaline electrolyzer, and a gas hydrogen storage tank. When the sun shines, PV power is available and directly supply the load. By this power electrolyzer produces hydrogen, which is delivered to the hydrogen storage tanks. When PV array cannot provide electricity, the 1.2 kW PEM fuel cell will begin to produce electricity. Hydrogen in storage tank prepares the feed of fuel cell for production of needed electricity [11].

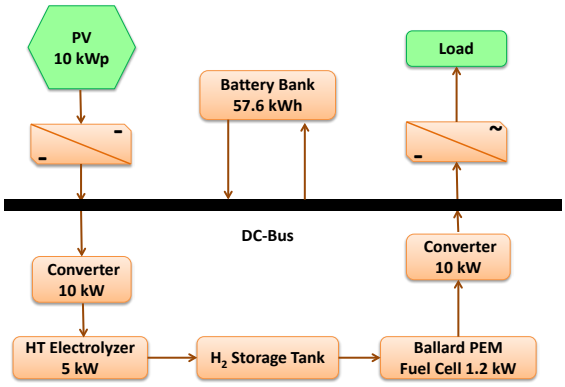

Fig. 1. Schematic of solar hydrogen energy system at the Taleghan site

Experimental results for the operation of directly coupled PV-electrolyzer in operating regime of electrolyzer for a sample day in summer are presented. The schematic of this energy system is given in Fig. 1.

3.2. Photovoltaic array

Solar energy is one type of the RE resources, which can be converted easily and directly to the electrical energy by PV converters. The PV module is a polycrystalline silicon type with maximum output of 45 W, an open circuit voltage of 20.5 V and 10 kW PV array consists of 224 solar panels MA36/45 modules installed at the Taleghan site. The PV array has a fixed inclination of 45 degree with horizontal and it is mounted such that the module is facing south direction [12]. Each module is 462 mm wide and 977 mm long for an area of 0.45 m^2 per module and total surface of 101.1 m^2 (2×7×16×0.45 ≈101.1 m^2). This angle corresponds to the optimum tilting in spring for the installed PV and is the latitude of Taleghan area. The power also depends on temperature, wind speed, and age of cells. The efficiency (η_e) of a solar cell is a function of the cell temperature (T_c) and it is defined as:

$$\eta_e = \eta_r\left[1-\beta(T_C - T_r)\right] \quad (1)$$

Where η_r is the efficiency of a solar cell at standard conditions, T_c the temperature of PV cell (^oC), T_r the PV cell reference temperature, and β is the temperature coefficient of a solar cell in STC (that for PV module is a polycrystalline silicon is 0.0004 $°C^{-1}$) [13-14].

Table 1.Parameters related to solar radiation, ambient temperature and power system vs. time

Time	Insolation (W/m^2)	Ambient temp. (^oC)	Module temp. (^oC)	Power system (kW)	Efficiency system (%)
6 a.m.	26	19	20	0.2989	11.45
7 a.m.	79	20	22	0.9045	11.41
8 a.m.	176	20	24	1.9988	11.32
9 a.m.	387	21	29	4.3236	11.13
10 a.m.	553	22	33	6.1016	10.99
11 a.m.	677	24	38	7.3760	10.86
12 a.m.	738	25	40	8.0086	10.81
13 p.m.	731	26	41	7.9306	10.81
14 p.m.	680	27	41	7.4087	10.86
15 p.m.	585	25	37	6.4277	10.95
16 p.m.	402	23	31	4.4912	11.13
17 p.m.	201	20	26	2.2642	11.22
18 p.m.	96	17	21	1.0770	11.32
19 p.m.	36	16	17	0.4138	11.45
20 p.m.	6	15	15	0.0692	11.50

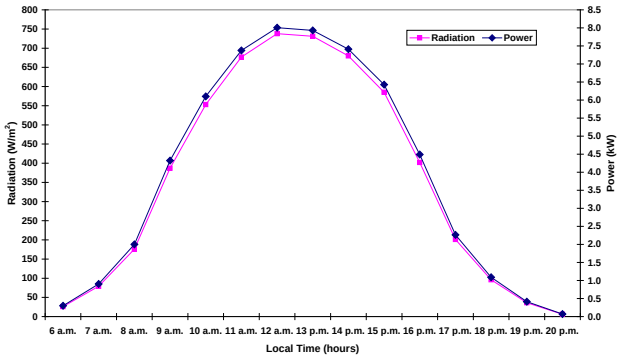

Fig. 2. Variations of the solar radiation intensity and power of 10 kW PV vs. time for a sample day

According to data received such as solar radiation intensity, ambient temperature, modules temperature, can be produced solar modules and system efficiency in the period 6 a.m. till

8 p.m. in sample day at Taleghan site was calculated. Parameters related to solar radiation intensity, ambient temperature, modules temperature, power system and solar cell efficiency versus time for sample day are given in Table 1. Variations of the solar radiation intensity, producing power system, efficiency and cell temperature of PV array against to time for a sample day are given Figs. 2 and 3.

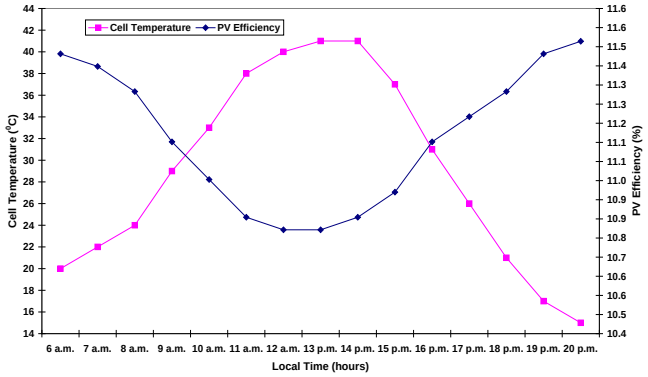

Fig. 3. Variations of efficiency of PV arrays and cell temperature vs. time for a sample day

3.3. Battery bank

It is known that a solar hydrogen system needs a storage system to provide energy for the cases of inappropriate weather conditions, instantaneous overload conditions, or demand for energy after sunset [15-16]. Sun irradiance is stochastic variables by nature. Energy storage such as in a battery is required for storing energy from PV array for the back up and stand by power source. The battery type is lead-acid because of the low cost and good electrical performance under various conditions [17-18]. The selection of a proper size of the battery bank for these types of applications requires a complete analysis of the battery's charge and discharge requirements [19-20]. The lead-acid batteries have the longest life and the least cost per amp-hour of any of the choices [21].The battery system is made up of forty-eight deep discharge lead-acid batteries which are installed at the capacity of 57.6 kWh (12V×100 Ah × 48 cell). Each battery has an average lifetime of five years. When the electrolyzer is turn off, the excess energy generated from PV array is used to charge the batteries. If electrolyzer needs more power, the rest of power for operation is supplied by the batteries.

3.4. Inverter

A 10 kW Sunny Boy 2500U model inverter is a single-phase AC power source that is connected between the battery bank and utility grid at 195-251 V_{AC}. The battery voltage decrease when the AC loads increase. The inverter is based on a power unit that operates with a very high efficiency and optimal reliability. For more specifications, see Table 2 [22].

Table 2. Inverter technical characteristics (Sunny Boy model 2500)

$P_{nominal}$	*2200 W_p*	Max. AC-power	*2500 W*
Max input voltage	*600 V*	Peak inverter efficiency (η_{max})	*93-94.4%*
Max input current	*11.2 A*	AC input frequency	*49.8-50.2 Hz*
PV-voltage range MPPT	*250-600 V*	V_{AC}	*198-251 V*

3.5. Hydrogen unit

Water electrolysis technology has the highest energy efficiency in non-fossil fuel based hydrogen production and is ideally suited for coupling with intermittent renewable energy resources [19]. In general, there is a good match between the polarization curves of PV cells

and water electrolysis. However electricity from PV is expensive and hydrogen produced from such electricity is even more expensive, but this technology is well developed and matured for a large scale electricity and hydrogen generation [23]. The decomposition of water into hydrogen and oxygen can be achieved by passing an electric current between two electrodes separated by an aqueous electrolyte. The total reaction for splitting water is [24]:

$$H_2O(l) + \text{Electrical Energy} \rightarrow \mathrm{H_2(g)} + \frac{1}{2}O_2(g)$$

In this pilot, the electrolyzer is a bipolar and alkaline type manufactured by the Hydrotechnik (Germany). The electrolyzer module consists of 10 cells in series. The nominal operating point is rated load, 250 amperes and rated voltage, 25 V_{max}. The electrolyte (KOH) concentration inside the cells is about 28 wt. %.; the amount of hydrogen produced in one hour by the electrolyzer is found by the formula:

$$\nu = 0.000419 \times I_e \times A \times n = 4.12 \times 10^{-3} . I_e \quad (\mathrm{m^3/hr}) \qquad (2)$$

where I_e is the current (in Ampere), A is a coefficient, n is number of electrolytic cells, and ν is the hydrogen production in m^3/hr. Hydrogen is stored at 10 bars in a tank to feed the fuel cell at low solar radiation levels and hence supply the required load power [25]. The maximum stable rate of hydrogen production was about 1 Nm^3/hr. The electrolysis efficiency is about 70 %, based on the HHV (Higher heat Value) [26].

$$P_{out} = 1\left(\frac{m^3}{hr}\right) \times \frac{1(\mathrm{mol\,H_2})}{22.4(lit)} \times \frac{285830(J)}{1(\mathrm{mol\,H_2})} \times \frac{1(hr)}{3600(\mathrm{sec})} \times \frac{1000(lit)}{1(m^3)} = \frac{285830000}{80640} = 3544\mathrm{W}$$

$$\eta = \frac{P_{out}}{P_{in}} = \frac{3544(W)}{5000(W)} = 0.7089 \qquad (3)$$

The oxygen output still contains small amounts of hydrogen gas and vast amounts of water vapor. It was not used in this system and was released into the atmosphere [27]. The hydrogen from the electrolyzer is sent into a low pressure tank (buffer tank) that is kept at a pressure lower than the hydrogen output pressure of the high pressure tank as shown in Fig. 4.

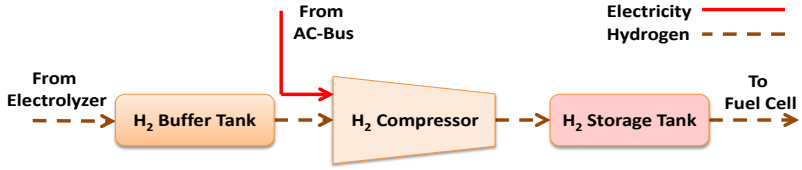

Fig. 4. Schematic of hydrogen storage system

Compression occurs during compressor cycles in which the hydrogen is continuously removed from the low-pressure tanks beginning at the current pressure of the low-pressure tank and ending when the pressure drops to a specified minimum supply pressure. The volume of hydrogen vessel is 1 m^3 and maximum pressure is 10 bars. It is known that a stand-alone photovoltaic system needs a storage system to provide energy for the cases of inappropriate weather conditions, instantaneous overload conditions, or demand for energy after sunset [28]. Due to simple operation, high efficiency and ability to provide power quickly from a standby configuration, a PEM fuel cell was chosen for this project. This system manufactured by Ballard power system Inc.(Canada) that has 30 cells and provides up to 1.2 kW of unregulated DC power at a nominal output voltage. The output voltage varies

with power, ranging from about 43 V at system idle to about 26 V_{DC} at full load. It has the capability to operate at low temperature and has short start-up period [29] .Overall system efficiency for the direct coupling system calculated according to the following equation:

$$\eta_{overall} = \frac{Q \cdot E}{S \cdot A} \quad (4)$$

where A is the PV array total surface (m^2), Q is hydrogen production rate (ml/sec), E is the calorific value of hydrogen (J/ml), and S is solar radiation (W/m^2) [30].

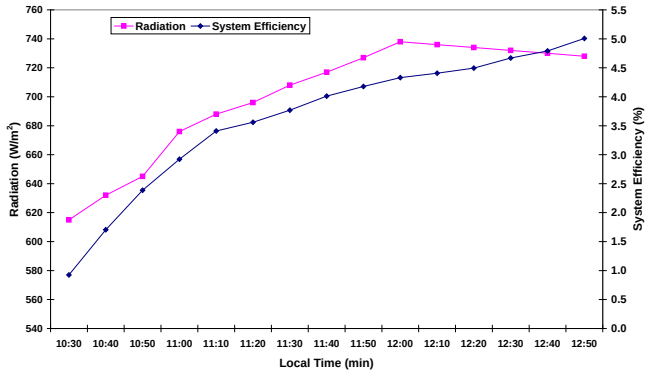

Fig.5. Variations of solar radiation intensity and solar hydrogen efficiency for a sample day

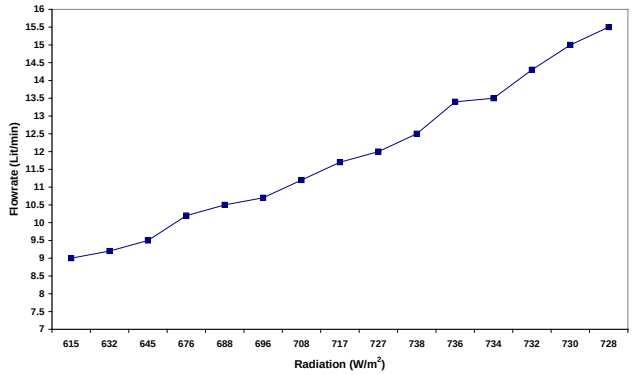

Fig.6. Variations of HPR vs. solar radiation

Hydrogen gas has the highest calorific value. When one gram of hydrogen is burnt completely, it produces 150 kJ. Thus the calorific value of hydrogen is 150 kJ/g (≈12.6 J/mol) [31]. We assumed that water electrolysis operated during a s ample day in summer season during 150 minutes (10:30 a.m. until 12:50 a.m.).

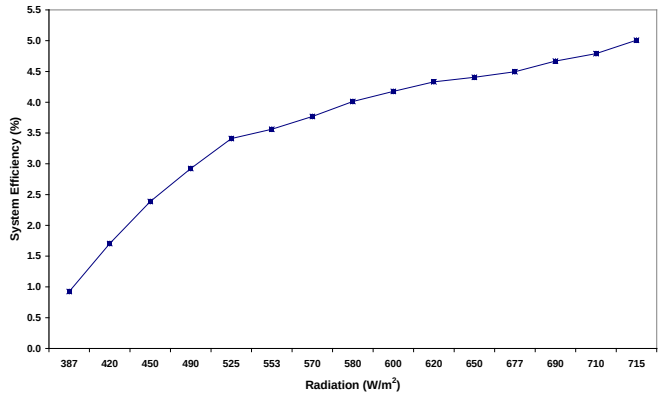

Fig.7. Variations of solar hydrogen system efficiency vs. solar radiation

Overall efficiency of solar hydrogen system in this time is shown that in Table 3; also variations of the solar radiation intensity and solar hydrogen efficiency versus time are shown in Fig. 5 a nd variations of hydrogen production rate and solar hydrogen energy system efficiency versus solar radiation intensity are shown in Figs.6 and 7. The effects of hydrogen production rate and solar radiation on the overall efficiency system are also given in Table 3 and are plotted in Fig. 7. The increase in overall efficiency was from 0.93 to 5.01 % with the increase in current from 25 t o 250 amperes, module temperature from 34 to 41^{o}C and hydrogen production rate from 9 to 15.5 lit/min.

Table 3. Parameters related to solar radiation, ambient temperature and power system vs. time

Time	Voltage (V)	Current (A)	Hydrogen Production rate (lit/min)	Insolation (W/m^2)	Ambient Temp. (^{o}C)	Module Temp. (^{o}C)	Overall Efficiency System (%)
6 a.m.	20.2	25	9.0	615	23	34	0.93
7 a.m.	21.4	50	9.2	632	23	35	1.70
8 a.m.	21.8	75	9.5	645	23.5	36	2.39
9 a.m.	22.3	100	10.2	676	24	38	2.92
10 a.m.	22.6	125	10.5	688	24	38.5	3.41
11 a.m.	22.7	137.5	10.7	696	24.5	39	3.56
12 a.m.	22.8	150	11	708	24.5	39	3.77
1 p.m.	22.9	162.5	11.5	717	24.5	39.5	4.01
2 p.m.	23	175	12	727	25	40	4.18
3 p.m.	23.1	187.5	12.5	738	25	40	4.33
4 p.m.	23	200	13	736	26	40	4.41
5 p.m.	22.8	212.5	13.5	734	26.5	40	4.49
6 p.m.	22.7	225	14	732	26.5	40	4.67
7 p.m.	22.4	237.5	15	730	27	40.5	4.79
8 p.m.	21.7	250	15.5	728	27	41	5.01

4. Conclusions

- The coupling of PV filed and an electrolyzer allows converting renewable electricity into time-stable storage. The time of storage can be unlimited and there is no loss of energy in stored energy. Using a fuel cell provide a silent electricity generator which has no environmental impact.
- The replacement of conventional technologies like batteries by new hydrogen technologies including using fuel cells in RE based stand-alone power systems is technologically feasible. It reduces emissions, noise and fossil fuel dependence and increases renewable energy penetration.
- New energy generators for stand-alone applications are expected to increase the comfort of people. The actual solutions are either limited by a low autonomy inducing reduction of the electricity consumption during worst seasons or noisy and using fossil energy.
- Iran country located on solar belt and has a great potential in direct natural solar radiation. Solar energy required high initial investment, so converting solar energy to other types of energy with high efficiency systems is vital.

References

[1] K. Ro, S. Rahman, IEEE Transactions on Energy Conversion 13(3), 1998, pp. 276-281.

[2] A.M. Ramirez, P.J. Sebastian, S.A. Gamboa, M.A. Rivera, O. Cuevas, J. Campos, Int J Hydrogen Energy 25, 2000, pp. 267-271.

[3] W. Isherwood, J.R. Smith, S.M. Aceves, G. Berry, W. Clark, R. Johnson, D. Das, D. Goering, R. Seifert, Solar Energy 25, 2000, pp. 1005-1020.

[4] M. Momirlan, T.N. Veziroglu, Renewable and Sustainable Energy Reviews 3, 1999, pp. 219-231.

[5] M. Momirlan, T.N. Veziroglu, Renewable and Sustainable Energy Reviews 6, 2002, pp. 141-179.

[6] A. Midilli, M. Ay, I. Dincer, M.A. Rosen, Renewable and Sustainable Energy Reviews 9, 2005, pp. 255-271.

[7] G.J. Conibeer, B.S. Richards, Int J Hydrogen Energy 32, 2007, pp. 2703-2711.

[8] Ø. Ulleberg, Solar Energy 76, 2004, pp. 323-329.

[9] J. Nowotny, C.C. Sorrell, L.R. Sheppard, T. Bak, Int J Hydrogen Energy 30, 2005, pp. 521-544.

[10] S. Galli, M. Stefanoni, Int J Hydrogen Energy 22(5), 1997, pp. 453-458.

[11] D.B. Nelson, M.H. Nehrir, C. Wang, Renewable Energy 31, 2006, pp.1641-1656.

[12] Technical Catalogue of Solar Module, MA36/45, Optical Fiber Fabrication Co, Iran.

[13] M.D. Siegel, S.A Klein, W.A. Beckman, Solar Energy 26, 1981, pp. 413-418.

[14] C. Soras, V. Makios, Solar Cells 25(2), 1988, pp. 127-142.

[15] B. Wichert, M. Dymond, W. Lawrance, T. Friese, Renewable Energy 22(1-3), 2001, pp. 311-319.

[16] E. Koutroulis, K. Kalaitzakis, Renewable Energy 28(1), 2003, pp. 139-152.

[17] A. Urbina, T.L. Paez, R.G. Jungst, Intersociety Energy Conversion Engineering Conference and Exhibit, 2000, pp. 995-1003.

[18] P.C. Butler, J.T. Crow, P.A. Taylor, the 19th International INTELEC, 1987, pp. 311-318.

[19] K.E. Cox, K.D. Williamson, Hydrogen: its technology and implications, Ohio: CRC Press Inc, 1977.

[20] G.W. Vinal, Storage Batteries, 4th edition, New York, N.Y.: John Wiley, 1967.

[21] Solar Electric Products Catalog, 2005.

[22] www.SMA.de.

[23] S.A. Sherif, F. Barbir, T.N. Vezirouglu, Solar Energy 78, 2005, pp. 647-660.

[24] M.J. Khan, M.T. Iqbal, Renewable Energy 30, 2005, pp. 421-439.

[25] Th.F. El-Shatter, M.N. Eskandar, M.T. El-Hagry, Renewable Energy 27, 2002.

[26] Instruction for erection operation and maintenance for hydrogen generation and compression plant EV05/10 system DEMAG, 1998.

[27] R. Perez, Home Power 22, 1991, pp. 26-30.

[28] E. Koutroulis, K. Kalaitzakis, Renewable Energy 28(1), 2003, pp. 139-152.

[29] Nexa™ (310- 0027) Power Module User's Manual, MAN5100078, 2003.

[30] G.E. Ahmad, E.T. El-Shenawy, Renewable Energy 31, 2006, pp. 1043-1054.

[31] http://home.att.net/~cat6a/fuels-VII.htm.

Demonstration project of the solar hydrogen energy system located on Taleghan-Iran: Technical-economic assessments

Abolfazl Shiroudi[1], Seyed Reza Hosseini Taklimi[2,*]

[1]*Ministry of Energy-Renewable Energy organization of Iran (SUNA), Tehran, Iran*
[2] *Linkoping University of Technology, Linkoping, Sweden*
** Corresponding author. Tel: +46 760830785, E-mail: seyho130@student.liu.se*

Abstract: One of the most attractive features of hydrogen as an energy carrier is that it can be produced from abundant material like water. The use of electrolysis to produce hydrogen from water is an efficient method from small to large scales. Energy for supplying water electrolysis systems can be provided by photovoltaic arrays. During the daylight hours, the sunlight on the photovoltaic arrays converts into electrical energy which can be used for electrolyzer. The hydrogen produced by the electrolyzer is compressed and stored in hydrogen vessel and provides energy for the fuel cell to meet the load when the solar energy is insufficient. This study investigates a stand-alone power system that consists of 10 kW PV arrays as power supply and 5 kW electrolyzer. They have been integrated and worked at Taleghan site in Iran. Result was simulated and optimized by using HOMER simulation tools and techno-economic analysis of system presented in this paper.

Keywords: *Hydrogen, PV array, Electrolyzer, Fuel cell, HOMER*

1. Introduction

Renewable energy (RE) sources are attracting more attention as alternative energy sources nowadays. Depletion of energy sources and global warming play big role in this movement [1]. RE sources can open a new ways to solve these environmental issues. They usually free of pollution during development and operation for power generation [2]. Integration of RE with energy storage would provide a better system reliability making it suitable for remote stand-alone applications [3]. Among these sources, solar energy is an important kind of them. Solar photovoltaic (PV) energy has been widely utilized in small size application and is the most promising candidate for research and development for large-scale use, as the fabrication of less costly PV devices becomes a reality [1]. Seasonal solar energy which stores in the form of hydrogen can provide the basis for a completely renewable energy system. One of the most promising applications is stationary stand-alone power systems, particularly those located in remote areas where the cost of transporting fuel is high [4]. There is a growing awareness that hydrogen is the fuel of the future. Solar hydrogen is a leading candidate for a renewable and environmentally safe energy carrier [5]. Iran with more than 4.5 kWh/m^2.day radiations has a great potential for attracting and converting it to electricity. One of the efforts done in the field of constructing and utilization solar hydrogen plant is constructing stand-alone power system PV- electrolyzer- fuel cell in Taleghan site. The current paper evaluates the techno-economic aspects of PV-Electrolyzer-Fuel cell system. Hybrid optimization model for electric renewable (HOMER) was used as the simulation and optimization tools. The schematic of the plant at Taleghan site is given in Fig. 1.

2. Methodology

Hybrid systems based on the synergy between RE sources and conventional energy systems can be a reliable solution for remote sites to provide their need of energy. In this study, first PV cells hourly data of Electricity production gathered. Specification of each units in system such as PV array, water electrolysis, hydrogen storage tank, a fuel cell and a Power Management Unit (PMU) collected and they used for design and calculating primary model of HOMER. Then model optimized by software and the results of techno-economic analysis of

integration between PV panels, alkaline water electrolysis and hydrogen storage tank are presented.

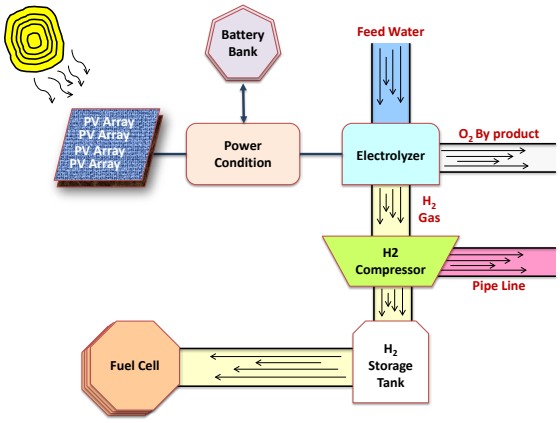

Fig. 1. Schematic of the PV-Electrolyzer-Fuel cell energy system at the Taleghan site

3. Result

3.1. Description of the system

This stand-alone energy system is located in altitude 1700 m and consists of a 10 kW_p PV array coupled to a 5 kWe bipolar, alkaline electrolyzer, a gas hydrogen storage tank (1 m^3), battery banks, converters DC/AC and a PMU. When the sun shines, PV power is available and it used directly to supply the load. Then electrolyzer turns on for producing hydrogen, which is delivered to the hydrogen storage tanks. In absent of solar the 1.2 kW Proton Exchange Membrane (PEM) fuel cell will begin to produce energy for the load using hydrogen from the hydrogen storage tank to produce the necessary electricity [6]. The PMU is in charge of the conversion and the dispatching of the energy between each component. It is composed of many converters and an inverter as well as a PLC, programmed to optimally switch on or off system components [7].

3.1.1 PV array

Solar energy is one type of the RE resources, which can be converted easily and directly to the electrical energy by PV converters. The PV array consists of 224 solar panels MA36/45 modules configured into 14 independent sub arrays. The array is broken into sub arrays that are each individually controlled. Each sub-array consists of 16 modules, which connected in parallel of seven modules in series. The nominal power rating for the array is 10 kW_p. The PV module is a polycrystalline silicon type with maximum output of 45 W. Each module is 462 mm wide and 977 mm long for an area of 0.45 m^2 per module and total surface of 101.1 m^2 ($2\times7\times16\times0.45=101.1$ m^2).

Table 1. Photovoltaic Module Electrical characteristics (MA 36/45)

Nominal power	*45 W*	Short circuit current	*2.96 A*
Nominal load voltage	*20.5 V*	Current at maximum power point	*2.74 A*
Voltage in maximum power point	*16.7 V*	Nominal efficiency	*0.115*

The tilt angle is fixed at 45 degree with horizontal in south direction [8]. The specifications of the modules in the standard condition (1000 W/m^2 radiation & 25 °C temperature), are listed in Table 1 [9].

3.1.2 The Battery Bank

Due to the stochastic nature of photovoltaic system, energy storage is needed to supply the load "on demand" by storing energy during periods of high bright sun. When the total output of the PV array is more than the energy demand, the battery bank is charged. The battery used in this system consists of 57.6 kWh (12V×100Ah×48cell). The 48 V battery bank originally consisted of 57.6 kWh of storage in (12×4) sealed, valve-regulated, deep-cycle batteries.

3.1.3 The Inverter

These units turn DC power into conventional AC power, as well as offer the ability to provide backup power during a power outage. When you need to use an electrical appliance, but only have access to DC power, an inverter is perfect. The inverter used in this project is a Sunny Boy model 2500U. It is based on a power unit that operates with a very high efficiency and optimal reliability. It is designed for strings with 18 to 24 standard modules connected in series. For more detailed specifications, see Table 2 [10].

Table 2. Inverter technical characteristics (Sunny Boy model 2500)

$P_{nominal}$	*2200 W_p*	Max. AC-power	*2500 W*
Max input voltage	*600 V*	Peak inverter efficiency (η_{max})	*93-94.4%*
Max input current	*11.2 A*	AC input frequency	*49.8-50.2 Hz*
PV-voltage range MPPT	*250-600 V*	V_{AC}	*198-251 V*

3.1.4 Electrolyzer

Water electrolysis technology has the highest energy efficiency in non-fossil fuel based hydrogen production and is ideally suited for coupling with intermittent RE sources. In this method, electricity is used to split water into hydrogen and oxygen [11]. Water electrolysis is particularly suitable to be used in conjunction with PV array. The electrolyzer used in this project is a bipolar alkaline type. The electrolyzer module consists of 10 cells in series. The nominal operating point is rated load, 250 amperes and rated voltage, 25 V_{max}. The electrolyte (KOH) concentration inside the cells is about 28 wt. %. It had a maximum power of 5 kW and yielded about 1 Nm^3/h hydrogen at normal conditions and a purity of 99.9 %. Under nominal condition, the efficiency of system is 70 %.

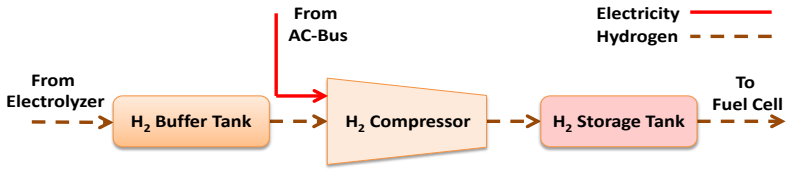

Fig. 2. Schematic of hydrogen storage system

The oxygen gas is far from pure as it leaves the electrolyzer's cells. The oxygen output of the electrolyzer still contains small amounts of hydrogen gas and vast amounts of water vapor [12-13]. The hydrogen from the electrolyzer is sent into a low-pressure tank (buffer tank) that is kept at a pressure lower than the hydrogen output pressure of the high-pressure tank as shown in Fig. 2. The intermediate reservoir system is used so that the compressor is only run when sufficient excess energy is available eliminates the use of energy from the fuel cell or enlargement of the battery bank to power the compressor. Compression occurs during compressor cycles in which the hydrogen is continuously removed from the low-pressure tanks beginning at the current pressure of the low-pressure tank and ending when the pressure

drops to a specified minimum supply pressure. The hydrogen gas is then compressed by about 10 bars by the compressor and sent for storage to hydrogen vessel.

3.1.5 Fuel cell

A fuel cell is an energy conversion device, which converts the chemical energy of a fuel and oxidant, often hydrogen and oxygen, to electrical energy fuel cells are similar to batteries, however, unlike battery a fuel cell must be continuously provided with fuel, rather than deriving energy from materials contained within the cell, and the products of the electrochemical reaction must be removed the cell. They can achieve operating efficiencies approaching 60 % nearly twice the efficiency of conventional internal combustion engines [14]. The outputs of the fuel cell are DC electricity and water. Fuel cells are a very attractive option to be used with intermittent sources of generation like the PV. Their feasibility in coordination with PV systems has been successfully demonstrated for both grid-connected and stand-alone applications [15]. A PEM fuel cell was chosen because of its passive operation, high efficiency, silent and its ability to provide power quickly from a standby configuration. In this project, The Nexa ™ system has 30 cells and provides up to 1.2 kW of unregulated DC power at a nominal output voltage of 26 V_{DC}. The output voltage varies with power, ranging from about 43 V at system idle to about 26 V at full load [16].

3.1.6 Hydrogen Storage

Hydrogen as an energy carrier must be stored to overcome daily and seasonal discrepancies between energy source availability and demand. Hydrogen storage has an economic advantage over lead acid batteries for long-term storage. Currently, pressurized tanks are still the most cost-effective means of hydrogen storage for most applications [17]. It is known that a stand-alone energy system needs a storage system to provide energy for the cases of inappropriate weather conditions, instantaneous overload conditions, or demand for energy after sunset [18]. In this project, hydrogen gas produced in the electrolyzer at 10 bars. This gas is stored in one hydrogen storage tank (1 m^3) with a rated working pressure of 10 bars.

3.2. Advantages of the PV-Electrolysis system

There are three main reasons why the PV efficiency is lower than we had hoped. First, the MA36/45 modules are rated at 45 W but when we tested them, the average output was lower than the manufacturer claimed. Second, the various wiring connections required by code add up to an appreciable voltage drop. And finally, the electrolyzer operating voltage usually doesn't exactly match the maximum power voltage of the array. The match between the electrolyzer and PV array is an important aspect of solar hydrogen system design [19]. Advantages of the PV-Electrolysis system:

- PV modules are sold with a warranty that guarantees the power generation for typically 25 years [10].
- PV modules are an ideal power supply for an electrolyzer. The output voltage of a PV array is DC and is roughly constant with illumination level. This is a good match to the electrolyzer, which requires a c onstant voltage of at least 1.9 V_{DC} (for the generic considered). Increasing PV current would increase the overall volume of hydrogen produced, although it would also slightly lower the production efficiency [20].
- The water electrolysis and PV array can be sized independently and located separately.

In this system, consumption power consists of 5 kW water electrolysis and 1.5 kW hydrogen compressors. In eight hours continuous working of electrolyzer, hydrogen compressor work just three hours; therefore total of demand energy in one-work days equal to:

$$E_{total} = (P_{elec} \times h_1) + (P_{pump} \times h_2) = [(5kW) \times (8hours)] + \left[(1.5kW) \times (6 \times \frac{1}{2} hours) \right] = 44500Wh/days \quad (1)$$

The average annual global radiation for Taleghan region is 4.5 kWh/m^2; Therefore power of PV system in this pilot equal to:

$$P_{PV} = \frac{44500Wh/days}{4500Wh/m^2} = 9.88kW \approx 10kW \quad (2)$$

The Depth of discharge (DOD) is defined as the amount of energy that has been removed from a battery or battery pack and usually expressed as a percentage of the total capacity of the battery. In this case, 30 % DOD means that 30 % of the energy has been discharged, so the battery now holds only 70 % of its full charge [21]. In this pilot, we used type of sealed lead acid with technical properties, 12 V and 100 Ah.

$$\text{Bank capacity} = 44500(Wh/days) \times \%130(DOD) = 57850Wh \quad (3)$$

$$\text{Bank capacity} = \frac{57850\text{Wh}}{12\text{V}} = 4820Ah \quad (4)$$

$$No.Battery = \frac{4820Ah}{100A} = 48.2 \approx 48 \quad (5)$$

3.3. Simulation solar hydrogen system with HOMER tools

National Renewable Energy Laboratory's software HOMER is used to select an optimum energy system. It also performs sensitivity analysis to evaluate the impact of a change in one or more of input parameters. Some required input information for HOMER are electrical loads, renewable resources, component technical/costs, constraints, controls, type of dispatch strategy, etc. [22]. The schematic of this system is shown in Fig. 3. Several simulation have been made by considering different capacities of PV panels, hydrogen tank, electrolyzer, battery bank, converter, fuel cell and primary load that the results of simulation, optimization and analysis for this system are described in the following sections:

- A cost of 342 $/45 W was used, resulting in a total capital cost of 76000 $ for a 10 kW PV array. PV array operation and maintenance (O&M) cost is considered practically zero and their lifetime is 20 years. After some preliminary runs with HOMER, it was decided that the most suitable PV size to be considered was 10 kW.
- A battery bank with a capacity of 1200 Ah (12 V, 100 A) per unit was installed. The total capacity of batteries installed was 57.6 kWh and the estimated lifetime was 5 years. The total capital cost of the battery bank was 4896 $. Sizes of batteries considered in the optimization were: 48 and 0 kWh (no batteries).
- An AC-DC power converter unit has been installed in PV-Hydrogen system of Taleghan site. Power conditioning capital cost is around 600-800 €/kW [23]. A cost of 1350 $/kW was chosen for Taleghan site. A lifetime of 20 years was assumed and a converter efficiency of >94%.
- The cost of hydrogen production unit integrated to the proposed PV-hydrogen cost was 2700 $ per Nm^3/h H_2. The introduction of this unit sizes (0-6.5 kW) was investigated with HOMER. The lifetime of this unit was considered as equal to 10 years.
- The capital cost of Nexa system (1.2 kW) is 5000 $/kW for the stand-alone energy system in Taleghan site (because of its very small-scale). Fuel cell lifetime was 1500 operating

hours. Three different PEM fuel cell size (1-1.2 kW) were considered in the calculations performed with HOMER and electrical efficiency assumed constant at 38 %.

- Compressed gas storage is used for this study. Small-quantity prices are around 1500 $/kg. A hydrogen storage tank options was investigated in the optimization process, namely 1 Nm^3 (≈1kg) and the lifetime were also considered 20 years [23].
- This system has an average AC load of 31 kWh/days, with the peak load of 2.9 kWh/days. HOMER allows input of the operating reserve for the system. Result of here required the operating reserve to be 10 % of the hourly load, plus 25 % of PV power output.

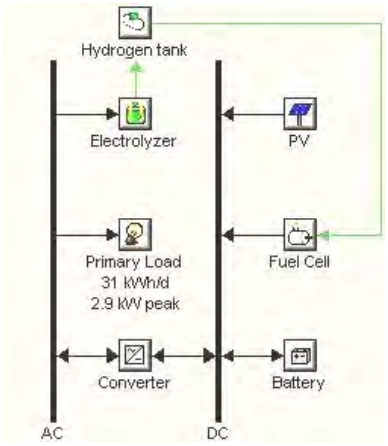

Fig. 3. Schematic of PV-Electrolyzer-Fuel cell power system

3.4. PV-hydrogen system optimization results

Actual load profile and meteorological data from the operation of the PV-fuel cell system in Taleghan site were used in this study. Hourly solar radiation measurements for a period of one year were imported into HOMER tools in order to calculate monthly average values of clearness index and daily radiation [24]. According to data from Taleghan area, the solar radiation is high, especially between June and August. The annual average global radiation is 4.5 kWh/m^2.day with an annual average clearness index of 0.62 a nd the average daily radiation is 5.095 kW h/m^2. The existing system was simulated in order to evaluate its operational characteristics, namely annual electrical energy production; annual electrical loads served, excess electricity, RE fraction, capacity shortage, unmet load etc. some environmental impact parameters of the system. A load-following control strategy was followed in the simulation. Under this strategy, whenever a power generator in needed it produces only enough power to meet the demand. Load following strategy tends to be optimal in systems with a surplus of renewable energy. An annual interest rate of 10 % and a project of 20 years were used in the economic calculations [24].

Table 3. Electrical production and demand for the stand-alone system

Annual Electric Energy Production		Annual Electric Energy Consumption		Other	
PV Array	*18025 kWh (99%)*	AC Primary Load	*11116 kWh (98%)*	Excess Power	*4109 kWh/years*
Fuel Cell	*101 kWh (1%)*	Electrolyzer Load	*392 kWh (2%)*	Capacity Shortage	*157 kWh/years*
Renewable Fraction	*100%*	Total	*11508 kWh*	CO_2 Emissions	*0.0619 kg/year*

The results of the simulation showed that this system had a total annual electrical energy production of 18126 kWh, the RE fraction of which was ≈1 (i.e. 18025 kWh were produced

by the PV array). All results related to the electric energy production and electric energy consumption is summarized in Table 3. Latter is attributed to high nighttime load, which enable the operation of fuel cell because PV energy stored in batteries is not adequate to serve the load overnight. To increase renewable energy penetration excess energy can be stored in the form of compressed hydrogen and drive a PEM fuel cell.

Table 4. Distribution of annualized costs for the main components of the stand-alone energy system

Component	Initial Capital ($)	Annualized Capital ($/year)	Annualized Replacement ($/year)	Annual O&M ($/year)	Annual Fuel ($/year)	Total Annualized ($/year)
PV Array	76000	8927	0	0	0	8927
Fuel Cell	5000	587	88	12.1	0	687
Battery	4896	575	320	0	0	895
Converter	13650	1603	0	0	0	1603
Electrolyzer	8100	951	272	0	0	1223
Hydrogen Tank	1500	176	0	0	0	176
Other	0	0	0	0.2	0	0

The Electrical production and demand of this system are listed in Table 3. When excess PV energy is available, power is supplied first to the batteries, and then to an electrolyzer, which generate hydrogen for storage. By using HOMER it can be decided whether to use energy from the battery, fuel cell, or both based on the replacement cost and O&M of the devices. PV-Hydrogen system components are described in more detail in the following sections. Total annualized costs for each component of the stand-alone energy system are shown in Table 4. This is attributed to the fact that the lifetime of batteries is only 5 years, and the system lifetime is 20 years. Therefore the battery bank needs to be replaced several times during the project. The total net present cost (NPC) of this system at Taleghan site is around 115034 $ and cost of energy (COE) of the proposed hydrogen system is 1.216 $/kWh.

4. Conclusions

The replacement of conventional technologies, namely batteries by hydrogen technologies including fuel cells in RE resources based stand-alone power systems is technologically feasible. It reduces emissions, noise and fossil fuel dependence and increases RE penetration. The coupling of PV field and electrolyzer allows converting at high efficiency renewable electricity. There is no loss whatever the storage time and no need of consumption to avoid storage destruction. Using a fuel cell to get back to electricity induces a low efficiency but allows building a silent energy generator consuming no materials. New energy generators for stand-alone applications are expected to increase the comfort of people. The actual solutions are either limited by a low autonomy inducing reduction of the electricity consumption during worst seasons or noisy and using fossil energy. The coupling of a PV field and an electrolyzer allows converting at high efficiency renewable electricity into time-stable storage from pure water. Using a fuel cell to get back to electricity allows building a noiseless energy generator consuming no materials. The gas storage induces a complete autonomy during all the years and should increase the use of the renewable production. Iran country located on solar belt, so it has great potentional in direct natural insolation for consuming and converting it to other types of energy. Using solar energy required high initial investment, so converting solar

energy to other types of energy with high efficiency systems is vital. Photovoltaic technology provides a reliable energy for producing hydrogen by electrolysis. Constructing this project illustrates photovoltaic system reliability, availability and being disputable in rural areas and end point of electricity yield. (Conclusion extract from) system operation conclusions shows equal real outputs, which calculated data and this, will be a start for gathering and processing information from operational parameters, in software.

References

[1] K. Ro, S. Rahman, IEEE Transactions on Energy Conversion 13 (3), 1998, pp. 276-281.

[2] A.M. Ramirez, P.J. Sebastian, S.A. Gamboa, M.A. Rivera, O. Cuevas, J. Campos, Int J Hydrogen Energy 25, 2000, pp. 267-271.

[3] W. Isherwood, J.R. Smith, S.M. Aceves, G. Berry, W. Clark, R. Johnson, D. das, D. Goering, R. Seifert, Solar Energy 25, 2000, pp. 1005-1020.

[4] Ø. Ulleberg, Solar Energy 76, 2004, pp. 323-329.

[5] S.A. Sherif, F. Barbir, T.N. Vezirouglu, Solar Energy 78, 2005, pp. 647-660.

[6] D.B. Nelson, M.H. Nehrir, C. Wang, Renewable Energy 31, 2006, pp. 1641-1656.

[7] S. Busquet, F. Domain, R. Metkemeijer, D. Mayer, Ecole des Mines de Paris-Centre d'Energétique, Rue Claude Daunesse, Les Lucioles-BP 207, F-06904 Sophia Antipolis.

[8] Technical Catalogue of Solar Module MA36/45,Optical Fiber Fabrication Company, Iran

[9] H. Moghbelli, R. Vartanian, International Conference on Renewable Energy for Developing Countries, 2006.

[10] www.SMA.de

[11] K.E. Cox, K.D. Williamson, Hydrogen: its technology and implications, Ohio: CRC Press Inc., 1977.

[12] P. Hollmuller, J. Joubert, B. Lachal, K. Yvon, Int. J. Hydrogen Energy 25, 2000.

[13] R. Perez, Home Power 22, 1991, pp. 26-30.

[14] Fuel Cell Handbook, 6th ed., National Energy Technology Lab, U.S. DOE, Pittsburgh, PA, 2002.

[15] S. Rahman and K. Tam, IEEE Transactions on Energy Conversion 3 (1), 1988, pp. 50-55.

[16] Nexa™ (310-0027) Power Module User's Manual, MAN5100078, 2003.

[17] J. Cotrell, W. Pratt, NREL/TP-500-34648, 2003.

[18] E. Koutroulis, K. Kalaitzakis, Renewable Energy 28 (1), 2003, pp. 139-152.

[19] P. Lehman, C. Parra, Solar Today, the American solar energy society, 1994, pp: 20-22

[20] N. Nagai, M. Takeuchi, T. Kimura, T. Oka, Int. J Hydrogen Energy 28, 2003, pp. 35-41.

[21] Solar Electric Products Catalog, August 2005.

[22] NERL. Hybrid Optimization Model for Electric Renewable (HOMER) Available freely at (http://www.nrel.gov/international/tools/HOMER/homer.html).

[23] E.I. Zoulias, N. Lymberopoulos, Renewable Energy 32, 2007, pp. 680-696.

[24] RETScreen™ database, URL: www.retscreen.net.

Two Dimensional PEM Fuel Cell Modeling at Different Operation Voltages

Mohammad Ameri*, Pooria Oroojie

Energy Eng. Department, Power & Water University of Technology, Tehran
** Tel: +98 2173932653, Fax: +98 2177311446, E-mail: ameri_m@yahoo.com*

Abstract: This paper presents a comprehensive, consistent and systematic mathematical modeling for PEM fuel cells that can be used as the general formulation for the simulation and analysis of PEM fuel cells. As an illustration, the model is applied to an isothermal, steady state, two-dimensional PEM fuel cell at different operation voltages to investigate the fuel cells performance parameters such as the mass concentration, the velocity distribution of reactant, current density distribution, and polarization curve. The model includes the transport of gas in the gas flow channels, electrode backing and catalyst layers; the transport of water and hydronium in the polymer electrolyte of the catalyst and polymer electrolyte layers; and the transport of electrical current in the solid phase. Water and ion transport in the polymer electrolyte has been modeled using the generalized Stefan–Maxwell equations. Moreover, the reactant gas flow in the gas channel has been modeled by continuity and the steady state incompressible Navier-Stokes equations. All of the model equations are solved with finite element method using commercial software package COMSOL Multi physics. The results from PEM fuel cell modeling at different operation voltages are then compared with each other and finally according to the results, the strategy to improve fuel cell performance with the target of reducing cost is introduced.

Keywords: *PEM fuel cell, Mathematical modeling, Finite element, COMSOL multi physic*

1. Introduction

Fuel cells and hydrogen technology represent the most promising alternative pathway for automotive and stationary applications. The PEMFC offers low to zero emission from sub-watt to megawatt power generation, for applications in transportation, industries and portable supplies units [1, 2]. In this paper, we focus on the role of computational tools in order to verify some experimental results and demonstrate the better performance of PEMFC constructed by application of optimizations techniques. Experimental research and numerical simulation have been used in fuel cell design in order to improve the performance of fuel cells. The experimental data will be useful to validate the model.

The search for reliable computational models is a challenge because it involves several transport phenomena: multi-component, multi phase and multi-dimensional flow processes, electrochemical reactions, convective heat and mass transport in flow channels, diffusion of reactants through porous electrodes, transport of water through the membrane and transport of electrons through solid matrix. The Computational Fluid Dynamic (CFD) is a very useful tool to simulate hydrogen and oxygen gases flow channels configurations, reducing the costs of bipolar plates' production and optimizing mass transport [3-5].

The computational models are efficient in predicting the cell performance under a variety of design parameters. Fuel cell models can be classified into 1D, 2D and 3D according to dimensions. The accuracy of 1D model [6,7] is sacrificed due to some assumptions made in order to simplify the problem to 1D. A 3D model simulates the reactant gas flow in the directions along the flow channel and perpendicular to the flow channel simultaneously, which results in more accurate results but requires longer computational time and larger computing capacity facility [8, 9]. A 2D fuel cell model [10,11] combines the benefits of 1D and 3D models and gains its popularity in PEM fuel cell modeling due to its higher computational efficiency compared to 3D models and better simulation accuracy compared to 1D model. A two-dimensional mathematical model of a PEM fuel cell can be conducted in two different modes: parallel or perpendicular to the gas flow direction in the gas channel

while the other modeling dimension is across the membrane in both cases. Models conducted in the first mode (parallel to the gas flow direction) consider the influence of fluid behavior in the channel; while in the second mode (perpendicular to the gas flow direction) the interdigitated flow pattern can be easily investigated. The goal of the present work is to develop 2D isothermal, steady state PEM fuel cell models in perpendicular to the gas flow direction to investigate the performance of fuel cells such as the mass concentration and velocity distribution of reactants, polarization curve, output power density at different operation voltages so that one can examine the influence of operation voltage on those items.

2. Modeling

Fig. 1 schematically shows a 3D single PEMFC and its various components including the membrane, flow channels, gas diffusion layers and catalyst layers on both anode and cathode sides. To conduct a 2D simulation, there are two options to choose the modeling geometry: one is in x-z plane as shown in Fig. 2(a), and the other is in x-y plane as shown in Fig. 2(b). The geometry which is shown in Fig.2 (b) will be studied in this paper.

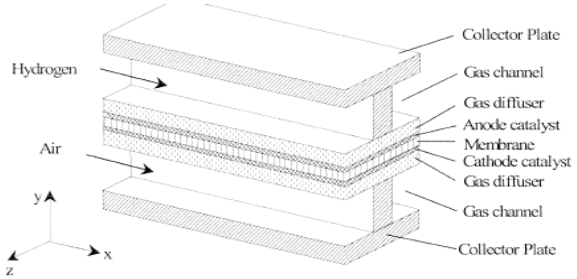

Fig.1. Three dimensional diagrams of a PEMFC and its various components.

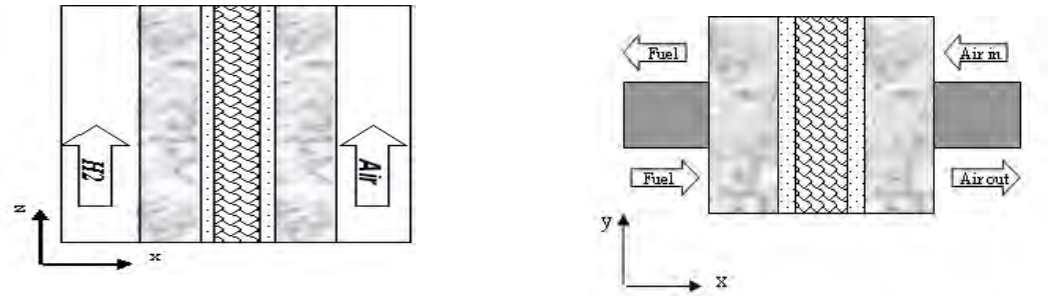

(a) x-z plane model geometry *(b) x-y plane model geometry*

Fig.2. Two-dimensional PEM fuel cell modeling geometry.

2.1. Model Definition

The modeled section of the fuel cell consists of three domains: an anode (Ω_a), a proton exchange membrane (Ω_m), and a cathode (Ω_c) as indicated in Fig. 3(a). Each of the porous electrodes is in contact with an interdigitated gas distributor, which has an inlet channel ($\partial\Omega_{a,\,inlet}$), a current collector ($\partial\Omega_{a,\,cc}$), and an outlet channel ($\partial\Omega_{a,\,outlet}$). The same notation is used for the cathode side. The model geometry is shown in Fig. 3(b).

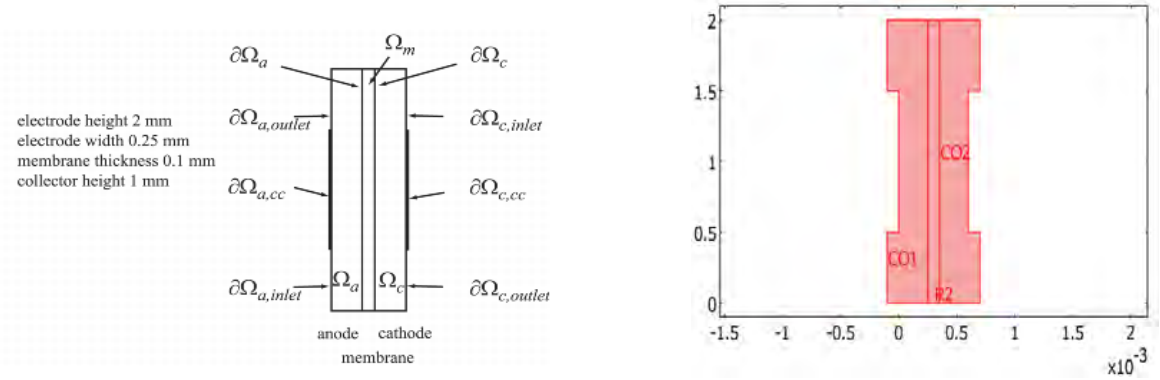

(a)Sub domain and boundary labels *(b) Model geometry*

Fig.3. Model geometry with sub-domain and boundary labels.

2.2. Governing Equations

2.2.1. Flow Channels

Based on the model assumptions, the reactant gas flow in the gas channel is governed by the continuity equation to insure the mass conservation as well as the steady state incompressible Navier-Stokes equation to describe the momentum conservation of Newtonian fluids. The multi-component diffusion and convection in flow channels are described by the Maxwell-Stefan equation. It solves for the fluxes in terms of mass fraction. The general form of the Maxwell-Stefan equation is shown below.

$$\frac{\partial}{\partial t}\rho\omega_l + \nabla.[-\rho\omega_l \sum_{j=1}^{N} D_{ij}\{\frac{M}{M_j}(\nabla\omega_j + \omega_j\frac{\nabla M}{M}) + (x_j - \omega_j)\frac{\nabla P}{P}\} + \rho\omega_l u] = R_i \quad (1)$$

Where D_{ij} (m^2/s) is the diffusion coefficient; R_i (kg/m^3.s) is the reaction rate and it is zero in the flow channel; x is the mole fraction; ω is the mass fraction; M (kg/mol) is the molecular mass; The subscript i (or j) represents each species of hydrogen and water on the anode side, and oxygen, water, nitrogen on the cathode side. On the cathode side, the transport equations are solved for two species since the third species can always be obtained from the mass balance equation given as the following:

$$w_{N_2} = 1 - w_{O_2} - w_{H_2O} \;;\quad w_{H_2O} = 1 - w_{H_2} \quad (2)$$

2.2.2. Gas diffusion layers and catalyst layers

Since gas diffusion layers (GDL) and catalyst layers are porous media, the velocity distribution is therefore formulated by Darcy's law and mass conservation equation.

$$u = -\frac{\kappa}{\mu}\nabla p \quad (3)$$

$$\nabla.(\rho u) = S \quad (4)$$

Where κ (m^2) is the permeability; and μ (Pa.s) is the dynamic viscosity. S is the source term, kg/ (m^3.s). The continuity equation for the gas flow mixture describes the sum of all the involved gas species at each side. The source term, S, accounts for the total consumption and

production during the electrochemical reactions. In the catalyst layer, the reaction rate R_i corresponding to each species is given as:

$$R_{H2} = -\frac{j_a}{2F} M_{H2} \; ; R_{O2} = -\frac{|j_c|}{4F} M_{O2}; \; R_{H2O} = \frac{|j_c|}{4F} M_{H2O} \tag{5}$$

2.2.3. Current transport

The continuity of current in a conducting material is described by:

$$\nabla.i = \nabla.i_s + \nabla.i_e = 0 \tag{6}$$

Protons travel through the ionic conductor (the membrane) to form an ionic current denoted by i_e while electrons can only be transferred through the solid matrix of electrodes which results in an electronic current denoted by i_s. The potential equations for both solid and electrolyte phases are obtained by applying Ohmic's law to Eq. (6).

$$\text{Electron transport: } \nabla.(-\sigma_s \nabla \phi_s) = S_s \; ; \; \text{Proton transport: } \nabla.(-\sigma_e \nabla \phi_e) = S_e \tag{7}$$

Where φ is the phase potential, V; σ (s/m) is the effective electric conductivity; S (A/m^3) is the current source term; the subscript s denotes the property of a solid phase and e denotes the property of an electrolyte phase. The source terms in the electron and proton transport equations, result from the electrochemical reaction occurring in the catalyst layers of anode and cathode sides.

$$\begin{aligned} &Anode \text{ Catalyst Layer: } S_e = j_a \; ; \quad S_s = -j_a \; , \\ &\text{Cathode Catalyst layer: } S_e = j_c \; ; S_s = -j_a \end{aligned} \tag{8}$$

Where j_a and j_c are the transfer current density corresponding to the electrochemical reaction at the anode and cathode catalyst layers, which is formulated by the agglomerate model. In the catalyst layers, the agglomerate is formed by the dispersed catalyst, and this zone is filled with electrolyte. Oxygen is dissolved into the electrolyte and reaches the catalyst site. The agglomerate model describes the transfer current density as following [12]:
Anode:

$$\begin{aligned} j_a = &-\frac{6(1-\varepsilon)FD_H{}^{agg}}{(R^{agg})^2}(C_H{}^{agg} - C_H{}^{ref} \exp(-\frac{2F}{RT}\eta). \\ &(1-\sqrt{\frac{j_{o,a^s}}{aFC_H{}^{ref} D_H{}^{agg}}} R^{agg} \coth \sqrt{\frac{j_{o,a^s}}{aFC_H{}^{ref} D_H{}^{agg}}} R^{agg}) \end{aligned} \tag{9}$$

Cathode:

$$\begin{aligned} j_c = R\, &\frac{12(1-\varepsilon)FD_O{}^{agg}}{(R^{agg})^2} C_O{}^{agg} .(1-\sqrt{\frac{j_{o,c^s}(R^{agg})^2}{4FC_O{}^{ref} D_O{}^{agg}} \exp(-\frac{0.5F}{RT}\eta)}). \\ &\coth \sqrt{\frac{j_{o,c^s}(R^{agg})^2}{4FC_O{}^{ref} D_O{}^{agg}} \exp(-\frac{0.5F}{RT}\eta)} \end{aligned} \tag{10}$$

where C^{agg} (mol/m^3) is the gas concentration at the surface of the agglomerates; C_{ref} (mol/m^3) is the dissolved gas concentration at a reference state;; D^{agg} (m^2/s) is the diffusion coefficient of the dissolved gas inside the agglomerate; R^{agg} (m) is the agglomerate radius; j_0 (A/m^2) is the exchange current density; s (m^2/m^3) is the specific surface area; η (V) is the electrochemical over potential which is expressed by the potential difference between solid matrix and electrolyte and is defined as:

$$\begin{aligned} &Anode\ \text{side}: \eta = \phi_s - \phi_e\ ;\ \text{Cathode side}: \eta = \phi_s - \phi_e - U_{OC} \\ &\text{Open-Circuit Potential}: U_{OC} = 1.23 - 0.9\times10^{-3}(\text{T-298}) \end{aligned} \quad (11)$$

The dissolved gas concentration at the surface of the agglomerates is corresponding to the molar fraction in the gas phase through Henry's Law:

$$C^{agg} = \frac{C_{gas}P}{H} \quad (12)$$

Where H ($pa.m^3/mol$) is the Henry's constant.

2.3. Numerical Procedure

COMSOL Multiphysics, which is a commercial solver based on the finite element technique, is used to solve the governing equations. The stationary nonlinear solver is used since the source terms of the current conservation equation make the problem non-linear. Furthermore, the convergence behavior of this non-linear solver is highly sensitive to the initial estimation of the solution. To accelerate the convergence, the following procedures are adopted. The Conductive Media DC module is firstly solved based on the initial setting. Secondly, Darcy's Law and Incompressible Navier-Stokes modules are solved together using the results from the previous calculation as initial conditions. After the previous two modules converge, all the coupled equations including Maxwell-Stefan Diffusion and Convection module are solved simultaneously until the convergence is obtained.

3. Results and Discussion

Using the aforementioned procedures, the x-y geometry as described in Fig. 2(b) simulated in different voltages. The parameters values that used in this study are extracted from [13]. The x-y model represents the PEM fuel cell with interdigitaed channels on the bipolar plate. Fig.4 shows the current density curve obtained from the x-y model at the anode active layer for a given operation voltage of 0.7.

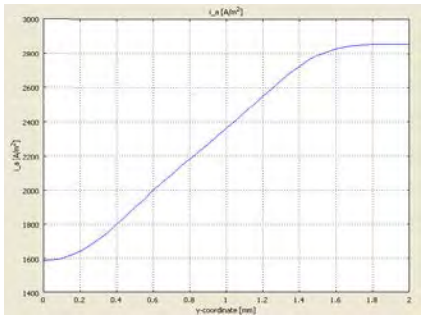

Fig.4. Current-density distribution at the anode active layer.

The current density is uneven with the highest density in the cell's upper region. This means that the oxygen-reduction reaction rate in the cathode determines the current-density distribution. The maximum current density arises close to the air inlet. Figure 5 shows the current distribution in the PEM fuel cell for a given operation voltages of 0.7 and 0.6. There are significant current spikes present at the corners of the current collectors and this trend will be more sensible at low voltages. The convective fluxes generally dominate mass transport in the cell. To study the convective effects, the velocity field is plotted in Fig.6. The flow-velocity magnitude attains its highest values at the current collector corners and it is more evident at lower operation voltages.

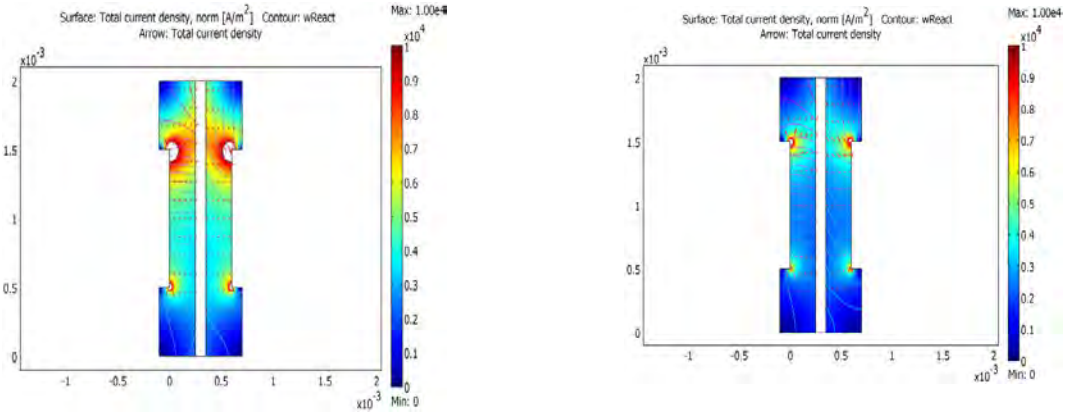

(a) 0.6 voltages *(b) 0.7 voltages*

Fig.5. Current density (surface plot) and current vector field (arrow plot).

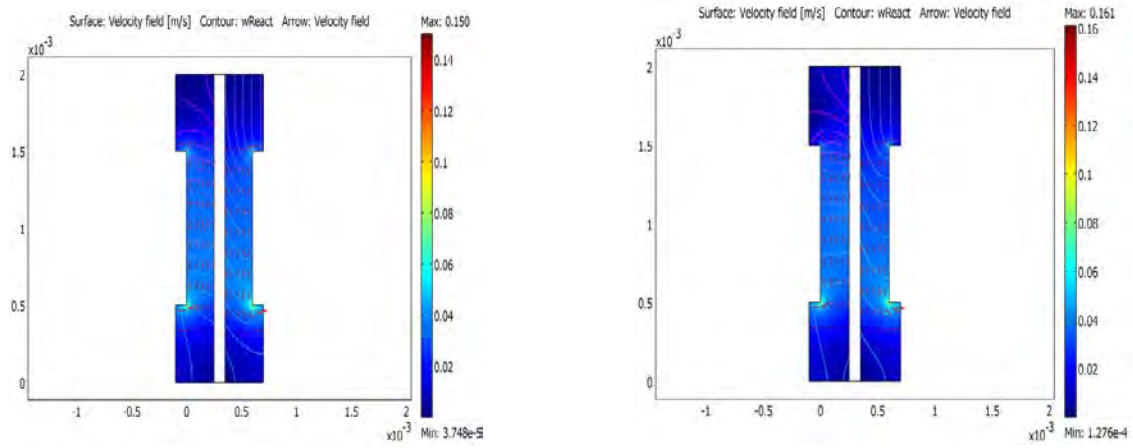

(a) 0.6 voltages *(b) 0.7 voltages*

Fig.6. Gas velocity field in the anode and cathode compartments.

Figure 7 shows the reactant (oxygen and hydrogen) weight fractions in the cathode and anode gases. It is interesting to note that the hydrogen fraction increases as the anode gas flows from the inlet (at the bottom) to the outlet (at the top). This is the result of the electro osmotic drag of water through the membrane, which results in a higher flux than the consumption of hydrogen. This means that the resulting convective flux of anode gas towards the membrane causes the weight fraction of hydrogen to go up. In the cathode gas, there is an expected decrease in oxygen content along the flow direction and a small change in the oxygen flow gives a substantial change in cell polarization. Figure 8 depicts the water mass fraction in the anode and cathode gases as well as the diffusive flux of water in the anode. It is clear that water is transported through diffusion and convection to the membrane on the anode side.

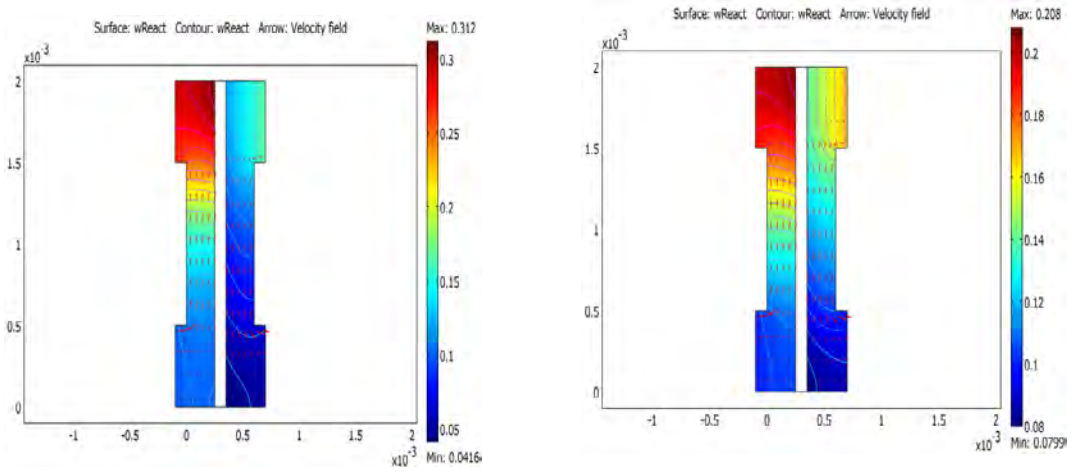

(a) 0.6 voltages *(b) 0.7 voltages*

Fig.7.Normolized Reactant mass fractions, on the anode side (left) and cathode side (right).

The results show a minimum occurs at the upper corner of the membrane on the anode side that limit fuel cell performance. If the anode gas becomes too much dry, the membrane dries out, resulting in a decrease in ionic conductivity and failure of fuel cell. On the other hand, at the cathode side the water levels increase with the direction of flow and a local maximum in water current occurs at the lower corner of the membrane. This may also be critical since the water droplets can clog the pores and effectively hinder gas transport to the active layer.

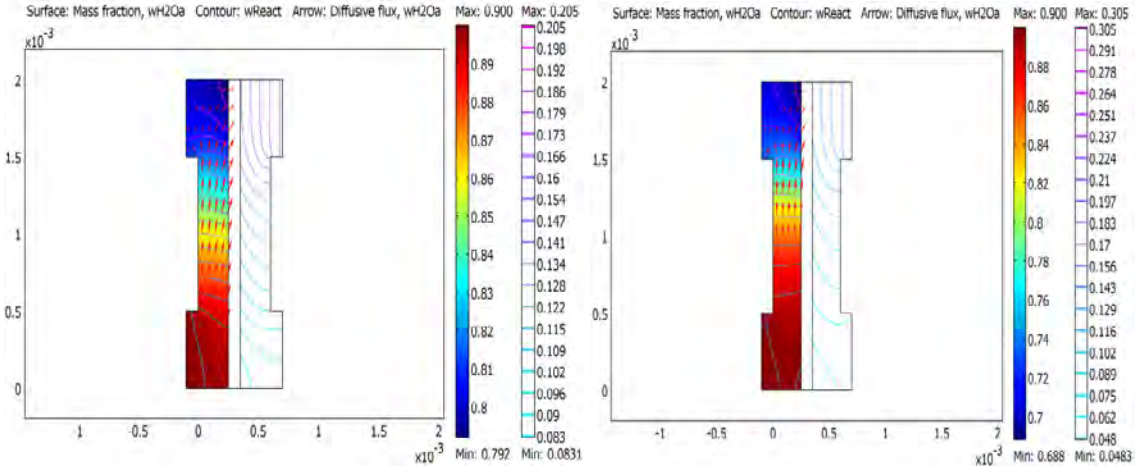

(a) 0.6 volt voltages *(b) 0.7 volt voltages*

Fig.8. Water mass fraction in the anode (left, surface plot) and the cathode (right, contour plot). The arrows visualize the diffusive flux vector field on the anode side.

4. Conclusion

Two-dimensional, single-phase and isothermal models of PEM fuel cells have been developed at two different operation voltages. The model is able to investigate the transport phenomena and electrical potential distribution for the various PEM fuel cell components including the gas channels, gas diffusion layers, catalyst layers and membrane. The current density curve has been presented. The x-y model used to study the fuel cell with interdigated channels design, shows that the fuel mass fraction decreases faster when the cell works at low voltage and high current density. The potential distribution indicates a major potential drop across the membrane. Moreover, a higher over potential on the cathode catalyst layer is noted. A minimum water mass fraction at upper corner of the membrane on anode side, reveals that

this phenomenon is more sensible at low voltages. The flow velocity magnitude attains its highest value at the current collector corners and it is more intensified at low voltages.

References

[1] N. Djilali, Computational modeling of polymer electrolyte membrane (PEM) fuel cells, Challenges and Opportunities Energy, 2006, pp.1006-1016.

[2] E.F. Cunha, A.B. Andrade, E. Robalinho, M.L.M. Bejarano, E. Cekinski, M. Linardi, Modeling and simulation of PEM fuel cell's flow channels us ing CFD techniques, Proceeding of International Nuclear Atlantic Conference, 2007, pp.107-123.

[3] P.T. Nguyen, T. Berning, N. Djilali, Computational model of P EM fuel cell with serpentine gas flow channels, Journal of Power Sources, 130, 2004, pp.149-157.

[4] S. Karvonen, T. Rottinen, J. Saarinen, O. Himanen, Modeling of flow field in polymer Electrolyte membrane fuel cell, Journal of Power Sources, 161, 2006, pp. 876-884.

[5] G. Squadrito, O. Barbera, I. Gatto, G. Giacoppo, F. Urbani, E. Passalacqua, CFD analysis of the flow field scale-up influence on the electrodes performance in a PEFC, Journal of Power Sources, 152, 2005, pp. 67-74.

[6] T.E. Springer, T.A. Zawodzinske, S. Gatteadold, Polymer Electrolyte Fuel Cell Model, Journal of Electrochem Soc., 138, 2000, pp. 2334-2342.

[7] V. Gurau, F. Barbir, H. Liu, An Analytical Solution of a Half-Cell Model for PEM Fuel Cell, Journal of the Electrochemical Society, 147, 2000, pp. 2468-2477.

[8] T. Berning, D.M. Lu , N. Djilali, Three-dimensional computational analysis of transport phenomena in a PEM fuel cell, Journal of Power Sources, 106, 2004, pp. 284-294.

[9] K. Haraldsson, K. Wipke, Evaluating PEM fuel cell system models, Journal of Power Sources, 126, 2004, pp. 88-97.

[10] D.J. Nelson, M.R. Spakovsky, Single domain PEMFC model based on Siegel Siegel agglomerate catalyst geometry, Journal of Power Sources, 115, 2003, pp. 81-89.

[11] A. Biyikoglu, Review of proton exchange membrane fuel cell models, International Journal of Hydrogen Energy, 30, 2007, pp. 1181-1212.

[12] K. Broka, Characterization of the Components of the Proton Exchange Membrane Fuel Cell, Technical licentiate Thesis, Royal Institute of Technology, Stockholm, Sweden, 1995, pp. 93-107.

[13] H. Meng, C.Y. Wang, Model of Two Phase Flow and Flooding Dynamics in PEMFC, Journal of the Electrochemical Society, 152, 2005, pp.1733-1741.

Effect of type and concentration of substrate on power generation in a dual chambered microbial fuel cell

A.A. Ghoreyshi[1,*], T.Jafary[1], G.D. Najafpour[1], F.Haghparast[1]

[1]*Chemical Engineering Department, Babol University of Technology, Babol, Iran*
** Corresponding author. Tel: 00981113234204, Fax: 00981113234204, E-mail: aa_ghoreyshi@nit.ac.ir*

Abstract: Microbial fuel cell, as a new technology for energy generation, has gained a lot of attention in converting a wide range of organic and inorganic substrates to bioelectricity in recent years. Substrate as the fuel of MFCs has an effective role on the performance of MFCs. To investigate the effect of type and concentration of substrate on the MFC performance, glucose and date syrup were examined over a concentration range of 2-20 $g.l^{-1}$. Date syrup or any waste of date could be used as a natural substrate while glucose is considered as a synthetic carbon source. In this research a two-rectangular chambered MFC separated by a Nafion 112 proton exchange membrane, was constructed. The anodic compartment was inoculated by *saccharomyces cerevisiae* as biocatalyst. 200 $\mu mol.l^{-1}$ of neutral red as the anodic mediator and 300 $\mu mol.l^{-1}$ of potassium ferricyanide as oxidizer were added to anode and cathode chambers, respectively. The results has shown that 3 $g.l^{-1}$ date syrup-fed- MFC had the highest power density, 51.95 $mW.m^{-2}$ (normalized to the geometric area of the anodic membrane, which was 9 cm^2), corresponding to a current density of 109.0384 $mA.m^{-2}$ and a MFC voltage of 967 mV.

Keywords: *Microbial fuel cell, Substrate, Glucose, Date syrup, Power density.*

1. Introduction

The microbial fuel cells convert the chemical content in organic and inorganic compounds to electricity via catalytic activity of microorganisms as the biocatalyst. Oxidation of substrate in anode chamber by microorganisms results in proton and electron production. Protons are transferred to cathode chamber through proton exchange membrane [1-3] . Depending on the type of electron transfer mechanisms, MFCs are categorized to two main groups, i.e. MFCs using mediator and mediator less MFCs [4].

Proton exchange system [5], electrode type and distance [6], temperature [7], pH [8], inoculums [9] and substrate [10, 11] as the main effective parameters on MFCs performance were investigated by many researchers. The substrate, as a key parameter, influences the integral composition of the bacterial community in the anode biofilm, and the MFC performance including the power density (PD) and Coulombic efficiency (CE) [12]. MFCs have been solely considered as a bioelectricity generation method, until different wastewaters were utilized as the fuel in anode chamber for the wastewater treatment [13]. Wide varieties of substrates ranging from pure compounds to complex mixture of organic matters present in wastewater have been used in MFCs as the carbon source for bioelectricity generation as well as wastewater treatment purposes. Acetate [14] and glucose [15] as the most common substrates, sucrose [16], xylose [17] and varios types of wastewater like synthetic [18], domestic [19], brewery [20], swine [21] and paper recycling wastewater [22] with different concentrations have been studied by many researchers. But it is difficult from literature to compare MFCs performances, due to different operating conditions such as surface area, type of electrodes and different microorganisms used. The main purpose of this article was to investigate the effect of two types of substrates, i.e. glucose and date syrup, as well as their concentration on the MFC electrical performance in a dual chambered fuel cell. Date is one of the main products of desert regions and its application as a substrate for MFCs in environmental biosensors in remote areas could be considered. A comparison was made by

the measurement of polarization curve under various concentrations for both types of substrates. Different concentrations ranging from 2- 20 $g.l^{-1}$ were chosen, while all other conditions kept constant.

2. Methodology

Saccharomyces cerevisiae PTCC 5269 was supplied by Iranian Research Organization for Science and Technology, Tehran, Iran. The microorganisms were grown in an anaerobic jar. The general medium for seed culture of both, Glucose-fed and date syrup-fed MFCs, consisted of yeast extract, NH_4Cl, NaH_2PO_4, $MgSO_4$ and $MnSo_4$: 3, 0.2, 0.6, 0.2 and 0.05 $g.l^{-1}$, respectively. Glucose and date syrup as the carbon sources were added to this medium in a range 1-20 $g.l^{-1}$. Due to high concentration of date syrup, date syrup was pretreated with different methods to break all its complex mixture to glucose. It was diluted, hydrolyzed with hydrochloric acid and then autoclaved for several times till getting constant sugar content. These processes convert all its sugar content to glucose. The medium then was sterilized, autoclaved at 121°C and 15psig for 20 min.

The medium pH was initially adjusted to 6.5 and the inoculum was introduced into the media at ambient temperature. The inoculated cultures were incubated at 30°C. The bacteria were fully grown for the duration of 24 hours in 100 ml flux without any agitation. Substrate consumption was calculated based on determination of the remained sugars in the culture. All chemicals and reagents used for the experiments were analytical grades and supplied by Merck (Germany). The pH meter, HANA 211(Romania) model glass-electrode was employed for the pH measurements of samples in the aqueous phase. The initial pH of the working solutions was adjusted by addition of dilute HNO_3 or 0.1M NaOH solutions. DNS reagent was developed to detect and measure substrate consumption using colorimetric method [23] and cell growth was also monitored by optical density using spectrophotometer (Unico, USA).

The fabricated cells in the laboratory scale were made of Plexiglas material. The volume of each chamber (anode and cathode chambers) was 800 ml with working volume of 600 ml (75% of total volume). The sample port was provided for the anode chamber, wire point inputs and inlet port. The selected electrodes in MFC were graphite felt in size of $50\times35\times2$ mm. Proton exchange membrane (PEM; NAFION 112, Sigma–Aldrich) was used to separate two compartments. The Nafion area separated the chambers was 3.79 cm^2. Nafion as a proton exchange membrane was subjected to a course pretreatment to take off any impurities that was boiling the film for 1h in 3% H_2O_2, washed with deionized water, 0.5 M H_2SO_4, and then washed with deionized water. The anode and cathode compartments were filled by deionized water when the biological fuel cell was not in use to maintain membrane for good conductivity. Natural Red and Ferricyanide were supplied by Merck (Germany). These chemicals in optimum concentrations (200 $\mu mol.l^{-1}$ & 300 $\mu mol.l^{-1}$) were used as mediators in anode and cathode of MFC, respectively.

S.cerevisiae used as a biocatalyst in microbial fuel cell for production of bioelectricity from carbohydrate source. This microorganism was grown under anaerobic condition in biofuel cell. Fixed incubation time and enriched media was used. The obtained data has shown that *S.cerevisiae* had good ability for consumption of substrate at anaerobic condition

The schematic diagram and illustration of the fabricated experimental set up with auxiliary equipments are shown in Fig. 1.

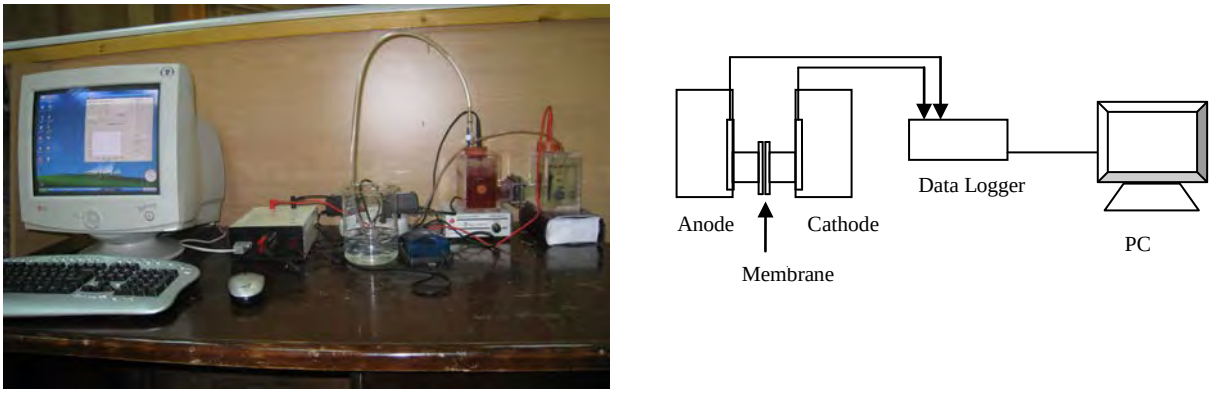

Fig. 1. The schematic diagram and illustration of the fabricated experimental set up with auxiliary equipments

3. Results and discussion

As the MFC were inoculated with *S.cerevisiae*, the voltage was continuously monitored by a data acquisition system to reach the constant open circuit voltage (OCV). It took 42, 57, 67, 65, 58, 48 and 30 hours for glucose with concentration of 1, 3, 5, 7, 10, 20 and 30 $g.l^{-1}$ to reach constant voltage of 922, 957, 970, 955, 920, 800mV respectively, These results were 64, 67, 72, 68, 64, 52 and 40 hours for the same concentrations of date syrup with the constant OCV of 988, 985, 948, 922, 916, 656 mV respectively. The results indicated that an increase in the substrate concentration increased the time needed to reach constant OCV at low concentration of 1-5 $g.l^{-1}$ for glucose and 1-3 $g.l^{-1}$ for date syrup.

Polarization curves were recorded by the data acquisition system after the mentioned time duration when the constant OCV was achieved. Fig. 2 shows polarization curves of the MFC at the glucose concentration range of 1-20 $g.l^{-1}$. As the glucose concentration increased from 1 to 5$g.l^{-1}$, power and current density gradually increased. However when the glucose concentration increased from 7 to 20$g.l^{-1}$, it was observed that the power and current density were considerably decreased. That was because the most of glucose remained unconsumed at high concentrations. The increase in time duration to reach constant OCV at low concentrations of 1-5 $g.l^{-1}$ for glucose and 1-3 $g.l^{-1}$ for date syrup, and subsequently the decrease at higher concentrations, 7-20 $g.l^{-1}$ for glucose and 5-20 $g.l^{-1}$ for date syrup, can be also attributed to the substrate inhibition effect. Indeed, all carbon sources available in the substrate solution at low concentrations were consumed resulted in longer time for attaining constant OCV. However as the substrate concentration increased, the constant OCV was achieved earlier with lower outputs, due to limitation in consuming carbon content in the substrate at higher concentration by microorganisms.

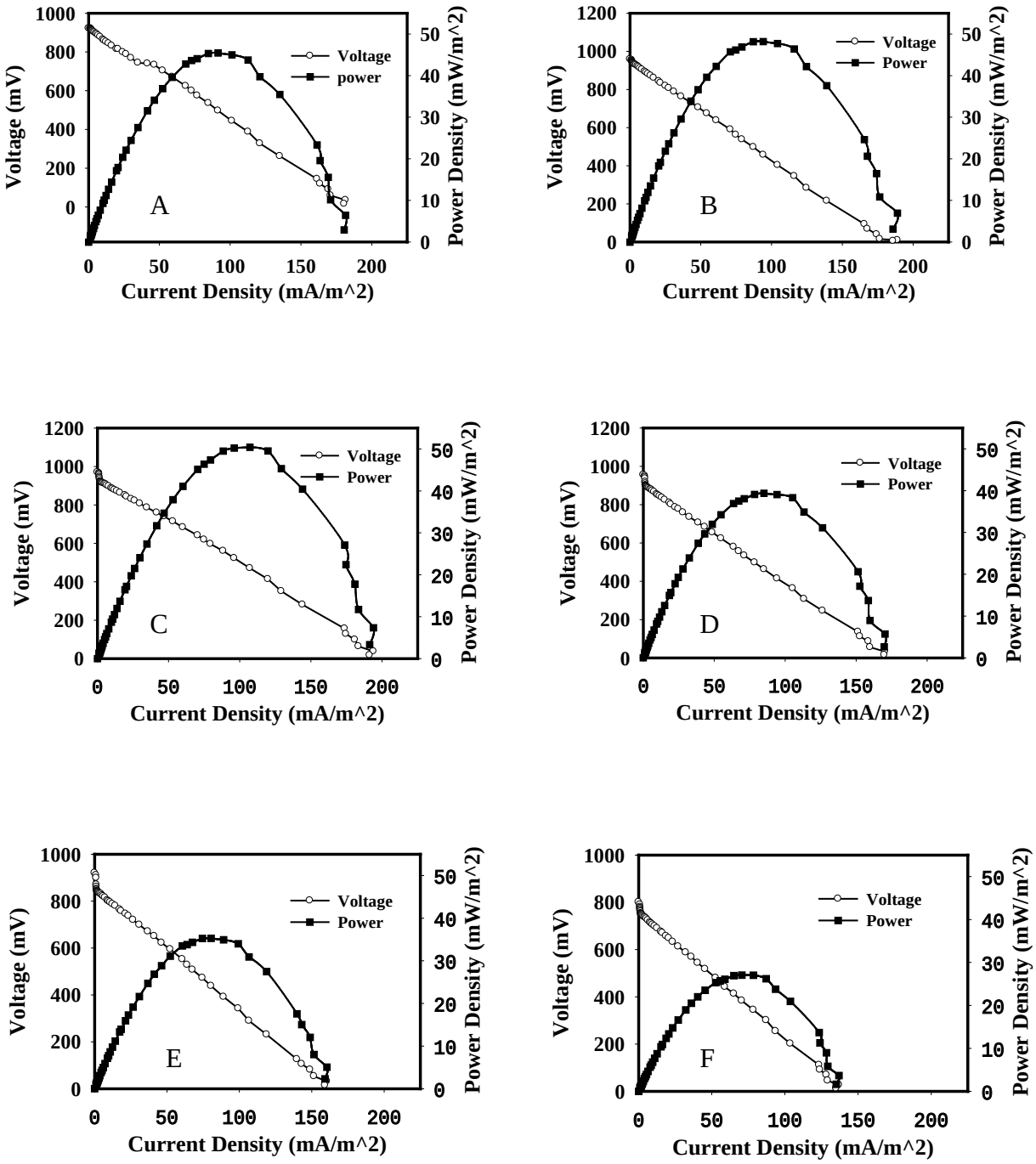

Fig. 1. Effect of different glucose concentrations on polarization curves
A) 1 g.l^{-1}, B) 2 g.l^{-1}, C) 5 g.l^{-1}, D) 7 g.l^{-1}, E) 10 g.l^{-1}, F) 20 g.l^{-1}

Fig. 3 shows polarization curves for the date syrup at the same concentration range. Comparing the results shown in Figure 2 and 3, the best results were achieved at the concentration 3 g.l^{-1} of date syrup with the maximum power 53.7031 mW.m^{-2} and current density 110.86 mA.m^{-2} .These results were followed by 5 g.l^{-1} of glucose (50.41 mW.m^{-2}, 107.16 mA.m^{-2}), 5 g.l^{-1} of date syrup (49.51 mW.m^{-2}, 195.19 mA.m^{-2}) , 3 g.l^{-1} of glucose (48.23 mW.m^{-2}, 94.16 mA.m^{-2}) and 1 g.l^{-1} of date syrup (47.36mW.m^{-2}, 104.12 mA.m^{-2}).

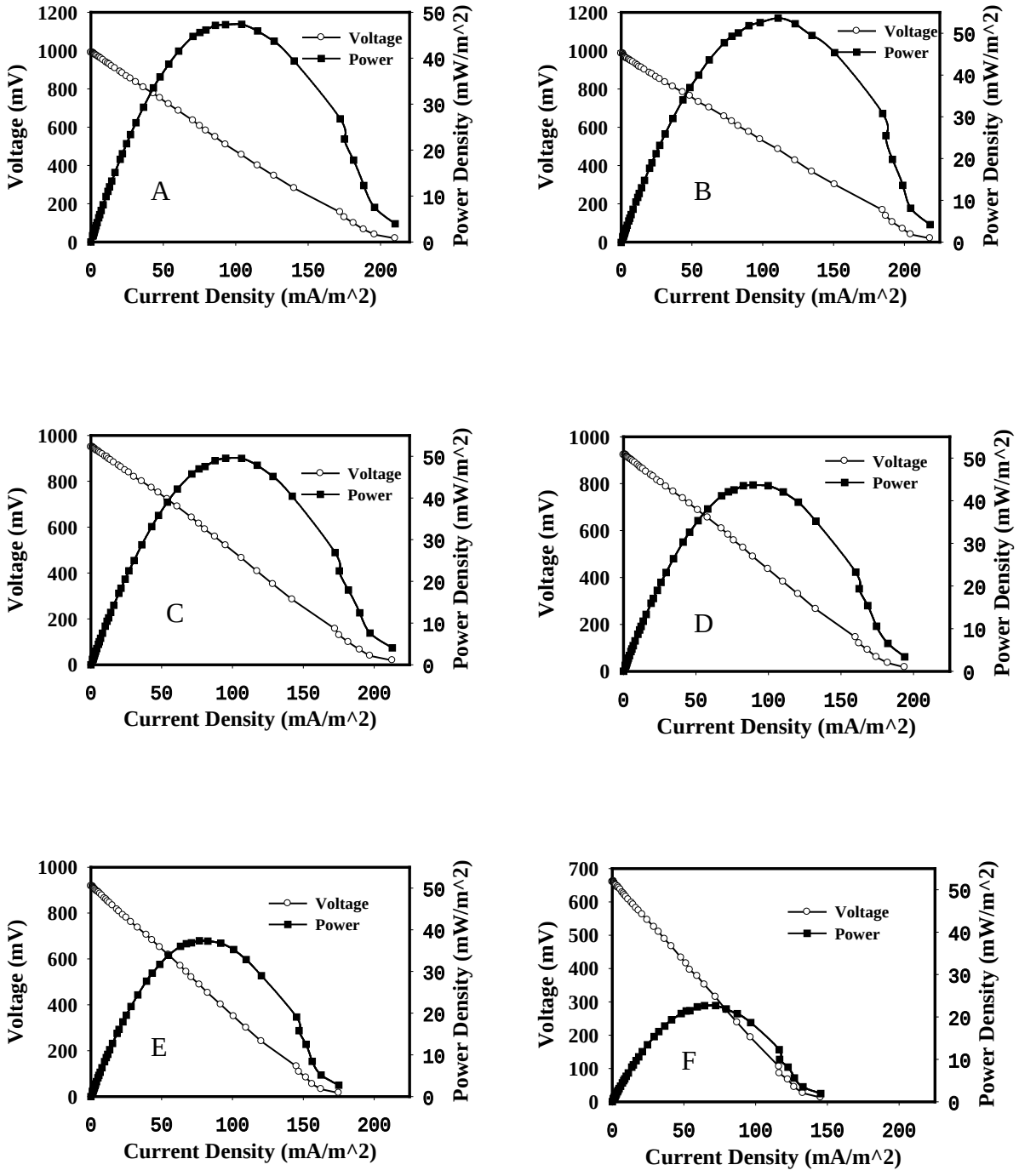

Fig. 3. Effect of different date syrup concentrations on polarization curves
1 g.l^{-1}, B) 2 g.l^{-1}, C) 5 g.l^{-1}, D) 7 g.l^{-1}, E) 10 g.l^{-1}, F) 20 g.l^{-1}

Fig. 4 compares the power and current output for the two types of substrates used in this study at their optimum concentration. The Figure indicates a superior electrical performance for the date syrup compared to the glucose.

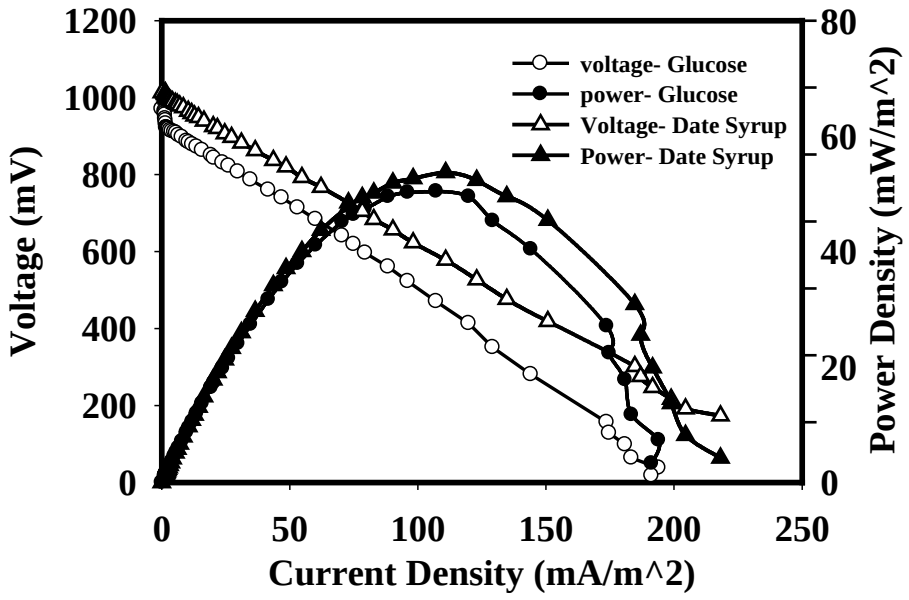

Fig. 4. Comparison of the MFC electrical performance working with glucose and date syrup as substrate at optimum concentration

4. Conclusions

In this study the effect of substrate type and concentration on the performance of microbial fuel cells was investigated. The glucose and date syrup were utilized as the carbon source for the production of electrical energy by means of *Saccharomyces cerevisiae* as the biocatalyst. Several concentrations of glucose and date syrup at the range of 1-20 $g.l^{-1}$ were experimented in a two-chambered fabricated MFC. The results revealed that the optimum concentration with the highest electrical performance were 3 $g.l^{-1}$ for date syrup and 5 $g.l^{-1}$ for glucose. Comparing the two types of substrates used in this study, date syrup has shown a superior electrical performance. The best results was achieved using the date syrup at optimum concentration of 3 $g.l^{-1}$ with the maximum power 53.7031 $mW.m^{-2}$ and current density 110.86 $mA.m^{-2}$. The results also indicated that the substrate inhibition effect may have a significant role in the performance of MFC at high concentration of glucose and date syrup.

References

[1] Z. D. Liu and H. R. Li, Effects of bio-and abio-factors on electricity production in a mediatorless microbial fuel cell, Biochemical Engineering Journal 36, 2007, pp. 209-214.

[2] M. S. Kim and Y. Lee, Optimization of culture conditions and electricity generation using Geobacter sulfurreducens in a dual-chambered microbial fuel-cell, International Journal of Hydrogen Energy 35, 2010, pp. 13028-13034.

[3] A. Larrosa, L. J. Lozano, K. P. Katuri, I. Head, K. Scott, and C. Godinez, On the repeatability and reproducibility of experimental two-chambered microbial fuel cells, Fuel 88, 2009, pp. 1852-1857.

[4] X. Tang, Z. Du, and H. Li, Anodic Electron Shuttle Mechanism Based on 1-Hydroxy-4-Aminoanthraquinone in Microbial Fuel Cells, Electrochemistry Communications 12, 2010, pp. 1140-1143.

[5] K. Chae, M. Choi, F. Ajayi, W. Park, I. Chang, and I. Kim, Mass Transport through a Proton Exchange Membrane (Nafion) in Microbial Fuel Cells†, Energy & Fuels 22, 2007, pp. 169-176.

[6] F. Li, Y. Sharma, Y. Lei, B. Li, and Q. Zhou, Microbial Fuel Cells: The Effects of Configurations, Electrolyte Solutions, and Electrode Materials on Power Generation, Applied biochemistry and biotechnology 160, 2010, pp. 168-181.

[7] A. Larrosa-Guerrero, K. Scott, I. M. Head, F. Mateo, A. Ginesta, and C. Godinez, Effect of temperature on the performance of microbial fuel cells, Fuel 2010, pp.

[8] Z. He, Y. Huang, A. K. Manohar, and F. Mansfeld, Effect of electrolyte pH on the rate of the anodic and cathodic reactions in an air-cathode microbial fuel cell, Bioelectrochemistry 74, 2008, pp. 78-82.

[9] I. Ieropoulos, J. Winfield, and J. Greenman, Effects of flow-rate, inoculum and time on the internal resistance of microbial fuel cells, Bioresource technology 101, 2010, pp. 3520-3525.

[10] K. Chae, M. Choi, J. Lee, K. Kim, and I. Kim, Effect of different substrates on the performance, bacterial diversity, and bacterial viability in microbial fuel cells, Bioresource technology 100, 2009, pp. 3518-3525.

[11] A. Thygesen, F. W. Poulsen, B. Min, I. Angelidaki, and A. B. Thomsen, The effect of different substrates and humic acid on power generation in microbial fuel cell operation, Bioresource technology 100, 2009, pp. 1186-1191.

[12] D. Pant, G. Van Bogaert, L. Diels, and K. Vanbroekhoven, A review of the substrates used in microbial fuel cells (MFCs) for sustainable energy production, Bioresource technology 101, 2010, pp. 1533-1543.

[13] W. Habermann and E. Pommer, Biological fuel cells with sulphide storage capacity, Applied microbiology and biotechnology 35, 1991, pp. 128-133.

[14] H. Liu, S. Cheng, and B. E. Logan, Production of electricity from acetate or butyrate using a single-chamber microbial fuel cell, Environ. Sci. Technol 39, 2005, pp. 658-662.

[15] S. Chaudhuri and D. Lovley, Electricity generation by direct oxidation of glucose in mediatorless microbial fuel cells, Nature Biotechnology 21, 2003, pp. 1229-1232.

[16] M. Behera and M. Ghangrekar, Performance of microbial fuel cell in response to change in sludge loading rate at different anodic feed pH, Bioresource technology 100, 2009, pp. 5114-5121.

[17] L. Huang, R. J. Zeng, and I. Angelidaki, Electricity production from xylose using a mediator-less microbial fuel cell, Bioresource technology 99, 2008, pp. 4178-4184.

[18] S. Venkata Mohan, G. Mohanakrishna, B. P. Reddy, R. Saravanan, and P. N. Sarma, Bioelectricity generation from chemical wastewater treatment in mediatorless (anode)

microbial fuel cell (MFC) using selectively enriched hydrogen producing mixed culture under acidophilic microenvironment, Biochemical Engineering Journal 39, 2008, pp. 121-130.

[19] X. Wang, Y. Feng, N. Ren, H. Wang, H. Lee, N. Li, and Q. Zhao, Accelerated start-up of two-chambered microbial fuel cells: Effect of anodic positive poised potential, Electrochimica Acta 54, 2009, pp. 1109-1114.

[20] Y. Feng, X. Wang, B. Logan, and H. Lee, Brewery wastewater treatment using air-cathode microbial fuel cells, Applied microbiology and biotechnology 78, 2008, pp. 873-880.

[21] B. Min, J. R. Kim, S. E. Oh, J. M. Regan, and B. E. Logan, Electricity generation from swine wastewater using microbial fuel cells, Water Research 39, 2005, pp. 4961-4968.

[22] L. Huang and B. E. Logan, Electricity generation and treatment of paper recycling wastewater using a microbial fuel cell, Applied microbiology and biotechnology 80, 2008, pp. 349-355.

[23] G. Chamberlin and G. Shute, Colorimetric chemical analytical methods, 1974

Bioelectricity power generation from organic substrate in a Microbial fuel cell using *Saccharomyces cerevisiae* as biocatalysts

T. Jafary[1], G.D. Najafpour[1,*], A.A. Ghoreyshi[1], F. Haghparast[1], M. Rahimnejad[1], H. Zare[1]

[1]*Biotechnology Research Lab., Faculty of Chemical Engineering, Noshirvani University, Babol, Iran,*
[*]*Corresponding author Email: najafpour@nit.ac.ir*

Abstract: In recent years, as a novel mode of converting organic matter into bioelectricity, Microbial fuel cells (MFCs) have gained significant attention. Among effective parameters in MFCs, substrate type and concentration play major role on MFC performance. In this study, a dual chamber MFC was used with a wide range of fructose concentrations: 10, 20 30 and 40 g/l. The MFC was inoculated with *Saccharomyces cerevisiae* as biocatalyst. A100µm of neutral red as mediator and also 100µm ferricyanide as oxidizer added to anode and cathode chambers, respectively. The MFC generated an open circuit voltage (OCV) of 690, 768, 548 and 507 mV with concentration of fructose from 10 to 40 $g.l^{-1}$, respectively. Maximum power density of 32.16, 23.7, 18.9 and 10.47 were obtained with substrate concentration of 10 to 40 $g.l^{-1}$, respectively. The maximum value of OCV and power density obtained with 10$g.l^{-1}$ of carbohydrate. To investigate resistance effect on MFC performance, for each substrate concentration data acquisition system was set at optimum value for the resistance which was resulted by the polarization curve. Then maximum power and optimum current density were recorded.

Keywords: *Bioelectricity, External resistance, Fructose, Microbial fuel cell, Saccharomyces cerevisiae*

1. Introduction

As fossil fuel sources are depleted, alternative energy sources are developed. Renewable energy is much eco-friendly such as biomass converted to fuel and energy in many alternative processes.

In the near future, the trends for new alternative renewable energies are gradually increasing.[1-4] Major efforts were devoted to develop alternative electricity generation methods.[5, 6] Among renewable alternatives, microbial fuel cell (MFC) created great interests for many researchers due to its possibility of directly harvesting electricity from organic wastes and renewable biomass.[7] MFC operates under very mild conditions and wide variable ranges of biodegradable materials are used as fuel.[8, 9] The bio base materials are oxidized by the microorganisms in the anode and the biocatalysts have the great potential to generate electrons. Biological systems possess number of advantages over the conventional chemical systems. Microbial fuel cell as the newest type of chemical fuel cells is a bioreactor that can generate electricity from what would be considered as organic wastes by means of microorganisms as biocatalysts. In this approach, bioelectricity generation and simultaneous waste treatment may take place in a cell; therefore the yield of newly developed system is much higher than any conventional processes. [10, 11]

A typical MFC consists of anodic and cathodic chambers partitioned by a proton exchange membrane (PEM). Microbes in the anodic chamber oxidize substrates and generate electrons and protons in the process. As an oxidative by-product, carbon dioxide is also produced. However, there is no net carbon emission because of the carbon dioxide originated from renewable biomass incorporated into photosynthetic process. Unlike in a direct combustion process, the electrons are absorbed by the anode and are transported to the cathode through an external circuit. After crossing a PEM or a salt bridge [12], the protons enter the cathodic chamber where they combine with oxygen to form water. Microbes in the anodic chamber generate electrons and protons in the dissimilative process of oxidizing organic substrates.[13, 14] Electric current generation is made possible by keeping microbes separated from oxygen

or any other end terminal acceptor other than the anode and this requires a separate anaerobic anodic chamber. In general, there are two types of microbial fuel cells: mediator and mediator-less microbial fuel cells.[15-18]

Among effective parameters on performance of microbial fuel cell, substrate type and concentrations had a significant effect on cell power.[19-22] The aim of this study was to investigate the effect of fructose, a monosaccharide that could be found in many fruit juices. Substrate concentrations were varied from 10 to 40 $g.l^{-1}$. Also, the influence of external resistance on production of bioelectricity in a dual chamber MFC was evaluated.

2. Methodology

Saccharomyces cerevisiae PTCC 5269 was supplied by Iranian Research Organization for Science and Technology (IROST), Tehran, Iran. The microorganisms were grown in an anaerobic jar. The prepared medium for seed culture consists of yeast extract, NH_4Cl, NaH_2PO_4, $MgSO_4$ and $MnSO_4$: 3, 0.2, 0.6, 0.2 and 0.05 $g.l^{-1}$, respectively. Fructose as carbon source was added to the medium with concentration in the range of 10-40 $g.l^{-1}$. The medium was sterilized, autoclaved at 121°C and 15psig for 20 min**.**

The medium pH was initially adjusted to 6.5 and the inoculums were introduced into the media at ambient temperature. The inoculated cultures were incubated at 30°C. The bacteria were fully grown for duration of 24 hours in 100 ml flask without any agitation. Substrate consumption was calculated based on determination of reduced sugars in the culture broth. All chemicals and reagents used for the experiments were analytical grades and supplied by Merck (Darmstadt, Germany). The pH meter, HANA 211(Romania) model glass-electrode was employed for pH measurements of the samples in aqueous phase. The initial pH of the working solutions was adjusted by addition of dilute HNO_3 or 0.1M NaOH solutions. DNS reagent was employed to detect and measure substrate consumption using colorimetric method and cell growth was also monitored by optical density using spectrophotometer (Unico, USA) at wave length of 620nm.

The fabricated cells in laboratory scale were made of Plexiglas material. The volume of each chamber (anode and cathode chambers) was 800 ml with working volume of 600 ml (75% of total volume). The sample port was provided for anode chamber, wire point inputs and inlet port. The selected electrodes in MFC were graphite felt in size of 50×35×2 mm. Proton exchange membrane (PEM; NAFION 112, Sigma–Aldrich) was used to separate two compartments. The Nafion area separated the chambers was 3.79 cm^2. Nafion as a proton exchange membrane was subjected to a course of pretreatment to take off any impurities. The membrane pretreatment started with boiling the film in 3% H_2O_2 for 1h, washed with deionized water, 0.5 M H_2SO_4, and then washed with deionized water. The anode and cathode compartments were filled by deionized water when the biological fuel cell was not in use to maintain and preserve the membrane for good conductivity. Natural Red and Ferricyanide were supplied by Merck (Germany). These chemicals with the concentrations of 100 $\mu mol.l^{-1}$ & 100 $\mu mol.l^{-1}$ were used as mediators in anode and cathode of MFC, respectively.

In the microbial fuel cell, *S. cerevisiae* was used as a biocatalyst for production of bioelectricity from carbohydrate source. This microorganism was grown under anaerobic condition in the biofuel cell. Fixed incubation time and enriched medium was used. The obtained data showed that *S. cerevisiae* had good ability to consume substrate under anaerobic

condition. The Fabricated cell for the experimental set up with auxiliary equipments is shown in Fig. 1.

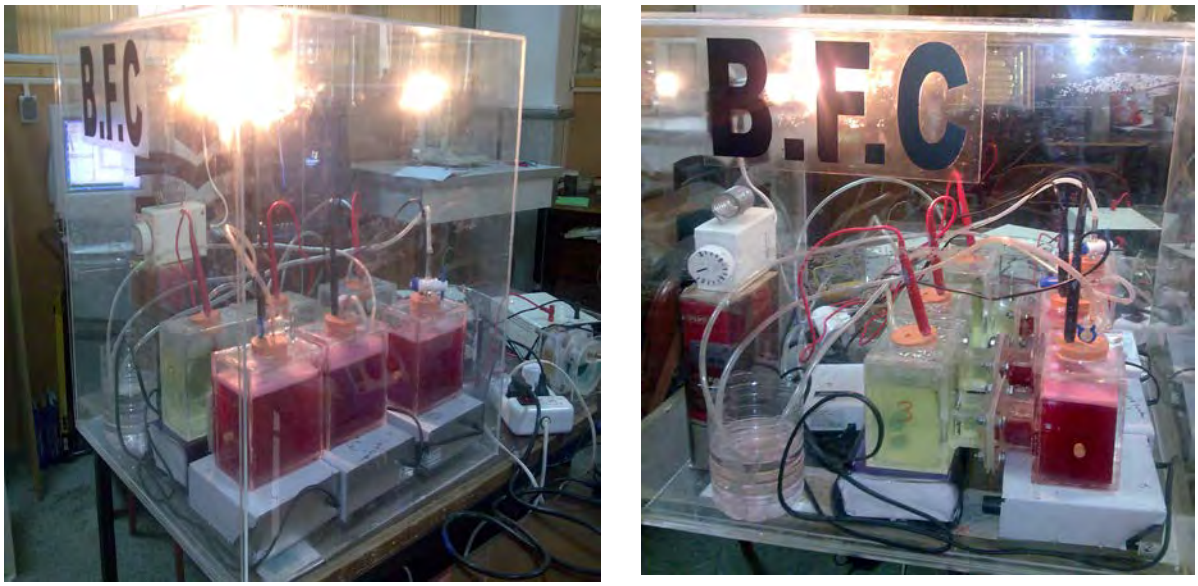

Fig. 1. The laboratory-scale MFCs with thermal controller in enclosed space

3. Result and Discussion

To start up the process, *S. cerevisiae* was inoculated into anode chamber. Fructose fed to microbial fuel cell with concentrations ranged from 10 to 40 $g.l^{-1}$. The output result in the form of open circuit voltage (OCV) was recorded by the data acquisition system. Biochemical activity of the microorganisms gradually increased electricity generation. At incubation time 64, 68, 59 and 57 hours after inoculation, the output OCV remained constant while the cell growth proceeded to stationary phase. The recorded voltages were 690, 768, 548 and 507 mV for 10, 20, 30 and 40 $g.l^{-1}$ of fructose, respectively. Due to stability of process operation after incubation time, the polarization curves were also recorded by data acquisition system in order to evaluate the performance of the MFCs. Fig. 2 shows the substrate concentration was increased (10 to 40 $g.l^{-1}$) the power and current density were decreased. With substrate concentration of 10 $g.l^{-1}$, maximum power and current density generated were 32.16 $mW.m^{-2}$ and 96.59 $mA.m^{-2}$, respectively.

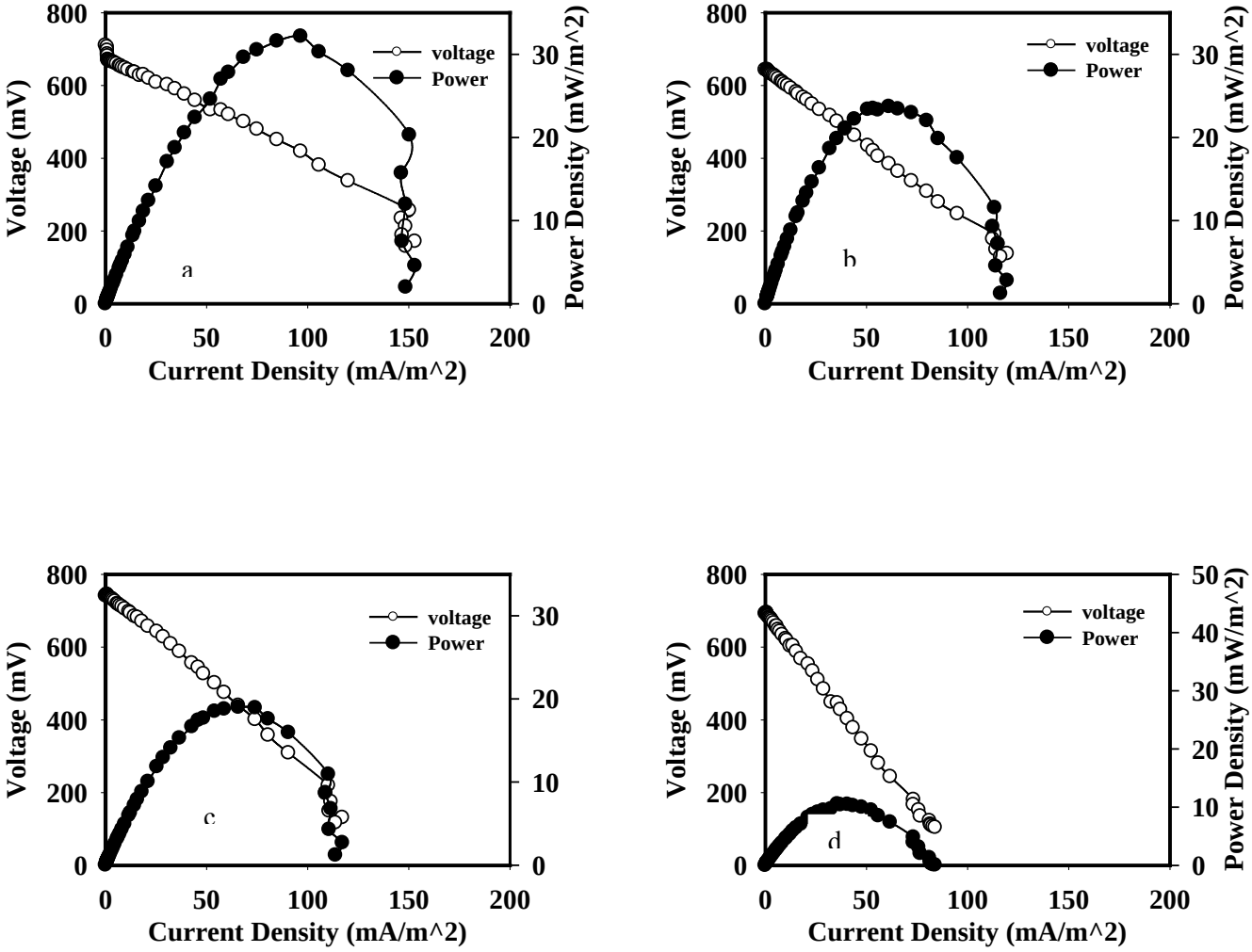

Fig. 2. Effect of different concentrations of fructose on polarization curves
a) 10 g.l^{-1}, b) 20 g.l^{-1}, c) 30 g.l^{-1}, d) 40 g.l^{-1}

As the electrical resistance applied to plot polarization curve varied in the range of 65535 to 0.1 kΩ, the pick point of the graph occurred at 3.88kΩ. Pick point demonstrated maximum power density and the optimum current density were proportional to applied resistance. The MFC performance is illustrated in Fig. 3. The cathode and anode of MFC were connected together through a circuit of 3.88kΩ as an external resistance. Due to presence of resistance, the power and voltage were considered as operational electricity (see Fig. 3).

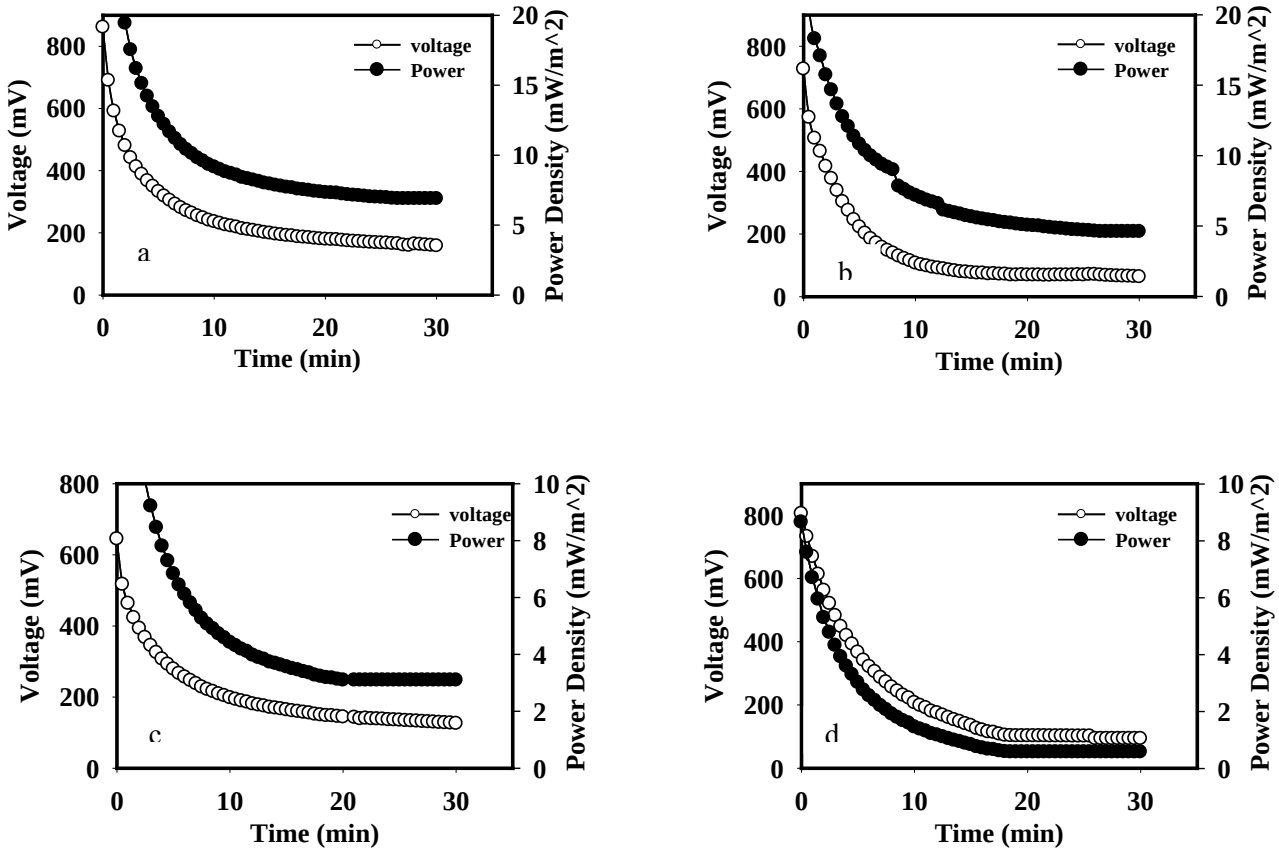

Fig. 3. Effect of external resistance on power density and voltage of MFC fed with a) 10 g.l^{-1}, b) 20 g.l^{-1}, c) 30 g.l^{-1} and d) 40 g.l^{-1} of fructose solution

The performance of MFC with respect to time was monitored. The voltage and power density in experimental runs for the course 30 minutes were obtained. In addition, current density was also recorded but due to complexity of presented plots the data are not shown. However the recorded data were averaged and summarized in Table 1.

Table1. Mean power and current density and mean voltage in presence of 3.88 kΩ as an external resistance

Fructose Concentration g.l^{-1}	Mean Power Density mW/m^{-2}	Mean Current Density mA/m^{-2}	Mean Voltage mV
10	11.26	56.25	196.02
20	9.8	39.17	248.2
30	5.86	36.88	165.7
40	2.3	15.86	145.9

4. Conclusions

The effect of substrate concentrations was investigated in a dual microbial fuel cell. Fructose was chosen as the simple carbon source with concentrations ranged from 1 to 40 $g.l^{-1}$. *S. cerevisiae* as the biocatalyst successfully oxidized the soluble substrate. The biocatalysts in the media with concentration of 10 $g.l^{-1}$ of substrate demonstrated the maximum power and optimum current density of 32.16 mW/m^{-2} and 96.59 mA/m^{-2}, respectively. The proportional resistance to the pick point of the polarization curve at 3.88 kΩ, was applied to the circuit as an external resistance in the operating system. The obtained averaged power and current density were 11.26 mW/m^{-2} and 56.26 mA/m^{-2}, respectively. The presented data were allocated to fructose with total sugar concentration of 10 $g.l^{-1}$.

References

[1] S. Meher Kotay and D. Das, Biohydrogen as a renewable energy resource--Prospects and potentials, International Journal of Hydrogen Energy 33, 2008, pp. 258-263.

[2] M. Dresselhaus and I. Thomas, Alternative energy technologies, Nature 414, 2001, pp. 332-337.

[3] R. Navarro, M. SЈnchez-SЈnchez, M. Alvarez-Galvan, F. Valle, and J. Fierro, Hydrogen production from renewable sources: biomass and photocatalytic opportunities, Energy & Environmental Science 2, 2009, pp. 35-54.

[4] M. Parikka, Global biomass fuel resources, Biomass and Bioenergy 27, 2004, pp. 613 - 620.

[5] A. Boudghene Stambouli and E. Traversa, Fuel cells, an alternative to standard sources of energy, Renewable and Sustainable Energy Reviews 6, 2002, pp. 295-304.

[6] B. Logan, Peer Reviewed: Extracting Hydrogen and Electricity from Renewable Resources, Environmental science & technology 38, 2004, pp. 160-167.

[7] D. Lovley, Microbial fuel cells: novel microbial physiologies and engineering approaches, Current opinion in biotechnology 17, 2006, pp. 327-332.

[8] M. Grzebyk and G. Pozniak, Microbial fuel cells (MFCs) with interpolymer cation exchange membranes, Separation and Purification Technology 41, 2005, pp. 321-328.

[9] F. Zhao, F. Harnisch, U. Schrder, F. Scholz, P. Bogdanoff, and I. Herrmann, Application of pyrolysed iron (II) phthalocyanine and CoTMPP based oxygen reduction catalysts as cathode materials in microbial fuel cells, Electrochemistry Communications 7, 2005, pp. 1405-1410.

[10] S. Patil, V. Surakasi, S. Koul, S. Ijmulwar, A. Vivek, Y. Shouche, and B. Kapadnis, Electricity generation using chocolate industry wastewater and its treatment in activated sludge based microbial fuel cell and analysis of developed microbial community in the anode chamber, Bioresource technology 100, 2009, pp. 5132-5139.

[11] H. Liu, R. Ramnarayanan, and B. Logan, Production of electricity during wastewater treatment using a single chamber microbial fuel cell, Environ. Sci. Technol 38, 2004, pp. 2281-2285.

[12] B. Min, S. Cheng, and B. Logan, Electricity generation using membrane and salt bridge microbial fuel cells, Water research 39, 2005, pp. 1675-1686.

[13] J. Jang, Construction and operation of a novel mediator-and membrane-less microbial fuel cell, Process Biochemistry 39, 2004, pp. 1007-1012.

[14] B. Logan and J. Regan, Electricity-producing bacterial communities in microbial fuel cells, TRENDS in Microbiology 14, 2006, pp. 512-518.

[15] H. Kim, H. Park, M. Hyun, I. Chang, M. Kim, and B. Kim, A mediator-less microbial fuel cell using a metal reducing bacterium, Shewanella putrefaciens, Enzyme and Microbial technology 30, 2002, pp. 145-152.

[16] G. Gil, I. Chang, B. Kim, M. Kim, J. Jang, H. Park, and H. Kim, Operational parameters affecting the performannce of a m ediator-less microbial fuel cell, Biosensors and Bioelectronics 18, 2003, pp. 327-334.

[17] D. Park and J. Zeikus, Electricity generation in microbial fuel cells using neutral red as an electronophore, Applied and environmental microbiology 66, 2000, pp. 1292.

[18] M. Nielsen, D. Wu, P. Girguis, and C. Reimers, Influence of Substrate on E lectron Transfer Mechanisms in Chambered Benthic Microbial Fuel Cells, Environmental science & technology 43, 2009, pp. 8671-8677.

[19] D. Pant, G. Van Bogaert, L. Diels, and K. Vanbroekhoven, A review of the substrates used in microbial fuel cells (MFCs) for sustainable energy production, Bioresource technology 101, pp. 1533-1543.

[20] J. Niessen, U. Schrder, and F. Scholz, Exploiting complex carbohydrates for microbial electricity generation-a bacterial fuel cell operating on starch, Electrochemistry Communications 6, 2004, pp. 955-958.

[21] M. Reddy, S. Srikanth, S. Mohan, and P. Sarma, Phosphatase and dehydrogenase activities in anodic chamber of single chamber microbial fuel cell (MFC) at variable substrate loading conditions, Bioelectrochemistry 77, pp. 125-132.

[22] Y. Zhang, B. Min, L. Huang, and I. Angelidaki, Electricity generation and microbial community response to substrate changes in microbial fuel cell, Bioresource technology 201.

Performance and economics of low cost clay cylinder microbial fuel cell for wastewater treatment

Siva Rama Satyam B[1], Manaswini Behera[1], Makarand M. Ghangrekar[1,*]

[1] *Department of Civil Engineering, Indian Institute of Technology, Kharagpur – 721302, India*
**Corresponding Author. Tel.:+91-3222-283440; Fax: +91-3222-282254*
E-mail: ghangrekar@civil.iitkgp.ernet.in

Abstract: Current wastewater treatment processes require large amount of power for various treatment units and most of the useful energy available in the wastewater remains unrecovered. With increase in demand for clean treatment technologies, Microbial Fuel Cell (MFC) technology is a viable option for treatment of wastewater, since simultaneous recovery of energy in the form of direct electricity with desired degree of treatment can be achieved in this process. Extensive research on MFCs is going on at laboratory scale but very few pilot scale studies have been reported. An attempt has been made to produce low cost scaled up MFCs fabricated using naturally available cheaper clay material as proton exchange membrane without involving any costly polymer membrane or noble metals for electrode fabrication. The results of the experimental study are promising and encouraging for further scaling up of MFCs.
Economic feasibility of MFCs for treating municipal wastewater having COD of 500 mg ·L-1 has been studied. The cost analysis shows that clay material may be suitable option as a membrane in scaling up of MFCs. It needs further study on strength of clay material as membrane to handle higher wastewater flows in larger reactor volume. Although, these clay MFCs were operated for more than six months, the life of this material without deteriorating its functional utility also need attention.

Keywords: *Earthen cylinder MFC, Proton exchange membrane, Power density*

1. Introduction

The global energy demand is increasing with exponential growth of population. Unsustainable supply of fossil fuels and the environmental concerns like air pollution and global worming associated with the use of fossil fuels are acting as major impetus for research into alternative renewable energy technologies. The high energy requirement of conventional sewage treatment systems are demanding for the alternative treatment technology which will require less energy for its efficient operation and recover useful energy to make this operation sustainable. In past two decades, high rate anaerobic processes such as up-flow anaerobic sludge blanket (UASB) reactors are finding increasing application for the treatment of domestic as well as industrial wastewaters. Although, energy can be recovered in the form of methane gas during anaerobic treatment of the wastewater, but utilization of methane for electricity generation is not attractive while treating small quantity of low strength wastewater and usually it is flared [1]. Therefore, other alternatives for simultaneous wastewater treatment with clean energy production are much desired.

Microbial fuel cell (MFC) is a promising technology for simultaneous treatment of organic wastewater and bio energy recovery in the form of direct electricity, which has gained much interest in recent years. Conventionally, MFC is made up of an anode chamber and a cathode chamber separated by a proton exchange membrane (PEM). MFCs are devices that use bacteria as the catalysts to oxidize organic matter and generate current. Electrons produced by the bacteria from the substrates i.e., organic matter present in wastewater in this case, are transferred to the anode. The electrons are transported to the cathode through an external circuit and protons are transferred through the membrane internally, where they utilize either oxygen to form water or other chemical oxidants to form reduced product.

The PEM used in MFC plays a substantial role in the power generation [2]. Despite of the rapid development of separators in recent years, there are limitations such as proton transfer limitation and oxygen leakage, which increase the internal resistance and decrease the MFC performance, and thus limit the practical application of MFCs [3]. Various materials are used by the researchers for separating anode and cathode chambers, including cation exchange membrane, anion exchange membrane, ultrafiltration membranes [4], bipolar membrane [5], microfiltration membrane [6], J-Cloth [7] and salt bridge [8], etc. The advances in separator materials and configurations have opened up new promises to overcome these limitations, but challenges remain for the practical full scale application of MFC for wastewater treatment using this material because of its high production cost and fouling of membrane expected requiring replacement. Recently successful treatment of synthetic and rice mill wastewater has been reported in MFC fabricated using earthen pot acting as membrane and its performance has been compared with MFC fabricated using Nafion membrane [9,10]. In terms of organic matter removal and power production it is reported that the earthen pot membrane MFC demonstrated better performance than the Nafion membrane MFC. Better performance of earthen cylinder MFC has been reported without employing commercially available PEM than that of MFC using Nafion as PEM [11]. Utilization of such low cost separator will drastically reduce production cost of MFC and it will help in enhancing its application for small wastewater treatment system.

Extensive research on MFCs is going on at laboratory scale but very few pilot scale studies have been reported. To bring this novel technology from laboratory to pilot scale, an attempt has been made for volumetric comparison of the performance of low cost mediator-less MFCs fabricated using naturally available cheaper clay material as proton exchange membrane instead of costly membrane and without using any catalysts. Economic feasibility of MFCs for treating municipal wastewater having COD of 500 mg $\cdot L^{-1}$ has been studied.

2. Methodology

2.1. Experimental set-up

The study was carried out in two laboratory scale up-flow dual chamber MFCs (MFC-1, MFC-2) with outer cathode chamber and inner cylindrical anode chamber without employing commercially available PEM. The anode chamber in both the MFCs was made up of earthen cylinder and the wall (5 mm thick) of the earthen cylinder itself was used as the medium for proton exchange. The working volume of anode chamber of MFC-1 and MFC-2 was 0.6 L and 3.75 L, respectively. The cathode chamber volume was 4.5 L and 16 L in MFC-1 and MFC-2, respectively. Earthen cylinder, made from locally available soil (elements present: Na-1.15 %, Mg- 1.52 %, Al-20.50 %, Si-53.52 %, K-4.74 %, Ca-1.15 %, Ti-0.94 %, Fe-16.48 %), was used in this study. The MFCs were operated under continuous mode. The wastewater was supplied to the MFCs from the bottom of the anode chamber with the help of peristaltic pump. The effluent leaving the anode chamber at the top was brought to the cathode chamber to work as catholyte, where it was given further aerobic treatment with the help of aerators. Stainless steel mesh having total surface area of 360 cm^2 and 2250 cm^2 was used as anode electrodes and graphite plates, having total surface area of 250 cm^2 and 1562.5 cm^2, was used as cathode electrodes in MFC-1 and MFC-2, respectively. The electrodes were connected externally with concealed copper wire through external resistance of 100 Ω.

2.2. MFC Operation

Synthetic wastewater containing sucrose as a source of carbon having chemical oxygen demand (COD) of about 500 mg $\cdot L^{-1}$ was used in this study. The sucrose medium was prepared using the composition given by Jadhav and Ghangrekar [12]. During start up, MFCs

were inoculated with anaerobic sludge collected from septic tank bottom after giving heat pretreatment [13] and required amount of sludge was added to the reactors to maintain the sludge loading rate at 0.1 kg COD ·kg VSS^{-1} ·d^{-1}. The influent feed pH was in the range of 7.2 to 7.8 throughout the experiments. These MFCs were operated at room temperature varying from 26 to 34°C. Both the MFCs were operated under continuous mode at hydraulic retention time (HRT) of 13 h and organic loading rate (OLR) of 0.923 kg COD ·m^{-3} ·d^{-1}.

2.3. Analyses and calculations

The suspended solids (SS), volatile suspended solids (VSS), and COD were monitored according to APHA standard methods [14]. The elemental composition of the earthen cylinder material was determined by Energy Dispersive X-ray analysis (EDX) scanning electron microscope with oxford EDX detector (JEOL JSM5800, Japan). The voltage and current were measured using a digital multimeter with data acquisition unit (Agilent Technologies, Malaysia) and converted to power according to $P = I*V$; where, P = power, I = current, and V = voltage (V). The Coulombic efficiency (CE) was estimated by integrating the measured current relative to the theoretical current on the basis of consumed COD [15]. Polarization studies were carried out at variable external resistances (10000-10 Ω) using 10 KΩ variable resistors. Internal resistance of the MFCs was measured from the slope of line from the plot of voltage versus current [16].

3. Results

3.1. Substrate degradation

The synthetic wastewater having COD of about 500 mg ·L^{-1} was treated anaerobically first in the anode chamber of the MFCs and further aerobic treatment was given to the anode chamber effluent in the cathode chamber. To achieve stable performance in terms COD removal efficiency MFC-1 took about 15 days and MFC-2 took about 13 days. Average COD removal efficiencies in the anode chambers of MFC-1 and MFC-2 were 77.5 ± 3.1% and 86.9 ± 2.65%, respectively. After aerobic treatment in the cathode chamber the total COD removal efficiencies of both MFC-1 and MFC-2 were 90.7 ± 4.2% and 93.12 ± 2.6%, respectively. The larger volume MFC (MFC-2) demonstrated higher COD removal efficiency when both the MFCs were operated at similar HRT and OLR. The higher COD removal could be due to better retention of sludge in larger reactor as compared to smaller reactor improving solid retention time, which favors higher substrate degradation rates.

3.2. Power generation

Electricity generation in both the MFCs increased gradually with time and got stabilized. Maximum open circuit voltage (OCV) of 0.698 V and maximum short circuit current (SC) of 6.04 mA were observed in MFC-1. Maximum OCV of 0.776 V and maximum SC of 27.6 mA were obtained in MFC-2. The average electrical output from these MFCs is presented in the Table 1. Sustainable power density (normalized to the anode surface area) of 12.84 mW m^{-2} and volumetric power (normalized to the working volume of anode chamber) of 770 mW ·m^{-3} (2.15 mA, 0.215 V) were generated at 100 Ω external resistance in MFC-1. MFC-2 generated sustainable power density and volumetric power of 12.11 m W ·m^{-2} and 727 mW ·m^{-3}, respectively. Sustainable volumetric current density with respect to working volume of anode chamber achieved in MFC-1 and MFC-2 were 3.6 A ·m^{-3} and 1.4 A ·m^{-3}, respectively. Maximum Coulombic efficiency of 5.43 % and 4.49 % was achieved in MFC-1 and MFC-2, respectively.

Table 1. Power generation in the MFCs at OLR of 0.923 kg COD ·m^{-3} ·d^{-1}

MFC	OCV (V)	SC (mA)	Voltage across 100 Ω (V)	Current density with 100 Ω (A ·m^{-3})	Power density with100 Ω (mW ·m^{-2})	Power/vol .with 100 Ω (mW ·m^{-3})	Max. Power/ vol. at optimum resistance (W ·m^{-3})	Internal resistance (Ω)
MFC-1	0.692	4.9	0.215	3.6	12.84	770.4	0.96	212.0
MFC-2	0.767	21.9	0.522	1.4	12.11	726.9	1.00	44.3

Although, the larger volume MFC (MFC-2) demonstrated slightly lower CE (4.49 %) as compared to MFC-1 (CE of 5.43 %), the volumetric power produced in both these MFCs was similar. This was due to 143 % higher working voltage demonstrated by MFC-2. This higher working voltage observed in MFC-2 could be due to higher working volume and hence having higher surface area of electrodes improving capacitance of the system. Also, the higher cathode surface area might have favored better cathodic reaction by reducing cathodic overpotential and improving voltage produced by this MFC as compared to MFC-1 with lower cathode surface area. Since oxygen is terminal electron acceptor in cathode, reduction of oxygen on cathode surface can occur in two different mechanisms at 25°C as:

$$O_2 + 4H^+ + 4e^- \longrightarrow 2H_2O \ (E_0 = 0.816 \text{ V})$$

$$2O_2 + 4H^+ + 4e^- \longrightarrow 2H_2O_2 \ (E_0 = 0.295 \text{ V})$$

Cathode potentials in MFC-1 and MFC-2 were 210 mV and 330 mV without employing any noble catalysts. The typical measured cathode potentials using oxygen as terminal electron acceptor is around 200 mV [15]. The higher cathode potential observed demonstrates the better performance of graphite plate cathode while using earthen material as membrane.

3.3. Polarization and internal resistance

Polarization studies were carried out for the MFCs by varying external resistance from 10000 Ω to 10 Ω. Maximum power densities observed during polarization were 15.97 mW ·m^{-2} at external resistance of 234 Ω in MFC-1 and 16.74 mW ·m^{-2} at external resistance of 45.5 Ω in MFC-2 (Fig. 1). Internal resistance of the MFCs measured from the slope of line from the voltage versus current plot of MFC-1 and MFC-2 were 212 Ω and 44.3 Ω, respectively. In spite of 6.25 times larger surface area of anode provided in MFC-2, it demonstrated slightly higher power density than the MFC-1 provided with lower anode surface area. Also, the larger MFC demonstrated very low internal resistance as compared to smaller MFC, indicating better substrate diffusion and less internal losses in larger MFC. This is particularly encouraging for scaling up of MFC and provides a scope for further increase in anode volume and surface area to obtain similar power density. This experience has demonstrated that, if properly designed, similar energy recovery efficiency can be obtained from the larger MFCs. This will facilitate reducing number of MFCs, to treat same wastewater volume or produce desired power, thus reducing its production cost and also operating complications and cost.

3.4. Cost Analysis for MFC

Preliminary cost analysis for MFCs treating municipal wastewater having COD of 500 mg ·L^{-1} with anode chamber volume of 20 liters and hydraulic retention time of 10 hours was performed. For 1 m^3 of wastewater treatment per day number of MFCs required are 21 and each will be treating wastewater flow rate of 48 L ·d^{-1}. With assumed COD removal efficiency of 75 %, cell voltage of 0.5 V and CE of 30 %, the power obtained from each cell is 0.3 W.

Reversal of voltage in stack of cells is not considered and maintenance cost of the cells and pumping costs are not included in the cost comparison. For treating wastewater flow of 1000 $m^3 \cdot d^{-1}$, total power achieved from MFC plant is 7.9 KW. Maximum power available in this wastewater is calculated based on 1g COD = 14.7 kJ [17]. Fig. 2 presents the power likely to be harvested from the MFCs treating 1000 $m^3.d^{-1}$ of wastewater flow rate at different Coulombic efficiencies. There is lot of scope for MFC to improve because from the theoretical calculations of power production at different flow rates with assumed voltage of 0.5 V, maximum power achieved from MFCs is 23.6 kW at CE of 90% and at flow rate of 1000 $m^3 \cdot d^{-1}$. Maximum power available in wastewater at similar conditions is 63.8 kW.

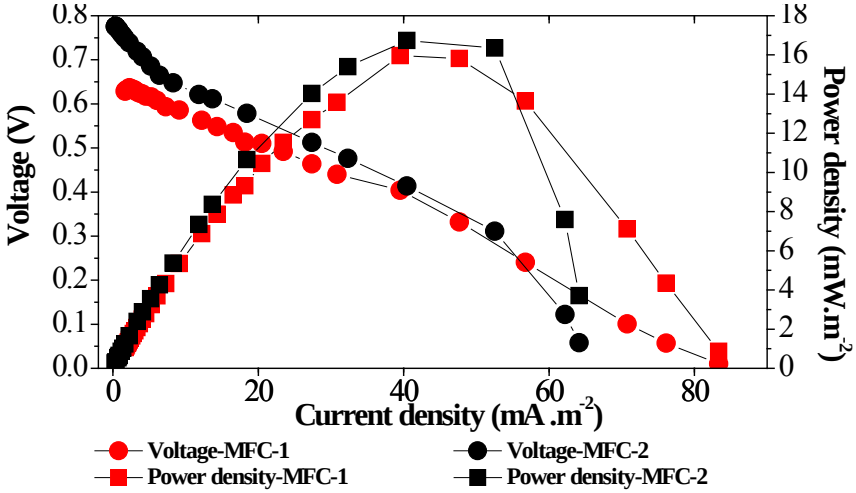

Fig. 1. Polarization curves for MFC-1 and MFC-2

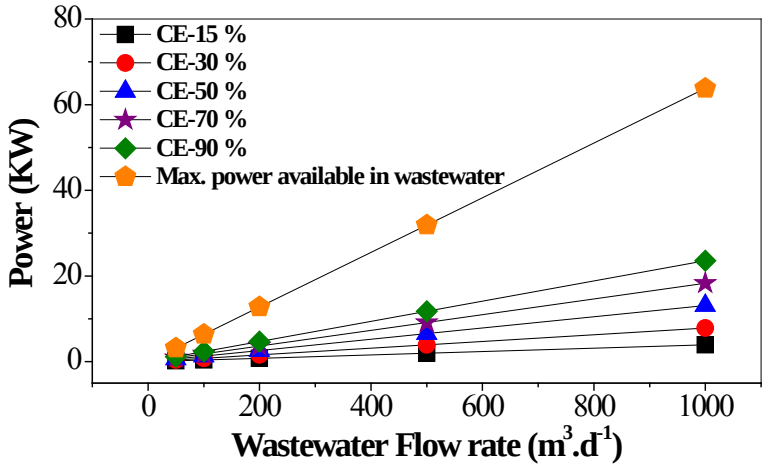

Figure 2 : Power achieved from the MFC treatment plant at different CE and different wastewater flowrates with assumed voltage obtained from each cell of 0.5 V and COD removal efficiency of 75 %.

The materials considered for cell construction are Stainless Steel (SS) mesh as electrode for both anode and cathode, Sintex[R] pipe for anode and cathode chamber in case of nafion membrane where 12 slits of 8 cm x 10 cm were considered on the circumference of anode chember wall for nafion membrane insertion (6 in bottom half and 6 in top half of anode chamber). In the second case, hollow cylindrical earthen pot was considered for fabrication of anode and the pot material acting as a membrane separating anode and cathode and Sintex[R] pipe was considered for fabrication of cathode chamber. Cost of each of these materials considered in this study is according to the prevailing Indian market. The approximate costing

of the MFCs for treatment of different wastewater flows is presented in the Table 2. MFC with earthen material as membrane is a sustainable option for its application in wastewater treatment because of low cost (79 % cost reduction compared to Nafion as membrane) and comparable power generation and treatment efficiency in terms of COD removal than Nafion as membrane. In addition to this no c hemical mediators are considered in this study to enhance the power production.

Table 2. Total capital cost comparison of MFC plant at different flow rates of wast water

Flow of wastewater ($m3 \cdot d^{-1}$)	Cost of MFC cells with Nafion membrane (Rupees)	Cost of MFC cells with earthen pot as membrane (Rupees)	% of cost reduction with earthen material than Nafion
1000	159,106,828	32,750,000	79
500	79,553,414	16,375,000	79
200	31,821,366	6,550,000	79
100	15,910,683	3,275,000	79
50	7,955,341	1,637,500	79

4. Discussions

The overall COD removal efficiency of both the MFCs were more than 90%, which demonstrates the feasibility of this configuration of MFC as an effective wastewater treatment technology and ensures better reliable effluent quality. It was observed that the power generation in the MFC did not change significantly when the volume of the reactor was increased from 0.6 L to 3.75 L. This result demonstrates that there is further scope in increasing the reactor size.

Jana et al. [11] have reported sustainable power density of 48.30 m W $\cdot m^{-2}$ in an MFC employing earthen cylinder of 0.6 L capacity as anode chamber. The power generated in MFC-1 was lower than that obtained by Jana et al. [11]. MFC-1 was in operation over 6 months prior to present study. The reduction in power generation might be due to fouling of earthen cylinder used as separator and decrease in the porosity of the earthen material, which probably has reduced the proton transfer and also due to the reuse of old graphite plate's electrodes. Recently we observed that by polishing the surfaces of graphite plates increased the power generation.

The internal resistance and overpotential losses of MFC-2 are less than MFC-1 which motivates further scaling up of microbial fuel cells with earthen cylinder as PEM. The study was carried out with synthetic wastewater. It needs further study on strength of clay material as membrane for higher wastewater flows and higher reactor volumes. The life of this material without deteriorating its functional utility also needs attention.

Rozendal et al. [18] have compared the anticipated costs of MFCs with the capital costs of the two most widely used conventional wastewater treatment systems, i.e., activated sludge treatment and anaerobic digestion. This comparison shows that, based on t he materials currently used in the laboratory, the capital costs of a full scale bioelectrochemical systems would be orders of magnitude higher than those of conventional wastewater treatment systems. The capital cost might be reduced significantly by improving the design and employing innovative materials, but because of the inherently complex design of bioelectrochemical systems, it is expected that the capital cost will always remain several times that of conventional wastewater treatment systems. However, for smaller wastewater flow such as from individual house or from the small group of housing, the cost of MFC may

become comparable with the other treatment methods and the advantage of direct electricity generation for powering certain onsite appliances can be gained. Also, this process can be best utilized for treatment of wastewater in remote area and generating the power in the form of direct electricity. Thus, the advantage of making electricity available can be utilized along with wastewater treatment in the remote area which is not connected with the electric grid.

The major drawback in MFC as compared to other processes is smaller volume required for anode chamber. Whatsoever the volume of anode, it will deliver maximum voltage of about 0.7 V and hence, smaller anode volume is desirable for integrating voltage by putting several MFCs in series. Whereas the single large anode of volume equal to that of summation of anode volumes in series will produce only about 0.7 V. Hence, while scaling up a trade-off need to be maintained while finalizing anode volume between the voltage and current recovered. If larger volume MFCs is able to demonstrate similar CE as smaller MFCs, higher current can be recovered from the MFC to maintain similar volumetric power densities. Therefore while scaling the geometrical arrangement and relative positions of the electrodes should be decided in such a way to obtain maximum Coulombic efficiency. Such large size MFCs will then be able to compete with the established alternative wastewater treatment processes in terms of capital investments.

5. Conclusions

Clay material was found to be a cheaper alternative to more commonly used expensive Nafion membrane in MFCs. It needs further study on strength of clay material as membrane for higher wastewater flows and higher reactor volumes. Although, these clay MFCs were operated for more than six months, the life of this material without deteriorating its functional utility also need attention. It remains to be demonstrated whether the results from this liter scale MFC can be extrapolated to more realistic scales for industrial applications. Full scale implementation of bioelectrochemical system is not straightforward as it includes certain microbiological, technological and economic challenges, which need to be resolved that have not previously been encountered in any other wastewater treatment systems.

Acknowledgement

The Grant received from the Ministry of Environment and Forest, Government of India (F. No. 19-35/2005-RE) is duly acknowledged.

References

[1] M.M. Ghangrekar, V.B. Shinde, Wastewater treatment in microbial fuel cell and electricity generation: a sustainable approach. Proceedings of 12th international sustainable development research conference, 2006, Hong Kong, pp. 1-9.

[2] Z. Du, H. Li, T. Gu, A state of the art review on microbial fuel cells: A promising technology for wastewater treatment and bioenergy, Biotechnology Advances, 25, 2007, pp. 464-482.

[3] W.W. Li, G.P. Sheng, X.W. Liu, H.Q. Yu, Recent advances in the separators for microbial fuel cells, Bioresource Technology, 102, 2011, pp. 244–252.

[4] J.R. Kim, S. Cheng, S.E. Oh, B.E. Logan, Power generation using different cation, anion, and ultrafiltration membranes in microbial fuel cells, Environmental Science and Technology, 41, 2007, pp. 1004-1009.

[5] A. Terheijne, H.V.M. Hamelers, V.D. Wildie, R.A. Rozendal, C.J.N. Buisman, A bipolar membrane combined with ferric iron reduction as an efficient cathode system in microbial fuel cells, Environmental Science and Technology, 40, 2006, pp. 5200-5206.

[6] J. Sun, Y. Hu, Z. Bi, Y. Cao, Simultaneous decolorization of azo dye and bioelectricity generation using a microfiltration membrane air-cathode single-chamber microbial fuel cell, Bioresource Technology, 100, 2009, pp. 3185–3192.

[7] Y. Fan, H. Hu, H. Liu, Enhanced Coulombic efficiency and power density of air-cathode microbial fuel cells with an improved cell configuration, Journal of Power Sources, 171, 2007, pp. 348–354.

[8] B. Min, S. Cheng, B.E. Logan, Electricity generation using membrane and salt bridge microbial fuel cells, Water Research 39, 2005, pp.1675-1686.

[9] M. Behera, P. S. Jana, M.M. Ghangrekar, Performance evaluation of low cost microbial fuel cell fabricated using earthen pot with biotic and abiotic cathode, Bioresource Technology, 101, 2010, pp.1183-1189.

[10] M. Behera, P. S. Jana, T. T., More, M.M. Ghangrekar, Rice mill wastewater treatment in microbial fuel cells fabricated using proton exchange membrane and earthen pot at different pH, Bioelectrochemistry, 79, 2010, pp. 228-233.

[11] P. S. Jana, M. Behera, M.M. Ghangrekar, Performance comparison of up-flow microbial fuel cells fabricated using proton exchange membrane and earthen cylinder, International Journal of Hydrogen Energy, 35, 2010, pp. 5681-5686.

[12] G.S. Jadhav, M.M. Ghangrekar, Improving performance of MFC by design alteration and adding cathodic electrolytes, Applied Biochemistry and Biotechnology, 2008, 151, pp. 319-332.

[13] M.M. Ghangrekar, V.B. Shinde, Performance of membrane-less microbial fuel cell treating wastewater and effect of electrode distance and area on electricity production, Bioresource Technology, 98, 2007, pp. 2879-2885.

[14] APHA, AWWA, WPCF, Standard methods for examination of water and wastewater, Washington, D.C., 20th Ed., 1998.

[15] B.E. Logan, B. Hamelers, R. Rozendal, U. Schroder, J. Keller, S. Freguia, P. Aelterman, W. Verstraete, K. Rabaey, Microbial fuel cells: methodology and technology, Environmental Science and Technology, 40, 2006, pp. 5181-5192.

[16] C. Picioreanu, I.M. Head, K.P. Katuri, M.C.M. van Loosdrecht, K. Scott, A computational model for biofilm-based microbial fuel cells, Water Research 41, 2007, pp. 2921-2940.

[17] I. Shizas, D.M. Bagley, Experimental determination of energy content of unknown organics in municipal wastewater streams, Journal of Energy Engineering, 130, 2004, pp. 45-53.

[18] R.A. Rozendal, H.V.M. Hamelers, K. Rabaey, J. Keller, C.J.N. Buisman, Towards practical implementation of bioelectrochemical wastewater treatment, Trends in Biotechnology, 26, 2008, pp. 450-459.

Development of laccase and manganese peroxidase biocathodes for microbial fuel cell applications

Sahar Bakhshian[1], Hamid-Reza Kariminia[1,*]

[1] *Department of Chemical and Petroleum Engineering, Sharif University of Technology, Tehran, Iran*
** Corresponding author. Tel: +98 21 66166426, Fax: +98 21 66166426, E-mail: kariminia@sharif.ir*

Abstract: In this study, we ivestigated how microbial fuel cell (MFC) performance can be affected by laccase and manganese peroxidase (MnP) enzymes as catalysts in the cathode compartment. Commercial laccase was immobilized by crosslinking on chitosan using glutaraldehyde. Immobilized enzyme was settled on graphite electrode previously covered with polymerized methylene blue. Application of this enzymatic electrode was investigated in the cathode chamber of a MFC. Output power density of the MFC in the mentioned situation was 100% higher than that for the graphite electrode. The MnP was first, produced from a white rot fungus isolate and was immobilized on the graphite electrode via adsorption. This modified electrode with MnP was utilized as cathode. The fuel cell with MnP modified graphite electrode and H_2O_2 as oxidizer yielded the maximum power density of 46 mW/m^2 at the current density of 109 mA/m^2. This augmentation of MFC performance was due to a higher cathode electrode potential with H_2O_2 rather than oxygen. The most important function of MnP was to catalyze the reduction of H_2O_2 and hence diminished activation overpotential loss of the cathode.

Keywords: *Biocathode, Laccase, Manganese peroxidase, Microbial fuel cell*

1. Introduction

Microbial fuel cells are devices that generate electricity by oxidation of organic substrates using bacterial metabolism. This technology is considered as a non-polluting and a new source of renewable energy [1,2,3].

Oxygen is a preferable oxidant in the cathode compartment of MFC because of its availability and its environmental friendly reduction product *i.e.* water [4]. Platinum has been applied as main catalyst to improve oxygen reduction rate in the cathode chamber; but it imposes high cost on MFC construction [5].

Application of biocatalysts as an inexpensive alternative to platinum is a potential solution [4]. Application of these components under moderate (ambient) temperatures and neutral pH are the main advantages of them over conventional catalysts [6]. Laccase, bilirubin oxidase and peroxidase like manganese peroxidase (MnP) has been used as biocatalysts in cathode of a MFC [6,7].

Laccase (E.C. 1.10.3.2, *p*-benzenediol: oxygen oxidoreductase) is a multi-copper oxidase enzyme in plants, fungi and some bacteria which can catalyze the oxidation of phenolic and other aromatic compounds resulting in four-electron reduction of oxygen to water [8]. The active site of laccase contains four cooper atoms as redox centers, classified in three types, T_1, T_2 and T_3. The T_1 site is reduced by oxidation of substrate or involving in polarized electrode. Four electrons are transferred from T_1 site to T_2 and T_3 sites where, O_2 is reduced to H_2O [9,4]. Palmore et al. have studied the application of fungal laccase in the cathode compartment of a dihydrogen/dioxygen biofuel cell. Reduction of dioxygen to water with laccase was mediated by redox mediator, 2,2'-azinobis (3-ethylbenzothiazoline-6-sulfonate). They concluded that a biocatalyst with specific activity of 10^3 U/mg has a higher catalysis rate than a platinum as catalyst in the cathode compartment [4].

Manganese peroxidase (MnP) (EC 1.11.1.13) is one of the major ligninolytic enzymes that can be produced by white rot fungi. This enzyme is a heme containing glycoprotein that uses hydrogen peroxide as oxidant and reduce it to water [10,11].

In this study, methylene blue was electropolymerized on graphite electrode as an electrical active polymer that can enhance electron transfer. Commercial laccase was immobilized by crosslinking on chitosan with glutaraldehyde. Immobilized laccase was settled on a graphite electrode covered with polymethylene blue and this enzymatic electrode was applied in a dual chamber MFC as cathode electrode. In another attempt, MnP produced from a white rot fungus isolate was immobilized on graphite electrode via adsorption. Effect of this biocathode electrode was also investigated on the MFC performance.

2. Methodology

2.1. Microbial fuel cell assembly

The MFC setup consisted of two 250 ml chambers joined through a short tube. Nafion 117 was utilized as membrane with 1.5 cm diameter separating two compartments. Pretreatment of the membrane was conducted by soaking it in a 0.1 M H_2SO_4 solution, H_2O_2 solution and deionized water, each for 60 min at 60°C. Anode and cathode electrodes were 6cm×2cm and 4cm×2cm graphite bars, respectively. These two electrodes were connected with a copper wire. The anode chamber was inoculated with anaerobic sludge and both chambers were mixed gently by a magnetic stirrer.

Nutrient medium (pH 7) utilized in the anode chamber consisted of molasses (1 g/l), K_2HPO_4, urea and trace elements (0.4 mg/l $FeCl_3$, 3 mg/l $MgSO_4$, 0.11 mg/l $CuSO_4.5H_2O$, 0.7 mg/l NaCl, 0.015 mg/l $ZnCl_2$, 4 mg/l $Na_2S_2O_5$, 0.254 mg/l $MnSO_4.H_2O$, 2.06 mg/l $FeSO_4.7H_2O$). All experiments were performed at the ambient temperature (28±1°C).

2.2. Microorganism and enzyme

Commercial laccase was prepared from AB Enzymes GmbH, Germany.
A lignolytic fungus isolated from rotted wood in Northern Iran was employed for the production of MnP. This isolate had indicated the capability to produce MnP as its main lignolytic enzyme. As much as 50 ml of the culture broth (30 g/l glucose, 10 g/l peptone, 5 g/l yeat extract and 0.1 mM Mn^{2+}, pH 4) was prepared in 250 ml Erlenmeyer flasks and autoclaved (121^0 C, 15 min). One mycelia piece of the isolated fungus was placed in the center of an autoclaved 3.9% potato dextrose agar plate and incubated at 32^0 C. After 7 days of cultivation, a mycelial plug (diameter 10 mm) of this culture was used as the inoculum. The cultivation was conducted in a rotary shaker with the rotation speed of 160 rpm at 32^0 C. After 14 days, when a maximum activity for the extracellular MnP was observed, the enzyme was collected from the culture broth by centrifugation (5,000 rpm for 30 min). The supernatant then was utilized for immobilization on the graphite electrode.

2.3. Preparation of enzymatic biocathodes

Electropolymerization of methylene blue was performed by cyclic voltammetery using a potentiostat – galvanostat EG&G PAR 273A, Princeton Applied Research, US from -0.5 to 1.2 V for 18 scans at a scan rate of 50 mV/s [13]. Electrolyte solution contained 0.01 M borate buffer (pH 9.1), 0.1 M $NaNO_3$ and 0.4 mM methylene blue. In another study, the optimal monomer concentration was found to be 0.4 mM. As basic electrolyte solution, 0.1 M $NaNO_3$ was used. Nitrate ions have catalytic role on electropolymerization of methylene blue. Graphite electrode (12 cm^2) was polished with emery paper and rinsed with distilled water

prior to use. The reference and counter electrodes were saturated calomel electrodes (SCE, 0.241 V vs. SHE) and platinum sheet (2 cm^2), respectively.

Crosslinking method was employed for laccase immobilization. The enzyme was immobilized on chitosan using glutaraldehyde [12]. A 5 g/l chitosan solution was prepared using a 2% acetic acid solution to dissolve chitosan. By addition of 2 M NaOH to this solution, a white flocculent deposit was formed and separated from the wet chitosan carrier. The flocculent was washed with distilled water several times and then 20 ml of a 5% glutaraldehyde solution was added. In order to associate the glutaraldehyde to the enzyme, the solution was mixed for 8 h and then left overnight. After that, the deposit was washed with water and added to 50 ml of a 20 g/l laccase solution. Then, 5 ml of acetate buffer (pH 4.4) was added to the solution, agitated for 16 h at room temperature and incubated at 4°C, overnight. The resulting settlement was immobilized laccase on chitosan. Then, 1 ml of the immobilized laccase on chitosan was pipetted onto the electropolymeried (polymethylene blue) graphite electrode and left to dry in a vacuum desiccator for 1 hour. Glutaraldehyde molecule includes two aldehyde group (-CHO) in its structure in which one of these groups react with amine group (-NH_2) of chitosn and crosslinking takes place. The free aldehyde group of glutaraldehyde bounds to an amine group of laccase, covalently. Therefore, glutaraldehyde plays the crosslinking agent role in the linkage of laccase to chitosan.
MnP was immobilized to the graphite electrode by adsorption. As much as 1 ml of the produced crude MnP was pipetted onto the graphite electrode and left to dry in a vacuum desiccator for 1 hour.

2.4. Laccase and MnP activity assay

Laccase activity measurement was performed spectrophotometrically at 25° C, using 2,2-azino-bis-(3-ethylbenzothiazoline-6-sulfonic acid) or ABTS as substrate. The mixture of reaction was contained 3 ml sodium acetate buffer (1 mM, pH 4.5), 0.1 ml ABTS (0.5 mM) and 0.1 ml enzyme solution. The reaction started by addition of ABTS solution (0.1 ml). The rate of $ABTS^+$ formation was measured spectrophotometrically at 420 nm. One unit of the enzyme activity (U) determined as the amount of the enzyme necessary to produce 1 μmol of oxidized ABTS per minute [14].

MnP was assayed by the formation of Mn^{3+} in 50mM sodium malonate buffer (pH 4.5), using 0.1 Mm H_2O_2 as substrate. The rate of complex formation between manganic ions Mn^{3+} and malonate was measured specrophotometrically at 270 nm. One unit of MnP activity defined as the amount of the enzyme necessary to produce 1 μmol of Mn^{3+} per minute at 25° C [15].

3. Results and Discussion

3.1. Electropolymerization of methylene blue on graphite

Methylene blue was polymerized on the surface of a graphite electrode. According to cyclic voltammogram of polymethylene blue on the graphite (Fig. 1), the picks appeared at high anodic potential (almost 1 V) are related to the irreversible oxidation of the monomer. Other picks are formed due to polymerization of formed cation radicals of methylene blue. Therefore, after oxidation of methylene blue and formation of radicals, chemical reaction related to the polymerization of these radicals had been taken place. Methylene blue which is an electroactive polymer was utilized as a mediator due to its high conductivity. Polymethylene blue could increase electron transfer from the electrode to active sites of the laccase. Therefore, electron access will be improved after polymerization of methylene blue

on the electrode surface. As a result, mediator utilization will influence oxygen reduction to water, catalyzed by the laccase in the cathode compartment.

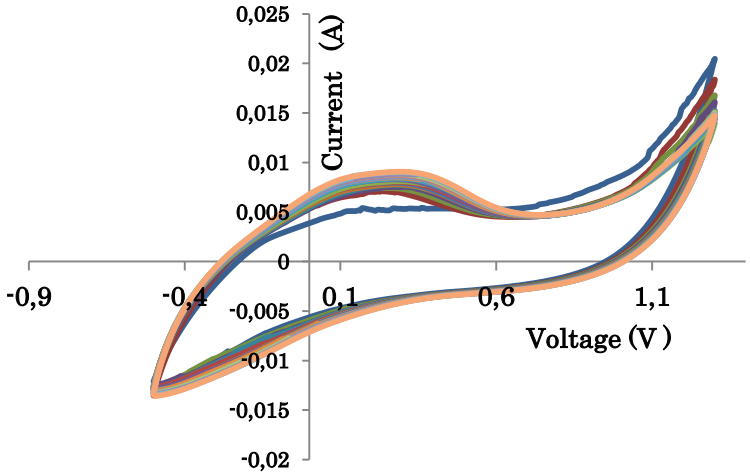

Fig 1. Cyclic voltagram of methylene blue on graphite electrode (Scan rate 50 mV/s).

3.2. MFC performance in the presence of laccase

The polarization curve that was obtained by changing the external load at the maximum output voltage of the MFC, indicates the cell voltage drop and power dependence on current. In general, power density increases to a maximum value against current density and then sharply decreases. Polarization and power curve of the cathode electrodes were plotted at the maximum voltage of the MFC when each of graphite, polymerized graphite or enzymatic electrode was used.

The polarization curves of graphite, polymerized graphite and laccase immobilized graphite are shown in Fig. 2. Maximum current density of the MFC for the polymerized graphite as cathode was 20% higher than that for the graphite electrode. This increase in the current density is due to electron transfer improvement because of improved conductivity of the polymerized graphite electrode.

The power curves of graphite, polymerized graphite and laccase immobilized graphite are indicated in Fig. 3. The maximum power density for the enzymatic electrode was 45.2 mW/m^2 at the current density of 175 mA/m^2, which was two folds of that for the graphite electrode (maximum power density of 22.3 mW/m^2 at current density of 106.9 mA/m^2). The maximum power density for the polymerized graphite electrode was 31 mW/m^2 at the current density of 140.6 mA/m^2. The power density improved 40% in comparison to the graphite electrode. The maximum power density for graphite, polymerized and enzymatic graphite occurred at the external load of 1.2, 98 and 92 kΩ, respectively. According to Ohm's law, at maximum power density, external load is equal to the internal load of MFC. Therefore, modification of graphite electrode through electropolymerization and enzyme immobilization causes a reduction in the internal resistance of the MFC. This phenomenon occurs due to the improvement of electron transfer when polymerized methylene blue or laccase is used on the graphite electrode and the internal resistance of the system decreases, accordingly.

Fig. 3 also indicates that the slope of polarization curve for the enzymatic electrode is milder than that for the graphite electrode at lower current densities. This observation suggests that the activation overpotential of the enzymatic electrode is less than the graphite electrode.

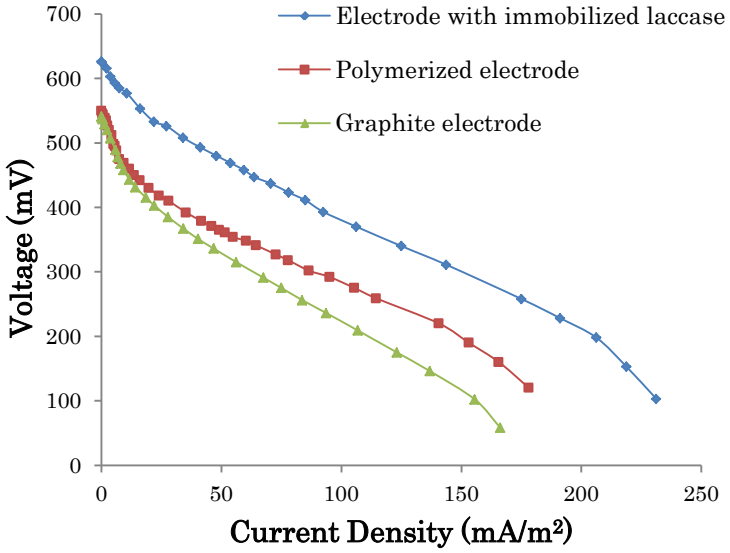

Fig. 2. Polarization curve of MFC with three different electrodes.

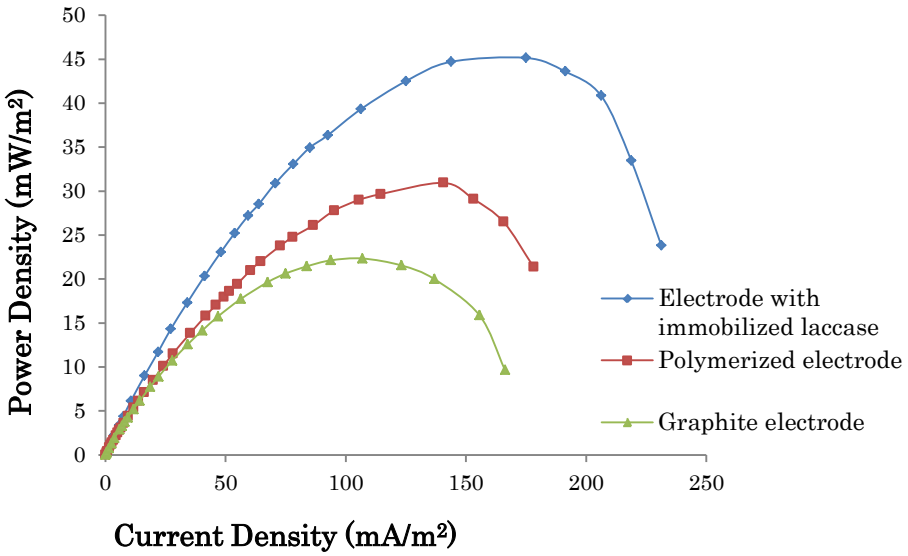

Fig. 3. Power density curve of MFC with three different.

3.3. MFC performance in the presence of MnP

The time course of open circuit voltage variation of the MFC after addition of H_2O_2 is shown in Fig. 4. After H_2O_2 addition, the voltage rapidly increased to a maximum value and then gradually decreased to a constant value. The voltage increase is related to a higher cathodic potential of H_2O_2 compared to oxygen potential. The MFC performance during this stable condition is shown in the polarization and power curves (Fig. 5 and Fig. 6). Maximum output power of 46 mW/m^2 was obtained at current density of 108.8 mA/m^2. This power density is 106% higher than that for a non-enzymatic cathode. The slope of polarization curve for MnP with immobilized MnP cathode at low current densities is 54% less than that for the non-enzymatic cathode. Therefore, MnP presence in the cathode reduces cathodic and overall activation overpotential which is attributed to the catalytic role of MnP in the cathode.

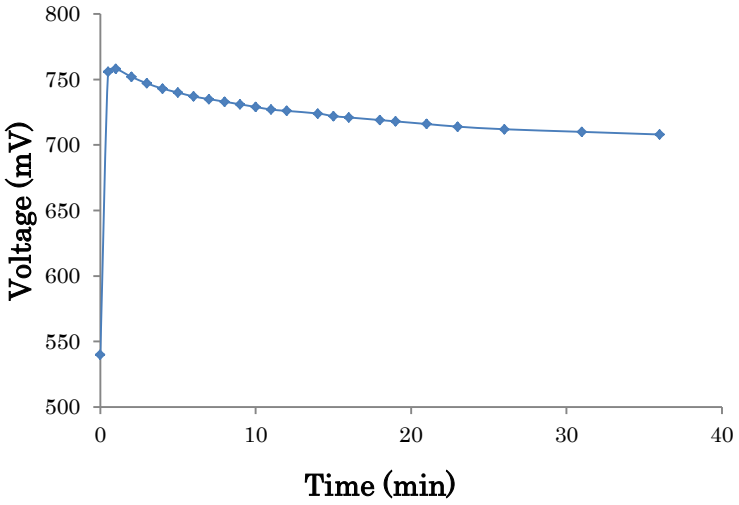

Fig. 4. Open circuit voltage-time curve of MFC after H_2O_2 addition to the cathode in the presence of MnP.

MnP can catalyze hydrogen peroxide reduction to water. Reduction of H_2O_2 causes the oxidation of heme group of the enzyme. The oxidized heme group needs to be reduced to keep its activity which can be fulfilled electrochemically or by an electron donor molecule. Here, Mn^{2+} acts as electron donor. Electrons generated through Mn^{2+} oxidation will be transferred to the active sites of the enzyme and will be utilized to reduce H_2O_2 to water. The produced Mn^{3+} ions extract electrons presented on the cathode surface. The cathodic reaction is catalyzed by MnP enzyme through repetition of the mentioned reactions, cyclically.

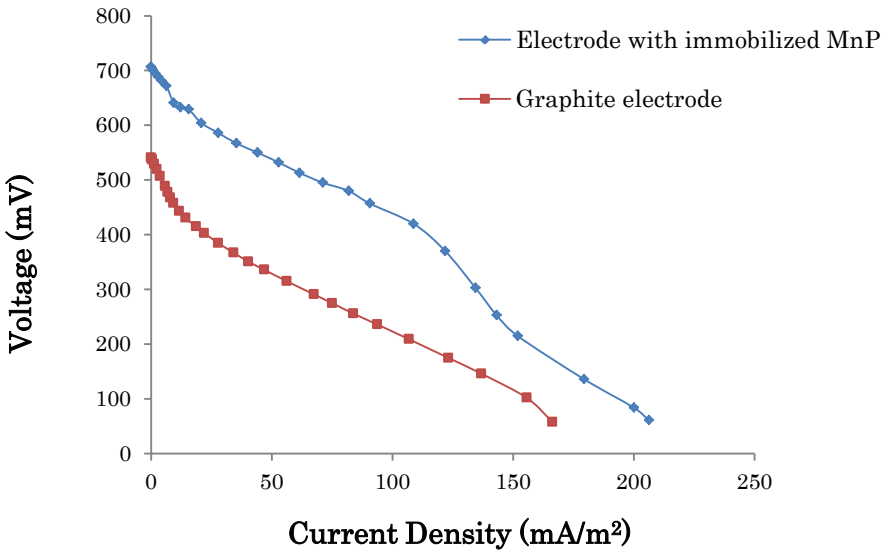

Fig. 5. Polarization curve of MFC with two different electrodes.

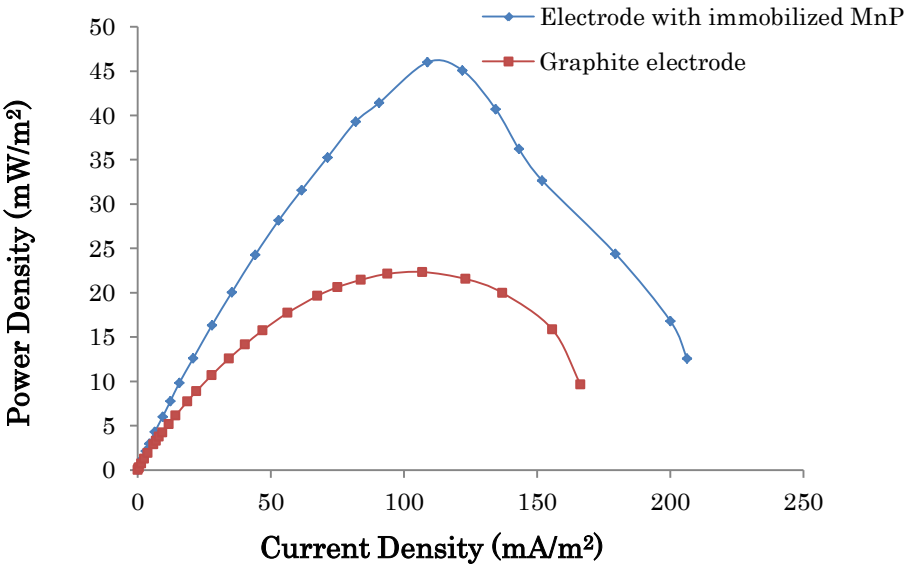

Fig. 6. Power density curve of MFC with three different electrodes.

4. Conclusion

Commercial laccase and MnP produced from a white rot fungus isolate were immobilized on graphite electrode and used as new renewable catalysts in the cathode compartment of a dual chamber MFC. Application of these electrodes in the cathode, enhanced the MFC performance. Output voltage and current density increased as two times as output voltage of the MFC with non-enzymatic cathode. Activation overpotential of MFC decreased due to the catalytic effect of laccase and MnP on reduction of oxygen and H_2O_2, respectively. Laccase and MnP can be proposed as innovative catalysts to be applied in MFCs in order to achieve higher performance via improvement of reaction kinetic in the cathode and therefore, reduction of its related overpotential.

References

[1] B.E. Logan, B. Hamelers, R. Rozendal, U. Schröder, J. Keller, S. Freguia, P. Aelterman, W. Verstraete and K. Rabaey, Microbial fuel cells: methodology and technology, Environmental Science and Technology, 2006, pp. 307-314.

[2] Z.-D. Liu, H.-R. Li, Effects of bio- and abio-factors on e lectricity production in a mediatorless microbial fuel cell, Biochemical Engineering Journal, 2007, pp. 209-214.

[3] R.D. Lovely, Microbial fuel cells: novel microbial physiologies and engineering approaches, Current Opinion in Biotechnology, 2006, pp. 327-332.

[4] G. Tayhas, R. Palmore, H.H. Kim, Electro-enzymatic reduction of dioxygen to water in the cathode compartment of a biofuel cell, Journal of Electroanalytical Chemistry, 1999, pp. 110-117.

[5] O. Lefebvre, W.K. Ooi, Z. Tang, Md. Abdullah-Al-Mamun, D.H.C. Chua, H.Y. Ng, Optimization of a Pt-free cathode suitable for practical applications of microbial fuel cells, Bioresource Technology, 2009, pp. 4907-4910.

[6] M. Smolander, H. Boer, M. Valkiainen, R. Roozemana, M. Bergelin, J. E. Eriksson, X. C. Zhang, A. Koivula, L. Viikari, Development of a printable laccase-based biocathode for fuel cell applications, Enzyme and Microbial Technology, 2008, pp. 93-102.

[7] R.A. Bullen, T.C. Arnot, J.B. Lakeman, F.C. Walsh, Biofuel cells and their development, Biosensors and Bioelectronics, 2006, pp. 2015-2045.

[8] N. Duran, M. Rosa, A.D. Annibale, L. Gianfreda, Application of laccases and tyrosinases (phenoloxidases) immobilized on different supports: a review, Enzyme and Microbial Technology, 2002, pp. 907-931.

[9] C. Vaz-Dominguez, S. Campuzano, O. Rudiger, M. Pita, M. Gorbacheva, S. Shleev, V. M. Fernandez, A.L.D. Lacey, Laccase electrode for direct electrocatalytic reduction of O_2 to H_2O with high-operational stability and resistance to chloride inhibition, Biosensors and Bioelectronics, 2008, pp. 531-537.

[10] H.-R. Kariminiaae-Hamedaani, A. Sakurai, M. Sakakibara, Decolorization of synthetic dyes by a new manganese peroxidase-producing white rot fungus. Dyes and Pigments, 2007, pp. 157-162.

[11] M. Hofrichter, Review: lignin conversion by manganese peroxidase (MnP), Enzyme and Microbial Technology, 2003, pp. 454-466.

[12] J. Zhang, Z. Xu, H. Chen, Y. Zong, Removal of 2,4-dichlorophenol by chitosan-immobilized laccase from *Coriolus versicolor*, Biochemical Engineering Journal, 2009, pp. 54-59.

[13] A.A. Karyakin, E.E. Karyakina, H.-L. Schmidt, Electropolymerized azines: a new group of electroactive polymers, Electroanalysis, 1999, pp. 149-155.

[14] X.Q. Yang, X.X. Zhao, C.Y. Liu, Y. Zheng, S.J. Qian, Decolorization of azo, triphenylmethane and anthraquinone dyes by a newly isolated *Trametes* sp. SQ01 and its laccase, Process Biochemistry, 2009, pp. 1185-1189.

[15] H. Wariishi, K. Valli, MH. Gold, Manganese (II) oxidation by manganese peroxidase from the basidiomycete *Phanerochaete chrysosporium*, Journal of Biological Chemistry, 1992, pp. 23688-23695.

Numerical Studies of PEM Fuel Cell with Serpentine Flow-Field for Sustainable Energy Use

Sang-Hoon Jang[1], GiSoo Shin[1], Hana Hwang[1], Kap-Seung Choi[1], Hyung-Man Kim[1,*]

[1] *Department of Mechanical Engineering & High Safety Vehicle Core Technology Research Center, INJE University, 607 Eobang-dong, Gimhae-si, Gyongsangnam-do 621-749, Republic of Korea*
** Corresponding author. Tel: +82 55 320 3666, Fax: +82 55 324 1723, E-mail: mechkhm@inje.ac.kr*

Abstract: This paper proposes the numerical analyses on performance for PEMFC in the aspects of water management and distribution of current density were performed to compare serpentine channel flow field of 5 passes 4 turns serpentine and 25cm^2 reaction surface between with and without sub-channel at rib. Through the supplement of sub-channel flow field, the improvement of water removal characteristic inside channel was confirmed from the numerical results because the flow direction of under-rib convection is changed into the sub-channel. Reacting gases supplied from entrance disperse into sub-channel flow field and electrochemical reaction occurs uniformly over the reaction surface. Therefore, it was also known that total current density distributions become uniform because retention time of reacting gases traveling to sub-channel flow field is longer than main channel. At the averaged current density of 0.6 A/cm^2, the results show that output power for the serpentine flow-field with sub-channel is 8.475 W which is decreased by about 0.35 % compared with 8.505 W for the conventional-advanced serpentine flow-field, whereas the pressure drops on the anode and cathode side for the serpentine flow-field with sub-channel are 0.282 kPa and 1.321 kPa which are decreased by about 22.95 % and 17.12 % compared with 0.366 kPa and 1.594 kPa for the conventional-advanced serpentine flow-field, respectively.

Keywords: *PEM Fuel Cell, Current density, Water management, Under-rib convection, Sub-channel*

1. Introduction

Proton exchange membrane fuel cell (PEMFC) has been considered one of the most promising alternative clean power generators because of its low to zero emission, its low temperature operation, high power density, and high efficiency [1]. Currently, many researchers have studied the bipolar plate considered performance and water management in the flow channel. Kanezaki [2] and Nam [3] have found that under-rib convection flow between adjacent channels. The under-rib convection is believed to increase the reactant concentration in the under-rib regions, facilitate liquid water removal from those regions, and enable a more uniform concentration distribution, thus explaining an experimental result of good cell performance.

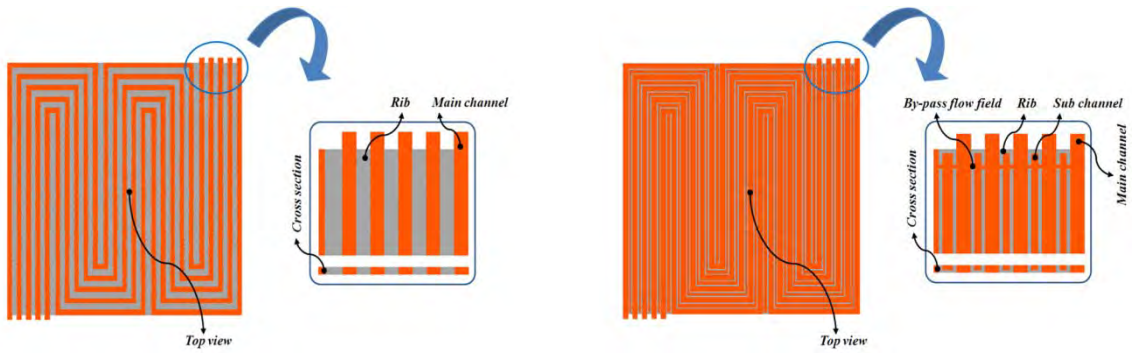

(a) case #1 (b) case #2

Fig. 1. Two 25cm^2 serpentine flow-field patterns; (a) case #1(without sub-channel); (b) case #2(with sub-channel).

This paper proposes the numerical analyses on performance for PEMFC in the aspects of water management and distribution of current density were performed to compare serpentine channel flow fields of 5-passes and 4-turns serpentine and 25cm^2 reaction surface between with and without sub-channel at rib. Two serpentine flow-field patterns are shown in Fig. 1.

2. Numerical model

In this study, CFD programs based on STAR-CD and ES-PEMFC were used to solve the fully coupled governing equations. The model assumes a steady state, ideal gas properties, and homogeneous two phase flows. Assuming that liquid film is formed on the electrode surface during liquid water condensation, the Henry's law of the solubility of gases in the liquid water is used to calculate the diffusion flux, electro-osmotic drag force, and water back diffusion [4, 5]. To improve the computational accuracy, grid cells were established by equalizing the node connectivity in each component and by using the hexahedron mesh. The number of computational cells used in the model varied with complexity of the model. For the case #1, the total cell number was 3.078 million cells, case #2 had 3.336 million computational cells. The present numerical model was validated by grid tests and numerical simulation results on 10cm^2 serpentine with single channel flow-field PEMFC [4].

3. Results and discussion

The parametric studies were conducted on 25 cm^2 serpentine channels that have the case #1 and case #2 configurations, all under the same operating conditions and inlet flow velocity as listed in Table 1 and Table 2. The performance-related parameters include membrane water content (λ), net water flux per proton (α), pressure drop, current density. They are investigated to generate the optimum serpentine flow-field that enhances the PEMFC performance. The net water flux per proton expresses the water transport between anode and cathode. If the net water flux per proton is greater than 0, the electro-osmotic drag is higher than the back diffusion, and water is transported from the anode to the cathode. On the other hand, the net water flux per proton is less than 0 mainly in the outlet area under the ribs, and water is transported from the cathode to the anode by the back diffusion. Back diffusion occurred due to the concentration of water on the anode is higher than on the cathode.

Table 1. Inlet conditions at Anode and Cathode.

Anode	Inlet conditions	Cathode	Inlet conditions
Gas	Hydrogen	Gas	Air
Stoichiometry	1.5	Stoichiometry	2.0
Inlet temperature (°C)	75	Inlet temperature (°C)	75
Inlet relative humidity (%)	100	Inlet relative humidity (%)	100
Mass fraction of hydrogen	0.078	Mass fraction of hydrogen	0.169
Mass fraction of water	0.561	Mass fraction of water	0.274

Table 2. Operating conditions at I_{ave} = 0.6A/cm^2.

Operating conditions	
%H_2 in reformate	75
Exit pressure (kPa)	101
H_2 exchange current density (A/cm^2)	2000
O_2 exchange current density (A/cm^2)	200
Open circuit voltage (V)	0.96
Cell temperature (°C)	75

Fig. 2 ~ Fig. 4 show the comparison of the membrane water contents (λ), net water flux per proton (α) and current density distributions at averaged current density of 0.6 A/cm^2.

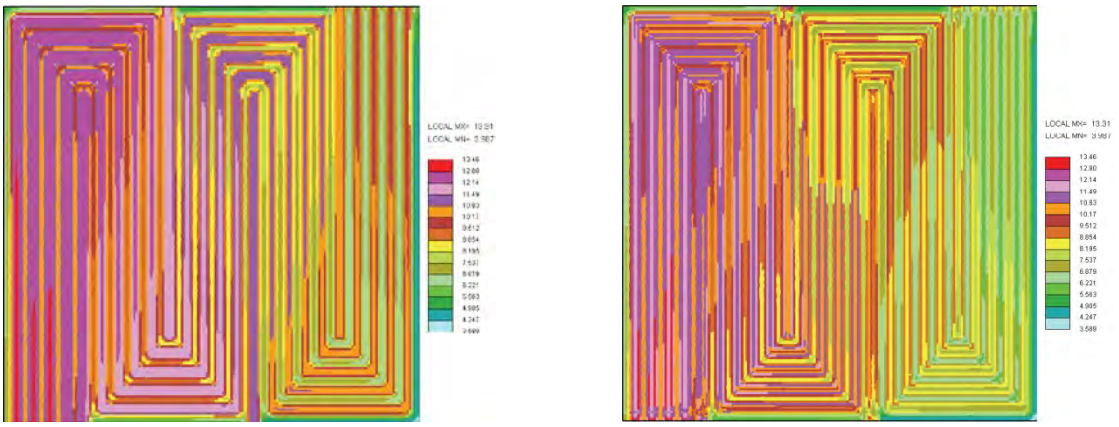

(a) case #1 (b) case #2

Fig. 2. Water content (λ) at I_{ave}=0.6 A/cm^2; (a) case #1; (b) case #2.

Fig. 2 shows the comparison of the membrane water contents between the case #1 and case #2 at the averaged current density of 0.6 A/cm^2. The membrane water content under the rib area is higher than that under the adjacent channel area because a lot of water produced at the cathode under the rib region can be absorbed into the membrane as shown in case #1. On the other hand, the membrane water content of the case #2 has smaller variation between the channel and rib than that of the case #1 because under-rib convection flow from channel to the adjacent rib and then flow from the inlet channel to the adjacent outlet channel, and liquid water gathers and discharges into sub-channel.

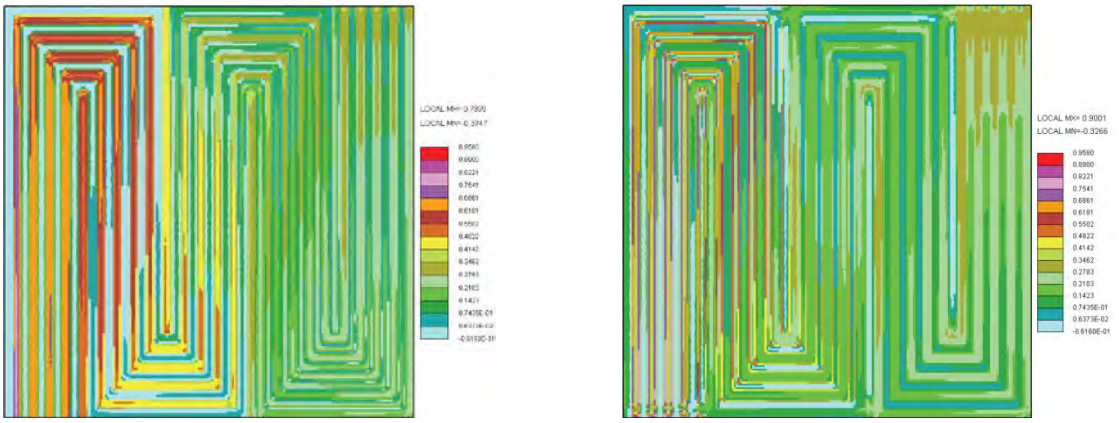

(a) case #1 (b) case #2

Fig. 3. Net water flux per proton (α) at I_{ave}=0.6 A/cm^2; (a) case #1; (b) case #2.

Fig. 3 shows the comparison of the net water flux per proton between the case #1 and case #2 at the averaged current density of 0.6 A/cm^2. The net water flux per proton is greater than 0 at the ribs and that is less than 0 at the channels as shown in case #1. The net water flux per proton is always greater than at the ribs because the hydrogen ions are transported from cathode to the anode with a lot of water. Case #2 shows that the net water flux per proton at the ribs is lower due to sub-channel than the net water flux per proton at the channels i.e. a lot of water is transported from cathode to the anode.

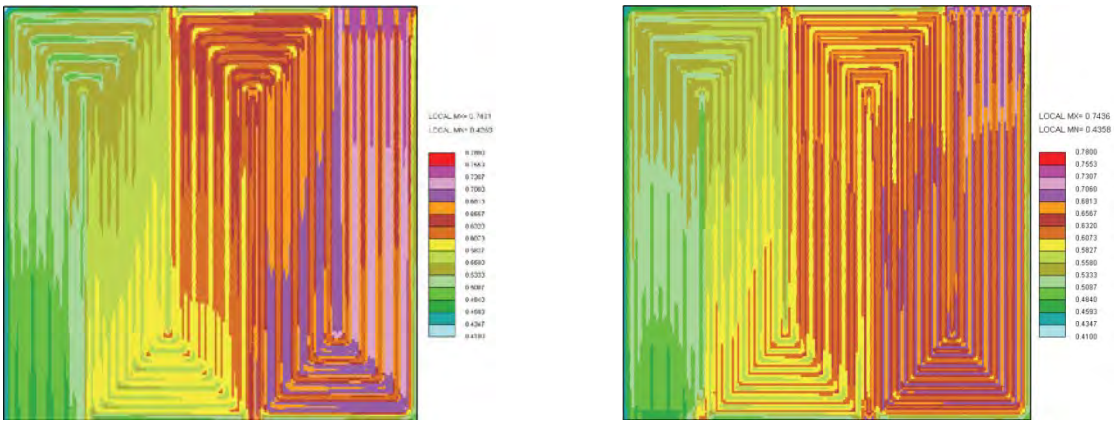

(a) case #1 (b) case #2

Fig. 4. Current density distributions at I_{ave}=0.6 A/cm^2; (a) case #1, case #2.

Fig. 4 presents the comparison of the current density distributions between the case #1 and case #2 at the averaged current density of 0.6 A/cm^2. The overall distributions show that the local current density is decreasing from the inlet toward the outlet due to the consumption of the reacting gases. Through the supplement of sub channel flow field, it is shown from the results that water removal characteristic inside channel improves because the flow direction of under-rib convection is changed into the sub channel. Therefore, case #2 shows that total current density distributions become uniform because retention time of reacting gases traveling to sub channel flow field is longer than to main channel.

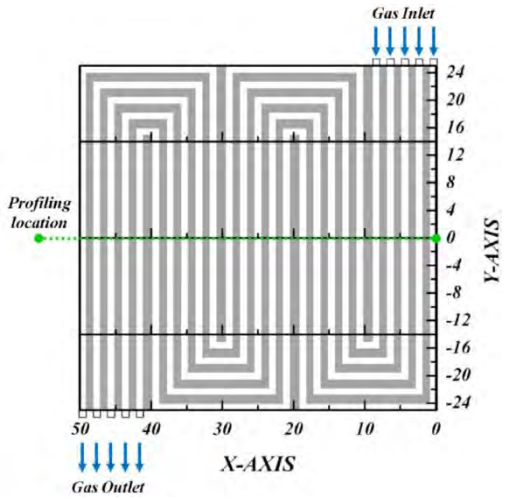

Fig. 5. Index and location of the serpentine flow-field.

Fig. 6 shows the comparison of the total pressures between the case #1 and case #2 at the averaged current density of 0.6 A/cm^2 and the same location as shown in Fig. 5. The pressure drops on the anode and cathode side for case #2 are 0.282 kPa and 1.321 kPa which are decreased by about 22.95 % and 17.12 % compared with 0.366 kPa and 1.594 kPa for case #1, respectively. The enhanced under-rib convection in both anode and cathode of case #2 decreases the pressure drop, which also contributes to the performance by reducing the power consumption of air blower.

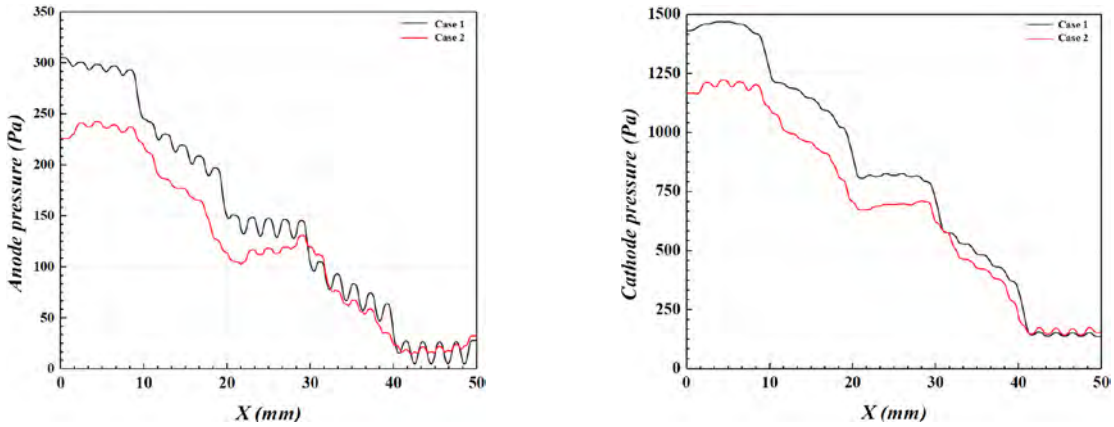

(a) Anode side (b) Cathode side

Fig. 6. The comparison of the total pressures between the case #1 and case #2 at I_{ave}=0.6 A/cm^2; (a) Anode side; (b) Cathode side.

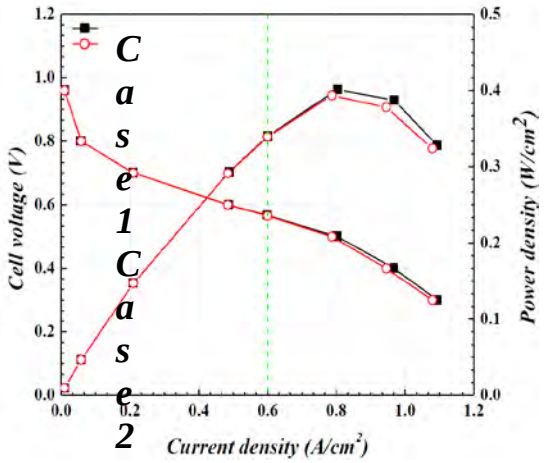

Fig. 7. The comparison of the polarization and power density curves between the case #1 and case #2.

To verify the maximization of power density among the performance-related parameters, the comparison of the polarization and power density curves between the case #1 and case #2 is given in Fig. 7. For the current density lower than 0.6 A/cm^2, the cell voltage and power density is independent of serpentine flow-field with and without sub-channel. For the current density greater than 0.6 A/cm^2, the cell voltages and power densities of case #1 and case #2 differ, the differences increase with the decreasing current density.

4. Conclusions

This study presents numerical analysis-based design of the serpentine flow field patterns to stimulate under-rib convection by adding sub-channel for improving the PEMFC performance. In the case of the case #2, under-rib convection flow from channel to the adjacent rib and then flow from the inlet channel to the adjacent outlet channel, and liquid water gathers and discharges into the sub-channel. Through the present numerical analysis-based design, the serpentine flow field with sub-channel enhances the performances of pressure drop, discharge of liquid water, and uniformities of current density.

Acknowledgements

This research was supported by Basic Science Research Program through the National Research Foundation of Korea (NRF) funded by the Ministry of Education, Science and Technology (No. 2009-0080496).

References

[1] F. Barbir, PEM Fuel Cells: Theory and Practice, Elsevier Academic Press, 2005.

[2] T. Kanezaki, X. Li and J.J. Baschuk, Cross-leakage flow between adjacent flow channels in PEM fuel cells, J. Power Sources 162, 2006, pp. 415 – 425.

[3] J.H. Nam, K.J. Lee, S.Sohn, C.H. Kim, Multi-pass serpentine flow-fields to enhance under-rib convection in polymer electrolyte membrane fuel cells: Design and geometrical characterization, J. Power Sources 188, 2009, pp. 14 – 23.

[4] D.H. Jeon, S. Greenway, S. shimpalee and J.W. Van Zee, The Effect of Serpentine Flow Field Designs on PEM Fuel Cell Performance, Int. J. Hydrogen Energy 33, 2008, pp. 1052 – 1066

[5] CD-adapco, ES-PEMFC Methodology and Tutorial Manual, CD-adapco Group, 2008, http://www.adapco.com.

Comparison of three anode channel configurations and their effects on DMFC performance

S.SH.Khoshmanesh[1,*], S.Bordbar[2]

[1] *Islamic Azad University, Khormoj branch, khormoj, Boushehr, Iran*
[2] *Petroiran company, Tehran, Iran*
** Corresponding author. Tel: +987726240716, Fax: +987726240286, E-mail: sharif.khoshmanesh@gmail.com*

Abstract: Here the 3D two phase homogenous CFD modeling for the anode channel and 1D two phase mathematical modeling for the porous media were considered. The challenging issue is to define the interface boundary conditions such as gradient of CO2 and methanol mass fraction between the diffuser layer and the anode channel. To overcome this difficulty, CFD modeling in the anode channel and mathematical modeling in the porous media were coupled. This combination models gives an accurate model to evaluate the cell performance and also to predict accumulation of CO2 in the channel and its negative effects on the cell performance. Output results of the combination's model are in very good agreement with the experimental data.
The distribution of CO2 in the anode channel shows that the accumulation of CO2 in the MSFF is less than SSFF and PFF configuration so the negative effect of CO2 decrease in the MSFF case relative to two other cases. Accumulation of CO2 is more in the channel rib relative to other places of channel. This is true for all three channel configurations.
The cell voltage-Current density graph shows that the MSFF performance is better than two other cases. Comparing MSFF configuration with the SSFF shows that the performance of MSFF is a little more than SSFF.

Keywords: *Direct methanol fuel cell, Anode flow configurations, CFD modeling, Mathematical modeling*

Nomenclature

C_0 *Average concentration of methanol at the channel/ADL interface…… molm^{-3}*
C_I *Concentration of methanol at the ADL/ACL interface…… molm^{-3}*
C_{II} *Concentration of methanol at the ACL/membrane interface…… molm^{-3}*
C *Molar Concentration ……kmolm^{-3}*
D *Diffusion coefficient …… ..... m^{2}s^{-1}*
X *Mass fraction*
F *Faraday's constant, 96,487…… Cequiv*
I_{Cell} *Cell current density……..Am^{-2}*
I_{Leak} *Leakage current density …… Am^{-2}*
$I_{o,ref}^{MeOH}$ *Exchange current density of methanol ……..Am^{-2}*
$I_{o,ref}^{O_2}$ *Exchange current density of oxygen …… …. Am^{-2}*
$N_{Cross\ Over}^{MeOH}$ *Methanol crossover ……..molm^{-2} s^{-1}*
P *Pressure ……..Pa*
T *Temperature…… K*
U_{MeOH} *Thermodynamic equilibrium potential of methanol oxidation……Volt*
U_{O2} *Thermodynamic equilibrium potential of oxygen oxidation…… Volt*
V_{cell} *Cell voltage…… Volt*
U_{O2} *Thermodynamic equilibrium potential of oxygen oxidation…… Volt*
M *Molecular weight ……km/kg*

Greek

α_A *Anodic transfer coefficient*
α_C *Cathodic transfer coefficient*
δ_{AC} *Anode Catalyst layer thickness…….m*
δ_{AD} *Anode diffuser layer thickness…….m*
δ_M *Membrane thickness……..m*
α *Void fraction*
μ *Dynamic viscosity……kgm^{-1}s^{-1}*
ρ *Density……kgm^{-3}*
η_A *Anode over potential……Volt*
η_C *Cathode over potential……Volt*
ξ^{MeOH} *Electro-osmotic drag coefficient of methanol*
κ *Ionic conductivity of the membrane ……Scm^{-1}*
x' *Quality*

Subscripts

ADL *Anode Diffuser Layer*
ACL *Anode Catalyst Layer*
M *Memberrane*

Superscripts

MeOH *Methanol*
O2 *Oxygen*
CO2 *Carbon dioxide*
K *Species*

1. Introduction

Direct methanol fuel cells (DMFCs) are currently being investigated as an alternative power source to batteries for portable applications such as cell phones, laptop computers and video recorders. DMFCs with advantages of high energy density, rapid startup and response, low operation temperature, zero emission and refueling instantly, stand out as a most promising candidate to the applications of present and next generation of portable electronic devices [1, 2].Regarding the DMFCs studies have been focused on two categories, materials of the cell and the anode electrochemical reaction. Water, methanol and gas management are the three main issues that some attempts have been investigated to optimize these effects on the cell performance. A good understanding of this complex, interacting phenomena to optimum the design parameters of system leads to numerous experimental and comprehensive mathematical modeling of cells.

Kulikovsky et al. [3] developed a vapor-feed two-dimensional DMFC model. Their model based on the mass conservation equations for concentrations of species and conservation equations of proton and electron currents, which govern the distributions of electrical potentials of the membrane and carbon phases. In his study, he neglected the methanol cross over the membrane.

Wang and Wang [4] presented a 2-D, two-phase model of liquid – feed DMFC. They extended their previous two-phase PEMFC model [5] to include two phase flow and transport phenomena in a liquid feed DMFC.1- D drift flow model was used to describe the methanol flow in the anode channel.

Here a comprehensive 3-D, homogenous two phase model for the anode channel and 1D two phase mathematical modeling for the porous region were considered. This combination model results in the easily managing and optimizing of effective parameters on DMFC.
A typical DMFC consists essentially of a membrane-electrode assembly (MEA) sandwiched between two bipolar plates which have a channel for distribution the fuel, an aqueous methanol solution in the anode and oxygen from air in the cathode, Figure (1).In an operation DMFC, methanol solution diffuses through one of the porous diffusion layer and is oxidize at the anode to produce carbon dioxide, protons and electrons. At the cathode, Oxygen diffuses through another porous diffusion layer and is reduced with the proton passing through the proton exchange membrane as well as electrons flowing through load from the anode to produce water, equations (1), (2) .

$$CH3OH + H2O \longrightarrow CO2 + 6\,H^{+} + 6\,e^{-} \quad (1)$$

$$3/2\ O2 + 6H^{+} + 6e^{-} \longrightarrow 3\ H2O \quad (2)$$

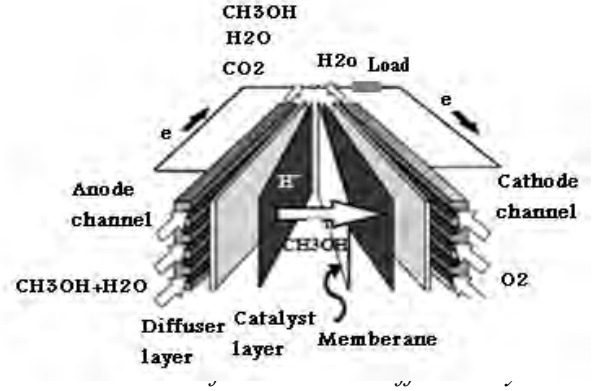

Fig. 1

2. Model description

Here 3-D homogenous, two phases, multi component flow for the anode channel and 1D two phase mathematical modeling for the porous regions were considered. For the anode channel

three type of flow patterns, parallel flow field (PFF), single-serpentine flow field (SSFF) and multiple serpentine flow field (MSFF) were considered, fig2.

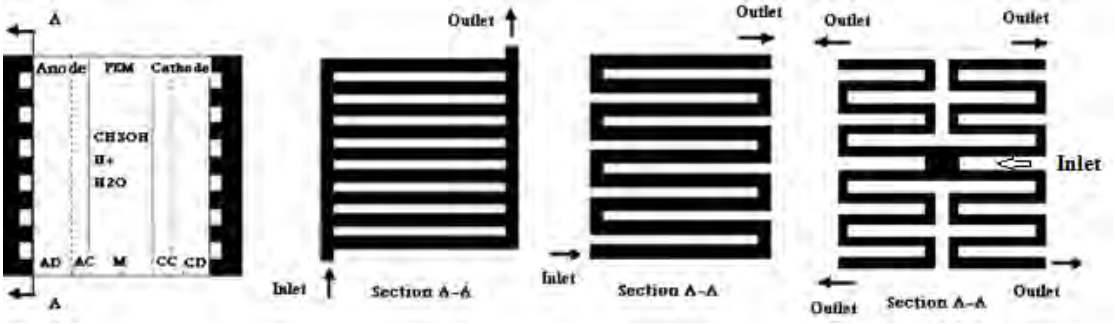

Fig. 2. Schematic view of DMFC with different anode configurations

The combination of CFD modeling and mathematical modeling has been shown in fig3.

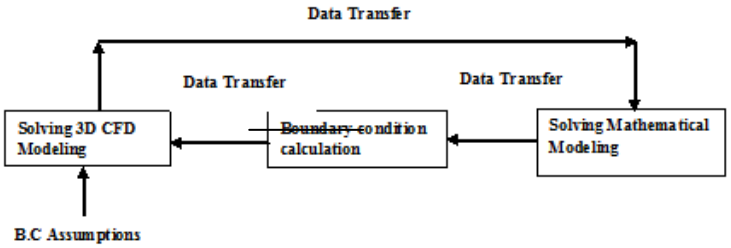

Fig. 3. Coupling CFD modeling and mathematical modeling

2.1. CFD modeling

In this study, two phase homogenous model have been used to describe the fluid flow in the anode channel. The study of Triplett [6], Fukano and Kariyasaki [7], showed that the homogeneous model is valid for two-phase bubbly flow because the tube diameter is smaller than 5.6 mm. In this model it is assumed that the thermodynamics equilibrium are available between the phases and two phases are well mixed and therefore travel with the same velocities so the mixture is treated as a pseudo-fluid that obeys the usual equations of single-phase flow.

$$\nabla.(\rho^{mix}\vec{U}) = 0 \quad (3)$$

$$\nabla.(\rho^{mix}\vec{U}\vec{U}) = -\nabla P + \nabla.\vec{\vec{T}} + \rho^{mix} g \quad (4)$$

$$T_{i,j} = \mu^{mix}\left(\frac{\partial u_i}{\partial x_j} + \frac{\partial u_j}{\partial x_i} - \frac{2}{3}\delta_{i,j}\frac{\partial u_n}{\partial x_n}\right) \quad (5)$$

$$\nabla.(\rho^{mix}\vec{U}C^k) = \nabla.(\rho^{mix}D^k\nabla \mathrm{C^k}) \quad (6)$$

$$\rho^{mix} = \alpha\rho_l + (1-\alpha)\rho_g \quad (8)$$

α is void fraction and related to quality x' by,

$$\alpha = \frac{1}{1 + (\frac{1-x'}{x'}\ \frac{\rho_g}{\rho_l})} \quad (9)$$

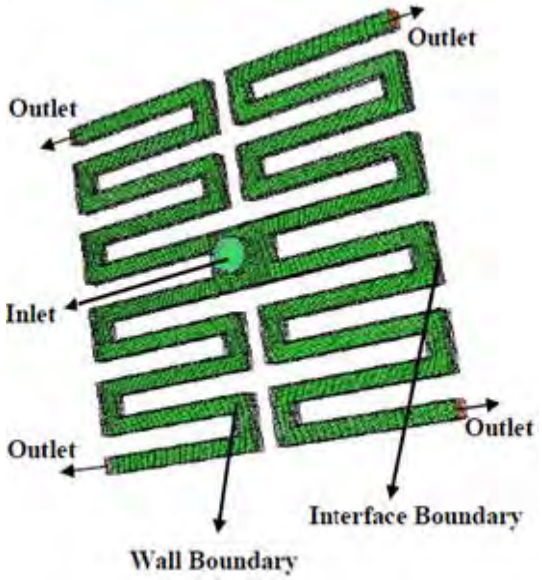

Fig. 4. MSFF configuration , boundary conditions and Meshing Scheme

$$x' = \frac{\rho_g(X_g^{CO2} + X_g^{H2O} + X_g^{MeOH})}{\rho_l(X_l^{H2O} + X_l^{MeOH} + X_l^{CO2})} \qquad (10)$$

The Isbin equations have been used to calculate the mixture viscosity [8].

$$\frac{1}{\mu^{mix}} = x' \frac{1}{\mu_l} + (1 - x') \frac{1}{\mu_g} \qquad (11)$$

2.2. Boundary Conditions

Fig 4 shows the view of MSFF with the different boundary conditions. In the inlet, mass flow rate of dilute methanol is defined. In the outlet, fully developed condition for the SSFF, MSFF and pressure outlet for the PFF is applied. In the boundary between the anode channel and diffuser layer the mass fraction of MeOH and CO2 are defined.

2.2.1. Channel/ Anode diffuser layer interface boundary conditions

Consumed methanol in the anode catalyst layer and methanol cross over the membrane are equal to methanol transfer due to convection and diffusion in Channel/ Anode diffuser layer,

$$\rho^{mix}\, \vec{U}.\vec{n} X^{MeOH} + \rho^{mix}\, D^{MeOH}\, \frac{\partial X^{MeOH}}{\partial X} = M^{MeOH}\, \frac{I_{cell}}{6F} + M^{MeOH} N_{Cross\ Over}^{MeOH} \qquad (12)$$

The consumptions of the methanol, water and methanol crossover are equal to the total mass flow rate that goes out of the interface, so

$$\rho^{mix} \vec{U}.\vec{n} = M^{MeOH}\, \frac{I_{cell}}{6F} + M^{MeOH} N_{Cross\ Over}^{MeOH} + M^{H2O}\, \frac{I_{cell}}{2F} \qquad (13)$$

If we replace the $\rho^{mix}\vec{U}.\vec{n}$ from equation (16) into the equation (15) it gives the diffusion flux from the channel into the diffuser layer.

$$\rho^{mix}\, D^{MeOH}\, \frac{\partial X^{MeOH}}{\partial x} = M^{MeOH}\, \frac{I_{cell}}{6F}(1 - X^{MeOH}) + M^{MeOH} N_{Cross\ Over}^{MeOH}(1 - X^{MeOH}) + M^{H2O}\, \frac{I_{cell}}{2F} X^{MeOH} \qquad (14)$$

For the carbon dioxide the diffusion flux, which comes into the channel via the diffuser layer is equal to the CO2 production in anode catalyst layer ,diffusion via convection neglected, so,

$$\rho^{mix} D^{co2}\, \frac{\partial X^{co2}}{\partial x} = M^{co2}\, \frac{I_{cell}}{6F} \qquad (15)$$

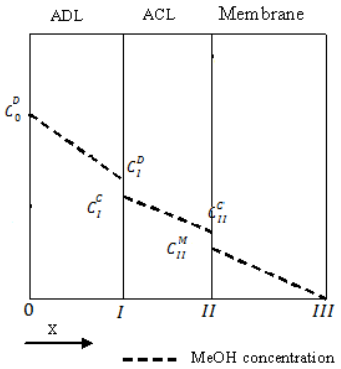

2.3. Mathematical modeling

The porous media regions are divided to the diffuser, catalyst and membrane layer, Fig4. Mathematical modeling has been studied in the detail by Brenda[9]. Here only the results have been shown,

$$C_{AC}^{MeOH} = \frac{I_{Cell}}{12F\delta_{AC}D_{AC}^{MeOH}} X^2 + C_1 X + C_2 \qquad (16)$$

$$C_1 = \frac{C_{II}^C - C_I^C}{\delta_{AC}} - \frac{I_{Cell}(2\delta_{AD} + \delta_{AC})}{12F\delta_{AC}D_{AC}^{MeOH}} \quad (17)$$

$$C_2 = C_I^C - \frac{(C_{II}^C - C_I^C)\delta_{AD}}{\delta_{AC}} + \frac{I_{cell}\delta_{AD}(\delta_{AD} + \delta_{AC})}{12F\delta_{AC}D_{AC}^{MeOH}} \quad (18)$$

$$C_I^C = \frac{\delta_{AC}D_M^{MeOH}K_{II}\left(D_{AD}^{MeOH}C_0^D - \frac{I_{cell}\delta_{AD}}{12F}\right) + \delta_M D_{AC}^{MeOH}(D_{AD}^{MeOH}C_0^D - (1 + 6\ \xi_{MeOH})\frac{I_{cell}\delta_{AD}}{6F})}{D_{AD}^{MeOH}K_I(\delta_{AC}D_M^{MeOH}K_{II} + \delta_M D_{ACL}^{MeOH}) + \delta_{AD}D_{AC}^{MeOH}D_M^{MeOH}K_{II}} \quad (19)$$

$$C_{II}^C = \frac{\delta_M(D_{AC}^{MeOH}D_{AD}^{MeOH}C_0^D - \delta_{AC}D_{AD}^{MeOH}K_I(1 + 12\ \xi_{MeOH})\frac{I_{Cell}}{12F} - \delta_{AD}D_{AC}^{MeOH}(1 + 6\ \xi_{MeOH})\frac{I_{cell}}{6F})}{D_{AD}^{MeOH}K_I(\delta_{AC}D_M^{MeOH}K_{II} + \delta_M D_{AC}^{MeOH}) + \delta_{AD}D_{AC}^{MeOH}D_M^{MeOH}K_{II}} \quad (20)$$

The operation conditions, geometry and physicochemical properties have been come in table 1 and 2.

Table 1. Operation and Geometry values

Parameters	Symbols	Values
Operation Temperature	T	60°c
Operation Pressure	P	1At
Rib Height	H	0.001 (m)
Rib Width	W	0.0013 (m)
Diffuser layer thickness	δ_{AD}	0.0015 (m)
Catalyst layer thickness	δ_{AC}	0.00023(m)
Membrane layer thickness	δ_M	0.0018 (m)

Table 2. Physicochemical properties

Parameters	Symbols	Values	Ref
Binary diffusion coefficient	$D_{\text{MeOH-Water}}$	1.74×10^{-6}	[11]
Binary diffusion coefficient	$D_{\text{CO2-Water}}$	3.19×10^{-6}	[11]
MeOH diffusion coefficient,diffuser layer	D_{AD}^{MeOH}	8.7×10^{-3}	[9]
MeOH diffusion coefficient,catalyst layer	D_{Ac}^{MeOH}	$2.8 \times 10^{-9}e^{2436(\frac{1}{353}-\frac{1}{T})}$	[12]
Methanol diffusion coefficient,memberane	D_M^{MeOH}	$4.9 \times 10^{-}e^{2436\left(\frac{1}{353}-\frac{1}{T}\right)}$	[12]
Thermodynamic potential of oxygen (Volt)	U^{O2}	1.24	[4]
Thermodynamic potential of methanol (Volt)	U^{MeOH}	0.03	[4]
Ref, exchange current density of anode (A/m2)	$I_{0,ref}^{MeOH}$	$94.25\ e^{\frac{35570}{R}(\frac{1}{353}-\frac{1}{T})}$	[4]
Ref, exchange current density of cathode (A/m2)	$I_{0,ref}^{O2}$	$42.22e^{\frac{73200}{R}(\frac{1}{353}-\frac{1}{T})}$	[15]
Anodic transfer coefficient	α_A	0.52	[4]
Cathodic transfer coefficient	α_C	1.55	[4]
Ionic conductivity of the membrane(S/Cm2)	κ	0.036	[11]
Electro-osmotic drag coefficient	ξ^{MeOH}	$2.5X^{MeOH}$	[14]
Partition coefficient	K_I	0.8	[13]
Partition coefficient	K_{II}	0.8	[13]

3. Performance Evaluation

To obtain the polarization curve the cell voltage of DMFC can be written as,

$$V_{cell} = U^{O2} - U^{MeOH} - \eta_A - \eta_C - \frac{\delta_{MEM} I_{Cell}}{\kappa} \quad (21)$$

The over potentials term η_A and η_C can be determined from the Tafel equations,

$$I_{Cell} = I_{0,ref}^{MeOH} \frac{C_{AC}^{MeOH}}{C_{MeOH,ref}} e^{\alpha_A \eta_A F/RT} = I_{0,ref}^{O2} \frac{C_{o2}}{C_{o2,ref}} e^{\alpha_C \eta_C F/RT} - I_{leak} \quad (22)$$

I_{leak} is the leakage current density due to the oxidation of the methanol crossover.

$$\frac{I_{leak}}{6F} = N_{Crossover}^{MeOH} = (-D_M^{MeOH} \frac{dC_M^{MeOH}}{dx} + \xi^{MeOH} \frac{I_{cell}}{F}) \quad (23)$$

4. Results

4.1. Effect of mass flow rate and inlet feed concentration on the cell performance

The model has been validated by comparison of the results from SSFF configuration with its experimental data from Q. Liao and X. Zhu [10].The cell performance have been calculated for the methanol inlet feed concentration of M=1, temperature of 60°c and two different inlet mass flow rate. As it can be seen the model results are in the good agreement with the experimental data. In the right figure the variation of cell voltage with the current density at different inlet feed concentrations have been shown and it is obvious that the cell performance will improve while the inlet feed concentration increase. The performance improvement from1M to 2M is more than from 0.5M to 1M. This can be attributed to increasing methanol concentration, which satisfies the additional requirement of the electrochemical reaction in the anode due to higher current densities.

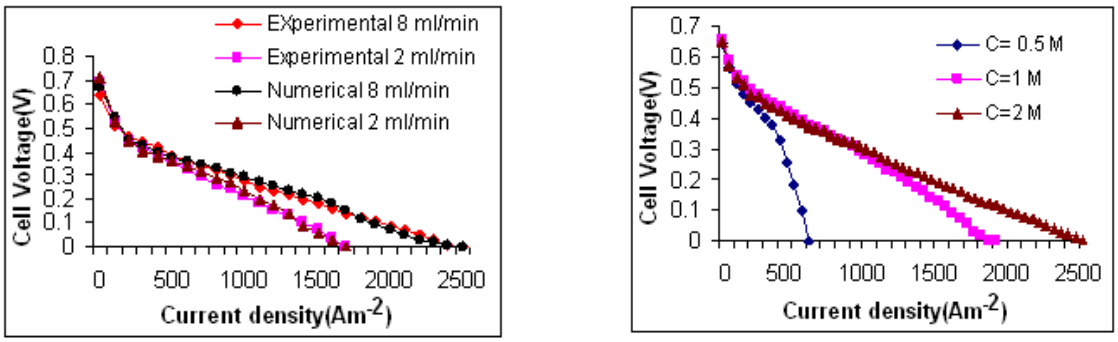

(6.a) *(6.b)*

Fig. 6. Numerical and experimental cell data performance for two different inlet mass flow rate (6.a) and Cell performance at different inlet feed concentration (6.b)

4.2. Effect of flow configuration on CO2 and methanol concentration

Distribution of CO2 molar concentration in the anode channel for different configurations at the inlet feed concentration and current density 2M, 1500A/m^2 respectively, have been shown in fig7.CO2 molar concentration increase incrementally from inlet to outlet and reach the maximum value 0.03 , 0.025 and .02 for PFF, SFF and MSFF respectively. Fig8 shows the distribution of methanol molar concentration. Here the methanol concentration decreases incrementally from inlet to outlet and reaches the minimum value of 0.5, 0.71 and 0.81 for PFF, SFF and MSFF respectively in the outlet of the channel. The distribution of the CO2 in

the MSFF is more smoothly relative to two other cases and the coalescence of gas bubbles in the corner of the ribs are less than other cases.

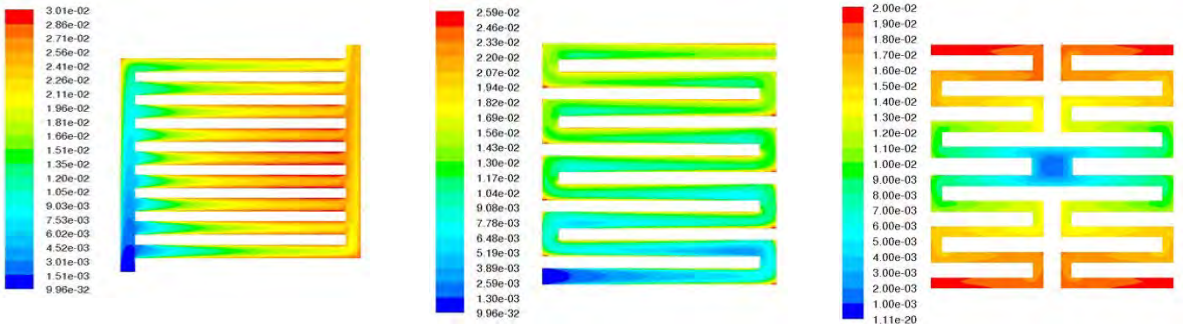

Fig. 7. Distribution of CO2 molar concentration for PFF, SFF and MSFF flow configuration

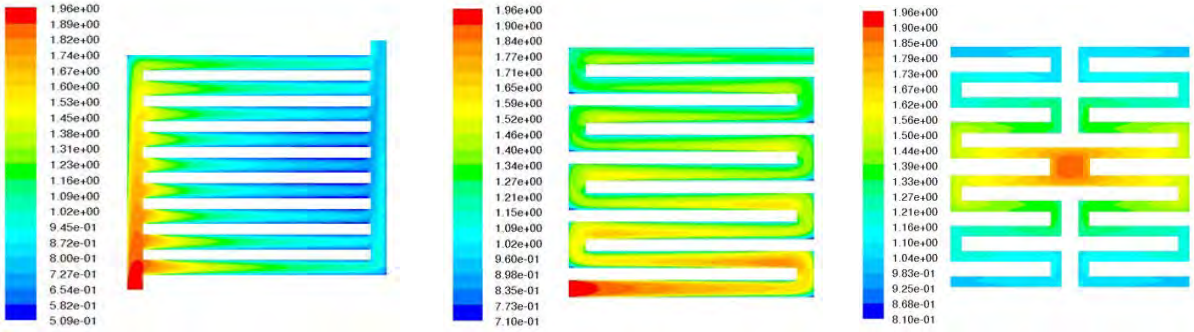

Fig. 8. Distribution of MeOH molar concentration for PFF, SFF and MSFF flow configuration

4.3. Effect of flow configuration and temperature on the cell performance

The performance of the cell is depended on the mass fraction of methanol in the catalyst layer that is depended on the average methanol mass fraction in the anode channel. By calculation the cell performance using mentioned combination method, it can be seen that the MSFF configuration has better performance relative two other cases fig9a. In the right picture9.b the effects of temperature on cell performance have been shown. As it can be seen with increasing the temperature the cell performance will increase, especially at high current density.

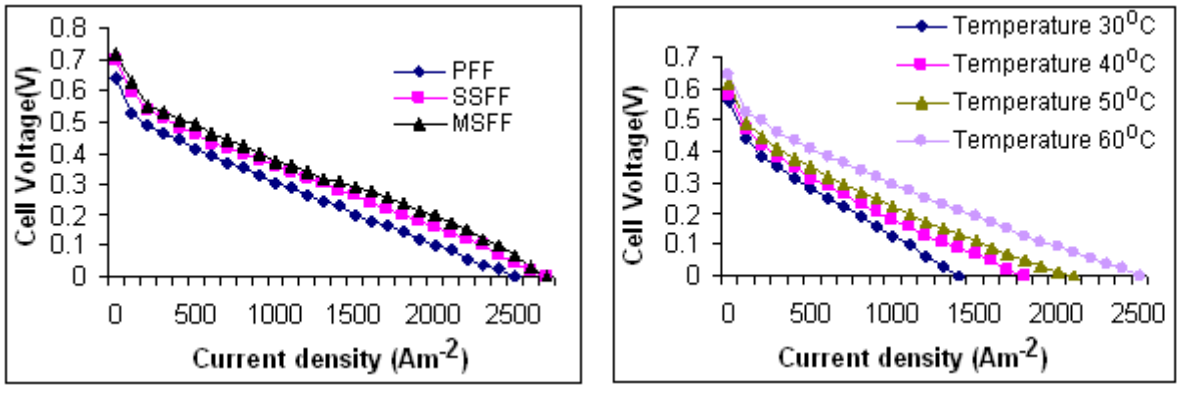

(9.a) *(9.b)*

Fig. 9. Comparison of anode configuration on cell voltage (9.a) and effects of temperature on cell performance (9.b)

5. Conclusions

DMFCs have the following advantages; easy fuel delivery and storage, no need for cooling or humidification, simpler system design and may even achieve higher overall energy efficiency than PEMFCs with further developments. This new modeling design is the way to find the exact cell performance with different geometry. From the results, MSFF flow configuration can give a better performance relative to two other cases so this kind of cell geometry can solve the problems regarding lower overall energy efficiency of DMFCs relative to PEMFCs.

References

[1] C.K. Dyer, Fuel Cells for Portable Applications, J. Power Sources 106 (2002) 31–34.

[2] K. Cowey, K.J. Green, G.O. Mepsted and R. Reeve, Portable and military fuel cells, Curr. Opin. Solid State Mater. Sci. 8 (2004) 367–371.

[3] A. Kulikovsky, J. Divisek and A.A. Kornyshev, Two-dimensional simulation of direct methanol fuel cells, a new type of current collector, J. Electrochem. Soc. 147 (2000) 953.

[4] Z.H. Wang and C.Y. Wang, Mathematical modeling of liquid-feed direct methanol fuel cells, J. Electrochem. Soc. 150 (4) (2003) 508–519.

[5] Z.H. Wang, C.Y. Wang and K.S. Chen, Two-phase flow and transport in the air cathode of proton exchange membrane fuel cells, J. Power Sources 94 (2001) 40–50.

[6] K.A. Triplett, S.M. Ghiaasiaan, S.I. Abdel-Khalik, A. LeMouel and B.N.Mc- Cord, Gas–liquid two-phase flow in microchannels, Part II, Int. J. Multiphase Flow 25 (1999) 395.

[7] T. Fukano and A. Kariyasaki, Characteristics of gas–liquid two-phase flow in a capillary tube, Nucl. Engng. Des 141 (1993) 59.

[8] H.S. Isbin, R.H. Moen, R.O. Wickey, D.R. Mosher and H.C. Larson, Two-phase Steam Water Pressure Drops, Nuclear Science and Engineering, Conference, Chicago,1958

[9] G.L Brenda , A.S. Vijay, J.W. Weidner and R. E. White, Mathematical Model of a Direct Methanol Fuel Cell Journal of Fuel Cell Science and Technology Nov, 2004, Vol. 1 /Pp 43-48

[10] L. Qiang, Z. Xun , Z. Xueyan and D. Yudong, Visualization study on the dynamics of CO2 bubbles in anode channels and performance of a DMFC, Journal of Power Sources 171 (2007) 644–651

[11] A. A. Kulikovsky, J. Divisek, and A. A. Kornyshev, Two-Dimensional Simulation of Direct Methanol Fuel Cell A New (Embedded) Type of Current Collector, Journal of the Electrochemical Society, 147 (3) 953-959 (2000)

[12] K. Scott,W. Taama and J. Cruickshank, Performance and Modeling of a Direct Methanol Solid Polymer Electrolyte Fuel Cell, J. Power Sources 65(1-2),1997, pp. 159-171.

[13] S.F. Baxter, V.S. Battaglia and R.E. White, Methanol Fuel Cell Model: Anode, Journal of the Electrochem Society, 1999, 146(2), pp. 437-447.

[14] X. M. Ren, T. E, Springer, T.A. Zawodzinski and S.Gottesfeld, Methanol Transport through Nafion Membranes, J. Electrochem Society, 2000. 147(2), pp. 466-474.

[15] A. Parthasarathy, S. Srinivasan, A.J. Appleby and C. R. Martin,Temperature Dependence of the Electrode Kinetics of Oxygen Reduction at the Platinum/Nafion Interface, a Microelectrode Investigation, J. ElectrochemSociety, 1992, 139(9), pp. 2530-2537.

Investigation of electrical, structural and thermal stability properties of cubic $(Bi_2O_3)_{1-x-y}(Dy_2O_3)_x(Ho_2O_3)_y$ ternary system

Refik Kayali[1,*], Murivet Kasikci[1], Semra Durmus[2], Mehmet Ari[2]

[1]*Department of Physics, Science-Literature Faculty, Nigde University, Nigde, Turkey*
[2]*Department of Physics, Science-Literature Faculty, Erciyes University, Kayseri, Turkey*
** Corresponding author. Tel: +90 388 225 4069, Fax: +90 388 225 0180, E-mail: refikkayali@nigde.edu.tr*

Abstract: In the scope of this work, $(Bi_2O_3)_{1-x-y}(Dy_2O_3)_x(Ho_2O_3)_y$ ternary system (x=1,3,5,7,9,11 mol % and y=11,9,7,5,3,1 mol %, dopant concentrations) sample materials were developed using solid state reaction method sintering each of them at 650, 700, 750, 800 °C for 48 hours. Structural, electrical and thermal properties of these samples which are candidate of electrolyte for solid oxide fuel cells (SOFCs) have been evaluated by means of XRD, four-probe method, and TGA / DTA. XRD measurements showed that except the samples annealed at 650 ^oC, all the other samples have stabilized δ- Bi_2O_3 phase. It was seen that duration of sintering time and temperature was rather effective on the formation of the stabilized sample materials and their other properties, such as electrical and structural properties. It was seen that the electrical conductivities of all the examples developed sintering at 700, 750 a nd 800 °C for 48 hours increases with the increasing temperature having numerical values varying in the range of $7{,}65x10^{-2}$ $\Omega.cm^{-1}$ - $6{,}11x10^{-1}$ $\Omega.cm^{-1}$. Activation energy of the sample A6 was calculated and it was found 0.97 eV. On the other hand, the main purpose of this study is to find an electrolyte which does not have any degradation in its properties with time; this maybe caused either interaction between the different electrochemical cell materials or by instability of the ionic conductor under operation conditions. During the heating/cooling process, the four-point probe conductivity measurements have been performed. The hysteresis curve was obtained for this sample due to time interval difference of heating/cooling processes. It was observed that there is no gradation in the structure of the sample.

Keywords: *Electrolyte, Solid state reaction, Fuel cell, Electrical conductivity, XRD, Four- probe point method*

1. Introduction

Recently, it has been known that bismuth oxide based and doped with the other two ceramic oxides are ternary materials with the properties showing promise of utility in SOFC's [1-7]. In addition, the need to develop oxide ion conductive materials with high conductivity and desired structure stability at low temperature directs most of the research toward solid oxide electrolyte materials. Among these electrolyte materials, Bi_2O_3 - based solid oxide electrolyte materials with δ-phase fcc fluorite type crystal structure are of interest for use in solid oxide fuel cell (SOFC) due to their high oxide ion conductivity [8,9]. The fluorite type phase of pure Bi_2O_3, known as the most highly conductive oxide-ion conductor, has a conductivity of about 1 Scm^{-1} at 750 °C. But, δ-phase Bi_2O_3 is stable only between 730 °C and 825 °C and cannot be quenched to room temperature [10]. However, the δ-phase can be obtained at room temperature by doping with some transition metal (Nb, Ta, V and W) and rare earth(Sm-Lu). It is also possible to use combination of oxides, so called double doping, to obtain the δ fluorite type phase. Fluorite type δ–phase materials displays very high oxide ion conductivity which is attributed to the highly polarisable Bi^{3+} cations and highly disordered structure of sublattice [11-15]. Structural and conductive properties of a solid material during the various temperature ranges determine its suitability as an electrolyte in the practical use. If an electrolyte material has a high conductive behavior over a long period of time at reasonably low temperature, it is possible to use at operation of a SOFC. Many researchers were reported that the fluorite type δ–phase Bi_2O_3 cannot be stabilized [11-13]. Some these kinds of materials had completely transformed into mixture phases after annealing for long time period. In addition, the conductivity decay can also occur for the fluorite type materials without changing its structure. The rate of conductivity decay is dependent on a nnealing temperature, long ordering oxide-ion sublattice and amount of doped cations.

2. Experimental

2.1. Sample preparation

We have tried to stabilize the fluorite type δ-phase in the ternary system $(Bi_2O_3)_{1-x-y}(Dy_2O_3)_x(Ho_2O_3)_y$. As a result, we could obtained a stabilized δ-phase in limited compositional range of x and y.

The desired proportions of the samples were accurately weighed and thoroughly mixed. The mixture was heated in an alumina crucible at 750 °C for 10 h and quenched to room temperature by air stream. Next, the samples were examined by XRD using CuKα radiation. Then, the prepared pellets were annealed at 650, 700, 750 and 800 °C for 48 h followed by air quenching. The same heat treatment was repeated several times in order to get its equilibrium state, after the conductivity measurements were performed in air. Finally, thermal behavior of the samples was taken the differential thermal analysis (DTA) measurements in order to find out whether any phase transition exists or not, after each measurement.

2.2. XRD measurements

Powder XRD measurements is carried out by using Bruker AXS D8 Advance type diffractometer with an interval $2\Theta = 10^o–90^o$, scanning $0{,}002^o$/min, and Cu-Kα radiation for the determination of the crystal structure of the samples at room temperature. These measurements were repeated for the powders of the samples obtained after every sintering process. Then, Diffrac Plus Eva packet program was used to analyze the unit lattice cell parameters (a, b, c, α, β, γ), Miller indexes, and the distance between the layers, d. On the other hand, Win-Index Professional Powder Indexing packet program was used for the indexing of the diffraction peaks in the powder patterns of the samples.

2.3. Electrical measurements

Conductivity of the samples was measured using four-point probe method. The pellets of the samples with 13 mm diameter and 2 mm thick were obtained by using a conventional press and then the pellets were being air-quenched after sintering. All of the measurements in this work were carried out by means of Data Acquisition Control System associated with a PC, interface card IEEE-488.2, multimeter with scanning card (Keithley 2700, 7700-2), programmable power supply (Keithley 2400), and computer program written for this purpose. These measurements were repeated for several times because of the electrical conductivity measurements performed during the first heating process are not enough to represent the complete electrical behavior of the samples.

2.4. TG/DTA measurements

The thermal behavior of the annealed materials was investigated by DTA/TG by means of DIAMOND TG/DTA-PERKIN ALMER Marck system. The samples whose masses are about 20-50 mg were heated at 200 °C min^{-1} in an alumina crucible and cooled quickly to room temperature under a stream of air.

3. Results and discussion

3.1. XRD measurement results

Figure 1 shows the comparisons of the XRD spectra of the samples annealed at 650 °C for 48 hours. As seen from this figure, all the samples do not have completely monoclinic-α phase, but some of them have also δ-phase. As a result, the samples prepared at this temperature have a mixed phase and the formation of the δ-phase also exhibits at this stage.

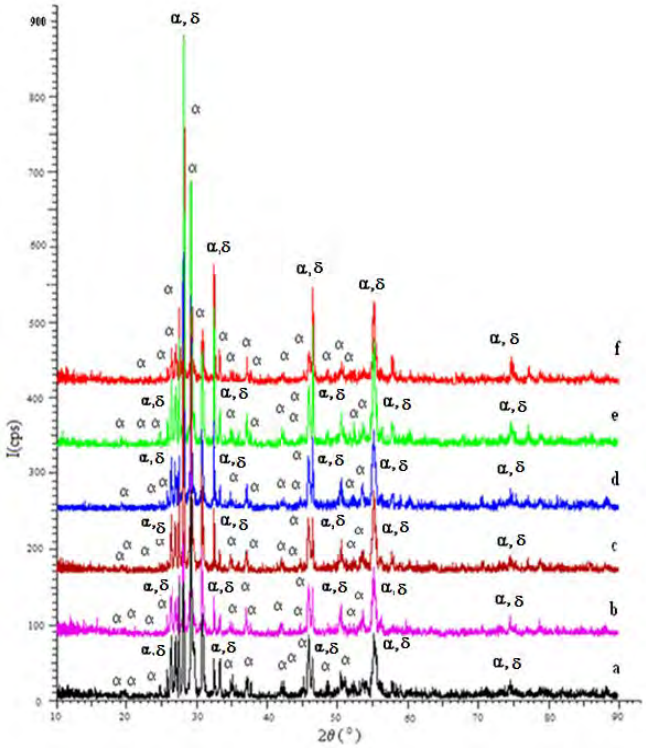

Fig.1. Comparisons of the XRD spectra of the samples annealed at 650 °C and for 48 hours and having α+δ-Bi_2O_3 phase (a) A1, (b) A2, (c) A3, (d) A4, (e) A5 and (f) A6

Figure 2 shows the comparisons of the XRD spectra of the samples annealed at 750 °C for 48 hours. From this figure, it is observed that all the samples except A1 have only δ-phase. Two peaks at the right and left side of the most intensive peak of the sample A1 are seen and they are belonging to the α-phase. No significant modification of the intensity of the XRD pattern can be detected, which means that the δ-phase of the samples has not been decomposed into the other low conductivity phases by changing amount of the doped materials.

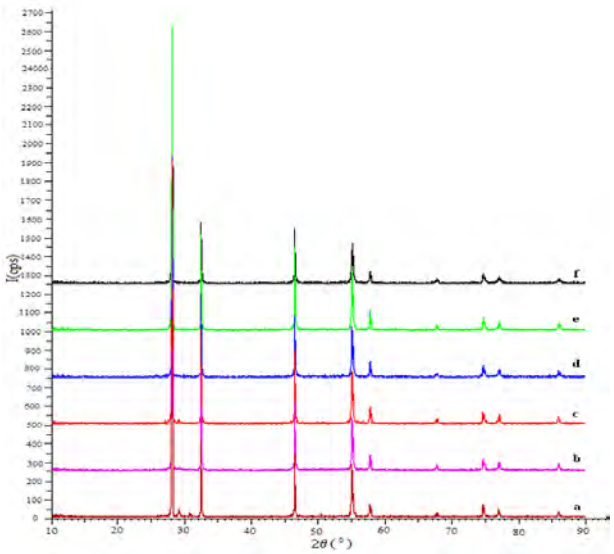

Fig. 2. Comparisons of the XRD spectra of the samples annealed at 750 °C and for 48 hours and having fcc δ-Bi_2O_3 phase (a) A1, (b) A2, (c) A3, (d) A4, (e) A5 ve (f) A6

Also, there is no transformation of the quenched δ-phase is evidenced on the XRD patterns. The fluorite type δ-phase is obtained at the end of the process. The first generated δ-phase has

been kept stable during the electrical measurement annealed at 700, 750, 800 °C for all the samples.

Summary of the observed phases from XRD measurements of the $(Bi_2O_3)_{1-x-y}(Ho_2O_3)_x(Dy_2O_3)_y$ ternary-systems with different dopant ratios and developed at different temperatures mentioned above is given in Table 1. As seen from this table, all the samples except the samples annealed at 650 °C have stable fcc δ-phase.

Table 1. Observed phases for $(Bi_2O_3)_{1-x-y}(Ho_2O_3)_x(Dy_2O_3)_y$ ternary-systems with different dopant ratios and developed at different temperatures

Synthesing temperature (°C)	Synthesing time (hour)	$(Ho_2O_3)_x(Dy_2O_3)_y(Bi_2O_3)_{1-x-y}$ (*x,y = mol %)*					
		x=1 y=11	x=3 y=9	x=5 y=7	x=7 y=5	x=9 y=3	x=11 y=1
650	48	α+ δ	α+ δ	α+ δ	α+ δ	α+ δ	α+ δ
700	48	δ	δ	δ	δ	δ	Δ
750	48	δ	δ	δ	δ	δ	Δ
800	48	δ	δ	δ	δ	δ	Δ

3.2. Electrical conductivity measurements

The conductivity measurements were performed on the samples $(Bi_2O_3)_{1-x-y}(Dy_2O_3)_x(Ho_2O_3)_y$ ternary system (x=1,3,5,7,9,11 mol % and y=11,9,7,5,3,1 mol %). Conductivity measurements were only carried out up to 850 °C in order to ensure that melting does not occur. In this report, we have presented only the electrical measurements of the samples developed at 750 °C, since it has the best conductivity. The conductivity of this sample is 0.6 $(\Omega.cm)^{-1}$ placing it among the most highly conductive materials known.

Figure 3 shows the graphics of the conductivity of the samples versus to 1000/T K. As seen from this figure, all the curves are similar with each other. It is the expected result since all of them have stable fcc δ-phase. These results were supported by the XRD patterns of the samples which have been given in Fig.3 too.

The Ho_2O_3 rich samples show higher electrical conductivity than the Dy_2O_3 rich materials. The conductivity results show that an intermediate fast changing conductivity region separated by linear evolution zone. The sharp rise of the conductivity is indication of an order-disorder transition.

Increase in the conductivity of the materials with increasing amount of Ho_2O_3 is attributed to the increase in the proportion of highly polarisable cations and in the number of oxide ion vacancies. It can be noticed that the conductivity slightly increases with increasing the Ho_2O_3 proportion, reaching highest values 0.6 $(\Omega.cm)^{-1}$ for x=11 an y=1 %mol (A6). This can simply be explained that can be attributed to the increase in the concentration of vacancies by the Ho cations located on the host sub-lattice, which are available for oxide ion migration. The distribution of vacancies affects the long range migration of oxide ions and therefore the conductivity increases. Since dopant cations and oxide ion vacancies have negative and positive charges, attractions between them are likely to be mainly responsible for the high activation energy. As a result, it can be said that an electrical conductivity rise has been observed for all samples when the proportion of the Ho^{3+} cation is increased.

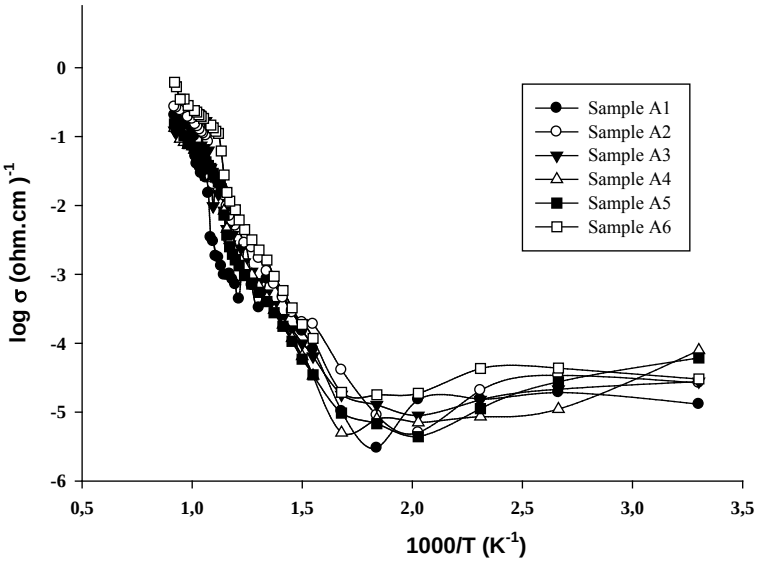

Fig. 3. Oxygen conductivity, as a function of temperature, for the samples A1, A2, A3, A4, A5, A6 obtained at 750 °C for 48 hours

Figure 4 shows the graphic of the conductivity of the sample A6 versus to 1000/T K at different annealing temperatures. As seen from this figure, two distinct regions observed on the curves corresponding to an order-disorder δ-phase transition which exhibits similar activation energy at these two regions. The characteristics of the conductivity curves are similar for all the samples. The conductivity values slightly increase with decreasing the annealing temperature especially at high temperature region.

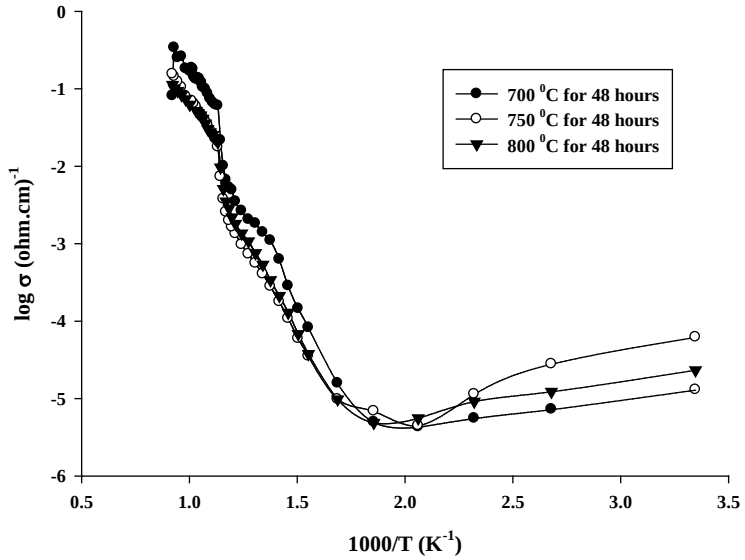

Fig. 4. Oxygen conductivity, as a function of temperature, for the sample A6

Activation energies of the samples can be obtained from the Arrhenius equation. As mentioned previously two distinct regions are observed for all samples corresponding to an order-disorder δ-phase transition which exhibits similar activation energy at these two regions. Activation energy calculated for sample A6 corresponding to the high temperature region is found 0.97 eV. And also, the conductivity results are in good agreement with these

already revealed by XRD and DTA/TG measurements. The samples which exhibit the lowest activation energy is associated the structure characterized by the fluorite type fcc lattice is likely responsible for opening of migration pathways for the oxide ions, and consequently to a decreasing of the activation energy.

The main purpose of this study is to find an electrolyte which does not have any degradation in its properties with time; this maybe caused either interaction between different electrochemical cell materials or by instability of the ionic conductor under operation conditions. So this sample has been firstly heated from room temperature to 650, 700, 750 and 800 °C in 48 hours and cooled from this temperature to room temperature in the same time. After this process, the four-point probe conductivity measurements have been performed.

Figure 5 shows the hysteresis curve obtained for the sample A6. This sample has been firstly heated from room temperature to 800 °C in 2 hours and cooled from this temperature to room temperature within the 4 hour s. During this process, the four-point probe conductivity measurements have been performed. The hysteresis curve was occurred for this sample due to time interval difference of heating/cooling processes. From this figure, the slopes of these curves nearly are the same. It means that there is no gradation in the physical and chemical properties of this sample after applying the operation condition.

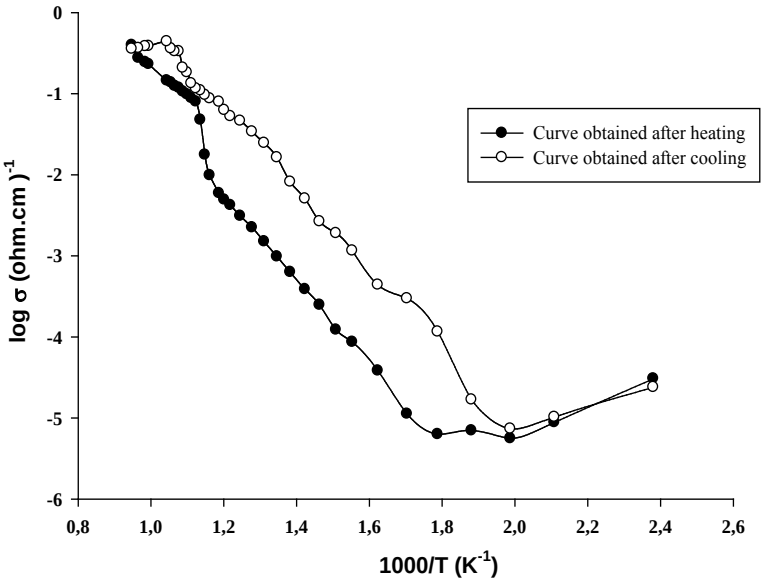

Fig. 5. Conductivity hysteresis curve obtained for the sample A6 obtained approximately 5 hours being heated from room temperature to 800 °C and cooled to room temperature

TG/DTA measurements of the samples have been carried out after the conductivity measurements of the samples using the same pellets. In figure 6, TG/DTA graphics of the sample A6 annealed at 750 °C and for 48 hours are given. From this figure, a wide range of exothermic peak is seen in a temperature range between 325-415 °C for A6 sample in DTA curve. Similar variation is seen between the same temperature ranges in TGA curve whose slope is changing during heating treatment. In this case, this peak results from the order/disorder transformation in the structure of the sample rather than the phase transformation. During the cooling process, there are no exothermic peak and slope changes because of long cooling time interval. This transformation is seen in the conductivity graphics of the same sample and its hysteresis curve (Fig. 5) too.

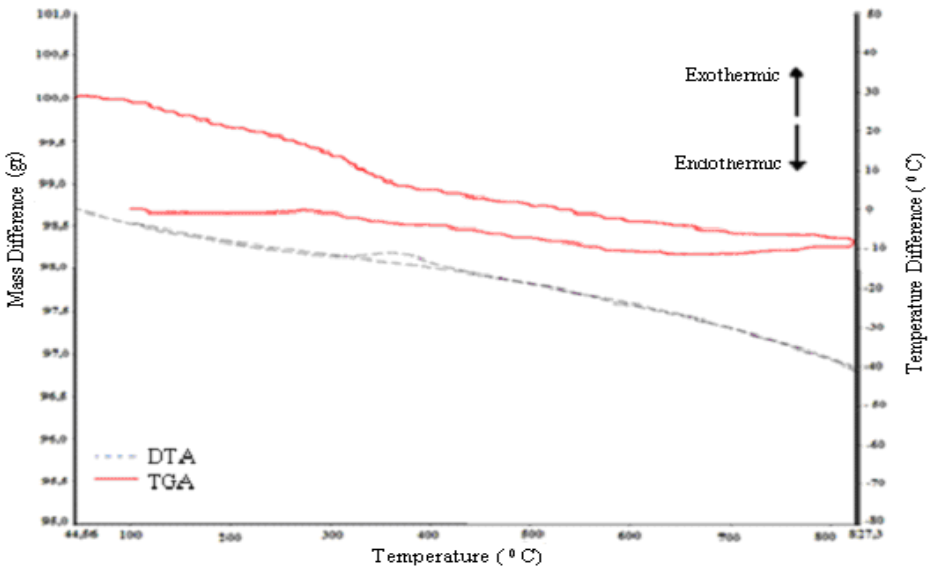

Fig. 6. TG/DTA graphics of sample A6 developed at 750 °C and for 48 hours

4. Conclusion

In this work, data obtained from XRD, DTA, TGA and four probe point method measurements for $(Bi_2O_3)_{1-x-y}(Ho_2O_3)_x(Dy_2O_3)_y$ (x=1, 3, 5, 7, 9, 11 mol%, y=11, 9, 7, 5, 3, 1 mol %) ternary system samples synthesized at different temperatures by solid state reaction method has been investigated in detail and some important results have been obtained for the chosen sample A6 as following:

- According to the obtained XRD results, all the samples synthesized at 700 °C, 750 °C and 800 °C for 48 hours have dominantly homogeneous face centered cubic δ-Bi_2O_3 phase. The samples annealed at 650 ^{0}C have mixed phases composed from monoclinic α-Bi_2O_3 phase and fcc δ-Bi_2O_3 phase.
- According to conductivity measurements, all the samples, having stable δ-Bi_2O_3 phase and synthesized at 700 °C, 750 °C, and 800 °C for 48 hours, have a good oxygen ion conductivity property.
- It has been observed that the electrical conductivity of all the samples increases while the percentage of the Ho_2O_3 doping materials increases.
- The best electrical conductivity has been observed for the sample A6 synthesized at 750 °C for 48 hours and having doping ratios % 11 mol for Ho_2O_3 and % 1 mol for Dy_2O_3 and maximum conductivity value has been measured as $6.11x10^{-1}$ $(\Omega.cm)^{-1}$.
- Stable δ-phase of $(Bi_2O_3)_{1-x-y}(Ho_2O_3)_x(Dy_2O_3)_y$ ternary system has been observed firstly in this study in operation conditions of an SOFC.

Comment

We are planning to perform resistance tests for this material for long time periods under the operation conditions to show that this material can be used as an electrolyte in SOFCs.

References

[1] D. Music, S. Konstantinidis and J. M. Schneider, Equilibrium structure of δ-Bi_2O_3 from first principle, J. Phys.: Condens. Matter, 21, 2009, 175403-175480.

[2] C. –Y. Hsieh, K.-Z. Fung, Crystal structure and electrical conductivity of cubic fluorite-based $(YO_{1.5})_x(WO_3)_{0.15}(BiO_{1.5})_{0.85-x}$ ($0 \leq x \leq 0.4$) solid solutions, J. Solid State Electrochem, 13, 2009, 951-957.

[3] P.K. Cheekatamarla, M. F. Caine, and J. Cai, Internal reforming of hydrocarbon fuels in tubular solid oxide fuel cells, Internatıonal Journal of Hydrogen Energy, 33, 2008, 1853-1858.

[4] S.R Xiao-Feng Ye, Z.R Wang, L. Wang, X.F Xiong, T.L. Sun Wen, Use of a catalyst layer for anode-supported SOFCs running on ethanol fuel, Journal of Power Sources, 177, 2008, 419-425.

[5] M. Wang, and K. Woo, Impact of Sr_2MnO_4 preparation process on its electrical resistivity, Energy Conversion and Management, 49, 2008, 2409–2412.

[6] S.H. Jung, E.D. Wachsman and N. Jiang, Structural Stability and Conductivity of Cubic $(WO_3)_x$-$(Dy_20_3)_y$-$(Bi_20_3)_{l.x.y}$, International Journal of Ionics, Volume 8, Numbers 3-4, 2002, 210-214.

[7] M. Benkaddour, M.C. Steil, M. Drache, and P. Conflant, The Influence of Particle Size on Sintering and Conductivity of $Bi_{0.85}Pr_{0.105}V_{0.045}O_{1.545}$ Ceramics, Journal of Solid State Chemistry, 155, 2000, 273-279 .

[8] N.M. Sammes, G.A. Tompsett, H. Nafe and F. Aldinger, Bismuth based oxide electrolytes structure and ionic conductivity, Journal of Europan Ceramic Society, 19, 1999, 1801-1826.

[9] N. Jiang, E.D. Wachsman and S.H. Jung, A higher conductivity Bi203-based electrolyte, Solid State ionics, 150, 3-4, 2002, 347-353.

[10] H.A. Harwing, On the Structure of Bismuthsesquioxide: The α, β, γ, and δ-phase, Z. Anorg. Allg. Chem., 444, 1978, 151-166.

[11] A. Watanabe, Is it possible to stabilize δ-Bi_2O_3 by an oxide additive?, Solid State Ionics, 40-41, 1990, 889-892 .

[12] N. Jiang, R.M. Buchanan, F.E.G. Henn. A.F. Marshall, D.A. Stevenson, E.E. Wachsman, Aging phenomenon of stabilized bismuth oxides, Mater. Res. Bull., 29, 1994, 247-254.

[13] E.D. Wachsman, S. Boyapati, M.J. Kaufman, N. Jiang, Modeling of Ordered Structures of Phase-Stabilized Cubic Bismuth Oxides, J. Am. Ceram. Soc., 83, 2000, 1964-1968.

[14] E.D. Wachsman, G.R. Ball, N. Jiang and D.A. Stevenson, Structural and defect studies in solid oxide electrolytes, Solid State Ionics, 52, 1992, 213-218.

[15] S. Boyabati, E.D. Wachsman and B.C. Chakoumakos, Neutron diffraction study of occupancy and positional oxygen ions in phase-stabilized cubic bismuth oxides, Solid state Ionics, 138, 2001, 293-304.

Alkaline Fuel Cell (AFC) engineering design, modeling and simulation for UPS provide in laboratory application

L. Ariyanfar[1,*], H. Ghadamian[2], R. Roshandel[3]

[1,2].*Department of Energy Engineering, Science and Research Campus, Islamic Azad University, Tehran, IRAN*
[3]. *Energy Engineering Department, Sharif University of Technology, Tehran, IRAN*
** Corresponding author. Tel: +98 21 44240042, Fax: +98 21 44232205, E-mail: Leyliariyan@gmail.com*

Abstract: In the presented research, a feasibility study to cover a mobile electrolyte alkaline fuel cell behaviors and characteristics (which the electrolyte has system cooling role) for UPS (Uninterruptable Power Supply) application is provided to use in an energy laboratory. Electrochemical modeling and computations for irreversiblities led to optimization of cell voltage, current & power densities and the results are found to be 0.566V, 574.3 mA/cm^2, 325.2 mW/cm^2 respectively. By using mentioned quantities, ideal thermodynamic efficiency, real thermodynamic efficiency and electrical efficiency concluded 80%, 38% and 34% respectively. Preliminary electrochemical studies in this research are combined with engineering designs in complementary stage of research. At the next stage, considerations on heat and mass transfer and contributed models lead to approve a double pipe heat exchanger as energy sink. Then the cost model is also determined and the optimization codes are developed to propose best operation point of system with minimizing total cost and determining the heat exchanger dimensions, flow rates and temperatures. Furthermore, parametric analysis for variation of temperature, electrolyte cooling rate and cost of planned AFC has been studied for energy efficiency and performance improvement.

Keywords: *Alkaline Fuel Cell (AFC), Irreversibilities, Heat Transfer, Cost Model, Parametric Analysis.*

1. Introduction

Fuel cell is an electrochemical system that converts energy of the chemical reaction to useful electrical energy and is made of anode, cathode and electrolyte. Fuel cells classified according to practical temperature, type of electrolyte and constitutive materials; and alkaline fuel cells or AFCs are one of low temperature systems with an alkaline solution as the electrolyte. Alkaline fuel cell is the oldest type of fuel cells, which had described in 1902 and have used in spatial applications [1]. AFC produce electricity through oxidation - reduction reactions between oxygen and hydrogen. In the fuel cell reaction water is generated, and two electrons are released. The electrons flow through an external circuit, and have returned to the cathode to reduce oxygen in an electrochemical reaction and thus hydroxide ions are produced. Electricity and heat are made as byproducts of this product [2]. This system usually has peripheral equipment. Wide studies have done about alkaline fuel cells; but what had not enough attention is specialty study with practical and all purpose approach. Although the central system produce the power, but peripheral equipment also use and effect on whole system performance and the total cost. In this research has been trying to design system and accessories in the optimal mode of increasing efficiency and reducing costs are assessed.

2. System configuration

An energy laboratory is designed, which part of its power provide from fuel cell systems with ancillary performance and specific aims. Several different objects in correlation with together are contemplated in this laboratory that each has its survey. The typical plan of laboratory is shown in Fig.1. As seen a 100W AFC has chosen for UPS provider of this laboratory. In these cells the electrolyte is alkaline solution and how to use of is an issue. It can be in mobile electrolyte, static electrolyte and dissolved fuel alkaline fuel cells modes [1]. What are discussed in this research are electrochemistry calculations, engineering design and heat transfer of an alkaline fuel cell system with system optimization aim.

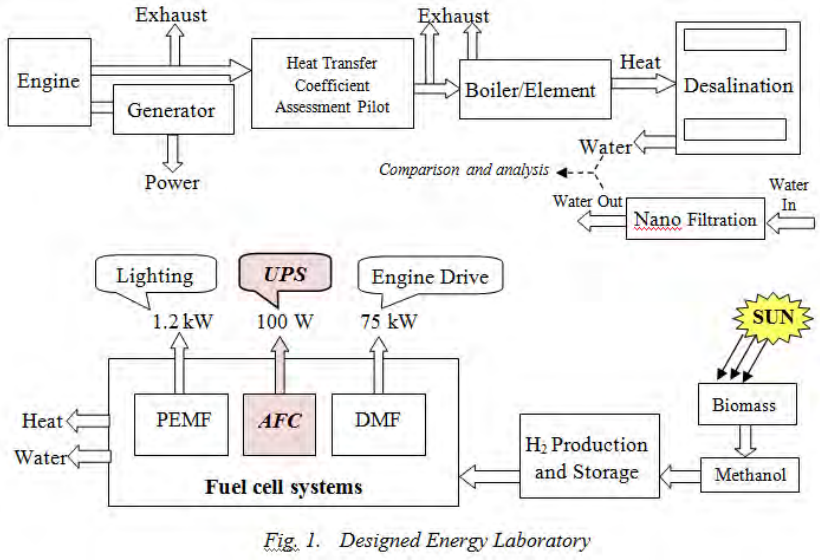

Fig. 1. Designed Energy Laboratory

Fig. 1. Designed Energy Laboratory

The basic structure design for mobile electrolyte AFC system [3] is shown in Fig.2.

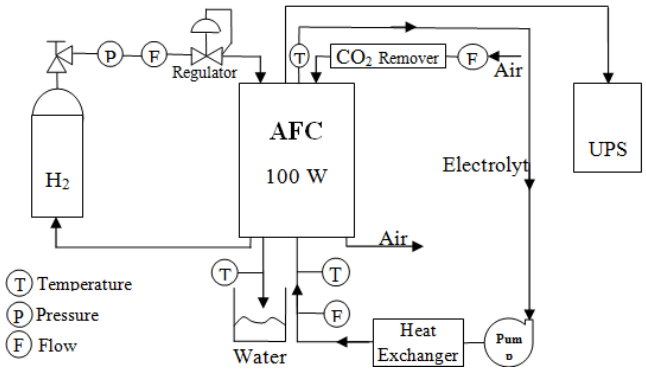

Fig. 2. Alkaline fuel cells with mobile electrolyte system and peripheral equipments

Procedures in this type of systems is so that the electrolyte flow between the anode and cathode plates in addition ion transfer and electric current; with its circulation led the excess heat of system to the outside and before re-entry into the system shall pass within a heat exchanger for cooling. Electrolyte needs pumping system us to held circulating [1].

2.1. Electrochemistry

According to voltage losses [4] in a fuel cell system, optimum current is achieved so that losses would be minimum, and thus optimal power and voltage are obtained [5,6]. Types of efficiencies that are considered in this system are ideal and actual thermodynamic efficiency and electrical efficiency that can be helpful to evaluation of system.

2.2. Engineering design

Hydrogen and air consumption, and water, electricity and heat production flow rates are calculated. A fuel cell stack consists of many separate cells. Design of stack and cells arrangement (after obtain the whole required surface) can has different modes. According to the desired power, energy demand and circumstances can decide regarding choice of optimized mode.

2.3. Heat Transfer

In mobile electrolyte systems, the cooling process is done by electrolyte. So according to the rate of heat production in electrochemical reactions and selected materials [7,8], electrolyte flow rate can set somehow that eject the waste heat from system and kept system performance in ideal temperature [9,10]. Overall fuel cell system heat transfer can be done through conduction, convection and radiation. Since the alkaline fuel cell systems have low operation temperature, radiant heat transfer can be waivered [11].

3. System Modeling

To begin calculations, considering series of assumptions and initial conditions are necessary [12]. The system is considered to produce 100 watt in atmospheric pressure. It is assumed that produced water is in liquid form. Electrochemistry relations have scrutinized with optimization voltage and current using GAMS software. The optimum solution determined efficiency values and input and output flow rates. According to the steps of stack and cells arrangement [13], algorithm of Fig.3 can be used in modicum number studies.

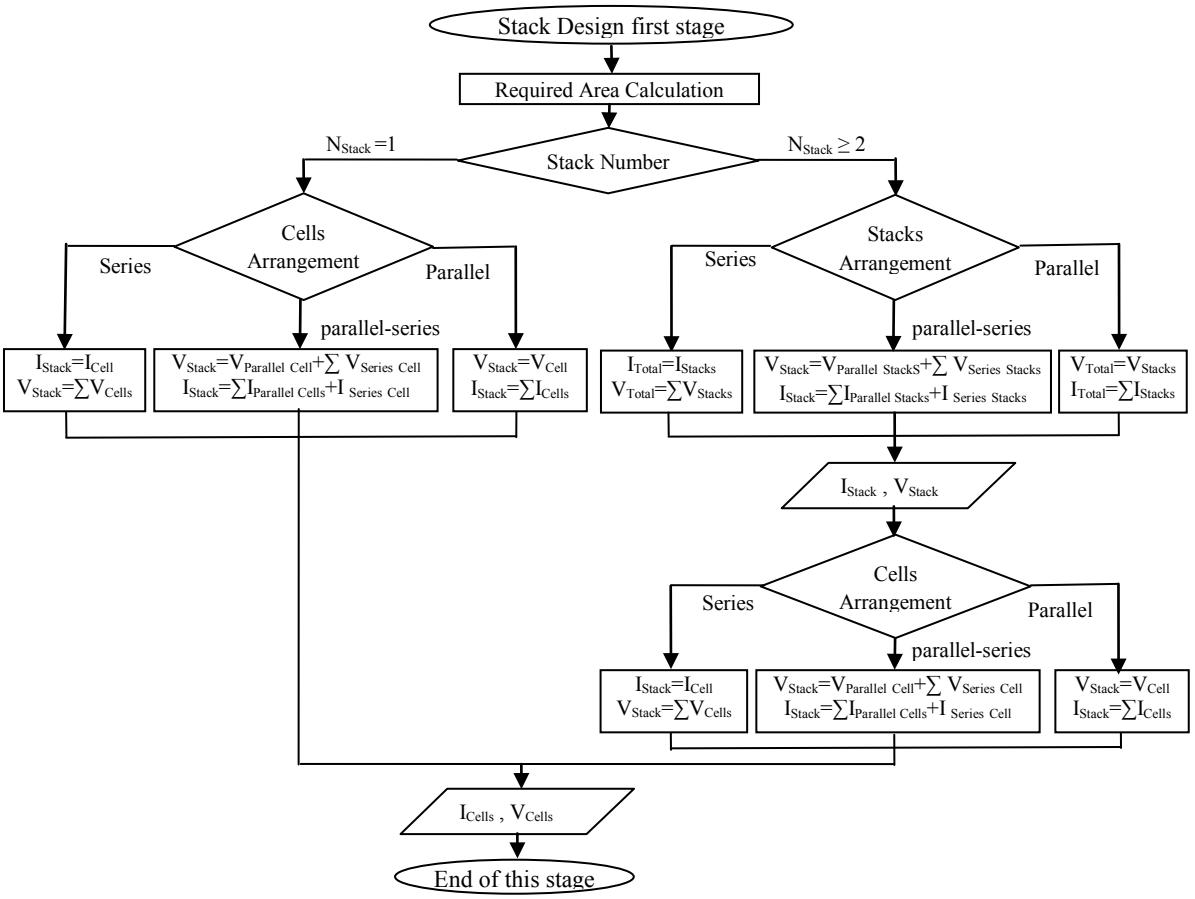

Fig. 3. Stack design algorithm

To evaluate heat transfer of system, anode, cathode and the whole of system are considered as three distinct control volumes, and heat and mass transfer relationships are extracted [14,15]. As noted, according to system description, a heat exchanger is required. For this purpose a double pipe heat exchanger is designed which electrolyte as the warm fluid have streaming in the inner tube and water consider as cooling fluid within the external tube [16]. In order to having a circulating electrolyte stream a proportional pump should be applied.

3.1. Cost model

A mobile alkaline electrolyte fuel cell system requires peripheral equipment such as hydrogen storage tank, circulating pump to provide the electrolyte driving force, heat exchanger and series of additional process such as hydrogen production. So in addition to the fuel cell cost, there are other equipments that should be considered. Thus, if consider the computing for 1000 hours annual performance, five years of application, and 15% inflation rate, with determining costs equation and set values also using the equations of heat transfer section and the heat exchanger design, it could be possible to optimize the overall system performance. For this purpose, GAMS code was developed, using heat transfer, heat exchanger design and the cost model equations the aim to minimize required cost to obtain the optimal heat exchanger area, rate of input and output flows and temperatures in the heat exchanger.

If design and calculation steps collect in an algorithm and associate them with each other, algorithm of Fig.4 will be obtained:

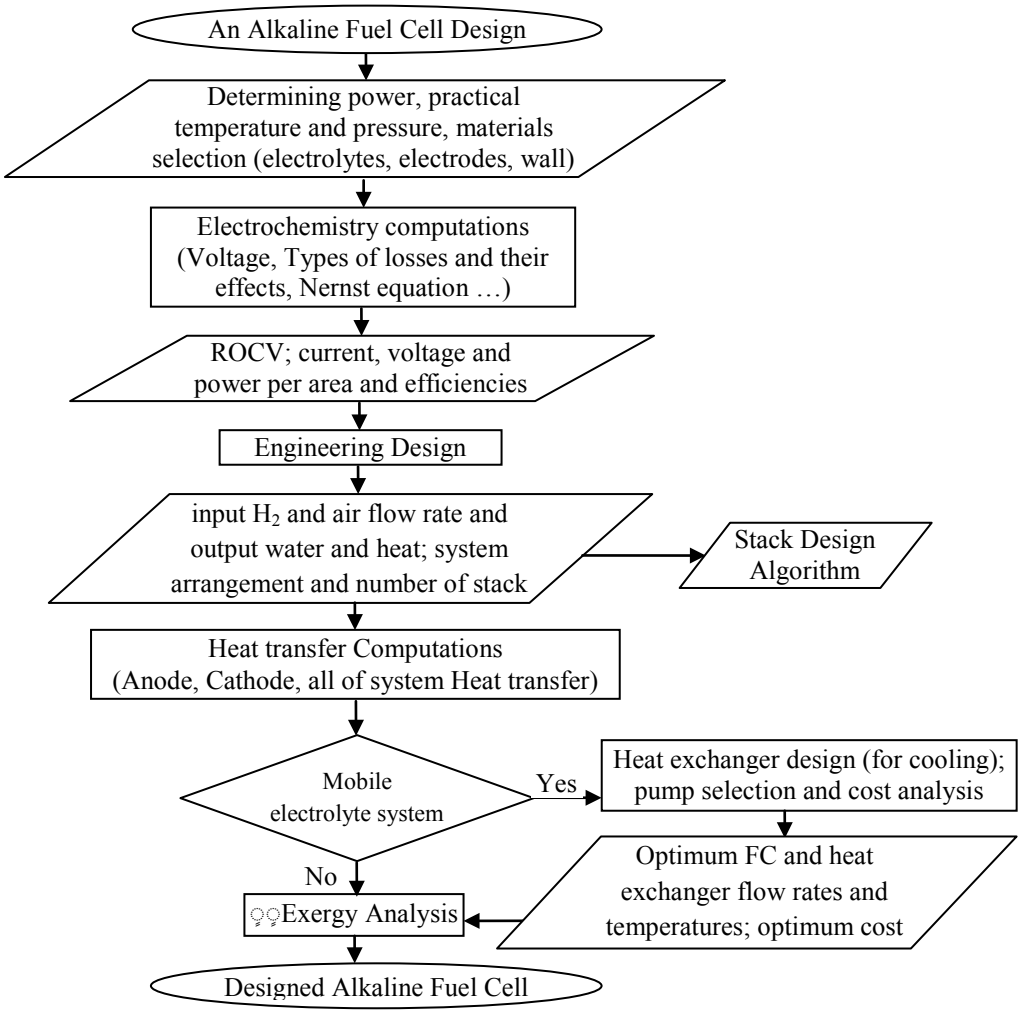

Fig. 4. Main steps of system design algorithm

4. Results

The results of electrochemical section and codes are presented in Table 1 and Fig.5 :

Table 1. Optimum electrochemical results

Voltage *(V)*	Current Density *(mA/cm^2)*	Power *(mW/cm^2)*
0.566	574.316	325.19

Required area for desired power is 308cm^2. Relation between voltage and current density [17, 18] is affected by irreversibilities and when cell current [19] increases, voltage of cell drops [20] because of activation, ohmic and mass transfer losses.

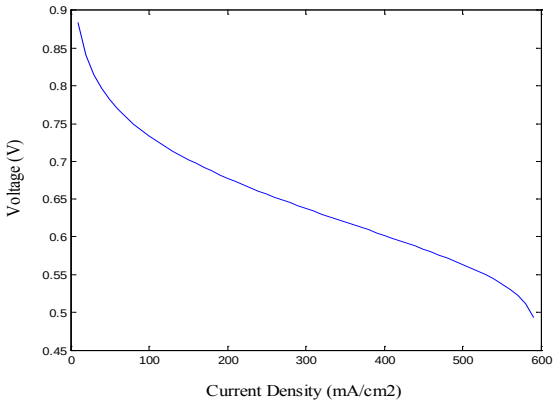

Fig.5. Voltage-Current graph

Designed system performance is presented in Table 2.

Table 2. Amount of efficiencies

Ideal thermodynamic efficiency	Actual thermodynamic efficiency	Electrical efficiency
80%	38%	34%

In engineering design step inlet and outlet flow rates are calculated as Table 3.

Table 3. Electrochemical flow rates

Hydrogen	Oxygen	Inlet air	Outlet air	Produced water	
1.85×10^{-6}	1.48×10^{-5}	1.26×10^{-4}	1.12×10^{-4}	1.65×10^{-10}	(kg/s)

Also it is concluded that for 100W power, overall 263W energy is generated. So it is seen that power to overall energy ratio is exactly 38%; and this is equal with calculated actual thermodynamic efficiency. Estimated cost for designed system in five years of operation is 2560 $. Obtained temperature, required area and flow rates in optimal mode are as Table 4:

Table 4. Optimum temperature, required area and flow rates

Electrolyte inlet to heat exchanger and outlet of cell temperature	40 (^{0}C)
Mass flow rate of electrolyte	1.6×10^{-4} (Kg/s)
Electrolyte outlet of heat exchanger and inlet to cell temperature	73 (^{0}C)
Cold fluid mass flow rate (Water)	2.827×10^{-4} (Kg/s)
Cold fluid outlet temperature (Water)	25 (^{0}C)
Area of heat exchanger	0.07 (m^2)
Pressure drop	5.2×10^{-4} (Pa)
Total Heat rate	121.7 (W)

The performance of cell is under influence of different factors, such as temperature. In order to peruse the effect of temperature on cell and all of system (cell and peripheral equipment), the graphs of difference efficiencies toward temperature are depicted in Fig.6. It is found that

because of reducing sensitivity of total system toward temperature with existing cooling section, its gradient is less than ideal performance of cell.

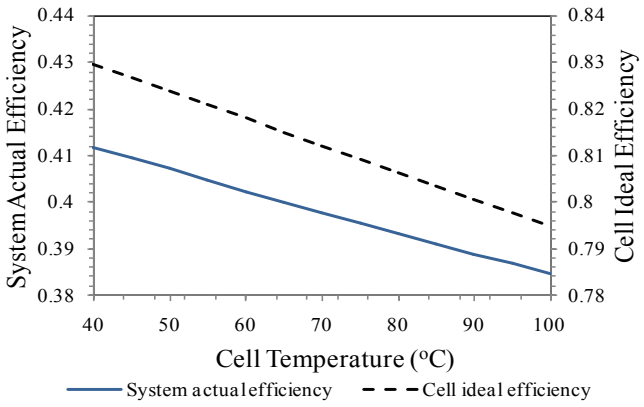

Fig. 6. Difference efficiency toward performance temperature

Nether graph is depicted to survey the effect of parameters variations toward electrolyte outlet temperature from AFC. As seen in Fig.7, with increasing temperature, flow rate of electrolyte and its pressure drop that depend on circulating flow rate, moreover the actual efficiency of system, are decreased. However, required heat exchanger area increases; because it should cool the warmer electrolyte. The minimum value of system total cost, which is obtained from system optimization GAMS codes, has been shown in this graph.

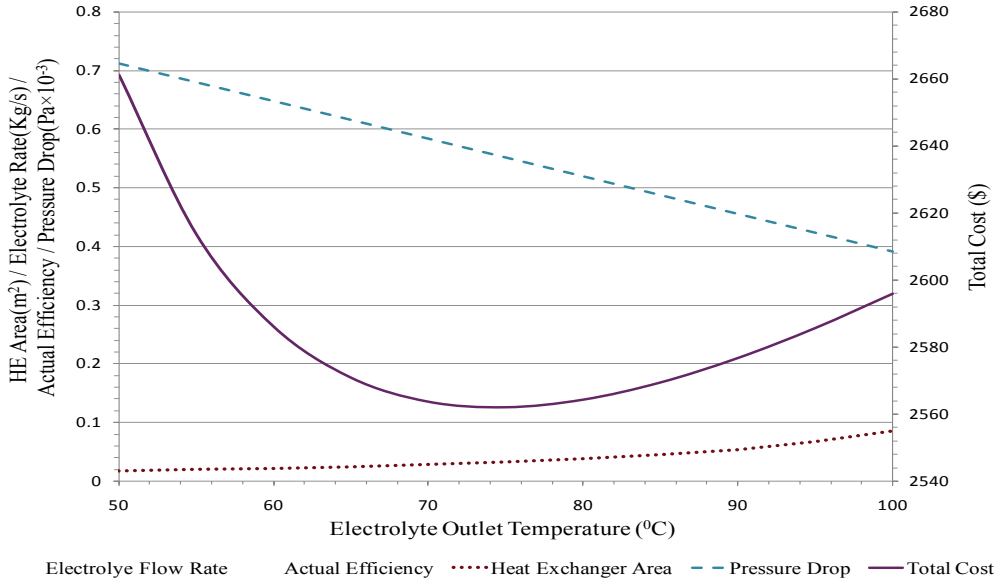

Fig. 7. Change of parameters toward electrolyte outlet temperature

Considering the gradient of cost in Fig.7, by temperature reducing before minimum cost, increasing of cost is more strongly; But after minimum cost by rising of temperature cost increasing is milder; And this suggests that circulating system is more effective than cooling system on total cost (Fig.8 confirm this matter, too).

Fig.8 is depicted to survey parameters variations toward electrolyte inlet temperature to AFC. As seen, with increasing temperature, flow rate of electrolyte and its pressure drop increase; because the electrolyte with increasing the circulation rate can compensate additional heat. Similar to Fig.7, increasing temperature of cell has led to decrease the actual efficiency of

system. Also required heat exchanger area is decreased; because it does not need to cool electrolyte to lower temperature and it needs lesser area.

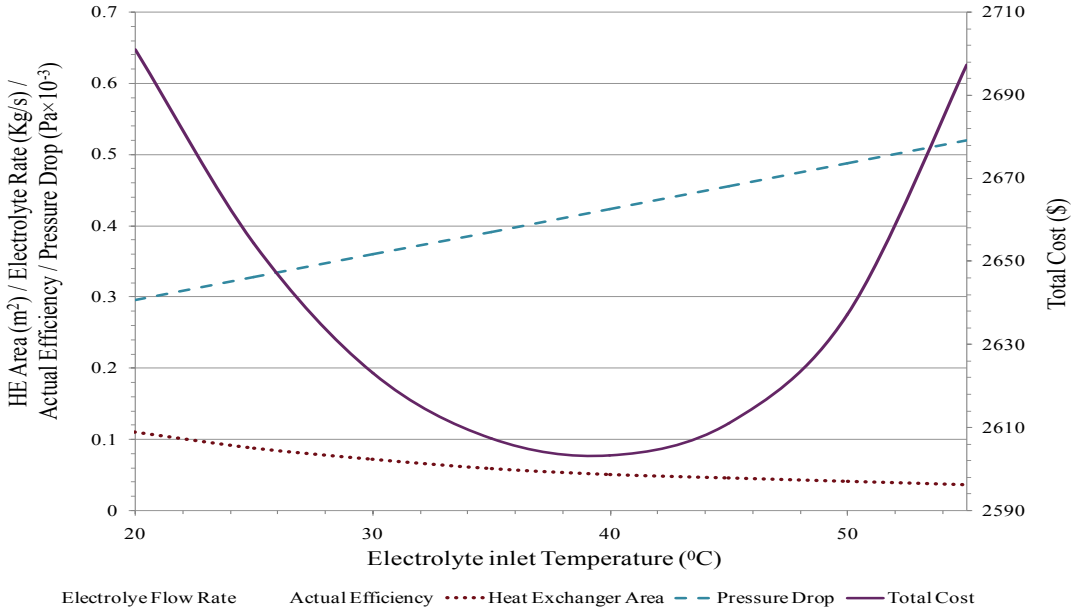

Fig. 8. Change of parameters toward electrolyte inlet temperature

According to the influential parameters plotted in the graphs and change quantities, from it is seen quality viewpoint that priority of items that effect the composite AFC system are for electrolyte pressure drop, electrolyte flow rate and heat exchanger area, respectively and two first items are running cost type, and third item is fixed cost type.

In Fig.7 and Fig.8, the effect of electrolyte input and output temperatures have been evaluated, hence with combining them the effect of ΔT changes can be deduced. Except actual efficiency of system, the changes sense is same with flow rate, pressure drop, heat exchanger area at all values, and also with total cost before and after the minimum point.

5. Conclusions

In the presented research, a 100W alkaline fuel cell with mobile electrolyte and its peripheral equipment have been designed in determined steps to achieve a design model. Presented model has been optimized using GAMS codes to find optimum values of cost model, electrochemical and heat transfer equations.

It was concluded that electrolyte flow rate and its inlet and outlet temperatures, pressure drop, heat exchanger area are some of parameters that effect on cell performance and total cost. Also the efficiency of system reduces toward temperatures rising.

Change of total cost is more sensitive toward input electrolyte temperature rather than output electrolyte temperature. Because input flow controls by peripheral systems; but outlet temperature is a function of fuel cell operation.

Also it was found that running cost is more effective parameter than the fixed cost, in the total cost of systems with similar capacity.

References

[1] J. Larminie, A. Dicks, Fuel Cell Systems Explained, Second Edition, 2002.

[2] M.C. Williams, EG&G Technical Services, Fuel Cell Handbook, Seventh Edition, 2004.

[3] E. Brillas, F. Alcaide, P. Cabot, A small-scale flow alkaline fuel cell for on-site production of hydrogen peroxide, Journal of Electrochimica Acta, 2002.

[4] M. Shen, K. Scott, Power loss and its effect on fuel cell performance, Journal of Power Sources, 2005.

[5] H. ghadamian, Quantitative analysis of irreversibilities causes voltage drop in fuel cell (simulation & modeling), Journal of Electrochimica Acta, 2004.

[6] N. Sammes , Fuel Cell Technology, 2006.

[7] F. Bidault, D.J.L. Brett, P.H. Middleton, N. Abson, N.P. Brandon, A new application for nickel foam in alkaline fuel cells, Journal of Hydrogen Energy, 2009.

[8] M. Schulz, E. Gulzow, G.Steinhilber , Activation of nickel-anode for alkaline fuel cells, Journal of applied surface science, 2001.

[9] G.F. McLean ∗, T. Niet, S. Prince-Richard, N. Djilali, An assessment of alkaline fuel cell technology, Journal of Hydrogen Energy, 2002.

[10] C. Siegel, Review of computational heat and mass transfer modeling in polymer-electrolyte-membrane (PEM) fuel cells, Journal of Energy, 2008.

[11] J. Holman, Heat Transfer, ninth Edition, 2002.

[12] M.W. Davis, Proposed Testing Methodology and Laboratory Facilities for Evaluating Residential Fuel Cell Systems, 2002.

[13] F. Barbir, Fuel cell stack design principles with concepts of micro-mini fuel cells, 2008.

[14] R.E. Sonntag, C. Borgnakke, G.J. Van Wylen, Fundamentals of Thermodynamics, Sixth edition, 1973.

[15] I. Verhaert, M.D. Paepe, G. Mulder, Thermodynamic model for an alkaline fuel cell, Journal of Power Sources, 2009.

[16] E.A.D. Saunders, Heat Exchangers (Designing for heat transfer), 1988.

[17] Yu. G. Chirkov, V. I. Rostokin, Alkaline fuel cells: calculating and comparing overall currents of hydrophobized cathodes with thin regular-structure and thick stochastic-structure active layers, Russian Journal of Electrochemistry, 2008.

[18] P. Gouérec, L. Poletto, J. Denizot, E. Sanchez-Cortezon, J.H. Miners, The evolution of alkaline fuel cells with circulating electrolyte, Journal of Power Sources, 2004.

[19] X.H. Wang, Y. Chen, H.G. Pan, R.G. Xu, S.Q. Li, L.X. Chen, C.P. Chen, Q.D. Wang, Electrochemical properties of $Ml(NiCoMnCu)_5$ used as an alkaline fuel cell anode, Journal of Alloys and Compounds, 1999.

[20] J.H. JO, S.K. MOON and S.C. YI, Simulation of influences of layer thicknesses in an alkaline fuel cell, Journal of Applied Electrochemistry, 2000.

Volume 5

Goethermal Applications

Energetic performance evaluation of an earth to air heat exchanger system for agricultural building heating

Onder Ozgener[1,*], Leyla Ozgener[2]

[1]*Solar Energy Institute, Ege University, Bornova, Izmir, Turkey*
[2]*Department of Mechanical Engineering Faculty of Engineering,*
Celal Bayar University, Muradiye, Manisa, Turkey
** Corresponding author. Tel: +90 232 3111232, Fax: +90 232 3886027, E-mail: Onder.Ozgener@ege.edu.tr*

Abstract: The main objective of the present study is to investigate the performance characteristics of an underground air tunnel (**E**arth to **A**ir **H**eat **E**xchanger) for greenhouse heating with a 47 m horizontal; 56cm nominal diameter U-bend buried galvanized ground heat exchanger. This system was designed and installed in the Solar Energy Institute, Ege University, Izmir, Turkey. Based upon the measurements were made in the heating mode. The system COP was calculated based on the amount of heating produced by the air tunnel and the amount of power required to move the air through the tunnel.

Keywords: *Energy, earth to air heat exchangers, COP, sustainable resources*

Nomenclature

COP, heating coefficient of performance of the system
D *pipe diameter*
f *fraction losses coefficient*
$h_{a,i}$ *specific enthalpy at underground air tunnel inlet*
$h_{a,0}$ *specific enthalpy at underground air tunnel outlet*
$h_{b,i}$ *specific enthalpy at blower input*
$h_{b,o}$ *specific enthalpy at blower output*
$h_{v,i}$ *specific enthalpy of water vapor at underground air tunnel inlet*

T_f *arithmetic average temperature of air flowing in buried pipe*
U *Velocity*
V *volumetric flow rate of air*
w_i *absolute humidity at underground air tunnel inlet (kg moisture per kg dry air)*
w_0 *absolute humidity at underground air tunnel outlet (kg moisture per kg dry air)*

$\dot{W}_b$ *work input rate to the blower*
$h_{v,0}$ *specific enthalpy of water vapor at underground air tunnel outlet*
$\bar{h}_a$ *convective heat transfer coefficient of air*
k *coefficient of thermal conductivity of pipe*
L *pipe length*
$\dot{m}_a$ *mass flow rate of air*
Nu *Nusselt number*
Pr *Prandtl number*
Re *Reynolds number*
$\dot{Q}_r$ *extracted heat (underground air tunnel load)*
T_w *measured temperature of pipe surface.K, ºC*

Greek letters

η_{mec} *mechanic efficiency of fan*
ΔP *pressure loss*
ζ *particular resistance losses of pipe line*
ρ *density of air*

1. Introduction

Although various studies [e.g., 1-6] were undertaken to evaluate the performance of underground air tunnel, as described previously, to the best of authors' knowledge, except authors' previous works [1-5] no studies on the performance testing of an underground air tunnel with a 47m, 56cm nominal diameter U-bend horizontal galvanized ground heat exchanger for greenhouse cooling have appeared in the open literature under Turkey's conditions. This study consists of an alternative to heating greenhouses with the utilization of an underground air tunnel system. The present study undertakes performance evaluation of underground air tunnel systems –earth to air heat exchangers (EAHE)- and applies to a local one in Turkey. Namely, thermodynamics performance of an EAHE has been evaluated in a demonstration in Solar Energy Institute of Ege University, Izmir, Turkey.

2. System Description

2.1. Experimental set-up

This system mainly consists of two separate circuits: (i) the fan (blower) circuit for greenhouse cooling, and (ii) the ground heat exchanger (GHE) (underground air tunnel). The underground air tunnel system studied was installed at the Solar Energy Institute of Ege University (latitude 38^o 24' N, longitude 27^o 50' E), Izmir, Turkey. Solar greenhouse was positioned towards the south along south-north axis. The greenhouse will be conditioned during the summer and winter seasons according to the needs of the agricultural products to be grown in it. A positive displacement type of air (twin lobe compressor) blower of 736 Watt capacity and volumetric flow rate of 5300m^3/h was fitted with the suction head positioned in the southwest corner of the greenhouse [1-5].

2.2. Measurements

Experiments were performed at the Ege University, Izmir, Turkey. A galvanized pipe of 56cm in diameter 47m in length was buried in the soil at about 3m in depth, a galvanized pipe of 80cm in diameter 15m in length. The three main reasons for this (i) air blowing speed is advised to be 0-3m/s in greenhouses in terms of efficient grow crop from unit area, (ii) blower power consumption rate was reduced due to low pressure losses, and (iii) pipe works as a heater. It is well known that increasing surface area of heater leads to increasing convection heat transfer rate. Due to the reasons listed, pipe diameter was selected as large. The soil at site was a mixture of clay, sand and small rocks. A sample of the soil taken from 3m depth was tested for thermal properties. Thermal conductivity was estimated to be 2.850W/mK.Temperatures of air, galvanized pipe surface, and soil at different locations was measured using PT-100 resistant thermometers. The temperatures of the air were measured at distances of 0, 4.2m, 8.4m, 12.6m, 16.8m, 21.2m, 25.6m, 29.8m, 34m, 38.2m, 42.4m, and 47m from the inlet end. Since the resistant thermometers used to measure the air temperature in the pipe were not shielded, there would be a small error in the air temperature measurement because of infra red radiative transfer between the resistant thermometers and the pipe surface and line voltage drop between measuring point and display. To measure soil and pipe surface temperatures, the resistant thermometers was positioned in the soil at the 25.6m length of the pipe. Air velocity in the pipe measured about 1m from the entrance; these measurements were subject to error because of entry length. To minimize the errors, air velocity was at several points on four different points and then averaged [1-5].

3. Analysis

In this context, two different ways of formulating heat extraction rate. The first form of the rate of heat extraction by the underground air tunnel in the heating mode $\dot{Q}_r$ is calculated from the following equation [1-5]

$$\dot{Q}_r = \dot{m}_a\left(h_{a,i} - h_{a,o}\right) \qquad (1)$$

where

$h_{a,i} = \left(h_a\right)_i + w_i\left(h_v\right)_i$ and $h_{a,o} = \left(h_{a,o}\right) + w_o\left(h_{v,o}\right)$.

Note that here; the values of $h_{a,i}$ and $h_{a,o}$ can be directly obtained from the psychometric chart. The second form of the rate of heat extracted by the underground air tunnel can be written as follows:

$$\dot{Q}_r = \bar{h}_a A\left(T_w - T_f\right) \qquad (2)$$

with

$$\bar{h}_a = \frac{Nuk}{D}, \qquad (3)$$

$$Nu = 0.023\,\mathrm{Re}^{0.8}\,\mathrm{Pr}^{1/3}, \qquad (4)$$

where $\bar{h}_a$ is the convective heat transfer coefficient of air, A is the surface area of the underground air tunnel (galvanized pipe), T_w is the temperature of pipe surface, T_f is average temperature of air flowing in buried pipe (U-tube), k is the coefficient of thermal conductivity of the pipe, and D is the pipe diameter. The convective heat transfer coefficient " $\bar{h}_a$ " in the above equations depends on the Reynolds number, the shape and roughness of the pipe for turbulent flow. The work input rate to the blower is

$$\dot{W}_b = \frac{\dot{m}_a\left(h_{b,i} - h_{b,o}\right)}{\eta_{mec}} \qquad (5)$$

or

$$\dot{W}_b = \frac{\Delta P V}{\eta_{mec}} \qquad (6)$$

where ΔP is the pressure loss, V is the volumetric flow rate of air, and η_{mec} is the mechanic efficiency of the blower. ΔP is written as follows:

$$\Delta P = 0.5 f \frac{L}{D}\rho U^2 + \Sigma\zeta \qquad (7)$$

where U is the velocity, f is the fraction losses, ζ is the particular resistance losses and L is the pipe length. Hence, the COP of the system can be calculated as

$$COP = \frac{\dot{Q}_r}{\dot{W}_b} \qquad (8)$$

The coefficient of performance of the overall heating system *(COP)* is the ratio of the greenhouse heating load (heat extracted by the underground air tunnel, $\dot{Q}_r$) to work consumption of the blower ($\dot{W}_b$). It can be noticed that the heat generated by the fan goes into the heated space.

4. Results and Discussion

In the present study, the results obtained from the experiments were evaluated to determine the overall performance of the system. The minimum ambient air temperatures varied between 4.7 and 13 ^{o}C during the experimental studies. If the system is operated, the maximum greenhouse temperatures changes between 13.1 and 25.2 ^{o}C. The average values of the temperature for the ambient air and the greenhouse are obtained to be 12.98 ^{o}C and 20.2 ^{o}C, respectively. When the system operates, the greenhouse air is at a minimum day temperature of 13.1^{o}C with a relative humidity of 32%. The maximum COP of the underground air tunnel system occurred at approximately 07:31 AM on November 29, 2009. For example, the maximum heating power of 4.5 kW could be realized at 07:31 PM for the buried pipe with the radius of 0.28m. Fig. 1 shows the COP and heating capacity variations of the underground air tunnel system of 0.28m radius, and illustrates the hourly variations of COP for the period studied. The maximum heating coefficient of performance of the underground air tunnel system is about 6.42, while its minimum value is about 0.98 at the end of a cloudy and cold day and fluctuates between these values at other times. The total average COP in the heating season is found to be 5.16.

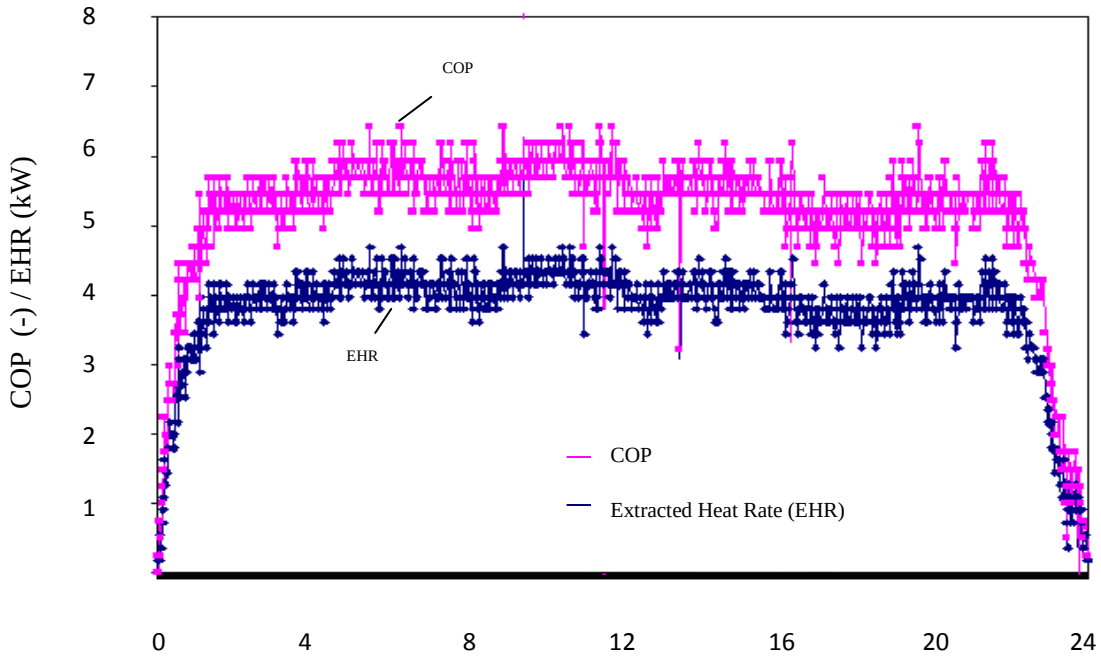

Fig. 1. Hourly variations of heating capacity and COP of the underground air tunnel system [4]

5. Conclusions

The experimental results indicate that this system can be used for greenhouse heating in the Mediterranean and Aegean regions of Turkey. During this test the underground air tunnel was able to provide 60.8 percent of the design heating load cold winter days. In spite of difficulties primarily encountered in coupling geothermal energy with conventional space heating and cooling equipment, underground air tunnels seem to be an exciting alternative [4].

Acknowledgements

The authors are grateful to Ege University Research Fund due to their financial supports.

References

[1] O. Ozgener, L. Ozgener, Exergoeconomic analysis of an underground air tunnel system for greenhouse cooling system, International Journal of Refrigeration 33(5), 2010, pp. 995-1005.

[2] O. Ozgener, L. Ozgener, Exergetic assessment of EAHEs for building heating in Turkey: A greenhouse case study, Energy Policy 38(9), 2010, pp. 5141-5150.

[3] L. Ozgener, O. Ozgener., Experimental study of the exergetic performance of an underground air tunnel system for greenhouse cooling, Renewable Energy 35(12), 2010, pp. 2804-2811.

[4] L. Ozgener, O. Ozgener, Energetic performance test of an underground air tunnel system for greenhouse heating, Energy 35(10),2010, pp. 262-268.

[5] O. Ozgener, L. Ozgener, D.Y. Goswami, Utilization of earth air heat exchangers for solar greenhouses pre heating and performance analysis. Project no: 09GEE003, supported by Ege University Research Fund , 2009, Continuing Project

[6] D.Y. Goswami, S. Ileslamlou, Performance analysis of a closed loop climate control system using underground air tunnel. Journal of Solar Energy Engineering 112, 1990, pp. 76-81.

An adaptive design approach for a geothermal plant with changing resource characteristics

M. Imroz Sohel[1,*], Mathieu Sellier[2], Susan Krumdieck[2]

[1] *Scion, Te Papa Tipu Innovation Park, 49 Sala Street, Rotorua, New Zealand*
[2] *Department of Mechanical Engineering, University of Canterbury, Private bag 4800, Christchurch, New Zealand*
** Corresponding author. Tel: +64 7 3435730; fax: +64 7 3435375; E-mail address: mohammed.sohel@scionresearch.com*

Abstract: Geothermal power plants are designed for optimal utilization of geothermal resource. However, geothermal fields typically undergo significant changes in resource characteristics such as pressure, temperature and steam quality over their life span. With appropriate reservoir modelling it is possible to predict the future resource characteristics of a geothermal field to a reasonable degree of accuracy. We propose a new adaptive design approach that would allow geothermal power plants to take into account the change of resource characteristics that occur over a 30-40 years time horizon based on the results of reservoir modelling. Currently, it is difficult and expensive to modify or renovate an existing plant due to space constraints, piping arrangements, transportation of machinery etc. The adaptive design approach would allow cost effective modifications in operation and equipment to adjust to changes in resource characteristics in the future. A simple model for a typical combined cycle geothermal power plant is considered as a test case for the adaptive design approach. Simulation is carried out using changes in both wellhead specific enthalpy and mass flow rate. There are four case studies presented in this paper that analysed various possible options of the hypothetical power plant depending on the changes in resource characteristics. Taking into account the results of the simulation, alternative plant designs are presented and improvements in performance are discussed. Although, the initial investment cost might go up as a consequence of adaptive design, over the life span of the plant the total benefit may be greater.

Keywords: *Geothermal power, resource characteristics change, adaptive design, low temperature power source.*

1. Introduction

We are at a point of time when on one hand, the negative effects of anthropogenic atmospheric alteration are more evident than ever, and on the other, the demand for energy is ever increasing. Although it claimed that there exists a vast reserve of fossil fuel, field by field petroleum production is decreasing [1]. The huge challenge of emission reduction, growing energy demand and peak oil can be approached in two ways. Firstly, by improving energy conversion efficiency of traditional energy sources and secondly, switching to more and more renewable energy sources. Unfortunately, most renewable energy sources are dependent on climatic variation and are not suitable for base load operations. Geothermal energy, on the contrary, provides a clean, reliable source of renewable energy. Energy concentration in geothermal sources is much higher than in many other renewable sources. Moreover, geothermal power plants are considered to have significant lower CO_2 emissions than a standard combined cycle power plant or a pulverized coal fired power plant [2].

Current research and development trends towards geothermal power generation, specifically, low temperature power cycles are noticeable [3-12]. Geothermal power plants are generally designed based on constant resource characteristics. However, it has been observed in many plants that the resource characteristics change significantly throughout the lifetime of the plant [13]. Consequently, deterioration of plant performance and unplanned design changes occur. However, geothermal power plants are very capital intensive and it is not very easy to change a plant to adapt to resource characteristics different from the original design.

By appropriate reservoir modelling, it is possible to predict future resource characteristics depending on various parameters including the rate of resource utilization, the percentage of brine reinjection etc [14]. In this paper we propose an adaptive design approach where provisions are kept for a plant to adapt to resource characteristics changes at the time of building which may save a great deal of effort and money in the long run. We have presented several case studies to demonstrate the benefit of the adaptive design approach.

2. Methodology

We have taken a hypothetical combined cycle geothermal power plant for our study. The geothermal fluid is a mixture of steam and brine. Steam is separated from the brine in a suitable separator then used to power a steam turbine. The exhaust steam from the steam turbine is used to power bottoming organic Rankine cycle units (BOT-ORC). The separated brine is also used in other organic Rankine cycle units (BRN-ORC). After the heat recovery, both condensed steam and geothermal brine are mixed together and reinjected to the reservoir. Pentane is used as the working fluid in the binary cycles. Fig. 1 shows a schematic of the hypothetical power plant. The base case considered here has four BOT-ORCs and two BRN-ORCs as presented in Fig. 1.

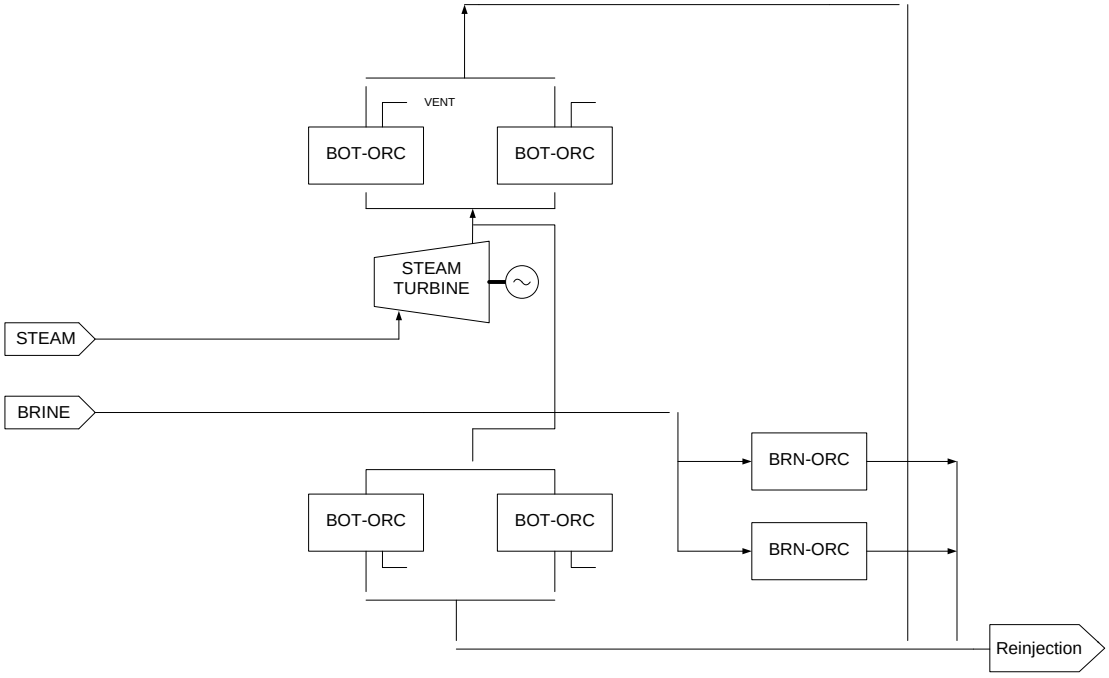

Fig. 1. Schematic diagram of the combined cycle geothermal power plant.

2.1. The component model

Simple models have been used for the analysis presented here. Independent component modules are developed in Matlab/Simulink [15] which can be connected later to develop a system model. The thermo-physical properties are calculated using the REFPROP [16] database. The working fluid flow round the cycle and each process may be analysed using the energy conservation, mass conservation and entropy generation applied to a system boundary around each system component. Changes in kinetic energy and potential energy may be neglected and equilibrium conditions can be assumed at the cross-sections of both inlet and outlet. Detailed discussion on the modelling of these ORCs is available in our previous work [9].

2.2. The Resource Affected Performance Model

A geothermal field passes through four different phases or periods [13]: (1) development, (2) sustainment, (3) decline and (4) renewable. During the last phase, a geothermal resource approaches the ideal of a sustainable and renewable resource. To attain this pahse requires prudent management of the resource. In a Resource Affected Performance Model (RAPM) we change the geothermal resource characteristics and observe the effect on plant performance. We assume that the reservoir modelling predicts that the geothermal resource enthalpy will increase from about 1400 kJ/kg to 2000 kJ/kg over the life time of the power plant. An adaptive design approach is discussed here which keeps provision for this change in resource characteristics.

Applying conservation of mass at the well head

$$\dot{m}_T = \dot{m}_b + \dot{m}_s \tag{1}$$

where, $\dot{m}_T$ is the total mass flow rate at the well head, $\dot{m}_b$ is the brine mass flow rate and $\dot{m}_s$ is the steam mass flow rate. Dividing Eq. (1) with $\dot{m}_T$ yields

$$1 = C_b + C_s \tag{2}$$

where, C_b is defined as brine content and C_s is defined as steam content. It is advantageous to express resource characteristics as steam content (C_s). Applying energy balance at the well head

$$\dot{m}_T h_R = \dot{m} h_b + \dot{m} h_s \tag{3}$$

where, h_R is the resource enthalpy, h_b is the enthalpy of the brine (saturated liquid) and h_s is the enthalpy of the steam (saturated vapour). The reinjection temperature is calculated from the energy balance of mixing of brine and condensate before reinjecting to the geothermal field.

$$\dot{m}_T h_{RNG} = \dot{m}_b h_b + \dot{m}_c h_c \tag{4}$$

where *RNG* stands for reinjection, *b* stands for brine and *c* stands for condensate.

From Eq. (2), if the steam content of a geothermal field (C_s) increases, the brine content (C_b) must be reduced and vice versa. If we want to keep $\dot{m}_b$ and h_b unchanged as C_s increases or decreases, we must manipulate parameters of the left hand side of Eq. (3). Since, h_R is the parameter characterised by geothermal resource, we may not want to manipulate it. The only suitable solution would be to control the geothermal fluid flow rate ($\dot{m}_T$). When C_s increases, we can keep $\dot{m}_b$ constant by using condensate recirculation and increased geothermal fluid flow rate ($\dot{m}_T$). If we are interested only on the constant heat transfer in the vaporizer, the reinjection temperature (i.e. brine outlet temperature) can be lowered. The following assumptions are made for the RAPM.

1. Operating state points of the geothermal power plant remain unchanged i.e., the change in mass flow rate in steam and brine are only responsible for the change in overall heat transfer coefficient.
2. To control the vaporizer steam outlet condition, excess steam is vented to the atmosphere.
3. The off-design well-head condition is always within the wet-steam zone i.e., there is no change in temperature at the well head and the geothermal fluid is a mixture of steam and brine.

3. Results

There are four case studies presented which analyze adaptive design approach to address the change in geothermal resource characteristics. These case studies present four possible solutions for the assumed future resource characteristics.

3.1. The base case

Normally, each turbine has an operating limit and for the steam turbine it has been fixed to 37 MW. For the pentane turbine the maximum power is fixed at 7 MW. Fig. 2 shows the plant output in the base case as the resource enthalpy increases. With increasing steam content from about 25% (1400 kJ/kg) to about 35%, the steam turbine reaches its maximum and produces the same power thereafter. Since the steam turbine is unable to utilize the excess steam, the bottoming cycle is receiving condensate at an elevated mass flow rate. Therefore, the power output of the BOT-ORC increases and owing to a lack of brine, the BRN-ORCs are producing much less than their capacity.

3.2. Case study 1: increased geothermal fluid flow rate

The reduced brine flow problem can be tackled in many ways. If one uses excess geothermal brine to reheat the condensate collected from the BOT-ORC, an increased mass flow of brine can be ensured for the BRN-ORC. Fig. 3 presents a schematic diagram of such a design. Here, more power is being produced at the expense of more geothermal fluid, which means the resource is being utilized at a higher rate; not necessarily ensuring optimum utilization. Fig. 4 shows a corresponding improvement in plant performance by adopting this approach. It is noticeable from Fig. 4 that the BRN-ORC produces gradually less power from 25% steam content to 35% then its power production is independent of steam content. Since, it is more efficient to directly expand steam in a turbine to produce power than in bottoming cycle, one should utilize as much steam as possible in the steam turbine within its manufacturing limit. By increasing the geothermal fluid flow rate, the brine reinjection temperature does not change much.

3.3. Case study 2: upgrading the steam turbine

Fig. 5 shows the performance of the geothermal power plant with increasing steam content when the original steam turbine is replaced with a higher capacity. The rated capacity of the new turbine is assumed 42 MW with the maximum power 47 MW. It is evident from the figure that such an upgrade results in significant improvement in power output. However, it is associated with large capital investment.

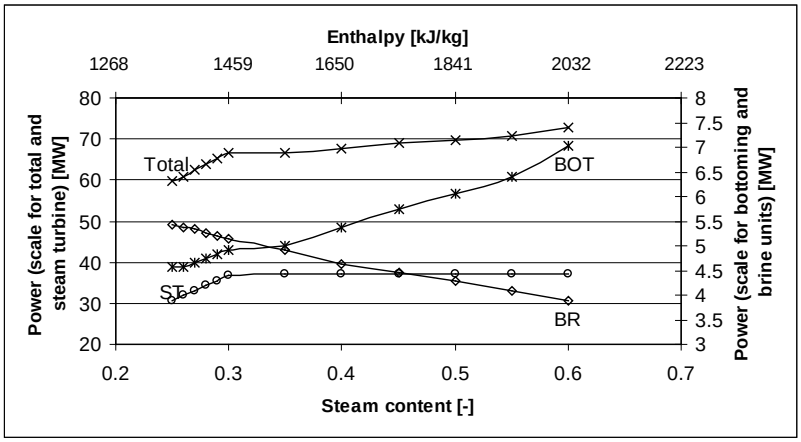

Fig. 2. Theoretical power for the base case as a function of resource enthalpy

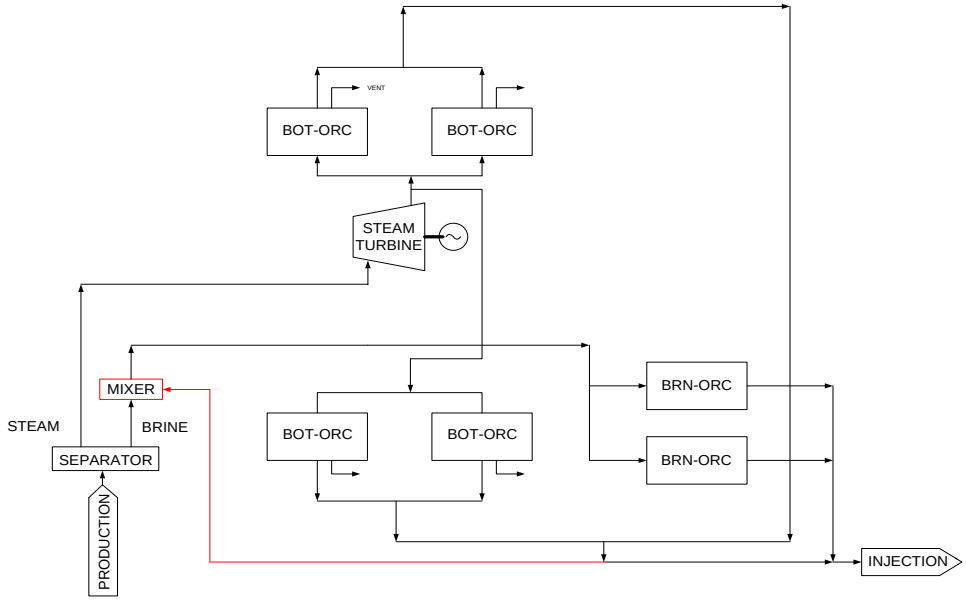

Fig. 3. Adaptive design for an increased flow of geothermal fluid

3.4. Case Study 3: constant flow of geothermal fluid and lowered reinjection temperature

In case 1, more geothermal fluid was used to overcome the problem of reduced brine in BRN-ORCs which results in utilization of the resource at a higher rate. The reinjection temperature of the geothermal brine is not affected much. In the base case, the reinjection temperature is about 125°C. The minimum recommended reinjection temperature of the site is about 80 ºC to prevent silica formation. So there is a possibility of further extracting heat from the reinjected brine.

The alternative design would look the same as Fig. 3. However, the geothermal resource is utilized at constant rate i.e. mass flow of geothermal fluid to the plant is the same as the base case. The plant performance would look like the same as Fig. 4 but the reinjection temperature will change. Fig.6 shows the corresponding reduction in reinjection temperature. It is clear from Fig. 6 that it is possible to stabilize the brine flow rate of the BRN-ORCs and consequently power output by keeping the reinjection temperature within an acceptable limit (80 ºC).

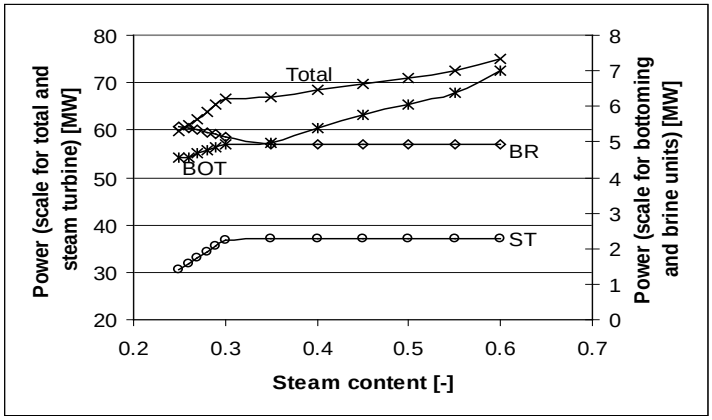

Fig. 4. Theoretical power for base case with increased mass flow of geothermal brine to keep the brine flow rate constant for the BRN-ORC as function of resource enthalpy

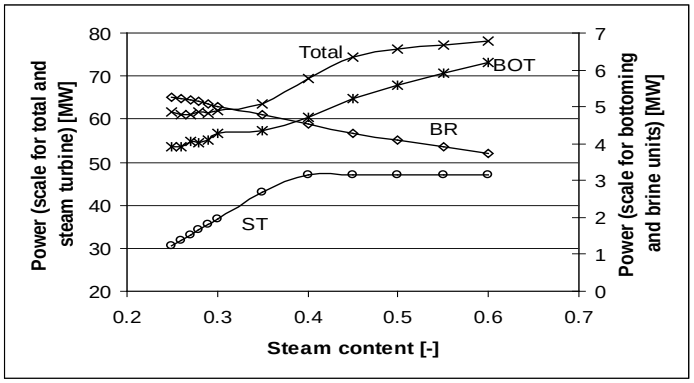

Fig. 5. Theoretical power of the geothermal power plant with a higher capacity steam turbine

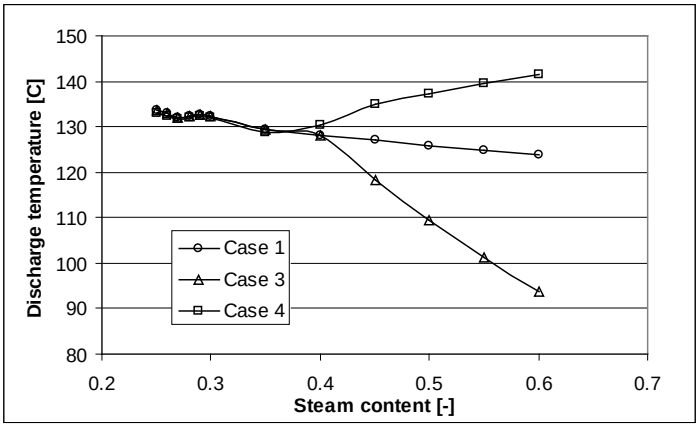

Fig. 6. Theoretical reinjection temperatures for case 1, case 3 and case 4

3.5. Case study 4: constant flow of geothermal fluid with excess steam (50/50)

It was stated earlier that the steam turbine has a power producing limit. Beyond this limit, the steam turbine cannot utilize the excess steam and the consequence is a higher discharge enthalpy. Another possible alternative is depicted in Fig. 7. The excess steam can be bypassed and used to reheat the condensate collected from the BOT-ORCs. The results of mixing excess steam (50%) and condensate (50%) are presented in Fig. 8. It is clear from Fig. 8 that

the reheating of the condensate by excess steam mitigates the reduced brine for the BRN-ORCs. The reinjection temperature is not reduced by this approach (Fig. 6).

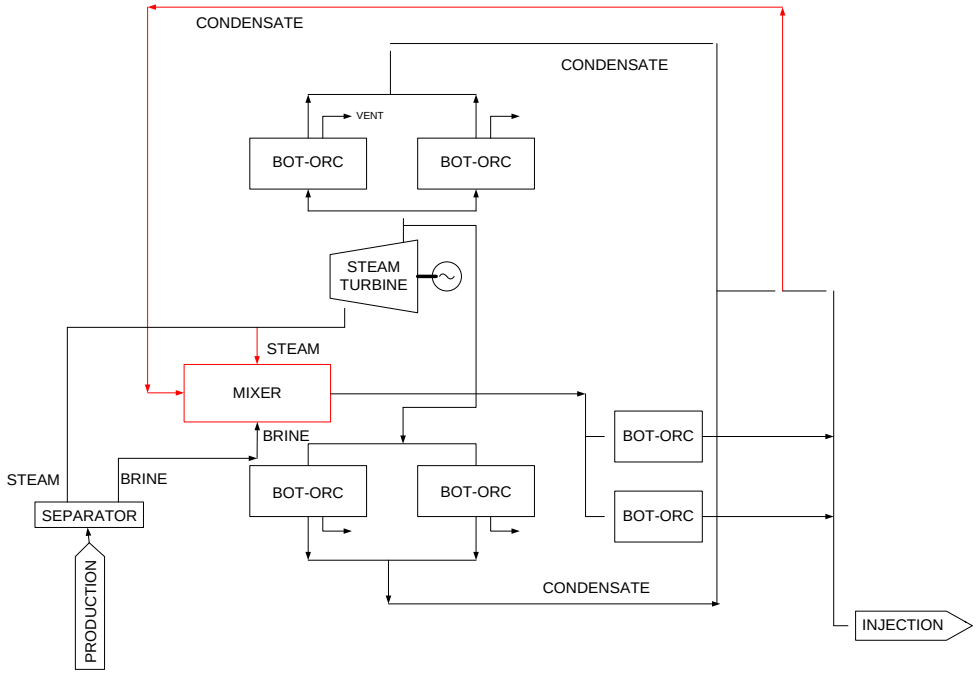

Fig.7. Adaptive design for a constant flow of geothermal fluid and regenerative heating

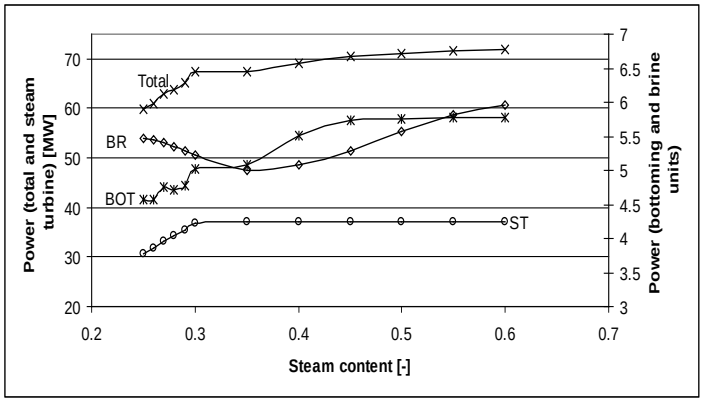

Fig. 8. Theoretical power of the geothermal power plant and constant mass flow of geothermal brine with regenerative heating of the brine by excess steam

4. Discussion and conclusion

This paper has introduced an alternative design approach that takes into account possible changes in future resource characteristics. As geothermal power plants are very capital intensive and it is not very easy to change a plant to adapt to resource characteristics different from the original design, keeping provision for future resource characteristics can be very effective. Although, the initial investment cost might go up as a consequence of adaptive design, over the life span of the plant the total benefit may be greater. A proper cost benefit analysis is necessary to identify the economic benefit. There are four case studies presented in this paper that analysed various possible options of the hypothetical power plant depending on the hypothetical changes in resource characteristics. The results show provisions that could be kept in the plant for future resource characteristics. The next phase is to do a cost benefit

analysis of these options and select the optimum option. In this paper we have only discussed adaptive design approach for increasing resource enthalpy. Similarly, adaptive design for a decreasing resource enthalpy can also be carried out which will provide different provision for the geothermal power plant. One such provision is that one or more of the BOT-ORCs can be designed in such a way that they can be used as BRN-ORCs when geothermal resource enthalpy reduces to utilize the increased brine available.

References

[1] IEA, World Energy Outlook. 2008: International Energy Agency.

[2] Barbier, E., Geothermal energy technology and current status: an overview. Renewable and Sustainable Energy Reviews, 2002. **6**(1-2): p. 3-65.

[3] DiPippo, R., Second Law assessment of binary plants generating power from low-temperature geothermal fluids. Geothermics, 2004. **33**(5): p. 565-586.

[4] Chen, H., D.Y. Goswami, and E.K. Stefanakos, A review of thermodynamic cycles and working fluids for the conversion of low-grade heat. Renewable and Sustainable Energy Reviews, 2010. DOI:10.1016/j.rser.2010.07.006

[5] Bombarda, P. and M. Gaia. Geothermal Binary Plants Utilising an Innovative Non-Flammable Azeotropic Mixture as Working Fluid. in Proceedings 28th NZ Geothermal Workshop. 2006.

[6] Madhawa Hettiarachchi, H.D., et al., Optimum design criteria for an Organic Rankine cycle using low-temperature geothermal heat sources. Energy, 2007. **32**(9): p. 1698-1706.

[7] DiPippo, R., Ideal thermal efficiency for geothermal binary plants. Geothermics, 2007. **36**(3): p. 276-285.

[8] Sohel, M.I. and M. Jack, Efficiency improvements by geothermal heat integration in a lignocellulosic biorefinery. Bioresource Technology, 2010. **101** p. 9342-9347.

[9] Sohel, M.I., et al., An iterative method for modelling the air-cooled organic Rankine cycle geothermal power plant. International Journal of Energy Research, 2010. DOI: 10.1002/er.1706

[10] Sohel, M.I., et al., Dynamic Modelling and Simulation of an Organic Rankine Cycle Unit of a Geothermal Power Plant. Proceedings World Geothermal Congress 2010 Bali, Indonesia, 25-29 April 2010.

[11] Atrens, A.D., H. Gurgenci, and V. Rudolph, Electricity generation using a carbon-dioxide thermosiphon. Geothermics, 2010. **39**(2): p. 161-169.

[12] Atrens, A.D., H. Gurgenci, and V. Rudolph, CO2 Thermosiphon for Competitive Geothermal Power Generation. Energy & Fuels, 2008. **23**(1): p. 553-557.

[13] DiPippo, R., Geothermal Power Plants: Principles, Applications and Case Studies. 2005: Elsevier Ltd.

[14] RJVL, ROTOKAWA GEOTHERMAL DEVELOPMENT Resource Consent Applications and Assessment of Environmental Effects. 2007, Rotokawa Joint Venture Limited, C/- Mighty River Power Limited, 160 Peachgrove Road, PO Box 445, HAMILTON, New Zealand.

[15] MathWorks, www.mathworks.com. 2008.

[16] REFPROP. National Institute of Standards and Technology (NIST), 2007. Available from: http://www.nist.gov/.

Managing Sustainable Design for Geothermal Plants: the Engineer's Perspective

Chun Chin[1,*], Joshua Gunderson[1], Joe Stippel[1], Matt Fishman[1], Gudrun Saevarsdottir[2], William Harvey[2]

[1] *POWER Engineers, Hailey Idaho, USA*
[2] *Reykjavik University, Reykjavik, Iceland*
** Corresponding author. Tel: +001 2087880527, E-mail:cchin@powereng.com*

Abstract: The fast pace of project development, design, and execution of power generation projects, together with the nature of Engineering-Procurement-Construction (EPC) contracts popular in the industry and to banks, often make sustainability considerations a grudging afterthought to the contractor or owner. Although careful consideration of technical, environmental, and social impacts may have been part of the up-front permitting process, the control wielded by skilled engineers during the detailed design process, if implemented in an educated and structured fashion with the owner, and in an EPC environment, with buy-in from the contractor, can result in plant designs that better benefit the local community in dimensions beyond thermal efficiency. This paper will present a structured review process developed by the authors, which is targeted toward the specific considerations of geothermal power projects. This procedure may be applied to other renewable projects, especially those with similarly complex processing systems such as biofuel refineries or solar thermal projects. The review process is performed with the owner and is documented to demonstrate upon completion the project's commitment to sustainable principles. These audit principles provide a platform to educate owners on topics such as alternative methods of construction best suited to the local conditions, workforce, and carbon footprint; project management structures to maximize local content and knowledge transfer, and assessment of all resource and revenue streams from the plant in addition to electrical production. The paper describes the way in which geothermal plants have and require a closer relationship with the local community, and strengthening this relationship is the goal of these processes.

Keywords: *Geothermal, Sustainability reviews, Local content, Project management.*

1. Introduction

The nature of geothermal projects, with their wide range of resource conditions and variety of material and revenue streams, render them more complex cases than many other "plug and play" fossil or renewable generation options. While careful consideration of technical, environmental, and social impacts may have been part of the up-front environmental and local permitting processes, these are often managed by developers and government agencies more focused on establishing the viability of the overall project than optimization of sustainability features. These features may include selection of equipment with lower energy requirements or greater local involvement, such as materials of construction for cooling towers, or use of byproduct streams for maximum benefit, such as recovered sulphur for fertilizers. The time and incentive to focus on sustainability features is diminished by the tendency for many of these projects to be executed under financing structures that discourage value engineering. This paper presents a method to integrate sustainability considerations more systematically into plant design.

This paper presents a structured audit and review process developed by the authors, based on the principles of sustainable development and their experience with geothermal projects, with case studies from locations in the developing world. The review process is targeted toward the specific considerations of geothermal power projects, performed with the owner, and documented to demonstrate upon completion the project's contributions to sustainable principles and community acceptance. These audit principles provide a platform to educate owners on topics such as alternative methods and materials of construction best suited to the

local conditions, best integration of local workforce for initial construction and O&M activities; reducing carbon and land footprint; project management structures to maximize local content and knowledge transfer, and assessment of multiple potential resource and revenue streams from the plant. This process represents a minor investment for the owner, makes best use of the talent available in the design phase, and is executed in the appropriate stage of development for greatest impact at least cost. Pitfalls will be discussed along with ways in which the review can be customized to suit the needs of various owners. Structured sustainability reviews will result in designs that harness the resource more fully, respect the owner's constraints, and contribute to greater project success.

The remainder of the Introduction section will discuss considerations of project execution and financing constraints specific to geothermal plants. The Methodology section will describe the timing and structure of sustainability audits developed by the authors for geothermal projects. The Results section will describe several case studies of how these audit principles have been applied successfully.

1.1. Geothermal Project Development

Geothermal plants, while lacking the aerodynamic sleekness of wind projects or the cutting edge science of photovoltaics, nevertheless can be major contributors to a country's renewable energy portfolio, providing dispatchable, reliable baseload power unaffected by the vagaries of fuel costs and environmental conditions. In developing countries such as Nicaragua and Kenya, geothermal offers the potential to completely displace fossil fuel generation as the lowest cost alternative.

While the capital costs of these projects may be substantial – perhaps $3,000 to $5,000 per kW of installed capacity – they also include the up-front "fuel costs" of well drilling. This high initial cost is further mitigated by the fact that geothermal plants operate at high capacity factors, routinely exceeding 90%.

A typical geothermal project encompasses three major areas:

- the reservoir, from which the hot geofluid (steam or water) is drawn and spent fluid returned,
- the gathering system, where the collected geofluid is conveyed from production wells to the plant and returned to injection wells, and
- the power plant, where power is generated from the geofluid by a variety of methods, most commonly flash (directly driving steam through a turbine) or binary (using the geofluid to vaporize a secondary working fluid, often a hydrocarbon, which passes through the turbine).

The characterization and exploration of the geothermal reservoir is a task that may take years and require the efforts of a dedicated team of geoscientists. Even with the best estimates, the production capacity of a geothermal field is generally uncertain until several wells have been drilled and proven. Until sufficient capacity has been proven, often to a significant percentage of the required plant capacity and typically above 50%, banks are generally unwilling to finance the project. For this reason, exploration is generally funded with equity from a developer which may amount to a considerable sum; a typical 50 MW plant may require an investment of $15 million of equity before loans can be obtained [1]. However, with proven wells and the requisite permits in place, the developer turns quickly to the challenge of designing and financing the project in preparation for construction.

1.2. Project Structures for Execution

The traditional structure for utility projects has historically been a Design-Bid-Build (D/B/B) approach, where the Owner will engage an Engineer to carry out the detailed design. The Owner and Engineer work collaboratively to define the design criteria, design the process, and specify equipment. Purchase orders for equipment are placed by the Owner. After approximately 60% of the design is complete, construction specifications for bidding by Contractors are prepared, where the Contractor will place orders for bulk materials and carry out the requisite work. The advantages of the D/B/B approach are that the Owner maintains firm control over the design process, avoids Contractor markups on major equipment, and the project schedule can be shorter than alternative project delivery methods. One disadvantage is that the firm project cost is not known until later in the process, which makes D/B/B less appealing for financiers. The Engineer might prefer a D/B/B approach because it leaves more room for value engineering and sustainability considerations in collaboration with the Owner. However, narrowly focused financial considerations are leading to an increase in projects that must be executed under an "EPC" approach, discussed next.

An Engineering-Procurement-Construction (EPC) approach is more favored by financiers, although the financial benefits are balanced by certain complications. The Owner begins by preparing a fairly detailed performance specification. An EPC Contractor then gives a firm lump sum bid backed by schedule and performance guarantees. This process is time intensive, leading to EPC projects generally being at least 4-6 months longer than a well executed D/B/B approach. Next, the Contractor engages an Engineer to perform the detailed design and the Contractor places the purchase orders for major equipment. The advantage of the EPC approach is ease of financing due to the Owner's financier having a firm price and performance/schedule guarantees at the beginning of the project. Disadvantages include less Owner control over the evolution of the design, since it is constrained only by the initial specifications; higher cost, due to additional markups and risk burden on the Contractor; and generally longer schedule due to the lengthier contract negotiations and some redundancy in design effort between the Owner and Contractor.

The initial phase of conceptual design by an EPC Contractor/Engineer team generally consists of several months of equipment specification and procurement, the goal being to award purchase orders for the critical path items that define the overall project schedule and impact the design of foundations and supporting subsystems. These major plant items include the turbine/generator, condenser, cooling tower, non-condensible gas removal system, and major pumps. These all will be ordered generally within four to six months after EPC contract award.

The opportunity to explore plant improvements that would improve sustainability attributes can be inhibited by the EPC approach. The contract is generally awarded to the lowest bidder; discouraging the search for solutions that may have greater long-term value. After award, the Contractor generally faces liquidated damages for schedule delays, hence they and the Engineer are considerably motivated to avoid proposing investigation of upgrade opportunities. Finally, the lump sum contract would require renegotiation in the event that the Contractor proposes investments in upgrades. All these, along with the rapid pace of design and construction, are disincentives to thoughtful plant optimization under the EPC approach.

2. Methodology

2.1. Timing of the Sustainability Review

The Engineer faces the challenge of how to incorporate sustainability considerations swiftly, appropriately, and in a win-win approach with the Owner and Contractor, which may have competing interests. The methodology developed by the authors incorporates a Sustainability Review into a natural Owner and Contractor design review process that generally occurs after 3-4 months for a typical project. In this design review the conceptual-level documents are reviewed for adequacy and conformance with the project specifications. At this time it is also common to hold a Process Hazard Analysis (PHA), or Hazard and Operability Study (HAZOP), which is a structured "what-if" review of the conceptual documents to explore the possibilities to improve safety. HAZOP reviews were originally developed for the chemical industry, and conducting these is often an Owner or regulatory requirement for a complex processing plant, such as a geothermal project, with its multitude of fluids and flows. The expansion of 'binary' technologies, which can be used in geothermal, ocean thermal, and solar thermal projects, generally call for HAZOPs since they often incorporate hydrocarbon working fluids. The Sustainability Review we have developed is scheduled at the same time and has a similar structure to the HAZOP.

2.2. Objectives of the Sustainability Review

The Bellagio Principles [3] are used as guidance, which emphasize among others clear goal setting, a holistic perspective, considerations of economic and non-economic principles, local and regional effects, short and long-term effects, and a focus on practical goals. The objective of the Sustainability Review is to emerge from the process with:

- Clear direction from the Owner and agreement with Contractor on any specification, contract, or schedule modifications required to enhance sustainable attributes.
- Written documentation describing the steps Owner, Contractor, and Engineer have taken to be mindful of sustainability considerations, in a format suitable for dissemination to the public if the Owner so chooses.
- An expectation that future changes will be minimized so as to protect the Contractor's project schedule and ongoing design.

2.3. Structure of the Sustainability Review

The proposed Sustainability Review process can be submitted to proposed EPC clients as part of the proposal documentation for consideration according to their green values. This is treated as a value-adding cost option, so that it is appreciated in its own right, and yet does not jeopardize winning an EPC project by building in costs that other bidders may not have allocated. If the project is a win, the Engineer works with the Owner and Contractor to make selections consistent with their philosophy on sustainability.

During the initial conceptual design phase, a preliminary project sustainability report is generated; typically at around the 3 month time frame and prior to the Design Review/HAZOP/Sustainability Review sessions. This provides an agenda and some suggested topics of discussion for the Review. Each proposed aspect should be developed with the following considerations in mind:

1. The Engineer's role is to educate and inform; the Owner and Contractor will be the final arbiters.
2. Must be mindful of the client's own sustainable charter.

3. Must sell on its own merit such that cost benefits, positive environmental impacts, better integration with the surrounding community and other intangible benefits make the program attractive.
4. Must be easy to understand, clearly defined (can be organized by system, discipline or combination thereof) and practical for implementation.
5. Positive impacts to the environment as well as a business case and cost justification must be measurable and presentable to both the Owner and Contractor
6. Flexibility in the program will allow clients to have the freedom to choose the weighted aspects of sustainability they want their project to possess.
7. Conduct risk assessments and comparative studies to show how an innovative technology compares with traditional technologies.

Following the Sustainability Review, a Sustainability Report is generated as part of the project record documentation, identifying the areas of positive impact and stating both one time and recurring benefits.

The effort involved in preparing for and executing the Sustainability Review is not inconsiderable, but the impact on even small subsystems can be substantial. Compare a scenario where 10 workdays are spent in preparation, 20 workdays for an attendance of ten representatives for two days of the review, and 10 workdays for preparation of the summary report. This may come to some tens of thousands of dollars for a dedicated review. Yet, identifying even small efficiency upgrades or locally, less expensive materials can be tremendously impactful. Plant output may be assessed with net present values in the $4000/kW range, meaning a 1% identified efficiency improvement on a 1000 kW pump/motor may cover the cost of the study. Similarly, the cost of a single imported stainless steel large diameter flange may exceed $20,000; alternative materials, layouts, or suppliers permitted by the Owner may result in significant cost savings. Also, design modifications that reduce environmental impact may have long term value for the Owner in terms of local acceptance of the project.

2.4. Methodology of the Sustainability Review

Similar to a HAZOP study, the Sustainability Review is designed to promote discussion and generation of ideas by being open ended. Specific suggestions may be covered in the preliminary report, if some research is required, but other ideas may be generated by the participants during the meeting. A full and comprehensive review meeting may last for several days and require an interdisciplinary and interparty team of 5-15 people, but an abbreviated review can be performed with a smaller group of stakeholder participants.

Natural divisions consistent with plant design may be used to facilitate an organized search for potential sustainability features. Primary divisions may be based on engineering disciplines such as Architectural, Civil, Structural, Mechanical, Electrical, and Controls. Each discipline brings to the review key deliverables such as Process Flow Diagrams, Electrical One-Line Diagrams, or General Arrangement Drawings. A set of key plant areas, systems, or equipment that merits study is developed. The team brainstorms to come up with alternative configurations within the area/system/equipment. Then each alternative is evaluated with regard to sustainability attributes and metrics. The following are sample parameters to be discussed and assessed with a weighted score.

- Environmental: Green/LEED structures, provide animal crossings, minimize chemical waste streams or improve disposal practices.

- Social: Use local labor and locally supplied materials. Innovative designs that appeal to the public while improving sustainability (geothermal heating, energy efficient lighting, passive solar, novel waste heat utilization), reduce noise levels.
- Health & Safety: Minimize use of hazardous materials. Use safer construction practices and materials.
- Diversity: Consider how alternatives may contribute to the diversity of organisms or institutions that benefit from its application.
- Natural Resources: Minimize land use. Minimize water use. Utilize waste streams.
- Human Resources: Make changes to facilities to improve workforce morale (covered walkways, breakrooms, better maintenance access ways, etc.)
- Engineering and Procurement: Increase efficiency due to alternative materials, equipment type, layout, or other design parameters. Improve off-design and turndown capabilities. Shorten the procurement cycle.
- Construction: Compress project schedule with changes to equipment, layout, materials, etc. Use locally available materials and construction techniques.
- Availability: Add equipment redundancy where appropriate. Review single points of failure.
- Operations: Consider alternatives to improve operator experience, ease of troubleshooting, etc.
- Maintenance: Evaluate impact on maintenance frequency, cost, need for specialists.

A typical Sustainability Review process is outlined in the appendix. Each suggestion for improvement is reviewed against the tender specifications to verify that it is not already a mandatory requirement. The cost of any suggested enhancement is assessed or tagged for further study. Within several weeks the facilitator prepares a report of the suggested upgrades, the proposed costs, and any schedule adjustments. Those options that are implemented and other observations such as plant benefits to the local community are documented in the report in a manner sufficient for use by the Owner to demonstrate their commitment to sustainable principles. The usefulness of this procedure would not necessarily be limited to powerplants; other similar renewable energy projects such as a biofuel synthesis facility could be studied with these techniques.

3. Case Studies

Through reviews such as these, several modifications leading to improved sustainability aspects have been successfully implemented in geothermal projects around the world.

Darajat II, Indonesia: This 110 MW geothermal plant houses the world's largest single pressure geothermal turbine. During reviews between the Owner, Contractor, and Engineer of the Darajat II project, it was revealed that several workers had died during the construction of the Darajat I concrete cooling tower some years earlier by a different team. Although a change in the style of construction of the tower was not a contract requirement, the Contractor and Engineer shifted from a cast-in-place concrete cooling tower to a precast design, where forms were set on grade and pieces lifted into place similar to the erection of a massive log building. This had not been attempted before on a geothermal project, and posed POWER Engineers and the cooling tower manufacturer, SPX, with several new challenges. Nevertheless, the tower was constructed without a major construction incident. Ironically the Contractor's project manager, who proposed the modification, lost his life due to illness during the project; the tower is a memorial of sorts.

Germencik, Turkey: This 47.4 MW unit is the largest geothermal plant in Turkey. A decision was made in the design phase to maximize the use of local subcontractors and materials, with consideration that in Turkey little geothermal-specific design expertise existed. A division of labor for the systems was developed that allowed specialist firms to design such items as the powerhouse layout and structural steel required to support equipment and piping, given certain critical loads, while Turkish firms familiar with locally available architectural styles and fixtures completed the detailed design of the façade. A list of structural shapes commonly available in Turkey was provided to POWER Engineers and preferentially used in the steel design to minimize the need for importation [4].

San Jacinto II, Nicaragua: These 2 x 38.5 MW flash plants currently under construction will add 10% of renewable capacity to Nicaragua's total generation of 750 MW, displacing about one million barrels of diesel fuel per year. Due to challenging construction conditions and a local scarcity of construction equipment such as augers, several modifications were made to reduce the size and depth of foundations associated with the major pumps, shortening the construction period and reducing concrete quantities. A shift was made from galvanized steel structures to wider use of painting to resist corrosion, in a desire to reduce imports due to a local scarcity of galvanizing facilities.

4. Conclusion

The rushed pace of project execution, especially for EPC contracts, make incorporation of sustainability considerations a challenge for the engineer. However, the customization of each geothermal plant, required due to the unique nature of each resource, means some time should be allocated to explore new opportunities for each project. Addressing these at the appropriate time during the conceptual design phase or early detailed design phase, and doing so with a structured process between the Owner, Contractor, and Engineer, is necessary for the right ideas to find expression in the plant design. The metrics to be applied and the appropriate weightings are parameters that may change for each project; better quantifying and handling of these is an avenue for future work. Documenting the decisions made and the potential positive impacts the plant can bring to the local community can improve the relationship between the Owner and local resources including workers and policy makers, making ongoing plant modifications or expansions (a common occurrence when new fields are incrementally developed) a smoother process. The review process suggested here is intended to bring more of these considerations into the awareness of the various parties, and may be extended for use to other sorts of analogous renewable projects.

References

[1] Deloitte, Geothermal Risk Mitigation Strategies Report, Prepared for the DOE Office of Energy Efficiency and Renewable Energy Geothermal Program. 2008.

[2] P. Hardi and T. Zdan, Assessing Sustainable Development: Principles in Practice, International Institute for Sustainable Development, 1997.

[3] International Hydropower Association, Sustainability Assessment Protocol, 2006.

[4] T. Dunford, M. Fishman, K. Wallace, M. Ralph, and W. Harvey, Engineering Local Value: Case Studies from Olkaria and Beyond. GRC Transactions, Vol. 34, 2010, pp. 186-190.

Appendix: Sample Sustainability Audit Process

1 DEFINING REVIEW AREAS

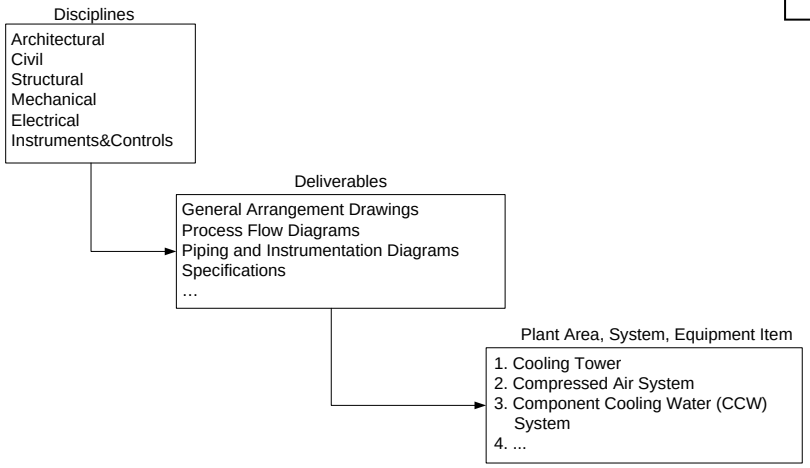

2 IDENTIFYING ALTERNATIVES

ID	Base Case	Alternative Design	Primary Incentive
S01	Fixed speed CCW pumps with control valves	VFD CCW pumps	Increased efficiency and reduced LCC for increased capital cost
S02	Restrictive Orifice used for CCW pump recirculation	Replace Restrictive Orifice with Control Valve	Increased efficiency and reduced LCC for increased capital cost
S03	Standard routing of CCW return to cooling tower	Reroute CCW through parking lot to melt snow in winter	Worker, visitor, community satisfaction and increased safety for increased capital cost
S04	…		

3 ASSESSING ALTERNATIVES

Project No./Name:	Sample Geothermal Project
Base Case:	Traditional CCW Routing
Alternative Design:	Route CCW through parking lot for winter snow melting

Category	C	Q	Description
Environmental			Reduced emissions by snow removal equipment, reduced water used at cooling tower in winter
Social			Will be appreciated by visitors, public relations during startup
Health & Safety			Increased safety in winter
Diversity			
Natural Resource			Reduced fossil fuel use by snow removal equipment, increased materials used for piping, increased equipment use during construction.
Human Resource			Workers will appreciate lack of snow accumulation in lot
Engineering and Procurement			Increased costs, increased engineering effort to properly size system
Construction			Increased costs, pipe must be buried shallow requiring additional protection from surface loads.
Availability			Slight increase in failure probability due to surface loads and increased pipe run length
Operations			
Maintenance			Reduced access to piping under parking lot
Totals (Σ_C,Σ_Q)			

C = Costs (Quantitative Impacts)
Q = Qualitative Impacts

4 SUMMARY AND ACTIONS

ID	Alternative Design	Σ_C	Σ_Q	Proposed Action
S01	VFD CCW pumps			
S02	Replace Restrictive Orifice with Control Valve			
S03	Reroute CCW through parking lot to melt snow in winter			
S04				

Numerical simulation of Northwest Sabalan geothermal reservoir, Iran

Younes Noorollahi[1*], Ryuichi Itoi[2]

[1]*Dep. of Environmental and Energy, Sciences and Research Branch, IAU, Pounak, Tehran, Iran*
[2]*Dep. of Earth Resources Engineering, Kyushu University, Fukuoka, Japan*
** Corresponding author. Tel: +98 21 44865320, Fax: +98 21 44865002, E-mail: hashtroudi@srbiau.ac.ir*

Abstract: A three dimensional numerical model of the northwest Sabalan geothermal system was developed on the basis of a conceptual model drawn from the analysis of the available field data. A numerical model of the reservoir was expressed with a grid system of a rectangular prism of 12km × 8km with 4.6km height, giving a total area of 96km^2. The model has 14 horizontal layers ranging in thickness between 100m to 1000m extending from a maximum of 3600 to -1000m a.s.l. Fifteen rock types were used in the model to assign different horizontal permeabilities from 5.0×10^{-18} to 4.0×10^{-13} m^2 based on the conceptual model. Natural state modeling of the reservoir was performed, and the results indicated good agreements with measured temperature and pressure in wells. Numerical simulations were conducted for predicting reservoir performances by allocating production and reinjection wells at specified locations. Two different exploitation scenarios were examined for sustainability of reservoir for the next thirty years. Effects of reinjection location and required number of makeup wells to maintain the specified fluid production were evaluated. The results showed that reinjecting at Site B is most effective for pressure maintenance of the system.

Keywords: *Geothermal, Reservoir, Simulation, Capacity, Sabalan, Iran*

1. Introduction

In this study, simulation for natural state and capacity assessment of the reservoir were undertaken for the primary purpose of predicting and assessing the response of the NW Sabalan geothermal reservoir to the planned development scenarios. The computer codes of TOUGH2 [1] and AUTOUGH2 [2] were used with the equation of state of water and steam (EOS1). Different production scenarios were examined by numerical simulations for evaluating the reservoir responses, and consequently the optimum future development scenario was defined. Three exploration wells, NWS1, NWS3 and NWS4, were drilled in the study area based on the results of geological, geochemical and geophysical studies. According to the geophysical surveys, deep geothermal reservoir may extend from northeast to southwest where exploration wells were drilled along this suitability area [3, 4, 5].

2. Conceptual model of NW Sabalan reservoir

Before a numerical simulation model of a given geothermal field being set up, a conceptual model must be developed. The model is usually represented by sketches showing a plan view and vertical sections of the geothermal system. On these sketches the most important features such as geothermal surface manifestations, hydrological boundaries, main geologic features such as faults and geological layers, zones of high and low permeabilities, location of deep inflows and boiling zones need to be involved. Thus, developing a conceptual model requires the synthesis of information from a multi-disciplinary team. The geological map of the Sabalan area with main surface manifestation, geological structures shown in Figure 1. A conceptual model of the study area was drawn along AB line in Figure 1, with 12km length, from north to south. Three drilled exploration wells were projected on the AB line [6] and Subsurface geology of the area is described along cross section AB, using geological data and information from three deep and two shallow exploration wells. In the central part of the model, Dizu formation presents and extends to the depth of about 200m a.s.l. This formation clearly exposed in the area where Wells NWS1 and NWS3 are located throughout the Valhezir formation reaches to the surface in the east of Well NWS4 and extends to 700 m

depth in the whole study area from top or below Dizu formation. In the northern part of the area where Well NWS3 was drilled, geological unit is comprised of andesitic lava flows, tuff and tuff breccia that belong to Dizu formation of Neogene to Quaternary and Mejendeh metamorphics of Paleozoic in descending order down to 1000 m below sea level. Magnetotelluric (MT) survey was carried out in 1998 with 212 stations [6]. Nineteen measurement stations were located along the AB line, and the results were analyzed which shows two anomalies of low resistivity in south and north part and a high resistivity in the central part which can represent the location of an intrusive body beneath Well NWS4. Temperature contours are drawn using measured temperatures in exploration wells. The temperature increases from north to south which suggests that an upflow zone of high temperature fluid likely presents in the southern part of the field. Thus, Faults NW3, NNW5, NE5, NNW2 and NW4 play as upflow zone of the system. By integrating the subsurface geology from the wells with resistivity and temperature data, the conceptual model of the system can be illustrated in Figure 2. Differences of subsurface geology revealed from drilling between Wells NWS4 and NWS3 support the presence of Fault NE2. Temperature profiles of these two wells also show differences, which implies that Fault NE2 plays as an impermeable or low permeable boundary. The presence of slightly high resistivity zone beneath Site B can be interpreted as the existence of a diorite porphyry intrusive body. It has been assumed that geothermal fluids ascend through Faults NW3, NNW5, NE5, NNW2 and NW4. This faulted area can be an upflow zone of the system. The fluids would ascend through this fault zone to higher elevations and then flow horizontally in shallow layers to the northward due mainly to gravitational force and discharge through hot springs in lower elevations.

3. Development of numerical model

3.1. Grid system and rock type and properties

The NW Sabalan geothermal system was modeled with a rectangular prism 12km long, 8km wide and 4.6km depth. The model has 14 horizontal layers, AA to PP, ranging in thickness between 100 to 1000m extending from a maximum of 3600 to -1000m a.s.l with 2595 grid blocks in total. For neglecting water-air unsaturated zone, first two top layers, AA and BB, were discarded from the model. Each layer has 192 grid blocks 500×500 and 1000×1000m. The exploration drilling area is located in the center of the model, covering an area of 3×5km. Permeability values were given to the model in ranges from 5.0×10^{-17} to 4.0×10^{-13} m^2**,** with the maximum value in the shallow permeable horizon on depth between 1900 and 1400 m a.s.l (Figure 3). Sixteen rock types were used mainly for assigning different permeability. Porosity, rock density and thermal conductivity were 0.1, 2500kg/m^3 and 2.5W/$m^{2\circ}$C to all rocks. Rock parameters corresponding to the optimum natural state model are summarized in Table 2. The rock types CAP01, TOP01 and TOP02 with lowest permeability were assigned to layers CC, DD and EE which represent the cap rock of the system. The MAKH0 with low permeability was assigned to the northern part of the field below Site C to layers FF, GG, HH, and II. The rock LOW01 was given to the deep part in C area from 1400-500m a.s.l. corresponding to the metamorphosed rocks appeared in Well NWS3. The TOP04 was assigned to the area beneath Site B and surroundings for representing the conductive temperature profile observed in Well NWS4. This rock types appears in elevation from 2000-1400m a.s.l. belong to the layers EE, FF, GG, HH and II. The MAKH1 rock type with high permeability was for the layer MM in Site B. The MAKH2 was assigned to the layers EE, FF, GG, HH and II from elevation of 2000-1400m a.s.l. according to information from Wells NWS1 and NWS4 as high permeable rock formations were found in these horizons. The LOW02 was used to the grid blocks in the layers KK and LL in the southern and central part and represent low permeability between two high permeable layers. The UPFLO rock type indicates the upflow zone with high vertical permeability. Six grid blocks (500×500m) in

southern part were assigned with this rock type from layer PP to GG. Information from two wells, NWS1 and NWS4 indicates that there are two main permeable horizons in the reservoir: a shallow zone between 1800 and 1400m a.s.l. in southern part, and a deeper zone between 500m a.s.l. and sea level in both wells. In the computational grid system, the uppermost high permeable horizon in the reservoir was therefore subdivided into four layers (FF, GG, HH and II). The layer MM denotes the deep permeable horizon. The layers AA and BB represent the unsaturated zone, which were discarded from computing. This geothermal field is located in an arid area and two top layers are unsaturated. We can model such condition by using EOS3 with all layers or EOS1 be neglecting unsaturated zone.

Table 1 Rock parameters of the best natural-state model

Rock type	Density (kg/m^3)	Porosity (%)	Permeability (m^2)			Thermal cond. ($W/m^2°C$)	Specific heat ($J/kg°C$)
			Kx	Ky	kz		
ATMOS	2500	99	2.5×10^{-14}	2.5×10^{-14}	2.5×10^{-14}	2.50	9.0×10^{5}
CAP01	2500	10	2.0×10^{-16}	2.0×10^{-16}	7.0×10^{-17}	2.50	1.0×10^{3}
BASE1	2500	10	6.0×10^{-15}	6.0×10^{-15}	3.0×10^{-15}	2.50	1.0×10^{3}
BOND1	2500	10	9.5×10^{-16}	9.5×10^{-16}	6.6×10^{-16}	2.50	1.0×10^{3}
TOP01	2500	10	5.5×10^{-16}	5.5×10^{-16}	1.1×10^{-16}	2.50	1.0×10^{3}
TOP04	2500	10	5.0×10^{-15}	5.0×10^{-15}	1.1×10^{-15}	2.50	1.0×10^{3}
BASE3	2500	10	1.0×10^{-17}	1.0×10^{-17}	5.0×10^{-18}	2.50	1.0×10^{3}
LOW01	2500	10	6.0×10^{-14}	6.0×10^{-14}	1.0×10^{-14}	2.50	1.0×10^{3}
MAKH3	2500	10	2.0×10^{-13}	2.0×10^{-13}	5.0×10^{-14}	2.50	1.0×10^{3}
MATRX	2500	10	5.0×10^{-15}	5.0×10^{-15}	1.0×10^{-15}	2.50	1.0×10^{3}
TOP02	2500	10	5.0×10^{-16}	5.0×10^{-16}	2.0×10^{-16}	2.50	1.0×10^{3}
MAKH0	2500	10	5.0×10^{-15}	2.0×10^{-15}	5.5×10^{-16}	2.50	1.0×10^{3}
LOW02	2500	10	7.0×10^{-16}	7.0×10^{-16}	1.5×10^{-16}	2.50	1.0×10^{3}
MAKH1	2500	10	1.0×10^{-15}	1.0×10^{-15}	5.0×10^{-16}	2.50	1.0×10^{3}
MAKH2	2500	10	4.0×10^{-13}	4.0×10^{-13}	7.0×10^{-14}	2.50	1.0×10^{3}
UPFLO	2500	10	3.0×10^{-13}	3.0×10^{-13}	3.0×10^{-13}	2.50	1.0×10^{3}

3.2. Initial and boundary conditions

The peripheral boundaries are impermeable for mass and adiabatic for heat. Grid blocks were filled with 15°C of water and pressure was equilibrated as an initial condition. High temperature fluid recharges at a rate of 90kg/s of 1159kJ/kg from the bottom layer was given through regional faults in the southwest region. The temperature of inflow geothermal fluid was calculated using geochemical geothermometers [6] and also slightly changed by trial and error manner through iterative process of natural state simulation. According to a vertical temperature distribution across AB cross section using data from the wells an upflow zone may present about 2.5 km to the southeast of Well NWS1. The recharge was assigned to the grid blocks of 89, 92, 103, 105, 109 and 111 in PP layer. A flow rate of 8kg/s of low temperature, 130°C, inflow was assigned to the grid 4 in northwestern part to simulate the temperature and pressure condition of the northern part close to Well NWS3. Natural discharge from the field was modeled using deliverability method. The productivity index (PI) was calculated on deliverability model [1] and well bottom pressures (P_{wb}) were obtained by trial-and-errors manner. Mass flow rate on deliverability is proportional to the pressure difference between the grid block and a prescribed pressure that is lower than that of the block. There are several hotspring with surface temperatures from 25 to 85°C and the flow rate of about 50kg/s. In order to reproduce the hot spring activity in the numerical model,

fluid production based on deliverability was utilized in three blocks in layers FF (51, 78, and 183) and one block in layer II (130). Heat flux was given to the blocks in the bottom layer, PP, of the model as a conductive heat supply. A heat flux of 200mW/m^2 was used as the initial basis for calculating the heat inflow in southern and central parts.

3.3. Wells data matching and model validation

The validation process normally involves comparing the computed results against measured temperature and pressure in three wells. This pressure are measured as stationary pressure measurement of single major feed zone during well testing. The matches between the measured and computed values were improved primarily by adjusting the permeability, fluid flow rate and specific enthalpy of the high-temperature recharge assigned to the bottom six grid blocks. Also the lower temperature in Well NWS3 was reproduced in the model by assigning an inflow from grid block 4 in the northwestern part.

4. Production prediction simulations

Once a reasonable numerical model of the natural state of reservoir has been developed, it can be used as an initial model for future prediction performances upon various exploitation scenarios. Main concern of prediction in terms of reservoir management is to examine whether the reservoir can produce required steam for specified period of the present state or is able to produce more steam within acceptable effects or changes in reservoir conditions. Two different exploitation scenarios are designed and then examined for future reservoir performances in this field. Wells on deliverability have been used for evaluating production rate of wells during prediction calculations. The well productivity depends on the well bottom pressure (P_{wb}) where the reservoir pressure will decreases during production, and if the reservoir pressure draw down to equal to the P_{wb}, the well cannot produce the fluid. Numerical simulations were carried out using the AUTOUGH2 simulator for 30 years from year 2015. Numerical simulations were conducted for predicting reservoir performances by assigning production and reinjection wells. The production zones are located in the southern area on Sites A, D and E (Figure 1). These areas situated in a junction of Faults NNW2, NNW3, NNW5, NE5, NE6, NW3, NW4 and NW5 where high permeable fractured zones can be developed along these faults. The northern part of the field with lower elevation was recommended for reinjection. Reinjecting geothermal waste water to these localities with different arrangement was examined on production scenarios. The simulations were run for 30 years of production. The recharge flow rate of the high temperature fluid to the system may increases upon production due to reservoir pressure drop. In prediction simulations, however, constant recharge flow rate was assumed as same as the natural state (98 kg/s). Prediction for NW Sabalan geothermal projects was simulated for two different cases for two power output scenarios; **Scenario II: 50MW; Case 1**: with drilling makeup wells and; **Case 2**: without drilling makeup well and; **Scenario III: 100MWe; Case 1**: with drilling makeup wells and **Case 2**: without drilling makeup well. In these scenarios, declines of pressure, temperature, enthalpy and mass rates of fluid and steam productions of wells were evaluated. The mass production rates of fluid and steam were calculated from fluid discharges of production blocks at a separator pressure of 5.5bar. The reinjection rate of wastewater and its enthalpy into reservoir were given as that of the separator pressure and temperature of 155°C. On the basis of discharge data from Well NWS4, required amount of geothermal fluid for a proposed single flash power plant was calculated [7]. The input parameters are; produced fluid enthalpy 985kJ/kg, separation pressure 5.5 bar, condenser pressure, 0.1bars, outlet temperature 46°C and isentropic efficiency of the turbine 0.78. By assigning these inputs and output information, required production rate of geothermal fluid for different scenarios and number of wells are summarized in Table 2.

4.1. Scenario II: 50 MWe power production

In this scenario for 50MWe generation, total amount of 690kg/s of the geothermal fluid is required. This amount of geothermal fluid was assigned to produce initially from 13 production wells which are fed from the layer MM. For reinjection of the wastewater, seven wells were allocated in the northern and central parts (Site B area) of the field. Two different cases in this scenario were simulated and the effects of production on total mass and steam productions, reservoir pressure, temperature, average flowing enthalpy and natural discharge rates were evaluated. To optimize the production scheme two production and injection cases were designed for this scenario including; **Case 1** : 50 MWe steady power production with makeup wells and **Case 2**: 50 MWe power production without makeup well.

Table 2 Characteristics of the production scenarios

Item	Scenario II Case1	Scenario II Case2	Scenario III
Power output (MWe)	50	50	100
Total production (kg/s)	690	690	1380
Steam production (kg/s)	106	106	212
Brine production (kg/s)	584	584	1168
Number of prod. well	13	13	35
Number of reinj. well	7	7	16
makeup wells	7	0	5

In Case 1; the base level was designed to produce 50MWe over 30 years. Because of pressure drop during production, steam flow rate as well as total production rate decrease. When the steam production rate decreases to 90% of the designated level or power generation drop below 45MWe, new makeup wells start to production for maintaining the total production rate. In Case 2 no makeup well was assigned and the production from 13 wells was maintained over 30 years and the behavior of the reservoir was monitored. Table 5 summarizes the production and reinjection flow rates and grid blocks.

4.1.1. Steam flow rates

Steam flow rates versus time for two cases in Scenario II are presented in Figure 4. In early times, production rates rapidly decease with time in both cases. In Case 1, steam production rate decreases below 95kg/s after 3 years of production and then a makeup well starts to production. This new well can keep the power production more than 45MWe for two years and another new makeup well was required. In this scenario seven makeup wells in total were required in years at 2018, 2020, 2023, 2026, 2029, 2033, and 2038 to keep the power generation of 45MWe for 30 years. In Case 2 the makeup well was not assigned and production was continued by 13 initially drilled wells over 30 years. The steam production rate decreases rapidly in the first 5 years with an average of 3.5% per year. From the year 2020 to 2030 the decline rate is moderated to 1.2% per year and in the next 15 years (2030-2045) the steam flow reduces only 0.31% per year. It can be concluded that the production rate eventually stabilize after 15 years of production. In this case, total production rate drops by 34% in 30 years.

4.1.2. Predicted pressure and temperature

Pressure and temperature changes of the reservoir were monitored while running this production scenario for 30 years. Changes of the pressure and temperature from their initial

values at shallow and deep layers are evaluated. Temperature drops in layers HH and MM for Case 1. In Layer HH temperature drop is less than 1°C. In the main producing layer of MM, cooling occurs in the northern part of the reservoir in reinjection area. Decrease amount of temperature shows up to 60°C in the central part of the reinjection zone and the area of 10°C cooling extends over 4.5km^2. Low temperature front moves from reinjection area to the southward of production zone. Actually, the temperature drop in production zone is only about 1°C. As shown in the figures cooling in main production and reinjection layer, MM, is more apparent than layer HH. Pressure changes also occurred in layers HH and MM. Pressure drops at layer HH are in the range of 4-11 bard . Largest pressure drop occurs in the main production zone in the southern part. In Layer MM the pressure drop in production zone is larger than that in Layer HH, and reaches up to 12 bar of pressure drop in the central part of the production zone. In reinjection area, pressure increases up to 50bar due to reinjection of large amount of the waste water.

4.2. Scenario III: 100 MWe power production

The largest power generation of 100MWe was examined for Scenario III. This requires a production of 1380kg/s of the geothermal fluid. For this scenario, total number of 35 production and 16 reinjection wells were assigned. The grid number corresponding to each production and reinjection wells and assumptions of the scenario is presented in Table 5. However, thirty five production wells is a large number, and it causes higher cost per kW of electricity generation. This scenario was given to evaluate the maximum production capacity of the field. As one well can be assigned in one grid, the maximum number of production wells being allocated is forty in the production zone. Thus, five wells can be allocated as the maximum number of makeup wells. One makeup well was allocated every 5 years for this scenario.

4.2.1. Total flow rate and flowing enthalpy

Figure 5 presents the total production rate with time. By starting the simulation with total flow rate of 1380kg/s the flow rate declines rapidly in both cases in 5 years. The result clearly indicates that adding five makeup wells do not increase the total production rate. The total production rate decreases to 600kg/s after 10 years. This corresponds to steam production for electricity generation of 47MWe. Based on the currently available subsurface information this field can produce 100MWe electricity for a short period, 5 years, and then decline to about 50MWe in following years. Total number of 35 production wells of 3000m depth makes the total length of 100km of drilling in this field. Consequently, electricity generation rate can be 1MWe per one kilometer of drilling in early stage of the production, but it is predicted to be decreased in the later years. World average rate is 2-5 MWe/km [8,9] which is much higher than this value. To evaluate the effects of total number of wells on average well output the simulations were carried out with different number of wells, from 5 to 35 wells. The results show that average production rate of each well decrease with an increase of the total number of the wells. Figure 6 illustrates relationship between average well output and the total number of the production well. For 5 to15 wells the average well output is 1.3MWe/km, which is still lower than the world average but output reduces to 0.8MWe/km by increasing the number of wells. This is considerably low and results in an increase of the electricity production cost. The simulation was run for 100 years to find out the reservoir capacity that can deliver steam at stabilized rate. Results show that after 20 years the steam flow rate reaches stable with rate of 98 kg/s which can generate 45-50MWe of electricity over 100 years. The flowing enthalpy does not change significantly during simulation period in both cases and the average flowing enthalpy of the produced fluid shows 998 kJ/kg.

4.2.2. Predicted pressure and temperature

The temperature and pressure changes for scenario III were examined for Layers MM. Cooling occurs in the northern part of the reservoir where reinjection wells locate. Temperature drops by 80°C from the initial in the central part of the reinjection zone, and more than 10°C cooling can be seen over an area about 7km^2 which is 4.5km^2 in Scenario II. In Layer MM the pressure drop in the production zone is large and shows up to 30bar in the central part of the production zone. This pressure drops can cause the production rate decline. Larger pressure drop in Layer MM occurs in a wider area compared with that of Scenario II. In the reinjection area, pressure increases due to the reinjection of large amount of waste water. In reinjection area pressure increases up to 80bar.

5. Conclusions

A three dimensional numerical model of the NW Sabalan geothermal field was developed and calibrated by numerical simulations. Prediction simulations of reservoir behaviors were also carried out using the numerical model developed. Two hypothetical development scenarios were evaluated for production capacity assessment and reinjection effects on fluid production. The conclusions are summarized as follows:

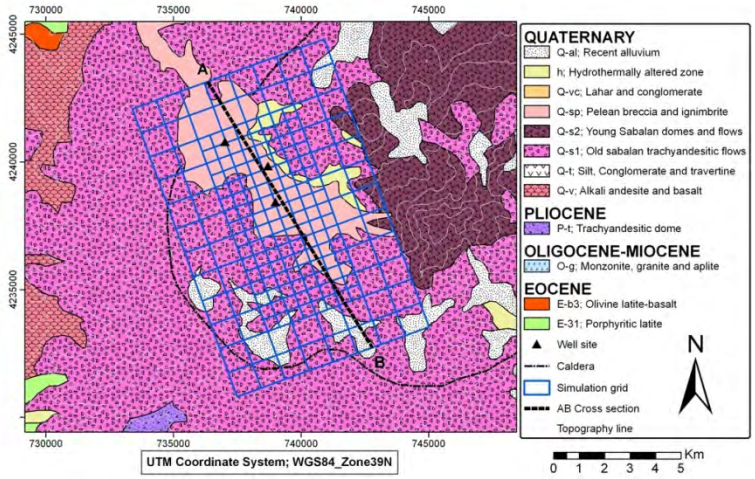

Figure 1 Geological map of the Sabalan area with grid system

The results of natural state simulation using the AUTOUGH2 simulator indicated good agreements in temperature and pressure profiles of three deep wells with measurement. Reinjection of the waste water is effective for moderating reservoir pressure drop. The immediate adjacent area, north to the production area, named as Site B is recommend for locating reinjection wells because of more effective on the pressure support compared with reinjection at further north area, Site C. Based on existing data and assumptions reservoir can sustain steam production equivalent to 50 MWe of electricity for 30 years or more. The reservoir can produce in maximum capacity for production of 90-100MWe for short period of time (5 years), but the production rate decreases gradually to the level of 50MWe after 20 years. The reservoir can sustain steam production for 50MWe over 100 years.

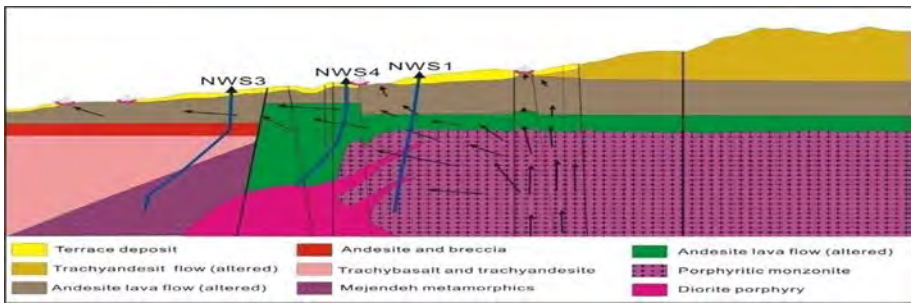

Figure 2 Conceptual model of the NW-Sabalan geothermal field

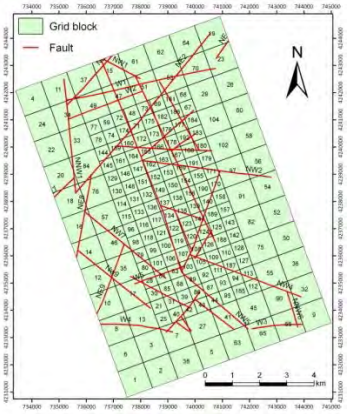

Figure 3 The grid system and faults in study area

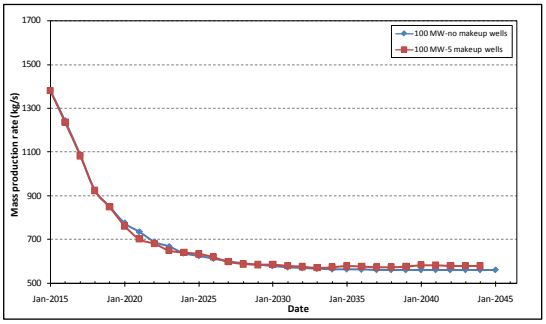

Figure 5 Total production rate over 30 years for Scenario III

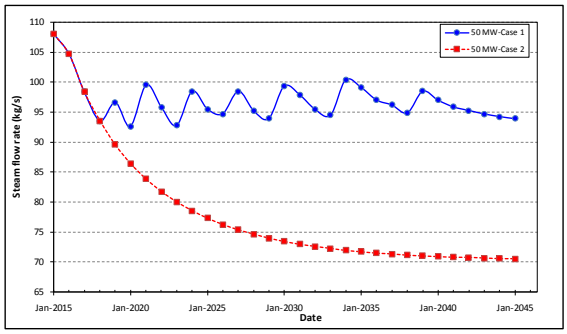

Figure 4 Steam flow rate change with time for Scenario II

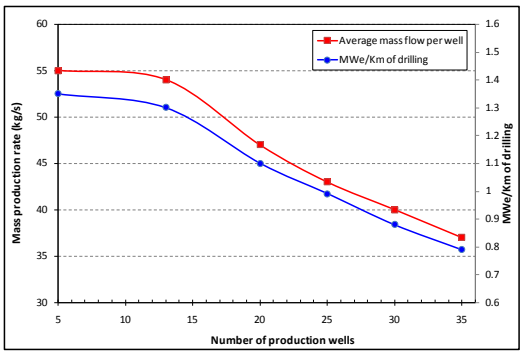

Figure 6 Relationship between average well-output and power generation per km of drilling and number of the production well

References

[1] Pruess, K.,TOUGH2-A General Purpose Numerical Simulator for Multiphase Fluid and Heat Flow, Earth Science Division, Lawrence Berkeley Laboratory, Berkeley,1991,102p

[2] O'Sullivan, MJ., AUTOUGH2 Notes, Department of Engineering Science, University of Auckland, 2000,18 pp

[3] SKM, Report on completion tests and heat up surveys of well NWS1, SUNA Co., 2004a

[4] SKM, Well NWS3 drilling completion report, SUNA Co., 2004b,47 pp

[5] SKM, Well NWS4 drilling completion report, SUNA Co., 2004c, 43 pp

[6] SKM, Sabalan geothermal project, Stage1- surface exploration, final exploration report, report number. 2505-RPT-GE-003, SUNA Co., 1998,83 pp

[7] Beckman, W. and Klein, S., Engineering Equation Solver Professional Versions user manual, F-Chart Software, 2007, pp. 312

[8] Stefansson. V., Investment cost for geothermal power plants, Geothermics, Vol. 31, 2002, 263-272

[9] Stefansson. V., Success in geothermal development, Geothermics, Vol. 21, 1992, 823-834

Utilisation of hydrogeothermal energy by use of heat pumps in Serbia – current state and perspectives

Dejan Milenic[1*], Ana Vranjes[1]

[1]*Univesity of Belgrade, Faculty of Mining and Geology, Department for Hydrogeology, Belgrade, Serbia*
[*]*Tel/fax: +381 11 3346 000, , E-mail: dmilenic@yahoo.ie*

Abstract: The development strategy of the energy sector in Serbia anticipates the intensive utilisation of renewable hydrogeothermal energy sources by using energy efficient technologies. The main aim of the paper is to perceive, for the first time, quantities and possibilities of the utilisation of available hydrogeothermal energy accumulated in groundwater with the temperature up to 30 ^{o}C in the concept of the substitution of fossil fuels by renewable en ergy sources in the Republic of Serbia. The available quantities of groundwater have been observed by regions whose borders correspond with hydrogeological characteristics of the terrain and conditions of groundwater formation. The territory of the Republic of Serbia is divided into eastern part, to which there belong estimated quantities of about 7400 $l \cdot s^{-1}$, namely the available heat power amounts about 200 MW, central and western parts of the territory (to which the capital city Belgrade also belongs) have about 14900 $l \cdot s^{-1}$, which is adequate to about 400 MW of heat power, and northern part of the territory with available 6600 $l \cdot s^{-1}$, namely about 180 MW of heat power. If we take into account the territory of the whole Republic, the available resources of subgeothermal energy amount about 28$m^3 \cdot s^{-1}$, namely over 770MW of heat power.

Keywords: *Hydrogeothermal energy, Subgeothermal energy, Groundwaters, Serbia*

1. Introduction

According to development plans in the field of energetics and energy efficiency of the Republic of Serbia, hydrogeothermal resources belong to renewable energy sources whose application and utilisation, namely the verification of reserves is in its initial phase. The potential and reserves are not examined and explorations of this kind of renewable energy have become significant lately. The strategy of energy development in Serbia anticipates the intensive utilisation of renewable hydrogeothermal energy sources, especially low temperature groundwater via the energy efficient technologies by using heat pumps.

The main aim of the paper is to perceive, for the first time, quantities and possibilities of the utilisation of available hydrogeothermal energy accumulated in groundwater with the temperature up to 30 ^{o}C (subhydrogeothermal energy) in the concept of the substitution of fossil fuels by renewable energy sources in the Republic of Serbia. In the past three years subhydrogeothermal energy resources have been classified in Serbia for the first time (Milenic et.al. 2010, V ranjes 2008), as well as the valorisation of available resources of subhydrogeothermal groundwaters (Stevanovic et al.2010). Hydrogeothermal resources of low enthalpy (fluid temperature to 100ºC) have been classified as the sub(hidro)geothermal energy (fluid temperature to 30ºC) and hydrogeothermal energy in the narrow sense (fluid temperature from 30ºC to 100ºC). Further in the text, for the sake of simplification, the notion: "sub(hydro)geothermal energy" will be used as subgeothermal energy.

On the basis of the mentioned explorations, the definition of subgeothermal energy sources has been deduced: "subgeothermal energy sources are a kind of hydrogeothermal energy of low enthalpy accumulated in groundwaters of the temperature scope to 30 ^{o}C, a nd whose exploitation and utilisation are conditioned by the application of geothermal heat pumps".

Consequently, groundwaters with the temperature of 30^{o}C are significant subgeothermal resources, especially in alluvial plains and Neogene basins in the Republic of Serbia. On the basis of classifications stated in this way, the scientific-research project initiated in the year

2008 (Stevanovic et al.2010), evaluated the availability of groundwater resources which can be used as sources of subgeothermal energy (SGTE) as a kind of hydrogeothermal energy of low enthalpy.The obtained results point out the enormous potential of groundwater in the concept of utilisation as a renewable energy source. However, a small number of subgeothermal systems worked out so far points out the necessity of wider engagement of both the state and independent experts in the sense of awareness are using of the significance of this kind of renewable energy.

The significance of explorations and the utilisation of subgeothermal energy can be seen in the following: groundwater is "easy" for taping and the energy resource is inexpensive for development and exploitation, a l ocally available resource is used via relatively simple technology, the conservation of fossil fuels (oil, natural gas) by the renewable energy source, the increase of self-sufficiency and the sustainability of energy consumption, the increase of environmental quality through the decrease, namely the reduction of the emission of hazardous gases, such as CO_2 (up to 75% in relation to a conventional heating procedure) the improvement of image in public, financial savings due to the reduced purchase of fossil fuels, and the introduction of the principle of "sustainable development".

2. Applied methodology

Hydrogeological and hydrogeothermal explorations in this field are of a highly multidisciplinary character and imply the engagement of researchers from the field of hydrogeology (geothermal resource provision), mechanical engineering (thermo engineering part, the utilization of SGTE), and architecture (the increase of energy efficiency and the correct utilization of SGTE in building).

Hydrogeological explorations imply the evaluation of resource availability, as to:

1. Quantity defining:
    i) hydrogeological regionalisation of the territory of Serbia
    ii) defining of aquifer types within each hydrogeological region
    iii) carrying out of pumping tests at the existing wells within the particular aquifer type
    iv) yield measurements at springs within the particular aquifer type
    v) collecting and synthesis of results of past explorations in the field of hydrogeology
2. Defining of aquifer hydrodynamic characteristics:
    i) calculation of environmental basic parameters
    ii) workingout of aquifer hydrodynamic model
3. Defining of physic-chemical characteristics:
    iii) determining of ground water temperature regime
    iv) determining of qualitative regime
    v) basic chemical composition of ground water
    vi) water aggressiveness (corrosiveness /inscrutability)

After available quantities of subgeothermal energy had been defined, the data obtained in additional explorations were used in discussions, first of all:

Thermodynamic and energy explorations, i.e. calculation of required energy quantity for the heating building / buildings (building energy consume) and techno-economical analyses, i.e. the economical analysis of the investment cost-efficiency in the utilisation of renewable

energy resources comparative analysis of expenses for various fuels and the period of investment cost-efficiency.

The aim of the work methodology set in this way was, first of all, hydrogeological. The paper did not deal, in details, with the efficiency of the utilisation of heat pumps, the analysis of COP, etc. As regards that the utilisation of heat pumps in Serbia is in its initial state, it is not possible to give any detailed analyses of the mentioned parameters of the heat pump work.

3. Survey of subgeothermal potential in Serbia

The Republic of Serbia is pronouncedly rich in hydrogethermal resources (Fig.1a). The waters of Vranjska Banja Spa (96^{o}C), Josanicka Banja Spa (78^{o}C) and some others have the highest temperature. Groundwater with the temperature over 30^{o}C is relatively well utilised. Unlike them, groundwater with temperatures up to 30^{o}C (subgeothermal energy) has not been the subject of explorations from other points of view, except for the needs of water supply. Development of heat pump systems, their growing commercialisation and application in the world, have resulted in increased possibilities of multipurpose utilisation of this water.The availability of subgeothermal groundwater resources is mainly related to depth up to 200m from the surface of the terrain and, on the territory of Serbia it is not evenly spaced. The largest quantities of this kind of energy are related to alluvions of big rivers, especially in towns they run through. Due to the heat island effect, temperatures of groundwater in towns are higher in relation to rural environment, thus the energy potential is higher. On the basis of carried out preliminary explorations of the assessment of groundwater resources with the temperature up to 30°C, the territory of the Republic of Serbia is a highly prospective one, from the point of view of the utilisation of subgeothermal energy. The available quantities of groundwater have been considered by regions, whose boundaries are adequate to hydrogeological characteristics of the terrain and conditions of groundwater formation. Available heat power of low enthalpy hydrogeothermal energy was calculated from the following equation (Eq.1):

$$E = C_p \cdot Q \cdot \Delta T \qquad (1)$$

where:

E - available heat power (KW, MW)

C_P - the specific heat of water (constant, $4.2 KJ \cdot kg^{-1} \cdot °C^{-1}$)

Q - yield of the wells ($kg \cdot s^{-1}$, the same as $l \cdot s^{-1}$)

ΔT - temperature reduction which can be realised in the heat pump (^{o}C)

The areas of big towns in Serbia have special potential, which due to the hot island effect have the most favourable subgeothermal characteristics with raised temperatures of groundwater even to 5^{o}C in relation to the remaining territory. The "heat island" effect is a consequence of urbanisation, leading to micro climatic changes expressed as air temperature raising. This temperature increase can reach 5^{o}C, in relation to inurbane suburbs. Being highly urbanised the City of Belgrade (the city core covers an area of over 10km^2, with more than 1,500.000 inhabitants) has all predispositions for heat island effect occurrence. The geological characteristics of the Belgrade area conditioned the existence of significant quantities of ground waters where heat effect is induced as temperature anomaly.

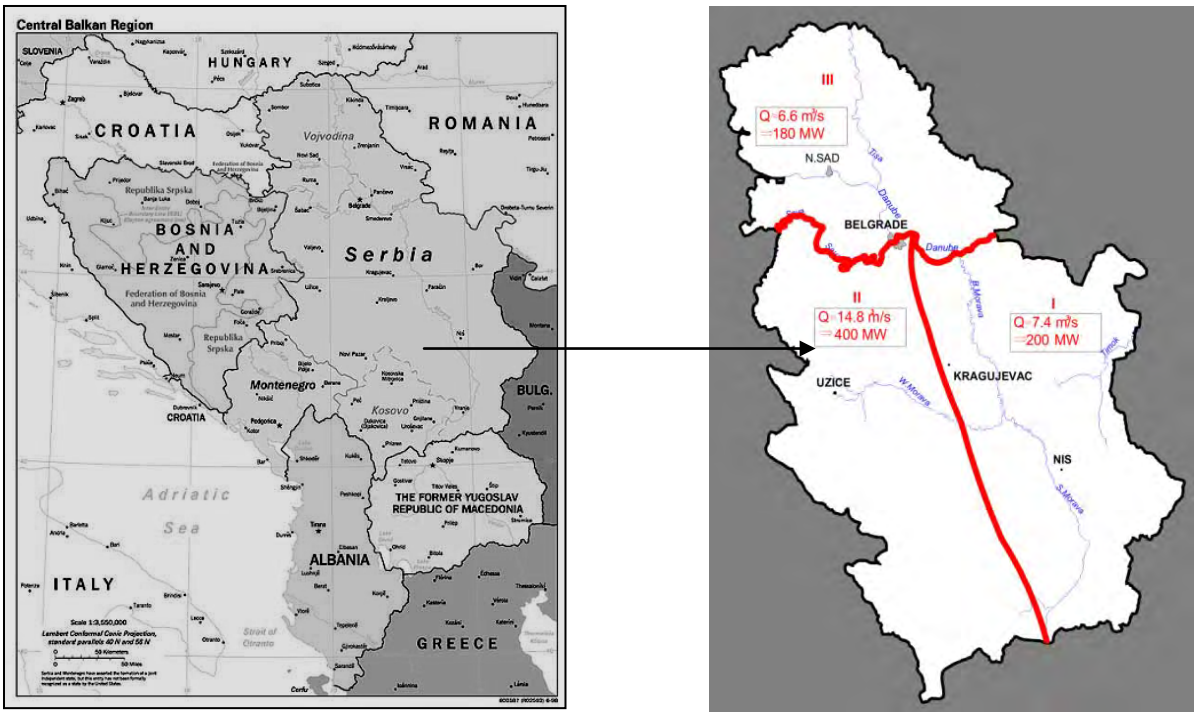

Fig. 1. a)Geographical position of the study area, b)Partition of the investigation area

The available energetic potential of ground water on carried out test exploited wells in New Belgrade goes over 0.5 MW for an individual well. This record was obtained by using minimal well yield of about 1,000- 1,500 m^3/daily and minimal temperature of ground water of 13 to 15°C. Hydroisotherms point out clearly that the groundwater temperature in lesser urbanised areas amounts 13-14°C. Moving to central and highly urbanised parts of New Belgrade the groundwater temperature reaches even 20°C (in summer months), i.e. the groundwater temperatures are higher from 3 to 6 °C. Fig 2.

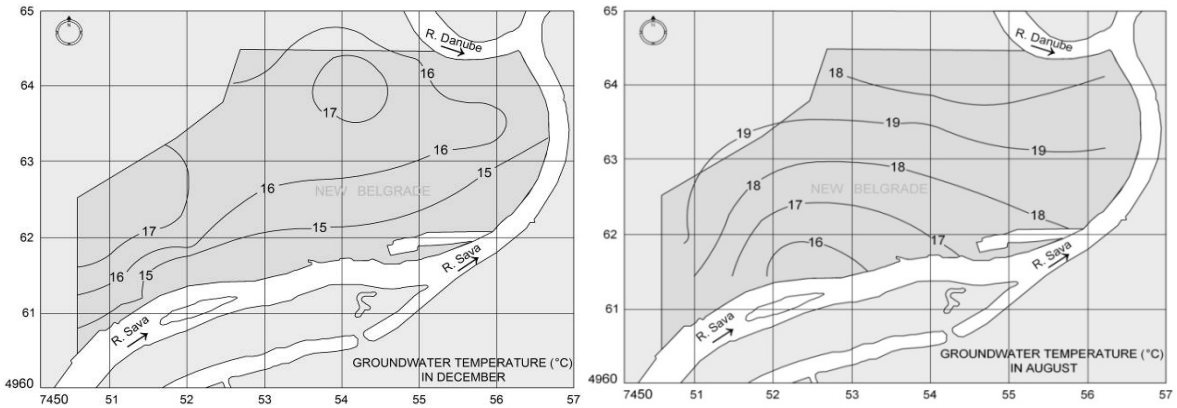

Fig. 2. Hydroisotherm maps of the territory of New Belgrade

The available quantities of groundwater have been observed by regions whose borders correspond with hydrogeological characteristics of the terrain and conditions of groundwater formation. The territory of the Republic of Serbia is divided into eastern part, central and western parts of the territory (Table 1).

Table 1.

	Estimated quantities of groundwaters for all purposes ($l \cdot s^{-1}$)			Total ($l \cdot s^{-1}$)	Total* heat power (MW)	Available quantities for SGTE ($l \cdot s^{-1}$)			Heat power for SGTE (MW)
	Groundwater temperature (°C)					Groundwater temperature (°C)			
	10-16	16-22	22-30			10-16	16-22	22-30	
	1	2	3	4	5	6	7	8	9
Eastern Serbia									
Alluvial deposits	15750	0	0	15750	388	5510	0	0	138
Neogene aquifer	2090	340	200	2630	73	730	155	105	34
Karstic aquifer	5080	130	50	5260	110	725	48	25	23
Fractured aquifer	200	60	50	310	11	71	28	25	5
TOTAL	23120	530	300	23950	582	7036	231	155	200
Central and western Serbia (Including Belgrade)									
Alluvial deposits	29000	0	0	29000	728	10150	0	0	255
Neogene aquifer	4700	350	320	5370	159	1645	150	140	60
Karstic aquifer	7000	380	130	7510	205	2450	150	45	73
Fractured aquifer	250	90	60	400	15	88	45	30	7
TOTAL	40950	820	510	42280	1107	14333	345	215	395
Northern Serbia									
Alluvial deposits	12100	0	0	12100	304	4235	0	0	107
Plioquaternary deposits	5100	200	100	5400	146	1785	100	50	54
Neogene aquifer	800	200	100	1100	38	280	100	50	16
Karstic aquifer	0	0	0	0	0	0	0	0	0
TOTAL	18000	400	200	18600	617	6300	200	100	177
TOTAL TERRITORY	82070	1750	1010	84830	2306	27669	776	470	770

***** Groundwater temperature 10-16 °C, ΔT=6 °C
Groundwater temperature 16-22 °C, ΔT=12 °C
Groundwater temperature 22-30 °C, ΔT=18 °C

4. Discussion

As can be seen from Table 1, the territory of the Republic of Serbia is divided into eastern part to which there belong estimated available quantities for SGTE of about 7400 $l \cdot s^{-1}$, namely the available heat power amounts about 200 MW, central and western parts of the territory (to which the capital Belgrade also belongs) have about 15000 $l \cdot s^{-1}$, which is adequate to about 400 MW of heat power, and northern part of the territory with available 6600 $l \cdot s^{-1}$, namely about 180 MW of heat power. Taking the whole territory of the Republic into account, the total estimated quantities of groundwaters for all purposes amount about 85 $m^3 \cdot s^{-1}$, the total heat power is about 2306 MW, the available resources of subgeothermal energy amount about 29 $m^3 \cdot s^{-1}$, namely over 770MW of heat power (Figure 1b).

If the obtained data are crossed according to types of water bearing structures, it can be seen that intergranular environments in alluvial deposits are far the most abundant. The positions-locations of the biggest towns in Serbia correspond with these environments, thus the possibilities of applications in them are the highest.

If the temperature of groundwater is observed as a parameter, it can be seen that groundwaters with the temperature range of 10-16^oC are most widely distributed. Waters of this temperature in the areas of big towns can be affected by the heat island effect being the most convenient ones for the use of heat pumps.

Utilisation has been mostly related to the territory of the city of Belgrade so far occurring individually, not organized. According to recorded users on the territory of Belgrade, for the needs of climatization of buildings, overall 100 $l \cdot s^{-1}$ of groundwater of 12ºC to 16ºC has been used, while on the territory of whole Serbia the quantities do not exceed 250 $l \cdot s^{-1}$ (overall about 100 users).

On the basis of the stated data, the great potential of subgeothermal resources in Serbia is obvious. The current energy crisis and increasing costs of fossil fuels used for heating(it is primarily related to natural gas whose price rises every year) impose the necessity to take seriously into account the utilisation of subgeothermal resources instead of ignoring it.

The significance of such a way of heating/cooling (by utilisation of SGTE) in building has been highly recognized in the EU. At the end of the last century the member states of the EU completed projects of rehabilitation of the existing housing in order to save energy tending to consume energy for heating lower than 80-100 $kWh \cdot m^{-2}$ annually. In Serbia, the state is still significantly different. The existing buildings are one of the highest consumers of energy in the Republic. Almost 50% of the consumed energy in Serbia is used in buildings, among which 65% for building heating. Almost the third of overall energy needs of Serbia is related to heating of residential and office buildings. According to estimation, the annual energy consumption for residential heating in Serbia ranges from 150 to 250 $kWh \cdot m^{-2}$ depending on the age and the state of buildings. The structure of energy consumption is exceptionally unfavourable: 26% of flats are connected to heating plants; 30% of households use electrical energy; 20% of them use firewood; 15% coal; <6% gas.

Consequently, for the lowest level of consumption (heating) the most qualitative energy (electrical energy) is mostly consumed. The aim of the applied measures is to achieve the reduction of energy consumption in office buildings and public facilities of 80-100$kWh \cdot m^{-2}$ / annually and in individual houses to 70-90$KWhm^2$/ annually, and in flats for collective dwelling to 65-80 $kWh \cdot m^{-2}$ /annually.

Buildings in Serbia are real energy wasters. Over 70% of existing residential buildings were constructed before passing the first serious regulations on thermal protection in the eighties of the last century. Bearing in mind that, annually, only 1% of the existing residential buildings is constructed, it is obvious that the basic resource for applications of energy efficiency measures of any sorts are the existing residential buildings. If only urban area is rehabilitated, i.e. 1.6 million of flats, in the period of the following ten years, that is the work worth 4.5 milliard € or 450 million € annually. Such a wide action would result in the fast creation of conditions for the application of SGTE for due to considerably reduced needs for energy far larger number of facilities could use these resources.

Accordingly, there also goes the comparative analysis of expenses required for the production of 1 MWh of heat energy in relation to the kind of the energy resource, the price of the energy resource, and the manufacturing price in the Republic of Serbia in the season 2010/2011 indicating the highest cost-efficiency of the subgeothermal energy utilisation (Table 2). The analysis has been carried out in relation to the following parameters: natural gas is imported from Russia, the kind of coal is lignite, the approximate price of a pellet is 140 € /t, hydrogeothermal energy is from heat pumps with the approximate COP 1:4, and the price of electrical energy of 0.05 € /KWh.

Table 2. Comparative analysis of expenses required for production of 1MWh of heat energy in relation to kind of energy resource, price of energy resource, and manufacturing price in Republic of Serbia in December 2010

Kind of energy resource	In relation to energy resource price (€)	Manufacturing price (€)
Natural gas	52	72
Mazut	48	68
Coal	32	52
Pellet	38	58
Hydrogeothermal energy (SGTE)	15	35

Nowadays, in Serbia, about 50-55% of overall energy consumption is used in building and about 70% out of that for heating and cooling. By correct investment, with energy savings, energy consumption could be even halved, with invested money refund in the period of five years. The first step is the reduction of loss with final consumers -in flats. The energy rehabilitation of an average flat in Serbia with the surface of 70 m^2 requires about 3000-4000 €. By such investment from 100 to 150 $kWh \cdot m^{-1}$ would be saved annually, meaning 400-600 € annually at nowadays' prices. In this way such investment is repayed in the period of four to seven years.

In order to establish economic justifiability of the SGTE system in new buildings it should be compared to conventional heating systems with regard to initial investment, maintenance expenses, system duration, and cost price of heating resources. Experiences indicate that initial investment in subgeothermal systems (capable to deliver 1 KW of thermal power) ranges within the scope of 850 € per kWh for heating, and up to 1000€ per kWh for combined heating and cooling systems. The initial investment prices in conventional systems are generally lower to some extent than in hydrogeothermal ones being about 40% in heating systems, namely 20% in combined cooling and heating systems. It should be stated that in recent years the prices of STGE systems have dropped significantly approaching those of conventional ones. Unlike the initial investment, the maintenance prices are lower in hydrogeothermal systems, about 50% in combined cooling and heating systems. The use of STGE in Serbia is not charged, once obtained licence for groundwater exploitation is renewed

every five years. Taking into account significant raising of prices of all kinds of fossil fuels, the economic cost-efficiency of this kind of heating is obvious.

Besides, we should bear in mind the reduction of CO_2 emission into atmosphere. As Serbia has signed the Kyoto Protocol, via the system of "quota trade" compensation financial means are obtained on behalf of "preserved" thousand tonnes of CO_2 emission into atmosphere. The current Law on Energetics introduces categories of privileged users, namely legal persons using renewable energy resources anticipating a set of benefits and facilities for them (tax free import of heat pumps, etc.).

References

[1] Milenic, D., Vasiljevic, P., Vranjes, A.: Criteria for use of groundwater as renewable energy source in geothermal heat pump systems for building heating/cooling purposes, Elsevier, Energy and Buildings, 2010, pp. 649-657

[2] Milenic, D., Vranjes, A., Savic, N., Veljkovic, Z.: Indicators of impact of heat island effect on ground water energetic potential on the territory of New Belgrade, Serbia, Europe, Proceedings of the XXXVI IAH Congress,Toyama, Japan,2008

[3] Milenic, D., et al: Exploration and application of renewable subgeothermal groundwater resources in the concept of energy efficiency increase in building, Project Number 33053, Strategic project for technological development for R.Serbia, 2011-2014 (in Serbian)

[4] Stevanovic, Z., Milenic, D., Dokmanovic, P., Martinovic, M., Saljnikov, A., Komatina, M., Antonijevic, D., Vranjes, A., Magazinovic,S.,: Optimization of energy utilization of subgeothermal water resources, Project Number 18008, Strategic project for technological development for R.Serbia, 2008-2010 (in Serbian)

[5] Vranjes, A., 2008: Hydrogeothermal resources of the city of Belgrade territory, phD project, University of Belgrade, Faculty of Mining and Geology

[6] Water management basics of Serbia, 2000

Geothermal Energy Utilization in the United States of America

J. Lund

National Renewable Energy Laboratory, Golden, Colorado, USA
**Tel: +1 541-891-2977, Fax: +1 541-885-1320, E-mail: john.lund@nrel.com*

Abstract: Geothermal energy is used for electric power generation and direct utilization in the United States. The present installed capacity (gross) for electric power generation is 3,087 MWe with about 2,024 MWe net delivering power to the gird producing approximately 16,600 GWh per year for a 94% net capacity factor. Geothermal electric power plants are located in Alaska, California, Hawaii, Idaho, Nevada, New Mexico, Oregon, Utah, Wyoming. The direct utilization of geothermal energy including the heating of pools and spas, greenhouses and aquaculture facilities, space heating and district heating, snow melting, agricultural drying, industrial applications and ground-source heat pumps. The installed capacity is approximately 12,610 MWt and the annual energy use is about 56,550 TJ or 15,700 GWh. The largest application is ground-source (geothermal) heat pumps (84% of the energy use). The largest direct-use (excluding geothermal heat pumps) is fish farming (34%), spa and swimming pool heating (28%), and space and district heating (23%). The energy savings from all geothermal use is about 48.5 million barrels (7.3 million tonnes) of equivalent fuel oil per year and reduces air pollution by about 6.65 million tonnes of carbon annually (compared to fuel oil).

Keywords: *geothermal energy, electric power, direct-use, geothermal heat pumps*

1. Introduction

Geothermal resources capable of supporting electrical generation and/or direct use projects are found primarily in the Western United States, where most of the recent volcanic and mountain building activity have occurred. The San Andreas fault running through California from the Imperial Valley to the San Francisco area, and the subduction zone off coast of northern California, Oregon and Washington along with Cascade volcanism are the source of much of the geothermal activity in the United States. However, geothermal (ground-source) heat pumps extend the utilization to all 50 states. The total identified potential for electrical production is estimated at 21,000 MWe (above 150^{o}C) and 42 EJ (between 90^{o} and 150^{o}C) of beneficial heat [1], and a recent estimate by the U.S. Geological Survey estimates a mean probability of electrical power generation from identified geothermal resources in12 western states during the next 30 years of 8,866 MWe, which would nearly triple the existing electrical capacity. Currently, the geothermal electrical generation installed capacity is 3,048 MWe (gross), 2,024 MWe (net), and the annual energy produced is 16,603 GWh/yr.

Geothermal direct-use is currently estimated at 9,152 TJ/yr (2,542 GWh/yr) with an installed capacity of 611 MWt. Geothermal heat pumps contribute 47,400 TJ/yr (13,167 GWh/yr) with an installed capacity of 12,000 MWt. The total of all direct utilization in the United States is 56,552 TJ/yr (15,709 GWh/yr) with an installed capacity of 12,611 MWt. A total of 20 new direct-use projects have come on line over the past five years, but this increase has been partially offset with closing of one agricultural drying plant and two small district heating projects. Geothermal heat pumps have seen the largest gain, growing at slightly over 10 percent a years with installed units.

This paper is based on material present at the World Geothermal Congress 2010, Bali, Indonesia [2].

1.1. Summary of Electric Power Generation

Even though the United States is the world leader in geothermal electric power generation, geothermal energy remains a small contributor to the electric power capacity and generation in the United States. In 2009, geothermal plants constituted about 0.27 percent of the total operable power capacity, and those plants contributed an estimated 0.48 percent of the total generation.

Since 2005 gross geothermal electrical production capacity has increased in the United States by approximately 500 MWe to a total an installed capacity of 3047.7 MWe and a net running capacity of 2,023.5 MWe due to derating of plants in The Geysers, producing 16,603.4 GWh/yr for a gross capacity factor of 0.62 and a net of 0.94. The low net value is due to plants, especially in The Geysers, operating in a load following mode rather than in a base load mode and due to a reduction in pressure and output of the steam field. The geothermal electric power generation accounted for 4% of the total renewable based electricity consumption in the United States. On a state level, geothermal electric generation is a major player in California and Nevada. The period 1990-2004 also saw a reduction at The Geysers geothermal field in northern California from 1,875 to around 1,529 MWe installed capacity and 945 MWe running capacity. Today, the installed capacity is 1584 MWe and 844 MWe running capacity. This was due to the closing of four units and a reduction in the steam availability. Some capacity has been restored due to the construction of two effluent pipelines, one from Clear Lake and the other from Santa Rosa, that brings about 72,000 tonnes of water per day (19 million gallons/day) to The Geysers for injection. This has restored an estimated 200 MWe of capacity to the field.

1.2. Summary of Direct Utilization

Direct-use, other than geothermal heat pumps, has remained static with increases being balanced by closing of some facilities. The main increases has been in expanding the Boise City District Heating System from 48 to 58 buildings; adding additional wells for space heating in Klamath Falls; expanding the snow melting system on the Oregon Institute of Technology campus from 316 m^2 to 3,753 m^2, increasing the amount of aquaculture product being produced, mainly Tilapia; starting two biodiesel plants; adding an absorption chiller for keeping the Ice Museum at Chena Hot Springs in Alaska intact during the summer months, and adding additional space heating to the Peppermill Casino in Reno. Losses have been the closing of the district heating systems at the California Correctional Center (now using natural gas) and the New Mexico University heating system (due to difficulty with maintenance), and the closing of the Empire onion dehydration plant (due to competition with imported garlic from China) near Gerlach, Nevada.

Geothermal heat pumps have seen the largest growth, increasing over the past five years from an estimated 600,000 to 1,000,000 equivalent 12 kW installed units. The estimated installation rate is from 100,000 to 120,000 units per year, or about a 12 to 13 percent annual growth, with most of the growth taking place in the mid-western and eastern states. A few states have tax rebate programs for geothermal heat pumps, and Congress has established a tax credit of 30% of costs up to $1,500 for installations. Otherwise, there is little support for implementing direct-use projects.

1.3. Enhanced (Engineered) Geothermal Systems

Enhanced (Engineered) Geothermal Systems (EGS) is the current R&D interest of the U.S. Department of Energy, Office of Geothermal Technologies as part of a revived national geothermal program. EGS includes the earlier hot dry rock technology, but now includes any

other method in which to improve geothermal reservoir performance. EGS is associated with both magmatic and high heat producing crustal sources of geothermal energy commonly at depths of about 4 to 5 km to reach 200^{o}C, but also having applications with normal gradient resources. However, EGC projects are currently at an early experimental demonstration stage. Several technological challenges need to be met for widespread efficient use of EGS. The key technical and economic changes for EGS over the next two decades will be to achieve economic stimulation of multiple reservoirs with sufficient volumes to sustain long term production, with low flow impedance, limited short-circuiting fractures and manageable water loss [3].

2. Production of Electricity

The total geothermal electrical installed capacity at the beginning of 2010 was 3,048 MWe producing 16,603 GWh/yr from a running capacity of 2,024MWe. A total of about 514 MWe has been installed in the last five years, amounting to a 20 percent increase or 3.7 percent annual increase.

2.1. Installed and Future Capacity Update

2.1.1. Alaska

Alaska's first geothermal power plant came online in 2006 in Chena Hot Springs. It is a small organic Rankine cycle (ORC) unit (250 kW gross) and produces electricity from the area's low temperature (74^{o}C) geothermal resource. Since coming online the power plant has added another 250 kW unit as well as a 280 kW unit, bringing total production capacity to 730 kW (gross).

Alaska currently has 70 to 115 MW of planned geothermal production coming down the pipeline. Of projects with potential to come online, the Southwest Alaska Regional Geothermal Energy Project 25 MWe, is in an exploratory drilling and resource confirmation phase. Other notable projects are Tongass (20 MWe), Unalaska (10–50 MWe), Pilgrim Hot Springs (10 MWe), and Chena Hot Springs II (5-10 MWe).

2.1.2. California

Current geothermal electricity grossproduction capacity in California is approximately 2497 MWe (1,627 MWe net). In 2010, 4.5% of California's electricity generation came from geothermal power plants, amounting to a net total of 13,605 GWh. The 50 MW North Brawley facility is the state's most recent geothermal power plant addition. Generally, geothermal power generation remains concentrated in California with the majority of production occurring at The Geysers in the north and Imperial Valley in the south.

California has approximately 1,555 – 19,39 MWe of planned geothermal resource production in various stages of development. Production drilling and facility construction are underway at Western GeoPower Corp.'s Unit 1 (35 MWe) at the Geysers as well as CHAR, LLC's Hudson Ranch I (49.9 MWe). Final permitting and PPA's are being secured for Ormat Technologies East Brawley project (30 MWe), Calpine Corporations Buckeye-North Geysers (30 MWe) and Wildhorse-North Geysers (30 MWe) projects, and CalEnergy's Black Rock 1, 2, and 3 units (53 MWe each).

2.1.3. Hawaii

There is only one geothermal power plant in all of Hawaii. Located on the big island, the Puna Geothermal Venture facility has a 35 MWe nameplate capacity and delivers 25–35 MWe of energy on a continuous basis and supplies 20% of the electricity needs of the big

island. Ormat is in the process of securing a PPA and final permitting for an 8 MWe expansion of its Puna project. The 10 units consist of a flash steam plant with a binary bottoming cycle plant.

2.1.4. Idaho

Idaho's first geothermal power plant, Raft River, came online in January 2008. Raft River is a binary plant that uses a 150^{o}C resource and has a nameplate production capacity of 15.8 MWe. Current net production output is between 10.5 and 11.5 MWe. US Geothermal is securing a PPA and final permitting for a 13 – 26 MWe expansion of the Raft River plant.

Another geothermal company, Idatherm, is developing a number of projects throughout Idaho. Idatherm has begun exploratory drilling and resource confirmation operations for its Willow Springs project (100 MWe). It is also planning to develop its China Cap (100 MWe), Preston Area Project (50 MWe), and Sulfur Springs (25 – 50 MWe) resources but is still in the process of conducting initial exploratory drilling and securing rights to resource. Total potential geothermal production for Idaho is 238 to 326 MWe.

2.1.5. Nevada

In 2008 Nevada had 18 geothermal power plants with a total nameplate capacity of 333 MWe and with a total gross output of 10,791 MWh/yr. In 2009 Nevada increased its installed geothermal capacity with the addition of the Stillwater (ENEL, 47.3 MWe), Salt Wells (ENEL, 18.6 MWe), and the Blue Mountain "Faulkner 1" (Nevada Geothermal Power, 49.5 MWe) power plants. Currently Nevada has more developing projects than any other state and it is expected that gross capacity will increase significantly in the future. The following companies have begun production drilling and facility construction at various project sites: Vulcan Power (Salt Wells, 175 – 245 MWe), Presco Energy (Rye Patch, 13 MWe), and US Geothermal (San Emidio "Repower" Project, 8.4 MWe), Ormat (Jersey Valley, 18 – 30 MWe). Many other companies are in the process of securing PPA's and final permitting for a number of projects and other companies are in the early exploratory stages of developing numerous geothermal resources. Nevada currently has 1,776 to 3,323 MW of geothermal capacity in development.

2.1.6. New Mexico

In July 2008, a 0.24 MWe pilot installation project came online at Burgetts Greenhouses near Animas. The pilot installation is part of a larger project known as Lightning Dock that aims to bring a 20 MWe capacity geothermal power plant online in 2011.

2.1.7. Oregon

While there is only one small unit producing geothermal electricity, significant developments are forthcoming. The Oregon Institute of Technology (OIT) has installed a 280 kWe (gross) binary units and is currently producing power for use on campus – the first campus in the world to generate its own power from a resource directly under campus. OIT has also completed production drilling of a 1,600-m deep well and will install a 1.2 MWe binary power unit by 2012 using the 93ºC resource at 158 L/s. Davenport Power, U.S. Renewables Group, and Riverstone are securing a PPA and final permitting for their 120 MWe Newberry Geothermal project as is Nevada Geothermal Power for its 40 – 60 MWe Crump Geyser project. U.S. Geothermal, Inc. successfully completed the drilling of its second full sized production well at Neil Hot Springs (20 – 26 MWe) in October 2009. Overall there are 317 to 368 MWe of potential geothermal power capacity in planning in Oregon.

2.1.8. Utah

Currently, Utah has three power plants online. Unit 1 of the Blundell Plant has a gross capacity of 25 MWe and Unit 2 has a capacity of 11 MWe. Utah's third power plant came online in December 2008 and was the first commercial power plant in the state in more than 20 years. The Thermo Hot Springs power plant, a Raser Techologies operation, came online in 2009 and has a gross capacity of 14 MWe and is expected to generate with a net capacity of approximately 10 MWe. Shoshone Renaissance Geothermal Project. ENEL North America has begun exploratory drilling and resource confirmation operations at its Cove Fort (69 MWe) project site. Other companies have potential geothermal sites that are in the early stages of planning/development and overall Utah has 272 to 332 MWe of planned geothermal capacity for future production.

2.1.9. Wyoming

In August 2008, a 250 kWe Ormat organic Rankine cycle (ORC) power unit was installed at Rocky Mountain Oil Test Site (RMOTC) and a month later it began operating. As of January 2009, the unit had produced more than 485 MWh of power from 413,000 tonnes of hot water annually. The demonstration project is still in operation, and a United Technology Corporation 280 kWe plant is scheduled for operation in 2011. During operation these plants will be an evaluation of how to reduce fluctuations of power and to generate more than 250 kWe.

3. Geothermal Direct Utilization

3.1. Background

Geothermal energy is estimated to currently supply for direct heat uses and geothermal (ground-source) heat pumps 56,552 TJ/yr (15,709 GWh/yr) of heat energy in the United States. The corresponding installed capacity is 12,611 MWt. Of these values, direct-use is 9152 TJ/yr (2,542 GWh/yr) and 611 MWt, and geothermal heat pumps the remainder.

Most of the direct use applications have remained constant or decreased slightly over the past five years; however geothermal heat pumps have increased significantly. A total of 20 new projects have come on line in the past five years.

3.2. Space Heating

Space heating of individual buildings (estimated at over 2,000 in 17 states) is mainly concentrated in Klamath Falls, Oregon where about 600 shallow wells have been drilled to heat homes, apartment houses and businesses. Most of these wells use downhole heat exchangers to supply heat to the buildings, thus, conserving the geothermal water [4]. A similar use of downhole heat exchangers is found in the Moana area of Reno, Nevada [5]. Installed capacity is 140 MWt and annual energy use is 1361 TJ.

3.3. District Heating

There are 20 geothermal district-heating systems in the United States, most being limited to a few buildings. The newest is a small project in northern California [6]. In this rural community of Canby, geothermal heat is used for heating buildings, a greenhouse, and most recently driers and washers in a laundry. The city system in Boise, Idaho has added 10 buildings to their system and will be extended to Boise State University next year. Klamath Falls system has expanded by adding a brewery and an additional greenhouse. Installed capacity is 75 MWt and annual energy use is 773 TJ (215 GWh).

3.4. Aquaculture Pond and Raceway Heating

There are 51 aquaculture sites in 11 states using geothermal energy. The largest concentration of this use is in the Imperial Valley in southern California and operations along the Snake River Plain in southern Idaho. There is a report that some of the facilities in the Imperial Valley have closed, but reliable information is lacking. A large facility at Kelly Hot Springs in northern California has been expanding and now produces slightly over half a million kg of tilapia annually. Two unique aquaculture related projects are in operation in Idaho and Colorado – that of raising alligators [7]. Recent trends in the U.S. aquaculture industry have seen a decline in growth due to saturation of the market and competition from imports. Installed capacity is 142 MWt and annual energy use is 3074 TJ (854 GWh).

3.5. Greenhouse Heating

There are 44 greenhouse operations in nine states using geothermal energy. These cover an area of about 45 ha, have an installed heat capacity of 97 MWt and an annual energy use of 800 TJ/yr (222 GWh). The main products raised are potted plants and cut flowers for local markets. Some tree seedlings and vegetables are also grown in Oregon; however raising vegetable is normally not economically competitive with imports from Central America, unless they are organically grown. One unusual greenhouse product, started recently, is spider mites grown on lima bean plants at Liskey Farms south of Klamath Falls, Oregon. They are grown for their eggs which are then shipped south as feed for predator mites, which in turn are sold to farms to eat spider mites – a complicated process, as the mites and eggs are almost microscopic in size and difficult to see [8]

3.6. Industrial Applications and Agricultural Drying

Industrial applications have increased significantly due to the addition of two biodiesel plants (Oregon and Nevada). These plants primarily use geothermal energy for the distillation of waste grease from restaurants, but one also used canola oil. Small industrial uses include clothes driers and washer installed in Canby, California, and a brewery using heat from the Klamath Falls district heating system for brewing beer and heating the building [9]. The main loss is the closing of an onion/garlic dehydration plant at Empire, Nevada due to competition with imported garlic from China. The installed industrial capacity for these two applications is 40 MWt and the annual energy use 519 TJ/yr (144 GWh/yr) with nine facilities located in three states.

3.7. Cooling and Snow Melting

The two major uses of geothermal energy are for pavement snow melting, on the Oregon Institute of Technology (OIT) campus, and keeping the Aurora Ice Museum frozen year-round at Chena Hot Springs, Alaska. The installed capacity for this application is 4.8 MWt and the annual energy use is 68 TJ/yr (19 GWh/yr).

3.8. Spas and Swimming Pools

This is one of the more difficult applications to quantify and even to find all the actual sites, as most owners do not know their average and peak flow rates, as well as the inlet and outlet temperatures. There are 242 facilities in 17 states, with an estimated installed capacity of 113 MWt and annual energy use of 2,557 TJ/yr (711 GWh/yr).

3.9. Geothermal (Ground-Source) Heat Pumps

The number of installed geothermal heat pumps has steadily increased over the past 15 years with an estimated 100,000 to 120,000 equivalent 12 kWt units installed this past year.

Present estimates are that there are at least one million units installed, mainly in the mid-western and eastern states. The present estimates are that approximately 70% of the units are installed in residences and the remaining 30% in commercial and institutional buildings. Approximately 90% of the units are closed loop (ground-coupled) and the remaining open loop (water-source). The estimated full load hours in heating mode is 2000/yr, and in cooling mode is 1000/yr. The installation cost is estimated at US$6,000 per ton (US$ 1,715 per kW) for residential and US$7,000 per ton (US$2,000 per kW) for commercial. The units are found in all 50 states and are growing 12 to 13% a year. It is presently a US$2 to US$3 billion annual industry. The current installed capacity is 12,000 MWt and the annual energy use in the heating mode is 47,400 TJ/yr (13,168 GWh/yr). The largest installation currently under construction is for Ball State University, Indiana where approximately 4,000 vertical loops are being installed to heat and cool over 40 buildings.

3.10. Conclusions – Direct-Use

The growth of direct use over the past five years is all due to the increased use of geothermal heat pumps, as traditional direct-use development has remained flat. Unfortunately, there is little interest for direct-use at the federal level, as their interests are mainly in promoting and developing Enhanced (Engineered) Geothermal Systems (EGS) and co-produced systems using abandoned oil and gas wells. There are few incentives for the traditional direct-use development, but as mentioned earlier, there are tax incentives for geothermal heat pumps at the federal level and in some states such as Oregon. Since, most direct-use projects are small, there are few, if any, developers and/or investors who are interested in supporting these uses.

4. Energy and Carbon Savings

In total, the savings from present geothermal energy production in the U.S., both electricity and direct-use amounts to 48.5 million barrels (7.28 million tonnes) of fuel oil equivalent (TOE) per year, and reduces air pollution by 6.65 million tonnes of carbon annually. CO_2 reduction is estimated at 18.8 million tonnes.

5. Comparison to Other Countries

Based on data from the WGC2010 [10, 11], the following comparisons with the U.S. geothermal data are made:

5.1 Worldwide Geothermal Electric Power Generation (5 leading countries, except USA)

Country	Installed capacity (MWe)	Running capacity (MWe)	Annual energy produced (GWh/yr)
Philippines	1,904	1,774	10,311
Indonesia	1,197	1,197	9,600
Mexico	958	958	7,047
Italy	843	843	5,520
New Zealand	628	628	4,055
World (24 countries)	10,715	n/a	67,246

5.2 Worldwide Geothermal Direct Utilization (5 leading countries, (except USA.)

Country	Installed capacity (MWt)	Annual energy produced (GWh/yr)	Principal use
China	8,898	20,932	Bathing/district heating

Sweden	4,460	12,585	Geothermal heat pumps
Japan	2,100	7,139	Bathing
Turkey	2,084	10,247	District heating
Iceland	1,826	6,768	District heating
World (78 countries)	48,483	117,778	

As can be calculated compared to the worldwide figures, the United States has 28.8% of the installed capacity, and 24.7% of the annual energy produced for electricity generation; and 26.0% of the installed capacity, and 13.3% of the annual energy use. The low annual energy direct-use percentage for the U.S. is due mainly to the large number of geothermal heat pumps, which have a low capacity factor. In terms of MWe and MWt, the USA is the leader.

References

[1] L. J. P. Muffler (editor), Assessment of Geothermal Resources in the United States – 1978. U. S. Geological Survey Circular 790, U. S. Department of Interior, 1979.

[2] J. Lund, K. Gawell, T. Boyd, D. Jennejohn, The United States of America Country Update 2010, Proceeding World Geothermal Congress 2010, Bali, Indonesia, International Geothermal Association, 2010 (CD-ROM).

[3] J. Tester, B. Anderson, A. Batchelor, D. Blackwell, R. DiPippo, E. Drake (editors), The Future of Geothermal Energy - Impact of Enhanced Geothermal Systems on the United States in the 21st Century, U.S. Department of Energy, 2006, 358 p.

[4] G. Culver, J. Lund, Downhole Heat Exchangers, Geo-Heat Center Quarterly Bulletin 20/3, Oregon Institute of Technology, Klamath Falls, 1999, pp. 1-11.

[5] T. Flynn, Moana Geothermal Area, Reno, NV – 2001 Update, Geo-Heat Center Quarterly Bulletin 22/3, Oregon Institute of Technology, Klamath Falls, 2001, pp. 1-7.

[6] D. Merrick, Adventures in the Life of a Small District Heating Project or The Little Project That Could, Geothermal Resources Council Transactions 26, Davis, CA (CD-ROM).

[7] T. Clutter, Out of Africa – Aquaculturist Ron Barnes Uses Geothermal Water in Southern Oregon to Rear Tropical Fish from the African Rift Lake, Geo-Heat Center Quarterly Bulletin 23/3, Oregon Institute of Technology, Klamath Falls, 2002, pp. 6-8.

[8] L. Riley, Inside the Greenhouse: Geothermal Energy and Spider Mite Production, Geo-Heat Center Quarterly Bulletin 29/3, Oregon Institute of Technology, Klamath Falls, OR, 2010, pp. 15-18.

[9] A. Chiasson, From Creamery to Brewery with Geothermal Energy, Geo-Heat Center Quarterly Bulletin 27/4, Oregon Institute of Technology, Klamath Falls, 2006, pp. 1-3.

[10] R. Bertani, Geothermal Power Generation in the World 2005-2010 Update Report, Proceeding, World Geothermal Congress 2010, Bali, Indonesia (CD-ROM).

[11] J. Lund, D. Freeston, T. Boyd, Direct Utilization of Geothermal Energy 2010 Worldwide Review, World Geothermal Congress 2010, Bali, Indonesia (CD-ROM).

Performance Analysis of a Hybrid Solar-Geothermal Power Plant in Northern Chile

Ignacio Mir[1], Rodrigo Escobar[1]*, Julio Vergara[1], Julio Bertrand[2]

[1] *Departamento de Ingeniería Mecánica y Metalúrgica, Pontificia Universidad Católica de Chile, Santiago, Chile.*
[2] *Empresa Nacional del Petróleo, ENA, Santiago, Chile*
** Corresponding author. Tel: +562 3545478, Fax: +562 3545828, E-mail: rescobar@ing.puc.cl*

Abstract: Chile has introduced sustainability goals in its electricity law in response to increased environmental awareness and the need to achieve higher levels of energy security. In northern Chile, the Atacama Desert has a large available surface with high radiation level, while the tectonic activity along the entire country testifies an ample yet unexploited geothermal resource. The novel concept of hybridizing a geothermal power plant with solar energy assistance is presented here for the particular conditions of Northern Chile. A thermodynamic model is developed to estimate the energy production in a hybrid power plant for two different configurations of solar resource use: adding peak power for a constant geothermal output, and saving geothermal resources for a constant power output. The thermodynamic model considers a single-flash geothermal plant with the addition of solar heat from a parabolic trough field. The solar heat is used to produce superheated steam and to produce additional saturated steam from the separator whenever possible. Results indicate that the energy produced by a geothermal well can be increased up to 11.6% and achieve savings of up to 10.3% in the use of geothermal resources by adding solar assistance when using the single flash geothermal technology. Moreover, the optimal mass flow rate of the geothermal plant is decreased when adding solar assistance. It is recommended to exploit solar energy together with geothermal energy wherever possible, to take advantage of each other's strengths and mutually eliminate weaknesses.

Keywords: *Concentrated solar power, Geothermal Power Plant, Hybrid, Chile*

1. Introduction

Chile exhibits a large diversity of geographical features and climates which has a great impact on the availability of renewable energy sources and their proper assessment. The country has limited energy resources apart from hydroelectric capacity, with a negligible internal fossil fuel production, thus relies on fuel imports to meet its growing energy demand. Renewable energy sources in use by the country comprise only hydroelectricity and wood-based biomass, which combined, only account for 24% of primary energy consumption as of 2008, while non-renewable fossil fuels account for the remaining 76%. Primary energy (Ep) consumption has increased at a yearly rate of 5%, and it is projected to continue doing so as the country further develops [1]. The mechanism that is currently operating in Chile consists in the application of a mandatory renewable energy quota requiring a minimum of 5% of electricity generation starting in 2010 must come from renewable energy sources, excluding large scale hydroelectricity, with a gradual increase of the quota to reach a 10% in the electricity generation mix by 2024 [2]. Given the local distribution of renewable energy sources, northern Chile displays no potential whatsoever for hydroelectricity and biomass since the area is the driest desert in the world. Although there is considerable potential for solar and geothermal energy, none of them is currently contributing to the energy mix, mostly due to the high uncertainty and cost of geothermal exploration and the lack of proper solar radiation databases [3]. Here we propose to integrate both energy sources in a hybrid concept, in order to take advantage of each other strengths and eliminate possible weaknesses. Geothermal resources tend to supply saturated steam and thus are limited in temperature and efficiency, while solar resource is available in daily cycles unless thermal energy storage is used. The goal of the present study is to find the configuration of an hybrid power plant that result in the best combination of solar thermal and geothermal power cycles. The concept of harvesting

solar and geothermal energy together has been proposed in the literature [4, 5] although in those cases the solar energy is used to increase the dryness fraction of the geothermal brine. This approach has been demonstrated as flawed since it makes a less efficient use of the high-exergy, high-cost solar heat. It has been showed previously that the best combination is to utilize the solar energy to increase the temperature of the geothermal fluid by superheating it, with the use of binary cycles also been proposed as a useful alternative for using low-enthalpy geothermal sources [6, 7]. In what follows, we will first describe a power plant configuration with an only-geothermal plant as base case, and then a model of hybridized plant for comparison purposes, aiming to improve the cycle's thermal efficiency and to create synergies between the two energy sources. The results will compare the total electricity produced in a period, and the consumption of geothermal fluid which is related to well depletion.

2. Power plant models

This section presents the plant models under study, focusing on the thermodynamic cycles. First a base case of geothermal-only plant is presented, and then the hybrid Solar-geothermal plant is described.

2.1. Geothermal base cycle

The geothermal power plant model considered for this study consists on a single production well and the basic components of a single flash power plant: a steam separator, turbine, condenser, and re-injection well as shown in Fig. 1. We consider a demonstration plant which is fed by a single well reaching a nominal power of 3.974 MW.

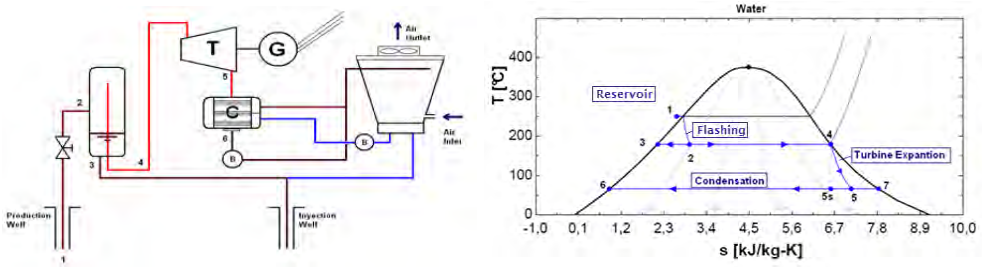

Fig. 1: Single flash plant and T-s diagram.

Numbers in the plant schematic match those from the T-s diagram. The letters T, C, and G stand for turbine, condenser and generator respectively. The conditions at the reservoir are considered to remain constant, while the behavior of the production well is be assumed to follow the productivity curve given by the polynomial expression that relates the mass flow rate with the wellhead pressure [6]:

$$\dot{m} = 44.333 - 0.3363 \cdot P - 0.1357 \cdot P^2 \qquad (1)$$

This fixes the conditions at the cycle beginning. The well head pressure is selected by optimizing the output power as $Max\{x_2 \cdot (h_5 - h_6)\}$, where the index numbers matches those on Fig. 1; therefore, by fixing the working pressure of the condenser, i.e. the pressure at the turbine's outlet, the geothermal power cycle is assumed completely determined. The condenser pressure used here is 0.01234 MPa, equivalent to a condensing temperature of 50°C. For all cases, it is assumed that the reservoir is at a constant temperature of 250°C. The steam fraction after the separator is given by $\dot{m}_{steam} = x_2 \cdot \dot{m}_{total}$, and the specific power from the turbine is $w_t = h_4 - h_5$, where h_5 stands for the enthalpy at the turbine outlet. If we

assume an ideal turbine, then we will have the ideal work produced by the turbine. Thus, we define the isentropic efficiency as the fraction between the real work produced by the turbine and the ideal work at the same conditions, considering h_{5s} as the isentropic enthalpy at the turbine outlet:

$$\eta_t = \frac{h_4 - h_5}{h_4 - h_{5s}} \quad (2)$$

The turbine efficiency is affected by the moisture level present in the steam during expansion. The larger the moisture present, the smaller is the turbine efficiency. This effect can be quantified using the Baumann's rule [8] which proposes that a 1% increase in moisture causes roughly a 1% drop in turbine efficiency. Adopting this rule, the isentropic efficiency is given by:

$$\eta_t = \eta_{td} \cdot \frac{x_4 + x_5}{2} \quad (3)$$

Where η_{td} represents the turbine isentropic efficiency working with dry steam, x_4 is the dryness fraction at the turbine inlet, assumed to be equal to one, and x_5 is the dryness fraction at the turbine outlet. It is assumed that the turbine isentropic efficiency for dry steam is constant and equal to 85%. The dryness fraction at the turbine outlet is calculated as:

$$x_5 = \frac{h_5 - h_6}{h_7 - h_6} \quad (4)$$

Where h_6 and h_7 are the enthalpies of saturated liquid and saturated vapor at the condenser pressure. As the dryness fraction at the turbine outlet depends on the isentropic efficiency, Eqs. (1) to (3) need to be solved simultaneously in order to determinate h_5 and therefore the specific power produced by the turbine. The mechanical power produced by the turbine is then calculated as $\dot{W}_t = \dot{m}_{steam} \cdot w_t$. The model considers that the generator efficiency is equal to 1, and that the parasitic loads are negligible. Finally, the heat rejected by the condenser after the turbine expansion is given by:

$$\dot{Q}_{cond} = \dot{m}_{steam} \cdot (h_5 - h_6) \quad (5)$$

With this the geothermal base cycle is defined and can be solved in order to obtain the steady-state power production.

2.2. Solar Field Modeling.

The solar field for the hybrid power plant is composed of parabolic trough collectors. The solar field sizing considers monthly means of solar radiation and the thermal energy demand. This demand depends on the characteristic of the thermodynamic cycle for each hybrid power plant configuration, depending on steam mass flow rate and the desired maximum temperature of the superheated steam being produced with solar heat. Once the thermal energy demand is determined, the field is sized for satisfying the demand by using a day modeled with the annual average radiation, which in northern Chile is within 20% of the annual maximum value. The sizing procedure includes an energy balance in which the collector area is determined as to ensure that the maximum desired temperature of the superheated steam is met after it passes through the heat exchanger system. The model utilizes Therminol VP1 as the solar field heat transfer fluid (HTF); its properties are obtained from the manufacturer, assuming a maximum working temperature of 400 °C [9]. Heat losses in the

receiver element are modeled based on correlations proposed by NREL [10] as a function of the temperature difference between HTF and the environment:

$$\dot{Q}_{loss} = 0.41 \cdot \Delta T + 1.21 \cdot 10^{-8} \cdot \Delta T^4 \quad (6)$$

A counter flow heat exchanger is used, considering an effectiveness of 95%. The energy balance in the heat exchanger is given by:

$$\eta_{HX} \cdot \dot{m}_{HTF} \cdot Cp_{VP1} \cdot (T_d - T_c) = \dot{m}_{AB} \cdot Cp_{AB} \cdot (T_a - T_b) \quad (7)$$

Where η_{HX} is the heat exchanger effectiveness, $\dot{m}_{HTF}$ is the HTF mass flow rate, C_pVP1 is the HTF heat capacity, T_D is the hot HTF temperature, T_C is the cold HTF temperature, $\dot{m}_{AB}$ is the water or steam mass flow rate, Cp_{AB} is the steam heat capacity, T_A is the sold steam temperature, and T_B is the hot steam temperature. Once the parabolic trough array is sized, it is possible to simulate the operating conditions for each hour of the year by using hourly solar radiation data. The solar field works in a similar way for all cases, varying the mass flow rate of the HTF to keep the outlet temperature constant at the design temperature independent of the actual radiation value. If the solar radiation in a given hour is higher than the design radiation, then it will have a HTF mass flow rate greater than the designed and vice versa. When solar energy exceeds the design value, the extra energy is used to increase the brine dryness factor.

2.3. Hybrid Power Plant

The hybrid Solar-Geothermal power plant consists of a geothermal power plant with assistance from a solar field. Two main scenarios for power production are used; the first aims to produce as much energy as possible without altering the basic operation of the geothermal component of the system, keeping the geothermal optimal mass flow rate from the reservoir fixed and producing extra power as function of solar radiation availability. The second scenario intends to keep the power production constant by reducing the geothermal mass flow rate while supplying extra heat from the solar field. The basic premise here is that saving geothermal fluid could result in extended well and reservoir lifetime, and as a result, decrease make up drilling costs without compromising the energy output rate. The input data are the geothermal well production curve and the solar radiation available (as in Eq. 1), and the prevailing climatic conditions at the chosen plant location. The solar radiation is obtained from pyranometer data available for the general area of Calama (22° 2S, 68° 5 W).

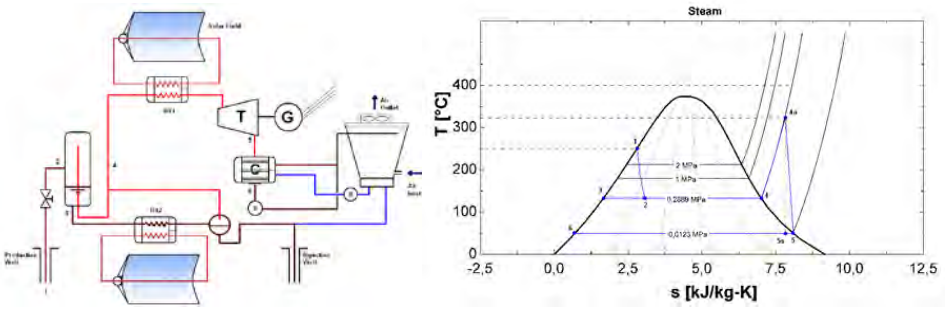

Fig. 2: Single flash Solar-Geothermal plant and T-s diagram.

2.3.1. Hybrid Solar-Geothermal, Scenario 1

A single-flash geothermal power plant is considered, with solar superheating after the separator. This scenario aims to increase production of the plant during the daylight hours

when electricity demand is higher and radiation is available. The geothermal well is kept working at constant mass flow rate, while solar thermal energy is added to increase output power. In this case, a superheating temperature of 320.8 °C is reached according with the thermodynamic conditions. With this temperature, using the radiation data for Calama and assuming an environment temperature of 15 °C, a solar field total aperture area of 4760 m^2 is obtained. If the solar radiation is higher than the design radiation (which is used to size the solar field as previously explained), then the excess is used to evaporate part of the saturated liquid stream from the separator and thus increase the main steam flow. If the solar radiation is lower than the design radiation, point 4a in the T-s diagram does not reach the maximum temperature, but it is instead located closer to point 4. In the limit with no solar radiation available, points 4 and 4a merge and fall in the saturated steam line. When point 4a is below the maximum temperature, expansion within the turbine will occur in two stages; the first is an expansion of superheated steam where the turbine isentropic efficiency is not affected by moisture, and a second stage where the expansion falls into the saturated steam zone, with moisture causing the turbine efficiency to be reduced according to the Baumann´s rule [8].

2.3.2. Hybrid Solar-Geothermal, Scenario 2

The second scenario aims to study a possible configuration that could reduce geothermal steam consumption and thus extend both well and reservoir life cycle. This can be achieved by replacing geothermal energy by solar energy when it is available, reducing the mass flow rate of geothermal fluid from the reservoir, and then using solar energy to compensate for the missing power by keeping the output power equal to the one obtained in the base scenario. The solar field sizing is done by fixing the turbine output at a value of 3.974 MW (equal to the base case, geothermal-only power plant), and then assuming that the design solar radiation is completely available. For this power output, the production curve of Eq. (1) indicates that the lowest extraction pressure is 0.9022 MPa, which results in a steam mass flow rate of 30.25 kg/s from the well, yielding 5.1 kg/s of saturated steam after the separator. The maximum steam temperature is limited to 400 °C, due to the HTF working range. This requires a power of 2505 kW in the heat exchanger number one (HX1, as in Fig. 3) and then a reheating step to take the steam back to 400 °C in the HX2 in order to deliver the 533.7 kW that are needed to reach the base case output power. This gives a total solar contribution of 3038 kW for the design conditions, resulting in a solar field collection area of 3685 m^2 in this scenario.

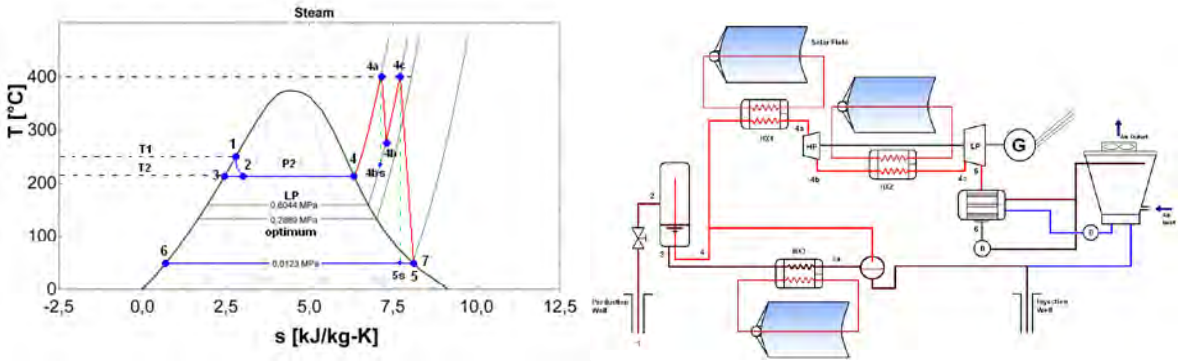

Fig. 3: Single flash Solar-Geothermal plant with reheating and T-s diagram.

An iterative process for the geothermal fluid mass flow rate is performed in order to determinate the thermodynamic states in the power plant model in an hourly basis during a 1-year period. The starting point is a given mass flow rate, which is reduced according to the available solar radiation. A decrease in the well mass flow rate results in a pressure increase at the separator inlet, thus allowing the superheating pressure value to be established. Solving

for the base case output power gives the amount of reheating needed. Again, the procedure is repeated in an hourly basis for the entire 1-year period.

3. Results

The main results obtained in this study are the hourly energy production of the base geothermal-only and the two scenarios of the Solar-Geothermal hybrid power plant, which can be integrated in a 1-year period to obtain the annual energy production of each plant.

3.1. Base Case

The first results correspond to the base case, a geothermal-only plant. By solving the equations that represent the thermodynamic cycle in Fig. 2 for a geothermal power plant, it is possible to obtain the optimum mass flow rate from the reservoir and the pressure at which the separator operates, thus achieving the maximum possible power output. The output power is 3974 kW, the total mass flow rate is 42.22 kg/s, the separator pressure is 0.2897 MPa, the energy produced for the entire year assuming a plant factor of 100% is 34.81 GWh, and the amount of extracted geothermal fluid in a year is 1331500 Tons, parameters which are established as the base case for our comparisons, corresponding to a plant that operates with a single well for a 3.974 MW power output.

3.2. Hybrid Solar-Geothermal, Scenario 1: Increased production

Even though the Chilean Desert offers a large number of clear days throughout the year, the daily radiation is subject to hourly variability as can be seen in days 1, 2, 5, and 9 of the 10-day sequence in Fig. 4. The different peaks in power output allow the plant to produce as much as 5.5 MW, an increase of more than 30% from the base power output. It can be seen that this scenario results in an annual increase of 11.36% on the total energy produced by the plant respect to the base case. An additional advantage of this configuration is that there is no need to regulate the mass flow rate of geothermal fluid from the reservoir, thus resulting in a much simpler plant operation scheme. However, the daily output power profile, where this scenario displays daily power production peaks make the power production variable and not easy to predict, which constitutes a disadvantage in terms of power dispatchability. Even though the difference between daily maximum and minimum varies only around 20%, the power curve is not as attractive as a flat curve. A positive point for these power production profiles is that, in general, the output power peak takes place during peak demand hours, thus resulting in highest spot prices that make this option attractive. The abnormality shown February is due to the altiplanic winter effect, where cloudy periods are present caused by the Amazonia wet season.

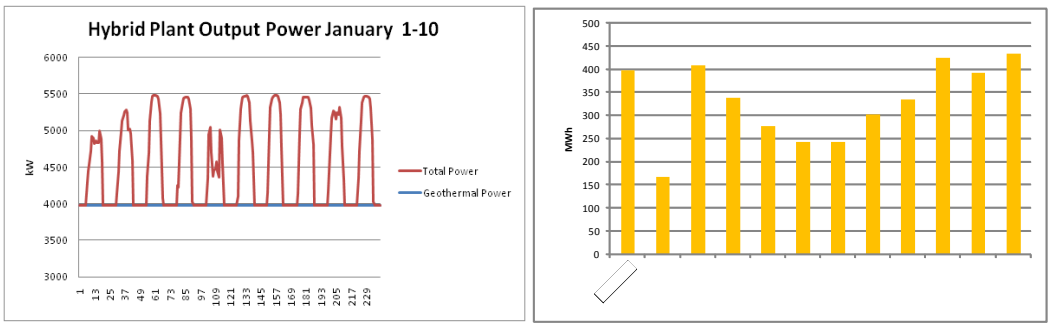

Fig. 4: Daily output power and monthly energy added, Solar-Geothermal plant Scenario 1.

3.3. Hybrid Solar-Geothermal, Scenario 2: Geothermal fluid savings

In this scenario the goal is to produce the same amount of energy as in the base case, by reducing the mass flow rate of geothermal fluid according to the availability of solar radiation, thus using solar heat to compensate for the reduced steam flow while maintaining the power output constant. Fig. 5 shows the power production profile for the same 10-day sequence as in Fig. 4, this time for the conditions corresponding to Scenario 2. The power production remains flat at a 3.974 MW value. The geothermal contribution, however, decreases as solar radiation becomes available. A significant reduction of 10.36% in geothermal fluid mass flow rate can be achieved for this particular conditions, which might translate into longer well and reservoir life, thus reducing the cost of exploring and drilling for new wells to replace those already depleted. An additional benefit is given by the flat power production profile, which makes this plant configuration attractive for sales contracts as is able to supply base load to the Chilean grid. This plant configuration also requires the smallest solar field sizes, due to the reduced solar heat required and the improved thermodynamic efficiency obtained in this scenario. The reduction of mass flow rate from the producing well implies a higher working pressure as per Eq. (1); adding this to the increased steam temperature achieved by the solar-superheated steam increases the efficiency of the thermodynamic cycle. Fig. 5 also displays the monthly total energy produced during a 1-year period. It can be seen that the solar contribution in this scenario is larger than that of scenario 1, thus effectively operating with an increased solar fraction.

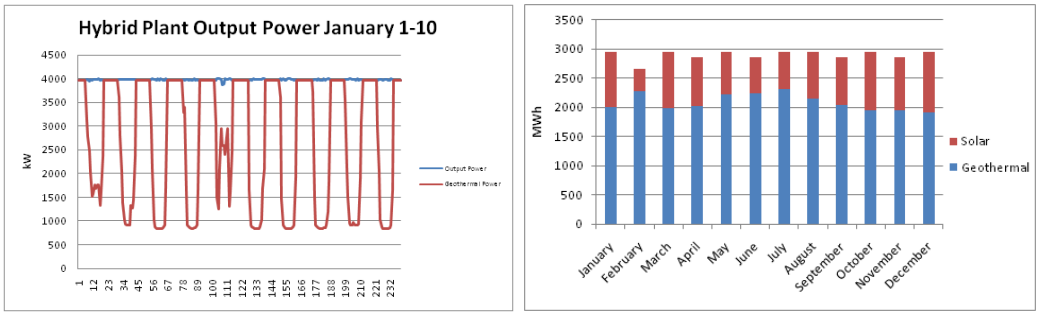

Fig. 5: Daily output power produced by the Solar-Geothermal plant, Scenario 2.

4. Conclusions

Chile faces several energy challenges as a country which is a net energy importer. The country exhibits ample potential for both solar and geothermal energy. Considering the variability of solar energy and the limitations that the use of saturated steam poses to geothermal energy, it is proposed to combine both energy sources into an hybrid power plant concept, with the general goal of taking advantage of each other strengths and mitigate their weaknesses. The hybrid Solar-Geothermal power plant models being presented consider a single flash geothermal plant with the addition of a parabolic trough collector solar field used for steam superheating. In this way the hybrid plant increases its maximum operating temperature and operates with superheated steam expansion in the turbine, as opposed to saturated steam expansion in the original, geothermal-only plant. Simulations of the plant operation in 1-year periods are performed based on hourly databases of available solar radiation for Northern Chile. Two different scenarios are proposed. The first allows the solar heat to increase the power production from the base case geothermal plant, while the second maintains a constant power output, instead utilizing the solar heat to reduce the geothermal fluid mass flow rate. It is found by the authors that the first scenario allows producing as much as 12% more energy than the base case due to the use of solar energy, producing an output power profile with daily peaks following the daily solar radiation availability. These power production peaks coincide with the peak energy demand hours, thus allowing the sale

of electricity at a larger price in the spot market. The main advantage of this generation scheme is the simplicity of its operation, where geothermal components operate the same way they do in a conventional geothermal power plant, allowing the solar radiation to add a contribution whenever available. The second scenario intends to use the available solar radiation as a way to save geothermal fluid mass flow rate. The basic premise is that reducing the well mass flow can result in an extended well and reservoir life, thus saving on exploration and perforation costs. This scenario produces a flat power output profile and therefore the same amount of energy produced than the geothermal-only base case, with lower geothermal fluid utilization. Reductions of more than 10% of geothermal fluid utilization were achieved when comparing to the base case. The operation of a power plant under this scenario requires constant monitoring of the well mass flow rate according to the availability of thermal energy coming from the solar field, which in practice is complex and has never been done before. It is also not known at the present time if the geothermal reservoir can be managed in such a way. The geothermal solar hybrid concept represents an interesting prospect for the Chilean electricity market, with the potential of providing base load energy with a high capacity factor from emissions-free and environmentally friendly sources. Further analyses are being performed for developing an economic model and assess in more detail the feasibility of this concept

Acknowledgements

Proyect FONDECYT 1095166 provided the computational platforms and simulation software, while Project FONDEF D08i1097 provided the solar radiation data.

References

[1] Comisión Nacional de Energía, CNE (2010). Balance Nacional Enegético 2008. Last accessed at http://www.cne.cl/cnewww/opencms/06_Estadisticas/Balances_Energ.html on August 13, 2010.

[2] Ministerio de Economía. Ley general de servicios eléctricos, Decreto con fuerza de ley n°4, Art. único Nº 2, D.O. 01.04.2008. Santiago, February 2007.

[3] Ortega, A., Escobar, R., Colle, S., Abreu, S. (2010). The State of Solar Energy Resource Assessment in Chile. *Renewable Energy*, 35, 11, 2514-2524.

[4] Handal, S., Alvarenga, Y., & Recinos, M. (2008). *Solar* Steam Booster in the Ahuachapán Geothermal Field. El Salvador.

[5] Lentz, & Almaza. (2003). Parabolic troughs to increase the geothermal wells flow enthalpy. Mexico.

[6] DiPippo, R. (2008). Geothermal Power Plants; Principles, Applications, Case Studies and Enviromental Impact, Second Edition. London: Elsevier.

[7] Tester, J. et al, Massachusetts Institute of Technology (MIT) (2006). The future of geothermal Energy. Retrieved Jan, 2010. Last accessed on August 13, 2010 at: http://geothermal.inel.gov/publications/future_of_geothermal_energy.pdf.

[8] Leyzerovich, A. (2005). Wet-Steam Turbines for Nuclear Power Plants. New York: PennWell.

[9] Therminol. (2009). *Therminol*. Retrieved 2009, from www.therminol.com

[10] National Renewable Energy Laboratory *NREL*. (2009). *TroughNet, Parabolic Trough Solar Field Technology* Retrieved 2009, from: http://www.nrel.gov/csp/troughnet/solar_field.html.

Potential use of geothermal energy sources for the production of lithium-ion batteries

Pai-chun Tao, Hlynur Stefansson, William Harvey, Gudrun Saevarsdottir*

[1] *Reykjavik University, Reykjavik, Iceland*
** Corresponding author. Tel: +354 599-6345, Fax: +354 599-6201, E-mail: gudrunsa@ru.is*

Abstract: The lithium-ion battery is one of the most promising technologies for energy storage in many recent and emerging applications. However, the cost of lithium-ion batteries limits their penetration in the public market. Energy input is a significant cost driver for lithium batteries due to both the electrical and thermal energy required in the production process. The drying process requires 45~57% of the energy consumption of the production process according to a model presented in this paper. The model is used as a base for quantifying the energy and temperatures at each step, as replacing electric energy with thermal energy is considered. In Iceland, it is possible to use geothermal steam as a thermal resource in the drying process. The most feasible type of dryer and heating method for lithium batteries would be a tray dryer (batch) using a conduction heating method under vacuum operation. Replacing conventional heat sources with heat from geothermal steam in Iceland, we can lower the energy cost to 0.008USD/Ah from 0.13USD/Ah based on average European energy prices. The energy expenditure after 15 years operation could be close to 2% of total expenditure using this renewable resource, down from 12~15% in other European countries. According to our profitability model, the internal rate of return of this project will increase from 11% to 23% by replacing the energy source. The impact on carbon emissions amounts to 393.4-215.1g/Ah lower releases of CO_2 per year, which is only 2-5 % of carbon emissions related to battery production using traditional energy sources.

Keywords: *Lithium ion battery, Geothermal energy, Energy cost, Carbon emission*

1. Introduction

The exponential growth in the use of portable electronic devices and electric vehicles has created enormous interest in inexpensive, compact, light-weight batteries offering high energy density. Clearly, the lithium-ion battery is one of the most appealing technologies to satisfy this need. It is estimated that the global market for lithium-ion batteries could grow from $877 million in 2010 to $8 billion by 2015[1]. However, cost limits their penetration in the global market. Energy is a significant cost driver for lithium batteries as both electrical and thermal energy is required in the raw materials processing and battery manufacturing and assembly. As energy use is significant in the process, the sustainability of the energy source influences the overall carbon footprint for the battery production. Iceland offers a number of potential avenues for cost and carbon emissions reductions in the manufacturing process, due to readily available medium grade thermal energy from geothermal or industrial sources, access to inexpensive renewable electricity, and a skilled workforce. The purpose of this paper is to quantify the economic advantages and carbon emission reductions to be gained by locating a lithium iron phosphate ($LiFePO_4$) factory in Iceland close to geothermal heat sources, versus sites in other locations where fossil sources of energy must be used. Furthermore, we will also present the sensitivity of profitability to energy cost.

2. Methodology

The presented work consists of three main tasks: 1) Collection of relevant data and information. 2) Estimation of energy consumption and temperature levels at various steps in the production process and 3) Assessment of profitability and impact on carbon emissions. Firstly, the literature review, including interview data, provides us with information to draw a complete production process map of the lithium iron phosphate battery manufacturing process. Unfortunately, detailed energy consumption data from each step in the lithium

battery production is not readily available from factories due to confidentiality reasons in this competitive market. Consequently, we build a theoretical energy consumption model for the drying process based on the thermal properties and moisture content of materials in the batteries, basic physical formulas, and industrial experience. There are some uncertainties in this model, as energy efficiency, and heat loss, are based on educated assumptions. The results from the model are therefore not data from an actual factory, but should be informative none the less. In reality, it could be lower or higher depending on de sign of industrial equipment components. For the profitability assessment, common standards of estimating the profit of an investment, for example, net present value (NPV) and the internal rate of return (IRR) are applied. Consequently, we build a comprehensive profitability assessment model for building a new lithium iron phosphate battery factory in Iceland. Most cost data are obtained directly from suppliers or publicly available information. The main assumptions are listed in Table 2.1. In the model, we make several financial assumptions, such as interest rate, capital structure and discount rate of based on current conditions in Iceland. The profitability calculation and Monte Carlo analysis are performed by Microsoft Excel plug in with @Risk5.7.

Table 2-1 Main assumptions of profitability model

Items	Value
Interest rate of loan	12%
Sale price	1.44 (USD/Ah) with 3% annual decreasing trend
Raw material price	0.69 (USD/Ah) with 2.75% annual decreasing trend
Initial investment	9612 million ISK
Discount Rate	15%
Capital structure	70% loan, 30% equity
Exchange rate	156 (ISK/Euro) 112 (ISK/USD)
Salary for workers	Iceland: 238,000 (ISK/Month) Germany: 1944 (€/Month)

3. Energy consumption of Lithium Iron Phosphate battery production process

3.1. Energy consumption of entire process

Energy consumption in lithium iron battery production is not openly available information from this emerging industry. Lifecycle analysis of lithium iron battery by Mats Zackrisson and Lars Avellán in 2010 claims that the total energy consumption corresponds to 11.7 kWh electricity and 8.8 kWh of thermal energy from natural gas per kg lithium-ion battery [2]. This corresponds to an energy consumption for 1Ah battery of approximately 0.68KWh, assuming that one kg lithium-ion provides 30Ah capacity of battery. In addition, energy consumption data were obtained from Matti Nuutinen, who reported data from a Chinese lithium iron phosphate battery factory and for European Batteries Oy[3]. In this report, Nuutinen shows that 5000kw electric power is required to produce 80MAh battery per year. This equates to energy consumption for producing 1Ah battery is approximately 0.54KWh. Based on these sources the energy consumption could range from 0.54 to 0.68 KWh/Ah according to our investigation.

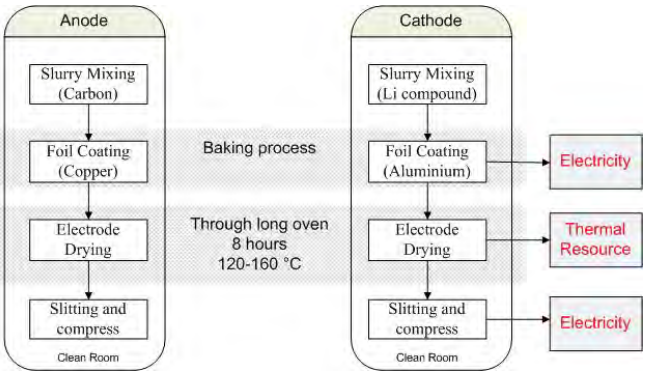

Figure 3-1 Production process map of Part 1

3.2. Production process map

In general, our analysis of the lithium iron battery production process starts with the various raw materials and components from suppliers. The overall process can be divided into two parts: preparation of electrodes and cells assembly. Fig 3-1 shows the main steps in first part of the production process. In first part, the first step is to mix anode and cathode powders with solvent and binder, coat them on the respective foils, and dry them in the vacuum oven at around 120˚C for 8 hours. Traditionally the heat applied at each of the drying steps is obtained by electric heating. However, since the temperature needed in the vacuum oven is relatively low, we might be able to replace electric heating with heat exchangers using geothermal steam as a thermal source. After this drying step the electrode disks would be cut into suitable sizes and compressed thinner by automatic machines. At this stage, the individual electrode is ready for assembly.

Fig 3-2 shows the second part, which is to assemble the various components, such as the separators, internal circuits, anodes and cathode altogether. In this step, the electrodes can be stacked and clamped first and put into a metal packing case. Afterwards, the battery cells are placed in the core drying machines. The purpose of this step is to remove the remaining moisture from electrodes completely. This is the most energy intensive step of the whole process. In principle it would seem feasible to accelerate this drying step by increasing the temperature in the oven. However, the melting point of the binder (PVDF) is around 170°C, so the temperature in the vacuum oven must be kept below 170°C. As an alternative the process is accelerated by lowering the pressure in the oven in order to efficiently remove the vapor formed. Thereby the boiling point of water and solvent is decreased in order to shorten the drying process. In the end, the moisture content rate in the electrodes is reduced to 500ppm [4]. After the core drying process, the electrolyte is injected into cell and it is sealed completely. Since the electrodes are very sensitive to moisture, those processes are usually operated in a room, where the humidity is kept at an acceptable level. In principle, the battery pack is ready for use at this stage. However, most producers test their products several times in order to ensure its performance and collect data before shipping the product to consumers.

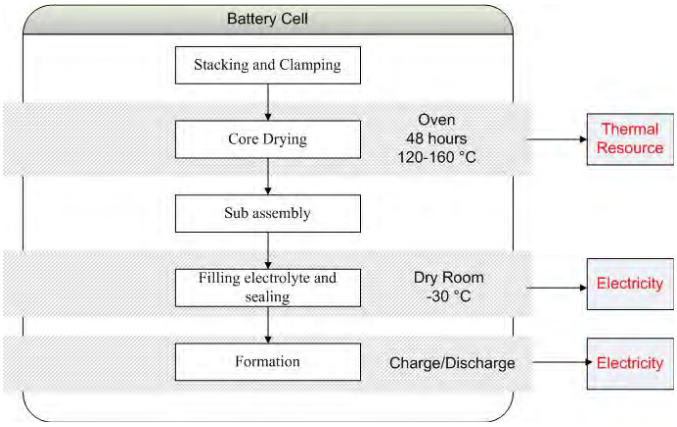

Figure 3-2 Production process map of Part 2

3.3. Energy consumption of the drying process

Through production analysis, the approximate energy consumption figure has been already addressed in the previous text. But, we need to know the energy consumption of the drying process, if we want to consider alternative energy resources for the drying process. Consequently, we build a theoretical calculation model. It is not perfect, but a reasonable approach to figure out the approximate energy consumption of the drying process. The first step of building an energy consumption model of drying is to collect the weight percentage and thermal properties of component materials. Table 3-1, shows the physical thermal properties of each material in the lithium iron battery.

Table 3-1 Physical properties of component material

Information of 1 kg lithium iron battery component material			
Cathode Composition	Weight (g)	Heat capacity	Others
$LiFePO_4$	422 g [2]	C_v: 0.9 J/g-K [2]	Melting point: 223°C
Al foil	19 g [2]	C_P(25°C) 0.89 J/g-K	Melting point: 660.3°C
Carbon black	27 g [2]	C_P(25°C): 0.71 J/g-K	Melting point: 3500°C
Binder (PVDF)	28 g [2]	C_v: 1.9J/g-K [5]	Melting point: 170 °C
NMP solvent	Initial: 244.2 g Outlet: 10g[6]	C_v: 1.76 J/g-K [7]	Boiling point: 202°C Heat of vaporization, 20°C: 550.5 KJ/g [6]
Anode Composition			
Graphite	169 g [2]	C_P(25°C): 0.71 J/g-K	Melting point: 3500°C
Cu foil	46 g [2]	C_p(25°C): 0.385 J/g-K	Melting point: 1084.6°C
NMP solvent	Initial: 116.2 g Outlet: 4.8g [6]	C_v: 1.76 J/g-K [7]	Boiling point: 202°C Heat of vaporization, 20°C: 550.5 KJ/g [6]
Total moisture	Initial: 4.5g Outlet: 0.5g [4]	C_v (25°C): 4.18 J/g-K C_v(100°C, steam): 2.08	Evaporation energy: 2270 KJ/g)

The model predicts how much thermal energy we need in order to remove the moisture and NMP from the electrodes. It is accompanied with the increasing temperature of other materials and some heat lost to environmental. The thermal energy consumption of the drying process calculation could be divided into two parts. (1) The energy for increasing the temperature of all component materials. (2) The energy for evaporating the moisture and NMP away from the feedstock. Through the thermal properties and some basic physical formulas, we obtain theoretical results for both parts respectively. And then, we take the empirical energy efficiency of the vacuum dryer into account to get more realistic data. The energy required for heating the materials to the dryer temperature would is 128.62kJ/kg. The second part is the energy consumption of evaporation. It dominates the energy consumption of drying process. The overall energy consumption of evaporation is 198197.8kJ/kg. The key factors in this calculation are the initial weight and outlet weight of moisture because the heat of evaporation of water and solvent dominates as compared to the sensible heat. However, the energy efficiency is not 100%. Based on the literature we assume that the energy efficiency of the vacuum dryer is 0.6 according to the Handbook of Industrial Drying [8]. In this case, the practical energy consumption would be 0.186/0.6 = 0.26 KWh/Ah. As a consequence the energy required is approximately 0.31 KWh thermal to dry 1Ah of lithium iron phosphate battery. This number does not include the electricity for vacuum machines and drying rooms, which are also part of the drying system. It only focuses on the thermal energy that can be replaced by geothermal steam. According to the energy consumption data in previous research, the whole energy consumption of producing 1Ah lithium battery would raised from 0.54~0.68 KWh. Based on this information 45~57% of the energy consumed by the process can be replaced by an alternative thermal source.

3.4. Alternative drying technology

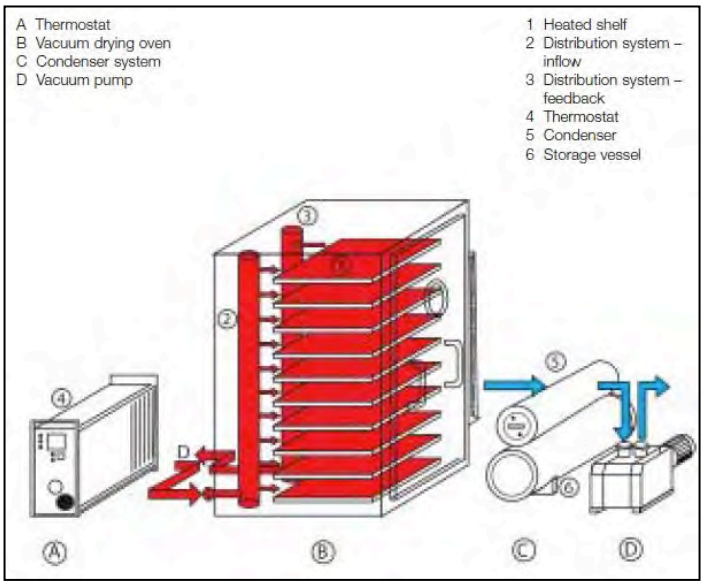

Figure 3-3 Schematic model of vacuum oven could use working fluid as thermal resource [9]

The volatile components targeted in drying are moisture and organic solvent (NMP) that are a part of the cathode or anode paste. The oven provides thermal energy to the feedstock continuously by convection, conduction or radiation in order to remove the targeted compounds from the battery components. In Iceland, geothermal power plants are typically operated with steam at 10-12 bar, but in some cases, a higher pressure up to 18 bar is applied. In this case we consider Reykjanes as a location due to the power plants proximity to a harbor and a developed industrial area, so geothermal steam at 18 bar 207°C is used as a thermal resource for the analysis. However a resource at 9 bar and 173°C, which would be more widely available, is quite sufficient for this process. As the factory is located close to the geothermal power plant, steam from two-phase separators could be applied directly. The power company, Hitaveita Sudurnesja, has offered 20 bar steam to other customers at 4USD/ton and 6 bar at 3 USD/ton in 1995[10]. As a comparison a diatomite processing plant at Lake Myvatn that was in operation until 2004 paid 1 USD/ton for geothermal steam. In this model, a steam price of 4 USD/ton is assumed. In reality, this price highly depends on the negotiation with power companies. The optimal dryer technology for lithium ion battery production is a tray dryer (batch) using conduction heating method under vacuum conditions. Although the geothermal steam from well contains some deleterious materials, most of them would be contained within the liquid phase in the separators. Thus, we would be able to fill the geothermal steam into the entire cavity of shelves directly. As you can see in Fig 3-3, while the feedstock is placed on the shelves, the thermal energy is transferred to products by conduction. In addition to the conduction, it also could be combined with irradiative heating in order to accelerate the drying rate. We assume the new type of dryers will cost 20% more than normal electric dryers. As the cost of dryers is only 14% of production lines, it does not affect the overall cost of production significantly.

4. Reduction in carbon emissions

From the data shown in Table 3-2, we can see that the energy structure of each country has different features. Based on that data, the average emission from electricity generation for each energy profile is calculated. If we build a lithium iron phosphate battery production facility with 10MW power requirement in other countries, it will emit 36247~64771 tons of CO_2 per year depending on the country's electric energy production profile. In Iceland, approximate 50% of energy consumption is still electricity, which emits 23.5 g/KWh CO_2 on average [11]. The rest of the energy consumption will be replaced by geothermal steam, which emits 18g/KWh CO_2 in this case. Thus, the total CO_2 emission in Iceland would be around 1818 tons of CO_2 per year. In summary, this project in Iceland has 393.4-215.1 g/Ah lower CO_2 emission advantage compare to other countries. However, we have to put it in mind that most of carbon dioxide is emitted naturally from geothermal area in Iceland. The

emission from geothermal plants is already part of CO_2 cycle, no new CO_2 is being produced as is in the case of fossil fuel.

Table 4-1 Comparison of carbon emission for Li-ion factories with 10MW power requirement located in different countries [12].

Various Resource	Average CO2 emission (g/kwh)	China	USA	Germany	Japan
Renewable	50	0.4%	2.8%	11.6%	2.7%
Oil	400	0.6%	1.3%	1.4%	12.8%
Gas	430	0.9%	20.9%	13.7%	26.1%
Nuclear	6	1.9%	19.2%	23.3%	23.8%
Hydro	4	16.9%	6.4%	4.2%	7.7%
Coal	925	79%	49%	45.6%	26.6%
Total		100%	100%	100%	100%
Average CO2 emission from electricity (g/kwh)		738.9	552.1	494.2	413.51
Total emission from this project per year (87.66 GWh)		64771.9	48402.3	43321.5	36247.4

5. Profitability assessment

We built a comprehensive model containing cost analysis, investment, operation, cash flow, profitability and sensitivity analysis in order to estimate the profitability of building a lithium iron phosphate battery factory using renewable energy in Iceland. We calculate NPV and IRR based on the current cost data on the market and some financial assumptions. The main results of this model are presented in the following text.

5.1.1. Net present value

Fig 5-1 shows that the NPV of total cash flow (for loan and equity) with 15% discount rate is 48.16 m illion USD after 15 years operation time. Also, NPV net cash flow (only for equity) with 15% discount rate is 52.57 million USD. The value of NPV of total cash flow and net cash flow take 9 and 8 years to turn positive, respectively. From the point of view of NPV, it seems a reasonably profitable business in Iceland. Building the factory at another location in Europe with similar operating environment, the accumulated net present value might turn negative due to much higher prices of industrial electricity. Applying European electric prices, the accumulated NPV of net cash flow will be -20.6 million USD, as shown in Fig 5-1. Other cost contribution might vary slightly depending on location but it is observed that energy price significantly affects net present value. The energy price will play more substantial part of the total variable as raw material prices are predicted to fall in the next 10 years.

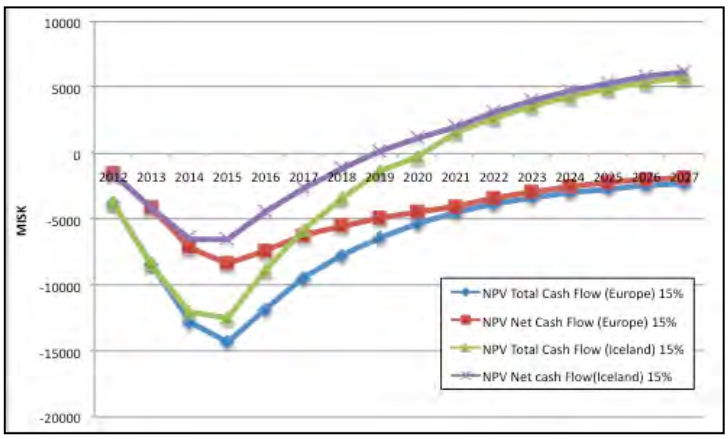

Figure 5-1 Accumulated NPV comparison between Iceland and other European countries.

5.1.2. Internal rate of return

In terms of internal rate of return, it is used in capital budgeting to measure and compare the profitability of the investment. Fig 5-2 shows the internal return rate of total cash flow and net cash flow in Iceland is 22% and 27%, respectively. On the other side, the internal return rate of total cash flow and net cash flow in Europe is 11% and 12%, respectively. Although there is some risk and uncertainty in this project, IRR is higher than the cost of capital in the normal situation in Iceland. To compare to a common investment, it has a relatively high internal rate of return based on the assumption. However, 11~12% of IRR is a normal and acceptable result for an investment project in other European countries.

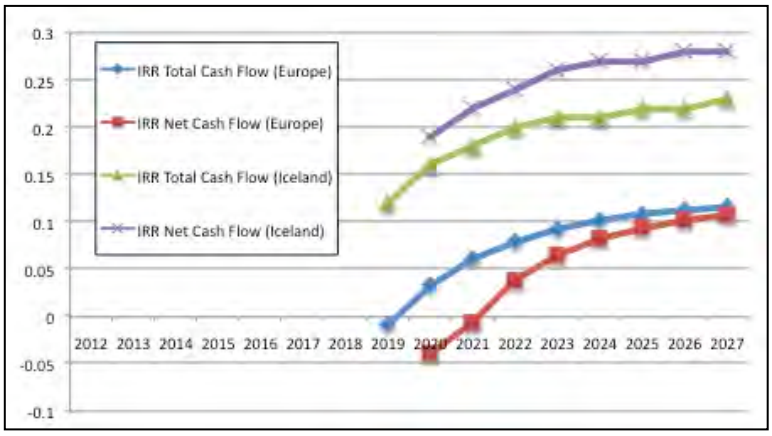

Figure 5-2 IRR comparison between Iceland and other European countries

6. Conclusion

With the anticipated reduction in material cost for Lithium-ion batteries, the energy cost for battery production will play a more important role in the overall cost of lithium ion batteries. According to our investigation, the energy consumption could range from 0.54 to 0.68 KWh/Ah depending on the factory's design and production process. Although we did not get access to first-hand energy consumption data of each step from factories directly, we can infer that the main energy consumption steps in the procedure are drying room, vacuum dryers, and testing equipment from our production process analysis, and create a process model. In locations with access to geothermal heat, such as Iceland, it is possible to replace the electricity used as a heat source for the drying processes by geothermal steam, reducing energy cost in combination with reasonably priced electricity. According to the model, the energy consumption of removing the moisture content in 1 Ah battery is 0.31 KWh, which is around half of the total energy consumption. The variable energy cost in Iceland could be reduced to 0.012 USD/Ah (0.007 USD for electricity; 0.005 for geothermal steam) if geothermal steam is used for drying. In this study Reykjanes in Iceland is considered as a location so geothermal steam at 18 bar 207°C is used as it is the available resource from an existing geothermal power plant. However a resource at 9 bar and 173°C, which would be more widely available, is quite sufficient for this process. In this case, the ideal type of dryer and heating method for lithium batteries would be a tray dryer. A profitability model was built using current cost data based on operating environment in Iceland. According to this model, the accumulated NPV for equity with a 15% discount rate is 52.5 million USD and internal rate of return is 27%. On the other hand, if we move the factory to other European countries with higher energy price (0.18€ /KWh[13]) and the same cost assumption, the NPV for equity will fall down to -20.6 million USD. The internal rate of return will fall from 27% to 11%. Moreover, with current feedstock prices the energy cost is estimated to be 1% with the Icelandic cost structure, while it would amount to 12~15% in other European countries based on average energy prices. The lower energy cost in Iceland results in an NPV less sensitive to fluctuation of energy prices. The geothermal resource seems to have a great economic advantage for lithium ion battery production due to lower energy prices, whether it is electric

energy or direct use of geothermal heat. Another feature of even more importance is that the lower carbon footprint of geothermal heat and renewable electricity, will result in 34429-62953tons lower CO_2 emissions per year from running a battery factory with 10 MW power consumption and 160MAh production capacity, compared to the emissions where a t he electric production profile is more traditional as would be the case in Europe or China. That means that only 2-5% percent of the carbon dioxide would be emitted as a result from this process as compared to traditional energy usage. This could bring some practical carbon emission credit value or an advantageous position on g reen marketing. Although most of battery companies still focus on reducing the cost of raw material at this moment, the energy cost will become more and more critical in the entire cost structure with future price reductions of raw material. The trend for companies planning to develop production in Europe will be a higher emphasis on selecting a location with reasonably priced renewable sources for heat and electric energy. The access to low cost low emission energy sources should be a significant factor when selecting a location for Lithium ion battery production.

References

[1] Pike Research, "Asian Manufacturers Will Lead the $8 B illion Market for Electric Vehicle Batteries", Retrieved 10.01.2010, from Pike Research: http: //www.pikeresearch.com/ newsroom/asian-manufacturers-will-lead-the-8-billion-market-for-electric-vehicle-batteries

[2] Zackrisson M & Orlenius J, Life cycle assessment of lithium-ion batteries for plug-in hybrid electric vehicles e Critical issues. Journal of Cleaner Production, 2010, pp.1517-1527.

[3] Nuutinen, M, Lithium-ion battery factory relocation from China to Finland. Material science and engineering. Helsinki: Helsinki university of technology, 2007, pp.68-69.

[4] She Haung Wu and Yang-Ting Lai, The effects of the moisture content of LiFePO4/C cathode and the addition of VC on the capacity fading of the LiFePO4/MCMB cell at elevated temperatures. The electrochemical Society, 2007.

[5] Dr. Michael Eastman, Smart Sensors Based on Piezoelectric PVDF, 2010, pp-6

[6] LICO Technology Corporation, LHB-108P Hydrophilic Binder, 2008, pp-6

[7] Taminco Co, N-Methylpyrrolidone Electronic grade Technical Data Sheet, 2004, pp-1

[8] Mujumdar A. S, Handbook of Industrial Drying. Taylor & Francis Group LLC, 2006, pp.1108-1109.

[9] Weiss Gallenkamp, Vacuum oven and drying oven VVT, 2010, pp-4.

[10] Invest in Iceland Agency, Doing business in Iceland 8 E dition. Reykjavik: Iceland investment agency, 2010.

[11] Landssvirkjun, Landssvirkjun's carbon footprint, Reykjavik: Landssvirkjun, 2009, pp-11.

[12] World Energy Council, World Energy council. Retrieved 10 1, 2010, from World Energy council:http://www.worldenergy.org/publications/survey_of_energy_resources_2007/geothermal_energy/737.asp

[13] Europe's Energy Portal, Industrial Electricity Rate, November 2009, http://www.energy.eu/#Industrial

Energy and exergy analysis and optimization of a double flash power plant for Meshkin Shahr region

Mohammad Ameri [1,*], Saman Amanpour [2], Saeid Amanpour [3]

[1] *Energy Eng. Department, Power & Water University of Technology, Tehran, Iran*
[2] *Department of Aerospace and Mechanical Engineering, Shiraz University, Shiraz, Iran*
[3] *Department of Electrical Engineering, University Teknologi Malaysia, Johor Darul Takzim, Malaysia*
** Corresponding author. +9821-73932653, Fax: +9821-77311446, E-mail: ameri_m@yahoo.com*

Abstract: One of the most influential improvements in geothermal industries has been the application of double flash power plants which can produce more power in comparison with single flash one. Although it is more expensive, however it is a reasonable option as the additional output power can justify the prices. The aim of this study is to represent a methodology in which a double flash power plant is thermodynamically designed and optimized in order to maximize the output power, and make a comparison with other possible type of geothermal power plant (single flash) for Meshkin Shahr region. Besides it represents the study of exergy and energy analysis for plant components through the optimization process, which can guide one to assess the operating status of plant components. It has been shown that flash vessels are the greatest exergy dissipaters and double flash power plant can be more efficient than single flash for this region.

Keywords: *Double Flash Power Plant, Geothermal Power Plant, Energy Analysis, Exergy Analysis, Optimization.*

Nomenclature

c	*specific heat of water* ..... *J/(kg K)*	*BF*	..... *Brute Force*
$\dot{E}$	*Exergy* ..... *kJ*	*Cond*	..... *condenser*
e	*specific exergy* ..... *kJ/kg*	*cw*	..... *cooling water*
h	*specific enthalpy* ..... *kJ/Kg*	*FV*	..... *flash vessel*
$\dot{m}$	*mass flow rate* ..... *kg/s*	*FUN*	..... *functional*
T	*temperature* ..... *°C*	*lp*	..... *low pressure*
w	*specific work* ..... *kJ/kg*	*t*	..... *turbine*
x	*quality or dryness fraction* ..... $m \cdot s^{-1}$	*W*	..... *work*
ρ	*density* ..... $kg \cdot m^{-3}Q$		

Subscripts

Greek Letters

η	*efficiency*
Δ	*difference*

1. Introduction

Increasing oil price and environmental concerns about pollution and global warming in recent years has doubled geothermal energy use as a clean source of energy [1]. Today three major types of geothermal power plants are being utilized: dry steam plants, flash steam plants and binary cycle plants [2]. DiPippo has presented some information about new geothermal power plant designs [3]. Flash power plants are likely in liquid-dominated fields with temperature greater than 182° C [4]. An important concern in engineering field of geothermal energy is thermodynamic design and optimization of an energy system, especially a power plant, which can reduce the expenses significantly. The application of double flash power plant is not rational for all projects, since the conversion system is more complex and of course more expensive. Stefansson depicted a strategy for the investment costs of geothermal power plants and estimated investment cost level in unknown fields [5]. Therefore, it is important to assess the performance of geothermal plants based on an optimized thermodynamic scheme with respect to the surrounding conditions and thermodynamic state of geothermal reservoir, before putting the plan into action [6]. This can help the designer in better understanding of

the occasion so that a precise decision can be made to select either a single flash or a double flash plant with respect to costs. Ozcan and Gokcen managed a thermodynamic assessment of single flash power plant and studied the effect of non-condensable gases on plant performance [7]. Dagdas et al. carried out a thermodynamic optimization for a geothermal power plant based on real data and results revealed that 93.2% more power can be obtained [8]. Franco and Villani found that optimization of binary cycle power plants can yield to reduction of brine specific consumption in a significant way up to 30-40% [9].

The study of energy and exergy analysis, based on Second Law of Thermodynamics, helps to evaluate the performance of a geothermal power plant in order to eliminate excess energy loss and improve the overall efficiency of the plant [6]. Kanoglu performed an exergy analysis of a binary geothermal power plant using actual plant data and studied the causes of exergy destruction [10]. DiPippo also made comparisons between different cycles of binary plants for low-temperature geothermal fields based on Second Law of Thermodynamics [11].

Bodvardson and Eggers made a comparison between single flash and double flash power plants taking advantage of their exergy tables, as denoted by Yari [1]. Kanoglu and Bolatturk performed an exergy analysis of a binary geothermal power plant, applying actual plant data [2]. Cerci evaluated the performance of a single flash power plant in Turkey by using exergy analysis based on actual plant operation data [12]. He had a debate in the form of response to Serpen who made some comments on performance evaluation of the same project in Turkey concluding that the performance of a geothermal power plant is affected by the chemistry of reservoir [13, 14, 15]. Serpen believed that the design and evaluation of geothermal power plants are subjected to profound study of the geothermal reservoir [13]. Madhawa et al. presented a criterion for cost effective optimum design of organic Rankine cycles based on low temperature geothermal heat sources [16]. Kanoglu et al. did a comprehensive survey on different power cycles including geothermal power plants and presented energy as well as exergy based efficiencies with some illustrative examples [17]. DiPippo also investigated different types of geothermal power generating systems and he applied the exergy analysis to geothermal power systems [3]. Yari did a comparative study of different geothermal power plants based on exergy analysis [1].

This paper represents a two dimensional optimization of a double flash power plant for Meshkin-Shahr region in which the pressure of the first and the second flashing process are optimized by help of a FORTRAN code in order to reach the maximum output power; and the results are sketched in form of 3D surfaces. Moreover, the isentropic efficiency of turbine, brute force and functional efficiency, and exergy dissipation of each plant components are calculated simultaneously in each step of optimization process.

Meshkin-Shahr, a region in the Moil valley which is located on the western slopes of Sabalan Mountain, is a potential geothermal field for power generation. It is the place where the first Iranian geothermal power plant is going to be installed [4]. According to the reservoir type of this region, flash power plants are valid cases for utilization of geothermal energy.

2. Methodology

2.1. Energy and exergy analysis

Exergy analysis is a thermodynamic analysis technique which is based on second law of thermodynamics. It presents a bright way for evaluation and comparison of processes and systems [18]. This method can be used to estimate the performance of any energy system and

the combination of this method with energy analysis can assist in elimination of excess energy loss in order to improve the overall efficiency [6]. All the processes in double flash power plant are assumed to be steady state processes. Therefore, the balance equations can be employed to calculate output power, exergy of flow streams and energy and exergy efficiencies. Neglecting the change in kinetic and potential energies, the First Law of Thermodynamics and mass balance equations can be written as:

$$\dot{Q} - \dot{W} = \sum\left(\dot{m}_e h_e - \dot{m}_i h_i \right) \tag{1}$$

$$\sum \dot{m}_i = \sum \dot{m}_e \tag{2}$$

The second law of thermodynamics for a perfect reversible process and the specific exergy of a fluid stream associated to dead state condition can be stated by Eq. (3) and Eq. (4) respectively. The subscribe "0" represents dead state condition at 20° C and 1 atm.

$$\sum\left(\dot{m}_e s_e - \dot{m}_i s_i \right) - \frac{\dot{Q}_0}{T_0} = 0 \tag{3}$$

$$e = h - h_0 - T_0(s - s_0) \tag{4}$$

2.2. Thermodynamic nature of processes in double flash power plants

Double flash power plant as a choice of energy conversion system for liquid-dominated fields, constitute about 14% of all geothermal plants with the power capacity ranges from 4.7 MW to 110 MW [3]. A T-S schematic diagram of a double flash power plant is shown in Fig. 1.

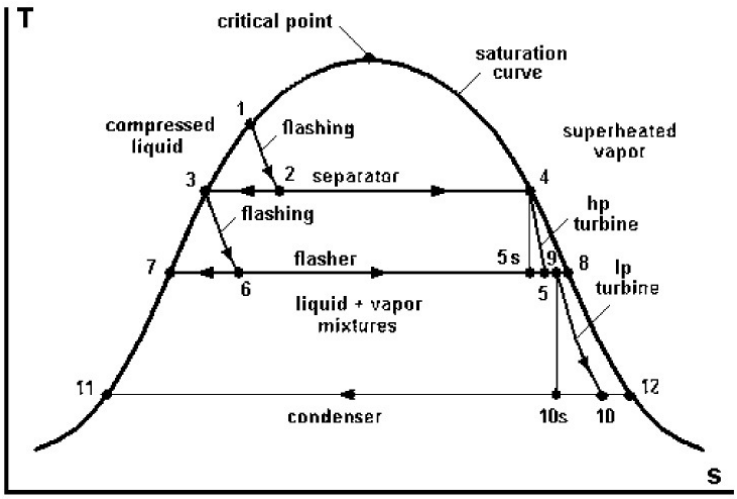

Fig. 1. Temperature-Entropy diagram of a double flash power plant.

Two phase fluid from geothermal wells is pumped to power plant on the ground surface at condition near saturation and it can be assumed as pressurized liquid (point 1 in Fig. 1). The pressurized liquid undergoes the first flashing process by passing through a throttle valve so its pressure falls in an isenthalpic process, where a two phase fluid is produced (point 2 in Fig. 1). These two phases are separated in a high pressure separator where the steam is guided to

drive the high pressure turbine (point 4 in Fig. 1) and the liquid phase undergone the second flashing process (point 3 in Fig. 1) and the two phases are separated efficiently. The low pressure steam of this process is guided toward a dual-admission turbine or it is guided toward a separate low pressure turbine (point 9 in Fig. 1) and the liquid phase is disposed to the injection wells (point 7 in Fig. 1). The two phased mixture of turbine exhaust will be then condensed in a condenser and disposed into injection wells (point 11 in Fig. 1). The enthalpy of actual turbines' processes can be easily calculated by incorporating fluid properties at state 5s and 10s and the efficiency of turbines as well as the Baumann rule. This rule states that since the turbine processes take place in wet region, there would be a 1% drop in efficiency of turbines per every percent of average moisture. Thus for low pressure turbine one may write:

$$h_{10} = \frac{h_9 - 0.425\left(h_9 - h_{10s}\right)\left(x_9 - \dfrac{h_{11}}{h_{12} - h_{11}}\right)}{1 + \dfrac{0.425\left(h_9 - h_{10s}\right)}{h_{12} - h_{11}}} \tag{5}$$

Properties at state 9 can be easily gained by combination of First Law of Thermodynamics and mass conservation and the condensation process is assumed to take place in a constant pressure process, and effects of non-condensable gases are neglected.

2.3. Exergy efficiencies and exergy dissipations of double flash power plant

There are two different approaches for the definition of exergy efficiencies. Brute force efficiency, defined as the sum of all output exergy terms divided by the sum of all input exergy terms, and functional efficiency, defined as the exergy of desired energy output divided by the exergy spent to achieve the desired output [3]. According to Fig.1, exergy dissipations and exergy efficiencies of a double flash power plant's components can be expressed as follows, for brevity we just point out some of the relations and others can be written in a similar way [3].

$$\Delta \dot{E}_{FV2} = \dot{m}_3 e_3 - \dot{m}_7 e_7 - \dot{m}_9 e_9 \tag{6}$$

$$\eta_{FV2,BF} = \frac{\dot{m}_7 e_7 + \dot{m}_9 e_9}{\dot{m}_3 e_3} \tag{7}$$

$$\eta_{FV2,FUC} = \frac{\dot{m}_9 e_9}{\dot{m}_3 e_3} \tag{8}$$

$$\eta_{tlp,BF} = \frac{w_{lp} + e_5}{e_4} \tag{9}$$

$$\eta_{tlp,FUN} = \frac{w_{hp}}{e_4 - e_5} \tag{10}$$

The functional efficiency for condenser can be estimated by two different approaches based on the nature of unit [3].

3. Results

The methodology which is used in this paper is based on assumptions pointed out in table 1 and piping losses are assumed to be negligible. "Equal-temperature-split" rule [3] is a usual method for the selection of temperature (or pressure) of separation process in order to approach the optimum state which leads to maximum output power. This rule cannot define the exact pressure since processes take place in two phase region. However, it can lead one to the verge of best option. The precise pressures require a two-dimensional optimization on vicinity of pressures estimated by "equal-temperature-split" rule. Fig. 2 illustrates a two-dimensional optimization in form of a saddle shaped surface where the maximum vertical point illustrates the maximum output power which is equal to 67793.04 KJ. This power is the total power produced by high pressure and low pressure turbines and it seems that double flash power plant can produce about 13-14% more power than single flash one [6]. The related pressures to this point are 0.67 MPa and 0.1 MPa for the first and second separation processes respectively. It is worth to mention that P2 and P6 in the following figures are adopted from Fig. 1.

Table 1. Fixed and variable parameters.

Parameter	Status	Possible range
Inlet temperature	225˚C (based on reservoir condition)	Temperatures greater than 180˚C [4]
Inlet mass flow rate	700 kg/s	-
Separators' pressure	Variable (optimized)	100-1000 KPa [19]
Condensation pressure	Fixed at 10 KPa	Recommended 8-10 KPa [19]

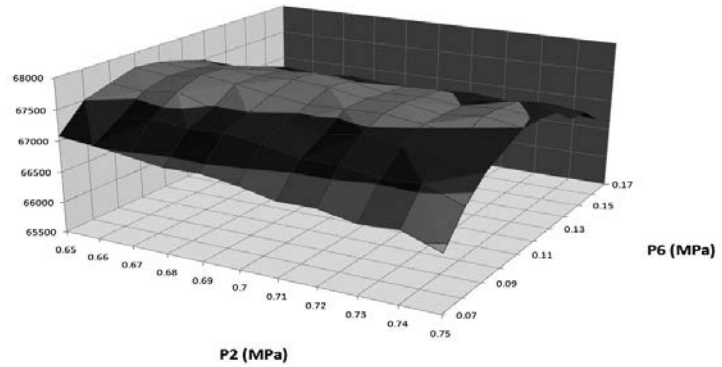

Fig. 2. Two dimensional optimization for output power (KJ).

Fig. 3 shows the effect of pressure change on the isentropic efficiencies of high pressure and low pressure turbines. It is obvious that the effect of separation pressures on isentropic efficiency of high pressure and low pressure turbines is somehow in opposite directions. Total exergy dissipations of turbines, flash vessels and condenser are illustrated in Fig. 4 and Fig. 5. It seems flash vessels are the greatest exergy dissipators in power plant and small changes in pressures can lead to a dramatic change in exergy dissipation of flash vessels.

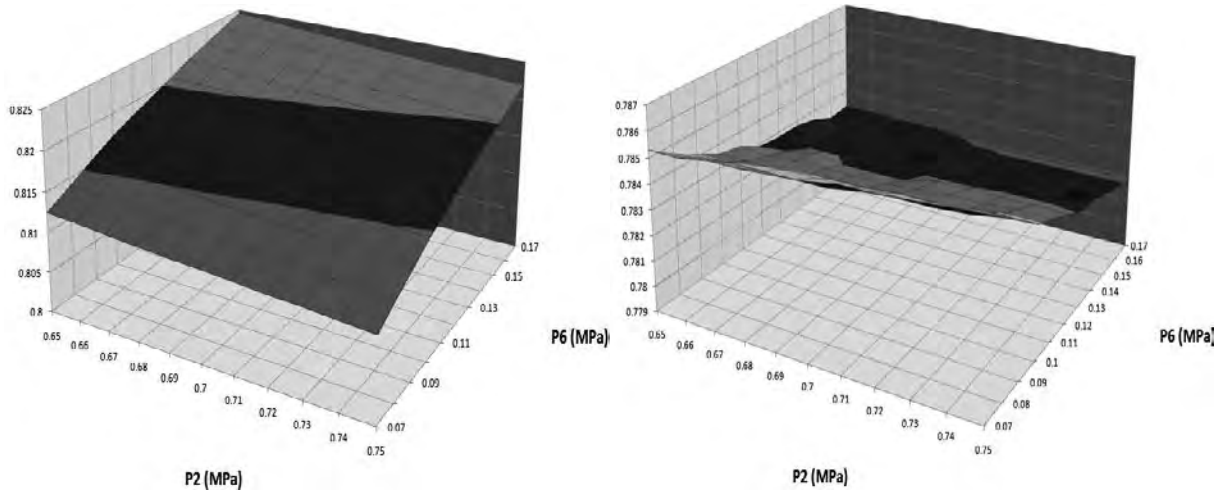

(a) *(b)*

Fig. 3. Isentropic efficiency for (a) High pressure turbine (b) Low pressure turbine.

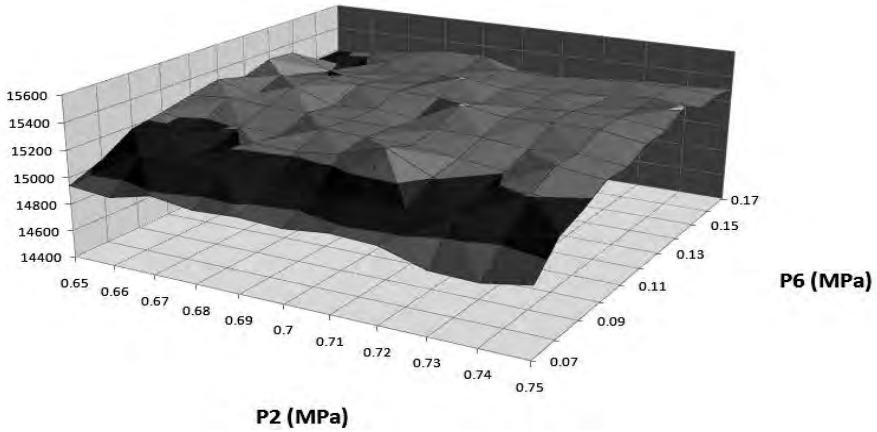

Fig.4. Total exergy dissipation of turbines (KJ).

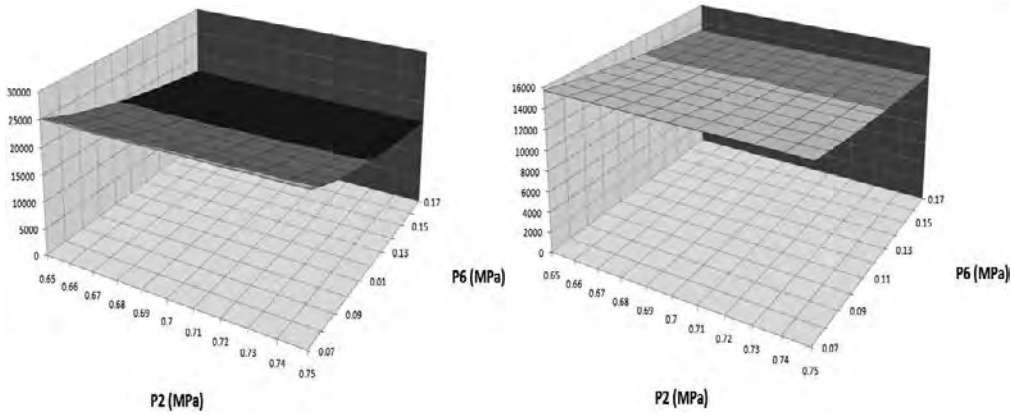

(a) *(b)*

Fig. 5. Total exergy dissipation (KJ) (a) Flash vessels (b) Condenser.

4. Discussion and Conclusions

As there is no data available for Meshkin-Shahr power plant, the validation of this study is done for a geothermal power plant in Turkey [19]. It shows good agreement. However, the validation is limited to annual net output power. The results of our study demonstrate that the exergy efficiencies of high pressure and low pressure turbines change in opposite directions. Brute force efficiency can reveal how much exergy of incoming flow is utilized and how

much is lost. On the other hand functional efficiency can disclose how much of incoming exergy is conserved in flow stream and how much leaves the component.

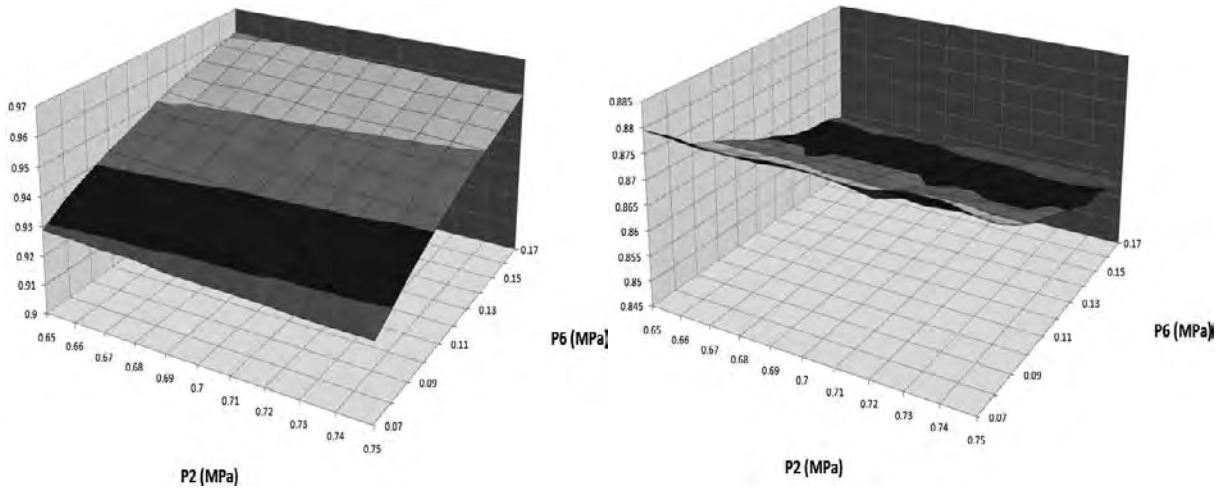

(a) (b)

Fig. 6. Brute force efficiency (a) High pressure turbine (b) Low Pressure turbine.

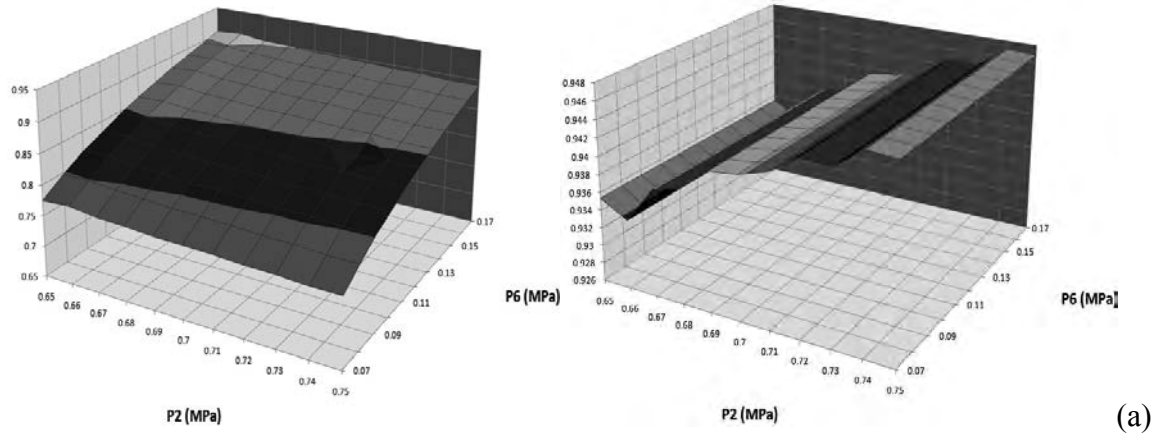

(a)

(b)

Fig. 7. Brute force efficiency (a) Low pressure flash vessel (b) High pressure flash vessel.

The suffered brute force and isentropic efficiencies of low pressure turbine in comparison with high pressure turbine is due to the fact that more amount of incoming exergy has left the turbine. A more profound study of Fig. 6 and having in mind that in double flash power plants low pressure turbines have greater portion in output power production, one can easily find why the optimum point for pressures is situated in the intersection of 0.67MPa and 0.1MPa. Since the pressure of incoming flow to high pressure flash vessel is constant, one can easily understand why the brute force efficiency surface is like sets of stairs.

References

[1] M. Yari, Exergetic analysis of various types of geothermal power plants, Renewable Energy 35, 2010, pp. 112-121.

[2] M. Kanoglu, A. Bolatturk, Performance and parametric investigation of a b inary geothermal power plant by exergy, Renewable Energy 33, 2008, pp. 2366-2374.

[3] R. DiPippo, Geothermal power plants, Elsevier Ltd, 2nd E dition, 2007, pp. 191 -251 & 102-104 & 241-247.

[4] M. Ameri, S.R. Shamshirgaran, M. Pour Yousefi, The Study of Key Thermodynamic Parameters Effect on the Performance of a Flash Steam Geothermal Power Plant, Proceeding of 2nd Joint Int. Conference SEE 2006, Bangkok, 2006, B-004 (O).

[5] V. Stefansson, Investment cost for geothermal power plants, Geothermics 31, 2002, pp. 263-272.

[6] M. Ameri, S. Amanpour, S. Amanpour, Energy and exergy analysis of Mehkin-Shahr single flash geothermal power plant, Proceeding of 10th International Conference on Clean Energy (ICCE-2010), 2010, No. 12-08.

[7] N. Y. Ozcan, G. Gokcen, Thermodynamic assessment of gas removal systems for single-flash geothermal power plants, Applied Thermal Engineering 29, 2009, pp. 3246-3253.

[8] A. Dagdas, R. Ozturk, S. Bekdemir, Thermodynamic evaluation of Denizli Kizildere geothermal power plant and its performance improvement, Energy Conversion and Management 46, 2005, pp. 245-256.

[9] A. Franco, M. Villani, Optimal design of binary cycle power plants for water-dominated, medium-temperature geothermal fields, Geothermics 38, 2009, pp. 379-391.

[10] M. Kanoglu, Exergy analysis of a dual-level binary geothermal power plant, Geothermics 31, 2002, pp. 709-724.

[11] R. DiPippo, Second Law assessment of binary plants generating power from low-temperature geothermal fluids, Geothermics 33, 2004, pp. 565-586.

[12] Y. Cerci, Performance evaluation of a single-flash geothermal power plant in Denizli, Turkey, Energy 28, 2003, pp. 27-35.

[13] U. Serpen, Comments on Performance evaluation of single-flash geothermal power plant in Denizli, Turkey, Energy 29, 2004, pp. 1219-1223.

[14] Y. Cerci, Response to comments on "Performance evaluation of single-flash geothermal power plant in Denizli, Turkey", Energy 29, 2004, pp. 1225-1226.

[15] U. Serpen, Reply to the author's response to comments on "Performance evaluation of single-flash geothermal power plant in Denizli, Turkey", Energy 29, 2004, pp.1227-1229.

[16] H.D. Madhawa Hettiarachchi, M. Golubovic, M. Worek William, Y. Ikegami, Optimum design criteria for an Organic Rankine cycle using low-temperature geothermal heat sources, Energy 32, 2007, pp. 1698-1706.

[17] M. Kanoglu, I. Dincer, A. Rosen Mark, Understanding energy and exergy efficiencies for improved energy management in power plants, Energy Policy 35, 2007, pp. 3967-3978.

[18] I. Dincer, M. Rosen, Exergy, Elsevier Ltd, 2007, pp. 23-24.

[19] N. YILDIRIM OZCAN, modeling, simulation and optimization of flashed-steam geothermal power plants from the point of view of non-condensable gas removal systems, PhD thesis, Graduate School of Engineering and Science of Izmir Institute of Technology, 2010, pp. 82-83 & 149-150.

Thermoeconomic evaluation of combined heat and power generation for geothermal applications

Florian Heberle*, Markus Preißinger, Dieter Brüggemann

University of Bayreuth, Germany
** Corresponding author. Tel: +49 921 557163, Fax: +49 921 557165, E-mail: lttt@uni-bayreuth.de*

Abstract: In this study a thermoeconomic analysis of combined heat and power generation (CHP) for geothermal applications is presented. Different working fluids and power plant concepts are investigated for power generation by Organic Rankine Cycle and additional heat generation. For geothermal conditions in Germany, process simulations of series, parallel and hybrid circuits compared to sole power generation are performed. The results show that for power generation fluids with low critical temperature, like R227ea or isobutane, are suitable. In general, an additional heat generation decreases the averaged costs of electricity generation. In case of a source temperature of 120 °C the costs can be reduced from 25 ct/kWh to 16 ct/kWh compared to power generation. For CHP applications fluids with higher critical temperature and series or hybrid circuits are the most efficient concepts. With increasing temperature of the geothermal water an increase of supply temperature of the heating system has less influence on the costs of electricity generation. A doubling of mass flow of the geothermal water decreases the averaged costs of electricity generation in the range of 28 % and 43 % depending on power plant concept and boundary conditions.

Keywords: *Geothermal energy, Organic Rankine Cycle, cogeneration, thermoeconomic analysis*

Nomenclature

c	*cost of electricity generation* ct/kWh	n	*contract period* a
C	*costs* €	N	*produced amount of electricity* kWh
e	*specific exergy* kJ/kg	p	*pressure* Pa
$\dot{E}$	*exergy flow rate* kW	P	*mechanical power* kW
h	*enthalpy* J/kg	s	*entropy* J/(kgK)
i	*interest rate* %	T	*temperature* °C
$\dot{m}$	*mass flow rate* kg/s	η	*efficiency* %

1. Introduction

Regarding base load capacity, geothermal resources play an important role for renewable energy generation. For temperatures of the geothermal water below 180 °C direct expansion or flash processes are not suitable under thermodynamic and economical aspects [1]. Instead binary power plants like the Organic Rankine Cycle (ORC) or the Kalina Cycle are used. Therefore thermal energy of the geothermal water is coupled with the secondary thermodynamic cycle. Concerning the ORC, there are different possibilities, like selection of the working fluid, supercritical cycle or multi-stage expansion, to raise the electric efficiency [2-5]. Another interesting strategy to improve the second law efficiency and economic aspects is combined heat and power generation (CHP). In case of geothermal applications, previous exergoeconomic and thermoeconomic investigations are restricted to sole power generation or district heating [6-8]. In this study potential ORC fluids, isobutane, isopentane, R227ea and R245fa are investigated for power generation. In case of additional heat generation, parallel, series and hybrid circuit are considered. Second law efficiency and costs of electricity generation are calculated for an assumed heat demand and typical geothermal conditions in Germany. Detailed simulations are performed for variations of mass flow of the geothermal water and supply temperature of the heating system. The results provide basic criteria for fluid selection under thermoeconomic aspects in case of power generation by ORC and CHP.

2. Methodology

2.1. Simulation

Process simulations are done by the software tool Cylce Tempo and fluid properties are calculated by REFPROP Version 8.0 [9,10]. The process scheme of the ORC for sole power generation (SPG) and the corresponding *T,s*-diagram for isopentane at standard conditions are shown in Fig.1.

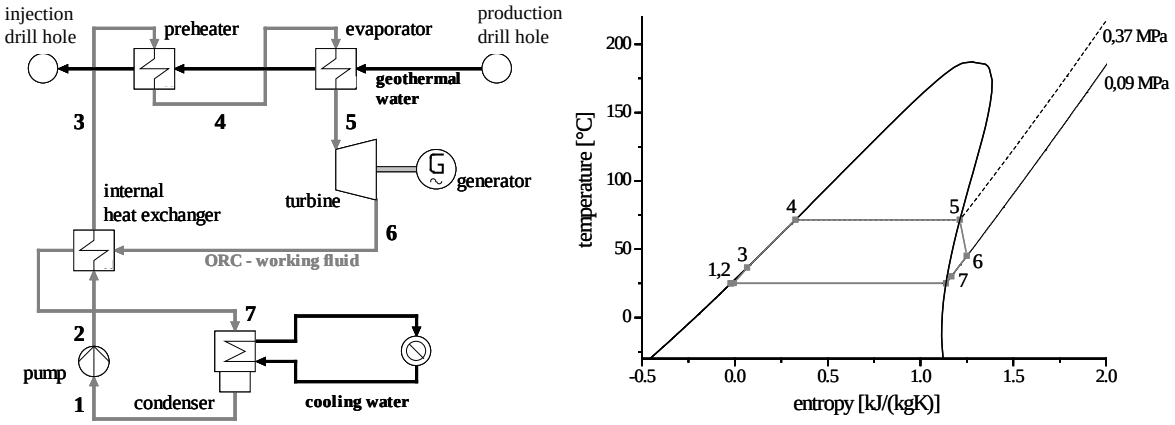

Fig. 1. Scheme of a geothermal ORC-power plant and corresponding T,s-diagram of isopentane.

The liquid fluid is compressed by the pump to maximum process pressure. The heat supply takes place in three steps. First the internal heat recovery, followed by the coupling with the geothermal heat source in the preheater and finally in the evaporator. As the analyzed fluids show a negative slope of the dew line in the *T,s*-diagram, so-called dry fluids, superheating is not necessary [11]. After the expansion the fluid is cooled down in the internal heat exchanger and condensed in the condenser. For the standard case, process parameters and boundary conditions of the heat source and sink are listed in table 1.

Table 1. Standard parameters of the ORC process simulation

parameter	
temperature of geothermal water	120 °C
mass flow of geothermal water	65.5 kg/s
ΔT-pinch-point (evaporation / condensation)	5 K
ΔT of the cooling water	5 K
cooling temperature	15 °C
maximum pressure ORC	$0.8 \cdot p_C$
isentropic efficiency (turbine / feed pump)	0.75

Regarding the additional heat generation, three concepts are investigated. Fig. 2 shows the series (SC), parallel (PC) and hybrid circuit (HC). As standard parameters of the heating system a supply temperature of 75 °C and a return temperature of 50 °C are assumed. The minimum temperature difference between heating system and geothermal water is 5 K. The supposed annual demand of thermal power is simulated in four steps: 10 MW for 1000 operating hours, 7.5 MW for 1500 operating hours, 5 MW for 2500 operating hours and 2.5 MW for another 3500 operating hours.

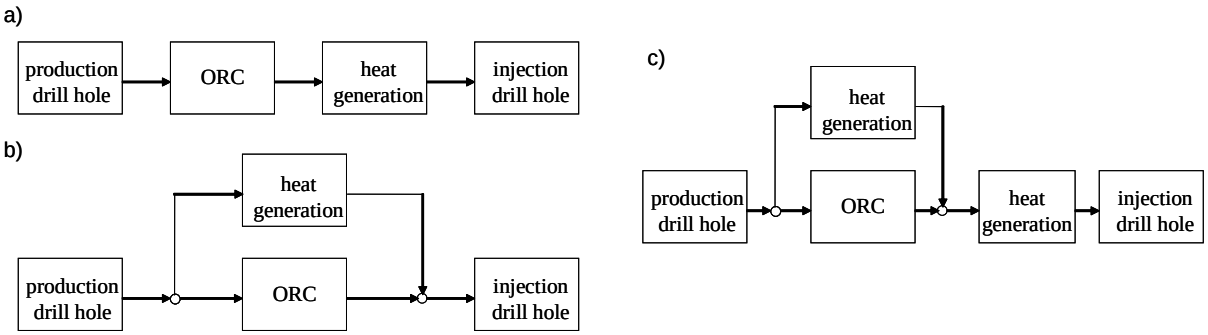

Fig. 2. Series circuit (a), parallel circuit (b) and hybrid circuit (c) as concepts for CHP

In case of series circuit the temperature of the geothermal water at the outlet of the ORC must be adapted to the peak load of the heat demand. For parallel circuit fluctuations in heat demand can be adjusted by varying the ratio of mass flow of the geothermal water. The hybrid circuit describes a coupling of series and parallel circuit.

2.2. Second law analysis

The simulations of the power plant are performed by solving a system of equations, consisting of energy balances of the heat exchangers units. Pressure and heat losses are not considered in the process components and pipes. As an example the energy balance of the preheater is given by

$$\dot{m}_{GW}(h_{GW,in}\text{-}h_{GW,out})_{PH} = \dot{m}_{ORC}(h_4 - h_3) \tag{1}$$

where $\dot{m}_{GW}$ corresponds to the mass flow of the geothermal water, $h_{GW,in}$ and $h_{GW,out}$ to the enthalpy of the geothermal water at the inlet and outlet of the preheater. The mass flow of the ORC is described as $\dot{m}_{ORC}$, h_3 and h_4 correspond to the enthalpies of the working fluid at the inlet and outlet of the preheater. A detailed formulation of the simulation model can be seen in Heberle and Brüggemann [12]. By using a user subroutine the outlet temperature of geothermal water is adapted to the maximum power output of the ORC in case of power generation. The second law efficiency for sole power generation is calculated by

$$\eta_{II,el} = \frac{\left|P_T + P_P\right|}{\dot{E}_{GW}} \tag{2}$$

where P_T is the power of the turbine and P_P corresponds to the power of the pump. The maximum power output of geothermal source, the exergy flow $\dot{E}_{GW}$, is obtained by multiplying the specific exergy e with the mass flow of the geothermal water:

$$\dot{E}_{GW} = \dot{m}_{GW} e \tag{3}$$

The specific exergy is calculated by:

$$e = h - h_0 - T_0(s - s_0) \tag{4}$$

The state variables T_0, p_0 and s_0 are related to ambient conditions. In the case of additional heat generation, the numerator from Equation 2 is extended with the exergetic value $\dot{E}_Q$

$$\eta_{II,tot} = \frac{\left|P_T + P_P\right| + \dot{E}_Q}{\dot{E}_{GW}} \tag{5}$$

where the exergy flow of the thermal energy coupled to the heating system $\dot{E}_Q$ can be calculated by

$$\dot{E}_Q = \dot{m}_{HS}\left(e_{out} - e_{in}\right)_{HS} \tag{6}$$

where $\dot{m}_{HS}$ is the mass flow of the heating system. The specific exergy at the inlet and outlet of the heat transfer unit of the heating system are e_{in} and e_{out}.

2.3. Economic analysis

The assumed parameters for the economic analysis, like exploration costs or specific costs for the ORC module and heating system, are listed in table 2 **[13]**. PRIVATE EQUITY AND STATE FUNDING ARE NOT CONSIDERED FOR THE CALCULATIONS.

Table 2. Economic boundary conditions for geothermal CHP

parameter	
exploration costs	18 000 000 €
other (building, insurance, etc.)	4 000 000 €
power plant (ORC)	4 000 €/kW
heating system	150 €/kW
costs of heating pipeline	150 €/m
heating price	40 €/MWh
rise in price rate (heating price)	1,5 %/a
operating and maintenance (O&M) costs	750 000 €/a
rise in price rate (O&M)	2 %
interest rate *i*	7 %
contract period *n* for consumption of fixed capital costs	20 a

The annual costs C_A of the power plant consist of capital consumption C_C, imputed interest C_I, and O&M costs $C_{O\&M}$. The imputed interest $C_{I,t}$ for the year t is calculated by

$$C_{I,t} = \frac{R_{t-1} + R_t}{2} \cdot i \qquad \text{with } t = 1,\ldots,n \tag{7}$$

where R_t is the residual value and R_0 corresponds to the initial investment costs. The costs of electricity generation c_t at year t are calculated by

$$c_t = \frac{C_{A,t}}{N} = \frac{C_{C,t} + C_{I,t} + C_{O\&M}}{N} \tag{8}$$

where N is the annual produced amount of electricity. In the following the averaged costs of electricity generation c are calculated for the economic analysis by:

$$c = \frac{\sum_{t=1}^{n} c_t}{n} \tag{9}$$

3. Results

3.1. Second law efficiency for power generation

The second law efficiency for sole power generation as a function of inlet temperature of the geothermal water is shown in Fig. 3 for the investigated working fluids.

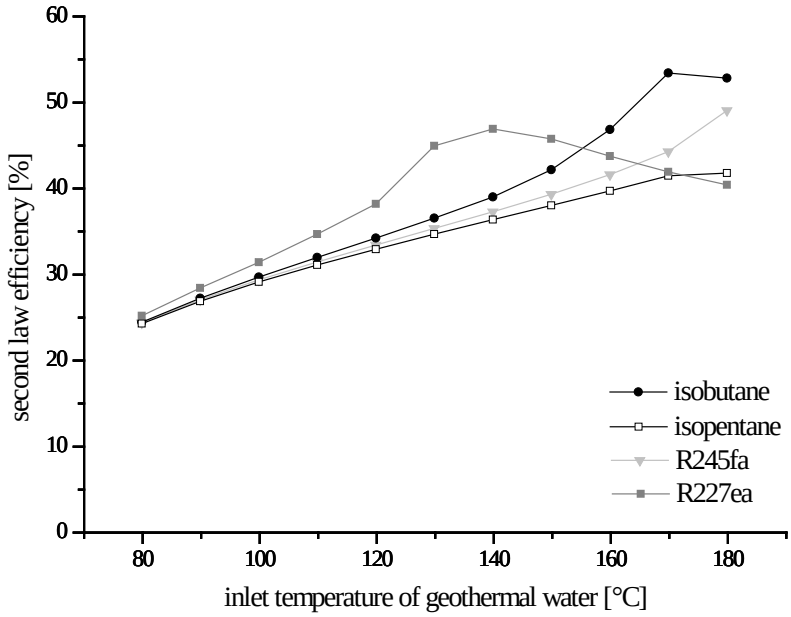

Fig. 3. Second law efficiency for the investigated working fluids as a function of temperature of the geothermal water

The results show obvious differences in efficiency depending on inlet temperatures. For low temperatures R227ea is a suitable working fluid, for temperatures higher than 150 °C isobutane should be favored. The local maxima for R227ea and isobutane are due to the shift of the pinch point from the inlet of the evaporator, state point 4, to the inlet of preheater, state point 3. The effect occurs, because the maximum process pressure of the ORC fluid is reached, which leads to a high amount of thermal energy coupled to the cycle. As a result the outlet temperature of the geothermal water decreases significantly. In case of the less efficient fluids, like R245fa and isopentane, the second law efficiency increases linear with inlet temperatures. For these fluids the outlet temperatures of the geothermal water are higher compared to R227ea or isobutane. At 120 °C inlet temperature isopentane leads to an outlet temperature of 64.3 °C compared to R227ea with 59.7 °C. The difference becomes apparent for 160 °C with outlet temperatures of 73.2 °C and 36.5 °C. A detailed explanation and graphical description of these correlations can be found in Heberle and Brüggemann [12].

3.2. Second law efficiency for CHP

Fig. 4 shows the second law efficiency for CHP as a function of thermal power of the heating system compared to sole power generation at standard conditions for isopentane and R227ea.

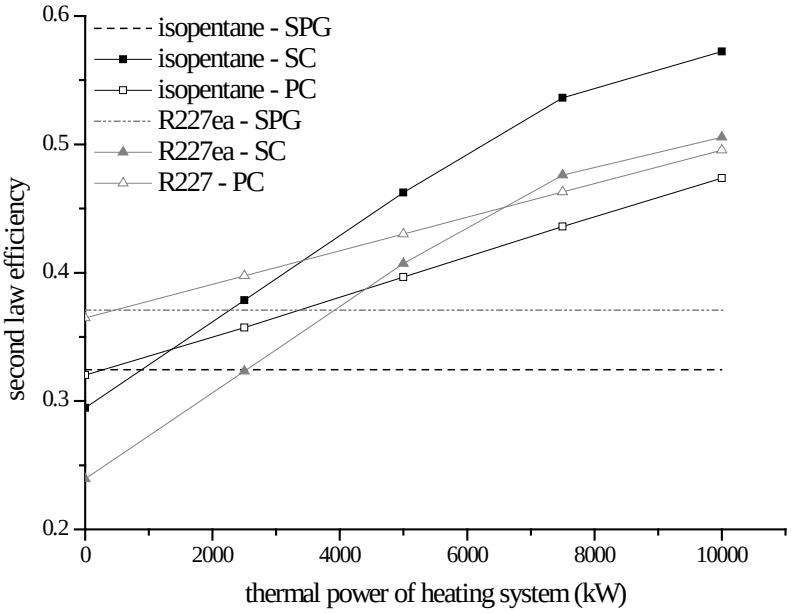

Fig. 4. Second law efficiency depending on thermal power coupled to the heating system

An additional heat generation improves the second law efficiency of the analyzed system. In case of isopentane the efficiency increases up to 24.8 % compared to sole power generation. For R227ea the raise is 15.5 % in case of 10 MW thermal power coupled to the heating system. Another interesting aspect is the comparison of the different concepts and working fluids. In the range of 1 MW to 10 MW thermal power the series circuit is the most efficient concept for isopentane as an ORC working fluid. In case of R227ea only for a thermal power higher than 7 MW the series circuit leads to slightly higher efficiencies compared to parallel circuit. The different behaviour of the working fluids corresponds to the outlet temperatures of geothermal water, which has to be adjusted to the temperatures of the heating system in case of series circuit. For R227ea, this adjustment shows higher losses in power generation compared to isopentane.

3.3. Averaged costs for electricity generation depending on power plant concept

In the following sections only the results for R227ea and isopentane are presented, to guarantee well-arranged analyses. The Southern German Molasse Basin and the Upper Rhine Rift Valley with temperatures of 120 °C and 160 °C for the geothermal water are chosen as geothermal reservoirs. In Fig. 5 the averaged costs of electricity generation depending on power plant concept and geothermal conditions are presented. Corresponding to the second law analysis R227ea is more suitable for power generation in comparison to isopentane. In case of 120 °C the costs are 25 ct/kWh, for 160 °C they are reduced to 15 ct/kWh. The difference to isopentane decreases with increasing temperature of the heat source. In general CHP leads to a decrease of averaged costs of electricity generation. In case of R227ea and 120 °C they are reduced to 18 ct/kWh by parallel circuit. The most economic concept for 120 °C is isopentane in conjunction with series circuit. For 160 °C the working fluid isopentane and the hybrid circuit with averaged costs of electricity generation of 9 ct/kWh should be preferred. In general the hybrid circuit only makes sense for working fluids with high outlet temperatures of the geothermal water, like R245fa or isopentane.

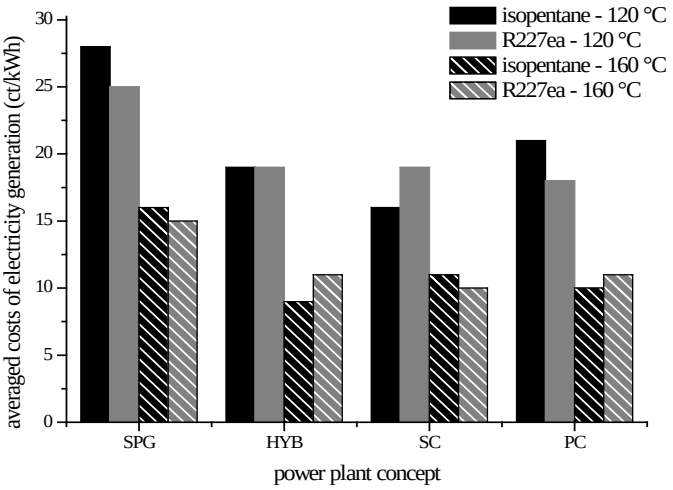

Fig. 5. Averaged costs of electricity generation depending on power plant concept

3.4. Variation of supply temperature of the heating system and mass flow of the geothermal water

Table 3 shows the averaged costs of electricity generation as a function of supply temperature of the heating system and mass flow of the geothermal water for isopentane in case of SPG and SC. In this case the duration curve of heat demand is analyzed more detailed in 11 steps.

Table 3. Averaged costs of electricity generation depending on supply temperature of the heating system and mass flow of the geothermal water

heating system supply temperature	SC – 120 °C (ct/kWh)	SPG – 120 °C (ct/kWh)	SC – 160 °C (ct/kWh)	SPG – 160 °C(ct/kWh)
75 °C	20	28	11	14
85 °C	24	28	11	14
95 °C	32	28	12	14
mass flow				
65.5 kg/s	20	28	11	14
100 kg/s	15	19	8	11
120 kg/s	13	16	8	10

In case of 120 °C an increasing supply temperature has a significant influence on the averaged costs of electricity generation. Since the outlet temperature of the geothermal water has to be increased for higher supply temperatures the losses in electrical power generation rise. For 95 °C supply temperature, the CHP concept leads with 32 ct/kWh to higher costs than sole power generation with 28 ct/kWh. For 160 °C the increase in supply temperature has only a marginal influence on economic aspects. A rise in mass flow of the geothermal water leads to a higher power output and lower costs of electricity generation. At a source temperature of 120 °C an increase from 65.5 kg/s to 120 kg/s leads to a reduction of costs from 28 ct/kWh to 16 ct/kWh in case of power generation and for series circuit from 20 ct/kWh to 13 ct/kWh. In case of 160 °C, costs are reduced up to 28 %.

4. Discussion

A thermoeconomic analysis for combined heat and power generation in case of geothermal heat sources below 180 °C was performed. For power generation the ORC with different

working fluids was investigated. The second law efficiency and the costs of electricity generation were calculated for three concepts of heat generation and two typical geothermal conditions in Germany. The following conclusions can be summarized:

- Second law efficiency and economic aspects can be enhanced by CHP.
- For power generation working fluids with low critical temperatures, at the shift of the pinch point, should be selected.
- R227ea leads with 25 ct/kWh and 15 ct/kWh to low costs for sole power generation.
- In case of CHP, working fluids with higher critical temperatures are suitable.
- Isopentane in conjunction with series and hybrid circuit is the most economic concept for CHP. In case of 120 °C and series circuit the costs of electricity generation are 16 ct/kWh and for 160 °C and hybrid circuit the costs are 8 ct/kWh.

References

[1] R. DiPippo, Small geothermal power plants: design, performance and economics, GHC Bulletin, June 1999.

[2] B. Saleh, G. Koglbauer, M. Wendland, J. Fischer, Working fluids for low-temperature organic Rankine cycles, Energy 32, 2007, pp. 1210-1221.

[3] U. Drescher, D. Brüggemann, Fluid selection for the Organic Rankine Cycle (ORC) in biomass power and heat plants, Applied Thermal Engineering 27, 2007, pp. 223-228.

[4] S. Karellas, A. Schuster, Supercritical fluid parameters in Organic Rankine Applications, International Journal of Thermodynamics 11, 2008, pp. 101-108.

[5] Z. Gnutek, A. Bryszewska-Mazurek, The thermodynamic analysis of multicycle ORC engine, Energy 26, 2001, pp. 1075-1082.

[6] O. Arslan, Exergoeconomic evaluation of electricity generation by the medium temperature geothermal resources, using a Kalina cycle: Simav case study, International Journal of Thermal Sciences 49, 2010, pp. 1866-1873.

[7] O. Arslan et al., Exergoeconomic evaluation on the optimum heating circuit system of Simav geothermal district heating system, Energy and Buildings 41, 2009, pp. 1325-1333.

[8] A. Hepbasli, A review on energetic, exergetic and exergoeconomic aspects of geothermal district heating systems, Energy Conversion and Management 51, 2010, pp. 2041-2061.

[9] N. Woudstra, T.P. van der Stelt. Cycle-Tempo: a program for the thermodynamic analysis. Energy Technology Section, Delft University of Technology, The Netherlands, 2002.

[10] E.W. Lemmon, M.L. Huber, M.O. McLinden. NIST Standard Reference Database 23 – Version 8.0. Physical and Chemical Properties Division, National Institute of Standards and Technology, Boulder, Colorado, US Department of Commerce, USA, 2002.

[11] P. Mago, L. Chamra, K. Srinivasan, C. Somayaji, An examination of regenerative organic Rankine cycles using dry fluids, Applied Thermal Engineering 28, 2008, pp. 998-1007.

[12] F. Heberle, D. Brüggemann, Exergy based fluid selection for a geothermal Organic Rankine Cycle for combined heat and power generation, Applied Thermal Engineering 30, 2010, pp. 1326-1332.

[13] B. Görke, A. Sievers, Gewinnbetrachtung von strom- und wärmegeführten Geothermie-Projekten unter Berücksichtigung der aktuellen EEG Novelle, Tagungsband Geothermiekongress, 2008, Karlsruhe (D), pp. 157-156.

Energy supply in buildings: heat pump and micro-cogeneration

Marta Galera Martínez, Laura Cristóbal Andrade, Pastora M. Bello Bugallo*, Manuel Bao Iglesias

Department of Chemical Engineering and Seminar of Renewable Energy (Aula de Energías Renovables), University of Santiago de Compostela, Spain
** Corresponding author. Tel: +34 881816757, Fax: +34981528050 , E-mail: pastora.bello.bugallo@usc.es*

Abstract: Heat pumps and micro-cogeneration technology for residential applications are an alternative for energy saving and for improving the energy efficiency. Nowadays, several nomenclatures are used for these technologies, creating confusion within this field. This situation causes that the commercial brands could not offer their products clearly to the market as the concepts and terminology they use are usually incorrect. This paper clarifies these concepts using thermodynamics, and provides clear classification criteria considering the heat pump and the power cycle as the starting point. Therefore, this paper provides an update review of heat pumps and micro-cogeneration which could be of great importance in the future for achieving the goals of the European legislation, especially those related to energy supply in buildings. It emphasizes the principles of operation and the advantages of the different devices as well as the consideration of this technology as renewable energy.

Keywords: *Energy Efficiency, Heat Pump, Micro-cogeneration, Distributed Generation*

1. Introduction

Buildings have an impact on long-term energy consumption. According to data from 2010, buildings account for 40% of the total energy use in the European Union (EU) [1]. Around the same percentage of all greenhouse gas emissions in developed countries have their origin in building equipments, where approximately 60% are produced by cooling and heating systems [2]. However, the energy use of any residence largely depends on its architectural design. All these factors are included in the Directive 2002/91/EC on the energy performance of buildings [3], which states that the calculation methodology must take into account insulation, technical and installation characteristics, design and positioning in relation to climatic aspects, solar exposure and influence of neighboring structures, own-energy generation and other factors such as indoors climate, which influences the energy demand. Directive 2009/28/CE on the promotion of the use of energy from renewable sources similarly talks about passive energy systems which use building design to harness energy [4]. This directive also requires that, before the end of 2014, Member States enforce the use of minimum levels of energy from renewable sources in buildings. This requirement may be fulfilled through heating and cooling systems that use a significant percentage of renewable energy sources [4].

Heat pumps (HP) and micro-cogeneration technologies for residential applications are an alternative for energy saving and for improving energy efficiency. Consequently, these technologies allow reducing the greenhouse gas emissions and can reduce energy dependence.

This paper clarifies these concepts using thermodynamics, and provides clear classifications considering the HP and the power cycle as the starting point. Therefore, this paper provides an update review of HPs and micro-cogeneration which could be of great importance in the future for achieving the goals of the European legislation. It emphasizes the principles of operation and the advantages of the different devices.

2. Heat pumps

2.1. Foundations

HP is a system that undergoes a thermodynamic cycle while thermally communicating with two bodies located in the surroundings or thermal reservoirs. They are devices designed to utilize low temperature sources of energy to heat a space to higher temperatures. The low temperature source may be the atmospheric air, the ground or a nearby body of water (lake or river). This energy comes from the solar radiation reaching the surface of the earth and its use constitutes therefore an indirect use of solar energy [5]. On the other hand, the space to be heated corresponds to the circuit for space heating, usually water or air. Net work input is needed to be provided by electricity, though it may also be provided by a mechanical engine. The components of a HP cycle, namely vapor compression HP, are: evaporator, condenser, compressor and expansion valve (Fig. 1).

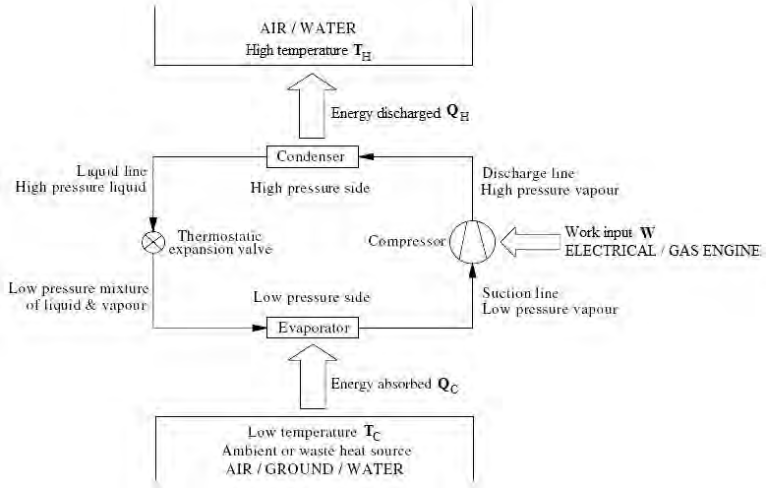

Fig. 1. Typical HP schematic.

$$W = Q_H - Q_C \quad (1)$$

$$COP = \frac{Q_H}{W} \quad (2)$$

$$COP = \frac{Q_H}{Q_H - Q_C} \quad (3)$$

$$COP_{máx} = \frac{T_H}{T_H - T_C} \quad (4)$$

The objective of a HP is to maintain the temperature *above* that of the surroundings. According to energy flows, the energy balance is defined by Eq. (1). Therefore, the Coefficient of Performance (COP) of a HP is calculated as the amount of energy discharged from the cycle system to the hot reservoir by the net work input needed to accomplish this effect (Eq. (2)). As Q_H is greater than Q_C, COP is never less than unity but it is also limited to a maximum value. The maximum COP of a reversible HP cycle is obtained in terms of reservoirs temperatures (Eq. (4)). In any case, and in spite of these limitations, it is desirable to obtain high values of COP.

2.2. Heat pumps classification

2.2.1. Thermodynamic cycle type

The foundations of HPs are used to give a first qualitative classification depending on the thermodynamic cycle. Accordingly, there are mainly three types of HPs (Fig. 2). Vapor-Compression Heat Pumps (VCHPs) are commonly used for space heating applications. Its compressor is mechanical, so it requires mechanical drive energy. Vapor Absorption Heat Pumps (VAHPs) are also used for space heating and require thermal drive energy. Both systems involve changes in phase, whereas in gas refrigeration systems the working fluid stays as a gas throughout. The Brayton refrigeration cycle illustrates an important type of gas refrigeration system [6] and consequently it can be also worked as a HP [7].

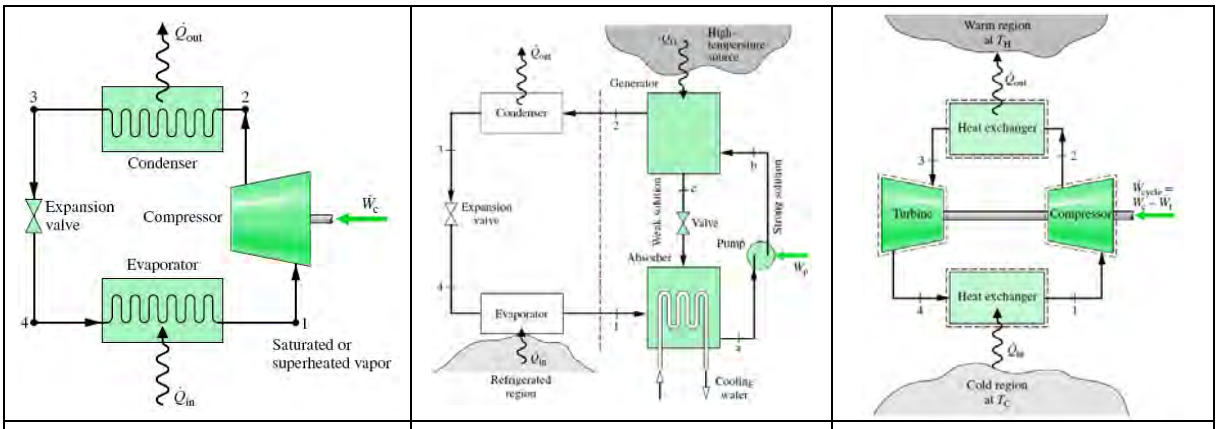

Vapor-compression cycle	Absorption cycle	Brayton cycle

Fig. 2. Diagrams of principal refrigeration or heat pump cycle [6].

2.2.2. Equipment

According to Fig. 1, and depending on the type of equipment that the HP uses to operate, different classifications can be considered.

- Evaporator. Depending on the type of equipment used to evaporate the refrigerant fluid, a classification can be made including any type of heat exchanger, as differently disposed shell-and-tube heat exchangers, solar collectors, etc. That depends on the cold reservoir. As a particular case, the Solar Assisted Heat Pump (SAHP) system mixes HP and solar technology, using solar radiation as evaporating heat source. This allows an improvement of the COP of the HP and, therefore, of the energy conversion efficiency. In Spain, a commercial term "thermodynamic solar cell" appears around 2006. From a commercial point of view, it is more socially impactful taking about "solar cells" than "HP", as solar cell is a term associated with positive connotations (ecologic, renewable, etc), which are not used when talking about HPs. However, the reality is that a "thermodynamic solar cell" is a SAHP. Ozgener et al. [8] have done a classification of SAHP according to the literature: (i) SAHPSs for water heating, (ii) SAHPSs with storage (conventional type) for space heating, (iii) SAHPSs with direct expansion for space heating, and (iv) Solar-Assisted Ground Source Heat Pump Greenhouse Heating System (SAGSHPGHS). Ji et al. [9] proposed in 2007 a novel Photo-Voltaic Solar Assisted Heat Pump (PV-SAHP) system capable of providing space cooling-heating and domestic water-heating. The solar panels are actually an assembly of PV cells laminated onto the evaporator-collector plate, allowing the direct solar energy absorption and, therefore, improving the protection of the evaporator from frosting in winter. Through experiments, the maximum COP (10.4) was obtained when the solar irradiance was also the highest. Then, they concluded that PV-SAHP system is better than the conventional HP systems.

- Compressor. Gas Engine Heat Pumps (GEHPs) have the compressor driven by a gas (natural gas, propane or LPG) fuelled internal by a combustion engine instead of electricity.

- Valve. There are two types: reversible (inverter) and irreversible, depending of the type of valve (four or two-way valves).

2.2.3. Net work input

HPs require energy (net work, W) for operating, so they can be basically divided into Electric-driven Heat Pumps (EHPs) and the Gas Engine Driven Heat Pump (GEHPs).

2.2.4. Cold reservoir

Directive 2009/28/CE enables HPs to use aerothermal, geothermal or hydrothermal heat. HPs are formally classified as air source, ground source or water source depending on the thermal reservoir they use. But there are hybrid HPs which combine, for example, ground source/air source units, and solar assisted and solar boosted air source and water source units.

2.2.4.1 Air-source HPs

The most common type of HP is the air-source HP. This category includes the air-to-air and air-to-water HPs. The solar energy is stored in the air, so this HP indirectly uses solar energy. They operate using fans to draw air across the evaporator. The inconvenient is their efficiency is influenced by the variation in ambient air temperature. If this temperature drops below 4 ºC, ice may appear in the evaporator, so efficiency decreases. The main advantage if compared with Ground Source Heat Pumps (GSHPs) is the relatively low capital cost.

2.2.4.2 Ground-source heat pumps (GSHPs)

GSHPs are also known as Geothermal Heat Pumps (GHPs). Yang et al. [10] classified these systems according to the source where they absorb the energy. This means that the cold reservoir could be the ground, ground water or surface water, and based on the type of reservoir there are basically three categories: (i) Ground-Coupled Heat Pump (GCHP) systems, (ii) Ground Water Heat Pump (GWHP) systems and (iii) Surface Water Heat Pump (SWHP) systems. They may be also classified according the loop: open loop (ground coupled) or closed loop (water source) [8]. The great advantage is the underground temperature remains fairly constant during the year, so this technology offers higher energy efficiency. However, in the case of SWHP the surface water temperature is influenced by weather condition. The pipes are buried in the ground horizontally or vertically. The horizontal system installation is less expensive than vertical one, but it requires much more ground area and it is more influenced by ambient air temperature.

2.2.4.3 Water-source heat pumps (WAHPs)

WAHPs, as the term implies, obtain heat from a large body of water source. As it uses water from the Earth as their energy source, WSHPs are incorporated in ground-source HPs. The classification has been shown before in 2.2.4.2, where SWHP employed a lake loop instead of water wells used in GWHP.

2.2.5. Hot reservoir

It is not usual to classify HPs according to the hot reservoir. It is more common to consider the relation between the cold and hot reservoir, which is explained in the next epigraph.

2.2.6. Cold reservoir-Hot reservoir

The types of HPs are usually determined by the combination of the heat source and the heat sink (where the heat is absorbed and where the heat is discharged) [11]. The cold reservoir is employed as heat source, and it may be the air, the ground or water. Depending on the nature of the hot reservoir, there are two possibilities: air or water, according to the objective. For example, air-to-water HP transfers heat from ambient air, which is used as cold reservoir, to water for space heating (radiators or an under floor heating system) or for domestic sanitary hot water [12]. On the other hand, air-to-air HP works transferring heat from the air outside to inside the building, where it is distributed by moving air. In the same way there are other systems [13]: ground-to-water, ground-to-air, water-to-water and water-to-air. It is observed

that this nomenclature is more used in the commercial sector, though it can also be found in scientific papers. In the commercial sphere there may also be found combinations like sun-water and sun-air, when a solar collector is used to obtain the heat [14].

3. Micro-cogeneration

Micro-cogeneration, also termed Micro-Combined Heat and Power (MCHP) or residential cogeneration, is a technology that has the ability to produce both useful thermal energy and electricity from a single source. Fuel is used more efficiently (Fig. 3), as a heat exchanger recovers waste heat from the engine and/or exhaust gas to produce hot water or steam [15].

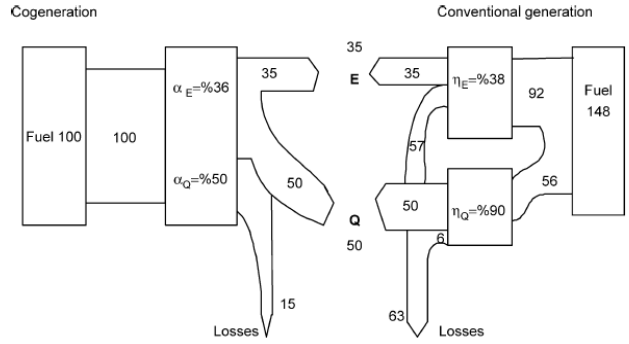

α_E, part of the energy transformed into electricity in a cogeneration unit.

α_Q, part of the energy transformed into usable heat in a cogeneration unit.

η_E, electrical yield of an electrical power plant (electricity production only).

η_Q, yield of a boiler (heat production only).

E, electricity demand.

Q, heat demand.

Fig. 3. Difference of primary energy consumption required for producing the same amount of heat and power using conventional fossil fuel fired electricity generation and boiler system compared to a cogeneration system [14].

The small-scale implementation (<10kW) or cogeneration is a solution that provides all the advantages of cogeneration, as controlled and predictable energy savings and emissions, energetic decentralization, supply security, etc [16].

3.1. Micro-cogeneration classification

A variety of types of cogeneration systems are commercially available (Table 1). The choice of the system depends on factors such as the demand of power and thermal energy, the choice of prime mover, capital installation and maintenance, etc. Some systems have been developed for micro-cogeneration, and their actual conditions are shown in Table 2.

Table 1. Cogeneration technologies [17].

Cogeneration Technology		
Combined cycle gas turbines	Steam turbine plants	Stirling engines
Steam condensing extraction turbine	Gas turbines with recovery boilers	Steam engines
Internal combustion engines	Microturbines	Fuell cells
		Organic Ranking cycles

Table 2. Status of micro-cogeneration technologies [18].

Technology	η_E (%)	η_Q (%)	η_T (%)	Minimal load (%)	T (ºC)	Noise (dB)	Fuel
Gas turbine	15-35	40-59	60-85	75	450-800	62-75	Natural gas
Alternative internal combustion engines	25-45	40-60	70-85	50	300-600	52-56	Gas, diesel, biofuel
Stirling engines	25-50	40-60	70-90	50	300-600	56	All
Fuel cells	35-55	40-60	70-90	No limit	250-550	Low	H_2

η_E: electric yield; η_Q: thermal yield; η_T: total yield; T: temperature

3.1.1. Reciprocating internal combustion engine

Reciprocating internal combustion engines are classified by their method of ignition: compression ignition (Diesel) engines and spark ignition (Otto) engines. Spark ignition engines are used typically for micro-cogeneration due to their heat recovery system producing up to 160°C hot water compared to diesel engines, where the temperature is often lower. Their efficiencies range from 25 to 45%. The main advantage is that their technology is mature and well-understood. It can be designed for different fuels but it needs frequent maintenance. On the other hand, as this technology burns fossil fuel there are emissions of pollutants such as oxides of nitrogen (NOx), carbon monoxide (CO), and volatile organic compounds (VOCs—unburned, non-methane hydrocarbons).

3.1.2. Micro-turbines

The basic components are the compressor, turbine generator and the recuperator. The thermodynamic process involves the pressurization of intake air by the compressor. The compressed air and a suitable fuel are mixed and ignited in a combustion chamber. The resulting hot combustion gas expands turning the turbine, which drives the compressor and provides power by rotating the compressor turbine shaft. With the recuperator, the hot exhaust gas helps pre-heat the air as it passes from the compressor to the combustion chamber. This increases the efficiency of the system. At first, micro-cogeneration competes with HP technologies but actually they may complement each other. For example, the remaining electricity generated from micro-cogeneration system is to meet a portion of the heating and cooling needs through the use of HPs. Ehyaei et al. [19] show how the excess electricity generated by the micro-turbines can to be used in a HP. This technology offers a high-grade of waste heat and other advantages such as a compact size, low weight, low maintenance requirements and lower noise. However, in the lower power ranges, reciprocating internal combustion engines have higher efficiency. It also produces pollutants (but in minor amount than the reciprocating internal combustion engine) as NOx, CO and unburnt hydrocarbons, and insignificant amounts of SO_2.

3.1.3. Fuel cells

Fuel cell technology is an emerging technology with a potential for cogeneration applications and is currently being developed for use in residential applications (3-10 kW). It can run independently or in parallel to a power grid [20]. The electrochemical reaction of hydrogen and oxygen in the presence of an electrolyte produces electricity without combustion and mechanical work. Water and heat are the only byproducts. Fuel cells normally run with hydrogen but can also be used with natural gas, propane or other fuels by external or internal reforming or through the electrolysis of water too. The advantages include low noise level, potential for low maintenance, low emissions and potential to achieve an overall efficiency of 85–90% even with small units. The fuel cell is the most promising technology and gradually becomes available, but it still has a problem with its high cost and relatively short lifetime.

3.1.4. Stirling engine

Stirling engine is an *external* combustion engine operated on the Stirling cycle, not totally developed yet. The cycle consists on four internally reversible processes in series: isothermal compression at constant temperature, constant-volume heating, isothermal expansion at constant temperature, and constant-volume cooling. The Stirling cycle engine can use different types of renewable sources of energy including biomass, solar and geothermal energy [21], so it offers opportunities for high efficiency with reduced emissions. It can be operated with a wide variety of fuels, the maintenance may be low and the life is usually long.

The major disadvantage is its high cost. Stirling engines can be classified according to their arrangement: the Alpha, Beta and the Gamma. This technology and fuel cell for cogeneration systems seem promising for residential and small-scale commercial applications.

4. Conclusions

HPs offer an energy-efficient and economical alternative to HVAC (Heating, Ventilating and Air Conditioning) systems for residential applications. According to recently published European legislation, HP can be considered as a renewable energy technology, since it is based on the essential feature of these unlimited sources, such as the water, air and ground. The micro-cogeneration is an emerging technology that produces useful thermal energy and electricity from a single resource of fuel, in the same place of consumption or close to it. Even though HP and micro-cogeneration technologies require less than conventional devices, they do require energy, usually obtained from the power distribution system where fuel is mainly converted to electrical energy at power plants and the waste heat is discharged to the environment. So it is not exactly correct to state that they are renewable energy technologies. For example in Spain, renewable companies offer geothermic energy for building, but generally is a "false" geothermal energy because it uses solar energy absorbed from the ground surface. Real geothermal energy uses the thermal energy stored into the Earth. Nevertheless, they are really efficient technologies that could involve a great change in the current power distribution system of centralized generation and could give way to distributed generation. This will minimize energy losses due to electrical transmission and distribution system. These will allow having fuel conversion systems close to consumption points, and energy efficiency could become higher. In addition, the waste heat of fuel combustion can be recovered by approximately 80%.

Considering the electrically driven HP technology within power distribution system of distributed generation and renewable supply like photovoltaic solar energy will be a great choice. This may be an alternative for Europe since their solar energy potential [22], especially of Southern Europe.

According to the Spanish regulation, the technologies presented are a good alternative. Moreover, these technologies provide a chance to change the current power distribution system (based on large electrical generation plants far from consumption points) by becoming a generation system where the electricity is generated and consumed in the same site or nearby. The distributed generation has the potential to reduce losses due to electrical transmission and distribution inefficiencies and to alleviate utility peak demand problems.

The possibilities of these technologies that use renewable energy suppose a great chance. The CHP (Combined Heat and Power) plants can be integrated with other fuels/technologies such as biomass, geothermal energy or solar collectors. But this makes no sense outside a bioclimatic construction field.

References

[1] EU, Directive 2010/31/EU on the energy performance of buildings, Official Journal of the European Communities L153, 2010, pp. 13-35.

[2] N. Pardo, A. Montero, J. Martos, J.F. Urchueguía, Optimization of hybrid – ground coupled and air source – heat pump systems in combination with thermal storage, Applied Thermal Engineering, 30, 2010, pp. 1073-1077.

[3] EU, Directive 2002/91/EC on the energy performance of buildings, Journal of the European Communities L1, 2002, pp. 65-71.

[4] EU, Directive 2009/28/EC on the promotion of the use of energy from renewable sources, Official Journal of the European Communities L140, 2009, pp. 16-62.

[5] L. Aye, W.W.S. Charters, Electrical and engine driven heat pumps for effective utilisation of renewable energy resources, Applied thermal engineering, 23, 2003, pp. 1295-1300.

[6] M.J. Moran, H.N. Shapiro, Fundamentals of engineering thermodynamics, Wiley, 5th edition, 2006.

[7] L. Chen, N. Ni, C. Wu, F. Sun, Performance analysis of a closed regenerated Brayton heat pump with internal irreversibilities, International Journal of Energy Research, 23, 1999, pp. 1039-1050.

[8] O. Ozgener, A. Hepbasli, A review on the energy and exergy analysis of solar assisted heat pump systems, Renewable & Sustainable Energy Reviews, 11, 2007, pp. 482-496.

[9] J. Ji, G. Pei, T. Chow, K. Liu, H. He, J. Lu, C. Han, Experimental study of photovoltaic solar assisted heat pump system, Solar energy, 82, 2008, pp. 43-52.

[10] H. Yang, P. Cui, Z. Fang, Vertical-borehole ground-coupled heat pumps: A review of models and systems, Applied energy, 87, 2010, pp.16-27.

[11] HPs as a renewable energy (in Spanish), *El instalador* magazine, 458, 2008, pp. 5-8.

[12] Toshiba, Air to water heat pump system, (available at http://www.toshiba-aircon.jp).

[13] A. Pither, N. Doyle, UK Heat Pump Study, 2005 (available at Energy Efficiency Partnership for Homes, http://www.eeph.org.uk).

[14] H.I. Onovwiona, V.I. Ugursal, Residential cogeneration systems: review of the current technology, Renewable and sustainable energy reviews, 10, 2006, pp. 389-431.

[15] M. Goodell, About the Renewable Energy Institute, Climate Science & America's Clear and Present Danger, 2010 (available at http://cogeneration.net/).

[16] D. Arzoz del Val, Energy saving in buildings by small-scale cogeneration (in Spanish), *El instalador* magazine, 466, 2009, pp. 70-72.

[17] European Commission, Reference Document on Best Available Techniques for Energy Efficiency, Institute for Prospective Technological Studies (IPTS), 2009.

[18] Energylab, Electricity micro-cogeneration: concepts, typology and results (in Spanish), Plenary Conference on the Electricity micro-cogeneration Seminar, 2010.

[19] M.A. Ehyaei, M.N. Bahadori, Selection of micro turbines to meet electrical and thermal energy needs of residential buildings in Iran, Energy and Buildings, 39, 2007, pp. 1227-1234.

[20] US Fuel Cell Council, www.usfcc.com.

[21] D. Scarpete, K. Uzuneanu, N. Badea, Stirling Engine in Residential Systems Based on Renewable Energy, (available at http://www.wseas.us).

[22] M. Šúri, T.A. Huld, E.D. Dunlop, H.A. Ossenbrink, Potential of solar electricity generation in the European Union member states and candidate countries, Solar Energy, 81, 2007, pp. 1295–1305(available at http://re.jrc.ec.europa.eu/pvgis/).

Study on the performance of air conditioning system combining heat pipe and vapor compression based on ground source energy-bus for commercial buildings in north China

Yijun Gao, Wei Wu, Zongwei Han, Xianting Li*

Tsinghua University, Beijing, China
** Xianting Li. Tel: +86 01062785860, Fax: +86 01062785860, E-mail: gaoyj08@mails.tsinghua.edu.cn*

Abstract: After introducing the application status and problems of geothermal air conditioning system in China, a new kind of ground source air-conditioning system (EBCS) is put forward. The system consists of distributed air-conditioners combining heat pipe and vapor compression, fresh air handling unit with large enthalpy difference and ground source water loop. Geothermal energy is transported to the combined air-conditioners for heating and cooling by water loop. The combined air-conditioner can be operated at heat pump condition or heat pipe condition for air conditioning. In winter and transition season, the cooling energy in ground can be directly used for the cooling in inner zone by heat pipe mode, while the recovered heat is used for heating in peripheral zone.

To analyze the performance of proposed system, a commercial building in north China has been taken as the research object, and the annual energy use is simulated. It is shown that the new system can save 21.7% energy compared to the traditional ground source heat pump system, and may be a potential air conditioning system for commercial buildings in north China.

Keywords: *Building energy efficiency, Ground source, Heat pipe, Water loop, fresh air handing unit, air conditioning.*

1. Introduction

The ground source heat pumps (GSHP) are widely used in China. The building areas that use this system exceed 10,000,000 m^2 in 2008, and it continues to keep a rapid growth [1]. The ground source heat pump is a heating and air-conditioning system which uses the shallow geothermal energy on the surface of the earth. The shallow geothermal energy is regarded as a renewable energy source [2]. In summer, the soil temperature is lower than the ambient temperature, which contributes to improve the COP of heat pumps. At the same time, the waste heat of buildings in summer can be stored in the soil to supply heat in winter. Thus, heat is transferred over seasons. The waste building heat rejected in summer and the primary energy demands for heating in winter are decreased greatly, which is good for environment protection. However, the COPs, especially the cooling COPs of many GSHP projects in China are proved to be not higher, or even lower than that of the traditional water-cooled systems with cooling towers. The existing problems in the GSHP systems are analysed and a novel central air conditioning system using geothermal energy is put forward.

2. Analysis on the existing problems in traditional GSHP systems

The traditional GSHP system consists of cooling water pumps, underground heat exchanger, heat pump unit, chilled and hot water pumps and terminal fan-coil units. The GSHP produces chilled water in summer and hot water in winter which is then transported to terminal fan-coil units to realize cooling and heating. At the same time, cooling water, the heat and cold source of the GSHP unit, is transported through underground heat exchanger. In this way, the ultimate energy transfer of the system is realized.

The main problems of traditional GSHP systems are listed as follows:

1) The centralized producing chilled water and hot water in summer and winter increases the energy transfer links of systems. So the improvement of COP is restricted. Besides, it is very common that the COP of heat pump is low under partial load, which leads to huge energy use.

2) In order to transport chilled water and hot water, the energy use of water circulating pumps of GSHP system is very high.

3) In the existing GSHP systems, usually, the switch of cooling and heating is realized by switching the cooling water circulation. The control is difficult because of the complexity of cooling water systems. In winter and transition season, when the cooling and heating is demanded simultaneously, it needs to produce both chilled and hot water.

How to improve the COP of GSHP systems? Based on the analysis above, some factors below should be taken into consideration.

Firstly, the centralized chilled and hot water should be cancelled. Cold or heat in cooling water can be transferred to the room air directly by distributed terminal cooling and heating units. So the energy transfer links are reduced, and the chilled and hot water pumps are cancelled. Consequently, the energy use of water pumps is reduced. On the other hand, the advantage of flexible adjustment of distributed terminal units can improve the cooling and heating COP under partial load.

Secondly, make the best use of the low temperature advantage of geothermal energy. The shallow soil temperature is lower than the demanded room temperature most of the year. So, it will obviously reduce the cooling energy use of a compressor if the temperature difference is used for natural cooling. But the system must be able to flexibly switch between natural cooling and compression refrigeration. When the natural cooling mode cannot meet the demand, it can easily be changed to compression mode.

3. Introduction of the new energy-bus air conditioning system

A new energy-bus central air conditioning system (EBCS) based on ground source is proposed according to the analysis above.

3.1. Composition construction and key equipments of EBCS

The new system, which is put forward by Xianting Li et al [3], professor of Tsinghua University, consists of water loop, water-cooled air conditioners combined with heat pipe, and fresh air handling unit with large enthalpy difference. The cooling water is transported to the terminal air-conditioners combined with heat pipe and fresh air handing units for heating, cooling by the water loop. The terminal air-conditioners combined with heat pipe can realize natural cooling in heat pipe mode or vapour compression cycle in heat pump mode depending on the water loop temperature. The fresh air handing unit with large enthalpy difference has a strong ability of dehumidification, which makes it capable of carrying much more building latent heat load in summer. The key equipments are introduced as follows.

Cooling-only type terminal unit with natural cooling function

The schematic diagram is showed as *Figure 1*. It combines the compression refrigeration circulation and separated heat pipe technique, which can realize switching between the two operating modes. When there is a temperature difference between the water loop and the room air, the compressor can stop working and the heat pipe starts to operate natural cooling circulation. When the water loop temperature is higher than the room air temperature, the

vapour compression refrigeration mode is activated. This unit is suitable for buildings with inner zones that need cooling throughout a year.

Heat pump type terminal unit with natural cooling function

The schematic diagram is showed as *Figure 2*. Compared to the cooling-only type unit, there is an additional four-way valve in heat pump type unit. Thus, the compressor is able to produce heating. So this unit can meet the demand of cooling as well as heating in the peripheral zones all year round.

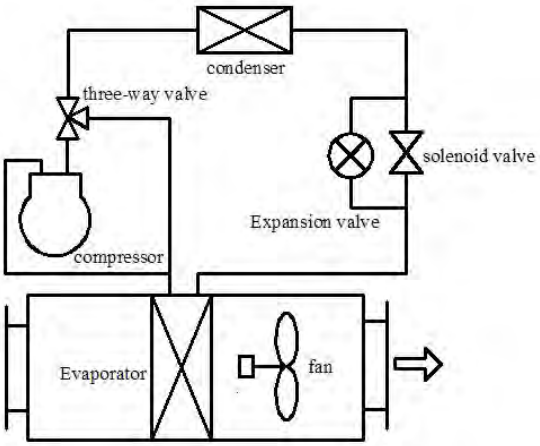

Figure 1 Cooling-only type terminal unit with natural cooling used in inner zone

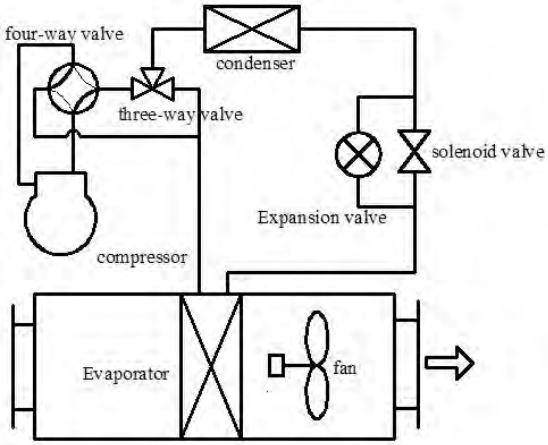

Figure 2 Heat pump type terminal unit with natural cooling used in peripheral zone

Direct evaporative fresh air handing unit with large enthalpy difference

The schematic diagram of direct evaporative fresh air handing unit with large enthalpy difference is showed as *Figure 3*. With the sensible heat exchanger, this unit can realize the sensible heat exchange between the fresh air handled by evaporator or condenser and non-handled fresh air. So the fresh air can be pre-cooled and the refrigeration system mainly carry the latent heating load in summer, which consequently reduces the energy use of the fresh air handling system. In winter, the non- handled fresh air can be pre-heated by the handled hot fresh air so as to solve the problem that compressor cannot work because of too low condensation pressure. It makes sure that the system can still work normally in cold weather.

Compared with the traditional fresh air unit, the fresh air handing unit with large enthalpy difference has a strong ability of dehumidification. So the fresh air handling unit is used to carry the latent load while the heat pipe combined air-conditioner is used to undertake the sensible heat load.

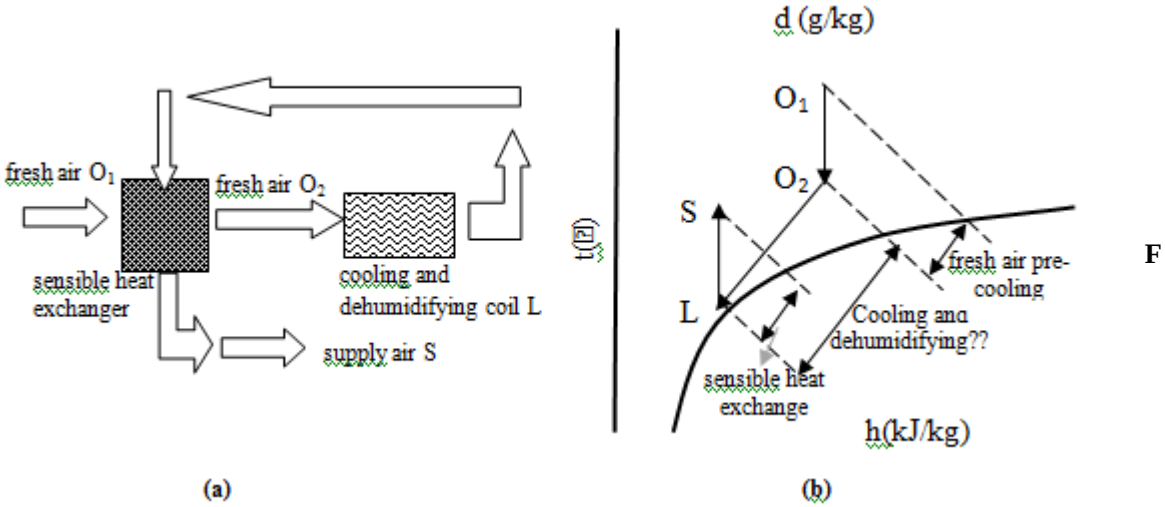

Figure 3 Direct evaporative fresh air handing unit with large enthalpy difference the schematic diagram (b) the psychrometric chart of air handling process notes : O_1 is the outdoor air condition, S is supply air condition Example in chart has no dehumidifying

3.2. The working principals of EBCS

In cooling season, the water-cooled air conditioners combined with heat pipe can realize switch between heat pipe mode (natural cooling) and air conditioning mode. At the beginning of cooling season, the soil temperature is low and the building load is small. So the terminal units can completely provide natural cooling under heat pipe mode. The heat is released to water loop and then stored in the soil through underground heat exchanger. When the heat pipe mode is insufficient to meet the cooling demand and the room temperature is higher than the maximum set value, the air conditioning mode is activated. When the room temperature is lower than the minimum set value, the compressor stops working and the heat pipe mode is activated. The switch between two operating modes can greatly reduce the compressor's working time.

In winter, the natural circulation of heat pipe mode is operated for cooling in the inner zones while the heat pump mode is operated for heating in the peripheral zones. If there is an unbalance between heat released to the soil and absorbed from it, heat compensation is needed. So this system can also recover the waste heat of inner zones for heating.

4. Energy saving and economic analysis of the new system

In order to evaluate the energy saving potential of the new system, a building model is built to simulate the annual energy consumption of the system which starts to operate from the summer cooling term. And then the energy use of the EBCS system and a traditional GSHP system are compared. Beijing, with a year average temperature of 11.4 ℃, is chosen as the simulation city. Both the EBCS and traditional GSHP system use underground heat exchangers as cold and heat source.

4.1. Building model

The building model is obtained from a research office building in Beijing after suitable simplification. There are 5 floors, and the drawing of standard floor is showed as *Figure 4*.

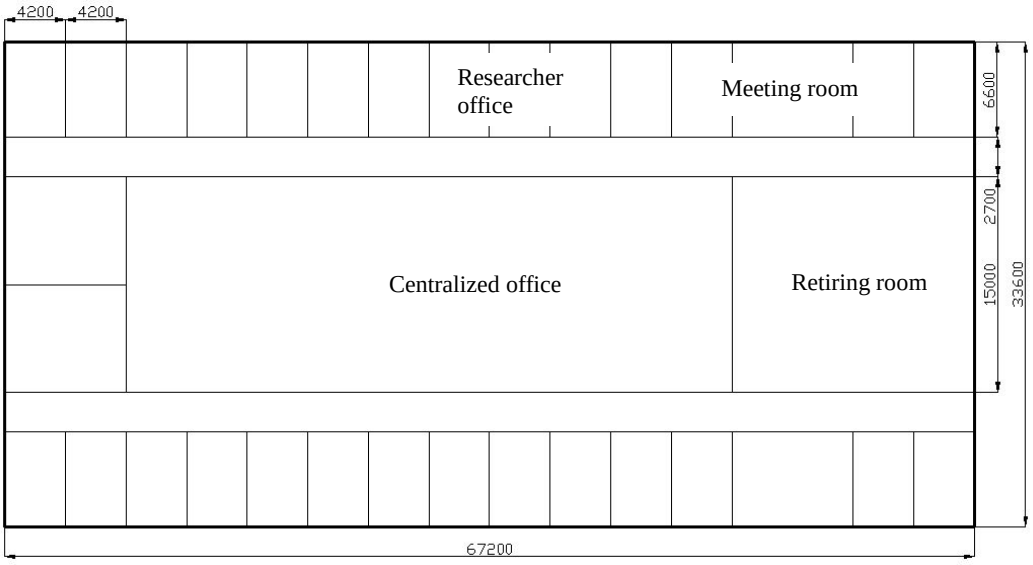

Figure 4 Standard floor of the building model

The area of each floor is 2258 m^2 and the total building area is 11290 m^2. The heat transfer coefficient of outside wall and roof is 0.8 W/m^2·K.The windows are doble-glazed with a 12 mm air layer and its heat transfer coefficient is 3.9 W/ m^2·K. The shading coefficient of the window is 0.83 and the inner shading is used. The window-wall area ratio is 0.65 in the south and north side and 0.9 in the east and west side.

The average minimum fresh air flow rate for each person in the building is 30m³/h. The room temperature is set within 24~26℃ in summer and 20~24℃ in winter. The software DEST-c is used to calculate the whole year hourly building load [4]. The calculation results are showed as *Table 1* and *Table 2*.

Table 1 The total building load

	Load
peak heating load	730.4(kW)
peak cooling load	895.3 (kW)
annual accumulated heating load	787.4 (MWh)
annual accumulated cooling load	844.3(MWh)

Table 2 The peak load of typical room

Typical room	area (m^2)	peak room cooling load (kW)	fresh air cooling load (kW)	peak room heating load (kW)	fresh air heating load (kW)
centralized office in inner zone	630.00	52.68	29.29	-4.90	29.17
office in outer zone	27.70	1.75	0.93	2.05	0.66

Notes: the humidification load is not included.

4.2. Simulation method for the energy use

The GSHP unit, fan-coil unit, fresh air handling unit, air conditioners combined with heat pipe and circulation water pump are chosen based on the total building load and peak cooling and heating load of typical room. The underground heat exchanger is designed to have 105 pipes with a 5.5 m interval and an 80 m depth. The U-bend heat exchanger is used in the simulation. Usually, the average transferring heat per unit of borehole depth is about 56w/m in Beijing. The U-bend is regarded to be equivalent to a vertical single pipe, and is numerically discreted by the inner node control volume method [5].

The method to calculate the energy use of GSHP unit or air conditioners combined with heat pipe is as follows [6] [7]:

$$N_c = \sum \frac{Q_{ci}}{EER_i} + \sum \frac{Q_{hi}}{COP_i} \quad (1)$$

Where N_c is the electricity consumption of GSHP unit or air conditioners combined with heat pipe, kWh. Q_{ci}, Q_{hi} is the building cooling load and heating load respectively in hour i, kWh. EER_i, COP_i is the energy efficiency ratio of GSHP unit/ air conditioners combined with heat pipe unit respectively in hour i.

The method to calculate the energy use of fans is as follows:

The total electricity consumption of fans in each system includes fan consumption in fresh air unit, fan-coil and air conditioners combined with heat pipe unit.

$$N_f = N_m \times \tau \quad (2)$$

Where N_m is the rated power of fans which are chosen based on the peak cooling load. τ is the annual running time of the air-conditioning system.

The method to calculate the electricity consumption of water pumps is as follows:

$$N_s = \sum N_w \times n_i \quad (3)$$

Where N_w is the rated power of a water pump. 3 chilled water pumps, 3 cooling water pumps and 3 hot water pumps are chosen with 2 in usage and 1 as backup. The selection of pumps is based on the peak cooling and heating load in the whole year. n_i is the number of pumps that should run in hour i.

4.3. The simulation results for annual energy use

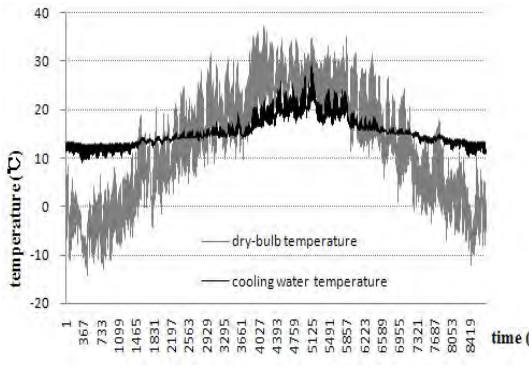

Figure 5 Hourly dry-bulb temperature and cooling water temperature

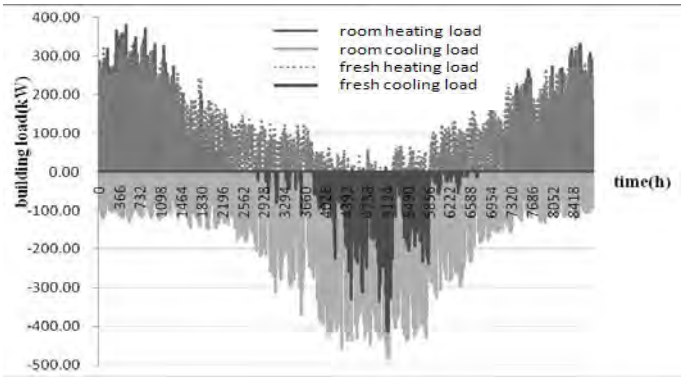

Figure 6 The calculated hourly building load for the whole year

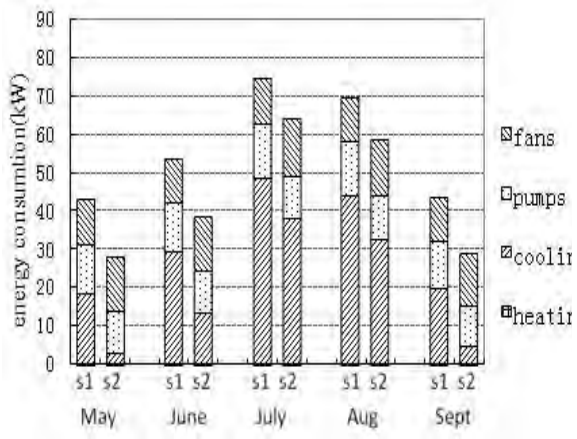

Figure 7 The comparison results of system energy use in summer

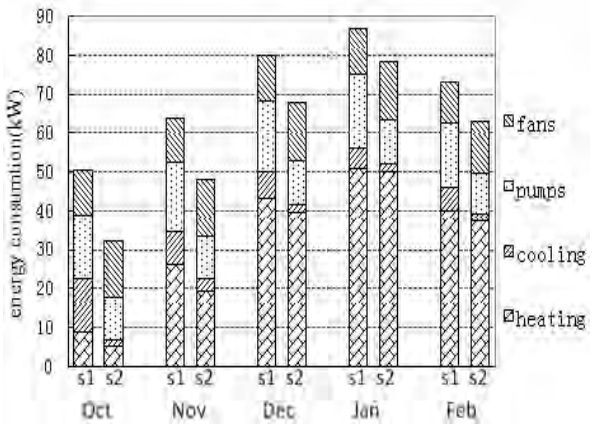

Figure 8 The comparison results of system energy use in winter and transition season

Notes: "s1" represents the GSHP and "s2" represents the EBCS, "heating" is the electricity consumption of compressors and in the GSHP and EBCS for heating, and "cooling" is the electricity consumption of compressors and heat pipe fans in the GSHP and EBCS for cooling.

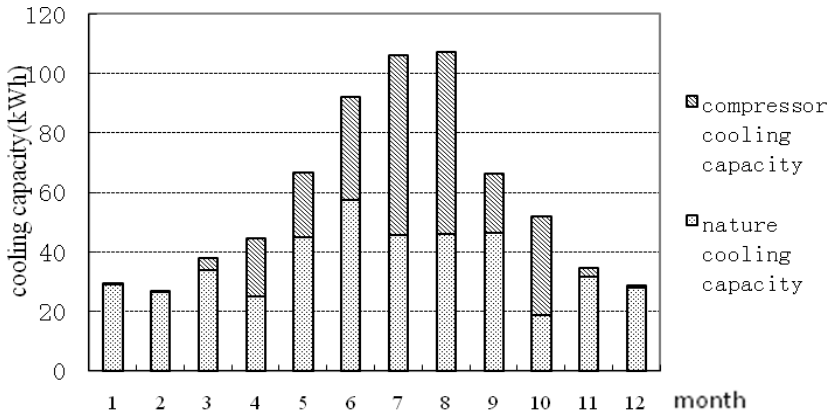

Figure 9 The annual accumulated natural cooling capacity analysis

From the energy use comparison, it can be concluded that:

1) The energy saving potential of EBCS is 21.7% compared to the traditional GSHP system. In EBCS, the air conditioners combined with heat pipe and water pumps use less energy while the fans use a little more energy.

2) Air conditioners combined with heat pipe contribute the most of energy saving because of natural cooling. With the heat pipe, the natural circulation mode can undertake almost all the cooling load in winter and transition season. Even in summer, it can undertake more than 30% cooling load. In the whole year, the natural circulation mode undertakes more than 60% cooling load totally.

3) In heating season, the EBCS has an obvious energy-saving advantage under partial load. It indicates that decentralized heating terminal units have higher energy efficiency at partial load.

4) Since the chilled and hot water pumps are cancelled in the EBCS, the annual electricity consumption of pumps is 30% lower in EBCS, even if the water head of pumps are higher than the cooling pump in the GSHP system.

5. Conclusions

The existing problems of the traditional GSHP systems are analyzed. A novel central air conditioning system based on ground source is proposed. The new system consists of decentralized terminal air conditioners combined with heat pipe, fresh air handing unit with large enthalpy difference and water loop. The chilled and hot water systems are cancelled. And the cooling water is transported to the terminal air-conditioners and fresh air handing units for heating and cooling by water loop. The air conditioners combined with heat pipe have two operating modes: natural cooling circulation and heat pump mode (compression refrigeration/heating). The air conditioners can switch between these two modes. The fresh air handing unit with large enthalpy difference has a strong ability of dehumidification, so it can be used to undertake the major latent load.

Based on the theoretical analysis, the annual energy consumption of an office building in Beijing is simulated. The calculation results show that EBCS can reduce much energy consumption for cooling compared to the traditional GSHP system. That's because the new system can realize natural circulation which can undertake 60% of the annual cooling load in the whole building. At the same time, EBCS also has obvious energy saving advantage in heating and transportation (pumps and fans) consumptions. The total energy saving potential in the whole year can reach 21.7%. Besides, the system form is simple and the control is easy. The terminal units can flexibly realize cooling and heating depending on the room demand, the same as the four-pipe type system. All this advantages can better ensure the temperature and humidity comfort all year round with much less energy use.

References

[1] W. Yang, J. Zhou, W. Xu, and G, Zhang. Current status of ground source heat pump in China. Energ. Policy, vol. 38, 2010: 323-332.

[2] Tao Meng. Yanqing Di, Li Liu, et al. Research of ground heat balance of ground source heat pump. 2009 International Conference on Energy and Environment Technology, 2009: 777-781.

[3] Xianting Li, Yijun Gao, Zongwei Han, et al. A new central air conditioning system combining heat pipe and vapor compression based on energy-bus. HEATING VENTILATING & AIR CONDITIONING, Vol.41, No.2, 2011: 1-6.

[4] Chen Feng, Deng Yuchun, Xue Zhifeng and Wu Ruhong. Toolpack for building environment simulation. HEATING VENTILATING & AIR CONDITIONING, Vol.29, No.4, 1999: 58-63.

[5] Zongwei Han, Maoyu Zheng, Fanhong Kong. Simulation research on solar-assisted ground source heat pump heating system with seasonal soil thermal storage in severe cold area. ACTA ENERGIAE SOLARIS SINICA. Vol.29, No.5, 2008: 574-580.

[6] Liu Tianwei, Du Kai. Research on the energy saving of water loop heat pump system applied to office buildings. HEATING VENTILATING & AIR CONDITIONING, Vol.40, No.3, 2010: 63-67.

[7] Huang Bing,Yang Chang-zhi. Resarch on simulation and economic assessment of ground source heat pump system. FLUID MACHINERY, Vol.38, No.1, 2010: 75-80.

Economic performance of ground source heat pump: does it pay off?

Laura Gabrielli[1,*], Michele Bottarelli[2]

[1] *University of Ferrara, Italy*
[2] *University of Ferrara, Italy*
** Corresponding author. Tel: +39 0532 293671, E-mail: laura.gabrielli@unife.it*

Abstract: A DCF model (discounted cash flow model) is implemented in order to investigate the economic aspects of GSHP (ground source heat pump) for heating and cooling, in comparison to traditional CB (condensing boiler). The DCF model allows the analysis of investment costs, operating costs and revenues of the two different systems in order to understand if the GSHP outperform its conventional counterpart in coming years, explicitly taking account for factors as price/cost growth. The whole analysis is performed adopting a parametric approach, in which all the previous terms are linked to energy labels, degree-days and EMRs (Energy Mix Ratios), the latter obtained as ratio between the full unit cost of electricity and natural gas paid by the householder. Relating to different EMRs, the DPBPs (Discounted Pay Back Periods) are presented in decision support matrixes in which energy labels and degree-days are the row/column variables, to confront the benefits of choosing between GSHP versus CB. Some considerations are also presented in order to express the environmental aspects. The results show that all higher energy labels have a good profitability ratio between costs and payback periods and demonstrate that GSHP system does pay off. Lower labels become interesting when the EMR drops to 0,25 and the gas price goes up 0,70 €/Nm^3.

Keywords: *ground source heat pump, discounted cash flow models, energy mix ratio, decision support matrixes*

1. Introduction

Heat pumps (HPs) are a reliable technology for space heating and cooling in commercial, industrial and residential buildings. In ground source heat pumps (GSHPs), the ground is used as heat source or sink; when compared to external air, it has smaller temperature variations during both heating and cooling season, and more advantageous thermal properties. For these reasons, GSHPs become an attractive alternative to conventional heating and cooling systems [1], owing to their higher energy utilization efficiency and reduction in greenhouse gases emission [2]. Economic evaluations were approached to exploit low temperature geothermal energy for buildings. In [3], the net present value is developed, showing a payback period of just a few years. Here, a discounted cash flow model (DFC) is implemented to assess the payback period for a GSHP application in comparison to traditional condensing boiler (CB), where the ground heat exchanger is the horizontal flat panel presented in [4].

2. Methodology

The goal is to calculate the payback period for a ground GSHP versus a CB, in connection with degree-days and energy building labels. The climate aspect and energy label are taken from the Italian law, but they can be easy extended to any other country setting different degree-days and energy requirements. To define the climate condition, a function was performed for the time series air temperature. Calibrating this function to obtain specific degree-days, it was possible to consider different climate zones. For both air conditioning systems it is supposed the same indoor distribution plant working at the same fixed low temperature (44 °C), keeping the analysis free from this part. The GSHP is supposed a vapor compression type heat pump coupled to a horizontal ground heat exchanger (Fig. 1). The CB is taken as boiler with high performance. For the GSHP, the coefficient of performance (COP) basically depends from the temperature at the evaporator, if the temperature at the condenser is taken fixed, like in this case. Anyway, the evaporator temperature is depending from the climate and the thermal behaviour of the HGHE and surrounding soil, so that this last

behavior is the key to approach correctly the problem. A solution for the HGHE behaviour was fund implementing a numerical model in unsteady state, and adopting a combination of degree-days and energy requirements. The results was achieved forcing the behavior of an exchanger five meters long to reach on average 0 °C in the ground surrounding the exchanger, to exclude groundwater icing. The combination between degree-days and maximum power for exchanger unit length represents the limit that each other combination must respect. So, all the other cases were gathered as different combinations among climate zones and energy requirements. The thermal analysis has made all the results for next economic valuation. Here, installation and operation costs were considered to achieve a full price for unit building volume. The economic analysis was performed adopting different ratio between the full unit cost of natural gas and electricity, and their potential trend, to link the payback and pay off to an energy mix ratio (EMR). In the following sections, the former steps are reported to explain the approach.

2.1. Building energy requirements and thermal behaviour

The Italian law defines the limit for building energy requirements in heating (EP_i), according to a country classification in seven degree-days climate zones (*A,B,C,D,E,F*), and to a building shape ratio (*S/V*). Moreover, the daily heating time is defined for each climate zone, but its observance is difficult to verify. The energy labeling weights the limit energy requirements to define eight energy classes (a^+,*b,c,d,e,f,g*), adopting *K* factors from 0,25 to 2,50 applied to EP_i. Generally, the heat exchange power ($\delta q_V/dt$) in steady state and for unit volume can be estimated for a given thermal difference *dT* occurred in time step *dt*, as:

$$\frac{\delta q_V}{dt} = \frac{1}{V}\frac{\delta Q}{dt} = U \cdot \frac{S}{V} \cdot dT \tag{1}$$

If its integral is extended to the full heating season, the product between *dT* and *dt* would represent the degree-days (*dd*) multiplied by the daily heating hours (*hh*). If as q_V it is taken $K*EP_i$ for a given climate zone and shape ratio, the previous transmittance would give the global behaviour of the whole building, inclusive of all heat exchanges (heat transfer through shell, air ventilation, free heating, …). So, it could be assumed as all-inclusive *"equivalent transmittance"*, and estimated as:

$$\overline{U} = \frac{EP_i}{\frac{S}{V} \cdot dd \cdot hh} \tag{2}$$

The former definition becomes usefully to approach heat transfer in a closed thermodynamic system by lumped parameters. Here, the building could be simplified in a homogenous body, whose internal energy variation occurs owing to the heat transfer belong its shell. The global mass is basically express only from walls, roof and foundation, because the air contribute is absolutely marginally. Knowing the building volume (*V*), the average density (ρ) and specific heat (*c*), and the ratio (*r*) between plenum over building volume, the integral of the energy balance between two time step becomes easy to do, assuming the air temperature independence from this heat exchange:

$$r \cdot \rho \cdot V \cdot c \cdot dT = -\overline{U} \cdot S \cdot \left(T - T^{air}\right) \cdot dt \quad \Rightarrow \quad \int_{T_0}^{T} \frac{d(T - T^{air})}{T - T^{air}} = -\int_{t_0}^{t} \frac{\overline{U} \cdot S}{r \cdot \rho \cdot V \cdot c} \cdot dt \tag{3}$$

where T_0 is the indoor air temperature at time step t_0. The indoor temperature becomes also:

$$T = T^{air} + \left(T_0 - T^{air}\right) \cdot e^{-\frac{\overline{U} \cdot S \cdot (t - t_0)}{r \cdot \rho \cdot V \cdot c}} \tag{4}$$

When the air conditioning plant is turned off, the function (4) calculates the indoor air temperature in time related to the changing outdoor air temperature. When the plant is switched on, a constant target value for the indoor temperature can be assumed, and the heat of the air conditioning plant can be calculated by the equation (1). For simplicity, we assume the plant is able to reach the target temperature in a single time step. To generalize the climate zones, a time series for air temperature was defined, so that knowing its trend during days and seasons, the degree-days are known and also the energy requirements according to the former equation (4) and (1). The time series was conceptualized as a sinusoidal trend, representing the seasonal temperature variation for daily maximum and minimum temperature, with a smaller sinusoidal oscillation superimposed, representing the hourly temperature variation with a daily time shift. In Fig 4 the air temperature is showed for a whole year; for each other details we remand to [4], where the method is presented.

2.2. Defining the Coefficient Of Performance for the heat pump

According to the previous considerations, the minimum fluid temperature leaving the indoor circulating pump is set to 44°C. Hence, it defines the temperature at the heat pump condenser, which can be supposed only few degrees higher (46 °C) than the first one, to perform suitably the heat exchange during condensation process. Neglecting the superheating after the evaporation and considering irreversibility coefficients to take into account the real processes, the thermodynamic cycle only depends from the temperature at the evaporator, which remain linked to the GHE. Therefore, even the COP only is depending to the fluid temperature leaving the GHE. It shouldn't drop too below 0 °C to exclude groundwater icing problem, and shouldn't go up 25÷30 °C, to limit environmental effects. If we adopt the refrigerant R134a, the thermodynamic cycle is laid in the Pressure-Enthalpy chart, where it is easy to estimate working relationships between enthalpy and temperature. According to the Fig.1 and [5], we have estimated the most important functions for the working temperature supposed at the condenser (46 °C), whose saturated pressure is 1,20 MPa. The compressor work is defined by the adiabatic *12* and then correct with a irreversibility coefficient η_{12}. The heat exchange at the condenser can be calculated knowing h_2 and h_3, and adopting a heat transfer coefficient η_{23}. Here, the performance at the compressor and at the condenser are taken 0,85 both. So, the COP becomes i.e. 4,01/5,35 at 0/10 °C. The expressions are reported in Fig. 2 and hold very high variances (R^2 >0,96).

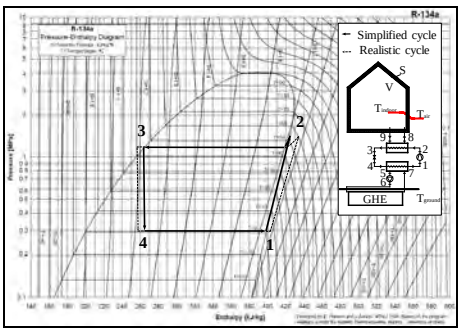

Figure 1: Thermodynamic cycle for R134a (E. Hansen & I. Aartun, NTNU 1999)

Quantity	Temperature at the condenser 46°C
h_1	$-0{,}0013 \cdot T^2 + 0{,}5774 \cdot T + 397{,}3$
h_2	$0{,}0012 \cdot T^2 - 0{,}1988 \cdot T + 426{,}2$
h_3, h_4	265,6
l_{12}	$0{,}0025 \cdot T^2 - 0{,}7762 \cdot T + 28{,}9$
q_{23}	$0{,}0012 \cdot T^2 - 0{,}1988 \cdot T + 160{,}6$
COP^*	$0{,}0012 \cdot T^2 - 0{,}1988 \cdot T + 160{,}4$
COP	$\dfrac{0{,}0012 \cdot T^2 - 0{,}1988 \cdot T + 160{,}4}{0{,}0025 \cdot T^2 - 0{,}7762 \cdot T + 28{,}9}$
	$\eta_{12} \cdot \eta_{23} \cdot COP^*$

Figure 2: Relationships in temperature adopting R134a (ASHRAE Trans., 1988, vol.94)

2.3. Benchmark for geothermal outlet loop temperature

The evaluation of the GHE performance was carried out as reported in [4]. There, the solution was conducted via the implementation of the unsteady-state three-dimensional numerical finite element code FEFLOW®, which allows determining the groundwater flow and temperature fields in saturated/unsaturated porous media, considering both conductive and convective heat transport. The HGHE used herein consists in a flat panel 0.80 m high, 0.02 m wide and 5.0 m long, buried vertically in a trench 6.0 m long, 0.30 m wide and 2.49 m deep. The overall computational domain is subdivided into 23 horizontal layers (Fig. 4) and the groundwater flow was imposed parallel to the HGHE direction with a piezometric gradient of 0,2%. The hydraulic and thermal properties attributed to the different materials constituting the domain (fluid within the panel, backfill, and surrounding soil) are assumed to be homogeneous are typical for sandy silts, bentonitic clay and water, within the ranges usually cited in [4]. Thermal boundary conditions are given at the soil surface in the form of a temperature time series, applying a coefficient at the previous sinusoidal function for air temperature, set to 0,6. The GSHP operation hours are selected to represent frequent working conditions, 5 AM - 9 AM and 5 PM - 10 PM from Monday to Friday, 7 AM - 11 PM on weekends. The heating operation is allowed from October 15th to April 30th, the cooling from June 1st to Septemebr 30th. During on time, the HP is activated in heating/cooling mode to maintain the indoor target temperature (20/26 °C), supplying for each time step the heat estimated according (1) and (4). For simplicity, we assume that this heat and the related power is the same requested at the HGHE, and the compressor works only to raise it to the requested temperature. This hypothesis overrates the heat required from the HGHE for a rate linked to the heat pump COP at the working temperature. The flow rate into the HGHE is calculated for flushing water with 3 °C between the inlet and outlet temperature. To do so, a specific numerical loop was supplied directly from the FEFLOW's producer [6]; this is the most important difference with [4], where the inlet temperature was fixed to 4°C in heating and 35°C in cooling. The resulting temperatures are showed in Fig. 3, with two independent temperatures at 1,4 and 2,5 m deep from soil surface. The minimum temperature at the soil near the inlet reached almost 0 °C at 70th day; no less temperature is accetable without icing problem. It means that no higher power is possible for this configuration, according to initial soil temperature, degree-days, energy requirements and type and length of HGHE. The maximum power was 36 W/m in heating mode for each meter of HGHE; the medium one 27 W/m. The soil volume surrounding the HGHE whose temperature varies by more than 0,5 °C from initial condition is almost 80 m^3.

The run for a full year needed very long computational time (more than six days). To avoid the time for running 29 cases, we examined each configuration according to the previous limit, and assuming the following hypothesis and observations:

1. the maximum heat extractable from the soil for heating time depends from the initial soil temperature and the maximum soil volume involved at same time;
2. the HGHE rate flow depends from the energy balance defined previously;
3. the HGHE outlet temperature for each different case can be estimate scaling the temperature time series resulting from the numerical solution for the limit case, using the difference between the two initial soil temperatures;
4. the difference of soil temperatures between two cases is equal to the difference of the yearly average air temperatures, because the sinusoidal functions are in phase;
5. the major or minor maximum power of a different case requires a proportional HGHE length for getting the same maximum power for unit length of limit case.

So, the heat transfer for each new case *"N"*, only can be equal to that of the limit case *"L"*:

$$c_t\rho_t V_t \cdot \left(\overline{T}_{i,N}^{soil} - \overline{T}_{f,N}^{soil}\right) + c_w\rho_w \dot{V}_N^w \Delta T_e \Delta t_N = c_t\rho_t V_t \cdot \left(\overline{T}_{i,L}^{soil} - \overline{T}_{f,L}^{soil}\right) + c_w\rho_w \dot{V}_L^w \Delta T_e \Delta t_L \quad (5)$$

As the final energy state of the involved soil volume must be the same for both cases, even their final average temperatures must be the same ($\overline{T}_{f,N}^{soil} \equiv \overline{T}_{f,L}^{soil}$), then, recording the phasing $\left(\Delta t_L \equiv \Delta t_N\right)$:

$$\dot{V}_N^w = \dot{V}_L^w + \frac{c_t\rho_t V_t}{c_w\rho_w \Delta T_e \Delta t_L} \cdot \left(\overline{T}_N^{air} - \overline{T}_L^{air}\right) \quad (6)$$

$$T_N = T_L - \left(\overline{T}_N^{air} - \overline{T}_L^{air}\right) \cdot \left(1 - \frac{t}{\Delta t_L}\right) \quad (7)$$

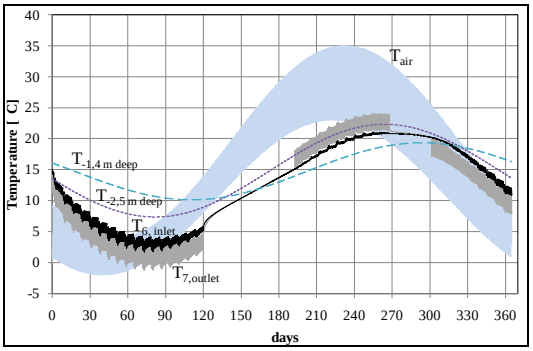

Figure 3: Time series for temperatures

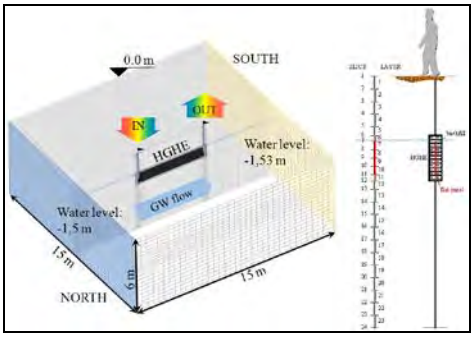

Figure 4: Computational finite elements domain

2.4. Pay back approach in Discounted cash flow analysis

The economic analysis was undertaken using the discounted cash flow (DFC) approach in order to compare the different hypothesis. Typically the investment feasibility calculations are carried out using DCF where all the present and future inflows and outflows are discounted to obtain the net present value (NPV), the internal rate of return (IRR) or the discounted payback period (DPBP). The net present value represents the present value of all incomes and costs during the period of analysis of the investment. If the present value gives us a number larger than zero, then the project can be accepted. If the NPV is negative, the project must be rejected or modified. The IRR is the discount rate that makes the net present value equal to zero, so when the net present value of all costs equals the net present values of all incomes or revenues of the project. Usually the IRR must exceed the cost of capital. The discounted payback period for a project is the time it takes to recover the cost of investment. The cash flows are added up after taking account of the time value of money. The decision is based on comparing the different pay back periods with a predetermined cut off period decided by the decision maker. [7] In our analysis we considered the DPBP in order to verify if the GSHP pays off in comparison to a traditional heating system. To undertake the economic analysis, it needs to identify all the critical variables and assign appropriate values to them based on an analysis of the current market. The variables identified are listed in Tab. 1. Four scenarios (*1*,*2*,*3*,*4*) where tested in order to consider the different cost of electricity and natural gas, which gives us a diverse energy mix ratio (EMR). The energy cost is expected to grow at a rate of 3% per year (in real term), inflation is considered at 2% per year. The rates were extrapolated considering the historical trends in the Eurozone [8]. To discount the future cash flows a weighted average cost of capital approach was used, considering a Debt/Equity ratio of 0.60/0.40; the cost of debt is set at 5% and the cost of equity is assumed at 7%. Sinking

funds formula has been used to build up a sum of money to replace the systems after their usable life. The formula is:

$$a = Ci\frac{r}{q^n - 1} \tag{8}$$

Where *a* is the annual deposit. The final value is used to replace the equipment at the cost *Ci*. All costs were discounted considering an inflation rate plus a growth rate of energy costs, which gave us:

$$C = \sum_{t=1}^{n} \frac{C_t(1+i+g)^t}{(1+r)^t} \tag{9}$$

Where *C* are the costs, *i* is the inflation rate, *g* is the growth rate, *r* is the discount rate. The same approach was used by [3]. The discounted payback period is finally calculated as:

$$DPBP = \frac{(Ci_{GSHP} - Ci_{CB})}{(C_{ECB} - C_{EGSHP})} \tag{10}$$

where:

Ci_{GSHP} : cost of installment (or investment) for GSHP system;
Ci_{CB}: cost of installment (or investment) for CB system;
Ce_{GSHP}: running costs (maintenance and electricity costs) for GSHP system;
Ce_{CB}: running costs (maintenance and natural gas costs) for CB system.

Table 1: Economic data

Description	*Value*	*Units*	*Life cycle*	Scenarios	A	B	C	D	Units
Indoor circulating pump	2,000	€/W_e	*10 years*	NATURAL GAS	1,0	1,0	0,7	1,2	€/Nm^3
GSHP	0,700	€/W_e	*15 years*	ELECTRICITY	0,5	0,25	0,175	0,24	€/kWh
Stack	0,100	€/W_t		EMR	0,50	0,25	0,25	0,20	
CB cost of maintenance	0,100	€/m^3*year		INFLATION RATE (i)	2%	2%	2%	2%	%
GSHP cost of maintenance	0,010	€/m^3		GROWTH (g)	3%	3%	3%	3%	%
CB	0,100	€/W_t	*15 years*	DISCOUNT RATE (r)	5,50%	5,50%	5,50%	5,50%	%
Pollution check	0,100	€/m^3*year							
Major supply cost	0,003	€/W_e*year							
GHE	40,000	€/m	*30 years*						

2.5. Results

The thermal analysis calculated all the necessary data to perform the economic analysis, adopting shape building ratio *S/V=0,5* and excluding climate zone *A* and energy labels *a+* and *g* of the Italian law, as they are very expensive or rare. In Tab. 2 are presented the most important entry data for calculating the payback period. In all next tables, data are given adopting energy labels (*a*/*b*/*c*/*d*/*e*/*f* as 0,37/0,63/0,88/1,13/1,50/2,13 part of EP_i) and climate zones (*B*/*C*/*D*/*E*/*F* as 750/1150/1750/2550/3550 degree-days) for rows and columns ($_L{}^Z$). The primary energy requirements are showed in Tab. 3 and 4, and from Tab. 5 to Tab. 8 payback periods are displayed for different scenarios (*1*/*2*/*3*/*4*). If we consider a predetermined cut off period of 30 years, in scenario *1* a large number of solutions overcame that period (indicated with *nc*). Considering a suitable payback for an householder of 10 years, all scenarios show that *a* energy label is the best option, not depending from the EMR and the gas price. When

we change the EMR from 0,50 to 0,25 keeping the gas price fixed into 0,7÷1,0 €/Nm^3, we can also include the *b* label as good opportunity for the GSHP technology. In scenario *4* almost the solutions give positive results as quicker payback periods, excluding the worst energy label *f*, which do not perform in terms of recovering the initial investments. In Fig. 4 is showed the EMR given by natural gas price for EU27 and used in our scenarios to identify their equivalence with Europe countries. Finally, in Fig. 5 is reported the payback period related to the energy requirements for each scenario, excluding the energy label *f*, for which the Italian low forces a fixed energy requirements. The scenario *1* shows higher slope, which can be taken as sign of instability with energy requirements. The scenario *4* mirrors the opposite case, where the low slope reflects almost the independence between payback period and energy requirements.

Table 2: Climate zones variables, shape building ratio S/V=0,5

Data	*Unit*	*B*	*C*	*D*	*E*	*F*
Daily heating hours	*hours/day*	7.2	8.0	9.0	9.6	10.5
Potential heating days	*day/season*	200	200	200	200	200
EP_i	$kWh_t/m^3 year$	8.1	11.2	15.4	20.4	22.9
Seasonal heating COP	-	6.3	6.1	5.9	5.6	5.3

Table 3: Electricity, kWh/m^3·year

L^Z	*B*	*C*	*D*	*E*	*F*
a	0.552	0.834	1.285	1.647	1.884
b	0.949	1.442	2.194	2.825	3.230
c	1.342	2.030	3.098	3.964	4.503
d	1.742	2.641	4.016	5.148	5.833
e	2.343	3.552	5.397	6.908	7.807
f	3.396	5.146	7.784	9.959	11.182

Table 4: Natural gas, Nm^3/m^3·year

L^Z	*B*	*C*	*D*	*E*	*F*
a	0.305	0.455	0.687	0.858	0.946
b	0.524	0.788	1.174	1.473	1.622
c	0.742	1.111	1.658	2.067	2.262
d	0.964	1.446	2.150	2.686	2.931
e	1.298	1.947	2.892	3.606	3.923
f	1.883	2.824	4.174	5.202	5.621

Table 5: Payback period, scenario 1

L^Z	*B*	*C*	*D*	*E*	*F*
a	0	3	6	10	8
b	4	9	13	20	18
c	7	15	21	nc	31
d	11	21	30	nc	nc
e	17	nc	nc	nc	nc
f	29	nc	nc	nc	nc

Table 6: Payback period, scenario 2

L^Z	*B*	*C*	*D*	*E*	*F*
a	0	3	4	7	5
b	3	6	8	10	8
c	5	9	10	12	10
d	7	11	12	14	12
e	10	14	14	16	13
f	13	17	16	19	15

Table 7: Payback period, scenario 3

L^Z	*B*	*C*	*D*	*E*	*F*
a	0	3	5	7	6
b	3	7	9	12	10
c	9	10	12	15	12
d	8	13	15	18	15
e	11	17	18	21	17
f	16	22	22	25	21

Table 8: Payback period, scenario 4

L^Z	*B*	*C*	*D*	*E*	*F*
a	0	3	4	6	5
b	3	6	6	8	7
c	5	8	8	10	8
d	6	9	10	11	9
e	8	11	11	12	10
f	11	13	12	14	11

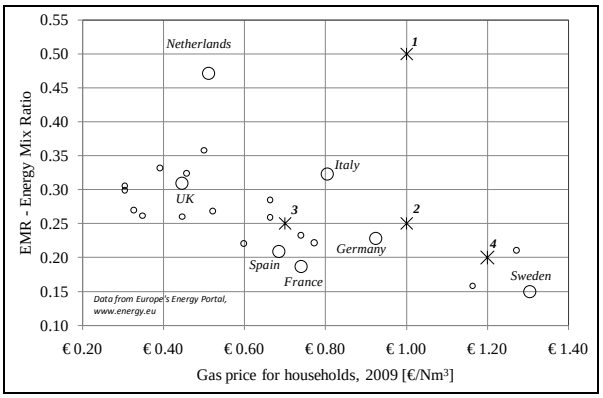

Figure 4: EMR given by gas price in EU27

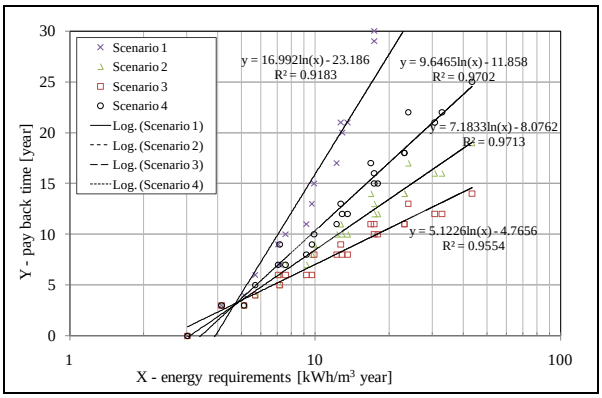

Figure 5: Regression analysis for the scenarios

3. Conclusions

We calculated the payback time for a ground source heat pump (GSHP) in comparison with a condensing boiler (CB), in connection with degree-days, energy building labels and an energy mix ratio (EMR), reflecting energy prices due to different combinations of primary energy. EMR is obtained as ratio between electricity and gas price. A numerical model was used to value the soil temperature modified from the HGHE, and this solution was scaled to approach the other combinations among climate zones and energy labels. The results show that all higher energy labels have a good profitability ratio between costs and payback periods, and demonstrate that GSHP system does pay off. Lower labels become interesting when the EMR drops to 0,25 and the gas price goes up 0,70 €/Nm^3. Further investigations should consider also environmental aspects (reductions of diffuse emissions, urban pollution control), potential raising energy label for retrofit action and different growth rate of energy price.

References

[1] A.D. Chiasson, Advances in modeling of ground-source heat pump systems, M. SC. Thesis, 1999, Oklahoma State University

[2] L. Rybach and W.J. Eugster, Sustainability aspects of geothermal heat pumps, Proceedings of 27th Workshop on Geothermal Reservoir Engineering, 2002

[3] Kulcar B., Goricanec D. Krope J. Economy of exploiting heat from low-temperature geothermal sources using a heat pump, Energy and buildings, 40, 2008, pp. 323 - 329

[4] Bottarelli M., Di Federico V., Adoption of flat panels in soil heat exchange, Proceedings of 11th World Renewable Energy Congress, 2010, pp. 330-335

[5] Y.A. Cengel, Termodinamica e trasmissione del calore, McGraw-Hill, 1st Ed., 1998, pp. 659-663

[6] DHI-WASY GmbH, OpenLoop IFM Module, Copyright 2009, Berlin

[7] G. Brown, G. Matysiak, Real estate investment, a capital market approach, Prentice Hall, 2000

[8] Europe's Energy Portal, 2010, www.energy.eu

Comparing Geothermal Heat Pump System with Natural Gas Heating System

Emin Acikkalp[1], Haydar Aras[2*]

[1]*Department of Mechanical and Manufacturing Engineering, Engineering Faculty, Bilecik University, Bilecik, Turkey*
[2]*Department of Mechanical Engineering, Engineering and Architecture Faculty, Eskisehir Osmangazi University, Eskisehir, Turkey*
** Corresponding author. Tel: +90 222 239 3750 / 3351, Fax: +90 222 239 36 13, E-mail: h_aras2002@yahoo.com, haras@ogu.edu.tr*

Abstract: In this study, approximately 150 m2 of floor space Eskisehir-Turkey have been investigated in a 2-story home. The building is heated with natural gas and heat loss is 24,172 kW. 3000 m 3 / year to meet the heat loss and the cost of natural gas consumed in 1620 U.S. dollars / year. Only the heat pump system under study is replaced by natural gas boilers, home heating system has not been any other changes. Thermodynamic analysis is applied, first, both the system and exergy loss of energy expenditure were calculated. Second, the environmental values were calculated for both systems. Finally, the results were compared between the two systems.

Keywords: *Geothermal heat pump, Exergy and energy analysis, Environmental aspects, Renewable energy*

1. Introduction

Due to the depletion and the environmental damages of the fossil fuels, use of alternative energy sources has become a necessity. Sustainable energy sources are divided into two parts as ground-source and atmosphere-source. Ground-source geothermal energy is stored heat energy in the earth's 0 to 10 km depth. This energy is 245.106 EJ in areas of high flux and 181.106 EJ low flux areas respectively. Considering the use of 1% of this energy is able to meet the world's current energy needs. It is predicted that Turkey has geothermal reserves that provide 50 EJ energy [1]. 31,500 MWh of thermal energy in Turkey and 2000 MWe/year of electrical energy can be achieved with this source. In the world, Turkey is the 5th among the best geothermal energy potential countries. Turkey has the geothermal energy potential to meet 30% thermal or 5% of electrical energy of it [2]. A significant portion of world energy consumption to the domestic heating and cooling is attributable. Heat pump and widely used in many applications are preferred due to their high utilization efficiencies Compared to conventional heating and cooling systems. There are two common types of heat pumps: air-source heat pumps and ground-source heat pumps (GSHPs), also known as geothermal heat pumps (GHPs). Several Advantages over or GHPs have GSHPs air source heat pumps as: (a) They're consumes less energy to operate. (b) They tap the earth or groundwater, a more stable energy source than air. (b) They require supplemental heat during extreme low outside temperature not do. (d) They're less refrigerant use. e) They have a simpler design and consequently less maintenance. (f) Require the unit to be located, where they're not do it is exposed to weathering. Their main disadvantage is the higher initial capital cost, being about 30-50% more expensive than air source units. This is due to the extra expense and effort to bury heat exchangers in the earth or providing a well for the energy sources. However, once installed, the annual cost is less over the life of the system, resulting in a net savings [3].

Eskisehir in Central Anatolia region of Turkey has a continental climate and has rich geothermal resources. Eskisehir water temperatures 25 ^{o}C - 55 ^{o}C has a range from 10 geothermal areas [1]. Geothermal resources in Eskisehir hotels, public baths and hot springs

are also used and not used in another application. This study investigated the geothermal heat source for a building.

2. Methodology

First and second law is basic laws for thermodynamics. First law is conservation of energy and the second law deals with the nature and quality of energy. In this study, heat pump and natural gas systems analyzed for first and second law of thermodynamic, and then environmental impacts of them has been attached and the results were then compared with each other finally.

2.1. Description of Systems

Application made for a house about 150 m^2 floor areas in Eskisehir-Turkey. Home is heated with natural gas and the heat loss is 24.172 kW. The study period was considered to be 6 months. In this time, 3000 m^3 of natural gas has been spent in and it cost $ 1,620 / year. R-134 was used as a refrigerant in heat pump. Natural gas boiler and heat pump system are shown in figure 1 and figure 2.

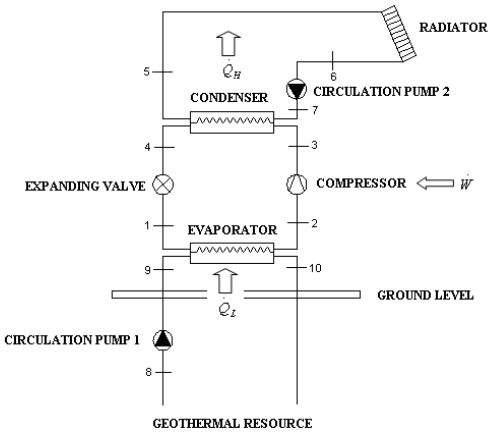

Figure 1. Investigated heat pump system.[3]

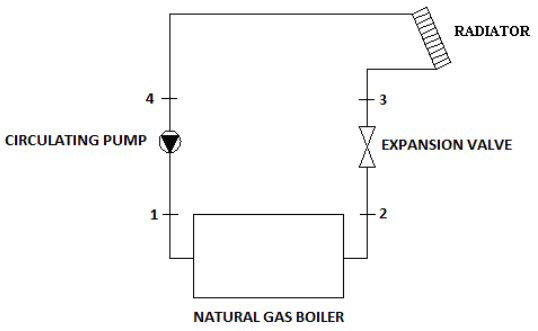

Figure 2. Natural gas boiler system

The assumptions for the system are as follows:

• All systems are adiabatic to the environment.

• Minimal and the average temperature during the heating period for Eskisehir are -12 ^oC and 5 °C respectively.

• Geothermal resource temperature is 40.5 ^oC [4].

• Radiator inlet and outlet temperature are 90 ^oC and 70 ^oC, respectively.

• Geothermal water depth is 79 m [4].

• Average daily heating period is 12 hours.

2.2. Thermodynamic Analysis

In this section, thermodynamic analysis was made detailed for first law (energy terms) and second law (exergy terms), also additional parameters have been added that allows evaluation system of the thermodynamically.

2.2.1. 2.2.1 Energy terms

Energy balances for any control volume at steady state can expressed as following [5],

$$\dot{Q} + \dot{W} = \dot{E}_Q + \dot{E}_W = \sum_o \dot{E}_o - \sum_i \dot{E}_i \quad (1)$$

In the absence of nuclear, magnetism, electricity and surface tension effects in the thermal systems and in this present study, the changes in the kinetic energy and potential energy are assumed to be negligible. The total energy for a flow of matter through a system can be expressed as [6];

$$\dot{E} = \dot{E}_{ph} + \dot{E}_{ch} \quad (2)$$

The physical energy for air and combustion gaseous with constant specific heat may be written as [6];

$$\dot{E}_{ph} = \dot{m}\left(h_{(T)} - h_o\right) \quad (3)$$

Given work to the pumps is;

$$\dot{W}_p = \dot{m}.g.H \quad (4)$$

Fuel's energy is given [5];

$$\dot{E}_F = \dot{m}_f LHV \quad (5)$$

LHV and molecule weight of natural gas is 44661 kJ/kg and 16,28 kg/kmol respectively [7,8]. *COP* of heat pump can be defined as the ratio of the energy output to energy input [6];

$$COP = \frac{\dot{Q}_{cond}}{\dot{W}_{comp} + \dot{W}_{pump,1} + \dot{W}_{pump,2}} \quad (6)$$

The energy efficiencies are calculated by [6];

$$\eta = \frac{\dot{E}_o}{\dot{E}_i} \quad (7)$$

2.2.2. 2.2.2 Exergy terms

Exergy balances for any control volume at steady state can expressed as following [5],

$$\sum\left(1-\frac{T_o}{T_k}\right)\dot{Q}_k+\dot{E}x_W+\sum_i\dot{E}x_i-\sum_o\dot{E}x_o=\dot{E}x_D \tag{8}$$

In the absence of nuclear, magnetism, electricity and surface tension effects in the thermal systems, and in this present study, the changes in the terms of kinetic exergy and potential exergy are assumed to be negligible, the total exergy for a flow of matter through a system can be expressed as [6];

$$\dot{E}x=\dot{E}x_{ph}+\dot{E}x_{ch} \tag{9}$$

The physical exergy of the liquid and gas is calculated by [9];

$$\dot{E}x_{ph}=\dot{m}\left[\left(h-h_o\right)-T_o\left(s-s_o\right)\right] \tag{10}$$

An approximate formulation for the chemical exergy of gaseous hydrocarbon fuels as C_aH_b is given as [10];

$$\frac{\dot{E}x_{ch,NG}}{\dot{m}_{NG}LHV_{NG}}=\gamma_{NG}\cong 1.033+0.0169\frac{b}{a}-\frac{0.0698}{a} \tag{11}$$

γ_{NG} is equal to 1.0308 for the natural gas(NG) composition given in Table 2.
The fuel exergy is equal to chemical exergy of fuel. The exergy efficiencies are calculated by [6];

$$\psi=\frac{\dot{E}x_o}{\dot{E}x_i} \tag{12}$$

2.2.3. Other Thermodynamic Evaluation Parameters

Fuel exergy depletion ratio can be defined as [5];

$$\alpha_k=\frac{\dot{E}x_{C,k}}{\dot{E}x_{TF}} \tag{13}$$

Relative exergy consumption ratio is calculated from [5];

$$\beta_k=\frac{\dot{E}x_{C,k}}{\dot{E}x_{TC}} \tag{14}$$

The exergetic improvement potential can be expressed following [5];

$$ExIP_k = (1-\psi)\, Ex_{C,k} \quad (15)$$

Similar parameters can be defined for energy terms. Fuel energy depletion ratio can be defined as [5];

$$\phi_k = \frac{\dot{E}_{L,k}}{\dot{E}_{TF}} \quad (16)$$

Relative energy loss ratio [5];

$$\Theta_k = \frac{\dot{E}_{L,k}}{\dot{E}_{TL}} \quad (17)$$

Energetic improvement potential [5];

$$EIP_k = (1-\eta)\, E_{L,k} \quad (18)$$

2.3. Environmental Aspects

In this section, environmental impacts were evaluated for CO_2 emissions released into the environment. Combustion equation of natural gas is showed as following;

0.9334 CH_4 + 0.00211 C_2H_6 + 0.00029 C_3H_8 +0.00012 C_4H_{10} + 0.06408 N_2 + 26.675 (0.7448 N_2 + 0.20509 O_2 + 0.0003 CO_2 +0.019 H_2O) 0.9469725 CO_2 + 4.76343 H_2O + 2.425 O_2 +19.93162 N_2 [7,8]

(19)

Rate of CO_2 mass to total mass [11];

$$M_{CO_2} = \frac{0.9469725 CO_2}{M_F} \quad (20)$$

Mass of CO_2 releasing to air [11];

$$M_{CO_2} = \frac{0.9469725 CO_2}{M_F}.m_F \quad (21)$$

3. Results

In this part, results of the energy and exergy values of the systems were submitted firstly. Then the results are presented in terms of environmental impacts.

3.1. Energy and Exergy Results for Both Systems.

Some important results can be summarized as follows. The largest loss of energy for natural gas and heat pump systems is in radiator. The largest exergy destruction is at natural gas system for boiler for natural gas system and at compressor for heat pump. The highest energy efficiencies are at condenser and evaporator for heat pump system and at natural gas boiler for natural gas system. The highest exergy efficiencies are at condenser for heat pump system and at radiator boiler for natural gas system. All thermodynamic values in the two systems can be shown in table 3-6.

Table 1. Heat pump system pressure, temperature, energy rate and exergy rate

Point	Fluid	Temperature (K)	Pressure (kPa)	Mass flow (kg / s)	Energy rate (kW)	Exergy rate (kW)
0	water	278.15	100			
0	refrigerant	278.15	100			
1	refrigerant	282.09	400	0.142	11.56	27.60
2	refrigerant	282.09	400	0.142	27.78	27.83
3	refrigerant	373.15	1400	0.142	38.81	33.01
4	refrigerant	347.15	1400	0.142	14.91	15.99
5	water	363.15	100	0.29	54.546	3.349
6	water	343.15	100	0.29	78.870	7.547
7	water	343.16	100	0.29	78.970	8.020
8	water	313.65	100	0.87	129.35	7.620
9	water	313.75	100	0.87	129.71	7.670
10	water	308.15	100	0.87	109.32	5.500

Table 2. Calculated values for heat pump system in terms of energy

Component	Energy input (kW)	Energy output (kW)	Energy loss (kW)	η	ϕ	Θ	EIP (kW)
Circ. pump 1	0.680	0.360	0.320	0.530	0.010	0.008	0.150
Circ. pump 2	0.142	0.100	0.042	0.700	0.001	0.001	0.012
Compressor	30.000	23.900	6.100	0.800	0.200	0.162	1.220
Condenser	137.300	136.670	0.630	0.990	0.021	0.016	0.006
Evaporator	118.070	117.900	0.170	0.990	0.006	0.004	0.002
Expansion valve	14.860	8.920	5.940	0.600	0.200	0.158	2.376
Radiator	78.870	54.546	24.324	0.691	0.801	0.548	7.516
All system	379.922	342.396	37.542	0.901	1.251	1.000	3.491

Table 3. Calculated values for heat pump system in terms of exergy

Component	Exergy input (kW)	Exergy output (kW)	Exergy destruction (kW)	ψ	α	β	ExIP (kW)
Circ. pump 1	0.680	0.050	0.630	0.080	0.021	0.028	0.630
Circ. pump 2	0.142	0.030	0.112	0.210	0.004	0.005	0.112
Compressor	30.000	17.020	12.980	0.570	0.432	0.571	12.980
Condenser	15.480	15.050	0.430	0.970	0.014	0.019	0.430
Evaporator	7.520	5.890	1.630	0.780	0.054	0.072	1.630
Expansion valve	1.870	0.120	1.750	0.070	0.058	0.077	1.750
Radiator	7.547	3.349	4.198	0.443	0.173	0.228	2.338
All system	63.262	41.509	21.73	0.670	0.752	1.000	7.448

Table 4. Natural gas system pressure. temperature. energy rate and exergy rate

Point	Fluid	Temperature (K)	Pressure (kPa)	Mass flow (kg / s)	Energy rate (kW)	Exergy rate (kW)
0	water	278.15	100			
1	water	343.16	100	0.29	78.97	8.02
2	water	363.15	300	0.29	103.21	13.18
3	water	363.15	100	0.29	103.21	13.18
4	water	343.15	100	0.29	78.87	7.99
Fuel	Natural gas	-	300	0.00065	28.630	29.97

Table 5. Calculated values for natural gas system in terms of energy

Component	**Energy input (kW)**	**Energy output (kW)**	**Energy loss (kW)**	**η**	**ϕ**	**Θ**	**EIP (kW)**
Circ. pump	0.14	0.1	0.04	0.7	0.002	0.002	0.012
Exp. valve	103.21	103.21	0	-	-	-	-
Nat. gas boiler	28.63	24.34	4.29	0.85	0.001	0.001	0.001
Radiator	78.870	54.546	24.324	0.691	0.801	0.548	7.516
All system	210.71	192.196	15.554	0.912	0.543	1.000	1.369

Table 6. Calculated values for natural gas system in terms of exergy

Component	**Exergy input (kW)**	**Exergy output (kW)**	**Exergy destruction (kW)**	**ψ**	**α**	**β**	**ExIP (kW)**
Circ. pump	0.140	0.030	0.110	0.210	0.004	0.004	0.087
Exp. valve	13.180	13.180	0.000	-	-	-	-
Nat. gas boiler	29.97	5.160	24.810	0.172	0.797	0.797	20.543
Radiator	7.547	3.349	4.198	0.443	0.173	0.228	2.338
All system	50.837	21.719	29.118	0.427	0.974	1.000	16.678

3.2. Result of Environmental Aspects

Natural Gas system release 4.64 kg/h CO_2 to air, while heat pump system doesn't release CO_2 emissions to the environment.

4. Conclusions

Considering energy need and environmental troubles, importance of saving large amount energy used heating in the world can be better understood. In this study, natural gas heat and pump systems compared with in terms of energy, exergy and environmental aspects. Some important results obtained are as follows; Heat pump COP value is 4.5, ie 4.5 unit heat energy corresponds to a unit to electrical energy can be obtained. According to energy analysis the energy consuming of natural gas system are 5.46 times more than heat pump system. Heating a building with heat pump is environmentally friendly. Because, using natural gas system causes releasing 4.64 kg/h CO_2 to air, on the contrary, in case heat pump using there is no emission to environment. According to exergy analysis the total exergy destruction of natural gas system are 3.82 times more than total exergy destruction of heat pump system, exergy efficiency heat pump system is 0.67, while 0.47 for the natural gas system. Energy development potential is 3.491 kW for the heat pump system, while 3.522 kW for the natural

gas system and the exergy development potential of the heat pump system is 7.448 kW, while 16.049 kW for the natural gas system.

According to the results seen above, energy, exergy and environmental assessments seems to be more suitable for the use of heat pump system. In addition, a review of the whole system in detail what is the weak and strong aspects of the system clearly seems possible. On this basis, these criteria should be considered when designing systems. Finally, it can be said geothermal source heat pump is suitable for places has rich geothermal resources such as Eskisehir.

References

[1] DPT. Sekizinci bes yıllık kalkınma planı DPT 2609 – ODK 620 (in Turkish) . Madencilik ozel ihtisas komisyonu raporu enerji hammaddeleri alt komisyon jeotermal calısma grubu Ankara. Turkey. 2001

[2] Jeotermal Enerji Derneği. http://www. jeotermaldernegi.org.tr.

[3] Hepbasli A.. Balta Tolga M. A study on modeling and performance assessment of a heat pump system for utilizing low temperature geothermal resources in buildings. Building and environment 42. 2006. pp. 3747-3756

[4] Demirkazıksoy M.A. Eskisehir civarı Jeotermal enerji potansiyeli kullanımı ve gelistirilmesi. A Thesis Submitted to The Graduate School of Natural and Applied of Anadolu University Eskisehir. Turkey; 2004.

[5] Balli O. Aras H. Hepbasli A. Thermodynamic and thermoeconomic analyses of a trigeneration (TRIGEN) system with a gas–diesel engine: Part I – Methodology. Energy Conservation and Management 51. 2010. pp. 2252- 2259.

[6] Moran MJ. Shapiro HN. Fundamentals of Engineering Thermodynamics. Wiley. 5th edition. 2006. pp. 121-315.

[7] Balli O. Aras H. Energetic and exergetic performance evaluation of a combined heat and power system with the micro gas turbine (MGTCHP). International Journal of Energy Research; 37. 2007. pp. 1425-1440.

[8] Balli O. Aras H. Hepbasli A. Energetic analysis of a combined heat and power system (CHP) in Turkey. Energy Exploration and Exploitation 25. 2007. pp. 139- 162

[9] Moran MJ. Sciubba E. Exergy analysis: principles and practice. Journal of Engineering Gas Turbines Power 116. 1994. pp. 285-290.

[10] Moran MJ. Availability analysis: a guide to efficient energy use. ASME press. 1st edition. 1989. pp. 146-180.

[11] Sisman N. Kahya E. Aras N. Aras H. Determination of optimum insulation thicknesses of the external walls and roof (ceiling) for Turkey's different degree-day regions. Energy Policy, 35 (10) 5151-5155, 2007

Optimization of a Hybrid Ground Source Heat Pump using the Response Surface Method

Honghee Park[1], Wonuk Kim[1], Joo Seoung Lee[1] and Yongchan Kim[2*]

[1] *Graduate School of Division of Mechanical Engineering, Korea University, Anam-Dong, Sungbuk-Gu, Seoul, 136-713, Korea*
[2] *School of Mechanical Engineering, Korea University, Anam-Dong, Sungbuk-Gu, Seoul, 136-713, Korea*
** Corresponding author. Tel.: +82 2 3290 3366, Fax: +82 2 921 5439, E-mail: yongckim@korea.ac.kr*

Abstract: A hybrid ground source heat pump (HGSHP) has been recommended as a low cost alternative of a ground source heat pump (GSHP) which has higher initial costs with increasing the size of ground heat exchanger (GHX) for imbalanced load conditions. HGSHP systems incorporate both GHX and supplemental equipments, such as cooling towers and/or boilers. The main issues of HGSHP are the optimal size design and control strategies of supplemental equipments. The objective of this paper is to optimize the size and control strategies using an optimization methodology called as the response surface method (RSM) to decrease the system's total initial cost (IC) and/or life cycle cost (LCC) and/or annual energy use (AEU) of HGSHP systems. The simulation data used in this research was originated from Yavutzurk et al. and integrated with the RSM. Commercial software, which is Minitab 15, has been adopted to draw contour plots, surface plots and overlaid contour. With using response optimizer, the optimal size design and control strategies of supplemental equipments were determined individually and the results were compared with the results of Yavutzurk et al. The optimal size and control strategies have been successfully determined using the optimization tool of the RSM.

Keywords: *Hybrid ground source heat pump, Supplemental equipment, Optimization, Response Surface Method*

Nomenclature

EFT	*entering fluid temperature.....K*	*IC*	*initial cost.....$*
ExFT	*exiting fluid temperature .....K*	*LCC*	*life cycle cost .....$*
GHXL	*ground heat exchanger length.....ft(m)*	*PV*	*present value cost.....$*

1. Introduction

The remarkable advantage of a ground source heat pump (GSHP) is its energy saving potential. The GSHP can save up to 50% of the energy that would be used by conventional systems [1]. The prominent disadvantage of GSHP is higher initial costs which make short-term economics unattractive, although long-term economics is attractive because of lower operating costs caused by higher system performance. Furthermore, for imbalanced load conditions, it is inevitable to increase the size of ground heat exchanger (GHX) or the distance between adjacent GHX boreholes to postpone heat buildup caused by the difference between cooling and heating. A hybrid ground source heat pump (HGSHP) has been recommended as a low cost alternative of GSHP, which can reduce GHX size and give more efficient operation. The HGSHP can effectively balance the ground thermal loads by incorporating supplemental equipments, such as cooling towers and/or boilers into the GSHP system. The design and operation of HGSHP are more complex than GSHP. Fig. 1 shows the schematic diagram of HGSHP system comprising serial and parallel arrangement of GHX and supplement equipment such as cooling tower and/or boiler. In this paper, the comparison between serial and parallel arrangement would not be conducted.

ASHRAE [2] sizes the supplemental heat rejecter capacity based on the difference between monthly average heating and cooling loads of the building rather than the peak loads. General

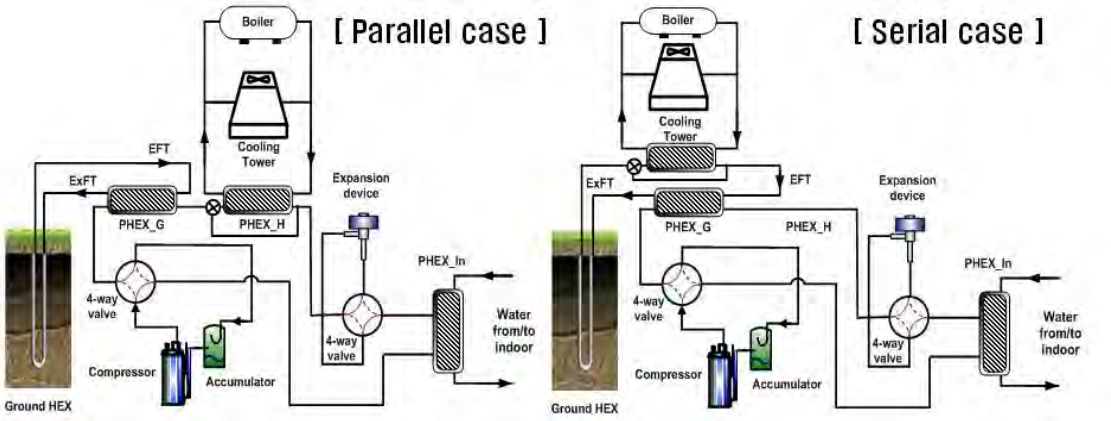

Fig. 1. Schematic diagram of hybrid ground source heat pump system.

guidelines for the integration of the heat rejecter into the system piping were presented. Kavanaugh and Rafferty [3] discuss HGSHP systems within the framework of GHX design alternatives. The sizing of the supplemental heat rejecter is based on the peak block load at the design condition. The nominal capacity is calculated based on the difference between the GHX length required for cooling and heating. Kavanaugh [4] revises and extends the existing design procedures as recommended in the above two publications. In addition, a control method is proposed for balancing the cooling and heating loads on the ground heat exchanger to limit long-term temperature rise. The revised procedure is applied to an office building in three climates, and initial cost and operating cost issues are discussed. Yavutzurk and Spitler [5] present a comparative study investigating several control strategies for HGSHP systems. The strategies investigated include set point control (operating the supplemental rejecter whenever the heat pump entering or exiting fluid temperature exceeds a set temperature, differential temperature control (operating the supplemental rejecter whenever the difference between heat pump fluid temperature and ambient air temperature exceeds set value), and operation of the supplemental rejecter to remove heat from the GHX field during nighttime hours. A 20-year life-cycle cost (LCC) analysis is conducted to compare each control strategy. Singh and Foster [6] explored first-cost savings resulting from HGSHP designs in two building-an office building and an elementary school. Ramamoorthy et al. [7] reported on a similar study that used a cooling pond as a supplemental heat rejecter. Using a differential temperature control strategy, a limited optimization of GHX size and pond size was performed. Chiasson and Yavutzurk [8] used the same system simulation approach to identify scenarios where the HGSHP system with a supplemental heat source is beneficial, in particular schools in heating-dominated climates, where the school was not operated during the summer. The supplemental heat sources investigated were solar thermal collectors and the approach was shown to be economically feasible.

Therefore, the main issues of HGSHP are the optimal size design and control strategies of supplemental equipments to minimize total initial cost or life-cycle cost or operating cost with satisfying designed range of entering or exiting fluid temperature to or from heat pump respectively which assures high performance of HGSHP. To size design of supplemental equipment depends on the size of GHX and its operating hours, and it means that smaller supplemental equipment should operate itself for longer hours. To size supplemental equipments and select its control strategies are coupled.

The objective of this paper is to optimize the size and control strategies using an optimization methodology called as the response surface method (RSM) to decrease the system's total

initial cost (IC) and/or life cycle cost (LCC) and/or annual energy use (AEU) of HGSHP systems.

2. Optimization Method

2.1. Control Strategies

The strategies investigated include 3 kinds of control logics. Set point control (Control 1) means that the cooling tower is activated when the heat pump entering or exiting fluid temperature exceeds a set temperature such as 96.5F (35.8C). Differential temperature control (Control 2) means that the supplemental rejecter is operated whenever the difference between heat pump fluid temperature and ambient air temperature exceeds set value such as 3.6F (2.0C) and is turned off when the difference is less than 2.7F (1.5C). Cool storage control (Control 3) means that the cooling tower is operated during nighttime hours to remove heat from the GHX field. For more detailed information, it could be found out in Yavutzurk and Spitler [5].

2.2. Simulated data used

This paper focused on the adoption of RSM as optimization method of HGSHP and so previously published data was used not to verify the building simulation results and to decide whether it is possible to solve this kind of optimization problem with RSM method or not. Used simulation data from TRNSYS simulation were originated from Yavutzurk and Spitler [5] of which building's total area is approximately 14,205 ft^2 (1320 m^2). A 20-year life-cycle cost (LCC) analysis is conducted to compare each control strategy. The detailed information about the annual building loads was skipped. The simulated data is summarized in Table 1.

2.3. RSM method and Objective function

RSM is a kind of optimization methodology determining the range of main factors for optimizing responses and statistical approximation method for coupled design factors problem. Using minitab software, all RSM process can be conducted and several kinds of plots can be drawn. First of all, the definition of design factors and responses should be conducted. In this paper, determined design factors are ground heat exchanger length (GHXL) and control

Table 1. Simulated data used.

Control	GHXL , ft(m)	Total Initial Costs($)	Total Present Value Costs($)	Annual Energy Use(kWh)
1	3000 (914)	26,662	46,075	24,179
	2625 (800)	23,036	40,783	22,200
	2250 (686)	19,505	35,493	19,913
2	3000 (914)	22,427	38,438	19,941
	2625 (800)	19,774	35,254	19,230
	2250 (686)	17,195	32,171	18,563
3	3000 (914)	21,272	41,845	25,623
	2625 (800)	18,175	37,259	23,800
	2250 (686)	15,078	32,672	21,914

Table 2. Coefficients of response surface regression.

Terms	Coefficients		
	Total Initial Costs($)	Total Present Value Costs($)	Annual Energy Use(kWh)
Constant	4417.81	19752.2	17924.8
a (GHXL)	8.40058	12.4643	6.14636
b (CONTROL)	-4061.50	-14267.7	-13042.8
c (GHXL*GHXL)	0.000217625	0.00018660	-2.37487E-04
d (CONTROL*CONTROL)	825.103	3742.74	3714.60
e (GHXL*CONTROL)	0.642000	-0.939333	-0.371333

strategies with which supplemental equipment such as cooling tower is operated, and selected responses are the size of supplemental equipment, total initial costs, total present value costs and annual energy use. The objective function was defined as minimization of total initial costs and/or total present value costs and/or annual energy use. After analyzing design of experiment, response surface analysis was conducted and several kinds of plots such as contour plots, surface plots and overlain plots for multiple responses were drawn as well as response surface regression. Finally, the optimized values of GHXL and Control strategy were obtained to satisfy the objective function.

3. Results and Discussions

3.1. Response surface regression

Response surface regression was conducted using software of Minitab 15 as shown in Eq. 1. The regression curves were deducted in terms of 'GHXL' and 'CONTROL' comprising second order terms such as 'GHXL*GHXL' and 'CONTROL* CONTROL' and interaction term of 'GHXL* CONTROL' for the responses (Y) such as total initial cost, total present value costs and annual energy use. The regression coefficients are listed in Table 2. The calculated R-Square values of total initial costs, total present value costs and annual energy use are 99.28%, 97.61%, 96.51% respectively.

$$\begin{aligned} Y = \text{Constant} + a\times(\text{GHXL}) + b\times(\text{Control}) + c\times(\text{GHXL}\times\text{GHXL}) \\ + d\times(\text{Control}\times\text{Control}) + e\times(\text{GHXL}\times\text{Control}) \end{aligned} \quad (1)$$

3.2. Surface plots and Contour plots

As it is shown in Fig. 2, Surface plots and Contour plots for 3 responses were drawn. Contour plot is two dimensional and Surface plot is three dimensional. With these plots, optimization direction could be obtained. To decrease total initial costs, total present value costs and annual energy use, GHXL size should be decreased which means increasing cooling tower size in all cases. As for the control strategies, in the case of total initial costs, control strategy should approach Control 3 which means cool storage control to minimize total initial costs, and in the case of total present value costs, control strategy should come close to the middle point between Control 2 which means differential control and Control 2.5 which means the mixed control of 50% Control 2 and 50% Control 3 for minimizing total present value costs. As we can see, the control strategy for annual energy use should approach Control 1.8 to minimize annual energy use.

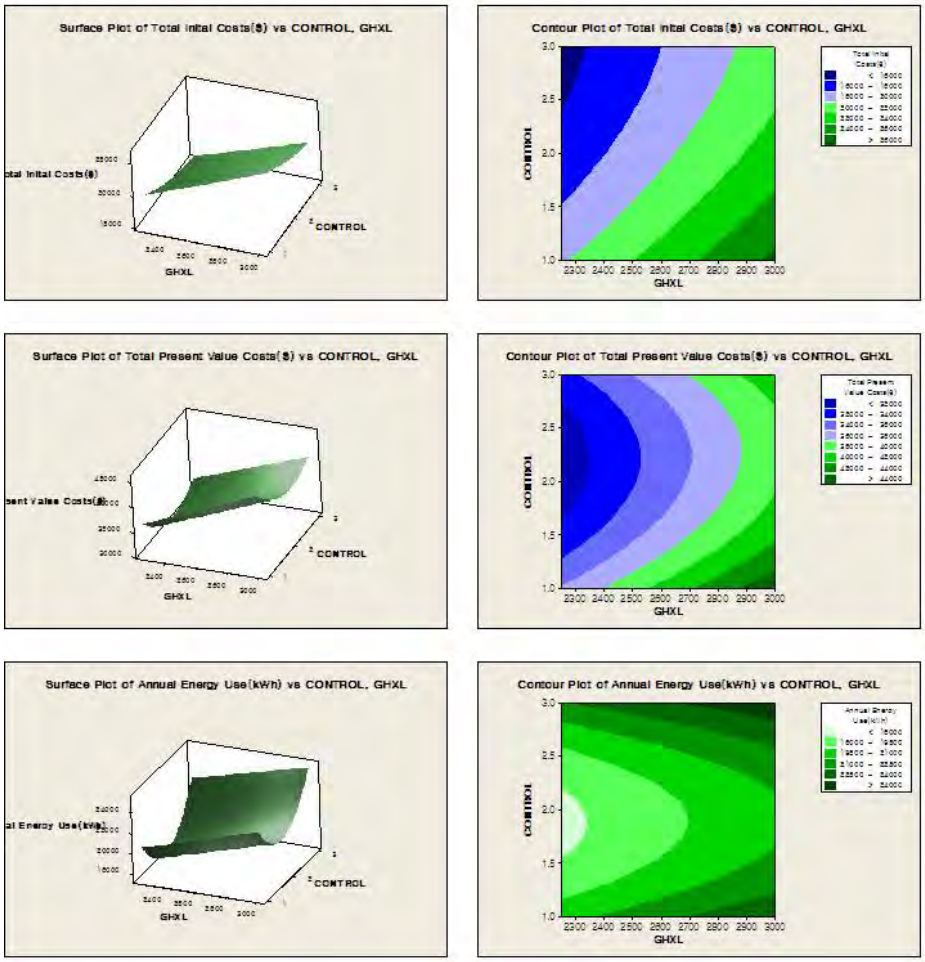

Fig. 2. Surface plots and Contour plots for 3 responses.

3.3. Overlaid contour

To draw overlaid contour, the ranges of 3 responses were determined as it is in Fig. 3 such as 15,000~18,000 ($) for total initial costs and 32,000~35,500 ($) for total present value costs and 18,500~19,900 (kWh) for annual energy use.

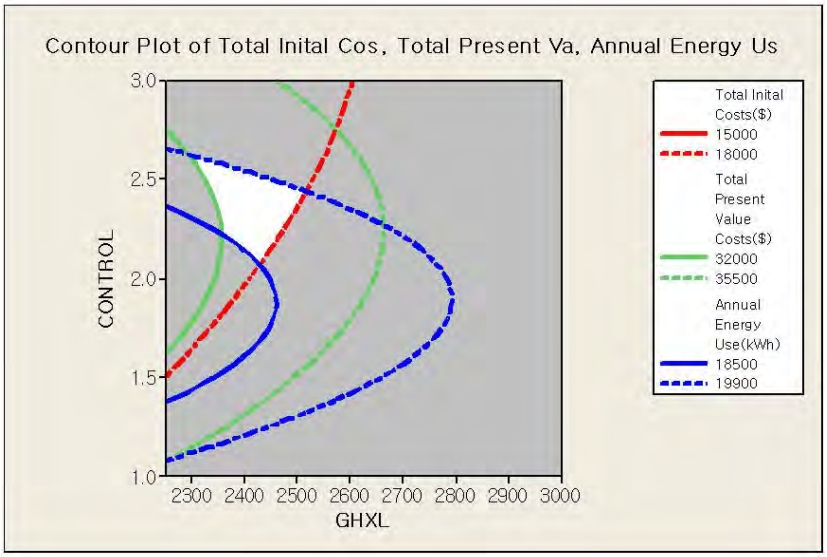

Fig. 3. Overlaid contour for 3 responses.

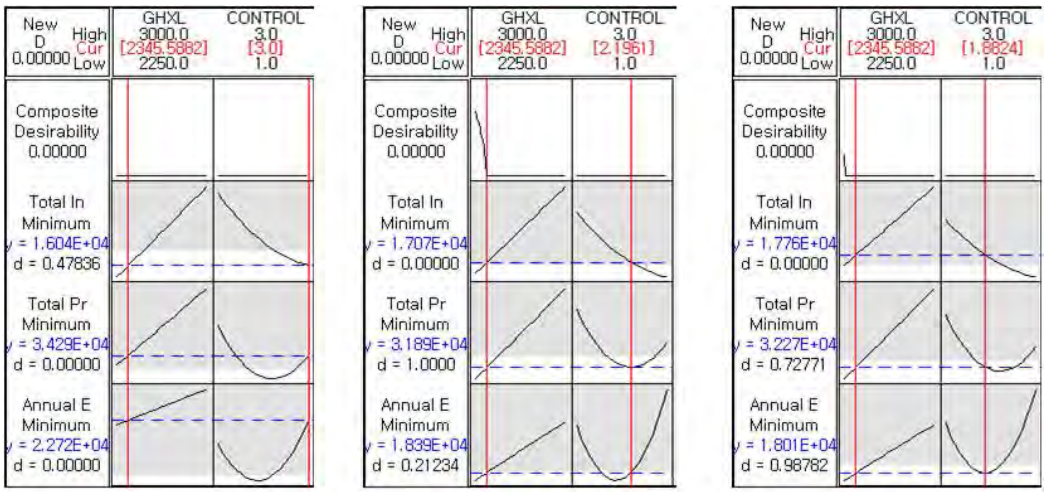

Fig. 4. The result of response optimizer for minimizing 3 responses

In Fig. 3, the bright region enclosed 3 pair of curves satisfies 3 conditions given and it means that the optimal values of factors and responses are within the bright region. For the purpose of determining optimum value of GHXL and Control to minimize individually each response, the response optimizer should be conducted.

3.4. Results from Response optimizer

In Fig. 4 the left figure presenting response optimizer result is for total initial costs and optimum value of GHXL and Control strategy are 2,345 ft (715 m), 3.0 respectively and minimum total initial cost is 16,040 $. The middle figure is for total present value costs and optimum value of GHXL and Control strategy are 2,345 ft (715 m), 2.2 respectively and minimum total present value cost is 31,890 $. The right figure is for annual energy use and optimum value of GHXL and Control strategy are 2,345 ft (715 m), 1.9 respectively and minimum annual energy use is 18,010 (kWh). The individual desirability and composite desirability were checked. These results are listed in Table 3 and compared with the previous results from Yavutzurk and Spitler [5]. With RSM, 17% decrease of total present value costs and 10% of annual energy use compared with Yavutzurk and Spitler [5] were obtained, though there was 7% increase of total initial costs.

4. Conclusions

The objective of this paper was to optimize the size and control strategies using an optimization methodology called as the response surface method (RSM) to decrease the system's total initial cost and/or life cycle cost and/or annual energy use of HGSHP systems.

Table 3. Results Comparison between RSM and Yavutzurk and Spitler [5].

Terms	RSM	Yavutzurk and Spitler [5]	Difference (±%)
Total Initial Costs ($)	16,140 ($)	15,078 ($)	+1,062 (+7%)
Total Present Value Costs ($)	31,890 ($)	38,438 ($)	-6,548 (-17%)
Annual Energy Use (kWh)	18,010 (kWh)	19,941 (kWh)	-1,931 (-10%)

In this paper, determined design factors were ground heat exchanger length (GHXL) and control strategies with which supplemental equipment such as cooling tower is operated, and selected responses were the size of supplemental equipment, total initial costs, total present value costs and annual energy use. The objective function was defined as minimization of total initial costs and/or total present value costs and/or annual energy use. Using minitab software, all RSM process was conducted and response surface regression and several kinds of plots such as surface plots, contour plots and overlaid contour were drawn.

With RSM, 17% decrease of total present value costs and 10% of annual energy use compared with Yavutzurk and Spitler [5] were obtained, though there was 7% increase of total initial costs. The optimal size and control strategies have been successfully determined using the optimization tool of the RSM.

Acknowledgement

This research was sponsored by the Korea Institute of Energy and Resources Technology Evaluation and Planning (Grant No. 2008NBLHME0900002008).

References

[1] United States Department of Energy, Energy Efficiency and Renewable Energy homepage, September 2007, http://www1.eere.energy.gov/geothermal/history.html.

[2] ASHRAE, Commercial/institutional ground-source heat pumps engineering manual, Atlanta: American Society of Heating, Refrigerating and Air-Conditioning Engineers, Inc., 1995.

[3] S.P. Kavanaugh and K. Rafferty, Ground-source heat pumps: Design of geothermal systems for commercial and institutional buildings, Atlanta: American Society of Heating, Refrigerating and Air-Conditioning Engineers, Inc., 1997.

[4] S.P. Kavanaugh, A design method for hybrid ground source heat pumps, ASHRAE Transactions 104 (2), 1998, pp. 691-698.

[5] C. Yavuzturk and J.D. Spitler, Comparative Study to Investigate Operating and control Strategies for Hybrid Ground Source Heat Pump Systems Using a Short Time-step Simulation Model, ASHRAE Transactions 106(2), 2000, pp.192-209.

[6] J.B. Singh and G. Foster, Advantages of Using the Hybrid Geothermal Option, The Second Stockholm International Geothermal Conference, The Richard Stockton College of New Jersey, 1998.

[7] M. Ramamoorthy et al., Optimal Sizing of Hybrid Ground- Source Heat Pump Systems that use a Cooling Pond as a Supplemental Heat Rejecter – A System Simulation Approach, ASHRAE Transactions 107(1), 2001, pp. 26-38.

[8] A.D. Chiasson and C. Yavuzturk, Assessment of the Viability of Hybrid Geothermal Heat Pump Systems with Solar Thermal Collectors, ASHRAE Transactions 109(2), 2003, pp. 487-500.

Experimental ground source heat pump system to investigate heat transfer in soil

Hakan Demir*, Ş. Özgür Atayılmaz, Özden Ağra

Yıldız Technical University, Istanbul, Turkey
** Corresponding author. Tel: +90 212 383 28 20, Fax: +90 212 261 66 59, E-mail: hdemir@yildiz.edu.tr*

Abstract: The earth is an energy resource which has more suitable and stable temperatures than air. Typical values for Coefficient of Performance (COP) of Ground Source Heat Pumps (GSHPs) are up to 8 while it is 4 of air source heat pumps. GSHPs were developed to use ground energy for residential heating. The most important part of a GSHP is the Ground Heat Exchanger (GHE) that consists of pipes buried in the soil and is used for transferring heat between the soil and the heat exchanger of the GSHP. Soil composition, density, moisture and burial depth of pipes affect the size of a GHE. Design of GSHP systems in different regions of US and Europe is performed using data from an experimental model. However, there are many more techniques including some complex calculations for sizing GHEs. An experimental study was carried out to investigate heat transfer in soil. Measured fluid inlet temperatures were used in the numerical simulation and the fluid outlet temperatures were calculated. A parametrical study was conducted to investigate effects of soil thermal properties and geometrical parameters on heat transfer from ground heat exchanger. It is seen that the soil thermal conductivity has great importance on heat transfer. Also, burial depth and distance between pipes are other parameters to be considered for sizing GHEs.

Keywords: *Ground source heat pump, Parallel pipe horizontal ground heat exchanger, Numerical solution*

1. Introduction

The GHE is an important part of GSHP systems and its dimensions and burial depth should be calculated with an effective method. Particularly, the cost of assembly of GHE affects the choice of these systems. In the literature, there are two kinds of analytical approaches: Kelvin Line Source Theory and Cylindrical Source Theory. In addition, there are many studies using two or three dimensional steady state and time dependent numerical techniques [1-7], [8-11, 12]. Kelvin Line Source and Cylindrical Source theories find only symmetrical soil temperature distributions around the pipe. Metz [7] has been suggested an analytical model to find temperature distribution in the soil by dividing ground into blocks around the coil and done some modifications to Line Source theory. Mei [6] has been included the effects of seasonal ground temperature variation, pipe material, circulating liquid properties and compared his work with modified line source and simple line source models. A simplification of boundary conditions to solve equations analytically causes some error on results especially shorter simulation times. Analytical models do not consider the temperature change of soil by depth and the surface effects such as radiation, convection and surface cover. The effects of the convection on the ground surface were included in some of the models [1, 2]. A more complicated model for heat transfer of buried pipes was performed by Negiz, Hastaoglu and Heidemann for petrol transferring pipes [4, 9, 10]. Piechowsky was included mass transfer in his model to take into account the effects of the soil moisture [11, 13]. In this study, a numerical model was suggested with realistic boundary conditions. In order to validate the new model a big scale experimental set area was built.

2. Experimental study

A GSHP having 4 kW heating and 2.7 kW cooling capacity is used for experimental study. The ground heat exchanger consists of three parallel pipes which have 40 m length and ½" diameter buried in soil at 1.8 m depth. The distance between the parallel pipes is 3 m. Experimental GSHP system is installed at Yıldız Technical University Davupaşa Campus on

800 m^2 surface area with no special surface cover. Temperature data were collected using T-type thermocouples buried in soil horizontally and vertically at various distances from the pipe center and at the inlet and outlet of the ground heat exchanger. All the thermocouples are connected to a 64 c hannel PLC system capable of saving data of hourly temperature measurements for 8 days. Figure 1 and 2 represents the experimental setup.

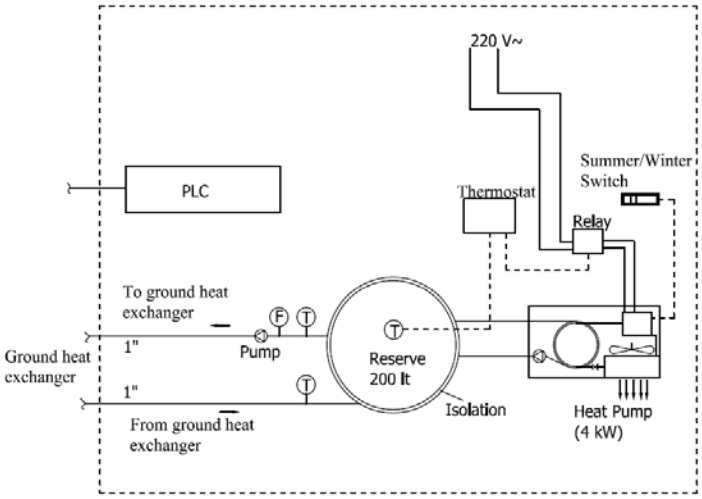

Figure 1 Experimental setup (heat pump and measuring system) [14]

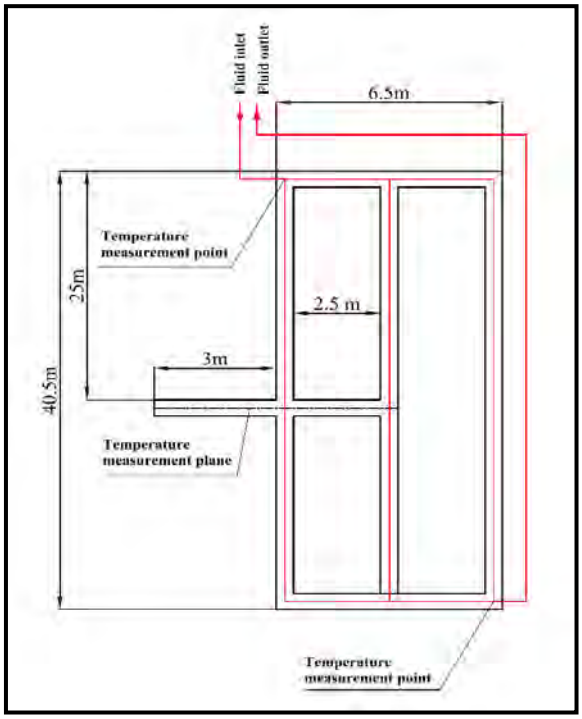

Figure 2 Experimental setup (ground heat exchanger and thermocouple locations) [14]

3. Numerical study

Aiming to find three dimensional temperature distributions in the soil, a new model with realistic boundary conditions was suggested. Heat transfer in the soil is time dependent three dimensional heat conduction. Temperature gradient along the pipe axis is so small that it can be neglected and the heat conduction equation can be solved using dynamical boundary conditions in two-dimensional geometry. The solution domain and boundary conditions was prepared as in Figure 3.

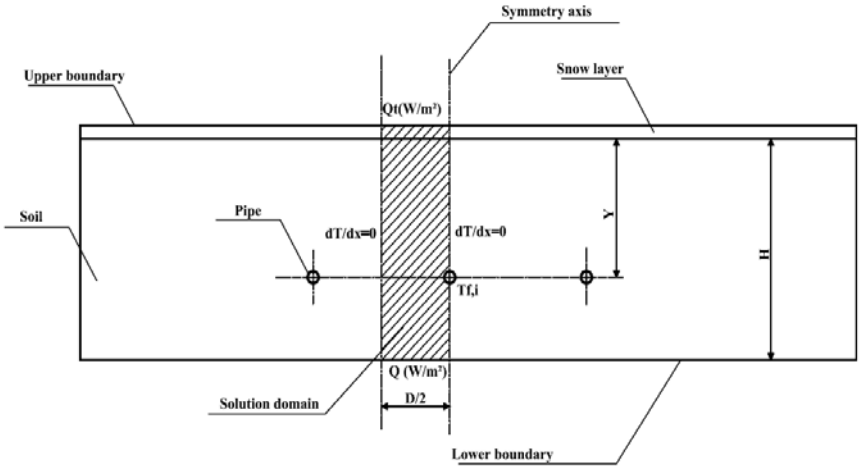

Figure 3 Parallel pipe horizontal GHE and solution area in the soil [14]

The model consists of parallel pipes buried at the depth of Y. Distance between pipes is D. Region shown in Figure 4 is taken as solution domain. This is two dimensional and presented in Cartesian coordinate system.

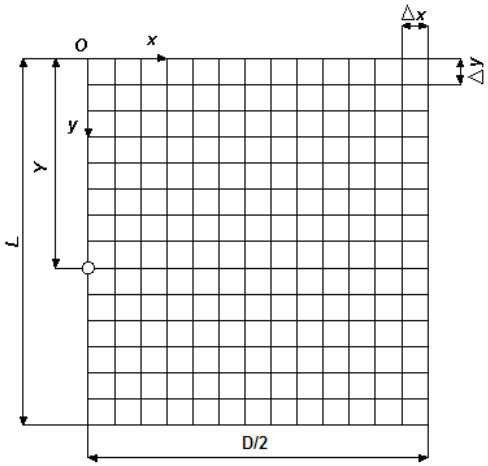

Figure 4 Computational solution domain [14]

Two-dimensional time dependent heat conduction and boundary conditions of problem are of the form;

$$\frac{\partial^2 T}{\partial x^2} + \frac{\partial^2 T}{\partial y^2} = \frac{1}{\alpha}\frac{\partial T}{\partial t} \tag{1}$$

$$T_i = T(x,t) \quad @t = 0 \tag{2}$$

$$\left.\frac{\partial T}{\partial x}\right|_{x=D/2} = 0 \tag{3}$$

$$\left.\frac{\partial T}{\partial x}\right|_{x=0} = 0 \tag{4}$$

$$Q(W/m^2) \quad @y = L \tag{5}$$

$$Q_t(W/m^2) \quad @y = 0 \tag{6}$$

$$T_{f,i} = C \tag{7}$$

Where Q_t is total heat transfer rate at the surface and $T_{f,i}$ is the fluid inlet temperature. Because of the complexity of the boundary conditions, the heat conduction equation has been solved numerically using Alternating Direction Implicit (ADI) Finite Difference formulation. ADI method is stable for every time step and grid size and the resulting matrix system is tri-diagonal. Tri-diagonal matrix systems can be solved easily using the Thomas algorithm. For this purpose, software was developed in MATLAB environment and the effects of solution parameters on the results were investigated. Details of the numerical model and solution procedure can be found in Demir et.al. [14]. The simulation results were acceptable when a mesh size of 0.1 m in x and y directions, 1 m in z direction and 1800 s as time step were used. Parameters from experimental study used in numerical simulation as below:

- Start date 13th December
- Volumetric flow rate, $V_f = 0.42768$ m^3/h
- Soil thermal conductivity, $k_s = 2.18$ W/m K
- Soil thermal diffusivity, $\alpha_s = 0.00000068$ m^2/s
- Pipe outer/inner diameter, $d_o/d_i = 20/14.6$ mm
- Pipe thermal conductivity, $k_p = 0.8999$ W/m K
- Length of parallel pipes, L = 40 m
- Distance between pipes, D = 3 m
- Burial depth, Y = 1.8 m
- Working fluid is water
- Pipe material = PPRC
- Number of parallel pipes, n = 3

4. Results

The experimental fluid inlet/outlet and theoretical fluid outlet temperatures are shown in Figure 5. It is seen that the experimental and numerical results are in good agreement.

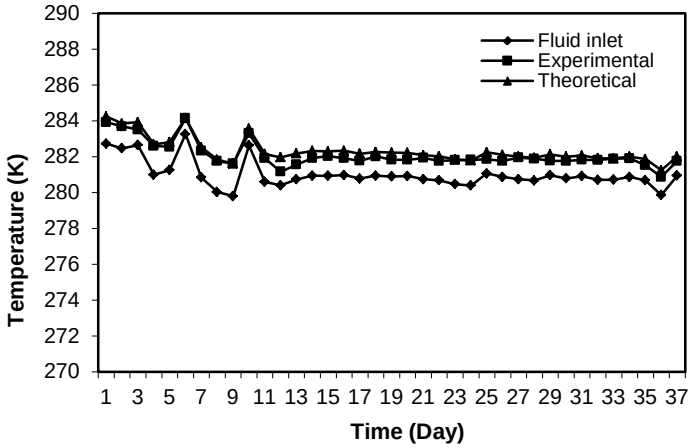

Figure 5 Experimental fluid inlet and experimental/theoretical fluid outlet temperatures [14]

The effects of the parameters, soil thermal conductivity, burial depth and distance between pipes were investigated numerically. Figure 6 and 7 s how the effects of soil thermal conductivity on fluid outlet temperature and horizontal temperature distribution in soil. Fluid outlet temperature increases with increasing thermal conductivity while has no e ffect on horizontal temperature distribution after 250 h of simulation time.

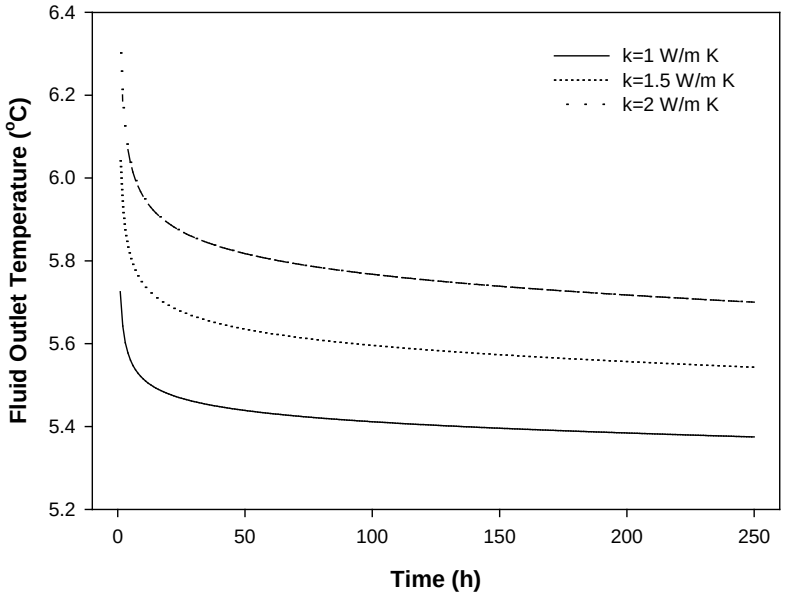

Figure 6 Effects of the soil thermal conductivity on fluid outlet temperature

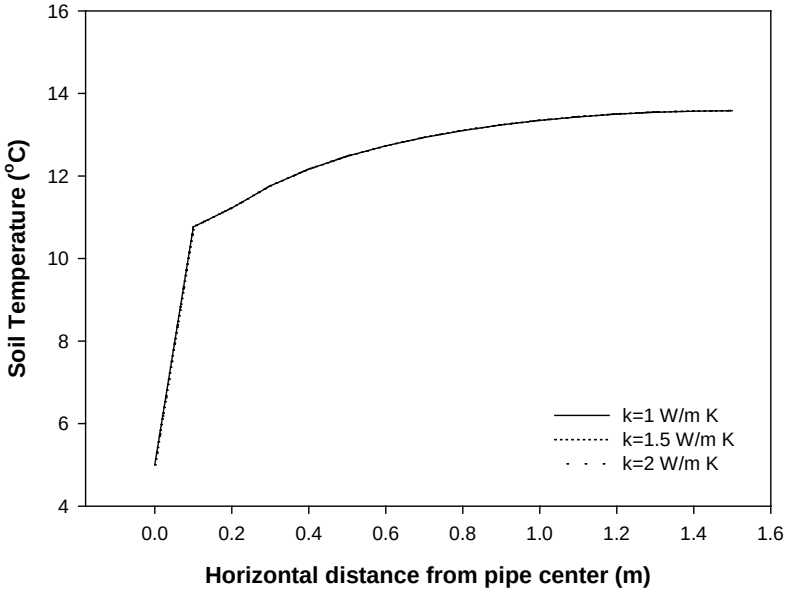

Figure 7 Effects of the soil thermal conductivity on horizontal temperature distribution in soil

In Figure 8 and 9, the effects of the distance between pipes on fluid outlet temperature and horizontal temperature distribution in soil are presented. Fluid outlet temperature increases with increasing distance. Also, it is seen from Figure 9 that increasing the distance between pipes affects the unaffected soil region and heat transfer characteristics. Smaller distances cause decrease of the temperature of the soil in the vicinity of the pipes and reduces heat transfer rate.

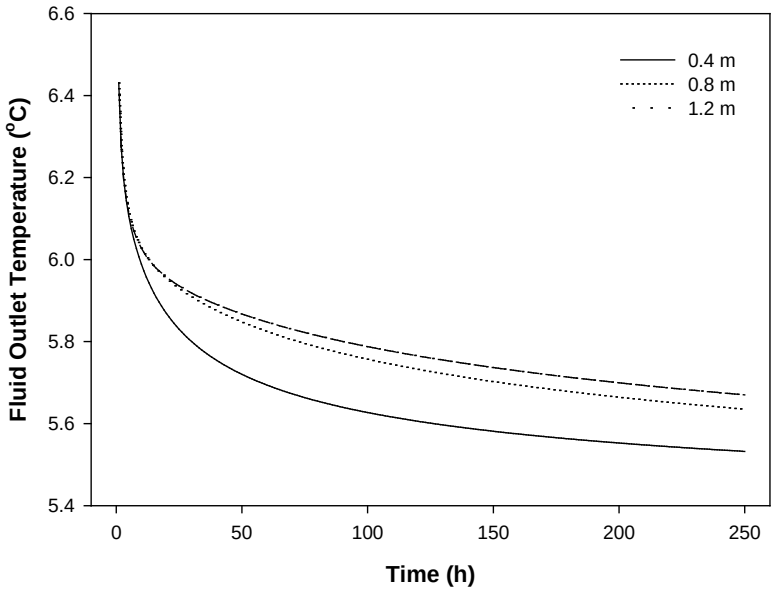

Figure 8 Effects of the distance between pipes on fluid outlet temperature

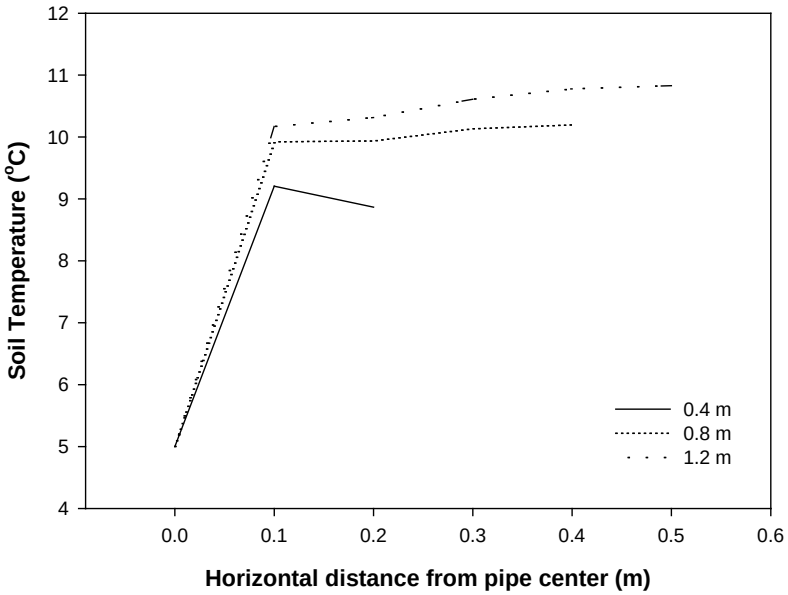

Figure 9 Effects of the distance between pipes on horizontal temperature distribution in soil

In Figure 10 and 11, the effects of the burial depth on fluid outlet temperature and horizontal temperature distribution in soil are shown. Fluid outlet temperature increases with increasing burial depth. It is easily seen the effects of surface temperature variations on the fluid outlet temperature for the burial depth of 0.5 m. Therefore, it is recommended that the minimum burial depth must be 1 m for horizontal ground heat exchangers. Also, increasing the burial depth increases the fluid outlet temperature as the temperature of the soil increase with depth.

5. Conclusions

In this study, the numerical model including all weather conditions was suggested and verified with the experimental study. The most important advantage of the model is implementation of meteorological data to numerical model. It is seen that the maximum deviation between calculated and experimental fluid outlet temperatures is 10.5%. It is

possible to simulate whole year operation of ground heat exchanger providing the meteorological data.

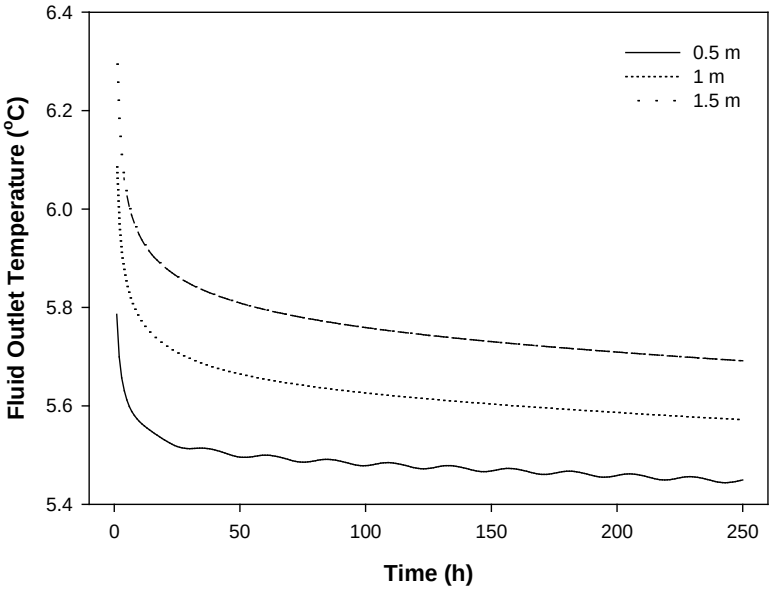

Figure 10 Effects of the burial depth pipes on fluid outlet temperature

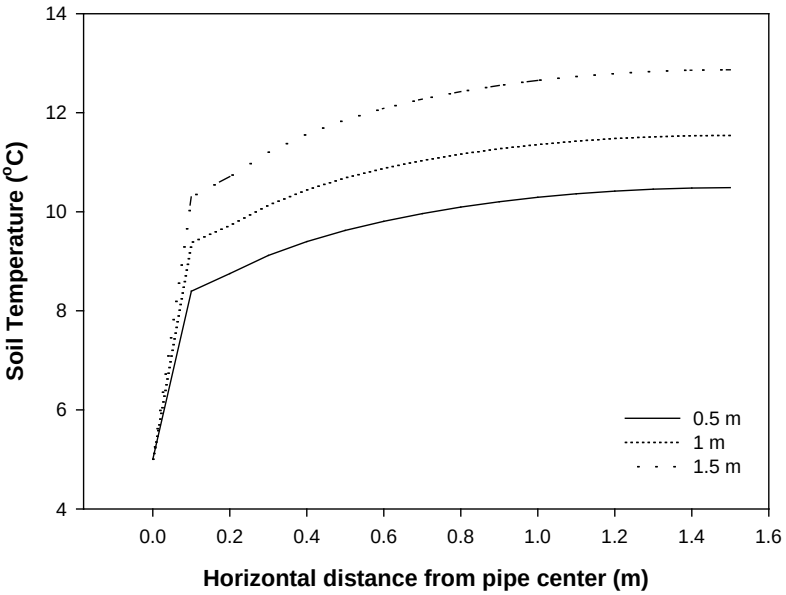

Figure 11 Effects of the burial depth pipes on horizontal temperature distribution in soil

After validating the numerical model, a parametrical study was conducted to investigate effects of the geometrical parameters and soil properties. It is determined that the fluid outlet temperature is strongly depends on soil thermal conductivity. The heat transfer characteristics of the soil in the vicinity of the pipes can be improved by using backfill material. Other important parameters are burial depth and distance between the pipes. Pipes should be buried in the soil below 1 m from the free surface in order to eliminate surface effects such as temperature variation, radiation, snow and rainfall. Also, the distance between pipes should not less than 0.8 m considering the required surface area.

To improve the accuracy of the model neural network approach may be used for modeling soil, air temperature and solar radiation. Also, moisture transfer and variation of soil thermal conductivity with soil moisture content and temperature can be modeled for further studies.

References

[1] B. Bohm, On transient heat losses from buried district heating pipes, Int. Journal of Energy Research 24 (2000), pp. 1311-1334

[2] M. Chung, P.S. Jung, R.H. Rangel, Semi-analytical solution for heat transfer from a buried pipe with convection on t he exposed surface, Int. Journal of Heat and Mass Transfer 42 (1999), pp. 3771-3786

[3] Y. Gu, D.L. O'Neal, An analytical solution to transient heat conduction in a composite region with a cylindrical heat source, Transactions of the ASME 117 (1995), pp. 242-248

[4] M.A. Hastaoglu, A. Negiz, R.A. Heidemann, Three-dimensional transient heat transfer from a buried pipe – part III comprehensive model, Chemical Engineering Science 50 (1995), pp. 2545-2555

[5] T.K. Lei, Development of a computational model for a ground-coupled heat exchanger, ASHRAE Transactions: Research 99 (1993), pp. 149-159

[6] V.C. Mei, Heat transfer of buried pipe for heat pump application, Journal of Solar Energy Engineering 113 (1991), pp. 51-55

[7] P.D. Metz, A Simple computer program to model three-dimensional underground heat flow with realistic boundary conditions, Transactions of the ASME 105 (1983)), pp. 42-49

[8] S. Mukerji, K.A. Tagavi, W.E. Murphy, Steady-state heat transfer analysis of arbitrary coiled buried pipes, Journal of Thermophysics and Heat Transfer 11 (1997), pp. 182-188

[9] A. Negiz, M.A. Hastaoglu, R.A. Heidemann, Three-dimensional heat transfer from a buried pipe – I. laminar flow, Chemical Eng. Science 48 (1993), pp. 3507-3517

[10] A. Negiz, M.A. Hastaoglu, R.A. Heidemann, Three-dimensional transient heat transfer from a buried pipe: solidification of a stationary fluid, Numerical Heat Transfer 28 (1995), pp. 175-193

[11] M. Piechowsky, Heat and mass transfer of a ground heat exchanger: theoretical development, Int. Journal of Energy Research 23 (1999), pp. 571-588

[12] A.D. Chiasson, Advances in Modeling of ground source heat pump systems, MSc Thesis, Oklahoma State University, 1999

[13] M. Piechowski, A ground coupled heat pump system with energy storage, PhD Thesis, The University of Melbourne, 1996

[14] H. Demir, A. Koyun, G. Temir, "Heat Transfer of Horizontal Parallel Pipe Ground Heat Exchanger and Experimental Verification", Applied Thermal Engineering 29 (2009), pp. 224-233

Influence of Undisturbed Ground Temperature and Geothermal Gradient on the Sizing of Borehole Heat Exchangers

Tomislav Kurevija[1,*], Domagoj Vulin[1], Vedrana Krapec[1]

[1] *Faculty of Mining, Geology and Petroleum Engineering, University of Zagreb, Zagreb, Croatia*
** Corresponding author. Tel: +385 1 5535843, Fax: +385 1 4836074, E-mail: tkurevi@rgn.hr*

Abstract: Undisturbed ground temperature is one of the most crucial thermogeological parameters needed for shallow geothermal resources assessment. Energy considered to be geothermal is energy stored in the ground at depths where solar radiation has no effect. At depth where undisturbed ground temperature occurs there is no influence of seasonal variations in air temperature from surface. Exact temperature value, and depth where it occurs, is functionally dependent on surface climate parameters and thermogeologic properties of ground. After abovementioned depth, increase of ground temperature is solely dependent on geothermal gradient. Accurately determined values of undisturbed ground temperature, and depth of occurrence, are beneficial for proper sizing of borehole heat exchangers and ground source heat pump system as a whole.
On practical example of building being heated and cooled with shallow geothermal resource, via heat pump system, influence of undisturbed ground temperature and geothermal gradient on size of borehole heat exchanger is going to be presented. Sizing of borehole heat exchanger was calculated with commercial software Ground Loop Designer (GLD), which uses modified line source and cylinder source solutions of heat conduction in solids.

Keywords: *Borehole heat exchanger, Shallow geothermal energy, Geothermal heat pump, Undisturbed ground temperature, Geothermal gradient*

1. Introduction

Today most of the commercially available simulation software packages that are used for sizing of geothermal heat pumps systems with borehole heat exchangers apply one of two (or both) theoretical heat transfer models. The first model is based on the cylindrical source model and allows for quick but accurate length or temperature calculations based on limited data input. The second model is based on a simple line source theory, but is more detailed in its ability to generate monthly temperature profiles over time given monthly loads and peak data. Although the solutions of the two models do not always agree, and strongly differ on valuation of thermal interferences effect, they do give the engineer more information on which to base a final borehole heat exchanger system design.

The vertical bore length equations used in the first model, also known as ASHRAE/Kavanaugh model, are based upon the solution for heat transfer from a cylinder buried in the earth. The method was developed and tested by Carslaw and Jaeger (1946). The solution gives a temperature difference between the outer cylindrical surface and the undisturbed ground temperature. Ingersoll suggested using the equation and its solution for the sizing of borehole heat exchangers in cases where the extraction or rejection of heat occurs in periods of less than six hours, where the simple line source model fails (Ingersoll, 1954). The model was further improved by solution of Kavanaugh and Deerman (1991) who arranged the methods of Ingersoll to account for U-pipe layout and hourly heat variations. For the first model, the most complete description of method and input data can be found in reference Kavanaugh and Rafferty (1997).

The second model, also known as Lund/Swedish model, is based on the solution to the solely heat conduction in a homogenous medium, which was solved by approximating the borehole as a finite line sink using superposition principle (Eskilson, 1987). The steady state solution

relates to the case where heat is extracted continuously from the borehole without ever exhausting the heat source, making it a fully renewable source of energy. The difference between the second model and the first one is that with the second model it is possible to calculate the evolution of the borehole wall temperature over time when a constant heat rate is extracted from the borehole. It makes use of a dimensionless *g-function* method to model the temperature variations, taking into account the ratio of the borehole radius and length and the physical layout of the bore field.

However, both of those models are not particularly considering geothermal gradient in their analysis, claiming that impact of geothermal gradient on overall borehole length needed for heat transfer is rather small and therefore should be neglected. This paper will discuss difference in results of borehole grid array design, obtained by applying Eskilson/Lund model in simulation process of geothermal heat pump system. Model will include two separate ground temperature inputs: one with entering solely undisturbed ground temperature at the site, and the other by entering effective ground temperature with applied geothermal gradient.

2. Influence of Undisturbed Ground Temperature and Geothermal Gradient

Ground surface is exposed to the solar radiation effect to the certain depth. The intensity of solar radiation is different because of geographic location, morphology and plant diversity. Ground temperature is generally a function of solar heat transferred by radiation, convection and conduction. Undisturbed ground temperature could be considered to occur at depth where annual ground temperature amplitude becomes as low as 0,1°C. Undisturbed ground temperature in fact represents temperature at the depth where exists equilibrium from solar radiation from surface and geothermal heat flow from Earth's crust.

Eskilson (1987), states that only an average undisturbed ground temperature is of importance for the heat extraction analysis while geothermal gradient and surface variations are neglected. This average temperature is normally with good accuracy equal to the undisturbed ground temperature at the mid-depth of the borehole. Experimentally, it is determined by circulating the heat carrier fluid without heat extraction or injection (prior Thermal Response Test). The circulating fluid assumes after a short transient period a steady temperature. Heat is then flowing to the lower half of the borehole from the surroundings, which have a temperature above average undisturbed ground temperature, and the same amount of heat is flowing from the borehole to the somewhat colder surroundings in the upper half. Ekilson (1987) also shown that the errors in heat extraction performance, when the simplified initial and boundary conditions are used (average undisturbed ground temperature on mid-depth of bore) instead of more precise ones which include geothermal gradient and temperature variations at surface, are characteristically less than 1%. This analysis was carried out with geothermal gradient of 0,0162°C/m which is common value for northern regions of Europe. Question emerges what would be effect of geothermal gradient on heat transfer in areas where this value is significantly higher. As shown on Figure 1, northern part of the Republic of Croatia posses much higher geothermal gradients in range between 0,04 - 0,07 °C/m. For example, capital city Zagreb, which is located in northwest part of Croatia has average gradient of 0,05 °C/m.

To also include surface temperature variations in analysis of determining average ground temperature through the borehole and simulate heat transfer between geothermal heat pump systems it is necessary to determine real depth where undisturbed ground temperature occurred. Long-term temperature measurements from 2 cm up to 100 cm are conducted on the points of observation by the Meteorological and Hydrological Service of the Republic of

Croatia (DHMZ). Maximum yearly amplitudes (25,1°C) in the ground temperature were observed at the depth of 2 cm in city of Zagreb. Annual amplitudes are decreasing to 15,1°C at 100 cm depth. By analyzing damping of temperature amplitudes, analytical solution by means of extrapolation of a ground temperature versus depth is possible, as published in previous research paper (Kurevija 2010.). If there are no measured data, yearly temperature oscillation at some depth can be estimated with sinusoidal function solving the differential equation as described by Hillel (1982).

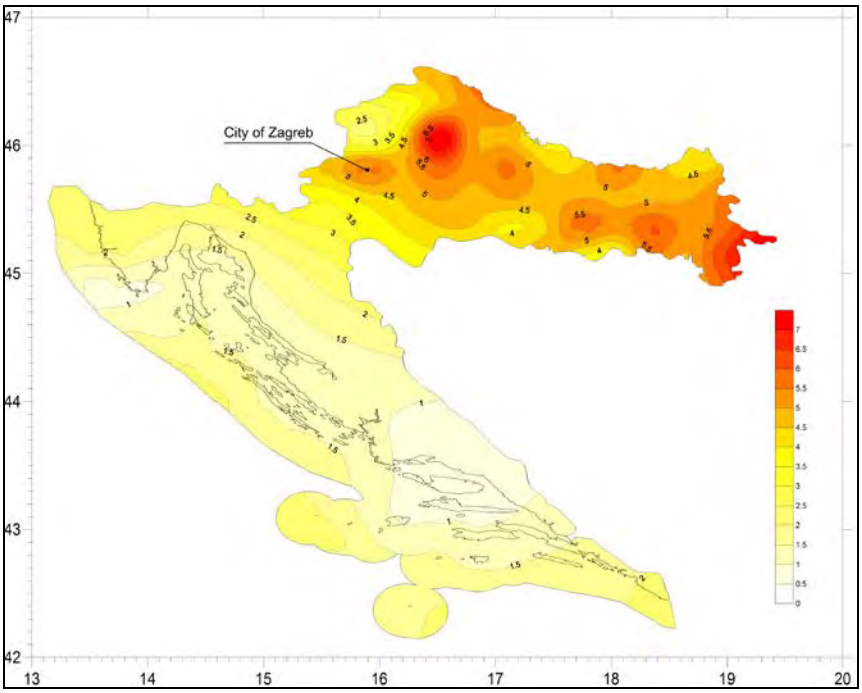

Fig. 1. Geothermal gradients in the Republic of Croatia

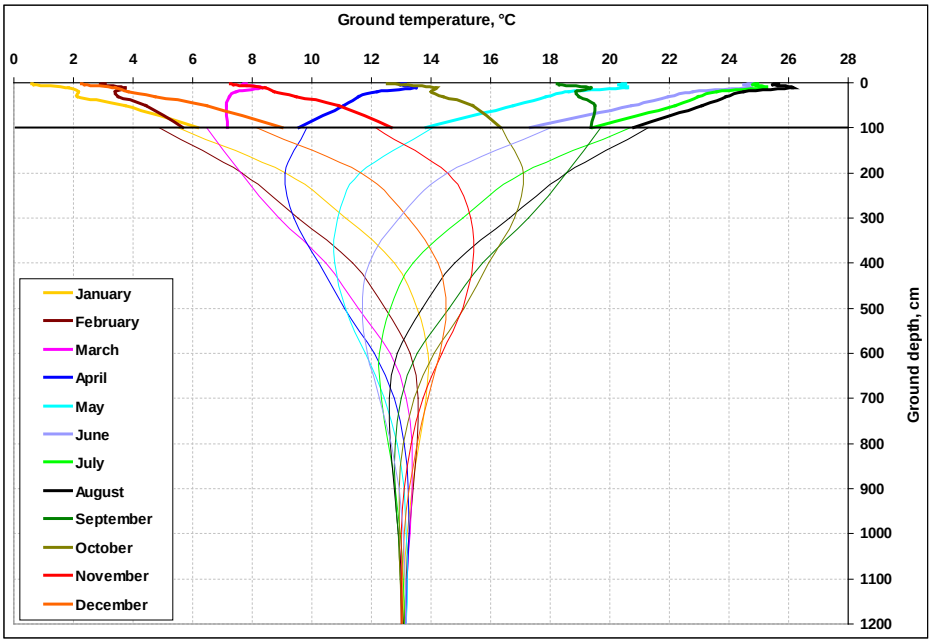

Fig.2. Measured average monthly ground temperatures up to 100 cm and calculated monthly ground temperature oscillations (100-1200 cm) for a meteo station Zagreb-Maksimir (Kurevija, 2010)

By solving the sinusoidal temperature amplitude damping function it can be perceived from Fig.2. that for depth of 1200 cm ground temperature amplitude amounts 0,1°C, and undisturbed ground temperature equals 13,1°C. This value is one of the most important parameters in modeling of borehole heat exchanger.

3. Analysis of Geothermal Heat Pump with Borehole Heat Exchanger Field

After determining undisturbed ground temperature and geothermal gradient in Zagreb location, analysis of ground heat exchanger will be carried out to determine impact of those two parameters. As an example, building with total area of 2500 m^2 and completely heated and cooled with shallow geothermal resource will be discussed. Numerical computation and sizing of borehole heat exchanger will be done with commercially available software *Ground Loop Designer (GLD)* which uses both heat transfer models described in introduction chapter. Second model will be applied (simplified line source heat transfer theory - Swedish/Lund method) because it gives more detailed evolution of the borehole wall and carrier fluid temperatures over long-term period.

Analysis will be based on fixed number of bores in borehole heat exchanger field. Two boreholes array grid will be discussed to determine effect of thermal interferences over long-term period of utilization, one rectangular shaped and compactly arranged in form 5x4, which is presumed to have significant borehole thermal interference effect on loop sizing, and one rectangular shaped in form of 10x2 which is presume to have smaller interferences. Both grids will be simulated in two modes: first one by importing only undisturbed ground temperature (if there is lack of data from circulating carrier fluid through bores prior Thermal Response Test - this is usually done for first approximation in pre-feasibility studies) and second one by importing effective ground temperature (mean ground temperature through the bore depth calculated by including surface variations in first few meters of soil and geothermal gradient which describes temperature rise versus depth). Table 1 shows input data from building annual energy consumption. This was simulated using building energy balance software *KI Expert* which incorporates Croatian directives regarding rational use of energy in buildings and prescribes allowable thermal conductivity factors.

Table 1. Building energy balance

Month	**Heating**	**Cooling**
January	40 633	195
February	25 544	311
March	13 288	764
April	4 003	2 499
May	418	6 403
June	14	10 190
July	0	13 170
August	3	10 261
September	398	4 392
October	6343	1 284
November	21 831	341
December	37 859	289
Total, kWh	**150 355**	**50 096**
Heating/Cooling ratio	3,00	
Peak load 8 hours, kW	99,2	95,8
Annual full load hours	1 516	523

From Table 1 it can be seen that the ratio between energy used during heating season and energy used during cooling season is 3,0. This indicates that more heat would be extracted to the ground than it would be rejected to it (in cooling mode total rejected heat to the ground is the sum of heat rejected from the building and the heat of compression from heat pump) which doubtlessly would cause some cooling of the ground in long-term period of utilization. Borehole input parameters and thermogeological characteristics of the ground at the location can be seen from Table 2. Value of ground thermal conductivity was taken from in-situ measurements conducted on 100m bore (Soldo 2010). Table 3. shows example of designed input parameters for the heat pump system (Waterfurnace EKW130 was used for purpose of this analysis). Building is presumed to have floor heating system with leaving load temperature (LLT) of 40,8°C with entering load temperature (ELT) to the heat pump of 37,8°C. Loop side is set with entering source temperature (EST) of 0°C and leaving source temperature (LST) of -2,3°C.

Table 2. Borehole heat exchanger and thermogeological ground parameters at the site

Loop solution properties	**-Water 76,5% - Propylene glycol 23,5% mixture;** **-Freezing point: -9,4°C** **-Specific heat capacity: 3,992 kJ/kg°C;** **-Density 1024,5 kg/m^3**
Polyethylene single U-pipe parameters	-Pipe size 1" (27,41mm ID/33,40mm OD); -Pipe type SDR11; -Thermal resistance: 0,060 m °C/W; -Average radial pipe placement inside bore
Borehole parameters	-Diameter 130 mm; -Grout thermal conductivity: 2,13 W/m °C; -Borehole eq. thermal resistance: 0,121 m °C/W -Separation distance in grid array: 6,0 m
Ground properties	-Lithology: mostly brown wet clay and unconsolidated coarse sand with thin layers of gravel and marl -Mean volume-specific heat capacity: 2,77 MJ/m^3°C -Undisturbed ground temperature: 13,1°C -Mean thermal conductivity: 1,70 W/m°C -Mean thermal diffusivity: 0,053 m^2/day

Table 3. Example of heat pump system designed input parameters used in ground loop simulation for grid array 5x4 with geothermal gradient included in analysis

Grid array 5x4 with included geothermal gradient	**Heating**	**Cooling**
Source side fluid temperatures, °C	0/-2,3 (EST/LST)	23,6/27,4 (EST/LST)
Load side fluid temperatures, °C	37,8/40,8 (ELT/LLT)	12,0/8,5 (ELT/LLT)
Total unit capacity, kW	99,2	114,6
System peak load, kW	99,2	95,8
Compressor peak demand, kW	28,3	18,8
Heat pump COP, kW/kW	3,5	5,1
Heat extracted/rejected from/to ground	70,9	114,6
Heat pump partial load factor	1,00	0,85

Investigations carried out in relevant literature (Kavanaugh 1984, Eskilson 1987) suggest that geothermal heat pump systems should be sized for at least 30 years period of operation to minimize thermal interferences effects and account sub-cooling of the ground. Principle of multi-year sizing is not to allow minimum temperature of the carrier fluid during peak-load conditions to approach its freezing point during that time and to assure that average fluid temperature of the solution inside the loop be near designed 0°C even after 30 years of operation. If the geothermal system is designed just for 1 year operation, result would be rather small and 'economic' loop size but after multi year of operation loop solution temperature would significantly drop, due to thermal interferences and sub-cooling of the ground, resulting in that way in very inefficient and troublesome system.

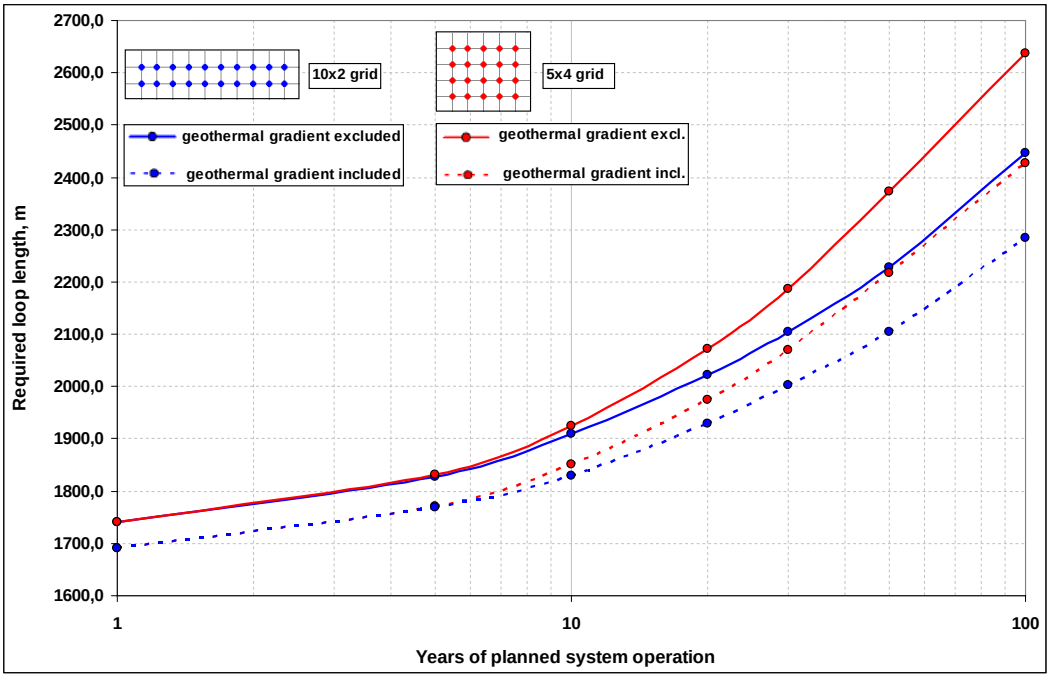

Fig.3. Results of sizing ground loop according to years of planned system operation and various array grids with input data presented in Tables 1,2 and 3 with borehole spacing distance of 6,0m

On Fig.4. results of ground loop simulation are presented. As mentioned, ground loop was simulated for two different grids, compact rectangular 5x4 grid and rectangular 10x2 grid. For both grids variations where calculated inserting in model firstly undisturbed ground temperature of 13,1°C for Zagreb location and then secondly effective ground temperature, which was influenced by geothermal gradient. Variations for different borehole separation distances were introduced to evaluate effect of thermal distances. It can be seen that for low separation distances (below 6,0 m) loop size drastically arises to compensate effect of thermal interferences of an adjacent bores. Also, it can be perceived that geothermal gradient, if introduced in effective ground temperature calculation, significantly influences loop size. For instance, if 5x4 array grid with bores separation distance of 6,0 m is observed, as shown in results from Table 4, it can be seen that analysis which included geothermal gradient in effective ground temperature calculation has 5,3% reduction in loop length, as oppose to analysis which included only undisturbed ground temperature.

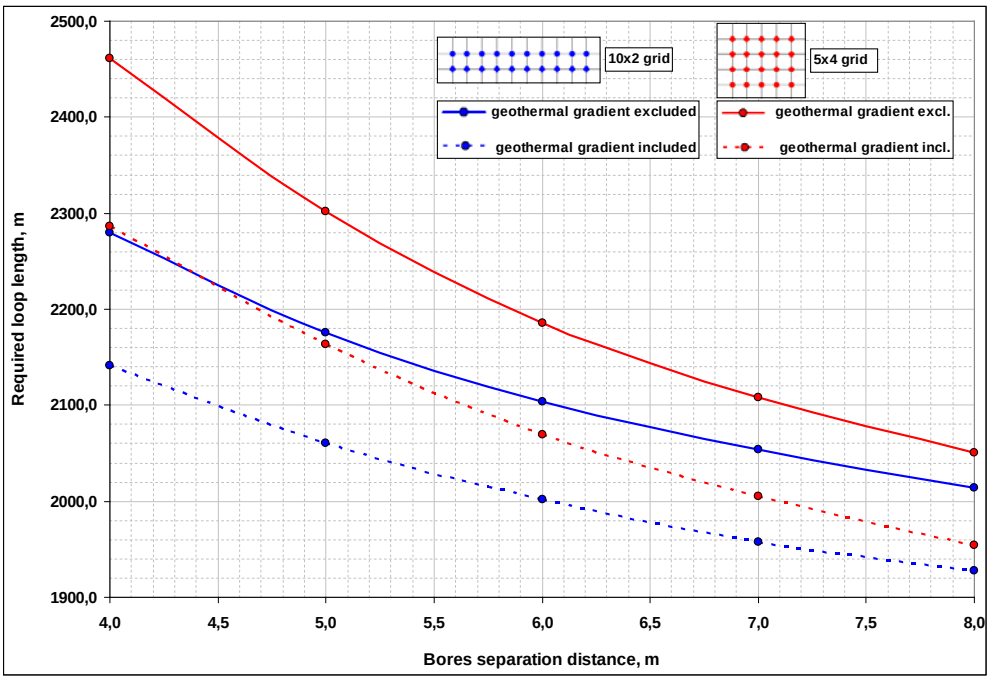

Fig.4. Results of sizing ground loop according to different borehole separation distances and various array grids with input data presented in Tables 1,2 and 3 for 30 years of operation

Table 4. Results of sizing borehole ground loop with calculated changes in loop size due to influence of geothermal gradient

Borehole spacing distance, m	Loop size (Gradient excluded 13,1°C), m	Loop size (Gradient included), m	Change in loop size, %	Depth per bore, m	Effective ground temperature with gradient included, °C	Ground temperature difference, °C
5x4 Borehole Array Grid						
4,0	2460,9	2286,3	7,1	114,3	14,15	1,05
5,0	2301,8	2163,1	6,0	108,2	13,99	0,89
6,0	2186,1	2069,5	5,3	103,5	13,89	0,79
7,0	2107,7	2005,7	4,8	100,3	13,82	0,72
8,0	2050,9	1954,7	4,7	97,7	13,73	0,63
10x2 Borehole Array Grid						
4,0	2279,9	2141,4	6,1	107,2	13,97	0,87
5,0	2175,1	2060,4	5,3	103,0	13,89	0,79
6,0	2103,7	2001,8	4,8	100,1	13,81	0,71
7,0	2053,8	1957,2	4,7	97,9	13,78	0,68
8,0	2014,2	1927,5	4,3	96,4	13,73	0,63

On Fig.5. results of long-term ground loop operation simulation are presented. It can be seen that if loop is sized for 30 years of operation, first years of operation would be most efficient for the geothermal system, as it benefits from 'oversized' loop. After 30 years some indication of steady state appearance can be noticed in loop solution temperatures.

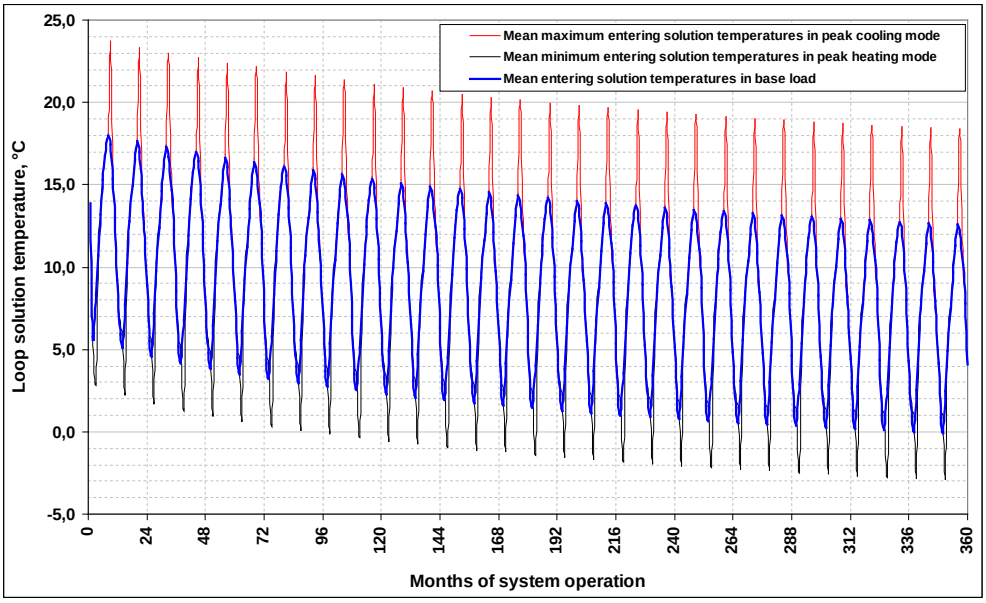

Fig.5. Changes in loop solution temperatures for 30 years of operation for array grid 5x4 and included geothermal gradients, with input data seen in Tables 1 to 4.

4. Conclusion

Analysis of geothermal gradient influence on borehole heat exchanger system showed that for regions where gradients are significantly higher than average, as it is case for northern part of Republic of Croatia, special care should be taken when defining parameters for simulation software input file. As seen from presented results in Fig.4 and Table 4. if only undisturbed ground temperature is entered, which in case of Zagreb location is equal to 13,1°C, and not effective ground temperature that for same location, in 5x4 array grid with 6,0 m bores spacing distance and 103,5m per bore depth, is equal to 13,9°C loop length differs 5,3%. Therefore, this percentage could not be neglected in pre-feasibility project analysis.

References

[1] Carslaw, H. S.; Jaeger J. C. 1946. Conduction of Heat in Solids, Oxford,Claremore Press.

[2] Ingersoll, L.R.; Zobel, O.J.; Ingersoll, A.C. 1954. Heat Conduction with Engineering, Geological and Other Applications. Madison, WI: The University of Wisconsin Press.

[3] Kavanaugh, S.P.; Rafferty, K. 1997. Ground-source Heat Pumps: Design of Geothermal Systems for Commercial and Institutional Buildings. American Society of Heating, Refrigeration and Airconditioning Engineers, Inc., Atlanta, GA.

[4] Eskilson, P. 1987. Thermal Analysis of Heat Extraction Boreholes. Doctoral Thesis, University of Lund, Department of Mathematical Physics. Lund, Sweden.

[5] Kurevija, T.; Vulin, D. 2010. Determining Of Undisturbed Ground Temperature As The Part Of Shallow Geothermal Resources Assessment, The Mining-Geological-Petroleum Bulletin, Faculty of Mining, Geology and Petroleum Engineering, Vol.22, p.27-36

[6] Soldo, V.; Rusevljan, M.; Curko, T.; Grozdek, M. 2010. Ground-source heat pump with a 100 m deep borehole heat exchanger – start up and first results, IIR/Eurotherm Sustainable Refrigeration and Heat Pump Technology Conference, Stockholm

Utilization of geothermal heat pumps in residential buildings for GHGs emission reduction

Farideh Atabi[1*], Seyed Mohammad Reza Heibati[2], Arash Rasouli[3], Ali Poursaeed[4]

[1*] *Assistant Prof., Graduate School of Energy and the Environment, Science & Research Branch, Islamic Azad University, Tehran, Iran*
[2] *Faculty Member of Islamic Azad University, Pardis Branch, Iran*
[3] *B.Sc. Student in Mechanical Engineering, Science & Research Branch, Islamic Azad University, Tehran, Iran*
[4] *B.Sc. Student in Mechanical Engineering, University of Tehran, Iran*
[*] *Corresponding author: Tel: +9821 22292909, E-mail: far-atabi@jamejam.net*

Abstract: This study aims to reduce energy consumption by application of geothermal heat pumps in residential buildings and reduction of Greenhouse Gases (GHGs) emissions under Clean Development Mechanism (CDM) project. In this approach, the required thermal load of a typical four-floor 12-units residential building located in Tehran city has been considered and calculated separately based on the actual operational data. According to the thermal properties of soil and the annual average temperature of the area, the appropriate geothermal heat pump system has been taken into consideration. Subsequently, three scenarios based on transaction of Certified Emission Reductions (CERs) as Primary, Secondary and Unilateral types of CDM projects were created considering the primary costs of purchase and installment of geothermal heat pump system and its electricity consumption. Technical, economical and environmental feasibility study of this project has been assessed through using Proform software in three different scenarios based on global carbon credit market.

The results show that in the optimum scenario in case of replacing the boiler system with vertical geothermal heat pump system in the residential building, could conserve 67,000 GJ of natural gas during the project implementation period and 3,759 tons of CO_2 equivalent emissions would be reduced. Results demonstrate also the favorable economic and environmental impacts that can be achieved by CDM.

Keywords*: Geothermal Heat Pump, GHGs Emission, Residential Building, Carbon Credit*

1. Introduction

Geothermal energy use avoids the problem of acid rain, and it generally reduces greenhouse gas emissions and other forms of air pollution. A continuing strong market for geothermal heat pumps is anticipated as a result of the increasing interest in controlling atmospheric pollution because of the spreading concern about global warming and because of their reliability, high level of comfort, low demand, and low operating costs. Ground source heat pumps (GSHPs), also known as geothermal heat pumps (GHPs), are attractive alternatives for both conventional heating and cooling systems because of their higher energy efficiencies. However, GSHP systems have recently been applied to many residential and a few commercial buildings for heating/cooling purposes [1,2]. These systems have had the largest growth since 1995, almost 59 or 9.7% annually in the United States and Europe. The installed capacity is 6850 MW and annual energy use is 23,214 TJ/year in 26 countries. The actual number of installed units was around 500,000 in 2000. It is also estimated that there are over a million today (e.g. [3,4-9]).

GSHPs have several advantages over air source heat pumps, as given by Lund and Freeston [10]: (a) they consume less energy to operate; (b) they tap the earth or groundwater, a more stable energy source than air; (c) they do not require supplemental heat during extreme low outside temperature; (d) they use less refrigerant; (e) they have a simpler design and consequently less maintenance; and (f) they do not require the unit to be located where it is exposed to weathering. The main disadvantage is the higher initial capital cost, being about 30-50% more expensive than air source units. This is due to the extra expense for burying heat exchangers in the earth or providing a well for the energy sources. However, once

installed, the annual cost is less over the life of the system, resulting in a net savings. In a comprehensive study conducted by Lund et al. [11], it is reported that GSHPs have the largest energy use and installed capacity according to the 2005 data, accounting for 54.4% and 32.0% of the worldwide capacity and use. The installed capacity is 15,384 MW_t and the annual energy use is 87,503 TJ/year, with a capacity factor of 0.18 (in the heating mode) [12].

The concept of GHP is not new. However, the utilization of GHPs in residential buildings is very new in Iran, although they have been in use for years in developed countries and the performance of the components is well documented. Worldwide GSHPs account for 12% of the geothermal energy used for direct applications, amounting to approximately 16,500 TJ (4580 GWh) annually. Present estimates indicate that there are over 150,000 groundwater and 250,000 ground coupled (55% vertical) heat pump installations in the USA [13]. According to the Kyoto Protocol, industrialized countries have agreed to reduce their overall emission of greenhouse gases (GHGs) by at least 5 percent below 1990 levels in the commitment period 2008–2012 (United Nations, 1998). In order to minimize the compliance cost, three flexible mechanisms are defined: the Clean Development Mechanism (CDM), Joint Implementation (JI), and Emission Trading (ET). CDM is the only mechanism applicable to the developing countries. Certified Emission Reductions (CERs) is a unit of GHGs reductions issued pursuant to the Clean Development Mechanism of the Kyoto Protocol, and measured in metric tons of carbon dioxide equivalent. One CER represents a reduction in greenhouse gas emissions of one metric ton of carbon dioxide equivalent. Primary CDM is the transaction of CERs between the original owner of the carbon asset and a buyer in the market. Depending on the amount of risks taken by the buyer and the seller, the price of CERs is agreed upon, which is lower than the secondary CDM prices. Secondary CDM is the transaction where the seller is not the original owner of the carbon asset. Usually, the seller and the buyer of secondary CDM are Annex I countries. Secondary CERs have higher prices than primary CERs due to its minimal risks imposed on the buyer. Unilateral CDM is the type of CDM project that an Annex I country is not involved and the developing country accepts all the risks and expenses in order to sell the CERs with higher prices in the market [14]. However, the developing country requires past experience in development and marketing of CDM projects. The present study deals with technical, economical and environmental feasibility assessment of a four-floor 12-units residential building, located at east of Tehran city, capital of Iran in which a boiler system is replaced by vertical ground source heat pump system under Primary, Secondary and Unilateral CDM projects.

2. Methodology

The residential building under study is a 12-unit complex located at east of Tehran city with four floors and the area of 565m^2 at each floor. The required heating and cooling loads of the building was calculated based on number of residents. Then considering the geographical position, thermal properties of the soil and the climate conditions, for supply of air and water heating, a vertical GSHP system was introduced to replace the present boiler. The reasoning for choosing the vertical type was land limitation, the necessity of keeping the private boundaries of the neighbors and also having the possibility of penetration into depth under ground in order to achieve a rather stable temperature all throughout the year. Then based on the global carbon market, by using Proform software, three scenarios based on Primary, Secondary and Unilateral types of CDM projects were created considering the primary costs of purchase and installment of GSHP system to replace the boiler system. Table (1) shows the specifications of the present heating system of the building.

Table 1. Specifications of the present heating system (boiler)

System Type	Efficiency (%)	Fuel Type	Annual Gas Consumption (GJ/y)
Boiler	75	Natural Gas	16750

For replacing the boiler system by GSHP system and in order to supply the required heating loads in the residential building, some required information and specifications are shown in Table (2).

Table 2. Required information and specifications for choosing proper geothermal heat pump for the desired building

Isentropic Compressor Efficiency (%)	75	Heating load(kW)	220
Electrical Compressor Efficiency (%)	80	Cooling l(kW)	184.4
Pump Efficiency (%)	80	total time of heating operation mode (h/y)	2880
Pump motor Efficiency (%)	80	System function of time for full time(h/y)	1350
Condenser internal diameter (m)	0.0318	System lifetime (year)	10
Condenser external diameter (m)	0.0348	Interest rate (%)	10
Thermal conductivity coefficient of condenser tube (kW/m°C)	0.398	Coefficient of thermal conductivity of soil (W/m°C)	4.2
Inner diameter tube evaporator(m)	0.0318	Earth temperature (°C)	16
Outer diameter tube evaporator (m)	0.0348	Overall heat transfer coefficient in soil (W/m2°C)	12
Heat pipe thermal conductivity coefficient (W/m°C)	0.3979	Thermal conductivity coefficient of evaporator tubes (kW/m°C)	0.398

According to Table (2) and the specifications provided by the manufacturer of different types of geothermal heat pumps [15], and by applying the correlations offered in the reference No.16, the vertical GSHP system with the specifications given at Table(3) was chosen for supplying the required air and water heating.

Table3. Technical specifications and costs of the chosen GSHP system in the building under study

Vertical pipe length converter (m)	9000	Compressor power consumption (kW)	3900
Type of pipe	polyethylene	Power pump (kW)	5.5
The initial investment cost (US$)*	28073.67	Deep wells (m)	111.8
Electricity consumption (MWh/y)	60	Coefficient of performance(COP)**	4.94

*Cost of initial investment is: cost of pump + cost of compressor + cost of operator + cost of condenser + cost of excavation + cost of piping + cost of vertical land converter + cost of installation and launching.

**The temperature dependence of the efficiency has been neglected.

2.1. Technical, Economical and Environmental Assessment of GSHP System

Technical, economical and environmental feasibility study of the chosen GSHP system in the residential building has been implemented by Proform software. Some required information about the present boiler system and new system (GSHP) are offered at Tables (4) and (5). Based on the international carbon credit market, three scenarios were created according to the data on Table (6) and compared by Proform software.

Table 4. Technical data provided as input for Proform software

Depreciation period (Years)	GSHP Capacity (kW)	Coefficient of performance (%) GSHP	Life time GSHP (Years)	GSHP energy consumption (MWh/y)	Boiler efficiency (%)	Type of fuel consumed by the boiler	Old system energy consumption (boiler) (MWh/y)
10	220	4.95	10	60.053	75	Natural gas	465.2

Table 5. Financial and economical data provided as input for Proform software

Discount rate (%)	Income tax rate (%)	Initial investment cost of the GSHP system (US$)	Inflation rate* (%)	Annual interest rate of electricity price (%)	Annual interest rate of natural gas price (%)	Natural gas consumption ** (US$/Gj)	Electricity price (US$/kWh)
16	15	28073.67	20.2	21	5.6	0.271	0.011

*Annual inflation rate based on the report of Central Bank of Islamic Republic of Iran, General Director of Economic Statistics, May 2009.
** Energy Balance, 2008, each m^3 of natural gas GJ 0.03726 and price of natural gas [17].

Table 6. Scenario Analysis based on carbon credit defined by World Bank

Scenarios	Value of carbon credits reduction CO_2 (US$/ton CO)	Price Growth Rate (%)	Sales income tax (%)
Scenario A	10	15	0
Scenario B	15	15	0
Scenario C	20	20	0

As shown in Table (6), carbon credit in scenario A (Primary CDM) is US$ 10/tonCO_2, in scenario B (Secondary CDM) is US$ 15/tonCO_2 and in scenario C (Unilateral CDM) is US$ 20/tonCO_2. In case of taking no action for sale of carbon credit, the results of such case was also compared with the scenario analysis results. The depreciation rate considered in accordance with statistics of balance sheet in the year 2008 is equivalent to 16%. Also income tax rate was considered to be 15%, but the income generated by sales of carbon credit is free from any tax.

3. Results and Discussions

Replacing the boiler system by GSHP system could conserve 67,000 GJ of natural gas (601 MWh/10yr electricity). In Table (7), the amounts of GSHP electricity consumption and decrease in fossil fuel consumption caused by implementation of the project have been shown.

Table7. Amounts of electricity consumption and decrease in fuel consumption over the life of the GSHP system

	Power consumption by GSHP (MWh)	Natural gas consumption rate (GJ000)
Average Annual	60.053	7
Total Project (10 yr)	601	67

As shown in Table (8), in scenario A, taking all the initial investment costs as well as the installment and operation costs fro replacing the boiler by GSHP system into account , the pay back period is 3.9 years. Moreover, net present value (NPV) without tax is estimated to be about US $ 17,000 and the internal rate of return (IRR) is about 27.45%. In case of tax being included, NPV is US$ 15,000, the IRR is 25.88%. In scenario B, the pay back period is 3.1 years. Taking tax into account, the NPV is US$ 30,000 and IRR is 34.66%, however without considering tax, NPV is US $ 33,000 and IRR is 36.11%. In scenario C, before tax, NPV is US $ 62,000 and the pay back period is in 2.6 years and the IRR is 47.66%. In case of considering tax, NPV is US $ 59,000 and IRR is 46.38%. Since the IRR is more than the interest rate (16%), the project is proven to be cost-effective in this case. In case of taking no action for sale of carbon credit, the results show minus profit.

Table 8. Economic assessment of different scenarios A, B, C

Scenarios	Before tax			After Tax	
	Simple pay back (year)	Net present value (NPV) (US$)	Internal rate of return (IRR) (%)	Net present value (NPV) (US$)	Internal rate of return (IRR) (%)
Scenario A	3.9	17000	27.45	15000	25.88
Scenario B	3.1	33000	36.11	30000	34.66
Scenario C	2.6	62000	47.66	59000	46.38
Without considering the sale of carbon credit	8.8	-14000	2.74	-16000	-

Net present values in different scenarios before and after tax have been compared over the life of the GSHP system (10 years) and according to Fig. (1) The scenario C in comparison to other scenarios has higher profit making.

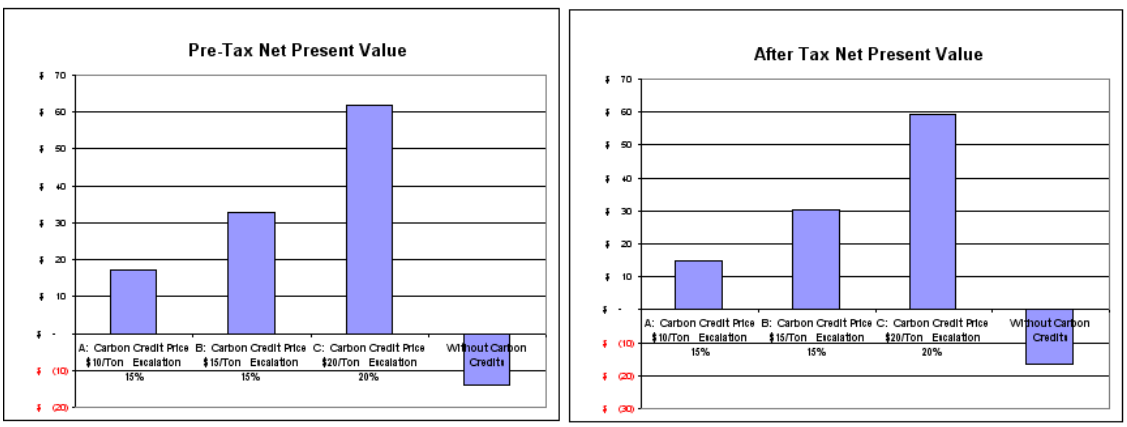

Fig.1. Comparing net present values in different scenarios before and after tax

Table (9) shows the annual income gained by sales of carbon credit in the three scenarios, so that if in the first year (year 0) the amount of US $ 30,000 is invested in the project, the amount of profit during the next year (year 1) in scenario A will be US $ 7,000, in scenario B will be US $ 9,000 and in scenario C will be US $ 10,000. While, in case of non selling of carbon credit, only US $ 3,000 profit in one year will be gained which makes the implementation of the whole project economically non feasible and non profitable. Furthermore, in the next coming years over the life of the project (10 years) the annual cash flow is compared and shown in the Table(9).

Table 9. Annual profit gained by sale of carbon credit in three scenarios during 10 years

Annual Cash Flow (US$000) Before Taxes				
	Without sale of Carbon Credit	Carbon Credit (Scenario A)	Carbon Credit (Scenario B)	Carbon Credit (Scenario C)
Year 0	-30	-30	-30	-30
Year 1	3	7	9	10
Year 2	3	7	10	12
Year 3	3	8	11	14
Year 4	3	9	12	16
Year 5	3	10	13	19
Year 6	4	11	15	22
Year 7	5	12	17	26
Year 8	5	14	19	31
Year 9	5	16	21	36
Year 10	6	17	24	43

Results of Proform software show that the elimination of natural gas consumption in the building reduces green house gases emission by 658 tons of CO_2 equivalent per year and by 3759 tons of CO_2 equivalent during the whole period of implementing the project. As shown in Fig. (2), the rate of CO_2 emission reduction is going up over the time.

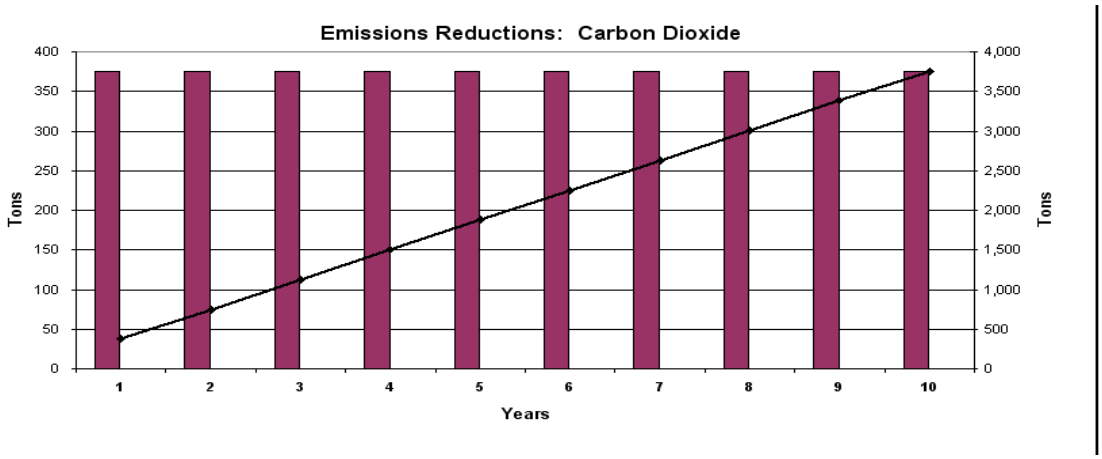

Fig. 2. CO_2 emission reduction during different years of the project implementation

4. Conclusion

In the present study a four-floor 12 unit residential building located at east of Tehran was assessed in the case of replacing the present boiler system by a vertical geothermal heat pump system. Based on the global carbon credit market, by using Proform software, three scenarios were considered on the basis of the primary costs of purchase and installment of GSHP

system to replace the boiler system. In scenario A considering all the investment expenses as well as the installment and operation costs of the geothermal heat pump and replacing boiler with it, the pay back period is 3.9 years. Moreover, considering tax, NPV is estimated to be US $ 15,000 and the internal rate of return (IRR) is about 25.88%. In scenario B the pay back period is 3.1 year. Considering tax, NPV is US $ 30,000 and IRR is 34.66%. In case of implementing scenario C, the NPV is US $ 59,000 and the pay back period is 2.6 years. Furthermore, IRR is 46.38%. Therefore, it is suggested that this project be implemented according to scenario C in which IRR is more than the other two scenarios. The results show that in the optimum scenario in case of replacing the boiler system by vertical geothermal heat pump system under the CDM project in the residential building could conserve 67,000 GJ of natural gas during the project implementation period (10 years) and 3,759 tons of CO_2 equivalent emissions would be reduced. Thus, the results clearly demonstrate that increasing geothermal utilization results to GHG emission reduction while helping to meet increasing power demand. It demonstrates also the favorable economic and environmental impacts that that can be achieved by CDM. The message is that the utilization of GSHP without carbon credit is economically not feasible. However, significant opportunities for GSHP CDM projects are likely to extend into future decades.

References

[1] Kavanaugh SP. Field test of vertical ground-coupled heat pump in Alabama. ASHRAE Transactions, 1992,98:60716.

[2] Hepbasli A, Akdemir O. Energy and exergy analysis of a ground source (geothermal) heat pump system. Energy Conversion and Management 2004,45:73753.

[3] Lund J.W. Ground source (Geothermal) heat pumps. Course on heating with geothermal energy: conventional and new schemes, Convener Paul J Lienau, WGC 2000 Short Courses Kazuno, Thoku District, Japan 810 June, 2000, p. 20936.

[4] Lund J. W. Geothermal heat pumps-trends and comparisons. Geo-Heat Center Q Bull 1989,12(1):16.

[5] Lund JW, Freeston DH. World-wide direct uses of geothermal energy 2000. Proceedings world geothermal 587 congress 2000, Kyushu-Tohoku, Japan, May28 - June 10, 2000, p. 121.

[6] Lund JW, Freeston DH. World-wide direct uses of geothermal energy 2000. Geothermics, 2000,30:2968.

[7] Lund JW. Direct use of geothermal energy in the USA. Appl Energy 2003,74:3342.

[8] Lund JW. Geothermal heat pump utilization in the United States. Geo-Heat Center Q Bull 1988,11(1):507.

[9] Lienau PJ, Lund JW. Geothermal direct use. Testimony presented at the house subcommittee on environment, July 30. Geo-Heat Center, Klamath Falls, OR; 1992.

[10] Lund JW, Freeston DH. World-wide direct uses of geothermal energy 2000. Proceedings world geothermal congress 2000. Kyushu-Tohoku, Japan, May 28June 10, 2000. p. 121.

[11] Lund JW, Freeston DH, Boyd TL. Direct application of geothermal energy: 2005 worldwide review. Geothermics 2005,34(6):691727.

[12] Akpinar E. .K , Hepbasli A., A comparative study on exergetic assessment of two ground-source (geothermal) heat pump systems for residential applications, Building and Environment, 2007, 42 :20042013

[13] Lund JW. Geothermal heat pump utilization in the United States. Geo-Heat Center Q Bull 1988,11(1):507.

[14] United Nations Development Program (UNDP), Human & Income/Poverty in Developing Countries, 2008.

[15] http://www.fhp-mfg.com/aecinfo/1/company/09/09/81/company_1.html

[16] Sanaye S., Niroomand B., "Thermal economic modeling & optimization of vertical ground coupled heat pump", Energy Conversion & Management, 2000, 50, 1136 - 1147.

[17] Ministry of Energy, Energy Balance, Iran Energy optimization Organization, 2008.

Volume 6

Hydropower Applications

Low Head Pico Hydro Turbine Selection using a Multi-Criteria Analysis

S.J. Williamson*, B.H. Stark, J.D. Booker

Faculty of Engineering, University of Bristol, Bristol, UK
** Corresponding author, Tel: +44 (0)117 954 5499, E-mail: sam.williamson@bristol.ac.uk*

Abstract: Turbine types suit specific ranges of head, flow rate and shaft speed and are categorised by specific speed. In the pico range, under 5kW, the requirements are often different to that of larger scale turbines and qualitative requirements become more influential. Pico hydro turbines can be applied beyond these conventional application domains, for example at reduced heads, by using non-traditional components such as low speed generators. This paper describes a method to select which turbine architecture is most appropriate for a low-head pico hydro specification using quantitative and qualitative analyses of 13 turbine system architectures found in literature. Quantitative and qualitative selection criteria are determined from the particular requirements of the end user. The individual scores from this analysis are weighted based on perceived relative importance of each of the criteria against the original specification and selects a turbine variant based on the total weighted score. This methodology is applied to an example of a remote site, low head and variable flow specification and used to select a propeller turbine variant or single-jet Turgo turbine for this specification.

Keywords: *Pico hydro, Turbine selection, Low head, Application Range, Turgo*

1. Introduction

Typically, selecting hydro turbines is based on the specific speed of the turbine, a non-dimensional parameter that includes head, output power and output shaft speed [1]. From this, the commonly used application domain for turbines is used to aid selection, as in Fig. 1, which has been compiled from [2], [3] and [4]. This leads to the choice of Pelton and Turgo turbines at high heads, crossflow and radial (Francis) turbines at mid heads and propeller turbines and waterwheels at low heads. This is also reflected in the commercially available turbines for these heads.

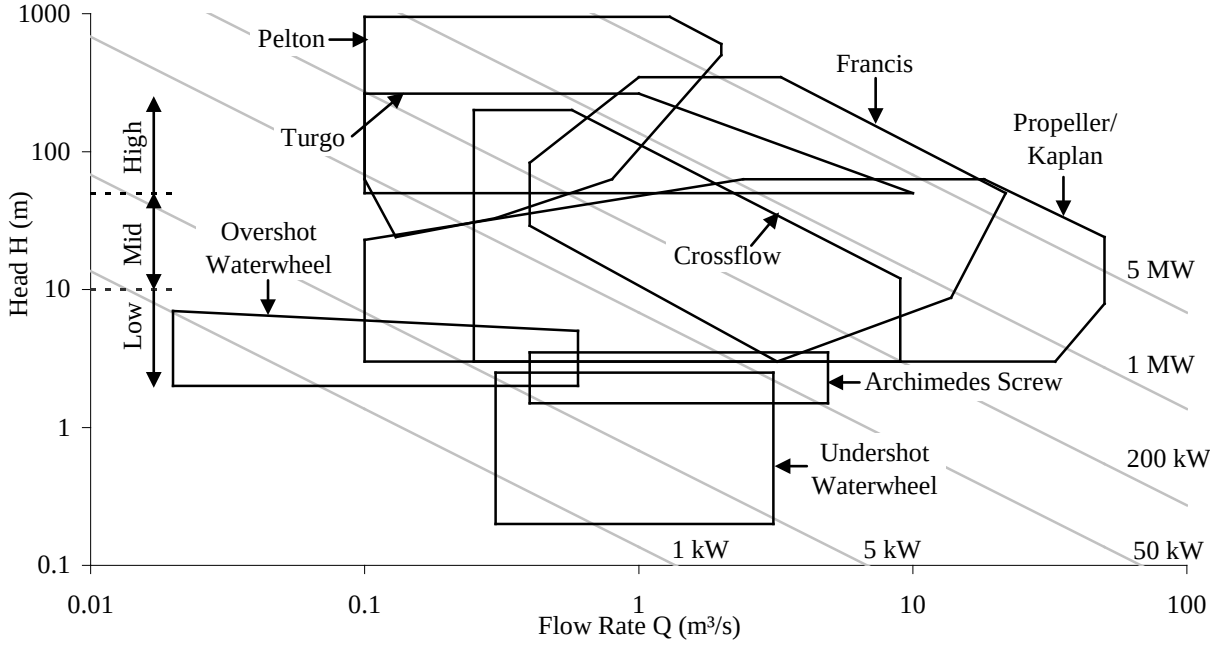

Fig. 1. Turbine application range chart, adapted from data in [2], [3] and [4].

As can be seen in Fig. 1, the pico range, under 5 kW generation, appears to be sparsely covered by reported application domains. There are several commercially available pico hydro products at high, mid and low head, and these tend to follow the topology of the larger scale turbines. The use of traditional 4 or 6-pole generators and direct generator-grid interfaces restricts the application domains for pico hydro turbines. However, introducing technologies such as low speed generators or inverter based grid interfaces generally extends a turbine's application domain, thus providing alternative turbine solutions. In addition, the requirements on a pico hydro turbine tend to be different to those of a larger scale turbine; pico hydro generators cannot carry the cost of unique designs for each location, requiring instead off-the-shelf solutions. It can be located in remote locations, several hours walk from the nearest road and have no skilled labour locally to operate and maintain the system. The application domain selection method of turbine selection does not take these more qualitative factors into account. The method proposed in this paper is used to select a pico hydro turbine for a low head specification using both quantitative and qualitative criteria.

2. Methodology

2.1. Selection Criteria

Each turbine system will have a set of requirements and specification. This will include either site conditions, such as head and flow rate, or output power requirements. There will be environmental requirements, for example the site may be in an inaccessible location, be subject to extremes in temperature or have to comply with fishery regulations. The turbine may be able to have regular maintenance checks from an onsite operator, or it may be required to be operated remotely and therefore should require minimal maintenance and have a high reliability. Using the requirements, a set of selection criteria can then be developed. Table 3 shows the selection criteria used in the method example in Section 3. Some of the criteria can be assessed through a quantitative analysis, whilst others are less quantifiable, and so will require a qualitative analysis. These analyses are then combined to give each turbine type a final score.

2.2. Quantitative Analysis

Basic fluid flow equations are used to derive simple performance characteristics about the turbine option for the quantitative analysis. The performance variables are turbine power P, overall turbine system efficiency η, flow rate Q, and gross head H_g, two of which will need to be defined, leaving two unknowns. These variables are combined using Eq. (1) [1] for a general turbine system.

$$P = \eta \rho g Q H_g \tag{1}$$

where ρ is density and g is the gravitational constant. The two unknowns are solved using a second equation, which is derived from further analysis of the turbine torque generation mechanism. This analysis may result in the power available at a specific site and the turbine system efficiency or the efficiency and flow rate required to produce a specified power depending on the variables defined. There are 13 turbine types commonly used which are divided into 4 categories: Impulse, Reaction, Archimedes Screw, and Waterwheel. Each category has a different torque generation mechanism and is analysed in a different manner, as summarised in the following Sections. The performance modelling used here is simplified, neglecting fluid mechanic non-linearities, and assumes linear geometric scaling. For some turbines considered, impractical geometries are generated at the extremes of their head range.

2.2.1. Impulse Type – Pelton and Turgo (single and multiple jet), Crossflow

Velocity triangles of the water jet impacting with the blade of the turbine are used to analyse the impulse turbines [1]. The head loss in the penstock H_{l1} reduces the inlet jet velocity. The change in whirl velocity Δv_w is used to calculate the rate of change in momentum of the water, generating a force at the blade. The force is concentrated at the jet impact point, radius r, assuming the flow enters and exits at the same radius, which causes a torque T on the wheel. The power is then the product of the rotational speed at maximum power ω by the torque

$$P = T\omega = Q\rho\Delta v_w r\omega \,. \tag{2}$$

2.2.2. Reaction Type – Axial, Radial

The gross head H_g in Eq. (1) is reduced by head losses in the penstock H_{l1}, the draft tube H_{l2}, and from the outflow kinetic energy H_{l3}. These head losses are functions of the speed of the water passing through the component and a factor dependent on the geometry of the component [1]. The power generated is then dependent on the net head and the estimated turbine hydraulic efficiency η_t, which is different to η in Eq. (1),

$$P = \eta_t \rho g Q\left(H_g - H_{l1} - H_{l2} - H_{l3}\right). \tag{3}$$

2.2.3. Archimedes Screw

The Archimedes screw operates on a hydrostatic pressure difference across the blades [5]. The efficiency η is a function of the geometry of the screw n, the diameter D, and the flow passing through it Q

$$\eta = \left(\frac{2n+1}{2n+2}\right)\left(1 - \frac{0.01125D^2}{Q}\right). \tag{4}$$

2.2.4. Waterwheels – Overshot, Breastshot, Undershot

The analysis for the waterwheels is based on the losses in the system, as described in [6]. For the Overshot and Breastshot Waterwheels it is assumed that the losses are only the kinetic energy loss from the water entering the wheel H_{l4}, and the swirl in the water on the exit of the wheel H_{l5}, and the efficiency is then

$$\eta = \left(\frac{H_g - H_{l4} - H_{l5}}{H_g}\right). \tag{5}$$

For an Undershot Waterwheel, two efficiency losses are considered. First the inlet efficiency η_{th} represents the non-ideal flow entrance due to fixed wheel geometry, second the friction on the water bed h_{l6} ($=H_{l6}/H_g$), which models friction loss as a function of inlet water velocity. The efficiency is then

$$\eta = \eta_{th} - h_{l6} \,. \tag{6}$$

2.3. Qualitative Analysis

The qualitative analysis uses clearly defined criteria to score the qualitative aspects of the turbine selection, as in [7]. Each criterion is given an unambiguous definition and a defined scoring system between 1 (poor) and 5 (excellent). Each turbine is then scored against this scoring system as a part of a team discussion. An example of the scoring system is shown in Table 1, which was developed as part of the research methodology and used in Section 3.

Table 1. Example qualitative scoring definition and criteria.

Scope for Modularity

Definition - Modules that allow the system to be broken into carryable/shippable units and allow line replaceable for easy servicing and fault identification, with the ability to interchange identical modules.

Scoring Criteria	**Score**
Few, but standard, interfaces; few system elements; simple coupling mechanisms between elements; simple element architecture orientation	5
Few non-standard interfaces, some standard interfaces; manageable architecture; some non-standard coupling between system elements	3
Many non-standard interfaces; many separate system elements; complex coupling mechanisms between system elements; unusual element architecture orientation	1

A scoring system is defined for each of the different selection criteria. If within a criterion there are several different aspects, then sub criteria are used to fully define all the different aspects. These are combined to form a single score for the criterion, through either an arithmetic or weighted mean.

2.4. Combining Analyses

The results from the quantitative analysis are normalised against the maximum value, and the qualitative scores are normalised against the maximum value, 5. A weighting for each of the criteria is decided by project stakeholders, as recommended by [7]. These weightings are multiplied by normalised scores from the quantitative and qualitative analyses to give a final score for each turbine solution. The scores can then be analysed and an appropriate solution chosen. In the following Sections, the method described above is shown through an example.

3. Example of Pico-Hydro Turbine Selection Using Multi-Criteria Analysis

The village of Bhanbhane in central Nepal has several low head sites for turbines. The heads at the sites vary from 0.5 m to 3.5 m, the flow available at the sites also varies depending on the season and the location in the river. There are two different rivers that would supply the sites. The villagers would like to install the same turbine in all of the locations, making savings in bulk buying and allowing them to stockpile spares. At each turbine site, they do not require more than 1 kW of electric power, so allowing for inefficiencies in the system, such as drive and generator losses, the turbine should produce 1.3 kW of mechanical power. Bhanbhane is a rural village, and the sites lie several kilometres from the nearest road, so the units need to be portable, ideally able to be carried by villagers. Also, with the rural location and the distance from a road, cement is expensive and difficult to obtain, therefore the civil works should be minimised. The villagers intend to carry out on-site maintenance and servicing themselves, so the unit should be simple to maintain and have a modular design allowing faulty modules to be easily identified and replaced. Any faulty modules that cannot be repaired onsite are to be returned to the manufacturer or a service centre for repair. It is

assumed that the generator output is 50 Hz, with a direct interface to the distribution system. From this, the specification for the turbine is derived (Table 2), and the selection criteria developed (Table 3).

Table 2. Turbine specification

Power:	1.3 kW
Head:	Range from 0.5 to 3.5 m
Portability:	Able to be transported to locations with limited transport infrastructure
Reliability:	High reliability for low maintenance operation
Output Frequency:	50 Hz output from generator
Maintenance:	Maintenance and servicing carried out by unskilled labour
Flow rate:	Large variation across the seasons
Modularity:	Turbine in modules to allow for easy fault identification and module replacement
Civil works:	Small civil works

Table 3. Selection criteria

Efficiency:	Efficiency of the unit at rated flow/head and at part flow/part head
Power:	Power of the unit must be 1.3 kW
Portability:	Minimised volume for easy transportation
Civil Works:	Minimised civil works – concrete sparsely available in site locations
Modularity:	Scope to incorporate modularity into the design for line replaceable units and to disassemble the unit for ease of portability
Maintenance & Serviceability:	The ease of maintaining and servicing the unit, especially with unskilled labour.

Here, power and head are the known variables, with the efficiency and flow rate required from the quantitative analysis. The volume of the unit is estimated as a function of the flow rate and using existing designs and rules, for example [8]. The portability and power are dealt with by deriving a power density metric (rated power/volume) which provides the volume required to generate 1.3 kW. This volume includes the penstock, turbine and casing. The power density and rated flow efficiency are thus treated by the quantitative analysis, whilst the part flow/part head efficiency, civil works, modularity and maintenance will be analysed qualitatively. The quantitative analysis designs a set of turbines for heads from 0.5 m to 3.5 m in 0.5 m steps. Power density is chosen to be the most important criterion, as if the unit is too large and unwieldy then the villagers will not be able to implement it in their chosen sites. The maintenance and serviceability and modularity in the design are considered less important, which is reflected in the weightings, shown in Table 4.

Table 4. Weighting scheme for example.

Selection Criteria	**Weighting**
Power Density	0.30
Rated Flow Efficiency	0.25
Part Flow, Part Head Efficiency	0.20
Civil Works	0.15
Maintainability & Serviceability	0.05
Scope for Modularity	0.05

The turbines assessed represent the four main different turbine types described in Section 2.2. Impulse and reaction turbines require a penstock, which is assumed to have a 5% head loss.

The multiple jet turbines are assumed to have four jets which give it a volume and efficiency penalty. It is assumed that the turbine is connected to a generator that can produce 50 Hz as long as the rotational speed is between 200 and 3000 rpm (commercially available generators). If the rotational speed is less than or greater than these limits, a gearbox is required to bring the speed within these limits and so gearbox efficiency is taken into account.

4. Results

The results from the quantitative analysis are shown in Fig. 2. The summary of the results from the combined analysis are shown in Fig. 3 and 4.

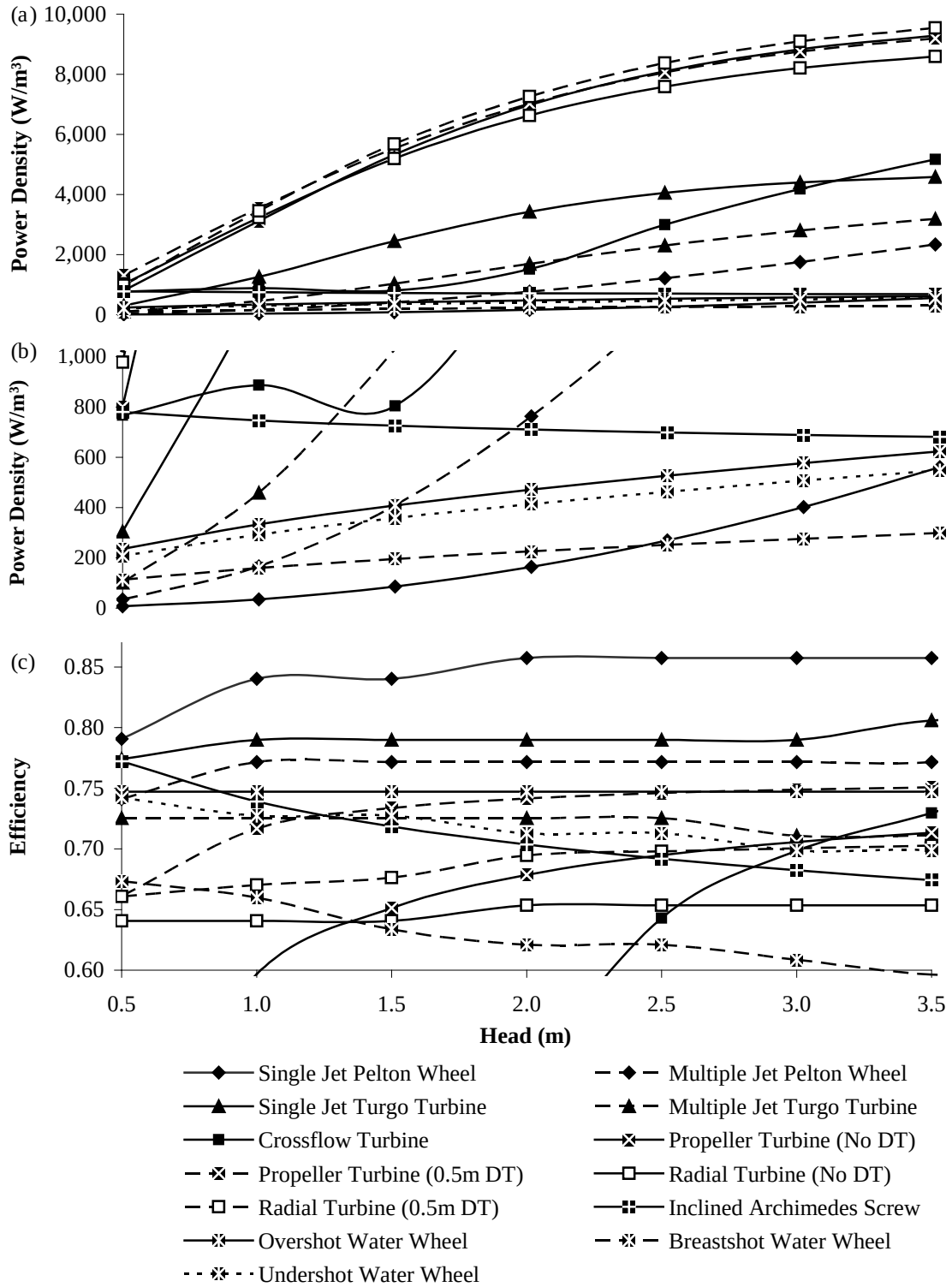

Fig. 2. The output of the quantitative analysis: (a) power density (b) power density zoomed in at low power density (c) efficiency variation over the head range 0.5 to 3.5m, 'DT'=Draft Tube.

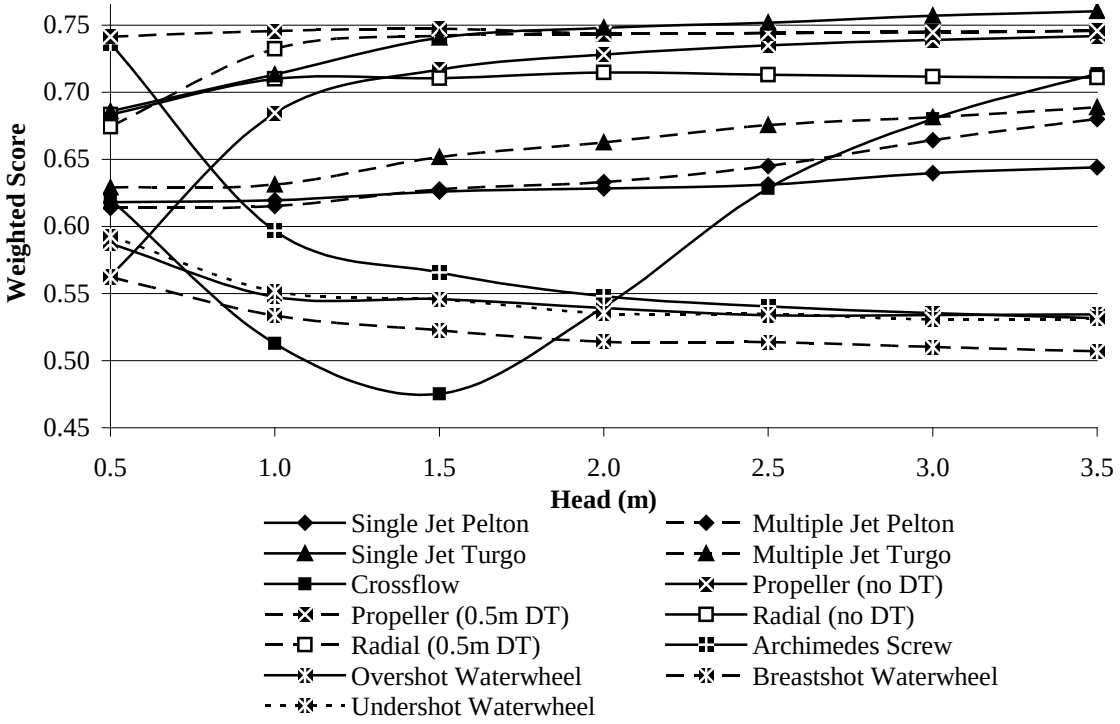

Fig. 3. The weighted scores for the 13 turbine choices over the head range 0.5 to 3.5m, 'DT'=Draft Tube.

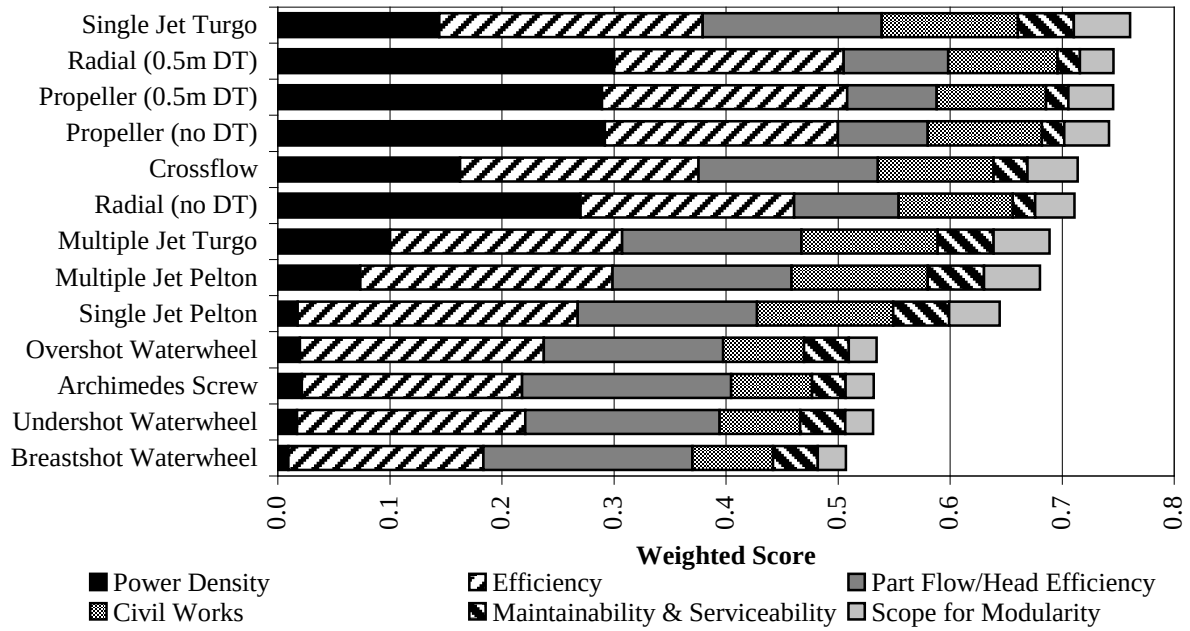

Fig. 4. The weighted score at 3.5m head for the 13 turbine choices with the contributions from each of the different selection criteria, 'DT'=Draft Tube.

Using this selection method and the specification in Table 2, the propeller turbine with draft tube (DT) should be selected if the typical head is between 0.5 and 1.5 m, and the single-jet Turgo turbine should be selected if the typical head is between 1.5 and 3.5 m.

5. Discussion

Fig. 2 (a) shows that the reaction turbines have a superior power density. As the head increases, the power density of the impulse turbines and waterwheels improves, whilst that of

the Archimedes Screw decreases. The conventional solution of adding multiple jets for Pelton and Turgo turbines at low heads is penalised in the power density, as the extra pipe work required to feed the jets takes up a large amount of volume. The efficiency of the single jet impulse turbines is superior to all the other turbines, as shown in Fig. 2 (c). As the head increases then the speed of the impulse turbine increases, so removing the need for a gearbox, increasing the overall efficiency of the turbine. Fig. 3 shows the variation in the weighted scores over the head range. This shows that a propeller turbine with a draft tube is the most suitable solution between 0.5 and 1.5 m typical head, with the single-jet Turgo turbine the best solution above 1.5 m typical head. The propeller and radial turbines with draft tubes have a similar weighted score to the single-jet Turgo turbine above 1.5 m head and therefore are viable choices for the specification. The reaction turbine result is expected, as many of the low head commercial turbine systems available are propeller turbines with draft tubes. The surprising result in this analysis is the Turgo turbine which is usually only used in medium to high heads – as indicated in the application range graph in Fig. 1, and stated in several literature resources such as [2]. However, as Harvey points out in [8], the Pelton turbine, and therefore the Turgo turbine, can be used in low heads if low speed and runner size do not pose problems. Using the calculations in the previous section, the runner diameter for a single-jet Turgo turbine generating 1.3 kW at 3.5 m head would be 435 mm, which would therefore not pose a portability problem in rural areas.

6. Conclusion

This research is part of a project to develop a low head pico-hydro off-grid network. The turbine selection is the first phase of the project which will look at developing the network technology requirements. This paper has presented a method of selecting low head pico hydro turbines through a multi-criteria analysis, using the specification of the turbine to assess the turbine types through quantitative and qualitative analyses. Using this method, a propeller turbine with a draft tube or a single-jet Turgo turbine has been shown to be the best solution for a given low head, variable flow specification.

Acknowledgements

This research is funded by Renishaw plc, and supported by Engineers Without Borders, UK.

References

[1] B. Massey, Mechanics of Fluids, Stanley Thornes Ltd, 7th Edition, 1998.

[2] O. Paish, Micro-hydropower: status and prospects, Proceedings of the Institution of Mechanical Engineers, Part A: Journal of Power and Energy, 216(1), 2002, pp.31-40.

[3] G. Muller and K. Kauppert, Old Watermills - Britain's new source of energy?, Proceedings of the ICE: Civil Engineering, 150, November 2002, pp.178-186.

[4] European Small Hydropower Association, A Layman's Guidebook on How to Develop a Small Hydro Site, 2nd Edition, 1998.

[5] G. Muller and J. Senior, Simplified Theory of Archimedean Screws, Journal of Hydraulic Research, 47(5), 2009, pp.666-669.

[6] F. C. Lea, Hydraulics for Engineers and Engineering Students, Edward Arnold, 1945.

[7] S. Pugh, Total Design, Prentice Hall, 1st Edition, 1991.

[8] A. Harvey et al, Micro-Hydro Design Manual, ITDG Publishing 1st Edition, 1993.

Small scale hydropower: generator analysis and optimization for water supply systems

Guilherme A. Caxaria[1,*], Duarte de Mesquita e Sousa[2,**] , Helena M. Ramos[3,***]

[1] *Electrical and Computer Engineering Department, Instituto Superior Técnico, Technical University of Lisbon, Lisbon, Portugal.*
[2] *Electrical and Computer Engineering Department and CIE[3], Instituto Superior Técnico, Technical University of Lisbon, Lisbon, Portugal.*
[3] *Civil Engineering Department and CEHIDRO, Instituto Superior Técnico, Technical University of Lisbon, Lisbon, Portugal.*
** Av. Rovisco Pais, 1049-001, Lisbon, Portugal , E-mail: gui.caxaria@gmail.com*
*** Av. Rovisco Pais, 1049-001, Lisbon, Portugal , E-mail: duarte.sousa@ist.utl.pt*
**** Av. Rovisco Pais, 1049-001, Lisbon, Portugal , E-mail: helena.ramos@civil.ist.utl.pt*

Abstract: This work focuses on the analysis of the power generation feasibility of both a pump as turbine (PAT) and an experimental propeller turbine, when applied to water supply systems. This is done through an analysis of the electrical generation aspects of the PAT's induction motor and of a permanent magnet DC motor, which was connected to the propeller turbine. The collected data allows for parameter optimization, adequate generator choice and computational modeling. These tests constitute a good sample of the range of applicability of small scale turbines as valid solutions for micro-hydro. It is also possible to consider multiple scenarios, such as rescaling/resizing, for larger turbines and systems, and the use of power electronics for further efficiency enhancing.

Keywords: *Small-scale hydropower, water supply systems, low power turbines, behavioral analysis*

1. Introduction

Starting from a scientific research base in the field of hydraulics, the objective of this work is to study the applicability and performance of electrical generators when connected to low power hydro turbines, for use in water supply systems (and others with similar characteristics). The generated power has a broad range of application, namely in the field of decentralized production (either on or off-grid) for use in rural or isolated areas, as well as in urban areas. It is possible to use the generated power to supply devices related with the small-scale industry (e.g. hydro-mechanical systems in pumping stations), communication stations, data acquirement, control or telemetry systems, or even observation posts in isolated areas.

Through the use of computer models, laboratorial tests and prototype analysis, a solution for a certain micro-hydro scheme is chosen. Behavioral analysis is then undertaken, allowing for further generator parameter optimization.

1.1. Water supply systems

Water supply systems aren't built with a power generation purpose. However, due to the type of infrastructure which is used for their normal operation (pressure reducing and flow control valves, reservoirs, pumps, and piping), they offer a multitude of power generation scenarios while assuring an almost constant flow rate 24h/day. It is then possible to generate power in the following manners: replacing (or assembling a joint installation with) pressure reducing valves; taking advantage of the hours where there's an increased demand for water (hours which coincide with an increase in demand for electrical power); piping water between

reservoirs, in hours of lower demand, and storing the produced energy. All of these are subject to the installation of adequate equipment in the piping.

1.2. Micro-hydro turbines

The existing micro-hydro conversion equipment is based on impulse turbines (i.e. *Pelton*, *Turgo*, and *Cross-flow*) and on reaction turbines (i.e. *Francis* and *Kaplan/propeller*). Their main problem is the low efficiency values (typically 30% to 60%) that are obtained regarding small scale schemes. In this case optimization is needed, in order to increase their efficiency. This type of work, however, will not be discussed in depth in this document.

The application of commercially available small scale turbines to water supply systems is conditioned by a series of restrictions, namely head, flow, pressure, and the need for piping adaptation, which can make them unsuitable for application in a vast majority of sites. Therefore, it is necessary to optimize and/or develop power generation solutions for water supply systems.

2. Pump as Turbine (PAT)

Given the information in the introductory chapter, a PAT was the first of the two solutions that have been considered for power generation in water supply systems. This was due to its simplicity in installation, only requiring small adaptation procedures. In water supply systems, a PAT is to be installed in a bypass circuit.

2.1. Theoretical considerations

Pumps as Turbines have, for the past three decades, been tested and considered for micro-hydro generation. This is due to a number of arguments, those being that PATs are mass produced, for various operating conditions, such as flow, drop, dimensions and rotating speeds. The electromechanical converters that usually equip a PAT are asynchronous machines, optimized for pumping operation, which, as previously mentioned, help to reduce acquisition costs, which, in turn, increase the competitiveness of a PAT in a power generation scenario. Another advantage in the use of a PAT is that its technology is vastly explored and with proven results, adding to the fact that these allow for power values starting at 50W [6].
The main disadvantage in the use of a PAT is that its operation is highly dependent on flow rate, not allowing for medium and high variations of flow. In situations where multiple flow values exist, it is possible to consider the use of two or more PATs [2].

2.2. Laboratorial testing

For laboratorial testing, a PAT (WITH $N_{SPT(M,M^3/S)} = 21\,\text{RPM}$ AND $N_{SPT(M,KW)} = 51\,\text{RPM}$) was acquired, and inserted in a laboratorial system that allowed for head and flow variation, and for grid-connected excitation. The electrical machine that equips the PAT is a six-pole (i.e. with a synchronous speed of 1000rpm) 550W induction motor. The objective was to test the power generation feasibility of the PAT when connected to the grid (i.e. with no additional equipment, such as capacitors for excitation), along with testing the transient response of the induction machine when a hydraulic transient regime occurred (e.g. the closing of a valve). Also analyzed was the behavior of the PAT under runaway conditions.

2.2.1. Power generation testing

Regarding power generation, the results are presentED in Figure 1. Values up to 160W (at a flow of 4.4l/s) were registered. However, due to the fact that the machine was excited

resorting to the main grid, the excitation required 240W of power; this meaning that, in fact, the generator never generated enough power to "counter" the excitation, and thus, the load flow was always done from the grid to the generator.

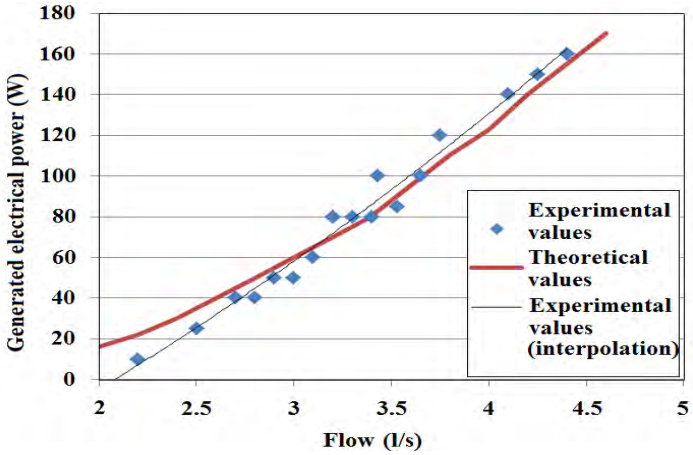

Fig. 1. PAT Power/Flow characteristics.

2.2.2. Transient response analysis

Transient analysis, either electrical or hydraulic, at a micro-hydro scale, is a field of research that is rather unexplored. This field of research, however, is of extreme importance, in order to properly dimension electrical protection methods. In this particular case, a h ydraulic transient regime was created by the sudden closure of a valve which, in turn, originated an electrical transient regime. The testing results are presentED in Figure 2.

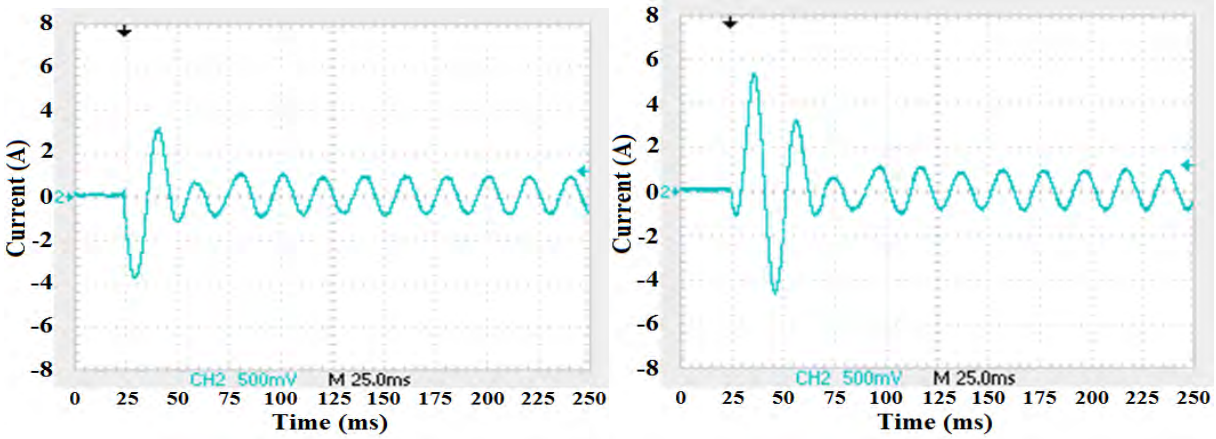

Fig. 2. Electrical transient regimes in the PAT, derived from pressure surges in the piping.

According to the work of [5], it is possible to verify that waterhammer effects induce electrical transients in the generator, thus influencing the power generation. However, it is possible to observe that the duration of the transient regime is, on both cases, under 100ms. Attending to the values of the time constants that are present in the used hydraulic systems, it is possible to claim that the generator doesn't introduce additional dynamic restrictions to the global system.

2.2.3. Runaway conditions analysis

Testing of runaway behavior was also undertaken, in order to properly apply control methods to the system. The results of the mentioned testing are presentED in Figure 3.

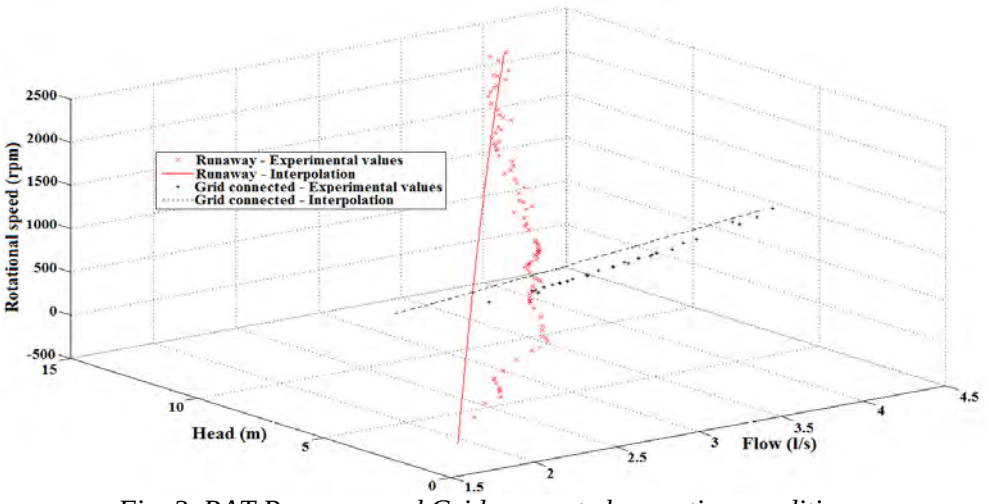

Fig. 3. PAT Runaway and Grid connected operating conditions.

It is possible to observe that, in runaway conditions, for the same flow rate value, pressure surges occur (here described by an increase in the available head). This is coincident with the work of [3] where it is shown that turbines with low specific rotating speeds induce high pressure surges in the piping

2.3. Computational model: control simulation

Given the results obtained in laboratorial testing and due to the nature of water supply systems, the chosen (and simulated) control method was the one resorting to flow control valves. The objective of these simulations was to control and avoid a runaway situation, which results from a load withdrawal on the generator. *MATLAB/Simulink* was used. The control scheme is described in fig 4 and the simulation results are presented in fig 5.

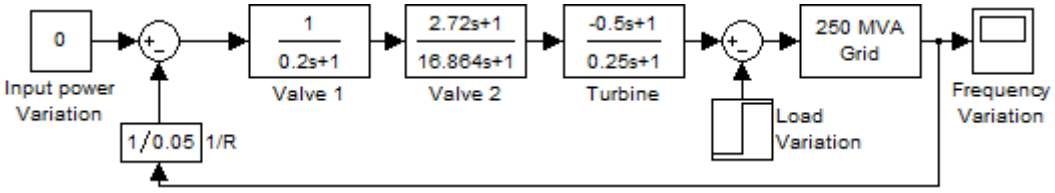

Fig. 4. Control scheme used for the PAT simulations.

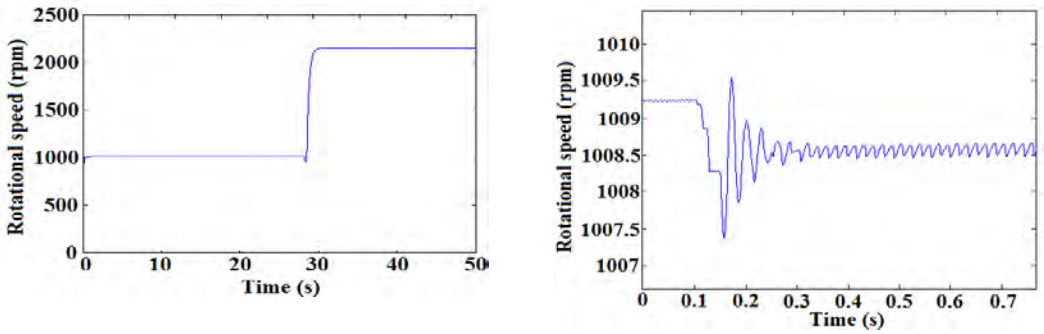

Fig. 5. Simulation results for full and uncontrolled (left), and partial and controlled (right) load removal on the PAT.

3. Five blade propeller turbine (5BPT)

A propeller turbine was the second of the two solutions chosen for micro-hydro generation in water supply systems. Again, equipment and installation simplicity were key factors regarding the choice.

3.1. Theoretical considerations

Propeller turbines are axial turbines, adequate for operation under low head (up to a minimum of 1.5m) and high flow rates. These have been mainly used in small (<10MW) and mini (<2MW) hydro schemes. Only recently, due to developments in scientific research (which, in turn, have resulted in an increase of the turbines' efficiency), has the application been extended to the field of micro-hydro.

Given the difficulties on applying commercially available micro-hydro turbines to water supply systems, a 100mm diameter prototypical propeller turbine was developed specifically for this purpose (under the HyLow project of the 7th Framework Program of the European Union) and (through the work of [7]) optimized for small scale (i.e. blade shape, number, and orientation). This type of turbine can be installed in either a bypass to, or directly in the main piping circuit. Its main disadvantages are that it is still experimental equipment, and there's very little knowledge regarding its long time operation in water supply systems.

3.2. Laboratorial testing

For laboratorial testing, similarly to what was done with the PAT, the 5BPT (with $N_{SPT(M,M^3/S)} = 238\,\text{RPM}$ AND $N_{SPT(M,KW)} = 118\,\text{RPM}$) was inserted in a laboratorial system that allowed for head and flow variation, and that mimicked the conditions found on a real water supply system. Being experimental equipment, the maximum obtained speed was of 1550rpm. For power generation purposes a 500W DC permanent-magnet machine, derived from an electrical scooter, was acquired. Due to the nature of the generator, and to the lack of additional power electronics, no grid connection was done. The turbine's characteristic curves are shown in Figure 5, the DC machine's characteristics and curves are shown in Table 1 and Figure 6.

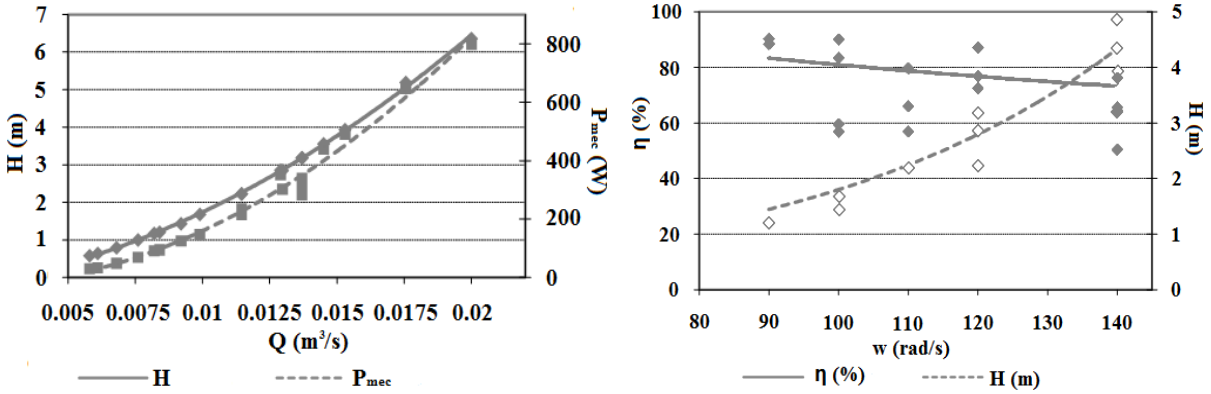

Fig. 6. Five blade propeller turbine characteristic curves

Table 1. DC motor manufacturer's parameters

Rated voltage (V)	Rated power (W)	No-load Current (A)	No-load Speed (rpm)	Rated Torque (N.m)	Rated Speed (rpm)	Rated Current (A)	Rated efficiency (%)
36	500	2.2	3150	1.9	2500	17.8	78

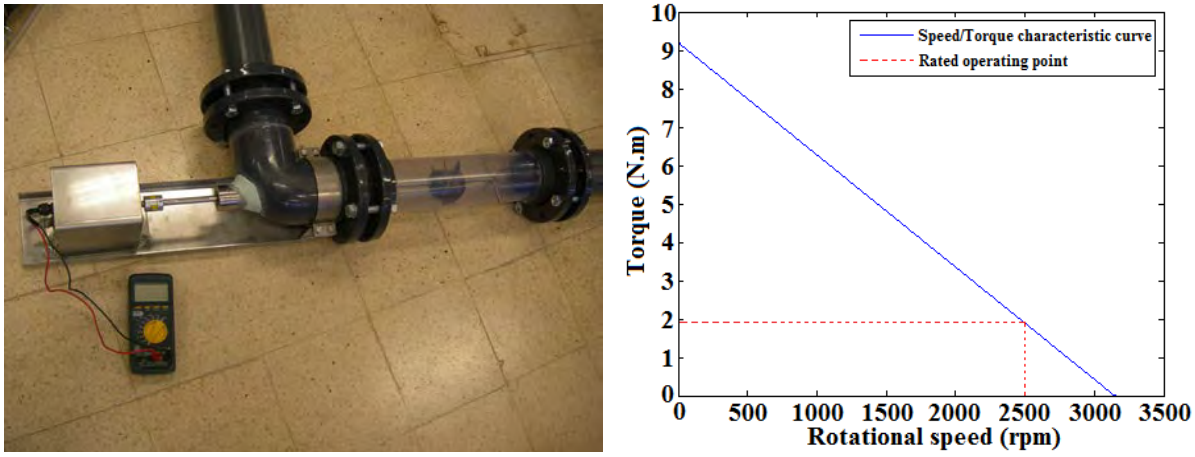

(a) *(b)*

Fig. 7. (a) The turbine+generator group (b) DC motor manufacturer's Torque/Speed curve.

From the data provided by the manufacturer, it was possible to calculate the machine's theoretical characteristic parameters, namely the armature resistance and the k_ϕ constant, to be used for computational simulations:

$$k_{\phi(manufacturer)} = 0.1091 \qquad R_{a(manufacturer)} = 0.4267\Omega$$

3.2.1. Power generation testing

For power generation testing purposes a 6Ω, 16A rheostat was used, in order to emulate the behavior of "normal" electrical loads. The testing was done by varying the resistive load while maintaining a fully open admission valve. The testing was done in three separate sessions, being that, on the first session, there was a constraint in terms of head and flow, and on the second and third sessions, that constraint was eliminated. The best efficiency points for the experimental sessions are presentED in Table 2.

Table 2. Best efficiency points for the three experimental sessions.

Experimental session	Maximum Generated power (W)	Rotational speed (rpm)	Flow rate (l/s)	Generator efficiency (%)	Overall efficiency (%)
#1	3.64	182.5	3.6	35.6	32.8
#2	34.4	719.7	8.8	50.3	46.8
#3	36.2	619.8	10.4	68.2	60.7

From the testing results, it w as possible to calculate the machine's real characteristic parameters, and while the armature resistance corresponded to the manufacturer's value, the k_ϕ constant greatly differed:

$$k_{\phi(experimental)} = 0.1443 \qquad R_{a(experimental)} = 0.4267\Omega$$

3.2.2. Computational model: power generation simulations

Given the obtained conclusions regarding the DC machine's characteristic parameters, simulation was undertaken, again using *MATLAB/Simulink*, in order to test the power generation under optimal conditions (i.e. with $k_\phi = k_{\phi(manufacturer)}$). Due to the nature (i.e. size)

of the turbine, a transfer function similar to the Pat's was used. The simulation results are presented in figures 7 and 8.

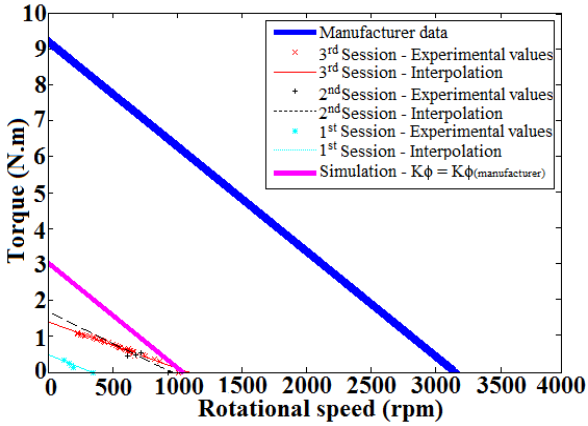

Fig. 8. Manufacturer's, experimental, and simulation Torque/Speed curves

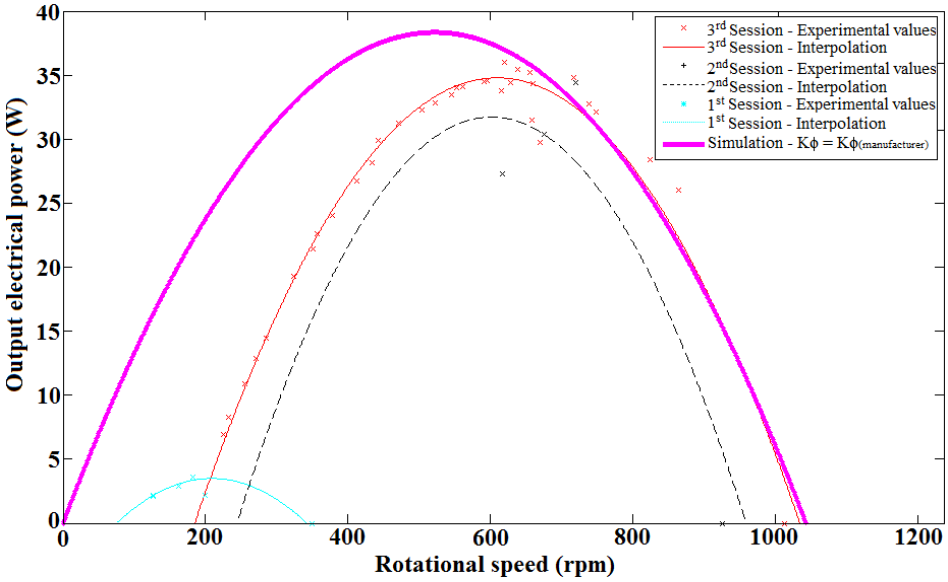

Fig. 9. Simulation and experimental turbo-generator group Output power/Speed curves

4. Conclusions and recommendations

4.1. Pump as Turbine

4.1.1. Main conclusions

From the power generation testing results, it is possible to conclude that the application of PATs for micro-hydro generation in water supply systems is viable. However, using grid-connected excitation may not be viable in all cases, namely the ones regarding lower power values. Control methods using valves, although efficient, may not be viable, namely in situations where there's a g eneration scheme directly applied to the main piping. In these cases, reducing the water flow, for control purposes, in hours of greater water need, may be prejudicial for the populations.

4.1.2. Recommendations

To avoid the excitation related issues, and according to [2] and [11], using "motor run" capacitors (either star, delta, or C-2C connected) for excitation purposes is an alternative, and more efficient way, than resorting to the main grid. As mentioned, for main piping connected

generation schemes, control methods using ELCs, or other electronic devices, may eliminate the issues related with control methods using valves.

4.2. Five blade propeller turbine

4.2.1. Main conclusions

Despite the power values that were generated, the 5BPT, regarding its use in water supply systems, is a very promising solution, with high hydro-mechanical efficiency values. The generated power values using the DC machine, although low, are still viable in a battery charging, or in a low power consumption equipment supply context. The turbo-generator group, when applied to water supply systems, doesn't interfere with the normal flow behavior in the piping.

4.2.2. Recommendations

Regarding power generation in a real system (opposed to a laboratorial one), for testing purposes, a permanent-magnet synchronous generator (or an induction motor) should be used. For laboratorial purposes, a lower power generator should be used, more adequate to the rotational speed and torque values present in the experimental piping system. Testing under better flow and head conditions, for improved power generation, is also recommended for future work.

References

[1] A. Williams, Pumps as Turbines: a user's guide, 2nd Edition, Practical Action Publishing, 2003.

[2] H. Ramos, Guidelines for design of small hydropower plants, 2000, WREAN/DED, ISBN 972-96346-4-5.

[3] H. Ramos, A.B. Almeida, Dynamic effects in micro-hydro modeling, 2003, pp. Water Power & Dam Construction, ISSN 0306-400X.

[4] H. Ramos, A.B. Almeida, Parametric analysis of waterhammer effects in small hydropower schemes, 2001, Journal of Hydraulic Research, IAHR, Vol. 39 (4), pp. 429-436, ISSN-0022-1686.

[5] H. Ramos, A. Borga, Pumps as turbines: unconventional solution to energy production, Urban Water International Journal, Elsevier Science Ltd, 2000, pp.261-265.

[6] H.M. Ramos, A. Borga, M. Simão, New design solutions of low power for energy production in water pipe systems, Water Science and Engineering, 2009, 2(4): 69-84, doi:10.3882/j.issn.1674-2370.2009.04.007.

[7] H.M. Ramos, M. Mello, P. De, Clean power in water supply systems as a sustainable solution: from conceptual to practical analysis, IWA Publishing, Water Science and Technology, 2010.

[8] H.M. Ramos, F. Vieira, D. Covas, Energy efficiency in a water supply system. Water Science and Engineering, 2010, pp.331-340.

[9] J.S. Ramos, H.M. Ramos, Sustainable application of renewable sources in water pumping systems: optimized energy system configuration, 2009, (doi:10.1016/ j.enpol. 2008.10.006), Energy Policy 37, 633-643.

[10] N. Smith, Motors as generators for micro-hydro power, 2nd Edition, Practical Action Publishing, 2008.

Performance evaluation of cross-flow turbine for low head application

Bryan Ho-Yan[1], W. David Lubitz[1,*]

[1] *School of Engineering, University of Guelph, Guelph, Ontario, Canada. N1G 2W1*
** Corresponding author. Tel: +1-519-824-4120 ext. 54387, Fax: +1-519-836-0227, E-mail: wlubitz@uoguelph.ca*

Abstract: Pico hydro generators are a promising means of providing cost-effective electricity to locations with limited or no availability of grid-supplied electricity. The Firefly design has been employed throughout rural areas of Cameroon and used as a light battery charger. It is hoped to extend the turbine capacity to provide steady baseload output between 100-500 W operating at low head sites (2-10 m). Suitability of the Firefly under these conditions is currently unknown, and the turbine has not been evaluated under conditions of very low head. The study objective was to characterize the performance through laboratory testing under conditions of low head and variable flow rate, in order to determine if the Firefly turbine meets the requirements of users in Cameroon. At this time, construction has been completed of the Firefly turbine and testing apparatus. The testing process and initial Firefly performance results, as well as lessons learned to date, are the focus of this paper. This is the first phase of a larger project seeking to design an optimized pico hydro turbine that balances performance, reliability and ease of manufacture and installation. The Firefly results will be used as a baseline in comparisons to new turbine designs.

Keywords: *Pico hydro, Cross-flow turbine, Low head, Remote power generation, Firefly.*

1. Introduction

Rural electrification enhances welfare through increased productivity, health, media access, and education. Studies by the Independent Evaluation Group of the World Bank (2008) have demonstrated this empirically and have also found that the benefits from rural electrification outweigh the cost of investment.

1.1. Introduction

Pico hydro systems harness the energy in flowing water at capacities smaller than 5 kW. They are recognized as a viable option to electrify remote areas with regard to economical, environmental, and social perspectives. Pico hydro yields one of the lowest generating costs amongst off-grid energy options (Williams & Simpson, 2009). Unlike large scale hydropower, there is low environmental impact with pico hydro systems, mainly due to the exclusion of large water containment. Associated large civil works and the displacement of habitats are not required for the commissioning of pico hydro systems. In addition, negative impacts of large reservoirs such as siltation, increased mercury levels, and off-gassing of green house gases from submerged decomposing organic material are avoided (Gunkel, 2009).

1.2. GREEN STEP e.V in Cameroon

GREEN STEP e.V. (http://www.green-step.org) is a non governmental organization originating from Germany with the objective to improve rural livelihoods through providing training and co-financing of renewable energy projects, building environmental awareness through education, and sustainable agriculture extension. In 2007, the organization connected with the M'muock village situated in south western Cameroon. The majority of the 70,000 residents of M'muock to do have access to grid-supplied electricity.

Pico hydro technology has been one of the main focuses and to date, 40 craftsmen have been trained and nearly 10 turbines successfully built. However, after a year in use, only 2 turbines remained in operation at a limited capacity. Observations (Hertlein, 2010) made from these implemented systems include:

- Concerns regarding ownership have arisen, especially in situations where multiple stakeholders (ie. community or multiple household ownership) are involved. The need for smaller systems targeted towards single dwellings has been identified as lines of responsibility are defined more clearly and free-rider issues are mitigated.
- Improvements are needed to reduce the complexity of the design and also increase robustness. End-users may not be made aware of the importance of maintenance; in addition, distances to workshops are far.
- The current systems employ expensive car alternators, car batteries and inverters. These components are also prone to failures, with the wearing down of alternator brushes being the main concern.
- The willingness-to-pay for a pico hydro system is estimated to be €150.
- Training is required for local construction of pico hydro systems.

Based on the above lessons-learned, the overall project objective is to design a robust and reliable pico hydro system that is affordable at the household level, suitable for household electricity demand, uses locally sourced materials, and can be manufactured locally at a small industrial scale. The operational range is to be 2 m to 10 m head, with flow rates of 5 L/s to 100 L/s, and electrical output in the range of 100 W to 500 W. The initial phase of the project is to characterize the performance of the existing systems at 2-10 m head and variable flow rates, in order to determine the degree to which the current Firefly turbine meets the targets that are required by users in Cameroon, and provide a baseline for comparisons to future designs.

1.3. Purpose

The purpose of this report is to present the low-head and variable-flow-rate laboratory test rig implemented at the University of Guelph (Canada) that is used for testing a pico hydro system built to the same specifications as those used in Cameroon. Results from the tests are tabulated. In addition, lessons learned from the Firefly construction process, and recommendations for improving the testing process are identified.

2. Methodology

The existing pico hydro systems employed by GREEN STEP e.V. in the field are known as the "Firefly" design. A Firefly unit was constructed in Guelph (Canada) for laboratory testing, according to the instructions of Portegijs (2003). Laboratory testing was conducted on a rig with the ability to vary flow rates and heads within the low head range. Focus was placed on the low head range as the Firefly documentation did not provide performance for heads below 3 m (Portegijs, 2003).

2.1. Firefly

The Firefly was designed by Jan Portegis for use in rural Philippines. It consists of a cross-flow turbine attached to a car alternator, and was intended strictly for battery charging.

The turbine has 27 blades supported by circular side plates with a 75 mm diameter and turbine height of 55 mm (Fig. 1). A 51 mm wide nozzle guides the flow to the turbine. The range of operating head is 3 m to 7 m, and 8 m to 25 m with governed flow (Portegijs, 2003).

In the original Firefly design, the field current of the alternator is controlled by 4 incandecsent light bulbs (3 x 20 W and 1 x 10 W) and switches connected in parallel. Six different resistance values are possible, which allows for optimization of the field current (Portegijs, 2003).

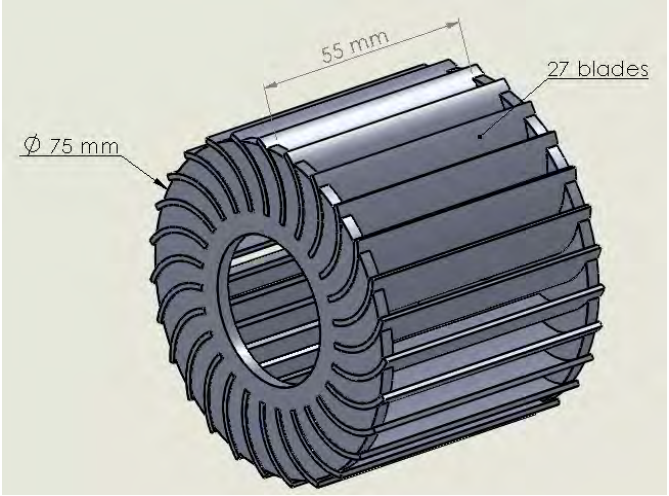

Fig. 1. Runner assembly.

2.2. Firefly construction

Construction of the Firefly for testing in Guelph generally followed the design manual (Portegijs, 2003). The cross-flow sidewalls were laser cut rather than hand cut. The blades were manually sheared and formed as per instructions. The turbine assembly was welded instead of soldered, as detailed in the design manual, however this is in agreement with practices used for the Cameroonian units. The nozzle and frame were also fabricated as per instructions. The casing was excluded as the test unit would not be exposed to a harsh field environment. A Valeo model AB180128 automobile alternator was used. All construction (except for laser cutting) took place within the engineering machine shop facilities at the University of Guelph.

Considerable lessons were learned from the build process. Significant skill on the part of the fabricator is required to build these units. Difficulty would be further accentuated by limited resources. The use of jigs, especially for blade cutting and bending, could improve consistency from blade to blade and simplify the turbine assembly: additional practical advice on fabrication would be a useful addition to an updated construction manual. The turbine sidewall fabrication involves cutting multiple curved slots for the attachment and soldering/welding of the curved blades. Consistently cutting the curved slots in the side walls is extremely difficult for unskilled workers (such as university students), which lead us to laser cut these components. It should be noted that skilled workers with metal working experience using appropriate jigs could mitigate much of this concern.

Variability between individual Firefly is also introduced if different models of alternators are used. For example, the joining of the turbine to the alternator shaft differs slightly between the Guelph unit and the instruction manual, owing to a different configuration of the alternator

shafts. This need to adapt to different alternator models affects the standardization of the build process, complicating construction by forcing builders to veer away from the design manual.

2.3. Test Apparatus

The Guelph laboratory test apparatus (shown in Fig. 2) consists of an 1135 L (0.9 m x 1.9 m plan, 0.6 m height) reservoir elevated on a 3.3 m high platform. A 10 cm (4 in) diameter ABS plastic penstock connects the drainage hole at the base of the reservoir to the Firefly. The total length of the penstock pipe from the reservoir to the Firefly is approximately 4 m. The Firefly is located above a receiving reservoir. An electric pump is used to return water to the supply reservoir between tests. With the Firefly in place, the system has a nominal head of 3 m, however, the head can be varied by changing the height of the Firefly while adjusting the length of the penstock.

The Firefly's alternator field circuit was connected to a high capacity 12 V deep discharge lead acid battery. A resistor was included in the circuit. Changing the resistance of this resistor allowed the field strength to be varied. The power output of the alternator was directly connected to a 2.0 ohm dynamic braking resistor with a 2 kW capacity.

A Medusa Scientific PowerPro power meter capable of measuring voltage, current and power was connected to the alternator. The PowerPro was connected to a desktop PC, which recorded data at a rate of 4 Hz.

Flow rate is controlled by throttling a needle valve installed at the penstock inlet at the base of the reservoir. Instantaneous reservoir level, and by extension, flow rate out of the reservoir, is measured using a float connected to an ultra-low friction potentiometer (adapted from an anemometer) by a swing arm. The potentiometer is connected to the PowerPro via a voltage divider circuit, so that head and flow rate are recorded simultaneously with voltage, current and power. Before testing, the output of the float sensor is calibrated and a transfer function is derived that outputs reservoir level as a function of the recorded signal.

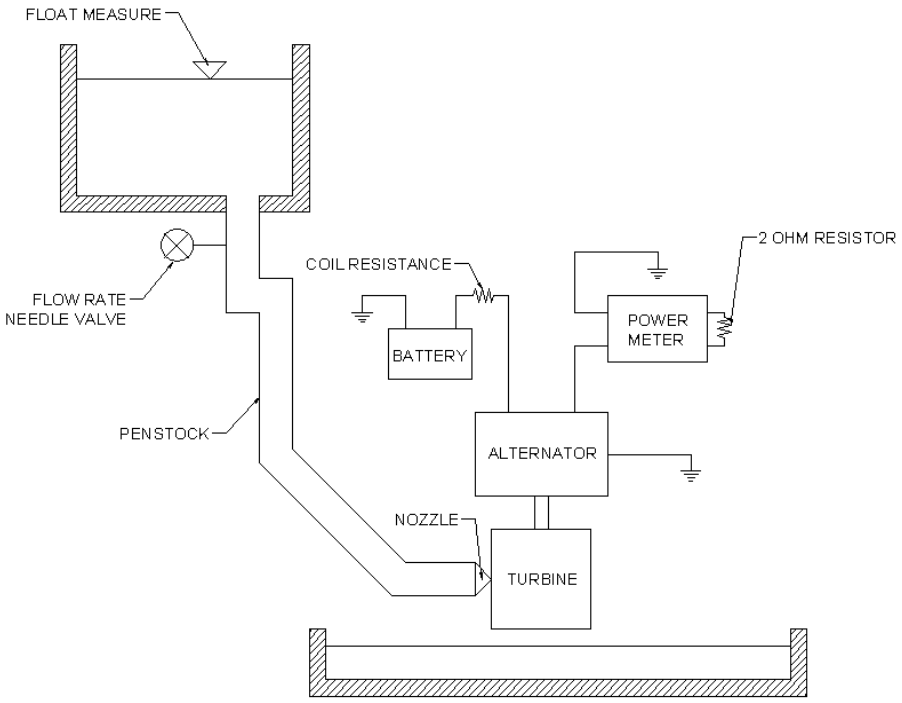

Fig. 2. Layout of test apparatus.

2.4. Test Method

Tests were conducted with flow rates ranging from 5.52 to 5.81 L/s and average heads of 3.4 m. The field circuit resistance was varied to determine the optimum resistance to include in the field coil circuit. Resistances used were 0, 5, 10, 20, and 47 ohm.

3. Results

The results of the tests are tabulated below in Table 1. Power output from the Firefly under a generally consistent flow rate and head is reported, with varying field resistance.

Table 1. Experimental results

Coil Resistance [ohm]	Flow Rate [L/s]	Average Head [m]	Average Power Output [W]	Efficiency
0	5.61	3.40	9.39	4.8%
5	5.81	3.39	12.15	5.9%
10	5.52	3.39	11.60	6.0%
20	5.73	3.39	10.70	5.3%
47	5.58	3.39	10.14	5.2%

Based on the test results, a 5 ohm to 10 ohm field circuit resistance was observed to be the optimal resistance, resulting in a higher average power output than was achieved with higher or lower resistances in the field circuit. The field current control recommended in the design manual is calculated to range from 2.1 ohm to 14.4 ohm, which is consistent is consistent with these test results.

Over the entire range of resistances, power output and efficiencies were lower than the predictions of Portegijs (2003). Portegijs predicted but could not test that the Firefly would produce 46 W at 3 m head and 5.3 L/s. It should be noted that a typical alternator would be below its normal operating range, and likely to underproduce the predicted value. Portegijs identified this as a concern, and suggested that his calculated values would be high because of this, for the combination of head and flow rates tested here. This is believed to be one reason for the lower than expected performance during testing.

4. Discussion

Given the lower than expected power outputs and efficiency, it is believed that the test Firefly requires modifications to enhance the test results. Construction of the Guelph Firefly must be revisited: it appears that the gap between the nozzle and turbine is higher than other examples of the Firefly. Inspection of the unit after testing showed that realignment is needed of the nozzle with respect to the cross-flow turbine, and that a small amount of nozzle movement was possible. This is considered to be the root of the matter. This demonstrates the criticality of construction training and the need for simplistic designs.

The test results also confirm that at the combinations of head and flow rate tested, the direct drive automobile alternator may not be the ideal type of generator to utilize, due to inefficiencies when operating at low rotational speed, and utilization of a large fraction of the power generated to energize the coils that provide the magnetic field. One recommendation is to consider the use of a permanent magnet alternator that can provide power over a greater range of rotation speeds, and critically, not consume power in its operation.

5. Conclusions

Following adjustments to nozzle position and mounting of the Guelph Firefly unit, testing will recommence with varied flows and heads.

Modeling the alternator is difficult: in addition to rotation speed and torque, performance is impacted by field strength. This makes it difficult to separate the effects of alternator performance from turbine performance. Future testing will separate the Firefly from the alternator. The Firefly turbine will be characterized by testing on a dynamometer over a range of torque and rotation rates. Separate dynamometer testing of the alternator will allow determination of the relative importance of alternator optimization (e.g. field strength) compared to turbine configuration (e.g. nozzle alignment). Alternative turbines of different configurations and lower parts counts will also be designed and tested, and compared to the Firefly.

This paper has described the initial stages of this research project. Additional testing of the current Firefly unit is currently being conducted, and work has begun on the design of different turbines with the goal of further optimizing ease of construction, performance and reliability. The results of the continued testing will be used to draw conclusions on the appropriateness of the current Firefly, and improved designs, in M'muock, Cameroon.

References

[1] International Evaluation Group – World Bank, The Welfare Impact of Rural Electrification: A Reassessment of the Costs and Benefits, 2008, URL: http://siteresources.worldbank.org/EXTRURELECT/Resources/full_doc.pdf [last accessed January 11, 2011].

[2] A.A. Williams and R. Simpson, Pico hydro – Reducing technical risks for rural electrification, Renewable Energy 34, 2009, pp. 1986 – 1991.

[3] G. Gunkel, Hydropower - A green energy? Tropical reservoirs and greenhouse gas emissions, Clean - Soil, Air, Water 37 – 9, 2009, pp. 726 – 734.

[4] J. Hertlein, Project start document – Small Scale Water Turbine for Cameroon. Report. Green Step e.V., 2010.

[5] J. Portegijs, J. The Firefly Micro Hydro System, 2003. URL: http://www.microhydropower.net/mhp_group/portegijs/firefly_bm/ffbm_index.html [last accessed January 11, 2011]

Water supply lines as a source of small hydropower in Turkey: A Case study in Edremit

S.Kucukali[1,*]

[1] *Cankaya University, Department of Civil Engineering, Balgat, 06530 Ankara, Turkey*
** Corresponding author. E-mail: kucukali78@hotmail.com*

Abstract: Hydropower has the highest share among the renewable energy sources of Turkey by 94% with a total installed capacity of 14,553 MW for the year 2009. Turkish government has based its energy policy on maximizing hydropower potential to be evaluated in next 15 years. In this context, private sector is expected to build hydroelectric power plants having a total capacity of 27,500 MW. Besides these hydropower plants, there is also a considerable hydropower potential in existing water supply systems. The most convenient locations for hydropower generation in water supply systems are water supply lines located before the water treatment or distribution network. In water supply lines, the excess pressure is dissipated by creating water jet in the pressure reduction tank. However, the excess pressure can be removed from the system by installing a hydro-turbine and it can be converted into useful energy by means of electricity. For a case study, the hydropower potential of the water supply system of Edremit in Turkey has been analyzed. There are 12 pressure reduction tanks along the water supply line of the city and the system has an electric energy potential of 4.08 GWh/year, corresponding to about 560,000 Euro/year economic benefit.

Keywords: *Hydropower, Water supply lines, Turkey.*

1. Introduction

The need for saving water and energy has grown as one of the world main concerns over the last years and it will become more important in the near future. Increase in oil and natural gas prices by 500% in last 15 years has made renewable energy sources become important than ever. Hydropower is a renewable energy source most widely used all around the world [1]. Installation of hydropower plants on water supply network has found a wide usage area in Europe (Table 1). For example, in Switzerland 90 small hydropower plants were installed on the municipal water supply network of the country (Table 2). The advantages of these facilities compared to river-type hydropower plants could be summarized as follows: (i) all civil works are present, which will reduce the investment cost in the order of 50% [2], (ii) the facility has no significant environmental impacts and it has a guaranteed discharge through the year, (iii) the generated electricity is used in the water supply system and the excess electricity is sold to the government, (iv) there is no land acquisition and significant operating costs [3]. In this context, this study aims to show the possible benefits of the installation of a water turbine in water supply line. This could be an alternative clean energy solution to reduce the consumption of energy supplied by the national electric grid mostly fed by fossil fuels and to induce the minimization of CO_2 emissions to the atmosphere. In the present study, utilization of the hydropower plants in existing water supply systems has been discussed. As a case study, the hydropower potential of the water supply system of Edremit, Turkey has been analyzed in detail.

Table 1. Some examples of hydropower plant installation on water supply lines in Europe. Data source: [1]

Plant Name	Country	Design discharge (m^3/s)	Gross head (m)	Output (kW)	Production (MWh/year)
Vienna Mauer	Austria	2	34	500	364
Mühlau	Austria	1.6	445	5750	34000
Shreyerbach	Austria	0.02	391	63	550
Poggio Cuculo	Italy	0.38	28	44	364
La Zour	Switzerland	0.30	217	465	1800

Table 2. Multipurpose schemes in Switzerland: operating and remaining potential. Data source: [1]

Water network type	Potential type	Number of sites	Output (MW)	Production (GWh/year)
Drinking water	Operating	90	17.8	80
	Remaining	380	38.9	175
Treated waste water	Operating	6	0.7	2.9
	Remaining	44	4.2	19

2. Methodology

A typical water supply system is composed of water source and storage, supply lines, water treatment plant, storage tank and distribution network (Fig. 1). The objective of water supply systems is to guarantee the delivery of adequate amount of good quality water to the inhabitants of the region. However, energy is needed to achieve this objective which requires operate water pumping and operation of treatment plants. The supply lines transport the water from storage to treatment facilities and treated water to storage tanks. It should be noted that the supply lines have limitations for pressure. For example, In Turkey, the static pressure should be in the range of 20-80 m head [4] and if the upper limit of the pressure is exceeded along the pipe line, pressure reduction valves or tanks are used to dissipate the excess pressure head. Based on the estimations of Bank of Provinces, there is a 30 MW hydropower potential in the existing pressure reduction and storage tanks in Turkey.

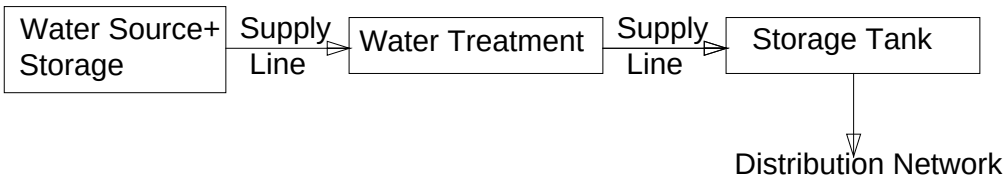

Fig. 1. Flow diagram of a typical water supply system

The shares of water supply sources in Turkey, with a capacity of 5.16 billion m^3 in 2006, are as follows: 36% dam reservoirs, 27% groundwater reservoirs, 27% springs, %6 rivers and 4% lakes [5]. The domestic water demand is expected to increase from 6.2 billion m^3 in 2007 to 26 billion m^3 in 2030 (Fig.2). There are totally 43 municipal water supply dams in operation and the distribution of these dams across the country is shown in Fig.3. The municipal dams

are distributed over 23 cities and the most of them are in the big cities like Ankara, Istanbul and Izmir [6].

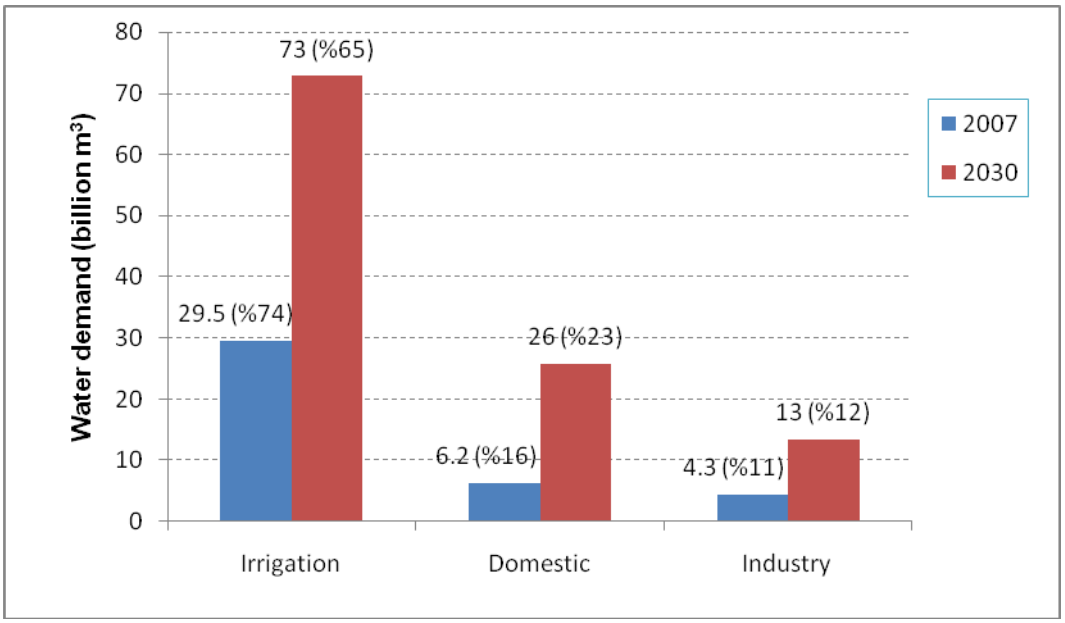

Fig. 2. Water demand of Turkey by sectors for 2007 and 2030 (projection by DSI)

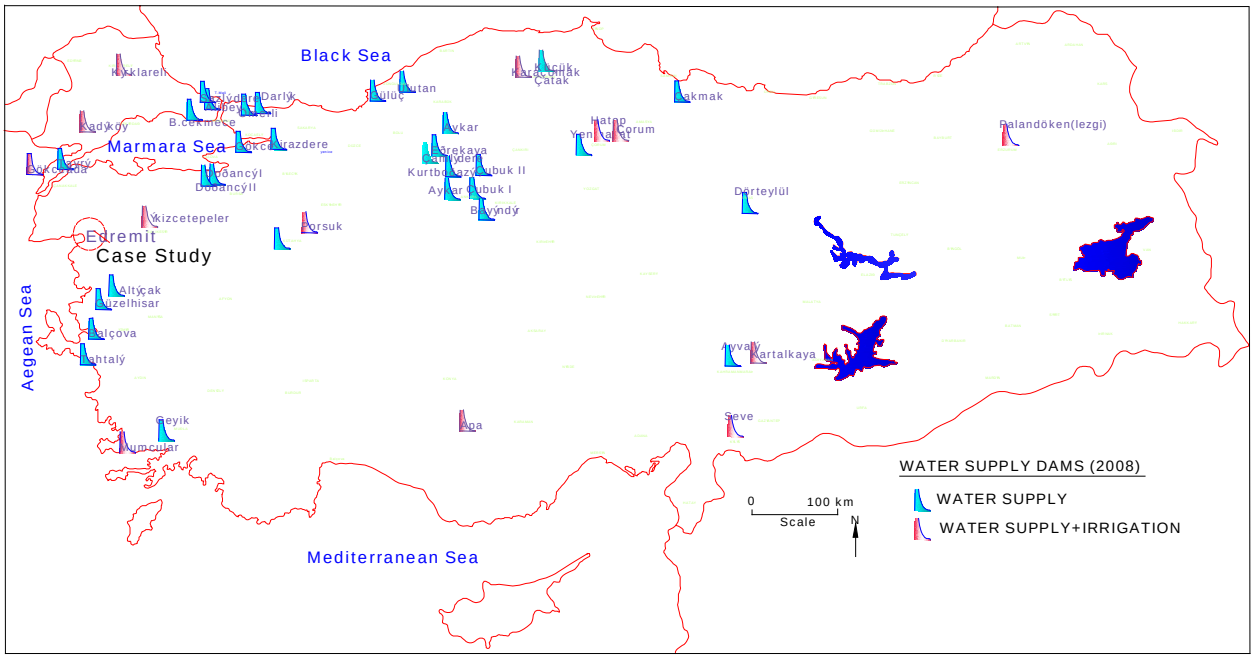

Fig.3. Municipal water supply dams in Turkey by 2008 and the location of the case study.

Hydro-turbines convert the water pressure into mechanical shaft power, which can be used to drive an electricity generator, or other machinery. The available power is proportional to the product of pressure head and water discharge. Modern hydro-turbines can convert as much as

90% of the available energy into electricity. The installed capacity P (kW) of a hydropower plant is calculated from

$$P = \gamma \times Q \times H_n \times \eta \quad (1)$$

where γ is the specific weight of water, Q (m^3/s) is the discharge, H_n (m) is the net head (m), η is the sum of the turbine and generator efficiency. The annual energy generation E (kWh/year) of a hydropower plant is obtained from

$$E = P \times t \quad (2)$$

where t is the operating hours in a year. The most convenient locations for hydropower generation in water supply systems are water supply lines located before the water treatment or distribution systems. In water supply lines, using the Bernoulli energy equation between sections 1 and 2 (Fig.4) and employing a velocity head correction factor of 1 gives

$$\frac{U_1^2}{2g} + \frac{p_1}{\gamma} + z_1 = \frac{U_2^2}{2g} + \frac{p_2}{\gamma} + z_2 + \Delta H \quad (3)$$

where, U is the average velocity, p is the pressure, z is the elevation above an arbitrary datum, g is the acceleration of gravity, ΔH (m) is the hydraulic head loss between 1 and 2. The head loss occurs because of the frictional and local energy losses. The velocity head is constant through the supply line and the excess pressure head equals to

$$\Delta H = \frac{p_1 - p_2}{\gamma} + (z_1 - z_2) \quad (4)$$

In water supply lines, the pressure head increases rapidly in the system where the elevation difference between two points is high and the excess pressure head is dissipated in pressure reduction tanks. In these structures, the pressure head is dissipated to atmospheric pressure by creating water jets. However, the pressure head could be removed from the system by installing a hydro-turbine. Then, the excess energy will be converted into useful energy by means of electricity.

3. Edremit Water supply System: A Case Study in Turkey

Edremit is situated on the north Aegean coast of Turkey (Fig. 4). Edremit's economy relies largely on the production of olives and tourism. The water used in the city is supplied from a spring located at Mount Ida and the supply line has an elevation range between 80-868 m. Water is carried at a rate of 0.16 m^3/s by a polyethylene pipeline which has a diameter of 450 mm and a length of 32.7 km (Fig.3). There are 12 pressure reduction tanks along the supply line to regulate the pressure of the flow. The pressure heads of the pressure reduction tanks are presented in Table 3.

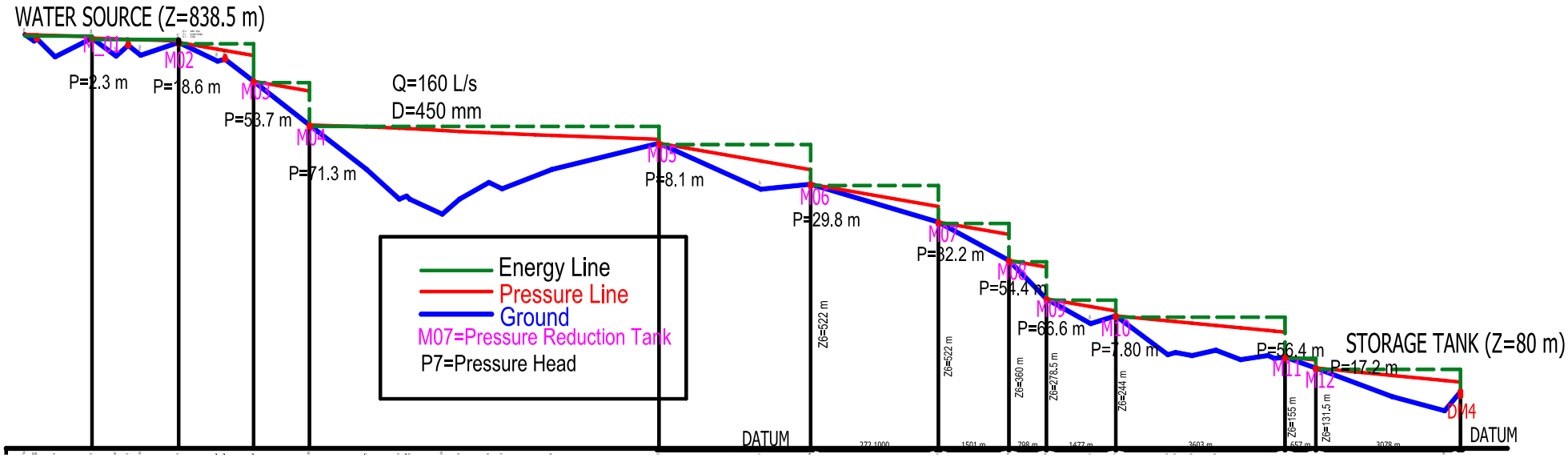

Fig.4 Water supply system of Edremit and the variation of pressure along the supply line

Table 3. Hydropower design characteristics of pressure reduction tanks of Edremit

Tank No	Head (m)	Discharge (m^3/s)	Output (kW)	Energy (kWh/year)	Benefit (Euro/year)
1	2.3	0.16	3	24,524	3,433
2	18.6	0.16	25	198,321	27,765
3	53.7	0.16	72	572,571	80,160
4	71.3	0.16	95	760,229	106,432
5	8.1	0.16	11	86,365	12,091
6	29.8	0.16	40	317,740	44,484
7	32.2	0.16	43	343,329	48,066
8	54.4	0.16	73	580,035	81,205
9	66.6	0.16	89	710,116	99,416
10	7.8	0.16	10	83,167	11,643
11	56.4	0.16	75	601,359	84,190
12	17.2	0.16	23	183,393	25,675

The excess pressure heads are dissipated to the atmospheric pressure by creating free water jets in these tanks (Fig. 5). However, the excess pressure can be removed from the system by installing a hydro-turbine and it can be converted into useful energy by means of electricity (Fig.6). The pressure head of the pressure reduction tank was taken as design head for the hydro turbine installation and the design discharge is selected as 0.16 m^3/s (Fig.7). The electricity price is about 14 Eurocent/kWh in Turkey for the May 2010 and the price was used in determining the economic benefit of the hydropower schemes. The operation of water supply system already exists. So there will be no e xtra operation cost. The annual maintenance cost is estimated to be 1% investment cost of hydropower plant [7]. This cost has been considered in the calculations of economic benefit in Table 4.

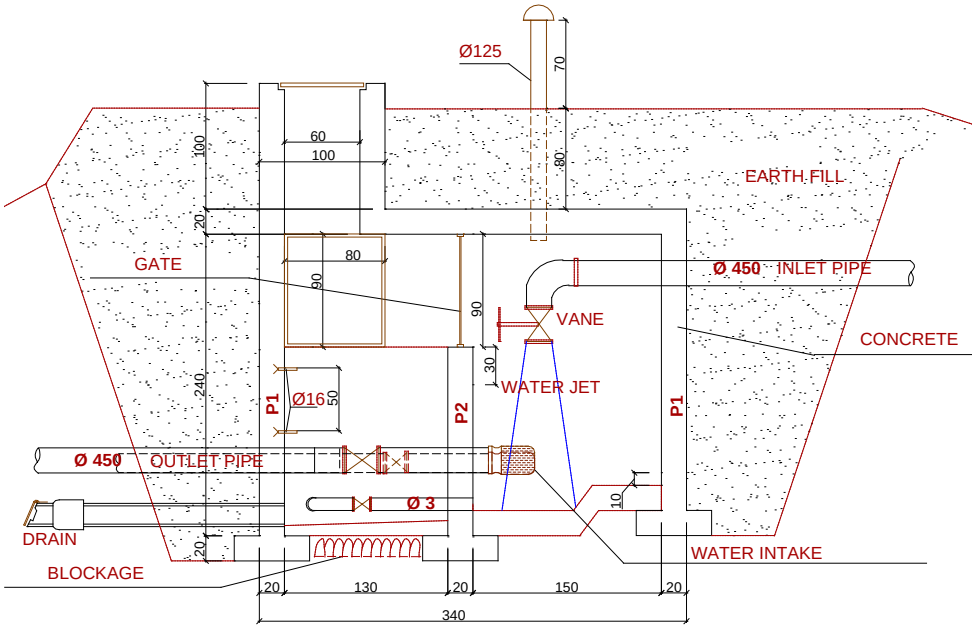

Fig.5 Longitudinal profile of the pressure reduction tank.

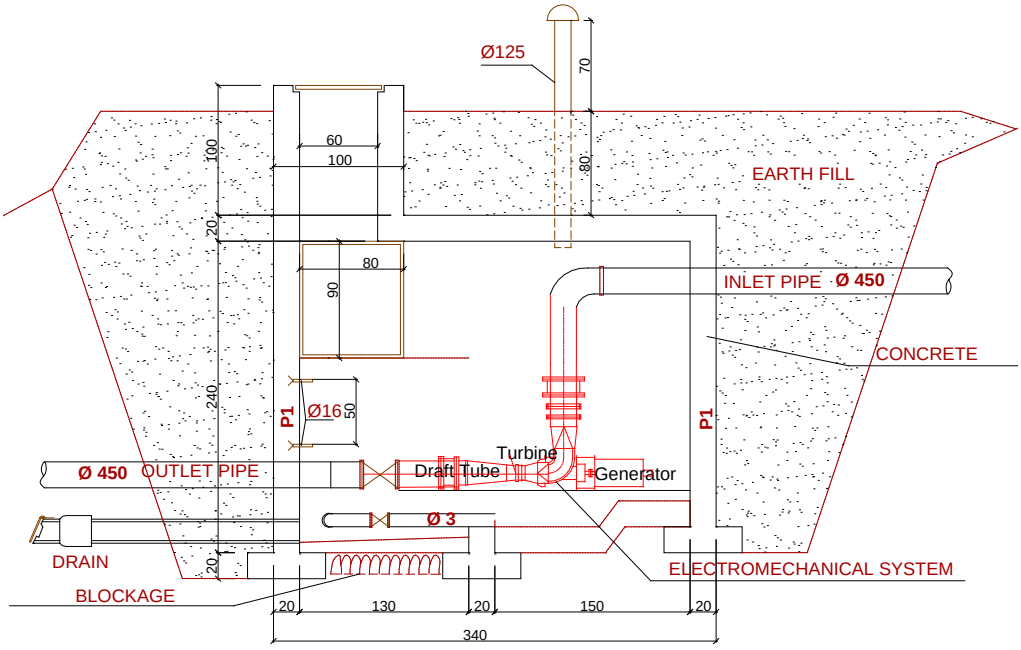

Fig.6 Hydropower generation in the pressure reduction tank.

The water supply system of Edremit has an electric energy potential of 4.08 GWh/year, corresponding to about 560,118 Euro/year economic benefit. The financing of the project would be supplied from international funding organizations like World Bank and European Union.

Table 4.Economic Analysis of The Proposed Project

Total Installed Capacity (kW)	559
The hours in operation (h/year)	7300
Annual Energy (kWh/year)	4,080,700
Cost of the investment (EUR)	1,118,000
Annual Benefit (EUR)	560,118
Payback period (year)	2.00

4. Conclusions

Utilization of the existing hydropower potential in water supply networks has been analyzed. The proposed facility has numerous advantages compared to river-type hydropower plants. The new energy laws and the economic aspects of Turkey create opportunity to develop this potential. For a case study, the water supply system of Edremit has been investigated in a detailed manner. There are 12 pressure reduction tanks along the water supply line and they have an power capacity of 559 kW. The proposed project is ecologically sustainable and it will produce clean and feasible energy.

References

[1] ESHA-European Small Hydropower Association, Energy Recovery in Existing Infrastructures with Small Hydropower Plants: Multipurpose Schemes-Overview and Examples, 2010.

[2] Kucukali, S. and Baris, K., Assessment of small hydropower (SHP) development in Turkey: Laws, regulations and EU policy perspective, *Energy Policy,* 37, 2009**,** 3872-3879.

[3] Kucukali, S., Municipal water supply dams as a source of small hydropower in Turkey, *Renewable Energy*, 35(9), 2010, 2001-2007.

[4] Bank of Provinces, Regulation on the Preparation of Water Supply Projects for Cities and Towns, 1992.

[5] Turkstat, Turkish Statistical Institute, 2009. (www.turkstat.gov.tr).

[6] DSI- General Directorate of State Hydraulic Works, Dams and hydroelectric power plants in Turkey**.** DSI**,** Ankara, 2005.

[7] Linsley, R.K., Franzini, J.B., Freyberg, D.L., Water Resources Engineering. McGraw-Hill Publications, 1992.

Concept-H: Sustainable Energy Supply

Jure Margeta[1], Zvonimir Glasnovic[2,*]

[1] *University of Split, Faculty of Civil and Architectural Engineering, 21000 Split, Matice Hrvatske 15, Croatia,*
[2] *University of Zagreb, Faculty of Chemical Engineering and Technology, 10000 Zagreb, Savska 16, Croatia,*
[*] *Corresponding author. Tel.: +385-1-4597108; Fax: +385-1-4597260, E-mail: zvonglas@fkit.hr*

Abstract: The paper presents an innovative solution that combines Pump Storage Hydroelectric (PSH) with power plants that use only Renewable Energy Sources (RES) into a unique energy producing technological system, called *Concept-H*, which combines PV, solar thermal and wind power plants with PSH. The basic difference between *Concept-H* and the previous use of RES, where output energy depends on the fluctuating input energy, lies in the fact that such new concept can continuously and safe supply a consumer with electric energy and power. In this sense RES are put in equal position with conventional energy sources and *Concept-H* promises to be the important building element of the future *sustainable power system* as a *green strategy* of electric energy production. The application of *Concept-H* creates a significantly lower risk for humans and the environment, than when using conventional technologies, especially in possible incidental situations. The proposed solution is flexible for realization and can be applied in different climatic, hydrological and physical conditions where people live.

Keywords: *Concept-H, Renewable Energy, Hydroelectric Energy, Sustainable Energy Supply, Green Energy Scenario*

1. Introduction

This paper analyses the possible development of the renewable electricity scenario, based on the strategy of the use of Renewable Energy Sources (RES), called *Concept-H* [1]. This concept is based on the use of renewable resources and the use, directly or indirectly, of water storage of hydroelectric (HE) plants as energy storage in addition to other technological possibilities which increase continuity of supplies of RES energy to Electric Power System (EPS). In addition to direct connection of RES with EPS and the users, Fig. 1 (a), the proposed approach in the development of continuous green energy supply also requires indirect connection by use of hydro energy power production unit, similar to Pump Storage Hydroelectric Plant (PSH), Fig. 1 (b).

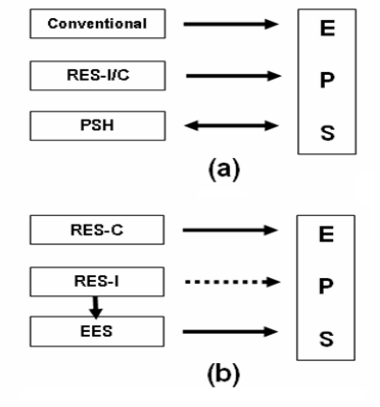

Figure 1. (a) Conventional connection of energy source and storage; (b) principle concept which would enable the green energy scenario (RES-I: intermittent RES; RES-C: continuous RES; EES: Electric Energy Storage, i.e. water storage).

Thus, the approach that enables the realization of green energy scenario would mostly be based on the concept of serial connection between green energy source and EPS through water storage of HE power plant, i.e. PSH, as shown in Fig. 1 (b). In this sense the future sustainable EPS or specific users, i.e. those based solely on RES, would have the configuration as in Figure 2. Solar (PV and solar thermal) and wind power plants, including

other non-continuous energy sources, would connect serially/indirectly to EPS and users through Electric Energy Storage (EES), i.e. water storage, while HE, geothermal and biomass power plants would connect directly, because they can provide continuous supply to consumers.

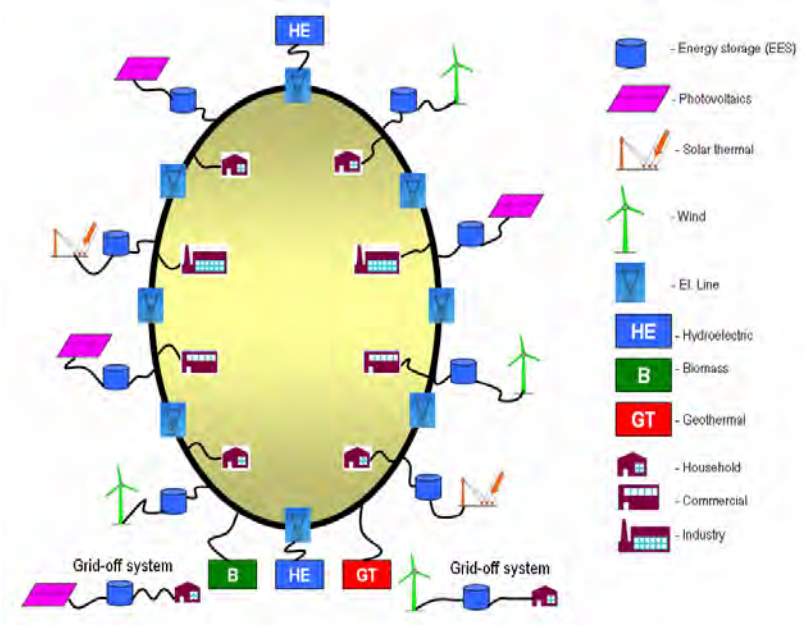

Figure 2. Vision of the future fully sustainable electric power system.

Renewable energy sources with occasional work will also be used directly through global and regional electric supply network, if and when it is acceptable for the electric power system. In this way water storage of hydroelectric power plants has the most significant role in realization of the green system, [2]. Numerous technologies of energy storage are known today (batteries, flywheel, pressure vessels, etc.), which differ in: size, energy storage costs, efficiency, lifetime, costs per cycle, etc., [3, 4]. It is well known that none of the present-day technologies could, in terms of ratings, be compared to storage by PSH, [4]. Precisely because of that, the concept of PSH is still the most significant EES today, which is a mature technology with large volume, long storage period, high efficiency and reliability, while capital cost per unit of energy is low, [5]. For this reason, with the present-day technology, it is possible to achieve the vision of continuous green energy production through *Concept-H* [1].

Implementation of this concept will depend primarily on the policy towards renewable energy sources, RES technological development, and economic conditions. Energy produced from RES is still significantly more expensive than conventional and therefore its production is subsidized. Therefore, the *Concept-H* in its initial implementation should be used primarily for daily energy peak shaving with a tendency towards daliy load leveling. Such implementation strategy would have the greatest ecological and economic effect.

2. Main settings of the proposed concept

2.1. Main elements of Concept-H

In the green scenario (Figure 2) continuous renewable energy sources (RES-C) are exploited directly, while intermittent energy sources, such as marine, wind and solar renewable energy sources (RES-I) are exploited indirectly through *Concept-H*. RES-I power plants deliver their energy to the Pump Station (PS) which pumps water into storage of HE power plants which then serve for daily, weekly and seasonal energy storage, while the consumer is supplied from

the associate PSH power plants, transforming intermittent energy supply into continuous and manageable energy supply as conventional storage of HE power plants, [6, 7]. Serial connection is based on two pipelines in classical concept of PSH. One pipeline pumps water from lower water resource into upper storage when RES produce energy and the other conveys water from the upper storage to turbines for production of hydro energy in accordance with the consumers' needs. In this way intermittent operation of RES-I does not affect hydro energy production according to the consumers' needs. In the proposed *Concept-H*, PSH is used for continuous production of energy, or energy storage for daily and seasonal peak load shaving.

The key driving elements of the solution are: (i) RES-I; (ii) energy storage unit (pump station and water storage); (iii) HE. Production and consumption balancing is performed in upper storage based on balance equation of storage volume and HE productivity, Figure 3. RES power plants are also in parallel (direct) connection with the regional EPS, because it is logical that RES-I power plant will directly deliver its energy excesses into the system, i.e. when the upper storage is full. It is also logical that energy surpluses in EPS are used for PSH operation.

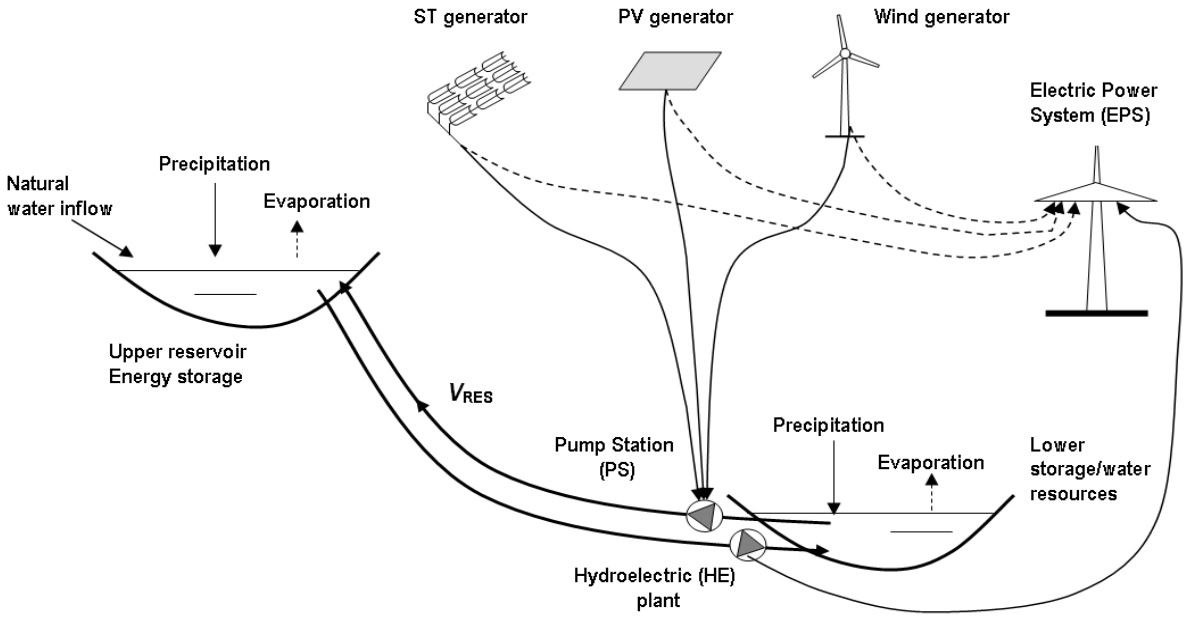

Fig 3. Concept-H: Hybrid power unit as the main building element of the future green energy scenario.

In this concept, water storages in energy power systems operate as energy storage. Hydroelectric power plants are very flexible and manageable in their work and quickly adapt to the needs of EPS. The biggest problems occur when hydrological conditions are not satisfactory. This problem is solved with the proposed *Concept-H,* because new non-natural water resources are created.

The basic unit for continuous production of energy is the hybrid power plant RES-PSH (i.e. *Concept-H)*. Hybridization can be applied to all RES-I energy sources, the most promising being with solar energy because, unlike wind power plants, it is a reliable source of energy, available at all locations where people live. In addition, solar energy enables rational daily balancing of energy production and consumption and thus the need for construction of small storage of PSH. Hybridization can be carried out with other sources of RES indirectly through energy system network.

The proposed solution is characterized by balance of energy and water. Energy balance of the hybrid electric power plant or the single time step is:

$$E_{hyb(i)} = E_{hyb(i-1)} + E_{PSH(i)} + E_{DRES(i)} \quad (1)$$

Where $E_{\mathrm{hyb(i)}}$ and $E_{\mathrm{hyb(i-1)}}$ are hybrid energy production in time stage i and i-1 respectively, $E_{\mathrm{PSH(i)}}$ is energy produced from PSH/HE, $E_{\mathrm{DRES(i)}}$ is energy which RES source supply directly to the energy power system in time period i. However, unlike $E_{\mathrm{PSH(i)}}$ which is reliable and manageable energy production, this energy supply is random, independent and uncontrollable energy production and thus is of minor importance for the EPS. Total energy production is:

$$E_{hyb} = \sum_{i=1}^{T} E_{hyb(i)} \quad (2)$$

Where T is total period used for production of energy (year).

Losses occur in energy transfers from one to the other ($E_{RES\text{-}I}$ into E_{PSH}), as well as in transport from the source to EPS. Total production losses ΔE period T are:

$$\Delta E = E_{RES-I} - E_{PSH} - E_{DRES}\,. \quad (3)$$

Losses due to energy transfer are inevitable and are the price paid for the sustainable and new quality in green energy production, Figure 3.

Water is the second resource needed for constant plant work. Water is necessary for filling of the system and compensation of losses due to evaporation, leakage and the like. Once fully filled, the system needs regular compensation of losses. Given that the system is integrated in the surroundings, part or all losses can be compensated by natural hydrological processes (precipitation, water inflow from catchment areas, etc.), or improved in special situations by external transfer of water mass inflow in the upper storage.

2.2. Water storage as energy storage

The equivalent reservoir energy balance for a single time step i is expressed as:

$$E_{PSH(i)} = E_{PSH(i-1)} + E_{nat(i)} + E_{RES(i)} - E_{prod(i)} - E_{evap(i)} - E_{loss(i)} \quad (4)$$

Where $E_{\mathrm{PSH(i)}}$ is the total equivalent reservoir stored energy in time period i and i-1 (MWh); $E_{\mathrm{nat(i)}}$ is the total natural potential energy inflow over time period i (MWh); $E_{\mathrm{RES(i)}}$ is the total energy inflow over time period i (MWh) generated (pumped) by energy from RES; $E_{\mathrm{prod(i)}}$ is the decision variable or the total energy outflow over time period i (MWh); and $E_{\mathrm{evap(i)}}$ and $E_{\mathrm{loss(i)}}$ is the energy outflow corresponding to the losses (evaporated volume and other losses) from the equivalent reservoir over time period i (MWh).

$E_{\mathrm{nat(i)}}$ during time period i is the sum of all reservoir natural potential energy inflows (river, rain). For a single reservoir, it is calculated by multiplying the natural water inflow discharge ($Q_{\mathrm{nat(i)}}$) by its mean productivity (ξ). Consumptive use water discharges (QC) must be subtracted from the natural inflows. Thus $E_{\mathrm{nat(i)}}$ is expressed as:

$$E_{nat(i)} = \xi(Q_{nat(i)} - QC_{(i)})\,. \quad (5)$$

$E_{\mathrm{RES(i)}}$ during time period i is the sum of all reservoir artificial potential energy inflows (RES). For a single reservoir, it is calculated by multiplying the artificial-RES water inflow discharge ($Q_{\mathrm{RES(i)}}$) by its mean productivity:

$$E_{RES(i)} = \xi \cdot Q_{RES(i)}\,, \tag{6}$$

$$Q_{RES(i)} = \frac{E_{RES}}{CF \cdot t \cdot (\rho \cdot g \cdot H_{n(PS)} \cdot \eta_{PS} \cdot \eta_{INV})} = \frac{E_{RES}}{CF \cdot t \cdot \xi_{MPI}}\,, \tag{7}$$

where $H_{n(PS)}$ is net head of pump station, η_{PS} is total available efficiency of pump station, η_{INV} efficiency of inverter and ζ_{MPI} is motor, pump and inverter productivity and t is time period. The energy outflow from the equivalent reservoir is the decision variable in the optimization problem, i.e. the desired energy production.

2.3. Relation between electric power of the RES generator and storage

The calculation of nominal power P_{el} for pumping water into upper storage and covering the demand for energy in a PSH in time step i is performed according to the characteristics of RES-I power plants (wind, PV and solar thermal). The equation for electric power of a RES-I generator (PV, ST or W) is derived from the equation used for dimensioning of the PV generator, presented in the paper [6] and which can generally be expressed as follows:

$$P_{el(i)} = \frac{2.72 \cdot 10^{-3} \cdot p_{RES} \cdot H_{TE(i)}}{\eta_{RES(i)}(T_a, v, \rho, \varphi) \cdot \eta_{MPI} \cdot E_{RES(i)}} \cdot V_{RES(i)}\,, \tag{8}$$

where p_{RES} (W/m^2) is equivalent value of RES-I power reference value (for solar systems it is 1000 W/m^2); η_{MPI} is efficiency of motor-pump unit and inverter; $\eta_{RES(i)}(T_a,v,\rho,\varphi)$ is exploitation efficiency of a RES, which depends on air temperature T_a, density ρ, wind velocity v and air humidity φ; $H_{TE(i)}$ (m) is total head, $V_{RES(i)}$ (m^3) is total water volume to be pumped by RES-I power plant into upper storage in order to satisfy daily energy consumption; $E_{RES(i)}$(kWh/m^2/day) is average daily energy from RES-I, available for energy production. Optimal power P_{el}* could be calculated in the similar way as is shown in the paper [6].

Apart from E_{RES} and the size of the consumer, expressed in Eq. (8) by $V_{RES(t)}$, it can be seen that upper storage volume V also has a dominant effect on P_{el}. The dependence of P_{el} on operating volume V of the upper storage is:

$$P_{el} = -a \cdot Ln(V) + b\,, \tag{9}$$

Where P_{el} is power of RES-I (W), V is operational volume storage (m^3), a,b – coefficients based on location and technological features. This relationship has been determined by the previous papers for PV and ST hybrid power plants, such papers have not yet been made for the wind power plants.

The interval $V_{min} < V < V_{max}$ which is called the boundary layer, serves as transition from the P_{max} value to the value P_{min}. Minimal value P_{min} is conditioned by the possibility of construction of storage (V_{max}) at a location. Therefore:

$$P|_{V=Vmax} = P_{min}\,. \tag{10}$$

As the period of daily insolation is always shorter than the daily period of planned energy production (24 hours), the minimum period of daily insolation, compared to the planned production of energy, determines the minimum dimensions of the storage volume and thus the maximum required power of solar power plant is:

$$P|_{V=Vmin} = P_{max}\,. \tag{11}$$

The boundary layer defines the size of storage volumes necessary to ensure the continuity of the planned production.

The constant "*b*" represents the maximum power of the plant that provides the total energy needed in the critical time step of the analysis period. The constant "*a*" represents the cumulative impact of factors for production of solar energy (technological and climate) in the period considered.

P_{el} and V are optimized according to characteristics of the problem. Based on the results of modelling it is possible to obtain more detailed information of interest to decision-making. Since the functional relationship between P_{el} and V is known (equation (9)), as well as the relationship between P_{el} and the area of collector field A of PV generator, it is possible to obtain the connection between the required A and V, according to:

$$A = \frac{P_{el}}{1000 \cdot \eta_{oc}} = \beta \cdot \left(-a \cdot Ln(V) + b\right) \ (\mathrm{m}^2) \qquad (12)$$

Where η_{oc} is PV generator efficiency.

In this way, relations are obtained for the size of the three key structures of the hybrid PV-PSH power plant, the area of the collector field (A), power of the PV generator (P_{el}) and the working volume (V). The results for Solar Thermal (ST) power plant can be obtained in the similar way.

Other objects of interest for the sizing of the system are pumping station PS and HE. The capacity of pump station Q_{PV} is obtained based on modelling results as dependent variable used for evaluating the performance of the system, and HE capacity is set by building objectives.

The relation between P_{el} and V can also be observed through the required reserve power supply in the system. It is obvious that the upper storage has the key role in the proposed hybrid power plant management. Relation between P_{el} of RES-I power plants (PV and ST) and reservoir volume V and the required P_{el} depending on power supply reserve, Figure 4.

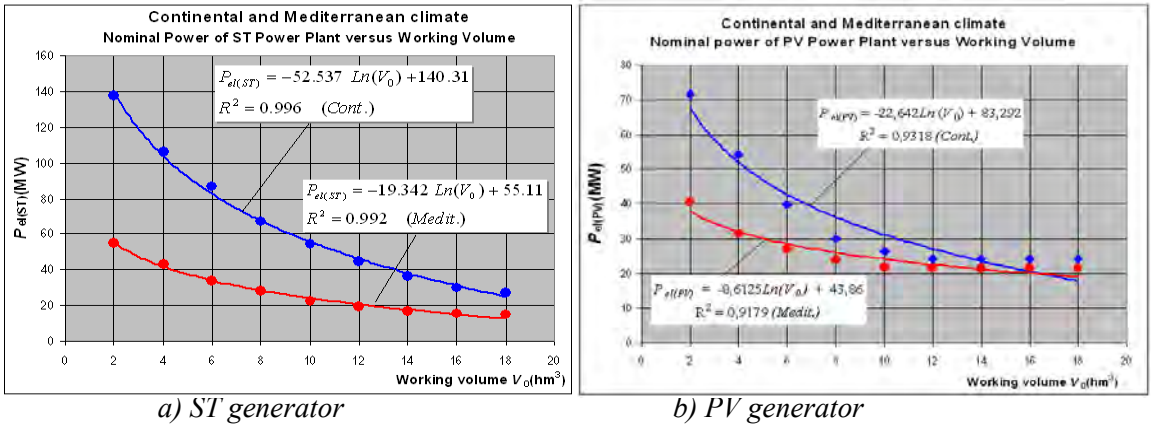

a) ST generator *b) PV generator*

Fig 4. Characteristic curves P_{el}=f(V) for ST and PV power plants for two climates areas.

3. Possible applications

Since this is a completely innovative solution, there are no practical results and the basic relationships of interest for the development and application can be obtained on the basis of previous research, basic theoretical assumptions and literature data. Key data relate to the

basic dimensions of power plant and its parts, production features, as well as economic, social and environmental impacts. Previous research [6, 7] shows that for Mediterranean climate (Island of Vis in Croatia) and continental climate conditions (Osijek, Croatia), the size of the hybrid system in the case of PV generator for these areas can be determined based on equations:

$$P_{PV\,(Medit.)} = -10.497\,Ln(V) + 44.21 \quad (13)$$

$$P_{PV\,(Cont.)} = -19.904\,Ln(V) + 65.123 \quad (14)$$

If these results were applied to the EPS, a general framework and dimensions of the solution could be obtained, using the *Concept-H*. The same was done in the case of Croatia [8], so that the reality of achievement of green energy policies [8] could be seen in Figure 5.

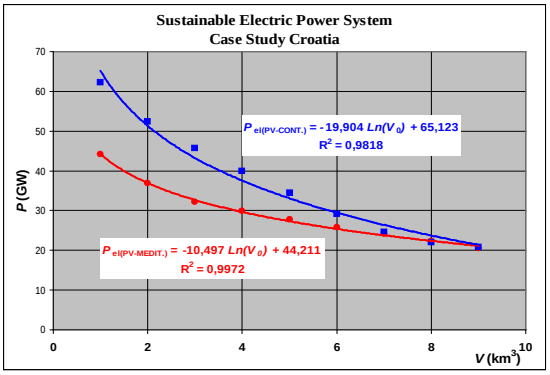

Fig 5. Scenario for Croatia.

In this way the possible applicability of the *Concept-H* at different locations and regions could be analyzed. The proposed *Concept-H* locally imitates the natural hydrological process, essentially generated by the same natural forces (solar energy and gravity), and, as a mostly closed system based on the use of natural renewable solar energy, it has a significantly smaller impact on the environment than other energy sources. In its operation it does not consume water, organic or other substances, does not create harmful residues and CO_2, and therefore provides opportunities to achieve sustainability objectives.

4. Comments and conclusions

This paper points to the possibility of realization of green energy scenario [8, 9, 10] by a concept, the so-called *Concept-H* [1]. It is a technological concept of hybrid RES-PSH systems which provides continuous energy production, the same as conventional energy sources. The solution in the proposed hybrid concept RES+PSH represents a production unit of sustainable energy supply based on natural resources which are free of charge and constantly available. The concept is very flexible in operation and construction. The accent is on hydroenergy, i.e. PSH as the main building unit, because this concept is flexible in implementation and provides continuous supply of „green“ energy and can be built in a wide range of climate areas, locations and water resources (fresh water, water with temporary flow, as well as on the sea). It can be implemented on the existing HE. The proposed production unit usually has very small impacts on the environment because it causes minimal changes in local and global hydrology and eco systems, and has a low level of potential danger for people and environment in case of incidental situations. Starting from the expected progress in the development of RES, especially PV [11], the proposed *Concept-H* may be one of the most promising solutions for achieving sustainable green energy scenario.

References

[1] Z. Glasnovic, J. Margeta, Vision of total renewable electricity scenario, Renewable and Sustainable Energy Reviews, (2011), doi: 10.1016/j.rser.2010.12.016 (in press).

[2] B. Lee, D. Gushee, Massive electricity storage, An AIChE White Paper, American Institute of Chemical Engineers, 3 Park Avenue, New York, NY 10016, 2007.

[3] H.Chen, T.N. Cong, , W. Yang, C. Tan, Y. Li, Y. Ding, Progress in electrical energy storage system: A critical review. Progress in Natural Science, 19, 2009, pp. 291-312.

[4] ESA, Electricity Storage Association, Energy storage technologies. Technologies & Applications – Technology Comparisons, 2009.

[5] J.P. Deane, B.P. Ó Gallachóir, E.J. McKeogh, Techno-economic review of existing and new pumped hydro energy storage plant, Renewable and Sustainable Energy Reviews, 14, 2010, pp. 1293-1302.

[6] Z. Glasnovic, J. Margeta, The features of sustainable Solar Hydroelectric Power Plant, Renewable Energy 34, 2009, 1742-1751.

[7] J. Margeta, Z. Glasnovic, Feasibility of the green energy production by hybrid solar + hydro power system in Europe and similar climate areas. Renewable and Sustainable Energy Reviews, 14, 2010, pp. 1580–1590.

[8] Z. Glasnovic, J. Margeta, Sustainable Electric Power System, Is It Possible? - Case Study Croatia, Journal of Energy Engineering 136, 2010, pp. 103-113.

[9] EREC, European Renewable Energy Council, 2004. Renewable Energy Target for Europe 20% by 2020. <http://www.erec-renewables.org/fileadmin/erec_docs/Documents/Publications/EREC_Targets_2020_def.pdf>

[10] EREC, European Renewable Energy Council, 2006. Renewable Energy Scenario to 2040, Half of the global energy supply from renewables in 2040. <http://www.censolar.es/erec2040.pdf>

[11] M. A. Green, K. Emery, Y. Hishikawa, W. Warta, Solar cell efficiency tables (Version 36), Progress in Photovoltaics: Research and Applications, 18, 2010, pp. 346–352.

Environmentally compatible hydropower potential in the estuary of the river Ems - Analysis for a floating energy converter

Steffi Dimke[1*], Frank Weichbrodt[1], Peter Froehle[1]

[1] *University of Rostock, Coastal Engineering Group, Germany*
** Corresponding author. Tel: +49 381 4983687, Fax: +49 381 4983682, E-mail: steffi.dimke@uni-rostock.de*

Abstract: Within the EC-funded research project *HYLOW - Hydropower converters for very low head differences* a floating energy converter - a so called Free Stream Energy Converter (FSEC) - for the energetic utilisation of currents with slow flow velocities (< 2.0 m/s) has been developed and will be optimized until 2012. In order to estimate the hydropower potential in case of deployment of the *FSEC*, a p otential analysis exemplarily for the northern part of the river *Ems,* at the border between *Netherlands* and *Germany,* was performed. Here, the *environmentally compatible hydropower potential* has a special importance. As expected, *this potential* is much lower than the *theoretical hydropower potential*. In addition to the efficiency of the energy converter, also the required water depth, existing protection areas and other uses are the main reason for the difference between the mentioned potentials in this investigation area.

Keywords: *Estuary River Ems, Environmentally compatible hydropower potential, Flow velocity*

Nomenclature (Optional)

P	*theoretical power* ... *W*	η	*efficiency factor* ... -
A	*flow trough area* ... *m²*	d	*water depth* ... *m*
ρ	*density of water* ... *kg/m³*	$L_{obstruct}$	*length of the obstructed area* ... *m*
v	*flow velocity* ... *m/s*	L_{demand}	*length of the demanded area* ... *m*
n	*number of energy converter like FSEC* ... -	w_{FSEC}	*width of energy converter as FSEC* ... *m*

1. Introduction

According to the European Small Hydropower Association (ESHA) in European rivers an unused small hydropower resource of 5 GW exists. An essential amount of this resource is available in terms of free stream energy with low flow velocities. The utilisation of this hydropower resource still constitutes an unsolved problem, because most current technologies are not cost effective (for low flow velocities and low discharge) and pose ecological risks to fluvial ecosystems due to blocking of the streaming water.

Within the EC-funded research project *HYLOW - Hydropower converters for very low head differences* a floating energy converter - a so called *Free Stream Energy Converter (FSEC)* - for the energetic utilisation of currents with slow flow velocities (< 2.0 m/s) has been developed and will be optimized until 2012. One important objective of the investigation with the *FSEC* is the development of an economic hydropower converter, which minimises the well known adverse ecological effects of small hydropower devices, since the proposed technique should be able to comply with the requirements of the European Water Framework Directive.

To estimate the hydropower potential in case of the deployment of a number of *FSEC´s* a hydropower potential analysis has been performed exemplarily for the northern part of the river Ems. One of the main objectives was the determination of the *environmentally compatible hydropower potential*. In the following paper, first the *FSEC* and the investigation area are described. After this, the results of the performed hydropower potential analysis are

described, the estimation results of the *theoretical* and the *environmentally compatible hydropower potential* are shown.

2. Free Stream Energy Converter

As mentioned before, the *Free Stream Energy Converter (FSEC)* is a floating energy converter for the energetic utilisation of currents with slow flow velocities. It consists of a Hydraulic Pressure Wheel (HPW), which is installed between two floating bodies. The floating bodies are connected with a bottom blade (Fig. 1). The *FSEC* has a length of 8 m, a width of 2.5 m and a draught of approx. 1 m. The width of the HPW is 1.2 m. This results in a flow trough area of 1.2 m². The design velocity is about 1 m/s - 2 m/s. The combined effect of the HPW, the floating bodies and the bottom blade should increase the efficiency by creating a small head differences between up- and downstream of the blade. Therefore, the hydrostatic pressure difference can be used for power generation in addition to utilisation of currents. [1].

Furthermore, within the *HYLOW* project, the expected influences of the *FSEC* on the environment were theoretically assessed and are investigated in field tests. Compared to conventional technologies, the operation of *FSEC* is environmental friendly. For example, the *FSEC* does not occupy the total river cross section, therefore the fauna and flora can migrate as well as sediment can be transported. As first measurements show, the water discharge and the flow conditions around the energy converter is changed only in a minor range. The *FSEC* also does not effect any pollution of the water. Because of that, the FSEC fits better with the ecological requirements according to the Water Framework Directive than the conventional technologies.

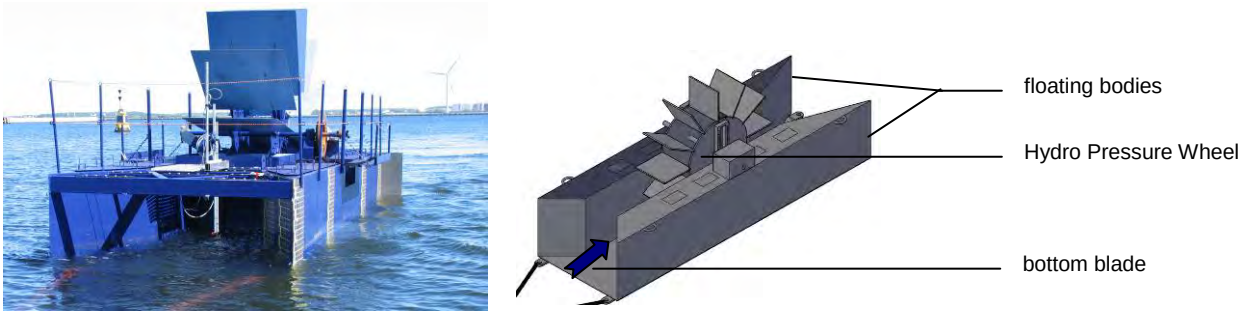

Fig. 1: Free Stream Energy Converter; length = 8 m, width = 2.5 m, draught = approx. 1 m

3. Categories of small hydropower potential

To characterize the areas for potential hydropower sites, different hydropower potentials are described. In publications different definitions for hydropower potential are available. In general the potential is divided into *theoretical, technical* and *realistic potential*. Several further sub-classifications exist.

The total availably energy is the *theoretical hydropower potential*, which can be calculated with following equation, (in which the efficiency factor is 1 for the theoretical potential):

$$P = \frac{1}{2} \cdot A \cdot \rho \cdot v^3 \cdot \eta \qquad (1)$$

The *technical hydropower potential* is only a part of the *theoretical hydropower potential*, which is realizable with existent techniques, at possible sites und complied with legal

regulations. In the range between the *technical* and *realisable hydropower potential*, the *environmentally complaint hydropower potential* and the *environmentally compatible hydropower potential* can be gradated, exemplarily. The definition criteria of mentioned potentials by [2] are mentioned in Fig. 2.

For our investigation within the *technical hydropower potential*, efficiency of the energy converter, requirements caused by dimension and operation of the *FSEC* and existing water uses are considered. The protection areas are taken into account in the *environmentally complaint hydropower potential*. Within the *environmentally complaint hydropower potential,* the impacts on the environment were considered (see chapter 6).

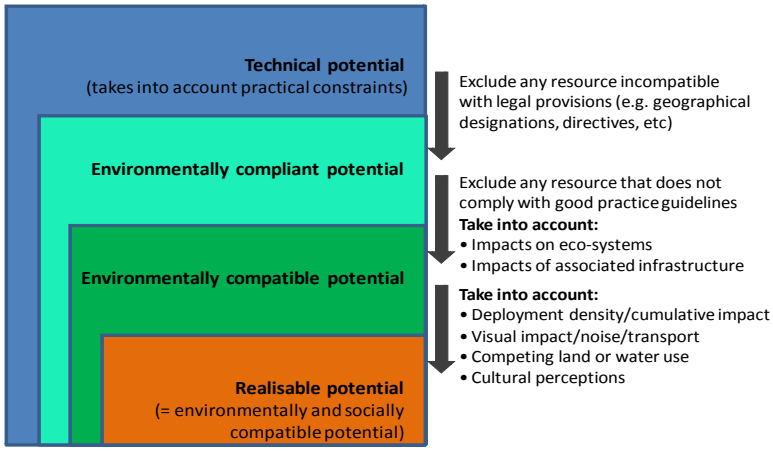

Fig. 2: Constraints to take into account when calculating the hydropower potential (after [2])

4. Investigation area – northern part of river Ems

4.1. Description of the investigation area

The investigation area is in the northern part of the river *Ems*, at the border between Netherlands and Germany. The river *Ems* has a typical river estuary which ends in the *North Sea* (Fig. 3). The river *Ems* is a typical European tidal river with mean tidal range of approx. 3.8 m and a distinctive river estuary. The average annual discharge is much higher than the average annual discharge of the river run-off, therefore not the river run-off but the discharge caused by the astronomical tide is the most important part of the total discharge and, hence, the most important factor influencing the flow velocities, too. The potential analysis for the river *Ems* can be stated to be exemplary for several rivers with tidal impact.

Fig. 3: Overview – investigation area (source: Google earth, modified)

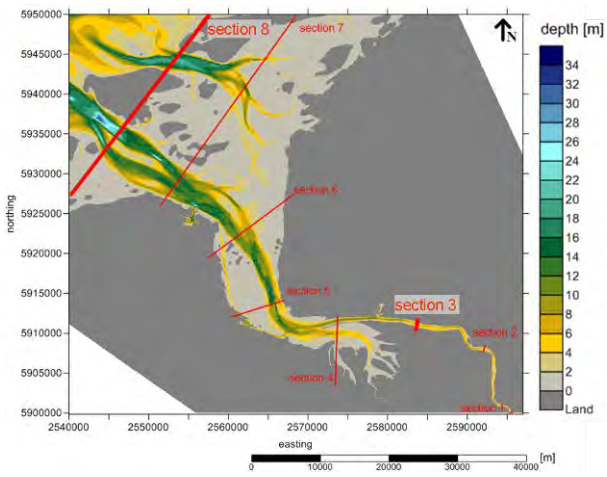

Fig. 4: sections for more detailed investigation, data source BAW

Within a detailed analysis, hydropower potentials were considered along 8 selected cross sections (see Fig. 4). Exemplarily, the investigation is described for the cross section 3 and 8. Section 3 is a typical river section. At this section the river *Ems* has a maximum depth of d = 7.2 m and a width of w = 560 m. The section 8 is typical for an estuary near the sea. The width of this section is about w = 28.000 m and the highest depth is about d = 22 m. Section 8 crosses the border area between Netherlands and Germany and is mainly situated in a protection area, as well as section 4 to section 7.

4.2. Data base

The data for the potential analysis at the *Ems* area is based on results of the Mathematical Model UnTRIM. The Federal Waterways Engineering and Research Institute used this numerical model to emulate and forecast the hydrodynamic conditions in the river *Ems* [2].

For the hydropower potential analysis the results of the simulation scenario with a constant mean run-off of 90 m³/s (average conditions) were used. The available results are representing the mean conditions of the astronomical tide and are available for approx. one day with a temporal resolution of Δt = 10 min and a spatial resolution of Δs = approx. 30 m x 30 m. For the potential analysis the temporal resolution was reduced to Δt = 1 hr and a spatial resolution of Δs = 50 m was used.

It can be assumed that the temporal variability of the natural flow conditions in the river, e.g. neap-spring differences, seasonally changing river run off have only negligible effects on the results of the potential analysis. Hence, the selected average conditions are extrapolated to assess the yearly potential.

4.3. Flow velocity

The mean tidal range is approximately 3.8 m and is varying along the river. The flow velocity varies with the tide and is in maximum about 2 m/s in the whole selected investigation area. Obviously, the flow direction varies also with the tide. The tidal wave is nearly totally reflected in the investigation area which means, that between low tide and high tide, the flow is directed in the upstream direction and between high tide and low tide the flow is directed in the down-stream direction. The mean (surface) flow velocities (on basic of one day) are shown in Fig. 5. As expected, the maximum flow velocities occur in the deep flow channels of the river and, correspondingly, the flow velocities are comparatively low in the shallow water areas.

Because of the bathymetry, the tidal range at section 1 with about 3.8 m is higher than the tidal range at section 8. The tidal range at section 8 is about 2.75 m. At both sections, the highest flow velocities are around v = 1.6 m/s. The flow velocity curves are proportional to the water depth at both sections. Hence, the highest flow velocities are at the sites with high water depth. The mean flow velocity varies along the cross section. A cross section sites with a water depth higher than 4 m, the mean flow velocities are about 1 m/s in section 3 as well as in section 8.

5. Theoretical hydropower potential

The *theoretical potential* is assessed as areal potential and based mainly on the flow velocity. The power output is determined for each grid on basis of the mean flow velocities with equation 1. For the comparison with other results, the flow trough area is defined with 1 m² and the efficiency factor is defined with 1. A bi-directional converter is assumed, which is

able to use the flow in both flow directions of the tide. In Fig. 6 the estimated *theoretical hydropower potential* for the investigation area is displayed. At several locations the estimated power output is higher than 1.2 kW. For most of the areas, the estimated theoretical power is between 0.2 kW and 0.8 kW.

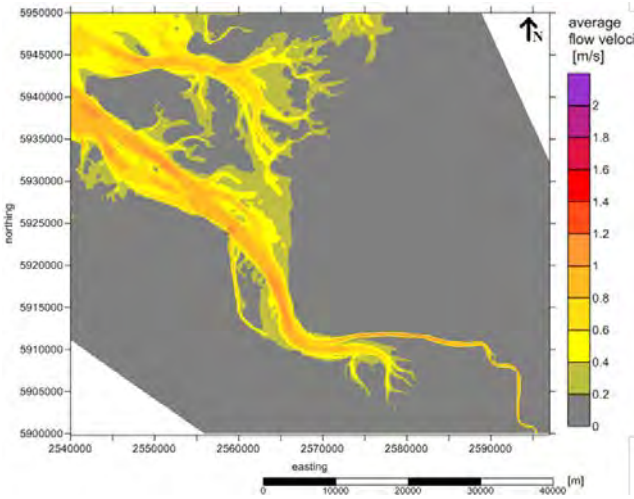

Fig. 5. average flow velocity, data source BAW

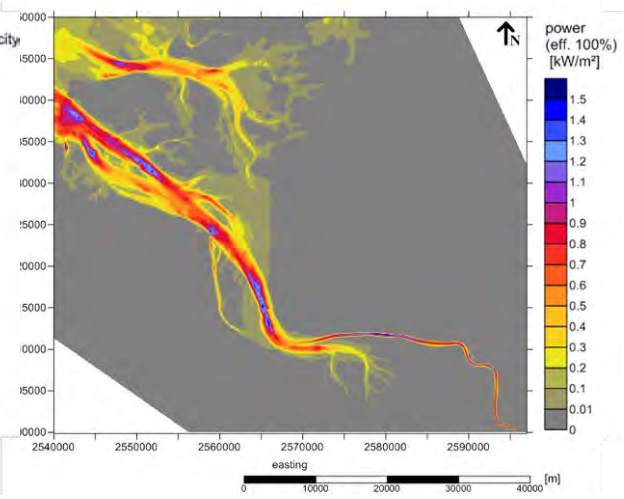

Fig. 6: theoretical power for the investigation area

An assumed realistic efficiency factor leads to decreasing estimates for the technical power. The definition of the efficiency factor for the *FSEC* is an objective of currently investigation and is not determined finally until now. With an assumed efficiency of 30%- 40% the maximum power is about 0.4 kW to 0.5 kW, with is in the range of the *technical hydropower potential*. The further factors, as water depth, other uses of the river or yearly operating hours are neglected, here. It will be considered in the following chapter.

6. Environmentally compatible hydropower potential

6.1. Considered aspects

As mentioned above, the *technical hydropower potential* considered the practical aspect, whether a deployment is possible regarding the technical requirements and other exiting site-uses (see chapter 3). One important aspect is the required space for the energy converter. All 8 considered cross sections are width enough to deploy a *FSEC*. For the *FSEC* (Fig. 1) the depth of the river is a restrictive factor (practical constraint). For the necessary river depth the draught of the *FESC* (1 m), the low water level and a necessary distance between river bottom and *FSEC* ("under keel clearance") have to be considered. The distance between bottom and *FSEC* is necessary, to ensure the floating behaviour of the *FSEC* and also to ensure the pass for the aquatic fauna and sediment below the *FSEC*. Its minimum is defined with 1 m. The low water level is strongly dependent on the local tidal range. The highest tidal range of the section is approx. 4 m, in section 1. Thus, the low water level is defined with -2 m NN. In the sum the required average water depth is 4 m including all sections of the river with river beds lower than -4 m NN.

In addition to the restrictive factor "required depth" existing uses of the river (competitive water uses) reduce the area to deploy the energy converter. In the investigation area, existing uses are mainly the use of the river as a waterway. In addition, uses like roadstead and spoil ground are of importance. The deployments of energy converter in the navigation canal are prohibited, in order to protect the navigation. A permission of hydropower deployment

outside of the navigation canal will be decided individually under consideration of the energy converter and the chosen deployment site.

Areas which are identified by a legal restriction, e.g. protection areas, or other environmental designation will be considered by the *environmentally compliant hydropower potential* (see chapter 3). A large part of the investigation area is defined as natural protected area.

At the latest by the implementation of the Water Framework Directive (WFD) it is not licensable to obstruct the whole river section with anthropogenic water uses. Also within the *environmentally compatible hydropower potential* the impact of uses is considered (see chapter 3). As mentioned above, the operation of the *FSEC* has only a minor effect on the environment. As a result, the use of the environmental friendly converter, like the *FSEC*, is a contribution for the *environmentally compatible hydropower potential.*

It is conceivable to deploy several energy converters in some converter fields. In this case, a distance between the single energy converters is required; especially in order to provide the river continuity, which is a main objective in the WFD. For the following analysis it is assumed that uses of 25 % of the river section is a minor impairment of the water bodies and therefore licensable. To not influence the operation mode and therefore the power output negatively, the distance between the single converters or to other uses and boundary are also important. Rightly this aspect is part of the *technical hydropower potential*.
The lateral distances between energy converters or to other uses/users or any other boundaries is chosen to 2 times of the converter width and is 5 m. In this paper the hydropower potential is only described along cross sections, therefore, the distance between the converter in down or upstream direction is not described.

It is distinguished between the demand of area for the deployment of the *FSEC* and the obstructed area caused by an *FSEC*. The obstructed area includes only width of the *FSEC*. The demanded area includes over more to the width of an *FSEC* the required distance between two successive energy converters, to other uses or to banks. For the calculation of the obstructed areas and for the demanded area the equation (2) and (3) are used, respectively.

Obstruct area: $L_{obstruct} = n \cdot w_{FSEC}$ (2)

Demand of area for deployment: $L_{demand} = n \cdot w_{FSEC} + 2 \cdot (n+1) \cdot w_{FSEC}$ (3)

In the following chapter it is determined how many energy converters like e.g. *FSEC* or other similar converters could be deployed along selected sections.

6.2. Results

The application of the mentioned aspect and the determination of the different hydropower potentials are described exemplarily along cross section 3 and 8 (see chapter 4). The power was determined based on the mean flow velocity and only at sites with water depths greater or equal to 4 m. The determined power and competitive uses along section 3 and section 8 are displayed in Fig. 7 and Fig. 8.

In case of section 3, the waterway utilizes 125 m of the total section of approx. 560 m. An average water depth higher than d = 4 m is available along a 410 m stretch of the section. More upstream of the river *Ems*, almost the total cross section length with a water depth

higher than d = 4 m is used by the waterway (e.g. section 1), therefore a deployment of the *FSEC* is not possible, there. The section 8 has a length of approx. 28,000 m. Thereof, approx. 13,500 m are land areas, for example the island *Borkum*. Only along approx. 7,000 m of the section length the average water depth is higher than 4 m. In addition, approx. 4,400 m of the remaining approx. 7,000 m are already in use or are protected areas. Along both sections possible deployment sites for the *FSEC* are remained (green lines in Fig. 7 and Fig. 8).

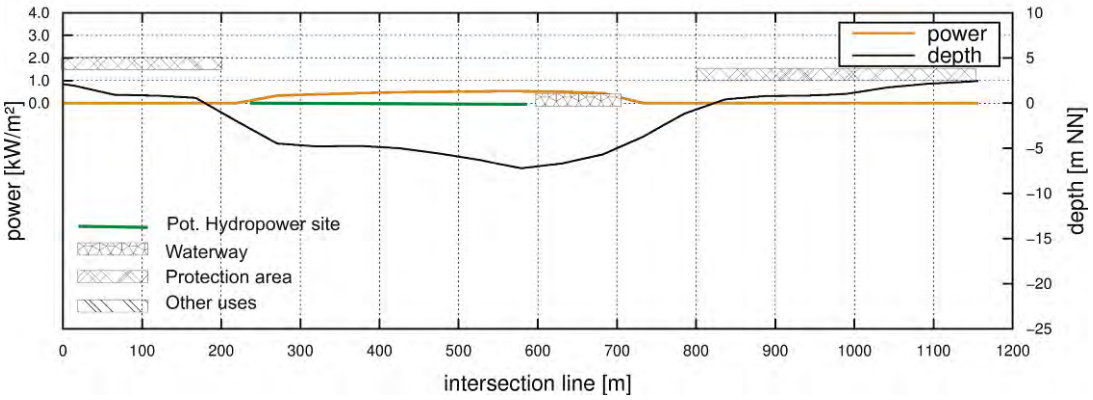

Fig. 7: Potential sites for hydropower uses and competitive uses, section 3 (power based on mean flow velocities)

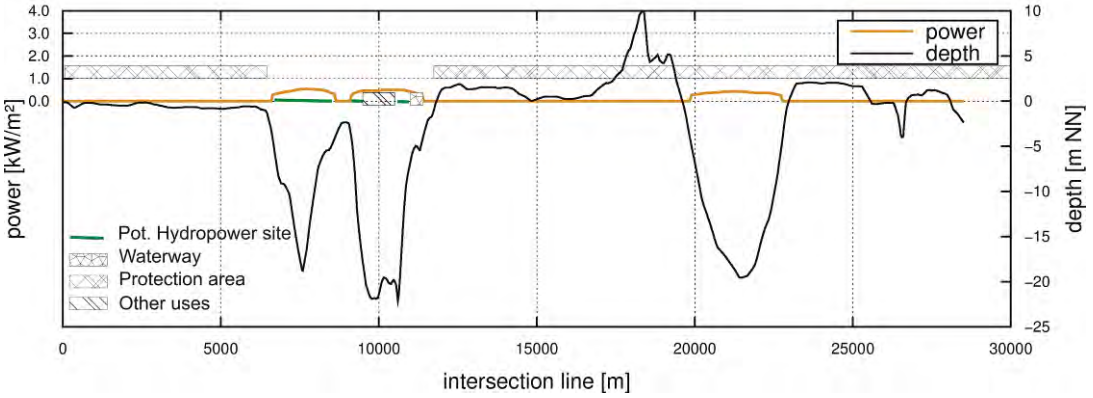

Fig. 8: Potential sites for hydropower uses and competitive uses, section 8 (power based on mean flow velocities)

Tab. 1: Properties of the sections

	Section 1	Section 8
Length of river cross section, only water areas (m)	560	16,590
Length of river cross section with existing uses/ protections area (m)	125	4,424
Length of river cross section d > 4 m (m)	411	7,003
25 % of river cross section length (m)	141	4,147

In Tab. 1 and Tab. 2 the properties and the *environmentally compatible potential* for the selected sections are presented. Along section 3 approx. 300 m and in the section 8 approx. 2,600 m could be used for the deployment of hydropower converters like the *FSEC*. Along all sections the obstructions of the river because of already existing uses are only minimal and therefore neglected. These results, that converter fields of possible 37 energy converters along section 3 and possible 343 energy converters along section 8 could be deployed. Accordingly, 16% of the river cross section 3 and 5% of the river cross section 8 would be obstructed.
For these possible energy converters fields the *environmentally compatible hydropower potential* is estimated with equation (1) on the basis of the assumptions that: all possible number of energy converter are installed, the average flow velocity v = 1 m, the flow through

area A_{FSEC} = 1.2 m² and the efficiency factor η = 0.3. If all 37 energy converters along section 3 and all 343 energy converters along section 8 could be installed, the potential is estimated with 7 kW and 62 kW (see Tab. 2). The operation period depends mainly on maintenance periods and weather conditions. With a realistic 5000 ope rating hours per year, the *environmentally compatible hydropower potential* is estimated with 33 MW/y for section 3 and 308 MW/y for section 8.

Tab. 2: useable resources of sections

	Section 1	Section 8
Length of river cross section d > 4 m minus length of other uses/ protections area (m)	287	2,579
25 % of river cross section length minus length of other obstructing uses (m)	141	4,147
Possible number of energy converters	37	343
Ratio: obstructed length / river cross section length (%)	16	5
Potential based on v_m = 1 m/s, A_{FSEC} = 1,2 m², η = 0.3 (kW)	7	62

7. Conclusion

The *realistic hydropower potential* will be lower than the afore-determined *environmentally compatible hydropower potential*. Furthermore the economical aspect was not considered in the paper. After the optimization procedure, the investigation costs will be calculated and put in relation with the expected power output. The estimated yearly performance per *FSEC* of approx. 890 kW/y is - compared to conventional energy converters - relatively low, but the advantage of *FSEC* is, that it has only small influences on the environment. The river *Ems* is an appropriate area for the deployment of the *FSEC*, because energy converters could be deployed in many sites and the flow conditions are continuous over the year. For example the discharge in rivers without tidal impact is seasonally different and depends of precipitation. In several rivers the flow velocity or the water depth are too low.

Acknowledgments

The research leading to these results has received funding from the EuropeanCommunity's Seventh Framework Program [FP7/2007-2013] under grant agreement° 212423.

References / Data sources

[1] Mueller G. and Senior J. (2007): The hydrostatic pressure machine with free surface – a novel energy converter for very low head differences. In: Zehntes Internationales Anwenderforum Kleinwasserkraftwerke 2007, Regensburg

[2] Landy, M. (2008): A methodology to quantify the environmentally compatible potentials of selected renewable energy technologies. ETC/ACC Technical Paper 2008/16, Harwell.

[3] BAW - Waterways Engineering and Research Institute (2004). Technical Report, Mathematical Model UnTRIM, Validation Document, Version June 2004 (1.0), http://www.baw.de/vip/abteilungen/wbk/Methoden/hnm/untrim/PDF/vd-untrim-2004.pdf.

[4] Hydrodynamic data for the river Ems: results of the “Mathematical Model UnTRIM”, Federal Waterways Engineering and Research Institute

Investigation on Effect of Aged Pumped-Storaged Component Replacement on Economic Profits Considering Reliability and Economic Efficiency

Jong Sung Kim[1,*]

[1] *Sunchon National University, Suncheon, Republic of Korea*
** Corresponding author. Tel: +82 617503537, Fax: +82 617503530, E-mail:kimjsbat@sunchon.ac.kr*

Abstract: Recently, availability decrease due to increase of midnight electric power demand has risen necessities to improve economic efficiency of the pumped-storage power plants in South Korea. The necessities cause to extend a preventative maintenance cycle, especially an overhaul cycle. But, unconditional extension cannot be implemented because it may generate unanticipated failures due to insufficient maintenance. So, first, in this study, possibility of extension of the preventative maintenance cycle is identified via investigation on preventative maintenance situation of overseas and domestic hydropower plants. Second, a methodology to optimize the preventative maintenance cycle considering both reliability and economic efficiency is presented via review of the previous reliability studies and considering characteristics of the pumped-storage power plant. The methodology consists of the eight parts including selection of principal components and subcomponents, identification of damage mechanisms in the principal components/subcomponents, FMEA(failure mode effect analysis), derivation of replacement and repair time of the principal components/subcomponents, design of preventative maintenance cycle plan, reliability analysis, economic assessment, and derivation of the optimized preventative maintenance cycle. Also, as a result of application of the methodology to an aged pumped-storage power plant in South Korea, the overhaul cycle has been extended from 4 years to 7.5years. Last, effect of replacement of some aged principal subcomponents such as rotor runner and generator stator on economic profits is investigated via application of the methodology to the aged pumped-storage power plant.

Keywords: *Pumped-Storage Power Plants, Replacement, Preventative Maintenance, Reliability, Economic Efficiency*

1. Introduction

Recently, it has been reported that availability of pumped-storage power plants decreases due to increase of midnight electric power demand in South Korea[1]. This low availability has been risen necessities to improve economic efficiency of the pumped-storage power plants. The necessities cause to extend a preventative maintenance cycle, especially an overhaul cycle. But, unconditional extension cannot be implemented because it may generate unanticipated failures due to insufficient maintenance.

All over the world, some studies has been performed about life extension, modernization and preventative maintenance of hydro and pumped-storage power plants[2-12]. In South Korea, life extension and modernization methodology for hydro power plants was established and applied to the aged hydro power plants several years ago but the methodology to optimize systematically an overhaul cycle wasn't developed[2]. The previous studies didn't investigate effect of aged pumped-storaged component replacement on economic profits considering reliability and economic efficiency.

Therefore, first, in this study, possibility of extension of the preventative maintenance (overhaul) cycle is identified via investigation on preventative maintenance situation of overseas and domestic hydropower plants[3-8]. Second, a methodology to optimize the preventative maintenance cycle considering both reliability and economic efficiency is presented via review of the previous reliability studies[6, 9-12] and considering characteristics of the pumped-storage power plant. Also, the optimized overhaul cycle is derived via application of the methodology to an aged pumped-storage power plant in South Korea. Last, effect of replacement of some aged principal subcomponents such as rotor runner and

generator stator on economic profits is investigated via application of the methodology to the aged pumped-storage power plant.

2. Investigation of Preventative Maintenance Situation

Table 1 presents the preventative maintenance cycles of hydro or pumped-storage power plants in some countries[3-8]. A class means complete overhaul for all components and B class means partial overhaul for some components. From the table, it is found that the preventative maintenance cycles of pumped-storage power plant in South Korea are shorter than those of other countries. It is identified that the A class preventative maintenance cycles of TEPCO and J-POWER have been gradually increased from 6years and will be 15years in the future by interview with working staff of TEPCO and J-POWER[7]. Also, It is confirmed that the recent availability of pumped-storage power plants in Japan is less than 10% similarly with South Korea. In some cases, Japan industries have taken and repaired the damaged principal components such as turbine runner, guide vane and generator rotor at maker's fabrication shops out of the site during A class overhaul period in order to improve their reliability to level of new products, but South Korea industries have repaired all the damaged principal components at the site.

As a result of this investigation, it is possible to extend the A class preventative maintenance cycle of pumped-storage power plants in South Korea like Japan. But, it is necessary to review in more detail and extend sequentially the cycle in order to extend to 10~15 years because there is difference in preventative maintenance method between South Korea and Japan.

Table 1. Preventative maintenance cycles of South Korea and overseas pumped-storage power plants.

Classification			A Class Preventative Maintenance Cycle (years)	Standard Period (days)	
South Korea/other countries	Company	Power Plant		A	B
South Korea : pumped-storage[3]	A	L	4 (A-B-A)	80	18
	B	M	4 (A-B-B-A)	76	12
	C	N	5 (A-B-A)	80	18
	D	O	4~6 (A-B-B-B-A)	80	16
	E	P	4 (A-B-A)	80	18
South Korea : hydro	KHNP[4]	-	4 (A-B-A)	-	-
	K-Water[5]	-	5 (A-B-A) or 6 (A-B-B-A)	-	-
Japan : hydro including pumped-storage[6]	-	-	9~15 or depends on equipment condition	-	-
Japan : pumped-storage[7]	TEPCO	Tamhara	12~18 (20,000hours)	150~180	21~28
	J-Power	Okki	15	125	8~10
USA : pumped-storage[8]	-	-	Average 10 (5~16)	75~150	-

3. Review of the Previous Studies about Reliability Assessment

Fig. 1 shows an optimization result of Snowy Mountains Hydro-electric Authority[9] for the complete overhaul cycle of hydro power plants by using the commercial program, RCM Turbo[13]. As shown in the figure, cost of unplanned maintenance increases drastically due to increase of breakdown probability with time span between planned activity while cost of

planned maintenance decreases continuously with the time span. So, sum of two costs has minimum value and the time corresponding to the value is an optimum overhaul cycle. However, this methodology cannot consider reliability reduction according to operation time beyond unit preventative maintenance cycle.

Japan Electricity Association presented a methodology to determine economic maintenance cycle of hydro-electric power equipments[6]. The methodology uses the same concept with Fig. 1.

Fig. 2 presents Vasilevski et al.'s methodology to investigate change of reliability with preventative maintenance cycle in order to determine optimal overhaul cycle and re-construction time[10]. As shown in Fig. 2, reliability reduction trend vs. operation time is changed with overhaul cycle, re-construction should be carried forward before reliability reaches critical value, and it mean that the overhaul cycle has to be adjusted as late as possible to be re-constructed. But, this study didn't present the method to set up critical failure probability and didn't consider economic efficiency so has practical problem.

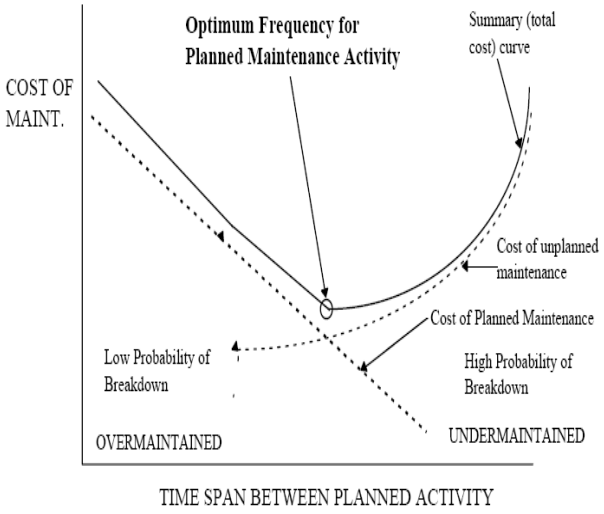

Fig.1 Maintenance cost optimization curve of Snowy Mountains Hydro-electric Authority[9].

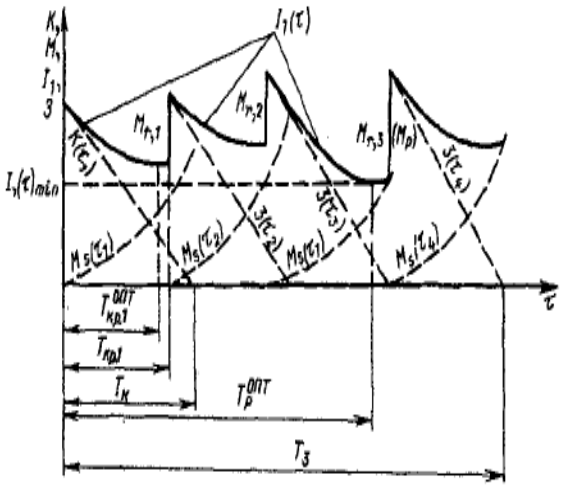

Fig.2 Vasilevski's methodology to determine optimal overhaul cycle and re-construction time[10].

EPRI TR-111488 presented outline of SRCM(streamlined reliability-centered maintenance) program for hydroelectric power plants instead of RCM(reliability-centered maintenance) that requires huge amounts of data and information[11]. EPRI TR-114160[12], which is a follow-up report of EPRI TR-1114888, presented three key factors(sound/cost-effective SRCM process, a software tool to manage consistently/effectively SRCM data and project management/working culture change) to succeed in performing SRCM and explained requirements for three key factors. However, purpose of the EPRI studies[11, 12] isn't optimization of overhaul cycle but deduction of preventative maintenance tasks for reliability improvement.

4. Methodology to Optimize Overhaul Cycle

Based on the review results of previous studies, this paper presents a methodology to optimize overhaul cycle considering both reliability and economic efficiency. Basic assumptions are used to develop the methodology as follows:

- Reliabilities of component and system should be drastically increased by A class preventative maintenance(overhaul).
- In cases of subcomponents or components applied only to B class preventative maintenance, effect of B class preventative maintenance on reliabilities of component/ system is insignificant.

Fig. 3 depicts overall flow chart of process to optimize overhaul cycle of pumped-storage power equipments. As depicted in the figure, item "task selection and comparison" of the RCM/SRCM methodology is removed because purpose of the methodology is to determine optimal overhaul cycle. Also, FFA(functional failure analysis) is performed including in FMEA(failure modes and effects analysis). Overall process consists of selection of target subcomponents/components, derivation of aging related damage mechanisms for the target subcomponent/components FMEA, calculation of repair/ replacement years, planning of preventative maintenance scenario, reliability analysis, economic efficiency analysis, and derivation of optimal overhaul cycle.

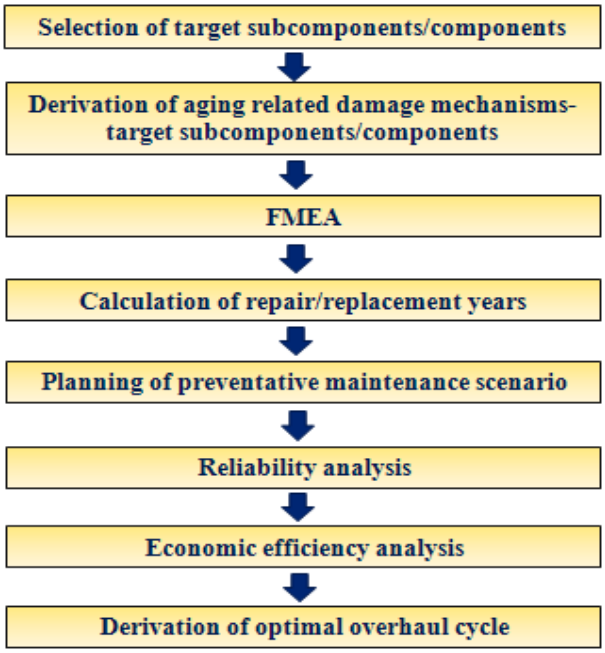

Fig.3 Overall flow chart of process to optimize overhaul cycle of pumped-storage power equipments.

Fig. 4 presents flow chart to select the target subcomponent and components. As presented in the figure, the subcomponents and components subject only to B class preventative maintenance are exclude from target in accordance with the basic assumption about effect of B class preventative maintenance on reliability. Fig. 5 shows flow chart to derive the aging related damage mechanisms for the target subcomponent and components.

Fig. 6 depicts flow chart of FMEA process. First, effect of each damage mechanism on intended function (e.g. structural integrity or performance) of subcomponent is evaluated. Second, based on the evaluation results, effect of the damage occurred on subcomponent on

component/system is evaluated. Third, next step, check whether subcomponents or components can be repaired or replaced during B class preventative maintenance or not. Last, if repair or replacement is impossible during B class preventative maintenance, draw up a final list of the relevant aging damage mechanisms for the target subcomponents/components.

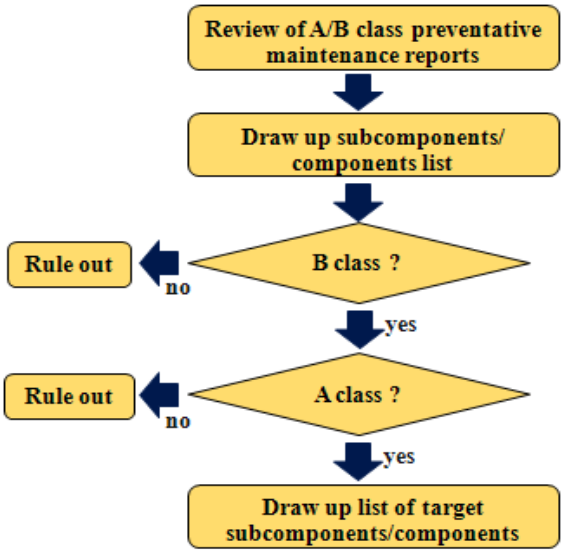

Fig. 4 Flow chart to select target subcomponents and components.

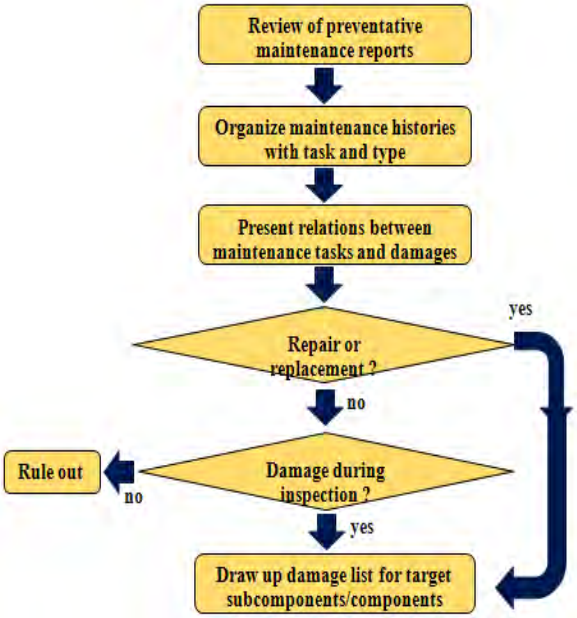

Fig. 5 Flow chart to derive the aging related damage mechanisms for the target sub-components/components.

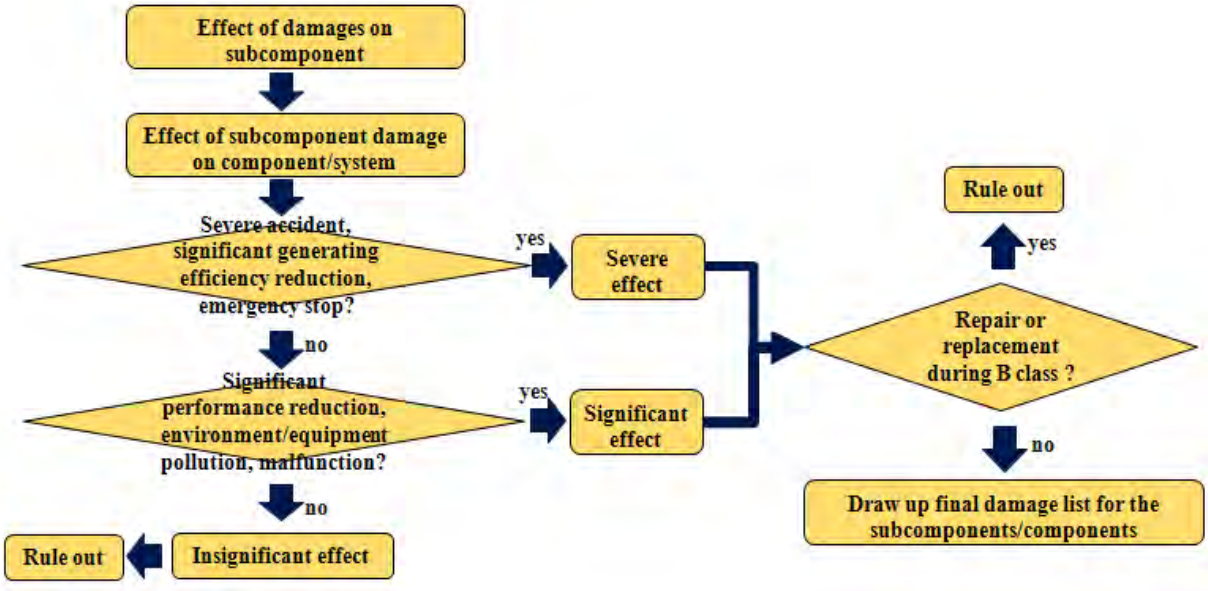

Fig. 6 Flow chart of FMEA.

Analyzing A and B class preventative maintenance histories for the final list derived via the process presented in Fig. 6, real repair/replacement cycles(minimum/mean) for the subcomponent-damage mechanism are derived. These repair and replacement cycles are used as an input for derivation of CHRF(cumulative hazard rate function) coefficients.

A preventative maintenance scenario has to be prepared because reliability has variation with order of maintenance class and number within unit cycle. For example, A-B-A, A-B-B-A, A-B-B-B-A, etc.
Fig. 7 shows flow chart of reliability analysis. If repair and replacement data are enough to evaluate, CHRF coefficients of equation (1) are directly derived via the numerical analysis using the repair and replacement cycles.

$$H(t) = a_0 + a_1 t + a_2 t^2 \quad (1)$$

$$R(t) = exp(-H(t)) \quad (2)$$

$$F(t) = 1-R(t) \quad (3)$$

where $H(t)$ is CHRF, $R(t)$ is reliability function, $F(t)$ is CDF(cumulative damage function) for failure time. If repair and replacement data are not enough to evaluate, CHRF coefficients are derived by using real repair/replacement data, reference reliability curve[14] or database[15], and Bayesian updating technique.

Finally, the overhaul cycle to derive minimum CPUT(cost per operating unit time) value at the target period is determined as an optimal overhaul cycle. CPUT for each preventative maintenance scenario is calculated by equation (4).

$$CPUT(t) = \frac{t_p[C_P R_{min} + C_U(1-R_{min})]}{t\int_0^{t_p} R(s)\,ds} \quad (4)$$

where C_p is preventative maintenance cost, C_u is post-accident preservation cost, t_p is unit cycle time, t is target period of scenario, R_{min} is minimum reliability within unit cycle.

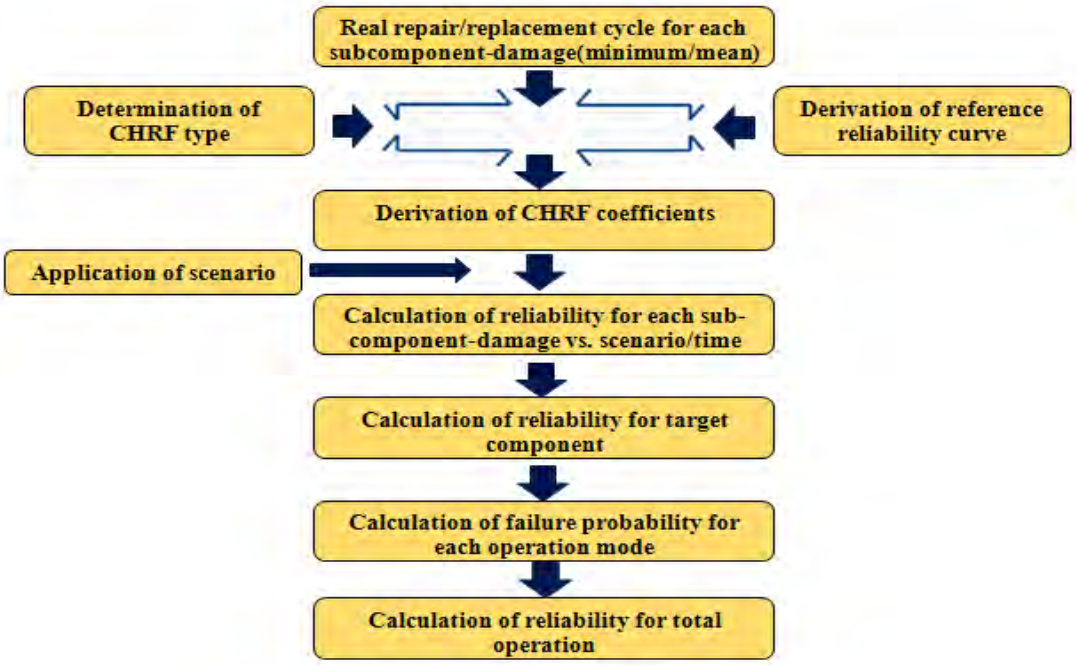

Fig. 7 Flow chart of reliability analysis.

5. Application Results

Table 2 presents overview of a pumped-storage power plant for application of the developed optimization methodology.

Table 2 Overview of a pumped-storage power plant for application of the methodology.

Items		Unit	Generation	Pumping
Operating time		years	24	
Capacity		MW	300×2	370×2
Pump turbine	Type	-	Francis	
	Max./min. head	m	345/288	355/310
	Max. output	kW	310,000	370,000
Generator/ Motor	Type	-	Vertical Inductive	
	Output	kVA	335,555	294,752
	Voltage/current	kV/A	18/10,763	18/10,763
Pony motor	Type	-	-	Vertical Inductive
	Output	kW	-	12,000
	Revolution speed	rpm	-	300
	Voltage/current	V/A	-	6,600/1,712

Fig. 8 depicts variation of reliability vs. time for various overhaul cycles of scenario 1(A-B-B-A). As depicted in the figure, reliability decreases continuously with time but increases after B or A class preventative maintenance. It is identified that improvement of A class is greater than B class in the viewpoint of reliability. Also, the overhaul cycle becomes longer, reduction degree of reliability is greater.

Fig. 9 shows CPUT variation vs. target operating time after the first overhaul completion for various overhaul cycles of scenario 1. As shown in the figure, the target operating time increases, CPUT value decreases irrelevantly to overhaul cycle. It is identified that CPUT has a minimum value at overhaul cycle, 7.5years when the target operating time for scenario 1 is more than 10 years. In other words, if the target operating time for scenario 1 is more than 10 years, optimal overhaul cycle is 7.5years. As a result of application of the methodology to an aged pumped-storage power plant in South Korea, the overhaul cycle has been extended from 4 years to 7.5years.

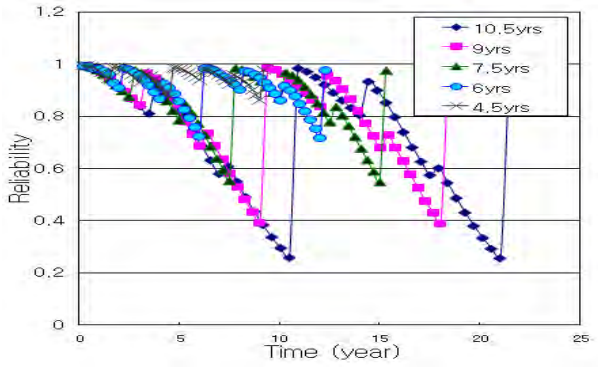

Fig. 8 Reliability of unit vs. time according to various overhaul of scenario 1.

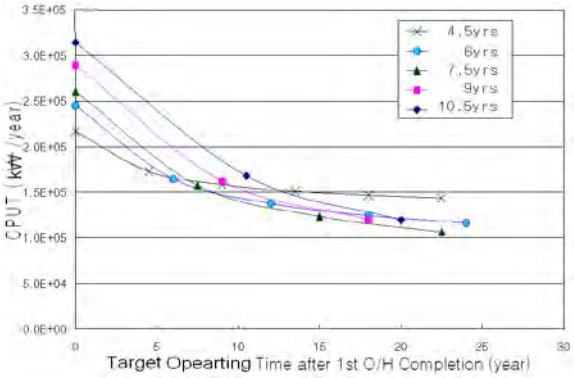

Fig. 9 CPU of unit vs. target time according to various overhaul cycles of scenario 1.

Table 3 presents CPUT variation according to replacement of principal components such as runner and generator. From the table, it is found that generator replacement has greater effect than runner replacement. When replaced with the runner and the generator to bring more economic benefits.

Table 3 CPUT variation according to replacement of runner and generator.

Component	Nothing	Runner	Generator	Runner & Generator
CPUT(kW/year)	1.2349×10^5	1.1611×10^5	1.1352×10^5	1.0491×10^5

Note) Scenario 1, Overhaul cycle: 7.5years, Target operating time: 15years

6. Conclusions

From the study to optimize overhaul cycle of pumped-storage power plants, the following findings are derived:

- As a result of this investigation, it is possible to extend the A class preventative maintenance cycle of pumped-storage power plants in South Korea.
- A methodology to optimize the preventative maintenance cycle based on the reliability and economic efficiency is presented, which can investigate variation of reliability and economic efficiency of generating unit vs. overhaul cycle.
- As a result of application of the methodology to an aged pumped-storage power plant in South Korea, the overhaul cycle has been extended from 4 years to 7.5years.
- When replaced with the runner and the generator to bring more economic benefits.

Acknowledgments

This work has been supported by KESRI-09310, which is funded by Korea Western Power Co. Ltd. and KHNP(Korea Hydro and Nuclear Power) Co., Ltd.

References

[1] http://news.naver.com/main/read.nhn?mode=LSD&mid=sec&sid1=0000070659.

[2] J.S. Kim, et al., Transaction of KSME, A, Vol.33, No.10, pp.1171-1176.

[3] Korea Western Power Co., Ltd., 2009, Planning Report to Optimize Preventative Maintenance of Pumped-Storage Power Plant.

[4] Korea Hydro & Nuclear Co., Ltd., 1976~2006, Electricity Generation Chronicles.

[5] K-Water, 2008~2010, Electricity Generation Chronicles.

[6] Japan Electricity Association, 2004, Investigation on Diagnosis Methods and Measures for Aging of Hydro Turbine.

[7] J.S. Kim, 2009, Overseas Business Trip Report for Investigation on Preventative Maintenance Situation of Japan Pumped-Storage Power Plant.

[8] EPRI, 1991, EPRI GS-7325.

[9] http://www.strategicorp.com/news%20case%20studies / rcm01.pdf.

[10] A.G. Vasilevski, et al., 1995, Power Technology and Engineering, Vol.29, No.1.

[11] EPRI, 1998, EPRI TR-111488.

[12] EPRI, 1999, Guidelines for RCM in the Hydro Power Industry, EPRI TR-114160.

[13] http://www.pinnaclesystems.us/solutions/manuf-reliability-mro-solutions/rcm-turbo.

[14] USACE, 1998, IWR Report 98-R-6.

[15] IEEE, 1984, IEEE Standard Reliability Data for Pump and Drives, Valve Actuators, and Valves, ANSI/IEEE Std 500-1984 P&V.

Risk assessment of river-type hydropower plants by using fuzzy logic approach

S.Kucukali[1,*]

[1] *Cankaya University, Department of Civil Engineering, Balgat, 06530 Ankara, Turkey*
** Corresponding author. E-mail: kucukali78@hotmail.com*

Abstract: In this paper, a fuzzy rating tool has been developed for river-type hydropower plant projects risk assessment and expert judgments have been used instead of probabilistic reasoning. The methodology is a multi-criteria decision analysis which provides a flexible and easily understood way to analyze project risks. The external risks, which are partly under the control of companies, have been considered in the model. The eleven classes of risk factors were determined based on the expert interviews, field studies and literature review as follows: site geology, land use, environmental issues, grid connection, social acceptance, financial, natural hazards, political/regulatory changes, terrorism, access to infrastructure and revenue. The relative importance (impact) of risk factors was determined from the survey results. The survey was conducted with the experts that have experience in river-type hydropower projects. The survey results revealed that the site geology and environmental issues were considered as the most important risks. The new risk assessment method enabled a Risk Index (R) value to be calculated, establishing a 4-grade evaluation system: low risk having R values between 1.2 and 1.6; medium risk, between 1.6 and 2; high risk, between 2 and 2.4; extreme risk, between 2.4 and 2.8. Applicability of the proposed methodology was tested on a real case hydropower project namely Kulp IV which was constructed on Dicle River in East Anatolia in Turkey. The proposed risk analysis will give investors a more rational basis on which to make decisions and it can prevent cost and schedule overruns.

Keywords: *Hydropower, Risk Analysis, Fuzzy Logic.*

1. Introduction

Renewable energy projects life cycle is full of various risks which will cause cost and schedule overrun or project failure. The surveys conducted by Gronbrekk et al. [1] and Komendantova et al. [2] identified the highest risk as political and regulatory changes for renewable energy projects in developing countries. Similarly, Ernst and Young [3] identified the most important business risk for 2010 as regulation and compliance.

Construction of river-type hydropower plants involves uncertainties because of various external factors such as site geology, grid connection, and environmental issues. These factors increase the construction costs and duration. For example, in one of the river-type hydropower plant in Turkey, namely Kulp IV, the cost of civil works increased by a factor of two because of unpredicted geologic structure at the tunneling site. In another example, the judges have ruled against hydroelectric power plants in 33 completed cases in Turkey, issuing a stay of execution decision or canceling the construction altogether because of the environmental issues.

In the literature there are several studies considering the risk analysis in construction projects [4] but risk analysis in renewable energy projects, especially for hydropower plants is very limited. In classical project risk analysis techniques, risk rating values are calculated by multiplying impact and probability values and direct analysis of these linguistic factors is often neglected [5]. Most existing risk analysis models, such as Monte Carlo simulation and tornado chart, are based on quantitative techniques which require numerical data. Kangari and Riggs [6] note that probabilistic models suffer from detailed quantitative information which is not normally available in the real construction world. However, much of the information related to risk analysis is not numerical [7]. Rather, this information is expressed as words or

sentences in a natural language. These conceptual factors can be expressed in linguistic terms that are, so called fuzzy information [8]. Uncertainty factors such as "poor geology" or "unstable policy" fall into this category. The aim of this paper is to introduce a new approach for hydropower projects risk assessment through the fuzzy set concepts.

2. Methodology

The eleven classes of risk factors were determined based on the expert interviews, field studies and literature review. The risk factors and their evaluation criteria are listed in Table 1. The risk factors are: site geology (geotechnical properties of the construction site), land use (right to use of the land for the construction of hydropower scheme), environmental issues (impact on ecosystem), grid connection (connection to the power system), social acceptance (impact on local community who use the river or the surrounding lands), financial (the status of the inflation and interest rate), natural hazards (earthquake, flooding and landslide), political/regulatory changes (level of political stability), terrorism (human-made disasters), access to infrastructure (road, electricity and water), revenue (cash flow). It should be noted that the financial, political/regulatory changes and terrorism were regarded as risks related to country conditions and their evaluation were done based on [9], [10].

In order to determine the relative importance (impact) of the risk factors, a survey was conducted with the experts from the banks and companies that have experience in the construction of river-type hydropower schemes. 14 experts were participated to the survey. The participants were asked to grade the importance of the risk factors regarding their importance and seriousness of concern. They graded the risk factors using a scale between 1-4, where 1 represents "low" and 4 "very high". The experts ranked site geology and environmental issues as the most important risks for river-type hydropower plants (Fig.1).

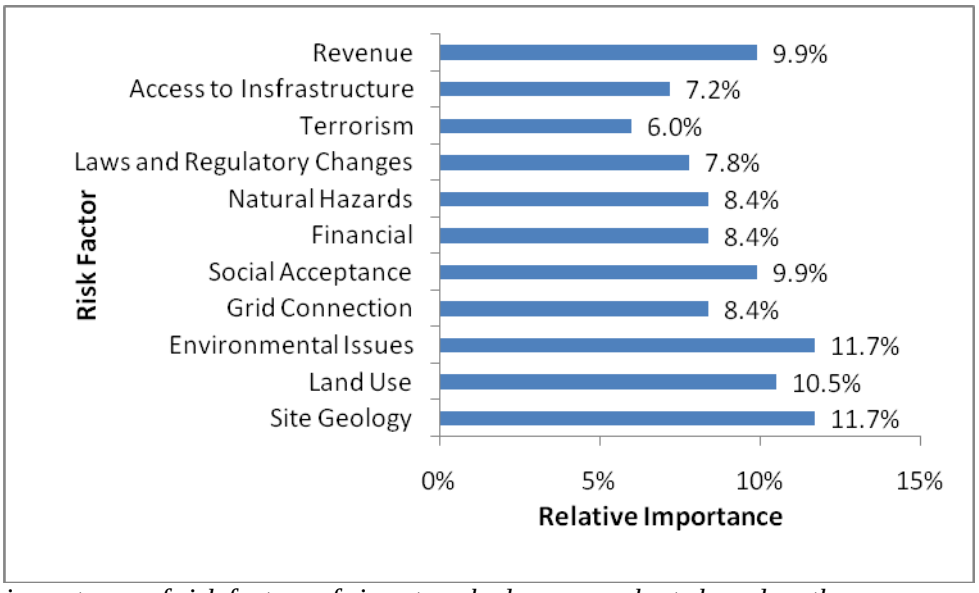

Fig.1 The importance of risk factors of river-type hydropower plants based on the survey results

Table 1. Evaluation criteria of risk factors in river type hydropower plants

Risk Factor	Score (1)	Score (2)	Score (3)	Score (4)
Site Geology	Rock mass quality is very good-good: RQD=%60-100	Rock mass quality is fair: RQD=%40-60	Rock mass quality is poor-very poor: RQD=%0-50	Soil with high ground water level
Land use	Property of Treasury	Forest	Private property: Agricultural land	Private property: Residential area
Environmental Issues	Project has detailed Environmental Impact Report	Project has Environmental Impact Report	Project has no Environmental Impact Report	Project is in an ecological sensitive area.
Grid Connection	Close to power system	Near to power system	Far to power system	Connection to the power system has some limitations
Social Acceptance	Project has detailed Social Impact Report	Project has Social Impact Report	Project has no Social Impact Report	Local community benefit from the river or the surrounding lands
Financial[a]	Economic performance of country is very high	Economic performance of country is high	Economic performance of country is medium	Economic performance of country is low
Natural Hazards	Low risk	Medium risk	High risk	Very high risk
Change in Laws and Regulations[a]	Political risk of country is low	Political risk of country is medium	Political risk of country is high	Political risk of country is very high
Terrorism[b]	Terror risk index of country is low	Terror risk index of country is medium	Terror risk index of country is high	Terror risk index of country is extreme
Access to Infrastructure	Very easy	Easy	Difficult	Very difficult
Revenue	Design discharge is high reliable	Design discharge is medium reliable	Design discharge is low reliable	Design discharge is unreliable

[a] country related risk and its evaluation is based on [9], [b] terrorism risk index is based on [10]

For each 11 parameter, an 1x4 input matrix was developed, each column corresponding scores 1- 4. If the score for a parameter is 3 and the input matrix (*I*) for the parameter is:

$$I = \begin{bmatrix} 0 & 0 & 1 & 0 \end{bmatrix} \quad (1)$$

Each parameter has an identical membership grading matrix. The fuzzy grading matrices were developed considering the degree of error a scoring observer may cause due to subjectivity and bias in the assessment process [11], [12]. Eq. (2) shows the fuzzy grading matrix (*FG*) used in this study:

$$FG = Score \begin{matrix} 1 \\ 2 \\ 3 \\ 4 \end{matrix} \begin{bmatrix} 1 & 0.4 & 0 & 0 \\ 0.2 & 1 & 0.2 & 0 \\ 0 & 0.2 & 1 & 0.2 \\ 0 & 0 & 0.4 & 1 \end{bmatrix} \quad (2)$$

The fuzzy assessment matrix (*FA*) was obtained by multiplying input matrices (*I*) with fuzzy grading matrix (*FG*) of the parameter,

$$FA_j = I_j \times FG_j \quad (j = 1\,to\,11) \quad (3)$$

where, j is the row number of the fuzzy assessment matrices. The membership degree matrix (*MD*) was obtained by multiplying weight of parameters (*w*) with fuzzy assessment matrix (*FA*) and summing the columns resulting in a one row matrix;

$$MD = w \times FA \quad (4)$$

A decision parameter computation was agreed upon f rom several scenarios considering membership degree versus attributes curves and formulation of Risk Index (R) was given as

$$R = \frac{1 \times A_{12} + 2 \times A_{23} + 3 \times A_{34}}{A_T} \quad (5)$$

where the area under the curve between the attributes i and j is named A_{ij} with: i =1,2, 3, and j = 2, 3, 4, . The total area under the curve is A_T. This enabled a R isk Index (*R*) value to be calculated, establishing a 4-grade evaluation system: Low risk having R values between 1.2 and 1.6; medium risk, between 1.6 and 2; high risk, between 2 and 2.4; extreme risk, between 2.4 and 2.8. The risk scale index represents the minimum and maximum values calculated by Eq.(5).

3. Investment Costs of Hydropower Schemes

Hydro power is the backbone of carbon dioxide free energy generation, about 22% of the world's electricity production comes from hydropower installations [13]. Hydropower plants can be classified into two categories: storage and river-type. In storage type hydropower plants, dams are used to retain river flow in a reservoir. A river-type hydropower plant diverts a portion of river through a channel or tunnel (Fig.2). River-type hydro power plants are dependent on the prevailing flow rate and can present problems of reliability if the flow varies greatly with time of the year or the weather [14]. Small hydropower (SHP) plants are mostly included in this category.

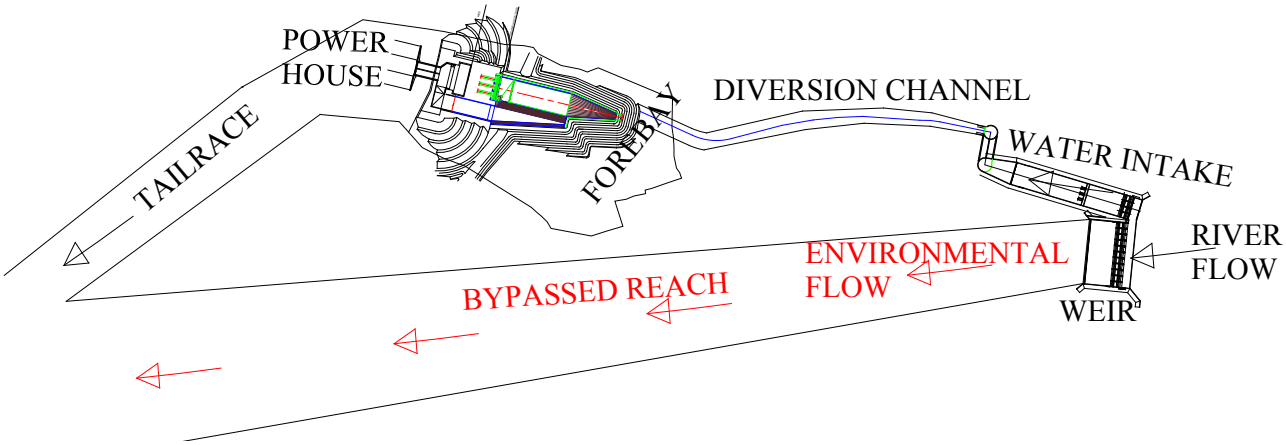

Fig.2 Site plan and components of a river-type hydropower plant

Hall et al. [15] determined the specific investment cost (total investment cost of the project divided by the installed capacity) of river-type hydropower plant in USA in the range of 2000-4000 $/kW. Also, they reported that the civil works account for 65-75% of capital cost. Each hydropower project is site specific that can explain the wide range of investment costs. Gordon [16] identified the main factors which can lead to cost overrun as the rate of inflation and site geology. The specific investment cost (SC) of a hydro power plant is the function of the net head (H) and installed capacity (P). It is well known from the literature that the SC increases as the head and installed capacity decreases [17], [18]. The investment cost a hydropower plant can be classified as follows: project design, land use and permits, financial, civil works, electro and hydro mechanical equipment, and grid connection (Table 3).

4. An Application of the Proposed Methodology

The developed risk assessment technique was applied to a real-time hydropower project namely Kulp IV which was constructed on Dicle River in Diyarbakır in East Anatolia. The characteristics of the project are as follows: Gross head=77 m, discharge=20 m^3/s, output=12.68 MW, energy=36.64 GWh/year, tunnel length=1885 m. Table 3 presents the investment cost analysis of Kulp IV hydropower plant. Actual cost of civil works and grid connection increased by a factor of two because of the poor geology and the technical demands by TEIAS, respectively. Table 4 shows the application of the risk assessment to the hydropower project. In the assessment fuzzy grading matrix provides more room for the justification of relationships between variables on the basis of fuzzy words. The project risk evaluation was done based on the criteria presented in Table 1. For example, Turkey has been ranked as extreme for Terrorism Risk Index by Maplecroft [9]. Therefore the risk factor of terrorism has a score of 4 for the project. Yet, project has no Environmental impact report, which yields the score of environmental issues as 4. By applying this method to other risk factors, the Kulp IV hydropower project Risk index was calculated as 2.26 which means project involves high risk.

Table 3. Analysis of the investment cost of Kulp IV hydropower plant (P=12.7 MW)

Description	Estimated Cost ($)	Actual Cost ($)	Rate of Increase	Share of Total Cost	Reason
Project design	1,090,000	1,180,000	8.3%	2.2%	Additional project designs
Civil works	12,500,000	25,700,000	105.6%	48.6%	Poor geology (serpentine) at the tunneling site
EME[a]	6,790,000	7,490,000	10.3%	14.2%	Under estimated costs of Technical equipment demand
HME[b]	8,900,000	4,800,000	-46.1%	9.1%	The prices of DSI are very high compared to the market.
Grid connection	2,600,000	5,400,000	107.7%	10.2%	Technical demands by TEIAS and length of the power supply line was increased
Land Use and Permits	2,200,000	2,600,000	18.2%	4.9%	The cost of the forest usage permit was not taken into account
Financial	3,100,000	5,700,000	83.9%	10.8%	Increase in interest rates because of the financial crisis

[a] Electro mechanical equipment, [b] Hydro mechanical equipment

Table 4. Fuzzy risk assessment rating tool application for Kulp IV Hydropower Plant

Risk Assessment																	
No	Risk Factor	Score	Relative Importance (W)	Input Matrix (*I*)				Fuzzy Logic Evaluation									
									Fuzzy Grading Matrix (*FG*)					Fuzzy Assessment Matrix (*FA*)			
														Membership Degree			
														1	2	3	4
1	Geology	3	0.117	0	0	1	0	*FG=f(I)*	0.00	**0.20**	**1.00**	**0.20**	*FA=FG*W*	0.000	**0.023**	**0.117**	**0.023**
2	Land Rent	3	0.105	0	0	1	0		0.00	**0.20**	**1.00**	**0.20**		0.000	**0.021**	**0.105**	**0.021**
3	Environment	3	0.117	0	0	1	0		0.00	**0.20**	**1.00**	**0.20**		0.000	**0.023**	**0.117**	**0.023**
4	Grid Connection	3	0.084	0	0	1	0		0.00	**0.20**	**1.00**	**0.20**		0.000	**0.017**	**0.084**	**0.017**
5	Social Acceptance	2	0.099	0	1	0	0		**0.20**	**1.00**	**0.20**	0.00		**0.020**	**0.099**	**0.020**	0.000
6	Financial	3	0.084	0	0	1	0		0.00	**0.20**	**1.00**	**0.20**		0.000	**0.017**	**0.084**	**0.017**
7	Natural Hazard	2	0.084	0	1	0	0		**0.20**	**1.00**	**0.20**	0.00		**0.017**	**0.084**	**0.017**	0.000
8	Political Changes	3	0.078	0	0	1	0		0.00	**0.20**	**1.00**	**0.20**		0.000	**0.016**	**0.078**	**0.016**
9	Terorism	4	0.060	0	0	0	1		0.00	0.00	**0.40**	**1.00**		0.000	0.000	**0.024**	**0.060**
10	Access to Insfrastructure	3	0.072	0	0	1	0		0.00	**0.20**	**1.00**	**0.20**		0.000	**0.014**	**0.072**	**0.014**
11	Revenue	3	0.099	0	0	1	0		0.00	**0.20**	**1.00**	**0.20**		0.000	**0.020**	**0.099**	**0.020**
Membership Degree Matrix (MD)														**0.037**	**0.335**	**0.817**	**0.211**
														0.19	**0.58**	**0.51**	**1.28**
														A_{12}	**A_{23}**	**A_{34}**	**A_T**
Decision Parameter (R)														**R = 2.26**		**High Risk**	

5. Conclusions

In this research, a new methodology is proposed for risk rating of river-type hydropower plant projects. The relative importance of the risk factors was determined from the expert judgments. The survey results showed that the most concerned risks are site geology and environmental issues. These results are in agreement with the Gordon [16].

Applicability of the proposed methodology has been tested on a real case. Findings of the case study demonstrate that the proposed methodology can be easily applied by the professionals to quantify risk ratings. The advantage of the proposed methodology is it will give investors a more rational basis on which to make decisions and it can prevent cost and schedule overruns. Forecasting the measure of risk of a river-type hydropower plant can be made by any decision maker with the help of the fuzzy rating tool described in this paper.

References

[1] Gronbrekk, W., Barton, H., and Khoury, R.H., International sustainability tools for hydropower role, relevance and industry reporting trends. Proc., Hydro 2010 C onf., Lisbon, Portugal, 2010.

[2] Komendantova, N., Patt, A., Barras, K. and Battaglini, A., Perception of risks in renewable energy projects: The case of concentrated solar power in North Africa, Energy Policy, 2011**,** In press.

[3] Ernst and Young, Business Risk Report, 2010. (www.maplecroft.com)

[4] Zavadskas, E.K., Turskis, Z., Tamosaitiene, J., Risk assessment of construction projects, J. Civil Engineering and Management, 16, 2010, 33-46

[5] Dikmen, I., Birgonul, M.T., Han, S., Using fuzzy risk assessment to rate cost overrun risk in international construction projects, Int J Project Management, 25, 2007, 494-505.

[6] Kangari, R. and Riggs, L.S., Construction risk assessment by linguistics, IEEE Transactions on Engineering Management, 36, 1989, 126-131.

[7] Mustafa, M.A., and Al-Bahar, J.F., Project risk assessment using the analytic hierarchy process, IEEE Transactions on Engineering Management, 38, 1991, 46-52.

[8] Kucukali, S., Baris, K., Turkey's short-term gross electricity demand forecast by fuzzy logic approach, Energy Policy, 38(5), 2010, 2438-2445.

[9] ECR-Euro Money Country Risk, 2010. (www.euromoney.com)

[10] Maplecroft , Terrorism Risk Index, 2010. (www.maplecroft.com)

[11] Karakaya, S.T., Coastal Scenic Evaluation by Application of Fuzzy Logic Mathematics, Msc. Thesis, METU,The Graduate School of Natural and Applied Sciences, Dept.of Civil Eng., Ankara, Turkey, 2004.

[12] Sahin, F., Scenic Evaluation of the Western Black Sea Coasts Using Fuzzy Logic, Msc. Thesis, ZKU, Graduate Sc. Of Natural and App. Sci., Dept. of Civil Eng., Zonguldak, Turkey, 2008 (inTurkish).

[13] Boyle, G., Renewable Energy: Power for a Sustainable Future. Oxford University Press, 2004.

[14] Kucukali, S. and Baris, K., Assessment of small hydropower (SHP) development in Turkey: Laws, regulations and EU policy perspective, Energy Policy, 37, 2009**,** 3872-3879.

[15] Hall, D.G., Hunt, R.T., Reeves, K.S. and Carroll, G.R., Estimation of Economic Parameters of U.S. Hydropower Resources, Idaho National Engineering and Environmental Laboratory, 2003.

[16] Gordon, J.L., Hydropower costs estimates, J Water Power Dam Constr, 35, 1983, 30-37.

[17] Gordon, J.L. and Noel, C.R., The economic limits of small and low-head hydro, J Water Power Dam Constr, 38, 1986, 23-26.

[18] Aggidis, G.A., Luchinskaya, E., Rothschhild, R. and Howard, D.C., The costs of small-scale hydropower production: Impact on t he development of existing potential, Renewable Energy, 35, 2010, 2632-2638.

Pump as turbine: dynamic effects in small hydro

Pedro A. Morgado[1,*], Helena M. Ramos[2,**]

[1, 2] *Civil Engineering Department and CEHIDRO, Instituto Superior Técnico, Technical University of Lisbon, Portugal.*
** Av. Rovisco Pais, 1049-001, Lisbon, Portugal , E-mail: plmorgado@gmail.com*
*** Av. Rovisco Pais, 1049-001, Lisbon, Portugal , E-mail: helena.ramos@civil.ist.utl.pt*

Abstract: This work focuses on the hydraulic aspects of a Pump as Turbine (PAT) when subjected to different working conditions, including accidental situations. This will provide useful information for the choice of the most adequate solution and will ensure a correct design and safe operation of the installed equipments. This work is supported by experimental data obtained in a series of tests performed at the university's laboratory and by calibrated computational modelling. The obtained data was used to perform a sensitivity analysis on the relation between discharge variation, runaway time and rotational speed and make inferences about the expected peak overpressure in an accidental situation. Based on the results, the hydropower system may be characterized by a relevant set of calculated parameters that are of extreme utility in the construction and calibration of a computational model capable of accurately predicting different scenarios and alternatives.

Keywords: *Dynamic effects; Reversible hydro; Safety solutions; Hydraulic transients.*

1. Introduction

In the operation of hydropower systems it is inevitable the occurrence of variations in the flow, being true either in routine manoeuvres, either in accidental or exceptional unforeseen events. To ensure the safety and reliability throughout the system life, it is very important that these dynamic effects and the associated risk factor are considered in the early stages of each design and the overpressures are accurately estimated [1, 2]. A detailed analysis for each operating situation is vital for understanding the dynamic behavior of hydro-mechanical equipment and their interaction with the flow and hydraulic circuit. This study is based on a parametric characterization of the different components of a hydro system as a support for a CFD modeling.

2. Methodology

2.1. Simulation-based modelling

2.1.1. Method of Characteristics

The quantitative analysis of unsteady flow through long conveyance systems is based on the fundamental hydrodynamic principles described by the dynamic (Eq. (1)) and continuity (Eq. (2)) equations [3]:

$$\frac{\partial V}{\partial t} + g\frac{\partial H}{\partial x} + \frac{fV|V|}{2D} = 0 \qquad (1)$$

$$\frac{\partial H}{\partial t} + V\frac{\partial H}{\partial x} + \frac{c^2}{g}\frac{\partial V}{\partial x} = 0 \qquad (2)$$

The previous equations can be used given the following conditions: the fluid in the pipe is homogeneous and mono-phase; the flow is mainly one-dimensional and the velocity profile is considered uniform through the cross-section of the pipe; the pipe axis remains static; the fluid and the pipe walls have physical linear elastic properties. For each calculation time step,

each pipe will be divided in a finite number of stretches bounded by the calculation sections building the rectangular mesh presented in Figure 1.

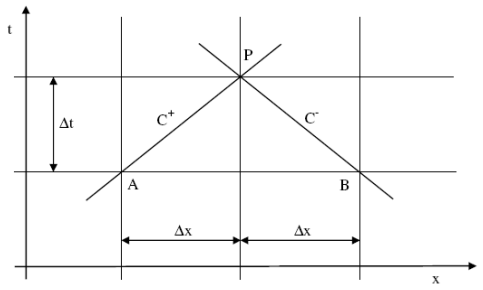

Figure 1 - Method of characteristics calculation grid.

The positive and negative characteristic equations can be written as follows:

$$Q_P = C_P - C_a H_P \tag{3}$$

$$Q_P = C_n + C_a H_P \tag{4}$$

in which:

$$C_P = Q_A \frac{gA}{c} H_A - \frac{f\Delta t}{c} Q_A |Q_A| \tag{5}$$

$$C_n = Q_B \frac{gA}{c} H_B - \frac{f\Delta t}{c} Q_B |Q_B| \tag{6}$$

and:

$$C_a = \frac{gA}{c} \tag{7}$$

Eq. (3) and Eq. (4) are only valid along the positive and negative characteristic lines, respectively. The values of C_P and C_n are known for each time step, although for the interior points of the mesh there are two unknowns, Q_P and H_P. These values can be determined by solving simultaneously Eq. (3) and Eq. (4):

$$Q_P = 0.5(C_P + C_n) \tag{8}$$

At both ends of each pipe it is only possible to define one characteristic line, so in order solve the system another equation is needed. This additional information may be obtained through the introduction of a boundary condition. Depending on the simulated system this boundary may be another pipe (with different characteristics), a reservoir, a turbine, a pump, a valve, a protection device or any other component analytically describable.

2.1.2. Turbine

The functioning of a turbogenerator can be characterized by a specific valve-type with adapted characteristics associated to customized closure maneuvers. Even though this solution may roughly simulate the vast majority of systems and situations, it does not consider the

specific parameters of the turbine, nor does it consider the overspeed of the turbine wheel and its complex interaction with the conveyance system. On this matter an innovative formulation was proposed for the simulation of the dynamic behavior of a turbogenerator based on a set of significant parameters that characterize a turbogenerator, allowing the evaluation of overspeed induced extreme upsurges and its propagation along the hydraulic circuit [4, 5, 6, 7, 8, 9] . This methodology simulates the turbine as a hydraulic resistive element, where the head lost by the flow is characterized by the basic formula of a hydraulic orifice equipped with dynamic discharge and rotational speed coefficients:

$$Q_P = C_g Q_R \left[1 + \frac{\alpha_R - 1}{\beta_R - 1} \left(\frac{N}{N_R} \sqrt{\frac{H_R}{H_u}} - 1 \right) \right] \sqrt{\frac{H_u}{H_R}} \tag{9}$$

in which q_P and h_P are respectively the relative flow through the orifice and available head at a certain time step. The factor C_g is the gate opening coefficient that defines the maximum discharge for a given head and rotational speed, as a function of the gate opening. The factor C_S accounts for the runner's rotational speed, adjusting the flow in each time step accordingly with the following formulation:

$$C_S = 1 + \frac{\alpha_R - 1}{\beta_R - 1} \left(\frac{n}{\sqrt{h}} - 1 \right) \tag{10}$$

where n stands for the dimensionless value of the rotational speed. The parameters $\alpha_R = \frac{Q_E}{Q_0}$ and $\beta_R = \frac{N_E}{N_0}$ are established for each turbomachine and represent the relation between the runaway situation and rated conditions, respectively for the flow and rotational speed. These values may be obtained from the manufacturers of the turbo equipments. The variation of the rotational speed for each time step depends on the inertia of the rotating masses, I, and the equilibrium between the hidraulic torque, T_H, and the magnetic torque, T_M. This relation may be expressed through the rotating mass equation:

$$\frac{d\omega}{dt} = \frac{60}{2\pi} \left(T_H - T_M \right) \tag{11}$$

in which ω is the angular speed (rpm). From Eq. (11), it is possible to conclude that for T_M = 0, the acceleration of the runner depends only on the hydraulic torque (T_H) and the inertia of the rotating masses, I. The hydraulic torque actuating in the rated operating conditions is given by the following equation:

$$B_{H,0} = \left(\frac{60}{2\pi} \right) \frac{\gamma \eta_0 Q_0 H_0}{N_0} \tag{12}$$

in wich η_0 = rated efficiency; Q_0 = rated flow; H_0 = rated net head; N_0 = rated runner speed. Assuming a linear variation of the discharge with the rotating speed under runaway conditions, the hydraulic torque at each timestep may obtained by multiplying the initial torque by a corrective factor, b, given by the following equation where $e = \frac{\eta}{\eta_0}$:

$$b = \frac{B_H}{B_{H,0}} = h^{3/2} C_g \frac{e}{n}\left[1 - \frac{\frac{n}{\sqrt{h}} - 1}{\beta_R - 1}\right] \tag{13}$$

The evaluation of the efficiency is a complex matter that depends on a vast set of parameters. This value may be considered to vary accordingly to the following approximate equations [4, 9].

$$\begin{cases} \eta_0 \dfrac{N}{N_0} & \text{for } N<N_0 \\ C_g\left(\dfrac{N_E}{N_E - N_0} - \dfrac{N}{N_E - N_0}\right)\eta_0 & \text{for } N>N_0 \end{cases} \tag{14}$$

2.1.3. Pumping system

The pump operation may be accurately simulated using the method of characteristics incorporating specific boundary conditions. Pump manufacturers generally provide the characteristic curves for their pumps as a function of the wheel diameter. These curves relate flow, manometric head, efficiency and power for a specific rotational speed and can be approximately represented in the first quadrant of operation (H,Q) by a second degree polynomial (Eq. (15)) [10]. Should this methodology be applied, a check valve should be installed at the downstream pump section to avoid reverse flow.

$$H_0 = AN^2 + BNQ - CQ^2 \tag{15}$$

The values A, B and C are constants and can be estimated from three known pairs of values (*Q, H*) of the pump characteristic curve. If correct data is available, a higher degree polynomial may be considered to enable a multi operating zone simulation. Although pump characteristic curves in the pumping zone operation are usually easy to obtain, the same is not true for the remaining zones. Figure 2 presents a schematic of a pump with the upstream and downstream connecting pipes and hydraulic grade line.

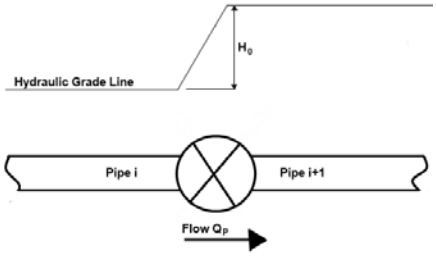

Figure 2 - Schematic drawing of a pump.

Referring to Figure 2 and considering the continuity equation, the relation, $Q_{P,i} = Q_{P,i+1}$, can be written. If the losses at the junctions are neglected, Eq. (16) gives the relation between head and discharge, in which *N* is the rotational speed:

$$H_{P,i+1} - H_{P,i} = AN^2 + BNQ - CQ^2 \tag{16}$$

when $A_i = A_{i+1}$, substituting Eqs. (3) and (4) into Eq. (16) the following polynomial is obtained, which can be solved for Q_P.

$$CC_a Q_P^2 + (BNC_a - 2)Q_P + \left(AC_a N^2 + C_n + C_P\right) = 0 \quad (17)$$

Once the flow Q_P is known, the heads $H_{P,i}$ and $H_{P,i+1}$ can be calculated for each time step. The total or partial shutdown of the pump as the cause of severe transient regimes may also be simulated. In this case the variation of the runner speed is given by Eq. (11) in which the hydraulic torque can be calculated based on efficiency data provided by the manufacturer.

2.1.4. Valve

Valves are installed in hydro systems to regulate the flow (or the pressure) by opening, closing or partially obstructing the pipe section. They can also be utilized to isolate system components in order to enable maintenance procedures or even their replacement. Figure 3 presents the schematic of a valve in hydraulic ciruit.

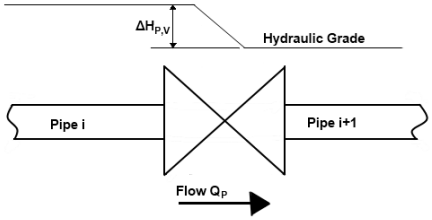

Figure 3 - Schematic of a generic valve.

The boundary condition for a valve can be written based on steady state head loss equation. The flow through the valve, Q_P, remains constant and the head loss can be written as the difference between the head at upstream and downstream valve section:

$$\Delta H_{P,V} = H_{P,i} - H_{P,i+1} = K_V \frac{Q_P^2}{2Ag} \quad (18)$$

in which K_V is a head loss coefficient obtained experimentally that depends on the Reynolds number, the type of valve and its opening at each time step. Substituting Eq. (3) or (4) in Eq. (18) a second degree polynomial equation is obtained:

$$\frac{K_V C_a}{2gA^2} Q_P^2 + 2Q_P - \left(C_P + C_n\right) = 0 \quad (19)$$

Solving for Q_P, the flow through the valve is obtained for each instant of simulation and subsequently the upstream and downstream head. For the situation where the valve is fully open, the head loss may be neglected and the flow can be determined by solving Eq. (8) or a fixed value should be considered. For the determination of the parameter K_V, a set of empirical results for each type of valve is presented in [11].

2.2. Model validation

Some supporting experimental tests were carried out in the Hydraulic lab of DECivil/IST, in order to analyze the behaviour of a reaction type turbomachine in different operation conditions. The hydraulic circuit is composed by a pipe of High-density polyethylene (HDPE), with an internal diameter of *0.043 m* and a length of *100 m*, which connects the pressurized vessel to the turbomachine. At the downstream end the water is discharged into a free surface tank. Both the air vessel and the free surface reservoir are responsible for

imposing a constant head respectively on t he upstream and downstream section. An intercalated pump is responsible for setting a recirculated constant flow. The turbomachine is a horizontal, single-stage pump-as-turbine, PAT*, KSB model Etanorm 32-125*. The generator was connected to the national grid via a l arge electrical transformer. Figure 4 presents a comparison between experimental pressure head variation and the corresponding simulation in the event of a full load rejection followed by a valve actuation.

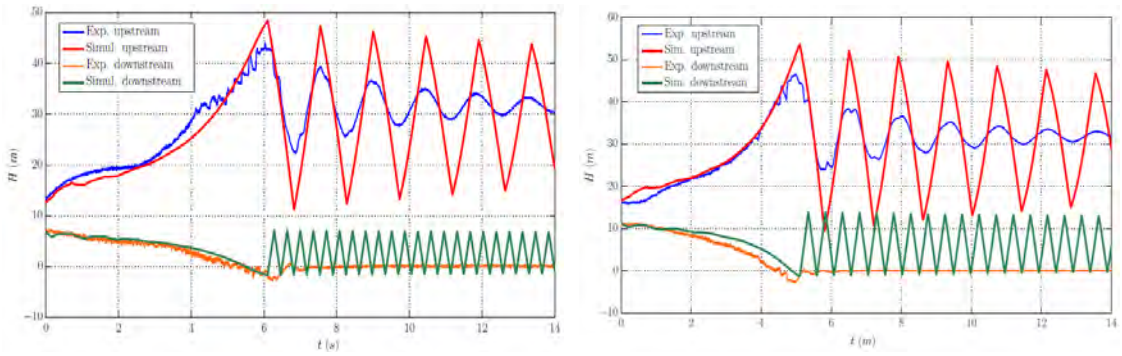

Figure 4 - Comparison between simulation and experimental results for Q = 4.2 l/s and Q=3.9l/s

3. Overspeed and dynamic effects

Based on a general hydropower system, a detailed analysis of the runaway effect without the interference of the closure of the flow control shutter (e.g. guidevane) or any special protection device was established. This was done in order to fully isolate and better understand the phenomenon under analysis. Under these conditions several independent computer simulations were carried out for a broad set of pairs of values of inertia, I, and specific speed, n_S. Figure 5 shows the upsurge on the upstream section of a turbine for the different combinations of parameters. For the lower values of n_S, the overspeed results in a flow reduction, causing an upsurge in the hydraulic system. On the other hand, turbines with high specific speeds are associated to an increase in flow when a load rejection occurs, resulting in sub-atmospheric pressures in the pipeline.

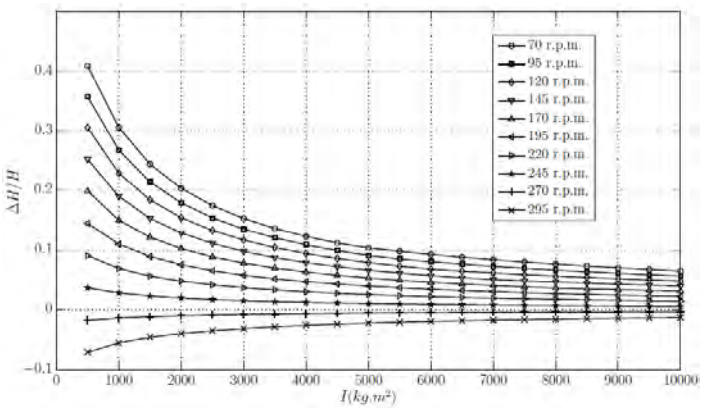

Figure 5 - Extreme relative pressure head as a function of I and n_S.

4. Load rejection and closure of flow control device

From the different emergency operations a hydropower system endures throughout its service life, the full load rejection followed by the actuation of a discharge shutter may stand among the most severe situations. Considering the same turbomachine used in the paragraph 3, the influence of the length, L, of the pipeline and its interaction with the safety valve closure time, t_C, was studied. For this purpose, a set of simulations were carried out in order to

calculate the maximum upsurge for different combinations of values, obtaining the results presented in Figure 6.

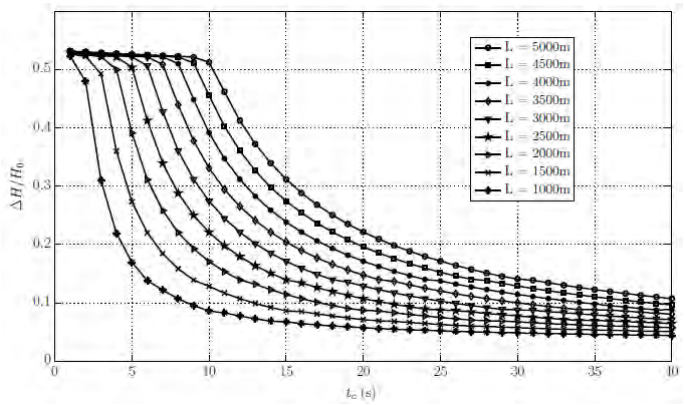

Figure 6 - Maximum relative overpressure for different combinations of L and t_C.

For all pipeline lengths, when approaching the elastic time constant, T_E, the maximum values of ΔH rise very quickly. It should be noted that below a certain value of t_C, for each different penstock length, all the curves tend to a common maximum value. This is the domain of what is called a fast manoeuvre, $t_C < T_E$, in which the transient peak overpressure depends only on the celerity of the elastic waves, c, and the mean flow velocity, U_0, given by the Frisel-Joukowsky formula.

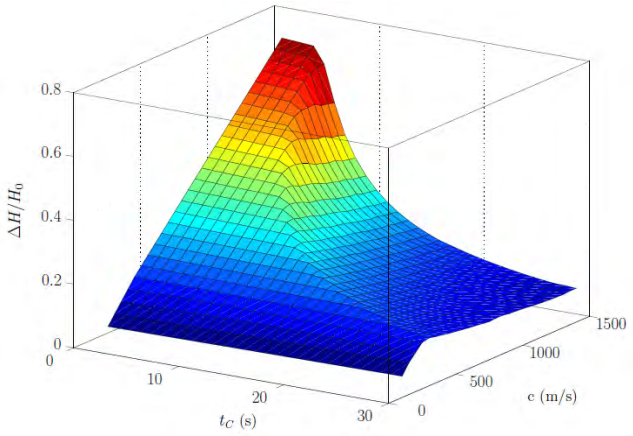

Figure 7 - Maximum relative overpressure for different combinations of c and t_C

Figure 7 was generated by utilizing the developed computational model, to show the maximum overpressure reached for different combinations of values of the celerity, c, and closure durations, t_C, for a fixed penstock length $L = 4000m$. When observing closely, it becomes evident that the classification of a closure manoeuvre as fast ($t_C < T_E$) or slow ($t_C > T_E$) is a relative concept that depends on the celerity of the elastic waves, thus on the pipe properties. In fact, the lower the value of c, the bigger the value of t_C must be in order to perform a slow closure manoeuvre. For a slow manoeuvre, the maximum pressure head depends essentially on the mean fluid velocity and on the flow control valve closure time. The maximum value can be estimated based on the by Michaud formula. Unlike what happens in a fast manoeuvre, the maximum overpressure is independent from the wave speed celerity.

5. Results

Both the experimental and the simulation results demonstrate the turbine load variation, in particular the runaway condition has a relevant impact on the discharge and, given the right circumstances, can be the sole cause of severe transients in hydropower systems. This is

especially evident for certain combinations of values of n_S and I that can result in a significant flow reduction during a short time interval. The comparison between the developed model and the experimental test results suggests a good estimation for the maximum transient overpressures, presenting conservative values valid for hydro and pumping design. This formulation based on modular linkable components proved to be flexible enough to allow the easy setup of a v ast set of different scenarios that are able to simulate the majority of situations. This methodology has the ability of predicting the runner overspeed of turbogenerators, as well as pumping stoppage and its effect on the flow along the pipe system.

References

[1] Ramos, H., Guidelines for Design of Small Hydropower Plants. Book published by WREAN (Western Regional Energy Agency and Network) and DED (Department of Economic Development - Energy Division). Número de páginas: 205. Belfast, North Ireland. ISBN 972-96346-4-5, 2000.

[2] Morgado, P.; Ramos, H., "Renewable Energy Production Integrated in Water Supply Systems: Dynamic Effects Analysis*" in Seminario Iberoamericano sobre Planificación, Proyecto y Operación de Sistemas de Abastecimiento de Agua,* Valência (Espanha), 24-27 de Novembro de 2009 (in Portuguese).

[3] Streeter, VL e Wylie, EB, *Hydraulic Transients*. New York, McGraw-Hill Book Co., 1967.

[4] Ramos, H., Simulation and Control of Hydraulic Transients in Small Hydro. Modelling and Analysis of Induced Effects by Turbogenerator Overspeed (in Portuguese). Ph. D. Dissertation in Civil Engineering. Portugal, Instituto Superior Técnico, 1995.

[5] Ramos, H.; Almeida A.B, *Experimental and C omputational Analysis of Hydraulic Transients Induced by Small Reaction Turbomachines* (in Portuguese). APRH, LNEC. Lisboa, 2001.

[6] Ramos, H., Unconventional Dynamic Effects in Pressurized Hydraulic System (in Portuguese). Support document for the subject Transients in Elevation and Hydroelectric Systems from the PhD in Hydraulics and Water Resources. IST, DECivil, 2004.

[7] Ramos, H. and Almeida, A. B., Parametric Analysis of Waterhammer Effects in Small Hydropower Schemes. HY/1999/021354. ASCE - Journal of Hydraulic Engineering. Volume 128, 7, pp. 689-697, ISSN 0733-9429, 2002.

[8] Ramos, H; Almeida, A. B., Dynamic orifice model on waterhammer analysis of high and medium heads of small hydropower schemes. Journal of Hydraulic Research, IAHR, Vol. 39 (4), pp. 429-436, ISSN-0022-1686, 2001.

[9] Morgado, P.; Ramos, H., "Dynamic Effects Analysis in Hydropower Systems" (in Portuguese), 10º Congresso da Água (Portugal), 2010

[10] Ramos, H., Support document for the subject Elevation and Hydroelectric Systems Subject of the Hydraulic and Water Resource Msc. IST, DECivil, 2003.

[11] Lencastre, A. – General Hydraulic (in Portuguese). Hidroprojecto, 1983.

Acoustic impact of an urban micro hydro scheme

Neil Johnson[*1], Jian Kang[1], Steve Sharples[1], Abigail Hathway[2], Papatya Dökmeci[1]

[1] *School of Architecture, University of Sheffield, Sheffield, UK*
[2] *School of Civil and Structural Engineering, University of Sheffield, Sheffield, UK*
** Corresponding author. Tel: +44 7534916870, E-mail: arq09nj@sheffield.ac.uk*

Abstract: Micro hydro systems can be regarded as a renewable energy source resulting from the natural hydrological cycle, it is by some considered sustainable due to the lack of impoundment of water and assumed negligible environmental impact. Experience with wind energy has highlighted that as the uptake of renewable energy technologies increases so government policies need to keep pace if public complaints and rejection of these technologies is to be averted. Studies on micro hydropower, particularly in an urban setting where propagation of noise is a planning issue, have been very limited. This paper focuses on the acoustic environmental impacts of micro hydropower considering a Reverse Archimedean Screw (RAS). Acoustic samples were taken directly above the RAS, and on a 5m interval along a transect and then at, 30m and 60m along another transect. Two further transects were considered and sampling was made at 30m and 60m. Initial results indicate that during normal operation at 25kW the screw would be barely perceptible beyond 60m; the weir provides significant masking of the turbine noise. It also shows that the noise generated is directional in nature at this site.

Keywords: *Micro hydro, Acoustics, Noise, Renewable energy, Environmental impact.*

1. Introduction

It is widely recognised that worldwide energy demand and use is continuing on an apparent, unceasingly ascending trend as, rapid population growth, economic development and therefore inherent demand for fuel increases [1, 2]. The world energy mix is depicted by the International Energy Agency (IEA). According to their *World Energy Outlook* (2008) [3]; renewables accounted for around 13% of global energy in 2006. This figure is predicted to rise to around 14% in the IEA 2030 reference scenario; and 24% in the IEA 450 (2030) policy scenario (based on policies under consideration). Oil and gas shares are predicted to be around 50% in both 2030 scenarios whilst coal lost some of its market share to an increase in the use of renewables (including biomass and waste), and nuclear energies.

The role of hydropower as a renewable resource varies dependent on the scale of the installation. As discussed by Frey and Linke [5], many legislative organisations do not consider large-scale hydro power to be a renewable resource when determining eligibility for government support. However, as argued in the paper, this is not a question of renewability but of sustainability. Although micro and pico hydro systems are assumed to be more environmentally friendly due to the lack of impoundment of water and assumed negligible environmental impact [4-6] emerging literature indicates that detrimental environmental impacts can be caused by smaller scale schemes [4].

Paish (2002) [4] indicates that small scale hydro developments in Europe will be the main area for hydro development in the future as the majority of large scale sites have already been exploited and micro hydro schemes seem to be growing in development and government support in the UK [2, 6]. In the urban setting, the issue of noise generation from visible systems can be a significant factor in the viability of the scheme, and the time period over which it is run. As part of a wider on-going research on the above issues, this paper will focus on initial results from a study of the impacts of a hydro scheme on the acoustic environment.

As there is recognised potential for hydro schemes in cities due to existing infrastructure, it would appear that there is need for such a study.

Three sites (semi-rural) within the UK using a Reverse Archimedean screws (RAS) to generate electrical power have already been identified as causing a noise nuisance. However, this tends to be associated with poor installation/design faults rather than general noise nuisance during normal operation. Any noise nuisance, whether design faults or operational, may be escalated within a densely populated and built-up urban setting. If micro-hydro is to penetrate into our cities then noise evaluation will become a key issue in the planning and design of such schemes. An extensive but not exhaustive literature search has demonstrated that this type of research has yet to be undertaken. Government policies may need to change to support these technologies and make them more viable; however, evidence is required to enable the government to establish the true impact on the environment of such technologies.

It is known that hydropower sites are most efficient at a particular speed, head and flow [4]. However, the relationship between the power output, river flow and sound power levels is not known. The following study will present measurements taken in the field to evaluate the sound generated from a RAS scheme in New Mills, running at a power output of 25kW, with a total head of 3+ metres, and in comparison to the existing sound produced by water flowing over a weir.

2. Methodology

Acoustic measurements were carried out around a 2.6 x 11m tri-blade RAS, with a fixed rotation of 28.03min^{-1} generating at 25kW and a river flow of around 2.17cumecs, located in a parkland setting, within an urban environment. *Figures 1 and 2* show plans, and photos of the site respectively. There do not appear to be any standards, or current methods for acoustic sampling of micro hydro turbines in the field in the UK possibly the world. It was therefore prudent to utilize BS 7445 and BS 4142 and the field site's complex geography to design a sampling strategy. Acoustic samples were taken along transects shown in *figure 1*. All samples were taken at 1.4m above the ground surface and where possible over 3m away from any facades. Acoustic samples were also taken directly above the RAS to enable the sound power level to be derived. On transects (a), (b) and (c) samples were taken at 30m and 60m from the RAS. Transects (b) and (c) also included a sample at 90m. Samples were then taken at 5m intervals along transect (d). Sampling directly to the side of the RAS was deemed unsuitable due to the presence of a wall. *Figure 2* is a photo of the site taken from above; the right hand image shows the bridge from which it was taken

After numerous visits, it was determined that the site's acoustic characteristics do not alter significantly over time. However, a sample of the acoustic environment was carried out using WinMLS (Windows Maximum Length Sequence), at a fast sampling rate to determine the required acoustic sampling time at each sampling instance. Two minute samples were deemed sufficient for this study.

In addition to the acoustic sampling, *figure 1 also,* shows the location of two pressure gauge sensors, which have been installed to allow future work on river flows, efficiency and acoustic impacts of the turbine at this site.

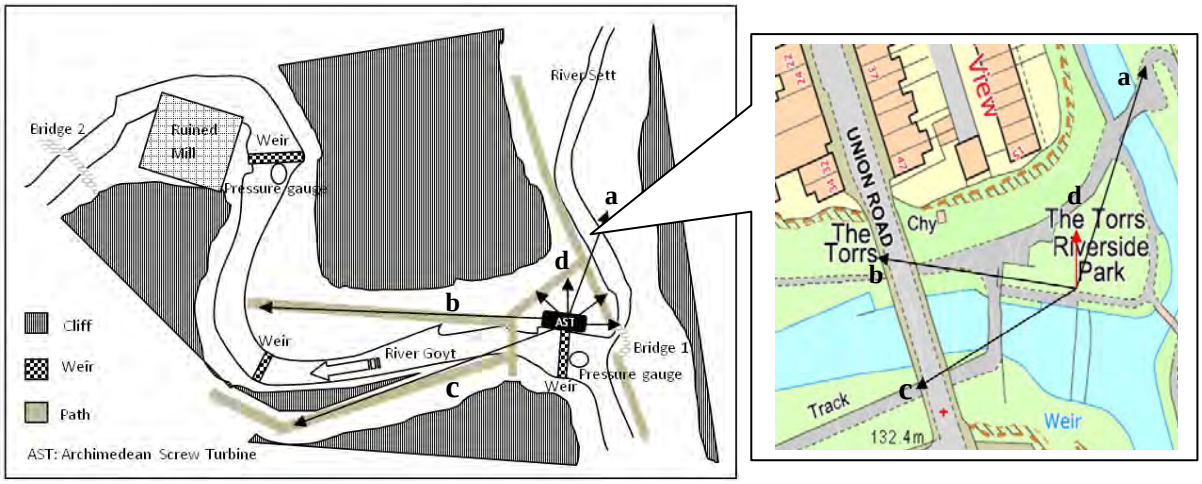

Figure 1. Location of the RAS studied, including the positions of the sampling transects (arrows) a, b and c, short red arrow is transect d. also shown is the positions of the pressure gauge sensors (for future work), and the location of the injection (Bridge 1), and sampling points (Bridge 2)

Figure 2. (Left) plan view photo of the RAS at New Mills and (right) a photo looking across the top of the weir to the angled transect (left-hand arch) and same axis (second arch in from right) NB: the bridge is indicative of the stone cliff heights around the site.

Sound Pressure Level (SPL) samples were taken (unweighted Leq) at each point along the transects using Class 1, MP231 microphones and WinMLS 2008. This was repeated when the RAS was running, and when all the water was diverted over the weir and the fish pass. A laser range finder and tape measure were used to give accurate distance of the sampling points from the weir and RAS for accurate sound propagation calculations and soundscape analysis. Processing of the acoustic samples was undertaken in the lab using WinMLS 2008. The main acoustic assumption is that the background soundscape is the same as when the screw is operational.

3. Results & Discussion

It is noted that in this paper, only limited results available are presented, and further measurements are being made. However, the results are of interest as there is no known data published for the sound propagation from RASs in the literature.

At a distance of 90m, the effects of other weirs downstream from the site were found to mask the sound from the RAS. Therefore, data from the 90m samples are not analysed further. *Figure 3* shows the SPL at increasing distances from the RAS along transect (d). As expected,

higher frequencies attenuate at a greater rate, see *figure 3*. The attenuation along distance is significant, and at a typical frequency, 500Hz, the SPL attenuation is about 10dB.

Observations of 1/3 octave plots and signals, *figures 4, 5 and 6* and recordings from the near field, transect (d); indicate a near white noise soundscape environment. By this, it is meant that the sound environment sounds like white noise. This near white noise is generated mainly by the water falling over the broad crest weir. Further to this a noticeable drop in amplitude in the signal can be observed with distance and between on and off, though less so. The spectrum plots of zero metres from screw, *figure 4*, indicate that there is a 3dBA difference between the screw being off and on which in acoustic terms contributes a barely legible amount [7].

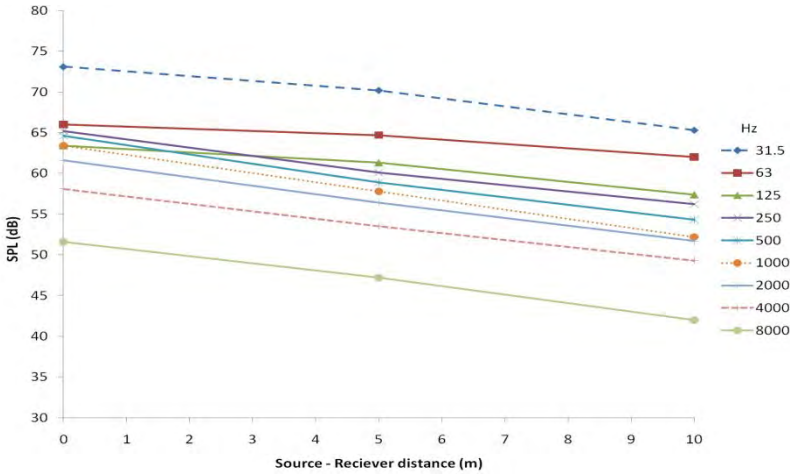

Figure 3. Background SPL when the flow is diverted from the RAS over the weir. Measurements taken along transect d (red arrow, figure 1) of SPL at a range of frequencies with increasing source - receiver distance.

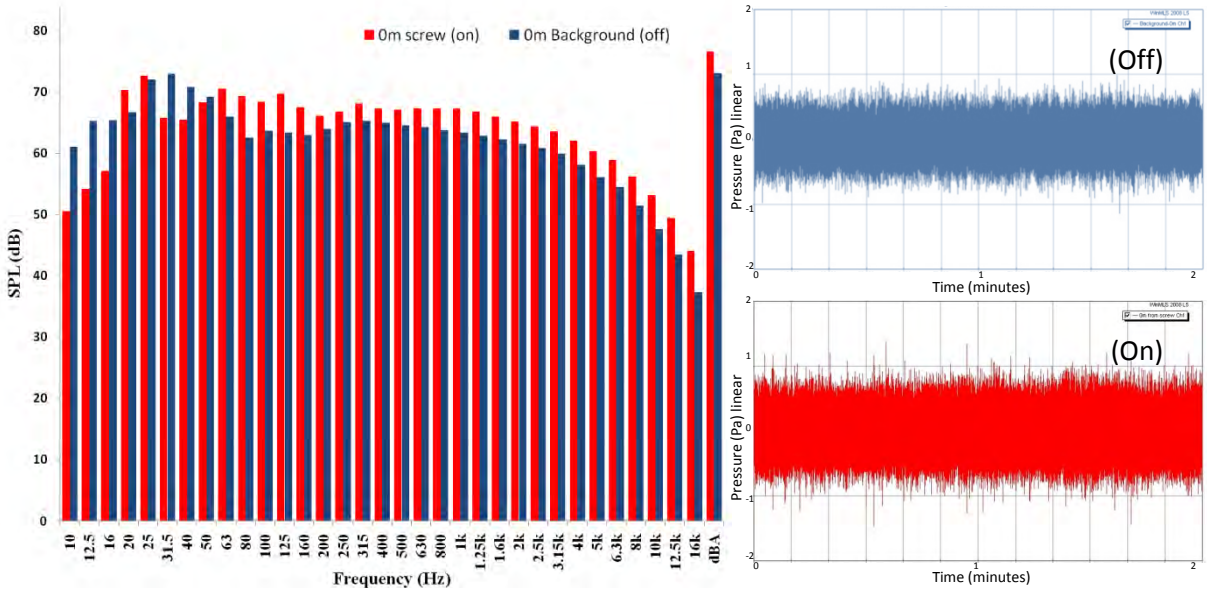

Figure 4. 1/3 octave spectrum plots of the SPL with 2 minute signal, when the RAS is operational at 25kW (red) and when the RAS is off, flow is diverted over the weir (blue) taken from directly above the RAS zero metres from screw.

At lower frequencies, the SPL with the RAS being off is 7-10dB higher. This might be due to the reduced volume of water falling over the weir when the RAS is running at 25kW,

reducing the low frequency component as less water falls into the weir pool. This may also explain the increase in SPL in the mid ranges. A similar pattern can be observed in the plots of samples taken 5m from the RAS, *figure 5*; and again at 10m, *figure 6*. However, there is less of a difference between the dBA results; with a difference of around 1dB and the mid to high frequency ranges being of a similar nature. However, lower frequencies are higher in amplitude during the background sampling than when the screw is operational, which may also be due to reflections from surrounding walls or being more exposed to the weir through an opening in the wall next to the screw and a function of directivity. *Figures 4-6* show a decrease in signal amplitude with distance.

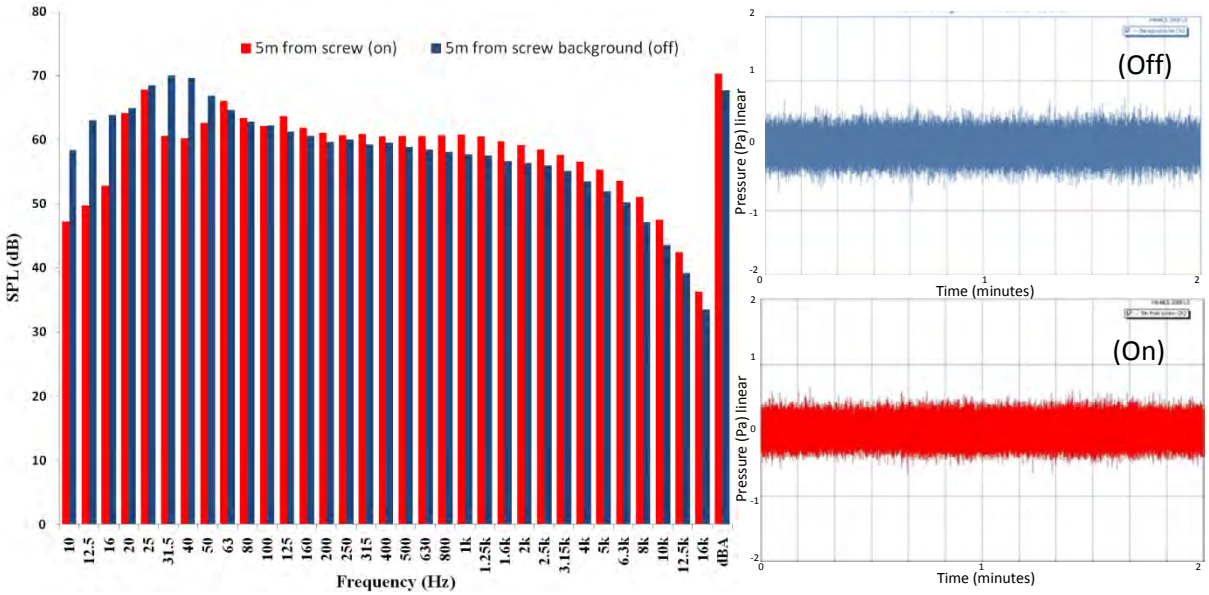

Figure 5. 1/3 octave spectrum plots of the SPL and 2 minute signal, when the RAS is operational at 25kW (red) and when the RAS is off, flow is diverted over the weir (blue) at 5m from screw.

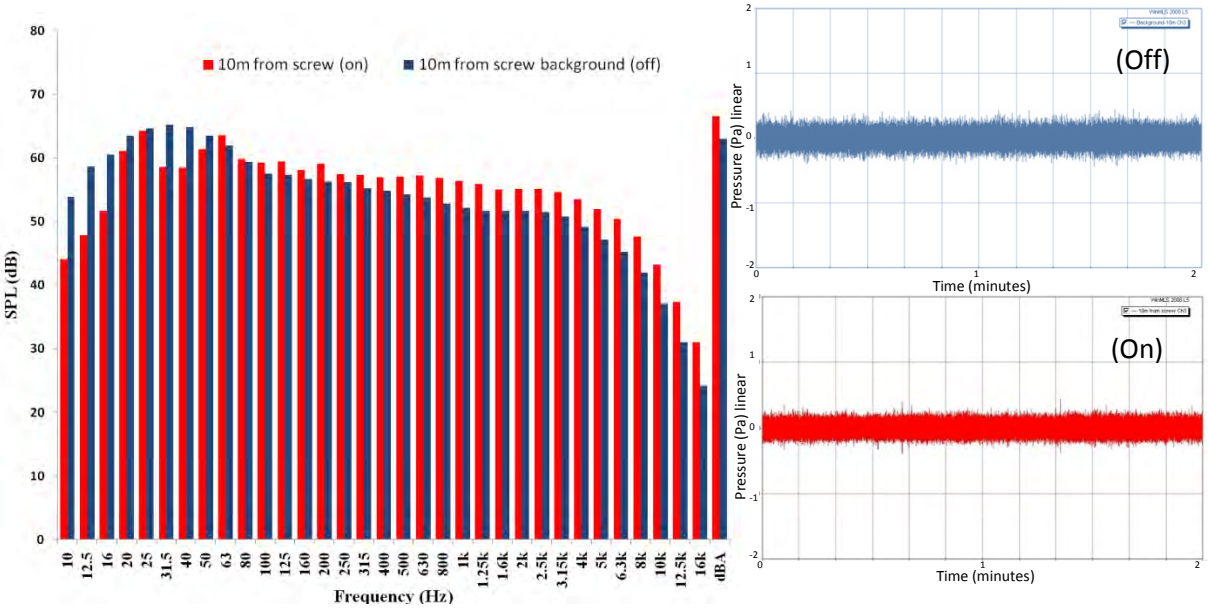

Figure 6. 1/3 octave spectrum plots of the SPL and 2 minute signal when the RAS is operational at 25kW (red) and when the RAS is off, flow is diverted over the weir (blue) at 10m from screw.

Table 1 and figure 7 show the SPL with increasing distance from the RAS along the three different transects a - c when the flow is diverted over the weir and the RAS is off. The

amplitudes are higher along transect (c) than (a) or (b), however this transect is located 10m from a stone cliff and road bridge, and it was noted on site that reflections were audible. The background data was all collected within a 40 minute period.

Table 1. Sample of background full octaves, SPL (dB) by frequency and transect distance figure 7, includes the frequencies not shown in this table.

Frequency [Hz]	SPL (dB) transect a 30 m	SPL (dB) transect b 30 m	SPL (dB) transect c 30 m	SPL (dB) transect a 60 m	SPL (dB) transect b 60 m	SPL (dB) transect c 60 m
250	51.8	55.0	61.4	44.3	53.1	55.3
1000	49.9	53.3	57.7	47.5	52.3	55.0
4000	46.1	49.7	53.6	40.7	45.5	50.5
dBA	60.3	63.6	68.1	56.5	61.5	64.6

At 30m on transect (b); there is a swash noise from water flowing over irregular rocks in the river next to the sample point. There are similar geographical features at this sample point to transect (c), which may increase the reflections in the area, including the large stone bridge, ruined walls and stone cliffs, though these cliffs are situated further away, and the ground is generally softer and grass covered between. There is an increase at 125Hz between the 30m and 60m sampling points on this axis (b). This may be related to other sound sources in the area, such as weirs present further downstream, or reflections in the area. It should also be noted that the large stone bridge near to the sampling point (*Figure 2*), is a road traffic bridge and this may explain the greater SPL low frequency results.

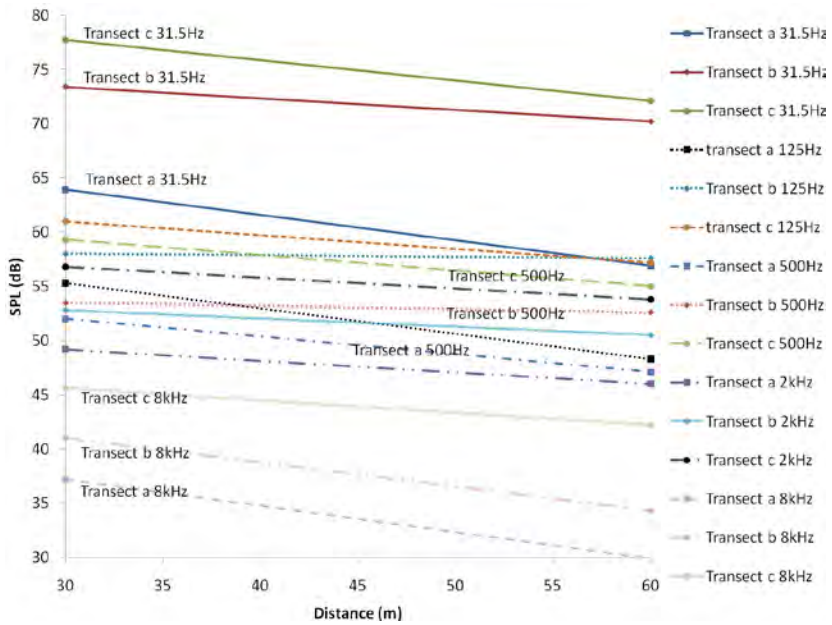

Along transect (a), running perpendicular to the RAS, the results taken at 30m and 60m sample points are noticeably lower in amplitude than (b) and (c) see *figure 7 and table 1*. As with the previous background plots *figures 3, 7 & 8*, the SPL of 31.5Hz is higher than that with the screw operational, see *figure 9*. *Figures 8* and *9* compare the SPL measured along transect (d) when the RAS is both on and off.

Figure 7. Example frequencies of the observed attenuation and SPL along transect a, b and c while the turbine is off. Lines between points are for demonstration purposes only and to aid pattern identification. The standard equation for attenuation of a line source with distance [11] was performed at 45m and it was found that deviation from the theoretical values is -1.6 to +2.1dB.

With a doubling of distance between 30 and 60m, in free-field conditions attenuation would be 3dB. Half the frequencies measured have higher attenuation levels than the 3dB whilst the other frequencies attenuate at a lower rate. It is thought that these differences are a function of the sampling environment as no corrections were added to the data, e.g. surface roughness differences or directivity. The variation in SPL differs depending on the frequency from

0.1dB to 9.1 dB, with an average difference between background frequencies and operational frequencies of 4.5dB at 0m, 3.3dB at 5m and 1.6dB at 10m. At 31.5Hz the SPL when the RAS is not operational is greater than when it is. These results are for a period when river flow enables the RAS to produce 25kW; further research is required to understand the generation of noise at a range of flows and electrical power outputs, and to validate the results presented.

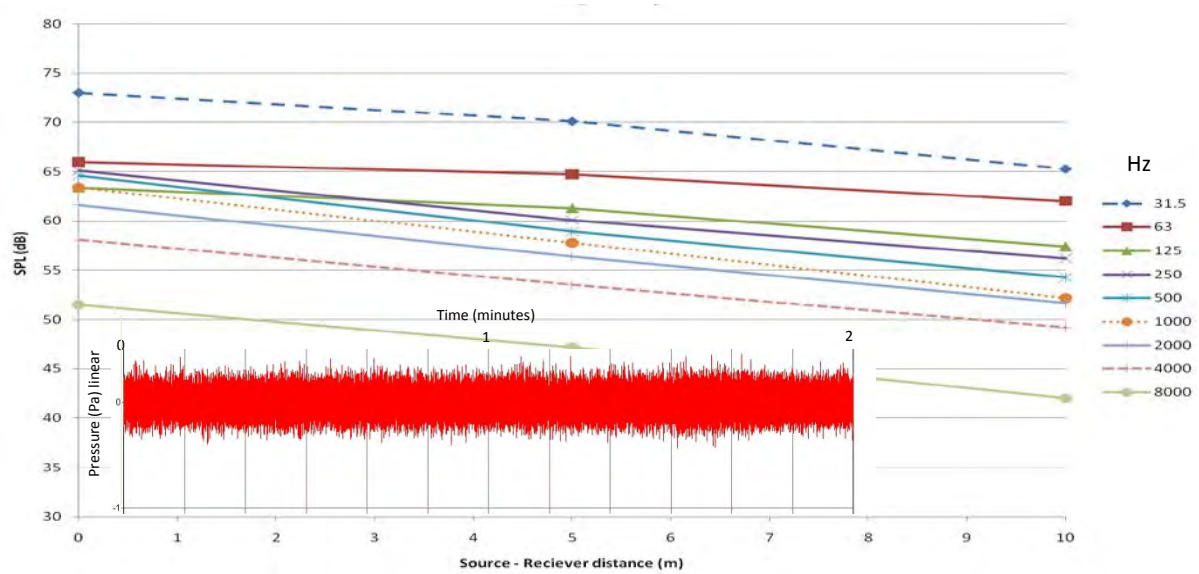

Figure 8. SPL by frequency from 0-10 whilst the turbine is off along transect a, where the insert is the 2 minute sample of the signal measured at 0m.

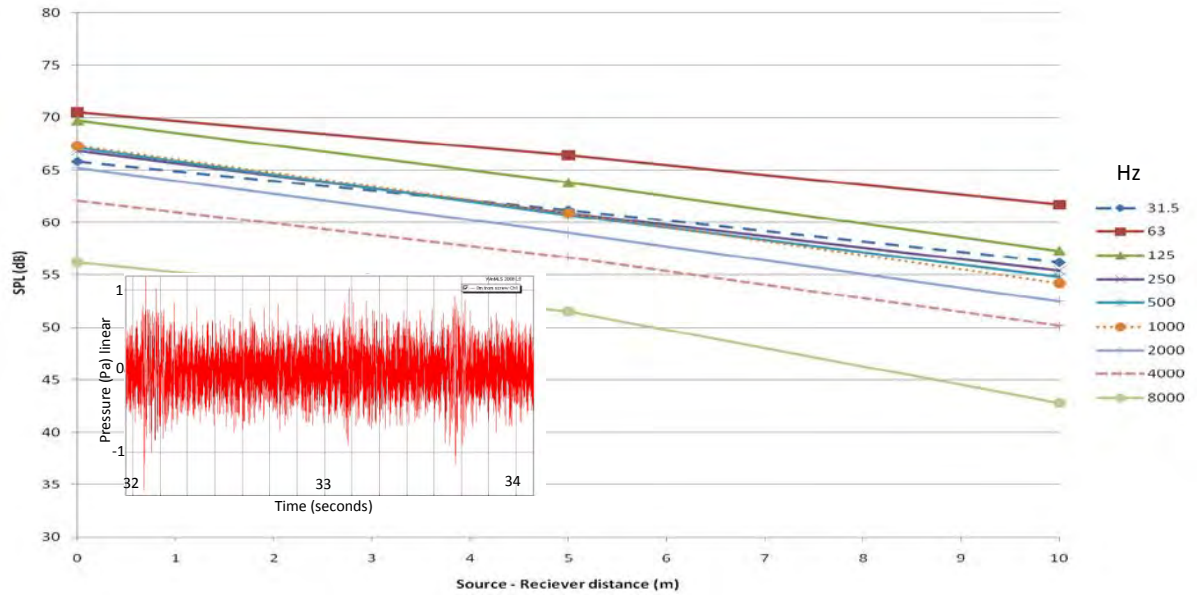

Figure 9. SPL by frequency from 0-10m whilst the turbine is switched on along transect a, where the insert is a 2 second sample of the signal measured at 10m between 32 and 34 seconds. A cyclic impulse can be seen within the signal plotted less than 2 seconds apart. This fits with the tri-blade rotational speed of the RAS which would include the blades entering/exiting the water.

4. Conclusions & Future Work

Initial results indicate that during normal operation at 25kW the screw would be barely perceptible beyond 60m, and adds just 3dB to the background environment and thus in many cases have negligible urban environmental impact running at 25kW. The weir has a significant masking effect on the RAS sound output. Further to this, the results indicate a directional aspect to the sound propagation from a RAS. However, whether this is a feature of the site or a feature of the RAS design is yet to be determined.

The RAS is not operational below 20kW, and therefore this study demonstrates the noise propagation at low flows. Future work will consider a range of flows from this increasing to the RAS design capacity of 53kW. Future work will also include a more detailed study of the RAS at New Mills with greater near field sampling and over shorter sampling periods to limit any extraneous noise sources from the results. Evaluation of other RAS sites will be carried to enable modeling and validation of the sound propagation. This will be used to assess the effect of various interventions in reducing noise nuisance from a RAS in an urban setting. Some further results will be presented at the conference.

References

[1] Driscoll, H.J.R., Micro-hydro power in Dorset: A re-assessment of potential installed capacity. Earth & E-nvironment, 2008. 3: p. 52-114.

[2] Lior, N., Energy resources and use: The present (2008) situation and possible sustainable paths to the future. Energy, 2009. 35: p. 2631-2638.

[3] International Energy Agency, World Energy Outlook 2008. IEA 2008.

[4] Paish, O., Small hydro power: technology and current status. Renewable & Sustainable Energy Reviews, 2002. 6(6): p. 537-556.

[5] Frey, G.W. and Linke, D.M., Hydropower as a renewable and sustainable energy resource meeting global energy challenges in a reasonable way. Energy Policy, 2002. 30(14): p. 1261-1265.

[6] Yi, C.-S., Lee, J.-H. and Shim, M.-P., Site location analysis for small hydropower using geo-spatial information system. Renewable Energy, 2010. 35(4): p. 852-861.

[7] Watson, R. and Downey, O., The Little Red Book of Acoustics: A Practical Guide. 2nd ed. 2008: Blue Tree Acoustics.

A Piezoelectric Energy Harvester Based on Pressure Fluctuations in Kármán Vortex Street

Dung-An Wang[1,*], Huy-Tuan Pham[1], Chia-Wei Chao[1], Jerry M. Chen[2]

[1] *Graduate Institute of Precision Engineering, National Chung Hsing University, Taichung 40227, Taiwan, ROC*
[2] *Department of Mechanical Engineering, National Chung Hsing University, Taichung 40227, Taiwan, ROC*
** Corresponding author. Tel: +886 422840531, Fax: +886 422858362, E-mail: daw@dragon.nchu.edu.tw*

Abstract: We have developed a new energy harvester for harnessing energy from the Kármán vortex street behind a bluff body in a water flow. It converts flow energy into electrical energy through oscillation of a piezoelectric film. Oscillation of the piezoelectric film is induced by pressure fluctuation in the Kármán vortex street. Prototypes of the energy harvester are fabricated and tested. Experimental results show that an open circuit output voltage of 0.12 V_{pp} and an instantaneous output power of 0.7 nW are generated when the pressure oscillates with an amplitude of ~0.3 kPa and a frequency of ~52 Hz. This approach has the potential of converting hydraulic energy into electricity for powering wireless devices. The low output power of the device can be improved by an optimization design procedure or by adopting a piezoelectric material with higher piezoelectric constants. An array of these devices with multiple resonant frequencies may be considered for energy harvesting from ambient flow sources.

Keywords: *Energy Harvester, Piezoelectric, Kármán vortex street*

1. Introduction

Recent development of wireless sensor networks allowing real-time industrial process monitoring, machine health monitoring, environment monitoring, healthcare applications, and traffic control demands an economical source of energy not requiring fuel or replacement of finite power stores. Considerable effort is focused on use of renewable energy coming from natural resources such as flowing water, rain, tides, wind, sunlight, geothermal heat and biomass. Renewable energy from small-scale hydro, modern biomass, wind, solar, geothermal and biofuels accounted for 2.7% of global final energy consumption in 2008 and is growing very rapidly [1].

Small hydro systems using turbines/wheels can be used to convert mechanical energy from water flow into electricity. Krähenbühl et al. [2] designed an electromagnetic harvester based on a turbine driven by water pressure drop in throttling valves and turbo expanders in plants that outputs 150 W power with a rotation speed of 490000 rpm. Their device comprises a turbine and a permanent generator. A detailed electromagnetic machine design, rotor dynamics analysis and a thermal design were required to construct their energy harvester. Holmes et al. [3] reported an electromagnetic generator integrated with a microfabricated axial-flow microturbine. The power output of the fabricated microdevice can be as high as 1.1 mW per stator when operated at a rotation speed of 30000 rpm, but the fabrication processes for their prototype involve deep reactive ion etching, multilevel electroplating, SU8 processing and laser micromachining. Herrault et al. [4] presented a rotary electromagnetic generator to harvest the mechanical energy of an air-driven turbine. The fabrication of their device requires electroforming, magnet demagnetization and laser machining. A maximum output power of 6.6 mW is attained when their device is driven at a rotation speed of 392000 rpm by an air turbine. The devices of Krähenbühl et al. [2], Holmes et al. [3] and Herrault et al. [4] require elaborate techniques for fabrication of their stator-rotor subcomponents and high rotation speeds for efficient energy harvesting. A device with simpler structure design

and ease of application may be needed to extract energy from fluid motion for microsensor and communications applications.

Installations with miniaturized pipe-line systems may provide an alterntive for harvesting small scale water flow energy. Sanchez-Sanz et al. [5] assessed the feasibility of using the unsteady forces generated by the Kármán street around a micro-prism in the laminar flow regime for energy harvesting. They presented design guidelines for their devices, but fabrication and demonstration of the proposed device are not shown in their work. Allen and Smits [6] used a piezoelectric membrane placed behind the Kármán vortex street formed behind a bluff body to harvest energy from fluid motion. They examined the response of the membrane to vortex shedding. The power output of the membrane is not presented. Taylor et al. [7] developed an eel structure of piezoelectric polymer to convert mechanical flow energy to electrical power. They have focused on characterization and optimization of the individual subsystems of the eel system with a generation and storage units in a wave tank. Design and deployment of the eel system need further investigation. Tang et al. [8] designed a flutter-mill to generate electricity by extracting energy from fluid flow. Their structure is similar to the eel systems of Allen and Smits [6] and Taylor et al. [7]. They investigate the energy transfer between the structure and the fluid flow through an analytical approach. These authors utilized the flow-induced vibrations of fluid-structure interaction system to extract energy from the surrounding fluid flow [9]. The eel structures of Allen and Smits [6], Taylor et al. [7] and Tang et al. [8] have the potential to generate power from milli-watts to many watts depending on system size and flow velocity, but a power-generating eel has not been demonstrated.

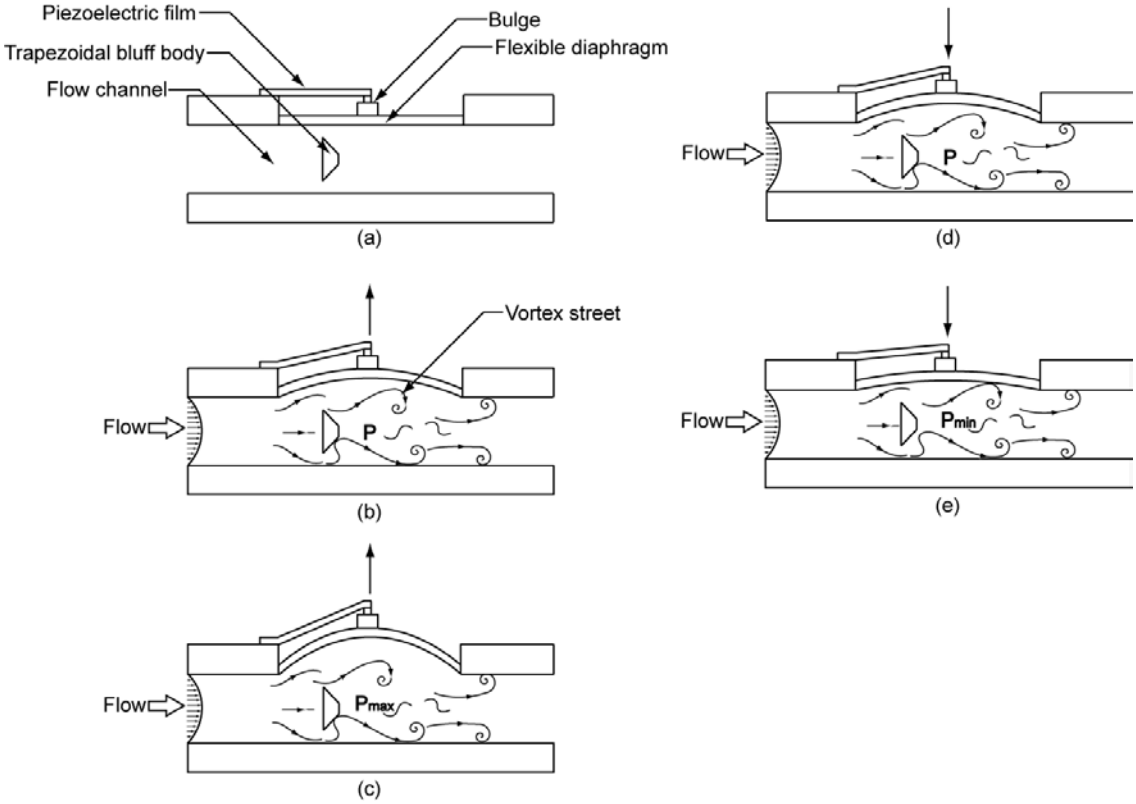

Fig. 1. Operation of a piezoelectric energy harvester.

In this report, we demonstrate a new device for energy harvesting from pressure fluctuations in the Kármán vortex street, where a piezoelectric film is placed on top of a flexible

diaphragm, which is located in the wake of a bluff body. The piezoelectric film oscillates on a flexible diaphragm due to the vortices shed from the bluff body in a water flow. As illustrated in Fig. 1(a), a flow channel with a flexible diaphragm is connected to a flow source. A piezoelectric film of a cantilever type is glued to a bulge affixed to the top surface of the flexible diaphragm. A bluff body is placed in the flow channel. Pressure in the flow channel behind the bluff body may fluctuate with the same frequency as the pressure variation caused by the Kármán vortex street. Fig. 1(b) shows that the pressure in the channel causes the diaphragm and the piezoelectric film to deflect in the upward direction. As the pressure increases to the maximum, the diaphragm reaches its highest position (Fig. 1(c)). When the pressure drops, the diaphragm and the piezoelectric film deflect downward (Fig. 1(d)). As the pressure decreases to the minimum, the diaphragm reaches its lowest position (Fig. 1(e)). Thus, by placing the energy harvester in a flow source, the oscillating movement of the diaphragm with the cantilever piezoelectric film attached to it makes the energy harvesting possible.

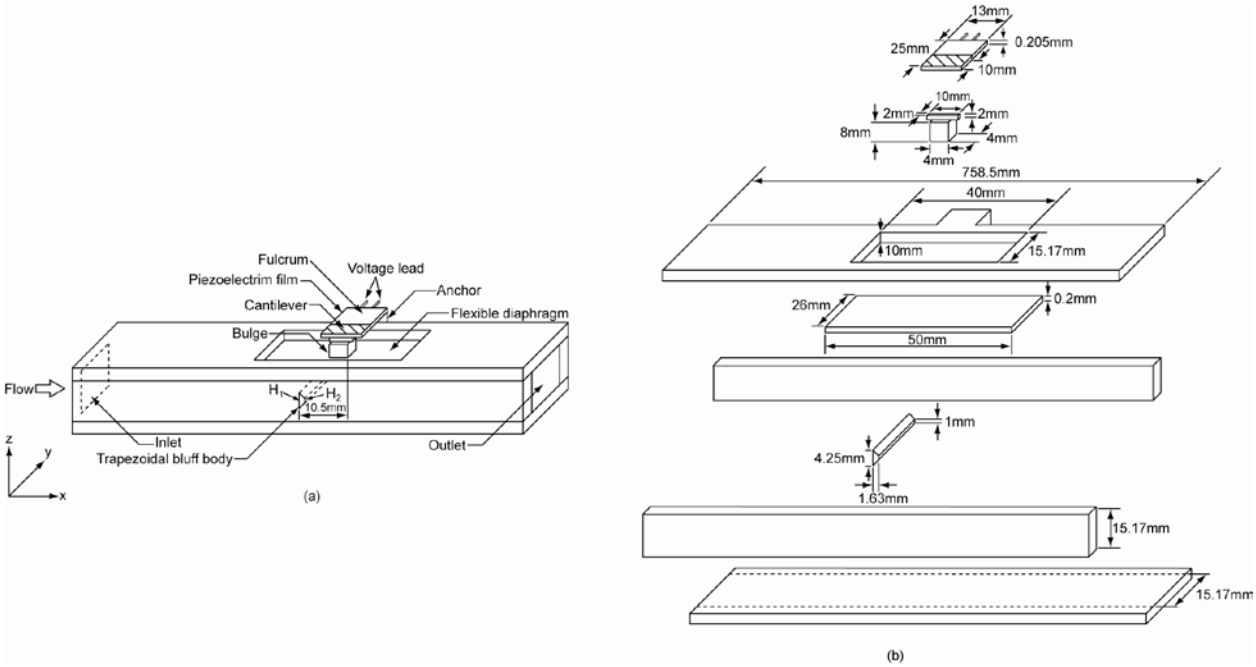

Fig. 2. (a) An assembled energy harvester. (b) Components of the energy harvester..

2. Methodology

2.1. Operational principle

A piezoelectric energy harvester considered in this investigation is shown in Fig. 2(a). Fig. 2(b) is an exploded view of the energy harvester. The dimensions of the energy harvester are indicated in Fig. 2(b). It consists of a flow channel, a bluff body, a polydimethylsiloxane (PDMS) diaphragm bonded to the channel, and a piezoelectric film attached to the PDMS diaphragm through a bulge made of acrylic blocks. Flow past a bluff body creates an unstable wake in the form of alternating vortices and induces periodic pressure variation [10]. The frequency at which the vortices are shed from the bluff body is given by the Strouhal number, St, $St = \omega \ell / U_\infty$ [11], where ω is the frequency of oscillating flow, ℓ is the characteristic length, and U_∞ is the free-stream velocity. Vortex shedding from a circular cylinder immersed in a steady flow occurs in the range $10 < Re < 10^5$, where Re is the Reynolds number, with an average Strouhal number $\omega d / 2\pi U_\infty \approx 0.2$ [12]. For a trapezoidal bluff

body, the Strouhal number is given as $S = \omega H_1 / U_\infty$ [13], where H_1 is the height of the front side of the trapezoidal cylinder. The front height H_1 and rear height H_2 of the trapezoidal cylinder are denoted in Fig. 2(a).

The piezoelectric film (LDT0-028K/L, Measurement Specialties, Inc., US) is a laminate including a polyvinylidene fluoride (PVDF) film, two silver electrode layers and a polyester (PE) layer. The PDMS flexible diaphragm has a thickness of 200 μm. The electrode layers with a thickness of 28 μm are attached to the top and bottom surfaces of the PVDF film of 24 μm. A 125 μm PE layer is laminated to the top surface of the top electrode layer. The values of d_{31} and d_{33} of the PVDF are 23 and -33 $pm \cdot V^{-1}$, respectively. The capacitance of the PVDF film is 380 $pF \cdot cm^{-2}$. The Young's modulus and Poisson's ratio of the PVDF are 3 GPa and 0.35, respectively. When used in a bending mode, the laminated piezoelectric film develops much higher voltage output when flexed than a non-laminated film. The neutral axis is in the PE layer instead of in the PVDF film so the film is strained more when flexed.

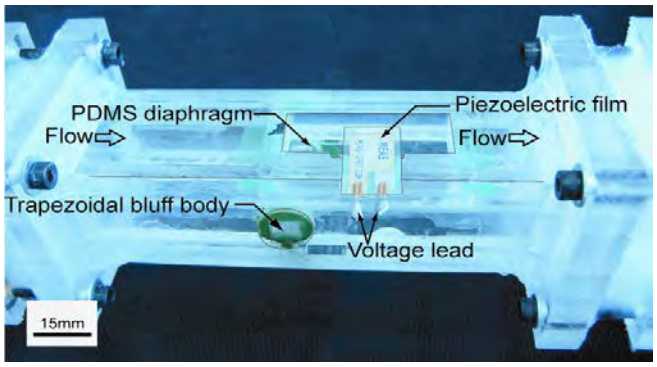

Fig. 3. Assembled energy harvester.

2.2. Fabrication and Experiments

In order to verify the effectiveness of the proposed energy harvesting device, prototypes of the energy harvester were fabricated. Fig. 3 is a photo of an assembled energy harvester. Its dimensions are indicated in Fig. 2(b). Fig. 4 is a photo of the experimental apparatus for testing of the fabricated device. The energy harvester is placed on an optical table for vibration isolation. From the bottom of a storage tank, an inlet pipe is run down to the inlet of the energy harvester. The water level in the storage tank is kept constant for a steady water flow at the inlet of the flow channel. Using gravity, water is forced into the inlet of the energy harvester. Tap water is pumped into the storage tank through a pump located in a recycle tank. An outlet pipe extending between the outlet of the energy harvester and the recycle tank provides a continuous supply of water. The oscillating deflection of the piezoelectric film is measured by a fiberoptic displacement sensor (MTI-2000, MTI Instruments Inc., US). The generated voltage of the piezoelectric film is recorded and analyzed by a data acquisition unit (PCI-5114, National Instruments Co., US). The pressure in the pressure chamber is measured with a subminiature pressure sensor (PS-05KC, Kyowa Electronic Instruments Co. Ltd., Japan) embedded in the bottom plate of the flow channel. The pressure sensor is connected to a data acquisition unit (DBU-120A, Kyowa Electronic Instruments Co. Ltd., Japan).

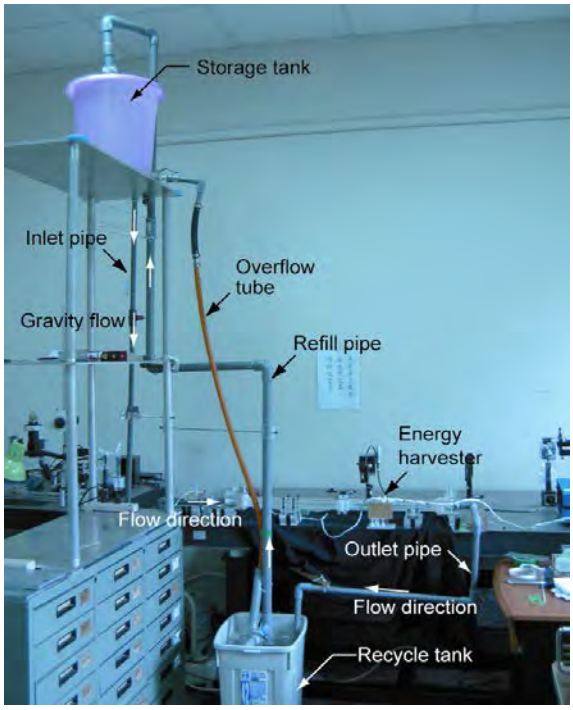

Fig. 4. A photo of the experimental setup.

3. Results

The experimental results are shown in Fig. 5. Fig. 5(a) shows the pressure history in the flow channel behind the bluff body, where the pressure oscillates with an amplitude of nearly 0.3 kPa and a frequency of 52 Hz. The measured deflection history of the free end of the piezoelectric film is shown in Fig. 5(b). The film oscillates with an amplitude of about 20 μm. The measured open circuit voltage generated by the piezoelectric film is shown in Fig. 5(c). The output peak-to-peak voltage is nearly 120 $\mathrm{mV_{pp}}$. The results shown in Figs. 5(a-c) are typical of those obtained over 20 seconds of measurements. Figs. 5(d-f) are the power spectral density corresponding to Figs. 5(a-c), respectively, but are based on all 20 seconds of measurements. Fast Fourier transform is used to compute the power spectral density. It can be seen from Figs. 5(d-f) that there is one obvious peak value of 52 Hz, caused by the pressure fluctuation in the flow channel. The low-frequency noise, below 20 Hz, observed in Figs. 5(d-f) can be attributed to the fact that flows in the experimental setup are always contaminated by ambient noise sources, and the geometry of the bluff body and the walls of the flow channel are not perfectly symmetric and smooth.

The average free-stream velocity U_∞ measured in the experiments is 1.083 m/sec. The Reynolds number Re of the flow can be determined by $\mathrm{Re} = \rho U_\infty D_h / \mu$, where μ is the dynamic viscosity of the water, 1.002×10^{-3} Pa·sec, and D_h is the hydraulic diameter, which is 15.17 mm for the flow channel considered. The calculated Re is 1.64×10^4, which is turbulent. The frequency of the pressure fluctuation is nearly 52 Hz (Fig. 5(d)), which is the rate at which the vortices are shed from the bluff body. Using the equation $\mathrm{St} = \omega H_1 / U_\infty$, the corresponding value of St is estimated as 0.204. White [12] reported an average St about 0.21 for the shedding from a circular cylinder immersed in a steady flow occurring in the range $10^2 < \mathrm{Re} < 10^3$. The estimated value of St for a trapezoidal bluff body of the experiments is reasonable compared with the value 0.21 reported by White [12]. The experimental values of

St for trapezoidal cylinders with the height ratio, H_2/H_1, ranging from 0.3 to 1.0 and the Re values of 100, 150, and 200, have a range from approximately 0.135 to approximately 0.155 [13]. Based on the work of Norberg [14] for a circular cylinder, the variations in St are within the limit 0.1 9 2 0.0 1 for the Re ranging from 250 t o 3×10^5. Ho and Huerre [15] commented that the values of St changes from 0.016 for a laminar flow to 0.022-0.024 for turbulent flow. Based on the reported experimental data [12-15], the estimated value of St, 0.204, based on the experiments carried out in this investigation could be acceptable.

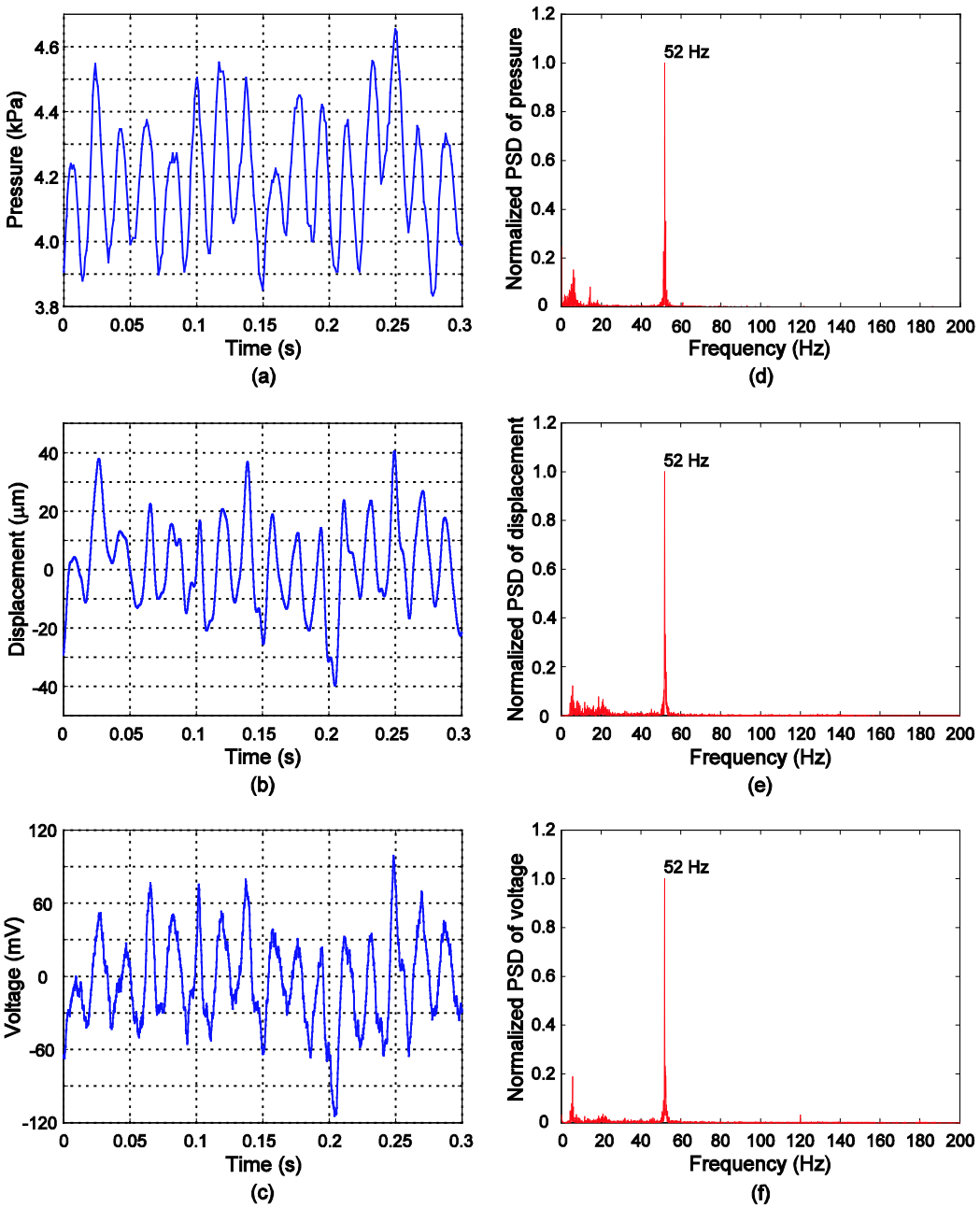

Fig. 5. Experimental results. (a) Pressure variation in the pressure chamber. (b) Deflection of the free end of the cantilever piezoelectric film. (c) Output voltage of the piezoelectric film. (d-f) Power spectral density corresponding to (a-c).

A matched load can be connected to the device to evaluate the power output of the device. The internal electrical resistance of the device is measured by a LCR meter (WK 4235,

Wayne Kerr Electronics, Ltd., UK). The instantaneous power can be expressed as $P = (\sqrt{2}\widetilde{V})^2 / R$, where R is the resistance value of the matched load and $\widetilde{V}$ is the root-mean-square value of the voltage drop across the matched load. By connecting the matched load of 655 kΩ to the device and detecting the voltage drop across the matched load, 14.89 mV_{rms}, the instantaneous power is determined as 0.7 nW.

4. Discussions

The output power of the device is relatively low, given the structure design of the flow channel, the bluff body and the cantilever piezoelectric film. In order to obtain a higher output power of the piezoelectric energy harvester, the dimensions and structure of the device can be optimized, and a piezoelectric material with higher piezoelectric constants can be adopted. In this investigation, the device is not operated at its resonance frequency. Most energy harvesting device based on piezoelectric effects have focused on single-frequency ambient energy, i.e. resonance-based energy harvesting [16]. The resonance frequency of the energy harvesting device can be tailored to the shedding frequency of the Kármán vortex street in order to increase the output power of the device. For random and broadband ambient flow sources, such a device may not be robust. A structure with multiple resonant frequencies may also be considered for energy harvesting from random vibrations with multiple resonant peaks, for example a segmented composite beam with embedded piezoelectric layers [17].

In order to generate the pressure fluctuation of the Kármán vortex street in the channel, a flow source assisted by gravity is used to force tap water into the flow channel in the laboratory environment. Energy can be harvested from pipe flows, blood flow in arteries [18,19], or air flow in tire cavities. The proposed device can be deployed on slopes to provide electricity for wireless sensor networks for detection of landslides. Landslides are usually preceded by heavy rainfalls, and the device can harvest the energy of the water flow along slopes due to rainfall. Energy harvesting from regular, periodic shedding can be integrated into tire pressure monitoring systems to harness the energy of air flow in tire cavities, or self-powering implantable and wireless devices in human bodies to convert the hydraulic energy of flow of body fluid.

References

[1] REN21, Renewables 2010 Global Status Report, 2010, pp. 15-16.

[2] D. Krähenbühl, C. Zwyssig, H. Weser, J.W. Kolar, Theoretical and experimental results of a mesoscale electric power generation system from pressurized gas flow, Journal of Micromechanics and Microengineering 19, 2009, 094009.

[3] A.S. Holmes, G. Hong, K.P. Pullen, Axial-flux permanent magnet machines for micropower generation, Journal of Microelectromechanical Systems 14, 2005, pp. 54-62.

[4] F. Herrault, C.-H. Ji, M. G. Allen, Ultraminiaturized high-speed permanent-magnet generators for milliwatt-level power generation, Journal of Microelectromechanical Systems 17, 2008, pp. 1376-1387.

[5] M. Sanchez-Sanz, B. Fernandez, A. Velazquez, Energy-harvesting microresonator based on the forces generated by the Kammon street around a rectangular prism, Journal of Microelectromechanical Systems 18, 2009, pp. 449-457.

[6] J.J. Allen, A.J. Smits, Energy harvesting eel, Journal of Fluid and Structures 15, 2001, pp. 629-640.

[7] G.W. Taylor, J.R. Burns, S.M. Kammann, W. B. Powers and T. R. Welsh, The energy harvesting eel: A small subsurface ocean/river power generator, IEEE Journal of Oceanic Engineering 26, 2001, pp. 539-547.

[8] L. Tang, M.P. Païdoussis, J. Jiang, Cantilevered flexible plates in axial flow: Energy transfer and the concept of flutter-mill, Journal of Sound and Vibration 326, 2009, pp. 263-276.

[9] R.D. Blevins, Flow-induced vibration, Van Nostrand Reinhold, ed. 2, 1990.

[10] R. Violette, E. de Langre, J. Szydlowski, Computation of vortex-induced vibrations of long structures using a wake oscillator model: Comparison with DNS and experiments, Computers and Structures 85, 2007, pp. 1134-1141.

[11] D.F. Young, B.R. Munson, T.H. Okiishi, A brief introduction to fluid mechanics, John Wiley & Sons, 2001.

[12] F.M. White, Fluid Mechanics, McGraw-Hill, 1986.

[13] Y.J. Chung, S.-H. Kang, Laminar vortex shedding from a trapezoidal cylinder with different height ratios, Physics of Fluids 12, 2000, pp. 1251-1254.

[14] C. Norberg, An experimental investigation of the flow around a circular cylinder: influence of aspect ratio, Journal of Fluid Mechanics 258, 1994, pp. 287-316.

[15] C.M. Ho, P. Huerre, Perturbed free shear layers, Annual Review of Fluid Mechanics 16, 1984, pp. 365-422.

[16] S. Adhikari, M.I. Friswell, D.J. Inman, Piezoelectric energy harvesting from broadband random vibrations, Smart Materials and Structures 18, 2009, 115005.

[17] S. Lee, B.D. Youn, B.C. Jung, Robust segment-type energy harvester and its application to a wireless sensor, Smart Materials and Structures 18, 2009, 095021.

[18] C. Mo, L.J. Radziemski, W.W. Clark, Experimental validation of energy harvesting performance for pressure-loaded piezoelectric circular diaphragms, Smart Materials and Structures 19, 2010, 075010.

[19] Z.L. Wang, J. Song, Piezoelectric nanogenerators based on zinc oxide nanowire arrays, Science 312, 2006, pp. 242-246.

Low head hydropower – its design and economic potential

Jana Hadler[1,*], Klaus Broekel[1]

[1] *University of Rostock, Institute of Engineering Design, Rostock, Germany*
** Corresponding author. Tel: +49 381 4989181, Fax: +49 381 4989172, E-mail: jana.hadler@uni-rostock.de*

Abstract: The large scale model of a Free Stream Energy Converter (FSEC) is built, and can be installed in protected as well as in tidal areas. This is one of the determined objectives of the EU-Project HYLOW, funded by the FP7. First field tests with rope winch and towing boat were done; further, in a protected area near Rostock, and the installation in the River Ems under tidal conditions and ship traffic, are planned for the first half of 2011. Besides, the permanent design control for the FSEC is as necessary as the monitoring of the behaviour of the model positioned in all the sites. If design changes or modifications are necessary, these can be done directly on site, respectively in the Steel Construction Company nearby. Whether it is suited for practice, however, is still dependent on other factors. The investigations are primarily limited on technical and ecological level. It is now necessary to look at the cost-sided development, too. Starting with considerations for the financing and economic efficiencies about expressive cost-benefit analyses up to design and material costs, the European need should be determined in hydropower for low potentials. Realization of hydropower plans takes a long period.

Keywords: *Low head differences, Free Stream Energy Converter, EU-Project, Hylow, Cost-benefit analysis.*

1. Introduction

One reason for the Hylow project is the rising demand for energy. Another one is the necessity to implement renewable energies, because of undeniable importance in view of declining natural resources. Small hydropower is a possible substitute for fossil fuels which are already limited. The European committee has fixed specific targets with a view to initiating change towards renewable energy. In order to achieve these objectives, energy generating systems, which were economically unattractive, are given greater priority.
The Hylow project focuses on the development of a mobile energy converter for low head differences – a topic which is usually neglected, because of missing significant results.

2. Motivation for hydropower

Compared to wind power and photovoltaic, small hydropower is often undervalued - at least in the public perception. In theory the worldwide demand for energy could be covered by hydropower. But it will not be economically practical, because of the uneven distribution of water resources on world territory.

2.1. Strong arguments

The power source “hydropower” offers many advantages.
Minimal emissions occur just in the installation period and in the first running period, when converters have to be stabled. A running energy converter does not need a great number of additional materials or energy. In sum there are low CO_2 emissions during operating time.

Hydropower requires no primary energy – therewith the respective countries relieve their own energy bills as well as they increase the security of energy supply. Furthermore, hydropower depends neither on the natural rhythm of the sun nor on the strength of the wind. This allows a permanent and continuous electricity generation.

There is a significant potential for hydropower in the EU and worldwide. However, the availability of use is limited by specific features of energy supply, such as localization, use of sites, power supply and current collection.

2.2. Background of Hylow

Small hydropower plants are close to nature; their design is often environmentally compatible. This applies to Hylow also. The floating Large Scale Model (LSM) of the FSEC is nearly 7,800 mm in length, 2,400 mm in width, and 3,500 mm in height. The wheel diameter is 3,200 mm and 1,100 mm in width (see Figure 1).

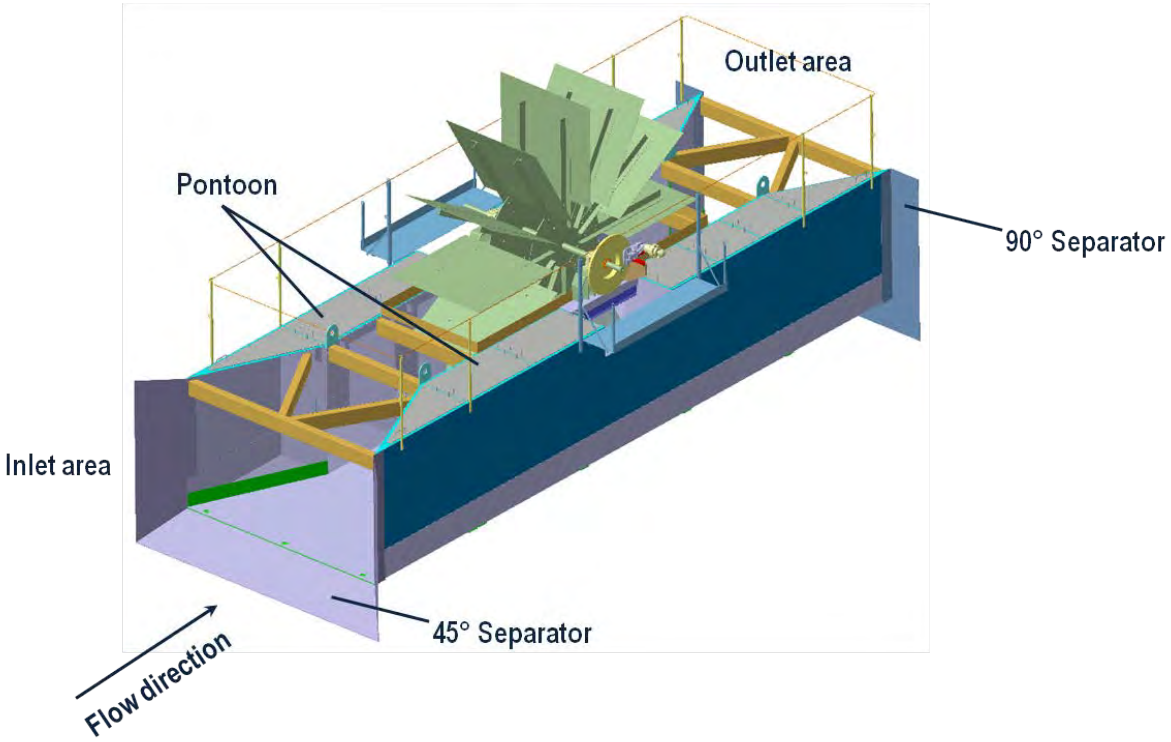

Fig. 1. The CAD model of the LSM, separators included.

The LSM will be placed in running waters with flow velocities of up to 1.5 m/s. The model is dimensioned for exceptional situations, in which the velocity rises, such as floodwaters or strong winds. To realize test runs with the LSM in protected areas no lubricants or other persistent products will be used. The power take-off is envisaged as a friction-type brake, and works without any liquids, so that even in the average case the environment takes no damage. For later applications and for deployment in developing countries to energy production, the brake system will be substituted with a generator solution which is adapted in ecological respects. [1]

3. Product development

Essential for product development activities, besides the idea, are calculations. These start with the power output to be expected. In addition, all forces, which appear, are to be taken into consideration.

3.1. Free Stream Energy Converter

The first geometry of the pontoon was given by calculations and basis tests done with simplified and down scaled configurations. The outline geometry consists of two hulls which

are connected via a base. The hulls in the inlet area are v-shaped, so that the channel will get narrowed, and the flow velocity accelerates. This procedure corresponds to the Venturi principle. [1]

Fig. 2. The LSM on the first deployment – the naval base in Rostock.

During the whole project three field tests with the LSM at different locations (with expected flow velocities between 0.4 and 1.5 m/s) are planned. The first deployment site was envisaged for towing tests; these tests have been successfully completed in autumn, 2010 (see Figure 2). The second and third test sites are in a protected area near Rostock, and in the River Ems in Northern Germany.

Initial towing tests were meant to demonstrate the model behaviour during operational conditions. In addition, the floating behaviour of the model with different velocities and geometries (additional separators) should be tested. The LSM delivered an electric power output up to 500 W.

The towing tests show that something has to be changed concerning the geometry of the LSM. The best results in the first deployment site were achieved with separators at both ends of the LSM. In the inlet area works the separator as a scoop with an angle of 45°, and in the outlet it has 90°. In order to limit the costs several models have to be analysed with the computational fluid dynamics (CFD) software FLOW-3D [3]. See first results in Figure 3.

The FLOW-3D tests are useful for the fine adjustment of length, arrangement and angular size of the separators. Moreover, the trim angle of the FSEC can be adjusted according to the waterline (horizontal alignment in the flow). Figure 3 shows three situations in FLOW-3D with different arrangements of the separators. The set velocity is determined with 1 m/s, and it changes as expected in several areas of the flow pattern – in narrowed parts of the channel are higher velocities than in the widened areas. The simulations are ongoing; final results are expected in spring, 2011.

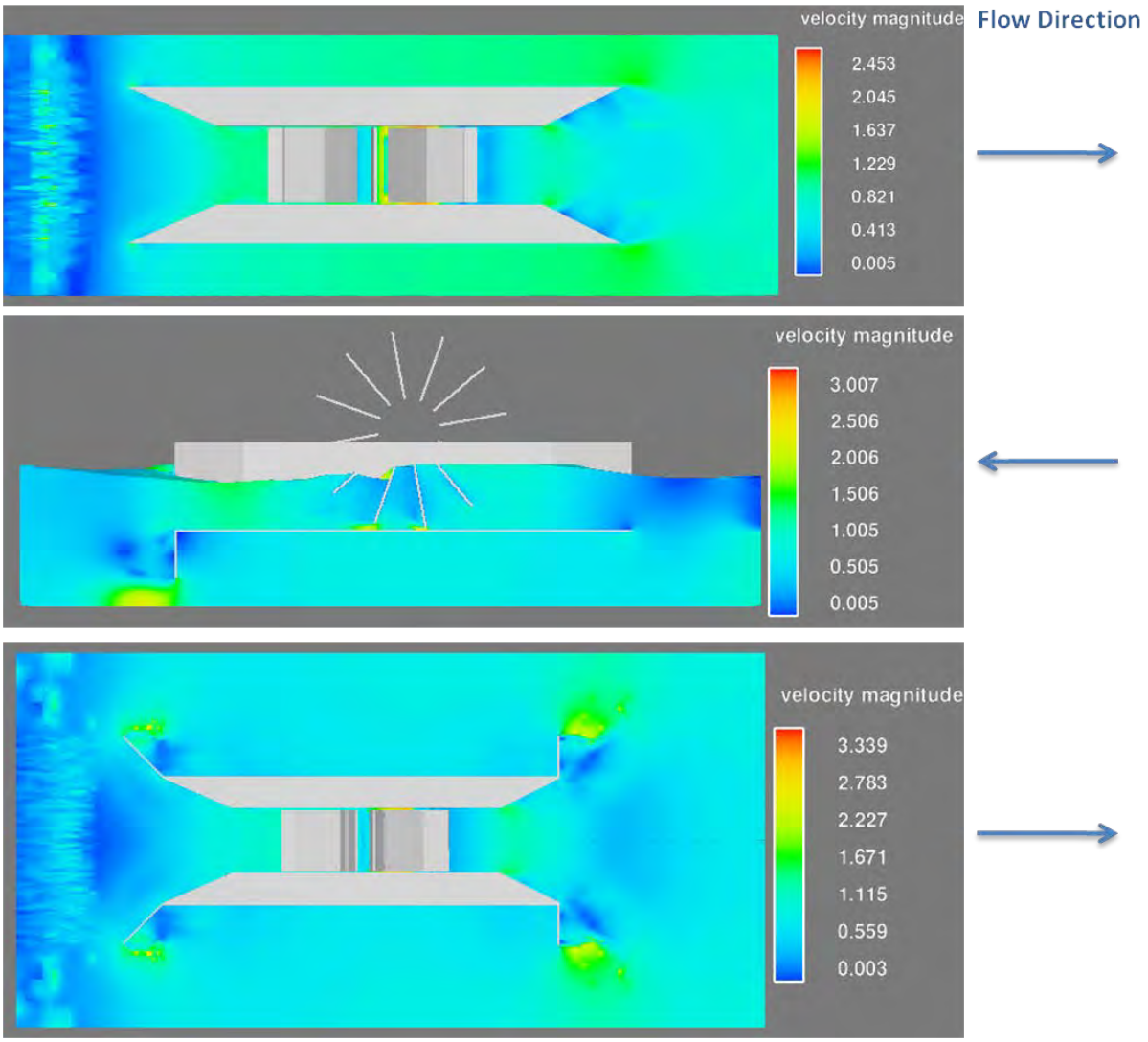

Fig. 3. Geometry tests with FLOW-3D.

3.2. Cost report of the FSEC prototype

To check the efficiency of the FSEC the annual costs are compared with the benefit. The benefit will be calculated from the sale of electricity to the energy companies. Thus, the investment can determine the annual profit, as the difference between the yields and costs. For the considerations, the average values of all costs and yields are used.

The total costs of the energy converter arise from different cost types. A calculation basis of these are the given production costs of the prototype which consist as follows (table 1):

Table 1. Production costs for prototype.

Cost type	**Total** [€]
Personnel costs	30,491.00
Material, standard parts & consumables	24,750.00
Indirect costs (20 % of direct costs)	11,048.20
Manufacturing costs	66,289.20

In these costs no costs for research and development included. Because of the prototype, no values of experience have still integrated into the production procedure. Moreover, detailed

values of wear behaviour are neglected, because there are no empirical values for this special case exist.

4. An FSEC in Europe – where conditions are most favorable

The benefit of the FSEC consists in the production of electrical energy using the potential of flowing water. For the feed in existing electrical grids there are fixed feed-in tariffs which mostly have a limited duration. In addition, a purchase obligation by the energy groups exists in several European countries.

4.1. Feed-in tariffs

Table 2 shows height and duration of the feed-in tariffs for selected European countries. To calculate the annual yield the payment must be multiplied by the energy generated in the year. It is assumed that the FSEC works continually without interruption 8,760 hours per year. The electrical energy is the product of the expected average electric power (assumption = 3 kW) and the annual power consumption in hours.

In case of permanent consumption the electrical energy for 3 kW power output will be 26,280 kWh. The resulting annual yields are given in the right column of table 2 [3]. The countries are sorted according to the amount of feed-in tariffs, starting with the highest.

Table 2. Feed-in tariffs and their time limits in Europe.

European country	**Amount of feed-in tariff**	**Duration of feed-in tariff***	**Annual yield**
	[€/kWh]	[years]	[€]
Great Britain	0.23	-	6044.40
Italy	0.22	15	5781.60
Germany	0.1267	20	3329.68
Netherlands	0.125	15	3285.00
Latvia	0.11	10	2890.80
Slovenia	0.105	15	2759.40
Czechia	0.081	30	2128.68
Denmark	0.0803	10	2110.28
Luxembourg	0.079	15	2076.12
Spain	0.077	25	2023.56
Portugal	0.075	20	1971.00
Ireland	0.072	15	1892.16
Greece	0.07	10	1839.60
Lithuania	0.07	-	1839.60
Slovakia	0.066	15	1734.48
France	0.06	20	1576.80
Estonia	0.051	12	1340.28
Belgium	0.05	-	1314.00
Bulgaria	0.045	15	1182.60
Austria	0.0378	13	993.38
Hungary	0.029	payoff time	762.12

* Some values are not known; duration is unlimited.

The European countries of the first rows have a good chance to invest in the small hydropower market. Therefore the use of the energy converter is determined as a value size. Now as a comparison the costs are considered.

4.2. Overview to cost covering

Thus, the production costs fall with renewed individual manufacture on 70%, because the development is concluded and is possible for a shorter manufacturing time by experience-guided, structured work.

With a small batch production of five energy converters, a cost reduction on 60% (according to the manufacturer) is to be achieved. With these estimates the manufacturing costs change as follows (table 3):

Table 3. Types of production series.

Manufacturing costs for	**Price per unit** [€]
Prototype	66,289.20
Individual production	46,402.44
Batch production (5 pieces)	39,773.52

It is assumed that steady wear behaviour during utilisation exists. The amount of annual depreciation may be calculated according to the linear method. Thereby in every period the same depreciations are created. If the lifespan is 20 years, than the following results can be represented (table 4):

Table 4. Cost structure for all considered production series.

	Prototype **100%**	**Individual production** **70%**	**Small batch production** **60%**
	[€]	[€]	[€]
Personnel costs	30,491.00		
Direct costs	24,750.00		
Indirect costs	11,048.20		
Total manufacturing costs*	***66,289.20***	***46,402.44***	***39,773.52***
Imputed depreciations**	3,314.46	2,320,12	1,988.68
Imputed interests***	1,756.66	1,229.66	1,054.00
Imputed costs of capital	***5,071.12***	***3,549.78***	***3,042.68***
Leasing costs	200.00	200.00	200.00
Maintenance costs	253.56	177.49	152.13
Insurance, taxes, administration	530.31	371.22	318.19
Annual costs	***6,054.99***	***4,298.49***	***3,713.00***

* Total manufacturing costs = A_0
** A_0 / lifespan
*** A_0 / 2 * 5.3% (discount rate of German Central Bank) [4]

The imputed costs of capital are divided into imputed depreciation and imputed interests. The imputed depreciations are the costs for losses in value. Whereas the imputed interests are the interests due on the amount of money lent over the maturity of the operation period.
The amount of the leasing costs depends on the plant size and the location. It varies from country to country, therefore it was assumed that the leasing costs are 200 € per year (average value in Germany). The maintenance costs are 5% of the imputed costs of the capital. The costs for insurance, taxes and administration are 0.8% of the total manufacturing costs.

Concluding, the following table 5 gives an overview to the first five European countries and the profit per annum (annual yield minus costs).

Table 5. Profit per annum for all considered production series.

European country	**Prototype 100%**	**Individual production**	**Small batch production**
	[€]	[€]	[€]
Great Britain	-10.59	1,745.91	2,331.40
Italy	-273.39	1,483.11	2,068.60
Germany	-2,725.31	-968.81	-383.32
Netherlands	-2,769.99	-1,013.49	-428.00
Latvia	-3,164.19	-1,407.69	-822.20

The profit table clearly shows that the prototype is not profitable in the next 20 years. With the other production forms the FSEC under described conditions could be a lucrative business.

5. Summary

The FSEC is able to convert the kinetic energy of flowing waters into electricity. By means of low head differences and by applications of separators power outputs of at least 3 kW are expected. To attain this objective a lot of additional research is needed. Initial results of the ongoing FLOW-3D trials show how the design of the FSEC might essentially change.

The presented cost report demonstrates that only in a few European countries the balance between annual costs and benefit can be achieved. The most important criterion is how long the payback period is. The other item to note is that all the assumptions are defined as cases with ideal conditions. It is still uncertain how long an FSEC in this form will work.

In the manufacture of the FSEC prototype, personnel and material costs is the biggest cost block by far. As a result of batch production and growing experience the personnel costs will be reduced. It is to think about moving the production of further plants in countries which have lower production costs to cover the risk of rising material costs, because of the development in the steel market. It is expected that the steel price and in this connection the material costs for the converter will increase. The saving in materials has direct impacts on the operating earnings, especially when using alternative materials such as wood or glass fibre plastics (GRP) [2].

Acknowledgements

The research leading to these results has received funding from the European Community's Seventh Framework Programme [FP7/2007-2013] under grant agreement n° 212423.

References

[1] J. Hadler and K. Broekel, (2010), Development and design of low potential hydropower converters in protected areas, in Proceedings of hidroenergia 2010, Lausanne, June 16 – 19, 2010.

[2] J. Hadler and K. Broekel, (2011), Cost-benefit analysis for low potential hydropower converters, in Proceedings of 34th IAHR World Congress 2011, Brisbane, June 26 – July 1, 2011 (not yet published).

[3] http://www.energy.eu (*20.11.2010*).

[4] http://www.bundesbank.de (*25.11.2010*).

On the Large Scale Assessment of Small Hydroelectric Potential: Application to the Province of New Brunswick (Canada)

Jean-François Cyr, Mathieu Landry, Yves Gagnon*

K.C. Irving Chair in Sustainable Development, Université de Moncton, Moncton (NB), Canada
** Corresponding author. Tel: +1 506 858 4152, Fax: +1 506 863 2110, E-mail: yves.gagnon@umoncton.ca*

Abstract: The mapping of the small hydropower (SHP) resource over a given territory is indispensable to identify suitable sites for the development of SHP renewable energy projects. In this study, a straightforward method to map the SHP potential over a large territory is presented. The methodology uses a synthetic hydro network (SHN) created from digital elevation models (DEM) to ensure precise hydro head estimations. From the SHN, hydro heads are calculated by subtracting the minimum from the maximum elevation of synthetic stream segments. Subsequently, stream segments with low hydro heads over a specified maximum distance are removed. Finally, the method uses regional regression models to estimate the annual baseflow for all drainage areas in the study area. The technical SHP potential can then be estimated as a function of the hydro head and maximum penstock length. An application of the method is made to the province of New Brunswick, Canada, where SHP maps have been developed to promote the development of the SHP energy sector in the province. In terms of the SHP opportunity, it is shown that the province of New Brunswick (71,450 km^2) has a good SHP resource. Using a representative hydro head (10 m) and penstock length (3,000 m) for the region, 696 potential sites have been identified over the territory. Results show that the technical SHP potential for New Brunswick is 368 MW for the conventional hydroelectric reservoir SHP configuration.

Keywords: *Small hydropower (SHP), Resource assessment, Hydroelectric power potential, Mapping*

1. Introduction

The definition of small hydropower (SHP) varies according to jurisdictions; in some instances, hydroelectric generating stations having installed capacities of up to 15 MW are generally characterized as SHP [1], while in Canada, hydroelectric generating facilities with installed capacities of up to 50 MW are considered as SHP [2]. Similarly to other renewable energy sources, such as wind power, the mapping of the SHP resource over a given territory is indispensable to identify suitable sites for the development of SHP renewable energy projects.

Large scale SHP assessments for pre-feasibility studies have been done in the United States [3], where data from hydrological regions were used to estimate the annual average streamflow for ungauged drainage areas; the estimated annual average streamflow was then used in conjunction with digital elevation models (DEM) to determine the hydropower potential for sites situated in ungauged natural streams in the corresponding regions. In Canada, even though the province of British Columbia is the only province to have developed an official map of the SHP resource [4], many Canadian SHP sites have been mapped in the International Small-Hydro Atlas [5]. However, the latter was developed with information from ref. [6-10] which are generally based on a combination of historical data and observations from field research; modern mapping techniques have only been implemented in a few of these studies.

In this paper, a methodology for the large scale assessment of small hydroelectric potential is presented along with an application to the province of New Brunswick, Canada. In the first instance, a method is described to find the available hydro head on the hydrographic network of a study area. Secondly, the annual streamflow is calculated, as a function of the hydro head and maximum penstock length, for each available hydro head sites. The technical

hydropower potential is then calculated and the study results are presented in the form of a SHP map.

2. Hydropower Potential Modeling

At a given site, the hydropower potential, P, can be calculated as

$$P = \rho Q g h \eta \quad (1)$$

where ρ is the density of water (kg/m^3), Q is the volumetric fluid flow rate (m^3/s), g is the gravity constant (9.81 m/s^2), h is the height (m) of the drop (gross hydro head), and η is the efficiency coefficient. In this study, the density of water is assumed constant at 1,000 kg/m^3, the efficiency coefficient is set to 0.8 while the hydro head is defined as the height difference between the intake and the generating station. Thus, with these assumptions, only two remaining parameters, Q and h, are needed to determine the hydropower potential for any site in a given study area. A third indirect parameter, the penstock length, can also be used in the determination of the gross hydro head.

2.1. Hydro head modeling

Assuming that a drainage area generates enough streamflow to be considered as a potential site, the first phase of large scale SHP mapping is to locate every potential hydro head on all stream segments of the hydrographic network. To this end, a synthetic hydro network (SHN) using DEM is created to ensure relatively precise hydro head estimations. This is done because spatial entities in the National Hydro Network (NHN) are based on existing data of different agencies [11] and do not perfectly match with the DEM. Since the SHN perfectly matches the DEM, the interoperability between information layers is assured. GIS software tools such as the TauDem tools [12], along with algorithms based on the previous works [13-15] are used to create the SHN from the DEM. The SHN is then validated with the NHN and all stream segments present in the SHN that does not correspond to a NHN stream segment are excluded. From the SHN, hydro heads are calculated by subtracting the minimum from the maximum elevation of the synthetic stream segment. Subsequently, because the penstock length represents an important capital cost of the total civil work costs for SHP projects, a limit is imposed on the Euclidian distance between the highest and lowest node of a SHN stream segment, which is used to represent the penstock length. In this work, the maximum penstock length is established at 3,000 m and all stream segments up to the maximum penstock length having hydro heads of less than 10 m are removed from the model, due to the altitudinal precision of the DEM (± 5 m, 90 % of the time).

2.2. Streamflow modeling

A regional regression model based on the work of Vogel et al. [16] is used to estimate the annual streamflow for all drainage areas in the study area, namely:

$$Q = e^{C_0} X_1^{C_1} X_2^{C_2} \ldots X_n^{C_n} e^{\varepsilon} \quad (2)$$

where Q is the observed annual streamflow or baseflow in a gauged basin (m^3/s), X_i are the various drainage area characteristics (climatic and physical attributes such as average annual temperature, average annual precipitation, elevation and drainage area), C_i are the ordinary least square regression coefficients and ε is the residual of the model.

In order to evaluate the efficiency of the regional regression model between the estimation results and the observation data, a goodness of fit statistical model, known as the Nash and Sutcliff efficiency index [17], E, is used and is given by:

$$E = 1 - \left[\sum_{t=1}^{T} \left(Q_0^t - Q_m^t \right)^2 / \sum_{t=1}^{T} \left(Q_0^t - \overline{Q_0} \right)^2 \right] \quad (3)$$

where Q_o is the observed streamflow at a given time t and Q_m the modeled streamflow. The Nash and Sutcliff efficiency index ranges from -∞ to 1, where 1 represents a perfect match between the model results and the observed data.

2.3. A case study: Province of New Brunswick, Canada

As an application of the methodology proposed, and in order to promote the development of the small hydropower energy sector in the province, the large scale SHP assessment methodology for the conventional hydroelectric reservoir SHP configurations is applied to the province of New Brunswick (NB), Canada. The province of New Brunswick, one of the smallest of the Canadian provinces, both in size (71,450 km^2) and population (748,319), is part of the Maritime provinces on the eastern coast of Canada. The topography of New Brunswick consists in three major geographic regions. The north-west region is characterized by the Appalachian Mountains, which are dominated by Mount Carleton (820 m above sea level). The center of the province is composed of small rounded hills delineated by river valleys. Finally, the southern part of New Brunswick is composed of small hills sloping down to the Bay of Fundy, with the exception of the south-eastern part of the province which is composed of the Caledonia Highlands. In terms of climate, the province of New Brunswick is located within the Atlantic Ecozone, which is characterized by a continental climate due to eastward moving air masses. Although the moist climate provides an annual runoff varying from 600 to 1,000 mm, the annual runoff is more important in the southern region of the province, near the Bay of Fundy, due to higher precipitation events. The province's hydrographic network is composed of three major rivers: the St. John River, which drains the western part of New Brunswick, takes its source in the state of Maine, U.S.A. and discharges into the Bay of Fundy; the Restigouche River, which discharges into the Baie des Chaleurs, drains the northern part of New Brunswick; finally, the Miramichi River, which drains the eastern part of New Brunswick, discharges into the Gulf of Saint Lawrence.

2.3.1. Hydro head modeling input data

The DEM's used to generate the SHN are retrieved from the Canadian Digital Elevation Data (CDED) [11]. The raster dataset, at a 1:50,000 scale, has a minimum cell resolution of 0.75 arc seconds, which represents approximately 32 m^2 for the province of New Brunswick. The altitudinal precision of the dataset is ±5 m, 90% of the time. Furthermore, because some watershed areas are contiguous to the state of Maine, DEM covering corresponding sections of the state are also used. The dataset used to cover the corresponding watersheds are taken from the National Elevation Dataset (NED) 1 Arc Second of the United States Geological Survey (USGS) [18]. The NED dataset has a resolution of approximately 30 m^2 and is resized to match the CDED resolution. Finally, due to computing limitations, the DEM for the entire region is divided into 9 sub-regions, as shown in Fig. 1. These sub-regions are defined by using aggregates of sub-sub-drainage areas as delimited by the Water Survey of Canada (WSC) dataset [19], thus maintaining the topology of the SHN within each sub-region.

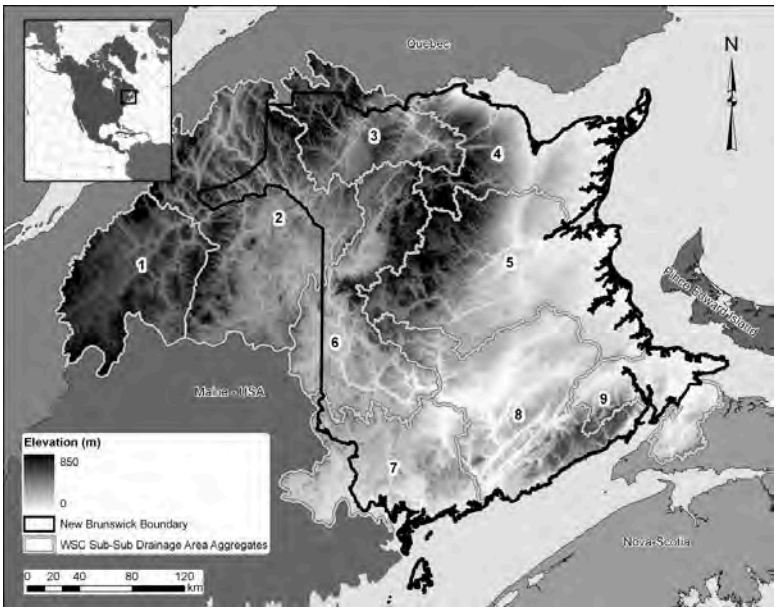

Fig. 1. Study area; sub-regions used for the extraction of the DEM.

2.3.2. Streamflow modeling input data

The climatic attributes such as average annual temperature and average annual precipitation used in several regional regression models tested in this study are taken from ref. [20-21]. In terms of the physical attributes used in the regional regression models, the majority of them, i.e. average slope, average elevation, elevation range, drainage area and eccentricity of the drainage area, are calculated from the DEM.

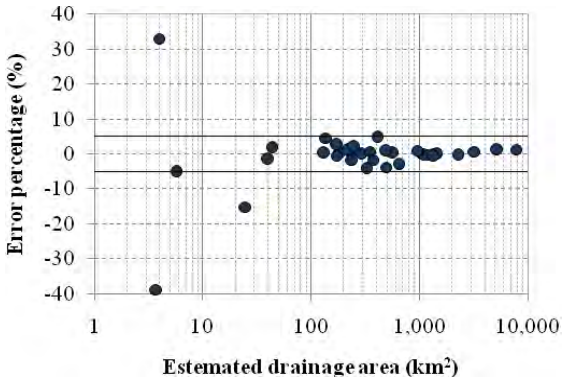

Fig. 2. Relative error between reference basin drainage areas and DEM-based basin drainage area estimation.

Previous research work in regional regression models has shown that the basin drainage areas provide good correlations in such models [16]. As is shown in Fig. 2, by comparing the DEM-based drainage area results for basins having hydrometric stations measuring natural flow to those of the Water Survey Canada as reference, it can be seen that the relative error decreases as the drainage area increases. In this work, a lower limit of 50 km^2 was imposed on drainage basins, such that hydro head having drainage areas with less than the lower limit where not considered. Finally, streamflow data from hydrometric stations [22], located across New Brunswick and having at least 30 years of continuous data, while being situated in basins with drainage areas larger than 50 km^2, are used in the various regional regression models tested.

3. Results

3.1. Hydro head modeling results

Results from the hydro head modeling showed that a total of 696 hydro heads in the province of New Brunswick satisfied the modeling constraints. In general, as in the case of other research in similar topography [23], because the topography is more variable in the upper part of a watershed area, stream segments with high hydro heads were generally located in the upper parts of a watershed area, while sites located in lower parts of a watershed area generally had lower hydro heads. Fig. 3 shows the distributions of hydro head sites by their characteristics.

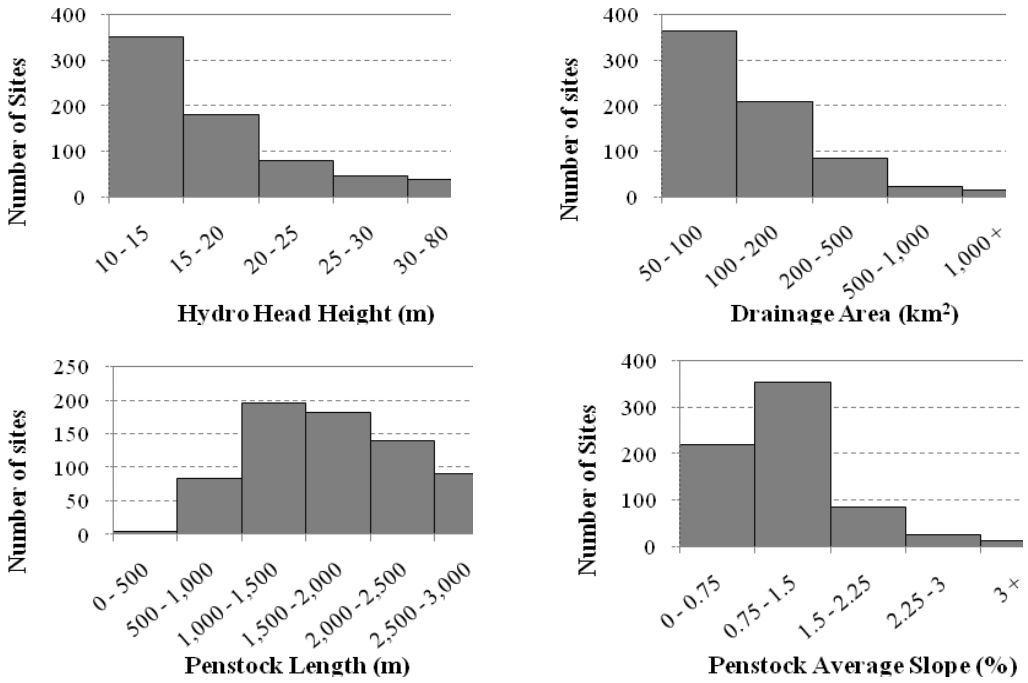

Fig. 3. Distribution of the hydro head sites.

3.2. Streamflow modeling results

In order to estimate the average annual streamflow for all basins in the study region, multiple regional regression models have been attempted in this work; the regional regression model having both the lowest average relative error (6.5%) and the highest Nash and Sutcliffe efficiency index (0.993) was chosen:

$$Q_m = e^{-16.552} A^{0.977} P^{1.733} D^{0.133} \quad (4)$$

where Q_m is the modeled streamflow (m^3/s), A is the drainage area (km^2), P is the average annual precipitation (mm) and D is the average elevation (m) of the drainage area.

3.3. Mapping results

While the methodology described in this paper can be used to estimate the SHP resource potential for both conventional hydroelectric reservoir and run-of-river SHP configurations, only results for the conventional hydroelectric reservoir SHP configuration are presented. Fig. 4 shows the mapping results of the SHP resource potential, for the conventional hydroelectric reservoir SHP configuration, in the province of New Brunswick. For this SHP configuration, the technical SHP potential for New Brunswick is 368 MW. The sites range in

SHP potential from 92 kW to 16.1 MW; the average potential for the 696 sites is 528 kW per site, while the median power potential is 303 kW.

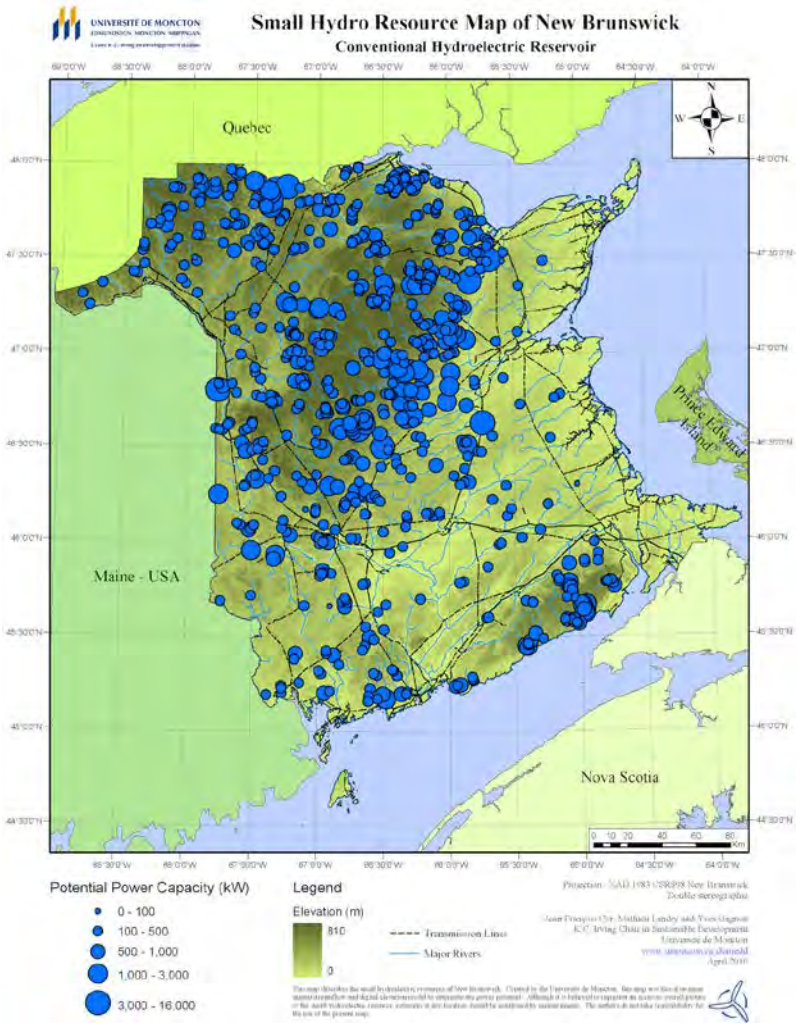

Fig. 4. SHP resource map of New Brunswick for conventional hydroelectric reservoirs.

4. Discussion and Conclusion

In this work, a straightforward method to map the small hydropower (SHP) potential over a large territory was presented. While the methodology presented in this paper is based on previous research work in this field of study, it contains several advantages which are not exclusive to this work but where their combination as a whole represents a significant advancement in this field. First, the methodology is general such that few variables are needed to perform a SHP study. Furthermore, the variables needed in the methodology are readily available at large scale for SHP studies in Canada or in other countries having publicly available GIS data. Secondly, the methodology can simultaneously evaluate and compare the SHP for both conventional and run-of-river configurations over a given area; this point represents a significant advancement in the field of study. Third, the methodology uses the gross hydro head, which significantly reduces the computational efforts of site selection. Fourth, the methodology is extremely fast and cost-effective when implemented using GIS-based software. However, the methodology introduces uncertainties in the estimation of the SHP resource potential which are due to the estimation of the efficiency of the SHP systems, the neglecting of SHP system head losses due to friction, and the use of yearly baseflow data

instead of monthly baseflow data. Finally, field measurements of terrain could be used to increase the accuracy of potential site locations.

An application of the method was made to the province of New Brunswick, Canada, where SHP maps were developed to validate the methodology and to promote the development of the small hydropower energy sector in the province. In terms of the SHP opportunity, it was shown that the province of New Brunswick has a good SHP resource. In comparison to the neighbouring state of Maine[1], a previous study [24] identified that there were over 5,883 sites in the state of Maine having a technical SHP potential capacity of 2,780 MW, thus giving an average SHP of 472 kW/site. In New Brunswick, results from this study have shown that there is a technical SHP potential capacity of 368 MW distributed on 696 sites; thus giving an average SHP of 528 kW/site.

Future work should focus on the elimination of potential sites that are not sustainable economically, environmentally or socially. To this end, potential sites that are located within federal and provincial park boundaries should be notably excluded. In addition, drainage basins having issues such as water supply, tourism, sport fishing, and the presence of species at risk should also be eliminated from the model.

Finally, the New Brunswick SHP map results have shown that the province of New Brunswick has a good small hydropower (SHP) resource which should be developed not only for its environmental benefits and attributes, but also for the social and economic benefits of its residents.

Acknowledgment

This research work was funded by the Natural Sciences and Engineering Research Council (NSERC) of Canada the Department of Energy of New Brunswick and the New Brunswick Innovation Foundation (NBIF).

References

[1] Renewable Energy Policy Network for the 21st Century (REN21), Renewables Global Status 2005 Update, Paris, 2005.

[2] Canada, Department of Natural Resources, Micro-Hydro Systems – A Buyer's Guide, Ottawa, 2004.

[3] United States, Department of Energy, Water Energy Resources of the United States with Emphasis on Low Head/Low Power Resources, Cat. No. DOE/1D-11111, Idaho National Engineering and Environmental Laboratory, 2004.

[4] BC Hydro & Power Authority and Canadian Cartographics Ltd., Energy Resources of British Columbia, Available at: www.canmap.com, 2002.

[5] International Small-Hydro Atlas, Available at: www.smallhydro.com, 2010.

[6] Monenco Limited, Identification of Environmentally Compatible Small Scale Hydroelectric Potential in Atlantic Canada, Phase 1, Vol. 1, Env. Canada, Halifax, 1984.

[7] Sigma Engineering, Small-Hydro Power Resource in the Provincial System, Ministry of Energy, Mines & Petroleum Resources, British Columbia, 1983.

[1] The number are for comparison only, both studies do not use the same methodology, nor the same definition for SHP and were made for different contexts.

[8] Sigma Engineering Ltd., Inventory of Undeveloped Opportunities at Potential Micro Hydro Sites in BC, Vancouver, British Columbia, 2000.

[9] Sigma Engineering Ltd., Green Energy Study for British Columbia Mainland Phase 2, Vancouver, British Columbia, 2002.

[10] Hatch Acres, Evaluation and Assessment of Ontario's Waterpower Potential, Ministry of Environmental Resources, Ontario, 2005.

[11] Geobase, National Hydro Network, Available at: www.geobase.ca, 2010.

[12] Utah State University, Terrain Analysis Using Digital Elevation Models (TauDEM), Available at: http://hydrology.neng.usu.edu/taudem/, 2009.

[13] S.K. Jenson, J.O. Domingue, Extracting Topographic Structure from Digital - Elevation Data for Geographic Information System Analysis, Photogrammetric Engineering and Remote Sensing, 54, 1988, pp.1593-1600.

[14] D.M. Mark, Network Models in Geomorphology, in: M.G. Anderson (Ed.), Modelling in Geomorphological Systems, John Wiley and Sons, New York, 1988, pp.73-97.

[15] D.G. Tarboton, A New Method for the Determination of Flow Directions and Contributing Areas in Grid Digital Elevation Models, Water Resources Research, 33, 1997, pp.309-319.

[16] R. Vogel, C. Bell, N. Fennessey, Climate, Streamflow and Water Supply in the Northeastern United States, Journal of Hydrology, 198, 1997, pp.42-68.

[17] J. E. Nash, J. V. Sutcliffe, River Flow Forecasting Through Conceptual Models. Part 1: A Discussion of Principles. Journal of Hydrology, 10 (3), 1970, pp.282–290.

[18] United States Geological Survey, The National Map Seamless Server, Earth Resources Observation - National Elevation Dataset (NED) 1 Arc Second, Available at: http://seamless.usgs.gov/products/1arc.php, 2008.

[19] Canada, Department of Natural Resources, GeoGratis - Atlas of Canada 1,000,000 National Frameworks Data, Hydrology Drainage Areas, Available at: www.geogratis.ca, 2009.

[20] Canada, Department of Environment, Canadian Climate Normals or Averages 1971-2000, Available at: http://climate.weatheroffice.ec.gc.ca/climate_normals/index_e.html, 2009.

[21] World Climate, Available at: www.worldclimate.com, 2005.

[22] Canada, Department of Environment, Water Survey, Available at: http://scitech.pyr.ec.gc.ca/waterweb/formnav.asp?lang=0, 2006.

[23] D. Nagel, J. Buffington, D. Isaak, Comparison of Methods for Estimating Stream Channel Gradien Using GIS, USDA Forest Service, Rocky Mountain Research Station Boise Aquatic Sciences Lab, Boise, Idaho, 2006.

[24] United States, Department of Energy, Feasibility Assessment of the Water Energy Resources of the United States for New Low Power and Small Hydro Classes of Hydroelectric Plants, Cat. No. DOE/1D-11263, Idaho National Laboratory, 2006.

Volume 7

Industrial Energy Efficiency

The effect of long lead times for planning of energy efficiency and biorefinery technologies at a pulp mill

Elin Svensson[1,*], Thore Berntsson[1]

[1] *Heat and Power Technology, Chalmers University of Technology, 412 96 Göteborg, Sweden*
** Corresponding author. Tel: +46 31 772 3016, Fax: +46 31 821 928, E-mail: elin.svensson@chalmers.se*

Abstract: The pulp and paper industry has many promising opportunities in the biorefinery field. To reach this potential, investments are required in new, emerging technologies and systems solutions which cannot be quickly implemented. In this paper, an approach to model the necessarily long planning times for this kind of investments is presented. The methodology used is based on stochastic programming, and all investments are optimized under uncertain energy market conditions. The uncertain cost development of the emerging technologies is also considered. It is analyzed using scenario analysis where both the cost levels and the timing for market introduction are considered. The effect of long lead times is studied by assuming that no investments can be decided on now and implemented already today, and only investments planned for today can be implemented in, for example, five years. An example is presented to illustrate the usefulness of the proposed approach. The example includes the possibility of future investment in lignin separation, and shows how the investment planning of industrial energy efficiency investments can be guided by using the proposed systematic approach. The example also illustrates the value of keeping flexibility in the investment planning.

Keywords: *Investment planning, Optimization under uncertainty, Process integration, Lignin separation, Pulp and paper industry*

1. Introduction

As a result of the increased climate concern in society, energy market conditions are bound to change, and energy and products based on renewable feedstock will gradually be valued higher. The pulp and paper industry, which already today is a large user and producer of biomass-based energy and materials, therefore has a large opportunity to increase and diversify its revenues through different biorefinery concepts, see e.g. [1–7]. For mills to become successful in this biorefinery arena, process integration investments are required to ensure energy efficiency of the combined pulp and paper production and biorefinery process. This also calls for investments in new, unproven technologies, with highly uncertain investment costs – for example, carbon capture, black liquor gasification, or lignin extraction.

Investments in these emerging technologies are not quickly implemented. Time is needed for analyzing different options, planning of construction including any shutdowns of the plant, contracting, and so on. This results in long lead times from the first decision to start planning for a certain technology path until the plant is finally run continuously at full load. This is true also for traditional options being evaluated in competition with emerging technologies.

Considering that new decisions cannot be immediately implemented if they have not previously been planned for, decision-makers need guidance – not only regarding what investments to make – but also, and more importantly, to what future investments should be planned for. Better tools to aid decision-makers in this field will hopefully lead to that more of these energy-efficiency and emission-reducing measures are carried out. The purpose of this work is therefore to further develop a methodology for process integration investment planning under uncertainty to consider these aspects of long-term decision-making. Here, we will also use the proposed approach to illustrate the effect of a five-year planning lead time in an example of a pulp mill that considers a future possibility of investing in lignin separation.

2. Methodology

The methodology used in this paper is based on a methodology for optimization of process integration investments under energy market uncertainty [8, 9]. In this work, we have used an approach which in addition allows the influence of the investment cost development for new, emerging technologies to be studied [10]. While investments are optimized under uncertainty in energy market parameters with a stochastic programming approach, the effect of different cost developments on the optimal solution is studied through sensitivity analysis. The solution to the optimization model will be an optimal investment plan with respect to the expected net present value (NPV) based on the information we have about the future today.

We model the investment optimization problem using AMPL [11] and solve it using CPLEX [12]. A strategic view of the analyzed investments is assumed, and the discount rate is therefore set to 9.3% over a 30-year-long planning horizon.

2.1. Long lead times for investment planning

Here, we use the expression 'lead time' to denote the time between the decision to invest and the actual implementation or installation of the technology invested in. This is simply modeled based on the assumption that it takes a few years to analyze, plan and prepare for these extensive process changes. When studying the effect of long lead times it is therefore assumed that it is too late now to decide about investments that should be implemented today, and the first investments will instead be implemented in five years.

Since there are costs associated with evaluation and planning of investments – mainly related to the time committed by engineers, consultants, etc. – a basic assumption is that it is not possible to plan for all investments that might be of interest. In this way, although the planning costs are not explicitly accounted for, they are implicitly considered in the proposed modeling approach. The idea of the proposed approach is then that investments planned for today will constrain what will be possible to implement in five years.

To find different planning alternatives, the approach is to start by optimizing the investment in each cost development scenario assuming that the first investment will be in five years. This will, however, lead to solutions where different investments should be made in five years depending on the cost and price development. Based on the solutions obtained, a matrix can be constructed that shows which investments will be possible to implement depending on what has been planned for. A general illustration of such a matrix is shown in Fig. 1.

The matrix could also contain other investment solutions based on experience from working with the model and the mill. The model will then be run for each of the planning alternatives, with possibilities for implementation as constraints. Thereby the results of different investment plans considering an initial lead time of five years can be analyzed, and the best one possibly identified.

Long lead times should also be modeled for later points in time, but this makes the model and especially the solution of the optimization problem hard. As a first step towards an improved understanding of the effects of lead times we therefore settle for the initial lead time. Experience shows, however, that for a majority of investment plans, very few investments are made at later points in time. Therefore, the modeling of later lead times should not be as important. Furthermore, the optimal solution will obviously result in a plan also for later investments, even though it is not considered that decisions have to be made years before the

actual implementation and hence possibly before future energy prices and cost reductions have been revealed.

		Possible to implement 2015				
		Technology 1	Technology 2	Technology 3	Technology 4	Technology 5
Plan 2010	Investment package 1	X	X			
	Investment package 2		X	X		
	Investment package 3		X		X	
	Investment package 4					X

Fig. 1. Generic matrix for investment planning.

3. Input data and assumptions

3.1. The pulp mill

We have applied the proposed approach to a pulp mill example that has previously been presented by the authors [10]. This mill is a computer model representing an average Swedish market pulp mill, producing 1000 tonnes per day of bleached Kraft pulp (see also [1, 13]).

Through process integration and more efficient technology, there is a potential to achieve a steam surplus at the mill of about 25%. The steam could, for example, be used to produce more electricity in a low-pressure turbine, or to produce district heating for a nearby community, or for cogeneration of both heat and electricity. District heating could also be produced from lower-quality excess heat at the mill. Except for these traditional ways of making use of the steam surplus, there are new, emerging technologies that might become promising alternatives. We will here look at the example of lignin extraction.

For energy conversion data and investment costs, the reader is referred to [10]. The cost development scenarios for the lignin separation process are presented in Section 3.3.

3.2. Energy market uncertainty model

The energy market model used in this study is the same as the one used in the previous study on the effect of uncertain investment cost developments for emerging technologies [10]. This uncertainty model was developed using the ENPAC tool [14]. The model consists of 28 scenarios for market electricity and fuel prices, see Fig. 2. The same probability has been assumed for each scenario.

3.3. The investment cost scenarios

For the cost development of the emerging lignin separation technology, six scenarios have been used. For this technology, we have assumed that market introduction might happen in 2015 or 2020. It is assumed that market introduction might happen at the base level (L), corresponding to the estimated cost of the N^{th} plant assumed in previous studies (see [10]), or at a higher cost level (H), here assumed to be 50% higher than the base cost level.

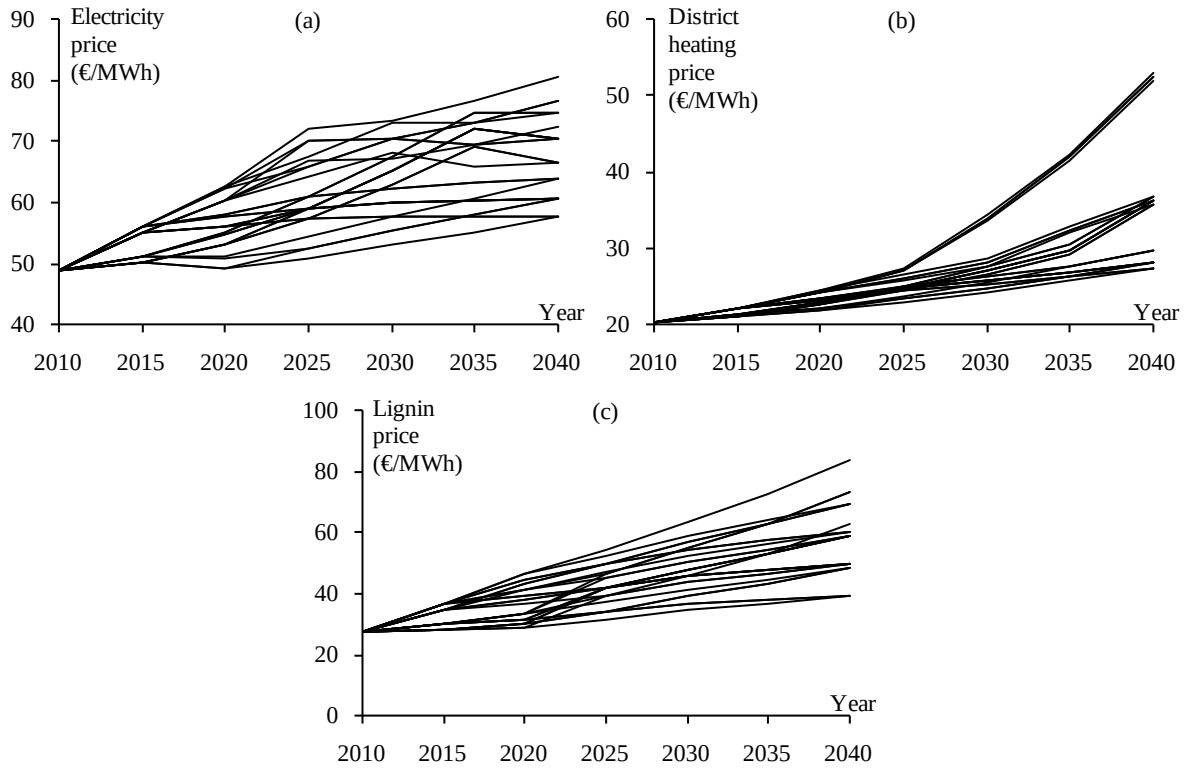

Fig. 2. a) Electricity price scenarios. b) District heating price scenarios. c) Lignin price scenarios.

Table 1 presents the different scenarios for the investment cost of the lignin separation plant. If the market introduction happens at the base cost level, the cost stays permanently at that level (Scenarios A and B). If, instead, market introduction happens at the higher cost level, the cost might stay at the higher level (Scenarios C and D), or it might drop later as a consequence of technological learning (Scenario E) if, for example, not very many plants are sold. There is also a possibility that the technology is never introduced to the market (Scenario F).

Table 1. Investment cost scenarios for the lignin separation plant.

Scenario & Market introduction (year)		2010	2015	2020	2025	2030	2035
A	2015 at base cost level	–	L	L	L	L	L
B	2020 at base cost level	–	–	L	L	L	L
C	2015 at higher cost level where cost is stabilized	–	H	H	H	H	H
D	2020 at higher cost level where cost is stabilized	–	–	H	H	H	H
E	2015 at higher cost level with drop to base cost level 2020	–	H	L	L	L	L
F	Never	–	–	–	–	–	–

–: Unavailability
L: Low cost / base cost level = Estimated cost of N^{th} plant
H: High cost / Higher cost level = 1.5L

4. Results

As described previously, the effect of long lead times is studied by assuming that no investments can be made already today, and that the first investments in five years must be planned for. Furthermore, we assume that the costs and personnel resources associated with planning of investment and implementation make it impossible to plan for every interesting

investment opportunity. To find a number of reasonable investment packages to plan for, the model was solved for one cost development scenario at a time with the constraint that the first investments could be made in five years. The solutions obtained are presented in Table 2.

Table 2. Optimal investments 2015 in different cost development scenarios.

Scenario	Optimal investment	
A, C, E	Lignin:	64 MW lignin
	Heat pump:	32 MW delivered heat
B, D	Cogeneration:	5MW elec. and 26 MW delivered heat
F	Cogeneration:	5MW elec. and 26 MW delivered heat
	Heat pump:	19 MW delivered heat

These three packages obviously differ regarding the lignin extraction investment, but also regarding the amount and means of district heating deliveries. The reason for this difference in district heating production is that the preferred way of generating district heating is by cogeneration from low-pressure steam, but when lignin is extracted as for Scenarios A, C and E, no low-pressure steam is available. In these scenarios, district heating is therefore generated by a heat pump instead. Also in the case of cogeneration, a heat pump might be interesting to further increase district heating deliveries as in Scenario F. By this solution, the mill is, however, locked into a district heating contract of substantial deliveries for which the production based on low-pressure steam is needed to fulfill the delivery requirement. In Scenarios B and D, later opportunities for lignin extraction might make it interesting to use the low-pressure steam for lignin extraction at a later point in time. Therefore, district heating deliveries are more limited, making it possible to replace the production from cogeneration with production from the heat pump.

In some mills, the power boiler and back-pressure turbine might be oversized. Under such conditions, it would probably be more beneficial to increase district heating deliveries by increasing the fuel input to the power boiler than to invest in a new heat pump. Here, however, the boiler is already assumed to be run at maximum capacity.

Fig. 3 is a matrix showing which investments can be made in 2015 depending on what investment package has been planned for. In addition to the alternatives from Table 3, we also added the alternative to plan for a condensing turbine and a heat pump. The alternative not to plan for any investment should obviously never be better than to plan for something, since there is always an option to avoid making an investment that has been planned for. However, the ‘no investment’ planning alternative was included for comparison. It might be interesting if costs and resources for planning are considered explicitly, which they are not here.

The X’s in the matrix represent that an investment is possible, though not required. That means, for example, that if a heat pump has been planned for, this possibility exists in 2015 but there is also always an option to withdraw from the investment. This option to abandon a planned investment is especially important for lignin extraction since this technology might not even be available on the market in 2015. Based on the matrix, the optimization model was solved for different planning alternatives. The expected net present value for the alternatives in the different cost development scenarios is shown in Fig. 4.

		Possible to implement 2015				
		Lignin	Heat pump	District heating from 145 and 100°C heat	Turbine (145-100°C)	Turbine (100-35°C)
Plan 2010	Lignin and heat pump	X	X			
	Cogeneration only			X	X	
	Cogeneration and heat pump		X	X	X	
	Condensing turbine and heat pump		X		X	X
	No investment					

Fig. 3. Matrix of possible technology implementations depending on what has been planned for.

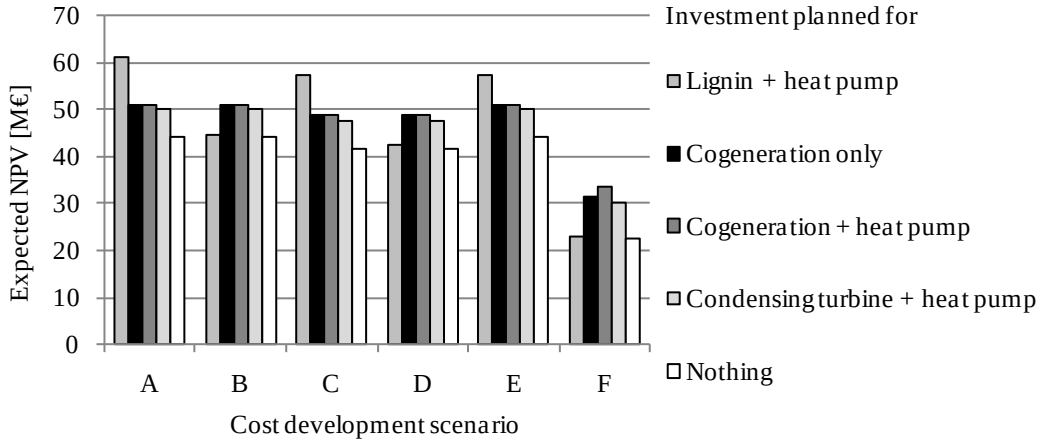

Fig. 4. Expected net present value for different planned investments in 2015.

As can be seen, depending on the cost development scenario, lignin extraction could either be by far the best or by far the worst alternative (at least except planning for nothing). This is explained by the large potential associated with this technology if it becomes a reality, which disappears if the technology has not yet become available for the pulp mill.

The good runner-up is instead cogeneration, which is either the best or the next best alternative in all scenarios. The difference is very small if you include the heat pump or not. Obviously, it is better to include the heat pump in the plan since there is no requirement of going through with the investment. In Scenario F where lignin extraction never becomes available on the market, the heat pump is slightly advantageous. As anticipated, the 'nothing' alternative is the worst one in all scenarios.

5. Discussion

In theory, the optimal planning alternative would include all different technology options, but this would obviously be difficult in practice. Principally, planning for everything means the

same as staying flexible and that should be striven for. However, the underlying assumption in this study was that this is too costly to achieve in reality. Nevertheless, the lack of flexibility obviously has a cost. The results show that if lignin extraction is not planned for, but cogeneration instead, the loss is 19% in expected NPV in Scenario A (17% and 12% in Scenarios C and E respectively). On the other hand, if the plan is for lignin extraction and a heat pump but the lignin separation technology does not become a possibility, the loss is 15%, 15% and even 46% in Scenarios B, D and F respectively. Considering that the use of expected NPV as investment evaluation measure partly hides differences in cash flows because of discounting and weighting of scenarios, these losses in expected NPV are quite important (see for example [10, 15] where differences in expected NPV are related to corresponding differences in annual net profits). These high values of staying flexible by planning for many different investment opportunities imply that, strategically, it should be worth committing more organizational resources to planning of these kinds of investments.

Nevertheless, if we assume that it is not possible to invest in anything else than what has been planned for, and if we further assume that it is not possible to plan for more than a few different new technologies, results like the ones presented in Fig. 4 can be used to evaluate different investment plans. In the example presented here, investment in lignin extraction involves both the highest potential and the highest risk, while cogeneration seems to be a more robust option. The best decision depends on the decision-maker's beliefs about the probabilities of the different cost development scenarios.

5.1. Limitations

The work presented in this paper provides a good starting point for an investment planning methodology where consideration is given to the long lead times that are often involved in these kinds of decisions. There are, however, some limitations which might make it difficult to use the methodology for some applications where these aspects are of importance. Further work with model development should focus on these issues. For example, the costs associated with evaluation, planning and detailed analyses of different investments and their implementation are not explicitly considered in this model. It should also be possible to differentiate these costs and the length of the planning lead time between different kinds of investment alternatives. Further work is needed, too, if not only the initial lead time but also the lead time for subsequent investment stages should be accounted for.

6. Conclusions

The proposed approach for modeling of long lead times for planning of industrial energy efficiency investments gives a more realistic representation of this kind of decision-making. An example illustrates how the planning of future investments can be guided by using this systematic approach considering uncertainties in future energy market conditions as well as in cost development of new technologies. The results clearly show the importance of considering the long lead times involved in the investment planning, since significant values are at stake by making the right or the wrong decision about which investments to plan for.

We have also shown how the proposed approach can be used to value flexibility in the planning of industrial energy efficiency measures. The example demonstrates that the value of this flexibility can be quite high. There is, however, a trade-off between the value of this flexibility and the associated planning costs required to obtain it. It is therefore important to continue the work regarding long lead times to incorporate these planning costs.

Acknowledgements

The project was financed by the Process Integration research programme funded by the Swedish Energy Agency and by the Södra Foundation for Research, Development and Education.

References

[1] M. Olsson, E. Axelsson, T. Berntsson, Exporting lignin or power from heat-integrated Kraft pulp mills: A techno-economic comparison using model mills, Nordic Pulp and Paper Research Journal 21, 2006, pp. 476–484.

[2] A. Van Heiningen, Converting a Kraft pulp mill into an integrated forest biorefinery, Pulp & Paper-Canada, 107, 2006, pp. 38–43.

[3] V. Chambost, J. McNutt, P.R. Stuart, Guided tour: Implementing the forest biorefinery (FBR) at existing pulp and paper mills, Pulp & Paper-Canada, 109, 2008, 19–27.

[4] S. Consonni, R.E. Katofsky, E.D. Larson, A gasification-based biorefinery for the pulp and paper industry. Chemical Engineering Research & Design, 87, 2009, 1293-1317.

[5] M. Marinova, E. Mateos-Espejel, N. Jemaa, J. Paris, Addressing the increased energy demand of a Kraft mill biorefinery: The hemicellulose extraction case. Chemical Engineering Research & Design, 87, 2009, 1269-1275.

[6] R. Fornell, Energy Efficiency Measures in a Kraft Pulp Mill Converted to a Biorefinery Producing Ethanol, Licentiate Thesis, Heat and Power Technology, Chalmers University of Technology, 2010.

[7] K. Pettersson, S. Harvey, CO2 emission balances for different black liquor gasification biorefinery concepts for production of electricity or second-generation liquid biofuels, Energy, 35, 2010, pp. 1101-1106.

[8] E. Svensson, A.-B. Strömberg, M. Patriksson, A scenario-based stochastic programming model for the optimization of process integration opportunities in a pulp mill, ISSN 1652-9715, no. 2008:29, Mathematical Sciences, Chalmers University of Technology, 2008.

[9] E. Svensson, T. Berntsson, A.-B. Strömberg, M. Patriksson, An optimization methodology for identifying robust process integration investments under uncertainty, Energy Policy, 37, 2009, pp. 680–685.

[10] E. Svensson, T. Berntsson, Planning future investments in emerging technologies for pulp mills considering different scenarios for their investment cost development, Submitted for publication, 2010.

[11] R. Fourer, D.M. Gay, B.W. Kernighan, AMPL: A Modeling Language for Mathematical Programming, Duxbury Press / Brooks/Cole Publishing Company, 2nd Edition, 2003.

[12] IBM ILOG, CPLEX: High-Performance Software for Mathematical Programming and Optimization, Version 12.1.

[13] E. Axelsson, M. Olsson, T. Berntsson, Heat integration opportunities in average Scandinavian Kraft pulp mills: Pinch analyses of model mills, Nordic Pulp and Paper Research Journal, 21, 2006, pp. 466–475.

[14] E. Axelsson, S. Harvey, Scenarios for assessing profitability and carbon balances of energy investments in industry, AGS Pathways report 2010:EU1, 2010.

[15] E. Svensson, T. Berntsson, Using optimization under uncertainty to study different aspects of process integration investment decisions – The example of lock-in effects, Proceedings of ECOS, 2010.

Energy use project and conversion efficiency analysis on biogas produced in breweries

LI Yingjian[1,*], QIU Qi[1], HE Xiangzhu[2], LI Jiezhi[3]

[1] *College of Chemistry & Chemical Engineering, Shenzhen University, 518060, Shenzhen, PR China.*
[2] *Hunan Energy Conservation Center,410007 Changsha, PR China*
[3] *Ecole centrale de Lyon, 69130, Lyon, France.*
* *Corresponding author. Tel.:+86 755-26538802; Fax: +86 755-26536141, E-mail address:szulyj@sohu.com*

Abstract: Electric power, steam and chilled water were consumed in beer brewing process. The process is intensive in energy conversion and utilization. The brewery wastewater can generate biogas of high methane content through anaerobic sludge fermentation. This high concentrated biogas could be an excellent choice employed in energy conversion and utilization. The reclaimed water, after proper treatment, could be employed to scrub CO_2 and H_2S in biogas. Through compression, the purified biogas could be stored as fuel for mechanical operation and further incorporated into the municipal LNG pipe network. According to biogas yield and energy requirements in breweries, energy usage efficiency and configuration of device for biogas Integrated Energy System (IES) were investigated. This paper introduced an Otto cycle internal combustion engine using biogas for power generation. With the biogas yield of 34.84m^3/h (standard state), the power efficiency of 28.45% could be generated with electricity of 70.0kW. Efficiency of combined heating and power (CHP) can reach 61.80% employing the excess heat of the engine exhaust. There are successful examples of combined cooling and power (CCP), combined cooling and heating (CCH) that has efficiency of over 60%.

Keywords: *Biogas produce, Purification process, IES conversion Using efficiency*

1. Introduction

In China, Biogas is not only new energy source, but also an important aspect of sustainable development for the renewable energy. The biogas is generated by industrial wastewater or municipal solid waste through degradation process of anaerobic digestion. Consequently, heat and electricity is generated through the biogas [1]. Adopting the technology of combined cooling, heating, and power (CCHP), this is also known as trigeneration, or integrated energy system (IES). CCHP is the simultaneous production of mechanical power (often converted to electricity), heating and/or cooling from one primary fuel, and is an extension of CHP (combined heat and power, also defined as cogeneration) by coupling with thermally activated cooling technologies that take the waste heat from CHP for producing cooling [2].

Moving parts of internal combustion engines and gas turbine contacts directly with burning gas, there need cleaner fuels, biogas as a biomass energy source by the removal of CO_2 and H_2S and combined with high conversion efficiency, low emission rates, suitable for CHP, CCH and CCP technology. Medium and small-scale units high exhaust temperature, heat recovery of flue gas is conducive to heat (cold) output, and improve unit efficiency.

Because the biogas contains a large share of the inert gas, emissions of oxides of nitrogen (NOx) were reduced relative to natural gas, while unburned hydrocarbons (CH) were increased, and exhibit penalties of performance compared with spark ignition engine of natural gas or gasoline [3].

Kautz et al. [4] studied a 100kW gas turbine recuperative cycle of exhaust to heat air and the influence of low calorific biogas on the combustion air ratio. Kim et al. [5] studied regenerative Brayton cycle using gas turbine recycling exhaust heat. Nwafor [6] examined the impact of advanced injection timing on the emission characteristics of dual-fuel engine.

Ahead of injection timing was intended to compensate for longer ignition delay and slower burning rate of fuelled natural gas engine, and there was a s lightly increase in the oil consumption accompanied with reduced emission of CO and CO_2.

Smith et al. [7] introduced an innovative domestic scale combined heat and power (CHP) plant incorporating a heat pump (HP). HP incorporating enhanced economy efficiency of domestic use of CHP equipment and satisfied flexibility of the family energy requirements.

Biogas was compressed to gather energy density and reduce storage capacity, the best method is biogas purified, then to compress [8]. For example, in New Zealand, both gas compressor and gas scrubber used in conjunction with, in Belgium, biogas produced from the livestock manure is being dried, scrubbed, compressed and stored in a steel tank with pressure of 4 bar in 0.2 m^3, so that is alternative fuels for CNG(compressed natural gas), gasoline, diesel and LPG (liquefied petroleum gas) [9].

2. Biogas process and energy demand in breweries

2.1. Biogas process

Brewery wastewater comes from various procedures, such as the cleaning process of the malt production, brewing, bottling, and the wastewater from cleaning the recycled beer bottle and the packaging sterilization, as well as the overflow, disqualified product, and filter back wash water. This wastewater is rich in carbohydrates, pectin, mineral salts, cellulose etc. Therefore, it is an organic wastewater with high BOD_5 and COD.

Aeration pond m ethod is the application of biological treatment earlier; because of aerobic bacteria have an allergic reaction to load fluctuations, not to deal with high carbohydrate and volatile components of beer wastewater. Use of the up-flow anaerobic sludge blanket (UASB) has a feature that of high organic loading, short hydraulic retention time, no filler in reactor, no sludge return and stirring device, low operation cost, can be inoculated directly with the sludge particles to produce biogas etc., and that is a wastewater treatment technology for sustainable development. It can not meet emission standards used alone. In most cases, the first need to treat beer wastewater by anaerobic digestion, the most of high concentration organic wastewater in UASB was degraded, and then, under the aerobic environment oxidize and decompose low concentration of pollutants in wastewater.

Fig.1 shows the brewery wastewater processing units and biogas generation set. The brewery wastewater discharged from workshop flows to the sump. Most of suspensions in waste water filter through the sieve grid. The pretreatment pool is necessary for wastewater with unqualified temperature and other physical/chemical conditions. Subsequently, the wastewater flows through the balance pool with the pH values adjusted by acid, alkali or $FeCl_3$. The adjusted water is pumped to UASB reactor in the reaction pool to decompose the organic first into acids, then to methane and CO_2. The three phase separator on top of the reactor could separate the biogas, mud and wastewater efficiently. Meanwhile, the methane bacteria could be effectively retained. The biogas is collected in gas tank after adsorption of H_2S through activated carbon. After anaerobic treatment, COD of beer wastewater dropped from about 2500 t o 500 mg / L. The use of air blower aerate for further processing in the aeration tank. Wastewater COD reduced to about 50 m g / L and then flow into the sediment pool. After suspended solid of aerobic fermentation were filtered, the reclaimed water qualified discharged to the sewer.

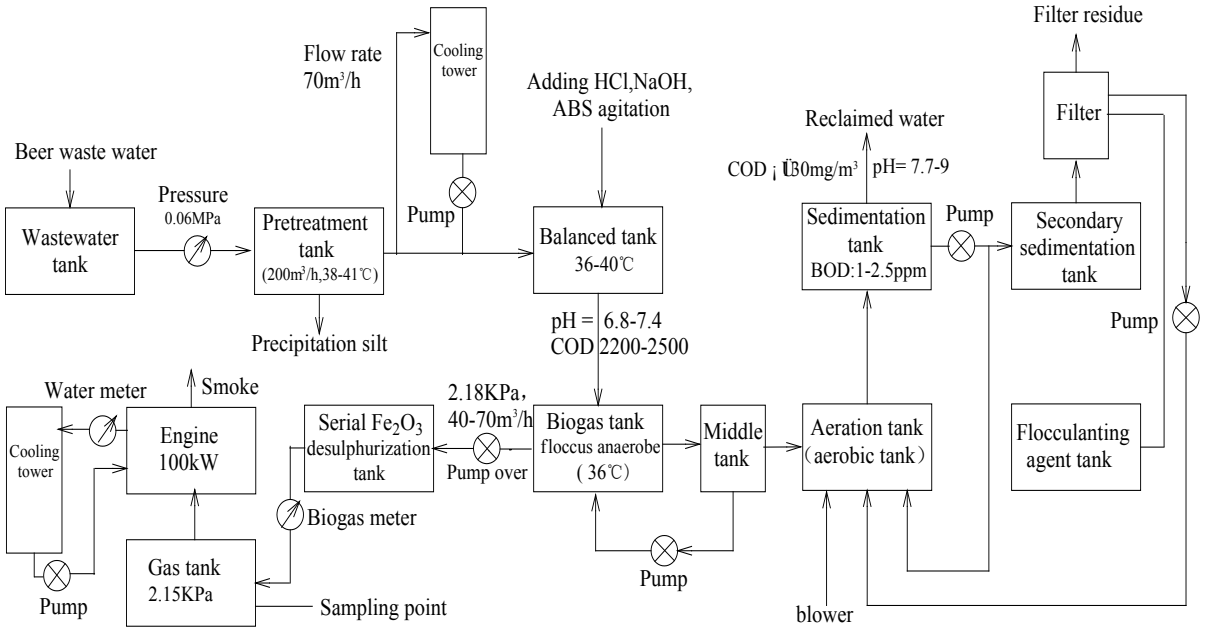

Fig.1. Schematic diagram of processing organic wastewater and generate electricity sets.

2.2. Energy requirement

The brewing process consumes a lot of electricity, steam and chilled water. This process is an intensive process of energy conversion and utilization. Therefore, energy consumption cost accounts for a large proportion of the production cost. Power workshop has 2 sets of 25t steam saturated boiler (burning oil and/or natural gas), steam pressure 7.0-8.0bar. 3 sets of ammonia compression refrigerator, cooling capacity of 496 RT, evaporator pressure of 3.7bar, chilled water supply 4°C, return 9°C. Fig.2 is energy flow diagram of steam and chilled water.

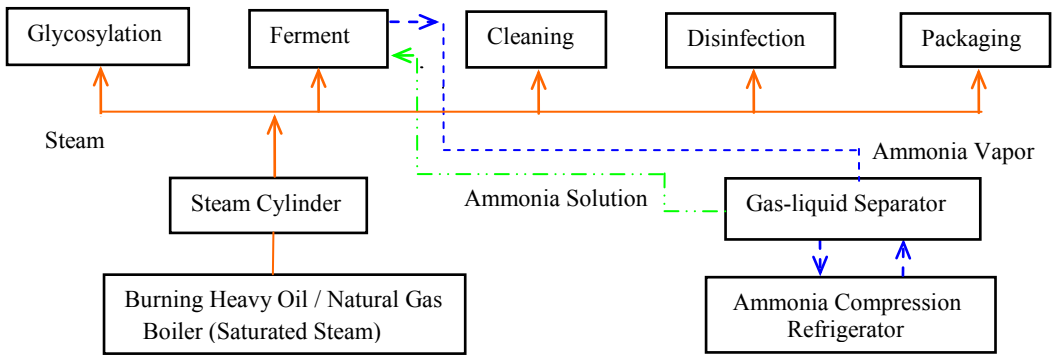

Fig.2. Energy flow diagram of steam and chilled water in breweries.

3. Status of biogas utilization

Shenzhen Kingway brewery (2 plants) and Shenzhen Tsingtao-Asahi brewery could treat beer brewery wastewater of 80-120m^3. The amount of biogas produced is 35-60 m^3 (maximum volume of 80m^3) per hour with the measured methane content of 71.2%. Table 1 shows the biogas composition with low heat value of about 25 426 kJ/Nm^3 and thermal capacity produced as 282.51-423.77kW per hour. Biogas power generation has been running for 1 year period, in order to prevent greenhouse gas emissions before it is used by the torch burning. The heat demand of beer production process provides a choice for biogas CHP and CCHP.

3.1. Engine power generation

Ignition engine was used for power generation in Shenzhen Kingway brewery, Table 2 was the spark ignition engine specifications. Biogas after the removal of H_2S could be generating 70kW (field test) per hour, efficiency of power generation was 28.45%. Table 3 was Composition of engine exhaust for the actual measurement.

Table1. Composition of the biogas

Component	Content (%)	Component	Content (%)
CH_4	71.2	H_2S	＞2500ppm
CO_2	17.1	H_2O,H_2	2.0
O_2	2.39	N_2*	7.31

* Air has leaked into biogas collection cavity over the silt anaerobic digestion pond.

Table2. Specification of 4 strokes and spark ignition engine.

Engine model	$Q6135DA_1$	Generator model	$90GFTA_1$
Rated power (kW)	83	Rated power (kW)	80
Rated speed (rpm)	1500	Rated speed (rpm)	1500
Arrangement/cylinder bore(mm)	6L /135	Rated voltage (V)	400
Displacement (L)	12.9	Nominal current (A)	162
Compression ratio	10.5	Nominal frequency (Hz)	50
Poston travel (mm)	150	Power factor	0.8
Exhaust temperature ($^{\circ}$C)	≤630	Fuel gas consumes (m^3/kW h)	≤0.33

Table3. Composition of the exhaust gas (volume percent).

Item	Test value	Reference value*	
		Gasoline	Diesel
O_2 (%)	6.24	0.3-0.8	2.0-18.0
CO_2 (%)	8.36	5.0-12.0	1.0-10.0
NO (ppm)	1793		
NOx (ppm)	1883	10^5-0.5×10^5	10^3-0.4×10^5
SO_2 (ppm)	32-0		
H_2O (%)	~8.8	3.0-5.5	0.5-4.0
N_2 (%)	~76.6	74-77	76-78

* Reference value from Table 4 of reference [10]

3.2. Heating boiler

There is a biogas fired boiler (model: FBA-080 F) in Shenzhen Tsingtao-Asahi Brewery with the parameters as follows: rated pressure: P = 1.04MPa (saturated steam), the amount of steam produced 1.25 t / h, e xhaust temperature 300°, biogas/ steam ratio = 2:1, boiler efficiency η = 80%. The actual operation pressure was 0. 6MPa.

4. Biogas processing

Because high temperature of biogas fire, slower burning speed, serious ignition delay and higher exhaust temperature, all that resulting in lower efficiency of biogas power generation. biogas purification (removal of CO_2 and H_2S), then compressed and stored as alternative

products of CNG, gasoline, diesel and LPG, showing the goods value of biogas through the transport.

4.1. Gas purification, compression and storage

Removal of H_2S in the biogas can be divided into ① dry and oxidation,② ferric oxide adsorption, ③ activated carbon adsorption, and④ liquid-phase oxidation process. A simple adsorption method using activated carbon was used in 3 breweries.

The amine solution of 10% mono-ethanolamine (MEA) and diethanolamine (DEA) are usually used to absorb CO_2. It takes 5min for the solution regeneration to be completed by boiling. The newer approach is the sulfolane method or the Sulfinol method composed by alcohol amine and sulfolane adding water. Method of reclaimed water which was beer wastewater treated when water pressure increased as the absorbent to remove CO_2 is the most simple and less expensive. Efficiency of the scrubber depends on that scrubber specifications, packing and gas pressure in scrubber, composition of raw biogas, the flow rate and purity of water used and so on.

The critical temperature and pressure required to liquefied biogas were: -82.58 $^{\circ}$C and 47.5 bar respectively. Purification biogas compressed by the compressor, according to different pressure stored in cylinders, which could be transported with long-distance, may be also build a small scale station on side.

4.2. Power fuel

After CO_2, H_2S and water vapor in biogas were removed, the methane (>90%, heat value equivalent to LNG), could be compressed and stored as fuel for car and other power machines.Table 4 is data of LNG imported to Guangdong province of China from Australia, kindly provided by the Shenzhen Gas Group.

Table 4. Data of physical and chemical for LNG.

Composition	(%)	Data (0℃,1atm)	Value
CH_4	87.59	HHV (MJ/Nm^3)	45.08
C_2H_6	8.13	LHV (MJ/Nm^3)	40.71
C_3H_8	3.2	Density (kg/Nm^3)	0.8318
C_4H_{10}	0.99	Specific volume (Nm^3/t)	1202
C_5H_{12}	0.05	LHV (MJ/kg)	48.92

Use of CNG instead of gasoline as a motor fuel, the emissions of CO, CH compounds and NO compounds can be decreased by 97%, 72%, and 39% respectively. Performance of resistance to blast for CNG equivalent to gasoline is about octane number of 130, and CNG does not release lead, benzene and other toxic substances all which can cause cancer. Forklift which using LPG as fuel made by Japan Fuji Co. in Shenzhen Tsingtao-Asahi brewery, may also use purified biogas as a substitute.

4.3. Incorporate into LNG pipe network

Due to lower productive rate of biogas, gas source instability, lower energy carrier demand load, difficult to manufacture equipment and operation and a long payback time as investment etc., biogas can no effectively use in the IES, so that, it could be considered incorporate into the municipal LNG Network pipe after the quality checked up.

5. Integrated energy system (IES) of biogas

Electricity is the high grade energy. According to the second law of thermodynamics, the electricity generated by biogas is of the highest efficiency, meanwhile, the exhaust gas could be employed for heating or cooling. IES of biogas would adopt the following technologies such as Otto cycle of ignition engine, Brayton cycle of gas turbine, power generation of fuel cells, absorption and adsorption refrigeration, high efficient combustion, high efficiency removal of H_2S and CO_2, as well as recovery and storage for thermal energy.

5.1. CHP project

Project 1: Engine + Heat tube exchanger of condensation type
(Shenzhen Kingway brewery)

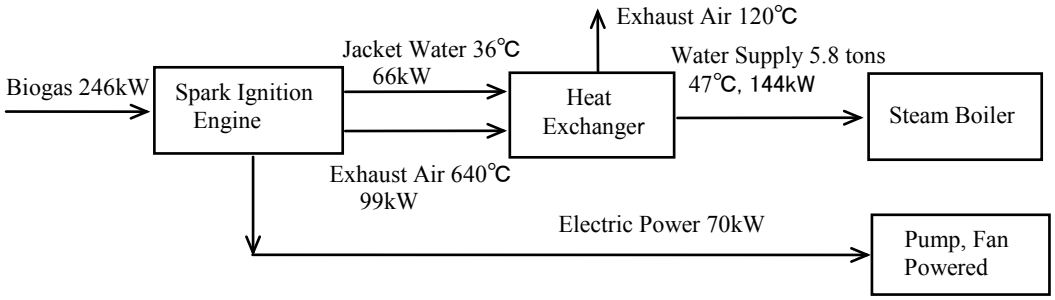

• Spark Ignition Engine of biogas fueled without removal of CO_2, generate electricity efficiency of 28.45%, discharged heat of 99kW by engine exhaust and of 66kW by jacket cooling water, dispersed heat of 2.8kW by convection and of 4.6kW by radiation.
• If heat of engine exhaust was utilized through heat tube heat exchanger to heat water supply and temperature was reduced to about 120℃, then, overall CHP efficiency may be reached 61.8%, and engine exhaust even could be discharged at the condensation temperature of 57℃.

5.2. CCP project [11]

Project 2: Micro Turbine (Honeywell) + Direct fired double effect chiller

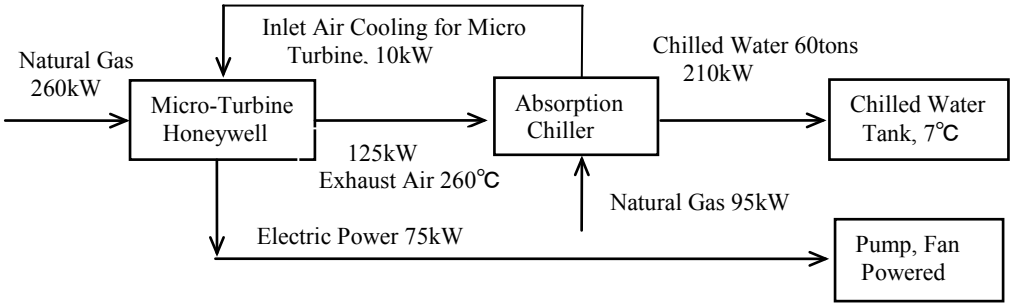

• Turbine efficiency 28.75%. Inlet air cooled to 16℃ to keep constant capacity of turbine.
• Broad absorption chiller using lithium bromide-water, direct fired double effect chiller with COP of 1. Chilled water temperature: supply 7.8-9.4℃, return 12.8-14.4℃.
Performance of MT Honeywell and absorption chiller were shown in Table 5 and Table 6.

Table 5. Performance parameters of MT (Honeywell).

Item	Parameter	
Rating power (kW)	75	15℃,1atm
NG wastage (m^3 /h)	27	≥0.62MPa(absolute)
Thermoelectricity efficiency (%)	28.5	15℃,1atm
Exhaust temperature (℃)	280	
Exhaust flux (kg/s)	0.67/0.76	
Emission of NO_X (ppm)	<13	15℃,1atm, full load

Table 6. Broad LiBr absorption chillers (Mode: BD7N280-15).

Item	Parameter	Item	Parameter
Capacity of refrigeration (USRT)	23	Produce heat (kW)	114
Chilled water outlet/inlet temp. (℃)	6.7/12.2	Warm water outlet temp.(℃)	50
Chilled water flux (m^3/h)	12.8	Warm water flux (m^3/h)	19.6
Cooling water outlet/inlet temp.(℃)	36/29.4	Inlet temp. of exhaust (℃)	280
Cooling water flux (m^3/h)	24.3	Match electricity (kW)	1.2

Project 3: Micro Turbines (Capstone) + Single effect chiller

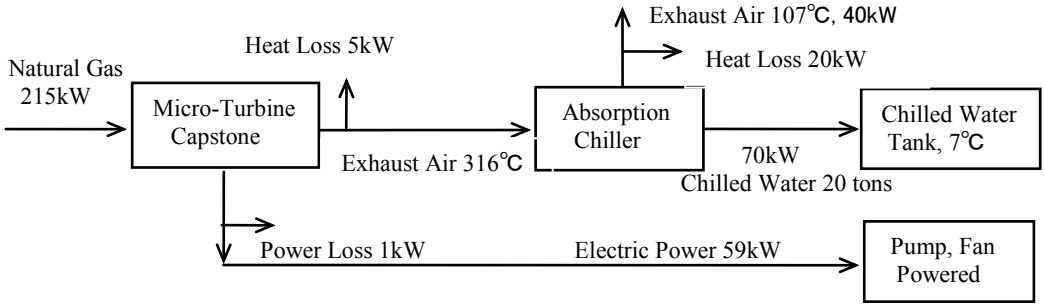

• MT Capstone efficiency 27.9%, with chiller 63.5%. Average exhaust inlet temp.℃271 , outlet temp.113℃.
• Broad absorption chiller driven only by MT exhaust. Single effect chiller with COP of 0.7, nominal capacity of chilled water is 20 tons. Parasitic power is 6.4kW.

5.3. CCH project

Project 4: Engine driven Goettl Units + Heat tube exchanger of condensation type

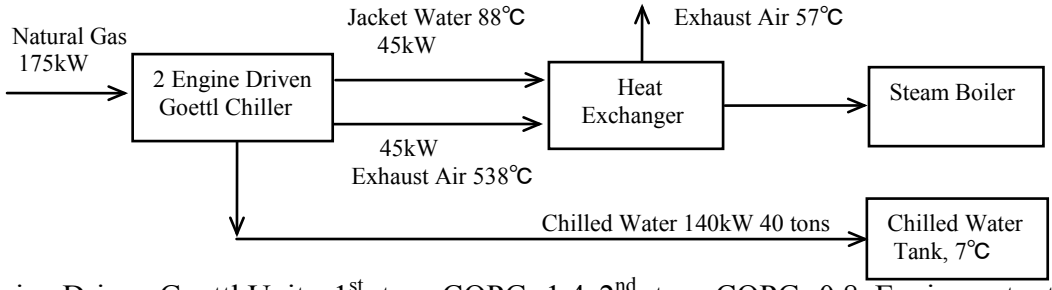

• Engine Driven Goettl Units. 1st stage COPG=1.4, 2nd stage COPG=0.8, Engine output 52kW, engine efficiency 30%.

6. Conclusion

This paper introduced and analyzed biogas utilization for the three large modern breweries, which is not perfect and irrational for use of biogas energy. Based on the current biogas technology and equipments, accordingly to the biogas yield and energy demand in breweries, analyzed and studied the energy utilization technology, equipment configuration, and conversion efficiency on the integrated energy system (IES) . The biogas purification process employs qualified reclaimed water from wastewater treated of the brewery to scrub CO_2 and H_2S in biogas. This process is simple with low operation cost. The resultant biogas is rich in methane content and efficient to improve the efficiency of IES. Both electricity generation and heating efficiency, as well as the cooling efficiency can reach as high as 60%.

Acknowledgements

This work was supported by public technological project of the Bureau of Science, Technology and Information of Shenzhen city, under Contract No.SY2008343.

References

[1] Pöschl M, Ward S, Owende P. Evaluation of energy efficiency of various biogas production and utilization pathways. Applied Energy. 87, 2010, pp. 3305–3321.

[2] Deng J, Wang RZ, Han GY. A review of thermally activated cooling technologies for combined cooling, heating and power systems. Progress in Energy and Combustion Science. 37, 2011, pp. 172-203.

[3] Crookes RJ. Comparative bio-fuel performance in internal combustion engines. Biomass and Bioenergy. 30, 2006, pp. 461-468.

[4] Kautz M, Hansen Ulf. The externally-fired gas-turbine (EFGT-Cycle) for decentralized use of biomass. Applied Energy. 84, 2007, pp.795-805.

[5] Kim KH, Perez-Blanco H. Potential of regenerative gas-turbine systems with high fogging compression. Applied Energy. 84, 2007, pp.16-28.

[6] Nwafor OMI. Effect of advanced injection timing on emission characteristics of diesel engine running on natural gas. Renewable Energy. 32, 2007, pp.2361-2368.

[7] Smith MA, Few PC. Domestic-scale combined heat-and-power system incorporating a heat pump: analysis of a prototype plant. Applied Energy. 70, 2001, pp. 215-232.

[8] Osorio F, Torresba JC. Biogas purification from anaerobic digestion in a wastewater treatment plant for biofuel Production. Renewable Energy. 34, 2009, pp. 2164–2171.

[9] Kapdi SS, Vijay VK, Rajesh SK, Rajendra Prasad. Biogas scrubbing, compression and storage: perspective and prospectus in Indian context. Renewable Energy. 30, 2005, pp. 1195–1202.

[10] Coronado CR, Carvalho JA, Yoshioka JT, Silveira JL. Determination of ecological efficiency in internal combustion engines:the use of biodiesel. Applied Thermal Engineering. 29, 2009, pp. 1887–1892.

[11] Garland PW.CHP for buildings integration: test centers at ORNL and University of Maryland. Oak Ridge National Laboratory, http://www.ornl. gov/sci/eere/PDFs/ garland_ seminar.pdf; 2003.

Thermoeconomic optimization of absorption chiller cycle

H. Mashayekh[1], G.R. Salehi [2]*, E. Taghdiri [3], M.H. Hamedi [3]

[1]*Islamic Azad University Science & Research Branch, Tehran, Iran*
[1]*Islamic Azad University Nowshahr Branch, Nowshahr, Iran*
[2] *KNToosi University of Technology, Tehran, Iran*
** Corresponding author. Tel: +989122031671, E-mail: rezasalehi20@gmail.com*

Abstract: In this paper, absorption chillers are modeled as four heat sources: the generator, the evaporator, the condenser, and the absorber and thermoeconomic issues are examined using the available relations. In order to simplify the calculations, all processes are assumed to be reversible. Since heat exchangers are expensive facilities, therefore, reducing the total heat transfer area is taken as the design criterion. In this paper, first the thermoeconomic criterion, taken as the total cost of unit of refrigeration which includes the capital cost and the energy cost, is defined. In the following, the available relationships are used to calculate the maximum value of the thermoeconomic criterion and the maximum refrigeration load. Next, optimal working conditions are specified for absorption chillers and after that, the effect of the thermoeconomic parameter on the maximum thermoeconomic criterion, coefficient of performance and the specific refrigeration load corresponding to the maximum value of the thermoeconomic criterion are investigated.

Keywords: *thermoeconomic performance, absorption chiller, optimization*

1. Introduction

Nowadays, costs of energy consumption and electricity compared to those of fossil fuels have caused engineers in most countries to consider using absorption chillers instead of compression chillers. However, fuel costs need to be controlled in some way and consequently, economical studies are carried out constantly on opt imization of absorption chillers and reducing their economical costs.

A new criterion has been used in the recent years to evaluate the degree of optimality of thermodynamic cycles. The thermoeconomic criterion economically investigates the phenomena. Capital costs and energy costs are considered in these investigations using thermodynamic relationships and working conditions are designed in a way that the operation is economically optimum. Chen and Schouten (1998) evaluated the optimal value of coefficient of performance in irreversible absorption chiller systems [1]. Next, Chen in 1999 evaluated the optimal value of coefficient of performance for the irreversible 4-heat exchange-surface absorption chiller in the maximum specific cooling load [2]. This was followed by other researches with the aim of optimization of absorption chiller processes and other processes similar to those, including thermoeconomic optimization of the reversible sterling heat pump cycle by Tyagi, Chena, and Kaushikb[3].

The largest portion of capital cost of absorption chiller pertains to the heat exchangers used in the generator, condenser, evaporator, and the absorber.

2. Modeling of the cycle and its relationships

In order to simplify the calculations, absorption chiller cycle is assumed to consist of four heat sources including the absorber, the generator, the evaporator, and the condenser, as illustrated in figure 1. We assume that the processes take place reversibly. It is also assumed that the flow is constant in working parts of the cycle and heat transfer between the elements and heat sources during the time of a complete cycle τ, happen at temperatures T_a, T_c, T_e, T_g, respectively. There are thermal resistances between the external components and the

operating elements of the cycle. Temperatures of working components in the generator, evaporator, condenser and the absorber are respectively T_4, T_3, T_2, T_1. Heat transfer coefficients are accordingly U_4, U_3, U_2, U_1. Moreover, heat transfer surfaces are A_4, A_3, A_2, A_1, in the generator, the evaporator, the condenser and the absorber, respectively. The work input for the pump in the cycle Is taken as negligible compared to the heat input to the generator.

It is assumed that the heat transfer between the operating components of the cycle and the external heat sources follows the linear (Newtonian) heat transfer mode and the four processes take place isothermally. Thus, heat transfer equations of all the four processes are written as follows:

$$Q_1 = U_1 A_1 (T_g - T_1)\tau \quad (1)$$
$$Q_2 = U_2 A_2 (T_e - T_2)\tau \quad (2)$$
$$Q_3 = U_3 A_3 (T_3 - T_c)\tau \quad (3)$$
$$Q_4 = U_4 A_4 (T_4 - T_a)\tau \quad (4)$$

Where Q_4, Q_3, Q_2, Q_1 are heat transfers in the generator, the evaporator, the condenser and the absorber, respectively, From the first law of thermodynamic we have:

$$Q_1 + Q_2 - Q_3 - Q_4 = 0 \quad (5)$$

Considering the second law of thermodynamic and the reversibility of the cycle we have:

$$\frac{Q_1}{T_1} + \frac{Q_2}{T_2} - \frac{Q_3}{T_3} - \frac{Q_4}{T_4} = 0 \quad (6)$$

Since the heat exchangers are the expensive component in the cycle, reduction of the heat transfer area (A) is taken as the design criterion. Therefore, by optimizing the total heat transfer area we can obtain optimality.

$$A = A_1 + A_2 + A_3 + A_4 \quad (7)$$

The parameter (a) is defined as the total distribution rate between the condenser and the absorber:

$$a = \frac{Q_3}{Q_4} \quad (8)$$

According to the standard definitions of coefficient of performance (COP) and specific cooling load (r) and equations (1) to (8), coefficient of performance can be obtained as follows:

$$\varepsilon = \frac{Q_2}{Q_1} = \frac{T_4^{-1} + aT_3^{-1} - (1+a)T_1^{-1}}{(1-a)T_2^{-1} - T_4^{-1} - aT_3^{-1}} \quad (9)$$

And the specific cooling load is obtained as follows:

$$r=\frac{Q_2}{A\tau}=\left\{\frac{1}{U_2\left(T_e-T_2\right)}+\frac{T_2^{-1}-T_4^{-1}+a\left(T_2^{-1}-T_3^{-1}\right)}{U_1\left(T_g-T_1\right)\left[T_4^{-1}-T_1^{-1}+a\left(T_3^{-1}-T_1^{-1}\right)\right]}\right.$$
$$\left.+\left[\frac{1}{U_4\left(T_4-T_a\right)}+\frac{a}{U_3\left(T_3-T_c\right)}\right]\frac{T_2^{-1}-T_1^{-1}}{T_4^{-1}-T_1^{-1}+a\left(T_3^{-1}-T_1^{-1}\right)}\right\}^{-1} \quad (10)$$

Equations 9 and 10 are the general relationships for absorption chillers with four reversible heat sources. These relationships can be used to obtain thermoeconomical optimum performance for this type of absorption chillers.According to the studies carried out by Kodal and Shahin as given in [5], the thermoeconomic criterion for absorption chillers with four reversible heat sources is defined as the total price of unit cooling load which includes both capital and energy costs. Therefore, the function which is to be optimized is as follows:

$$F=\frac{\frac{Q_2}{\tau}}{C_i+C_e} \quad (11)$$

Where C_i, C_e are capital and energy costs in the unit of time, respectively. The capital cost of absorption chillers is assumed to be proportional to its total heat transfer area:

$$C_i=k_1 A \quad (12)$$

Where k_1 is the capital recovery factor, the capital cost for the unit heat transfer area. Energy consumption cost is directly proportional to the rate of heat input:

$$C_e=k_2\frac{Q_1}{\tau} \quad (13)$$

Where k_2 is the unit cost of energy. By substituting equations 12 and 13 in 11, we obtain:

$$F=\frac{Q_2/\tau}{(k_1A+k_2Q_1/\tau)}=(k_1r^{-1}+k_2\varepsilon^{-1})^{-1}. \quad (14)$$

By defining $k=\frac{k_1}{k_2}$ as the thermoeconomic parameter having the dimension $\frac{KW}{m^2}$, when the capital cost increases and the cost of energy consumption reduces, the thermoeconomic parameter k goes up. The optimal relationship for the total refrigeration load and the COP of absorption chillers is as follows:

$$r=U_2\left[T_eT_c+aT_eT_a-(T_g\varepsilon+T_e)\frac{T_cT_a(1+a)}{T_g(1+\varepsilon)}\right]$$
$$\times\left\{\left[(1+b_2)^2T_c+a(1+b_3)^2T_a-\frac{a}{1+a}(b_2-b_3)^2T_e\right]-(1-b_1)^2\frac{(1+a)T_aT_c}{(1+\varepsilon)T_g}\right. \quad (15)$$
$$\left.+\frac{T_e}{\varepsilon T_g}\left[(b_1+b_2)^2T_c+a(b_1+b_3)^2T_a-\frac{a}{1+a}(b_2-b_3)^2T_g\right]\right\}^{-1},$$

Where: $b_1 = \sqrt{\frac{U_2}{U_1}}$ (16)

By combining (14) and (15), the ration of the optimal value of the thermoeconomic criterion and the COP of absorption chillers with four reversible heat sources is obtained as follows:

$$k_2F = \left\{ \frac{k}{U_2}\left[T_eT_c + aT_eT_a - (T_g\varepsilon + T_e)\frac{T_cT_a(1+a)}{T_g(1+\varepsilon)}\right]^{-1} \times \left[(1+b_2)^2T_c + a(1+b_3)^2T_a - \frac{a}{1+a}(b_2-b_3)^2T_e\right] - (1-b_1)^2\frac{(1+a)T_aT_c}{(1+\varepsilon)T_g} + \frac{T_e}{\varepsilon T_g}\left[(b_1+b_2)^2T_c + a(b_1+b_3)^2T_a - \frac{a}{1+a}(b_2-b_3)^2T_g\right] + \varepsilon^{-1}\right\}^{-1}. \quad (19)$$

Equation 19 gives the optimum thermoeconomic criterion for a given value of COP and also the optimum coefficient of performance for a given thermoeconomic parameter in reversible absorption chillers. Using equation19, we can evaluate other characteristics of thermoeconomic operation of reversible absorption chillers which obey the linear (Newtonian) heat transfer law.

Equation 19 demonstrates that for the thermoeconomic parameter we have $F = 0$ when $\varepsilon = 0$ or $\varepsilon = \varepsilon_c$, where:

$$\varepsilon_c = \frac{T_a^{-1} + aT_c^{-1} - (1+a)T_g^{-1}}{(1+a)T_e^{-1} - T_a^{-1} - aT_c^{-1}}, \quad (20)$$

is the coefficient of performance for an absorption chiller with four reversible heat sources. When $\varepsilon < \varepsilon_c$, the maximum thermoeconomic criterion is derived. Using (19) and the final condition $\frac{d(k_2F)}{d\varepsilon} = 0$, we can evaluate $COP(\varepsilon_r)$ for the maximum value of the maximum thermoeconomic criteria $(F_{\max})$:

$$\varepsilon_F = \left[1 - \sqrt{1 - \frac{(1+a)T_g^{-1} - T_a^{-1} - aT_c^{-1}}{T_a^{-1} + aT_c^{-1} - (1+a)T_e^{-1}}d_1}\right]d_1^{-1} \quad (21)$$

Where

$$d_1 = \frac{(1+a)(T_g - T_e)d_2}{T_e^2[T_a^{-1} + aT_c^{-1} - (1+a)T_e^{-1}]\{d_3 + [T_cT_g + aT_aT_g - (1+a)T_aT_c]U_2/k\}} + \frac{(1-b_1)^2(1+a)T_aT_c - d_3T_e - [T_eT_c + aT_eT_a - (1+a)T_aT_c]T_gU_2/k}{T_e\{d_3 + [T_cT_g + aT_aT_g - (1+a)T_aT_c]U_2/k\}} \quad (22)$$

$$d_2 = (1+b_2)^2T_c + a(1+b_3)^2T_a - (b_2-b_3)^2T_ea/(1+a) \quad (23)$$

$$d_3 = (b_1+b_3)^2T_c + a(b_1+b_3)^2T_a - (b_2-b_3)^2T_ga/(1+a) \quad (24)$$

Substituting (21) in (19), we can obtain the maximum thermoeconomic limit for a reversible absorption chiller. Substituting (21) in (15), we can obtain the specific refrigeration load (r_F) for the maximum thermoeconomic criterion. Three parameters $F_{\max}, r_F, \varepsilon_F$ are important for the optimum design of reversible absorption chillers. These parameters result in the lowest value of COP and the lowest value of the characteristic refrigeration load and the top limit of the thermoeconomic criterion [5,6,7].

3. Investigation and conclusion

In order to examine the thermoeconomic of the cycle and the impact of its different parameters, a case study was analyzed and the obtained circumstances were compared with each other. The following data were known for the aforementioned case study.

$$T_g = 403K, T_e = 293K, T_c = 313K, T_a = 305K, a = 1, U_1 = U_2 = U_3 = U_4 = 0.5\frac{KW}{K.m^2}$$

By changing any of the following parameters, we take other parameters as constant and equal to the values mentioned above. The characteristic charts of the problem at hand were obtained using the above data. Figure 2 shows the thermoeconomic criteria versus the coefficient of performance of a reversible chiller with $k = 1\frac{KW}{m^2}$. The value of the maximum thermoeconomic criterion $(F_{\max})$ can be obtained from this curve. As you can see, this chart consists of two sections with negative and positive slopes. The part which has a negative slope represents the optimum region for operation of absorption chillers. In figure 3, variations of the thermoeconomic criterion in terms of the characteristic refrigeration load is shown. Here too, we have $k = 1\frac{KW}{m^2}$. From this curve one can easily obtain the maximum value for the thermoeconomic criterion $(F_{\max})$ and the maximum refrigeration load $(r_{\max})$. This curve has three parts. It is obvious that the optimum working conditions for absorption chillers are in the region with negative slope.

Figures 2 and 3 can help one find the optimum region for operation of absorption chillers, which are the regions with negative slopes. This region should abide by the following conditions:

$$F_r \leqslant F \leqslant F_{\max} \quad (25) \qquad \varepsilon_F \leqslant \varepsilon \leqslant \varepsilon_r \quad (26) \qquad r_F \leqslant r \leqslant r_{\max} \quad (27)$$

Where F_r the thermoeconomic criterion for the maximum refrigeration is load $(r_{\max})$ and ε_r is the COP for the maximum value of characteristic refrigeration load for the reversible absorption chiller which can be obtained from the following equation:

$$\varepsilon_r = \left[1 - \sqrt{1 - \frac{(1+a)T_g^{-1} - T_a^{-1} - aT_c^{-1}}{T_a^{-1} + aT_c^{-1} - (1+a)T_e^{-1}} d_4}\right] d_4^{-1} \quad (28)$$

Where:

$$d_4 = \frac{(1+a)\{(1-b_1)^2[T_e T_c + aT_e T_a - (1+a)T_a T_c] + (T_g - T_e)d_2\}}{T_e^2[T_a^{-1} + aT_c^{-1} - (1+a)T_e^{-1}]d_3} - 1 \quad (29)$$

Substituting 28 in 19, we can obtain the maximum value for the characteristic refrigeration load. Moreover, by substituting 28 in (15), we can obtain the value of the thermoeconomic criterion for the maximum characteristic refrigeration load, (F_r). The values of the parameters which influence the operation of the cycle are changed and their effects on the cycle are compared. Figure 4 shows the characteristic curve of the thermoeconomic criterion-coefficient of performance for four different values of the thermoeconomic criterion (k) and figure 5 shows the characteristic curve of the thermoeconomic criterion – refrigeration load for the same four values of the thermoeconomic criterion. We can deduce from these curves that the optimum thermoeconomic criterion for a known value of COP, the thermoeconomic criterion for a specific capacity of refrigeration and optimum coefficient of performance and characteristic refrigeration capacity for a known value of the thermoeconomic criterion, all reduce by increasing the thermoeconomic parameter (k). Figure 6 shows the characteristic thermoeconomic parameter- coefficient of performance curve for four different values of total rate of distribution on heat output (a) and figure 7 shows the characteristic thermoeconomic criterion-refrigeration load curve for the same four values of the total rate of heat output.

It can be deduced from these curve that the optimum thermoeconomic criterion for a known value of COP, the thermoeconomic criterion for a special refrigeration capacity and the optimum coefficient of performance, and the characteristic refrigeration performance for a known value of thermoeconomic criterion all decrease by increasing the total heat output distribution rate (a). As it is evident from figure 7, t he maximum value for the thermoeconomic criterion and its corresponding coefficient of performance, reduce by increasing the thermoeconomic parameter (k) and the specific refrigeration load corresponding to the maximum thermoeconomic criterion increases by increasing the thermoeconomic parameter (k).

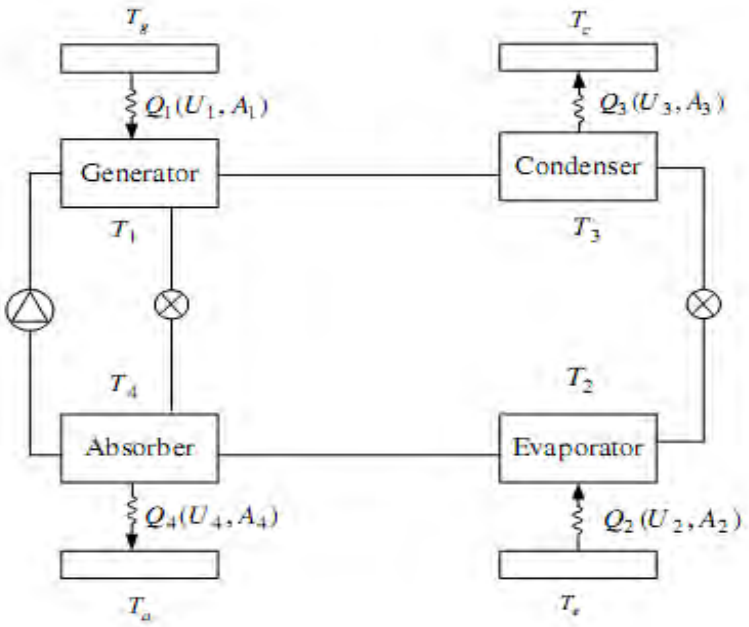

Fig 1: modeling of the cycle

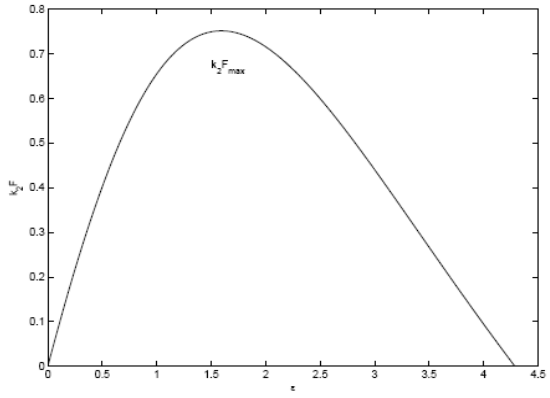

Figure 2: the thermoeconomic criterion in terms of coefficient of performance

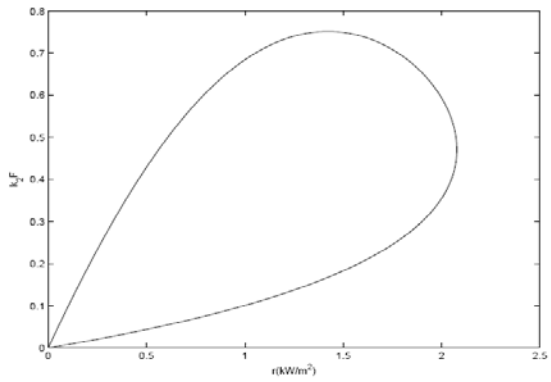

Figure 3: the curve of the thermoeconomic criterion in terms of the characteristic curve of the system.

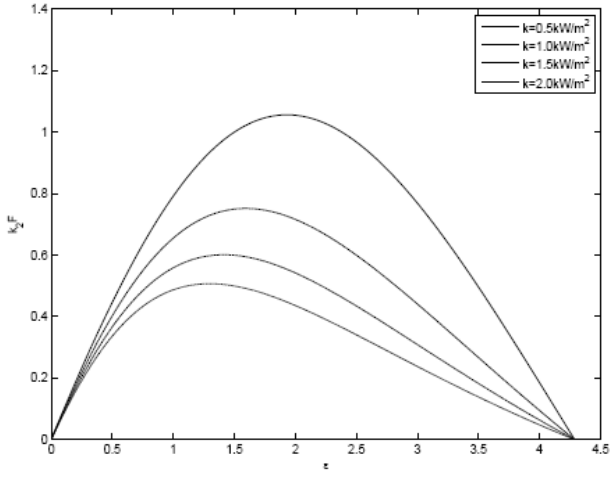

Figure 4: the effect of the thermoeconomic parameter on the ration of the thermoeconomic criterion and the coefficient of performance

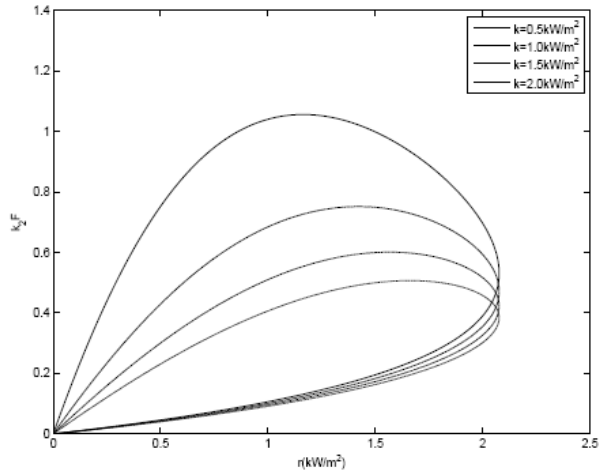

Figure 5: the effect of the thermoeconomic parameter on the thermoeconomic criterion and refrigeration capacity

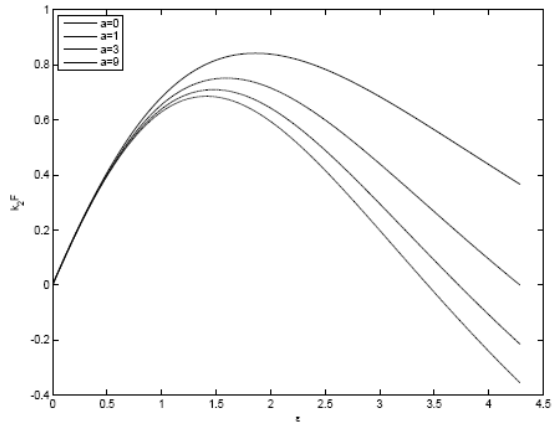

Figure 6: the effect of the total rate of heat output on the ratio of the thermoeconomic criterion and coefficient of performance

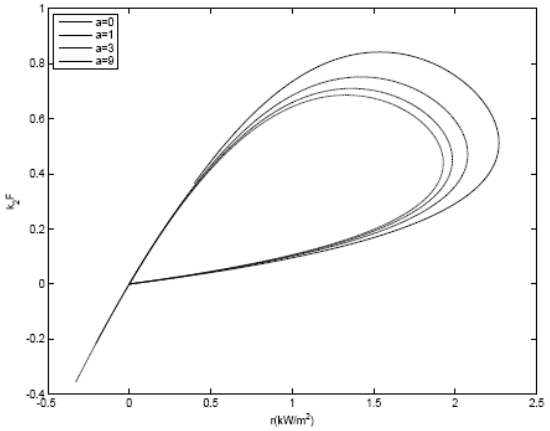

Figure 7: the effect of the total rate of heat output on the ratio of the thermoeconomic criterion and refrigeration capacity

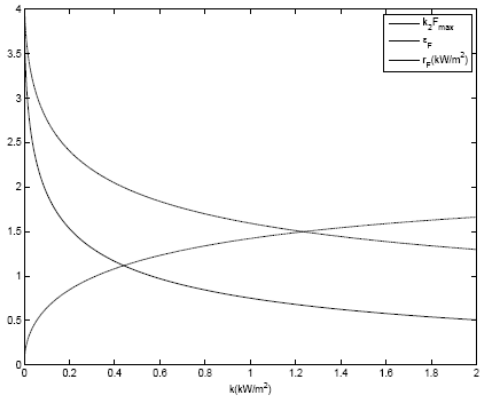

Figure 8: the effect of the thermoeconomic parameter on $F_{\max}, r_F, \varepsilon_F$

4. Conclusion

In this paper, the performance of absorption chillers with four reversible heat sources was analyzed and optimized with the existing relationships. The range of the important parameters for the absorption cooling cycle with four reversible heat sources for its optimum operation was determined. The obtained results can be used as a theoretic guide for further studies on the thermoeconomic optimization and further development of performance of absorption chiller cycles.

References

[1] Chen J, Schouten "A. Optimal performance-characteristic of an irreversible absorption-refrigerationsystem". Energy Convers Manage 1998

[2] Chen J. "The optimal performance-characteristic of a four-temperature-level irreversible absorption-refrigerator at maximum specific-cooling load". J Phys D: Appl Phys 1999

[3] S.K. Tyagi, Jincan Chena, S.C. Kaushikb "Thermoeconomic optimization and parametric study of an irreversible Stirling heat pump cycle"., International Journal of Thermal Sciences 43

[4] Wang S.K., "Handbook of Air Conditioning and Refrigeration" McGraw-Hill, 2nd Ed, New York, 2000.

[5] Kodal A, Sahin B, Ekmekci I, Yilmaz T. "Thermoeconomic optimization for irreversible absorption-refrigeration and heat pumps". Energy Convers Manage 2003.

[6] Sahin B, Kodal A. "Finite-time thermoeconomic optimization for endoreversible refrigerators and heat pumps. " Energy Convers Manage 1999;40(9):951–60.

[7] Chen L, Sun F, Chen W, Wu C. "Optimal performance coeffcient and cooling-load relationship of a three-heat-reservoir endoreversible refrigerator. " Int J Power Energy Sys 1997; 17(3):206–8.

Simulation and optimization of steam generation in a pulp and paper mill

Xiaoyan Ji[1,*], Joakim Lundgren[1], Chuan Wang[2], Jan Dahl[1], Carl-Erik Grip[1]

[1] *Division of Energy Engineering, Luleå University of Technology, 971 87 Luleå, Sweden*
[2] *PRISMA – Centre for process integration in steelmaking, Swerea MEFOS AB, 971 25 Luleå, Sweden*
** Corresponding author. Tel: +46 920492837, Fax: +46 920491074, E-mail: xiaoyan.ji@ltu.se*

Abstract: A mathematical process integration model for the steam generation part (recovery boiler, bark boiler, and turbine) was developed based on a pulp and paper mill in the Northern Sweden. The material and energy balances were calculated theoretically and then the operation data from a pulp and paper mill in the Northern Sweden were used to validate the simulation results. By implementing it into the whole plant, the effect of the operation conditions on the whole plant performance were investigated. The introductory studies were carried out with an objective function to minimize the energy cost. The influence of different parameters was rigorously studied. The correlation between economic and energy optima was discussed.

Keywords: *Pulp and Paper Mill, Steam Generation, Simulation, Optimization*

1. Introduction

The pulp and paper industry is a very energy-intensive industrial sector where it is crucial to improve the material and energy efficiency to the greatest possible extent. Process integration methods represent useful tools for evaluating possible process alternatives. Many process integration studies in the pulp and paper industry have previously been carried out mainly by using Pinch analysis[1,2] and mathematical programming[3,4]. However, the scope of modeling and simulation of the energy and material balances is not as complete as it is in other modern process industries. More detailed work is required especially as large efforts are currently put on turning pulp mills into bio-refineries.

Based on the mixed integer linear programming (MILP) combined with ReMIND[5] and CPLEX[6], mathematical process integration models of steelmaking industries have been developed in our research groups. The developed model has been successfully applied, for example to give suggestions on choosing a new blast furnace, to reduce the CO_2 emission by using alternative production routines, etc[7,8]. Recently, the research work has been extended to mining industries also[9,10].

To extend researches to pulp and paper mill, a complete plant model was developed based on a pulp and paper mill in the Northern Sweden and described briefly in our previous work[11]. In this work, a mathematical process integration model for the steam generation part (recovery boiler, bark boiler, and turbine) was developed in which the material and energy balances were performed theoretically and the operation data (measurements) from the mill were used to validate the model results, which was presented in detail. By implementing it into the complete plant model, the effects of the operation conditions in the steam generation part on the whole plant performance were investigated. Furthermore, introductory studies were carried out with the main objective to minimize the energy cost, and the correlation and differences between economic and energy were also discussed.

2. Process description and model construction

The pulp and paper mill in the Northern Sweden is illustrated in Fig. 1. The lignin is removed to produce the brightness pulp by passing through the digester, O_2 delignification, and

bleaching plant. Paper is produced from pulp in paper making section. The by-product extracted from pulping chips in the digester, i.e. the black liquor, is concentrated in a multi-effect evaporation plant and burned in a recovery boiler (RB) where the combustion of organics provides energy and recovers chemicals which are used to generate the solution of NaOH and Na_2S by passing through the causticizing plant. Bark boiler (BB) provides additional high pressure steam to satisfy the steam demand for the whole plant. The high pressure steam produced in the RB and BB is expanded in a steam turbine producing process steam of 10 and 4 bar. Steam of 30 bar is extracted from the turbine for soot-blowing in the RB and steam 10 bar is used for soot-blowing in the BB. Biomass in form of bark or forest residues and fuel oil are used in the BB. Fuel oil is also used to start up the RB.

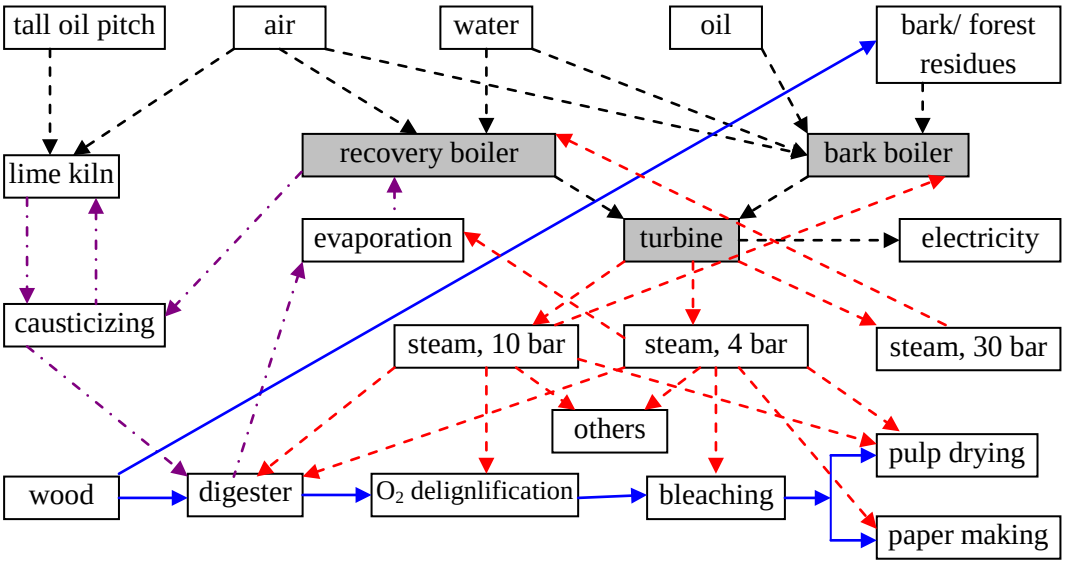

Fig. 1. Schematic representation of the pulp and paper mill.

To perform the process integration, each process unit was modeled as separate modules and thereafter linked. The construction of modules was based on a mathematical programming, i.e. mixed integer linear programming (MILP), and the equation editor used was a Java based programming — ReMIND[5]. In ReMIND, the model structure is represented as a network of nodes and branches, which represent process units and energy/material flows, respectively. The different nodes are connected depending on the input and output to/from each process unit. Each node contains linear equations to express the energy and mass balances required in the process unit. There are two options to express the energy and mass balances for each node, i.e. representing theoretically (option one), or obtaining an equation from the operation measurement under a set of conditions (option two). We chose the option one. The steam generation part including RB, BB, and back pressure turbine is the heart of energy utilization in the plant, and it was studied in the present work.

For RB and BB (boilers), the energy and mass balances were estimated from the chemical compositions of the fuels, the effective heat value of the fuels (H_{eff}) and the corresponding thermodynamic properties of all the related flows. This has been described in detail in literature[12] under operation conditions, such as the temperature of water, air, and flue gas, and the temperature and pressure of steam generated. From the chemical composition of the fuel and the amount of the excess air, the air demand and the amount of flue gas were calculated based on the mass balances. The fuel demand (ton fuel/ ton steam) was calculated from the air demand, the amount of the flue gas, the heat value of fuels together with

conditions for the air, flue gas, water and steam. The principle was briefly summarized in Fig. 2, and the brief description was given in the following text. The properties of the fuels and the related heat capacities were taken from public references and listed in Tables 1 and 2, respectively.

Table 1. Properties of fuels.

	C	H	O	S	Na	K	Slagg	N	H_2O	$H_{eff,dry}$, kJ/kg
black liquor	36.4	3.7	34	5.2	19.9	0.8	0	0	0	12400
fuel oil 5	85.9	11.4	0.9	1	0	0	0.03	0.3	0.5	40700
forest residues	51.9	6.15	40.5	0.02	0.05	0.3	0.86	0.22	0	19300

Table 2.Heat capacity.

substance	heat capacity (kJ/(kgK))		heat capacity (kJ/(Nm^3K))
black liquor	3.74	air	1.29
Na_2CO_3	1.09	flue gas	1.40
Oil	1.92		
bark	2.97		

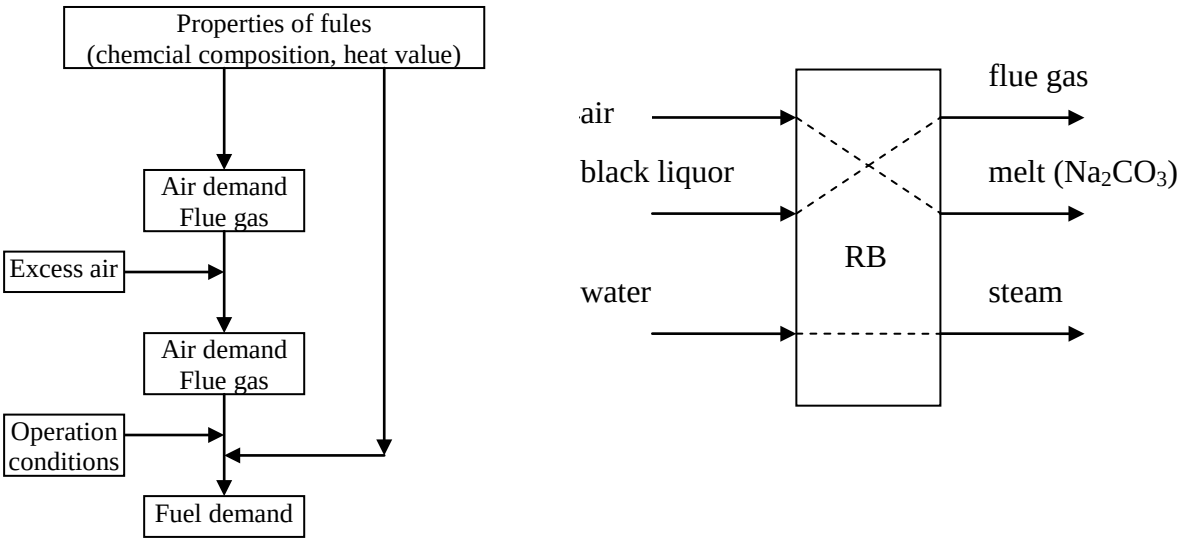

Fig. 2. Schematic representation of mass and energy balance for RB and BB.

$$f_{air,\min} = 22.7 \cdot \left(\frac{w_C}{12} + \frac{w_H}{2} + \frac{w_S}{32} - \frac{w_O}{32} \right) \quad (1)$$

$$f_{air} = f_{air,\min} \cdot (100 + c\%)/100 \qquad \text{m}^3\text{(n)/kg dry fuel} \quad (2)$$

$$f_{flue\ gas} = 22.7 \cdot \left(\frac{w_C}{12} + \frac{w_H}{2} + \frac{w_{H_2O}}{18} + \frac{w_S}{32} + \frac{w_N}{28} \right) + f_{air,\min} \cdot \left(\frac{0.791}{0.209} + c \right) \text{m}^3\text{(n)/kg dry fuel} \quad (3)$$

where f is the flow rate, w is the composition in mass fraction, and c is the excess air in percentage. The flow rate of the flue gas in Eq. (3) is based on the assumption that all the

elements of C, H, S, N will leave the boiler as the flue gas. However, in some case, some elements may leave the boiler more than one form. For example, in the recovery boiler, the elements of C and O leaves boiler as the flue gas and melt in the form of Na_2CO_3. In this case, the following equation was used:

$$f_{flue\ gas} = 22.7 \cdot \left(\frac{w_C}{12} + \frac{w_H}{2} + \frac{w_{H_2O}}{18} + \frac{w_S}{32} + \frac{w_N}{28} \right) + f_{air,\min} \cdot \left(\frac{0.791}{0.209} + c \right) - f_{CO,melt} \qquad (4)$$

where $f_{CO,melt}$ is the consumption part because the element of C and O leaves in the form of Na_2CO_3 (Na+C+O $\rightarrow$ Na_2CO_3). To calculate the flow rate of Na_2CO_3, the totally amount of Na is assumed to be the summation of those for Na and K. Based on the mass balance, we got Eq. (5) in which *TS*% is the dry content of black liquor, and we assumed the same flow rates for water and steam, i.e.: $f_{water} = f_{steam}$.

$$f_{Na2CO3} = 0.53 \frac{\left(w_{Na} + w_K \right)}{\left(1 + \frac{1 - TS\%/100}{TS\%/100} \right)} \qquad \text{(kg/kg wet fuel)} \qquad (5)$$

To represent the energy balance, the reference temperature was chose as 20 °C, and the enthalpy for the components except water and steam at a certain temperature was calculated with the Eq. (6) where *f* is the flow rate, C_p is the heat capacity, and *t* is the temperature in °C:

$$h = fC_p(t - 20) \qquad (6)$$

In ReMIND, the equation representing mass and energy balances should be linear, while the enthalpy of water or steam depends on both temperature and pressure. Therefore, the enthalpies of water/ steam at different temperatures and pressures were calculated firstly from the NIST online database[13] and then the calculated enthalpies were fitted to an equation that is a function of temperature and pressure by assuming the pressure effect is a linear. The fitted equation was input in the equation editor in ReMIND. For water, we obtained:

$$h = (4.2354t + 0.892) + (0.1008 - 2.51 \times 10^{-4} t)(P - 75) \qquad \text{(kJ/kg)} \qquad (7)$$

where *P* is the pressure in bar. For high pressure steam (60 bar), we obtained:

$$h = (2216.2 + 2.4309t) + (7.76 \times 10^{-3} t - 4.94)(P - 55) \qquad \text{(kJ/kg)} \qquad (8)$$

The total energy balance for the RB was:

$$h_{air} + h_{blackliquor} + f_{water} h_{water} + f_{blackliquor} \cdot h_{heatvalue} + h_{heatloss} = h_{fluegas} + h_{melt} + f_{water} h_{steam} \qquad (9)$$

For the BB, we neglected the energy in ash, and the flow rate of the flue gas was calculated with Eq. (3), and total energy balance was:

$$h_{air} + h_{fuel} + f_{water} h_{water} + f_{fuel} \cdot h_{heatvalue} + h_{heatloss} = h_{fluegas} + f_{water} h_{steam} \qquad (10)$$

The mass and energy balances for the turbine are much easier to generate compared to those for the boilers. The enthalpies of steams were obtained with the same method as those in the boilers, and results for medium pressure steam (30bar), low pressure steam at 10 bar, and low pressure steam at 4 bar were shown as Eqs. (11), (12), and (13), respectively.

$$h = (2313.5 + 2.3058t) + (1.395 \times 10^{-2} t - 7.15)(P - 28) \quad \text{(kJ/kg)} \quad (11)$$

$$h = (2400.1 + 2.1856t) + (2.910 \times 10^{-2} t - 11.00)(P - 9) \quad \text{(kJ/kg)} \quad (12)$$

$$h = (2443.9 + 2.1157t) + (8.06 \times 10^{-2} t - 20.5)(P - 3) \quad \text{(kJ/kg)} \quad (13)$$

The material and energy balances for the turbine were:

$$f_{60bar} = f_{30bar} + f_{10bar} + f_{4bar} \quad (14)$$

$$f_{60bar} h_{60bar} \eta = f_{30bar} h_{30bar} + f_{10bar} h_{10bar} + f_{4bar} h_{4bar} + EL + h_{loss} \quad (15)$$

where the flow rate of the 30 bar steam was obtained from the plant, and η is the mechanical efficiency, and h_{loss} is the heat loss, and EL is the electricity generation in MW.

3. Model validation and process integration

The developed model for the steam generation part was implemented into the complete plant model in our previous work[11]. By running the process integration model for the complete plant, the model results were compared with the operation measurements for the model validation. To run the process integration model, an objective function has to be set. In the present work, the objective function was the minimization of the energy cost for the studied pulp and paper mill, and the prices of fuels and electricity used were the same as those we set in our previous work[11].

3.1. Model validation

For the RB, by assuming the heat loss 3.5% and 5% excess air with a certain flow rate of black liquor, the process integration was carried out. The steam generation calculated from model is 220.9 ton/h which is 3.8% higher than the measurement from the mill. For the BB, by assuming the heat loss 3.5%, 5% excess air and 45% dry content of bark, the ratio of the steam generation to bark consumption (dry) calculated from the model is 5.15 ton steam/ ton dry bark, and the corresponding measurements from the mill is 6.07 (ton steam/ ton dry bark). The discrepancy for the BB may be from assumption of the dry content of bark. Generally, the dry content of the bark is from 40 to 50%, and the bark consumption increases with increasing water content of bark. For the turbine, by assuming the mechanical loss 5%, the model calculation agrees well with measurements.

3.2. Process integration

The running of the BB is to satisfy the process steam demand for the whole plant. The operation conditions in the RB will affect the energy consumption for the RB itself, and then affect the performance of the BB. While the operation conditions in the BB will only affect the performance of the BB.

For the RB, the temperature of the flue gas, the temperature of the liquid into the RB, the temperature of the water into the RB, the amount of the access air, the temperature of the air, the water content of the liquor, and the heat loss of the RB will affect the steam generation from the RB. Since the RB is insulated well, the heat loss may be in the range of 1 to 5%. Meanwhile, the amount of the excess air may be from 5% to 15%. The model calculation results show that the variations of these two operation conditions do not affect the performance of the RB a lot, and the discussions were not shown. In addition, the influence the water content of the liquor to the RB has been discussed in our previous work[11].

Fig. 3 illustrates the influence of the temperature of the flue gas on the performance of the RB and the BB. The utilization of the waste heat from the flue gas is very promising. If the temperature of the flue gas decreases from 250 to 125 °C by using heat exchanger to exchange the heat with flows to the RB, the steam generation will increase from 215 to 232 ton/h, and the corresponding bark consumption (wet basis) will decrease from 22.6 to 15.6 to/h. How to utilize the waste heat is a big challenge, and the following text will give the discussion.

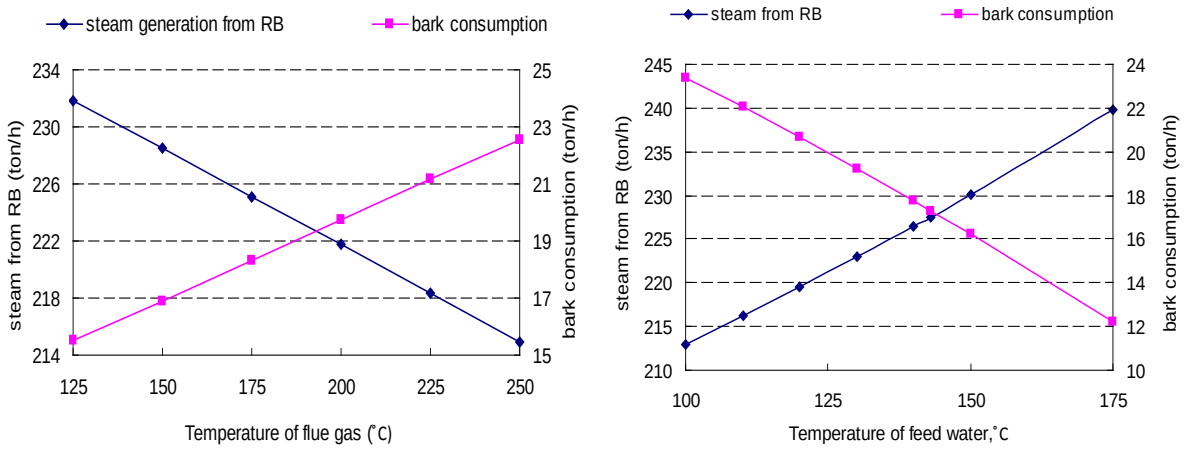

Fig.3. The effects of temperature of flue gas and feed water on the performance of the RB and the BB.

The influence of the temperature of the water on the performance of the RB is also shown in Fig. 3. If the temperature of water increases from 100 to 175 °C, the steam generation from the RB will increase from 213 to 240 ton/h, and the corresponding bark consumption will decrease from 23 to 12 ton/h. This is one possibility to utilize the waste heat in the flue gas. Sometimes, the waste heat from flue gas may not be enough to preheat water, which means that how to reasonably use the waste heat for the whole plant to preheat water is a vital issue to save the energy. On the other hand, the improvement of process performance by adding new heat exchangers and/or changing the existing routines always requires additional investment. It is worth or not? The model results can provide the possibility for the process improvement, and then make the cost estimation to help people to make a decision, which is just the goal of our work.

The temperature of the liquor to the RB will affect the performance of the RB and BB. When the liquor leaves from the evaporation plant, the temperature of the liquor is around 125 °C. From the energy point of view, if the temperature of the liquor can be further increased, the steam generation from the RB will be increased obviously as shown in Fig. 4. However, from the practice point of view, the temperature of the liquor should be lower than the boiling temperature of the liquor which is around 130 °C. Because of this reason, the insulation of the

pipe for the black liquor distribution from the evaporation plant to the RB is very important. For example, if the black liquor is cooled to 100 °C to enter the RB, the steam generation will decrease to 3.5 ton/h and the bark consumption will increase 1.5 ton/h compared to 130°C.

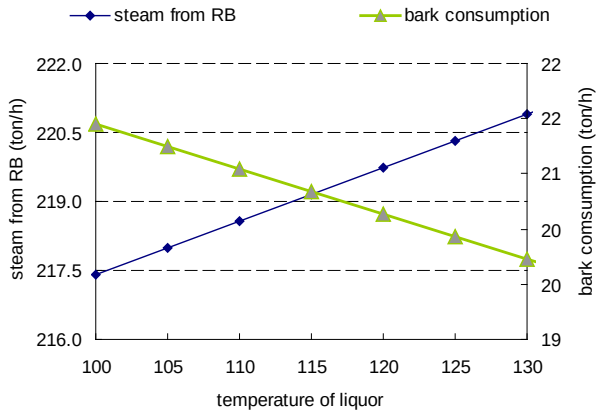

Fig.4. The effect of the temperature of the liquor on the performance of RB and BB.

For the BB, the influences of the temperature of the flue gas, the temperature of the water into the boiler, the amount of the excess air, the temperature of the air, and the heat loss of the boiler on the performance of the BB is the same as those for RB. The effects of the temperature and the water content of the bark are illustrated in Fig. 5, respectively. The increases of temperature of the bark will decrease the bark consumption. Although the energy saving is not so obviously, but it should be very easy to increase the temperature of the bark from 20 to 80 °C. On the contrary, the effect of water content on the bark consumption is considerable, and this explains the possible reason for the discrepancies of the model results from the measurement in model validation part.

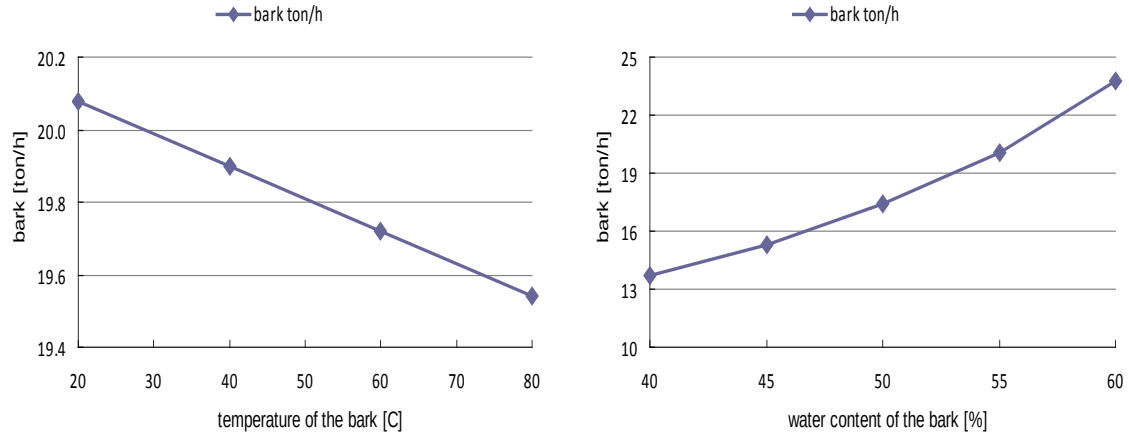

Fig.5. The effect of the temperature and water content of the bark on the performance of BB.

4. Conclusions

A mathematical process integration model for the steam generation part was developed. The material and energy balances were obtained theoretically. The model of the steam generation part was implemented into the previous developed whole plant model, and the model results of the steam generation part were validated with the operation data by running the process integration model with the low energy cost as the objective function. The effects of the operation conditions in the steam generation part on the whole plant performance were investigated. It shows that the utilization of the waste heat from the flue gas to increase the

temperature of the feed water into the boiler is an option to decrease the bark consumption, and the insulation of the pipes for the black liquor distribution from the evaporation plant to the RB is very important. For the BB, the water content of the bark affects the bark consumption considerably.

Acknowledgements

The authors gratefully acknowledge the Swedish Energy Agency, Billerud Karlsborg AB, and Bio4Energy for the funding and support of this work.

References

[1] P. Ruohonen, I. Hippinen, M. Tuomaala, P. Ahtila, Analysis of alternative secondary heat uses to improve energy efficiency-case: A Finnish mechanical pulp and paper mill. Resources Conservation and Recycling 54(5), 2010, pp. 326-335

[2] J. Persson, T. Berntsson, Influence of seasonal variations on energy-saving opportunities in a pulp mill. Energy 34(10), 2009, pp. 1705-1714

[3] A. Blanco, E. Dahlquist, J. Kappen, J. Manninen, C. Negro, R. Ritala, Use of modelling and simulation in the pulp and paper industry. Mathematical and Computer Modelling of Dynamical Systems 15(5), 2009, pp. 409-423

[4] S. Klugman, M. Karlsson, B. Moshfegh, A Swedish integrated pulp and paper mill-Energy optimisation and local heat cooperation. Energy Policy 37(7), 2009, pp. 2514-2524

[5] K. Nilsson, MIND — optimization method for industrial energy systems. Linköping: Linköping University: 1990; Vol. LiU-TEK-LIC-1990.

[6] http://www.ilog.com/products/cplex/.

[7] M. Larsson, C. Wang, J. Dahl, A. Wedholm, C. Samuelsson, M. Magnusson, H. O. Lampinen, F. W. Su, C. E. Grip, Improved energy and material efficiency using new tools for global optimisation of residue material flows. International Journal of Green Energy 3(2), 2006, pp. 127-137

[8] C. Wang, C. Ryman, J. Dahl, Potential CO2 emission reduction for BF-BOF steelmaking based on optimised use of ferrous burden materials. International Journal of Greenhouse Gas Control 3(1), 2009, pp. 29-38

[9] S. Nordgre, J. Dahl, C. Wang, B. Lindblom, In Process integration in an iron ore upgrading process system : analysis of mass and energy flows within a straight grate induration furnace, 18th International Congress of Chemical and Process Engineering Prague - Czech Republic, 24th - 28th August, Prague - Czech Republic, 2008.

[10] J. Sandberg, J. Dahl, In Adaptation and development of process integration tools for an existing iron ore pelletising production system, 18th International Congress of Chemical and Process Engineering Prague - Czech Republic, 24th - 28th August; Prague - Czech Republic, 2008.

[11] X. Ji, J. Lundgren, C. Wang, J. Dahl, C.-E. Grip, In Process Simulation and Energy Optimization for the Pulp and Paper Mill, PRES2010, Prague, Czech Republic, 28 August – 1 September; Prague, Czech Republic, 2010.

[12] SCPF, Energikompendium för massa- och pappersindustrin. 1985.

[13] http://webbook.nist.gov/chemistry/fluid.

A simplified energy management system towards increased energy efficiency in SMEs

Adnan Hrustic[1], Per Sommarin[1,*], Patrik Thollander[2], Mats Söderström[2]

[1] *Swerea SWECAST AB, Jönköping, Sweden*
[2] *Department of Management and Engineering, Linköping University, Linköping , Sweden*
** Corresponding author. Tel: +46 036301225, Fax: +46 036166866, E-mail: per.sommarin@swerea.se*

Abstract: Swedish companies have since 2003 been able to get certified by an energy management system (EEMS) and companies that have been certified, can now show savings in energy use. The downside of today's EEMs is that too few small and medium-sized enterprises (SMEs) have chosen to certify such a system in the organization. To increase awareness and interest among SMEs, a simplified version of the EEMS would be desirable. This article presents a simplified EEMs for SMEs developed from the original European standard (SS-EN 16 001). The article describes how the simple EEMS was developed and how the system was validated, i.e. how different companies responded to test-runs of the developed simplified EEMS. By testing the simplified EEMS in practice among various SMEs, different needs from the industry have been documented. The requests that were of greatest importance was how different incentives can be designed to increase the certification level, e.g. tax exemptions etc. The Swedish LTA for energy-intensive industries includes tax exemptions, as well as the certification of the European EEMS standard, and has shown to lead to large energy savings. An examples of a future energy policy could thus be a Long-Term Agreement (LTA)s program for SMEs including the simplified EEMS.

Keywords: *Energy management, SME, Industrial energy efficiency, PFE*

1. Introduction

Increased global warming is posing a major threat to global environment. The industry is a large emitter of carbon dioxide emissions, the major green house gas, and accounting for about 78 percent of the world's annual coal consumption, 41 percent of the world's electricity use, 35 percent of the world's natural gas consumption, and nine percent of global oil consumption [1]. Industrial energy efficiency is one of the most significant means of reducing the threat of increased global warming [2]. During the last decade, energy prices rose significantly for the Swedish industry. Between 2000 and 2006, electricity prices in Swedish industry almost doubled and oil prices rose by about 70 percent [3]. Even more price increases are to be expected, not least as a consequence of planned tax increases in the nation. The electricity price increase has partly been due to the liberalization of the European electricity markets. The liberalization caused the domestic markets to converge and Sweden has for a long time enjoyed one of the lowest electricity prices in Europe, see, e.g. [4]. Oil price increases may not create competitive disadvantages solely for Swedish industry. Electricity price increases on the contrary most likely will. This is particularly related to the Swedish industries and the fact that the historically low electricity prices have resulted in a higher use of electricity than for their European competitors in many Swedish industrial sectors, see [4] for a comparison in the European foundry industry.

Two main means exist of overcoming the threat of rising energy prices for the Swedish industry. One is to focus on managing the energy supply side with diversified portfolios etc. and, the other means is energy management focusing on a reducing energy end-use at the company. In regard to the latter, an EnErgy Management System (EEMS) may be a tool supporting companies in this important work. However, for most companies, not the least small- and medium-sized enterprises (SMEs), the certification of an EEMS is far too costly. The cost for an EEMS certification in Sweden is approximately 8 000 EUR. The need for

developing an EEMS for SMEs can thus not be understated. The aim of this study has been to develop an EEMS for SMEs. The conducted research has been inspired by the European standard for EEMS but is a stand-alone product with a graphical interface. The paper is outlined as follows. Initially, the background to the paper (introduction) is presented, followed by a presentation of energy efficiency in SMEs, and a presentation of the methodology. After that, the developed EEMS is presented, and finally, results and major conclusions are presented.

2. Energy efficiency in SMEs

Even though energy management is stated to be an important means for reducing industrial energy costs and reducing negative environmental impact [5-6], with some exceptions, e.g. [5-10], energy management in industry may be considered a scarcely researched subject. In regard to SMEs having limited resources to work with energy efficiency and energy management, a full-scale, in-house energy management program may not be justifiable [11]. For example, the cost of an energy management program, e.g. certification of an EEMS etc., may be in parity with the annual energy cost at an SME. A simplified EEMS for SMEs could thus be a means for increased energy management practices.

In Sweden, a few studies on barriers to energy efficiency among SMEs have been conducted [4,12-13]. Major barriers include: lack of time or other priorities/other priorities for capital investments, lack of access to capital/lack of budget funding, cost of production disruption/hassle/inconvenience, technical risk such as risk of production disruptions, difficulty/cost of obtaining information on the energy use of purchased equipment [9,22-23]. High-ranked barriers to energy efficiency among SMEs such as lack of time and other priorities, outlines the need for support, support which should not be too costly due to the barriers lack of access to capital, and moreover should involve information (difficulty/cost of obtaining information) [9,22-23]. A simplified EEMS developed for SMEs may overcome many of the barriers to energy efficiency and facilitate the adoption and governance of energy management in the sector.

3. Methodology

Swerea SWECAST conducts a research project named ENIG (Energy Efficiency In Group) together with Swerea IVF and FSEK (Association of Swedish Regional Energy Agencies). Project ENIG includes a number of research and development tasks to promote energy efficiency in Swedish industry [14].

A task in the project ENIG is "To develop a simplified EEMS for SMEs ", which means that a system promoting industry for energy efficiency will be developed based on the existing European standard for energy management systems, EN 16001. The new EEMS will serve as guidance for companies in their work with management systems. Most companies that have adopted energy management are outside the definition of SMEs. The reason for this is that many companies lack the resources to establish management systems, but also the lack of incentives that could increase the level of certification within the SMEs.

At a later stage, there are expectations that the simple EEMS in turn could help SMEs with the introduction of the real European standard, EN 16001, or the coming international standard ISO 50001 [15] .

SIS Publishing Co. owns the copyright to SS-EN 16 001 and because of legal reasons, an interconnection with the original standard had to be excluded. The application has been developed considering that it could be upgraded meaning that SMEs could get certified according to SS-EN 16 001. The management system is based on the PDCA-method (Plan-Do-Check-Act-method). Figure 1 shows an illustration on the PDCA-method and how it leads to continuous improvement.

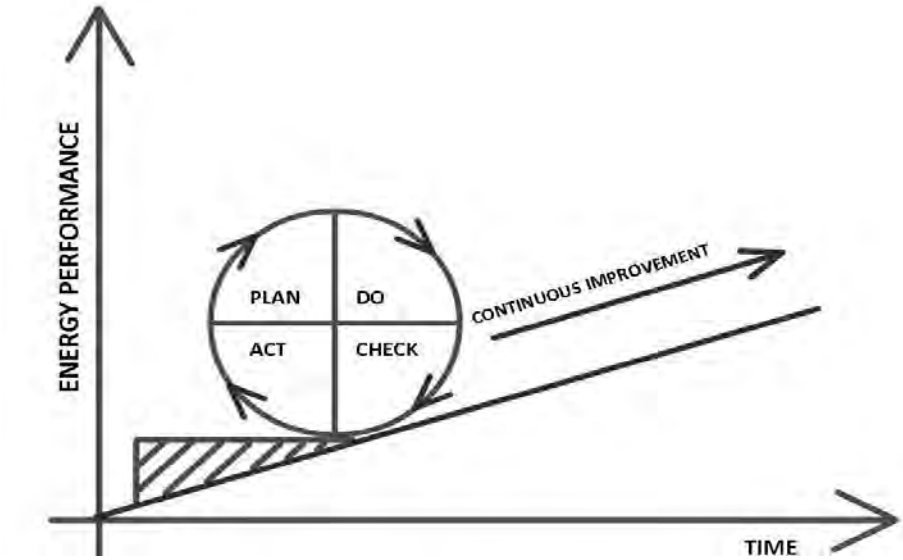

Figure 1: Continuous improvement with the PDCA-method. [16]

The simplified EEMS is built using lean production as a way of thinking when introducing energy use in EEMS [17] and its graphical interface is developed using Adobe Flash and Adobe Acrobat. It is developed as a presentation of the EEMS, and the SMEs should by working through the presentation; learn how to start working with EEMS. The simplified EEMS is more or less a self-learning system. To make the program more interesting and user-friendly, focus on how to build the interface resulted in the use of Adobe Acrobat. The EEMS program takes the user through the EEMS step by step by linking the slides with each other. The linking is made following the PDCA-method, see figure 2.

To improve the simplified EEMS even more, different companies in different sectors were visited and were asked to test-run the program. Interviews were held concerning how the SMEs would like to work with a management system and why they didn't certify in accordance with the original standard. During the test-run, the EEMS was demonstrated and a review on how it differed from the real standard was explained. The results were documented and from the testing results, changes were made in the EEMS. The testing of the simplified EEMS was divided into two phases, the first one with companies that have worked with EEMS for a while and have experience on how to organize their work with energy improvements. The second phase included SMEs, mainly without any experience with management systems. With results from the site visits and test runs, the EEMS could be developed even further and included a validation of the developed program, i.e. how compatible it was in practice for SMEs.

4. Results – simple EEMS program

SMEs can benefit from a simplified EEMS, because they usually have lack of resources and time to look for the best practices that are relevant to their sector [18]. Figure 2 shows how the system is built and how every part of the system is linked together.

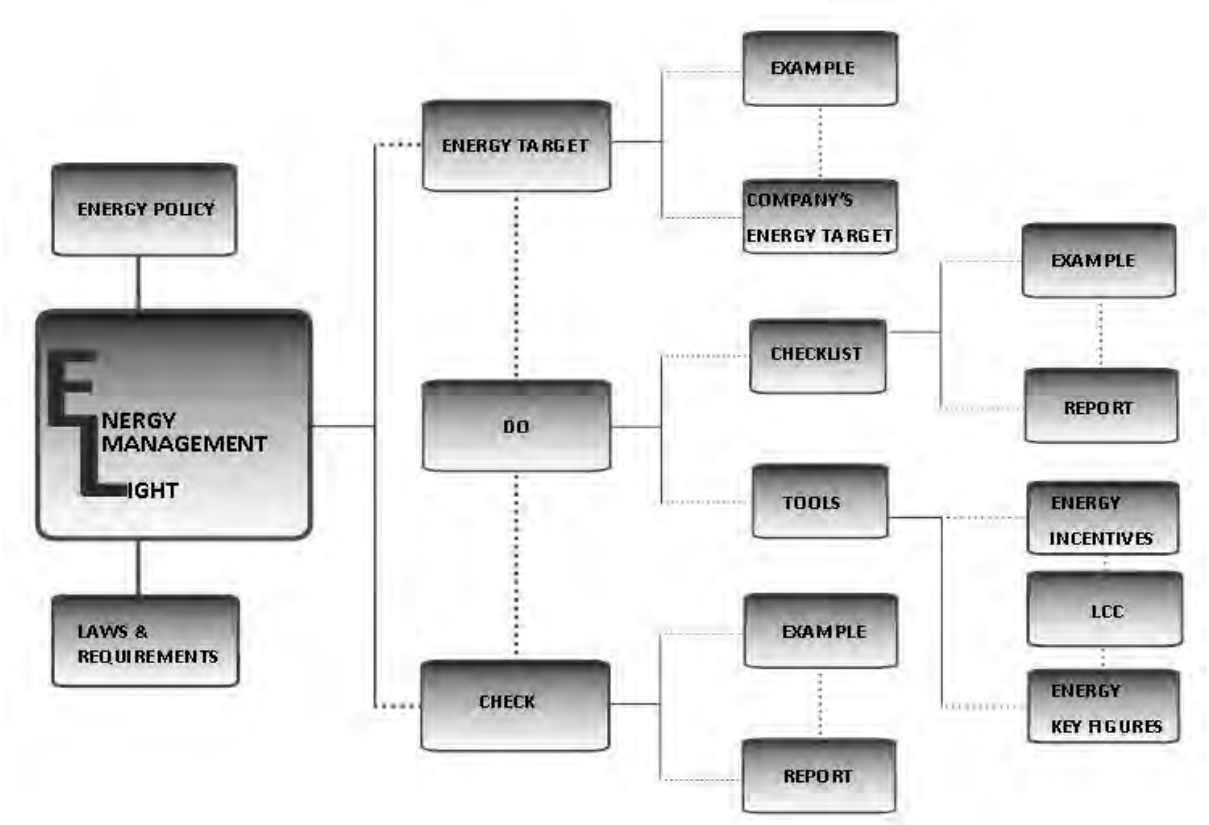

Figure 2: How the different parts from the simple EEMS are linked together.

To implement the simplified EEMS, companies should go through the management system in the following order:

1st. Energy Policy: The company should define an energy policy. Some requirements for an energy policy are that, it should be simple, easy and possible to communicate to everyone in the company. The Energy Policy will be the document that is published and it shows how the company plans to work with energy efficiency. It is important to write an easily understandable to understand policy and it is desirable that all the staff from the company agrees on what is expressed in the policy.

2nd. Laws and standards: Update the laws and requirements that could affect the company's work. Documenting a record of national, but also international laws and standards is a way to identify what rules the company should adjust its energy use for. The laws and requirements that concern the company will be documented and saved for future monitoring.

3rd. Implementation: The implementation part of the EEMS consists of two parts, checklist and energy tools. Introducing a checklist could be used as guidance for companies in their energy use, see figure 3. By introducing different energy tools in the company, they will have more alternatives to improve the work with energy efficiency. The energy tools that the company could use in their energy work are energy incentives, LCC and key energy figures etc.

4th. Follow up: In the follow-up, companies should review their results, through a review of the energy management practices conducted. The review should address the energy policy and work with energy efficiency at the company. In order to facilitate the revision an example

paper was developed to show which parts that are the most important to review. A proper follow up of the management system should find different discrepancies that exist in the energy targets. By eliminating the discrepancies, companies could improve their level of energy efficiency.

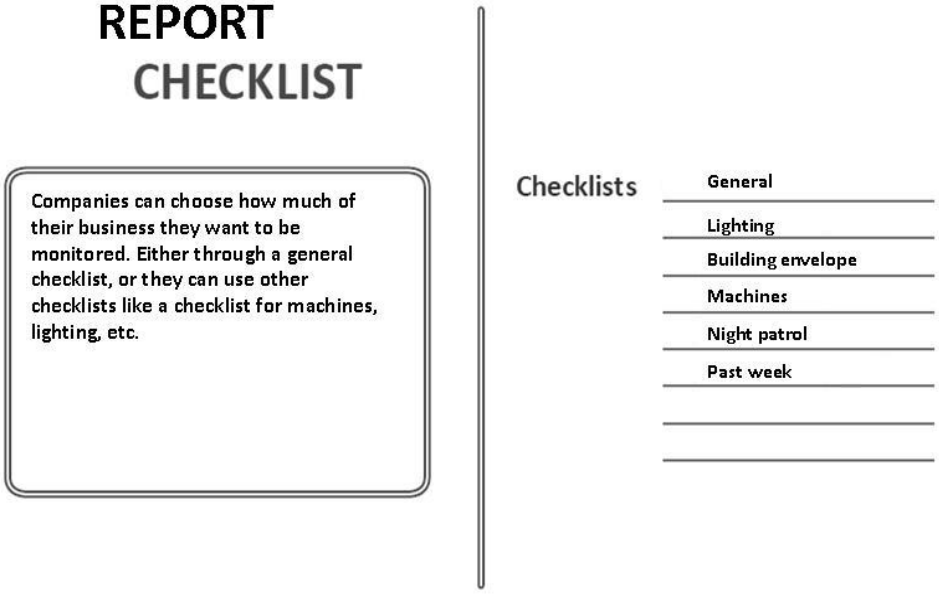

Figure 3: How EEMS presents the different checklists.

5th. Continuous improvement: The companies should always work with continuous improvement of the simple EEMS, see figure 4.

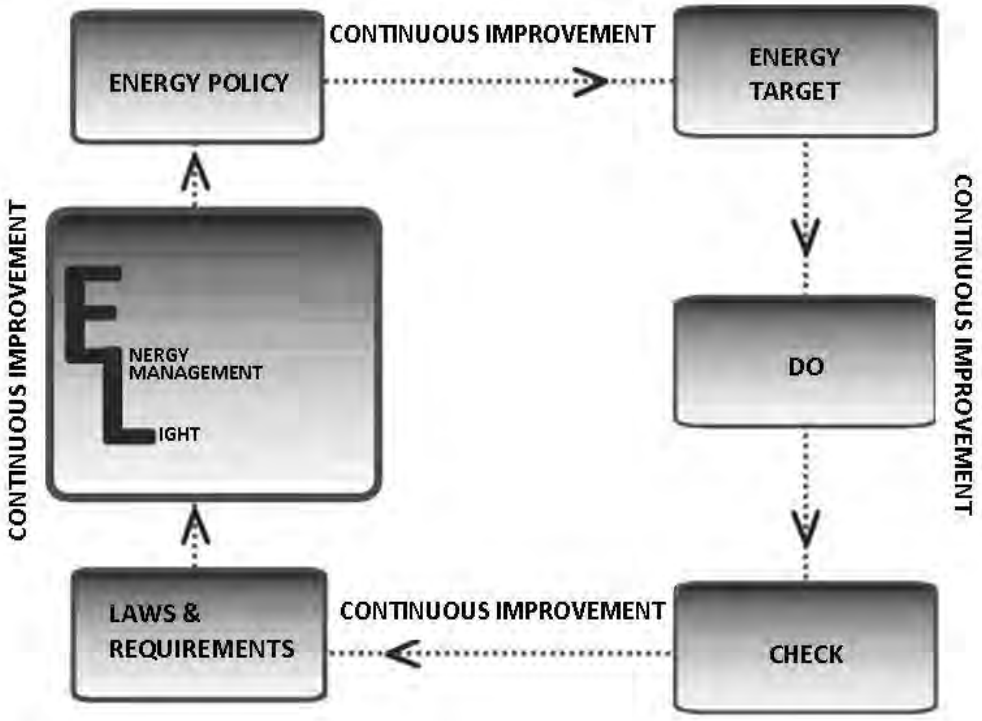

Figure 4: Continuous improvement of the simple EEMS.

If the company wants to do an effective work with their management system they have to dare to act and improve. In order to improve the simplified EEMS, anomalies in the system could be reduced and the the energy efficiency could be increased.

4.1. Validation of the developed EEMS program

Test runs of the simple EEMS have contributed to a continuous improvement of the program on how they would like to use an energy management system.

In early development of the simple EEMS, people with a greater insight on how to work with management functions were visited. The people who attended the first testing may be seen as either energy experts at the Swedish Energy Agency or staff from large industries with a well-known reputation from decades of successful energy management practices.

The improvements that were made during the test runs in the first phase were how the simplified EEMS could be more easily understood and user friendly. An idea from one of the industrial respondents was that if companies were trying to work according to the lean-production philosophy, they would automatically understand how EEMS is supposed to work. By implementing a presentation on how lean production and EEMS are linked together a more user friendly approach could thus be achieved.

During the meeting with respondents from the Swedish Energy Agency, ideas resulted in adapting checklists in the simplified EEMS, arguing that a checklist is an easy way to do an energy audit of the energy use in a SME. The meeting with another industry respondent helped to develop an EEMS towards a more user-friendly interface. The respondent working full time with certified environmental and energy management systems could contribute with thoughts and ideas about how the workflow should be improved.

After the site visits and meetings with respondents at the Swedish Energy Agency, the EEMS was now ready to go into phase two, which was testing the EEMS among SMEs. Four companies were visited during the test phase.

Feedback from the test runs in phase two was solely positive. The test-runs gave a useful view on how the SMEs would like to work with an EEMS. All of the four companies thought that the simplified EEMS was easier to use, smoother, based on common sense and required less resources to implement than the original SS-EN 16 001.

The Swedish LTA for energy-intensive industries includes tax exemptions, as well as the certification of the European EEMS standard (SS-EN 16 001), and has shown to lead to large energy savings (about 1.4 TWh electricity annually). A request from one of the company respondents test runs was to use the simplified EEMS in an LTA (Long-Term Agreements) specially tailored for SMEs in the future. The main reason why the company participating in the test-run did not participate in the current LTA was due to too high certification EEMS costs.

5. Conclusion

This work together with previous research by Thollander and Dotzauer (2010) [11], indicates that a simple and less costly version of an EEMS is desirable among SMEs. By developing an EEMS suited for smaller organizations, it could help companies to increase their level of knowledge on how to organize their business in regard to energy management, and thus enabling increasing levels of energy efficiency in the company. Increased understanding of

energy management could contribute to more companies seeing the potential for energy efficiency and energy management.

Even if companies do not consider that they need an EEMS, a shorter training or insight into the simplified EEMS would help companies to realize the importance of organizing their energy management work. By trying to reduce inventories, increase productivity, improve quality, they can become more competitive and (energy) efficient in their business. Moreover, by increasing awareness on how production is managed, this may contribute to a reduction of energy use.

One incentive could be an LTA with tax exemption if companies used the simplified EEMS, like the Swedish PFE for energy-intensive industries.
PFE was found to show large energy savings among the participating companies and the project showed that companies succeed in saving energy through certification of an EEMS. However, PFE for SMEs should have greater demands for education and training in management systems and a required implementation of an energy audit. By informing companies how to use an EEMS, they could implement routines on how to use the data they receive through an energy audit.

According to the company-visits, the simplified EEMS program proved easy to use, none of the visited SMEs who made test-runs of the program thought it was inconceivable. However, more test-runs are needed to further shape the program into a final form. The estimation is that about 20 test runs would be needed to get an insight into how well the simplified EEMS performs among SMEs. Another interesting test-run, which was not performed, is to let a few companies use the simple EEMS for a longer period. This test run could be a good feedback on how well a simple EEMS actually works for a longer period and if the companies can achieve savings in their energy use.

A final conclusion is that a simplified EEMS can help companies to start implementing the measures that are deduced from an energy audit. An obstacle for energy audits to become useful is that they may end up in a "desk drawer", i.e. the company has not been able to use the new information. The main reason is that companies lack tools for how to deal with all of the new data obtained from an energy audit. By using a simplified EEMS, companies have now a tool that creates routines that measure and document their use of energy and their work to increase energy efficiency. Thus, companies can, through the developed program, achieve a support to spot inefficiencies in their energy use and realize that they can increase profits by reducing their energy use.

References

[1] IEA (International Energy Agency), 2007. Key world energy statistics 2007, Paris. Retrieved January 8, 2008, from: http://195.200.115.136/textbase/nppdf/free /2007/key_stats_2007.pdf

[2] IPCC, 2007. Contribution of Working Group III to the Fourth Assessment Report of the Intergovernmental Panel on Climate Change. Summary for Policymakers. Retrieved October 8, 2007, from: http://www.ipcc.ch/SPM0405 07.pdf

[3] Johansson, B., Modig, G., Nilsson, L.J., 2007. Policy instruments and industrial responses - experiences from Sweden. In: Proceedings of the 2007 ECEEE summer study “Saving energy - just do it”, Panel 7, 1413-1421.EEPO (2003)

[4] Rohdin, P., Thollander, P., Solding, P., 2007. Barriers to and drivers for energy efficiency in the Swedish foundry industry. Energy Policy;35(1):672-77.

[5] Thollander, P., Ottosson, M., 2010. Energy Management practices in Swedish energy-intensive industries, Journal of Cleaner Production 18(12):1125-1133.

[6] Worrell, E., Bernstein, L., Roy, J., Price L., and Harnisch, J., 2009. Industrial energy efficiency and climate change mitigation. Energy Efficiency 2:109–123.

[7] Christoffersen, L.B., Larsen, A., Togeby, M., 2006. Empirical analysis of energy management in Danish industry. Journal of Cleaner Production;14(5):516-26.

[8] McKane, A., Williams, R., Perry, W., T, L., 2007. Setting the Standard for Industrial Energy Efficiency Retrieved, December 9, 2009, from: http://industrial-energy.lbl.gov/node/399

[9] Caffal, C., 1996. Energy management in industry. Centre for the Analysis and Dissemination of Demonstrated Energy Technologies (CADDET). Analysis Series 17. Sittard, The Netherlands.

[10] Bunse, K., Vodicka, M., Schönsleben, P., Brülhart, M., Ernst, F.O., 2011. Integrating energy efficiency performance in production management – gap analysis between industrial needs and scientific literature. Journal of Cleaner Production, In Press.

[11] Thollander, P., Dotzauer, E., 2010. An energy efficiency program for Swedish industrial small- and medium-sized enterprises. Journal of Cleaner Production 18(13):1339-1346.

[12] Thollander, P., Rohdin, P., Danestig, M., 2007. Energy policies for increased industrial energy efficiency: Evaluation of a local energy programme for manufacturing SMEs. Energy Policy;35(11):5774-83.

[13] Rohdin, P., Thollander, P., 2006. Barriers to and Driving Forces for Energy Efficiency in the Non-energy Intensive Manufacturing Industry in Sweden. Energy;31(12):1836-44.

[14] Swerea, SWECAST. Project ENIG. http://www.swerea.se/enig/. Taken 2011-02-30

[15] SIS Förlag, SS-EN 16001, Energy management systems – Requirements with guidance for use, European Committee for Standardization published 2009-07-01

[16] Arveson, P. Lacknerl, P & Holanek, N. Step by step guidance for implementation of energy management, Benchmarking and Energy Management Schemes in SMEs. Rapport, published 2007-01-01

[17] Johansson, P-E., 2011. Lean production. Dynamate, Sweden.

[18] Shipley, A.M., Elliot, R.E., 2001 Energy Efficiency Programs for Small and Medium Sized industry. In: Proceedings of the 2001 ACEEE summer study on energy efficiency in industry, vol. 1, 183-196.

Pinch Analysis of a Partly Integrated Pulp and Paper Mill

Elin Svensson[1], Simon Harvey[1,*]

[1] *Dept. of Energy and Environment, Chalmers University of Technology, Göteborg, Sweden*
** Corresponding author. Tel: +46 31 772 8531, Fax: +46 31 821 928, E-mail: simon.harvey@chalmers.se*

Abstract: The pulp and paper industry, with its wood biomass feedstock, has promising opportunities to become a key player in the biorefinery arena. A successful implementation of biorefinery pathways requires optimization of the energy system through process integration, and can lead to both increased and diversified revenues as well as a reduction of global CO_2 emissions. This paper presents the results from a pinch analysis of a partly integrated Kraft pulp and paper mill. The objective was to identify the potential for energy efficiency improvements, focusing on possibilities to save steam. Another objective was to identify practical retrofit solutions for the mill heat exchanger network and to estimate the costs for the required investments. The potential for energy savings at the mill is estimated at 18.5 MW, i.e. 12% of the current steam demand. Two alternative retrofit options are presented in the paper. A straightforward retrofit that is easy to implement enables 5.8 MW of steam to be saved at a cost of €0.13 million per MW of saved steam. A second more extensive retrofit option is also presented which could achieve steam savings of 11 MW at a cost of €0.14 million per MW of saved steam. Assuming that the steam savings lead to a reduced use of bark fuel in the power boiler, the pay-back period of both energy saving retrofit investments is estimated to be less than about 16 months.

Keywords: *Pinch analysis, Pulp and paper industry, Retrofit, Steam savings.*

1. Introduction

Extensive research aiming at improving energy efficiency and heat integration of pulp and paper plants has been conducted during the past decades. The pulping industry, with its wood biomass feedstock, has clear opportunities to become a key player in the biorefinery arena. Successful implementation of biorefinery concepts requires maximized heat integration, and can lead to increased and diversified revenues as well as reduced global CO_2 emissions.

There are many possible biomass conversion paths in biorefineries, including thermo-chemical, biochemical, mechanical and chemical processes. Thermo-chemical conversion usually involves gasification, pyrolysis or direct combustion, with significant excess heat flows at different temperature levels. Pinch analysis is an essential tool for investigating opportunities for heat integration both within the thermo-chemical biorefinery plant, and between the thermo-chemical biorefinery plant and other nearby industrial process plants with significant heat flows, such as a Kraft pulp mill.

Integration of biorefinery operations within a pulp and paper plant is a typical application of heat cascading, whereby heat for one plant is supplied by excess heat from another. Opportunities for biorefinery-related heat-cascading in the pulping industry have been widely discussed in the literature. A review report published in 2008 [1] discusses general issues for process-integrated biorefineries and also discusses the following specific examples:
Drying of biomass (e.g. forest residues, bark)
Pelletizing in connection with drying and forest residues leaching
Energy combine with ethanol production
Energy combines with other industries
A chemical market pulp mill with optimized energy consumption could achieve a surplus of energy which can be utilized to produce electricity, enable decreased firing of bark fuel in the mill's power boiler which can be dried and sold on the biomass fuel market, or enable

integration of appropriate biomass energy combine process concepts. An integrated chemical pulp and paper mill, on the other hand, needs to import energy, since the paper machine is a large consumer of heating steam. However, energy savings within an integrated mill also lead to economical savings and decreased environmental impact since they provide a way to reduce the fuel import demand. The mill studied here is a partly integrated pulp and paper mill which means that part of the produced pulp is sold as market pulp and the rest is used to produce paper. One objective of this study was therefore to contribute to the knowledge base about the energy situation in such a partly integrated pulp and paper mill. It is important to note that very few published studies in the literature address energy efficiency at partly integrated pulp and paper mills based on the Kraft process. Therefore, it is important to contribute to further development of the knowledge about the energy situation in this type of mill. The main objective of this work was to identify potential energy savings through pinch analysis at a partly integrated pulp and paper mill. The aim was also to suggest practical retrofit solutions for how to achieve a reduced energy demand, or alternatively, how to release excess heat at higher temperatures. The costs of the proposed measures were also estimated.

The results presented in this paper are based on the results of an MSc thesis project conducted by two students at Chalmers University of Technology in close co-operation with mill personnel at the Billerud Karlsborg mill. The thesis report by Eriksson and Hermansson, *Pinch analysis of Billerud Karlsborg, a partly integrated pulp and paper mill* [2] provides a detailed description of the work and results of the energy systems analysis.

The pinch study was part of a larger project conducted in co-operation between research groups at several Swedish universities[1], the Swerea MEFOS Research Institute and the pulp and paper mill Billerud Karlsborg. The aim of the project, hereafter called the Billerud project, was to establish a framework for process integration studies with a regional perspective in the pulp and paper industry. One of the objectives of the project was to improve co-operation between different institutions and actors who use and develop process integration tools such as pinch technology and reMIND (see for example reference [9]). The results of the pinch analysis presented in this paper are therefore planned to be used in connection with other models developed within the project. The opportunities for this model interaction are discussed in Section 5.2.

2. Methodology

This study was conducted using pinch technology, and it is assumed that the reader is familiar with the basic concepts. For a comprehensive description of the theory, the reader is referred to references [3] and [4]. The principal steps of the methodology are described below [5]:
Define the process stream system to be investigated with respect to opportunities for improved energy efficiency.

Extract stream data and establish energy saving targets using pinch analysis.
Analyze the existing heat exchanger network in order to identify pinch rule violations.
Make changes to the existing network so as to solve some of the pinch violations.
Evaluate the profitability of the proposed changes to the heat exchanger network.
Process data representing typical average winter operation was retained for the study. Most of the data required was available directly in the plant's process data-log, but some additional

[1] Energy Engineering at Luleå University of Technology, Business Administration and Social Sciences at Luleå University of Technology, Energy Systems at Linköping University, School of Natural Sciences, Linnæus University and Heat and Power Technology, Chalmers University of Technology.

measurements were needed. Manufacturer specifications, engineer estimations, and mass and energy balances were also used to complete the data set required. Stream-specific minimum temperature differences for heat exchanging and heat transfer coefficients were used in accordance with previous studies [5].

The costs of the proposed heat exchanger network retrofits were calculated based on area requirements, with surface area costs taken from recent pinch studies of similar mills [6]. The cost of piping was estimated at 50% of the installed heat exchanger cost based on typical cost estimation factors presented in [4], since the distances between streams were not investigated. Additional costs for e.g. instrumentation, control and pumping costs were also neglected.

3. Mill description

The studied mill is a partly integrated Kraft pulp and paper mill situated in northern Sweden, producing 300 000 tonnes/year of pulp and paper (40% pulp and 60% paper). Electricity is cogenerated in a back-pressure steam turbine unit. The mill was built over 80 years ago, but the main parts still in use were built in the early 1980's. Continuous energy improvements have been made during the lifetime of the plant. However, given the availability of new research results and the continuous changes of energy market conditions, it is of interest to re-investigate the potential for process integration and energy savings on a regular basis. Pinch analysis provides a good tool for this type of investigation and has now been used at the Billerud Karlsborg mill for the first time.

4. Results

4.1 *Theoretic potential for energy savings*

A large number of heat exchangers supplying heating or cooling to mill process streams were identified (27 cold and 35 hot streams). Adopting stream-specific values of $\frac{1}{2}\Delta T_{min}$ for different stream types, ranging from 0.5 K for utility steam to 8 K for air, the process pinch temperature is 148˚C. This means that the mill has a net deficit of heat above 148˚C and a net surplus below. The theoretical minimum external heating requirement is 135.4 MW.
The composite curves for the mill are shown in Fig. 1. The potential internal heat exchange is illustrated by the overlap of the hot and cold curves. In a theoretical case with maximum heat exchange between the curves, the hot streams should be able to provide all heat to the process except for the actual steam demand. Achieving this for a retrofit design would, however, require far too many new heat exchangers to be profitable.

In the grand composite curve (Fig. 2), the composite curves are merged. The horizontal line below the pinch represents the surface condensers, which provide about 41 MW of heat at 60˚C. This heat is currently used for warm water production from raw water. This heat could be released by making use of the hot streams in the heat pocket below the surface condensers' temperature. These streams are hot effluents from the evaporation and bleaching plant and outgoing air from the pulp dryer and the paper machine. There is also a heat pocket at around 70˚C which could enable heat integration for several streams in this region.

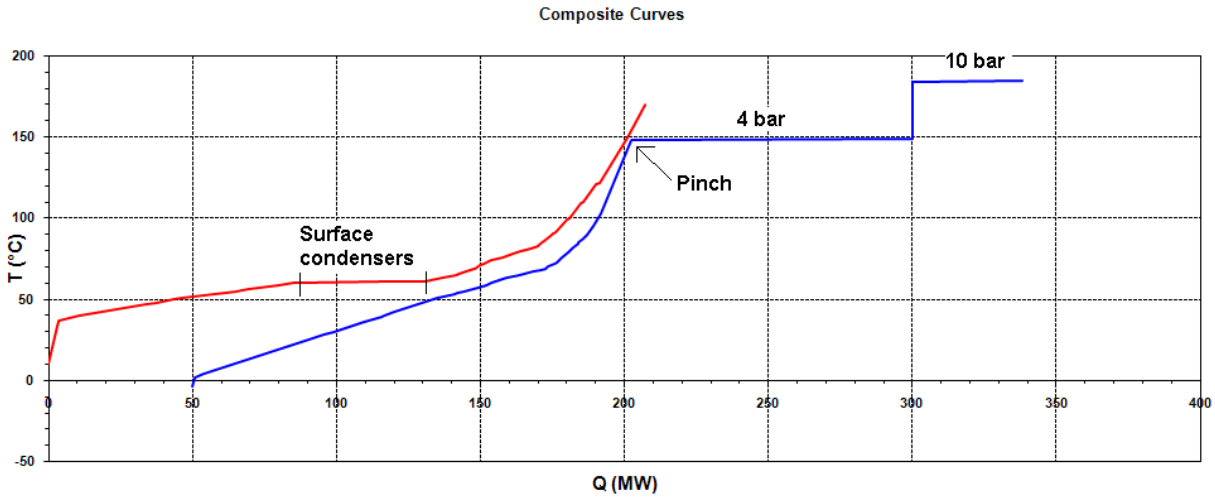

Fig. 1. Composite curves for the process.

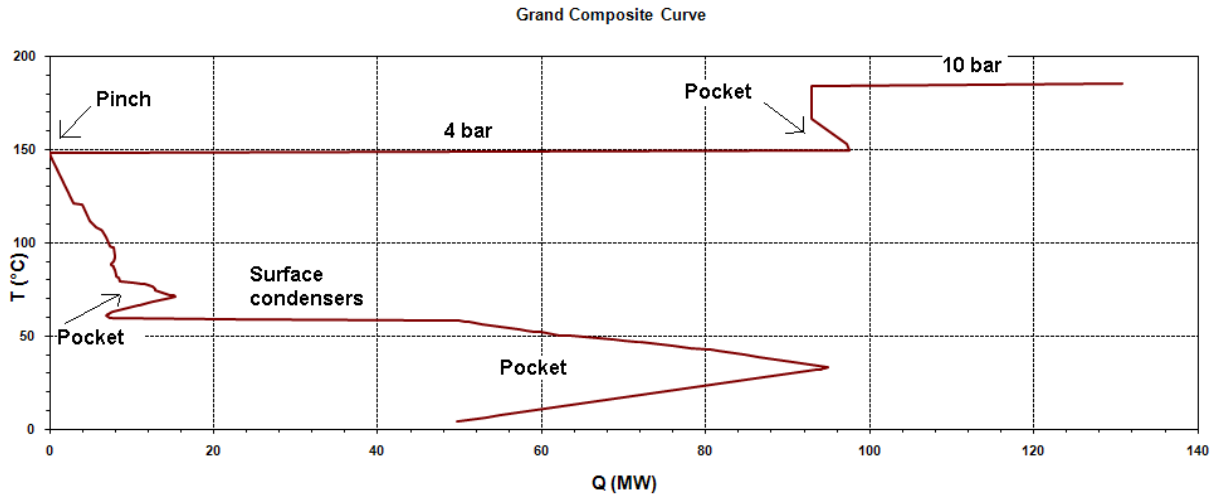

Fig. 2. Grand composite curve for the process.

4.2 *Pinch violations*

The difference between the actual steam demand and the minimum demand for hot utility is due to pinch violations i.e. non-optimal heat exchange. With a minimum hot utility of 135.4 MW and a current steam demand of 153.9 MW, the resulting pinch violations for the plant are 18.5 MW. This corresponds to a theoretical steam-saving potential of 12% of the current steam demand. All violations are due to heating below the pinch.

4.3 *Retrofit suggestions*

In this section, two retrofit options are presented: Retrofit I involves relatively straightforward changes whereas Retrofit II is more extensive. The focus of both retrofit options is on eliminating steam users below the pinch temperature. This could be achieved by improved heat recovery from high temperature water effluent streams in drains or by heat exchanging streams differently in the network. The major difference between the proposals is that in Retrofit I only changes that do not affect the hot and warm water system (HWWS) are considered, whereas in Retrofit II this process section is included.

4.3.1 *Retrofit I*

In Retrofit I, the main focus has been to save as much steam as possible without interfering with the HWWS. This retrofit could achieve steam savings of 5.8 MW of low-pressure (LP) steam, which corresponds to 4% of the present steam demand and 32% of the pinch violations. In Table 1, the cold streams are presented together with the hot stream that, according to the proposal, should replace the LP steam that is currently used. The resulting steam savings are also indicated. In this proposal, steam is replaced by condensate streams and hot effluents from the evaporation plant. Costs for new heat exchangers include costs for new heat exchanger area and piping. The total cost for the Retrofit I proposal is estimated at €759 000 and the resulting specific cost is €130 000 per MW.

Table 1. Steam savings resulting from retrofit measures in Retrofit I.

Cold stream	**New hot stream**	**Steam saved (MW)**
E2 filtrate	Condensate from stripper	1.0
E2 filtrate	Condensate from stripper	1.3
White water for pulp dryer and paper machine	B-condensate	2.1
White water for paper machine	Condensate cooling pulp dryer	1.5
Total		**5.8**

4.3.2 *Retrofit II*

The more extensive heat exchanger network retrofit results in larger energy savings than Retrofit I. In addition to the steam savings of Retrofit I, changes that affect the HWWS are also included in Retrofit II. The replaced steam users are shown in Table 2. In total it is possible to save approx. twice as much steam as in Retrofit I, i.e. about 11 MW of LP steam. This corresponds to 7% of the present steam demand and 60% of the pinch violations. The total cost of the Retrofit II proposal is estimated at €1 580 000, or €143 000 per MW.

Table 2. Steam savings resulting from retrofit measures in Retrofit II.

Cold stream	**New hot stream**	**Steam saved (MW)**
E1 filtrate	Liquor cooling	1.6
E2 filtrate	Condensate from stripper	1.0
E2 filtrate	Condensate from stripper	1.3
D0 filtrate	Hot water	2.6
White water for pulp dryer and paper machine	B-condensate	2.1
Local heating	Digester liquor	1.0
White water for paper machine	Condensate cooling pulp dryer	1.5
Total		**11.0**

In addition to the changes made in Retrofit I, it is necessary to modify or build seven additional heat exchangers. When replacing a heat exchanger in the HWWS it is important that the new network still can achieve the same temperatures in the hot and warm water tanks.

4.4 *Other findings from the pinch study*

4.4.1 *The paper machine*

There is a lack of information regarding how the heat recovery in the paper machine is currently implemented. A thorough investigation of the heat recovery system would most

probably identify further opportunities for improvement. Using a system similar to the one used in the pulp dryer, with a fluid transferring heat from the outgoing air to the incoming air, could improve efficiency and provide operational flexibility with respect to outdoor temperature. At present, there are large amounts of energy released to the surrounding with the outgoing air effluent stream due to its high humidity content.

4.4.2 *Bleaching plant*

The bleaching plant is the largest user of hot water in the mill. A comparison with other mills indicates that there is a potential for energy savings at the studied mill and that there are reasons to investigate the bleaching plant more thoroughly. Using presses instead of filters when washing the pulp and keeping the temperature at a more even level between the bleaching steps are two ways of lowering the demand for steam and hot water and thus improving the energy efficiency.

4.4.3 *Hot and Warm Water System (HWWS)*

It would be possible to reach a higher temperature in the hot water tank with some changes in the heat exchanger network. This would lead to lowered steam demand in the subsequent hot water users. This option was not included in the study, since traditional pinch analysis is not the best approach to such tank temperature optimization. It would, however, be interesting to further analyze this opportunity.

4.5 *Economic evaluation*

There are several ways for the mill to benefit from potential energy savings. The most obvious and straightforward is to simply reduce the amounts of oil and bark fired in the power boiler. Due to large seasonal variations it is, however, not possible to reduce the boiler load during all parts of the year, since during summer, it already runs at minimum load. Other options include investing in a condensing turbine, delivering district heating or integrating a biorefinery process.

To make an initial assessment of the profitability of the proposed energy-efficiency measures, a simple calculation was performed for the option of bark savings. Assuming bark savings can be achieved during two thirds of the year, the economic savings will be €107 000 per MW and year and hence the payback period will be less than 16 months for both proposals. Considering that the fuel reduction is likely to be oil rather than bark during parts of the year, the payback period could well be even lower.

5. Discussion

5.1 *Seasonal variations*

The study was carried out for winter operating data. The summer steam demand is lower because of increased ambient temperatures. Therefore this study is not representative for the whole year.

No detailed investigation of possible economic benefits through, for example, reduced burning of bark or district heating delivery were made. To analyze these options, more information regarding yearly variations in bark boiler firing, steam system and demand of heating and cooling in general are required. The effect of these seasonal variations on the steam-saving potential could, however, be estimated using the results of previous studies [6]. The effect on the overall energy balance of the mill could, for example, be studied using the

reMIND tool, thereby connecting the results from this pinch analysis to other studies within the Billerud project.

5.2 *Pinch-reMIND interaction*

It is possible to use the results of the pinch analysis presented in this paper in an energy system model developed using the reMIND simulation and optimization tool (see e.g. [7]). This model interaction is based on what has previously been shown to be a good way to use the results from pinch analysis in optimization studies using reMIND, see for example [8] and [9]. For a more general discussion of the role of optimization for efficient implementation of process integration measures in industry, see [10].

In reMIND, optimization is carried out by using mixed integer linear programming in order to minimize the system cost. The system cost includes amongst others, the investment costs of different measures that can be taken to change the system. The structure of the energy system is represented as a network of nodes and branches where branches represent energy or material flows. One node may represent, for example, a process line or a single equipment unit. It may also represent a possible steam-saving investment which will be the case when representing the results from the pinch analysis. Multi-period optimization can be modelled in reMIND which makes it possible to consider seasonal variations in the overall energy system studied.

The two retrofit alternatives identified in the pinch analysis could, for example, be modelled as two different investment options in the reMIND model, each resulting in a certain steam saving2 which can be achieved for a specified investment cost.

6. Conclusions

The theoretical potential for energy savings at the studied mill was estimated at 18.5 MW, corresponding to 12% of the current steam demand. Two retrofit proposals to accomplish parts of this theoretical potential were suggested. Assuming that the steam savings lead to a reduced use of bark in the power boiler, the pay-back period of the energy savings investment is estimated to be less than about 16 months.

Acknowledgements

The excellent work of Lina Eriksson and Simon Hermansson who conducted the pinch study during their MSc thesis work is gratefully acknowledged. We would also like to thank Monika Resin, process engineer at Billerud Karlsborg, who co-supervised their work and of course also the rest of the staff at the mill who contributed to the study. Professor Thore Berntsson (examiner of the MSc thesis and supervisor to the first author of this paper) is also acknowledged for his contributions to this work.
This research project was led by the Energy Engineering group at Luleå University of Technology with funding provided by the Swedish Energy Agency, Billerud Karlsborg AB and Billerud Skog.

References

[1] T. Berntsson. Swedish Pulp Mill Biorefineries - A vision of future possibilities. Swedish Energy Agency, report nr ER 2008:26, ISSN 1403-1892, 2008.

[2] The steam saving measure could, for example, be modelled as a fictitious steam production unit, i.e. as one option to partly cover the steam demand at the mill.

[2] L. Eriksson, S. Hermansson. Pinch analysis of Billerud Karlsborg, a partly integrated pulp and paper mill. Master's thesis, Heat and Power Technology, Energy and Environment, Chalmers University of Technology, Göteborg, 2010.

[3] I.C. Kemp. Pinch Analysis and Process Integration: A User Guide on Process Integration for the Efficient Use of Energy, Butterworth-Heinemann, Oxford, UK, 2007.

[4] R. Smith. Chemical Process Design, McGraw-Hill, Inc, New York, 1995.

[5] E. Axelsson, M. Olsson, T. Berntsson. Heat integration opportunities in average Scandinavian kraft pulp mills: Pinch analyses of model mills. Nordic Pulp and Paper Research Journal. 21 (2006) 466–475.

[6] J. Persson, T. Berntsson. Influence of seasonal variations on energy-saving opportunities in a pulp mill. Energy. 34 (2009) 1705–1714.

[7] M. Karlsson, P. Sandberg. The MIND method: a decision support system based on MILP. Paper 8 in Sandberg, P., 2004. Optimisation and Co-operative Perspectives on Industrial Energy Systems. PhD Thesis, Division of Energy Systems, Department of Mechanical Engineering, Linköping University, Sweden. 2004.

[8] I.-L. Svensson, J. Jönsson, T. Berntsson, B. Moshfegh. Excess heat from kraft pulp mills: Trade-offs between internal and external use in the case of Sweden – Part 1: Methodology. Energy Policy. 36 (2008) 4178–4185.

[9] C. Bengtsson, M. Karlsson, T. Berntsson, M. Söderström. Co-ordination of pinch technology and the MIND method--applied to a Swedish board mill. Applied Thermal Engineering. 22 (2002) 133–144.

[10] J. Klemes, F. Friedler, I. Bulatov, P. Varbanov. Sustainability in the process industry – Integration and optimization. McGraw-Hill, New York, 2010.

Power Yield Processes: Modeling, Simulation and Optimization

P. Kuran[1,*], and S. Sieniutycz[1]

[1] *Warsaw University of Technology, Warszawa, Poland*
** Corresponding author. Tel: +48 22 8256340, Fax: +48 22 8251440, E-mail: kuran@ichip.pw.edu.pl*

Abstract: Classical thermodynamics is capable of determining limits on energy production or consumption in terms of the exergy change. However, they are often too distant from reality. Yet, by introducing rate dependent factors, irreversible thermodynamics offers enhanced limits that are closer to reality. Thermodynamic analyses lead to important formulas for imperfect efficiencies. In this paper power limits for generation or consumption of thermal, solar, chemical energy are obtained by application of the optimal control theory.

Power limits define maximum power released from energy generators and minimum work supplied to separators or heat pumps. In this research we consider power limits for both devices of energy generator type (engines and fuel cells) and of energy consumer type (heat pumps, separators and electrolysers). Each process is driven either by a simple heat exchange or by the simultaneous exchange of energy and mass fluxes. We stress the link of these problems with the classical problem of maximum work. Particular attention is devoted to fuel cells as electrochemical flow engines. Amongst a number of new results, notion of certain special controls (Carnot variables) plays an important role. In particular, we demonstrate their role in the analysis of heat and radiation engines, chemical power generators and fuel cells.

Keywords: *efficiency, power generation, entropy, thermal machines, fuel cells.*

Nomenclature

A_v *generalized exergy per unit volume*.....Jm^{-3}
a_0 *constant related to the Stefan-Boltzmann constant*.....$Jm^{-3}K^{-4}$
a_v *total area of energy exchange per unit volume*..... m^{-1}
$\dot{G}$ *resource flux*.....gs^{-1}, $mols^{-1}$
g *conductance*.....$Js^{-1}K^{-a}$
h *numerical value of Hamiltonian*.....$Jm^{-3}K^{-1}$
n *flux of fuel reagents*.....gs^{-1}, $mols^{-1}$
q *heat flux between a stream and pow er generator*.....Js^{-1}
Q *total heat flux involving transferred entropies*.....Js^{-1}
S_σ *entropy produced*.....JK^{-1}
s_v *volumetric entropy*.....$J\,K^{-1}m^{-3}$
T *variable temperature of resource*.....K
$T_{1,2}$ *bulk temperatures of reservoirs1 and 2* ...K
$T_{1',2'}$ *temperatures of circulating fluid*.....K
T' *Carnot temperature control*.....K
t *physical time*.....s
W *work produced, positive in engine mode*...J
w *specific work at flow or power per unit flux of a resource*.....J/mol
α *heat coefficients*..... $Jm^{-2}s^{-1}K^{-1}$
ε *total energy flux*.....Js^{-1}
μ *chemical potential*.....$Jmol^{-1}$
μ' *Carnot chemical potential*.....$Jmol^{-1}$
Φ *factor of internal irreversibility*..... -
σ *Stefan-Boltzmann constant*..... $Jm^{-2}\,s^{-1}K^{-4}$
σ_s *entropy production of the system*..... $JK^{-1}s^{-1}$
ζ *chemical efficiency*..... -

1. Introduction

In a previous work (Sieniutycz 2003 [1]) we discussed basic rules for modeling power production and energy limits in purely thermal systems with finite rates. In particular, radiation engines were analyzed. In the present work we treat generalized systems in which temperatures T and chemical potentials μ^k are essential. This is associated with engines propelled by fluxes of both energy and substance. When one, say, upper, reservoir is finite, its thermal potential decreases along the stream path, which is the consequence of the energy balance. Any finite reservoir is thus a resource reservoir. It is the resource property or the finiteness of amount or flow of a valuable substance or energy which changes the upper fluid properties along its path. Then, in the engine mode of the system, one observes fluid's

relaxation to the equilibrium with an infinite lower reservoir, usually the environment. This is a cumulative effect obtained for a resource fluid at flow, a set of sequentially arranged engines, and an infinite bath Downgrading or upgrading of resources may occur also in electrochemical systems of fuel cell type. Fuel cells working in the power production mode are electrochemical flow engines propelled by chemical reactions.

In a process of power production shown in Fig. 1 two media differing in values of T and μ interact through an energy generator (engine), and the process is propelled by diffusive and/or convective fluxes of heat and mass transferred through 'conductance' or boundary layers. The energy flux (power) is created in the generator between the resource fluid ('upper' fluid 1) and, say, an environment fluid ('lower' fluid, 2). In principle, both transfer mechanisms and values of conductance of boundary layers influence the rate of power production (Curzon and Ahlborn 1975[2]; De Vos 1994 [3], Sieniutycz and Kuran 2005 [4], 2006 [5]).

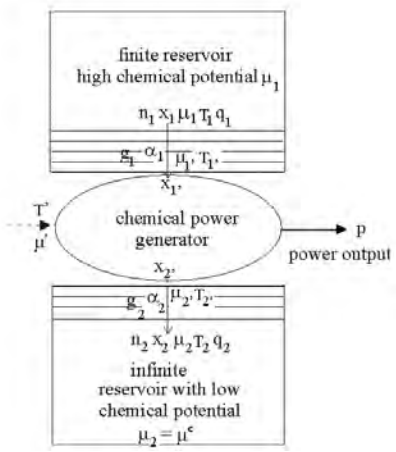

Fig. 1. A scheme of chemical and/or thermal engine.

2. Carnot Control Variables in Power Systems

Diverse controls can be applied in power systems to represent the propelling fluxes of heat and mass transfer. Here we shall recall and then use definitions of Carnot control variables (Carnot temperature and chemical potential) whose derivations and applications were originated in our previous work (Sieniutycz 2003 [8]). We begin with the simplest case of no mass transfer, i.e. we shall consider a steady, internally reversible ('endoreversible') heat engine with a perfect internal power generator characterized by temperatures of circulating fluid $T_{1'}$ and $T_{2'}$, Fig.1. The stream temperatures, attributed to the bulk o each fluid are T_1 and T_2. The inequalities $T_1 > T_{1'} > T_{2'} > T_2$ are valid for the engine mode of the system. With an effective temperature called Carnot temperature

$$T' \equiv T_2 \frac{T_{1'}}{T_{2'}} \tag{1}$$

entropy production of the endoreversible process, takes the following simple form

$$\sigma_s = q_1 \left(\frac{1}{T'} - \frac{1}{T_1} \right) \tag{2}$$

This form is identical with the familiar expression obtained for processes of purely dissipative heat exchange between two bodies with temperatures T_1 and T'. In terms of temperature T' of Eq. (1) thermal efficiency assumes the classical Carnot form containing the temperature in the bulk of the second reservoir and temperature T':

$$\eta = 1 - \frac{T_2}{T'} \tag{3}$$

This property substantiates the name "Carnot temperature" for control variable T'. In terms of T' description of thermal endoreversible cycles is broken down to formally "classical" equations which contain T' in place of T_1. In irreversible situations Carnot temperature T' efficiently represents temperature of the upper reservoir, T_1. Yet, at the reversible Carnot point, where $T_{1'} = T_1$ and $T_{2'} = T_2$, Eq. (1) yields $T' = T_1$, thus returning to the classical reversible theory. These properties of Carnot temperature render descriptions of endoreversible and reversible cycles similar. They also make the variable T' a suitable control in both static and dynamic cases (Sieniutycz 2003 [8]).The notion of Carnot temperature can be extended to chemical systems, where also the Carnot chemical potential emerges (Sieniutycz 2003 [8]), where instead of pure heat flux q the so called total heat flux (mass transfer involving heat flux) Q is introduced. The heat flux equals the difference between total energy flux ε and flux of enthalpies of transferred components, $q = \varepsilon - h$, satisfying an equation

$$Q \equiv \varepsilon - \mu_1 n_1 ... \mu_k n_k ... - \mu_m n_m . \equiv \varepsilon - G \tag{4}$$

where G is the flux of Gibbs thermodynamic function (Gibbs flux). The equality $\varepsilon = Q + G$ is fundamental in the theory of chemical engines; it indicates that power can be generated by two propelling fluxes: heat flux Q and Gibbs flux G, each generation having its own efficiency. The related driving forces are the temperature difference and chemical affinity. Assuming a complete conversion we restrict to power yield by a simple reaction $A_1 + A_2 = 0$ (isomerisation or phase change of A_1 into A_2). We have a chemical control variable

$$\mu' = \mu_2 + \mu_{1'} - \mu_{2'} \tag{5}$$

which has been used earlier to study an isothermal engine (Sieniutycz 2008 [9]). After introducing the Carnot temperature in accordance with Eq. (1), total entropy production of the endoreversible power generation by the simple reaction $A_1 + A_2 = 0$ takes the following form

$$\sigma_s = Q_1 \left(\frac{1}{T'} - \frac{1}{T_1} \right) + n_1 \frac{\mu_1 - \mu'}{T'} \tag{6}$$

where $Q_1 = q_1 + T_1 s_1 n_1$ is the total heat flux propelling the power generation in the system. The resulting equation is formally equivalent with a formula obtained for the purely dissipative exchange of energy and matter between two bodies with temperatures T_1 and T' and chemical potentials μ_1 and μ'.

3. Energy Systems with Internal Imperfections

Carnot variables T' and μ' are two free, independent control variables applied in power maximization of steady and dynamical generators. Ideas referring to endoreversible systems may be generalized to those with internal dissipation. In such cases a single irreversible unit can be characterized by two loops shown in Fig. 2 which presents the temperature–entropy

diagram of an arbitrary irreversible stage. Each stage can work either in the heat-pump mode (larger, external loop in Fig. 2) or in the engine mode (smaller, internal loop in Fig. 2).

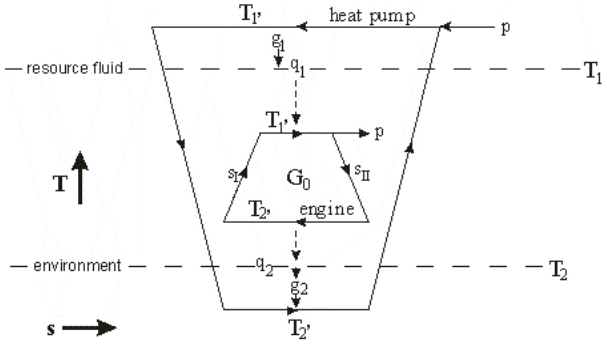

Fig. 2. Two basic modes with internal and external dissipation: power yield in an engine and power consumption in a heat pump. Primed temperatures characterize the circulating fluid.

The related analysis follows the earlier analyses of the problem which take into account internal irreversibility by applying the factor of internal irreversibility, Φ. By definition, $\Phi = \Delta S_{2'}/\Delta S_{1'}$ (where $\Delta S_{1'}$ and $\Delta S_{2'}$ are respectively the entropy changes of the circulating fluid along the two isotherms $T_{1'}$ and $T_{2'}$ in Fig. 2) equals the ratio of the entropy fluxes across the thermal machine, $\Phi = J_{s2'}/ J_{s1'}$. Due to the second law inequality at the steady state the following inequalities are valid: $J_{s2'}/J_{s1} > 1$ for engines and $J_{s2'}/J_{s1} < 1$ for heat pumps; thus the considered ratio Φ measures the internal irreversibility. In fact, Φ is a synthetic measure of the machine's imperfection. Φ satisfies inequality $\Phi > 1$ for engine mode and $\Phi < 1$ for heat pump mode of the system. A typical goal is to derive efficiency, entropy production and power limits in terms of Φ.

3.1. Power yield and entropy production in systems with internal imperfections

The thermal efficiency component of any endoreversible thermal or chemical engine can always by written in the form $\eta = 1 - Q_2/Q_1$. After defining the coefficient $\Phi = 1 + T_{1'}\sigma_S^{int}/Q_1$ called the internal irreversibility factor the internal entropy balance takes the form usually applied for thermal machines

$$\Phi \frac{Q_1}{T_{1'}} = \frac{Q_2}{T_{2'}} \qquad (7)$$

One can evaluate Φ from averaged value of the internal entropy production that describes the effect of irreversible processes within the thermal machine. Clearly, in many cases Φ is a complicated function of the machine's operating variables. In those complex cases one applies the data of $\sigma_s^{int} = dS_\sigma^{int}/dt$ to calculate averaged values of the coefficient Φ. In our analysis the quantity Φ is treated as the process constant. This corresponds with the observation that it is an average value of Φ, evaluated within the boundaries of operative parameters of interest which is used in most of analyses of thermal machines. In terms of the Carnot temperature T' and factor Φ the efficiency η , Eq. (7), assumes the simple, pseudo-Carnot form which is quite useful and general enough to describe thermal, radiative and chemical engines:

$$\eta = 1 - \Phi \frac{T_2}{T'} \qquad (8)$$

A particularly interesting role of the above formulas is observed for radiation engines which are energy systems driven by black radiation. In these systems Gibbs flux $G = 0$, whereas total heat flux Q is identical with the energy flux ε, i.e. $Q = \varepsilon$. The majority of research papers on power limits published to date deals with systems in which there are two infinite reservoirs. To this case refer steady-state analyses of the Chambadal-Novikov-Curzon-Ahlborn engine (CNCA engine) in which energy exchange is described by Newtonian law of cooling, Curzon and Ahlborn 1975 [2], or of the Stefan-Boltzmann engine, a system with the radiation fluids and energy exchange governed by the Stefan-Boltzmann law (De Vos 1994 [3]). In a CNCA engine the maximum power point may be related to the optimum value of a free (unconstrained) control variable which may be efficiency η, heat flux q_1, or Carnot temperature T'. When internal irreversibility within the power generator play a role, the pseudo-Carnot formula (8) applies in place of Eq. (3), where Φ is the internal irreversibility factor (Sieniutycz and Kuran 2006 [5]). In terms of bulk temperatures T_1, T_2 and Φ one finds at the maximum power point

$$T'_{opt} = \left(T_1 \Phi T_2\right)^{1/2} \qquad (9)$$

For the Stefan-Boltzmann engine exact expression for the optimal point cannot be determined analytically, yet, this temperature can be found graphically from the chart $p = f(T')$. A pseudo-Newtonian model, Sieniutycz and Kuran 2006 [5], Kuran 2006 [6], which treats the state dependent energy exchange with coefficient $\alpha(T^3)$, omits to a considerable extent analytical difficulties associated with the use of the Stefan-Boltzmann equation.

4. Dynamical Energy Yield

4.1. General Issues

When resources are finite and/or the propelling fluid flows at a finite rate, the Carnot and resource temperatures decrease along the process path. The previous (steady) analysis is replaced by a dynamic one, and the mathematical formalism is transferred from the realm of functions to the realm of functionals. Here the optimization task is to find an optimal profile of the Carnot temperature T' along the resource fluid path that assures an extremum of the work consumed or delivered and – simultaneously – the minimum of the integral entropy production. Dynamical energy yield requires the knowledge of an extremal curve rather than an extremum point. This leads us to variational methods (to handle extrema of functionals) in place of static optimization methods (to handle extrema of functions). For example, the use of a pseudo-Newtonian model to quantify the dynamic power yield from radiation, gives rise to a non-exponential optimal curve describing the radiation relaxation to the equilibrium. The non-exponential shape of the relaxation curve is the consequence of nonlinear properties of the radiation fluid. Non-exponential are also other curves describing the radiation relaxation, e.g. those following from exact models involving the Stefan-Boltzmann equation (Kuran 2006 [6], Sieniutycz and Kuran 2005 [4], 2006 [5]). Optimal (e.g. power-maximizing) state $T(t)$ is accompanied by optimal control $T'(t)$; they both are components of the dynamic optimization solution.

Energy limits of dynamical processes are inherently connected with exergies, the classical exergy and its rate-dependent extensions. To obtain the classical exergy from work functionals it suffices to assume that the thermal efficiency of the system is identical with the

Carnot efficiency. On the other hand, non-Carnot efficiencies, influenced by rates, lead to 'generalized exergies'. The benefit from generalized exergies is that they define stronger energy limits than those predicted by classical exergies (Berry *at al* 2000 [7]).

4.2. Radiation Systems

Radiation engines are thermal machines driven by the radiation fluid, a medium exhibiting nonlinear properties. Energy transfer rates in reservoirs containing nonlinear media can be described by various models. Usually one assumes that the energy transfer in a reservoir is proportional to the difference of absolute temperatures in certain power, a. The case of $a = 4$ refers to the radiation, $a = -1$ to the Onsagerian kinetics and $a = 1$ to the Fourier law of heat exchange. As the first case of the radiation engine modeling we consider a "symmetric nonlinear case" in which the energy exchange process in the energy exchange in each reservoir satisfies the Stefan-Boltzmann equation. Next we consider "hybrid nonlinear case" in which the upper-temperature fluid is still governed by the kinetics proportional to the difference of $(T^4)_i$ whereas the kinetics in the lower reservoir is Newtonian.

Here are equations of *symmetric nonlinear case*. For the "symmetric" kinetics governed by the differences in T^a, the Carnot representation of the total entropy production has the form

$$\sigma_s = g_1 g_2 \frac{T_1^a - T'^a}{\Phi g_1 \left(T'/T_2\right)^{a-1} + g_2} \left(\frac{(\Phi - 1)}{T'} + \left(\frac{1}{T'} - \frac{1}{T_1} \right) \right) \qquad (10)$$

Superiority of Carnot control T' over the energy flux control ε_1 may be noted. Analytical expressions for the energy-flux representation of the entropy production or the associated mechanical power p cannot generally be found in an analytical form. The work expression to be minimized is

$$W = \int_{t^i}^{t^f} \varepsilon_1 \eta dt = \int_{t^i}^{t^f} g_1 g_2 \frac{T_1^a - T'^a}{\Phi g_1 \left(T'/T_2\right)^{a-1} + g_2} \left(1 - \Phi \frac{T_2}{T'} \right) dt \qquad (11)$$

In the case of analytical difficulties which occur for a different from the unity the maximization can be performed numerically by dynamic programming using Carnot T' as the free control.

We consider now *hybrid nonlinear case*. It involves the radiative heat transfer ($a = 4$) in the upper reservoir and a convective one in the lower one. To obtain an optimal path associated with the limiting production or consumption of mechanical energy the sum of the above functionals i.e. the overall entropy production

$$S_\sigma = -\int_{\tau^i}^{\tau^f} c(T_1) \left(\frac{\Phi}{\left(T_1^a + \dot{T}_1^a\right)^{\frac{1}{a}} + \dot{T}_1 \Phi g_1 / g_2} - \frac{1}{T_1} \right) \dot{T}_1 d\tau_1 \qquad (12)$$

has to be minimized for a fixed duration and defined end states of the radiation fluid. The most typical way to do accomplish the minimization is to write down and then solve the Euler-Lagrange equation of the variational problem. Analytical solution is very difficult to obtain, thus one has to rest on numerical approaches.

5. Finite Rate Exergies and Finite Resources

We are now in position to formulate the Hamilton Jacobi Bellman theory for systems propelled by energy flux ε. Two different kinds of work: first associated with the resource downgrading during its relaxation to the equilibrium and the second – with the reverse process of resource upgrading, are essential. Total power obtained from an infinite number of infinitesimal stages representing the resource relaxation is determined as the Lagrange functional.

5.1. Some Hamilton Jacobi Bellman Equations for Energy Systems

We shall display some Hamilton Jacobi Bellman (HJB) equations for radiation power systems. A suitable example is a radiation engine whose power integral is approximated by a pseudo-Newtonian model of radiative energy exchange. For the *symmetric* model of radiation conversion (both reservoirs composed of radiation), where $\Phi' \equiv \Phi g_1/g_2$ and coefficient $\beta = \sigma a_v c_h^{-1}(p_m^0)^{-1}$ is related to molar constant of photons density p_m^0 and Stefan-Boltzmann constant σ, we obtain a HJB equation

$$\frac{\partial V}{\partial t} = \max_{T'(t)}\left\{\left(\dot{G}_c\left(1-\Phi\frac{T^e}{T'}\right)+\partial V/\partial T\right)\beta\frac{T^a - T'^a}{\left(\Phi'(T'/T_2)^{a-1}+1\right)T^{a-1}}\right\} \qquad (13)$$

For *a hybrid model* of the radiation conversion (upper reservoir composed of the radiation and lower reservoir of a Newtonian fluid the related Hamilton-Jacobi-Bellman (HJB) equation is

$$-\frac{\partial V}{\partial t^f}+\max_{T'(t)}\left\{-\left(\dot{G}_c(T)(1-\frac{\Phi T^e}{T'})+\frac{\partial V}{\partial T^f}\right)u\right\}=0 \qquad (14)$$

5.2. Chemical Power Systems

The developed approach can be extended to chemical and electrochemical engines. Here we shall make only a few basic remarks. Yet, as opposed to thermal machines, in chemical ones generalized streams or reservoirs are present, capable of providing both heat and substance. Large streams or infinite reservoirs assure constancy of chemical potentials. Problems of extremum power (maximum of power produced and minimum of power consumed) are static optimization problems. For a finite "upper stream", however, amount and chemical potential of an active reactant decrease in time, and considered problems are those of dynamic optimization and variational calculus. Application of chemical Carnot control μ' in terms of fuel flux n_1 and its mole fraction x to the Lagrangian relaxation path leads to a work functional

$$W = -\int_{\tau_1^i}^{\tau_1^f}\left\{\zeta_0 + RT\ln\left(\frac{X/(1+X)+dX/d\tau_1}{x_2 - jdX/d\tau_1}\right)\right\}\frac{dX}{d\tau_1}d\tau_1 \qquad (15)$$

whose maximum describes the dynamical limit of the system. Here X = x/(1-x) and j equals the ratio of upper to lower mass conductance, g_1/g_2. The path optimality condition may be expressed in terms of the constancy of the following Hamiltonian

$$H(X,\dot{X}) = RT\dot{X}^2\left(\frac{1+X}{X}+\frac{j}{x_2}\right) \qquad (16)$$

For low rates and large concentrations X (mole fractions x_1 close to the unity) optimal relaxation rate of the fuel resource is approximately constant. Yet, in an arbitrary situation optimal rates are state dependent so as to preserve the constancy of H in Eq. (16).

6. Concluding Remarks

This research provides data for power production bounds (limits) which are enhanced in comparison with those predicted by the classical thermodynamics. As opposed to the classical thermodynamics, these bounds depend not only on changes of the thermodynamic state of participating resources but also on process irreversibility, ratios of stream flows, stream directions, and mechanism of heat and mass transfer. The methodology familiar for thermal machines has been extended to chemical and electrochemical engines. Extensions are also available for multicomponent, multireaction units (Sieniutycz 2009 [10]).

The generalized bounds, obtained here by solving Hamilton Jacobi Bellman equations, are stronger than those predicted by thermostatic. They do not coincide for processes of work production and work consumption; they are 'thermokinetic' rather than 'thermostatic' bounds. Only for infinitely long durations or for processes with excellent transfer (an infinite number of transfer units) the thermokinetic bounds reduce to the classical thermostatic bounds. A real process which does not apply the optimal protocol but has the same boundary states and duration as the optimal path, requires a real work supply that can only be larger than the finite-rate bound obtained by the optimization. Similarly, the real work delivered from a nonequilibrium work-producing system (with the same boundary states and duration but with a suboptimal control) can only be lower than the corresponding finite-rate bound. This is a direction with many open opportunities, especially for separation and chemical systems.

References

[1] S. Sieniutycz, Thermodynamic Limits on Production or Consumption of Mechanical Energy in Practical and Industrial Systems, Progress in Energy and Combustion Science, 29, 2003, pp. 193 – 246.

[2] F.L. Curzon, B. Ahlborn, Efficiency of Carnot engine at maximum power output, American J. Phys., 43(1), 1975, pp. 22 – 24.

[3] A. De Vos, Endoreversible Thermodynamics of Solar Energy Conversion, Oxford University Press, 1994, pp. 30 – 41.

[4] S. Sieniutycz, P. Kuran, Nonlinear models for mechanical energy production in imperfect generators driven by thermal or solar energy, International Journal of Heat and Mass Transfer, 48(3-4), 2005, pp. 719 – 730.

[5] S. Sieniutycz, P. Kuran, Modeling thermal behavior and work flux in finite-rate systems with radiation, Int. Journ. of Heat and Mass Transfer, 49(17-18), 2006, pp. 3264 – 3283.

[6] P. Kuran, Nonlinear Models of Production of Mechanical Energy in Non-Ideal Generators Driven by Thermal or Solar Energy, Thesis (PhD), Warsaw University of Technology, 2006.

[7] R. S. Berry, V. A. Kazakov, S. Sieniutycz, Z. Szwast, A. M. Tsirlin, Thermodynamic Optimization of Finite Time Processes, Chichester, Wiley, 2000, p. 197.

[8] S. Sieniutycz, Carnot controls to unify traditional and work-assisted operations with heat & mass transfer. Intern. Journal of Applied Thermodynamics, 6(2), 2003, pp. 59 – 67.

[9] S. Sieniutycz, An analysis of power and entropy generation in a chemical engine, International Journal of Heat and Mass Transfer, 51(25-26), 2008, pp. 5859 – 5871.

[10] S. Sieniutycz, Complex chemical systems with power production driven by mass transfer, International Journal of Heat and Mass Transfer, 52(10), 2009, pp. 2453 – 2465.

Application of oxygen enrichment in hot stoves and its potential influences on the energy system at an integrated steel plant

Chuan Wang[1,*], Jonny Karlsson[2], Lawrence Hooey[1,3], Axel Boden[1]

[1]*Centre for process integration in steelmaking, Swerea MEFOS AB, 971 25 Luleå, Sweden*
[2]*SSAB EMEA, SE-97188 Luleå, Sweden*
[3]*University of Oulu, PL 4000, 900014 Oulun Yliopisto, Finland (Adjunct Professor)*
** Corresponding author. Tel: +46 920200223, Fax: +46 920255832, E-mail: chuan.wang@swerea.se*

Abstract: The purpose of the presented paper is to investigate oxygen enrichment in hot stoves for an integrated steel plant. The application of oxygen enrichment in hot stoves will lead to lower coke or PCI rate by increased blast temperature. With oxygen enrichment, the high calorific value COG, could be saved while keeping the same blast temperature. Several alternatives of using the saved COG are presented. Furthermore, an analysis of how oxygen enrichment into hot stoves will have influence on the whole energy system has been carried out by means of an optimization model. Different strategies have been suggested to minimize the total energy consumption at the studied steel plant and the nearby CHP plant.

Keywords: *Oxygen enrichment, Hot stoves, Blast furnace, Energy system*

1. Introduction

In the process of iron-making, hot stoves (HS) are used to preheat air used in the blast furnace (BF). The preheated air is called hot blast. A higher blast temperature will lead to lower coke consumption in BF operation, hence, the energy consumption and CO_2 emission from BF will be reduced. Hot stoves work as counter-current regenerative heat exchangers. Hot stoves typically use low calorific blast furnace gas (BFG) combined with higher calorific value coke oven gas (COG). BFG is generated from BF when producing hot metal. COG is a valuable fuel being high in hydrogen (H_2) and methane (CH_4). At an integrated steel plant, COG is often delivered from the coking plant.

Basically, using oxygen enrichment in the air for combustion in the hot stoves offers three advantages. First, the hot blast temperature may be increased due to higher flame temperature which reduces the blast furnace reductant consumption. Secondly, the lower volume of flue gas reduces the loss of sensible heat via the flue gas. Thirdly, COG or other higher value fuels could be used more effectively elsewhere.

The purpose of this paper is to investigate the application of oxygen enrichment in hot stoves and its potential influences to the total energy system at an integrated steel plant. This is done by performing calculations of mass and heat balance for the HS-BF system, and also by means of an optimization model.

In next section, the HS-BF system is described followed by the description of BF performance with oxygen enrichment in hot stoves. In section 4, an optimization model has been applied to present the potential influences on the total energy system of the studied steel plant and a nearby combined heat and power plant (CHP). Finally, in section 5 concluding remarks are made based on the presented work including some recommendations.

2. Description of hot stove – blast furnace system

The hot stove often includes two separate parts, a combustion chamber and a check chamber. They work as a counter-current regenerative heat exchanger. The fuel gas is first combusted

in the combustion chamber. The flue gas passes through the check chamber and heats it up, then leaves the stack to the ambient. This progress is often called on-gas time. When the check chamber is fully heated up during on-gas time, the blast time is started. During the blast time, the cold blast is blown into the system in opposite cycle and is heated by the check chamber. It then passes through the combustion chamber. Before blowing into the blast furnace, it is often mixed with cold blast to get the required and stable hot blast temperature. BFG is a process gas with low calorific value. It has to be blended with COG to get a higher calorific value before entering the combustion chamber. After blending, the average heating value is around 4.3 MJ/Nm^3.

Traditionally the combustion air is used in hot stoves for fuel combustion. For the studied plant, the hot blast produced is 254 kNm^3 per hour with a temperature of 1104 °C, which is required by the blast furnace to produce hot metal with a production rate of 275 tonnes per hour during the reference period.

The combustion air can be enriched with gaseous oxygen, oxygen enrichment. Compared to traditional combustion, less N_2 will be generated which will absorb less reaction heat from combustion. This will lead to a higher adiabatic flame temperature (AFT) with the same amount of fuel gas. As for the hot stove, therefore, a higher blast temperature can be achieved. On the other hand, the low caloric value fuel gas can also be combusted alone without mixing with any enrichment gas to get the same flame temperature with the use of oxygen enrichment instead. The common enrichment gases used at hot stoves are, for example COG, LPG or NG.

3. BF performance with oxygen enrichment in hot stoves

In the studied steel plant, the hot stoves are fuelled with BFG together with some amounts of COG. The calculations for oxygen enrichment in HS-BF system were carried out by using a spreadsheet model [1].

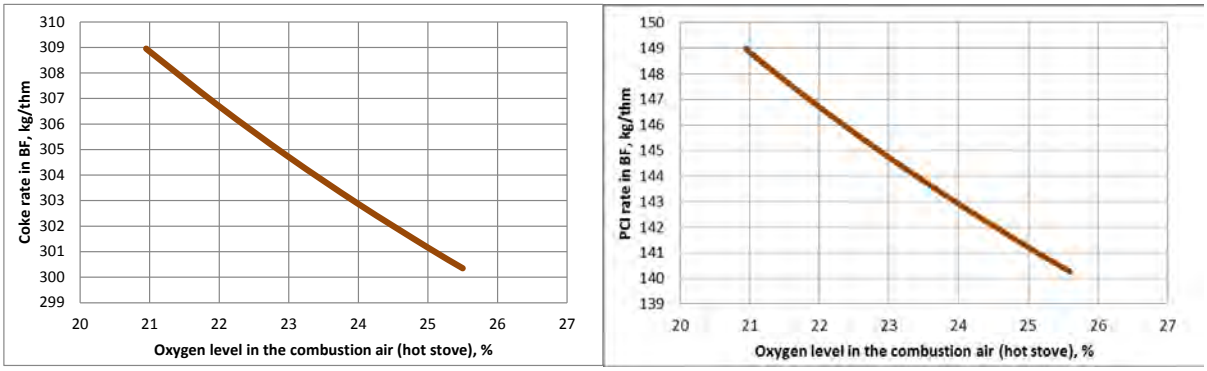

Fig. 1. The correlation between oxygen level in the air and coke rate (left) and PCI rate (right) in BF.

3.1. Increased blast temperature with oxygen enrichment

For the studied hot stoves, the hot blast temperature is assumed to increase to 1200 °C with the enriched oxygen in the combustion air. A higher hot blast temperature will lead to a lower reductant in the blast furnace. In the studied BF blast furnace, coke is used as reductant and charged from the top with other burden materials such as iron ore pellet and fluxes. Besides coke, pulverized coal (PCI) is also injection into BF via tuyers as fuel and reductant. Therefore, it's interesting to study the potential coke and PCI saving due to a higher hot blast temperature. Fig. 1 presents potential coke and PCI saving with enriched oxygen in the

combustion air, which corresponds to 9.01 kg coke or 9.15 kg PCI with per ton hot metal per increased 100 °C blast temperature, respectively.

3.2. COG saved with oxygen enrichment

At a fixed blast temperature, increased oxygen level in the combustion air will lead to decreased COG flow in hot stoves, while BFG flow rate has to increase to provide enough energy, as shown in Fig.2. The high caloric value COG can be saved and used for other purpose.

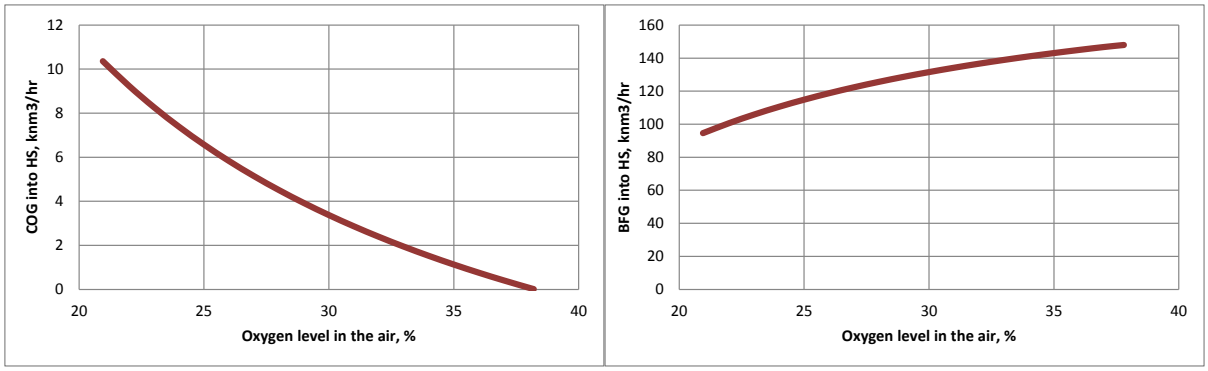

Fig.2. The correlation between oxygen level in the combustion air and COG (left) and BFG (right) flow in the hot stoves.

Previous studies showed that a lower reducant in BF could be achieved by injecting COG through tuyers [1-3]. Fig.3 shows the potential coke or PCI saving if saved COG in hot stoves instead is injected into BF via tuyers.

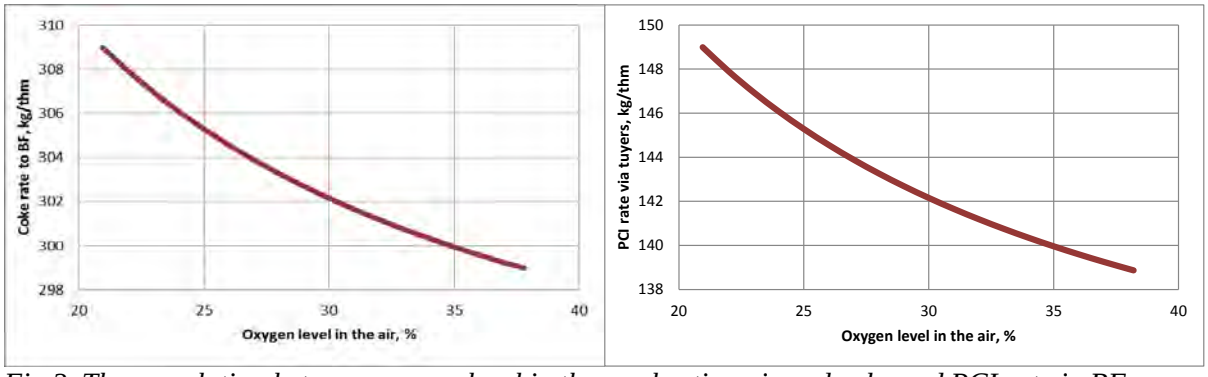

Fig.3. The correlation between oxygen level in the combustion air and coke and PCI rate in BF.

Table 1 gives a summary of key parameters for all scenarios discussed above. It's been noticed that a higher amount of BFG could be generated when COG is injected into BF via tuyers. At the same time, this will also lead to a higher heating value of BFG.

For the studied steel plant, there is another scenario to utilize the saved COG from the hot stove. That is to use it at the nearby combined heat and power (CHP) plant, which corresponds to Scenario 4 in Table 1. This will be presented in Section 4.

Table 1. Key parameters in hot stove – blast furnace system for different scenarios.

	Unit	Ref. case	Fixed COG_coke saving	Fixed COG_PCI saving	Fixed BLT_to PP	Fixed BLT_coke saving	Fixed BLT_PCI saving
	Scenarios	Scenario 1	Scenario 2	Scenario 3	Scenario 4	Scenario 5	Scenario 6
Coke	kg/thm	309.0	300.4	309.0	309.0	299.0	309.0
PCI	kg/thm	149.0	149.0	140.3	149.0	149.0	138.9
COG to BF via tuyers	MJ/thm	0.0	0.0	0.0	0.0	642.6	642.6
BFG generated	knm3/thm	1.47	1.43	1.43	1.47	1.51	1.50
Heating value	MJ/Nm^3	2.97	2.97	2.96	2.97	3.08	3.07
Blast generated	Nm^3/thm	924.2	886.5	885.5	924.2	917.7	916.4
Blast temperature	°C	1104	1200	1200	1104	1104	1104
BFG consumed in HS	nm^3/thm	332.9	358.2	358.6	332.9	524.7	525.5
COG consumed in HS	MJ/thm	642.6	642.6	642.6	0	0	0
O_2 in combustion air	Nm^3/thm	0	14.8	15.0	39.0	32.8	33.1

4. System analysis of the energy system in the studied steel plant

The studied integrated steel plant consists of the following main process units: coking plant (CP) → blast furnace (BF) → basic oxygen plant (BOF) → secondary metallurgy (SM) → continuous casting (CC). The final product is slab from CC. In addition, there are also some other process units, a lime kiln for lime production, an oxygen plant and a combined heat and power plant (CHP). All these process units are connected through material flows and a process gases network. Besides COG and BFG, there is also recovered process gas from the BOF, called basic oxygen furnace gas (BOFG). Fig. 4 shows the structure of the process gas network

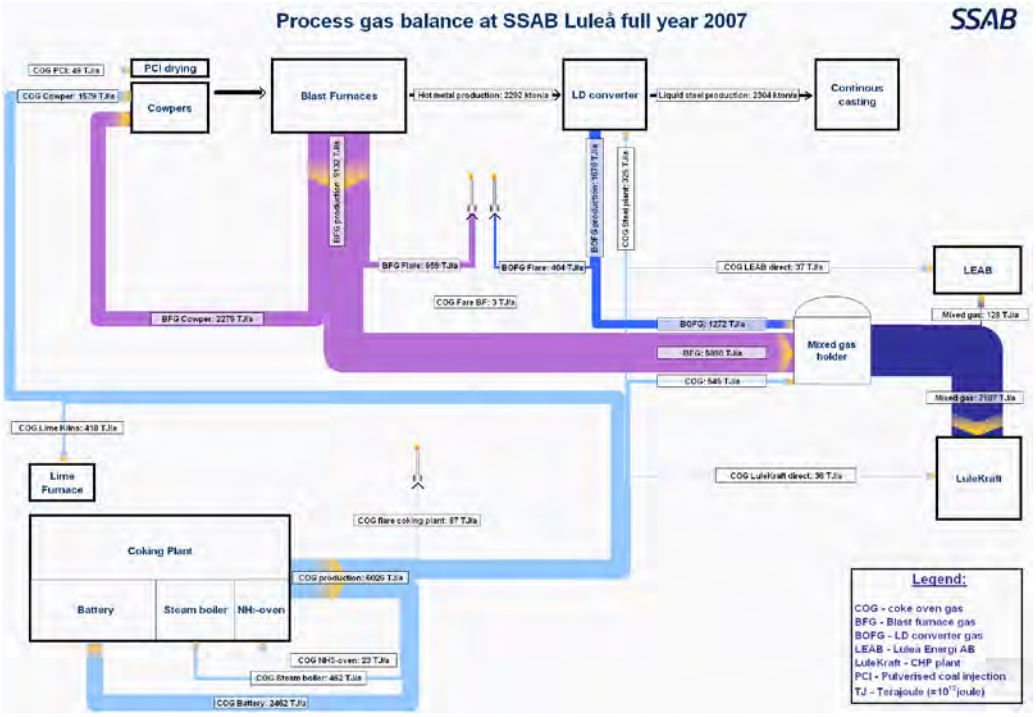

Fig. 4. The structure of process gas network at the studied plant

An optimization model has been applied to analyze the energy system in the studied steel plant. More details about the model can be read in previous publications [4-5]. The objective function set in the model is to minimize energy consumption for the total steel plant. There are two driving forces to run the model. The first is to produce the final product slabs, at 263 ton/hour as a year average. The second is to produce hot water at the CHP plant to the district heat network used by the nearby city. The CHP plant also produces electricity which is used at different process units within the plant. Therefore, it also provides electricity for oxygen

production at the oxygen plant. When there is excess electricity generated from the CHP plant, the extra electricity is sold externally to the grid.

Before entering the CHP plant, the process gases of BFG, COG and BOFG are blended in the mix gas holder to get the required heating value and a stable gas flow before entering the boiler. Oil is used when heat load is higher or when there is lack of mixed gases. The electricity can be generated from the steam turbine by two different modules, a back pressure module and a condenser module, mainly depending on the heat demand from the district heat network. The alpha value of the back pressure module is 0.44 ($\alpha = P_{el}/P_{heat)}$), and the electricity efficiency of the condenser module is 0.32. The boiler efficiency, η, is 0.9. In the model, the maximum fuel limitation for the boiler is 350MW, which is set by the regulation to control emissions, e.g. NO_x, SO_x and CO_2. The other limitation set for the boiler is the maximum flow rate of process gas, 90 Nm^3/s.

Fig. 5 illustrates the heat demand curve versus the out-door temperature. As shown in the figure, the maximum heat supply from the CHP plant is 220 MW, and the minimum heat supply is 20 MW. When the out-door temperature varies in the internal of [-18;16] °C, the heat demand curve can be linearized.

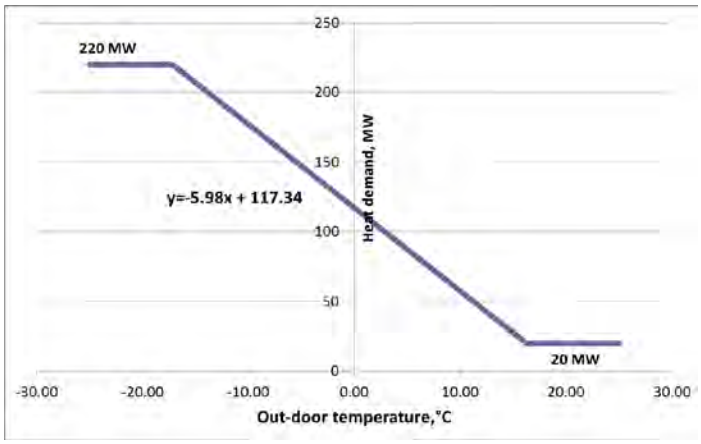

Fig.5.The correlation between out-door temperature and heat demand in the district heat network.

The optimization model is based on hourly data with a time span of one full year for the reference period. For example, the average heat demand is 85.7 MW, corresponding to an average out-door temperature of 5.3 °C. However, to illustrate how heat demand changes will have influence on the process gas network, the average value cannot be used because it varies with the seasonal out-door temperature especially in the Nordic region. Therefore, in this presented work 5 different values of heat demand are chosen: 20, 70, 120, 170 and 220MW respectively.

The model is set to run for the reference case and the optimized case to minimize the energy use for the total energy system. The energy content of the used energy carriers are presented in Table 2.

For the reference case, the model is run based on the operational data during the reference period to simulate for different heat demand levels. For the optimized case, the model will choose one scenario and combined scenarios listed in Table 1 (Scenario 1-6). Compared to the reference case, more freedoms are given in coal blending in the coke plant in the

optimized case. Stable production is assumed, meaning there are no variations in each process unit, except for the CHP plant.

Table 2. Key parameters in hot stoves, GJ/ton.

Energy carrier	Value	Energy carrier	Value
TCMT petcoke coal	35.9	Bachatsky PCI coal	28.7
Peak downs coal	29.6	El Cerrejon PCI coal	27.0
Riverside coal	29.3	External coke	40.9
Massey powellton coal	30.2	PCI	28.2
Rocklick Eagle coal	30.4	Oil, GJ/MWh	3.6
Gonyella coal	29.2	Electricity, GJ/MWh	3.6
Gusare PCI coal	28.2	Flaring, GJ/unit	1.0

Fig. 6 shows the specific energy consumption (SEC) both for the reference and the optimized case. It indicates that a lower SEC will always be achieved in the optimized case. It's been found that BF behaviors in the optimized case are changing when heat demand is increasing at the CHP plant. The model prefers oxygen enrichment for COG saving to get the fixed BLT the same as the reference into BF. However, the way to use the saved COG varies between the scenarios of injecting into BF for coke saving (Scenario 5) and delivering to the CHP plant (Scenario 4) to avoid oil consumption in boiler. As indicated in Fig. 8 (right), before the heat demand is increased to 153.3 MW which corresponds to an out-door temperature of -6°C, BF will always be operated as Scenario 5. Scenario 4 starts when heat demand is greater than 153.3 MW. The percentage of Scenario 4 operation increases to 100% when the heat demand rises to 183.8 MW, meanwhile, operating of Scenario 5 decrease from 100% to 0%. The model will keep running Scenario 4 when heat demand is higher than 183.8 MW to get the minimum energy consumption.

The comparison between reference case and optimized case at a same level of heat demand may explain why minimum energy consumption could be achieved for the model. The following factors contribute for this. First in the coke plant, the coal blending is changed. In principle, the types of coal chosen are with lower volatile energy content. Lower volatile content coal will lead to a higher coke production rate, which will also lead to a lower amount of coking coal required in the coke batteries to produce the same amount of coke as the reference case. Thus, the energy consumption from the coke plant could keep as low as possible. Lower volatile type coal will generate less COG, consequently there will less COG to the CHP plant. However, this will compensate when saved COG from hot stoves instead is injected into BF to have a lower coke rate in BF. This has been proved when comparing the purchased coke amount between reference case and optimized case for example at the heat demand level of 20 MW. This solution will be kept the same until the heat demand is up to 153.3 MW at which point the model has to adopt a strategy of mixing Scenario 5 and Scenario 4 with a varying weighting ratio in order to keep the minimum energy consumption for the total energy system. At the point of 183.8 MW, the solution is completely switched to 100% of Scenario 4 because at such a high level heat demand it is more energy effective to use the saved COG in the CHP plant instead of injecting into BF and by that avoiding use of oil at the CHP plant. However, some amount of oil has to be used even in the optimized case when the heat demand is over 185.7 MW.

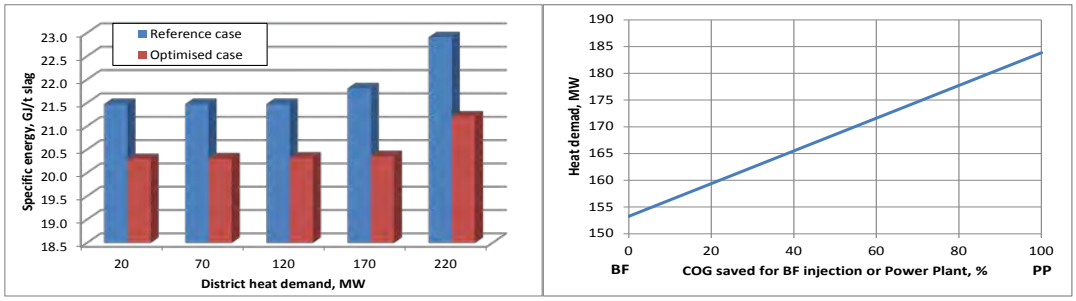

Fig.6. Left: Comparison of SEC between reference case and optimized case;
Right: BF behavior in the optimized case.

Fig. 7 illustrates the comparison of heat supply from the CHP between the reference case and the optimized case. It is found that oil will be replaced by COG in the optimized case at a high levels of heat demand. However, some amount of oil is still needed when the out-door temperature is lower than -11 °C.

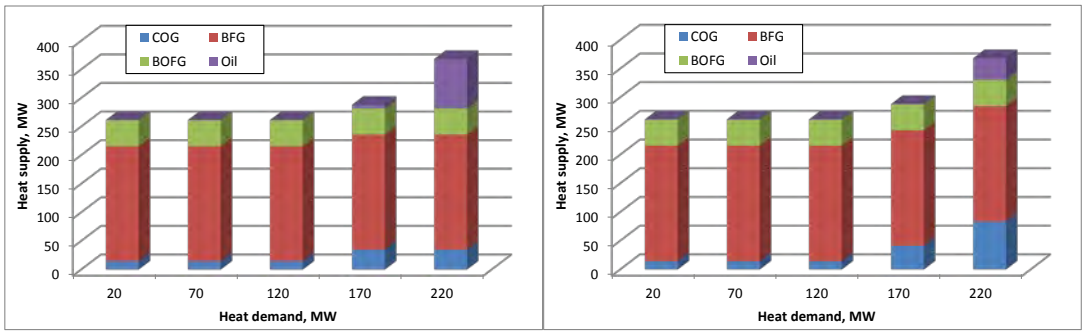

Fig.7. Left: Heat supply in the reference case; Right: Heat supply in the optimized case.

5. Concluding remarks

The presented work shows that the application of oxygen enrichment into hot stoves could lead to a lower coke or PCI rate in BF if the blast temperature is allowed to increase. High calorific value COG can also be saved by use of oxygen enrichment. Therefore, it is possible to use the saved COG in other process units. For the studied steel plant, the alternatives are, for example, inject COG into BF via tuyers or deliver it to the nearby CHP plant for district heat and electricity production. There are also other alternatives to use COG, such as at the reheating furnace in the rolling mill, or in the electric arc furnaces (EAF) to replace other fuels such as natural gas, LPG or oil. However, this depends on the site specific and is not applicable on the studied site.

An analysis of how oxygen enrichment into hot stoves will influence the total energy system has been carried out by means of an optimization model. Different strategies have been suggested from the model to achieve the minimum energy consumption for the studied steel plant and the nearby CHP plant.

The optimization made for the studied plant is to minimize the energy consumption for the total energy system. However, it does not mean that optimal solutions also are cost effective, which in fact is interesting to study.

In the current model, the availability of process gases and their flaring are set at a fixed value, based on hourly average value with a yearly time span. In addition, each process unit is assumed operating continuously and steadily. However, in reality there is normal varations.

Therefore, it might be of importance to take these factors into account for energy system optimization.

As for the CHP plant, only a few heat demand corresponding to a few out-door temperatures, are included in this optimization work. The performance of CHP plant, such as heat loads curve, is therefore limited. Solution space based optimization can provide a better resolution for the studied energy system [6].

The HS-BF system is a very important part in the optimization model, and it's also the most complicated process unit in an integrated steel plant with the BF-BOF route. The mass and energy balance for HS-BF system are first carried out in a spreadsheet, key operating parameters generated from the spreadsheet then put into the HS-BF sub-model of the optimization model. Different operating conditions generate a list of key operating parameters as input to the model. Thus, the optimal solution from this sub-model can either be one case or a mixed case. This, however, may lead to less dynamic. For instance, the model only shows the oxygen amount into hot stoves at which COG will be fully substituted by BFG. What happen in between oxygen enrichment starting and maximum level cannot be predicted in model. Therefore, it could not show the results if the optimum level of oxygen enrichment is in between when modeling the total energy system although it may not be the case. Further model improvement in HS-BF system is needed towards a dynamic response.

Acknowledgements

We would like to thank the Centre for Process Integration in Steelmaking (PRISMA) and SSAB EMEA for the possibility to present this work. PRISMA is an Institute Excellence Centre supported by the Swedish Agency for Innovation Systems, the Knowledge Foundation, and eight industrial partners within the iron- and steel industry.

References

[1] P. Hooey, A. Boden, C. Wang, C. Grip and B. Jansson. Design and application of a spreadsheet-based model of the blast furnace factory, ISIJ International 50(7), 2010, pp. 924-930.

[2] A. Babich, S. Yaroshevskii, A. Formoso, A. Cores, L. Garcia and V. Nozdrachev. Co-injection of Noncoking Coal and Natural Gas in Blast furnace. ISIJ International 39 (3), 1999, pp. 229-238.

[3] J.C. Agarwal, F.C.Brown, D.L. Chin and G.S. Stevens, Results of Ultra High Rates of Natural Gas Injection into the Blast Furnace at Acme Steel Company, ISCTI/Ironmaking Conference Proceedings 57, 1998, 443-461.

[4] M. Larsson and J. Dahl, Reduction of the specific energy use in an integrated steel plant – the effect of an optimization model, ISIJ International 43, 2003, pp. 1664-1673.

[5] C. Wang, C. Ryman, Larsson M, Wikström J-O and Grip C-E. A model on CO_2 emission reduction in integrated steelmaking by optimization methods. International Journal of Energy Research 32, 2008, pp.1092-1106.

[6] J. Sandberg, M. Larsson, C. Wang, S. Lahti and J. Dahl. Solution space based optimization for increased resolution in energy system modeling, 2010, Manuscript to be submitted.

Economical analysis of a chemical heat pump system for waste heat recovery

Hakan Demir*, Özden Ağra, Ş. Özgür Atayılmaz

Yıldız Technical University, Istanbul, Turkey
** Corresponding author. Tel: +90 212 383 28 20, Fax: +90 212 261 66 59, E-mail: hdemir@yildiz.edu.tr*

Abstract: Industrial chemical heat pumps (ICHPs) provide an ability to capture low - grade heat rejected from industrial sources and to reuse the heat increased temperature in industrial processes. Also it can be used for residential heating, cooling, water heating and energy storage. Several temperature boost levels can be obtained according to chemical reaction couple chosen. It can be either single source system or dual source system connected with available reject heat source. Dual source system is more effective than single source system and higher output temperature levels can be obtained. Reject heat source temperature and desired temperature boost are important in chemical reaction couple selection. Chemical reaction couple must be chosen carefully to provide the highest efficiency in all candidate systems. Economical feasibility of industrial chemical heat pump can be determined after calculations according to heat pump capacity. In this study, economical analysis of an industrial chemical heat pump system was accomplished compared with a steam boiler. Economical calculations was carried out and curves that show the relations between investment cost and capacity of chemical heat pump, investment cost and capacity of steam boiler, reject heat capacity and net savings were obtained for waste heat capacities below 2000 kW. It is determined that the chemical system is feasible if the waste heat capacity is higher than a certain value according to economical parameters and lifetime. Also, net gain increases almost linearly with increasing waste heat capacity.

Keywords: *Chemical heat pump, Economical analysis, Waste heat*

1. Introduction

Industrial chemical heat pumps can utilize waste heat at lower temperatures and use it at increased temperatures for industrial processes. An extensive literature study was performed by Wongsuwan et. al. [1]. Industrial chemical heat pumps requires up to one-fifteenth of electrical power input when compared to conventional vapor compression cycle heat pumps [2]. Chemical heat pumps consist of two different reactions which run at two different temperature levels [3]. For this aim, dehydrogenation of alcohols and hydrogenation of acetone can be used in chemical heat pumps [4]. The feasibility of the isopropanol/acetone/hydrogen chemical heat pump system was investigated theoretically by Gastauer and Kameyama [5]. Reverse reaction for isopropanol/acetone/hydrogen chemical heat pump system is

$$CH_3\text{-}CHOH\text{-}CH_3 \leftrightarrow CH_3\text{-}CO\text{-}CH_3 + H_2 \quad (1)$$

Dehydrogenation of isopropanol is endothermic reaction which occurs at 55-85 ^oC in liquid phase and hydrogenation is exothermic reaction and occurs at maximum 202 ^oC in gas phase. A typical isopropanol/acetone/hydrogen heat pump is given in Figure 1. In this study a comparative economical analysis was performed. Maximum $COP_t=Q_{out}/Q_{in}$ of the isopropanol/acetone/hydrogen heat pump is 18.2% depending on isopropanol concentration [6].

In this study, an economical analysis was conducted as a function of waste heat flux. Total costs including investment and operational and maintenance costs of the chemical heat pump system and the steam boiler is obtained. Net gain is defined as the difference between the total costs of the chemical heat pump system and the steam boiler.

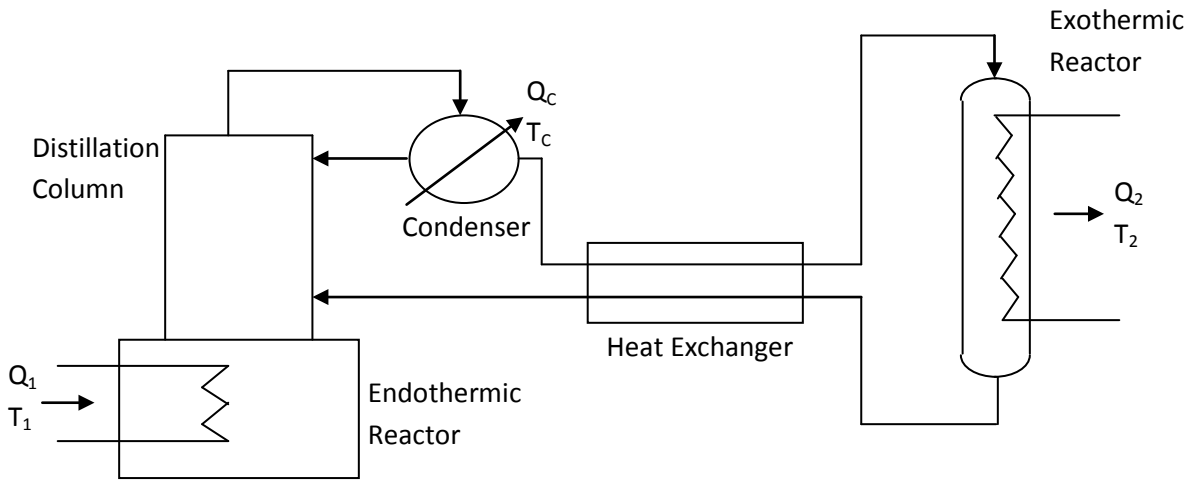

Figure 1 Isopropanol/acetone/hydrogen chemical heat pump flow diagram [5]

2. Economical Analysis of Chemical Heat Pump System

2.1. Investment Cost

Figure 2 derived from [7] can be used for determination of the investment cost of the chemical heat pump system.

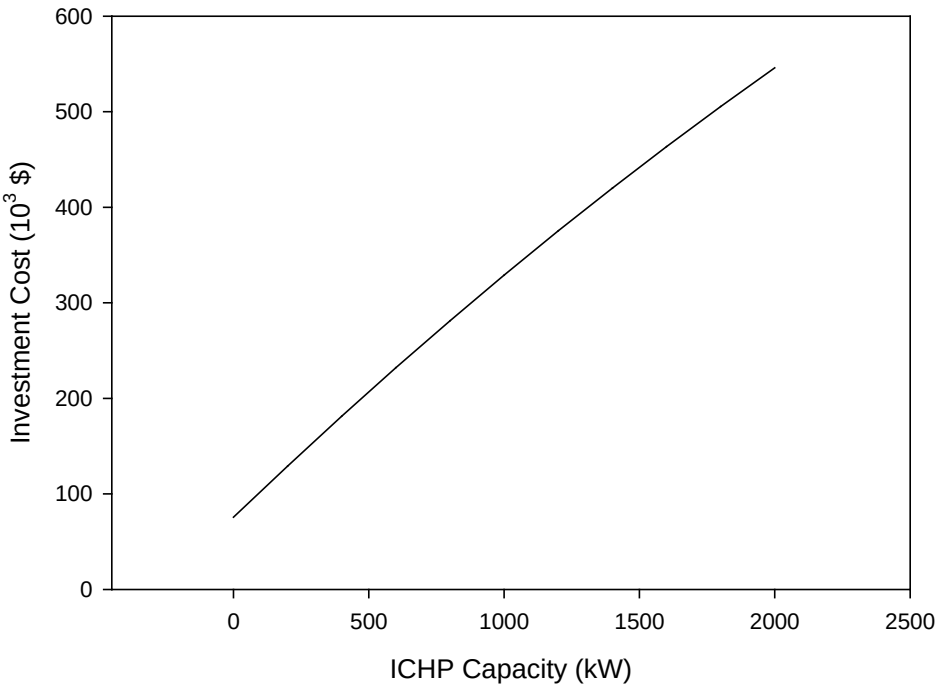

Figure 2 Relationship between industrial chemical heat pump capacity and investment cost

The equation that gives the function in Figure 2 is of the form

$$I_{CO} = -0.01832Q^2 + 271.77Q + 75567.3 \quad (2)$$

where ICO is the investment cost ($) and Q is the capacity (kW).

Figure 2 was obtained using economical values for 1988. In order to use it for the present calculations, it is required to make some modifications. For this aim a correction factor was defined as below:

$$f = (1 + i_1)(1 + i_2)(1 + i_3) \ldots\ldots (1 + i_n) \quad (3)$$

where i represents the inflation rate in corresponding year after 1988.
If the inflation rate is constant for all years from 1988 to the present, in that case;

$$f = (1 + i)^n \quad (4)$$

n is the number of the years from 1988 to present. Then, the investment cost of the chemical heat pump system in the present year, I_C ($), is calculated from

$$I_C = f.I_{CO} \quad (5)$$

2.2. Equivalent Annual Cost

Equivalent annual cost is obtained as a function of interest rate, i and lifetime of investment, n (year) from

$$EAC = I_C \frac{i(1+i)^n}{(1+i)^n - 1} \quad (6)$$

2.3. Operating and Maintenance Cost

Operating and maintenance cost of the chemical heat pump is calculated from [7]

$$OM = \frac{ES.CE.OT}{16} + 0.05 I_C \quad (7)$$

Here, ES, CE and OT are equipment size (kW), cost of electricity ($/kWh) and operating time (h) respectively. The number 16 is used for industrial chemical heat pump which uses a fan to operate a cooling tower. If groundwater is used for cooling then a value of 20 should be used [7]. Maintenance cost is assumed 5% of investment cost.

2.4. Total Cost

Total cost is the sum of the equivalent annual cost and operating and maintenance cost.

$$TC = EAC + OM \quad (8)$$

3. Economical Analysis of Boiler

3.1. Investment Cost

Investment cost is the price of a boiler which has the same thermal capacity as the chemical heat pump system. The investment cost of boiler was derived from present steam boiler prices available in the market. The variation of the boiler price ($) with thermal capacity (kW) is given in Figure 3 and can be calculated from the Eq. 9 as a function of boiler capacity Q (kW) for the capacities up to 2000 kW.

$$I_C = -0.00453216Q^2 + 21.9991Q + 3367.2 \quad (9)$$

3.2. Equivalent Annual Cost

Equivalent annual cost is obtained as a function of interest rate, i and lifetime of investment, n (year) from

$$EAC = I_C \frac{i(1+i)^n}{(1+i)^n - 1} \tag{10}$$

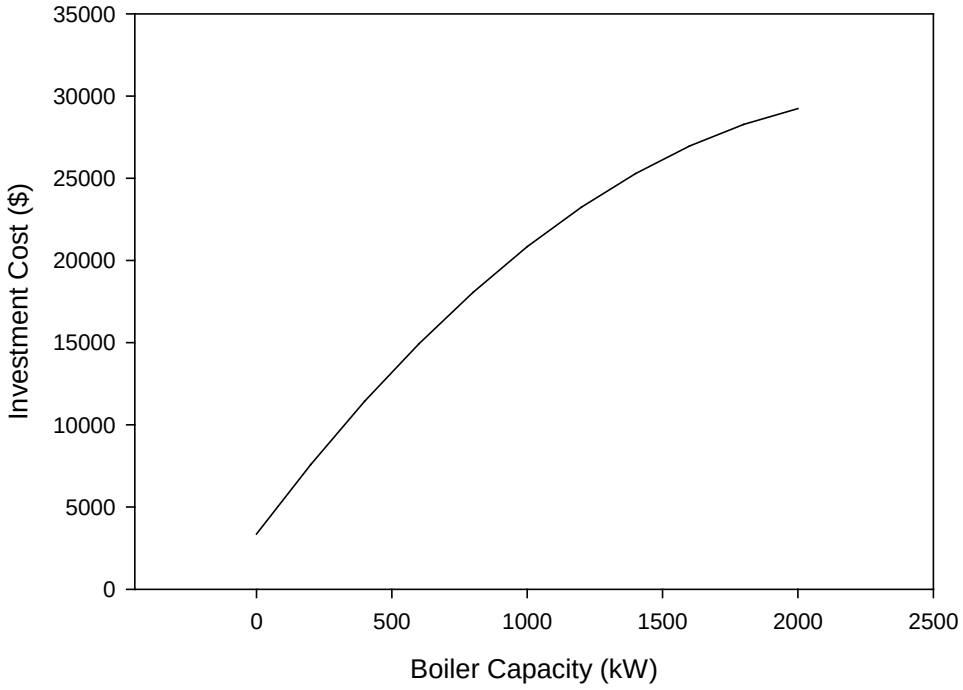

Figure 3 Relationship between boiler capacity and investment cost

3.3. Annual Energy Consumption

Annual energy consumption is the amount of fuel which is consumed during the operation of boiler and can be calculated from

$$AEC = \frac{Q.OT}{\eta_B.LHV} \tag{11}$$

where η_B is the boiler efficiency and LHV is the lower heating value of fuel (kJ/kg). The cost of the annual energy consumption is

$$AC = AEC.CF \tag{12}$$

and CF is the cost of the fuel ($/kg).

3.4. Operating and Maintenance Cost

Operating and maintenance cost of the boiler is calculated from

$$OM = AC + 0.05I_C \tag{13}$$

Maintenance cost is assumed 5% of investment cost.

3.5. Total Cost

Total cost is the sum of the equivalent annual cost and operating and maintenance cost.

$$TC = EAC + OM \tag{14}$$

4. Results

Net gain is calculated from the difference between total costs of the chemical heat pump system and the boiler.

$$NG = TC_{CHP} - TC_B \tag{15}$$

where TC_{CHP} and TC_B are total annual costs of chemical heat pump and boiler respectively. The parameters used in the analysis are as below:

Waste heat flux, 550 – 11200 kW
Effectiveness of chemical heat pump, 18% [6]
ICHP capacity, 100 – 2000 kW
Boiler efficiency, 90%
Fuel, Fuel-Oil
Lower heating value of fuel, 39774.6 kJ/kg
Fuel price, 0.87 $/kg
Electricity price, 0.125 $/kWh
Inflation rate, 8%
Operating time, 5475 h/year
Lifetime, 6 – 15 years

Figure 4 represents the relation between ICHP capacity and net gain. It is seen that net gain increase almost linearly with increasing ICHP capacity.

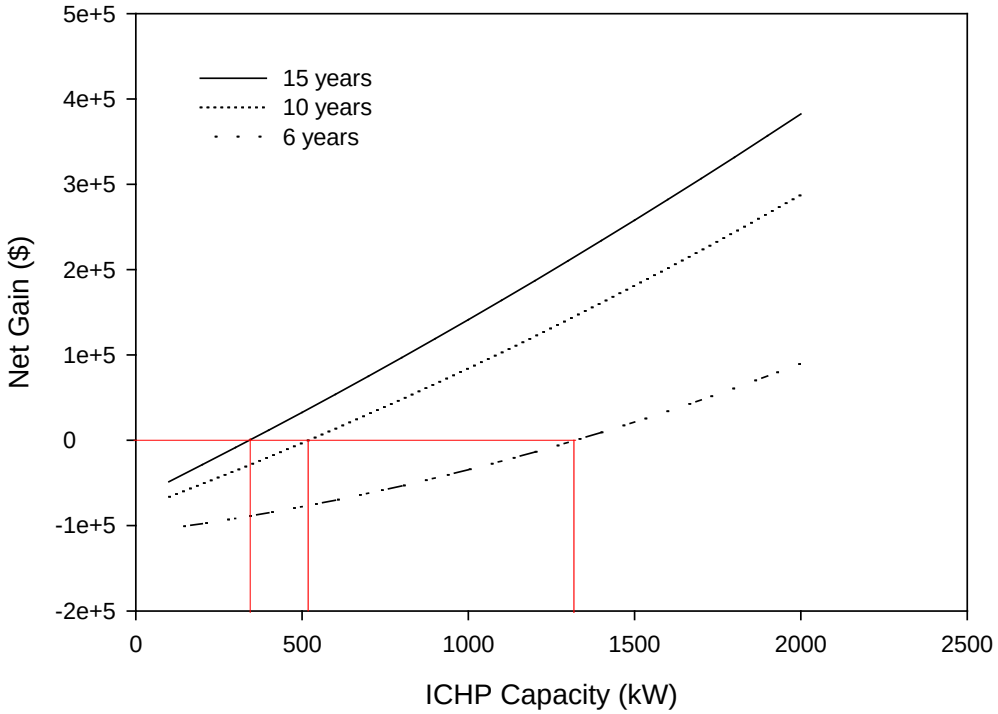

Figure 4 Relationship between ICHP capacity and net gain for lifetime 6, 10 and 15 years

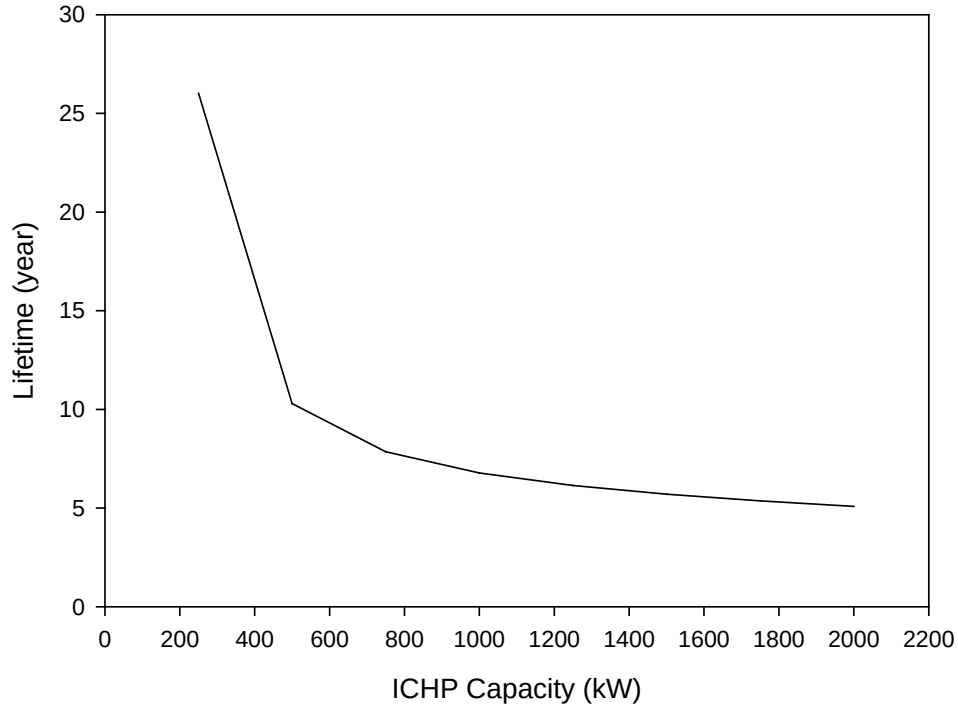

Figure 5 Relationship between ICHP capacity and lifetime where the net gain is zero

Figure 5 shows the relation between ICHP capacity and lifetime for zero net gain. It is seen that if the ICHP capacity is higher than 1000 kW, lifetime is asymptotically approaches 5 years.

5. Conclusion

Economical feasibility of industrial chemical heat pumps can be determined after calculations according to heat pump capacity. Economical calculations were carried out and curves show the relations between investment cost and capacity of chemical heat pump, capital cost and capacity of steam boiler, ICHP capacity and net savings were obtained. It is determined that the chemical system is feasible if the waste heat capacity is higher than a certain value according to lifetime of investment. Also, net gain increases linearly with increasing waste heat capacity. In Figure 5, the upper region of the net gain zero curve shows the feasible zone and it is seen that the payback period is almost constant for the capacities higher than 1000 kW.

References

[1] Wongsuwan, W., Kumar, S., Neveu, P., Meunier, F., A review of chemical heat pump technology and applications, Applied Thermal Engineering 21, 2001, pp. 1489-1519

[2] Clark , E . C., Industrial Chemical Heat Pumps: Chemically Driven, Rocket research Company, Washington, 1982

[3] Raldow, W. M., Wentworth , W . E., Chemical Heat Pumps - A Basic Thermodynamic Analysis, Solar Energy 23, 1979, pp. 75-79

[4] Prevost, M. ve Bugarel, R., "Chemical Heat Pumps: System Isopropanol - Acetone - Hydrogen" , Instut du Genie Chimique

[5] Gastauer, P., Kameyama, H., The thermal efficiency of the isopropanol/acetone/hydrogen chemical heat pump: analysis and improvement, Proceedings of International Hydrogen and Clean Energy Symposium 1995, pp. 317-320

[6] Demir, H., Industrial Chemical Heat Pumps, MSc Thesis, Yıldız Technical University, 1999

[7] Clark , E. C., ICHP Economic Analysis, Rocket research Company, Washington, 1990

[8] Aybers , N., Şahin , B., Enerji Maliyeti, Yıldız Technical University, 1995

Avoiding loss of energy in a petrochemical industry, operation and design

S. Ávila[1,*], A.Kiperstok[1], B.Braga[1], R. Kalid[1]

[1] *Federal University of Bahia, Salvador, Brazil*
** Corresponding author. Tel: +00557188977855, E-mail:avilasalva@gmail.com*

Abstract: The challenge of economic and environmental sustainability demands a better way to manage production in the industry when treating energy consumption and emission of greenhouse gases. The reduction of greenhouse gases promoters are using: renewable energy matrix that can capture the CO_2, renewable energy resources and, production activities with better efficiency in thermal systems. The industry segment contributes over 33% for CO_2 emissions and it can be reduced through: energy integration in designs, intensifying the process and, better efficiency of utilities in the routine. The objective is demonstrates that, if global industry reduce at least 25% of thermal energy losses, 20% of losses of steam, and if change combustible oil to renewable in 33,8% proportion, the greenhouse effect reduce in 33%. The methodology to achieve reduction of CO_2 emission includes: Preliminary assessment, Strategies, Specific Programs, Restrictions analyzes and measurement of results. Between strategies are actions on operation, design and business chain. Between programs there are: evaluations about utility control and management; biomass economic chain viability; and, actions to recover steam losses on design. The restrictions are to implement politic programs in society and industry segment to change patterns becoming possible thermal energy reduction and renewable combustible substitution. The projected results on reduction of CO_2 in industry emissions are summed and almost overcome target of 21,6 (20,4) GTY. The segments of society can prepare similar programs and transform exercise in practice giving better quality of life for earth population.

Keywords: Energy efficiency, Utility management, Industry Sustainability

Nomenclature

GTY Giga ton per year
IEA International Energy Agency
BRIC Brazil, Russia, India and China
MMI Man Machine Interface
CW Cooling Water
Biom Biomass

1. Introduction

This paper aims to demonstrate that, integrated actions of industries can achieve the target reduction in CO_2 generation by greater energy efficiency in unit operations and by replacing the oil and gas fuels by biomass. After discussion about the industrial segment impact causing the greenhouse effect, topics of thermal efficiency and renewable energy resources are discussed. Then some activities and calculation methods are suggested for achieving the goals of reducing the generation of CO_2.

According to Johan Rockstrom and others [1] [2] the challenges to sustaining life on planet earth (sustainable) depend on the care of large environmental requirements. These requirements are conditions for the stabilization of the atmosphere and return to equilibrium between the species and nature as they did before the uncontrolled growth of world economy. Climate change is one of the uncontrolled factors indicating the need for urgent action to reduce emissions of CO_2, the main reason. Several programs and initiatives such as the gradual change of the current oil energy by renewable resources should be performed to prevent the growth and maintenance of the economy causing uncontrolled situations in nature and in particular in global climate.

To avoid the impact of gases contributing to air pollution, scientists seek to reduce its generation at source and reduce its inventory too. So they propose a series of actions resulting from studies that treat about the possible sources of energy and energy transformations, from

2010 to 2050, by IEA - International Energy Agency [3]. According to the IEA study, in 2005 CO_2 emissions to the atmosphere were the order of 28 GTY (Giga Ton per year), and imagining that, with the growth of global economies and emerging countries especially BRIC, the issue will be 62 GTY CO_2. With the work proposed here and in several initiatives by the conscious world, we intend to achieve by 2050 a situation of greater sustainability by reducing CO_2 emissions to around 14 GTY, or, half emission of 2005. Humanity needs to cut emissions from 2010 to 2050 on 48 GTY of CO_2 (considering that very little was achieved from 2005 to 2010). Scientists from IEA [3] estimated options about contribution of human activities to emission reduction. From this study, the opportunities to reduce inventory of CO_2 on atmosphere are located in different sectors of the economy. Energy sector has more potential for reduction with 20 GTY of CO_2, industrial sector with half the quota, 10 GTY of CO_2, transportation sector with 13 GTY, and urban areas with 15 GTY of CO_2.

Within the industrial sector, the opportunities to reduce CO_2 generation are: end-use efficiency of fuel utilization and use of new renewable energy resources, using as knowledge base some researches and services in petrochemical, refine and metallurgical industries in Brazil at TECLIM, clean technology research group inside UFBA, Engineering School. These issues are very important to the industry and can be classified as strategic to their survival. The best efficiency in the end-use of fuel is due reductions achieved from thermal energy consumption in furnaces and boilers allowed by new criteria to control these operations proposed to petrochemical industry. New scenery of combustible changing is constructed with substitution of oil by regional biomass in petrochemical industry (thermal-power facility).

2. Methodology

The Methodology to achieve the reduction of this green house gas presented in Figure 1, is divided in: definition of target (total quantity of emission that will be reduced), preliminary assessment, principal strategies, for each strategy definition of a program to be implemented at industrial segment, restrictions analyzes, and, expected results and respective measurement tools. This paper develops programs that treat these strategies: (1) reduction of thermal energy consumption and (2) use of biomass to decrease emissions of CO_2.

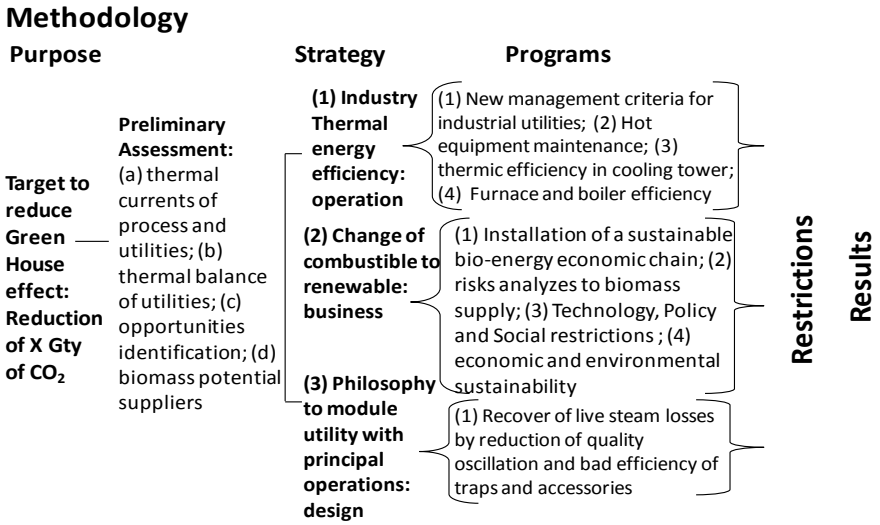

Figure 1. Methodology to investigate about reduction of CO_2 emission by energy control

In these exercises the responsibility to exchange energy type and reduction of thermal energy loss causing reduction in fuel use are of industry. These exercises can point the way for new business with respect to energy consumption and reduction in CO_2 generation. It means that

industry intends to achieve a reduction of 12 GTY of CO_2 from burning fuel and 8.4 GTY of free captured CO_2 by photosynthesis after CO_2 balancing with burning biomass.

2.1. Strategy 1: Thermal Energy Efficiency at Industry, a research case

The methods to increase energy efficiency depend on knowledge about energy balance and tasks related to control of thermal energy, cooling and heating systems at industry. Apart from knowledge availability and tasks well-planned, it is important reviewing conduct of the technical groups about management of utilities in the industry. A research about energy control was performed in a local Petrochemical Company [8] and proposes activities: (1) Planning and programming of Production allowing best decision-making in production scheduling (distribution of energy to activity); (2) Greater efficiency in cooling towers and systems allowing reduction of volatile products and hot energy consumption (temperature profile of separation columns); and (3) Efficiency of heat transfer in hot systems (boilers, furnaces, steam distribution, traps, condensate, and turbines) due to criteria of: projects, assemblies, operation, and thermal charge not compatible with the scale causing heat stress.

Although some of these issues involve the operation and maintenance of plants, the criteria of new projects must be adjusted using above standards, leading to a lower investment, to achieve the goal of greater efficiency in the use of fuel at industry and services. The article by Richard Doornbosch [3] present that the part concerning the reduction of fuel consumption is 12 GTY of CO_2, reference number for the industrial sector. The purpose is to work in a more efficient use of cold and hot energy to reduce consumption combustible thus generating smaller quantity of CO_2 into the atmosphere.

To achieve better thermal performance in cooling and heating systems, heat balances were made in research cases at petrochemical [8], oil and metallurgical industry, where: (A) in the balance of the cooling towers are pointed out possibility of recovery losses, improving the thermal performance; (B) in the balance of boilers was identified recovery energy due to: incomplete burning, and failure on steam generation (bad operational procedures ➔ low availability); (C) in the balance of furnace, the heat is too large by radiation, and the use of thermal energy to heat the reaction depends on: configuration of the tubes, complete burning of the furnace, and good insulation to prevent passage of heat through the equipment walls. Figure 2 descript part of topologies to study thermal performance.

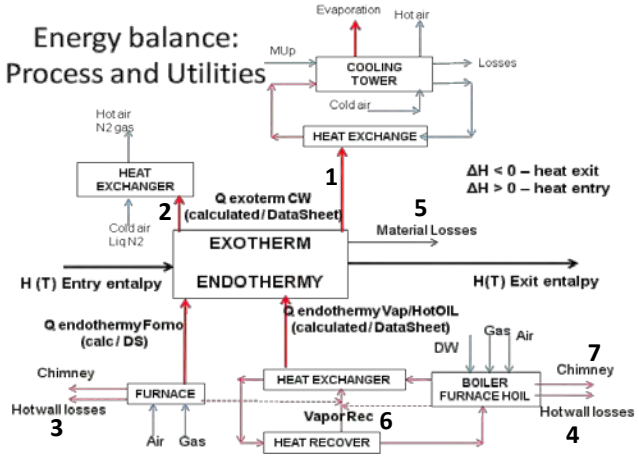

1 - Quality of CW and reflux; 2 - Removal of excess heat - thermal inadequate planning; **3 - Losses at wall furnace** due to ingress of cold process fluid; **4 - Losses at wall boiler** and operational inefficiency in purges; **5 - Losses due flare materials** by higher volatile content at the top of separation equipment; **6** - Traps, separators, process control, incorrect scale of equipments causing **loss of alive steam**; **7 - Losses in chimneys** by not recover of residual heat.

Figure 2. Topology of direct and indirect heat transfer [9]

2.2. Strategy 2: Energy substitution, combustible mineral oils by biomass, a case

With the forecast that world oil reserves are exhausted in about 100 years, there will be, in the medium and long term, environmental and economic viability to greater utilization of available biomass energy and currently is found in nature generating methane, most striking than carbon dioxide to the greenhouse effect. The total use of biomass as fuel for industry depends on some difficult to be worked as: complicated logistics, model of business, and need to increase the efficiency of combustion in furnaces and boilers. Biomass has the advantage of being a natural process that performs photosynthesis where the removal of CO_2 occurs from the atmosphere, thus promoting favorable carbon balance. Assuming that each kilogram of CO_2 generated from burning of biomass has direct equivalence for each kilogram of CO_2 captured from atmosphere, we try to relate in Table 1, different types of Brazilian biomass.

Table 1- Comparison between different biomass and diesel

Biomass	gCO_2/kg Biom	MJ/kg Biom	Quantity Biom GTY	*CO_2 GTY
Sugar can bagass	0,075	15,49	200 E-3	0,08
Black liquor	998,79	13,40	2 E-3	0,002
Coconut fiber	1310,87	17,59	0,42 E-3 (peel, fiber)	0,0002
Cake/ Glycerin	1885,77	25,30	2,2 E-3 (5% biofuel)	0,0023
Total			204,62 E-3 = 0,2 GTY	0,0845

The biomasses chosen are present in abundance in Brazil, due to the large production of sugar cane industry, producing about 200 million tons of bagasse, the pulp industry producing about 9 million tons of black liquor, and the incipient biodiesel industry that generates about 2 million tons per year of glycerin and cake. The marketing of coconuts is quite common in Brazil and the waste generated, coconut peel and fiber, are good source of biomass.

2.3. Proposed activities to be performed

The Programs to increase Energy Efficiency and Mineral Combustible Replacement in the Industrial Segment are presented in table 2 and 3 to discussions.

Table 2 – Energy Efficiency Program

- ✓ Energy balance for process integration and definition of production scheduling;
- ✓ Thermal performance in cooling systems and towers to reduce the temperature of water;
- ✓ Thermal performance in heating systems, boilers, furnaces, steam / condensate and oil, in an attempt to reduce wall losses, loss of live steam, the reuse of energy, equipment reliability through proper drainage, and additional measures;
- ✓ Review the criteria for equipment design in operation by reducing the size of the plants and allowing to work with adjusted modules and not unequal growth of utilities;
- ✓ Review the criteria for management of maintenance and operation (tasks with more human reliability) in industrial plants intending to increase the operational availability of systems for cooling and heating.

Table 3 – Renewable biomass replacement program

✓ Mapping the biomass availability;	✓ Installation of local clusters by biomass type;
✓ Installation of processing plants to adequacy the biomass;	✓ Define national and global economic architecture for using biomass;
✓ Prepare managers in biomass area;	✓ Promote the establishment of cooperatives;
✓ Construct logistics scheme;	✓ Training the cooperative managers.

3. Program of activities to increase thermal energy efficiency, Strategy 1, research case

Assuming that the petrochemical plants and industry in general are in high charge/load, under thermal stress, the plants need to install additional equipment, or practicing high reflux flow in the distillation unit operations or similar. After performance tests conducted in the thermal cooling systems, some recommendations about proper operation can reduce by 15% or more, the temperature of cold water. Thus, fitting temperatures at the top of the decanter vessels, it reduces the reflux without losing the quality of final products, in bottom and top of equipments. If the premise that the proportion of decreasing the need for reflux ratio is equivalent to decreasing for hot utility at the bottom of the equipment, means that the reduction of steam consumption achieve the same, 15% (%RTEP1).

Some investigations are performed to reduce top temperature as result of cooling system (based on research case [9] and services): audit programs, calculations, process and operation investigations, and thermal performance tests discussed in Figure 3. The probably activities suggested are: change distribution of top cold pool, maintenance of top valves, vibration analyzes of fans, installation of side filters, temperature control measure with minimum of one decimal, calculation of concentration cycle based on good precision parameters, check of humidity of atmosphere and others. Other possibilities to reduction of losses are due to recovering of energy from: better insulation of hot equipment wall, increase of continuity in furnaces and boilers caused by increasing of human and operational reliability, diminish of mass losses to flare with cold temperature at column top, diminish of loss on energy recovery systems (condensate) by better control of steam quality. All these possibilities can increase the yield from 88% to 93%, saving 10% of fuel consumption to generate steam and fuel consumption in furnaces (%RTEP2). Summing possibilities of energy economy from cooling tower (15%) with better operation and design of hot systems (10%), we can achieve 25% of decreasing of combustible consumption (%RTEP=%RTEP1+%RTEP2).

The hot utility project (steam and condensate) have flexibility to increase 15% when compared with the design capacity, different from the case of large equipment (cooling towers, reactors, separators, heat exchangers and others) with the possibility to lift charges between 50 to 80% more than project charge. Thus, in debottlenecking design, the review of projects is poorly made for utilities generating non conformities with loss of live steam above 25% (%RSE). We consider, in the calculations, the possibility of recovery at least of 25% of live steam lost to the atmosphere.

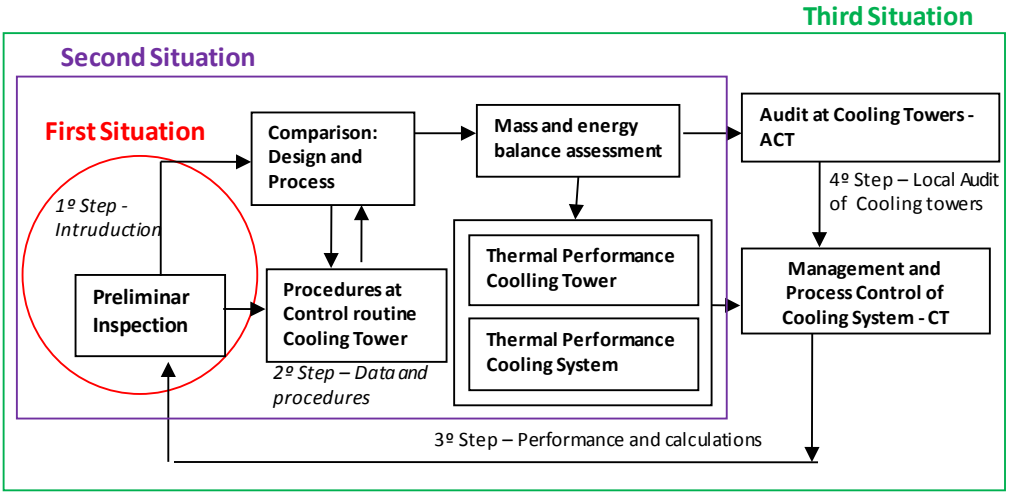

Figure 3. Energy management and audit of cooling system, based on research cases/services

Join knowledge from operation of equipments with technology, including knowledge about human factors in MMI of equipments and including process intensification concerns, is possible to change the design criteria for equipment and processes increasing certainty and decreasing rate of the flexibility of capacity (reducing the engineering coefficients of ignorance in design). So with project of smaller equipments in conjunction with the project of appropriate utility systems increase the load of plant in industrial modules instead of debottlenecking, reducing than, the losses of live steam and reducing factory investment.

Estimation based on Petrochemical Industry X in Brazil and Global Ones (Table 4). Based on data from large petrochemical X in Brazil, the annual production of ethylene is around 142,000 tons per year, and global ethylene production in 2010 was 142 million ton per year [4]. Thus, the calculation of fuel oil consumption and CO_2 generation for petrochemical industries can be multiplied, for exploratory calculations, by 1000 (thousand) that represents all the petrochemical companies worldwide. Thus, for the production of plant X of 260 thousand tons/year and consumption index 16.5 GJ / ton, this means all the energy consumption of around 4.3 million GJ/year. Whereas the average fuel PCI is (43000 KJ/Kg) 43 GJ per ton of fuel for the plant X. Annual consumption of fuels is 100 thousand tons of fuel per year for one plant in place X (*0,0001 Gton/Y).* For calculation to all petrochemicals, in exploratory way, it is considered *0,1 GTY* of fuel.

Table 4 – Data an formula for calculation Petrochemical Industry (Local X and Global)

Pet EGP (Ethylene Global production) = 142.000.000 ton per year	
Pet EXP (Ethylene Local production X) = 142.000 ton per year	
RelG/X (Relation Global/Local) = PetEGP/PetEXP=1000 petrochemical estimated world	
PPetX (Production of Petrochemicals at X) = 260.000 Ton/Y	
CIPetX (Consumption Energy/Mass Index, Petrochemical X) = 16,5 GJ/Ton	
*CcombX (Consumption of combustible per year at X) = PPetX * CIPetX= 4.300.000 GJ/Y*	
COPCI (Combustible Oil - PCI) = 43 GJ/Ton of oil	
FCPetX (Consumption of fuel to Petrochemical X) = CcombX/COPCI= 100.000 Ton of oil/Y	
FCPetX = 0,0001 Gton/Y =1E-4 Gton/Y	
FCPetGlobal(Global Consumption fuel to 1000 Petrochemical)=100.000.000 Ton/Y=0,1GTY	
RelG/X= PetEGP/PetEXP	*(1)*
*CcombX = PPetX*CIPetX*	*(2)*
FCPetX = CcombX/COPCI	*(3)*
*FCPetGlobal = FCPetX * RelG/X*	*(4)*
General Equation to consumption fuel at Global Petrochemicals indystries	
*FCPetGlobal = ((PPetX * CIPetX) / COPCI))* (PetEGP / PetEXP)*	*(5)*

Estimation based on Global Industry (Table 5). Considering that 1 kg of Carbon (C) generates 3 kg of CO_2, giving approximately 2.5 kg of CO_2 per kg of fuel. Thus 0,1 GTY of fuel generates 0,25 GTY of CO_2. If we consider that 1% of industry is of petrochemical type [8] then total industry generates 25 GTY of CO_2. If recovery of 25% of CO_2 by thermal efficiency and recovered is equivalent to 6.25 GTY, fulfilling the quota of efficiency in fuel consumption (12 GTY) for 1000 of petrochemicals X. This recovery is possible with better thermal performance of the separators from better operation of cooling systems and reduction of heat stress. If you consider the projected area, where you can recover 50% of live steam lost in the area, is reduced 25% of total CO_2, since no generation of 12.5 GTY which is higher than the target of 25% from 25 GTY of CO_2, or 6.25 GTY.

Table 5 – Data an formula for calculation Global Industry and decrease of CO_2

GICCO2 (Generation Index CCO2) = 3 kg CO_2/ 1 kg of Carbon
GICO2Fuel (Generation Index CO2Fuel) = 2,5 kg CO_2/1 kg fuel= 2,5 ton CO_2/ ton fuel
*PCO2PetX (Production of CO2 at X) = GICCO2Fuel * FCPetX = 2,5 E-4 Gton CO_2/Y*
PCO2GTotalIndX (Total Ind Production of CO_2 at X) = 2,6 E-2 Gton CO_2/Y [1][8]
Relation (Pet/Total Ind X)= (PCO2PetX/ PCO2GTotalIndX) = 1%
*PCO2PetG (Production of CO_2) = FCPetGlobal * GICO2Fuel= 0,25 Gton/Y of CO_2*
PCO2IndG (Prod of CO_2) = PCO2PetG/ Relation = 25 GTY
%RTEP = %RSE = 25% (recovered steam by thermal programs – operation and design)
*RTEP, Recovered by Thermal Energy Production= (%RTEP*PCO2IndG) = (25% * 25 GTY) = 6,25 GTY of CO_2; RSE (Recovered by Steam economy) = production and design = (%RSE*PCO2IndG) = (25%*25 GTY)=6,25 GTY of CO_2; Total Recovered (TR)=12,5 GTY*
TR ={*(%RTEP+%RSE)*[(FCPetGlobal*GICO2Fuel)/(PCO2PetX/PCO2GTotalIndX)] }(6)

4. Program of Activities to combustible substitution: biomass related to strategy 2

Brazil [5] [6] [7] is an agricultural country and has large area of land available for food crops, has ample opportunity to use the biomass generated as a natural substitute of petroleum. Because of this trend, in very near future, there is a need for the government to invest in productive arrangements to provide this biomass for energy and industrial segment. For this change in the energy supply chain, it is required to mapping sources of biomass, defining the inventory economically feasible to tie their strategies, including political, technical, economic, environmental, ethical and seasonal risks. This Petrochemical Industry in study intends to meet the environmental paradigms to reduce greenhouse gases (carbon balance favorable due to increased carbon sequestration), and meet global energy demand.

There are some steps that the government, together with the industries and society in general must accomplish: • Develop network of institutions and companies with roles to enable installation of a sustainable bio-energy economic chain; • Analyze risks to regular supply of biomass; • Identify restrictions in: Technology, Policy and Social aspects; • Ensure the economic and environmental sustainability. Between policy challenges, there are: prepare economic local clusters, check on the participation of society (cooperatives in logistics and sorting) in this new economic activity, and development of technology to Bio-energy.

5. Discussion of results

In the global, if it is possible to reduce 25% of fuel consumption resulting from energy efficiency program and reduces 20% absolute of live stream to atmosphere is sufficient to meet the challenge posed by the IEA, a reduction of 12 GTY. In the biomass, considering the estimated of last four cases (sugar can bagass, coconut, cake/glycerin from biodiesel, and black liquor), achieves a 0.0845 GTY of CO_2, needing a biomass matrix at least 100 times bigger, including other biomass and other countries like China and India in trying to reduce carbon emissions into the atmosphere. If you reach this goal, with 8.45 GTY versus 9.6 GTY CO_2, quota demanded to be reduced. As mentioned before, the industry emits 25 GTY of CO_2 from fuel combustion, is intended to reduce 8.45 equivalent to 33.8% of the diesel currently used, when you know that above the goal number of 10 %, a third part of necessity, demanding strong economic and political organization and efforts around the biomass.

[1] * General Relation Industry/Petrochemical in Bahia/BR, place X, [8]

6. Conclusion and Restrictions

Work with energy efficiency is simple when Industry management gives importance to utilities as: steam (generated by water and heat from combustible), direct heat to furnace (generated by heat from combustible burning), and cooling water (that depends of cooling tower work). The difficulties are to change managers' decision model that analyze short term problems and does not work to increase human and operational reliability. One other concern is about the necessity to change design criteria preparing factories in smaller size.

Despite the great potential of Brazil to the wide use of biomass, it is not still efficient to process and distribute products in biomass segment; it depends of governments' infrastructure in logistics area. Although there are many searches for new technologies in which the fuel is biomass, it does have large-scale policies or actions that make the distribution of this form of biomass for industry, already ready for use. Therefore, it is necessary to analyze the economics chain in the vertical form, including all activities in the life cycle of different biomasses. For the energetic matrix change to renewable one, some multi-attributes assessment (environment, economic, ethical, policy, social) to choice biomass must be done. The criteria for choice of matrix must be analyzed in biomass to prevent, for lack of planning, the projects unviable after long-term, development policy for biomass, availability of materials, supply guarantees, social and environmental benefits.

References

[1] Johan RockstrOm et al. A safe operating space for humanity. Macmillan Publishers: Nature, vol 461, p. 472/475. 2009.

[2] Johan RockstrOm et al. Planetary Boundaries: Exploring the safe operating space for humanity. Ecology and Societ. 36 p. 2009.

[3] Richard Doornbosch et al. Round Table on Sustainable Development: Mobilizing Investments in LowEmission Energy Technologies on the Scale Needed to Reduce the Risks of Climate Change. Organisation Economic Cooperation /Development. 53p. 2008.

[4] Global Industry Analysts. World ethylene market to cross 160 million tons by 2015, according to new report by global industry analysts. Researched on January 2011. http://www.chemicalonline.com/article.mvc/World-Ethylene-Market-To-Cross-160-Million-0001. 2008.

[5] Painel Florestal. Brasil cresce 7,3% na produção de celulose e fortalece investimentos. Researched on 2010: http://painelflorestal.com.br/noticias/celulose/9721/brasil-cresce-7-3-na-producao-de-celulose-e-fortalece-investimentos. Original source: Bracelpa. 2010.

[6] Biodieselbr.com. Biodiesel no Brasil. http://www.biodieselbr.com/biodiesel/brasil/biodiesel-brasil.htm. 2011.

[7] John Deere. Cana/açúcar/alcool: preços firmes no curto e no longo prazo. Original source: Carlos Cogo Consultoria Agroeconômica. http://www.deere.com.br/pt_BR/ag/veja_mais/info_mercado/sugar_cane.html

[8] IBGE – Instituto Brasileiro de Geografia e Estatística - IBGE. Sustainable Development Indexes of Brazil – Greenhouse gas emissions. 443 p. 2010.

[9] Teclim Research EcoBraskem - UFBA. Final Report: Thermal Energy Balance at UNIB/ Braskem. 2009.

Integration of biogas plants in the building materials industry

M. Ellersdorfer[1,*], C. Weiß[1]

[1] *Institute of Process Technology and Industrial Environmental Protection, Mining University Leoben, Austria*
** Corresponding author. Tel: +4338424025006, Fax: +4338424025002, E-mail: markus.ellersdorfer@unileoben.ac.at*

Abstract: The paper quantifies the synergy-effects of an areal combination of biogas-plants with plants of the building materials industry (e.g. cement plants) from the energetic and economical point of view. Therefore a model biogas and cement plant are defined and the effects of a combination of both plants in terms of energetic efficiency, investment and operating costs, greenhouse gas emission reduction and overall energy production costs are quantified. The main benefits of this combination are the utilisation of low temperature excess heat sources from the cement plant for fermenter heating and the direct thermal utilisation of unprocessed biogas as a valuable, CO_2-neutral fuel for combustion processes for instance clinker burning. Due to the combination, the energetic efficiency of the biogas plant, defined as utilisable energy output in relation to the energy content of the produced biogas, significantly increases from 63.0% to 83.8%. Concurrently the energy production costs are reduced, turning biogas into a competitive source of energy without the need for federal sponsorship. Calculations show, that from a plant size of around 90 m^3_{STP}/h biogas production costs in combined plants are even lower than the actual market prize of natural gas.

Keywords: *biogas, cement plant, thermal utilisation, excess heat recovery*

Nomenclature

volumetric flow rate (standard temperature and pressure)	m^3_{STP}/h
energy (general)	kWh
electrical energy	kWh_{el}
thermal energy	kWh_{th}
European currency	*€, ct*

1. Introduction

The anaerobic fermentation of biogenic material presents a well known technology in waste treatment and agriculture. Furthermore the specific production of biogas out of renewable resources provides an opportunity to integrate CO_2-neutral energy sources in the power supply chain. Nevertheless state of the art concepts of biogas utilisation like electricity generation in combined heat and power plants (CHPs) or processing of the raw biogas to inject it in existing gas supply systems are still in need of improvement. Energy losses due to processing and compression steps or the production of a significant amount of excess heat reduce the percentage of useable energy from the raw biogas.

In view of this problem, an alternative way of gas utilisation would be desirable. The combination of biogas plants with plants of the building materials industry especially cement plants, presents a unique opportunity to meet these demands [1]. The main benefits are:

- utilisation of excess heat from the cement plant for fermenter heating
- raw biogas as CO_2-neutral fuel without the need of processing
- ammonia recovery from the digestate and use as reducing agent in DeNOx-processes

High temperature processes in the cement, lime and magnesia industry are a source of waste heat at various temperature levels. The use of this energy for heating a mesophillic biogas fermenter (~35°C) allows the utilisation of excess heat at temperature levels beyond 100°C, which presents a problem for other state-of-the-art solutions.

The average calorific value of biogas with 21 MJ/m³ (60% methane, [2]) is sufficient for a direct use as fuel in cement and clinker burning. Primary fuel combustion in the rotary kiln and secondary combustion in the precalciner can be adjusted to work with natural gas as well as biogas [3]. The demands in terms of gas composition for direct burning are not that strict as for CHP plants or injection in natural gas supply systems. Compression of the gas to the pipeline pressure (30 to 80 bar) is not necessary. Hence, raw biogas can be used directly for burning without processing steps like desulphurisation and NH_3-removal. H_2S in the biogas is oxidised to SO_2 during combustion, which reacts to alkalisulphates with the clinker in the preheating and calcining system [4]. The fate of NH_3 has to be investigated.

The application of biogas reduces the greenhouse-gas emissions of the cement plant due to the substitution of fossil fuels. On the other hand the combination offers the possibility to improve the partially negative ecobalance of some biogas production ways [5].

The third benefit is the potential recovery of ammonia from the digestate. The output of digestate as a fertiliser for agricultural areas is limited to certain times of the year due to ammonia emissions. Processing of digestate and ammonia recovery can solve the problem of temporal dependency with the concurrent benefit of producing a NO_x-reducing agent for cement plants. By decreasing the ammonium concentration in the effluent for example by steam-stripping, the recycling of the liquid phase into the fermenter might be possible.

2. Methodology

To quantify the synergy effects of the areal combination of biogas and cement plants, an Excel-model was developed, in which conventional biogas plants with CHP are compared to the corresponding combined plant in regard to energetic efficiency, CO_2-savings, energy production costs and plant feasibility. The biogas plant scale can be adjusted by varying the amount of substrates. For the actual calculations a substrate mix with 90% manure and 10% co-substrates (4% food leftovers, 3% glycerine and 3% flotate sludge) was chosen.

The energy balances and costs of combining a conventional biogas plant with a production of 250 m^3_{STP}/h respectively 550 kW_{el} installed electrical power with a cement plant with a production capacity of 440 000 $t_{clinker}$/a are presented in detail. Both plants represent a mean plant size in Austria derived from overall production data divided by the number of plants [6, 7]. In biogas production the trend goes to larger plant sizes, wherefore the mean biogas plant size derived from literature data (270 kW_{el}/plant) was doubled. Based on averaged data of numerous existing biogas-plants [8, 9] in combination with data from CHP evaluations [10] a basic energy balance for a model biogas-plant was determined. To quantify the main excess heat sources of a model cement plant, the mean thermal energy balance was calculated from averaged literature data for Austrian cement plants [11].

Investment and operating costs of the conventional plant were calculated with four different literature models [2, 9, 12, 13] to prove consistency. The estimations were converted to actual costs on the basis of 2009 by correction with the harmonised index of consumer prices in Austria. The most suited model due to its modular configuration (FNR, 2008) was chosen for the economical comparison of conventional and combined plants. Based on the published FNR-data, compensating curves for specific investment and operating costs were implemented to calculate the scale dependent energy production costs. Investment and operating costs of the combined plant do not comprise expenses for CHP and desulphurisation units but an additional cost factor for the combination (burner, gas pipeline, excess heat utilisation). This factor is made up of fixed costs and scale dependent additional costs

(investment costs combination in € = 30000 + (actual plant size [m^3_{STP}/h] / 500) * 100000). It is assumed that substrate and digestate processing costs are the same for both plants, wherefore these expenses remain unaccounted for.

The determined operating costs together with the depreciation charges result in mean energy production costs in ct/kWh, when divided by the useable energy output. Depreciation charges were calculated on the basis of an annuity factor for 16 years deprication period and an imputed interest rate of 6%. The income of the conventional biogas plant comprises the sale of electricity and thermal energy according to the renewable energy feed-in tariff of the ÖSVO 2010 [14]. In case of the combined plants, the income is considered to result from cost savings for fossil fuels (natural gas and fuel oil) [15] and CO_2-savings valuated with an actual emission certificate price of 15 €/t CO_2. Electrical energy to cover the internal demand of the combined plant has to be bought on the market [16]. Based on these data the ROI and payback-period for the conventional and combined plant can be calculated.

The determination of the CO_2-savings is based on a representative mixture of cement plant fuels from literature [6]. It is assumed, that first natural gas and then fuel oil are replaced by biogas, as far as the produced amount of biogas can cover the demands of these fuels. Mean CO_2-savings were calculated from literature data for CO_2-emission rates of fossil fuels [17]. The electrical energy demand of the combined plant is covered by electricity from national power networks, which decreases the CO_2-savings due to emission of greenhouse gases during the production of conventional electrical energy [18].

3. Results

The basic energy balance of a 250 m^3_{STP}/h model biogas plant is visualised in figure 1.

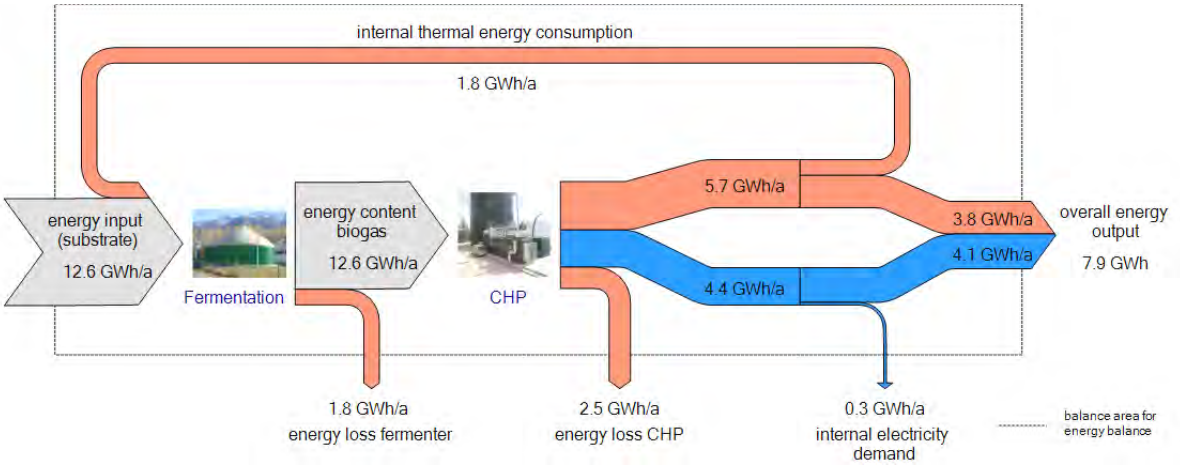

Fig. 1. Energy balance of a conventional biogas plant (250 m^3_{STP}/h) with combined heat and power unit (CHP, 550 kWh_{el} installed electrical power); for detailed data see table 2.

Figure 1 shows that only 35% of the input energy of 12.6 GWh/a can be converted to electrical energy with 45% low temperature excess heat from the CHP. After deduction of the internal electrical and thermal energy demand, 30.5% thermal energy and 32.5% electrical energy remain, giving an overall energetic plant efficiency of 63%. The high amounts of energy needed for fermenter heating and a CHP efficiency of 80% significantly decrease the overall plant efficiency. Moreover, this calculation represents the ideal case, where 100% of the available thermal energy is utilised for example for drying processes or district heating.

The thermal energy balance of the model cement plant (440 000 $t_{clinker}$/a) is visualised in figure 2.

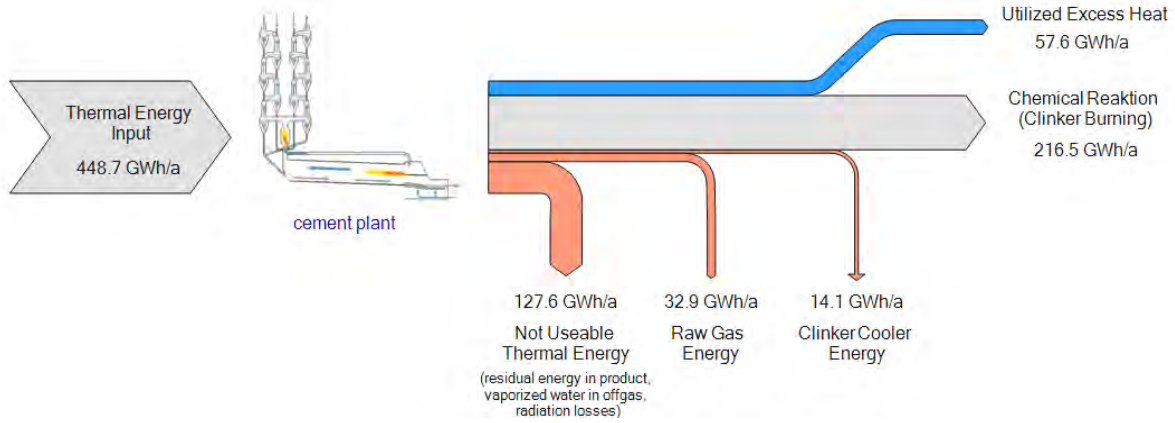

Fig. 2. Thermal energy balance of a conventional cement plant (440 000 $t_{clinker}$ /a)

Not useable thermal energy like the remaining energy content in the product, vaporised water in the offgas and thermal radiation turn out to be the main excess heat sources. The residual energy in the cooling air after the clinker cooler and the energy in the raw gas after the raw mill can easily be utilised for fermenter heating by adequate heat recovery concepts, for example the installation of gas/fluid heat exchangers as shown in figure 3.

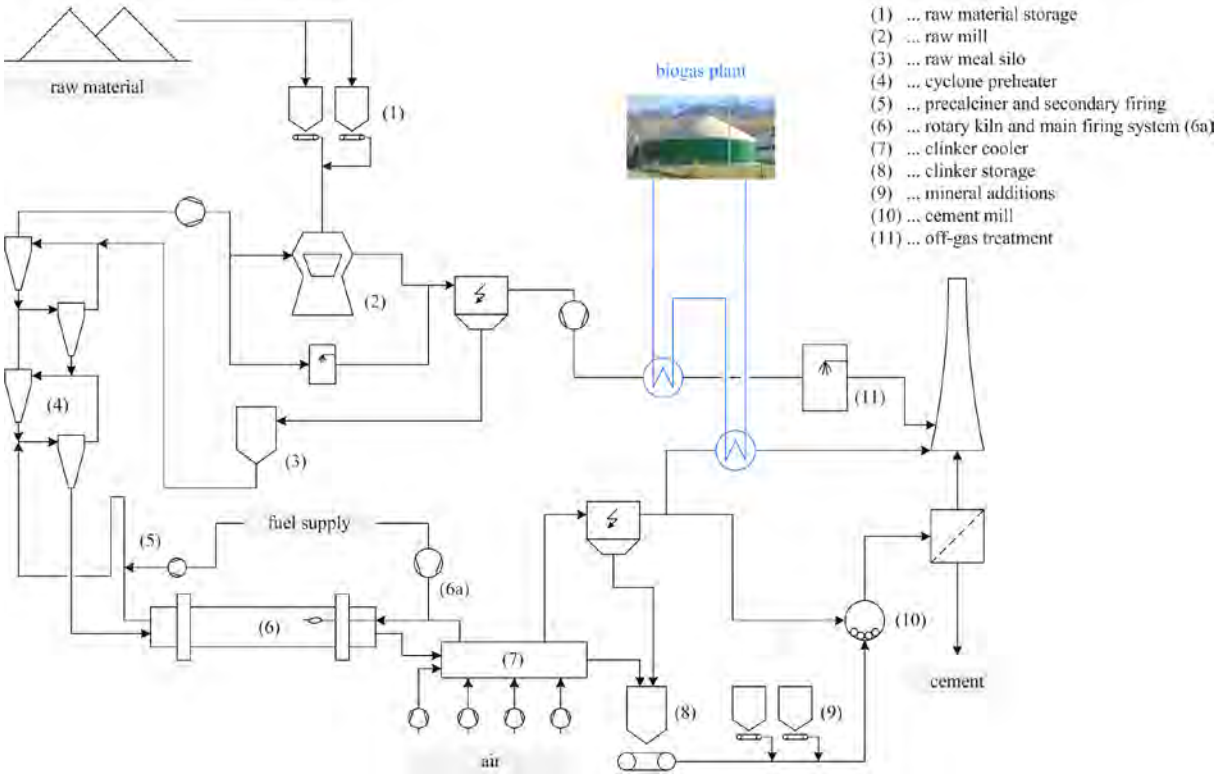

Fig. 3. Process flowchart of a combined biogas and cement plant.

Figure 4 illustrates the effects of this combination on the energy balance of a 250 m^3_{STP}/h biogas plant. Clinker cooler and raw gas excess energy together offer nearly the 27-fold amount of energy needed for fermenter heating. Electrical energy has to be bought in addition. The direct use of raw biogas enhances the utilisable energy of the biogas plant,

leading to a major increase from 63.0 to 83.8% in the overall plant efficiency (cf. table 2). The thermal efficiency of the cement plant only slightly increases from 61.3 to 61.5% due to its large excess heat production compared to the energy demand of the biogas plant. On the basis of the above defined plants scales, 2.7% of the thermal energy consumption of the cement plant can be replaced by raw biogas, resulting in a decrease in greenhouse gas emissions of around 2860 t CO_2/a or 0.8% of the annual CO_2-emissions of the cement plant.

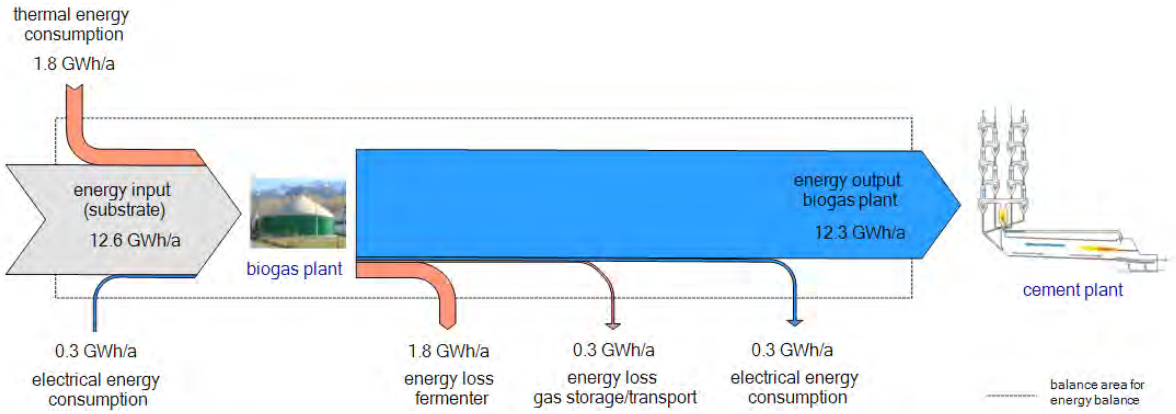

Fig. 4. Energy balance of a combined plant; biogas plant (250 m^3_{STP}/h) coupled with a cement plant (440 000 $t_{clinker}$/a)

Table 1 comprises the estimated investment costs for a conventional biogas plant (250 m^3_{STP}/h) with biogas utilisation via a CHP. The results of the models generally fit together, with the FNR model being the closest to the mean investment costs of 1,750,819€ derived from all models.

Table 1. Investment costs for a conventional biogas plant (250 m^3_{STP}/h) based on different models

		FNR [12]	KTBL [9]	LfU Bayern [2]	Hornbacher* [13]
plant investment costs	[€]	1,172,538	943,757	-	1,578,733
CHP investment costs	[€]	493,729	626,819	-	336,284
total investment costs	**[€]**	**1,666,267**	**1,570,577**	**1,851,414**	**1,915,017**

* estimation excl. CHP, CHP costs estimated with different model (ASUE [10])

Table 2 shows the results of the energy balance as well as the energy production costs and plant feasibility calculations of a conventional plant compared with the combined alternative.

Investment and operating costs of the combined plant are considerably lower because of the missing CHP plant. Together with the higher amount of energy output in terms of fuel, the production costs of energy in a combined plant are around 3.2 ct/kWh compared to 7.0 ct/kWh for a conventional plant, in which 100% of the thermal energy output of the CHP are utilised. Electricity production costs without thermal energy utilisation are 13.5 ct/kWh_{el}. The ROI of the combined plant is somewhat higher and the payback period shorter because of the lower investment and operating costs compared to the conventional plant.

Table 2. Base data of a conventional biogas plant compared with an equally scaled combined plant

		FNR conventional plant	FNR combined plants
biogas production	[m^3_{STP}/h]	250	250
plant energy input	[kWh/a]	12,580,295	14,718,946
electrical energy output	[kWh_{el}/a]	4,088,596	0
thermal energy output	[kWh_{th}/a]	3,836,990	0
utilisable energy output	[kWh/a]	7,925,586	12,328,,689
overall plant efficiency	**[%]**	**63.0**	**83.8**
total investment costs	[€]	1,666,267	1,175,732
operating costs	[€/a]	387,181	281,055
annual depreciation	[€/a]	164,881	116,341
total variable costs	[€/a]	552,062	397,396
energy production costs*	**[ct/kWh]**	**7.0**	**3.2**
electrical energy costs	[ct/kWh_{el}]	13.5	-
cost savings fossil fuels	[€/a]	0	471,895
cost savings CO_2-emissions	[€/a]	0	45,598
electrical energy income	[€/a]	506,986	0
thermal energy income	[€/a]	92,088	0
total income	[€/a]	599,074	517,494
total profit	[€/a]	47,012	120,098
ROI (profit/investment)	[%]	2.8	10.2
payback period (debt-repayment method)	[a]	11.0	6.1

* 100% utilisation of thermal energy

The depiction of the energy production costs of the conventional and combined plant over the plant scale shows the typical decrease in production costs with increasing plant size (figure 5).

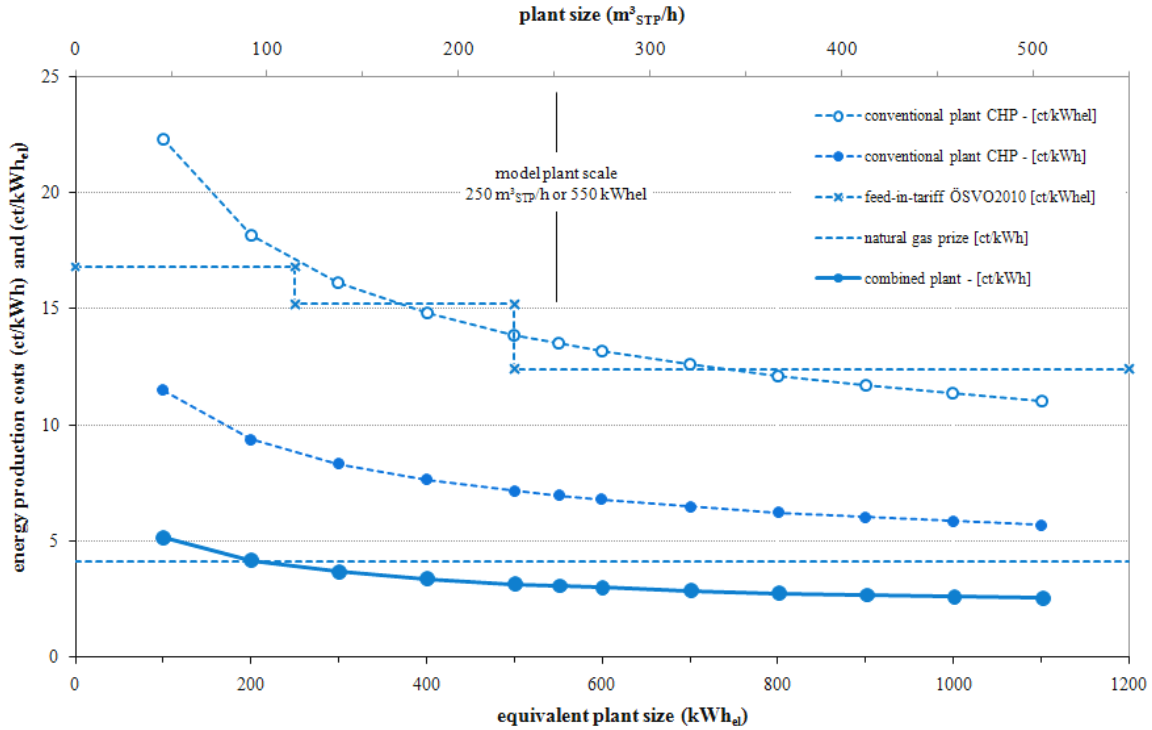

Fig. 5. Energy production costs (electrical and thermal energy) for various plant sizes.

Conventional biogas plants without thermal energy utilisation have electrical energy production costs from 20 to 12 ct/kWh$_{el}$. The simultaneous use of 100% of the CHPs thermal energy output can decrease the energy production costs to values between 11 and 6 ct/kWh but is difficult to implement. Compared to the feed-in-tariff in accordance with the ÖSVO 2010 [14] one can see, that the combined use of thermal energy is essential for the feasibility of a conventional biogas plant. The energy production costs of combined plants (~ 5 and 2.5 ct/kWh) are well below conventional plants due to the higher amount of energy utilised as fuel for clinker burning. From a plant size of 200 kWh$_{el}$ (~ 90 m$^3_{STP}$/h) the production costs of biogas in combined plants actually fall below the costs for natural gas [20].

4. Conclusions

The combination of a biogas plant with a cement plant is a possibility to significantly increase the overall efficiency of a biogas plant. The use of unprocessed biogas as a fuel for clinker burning and the utilisation of excess heat from the cement plant enables biogas costs to be competitive to natural gas costs even without federal sponsorship.

Nevertheless, there are still points that have to be investigated, first and foremost the fate of H_2S and NH_3 in the clinker burning process and their contribution to NOx and SO_2 emissions of the cement plant. Moreover, solutions for the gas utilisation during maintenance periods of the cement plant have to be found. Whereas these periods might also be used for servicing the biogas plant, concepts must be developed for a controlled diminishing of the biogas production rate by reducing or altering the substrate feed and concurrent burning of biogas. Thereby, the internal thermal energy demand of the biogas plant can be covered temporarily.

The recovery of ammonia from the digestate for DeNOx-processes would be a major benefit for the cement plant. Potential technical solutions like steam-stripping of liquid digestate have to be investigated. Especially substrates with the potential to cause ammonia inhibition of the fermentation process might be processed in combined plants, if ammonia recovery is feasible. The practicability also strongly depends on the type of substrates, which have to be suited for fermentation but not for direct burning. Important parameters for waste fuels in cement plants are calorific value along with the content of water, ash, sulphur, chlorine and heavy metals as well as the suitability for the burners [3]. Examples for substrates with limited applicability are liquid manure and brewery and agricultural residues due to the high water content. The inhomogeneity of food residues as well as slaughterhouse waste and similar materials impede direct burning, but otherwise present wastes high in biogas production.

Due to sufficiently available waste heat energy and the huge fuel consumption of cement plants, the share of fuel provided by biogas can be increased almost arbitrarily, resulting in cheaper biogas production costs and significant CO_2-savings. One 2 MW biogas plant can substitute over 10% of the energy consumption of a 440 000 t$_{clinker}$/a cement plant and save around 13 000 t CO_2/a. The substitution is only limited by the available amount of substrates for the biogas plant. Nevertheless, also small scale options are possible, because any industrial plant with high temperature processes and utilisable excess heat, high fossil fuel consumption and the need of a denitrification system is a potential site where biogas plants can be installed. In many cases this combination would be the better alternative compared to biogas plants in the open countryside. With the developed model, site specific questions like maximum substrate and transport costs for economical plant operation can be estimated. Thereby, the number of potential biogas plant sites increases and the role of biogas as CO_2-neutral fuel in power supply can be strenghtened due to the installation of sustainable energy systems.

References

[1] M. Ellersdorfer, W. Kepplinger, Utilisation of Biogas, in: 13th International Tuzla Summer University, Symposium Rational Energy Usage, Energetic Efficiency and Sustainable Ecological Development, 2008, p. 45 – 48.

[2] Bayerisches Landesamt für Umwelt (Hrsg.), Biogashandbuch Bayern - Materialienband, Kap. 1.7, Stand Mai 2007, p. 20.

[3] European IPPC Bureau (Hrsg.), Reference Document on Best Available Technique in the Cement, Lime and Magnesium Oxide Manufacturing Industries, Feb. 2009, pp. 26 – 32.

[4] Verein Deutscher Zementwerke e.V., Umweltdaten der deutschen Zementindustrie 2009, 11. Ausgabe, 2010, p. 21.m

[5] R. Zah et. al., Ökobilanz von Energieprodukten: Ökologische Bewertung von Biotreibstoffen, Schlussbericht, Empa (Hrsg.), 2007, pp. 92 – 94.

[6] G. Mauschitz, Emissionen aus Anlagen der österreichischen Zementindustrie Berichtsjahr 2009, Vereinigung der österreichischen Zementindustrie (Hrsg.), 2010, p. 4.

[7] B. Baumgartner, M. Kupusovic, H.T. Blattner, National Report on current status of biogas/biomethane production – AUSTRIA, WP5 – deliverable 5.1, Feb. 2010, p. 4.

[8] Fachagentur Nachwachsende Rohstoffe e.V. (Hrsg), Biogas-Anlagen, 12 Datenblätter, www.fnr.de, 2004, pp. 7 – 39.

[9] H. Döhler et. al., Faustzahlen Biogas, Kuratorium für Technik und Bauwesen in der Landwirtschaft e.V. (Hrsg.), 2. Auflage, 2009, p. 187 – 199.

[10] ASUE Arbeitsgemeinschaft für sparsamen und umweltfreundlichen Energieverbrauch e.V. (Hrsg), BHKW-Kenndaten 2005, Verlag rationeller Erdgaseinsatz, 2005, p. 14.

[11] H. Berger, V. Hoenig, Energieeffizienz der österreichischen Zementindustrie, Vereinigung der österreichischen Zementindustrie (Hrsg.), 2010, pp. 18 – 44.

[12] Institut für Energetik und Umwelt GmbH, Studie Einspeisung von Biogas in das Erdgasnetz, Fachagentur Nachwachsende Rohstoffe e.V. (Hrsg), 2. Auflage 2006, pp. 127 – 159.

[13] D. Hornbacher, Online Planung einer Anlage zur Biogas-Netzeinspeisung, www.biogas-netzeinspeisung.at, 2010.

[14] Bgbl.II Nr.42/2010, Ökostromverordnung 2010 – ÖSVO 2010 Teil II, www.ris.bka.gv.at.

[15] Statistik Austria (Hrsg.), Jahresdurchschnittspreise und –steuern für die wichtigsten Energieträger 2009, www.statistik.at, 2009, pp. 1.

[16] Energie-Control GmbH (Hrsg.), Auswertung der Industriepreiserhebung Strom Jänner 2010, www.e-control.at, 2010, pp. 2.

[17] Bayerisches Landesamt für Umwelt (Hrsg.), Leitfaden für effiziente Energienutzung in Industrie und Gewerbe, 2. überarbeitete Auflage, Stand November 2009, p. 27.

[18] International Energy Agency, CO_2 Emissions from Fuel Combustion Highlights, IEA Statistics, 2010 Edition, p. 107.

[20] Energie-Control GmbH (Hrsg.), Auswertung der Industriepreiserhebung Gas Jänner 2010, www.e-control.at, 2010, p. 2.

Improvement of energy utilization in natural gas liquid plant through using self-refrigeration system

H.Farzaneh*, B.Abbasgholi

Science and Research Branch, Islamic Azad University, Tehran, Iran
** Corresponding author. Tel: +982144865320, Fax: +982144865003, E-mail: info@hfarzaneh.com*

Abstract: In recent years, there has been great incentive to improve the energy utilization with which the existing capital in offshore and onshore surface facilities is utilized. One of the most energy intensive processes in oil upstream industry is natural gas liquid or NGL recovery plant. The main gorge of energy consumption in conventional NGL plants is propane refrigeration. Hence, more attention should be focused on the effective utilization of propane chillers in a NGL plant. In this study, a novel process configuration for recovery of natural gas liquids in NGL plant is purposed. The required refrigeration in this configuration is obtained by a self-refrigeration system. In summary, the novel scheme generates refrigeration internally, decreasing cooling load of propane chiller and providing additional refrigeration for inlet gas cooling due to plant capacity increase. Besides, the recycled stripping gas also eliminates the need for external reboiler heat. The warmer the stripping gas, the less demand is placed upon the bottom reboiler, thereby saving fuel and energy cost. In this investigation, a simulation model has been developed on the basis of using novel configuration in Gachsaran NGL1200 in south of Iran. The model has been applied for evaluating of energy utilization in this plant. Results of the model show decreasing in total electricity demand of the plant from 268 kWh/t_{NGL} to 175 kWh/t_{NGL} by decreasing cooling load and electricity consumption in propane chiller. Also, the need for reboiler heat is satisfied and efficacy of demethanizer column is improved from 72% to 84% by more NGL recovery. Finally, economical analysis of the new retrofit has been studied.

Keywords: *NGL plant, self-refrigeration, SGR, energy utilization*

1. Introduction

Natural Liquid gas factories which produce NGL are one of the important and energy intensive units of offshore industries. In these units, natural gas liquids are separated from the sweet gas which has been sweetened in gas sweetening units before. Recovery of natural gas liquids (NGL) components in gas not only may be required for hydrocarbon dew point control in a natural gas stream, but also yields a source of revenue, e.g., natural gas may include up to about fifty percent by volume of heavier hydrocarbons recovered as NGL [1].

Most of the NGL plants in operation today use conventional single-stage turbo expander technology for moderately high ethane recovery. Based on this technology, after the inlet gas is treated to remove water and other contaminants, it's cooled by cold residue gas in gas/gas exchangers. Propane refrigeration is often required to help in condensing the heavy components for a rich gas. Then, liquid condensed from the inlet gas is separated and fed to the tower for further fractionation after being flashed to the tower pressure. The remaining non-condensed vapor portion is subject to turbo-expansion to the top section of the demethanizer column, with the cold liquids acting as the top reflux to enhance recovery of heavier hydrocarbon components.

The growing economic opportunities offered by the markets associated with natural gas liquids determined the development of using different technologies in NGL recovery units. The difference between the various technologies lays in the energy recovery strategies that each of them utilizes [2].

One of the most attractive technologies for reducing energy intensity in NGL recovery unit is Stripping Gas Refrigeration (SGR) method. SGR is a self-refrigeration system is widely

applicable not only for new, grass-root plants but for revamping old, existing plants. This technology utilizes a slipstream from the demethanizer bottom. This stream is totally or partially vaporized, providing additional refrigeration for inlet gas cooling. The flashed vapor generated from the self-refrigeration cycle is recycled back to the column, where it serves as stripping gas. Stripping gas increases the critical pressure thus enhancing the relative volatility.

This paper focuses on revamping existing plants using the stripping gas refrigeration scheme. To this aim, factory of NGL 1200 in south of Iran is selected as case study. The results show the economic return on retrofit investment is much more attractive and also, there are opportunities for upgrading the performance of the plant, e.g., plant capacity increases and energy intensity decreases over the time [3].

2. NGL recovery process

The process flow diagram of a NGL plant based on the simulation of NGL1200 by HYSYS software is depicted in figure (1). According to this figure, inlet sweet gas flows into the two stages of gas to gas heat exchanging process (E_1 and E_3) and exchanges its heat with separated gas stream form the three phases separator (E_6) and therefore, its temperature is decreased from 65^{0C} to 25^{0C}. Then, outflow stream from second heat exchanger enters into two stages of propane chilling system (E_4 and E_5) and it is cooled to temperature lower than -29 centigrade degrees to condense out the liquids. At the exit point of chilling system, gas has two phases condition and therefore liquid and vapor phases should be separated by separator (E_6). The vapor phase returns to the heat exchanger (E_3) and the liquid phase is then fed into the demethanizer column which has 9 trays to stabilize gas liquids and separate light compounds. Demethanizer column also has a kettle reboiler for providing required heat in the bottom section of the column for vaporizing heavy product and recycling it to the column. Overhead flow of column which has more methane and ethane will be recompressed by compressor (E_{11}) and will be returned to the gas injection unit; propane, butane and condensates are separated as bottom product and sent to the pressurized refrigerated storage vessels to await transportation to market [4].

Table (1) represents physical properties of streams which have been approximated by the Peng-Robinson equation of state formula through developing simulation model by HYSYS software. The aforementioned simulation model has been applied for analysis of performance of the factory of NGL1200 and estimation total energy intensity and efficiency of this plant [5].

According to results of simulation, total performance and energy intensity of NGL1200 are represented in table (2). Also, major energy intensive equipments of NGL1200 are reported in table (3).

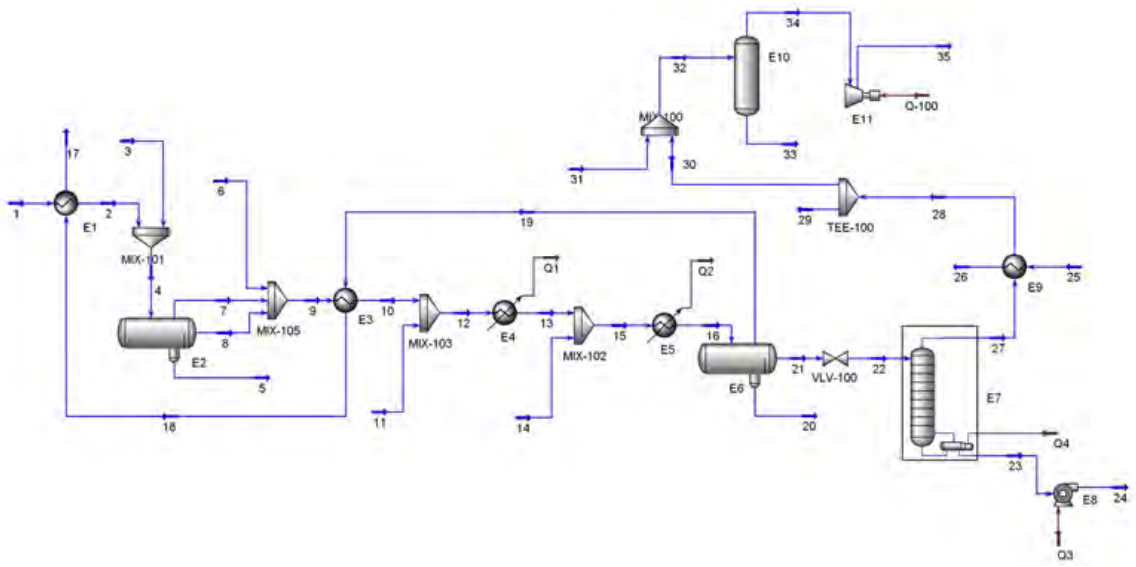

Fig. 1 Process flow diagram of NGL1200

3. Self-refrigeration method

Self- refrigeration method is a modern method to increase NGL plant capacity, to decrease plant electricity consumption and to eliminate the need for external reboiler load. Also, application of this method increases critical pressure and volatility of demethanizer column and therefore, efficacy of column will be improved. This method is known as Stripping Gas Refrigeration (SGR) method [6].

SGR method generates internal refrigeration by expanding a liquid stream from the bottom of the demethanizer column. Simulated process of SGR method and its application in NGL1200 is represented in figure (2)**.** According to this figure, liquid stream from the bottom of the column (stream 39) is then heated by indirect heat exchange with inlet sweet gas to generate a two-phase stream. The two-phase stream (stream 42) is flashed in a separator. The flashed vapor (stream 44) is compressed and recycled to the demethanizer as a stripping gas, which increases the ethane and propane concentration in the column. The flashed liquid stream (stream 43) is pumped and mixed with other NGL product streams.

Three major advantages of using SGR method in a NGL plant may be concluded by following items [7]:

1) Increasing production level up to 20%.
2) Increasing recovery of ethane. Concentration of ethane and propane will be increased in the column and heat profile on the trays will be decreased significantly.
3) Increasing operational pressure of the column is one of the other advantages of this method which increases volatility of propane and ethane and then separation efficacy of column will be increased.

Modification of physical properties of streams after using SGR method in NGL1300 is represented in table (4) [8].

Table1. Physical properties and flow rate of streams

Stream line	1	2	3	4	5	6	7
Temperature (C)	60.5	37	62.1	38.3	38.3	25	38.3
Pressure (kPa)	3690	3680	3770	3680	3680	4300	3680
Mass flow (t/h)	200.6	200.6	12.8	213.4	0.47	2.3	211.5
Stream line	8	9	10	11	12	13	14
Temperature (C)	38.3	38.3	24	25	24	-5	25
Pressure (kPa)	3680	3680	3670	4300	4300	3655	4300
Mass flow (t/h)	1.4	215.2	215.2	2.2	217.4	217.4	2.2
Stream line	15	16	17	18	19	20	21
Temperature (C)	-5	-29	47	-10	-29	-29	-29
Pressure (kPa)	3655	3640	3510	3640	3640	3640	3640
Mass flow (t/h)	219.6	219.6	113	113	113	7	99.6
Stream line	22	23	24	27			
Temperature (C)	-38	33.3	35	-38			
Pressure (kPa)	2000	2000	3910	2000			
Mass flow (t/h)	99.6	78	78	21.6			

Table2. Performance and energy intensity of NGL1300

Inlet gas flow rate	206 t/h
NGL production	78 t/h
Lean gas production	128 t/h
Electricity intensity	268.5 kWh/t
Thermal heat intensity	56.4 kWh/t
Demethanizer Efficacy	72%

Table3. Specification of energy intensive equipments of NGL1200

	Electrical power (kW)	Heat load (kW)
Propane pre chiller (E_4)	3673	7014
Propane main chiller(E_5)	3673	6153
Reboiler	-	4411
Lean Gas Compressor	531×2	-

Table4. Physical properties of main streams after using SGR

Stream line	Flow rate t/h	Pressure kPa	Temperature C
External gas line from two phase heat exchanger (15)	9	3650	7.7
The last external line from two phase heat exchanger (42)	104	1900	16
The last internal line to two phase heat exchanger (39)	104	2000	-26
External line from compressor to demethanizer column(45)	9	1900	16

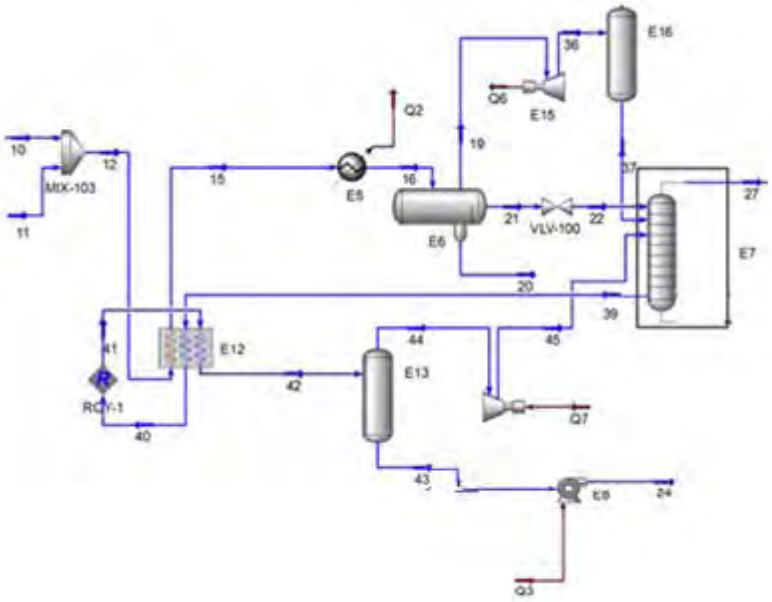

Fig. 2 Using SGR method in NGL1200

4. Results and Discussions

Comparison between results of simulation of NGL1200 before and after using SGR method is represented by table (5).

Table5. Comparison between obtained results before and after using SGR method

	Before	After
NGL production rate (t/h)	78 t/h	92.8
Electricity intensity (kWh/t_{NGL})	268.5	175
Thermal energy intensity (kWh/t_{NGL})	56.4	0
Demethanizer efficacy (%)	72	84

The results indicate that, application of self-refrigeration method reduces electricity intensity of the plant up to 34.7 % and also eliminates the need for reboiler heat load completely. Decreasing in electricity intensity is obtained directly from replacing cooling load of propane per-chiller by heat exchanging of liquid stream from the bottom of demethanizer column with inlet sweet gas. Required capital investment for improving this novel configuration in Gachsaran NGL1200 is represented in table (6).

Table6. Capital investment of SGR method

Item	Capital Investment (10^3 $)
Expander	256
Separators	21.6
Compressor	25.6
Pump	15
Two phase heat exchanger	336
Installation	182

The results of feasibility study show payback period of total investment of project will be lower than 2 years when the unit price of electricity and NGL is considered consequently, 4 cent per kWh and 500 cent per kg [10].

5. Conclusion

The objective of this research work has been to introduce a novel configuration in NGL plants which is obtained by a self-refrigeration system name as Stripping Gas Refrigeration (SGR). SGR scheme provides overall energy integration and replaces propane refrigeration system. The main results of using this configuration may be concluded as decreasing propane refrigeration, eliminating external heat source of reboiler, decreasing compression hoarse power of the plant. Also, using this method is accompanied with lower capital and operating cost with less impact to the existing equipment of the plant. With purposing total capital investment around 836 thousands dollars including, net present value (NPV) of project may be estimated at 5.6 millions dollars through 15 years operation of the system and its economical feasibility will be supported [11].

Acknowledgment

We take this opportunity to thank Iranian Fuel Conservation Company for attending in this paper.

References

[1] J.Bibler, J.S.Marshall, C.Raymond, Status of worldwide coal mine methane emissions and use, International Journal of Coal Geology, 1998, pp.283–310

[2] B.Tirandazi, M.Mehrpooya, A.Vatani , Effect of the valve pressure drop in exergy analysis of c_2+ recovery plants refrigeration cycle , International journal of electrical power and energy systems engineering, 2008, pp.4-8.

[3] L.Roger, J.Chen, Retrofit for NGL Recovery Performance Using a Novel Stripping Gas Refrigeration Schem, IPSIllc, Hostune, Texas USA, 2007

[4] W.C. Lyones, Standard Hand Book Of petroleum & Natural Gas Engineering, Elsevier, 2007

[5] M.Kamaruddin A.Hamid, HYSYS An Introduction to Chemical Engineering Simulate, Department chemical engineering Maleysia,Thirth edition, 2006.

[6] G.Yao, J.J.Chen, S.Land , D.G.Elliot, Enhanced recovery process, 1999, patent 5,992,175.

[7] J.Lee, Y.Z.Jame, S.Y.Juh, D.G.Elliot, International refrigeration for enhanced NGl recovery, 2006, patent 150,627

[8] A. J. Kidnay, W. Parrish, Fundamental Natural Gas Processing, GPP.INC, 2006.

[9] W.County, N.Dakota, Natural gas engineering, McGraw-Hill, Second edition, 2007.

[10] A.J.Kinday, W. R.parrish , Fundamentals of natural gas processing , Taylor and Francis Group , Boca Raton , London, New York, 2006

[11] S.Peters, K.B.Time, R.West, Plant Design &Economics For Chemical Engineering McGraw-Hill ,Forth edition, 2007.

Analysis of optimal application for exhaust gas in thermal oxidizers with case studies

Naser Hamedi[1,*], Arzhang Abadi[2], Ramin Imani Jajarmi[3]

[1,3] *Linköping University, Linköping, Sweden*
[2] *Urmia University, Urmia, Iran*
** Corresponding author. Tel: +46 (0)762 27 40 78, E-mail: nasha244@student.liu.se*

Abstract: There is potential for optimizing thermal oxidizer plants to increase industrial energy efficiency results in environmental and economic dimension of sustainability. In the present work, genetic algorithm is implemented for three thermal oxidizer cases in three different petrochemical plants to optimize the fuel cost for the three Heat Recovery Steam Generators (HRSG's) which are going to be used for the recovery of the heat from the outlet of the thermal oxidizer units. Generally, thermal oxidizers are used in petrochemical plants to burn waste gases in the plant to reduce the environmental impact of the off-gases of plant and normally the waste heat are released to the atmosphere via a stack. The optimization results have been compared for three cases. Five decision variables have been selected and the objective function was optimized. By increasing the fuel price, the values of thermo-economical decision variables tend to those thermodynamically optimal designs.

Keywords: *Heat Recovery Steam Generator (HRSG), thermo-economics, Optimization, Thermal Oxidizer, Genetic Algorithm, Low Density Polyethylene (LDPE) Plant.*

Nomenclatures

c	*Cost per exergy unit*…….. $\$.MJ^{-1}$
c	*Cost of fuel per energy unit*… $\$.MJ^{-1}$
$\dot{c}$	*Cost flow rate*…….. $\$.sec^{-1}$
c_p	*Specific heat at constant Pressure*…… $KJ.Kg^{-1}.K^{-1}$
CRF	*Capital recovery factor*
h	*Enthalpy*…… $KJ.Kg^{-1}$
LHV	*Lower heating value*…… $KJ.Kg^{-1}$
$\dot{m}$	*Mass flow rate*…… $Kg.s^{-1}$
r_c	*Compressor pressure ratio*
T	*Temperature*……K
Z	*Capital cost of a component*……$
$\dot{Z}$	*Capital cost rate*…… $\$.sec^{-1}$
ΔP	*Pressure loss*
η_{ac}	*Compressor isentropic efficiency*
η_{cc}	*Combustion chamber first law efficiency*
γ	*Specific heat ratio*
φ	*Maintenance factor*
EA	*Evolutionary algorithm*
GA	*Genetic algorithm*
P,/Pr,	*pressure ratio of compressor*
r_{ih}	*Inlet humidity percent*
η_{to}	Thermal efficiency of thermal oxidizer
$\dot{W}$	Work…….KW

Subscripts

ac	*Air compressor*
a	*Air*
cc	*Combustion chamber*
ev	*Evaporator*
ec	*Economizer*
f	*Fuel*
F	*Fuel for a component*
g	*Combustion gasses*
j	*Stream*
k	*Component*
s	*Steam*
P	*Product of a component*
Pinch	*Pinch point*

1. Introduction

One of the important ways to reduce the effects of environmental impacts of industrial plants is increasing energy efficiency of the plants. Developing techniques for designing efficient and cost-effective energy systems is one of the foremost challenges of energy engineering face. In a world with finite natural resources and increasing energy demand by developing countries, it becomes increasingly important to understand the mechanisms which degrade energy and resources and to develop systematic approaches for improving the design of

energy systems and reducing the impact on t he environment. The second law of thermodynamics combined with economics represents a very powerful tool for the systematic study and optimization of energy systems. This combination forms the basis of the relatively new field of thermo-economics.

Ethylene is the main feed of LDPE (Low density polyethylene) plant to produce LDPE product(s) in high pressure. By using a compressor system, excess ethylene in different units of the plant, some traced gases like Methane and Propane, small quantity of water and air are forced to a multi channel combustion chamber of thermal oxidizer unit to burn and diminish the concentration of pollutant, as consequences of imposed environmental limitations that exist for the petrochemical off-gases. After burning the off-gases in the combustion chamber, the considerable medium quality waste gas is released to atmosphere via vent stack. In practise, in most of the petrochemical plants the thermal oxidizer units work continuously as a matter of excess amount of ethylene and other mentioned substances.

For a medium LDPE plant, maximum volume off gases reaches 55000 kg/h with constant steady state pressure. This flow produces an average thermal caloric value of 45000 KJ/kg with average 300 °C flue gas.

The structure of a common thermal oxidizer is illustrated in figure 1. The installation consists of two compressor systems, multi channel combustion chambers, fuel supply and burner systems. In current models for the environmental condition the following are considered (T = 298.15 K and P = 1.013 bar). The operating fuel for the total plant is natural gas (taken as methane) with a lower heating value (LHV) equal to 50000 kJ/kg.

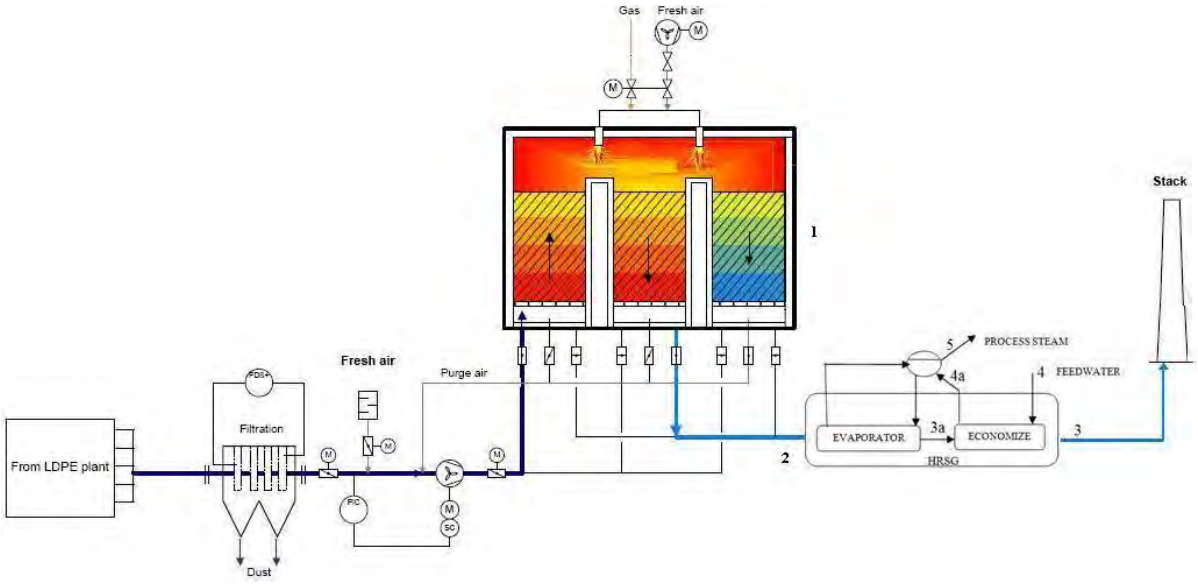

Fig. 1. Schematic sketch of thermal oxidizer with HRSG

In the current research, a part of waste heat energy system (thermal oxidizer) in LDPE (Low Density Polyethylene) plant is optimized according to some decision variables. The hot gases from the combustion chamber are conducted to a HRSG (Heat Recovery Steam Generator) to be utilized for producing steam and hot water. This steam and/or hot water can be used in different ways in this plant (LDPE Plant) or other adjacent industrial plants. Moreover, in this investigation three different thermal oxidizers units were studied and data obtained are analysed for research validation. The models used in this paper are realistic but incomplete

from an engineering point of view since the object of this study is to present distinct models of thermoeconomic optimization. Therefore, it would be unreasonable to use an excessively complicated mathematical model to describe the performance of the plant.

2. Methodology

For modelling the system three categories of equations have been considered, the equations which describe the behaviour of the system (physical model), the equations for calculating the capital costs of the components (economic model) and the equations which has been used to calculate the thermodynamic properties (thermodynamic model) [1,2]. The decision variables selected for the optimization are the compressor pressure ratio P,/Pr, the isentropic efficiencies of the compressor (η_c), inlet humidity percent (r_{ih}), the temperature of the combustion gas at the HRSG inlet (T_2) and thermal efficiency of thermal oxidizer (η_{to}).

The following models are formulated as a function of these decision variables. To simplify these models without loss of methodological generality, the following assumptions are made: (1) The air and the combustion gases behave as ideal gases with constant specific heats. (2) For combustion calculations, the fuel is taken to be methane CH4 (3) All components, except the combustion chamber, are adiabatic. (4) Reasonable values are chosen for the pressure loss of the air and gas flows in the combustion chamber and recuperate boiler.

Our optimization program that is based on evolutionary algorithm has good convergence and better results due to using three input category data from three different petrochemical plants. As we know the optimization procedure is so crucial in engineering fields, especially mechanical engineering. Among the various techniques evolutionary algorithms (EAs) are of the greatest importance because of their convergence rate. Among EA algorithms, the Genetic Algorithm is the best option due to its less time consuming for iteration time as well as satisfying the several constraints. Besides, at the end of this study the influence of alteration in the demanded steam on the design parameters has been also studied.

In this paper, after thermodynamic modelling of the system and formation of the objective function, a cogeneration unit with thermal characteristics of well known problem [1,3,4,5] are simulated, optimized, and its results are compared to the results of other cases; in order to ensure the validity of our physical modelling and optimization procedure. Subsequently, parameters of problem are modified to match the conditions and requirements of the present work.

2.1. Thermodynamic modeling of thermal oxidizer with HRSG

Having known the values of decision variables (r_c, η_c, η_{to}, T2 and r_{ih}) for a set of fixed demands of process steam, the values of temperature and pressure in all lines of system was computed. Consequently, the value of fuel mass flow rate $\dot{m}_f$, which should be expressed in terms of decision variables, is determined. The relations of thermodynamic modelling are as follows:

Air compressor

$$T_{out} = T_{in}\left\{1+\frac{1}{\eta_{AC}}\left[r_c^{\frac{\gamma_a-1}{\gamma_a}}-1\right]\right\}, \quad (1)$$

$$\dot{W}_{ac} = \dot{m}_a.c_{p,a}(T_{out}-T_{in}) \quad (2)$$

Combustion chamber

$$\dot{m}_a h_1 + \dot{m}_f \, LHV = \dot{m}_g h_2 + (1-\eta_{cc})\,\dot{m}_f \, LHV \quad (3)$$

$$\frac{P_2}{P_1} = (1 - \Delta P_{cc}) \quad (4)$$

Heat recovery steam generator

$$\dot{m}_s (h_5 - h_4) = \dot{m}_g (h_2 - h_3) \quad (5)$$

$$\dot{m}_s (h_5 - h_{4a}) = \dot{m}_g (h_2 - h_{3a}) \quad (6)$$

2.2. Objective function

The objective function is defined as the sum of two parts; the operational cost rate, which is related to the fuel expense, the rate of capital cost which stands for the capital investment and maintenance expenses. Therefore, the objective function represents total cost rate of the plant in terms of dollar per unit of time.

$$Obj.Func. = c_f \dot{m}_f LHV + \sum \dot{Z}_k \quad (7)$$

Since the amounts of ultimate products (process steam) are fixed, the objective function is to be minimized so that the values of optimal design parameters would be obtained. For calculating the rate of operating cost equation, we have:

$$\dot{c}_f = c_f \dot{m}_f LHV \quad (8)$$

In which c_f = 0.003 $/MJ is the regional cost of fuel per unit of energy,$\dot{m}_f$ is the fuel mass flow rate, and LHV = 50000 kJ/kg is the lower heating value of Methane.

For expressing the purchase cost of equipment in terms of design parameters, several method have been suggested [2, 7-11]. In this paper, we used the cost functions mentioned in ref [2]. However, some modifications were made to tailor these results to the regional conditions in Iran and taking into account the inflammation rate. For converting the capital investment into cost per time unit:

$$\dot{Z}_k = Z_k . CRF . \varphi / (N \times 3600) \quad (9)$$

Where, Z_k is the purchase cost of component in dollar, CRF (18%) is the capital recovery factor, N is the annual number of the operation hours of the unit (7500 hr), and φ (1.06) is the maintenance factor.

2.3. Optimization Procedure

Minimizing the objective function Eq.7 is a nonlinear optimization problem. In order to achieve feasible design parameters some physical constraints should be considered seriously. The list of these constraints and their reasons are briefed in table 1. Moreover, the following inequality constraints should be satisfied in heat exchangers (air pre-heater and heat recovery steam generator).

$$T_2 > T_1, \quad T_2 > T_5, \quad T_{3a} > T_5 + \Delta T_{pinch,\,min} \tag{10}$$

In the present work a genetic algorithm code is developed in Matlab Software Programming.

Table1. The list of constraints

Constraints	Reason
$T_2 \le 1600^{\circ} K$	Material limitation
$r_c \le 16$	Commercial availability
$\eta_{ac} \le 0.9$	Commercial availability
$\eta_{to} \le 0.96$	Commercial availability
$T_3 \ge 400^{\circ} K$	To avoid formation of sulfuric acid in exhaust gases
$T_{4a} = T_5 - 15^{\circ} K$	To avoid evaporation of water in HRSG economizer

2.4. Evolutionary algorithm (Genetic Algorithm)

Such algorithms simulate an evolutionary process where the goal is to evolve solutions by means of cross over, mutation, and selection based on their quality (fitness) with respect to the optimization problem at hand. Evolutionary algorithms (EAs) are highly relevant for industrial applications, because they are capable of handling problems with non-linear constraints, multiple objectives and dynamic components properties that frequently appear in real-world problems. Moreover the input and output values for Genetic Algorithm method used in this study are shown in tables 2, 3.

Table 2. Genetic algorithm input

Tuning Parameters	Value
Population size	500
Maximum number of generation	1000
PC(Probability of Crossover) %	70
Pm (Probability of mutation) %	1
Number of crossover	2
Selection in process	Tournament
Tournament size	2

3. Discussion and result

The numerical values of the optimum design parameters of the thermal oxidizer with HRSG are listed in table 3. Moreover, the constraints of the problem are listed in table 1. These

results are compared with other case's results. Figure 2 depicts the changes in the objective function versus generation in the developed genetic algorithm code.

Table 3. The comparison of simulation and optimization numerical output for three mentioned cases.

Decision variable	Optimum design	Optimum design	Optimum design
r_c	8.597	8.523	8.504
η_C	0.8465	0.8468	0.83292
η_{to}	94.5	95	95.4
T_2 (K)	504	573	642.3
r_{ih} (K)	80	70	65
Objective Function	0.362 ($/s)	0.3617 ($/s)	0.3294 ($/s)

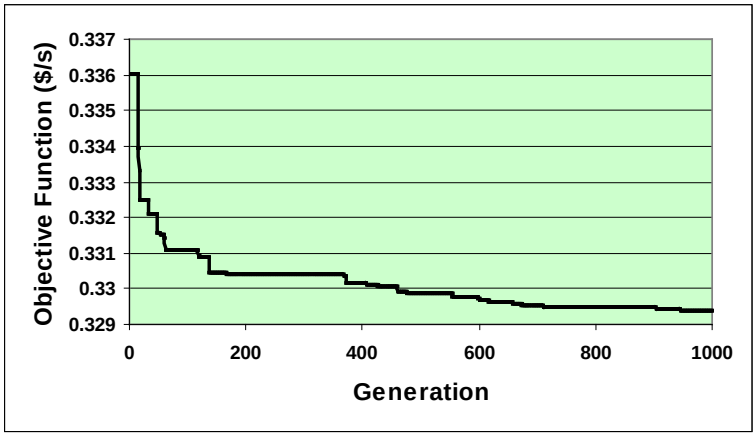

Fig. 2. Variation of Objective Function of the system with Generation (CE=.003$/MJ).

Study of the variation of the optimal decision variables versus fuel unit cost reveals that by increasing the fuel cost optimal decision variables generally shift to thermodynamically more efficient design. As it can be clearly seen the values of decision variables r_p, η_{ac}, and HRSG inlet temperature (T_2) increase with increasing fuel unit cost. It is worthy to mention that while increasing combustion inlet temperature (T_1) reduces the exergy destruction in combustion chamber and heat exchangers (HRSG), due to the exhaust gases constraint ($T_3 >$ 400K); it decreases with increasing the fuel unit cost. It should be noted that for each T_2 there exists a T_1 in which the best thermodynamical efficiency may be achieved. Moreover, an increase in HRSG inlet temperature reduces the exergy destruction in combustion chamber; and since increasing T_2 results in higher exhaust temperature of exhaust gases, the constraint $T_3 >$ 400K does not cause any limitation for rising T_2. Due the fact that any increase in T_2 will dramatically affects the HRSG investment cost, figures 3-5 show the influence of the unit cost of fuel on the values of some the optimal decision variables. Figure 5 shows that when the fuel price increased the combustion chamber fuel mass flow rate decrease for minimizing the objective function. Due to uncertainty of capital investment data, it is imperative to study the results of capital expense variation on the optimal values of decision variables.

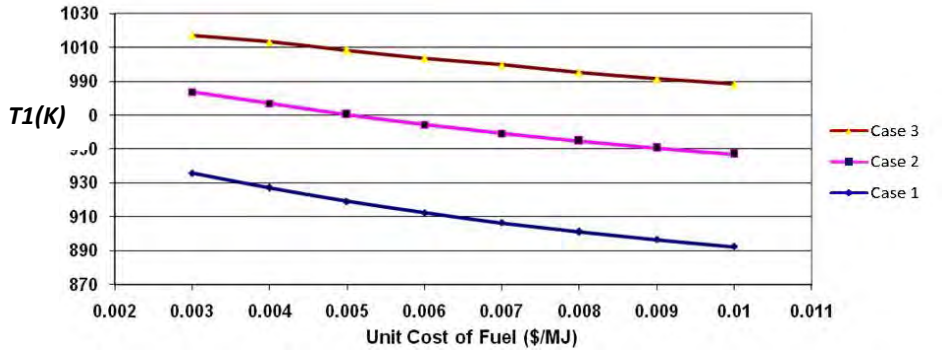

Fig. 3. The effects of fuel unit cost on the optimal value of combustion chamber inlet temperature, T1

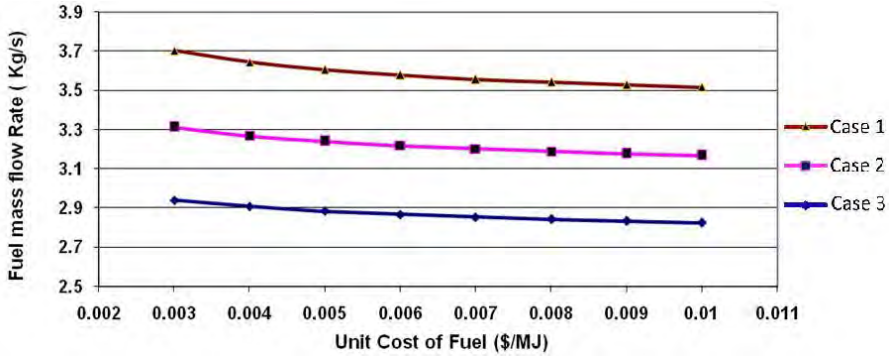

Fig. 4. The effects of fuel unit cost on the optimal value of Fuel Mass Flow Rate, mf

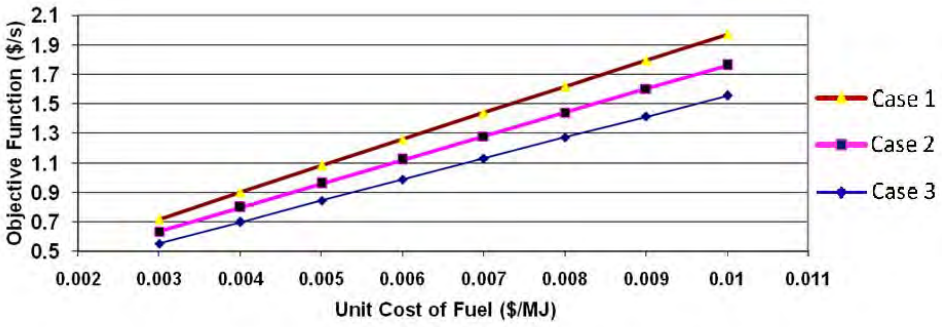

Fig. 5. The effects of fuel unit cost on the optimal value of Objective Function ($/s)

4. Conclusion

The determined optimum design parameters for thermal oxidizer with HRSG apparently show a trade-off between thermodynamically and economically optimal designs. For example, from thermodynamic point of view, the decision variable η_c should be selected as high as possible while this leads to an increase in capital cost. It should be noted that any change in the numerical values of a decision variable not only affects the performance of the related equipment but also all the performance of other equipments as well. It can be deduced from the figures 3-5 that by increasing the fuel price the values of decision variable in thermo-economically optimal design tend to those of thermodynamically optimal design.

Using heat recovery, thermal oxidizers cause more energy efficiency and decrease the level of green house gases accordingly. In spite of the fact that utilizing these types of technologies

categorized as an end-of-pipe solution, nevertheless according to the three pillars of sustainability it contribute to both environmental dimension and economic dimension of sustainability.

References

[1] Valero, A., Lozano, Miguel A., Serra, L., Tsatsaronis, G., Pisa, J., Frangopoulos, C., and Von Spakovsky, M. R., 1994, " CGAM Problem: Definition and Conventional Solutions," Energy-The International Journal, 19, pp. 279-286.

[2] Bejan, A., Tsatsaronis, G., Moran, M., 1996, Thermal design & optimization, John Wiley & Sons Inc.

[3] Ghaffarizadeh, A., 2006, Investigation on Evolutionary Algorithms Emphasizing Mass Extinction, B.Sc thesis, Shiraz University of Technology, Shiraz, Iran.

[4] Frangopouls, C. A., 1994, "Application of the Thermoeconmic Functional Approach to the CGAM problem," Energy-The International Journal, 19, pp. 323-342.

[5] Tsatsaronis, G., and Pisa, J., 1994, "Exergoeconomic Evaluation and Optimization of Energy Systems- Application to the CGAM Problem, Energy-The International Journal, 19, pp. 287-321.

[6] Valero, A., Lozano, M.A., Serra, L., Torres, C., 1994, "Application of the Exergetic Cost Theory to the CGAM problem, Energy -The International Journal, 19, pp. 365-381.

[7] Spakovsky, M.R., 1994, " Application of Engineering Functional Approach to The Analysis and Optimization of the CGAM problem," Energy- The International Journal, 19, 343-364.

[8] Moran, M.J., 1989, Availability Analysis: A Guide to Efficient Energy Use, ASME Press, New York.

[9] Horlock, J.H., 1987, Cogeneration-Combined Heat and Power (CHP), Thermodynamics and Economics, pergamon press.

[10] Kotas, T.J., 1995, The exergy method of thermal plant analysis, Krieger Pub. Co., Florida.

[11] Szargut, J., Morris, D.R., Steward, F.R., 1988, Exergy analysis of thermal, chemical, and metallurgical processes, Hemisphere Pub. Co., New York.

Evaluation of repowering in a gas fired steam power plant based on exergy and exergoeconomic analysis

Mohammad Baghestani[1], Masoud Ziabasharhagh [1*], Mohammad Hasan Khoshgoftar Manesh[1]

[1]*Mechanical Engineering Faculty K.N.Toosi University of Technology, Tehran, Iran*
** Corresponding author. Tel: +982184063255, E-mail: mzia@kntu.ac.ir*

Abstract: Increased competition among power generating companies, changes in generating system load requirements, lower allowable plant emissions, and changes in fuel availability and cost accentuate the need to closely assess the economics and performance of older electric generating units. Generally, decisions must be made as to whether these units should be retired and replaced with new generation capacity, whether capacity should be purchased from other generation companies, or if these existing units should be repowered. These decisions usually require the evaluation of many factors. The analysis is usually complicated due to the interaction of all the factors involved. In this paper, evaluation of a 156MW steam power plant and proposed repowered scenario has been performed. The exergy and exergoeconomic analysis method was applied in order to evaluate the proposed repowered plant. Simulation of each case has been performed in Thermoflow software. Also, computer code has been developed for exergy and exergoeconomic analysis. It is anticipated that the results provide insights useful to designers into the relations between the thermodynamic losses and capital costs, it also helps to demonstrate the merits of second law analysis over the more conventional first law analysis techniques.

Keywords*: Repowering; Combined cycles; Gas turbines; Steam injection*

Nomenclature

c *cost per unit exergy ($/MW) .....($/MW)*
C *cost flow rate .....($/hr)*
e *exergy rate per mass.....(MW/kg)*
E *specific exergy .....(MW)*
Z *capital cost rate of unit.....($/hr)*
GT *…….gas turbine*
CRF …….capital recovery factor
PWF …….Present worth factor
LHV……..Lower heating value
PW……Present worth

1. Introduction

Deregulation and competition are further fueling the demand for new power generation equipment worldwide. Due to the availability and cleanliness of gas, and the ease of consent, gas turbine applications have increased over the last few years. This development is driven by the addition of capacity, but also by major replacement programs.[1] Almost all industrialized countries are now facing some degree of electric power shortage. The major problem is probably the lack of suitable sites for building new power plants of whatever type or size. Moreover, increasing environmental awareness has resulted in more demanding requirements in terms of preliminary analysis, prolonging and complicating the plant commissioning process. All these problems have led many utilities to consider extending the life of existing plants by repowering. Basically, these interventions have been done on gas fired steam plants by addition of a natural gas fired turbine. This reduces specific emissions of the existing steam plant while maintaining or even slightly improving its efficiency. As a rule, a repowered plant can be expected to give a lower cost per kW h produced as well as per kW installed repowering of steam plants can be achieved in two ways: feed water repowering and boiler repowering. The first option uses heat from the turbine exhaust to raise the feed water temperature instead of bleeding steam. This means that increased steam flow has to be managed by the low pressure section of the original steam turbine, requiring either extensive modification of the steam turbine or impairing the repowered plant performance. The other

option, boiler repowering, entails major steam generator redesign[2]. Energy systems involve a large number and various types of interactions with the world outside their physical boundaries. The designer must, therefore, face many issues, which deal primarily with the energetic and economic aspects of the system. Thermodynamic laws govern energy conversion processes, costs are involved in obtaining the final products (expenses for the purchase of equipment and input energy resources, operation and maintenance costs), and the effects of undesired fluxes to the ambient must be evaluated in order to answer environmental concerns. Second law analysis has been widely used in the last several decades by many researchers. Exergy analysis usually predicts the thermodynamic performance of an energy system and the efficiency of the system components by accurately quantifying the entropy-generation of the components [3]. Furthermore, exergoeconomic analysis estimates the unit cost of products such as electricity, steam and quantifies monetary loss due to irreversibility. Also, this analysis provides a tool for the optimum design and operation of complex thermal systems [3], [4], [5].

In this study, exergetic, thermoeconomic and exergy analyses have been performed for 156MW steam cycle and repowered gas fired steam power plants. In these analyses, mass and energy conservation laws were applied to each component. Quantitative balance of the exergies and exergy costs for each component and for the whole system was carefully considered. The exergy-balance equation developed by Oh et al. [6] and the corresponding exergy cost-balance equations developed by Kimet al. [7] were used in these analyses. In this regard, computer program has been developed for energy, exergy, exergoeconomic and exergy analysis of both of cases in different load conditions. Furthermore, it can also used to study plant characteristics, namely, thermodynamic performance and sensitivity to changes in process and/or component design variables. In this paper, the authors evaluate and compare repowered power planet and steam power plants in view of exergy and thermoeconomic analysis.

2 Process description

In this paper, GHAZVIN steam cycle power plant has repowered and compared with old steam cycle. The steam cycle power plant encompasses three turbines, that work with three different pressures and 6 feed water heaters. The Steam cycle has been modeled by MATLAB code and STEAM PRO (THERMOFLOW). Results of modeling steam cycle have been introduced and compared with real data in table.1.

Table1. Compare result of modeling steam cycle

	THERMOFLOW	Simulation code	Real
Plant Gross power(kW)	156300	156305	156294
Plant Gross Heat Rate(kJ/kWh)	9010	9120	8976
Plant Gross Efficiency (LHV)	39.9%	39.4%	40.1%
Superheater Capacity(kg/s)	133	130	136
Reheater Capacity(kg/s)	115	114	117

3. Repowering

There are several alternatives to combine and integrate a gas turbine into an existing steam power plant. For 156MW steam power plant unit in Iran, the best alternative is full repowering because its boiler is very old and boiler life time is concluded. Full repowering is defined as complete replacement of the original boiler with a combination of one or more gas turbines (GT) and heat-recovery steam generators (HRSG), and is widely used with very old

plants with boilers at the end of their lifetime. It is considered as one of the simplest ways of repowering for existing plant.
For this power plant, Full Repowering with SGT5-4000F (formerly known as CC 2.V94.3A) with triple pressure reheat cycle was found to be the most economic approach.
Schematic flow diagram of combined cycle with the components is shown in Fig. 2. The gas cycle is selected as a topping cycle. The heating devices in the HRSG are arranged from the high temperature (HT) to the low temperature (LT) exchangers in the flue gas path to get the minimum temperature difference between the flue gas and the water/steam.

4. Exergoeconomic Analysis

All costs due to owning and operating a plant depend on the type of financing, the required capital, the expected life of a component, and so on. The annualized (levelized) cost method of Moran [9] was used to estimate the capital cost of system components in this study. The amortization cost for a particular plant component may be written as:

$$PW = C_t - S_n PWF(t,n) \quad (1)$$

$$\dot{C}(\$/year) = PW \times CRF(t,n) \quad (2)$$

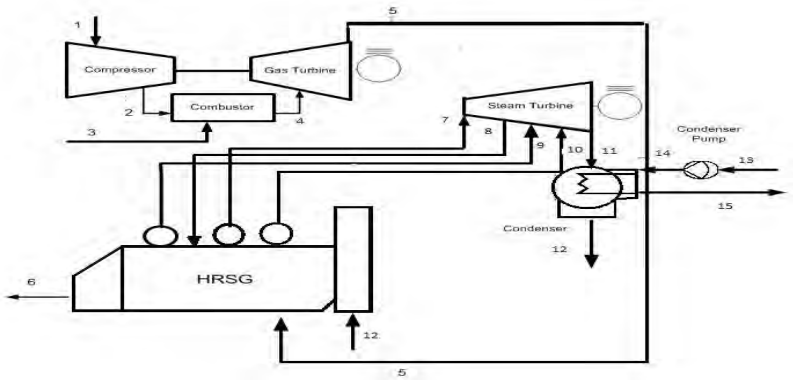

Fig 1.- combined cycle power plant

The present worth of the component is converted to annualized cost by using the capital recovery factor CRF(*i*,*n*), i.e [4]. Dividing the levelized cost by 8000 annual operating hours, we obtain the following capital cost for the *k*th component of the plant.

$$Z_k = \Phi_k \dot{C}_k/(3600 \times 8000) \quad (3)$$

The maintenance cost is taken into consideration through the factor $\Phi_k = 1.06$ for each plant component whose expected life is assumed to be 15 years [6].

4.1 Thermoeconomic Modeling

The results from an exergy analysis constitute a unique base for exergoeconomics, an exergy-aided cost reduction method. A general exergy-balance equation, applicable to any component of a thermal system may be formulated by utilizing the first and second law of thermodynamics [4].
The cost balance expresses that the cost rate associated with the product of the system (C_P), the cost rates equals the total rate of expenditure made to generate the product, namely the fuel cost rate (C_F), the cost rates associated with capital investment (Z^{CI}), operating and

maintenance (Z^{OM}) [12].In a conventional economic analysis, a cost balance is usually formulated for the overall system (subscript tot) operating at steady state [11]:

$$\dot{C}_{P,tot} = \dot{C}_{Ftot} + Z_{tot} \quad (4)$$

Accordingly, for a component receiving a heat transfer and generating power, we would write [4]:

$$\sum_e \dot{C}_{e,k} + \dot{C}_{w,k} = \dot{C}_{q,k} - \sum_i \dot{C}_{i,k} + Z_k \quad (5)$$

To solve for the unknown variables, it is necessary to develop a system of equations applying Eq. (5) to each component, and it some cases we need to apply some additional equations, to fit the number of unknown variables with the number of equations [12]. A general exergy-balance equation, able to any component of a thermal system may be formulated by utilizing the first and second law of thermodynamics. In a conventional economic analysis a cost balance is usually formulated for the overall system operating at steady state. To derive the cost balance equation for each component, we assigned a unit cost to the principal product for each component. Depending on the type of fuel consumed in the production process different unit cost of product should be assigned [13].

Table2. Combined cycle results

	Repowering
Gas Turbine(kW)	278041
Steam Turbine(kW)	125655
Plant Total (kW)	403695
Plant net LHV efficiency (%)	55.27
Plant net LHV heat rate(kJ/kWh)	6514
Gas turbine LHV efficiency (%)	39.05
Steam turbine efficiency (%)	34.59

5. Results and discussion

In this paper, computer codes have been developed for thermodynamic simulation and analysis of 156-MW old steam cycle and 400-MW repowered combined power plants. The enthalpy and entropy of non-interacting gas species were calculated by using appropriate polynomials fitted to the thermophysical data in the JANAF Tables [14]. Also the values of physical properties such as enthalpy and entropy for water and steam were evaluated by using equations suggested by the International Association for the Properties of Water and Steam IAPWS-IF97) [14].

Table 2 indicates specification of repowered plant. It shows that, 68% of total power is produced by gas turbine cycle with 39% efficiency, in addition remained power are produced by steam cycle with 34% overall efficiency. Repowered cycle produces 250MW more than old power plant. Heat rate in repowering power plant is 6500(KJ/KWh) and 1500(KJ/KWh) more than old power plant. As a result of repowering, overall efficiency rises 15% and new power plant produce net power with less reduction of energy. The combined cycle results have been developed for gas turbine partial load. Load condition varied from 30% to 100% of full load and figure 2 presents load variation and net power of cycles. Further, entire rate of

exergy destruction has been shown in this figure. However full load has the most exergy destruction, ratio of exregy destruction to supplied energy is less than partial load. In figure 3 efficiency of combined cycle accompaniment gas turbine cycle and steam cycle exhibited. Gas turbine efficiency severely depends on design load and it is decreased when works at partial load states. Since supplied energy for steam cycle depends on exit flow stream of gas turbine, steam cycle efficiency is just independent of load condition. Combined cycle efficiency varied from 40% to 55% and deteriorates with variation from design load.

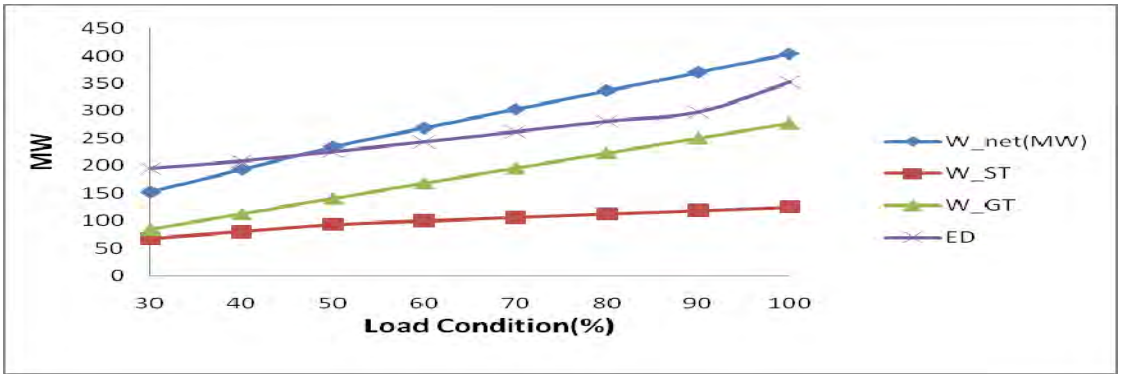

Fig 2. Variation of output power

In this regard, exergy flow and cost flow rates of exergy with and without considering capital investment for each stream in old power plant and repowering plant have been calculated. Also, Table 3 and 4 show Exergy destruction and cost fuel and product rates of exergy with and without considering capital investment for each component in old and repowered power plants. These results represent that boiler in old steam power plant and that combustion chamber and heat recovery steam generator in repowered combined cycle has most exergy and exergy cost destruction due to nature of combustion; however combustor in gas fired combined cycle plant shares about 51% TED, 44% TCD0 and 43% TCD. In next steps, compressor and steam generator of repowered have most exergy and exergy cost destruction. Cost product of steam turbine and gas turbine for combined cycle with and without considering capital investment at various load conditions has been presented in figure 4. As results shown, CP_0 and CP increase when load condition reduces because the thermal efficiency decreases. Therefore full load has the best and minimum cost product. In figure 5 rate of total cost exergy destruction has been shown at different load. As results shown, TCD0 and TCD0 reduce when load condition decreases and vice versa because the fuel consumption decreases when load condition reduces and vice versa, so TCD0 and TCD have direct relation with load conditions. In steam cycle power plant 430 MW exergy is destructed and more than 85% of exergy destruction happened in boiler. However combined cycle produced 250 MW net power more than steam cycle, Total exergy destruction in combined cycle is 296 MW and 70% of steam cycle exergy destruction. Since cost product of gas turbine in combined cycle is less than steam turbine and majority of output power produced with gas turbine, combined cycle cost product is reasonable. Therefore repowered power plant generated more power than old power plant with recuperated efficiency and more reasonable cost product.

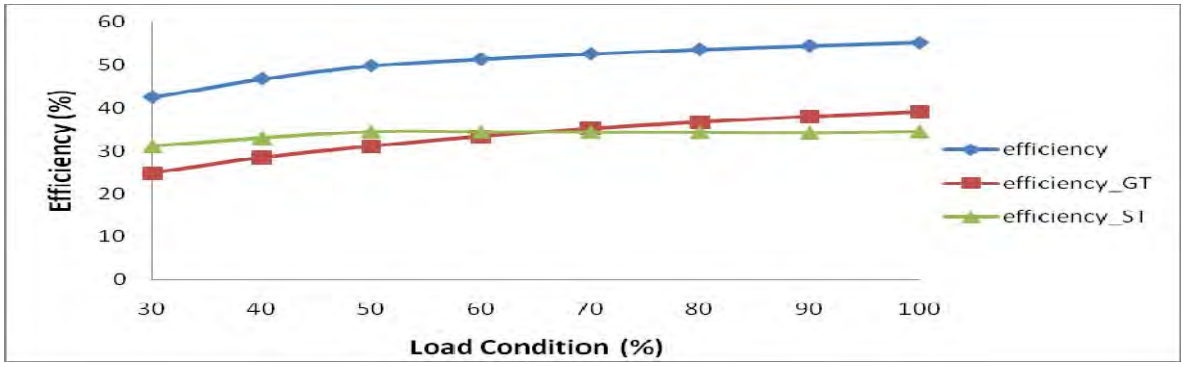

Fig 3. Partial load efficiency

Table 3. Exergy destruction and cost fuel and product rates of exergy with and without considering capital investment for each component in steam cycle power plant

Component	Exergy Destruction	CF0 ($/MW)	CP0 ($/M	CD0 ($.s)	CF ($/MW)	CP ($/MW	CD ($/s)
FWH1	1.2437	0.0054	0.0086	0.0067	0.0056	0.009	0.0069
FWH2	0.3984	0.0054	0.0059	0.0021	0.0056	0.0062	0.0022
FWH3	0.3295	0.0054	0.0399	0.0017	0.0056	0.0414	0.0018
FWH4	0.5141	0.0187	0.0193	0.0096	0.0196	0.0203	0.0100
FWH5	0.539	0.0055	0.0062	0.0029	0.0057	0.0065	0.0030
FWH6	0.5659	0.0057	0.006	0.0032	0.0059	0.0064	0.0033
CONDENSER	6.0506	0.0054	0.0103	0.0326	0.0056	0.0109	0.0338
LP St Turbine	9.1386	0.0057	0.0068	0.0520	0.0059	0.0072	0.0539
IP St Turbine	2.4625	0.0054	0.0056	0.0132	0.0056	0.0059	0.0137
HP St Turbine	18.5699	0.0054	0.0061	0.1002	0.0056	0.0064	0.1039
Boiler	388.9632	0.0014	0.0043	0.5445	0.0014	0.0044	0.5445
CP	0.3484	0.003	0.0038	0.0010	0.0031	0.004	0.0010
FPT	1.3422	0.003	0.0042	0.0040	0.0032	0.0045	0.0042

6. Conclusion

In this paper, an exergy-costing method has been applied to both cases to estimate the unit costs of electricity produced from steam turbines. The computer program that was developed which shows that the exergy and the thermoeconomic analysis presented here can be applied to any energy system systematically and elegantly. If correct information on the initial investments, salvage values and maintenance costs for each component can be supplied, the unit cost of products can be evaluated.

Table 4. Exergy destruction and cost fuel and product rates of exergy with and without considering capital investment for each component in repowered power plant

Component	Exergy Destruction(MW)	CF0 ($/MW)	CP0 ($/MW)	CD0 ($.s)	CF ($/MW)	CP ($/MW)	CD ($/s)
COMP	46.2489	0.0061	0.0073	0.2821	0.0064	0.0078	0.2959
COMB	152.5663	0.0049	0.0059	0.7475	0.0051	0.0061	0.7780
GT	17.0101	0.0059	0.0061	0.1003	0.0061	0.0064	0.1037
ST	36.2881	0.0083	0.0092	0.3011	0.0089	0.0101	0.3229
HRSG	38.6824	0.0063	0.0073	0.2436	0.0065	0.0078	0.2514
COND	4.8385	0.0083	0.2376	0.0401	0.0083	0.2603	0.0401
FWP	0.0236	0.0064	0.0113	0.0001	0.0064	0.0177	0.0001
CWP	0.6226	0.0064	0.0006	0.0039	0.0064	0.0007	0.0039

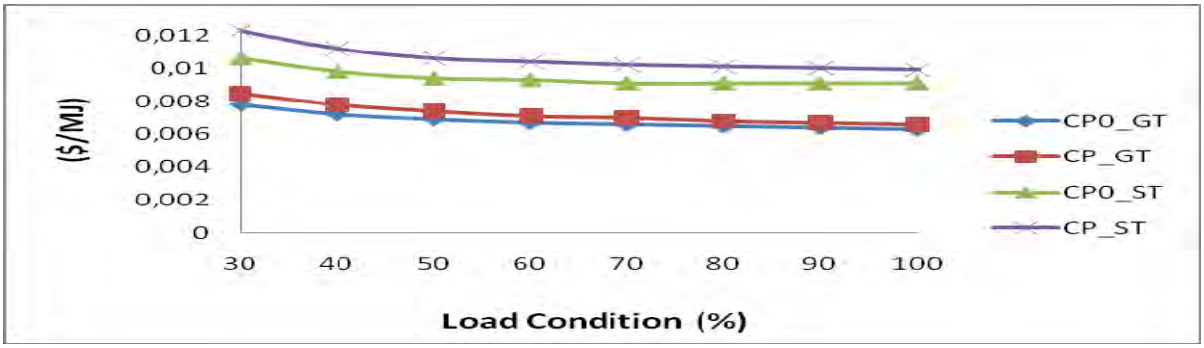

Fig4. C_p and C_{P0} of repowered power plants at different loads

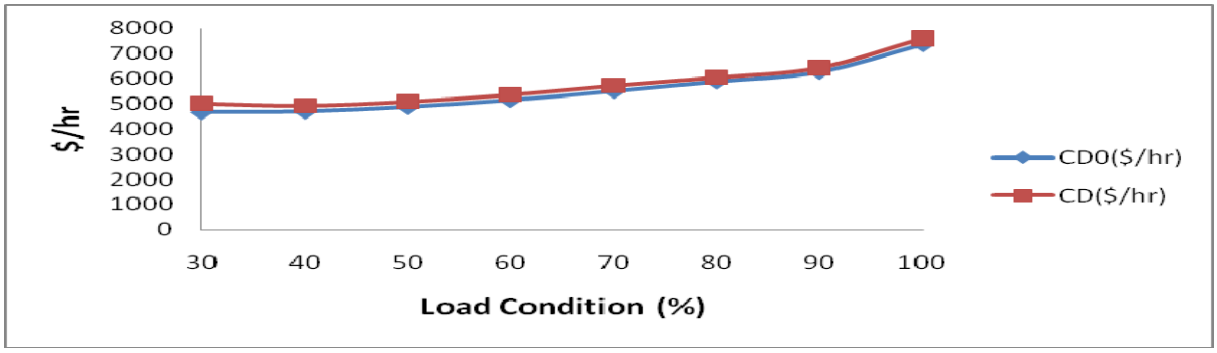

Fig 5.CD, CD_0 of repowered power plants at different load

Although the overall picture of a system can be shown and major directions for improving the system performance can be identified from the above two levels of analysis, the maximum potential or the limit of improvement for individual units and processes are still uncertain, since the exergy loss analysis so far is based on the concept of total exergy loss. In some cases, the suggestions for promising modifications based on the total exergy loss may be misleading, since they do not consider the minimum exergy loss which is required to operate a process.

References

[1] M.Frankle. The standardized repowering solution for 300 MW steam power plants in Russia. Siemens AG 2006.

[2] R.carapellucci, A.Milazzo. Repowering combined cycle power plant by a modified STIG configuration . Energy Conversion and Management 48 (2007) 1590–1600.

[3] Sanjay Y, Singh O, Prasad BN. Energy and exergy analysis of steam cooled reheat gas–steam combined cycle. *Applied Thermal Engineering* 2007; 27: 2779–2790.

[4] Chao Z, Yan W. Exergy cost analysis of a coal fired power plant based on structural theory of thermoeconomics. *Energy Conversion and Management* 2006; 47:817–843.

[5] Modesto M, Nebra SA. Analysis of a repowering proposal to the power generation system of a steel mill plant through the exergetic cost method, *Energy* 2006; 31: 3261–3277.

[6] Cziesla F. Produktkostenminimierung beim Entwurf komplexer Energieumwandlungsanlagen mit Hilfe von wissensbasierten Methoden, no. 438 in Fortschr. -Ber. VDI, Reihe 6, VDI Verlag, D¨usseldorf, 2000.

[7] Cziesla F, Tsatsaronis G. Iterative exergoeconomic evaluation and improvement of thermal power plants using fuzzy inference systems. *Energy Conversion and Management* 2002; 43: 1537–1548.

[8] Uhlenbruck S, Lucas K. Exergoeconomically-aided evolution strategy applied to a combined cycle power plant. *International Journal of Thermal Science* 2004; 43: 289–296.

[9] Bejan A, Tsatsaronis G, Moran M. Thermal design and optimization. New York: Wiley; 1996.

[10] Dobrowolski R, Witkowski A, Leithner R, Simulation and optimization of power plant cycles, in: G. satsaronis, M. Moran F. Cziesla T. Bruckner (Eds.), ECOS 2002, Proceedings of the 15th International Conference on Efficiency, Costs, Optimization, Simulation and Environmental Impact of Energy Systems, Berlin, Germany, 2002, pp. 766–772.

[11] Nafey AS, Fath HES, Mabrouk AA. Exergy and thermoeconomic evaluation of MSF process using a new visual package. *Desalination 2006;* 201: 224-240.

[12] Dobrowolski R, Witkowski A, Leithner R. Simulation and optimization of power plant cycles. ECOS 2002, Proceedings of the 15th International Conference on Efficiency, Costs, Optimization, Simulation and Environmental Impact of Energy Systems, Berlin, Germany, 2002, pp. 766–772.

[13] Emmerich M, Grotzner M, Schutz M. Design of graph-based evolutionary algorithms: A case study for chemical process networks. Evolutionary Computation 2001; 9 (3): 329–354.

[14] Joint Army-Navy–Air Force Thermochemical Tables. NSRDS-N3537, Washington, DC: National Bureau of Standard Publications; 1985.

An Inquiry into the Sources of Change in Industrial Energy Use in the Japanese Economy: Multiple Calibration Decomposition Analysis

Makoto Tamura[1,*], Shinichiro Okushima[2]

[1] *Ibaraki University, Mito-city, Japan*
[2] *University of Tsukuba, Tsukuba-science-city, Japan*
** Corresponding author. Tel: +81 292288817, Fax: +81 292288817, E-mail: tamura@mx.ibaraki.ac.jp*

Abstract: Decomposition methodologies are necessary to examine the causal factors of energy use trends in an economy. This paper suggests a new approach -the Multiple Calibration Decomposition Analysis (MCDA)- to investigate the sources of change in industrial energy use in the Japanese economy. The multiple calibration technique is utilized for an *ex post* decomposition analysis of structural change between periods, enabling distinction between price substitution and technological change for each sector. This paper explains the theoretical properties of MCDA and applies it to an empirical case -the change in energy use in Japanese industry from 1970 to 1990. This paper clarifies how industrial energy use was affected by price substitution or technological change through the experience of the two oil crises, focusing on energy-intensive industry. The paper shows that technological change played an important role in reducing industrial energy use in the Japanese economy. Remarkably, oil-saving technological change advanced by 60% or more in energy-intensive industry during the 1980s.

Keywords: *calibration, decomposition, industrial energy efficiency, price substitution, technological change*

1. Introduction

New interest has arisen in energy demand analysis, reflecting the rapid fluctuation of oil prices, and by the same token the problem of climate change (e.g., Dowlatabadi and Oravetz [1], Metcalf [2], Sue Wing [3]). From a historical point of view, discussions of energy demand analysis have been lively since the oil crises of the 1970s. A vast amount of literature has been devoted to such analyses, including classic works by Hudson and Jorgenson [4] Berndt and Wood [5], Manne [6], Borges and Goulder [7], and Solow [8].

Change in energy use is caused by various factors, including price substitution and autonomous technological development. Determining the contribution of these factors to energy use trends is a difficult but necessary quest, for which decomposition techniques are required. In this context, many decomposition methodologies have been accepted for the quantification of causal factors: for example, Index Decomposition (ID; see, e.g., Ang and Zhang [9], Hoekstra [10]) and Structural Decomposition Analysis (SDA; see, e.g., Rose and Casler [11], Rose [12], Hoekstra [10]), which are well-established decomposition methodologies for this purpose.

This paper proposes a new approach -the Multiple Calibration Decomposition Analysis (MCDA)- to investigate the driving forces of change in industrial energy use in the Japanese economy. The MCDA methodology was originally proposed by Okushima and Tamura [13]. The multiple calibration technique is applied to an *ex post* decomposition analysis of structural change between periods, enabling distinction between price substitution and technological change for each sector. This approach has sounder microtheoretical foundations than conventional methods.

In this paper, the MCDA methodology is applied to the decomposition analysis of change in industrial energy use following the oil crises of 1970-1990, focusing on energy-intensive industry. This period includes two oil crises, during which a rise in oil prices influenced the

Japanese economy to an enormous extent. Moreover, energy use by industry, especially energy-intensive industry, is a key factor of change in energy use in the economy. This is an appropriate area to apply this method to evaluate the extent to which industrial energy use was affected by price substitution or technological change. Besides that, this kind of analysis may add to our stock of information for future Japanese energy or environmental policy.

The remainder of the paper is structured as follows. Section 2 explains the MCDA methodology. Section 3 applies the method to an empirical case, energy use in Japanese industry from 1970 to 1990. The final section provides concluding remarks.

2. Methodology

This section outlines a new decomposition methodology -the Multiple Calibration Decomposition Analysis (MCDA)- originally proposed by Okushima and Tamura [13]. The method explicitly defines two-tier constant elasticity of substitution (CES) production functions as an underlying model to separate price substitution effects from other types of technological change. For more information on CES functions, see, e.g., Shoven and Whalley [14]. The MCDA decomposes structural change in the economy, shown by the change in factor inputs per unit of output between periods (CFI), into two parts: one attributable to price substitution (PS) and the other attributable to technological change (TC).

This paper assumes the model structure in the MCDA to be as shown in Fig. 1. The two models which are identical except for the number of sectors are employed in the following section. The production functions are given by two-tier constant-returns-to-scale CES functions. The model comprises capital *K*, labor *L*, energy aggregate *E*, and material aggregate *M*, as well as energy and material inputs. Capital *K* and labor *L* are the primary factors of production.

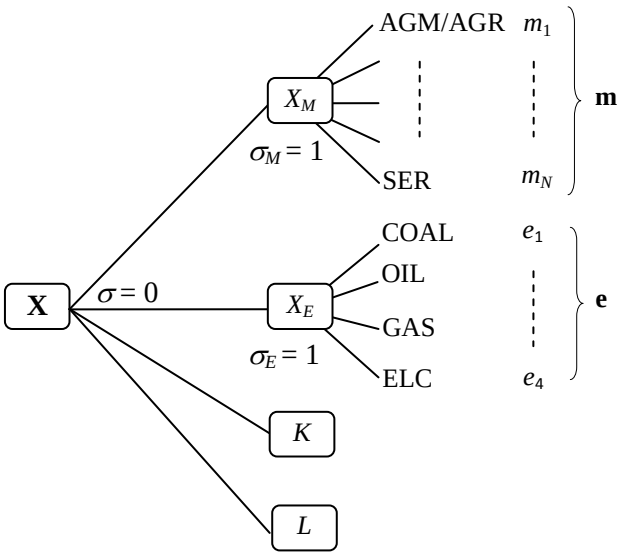

Fig. 1. The model (N = 5 in the 9-sector model and N=14 in the 18-sector model)

Fig. 2 illustrates the MCDA methodology. The MCDA can exactly decompose the CFI into PS and TC. PS, which depends upon the elasticity of substitution (σ) and the change in relative prices between the periods ($p^{t-1} \to p^t$), represents the price substitution effects, while TC represents those portions of the factor input change that cannot be interpreted by the price substitution effects ($\lambda^{t-1} \to \lambda^t$), including autonomous technological development. The

counterfactual points of the MCDA mean the junctures into which the effects of the relative price change between the initial and terminal periods are incorporated. From a theoretical perspective, PS means a change in factor inputs along the production function, while TC refers to shifts in the production function. Therefore, the decomposition of the MCDA is consistent with production theory in microeconomics. The method has clear microtheoretical foundations; then, the decomposition components can be interpreted in a theoretically meaningful way. For more details of the MCDA methodology, see Okushima and Tamura [13].

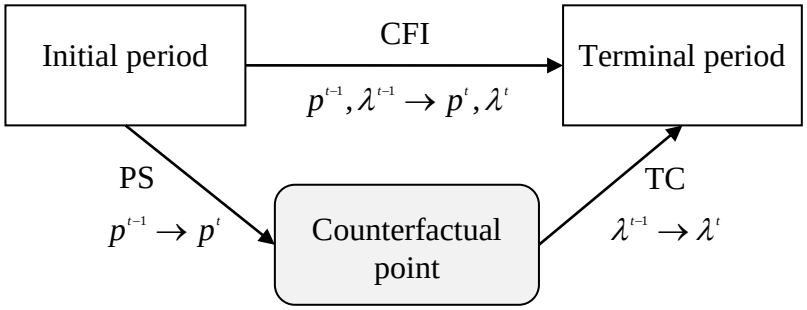

Fig. 2. The methodology

3. Empirical results

This paper applies the Multiple Calibration Decomposition Analysis (MCDA) to investigate the sources of change in industrial energy use in Japan. While Okushima and Tamura [13] is a comprehensive study of changes in energy use and carbon dioxide emissions in the Japanese economy from 1970 to 1995, this paper centers on the change in industrial energy use, especially energy-intensive industry, in the 1970-1990 period. This period includes two oil crises: one in 1973 and a second in 1979. It is widely recognized that skyrocketing oil prices had a huge influence on the Japanese economy during this time, and that the structural changes had a great impact on manufacturing energy use (see, e.g., IEA [15]). This situation presents a typical context in which to apply the method, which can provide a detailed analysis of how change in industrial energy use was caused by price substitution or technological change.

This section analyzes the change in industrial energy use, using data from 1970 to 1990. Nominal outputs (factor inputs) are obtained from the 1970-75-80 and 1985-90-95 Linked Input-Output Tables (Management and Coordination Agency). Real outputs (factor inputs) are obtained by deflating the nominal values by the corresponding prices. Prices of goods and services are from the Domestic Wholesale Price Index (Bank of Japan) or Deflators on Outputs of National Accounts (Economic Planning Agency). Capital and labor prices are estimated following Ito and Murota [16]. In the MCDA, these prices are normalized such that the prices in the initial period are at unity. This units convention, originally proposed by Harberger [17] and widely adopted since (Shoven and Whalley[14], [18], Dawkins et al. [19]), permits the analysis of consistent units across time. The elasticities of substitution are assumed, for the purposes of simplicity, to be $\sigma = 0$ and $\sigma_E, \sigma_M = 1$ as in Fig. 1; nevertheless, these estimates are not significantly different from those in the previous literature that econometrically estimates these elasticities for the Japanese economy (see, e.g., Okushima and Goto [20]).

As in Fig. 1, the sectors are classified into five industries and four energy inputs in the 9-sector model. On the other hand, the sectors are classified into fourteen industries and four

energy inputs in the 18-sector model. Please see the notes accompanying Table 1 and Table 2 for the sector classification.

First, Fig. 3 is a summary of the trends in Japan's energy use (see, e.g., IEA[15]). Energy use in the Japanese economy has continuously increased in volume since the 1970s. However, the growth rate in the early 1980s after the oil crises was lower than in other periods. It is recognized that Japan succeeded in the field of energy conservation and substitution from oil as a result of the lessons of the oil crises (see, e.g., Gregory [21]). The proportion of oil in both primary supply and final consumption has decreased after the oil crises, while the proportions of gas and electricity have increased, mainly owing to the use of natural gas and nuclear power. The primary supply of coal, such as for power generation, is gradually increasing while final consumption has remained almost unchanged, and its share of final consumption is diminishing. Following the trend of final energy consumption, the changes in factor inputs (CFIs) also reflect this experience. Table 1 shows that the CFIs for coal and oil are mostly negative while those for gas and electricity are the opposite. The CFIs should be caused by various effects such as price substitution or technological change.

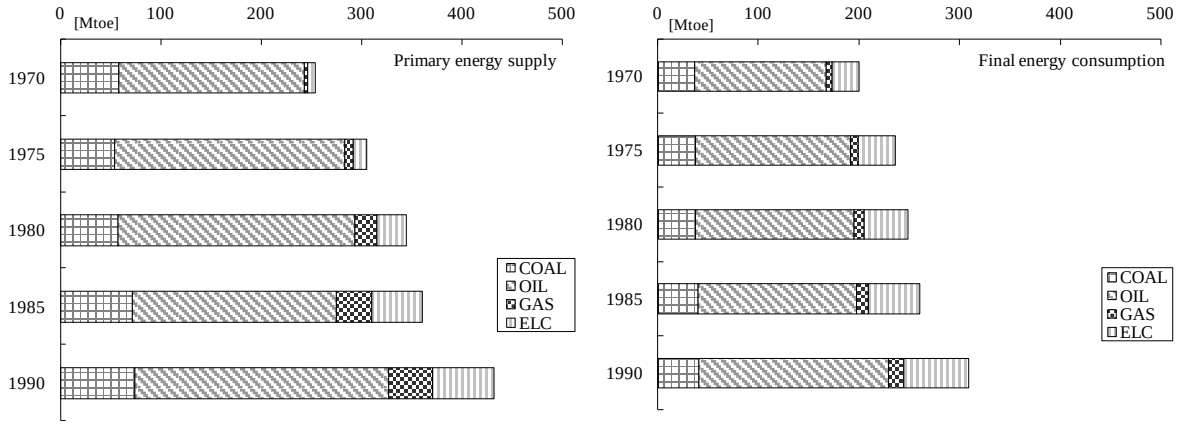

Fig. 3. Primary energy supply and final energy consumption in Japan (Source: IEA[22])

Table 1 illustrates the decomposition of the CFIs by the MCDA with the 9-sector model. The MCDA decomposes the CFI into technological change (TC) and price substitution (PS). The advantage of the method is that it can evaluate these causal factors in terms of types of energy, sectors, or periods, respectively. Table 1 demonstrates that in the 1970s the PSs for oil are negative in all sectors while those for the other types of energy are mostly positive. This means that the rise in oil prices decreased the factor inputs of oil while the demand for coal, gas, and electricity increased because of relatively low prices. Conversely, the PSs for oil become positive in the 1980s, reflecting the fall in oil prices, while those for other types of energy, coal and electricity, become negative. It is remarkable that the PSs for coal form a sharp contrast with those for oil. The PSs for gas are mostly positive. This indicates that the industries had expanded their use of gas because of its price advantage. Thus, the MCDA can clearly show the price substitution effect consistent with the production theory; that is, substitution from inputs with higher prices to those with lower prices.

Table 1 also reveals that the TCs for oil are largely negative in the 1980s. Theoretically, this means that the CFIs for oil had decreased to a greater degree than was expected from the price substitution effect (PS). This is consistent with other empirical studies, such as Han and Lakshmanan [23] and Unander et al. [24], which suggest that improvements in energy efficiency took place in the period even without higher prices. The result indicates that oil-

saving technological change had occurred primarily in the 1980s rather than in the 1970s. In addition, the TCs for coal are almost all negative throughout the periods. The result shows the importance of technological change in reducing industrial energy use.

Table 1. Decomposition of the changes in energy inputs

	Sector														
Input/	AGM			EII			MAC			OMF			SER		
Period	CFI	TC	PS	CFI	TC	PS	CFI	TC	PS	CFI	TC	PS	CFI	TC	PS
COAL															
(i)	-59.5	-89.7	30.2	29.6	22.9	6.7	-70.1	-77.6	7.5	-43.6	-50.8	7.1	-5.2	-22.6	17.4
(ii)	-23.6	-67.4	43.8	-31.7	-54.3	22.6	-19.2	-52.6	33.4	-14.1	-49.1	35.0	-0.3	-36.4	36.0
(iii)	-68.5	-59.4	-9.1	-36.1	-29.9	-6.2	-60.1	-52.7	-7.4	-36.8	-29.4	-7.4	-32.7	-24.8	-7.8
(iv)	32.2	57.8	-25.6	-25.4	-6.4	-19.0	-3.6	18.1	-21.7	-22.5	-0.4	-22.1	-19.3	3.9	-23.2
OIL															
(i)	-9.2	-5.2	-4.0	0.6	21.9	-21.3	-51.0	-30.3	-20.7	-6.6	14.4	-21.0	-22.0	-8.5	-13.4
(ii)	-1.5	-0.5	-1.1	-8.2	7.4	-15.7	-36.8	-28.6	-8.2	7.6	14.8	-7.1	-23.2	-16.8	-6.4
(iii)	-43.2	-43.6	0.3	-23.9	-27.5	3.5	-28.0	-30.2	2.2	-38.8	-41.0	2.1	-15.2	-16.9	1.7
(iv)	-4.1	-5.2	1.1	-32.0	-41.9	9.9	-41.8	-48.2	6.3	-31.1	-36.9	5.8	-22.9	-27.2	4.4
GAS															
(i)	14.3	-33.0	47.3	2.8	-17.9	20.7	-36.3	-57.9	21.6	-13.2	-34.4	21.2	49.1	16.3	32.8
(ii)	30.6	2.6	27.9	34.0	25.0	9.0	-13.4	-32.0	18.7	62.0	41.9	20.1	15.4	-5.6	21.0
(iii)	-24.7	-23.8	-0.9	-51.0	-53.3	2.3	-42.8	-43.8	1.0	84.7	83.8	0.9	-17.8	-18.3	0.5
(iv)	-40.2	-43.6	3.4	88.3	75.8	12.4	-41.9	-50.6	8.8	19.0	10.8	8.2	-15.5	-22.2	6.7
ELC															
(i)	7.5	-32.8	40.3	12.9	-2.1	15.0	-17.9	-33.8	15.9	20.9	5.5	15.5	21.0	-5.5	26.5
(ii)	23.3	12.4	10.9	-9.1	-3.6	-5.4	-16.4	-19.3	2.9	19.2	15.1	4.1	1.3	-3.6	4.9
(iii)	-24.5	-21.2	-3.2	-7.7	-7.5	-0.1	37.0	38.4	-1.4	-6.3	-4.9	-1.5	-2.9	-1.0	-1.9
(iv)	25.8	33.0	-7.2	0.5	-0.4	0.9	-24.0	-21.7	-2.4	-6.1	-3.3	-2.8	8.3	12.5	-4.2

Note: (1) The values are percentage changes.
(2) Classifications are as follows.
AGM: Agriculture, forestry, fishery, and mining; EII: Energy-intensive industry (paper and pulp, chemical, ceramics, and iron and steel); MAC: Machinery; OMF: Other manufacturing; SER: Services and others (including construction); COAL: Coal and coal products; OIL: Oil and oil products; GAS: Gas; ELC: Electricity.
(3) Periods are as follows. (i): 1970-75; (ii): 1975-80; (iii): 1980-85; (iv): 1985-90.

Next, this paper investigates the details of energy use in energy-intensive industry (EII), using the 18-sector model. Here, EII represents the following four industries: paper and pulp (PAP), chemical (CHM), ceramics (CRM), and iron and steel (IAS). These industries account for a large proportion -i.e., about seventy percent- of the industrial energy use in the Japanese economy. It is widely known that EII contributed greatly to the reduction of energy consumption in the period. METI [25] shows that energy efficiency rose dramatically by 42% in PAP, 34% in CHM, 26% in CRM, and 17% in IAS between 1973 and 1990 (see also, e.g., Toichi [26]). Unander et al. [24] examines such improvements in energy efficiency and implies that both price change and other factors induce it. The MCDA has the advantage of enabling the decomposition of CFI, i.e., the change in energy efficiency, into PS and TC. Hence, this section examines the energy use of EII more closely using the MCDA.

Table 2 illustrates the decomposition result. The PSs for oil are negative in all sectors in the 1970s, while they all become positive in the 1980s. Among the other types of energy, coal shows a clear contrast in terms of PSs during these periods. This shows an offsetting effect of a demand for coal as a substitute for oil, because of its price advantage. The trend in PSs nearly corresponds with that of the EII total in Table 1.

Table 2 also shows that the TCs for oil are strongly negative in the 1980s. Corresponding with the above result in Table 1, oil-saving technological change was primarily developed in the 1980s for those industries. These results are supported by engineering studies indicating that energy conservation was attained by means of an improvement in operations in the 1970s, while full-scale energy conservation was advanced by the introduction of various kinds of energy-saving technology in the 1980s after the second oil crisis (see, e.g., the Study Group on Energy and Industry [27]). In fact, multifarious technological innovations took place during that period; specifically, the continuous casting or waste heat recovery in IAS, and the waste heat recovery equipment of plants in CHM (see, e.g., METI [25]).

There is a point of contrast regarding PAP and CRM: the TCs for coal in these industries from 1975 to 1985 are sizably positive, although those in other EIIs are mostly negative. At this point, engineering studies indicate that PAP and CRM increased the use of coal by installing new combustion equipment in that period (see, e.g., the Study Group on Energy and Industry [27], METI [25]). The trend is reflected in these backgrounds. As a result, the CFIs for coal in PAP and CRM greatly increased; the TCs also increased without regard to the trend of PSs. The results in this section indicate that technological change is important for diminishing industrial energy use.

Table 2. Decomposition of the changes in energy inputs in energy-intensive industry

	Sector											
Input/	PAP			CHM			CRM			IAS		
Period	CFI	TC	PS	CFI	TC	PS	CFI	TC	PS	CFI	TC	PS
COAL												
(i)	-89.4	-92.6	3.2	-20.0	-34.9	14.9	-51.9	-65.2	13.3	25.2	23.9	1.3
(ii)	158.6	125.6	33.1	-13.3	-51.2	37.9	333.6	295.5	38.1	-31.1	-42.4	11.3
(iii)	277.7	285.3	-7.6	-4.1	4.2	-8.3	10.4	17.9	-7.5	-32.6	-29.1	-3.6
(iv)	-14.5	8.4	-22.9	-26.1	-2.7	-23.4	-24.6	-3.3	-21.4	-16.5	-4.8	-11.6
OIL												
(i)	-28.8	-4.8	-23.9	2.6	17.9	-15.3	17.8	34.3	-16.5	-5.1	20.2	-25.3
(ii)	81.5	90.0	-8.4	-12.2	-7.1	-5.1	-25.6	-20.7	-5.0	-28.6	-5.2	-23.4
(iii)	4.7	2.7	2.0	-31.4	-32.6	1.2	-28.0	-30.1	2.1	-47.4	-53.9	6.4
(iv)	-59.1	-63.8	4.7	-31.2	-35.3	4.1	-40.5	-47.3	6.8	-40.4	-60.4	20.0
GAS												
(i)	1.7	-15.0	16.7	6.8	-23.2	30.0	-11.5	-39.6	28.2	16.1	1.5	14.6
(ii)	-16.7	-35.0	18.4	-5.0	-27.7	22.7	-3.8	-26.7	22.9	181.2	182.2	-1.0
(iii)	21.6	20.8	0.7	-66.0	-65.9	-0.1	6.5	5.6	0.9	-62.3	-67.4	5.1
(iv)	7.8	0.7	7.1	71.6	65.1	6.4	78.2	69.0	9.2	173.7	150.9	22.8
ELC												
(i)	17.8	6.6	11.2	2.7	-21.1	23.8	26.9	4.8	22.1	13.4	4.3	9.2
(ii)	-14.1	-16.8	2.7	-24.2	-30.6	6.4	5.4	-1.2	6.6	-5.4	8.7	-14.1
(iii)	-15.0	-13.4	-1.6	7.0	9.4	-2.4	-26.5	-25.0	-1.5	-6.6	-9.3	2.7
(iv)	9.2	13.1	-3.9	-14.3	-9.8	-4.5	-6.8	-4.8	-1.9	15.8	5.6	10.2

Note: (1) The values are percentage changes.
(2) Classifications are as follows.
PAP: Paper and pulp; CHM: Chemical; CRM: Ceramics; IAS: Iron and steel.
(3) Periods are as follows. (i): 1970-75; (ii): 1975-80; (iii): 1980-85; (iv): 1985-90.

4. Conclusions

This paper suggests a new approach -the Multiple Calibration Decomposition Analysis (MCDA)- to investigate the sources of change in industrial energy use in the Japanese economy during the 1970-1990 period. The primary contribution of this paper is to use the new methodology to examine the causal factors of energy use change in energy-intensive

industry (EII) following the oil crises. The MCDA can decompose the change in factor inputs per unit of output (CFI) into price substitution (PS) and technological change (TC) in a multisector general equilibrium framework. The empirical result in Section 3 shows how industrial energy use was influenced by price substitution or technological change through the experience of the two oil crises. It illustrates that price substitution from oil to other types of energy occurred in the 1970s, while the reverse occurred in the 1980s. Nevertheless, factor inputs of oil decreased in the 1980s, because oil-saving technological change primarily occurred in that period. Notably, oil-saving technological change in EII advanced by 60% or more in the 1980s. This paper casts light on EII and investigates the details of its contribution. The results show the important role of technological change in curtailing industrial energy use in the Japanese economy.

This study presents the MCDA, which could serve as a practical tool for energy analysis. Finally, it clarifies the assumptions upon which the MCDA depends. It is notable that the method employs a deterministic procedure, and the reliability of empirical results depends on the empirical validity of elasticity parameters. Hence, the MCDA has similar defects to applied general equilibrium analysis. In practice, there are still problems in acquiring reliable elasticity parameters. Nevertheless, the method would be a great help in energy analysis with the support of other conventional methods.

Acknowledgments
The earlier version of this paper was presented at the 5th Dubrovnik Conference on Sustainable Development of Energy, Water and Environment Systems. This research was supported by the Grant-in-Aid for Scientific Research and Environment Research and Technology Development Fund of the Ministry of the Environment (S-8) in Japan.

References

[1] H. Dowlatabadi, M.A. Oravetz, U.S. long-term energy intensity: backcast and projection, Energy Policy 34(17), 2006, pp. 3245-3256.

[2] G.E. Metcalf, An empirical analysis of energy intensity and its determinants at the state level, Energy Journal 29(3), 2008, pp. 1-26.

[3] I. Sue Wing, Explaining the declining energy intensity of the U.S. economy, Resource and Energy Economics 30(1), 2008, pp. 21-49.

[4] E.A. Hudson, D.W. Jorgenson, U.S. energy policy and economic growth, 1975-2000, Bell Journal of Economics and Management Science 5(2), 1974, pp. 461-514.

[5] E.R. Berndt, D.O. Wood, Technology, prices, and the derived demand for energy, Review of Economics and Statistics 57(3), 1975, pp. 259-268.

[6] A.S. Manne, ETA: a model for energy technology assessment, Bell Journal of Economics 7(2), 1976, pp. 379-406.

[7] A.M. Borges, L.H. Goulder, Decomposing the impact of higher energy prices on long-term growth. In: H.E. Scarf, J.B. Shoven, editors, Applied general equilibrium analysis, Cambridge: Cambridge University Press, 1984, pp. 319-362.

[8] J.L. Solow, The capital-energy complementarity debate revisited, American Economic Review 77(4), 1987, pp. 605-614.

[9] B.W. Ang, F.Q. Zhang, A survey of index decomposition analysis in energy and environmental studies, Energy 25(12), 2000, pp. 1149-1176.

[10] R. Hoekstra, Economic growth, material flows and the environment: new applications of structural decomposition analysis and physical input-output tables, Cheltenham: Edward Elgar, 2005.

[11] A. Rose, S. Casler, Input-output structural decomposition analysis: a critical appraisal, Economic Systems Research 8(1), 1996, pp. 33-62.

[12] A. Rose, Input-output structural decomposition analysis of energy and the environment. In: J.C.J.M. van den Bergh, editor, Handbook of environmental and resource economics, Cheltenham: Edward Elgar, 1999, pp. 1164-1179.

[13] S. Okushima, M. Tamura, Multiple calibration decomposition analysis: energy use and carbon dioxide emissions in the Japanese economy, 1970-1995, Energy Policy 35(10), 2007, pp. 5156-5170.

[14] J.B. Shoven, J. Whalley, Applying general equilibrium, Cambridge: Cambridge University Press, 1992.

[15] IEA (International Energy Agency), Oil crises and climate challenges: 30 years of energy use in IEA countries, Paris: OECD/IEA, 2004.

[16] K. Ito, Y. Murota, A macro economic modeling by using translog cost function, Journal of Japan Economic Research 13, 1984, pp. 31-41 (in Japanese).

[17] A.C. Harberger, The incidence of the corporation income tax, Journal of Political Economy 70(3), 1962, pp. 215-240.

[18] J.B. Shoven, J. Whalley, Applied general-equilibrium models of taxation and international trade: an introduction and survey, Journal of Economic Literature 22(3), 1984, pp. 1007-1051.

[19] C. Dawkins, T.N. Srinivasan, J. Whalley, Calibration. In: J.J. Heckman, E. Leamer, editors, Handbook of econometrics, vol.5, New York: Elsevier, 2001, pp. 3653-3703.

[20] S. Okushima, N. Goto, Production structure and energy substitution responses in Japan: evaluation of the economic effects of policies for preventing global warming, JCER Economic Journal 42, 2001, pp. 228-242 (in Japanese).

[21] G. Gregory, Energy for Japan's new industrial frontier, Energy 8(6), 1983, pp. 481-490.

[22] IEA (International Energy Agency), IEA statistics 1998, Paris: OECD/IEA, 1999.

[23] X. Han, T.K. Lakshmanan, Structural changes and energy consumption in the Japanese economy 1975-1985: an input-output analysis, Energy Journal 15(3), 1994, pp. 165-188.

[24] F. Unander, S. Karbuz, L. Schipper, M. Khrushch, M. Ting. Manufacturing energy use in OECD countries: decomposition of long-term trends, Energy Policy 27(13), 1999, pp. 769-778.

[25] METI (Ministry of Economy, Trade and Industry), White paper on energy 2007, Tokyo: Yamaura Print Co., 2007 (in Japanese).

[26] T. Toichi, Present state of energy conservation and government policy in Japan, Energy 8(1), 1983, pp. 97-106.

[27] The Study Group on Energy and Industry, 30 years after the oil crises: an examination of energy policy, Tokyo: Energy Forum Co., 2003 (in Japanese).

Simulation of energy recovery system for power generation form coal bed gas of Tabas coal mine of Iran

H.Farzaneh*, M.Fahimi

Science and Research Branch, Islamic Azad University, Tehran, Iran
** Corresponding author. Tel: +982144865320, Fax: +982144865003, E-mail: info@hfarzaneh.com*

Abstract: Coal mine methane is a general description for all methane released prior to, during and after mining operations. As such, there is considerable variability in flow rate and composition of the various gas emissions during mining operations. It would be highly desirable to recover energy from emitted methane of coal mine to generate electricity. Hence, more attention should be focused on the effective utilization of emitted methane in coal mines. The energy recovery system, as one of the promising technologies, has been attracting increased attention to generate electricity from emitted methane in Tabas mine. Some energy recovery systems with different configurations may be proposed such as gas turbine and gas engines. In this investigation, a simulation model has been developed in Hysys software environment to predict generated power from combination of ventilation air and drainage gas (mixture with 1.6 % methane concentration) form Tabas mine by using a lean-burn gas turbine.

Keywords: *Coal bed gas, energy recovery system, lean-burn gas turbine, simulation*

1. Introduction

New natural gas reserves are vital to guaranteeing a steady supply of affordable fuel to generate electricity and preserve quality of life. Coal bed gas is a form of natural gas reserve which is extracted from coal beds. In recent decades it has become an important source of energy in many countries of the world. It is mainly composed of methane with variable amounts of ethane, nitrogen, and carbon dioxide [1].

A large portion of the methane emitted from coal mines comes from gob areas (collapsed rock over mined-out coal). Coal mines frequently do not use medium-quality gas from gob wells and instead vent the gas to the atmosphere, contributing to global warming. However, gas with a methane concentration exceeding 35% can in fact be used as a fuel for on-site power generation [2]. Given their large energy requirements, coal mines can recover methane and generate electricity with energy recovery systems to realize significant economic savings and reduce greenhouse gas emissions. Generating electricity is an attractive option because most coal mines have significant electricity loads. Electricity is required to run nearly every piece of equipment including mining machines, conveyor belts, desalination plants, coal preparation plants, and ventilation fans [3].

Coal bed gas methane is emitted in two streams: (1) mine ventilation air (0.1–1% CH4) and (2) gas drained from the seam before and after mining (60–95%) CH4. Drainage gas can be utilized to generate electricity directly [4]. For example, internal combustion engines, such as compression fired diesel engines and compression ignition engines modified to be spark-fired engines commonly use drainage gas to generate electricity[5]. The main problem of using drainage gas is related to its periodic extraction from the mine. Also, ventilation air methane is the most difficult source of methane to use as an energy source, as the air volume is large and the methane resource is dilute and variable in concentration and flow rate. Because of low concentration of methane in mine ventilation air, effective technology will be required to utilize it and generate electricity. As brilliant idea, it will be possible to combine ventilation air and drainage gas and produce mixture with sufficient concentration of methane. The

mixture then can be used as fuel in low concentration methane combustion process such as lean-burn gas turbine for on-site power generation in the mine location [6].
In this investigation, a simulation model has been developed in Hysys software environment to predict generated power from combination of ventilation air and drainage methane in an energy recovery system. To this aim, Tabas mine is considered as case study. The results of the simulation model show that the large portion of total electricity demand of the Tabas coal mine can be supplied from the coal bed gas.

2. Materials and Methods

2.1. System description

There are several technologies that can be used for stationary power generation by directly using drainage gas, namely conventional gas turbines and gas engines or every internal combustion engine. However, it would be expected that variation of methane concentration and amount of the drainage gas should affect the continuous and stable operation of the power generation units.
The mechanism for generation power from ventilation air may be considered in two categories: 1) Catalytic oxidation 2) Thermal oxidation. In general, catalytic combustion is a multi-step process involving diffusion methane to the catalyst surface, adsorption onto the catalyst, reaction, and release of the product species from the catalyst surface and diffusion back into the bulk [7].

Thermal oxidation can be occurred in combustion chamber of lean-burn gas turbine. The lean-burn gas turbine is a recuperative gas turbine, which uses heat from the combustion process to preheat the air containing methane to the auto-ignition temperature (in the range 700–1000 C), with the combusted gas being used to drive a turbine. This gas turbine can operate continuously when the methane concentration in air is above 1.6%, which leads to the air being preheated to 700 C before combustion. Therefore, it requires the addition of substantial quantities of methane to the ventilation air to reach adequate methane concentrations from drainage methane. The mixture is preheated by a recuperator to 450 C. Then a recuperative combustion chamber uses the hot combustion products to further heat the fuel–air mixture to a point where ignition occurs. The fuel and air mixture is injected through stainless steel tubes into the combustion region. The burnt gas then passes up the outside of the stainless steel tubes to heat incoming air, and then enters into the turbine inlet to drive the turbine. This heat exchange reduces the exit temperature of air to 850 C, which is the same as the standard Centaur turbine. With this design, there is a need to use a turbine that has a low combustion temperature [8].

In this paper, Tabas mine is considered as a case study. Tabas mine is located in Yazd Province, 80 km south of Tabas City of Iran. This mine is the first mechanized coal mine of Iran that is designed by room and pillar method. Overall specifications of the mine are represented in table (1).

Table1. Overall specifications of Tabas Mine

Total production per year (2009)	1.2 Millions tones
Ventilation air flow rate (0.18 % CH4 by volume)	360000 Nm^3/h
Drainage gas flow rate (76.5% CH4 by volume)	2271 Nm^3/h
Total installed electricity demand	10.8 MW

Concentration of methane in ventilation air is available by on site measuring system. Figure (1) shows the variation of methane concentration in ventilation air flow during 7 months.

According to this figure, the higher peak and average value of methane concentration are measured around 0.25% and 0.18% respectively. It is clear that, the concentration of methane in ventilation air is not sufficient for burning in combustion chamber of lean-burn gas turbine. Therefore, mixing of certain amount of drainage gas will be required to improve the level of methane concentration up to 1.6%.

Schematic of energy recovery system which may be used for methane recovery in Tabas coal mine is depicted in figure (2). According to this figure, ventilation air and drainage gas are mixed together in the mixer storage and with suitable concentration will be fed into the lean-burn gas turbine. It may be possible to use remainder amount of drainage gas in a gas engine for generating excess electricity.

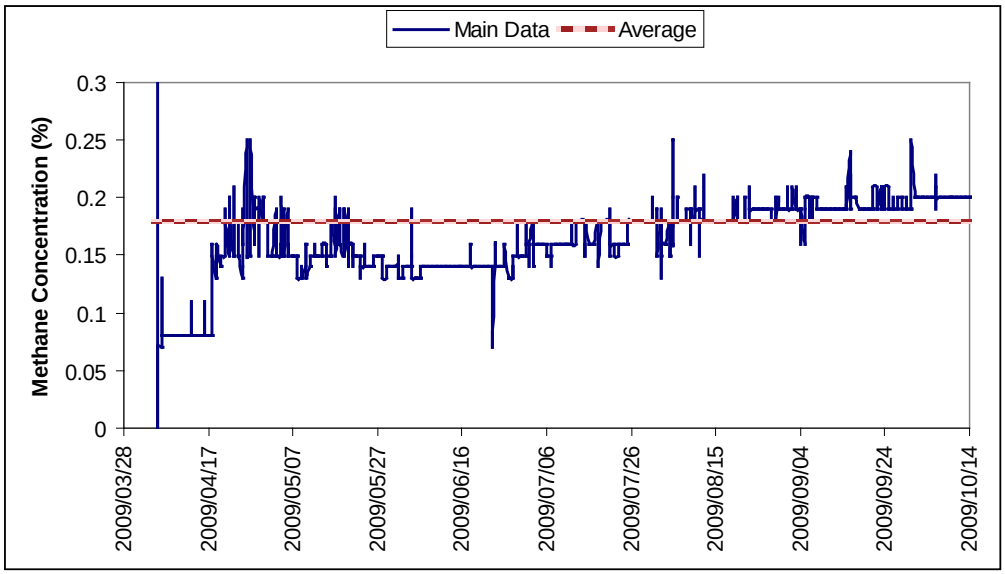

Fig. 1 Variation of methane concentration of ventilation air in Tabas mine

2.2. Methodology

The simulation model has been found on the theoretical principles of first and second lows of thermodynamics and it has been tailored to identify the design condition of specified energy recovery system for power generation in Tabas coal mine. To this aim, HYSYS simulator is used. Simulated framework of the energy recovery system in Tabas coal mine is represented in figure (3). While, the methane concentration of ventilation air of Tabas mine is very low, total amount of drainage gas should be consumed for generating power in lean-burn gas turbine cycle. Therefore, no gas engine will be required for excess power generation. Physical properties of streams are approximated by the Peng-Robinson equation of state formula through developing simulation model by HYSYS software [9].

3. Results and Discussions

The aforementioned simulation model has been applied for performance analysis of the energy recovery system and estimation total generated power form the energy recovery system in Tabas coal mine. According to represented results in table (2), 6.193 MW power can be generated by the energy recovery system. The thermal efficiency of the cycle is obtained at 24.74% because of low concentration of methane in the inlet feed of combustion chamber of lean-burn gas turbine.

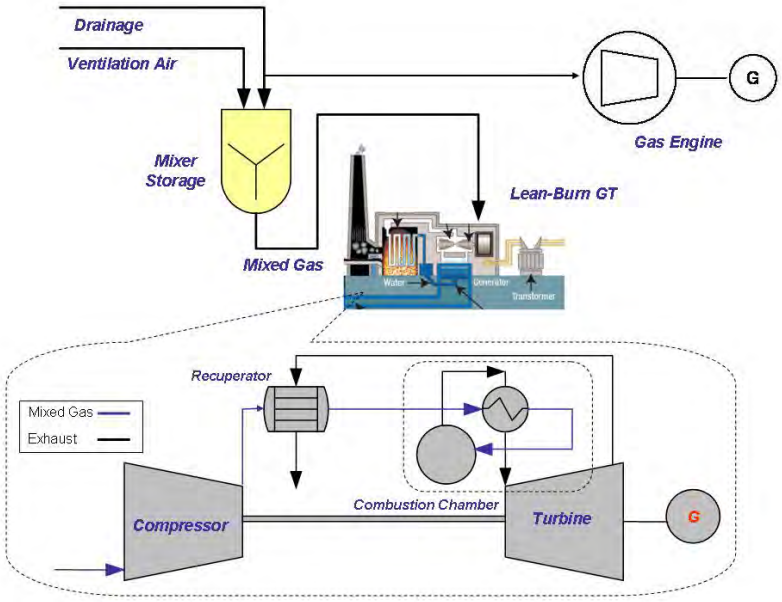

Fig. 2 schematic of energy recovery system in coal mine

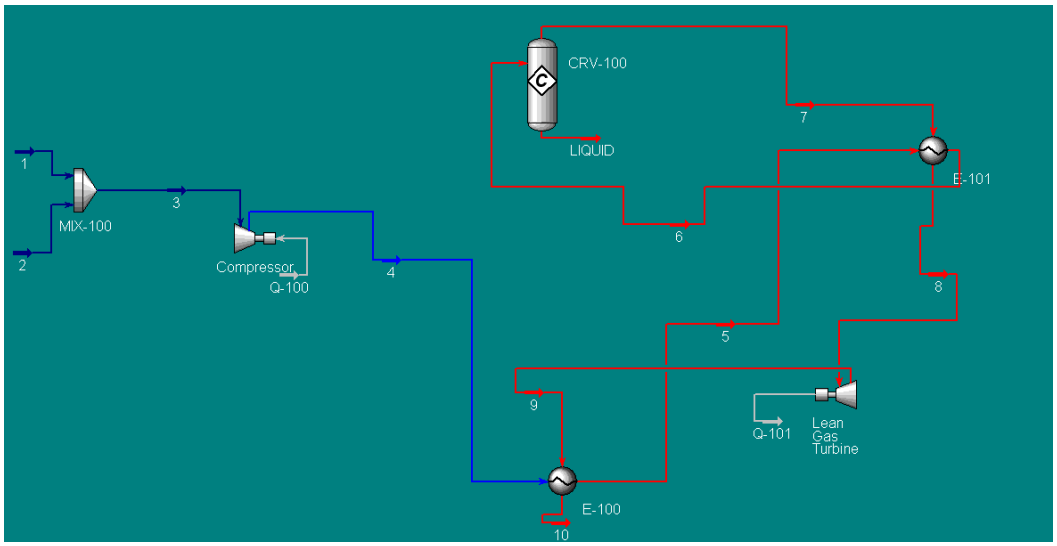

Fig. 3 Simulated frame work of energy recovery system in HYSYS simulator

Table2. Simulation results

Turbine power generated (MW)	12.60
Compressor power consumed (MW)	6.407
Net power generated by cycle (MW)	6.193
Thermal efficiency of cycle (%)	24.74
Usage percentage of ventilation air (%)	54
Usage percentage of drainage gas (%)	100

According to simulation results, physical properties and flow rate of streams are represented in table (3). Also, compositions of main streams are reported in table (4).

Table3. Physical properties and flow rate of streams

Line	1	2	3	4	5
Temperature(C)	50	25	25.57	139.3	352
Pressure(kPa)	150	150	150	400	350
Flow(kg/h)	2503	194000	196503	196503	196503
Line	6	7	8	9	10
Temperature(C)	773.5	1137	738.1	538.5	334.5
Pressure(kPa)	300	300	297	106	100
Flow(kg/h)	196503	196503	196503	196503	196503

Table4. Composition of main streams

(Mole Fraction)	**1**	**2**	**3**	**7**	**8**	**10**
Oxygen	0.006	0.2116	0.2078	0.176	0.176	0.177
Nitrogen	0.16	0.7766	0.7651	0.7651	0.7651	0.764
Ethane	0.020	0	0.0004	0.0004	0.0004	0.0003
H_2O	0	0	0	0.0317	0.0317	0.0317
CO_2	0.048	0.010	0.0107	0.0266	0.0266	0.0263
CH_4	0.765	0.0018	0.0160	0.0002	0.0002	0.0002

Figure (4-a) shows variation of the thermal efficiency with the compression ratio. It is clear that the thermal efficiency will be increased with increasing of compression ratio in compressor. It can be observed in this figure that, the thermal efficiency of cycle reaches to its maximum point at each selected value of compression ratio by increasing methane concentration in inlet fuel mixture of lean-burn gas turbine. As shown in figure (4-b), increasing of the compression ratio is accompanied with increasing of the methane concentration in the intake feed at each turbine inlet temperature (TIT). However, it can be observed from combination of figure (4-a) and (4-b), at the same pressure ratio, higher thermal efficiency may be obtained at higher TIT and higher concentration of methane.

4. Conclusion

The objective of this research work has been to introduce an energy recovery system for power generation from coal bed gas of Tabas coal mine of Iran. With the aim of developing more efficient, cost-effective technologies for mitigating and utilizing the diluted coal mine, this paper studied a novel energy recovery system, which can be powered with about 1.6 % methane (volume) in intake mixture. The results indicate that, the methane concentration of ventilation air and also temporal availability of drainage gas should be considered as main factors for developing any power generation system in a coal mine. Based on the obtained results from simulation, 6.193 MW power may be generated from coal bed gas recovery in Tabas coal mine. Therefore, 57% of total electricity demand of the mine can be supplied by the on-site power generation in this mine. If electricity unit price is considered as 0.09 $/kWh and with purposing total capital investment around 6.7 millions dollars including lean-burn gas turbine, ventilation fan, drainage fan, mixer and piping, internal rate of ratio (IRR) and net present value (NPV) of project may be estimated at 41% and 14.6 millions dollars respectively and its economical feasibility will be supported.

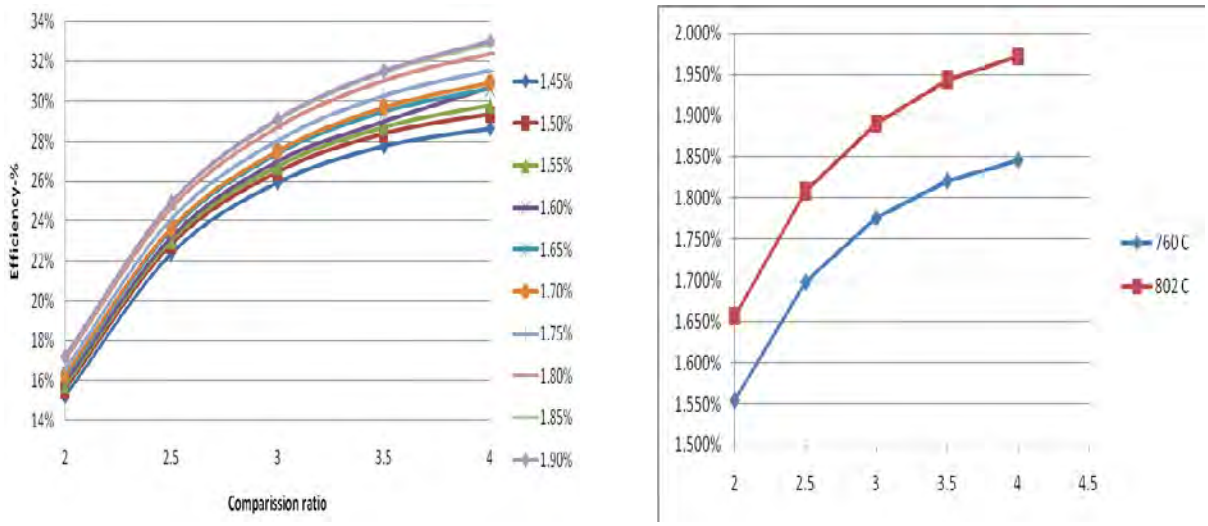

Fig. 4: a) Variation of thermal efficiency with compression ratio b) variation of TIT with compression ratio and different methane concentration

References

[1] C.J.Bibler, J.S.Marshall, R.C.Pilcher, Status of worldwide coal mine methane emissions and use. International Journal of Coal Geology, 1998, pp.283–310

[2] S.Su, T.Ren, R.Balusu, A.Beath, H. Guo, C.Mallett, Development of Two Case Studies on Mine, Methane Capture and Utilization in China, CSIRO Exploration and Mining report, 2006

[3] K.Markowski, Coalbed methane resource potential and current prospects in Pennsylvania, Int. journal of Geology, 1998, pp.137–159

[4] S.Su, H.Chen, P.Teakle, S.Xue, Characteristics of coal mine ventilation air flows. Journal of Environmental Management, 2008, pp. 44–62

[5] J.Yin, S.Su, X.Xiang Y.Yiwu, Thermodynamic characteristics of a low concentration methane catalytic combustion gas turbine, Applied Energy, 2010, onsite available

[6] L.Chuan-tong, L.Fa-yangb, S.Jin-di, Thermal economy analysis of utilizing coalmine methane energy, journal of Procedia Earth and Planetary Science, 2009,pp. 1343–1350

[7] S.Su, J.Agnew, Catalytic combustion of coal mine ventilation air methane. Journal of Fuel 2006, pp. 1201–1210

[8] A.Beath, C.W.Mallett. An assessment of mine methane mitigation and utilization technologies. Journal of Progress Combustion Science, 2005, pp.31:123–70.

[9] P.Robert, P. Hesketh, HYSYS – Inductive Method, AspenTech Report, 2003

Possibilities and problems in using exergy expressions in process integration

Carl-Erik Grip [1,*], Erik Elfgren[1], Mats Söderström[2], Patrik Thollander[2], Thore Berntsson[3], Anders Åsblad[4], Chuan Wang[5]

[1] *LTU (Luleå University of Technology) Division Energy Technology, Luleå, Sweden*
[2] *LIU (Linköping University), Division Energy Systems, Linköping, Sweden*
[3] *Chalmers University of Technology, Division Heat and Power Technology, Gothenburg, Sweden*
[4] *CIT Industriell Energi, Gothenburg, Sweden*
[5] *Swerea MEFOS, Luleå Sweden*
** Corresponding author. Tel: +46 920 49 14 72, Fax: 46 920 49 10 74, E-mail: carl-erik.grip@ltu.se*

Abstract: Industrial energy systems are complicated networks, where changes in one process influence its neighboring processes. Saving energy in one unit does not necessarily lead to energy savings for the total system. A study has been carried out on the possibility to use the exergy concept in the analysis of industrial energy systems. The exergy concept defines the quality of an amount of energy in relation to its surrounding, expressing the part that could be converted into work. The study consists of literature studies and general evaluations, an extensive case study and an interview study. In the latter it was found that non technical factors are major obstacles to the introduction of exergy.

Keywords: *Energy efficiency, Exergy, Process integration, User acceptance, Industrial energy system*

1. Introduction

1.1. The need and development of process integration in Swedish industry

Energy use in Swedish industry amounts to more than 40% of the national energy use. The three most energy-intensive industrial branches in Sweden, pulp and paper, iron and steel and chemical industries use more than two thirds of industrial energy use. Over the years a large effort has been made to increase industrial energy efficiency. This includes measures to increase energy efficiency as well as increased use of excess energy in other branches, e.g. for heat and electricity generation.

One problem is that industrial energy systems are complicated networks where changes in one process, influence its neighboring processes. Thus saving energy in one unit does not necessarily lead to an energy saving for the whole system. A system approach is needed to avoid sub optimization. One early attempt to make a more systematic analysis of this type of problems, the Pinch analysis, was made at Manchester University [1] during the 1970s. A method, pinch analysis, was developed, where the heat-carrying media are categorized as either cold streams (media that are heated during the process) or hot streams (media that are cooled down during the process). They are then added to one hot and one cold stream. The system could be characterized by the point where the composite streams are closest to each other, the pinch point. Exergy analysis [2] and mathematical programming, e.g. the MIND method [3], have been developed for industrial energy system studies starting in the 1980s. A national program to support research, development and use of process integration in Sweden was initiated and financed in cooperation between the Swedish Energy Agency and the Swedish energy-intensive industry [4],[5]. It started 1997 and ended in 2010.

The energy systems of the steel industry are characterized by large high temperature flows of molten solid and gaseous materials, as well as energy intensive chemical reactions. Mathematical programming was considered most suitable for that type of system. A methodology, reMIND, was developed and implemented for practical steel plant use (ref [6]-

[9]). Based on successful industrial applications three research supporting agencies and a group of Scandinavian steel- and mining companies decided to start and finance an excellence center for process integration in the steel industry, PRISMA which is located at Swerea MEFOS AB in Luleå.

The national program focused on three process integration technologies: Pinch analysis, mathematical programming and exergy analysis. When the work was summarized, it was seen that the main part of research was on mathematical programming and pinch analysis, whereas only a very limited work was made on exergy studies. Considering this, the Process Integration Program of the Swedish Energy Agency has supported a special study on the usefulness of the exergy concept, as well as its limitations and obstacles to future use.

1.2. What is exergy?

Energy balances are a common tool in technical energy studies. In these balances energy input equals energy output. This is based on the first law of thermodynamics: energy can neither be destroyed nor be created. The balances also include energy losses. The lost energy has not disappeared; it is converted into a practically useless flow of low-value energy, e.g. used cooling water or waste gas. This indicates the need of a way to describe also the quality of energy flows. The exergy concept defines the quality of an amount of energy in relation to its surrounding, expressing the part that can be converted into work. It is based on the second law of thermodynamics: the entropy of an isolated system never decreases. A certain media can produce work only if there is a difference e.g. in temperature and pressure versus the surrounding. The exergy expression describes the theoretically possible production of work as a function of that difference:

$$E = \Delta H - T_0 * \Delta S \quad (1)$$

Where E = exergy, H = enthalpy, S = entropy, ΔH and ΔS are differences from the reference state (the surroundings) and T_0 = the absolute temperature at the reference state.

For a non compressible liquid or solid with constant specific heat the entropy difference can be calculated as

$$\Delta S = m * c_p * \ln\left(\frac{T}{T_0}\right) \quad (2)$$

And for an ideal gas as

$$\Delta S = m * \left(c_p * \ln\left(\frac{T}{T_0}\right) + R * \ln\left(\frac{p_0}{p}\right)\right) \quad (3)$$

Where m and c_p are mass and specific heat, T and p are absolute temperature and pressure of the substance and T_0 and p_0 are temperature and pressure at the reference state.

1.3. Scope of paper

The main scope is to improve the knowledge of when and how exergy analysis is useful on its own or in combination with other methods and methodologies, as well as on the improvements needed to increase the use of exergy analysis in process integration projects. It was considered important to cover both technical and nontechnical limitations to an improved use. The work was structured in the following parts: literature study, analysis, interview study, case study and synthesis.

2. Methodology

The study was carried out in five steps

Step 1. A literature study with the aim to provide an overview on the utilization and advantages of the exergy analysis method in several systems, especially in industrial ones.

Step 2. An analysis where literature data and experience of the project partners were used to define subsystems where exergy can be used as well as identifying problems and unanswered questions.

Step 3. An interview study with the aim to find the reasons why Exergy was used or not used by different actors. The method was based on a combination of in-depth, semi-structured interviews and a more straight-forward questionnaire [10]. Both technical and non-technical aspects were studied. The questions were formulated using the results of the analysis study

Step 4. A case study to demonstrate the practical application on an industrial system. The case chosen was the Luleå Energy: The SSAB steel plant, CHP (combined heat and power plant) and district heating. Collected production data were used for exergy calculations both for the total system and some subsystems

Step 5. A synthesis based on the results from step 1-4 with the aim to answer the following questions: Which criteria for comparison should be used? Should the methodology be used in combination with other methods? Should there be increased dissemination? When should the exergy concept be used? Is exergy research worthwhile? Could the formulation of the exergy concept be explained in a better way? When should the exergy concept and exergy studies be used? Is there a need for exergy research

3. Results

3.1. Literature study

155 references were included, and 115 of these were described in some detail. The distribution between publication categories is illustrated in Fig. 1 a. The main part of material is distributed almost evenly between journal and conference publications.

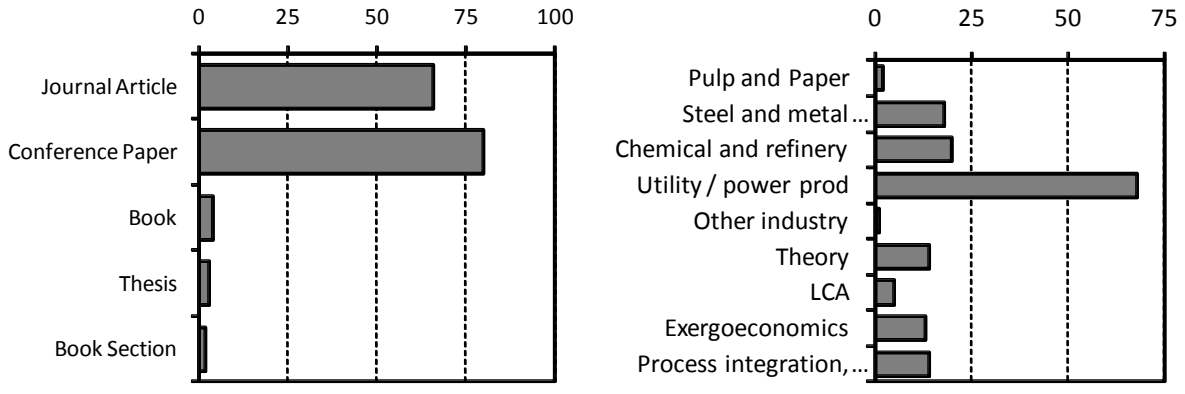

a) Category of publication *b) Subject of publication*

Fig. 1 Distribution of literature references between publication types and subjects. The diagrams show the number of references per category

The collected references described the use in different industrial branches and for specific equipment, some more sophisticated uses, e.g. in LCA or exergoecoonomics, as well as some general studies. The distribution between these subjects is illustrated

The use is relatively small in the pulp and paper industry. The reason is probably that the transport and exchange of thermal energy is a dominant part of the energy system, which gives a preference for pinch analysis. A higher frequency of references is shown for steel and chemical industry where chemical reactions and energies are important. The power industry and utilities show the highest frequency in Fig. 1 b. A reason can be that components like boilers, turbines, valves and heat exchangers usually entail large exergy destruction rates. The solutions proposed to minimize these losses are often to change operation parameters or to install new equipment with different operating characteristics. The most common action proposed to increase exergy efficiency is to decrease the temperature difference in heat transfer equipment. Since this decreases the driving force, investment costs are likely to increase.

In a system of nodes and streams, exergy analysis is applied to the efficiency of nodes. This can lead to more capital-intensive suggestions e.g. change of process technology.

Several authors suggest using combined pinch and exergy analysis to achieve better results. Pinch analysis could be used to determine minimum cooling and heating demands, thereafter exergy analysis could be used to detect inefficiencies. Finally, the design capabilities of pinch analysis could be used to synthesize a heat exchanger network.

3.2. Analysis

The usefulness of the Exergy concept was analyzed separately in pulp and paper, steel industry, mining industry, cement industry, use for electricity generation and for regional cooperation. The result varied between branches. Two interesting uses can be: energy quality to compare subsystems and recovering excess energies. Presently there is a lack of comparison data. Creating a BAT (Best Available Technology) database for energy efficiency and exergy destruction could be interesting. This study also produced parameters for the interview study

3.3. Interview study

The aim was to observe the effect of technical and non-technical factors which were of great importance for the introduction of exergy studies as well as for failure or success in the application. The interview form consisted of an interview part where questions were answered in words and a short questionnaire part, where the respondents could rank different obstacles to each other. Fig. 2 illustrates the weighted summary of important obstacles in the questionnaire part. The most important factor seems to be the lack of strategy. Points like lack of time, priorities, lack of capital and slim organization got a low priority. A comment when these points were discussed was: “When we get the job to make an energy analysis the priority is always very high, so those limitations (to the use of exergy analysis, author’s remark) are not relevant”.

Fig. 2 Weighted summary of obstacles for exergy analysis. Often important =1, sometimes important =0.5, seldom Important = 0.

The answers to the in-depth interview questions indicated that one reason for the low rate of applications of exergy analysis is that most missions in the industry, according to respondents, do not require this type of tool, e.g. studies for small and medium-sized businesses. Only about 600 of 59 000 manufacturing companies in Sweden are defined as energy-intensive. This can be linked to the obstacles heterogeneity, i.e. the method is not considered by respondents to be applicable in most industries. One reason for the low level of potential applications, however, seems to be that several respondents felt that exergy was difficult to use. One conclusion from this is that the development of software for exergy could promote its use. The major obstacle to exergy analysis that was detected in the interview study was heterogeneity in the technical system level and information imperfections and asymmetries in the socio-technical systems level. (The heterogeneity refers to the fact that different companies have differing conditions for the use of exergy. Imperfections refer to lack of sufficient information and asymmetry to differences in information between different actors.) The highest ranked obstacle to the use of exergy analysis was a lack of strategy. This can be linked to one respondent who indicated that exergy often competes with cost analysis. One conclusion from this is that the tool should be competitive in the analysis of large technical systems where it can be used as decision support for industries or society.

3.4. Case study

The case study was made for the Luleå energy system. Existing data for the steel plant site, see ref [11] were extended by data collected from the CHP plant and District heating network.

An example of Sankey diagrams showing energy and exergy flows from the SSAB study 2005 is shown in Fig. 3. In the energy diagram for the blast furnace there is an energy input of 100%, whereas the output is 86.7 % export and 13.3 % losses. The sum of input flows is equal to the sum of the output flows because energy is indestructible according to the first law of thermodynamics. If we instead look at the exergy diagram, both the export and the heat loss flows are lower because the energy consists of energy forms of lower exergy value. Also the

output exergy is lower than the input exergy. The difference is irreversibly destroyed and corresponds to the entropy increase.

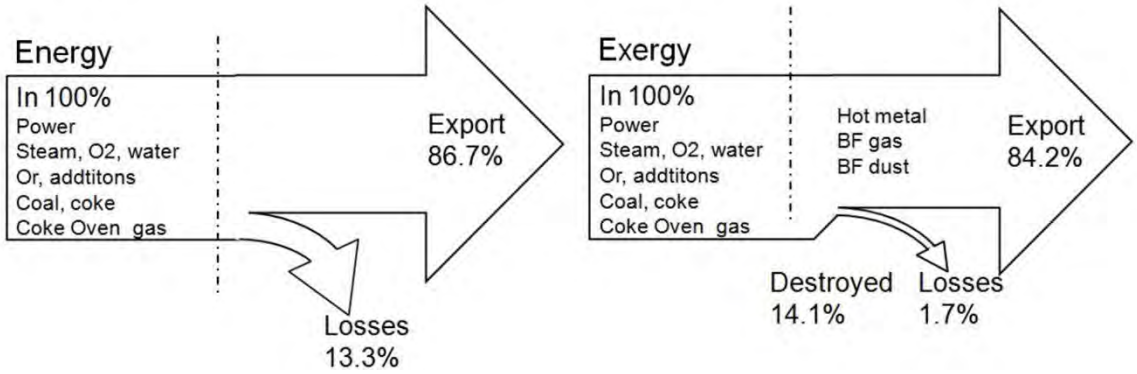

Fig. 3 SSAB Study 2005, Example on Energy-Exergy Diagrams for the blast furnace [12].

The destroyed exergy is a measure of the inefficiency of the unit in question. The heat loss exergy is a measure on the energy that could possibly be recovered.

Fig. 4 shows similar values for the heat and power plant. There are comparatively small heat loss flows, but a relatively high amount of destroyed exergy. The destruction rate is quite different between the units in Fig. 4. It is highest for the boiler and more moderate for the heat exchanger and turbine.

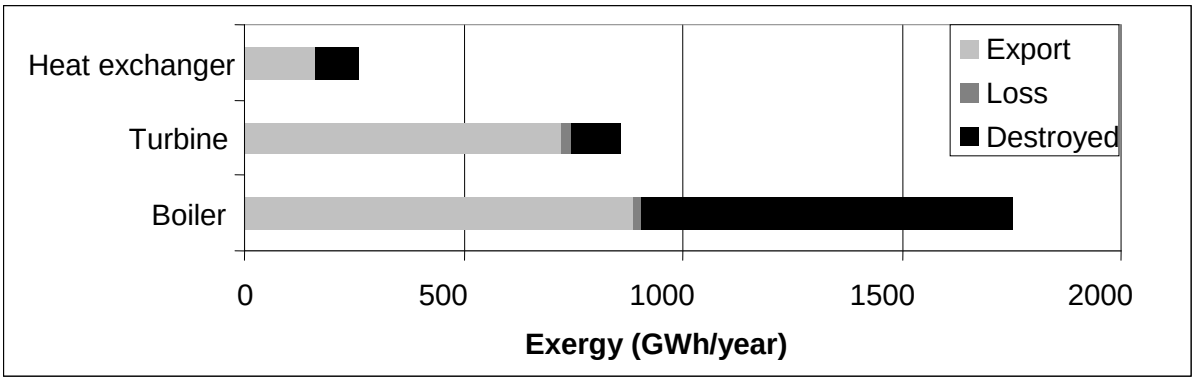

Fig. 4 Example on Exergy balances for the heat and power plant.

The reason for the higher destruction rate in the boiler is that it converts fuel energy (in principle 100% exergy) into high pressure steam with an exergy content that is roughly 50% of the enthalpy. It does not indicate a problem with the boiler; the boiler simply has a function where exergy destruction is inevitable. An important conclusion of this is that exergy destruction rate (or exergy efficiency) can be a tool to find out where to look. However, if it is to be used to judge bad or good function a reference value is needed. This could be previous data from the unit or published data. A catalogue for reference exergy data could perhaps be of interest.

Fig. 5 shows a Sankey diagram for the total system: Steel plant – Heat and power plant – District heating. The exergy in heat loss flows was relatively small in Fig. 3 but has increased when all steel plant units are increased. This flow represents energy that theoretically could be recovered as higher forms. These results have initiated quantitative studies on recovery e.g. by ORC turbine It can be seen that the exergy is destroyed stepwise through the system. The low amount of exergy in the district heating indicates that a large amount of energy sent to users with a low exergy demand. This can be a potential use for energy recovery from the steel plant. This can be expected to produce media flows with low or moderate exergy content.

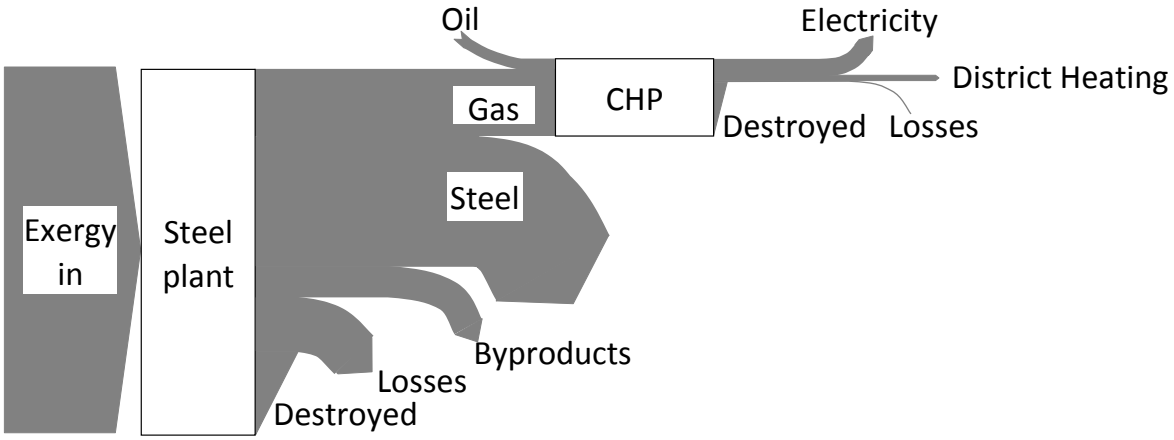

Fig. 5 Exergy flows through the total system

4. Synthesis, Discussion and Conclusions

In the project it was shown that:

- Exergy analysis is most competitive for industrial systems dominated by chemical conversions and energies other than thermal energies, e.g. chemical energy. Good examples are the steel industry and the chemical industry, especially refineries. Another important use is systems with different pressures and where production of electricity is of interest.
- Exergy expressions can be used to study process efficiency, possible modifications and mapping possibilities for excess energy recovery.
- Relatively much exergy is used for heating with a low need for exergy, compare Fig. 5. A study to decrease the imbalance using a modified system temperature is planned. Variations in the hot water balance for district heating are also influencing the energy efficiency.
- It is probably better to use a combination of Process integration methods than to only focus on one.
- Inclusion of exergy calculations in the mathematical programming tool reMIND was explored in the case study [15]. Continued work is interesting.
- Non-technical factors are responsible for the slow adoption of exergy analysis, e.g. lack of strategy, heterogeneity, information imperfections and asymmetries.
- The interview study has given an insight into the effect of non-technical parameters. The present technique has a relatively broad spectrum of questions which gives a good result even with a limited amount of respondents.
- Exergy studies are becoming established for system studies in the steel industry. Extension to further sites is being planned.
- A catalogue of reference data would be of interest for better interpretation of results

Acknowledgements

The authors would like to thank the Swedish Energy Agency for financing the project. We would also like to thank the many interviewees who kindly answered our questions and the people at SSAB, Lulekraft and Luleå Energi who have helped with data collection.

References

[1] Linnhoff B. & Flower J.R., "Synthesis of Heat exchanger Networks I. Systematic generation of energy optimal networks", Aiche Journal 24 (4), 1978, pp. 633-64

[2] G. Wall, "Exergy Flows in a Pulp and Paper Mill and in a Steel Plant and Rolling Mill", The Fourth International Symposium on Second Law Analysis of Thermal Systems, Rome, 25-29 May, 1987, pp. 131-140, ASME.

[3] Nilsson K. and Söderström M., "Optimising the operation Strategy of a pulp and paper mill using the MIND Method", Energy, vol. 17 (10), 1992, pp. 945-953

[4] Grip C.-E. and Thorsell A., "Swedish national research program for energy saving by means of process integration", Scanmet II, 2nd International Conference on Process Development in Iron and Steelmaking, June 6-9, 2004, Luleå, Sweden

[5] Grip C.-E., Söderström M., Berntsson T., "Process integration as a general tool for energy intensive process industry. Development and practical applications in Sweden", SCANMET III (3rd International Conference on Process Development in Iron and Steelmaking), June 8-11, 2008, Luleå, Sweden

[6] Larsson M., Doctoral thesis, Luleå University of Technology, 2004, No.:2004:63, ISSN: 1402-1544

[7] Larsson M., Sandberg P., Söderström M., Vuorinen H., "System gains from widening the system boundaries: analysis of the material and energy balance during renovation of a coke oven battery", Int J Energy Res., 2004, pp. 1051-1064

[8] Larsson M., Grip C.-E., Ohlsson H., Rutqvist S., Wikström J.-O., Ångström, S., "Comprehensive study regarding greenhouse gas emission from iron ore based production at the integrated steel plant SSAB TUNNPLAT AB", International journal of green energy. vol. 3, nr. 2, 2006, pp. 171-183

[9] Wang C., Doctoral thesis, Luleå University of Technology, 2007, No:2007:28, ISSN print):1402-1544

[10] Thollander P., Trygg, L., Svensson, I.-L., "Analyzing variables for district heating collaborations between energy utilities and industries", Energy 35 (9), 2010, pp. 3649-3656

[11] Zetterberg L., "Flows of Energy and Exergy in the Steelmaking process at SSAB Luleå", Master Thesis SSAB and Chalmers, Gothenburg, 1989

[12] Verbova M., "Energy and Exergy flows in Steelmaking Processes at SSAB Strip Products Division in Luleå", Master Thesis SSAB and LTU, 2007:080

[13] Grip, C., Dahl, J., Söderström, M., "Exergy as a means for process integration in integrated steel plants and process industry". Stahl und Eisen, 129, 2009, pp. S2–S8

[14] Malmström, S., "Efficient use of waste energy in the steel industry", Luleå University of Technology, Master Thesis SSAB and LTU, 2009:110

[15] Elfgren E, Grip C, Wang C and Karlsson J. Possibility to combine exergy with other process integration methods for a steelmaking case. 13th Conference on Process Integration, Modelling and Optimisation for Energy Saving and Pollution Reduction (PRES'10), 28 August – 1 September 2010, Prague, Czech Republic

Exergy Analysis applied to a Mexican flavor industry that uses liquefied petroleum gas as a primary energy source

P. Burgos-Madrigal[1,*], V.H. Gómez[2], R.Best[2]

[1] *Posgrado en Ingeniería (Energía), Universidad Nacional Autónoma de México, México D.F., México.*
[2] *Centro de Investigación en Energía, Universidad Nacional Autónoma de México, México D.F., México.*
** Corresponding author. Tel: +52 7773620090, Fax: +52 5556229791, E-mail: pabum@cie.unam.mx*

Abstract: An exergy analysis to a Mexican flavor industry, which uses liquefied petroleum gas as a primary energy fuel in their process equipment was carried out. .
The analysis used a proposed method that quantifies efficiency by means of exergetic indicators. To apply it to this case study equipment, the system or process was assumed to be a block that interacts with the surroundings in three ways: heat, work and mass transfer. The analyzed blocks were boilers, a thermal oxidizer, dryers, a distillation tower and extractors. Work and heat needs were covered by liquefied petroleum gas.
The exergy indicators quantify the degradation of energy by determinining the difference between the actual operation efficiency of the block and the maximum operation, both of them obtained from second law point of view. These indicators were exergy loss, efficiency, effectiveness, performance and potential of improvement.
Following the exergetic method application, it was found that the indicators of the effectiveness and performance in all blocks analyzed are near zero. This means that the process equipments are using a high exergy source to perform their function and also in large quantity. The results show that the oxidizer presented the major irreversibilities, and it is the equipment with the greatest potential for improvement and the key to reducing fuel consumption.

Keywords: *Optimization, Efficiency, Indicators, Block, Quantify*

Nomenclature

Latin Symbols

Efl	*effluents exergy losses*	*kJ/kg*
Ex	*exergy*	*kJ/kg*
H	*enthalpy*	*kJ/kg*
Irr	*Irreversible exergy losses*	*kJ/kg*
S	*entropy*	*kJ/kg K*
Pot	*Improvement potential*	*kJ/kg*

Greek symbols

ε	*Effectiveness*
ζ	*Performance*
η	*Efficiency*
Δ	*difference*

Subscripts

ntp	*net produced*
nts	*net supplied*
tte	*total input*
tts	*total output*
uts	*useful outlet exergy*
0	*reference, dead state*

1. Introduction

The industry sector is sensitive to the variability of the energy prices; as a result it adjusts the production priority to an efficient energy consumption to obtain advantages in cost. The economic factor is not the only reason to reach an efficient energy consumption in a country. The environmental negative impact as a result of an inefficient use of an energy resource is important as well [1,2].

Efficient energy use in the industry sector is possible with energy consumption analysis. Two problems promptly arise: the scarce information about an optimum use of energy in the industrial processes and the use of inefficient technology. [3,4].

The exergy analysis is especially useful when it is necessary to detect equipment, systems or processes that use a high quality energy source that is unnecessary for the objective, because

in this case important exergy losses arise [3]. Exergy analysis has been applied since the early 1970's with the aim of finding the most rational use of energy, which means at the same time reducing fossil fuel consumption, applying energy efficiency and matching the quality levels of the energy supplied and demanded [5]. The exergy method is useful for improving the efficiency of energy-resource use, for it quantifies the locations, types and magnitudes of wastes and losses. Also it is useful in identifying the causes, locations and magnitudes of process inefficiencies [6].

This paper discusses an exergy analysis of a flavoring industry plant (FIP) located in Morelos, Mexico. The monitoring of energy utilization of different equipments used in the process was necessary in order to investigate, analyze, verify and compare the data so as to try to understand the actual condition. The monitoring and data collection lasted from March to December, 2009. Table 1 shows the analyzed equipment:

Table 1. Identify and capacity of the analyzed equipment.

Identification	Capacity	Units
Distillation column A-001	700	l
Distillation column A-002	700	l
Distillation column A-004	70	l
Distillation column A-009	1900	l
Extractor A-103	2734	l
Extractor A-104	2734	l
Extractor A-106	7570	l
Extractor A-107	7570	l
Dryer S-01	30	kg/h
Dryer S-02	40	kg/h
Dryer S-03	150	kg/h
Dryer S-05	100	kg/h
Boiler CA-01	250	hp(S)
Boiler CA-02	100	hp(S)
Oxidizer		

l: liters, kg/h: kilograms per hour, hp(S) Boiler horsepower

These five kinds of equipments have the following function in the FIP:

- *Distillation column*: To separate mixtures based on differences in their volatilities in a boiling liquid mixture.
- *Extractor*: To separate a substance from a matrix. In the case of the FIP we refer to solid phase extraction.
- *Dryers*: To eliminate the liquid in a substance. The powder production starts by atomizing the emulsion in a hot air stream inside the dryer chamber in which the liquids evaporate instantly. The active material in the emulsion is encapsulated inside the film material.
- *Boiler*: To generate steam with the liquefied petroleum gas (LPG) combustion. The liquid water changes to vapor phase due to the high temperatures obtained.

2. Methodology of exergetic analysis

Exergy is defined as the maximum theoretical work obtainable from the interaction of a system with its environment until the equilibrium state between both is reached [7], it can also be seen as the departure state of one system from that of the reference environment [8]. Therefore, exergy is a thermodynamic potential dependent on the state of the system under

analysis and its surrounding environment, so called "reference state". The environment is regarded as a part of the system surroundings, large in extent so that no changes in its intensive properties, pressure P_0 and temperature T_0 mainly, occur as a result of the interaction with the system considered.

The exergy method quantifies the energy degradation using six different indicators. We assume the equipment, system or process to be a block that is interacting with the surroundings through heat, work and mass transfer. The work and the heat refer to the energy such as electricity solar radiation, mechanic work, etc. The mass transfer is the inflow and outflow of chemical substance, flows like vapor and fuel [9]. In the analyzer equipments in the flavor industry, the required work and heat are provided by LPG.

The exergy is the quality of energy in the block and is defined as:

$$Ex = (H - H_0) - [T_0(S - S_0)] \quad (1)$$

In Eq (1), the first term is the total enthalpy of the system that includes the thermal, mechanical, chemiscal, kinetic and potential energy. The second term, on the right -hand side, is the total entropy. The enthalpy (H_0) and entropy (S_0) of the reference state are defined by its pressure, composition, velocity, position and temperature.

2.1. Exergetic indicators

In order to quantify the energy degradation of the block, a series of exergy indicators were used. These indicators were: exergy losses (Irr), efficiency (η), effectiveness (ε), performance (ζ), potential of improvement (*Pot*). These are the relationship between the reality and the ideality expressed by fraction or percentage [4]. Table 2 shows the corresponding indicators:

Table2. Exergetic indicators to quantify the energy.

Exergy indicator	Equation
Exergy losses	$Irr = \sum (Ex_{tte} - Ex_{tts})$
Efficiency	$\eta = \frac{\sum Ex_{tts}}{\sum Ex_{tte}}$
Effectiveness	$\varepsilon = \frac{Ex_{ntp}}{Ex_{nts}}$
Performance	$\zeta = \frac{Ex_{uts}}{Ex_{tte}}$
Potential improvement	$Pot = Irr(1-\varepsilon) + Efl$

Below is a brief explanation of each indicator:

- *Exergy losses.* The measure of the total exergy provided by the inflow such as fuel and raw material, and the total exergy at the outlet such as products and effluents.
- *Efficiency.* The ratio of the total exergy at the outlet of the block in relation to the total exergy of the inlet.
- *Effectiveness.* It evaluates if the analyzed block satisfies its function, considering the term "net" means difference (Δ). The net exergy produced is the one obtained by the products and the net exergy supplied is provided by the energy resource, for instance LPG.
- *Performance.* Relation of the useful outlet exergy and total entrance exergy.

- *Potential improvement.* It is the measurement of block improvement. The equation has been obtained through the combination by exergy losses and the system effectiveness. The exergy losses are due to two different sources, the first one derives from the internal use of the block and is referred to as irreversibilities (Irr) and the last one arises from the effluents (Efl), that are released into the environment like wastes.

To obtain the reference temperature, the actual hourly temperature in the process plant was registered for a week. The value was 29.3 ºC±1.9°C. The pressure was considered constant at 101.325 kPa.

2.2. Blocks

As mentioned in the introduction, five different equipments were analyzed. The exergetic balance of each equipment was different and depended on the way that it operated, the energy quantities they require, and the energy wasted in irreversibilities, so it was necessary to consider an exergetic balance for each case.

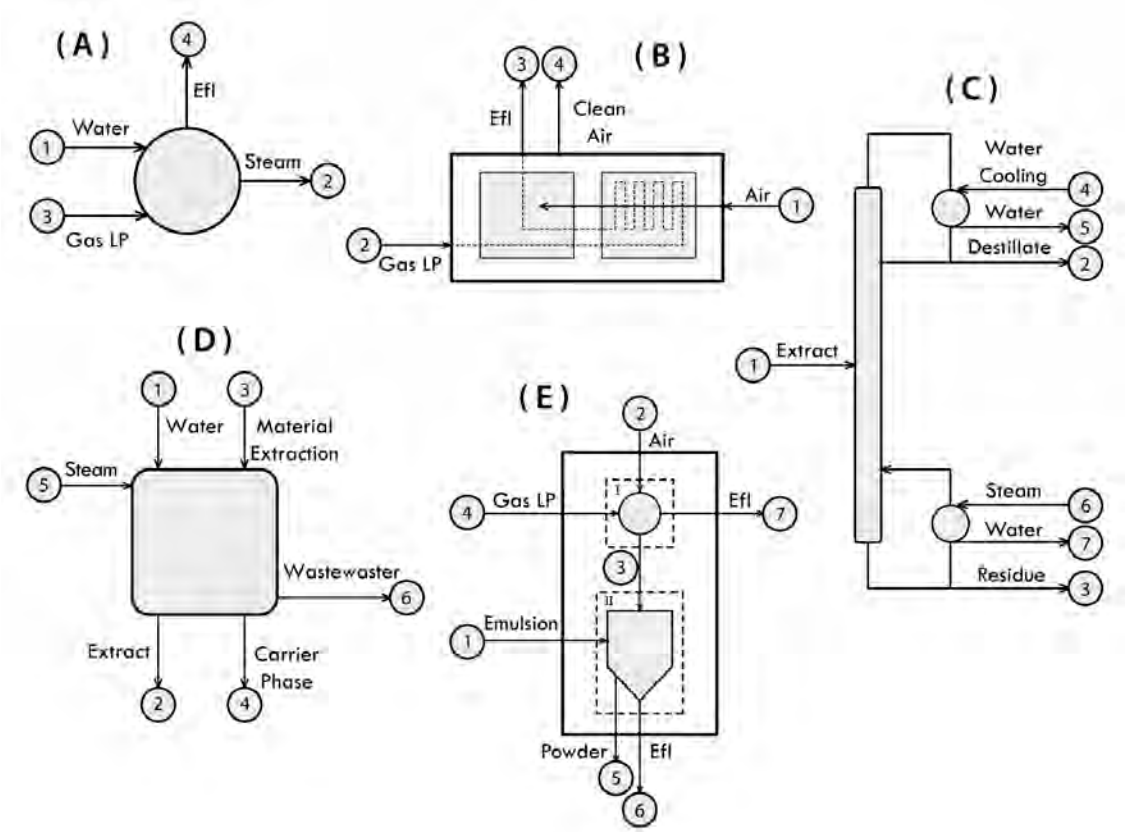

Fig. 1. Diagrams of the blocks. Boiler (A), Oxidizer (B), Distillation tower (C), Extractor (D) and Dryer (E)

Figure 1 shows the diagrams of the different blocks to be analyzed. The numbers represent the process streams of each case. When the arrows point inwards, it refers to the stream with the exergy that enters the equipment; it could be fuel, vapor or fluid. Conversely, when the arrow points outwards, it refers to the stream with the exergy that goes to the environment, such as products, effluents or wastes. Table 3 shows all the exergetic balances obtained for the blocks.

Table 3. Exergetic balance

Block	Ex_{tte}	Ex_{tts}	Ex_{nts}	Ex_{ntp}
Distillation tower	$Ex_1 + Ex_4 + Ex_6$	$Ex_2 + Ex_3 + Ex_5 + Ex_7$	$(Ex_6 - Ex_7) + [Ex_1 - (Ex_2 + Ex_3)] + (Ex_4 - Ex_5)$	$(Ex_2 + Ex_3) - Ex_1$
Extractor	$Ex_1 + Ex_3 + Ex_5$	$Ex_5 + Ex_4 + Ex_6$	$Ex_5 - Ex_6$	$(Ex_2 + Ex_4) - (Ex_1 + Ex_3)$
Dryer	$Ex_1 + Ex_2 + Ex_4$	$Ex_5 + Ex_6 + Ex_7$	$Ex_4 - Ex_7$	$Ex_5 - Ex_1$
Boiler	$Ex_1 + Ex_3$	$Ex_2 + Ex_4$	$Ex_3 - Ex_4$	$Ex_2 - Ex_1$
Oxidizer	$Ex_1 + Ex_2$	$Ex_3 + Ex_4$	$Ex_2 - Ex_3$	$Ex_4 - Ex_1$

Finally, with the exergy balance of each block it is necessary to calculate the exergetic indicators with the equations presented in Table 2.

3. Results

The values of the indicators in all the equipments studied were plotted with the objective of analyzing and comparing the behavior in the FIP.

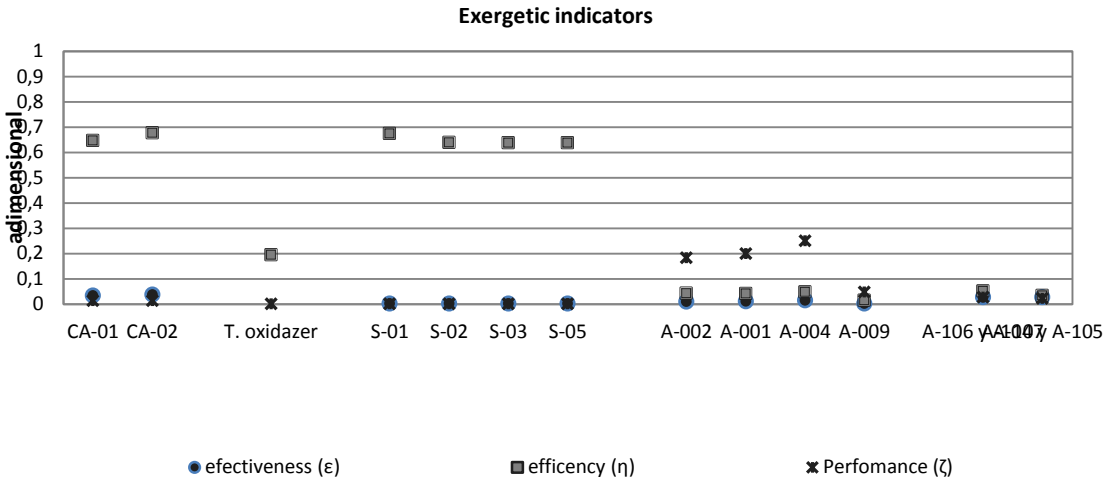

Fig. 2. Effectiveness, efficiency, performance of the analyzer blocks in the FIP

Figure 2 presents the dimensionless indicators: the effectiveness, efficiency and performance. The effectiveness is near a zero value in all the blocks as a consequence of the important quantity of exergy required to carry out their objective. This happens commonly with old equipment where the design does not have priority on saving fuel. The performance is larger in the distillation columns 0,2 to 0,3 because they do not require high temperatures for their function and the effluents are smaller than in others blocks. The efficiency of the combustion equipment is estimated at 0.7 which shows a large amount of effluent in the total output exergy, with up to 65% of exergy provided by the LPG thrown into the atmosphere as combustion gases.

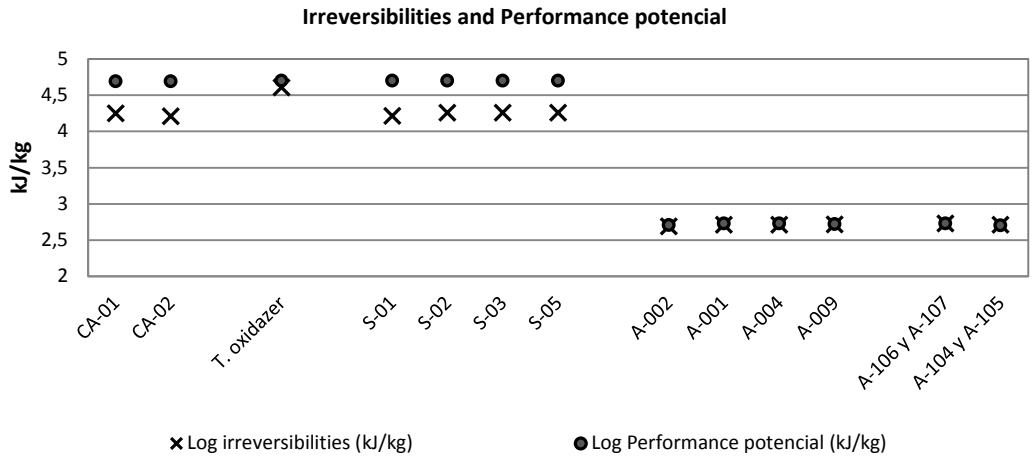

Fig. 3. Irreversibility and improvement potential of the analyzer blocks in the FIP

In Figure 3, the distillations columns and extractors present similar improvement potential values and irreversibilities due to the fact that the effluents are insignificant, a slight flow of water between 60°C to 80°C from the steam used to obtain the process temperature circulating in the insulation of the equipments. In contrast in the combustion equipment their improvement potential is higher than the irreversibbilities because of the large quantity of effluents, 33000 kJ/kg. These blocks have an important feasibility of optimization, by recovering heat from the effluents to preheat the water used in the boiler.

As a result of the method, the global exergy flow of the plant can be represented with a Sankey diagram; this diagram is a summary of the exergy analysis of all equipments of the FIP. The width of the arrow gives the flow, specifies the effluents (arrows pointing upwards), irreversibilities (arrows pointing downwards) and the net exergy produced (arrows pointing to the right), the numbers outside the arrows in parenthesis describe the percentage of the total exergy in the FIP, and the numbers inside the blocks in parenthesis describe the quantity of equipment that represents each block. The indicators represent a specific aspect of the equipment and the Sankey diagram the interaction of all the blocks in the FIP. In Figure 4, an expansion in scale from the steam of the oulet of the boilers to the inlet of the extractors and distillation tower was necessary, because only the 0.35% is the net produced exergy as steam.

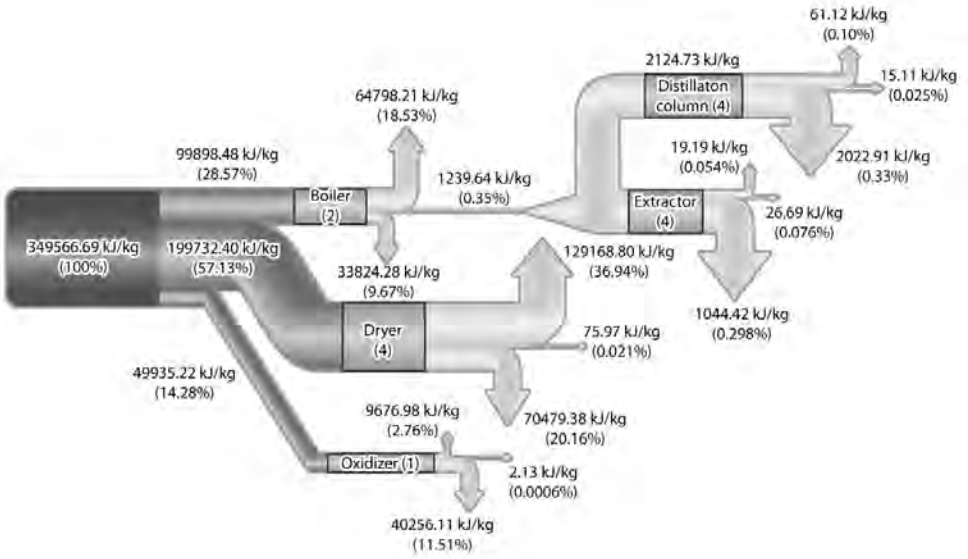

Fig. 4. Sankey diagram for the global exergy flow in a FIP

The diagram shows that the exergy provided by the LPG energy source is 349,566 kJ/kg, and is distributed to the process blocks. Over half of the exergy 57.1% is used for the driying process in which only 0.021% of the net exergy produced is obtained as powder.

The distillation columns and extractors have small effluents of approximately 20 kJ/kg per equipment, compared with the combustions blocks with 33000 kJ/kg. On the other hand. they have more important irreversibilities, as compared to the combustion blocks. To optimize these equipments it is necessary to analyze how they operate and find an improvement in their design. [10].

4. Conclusions

In this paper a second law analysis in a flavor industry was carried out. The process blocks with higher efficiency, close to 0.7, were the boilers and the dryers. This is to the fact that the total output exergy includes the effluents, that represent 90% of the total of the exergy that is provided by the fuel.

The thermal oxidizer does not present important losses in effluents (9,676.98 kJ/kg), but its irreversibilities are the largest with 40,256.11 kJ/kg and an effectiveness close to zero. As a result, this block has the highest performance potential 49,933.6 kJ/kg and is the main equipment in which to focus in order to achieve a low fuel consumption. It is possible to use other kind of equipment for the same objective (eliminates unpleasant odor) without using combustion.

The distillation towers and extractors present low effluents (20 kJ/kg) per equipment approximately as compare with combustion blocks (33,000 kJ/kg). This means that the energy is degraded in the distillation columns due to the presence of significant irreversibilities. To optimize these equipments it is necessary analyze their performance and find a design improvement, owing to the fact that they are more than 30 years old with no technological improvements. The best solution is to upgrade the equipments.

The indicators in all equipments such as efficiency, effectiveness, and performance are close to zero. This means that the FIP requires a high exergy source and a large quantity forcarried out its objective, approximately 350,000 kJ/kg. This consumption decrease at least 68% applying waste heat recovery of the effluents of the combustion equipments, like boilers, dryers and oxidizer, to warm currents in other processes such as in the extractors where the optimal temperature is 60 °C. [10].

5. Acknowledges

The authors thank CONACYT and Posgrado UNAM for their support. Thanks to the FIP for accepting do the analysis and providing the necessary access and information. Finally we want to thank the graphic designer, Hernán A. Perez for making the diagrams necessary for the paper.

References

[1] G.P. Hammond, Industrial energy analysis, thermodynamics and sustainability, Applied Energy 84, 2007, pp 675-700.

[2] M.A. Rosen, D.S. Scott, A methodology based on exergy, cost, energy and mass for the analysis of systems and processes, In: Proceedings of the Meering of International Society for General Systems Research, 20-22 May, Toronto, p. 8.3.1-13.

[3] R. Rivero, Programas Integrales de Ahorro de Energía (exergia) en la Industria Petrolera, Instituto Mexicano de Ingenieros Químicos A.C., 1996, pp 7-9.

[4] C. Palanichamy, N. Sundar Babu, Second stage energy conservation experience with a textile industry, Energy Policy 33, 2005, pp. 603-609.

[5] H. Torío, A. Angelotti, D. Schmidt, Exergy analysis of renewable energy-based climatisation systems for buildings: A critical view, Energy and Buildings 41, 2009, pp.248-271.

[6] M.A. Rosen, I. Dincer, M. Kanoglu, Role of exergy in increasing efficiency and sustainability and reducing environmental impact, Energy Policy 36, 2008, 128-137.

[7] M.J. Moran, H.N. Shapiro, Fundamentals of Engineering Thermodynamics, 3rd ed, John Wiley & Sons, New York, USA, 1998.

[8] A. Bejan, G. Tsatsaronis, M. Moran, Thermal Design and Optimization, John Wiley and Sons, New York, USA, 1996.

[9] R. Rivero, El análisis de Exergia", Instituto Mexicano de Ingenieros Químicos A.C 11,1994, pp14-27.

[10] P. Burgos, Análisis exergético de procesos que utilizan gas LP en una industria de saborizantes: Calderas y secadores, Tesis de Maestría-UNAM, 2010.

Thermal cooling basin exploration for thermal calculations

Peteris Shipkovs[1], Kaspars Grinbergs[2]

[1] *Institute of Physical Energetics, Energy Resources Laboratory, Riga, Latvia*
[2] *Riga Technical University, Riga, Latvia*
** Corresponding author. +371 67553537, Fax: +371 67553537,, E-mail: shipkovs@edi.lv*

Abstract: There are a number of cooling systems known across the world. For decades they have undergone development, changing coolants and their chemical composition, but water has, thanks to its universal properties, remained an undying presence in this technology. Water is used as a carrier heat or cold for cooling spaces and some cooling equipment itself, for accumulating and radiating heat to an environment with lower heat potential, for heat evaporation, and as a solvent which is great at dissolving substances we know as cooling agents.
Pools are an especially practical and aesthetically appealing execution of a co oling system – provided appropriate temperature modes and external air temperature during the operational season. In centralised heat supply conditions, heat production companies choose to install cogeneration engines to increase energy production efficiency and profitability, allowing both electricity and heat to be produced from one type of fuel. However, the world at large has also seen trigeneration systems: such large urban areas as New York and Tokyo have long been using one type of fuel to produce electricity and, adjusting to weather patterns, either heat or cold energy. Of course, these enormous cities and their energy delivery patterns cannot be compared to those of small cities and rural towns which are common in the Baltic and CIS countries. Conversion of heat into cold energy takes place at heat absorption cooling facilities. Heat absorption facilities require a fluid overcooling cycle to store a concentrated fluid. The temperature modes of this cycle (which vary between producers) produce low-potential heat which cannot be reused to produce heat energy, e.g. 35-29*C. To support such a temperature schedule, producers generally recommend installing heat evaporation towers, but they are expensive and will often clash visually with the landscape. A cooling pool may be used instead for both practical and aesthetic reasons, using water sprayers to promote evaporation. Water spraying is necessary to increase the surface area of water-to-air contact: this way, the surface area is equal to the combined areas of all water droplets. The depth of a pool must be no less than 1.5 m, preventing heating by sun rays. Pool cooling properties improve with finer droplet size, although this carries higher electricity expenses to produce adequately high pressure before pulverisation. Such pools may use fountains which serve both as a cooling facility and an attractive landscaping piece. An evaporation pool is also significantly cheaper to build than an evaporation tower, although water loss may be higher.
In consideration of the facts described above, a pool with a water spraying device was built for this research project. With appropriate air temperature, pressure and relative humidity, heat yield and yield changes were measured.
The goal of this study was to compare the research and experimental parts of the project to similar studies performed previously, in order to determine the practical viability of using heat evaporation pools as well as to develop a complete prototype which may be used as the basis for building similar structures.

Keywords: *cooling systems, heat evaporation pools*

1. Introduction

Latvia is located in a climate region where heat is necessary not only for improving quality of life, but also as a prerequisite for survival during the winter, which lasts for about 200 calendar days. Therefore, heat supply is a particularly important part of Latvia's power industry, as evident from the fact that over 60% of the country's energy resource consumption goes into heating. Increasing the efficiency of heat supply, especially centralised heat supply, which provides 30% of the heat required within the country by households and technological facilities (the proportion of centralised heat supply in the housing sector exceeds 45%). Increasing the efficiency of centralised heat supply systems also has a d eciding role in ensuring the competitive ability of heat supply companies, which in turn is a requirement for using the possibilities and advantages of centralised heat supply systems. In the large part of country (one-third of the primary energy consumption) as the raw material for the energy

production (including centralized heating) is used natural gas. It increases the dependence of the energy import and the energy purchase price. There is as a large potential of renewable energy in Latvia, it could be used in energy production, but in many cases necessary investment for communication shift are hardly to attract, that's way there musts be done everything to improve current centralised heat supply, to make maximum benefit for the energy supplier ad it's user.

2.1. Purpose of Introducing a Trigeneration System

One of the solutions for improving the efficiency of the centralised heat supply system might be introducing a trigeneration system in the centralised municipal heat supply system. Traditional producers of electricity produce electricity from fuel, such as fuel oil, diesel or natural gas, however this process is inefficient: it produces waste heat, which may be converted into various types of energy and put to use. At cogeneration facilities, this heat is used to supply nearby household or industrial demand. In case of trigeneration, fuel is used to produce electricity, heat, and, if necessary, convert the heat into cold energy, to be used for household or industrial cooling; additional heat is removed from smoke and gas before they are emitted into the atmosphere, producing additional heat for heating or cooling of spaces. Trigeneration systems in large urban areas as New York and Tokyo have long been using one type of fuel to produce electricity and, adjusting to weather patterns, either heat or cold energy, but it is a great challenge to adjust this system in areas that do not requires such great energy consumption.
Purpose of introducing a trigeneration system:

- Consumption of heat load during the summer period
- Economically advantageous conditions for using the heat source
- Constant loading of the cogeneration facility year-round
- Potential for reducing heat energy tariffs

The centralised heat supply system works according to a specific temperature schedule adapted to changes in external air temperature. The city boiler house works according to such a temperature schedule. The boiler house generally services not only tenement and private houses, but also office spaces, utility consumers and often production facilities interested in heat absorption capacities for their cooling equipment during the summer. There is no need for heating inside the city's residential spaces; the heat supply system works according to a 65-40°C temperature schedule (not Riga). The heat producer considers the issue of profitable heat carrier temperature during summer months – it is well known that with increased heat carrier temperature, heat carrier surface heat loss increases as well (the temperature schedule for trigeneration heat absorption equipment is 95-70°C). Here, one must consider the usefulness of maintaining adequate heat carrier temperature for heat absorption equipment, while at the same time providing the same temperature to tenement houses, which only use hot water. On the other hand, it is useful because cogeneration facilities may be operated at higher loads during the summer period. An assessment of issues related to introducing a trigeneration system must consider the possibility of dividing the heat supply network into primary and secondary circuits. This means that a heat source would produce heat both for delivering hot water to consumers during the summer period and for cooling spaces. The principal layout of a trigeneration system is shown in Figure No. 1. However, the following obstacles complicate the introduction of a trigeneration system:

- Heating network configuration must be adjusted
- A heat supply and temperature schedule must be specified for consumers
- Daily heat consumption patterns must be analysed
- Strategic choice of absorption equipment (centralised, decentralised)
- **Building an evaporation tower**

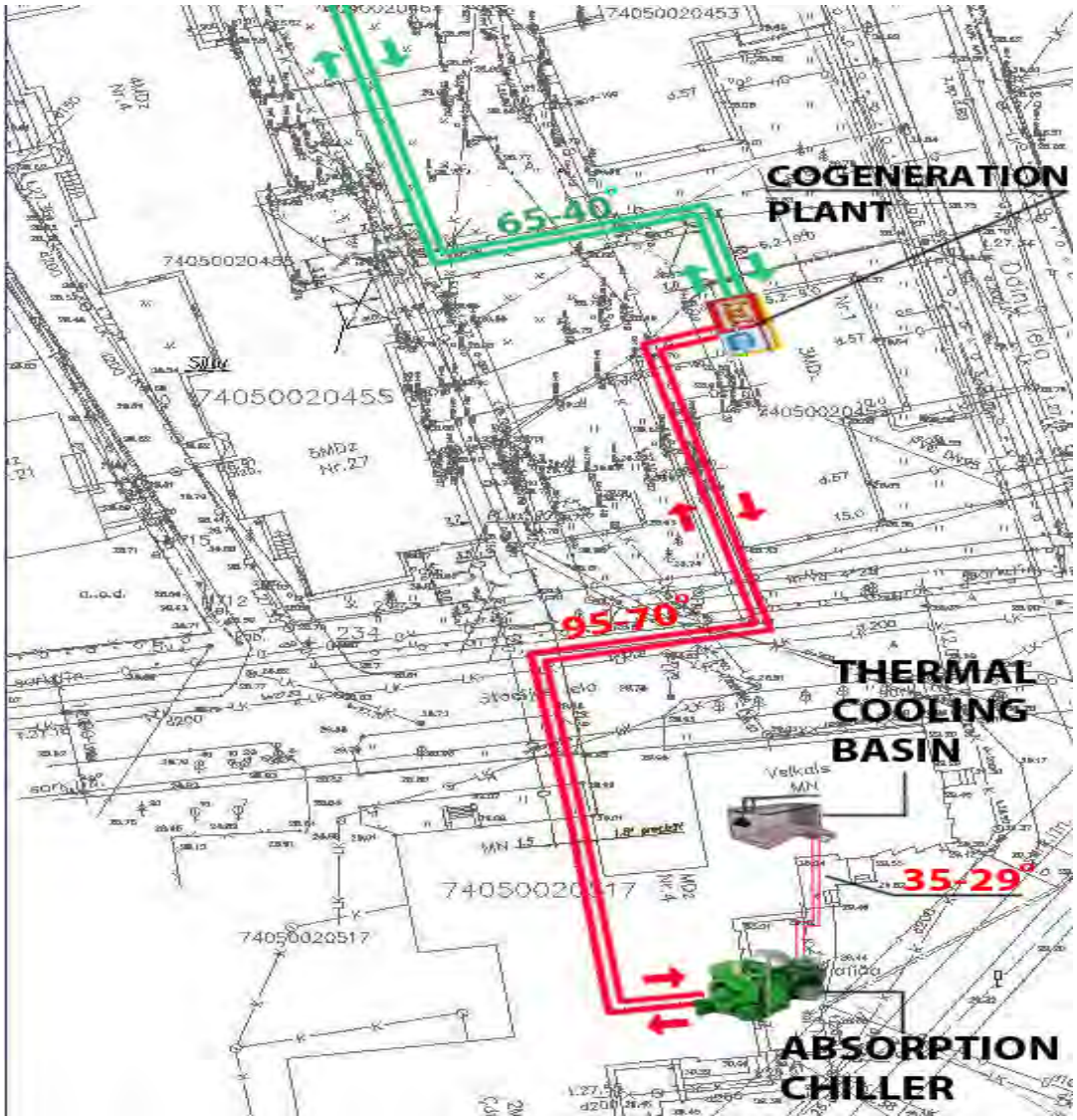

Fig. 1. Principal layout of a trigeneration system

2.2. Heat Evaporation Pools as an Alternative to Cooling Towers

Heat conversion into cold energy takes place at heat absorption chillers. A heat absorption chiller can be seen in Figure No. 2. Two connection points to the cooling tower are shown on the layout, the heat absorption facility may instead be connected to a heat evaporation pool. In order to contain a concentrated fluid, heat absorption facilities require a fluid supercooling cycle. The heat carrier temperatures within this cycle (depending on the manufacturer, this value may vary) are usually low, such as 35-29°C. In order to ensure a temperature schedule for such a cycle, the manufacturer usually recommends building heat evaporation towers, although these are expensive and often clash with the landscape. For practical as well as aesthetic reasons, a heat evaporation pool may be used here, employing water sprinklers to boost cooling efficiency. Water sprinkling is necessary for increasing the area of contact between water and air because the area of contact is equal to the sum of the areas of all airborne droplets of water.

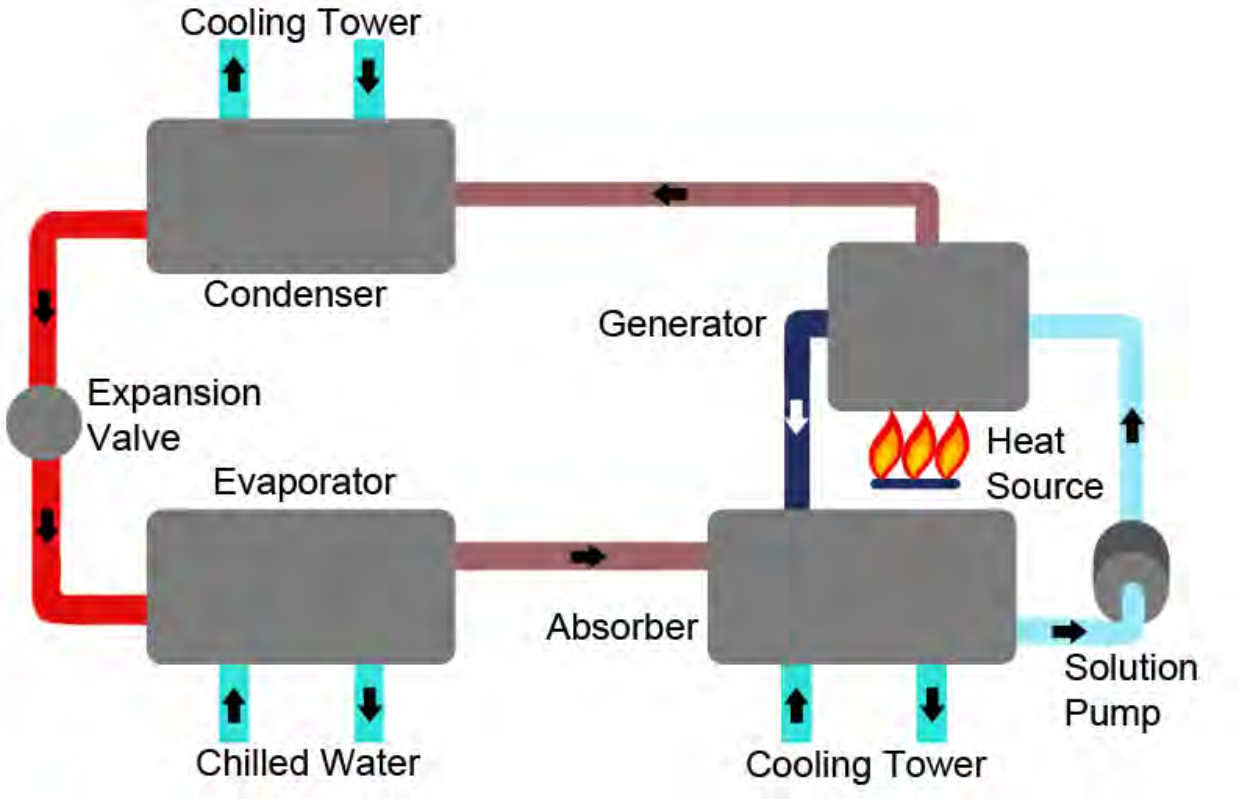

Fig. 2. Heat absorption chiller

The pool may not be shallower than 1.5 m, to prevent heating by solar rays. The cooling properties of the pool will improve with sprinkling of finer droplets, although this leads to higher water losses as well.
A heat evaporation pool (as seen in figure No. 3) may be a heat engineering structure; its advantages include:

- A heat evaporation pool is much cheaper to build than an evaporation tower
- An evaporation pool is a closed system which may therefore be located in public areas
- An evaporation pool is a significantly smaller structure than a tower
- An evaporation pool is more visually appealing and landscape-friendly than an evaporation tower.

2.3. Analysis of Heat Evaporation Pools for Heat Engineering Calculations

The purpose of this research is to perform a study and compare the experimental data to similar studies done previously across the world in order to determine the possibility of practically implementing a heat evaporation pool, as well as to develop a full prototype that would make the basis for building similar structures. In the past sever Russian scientist's worked at this scope, thermal cooling basins where located nearby nuclear and thermal power plants because turbine cooling required heat potential reduction. Those pools where open systems without heater. Water from turbines was supplied directly to the basin and sprinklers. In such a system it's easier to cool because heat potential is usually much higher than the outdoor air temperature (the coolant temperature is considerably higher). Remove maximum heat from the heater and refrigerate with the sprinkler spray in sufficient quantity within the prescribed limits is a challenge in closed – cycle refrigeration. Closed system allows locate

basins in public places because the cooling circuit is protected against pollution.The research stand visualisation is provided in Figure No. 3.

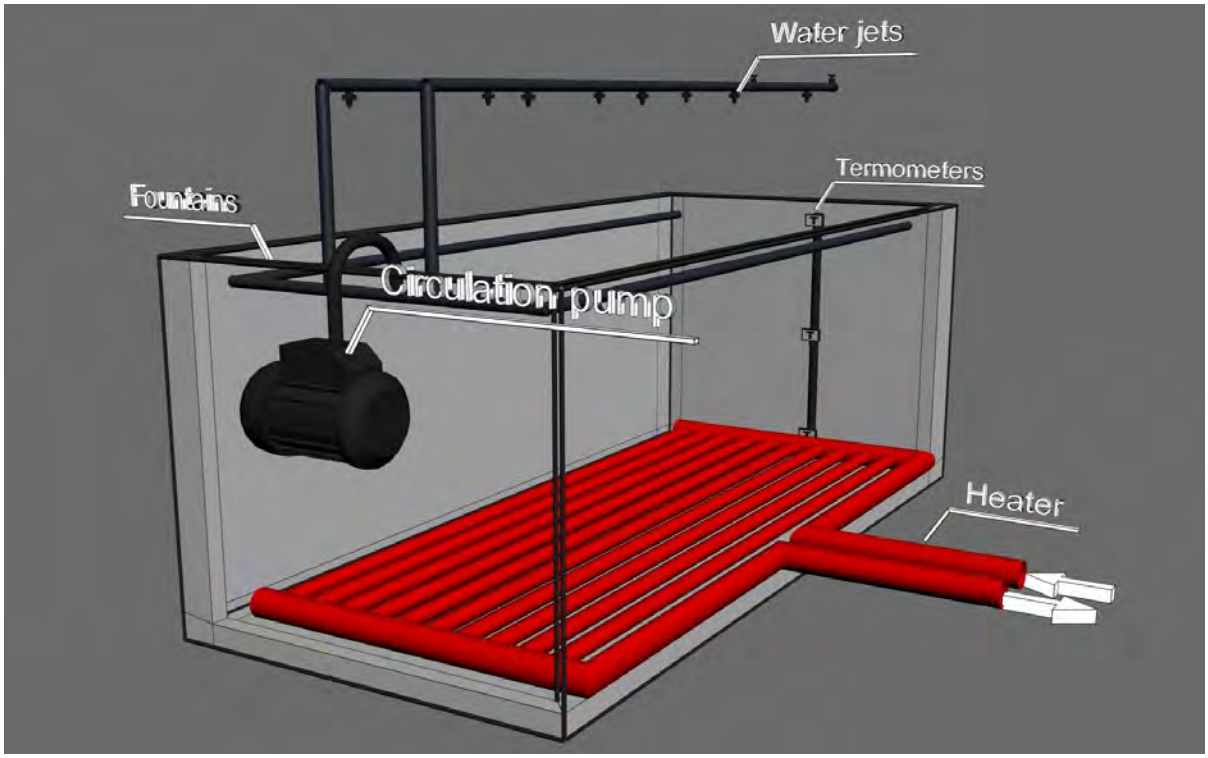

Fig. 3. Visualisation of Heat Evaporation Pool

The heat evaporation pool idea is based on the concept of uniting two systems; a heating element is placed inside the pool and a circulation pump is connected to deliver water inside the pool into sprinklers located above its surface. Compared to an evaporation tower, which is an open system, a pool is a closed system, which means that an evaporation pool may be located in inhabited areas, such as towns, parks, parking spaces etc.

Circulation pump: by adjusting the circulation pump's throughput, the intensity of droplet sprinkling may be adjusted, which will in turn be reflected in the cooling performance of the fluid. It should be considered that the cooling performance of a pool is also affected by a number of outside conditions, such as external air temperature, relative humidity, external wind speed; these parameters must are measured during the experiment, and the parameter value will be applied to the results of the heat engineering calculations. The heat transfer ratio must be adjusted depending on external air parameters. Near the basin is located weather detection station to obtain ear condition data during the experiment, up to now fully equipped experiment has lasted only for days in October 2010, when the outdoor air temperature at the ranged from +7 till +12° C per day. It was clear after comparing the temperature curves that at low outdoor air temperature cooling capacity was directly related the outdoor air temperature fluctuations, it can be seen in Figure No. 4. Graf shoes that basin cooling properties increases when outdoor temperature drops, it cannot be observed literally because of a heat storage. The other parameters made a minor impact on cooling capacity, except wind speed, it increases cooling properties and water loss. There are three thermometers placed in the basin to determine temperature changes in different strata. First is placed 0.3 m above the heater, the second 0.5 m below the air / water contact surface, the third is already over the air and water contact surface. All of these thermometers show the different temperatures.

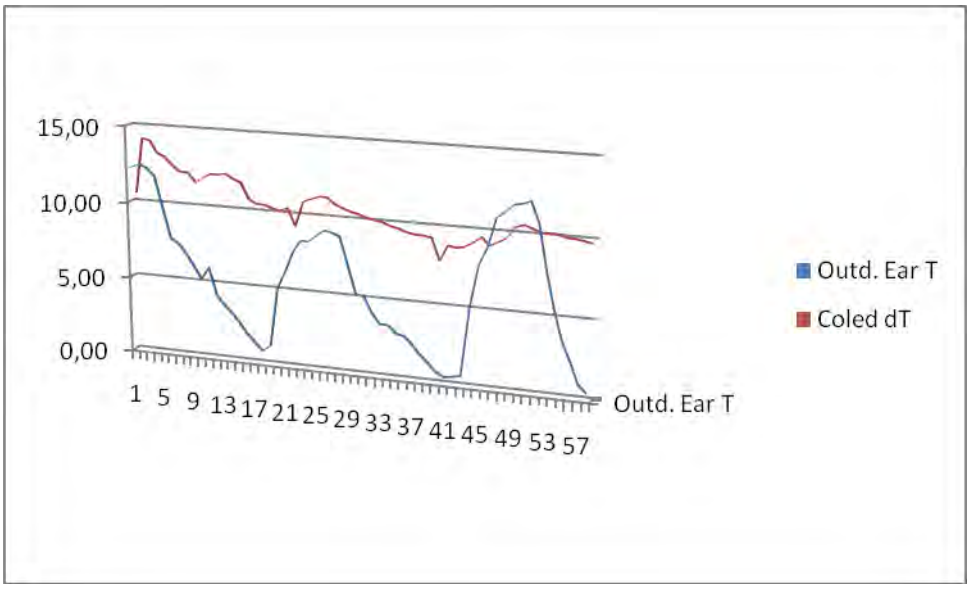

Fig. 4. *Outdoor air temperature impact on the cooling basin properties*

Heating element: a heating element is placed inside the pool, adapting it to the shape and area of the pool – in any case, the configuration of the heating element must be selected so as to create maximum heat carrier resistance and heat loss both as radiation and as hydraulic loss. The pool in question is connected to the boiler room's heat exchanger, which allows adjustment of heat carrier input temperature as well as heat carrier throughput.

The purpose of the heat evaporation pool is to retain the installed cooling parameters regardless of fluctuating external conditions.

Thermal cooling basin exploration for thermal calculations:

- Basin size $S = 11\text{m}^2$;
- Basin volume $v = 22\text{m}^3$;
- Basin temperature Schedule 35° – 29°C;
- Basin heat input $Q = 3.20\ \text{m}^3/\text{h}$;
- Circulation pump yield $Q = 8\ \text{m}^3/\text{h}$;
- Heat transition coefficient K kJ/m^2;
- Spray jet yield V m^3/s;
- Spray jet diameter $F = 0{,}001$m;
- Relative water weight $\alpha_p = 1\text{kg/m}^3$;
- Yield coefficient η - (0,6 – 0,75)
- Nozzle pressure drop $\Delta P = 0{,}00032$ kg/m^2
- Gravitational force $g = 9{,}8$ m/s^2;
- Pressure supply in lines 3,2 atm, 324240Pa;
- Relative air pressure P_g, Pa;
- Outdoor air temperature T_a, °C;
- Air relative moisture d, %;
- Wind speed v, m/s;

Water loss, depending on the outdoor temperature, coefficient k values shown in Table 1.

$$\Delta = k \cdot \Delta T, \% \qquad (1.)$$

Table 1. Coefficient k value depends on air temperature [2]

Air temperature, °C	0°	10°	20°	30°	35°
Coefficient *k*	0,10	0,12	0,14	0,16	0,17

Guided thermal basin volume:

$Q_{heat}=M\cdot C\cdot(T1 - T2)$; [3] (2.)

$Q_{heat}=22.34$ kW/h ;

Heat transition coefficient:

$K = Q/S \cdot \Delta T$; [3] (3.)

K= 0,33kW/m^2;

Sprayed water volume, changes depending on weather conditions:

$V = \eta \cdot F \cdot \sqrt{(2g)} \cdot \Delta P / \alpha_p$; [1] (4.)

$V = 1.5\cdot10^{-6}$ m^3/s;

3. Conclusions

Experimented will be repeated and basins cooling properties measured according with whether when the cooling is necessary – in summer.

Graf shoes there is minor influence on the basins cooling properties by wind speed, there must be assurance that fluctuating is insubstantial in suitable weather conditions.

Water jets and fountains musts be located to exclude terrorism danger.

There is a slight difference between the first and second thermometer readings, but significant deferent's with third thermometer readings because its located above ear and water contact area, but the deferent's between first and second thermometer is called by location, first thermometer located 0.3m above the heater and readings are 0.2-0.5°C higher, but when the heater is shut down readings shift and the second thermometer shoes 0.1-0.2°C higher temperature, this indicates heat flow change and basin heats from the outdoor ear and sunlight when the heater switched on basins heat potential is higher and heat flow changes.

The sprinkling intensity is determined and the heat transfer ratio is adjusted depending on external air parameter fluctuations in order to keep the Δ T value above the installed minimum.

The influence of external air parameters on Δ T changes must be determined during the study.

The most profitable sprinkling intensity must be determined considering the results.

Water volume has properties for heat accumulation, that's why after water jets are shouted down basins retains its cooling properties, for a while.

There musts be investigation before adapt thermal cooling basin to certain system, basins cooling properties changes depending on weather conditions.

Thermal cooling basin could be combined with equipment with absorption and compression cycles, solar collectors, PV and PVT solar cells.

Experiment will be continued and the results will be published.

References

[1] П .Д. Лебедев Расчеты и проектирование сушки устройств, Государственное энергическое Издательскmво, Москва, 1963, 142pp;

[2] Т. Х. Маргуглова, Атомные электро станции, Государственное энергическое Издательство, Москва, 1975, 205pp;

[3] Gedrovičs M., Nekustāmā īpašuma pārvaldnieks,: Biznesa augstskola Turība, Riga, 2002, 287 pp;

[4] Osipovs L., Ķīmijas tehnoloģijas pamatprocesi un aparāti,: Zvaigzne, Riga, 1991, 98, pp;

Development of a tool for the evaluation and improvement of the energy management in small and medium enterprises (SMEs)

I. Morales[1,*], J.P. Jiménez[2]

[1] *Andalusia Institute of Technology, Málaga, Spain*
[2] *Andalusia Institute of Technology, Málaga, Spain*
** Corresponding author. Tel: +34 952 02 87 10, Fax: +34 952 02 04 80, E-mail: imorales@iat.es*

Abstract: A new tool is presented in this article. The main objective is the improvement of the small and medium companies' energy management systems in order to obtain energy savings and the adaptation of the organizations according to the recognized standard UNE-*EN* 16001:2010. The application of the tool lets companies reduce their energy consumption and improve their processes in an energy efficiency perspective. The methodology is based in questionnaires and tests which will report information in order to identify all standard requirements. In a near future, the expected benefits are going to be a knowledge about the companies' EMS situation, information to prioritize actions to improve, identification of critical areas, comparison between different EMS evaluation results (for example: company' EMS with industry average, etc.), improve companies knowledge about energy, energy efficiency, etc.

Keywords: *Energy, Management, System, software, companies.*

Nomenclature

EMS Energy Management System
SME: Small and medium enterprise
IAT: Instituto Andaluz de Tecnología (Andalusia Institute of Technology: company name).

1. Introduction

In the last few years, society, governments and companies have changed their philosophy in order to protect and preserve the environment. Nowadays, instead of being watched as an economical consumption, this philosophy has become in a competitive factor.

At the same time, laws have included topics related to environment which gives an answer to the general interest.

The purpose of this paper is to introduce a tool (named EVALENER) that offers companies the possibility of evaluating the management system focused on energy efficiency according to the recognized standard UNE-EN 16001:2010 "Energy Management System – Requirements with guidance for use´" (Spanish version of EN 16001:2009).

UNE-EN 16001:2010 [1] standard just became an European standard, so not many other evaluating software has been developed to help companies and no relevant result have been set. Even more so for SMEs. In Spain only few companies has got its EMS certified and most of them are big organizations.

The use of this tool will let companies reach both environmental and business benefits. Regarding environmental benefits the following goals could be achieved: CO2 emissions, global warming and climate change impact and exterior energetic dependence could be reduced. According to business benefits, companies will obtain financial savings (energy bills reduction), achieve legal requirements, social responsibility and corporate image improvement.

Another important aspect is the fact that the tool is focused to be applied in small and medium enterprises (SMEs) since they do not have as much economical resources as big companies have. So the tool's main objective is helping SMEs to achieve an effective EMS carrying out their own evaluations and measuring the impact of the development improvements in the organizations.

2. Methodology

EVALENER has been based in recognized standard UNE-*EN 16001:2010 'Energy Management Systems - Requirements with guidance for use'* that provided a model of excellent energy management to the organization to compare their energy management system with the model one.

The methodology for developing EVALENER has been the same following for the Instituto Andaluz de Tecnología (www.iat.es) to develop other evaluating tools that exist in its organization. IAT has wanted to provide companies (emphasized in small and medium companies) with a set of tools to evaluate different aspects into the organization with the same aspect and the same operation. The results are shown in the same way as well to help companies understand the results.

The methodology for developing the tool in order to evaluate the Energy Management System (EMS in advance) has been the following:

1.- A questionnaire has been developed to cover all standard requirements.

This questionnaire has several questions for each UNE-EN 16001 aspect. Each question is accompanied for evidences examples to help the evaluator to find into his/her organization what they are doing to compliance the aspect asked.

2.- Question weighting has been developed to reach a value for each standard requirement.

The evaluator will have to mark each question between 1 and 5 to show the maturity level as shown in Table 1.

Table 1:Marking of every Maturity level and sub-level for standard aspects

Maturity Level	Marking (Maturity sub level)		
	Basic	High	Advanced
1	1	1,4	1,7
2	2	2,4	2,7
3	3	3,4	3,7
4	4	4,4	4,7
5	5	5	5

To choose the value in this table 1, the evaluator will use first Table 2

Table 2:Maturity Level of every standard aspect

Maturity level	Approach	Performance	Improvement
1	It isn't very sound	It isn't done systematically and not always as planning.	It is done just to repair problems
2	It is sound and it is based in a recognized standard, model, etc.	It is done systematically and not always as planning.	Non conformities are detected in order to plan and to star improvement actions
3	It support the management policy and established targets	It is done regularly and in many relevant areas	Improvement actions are set to avoid future problems. Effectiveness of these actions is measured
4	It consider the influence of all management areas and relevant stakeholders.	It is done in nearly all relevant areas	Results are analyzed and compared with company targets in order to get information to improve activities, process, etc.
5	It is done considered internal and external data	It is done in all relevant areas to guarantee good results for all stakeholders	Best practices and comparison with other companies results are taken into account to set up improvement plans.

This table may be used to set the Maturity Level: The user will mark approach, performance and improvement levels (one mark in each columns). Maturity base level will be given by the lower value.

To find the maturity sub-level (Table 1) the following criteria are considered:

- Basic: the 3 marks in the array have the same level.
- High: one of the mark (approach, performance or improvement) is above the basic level.
- Advanced: 2 of the 3 marks are above the basic level.

By using both tables above, it can be obtained a value between 1 and 5 for each question. In an example both tables will be used as follows:

Set the maturity level: user will mark with a cross the maturity level of approach, performance and improvement (each column in Table 2). The maturity level will be the lower of these three values.

Table3:E.g. of setting Maturity level.

Maturity level	Approach	Performance	Improvement
1			
2		**X**	**X**
3	**X**		
4			
5			

Maturity level will be 2 in this example

Set the maturity sub-level: In the above example: sub-level is "high", therefore this question points with a value of 2,4 (Fig.1) using Table 1 to set it.

Maturity Level	Marking (Maturity sub level)		
	Basic	High	Advanced
1	1	1,4	1,7
2	2	2,4	2,7
3	3	3,4	3,7
4	4	4,4	4,7
5	5	5	5

Fig.1. Example of setting the question value

Thus, for each question the user get a value between 1 and 5.

3.- Some tests have been passed to the tool in order to identify errors and to check the smooth running of it.

4.- The tool has been validated in 15 real cases to assure it provides companies key focus areas and the possibility to compare its EMS evolution throughout the time.

EMS EVALUATION

User, during the evaluation, will answer several questions within each part of the standard. The screen layout of the tool for each question is the following (Fig. 2):

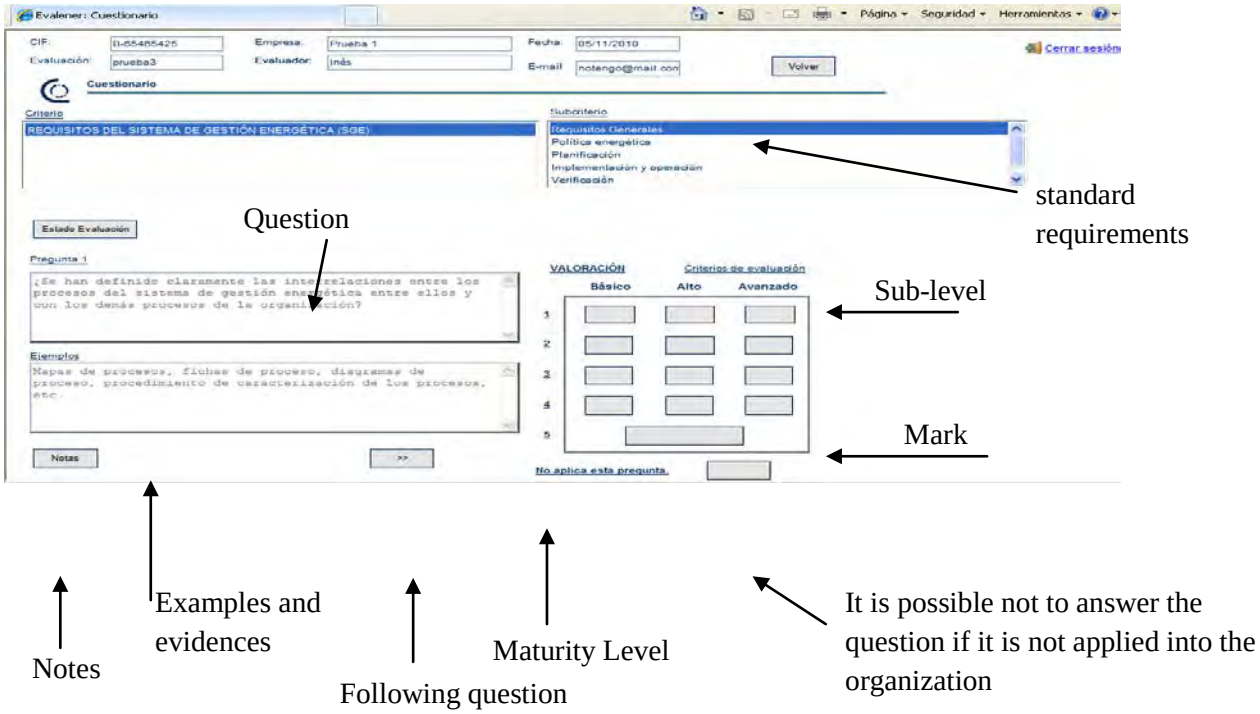

Fig.2. Screen layout of EVALENER

Furthermore, the user could highlight strengths and improvement areas by clicking the Notes button (Fig. 2), which will help detecting during the global analysis the most important areas to be improved. All this information will be shown in a report named “evaluator's notebook” (Fig. 3)

Fig.3. Example of Evaluator’s Notebook report

At the end of the evaluation, EVALENER offers a report with the obtained scores and the evolution from previous evaluations (if exist) as shown in Fig. 4.

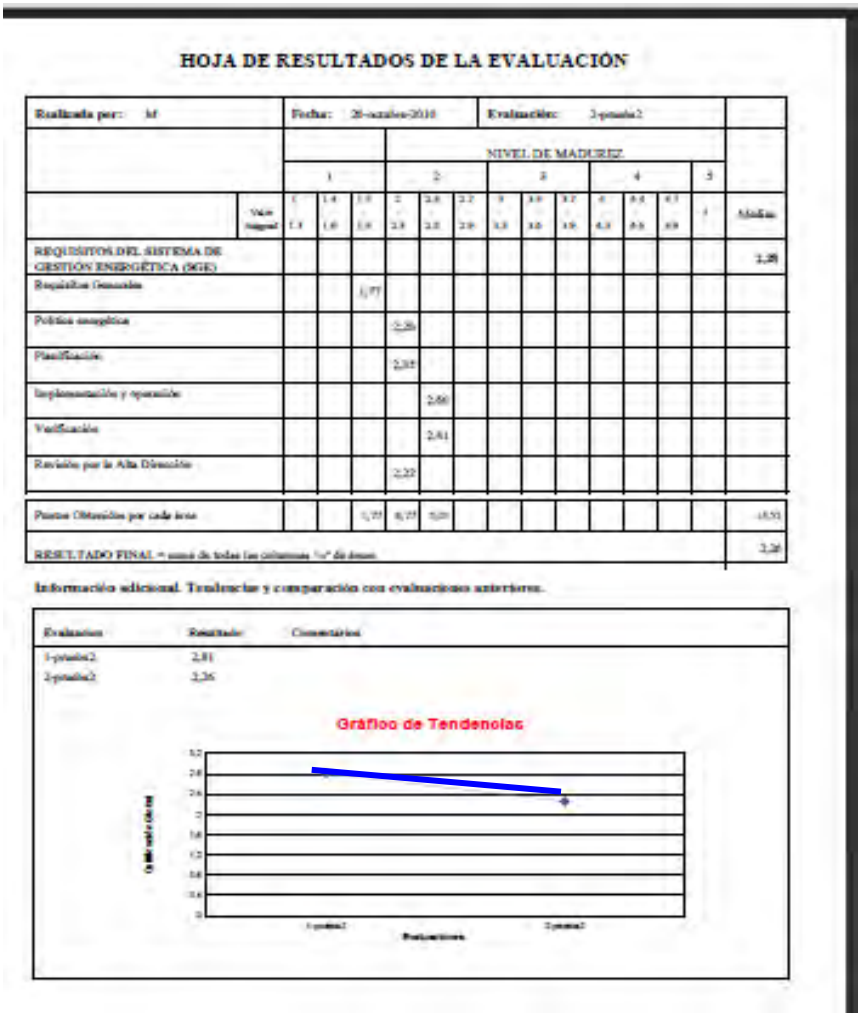

Fig.4. Example of Evaluation Report

3. Results

Companies that took part in this project were SMEs. Some of them have set their own environment management systems (according ISO 14001) but some others don't. None of them have got EMS, although some would consider its use in a future.

A varied set of companies participated during the tool's validation process, companies like a pharmacy, manufactures, or a health care company.

Those companies that have decided to become certified according to UNE-EN 16001:2010 standard want to show customers that these companies are consistent with their business (for example engineering and/or architecting firms that works with energy efficiencies) and others to get more points going to qualify for government public tenders.

Those which are using an environment management system have achieved better scores and found easier during the evaluation understanding the question and evidences compared to those companies that don't use any environment management system. The companies that don't use it even found hard to understand concepts like operational control and significant energetic aspects, besides they achieved low scores in the auto evaluation.

All of the participants used the experience to think about their use of energy, considering new metrics and, the most important, improvement areas in the aspects that they could afford given the current economical circumstances (change machines to other that consume less energy, change to LED technology, used better enclosures, changes in human behavior…)

4. Conclusions

SMEs in Andalusia are currently passing through an economical delicate moment, as in the rest of Spain but increased by a weakest regional and local industry.

In this scenario, an efficient energy management is a must in order of reducing costs and looking after the environment, taking part of the European compromises for reducing the greenhouse effect, consumption, etc.

The main obstacle for these SMEs is the access to information related with energy management, contracting experts to help with it or even economically afford some of the improvement options available in the market.

Because of the mentioned reasons, this tool tries to help small companies that cannot make use of any EMS because of a lack of resources. The software has been organized following the standard requirements with the purpose of helping companies approach to the standard and it has been adopted the question-evidences formula to ease its understanding.

The option of evaluator's notebook makes considerably easy bringing up improvement areas after finishing auto-evaluation as well as highlighting the strengths of the company.

Beside of evaluator's notebook, EVALENER offers the chance to de companies to compare evaluations and see the EMS evolution. This information will be useful to know how efficient were the improvement actions undertaken by the company and will help with the continuous improvement of the organization.

In any case, the system has to be improved because it has been revealed as not very flexible (it doesn't allow weighting each question or section) and not very intuitive in the use of both tables (Tables 1 and 2). The way of looking for the score for every question (Table 2) requires using an auxiliary paper sheet as it is not automated in the software, and makes it hard until further practice had been acquired. For this reason, this functionality should be improved in a second version of the tool (now developing by IAT and to be integrated with other evaluation tools that have been developed by IAT).

The software could be enhanced by adding help tags and screens to let the evaluator a better understanding of each question or standard aspect.

Despite all, the goal of approaching EMS to SMEs and letting them, in an affordable way, analyze and reflect on their way of use of energy and consider actions for improvement has been achieved.

The main advantage of this methodology is the used of a questionnaire to analyze that companies done about their EMS and to be able to get a goal easily to compare different situations (with other companies, with the own company after to carry out improvement actions, etc.). That is easy to use for SMEs and not require a lot of knowledge or experience.

References

[1] Standard UNE-EN 16001:2010 "Energy Management System – Requirements with guidance for use", AENOR, 2010

"Uncovering Industrial Symbiosis in Sweden" -exploring a possible approach

Sofia Persson [1,*], Jenny Ivner[1]

Linköping University, Linköping, Sweden
** Corresponding author: Sofia Persson. Tel: +46 13285613, Fax: +46 13149403, E-mail: sofia.persson@liu.se*

Abstract: Industrial Ecology (IE) is a relatively new field that is based on the ideology of nature. IE uses nature as a "reference" to study resource productivity and environmental burdens of industrial and consumer products and their production and consumption systems.

Industrial Symbiosis (IS) is a subset of Industrial Ecology with a particular focus on cyclical flows of resources through networks of businesses. One definition is that IS "engages traditionally separate businesses in a collective approach to competitive advantage involving physical exchange of materials, energy, water and/or byproducts. "The keys to IS are collaboration and the synergistic possibilities offered by geographic proximity" [1].

This paper presents a methodology that aims at developing a method for uncovering IS in the Swedish energy sector. The method is exemplified by district heating and consists of data collection of the occurring resource and energy flows to and from district heating plants in three different Swedish regions. The results show that the method presented in this article can be used in future and more comprehensive "uncovering" studies. The material from a broader, nationwide study is expected to make it possible to develop tools to facilitate the conditions for IS to be developed.

Keywords: *Industrial Symbiosis, Methodology, Uncovering*

1. Introduction

Industrial symbiosis (IS) has been defined as "engaging traditionally separate industries in a collective approach to competitive advantage involving physical exchange of materials, energy, water, and by-products"[1]. IS emerge as a self-organizing business strategy among firms that are willing to cooperate to improve their economic and environmental performance [2]. According to Chertow [1] "The keys to IS are collaboration and the synergistic possibilities offered by geographic proximity". Businesses that are collocated can, in accordance to IS, reach environmental benefits and competitive advantages by physical exchange of resources with each other or with residential areas [3]. In Sweden, the occurring identified cases of IS show fruitful collaboration and integration from the companies´ point of view as well as increased environmental performance [4, 5]. However, there is a gap of knowledge when it comes to an overview of the occurring IS in Sweden. It is currently not known how common these kinds of mutual exchanges and collaborations are.

In the United States Chertow [6] conducted an uncovering study that investigated IS in a broader perspective. In Sweden there have previously been single case studies of IS. Therefore there is both a knowledge gap about the occurrence of IS in Sweden and also when it comes to methodologies to systematically gather data in order to analyze whether IS occur or not.

1.1. Aim and research questions

This article presents a method for uncovering Industrial Symbiosis and how this method can be applied to the Swedish energy sector. The method is exemplified by district heating. The

aim is to illustrate and explain a method used to conduct an uncovering study of IS in Sweden and to discuss how the method can be used to create more in-depth knowledge about IS in Sweden when it comes to the extent of collaboration and mutual exchanges. The discussions are based on a pre-study where the method is tested on three Swedish regions.

2. Background

Efforts to understand and replicate Industrial Symbiosis in the form of inter-firm resource sharing like what was largely self-organizing in Kalundborg, Denmark have since 1989 followed many paths. The success has varied, some of the efforts have been very successful and some have not [6]. Chertow [6] describes the year of 1989 as "an inspirational year for industry and environment". The main reason behind the success is described as two key events following the Bruntland Commission report in 1987. The first was a seminal article in Scientific American illustrating "industrial ecosystems" in which "the consumption of energy and materials is optimized and the effluents of one process serve as the raw material for another process." The article was written by Frosch and Gallopoulos [7]. That same year the Industrial Symbiosis in Kalundborg was discovered as a concrete realization of the theory described by Frosch and Gallopoulos [7]. The cluster of intensively resource sharing companies from different industries in Kalundborg, Denmark was uncovered unexpectedly [6].

Previous research shows many, both public and private, benefits of IS as a result of "spontaneously co-location" of different businesses in industrial areas. Duranaton and Puga [8] describe these benefits as labor availability, access to capital, technological innovation and infrastructure efficiency. Key rationales for advancing IS projects as a way of trying to recreate the same types of collaboration and mutual exchanges include economic development, remediation of pollution associated with heavy industry, water and land savings, and greenhouse gas reductions [9]. Another reason for collaboration around energy savings and greenhouse gas reduction is the construction of shared visions and goal, which also makes projects less vulnerable [10].

Examples from previous research from Sweden and the Swedish forest industry show that there are several occurring cases of IS and that the conditions for implementing IS varies [5]. Also, these studies indicate that IS can have advantages both from an economic and environmental perspective [4]. Mapping these existing cases of symbiotic activity makes it possible to use the knowledge in the IS field to study and develop the partnerships further.

3. Method

As mentioned above, this article presents an approach to uncover industrial symbiosis in Sweden. The overall approach to these uncovering activities is data collection from several sources to obtain triangulation of data for each found case. This is an approach that strengthens the validity and to facilitate deeper analyses [11].

Yin [11] recommends four methods of analysis: Explanation–Building, Pattern–Matching, Time–Series Analysis and Program Logic Models. For this type of study, with large amounts of data, it is of great importance to have a fully functional database. In this case the database is designed to show the different flows that occur, as well as between which actors the flows occur. This gives a good overview and understanding of the situation within the studied regions.

Explanation–Building can mean two things: according to Yin [11] it primarily means building an explanatory narrative, which shows the causal relationship, it also can be about creating a coherent and credible overall picture of a phenomenon [12].

Pattern-Matching means that patterns that can be observed are compared to patterns that have been predicted or known from other cases. To analyse the cooperation and mutual exchanges between the studied district heating plants and related, nearby industries and companies within a specific cluster, comparison with previously known cases of similar character as an ideal type is a form of Pattern-Matching.

In the next step the various actors involved in the symbiosis cluster is studied deeper to understand the sequence in which the development of the cooperation and exchanges develop. Time–Series Analysis means clarifying the order in which events or actions occur, with what intensity they vary over time or how far they are in time.

As a last step the Program Logic Models is used to analyse the assumptions about the connections. In this case, the previous knowledge will enhance the understanding and of the elementary conditions for IS.

4. Methodology

To be able to map ongoing cases of IS empirical data about occurring collaboration and mutual exchanges needed to be collected. In order to test if the chosen approach to uncover IS is appropriate a diversity of empirical material is needed. Therefore three geographically diverse regions with different types of industrial conditions were selected for this study; one region with dominating forest industry, one with a dominating agricultural sector, and one with a diverse industrial sector including food industry, manufacturing as well as pulp and paper industry.

Investigating every single industry in these regions was not feasible for this pre-study, therefore district heating industry was chosen as the main actor to start empirical research from. The motive to choose district heating plants in order to uncover IS was that district heating occur in more or less all Swedish municipalities. In addition, activities from the business of district heating generate large flows of material and energy which are important prerequisites for IS.

The first step in process is to collect data of the occurring resource and energy flows to and from the different district heating plants within the three different regions. All of the district heating plants are also studied more in detail, one plant at a time, based on information from websites and additional interviews. All interviews were conducted via telephone and in semi-structured format, which means that the same question guide was used for all interviews, but the interviewer had the opportunity to ask supplementary questions. This type of interview is recommended since it helps structuring the interview [13]. However, this interview method also allows new and unforeseen issues to arise during the interview and hence is an effective tool for gathering information that is difficult to obtain otherwise [14].This method is expected to provide data that will show which of the studied district heating plants who has some kind of collaboration or mutual exchanges with other nearby business or industries.

To be able to identify and classify occurring cases of IS there is a need of a consequent definition with clear criterions. This study will use the same criterions as the previous study

"Uncovering Industrial Symbioses" made by Chertow [6]. Chertow defines the minimum criterion of IS as "3–2 heuristic". This means that at least three different entities must be involved in exchanging at least two different resources. An example of a 3–2 heuristic relationship within this study is industry 1 providing industry 2 with a flow of resource and industry 2, in turn, provides industry 3 with another flow of resource, figure 1.

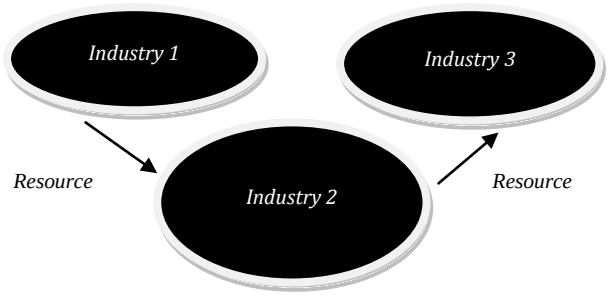

Figure 1. Example of a "3-2 heuristic" relationship. Inspired by Chertow [6].

4.1. Structuring the empirical data

The results from this study are stored in a database designed to address the collected data and to demonstrate the flows of different resources that occur between the actors involved in the detected clusters of symbiotic activity. The structure of the database is built on a model that makes it possible to link "plants" with different "flows" of resources in several steps. The database is also designed to be able to store specific information about the different flows of resources as well as the different plants involved. The information of the plants regards what type of plant it is, the size of the plant, the occurring ownership and the location of the plant. When it comes to the flows, the additional information regards what type of resource it is and of what amount, origin- and destination pant and if the specific resource is used as resource in the industrial process or functions as a utility, see figure 2. It is also possible to specify whether the resource originates as a main product (on which production the industry is based) or a byproduct (waste) from the industry. This information about each resource flow opens up for analyses about for example which kinds of exchanges are more common in relation to different kinds of plants. Martin [15] mean, for instance that by-product synergies are the most abundant type of synergies and that utility synergies in the form of shared use of energy and utilities are not as common.

The implementation of the data is done by two different formulas created in the database. The first formula manages data for each "plant" and the second formula manages data for each "flow" of a specific resource. The formulas are based on the tables within the database where the data is stored and they are created to facilitate the implementation of the collected data. Figure 2 shows the model and how the different data are related.

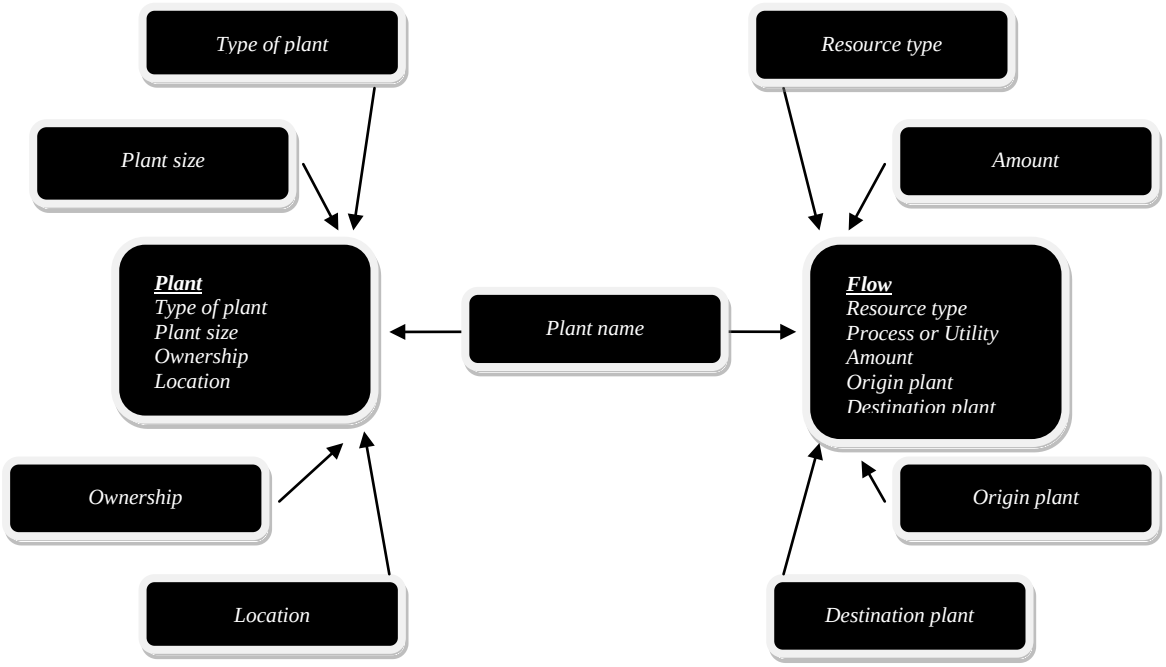

Figure 2. A model of an extract from the database demonstrating how the different data in the database are related.

5. Expected results

The collected data from the three different regions indicate that there is occurring cases of IS within these regions. The most common forms of collaboration is in the form of "3-2 heuristic" relationships, especially in the smaller municipalities. In some of the larger medium size municipalities, where the conditions of collaborations are better, the results show more complex ongoing cases of IS. One example is a forest industry and energy plant co-location, Figure 3. In this (fictional) case it is possible to define five different flows: wood, wood chips, sawdust, process steam and nutrients (ashes). Forestry, the sawmill and the district heating plants all pose as both origin and destination plants, depending on which resource flow is described. It is also possible to define both main products and by-products: wood is a main product from forest industry and ashes are by-products from incineration plants. Furthermore there are resources that pose as both process input and utilities to the destinations plants: sawdust goes into the main process at the main pellet producer and process stem is used as a utility. It is however too soon to draw general conclusions about the data material.

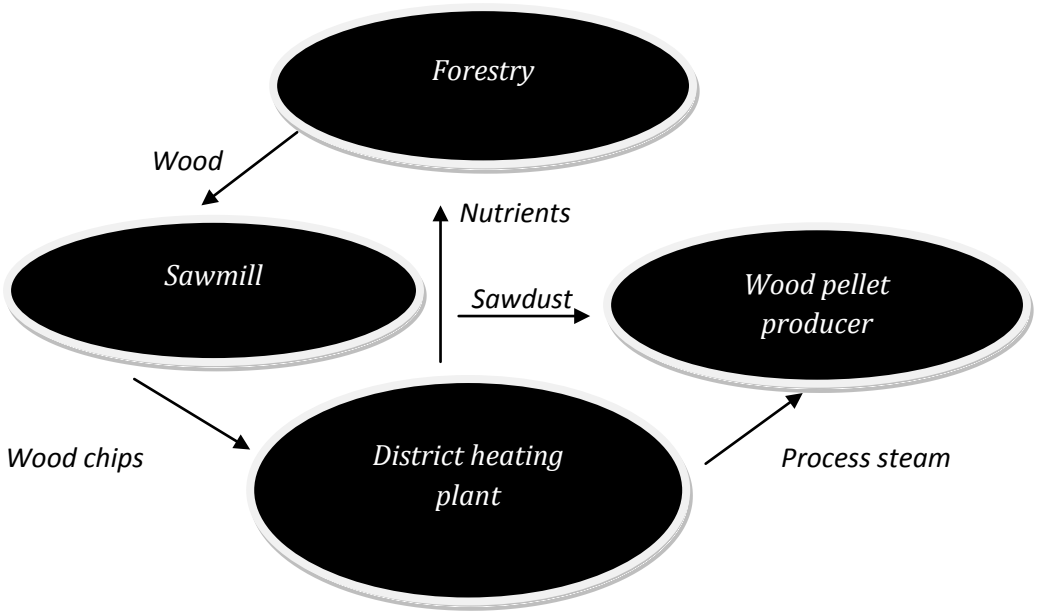

Figure 3. Example of resource flows that can be mapped in the described approach to uncovering industrial symbiosis.

The four methods of analysis described in the methods section can be used to analyze the collected data. This way of arranging the data creates a coherent and credible overall picture of the flows connecting the plants. When mapping the relationships between resource flows and plants is made for a whole region, it will be possible to analyze patterns of occurring collaborations. Thereafter observed patters can be compared to previous research but also to other regions or businesses. In this sense this will function in accordance to the Pattern-Matching as described by Yin [11]. As a continuation of the analysis, Time-Series Analysis can be used to clarify the order in which the different steps in the Symbiotic process occur, to understand the sequence in which the development of the cooperation an exchanges develop. This kind of analysis would however need additional empirical data.

When a deeper understanding of the development of discovered symbiotic activity has been created, it may be used to develop proposals on measures to improve the conditions and the facilitation of the implementation of IS in the future analogous to Yin's [11]the Program Logic Models.

6. Concluding discussion

This article has presented a method for uncovering Industrial Symbiosis and how it can be applied to the Swedish energy sector. Experiences so far have shown that the method for collecting data an organizing them in a database functions well. This method is probably suitable for uncovering IS, however it may be too demanding if it comes to cover large areas, for example the whole of Sweden. A broader, nation wide, study like that with more and broader data would probably need a less personnel intense method than semi-structured interviews with all actors. It is therefore a need to further develop the methods for uncovering industrial symbiosis to be able to expand the studies.

According to Chertow [6] the "Uncovering" of existing kernels of symbiotic exchanges has led to more sustainable development and designing of eco industrial parks. Knowledge about the occurring and ongoing cases of IS in Sweden is expected to provide the basis for more in-

depth knowledge of how these collaborations and mutual exchange evolved and what the important elements for them to arise and function are. Therefore it would be of great interest to develop the methods for uncovering industrial symbiosis in Sweden. This would help to create more in-depth knowledge about IS in Sweden when it comes to the extent of collaboration and mutual exchanges and subsequently the prerequisites for such collaboration. Such knowledge in turn can contribute to develop more efficient, environmentally adapted and prosperous business.

References

[1] Chertow, M.R., Industrial Symbiosis: Literature and Taxonomy, Annual Review of Energy & the Environment 25(1), 2000, pp. 313.

[2] Costa, I., G. Massard, and A. Agarwal, Waste Management Policies for Industrial Symbiosis Development: Case Studies in European Countries, Journal of Cleaner Production 18(8), 2010, pp. 815-822.

[3] Van Berkel, R., et al., Industrial and Urban Symbiosis in Japan: Analysis of the Eco-Town Program 1997â€“2006, Journal of Environmental Management 90(3), 2009, pp. 1544-1556.

[4] Wolf, A., Industrial Symbiosis in the Swedish Forest Industry. 2007, Linköping University: Linköping.

[5] Wolf, A., M. Eklund, and M. Söderström, Developing Integration in a Local Industrial Ecosystem - an Explorative Approach, Business Strategy and the Environment 16, 2005, pp. 442-455.

[6] Chertow, M., Uncovering Industrial Symbiosis, in School of forestry and environmental studies. 2007, Yale University.

[7] Frosch, R.A. and N.E. Gallopoulos, Strategies for Manufacturing, Scientific American 261(3), 1989, pp. 144.

[8] Duranton, G.a.P., D. Micro-Foundations of Urban Agglomeration Economics National Bureau of Econimic Research Working Paper. 2003

[9] Chertow, M.R. and D.R. Lombardi, Quantifying Economic and Environmental Benefits of Co-Located Firms, Environmental Science & Technology 39(17), 2005, pp. 6535-6541.

[10] Ling, E., K. Mårtensson, and K. Westerberg, Mot Ett Hållbart Energisystem. Fyra Förändringsmodeller. 2002, Malmö Högskola: Malmö.

[11] Yin, R.K., Case Study Research. Design and Methods. Second edition ed. Applied Social Research Methods Series. Vol. 5. 1994, Thousand Oaks: Sage.

[12] Stake, R., Case Studies, in Strategies of Qualitative Inquiry, N. Denzin and Y. Lincoln, Editors., Sage Publications1998.

[13] Bryman, A., Samhällsvetenskapliga Metoder. 2002, Malmö: Liber Ekonomi.

[14] Krag Jacobsen, J., Intervju. Konsten Att Lyssna Och Fråga. 1993, Lund: Studentlitteratur.

[15] Martin, M. (2010) Industrial Symbiosis for the Development of Biofuel Production. Licentiate Thesis. LIU-TEK-LIC-2010:12.

Towards increased energy efficiency in industry – a manager's perspective

Per-Erik Johansson[1,*], Patrik Thollander [2], Bahram Moshfegh [2]

[1] *DynaMate Industrial Services AB, Stockholm, Sweden*
[2] *Department of Management and Engineering, Linköping University, Linköping , Sweden*
** Corresponding author. Tel: +46 0852293373, Fax: +46 0852293373,*
E-mail: per-erik.johansson@dynamate-is.se

Abstract: Industry is one of the major users of fossils fuels resulting in emissions of GHG (Green House Gases), leading to global climate change. One means of promoting energy efficiency in industry is energy management. The aim of this paper is to outline a number of energy management related factors which affects energy management in industry positively. The paper is a result of collaboration between industry professionals and researchers within an ongoing research project and addresses the issue using a bottom-up energy management perspective. Results indicate that that the "soft" issues of energy management play a crucial role in the success (or not) of energy management in industry, e.g. the manager's role and attitude towards the employees cannot be understated. Instead it addresses that implementation is not only about technology but equally or even more important, concerns the diffusion and adoption of energy management practices and principals.

Keywords: *Industrial energy management, Organizational change, Industrial energy efficiency*

1. Introduction

Research indicates that global climate change resulting from the use of fossil fuels is one of the major challenges for future decision makers worldwide. Industry is one of the major users of fossils fuels resulting in emissions of GHG (Green House Gases), leading to global climate change. EU and other regions are now working proactively to reduce GHG emissions resulting from use of energy. One example is the 20-20-20-targets within the EU which in relation to energy means that each EU Member States should reduce the use of energy with 20% by reducing energy intensity with 3.3 % annually from 2005 to 2020. Industrial energy efficiency is one of the most efficient means of reducing GHG [1]. However, a number of barriers to energy efficiency exist in industry which inhibits adoption of energy efficient technologies and energy conservation [2-4]. One means of promoting energy efficiency in industry overcoming a number of barriers to energy efficiency is energy management [5-6]. Even though the potential is vast, research in the area is scarce [7]. One reason for this is its interdisciplinary character calling for interdisciplinary methods such as collaboration between researchers and industry professionals. The aim of this paper is to outline a number of energy management related factors which affects energy management in industry positively. The paper is a result of collaboration between industry professionals and researchers within an ongoing research project within Swedish industry and addresses the issue of promoting energy efficiency using a bottom-up energy management perspective. This paper is unique in the sense that is leaves the realm of focusing solely on energy efficient technologies when studying industrial energy efficiency.

2. Methodology

Previously, research has focused on energy management practices using questionnaires and in-depth interviews, e.g. [5] and [7]. In this study, the scope is to try to take the research on energy management in industry a leap further. Moving beyond questionnaire and in-depth interviews, an attempt is made to incorporate the manager's own ideas and concepts, not merely study an array of factors (using a questionnaire) or respondents' views and opinions (using interviews) on various themes or topics. As the applied method is narrowed down to

fewer respondents, it naturally may be more difficult to generalize results from this type of research, see Fig 1. A previous literature review on energy management [7], shows that this research, so far is lacking in the academic literature, as well as clear results on how to apply successful energy management practices. We therefore conclude that this type of methodological approach is needed.

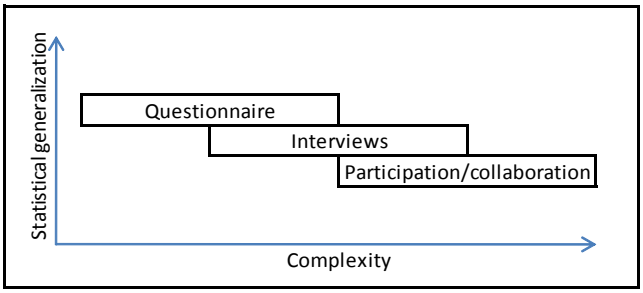

Fig. 1: Differences between participation/collaboration and interviews and questionnaires (Inspired by [8].

According to [8], systems may be categorized depending on degree of complexity. [8] state nine levels and write that research concerning social interaction, i.e. interaction between two individuals is the most complex system to study. He moreover criticizes management research for not moving beyond the lower system levels. In response to [8]'s critique on management research, we aim to move beyond the more common methodological approaches using questionnaires and interviews applying participation/collaboration. Naturally, this limits the ability to generalize results, compared with questionnaires and interviews, as these methods cover several respondents. On the contrary, participation/collaboration methodology enables research to move into the more complex levels of (energy) management. This paper has applied a participation/collaboration methodology where the researchers have collected the manager's ideas and philosophies of successful energy management practices, based on more than 20 years of experience in the field. In doing so, it is evident that this relies on relatively a few cases, and naturally faces an increased risk of being biased, compared with questionnaires and interviews. When analyzing results from this paper, it is therefore important to keep in mind the statement by [5] *"there is no one size fits all"* when it comes to energy management.

3. Results - driving forces for successful energy management practices

In the following section, a number of important factor for successful organizational change related to energy management practices are presented. The stated factors come from the participation/collaboration approach, i.e. a bottom-up energy manager's perspective, a perspective which is derived from the truck manufacturer Scania's more than 20 years of successful energy management practices.

3.1. Culture

An organization has its own culture which is created by a number of factors, such as individuals own values [4]. Culture is an important factor when striving to change an organization, as culture governs the behavior of the individuals of the group, and it is their behavior that creates the organization's results. If any major changes are to take place within the organization, the behavior among the individuals has to change. In the long run, this will change the organizational culture, a change which is needed, if the individuals within the organization are to maintain their changed behavior.

3.2. Will

The second factor of importance is that normally, people want to change things they are not satisfied with, while maintain that which one is satisfied with. The will to change is thus dependent on how dissatisfied a person is, and also how risk averse a person is. The importance for those who lead the change is to perceive that the challenge lies in that person's want the change to take place in their own way.

3.3. Acceptance and recognition

The third factor of importance is that people in general wants attention and positive recognition from personal achievements, from other persons. Many people can go a long way to receive recognition and acceptance. It can range anywhere from fame and compensation in the form of money for the effort one has made, to encouragement and a "thank you" for a good result that the person has accomplished. The former can never replace the encouragement from a manager, thanking the employee for good work. This holds in particular if the manager is also the informal leader, i.e. someone the employees look up to.

In general, people go to their work with a goal to be part of it as they wants to do a good job. If not, this creates discomfort, discouragement and frustration that often take the expression in unwillingness to cooperate, or an unwillingness to change situations at work. Paradoxically, people tend to do exactly the opposite of what it takes to get what one really wants. What this behavior gives in return is attention and an opportunity to be seen in the absence of recognition. Reasons why such an individual have lost sight can be, e.g. lack of attention, challenge or admission from those who are managers. It may also be due to an inadequate role and mission in the group the individual belong to. One may call this a deficiency in the organization caused by poor leadership.

The above three factors, culture, will and acceptance and recognition interact between each other and create the conditions one have in an organization, department and group. It is these challenges that the leader has to work with in order to achieve the expected results.

3.4. Establishing change within an organization

When a manager is leading a change in the organization, he or she can choose one of two main roads or paths. The difference between these two paths can be described by the following: To get from location A to B can be done in two principally different ways. The first option is to run in the sand at the water's edge. Although the road is long, it goes relatively quickly. The tracks in the sand are washed away rapidly and soon, no one else can, by the help of the first person's achievement, manage the very same way. Instead, each one has to take its own way to position B. The load to be moved from A to B depends on the individual's capacity and external conditions and circumstances. In summary, the first path is that of individuality, a path which does not help or support the persons that later wants to take the same path.

The second option is to build a road. It will take much more time, demands much more resources and effort, but when it is finished, there are clearly more people being able to travel from position A to position B. Moreover, people can get more loads with them on the road. The modes of transport can also be developed so that more cargo than was previously possible to carry can be included in each trip. The time to carry out the shipment may eventually be reduced. The load to be moved from A to B is through a road much less dependent on the individual's capacity and external conditions. In summary, the second path is that of the

standardization and continuous improvement, a path which help and support the persons that later wants to take the same path.

Road number one may be stated as to govern by results. This is a road which with the right leadership often creates positive results relatively quickly, but the lasting result is often not maintained. The way to influence behavior is by getting members of the group to do what they request. As the manager does not require how results are achieved, solutions often rely upon individual solutions, i.e. the employees own way. Moreover, duplication of these individual solutions is generally not possible. This, in turn, leads to the fact that structural capital is not being built up within the organization, department or group. The culture is affected only to a limited extent and the impact it does create takes time. There is great risks that if the leader loses focus, or change job, the good results will not last.

Road number two is to use what we define as method governing. This is about influencing the behavior by using good methods and approaches. The modified behavior provides better results both in the economic sense, but also regarding the conditions to do a good job of maintaining or improving quality and work environment. The positive change one gains may be linked to the group and the positive spiral which then creates the opportunity to influence the culture of the group. As method governing focuses on how the work is done, conditions for working with continuous improvement are established.

Things which can be improved are the methods, routines and instructions. These are always the same; everyone in the group performs the operations in a similar way and can contribute to the improvement of the method. This will benefit both the individual and the group, even if the work and the physical and psychological conditions of the work are continuously changing. Method governing thus, and unlike the first road, builds structure capital, and with the right leadership, in the long run, an improvement in the culture of the group is achieved. This also reduces the risk of a manager changing job. However, and this must not be understated, bad leadership will always be able to bring down an organization, independent on which road that is taken.

3.5. Successful organizational change

Fig. 2. displays how an organization may successfully be transitioned by the second road, method governing. If one choose to work after the second road, there are some fundamental principles that should be followed, e.g. focus on the organization's value stream and continuous improvements. These are presented in the coming sections.

3.6. Basis – the organization's value stream

Start from the company's product's value stream and the company's services and do not view energy management as a means which creates value by itself. All work which is done in the organization (be it external or internal) must be valued based on the product's value stream. This provides the ability to sort and evaluate, not based on function, but on value. What is waste and what is value? Waste can also be divided into that which is necessary but not value-adding and that which is simply waste. What is value adding is often of no reason to attack first. It only involves the risk of new losses.

That which is necessary but not value adding should be minimized. That which is solely waste must be eliminated as quickly and smoothly as possible. It usually does not cost so much, it is often achieved relatively quickly, and the risk is often low.

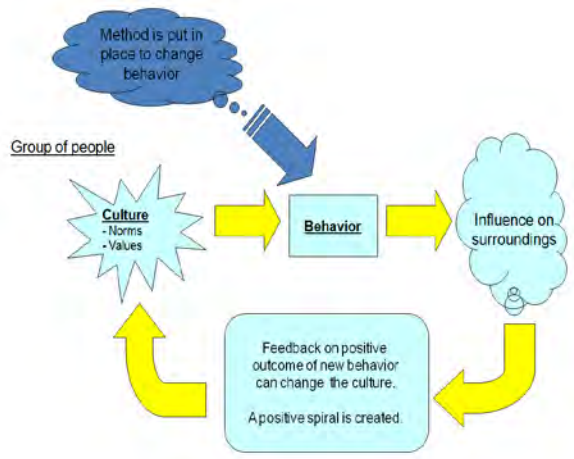

Fig. 2. Example of how an organization may be transitioned successfully based on method governing.

If the organization is a manufacturing company, it is important to understand how the production technologies, maintenance and energy management work is related. Increasing process efficiency is an effective way to reduce energy use for the product. To have a system perspective is necessary when improvements are carried out.

Moreover, aiming to achieve stable systems is of great importance. If for example, the shutdown of a machine or a process, leads to problems when the machine or process is being started, i.e. it may not work properly after shutting it down, employees may be unwilling to shutdown equipment. The root cause to this is not a system which is impossible to change, but rather an unstable system.

The eight types of waste which are relevant also in terms of industrial energy efficiency are: overproduction, unnecessary operations, transportation, discards, waiting, unnecessary movement, storage, and unused skills. Working to minimize and eliminate these both in the organization's value stream, but also in regard to the organizations energy use.

3.7. Basis – continuous improvements

The basis for long-term success is to work according to the principles of continuous improvement. This means that the leader must create an improvement culture within the group/company. The engine in the process of improvement is improvement groups and a systematic work with deviation.

To create an organization in which the principles of continuous improvement are used, and create a continuous improvement cycle, will not be made without effort. It demands leadership in order to be formed, kept active, and further developed. Fig. 3. visualize the above presented approach.

Work with improvement in small steps is of great importance, and one should aim to use all the tools for continuous improvement at disposal, such as deviation control. In order to be able to improve a system, one must be able to describe what the normal state or level is. If one does not know what the normal level is, improvements are not likely to take place. What is described and perceived as normal in the organization is what one can expect. When the outcome deviates from the expected normal state, the organization receives a signal that something has gone wrong. Detecing deviations may be achieved from, e.g. deviation management methods, the use of standards and routines etc. When a deviation from the

normal state has been detected, the system can be improved in small steps, which in turn slowly increase the normal state level.

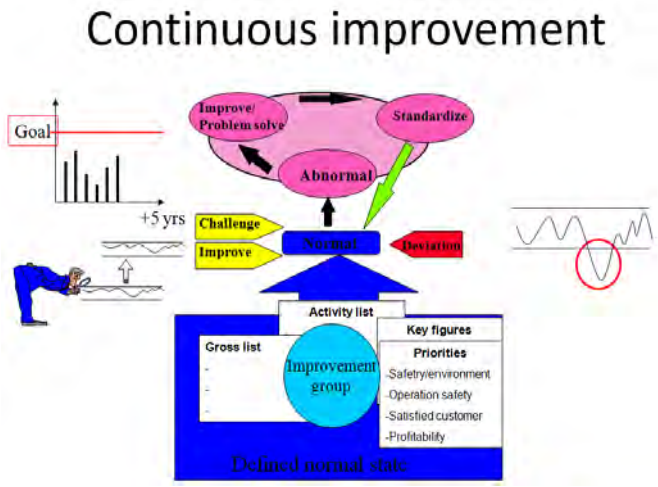

Fig. 3: Principles for continuous improvement in regard to energy efficiency.

Identify where the organization stand in terms of the performance it delivers. All phases have different needs for improvement. Improve from the defined normal state, do it with small steps but take steps often. Fig. 4. visualize the above presented approach.

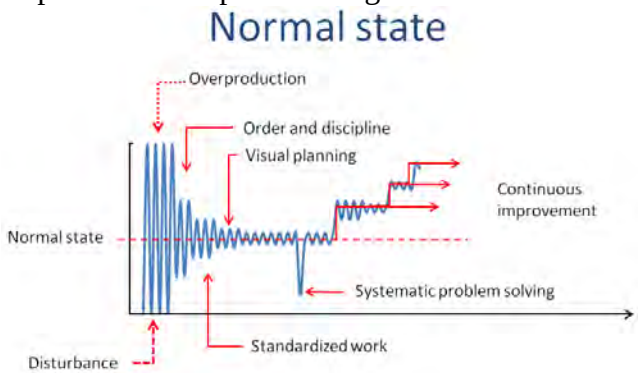

Fig. 4: Principles of defining and working with continuous improvement based on a normal state.

Ending improvement is as important as initiating them. Aim to try to find effective methods to evaluate when an improvement is "effective enough". Describe the new normal mode, implement it, and move on to the next improvement that gives the best effect on the overall efficiency.

Moreover, one should put focus on the flow (creating smooth flows, governed by demand, be sure to reduce the variance). Also, do not forget the work- and information flow. Otherwise, adequate conditions for improvements will not be established. Furthermore, one should focus on quality and time, and make sure to keep the correct delivery parameters, i.e. avoid variation and overproduction. Make sure to deliver on time and let demand govern as much as possible. By describing what is normal, delivery can be assessed, and the root cause for the deviation can be corrected.

Some general issues related to successful energy management practices are similar, no matter which one of the two main roads one chooses for implementing change. These are presented in the coming sections.

3.8. The role of leadership

The role of leadership is independent of which main road one chooses to take. Leaders must lead through visions and overall goals. The larger the group/organization is, the more important it becomes. One of the reasons that this is so universal is that it provides space for the group and its members to use their individual creativity to solve the tasks. It uses the collective expertise of the group. However, it requires that the leader, e.g.:

- Is willing to join and show how tasks must be carried out (if required). Moreover, the leader has to be so knowledgeable that he or she, if needed, can act as a role model. Notably, this does not mean that the leader should do all the work for the employees.
- Serve as the creator of contacts, not as problem solver.
- Work with the monitoring of agreed activities and targets. Send feedback and let the person who made the job receive recognition for the accomplishment. Focus on those in the group who have the ability to influence.
- Work with action plans developed by those who must do the job. Do not let the action plans run over a too long period of time. Half a year may often be a good time horizon. Make sure to keep activity plans short and prioritize what is most important. Working with gross list and make decisions on new items on the list if space is available. Follow up about this on a regular basis, e.g twice a month: provide support, feedback and encouragement when the data is completed. Be sure that the agreements on completion dates are kept. Measure and visualize the number of items completed on time. If events are "slipping", find the root cause to this. In principal, this is a leadership issue. However, it may also be due to that the employee does not fit for the specific assignment or lacks time. In general, it is not due to unwillingness from the employee.
- Create conditions for a rapid feedback of the key indicators chosen to measure. Use them to guide and evaluate the work. The feedback often needs to be done weekly or whether it is possible, in real time.
- Try to create a positive atmosphere where “anything is possible”. A positive spiral. It is therefore important to ensure that "easy victories", particularly early in the process, are achieved.
- When one set goals and prioritize activities always base this on the organization’s value stream flow. It is the value stream which should be improved and not primarily single processes. It is only from the basis of the organization’s value flow, ones effort can be measured correctly. Working with energy in general may not provide much value, but rather to be effective in reducing waste.
- Put effort into understanding the system links. There is always a larger improvement potential in a system than in a single component or process. Let the need control demand.
- Develops a strategy for how the plant should be operated in the long run. Do this in terms of the desired operational strategy, and the desired technology strategy, and how the desired system strategy should look like. When done, one can be flexible, and make changes when available opportunities occur in the business. Streamlining systems and components are not so costly when a major change is to be made but may be very costly if done as an operational acticity, e.g. lead to production disruptions.

4. Conclusion

This paper addresses that increasing industrial energy efficiency is not only about technology, but equally important concerns the diffusion and adoption of energy management practices. In particular, the three factors, *culture*, *will* and *acceptance and recognition* interact between each other and create the conditions one has in an organization, department and group. It is these challenges that the leader has to work with to achieve the expected results. Moreover, results may be achieved in principally two different ways, where method governing is the way advocated for in this paper as it builds structural capital in the organization. If one choose to work with method governing, there are some fundamental principles that should be followed, e.g. focus on the organization's value stream, normal situation, standardization and continuous improvements. It is also of importance to define the system's normal state. From that position, improvements may be carried out in small steps. If a manager follows these basic recommendations outlined in this paper, and allows employees to understand and see the connections, improved results are achieved in the long run. Energy management practices using these principals may lead to employees showing improvements far above what the manager or organization thought was possible.

The applied methodology was shown to contribute with increased knowledge on how energy management practices successfully can be carried. Further research in the field using the applied methodology is suggested.

In conclusion, a fully successful in-house management program is dependent on both sound leadership and adoption of sounds methods. If either one is lacking, the full embodied (energy efficiency) potential in the organization is not released.

References

[1] IPCC, 2007. Contribution of Working Group III to the Fourth Assessment Report of the Intergovernmental Panel on Climate Change. Summary for Policymakers. Retrieved October 8, 2007, from: http://www.ipcc.ch/SPM0405 07.pdf

[2] Thollander P, Ottosson M. An energy efficient Swedish pulp and paper industry – exploring barriers to and driving forces for cost-effective energy efficiency investments. Energy Efficiency 2008;1(1):21–34.

[3] Rohdin P, Thollander P, Solding P. Barriers to and drivers for energy efficiency in the Swedish foundry industry. Energy Policy 2007;35(1):672–7.

[4] Rohdin, P., Thollander, P., 2006. Barriers to and Driving Forces for Energy Efficiency in the Non-energy Intensive Manufacturing Industry in Sweden. Energy;31(12):1836-44.

[5] Christoffersen, L.B., Larsen, A., Togeby, M., 2006. Empirical analysis of energy management in Danish industry. Journal of Cleaner Production;14(5):516-26.

[6] Caffal, C., 1996. Energy management in industry. Centre for the Analysis and Dissemination of Demonstrated Energy Technologies (CADDET). Analysis Series 17. Sittard, The Netherlands.

[7] Thollander, P., Ottosson, M., 2010. Energy management practices in Swedish energy-intensive industries. Journal of Cleaner Production 18(2):125-133.

[8] Boulding, K.E., 1956. General System Theory - The Skeleton of Science. Management Science 2 (3): 197-208.

Comparison of repowering by STIG combined cycle and full repowering based on exergy and exergoeconomic analysis

Mohammad Baghestani[1], Masoud Ziabasharhagh [1*], Mohammad Hasan Khoshgoftar Manesh[1]

[1]Mechanical Engineering Faculty K.N.Toosi University of Technology, Tehran, Iran
** Corresponding author. Tel: +982184063255, E-mail: mzia@kntu.ac.ir*

Abstract: Nowadays, repowering is considered as the most common methods for improving status of current power plants. Repowering is the transformation of an existing steam power plant into a combined cycle system by adding one or more gas turbines and heat recovery capacity. It is a cost-effective way to improve performance and extended unit lifetime while adding capacity, reducing emissions and lowering heat rejection and water usage per kW generated. Each methods of repowering from "para repowering" to "full repowering" shall probably be the best choice for special national and economical power plant. In this paper different repowering methods have been introduced. The design concept consists in adding a gas turbine to the combined cycle, integrated by steam injection into the existing gas turbine. The steam is produced in a simplified heat recovery steam generator fed by the additional turbine's exhaust gas.
A 156MW steam cycle power plant has been chosen as a case study. Two repowering scenarios have been utilized for this case. Thermodynamics code has been supplied for combined cycle and STIG combined cycle and compare with each others. The exergy and exergoeconomic analysis method was applied in order to evaluate the proposed repowered plant. Also, computer code has been developed for exergy and exergoeconomic analysis. It is anticipated that the results provide insights useful to designers into the relations between the thermodynamic losses and capital costs, it also helps to demonstrate the merits of second law analysis over the more conventional first law analysis techniques.The efficiency of the STIG repowered plant compares favourably with repowered combined cycle.

Keywords*: Repowering, Gas turbines, Steam injection, exergy, Exergoeconomic*

Nomenclature (Optional)

c	*cost per unit exergy ($/MW).....($/MW)*	*f*	*..... fuel*
C	*cost flow rate .....($/hr)*	*a*	*.....air*
e	*exergy rate per mass .....(MW/kg)*	*GT*	*..... gas turbine*
E	*specific exergy.....(MW)*	*CRF*	*..... capital recovery factor*
Z	*capital cost rate of unit .....($/hr)*	*PWF*	*..... Present worth factor*
St	*.....steam*	*PW*	*.....Present worth*

1. Introduction

The country of Iran is experiencing in all fronts and areas and thus, consumption of electrical power is on the increase on a daily basis. Based on the ever increasing electrical energy consumption, changes in generating system load requirements, lower allowable plant emissions and changes in fuel availability, steam power plants repowering has been investigated much more as a method for energy conservation. Considering the increased electrical energy consumption and annual growth rate of 4.5 percent and according to the end of existing steam power plants life in Iran(like Montazer Ghaem power plant), repowering could be used as an economical method for increasing the output power with less investment than building a new power plant. Repowering of steam power plant can be achieved in several ways. In a full repowering, several gas turbines (GT) and heat recovery steam generators (HRSG) are installed in a parallel arrangement dispensing with the conventional boiler. Live steam from HRSG is used in the original steam turbine [1]. Industrial gas turbines are one of the well established technologies for power generation. Various additional cycle configurations such as reheating, regeneration, intercooling and steam injection have been

suggested [2, 3]. All of them offer increased performance and increased output compared to a dry gas turbine cycle. Several types of water or steam injection gas turbine cycle (STIG) have been proposed in previous studies and the performance characteristics of them investigated [4]. The exhaust gas from the turbine is used as an energy source in a heat recovery steam generator (HRSG) where energy is transferred from the exhaust gases to the boiler feed water. The high pressure steam is generated from HRSG. The steam is then injected into the combustor. Injection of steam increases the mass flow rate through the expander and so the power output and the efficiency of the turbine increase. Steam injection also helps in reducing the NOx emissions from the gas turbine [5]. Exergy analysis usually predicts the thermodynamic performance of an energy system and the efficiency of the system components by accurately quantifying the entropy-generation of the components [6]. Furthermore, exergoeconomic analysis estimates the unit cost of products such as electricity, steam and quantifies monetary loss due to irreversibility. Also, this analysis provides a tool for the optimum design and operation of complex thermal systems [7]. Combined and steam injected gas turbine cycle power plants are being installed all over the world as compared to other plants. The current emphasis is on increasing the plant efficiency and specific work while minimizing the cost of power production per kW and emission. In this paper, simple repowered combined cycle and combined cycle with added steam injected gas turbine have been modeled as a repowering design for 156MW steam power plant. For each cases exergy and exergoeconomic analysis has been studied and compared as a economical analysis for product cost estimation.

2. Process description

In this paper, 156MW steam cycle power plant has been selected as a case study for exploring two repowering methods and comparing with each other. The steam cycle power plant encompasses three turbines, that work with three different pressures and 6 feed water heaters. The Steam cycle has been modeled by MATLAB code and STEAM PRO (THERMOFLOW). Results of modeling steam cycle have been introduced and compared with real data in table.1.

Table1. Compare result of modeling steam cycle

	THERMOFLOW	Simulation code	Real
Plant Gross power(kW)	156300	156305	156294
Plant Gross Heat Rate(kJ/kWh)	9010	9120	8976
Plant Gross Efficiency (LHV)	39.9%	39.4%	40.1%
Superheater Capacity(kg/s)	133	130	136
Reheater Capacity(kg/s)	115	114	117

3. Repowering

There are several alternatives to combine and integrate a gas turbine into an existing steam power plant. As a result of ending boiler life time and exploring another aspect for this case, the best alternative is full repowering. Full repowering is defined as complete replacement of the original boiler with a combination of one or more gas turbines (GT) and heat-recovery steam generators (HRSG), and is widely used with very old plants with boilers at the end of their lifetime. It is considered as one of the simplest ways of repowering for existing plant.
For this power plant, Full Repowering with SGT5-4000F (formerly known as CC 2.V94.3A) with triple pressure reheat cycle has been considered as a first method for repowering old steam cycle power plant. Schematic flow diagram of combined cycle with the components is shown in Fig. 1. The gas cycle is selected as a topping cycle.

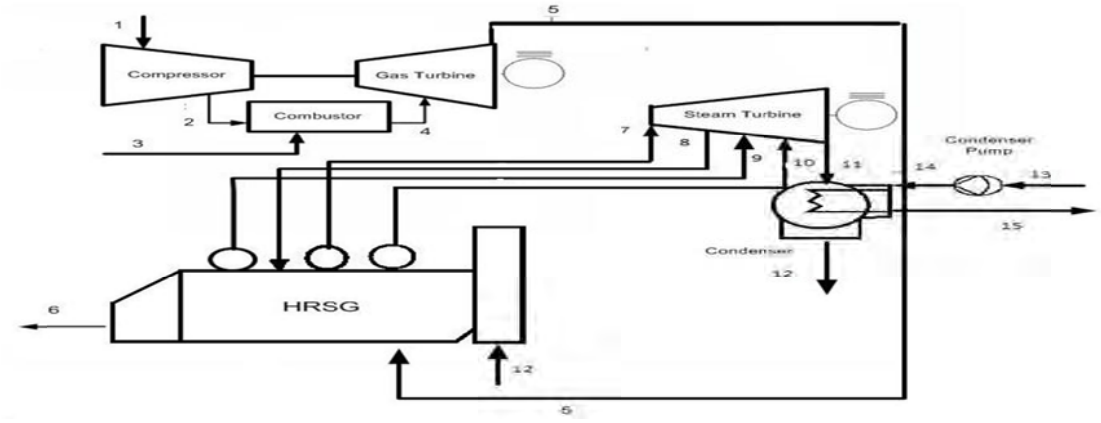

Fig 1. Combined cycle power plant (Repowering 1)

Second repowering scheme is based on the addition of a gas turbine and of a HRSG to a baseline of combined cycle. This method includes two main parts, the first part is combined cycle and the second part is a small gas turbine with a single pressure HRSG. These new components are integrated within the existing plant by injecting the steam produced by the additional HRSG into the existing gas turbine. The second part generates needed steam for injecting into main gas turbine of combined cycle in addition of producing extra power. In this way, the original turbine is transformed into a STIG (steam injected gas turbine), thereby increasing power. CC power augmentation is, thus, the sum of the power generated by the new gas turbine and the additional power of the original plant, comprising both the gas turbine and steam cycle. This scheme figure is shown in Fig.2.

As can be seen, the steam line feeding the original gas turbine connects the plant to the added section that comprises a gas turbine and a heat recovery steam generator. However, many other subsystems may be shared to reduce the repowering cost such as, for examples, flue gas treatment, electric power conditioning etc. One major addition to the plant is the water flow entering the new HRSG, which is inevitably lost at the stack. This can be a major drawback in certain situations and limits the applicability of the present scheme to sites with large fresh water availability, though the specific water requirements are fairly low, as will be shown later. If a low temperature thermal load is available nearby the power plant, the steam in the exhaust could eventually be condensed and the water could be recovered. Obviously, the very large size and the very low temperature level of such a heat sink restrict this option to quite uncommon cases, and its feasibility has to be carefully evaluated. Another significant feature of the proposed repowering scheme is its operational flexibility. Because of the inherent flexibility of the gas turbine, the entire additional section can be switched off in a short time, yielding part load efficiency equal to that of the original plant. At full load, the efficiency does not differ substantially, as will be demonstrated by the thermodynamic simulation. Fitting both the new and original gas turbines with variable intake guide vanes (IGVs) should provide a fairly wide operating range with efficiency close to rated.

4. Exergoeconomics analyses

All costs due to owning and operating a plant depend on the type of financing, the required capital, the expected life of a component, and so on. The annualized (levelized) cost method of Moran [9] was used to estimate the capital cost of system components in this study. The amortization cost for a particular plant component may be written as:

$$PW = C_i - S_n PWF(i,n) \quad (1)$$

$$\dot{C}(\$ / year) = PW \times CRF(i,n) \quad (2)$$

The present worth of the component is converted to annualized cost by using the capital recovery factor CRF (*i*,*n*), i.e [7]. Dividing the levelized cost by 8000 annual operating hours, We obtain the following capital cost for the *k*th component of the plant.

$$Z_k = \Phi_k \dot{C}_k / (3600 \times 8000) \quad (3)$$

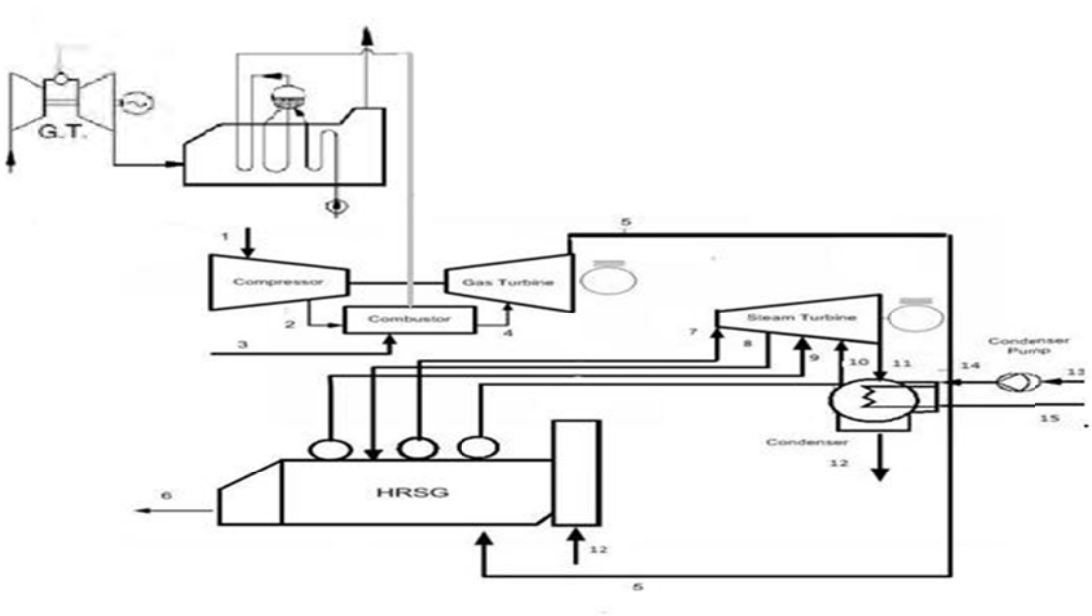

Fig 2. Combined cycle with STIG power plant (repowering2)

The maintenance cost is taken into consideration through the factor $\Phi_k = 1.06$ for each plant component whose expected life is assumed to be 15 years [9].

4.1. Thermoeconomic Modeling

The results from an exergy analysis constitute a unique base for exergoeconomics, an exergy-aided cost reduction method. A general exergy-balance equation, applicable to any component of a thermal system may be formulated by utilizing the first and second law of thermodynamics [10].

The cost balance expresses that the cost rate associated with the product of the system (C_P), the cost rates equals the total rate of expenditure made to generate the product, namely the fuel cost rate (C_F), the cost rates associated with capital investment (Z^{CI}), operating and maintenance (Z^{OM}) [12].

In a conventional economic analysis, a cost balance is usually formulated for the overall system (subscript tot) operating at steady state [12]:

$$C_{P,tot} = C_{F,tot} + Z_{tot} \quad (4)$$

Accordingly, for a component receiving a heat transfer and generating power, we would write [4]:

$$\sum_e \dot{C}_{e,k} + \dot{C}_{w,k} = \dot{C}_{q,k} - \sum_i \dot{C}_{i,k} + Z_k \quad (5)$$

To solve for the unknown variables, it is necessary to develop a system of equations applying Eq. (6) to each component, and it some cases we need to apply some additional equations, to fit the number of unknown variables with the number of equations [11].

A general exergy-balance equation, able to any component of a thermal system may be formulated by utilizing the first and second law of thermodynamics. In a conventional economic analysis a cost balance is usually formulated for the overall system operating at steady state. To derive the cost balance equation for each component, we assigned a unit cost to the principal product for each component. Depending on the type of fuel consumed in the production process different unit cost of product should be assigned [11].

5. Result and discussion

In this paper full repowering method for 156MW steam power plant has been applied. Table 1 indicates specification of repowered plant. It shows that, 68% of total power is produced by gas turbine cycle with 39% efficiency, in addition remained power are produced by steam cycle with 34% overall efficiency.

Repowered cycle produces 250MW more than old power plant. Heat rate in repowering power plant is 6500(KJ/KWh) and 1500(KJ/KWh) more than old power plant. Efficiency increases 15% for repowering model more than old power plant.

Table 2- combined cycle results

	Repowering
Gas Turbine(kW)	278041
Steam Turbine(kW)	125655
Plant Total (kW)	403695
Plant net LHV efficiency (%)	55.27
Plant net LHV heat rate(kJ/kWh)	6514
Gas turbine LHV efficiency (%)	39.05
Steam turbine efficiency (%)	34.59

Second proposed method uses STIG and adds a small gas turbine with single pressure HRSG. Result of this method with three model of gas turbine for producing steam injected, is shown in Table 2. For each three gas turbine model efficiency and exergy efficiency has been calculated. These results show that, increasing amount of injected steam mass flow can improve efficiency, but obviously only a limited amount of steam can be injected into the original gas turbine. This method can improve efficiency also increasing net power. In second stage, exergy and exergeoconimcs analyses are studied for both repowering method as an economical analyses. Table 3 and 4 show Exergy destruction and cost fuel and product rates of exergy with and without considering capital investment for each component in both repowered power plants.

Table 3- combined STIG cycle results

	V64.3A	V84.2	V84.3
Injected steam mass flow (kg/s)	26.2	49.2	53.2
added gas turbine power (MW)	68.7	108.2	138.2
Gas turbine power (MW)	306.1	330	334.5
Steam turbine power (MW)	123.8	140.2	142.1
Added gas turbine efficiency (%)	37.2	33.7	35.9
Gas turbine efficiency (%)	48.8	52.6	53.3
Steam turbine efficiency (%)	32.8	36.6	36.5
Net power (MW)	498.7	578.8	615
Efficiency (%)	61.2	60.32	60.8
Exergy efficiency (%)	59.6	58.6	59.1

Table 4-Exergy destruction and cost fuel and product rates of exergy with and without considering capital investment for each component in combined cycle

Component	Exergy Destruction(MW)	CF0 ($/MW)	CP0 ($/MW)	CD0 ($.s)	CF ($/MW)	CP ($/MW)	CD ($/s)
COMP	46.2489	0.0061	0.0073	0.2821	0.0064	0.0078	0.2959
COMB	152.5663	0.0049	0.0059	0.7475	0.0051	0.0061	0.7780
GT	17.0101	0.0059	0.0061	0.1003	0.0061	0.0064	0.1037
ST	36.2881	0.0083	0.0092	0.3011	0.0089	0.0101	0.3229
HRSG	38.6824	0.0063	0.0073	0.2436	0.0065	0.0078	0.2514
COND	4.8385	0.0083	0.2376	0.0401	0.0083	0.2603	0.0401
FWP	0.0236	0.0064	0.0113	0.0001	0.0064	0.0177	0.0001
CWP	0.6226	0.0064	0.0006	0.0039	0.0064	0.0007	0.0039

These results represented that combustion chamber and heat recovery steam generator in repowered combined cycle has most exergy and exergy cost destruction due to nature of combustion; however combustor in combined cycle plant shares about 51% TED, 44% TCD0 and 43% TCD. In next steps, compressor and steam generator have most exergy and exergy cost destruction.

Comparison of cost fuel and product of turbine for both schemes is shown in table 5. Gas turbine produce major of net power therefore cost product of gas turbine has important role in whole cost product. Gas turbine cost product for STIG combined cycle is less than ordinary combined cycle. However Cp of HPST in STIG cycle is more than ordinary combined cycle, HPST power is not as much important as other power product utility such as GT, LPST and IPST. Rate of total cost exergy destruction is specified in table 6.As shown, second repowering method can decrease TCD and TCD0 and therefore this scheme is more economical. Although exergy destruction increases in this method, ratio of exergy destruction to net power improves appreciably. Combined cycle with STIG can produce 498MW net power and has 356 MW exergy destruction but ordinary combined cycle produce 400MW net power with 346MW exergy destruction.

Table 4-Exergy destruction and cost fuel and product rates of exergy with and without considering capital investment for each component in STIG combined cycle

Component	Exergy destruction(MW)	Cf0 ($/MJ)	Cp0 ($/MJ)	CD0 ($/s)	Cf ($/MJ)	Cp ($/MJ)	CD ($/s)
Compressor	55.3869	0.0057	0.0073	0.3157	0.006	0.0079	0.3323
Combustion	120.8498	0.0049	0.0056	0.5921	0.0051	0.0058	0.6163
Gas Turbine	10.4329	0.0056	0.0057	0.0584	0.0058	0.006	0.0605
HPT	3.3937	0.0059	0.0078	0.0200	0.0074	0.0086	0.0251
IPT	21.4033	0.0069	0.0079	0.1476	0.0074	0.0087	0.1583
LPT	11.199	0.0069	0.0084	0.0772	0.0074	0.0093	0.0828
HRSG	38.2549	0.0056	0.0065	0.2142	0.0058	0.0069	0.2218
Condenser	9.6905	0.0069	0.202	0.0668	0.0074	0.2238	0.0717
CEP	0.0239	0.0069	0.0106	0.0001	0.0074	0.008	0.0001
deaerator	0.2376	0.0057	0.0074	0.0013	0.006	0.017	0.0014
LPFP	2.9043	0.0057	0.0067	0.0165	0.006	0.0151	0.0174
IPFP	0.4698	0.0057	0.0065	0.0026	0.006	0.0101	0.0028
HPFP	0.0878	0.0057	0.0063	0.0005	0.006	0.0075	0.0005
CWP	0.78	0.0057	0.0053	0.0044	0.006	0.0024	0.0046
added Comb	49.8	0.0051	0.0064	0.2539	0.0052	0.0066	0.2589
added Comp	15.8891	0.0064	0.0085	0.1016	0.0069	0.0091	0.1096
added GT	4	0.0064	0.0066	0.0256	0.0066	0.0069	0.0264
added HRSG	11.789	0.0066	0.0086	0.0778	0.0086	0.0089	0.1013

Table 5-comparsion of cost fuel and product with and without considering capital investment for both schemes

	combined cycle				STIG combined cycle				
	G.T.	HPST	IPST	LPST	G.T	HPST	IPST	LPST	added GT
Cf0 ($/MJ)	0.0064	0.0062	0.0074	0.0074	0.0056	0.0059	0.0069	0.0069	0.0064
Cf ($/MJ)	0.0065	0.0069	0.0083	0.0084	0.0057	0.0078	0.0079	0.0084	0.0066
Cp0 ($/MJ)	0.0065	0.0064	0.0078	0.0078	0.0058	0.0074	0.0074	0.0074	0.0066
Cp($/MJ)	0.0067	0.0073	0.0091	0.0092	0.0060	0.0086	0.0087	0.0093	0.0069

Table 6-comparsion of cost exergy destruction with and without considering capital investment for both schemes

	Exergy destruction(MW)	TCD0 ($/s)	TCD0 ($/h)	TCD ($/s)	TCD0 ($/h)
Simple C.C	346.2758	2.3209	8337.083	2.4188	8686.63
STIG C.C	356.5925	1.9771	7117.703	2.0925	7533.21

6. Conclusions

In this paper an old steam cycle has been chosen as a model for repowering. At first full repowering has been examined for this model and it changed into combined cycle that has 400MW net power. This repowering increases net power and improves efficiency. As a result of old boiler and power capacity for this model, full repowering is one of the useful an economical method. After that, a gas turbine and a single pressure HRSG added to combined cycle and it has been changed into STIG combined cycle. Net power increases with adding

new gas turbine and using STIG in this method. However increasing amount of mass flow steam injected can heighten net power, there is limitation for mass flow. Exergy and exergoeconomic methods have been applied for analysis and comparison both repowering method. An exergy-costing method has been applied to both cases to estimate the unit costs of electricity produced from steam turbines. The computer program that was developed which shows that the exergy and the thermoeconomic analysis presented here can be applied to any energy system systematically and elegantly. If correct information on the initial investments, salvage values and maintenance costs for each component can be supplied, the unit cost of products can be evaluated. These analyses shows that cost product of combined cycle with STIG is less than ordinary combined cycle. Also net power and efficiency of combined cycle with STIG is more than ordinary combined cycle. Although using water for steam injection is the most problem of this new method, there are some suggestions to recycle water and reused in the cycle.

References

[1]. M.Frankle. The standardized repowering solution for 300 MW steam power plants in Russia. Siemens AG 2006.

[2]. A.bouam, S.aissani. Combustion chamber steam injected for gas turbine performance improvement during high ambient temperature operation. Journal of Engineering for Gas Turbines and Power JULY 2008, Vol. 130 / 041701-1

[3]. T Srinivas, AVSSK S Gupta. Parametric simulation of steam injected gas turbine combined cycle. J. Power and Energy Vol. 221 Part A

[4]. R.carapellucci, A.Milazzo. Repowering combined cycle power plant by a modified STIG configuration. Energy Conversion and Management 48 (2007) 1590–1600.

[5]. Haselbacher, H. Performance of water/steam injected gas turbine power plants consisting of standard gas turbines and turbo expanders. Int. J. Energy Technol. Policy, 2005, 3(1/2), 12–23.

[6]. Sanjay Y, Singh O, Prasad BN. Energy and exergy analysis of steam cooled reheat gas–steam combined cycle. *Applied Thermal Engineering* 2007; 27: 2779–2790.

[7]. Chao Z, Yan W. Exergy cost analysis of a coal fired power plant based on structural theory of thermoeconomics. *Energy Conversion and Management* 2006; 47:817–843.

[8]. Modesto M, Nebra SA. Analysis of a repowering proposal to the power generation system of a steel mill plant through the exergetic cost method, *Energy* 2006; 31: 3261–3277.

[9]. Feng X, Zhu XX. Combining pinch and exergy analysis for process modifications. *Applied Thermal Engineering* 1997*;* 17: 250-260.

[10]. Durmayaz A, Yavuz Y. Exergy analysis of a pressurized water reactor nuclear power plant. *Applied Energy 2001;* 69: 39-57.

[11]. Nafey AS, Fath HES, Mabrouk AA. Exergy and thermoeconomic evaluation of MSF process using a new visual package. *Desalination 2006;* 201: 224-240.

[12]. Dobrowolski R, Witkowski A, Leithner R. Simulation and optimization of power plant cycles. ECOS 2002, Proceedings of the 15th International Conference on Efficiency, Costs, Optimization, Simulation and Environmental Impact of Energy Systems, Berlin, Germany, 2002, pp. 766–772.

[13]. Joint Army-Navy–Air Force Thermochemical Tables. NSRDS-N3537, Washington, DC: National Bureau of Standard Publications; 1985.

Possibilities to implement pinch analysis in the steel industry – a case study at SSAB EMEA in Luleå

Johan Isaksson[1,*], Simon Harvey[1], Carl-Erik Grip[2], Jonny Karlsson[3]

[1] *Div. of Heat and Power Technology, Chalmers University of Technology, Göteborg, Sweden*
[2] *Div. of Energy Engineering, Luleå University of Technology, Luleå, Sweden*
[3] *SSAB EMEA, Luleå, Sweden*
** Corresponding author. Tel: +46 31 772 3867, Fax: +46 31 821928, E-mail: johan.isaksson@chalmers.se*

Abstract: Steelmaking is an energy intensive industry. Much development work has been accomplished during the past years to make the processes more efficient. Process integration has come to play an important role for identifying efficiency measures, using mathematical programming as general tool. So far only a few minor process integration studies using pinch analysis have been made in this type of industry, and only on smaller sub-systems. This paper presents the results of a pinch targeting study that was conducted at the Swedish steel making company SSAB EMEA in Luleå. The pinch analysis methodology was originally developed to study heating, cooling and heat exchange in process systems with many streams. In the steel industry there are relatively few streams that are appropriate for heat exchange. This limits the use of pinch analysis. However, this study demonstrates that pinch analysis is a powerful tool for certain subsystems, especially the gas cleaning unit of the coke plant. The paper includes several suggestions for improved energy efficiency in this section of the steel plant.

Keywords: *Pinch analysis, Energy efficiency, Steel industry, Process integration*

1. Introduction

1.1. The steel industry

The steel industry sector is the second largest industrial user of energy in the world. In 2007 it used 24 EJ or 6700 TWh according to IEA [1]. Steel is an important construction material and the production has increased with the growth of the world economy. The development of the world production of steel is shown in Fig. 1.

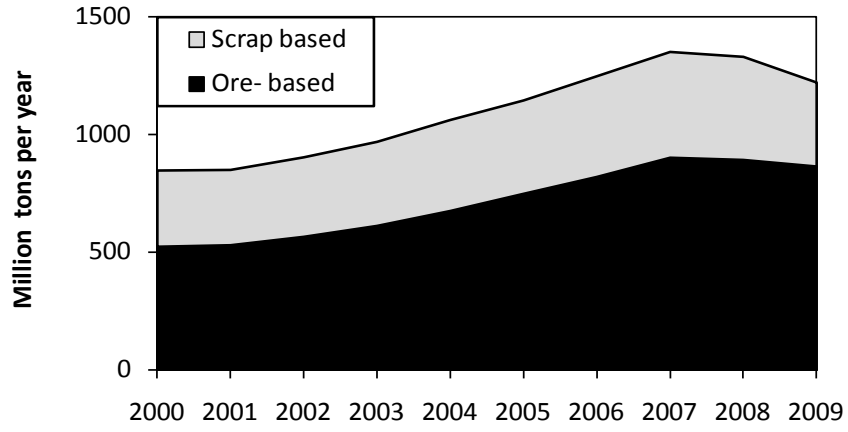

Fig. 1 Development of world steel production from ore and scrap based route[2]

The diagram shows a steady growth except from the recession years 2008-2009. A considerable part of reactants and fuels that are used in the processes are of fossil origin. The combination of production increase and use of fossil energy puts an emphasis on work to decrease energy consumption. One road to achieve this is to improve the processes to decrease their consumption. A large amount of work is and has been carried out in this area. It is, however, considered out of scope for this paper and not described here. A second road is to

improve the system efficiency, with process integration as one important tool. That type of work is the subject of this paper.

Steel is produced using two alternative routes: an ore based route where primary steel is produced from iron ore and a scrap based route where recycled steel (scrap) is re-melted (Fig. 2).

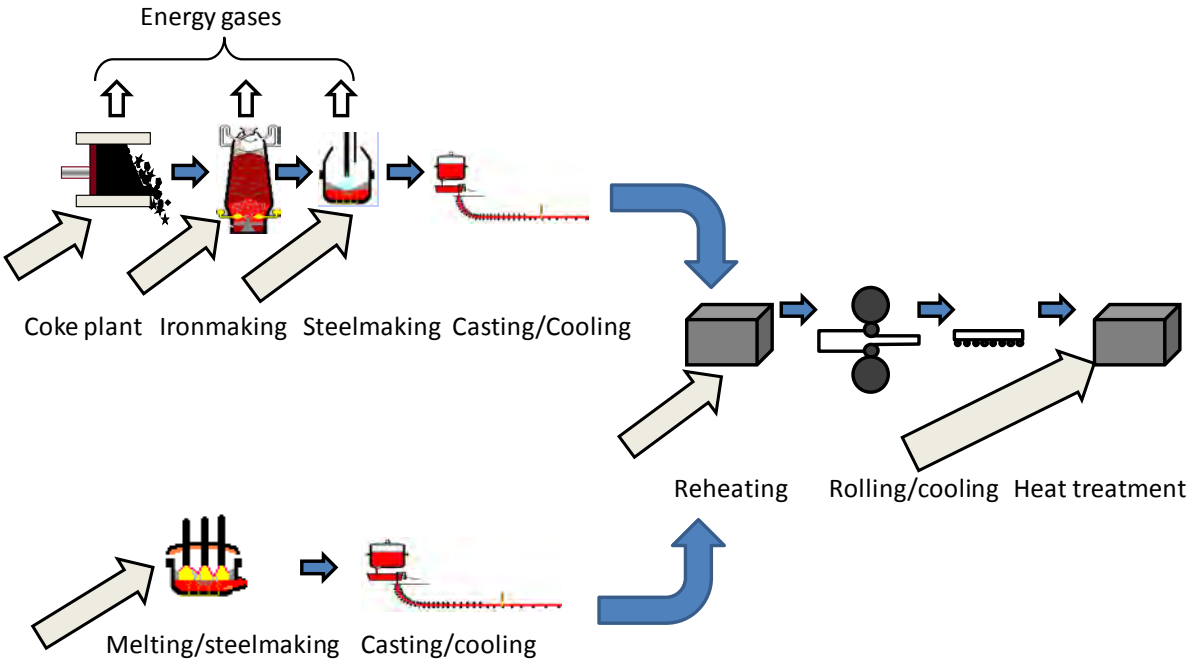

Fig. 2 Process route for ore and scrap based steel production

The upper branch in Fig. 2 illustrates the ore-based route. The production is based on coal and ore (mainly iron oxide). The coal is converted to coke by dry distillation in a coking plant. Approximately 25% of the weight is recovered as energy rich gas, tar and chemical products. The ore, e.g. in the form of pellets, is fed into the blast furnace along with coke and preheated blast air. The blast furnace produces a hot liquid metal with high carbon content. A combustible gas is obtained as a by-product. The hot metal is transformed into steel in an oxygen converter (BOF). An energy-rich gas is obtained as a by-product. After ladle treatment the steel is cast in a continuous casting machine. The semi-finished cast steel is cooled and transported to a rolling mill where it is heated to rolling temperature and rolled (or forged) into products and cooled on a cooling bed. Depending on the product, there may be additional treatment, such as heat treatment, cold rolling and metal coating (e.g. zinc). In most cases by-product energy gases from iron and steel-making are used in the reheating furnaces.

After some time the steel products are returned as scrap, and converted into new steel using the scrap based route (lower branch in Fig. 2). The scrap is melted and heated, usually in an electric arc furnace. The molten steel is then refined. This post-processing can be carried out in the furnace, in the ladle treatment or in a separate unit, e.g. refining with oxygen in a so-called AOD converter. Then the finished steel is cast and treated in the same way as in the ore-based route. This recirculation is an important part of the steel economy.

The system studied in this work is the SSAB EMEA steel plant in Luleå. This is an ore-based plant. The by-product energy gases cannot be used for preheating as the rolling mill is situated 800 km from the steel plant. Instead they are used in a local CHP plant, which co-produces electricity for the steel plant and district heating for the community (see Fig. 3 a.

1.2. Process integration and Pinch analysis

A typical process industry does not consist of independent process units. Instead, it is a network of units exchanging energy and energy media with each other. Very often the local community is also involved in the network, e.g., through power generation and/or district heating. The flowsheet and photo in Fig. 3 show the network that is studied in this paper.

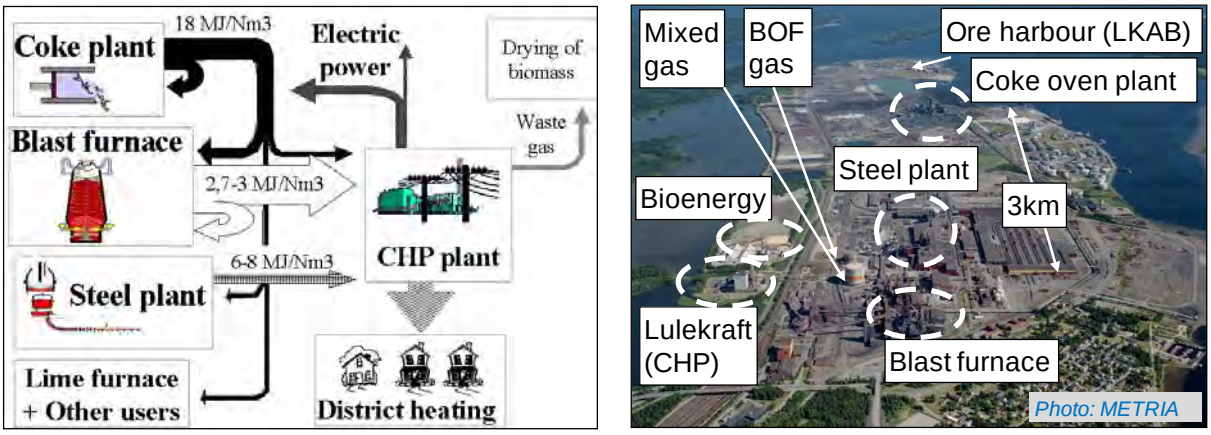

a) Flow sheet *b) Actual plant*

Fig. 3. Network of the Luleå energy system.

The different units exchange energy and material with each other. Changes in one unit have side effects on the other units. Energy saving in one unit does not necessarily lead to energy saving of the total system. A global approach is needed to avoid sub-optimization. A flowsheet does not tell the whole truth. At the actual plant site there is usually a great distance between some units, in this case up to 2-3 km (see Fig. 3 b). Some connections that would be optimal from an energetic point of view may be impossible from a practical and economic point of view. A good analysis tool should be able to select the solution that is technically and economically most attractive.

A first attempt to make a more systematic analysis of this type of problem using pinch analysis was made at Manchester University in the UK [3]. In this type of analysis, the heat-carrying media are categorized as either cold streams (media that require heating during the process) or hot streams (media that require cooling). Based on this information it is possible to construct *composite curves* in order to determine the minimum energy-consumption target for the process. The curves are profiles of the process' heat availability (hot composite curve) and heat demands (cold composite curve). The degree to which the curves can overlap for a specified value of minimum temperature difference for heat exchanging (ΔT_{min}) is a measure of the potential for heat recovery. The point of closest approach of the composite curves, i.e. where ΔT_{min} is reached, is known as the pinch point. The effect of different operations and/or process modifications can be studied using pinch analysis. The relative position of such operations in the composite curves with respect to the pinch point is often a determining factor. Further details are described in Section 2 (Methodology). Pinch analysis has since then become a wide-spread tool for process integration in many industrial systems. Ref [4] can be seen as an example.

Steel industry energy systems are characterized by large high temperature flows of molten, solid and gaseous materials, as well as by energy intensive chemical reactions. Mathematical programming is considered particularly suitable for optimizing energy flows in this type of system. A specific simulation and optimization tool (reMIND) was developed and

implemented for steel plant applications ([6], [7]) and has reached a position as standard process integration tool for those applications.

Pinch analysis was originally developed for large systems with many streams that require heating and cooling and that are suitable for heat exchanging. This makes implementation in the steel industry somewhat restricted as there are relatively few streams, and the ones with the largest energy content are in the form of molten metal, hot slag or as radiation from slabs, i.e. unsuitable for conventional heat exchanging. Only limited uses of pinch analysis in the steel industry are reported ([8], [9]). However, previously conducted system studies carried out in the steel sector and PRISMA indicate that there are subsystems where pinch analysis could be a powerful tool. The Swedish Energy Agency and the national program for process integration decided to carry out a study on the possibility to use pinch analysis in the steel and mining sector. A major part of that work was a smaller pinch targeting study of the Luleå Steel plant system.

1.3. Scope of paper

The main scope of this study is to describe the above mentioned targeting study and the conclusions on possible use of pinch analysis in the steel industry.

2. Methodology

The analysis procedure for one of the subsystems (the gas cleaning system of the coke oven plant) is described in more detail to illustrate the methodology.

Data was collected together with coke plant staff. The energy streams were compiled and characterized as hot or cold streams. The cold streams, or ”heating loads”, are shown in Table 1. A similar table (not shown here) was made for the hot streams.

Table 1 Heating loads in the coke oven gas cleaning area

Process part	Unit	T_{start} (°C)	T_{end} (°C)	Flow	Load (kW)
Ammonia stripper	DB 602 A/B	MP steam			5 852
	EB 605 cold side	6.8 [1]	63	22 t/h	≈1 500
Benzene stripper	EA 2363	LP steam			42.3
	DB 2362	LP steam			633
	EA 2361	178	178.1		950
	EB 2261 A-D cold side [2]	27	143	51.8 m^3/h	2 620
2nd feed water preheat	FL 1401	63	124	22 t/h	1 566
Sulfur stripper	EB 601 cold side	26	51	61.1 m^3/h	1 770

[1] Yearly average water temperature in Lule River

[2] Heat capacity of 2.13 kJ/kg K is used for the circulating oil (petroleum) Density = 881 kg/m^3. The load is the average value of the two streams: (3132 kW + 2108 kW)/2

Composite curves (CC) were constructed for the gas cleaning section of the coking plant, shown in Fig. 4, using the stream data. The minimum distance between the curves is set by ΔT_{min}, set at 10 K in this study. Internal heat recovery is theoretically possible where the curves overlap (shaded area). A larger ΔT_{min} would push the curves further apart, thus decreasing the overlap and cause an increasing demand for heating and cooling media ($Q_{H,minimum}$ and $Q_{C,minimum}$).

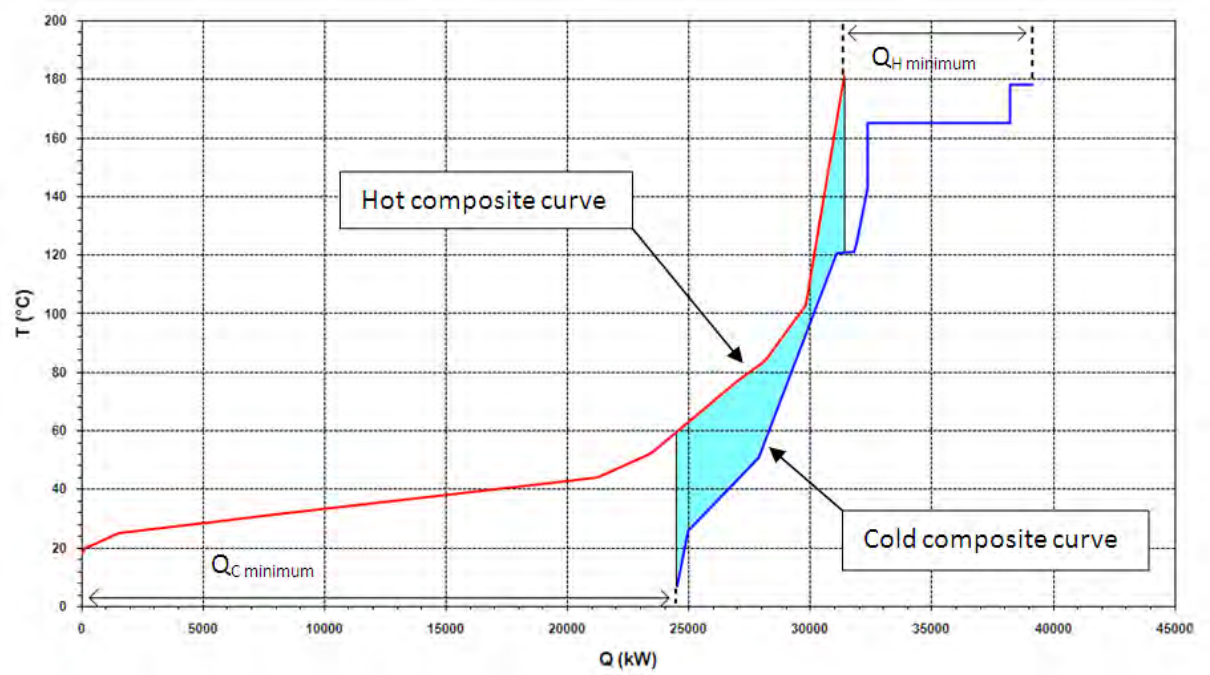

Fig. 4 Composite curves (CC) for the coking plant's gas cleaning area

The CC establish the energy targets (minimum hot and cold utility demand), but are not suitable for identifying appropriate utility steam levels and loads, or whether excess process heat can be used for hot water production instead of using cooling water. The Grand Composite Curve (GCC) is more appropriate for analyzing the interaction between the process and the utility system. Therefore a GCC was constructed for the gas cleaning area. To visualize the correspondence between CC and GCC, these are put next to each other in Fig. 5. The hot and cold composite curves are merged into one curve, i.e. the GCC, by calculating the net heat load in each temperature interval. A new interval can often be identified by a gradient change in the curve.

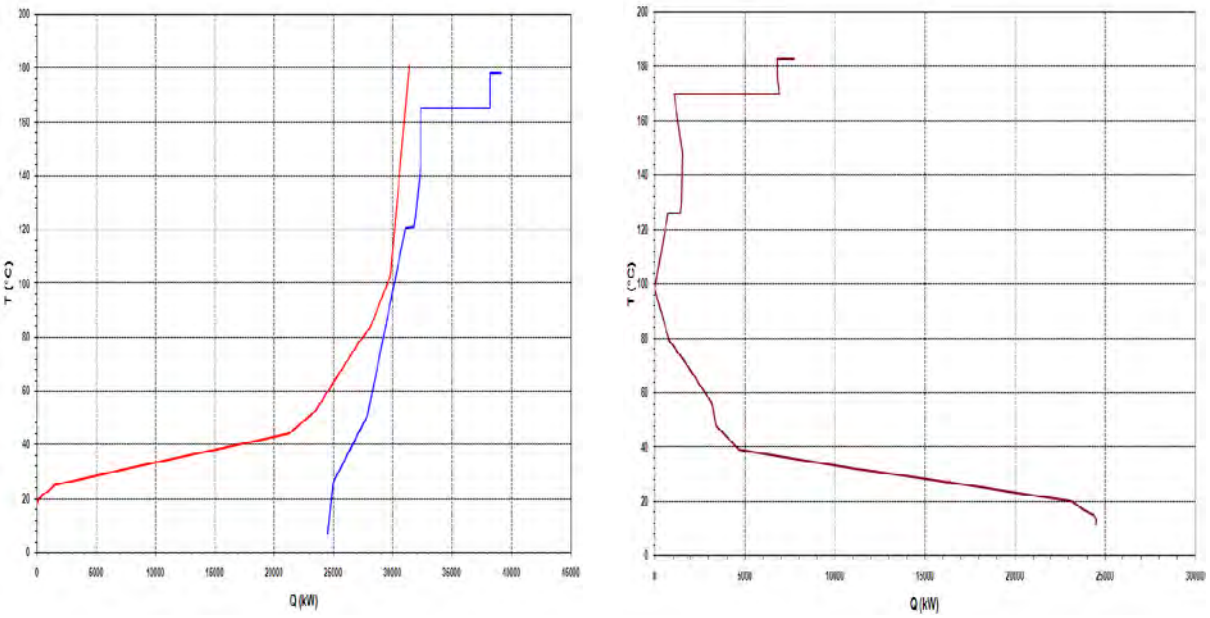

Fig. 5 Composite curves (CC) and corresponding grand composite curve (GCC) for the coking plant's gas cleaning area

A more detailed view of the GCC is shown in Fig. 6, enabling an analysis of different possible utility level setups.

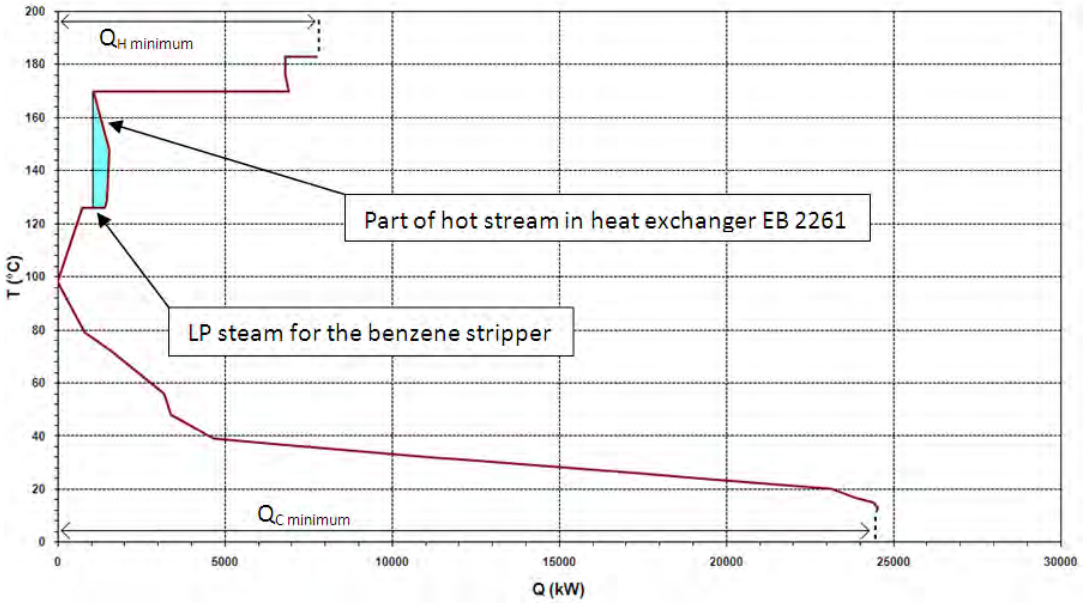

Fig. 6 Grand composite curve for the coking plant's gas cleaning area

One can for example examine whether there is any heat surplus (below the pinch) at useful levels, which could be used for steam generation, district heating, electricity production in a Rankine cycle, etc. The shaded part shows where internal heat exchange between temperature intervals is possible, i.e. a so-called pocket. The curve shows that part of the hot stream in EB 2261 is used to generate LP steam for the benzene stripper. The same methodology was used to analyze the other subsystems and the total plant.

3. Results

3.1. Coke plant

The analysis of the gas cleaning section of the coking plant (Fig. 4) shows that the demand for feed water preheating will decrease since less steam is needed in the process. The current preheating load is approximately 1500 kW in heat exchanger EB 605 and 1566 kW in FL 1401 (Current preheating load ≈3066 kW). The minimum preheating requirement turned out to be 2779 kW in total in this first step of the analysis of the coking plant. The horizontal parts of the lower line represent the demand for condensing steam in the strippers. The slope is determined by the flow multiplied by the heat capacity [kJ/°C] in each temperature interval. In all, the gas cleaning area currently uses 25.7 MW of cooling water whereas the minimum cooling demand, determined by pinch analysis, is 24.5 MW ($Q_{C,minimum}$ in Fig. 4). The process uses 9 MW of external heat, compared to 7.7 MW ($Q_{H,minimum}$.). This means that there is a 14% steam savings potential if a maximum energy recovery heat exchanger network were to be built, assuming ΔT_{min} = 10 K. The pinch temperature is 103°C for hot streams and 93°C for cold streams. That tells us, for example, that external heating media has to be at least 103°C and that the cooling media can be 93°C at the most, in order not to violate the ΔT_{min} of 10 K for heat exchange between utility and process streams.

An extended study (diagram not shown) was carried out to study the effect on heating and cooling loads in the total coking plant area assuming that steam is used at as low pressure as possible. This is particularly important if the steam is extracted from a turbine, in order to maximize electricity production. This showed a 1290 kW steam saving potential. The main

reason was elimination of the use of LP steam for feed water heating and avoiding heat exchange through the pinch.

A lot of heat at high temperature is wasted when washing water at around 70°C is used to cool the hot coke oven gas directly after it leaves the ovens. It should be possible to heat exchange the gas down to the tar dew point. A study was made to study what could be gained from such an arrangement. The dew point is between 350 and 150°C. An inlet temperature at a temperature of 450°C (i.e. significantly above the dew point) was assumed to give a safety margin. A gain of 9 MW was indicated if the heat is used to replace steam from the boiler.

3.2. Blast furnace and steel plant

A first attempt was made with separate studies of the blast furnace, the steelmaking converter plant, the ladle metallurgy and the continuous casting. However, limited availability of cold streams limited meaningful implementation of process integration based on pinch analysis. Since the distance between the units was not very large, a merged study of the Blast Furnace-Steel Plant system was tried. The analysis showed a potential hot utility savings of 2.7 MW that could be accomplished by using BOF steam for preheating the inlet gas to the cowper. This is further commented in the discussion chapter.

3.3. Total system

The study indicated that there actually is a match between the two sites, where the steel plant fits in the coking plant's "pocket". Flue gases and hot coke oven gas are in that case used to heat the blast air and steam from the BOF converters is used to run the strippers in the coking plant. There is a difference in load magnitude between the two sites, where the blast furnace and steel plant demand lots of external utility.

4. Discussion

4.1. General results

The expected result was that many sources of excess heat at hot water temperature level would be found. However, that is not the case assuming that this study shows the whole picture. Excess heat is available either at low temperatures, where utilization is more or less impossible, or at levels where steam could be generated. The dominating energy carrier suggested in this study is steam at fairly moderate pressure and temperature (below 200°C). Before heat recovery of that kind is realized, there must be heat sinks where the steam can be utilized. Several options are available but the simplest solution appears to be a steam turbine for electricity production.

4.2. System blast furnace + steel plant

The study in section 3.2 suggested that BOF steam should be used to preheat input cowper gas. For different reasons this is not technically feasible. However, it indicates another option that was not visible with the available stream data. A solution that has been used in some plants is preheating of the combustion air using a heat exchanger with the off-gas from those burners. The results confirm that this is interesting, although a different technical solution was suggested due to lack of detailed data regarding internal cowper streams.

4.3. Analysis of the total system

The analysis shows a large energetic gain by transportation of flue gases and steam between the sites. However, under present conditions this can be judged as less realistic due to the transport distances. Combining the two sites does not seem to be a feasible option just by

investigating integration possibilities. It would, however, add a degree of flexibility to have a common steam net.

4.4. Effect of process integration on sustainability

The effect is usually indirect, energy that would otherwise have gone to waste is used elsewhere, e.g. to replace consumption of fuel. Pinch analysis is useful where matches can be found at proper temperature between heat sinks and excess heat.

4.5. Future work

It would be interesting to carry out further studies at other plants. It is suggested that this is done as integrated projects where Pinch analysis is used together with other methods. Commonly available software and educational tools could increase industrial general awareness about pinch analysis.

5. Acknowledgments

The authors of this paper would like to thank Ida Engström and Rickard Broström at SSAB in Luleå, for guidance about the processes and for providing data to this work, and Chuan Wang, MEFOS, for valuable comments. We also would like to thank the Swedish Energy Agency for financing the study.

References

[1] Energy Technology Transitions for Industry- Strategies for the Next Industrial Revolution, OECD/IEA 2009, International Energy agency, Paris

[2] Steel Statistical Yearbook 2009, World Steel Association, Brussels Belgium, 2009

[3] Linnhoff B and Flower J.R. , "Synthesis of Heat exchanger Networks I. Systematic generation of energy optimal networks" , Aiche Journal 24 (4), 1978, pp 633-64)

[4] Klemeš J och Varbanov P S 2010, "Implementation and Pitfalls of Process Integration, Pres2010(13th Conference on Process Integration, Modelling and Optimisation)" , Prague, Czech Republic , 28 August – 1 September 2010.

[5] Nilsson K and Söderström M, 1992,Optimising the operation Strategy of a pulp and paper mill using the MIND Method ,Energy, vol17 (10)945-953

[6] Wang C, Ryman C, Dahl J, "Potential CO2 emission reduction for BF-BOF steelmaking based on optimised use of ferrous burden materials", International Journal of Greenhouse Gas Control (2009), 3:29-38

[7] Wang C, Larsson M, Ryman C, Grip C-E, Wikström J-O, Johnsson A, Engdahl J, "A model on CO2 emission reduction in integrated steelmaking by optimization methods", International Journal of Energy Research, 2008; 32:1092-11061987

[8] Clayton, R.W. Cost reduction at a steel works - Identified by a process integration study at Sheerness Steel plc, Department of Energy.

[9] Johansson, E., "Recovery of rest energy, a study on the potential for heat recovery in the tube mill at OVAKO steel in Hofors", Master thesis, Chalmers university of technology, Gothenburg, 2002.

Energy efficient dual command cycles in Automated Storage and Retrieval Systems

Antonella Meneghetti[1,*], Luca Monti[1]

[1] *DiEM – Dipartimento di Energetica e Macchine, University of Udine, Udine, Italy*
** Corresponding author. Tel: +39 0432 558026, Fax: +39 0432 558027, E-mail: meneghetti@uniud.it*

Abstract: Sustainable manufacturing claims for more energy efficient operations in warehouse management. In AS/RSs they can be pursued by optimizing storage and retrieval cycles so that the least energy is required to move the crane. While picking operations have been traditionally optimized in order to minimize picking times directly linked to the service level perceived by customers, a sustainable approach leads to change this perspective by optimizing storage and retrieval cycles to lower energy requirements. In this paper we propose an energy-based heuristic to re-sequence retrievals in order to perform dual command cycles with the least energy requirements. Impact on both energy savings and round trip times is assessed when moving from single command to dual command cycles, if storage and retrieval operations are combined by the common first-come first-served policy. Further improvements on energy and time performances achievable by adopting different re-sequencing heuristics are then investigated. Factors affecting energy consumption and round trip times such as the storage allocation strategy, the re-sequencing time-based or energy-based policies, the demand distribution, and the shape of the rack, are analyzed by a 2^4 factorial design of experiments.

Keywords: *energy efficiency, Automated Storage and Retrieval Systems, dual command cycles.*

1. Introduction

An automated storage and retrieval system (AS/RS) is a fully automated facility, where cranes running on rails between fixed storage racks pick up and drop off unit loads without the need of human operators.

AS/RSs have been recognized as sustainable facilities [1]. Since they allow to store inventory more densely and vertically than traditional warehouses, they reduce, in facts, energy consumptions to heat, cool, light and ventilate excess square footage. Furthermore, allowing storage of the same number of units in a smaller footprint, AS/RSs require less concrete, reducing carbon dioxide emissions.

From an operations management point of view, energy efficiency can be pursued in AS/RSs by optimizing also their storage and retrieval cycles, so that the least motion energy consumption can be achieved [2]. While picking operations have been traditionally optimized in order to minimize picking times directly linked to the service level perceived by customers [3], a sustainable approach leads to change this perspective by matching time performances with energy efficiency ones.

Dual command cycles couple a storage operation to a retrieval one into the same trip, in order to avoid idle travels of the AS/RS machine to/from the I/O station as in single command cycles, where only one operation (storage or retrieval) is performed at a time. In a dual command cycle, therefore, the AS/RS machine departs from the I/O station with a load on board and reaches the desired storage location, then it moves directly towards the selected retrieval location where the load is picked up, and then it comes back to the I/O station. The possibility of performing dual command cycles depends on the simultaneous availability of both storage and retrieval requests. When this occurs, dual command cycles have been recognized by literature to lead to significant time savings if compared to traditional single command ones in the order of 30% [4]. Adopting a sustainable perspective, the first question

to be addressed is therefore how much energy consumption can be reduced by adopting dual command cycles with respect single command ones.
Time savings are strictly related to the storage assignment policy adopted. Graves et al. [4] demonstrated by both analytical and enumeration analysis that maximum time savings are achieved by mandatory interleaving, that means performing dual command cycles whenever possible, with a full turnover strategy rather then the common random allocation. The full turnover strategy is a dedicated assignment policy, which exclusively assigns a given number of locations to a product, on the basis of its demand rate sorted by decreasing order. In this way the most frequently moved items are located to the most convenient positions with respect to the I/O station and maximum improvement on the selected performance is achieved. From the traditional time-based perspective convenience has been read in terms of minimum picking time, which has been the performance to be enhanced. Since it was found that interleaving time accounts for 30% of the total round trip time (equal to the sum of the travel time from the I/O station to the storage location + interleaving time from storage to the retrieval location + time to travel from the retrieval location to the I/O station), the time-based full turnover strategy allows to minimize the one-way travel component from/to the I/O station of a dual command cycle, thus is able to affect the 70% of total time.

In our opinion, when a sustainable perspective is adopted convenience should be read in terms of energy efficiency. Therefore, in order to assess the maximum energy savings achievable by dual command cycles, we introduce a full turnover strategy based on the least motion energy, that means assigning high turnover items to locations requiring the least energy to be served. Energy performance achievable by the energy-based full turnover policy can therefore be considered as upper bounds of energy savings achievable with other less performing but more easy to apply storage policies, such as the random allocation (i.e. each open location can be occupied by every item) or the class-based storage allocation. It was already shown in our previous work [2] how energy-based dedicated zones differs from time-based ones; from the traditional rectangular or L shapes of time-based approach, in fact, step-wise zones are identified by the energy-based one, with a general shift towards upper levels of the rack, due to exploitation of gravity.

Performance improvement gained by dual command cycles depends also on the capability of optimally combining storage and retrieval requests in order to optimize the interleaving phase. A common practice is to adopt a First-Come First-Served (FCFS) policy, which means processing storage requests in the exact sequence they arrive and combining each storage with the first available retrieval request respecting the order it has been inserted into the information system. While processing storage in FCFS order reflects the fact that in general input unit loads are moved by a conveyor to the I/O station of the AS/RS and therefore their sequence is fixed, retrieval requests can be considered as electronic messages, which can be rearranged in any desired sequence.

When a random allocation is performed, and only one open location is available at a time, Bozer et al. [5] explained that the dual command scheduling of AS/RSs can be formulated as a Chebyshev travelling salesman problem, which is known to be NP complete. When multiple open locations are available for storage, the problem involves finding the best storage locations other than coupling storage and retrieval requests and it is in general NP-hard [6]. This is the reason why several heuristics were developed to overcome such complexity. By analytical analysis, Han et al. argued that in order to gain an improvement in throughput greater than 10%, travel-between (i.e. interleaving time from storage locations to the retrieval ones under the hypothesis of rectilinear constant speed motion) must be reduced by over 50%

with respect to FCFS retrievals as it is achievable by the Nearest-Neighbor Heuristic [6]. The overall performance of this heuristic can be enhanced by adopting a class-based storage policy rather than a random one [7]. Near-optimal solutions can be achieved under random storage by the ε-optimum algorithm proposed by Lee and Schaefer [8]. An $O(n^3)$ heuristic for dedicated storage with one open location at a time (meaning that storage locations have been previously identified and no storage choice has to be performed) was also proposed by authors [9] with very good performance with respect to the optimal solution.

In this paper, a heuristic approach to couple storage and retrieval requests within a given time period aiming at minimizing motion energy requirements rather than picking time is proposed for the energy-based full turnover strategy. Time and energy are related by power, but it should be considered that due to simultaneity of movements along vertical and horizontal axes the Chebyshev metric applies to travel time (i.e. machine travel time is the maximum between x-time and y-time), while energy is the sum of the requirements of both the x motor and the y motor installed in the crane. This is the reason why energy savings potential could be different from time savings potential gained by dual command cycles and should be analyzed. Furthermore one can wonder to what extent energy-based dual command cycles overcome time-based ones as regards energy saving if compared to single command cycles and FCFS dual command ones.

Therefore, picking time and energy performances of dual command cycles identified by the proposed heuristic are compared to the commonly use First Come First Served combination approach and Lee Schafer time-based heuristic's one by simulation. Energy saving potential related to dual command cycle optimization is assessed as well as the impact of a sustainable approach on client service levels. Factors such as the shape of the rack affecting motion energy, the ABC demand curves affecting the turnover frequency or the type of full turnover strategy (time-based versus energy-based heuristics) are considered in other to analyze the amount of energy savings obtainable by optimizing both location assignment and picking cycles.

The paper is organized as following. In par. 2.1 the energy model developed in order to compute energy required for crane movements is described. In par. 2.2 an energy-based heuristic for combining storage and retrieval requests is proposed, while in par. 2.3 the design of simulation experiments is described. In par. 3 results are analyzed and conclusions on energy saving potential are collected in par. 4.

2. Methodology

To adopt the new perspective aiming at energy efficient manufacturing, new models and performance measures should be introduced in order to assess energy saving potential of different operation policies.

The first step is the development of an energy model so that motion energy required by the crane to reach each storage location of the AS/RS rack can be estimated. The second step is therefore an energy-based heuristic to combine storage and retrieval requests into dual command cycles. Finally, factors which are expected to affect energy efficiency performance of dual command cycles should be identified and a factorial design of simulation experiments provided. In the following subsections previously described steps are discussed.

2.1. The energy model

The crane movements along the horizontal axis (namely x) and the vertical one (namely y) are described as a rectilinear motion with constant acceleration. A trapezium speed profile is adopted, where three phases can be recognized: acceleration until the maximum speed is reached, constant speed motion, and deceleration in order to stop at the desired location in the rack. When the shift to be performed by the AS/RS machine isn't great enough to reach the maximum speed, a triangular speed profile with only symmetric acceleration and deceleration phases is adopted. The AS/RS machine movements are characterized by their simultaneity along the two axes, and therefore the Chebyshev metric has been applied in literature to calculate travel time. As regards energy, the crane in equipped with 3 independent motors per axis. Since fork cycle to insert and/or drop off unit loads from the rack is independent from their location and can be considered a fixed component of energy requirements, energy for the z axis is neglected in our model. New generation crane are controlled so that their movements along x and y axes not only start simultaneously, but also end at the same time. This allows to avoid the additional torque needed to maintain the load in position while completing the slowest movement as in traditional cranes. To adhere to market behavior, we slow down the fastest motion by decreasing the acceleration/deceleration times so that the maximum speed value achievable is lower than the nominal one, while keeping acceleration at nominal value, as described in [2].

Energy is then computed per axis on the basis of the torque provided at the motor shaft, supposed constant during acceleration due to A.C. 3-phase inverter duty motors. Torque has to counterbalance inertia of load and masses (motor + crane), friction and gravity (for the y-axis). It was so possible to assign to each location in the rack the value of energy required to store into or retrieve from by departing/arriving from/to the I/O station supposed at the lower left corner of the rack. Furthermore, the model allows to dynamically compute energy for interleaving between any pairs of locations in a dual command cycle.

2.2. The energy-based dual command cycle heuristic

We imagine to process storage requests in the same order they arrive, since unit loads are supposed to be moved to the I/O station of the AS/RS by a loop conveyor. Retrieval requests, instead, are re-sequenced in order to save motion energy. In order to limit computational time but also to adhere to a dynamic environment, the list of available retrievals requests is commonly split into blocks which are sequenced one at time [3]. We adopt blocks of 15 storages and 15 retrievals to be combined into N = 15 dual command cycles at time. In our computation we considered unchanged each block until all the pairs have been identified, thus adopting a static approach. In a very turbulent environment, however, it is possible to adopt a dynamic approach by updating the block with new retrievals requests at each iteration before selecting the successive pair of operations.

Let be L_S the list of N storage requests and L_R the list of N retrievals requests in the analyzed block. The energy-based heuristic consists of the following steps.

1. Assign to each element in L_S the open location with the lowest energy required to store the load moving from the I/O station. Let S the set of such locations.
2. Assign to each element in L_R the retrieval location among the available with the lowest energy required to pick the load to the I/O station. Let R the set of such locations.
3. For each pair (s, r) with $s \in S$, $r \in R$, compute energy requirements for moving from storage location s to retrieval location r;

4. Select the pair (s^*, r^*) $s^* \in S$, $r^* \in R$ with the minimum energy requirement and perform the related dual command cycle;
5. Set $S = S - \{s^*\}$, $R = R - \{r^*\}$;
6. Go to step 4 until $S = \varnothing$ and $R = \varnothing$.

The rationale of steps 1 and 2 is attempting to positively affect the one way travels from and to the I/O of a dual command cycle, so that the minimum energy is consumed for them. Steps 3-5 try to minimize energy required by interleaving, which is the only energy component that can be changed with a different combination of storage and retrievals requests. As it has been already assessed [4], in fact, given a block of N storage locations to be served and N retrieval ones, one-way travels from/to the I/O station are fixed both in terms of time and energy, since all the selected locations must be served anyway. The variable component remains the travel between a storage position and the coupled retrieval one in a dual command cycle, that strictly depends on how retrievals are re-sequenced. The above heuristic has a $O(N^2 \log_2 N)$ complexity, as shown in Appendix.

2.3. Simulation

By simulation experiments we compare energy consumption and round trip times of dual command cycles with single command cycles under different re-sequencing policies, namely FCFS, time-based, and energy-based ones. We consider only one side rack and one crane per aisle, since results can be modularly extended to all the fronts of an AS/RS. A reorder point replenishment policy is adopted and the size of each dedicated zone corresponds to the Economic Order Quantity (EOQ) of a given items. According to Graves et al. [4] EOQ is calculated assuming an equal ratio of inventory to order costs, so that the introduction of disturbing factors such as the supply policy can be avoided. In this way, zone size and frequency of access to a given location are affected only by demand distribution, as required by the full turnover strategy. Since the storage location policy has been showed in literature to significantly affect picking performances, we apply both the time-based full turnover strategy and the energy-based one. In this way we analyze whether adopting a sustainable perspective even when establishing dedicated zones could lead to significant energy savings with respect to the traditional time-based allocation.

In order to apply Lee-Schaefer heuristic to identify time-based dual command cycles, we need to first select storage and retrieval locations, since this heuristic applies only to re-sequencing of retrievals when locations involved in the decision process have been already established. We introduce a rule similar to step 1 of our energy-based heuristic, that is sorting all open locations dedicated to a given item by their one-way travel time from the I/O station and selecting at each iteration the position with the lowest time to be reached. Similarly to step 2 of the energy heuristic, all occupied locations of a given item are sorted by their one-way travel time to the I/O station and the position with minimum required time is selected for retrieval.

Since the adopted storage policy is strictly related to the ABC demand distribution curve of items stored in the analyzed AS/RS, we consider the ABC shape as a main factor in our analysis and select two levels: a 20-50 curve, meaning that the 20% of items account for the 50% of picking operations, and a more skewed one such as the 20-80 curve.

Nominal speed and acceleration of the crane, angular speed and inertia of motors etc. and shifts to be performed in order to serve locations are related to the shape of the AS/RS rack. Since all these quantities represent an input of the energy model as described in par. 2.1 and in previous research [2], we select also the shape of the rack as a factor of analysis. In particular

we compare a horizontally laid AS/RS with 99 columns and 10 levels to a more vertically developed one, characterized by 45 columns and 22 levels for a total amount of 990 available locations in both cases. We used actual data provided by System Logistics SpA, an international manufacturer of AS/RSs, to properly select a crane for each rack.

We first compare single command performances to First-Come First-Served dual command ones by a 2^4 factorial design, including the storage policy, the movement strategy, the ABC distribution and the rack shape as main factors to be analyzed, each at the two levels previously described. The rationale is to assess if dual command cycles can contribute to energy efficiency so significantly as they were proven to do for time reduction. This is the reason why the most actually used policy for re-sequencing retrievals, the FCFS one, is initially adopted. As regards the movement strategy, we mean how storage and retrieval locations to be served are selected before the coupling process based on the FCFS policy is performed. Empty locations for storages as well as available location for retrievals basically depend on the position of dedicated zones established by the storage strategy, but among these the selection of the order by which they will be served depends if movements are optimized by the time-based perspective or by the energy-based perspective. By the former, the location with the minimum one-way time from/to the I/O station is selected among the available, by the latter, instead, the location with the minimum motion energy requirement for the one-way travel from/to the I/O station is identified.

Once established if and how much FCFS dual command cycles overcome single command ones, an analysis on further improvements achievable by dual command cycles when replacing FCFS re-sequencing policy with time-based and energy-based heuristics is performed. A 2^4 factorial design of experiments with 4 factors (storage policy, re-sequencing policy, demand curve, and rack shape) at two levels is selected again. Main factors and related levels are summarized in Table 1.

Table 1.Factors and levels of the 2^4 design of experiments

Factors	**Low Level**	**High Level**
Re-sequencing policy	Time-based heuristic	Energy-based heuristic
Storage strategy	Time-based full turnover	Energy-based full turnover
Demand distribution	20-50 ABC curve	20-80 ABC curve
Rack shape	99×10	45×22

Simulation of 450 storage operations plus 450 retrievals is therefore performed. It is supposed that storage and retrievals operations can be always coupled, meaning that requests for both operations are available when planning the AS/RS machine cycles. Heuristics for re-sequencing retrievals are applied to block of 15 storage operations and 15 picking operations at time, for a total amount of 30 blocks to be analyzed. The size of the block is selected as a reasonable trade-off between opposite patterns. On one hand, in fact, computational effort increases as the block size is increased. Furthermore, if a dynamic approach should be adopted, meaning that the list of retrieval requests is updated as much frequently as possible to be aligned with client requirements, then the size of the block should be kept small in order to reduce the frozen window in the planning process. On the other hand, the capacity of really optimizing cycles in the whole planning horizon increases as the block size increases, since more operations are involved in the optimization process.

3. Results

Results from simulation runs show how dual command cycles gain significant performance improvements in comparison to single command cycles.
The average round trip time decreases of 29.7% when moving from single command to First-Come First-Served dual command cycles, in line with well-known results reported in literature.

Energy consumption to move the crane towards the desired storage and retrieval locations is lowered by a 26.6% on average, when storage and retrieval operations are combined into dual command cycles. Thus, dual command cycles are showed to be an effective operative mean to foster energy efficiency in warehouse management other than improve the service level perceived by client, for which they have been traditionally conceived. Main effects of the identified factors on lowering energy requirements are positive, but of limited importance. It comes that deleting one-way idle travels to/from the I/O station and replacing them with interleaving from a storage location to the coupled retrieval one leads itself to a significant improvement, which can be weakly affected by other characteristics of the system.

When replacing FCFS policy with heuristics to combine storage and retrieval requests into dual command cycles, a little improvement on the desire performance can be further achieved. Simulations analysis highlights how a 32.4% of improvement on round trip times is gained on average, and a 30.11% of energy savings can be obtained on average. As concern factorial analysis, the major effect on round trip time reduction if compared to FCFS policy is played by the time-based heuristic, whose implementation gains a 2.4% improvement with respect to the energy-based one. Concerning factorial analysis on motion energy savings when applying heuristics, instead, the major effect is achieved by applying the energy-based full turnover storage policy rather than the traditional time-based one, with a 1.7% increase. This confirms how the storage policy affects results obtainable successively by a proper management of AS/RS machine operations.

It is worthwhile to notice how adopting a full energy-based management of the AS/RS, meaning that both storage and re-sequencing are based on the least motion energy, leads to an energy saving increase of 30.77% with respect to single command cycles, but a time decrease of 30.78%. When a full time-based management is selected, instead, we obtain a 33.2% improvement of round trip times in comparison to single command cycles, and 29.61% improvement of energy requirements. It comes that if the most critical performance for a company is energy consumption, then an energy-based approach leads to the maximum benefit in terms of energy consumption, but renouncing to a 2.4% of improvement in times and the associated service level perceived by customers.

4. Conclusions

Sustainable manufacturing claims for more energy efficient operations in warehouse management. While AS/RS operations have been traditionally optimized in order to minimize picking times directly linked to the service level perceived by customers, a sustainable approach leads to change this perspective by optimizing storage and retrieval cycles so that the least motion energy is required to perform them.

Adopting dual command cycles instead of the more common single ones leads not only to reduce picking time, as traditionally expected, but also to strongly increase energy saving. Comparing single command cycles to dual command ones obtained by coupling storage and retrieval requests by the easy-to-use and largely applied First-Come First-Served policy, a

26.6% of energy saving was found on average. Further improvement of about 3.5% on energy saving can be achieved by implementing heuristics to optimize dual command cycles. In this case, current results show how the major benefit can be gained by a full energy-based approach, thus adopting both an energy-based full turnover storage strategy and an energy-based re-sequencing heuristic.

Appendix

For implementing step 3 of the energy-based heuristic described in par. 2.2, one can compute the N^2 energy values related to all the N^2 possible couples (s, r) and then choose the minimum. However, if an ordering of this N^2 length list is made, the following steps can be implemented faster.

Therefore, let E the ordered list of N^2 tuples (s, r, En(s, r)), where En is the interleaving energy requirement associated to (s, r). It can be computed in time $O(N^2\log_2 N^2) = O(N^2\log_2 N)$.

For each $s \in S$ we build a list L(s) pointing to those elements concerning s and a list L(r) pointing to $r \in R$. Then step 4 can be executed in constant time (the first cell of the list stores the minimum). We use the lists L(s) and L(r) for accessing E and remove the cells of the kind (s,..,...) or (..,r,…). This can be done in time $O(N)$. The loop is repeated N times, therefore the overall complexity is $O(N^2\log_2 N + 2N^2) = O(N^2\log_2 N)$.

Acknowledgements

We are grateful to Manuel Clocchiatti, Elisa De Zan, Paola Frisiero, and Carlo Ongaro for data processing.

References

[1] Material Handling Industry of America, Automated Storage Systems Make a Play for Sustainability, AS/RS quarterly report, fall 2009, available at www.mhia.org/industrygroups/as-rs/news.

[2] A. Meneghetti, Sustainable storage assignments in AS/RSs, Proceedings of the International Conference on Advances in Production Management Systems (APMS) 2010, ISBN 9788864930077.

[3] K.J. Roodbergen, I.F.A. Vis, A survey of literature on automated storage and retrieval systems, European Journal of Operational Research 194, 2009, pp. 343-362.

[4] S.C. Graves, W.H. Hausman, L.B. Schwarz, Storage-retrieval interleaving in automatic warehousing systems, Management Science 23 (9), 1977, pp. 935-945.

[5] Y.A. Bozer, E.C. Schorn, G.P. Sharp, Geometric approaches to solve the Chebyshev traveling salesman problem, IIE Transactions 22(3), 1990, 238–254.

[6] M.H. Han, L.F. McGinnis, J.S. Shieh, J.A. White, On sequencing retrievals in an automated storage/retrieval system, IIE Transactions 19 (1), 1987, pp. 56-66.

[7] A. Eynan, M.J. Rosenblatt, An interleaving policy in automated storage/retrieval systems, International Journal of Production Research 31(1), 1993, 1-18.

[8] H.F. Lee, S.K. Schaefer, Retrieval sequencing for unit-load automated storage and retrieval systems with multiple openings, International Journal of Production Research 34 (10), 1996, 2943–2962.

[9] H.F. Lee, S.K. Schaefer, Sequencing methods for automated storage and retrieval systems with dedicated storage, Computers & Industrial Engineering 32 (2), 1997, 351–362.

Energy system optimization for a scrap based steel plant using mixed integer linear programming

Johan Riesbeck[1,*], Philip Lingebrant[2], Erik Sandberg[1], Chuan Wang[1]

[1] *Centre for Process Integration in Steelmaking, Swerea MEFOS, Luleå, Sweden*
[2] *Höganäs AB, Höganäs, Sweden*
** Corresponding author. Tel: +46 920200208, Fax: +46 920255832, E-mail: johan.riesbeck@swerea.se*

Abstract: In this work a mathematic model to simulate and optimize the energy system of a scrap based plant has been developed. Scrap based steelmaking is an energy intense production system. The potential for energy saving by system optimization is therefore high, even if the percentage of saved energy is relatively small. The model includes scrap pre-treatment, electrical arc furnace, ladle furnace and continuous casting units. To estimate the chemical compositions of the scrap charged into the EAF a statistical model based on an existing EAF plant has been used to provide the inputs to the model. Distribution factors have been used to describe the distribution of elements and oxides between the steel, slag and off gas/dust. To calculate the energy consumption in the electrical arc furnace a combination of an empirical and theoretical energy formula has been used. The model represents a general description of the most common process in electric steelmaking. It is suited to be adapted for specific plants with adjustments to the model parameters. The model gives reasonable results which follow the chemical composition of steel and slag and yield. The model can be a powerful tool to optimize the scrap mix and injectants towards energy and costs.

Keywords: *Energy systems, optimization, steelmaking, EAF, MILP, linear programming*

1. Introduction

Energy has been and will always be one of the most important production factors in the iron- and steel industry. In Sweden approximately one third of the total steel production is produced in electrical arc furnaces (EAF) and two thirds in basic oxygen furnaces (BOF) [1].

In the steel industry system, several processes are often connected together. A change in one process unit may result in unpredicted changes in other parts of the system. A literature study has been made of the best available technique and state-of the-art processes to decrease the specific energy consumption in the electrical arc furnace steel making.

The purpose of this work is to create a mathematic model to simulate and optimize the energy system of an EAF plant. In the past similar work has been made on the integrated blast furnace route energy system [2]. It is likely to presume that the scrap based steelmaking will increase in the future and more efforts will be spent to optimize the energy used in this area.

For the scrap based steel plant, it is often difficult to know the exact chemical compositions of the scrap charged into the EAF. In this work a scrap material statistical model based on an existing EAF plant has been used to provide the inputs to the model. The process steps in scrap based steelmaking are raw materials handling, pre-treatment EAF scrap melting, steel and slag tapping, ladle furnace treatments and casting.

1.1. Scraped based steel plant

With respect to the end-products, distinction has to be made between production of ordinary, so-called carbon steel as well as low alloyed steel and high alloyed steel/stainless steel. In the EU, about 88 % of steel production is carbon or low alloyed steel.

1.1.1. Energy consumption in electrical steelmaking

Electric arc furnace steelmaking uses heat supplied from electricity that arc from graphite electrodes to the metal bath to melt the solid iron feed materials. Although electricity provides most of the energy for EAF steelmaking, supplemental heating from oxy-fuel burners and oxygen injection is used. To produce EAF steel, scrap is melted and refined, using a strong electric current. Several process variations exist, using either AC or DC currents and fuels can be injected to reduce electricity use.

EAF steelmaking can use a wide range of scrap types, as well as pig iron, direct reduced iron (DRI/HBI) and hot metal. The EAF operates as a batch melting process, producing heats of molten steel with tap-to-tap times for modern furnaces of 30 minutes [3]. Current on-going EAF steelmaking research includes reducing electricity requirement per ton of steel, modifying equipment and practices to minimize consumption of the graphite electrodes, and improving the quality and range of steel produced from low quality and low cost scrap.

The best practice EAF plant is state-of-the-art facility with eccentric bottom tapping, ultra high power transformers, oxygen blowing, and carbon injection. The “best practice” is to use as much scrap as possible, as melting of DRI/HBI requires more energy. An efficient electric steelmaking plant with 100 % scrap as iron bearers has an electrical energy consumption of 409 kWh/t liquid steel for the EAF and 65 kWh/t liquid steel for gas cleaning and ladle refining, as well as 42 kWh/ton liquid steel of natural gas and 8 kg/t liquid steel of carbon [4].

There are various techniques to decrease the energy consumption for scrap based steelmaking. The Best Available Technique (BAT) to consider is to preheat the scrap and to replace the continuous casting, hot rolling, cold rolling and finishing with thin slab casting, also called near net shape strip casting [5]. The two most common methods to preheat steel are the CONSTEEL process and the post combustion shaft furnace (FUCHS). The electricity savings reported are 60 and 100 kWh/t liquid steel respectively [6]. An example of a thin slab casting technique is the Castrip® process. Potential energy savings are estimated to be 80 to 90% over conventional slab casting and hot rolling methods [7].

2. Methodology

The method used in this work is a model for industrial systems where the process is described as a network of nodes (sub-processes) which are connected by energy and material flows. The potential of this method is that it enables a simultaneous representation of the total industrial system, and that it makes it possible to optimize the whole system, in contrast to the optimization of each sub-process individually. The method is described by Nilsson [8], and later developed for complex material production systems by others [9]-[11].

The method is based on Mixed Integer Linear Programming (MILP). The model described in this paper contains no integers. There are four main nodes that symbolize the different processes in the system. These are a pre-treatment node, an electric arc furnace node, a ladle furnace node and a continuous casting node. There are nodes that provide the main processes with resources such as raw material, slag formers, alloys, energy sources and destination nodes for products and by-products.

2.1. Scrap pre-treatment

The scrap pre-treatment nodes main function is to summarize the different ingoing elements and oxides from each scrap grade and slag former, and transport them to the EAF node. There

is one flow for each element or oxide. There is also a possibility to restrict the amount of each scrap grade or slag former going into the EAF. As well as it is possible to set boundaries on each scrap grade it is also possible to set a fixed scrap recipe. Fig. 1 describes the ingoing and outgoing flows for the scrap pre-treatment node.

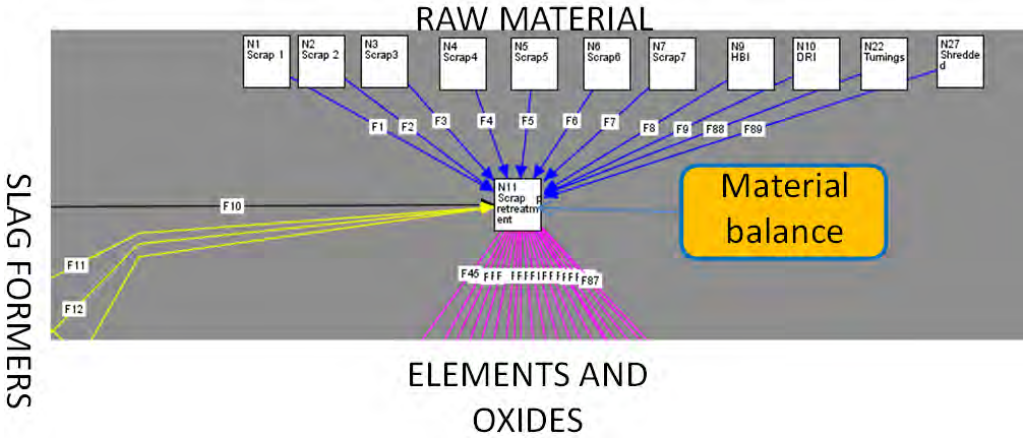

Fig. 1. Ingoing and outgoing flows for the scrap pre-treatment node

The chemical composition of scrap grades have a tendency to vary over a period of time as well as from heat to heat. For the raw material with well-known chemical composition the content are written according to that [12]-[14]. For scrap grades that have a more uncertain chemical composition the values have been estimated with multiple linear regression (OLS – Ordinary Least Squares) or "by hand".

Process data from approximately 1400 melts have been used in the OLS regression analysis. The data contained information about both scrap mix and steel analysis and an assumed distribution factor for each element/oxide to steel in the EAF for each element. From this information a material balance was made. The outgoing flows from the pre-treatment node represent the weight of each element and oxide and total weight of charged material.

2.2. Electric arc furnace

Ingoing raw material to the EAF node is the different amount of each element and oxide that is determined in the pre-treatment node. As ingoing material there are also three types of slag formers. Carbon and fuels in form of natural gas, LPG and oil are represented. The electrode consumption is also represented as an ingoing flow. The ingoing gases are nitrogen for stirring, oxygen from lance and air leakage from slag door and from off-gas duct opening after the 4th hole. There are three different flows for by-products; flue-gas, slag and dust. Fig. 2 describes the ingoing and outgoing flows for the electrical arc furnace.

All incoming elements and oxides from all sources are treated in a material balance. A very central part of this node is the distribution factor table between steel, slag and off-gas/dust. This table decides how much of each element that remains in the steel and how much that are transferred to the slag or off-gas. The distribution factor for an element/oxide applies for the sum of that element/oxide for all incoming flows. The distribution coefficients have been determined statistically by calculation of average weights and concentration of elements and oxides in steel, slag, dust and off-gas.

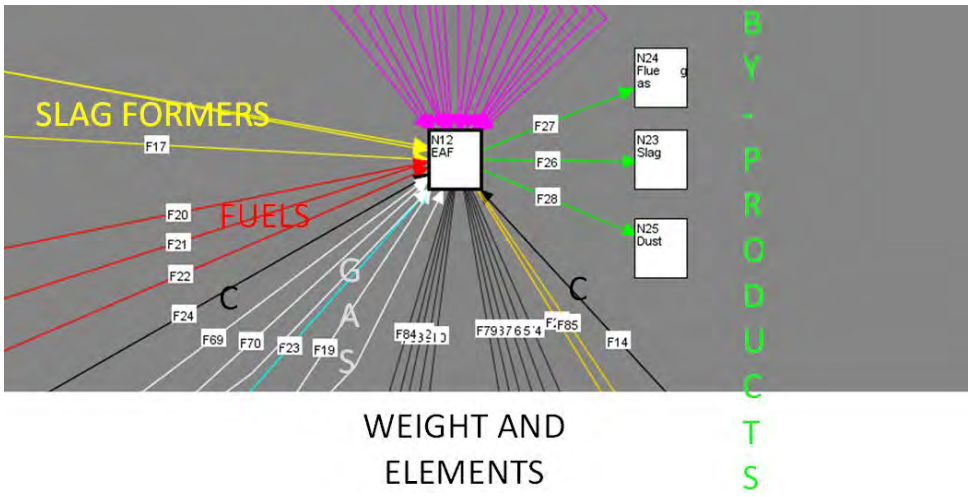

Fig. 2. Ingoing and outgoing flows for the EAF node

2.2.1. Energy calculation

For calculations regarding energy consumption for the electric arc furnace one empirical formula (Köhle-Formula) [3, 15] and a theoretical formula (Adams' formula) [16] has been used. Köhle's formula determines the electrical energy demand based on the use of other energy carriers, added materials, tapping temperature and tap-to-tap time. The Adams' formula determines the total energy consumption where quantities of non-electric energy are converted into kWh. The coefficients in the Adams formula have been used to assign "energy costs" for chemical fuel (kWh/kg or kWh/Nm^3) so that a "cost function" (kWh) for total energy consumption can be defined.

All the values that are needed for the formula are selected from the calculations or flows in the model. The values that are fixed constants are tapping temperature, power on time and power of time. Hot metal is not included in the model but there is a possibility to add it in the pre-treatment node along with the chemical analysis and also include it as a factor in the Köhle formula.

In the EAF-node there is an equation for pre-heating of scrap. The user can choose the preferred pre-heating end temperature of the charged scrap. If this function is activated this will also affect the electric consumption that is calculated. The energy added to the scrap is calculated with a fixed heating value (Cp) for the scrap mix. The Cp value has been estimated as the average value in the temperature range of 0 to 500 °C [17]. The reduced electric energy is calculated from the added energy value multiplied by the efficiency factor of the electric arc furnace.

2.2.2. Assumptions

It should be noted that factors for Oil and LPG are included in the Adams formula but not in the Köhle formula. Factors for Oil and LPG were therefore added to the Köhle formula as well. For calculation of these additional factors to the Köhle formula it was assumed that the heat transfer efficiency to the scrap/steel is the same for all kinds of chemical fuel (natural gas, oil and LPG). Then the factors for oil and LPG in the Köhle formula can be estimated as the factor for natural gas in the Köhle formula multiplied by the ratio of the factors for oil/LPG and natural gas in the Adams formula (11/10.5 for oil and 8/10.5 for LPG).

It is possible to set specifications for the steel chemistry. This is made by restricting the calculations to fit the minimum and/or maximum allowed concentrations of each element in

the steel. The slag weight must be greater than 7% of the steel weight and the amount of MgO in the slag must be greater than 8% of the slag weight. The slag basicity (CaO/SiO_2) is restricted to a constant that is determined by the user.

There are calculations regarding the off gas in two stages of the process, one calculation at the so called 4th hole and the other after the slip gap of the off gas duct. The calculations have been made in this way to show the post combustion energy potential of the off-gas before the air leakage in the slip gap. The calculations of the flue gas are depending on a number of assumptions. All C and H from the incoming flows leave the steel bath as CO and H_2 except the contribution from the burner fuel, which is completely combusted to CO_2 and H_2O. All Zn from ingoing flows that ends up in the dust leave the steel bath as Zn(g). These gases react with the air coming from the slag door and with the post combustion oxygen from the burners. At this point all the Zn(g) is oxidized to ZnO and the O_2 that is left reacts with CO and H_2 and generates CO_2 and H_2O. This reaction occurs according to a fixed distribution where a defined percentage of the remaining oxygen after Zn oxidation reacts with the CO and the rest with H_2. At the slip gap at the off gas duct it is assumed that there will be enough air flow for a complete combustion of the remaining CO and the H_2 in the off gas. The amount of excess oxygen in the flue gas after the slip gap is set to a constant.

2.3. Ladle furnace

The steel is going into the ladle furnace node with one flow for each element represented in the liquid steel. In this node there is a function where the user specifies the final steel weight. If a specified scrap weight and scrap mix is used there is a need to disable this function for the model to work properly. There is the opportunity to use the three slag formers that are used in the EAF node as well as a synthetic slag former. The model offers the user to add different kinds of alloys to the steel. The most common alloys that are available have been added but it is possible to add additional ones if that is needed. The chemical composition of the included alloys can also be changed. Fig. 3 describes the ingoing and outgoing flows for the ladle furnace.

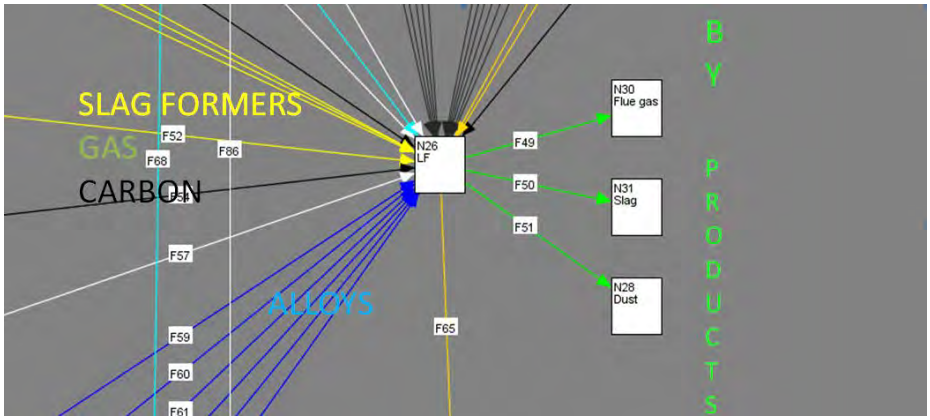

Fig. 3. Ingoing and outgoing flows for the LF node

The material balance in this node is as in the EAF node based on a distribution table between steel, slag and off gas/dust. The distribution coefficients have been estimated by empirical knowledge. The distribution coefficients refer to the materials that are added in the node. The contents of the ingoing steel are therefore not affected by any distribution factor. The exception from this is sulfur that has distribution coefficients also for the amount that is transferred with the steel into the ladle furnace node.

The ingoing temperature of the liquid steel to the ladle furnace is decided by the tapping temperature from the EAF which is reduced by a constant factor due to temperature loss during tapping of the EAF. The final temperature is decided by the demands of the following operation. It is also assumed that an average amount of slag is transferred along with the liquid steel from the EAF to the LF during tapping. There is a calculation of the electrode consumption that is based on a constant amount of electrode per kWh.

In the model it is assumed that argon is used for stirring the melt during the ladle furnace operation. The consumption is based on a fixed volume per ton of steel. This assumption is made from an average calculation from the process data. The amount of air that leaks into the system is also a constant per ton of steel.

2.3.1. Energy calculation

The electric energy consumption in the ladle furnace is based on the amount of steel and the increase in steel temperature needed to reach the final temperature. At first there is the difference between the ingoing temperature and the final temperature. But also the effect of the added material will contribute to a temperature drop. The temperature drop caused by each added material is based on an individual material constant. This constant determines how large the temperature drop, or in some cases a temperature raise, will be depending on the percentage of material added to the liquid steel. The temperature drop constants have been estimated by empirical knowledge.

2.3.2. Assumptions

It is possible to set specifications for the steel chemistry. This is made by restricting the calculations to fit the minimum and/or maximum allowed concentrations (wt. %) of each element in the steel. This is also possible in the EAF node so the user can choose if the specification is to be set at the LF or both. The slag weight is set to be greater than 2% of the steel weight and the slag basicity (CaO/SiO2) is restricted to a constant. The amount of elements and oxides in the off gas/dust that leaves the steel bath is calculated according to the same principles as the off gas in the EAF node. However, the reactions with infiltrated air are not considered.

2.4. Continuous casting

The continuous casting (CC) unit is treated in a simple way in the model. For the material flow, a material loss in percentage based on the total liquid steel amount from the LF unit is assumed when casting. A specific oxygen consumption (Nm^3 O_2/ton-slab) based on the final product (slab in this case) is assumed to calculate the total oxygen consumption. The oxygen is needed when cutting the slabs. For the electricity consumption in CC, it is based on assumed specific electricity consumption (MWh/ton slab).

3. Results

Simulations have been run in CPLEX with three different scrap mixes corresponding to average mixes for three different steel grades at Höganäs AB EAF plant in Halmstad. The model calculations in terms of chemical analysis of steel and slag and metallic yield have been compared with real data from Halmstad. The model calculates reasonable results which correspond well to real data.

An optimization test with the objective to minimize the total energy consumption (kWh) in the system (for a given quantity of a specific steel grade at Halmstad) was performed. During

the optimization scrap preheating function was turned off and the EAF tapping temperature was constant.

In the optimized solution, the use of shredded scrap is maximized because of the lower specific energy consumption for this scrap grade (-50 kWh/ton compared to "normal" scrap) in the Köhle formula [3]. The maximum amount of shredded scrap is limited by the quality restrictions (chemical analysis) of the steel grade. The use of HBI/DRI is minimized (zero consumption) because of their higher specific energy consumption (+80 kWh/ton compared to "normal" scrap) in the Köhle formula [5].

For all chemical fuels (oil, natural gas and LPG), the optimizer chooses zero consumption in the EAF This is because the energy content according to Adams [16] for natural gas (10.5 kWh/Nm^3) is higher than the reduction of electrical energy consumption it gives according to the Köhle formula (-8 kWh/ Nm^3) [3]. As the efficiency of oil and LPG in the EAF burners are assumed to be the same as for natural gas it follows that the energy content of all chemical fuels are higher than their reduction of electrical energy consumption in the EAF.

The optimizer chooses to add as much post combustion (PC) oxygen through the burners in the EAF as possible, because burner PC oxygen has zero energy content and will reduce the electrical energy consumption (-2.8 kWh/Nm^3) according to the Köhle formula. The limit of PC oxygen is set by the available amounts of post-combustible gases (H_2, CO and Zn) in the furnace, as the amount of these substances in the 4^{th} hole off-gas must be zero or higher. The amounts of post-combustible gases in turn are determined by the charge material mix and the amount of air leakage through the slag door.

The lance oxygen consumption is minimized in the optimized solution. This is because the energy development for oxygen injection (5.2 kWh/Nm^3) according to Adams [16] is higher than the reduction of electrical energy consumption that it gives according to the Köhle formula (-4.3 kWh/Nm^3) [3].

4. Concluding remarks

Scrap based steel plants around the world differs a lot in terms of scrap mixes and final products. The model described in this paper represents a general description which shall be adapted for specific cases. The model is built up to easy adjust to the processes of interest. To use the model correctly the incoming data needs to be correct and the model parameters (raw material analysis, slag basicity, air leakage, etc.) must be adjusted to represent the conditions of the specific plant. Then the model can be a powerful tool to optimize the scrap mix and injectants towards minimized energy consumption or production cost. In upcoming work the model will be used to optimize specific processes and plants.

The future work will also include further development of the scrap preheating function and move it to a separate node. A cost function for monetary units for all incoming flows will be added so that the total production cost can be optimized. Nodes for alternative solidification processes such as ingot casting and atomization will be considered and coefficients for specific energy consumption for different scrap grades in the EAF will be adjusted and added. Interaction with external systems like district heating can also be added.

Moreover different feeding and charging systems and a water cooling system for EAF are planned to be implemented and the processes after casting such as transport, heating and metalworking processes needs to added to complete the system.

Acknowledgement

We are grateful to the Centre for Process Integration in Steelmaking (PRISMA) and Höganäs AB for the possibility to present this work. PRISMA is an Institute Excellence Centre supported by the Swedish Agency for Innovation Systems, the Knowledge Foundation, and eight industrial partners within the iron- and steel industry.

References

[1] www.worldsteel.org

[2] M. Larsson, and Dahl, Reduction of the specific energy use in an integrated steel plant – The effect of an optimization model, ISIJ International 43(10), 2003, pp. 1664-1673.

[3] H. Pfeifer, M. Kirschen, J.P. Simoes, Thermodynamic analysis of EAF electrical energy demand, EEC 2005, May 9-11, 2005, Birmingham, England.

[4] E. Worrel, L. Price, M. Neelis, C Galitsky, Z Nan, World Best Practice Energy Intensity Values for Selected Industrial Sector. u.o.: Ernest Orlando Lawrence Berkely National Laboratory, February, 2008.

[5] Draft Reference Document on Best Available Techniques for the Production of Iron and steel, Institute for Prospective Technological Studies, European IPPC Bureau, July, 2009.

[6] The State-Of-The-Art Clean Technologies (SOACT) for Steelmaking Handbook, Asia Pacific Partnership for Clean Development and Climate, December, 2007

[7] www.castrip.com

[8] K. Nilsson, and M. Söderström, Optimizing the Operating Strategy of A Pulp and Paper Mill using the MIND Method, Energy – The International Journal 17(10), 1992, pp. 945-953.

[9] M. Karlsson, and M. Söderström, Sensitivity analysis of investments in the pulp and paper industry - on investments in the chemical recovery cycle at a board mill, International Journal of Energy Research 26(14), 2002, pp. 1253-1267.

[10] C. Ryman, and M. Larsson, Reduction of CO2 emissions from integrated steel-making by optimized scrap strategies: Application of process integration models on the BF-BOF system, ISIJ International, 46(12), 2006, pp. 1752-1758.

[11] M. Karlsson, The MIND method: A decision support for optimization of industrial energy systems - Principles and case studies, Applied Energy 88(3), 2011, pp. 577-589.

[12] www.rawmatmix.se

[13] www.ecn.nl/Phyllis

[14] Purchase specifications, Höganäs AB, Halmstad, Sweden

[15] S. Köhle, Einflussgrößen des elektrischen Energieverbrauchs und des Elektroverbrauchs von Lichtbogenöfen, Stahl und Eisen, 112(11), 1992, pp. 59-67.

[16] W. Adams, S. Alameddine, B, Bowman, N. Lugo, S. Paege, Stafford P., Total energy consumption in arc furnaces, MPT International 6, 2002, pp. 44-50.

[17] HSC Chemistry 6.1 (software), Outotech Research Oy, Antti Roine.

Environmental system effects when including scrap preheating and surface cleaning in steel making routes

Marianne Östman[1,*], Katarina Lundkvist[1], Mikael Larsson[1]

[1] *Swerea MEFOS, Luleå, Sweden*
** Corresponding author. Tel: +46 920201900, Fax: +46 920255832, E-mail: marianne.ostman@swerea.se*

Abstract: The main part of the steel manufactures producing alloyed steel use scrap as an essential raw material. To increase the corrosion resistance of steel a coating is often applied. The share of steel being coated and galvanized is today globally increasing, which is resulting that the amount of scrap with different types of coatings are increasing. This result in that more of the scrap used in steel making is contaminated with for example Zinc and organics. Scrap preheating is a known method for reduction of energy use in steelmaking. However due to environmental restrictions a widespread implementation of scrap preheating have not been achieved in the steel industry. Combined surface cleaning and scrap preheating is a way to handle the problem that coatings give rise to in the melting cycle and is a new concept suggested and developed at Swerea MEFOS. The pre-treated scrap (cleaned and preheated) is charged hot into the oxygen converters with direct savings of energy, as the demand of hot metal from the blast furnace decreases. The method opens for the possibility to widen the scrap base and to melt complicated scrap. Since the preheating process is a standalone solution, a large number of unwanted chemical components are removed prior melting resulting in that the dust generated from the melting process is easier to recover. In this paper the system effect of introducing a preheating and surface cleaning process for scrap in a Blast Furnace (BF) and oxygen converter (BOF) steelmaking route is analyzed according to energy and CO_2 emissions. The system analysis shows that surface cleaning of scrap makes it possible to use shredded scrap and ASR (automotive shredder residue) or other combustible waste to replace fossil fuels. The results from the analysis demonstrates that implementing surface cleaning leads to increased possibilities for recycling of otherwise non-recyclable material. The system model shows the interaction between different processes, which gives an overview picture including the whole steel making route. The model is used to investigate changes in process conditions from making use of shredded scrap and ASR as input material in the steel making process. The implementation of surface cleaning and preheating lead to both increased possibilities for recycling of scrap, and more efficient energy use in the steelmaking routes.

Keywords: *BOF, Scrap preheating, Surface cleaning, optimization, ASR*

1. Introduction

Currently, the blast furnace (BF), basic oxygen furnace (BOF) route is the dominating processes for iron ore steel making. The steel is produced from the hot metal produced in the BF by treatment in a BOF converter. In the converter process a surplus heat is generated during the oxygen blowing which is utilized for scrap melting. 15-20 % of the iron raw material input to the BOF is originated from scrap. Liquid steel (LS) from the converter is sent to an after-treatment station where the final adjustment of the steel analysis and temperature is performed before the casting procedure. Energy and material efficiency in a process system is closely linked together. A higher recycling rate and a minimization of landfill is energy efficient, since it decreases the demand of virgin materials.

The main part of the steel manufactures producing alloyed steel use scrap as an essential raw material. To increase the corrosion resistance of steel a coating is often applied. The share of steel being coated and galvanized is today globally increasing, which is resulting that the amount of scrap with different types of coatings are increasing. This result in that more of the scrap used in steel making is contaminated with for example Zinc and organics. In this paper the system effect of introducing a preheating and surface cleaning process for scrap in a Blast Furnace and oxygen converter (BOF) steelmaking route is analyzed according to energy and CO_2 emissions.

Scrap preheating is a known method for reduction of energy consumption for melting. However due to hazardous components generated in the exhaust, a widespread implementation of scrap preheating have been interfered due to the costly treatment required. A standalone combined surface cleaning and scrap preheating is a way to handle the problem that coatings on the scrap give rise to. This is a new concept suggested and developed at Swerea MEFOS [1]. The pre-treated scrap (cleaned and preheated) is charged hot into the oxygen converters with direct savings of energy, as the demand of hot metal from the blast furnace decreases. The method opens for the possibility to widen the scrap base and to melt complicated scrap. Since the preheating process also applies surface cleaning a large number of unwanted chemical components are removed prior melting resulting in that the dust generated from the melting process is easier to recover. [1-2]

1.1. Objective of the study

This study analyzes the system effect of introducing surface cleaning of scrap in a BF-BOF steel making route. An optimization model highlights the possibilities regarding cost and CO_2 emission. The model is used to do analysis on operation practice, scrap usage and cost. The intention of the study is to investigate the changes in the process system, when using shredded scrap in the scrap mix.

2. Methodology

The method used in this work is based on the MIND method [3]. The study is made in an optimization model of an integrated steel mill, where the process is described as a network of nodes (sub-processes) which are connected by energy and material flows. The potential of this method is that is enables a simultaneous representation of the total industrial system, and that is makes it possible to optimize the whole system, in contrast to the optimization of each sub-process individually. The optimization model of one integrated steel plant has been further developed with the requirements for scrap preheating [4-5]. The model used in this work is based on an existing energy optimization model designed for the iron and steel industry [6-8].

2.1. The optimization model

2.1.1. Objective function

This study uses two objective functions which are defined in the model as raw material and energy costs and CO_2 emission. Generally the objective function is imbedded within the optimization model but can in mathematical terms be written as follows.

$$\min z = \sum_{i=1}^{n} c_i x_i \qquad (1)$$

where z is the objective function for the minimization problem. It could be CO_2 emission and cost, depending on what objective is set for the optimization. x is studied variables and c is coefficients set for the corresponding objective function and depends on which objective function. The coefficients set for the corresponding objective functions are shown in Table 1.

Table 1. Coefficients used for different objective functions.

	Unit	Cost (SEK)	CO_2 emission (ton)
Iron ore pellet	ton	675	0.051
Lime stone (wet)	ton	128	0.856
Mn ore	ton	488	-
Quartz	ton	180	-
Lime stone	ton	124	0.856
Dolomite Lime	ton	600	0.466
Raw Dolomite Lime	ton	263	0.931
FeSi	ton/ton RS	4875	-
CaC_2	ton	3225	-
Coal and coke	ton	293-331	2.492-3.064
External coke	ton	1950	3.744
Pulverized coal injection	ton	205-525	2.488-2.916
External scrap	ton	2300	-
Shredded scrap	ton	2000	-
BOF sludge	ton	-	-
Oil	MWh	5550	3.126
External energy	MWh	-	0.6
Excess coke	ton	-1950	-3.744
Benzene	ton	-1600	-3.287
Sulphur	ton	-40	-
Tar	ton	-1300	-3.349

In Table 1, the costs analysis is limited to raw material and energy and thereby not including the cost for energy and landfill of material. Furthermore credits are made in the model for by-products. Market values for the different raw materials and energy sources fluctuate whereby the costs for raw materials and energy used in the model is mean values calculated over a conjuncture cycle. Values of costs are estimations based on figures from The London Bullion Market Association.

2.1.2. Boundary conditions and limitations

To make sure to get reasonable results, some necessary boundary are introduced. The boundary conditions, which can describe variations in the system, maximum and minimum for various variables can be expressed as follows.

$$x_i \le b_i, \quad i = 1,...,n \tag{2}$$

where the x_i variable could be the corresponding flow variables, and the boundaries b_i, are the corresponding restrictions. As a boundary condition the production of prime slabs is fixed in the model. The BOF charges has limitations, such as hot metal, pig iron, slag binders and scrap are set to the production parameters of liquid steel, to ensure the right quality for the final products.

2.2. Model description

In the iron and steel industry optimization models considering effects on the entire production process chain have been used for investigations of performance of different aspects like energy consumption, CO_2 emission, costs and environmental issues [4-8]. The system boundary of the whole system is to casted steel slab, the boundary of this study is to RS (Raw

Steel) from the BOF converter. The process units included are coking plant, blast furnace (BF), basic oxygen furnace (BOF), and continuous casting (CC), oxygen plant, and lime furnace, etc. [9]

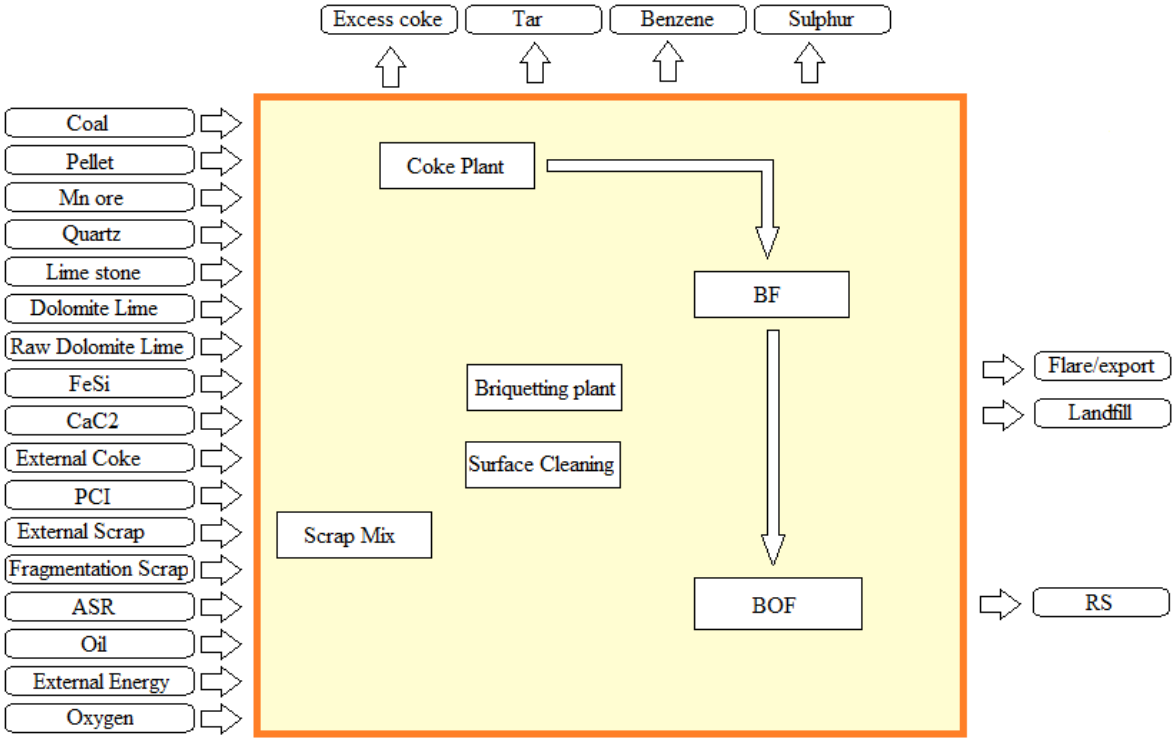

Fig. 1. Schematic outline of the modeled system.

The blast furnace is a very complex process and thus difficult to model. In this study different operational conditions for the blast furnace, which are feasible are defined. The model chooses and combines between these to overcome this problem. The prepared model is consisting of modules of process steps connected by mass and energy balances.

2.2.1. Operating conditions and modeling cases

The BF module is simulating the hot metal production in a Swedish BF with potential changes in briquette recipe and charged amounts. The BOF production process is described in the model by the mass and energy balance of the process. Different options can be optimized regarding the raw materials used due to the chemical composition. The coarse fraction of the generated BOF sludge is recycled through briquettes charged into the BF. The fine fraction of sludge from the BOF is normally land filled however it may be recycled in briquettes provided the zinc content is reduced sufficiently [10]. Including the scrap preheating unit in the system contributes to the scrap usage efficiency by the charging of preheated scrap. The introduction of the scrap surface cleaning unit in the model makes the use of shredded scrap as a scrap source to the BOF viable as it reduces the Zinc content in the scrap input to the BOF to zero. Scrap cleaning and preheating is performed on all the scrap charged to the BOF when the pre-treatment operation is implemented. Since the exhaust problem with the pre-treatment of scrap roughly identical with the combustion of many types of polluted fuels, Therefore the preheating process needs an advanced gas cleaning facility which gives that fossil fuel could be replaced with organic rest material. In this study ASR (automotive shredder residue) has been chosen as fuel in the preheating process since it has a good heating value and can be delivered in enough quantity to be interested for industrial use. Zinc sources

to the BOF sludge and dust in the model is the external scrap and the shredded scrap. Sources of Zinc to the BF come from the iron ore pellets and briquettes. The possible integration and effect of the preheating and surface cleaning operation is analyzed in five cases compared against a reference case, Table 2. The input of scrap to the BOF is limited to 17 % in the reference case, case 1 and 2, since it is a reasonable amount. To ensure that the use of internal scarp is preferred, the external scrap use is limited to maximum 5 % of the scrap charge into the BOF. The optimization cases have a higher degree of freedom on the BF operation and on the raw material input in the BOF.

Table 2. Case study.

Case	Comments
Reference Case	BF operation with briquettes
Case 1	BF operation with briquettes, scrap pretreatment implemented, otherwise as the Reference Case
Case 2	BF operation without by-product briquettes, otherwise as the Ref. Case
Case 3	Optimization of cost, Scrap preheating/surface cleaning available
Case 4	Optimization of CO_2, Scrap preheating/surface cleaning available

3. Results

3.1. System optimization

Data from the system modeling of production and differences in the analyzed cases is illustrated in Table 3. Regarding the coke making there are only minor differences between the reference production and the five different cases. The production rate of coke is the same in all five cases. Small change in coal mix volatile matter and ash result in small increase in COG production compared to the reference case. To increase recycling inside the steel plant by-product briquettes are used. Data from the system model of BF operation show that the HM (Hot Metal) production is higher in the reference case and in case 2 which is using no briquettes. Increased use of briquettes is positively affects the cost- and CO2 emission optimized cases by the lower lime stone and pellet consumption in the BF.

3.1.1. Iron ore pellet consumption

The use of iron ore pellets in the analyzed cases vary. Iron ore pellets has a CO_2 emission burden of 0.051 ton, as a comparison to scrap which has zero, se Table 1, since scrap is a recycled material origin from iron ore. In case 2 where no briquettes are produced the major amount of pellets is being utilized due to less recycling of iron bearing by-products. In the case 4, where CO_2 emission is the optimization target, the lowest amounts of pellets are used.

3.1.2. Scrap consumption

Producing steel from scrap is better from an environmental point of view since the energy demand for producing steel from iron ore is more than twice the energy required in scrap based production. Scrap usage for the cases is illustrated in Fig. 2. Shredded scrap may only be utilized in the cases when surface cleaning is implemented. The Reference case, case 1 and 2 has a limitation on the scrap usage to a maximum load of 17 %, where maximum of external scrap is 5 % in the BOF. The largest amount of scrap utilized is in case 4, which is the CO_2 emission optimization case. Since energy use and CO_2 emissions from integrated steelmaking is closely related, increased scrap utilization results in less CO_2 emissions.

Table 3. Optimization results coke making, Blast furnace and BOF route.

	Ref.	Case 1	Case 2	Case 3	Case 4
Coke plant					
Coke production (t)	84.5	84.5	84.5	84.5	84.5
COG production (GJ/t coke)	8.4	8.4	8.4	8.4	8.4
Coke yield, dry (t coke/t coal)	1.287	1.287	1.287	1.287	1.288
Excess coke (t)	0.00	0.00	0.00	0.00	0.00
Ash (%, dry basis)	9.12	9.12	9.12	9.12	9.14
Volatile matter (%, dry basis)	25.60	25.60	25.60	25.60	25.66
BF					
HM production (t/h)	250.1	244.4	250.1	246.6	246.4
BF slag production (t/t HM)	0.162	0.162	0.156	0.164	0.164
Pellet (kg/t HM)	1356	1356	1394	1339	1340
Coke (kg/t HM)	320	320	330	317	317
PCI (kg/t HM)	141	141	141	141	141
Lime stone (kg/t HM)	30	30	46	20	20
By product briquettes (kg/t HM)	59	59	0	84	82
BOF slag (kg/t HM)	46	46	46	46	46
Other (kg/t HM)	4	4	5	4	4
Blast (kNm^3/t HM)	0.98	0.98	0.98	0.98	0.98
BFG (GJ/Nm3 blast)	1.13	1.13	1.13	1.15	1.15
COG (GJ/Nm3 blast)	0.71	0.71	0.71	0.72	0.72
BOF					
RS (t/h)	257.5	257.5	257.5	257.5	257.5
BOF slag (t/h)	0.08	0.08	0.08	0.08	0.08
HM (kg/t RS)	879	859	879	867	866
Pellets (kg/t RS)	0	8	0	11	10
Scrap mix (kg/t RS)	175	188	175	179	225
Lime (kg/t RS)	27	26	27	26	25
Dolomite lime (kg/t RS)	23	23	23	23	22
Raw dolomite lime (kg/t RS)	4	4	4	4	4
O_2 blowing (Nm^3/t RS)	50.0	47.7	50.0	47.7	47.6
Scrap preheating on/off (1/0)	0	1	0	1	1
O_2 (Nm^3/t scrap)	37	37	37	37	37
ASR (kg /t scrap)	32	32	32	32	32

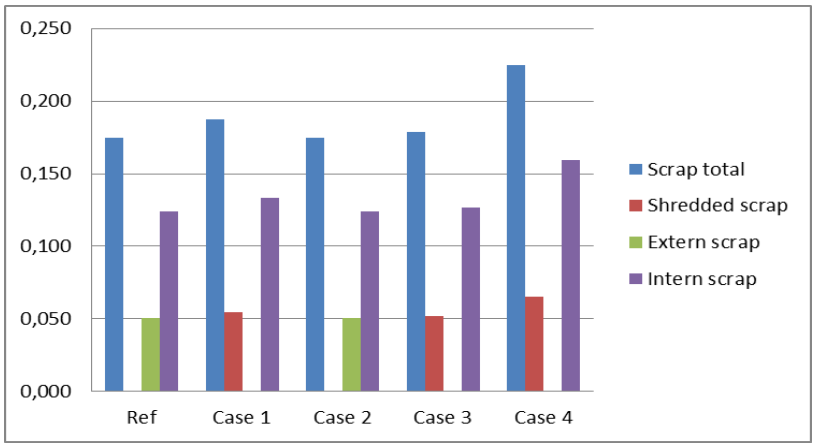

Fig. 2. Scrap consumption in the different cases, unit t/t RS.

4. Discussion and Conclusions

4.1. Results from the objective function analysis

Table 4. Results from the objective functions.

Case	Cost (SEK/t slabs)	CO_2 (t/t slabs)
Reference Case	1409	1.936
Case 1	1365	1.892
Case 2	1461	1.994
Case 3	1357	1.887
Case 4	1359	1.884

Comparison of the different cases with the reference regarding the cost objective is illustrated in Table 4. The results show that the cost optimization case followed by the case 1, where surface cleaning is utilized for the reference case, is generating the lowest production costs. The highest costs are shown to be generated in case 2, where no briquettes are produced. This shows that the use of briquettes and surface cleaning of scrap improves the cost analysis. In Cases 3 and 4, the cost decreases approximately 4 %, compared to the reference case. However the model only considers raw material cost related directly to the process and does not consider investment cost, salary, administration and other external costs. Furthermore no credits are made in the model for decreased landfill costs. Analysis of the results from using CO_2 emission as the object function demonstrates only minor differences between the cases, as seen in Table 4. The case with the highest CO_2 emission is Case 2 where no by-product briquettes are used; consequently an increased pellet and coke consumption generate higher CO_2 emissions.

4.2. Conclusions

The system model shows the interaction between different processes, which gives an overview picture of the whole steel making route. The model is used to investigate changes in process conditions from making use of shredded scrap and ASR as input material in the steel making process. The system analysis shows that surface cleaning of scrap makes it possible to use shredded scrap and ASR or other combustible waste to replace fossil fuels as a cost and environmental efficiency choice. The implementation of surface cleaning and preheating leads to both increased possibilities for recycling materials, which otherwise is difficult to recycle and a more efficient use of energy in the steelmaking routes. Increased recycling of materials is efficient ways to reduce the energy demand, since it often replace virgin materials. The optimization of the model shows that both cost and CO_2 can be decreased when scrap pretreatment is implemented, however none of the analyzed cases is simultaneous minimizing cost and CO_2 emission.

Acknowledgement

This work is part of the ongoing projects in the Centre for Process Integration in Steelmaking (PRISMA) for the possibility to present this work. PRISMA is an Institute Excellence Centre supported by the Swedish Agency for Innovation Systems, the Knowledge Foundation, and eight industrial partners within the iron- and steel industry. This study has also received funding form the SSF ProInstitute programme.

References

[1] M. Larsson, S. Ångström, A novel process for simultaneous scrap preheating and surface rinsing, SCANMET III, 3rd International Conference on Process Development in Iron and Steelmaking, June 8-11, 2008, Luleå, Sweden.

[2] J. K. S. Tee, D.J. Fray, Recycling of galvanized steel scrap using chlorination, Iron and Steelmaking, 2005, Vol. 32, No 6, pp. 509 – 514.

[3] K. Nilsson, M. Söderström, Optimizing the Operating Strategy of A Pulp and Paper Mill using the MIND Method, Energy – The International Journal, 1992, Vol. 17, No. 10, pp. 945-953

[4] M. Larsson, J. Dahl, Reduction of the specific energy use in an integrated steel plant- The effect of and optimisation model, ISIJ International, 2003, Vol. 43, No. 10, pp. 1664-1673

[5] C. Ryman, M. Larsson, Reduction of CO2-emissions from integrated steel-making by optimized scrap strategies: Application of process integration models on the BF-BOF system, ISIJ International, 2006, Vol. 46, No. 12, pp. 1752-1758

[6] C. Ryman, M. Larsson, Adaption of process integration models for minimization of energy use, CO2-emissions and raw material cost for integrated steelmaking, Chemical Engineering Transactions, 2007, Vol. 12, pp. 495 – 500.

[7] C. Ryman, C. Wang, M. Larsson, J. Dahl, C-E. Grip, Minimization of energy consumption and conversion cost for BF-BOF system based on optimized use of ferrous burden materials, 5th European Oxygen Steelmaking Conference, June 26-28, 2006, Aachen, Germany.

[8] C. Wang, M. Larsson, C. Ryman, C-E Grip, J-O. Wikström, A. Johnsson, J. Engdahl, A model on CO2 emission reduction integrated steelmaking by optimization methods, International journal of energy research, 2008, 32, pp. 1092-1106

[9] U.S. Department of Energy, Energy Efficiency and Renewable energy, Steel Industry Technology Roadmap. http://www1.eere.energy.gov/industry/steel/roadmap.html (accessed during Jan. 2010).

[10] F. Su, S. Rutqvist, K. Andersson, Recycling of iron-bearing sludge and technological development at SSAB Tunnplat, CSM 2007 Annual Meeting Proceedings, November 15-17, 2007, Chengdu City, China.

Potential of fossil and renewable CHP technology to reduce CO_2 emissions in the German industry sector

Marian Klobasa[1,*], Felipe Toro[2], Farikha Idrissova[2], Felix Reitze[2]

[1] *Fraunhofer Institute for Systems and Innovation Research, Karlsruhe, Germany*
[2] *Institute for Resource Efficiency and Energy Strategies, Karlsruhe, Germany*
** Corresponding author. Tel: +49 7216809-287, Fax: +49 6809-272, E-mail: m.klobasa@fraunhofer.de*

Abstract: Based on statistics about fuel demand in industry sectors a method is developed for the estimation of additional combined heat and power (CHP) potential in the main industry sectors. Electricity generation costs of several CHP technologies are then compared to the purchase of electricity on electricity markets. It is found that additional heat potential for CHP is limited in the chemical industry; additional potential is found in the paper industry, food industry and in the manufacturing industry. Additional electricity potential for CHP can be found in all sectors as electricity to heat share is 0.34 at the moment and can be increased with new installations to more than 0.7. The share of renewable fuels used in CHP is highest in the wood and paper industry, additional potential can be found in several branches, but costs are high at the moment.
Markets can pick up CHP electricity in the short term and installations are profitable when long operating hours can be reached. Looking in electricity markets with a higher share of renewable energy sources (RES), operation become more restricted making new operation strategies necessary. Times with electricity prices below short term generation costs of CHP installations increase in the future, so that operation will be less profitable.
In short term CHP can bring additional CO_2 reduction, specific emissions are below new combined cycle units. In the medium to long term additional use of RES fuels and adapted operation strategies will be necessary to lead to further CO_2 reductions.

Keywords: *Combined Heat and Power, Renewable energy, Electricity market, Industrial applications*

1. Introduction

Reduction of CO_2-emissions in all energy consuming sectors will be necessary to fulfill short and long term goals to stabilize climate change. The usage of combined heat and power technologies (CHP) is promising to provide cheap CO_2 reductions especially in the industry sector, but is questioned to be the right technology option regarding long term goals [1]. The EU commission tries to promote CHP technologies with the CHP directive 2004/08/EC [2]. Various support schemes has been implemented throughout Europe [3] and the member states have to report progress to the EU commission. So far progress in the German industry sector has been limited although potential is expected to be large [4]. The purpose of the work is to identify reduction potential in the German industry sector based on fossil but also on renewable fuels. Furthermore the work analysed the possibilities of selling CHP electricity on future power markets with increasing renewable electricity generation.

2. Methodology

2.1. Approach

Statistics of final energy demand in Germany's industrial sector and estimates of the electricity demand in the future were used as a basis for the identification of the industrial heat demand and industrial CHP potentials [5], [6]. The final energy consumption less electricity demand was applied as an indicator for the heat demand. Sector specific energy intensity and indicators of sectoral economic development served as important influencing factors for the estimation of the future heat demand of the German industry. With the help of estimated heat demand the technical potential which could be covered by CHP was then projected (Fig. 1). In this projection the evaluated distribution of heat demand according to

the temperature levels for different industry sectors and technical assumptions of conversion efficiency and CHP heat coverage were also integrated.

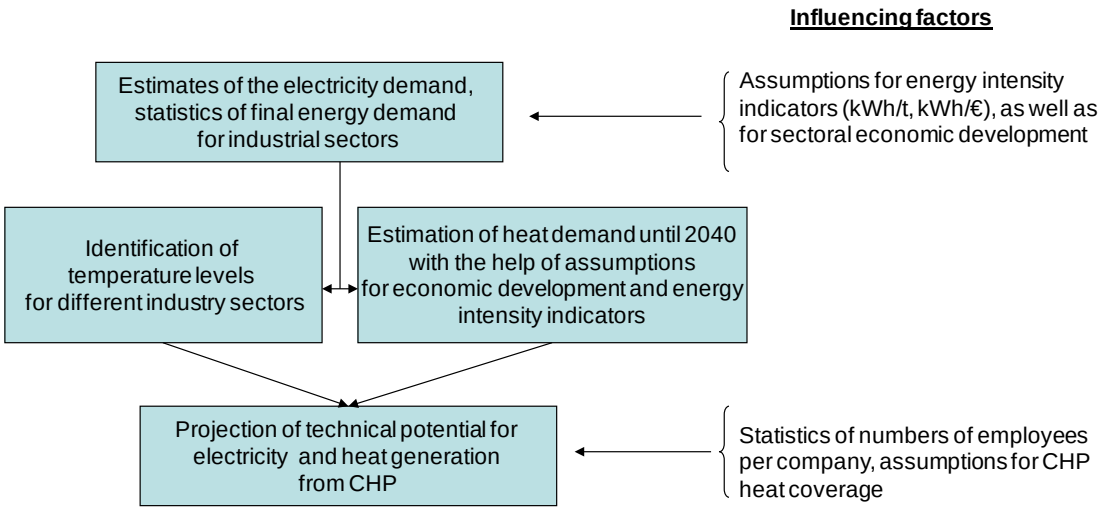

Fig. 1. Methodical approach for estimation of the heat demand in German industry and technical CHP potential.

The evaluation of heat demand according to the temperature distribution for different industry sectors was performed on the basis of previous estimations by Wagner et al. [7] as shown in Fig. 2. As one can see this temperature distribution provides indication for temperature levels of heat demand applicable for possible CHP generation. In this case the process heat at temperature levels lower than 500 °C and heat use for space heating and process water were of high relevance for the identification of the technical CHP potential.

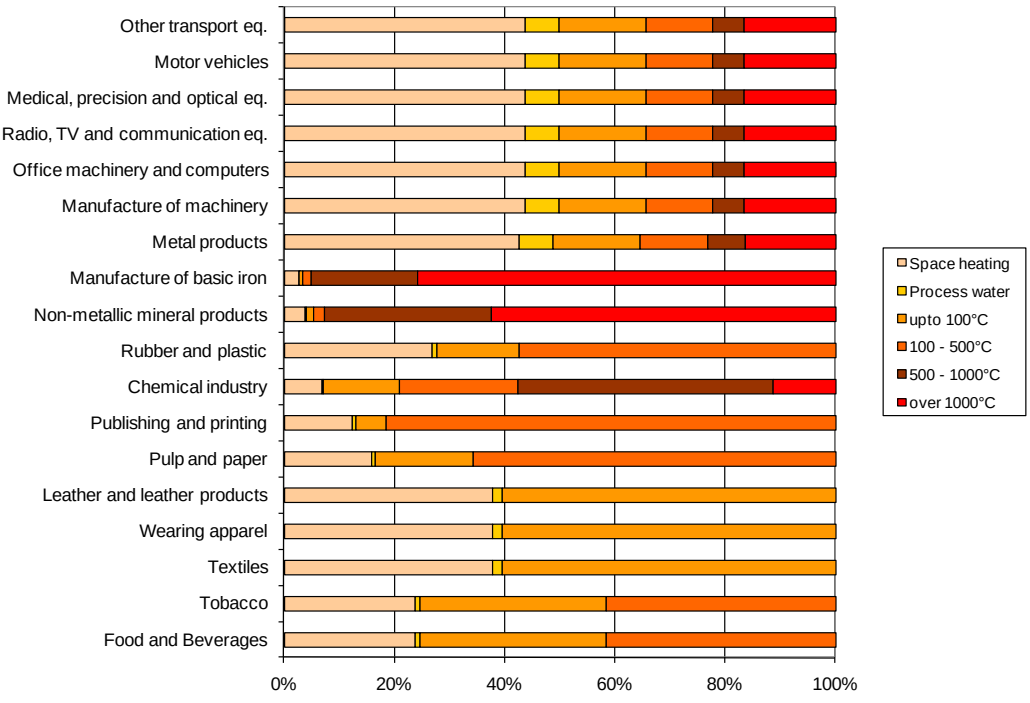

Fig. 2. Distribution of heat demand according to temperature levels and industry sectors in Germany in 2001.

Besides the technical potential also the economic (cost-effective) potential for CHP in the German industry is estimated. The parameters for the technical and economic potentials are defined as follows:

- Technical potential

The technical potential is derived from the useful heat demand applicable for CHP installations (< 500 °C). The conversion from fuel input (final energy) to useful energy is performed with the constant conversion efficiency factor of 90% which corresponds to the boiler efficiency of the separate heat generation. The CHP installation is assumed to apply for 75% of the heat demand. The rest of heat demand will always be generated via a peak load boiler.

- Economic (cost-effective) potential

Economic (cost-effective) potential is defined as a potential that can be supplied more economically attractive via CHP installation than with a separate electricity and heat generation. The base load price on the European Energy Exchange (EEX) served as a reference for electricity generation. The heat generation is considered via a heat bonus. These reference costs were calculated as saved fuel costs in case of separate heat generation. The life cycle of installations was assessed depending on installation type and was defined as 12 years for small installations and up to 20 years for large installations. The interest rate for calculations was set at 10%. Also the financial remuneration of CHP and grid access fees were taken into consideration. In Germany operators of CHP plants get a CHP premium on the electricity production guaranteed by law. The premium is paid to promote new installations of CHP power plants. It is typically between 1.5 and 2 €/MWh and is paid additionally to the revenues for the electricity production. The premium is paid for 4 to 6 years after the installation of the power plant. A comparison of costs and revenues is presented in Table 1.

Table 1. Costs and Revenues for identification of cost-effective CHP potential in the industry.

Costs	Revenues
Investment (life cycle of 12 – 20 years, 10 % real interest rate)	For electricity
Fixed operating costs	For heat
Variable operating costs	CHP premium
Fuel expenses	Avoided grid access fees
CO_2-allowances	

The impacts on the electricity markets are calculated using today's spot market prices from the EEX. Spot market prices for a future scenario with higher RES shares of 40 % have been calculated using the agent based electricity market model PowerACE [8].

2.2. Technical and economic specifications

The spectrum of industrial CHP technologies varies from CHP installations with 1 MW of electric power output to large power plants with several hundred MW of electric power output. In this research the complete spectrum of various CHP technologies available for combined heat and power generation was analysed. For that purpose so called reference installations were defined and their various technical and economic parameters were

described. In Table 2 one can see a clear cost decrease with growing power output of an installation.

Table 2: Parameters of CHP installations for output range from 2 to 220 MW (el).)

Parameters	**Unit**	**CC-GT**	**CC-GT**	**OC-GT**	**CC-GT**	**OC-GT**	**Gas Engine**
Power output [MW]	MW (el)	**220**	**100**	**90**	**20**	**10**	**2**
el. efficiency	%	47.6	47.1	33.0	44.4	31.0	39.0
heat efficiency	%	40.3	41.0	52.4	42.3	49.0	47.6
Efficiency total	%	87.9	88.1	85.4	86.7	80.0	86.5
Investment	€/kW (el)	742	756	722	820	700	800
fixed operating costs	€/kW/a % of Investment	37.1 7 %	37.8 7 %	33.3 6 %	57.4 7 %	42.0 6 %	16.0 2 %
other variable operating costs	€/ MWh_{el}	0.5	0.5	0.5	0.5	0.5	8

Source: own assumptions based on information from project developers, CC-GT: combined cycle gas turbine, OC-GT: open cycle gas turbine

3. Results

3.1. Additional technical CHP potential

Today the major industry sectors using CHP power plants are the chemical industry, the paper industry and the food industry in Germany (see Fig. 3). They provide around 74 % or more than 19 TWh of the CHP electricity production in the industry sector in 2009 [6]. Additional electricity generation is possible without an increase of the heat generation as the average electricity to heat factor of the CHP installations is only ca. 0.34. The modernization of old CHP devices can increase the electricity to heat ratio above 0.7 and double the electricity generation.

Next to modernization of old CHP generation units, there is also the possibility to find new heat sinks that can be supplied by CHP units. It is found that additional heat potential for CHP heat generation is limited in the chemical industry, some additional potential is found in the paper and food industry (see Fig. 4). Further additional heat potential is found in the manufacturing industry. Final energy demand in the industry sector has been 700 TWh in 2008 with around 214 TWh of low temperature heat. Around 45 % of this low temperature heat is already supplied by district heating or by CHP auto producers. The technical potential to increase CHP heat production is then around 118 TWh. Only a small part of it is a cost-effective and realizable potential. In some sectors like metal or glass industry a lot of high temperature heat is available that could be used first before new CHP units would be installed. In other sectors with small companies the installation of CHP units might not be profitable as only small units with shorter operation times could be used.

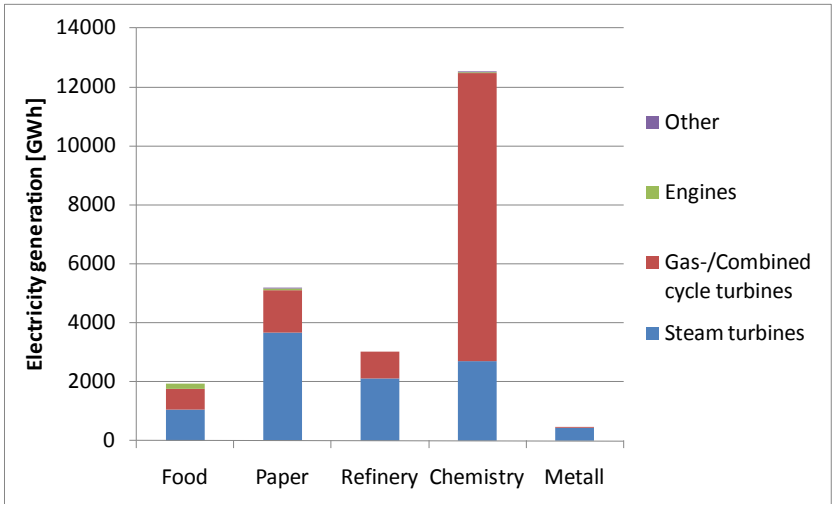

Source: [6]

Fig. 3. CHP electricity generation in major industry sectors related to the generation technology in 2009 in Germany

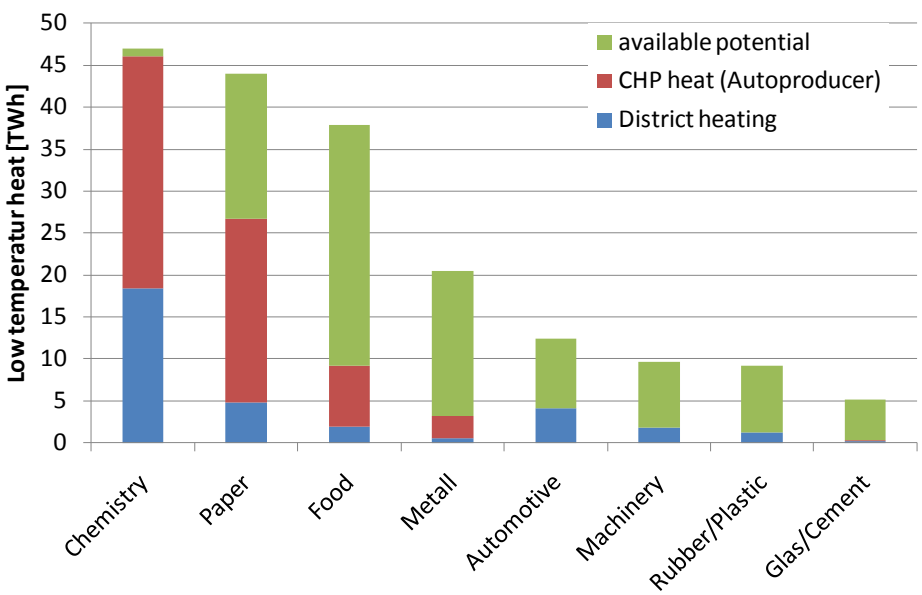

Source: Own figure based on [5, 6, 7]

Fig. 4. Provision of low temperature heat by CHP heat generation, district heating and available CHP heat potential in major industry sectors in 2008

3.2. Renewable fuel use in the industry sector

Until now renewable fuels have only a very limited share of 4 % in the industrial sector corresponding to around 27.5 TWh (final energy demand) in 2008 [5]. It increased from 15.5 TWh in 2003. Most of it is used in the wood and furniture industry followed by the pulp and paper industry (see Table 3). In this figure fuel use for heat production in CHP power plants is included. The fuel use for CHP electricity production is covered by the statistics for the power plant sector. The renewable fuel use for electricity production in industrial power plants was 7.8 TWh in 2008 (with 3 TWh in 2003).

Table 3. Distribution of renewable fuel use in major industry sectors in Germany 2008.

Sector	Wood/ furniture	Paper	Chemistry	Cements	Food	Other
Share [%]	37	27	22	8	3	3
Total [TWh]			27.5			

3.3. Renewable CHP generation

The share of renewable fuels used in CHP power plants is covered in the statistic [6] together with other fuels like waste (refuse-derived fuels, RDF). In the past the use of renewable and RDF fuels has slightly increased from 25.3 TWh in 2003 to 29.8 TWh in 2008 (see Fig. 6). In 2003 around 24 % (6 TWh) of the 25.3 TWh are renewable fuel due to statistics from EUROSTAT [9]. This corresponds to almost 5 % of the fuel used in CHP power plants. For 2008 no statistics are available. Under the assumption that the fuel use in CHP power plants has increased similar to the total renewable fuel use in the industry sector, it should be around 11 TWh in 2008. Progress in the sector is difficult to estimate, but there should have been some in the past.

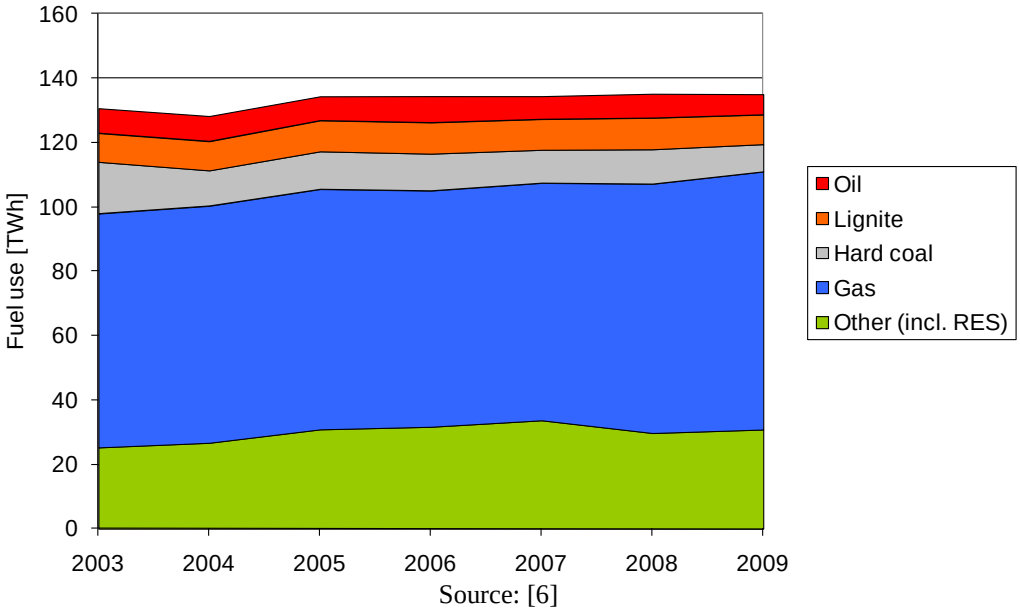

Fig. 5. Fuel use in CHP power plants from 2003 until 2008 in the industry sector in Germany

High shares of renewable fuel use in CHP power plants can be found in the wood industry and in the paper industry (see Fig.7). Renewable fuels are also used in the chemical industry. Additional potential in the wood and paper industry is very limited as the major waste material from production processes is already in use [10]. An increase of renewable fuels in CHP power plants can be done with external biomass like wood chips or pellets. Another option is the usage of biogas. Until now this option has not been used as renewable fuel costs were much higher than fossil fuel prices.

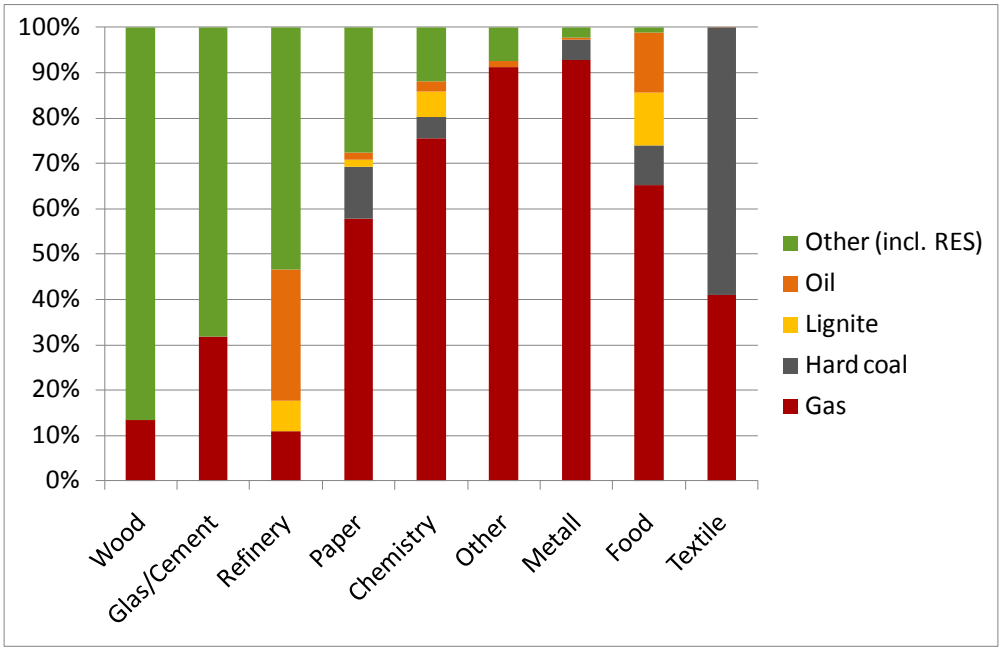

Source: [6]

Fig. 6. Share of renewable fuel use in CHP power plants in major industry sectors in Germany 2008

3.4. Economic potential and CO_2 savings

The economic assessment is driven by the size of the CHP units as investment costs typically decreases for larger units. Furthermore utilization decreases costs. Electricity production costs range between 10 Cent/kWh(el) for small CHP units (500 kW) and 6 Cent/kWh for big CHP units (400 MW), when units are in operation for 4000 h/a. If the value of the heat generation is estimated with saved fuel costs then electricity production costs are typically reduced by 2 to 4 Cent/kWh. In this case, CHP units are profitable compared to the electricity purchase. With a higher utilization the benefits typically increase.

Markets can pick up CHP electricity in the short term and installation are profitable when long operating hours can be reached. Profit margins are in the range of 13 to 25 €/MWh for more than 5000 hours per year.

Looking in electricity markets with a higher RES share of 40 %, operation become more restricted making new operation strategies necessary. Times with electricity prices below short term generation costs of CHP installations increase in the future, so that operation will be profitable in fewer hours than today. This is because natural gas and CO_2 allowances will be more expensive. This will be partly compensated by higher revenues for electricity, but the increase of electricity prices will be limited due to wind and solar power production. Typical profit margin increases up to 40 €/MWh, but can be reached only 2500 – 4000 hours per year.

The heat bonus for CO_2 emissions on the CHP heat generation is calculated using a reference heat technology. Assuming gas as fuel and a 90 % efficiency of the heat generation the heat bonus is 223 g CO_2/kWh(heat). Resulting CO_2-Emissions for the electricity generation reach 230 – 280 g CO_2/kWh(el) depending on the CHP technologies. Compared to the German electricity mix with specific emissions of 575 g CO_2/kWh(el) savings up to 60 % can be reached. A comparison with a modern combined cycle power plant, specific emissions are at 340 - 350 g CO_2/kWh(el), leads to a reduction of ca. 35 %.

4. Discussion and conclusions

In short term CHP can bring additional CO_2 reduction in the German industry sector as specific emissions are below the actual electricity mix and also below new combined cycle power plants with no heat or steam generation. As gas is already the dominant fuel source in the industry sector savings in the heat production are limited. Major reductions can be achieved by the substitution of fossil electricity generation outside the industry sector. Renewable fuel use is already done in sectors that have renewable waste from its production process. These potentials within the different sectors are already used today, so that an increase of renewable fuels can be mainly achieved by using additional renewable fuels like wood chips, pellets or biogas from outside the industry sectors. In the medium to long term additional use of RES fuels and adapted operation strategies will be necessary to lead to further CO_2 reductions.

References

[1] M. Horn, H-J. Ziesing, et al., Ermittlung der Potenziale für die Anwendung der Kraft-Wärme-Kopplung und der erzielbaren Minderung der CO_2-Emissionen einschließlich Bewertung der Kosten (Verstärkte Nutzung der Kraft-Wärme-Kopplung), Federal Environmental Agency, UBA 2007, pp. 18-27.

[2] European Commission,2004.Directive2004/8/EC on the promotion of cogeneration based on a useful heat demand in the internal energy market and amending Directive 92/42/EEC, 11February2004.

[3] Westner, G. and Madlener, R., 2010. The benefit of regional diversification of cogeneration investments in Europe: A mean-variance portfolio analysis. Energy Policy, 38(12), pp. 7911-7920.

[4] Eikmeier, B., J. Gabriel, et al. (2006). An analysis of the national potential for the application of high-efficiency cogeneration in Germany, Energie & Management.

[5] AGEB, Energy Balances for the Federal Republic of Germany from 1990 to 2008, Arbeitsgemeinschaft Energiebilanzen, www.ag-energiebilanzen.de, October 2009.

[6] Federal Statistical Office (DESTATIS), Erhebung über die Energieverwendung. Energieverbrauch nach Energieträgern. Berichtszeitraum 2008 sowie Stromerzeugungsanlagen 2008 der Betriebe im Bergbau und Verarbeitenden Bergbau. Brennstoffeinsatz für die Strom- und/oder Wärmeerzeugung nach Energieträgern, 2009, Wiesbaden.

[7] H.-J. Wagner, H. Unger, et al., Validierung und kommunale Disaggregierung des Expertensystems HERAKLES, Abschlussbericht, Ruhr-Universität Bochum, 2002, pp. 40-41.

[8] Sensfuß, F. (2008): Assessment of the impact of renewable electricity generation on the German electricity sector An agent-based simulation approach. Dissertation. Universität Karlsruhe (TH). Fortschritt-Berichte Reihe 16 Nr. 188. VDI Verlag, 2008 Düsseldorf.

[9] EUROSTAT, personal communication with A. Golbach

[10] G. Dehoust, U. Fritsche, et al., Material stream of biomass wastes for the optimization of organic wastes utilization, Report for the Umweltbundesamt (UBA), IFEU and Ökoinstitut, 2007, Dessau

Energy efficiency opportunities within the powder coating industry

Sofie Osbeck[1], Charlotte Bergek [1], Anders Klässbo[1,*], Patrik Thollander[2], Simon Harvey[3], Patrik Rohdin[2]

[1] *Swerea IVF AB, Mölndal, Sweden*
[2] *Department of Management and Engineering, Linköping Univeristy, Linköping, Sweden*
[3] *Department of Energy and Environment, Chalmers University of Technology, Göteborg, Sweden*
* *Corresponding author. Tel: +46 317066073, Fax: +46 31276130, E-mail: anders.klassbo@swerea.se*

Abstract: A new challenge to reduce energy usage has emerged in Swedish industry because of increasing energy costs. Energy usage in the Swedish powder coating industry is about 525 GWh annually. This industry has a long and successful record of working towards reduced environmental impact. However, they have not given priority to energy saving investments. Electricity and LPG, for which end-user prices are predicted to increase by as much as 50 – 60% by 2020, are the main energy carriers used in the plants. This paper presents the results of two detailed industrial energy audits conducted with the aim of quantifying the energy efficiency potential for the Swedish powder coating industry. Energy auditing and pinch analysis methods were used to identify possible energy housekeeping measures and heat exchanging opportunities. The biggest users of energy within the plants are the cure oven, drying oven and pre-treatment units. The energy use reduction by the housekeeping measures is 8 – 19% and by thermal heat recovery an additional 8 – 13%. These measures result in an average energy cost saving of 25% and reduction of carbon dioxide emissions of 30%. The results indicate that the powder coating industry has a total energy efficiency potential of at least 20%.

Keywords: *Powder coating, energy audit, pinch analysis, energy efficiency*

1. Introduction

The Swedish electricity market was liberalized 1996 in order to increase competition. The European electricity market deregulation was delayed until 2004 before it was liberalized for industrial consumers, which has led to increased electricity prices in Sweden [1]. Industry accounts for 40% of Sweden's total energy use, which is forecasted to increase due to greater industrial demand. Hopefully new eco-efficient technology as well as increased energy efficiency will reduce the rate of increase of energy usage in industry [2].

The 20-20-20-targets have been formulated by the EU commission in order to achieve their energy policy vision: competitiveness, sustainability and security-of supply. The targets represent 20% reduction in energy use and at least 20% share of renewable energy supply based on the 2005-levels and a 20% reduction in greenhouse gas emissions based on the 1990-level. Key areas of the EU targets are in the electricity and gas markets, renewable energy sources, consumer behavior and closer international cooperation. All EU countries are encouraged to act and coordinate activities in order to try to distribute the burden but also its future dividends. Policy instruments have been introduced in Sweden to achieve these goals and guide the energy use in a sustainable direction, and decrease emissions to reduce climate change. The instruments include energy, carbon and sulfur taxes but also the electricity certificate system, program for Energy Efficiency (PFE), the energy audit program, technology procurement, policy instruments for buildings and transport and information [3]. The end user prices of electricity and liquefied petroleum gas (LPG) is predicted to increase by as much as 50 - 60% by 2020 [4]. This is another driving force in implementing energy efficiency measures. Beside the environmental and economical benefits from making industrial energy usage more efficient there are also marketing benefits as customers begin to require energy-efficient production within the powder coating industry [5].

Experience from Swedish research in industry reveals that the energy saving potential among non energy-intensive companies ranges from 15-50% [6-7]. No figures are available for the energy saving potential in the energy-intensive powder coating industry. The aim of this paper is to quantify energy efficiency potential for the Swedish powder coating industry based on two thorough industrial energy audits. The research was conducted using multiple case study analysis, energy audit as well as pinch analysis.

The Swedish powder coating industry includes approximately 350 plants using more than one metric ton of coating powder. These currently accounts for a combined energy usage of 525 GWh/year, corresponding to 1,5 GWh/year per plant [5]. This sector has successfully implemented eco-technology as a result of legal requirements. However, so far they have not given priority to energy saving investments. A powder coating plant usually includes pre-treatment, drying oven, powder box and cure oven, e.g. see Fig. 6. In the pre-treatment unit, the parts that are to be coated are washed in a degreasing step with alkaline washing solution of around 60°C. The pre-treatment also includes a number of rinsing steps. The parts go through a drying oven that has a temperature of around 120–150°C. Then one layer of powder is applied in the powder box and at the end of the conveyor the parts go through a cure oven that has a temperature of 200°C. After the cure oven some plants have a cooling zone where cold air is blown over the parts to make them cool faster [8].

Two companies were selected for this multiple case study analysis [5]. Company A uses LPG as fuel for firing an immersed heater in order to heat their first pre-treatment bath. Company B uses district heating instead. Direct burners using LPG heat the drying ovens to a temperature of 150^{o}C and 120^{o}C respectively. The cure oven is heated by electricity to 200^{o}C at Company A while Company B uses LPG with direct burners. Company B also has a primer box, primer oven and cooling zone while Company A has a liquid finish box between the drying oven and the powder box. All components besides heating accessories are driven by electricity.

2. Methodology

The electricity use is based on instantaneous measurements for the different units of the process as well as on logging of selected components and it was performed during one week for each company. The values from the logging were used to evaluate how many hours the different parts of the process are in use each day as well as to get an average value for the electricity usage. The calculated energy use of electricity was compared with the electricity invoices. This comparison made it possible to extrapolate the logged and instantaneous measurements to the usage of one year. The usage of district heating and LPG was based on the monthly values for the consumption stated on the invoices. Invoices for one year were compared for all three energy carriers.

Pinch analysis is a tool to analyse industrial process systems and determine how much heat that must be added, how much excess heat must be removed and how much heat that can be recovered within the process. Pinch technology is also a useful tool to investigate how to design a heat exchanger network in order to achieve maximum heat recovery. In this project the heat content in the different streams was estimated based on process data and after this different possible options for heat exchange were investigated. The heat usage depends on the different production schemes, when the processes are used, for how long and the distance between them. In the end the options are weighed against each other based on energy cost savings and capital investment required.
The payoff period and the net present value (NPV) method were used to evaluate the investments. The payoff period quantifies the time period necessary for the investment's

energy cost savings to cover the initial investment cost. The net present value method evaluates the viability of an initial investment by comparing it with all future energy related cash flows. All future cash flows are discounted using the interest rate and a reference period of time. The net present value ratio (NPV divided by initial investment) is used to compare different investments. The investment with the maximum ratio is the most attractive. In the base case, the investments are analyzed assuming constant energy prices over the lifetime of the investment. In a sensitivity analysis, the analysis accounts for the development of energy prices during the years 2010 – 2020.

3. Results

The energy audit showed that 77 – 86% of total energy usage occurs in the core production processes, whereas 14 – 23% is connected to the support processes. The first graphs illustrate the electricity use during an average production day. As can be seen in Fig. 1a, company A has two peaks for the production processes during the day. This is because they operate with two shifts and they have a large variation of products. Company B, e.g. Fig. 1b, has a more homogeneous production and single-shift operation. Significant differences can be seen when analysing how the electrical power load is distributed between the process units during operating hours, e.g. Fig. 2. For Company A the cure oven is the largest consumer of electricity and for Company B it is the powder box. For Company A the cure oven can be used at three different temperatures due to combination of liquid finishing and powder coating. The powder box in Company B has a high ventilation requirement because of a more open construction and employees working inside compared to Company A. Figures 1 and 2 are comparable when production is at its full capacity.

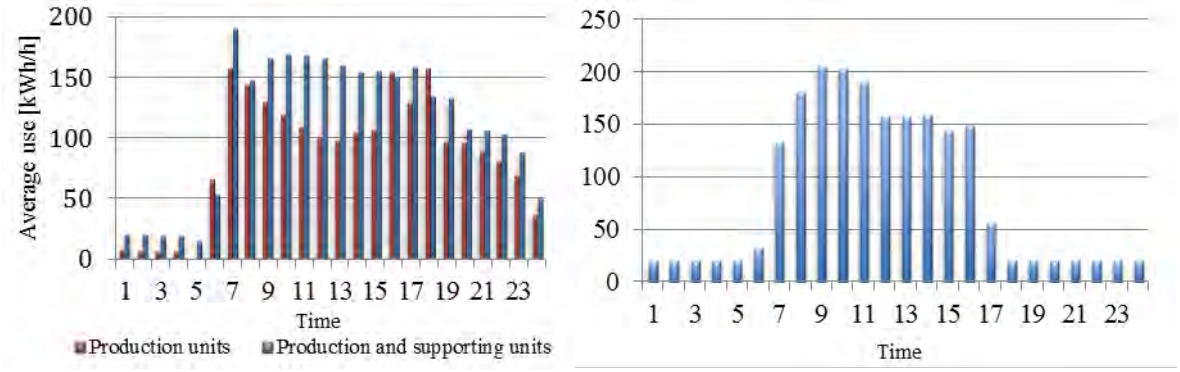

Fig. 1. Electricity use during an average production day for Company A (left) and B (right).

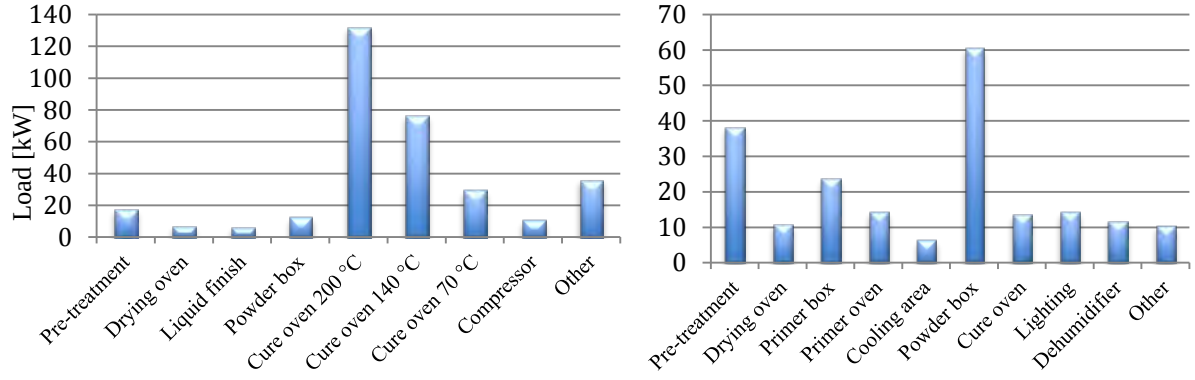

Fig. 2. Load balance for electricity during production for Company A (left) and B (right).

In the energy balance all energy sources are included, i.e. electricity and LPG for Company A and electricity, LPG and district heating for Company B, e.g. Fig. 3. As can be seen it is the pre-treatment, drying oven and cure oven that uses most energy. Together these three units

accounts for about 70% of the total energy supply for both companies. When using liquid finishing (65% of the time) the pre-treatment and drying oven are turned off for company A, which leads to a lower demand for LPG for this company. For company B it is the primer box, primer oven and cooling zone that can be turned off during periods.

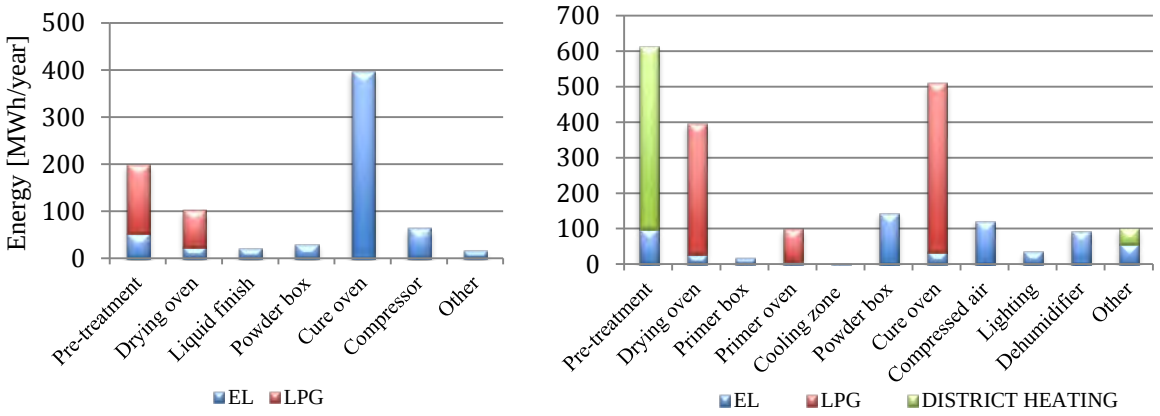

Fig. 3. Energy balance during one year for Company A (left) and B (right).

Figure 4 shows the total energy use for the two companies. Both companies have a significant use of electricity during downtime. This is due to that both have dehumidifiers that are on all the time as well as charging of trucks during the nights.

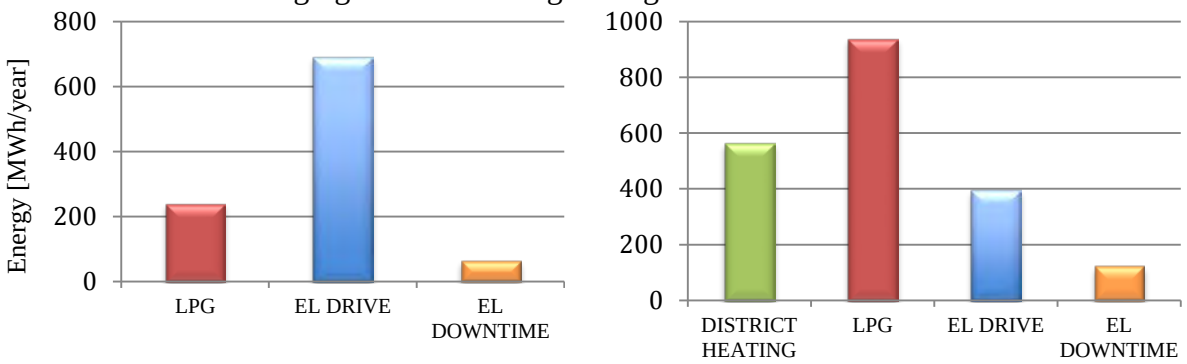

Fig. 4. Total energy use per year for Company A (left) and B (right).

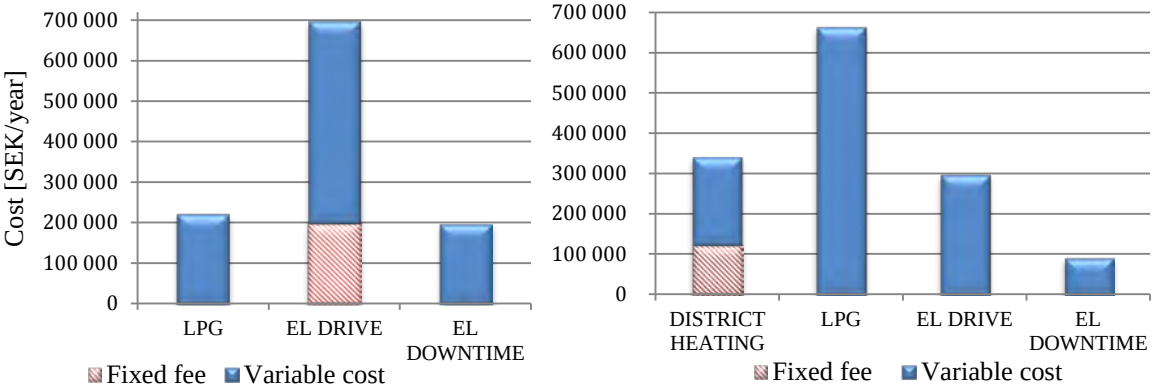

Fig. 5. Energy cost per year for Company A (left) and B (right).

The energy cost can be seen in Figure 5 above. Company A has a fixed fee for electricity but not for LPG. Company B has a fixed fee for district heating but not for the other energy sources. Electricity is the highest energy cost for company A while LPG is the highest cost for company B.

The specific energy usage indicators have been chosen based on a national project within Swedish industry named ENIG (EN in Groups), see Table 1. One main difference between the two companies is that Company A uses half as much energy per year but has twice as much

production time. This is because Company A combines other varnishing techniques and offers packing and masking. Company B only uses powder coating technology which is more energy demanding. Since the turnover is similar the second indicator depends mostly on the energy use. The mass flow of parts is more than twice as high for Company B compared to Company A, which affects the third indicator (specific energy usage per ton of product).

Table 1. Specific energy usage indicators.

Company	Energy use per		
	Production time [kWh/h]	Turnover [kWh/kSEK]	Parts [kWh/Ton]
Company A	230	47	185
Company B	973	107	135

The reduction of CO_2-emissions for the suggested measures are based on values of 234 kg CO_2/MWh of LPG, 770 kg CO_2/MWh of electricity and 0 kg CO_2/MWh for district heating. Electricity has a high value due to that it is assumed to be electricity on the margin and district heating has zero emissions due to production from biomass. The energy prices can be seen in Table 2. The prices for 2010 is stated on the companies invoices and the increase until 2020 is expected to be 60% for LPG, 50% for electricity and 30% for biomass [4].

Table 2. Energy prices for 2010 and 2020.

Company	Energy price [SEK/MWh]					
	El. 2010	El. 2020	LPG 2010	LPG 2020	DH 2010	DH 2020
Company A	735	1103	953	1525		
Company B	755	1133	707	1131	391	508

Energy housekeeping measures do not include heat exchanging and are primarily targeted at identifying better operational practices. The potential energy usage reduction, based on such measures was estimated at 8 – 19%, e.g. Table 3.

Table 3. Energy housekeeping measures (compared with the total energy use for each company).

Measure	Reduction potential		
Company A	Energy [MWh/year]	Running cost [SEK/year]	CO_2-emission [Ton/year]
Lighting	22	17 000	17
Standby	65	49 000	50
Production planning	100	74 000	77
Drying oven	8	6 000	2
Total	195 (19%)	147 000 (15%)	146 (23%)
Company B			
Lighting	18	14 000	14
Dehumidifier	31	24 000	24
Powder box’s ventilation	13	10 000	10
Production planning	44	33 000	34
Fans	16	12 000	13
New powder box	44	33 000	34
Total	166 (8%)	176 000 (9%)	129 (26%)

Lighting measures include switching to low energy lighting, removing it in areas where it is not necessary as well as turning off when not in use. Both companies have several

applications on standby during nights and weekends, for example compressor and dehumidifier. Complete shut-off of such equipment can lead to substantial energy savings. Company B can turn off the powder box ventilation during breaks. Production planning could reduce the energy usage by having one start per day and process unit. Using a lower temperature in the drying oven for Company A could decrease energy usage but it also generates a risk of lower coating quality. The fans to the drying oven and cure oven are oversized for Company B and changing them could reduce the plant's power load. If Best Available Technology (BAT) is adopted for the powder box, electricity use for the ventilation within the box could be reduced by 30% and the compressed air usage by 45%.

Pinch analysis was used to identify opportunities for heat recovery by heat exchanging. Two possible heat recovery cases were investigated, e.g. Table 4. Case 1 involves heat exchanging incoming and outgoing airflows in the cure oven and drying oven, e.g. Fig. 6.

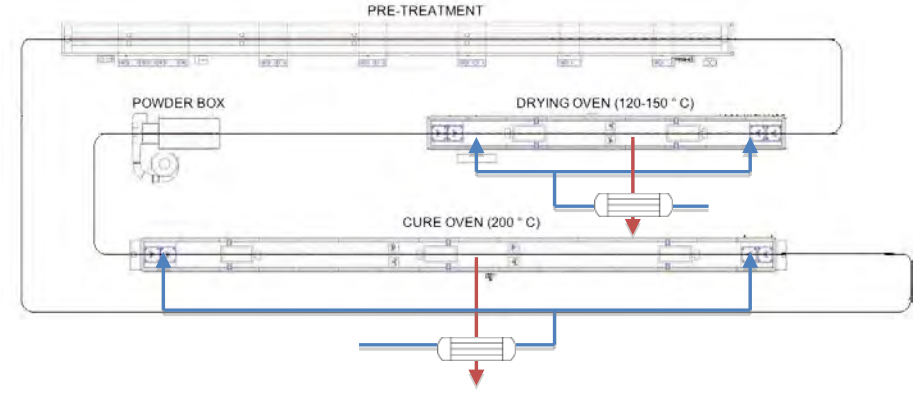

Fig. 6. Case 1 Proposed heat exchanging measures for powder coating process.

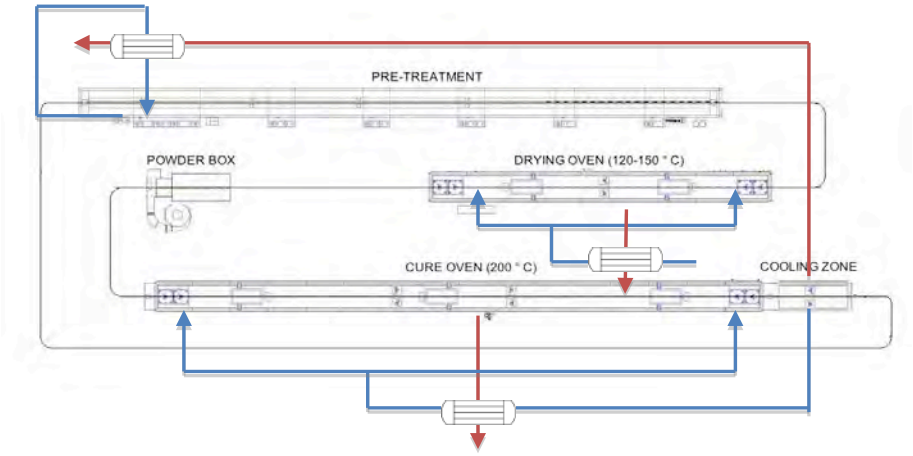

Fig. 7. Case 2 Proposed heat exchanging measures for powder coating process.

Table 4. Saving potentials for heat recovery cases.

Measure	Reduction potential		
	Energy [MWh/year]	Running cost [SEK/year]	CO_2-emission [Ton/year]
Case 1 Company A	121	90 000	76
Case 2 Company A	128	85 000	73
Case 1 Company B	140	100 000	33
Case 2 Company B	251	146 000	28

Case 2 includes a cooling zone after the cure oven. The large airflow from the cooling zone can be divided and used as preheated ingoing air to the cure oven as well as for heat exchanging to heat the pre-treatment bath. For the drying oven the heat exchange is the same as in Case 1, e.g. Fig. 7.

The economic assessment, e.g. Table 5, shows that the two cases for heat recovery are profitable for both companies. However, Case 1 has a much higher NPV and NPVR than Case 2. The total savings are presented in Table 6, showing that Company A has a higher potential for reduction of energy use due to more variations in the production as well as larger hot streams out from the ovens.

Table 5. Economic assessment with expected increased energy prices until 2020 for Company A (interest rate 10%) and Company B (interest rate 15%).

Measure				
Period 10 years	Investment cost [SEK]	Pay off period [year]	NPV [SEK]	NPVR
Case 1 Company A	135 000	0,9	795 000	5,90
Case 2 Company A	450 000	3,1	440 000	1,00
Case 1 Company B	150 000	1,2	460 000	3,08
Case 2 Company B	495 000	2,8	400 000	0,80

Table 6. Total savings for energy housekeeping measures plus thermal heat recovery cases (compared with the total energy use).

Measure	Reduction potential		
	Energy [MWh/year]	Running cost [SEK/year]	CO_2-emission [Ton/year]
EHK+Case 1 Company A	316 (32%)	237 000 (26%)	220 (35%)
EHK+Case 2 Company A	323 (33%)	232 000 (25%)	219 (34%)
EHK+Case 1 Company B	306 (16%)	276 000 (20%)	162 (26%)
EHK+Case 2 Company B	417 (21%)	322 000 (23%)	157 (25%)

4. Concluding discussion

The energy audit shows that the production processes use a substantial amount of energy 77 – 86% whereas the support processes use 14 – 23%. For the two companies investigated the energy usage can be reduced by 8 – 19% with energy housekeeping measures. Thermal heat exchange can reduce the energy use by an additional 8 – 13%. In total this gives energy savings of around 30% for company A and 20% for company B.

Improved production planning will make a large impact on energy usage. For company A this could lead to a reduction of the second electricity use peak, e.g. Fig. 1a. For company B turning on the primer part only once a day could save energy. Another measure for company A is to completely turn off equipment that is not used. For company B the powder box can be turned off during breaks. These are measures that can be implemented by changing the routines etc. within the companies. In this study, energy housekeeping measures have been shown to achieve the same or higher energy savings compared to thermal heat recovery.

Benchmarking shows that the most efficient way of heat exchanging is within the same part in the process. This will reduce the investment costs as well as contribute to a flexible process. Installing a cooling zone after the cure oven will be profitable but there are other investments

that are even more profitable. The fact that the cooling zone will give a better working environment should be taken into account. The benchmarking also shows that the airlocks from the ovens usually have too small heat content to be efficiently heat exchanged against ingoing air to the ovens. The contaminations that follow the airlocks also prevent using this air as ingoing air. Another reason is that there is a risk that to much air is pushed into the ovens if airlocks are used. However, there might be a possibility to use them for heat exchanging against facility ventilation air to reduce demand for space heating. To be able to implement thermal heat exchange further study is necessary in order to investigate the impact of contaminants released from the powders when cured in the cure oven. There is a possibility that these contaminants will stick in the heat exchangers and tests must be conducted to see if filters are required upstream from the heat exchangers. It should be noted that companies in Finland have successfully used the airlocks for space heating [5].

The economic results are based on an interest rate of 10% and 15% respectively. A lower interest rate would increase the net present value and the net present value ratio. The results in these projects show that Case 1 is the best investments from an economical perspective for both companies. However, Case 2 has other positive effects that are not accounted for in the calculations. For example a cooling zone would substantially improve the working environment by reducing the heat that is emitted to the facility. Results indicate, based on benchmarking between these two projects, that the powder coating industry may have an energy efficiency potential of 20% which corresponds to total energy savings of at least 105 GWh/year for the sector.

References

[1] B. Karlsson, Strategi för systemförändringar av industriell energianvändning, Linköpings universitet, 2001-05-02, pp 1-3.

[2] T. Kåberger, D. Andersson, Energiförsörjningen I Sverige – en korttidsprognos, Energimyndigheten, ISSN 1403-1892, 2009, pp 17-20.

[3] T. Kåberger, S. Lublin, A. Andersson, Energiläget 2009, Energimyndigheten, pp 8-12, 31

[4] Simon Harvey, Department of Energy and Environment, Chalmers University of Technology, 2010.

[5] Lars Österberg, Svensk Pulverlackteknisk Förening, 2010.

[6] Trygg, L., Karlsson B., 2005. Industrial DSM in a deregulated European electricity market - a case study of 11 plants in Sweden. Energy Policy 33 (11): 1445-1459.

[7] Thollander, P., Rohdin, P., Danestig, M., 2007. Energy policies for increased industrial energy efficiency: Evaluation of a local energy programme for manufacturing SMEs. Energy Policy;35(11):5774-83.

[8] Liberto, N., 2003. Users's guide to Powder Coating 4th edition,.

Case Study and Analysis of the Production Processes in a Steel Factory in Jordan

Jamil J. Al Asfar[1,*] and Ashraf Salim[2]

[1] *Assistant Professor, The University of Jordan, Amman, Jordan*
[2] *Assistant Professor, Philadelphia University, Jarash, Jordan*
** Corresponding author. Tel : +962 79 5568 716, E-mail: jasfar@ju.edu.jo*

Abstract: This work represents a true case study and analysis of the technical and energy managerial aspects of recommended designs of the production lines of a steel factory in Jordan. A modern structure of a control system based on SCADA (Supervisory Control And Data Acquisition) technology is proposed. Furthermore, the mechanical and electrical maintenance sections in the factory were reviewed due to their major effects on the production cost and energy consumption of the factory. This study was performed in two main phases: The first phase contains the collected data and process assessment that were undertaken by traditional direct observation and activity categorization, while the second phase gave details on the proposed control methodology in terms of design and architecture.
Moreover, a proposal on maintenance planning and procedure program was also included in this study in order to reduce the time and accordingly the cost of maintenance. The steel factory studied produces various steel products such as: Concrete Reinforcement Steel Bars (Rebars), Flat & Square Bars Section which includes standard flat bars, standard square bars, and plane round bars, in addition to Wire mesh in different sizes and steel billets. In steel production industries, two automation levels can, in general, be identified. The first level involves the electromechanical actuation of the devices in the production plant; this level of automation is currently available in every plant. The second level involves the supervision of the production process; this level of automation is less frequent and is generally only partial. In fact, steel production involves a variety of complex physical phenomena, described by sophisticated mathematical models which are rarely usable to derive real-time advice for process supervision and control. Most operators' support systems for steel production are represented by simple technologies such as microprocessor-based systems.
Based on the outcomes of this study, the factory purchased a new melting furnace of (60) tons capacity instead of the (30) tons capacity melting furnace used in the factory before the study. The factory is considering also the purchase of a scrap press in its new budget in order to improve scrap quality before melting it; in order to reduce the rate of consuming the furnace electrodes. Also, the maintenance section will be restructured by merging electrical and mechanical maintenance sections into one section headed by the deputy of the factory manager.

Keywords: *Steel Production Line, SCADA System, Maintenance Structure, Efficiency*

1. Introduction

To maintain an efficiently operating unit and avoid failure of critical equipment, especially modern steel industry equipment, the focus has clearly shifted over the years, from Breakdown Maintenance, i.e. repairing the equipment after its malfunctions, to Preventive Maintenance, i.e. fixing the equipment according to planned maintenance schedule. The next trend was Computerized Maintenance Management Systems (CMMS), and the latest trend encompasses asset management and maintenance, supported by various methods of Condition Based Maintenance Systems (CBMS) and in-service inspection processes. CBMS or Predictive Maintenance methods are an extension of preventive maintenance and have been proved to minimize the cost of maintenance, improve operational safety and reduce the frequency and severity of in-service machine failures. The basic theory of condition monitoring is to know the deteriorating condition of a machine component, well in advance of a breakdown, for proactive maintenance. A conventional integrated steel plant has a vast array of equipment. The plant is a conglomeration of smaller units, each in itself complete and self-contained. These constitute Coke Ovens, Coal Chemicals, Sinter Plants, Furnace, Steel Melting Shops, Continuous Casting Machine, Tonnage Oxygen Plants, Plate Mill, Hot Strip Mill, Cold Rolling Mill, other secondary mills, Captive Power Plants and a host of other

departments. Every piece of equipment needs special care and attention, characteristic to it. The Coal Chemicals unit has Gas Boosters and Exhausters that handle coke oven gas, a highly inflammable commodity, whereas Sinter Plant Blowers and Waste Gas fans handle air containing highly abrasive sinter dust. The Turbo Alternators of Captive Power Plant require round the clock vigilance involving a variety of parameters. Seemingly innocuous Forced Draft & Induced Draft fans of the Reheating Furnaces also assume significance because of their criticality in application. Failure of these fans may lead to cut down of Hot Strip Mill/ Plate Mill production by 33 - 50 percent. Under the current business environment, cost competitiveness of steelmakers has assumed a priority role. As a global phenomenon, effective maintenance management has been accepted as the key to corporate strategy for reduced costs. This has led to integration of maintenance management function with production and business problems, not just equipment problems. With this realization that maintenance management can cost 35 - 40 percent of revenues and, in most cases up to 15 percent of unit production cost, steel companies are increasingly opting for new maintenance technologies which can be effectively and relatively easily implemented for reduced costs and increased profitability. According to industry estimates, a 10 percent reduction in maintenance costs translates to a 30 percent increase in profitability.

From the previous discussion, the need for introducing new technologies to the steel production is definite. This study provided the factory with some state-of-the-art technologies which can be adopted into the steel production processes in order to improve the product quality, minimize the need for electrical energy and human resources, reduce maintenance time and cost, and increase reliability and real-time data accuracy. The Jordanian factory is located in Zarqa area, and employs (324) technicians, engineers and administration employees. The main function of the factory is to melt Scrap (collected used steel pieces) in an electric furnace of (30) tons capacity, then cast molten iron in moulds to obtain steel billets. The steel billets are then manufactured in a sister company factory to produce concrete reinforcement steel bars (Rebar) in different sizes using rolling and extrusion, flat and square bars, and wire mesh. This factory, which was manufactured by a Turkish company, is a new one that started production in 2008. The current production capacity is around 10,000 tons of steel billets per month.

Employing SCADA system into the melting and casting processes has a good impact on the product quality, minimizing the need for human resources, reducing maintenance time and cost; increasing reliability, and real-time data accuracy. This technology should provide the following:

- Continuous (momentarily) monitoring of the state of the process and of the plant;
- Displaying warnings and alarms, at a sufficiently high level of abstraction;
- Giving advice as needed to the metallurgical management of the process.
- Generating historical reports.

Nowadays, there are two main industrial processes to produce steel: The first one, which is known as integrated steel plant, produces steel by refining iron ore. This ore-based process uses a blast furnace. The other one, which is steel-making from scrap metals, involves melting scrap metal, removing impurities and casting it into the desired shapes. Although, originally the steel production in the electric arc furnaces (EAFs) was applied mainly to the special steel grades, the situation has changed with tap's size increase, and the high productivity that has been reached progressively. This has allowed significant cost reduction, diminishing consumption of energy, electrodes and refractory. At present, electric furnace combined with chemical additives, allows to make a very important part of the worldwide steel production on

the basis of the massive recycling of the iron scrap. Under the current business environment, cost competitiveness of steelmakers has assumed a priority role. As a global phenomenon, effective maintenance management has been accepted as the key to corporate strategy for reduced costs. This has led to integration of maintenance management function with production and business problems, not just equipment problems. With this realization that maintenance management can cost 35 - 40 percent of revenues and, in most cases up to 15 percent of unit production cost, steel companies are increasingly opting for new maintenance technologies which can be effectively and relatively easily implemented for reduced costs and increased profitability. According to industry estimates, a 10 percent reduction in maintenance costs translates to a 30 percent increase in profitability [1-3].

2. Methodology

This study reviewed the structure of the maintenance section in the factory in order to improve and develop the existing maintenance processes and reduce running production costs of consumed electrodes and electricity. The current bill of electricity consumption per month by the factory is around $0.5m, which is relatively high for a factory in a developing country. As mentioned above, the automatic control system and measures used to control the process of melting iron and steel scrap, was analyzed and reviewed in order to evaluate its effect on the mechanical and electrical maintenance of the factory. Many machinery parameters can be measured, trended and analyzed to detect imminent failure or onset of problems. Common among them are: Machinery vibration, Lube oil analysis including wear debris analysis, Infrared thermograph, Ultrasonic testing, Motor current analysis, Shock pulse measurement, …,etc. Additionally, operational characteristics such as flow rates, heat, pressure, tension, speed and so on can also be monitored to detect problems. In case of machine tools, product quality in terms of surface finish or dimensional tolerances is often an indication of problems. As all these techniques have value and merit, the application of any particular technique depends on the suitability and ease of implementation [1-4].

The control systems of the Electrical Arc Furnace (EAF) used in the factory need the following improvement and development in order to reduce the final product cost. In order to achieve this aim, analytical methods were followed to improve steel production process in the EAF. In order to do so, the study was divided into two phases that are sequential yet synergistic. The first phase used traditional methods of work measurement drawn from industrial engineering practice, such as process definition, development of flow charts, and data collection via time-and-motion studies, to obtain a complete, quantitative understanding of current system operational procedures, workflow patterns, and location of productivity constraints. The second phase was built upon the understanding gained during the first phase. In the second phase, opportunities to improve throughput was identified, with particular attention to those opportunities requiring relatively low capital investment. The principal analytical tools to be used for this phase were the operations research techniques of project management, to identify both critical paths within work flow and utilization imbalances among system resources.

2.1. Improving Maintenance Management

A working definition for various types of maintenance actions is as follows:

- Failure Maintenance: This relates to the policy of repair or replacement of a part or subsystem only upon failure of the named part or assembly.
- Block Maintenance: This relates to the policy of repair or replacement of all parts on subsystems (block) at a predetermined interval of time.

- Preventive Maintenance: This relates to the policy of repair or replacement of a subset of parts or subsystems, when another part of subsystem fails or is repaired/replaced after a certain length of service [5, 6].

Proper maintenance is essential to keep production equipment and capital assets at a state conducive to its output role in maintaining a level of production at a predetermined quality and quantity. Maintenance costs typically average from 5% to 7% of the value of fixed capital assets, hence the economic implications of reducing maintenance costs are very vast. Data can be collected on costs of repair, downtime and availability percent statistics, usage of spares inventory, etc. This information can be used to set budgets, make historic comparisons and in general be used as control information. A sensible combination of failure maintenance and preventive maintenance will ensure that these objectives are met. The equipment failure characteristics often determine the worthwhileness of preventive maintenance activities. Equipment that fail randomly due to unexpected and inexplicable overstress, generally do not lend itself to preventive maintenance. Equipment that fails due to wear and tear may lend itself to preventive maintenance. Thus the 1st step in maintenance planning consists of analysis of failure characteristics of the subsystems comprising the total system. Forecasting of equipment failures in a stochastic system (probabilistic) is based on studying the past performance of the equipment and its subsystems, and assuming that these characteristics will hold in the future. Past data of equipment failures like time to fail are analyzed with a view to find a statistical distribution which closely resembles with a confidence limit of 90% or more the actual failure distribution of the subsystem. Once this is determined, methods of statistical sampling can be used to predict times to failure in any analysis. Among the most common failure distribution applicable to electromechanical systems are the Exponential distribution, Normal distribution, Log Normal distribution, Gamma distribution and Weibull distribution.

Maintenance Procedure Program (MPP) system is a series of dynamically linked programs, each of which plays an important role in the effectiveness of the maintenance program. The system applies to both electrical and/or mechanical maintenance in the steel production line and provides the process of equipment inspection as well. The MPP is a manner of applying several maintenance concepts into a complete program. This program fully utilizes each concept while combining the efforts of all. Each program element can stand alone in its own right, yet together their strength is multiplied. The need of such a program came about after many attempts of installing only one concept of preventive maintenance. It became apparent that no one method would cover all the bases at any one time. Thus, building a structure which would take into account each facet of maintenance and combine the efforts of each into a master program became a reasonable task. In Maintenance Job Order System, information is fed into this system from the crew inspectors, the department inspectors, the nondestructive testing group, the operations department, and the electrical/mechanical maintenance group. This information is in the form of necessary work to be done as a result of inspections from the various sources. The equipment history files are also important inputs into the job order system. This history helps coordinate the jobs to be completed during planned outages. The next step is to open the job order. The job order can be opened or directed to the maintenance foreman or the departmental planner. If the order is directed to the foreman, the work is assigned to a crew for completion. Normally, work assigned to the foreman would be of a nature which could be completed with the line running or which would be done during an unscheduled interruption in the operation. If the job order is opened to the departmental planner, he will coordinate the job order with the central shops crafts department using a shops job priority system, the maintenance foreman, and the maintenance spares man. These people act as a team in organizing the manpower, spares, and other factors necessary to

complete the required job during the planned outage. After the completion of the job, the job order is closed.

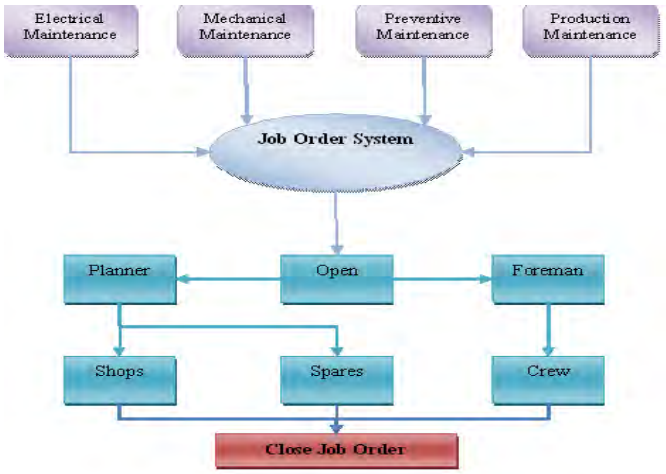

Fig 1: Maintenance Job Order System [5].

2.2. System Modelling

Fig.'s 2 and 3 show physical and electrical models of the existing EAF. In these models, three electrodes are moved vertically up and down with hydraulic actuators. Each of these electrodes weighs 0.4 tons and is 1.5m long. The ore is melted with a huge power surge from the electrodes. The actual product is denser than the scrap and thus falls to the bottom of the furnace creating the matte. Above the matte lies the slag where the electrode tips are dipped. The tremendous heat created by these electrodes causes the ore to liquefy and separate. Thereupon, more raw materials are placed in the furnace and the process repeats itself.

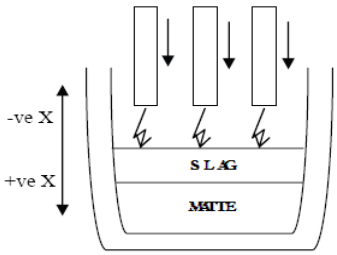

Fig. 2: Physical Model of the EAF [2].

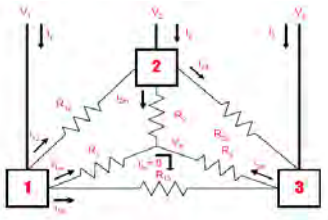

Fig. 3: Electrical Model of the EAF [2].

3. Results

The EAF operates on the principle of direct arc heating. Three graphite electrodes carry the three phase current into the furnace. An electric arc is generated between the electrodes and the metal charge which gives out heat. The charge gets melted by the direct impingement of the arc and also by the radiation from the roof and walls. A proper length of arc is to be maintained throughout the melting cycle. The furnace consists of a cylindrical steel shell

mounted on supporting rockets. There is a tapping spout for drawing molten metal and a slag door at the back for slag removal. A removable roof covers the shell. The three electrodes enter the shell through the holes on the roof and are carried by electrode holders on the electrode arm. The position of the electrodes is controlled by moving the mobile carriage over the electrode post which- is done by electrode hydraulic cylinders. The electrodes are water cooled at the point of entry into the furnace. A separate water storage tank with a centrifugal pump is provided for circulating cooling water for the shel1, electrode holder, roof and the slagging door. A control panel is provided for controlling power input to the furnace, for forward and backward tilting, to indicate the currents and voltages and for accurate lifting and lowering of the electrodes. The hydraulic cylinder used for electrode movement is controlled by PLC (S7 400) to maintain the arc impedance a constant for a given voltage, the charging of furnace is done by opening the roof by swinging it to one side. One of the main objectives of the three-electrode control study is to have the electrodes maintain constant power consumption. This is achieved by moving the electrodes to a given depth, obtaining the desired resistances (or conductance), which leads to a constant power consumption. To attain this goal, the open-loop system must be closed in order to create an error signal. The control principle is accomplished by minimizing this error signal with specific controllers. PID controller can be designed and optimized for best performance. For this system, controlling the current will lead to power control; since the power magnitudes are scalar multiples of the electrode currents. Employing SCADA system into the melting and casting processes has a good impact on t he product quality, minimizing the need for human resources, reduction maintenance time and cost, increasing reliability, and real-time data accuracy. This technology should provide the following:

- Continuous (momentarily) monitoring of the state of the process and of the plant;
- Displaying warnings and alarms, at a sufficiently high level of abstraction;
- Giving advice as needed to the metallurgical management of the process.
- Generating historical reports.

4. Discussion and Conclusions

Unfortunately, we found that the SCADA system in the factory is only used for continuous (momentarily) monitoring of the state of the process and of the plant. Therefore; it is highly recommended to activate the other three facilities of the plant. Moreover, the SCADA systems which are employed for the EAF, Ladle Furnace, and the Continuous Casting Machine (CCM) are not networked, which is causing an extra burden and difficulty in the management process [2].

Based on above analysis, great deal of improvements is suggested in order to implement an active control and analysis in order to reduce the cost of production and maintenance in this factory, including scrap management; since economic and competitive pressures force industrial and process engineers to seek continuous improvement in industrial production processes [1]. In a complex industrial system, as in an EAF, the ways to improve this process are diverse, such as selection and treatment of materials, the redesign of the facilities and new kinds of energetic contributions to the process. The evolution of electric furnaces is reflected mainly in the progressive reduction of specific consumption of energy, tap-to-tap times and improvement of the metallic yield [2]. A deep study, comparing energy consumed currently in the production of steel with theoretically needed energy, was made by the Carnegie Mellon University (Pittsburg, USA) for the US Department of Energy [3-8]. The principal analytical tools used for second phase were the operations research techniques of project management and heuristic scheduling [6]. Though the direct comparison of different EAFs is difficult due to the operational differences, the disparity between the theoretical energy and the consumed

energy contributes to the idea of potential improvement of these facilities which could be about 25% of the energy consumption. One of the pathways proposed to reach this yield improvement in EAF operation is the optimization of process sequencing by means of Programmable Logic Controllers (PLCs). Important effort has been directed towards further productivity improvements under EAF process. Much of this has focused on developing alternative energy sources to reduce the high cost of electrical energy, which means about 10-15% of EAF operation costs. Another two different types of costs that have impact on the total cost of EAF operation can be identified: the cost of the feed materials and the cost implication of not reaching control objectives. Feed materials are very conditioned by the final quality of steel to obtain (scrap substitutes are mainly used in the production of higher quality products) and the steel cost due to materials is mainly determined by the price of scrap in the world-wide market. Processing control optimization is another very important way for the reduction of the energy consumption. Because of knowledge lack of a suitable plant model, the operations in the furnace are only based on empirical knowledge. There are a large number of traditionally manually controlled variables. The furnace operator, in accordance with his own experience and in his particular way of working, has been taking the decisions. For example, he was deciding if it was necessary to inject more or less oxygen, coal or HBI (hot briquetted iron), or even stopping the process and measuring the steel temperature. The automation of these variables ensures better operation in EAFs [7-13].

Steel scrap is the most important raw material for electric steelmaking, contributing between 60% and 80% of total production costs. In addition, the degree of which the EAF process may be controlled and optimized is limited by fluctuations in scrap quality. Therefore quick estimations of properties of different steel scrap grades are very important for improving the control and optimization of the EAF process. Most countries have national classification systems for steel scrap, but there is also a European classification system that the EU-countries use for international scrap trade [13]. Steel scrap is usually graded in terms of size distribution, chemistry, density, and origin, and processing method. Some melt shops have internal classification systems that further divide the standard scrap grades into subtypes, and also a number of internal scrap grades (scrap produced within the steel plant). However, the scrap grading systems are designed for commercial purposes and the variation in scrap properties within each scrap grade is high. In general, scrap properties may be divided into two main categories, physicochemical properties and process related properties. Physicochemical properties (chemical composition, density, specific surface area, size distribution and melting temperature, specific heat capacity, metallic/ organic/oxidic content) are only dependent on the particular scrap grade and are best determined by controlled experiments in laboratories. Process related properties (yield coefficients, specific energy consumption, contribution to chemistry of steel and slag, contribution to basket and furnace filling degree, contribution to dust generation and off gas composition) depend on both the process conditions and the other materials in the scrap mix. Therefore, the process related properties for the same scrap grade may vary considerably between different melt shops. Chemical analysis, conductivity, metal content and size distribution may be measured or estimated for individual pieces of scrap and/or random samples but the fluctuation in scrap quality is often too large for these measurements to be representative for the whole population of a scrap lot on the scrap yard. Experimental design methods have been proposed to set up a series of experimental heating processes that can then be used to estimate the scrap thermophysical properties. However, because of the variation in process conditions and fluctuations in scrap quality each experiment would have to be repeated several times. The number of experiments needed to get estimations for all scrap grades can therefore be very high, depending on the number of scrap grades that are used, rendering this approach

unsuitable. An alternative to designed experiments is to firstly extract large quantities of data from process databases [3]. Advanced statistical methods can then be used to analyze the combined effect of scrap mix and process conditions on the end conditions, chemical analysis of the liquid steel, energy consumption and metal yield [2- 3, 13].

References

[1] Reeder, Thomas J. 1995. Take a Flexible Approach - Combine Project Management and Business Principles into Program Management. Industrial Engineering 27(3): pp. 29-35.

[2] E. Quation, Jose´ Manuel Mesa Ferna´ ndez_, Valeriano A ´ lvarez Cabal, Vicente Rodrı´guez Montequin, Joaquı´n Villanueva Balsera, Online estimation of electric arc furnace tap temperature by using fuzzy neural networks, Engineering Applications of Artificial Intelligence, 2007.

[3] Fruehan, R.J., Fortini, O., Paxton, H.W., and Brindle, R., 2000. Theoretical Minimum Energies to Produce Steel for Selected Conditions. Energetics, Inc., Columbia, MD, US Department of Energy Office of Industrial Technologies Washington, DC.

[4] Leu, Bor-Yuh., 1996. Simulation Analysis of Scheduling Heuristics in a Flow-Line Manufacturing Cell with Two Types of Order Shipment Environments. Simulation 66(2): pp. 106-116.

[5] McIlvaine, Bill. 1996. Planning and Scheduling Gets the Job Done. Managing Automation 11(8): pp. 24-30.

[6] Morton, Thomas E. and David W. Pentico. 1993. Heuristic Scheduling Systems with Applications to Production Systems and Project Management. New York: John Wiley & Sons.

[7] Mundel. Marvin E., and David L. Danner. 1994. Motion and Time Study Improving Productivity,7th edition. Englewood Cliffs, New Jersey: Prentice-Hall.

[8] Pegden, C. Dennis, Robert E. Shannon and Randall P. Sadowski. 1995. Introduction to Simulation Using SIMAN, 2nd edition. New York, New York: McGraw-Hill.

[9] Pinedo, Michael. 1995. Scheduling Theory, Algorithms, and Systems. Englewood Cliffs, .New Jersey:Prentice-Hall, Incorporated.

[10] Profozich, David M. and David T. Sturrock. 1995. Introduction to SIMAN/CINEMA. In Proceedings of the 1995 Winter Simulation Conference, eds. Christos Alexopoulos, Keebom Kang. William R. Lilegdon and David Goldsman: pp. 515-518.

[11] Raman, Narayan. 1995. Input Control in Job Shops. IIE Transactions 27(2): pp. 201-209.

[12] Seila, Andrew F. 1995. Introduction to Simulation. In Proceedings of the 1995 Winter Simulation Conference, eds. Christos Alexopoulos. Keebom. Kang, William R. Lilegdon, and David Goldsman, pp. 7-15.

[13] Seila, Andrew F. 1995. Introduction to Simulation. In Proceedings of the 1995 Winter Simulation Conference, eds. Christos Alexopoulos. Keebom. Kang, William R. Lilegdon, and David Goldsman, 7-15.

Applying process integration methods to target for electricity production from industrial waste heat using Organic Rankine Cycle (ORC) technology

Roman Hackl[1,*], Simon Harvey[1]

[1] *Chalmers University of Technology Göteborg, Sweden*
** Corresponding author: Tel: +46 31 772 3861, Fax: +46 31 821928, E-mail: roman.hackl@chalmers.se*

Abstract: This paper presents the results of an investigation of power production from low temperature excess process heat from a chemical cluster using Organic Rankine Cycle (ORC) technology. Process simulations and process integration methods including Pinch Technology and Total Site Analysis (TSA) are used to estimate the potential for electricity production from excess heat from the cluster. Results of a previous TSA study indicate that ca. 192 MW_{heat} of waste heat are available at 84 °C to 55 °C, a suitable temperature range for ORC applications. Process streams especially suitable for ORC power production are identified. Simulation results indicate that 14 MW_{heat} of waste heat are available from a PE-reactor, which can be used to generate ca. 1 MW_{el}. Costs of electricity production calculated range from 70 to 147 €/MWh depending on the cost for ORC integration. Economic risk evaluation indicates that pay-back periods lower than 4.5 years should not be expected at the electricity price and RES-E support (a European support system for renewable electricity) levels considered in this study. CO_2 emission reductions of up to 5900 tonnes/year were estimated for the analysed case.

Keywords: *Organic Rankine Cycle, Process integration, Total site analysis, Waste heat recovery.*

1. Introduction

1.1. Background

Growing awareness about the greenhouse effect combined with limited fossil fuel resources provide clear incentives for implementing energy savings measures and achieving CO_2 emission reductions in industry. One example to increase energy efficiency is the conversion of low temperature excess process heat into electricity using Organic Rankine Cycle (ORC) technology. The objective of this paper is to assess the potential for electric power generation from low temperature excess process heat at the chemical cluster in Stenungsund, Sweden. Results from a previously performed total site analysis [1] are used to determine the overall amount and the temperature levels of net excess heat from the cluster. Net excess heat is defined as heat that is available after all opportunities for process integration have been exploited and for which no other alternative use is available. Simulation of a selected ORC power cycle was conducted so as to quantify the power output and the overall performance of the system. A preliminary economic evaluation of a selected configuration is presented based on the simulations, supplier/literature data for ORC technology, engineering assumptions for ORC integration and scenarios for assessing profitability and carbon balances of energy investments [2]. The work aims at providing a basis for future projects to optimize energy usage and consequently lower costs and CO_2 emissions from the cluster.

1.2. ORC Technology

ORC is a technology to generate electricity from low temperature heat sources. Unlike in a conventional steam Rankine cycle, a low boiling point organic fluid is used as working fluid. In low temperature applications this technology offers advantages over conventional Rankine Cycles, and a higher heat recovery (efficiency) can be achieved [3]. ORC systems are mainly used in geothermal, solar and industrial waste heat recovery applications. Figure 1 illustrates the working principle of an ORC. The working fluid is pumped from a lower pressure level

(state 1) to a higher (state 2). Between states 2 and 3 the fluid exchanges heat with a waste heat stream in a heat exchanger and is evaporated. Contrary to Rankine cycle technology, the working fluid is usually not superheated after the evaporator. The vapour is then expanded in a turbine (state 4), which is connected to a generator to produce electricity. The expanded vapour is condensed by transferring heat to a cooling medium in the condenser (state 1). The cooling can be achieved by air coolers, cooling water or other heat sinks.

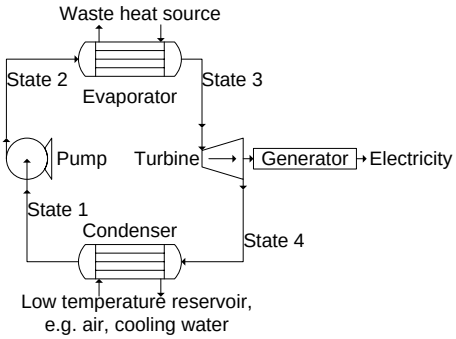

Fig. 1. Working principle of a simple ORC

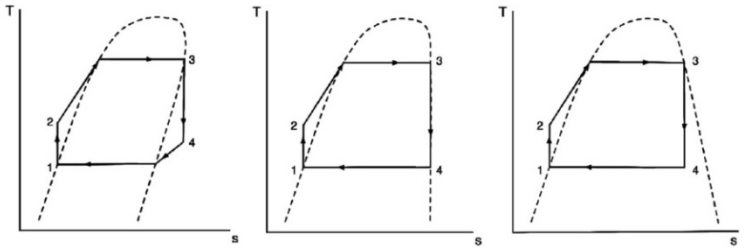

Fig. 2. Characteristic T-S process ORC diagrams for "dry", "isentropic" and "wet"-fluids [4]

The choice of the working fluid strongly influences the efficiency and economy of an ORC system. Working fluids can be divided into three different groups according to their behaviour in the thermodynamic cycle. Figure 2 shows the characteristic T-S diagrams for the three different types of working fluids. "Wet" fluids have a negative slope in the saturation vapour curve. Expansion in the turbine occurs entirely in the two-phase state, and the liquid fraction of "wet" fluids increases. The liquid droplets that form can cause blade erosion damage to the turbine. Condensation is easiest avoided by superheating of "wet" fluids. "Dry"-fluids have a positive slope (left), which means they do not condense during expansion since the degree of superheat increases as the expansion proceeds. Examples of such working fluids include organic substances such as benzene and refrigerants. The third group is "isentropic" fluids with quasi-vertical saturated vapour curves. Since the purpose of an ORC is to recover low temperature heat for electricity production, superheating is not appropriate. Therefore the working fluids used are either "dry" or "isentropic" [5]. Moreover, water has the disadvantage of having a higher specific volume compared to organic working fluids. This increases the size of the turbine, the height of the turbine's last stage blades and pipe diameters [3]. The working fluid should be selected with care so as to achieve a good match with the heat source characteristics and also the available cooling facilities. The following properties should also be considered: high thermal stability at the given operating conditions, low specific volume, low cost, low toxicity, low Ozone Depletion Potential (ODP) and low Global Warming Potential (GWP). The choice has to be based on careful analysis of the given conditions [6].

1.3. Results from total site analysis (TSA)

In a previous work the cluster was analyzed using TSA methodology [1]. The method is based on pinch technology and aims for integration of the heating and cooling demands of the different individual processes at a given site with a common utility system. In this way the amounts of hot utility generated and used by the combined individual processes, the amount of heat recovered in a common hot utility system, and the cogeneration potential can be determined [1]. The previous study [1] showed that the combined heating demand of process plants within the cluster is 442 MW of which 320 MW can be covered by heat recovery within the cluster, assuming that no changes are made to existing process utility levels. The

other 122 M W must be covered by hot utility, mostly in the form of boiler steam. Furthermore, the previous TSA study also showed that by making improvements to the overall utility system which enable increased energy collaboration between the companies it is possible to increase the amount of heat recovery at the site from 320 MW to 449 MW. As a result, boiler utility steam is no longer necessary. In addition a net surplus of 7 MW steam is achieved. The cooling demand of the cluster is then 506 MW at temperatures up to 84 °C.

These results are used in the present study to determine the maximum potential for power generation from low temperature excess heat within the cluster, using ORC technology. Because of the relatively low efficiency of low temperature heat-to-electricity conversion it is appropriate to only utilise net excess heat that cannot be utilised in another way [7]. The maximum potential for heat available for power production is estimated using TSA. Within the cluster available heat is estimated at Q_{ORC}=192 MW_{heat} at temperatures between 84°C and 55°C.

2. Methodology

2.1. Heat source selection

From the inventory of the excess process heat available, a selection is made to focus on streams with loads and temperature levels interesting for power generation and for which there is no alternative use. This temperature range was determined in a previous TSA study. The maximum heat source temperature for excess heat from the cluster is 84°C. The minimum allowable heat source temperature was selected as 55°C in order to achieve acceptable Carnot conversion efficiency values. Supplier information also confirmed this value of lower temperature limit [8].

2.2. ORC simulation

Literature data about ORC cycles only provided information about approximate efficiency values. Furthermore, it was necessary to evaluate different working fluids depending on the process conditions in order to achieve maximum efficiency. Therefore a simple ORC cycle was simulated in HYSYS. The cycle includes a pump, an evaporator, a turbine and a condenser. The tested working fluids are R134a, Propane, 1-Butene, Butane and Pentane as they are typical fluids for ORC applications at low temperature levels. The results are used as input for the economic evaluation.

2.3. Cost estimations

To determine the basic investment costs of the unit, the turbine capacity (in kW) is taken as the indicative size of the new unit. The equipment costs of a reference ORC-unit are estimated based on published data for a reference geothermal power plant located in Altheim, Austria with a capacity of 1 MW_{el} [9]. The equipment cost of this reference ORC-unit is 1.58 M€ (in 2000). This cost was updated using the Chemical Engineering Plant Cost Index (CEPCI) for 2010 and 2000, i.e. an update factor of 1.376 [10]. Furthermore, a scaling factor of 0.7 (widely used for electricity production) was used for estimating the investment costs of differently sized units [11]. The installed cost of the ORC unit can thereafter be calculated based on published cost data for an ORC plant in Lienz, Austria with an installation cost factor of 1.32 [12], which covers planning, installation and grid connection costs. Not included are the costs of integration in the considered process plant.

The costs for integrating the ORC into the process plant vary depending on the situation on-site, the process fluid, the location of the ORC-unit and other factors. Three examples of

projects presented by the ORC manufacturer Turboden [13] indicate integration cost factors ranging from 1.7 to 2.6. All projects include a thermal oil cycle which collects the heat from the waste heat source and delivers it to the ORC unit. For this reason those systems are more complicated and expensive than systems where the process stream is used directly, which might be the case for integration with a chemical cluster. Therefore integration cost factors from 1.1 to 2.6 were considered in this work. The annuity method is used for determining the annualized investment costs ($I_{\text{total annualized capital cost}}$) which are used to estimate the net Cost of Electricity (CoE) generation for the ORC plant. The assumed internal interest rate is 11 % (i_r). The economic lifetime (t_e) is assumed to be 15 years, as this is typical for CHP plants based on ORC technology [12]. The corresponding annuity factor is 0.14. Cost data for annual operating costs are assumed to be 3 % of the installed costs of the ORC plus the personnel costs (400 h/yr á 30 €/h) [12]. The CoE are calculated by Eq. (1)

$$\text{CoE} = \frac{I_{\text{total annualized capital cost}} + \text{Annual operating costs}}{\text{Annual electricity production}} \qquad (1)$$

CoE can then be compared with scenario values for electricity purchased from the grid. The economic value of the electricity produced is based on avoided costs of purchasing electricity. Five different grid electricity price scenarios are analysed, see Table 1.

In order to discuss the economic risk of investment in an ORC unit, the payback period for a new ORC investment is also calculated. The total annual savings take into account the avoidance of electricity purchased (equal to net power output of ORC) and the electricity saved by less cooling water pumping (2.5 % of net power output of ORC). When producing electricity from waste heat, which otherwise is cooled by cooling water, part of the cooling is saved. The main part of the cooling costs is the pump work in the cooling water system. In this study it is assumed that for each avoided MW of cooling, 0.025 MW_{el} are saved. These cost savings are calculated with the assumed electricity price and included in the annual cash flow to calculate the payback period (see below). An annual running time of 8000 h per year is assumed. The pay-back period for the ORC investment can then be calculated according to Eq. (2).

$$\text{Pay - back period} = \frac{I_{\text{total ORC}}}{(\text{Annual savings - Annual operating costs})} \qquad (2)$$

The scenarios were generated using the ENPAC tool, developed with the purpose of evaluating the performance of future or long-term energy investments at industrial sites using consistent scenarios. Scenarios chosen in this study include the current electricity price and two scenarios (high/low) for the years 2020 and 2030. RES-E support is currently not granted in Sweden for electricity production from waste heat with fossil origin. In this study both case (with and without support) will be shown in order to show its influence on the overall economic performance of ORC investments. By using a number of different scenarios that outline possible cornerstones of the future energy market, robust investments can be identified and the climate benefit can be evaluated. To obtain reliable results, it is important that the energy market parameters within a scenario are consistent. Consistent scenarios can be achieved by using a tool in which the energy-market parameters (e.g. energy prices and energy conversion technologies) are related to each other [14]. Table 1 shows the electricity prices, support levels for "green" electricity generation and CO_2 emissions from electricity production from the assumed long term marginal electricity production.

Table 1. Electricity prices, support for green electricity, CO_2 emissions from electricity production and marginal long term electricity production for the five scenarios [2]

Scenario		1	2	3	4	5
Year		2010	2020	2020	2030	2030
Fossil fuel price		2010	Low	High	Low	High
CO_2 charge	[€/ton]	20	15	58	15	58
Electricity price SPOT	[€/MWh_{el}]	51	46	74	45	81
RES-E support[1]	[€/MWh_{el}]	20	20	20	20	20
CO_2 emission from electricity production	[kg/MWh_{el}]	770	722	722	679	129
Long term marginal electricity production		Coal	Coal	Coal	Coal	Coal, CCS

[1]Premium paid to producers of electricity from renewable energy sources [2]

2.4. CO_2 emissions reduction

CO_2 emissions reduction by electricity produced with an ORC unit is calculated from CO_2 emissions data for future long term marginal electricity production in Table 1. It is assumed that electricity from the ORC unit replaces marginal electricity and that the waste heat used for electricity production has no alternative use (in this case the possibility to deliver waste heat to the district heating system close to the cluster is fully exploited).

3. Results

3.1. Heat source selection

One heat source is chosen as an example to carry out further investigations, including simulation of the ORC unit using HYSYS and economic assessment and calculation of CO_2 emissions reduction. The stream chosen is a loop reactor jacket cooling water stream with T_{start} and T_{target} of 78 °C and 68 °C, respectively. This results in a Carnot efficiency of 17 %. The heat load of the stream is 13970 kW.

3.2. ORC simulation

Simulations were carried out with different "dry" fluids appropriate for use in ORC systems. The main results are presented in Table 2. The turbine inlet and outlet pressure is chosen so that the boiling point of the working fluid is matched with the temperature profile of the heat source and the heat sink (cooling water at 20 to 25 °C) respectively. Among the five working fluids investigated, butane shows the best net electrical output and electrical efficiency. R134a and Propane are interesting cases, but the cycle needs to operate at higher pressure than the cycle with butane. Lower operating pressure should be preferred as increased pressure implies higher investment costs. Pentane is not suitable as the minimum pressure in the cycle is set to 0 bar(g), to avoid extra costs for vacuum operation. Pentane is more suitable for higher temperature heat sources. Butane has a slightly higher power output and efficiency compared to 1-Butene. The simulation with a mixture of pentane and butane does not show better results than with a single fluid, even though the temperature profiles of heat source and working media match better, which results in less exergy losses during evaporation. High performance is not reached with the mixture as the pressure difference for expansion in the turbine is not sufficient. Pentane limits the maximum and butane the minimum possible pressure in the given case (ΔT_{min} of 5 K in the evaporator and condenser). Butane was retained as working

fluid for the ORC unit. This cycle has a net electricity output of 958 kW_{el} (7.7 GWh/yr for 8000 hours/yr of operation), with 6.85 % electrical efficiency.

Table 2 Results from the simulation in HYSYS for an ORC unit using loop reactor cooling water heat source

	R 134a	Propane	1-Butene	**Butane**	Pentane	Butane +Pentane
$p_{turb,in}$ [bar(g)]	18.5	23	7.6	**6.2**	1.45	3.5
$p_{turb,out}$ [bar(g)]	6.7	9.8	2.5	**1.8**	0	0.6
$Q_{el,out}$ (net) [kW]	923	900	948	**958**	798	950
η_{el} [%]	6.6	6.4	6.8	**6.85**	5.7	6.8

3.3. Cost estimation

The results for the selected heat source stream are presented below. Costs calculations have been performed according to the procedure defined in Section 2.3. Table 3 shows simulation and economic results for the selected waste heat source assuming butane as working fluid

Table 3 Turbine capacity, basic equipment investment costs, installed costs and operating costs

Turbine output [kW]	Net power output [kW]	Equipment investment costs for ORC unit [€]	Investment costs ORC including installation [€]	Operating costs [€/yr]
993	958	2 163 489	2 855 806	97 674

The calculated CoE range from 70 to 147 €/MWh, depending on the integration cost factor, see Figure 3 and Figure 4. The electricity price scenarios in Figure 3 do not include RES-E support. It can be seen that at the current electricity price (Scenario 1: ca. 51 €/MWh) and without RES-E support, investing in an ORC is not profitable.

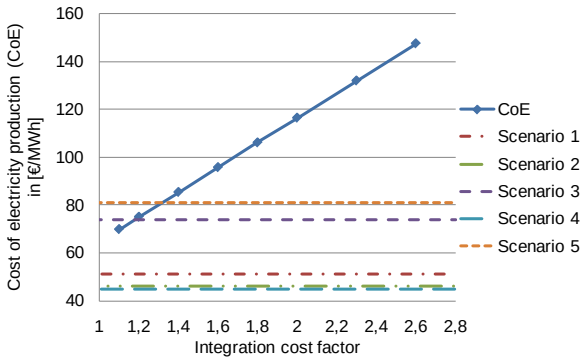

Fig. 3. CoE depending on the integration cost factor (with electricity price scenarios without RES-E support)

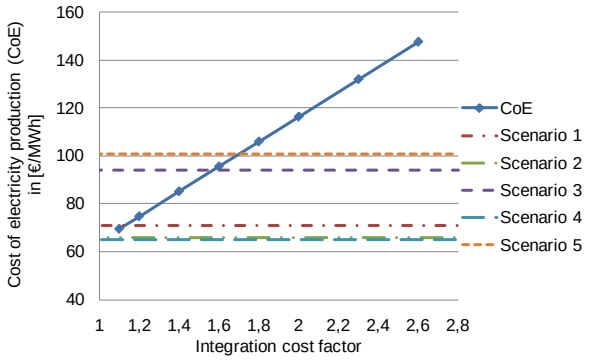

Fig. 4. CoE depending on the integration cost factor (with scenarios including RES-E support)

Without RES-E support, ORC electricity generation is only profitable for the two highest price scenarios (Scenario 3 and 5) considered in this study and at low costs of integration. If RES-E support is granted also more complicated integration is feasible at high electricity prices. At low integration costs even the current electricity price shows a feasible investment. Calculations on the pay-back period of an ORC investment show that without support for electricity production the pay-back period for the lowest costs of integration estimated (10 % of ORC installed costs) ranges from 5.8 to 12.3 years depending on the electricity price scenario. With RES-E support the pay-back period is decreased for the low integration factor

case to between 4.5 to 7.7 years. Even if RES-E support is considered, pay-back periods lower than 4.5 years should not be expected for ORC technologies at the electricity price and RES-E support levels considered in this study. On-site electricity production bears lower risks than other investments, as the produced electricity can be used on-site. This might justify longer pay-back periods. The scenarios used in this study include costs for CO_2 emissions from fossil-fuel fired power plants. It can also be seen that in the scenarios with low CO_2 emission charge (scenario 2 and 4) the costs of electricity production and pay-back period are highest, while high CO_2 emissions charge (scenario 3 and 5) shows lower values. Therefore CO_2 emissions charge is seen as an important parameter which has a large influence on the profitability of ORC investments.

3.4. CO_2 emissions reduction

Figure 5 shows the CO_2 emissions reduction in the different scenarios when electricity is produced with an ORC unit. It can be seen that the reduction is high if marginal electricity from coal power plants is replaced by electricity from the ORC unit, 5204-5902 tonnes-CO_2/year. The least reduction is achieved if marginal electricity is produced in coal power plants with carbon capture and storage (CCS) technology (989 tonnes-CO_2/year). This is the case because the electricity produced with an ORC replaces marginal electricity, which in the CCS case already has relatively low CO_2 emissions.

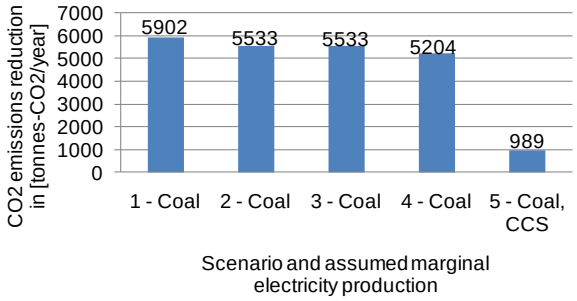

Figure 5 CO_2 emissions reduction associated with electricity production from excess process heat using ORC unit

4. Conclusions and Discussion

In this paper TSA methodology was used to identify the amount of net excess heat from a chemical cluster including the corresponding temperature levels suitable for low temperature heat-to-electricity production by ORC technology. For a more detailed analysis a suitable process stream was selected as heat source. Process simulation was used to determine the best working fluid for the suggested ORC unit, to calculate the net electricity output and the electrical efficiency of the unit. The simulation results were used for preliminary economic assessment and calculation of CO_2 emissions reduction potential based on different future energy market scenarios. From the TSA study it was found that there is 192 MW_{heat} at a temperature range between 84 °C and 55 °C available that can potentially be used for ORC applications. It was shown by process simulation that the selected ORC reaches an electrical efficiency of 6.85 % when converting ca. 14 MW_{heat} into 953 kW_{el}, using butane as working fluid. Economic assessment of the system shows a strong dependence of profitability to the costs for integration of the ORC unit in the process. Production costs were determined in a range between 70 and 147 €/MWh, indicating that at the current prices and without support an ORC project is not feasible and also only two out of seven scenarios showed feasibility without support. Depending on the scenario, pay-back periods between 5.8 to 12.3 years

assuming low costs of integration. RES-E support and CO_2 emissions charge were found to have a strong influence on profitability. Pay-back periods lower than 4.5 years should not be expected at the electricity price and RES-E support levels considered in this study, even if in the future support is granted for this kind of electricity production. Standardisation and technology improvements are expected to have a p ositive effect on the costs of ORC technology, leading to lower electricity production costs and pay-back periods in the future.

References

[1] R. Hackl, E. Andersson, and S. Harvey, "Targeting for energy efficiency and improved energy collaboration between different companies using total site analysis (tsa)," Chemical Engineering Transactions, vol. 21, pp. 301-306, 2010.

[2] S. Harvey and E. Axelsson, "Scenarios for assessing profitability and carbon balances of energy investments in industry," 2010. [Online]. Available: http://publications.lib.chalmers.se/cpl/record/index.xsql?pubid=98347. [Accessed: 24-Nov-2010].

[3] H. Legman and D. Citrin, "Low grade heat recovery," World cement, vol. 35, no. 4, pp. 111-116, 2004.

[4] P. J. Mago, L. M. Chamra, K. Srinivasan, and C. Somayaji, "An examination of regenerative organic Rankine cycles using dry fluids," Applied Thermal Engineering, vol. 28, no. 8, pp. 998-1007, Jun. 2008.

[5] T. C. Hung, T. Y. Shai, and S. K. Wang, "A review of organic rankine cycles (ORCs) for the recovery of low-grade waste heat," Energy, vol. 22, no. 7, pp. 661-667, Jul. 1997.

[6] B. F. Tchanche, G. Papadakis, G. Lambrinos, and A. Frangoudakis, "Fluid selection for a low-temperature solar organic Rankine cycle," Applied Thermal Engineering, vol. 29, no. 11, pp. 2468-2476, Aug. 2009.

[7] N. B. Desai and S. Bandyopadhyay, "Process integration of organic Rankine cycle," Energy, vol. 34, no. 10, pp. 1674-1686, Oct. 2009.

[8] Opcon, "Emission free electric power," 2010. [Online]. Available: http://www.opcon.se/www/files/oes/opcon_powerbox_eng.pdf. [Accessed: 07-Dec-2010].

[9] G. Pernecker and S. Uhlig, "Low-enthalpy power generation with ORC-turbogenerator, the altheim-project," in GHC BULLETIN, 2002.

[10] Chemical Engineering, "Economic Indicators," Chemical Engineering, vol. 117, no. 7 , pp. 59-60, Jul. 2010.

[11] B. Asp, M. Wiklung, and J. Dahl, Användning av stålindustrins restenergier för elproduktion: Ett effektivt resursutnyttjande för elproduktion. Luleå: Jernkontorets Forskning, 2008.

[12] I. Obernberger, P. Thonhofer, and E. Reisenhofer, "Description and evaluation of the new 1,000 kWel Organic Rankie Cycle process integrated in the biomass CHP plant in Lienz, Austria," Euroheat & Power, vol. 10, 2002.

[13] R. Vescovo, "ORC recovering industrial waste heat," Cogeneration and On-Site Power Production, vol. 10, no. 2, pp. 53-57, 2009.

[14] S. Harvey and E. Axelsson, Scenarios for assessing profitability and carbon balances of energy investments in industry. Chalmers University of Technology, 2010.

Modeling SOFC & GT Integrated-Cycle Power System with Energy Consumption Minimizing Target to Improve Comprehensive cycle Performance (Applied in pulp and paper, case studied)

H.A. Ozgoli[1,*], H. Ghadamian[2], N. Andriazian[3]

[1, 2, 3] *Department of energy, science & research campus, Islamic Azad University, Tehran, IRAN*
** Corresponding author. Tel: +98 9122449408, Fax: +98 21 44232205, E-mail: a.ozgoli@srbiau.ac.ir*

Abstract: This study has considered hybrid system SOFC/GT with the new approach. This cycle, as a power plant is designed to reduce losses and improve comprehensive cycle performance. In the first part cycle, fluidized bed system with biomass (wood chips) fuel using gas cleaning mechanism, produce combustible gases which are required fuel combustion chambers of steam reformer and the GT. Second part cycle, required hydrogen for SOFC system is supplied through external SR. In the third part, the treated bio syn-gas from the cleaning unit outlet, in conjunction with recycled exhaust gases of the cell's anode will feed SR and GT combustors. In the fourth part cycle, flue gas would pass through heat recovery steam generator. Thus, high pressure and low pressure steams with values 3.39&0.45 ton/hr, respectively are generated. In this study, SOFC and GT with a capacity of 1000 & 750.81 kW respectively are designed. Overall efficiency of power production 74.4% is obtained. In comparison with similar study done in 2008 at the University of Delft, that overall 47% efficiency, increasing the efficiency of such systems has been viewed.

Keywords: *Solid Oxide Fuel Cell (SOFC), Gas Turbine (GT), Bio syn-gas, Fluidized Bed (FB), Steam Reformer (SR), Comprehensive Cycle Performance*

1. Introduction

Recent studies have indicated that in integrated SOFC/GT cycles which employ natural gas, the overall efficiency of the system is estimated to be 50% to 60%. Burning and gasifying the biomass and combining the result with SOFC/GT system, enables the hybrid system to contribute to an efficient power plant [1], [2]. Generally, in order to generate power in a cost effective way and develop generating systems, distributed power generation has recommended an effective measure [3], [4]. The general prospect of the present study has been the integration of industries which normally generate combustible wastes and plants that consume such wastes. This study mainly focuses on de signing an integerated SOFC/GT power plant based on burning biomass in combustion chambers and reforming the natural gas in a steam reformer. The a-grade wood has been considered as the biomass in the planning and 1.75 MW of the electrical energy is expected to be generated. According to the field available technologies and the studies which have already been conducted in this field, our proposed cycle can be considered as a new approach in designing similar power plants in the future. A thorough analysis of energy in the system will determine and visualize the losses and realize the thermodynamically efficiency.

2. System Approach

2.1. Improving the efficiency

1- Trying to improve energy generation efficiency and enhancing energy transfer and distribution efficiency (utilizing CHP systems and cogeneration to maximize absorption and recovery).
2- Determining the essential fuel and each of the aforementioned units' efficiency.

2.2. Employing renewable form of energy

1- Calculation related to considerable amount of electrical energy by using renewable forms of energy (SOFC/GT).
2- Estimating a portion of required fuel by renewable forms of energy (Biomass gasification system).

2.3. Managing the industrial process products

1- Putting to use the by-products of industrial process (such as pulp and paper industry) to supply the fuel required for SR and GT systems [9].

2- Making use of hot flue gases and generated heat, for consuming in the comprehensive cycle and auxiliary units.

3. System Configuration

As it is illustrated in the figure 1, this system is comprised of different sections which have been pinpointed by the sections' names. These sections are as the following:

Fluidized bed system and gas cleaning, External Reforming SOFC system, GT system, HRSG[1] system, heat exchangers for pre heating fuel and air generating steam required for the reformer. Burning and gasification of the fuel biomass (wood) is usually preformed in the FB system. The gasifier operates at $500^{\circ C}$ and 4 bar. Heat is transferred by circulating the materials. Impurities within the components of the bed are separated from the gases by a C, SiO_2 separator [6], [7]. The gas which is exhausted from FB unit cannot be directly used within SR combustion chamber and GT. This is mainly due to the fact that the gas turbine. Therefore components such as H_2S, SO_2, COS and NH_3 are effectively removed from the exhaust gas [8]. Form chemical prospect, performing gas treatment, within the higher temperature ranges, seem to be able to be really demanding and imposes restriction treatment process. It is generally believed that the hot gas needs to be appropriately cooled down before being treated. Hot gas temperature is diminished to $500^{\circ C}$ in the heat exchanger [9], [10]. The cooled exhaust gas from cooling and treatment units is then mixed with hot exhaust gas from SOFC which mainly contain non-reacted steam and hydrogen. The mixture will then be transferred to GT and SR combustion chambers. The SR units have been employed to supply the fuel required for SOFC. This unit makes use of natural gas reformation to produce the fuel. The operating temperature and pressure of SR are considered to be $800^{\circ C}$ and 1 bar respectively [11]. The treated syn-gas from the cleaning unit outlet, in conjunction with recycled flue/exhaust gases of the cell's anode (off-gas), which contains some combustible remnants; will feed SR and GT combustors. The pressurized air is directed towards the cathode. Fuel cell with an external reformer (SOFC) is able to directly turn hydrogen, which is the product of already reformed natural gas method, in to electricity. The hot exhaust gas from the cathode (off-gas) is recycled to supply the gas turbine. The expanded flue gas has been used to recuperate the incoming air, after it had been pressurized. An air compressor attached to the turbine supplies the essential air for the integrated SOFC/GT system. Connecting the turbine to the generator, the second electrical current in the cycle is generated. HRSG system has been designed based on a dual pressure-mode in which both high and low steam pressures are generated, in order to improve the system performance and enhance steam generation rate. The results of the previous studies took the HRSG planning process into consideration. There is a feed water boiler in the methodology where the water supply after leaving LP (Low Pressure) economizer is split into two parts. One portion is directed

2- Heat Recovery Steam Generator

towards LP evaporator and another one to HP (High Pressure) economizer. Figure 2 illustrates the schematic performance mechanism of HRSG in the cycle [12].

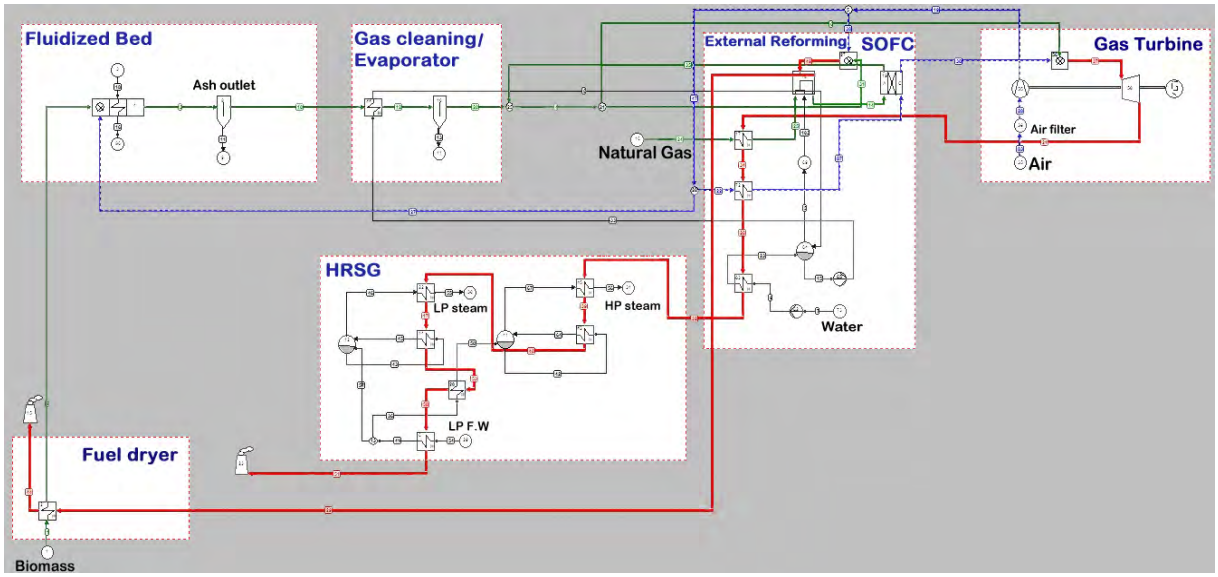

Fig. 1. Schematic of hybrid system

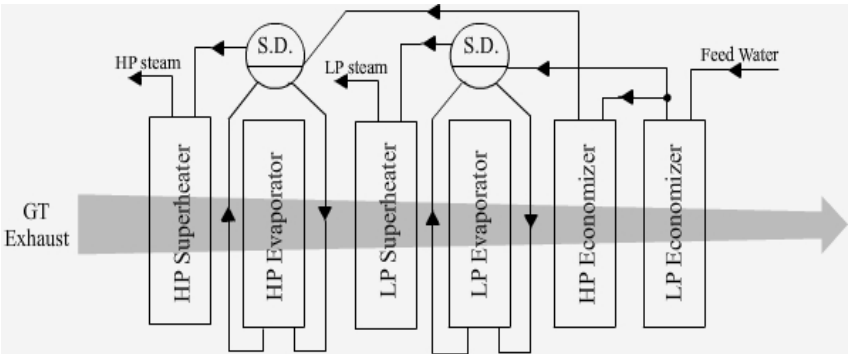

Fig. 2. Schematic of HRSG mechanism

4. System modeling

4.1. Model assumptions

In order to evaluate the system and obtain a balance between mass and energy of the cycle, Cycle-tempo software was employed. The main purpose of using such software was to create a model in the study state. Therefore a model consisting of subsystems has been created. Achieving a consensus on subsystem calculations is the prime objective in creating this model. There are some general assumptions which have been made in creating this model [13], [14].

- The whole system operates at steady state.
- In SR steam generating section, isentropic efficiency of the pump after the steam drum equals 75% and prior to the economizer is 85%.
- Isotopic efficiency of the compressor and gas turbine are 87% and 86% respectively.
- The mechanical efficiency for compressor and gas turbine is set to 99%.
- The generator efficiency is set to 98%.
- The pressure drop within the heat exchanger has been assumed to be zero. Pressure and temperature prior to the system have been listed in table 1.

Table 1. Pressure and temperature of fuels, air and water inlet to the system

Sink name	Pressure(bar)	Temperature(^{oC})
Biomass	4	15
Natural gas	1.18	15
Air	1.013	15
Water*	1.2	20

* Inlet water in SR system

The operational temperature of the fuel cell is 950^{oC} and the pressure is 3.45 bar. The fuel cell area is supposed to be 700 m^2 and the fuel cell resistance 0.75 $\Omega.cm^2$. The efficiency of the DC/AC converter is 96%.

Figure 1 illustrates the SOFC and GT integrated cycle power system schematically. Based on temperature and pressure, two different types of system are generated in HRSG unit. High pressure steam (50 bar) which is as hot as 470$^{°C}$ and low presser steam of 15 bar and 270$^{°C}$.

4.2. Preliminary discussion

With a view to reach a higher efficiency in SOFC/GT hybrid system, the following points should be considered in planning the cycle.

- The combustible gases which have been produced in FB can be directly used in SR and GT combustors.
- Making use of the released heat while cooling the gas leaving FB and prior to cleaning which can be used to supply the necessary steam for SR unit.
- Employing a portion of the gas turbine flue gas heat in pre heating the fuel (natural gas) and the air entering the SOFC system.
- Using the pressurized air by the gas turbine compressor in the cathode.
- Using a great deal of gas turbine flue gas heat to generate steam in HRSG.
- Making use of the exhaust heat from SR in drying biomass entering the system.

After considering the application of a SOFC system with a constant power of 1MW for reaching such power in GT, the present study adjusted reaction pressure and outlet pressure of the FB unit to 4 bar. The outlet pressure of the compressor was sent to 3.46. Minimizing fuel consumption was one of our other objectives.
Comparing this hybrid system with 1.75MW gas turbine system within similar temperature & pressure states, implies a considerable reduction in fuel consumption. Table 2 shows the comparison of these two systems.

Table 2. Comparison of fuel consumption in hybrid and GT systems with similar capacity

System type	Natural gas consumption (kg/hr)	Biomass consumption (kg/hr)
Hybrid system	159.41	129.6
Gas Turbine system	1396.8	-

In order to substitute the integrated system of heat and power generation, a pulp manufacturing plant which is also capable to be developed to produce pulp and paper (the 22Bahman particle board manufacturing company located in northern city of Behshahr in Iran) was considered. This plant is traditionally supplied by the regional electrical transmission network in tandem with burning fossil fuel, to run its manufacturing process. The main characteristics of this study are presented in table 3. The annual production of the

plant has been estimated to be 41438880 kg. The capacity which has been selected for the hybrid system is in congruity with electrical power consumption of the plant.

Table 3. Energy consumption comparison between the Traditional and integrated power generation

	Description	Energy unit
Traditional system	Electric power consumption	52753716 MJ
	Heat consumption	60802100 MJ
	Specific energy consumption (SEC)	5.28 MJ/kg
Hybrid system	Electric power generation capacity	1.75 MW
	Heat consumption	97136501 MJ
	Specific energy consumption (SEC)	2.34 MJ/kg

Based on the results from the study, the specific energy consumption shows a decrease of 2.94 MJ/kg. The first reason for such decrease is electrical power generation in the new system. The second reason to be mentioned is daily generation of 690.65 kg waste product which constitutes the 22% biomass fuel essential for hybrid system.

5. Results and conclusion

5.1. Quantitative approach

In the present model, according to the power generation capacity of the integrated SOFC/GT system which is 1.75 MW the mass flow rate entering biomass is set to be 129.6 kg/hr. The already generated gas leaved FB with 4 bar and 1543.04$^{\circ C}$. The main ingredients and their mole fractions have been shown in table 4.

Table 4. Mole fractions of FB exhaust gases

Component	Mole fraction (%)
H_2	7.07
N_2	49.72
CH_4	4.34
H_2O	18.45
CO_2	18.42
CO	1.37
AR	0.59

Here, 31.9 kg/hr ash leaves the system as mentioned earlier; the mixture contains some harmful gases which will affect the SR and GT system unless they are controlled. The gas which has undergone cleaning process is mixed with the gas leaving the fuel cell anode under a pressure around 3.45 bar. The hot flue gases (1200$^{\circ C}$) from the combustor enter SR. SR requires steam with a flow rate of 460.26 kg/hr. In view of the reactions occurred in SR, the convenient fuel with a mass flow rate of 619.67 kg/hr, are generated in SOFC. The fuel cell operating at 950$^{\circ C}$ produces 1000 kW of electrical energy. Not all fuel is converted in the SOFC stack; the fuel utilization is 85%. The SOFC characteristics for current & power densities are rendered 1963.04 A/m^2 & 1488.1 W/m^2 respectively. The TIT[1] is 1100$^{\circ C}$. Expansion of the mixture of gases entering the turbine 1276 kJ/kg generates power. Having

1- Turbine Inlet Temperature

preheated the fuel and air in the SOFC system, and also exchanged heat in SR steam generating economizer, the flue gas from the gas turbine enters HRSG; meanwhile its energy content and temperature are 3908.7 kW and 782.94$^{\circ C}$ respectively. Economizer outlet is split into two 183$^{\circ C}$ currents, which enter the LP and HP evaporators. The outlet pressures of HP and LP evaporators reach 15 bar and 50 bar respectively. The flow rate of steam leaving HP and LP super heater outlets are 0.45 ton/hr and 3.39 ton/hr respectively. Energetic HRSG efficiency equal to 92% was obtained. In table 5 the energy inputs and consumptions of the system for the conversion of biomass into electricity are presented.

Table 5. Energy input and consumption of the biomass gasifier and SOFC-GT hybrid system

	Biomass	Natural Gas	Fuel Cell	Gas Turbine
Absorbed power(kW)	670.32	1682.81	–	–
Delivered gross power(kW)	–	–	1000	750.81

5.2. Qualitative approach and recommendations

In the Figure 3, the nature of heat recovery and constant output is reasonable. Increase in bio fuel consumption is mainly due to FB system performance as a bottleneck. We have to cross out (as a decrease) in some of the objective to increase Bio. In reality if there is a necessity for increasing the bio fuel, right after that increase ash production rate is maximized to a great extent and puts a restriction on power generation and heat recovery.

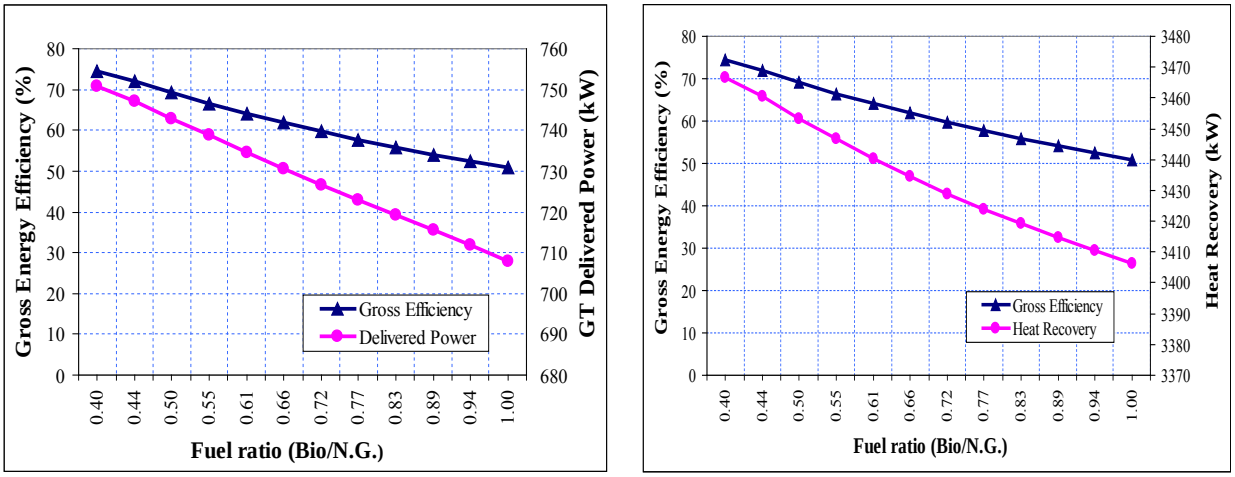

Fig. 3. Fuel ratio variations against hybrid system energy profiles

The point that is worth mentioning is that geometry of the bed and incoming fuel level can be increased but the thermal value and residence time, which is considered to be a more important factor, are limited. In Figure 4(a), the real difference in curves' tails is strongly depends on irreversibilities that taking place by more rated pressure in GT. (As GT's property, sacrificing efficiency against more power production is technically predicted).

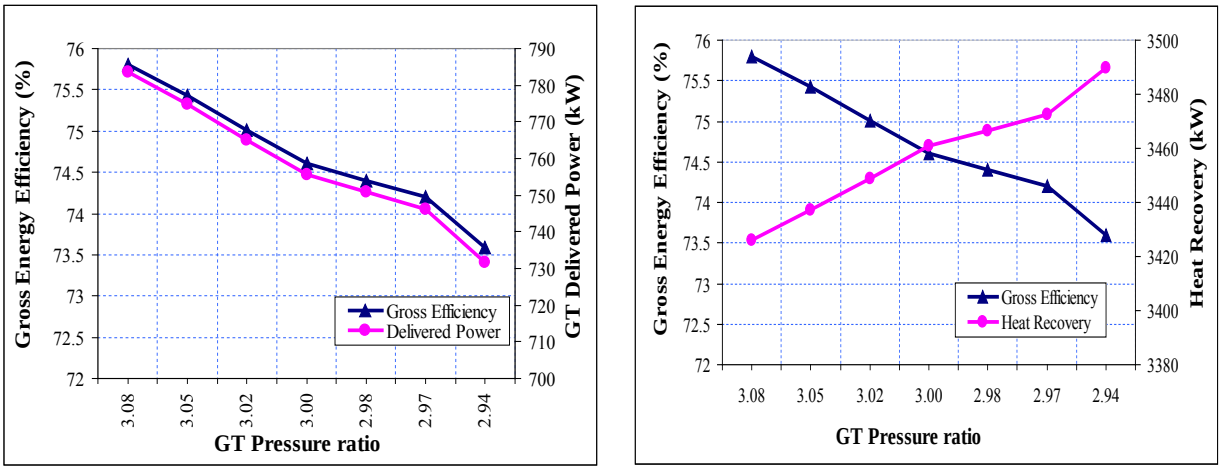

(a) *(b)*

Fig. 4. GT pressure ratio variations against hybrid system energy profiles

But in Figure 4(b), the pressure ratio in GT is working as a balancing element, which is correlated directly with GT delivered power and inversed with Heat recovery. These explanations are clearly demonstrated in mentioned graphs. In this stage a trade-off point is found at 3 for pressure ratio, which covers all two targets named GT delivered power and heat recovery. This point can be applied as a nominative reference for our designed system called best practice point in our modeling approach. In the comparison of graphs Nos. 4(a), 4(b) it can be observed that mentioned increased irreversibilities based on pr essure decreasing, would be transferred to stack as an increased source for heat recovery. The best proportion for electricity generation in an integrated SOFC/GT system is 60 to 40 [15]. Therefore the power which is expected to be generated by the system is planned in such a way that 1000 kW is generated by SOFC. Likewise according to the assumptions and calculations conducted, the power generated by GT equals 750.81 kW. As it c an be implied from table 5, the gross efficiency of the cycle is 74.4%. This can be compared with the gross efficiency of the similar study which had been conducted in university of Delft [3]. It is thus evident that an increase in gross efficiency has been fulfilled. Such increase can be attributed to the following reasons.

1. Direct burning of FB combustible gases output at GT combustion chambers and SR
2. Using natural gas (with a higher percentage of hydrogen) as fuel input SR system and its sense of more appropriate quality in fuel Sign for SOFC
3. Changes in the recovery position of SOFC gas combustible system, comes from SOFC process recycling by adding them to the purified gas cleaning unit (obviously, internal reforming itself is a part of the energy consumption indeed)

In order to obtain a h igher efficiency and higher steam mass flow rate generated by the system, some changes in heat exchangers' locations were applied. The pinch point which is located between the evaporator's outlet and inlet has been adjusted to be 10 ^{o}C. LP and HP steam produced in the cycle can be used for steam units placed side-consumer. Also adding a steam cycle power generation, steam production can be used to generate electricity. Thus, the overall efficiency of power production systems will increase.

References

[1] L. E. Fryda, K. D. Panopoulos, and E. Kakaras, Integrated Combined Heat and Power with Biomass Gasification and SOFC-micro Gas Turbine, VGB PowerTech 4, 2008, pp.66-72.

[2] F. Calise , M. Dentice d' Accadia , et al., Single-level optimization of a hybrid SOFC–GT power plant, Journal of Power Sources 159 ,2006, pp.1169–1185

[3] R. Toonssen, N. Woudstra, and A.H.M. Verkooijen, Reference System for a Power Plant Based on Biomass Gasification and SOFC, Delft University of Technology Energy Technology, Process & Energy department, 2008

[4] F. Calise, M. Dentice d' Accadia, et al., Full load synthesis/design optimization of a hybrid SOFC–GT power plant, Energy 32, 2007, pp.446–458

[5] M. Sucipta, S. Kimijima, and K. Suzuki, Biomass solid oxide fuel cell-micro gas turbine hybrid system: Effect of fuel composition, Journal of Fuel Cell Science and Technology 155, 2008, pp.B258-B263

[6] S. Baron, N. Brandon, et al., The impact of wood-derived gasification gases on Ni-CGO anodes in intermediate temperature solid oxide fuel cells, Journal of Power Sources 126, 2004, pp. 58-66.

[7] K.V. Van der Nat, N. Woudstra, Evaluation of several biomass gasification processes for the production of a hydrogen rich synthesis gas, Proceedings International Hydrogen Energy Congress and Exhibition IHEC 2005

[8] W. Doherty, A. Reynolds, D. Kennedy. Modeling and Simulation of a Biomass Gasification-Solid Oxide Fuel Cell Combined Heat and Power Plant Using Aspen Plus, Proc. 22nd International Conference on Efficiency, Cost, Optimization, Simulation and Environmental Impact of Energy Systems, 2009

[9] R. Toonssen, P. V. Aravind, et al., System Study on Hydrothermal Gasification Combined With a Hybrid Solid Oxide Fuel Cell Gas Turbine, Fuel Cells, 10, 2010, pp. 643–653

[10] S. Poulou, E. Kakaras, High tempera-ture solid oxide fuel cell integrated with no-vel allothermal biomass gasification: Part II: Exergy analysis, Journal of Power Sources 159, 2006, pp. 586-594

[11] A. Sordi, E. P. da Silva, et al., Thermodynamic Simulation of Biomass Gas Steam Reforming for a Solid Oxide Fuel Cell (SOFC) System, Brazilian Journal of Chemical Engineering 26, 2009, pp. 745-755

[12] N. Andriazian, off-design performance modeling of gas turbine cycles considering exergy-cost trade-off and CO2 capture, M.Sc thesis, IAU, 2008

[13] EG&G Technical Services Inc., Fuel Cell Handbook, U.S. Dept. of Energy Office of Fossil Energy National Energy Technology Laboratory, Morgantown, West Virginia, 2004

[14] L. Fryda, K.D. Panopoulos, and E. Kakaras, Integrated CHP with autothermal biomass gasification and SOFC- MGT, Energy Conversion and Management 49, 2008, pp. 281-290

[15] T.W. Song , J.L. Sohn, et al., Performance characteristics of a MW-class SOFC/GT hybrid system based on a commercially available gas turbine, Journal of Power Sources 158, 2006, pp.361–367

Studies of preferences as an extra dimension in system studies

Stina Alriksson[1,*], Carl-Erik Grip[2]

[1] *Linnaeus University, School of natural science, Kalmar, Sweden*
[2] *LTU (luleå University of technology) Dept Energy technology, Luleå, Sweden*
** Corresponding author. Tel: +46 480 446773, Fax: +46 480 447305, E-mail: stina.alksson@lnu.se*

Abstract: Industrial energy systems are complicated networks where changes in one process influence its neighboring processes. The network complexity increases if production/use of bio fuel is introduced in an existing system. Process integration can be a useful tool to study such systems and thus avoid sub optimization.

However, changes in an industrial complex do not only influence the technical values of energy and material efficiency. The social impact is also important and sometimes is comparable to that of technical factors.
A process integration project has recently been carried out for a paper mill in northern Sweden with a side view on future expansion with a bio refinery. An activity to study the social impacts were included through a Conjoint analysis, a stated preference method that combines statistics and interviewing technique.

The results indicate that the participants are divided in four groups, the largest group focusing on a change in the process towards a bio refinery, the second largest focusing on the local environment. The third and fourth group both look at the local forestry, one group wanting to increase local forest production, and one rejecting an increase.

Keywords: *process integration, bio refinery, conjoint analysis, social values.*

1. Introduction

1.1. Pulp and paper – development of energy efficiency and biofuel production

The Swedish wood industry is an important part of the Swedish economy and is responsible for 12 % of the Swedish export. Totally, it is the world's second largest exporter of total paper, pulp and sawn timber. The forest industry is Sweden's largest user of bio-energy and also the largest producer of bio energy. Presently this energy is used mainly internally [1]. A lot of effort is put on work to improve energy efficiency and sustainability. Also several large projects have been started on conversion of by-product into bio fuel e.g. green motor fuel [2].
A partly conversion of a paper producer into a bio refinery involves a lot of changes which will influence the rest of the mill, the employees, the surrounding society and the interaction with the actors involved in supply of wood raw material. It is important, in order to get a successful practical implementation, to consider also non-technical factors, like ete attitudes and reactions of these actors.

It was decided to test these ideas in a process integration project that was carried 2009-2010 in an existing pulp and paper mill. The project studied changes to improve energy efficiency as well as a hypothetical transformation to also include a bio refinery [3]. The project included several different methods and models. A process integration model of the paper mill was developed using the mathematical programming tool reMIND [4]. The results from this model was compared to a Pinch-analysis. The work also included a study on the effect on the wood suppliers and market prices of raw material, using the tool ReCOM, a regional economic market model. A study using the conjoint method [5] was included to study the effect of a plant conversion on attitudes and popular acceptance. Only plant employees were included as test group to limit the size of the first study.

1.2. What is conjoint

The choices people make are based on many things as previous experiences, training, attitude, habits, ethics etc. A person will choose the product or alternative that is most useful for this person (utility theory). The decision is formed by simultaneously considering multiple factors, a unique quality of the human brain. On a daily basis a person makes hundreds or possibly thousands of choices in this way, and this is what the method of conjoint analysis takes advantage of.

Conjoint analysis is a stated preference method, which can be used to assess people's preferences for a specific product, service or situation. It is used to evaluate the attributes of the product/service/situation and thereby makes it possible to determine which attribute is the most important in the evaluated situation. Individual or group level preferences can be estimated by decomposing the responses into part-worth's, thus the results come in quantitative measures which means that they can potentially be incorporated into other models such as process integration models and/or economic models. Studies have previously been made in which conjoint analysis results has been integrated in a Life Cycle Assessment (LCA) as weights in the environmental valuation phase [6]. There has been some attempts to integrate process integration with economic modeling [7] but to the best of out knowledge studies of social values has never been integrated in a process integration project. Further information on conjoint analysis can be found in [8-11].

The purpose of the study was to study the preferences of the employees when asked to compare local environment, global environment, increased local forest outtake and change of process from paper/pulp to paper/pulp and bio refinery. Another aim of the study was to find methods to integrate the result with the process integration result.

1.3. Scope of paper

The paper describes the conjoint method as such, the possibility to integrate the result with process integration models and economic models, as well as the possible use of the results as a basis for decision-making in the paper mill as well as for community decisions.

2. Methodology

The study was carried out through a web-based questionnaire where employees at a paper mill were asked to rank eight different alternatives where local and global environmental impact, local forestry and change in the process were altered in different ways. From the responses, individual as well ass average preferences have been estimated.

2.1. Conjoint analysis

In a conjoint study, the respondent is asked to evaluate a set of alternatives where the factors are varied in a fractional factorial design (reduced design), with two or three levels of each factor (attribute). The factors must be carefully chosen, and can be identified through group discussions, in depth interviews or expert elicitation. Each factor must be provided with two or more levels (high/low). The number of factors must be limited since respondents will not be able to maintain the same level of concentration if the number of evaluations is too large. Four to six attributes are often considered functional [11].

The alternatives that the respondents are asked to evaluate are created through an experimental plan. In order to keep the workload manageable for the respondents the number of alternatives to evaluate needs to be kept at a reasonable level.

The factors were chosen through discussions with Billerud Karlsborg AB in order to make the study relevant for the paper/pulp mill. Relatively early in the process it was decided that the study should be held internally at Karlsborg in order to avoid rumours and speculations in the surrounding society since a bio refinery is not planned in Karlsborg as of today. In the final design of the study, a fractional factorial design with four factors in two levels (2^4) were used, see table 1. The resolution of the design was IV, and only main effects were studied.

Table 1, The design of the study.

Alternative	Local forestry	Process	Emission of carbon dioxide	Local environmental impact
A	Same as now	Pulp/paper + bio refinery	Same as now	20% increase
B	Same as now	Pulp/paper	Same as now	Same as now
C	Same as now	Pulp/paper + bio refinery	Decrease	Same as now
D	Increased outtake	Pulp/paper + bio refinery	Decrease	20% increase
E	Increased outtake	Pulp/paper	Same as now	20% increase
F	Increased outtake	Pulp/paper + bio refinery	Same as now	Same as now
G	Same as now	Pulp/paper	Decrease	20% increase
H	Increased outtake	Pulp/paper	Decrease	Same as now

The study was distributed as a web questionnaire. A message was posted on the intranet to encourage employees to participate. The questionnaire consisted of three parts, first an introductory letter with information on the study and the factors, then the conjoint analysis where the respondents were asked to rank the alternatives in Table 1 from 1-8, and finally the participants were asked questions on residency, age, gender, educational level, work situation and any training in energy efficiency, environment, work environment and forestry.

All employees hand the opportunity to fill out the questionnaire, it was open for two weeks in order to cover all shifts. In all 61 persons answered the questionnaire and from these six responses had to be removed due to inconsistent answers, leaving 55 responses. There are 425 employees at the mill leaving us with a response rate of 13%.

2.2. Analysis of data

In this study two ways of analysing the data are used, first by calculating the main effects from the experimental plan, and then using partial least squares regression, PLSR.

Partial Least Squares Regression (PLSR) is a bilinear multivariate regression method that can simultaneously handle several response variables. PLSR is based on a linear transformation of the original variables to a limited set of latent variables (orthogonal factors), PLSR also attempts to maximize the covariance between the independent and dependent variables. The main advantage of PLSR is that the results can be presented graphically with all individual responses visible. Further information on this method can be found in [12]. The Unscrambler software was used to perform the PLS regressions in this survey [13].

Cluster analysis has proven useful to find segments among respondents in conjoint analysis studies [14-15]. The cluster analysis forms clusters of the respondents by putting respondents (samples) that are similar to each other into groups, at the same time as respondents that differ in response are kept apart. In this project, a hierarchical cluster analysis was applied to the individual main effects from the experimental plan (cluster method: between-groups linkage and interval measure: squared euclidean distance). The analysis was performed with the classification unit from the SPSS v. 17.0 software package [16].

3. Results

3.1. Respondents

Age and gender of the respondents can be seen in table 2. 22 respondents (40%) worked with operation of the mill, 12 respondents (22%) worked with maintenance, 9 respondents (16%) worked with process- and product development and 11 respondents (20%) worked with administration. 41 of the respondents (75%) worked daytime while 14 (25%) worked shifts.

Table 2, age and gender of the respondents in numbers.

Born	80's	70's	60's	50's	40's	No information	Sum
Men	3	6	9	18	6	2	44
Women	3	3	2	3	0	0	11

37 respondents (67%) lived 6-30 km from Karlsborg, 10 respondents (18%) lived in the vicinity, i.e. closer than 5 km and 8 respondents (15%) had more than 31 km to Karlsborg from their homes. 29 of the respondents (53%) were forest owners (or had someone in their closest family that owned forest), 25 respondents (45%) were not and 1 respondent (2 %) did not give any information on this question. 5 of the respondents (9%) had finished primary school, 27 respondents (49%) had finished secondary school and 23 respondents (42%) had a university degree.

3.2. Preferences

The average results are presented in Figure 1. It must be remembered that the number of respondents is small, only 55 complete responses, which means that the result could probably look different with more respondents.

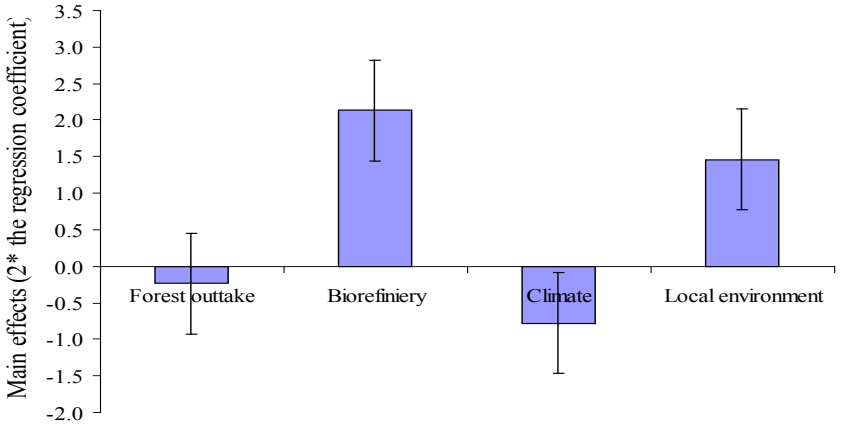

Figure 1. Averaged main effects with standard error for all respondents.

By using a PLSR-plot, individual results can be illustrated, see Figure 2. In the plot, the numbered marks represent individual respondents while the factors are marked with text. The PLSR plot is multi-dimensional, but here, only the first two latent variables are shown,

making the graph two-dimensional. The plot can be interpreted like a map, the closer a respondent lies to a factor, the more important the respondent regard the factor. The plot also reveals negative correlations when a respondent lies on the other end of the latent variable (axis) from a factor, she or he has a negative preference for the specific factor.

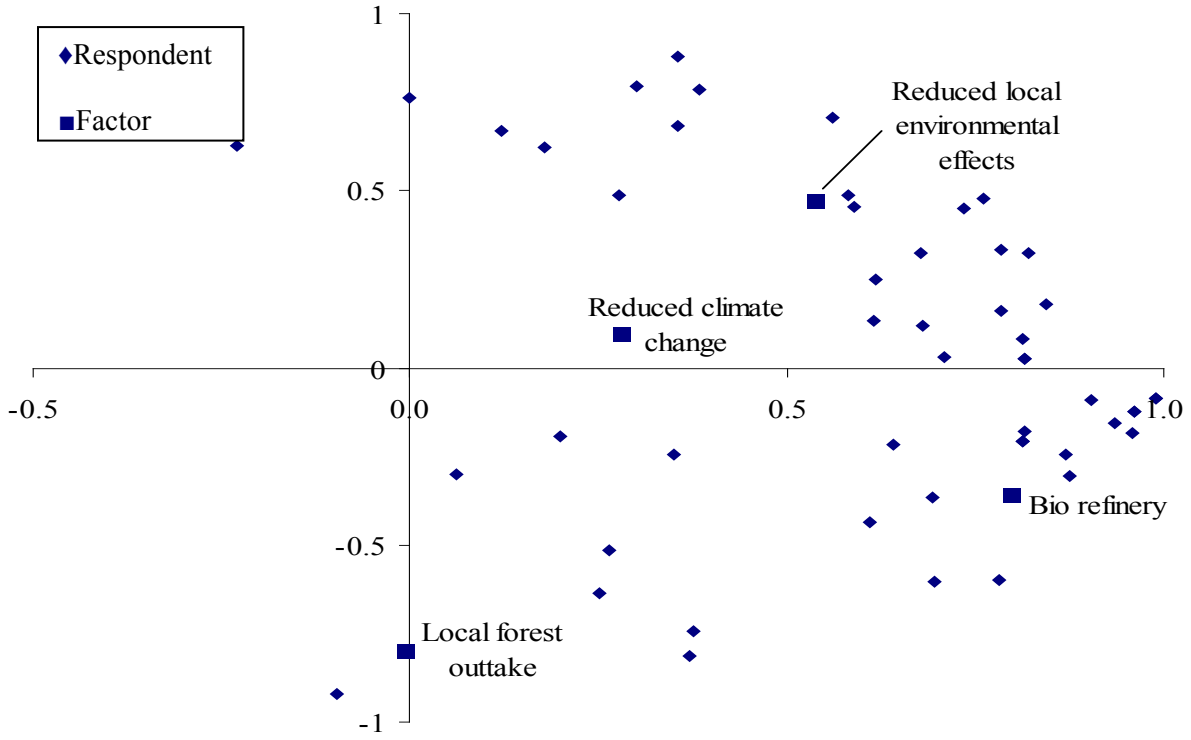

Fig 2. PLSR2. The first two latent variables explaining 65% of the total variance.

If the preferences are compared to the known facts on the respondents, from the information they left in the questionnaire, women are generally more concerned for the local environment than men (p=0.009). Age influence the view on local forestry (p=0.011). Preferences for the local environment are influenced by educational level (p=0.016) and whether or not the respondent or anyone in her/his close family own forest (p=0.010).

If respondents working with maintenance are compared to respondents working with process and product development, there is a significant difference in how they prioritize an increase in forest outtake (p=0.033), see Figure 3.

3.2.1. Training

Respondents with a university degree prioritise increased forest outtake more than respondents with primary and secondary school degrees (p=0.046). 10 respondents had taken part in three or four of the training subjects (forestry, energy, environment or work environment) and for these respondents preferences for forestry differed significantly from the others (p=0.010). The training subjects individually had no influence on the preferences at all. One more thing is interesting to notice, all educations correlate to each other, i.e. if a person has attended one education, she or he is more likely to attend educations in other areas as well.

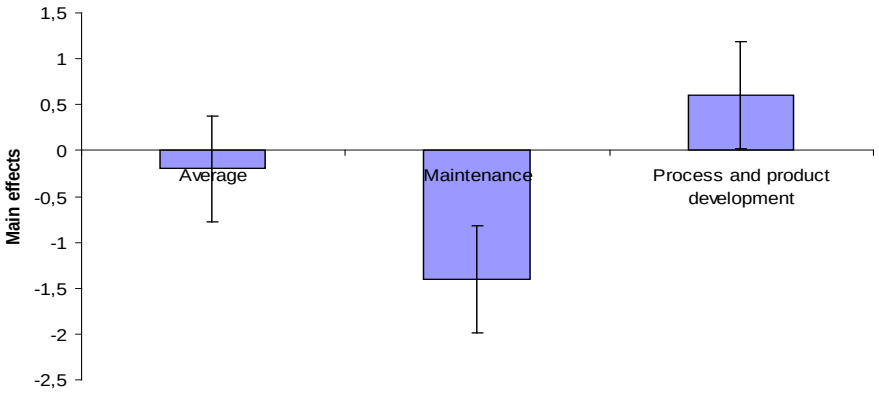

Fig 3. Averaged main effects for respondents working with maintenance (n=12) and process and product development (n=10).

3.2.2. Clusters

Through cluster analysis four clusters (groups) of respondents were formed, see Figure 5.

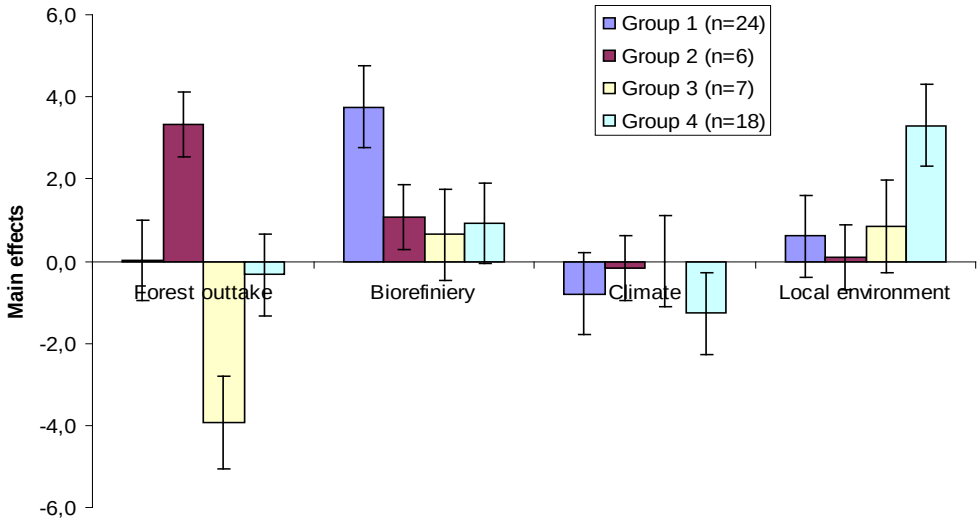

Fig 5. Groups created through cluster analysis.

The number of respondents in this study are to few to draw any further conclusions from the clusters, but in a large-scale study, the clusters could be analyzed for common characteristics such as educational level, occupation, gender etc.

4. Discussion and Conclusions

4.1. Discussion

The number of respondents were fewer than most favorable, probably due to many different reasons. The questionnaire was made available on the Billerud intranet for two weeks, in order to cover all shifts, but it would probably have needed further marketing for more employees to fill out the questionnaire. It would have been preferable to have at least 100 correct responses to the questionnaire.

The results from a conjoint analysis are quantitative. They can be averaged for the whole group or presented individually for each respondent. New groups can also be found through

cluster analysis (see Figure 5). Since the number of respondents are so small, it is not possible to draw any further conclusions on common features among the people in the same group (cluster), but with a larger set of samples (respondents) this would be possible. For the industry this means that it could be possible to pinpoint groups of employees that can be especially helpful in implementing new energy efficient processes, or groups that need extra information to be able to carry out new procedures in a correct way.

Conjoint analysis has been used to illustrate and discuss if the results from a conjoint analysis can be used together with a process integration tool such as a remind model and/or an economic model such as the ReCOM model.

The quantitative results can be used in process integration in several ways, see Figure 6.

A It can be used together with en economic model such as ReCOM as a means of choosing scenarios in the model. The factors in the conjoint analysis can be tailored to indicate how the market would respond in a hypothetical situation.

B Conjoint analysis can also be combined with economic theory and used to derive Willingness To Pay (WTP). This implicit pricing can also be used in economic models such as the ReCOM model. The economic model can be used to derive relevant levels to the factors of the conjoint analysis.

C Conjoint analysis can be used to weight different factors in the process integration model. The weighting can possibly also be used in the economic model. The factors will need to bee rather specific, for example emission of NOx from process XX.

D A process integration model can be used to derive relevant levels to the factors of the conjoint analysis.

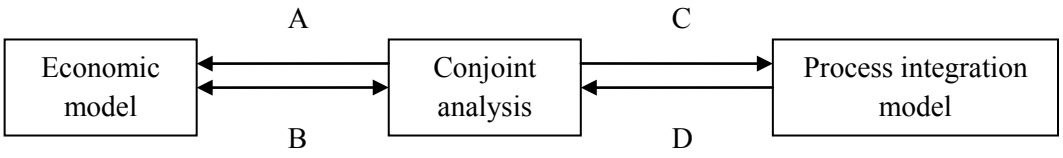

Figure 6. Possible exchanges between conjoint analysis, a process integration model such as a remind model and an economic model such as the ReMIND model.

4.2. Conclusions

Preference studies using Conjoint can be an important tool in studies and actions to improve energy efficiency and sustainability. It can be related in different ways to process integration models and economic models associated with them.

It is also interesting to notice that it is possible to find groups of respondents that were unknown previous to the study, as with the example with two groups of employees working with maintenance and process and product development. If an organisation wants to implement a change in the process conjoint analysis can be used to identify groups of participants with similar preferences and then tailor information to suit these specific groups.

The results of this study leave no clear information on the effect of training. If behaviour and attitudes of the employees are crucial for the full scale implementation of a process integration model, more research needs to be done on the effect of training. In this study, there were no significant connections at all between training and preferences.

Acknowledgements

The authors would like to thank the Swedish energy agency and the Billerud Karlsborg paper mill for financing the work. Also the people at Billerud Karlsborg are thanked for their cooperation in the work

References

[1] Home page of the Swedish forest industry, http://www.skogsindustrierna.org/ 2010-12-15

[2] Products from the forest – a natural choice- The Swedish Forest Industry's sustainability publication 2008–2009. http://www.forestindustries.se/web/Publications_and_surveys.aspx 2010-12-15

[3] Lundgren J. et. al. Development of a regional-economic process integration model for Billerud Karlsborg AB. 2010

[4] Ji X., Lundgren J., Wang C., Dahl J., Grip C-E. Process simulation and energy optimization of a paper and pulp mill. Presented at PRES, Prague, August 28 – September 1, 2010.

[5] Grip C-E, Lundmark R, Alriksson S. Possibilities for combined evaluation of social, economic energy/environmental values. Presented at the International Seminar on Society & Materials, SAM3, Freiberg 2009

[6] Itsubo, N., M. Sakagami, T. Washida, K. Kokubu and A. Inaba, Weighting across safeguard subjects for LCIA through the application of conjoint analysis, International Journal of Life Cycle Assessment 9, 2004, pp196-205.

[7] Sammons NE, Yuan W, Eden MR, Aksoy B, Cullinan HT, Optimal biorefinery product allocation by combining process and economic modeling, chemical engineering research and design 86, 2008, pp 800–808

[8] Green, P. E. and V. Srinivasan, Conjoint analysis in marketing: new developments with implications for research and practice, Journal of Marketing 54, 1990, pp 3-20.

[9] McCullough, D, A user's guide to conjoint analysis, Marketing Research 14,2002, pp 18-23.

[10] Gustafsson, A., A. Herrmann and F. Huber, Conjoint measurement – methods and applications, Springer Verlag, 2003, Berlin.

[11] Alriksson, S. and T. Öberg, Conjoint analysis for environmental evaluation – a review of methods and applications. Environmental Science and Pollution Research 15, 2008, pp 237-250.

[12] Martens, H. and M. Martens, Multivariate analysis of quality - an introduction. John Wiley & Sons Ltd, Chichester, England, 2001.

[13] CAMO, The Unscrambler v9.2, 2005, Oslo, Norway, CAMO Process AS.

[14] Bigsby, H. and L. K. Ozanne, The purchase decision: consumers and environmentally certified wood products. Forest Products Journal 52, 2002, pp 100-105.

[15] Narin, A., L. Ede and P. Naudé, Multivariate statistics in industrial marketing management: A practitioner tool kit, Industrial Marketing Management 33, 2004, pp 573-582.

[16] SPSS_Inc., SPSS 17.0.0., 2008.

Volume 8

Low-Energy Architecture

Earthen buildings for a low-cost high-energy performance social housing

Stefania Liuzzi[1,*], Pietro Stefanizzi[2]

[1]*Department of Architecture and Urban Planning, University of Politecnico di Bari, Italy*
[2] *Department of Architecture and Urban Planning, University of Politecnico di Bari, Italy*
** Corresponding author. Tel./ Fax: +39 080 5963474, E-mail: stefanialiuzzi@libero.it*

Abstract: A social housing project was carried out in a developing country (Benin, West Central Africa). A complex of twenty two-storey houses was designed in the city of Cotonou, in order to achieve the best architectural solution with the lowest cost. The project was carried out taking into account the bioclimatic and passive architectural devices in a h ot-humid climate site. By using the software ECOTECT V 5.50 the hygrothermal behavior of the buildings was assessed. Every building was supposed with a reinforced concrete structure, and unfired brick walls. The raw earth was also used as a filler layer in the floor and roof slabs. None HVAC was assumed. The simulation has led the best results in terms of thermal performances and indoor comfort conditions. A partial do-it-yourself building was also supposed in the project, allowing to bring down, with use of the earthen materials, the cost of the whole project of almost 30%.
Further investigations on the earthen materials were started at the Laboratory of Thermophysics of Materials (LTM), University of Politecnico di Bari. The aim of the study is to obtain a low-cost high-energy performance building material suitable to achieve a better hygrothermal comfort in sustainable buildings.

Keywords: *Earth, Hygrothermal behavior, Social housing*

1. Introduction

One of the most important issue in the developing countries is the very poor quality of the houses. Several people build by themselves their houses by using local available materials; producing in the most cases a very high level of indoor discomfort, moreover increasing the environmental pollution.

In terms of architectural design, a global policy attempts to invert this trend by increasing the energy efficiency of the building themselves [1].

Several authors [2,3] pointed out the importance to design a building in regards to the bioclimatic and passive architecture devices, taking into account the climate of the site besides the availability of the local resources. In the tropical climates, heat as well as moisture poses an important consideration that must be factored into design of suitable and affordable housing in such an environment [4].

It can be remarked that the temperature and the relative humidity of the indoor building environment are mainly related to the construction materials [5].

Many studies highlighted the importance of the earth, as an ancient eco-friendly building material, able to keep constant indoor temperature and relative humidity values [6,7,8,9]. Different earthen building techniques and several codes are used also in the hot-humid climate countries [10].

The main aim of the present work was to design in a developing country, Benin, an architectural complex of social affordable houses with the highest energy efficiency and the lowest economic cost. The project, started from the social and economic site analysis, has carried out following the bioclimatic and passive architecture devices and was analyzed by the software ECOTECT V 5.50.

2. Methodology

2.1. Site analysis

The work was carried out in the city of Cotonou, which belongs to the country of Benin, in Central West Africa. Before starting the project several social-economic and climatic aspects were taken into account in order to obtain a sustainable project. As refers by the lists of the UNDP [11] Benin is one of the poorest countries in the world; a study extracted by the Government of Benin [12] has demonstrated that 79,1% of the houses were built with metal sheet roofs in 2002.

According to Koppen's climate classification the city of Cotonou was characterized by a tropical wet climate. The main features of this climate are a very small annual temperature range, heavy rainfalls and wet-warm winds. During the year the average daily temperature is included between 27°C and 32°C; the relative humidity of the air is very high with frequent peaks of about 80%.

Several aspects of the prevailing winds were also taken into account: during the driest season (from November to April) the wind, named Harmattan, with direction North-East, is warm and dry. The wetter season (from April to July), instead, is characterized by the Monsoni winds; their speed can achieve 72 km/h.

2.2. Design of the residences

The project area was a popular zone of the city of Cotonou. The main objective to accomplish was to create an integrated design building form and material as a total system able to achieve the optimum indoor comfort with the best energy saving and the lowest economic cost. Twenty two-storey houses were designed. There were considered two types of residences: type A was supposed as a duplex house for two different low-income households of 4/5 people; type B was assumed as a simplex house for one medium-income household for 6 people.

Fig. 1. The project of the residences (From left to right: Urban layout; type A building; type B building)

None HVAC system was assumed in the buildings. Different passive cooling strategies were taken into account: prevailing winds and solar irradiation analysis, shape of the buildings in regard to the site climate, study of the shape of the single building respect to the whole architectural complex, set up of the internal spaces with the different functions and use of building materials suitable to keep constant indoor temperature and relative humidity values.
According to the bioclimatic architecture devices for the hot-humid climate [2] the buildings were designed along the East-West axis with a surface/volume ratio of 0,64.
All the residences were placed along North-South direction, at the sides of the area. Some "cooling corridors" were also created by using the vegetation and thus different sun path diagrams during the day were analyzed in order to study the daily percentages of shadow.

The layout of each house was built up by a starting modular grid of 6 m by 3,5 m; then some modules were staggered with the aim to produce some external cohorts which can allow to reduce the wind speed and work as sunscreens avoiding the overheating of the internal rooms. Furthermore in each building was created a central natural ventilation chimney [13] by using the stairwell; the sizes and the position of the windows were also taken into account to optimize the indoor comfort by studying the direction of the airflows.

Since the relative humidity rate was very high during the whole year, it was assumed that all the non load-bearing walls and some layers of the floor slabs and the roofs were made respectively of unfired bricks and unbaked earth layer. Several studies pointed out the good moisture buffering capacity of the loam as a building material [6,7,8,9].

3. Results

3.1. Analysis of the thermal performances

According to the EN ISO 13786 [14] the thermal transmittance ($W \cdot m^2/K$), the time lag (h) and the decrement factor of the walls and the floor slabs were evaluated (tab.1-2). Every building was assumed with a reinforced concrete structure. The non-load bearing walls were supposed with an air cavity of 7 cm, two internal and external layers of earthen bricks of 15 cm covered with common plaster layers of 1,5 cm. About the floor slabs the thermo-acoustic layer were supposed of a mixture of wood shavings and raw earth. Minke pointed out the excellent thermal capacity of the unbaked earth [15].

The results showed in the tables 1 suggest that by using the unbaked earth it can be achieved a good thermal inertia; thus it was possible to keep constant values in terms of indoor temperature during all the day even if high variation of external temperature values occur.
According to the EN ISO 13788 [16] the internal moisture of the walls was also verified by using the MC4 software. It can be seen by the figure 2 that during the whole year the saturation vapor pressure (red line) was higher than the vapor pressure (blue line) in each layer of the wall. This means that none internal moisture condensation is possible.

The performance of a passive cooling system through an underground duct was estimated. According to the EN ISO 13370 [17] the average annual ground temperature was assessed at a deepness of about 1 m. It was calculated that this allows to reduce the indoor temperature in a range between 1,5°C and 7,5°C during the summer.

Table 1.Thermophysical properties.

	Surface Mass (kg/m^2)	Thermal Resistance (m^2K/W)	Thermal Transmittance (m^2K/W)	Thermal lag (h)	Decrement factor (-)
External walls	306,1	2,246	0,445	14,69	0,136
Roof slab – type B	453,3	1,991	0,502	12,94	0,102

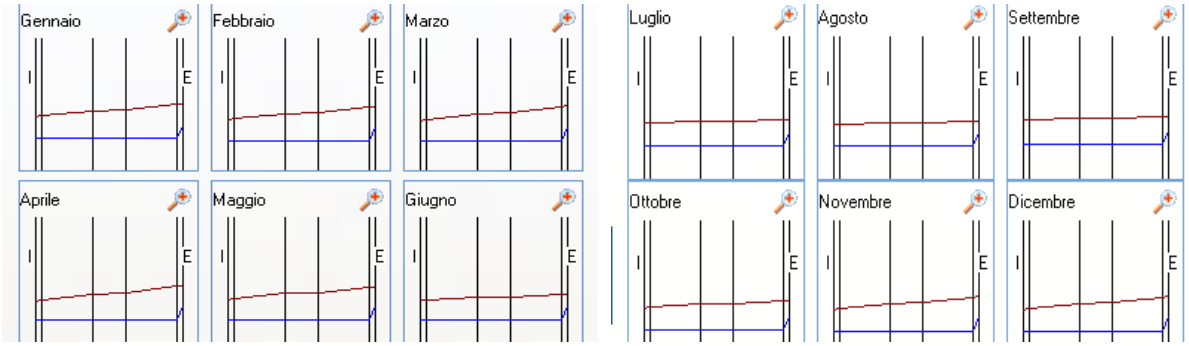

Fig. 2. Water Vapor Pressure profile in the external wall (in red the saturation vapor pressure, in blue the vapor pressure)

3.2. *Analysis of the energy performances with ECOTECT*

Both the two residences (type A and B) were assessed by the software ECOTECT V 5.50.
Each type of building was supposed as a block of different "thermal zones", each of one set with specific hygrothermal and physical properties as shown in the table 2. The database, previously calculated according to the EN ISO norms, was used to carry on the simulation.

Table 2. Hygrothermal and physical properties of the zones.

	Clo value	Air relative humidity (%)	Air speed (m/s)	Illumination level (lux)	Comfort Band (°C)	Latent - sensibile heat gain (W/m^2)
Living area	0.40	60	0.5	300	18-26	2.14-0.86
Night area	0.40	60	0.5	200	18-26	2.14-0.86
Bathroom	0.20	65	0.5	200	18-26	5-2
Kitchen	0.40	65	0.5	300	18-26	5-2
Corridor	0.40	60	0.5	150	18-26	5-2

3.2.1. Indoor temperature analysis

The graph 3 shows the annual temperature distribution of the main internal zones. The comfort band (in yellow) was considered included in the range between 18°C and 26°C.
The temperature of the living area (in red) is in the comfort band for 70% of the hours.
Moreover in the sleeping area (in green) the temperature is in the comfort area for 79% and 89% of the hours. This condition changes in regard to the floor in which the area is.
Conversely the warmest zones of the building are the corridors, the bathrooms and the kitchen.

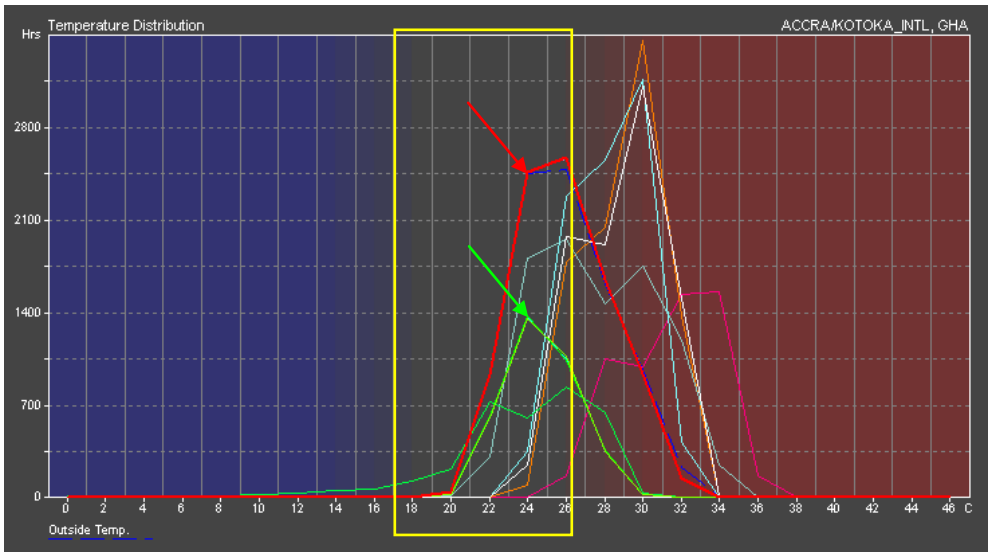

Fig. 3. Annual temperature distribution (in red the living area; in green the sleeping area, in yellow the comfort band)

3.2.2. Internal gain analysis

It was carried out, also, the annual and daily thermal gain and loss analysis due to the temperature gradient in the building.

Due to the solar radiation intensity the main daily gain, of about 1.760 Watts, was achieved during the first afternoon hours in the first and the last months, i.e the driest season of the year. In the night hours there were found the best indoor comfort conditions.

This is owing to the good thermal transmittance, the time lag and the decrement factor described above (table 1) of unfired brick walls.

3.2.3. Wind and solar radiation analysis

The passive ventilation is one of the most effective strategies to use in a hot-humid climate. This is the reason why the buildings were designed in regard to the direction and the type of the winds. The buildings were set with the direction North–South, using the opposite direction of the winds that allowed to dump the discomfort effect produced by the external relative humidity and temperature. On the other hand the design of the external cohorts could also reduce the speed of the air fluxes, when the wind speed is too high.

The design of the buildings was carried on taking into account the solar exposure. Fig. 4 shows the average daily absorbed solar radiation. It can be noticed that the roof is the part of the building mainly involved, with a value between 480 and 600 Wh/m^2. This is the reason why it was created a system of ventilate roof by an air cavity of 4 cm (type A) and a second upturned cover above the roof slab (type B).

The annual sun path diagrams were also studied in order to design the best solution in terms of passive sunscreens. The sun path diagram (Fig. 4) shows that each building is in the shady area for the most time during the whole year.

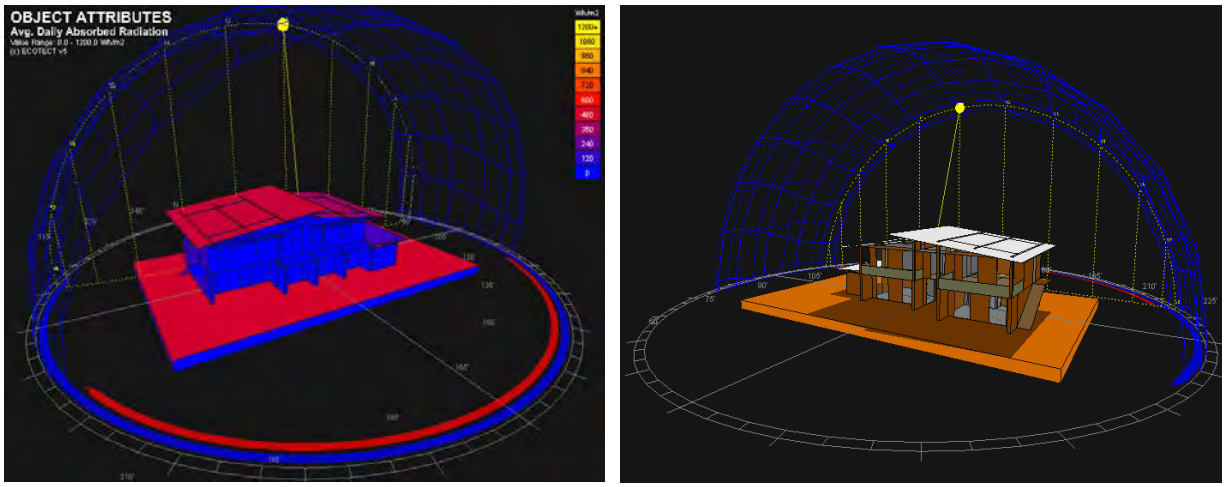

Fig. 4. Solar radiation analysis (Left: Absorbed Radiation; Right: Sun path diagram)

3.2.4. Indoor comfort analysis

According to the EN ISO 7730 [18] the PMV value (Predicted Mean Vote) was computed. The analysis was carried on considering the hottest and coldest days of the year. The graph in figure 5 refers to the warmest day of the year (April 21th) at midday. The main areas of the house, i.e the living and the night areas, show an average PMV value of 1.20. According to the software settings this value means a feeling of lightly warm.

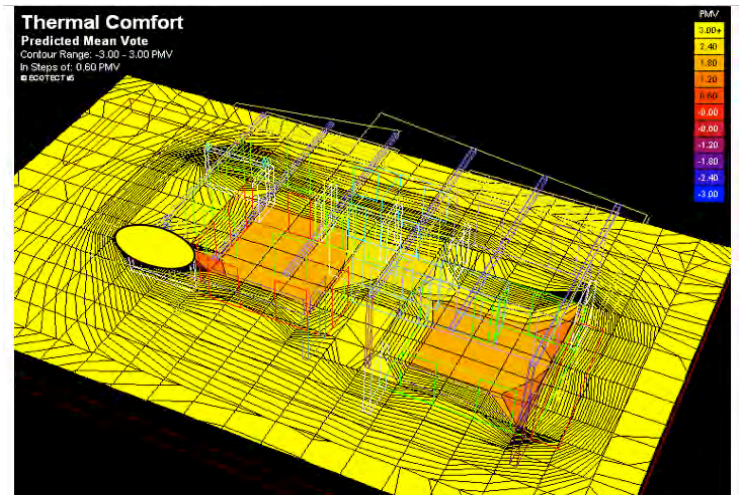

Vote	PMV	Feeling
+3	3.00+	Very warm
Up to 2	2.40 1.80 1.20	Lightly warm
Up to1	0.60 -0.00	Lightly warm
0	-0.60	impartial
Up to -1	-1.20	Lightly cold
Up to -2	-1.80 -2.40	cold
-3	-3.00	Very cold

Fig. 5. Thermal comfort – Predicted Mean Vote

3.3. Cost accounting and sustainability of the project

Several economic saving factors were taken into account in order to accomplish to low cost housing objective. The whole design of the architectural complex and the tree-shaped disposal of the buildings (fig. 1) can allow to suppose an expansion of the houses themselves in the future, solving one of the most pressing problem of a developing country: the uncontrolled population grow.

The structure of the buildings was supposed simple with a modular grid of 3,5 by 6 m. This allows to realize the housing typologies partially with do-it-yourself building, employing the future users.

In order to support the local economy, the use of many local building materials was assumed in the project. Thus it was used unbaked earth both as unfired bricks for non-load-bearing walls and as filler layer of the slabs.

A comparison between the use of fired bricks and unfired bricks was carried out; by the cost analysis it could be noticed that the unbaked earth as a building material allows to bring down the full economic cost of the project of almost 30%. As common strategy in a developing country, assuming the structure cost is at expense of the government, it was calculated that the total cost of a duplex house is about 16.900 euro and the total cost of a simplex house is about 8.500 euro at expense of the future users.

Moreover it was also calculated that with the do-it-yourself building it can be achieved a further lowering cost of about 30%; in this latter case for example the simplex house cost could be 6.000 euro at expense of the user.

4. Conclusion

The main objective of the work was to project an architectural complex of low cost houses in a developing country, characterized by a hot-humid climate. Several architectural devices and socio-economic aspects were taken into account.

The results obtained by the software analysis demonstrated that by using the unbaked earth as a building material it can be achieved a good thermal performance of the whole building envelope, in terms of thermal inertia.

Furthermore the use of many passive cooling strategies, starting from the shape of the buildings themselves up to the whole architectural configuration, have led to obtain excellent results in terms of indoor comfort.

In order to achieve a low-cost high-energy performance housing many economic strategies were also considered. Among these, the use of a local and sustainable material as unbaked earth, on the one hand, and the hypothesis of partial do-it-yourself building, on the other hand, have allowed to bring down the total housing cost of about 60% if compared with a common house built with fired bricks and traditional labor.

Several experimental investigations were started in the Laboratory of Thermophysics of Materials (LTM) (Politecnico di Bari) in order to study the hygrothermal behavior of the unbaked earth building materials.

Two different research lines are carrying on: the lightweight earth by using different additives, like straw and sawdust, and stabilized earth by the addition of the lime. The main objective of the ongoing research is to study how to optimize and obtain a sustainable building material suitable to reduce the energy consumption of the buildings with the lowest economic cost.

References

[1] J. A. Orosa, A. C. Olivieira, Energy saving with passive climate control methods in Spanish office buildings, Energy and Buildings 41, 2009, pp 823-828

[2] V.Olgyay, Design With Climate: Bioclimatic Approach to Architectural Regionalism, Princeton University Press, 1963

[3] N. Engin, N. Vural, S. Vural, M.R. Sumerkan, Climatic effect in the formation of vernacular houses in the Eastern Black Sea region, Building and Environment 42, 2007, pp 960-969

[4] N. Djongyang, R. Tchinda, D. Njomo, A study of coupled heat and mass transfer across a porous building component in intertropical conditions, Energy and Buildings 41, 2009, pp 461-469

[5] D. Allinson, M. Hall, Hygrothermal analysis of a stabilised rammed earth test building in the UK, Energy and Buildings 42, 2009, pp. 845–852

[6] M. Hall, D. Allinson, Assessing the moisture-content-dependent parameters of stabilised earth materials using the cyclic-response admittance method, Energy and Buildings 40, 2008, 2044-2051

[7] M. Hall, Assessing the environmental performance of stabilised rammed earth walls using a climatic simulation chamber, Building and Environment 42, 2007, 139-145

[8] M. Hall, D. Allinson, Analysis of the hygrothermal functional properties of stabilised rammed earth materials, Building and Environment 44, 1935-1942

[9] S. Liuzzi, M. Petrella, P.Stefanizzi, Building with earth, a sustainable material for efficient buildings, Proceeding of 37th international IAHS World Congress on housing, 2010

[10] M.C.J Delgado, I.C Guerrero, The selection of soil for unstabilised earth building: a normative review, Construction and building materials 21, 2007, pp. 237-251

[11] Human Development Report 2007-2008 available on http://hdr.undp.org

[12] Troisement Recensement General De La Population et de l'habitation, Institut National De La Statitique et de l'analyse economique, Benin, February 2002

[13] H.Y Chan, S. B. Riffata, J. Zhua Review of passive solar heating and cooling technologies, Renewable and Sustainable Energy Reviews 14, 2010, pp 781-789

[14] EN ISO 13786, Thermal performance of building components - Dynamic thermal characteristics - Calculation methods, 2007

[15] G. Minke, Building with earth. Design and Technology of a Sustainable Architecture. Birkhauser, 2006.

[16] EN ISO 13788, Hygrothermal performance of building components and building elements - Internal surface temperature to avoid critical surface humidity and interstitial condensation - Calculation methods, 2001

[17] EN ISO 13370, T hermal performance of buildings - Heat transfer via the ground - Calculation methods, 2007

[18] ISO EN 7730, Moderate thermal environments - Determination of the PMV and PPD indices and specification of the conditions for thermal comfort, 2005

Energy performance of residential buildings and their architectural configuration

İlknur Erlalelitepe[1], Kenan Evren Ekmen[2], Cihan Turhan[2], Manolya Akdemir[2], Gülden Gökçen Akkurt[3], Tuğçe Kazanasmaz[1*]

[1] *Izmir Institute of Technology, Department of Architecture, İzmir, Turkey*
[2] *Izmir Institute of Technology, Energy Engineering Program, İzmir, Turkey*
[3] *Izmir Institute of Technology, Department of Mechanical Engineering, İzmir, Turkey*
** Corresponding author. Tel: +907507063, Fax: +907507012, E-mail: tugcekazanasmaz@iyte.edu.tr**

Abstract: This study was conducted to determine a significant relationship between energy performance of residential buildings and their architectural configuration. It is known that there are high amount of energy expenses of residential buildings while they are in use. Utilizing knowledge to decrease costs in housing construction and energy consumption during their lifetime, it has been worth to study this subject here. Case study examples were selected from residential buildings in İzmir, Turkey, which were 5-11 storey-blocks with various construction dates. Utilizing architectural and mechanical production drawings, certain area-based ratios and building dimensions were determined as architectural configuration indicators. Energy performance of case buildings were determined by using a calculation method according to the Thermal insulation Requirements for Buildings-TS825. The significant relationship between architectural configuration aspects and energy performance of buildings were analyzed through statistical analysis and scatter charts. Findings were discussed on the basis of TS825. Thus, instead of renovation of existing buildings' energy performance by limited solutions (to add insulation material etc.), taking simple and inexpensive precautions in design process and their application might provide a wide energy saving potential.

Keywords: *Energy performance, Design efficiency, Architectural, Residential buildings.*

1. Introduction

Energy efficiency has been a critical issue to design residential buildings of good quality, all over the world, and in Turkey as well. It is a high indicator of thermal and visual comfort, and also a significant and powerful impact on energy costs. Due to sheltering needs of increasing population and providing a qualified habitat, the field of housing design is rife with proposals that lay claim in improving efficiency [1-3]. As the residential heating is the main source for energy and resource consumption in Turkey, residential design has gained utmost concern nowadays to reduce energy and resource consumption. Utilizing dwellings offering comfortable interior spaces, it would also be possible to reduce harmful gases released into the environment [4-6].

It is clear in literature that architectural configuration of buildings and design norms have direct impact on energy performance of buildings. Several studies have been conducted about thermo-physical characteristics of the exterior walls, building orientation and geometry, building location together with energy efficiency of buildings [7-10]. In a study, for example, optimum window dimensions and heat insulation with an optimum thickness together resulted in a high energy performance among case buildings [11]. In another study, the impact of glass types and overhangs on the heat conductance of wall and roofs were analyzed [12].

Studies on energy rating offered a variety of methods and software (design tools) to design and analyze energy efficient indoor environments [13-18]. Especially the attempt of construction sector consuming high energy in developed countries was to take measures and programs to

rationalize energy consumption in residential buildings. The main objective was to reduce energy consumption for heating [1-3]. To achieve this goal, the design and evaluation process should be in accordance with the proposed method [19]. Considering the lack of comprehensive studies on the relations of energy performance and architectural parameters of buildings in Turkey, a detailed research has been conducting in Izmir and the initial findings will be discussed here.

From the beginning of the 1990s, the Member States in Europe dealt with the legal regulations about energy consumption in order to reduce carbon dioxide emissions, according to Kyoto Protocol. Turkey is now responsible to provide regulations to comply for the latest European Energy Performance of Buildings Directive 2010/31/EC. [20]. In particular, the Thermal insulation requirements for buildings-TS825 and Heat Insulation Regulation (2000) were legally adopted in 2000: the latter is the complementary regulation of the former which offers the calculation method for the energy demand for heating in buildings [21]. Heat Insulation Regulation sets rules for all buildings to reduce heat loss, to provide energy saving and to determine application guideline [22]. Turkey complied with the rules by Directive 2010/31/EC, through Energy Efficiency Law (2007) and Building Energy Performance Regulation (2008). As regards these regulations, following actions were proposed: the evaluation for the energy consumption of buildings, the classification of buildings, determination of minimum energy performance requirements of existing buildings for their renovation [23,24]. "Standard Assessment Method for Energy Performance of Buildings" has been developed by The Ministry of Public Works and is expected to be published in January 2011. It will be legally adopted and will draft energy certificate and compare the energy performance of a building with ascertained energy limits. This method will include heating, cooling, domestic hot water production, lighting energy consumptions and CO_2 emissions. This study, however, included the calculation method which is currently in use.

Design efficiency in architecture is a concept to design and construct buildings and spaces inside more efficiently. It is derived from architectural configuration factors. By this way, it provides construction and maintenance costs at an optimum level. Energy performance is an indicator for the energy cost of the building and for the visual and thermal comfort conditions of users, as well. Again, Turkey, preparing legislations for energy performance, is responsible to ensure compliance of 2010/31/EC and these legislations offer to conduct several studies for new and existing buildings in a 10-year-period. In view of these resent research and ongoing knowledge, this study was constructed for residential buildings in İzmir, which is the third most populated city of Turkey to analyze their energy performance and architectural configuration. The objective is to determine relations between energy performance of residential buildings and their design efficiency. Energy performance of case buildings were determined by using a calculation method defined by TS825. The significant relationship between architectural configuration aspects and energy performance of buildings were determined through statistical analysis and scatter charts. To rank buildings according to their energy performance, the ratio of calculated energy demand to maximum allowed energy demand defined in TS825 were used.

2. Methodology

2.1. Residential buildings in İzmir

Case study examples were selected from İzmir which is situated in the western part of Turkey (latitude 38°25'N, longitude 27°08'E), along the Gulf of İzmir, by the Aegean Sea. İzmir has a

typical Mediterranean climate which is characterized by long, hot and dry summers; and mild to cool, rainy winters. The average minimum temperatures during winter months vary between 6 and 8°C. Average daytime temperatures, however, during summer months (May to October) are almost 25°C or higher.

To determine case buildings, Building Construction Statistics by Turkish Statistical Institute were analyzed. According to these, the number of multi-story residential buildings is 40% of the whole residential buildings constructed from 1960s to 2008, in İzmir. This rate tends to increase because of increasing population and lack of construction area. Thus, subject buildings in this study were defined to be 5-11 storey residential buildings. A total of 30 buildings were selected from three municipalities due to variation in zoning status and high construction rate. Among these, ten out of 30 were in Konak (designated as K1,K2, …), the other ten were in Karabağlar (designated as Ka1,Ka2…), and the rest in Balçova (designated as Ba1,Ba2…). Architectural and mechanical production drawings were obtained from archives of related municipalities. Buildings were classified with reference to zoning status, orientation, floor number, designer and construction year. The data obtained from drawings included address, construction year, number of flats, floor number, zoning status, designer's professional status, width and height of the building, total floor area, total floor area of common spaces, total volume, total area of façade. The principal aim of this study was to analyze existing residential buildings in İzmir with respect to their architectural configuration as a representative tool for their energy performance. It was also thought that results of this analysis would provide much-needed feedback for designers and professionals in İzmir and in other cities.

2.2. Architectural configuration indicators

Relevant attributes of the architectural configuration are basically building form, orientation, zoning status together with several building envelope factors and climate [7-11]. In addition to data cited in previous section, relevant areas of architectural configuration calculated from drawings in this study were the following: n*et-usable floor area (*inclusive of all internal areas left out from footprint area of all structural elements); e*xternal surface area(*calculated from external perimeter and the floor to ceiling height of residential building); n*et-usable common floor area (*the exclusive of all residential flats from net-usable floor area); w*indow area (*area where high amount of heat would be gained/lost); *external wall area* and e*xternal dimension*(width and length). Architectural configuration indicators, as shown in Table 1, were, then, offered to conduct the assessment for the occurrence of significant relations between energy performances and architectural configuration of buildings. These ratios derived from above areas are described below;

Ratio of external surface area to net usable floor area: This is an indicator that reflects form of building by its volume in zoning status. So it is highly related in exterior surface design and in cost efficiency of energy consumption by concerning surfaces. *Ratio of window area to external surface area:* This was viewed as the indicator for the equilibrium of solid-void, describing effects of void surfaces to hold minimum heat load. *Ratio of width to length:* This is an indicator of plan configuration. The objective here was to determine maximum utility spaces and building surfaces in suggested zoning plan. *Ratio of external wall area to net-usable area:* This ratio was used to define design efficiency indicator related flexibility, utility and cost efficiency of designed spaces. It is the one of the general design principle, creating minimum wall area and

minimum fragment plan scheme. *Ratio of net-usable common floor area to net-usable floor area:* Minimum common spaces have great potential on useful spaces to make them usable and generative. It is related in management cost of first and after construction.

Table 1 Architectural configuration indicators(Balçova:Ba, Konak:K, Karabağlar:Ka)

Build no.	building surface/ net-usable area	window area/ building surface	width /length	wall surface/ net-usable area	net-usable common floor area/ net-usable area
Ba1	1,86	0,22	0,54	1,45	0,11
Ba2	0,87	0,22	0,69	0,68	0,04
Ba3	0,50	0,35	0,88	0,32	0,06
Ba4	1,09	0,17	0,67	0,90	0,15
Ba5	1,02	0,13	0,88	0,88	0,06
Ba6	1,19	0,16	0,99	1,00	0,09
Ba7	0,74	0,21	0,29	0,59	0,09
Ba8	0,64	0,30	0,56	0,44	0,10
Ba9	0,90	0,19	0,51	0,57	0,07
Ba10	0,84	0,18	0,67	0,69	0,11
K1	0,59	0,16	0,52	0,50	0,10
K2	0,32	0,46	0,71	0,17	0,06
K3	1,09	0,15	0,40	1,15	0,02
K4	0,17	0,38	0,41	0,07	0,03
K5	0,55	0,32	0,61	0,37	0,04
K6	0,51	0,34	0,79	0,34	0,03
K7	0,50	0,57	0,59	0,21	0,06
K8	0,99	0,15	0,36	1,05	0,02
K9	0,74	0,31	0,80	0,51	0,10
K10	0,61	0,42	0,45	0,35	0,10
Ka 1	0,31	0,37	0,39	0,20	0,04
Ka 2	0,73	0,42	0,37	0,42	0,08
Ka 3	0,30	0,54	0,36	0,14	0,09
Ka 4	0,56	0,39	0,54	0,34	0,05
Ka 5	0,64	0,56	0,58	0,28	0,07
Ka 6	0,57	0,55	0,50	0,26	0,09
Ka 7	0,40	0,48	0,52	0,21	0,06
Ka 8	0,69	0,36	0,46	0,44	0,05
Ka 9	0,59	0,37	0,48	0,37	0,05
Ka 10	0,02	0,40	0,49	0,01	0,00

2.3. Thermal Insulation Requirements for Buildings -TS 825

TS 825 [21] "Thermal Insulation Requirements for Buildings" is an official obligatory standard of Turkey derived from DIN V 18599. TS 825 has been in use since 2000 which is revised in

2008 by lowering maximum allowable total heat transfer coefficient. Main purpose of TS 825 is to limit building's energy demand according to exposed area to volume (A/V) ratio. TS 825 uses solar radiation and outdoor air temperature values which are tabulated according to climatic regions specifically determined for Turkey using degree-day method. Heat demand is calculated monthly including specific heat loss, efficiency factor, internal and solar gains. Thermal bridging effect is taken into account with length of the element (I) and longitudinal heat loss coefficient (U_L) according to TS EN ISO 14683 (2004). In TS 825, internal gains are simplified as 5 W/m^2 for net floor area. Gain utilization factor (η) is used to correct the total of internal and solar gains to calculate average monthly useful gains in a statistical way. Calculation of yearly heat demand is followed by comparison of limiting values given in TS 825 according to A/V ratio. If the yearly heat demand is within the limits, the procedure is completed; otherwise properties of the building elements should be re-evaluated and re-calculated.

2.4 Statistical Analysis

The relations between variables, namely, ratio of external surface area to net usable floor area, ratio of window area to external surface area, ratio of width to length, ratio of external wall area to net-usable area, ratio of net-usable common floor area to net-usable floor area and energy performance ratio were tested by single-factor ANOVA at a 5% level of significance (α=0.05). Scatter plots were derived from paired values of variables, namely, heating energy demand, ratio of building surface area to net usable floor area, ratio of window area to external surface area, ratio of width to length, net-usable common floor area to net-usable floor area. These were constructed to understand the relation between architectural configuration indicators and heating energy demand.

3. Results and Discussion

3.1 Findings obtained from TS825.

The results of calculation method-TS825 were tabulated according to construction year, orientation and zoning status. Here, external surface area per volume, heat loss, solar gain, calculated energy demand, max. energy demand, energy performance ratio, and annual fuel demand were tabulated according to construction year as shown in Table 2. In the analysis, heat loss through ventilation and heat gain from internal environment were also calculated. Energy performance ratio of 9 buildings range from 0,94 to 1,00, while 11 of them were from 1,03 to 1,92. Rest of the buildings' energy performance ratio varies between 2,14 and 2,88. Most of the buildings with high energy performance were situated in Balçova. They were the recently constructed buildings according to construction year. However, buildings constructed mostly in 1970s in Karabağlar were having low energy performance.

3.2 Findings obtained from statistical analysis.

The null hypothesis was H_0:τ_i=0; there is no relation among energy performance according to ratio of window area to external surface area. Accordingly, H_0 was accepted at 5% level of significance. It was concluded that ratio of window area to external surface area did not varied significantly according to energy performance. All findings showed that there was no relation between architectural configuration indicators mentioned above and energy performance ratio. Scatter charts also supported this result.

Table 2 Building energy performance data obtained from TS825 according to construction year

Year	build. no	A/V	heat loss (W/K)	solar gain (W)	calculated energy demand (kWh/m^3)	max. energy demand (kWh/m^3)	energy per. ratio cal.energy/ max.energy	annual fuel demand (kg)
1960-1969	K9	0,42	1169,70	61276	18,00	9,36	1,92	7291,54
1970-1979	Ka 10	0,18	2638,28	94290	13,25	6,20	2,14	19721,04
	Ka 5	0,34	3761,00	371190	12,49	8,24	1,52	18721,95
	Ka 6	0,32	4874,74	307516	21,48	7,95	2,70	28624,84
	Ka 7	0,27	3531,69	161045	20,29	7,22	2,81	23744,44
	Ka 8	0,37	3681,05	155100	23,76	8,59	2,77	22747,55
	Ka 3	0,23	2078,27	104923	17,04	6,64	2,57	14156,78
	Ka 4	0,28	4106,35	224229	15,98	6,51	2,45	25889,27
1980-1989	BA1	0,37	2399,00	134625	13,48	8,67	1,55	16055,33
	BA2	0,44	2827,20	108958	21,04	9,65	2,18	19688,14
	K3	0,49	2144,20	101650	13,43	10,35	1,30	14323,37
	K4	0,19	1642,00	122282	9,25	6,20	1,49	10493,66
	K7	0,13	1945,20	191959	5,84	6,20	0,94	13818,38
	K10	0,28	2885,90	175195	9,83	6,22	1,58	8424,46
	K8	0,35	2325,10	101560	10,95	8,38	1,31	16829,06
	K6	0,29	3456,60	275989	9,05	9,05	1,00	21982,30
	K5	0,39	1540,40	156551	11,19	10,82	1,03	8507,13
	Ka 9	0,33	4362,80	198601	22,77	7,98	2,85	28731,50
	Ka 1	0,23	1724,94	62394	14,46	6,66	2,17	12817,99
	Ka 2	0,39	3912,23	209748	25,44	8,84	2,88	24115,27
1990-1999	BA3	0,23	3483,80	244071	9,77	6,60	1,48	10473,92
	K1	0,37	344,90	15174	9,90	8,63	1,15	2640,02
	K2	0,14	2247,30	113928	6,10	6,20	0,98	21462,84
2000-2009	BA4	0,61	441,09	38941	11,95	11,55	1,03	3370,58
	BA5	0,27	2655,97	39810	9,15	9,54	0,96	5470,00
	BA6	0,43	1047,77	32318	11,27	11,92	0,95	23250,00
	BA7	0,33	1909,56	114991	7,90	7,98	0,99	15003,07
	BA8	0,44	1001,88	74182	8,77	9,17	0,96	7239,95
	BA9	0,49	951,31	52132	9,86	10,24	0,96	6712,55
	BA10	0,73	464,34	38135	13,06	13,64	0,96	3412,85

4. Conclusions and Recommendations

The analyses of variance and scatter charts were applied to determine relation between architectural configuration indicators and energy performance of residential buildings. Energy demand calculations were constructed by TS 825. A number of results about architectural configuration indicators and their relationship with energy performance ratio were considered as noteworthy on their own merit. One was that the energy performance ratio was independent of

architectural configuration indicators, despite literature [7-14], showing distinct impact of architectural aspects on building energy performance. Another noteworthy observation was the independence of zoning status and orientation on the energy performance ratio. Several conditions may indicate such an anomaly. One is that the study included a limited number of sample buildings. The other one is that the calculation method is independent from orientation, building form. TS 825, as a static method, is well established to control overall heat transfer coefficient and limit heating energy demand of a building. However, using monthly average climatic values, single zone assumption, ignoring thermal mass, assuming continuous heating regime, lack of internal gain details and control of HVAC systems leads inaccurate results compared with measurements. Results of the static methods give an estimate of monthly heating load and idea about applicable measures to reduce the heat loss of the building. On the other hand, dynamic methods calculate gains and losses from different elements in a building, giving details about different zones and their interactions with the building. Therefore, once the dynamic method which has been developed for building energy performance for Turkey is released, this study will be repeated accordingly. The authors hoped that the new method will exhibit the relationship with building energy performance and architectural parameters. It is necessary to conduct further investigations with inclusion of high number of sample buildings in Turkey. Then, all findings which will be resulted by objective evaluations about existing buildings will be presented to all correspondings' knowledge and use.

Acknowledgements

The Scientific and Technological Research Council of Turkey (TÜBİTAK) funded this research and their contribution is gratefully acknowledged.

References

[1] M. Santamouris, Introduction On the Energy Rating of Buildings, in Energy Performance of Residential Buildings, James & James/Earthscan, UK, 2005.

[2] J. Smeds, and M. Wall, Enhanced Energy Conservation in Houses through High Performance Design, Energy and Buildings, 39, 2007, pp. 273–278.

[3] I. Borden, A. Leaman A. and M. Atkins, Energy efficient design, A Guide to Energy Efficiency and Solar Applications in Building Design, United Nations, New York, 1991.

[4] E. Berköz and G. Kocaaslan, Enerji ve Kaynak Tüketimini azaltan Konut ve Yerleşme Tasarımı, Konutta Kalite, Derleyen T. Aktüre, MESA, Ankara, 1994, pp. 141-156.

[5] M. Balamir, Kentleşme, Kentsel süreçler ve kent yapısı, ODTÜ Mimarlık Fakültesi, Ankara, 1982.

[6] V. İmamoğlu, Konutlarda Isı Konforu, Konutta Kalite, Derleyen; T.Aktüre, MESA, Ankara, 1994, pp. 105-116.

[7] R. Ünver, N.Y. Akdag,, G.Z. Gedik, L.D. Öztürk and Z. Karabiber, Prediction of building envelope performance in the design stage: an application for office buildings, Building and Environment, 39, 2004, pp. 143 – 152.

[8] G. K. Oral, A.K. Yener, N.T. Bayazit, Building envelope design with the objective to ensure thermal, visual and acoustic comfort conditions, Building and Environment, 39, 2004, pp. 281 – 287.

[9] G.K. Oral, and Z. Yılmaz, The limit U values for building envelope related to building form in temperate and cold climatic zones, Building and Environment, 37, 2002, pp. 1173 – 1180.

[10] G. Manioğlu and Z. Yılmaz, Energy Efficient Design Strategies in the Hot Dry Area of Turkey, Building and Environment, 43, 2008, pp. 1301–1309.

[11] M.N. İnanıcı and F.N. Demirbilek, Thermal Performance Optimization of Building Aspect Ratio and South Window Size in Five Cities Having Different Climatic Characteristics of Turkey, Building and Environment, 35, 2000, pp. 41-52.

[12] G.A. Floridesa, S.A. Tassoub, S.A. Kalogiroua and L.C. Wrobelb, Measures Used to Lower Building Energy Consumption and Their Cost Effectiveness, Applied Energy, 73, 2002, pp. 299–328.

[13] S. Alvarez, A. Blanco, J.A. Sanz, F.J. Sanchez, The Euroclass method-description of the software, in Energy Performance of Residential Buildings, Ed.M.Santamouris, James & James/Earthscan, UK, 2005.

[14] B. Poel, G. Cruchten, and C. Balaras, Energy performance assessment of existing dwellings, Energy and Buildings, 39, 2007, pp. 393–403.

[15] L. Pedersen, Use of different methodologies for thermal load and energy estimations in buildings including meteorological and sociological input parameters, Renewable and Sustainable Energy Reviews, 11, 2007, pp. 998–1007.

[16] TOBUS.About EPIQR.Visited on: January 6, 2007. Available at:

[http://tobus.cstb.fr/english/epiqr.htm].

[17] C.A. Balaras, K. Droutsa, A.A. Argiriou and D.N. Asimakopoulos, EPIQR surveys of apartment buildings in Europe, Energy and Buildings, 31, 2000, pp. 111-128.

[18] SAP2005, The Government's Standard Assessment Procedure for Energy Rating of Dwellings, 2005 Ed., Revision 1, Version 9.81, 2008.

[19] International Energy Agency (IEA), Integral Building Envelope Performance Assessment, Technical Synthesis Report IEA ECBCS Annex 32, Energy Conservation in Buildings and Community System, FaberMaunsell Ltd., United Kingdom, 2003.

[20] DIRECTIVE 2010/31/EC of the European Parliament and of the Council on the Energy Performance of Buildings, 2010.

[21] Anon. the Thermal Insulation Requirements for Buildings -TS825, Ankara: Turkish regulations, 1999 (in Turkish)

[22] Anon. Heat Insulation Regulation, Ankara: Ministry of Public Works, 2008 (in Turkish).

[23] Anon. Energy Efficiency Law, Ankara: Ministry of Public Works, 2007 (in Turkish).

[24] Anon. Building Energy Performance Regulation, Ankara: Ministry of Public Works,2008(in Turkish).

Existing buildings – users, renovations and policy

Kirsten Gram-Hanssen

Danish Building Research Institute, Aalborg University, Denmark
**Corresponding author: Tel: (+45) 23605653, E-mail:kgh@sbi.dk*

Abstract: This paper deals with the energy consumption of existing owner-occupied detached houses and the question of how they can be energy renovated. Data on the age of the Danish housing stock, and its energy consumption is presented. Research on the potential for energy reductions in the Danish housing sector is presented, and it is shown that there is a huge potential for reductions. It is a well-known problem that even if there are relevant technical means, and even if it is economically feasible, the majority of house owners do not energy renovate their homes. This paper intends to address what can be done with this problem. The paper draws on different sources of why, when, how, and why not people renovate their home. These results are then compared and discussed together with a presentation and discussion of the Danish policy measures that are put forward in order to encourage people to energy renovate their home. These policy measures include building regulations, energy tax and different types of incentives and information dissemination. The conclusion calls for new innovative policy measures to cope with the realities of energy renovations of owner-occupied houses.

Keywords: *Detached houses, Energy renovations, User practices, Energy policy.*

1. Introduction

In low-energy architecture focus is often on new buildings and their potential for reducing or eliminating energy consumption for heating purposes as is seen in zero-emission buildings and passive houses. Figure 1 shows the construction age of the Danish building stock in 2004. In the figure is seen that buildings typically have a lifetime of more than 50 years and if we envision the same level of construction activities for the next 20 years as seen for the last 10-20 years, for a very long time the majority of the Danish building stock will continue to be built before the era of low energy housing. This corresponds to British data suggesting that 70% of all homes that will exist in 2050 have already been built [1].

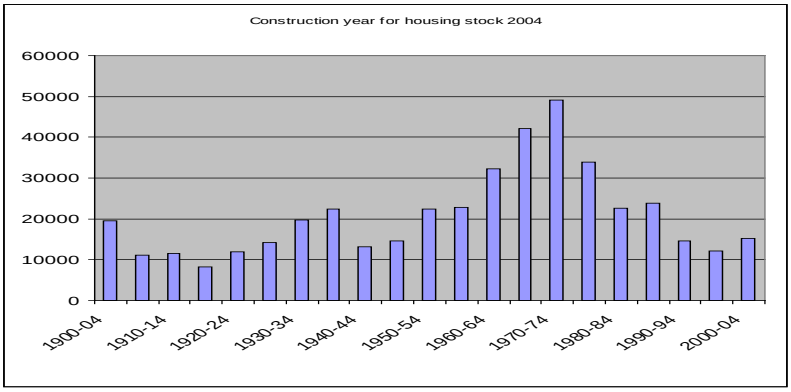

Fig. 1. The construction year of the Danish housing stock in 2004, source Statistics Denmark.

Questions have been raised whether it is better, from an environmental perspective, to demolish buildings and build new ones rather than to renovate, and a few case studies based on LCA analysis have been conducted; however, there does not seem to be agreement on the results [1], [2]. Furthermore there might be other arguments than energy and environment calling for renovating rather than demolishing, including the arguments of cultural heritage and people's personal relation to their homes.

Thus attention has to be paid to how energy reductions in existing buildings can be achieved. In 2009 the final energy consumption in households was 192,145 TJ, representing 30.4% of the total Danish energy consumption, and out of this approx. 83% was related to heating purposes in households [3]. Studies have documented the potential for energy savings if the existing building stock were proper energy renovated [4]. Here the Danish building stock is divided into five groups, including farm houses, detached houses, terraced houses, multi-storey buildings and commercial buildings. In a scenario where only energy renovations that have a payback time of less than 15-25 years are considered, the total amount of energy savings are calculated to 37 PJ, which corresponds to 23% of the annual energy used for the heating of buildings. The building type with the highest potential for energy savings is the detached house, which stands for 41% of the possible energy savings relating to energy renovation in all of the building stock. The reason for the high potential for energy savings in detached housing is a combination of the volume of this type of buildings - the majority of the Danish population lives in detached housing (the Danish housing stock consists of approx. 40% apartments, 46% single-family houses and 14% terraced houses) and these homes are typically considerably bigger compared with e.g. apartments in multi-storey buildings - and the fact that many of these houses were built in the 1960s and 1970s, or earlier, and thus before stricter energy requirements in the Danish Building Regulations came into force.

On the whole there are good arguments for having a closer look at how energy renovations of the existing housing stock, especially the detached owner-occupied housing, can be promoted. In the following, empirical investigations on why people renovate their home will be presented and compared with the policy measures that are put forward in Denmark to encourage energy renovation.

2. Methodology

Results presented in this paper have been conducted in two previously reported studies. The first study is from 2000 and focused on to what extent environment and architecture were considered when people renovated their homes [5]. This study deals with two middle class neighbourhoods from the 1960-70s and from the 1940-50s respectively and it contains a questionnaire survey and qualitative interviews with four house owners. Another study from 2005 included people who had bought a house within the last three years, and focused on what renovations they had so far carried out or planned to do, and to what extent the energy label on their home had influenced their buying of the home or the renovations they had done [6], [7]. This study included 10 qualitative interviews. All 14 interviews have been recorded, transcribed and analysed according to qualitative social science standards [8]. The survey questionnaire was mailed to approx. 350 households, approx. 50% of which responded, i.e. 170 house owners, and the answers have been analysed by the use of SPSS. The new approach in this paper is that these empirical findings are combined and analysed together with a review of Danish energy policy directed at house owners. Furthermore the majority of the empirical results have not been published in English before. As some of these data are more than 10 years old, they will be compared with more resent data on renovation, though, as will be shown, these types of data are rather scarce.

3. Results

The following will first present extracts from studies on house owners' renovation of their homes followed by a review of existing policy measures in Danish energy policy to induce energy renovations of detached single family housing.

3.1 Why, what and how households renovate their homes

According to the survey the renovations made by most of the house owners are kitchen and bathrooms, which 52% and 40% respectively of the house owners have done, whereas for example new windows or roof are only done by 32% and 22% respectively of house owners. Connection to district heating is also made by many of the house owners; however, this should be seen in light of Danish law where authorities can impose this connection. Furthermore Table 1 shows that more than one third of the households have insulated their house. Thus it is seen that renovations including the indoor aesthetics and functions are higher on the agenda than renovations which might save energy for heat consumption. Interviews with house owners supplement and support this: A new kitchen is something to dream about, make plans for and show to others. Renovation of the roof on the contrary is typically made because of necessity more than because of dreams and passion. In Figure 2 this tension is illustrated by an axis called Lifestyle vs. Wear and tear.

Table 1. Results from survey on what type of renovations the present house owners had made to their house. Results are divided between answers from the neighbourhood with houses built in 1960-70s, and in 1940-50s and show the overall percentages as well.

	1960-70s	1940-50s	Overall
Kitchen	44%	57%	52%
Bathroom	38%	41%	40%
Windows	21%	40%	32%
Extensions	30%	16%	22%
Roof	15%	27%	22%
Façade	15%	14%	14%
Patio	17%	8%	12%
Connection to district heating	48%	35%	40%
Radiators and pipes	22%	32%	28%
Insulation	34%	37%	36%
Electric installations	6%	21%	15%
Number of answering households	71	99	170

Table 2. Results from survey on the relation between how long people have resided in their house and whether they have made any renovations

How long have they lived in the house	Have not renovated	Have renovated
0-5 years	65%	35%
5-10 years	42%	58%
10-20 years	31%	69%
More than 20 years	19%	81%
Answers (numbers)	58	104

When looking at who is doing the renovations, the survey shows that in most cases the house owners do some or the majority of the renovations themselves and only in a minority of the houses are renovations made solely by craftsmen. Craftsmen might be involved in the DIY (Do-It-Yourself) renovations as well, because the house owners, or their friends or family helping them, are craftsmen as we heard in several interviews. Furthermore the survey shows that the longer people have lived in their house, the higher the possibility that they have done any renovations (see Table 2). This breaks with a myth indicating that when people buy a house, they renovate it before they move in. On the contrary, renovations are typically something that is done continuously during all the years people live in the house. Also from interviews we know that house owners often have a sort of imaginary list of renovations they

could do or would like to do, but as there is not always time, money or other resources, and as it is not always funny to live in a house that is being renovated, some renovations are postponed and others are carried out. From the interviews, however, we also know that for some families the renovations are not only a dull duty, it might be a creative task, which people appreciate. For several house owners it might even be part of the reason why they have bought a house that they wanted a house to work on and build and that renovating the house is an integrated part of living in it. This tension on the one hand between seeing renovations as something that is interesting in itself because of the process and on the other hand wanting to renovate the house primarily, because one is interested in the result of the renovation is shown in Figure 2, as the axis Process vs. Project.

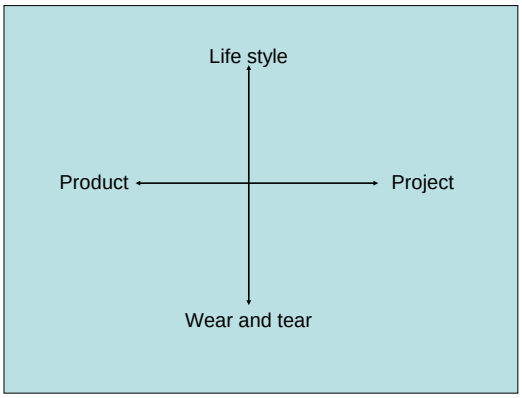

Fig. 2. Reasons for renovating. The figure distinguishes between whether house owners are primarily interested in doing the actual renovating (project) or in the result of (product) the renovation, or whether the renovation is primarily done because of necessity due to wear and tear or because house owners like to have something new (lifestyle). Different house owners, as well as different types of renovations, will be placed differently in the figure.

Different types of renovations thus might have to be interpreted in different terms. Some renovations are done because of aesthetics and dreams of having what friends or family have or what can be seen in catalogues. These renovations might best be understood within understandings of lifestyle, status and consumer choice [9]. This is often the case with kitchens and bathrooms that are renovated without it actually being necessary from a more functional perspective. Outdoor renovations like roofs and windows are more often done as maintenance resulting from wear and tear, though in some of the interviews there are also examples of this being done primarily because of aesthetics. In some families, an important aspect of why people renovate their house is that they actually like to work physically on their house, they enjoy the project and the process. This may include light maintenance like painting walls or it might include completely new construction work like building extensions etc. During these DIY projects people often feel that by working on their own house they get more attached to their home and feel that the house becomes more of a home, as compared with just buying a new and maintenance-free house. In other families, maintenance and renovation are, however, primarily seen as a dull duty that they would rather be without. When understanding this, it is important to see renovation as a part of the specific everyday life of every different family. For example, in some families and at some times living in a house being renovated is a big problem and at other times and families it is easily part of the everyday life. As an example, one of the interviewed families had just had quadruplets, and could thus envision not having any time at all for renovating for the next many years to come. Under other circumstances this family might have liked to renovate their house themselves, however, they had decided to have new windows installed by craftsmen before they moved in.

There might be different types of energy-related issues connected with the renovations. Renewing the windows or the roof most often also include improving the energy efficiency of the house, and renovating the kitchen might include buying new and more efficient technologies. However, in most of these cases energy concern is not part of the main reason for doing the renovation, even though the renovation includes improved energy efficiency. It is just something following from other wishes and dreams. On the other hand some renovations might also include higher levels of comfort, e.g. more heated square meters, a higher indoor temperature or bathrooms with spa, and thus involve increasing energy consumption.

As some of this empirical material is up to 10 years old, it is relevant to compare it with more recent results and with international results. A study comparing the residential building stock in eight European countries (AT, FI, FR, DE, NL, SE, CH, UK) observes that there is not any statistics on the renovation of the building stock in any of the countries [10]. Instead this study uses interviews with key stakeholders to estimate size and type of renovations, and they conclude that modernisation of kitchen and bathrooms is the most common renovation activity in all the studied countries, and furthermore that most of these modernisation activities take place before the end of the components' service life is reached. A recent German study based on a survey of 1000 households [11] and 44 qualitative interviews [12] gives a more solid base for comparison. In the qualitative studies as well as in the survey, it is found that the everyday life situation of the house owners is important for the decision to renovate, and that the reasons for renovating are diverse and include other arguments than a response to an urgent need and that the economy of energy renovation is not a main argument.

3.2 Danish energy policy directed at house owners

The following will present a review of the different elements of Danish energy policy which seeks to promote energy renovation of owner-occupied detached housing [13].

3.2.1 Danish Buildings Regulations

In 1979 for the first time, the Danish Building Regulations included minimum requirements for energy consumption for new buildings. Since then, the Building Regulations have been tightened several times and since 2006 they have also included provisions on the renovation of existing buildings. Here the Building Regulations distinguishes between whether activities include more or less than 25% of the building's physical surface or economic value. If it includes more than 25%, all renovation measures stated in the energy label that are economically profitable have to be implemented. Furthermore the U-values, as required in the Building Regulations for different types of building components, have to be kept, as well as do standards for heating supply etc. If the rebuilding includes less than 25% of the existing building, only the U-values and the standards for heating supply have to be kept.

3.2.2 Energy label and energy inspection schemes

The energy label system in Denmark dates back to the 1980s and since 2006 the labelling system follows the implementation of the EU Directive 2002/91 on the Energy Performance of Buildings (EPBD), which partly builds on the ideas and early experiences in Denmark with energy labels for buildings. The label has to be issued for houses sold as well as for new buildings, and the label includes grades from A1 to G, based on the calculated energy consumption, together with the grade that could be achieved if the house was renovated according to the recommendations. Recommendations are given in an energy plan where the proposals are divided into profitable improvements and "other improvements" respectively

and include estimates of necessary investments, annual savings from improvements (in DKK and energy units) and the payback period of investments.

3.2.3 Utilities' saving obligations

Utilities have been advising their customers on energy since the beginning of the 1990s, and the legal obligation for the utilities to promote energy savings has been part of the law since 1996. According to the energy agreement from 2009, the utilities are responsible for their costumers realizing 6.1 PJ in saved energy. Utilities are free to choose their methods which typically include different types of advice, communication and economic incentives. As regards heating consumption in detached housing, it is primarily the district heating companies that have had the responsibility to promote savings; however, as will be described later, they have primarily focused on change of type of heat supply, to more efficient technologies and to gas and district heating rather than electric heating. The energy authorities require documentation from the utilities that they actually reach these targets on energy savings.

3.2.3 Economic means

There have been energy taxes in Denmark since 1977, and today they represent a considerable amount of what households pay for their energy. Compared with other European countries, Denmark is among those with the highest energy taxes in per cent of GDP [14]. The Danish authorities estimate that over the last 30 years energy taxes have resulted in a 16% reduction in energy [14]. It must be assumed that this has been realized partly through energy efficient renovation.

Economic incentives to households have to a lesser degree been part of Danish energy policy towards households. Examples include a governmental "Growth Fond" with 1.5 billion DKK (200 million euros) to get the Danish construction sector going in 2009. The fond provided subsidy for renovation and building projects in private housing including energy renovations.

3.2.4 Information dissemination

Informative initiatives have been part of the utilities' saving obligations and obviously the energy label on buildings is also an example of an informative mean. However, there are also other initiatives in Denmark that use information as a means of promoting energy savings. Besides different types of campaigns aimed at households, throughout the years the most relevant to mention is a Knowledge Centre for energy savings in buildings. The purpose of the Knowledge Centre is to collect knowledge on how to reduce energy consumption in buildings and communicate it to the professional actors in the building sector, including craftsmen. In the years 2008-2011, 10 million DKK are allocated to the centre.

4. Discussion and Conclusions

As described in paragraph 3.1, energy renovations seen from the perspective of the house owner is an integrated part of living in and continuously renovating the house. Energy renovations are typically done as an integrated part of other renovations, and considering the tear and wear of e.g. roofs or windows, however, the renovation rate has so far been too slow, as the majority of the houses still lack sufficient insulation. This is partly because these types of renovations are prioritised lower than other renovations and according to available time, money and mental surplus. Most often indoor renovations of kitchen and bathroom are higher on the priority list, than renovations related to reducing energy consumption for heating. So a

relevant question is how to make people do more renovations on their home and how to make them prioritise those related to energy savings higher.

As described in paragraph 3.2, there have been political efforts over the last thirty years to make house owners energy renovate their homes. Apart from the mandatory elements of the Danish Building Regulations, all these efforts have focused on information on rational choices related to energy and economy and on economic incentives making it more economically attractive to choose the most energy efficient when renovating. Policy measures thus indirectly assume that economic and rational decision making is decisive when house owners decide what and how to renovate. As shown in paragraph 3.1 this is, however, not necessarily the case. Economy can be decisive in the sense that the amount of money that the house owner is able to, or interested in, spending on renovations is limited, though this does not imply that house owners also make an economic calculation on payback time. Kitchens and bathrooms do not pay back in any economic meaning of the word, and they are still at the top of the priority list. If the family has decided to change windows or renew the roof, then rational economic calculations on saved energy might be decisive for the decision on the amount of insulation material or the energy quality of the windows, however, when deciding to renovate or not, or what renovation to implement, economic payback time is very seldom included as grounds for decisions.

This can be elaborated by including Figure 2, summarising the different reasons that people have for doing renovations. Thus the majority of policy efforts so far can be said to have focused on the right bottom part of the figure: renovations done because of necessity owing to *wear and tear*, and because of an interest in the result (*product)* of the renovation, and on how it can be more economically attractive to include energy in this type of renovation. However, as the text in 3.1 describes and Figure 2 illustrates, there are other, and maybe stronger, reasons why people renovate their homes. They include that the house owner wants something new and more fashionable (*lifestyle*) and that they enjoy working on the house, and in this way appropriate it and make it their home (*project*). Based on the results presented in this paper, it is relevant to raise the question of how to make policy or in other ways to promote that energy renovation is also seen as something that is done because of fashion and lifestyle or because the project in itself is interesting.

I will conclude by giving two examples of what this might include. The first example comes from a Belgian project, which includes interviews with house owners having had an energy assessment [7]. Some of the interviewees indicated that they had thought about installing PVs, and they were rather disappointed because the energy adviser advised against it based on economy. These house owners found PVs interesting more from a lifestyle perspective than from an energy-economic perspective. PVs are visible from outside, you can show them to your neighbours and you can feel good about them – like a new kitchen. Insulation in comparison has none of these qualities. However, having an energy adviser arguing against installing PVs, made the house owners change their mind. This point to the need of energy advisers to be educated in other approaches than the simple economic rational approach as well as the informative materiel also appreciating lifestyle arguments for doing energy renovations. The other example calls for more user-oriented products in energy renovation. What would happen if insulation companies put more emphasis on developing new products with an explicit emphasis on making it interesting, fun and easy to insulate your building, and at the same time give people a possibility of putting a personal stamp on their home, through these products?

References

[1] A. Power, Does demolition or refurbishment of old and inefficient homes help to increase our environmental, social and economic viability? Energy Policy, 36, 2008, pp 4487–4501.

[2] A. Thomsen and K. van der Flier, Replacement or renovation of dwellings: the relevance of a more sustainable approach, Building Research & Information, 2009, 37: 5, pp 649 — 659.

[3] Danish Energy Authorities, Energy statistics, 2009.

[4] K. B. Witchen, Potentielle energibesparelser i det eksisterende byggeri, Hørsholm: Statens Byggeforskningsinstitut, SBI, 2009, 38 s.

[5] K. Gram-Hanssen, C. Bech-Danielsen, 2000, Renovering af enfamiliehuset - holdninger til økologi og arkitektur. SBI-meddelelse 134.

[6] K. Gram-Hanssen and O.M. Jensen, Notat om energimærkning af enfamiliehuse, 2005, Retrieved at http://www.sbi.dk/miljo-og-energi/livsstil-og-adferd/energimerkning-af-enfamiliehuse/

[7] K. Gram-Hanssen, F. Bartiaux, O.M. Jensen, & M. Cantaert, Do homeowners use energy labels? A comparison between Denmark and Belgium, Energy Policy, *35* (5), 2007, pp 2879-2888.

[8] S. Kvale, InterViews. An Introduction to Qualitative Research Inter-viewing. Sage Publications, Thousand Oaks, California, 1996.

[9] K. Gram-Hanssen and C. Bech-Danielsen, House, home and identity from a consumption perspective. Housing, Theory and society Vol. 21 No.1. 2004, pp. 17 – 26.

[10] F. Meijer, L. Itard and M. Sunikka-Blank, Comparing European residential building stocks: performance, renovation and policy opportunities, Building Research & Information, 37: 5, 2009, pp 533 — 551.

[11] I. Stieß, V. van der Land, Just another Business case? Enhancing the agency for energy-efficient refurbishment among private homeowners, Knowledge Collaboration & Learning for Sustainable Innovation, ERSCP-EMSU conference, Delft, The Netherlands, October 25-29, 2010

[12] I. Stieß, S. Zundel, J. Deffner, Making the home consume less – putting energy efficiency on the refurbishment agenda, In: Conference proceedings: ECEEE Summer Studies 2009, Ile Saint-Denis: ECEEE.

[13] K. Gram-Hanssen and T. H. Christensen. Energy efficiency in existing detached housing. Danish experiences with different policy instruments. SBI, 2011.

[14] Økonomi og erhvervsministeriet, Vækst, klima og konkurrenceevne, 2008.

An energy-autonomous home in Melbourne – myth or reality?

R.J. Fuller* and S.J. Loersch

School of Architecture and Building, Deakin University, Geelong 3217, Victoria, Australia
** Corresponding author. Tel: +61 352278300, Fax: +61 352278303, E-mail: rjfull@deakin.edu.au*

Abstract: Energy-autonomous buildings are possible. Completely energy self-sufficient houses can be found, for example, in Europe. If it is possible to cover the entire energy demand of a household from only renewable energy generated on site in a central European climate, what is required in a temperate climate, typical of southern Australia? This paper describes an investigation to broadly assess the technical, practical and financial feasibility of energy-autonomy for a hypothetical suburban house in Melbourne, Victoria. The findings firstly demonstrate the importance of reducing energy demand by using passive solar building strategies and energy efficient appliances to reduce demand to a reasonable level. The paper then discusses four scenarios and combinations of technologies to meet this reduced demand. The three scenarios which give energy autonomy increase the capital cost of a typical house by between 15% and 33%, and there would be insufficient roof area to accommodate the solar technologies required in two of the scenarios investigated. It is therefore concluded that while the goal of energy autonomy is technically feasible, it is not likely to be financially or practically acceptable. A fourth scenario of an energy-exporting house was also investigated and is shown to be a much more attractive option.

Keywords: *Energy autonomy, Housing, Melbourne, Conservation, Solar Technologies*

1. Introduction

Globally there is a long tradition in energy-autonomous housing. Examples include the Vale home built in 1974 [1] and more recently, the Solar House at Freiburg built in 1992 [2]. If energy-autonomous buildings can be realized in Europe, what does it take for residential housing in the temperate climate of southern Australia to be energy-autonomous? This paper explores the potential for an energy-autonomous home in the suburbs of Melbourne. The purpose is to broadly assess the available renewable energy (RE) technologies in terms of their likely cost and physical requirements in order to determine whether energy-autonomy is feasible and worthwhile. The current energy consumption of a hypothetical household has been analysed. The assumptions made to reduce this demand using accepted conservation strategies are then described. Various approaches to meet the remaining energy demand from renewable sources have then been assessed.

2. Residential energy consumption in Victoria

Residential energy consumption can be divided into five end-use groups (Fig. 1). Space heating accounts for 44.3 GJ per household per year or 58% of the total energy demand. Electrical appliances and water heaters are the next two major energy consumers, accounting for 20% and 18% of usage respectively. Energy used for cooking and space cooling is only 3% and 1% respectively, despite the large increase in the penetration of air conditioning since 1990 [3].

3. Energy conservation

Reducing the demand for energy for heating and cooling through energy conservation measures is crucial for an energy-autonomous building. Melbourne has a mild, temperate climate with cool winters and mean minimum temperatures of approximately 7° C. The summers are mild-to-hot with mean maximum temperatures of approximately 24°C from December until February. Peak temperatures, however, can exceed 40°C on occasions. The

average daily horizontal solar radiation levels in winter and summer are 2.0 and 6.4 kWh m^{-2} respectively. Proper passive design is essential to moderate internal temperatures within a dwelling to minimise the need for conditioning. In this study, it has been assumed that accepted passive design practices in terms of: house orientation and aspect ratio; magnitude of north-facing glazing; thermal mass and insulation; living room and bedroom location; provision for cross ventilation; summer shading; and reduced infiltration have all been followed. Minimum energy performance requirements for new homes in Victoria currently require an energy rating of 5-stars. This rating equates to using 165 $MJ.m^{-2}$ annually for heating and cooling the home. However, sections of the building industry are already demonstrating that much more efficient homes can be constructed. One commercial builder of mass housing has unveiled a 9-star home, which has a predicted energy consumption of 21.9 $MJ.m^{-2}$. This practice should mean that the heating and cooling demand can be reduced substantially. In this study, it has been assumed that heating demand can be reduced by almost 90% and that cooling can be achieved without air conditioning. For a 220 m^2 home, the energy consumption will therefore be 4818 MJ per annum (1338 kWh).

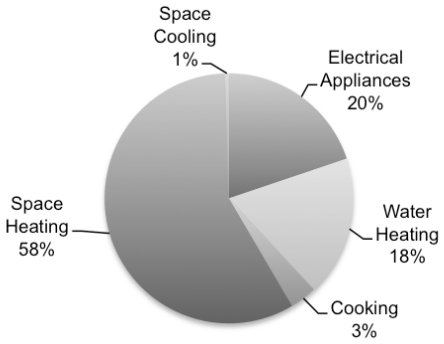

Fig. 1. Residential energy consumption by end use in Victoria (source: adapted from [3])

The average electricity demand of Victorian households in 2008 was 5,824 kWh per year or 16 kWh per day [3]. The electricity consumption of several families (three or four persons), who have made a conscious decision to reduce their energy use, shows that a daily use of 5 kWh is easily achievable without abandoning a modern and comfortable lifestyle [4][5]. Typical strategies to achieve this reduction include: choosing energy efficient appliances; reducing the size of the appliances e.g. the refrigerator to be appropriate to the demand; eliminating standby energy consumption (alone equal to about 10% of the total electricity use); and installing more efficient lighting. According to [6], most homes could reduce their energy use for lighting by 50 per cent or more by using more efficient technologies. In this study, it has been assumed that most or all of these strategies have been used to reduce annual electricity requirements to 1825 kWh i.e. 5 kWh per day.

In Victoria, 74% of household uses a gas cook top and 60% use an electric oven [3]. In an energy-autonomous home powered by RE, gas would not be used. The production of gas from biomass is an unrealistic proposition for a normal suburban household and therefore it has been assumed that electricity will be used for cooking using a combination of electric and microwave ovens, and an induction cook top. An induction cook top is about twice as efficient as a gas cook top [7]. In this study, a modest 5% reduction in energy required for cooking has been assumed because of the uncertainty of the usage patterns of the three cooking technologies to be employed.

The daily hot water usage of an average Australian household is about 193 litres i.e. 76 litres per person [8]; 57% of the hot water is used for showering, 11% for clothes washing and 32% for washing dishes and general household cleaning. High efficiency shower heads can reduce water usage in the shower to 7 litres per minute. Cold water clothes washing can reduce this hot water requirement by at least half. Although improvements in hot water system efficiency could produce further savings in the hot water energy use, this study has assumed that energy consumption for hot water will be achieved by a reduction in hot water usage alone and this will cut the demand down to 50 litres per day per person. Table 2 shows a summary of the current average and reduced annual energy demand for various tasks for a Victorian household.

Table 2: Current and reduced annual energy demand for a Victorian household [3]

	Average household consumption (kWh)	Reduced demand (kWh)
Electrical appliances	4,207	1,825
Water heating	3,851	2,460
Cooking	740	700
Space heating	12,292	1,338
Space cooling	109	0
Total	21,199	6,323

4. Renewable energy technologies

A wide range of technologies are available to harness RE sources. These technologies include solar photovoltaic and thermal systems, hydro, wave or tidal energy systems, wind turbines, biomass burners and digesters, and heat pumps. However, many of these systems are unsuitable either for a single residential dwelling or the RE sources are unavailable in an urban location. Micro-hydro, wave and tidal systems obviously cannot be employed in an urban area like Melbourne. Although wind turbine systems have been developed for rooftop installation in urban areas, wind energy technology is considered unsuitable for Melbourne [9].

Biomass burners in the form of woodstoves are currently used to heat Melbourne homes but their popularity is declining in preference to natural gas. It is predicted that residential energy supplied by wood will decline from 21% in 1990 to 8% by 2020 [3]. In Europe, high efficiency stoves burning pellets made from wood waste are used on a wide scale and encouraged. Although pellet stoves are still relatively new in Australia, pellets from plantation forests are set to become easily available in coming years in Australia. Whether pellet-burning stoves will reverse the preference for gas space heating is uncertain and therefore this technology is not considered in this study. Individual biogas digesters are also not considered because of the need for a reliable supply of feedstock, which is unrealistic for a suburban residence. Solar (electric and thermal) systems and heat pumps using geothermal energy are therefore considered to be the most suitable RE technologies for an energy-autonomous house in a Melbourne suburb and are discussed in more detail below.

4.1. Space heating

There two options for solar heating systems. One system is water-based i.e. hydronic, using radiators or coils in a concrete slab. A system capable of heating a 232 m^2 house would need eight 12-tube evacuated collectors and a 1200 litre storage tank [10]. The cost of the solar components of a hydronic system is estimated to be approximately A$19,000. However, the system would also provide domestic hot water, which would therefore reduce the cost by

about A$5,000. The other system is air-based and would consist of a solar air heater, fan and thermal storage. In the 1970s and 1980s, rockbeds or piles were the preferred thermal storage medium [11]. However, solar air heating systems have declined in popularity and few systems have been installed in recent times and were therefore not considered in this study.

A ground-source heat pump uses the year-round relatively-constant temperature of the earth at 2-3 m below the surface. In Melbourne, this is approximately 15°C. A heat pump uses the energy in the ground to heat the house in winter. In summer, the process can be reversed for cooling by transferring the heat from the building to the ground, using it as a heat sink. In the case of a well-designed house, cooling should not be required. The pipe heat exchanger system, containing water or refrigerant, can be installed either vertically or horizontally. Vertical pipes require boreholes of 30 to 120 metre in depth. A horizontal system requires more space, but it is cheaper to install the pipes at depths of 1-2 m. In addition to space conditioning, ground-source heat pumps can also be used for hot water production. Their main disadvantage is the higher first cost for the excavation work compared to conventional HVAC technologies. In this study, it is assumed that the pipe heat exchanger is installed vertically because of the space restriction of a small urban garden and that the installed price is approximately twice the price of the heat pump alone [12].

4.2. Hot water production

A 30-tube evacuated tube system with a 315 litre storage tank and electric booster has a recommended retail price of approximately A$6500 [13]. In Melbourne, a correctly-sized domestic solar water heating system is generally estimated to contribute about 60-65% of a household's hot water demand. In order to achieve a higher solar fraction and therefore greater energy autonomy, a larger area would be required.

4.3. Electricity generation and storage

Depending on the type of RE system, the electricity generation will vary depending on the daily and seasonal conditions. Compared to a grid-interactive system which uses the main electricity grid as backup, a stand-alone power supply has to provide the entire energy demand either from the generation system directly or from a storage system. This means that the system has to be larger to meet peak loads, and therefore will be oversized at other times. Stand-alone photovoltaic systems in particular require energy storage to enable the energy generated during the sunshine hours to be available for later use. The most common storage system in Australia for stand-alone systems is a large capacity battery bank.

Fuel cells, like batteries, are electro-chemical power sources but, unlike batteries which store energy, fuel cells transform energy, the primary fuel source being hydrogen. Hydrogen can be produced from water by electrolysis with low emissions, if the electricity used for the process is generated by a RE technology such as a photovoltaic array or wind turbine. Such a system could provide electricity on demand and therefore offers the potential to overcome the intermittence of RE sources. The system will require an RE electricity supply, an electrolyser, compressor, purification system, storage cylinders and a fuel cell. The feasibility of a similar system in Australia has been investigated [14] and although the load requirement was ten times greater, some of their findings are relevant to this study. The PV system was the least cost of any combination investigated, and the electrolyser represented about half of the system costs, which was over A$300,000. One manufacturer has sold its first 4 kW RE fuel cell systems and the price of these is approximately A$57,000 [15].

5. Methodology

The various RE technologies considered have been sized and their cost estimated using on-line calculators. To simplify sizing, various assumptions have been made. The energy demand for water heating, cooking and general electricity is assumed to be independent of ambient conditions. Because of the solar passive design features and energy conservation measures, space heating is required now only in the three main winter months i.e. June, July and August. Energy demand is assumed to be equally spread across these three months. Fig. 2 shows the energy demand for the proposed autonomous house throughout the year.

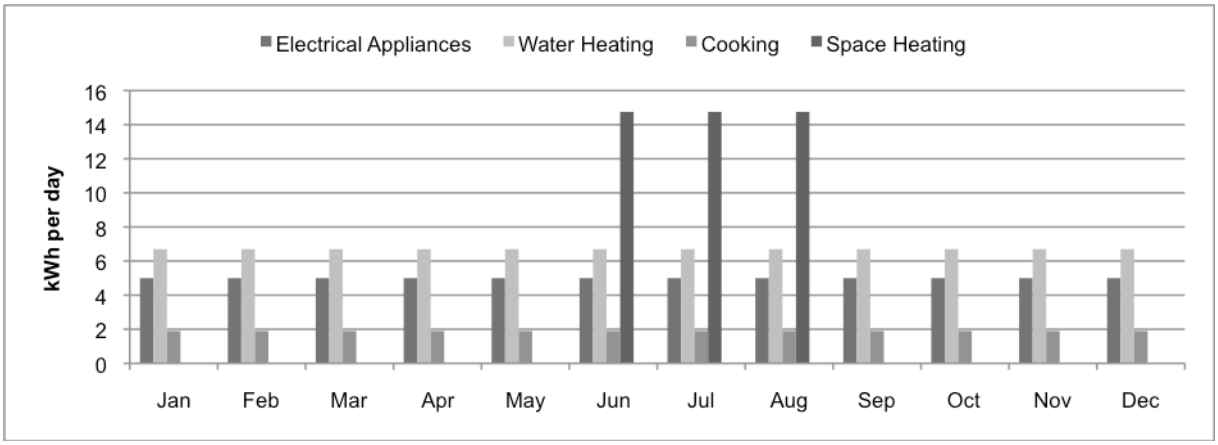

Fig. 2: Daily energy demand (kWh) throughout the year

6. Scenarios

Using different combinations of RE systems, three scenarios to provide the required energy to the autonomous house have been analysed. A fourth scenario using RE technologies in combination with conventional energy systems has also been included for comparison (Table 3). In each case, the house is a detached dwelling with a floor area of 220 m^2 and is occupied by three people. The assumed energy requirements for space heating, hot water and cooking are the 'reduced demands' shown in Table 2 and, depending on the technologies, the demand for electricity will increase above the requirements just for electrical appliances. In Scenario 1, 2525 kWh is required and spread evenly throughout the year. In Scenario 2, an additional 14.9 kWh per day are required in the winter months from the fuel cell. In Scenario 3, the heat pump will require electricity to provide hot water for both washing and space heating. Operating continuously in the winter months, it will therefore require an additional 5.3 kWh per day, assuming a COP of 4. In Scenario 4, only 1825 kWh is required because natural gas is used for cooking.

7. Results and discussion

In Scenario 1, a 17 m^2 evacuated tube array would provide both the space heating and water heating demand, although the system will be greatly oversized for the non-winter months. The photovoltaic system is sized to provide sufficient energy for the daily use in the winter months. A 6.6 kW system with a 1515 Ah battery bank to provide five days of backup is required to provide the electricity for cooking and appliance use [16].

Table 3: Scenarios of RE systems for energy-autonomous and grid-connected houses

End use	Scenario 1	Scenario 2	Scenario 3	Scenario 4
Space Heating	Solar hot water	Hydrogen fuel cell	Ground source heat pump	Solar hot water
Hot Water	Solar hot water	Solar hot water + fuel cell waste heat	Ground source heat pump	Solar hot water + gas booster
Cooking	Photovoltaics	Fuel cell - cooktop Photovoltaics - oven	Photovoltaics	Natural gas
Appliances	Photovoltaics	Photovoltaics	Photovoltaics	Photovoltaics
Energy Storage	Batteries	Hydrogen in storage cylinders	Batteries	Grid-connected

In Scenario 2 the output from the photovoltaic system can be used both directly and indirectly to meet the various energy demands. Electrical appliance use and oven cooking can be met directly. The heating system and the cook top use the PV electricity indirectly in form of electrolysis-produced hydrogen. For space heating the hydrogen is fed to a fuel cell. The cook top is powered by hydrogen gas. Assuming a combined efficiency of 0.74 for the electrolyzer and purifier [14] and a fuel cell hydrogen-electricity conversion efficiency of 0.5, Scenario 2 has an annual electricity demand of 6181 kWh. However, the PV array size required is smaller than Scenario 1. If the electricity generated from the solar panels is insufficient in the winter months, the household can draw from the excess hydrogen energy stored over the summer, thus obviating the need for battery storage and an overly-large PV array size designed to produce the daily requirements in winter. The 4.2 kW system requires an area of approximately 34 m^2 [16][17]. The solar thermal system in this scenario provides 70 per cent of the hot water demand. It consists of a collector area of 5 m^2 with evacuated tubes and a storage tank of 315 litres. When the solar hot water production is insufficient, the waste heat from the fuel cell can be used as a back-up system.

In Scenario 3, a 2.1 kW ground-source heat pump (A$12,000 installed) provides the household with domestic hot water and space heating; a total of 21.28 kWh per day during the winter months. Assuming a COP of 4, this means that 5.32 kWh per day must be generated by the PV array in addition to that required to provide energy for the appliances and cooking. An 11.4 kW system is therefore required. In Scenario 4, the space heating demand is covered by a solar thermal heating system, as in Scenario 1. The photovoltaic system is sized to cover the annual electricity demand, rather than the daily load. A 1.5 kW solar system would generate 2,132 kWh over the year providing an excess of 307 kWh [16]. Natural gas is used for cooking and also to back up the solar hot water system with a solar fraction of 0.65, thus using another 1,561 kWh in total. A 2.5 kW photovoltaic system with an annual output of 3,553 kWh would make the household a net energy-exporter.

8. Feasibility Assessment

Table 4 shows the estimated area requirements and cost for each scenario. The median price of a house in Melbourne in mid-2010 was approximately A$560,000 and a typical house of the size assumed would have a north-facing roof of approximately 50 m^2. In terms of the physical feasibility, Scenarios 1 and 3 require a larger roof area than is available and are therefore not practical unless alternative unobstructed north-facing areas are available. The

data in Table 4 also indicates that a fully energy-autonomous house would add between 15% and 33 % to the median price (Scenarios 1-3). However, a net-energy exporting house would only increase the price by 6%. It is acknowledged that the solar system costs are from one supplier only and lower prices may be available. In addition, the costs used do not include government rebates, which would also reduce the price, but only by approximately 10%. Reducing the number of days of battery storage would also reduce capital costs. The purpose of this exercise, however, is to achieve an order-of-magnitude assessment rather than detailed costing.

Table 4: Additional costs and roof area requirements for an energy-autonomous house

	Scenario 1	Scenario 2	Scenario 3	Scenario 4
Area (m^2)	SHD/HWS - 17 PV (6.6kW) - 48 Total = ~ 65	HWS - 5 PV (4.5 kW) - 34 Total = ~ 39	PV (11.4 kW) - 88 Total = ~ 88	SHD/HWS - 17 PV (2.5kW) - 19 Total ~ 36
Cost (A$k)	SHD/HWS ~ 19 PV(6.6kW) ~ 100 Total = ~119	HWS ~ 6.5 PV(4.5kW) ~ 22 H_2 ~ 57+ Total = ~86	HP ~ 12 PV(11.4kW) ~ 174 Total = ~186	SHD/HWS ~ 19 PV(2.5kW) ~ 15 Total = ~ 34

9. Conclusions

The purpose of this study was to broadly assess the technical, practical and financial feasibility of an energy-autonomous house in Melbourne. It is concluded that the energy-autonomous home in Melbourne is technically possible. With reduced demand, RE technologies are capable of providing a household's complete energy needs, but energy autonomy can only be achieved by installing over-sized systems, the output from which is not used much of the time. This means that very large and expensive systems are required, which are likely to be unacceptable to most homeowners. It is therefore concluded that the goal of energy-autonomy in a suburban Melbourne house is currently not worth pursuing. The alternative option of a low-energy house, which exports electricity produced from renewable sources to the grid offers many benefits in comparison to the autonomous version. Electricity storage systems are not necessary and the energy generating systems can be smaller and cheaper because seasonal differences can be balanced out by the grid. Furthermore, any excess energy produced in summer is not wasted but supplied to other grid users.

Acknowledgements

The authors would like to acknowledge the useful inputs from Dr Lu Aye and Tshewang Llendhup from The University of Melbourne during the preparation of this paper.

References

[1] B. and R. Vale, The Autonomous House – design and planning for self-sufficiency. Thames and Hudson, London, 1975.

[2] K. Voss, A. Goetzberger, G. Bopp, A Haberle, A. Heinzel and H. Lehmberg, The self-sufficient solar housing in Freiburg – results of 3 years of operation, Solar Energy, 58, 1-3, pp. 17-23.

[3] DEWHA Department of the Environment, Water, Heritage and the Arts (2008) Energy use in the Australian residential sector 1986 – 2020: Canberra.

[4] ReNew (2005). Smart house in a smart street. ReNew, 90, Jan-March, 41-44.

[5] ReNew (2006). Solar surplus, 10 years in a row. ReNew, 96, July-September, 19-21.

[6] Milne, G. and Riedy, C. (2008) Energy use in Australian Government (2008) Technical Manual, retrieved 2 August 2009, >http://www.yourhome.gov.au/technical/fs61.html<

[7] DOE (1997). Technical support document for residential cooking products. Volume 2: Potential impact of alternative efficiency levels for residential cooking products. U.S. Department of Energy, Office of Codes and Standards.

[8] Wilkenfeld, G. and Associates Pty Ltd (2004). NFEE – Energy efficiency improvement potential case studies, residential water heating. Report to the Sustainable Energy Authority Victoria. Feb, 18 pp.

[9] Webb, A. (2007). The viability of domestic wind turbines for urban Melbourne. Alternative Technology Association report for Sustainability Victoria, June, 53 pp.

[10] Harris, M. (2006). Use the sun to heat the house, ReNew, 9, 31-33.

[11] Fuller, R. (2003). Operational experiences with rockbed storage systems. Proc. Solar 03, Destination renewables: from research to market: 41st annual conference of the Australian and New Zealand Solar Energy Society, Australian and New Zealand Solar Energy Society, Maroubra, N.S.W., pp. 19-25.

[12] Begert, C. (2006). Heat pumps and environmental performance - assessing the potential of ground-source heat pumps, ATA Alternative Technology Association, December.

[13] ReNew (2009). Solar water heater buyers guide, ReNew, 106, 41-51, January-March.

[14] Shakya, B.D., Lu Aye and Musgrave, P. (2005). Technical feasibility and financial analysis of hybrid wind-photovoltaic system with hydrogen storage for Cooma. Int. Jnl. for Hydrogen Energy, 30, 1, 9-20.

[15] Fronius (2010). The stationary Fronius energy cell. Available from: http://www.fronius.com/cps/rde/xchg/SID-D253C5D6-02484037/fronius_international/hs.xsl/83_18098_ENG_HTML.htm. Accessed 13th December 2010

[16] Energymatters (2010) Renewable energy design tools. Available at: <http://www.energymatters. com.au/climate-data/> Accessed 12th December 2010.

[17] Solar Online Australia (2010). Remote area power system costs. Available at: <http://www.solaronline.com.au/solar_system_pricing/> Accessed 30th November 2010

Feasibility study on using solar chimney and earth-to-air heat exchanger for natural heating of buildings

Amin Haghighi Poshtiri[1,*], Neda Gilani[2], Farshad zamiri[3]

[1] *Guilan University, Rasht, Iran*
[2] *Tarbiat modares University, Tehran, Iran*
[3] *Sharif university of technology, Tehran, Iran*
** Corresponding author. Tel: +98 1316690273, Fax: +98 1316690271, E-mail: aminhaghighi_p@yahoo.com*

Abstract: Here, the capability of the SC-EAHE system to meet the required thermal needs of individuals and also the dependence of the system performance on environmental and geometrical issues, have been studied. To determine the heat transfer characteristics of the system, a mathematical model based on energy conservation equations has been developed and solved by an iterative method. The results of study for the effect of air gap size variation on the air change per hour (ACH) at various solar radiation values shows that this effect (air gap depth on the ACH) is significant up to 0.2 (m), and the ACH and room air temperature remains almost constant beyond the 0.2 (m). The results also revealed that the design of EAHE with the diameter of 0.5 (m) would lead to the best performance. It is found that, with proper insulation, SC system can provide thermal comfort condition even at the ambient temperature as low as 5 ^{o}C and the solar radiation intensity of 185 (w/m^2).

Keywords: *Solar chimney, Earth-to-air heat exchanger, Natural heating, Building.*

Nomenclature (Optional)

A	*area*	m^2
ACH	*air change per hour*	h^{-1}
C	*specific heat of air*	J/kgK
c	*pressure loss coefficient of fittings*	
d	*air gap depth, diameter*	m
H	*distance*	m
h	*convective heat transfer coefficient*	$W/m^2.K$
hr	*radiative heat transfer coefficient*	$W/m^2.K$
I	*total solar radiation on surface*	W/m^2
k	*thermal conductivity*	$W/m.K$
L	*length*	m
m	*mass flow rate of air*	kg/s
Q	*heat transfer to air stream*	W/m^2
R	*thermal resistance*	$m^2.K/W$
r	*radius*	m
T	*temperature*	K
t	*thickness*	m
U	*overall heat transfer coefficient*	$W/m^2.K$
u	*air velocity*	m/s
V	*volume of room*	m^3
x	*coordinate system*	m

Greek symbols

α	*absorbtion coefficient*	
γ	*constant in Eqs.(9) and,(10)*	
δ	*heat penetration depth*	m
ε	*emissivity*	
λ	*thermal diffusivity*	m^2/s
ξ	*friction factor*	
ρ	*density*	kg/m^3
ω	*frequency of temperature oscillation*	rad/s

Dimensionless terms

Nu	*Nusselt number*	$h_f.L/\mu_f$

Subscripts

a	*ambient*
abs	*absorber wall*
f	*air flow*
g	*glass*
hyd	*hydraulic*
i	*internal*
r	*room*
s	*soil*
su	*undisturbed soil*
t	*pipe*
o	*outlet*

1. Introduction

Traditional energy resources such as fossil fuels which lead to the greenhouse effect, global warming, are expected to dwindle gradually. As environmental regulations are becoming strict, further investigation on alternative solutions to meet the energy needs of residential

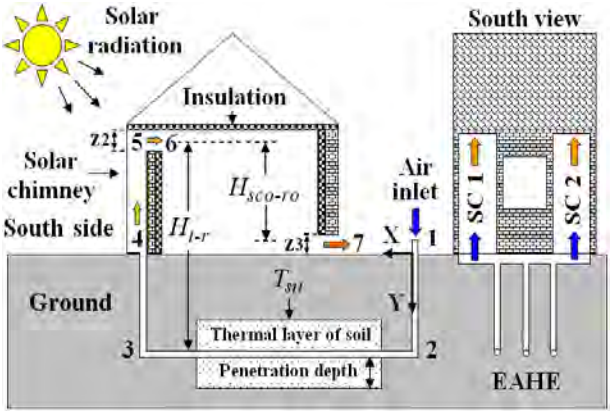

Fig. 1. Schematic diagram of integrated EAHE and SC.

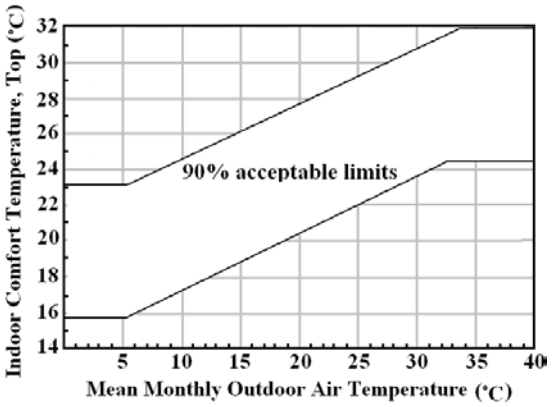

Fig. 2. Adaptive Comfort standard.

units as well as industrial ones is also on the table. The use of passive techniques is an effective tool for attenuating the growth of the energy consumption for air conditioning. Earth to air heat exchanger (EAHE) and solar chimney (SC) are passive heating systems which are commonly used for reducing energy consumption.

Many researches have been conducted on using EAHE for producing cool or warm air so far. Hollmuller [1] considered a periodic input for the air in the buried pipe, yielding a physical interpretation of the amplitude-dampening and the phase-shifting of the periodic input signal. Al-Ajmi et al. [2] developed a theoretical model of an EAHE for predicting the outlet air temperature and cooling potential of these devices. They showed that it have the potential for reducing cooling energy demand in a typical house by 30% over the peak summer season.

Solar chimneys have attracted much attention of researchers. Bansal et al. [3] analytically studied a solar chimney-assisted wind tower for natural ventilation in buildings. The estimated effect of the solar chimney was shown to be substantial in inducing natural ventilation for low wind speeds. Gan and Riffat [4] also investigated solar assisted natural ventilation with heat-pipe heat recovery in naturally ventilated buildings, using a CFD technique. Mathur et al. [5] analytically studied the effect of absorber inclination on the air flow rate in a solar induced ventilation system using roof solar chimney. The results showed that optimum absorber inclination depending upon the latitude of the location. Maerefat and Haghighi [6] introduced and investigated integrated EAHE-SC system. They showed that the solar chimney can be perfectly used to power the underground cooling system during the daytime, without any need for electricity. The review of the related literature shows that the combination of EAHE and SC as a heating system has not been fully investigated yet.

Fig.1 illustrates a schematic plan of the system. The solar chimney comprises a glass surface oriented to the south and an absorber wall which acts as a capturing surface. The EAHE consists of horizontal long pipe that is placed underground. The air is heated up in the SC by the solar energy, and by natural convection mechanism the outside air is sucked-in through the pipe. It will be shown that this system can provide good indoor condition in accordance with the Adapted Comfort Standard (ACS). The required indoor temperatures according to the adaptive comfort model are shown in Fig. 2. ACS does not recommend the ventilation rate [7]. Therefore, the minimum ventilation rate is set around 3 ACH [8].

2. Problem formulation

The modeling includes models of earth to air heat exchanger (Fig. 3) and solar chimney Fig. 4). The following assumptions are made in this analysis.

1. Only buoyancy force is considered, wind induced natural ventilation is not included.
2. The flows in the channels are hydro dynamically and thermally fully developed.

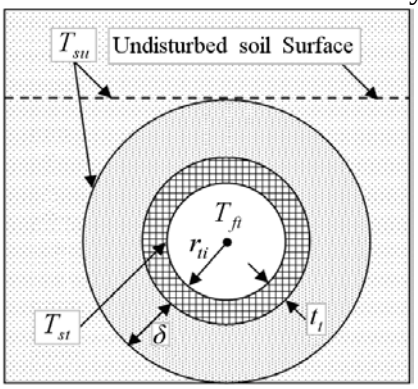

Fig. 3. Cross section of an EAHE.

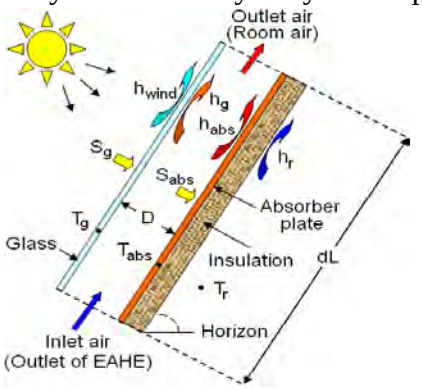

Fig. 4. Diagram of the heat transfer in the SC.

3. The glass cover is opaque for infrared radiation.
4. Thermal capacities of glass and absorber wall are negligible.
5. The air flow in the channel is radiation non-participating media.
6. The soil is homogeneous and the soil type does not change along the channel.
7. The system is at steady-state condition.

2.1. Mathematical modeling of EAHE

The cross section of EAHE used in the model is shown in Fig. 3. In order to impose the ground thermal loads as boundary conditions at the EAHE wall, the undisturbed soil temperature (T_{su}) has been used. The soil temperature is nearly constant at the penetration depth. It is defined when the surface of the soil is subjected to a periodic temperature [1].

$$\delta = \sqrt{2\lambda_s / \omega} \tag{1}$$

The air temperature through the EAHE is calculated by the following equation [6].

$$T_{ft}(x) = T_{su} + (T_a - T_{su}) exp\left(-x / \left(mC_{ft} R_{total}\right)\right) \tag{2}$$

Where R_{total} represents the overall thermal resistance and is given by [6]:

$$R_{total} = \frac{1}{2\pi L_t}\left(1/h_{ft} + \ln\left(\frac{r_{ti}+t_t}{r_{ti}}\right)/k_t + \ln\left(1+\frac{\delta}{r_{ti}+t_t}+\sqrt{\left(1+\frac{\delta}{r_{ti}+t_t}\right)^2-1}\right)/k_s\right) \tag{3}$$

2.2. Mathematical modeling of SC

An element of the model for SC is shown in Fig. 4. In principle and based on the energy conservation law, a set of differential equations are obtained along the length of SC [6].
The energy balance equation for glass cover is:

$$\alpha_g I A_g + hr_{abs-g} A_{abs}\left(T_{abs} - T_g\right) = h_g A_g\left(T_g - T_{fsc}\right) + U_{g-a} A_g\left(T_g - T_a\right) \tag{4}$$

The overall top heat loss coefficient from glass cover to ambient air U_{g-a}, can be written as:

$$U_{g-a} = h_{wind} + hr_{g-sky} + h_{g-a} \tag{5}$$

The convective heat transfer coefficient due to the wind is $h_{wind} = 2.8 + 3.0u_{wind}$ [9].

The radiative heat transfer coefficient from the outer glass surface to the sky and between absorber plate and glass cover may be obtained from [9]:

$$hr_{g-sky} = \sigma\varepsilon_g \left(T_g + T_{sky}\right)\left(T_g^2 + T_{sky}^2\right)\left(T_g - T_{sky}\right)/\left(T_g - T_a\right) \quad (6)$$

$$hr_{abs-g} = \sigma\left(T_g^2 + T_{abs}^2\right)\left(T_g + T_{abs}\right)/\left(1/\varepsilon_g + 1/\varepsilon_{abs} - 1\right) \quad (7)$$

Where, the sky temperature is $T_{sky} = 0.0552T_a^{1.5}$ [9].

The convective heat transfer coefficient is given by: [5]:

$$h = \mathrm{Nu}k_{fsc}/L \quad (8)$$

All property values are evaluated at average surface – air temperatures.

The energy balance equation for air flow in the chimney is:

$$h_{abs}A_{abs}\left(T_{abs} - T_{fsc}\right) + h_g A_g\left(T_g - T_{fsc}\right) = -mC_{fsc}\left(T_{fsc} - T_{fto}\right)/\gamma \quad (9)$$

The mean air temperature was experimentally determined to follow the non-linear form [10]:

$$T_{fsc} = \gamma T_{fsco} + (1-\gamma)T_{fscin} \quad (10)$$

Value of the constant γ is taken as 0.74 according to Ref. [10].

The energy balance equation for the absorber plate is written as:

$$\alpha_{abs}IA_{abs} = h_{abs}A_{abs}\left(T_{abs} - T_{fsc}\right) + hr_{abs-g}A_{abs}\left(T_{abs} - T_g\right) + U_{abs-r}A_{abs}\left(T_{abs} - T_r\right) \quad (11)$$

The overall heat transfer coefficient from the absorber wall to the room U_{abs-a} is given by:

$$U_{abs-r} = 1/\left(1/h_r + t_{ins}/k_{ins}\right) \quad (12)$$

In the above equation h_r has been taken as 2.8 W/m^2 K [10].

2.3. Room ventilation and temperature

The buoyancy pressure due to increasing air temperature in SC, sucks the air through the EAHE. The friction losses due to fluid flow through the channels and across the fittings, refrain from the fluid flow. If the buoyancy pressure overcomes the sum of all flow pressure losses, the natural ventilation may take place.

A mathematical model based on Bernoulli's equation has been used to estimate the system flow rate. Thus, the chimney net draft can be calculated by the following equation:

$$Draft_{sc} = \left(\rho_{fto} - \rho_{fsco}\right)gL_{sc} - \left(\sum_{j=5}^{6} c_j + \xi_{sc}\frac{L_{sc}}{(d_{hyd})_{sc}}\right)\left(\frac{\rho_{fsco}u_{sc}^2}{2}\right) \quad (13)$$

Where the c_j is the pressure loss coefficients at the locations which are indicated in Fig. 1.

The EAHE pressure loss ΔP_{EAHE} is:

$$\Delta P_{EAHE} = \left(\sum_{j=1}^{4} c_j + \xi_t\frac{L_{EAHE}}{d_{tin}}\right)\left(\frac{\rho_{ft}u_{ft}^2}{2}\right) \quad (14)$$

The chimney effects $Draft_{EAHE}$ and $Draft_{Room}$ can be expressed as:

$$Draft_{EAHE} = \left(\rho_{fa} - \rho_{ft}\right)g\left(H_{t-r} - L_{sc}\right) \quad (15)$$

$$Draft_r = \left(\rho_{fr} - \rho_{fsco}\right)gH_{sco-ro} \quad (16)$$

The required draft for heating system $Draft_{System}$ is the sum of the pipe pressure loss and the positive pressure $Draft_{EAHE}$ and $Draft_{Room}$.

$$Draft_{System} = \Delta P_{EAHE} + Draft_{EAHE} + Draft_r \quad (17)$$

Under steady-state conditions, we can write:

$$Draft_{System} = Draft_{sc} \quad (18)$$

The air mass flow rate at the chimney and EAHE are the same if there is no air infiltration:

$$m = \rho A u\Big|_{Chimney\ outlet} = \rho A u\Big|_{Chimney\ inlet} = \rho A u\Big|_{EAHE} \quad (19)$$

By expanding equation (18), the air velocity in the SC can be obtained as:

Table 1. Comparison of experimental and theoretical results for solar chimney included ACH No.

Solar radiation (W/m^2)	Absorber Length (m)	Inlet chim. Dimens (m×m)	Ambient temp. (K)	ACH			Errors of [10] (%)	Errors of present study (%)
				Exp. [10]	Theo. [10]	Theo. (present study)		
500	0.8	1.0×0.2	298-304	4.53	4.89	4.68	7.95	3.31
500	0.9	1.0×0.1	294-296	2.66	3.46	3.44	30.07	29.32
700	0.8	1.0×0.2	298-304	5.33	5.17	5.31	3.00	0.37
700	0.9	1.0×0.1	294-296	2.93	3.67	3.32	25.25	13.31

$$u_{sc} = \sqrt{Bouyancy\ Terms / Friction\ Terms} \quad (20)$$

$$Buoyancy\ Terms = 2\left\{\begin{matrix}\left(\rho_{fto} - \rho_{fsco}\right)gL_{sc} - \left(\rho_{fa} - \rho_{ft}\right)g\left(H_{t-r} - L_{sc}\right) - \\ \left(\rho_{fr} - \rho_{fsco}\right)gH_{sco-ro}\end{matrix}\right\} \quad (21)$$

$$Friction\ Terms = (c)_7\left(\frac{\rho_{fsco}A_{sco}}{\rho_{fr}A_{ro}}\right)^2\rho_{fr} + \left\{(c)_5 + (c)_6 + \xi_{sc}\frac{L_{sc}}{(d_{hyd})_{sc}}\right\}\rho_{fsco} + \left\{\left(\sum_{j=1}^{4}c_j + \xi_t\frac{L_t + 2(H_{t-r} - L_{sc})}{d_t}\right)\left(\frac{\rho_{fsco}A_{sco}}{\rho_{ft}A_t}\right)^2\right\}\rho_{ft} \quad (22)$$

The ACH is calculated under steady-state conditions by the following equation [10]:

$$ACH = 3600m/\left(\rho_{fsc}V\right) \quad (23)$$

The room air temperature which depends on room heat gain is given by:

$$T_r = T_{fscout} - Q_r/\left(mC_{fr}\right) \quad (24)$$

Where Q_r is sum of the heats that the room gains through the walls and the heat generated by internal heat sources.

The coupled governing equations (2), (4), (9), (11) and (20) are the full description of the system and have to be solved iteratively until convergence of the results.

3. Model validation

There is no experimental data to validate the results of theoretical model for the integrated system. So, the calculation has been carried out for SC and EAHE separately under same conditions of experimental studies of [10] and [11]. Table 1 shows the results of present model and the theoretical and experimental results of Mathur et al. [10]. The quantitative comparison shows a reasonable agreement between the results obtained by the present study and the published results of [10]. The results of present study are closer to the experimental results than the theoretical results of Ref. [10]. It should be noted that the calculation carried out at the same conditions of Ref. [10] in which the room volume is 27.0 (m^3). Fig. 5 shows the air temperature variation along the cooling pipe. The results of the present work are calculated at the conditions of experiments based on Ref. [11]. As the figure shows, there is good agreement between the present theoretical results and the experimental results of Ref. [11]. However, it is reasonable to conclude that the mathematical model can predict air temperature quite accurately and the calculated results are reliable.

4. Results and discussion

The following dimensions and specifications are used in the modeling. The room has size of

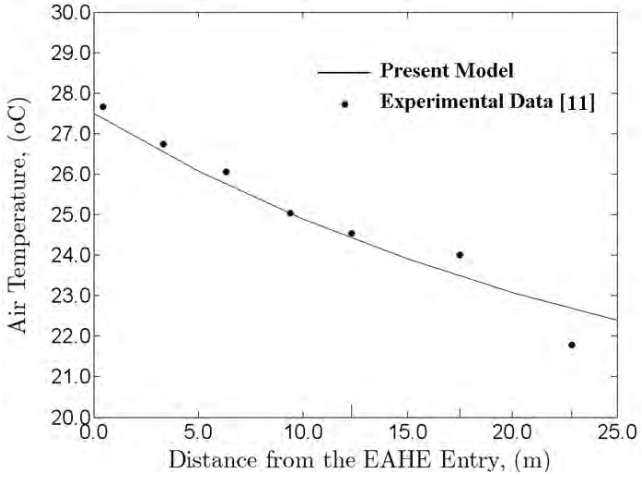

Fig. 5. Comparison present results with experimental data.

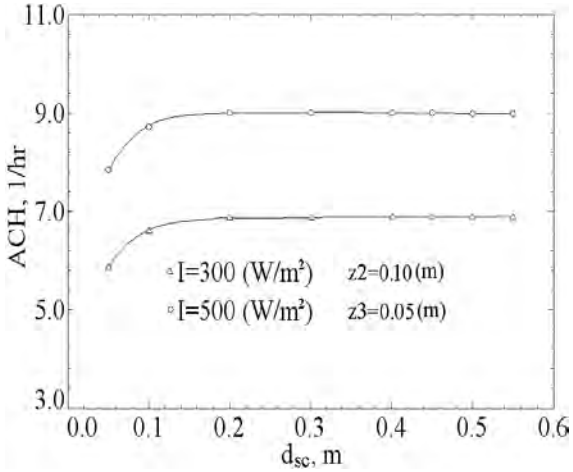

Fig. 6. ACH variation with changes of air gap depth of SC (T_a=10°C).

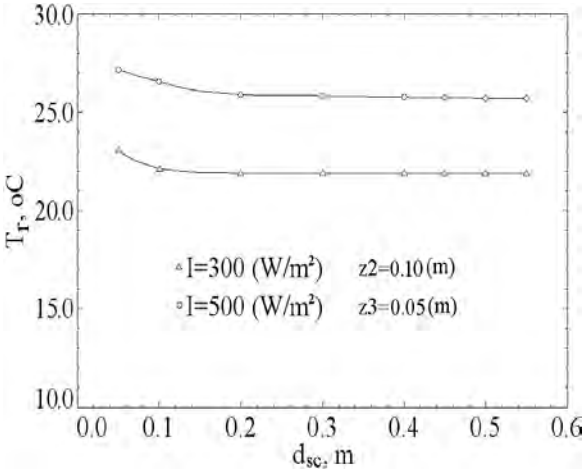

Fig. 7. Room air temperature variation with changes of air gap depth of SC (T_a=10°C).

4.0(m)×4.0(m)×3.125(m) without air infiltration. The heating demand is assumed to change within the range of 0.0-1000 (W) in the calculations. A solar chimney with the length of 3.125 (m), width of 4.0 (m) and air gap depth of 0.2 (m) is considered. The thickness and thermal conductivity of the insulation located in south wall of the room are 0.2 (m) and 0.046 ($Wm^{-1}K^{-1}$), respectively. The transmissivity of the glass wall is 0.84 and the absorber wall has an emissivity and absorptivity equal to 0.95. The outlet sizes of SC and room (Fig. 1) are 0.05(m)×4.0(m) and 0.1(m)×4.0(m) respectively. The heating pipe of EAHE is a PVC pipe with 25.0 (m) length, 0.01 (m) thickness, and inside diameter of 0.5 (m) and is buried 3.0 (m) below the soil surface. The initial soil temperature at it, is approximated to be 19°C for a dry shaded soil surface condition and it is considered to be the heat source temperature.

4.1. Effective dimensions of the system

There are many geometrical dimensions which affect the system performance: i) air gap depth of the SC, ii) heating surface area of the EAHE. Fig. 6 shows the effect of air gap size variation on the ACH. It shows that the effect of air gap depth on the ACH is significant up to 0.2 (m) and, the ACH remains almost constant beyond 0.2 (m). Fig. 7 shows that as the air

gap depth increases, the room air temperature decreases gradually. This decrease is due to the result of increasing the ACH which causes reduction in the energy gained by the absorber. A comparison between these figures shows that as the chimney air gap size increases up to almost 0.2 (m), any further increase does not have a significant effect on room air temperature and it is considered as an optimum required value of the air gap.

Table 2. Effects of diameter of EAHE on system performance.

Heating demand (W)	Solar radiation (W/m^2)	Ambient air temp. (^oC)	Length of EAHE (m)	Diameter of EAHE (m)	ACH	Room air temp. (^oC)	Number of SC and EAHE
0	300	10	25	0.3	3.82	27.2	1
0	300	10	25	0.5	6.85	21.9	1
0	300	10	25	0.7	7.72	20.7	1
500	300	10	25	0.3	Thermal comfort cannot be provided.		
500	300	10	25	0.5	5.04	20.0	1
500	300	10	25	0.7	5.74	18.5	1

Table 3. Effects of length of EAHE on system performance.

Heating demand (W)	Solar radiation (W/m^2)	Ambient air temp. (^oC)	Length of EAHE (m)	Diameter of EAHE (m)	ACH	Room air temp. (^oC)	Number of SC and EAHE
0	300	10	25	0.5	6.85	21.9	1
0	300	10	35	0.5	6.35	23.2	1
0	300	10	45	0.5	5.89	24.4	1
500	300	10	25	0.5	5.04	20.0	1
500	300	10	35	0.5	4.73	21.3	1
500	300	10	45	0.5	Thermal comfort cannot be provided.		

In order to increase the heating surface one may increase the diameter and/or the length of the pipe. Table 2 shows the effect of EAHE diameter on system performance. A comparative survey shows that that as the diameter of EAHE increases up to almost 0.5 (m), any further increase does not have a significant effect on ACH and room air temperature. Therefore this value is adopted as default value of diameter. Table 3 shows the effect of EAHE length on system performance. For the length of EAHE more than 35 (m), the comfort temperature may not be provided and smaller EAHE should be employed.

4.2. Effect of environmental conditions on the system performance

The results of Table 4 also show that when air temperature rises, thermal comfort can be achieved in lower solar radiation. It is also found that when the heating demand is high, thermal comfort can be achieved only at high solar radiation. However, with proper insulation and reduction of the heating demand, SC can provide good indoor condition in the poor solar intensity and low ambient air temperature. The results show that when the heating demand is low, SC can provide thermal comfort condition even when the ambient temperature and solar intensity are equal to 5 ^oC and 185w/m^2, respectively.

5. Conclusions

Natural ventilation and heating of a room which uses SC and an EAHE have been studied in this paper. The results show that there is an optimum size for air gap size of SC (0.2 (m)) and diameter of heating pipe (0.5 (m)). It has been found that the long EAHE with the length of

less than 35 (m) should be employed to provide the thermal comfort condition. The results also show that when the ambient temperature is low, although providing thermal comfort is difficult, proper configurations could provide good indoor condition even in the poor solar intensity.

Table 4. System performance at different indoor and outdoor conditions.

Heating demand (W)	Solar radiation (W/m^2)	Ambient air temp. (^oC)	Length of EAHE (m)	Diameter of EAHE (m)	ACH	Room air temp. (^oC)	Number of SC and EAHE
0	400	0	15	0.5	8.59	15.9	1
0	250	0	25	0.5	5.11	15.9	1
0	250	5	15	0.5	6.28	17.5	1
0	185	5	25	0.5	3.45	17.5	1
500	560	0	15	0.5	8.59	15.9	1
500	550	0	25	0.5	8.47	15.9	1
500	390	5	15	0.5	6.79	17.5	1
500	320	5	25	0.5	5.67	17.5	1
1000	-	0	15	Thermal comfort cannot be provided.			
1000	-	0	25	Thermal comfort cannot be provided.			
1000	500	5	15	0.5	6.26	17.5	1
1000	-	5	25	Thermal comfort cannot be provided.			

References

[1] P. Hollmuller, Analytical characterization of amplitude-dampening and phase shifting in air/soil heat exchangers. International Journal of Heat and Mass Transfer 46, 2003, pp.4303-4317.

[2] F. Al-Ajmi, DL. Loveday, VI. Hanby, The cooling potential of earth-air heat exchangers for domestic buildings in a desert climate, Building and Environment 41, 2006, pp. 235-244.

[3] NK. Bansal, R. Mathur, MS. Bhandari, A study of solar chimney assisted wind tower system for natural ventilation in buildings, Building and Environment 29(4), 1994, pp. 495-500.

[4] G. Gan, SB. Riffat, A numerical study of solar chimney for natural ventilation of buildings with heat recovery, Applied Thermal Engineering 18, 1998, pp. 117-187.

[5] J. Mathur, S. Mathur, Anupma, Summer-performance of inclined roof solar chimney for natural ventilation, Energy and Buildings 38, 2006, pp. 1156-1163.

[6] M. Maerefat, AP. Haghighi, passive cooling of building by using integrated earth to air heat exchanger and solar chimney, Renewable Energy 35, 2010, pp. 2316-2324.

[7] GS. Brager, RJ. De dear, A standard for natural ventilation, ASHRAE Journal 42(10), 2000, pp. 21-28.

[8] BIS, Bureau of Indian Standards, Handbook of Functional Requirements of Buildings 1997 ISBN81-7061-011-7.

[9] KS. Ong, A mathematical model of a solar chimney, Renewable Energy 28, 2003, pp. 1047-1060.

[10] J. Mathur, NK. Bansal, S. Mathur, M. Jain, Experimental investigations on solar chimney for room ventilation, Solar Energy 80, 2006, pp. 927-935.

[11] As. Dhaliwal, DY. Goswami, Heat transfer analysis in environmental control using an underground air tunnel, Journal of Solar Energy Engineering 107, 1985, 141-145.

Case study on the whole life carbon cycle in buildings

Howard J. Darby[1,*], Abbas A. Elmualim[2], Fergal Kelly[3]

[1] *Technologies for Sustainable Built Environments, University of Reading, Reading, UK*
[2]*School of Construction Management and Engineering, University of Reading, Reading, UK*
[3]*Peter Brett Associates LLP, Reading, UK*
Corresponding author. Tel: +44 (0) 118 987 5123, Fax: +44 (0) 118 031 4404,
E-mail: h.j.darby@pgr.reading.ac.uk

Abstract: The potential for reducing greenhouse gas emission from buildings comes from both operational and embodied emissions. To date the focus has been on reducing the operational element, although, it is suggested that it is also important to consider early embodied carbon reductions.
This paper describes a case study on the whole life carbon cycle of a building in the UK. Specific issues addressed are the relationship between embodied carbon (Ec) and operational carbon (Oc), the proportions of Ec from the structural and non-structural elements, carbon benchmarking of the structure, the value of 'cradle to site' or 'cradle to grave' assessments and the significance of the timing of emissions during the life of the building.
The case study indicates that Ec can be an important consideration and that the structure was responsible for more than half of the Ec.
An indicative structural benchmark for the building is between 260kgCO_2/m^2 and 286kgCO_2/m^2.
Weighting of future emissions appears to be an important factor to consider. The PAS 2050 reduction factors had only a modest effect but weighting to allow for future decarbonisation of the energy supply had a large effect.

Keywords: *Embodied carbon, Carbon emission, Building, Operational carbon, CO_2.*

1. Introduction

The potential for reducing greenhouse gas emission from buildings comes from both operational emissions, produced by buildings during use, and embodied emissions, produced during manufacture of materials and components, and construction and demolition of buildings.

To date the UK government has focused attention on reducing the, apparently, larger operational element. This is reflected in the current methods of environmental assessment of buildings, which allow the highest environmental ratings to be achieved without any consideration of embodied emissions. This, together with the lack of readily available and usable data on embodied emissions, has hampered the consideration of embodied carbon during building design.

UK Building Regulations are employing a phased approach to increasing energy conservation criteria, resulting in reduced carbon emissions, in the period up to 2020. However, this only applies to operational carbon.

In terms of meeting the UK carbon reduction targets of 34% by 2020 and 80% by 2050 (measured against the 1990 baseline), it may be equally, if not more, important to consider early embodied carbon reductions, rather than just future operational reductions. Future decarbonisation of energy supply and more efficient lighting and M&E equipment installed in future refits is likely to significantly reduce operational emissions, lending further weight to this argument. Methods of emission discounting to evaluate the present value of future emissions, may allow more realistic comparisons to be made between the embodied and operational elements.

Currently, there is lack of a consistent and accepted approach to the calculation of embodied emissions, the relationship and interaction between the embodied and operational elements is not well understood, and there is considerable uncertainty and variability in the available information on emission factors for building materials and processes. Work under the European Standards Mandate M350 'Sustainability of Construction Works' [1] seeks to remedy this by developing a harmonised approach to the measurement of embodied and operational environmental impacts of construction products and whole buildings, across the entire life cycle. At this stage, it is not clear when this will become available. In the meantime, PAS 2050 [2] is available, which builds on the life cycle analysis frameworks given in the BS EN 14040 [3] suite of standards and the Greenhouse Gas (GHG) Protocol [4] developed by the World Resources Institute and the World Business Council for Sustainable Development in 2004. PAS 2050 focuses exclusively on GHGs produced during the life of a product and services. However there is huge scope for variability in the data, life cycle boundaries selected, and assumptions made [5].

This paper describes a case study on the whole life carbon cycle of a book storage building in the UK. This is part of a research project aimed at producing data on embodied carbon for different types of building, components and forms of construction to assist designers in optimising building designs and minimising carbon emissions.

The paper investigates the following specific issues:
- the relationship between embodied carbon emissions (Ec) and operational carbon emissions (Oc)
- the proportions of Ec from the structural and non-structural elements, in order to determine the relative importance of Ec from the structure and to provide data for carbon benchmarking
- how 'cradle to site' and 'cradle to grave' based assessments compare
- the significance of considering when emissions occur during the life of the building.

2. Methodology

2.1. Description of the case study building

The case study building is a book storage facility, completed in October 2010, with a total internal floor area of 11,578m^2, designed to house around eight million volumes, in carefully regulated internal temperature and humidity conditions. It has a steel framed structure on mass concrete foundations, in-situ concrete floor and precast concrete insulated sandwich cladding panels to the external walls. The 12m-high main storage chamber has insulated metal deck roof cladding and the lower 7m high section has a composite concrete and metal deck roof to support the building plant and equipment. The building is well insulated, with high thermal mass provided by the external wall panels, and is well sealed, achieving an on-site air test result of 1.6m3/h/m^2.

2.2. Assumptions and procedure

In the majority of cases, available emission factors are for CO_2, and do not include the full basket of greenhouse gases (GHGs). Therefore, this study is based on CO_2 emissions only. It is estimated [6] that, for most building materials, CO_2 represents the vast majority of GHGs (e.g., around 95%), although for plastics other GHGs are more significant. It is anticipated that as materials data evolves and becomes more comprehensive, factors including all GHGs will become available.

A building life of 60 years has been assumed for the purposes of this study.

Ec values include emissions from materials and components ('cradle to gate'), transport to site and site construction ('cradle to site'), three M&E refits at 15, 30 and 45 years, a general building refurbishment at 30 years, demolition, transport and end of life treatment for demolished materials. End of life treatment has been assumed to be based on the following hierarchy: recycled where possible (e.g., steel); downcycled to a usable but lower grade material (e.g., concrete); incinerate for energy generation (e.g., timber); landfill.

Ec values for structural elements and non-structural have been calculated separately to assess their relative importance and to provide information for structural benchmarking. These are then compared with predicted Oc. This information can be valuable when assessing where to concentrate effort most effectively to reduce emissions.

Both 'cradle to site' and 'cradle to grave' assessments are carried out. The former is more straightforward to establish at the design stage. It is, therefore, useful to investigate if the additional effort required for a 'cradle to grave' assessment produces very different overall results. In this study 'cradle to site' also included site construction.

Previous studies [7] have shown that lifetime Oc is generally larger than Ec. However, Oc occurs over the lifetime of a building (generally 60 to 100years), whereas the vast majority of Ec occurs at the start of a building's life. In terms of the timeframe in which carbon reductions need to be made, it is possible that carbon savings made at the start of a building's life could be more valuable than predicted savings in the future. The effect of future decarbonisation of energy supply could have a profound effect on future emissions, as could more efficient lighting and M&E equipment installed in future refits. It is argued [8] that the cost of measures to mitigate climate change increase for every year the measures are delayed. For these reasons two methods of weighting future emissions are investigated, which may allow more realistic comparisons to be made between EC and OC.

The first is based on PAS 2050 [2] which accounts for the reduced period emissions are present in the atmosphere during a 100-year assessment period and the weighting factor is given by Eq.(1). This is a simplified version of the approach outlined by the IPCC[9].

$$Weighting\ factor = \frac{\sum_{i=1}^{100} X_i(100-i)}{100} \qquad (1)$$

Where i is the year in which emissions occur and X is the proportion of total emissions occurring in that year i.

The second approach is based on the UK Government Markal-Med model scenarios for decarbonisation of the electricity supply over the period 2010 to 2050 [10]. Mean values of the scenarios considered have been used to give reduction factors to be applied to each of the annual Oc and the future Ec. These factors apply to future electricity supply but for the purposes of this study they are applied to energy supply as a whole.

2.3. Operation emissions (Oc)

The predicted annual 'Building Emission Rate', provided by the building designers, is $20kgCO_2/m^2$. This gives a predicted annual Oc of $231tCO_2$ for the whole building.

2.4. Embodied emissions (Ec)

The process of determining embodied carbon, although simple in principle, is not straightforward in reality due to uncertainty and lack of information on emission factors for

all the materials and processes involved. There is considerable variability between the currently available databases for emissions from materials alone and there are a plethora of software tools and online 'carbon calculators' available purporting to provide whole life assessments. In many cases it is unclear exactly where the assessment boundaries have been drawn and which data sources have been used.

For these reasons Ec in this case study has been assessed using the authors own estimates of embodied CO_2 for materials from 'cradle to grave' using 'as constructed' data. Reference has been made to published UK and global figures from a variety of sources to achieve this [11], [12], [13], [14], [15], [16], [17], [18].

2.5. Transport

Transport emissions were determined using the UK Government published figures [19] and actual travel distances from suppliers to site, where this was known. Distances could be determined for the majority of the large quantity materials, but estimates were made where this information was not available.

2.6. Construction and demolition

Emissions from construction and demolition works on site were assessed using UK Environment Agency base data [12], the actual construction period and an estimate of the period required for demolition.

3. Results

3.1. Relationship between Ec (structure and non-structure) and Oc

Table 1 shows the relationship between Ec(structure), Ec(non-structure) for the different scenarios considered in the study.

Table 1. Case study building: proportions of Ec and Oc

	unweighted		PAS 2050		PAS 2050 + Markal	
	Cradle to site	Cradle to grave	Cradle to site	Cradle to grave	Cradle to site	Cradle to grave
Ec						
structure	17%	18%	19%	18%	35%	35%
non-structure	10%	14%	12%	14%	22%	22%
sub total	27%	32%	31%	32%	57%	57%
Oc	73%	68%	69%	68%	43%	43%
Total	100%	100%	100%	100%	100%	100%

The range of Ec as a percentage of the total emissions was found to be 27% to 57%, with structure 17% to 35%. Ec(structure) was always greater than Ec(non-structure).

The two extreme cases are shown as pie charts in Fig. 1 and Fig. 2 together with calculated values of tCO_2.

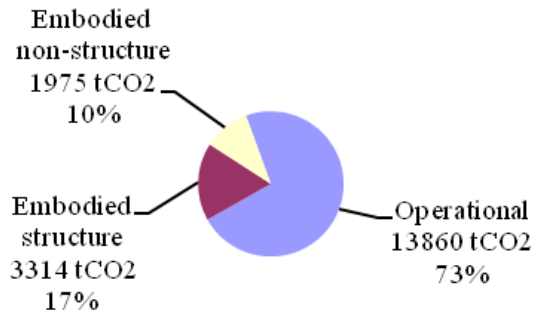

Figure 1. Case study building: embodied and operational emissions (cradle to site, unweighted)

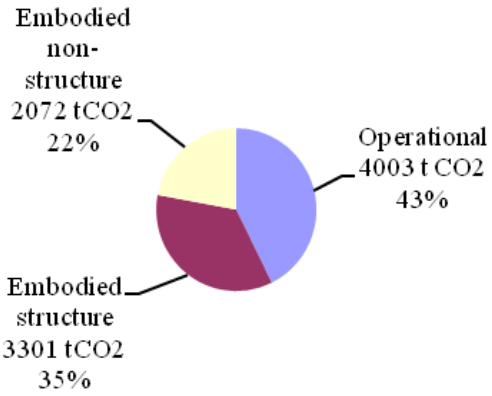

Figure 2. Case study building: embodied and operational emissions (cradle to grave, PAS 2050+Markal)

3.2. Structural benchmarkingc

The range of values of Ec(structure)/m^2 of floor area was found to be between 260kgCO_2/m^2 ('cradle to grave', unweighted) and 286kgCO_2/m^2 ('cradle to site', PAS 2050 and PAS 2050+Markal).

3.3. 'Cradle to site' and 'cradle to grave'

Overall percentage differences between 'cradle to site' and 'cradle to grave' were relatively modest with a maximum of 5% in the unweighted case. The differences reduced if future emissions were weighted. However, for a comparison of individual materials, the end of life scenario can be significant, which indicates that material choices base purely on 'cradle to site', can give misleading results.

3.4. Weighting of future emissions'

Fig 3 shows CO_2 emissions for the case study building lifetime phases.

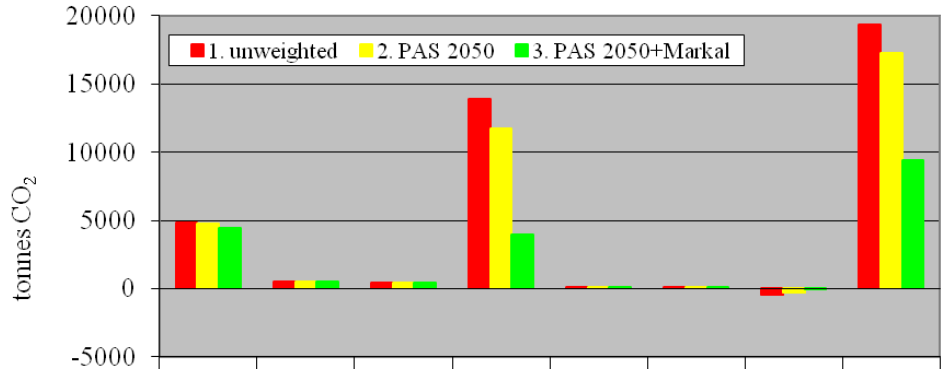

	Cradle to gate	Transport to/from site	Const-ruction	Oper-ation	Demo-lition	Transport to/from site	End of Life	Total cradle to grave
1. unweighted	4823	519	414	13860	52	102	-438	19332
2. PAS 2050	4756	518	413	11748	36	71	-307	17235
3. PAS 2050+Markal	4466	512	407	4003	2	4	-19	9376

Figure 3. Case study building: lifecycle CO_2 emissions

Applying the PAS 2050 reduction factors has a relatively small impact, whereas applying the PAS 2050+ Markal reduction factors has a large effect. The emission profiles over the building lifetime are clearly demonstrated in Fig. 4. This indicates that Ec is equivalent to approximately 23 and 25 years of Oc respectively in the unweighted and PAS 2050 cases and more than 60 years in the PAS 2050+Markal case.

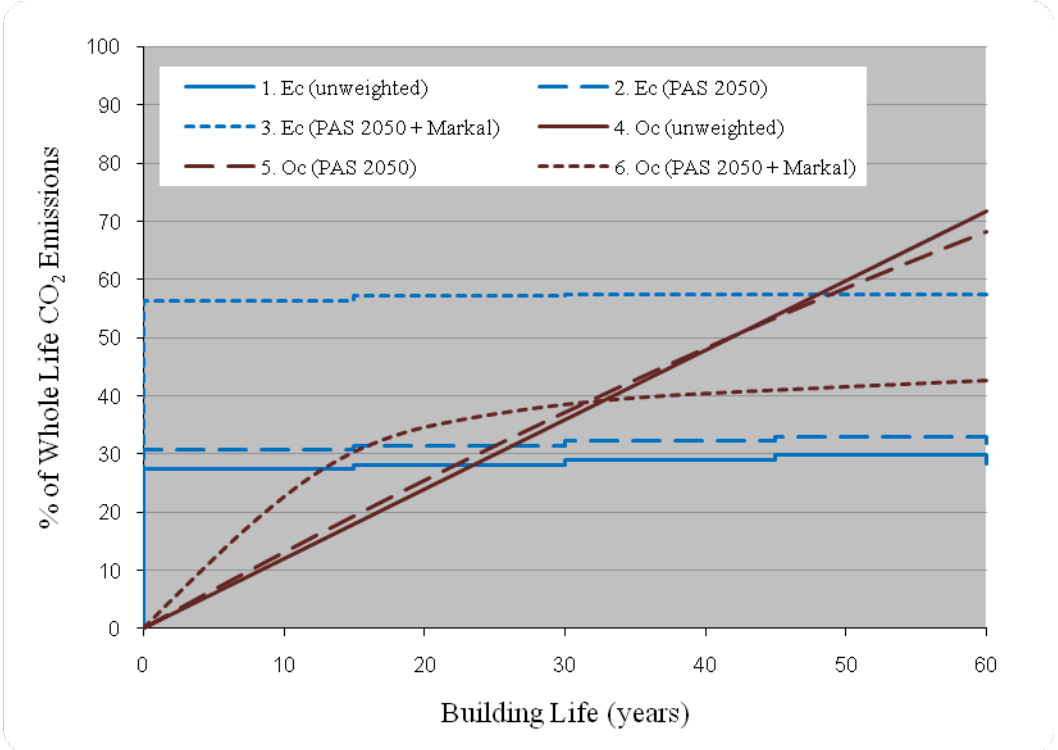

Figure 4. Case study building: Ec and Oc (cradle to grave) as a percentage of whole life emissions

4. Discussion and conclusions

The case study indicates that Ec can be an important consideration in lifecycle CO_2 emissions from buildings, and that in this case the structure was responsible for more than half of the Ec.

A review of other previous case studies [7] indicated that Ec varied between 79% and 108% of Oc for warehouse buildings and was as low as 2% for some other buildings. In this study the range was found to be between 27% and 57% demonstrating that different assumptions and boundary conditions can produce widely differing results and confirming the need for standardisation of Ec data and assessment methods. Assessment of lifecycle carbon emissions should not be considered a precise process due to the many uncertainties and assumptions that have to be made. Nevertheless, it can be a useful tool in assessing where emission reductions can be made most effectively.

An indicative structural benchmark for the building is between 260kgCO_2/m^2 and 286kgCO_2/m^2.

Oc in this case study is based on predicted values. The building was only completed in October 2010 and, therefore, there is currently no data available to assess their accuracy, although these will be available for future updates of the study.

Weighting of future emissions appears to be an important factor to consider. The PAS 2050 reduction factors, to reflect the period emissions are present in the atmosphere during a 100-year assessment period, had only a modest effect, possibly due to the relatively short building life. Longer life buildings would increase this effect but would conversely tend to reduce the Ec proportion of the whole life emissions. In contrast, weighting due to decarbonisation of the energy supply has a large effect, although a more detailed analysis of whether the rate of decarbonisation of the electricity supply will be reflected in the overall energy supply is required before the method used in this study can be validated. No attempt has been made to include discounting based on the cost of measures to mitigate climate change increasing with time but is considered that it would be useful to investigate this issue further.

It is considered that the results of this case study make a useful contribution to the overall bank of data on Ec in buildings.

References

[1] www.bsigroup.com/Standards-and-Publications/Committee-Members/Construction-committee-members-area/M350-Standards/?id=158921 (consulted May 2010).

[2] British Standards Institution, ”Publicly Available Specification PAS 2050:2008: Specification for the assessment of the life cycle greenhouse gas emissions of goods and services”, BSI, 2008.

[3] British Standards Institution, ”BS EN ISO 14040:2006: Environmental management – Life cycle assessment – Principles and framework”, BSI, 2006.

[4] World Resources Institute (WRI) and World Business Council for Sustainable Development, “The Greenhouse Gas Protocol, A Corporate Accounting and Reporting Standard, revised edition”, WRI&WBCSD, 2004.

[5] TRADA Technology Limited, “Construction briefings: PAS 2050: A Summary of the Standard and its Background”, TTL, 2009.

[6] G. Hammond, C. Jones, “Inventory of Carbon & Energy (ICE) Version 1.6a”, University of Bath, 2008.

[7] H. Darby, “The Carbon Life Cycle of Buildings: A Review of the Current UK Carbon Emissions Reduction Strategy for Buildings”, TSBE, University of Reading, 2010.

[8] www.hm-treasury.gov.uk/stern_review_report.htm "Stern Review on the Economics of Climate Change (2006)" (consulted 20/05/10).

[9] Solomon, S., D. Qin, M. Manning, Z. Chen, M. Marquis, K.B. Averyt, M. Tignor and H.L. Miller (eds.), "Contribution of Working Group I to the Fourth Assessment Report of the Intergovernmental Panel on Climate Change, 2007", Cambridge University Press, 2007.

[10] Department of Energy and Climate Change, "Analytical Annex The UK Low Carbon Transition Plan", DECC, 2009.

[11] Granta Design (software), "CES Selector 2010". Granta Design, 2010.

[12] Environment Agency (software), "Carbon Calculator, version 3.1.1", 2009.

[13] Hutchins, "UK Building Blackbook, The Capital Cost and Embodied CO2 Guide, Volume Two: Major Works", Franklin and Andrews, 2010.

[14] J. Anderson, D. Shiers, K. Steele, "The Green Guide to Specification, Fourth Edition", BRE, 2009.

[15] World Steel Association, "LCI Data for Steel Products" WSA, 2010.

[16] TRADA Technology Limited, "Construction Briefings: Timber carbon footprints", TTL, 2009

[17].BRE (software), "Envest, Environmental Impact and Whole Life Costs for Buildings", BRE, 2009.

[18] The Concrete Centre, "Concrete Structures 10", The Concrete Centre 2010.

[19] Department of Energy and Climate Change, "Guidelines to Defra / DECC's Greenhouse Gas Conversion Factors for Company Reporting", DEC, 2010.

From a passive to an active house

Charlotta Isaksson

Department of education, communication and learning, University of Gothenburg, Gothenburg, Sweden
Tel: +46709-708377, E-mail: charlotta.isaksson@ped.gu.se

Abstract: This paper presents a study on how the energy concept for passive houses is interpreted and used in the daily life of householders. It examines the gradual process by which householders both adapt to and shape passive house technology in their material and social context, thus creating a comfortable home. The theoretical concept of domestication was used in order to understand this process. The empirical material was based on qualitative interviews with residents of passive houses in Sweden. Two rounds of interviews were conducted with 22 informants from 16 households and 21 informants from 15 households. The results show that from a user perspective, the passive house is an active house. An active house has event-based heating. The indoor temperature changes in relation to the household's daily routines and rhythms, their everyday activities and use of appliances. Event-based heating creates different conditions for individual households and alters the meaning of many daily chores. Another result shows that domestication of the passive house concept is a dynamic and long-term process, where the view of indoor temperature and use of technologies change over time. Examining the domestication of passive houses leads to a more informed design process and an opportunity to educate new residents.

Keywords: *Passive houses, Domestication, Households, Space heating*

1. Introduction

Passive houses have been highlighted as an important solution to the problems associated with high energy use for heating in the built environment [1] [2]. The last ten years have witnessed a considerable increase in the market for passive houses in north and central Europe, which is proof of the value of this energy concept. In other words, it has passed the trials connected with its use. The energy use of passive houses has been found to be far below the average and papers have been published about satisfied residents, containing descriptions of comfortable climate conditions [3]. However, the results often show a static product which may be misleading for new residents. Expressed differently, a common impression is that the user simply and immediately adapts to what is offered. The users are seen as passive receivers of the technology. As with any new technology, residents of a recently acquired passive house are confronted by unfamiliar features, to which they have to accustom themselves in one way or another. This paper presents a study of how the energy concept for passive houses is interpreted and used in the daily life of householders. It examines the gradual process in which the householders both adapt to and shape the passive house technology in their material and social context, thus creating a comfortable home. The focus is on the energy concept for heating these buildings:

There are three main factors that affect the amount of energy required for heating a building: 1) the quality of the envelope of the building, including heat exchange. 2) The efficiency of the heating system and 3) the householders' activities, preferences and needs related to heating [4]. Considering the first factor, typical components and requirements for a passive house are a very well insulated and tight building envelope combined with a ventilation system equipped with an efficient heat exchanger. With regard to factor two, the heating of the building is supposed to be mainly managed by "passive" sources such as solar irradiation, human body heat and the residents' use of appliances and lighting [3]. In the case of the energy concept of passive houses, a grouping between factors two and three is made. Through their body heat and use of household appliances, the members of the household constitute a

major part of the heating system. The research questions are: How is the energy concept for heating the building interpreted from a user perspective? How do the residents become accustomed to the energy concept of passive houses? The paper specifically contributes to an understanding of the passive house concept from a user perspective. It provides an understanding of the dynamic yet gradual process of domesticating new technologies. The paper begins with an introduction of the concept of domestication, which is used to describe how passive house technology is gradually integrated into the everyday life of users. The next section outlines the empirical method and data. Thereafter, the results of the two research questions are presented. Finally, conclusions are drawn that highlight the importance of examining the gradual implementation of energy efficient technology.

2. Theoretical approach

This paper examines the domestication of the energy concept in passive houses. In the concept of domestication, the users are regarded as active agents in shaping the way technology is used and, in the long term, its future development [5]. In this paper domestication is regarded as a process, in which the individual both *adapts to* and *shapes* the novel technology in his/her social and material context [6] [7]. The user undertakes both practical and symbolic work in relation to the technology as well as learns how to handle it in an appropriate way. In this process, the reciprocal influence of the user and the technology is not totally predictable. Thus, the passive house concept leads to a change in how the heating of buildings is achieved. This change is ultimately manifested in the social environment where the technology is used and particular meanings are assigned [8].

In this process the users´ relationship to the technology changes over time. For instance, Silverstone et al. analysed the domestication of new technology by means of four non-discrete phases [5]. The first phase occurs when the technology is introduced to the domestic environment. The second is when the technology is assigned a physical space in the home, where norms and values attached to the technology are highlighted, and the initial use begins. The third phase emphasises the subsequent use of the technology and how it is incorporated and fitted into the routines of daily life. Finally, the fourth phase describes the communication between the household and the outside world. By demonstrating different phases, Silverstone et al. highlighted the integration of a new technology as a dynamic and changeable process, where the users´ relationship to and strategies associated with the technology vary. Thus, the interplay with technology is reviewed and reassessed over time [7]. In a similar vein, Lehtonen interpreted the domestication of new technologies, although he studied the phases of domestication as a set of trials in which the capabilities of the users and the technologies were tested in multiple ways [9]. For instance, one type of test is the process of learning what the technologies can do and what the user can do with them, while another is the process of judging that the technology is no longer of any value. In this paper, I will examine the gradual integration of the energy concept for passive houses in relation to the householders' previous situation and collective norms in society. Passive house technology provides a new way of heating buildings, and these features are compared with what the residents were used to in their former accommodation and the houses of others.

3. Methodology

In-depth interviews were conducted with residents living in the first passive houses in Sweden situated south of Gothenburg. The buildings, which were completed in 2001 and were sold as co-operative flats, consist of 20 terraced houses divided into four blocks. Each house is 120 m² and comprises a ground floor, an upper floor and an attic. The south side of the houses has

large window areas, while the north facing side has smaller windows. The passive house standard has a maximum space heating load of 10W/m² [10]. In these buildings a 900 W integrated heater connected to the supply air is intended to cover some of the space heating demand during cold periods. Moreover, solar collectors were installed on the roofs to cover parts of the hot water demand. The measured mean values from all of the passive houses during the second year, show an indoor temperature of 23 ºC (from two measuring points central in the buildings). The occupants stated that the average temperature was about 20-21ºC [11]. It is worth noticing that these temperatures do not say anything about the heat sources used.

The interviews were conducted in two sessions, 2002 and 2005, with 22 members of 16 households and 21 members of 15 households. (During both rounds of interviews one of the apartments was uninhabited and used for research and demonstration purposes). The interviews took place in the householders' homes and lasted between one and two hours, depending on how many family members were present. In six of the interviews, both in 2002 and 2005, two adults from each household were present, while one adult participated in the remaining interviews. In total, 31 informants took part in the study and 12 were interviewed twice. The interviews were audio-taped and later transcribed for analysis. A quoted informant is referenced by an assumed name and the interview year, since they participated anonymously in the investigation [12].

Qualitative interviews were chosen, since they are successful for promoting a user-centred approach where the point of departure is the residents' own perception of how they use and relate to the technology. The strength of qualitative interviews is their ability to capture a variety of opinions and provide a multifaceted and comprehensive picture of the phenomenon studied [13]. The main topic of the interviews was heat comfort and different ways of managing the heating in passive house apartments. Investigations and evaluations of heat comfort often fail to consider the residents' perceptions and activities, instead relying on physical measurements or different statistical standards. Thus, the users are seen as passive recipients of an indoor climate achieved by means of installations such as heating systems [14]. However, this paper is more in line with the so called "adaptive approach" where the residents actively adapt to certain conditions with the help of building technologies and other resources such as clothes, slippers, candles etc [15]. Moreover, the users' management of heating is situated in a social and cultural context that shapes their handling of the heating and what they consider to be an acceptable indoor temperature [14].

4. Result

In the energy concept of passive houses, the residents are explicitly described as being part of the heating system by means of their use of household appliances and human body heat. The first section briefly considers how this heating system is interpreted from a user perspective, whereas the second analyses its gradual integration into the everyday life of householders.

4.1. Event-based heating

When addressing how the households perceive indoor temperature, some dominant features become evident. One of them is *fluctuating* indoor temperatures [16]. The temperature in passive houses changes during the day. In the morning when the household wakes up, it is warmer on the second floor where the bedrooms are situated, but colder on the first floor where the living room and kitchen are located. Nevertheless, the temperature increases rather quickly when the family gathers on the first floor and household appliances are used for

making breakfast. The temperature decreases after the members of the household leave the building for work and school, but rises again shortly after they return to the building in the afternoon. Whether it is warmer on the second or first floor in the evening when everybody is at home appears on first sight to be an issue of where the family members *usually are*. This is interesting, as the passive house concept seems to change the way the indoor temperature is normally perceived to function.

In a cross-cultural study between Norway and Japan, Wilhite et al. identified differences in how buildings are heated [17]. Norwegians tend to heat the whole building and have a relatively constant indoor temperature, whereas the Japanese, only tend to heat the room they occupy. The culture in Sweden is closer to that of Norway, but the energy concept has led to a change. This partly means a shift from heating the whole building to heating the room in which one usually finds oneself. However, the indoor temperature in passive houses does not only fluctuate during the day. Another striking feature is the difference in temperatures *between the weekend and weekdays*, since to a large extent the members of the household are at home during the weekend: ”When one is at home and doing things, washing, using the dish washer, cooking and suchlike, I think that there is good heat circulation and it feels warm” (Frida 02). Frida’s description does not really coincide with the heating culture mentioned above. It indicates something different from generating heat for the rooms that the family members normally use, namely a heating system made up of human activities; an event-based heating system. Heat is supplied when they are engaged in daily activities such as cooking and cleaning, or when they have guests for dinner, thus the term “passive house” is misleading. From a user perspective, it is an *“active house”*, where the heat is generated from the everyday activities of the residents.

Two different tendencies can be discerned within event-based heating. One is that the more activities the household members engage in, the warmer it becomes. That is, people and their participation in everyday activities at home “add” heat for the benefit of each other. The other is that it becomes cooler when there is no one or only a few household members at home or at the times when the household members change location in the house to a place where they have not been for a long time. This mainly concerns going from the second to the first floor or vice versa, such as in the example above when the householders come down to the first floor in the morning.

The concept of domestication underlines the fact that the use and meaning of the technology is integrated and shaped by the social milieu, everyday rhythms and routines of the households [5]. Domestication of the energy concept for passive houses gives rise to an event-based heating that is highly dependent on the social milieu and activities of the households. An event-based heating *creates different conditions* for different households. Smaller households may not generate enough body heat or heat from human activities. Moreover, the result shows that households in which members perform many activities outside the home will have difficulty making the energy concept work adequately, i.e. it does not fit their daily routines and rhythms. In addition, there is a relatively large difference between living in an apartment located at the gable end and living in the middle apartment of the passive house, since heat was better retained in the middle one. In conclusion, the concept generally better fits a four-person household in a middle apartment when the residents spend a considerable amount of time at home. However, the individual conditions of those living in the apartment are also important to consider. For instance, an addition to the family means more body heat as well as increased use of household appliances, which makes it warmer indoors.

Simultaneously, the responsibility that comes with the new family member often leads to a demand for a warmer indoor climate.

4.2. Domestication of the energy concept for passive houses

The following subsections consider the gradual process by which householders both adapt to and shape the content of the event-based heating by means of four types of interplay between their previous experience and the new way of handling heating. In particular, the first three reveal how the householders use of technologies and their view of the indoor temperature changes over time.

4.2.1. Re-creating an acceptable heat comfort

In the 2005 interview session, when the residents looked back on their years in the passive houses, the first two were described as more troublesome, slightly cooler and sometimes too cold. The resources offered by the energy concept were simply not regarded as sufficient to create a comfortable indoor temperature at home. This led to frequent use of other resources – not compatible with the energy concept – such as external electric heaters: ”We used fan heaters. We had one downstairs and one upstairs with the timer set for three times per day. Because we didn’t have the temperature we wanted” (Maria 02). Maria’s family was used to a temperature of around 23-24ºC from her previous home, which she tried to *re-create* in the passive house with the aid of electric heaters. The term re-creating indicates that the difference between the new way of heating the building and the household members´ previous experience is large and also perceived as such and that the members somehow try to recreate the former conditions.

Furthermore, the resources used for re-creating a comfortable indoor temperature were not limited to external heaters. Domestication of technology may give rise to meaning and usage not intended by the producers [5]. One such consequence of the event-based heating is that it alters the meaning of many daily chores at home, such as washing dishes and drying clothes: “If I put the dishwasher on it gets warm” stated Hanna (05), one of the informants. The tumble drier is “really nice and warm” said Maria (02). The dishwasher and the tumble drier were not only appliances that could dry clothes and clean dishes, they also meant a warm and comfortable indoor temperature during the cold winter months. In general, this “double meaning” of the use of household appliances did not stimulate the conservation of energy and an opposite tendency was found. For example, households sometimes washed clothes or turned on the oven, not because they needed to wash or cook, but because the appliances contributed to a comfortable indoor temperature. Use of other resources compatible with the energy concept, such as extra clothing, was not acceptable to these residents.

4.2.2. Re-evaluation of the indoor heat

Thus during the first year, the households where unfamiliar with living in a passive house and many felt that the indoor temperature was to some extent too low. However, while the use of external radiators occurred relatively frequently during the first and second winter in many of the apartments, they became much less common in the following years. In addition, as time passed, the indoor temperature was perceived as normal. A change in how they related to the event-based heating obviously occurred: I think that I have got used to the temperature, that it’s a little cooler. It is really too hot at work” (Hannes 05). As Hannes put it, the change in perception also involved an aspect of *re-evaluation* of the indoor temperature where previous conditions were regarded as less favourable in the light of the present ones.

One interesting reason for this change can be found in what Berner defines as a "perceptual and bodily adjustment" [18]. Berner, who studied industrial workers´ interaction with machines, described it as a process where the human being is forced to "filter out" what one would normally notice in a new environment, such as smell, sound and the speed of new machines etc. It happens simultaneously, as one has to learn how to recognize and act on the basis of new phenomena of which one was previously unaware. The perceptual adjustment to event-based heating occurs by living in the passive house and noticing how the indoor heat changes in relation to the activities and daily rhythms of the household. Moreover, by comparing the heat generating capacity of various technologies and appliances, the household becomes aware of the most suitable method of heating the building. This was demonstrated by Nina who reported that "the effect is better with the candles than with household appliances" or when Johanna compared the use of candles with that of electric light, concluding that the former was more effective. Such comparisons probably facilitate the handling of the heating in the passive house. Other reasons for the change in how the energy concept of passive houses was interpreted are the household's increasing competence in handling the integrated heater in the ventilation system and improved functioning of the energy technology installations. (During the first two years, the ventilation system sometimes malfunctioned). Moreover, some of the informants mentioned the damp remaining from the construction of the houses, which they said gradually vanished. These issues are beyond the scope of this paper, but they all point to the fact that the interplay with technology is reviewed and reassessed by the residents over time [7].

4.2.3. Familiar circumstances

One explanation for their *re-evaluation* of what an acceptable indoor temperature should be is found in the references to other people's homes, and what is considered a normal indoor climate. "They [the cold floors] made me react a little at first but on the other hand they are cold in other houses too and I don't think they are colder here than in other terraced houses" (Caroline 02). Here, the *similarities* between the heat comfort in passive houses and other buildings were highlighted, pointing to the existence of *ordinary and familiar* aspects in the confrontation with the new way of handling heating. The term ordinary indicates that the routines for handling indoor comfort, such as the use of slippers and cardigans, as well as the perception of the indoor temperature are similar to what the household members are used to or are common in society in general.

4.2.4. Innovative ways of managing indoor heat

A re-evaluation of the indoor temperature also highlights positive differences. Although the differences between the household members' previous ways of handling heating and the passive house energy concept are large, they are not necessarily seen as negative. As Bakardjieva who studied the use of internet stated, technologies are often used as innovative tools for changing the present circumstances [19]. Thus, passive house technology becomes interpreted as an *innovative* tool for changing previous ways of handling indoor heat and creating a more pleasant and comfortable indoor temperature. For Paulina, this was the case from an early stage: "As I left a house that was really very warm I thought that it was more comfortable to live in a house where I can put extra clothes on instead of a house where it's too hot" (Paulina 02). The differences outlined above are overcome by the fact that the energy concept for passive houses leads to a desirable change. In addition, resources such as clothes, slippers and blankets are regarded as "nice and cosy" and as a prerequisite for a healthier and comfortable indoor climate.

Other examples of new routines, or new ways of thinking about indoor climate in buildings, are keeping the heat inside by quickly closing the door when entering and seldom airing. This is a new habit that is partly due to the limited possibilities of heating the passive house. Moreover, as highlighted above, the household appliances have become "producers of heat." Another aspect of this is that the householders utilized the heat from the appliances, for instance by facilitating the spread of heat by opening interior doors. These activities are not a "passive" adaptation to the circumstances in a passive house. From the perspective of the householders it is an active process and interpreted as the most appropriate way to handle indoor heat. Other desirable changes that come with the passive house energy concept are an improved economic situation as well as environmental protection. The former included feelings of participation in fulfilling the intentions of the product developers in the creation of an energy efficient home.

5. Conclusion

This paper has examined the domestication of the energy concept for passive houses. Using the term 'event based heating' I have highlighted some important features that newcomers to passive houses may encounter. The gradual process of getting used to the energy concept has been explored by means of four types of interplay between the householders' previous experiences and the new way of handling heating influenced by the energy concept. In a sense, these types reflect what users may be confronted by when leaving old technology behind and experiencing new. Some features are missing, which the householders try to compensate for, whereas others are improved or fairly similar to what they were used to. Nevertheless, their relationship to these features is changeable and might be re-evaluated over time. It is important to identify the content and development of the reciprocal influence between the energy related technology and the user. For instance, does living in passive houses give rise to non-energy efficient routines in relation to household appliances? The result of this study indicates that it does, which in part questions the establishment of a maximum space heating load of 10W/m². However, there are also long term tendencies that demonstrate the creation of a more environmentally friendly view of indoor temperature as well as routines in line with an energy efficient way of life. By examining the domestication of the energy concept in passive houses, an improved understanding of user practice in these buildings can be developed. This would lead to a more informed design process as well as an opportunity to provide information to new residents of passive houses.

References

[1] Statens offentliga utredningar, Vägen till ett energieffektivare Sverige. Slutbetänkande av Energieffektiviseringsutredningen, (Government official reports. The road to an energy-efficient Sweden. Final report of Energy-efficiency Inquiry), SOU 2008:110.

[2] European Parliament resolution of 31 January 2008 on an Action Plan for Energy Efficiency: Realising the Potential (2007/2106(INI)).

[3] J. Schnieders & A. Hermelink, CEPHEUS results: measurements and occupants´ satisfaction provide evidence for Passive Houses being an option for sustainable building, Energy Policy 34, 2006, pp 151-171.

[4] A-L. Lindén, Värme i bostäder. En kvantitativ analys av energiförbrukning. (Heating in homes. A Quantitative analysis of energy consumption) Elforsk rapport 07:61, 2007.

[5] R. Silverstone, E. Hirsch & D. Morley, Information and communication technologies and the moral economy of the household, in R. Silverstone & E. Hirsch (eds) Consuming technology: Media and Information in Domestic Spaces. Routledge, 1992, pp 15-31.

[6] M. Lie & K. H. Sørensen, Making technology our own, Scandinavian University Press, 1996.

[7] K. Sørensen, Domestication: the enactment of technology, in T. Berker et al. (eds) Domestication of Media and Technology, Open University Press, 2006, pp 40-57.

[8] C. Isaksson, Uthålligt lärande om värmen? Domesticering av energiteknik i passivhus, (Sustainable learning about indoor heat? Domesticating energy technology in passive houses.), Department of Thematic Studies- Technology and social change, Linköping University, Sweden, 2009.

[9] T. Lehtonen, The domestication of new Technologies as a Set of Trials, Journal of Consumer Culture 3, 2003, pp 363-385.

[10] W. Feist, J. Schnieders, V. Dorer. & A. Haas, Re-inventing air heating: Convenient and comfortable within the frame of the Passive House concept, Energy and buildings 37, 2005, pp 1186-1203.

[11] C. Isaksson & F. Karlsson, Indoor Climate in Low-energy Houses – An Interdisciplinary Investigation, Building and Environment 41, 2006, pp 1678-1690.

[12] Empirical data (2002 & 2005) Members from 20 households took part in the study: 1. Alva 02 & 05, Alf 02 & 05, 2. Gunilla 02**,** 3. Hanna 05, Hannes 05, 4. Lisa 05**,** 5. Karl 02, Karin 02 & 05**,** 6. Maria 02, Marcus 05**,** 7. Paulina 02 & 05**,** 8. Rickard 02 & 05**,** Rakel 02 & 05**,** 9. Ville 02 & 05**,** Vera 02 & 05**,** 10. Caroline 02, Christer 05**,** 11. Daniela 02, David 02**,** 12. Frida 02, Fredrik 05**,** 13. Elin 05, Edvin 05**,** 14. Ida 02 & 05**,** Isak 02 & 05**,** 15. Johanna 02**,** 16. Nina 02**,** 17. Sandra 05**,** 18. Oda 02 & 05**,** 19. Tea 02 & 05**,** 20. Ulla 02.

[13] S. Kvale, Den kvalitativa forskningsintervjun (The Qualitative research interview) Studentlitteratur, 1997.

[14] E. Shove, Comfort Cleanliness Convenience. The Social Organization of Normality, Berg, 2003.

[15] J.F. Nicol & M.A. Humphreys, Adaptive thermal comfort and sustainable thermal standards for buildings, Energy and buildings 34, 2002 pp 563-572.

[16] C. Isaksson, The Absence of a Conventional Heating System –From the Perspective of the Occupants, Proceedings ECEEE 2005 Summer study Energy savings: What Works and Who Delivers?, Panel 6, 2005, pp 1221-1230.

[17] H. Wilhite, N. Hidetoshi, T. Masuda, Y. Yamaga, & H. Haneda, A cross-cultural analysis of household energy use behaviour in Japan and Norway, Energy Policy 24, 1996, pp 795-803.

[18] B. Berner, Working knowledge as performance: on practical understanding of machines, Work Employment & Society 22, 2008, pp 319-336.

[19] M. Bakardjieva, Domestication running wild. From the moral economy of the household to the mores of a culture, in T. Berker, M. Hartmann, Y. Punie & J. K. Ward (eds), Domestication of Media and Technology, Open University Press, 2006, pp 62-79.

Numerical simulation of a PCM shutter for buildings space heating during the winter

N. Soares[1,*], A. Samagaio[2], R.Vicente[1], J. Costa[3]

[1] *Civil Engineering Department of the University of Aveiro, Aveiro, Portugal*
[2] *Environment and Planning Department of the University of Aveiro, Aveiro, Portugal*
[3] *ADAI – Mechanical Engineering Department of the University of Coimbra, Coimbra, Portugal*
** Corresponding author. Tel: +351 234370845, Fax: +351 234370094, E-mail: nsoares@ua.pt*

Abstract: The integration of Phase Change Materials (PCMs) into the building envelope provides a higher thermal inertia that, combined with the thermal insulation effect, can reduce the energy consumption.
Using a 2-dimensional simulation model based on the enthalpy formulation, a latent heat storage system has been numerically designed and parametrically optimized to take advantage of solar thermal energy for buildings space heating during the winter in Coimbra, Portugal. The main purpose of this study is to show the potential of incorporating PCMs in structural cells of shading elements associated to southward façade windows.
In view of the low thermal diffusivity of the Phase Change Material (PCM) chosen, the distance between metal fins is directly proportional to the energy storage/release capacity of the system. The results of the parametric study also show that solar radiation flux has a strong effect on the melting/charging process. On the other hand, the indoor temperature and the indoor heat convection transfer rate, during the night, play an important role in PCM solidification/discharging process.
In conclusion, an optimal thermal storage system – PCM shutter – can be designed for any given location and characteristic climatic data during the winter. The optimum depends strongly on the thermophysical properties of the PCM and on the internal boundary conditions considered.

Keywords: *Phase Change Material, PCM, Enthalpy formulation, Energy storage, Numerical modelling.*

Nomenclature

CM	*thickness of the metal fin* ..... *m*	L	*latent heat of fusion*..... $J\ kg^{-1}$
E	*total energy stored and released by the system during a day cycle*.....*kJ*	$\dot{q}_{rad}$	*solar radiation* ..... $W\ m^{-2}$
F	*total PCM melted fraction*.....*%*	$\dot{q}_{rad,ref}$	*reference solar radiation* ..... $W\ m^{-2}$
FL	*thickness of the system* ..... *m*	Rvi	*thickness of the metal liner*.....*m*
H	*enthalpy of the system*.....*kJ*	t	*time*.....*h*
h	*volumetric sensible enthalpy* .....$J\ m^{-3}$	t_m	*time needed to melt all the PCM volumes*
h_e	*external convection heat transfer coefficient* ..... $W\ m^{-2}\ ºC^{-1}$	T_e	*outdoor air temperature*.....*ºC*
		$T_{e,ref}$	*reference outdoor air temperature*.....*ºC*
h_i	*internal convection heat transfer coefficient* ..... $W\ m^{-2}\ ºC^{-1}$	T_i	*internal air temperature*.....*ºC*
		T_m	*PCM melting temperature*.....*ºC*
HL	*inter-fins distance*..... *m*		

1. Introduction

As referred by many authors [1-5], the thermal energy storage systems using PCMs have been recognized as one of the most advanced energy technologies to enhance the energy efficiency and sustainability of buildings. An interesting feature of PCMs is that they can store latent energy as well as sensible energy. Their high latent heat storage capacity combined with friendly energy systems employing endogenous energies, such as solar thermal energy, can reduce the energy consumption of buildings in a passive and sustainable way. The systems incorporating PCMs benefit also from the isothermal nature of the phase change process. For a review, see [1-5]. At the same time as the demand for thermal comfort in buildings in Portugal increases, so does the energy consumption for buildings' indoor environmental control, particularly, for space heating during the winter. The main goal of the present work is

to design a latent thermal energy storage system incorporating PCM, taking advantage of solar energy, which is an abundant resource in Mediterranean climates, for space heating during the winter season in Coimbra, Portugal. The numerical simulation of the system is performed using a code specifically developed for this purpose, based on a 2-dimensional model following the enthalpy formulation.

The enthalpy formulation has been extensively employed by many authors in the modelling of phase change problems [6-11] and it is one of the most popular fixed-domain methods for solving the Stefan problem [4]. The problem of predicting the behaviour of phase change is difficult due to its nonlinear nature at the moving interface and, in addition, to the fact that the material at the two phases has different thermophysical properties. When the PCM undergoes a phase change, both the solid and the liquid phases are present and are separated by a moving interface between them. The difficulty in solving a phase change problem is the presence of a moving boundary or region in which heat and mass balance conditions have to be met.

2. Methodology

2.1. System Descriptions

The scheme of the architectural configuration of the system is shown in Fig. 1a. It consists of 2 shutter panels, each 0.5 *m* by 1.5 *m* and composed of a set of several aluminium rectangular cavities filled with the PCM. The horizontal walls of the cavities are supposed to act as a fin arrangement and enhance the rate of heat transfer to the PCM. To compensate the low thermal conductivity of PCM, the use of metal fins in a latent heat storage system has been studied by many authors [7-11]. The insulation layer on the back surface of the shutter is essential to enable the control of the direction of the stored heat delivery, especially during the thermal discharge of the system.

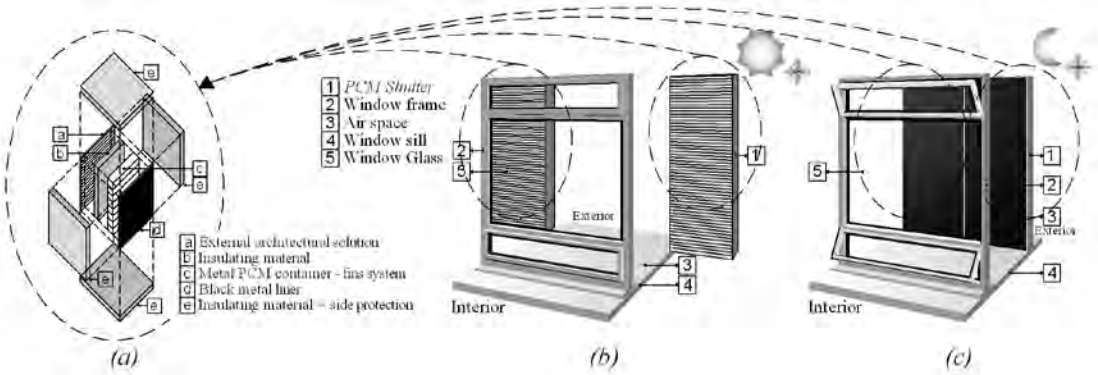

Fig. 1. (a) Schematics of the latent heat storage system; (b) Schematics of the functioning of the PCM shutter during a winter day – PCM charging when the system is opened; (b) Schematics of the functioning of the PCM shutter during a winter night – PCM discharging when the system is closed.

The rationale of the system operation during a consecutive day and night in winter is sketched in Figs. 1b and 1c. The system must operate cyclically, reflecting the ongoing cycles of the daytime and of the PCM phase change process (from solid to liquid and *vice versa*) and, at the same time, enabling the storage and release of thermal energy. The system is to be opened during the day to maximize the solar direct gains through the glass window and the charging of the system – PCM melting. During the night the system must be closed to minimize the heat losses through the glazing and to allow the discharging of the system by releasing the thermal energy indoors through the window arrangement – PCM solidification. During the night the window must be somehow opened to ensure the ventilation of the air cavity separating the window glass and the PCM shutter promoting the heat release indoors.

Many authors have considered the design and analysis of a system with the same goals as the one we propose here, particularly Costa *et al.* [7] and Brousseau and Lacroix [8]. Both works define and study latent heat thermal energy storage systems designed to store the off-peak electrical energy in the form of thermal energy via PCM phase change processes. Using off-peak electricity, a PCM can be melted to store electrical energy in the form of latent heat thermal energy, and the heat is then available when needed for space heating, during the period when the electricity is most expensive. The system proposed in this work aims to take advantage of the solar energy, instead of the electrical energy, to melt the PCM.

2.2. General Assumptions

The chosen PCM for this simulation is similar to an n-Octadecane – CH3(CH2)16CH3. The thermophysical properties of this PCM and of the heat exchanger material (aluminium) are given in Table 1. One uses all of n-Octadecane's thermophysical properties, except for the melting temperature, which shall be considered lower than that of n-Octadecane and closer to indoor comfort temperature in wintertime.

Table1. Thermophysical properties of the system materials.

Thermophysical properties	PCM	Aluminium
Latent heat of fusion ($J\ kg^{-1}$)	243500	-
Density – solid ($kg\ m^{-3}$)	865	2707
Density – liquid ($kg\ m^{-3}$)	780	-
Specific heat – solid ($J\ kg^{-1}\ ^oC^{-1}$)	1934	896
Specific heat – liquid ($J\ kg^{-1}\ ^oC^{-1}$)	2196	-
Thermal conductivity – solid ($W\ m^{-1}\ ^oC^{-1}$)	0.358	204
Thermal conductivity – liquid ($W\ m^{-1}\ ^oC^{-1}$)	0.148	-

The main reference outdoor conditions, Eq. (1), are the external air temperature, $T_{e,ref}$, and the solar radiation in a vertical South facing wall in Coimbra in January, $\dot{q}_{rad,ref}$, both calculated according to the climatic data of SOLTERM® during the period when the system must be opened – from 9 am until 5 pm. The external convection heat transfer coefficient considered is $h_e = 25\ W\ m^{-2}\ ^oC^{-1}$.

$$\begin{cases} T_{e,ref} = 8.2 - 5.5\sin\left(0.32t\right) \\ \dot{q}_{rad,ref} = 160.0 - 350.0\sin\left(0.385t\right) \end{cases}, \text{ with } t \text{ in hours and } \theta \text{ in rad} \qquad (1)$$

The indoor air temperature, T_i, is influenced by outdoor conditions, by the internal loads and by the buildings envelope constitution. However in this study, during the time when the system must be closed – from 5 pm until 9 am – the average indoor air temperature is considered fixed and equal to 15 ^oC. The internal convection heat transfer coefficient, h_i, can vary according to the model chosen for its determination, as explained below.

2.3. Numerical Simulation and Numerical Solution

The model was developed using the enthalpy formulation, as sketched in Fig. 2. In the discretized energy conservation equation, the volumetric sensible enthalpy, h, is the dependent variable and the latent energy rate involved in the phase change process is considered in the source term, which in turn is expressed in terms of the local fraction of melted PCM. The main advantages of this method are: (*i*) the dispense of a condition to be

satisfied at the solid-liquid interface (as it automatically obeys the interface condition), (*ii*) the existence of a mushy zone between the two phases in each control volume, (*iii*) the fact that the energy conservation equation is similar to the one of the pure heat diffusion model (without phase change) and (*iv*) that this method guaranties the isothermal nature of the phase change process. This model is meant to solve the problem of heat diffusion associated to the PCM phase change in a 2-dimensional domain. The differential equation governing the underlying physical phenomenon is integrated using the finite-volume method proposed by Patankar [12]. The system of equations is iteratively solved by a tri-diagonal-matrix algorithm and the evolution in time is modelled according to a totally implicit formulation. Further details concerning the numerical implementation of present enthalpy method may be found in the previous work of the authors [13].

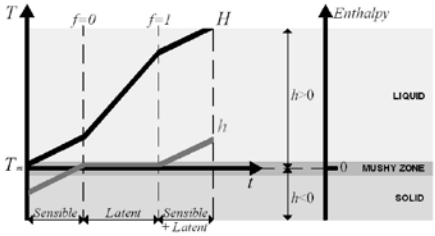

Fig. 2. Sketch of the enthalpy formulation.

3. Results and Discussion

This section is devoted to the identification of the optimal PCM volume, and of the optimal PCM melting temperature, T_m. The first part shows the existence of the optimum PCM volume and its calculation for a specific case. The following parts are concerned with the estimation of the impact of some parameters: outdoor condition, indoor conditions and PCM thermophysical properties. Finally, the optimal configuration is discussed.

3.1. Determination of the PCM volume

Case of: $\begin{cases} T_m = 18\ ^{o}C,\ L = 243500\ J\ kg^{-1},\ h_i \text{ estimated by natural convection over vertical surface} \\ T_i = 15\ ^{o}C, h_e = 25\ W\ m^{-2}\ ^{o}C^{-1}, T_e = T_{e,ref}, \dot{q}_{rad} = \dot{q}_{rad,ref}, CM = Rvi = 0.002\ m, FL = 0.03\ m \end{cases}$

In order to find the optimal PCM volume to incorporate in the shutter, a set of numerical experiments was held using the methodology presented in Section 2.3, for the test case described in Section 2.1 and for the values above. The optimum PCM volume corresponds to the one that can be totally melted during the charging period (daytime) and totally solidified during the discharging period. Due to the low thermal diffusivity of the PCM, the total volume melted and solidified is strictly related with the distance between the metal fins.

For a given inter-fins distance *HL*, the enthalpy of the system, *H*, and the total PCM melted fraction, *F*, were computed. Figure 3a shows that the PCM can be totally melted considering *HL* = 0.004 *m*. This means that the total volume of PCM with which the container described in Section 2.1 can be filled represents 40 % of the total volume of the system. Results with higher PCM volumes (larger distances between fins) are not so attractive because they cannot be totally melted during the day, and so, the enthalpy of the system is smaller (Fig. 3b) and the PCM potential as a latent heat material is overvalued. The results considered in Fig. 3a and in Fig. 3b were obtained for three consecutive day cycles numerically simulated, starting from a condition of no PCM melted and the whole system at a uniform temperature T_m.

For the PCM volume corresponding to $HL = 0.004\ m$ the discharging process is not completed during the night, which can mean that there will be an enduring melted PCM fraction overvaluing the potential of PCM as a latent heat material. In order to enhance the discharging of the system and the solidifying process of the PCM, indoor forced airflow must be induced in the air gap between the shutter and the glass to enhance heat convection in that period.

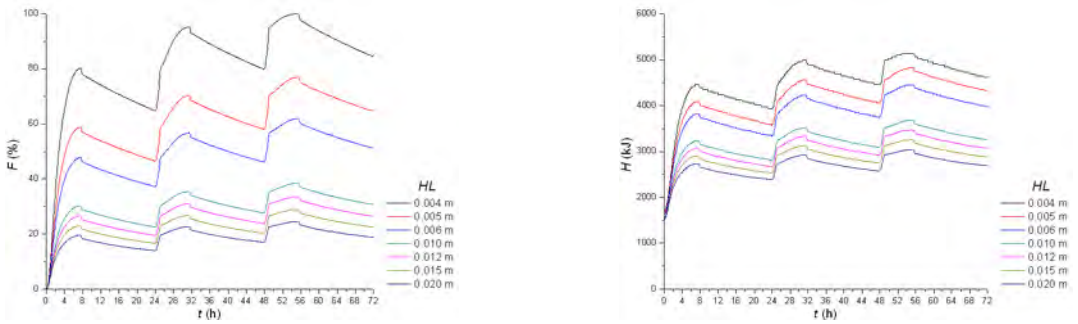

(a) *(b)*

Fig. 3. Evolutions (a) of the total PCM melted fraction, F, and (b) of the enthalpy of the system, H, during three consecutive day cycles simulated.

3.2. Impact of the internal heat transfer coefficient

Case of: $\begin{cases} T_m = 18\ ^{o}C,\ L = 243500\ J\ kg^{-1},\ T_i = 15\ ^{o}C,\ h_e = 25\ W\ m^{-2}\ ^{o}C^{-1} \\ T_e = T_{e,ref},\ \dot{q}_{rad} = \dot{q}_{rad,ref},\ CM = Rvi = 0.002\ m,\ FL = 0.03\ m,\ HL = 0.004\ m \end{cases}$

A set of numerical experiments was held in order to evaluate the influence of the h_i value on the total energy stored in the system via the PCM phase change from solid to liquid and released by the system to the indoor air via PCM phase change from liquid to solid. The different values for h_i considered in the simulations are shown in the legend of Fig. 4.

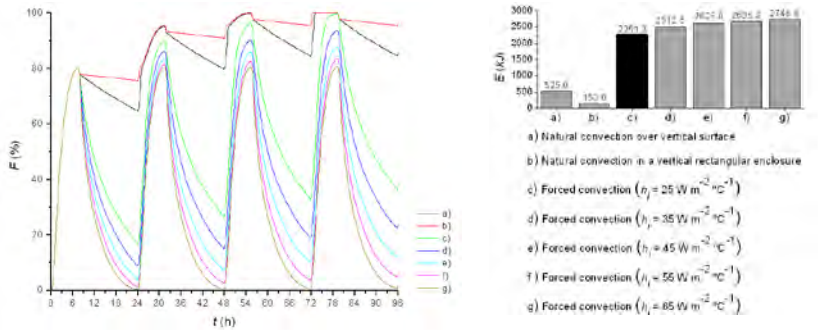

(a) *(b)*

Fig. 4. (a) Evolution of the F value, during the first four numerical cycles for different values of h_i; (b) Evaluation of the E value during the fourth simulated cycle for the different models considered for h_i.

The results presented in Fig. 4a were obtained for the first four numerical day cycles simulated, the point in time when steady cyclic behaviour was achieved. The values of the total energy stored and released indoors by the system during a complete day cycle, *E*, showed in Fig. 4b, correspond to those of the fourth day cycle simulated. By matching the results of Fig. 4a and Fig. 4b one can see that the *E* value is proportional to the fraction of PCM solidified during the discharging period. The larger the value of h_i the larger is the fraction of PCM solidified during the night and the heat released to the indoor space. For very large values of h_i the system is totally discharged but the PCM volume cannot be totally

melted during the day. Fixing $h_i = h_e = 25\ W\ m^{-2}\ ºC^{-1}$ one can enhance the performance of the system during the night without compromising the melted fraction during the day.

3.3. Impact of the indoor temperature

Case of: $\begin{cases} T_e = T_{e,ref}, \dot{q}_{rad} = \dot{q}_{rad,ref}, h_i \text{ estimated by natural convection over vertical surface} \\ h_e = 25\ \mathrm{W\,m^{-2}\ ºC^{-1}}, L = 243500\ J\ kg^{-1}, CM = Rvi = 0.002\ m, FL = 0.03\ m, HL = 0.004\ m \end{cases}$

In order to evaluate de impact of the indoor temperature considered, T_i, a set of numerical experiments was held with a range of values for T_i and T_m. The results are shown in Fig. 5. One can see that the E value grows proportionally to the difference between T_m and T_i. That is because the driving potential for the heat flow rate to the inside is enhanced and the release of energy during the night is improved while the PCM changes phase from liquid to solid.

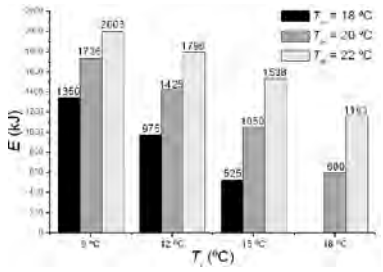

Fig. 5. Evaluation of the total energy stored and released by the system, E, during the fourth numerical day cycle for the different values considered for T_m and T_i.

3.4. Impact of the outdoor conditions

Case of: $\begin{cases} L = 243500\ J\ kg^{-1},\ T_m = 18\ ºC,\ h_i \text{ estimated by natural convection over vertical surface} \\ h_e = 25\ W\ m^{-2}\ ºC^{-1},\ T_i = 15\ ºC,\ CM = Rvi = 0.002\ m,\ FL = 0.03\ m,\ HL = 0.004\ m \end{cases}$

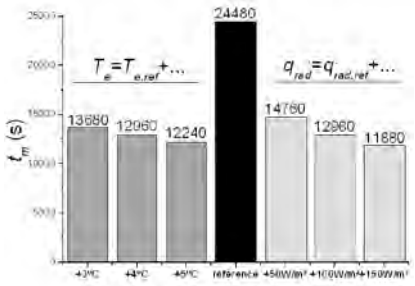

Fig. 6. Evaluation of the time needed to melt all the PCM volume, t_m, considering the reference outdoor conditions and 3 different sinusoidal swing approaches to calculate T_e and $\dot{q}_{rad}$ evolutions.

The impact of the outdoor air temperature, T_e, is evaluated through the time needed to melt all the PCM volume, t_m, using three different sinusoidal swing approaches to estimate the T_e evolution during the time when the system must be opened, and comparing them with the reference sinusoidal curve presented in Section 2.2. The same methodology is carried out for the solar radiation, $\dot{q}_{rad}$. The results are presented in Fig.6 showing that the higher the outdoor air temperature and the solar radiation are, the less time it takes to melt all the PCM volume.

3.5. Impact of the PCM melt temperature

Case of: $\begin{cases} L = 243500\ J\ kg^{-1},\ T_i = 15\ ºC,\ h_i = h_e = 25\ W\ m^{-2}\ ºC^{-1} \\ T_e = T_{e,ref},\ \dot{q}_{rad} = \dot{q}_{rad,ref},\ CM = Rvi = 0.002\ m,\ FL = 0.03\ m,\ HL = 0.004\ m \end{cases}$

The total energy stored and released by the system, *E*, is strongly influenced by the melt temperature of the PCM, T_m. When it is lower than the optimum T_m, the charging process is faster and less time is needed to complete it, thereby melting all the PCM mass. On the other hand, if the difference between T_m and T_i is very small, the discharging process of the system is compromised and the time needed to complete it is larger than the time available (period of system closed). When T_m is higher than the optimum temperature, the discharging process is more efficient. However, the charging (melting) process will not be completed in the time specified by the operating conditions. Figure 7 illustrates the influence of T_m in the *E* value.

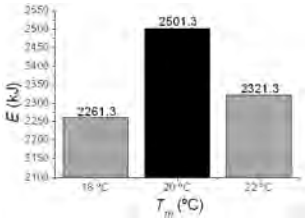

Fig. 7. Influence of T_m in the total energy stored by the system during the day-time and released to the interior during the night in a complete day cycle under the same operating conditions.

3.6. Existence of the optimum

Case of: $\begin{cases} T_m = 20\ ^{o}C,\ L = 243500\ J\ kg^{-1},\ T_i = 15\ ^{o}C,\ h_i = h_e = 25\ W\ m^{-2}\ ^{o}C^{-1}, \\ T_e = T_{e,ref},\ \dot{q}_{rad} = \dot{q}_{rad,ref},\ CM = Rvi = 0.002\ m,\ FL = 0.03\ m,\ HL = 0.004\ m \end{cases}$

The reference test case above shows an optimum configuration for the system. The total energy stored and released by the system, *E*, during a complete 24 hours day cycle is compared with that of other 0.03 *m* thick building materials under the same operating conditions. The results are shown in Fig. 8.

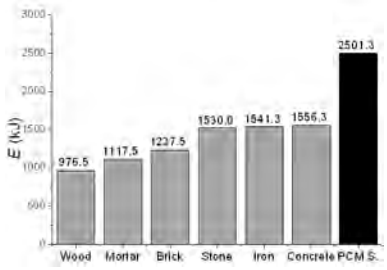

Fig. 8. Total energy stored and released by the system during a complete day cycle, E, compared it with that of other 0.03 m thick building materials under the same operating conditions.

4. Conclusions

The outdoor air temperature and the solar radiation flux play an important role during melting and consequently have a strong effect on the time needed to melt the PCM volume. On the other hand, the indoor temperature and the convection heat transfer rate on the inner side of the shading element, during the night, play an important role for the PCM solidification and have a strong effect on the energy release indoors. To enhance the discharging of the PCM a ventilator must be adjoined to the inner side to increase the internal heat transfer coefficient.
In conclusion, using the numerical simulation as carried out, an optimal system configuration, with an optimal PCM melting temperature, can be found for any given location and characteristic climatic data during the winter season. The results for stored and released energy in a complete day cycle, using a 0.03 m thick layer of different materials, show the

enhancement of the thermal inertia of the building envelope obtained by using the system described. The Tm value has a strong influence on the energy storage capacity of the system. The optimal melting temperature of the PCM to be incorporated in the system for the location of Coimbra is 20 ºC. According to the present predictions, the total energy stored and released by the optimum system during a complete 24 hours day cycle can reach 2501.3 kJ.

Further work has to be done to assess the behaviour of the system in a physical testing – prototype and cell test. A building dynamic simulation has also to be carried out to evaluate the influence of the latent heat loads in the thermal behaviour of the building.

References

[1] V.V. Tyagi & D. Buddhi, 'PCM thermal storage in buildings: A state of art', *Renewable and Sustainable Energy Reviews*, **11**, 2007, pp. 1146-1166.

[2] V.V. Tyagi, S.C. Kaushik, S.K. Tyagi & T. Akiyama, 'Development of phase change materials based microencapsulated technology for buildings: A review', *Renewable and Sustainable Energy Reviews*, 2010.

[3] B. Zalba, J.M. Marín, L.F. Cabeza & H. Mehling, 'Review on thermal energy storage with phase change: materials, heat transfer analysis and applications', *Applied Thermal Engineering*, **23**, 2003, pp. 251-283.

[4] A. Sharma, V.V. Tyagi, C.R. Chen & D. Buddhi, 'Review on thermal energy storage with phase change materials and applications', *Renewable and Sustainable Energy Reviews*, **13**, 2009, pp. 318-345.

[5] A. Pasupathy, R. Velraj & R.V. Seeniraj, 'Phase change material-based building architecture for thermal management in residential and commercial establishments', *Renewable and Sustainable Energy Reviews* , **12**, 2008, pp. 39-64.

[6] C.R. Swaminathan & V.R. Voller, 'On the enthalpy method', *International Journal of Numerical Methods for Heat & Fluid Flow*, **3**, 1993, pp. 233-244.

[7] M. Costa, D. Buddhi & A. Oliva, 'Numerical simulation of a latent heat thermal energy storage system with enhanced heat conduction', *Energy Conversion and Management*, **39**[3/4], 1998, pp. 319-330.

[8] P. Brousseau & M. Lacroix, 'Numerical simulation of a multi-layer latent heat thermal energy storage system', *International Journal of Energy Research*, **22**, 1998, pp. 1-15.

[9] C.R. Chen & A. Sharma, 'Numerical investigation of melt fraction of PCMs in a latent heat storage system', *Journal of Engineering & Applied Sciences*, **1**, 2006, pp. 437-444.

[10] A. Sharma, S.D. Sharma, D. Buddhi & L.D. Won, 'Effect of thermo physical properties of heat exchanger material on the performance of latent heat storage system using an enthalpy method', *International Journal of Energy Research*, **30**, 2006, pp. 191-201.

[11] C.R. Chen, A. Sharma, S.K. Tyagi & D. Buddhi, 'Numerical heat transfer studies of PCMs used in a box-type solar cooker', *Renewable Energy*, **33**, 2008, pp.1121-1129.

[12] S.V. Patankar, *Numerical heat transfer and fluid flow*, Hemisphere Publishing Corporation, Washington, 1980.

[13] N. Soares, R. Vicente, A. Samagaio & J. Costa, 'Investigation of a multi-layer latent heat solar thermal energy storage system with PCMs', Proceeding of 12th International Conference on Building Materials and Components, 2011.

Considering users' factors in sustainable building refurbishment projects

M.Agha-Hossein[1,*], A. Elmualim[2], M. Williams[2], A. Kluth[3]

[1]*Halcrow Group Ltd/TSBE, University of Reading, UK*
[2]*University of Reading, UK*
[3]*Halcrow Group Ltd, London, UK*
** Corresponding author. Tel: +44 7876040789, E-mail: AghahosseinM@Halcrow.com*

Abstract: Research shows that, as a result of poor energy efficiency, a significant amount of the UK's total energy expenditure is wasted. Changing building occupants' behaviour could help to prevent this energy loss and considerably cut carbon emissions per year. This paper presents an overview of the impact of occupants' behaviour on the energy performance of non-domestic buildings. It further introduces Halcrow's current research project on how to improve the energy performance of their recently refurbished and occupied Headquarters in London, while increasing the satisfaction and well-being of their employees. An employee benchmark survey was conducted at the pre-occupancy stage. The purpose of this survey was to identify the employees' level of satisfaction with their current workplace and, also, to indicate employees' motivation and energy awareness level. The mean score of 2.98 indicates that the majority of the respondents are neither satisfied nor dissatisfied with their current workplace. The results of this survey also show that employees who work in cellular offices on their own are less satisfied than those who work in open-plan offices. Regarding employees' sustainability awareness, most of the respondents said that they were not fully aware of Halcrow's sustainability targets. This paper provides the results of this survey in detail.

Keywords: *Energy Awareness, Non-domestic Building, Sustainability, Refurbishment, and Carbon Reduction*

1. Introduction

About one fourth (25%) of carbon emissions in the UK, which is about 100 million tonnes of CO2 per year, are generated by non-domestic buildings [1]. Considering the fact that 60% of the total non-domestic buildings in 2050 exist today [2], sustainable building refurbishment can significantly contribute to meeting the UK government's target. Every day about £7 million, which is about 21% of the UK's total energy costs, is wasted in UK industry due to poor energy efficiency [3]. In comparison, it is estimated that changing buildings users' behaviour could save this money for the companies and cut carbon emissions by 22 million tonnes per year [4].

It is argued that green technologies such as efficient lighting and advanced ventilating systems will enhance interior environmental quality and therefore be beneficial to human well being and productivity.[5]. Technologies which are designed to improve the energy efficiency of a building must engage with the users, or the building will underperform and energy savings will be limited [6]. Organizational scientists pay little attention to the physical environment, despite its impact on social behaviour [7]. Working space affects the user's performance [8], and productivity is also believed to be associated with the provision of high quality interior environments [9]. However, there is little understanding of how such benefits might be achieved by a satisfactory work environment.

Halcrow Group Ltd has recently refurbished a leased 1930's, 5-storey office building in Hammersmith, London. This building is now occupied by about 450 people who have moved from Halcrow's previous offices (Vineyard House (VH) and Shortlands) adjacent to the site. As staff satisfaction has a central place in social sustainability, Halcrow wishes to investigate innovative interventions currently available to reduce their energy consumption in their new HQ, while increasing their employee's satisfaction and well-being. To do this, a survey was carried out at the pre-occupancy stage to understand employees' needs and expectations

regarding their work environment. The findings from this questionnaire were considered at the design stage of the new building and also used as a benchmark for evaluating the new building's performance. This paper demonstrates some of the findings from the questionnaire.

2. Methodology

An employee survey was conducted to collect data regarding employee satisfaction, needs and expectations. This benchmark survey was used as a tool to enable the employees to confidentially express how they felt about their work environment. The first part of the questionnaire included items concerning demographic factors such as age, sex and employment status. Also, in this part, employees were asked to specify their modes of transportation to work and their willingness to work at home. In the second part, employees were asked to indicate their levels of satisfaction with their workplace physical environment, use of interior space, indoor facilities and current policies. For these questions, 5-point response scales were used, where: 1= Strongly Agree, 2= Agree, 3= Neither Agree nor Disagree, 4=Disagree and 5 = Strongly Disagree. In the latter part, employees were asked to state whether they were aware of Halcrow's sustainability targets and whether they felt personally responsible for contributing to Halcrow's sustainability objectives. This survey was sent via internet to all employees in Vineyard House (VH) and Shortlands buildings and stayed open for two weeks. Initially, 197 completed surveys were returned, (representing 34% response rate). Having excluded data from ineligible participants and questionnaires with missing data on more than 70% of items on "satisfaction with workplace" questions, the final sample consisted of 189, 162 from VH and 27 from Shortlands.

3. Results

This part of the paper illustrates the findings from the pre–occupancy employee survey, for VH employees only.

3.1. Demographic Questions

Over two-thirds of the 162 VH respondents were male, 32.7% (53) were female. Most respondents, 41% (66), were between 26 and 35 years old, 5.6% (9) were 25 years old and under, 23.6% (38) were between 36 and 45, 16% (26) were 46 and 55 and 13.7% (22) were over 55 years old. In terms of employment status, the majority of the respondents, 95.1% (154), were full-time. More than 70% respondents (115) indicated that they were based in VH 75%-100% of the time.

3.2. Mode(s) of Transport

About 98% (159) respondents answered this question. Their responses are shown in Table 1.

Table 1: Mode(s) of transport you normally use to commute to your office

	Frequency	Percent
Bus/Train/Underground/Foot/Bicycle	64	40
Car (in combination with other modes)	27	17
Bicycle (in combination with other modes)	32	20
Foot (in combination with other modes)	79	49
Bicycle (only)	5	3
Foot (only)	11	7
Car (only)	7	4

3.3. Working from Home

Of 154 respondents, 47.4% (73) indicated that they already worked occasionally from home; while 39% (60) said that they would consider working from home given the opportunity. Among the latter, 7 respondents reported driving to work for part, or the whole of their journey, with a total mileage of 9701.379 km per year.

3.4. Working in the Office after Office Working Hours

The majority of respondents, 57.1% (92), specified that they rarely worked after 7.00pm (0-1 evenings/ month). However, a good number - 40% (65), indicated that they needed to work in their office for 2-10 evenings/month. Only 2.5% (4) needed to work for more than 10 evenings/ month.

3.5. Using the Canteen in VH

About half the respondents (81) specified that they rarely used the canteen facilities in VH.

3.6. Office Set Up:' Where You Sit in the Office'

The majority of the respondents, 76.4% (123) worked in an open plan office with more than 5 people, 17.4% (28) worked in a multi-occupant cellular office (5 people or less), 5.6% (9) had their own single cellular office and only 0.6% (1) of the respondents hot-desked in an open plan office.

3.7. Employees' Satisfaction with Their Workplace

Physical Environment

Approximately 86% (139) of participants answered all the questions (8) in this category; the results are illustrated in Figure 1.

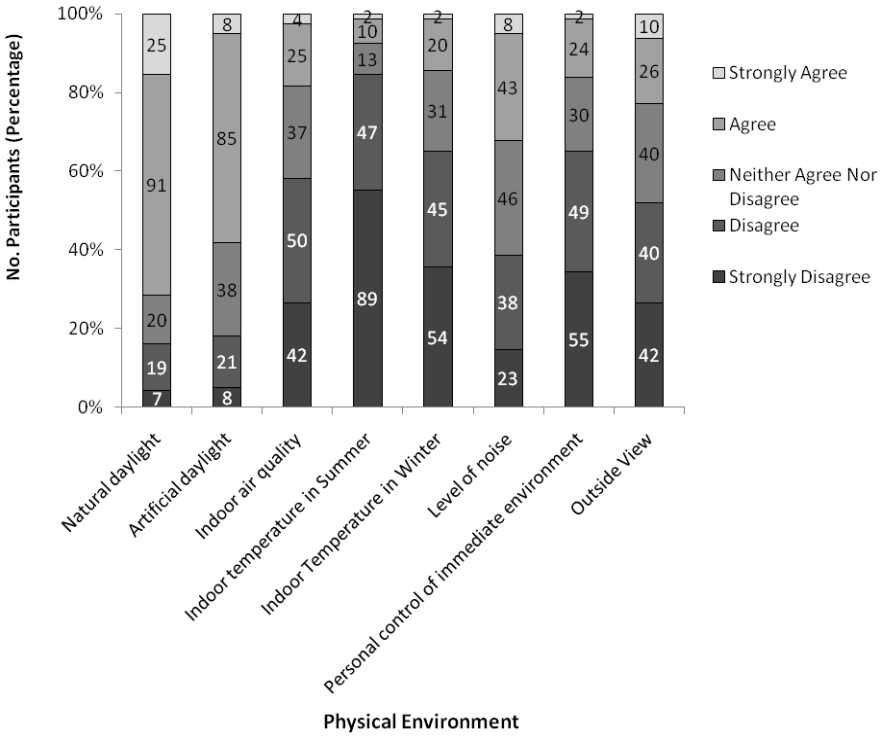

Figure 1: I feel satisfied with the physical environment of my workplace

Use of Interior Space

Approximately 84% (136) of the participants answered all the questions (13) in this category; the results are illustrated in Figure 2.

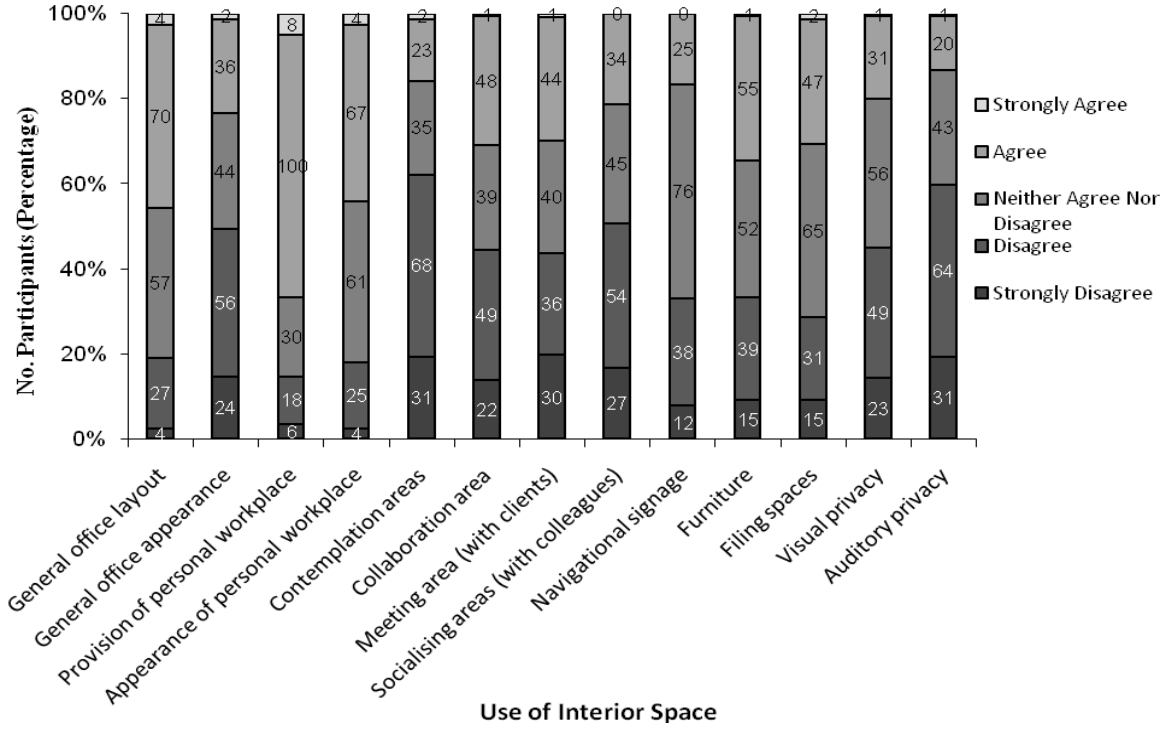

Figure 2: I feel satisfied with the use of interior space in my workplace

Indoor Facilities

Approximately 92% (149) of the participants answered all the questions (5) in this category; the results are shown in Figure 3.

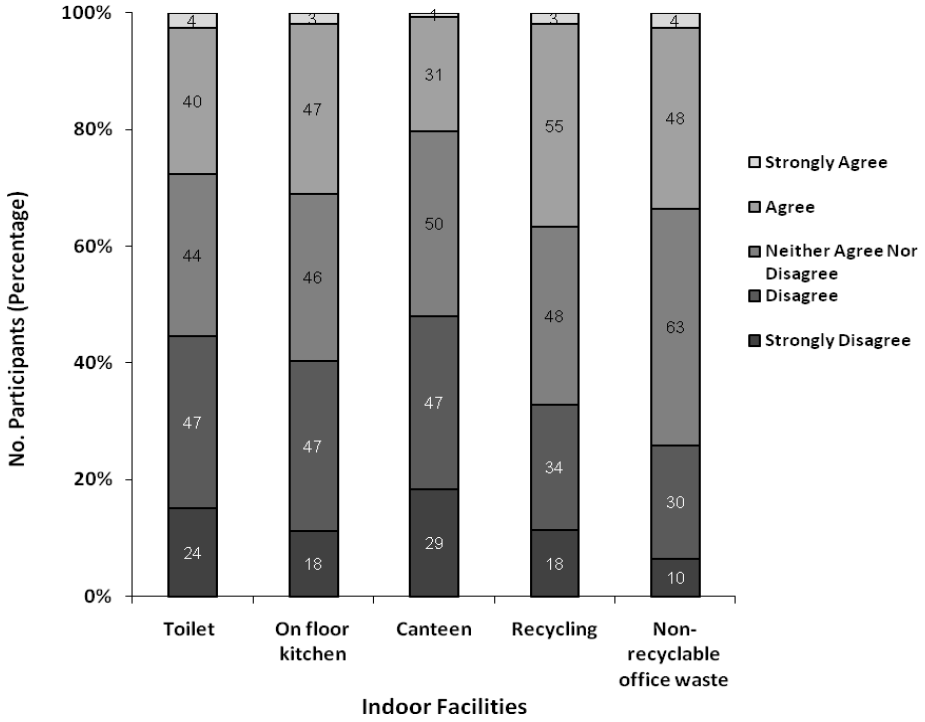

Figure 3: I feel satisfied about the indoor facilities in my workplace

The Policies

Approximately 98% of participants (159) answered this question; the results are shown in Figure 4.

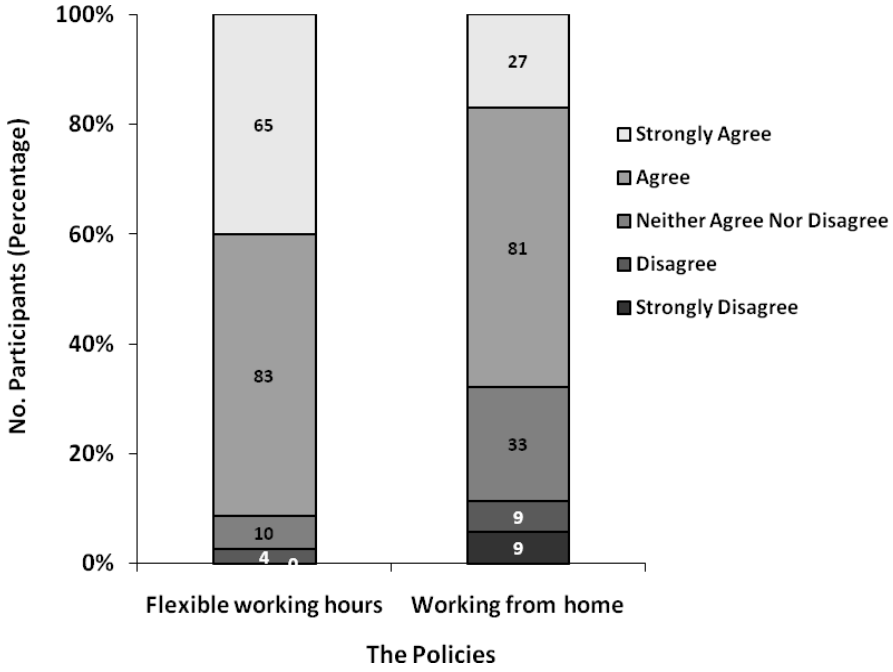

Figure 4: I feel satisfied with the policies available at my workplace

Table 2 shows the mean employees' satisfaction level in each category. The 4 items together showed a satisfactory level of reliability (Cronbach's alpha = 0.89), so overall satisfaction scores could be derived; overall satisfaction mean scores are also shown in Table 2.

Table 2: Mean Scores for Employee's Satisfaction

	Physical Environment	Use of Interior Space	Indoor Facilities	The Policies	Overall Employees' Satisfaction Level at VH
Frequency	139	136	149	159	111
Mean	3.45	3.18	3.20	2.02	**2.98**

Analysis was conducted to assess whether overall satisfaction differed between office set-ups (e.g. open plan, cellular offices, etc) (see Figure 5 overleaf). Overall satisfaction of respondents in single cellular offices (Mean=2.61, Std. Error of Mean=0.14) was higher than that of those in open-plan offices (Mean= 2.98, Std. Error of Mean=0.047). This difference was significant, t (92) = -2.104, p=0.038.

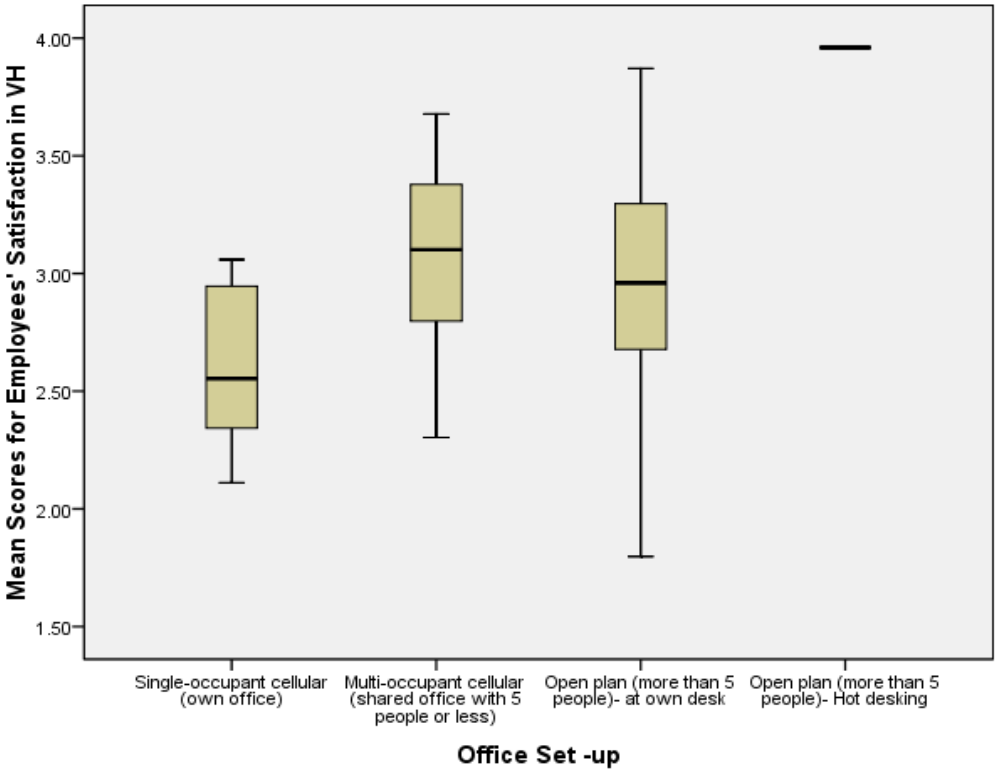

Figure 5: VH Employees' Satisfaction in different office set-ups.

3.8. The Positive Effect of Office Environment on Employees' Productivity, Well-being and Enjoyment

Figure 6 indicates the degree to which respondents felt that their current workplace had a positive effect on their productivity, well-being and enjoyment at work. The overall mean score (Cronbach's alpha = 0.902) was 3.07.

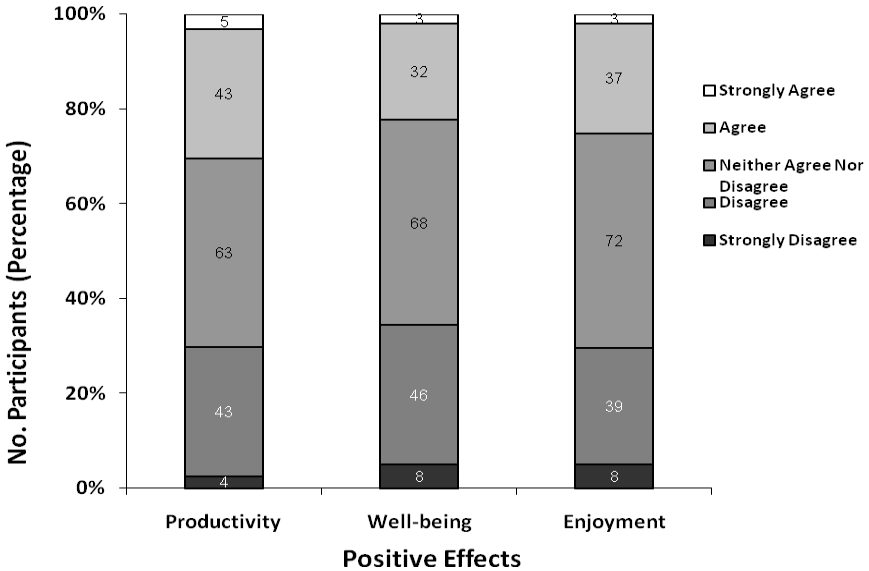

Figure 6: The Positive Effect of VH Environment on Employees' Productivity, Well-being and Enjoyment

An analysis was performed to assess the correlation between employees' overall satisfaction in VH and the positive effect of VH environment they perceived. A significant positive correlation ($r = 0.602$, $p < 0.001$) *was found*, indicating that satisfaction was positively associated with perceived positive effect

3.9. Employees' Awareness of, and Attitudes towards, Halcrow's Sustainability Targets

Figure 7 shows the level of employees' awareness of Halcrow's sustainability targets and whether they felt personally responsible for contributing to these targets.

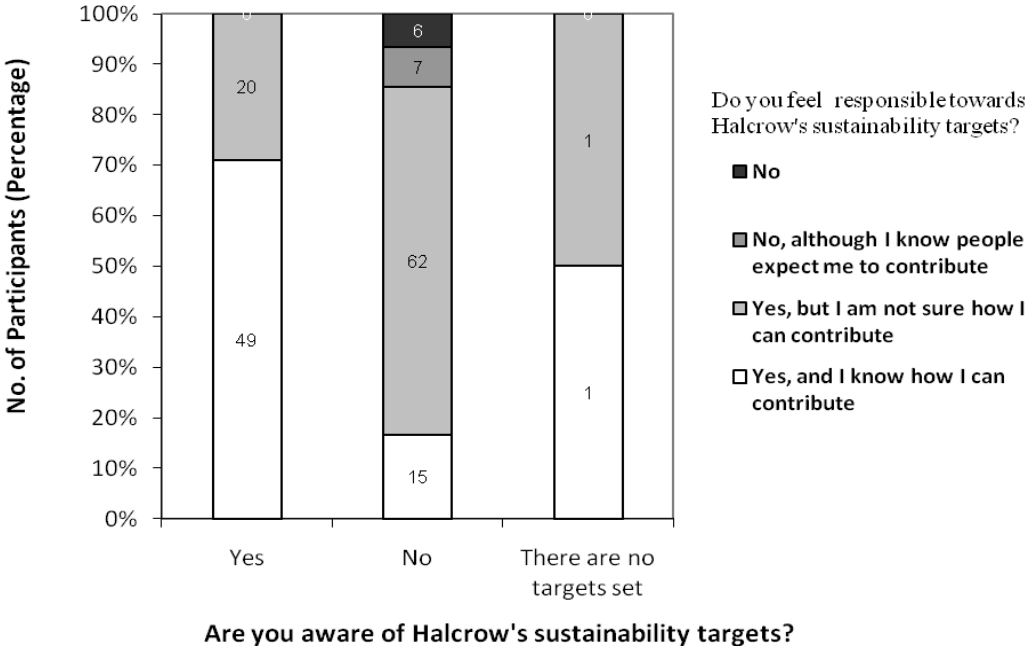

Figure 7: Employees' Awareness of and Attitudes towards Halcrow's Sustainability Targets

4. Discussion and Conclusions

A sustainable workplace is no longer just about technical fixes. Now, it is felt that behavioural intervention is perhaps going to be the key and that physical work environment might help drive certain behaviours. In this study, an employee survey was used as a tool to improve workplace sustainability by engaging the building's occupants.

The sample of respondents was broadly representative of the employees at VH, as indicated by responses to the demographic questions and the question regarding office set-up.

The overall employees' satisfaction score indicated that the respondents, on average, were neither satisfied nor dissatisfied with their workplace. Considering the four categories of employees' satisfaction separately, the respondents, (as was expected due to the poor air conditioning system in VH), were not satisfied with their workplace indoor temperature, indoor air quality and opportunity for personal control of the immediate environment. Inappropriate thermal conditions affect dexterity and increase physiological stress [10]; therefore, it was important to consider these issues in the building's refurbishment. Regarding the use of interior space, most of the respondents were not satisfied with the availability of contemplation areas and also with the auditory privacy of the individual workspace. Providing spaces for different work-styles, in the new building, was considered at the design stage.

The data presented in Table 1 (Modes of transport) indicate that the majority of the employees used sustainable modes of transport to commute to work. Giving the home-working opportunity to those who drive to work could save about 20.6 tCO2/year.

About half the respondents indicated that they rarely used the canteen facilities in VH. This was expected, as the canteen was too small to accommodate the number of the employees in VH and was not a welcoming place for the employees to socialize during their lunch breaks.

As is shown in Figure 5, and as confirmed by t-test, respondents who worked in single cellular offices were more satisfied than those who worked in open plan offices. However, it should be borne in mind that the sample size for single cellular offices was small compared to that for the open plan offices. Figure 7 indicated that the majority of the respondents did not know about Halcrow's sustainability targets and most reported that they did not know how to contribute towards Halcrow's sustainability objectives. This could be because the channels of communication were ineffective

This survey and the post-occupancy survey will indicate whether the refurbishment is meeting expectations that the new building is more sustainable than the old HQ building, and guide thinking on the need for new technical, behavioural and policy changes that are necessary to maximise sustainability performance within the budget and other practical constraints that have been identified.

References

[1] S. Ni Hogain, A New Energy Strategy: The second report of the Zero Carbon Britain project, Zero Carbon Britain 2030, CAT Publication, M. Kemp, Ed. 2010, pp.4.

[2] T. Delay, S. Farmer, T. Jennings, Building the future today-Executive summary-Transforming the economic and carbon performance of the buildings we work in, Carbon Trust, 2009.

[3] Carbon Trust, Management Guide: Creating an awareness campaign, Queen's Printer and controller of HMSO, 2005.

[4] Carbon Trust, Cited in Opus Energy 2010, Rising employee awareness, [online], Available from: http://electricityadvice.opusenergy.com/module/page-254/employee-awareness.cfm (Accessed 13/12/2010)

[5] W. Browning, J. Roman, Green and the Bottom Line: Increasing Productivity through energy efficient design, 1995.

[6] I. Gray, Technology Strategy Board: Driving Innovation, (11 August, 2010), Press release, [online], Available from: http://www.innovateuk.org/_assets/pdf/press-releases/11_aug_10_ucd.pdf (Accessed 13/12/2010)

[7] J.Heerwagen, K. Kampschroer, K. Powell, V. Loftness, Collaborative knowledge work

Environments, BUILDING RESEARCH & INFORMATION, 2004

[8] J. Myerson, 2008, Welcoming workplace, Royal College of Art

[9] J. Heerwagen, Green Building, Organizational Success, and Occupant Productivity, Building Research and Information, 2000, Vol. 28, pp 353-367

[10] Y. Zhang, P. Barrett, Findings from a post-occupancy evaluation in the UK primary schools sector", Facilities, 2010, Vol. 28, pp.641 - 656

Environmental impact of optimum insulation thickness in buildings

Özden Ağra[1,*], Ş.Özgür Atayılmaz[1], Hakan Demir[1], İsmail Teke[1]

[1] *Yıldız Technical University, Mechanical Eng.Dep., İstanbul, Turkey*
** Corresponding author. Tel: +90 212 383 2820, Fax: +90 212 261 6659 E-mail: oagra@yildiz.edu.tr*

Abstract: Environmental problems caused by energy usage threaten the world. High CO_2 emission emitted into the atmosphere by combustion of fossil fuels cause global warming. As a result of combustion of fossil fuels used for heating buildings, air pollution occurs. E ffective thermal protection in residential sector playsan important role towards the reduction of energy consumption for space heating. Insulation reduces fuel consumption, undesirable emissions from the burning of fossil fuels, and increases thermal comfort by minimizing heat losses from buildings. In this study, the four different cities of Turkey, Antalya, Istanbul, Eskişehir and Erzurum are selected to determine the optimum insulation thickness of the external wall of buildings. Optimum insulation thicknesses for two different energy sources (coal and natural gas) by using extruded polystyrene as an insulant are calculated and compared to each other. Annual savings in energy consumption and CO_2 emissions have been determined after optimization of insulation thickness. The result proved that when the optimum insulation thickness was used, the energy consumption and the emission of CO_2 decreased.

Keywords: *Environmental impact, Insulation thickness, Energy*

Nomenclature

A_{year}	*Difference of annual total heating cost ($/m² year)*
C_{fuel}	*Cost of the fuel, ($/m³, $/kg)*
$C_{insulation}$	*Cost of the insulant, ($/m²)*
$C_{totalinsulation}$	*Total heating cost of the insulated building, ($/m² year)*
C_{total}	*Total heating cost of the insulated building, ($/m² year)*
C_y	*Cost of the insulant ($/m³)*
C_{year}	*Annual heating cost for unit surface, ($/m² year)*
DD	*Degree-day value, (°C-days)*
g	*Inflation rate, (%)*
Hu	*Low heat value of the fuel, (J/kg)*
i	*Interest rate, (%)*
k	*Thermal conductivity, (W/mK)*
N	*Lifetime, (year)*
pp	*Pay-back period (year)*
PWF	*Present worth factor*
q	*Annual heat loss, (W/m²)*
R	*Thermal resistance, (m²K/W)*
R_d	*thermal resistances of the Outdoor, (m²K/W)*
R_i	*thermal resistances of the Indoor, (m²K/W)*
$R_{insulation}$	*Thermal resistance of the insulant, (m²K/W)*
$R_{wall\ total}$	*Thermal resistance of non-insulated wall, (m²K/W)*
T_b	*Base temperature (°C)*
T_0	*Mean daily temperature (°C)*
U	*Overall transfer coefficient, (W/m²K)*
x	*Insulation thickness, (m)*
η	*Efficiency of the combustion system*

1. Introduction

In recent years, the amount of the energy consumption is increasing depending on t he development of technology, social and economic life. Although this shows the welfare of the society level, increase in energy consumption has brought environmental problems. One of the most crucial impacts resulting of consumption of variety of energy resources is changing the global climate which is known as the greenhouse effect or the global warming. During the recent years, greenhouse gases concentration has occurred continuous increase in the atmosphere. Turkey has a dynamic economic development besides its rapid population growth and industrial developments. Therefore, energy consumption has dramatically increased. Both the increase in energy need and the environmental problems make it

necessary to utilize energy in the most efficient way. In the "climate change report" announced by the UN, it is indicated that global warming has been created in the last 50 years by the human being [1]. Among the order of countries emitting carbon dioxide- the US(5.5 billion tons), Russia(2.8 billion tons) and Japan(1.3) billion tons-, with carbon dioxide emmision of 294 million tons annually, Turkey was annnounced to be 13th. CO_2 emission in Turkey results 42% from industry, 30% from residences, 20% from transportation, 5% from agriculture and 3% from consumption out of the energy. The importance of environmental problems originating from residences will be better understood, when the amount of consumed energy for heating is considered in the portion of total energy. CO_2 emissions produced by the fuels for heating in residences will be reduced by insulating the buildings. When the insulation in optimum thickness is applied to the outer walls of the building, CO_2 emissions will be reduced 30% by status of uninsulated.

Dombaycı et al [1] calculated the optimum insulation thickness for Denizli by using two different insulants and five different fuel types. Dombaycı [2] further calculated the optimum insulation thickness of external walls of buildings in Denizli by using the expanded polystyrene insulant and coal. He determined that with a decrease of 46.6% in fuel consumption. CO_2 and SO_2 emissions dropped by 41.53%.

Çomaklı and Yüksel [3] calculated the optimum insulation thickness for Erzurum which is the coldest cities in the IV. degree-day zone of Turkey in accordance with the TS Standard no 825 on Rules of Heat Insulation in Buildings. He has been determined that CO_2 emissions amount decreased 50%

Ucar A. and Balo F.[4] calculated the optimum insulation thickness of the external wall, energy cost savings over a lifetime of 10 yr, and payback periods for the four different wall types in Elazığ. It is found that when the optimum insulation thickness is used, the amount of fuel consumption and the emissions of CO_2, SO_2, NO_x, and CO are decreased depending on the wall type.

For this purpose in this study, the optimum insulation thicknesses of external walls were calculated by using two different fuel types (coal and natural gas) for heating and expanded polystrene as the insulation material in buildings at selected cities of Turkey in four degree-day zones such as Antalya, Istanbul, Eskişehir and Erzurum, respectively. Annual savings in energy consumption and CO_2 emissions have been determined after optimization of insulation thickness.

2. Methology

Turkey is divided into four climatic zones depending on average temperature degree days of heating. Table 1 shows the degree-day values with reference to an equilibrium temperature of 18°C in provinces within the four degree-day zones of Turkey as per the TS Standard no 825 on Rules of Heat Insulation in Buildings [5].

Table 1 Degree-day values with reference to an equilibrium temperature of 18°C [6]

Region	Provinces	Degree-day value
I	Antalya	1083
II	Istanbul	1865
III	Eskişehir	3049
IV	Erzurum	4827

2.1. The Heat Loss Calculation For External Walls

Heat losses in buildings generally occur through external walls, windows, roof, floors and air infiltration. In this study, the optimum insulation thickness has been calculated in consideration of heat losses only occurring in the external walls.

The external wall of a building is an externally-insulated wall composed of a 2 cm internal plaster. 13 cm bricks, insulant and a 3 cm external plaster. Physical characteristics of constituents of the wall are given in Table 2. In calculations, only the heat losses occurring in external walls were considered to calculate the optimum insulation thickness.

Table 2 Physical properties of the materials of external wall

Constituent	Thickness(m)	k (W/mK)	R (m^2K/W)
Internal Plaster(Lime-based)	0.02	0.87	0.02
Bricks	0.13	0.45	0.28
External plaster(cement-based)	0.03	1.4	0.02
R_i			0.14
R_o			0.04
$R_{wall\ total}$			0.50

In the study, extruded polystyrene (k=0.032 W/mK) was used as an insulation material. The price of insulation material is 158 $/m3.

The heat loss per unit area of external wall is

$$q = U \cdot (T_b - T_0) \tag{1}$$

The annual heat loss in unit area,q, can be determined using the degree days,DD asoccurring in unit surface is calculated by using U and the degree-day value [6].

$$q_{year} = 86400 \cdot DD \cdot U \tag{2}$$

The annual energy requirement can be calculated by dividing the annual heat loss to the efficiency of the heating system η:

$$E_{year} = \frac{86400 \cdot DD.U}{\cdot \eta} \tag{3}$$

where U is the overall heat transfer coefficient for a typical wall that includes a layer of insulation is given by

$$U = \frac{1}{R_i + R_{wall} + R_{insulation} + R_o} \tag{4}$$

R_i and R_o are the the inside and outside air film thermal resistances respectively and R_{wall} is the total thermal resistance of wall layers without insulation. $R_{insulation}$ is the thermal resistance of the insulant and calculated as follows:

$$R_{insulation} = \frac{x}{k} \tag{5}$$

Total resistance of the non-insulated wall layer $R_{wall.\ total}$ is

$$R_{wall,total} = R_i + R_{wall} + R_o \tag{6}$$

As a result, the annual heating load is then given by

$$E_{year} = \frac{86400 \cdot DD}{\left(R_{wall,total} + R_{insulation}\right) \cdot \eta} \tag{7}$$

Annual energy cost for unit surface C_{year} is calculated with the following equation:

$$C_{year} = \frac{86400 \cdot DD \cdot C_{fuel}}{\left(R_{wall,total} + R_{insulation}\right) \cdot Hu \cdot \eta} \tag{8}$$

The price and lower heating values of fuels and efficiencies of heating systems used in these calculations are given in Table 3.

Table 3 The parameters used in calculations

Parameter	**Value**	**Parameter**	**Value**
Natural gas		**Coal**	
Chemical formula	CH_4	Chemical formula	$C_{7.078}\ H_{5.149}\ O_{0.517}\ S_{0.01}\ N_{0.086}$
Hu (J/kg)	$34{,}526.10^6$	Hu (J/kg)	$29{,}295.10^6$
η	0,93	η	0,65
C_{fuel} ($/m^3)	0,72	C_{fuel} ($/kg)	0,2216
Interest rate (i)		%7	
Inflation rate (g)		%10	
Life cycle (N)		10 years	
Present Worth Factor (PWF)		11.67	

The life cycle cost analysis method was used in calculating the optimum insulation thickness. Annual energy cost was calculated based upon t he present worth factor and the lifetime determined [1]. The interest rate adapted for inflation rate r is given by if

$$i > g \rightarrow r = \frac{i-g}{1+g}$$

$$i < g \rightarrow r = \frac{g+i}{1+i} \tag{9}$$

The present worth factor is calculated based upon the inflation and interest rates as follows:

$$PWF = \frac{(1+r)^N - 1}{r \cdot (1+r)^N} \tag{10}$$

Insulation cost is calculated as follows:

$$C_{insulation} = C_y \cdot x \tag{11}$$

Ultimately, the total heating cost of an insulated building as per the life cycle cost analysis is calculated as follows:

$$C_{insulation,\,total} = C_{year} \cdot PWF + C_y \cdot x \tag{12}$$

Energy savings ($/m^2) obtained dring the life time of insulation material can be calculated as follows:

$$A_{year} = C_{total} - C_{t\,ins} \tag{13}$$

where, C_{total} and C_{tins} are the total heating costs of the building when insulation is not and is applied, respectively.

Pay-back period

$$pp = \frac{C_{total}}{A_{year}} \tag{14}$$

the fuel consumption per year as follows:

$$M_F = \frac{86400.DD}{(R_{wall,\,total} + R_{insulation})\eta \cdot Hu}\,(Kg/year) \tag{15}$$

2.2. Calculation Of Annual Combustion Gases Amount

Building lose heat through the wall and insulation reduces this heat loss giving increased comfort conditions and fuel consumption reduced. The general chemical formula of combustion for fuel is given by

$$C_x H_y O_z S_p N_q + \alpha A(O_2 + 3.76N_2) \rightarrow xCO_2 + \left(\frac{y}{2}\right)H_2O + p.SO_2 + B.O_2 + D.N_2 \tag{16}$$

The constants A, B and D calculated from the oxygen balance formulas given in (17), (18)and (19) respectively:

$$A = a + \left(\frac{b}{4}\right) + e - \left(\frac{d}{2}\right) \tag{17}$$

$$B = (\alpha - 1) + \left(a + \frac{b}{4} + e - \frac{d}{2}\right) \tag{18}$$

$$D = 3.76\alpha\left(a + \frac{b}{4} + e - \frac{d}{2}\right) + \frac{f}{2} \tag{19}$$

Total emission of CO_2 products resulting from the burning 1 kg of fuel can be calculated by

$$M_{CO_2} = \frac{x.CO_2}{\dot{M}} = \text{kg } CO_2 / \text{kg fuel} \quad (20)$$

$\dot{M}$ is the weight of mol for fuel which can be calculated using,

$$\dot{M} = 12x + y + 16z + 32q + 14p \text{ kg / kmol} \quad (21)$$

2.3. Results

In this study, the optimum thickness of insulation with heating load for four different walls used for the buildings in turkey is determined. The effect of insulation thickness on total cost, fuel cost and investment cost for Antalya, Istanbul, Eskişehir and Erzurum province has been calculated. Optimum insulation thickness, pay-back period and energy saved over a period of 10 years calculated for two different fuel types are shown in Table 4. The effect of insulation thickness on the total cost over the lifetime of 10 year in Erzurum,which is the coldest city in Turkey, is given in Figure 1a-b. As shown in the figure 1, while the optimum insulation thickness for Erzurum with extruded polystyrene used for the insulation of the external wall within a natural-gas fuelled heating system is 14 cm, it is 9 cm when coal used as a fuel.

Table 4. Optimum insulation thickness, pay-back period and energy saving for different fuel types

	Insulant	**Extruded polystyrene**		
City	**Fuel type**	**Thickness (m)**	**Pay-back period (year)**	**Energy Saving (10 years) ($/m^2)**
Antalya	Coal	0.03	2.14	11.84
	Natural gas	0.05	1.67	29.22
Istanbul	Coal	0.05	1.73	25.28
	Natural gas	0.08	1.46	57.69
Eskişehir	Coal	0.07	1.51	47.22
	Natural gas	0.09	1.3 4	102.93
Erzurum	Coal	0.09	1.38	82.03
	Natural gas	0.14	1.26	173.5

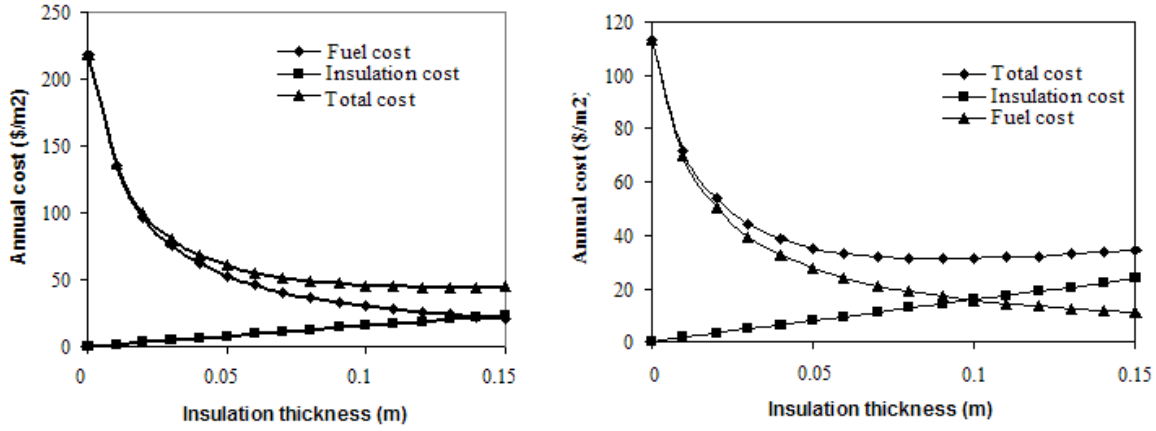

(a) (b)

Fig. 1 Effect of insulation thickness on total cost for Erzurum a) natural gas b) Coal

The variations of the emissions of CO_2 versus insulation thickness for a $1m^2$ external wall of a building for four different cities of Turkey are shown in Figure 2 a by using natural gas and 2.b by using coal respectively.

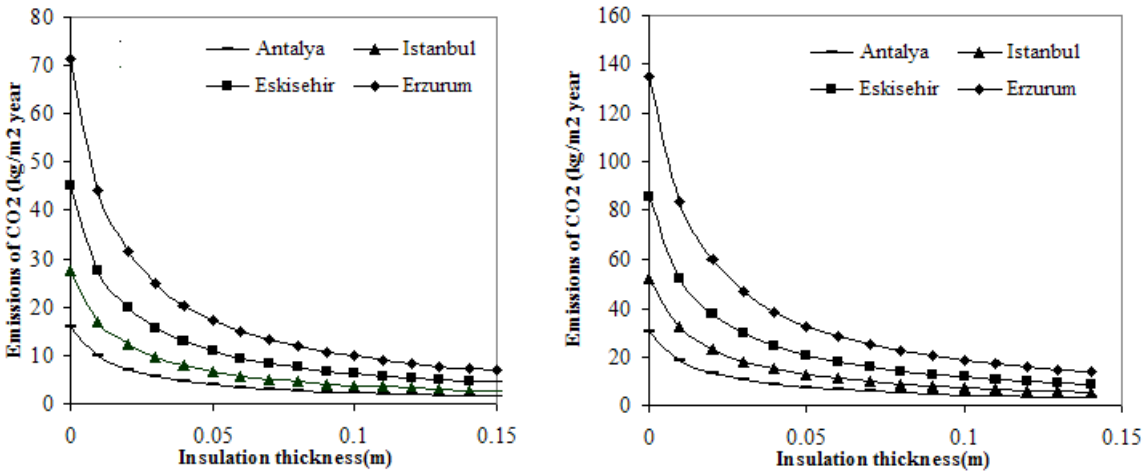

(a) (b)

Fig. 2 Emissions of CO_2 versus insulation thickness a)For natural gas b) For Coal

As shown in the figure 2, CO_2 emission release from coal is greater than the natural gas when the coal is fired in Erzurum, located in the 4th climate region.The use of low- quality coal will increase the air pollution in particular. CO_2 emissions produced by the fuels for heating in residences will be reduced by using insulate the buildings. As shown the figures 2a, if we apply 14 cm insulation, which was found to be the optimum when natural gas is burned, the emission rates of fuel 7 kg/m^2. If insulation was not applied, CO_2 emission rate would be 71 kg /m^2. Similary, if we apply 9 cm insulation, which was found to be the optimum when coal (Figure 2b) is burned, the emission rates of fuel 20 kg/m^2. If insulation was not applied, CO_2 emission rate would be 135 kg /m^2.

Conclusion

As energy sources of our country are limited and foreign-dependent, conservation and efficient use of energy particularly in housing sector where energy is intensively consumed, and heat losses are much gain more significance day by day. In this study, optimum insulation thickness for external walls with two different fuels in four climatic zones of

Turkey have been calculated. The life cycle cost analysis method has been used in the calculations. Though variable by the fuel used selected, pay-back period of insulations applied to buildings are usually too short. Investments in insulation shortly pay off and contribute to diminishing the dependency of our country in terms of fuel sources. At the present, where fuel and energy costs drastically increase, this situation becomes vitally important. It is found that when the optimum insulation thickness is used, the amount of fuel consumption and the emissions of CO_2 decreased depending on the fuel. The highest values of the CO_2 emission rates is reached for coal. The results indicate that the optimum insulation thicknesses show significant variation due to fuel and climatic conditions.

References

[1]. Dombaycı. Ö.A., "The environmental Impact of Optimum Insulation Thickness for External Walls of Buildings",Building and Environment 42 (2007) 3855-3859.

[2]. Gölcü. M., Dombaycı. A., Abalı. S., "Optimization of Insulation Thickness for External Walls Using Different Energy-Sources", Applied Energy, v 83,921-928, 2006

[3]. Çomaklı. K., Yüksel. B., "Enviromental impact of thermal insulation thickness in buildings, Applied Thermal Engineering, 24 (2004) 973-940.

[4] Ucar A.,Balo F., "Determination of environmental impact and optimum thickness of insulation for building walls" Environmental Progress & Sustainable Energy, DOI: 10.1002/ep.10448

[5] TS 825 T hermal insulation rules in buildings. Turkish Standart Institute, The official journal, 23745,1999

[6]. Bulut. H., Büyükalaca. O., Yılmaz. T., "Analysis of variable-base heating and cooling degree-days for Turkey", Applied Energy 69(4), 269-283, 2001

Overheating risk evaluation of school classrooms

Despoina Teli[1,*], Mark F. Jentsch[1], Patrick A.B. James[1], AbuBakr S. Bahaj[1]

[1] *Sustainable Energy Research Group, School of Civil Engineering and the Environment, University of Southampton, Southampton SO17 1BJ, United Kingdom*
** Corresponding author. Tel: +44 (0)2380592134, E-mail: dt1e09@soton.ac.uk*

Abstract: This paper presents a pilot study which considers the overheating risk of classrooms in school buildings. Four schools in Southampton in the South of the UK, constructed during the period of the 1950s-1980s were used as case study examples. The schools were studied in terms of the parameters or the combination of parameters that may drive classroom overheating. Topographic features, built-up area, urban density, adjacency to roads and parks and other characteristics such as building form and materials were assessed, looking at the urban, building and classroom scale. In addition to this a questionnaire survey was conducted to assess the teachers' perception of their classrooms' thermal environment. The survey responses are discussed and compared to the outcomes of the school parameter analysis, also considering the limitations of the survey approach. It was found that gaining an understanding of the occupants' perception of the thermal conditions in a school's classrooms is essential for developing recommendations for addressing overheating. The study appears to indicate that individual perception of overheating may outweigh the objective influence of urban design and construction parameters on the indoor thermal conditions.

Keywords: *School buildings, Overheating, Microclimate, Refurbishment, Classroom.*

1. Introduction

Over recent years, children and teachers in the UK have been experiencing uncomfortably warm thermal conditions inside school classrooms during non-heating periods [1]. This potentially has implications on learning outcomes since it has long been understood that an increase in the indoor temperature may lead to a decline in the productivity of students [2].

Some school buildings constructed between the 1950s and the 1980s are unsuitable for hot summer periods, due to characteristics such as low thermal mass and highly glazed facades. Building performance simulations of typical UK school building types have shown that their overheating risk is likely to be exacerbated under the predicted future climates [3]. Due to cuts in public budgets new school projects have been cancelled in the UK [4] and the life of the majority of the existing school building stock will have to be extended further. In terms of internal thermal comfort, summer overheating could be addressed by installing air conditioning systems, a solution which has been widely adopted in southern Europe over the past decades [5]. The adaptation of such a measure would however conflict with the goal to reduce building related greenhouse gas emissions [6]. It would also set a precedent where air-conditioning would become the expected norm.

The aim of this study is to investigate methodological approaches for evaluating the overheating risk of school buildings. It considers the schools' characteristics and the teachers' perception of their classroom's thermal conditions.

2. Parameters that drive overheating

The thermal conditions inside a building are determined by the interactions between the external climate and the building, the building shell and the internal space and the internal space and the occupants [7]. Accordingly, the parameters which influence the risk of overheating in buildings are:

- The external climatic conditions, i.e. the air temperature; solar radiation; rainfall; relative humidity and wind velocity.
- The microclimatic profile, i.e the local scale climate which is affected by the surrounding surfaces (albedo, thermal capacity); topography; vegetation; soil structure and urban form (industrial processes, transportation, buildings, human metabolism) [8].
- The building shape and form, i.e. the geometric relations (envelope area to volume ratio, building height) which determine the building's exposure to solar radiation and the ambient air [9].
- The building fabric properties, i.e. the thermo-physical properties of its construction materials (U-values, g-values and albedo, thermal capacity).
- Internal gains, i.e. the sensible and latent heat emitted by human bodies, lighting, computing and office equipment, electric motors and appliances [10].

During the last 30 years, there has been a trend towards warmer summers [11]. This trend is likely to continue as projections for the future UK climate in the 2020s, under a medium emissions scenario, predict about 1.5 ºC higher summer mean temperatures and up to 3 ºC higher summer mean daily maximum temperatures, relative to a modelled 1961–1990 baseline period [12]. This can be expected to further drive the occurrence of summer overheating in buildings.

3. Methodology for overheating risk assessment

Four primary schools in Southampton on the South coast of the UK were chosen as case study examples in order to evaluate overheating risks of existing school buildings. Primary schools were selected as the teachers and students remain in the same classroom during the school hours ensuring uniformity in terms of occupancy. The study consisted of two components: (i) an aerial photo analysis of the schools and their surrounding environment and (ii) a questionnaire survey of the teachers.

3.1. Aerial-photo analysis

The aerial photo analysis, which is highlighted in Fig.1 for three of the schools discussed in this paper, included:

- the surrounding urban environment (urban density level, building heights, adjacency to roads/parks/fields/water).
- the school ground (density level, greenery/hard surfaces, location of the building within the school ground, shape of the school ground in relation to the orientation)
- the building (form, shape, roof cover)
- the classrooms (materials, window/wall ratio, shading conditions)

The area within 100m around the schools was studied since the local microclimate of this area was considered as influential for the building performance.

3.2. Questionnaire survey

The teachers of the 4 schools were requested to complete an 11 question survey investigating their perception of their individual classroom's thermal environment. In case they had been in that classroom for less than 1 year, they were asked to answer for their previous classroom (within the same school). Most of the questions were closed type questions (fixed-response). The survey forms were filled in face-to-face with the respondents in an interview style. The aim of the questionnaire was to identify the following:

- when, where and under which circumstances overheating occurs
- the duration of overheating occurrences in the school/classroom
- the teachers' understanding of the factors which cause overheating
- the mitigation measures taken to date with respect to overheating
- the teachers' perceived impact of overheating on students

The pilot study of four schools has highlighted limitations of the survey which need to be taken into account in the analysis of the results. These limitations are:

- the subjective perception of individuals
- the possibility of an established view in each school about the thermal conditions in the classrooms
- the expectations of individuals based on their perception of the outside climatic alterations throughout the year.

4. Aerial photo analysis of the four investigated schools

The four schools used in this study are denoted as A, B, C and D in Fig.1. They share their school grounds in pairs and are surrounded by residential areas of a relatively low density with detached 2-storey houses. The schools are not shaded by surrounding buildings or trees. Vegetation is limited to grass surfaces with few trees in the school grounds. The outdoor space material surrounding the buildings is mainly tarmac, covering 58 and 68% of the open spaces for schools A, B and C,D respectively (excluding sports fields).

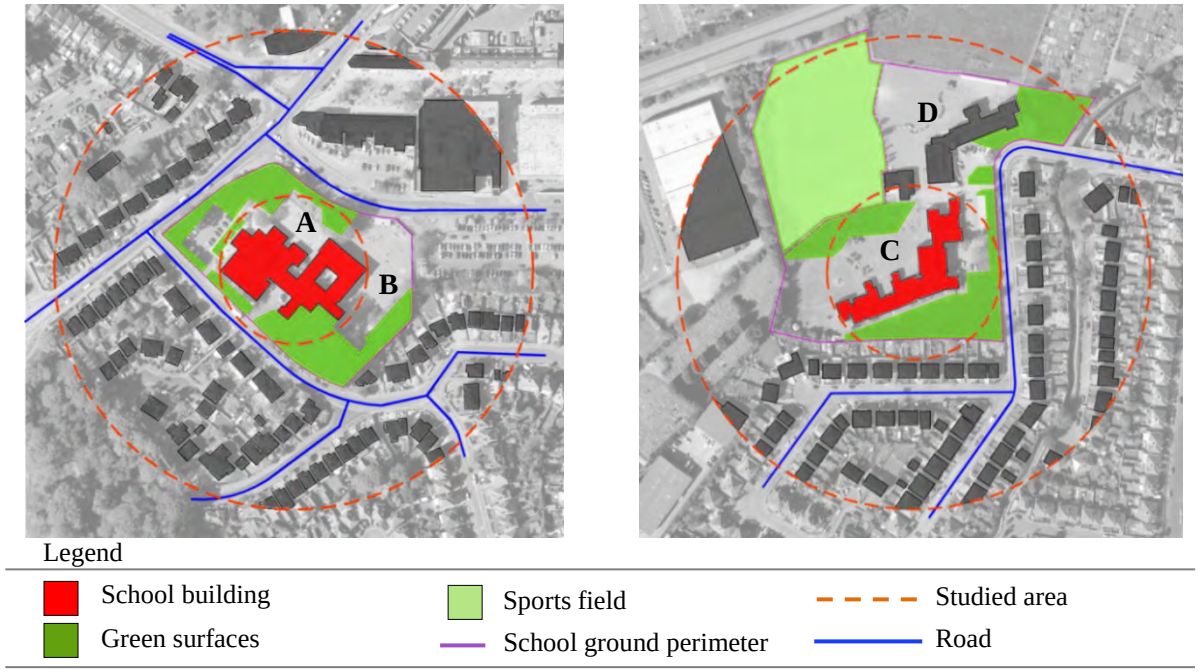

Fig. 1. Analysis of the main urban characteristics of three of the studied schools

School A is a compact one-storey building with an assembly hall in the centre and the classrooms located around it. School B consists of two parts which create an enclosed yard, a 2-storey L shaped building housing the classrooms and a 1-storey building with the remaining school spaces. Schools C and D both consist of linear sections. The building parts which face southeast (SE) accommodate the classrooms. In school D the classroom part has 2 storeys.

Schools A and B were built in 1978 using a light-weight construction with steel frames and pre-fabricated concrete panels. The other two schools (C and D) were constructed in 1950 using a brick cavity wall system. 40 to 60% of the façades are glazed in all four schools (Fig.2). Windows in schools A and B are single glazed whilst they are double glazed in schools C and D. All buildings are internally shaded with blinds or curtains. In schools C and D most classrooms face SE while in school A most classrooms open to two orientations and in school B half of the classrooms face northeast (NE) and half southeast (SE). This is shown in Fig.3.

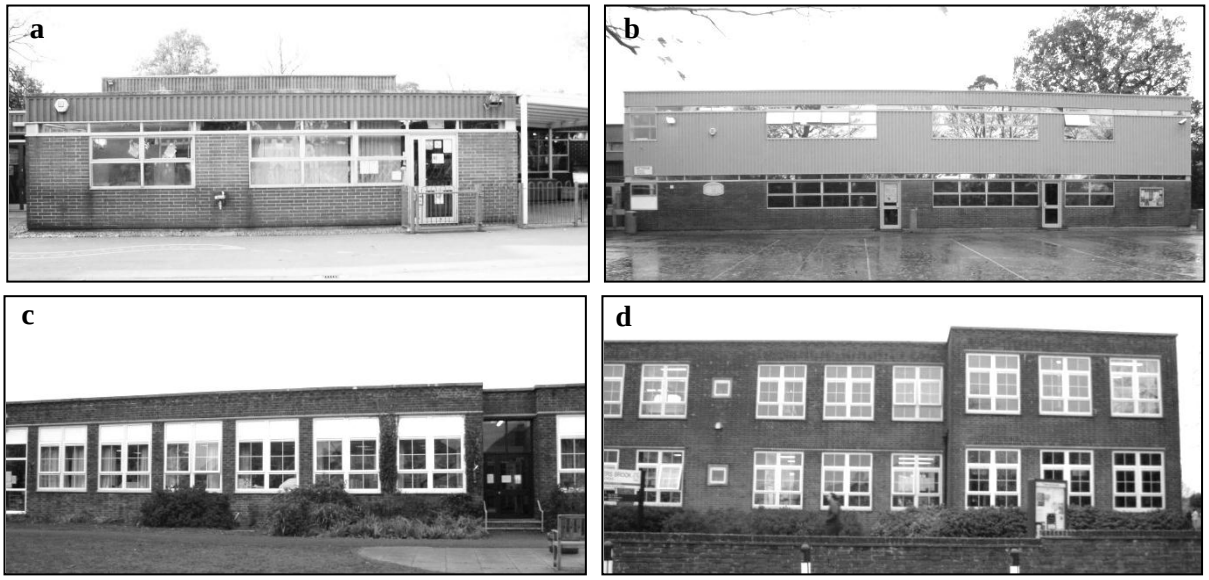

Fig. 2. Schools' facades: a. Northeast elevation of school A, b. Southeast elevation of school B, c. Southeast elevation of school C and d. Southeast elevation of school D.

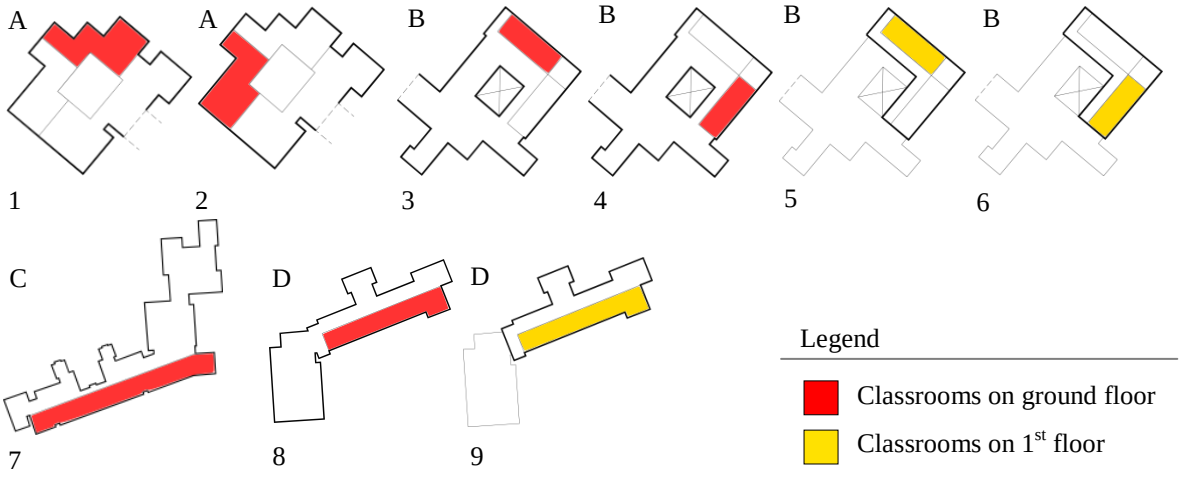

Fig. 3. Classroom clusters of the case study schools

From the aerial photo analysis 9 classroom clusters were identified based on construction, orientation, storey and surrounding environment (Fig.3). Clusters 5 and 6 (school B) appear to have the highest potential risk of overheating. Their NE and SE orientation in combination with the outdoor tarmac surfaces, a flat bitumen roof, a light-weight construction, single glazing and a lack of wind exposure are parameters which may drive overheating in the classrooms. Ground floor clusters 3 and 4 have the same characteristics like 5 and 6 apart from the missing heat absorption from the roof. In school A (clusters 1 and 2) the classrooms

benefit from 2 facades due to the building form which increases their ventilation potential. Cluster 2 is adjacent to a small green area and it is relatively exposed to prevailing SW winds. However, the light-weight construction, single glazing and flat roof indicate a high risk of summer overheating later in the day. Schools C and D (clusters 7-9) benefit from the cavity wall system and double glazing but the large SE oriented windows and the lack of ventilation and shading suggest high penetration of solar radiation.

5. Questionnaire survey results of the four investigated schools

50 teachers completed questionnaires across the 4 schools for their individual classroom. Their responses are analysed below and subsequently compared with the outcomes of the aerial photo analysis.

5.1. Thermal performance of the classrooms

The teachers were asked to evaluate their classroom's thermal performance for the occupancy period from April to October 2010. As shown in Fig.4, June and July are considered as the months with the greatest overheating occurrence, whilst in May and September are perceived as less problematic, yet with about half of the teachers stating that the classroom is either 'warm' or 'too warm'. April and October are generally perceived as acceptable. It should be noted however that the teachers might be influenced by the general perception of the climatic alterations throughout the year.

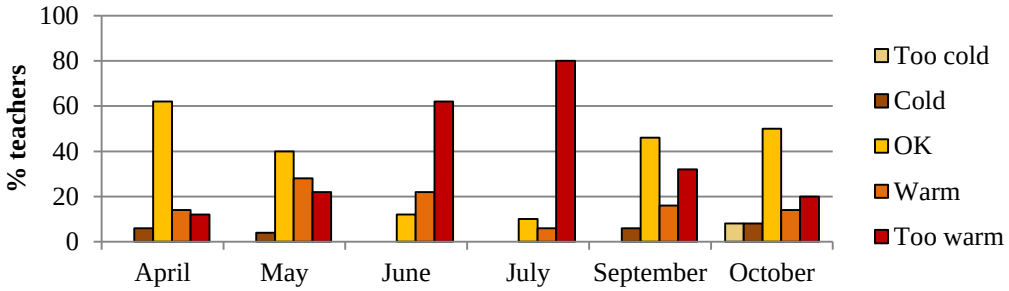

Fig. 4. Perceived classroom temperature conditions from April-October

When comparing individual responses in relation to the clusters described in section 4, a high variation in responses on a single façade orientation was identified for the months of April, May, September and October. In some cases the temperature of adjacent classrooms with exactly the same characteristics was assessed as 'OK' by one respondent and as 'too warm' by another. This suggests that in the spring and autumn months individual variation in perception appears to be more significant for overheating perception than absolute classroom temperatures.

5.2. Overheating occurrence

The teachers were asked about the magnitude and duration of overheating in their school and classroom. As shown in Fig.5, 80% of the teachers stated that in the non-heating season more than 60% of their school's classrooms experience overheating. In winter the responses vary. One of the reasons for this variation was found to be that in schools A and B the heating system is controllable and some teachers switch it off when temperatures are too high.

Almost 60% of the respondents answered that overheating occurrences in the non-heating season last for more than a week (Fig.6). For the heating season the responses are less clear. 30% of the teachers voted for 'not applicable' and about 25% for 'more than a week'.

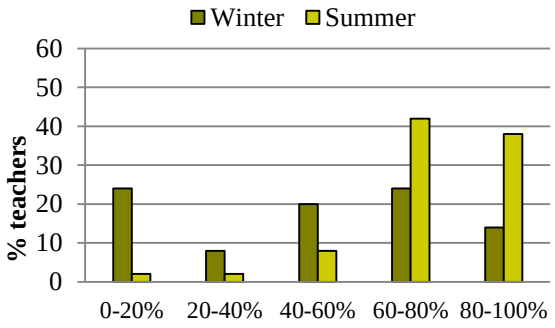

Fig.5. Perceived percentage of the school's classrooms that have experienced overheating

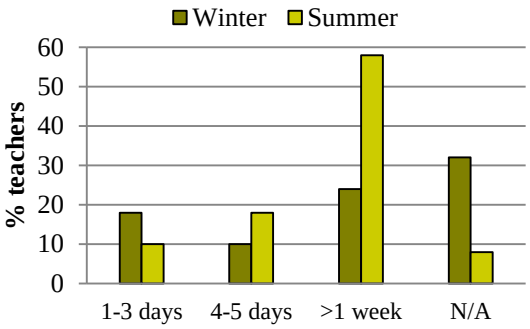

Fig.6. Perceived duration of overheating occurrences in the teachers' classrooms

The teachers were also asked to assess the frequency of overheating occurrences in various school spaces (Fig.7). For the classrooms, 80% of the teachers agreed that overheating occurs very often while for the assembly hall, circulation areas and library the responses are less pronounced. This difference in perception may be related to the characteristics of the classrooms (high occupancy density, large windows, small window openings, internal gains etc) but it may also be due to the stronger concern of the teachers for the spaces where most of the school activities take place.

Fig.8 shows the months which are perceived to cause greatest classroom overheating during the school occupancy periods. As expected, June and July were indicated by almost all respondents as the two months with the greatest overheating problems.

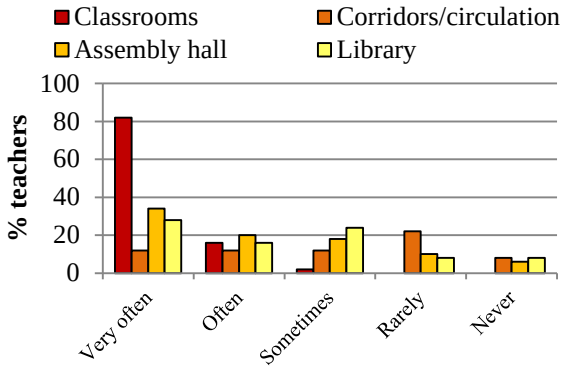

Fig.7. Perceived overheating occurrence in different school spaces

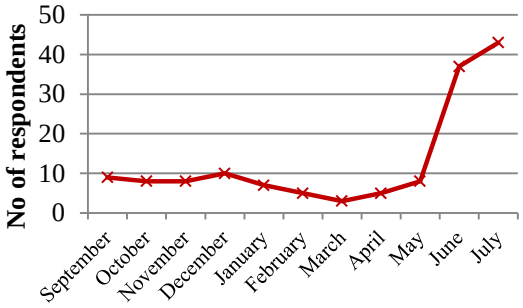

Fig.8. Months perceived to cause greatest overheating (School year: Sept '09-July '10)

5.3. Possible causes of overheating and mitigation measures applied by the teachers

In an open question the teachers indicated the factors which they believe to drive overheating in their classroom (Fig.9). Poor ventilation, a poorly controlled heating system and the number of students were the most frequent answers followed by room size and not-openable windows.

Achieving appropriate ventilation is a problem in many classrooms as cross ventilation is not possible. Also, in all 4 schools the windows open only to a certain extent and the internal shading obstructs the air flow. The heating system was often highlighted as an issue because some teachers cannot control it in their classroom or they weren't aware that they could.

The students' habits and behaviour towards heat stress were identified as a point of concern. According to some teachers, children may be clearly too warm and yet do not take off their jumpers or ask for help. Teachers felt that children's perception of heat is different from adults and that this should be taken into account when school buildings' thermal conditions are studied. This furthermore indicates that more research is needed addressing the perception of children, looking at temperature thresholds from a children's perspective and the implications of classroom overheating for their learning experience.

Fig.10 shows the measures taken by the teachers when overheating occurs. The question was fixed-response with the opportunity to add further measures. All teachers selected window opening and almost everyone drinking of water.

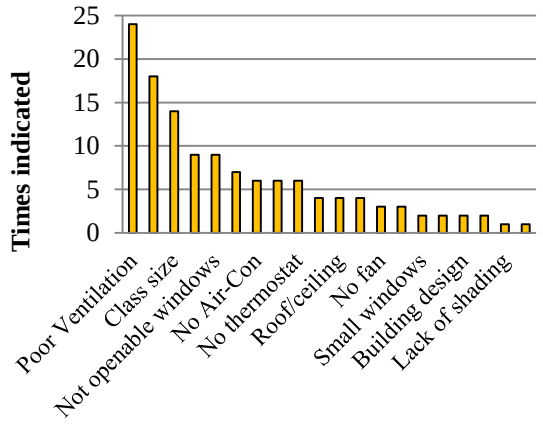

Fig. 9. Causes for overheating of their classroom according to teachers' responses

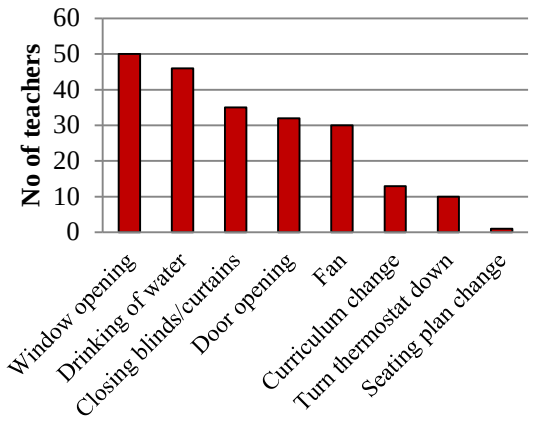

Fig. 10. Mitigation measures taken by teachers when overheating occurs

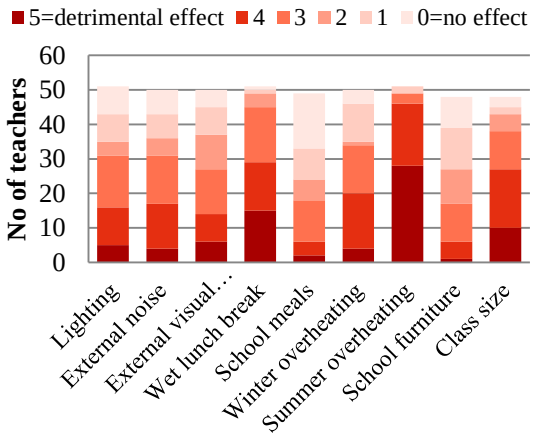

Fig. 11. Perceived effect of different factors on students' learning experience

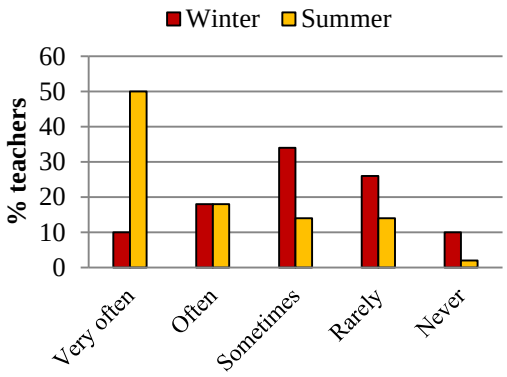

Fig. 12. Complains from children about excessively high temperatures in classroom

5.4. Impact on students

The teachers were asked to rate 9 factors in terms of their impact on students' learning experience, using a scale of 0-5, 0 representing no impact and 5 standing for a highly detrimental impact. As shown in Fig.11, summer overheating gathered the largest number of 5 and 4 rates. This is followed by a wet lunch break and the class size (number of occupants in classroom). However, it should be taken into account that this result may have been affected by the specific interest of the survey in summer overheating.

Teachers were also asked whether students have complained about excessively high temperatures (Fig.12). 50% of them said that this was 'very often' the case during the non-heating season and some noted that children may not complain even though they feel discomfort.

6. Discussion

This work investigated the overheating risk of four UK schools through an aerial photo analysis and a questionnaire survey of the schools' teachers. The aerial photo analysis suggested a high overheating risk within all 4 schools which was verified by the teachers' survey responses. However, a detailed comparison at the classroom level showed variations in individual responses for the spring and autumn months. This appears to indicate that the individual perception of thermal comfort may outweigh the impacts of the building's design and its surrounding landscape conditions on indoor temperatures. The teachers' observations that children may have a different thermal perception to adults suggest that more work is needed looking at the relation between children's perception and building overheating.

The study furthermore highlighted that teachers are often not aware of how their classroom operates (widow opening, heating system). Therefore, low-cost measures such as training may be an effective way to address hot classroom conditions and should be explored prior to taking any retrofitting measures.

References

[1] NASUWT, Safe to Teach? Health and Safety at Work, Birmingham, 2008.

[2] D. P. Wyon, Studies of Children under Imposed Noise and Heat Stress, Ergonomics 13, 1970, pp 598 - 612.

[3] D. P. Jenkins, A. D. Peacock, & P. F. G. Banfill, Will future low-carbon schools in the UK have an overheating problem?, Building and Environment, 44, 2009, pp 490-501.

[4] Hansard Parliamentary Debates, Vol. 513, col. 47, 5 July 2010.

[5] M. Santamouris, & D. Asimakopoulos, Passive cooling of buildings, James & James, London, 1996.

[6] UK-Parliament, Climate Change Act, The Stationery Office Limited, 2008.

[7] T.R. Oke, Boundary layer climates, Methuen, London, 1987.

[8] F. S. De La Flor, & S. A. Domínguez, Modelling microclimate in urban environments and assessing its influence on the performance of surrounding buildings. Energy and Buildings, 36, 2004, pp 403-413.

[9] B. Givoni, Climate considerations in building and urban design, Van Nostrand Reinhold, New York, 1998.

[10] CIBSE, Guide A-Environmental design, Chartered Institution of Building Services Engineers, London, 2006.

[11] G. J. Jenkins, M.C. Perry, M.J. Prior, The climate of the United Kingdom and recent trends, Exeter UK: Met Office Hadley Centre, 2008.

[12] G. J. Jenkins, J. M. Murphy, D. M. H. Sexton, J. A. Lowe, P. Jones & C. G. Kilsby, UK Climate Projections: Briefing report. Exeter, UK: Met Office Hadley Centre, 2009.

Energy retrofit and indoor environmental requalification of existing school buildings. Method and tools for operating procedures

Paola Boarin[1,*], Pietromaria Davoli[1]

[1] *University of Ferrara, Department of Architecture, Architettura>Energia Research Center, Ferrara, Italy*
** Corresponding author. Tel: +39 0532293631, Fax: +39 0532293631, E-mail: paola.boarin@unife.it*

Abstract: Within the existing building stock, schools occupy a large segment of public real estate but are rarely involved in widespread retrofit investment plans. For example, according to Italian statistics, two thirds of existing schools are hosted in buildings constructed between 1940 and 1990, many of which have not undergone substantial changes and transformations over time. Verifications made by Public Administrations and users demonstrate that these structures have many building problems related to the consumption of resources, the well-being and security of users and, not least, the management by local government units.
Operating substantially and in a scheduled way on existing school buildings, by adapting the physical environment and optimizing the use of resources, would, on the one hand, increase the quality of construction and conditions of use (and then last but not least the effectiveness of the educational system) and, on the other hand, improve the economic management of resources by local government units.

Keywords: *Existing educational buildings, Energy retrofit technologies, Indoor climate enhancement, Operating procedures.*

1. Introduction

Within the Italian existing building stock, schools occupy a large segment of public real estate (throughout the country there are about 42,000 schools). Schools host a very sensitive group, but currently don't provide the necessary well-being and use a large amount of resources. Nonetheless, they are rarely involved in widespread investment projects of national interest. The national annual reports provided by Legambiente [1] show that about 1 out of 3 buildings needs urgent maintenance because of many problems related to resource consumption, indoor environmental quality, security conditions and management by Public Administrations.

The present paper presents the results of a syudy aimed at establishing planned, systematic, substantial and integrated operating procedures for energy retrofit and indoor environmental quality enhancement on existing school buildings to increase construction quality, reduce energy consumptions and optimize economic management of resources by the Owner. Even if this topic has already been developed on the international landscape (IEA ECBCS Annexe 36 [2] is one of the most important experience), it hasn't found a pragmatic approach yet in Italy where, because of the low qualification of the public technical staff and of the few economical investments by the Owners, it is (and even more will be in the next few years) a real problem for Public Administrations from the economical, management and security points of view.

2. Methodology and phases

Given that the Ministry of Education or Local Goverments do not provide any comprehensive technological database concerning building elements and plant systems, it has been decided to directly investigate an existing school building stock by studying a sample of buildings that has been considered to be representative of the wider national situation (different climatic conditions, various building technologies and plant systems, different energy contracts and management). The survey procedure has been essential to define energy benchmarks and technological state of the art that has been compared with best practice projects, choosen from national and international landscape and concerning exemplary and innovative requalification

processes on existing school buildings. The direct results of the study sample survey have been compared with the performance requirements coming from national regualtions and lows that are considered to be the minimum level of success of the future retrofit strategies. Retrofit measures has been defined through: energy and environmental goals (from the previous survey and best practice analysis), needs-performance framework (from low and regulations) and best technical solutions for energy and quality enhancement (referring to the outcome state of the art of the surveyed study sample).

The operating procedure has been systematically developed to support decision-makers during the retrofit strategy choice, considering performance targets, technological (energy saving and environmental quality enhancement) and economical (payback period optimization) aspects, people involved (technical staff, Owners, Designers, Energy Managers) and in order to obtain an appropriate management of the existing school building stock.

3. State of the art: the technological point of view

The study sample has focussed on the municipalities and provinces of Rovigo, Ferrara and Modena and has been composed of 232 buildings. The abovementioned municipalities and provinces have been chosen because of the information available and their geographical location, in a temperate area requiring more attention in the building and plant system design. The survey shows that existing school buildings of the study sample are in a critical situation.

Table 1 List and geographical distribution of the study sample.

Municipality or Provincial Administration	Number of investigated buildings
Municipality of Ferrara	53
Province of Ferrara	27
Municipality of Rovigo	25
Province of Rovigo	24
Municipality of Modena	69
Province of Modena	34
Total	232

Table 2 Overview results of existing buildings actual technological features.

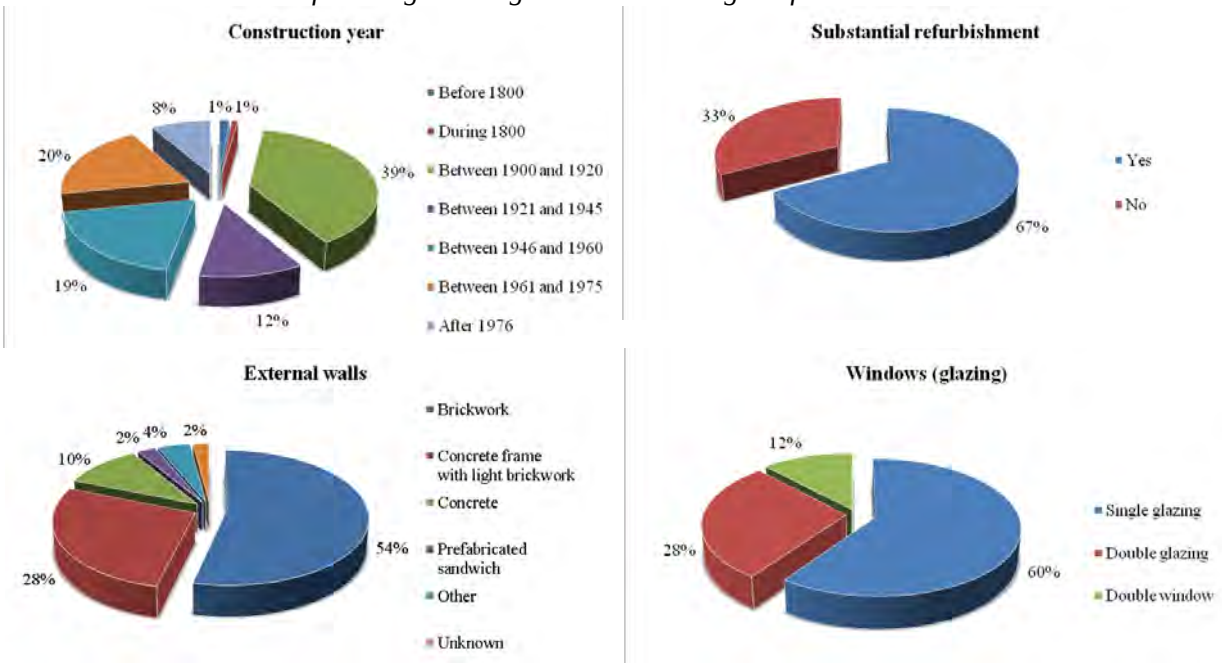

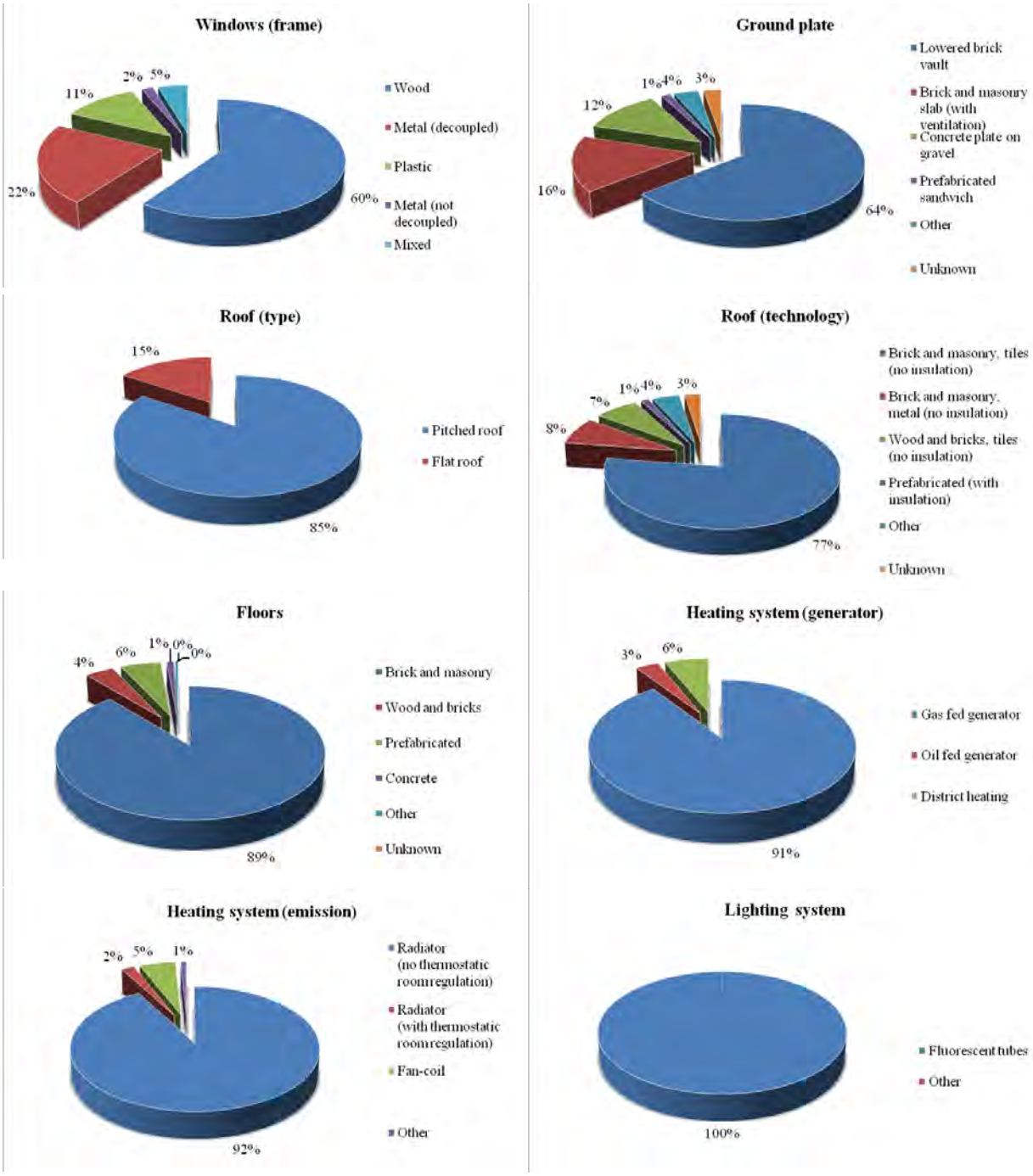

3.1. Building envelope

From an energy point of view, heat losses through the building envelope are mainly due to the lack of thermal insulation in walls, roofs and ground floors. Traditionally, Italian constructions have a strong brick enclosure, which can be single layered or combined with other materials (concrete blocks, plaster, stone and wood), and whose performance is particularly poor in buildings dating from the Fifties and Seventies.

Even windows and glazed systems have a very low performance. This aspect is particularly relevant because school buildings have many large window areas in order to archieve lighting targets. The study sample also has a low proportion of low-emissivity glass (most of the buildings are single-glazed) and frames, which are primarily wooden but without seals, or

metal but not thermally decoupled. Importantly, however, windows replacement is the owner's first item of intervention.

3.2. Heating system

Investigated school buildings have traditional heating plant systems (consisting of boilers which are mainly powered by natural gas) with no zoning. The output terminals in classrooms are large radiators, mostly made by cast iron, which, with rare exceptions, don't have any thermostatic control valves or any room regulation. Because of the amount of air to be heated, mechanical ventilation systems (without any heat recovery) or plants heaters (fan-coils) are often used in larger rooms (gymnasiums, lecture halls, laboratories). The employment of air heating system (air vents) is much more limited in classrooms, because of noise transmission, air movement and filter maintenance. Mechanical ventilation systems are also rarely used and are almost completely absent in the existing school buildings which have been evaluated.

3.3. Summer air conditioning system

Since school buildings are used in Italy from September to June, air conditioning systems are quite rare and the study sample has confirmed this trend. The only exceptions to be found are school staff offices where low-performance and high-consumption independent air conditioning units which are not connected to the centralized system have been installed.

3.4. Lighting system

The investigation demonstrated that schools are only lightened by fluorescent tubes without any occupancy sensor (for example in hallways or bathrooms) or automatic dimming of light intensity according to the amount and distribution of natural light in classrooms.
Beside the absence of energy saving devices, a comprehensive design based on different lighting needs in classrooms (especially to avoid glare and to promote a homogeneous distribution of natural light) and in other parts of school buildings is also lacking.

3.5. Energy sources

Natural gas is currently the most widely used energy source, but few buildings still use diesel. Usually, these are isolated buildings located in the outskirts of cities and villages which are not yet served by the distribution network because of local conditions. A good practice is the connection to the district heating network, but it is still incomplete and quite limited in some areas. Renewable energy sources (mainly photovoltaic and solar thermal) have begun to be used only in recent years, particularly in structures with continuous use and extra-curricular functions.

4. The operating procedure: application phases

Enery and environmental analysis of the study sample direct survey data have demonstrate how existing educational buildings are distant from the minimum performance requirements given by lows and how uncomfortable many scool buildings are for occupants. The operating procedure minimum level of success is the archievement of the minimum performance values given by national lows and regulations for the parameters that are responsible of considerable variations of energy consumption and environmental quality (air, temperature, humidity, lighting, noise). The further level of success is the archievement of the maximum level of energy saving and indoor environmental quality enhancement (increasing comfort perceived by occupants), together with the optimization of the Owner's economical investment.

Therefore, the operating procedure deals with several topics (technology, energy, economy, management, etc.) which are considered in subsequent and linked phases and should be seen as a decision support tool for recovery strategies of existing educational buildings.

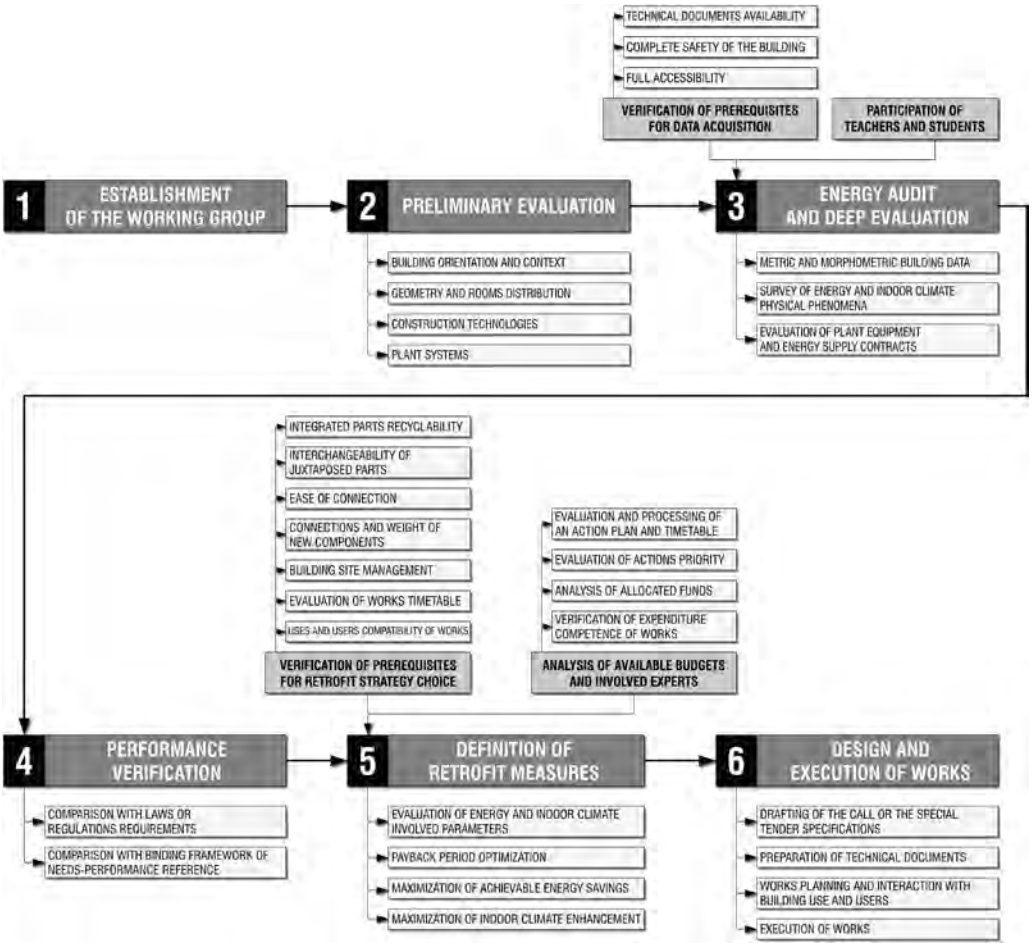

Fig. 1 Operating scheme of energy and indoor environmental refurbishment process.

4.1. Step 1: establishment of the working group

The first step of the procedure is the establishment of a working group composed of people involved in the management, design and educational process. At this stage, several stakeholders meet the Public Agency that promotes the intervention, which ca be the municipality or the province depending on the specific competences on the school building stock; the Educational Institution, that has the double task of informing about the critical problems related to the use and to initiate educational activities to raise awareness among students (for example, daily actions aimed at savings and at the management of energy resources); the Designer, who is tasked with drawing up the project and coordinating the activity; and the Energy Manager, who optimizes energy management in different building redevelopment stages.

4.2. Step 2: preliminary evaluation

The second phase is a preliminary evaluation of the existing building, aimed at identifying morphological features and general technologies which are useful to define the retrofit strategy to be adopted. In particular, the following aspects must be evaluated:

- building orientation and evaluation of the surrounding natural or urban elements that may affect energy and environmental behaviour (shading from adjacent buildings that limit solar direct gains, proximity to noise sources, presence of vegetation shielding, etc.);

- building type (geometry) and internal distribution of rooms. This can be done by reading the project plans with their subsequent modifications and implementations. This information is aimed at finding a first guidance for action based on the savings potential inherent in any type of building;
- existing construction technologies of technical element. Information in this regards can be retrieved in the project documentation submitted during the execution of works (if any), in owner's and manager's databases or through a direct visual examination;
- plants systems. This can be studied basing on the direct experience of Energy Managers or through visual inspection of books and equipment (in this case, the potential for savings depends not only on the optimization of the plant system, but also on the verification of the supply contracts, especially in the context of energy market liberalization).

The most critical part of this phase is the definition of the technological features, due to owner's or managers' lack of knowledge about construction techniques and plants systems of the building heritage. Public Administrations do not usually have any monitoring tools to manage the building stock and leave the transmission of information to the "historical memory" of the contractors carrying out maintenance.

4.3. Step 3: energy audit and deep evaluation

This phase may require external professional support to evaluate parameters that affect energy and environmental building behaviour. There are three main subtasks:

- determination of metric and morphometric building data for calculation of gross floor areas, heated volume and dispersant surface, aimed at energy evaluations;
- survey of physical phenomena related to energy and environmental building behaviour concerning the whole technological system (enclosures and internal partitions), by studying the main factors affecting energy consumption and indoor comfort (air, temperature, humidity, lighting, noise);
- evaluation of plant equipment and energy supply contracts (which may cause consumption not attributable to the efficiency of plant system).

Since this phase requires where direct investigations on the building several conditions must be met to be able to gather data, such as:

- full accessibility to different parts of the building, including basement, attics and spaces normally closed to the public;
- guarantee of the complete safety of the building;
- availability of technical original and subsequent versions of design documents, as a basis for the determination of the status quo.

4.4. Step 4: performance verification

The fourth phase, which is closely linked to the previous one, is a comparison between measured performance and laws or regulations requirements in relation to the parameters involved in energy consumption and indoor environmental quality. By comparing the actual performance and with the binding framework of needs-performance reference for each building element, the main critical elementsd of the existing building are identified.

4.5. Step 5: definition of retrofit measures

The people involved are the same as in the preliminary working group but the Designer is definitely the emerging personality. He is tasked with coordinating the different needs and defining technically and morphologically relevant design solutions.

Before planning any activity, the presence of some prerequisites has to be verified, as:

- compatibility of works with building uses and users;

- evaluation of the works execution timetable and its relationship with school activities;
- management of building sites (possibility of storage of materials, accessibility, etc.).
- connections and weight of the new components compared to existing structures;
- ease of connection of any new elements to existing structures;
- interchangeability of juxtaposed parts related to future opportunities for interventions;
- recyclability of integrated parts.

Apart from these considerations, the Designer shall, in collaboration with the Promoter, verify and analyze the available budget and experts involved through:

- a preliminary verification of expenditure competence of the works
- an analysis of the funds allocated by the local Administration or the Owner;
- the evaluation of the actions to be performed depending on the priority and urgency of interventions;
- the evaluation and development of an action plan accompanied by a timetable.

Once these steps are completed, the most appropriate intervention strategy can be chosen basing on the evaluation process (preliminary or in-depth), the issues raised during the performance evaluation (energy and environmental factors involved), the Owner's budget or investments availability and the main features of the building site. Given that these involved factor are several and complex, it has been decided in the study to define a panel of retrofit measures [3], aimed at finding the best technical solution for the specific case and based on the need-performance requirements. Therefore, the action to be identified are those which can optimize the payback period (expressed in years), maximize the energy savings (expressed by the percentage reduction of primary energy consumption compared with the previous condition) and enhance the environmental quality to the greater extent (expressed by an occupant's sensation scale from 0 – neutral to +2 – considerably perceived; action with negative influence on occupants' perceived comfort will not be taken into consideration).

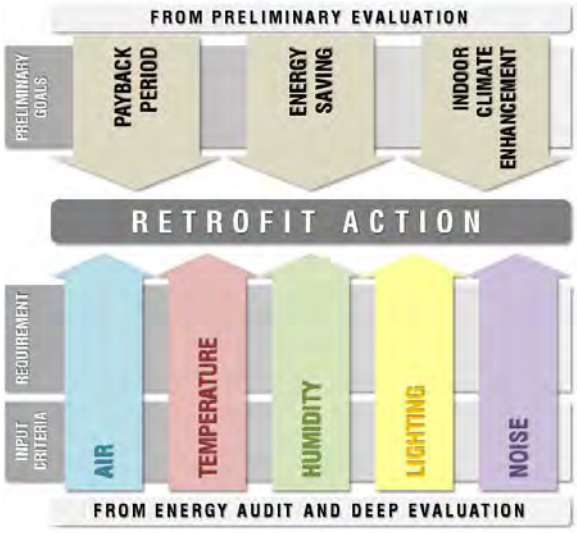

Fig. 2 Main criteria involved in the definition of operating procedure's retrofit actions, starting from preliminary or deep evaluation of existing educational building.

4.6. Step 6: design and execution of works

This phase includes the following:

- drafting of the call or of the special tender specifications;
- preparation of technical documents in collaboration with other experts and stakeholders involved (the document will be entirely drafted by the Administration in case of internal procedure, otherwise they will be contracted out to Designers);

- works planning taking possible interaction with building use and users into consideration;
- execution of works.

The drafting of the documents containing the technical specifications of the project and for the tender is the most critical point of this phase. This phase may be rather long because of the high number of experts to be involved and the unexpected prolongation of the timing of the tender. In addition, the organization of timing and of the different phases of the works, together with the potential overlapping with school activities, may lead to moving classes in other temporary structures, is another complex aspect in this phase.

5. Further suggestions

5.1. The potential of integrated and optimized procedures for morphometric and energy data collection on existing buildings

The current research in the field is even more focussed on the definition of integrated and optimized procedures for data gathering by integrating experimental acquisition methods and instruments (advanced survey). Consequently, proper planning and scheduling of all survey phases is crucial, with the aim of determining an optimized sequence of steps for acquisition, processing and management of data. Each phase is not independent and autonomous, but functional and closely related to the others. Thanks to technological innovation and economic competitiveness, the more advanced techniques are reaching levels that make them comparable with traditional ones, but with the addition of the features of the advanced survey, especially in terms of productivity because they significantly increase the amount of information gathered, reducing the time needed for the survey.

5.2. Importance of post occupancy evaluations and participatory management

Once works have been executed, it is essential to carry on with building management activities, i.e. all operation, maintenance and monitoring phases on the reskilled building aimed at comparing project design criteria to real performances obtained. They include:

- students awareness and training on how to use the building in a proper way in order not to waste energy that would result in a reduction of the achievable savings and, therefore, in the extension of the payback time.
- participatory management of the redeveloped building through the involvement of users;
- post-occupancy evaluation, also through the participation of users (even students and teachers) to data acquisition and monitoring of the building;
- periodic monitoring of contracts for energy management, consumption and counters, to be carried out by an Energy Manager.

References

[1] Legambiente, Ecosistema Scuola. Rapporto di Legambiente sulla qualità dell'edilizia scolastica, delle strutture e dei servizi, 2010, pp. 77, http://risorse.legambiente.it/docs/ECOSISTEMASCUOLA-2010.0000000962.pdf.

[2] IEA ECBCS - International Energy Agency - Energy conservation in buildings and community systems programme, Working group on energy efficiency in educational buildings. Final Report, 1996, pp. 108, www.annex36.com/index.html.

[3] Boarin P., Edilizia scolastica. Riqualificazione energetica e ambientale, EdicomEdizioni, 2010, pp.336.

Analysing the energy performance of secondary schools in N. Greece

Vagi F. [1], Dimoudi A.[1,2,*]

[1] *Hellenic Open University, MSc 'Environmental Design of Cities and Buildings', Patras, Greece*
[2] *Department of Environmental Engineering, Democritus University of Thrace, Xanthi, Greece*
** Corresponding author: Tel./Fax: +30.25410.79.388, E-mail: adimoudi@env.duth.gr*

Abstract: Aim of this paper is the analysis of the energy performance of secondary school buildings in North Greece and the investigation of proposals for their energy upgrade. The survey was carried out by monitoring the energy performance of 20 secondary school buildings in the prefecture of Evros in Thrace and by simulating representative school buildings. Energy data both for heating and electricity, together with other information concerning structural details and operational characteristics for a period of 5 years (2001-2005) were collected. The energy data for the secondary schools are presented and compared with data from other regions in Greece. The mean heating energy consumption of secondary school buildings in the prefecture is 70.6 kWh/m^2, with insulated buildings performing with 27% less energy consumption than non-insulated buildings. Simulation of representative school buildings in this area suggests that measures for natural lighting, reduction of infiltration losses, controlled ventilation during the winter, shading and natural ventilation during summer and the effective functioning of heating and lighting system are the major priority for the school building stock. Especially in the 'old school buildings', this type of interventions are necessary not only for achieving energy efficiency but for obtaining thermal comfort conditions in their interior.

Keywords: *Energy efficiency, Schools, Monitoring, Simulations*

1. Introduction

The mean annual energy consumption of buildings in Greece is allocated as : 406.8 kWh/m^2 in hospitals, 273 kWh/m^2 in hotels, 187 kWh/m^2 in offices, 152 kWh/m^2 in commercial buildings and 93 kWh/m^2 in schools [1]. Although the energy consumption in school buildings is lower than other building categories, the overall energy consumption at national level is considered high due to the big number of school units, and the fact that they mainly operate during the heating period - they operate about 9 months -, they are not equipped with cooling systems and the majority of energy is spent for heating. The inadequate energy design of existing buildings, their age (40.9% is older than 30 years), their initial design (87.3% designed for schools), their location and proximity with disturbance sources (33.5% with high traffic roads, 15.9% with manufacturing premises and polluting areas), lack of regular maintenance and refurbishment can lead to education spaces with low thermal, visual and noise comfort, at reduction of pupils educational perception and additionally, at considerable environmental implications as a result of the increased energy consumption [2].

School buildings, due to their specialized operational characteristics and their social/ educational character have special requirements for environmental design for heating, cooling, ventilation and daylighting of their buildings. Collection of reliable energy data can facilitate to creation of a national data base that is useful to support reliable energy certification of school buildings and also to facilitate national energy policy measures to be taken. Aim of this paper is the analysis of the energy performance of secondary school buildings in North Greece and the investigation of proposals for their energy upgrade.

2. Methodology

2.1 Energy Consumption in School Buildings

All school units in Greece are equipped with heating systems (99.9% during the school year 2003-04) and the majority has a central heating system (88.0%). According to the opinion of

the Master of the school units, a portion of 11.1% considered as inadequate the operation of the heating system and in only 1.5% there was lack of heating operation during the years 2003-04 [2]. The energy consumption of school units, irrespective of education level (primary, secondary) based on previous surveys carried out in school units around Greece is reported in table 1. School buildings in Greece consume electrical energy mainly for artificial lighting and during the lasts years, especially in secondary schools, for new technologies (e.g. PCs). The mean energy consumption for heating and electricity in school buildings in other European countries, based on data from EC (Energy, E. C, 2000) [7] and other literature sources [8, 9, 10] are presented in table 2:

Table 1. Mean annual energy consumption in school buildings in Greece

Region / Climate zone	Year of research	No of buildings	Mean heating energy (kWh/m^2)			Mean electrical energy (kWh/m^2)
All Greece [1]	1993	238		67	Difference 40%	26
All Greece [3]	2006	340		68		27
Evros / C Climate zone [4]	2001-2005	10 primary Schools	No-insulated 89.4	72.8 Insulated 56.65	Difference 37%	8.65
Grevena / D Climate zone [5]	2004	9	No-insulated 139	123.31 Insulated 115.38	Difference 17%	14.31
Kozani / D Climate zone [6]	2003-2007	11 nursery 10 primary		135.9 105.8		7.5 9.3

Table 2. Mean annual energy consumption in school buildings of the member states of the European Union [7, 8, 9, 10]

Member States of the European Union	Heating energy (kWh/m^2/ year)	Electrical energy (kWh/m^2 /year)	Mean annual (kWh/m^2/year)
England (Mean value)	137-189	20-27	
Secondary school (Gateshead)	177		
Denmark (Skive)			
Primary school	170-175		
Sweden (Karlskrona)			
Secondary school	210		
Portugal (Agueda/Crato)			
Secondary school	64 /67		
Ireland [8]			96
Italy [9]			110
Slovenia [10]			192

3. Energy monitoring of secondary school units in the prefecture of Evros

The energy monitoring survey was carried out in 20 secondary school units out of 45 in the prefecture of Evros (NE Greece) covering 10 Junior High Schools, that is the 42% of corresponding units in the prefecture and 10 High Schools, corresponding at 48% of the

majority of high schools in the prefecture. The 5 out of the 10 junior high schools were located at the municipality of Alexandroupolis (the capital of the prefecture) thus, corresponding at 83% of the units in the municipality. The 8 out of 10 high schools were also located at the municipality of Alexandroupolis, covering the 63% of high schools in the municipality. During the survey, energy data for 5 years were collected (2001-2005), both for heating and electricity, together with other information concerning structural details and operational characteristics (e.g. no of pupils, heating system operation schedule, etc).

Table 3: Total mean annual energy consumption in 10 junior high schools of Evros Prefecture during the period 2001-05

			Heating energy			Electricity		Total
No	Construction year	Heating floor area (m^2)	Oil cost (Euro)	Oil quantity (kg)	*Heating energy (kWh/m^2)*	*Cost (Euro)*	*Consumption (kWh/m^2)*	*Total energy (kWh/m^2)*
1	1964	2.048.62	6,834	13,524.84	78.69	2,510	12.90	91.59
2	1976	2,300	7,420	14,605.08	75.69	1,724	7.89	83.58
3	1978	2,214	4,835	9,746.52	52.47	1,809	8.60	61.07
4	1978/ 1992	3,089.6*	6,055	12,437.04	78.72	4,339	14.78	93.50
5	1980	902.23	4,761	9,476.04	125.19	975	11.38	136.57
6	1986	809	2,826	5,765.76	85.00	649	8.45	93.45
7	1990	2,745.54	6,318	12,588.24	54.65	2,250	8.63	63.28
8	1992	1,613.15	4,008	7,847.28	57.99	1,720	11.22	69.21
9	1996	2,398.5	5,414	10,887.24	54.11	2,023	8.88	62.99
10	1957/1995	2,348.96	5,350	11,340	57.55	1,928	8.64	66.19
		Total Mean Consumption:			72.00		10.14	82.14

* 1,883.15 (1978) + 1,206.45 (1992) = 3,089.6 m^2

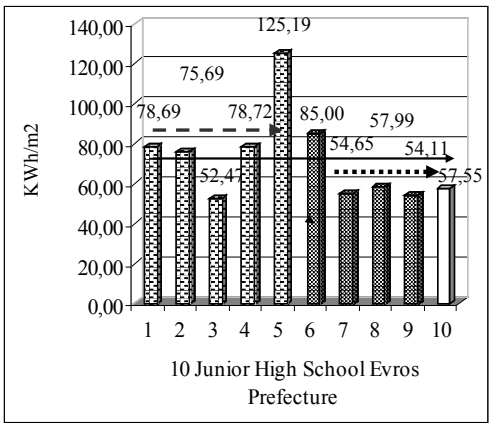

Fig. 1: Mean heating energy consumption in a sample of 10 junior high schools in the Prefecture of Evros for the period 2001-05

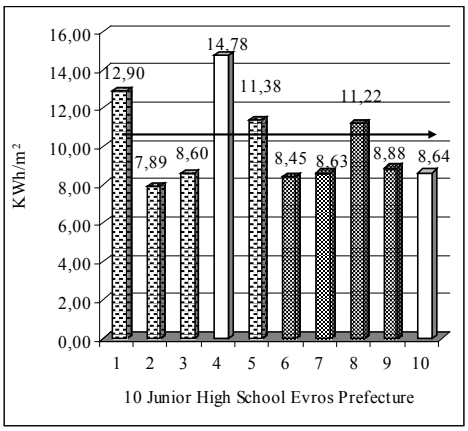

Fig. 2: Mean electrical energy consumption in a sample of 10 junior high schools in the Prefecture of Evros for the period 2001-05

Mean heating energy consumption for:

non - insulated junior high schools (1, 2, 3, 4, 5) :	82.16 kWh/m^2
insulated junior high schools (6, 7, 8, 9):	62.94 kWh/m^2
"Old" with "New" additions in junior high schools (4, 10) :	57.55 kWh/m^2
All junior high schools	72.00 kWh/m^2

The monitored energy consumption data, based on data of 5 years for the period 2001-2005, together with the construction year are summarized at tables 3 and 4 for the junior high schools and high schools respectively. The annual records for heating costs were available in each school and these values were quantified into energy consumption (in kWh/m^2) based on the mean annual price of diesel oil from the records of the Ministry of Development.

It is observed from figure 1 that the heating energy consumption in junior high schools ranges from 52.47 kWh/m^2 up to 125.19 kWh/m^2, with a mean value of 72 kWh/m^2, showing the higher values in 'old' buildings. Building 10 concerns an old building with an addition and its energy consumption is in the levels of the 'new' buildings. Junior high school no 4 is "old" with "new" additions, but the heating energy consumption concerns only the 'old' buildings while the electricity energy consumption both of them.

Table 4: Total mean energy consumption in 10 high schools of the Prefecture of Evros (2001-05)

			Heating energy			Electricity		Total
No	Construction year	Heating floor area (m^2)	Oil cost (Euro)	Oil quantity (Kg)	Heating energy (kWh/m^2)	Cost (Euro)	Consumption (kWh/m^2)	Total energy (kWh/m^2)
1	1970	3,300	10,828	21,215.04	76.63	4,104	13.09	89.72
2	1976	2,100	6,091	12,122.88	68.81	2,126	10.66	79.47
3	1976	4,405	20,103	40,057.92	108.39	7,032	16.8	125.19
4	1977	2,030	7,917	16,136.40	94.75	2,547	13.21	107.96
5	1981	3,500	18,799	39,170.88	133.4	6,595	19.83	153.23
6	1984	1,377	5,866	11,103.96	96.12	1,222	9.34	105.46
7	1985	2,716	7,768	15,333.36	67.3	2,969	11.51	78.81
8	1987	2,067.5	4,057	7,866.60	45.35	3,095	15.76	61.11
9	1996	1,404	3,609	7,203.84	61.16	2,009	15.06	76.22
10	1999	2,398.,5	6,646	12,701.64	63.12	3,523	15.46	78.58
		Total Mean Consumption:			81.50		14.10	95.60

Concerning high schools (fig 3), the heating energy consumption ranges from 45.35 kWh/m^2 up to 133.40 kWh/m^2 with a mean value of 81.5 kWh/m^2, showing the higher values in 'old' buildings. Energy consumption in units no 3 and 5 is increased (table 4 and fig. 3 και 4) as they concern technical high schools, which are equipped with different laboratories (mechanical, computers, horticulture sunspaces, etc), resulting at high energy consumption.

The mean electrical energy consumption is 10.14 kWh/m^2 in junior high schools 14.10 kWh/m^2 in high schools (tables 3 and 4) and 8.56 kWh/m^2 in primary schools in the prefecture of Evros [4]. The electrical energy corresponds only to about the 1/6th of the heating energy (fig. 5 and 6), mainly in the 'old' buildings', while in the new 'ones', electrical energy has a higher merit at the overall energy balance as the heating energy is reduced due to the improved building construction.

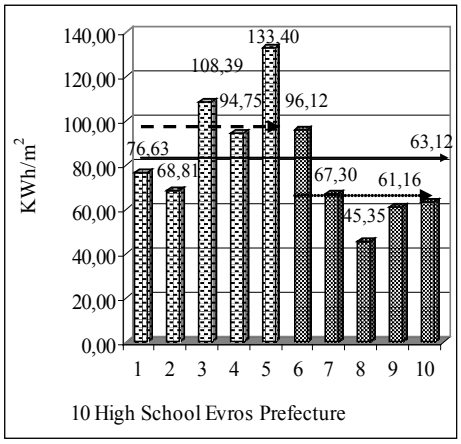

Fig. 3: Mean heating energy consumption in a sample of 10 high schools in the Prefecture of Evros for the period 2001-05

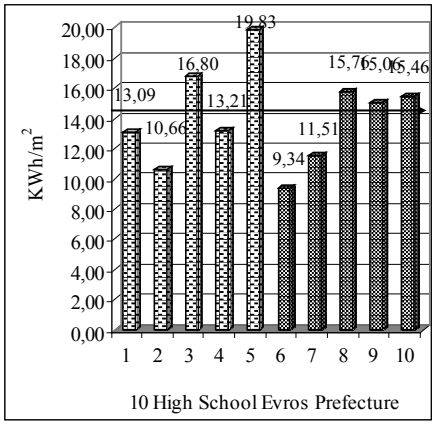

Fig. 4: Mean electrical energy consumption in a sample of 10 high schools in the Prefecture of Evros for the period 2001-05

Mean heating energy consumption for:

non-insulated high schools (1, 2, 3, 4, 5) :	96.40 kWh/m^2
insulated high schools (6, 7, 8, 9, 10):	66.61 kWh/m^2
All high schools	81.50 kWh/m^2

The mean heating energy of the school units in the region (Climatic zone C) corresponds at the 85% - 88% of the total energy consumption, compared to 72% that was recorded from previous studies [1] for all grades school buildings around Greece. This may attributed at the low temperatures recorded at this climatic zone and consequently the increased heating needs of the buildings, at the old age of buildings and lack of envelope insulation, at the fact that existing insulation in some buildings may be deteriorated, at the inadequate maintenance of the envelope and of the mechanical installations.

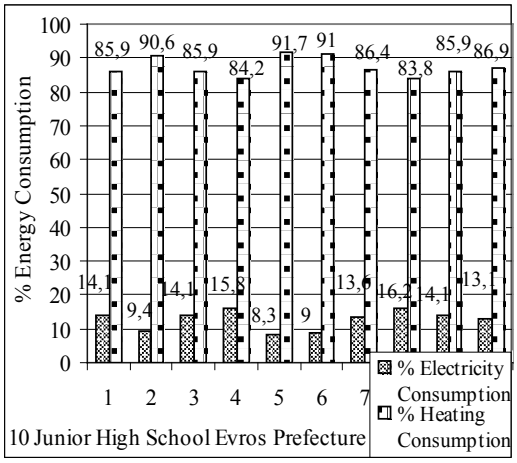

Fig.5: Mean energy consumption for heating and electricity (in %) in junior high schools in the Prefecture of Evros

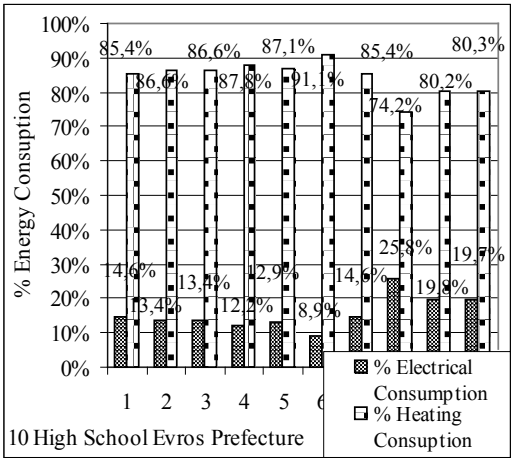

Fig. 6: Mean energy consumption for heating and electricity (in %) in high schools in the Prefecture of Evros

Analyzing the energy performance of all secondary school buildings in the prefecture of Evros (climate zone C) (fig. 7) the mean heating energy consumption is 70.6 kWh/m^2, with insulated buildings ('new') performing with 27% less energy consumption than non-insulated ('old') buildings. The 100% of insulated buildings show an energy consumption less than 100

kWh/m^2, compared to 70% of the non-insulated ones (table 3 & 4). In an older study of 180 insulated and 58 non-insulated school buildings in different climatic zones [1], the heating energy consumption differs between them by 40%, while the 88% of insulated buildings have energy consumption lower than 100 k Wh/m^2 compared to 79% of the 'non-insulated' buildings [1].

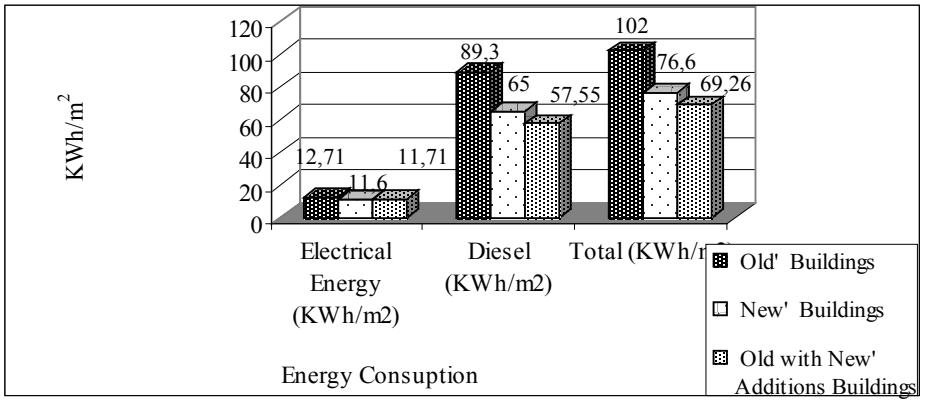

Fig. 7: Mean energy consumption according to the antiquity of 20 sschool buildings

4. Assessment of the thermal performance of 6 school buildings

For the thermal assessment of the school buildings, 6 units were chosen, 5 junior high schools and 1 hi gh school. The 4 junior high schools are located at the municipality of Alexandroupolis, representing 67% of junior high school buildings as well as the high school. From the 6 studied buildings, the 2 are 'old'ones constructed before 1981, and the 4 are 'new' ones, constructed after 1985. The thermal assessment of the studied school building and investigation of alternative energy saving measures was performed with the software tool XENIOS. The XENIOS is a European software tool that was developed in the frame of an Altener programme, partly financed by the EC DG on Energy and Transport. For each building the existing thermal performance was evaluated and alternative scenarios of energy upgrade were investigated.

4.1. Conclusions from the thermal analysis

4.1.1. Heating period

The following conclusions were drawn from the thermal analysis of the six buildings:

- Replacement of the windows with new ones and improving their overall transmittance of windows from 5.2 W/m^{2}K to 2.56 W/m^{2}K in the 'old' buildings resulted at reduction of the energy requirements during the heating period by about 12%. Improvement of the thermal properties of the windows in the 'new' buildings from 3.26 W/m^{2}K to 2.56 W/m^{2}K results at reduction from 1% up to 3%.
- Insulation of the external walls results at reduction of the energy consumption up to 12%.
- Insulation of the building envelope, with addition of insulation at the external walls, roof and windows replacement has an energy reduction up to 25% in 'old' buildings. In the 'new' ones a small energy reduction, in the order of 2% to 3% was observed.
- In most school buildings, the heating system is oversized, not well maintained and in the majority, there is no provision for control of their operation [12, p.25]. Improvement of the efficiency of the boiler up to 90% may bring energy savings up to 27% in all school buildings.
- Improvement of the efficiency of the distribution system, with appropriate pipes insulation, especially in they case they pass through unheated spaces, may bring considerable energy reduction, up to 15% in the studied buildings.

- Control of the indoor air temperature with thermostats in classrooms may lead to energy reduction up to 21% in all studied buildings. Installation of time-controllers, low control, room temperature sensors or external temperature based controllers or more advanced control systems (e.g. optimizers) achieving synchronization of the external and internal climatic conditions with the operation of the heating system can achieve indoor thermal comfort and energy savings. A thermostatic valve in the heating system is considered necessary for achieving the desired temperature in a space and achieving energy savings.
- The combined measures of improvement of the efficiency of the boiler and the distribution system and of the control of the indoor thermal conditions can increase the energy savings up to 52% both in the 'old' and the 'new' ones. Taking into account that in most school buildings, the heating system operates for a few hours, manually, with no room air temperature control, irrespective of indoor thermal conditions and outside climatic conditions and considering that the payback period for the improvement of the boiler and the distribution system efficiency is relatively low, it is considered imperative the replacement of the old systems with new ones.
- Applying all the proposed measures in the studied school buildings, an energy reduction from 53% up to 64% may be achieved.

4.1.2. Cooling period

- Insulation of the walls and of the roof would reduce energy cooling demands in 'old' buildings by about 2% in each case separately.
- Painting the outside surface of the external walls with a light colour reduces by 5% and by 3% the energy demand in cooling loads in the "old" buildings while in the "new" buildings only by 1%. The light colour on the roofs does not show a remarkable change in their thermal performance.
- The installation of interior blinds on all openings of the buildings, especially of southern, eastern and western orientation, may conserve energy of up to 61%.
- Installation of ceiling fans in the centre of each classroom, of power 100-200W, is sufficient to create the conditions for thermal comfort, provided that is combined with adequate shading and natural ventilation [12, p.30]. It may result in conservation of cooling energy up to 100% when combined with shading devices and light colored roof and walls. This is due to the fact that while the limit of thermal comfort in a natural cooled space is 27^{o}C, when a fan operates, the heat is dispersed because of air currents and the comfort level is raised over 29^{o}C.
- Also noctumal ventilation in schools is very effective especially during the hot days where the daily ventilation heats the building. It stores coolness in the thermal mass of the building, thereby reducing the thermal burden of the building during the next day. Schools are kept safe all night, so night ventilation can be applied without any risk.
- Energy conservation with implementation of all scenarios can reach up to 100%. At the same time, thermal comfort conditions are created in the classrooms that are considered necessary for the educational process and also contribute to reduction of air pollution with a lot of environmental and social benefits.

5. Conclusions

To ensure the efficient function of a school building and the reduction of problems that usually arise with time and the use of systems, the proper and regular maintenance of the building and its systems is essential. Collection and analysis of their energy data is essential for monitoring their energy performance and to react by taking the appropriate energy saving measures. In a national context, collection of energy data for different building categories can create reliable databases for certification of buildings and for prioritizing energy policy

measures. The assessment of the thermal performance of the school buildings in this study may provide useful conclusions for the actions to be considered in school building of the C' climatic zone in order to improve energy efficiency and achieve comfort conditions in the working space. Actions like planning and monitoring of an energy management plan, maintenance of the electromechanical installation and regulation procedures of natural lighting, reduction of losses from air infiltration, controlled ventilation for the winter period, shading and natural ventilation for the period of cooling and interventions in the exterior building structure particularly in the "old" school buildings are required, both to achieve thermal comfort and conservation of energy.

References

[1] M. Santamouris, C.A. Balaras, E. Dascalaki, A. Argiriou, A. Gaglia, Energy Consumption and the potential for energy conservation in school buildings in Hellas, Energy 19(6), 1994, pp 653-660.

[2] B. Koulaidis, Mapping of the educational system in school buildings, Athens, Educational Research Centre, 2005.

[3] M. Santamouris, G. Mihalakakou, P. Patargias, N. Gaitani, K. Sfakianaki, M. Papaglastra, C. Pavlou, P. Doukas, E. Primikiri, V. Geros, M.N. Assimakopoulos, R. Mitoula, S. Zerefos, Using intelligent clustering techniques to classify the energy performance of school buildings, Energy and Buildings 39, 2007, pp. 45-51.

[4] F. Vagi, A. Dimoudi, Investigation of energy and comfort conditions in Greek primary schools, Proceedings of the 3rd international Conference on P assive and Low Energy Cooling for the Built Environment, PALENC 2010 & EPIC 2010 & 1st Cool Roof Conf., Rhodes, 29 Sept. – 2 October 2010.

[5] A. Dimoudi, P. Kostarela, Energy monitoring and conservation potential in school buildings in the climatic zone of Greece, Renewable Energy 34, 2008, pp. 289-296.

[6] T.G. Theodosiou, K.T. Ordoumpozanis, Energy comfort and indoor air quality in nursery and elementary school buildings in the climatic zone of Greece, Energy and Buildings 40(3), 2008, pp. 2207-2214.

[7] Energy, European Communities, New Solutions in Energy Utilisation; The guide to sustainable energy technologies for school, European Communities, 2000.

[8] O. Hernandex, K. Burke, O. Lewis, Development of energy performance benchmarks and building energy ratings for non-domestic buildings: an example for Irish primary schools, Energy and Buildings 40(1), 2008, pp. 249-254.

[9] S.P. Corgnati, V. Corrado, M. Filippi, A method for heating consumption assessment in existing buildings: A field survey concerning 120 Italian schools, Energy and Buildings 40(1), 2008, pp. 801-809.

[10] V. Butala, P. Novac, Energy consumption and potential energy savings in old school buildings, Energy and Buildings 29(3), 1999, pp. 241-246.

[11] CRES, Guidelines for Heating-Lighting Comfort and Saving Energy in Primary Schools, Athens, 1996.

[12] S. Yiannas, Environmental Assessment Methods-Environmental Targets and Architectural Programme", in the "Bioclimatic Design of Buildings and Surrounding Space", Patra (Greece), Hellenic Open University, 2001, pp. 307-327.

Optimal design of Net Zero Energy Buildings

Ala Hasan[1,*]
[1] *Aalto University, School of Engineering, Department of Energy Technology, Finland*
** Corresponding author. Tel: + 358 9 470 23598, E-mail: ala.hasan@tkk.fi*

Abstract: The new recast of the Energy Performance of Buildings Directive (EPBD) calls for all new buildings to be nearly zero energy buildings by the end of 2020. Besides, there are many evolving new definitions of Net Zero Energy Building (NZEB) that need to be fulfilled. To achieve the above mentioned targets is quite challenging. In this paper the author presents his approach for the optimum deign method for NZEBs, which is by using combined simulation-optimisation. The method takes the problem as one-integrated design problem, where all possible components of the on-site renewable production, energy conversion, HVAC systems, building envelope and grid-connection are considered together as options in the design. It is a multi-objective problem, because it is to simultaneously minimise energy, CO2 emission, cost and indoor discomfort. Since these are conflicting objectives, thus it is an optimisation problem. An optimisation example is presented, which is solved by two methods: as a single objective problem and a two-objective problem.

Keywords: *NZEB, cost-optimal design, simulation, optimisation*

1. Introduction

The new recast of the Energy Performance of Buildings Directive (EPBD) calls for all new buildings to be nearly zero energy buildings by 31.12.2020 and two years prior to that for new public buildings. The rest of the energy is to be covered by renewable sources. Achieving the above mentioned targets is quite challenging. In order to fulfil the requirements for a Net Zero Energy Building (NZEB), it is to find the answers to the following question: What are the "best" components to be used in the building (materials of constructions, windows, air-tightness, insulation thickness, daylighting .vs. artificial lighting, shading type, etc), in the Heating, Ventilating and Air Conditioning (HVAC) systems (type of systems and equipments) and in the energy supply (including options for on-site renewable energy sources)? Those "best" components used to fulfil the energy target should not impose very high investment costs; otherwise the concept will not be economically viable. Besides, thermal comfort should also be kept on a high level. In addition, those best solutions will be different according to different definitions of the NZEB Concepts (e.g. NZ Site- Energy Buildings, NZ Primary Energy Buildings, NZ CO2 Emission Buildings, NZ Cost Buildings, etc). This leads us to think about: how to find the "best" components since there many targets to be achieved related to energy, cost, indoor-air comfort etc?

Then about the way to design a NZEB: the conventional way is to go first for minimising the energy demand on the building side and then to introduce on-site renewable energy. So is this the "optimum" approach?

In this paper an overview of the general method proposed by the EPBD, and as described by the Buildings Performance Institute Europe (BPIE), for finding cost-optimal solutions for nearly energy buildings is presented. Besides, the conventional method for designing buildings for the fulfilment of the NZEB definition according to the IEA-SHC Task 40 / ECBCS Annex 52 i s also presented. Then, the author presents his own approach for the optimum deign as a part of his position as a research-fellow of the Academy of Finland (2010-2015). The project aims for developing a combined simulation-optimisation tool for the optimal design of the NZEB's.

2. The EPBD recast 2010 and the IEA-SHC Task 40 Annex 52

2.1. The EPBD recast 2010 [1]

According to the recast of Energy Performance of Buildings Directive (2010/31/EU), all new buildings shall be "nearly zero energy buildings" as of end of 2020, and two years prior to that for the public sector. Such buildings should have very high energy performance. The nearly zero or very low amount of energy required should be covered to a very significant extent by energy from renewable sources, including energy from renewable sources produced on-site or nearby. Minimum energy performance requirements should be set for all existing buildings that undergo any energy relevant renovation. Besides it is to specify the level of minimum energy performance requirements for new buildings and renovations by developing benchmark method to achieve cost-optimal levels.

Overview of the cost-optimal method
The method in brief is:

- To define and select representative reference buildings (residential and non-residential, both for new and existing).
- To define combinations of compatible energy efficiency and energy supply measures to be applied to the reference buildings (packages of measures)
- To assess the delivered energy and primary energy of the selected building
- To find the corresponding global costs
- To develop cost curve(s) and derive an optimum.

The EPBD recast prescribes that the cost-efficiency of different packages of measures (combinations of compatible energy efficiency and energy supply measures) can be assessed by calculating and comparing the energy-related lifecycle costs. From the variety of specific results for the assessed packages, a cost curve (global costs .vs. primary energy) can be derived (Figure 1). Global costs are defined as the net present value of all costs during a defined calculation period (investment costs, maintenance and operating costs, earnings from energy produced and disposal costs). It is first to start with packages of measures that comply with the minimum performance requirements in force, and then to find ambition solutions beyond current minimum requirements up to and including nearly zero-energy buildings. The lowest part of the curve in Figure 1 represents the economic optimum for a combination of packages.

To establish a comprehensive overview, all combinations of commonly used and advanced measures should be assessed in the cost curve. The packages of measures should range from compliance with current regulations and best practices to combinations that realise nearly zero-energy buildings. The packages should also include various options for local renewable energy generation. The variety of solutions will form a "cloud" of data points from which a cost curve can be derived. The minimum energy performance requirements are represented by the portion of the curve that has the lowest cost in Figure 1. The part of the curve to the right of the economic optimum represents solutions that underperform in both aspects (environmental and financial). To prepare for higher energy or environmental targets related to 2020, certain Member States might choose even stricter requirements than the economic optimum (left part of the curve). The distance to the target for new buildings "nearly zero-energy buildings as from 2021" is shown in Figure 1.

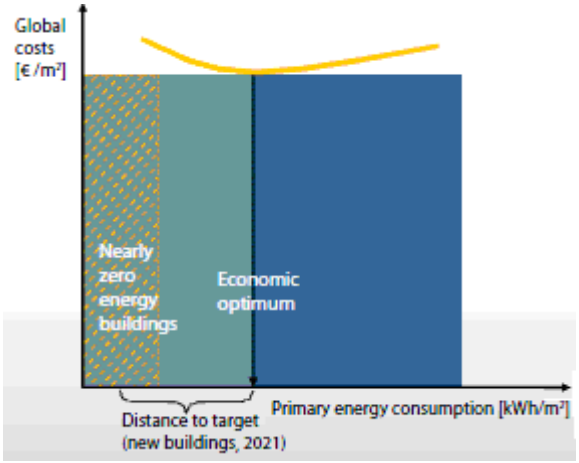

Fig. 1. Cost optimum and distance to target [1].

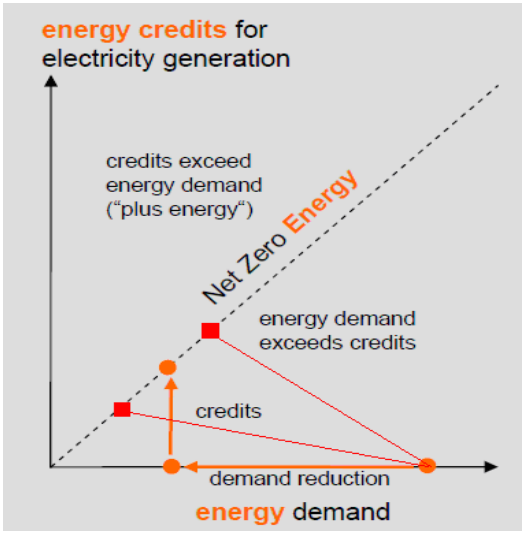

Fig. 2. Conventional way to achieve NZEB [2].

2.2. IEA-SHC Task 40 Annex 52 definition for NZEB [2]

For a NZEB, the balance between energy export (feed-in energy to the grid) and import (delivered energy from the grid) over a period of time must be zero or positive. The following inequality defines a NZEB:

$$Export - Import \geq 0.$$

The balance is normally calculated by means of some credits rather than directly on physical units of energy. The terms of the above inequality are expressed as follows:

$$Import = \sum_i delivered\ energy(i) \times credits(i)$$
$$Export = \sum_i feed\text{-}in\ energy(i) \times credits(i)\ ,$$ where i is the energy carrier.

The credits are therefore the metric used to calculate the balance. Figure 2 gives a graphical representation of the general pathway for the design of NZEBs in two steps (indicated by the orange circles): it is firstly to reduce the energy demand on the building side and secondly to generate renewable energy to get enough credits to achieve the balance.

2.3. Comments on the above mentioned methods

A crucial issue in the EPBD method is how to define the packages of measures (i.e. how can we say that for this package let us take x_1, x_2, x_3 and x_4 as the insulation thickness in the external wall, roof, floor, and the U-value of the window, respectively?). This is also pointed out by the IBPE publication [1]. On the other hand, and even for one package, searching for the optimum values and types of the design variables by making a comprehensive overview of all possible combinations of commonly used and advanced measures is not a simple task. This is because if we make an exhaustive search, the total number of combinations is a result of multiplication of the options for each variable. This will produce a huge number of combinations to be investigated. And then for both EPBD and IEA-Annex 52 methods, the approach should not be split into two steps, firstly reducing the energy demand to nearly zero energy and secondly introducing on-site renewable energy production. This is because if we apply this approach, we will first end-up with an extremely low-energy house or a passive-house before giving a very small chance for on-site renewable energy production to participate in the solution, which is not the best method for all cases (e.g. a case using micro-CHP).

3. Optimum Method for Designing NZEBs

The optimum method is to take the problem as a one-integrated problem, where all possible components of energy production (e.g. on-site renewables), energy conversion (e.g. via heat pumps), HVAC systems, building envelope and grid-connection are considered together as options. It is a multi-objective problem, because it is to simultaneously minimise the targets of energy (heating/cooling energy, primary energy), CO2 emission, cost (investment cost, operating cost, net present value costs), indoor discomfort, etc. Since these are mostly conflicting objectives, thus it is an optimisation problem, where optimal trade-off designs are searched. This holistic approach will produce a huge optimisation problem. However, it could be converted into a manageable size using e.g. problem specifying heuristics and considering most promising components in the building and the HVAC system. An optimisation problem is formulated by specifying the variables and objectives of the problem. The parameters are classified as fixed and variable parameters. These latter we call "design variables", are the ones we seek to find their optimum values that will make the best impact in achieving the objective functions (i.e. targets).

The implemented approach is "combined simulation-optimisation", which is made by coupling the dynamic building simulation program with optimisation algorithms, to find optimal values of the design variables. Figure 3 shows a typical combination of an optimisation program with a simulation program. To perform the optimisation, the optimisation program automatically writes the input files for the simulation program. Then it starts the simulation program, reads the value of the function to be minimised from the simulation result file and then determines the new set of input parameters for the next run. The whole process is repeated iteratively until a p re-defined criterion is fulfilled or a maximum number of iterations is reached. Two optimisation programs are implemented in our studies. In our implementations, we have modified those programs [3, 4], so that we are able to handle single and multi-objective function problems, with or without constraints, having continuous and discrete variables. Discrete design variables are very common in building designs (e.g. different types of windows, walls, shadings, HVAC equipments etc).

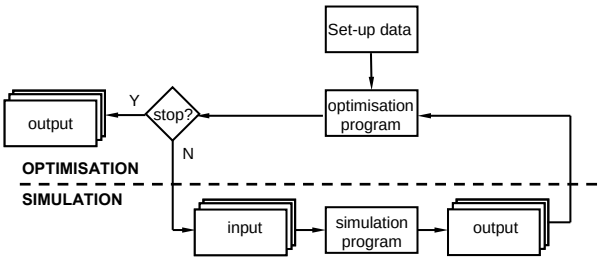

Fig. 3 Combined simulation-optimisation.

Table 1. Design variables and bounds.

	d$X_{extwall}$ (m)	dX_{roof} (m)	dX_{floor} (m)	U_{window} (W/m^{2}K)	*Eff.*
Min. (m)	0	0	0	1.0	07
Max. (m)	1.0	1.0	1.0	Or	or
Step (m)	0.05	0.05	0.05	1.4	0.8
Initial (m)	0	0	0	1.4	0.7

Min. is the lower bound value
Max. is the upper bound value
dX is the additional insulation thickness to be added to the standard
U_{window} is the window's thermal transmittance
Eff. is the efficiency of the heat recovery unit

3.1. Example

To demonstrate the method, a building design example is presented here. In this example, a detached house (floor area 147 m^2) designed according to the Finnish Building Standard-2003 is studied (Standard House). The task is to modify the house by finding optimal values for five design variables that will need minimum investment while making best impact on

lowering the operating energy cost. These variables are: three continuous variables as additional insulation thicknesses to be added to the Standard House (in the external wall, roof and floor) and two discrete variables (types of windows and ventilation heat recovery exchanger). The given bounds for the values of those variables are indicated in Table 1. The problem is solved in two ways, as a single objective problem and a two-objective problem. In this paper, data from [4 and 5] are reproduced to explain the implementation.

3.1.1. Solution as a Single Objective Problem

The objective is formulated as a single objective optimisation problem for minimising of one objective (ΔLCC) (€), the difference in the life cycle cost of the house discounted to net present value compared with its standard design. ΔLCC is defined as

$$\Delta LCC = \Delta IC + \Delta RC + \Delta OC$$

ΔIC difference in the investment cost (€) for the specified design variables
ΔRC difference in the replacement cost (€) due to replaced items (in the building envelope or system) in specified years due to shorter life of those items with respect to the building life.
ΔOC difference in the operating cost (€) due to difference in energy consumption

All above cost differences are with respect to those for the Standard House. This is an optimisation problem because it includes conflicting targets (i.e. increasing the investment cost will decrease the operating energy cost and vice-versa). An exhaustive search method to find the optimal values of the design variables will need a huge number of simulations even for this simple case. For example, if we assume that there is 1 cm step in the additional insulation thickness in Table 1, then the total number of possible combinations to be investigated is $100 \times 100 \times 100 \times 2 \times 2 = 4 \times 10^6$. The combined simulation-optimisation does it in much less number of simulations.

For this example, eight cases were studied [5] with different assumptions for the life-cycle span *n*, escalation in the energy price *e* and the source of the design variable prices. Figure 4 shows the optimisation-simulation iterations for one case (n = 20 years, e = 0.01 and real interest rate = 4.90 %). Only 241 simulations were needed to find the cost-optimal solution using a hybrid algorithm (PSO and Hooke-Jeeves). Each point in the figure is a full-year hourly dynamic simulation. From this figure, it can be seen that the solution has a minimum value of ΔLCC (−2102 €) as a result of the reduction made in the energy cost for space heating ΔOC (−4229 €) when investment is made in the insulations, windows and heat recovery including associated replacement costs ΔIC+ΔRC (+2127 €). Since ΔLCC for the Standard House is 0, therefore the negative value of ΔLCC means lower LCC cost is reached compared with the Standard House. The optimisation results give the optimised values of the five design variables to achieve this target. The simulation-iteration runs, when searching for the optimal solution, are indicated in Figure 5 as ΔLCC .vs. annual space heating energy. From this figure, we can conclude that there is no need to make an exhaustive search and draw the whole energy-cost curve to find the cost-optimal solution because the optimisation algorithm finds shortest ways to that. In addition to minimising the LCC, Figure 5 shows that the annual space heating energy demand at the cost-optimal solution is about 71 kWh/m^{2}a, which is 28% lower than that for the Standard House. This means that the obtained cost-optimal solution achieves both the financial and energy targets. By this method, the optimisation method took the problem as one investigation for minimisation of the LCC, which inherently accomplished the environmental target.

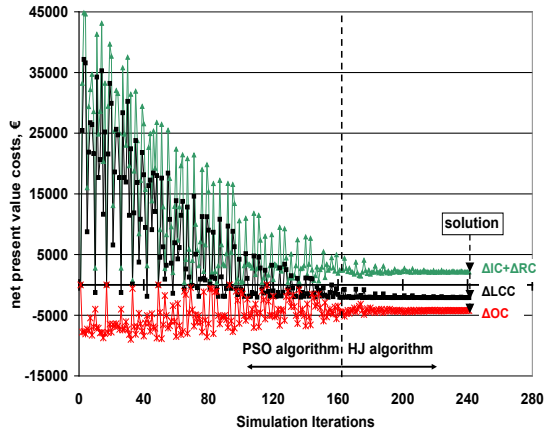

Fig. 4. Simulation-optimisation iterations.

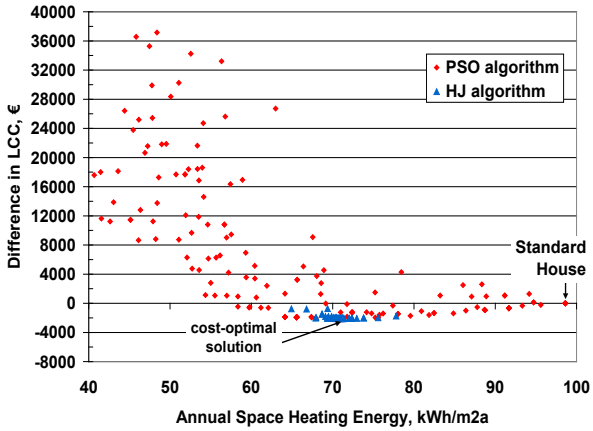

Fig. 5. Finding the cost-optimal solution.

3.1.2. Solution as a Multi-Objective Problem

By taking the problem as a multi-objective optimisation problem, we can draw the cost-curve, find the cost-optimal solution and specify other potential solutions towards nearly zero energy buildings, without making an exhaustive search. To explain this method, the previous example is converted into a two-objective optimisation problem where it is to simultaneously minimise both the difference in the investment cost (ΔIC) and the annual space heating energy demand. Figure 6 shows the optimisation solutions for this two-objective problem using combined simulation and a Genetic-algorithm optimisation [4]. In this figure, the results of an exhaustive search (Brute-force) made on preferable solutions are also shown. The Brute-force search is made by keeping the floor thickness according to the Standard House. This makes the number of variables four. Besides, a maximum value of 0.39 m is considered for ($dX_{extwall}$) and (dX_{roof}). Assuming a 1 cm step in the insulation thickness, the total number of Brute-force candidate solutions is 40×40×2×2 =6400 and as shown in Figure 6. These hints were concluded from the single-objective case results; otherwise a complete exhaustive search will be needed with 4×10^6 candidate solutions. It can be seen that the optimisation solution captures the optimal Pareto-front of the Brute-force, which is an indication of the high accuracy of the optimisation results. Figure 7 presents the difference in the life cycle cost (ΔLCC) based on the data from the optimisation solutions and the Brute-force results from Figure 6. It can be seen from Fig. 7 that the cost-curve is constructed and the cost-optimal solution can be found. In comparison with the single-objective solution, this two-objective solution facilitates assessing potentials for nearly-zero buildings (range of optimal solutions to the left of the cost-optimal in Fig. 7), which is a big advantage over the single objective approach. It is to note that a constraint of 6000 € was applied on (ΔIC) in the optimisation problem to obtain similar range of results as those got from the brute-force search in Fig. 6. We could have got a more complete cost-curve without such a constraint.

Similarly for the NZEB case, the optimisation method can find optimum solutions (indicated by the red squares in Figure 2) without going through the conventional two-step solution method.

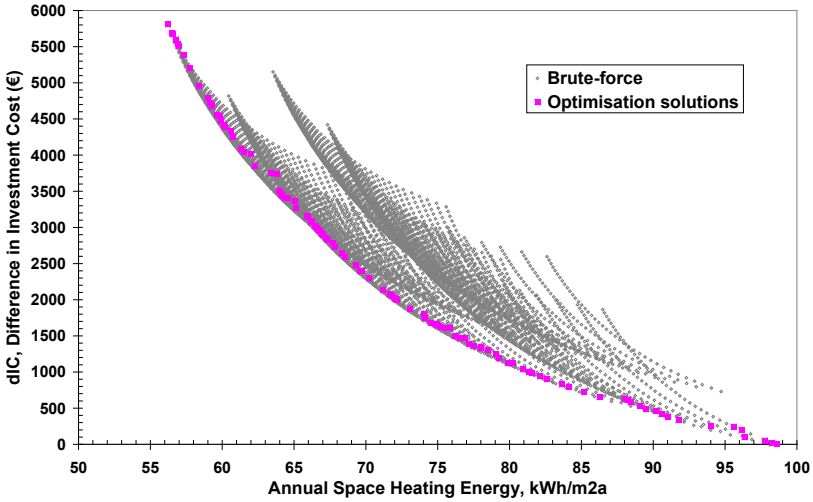

Fig. 6. Two-objective optimisation results and Brute-force candidate solutions [4].

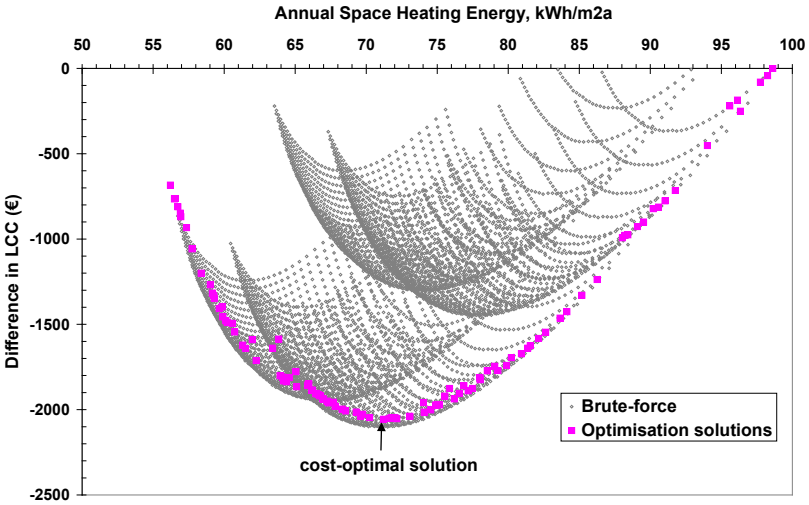

Fig. 7. Cost-curve and cost-optimal solution found from the two-objective optimisation results.

4. Conclusion

It is concluded that optimisation tools have to be combined with simulation tools for finding optimal designs of NZEBs. This is valid for the two methods discussed in this paper: the EPBD recast method and the IEA-Annex 52 NZEB definition. Otherwise it is very difficult for a designer to make a "good" guess at best candidate combinations of measures that will be compared for their cost-energy performance especially when there are many variables in the problem and also due to the nonlinear interaction between the variables. Another way is to make exhaustive searches for each case to define candidate packages, which will then need a huge number of simulation iterations.

The approach should not be split into two steps, firstly reducing the energy demand to nearly zero energy and secondly introducing on-site renewables. If we apply such approach, we will end-up with an extremely low-energy house before giving a very small chance for on-site renewables to participate in the solution, which is not the best method for all cases. For example a house with on-site energy generation from a micro-CHP dose not need to have high quality windows or very thick insulations because of the ample heat accompanied with the generation of electricity. Besides, the selection of the optimal measures should not be only dependent on achieving cost and energy targets, but indoor air comfort should be considered

as target in the problem as well, otherwise overheating could be faced when using more insulations and air-tight envelopes or overcooling could be faced when low-energy value sources are used for heating.

The optimum design method for NZEBs is by taking the problem as one-integrated problem (envelope + HVAC systems + en ergy supply including renewables) using combined simulation-optimisation. The optimisation tool will find the best combinations of measures that will fulfil the objectives of the problem. This approach was applied in the presented example. The problem was solved by two methods. In the first method, the problem was formulated as a single objective LCC minimisation problem, where search was done for finding the cost-optimal solution. In the second method, the problem was formulated as a two-objective problem, where search was done for minimising both energy and investment cost, from which the whole cost-curve was constructed and the cost-optimal and other alternative solutions were found.

Acknowledgment

The author would like to thank the Academy of Finland for funding this research.

References

[1] The Buildings Performance Institute Europe (BPIE), Cost optimality: How to identify cost-optimal levels when implementing energy efficiency in buildings? http://dl.dropbox.com/u/4399528/BPIE/BPIE_costoptimality_publication2010.pdf

[2] I. Sartoria, I Graabak, T. H. Dokka, Proposal of a Norwegian ZEB definition: Storylines and Criteria. zero emission buildings, proceedings of Renewable Energy Conference 2010, Trondheim, Norway.

[3] M. Palonen, A. Hasan, K. Sirén, A Genetic Algorithm for the Optimisation of Building Envelope and HVAC System Parameters. 11th International Building Performance Simulation Association (IBPSA) Conference, 27-30.7.2009, Glasgow.

[4] M. Hamdy, A. Hasan, K. Sirén, Combination of Optimisation Algorithms for a Multi-Objective Building Design Problem. 11th International Building Performance Simulation Association (IBPSA) Conference, 27-30.7.2009, Glasgow.

[5] A. Hasan, M. Vuolle, K. Sirén, Minimisation of life cycle cost of a detached house using combined simulation and optimisation. Building and Environment 43(12): 2022-2034.

[6] M. Hamdy, A. Hasan, K. Sirén, Applying a multi-objective optimization approach for design of low-emission cost-effective dwellings. Building and Environment 46 (2011):109-123.

Experimental performance of unglazed transpired solar collector for air heating

Hoy-Yen Chan[1,*], Saffa Riffat[1], Jie Zhu[1]

[1]*Department of Architecture and Built Environment, University of Nottingham, Nottingham, UK*
** Corresponding author. Tel: +44 115 951 3134, Fax: +44 115 951 31591, E-mail: laxhyc@nottingham.ac.uk*

Abstract: Unglazed transpired solar collectors are usually mounted on the side of the building that receives the most sunlight. It is a fan-assisted system, whereby air is drawn through the holes into the plenum and the warm air is then ducted into the building. The primary reason for using the unglazed transpired metal plate as the solar collector is not only to absorb the solar heat but also to reduce the convection heat loss. These in return will have higher heat exchange effectives and heating efficiency. Though many research have been carried out to study the Nusselt number correlations, heat exchange effectiveness, wind effects and pressure drop, yet only hand full of research that involved heat transfer study that including the vertical airflow in the plenum. This paper is to assess the heating performance of this system through experimental tests which involve the study of temperature rise along the vertical air flow in the plenum. Results show that the temperature of the air flowing vertically is increasing gradually from the bottom to the top of the plenum. This is contrast with the previous studies which assumed that the temperature of the air in the plenum is constant and same as the outlet air temperature at the top of the plenum. The temperature rise is increasing with solar radiation intensity. Temperature rise along the plenum contributes between 30 to 60% of the total temperature rise at a constant suction velocity. On the other hand, temperature rise is decreasing with suction velocity. Values of temperature rise along the plenum are between 30 to 50% of the total temperature rise for suction velocity of 0.03 to 0.05 ms^{-1} at 600Wm^{-2} of solar radiation. Therefore, this study has proved that heat transfer of vertical airflow in the plenum has a crucial heating effect.

Keywords: *Unglazed transpired solar collector, Air heating, Solar façade.*

Nomenclature

d *hole diameter* ..... *m*
D *plenum depth* ..... *m*
ΔP *pressure drop*..... *Pa G*
H *collector height* ..... *m*
I *solar radiation intensity* ..... $W \cdot m^{-2}$
L *collector width*..... *m*
Nu *Nusselt Number*
Pit *pitch*..... *m*
Re *Reynolds number*
Ta *ambiant temperature*.....*K*
Ti *air temperature at the bottom of the plenum also air temperature after pass through the hole* .....*K*
Tout *outlet air temperature (on top of plenum)* *K*
Tp *collector plate temperature* .....*K*
U_w *wind velocity*..... $m \cdot s^{-1}$
v_s *suction velocity* ..... $m \cdot s^{-1}$

1. Introduction

The heat transfer of the transpired plate occurs at the front-of-plate (the upstream-facing surface), the hole and the back-of-plate. The diameter, pitch and geometrical of the hole together with the porosity of the plate and suction velocity of airflow rate are the key factors for the heat transfer coefficient. However, there are limited studies on transpired plate heat transfer. Kutsher [1] has developed an empirical correlation of Nusselt number which is appropriate for thin transpired plates with porosity less than 2%, low suction flow rates and triangular hole arrays. To-date, this is the only study considering the porosity, hole diameter and crosswind conditions to reach the empirical correlation Nu. The correlation covers heat transfers from the front-of-plate, hole and back-of-plate but excludes the vertical airflow in the plenum. The author ignore heat transfer between the back surface and the vertical airflow because it is believed that the flow in plenum has little effect due to the injection effect on the

back-of-plate side and the air laminarization induced by acceleration. The numerical results show that the heat transfer that occurs at the front surface dominates heat transfer in the hole and on the back surface at suction flow rates of 0.02 to 0.07 kg $s^{-1}m^{-2}$. The crosswind data for the narrow transverse spacing are correlated as $Nu=2.75[(Pit/d)^{-1.2}Re^{0.43}+0.011PRe(U_w/v_s)^{0.48}]$ with $0.001\leq P\leq 0.05$ and $100\leq Re\leq 200$ [1]. Augustus and Kumar [2] use the same Nu correlation in their mathematical modelling of transpired solar collector performance. The assumptions made are the same as Kutscher's [1, 3] and Dymond's [4] studies. The plate is a mild steel absorber coated with black paint with input parameters as follows: $400\leq I\leq 900 Wm^{-2}$, $0.02\leq v_s\leq 0.03 ms^{-1}$, $25\leq \Delta P\leq 80 Pa$, $0.050\leq D\leq 0.150 m$, $0.012\leq Pit\leq 0.024 m$ and $0.00080\leq d\leq 0.00155 m$.

Gunnewiek et.al have studied the airflow in plenum but only considering the vertical direction by using 2D CFD model. The transpiration of air through the plate is modelled as a process occurring through discrete holes. The collector height range is $3.0 \leq H\leq 6.0$ m, and the plenum aspect ratio range is $10 \leq H/D \leq 50$. The results show that different settings of parameters yield different airflow profiles. The nature of the profile depends on whether the flow is dominated by buoyancy or by the forced-flow produced by the fan. When the flow is non-uniform, the code predicts that an important amount of heat transfer can take place from the back-of-plate to the vertical air in the plenum. The non-uniform flow is favoured in flows that are buoyancy dominated. Besides improving the efficiency, non-uniform flow is also keeping the fan power at a minimum, so there is a dual benefit [5]. Poor flow distribution occur in large building applications; this has been shown by infrared photographs [4]. Such poor distribution would cause penalties in performance due to greater radiation and convective heat losses at hotter, flow-starved surfaces. In order to study the uniformity of the airflow, Dymond and Kutsher [4] have developed a computer program to allow designers to predict flow uniformity and efficiency by applying pipe networks concept. The studied range of plenum depth, D is between 5 and 30cm. In terms of the energy balance the authors acknowledge additional heat transfer from the plate to the air in the plenum is possible, which has been indicated by Gunnewiek et. al [5] simulation results. However this part of heat transfer is ignored due to the absence of heat transfer correlation between the back-of-plate and the vertical airflow. Hence, it is assumed that the air temperature leaving a junction is the same as the perfectly mixed temperature of the air entering the junction. The overall results show that the air inside the collector plenum experiences three plenum pressure drops, i.e. acceleration, friction, and buoyancy. The larger the air flow through the collector, the better the heat is transferred away from the collector, which results in a higher collector efficiency.

Though there are quite a number of studies that ignored the heat transfer from the back of the plate, study [5] has proved that this part of heat transfer is possible and the authors [4, 6] also acknowledge this possibility if the collector is vertically tall. Thus, this paper is to discuss the heating performance of this system through experimental tests which involve the study of temperature rise along the vertical air flow in the plenum.

2. Methodology

A chamber is built inside a laboratory. Fig. 1 illustrates the schematic view of the experimental system. The wall of the façade that contacts with the ambient is a black painted aluminium transpired plate which adjuncts with three other solid walls, and so they form a plenum. As shown in Fig. 1. The sandtile wall is made of eight sandtile blocks with the dimension of 0.25m x 0.25m x 0.06m for a single block. The other two adjunction walls that attached to both aluminium plate and sandtile wall are rigid polyisocyanurate foam boards

with glassfibre of 0.07m of thickness and U-value of 0.023W $m^{-2}K^{-1}$. The opening of the air outlet is 0.23m x 1.0m. Two fans are installed at the air outlet. Nine K-type thermocouples are placed on each aluminium plate, the plenum and the sandtile wall as shown in Fig. 2. The locations of thermocouples between the wall and the plate (the plenum) are in line with the thermocouples on the sandtile wall except at the bottom they are in line with the first row of the holes from the bottom. The thermocouples are connected to a computer-controlled data logger. Temperatures data are started to be taken only after the test has begun for 2hours to reach a steady state. Air velocities are measured at the centreline of the plenum and at the outlet of the plenum.

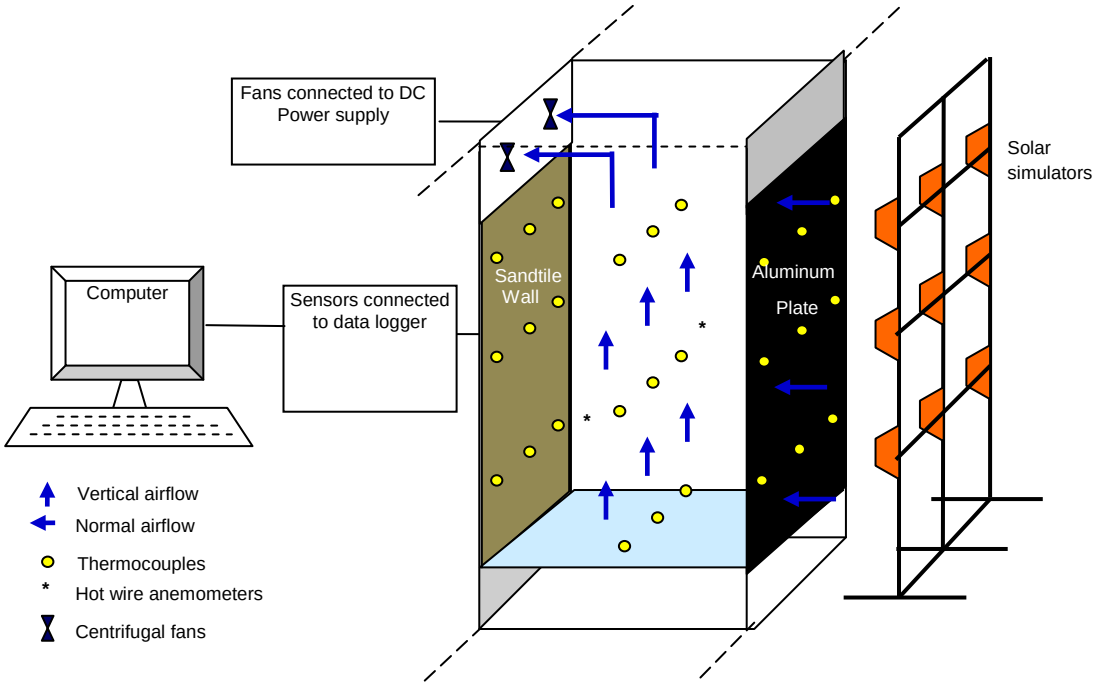

Fig. 1. Schematic view of experimental set up.

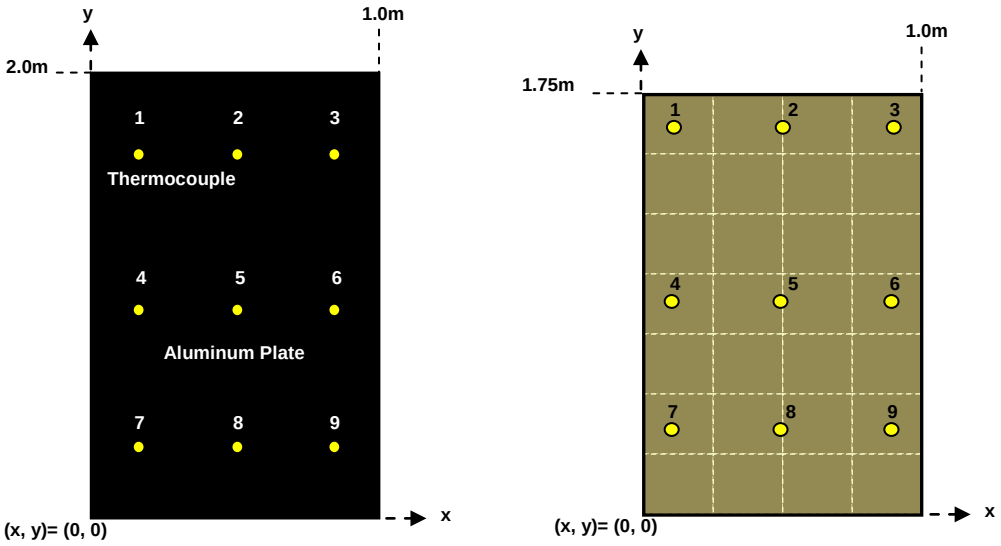

Fig. 2. Thermocouples' location on the plate and santile wall.

2.1. Test conditions and analytical parameters

The test conditions and some of the interested parameter to be investigated in this study are as shown in Table 1. The parameters that vary from one cycle to another of the tests are among solar radiation intensity and suction velocity. Only one design of the transpired plate is involved in this study, which the circular holes are arranged in triangular geometry. Pressure drops across the collector for all the tests are ensured to be at least 10 times greater than the pressure drops in the plenum and so as positive values of pressure coefficient. This step is to avoid outflow air from the plenum. The solar radiation that absorbed by the plate is assumed to be homogenous.

Table 1. Parameters for the experiment tests.

Parameter	Value/ range
Solar radiation intensity (I), Wm^{-2}	300-800
Suction velocity (v_s), ms^{-1}	0.03-0.05
Plenum depth (D), m	0.25
Pressure drop across the collector (ΔP), Pa	12-36
Pitch (Pit), m	0.012
Hole diameter (d), m	0.0012
Height of the collector (H), m	2.0
Width of the collector (L), m	1.0

3. Results

Effects of suction mass flow rate and solar radiation intensity have been studied and results are as discussed in the following sections.

3.1. Effect of suction airflow rate

Fig. 3 shows the temperature rise for different depths of the channel at different suction mass flow rates with a solar radiation intensity of 614Wm-2. The temperature rise of (Tout-Ta) is the overall temperature rise for the system, which is the temperature difference between the outlet air and the ambient air. The temperature rise of (Ti-Ta) is the temperature difference between the heated air after passing through the holes (normal flow) and the ambient air. Whereas the (Tout-Ti) is temperature change of the vertical flow from the bottom to the top of plenum. The values of these temperature rises decrease with the suction mass flow rate. Increasing the suction mass flow rate by about $0.02kgs^{-1}m^{-2}$, Tout-Ta decreases nearly 3K, while (Ti-Ta) and (Tout-Ti) decrease about 1K and 3K respectively. T he shares of temperature rises contributed from normal and vertical flows remain almost the same between 0.04 to $0.06kgs^{-1}m^{-2}$ (Fig. 3). The degrees of temperature decrease for the normal and vertical flows are about the same. Nonetheless, results shows that in term of percentage the vertical flow (Tout-Ti) contributes about 39-49% of the total air temperature rise (Tout-Ta). Thus the air temperature rise along the plenum should not be ignored.

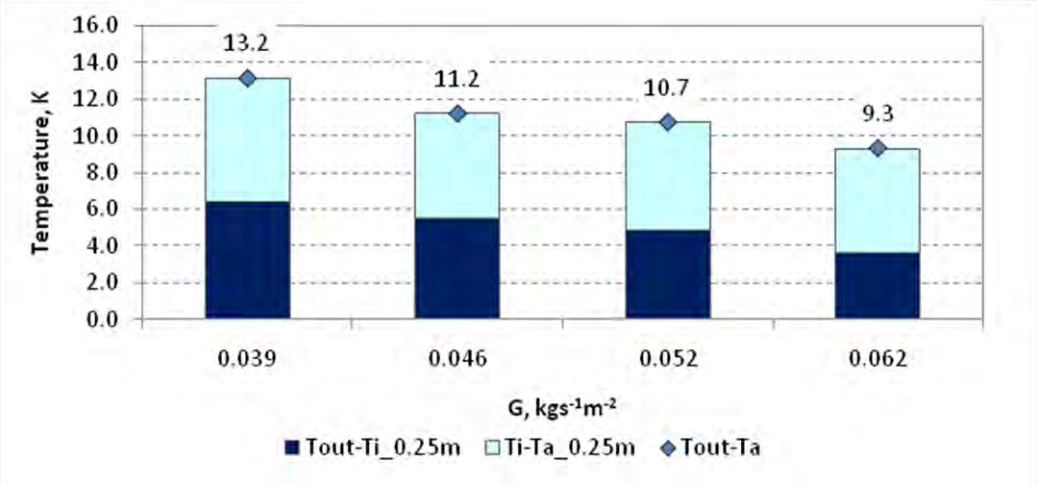

Fig. 3. Values of total, normal and vertical temperature rise at different suction mass flow rates.

3.2. Effect of solar radiation intensity

Fig. 4 shows the temperatures of the ambient, the plate and the air in the plenum for plenum depth of 0.20, 0.25 and 0.30m respectively, at a constant suction mass flow rate. The values of the temperatures increase with the solar radiation intensity and are as shown in Figure 8. The overall rise in temperature (Tout-Ta) from 307 t o 820Wm-2 is about 6 t o 18K, which approximately increases 3K for every increase of 100Wm-2. Thus, the solar radiation intensity plays an important role in the thermal performance of the system. Fig. 5 shows the shares of temperature rises contributed by the normal (Ti-Ta) and vertical (Tout-Ti) flows at constant suction mass flow rate and solar radiation intensity. In terms of percentage, vertical flow contributes 34% of total temperature rise at 307Wm^{-2} and increases to 58% at 820Wm^{-2}. Therefore, this indicates that the temperature rise in the plenum should not be ignored.

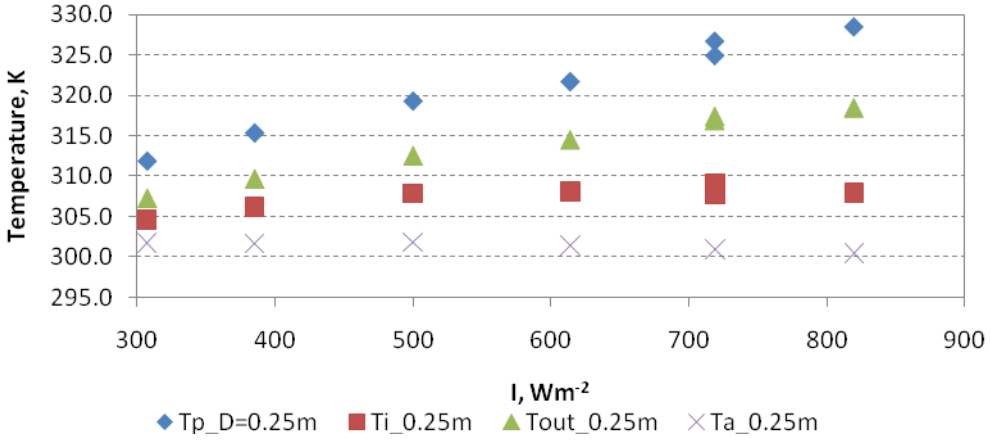

Fig. 4. Temperatures of ambient, at the plate, bottom of plenum and the outlet at a constant suction mass flow rate and different solar radiation intensities.

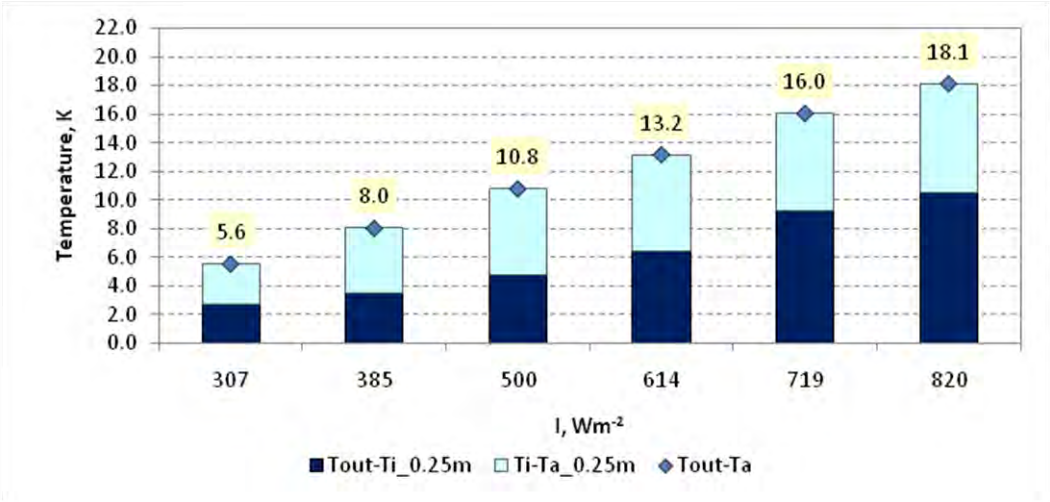

Fig. 5. Values of total, normal and vertical temperature rise at different solar radiation intensities.

4. Discussion and Conclusions

Experimental results show that the vertical flow contributes about 50% of the total air temperature rise. This is contrast with previous studies. As most of the transpired solar collector related studies adopt the same Nu heat transfer correlation [1] and lack of correlation between the plate and the air in the plenum, they accept the same assumption which is neglecting the heat transfer from the back of the plate to the air in the plenum. One of the possibilities for being disagreed with this assumption could be the height of the collector in Kutscher's study [6]. The height for the collector was 0.5m which is quarter of the height of present study. In the study, the author acknowledges that heat transfer from the back of plate might occur for tall vertical collector. Moreover, this could be due to buoyancy-dominated pattern of the vertical flow and causes heat transfer takes place from the back of the plate [5]. Present results show that vertical flow heat transfer is significant for the total air temperature rise. The air temperature rise from the bottom to the top of plenum is between 2 to 10K depends on the operating parameters. However the pattern of the vertical flow is beyond this study. A more precise correlation for vertically tall solar collector need to be developed which include the heat transfer along the plenum whether experimentally or through CFD simulation.

References

[1] Kutscher C. F, Heat exchange effectiveness and pressure drop for air flow through perforated plates with and without crosswinds, *J Heat Transfer* 116, 1994, pp. 391–9.

[2] M. Augustus Leon, S. Kumar, Mathematical modeling and thermal performance analysis of unglazed transpired solar collectors, *Solar Energy* 81, 2007, pp. 62-75.

[3] Kutscher, C.F., Christensen, C.B., Barker, G.M, Unglazed transpired solar collectors: heat loss theory, *ASME Journal of Solar Engineering* 115, 1993, pp. 182–8.

[4] Dymond C., and Kutscher, C., Development of a flow distribution and design model for transpired solar collectors, *Solar Energy* 60, 1997, pp. 291-300.

[5] L. H. Gunnewiek, E. Brundrett, K. G. T. Hollands, Flow distribution in unglazed transpired plate solar air heaters of large area, *Solar Energy* 58, 1996, pp. 227-37.

[6] Kutscher C. F., An investigation of heat transfer for air flow through low porosity perforated plates, Colorado: University of Colorado, 1992.

Improving thermal performance of offices in JUST using fixed shading devices

Ahmed A. Y Freewan*

Jordan University of Science and Technology , Irbid, Jordan
**. Tel: +962 796636130, Fax: +962 2 72010381, aafreewan@just.edu.jo (ahmedfreewan@hotmail.com)*

Abstract: Large windows and highly glazed façades have been increasingly used in new buildings, allowing the access to daylight, solar gain and external view. Solar gain through non-shaded windows and glazed facades extremely increases the air temperature in summer especially in hot climates regions, like Jordan. Therefore, it affects thermal comfort, increase the cooling load and become a s ource of glare which harms the visual environment. Generally, shading devices are used to protect inner spaces from direct solar gain through openings, windows and glazed surfaces. The current research examined the effect of using shading devices on thermal environment and air temperature in offices facing south-west façade at Jordan University of Science and Technology (JUST). I n such orientation windows required especial considerations to control solar gain in summer and winter. The research used real experiments to study effects of shading devices on thermal comfort. Three fixed shading devices; vertical fins and diagonal fins and egg crate, were installed in three identical offices. Thereafter, the air temperature was monitored and compared to non-shaded office. The results showed that the temperature in offices with shading devices compared to the office without shading devices was reduced to acceptable level. At the time of measurements diagonal fins perform better compared to other shading devices.

Keywords: *Shading devices, Thermal comfort, Cooling load.*

1. Introduction

1.1. Shading devices

Building around the world required a large amount of energy for cooling, heating and lighting. Well-building design requires integration of many factors, such as orientation shading devices and building form, to compromise energy consumption through a building. In additions windows, glazed façades and openings have an important role in building energy consumption whether for heating, cooling or lighting. Highly glazed façades and large windows have been increasingly used in new buildings, allowing the access to daylight, solar gain and external view. Therefore, their impact on cooling, heating and lighting demand in the building is significantly needed to be considered in building design. Proper shading design can contribute well to indoor illumination from daylight, improve thermal comfort, control solar heat gains and reduce glare at the same time as keep the view out.

Datta [1] studied the effect of using shading devices on thermal performances of buildings in Italy. The study used TRNSYS computer simulation to study many variables related to horizontal shading devices in different cities in Italy. It found that well shading devices could help save energy and improve thermal performance of buildings. Palmero-Marrero and Oliveira [2] studied the effect of using shading devices on thermal performance in many cities, around the world, with different latitude and climatic conditions using TRNSYS. The study showed that shading devices have a great impact on saving energy and improving thermal performance in offices in different climatic conditions. Bessoudo and other [3] and Tzempelikos and other [4, 5] studied how shadings devices effect the thermal comfort in offices with glazed façades in cold climate in Montreal-Canada. They studied interior glazing and shading devices temperature, operative temperature and radiant temperature under different variables such as: Venetian blind, roller shade, and blind rotated angles. The study showed that shading devices could improve the thermal condition in cold and sunny conditions. They also developed a transient building thermal model. However, many

researchers have studied the effect of using of shading devices on thermal comfort, energy consumptions and daylight performance of buildings [6-13].

The literature review has shown the need for studying the effect of shading devices on real building in regions with hot summer and cold winter like Jordan. The current research will investigate the effect of using of shading devices in south-west façade of offices in Jordan University of Science and Technology (JUST) on thermal conditions and air temperature.

1.2. Case Study

Jordan is classified as subtropical area, which is characterized by hot and dry summer and cold winter. Clear sky conditions dominate around the year with medium to overcast sky and moderate rainfall in winter. The average direct sun component is generally about eight hours a day. The major characteristic of Jordan's climate is the contrast between a relatively rainy season from November to April and dry weather for the rest of the year. The country has a long summer with a peak in August while January is the coolest month.

Jordan University of Science and Technology (JUST) is in Irbid (latitude 31.9˚ North, longitude 35.9˚ East) around 80 km to the north of Amman. The campus was designed by the Japanese architect Kenzo Tange. Buildings were constructed using prefab concrete panels and blocks. Office are on second floors, while ground and first floors used for lectures halls and labs respectively. The plan of the office levels, like wing A3 level 3, is double loaded corridor with offices at each side. The number of offices in south-west facade is 11 offices; each office is 3.5m width, 4.25m deep and 2.75m high as seen in figure (1). The façade height comprised three sections; 0.80m sills, 1m windows and 0.5m upper windows figure (2).

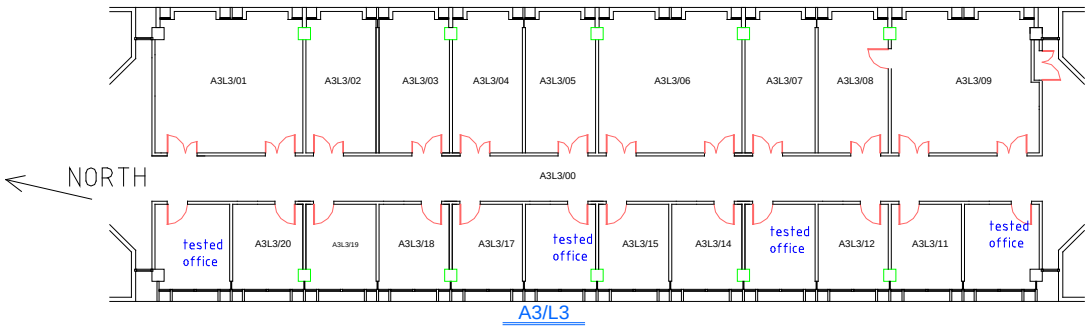

Figure 1 plan of offices level 3 wing A3 at JUST

Buildings oriented toward south-west with large windows area such office spaces in wing A3 at JUST suffer from uncontrolled solar gain throughout the year. In such orientation windows required especial considerations to control solar gain in summer and winter. The offices in wing A3-L3 at JUST expose to direct sunrays from noontime to sunset. The total hours of exposing is more than seven hours in summer raising the air temperature to intolerable level. Sunny area starts increasing gradually inside the offices from noontime to cover most of the office area thereafter as seen in figure (3).

1.3. Current situation

Author noticed that offices oriented to south-west such as offices in wing A3 experiencing high indoor temperature during sunny days at the same time lack of sufficient daylight due to occupants reactions.

Figure 2 office façade (left), single office' windows details (right)

Occupants' reactions to discomfort almost have negative impact from energy view. Users spontaneously used curtains to overcome the problems shaped by large glazing area, especially the increasing sunny area, to block the direct sunrays and to avoid glare figure (3). So, the daylight level inside the offices decreased that needed auxiliary artificial light to keep the light level up to the needed task level. Curtains are 40cm from the window because of architectural design details. Therefore, they could block the direct sunrays, but the heat gain inside the offices will remain with same rate. It will heat up the space between the curtains and the windows which automatically raise the temperature inside the whole office by direct gain, re-radiation and convection currents. F igure out a solution that overcoming such problems needs blocking the direct sunrays from outside before reaching the windows by shading device.

Figure 3 sunny area in the office without shading devices (left) the office with vertical fins (right)

2. Experiment set up

Three fixed temporary shading devices; egg-crate, vertical fins and diagonal fins, were installed in three offices. Thereafter, experimental measurements were conducted in three offices with different common shading devices, in addition to a base case office, an office without shading devices being installed. The offices are identical in all parameters like; area, geometry, orientation, windows design, glazing area and transmittance ratios, function, opening and surfaces material. The exposed façade of the tested offices is oriented to 12 south of the west.
Experimental measurements were taken in offices spaces on fully sunny days. Accordingly, measurements from tested offices fitted with the selected shading devices were compared to the measurement of the base case.

The dimensions and materials of these temporary devices were preliminary designed to keep the original building without major change to ease installing the devices in order to set the requirements of the permanent design. This is a part of long-term program aims at improving

environmental and climatic conditions of JUST buildings to improve thermal conditions, visual environment and reduce energy consumptions. The next step of the research will be to study natural lighting environment and thermal comfort to compromise between thermal comfort, visual environment and energy saving. And so, the current research will be an initial stage for the long-term program to design the permanent shades to compromise between building changes and energy saving. Indoor air temperatures were measured using pre-calibrated thermometer. Data were collected every five minutes using EXTECH thermometer.

Vertical slats of 10cm width were arranged with a small gap of 5cm between the slats to admit some light, provide a view and allow for ventilation. They were not adjustable or designed to be angled. Diagonal fins consist of vertical fins of 30cm width rotated at 45˚ with a gap of 17cm between the slats. Egg crate consists of verticals slats and horizontal louvers of 10cm width. Vertical slats were arranged with a gap of 15cm between the slats and horizontal parts with 7.5cm between the louvers. It could admit light, provide a view to outside and allow for ventilation.

3. Results

Figure 4 (left) shows the results of air temperature in office with vertical fins compared to the base case. Clearly, using vertical fins help reduce the inner temperature compared to non shaded office. It helped reduce air temperature up 17% in the afternoon with an average of 9%. In the morning the air temperature almost closed in both offices, while the difference start to increase gradually as the sunrays start reaching the windows as seen in figure (3). Generally verticals fins reduce the air temperature in the period from 1pm to 4pm by an average of 4C˚ with maximum reduction by 7C˚. On the other hand, diagonal fins as seen in figure 4 (right) reduced the air temperature by up to 21% compare to the base case with an average of 13%. The difference in the morning is neglected while it s tarts to increase dramatically from 12pm to 4pm. The maximum decrease occurred after 3pm by 8.5C˚. Figure 5 (left) shows how the egg–crate shading improves the thermal performance of the office. It reduced the air temperature by an average of 12% in the period from 12pm to 4pm compare to the base case. Between 3pm and 4pm it reduced the air temperature by 8C˚.

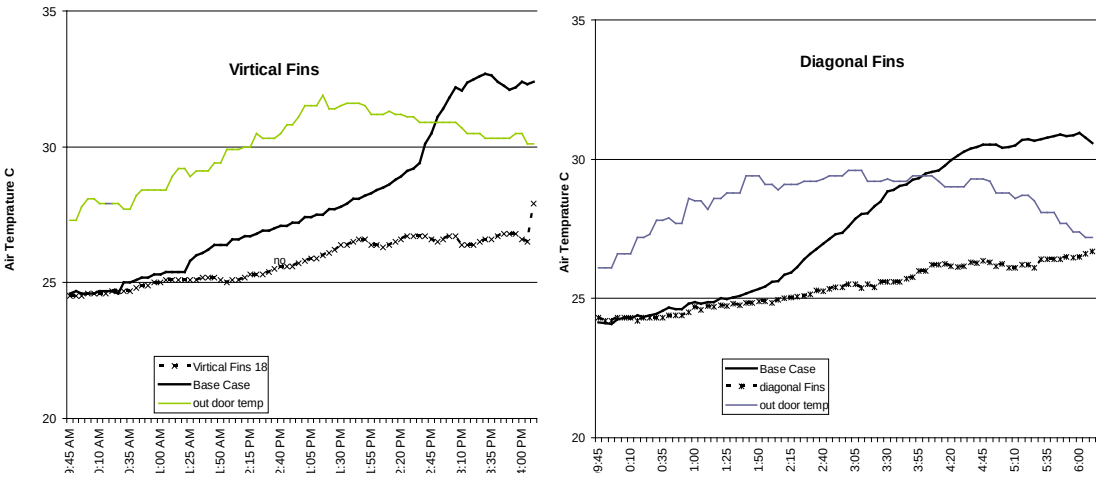

Figure 4 air temperature in office with vertical fins compared to the base case (left) air temperature in office with diagonal fins compared to base case.

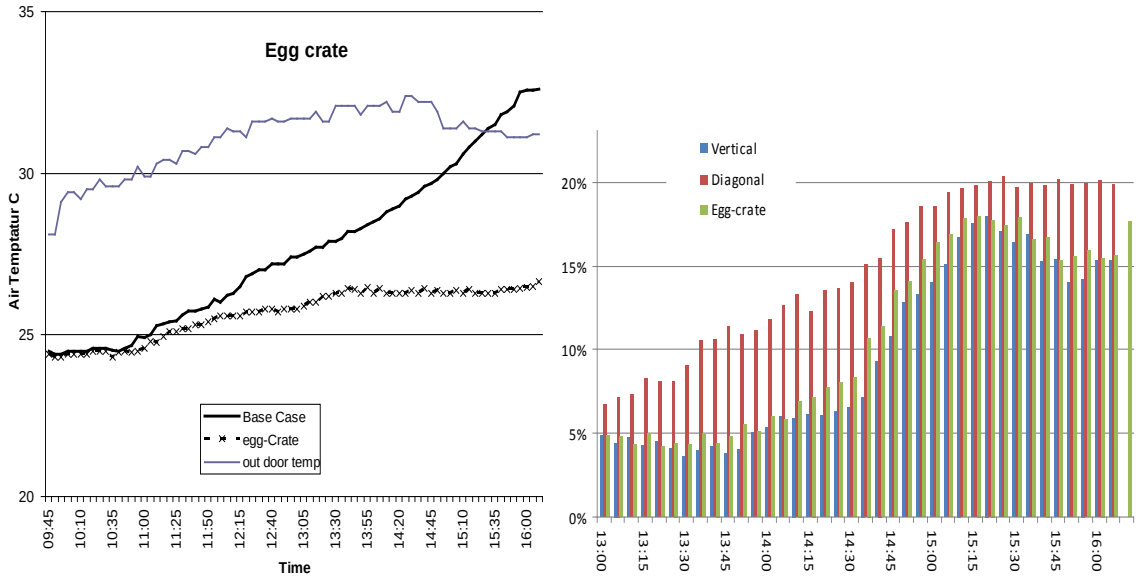

Figure 5 air temperature in office with egg-crate compared to base case and outdoor temperature (left) shows the percentage of reduction in air temperature as a result of using shading (right)

Figure 5 (right) shows the percentage of reduction in air temperature as a result of using shading compared to the base case office. It clearly can be inferred the diagonal fins performed better than verticals and egg-crate in the period from 1pm to 3pm during the period of measurement in September and October.

Graphically analysis of applying shading and shade angles on s undial diagrams show how each type of shading devices perform around the year. Table 1 shows how the shading devices will perform all the time according to solar angles, altitude and azimuth, during the time of the experiments. Diagonal fins will block all sun rays while vertical fins will block the sunrays in the period 12pm-1pm and 2pm to 4pm and allow the sunrays to enter the offices from 1pm to 2pm. Egg-crate shading will allow sunrays to enter the offices between 1:30pm to 3pm and block before and after that.

Studying the performance of shading devices around the year shows that verticals fins partially shade inner spaces in the period from October to February and allow sun to reach inner spaces after 2pm. In contrast, it allows the sunrays to reach the inner spaces in the hot period of the year, March to September, and in the hot time of the day from 1:30pm to 3:30 pm. Diagonal fins fully shade inner spaces in the period October to March and partially in the period April to September. It will block the sunrays only before 1 pm in the period from May to July when the shading are crucially needed. Egg-crate will perform well in hot period and allow for sun rays to enter inner spaces in such orientation in cold period. The analysis of the results show, that well shading design could help improve the thermal performance of the offices oriented to south-west.

Table 1 Installed shading devices and shading angles with sundial diagrams

	Installed shading devices	Shade angles	Sundial Diagrams
	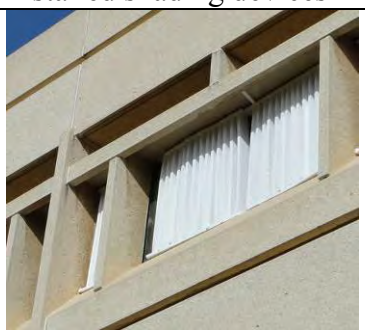	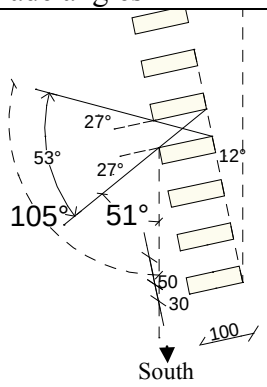	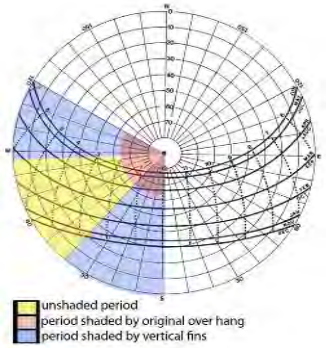
Diagonal Fins		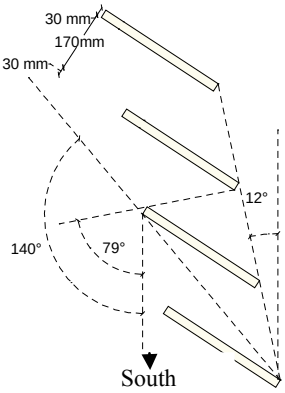	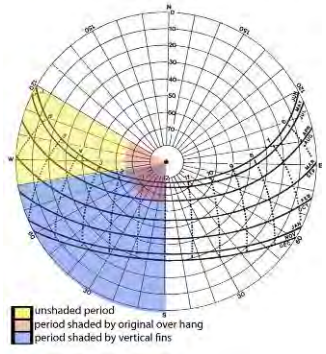
Egg-crate		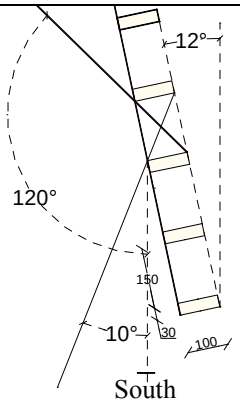	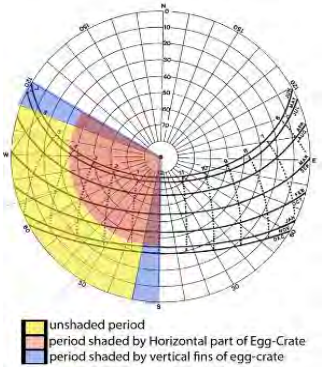

4. Discussion and Conclusions

This paper summarizes the experimental results of thermal environment and air temperature in highly glazed offices with shading devices. In general, results indicate a major influence of shading on s olar gains and thermal performance of offices. All shading devices helped improve the thermal environment in the offices in time of the experiments in September and October. It is clear that until 1pm all shading devices reduced the air temperature approximately with same rate. On the contrary, after 1pm the diagonal shading devices performed better as it helped block all the sunrays all the time. On the other side, vertical fins and egg-crate shading devices allowed some part of sun shine to enter the offices in the period 1pm-3pm.

Designing of shading devices requires taking into consideration around the year measurements in both hot and cold periods. Therefore, egg-crate shading devices could perform well around the year if the horizontal part extends to the outside by the half of the

current width. It will block the sunrays in hot period and allow it to enter in cold period. Diagonal fins will completely block the sun rays in the clod period when the sun is crucially required it cloud perform well in intermediate period such as in September. Moreover, diagonal fins block the view to outside while egg-crate will allow for kind of connections to outside. Modified egg-crate could go well with current situation, fewer modifications, as vertical slats of small width can be easily installed on the window sills and horizontal part can be fixed on vertical slats. Further studies are required to study the effect of shading devices on daylight, visual environment and view out.

References

[1] Datta, G., Effect of fixed horizontal louver shading devices on thermal performance of building by TRNSYS simulation. Renewable Energy 23, 2001, p. 497–507.

[2] Palmero-Marrero, A.I. and A.C. OLiveira, effect of louver shading devices on building energy requirements Applied Energy 87, 2010, p. 2040-2049.

[3] Bessoudo, M., et al., Indoor thermal environmental conditions near glazed facades with shading devices e Part I: Experiments and building thermal model. Building and Environment 45, 2010, p. 2506-2516.

[4] Tzempelikos, A., et al. the impact of shading devices on the thermal comfort conditions in perimeter zones with glass facades. in 2nd PALENC conference and 28th AIVC conference on building low energy cooling and advanced ventilation technologies in the 21st century. 2007, Crete Island, Greece,P 1072-1077

[5] Tzempelikos, A., et al., Indoor thermal environmental conditions near glazed facades with shading devices e Part II: Experiments and building thermal model. Building and Environment 45, 2010. p. 2517-2525.

[6] Freewan, A.A., L. Shao, and S. Riffat, Interactions between louvers and ceiling geometry for maximum daylighting performance. Renewable Energy 34, 2009, p. 223-232.

[7] Tzempelikos, A. and A.K. Athienitis, The impact of shading design and control on building cooling and lighting demand. Solar Energy 81, 2007, p. 369-382.

[8] Chou, C.-P., The Performance of Daylighting with Shading Device in Architecture Design. Tamkang Journal of Science and Engineering 7, 2004, p. 205-212.

[9] Dubois, M.C., Shading devices and daylight quality: an evaluation based on simple performance indicators. Lighting Research and Technology 35, 2003, p. 61-76.

[10] Lee, E.S., D.L. DiBartolomeo, and S.E. Selkowitz, Thermal and daylighting performance of an automated venetian blind and lighting system in a full-scale private office. Energy and Buildings 29(1), 1998, p. 47-63.

[11] Wong and I. Agustinus Djoko, Effect of external shading devices on daylighting penetration in residential buildings. Lighting Research and Technology 36, 2004, p. 317-333.

[12] Sutter, Y., D. Dumortier, and M. Fontoynont, The use of shading systems in VDU task offices: A pilot study. Energy and Buildings 38, 2006, p. 780-789.

[13] Yoo, S.-H. and E.-T. Lee, Efficiency characteristic of building integrated photovoltaics as a shading device. Building and Environment 37, 2002, P. 615-623.

The Assessment of Advanced Daylighting Systems in Multi-Story Office Buildings Using a Dynamic Method

Jianxin Hu[1,*], Jiangtao Du[2], Wayne Place[1]

[1] *College of Design, School of Architecture, North Carolina State University, Raleigh, USA*
[2] *School of Architecture, University of Sheffield, Sheffield, UK*
** Corresponding author. Tel: +01 919-4234955, Fax: +01 919-5158951, E-mail: jhu3@unity.ncsu.edu*

Abstract: The performances of light shelf systems are evaluated in the context of various interior configurations typical of multistory office buildings by using CBDM (climate-based daylight modeling). A physical scale model of one of the light shelf systems is tested in the first phase under real sky conditions in Raleigh, North Carolina, USA. The data collected from the experiments are used to validate the simulations by a computer-based dynamic daylighting research tool - DAYSIM which is based on the concept of CBDM (Radiance + Perez Sky Luminance Model + Daylight Coefficient). In the second phase, additional simulations utilizing the validated tool are conducted to study the effects of system geometries and interior space characteristics. Specifically, the following parameters are identified and assessed: light shelf length, ceiling height, and interior configurations typical of North American office building settings. The findings have displayed the impact of various system parameters and interior design approaches on daylighting performances. The limitations of the study include possible errors in both computational simulations and the physical testing, and errors caused by the process of generating the sky models from solar radiation data for DAYSIM.

Keywords: *Lightshelf, Ceiling Height, Interior Configuration, CBDM, Simulation*

1. Introduction

Although electric lighting has now assumed the role of being the primary means of illumination for many buildings, people generally express a strong preference for natural light in their work environment. There also has been an interest in daylighting as a means of reducing nonrenewable energy use. In multistory office building, one of the strategies for achieving the comfortable interior environment is to redirect daylight from primary surfaces, such as a light shelf, to secondary room surfaces (ceiling and walls), which in turn will illuminate horizontal work surfaces. A light shelf is a small area of horizontal reflecting surface mounted just below the daylight glazing in the façade. Typically, the designer of the building will have a high degree of control over the placement and optical properties of that reflective surface, which makes it a much better candidate light reflecting source than the ground plane. Furthermore, this reflecting surface can be placed above eyelevel for the building occupants, thereby avoiding the potentially severe glare effects of intense upward light in the eyes of occupants near the window. There are two functions to a light shelf system: To reflect light deeper into the building, thereby providing more light in the interior, and to block excessive light from entering spaces close to the perimeter wall.

There have been a limited number of studies on light shelves. The early studies focused on flat simple light shelves. Simple light shelf is referred to the system with interior shelf length of about 4-6 feet. In a study presented by Selkowitz, et al. [1], it was concluded that "in general, simple light shelf designs provide improvements in light penetration." This study did not assess the effects of changing the length of the shelf. Burt Hill Kosar Tittelmann Associates also presented a study on simple light shelves, showing that light shelves do improve the quality and quantity of light in perimeter zones. In this study, a fixed length exterior light shelf was investigated [2]. Advanced light shelf systems were also developed and tested. Some of these studies focused on ceiling configuration. Fardeheb found that exterior shelves in conjunction with a sloped ceiling were most effective among nine different

light shelf designs that they studied [3]. Another category of advanced light shelf research dealt with the shape and movement of the shelf. Place and Howard developed and assessed two advanced daylighting systems, one involving a static curved-mirror and the other involving a tracking flat-mirror system [4]. Based on the behaviors of the two systems in different seasons under different sun angles, design guidelines were developed. An external curved light deflector was designed and tested by Close as one of the three features of the daylighting system designed for a high-rise building in Hong Kong [5]. The performance of the system was simulated by computer and then verified against physical scale models. Finally, some researchers were interested in the effects of varying the reflectance of light shelf surfaces. Claros and Soler investigated the performances of two light shelves with different types of reflecting materials [6].

This list of studies generally delineates a picture of what has been covered by the efforts of previous researchers. It also introduces the three topics to be explored in this study:

- ***Length of light shelves*** - Throughout the literature there has been little effort to systematically assess the impact of light shelf geometries, especially, of longer light shelves (more than 6 feet).
- ***Ceiling height*** - Ceiling height is a crucial factor in daylighting design. This is also the area where "battles" tend to occur between daylighting designers and other members of the design team, such as the structural and mechanical engineers. It is thus important to quantify the importance of ceiling height for delivering light into a space.
- ***Interior configuration*** - Very few researchers have considered the impacts of interior partition designs (layout & material) on lighting environment. Almost all the experiments were performed in an open space. Modern office buildings take on a variety of interior layouts, which can drastically affect lighting performances.

2. Methodology

The traditional daylighting research approach – the Daylight Factor method, only addresses overcast conditions and leaves out important design factors, such as building orientation. Understanding daylight from a climate-based point of view would therefore be more practical to assess daylighting systems in areas with a highly luminous climate, in which case various types of sky conditions (e.g. clear sky or intermediate sky) are all taken into considerations. However, climate-based experimental testing can be time consuming, since monitoring design options in a full year is normally not feasible for most design projects. As an alternative, a dynamic Radiance-based simulation tool - DAYSIM can be adopted for carrying out Climate-Based Daylight Modeling (CBDM) using meteorological dataset [7, 8, & 9]. By the comparisons with experimental measurements, DAYSIM has been proven to be accurate for performing annual daylight predictions for regular daylit spaces [8]. However, it would be prudent to validate the tool before it is used for assessing any advanced daylighting systems, such as light shelves in conjunction with various interior design approaches in this study.

2.1. Validation of DAYSIM simulations by experimental measurements

A physical scale model (scale: 1:6) is established to represent a 30' x 40' (9.14M x 12.19M) portion of a typical office floor (Figure 1). A daylighting system incorporating a 6-ft (1.83 M) lightshelf and a 3-ft (0.92 M) overhang is integrated on the south elevation (Figure 2). The ceiling height is 11' (3.35M) and the top of view glazing is at 7'-2" (2.18M) above the finish floor. The surface reflectances are: ceiling and walls: 90%; floor: 20%; lightshelf top and bottom surfaces: 90%; overhang top and bottom surfaces: 15%; exterior ground reflectance is assumed at 20%; glazing transmittance: 70%. The interior space is divided into five equal

daylit zones. Annual daylight levels in each zone are predicted by both physical experiments and DAYSIM.

Fig. 1. Physical scale model being tested on a heliodon.

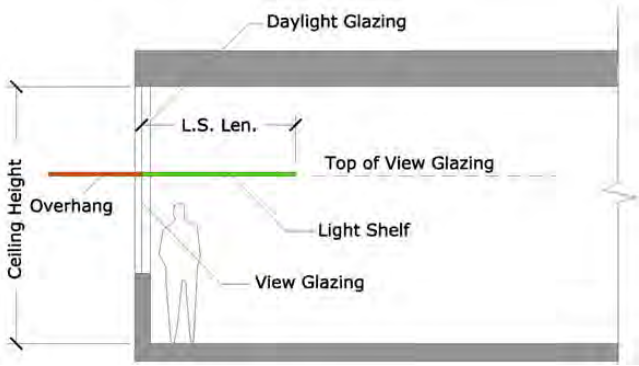

Fig. 2. The daylighting system with a light shelf and an overhang

2.1.1. Physical experiments

To simplify the experimental procedures, the model is only tested under a diffuse sky – a blue sky in this case (clear sky without the sun component), because a diffuse sky is a much more reliable light source than the sun. Sunlight is highly variable depending on seasons, solar angles and weather conditions. A Licor photocell sensor (Model 210L) is installed at the center of each daylit zone (Sensor Ez1 through Ez5). An exterior sensor (Ev) is mounted on a vertical plane facing the same direction as does the window. To simulate a blue sky condition on a clear day, the system designed for facing south is rotated so that it faces only diffuse sky (Figure 3). This approach allows for the system to be tested only under diffuse blue sky by eliminating the sun component. A Coefficient of Utilization can then be developed for each zone to establish the relationship between the sky and interior illuminances. Using Zone 1 as an example, the CU is calculated by the following formulas: CU1 = Ez1 / Ev. Note that a CU relates the interior illuminance to exterior vertical illuminance while a Daylight Factor relates the interior illuminance to exterior horizontal illuminance. Exterior horizontal illuminance only depends on solar altitude, which makes the factor of building orientation out of the question, whereas exterior vertical illuminance depends on both solar altitude and azimuth. Therefore, vertical illuminance is a better indicator of lighting conditions outside especially for assessing sidelighting systems. In addition, the exterior vertical illuminance (Ev), which is taken at the window surface, provides a direct measurement of how much light actually enters the room.

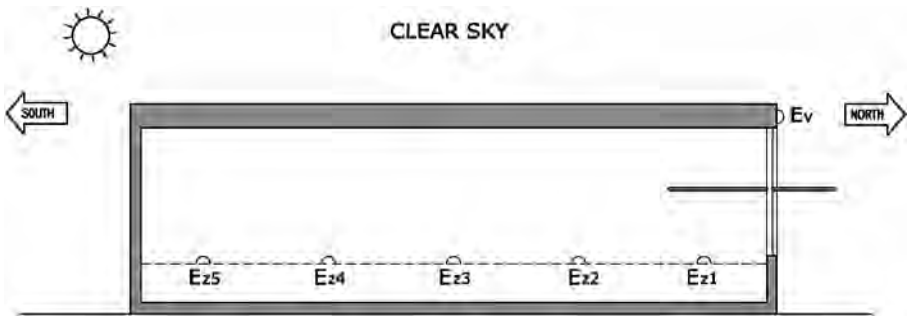

Fig. 3. Model being tested under blue sky. (The lightshelf system is designed for south-facing. However, it is rotated in the experiment to face away from the sun, towards diffuse sky light only)

Hourly daylight levels in Lux in all zones can be developed in a full year by multiplying the CUs by the annual exterior illuminance data (Ev), which were made available by the Daylighting Research Lab at NC State University. The data set, including hourly Ev values in a full year, was collected in a two-year period (1991 & 1992) in Raleigh, North Carolina [10]. Table 1 shows this process for the 1st day (From 7:00am to 5:00pm) of the year.

Table 1: Using CUs to predict hourly illuminances (Lux) for the 1st day of the year by multiplying CUs by the south-facing vertical sky illuminances (Ev in Lux) from the annual sky illuminance data set.

		CU	**0.0938**	**0.06647**	**0.05194**	**0.04342**	**0.04227**
Day	Time	**Ev**	Ez1	Ez2	Ez3	Ez4	Ez5
1	700	**66**	6	4	3	3	3
1	800	**3,074**	288	204	160	134	130
1	900	**7,804**	732	519	405	339	330
1	1000	**13,424**	1,259	892	697	583	567
1	1100	**12,617**	1,183	839	655	548	533
1	1200	**28,730**	2,695	1,910	1,492	1,248	1,214
1	1300	**29,434**	2,761	1,956	1,529	1,278	1,244
1	1400	**64,603**	6,060	4,294	3,355	2,805	2,731
1	1500	**52,715**	4,945	3,504	2,738	2,289	2,228
1	1600	**11,934**	1,119	793	620	518	504
1	1700	**528**	50	35	27	23	22

2.1.2. DAYSIM simulations

A virtual model of the building is built in a CAD tool, which coincided with the physical model. Similarly, five study points are placed along the center line of the daylit zones. The weather file of the site (Raleigh-Durham International Airport) is used as the climate data for the simulation. With a proper ambient parameter setting, the annual illuminance values are calculated by DAYSIM 3.0 and can be presented in the same format as in Table 1.

2.1.3. Comparison

Daylight Autonomy, the numbers of hours in which interior illuminances are above minimum light level for performing the designed tasks (500 Lux in this case), is used as the indicator to assess the two methods (Figure 4).

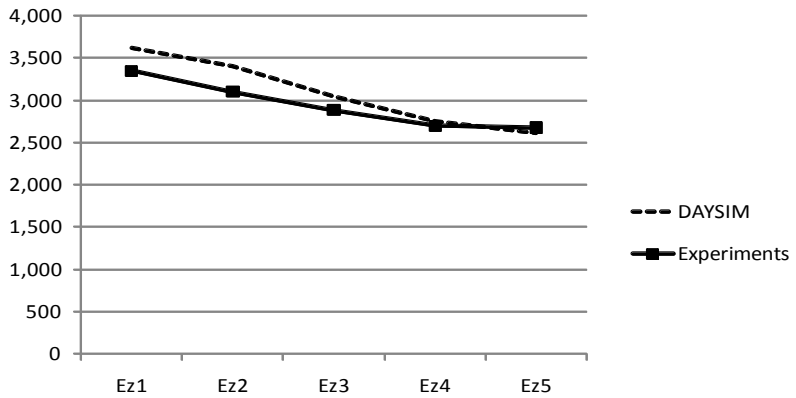

Fig. 4. The numbers of hours in which interior illuminances are above 500Lux predicted by DAYSIM and the experimental methods

To estimate how close the results are between DAYSIM and the experimental methods, the differences in percentage between the two methods are shown in Table 2. DAYSIM generates reasonably close predictions comparing with the experiments. The differences are below 9% in all five zones. For internal zones (Ez3 through Ez5) where daylight levels are lower, the results are even closer (5% and below).

Table 2: Daylight Autonomy values in each daylit zone and percentage of differences when comparing results from the experimental method with those from DAYSIM.

	Ez1	Ez2	Ez3	Ez4	Ez5
DAYSIM	3,615	3,405	3,044	2,747	2,609
Experiment	3,348	3,101	2,885	2,699	2,678
Difference	-7.39%	-8.93%	-5.22%	-1.75%	2.64%

2.2. Assessments of daylighting systems and interior configurations

The validation study reported in section 2.1 demonstrates the effectiveness of the computer-based simulation tool – DAYSIM for predicting climate-based performances of the light shelf system. The tool is then used for the following assessments of the parameters in various daylighting systems and interior configurations.

2.2.1. Length of light shelves

The light shelf lengths of 2', 4', 6', 8' 10', and 12' are simulated in DAYSIM respectively based on the model in Figure 3. Ceiling height, light shelf mounting height, overhang length, and all interior surface reflectances are kept constant. The interior space is open layout.

2.2.2. Ceiling height

Again, based on the model in Figure 3, ceiling heights of 9', 10', 11', and 12' are assessed assuming other systems parameters remain constant (Light shelf length is 6' long in this case).

2.2.3. Interior configuration

Four interior configurations typical of multistory office buildings are identified and compared by using the same method as in the above comparison studies (Figure 5). The same five daylit zones are incorporated in these plans, where there are always two measuring points in the private offices and three in the open area. These configurations are:

Configuration 0: Open office plan where there are no private offices. A section of this design is illustrated in Figure 3.

Configuration 1A: Private offices are located at the perimeter of the floor plate. The partition parallel to the window wall consists of a lower portion (7' high) and an upper portion. The lower portion is an opaque wall; the upper portion is clear glazing (transmittance: 90%). The partitions perpendicular to the window wall are opaque (Figure 5).

Configuration 1B: Same as 1A except that the lower portion of the partition parallel to the window wall is constructed with translucent glazing (transmittance: 50%) (Figure 5).

Configuration 2: Private offices are located at the core area of the floor plate. The lower portion of the partition parallel to the window wall is made of translucent glazing (transmittance: 50%); the upper portion is clear glazing (transmittance: 90%). The partitions perpendicular to the window wall are opaque (Figure 5).

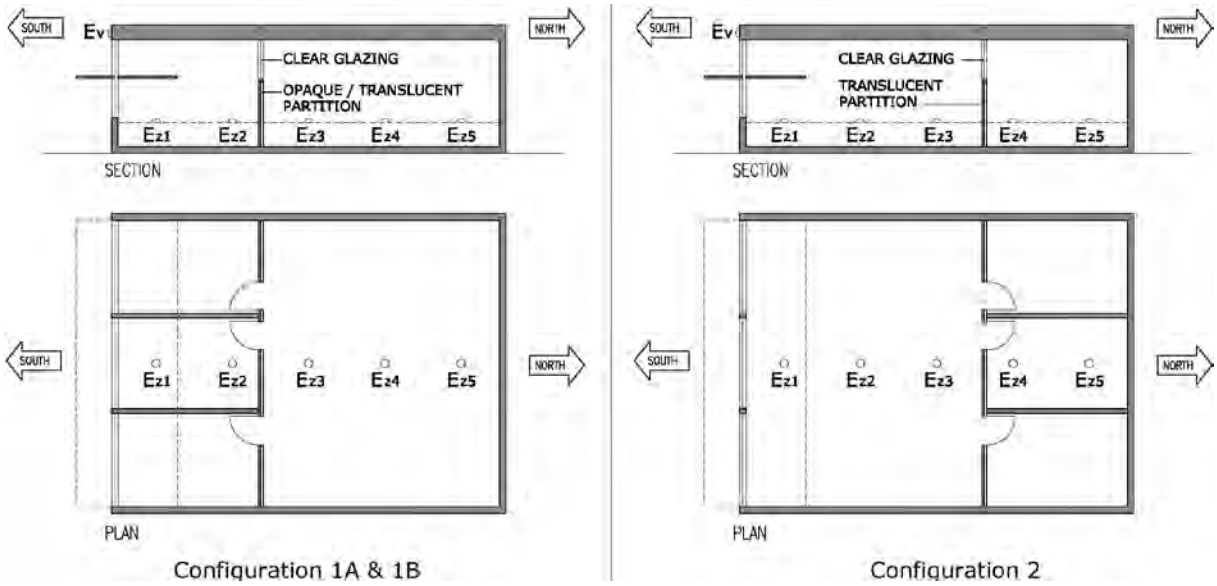

Fig. 5. Interior configuration 1A, 1B and 2.

3. Results & Discussions

Hourly illuminance data in each zone are generated for the above comparison studies. Daylight Autonomy data are then developed based on these values as performance indicators.

3.1. Length of light shelves

The performances of light shelves with various lengths (2' through 12' with 2' increment) are illustrated in Figure 6. For internal zones (Ez3 through Ez5), the 4-ft light shelf performs slightly better than the 6-ft version. However, the longer light shelf outperforms the shorter one for the purpose of blocking the direct sunbeam penetration through the daylight glazing (Figure 7). In general the 6-ft light shelf appears to be the optimal solution among all the lengths tested and will be used for later phases of the study.

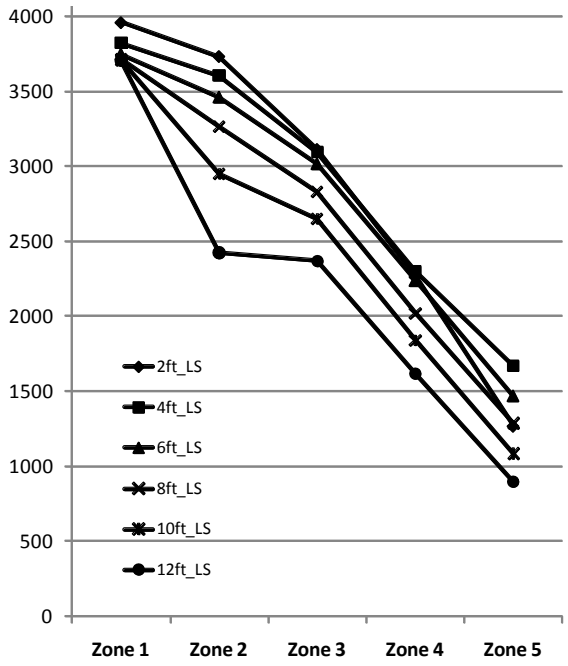

Fig.6. The numbers of hours in which interior illuminances are above 500Lux for light shelves with various lengths

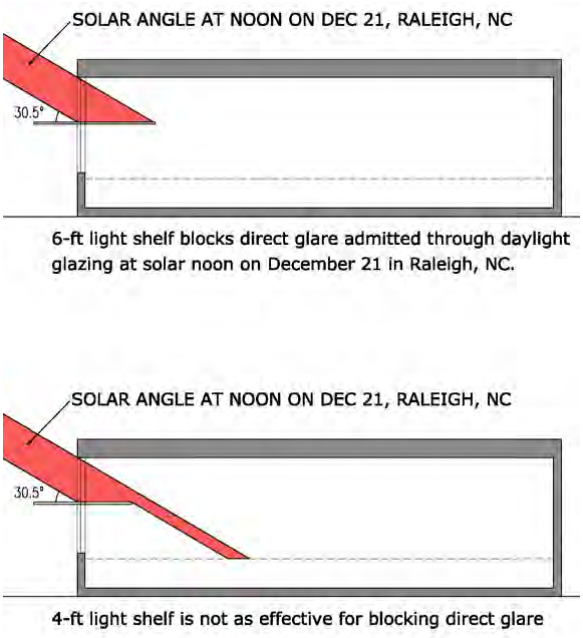

Fig.7. Direct glare admitted through daylight glazing with 4-ft and 6-ft light shelves. 6-ft version performs better for blocking direct glare

3.2. Ceiling height

The impact of ceiling height on light quantity is fairly significant as illustrated in Figure 8. In conjunction with the light shelves, higher ceilings are obviously desirable for the purpose of delivering daylight deeper in the space.

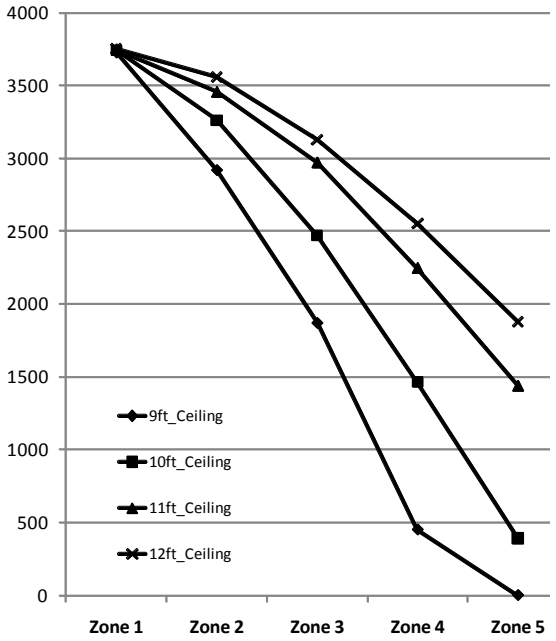

Fig.8. The numbers of hours in which interior illuminances are above 500Lux for interior space with different ceiling heights

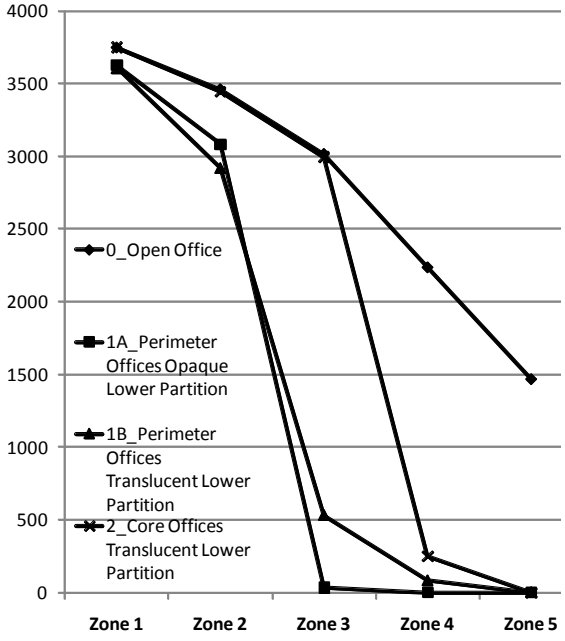

Fig.9. The numbers of hours in which interior illuminances are above 500Lux for different interior configurations

3.3. Interior configuration

As shown in Figure 9, among the four interior configurations proposed in section 2.2.3, open office layout (Configuration 0) certainly gives the best performances in that it maintains higher light levels across the space and produces a fairly uniform distribution without any abrupt change of light levels. Introducing private enclosed offices at the perimeter of the floor plate (Configuration 1A) dramatically lowers the daylight quantity in the inner open office. Switching the material from opaque to translucent for the lower portion of the partition that divides the perimeter offices and the open office improves the condition to some extent (Configuration 1B). However, if private offices have to be provided, relocating them to the core of the space and leaving the open office at the perimeter greatly (Configuration 2) improve the overall lighting conditions, especially at the open area which is occupied by more users. In addition, comparing the results between Configuration 0 and 1A, by adding partitions perpendicular to the window wall to define the private offices in 1A, the light levels in the perimeter zones (Zone 1 and 2) are lowered as well as in the inner open office.

4. Conclusions

Although light shelves generally help project daylight deeper in the space under certain solar angles, it is a misunderstanding that the longer a light shelf is, the better it performs. It is the proportion of the daylighting glazing height and light shelf length that determines the performance of the system. Therefore, the length needs to be optimized based on other geometries of the system, such as ceiling height and daylight glazing height, and the system needs to be evaluated in terms of both light quantity and quality. For the particular daylight system assessed in this study, the 6-ft light shelf is proven to be the optimal solution.

The benefits of raising the ceiling are significant. Even though there are many factors motivating towards lowering the ceiling, including construction cost, fire rating, accommodating structure, duct work, etc., a carefully designed and highly integrated building system needs to be in place to assure adequate ceiling height for daylighting.

Adding partitions that are either parallel or perpendicular to the south-facing window wall to divide open space into small offices creates a fairly big drop in the illuminance deeper inside the space. If private offices have to be incorporated in the floor plate due to programmatic requirements, it is recommended that the small offers be located at the core of the building. Comparing with opaque partitions, translucent partitions give superior illuminance levels deep inside the building and they also produce superior light quality in the form of less extreme luminance ratios in both interior and perimeter spaces. It is highly desirable to use clear glazing above the level required for visual privacy (e.g., from the top of the door up to the ceiling). It is also desirable to minimize the number and width of mullion elements, to allow as much light as possible through the partition.

References

[1] Selkowitz, S., Navvab, M. and S. Mathews, "Design and Performance of Light Shelves", International Daylighting Conference, Phoenix, AZ., 1983.

[2] Burt Hill Kosar Rittlemann Associates, "Thermal and Optical Performance Characteristics of Reflective Light Shelves in Buildings", NTIS PB 88160965, 1985.

[3] Fardeheb, F., "Effects of sloped versus horizontal ceiling combined with different light shelf designs", American Solar Energy Society, 11th National Passive Solar Conference, Boulder, CO., 1986

[4] Place, W., Howard, T., and S. Howard, Daylighting Classroom Buildings, North Carolina Alternative Energy Corporation, 1991.

[5] Close, J., "Optimizing Daylighting in High-rise Commercial Developments in SE Asia and the Use of Computer Programs as a Design Tool", WREC, 1996.

[6] Claros, S. and A. Soler, "Indoor Daylight Climate-comparison between Light Shelves and Overhang Performances in Madrid for Hours with Unit Sunshine Frantion and Realistic Values for Model Reflectance", Solar Energy, Vol.71, No.4, 2001.

[7] Mardaljevic, J., "Examples of Climate-Based Daylight Modelling", CIBSE National Conference 2006: Engineering the Future.

[8] Reinhart C F, Walkenhorst O, "Dynamic RADIANCE-based daylight simulations for a full-scale test office with outer venetian blinds." Energy & Buildings, 33:7 pp. 683-697, 2001.

[9] Reinhart C F, Herkel S, "The simulation of annual daylight illuminance distributions – a state-of-the-art comparison of six Radiance-based methods." Energy & Buildings, 32 pp. 167-187, 2000.

[10] Place, W., Howard, T., and S. Howard, Daylight Resource Data for Illuminating Building Interiors in North Carolina, North Carolina Alternative Energy Corporation, 1992.

Optimized Modular window as a sustainable and industrialized solution for indoor daylighting

P. Oteiza[1,*], S. Orozco[2], M. Pérez[2], C. Bedoya[2], J. Neila[2]

[1] *Department of Physics, School of Architecture, Universidad Politécnica de Madrid, Spain*
2 *Department of Construction, School of Architecture, Universidad Politécnica de Madrid, Spain*
**Corresponding author: Tel: +34 913366542, Fax: +34 913366554, E-mail: mariapilar.oteiza@upm.es*

Abstract: The objective of this paper is to present the computer simulation results that we have obtained with a new window design. This prototype is equipped with the elements necessary to capture and distribute natural daylight in an optimum way. The whole window system is able to be adapted to the weather conditions of most of the Iberian Peninsula. Its design contains elements to let the sunlight into the room, and elements to control it. The initial results of the daylight experimental analysis we have carried out so far, demonstrate the system´s overall efficiency, however, we continue to research about the light shelf´s optimal configuration in order to obtain the maximum and most flexible performance. There is demonstrated in this work that the Modular window with a top hollow of 40 cm, instead of 30 cm of the original one, improves the luminous conditions of the room. Once the preliminary analysis phase is concluded, the window will be installed in one of the two testing houses being constructed at Cáceres (Spain), so that real-scale conclusions can be obtained, and recommendations be set, aimed to improve the quality of the construction process, while maintaining the high standards of sustainability we pursue.

Keywords*: Windows, Daylighting, Solar Protection, Sustainability, Industrialization.*

1. Introduction

This paper summarizes the design process, and the final results, for the development of a Modular window, capable of effectively responding to the climatic conditions of the Iberian Peninsula. It is part of the INVISO research project (Industrialization of Sustainable Housing) under development at the ETSAM (Escuela Técnica Superior de Arquitectura de Madrid). It is being carried out by the Researching Group ABIO (Bioclimatic Architecture in a Sustainable Environment).

The design process started off with the definition of the objectives that the Modular window must achieve, which at the same time, determined it´s basic constitutive elements: a solar shading box, a light shelf for daylight projection into the inner parts of the room, direct light and solar radiation control elements, as well as phase change materials (PCM) for thermal lag profiting. With this basic component list, two 1:10 scale models were built and exposed to real external environmental conditions. Continuous light level measurements [1] were taken with these models, which, along with thermal balance calculations [2] and the simulations presented here, allowed us to correct of the original design until the current Optimized version. This Optimized Modular window consists of three vertically aligned apertures: the top one with a 0.40 m height and light shelf; the central one, with a 1.38 m height and low emissivity glazing; and the lower one with an 0.82 m height and an externally glazed Trombe wall with paraffin as PCM.

Partial prefabrication is intended to make the installation easier, and allow some flexibility in the aspect of the final result.

2. Design objectives

In order to reduce environmental impact associated with buildings envelope, external windows in medium latitude countries, as in the case of Spain, must keep a balance between

daylight entry and it´s implicated heat transfer [3,4]. The window must be industrializable, so its main elements will be pre-assembled in the factory and later brought to the building site. Materials employed will be light, safe, economic and, as far as possible, not aggressive with the environment.

The future objective of the present work is not only the prototype design, but it´s construction and installation in a housing building which will be used as a laboratory. Monitored data from the different thermal and daylighting parameters will be compared to those obtained in an identical building with conventional windows, so that real conditions results and conclusions can be obtained from them. In Cáceres (39º 28' N and 405 m.a.s.l) far from big water masses which would mild the value oscillations, temperature fluctuations per day and per year are very important. In a summer day up to a 15 ºC difference can be measured. Taking into account the annual behavior, external temperature differences can reach 25 ºC between a summer and a winter day. These marked fluctuations require different strategies of environmental conditioning. In summary, it can be said that in Cáceres, like in Madrid, cities of soft and large winters, there´s a need for a mechanical heating system during 73 % of the annual period, furthermore, the short and strong summers require cooling during the 27 % left. The dimensioning stage of the design process, has considered current regulations on daylight and ventilation minimal areas: the Modular Window has an area that accounts for the 22.30 % of the test room´s total floor area, which, by far, surpasses the value stated in the current regulation.

3. Components

The components that make this window an innovative product, Fig. 1, can be grouped in three zones: *Upper zone or clerestory.* It is 0.30 m high, its main function is to light the interior of the room by reflecting daylight on the shelf [5]. The light shelf is 0.9 m deep and it is covered on its upper side by a 90% reflectance mirror. The light shelf is partly inside the module (1/3 of its depth). The *Central zone, or window view.* It is 1.48 m high. Its main function is to allow observation and contact with the outside environment. It is also able to open and allow ventilation. And finally, the *Bottom zone,* 0.82 m high, and designed to integrate phase change materials in order to maximize thermal benefits. Besides, the Central zone and the Lower zone are surrounded by a frame which overhangs 0.6 m in order to reduce the direct sun radiation and also the diffuse sun radiation.

4. Experimental analysis of the Modular Window´s daylighting performance

In the previously undertaken experimental study, two 1:10 scale models were used. These were situated on an obstacle-free (no overshadowing) terrace in Madrid. One of the models was equipped with a simplified Modular window, consisting of its three basic parts: top light shelf, central shaded opening, and lower completely opaque box. The second model was equipped with a conventional window, without the light shelf, nor any shading device. This was used as the reference model. Continuous measurements were taken, for global horizontal illuminance using five photometric sensors Li-Cor 210SA, two scenarios were tested: the first one, allowing light only through the top opening (*clerestory* only), and the second one, allowing illumination through both the top, and central openings (*clerestory* and *view*). Los the results are summarized in the following statements:

- With the top section opened (clerestory), and the rest of the window shut (opaque), the sensor located furthermost from the window, registered higher illuminance values for the Modular window, during 75% of the time. Reaching a maximum difference value of 1.87 times in a Modular – Conventional comparison. Therefore, the light shelf on

the Modular window significantly contributed to a better illumination of the inner room area farther from the window.

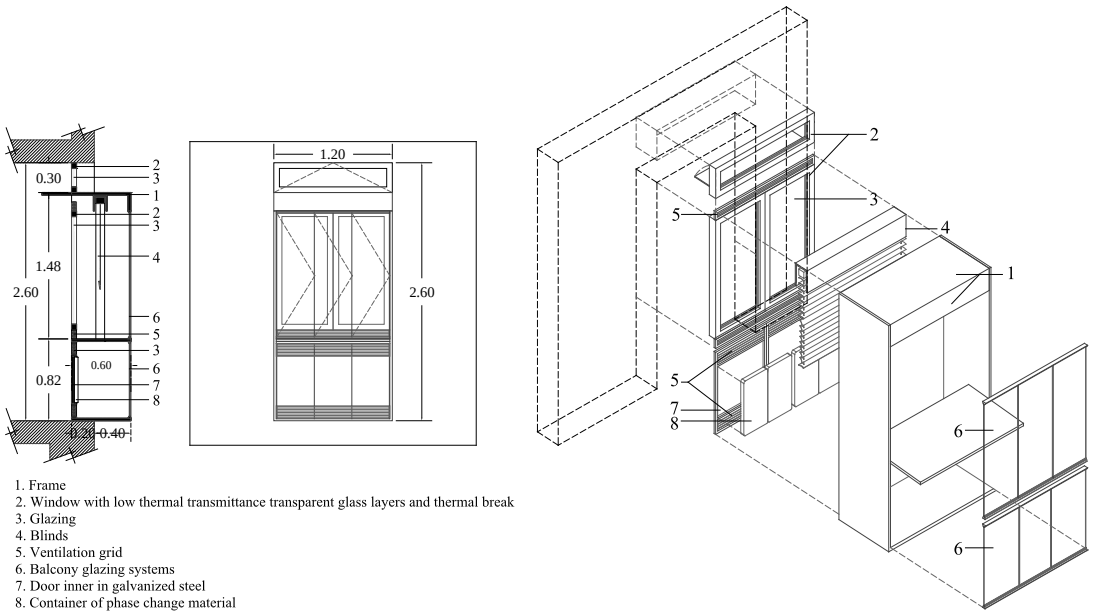

Fig. 1. The components of the original Modular Window

- When the two upper sections of the window (clerestory and view) were open on both models, the inner sensor (furthermost from window), registered higher illuminance levels for the Modular window during 21% of the time. The difference with the result mentioned on the previous statement is due to the effect of the solar shading box on the Modular window.
- The Modular Window improved the lighting conditions in the area closest to the window because the solar shading reduced the high illuminance values of that particular zone (especially during summer´s high solar angle period).
- The differences in illuminance levels obtained with the sensors located near and far from the window, were smaller in the Modular window equipped model. This demonstrates a more uniform daylight distribution in the room´s interior, and thus a significant glare reduction.

5. Clerestory modifications for the optimization of the Modular window

The study described so far, corresponds to the basic design of the Modular window, which had a 30 cm high top opening (clerestory). In order to improve the previously obtained results, we have carried out a brief comparative analysis with a variable clerestory dimension, ranging from 30, 35, 40, and 45 cm, Fig. 2. This range is derived from the limits established as acceptable: for starters a vertical dimension less than 30 cm is not constructively or functionally possible; on the other hand, the light shelf´s vertical position must correspond to a certain height that does not cast any direct reflexion at the occupant's eye level. Accordingly, with a 45 cm clerestory, the light shelf sits at a top height of 215 cm from the floor, which is enough to avoid any light reflexion related disturbances. This analysis has been developed with the use of the simulation tools Autodesk Ecotect, and LBNL Radiance[6]. In the first place, the annual periods with different thermal requirements have been defined, and consequently, their relationship with the window design. Based on the climatic records from the Spanish Weather for Energy Calculations (SWEC) [7] for the city of Madrid (very similar conditions to the ones found at Cáceres) and with the use of the Adaptive Comfort

Chart, developed by J. Neila, and his research group at ETSAM [8], we have defined a basic human comfort temperature range that goes from 18 ºC up to 26 ºC.

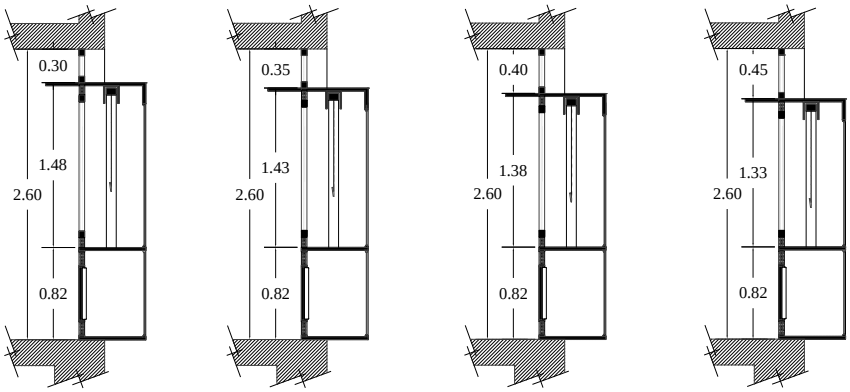

Fig. 2. Detail sections of the four dimensioning options analyzed for the clerestory(dimensions in m).

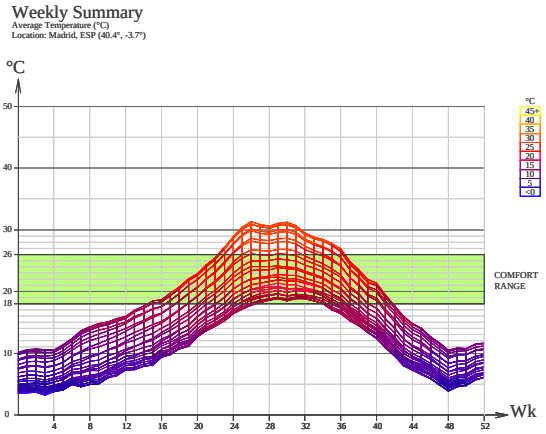

Fig. 3. Average temperature trend and human comfort range for the city of Madrid.

From here, the annual period with average temperature values under 18 ºC, has been established as “Heating Requiring Period”, and inversely, the period with average temperature values over 26 ºC, has been defined as ”Cooling Requiring Period”. Fig. 3 shows the average temperature trend throughout the year, along with the previously mentioned comfort range. Fig. 4 shows the monthly heating/cooling requirements as well as the solar radiation available so as to clearly observe each period and its thermal requirements. With the start-end dates established for each period, the clerestory´s dimension was analyzed so that it would allow the maximum collect of direct solar radiation during the underheated period, but at the same time, it would offer the maximum protection from possible heat gains during the overheated period.

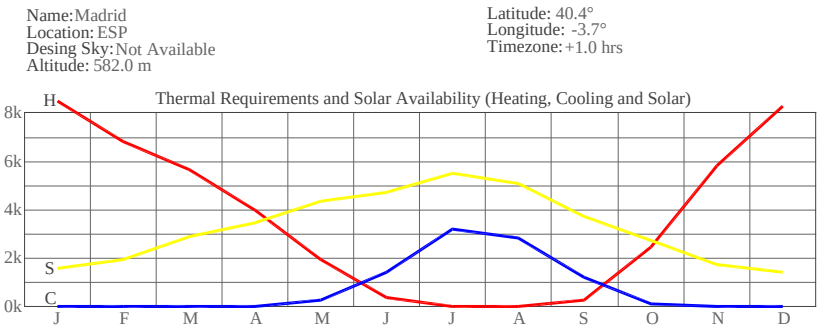

Fig. 4. Thermal requirement curves (heating: red ; cooling: blue) and solar availability (yellow) for the city of Madrid.

5.1. Shading coefficient analysis

In order to optimize the clerestory dimensions and ensure the light shelf´s máximum efficiency, the following premise has been set: a very small opening, offers a good protection (shading) during the overheated period, but limits the thermal contribution of solar direct radiation during the underheated period; in an opposite way, a very big opening maximizes thermal benefits during this cold period, but also contributes to interior space overheating during the warm period. To be able to objectively compare this factor, we have analyzed the Shading Coefficient value, which has been defined by the australian research group SquareOne[9] as: "*…an hourly averaged value that represents the shaded area of a vertical opening in relationship to the opening´s total area* ". The values of each dimensioning option have been studied considering a minimum inset of 18 cm (typical value of an unshaded window built with a conventional system). Fig.5 shows the respective performance in terms of the capture/protection balance described above. Amongst the multiple interpretations that can be made, the one we are more interested in is the one related to each of the openings behavior during the warm and cold periods. For instance, it is clear that all of the openings offer 100% shading during May, June, and July, however, the 45 cm opening considerably loses effectiveness during August and September, at a monthly ratio slightly superior to 15 %. In a similar way, the original 30 cm opening minimizes the heat gain profits during the cold period, with a minimal shading coefficient of 30 % year-round. For these particular reasons we have focused on the 35 cm and 40 cm openings, of which a very similar performance can be apreciated. Nonetheless, the 40 cm hole has an average shading coefficient 3% smaller than the 35cm hole one during the underheated period of the year (months with heating requirements). This results in a slightly better solar-thermal energy penetration and minor savings in heating-energy. Hence, the 40 cm hole has been selected to undertake the daylighting performance simulation analysis.

5.2 The use of Ecotect/Radiance for daylight simulation.

Having selected the optimized dimensions for the clerestory (40 cm), and keeping the original design dimensions (30 cm) as a reference, we carried out computational daylight simulations of interior luminous distribution. Furthermore, in order to visually determine the advantages of the proposed design, we have compared both Modular windows (original and optimized) with a conventional window. The simulation has been done using a software combination of Autodesk Ecotect + LBNL Radiance, and therefore all of the results obtained are subject to the accuracy and acknowledgement of these programs. All of the analysis have been undertaken in an hourly sequence, the luminous internal penetration and distribution results are presented for 13h (legal time), and accordingly there are three images for each date.

Fig. 6 shows the illuminance range for a date representative of the underheated period: December 21st (winter solstice). There are no remarkable differences between the three models (Conventional, Modular, and Optimized Modular), mainly due to the low angular rise of solar rays (23º at noon).

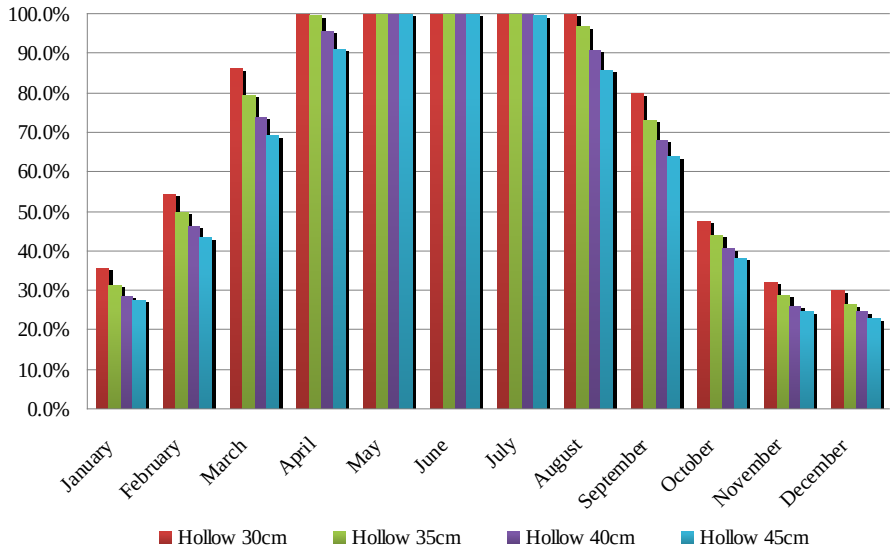

Fig. 5. Monthly shading coefficients comparison for the four dimensioning options.

The conventional window (on the left) shows the highest illuminance levels both during morning and evening hours, plus, it performs similarly to the Modular (center) and Optimized Modular (right) models during midday. In spite of this, a slightly better performance (more depth) can be observed for the Optimized Modular against the original design.

Fig. 7, shows the same analysis done for a date representative of the overheated period: June 22 (summer solstice). For this second series of analysis, a better performance on behalf of the Optimized Modular Window becomes quite evident: a deeper luminous penetration, along with a more uniform light distribution, and mainly a better shading protection against direct solar radiation during all day.

Finally, the last analysis series correspond to a “thermal neutrality” date: September 21 (fall equinox), Fig. 8. Clearly demonstrates the functioning of the three window models in a moderate solar height scenario. On top of a better overall illumination, the Optimized Modular Window offers the best shading against direct solar radiation and thus, it avoids as much as possible the potential glare effect.

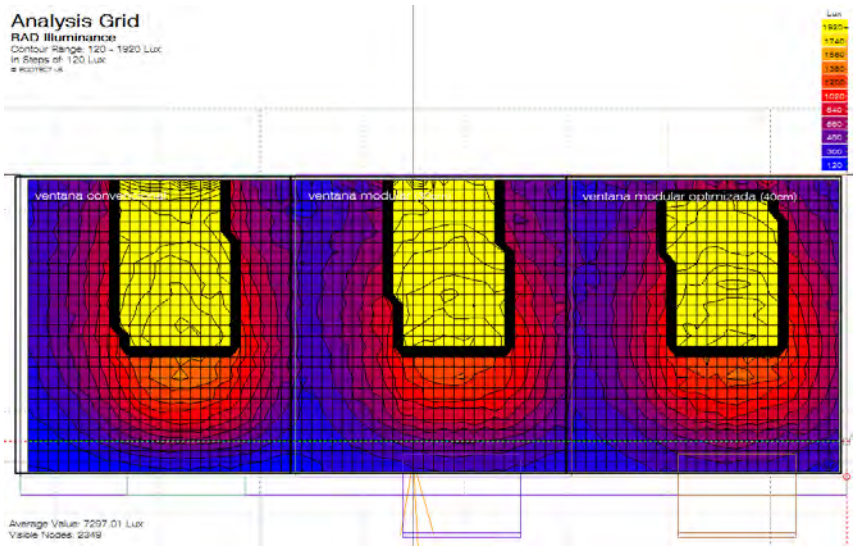

Fig. 6. Internal illuminance distribution (plan view of the room) for the three window: Conventional (left), Modular original (center), Modular optimized (right), during December 21st at 13 h.

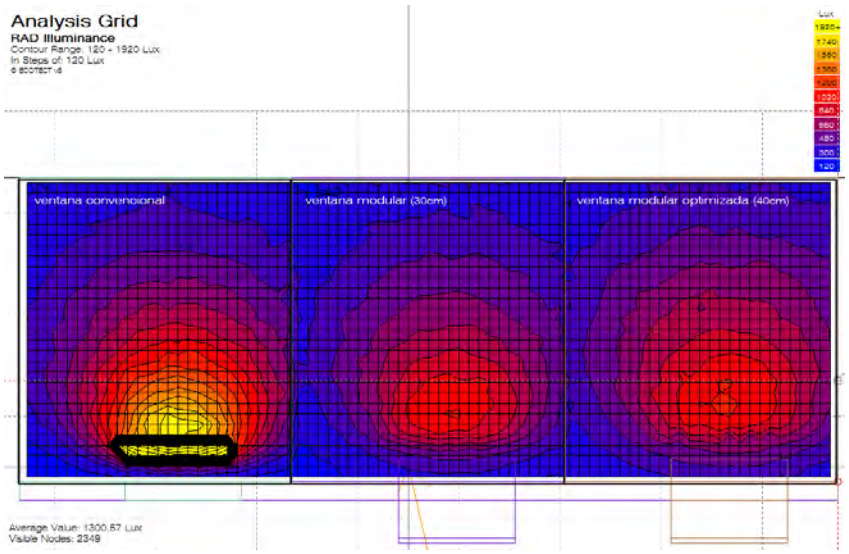

Fig. 7. Internal illuminance distribution (plan view of the room) for the three windows: Conventional (left), Modular original (center), Modular optimized (right), during June 22nd, at 13 h.

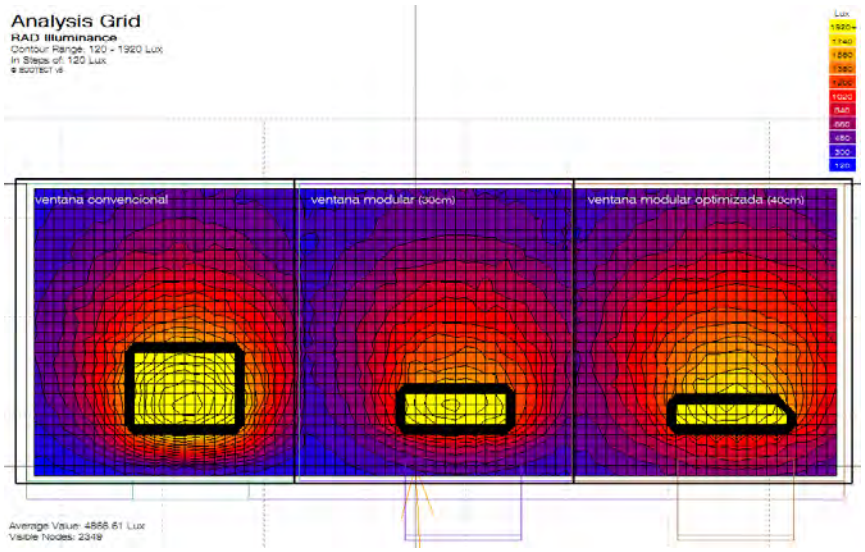

Fig. 8. Internal illuminance distribution (plan view of the room) for the three windows: Conventional (left), Modular original (center), Modular optimized (right), during September 21st at 13 h.

6. Conclusions

The Modular window consists of three parts: i) the top section, which is a 30 cm high opening equipped with a light shelf to improve the illumination of the inner room area, farthest from the window: ii) the central section, with a 148 cm high opening that not only pursues natural illumination and visual contact with the exterior surroundings, but also counts with the protective shading elements required by our climatic conditions; and iii) the lower section is an opaque, 82cm high element, that includes a trombe wall formed out of paraffin, which is an innovative building material that changes its physical state (solid-liquid) at specific predetermined temperatures, thus reducing and retarding the heat exchange through itself. In order to be able to test its luminous performance, a previous study was made with the use of scale models, for which the Modular window design was compared against a conventional unequipped window; this study demonstrated that the Modular window improved daylighting intensity in the inner part of the room, located farther from the window. However, since the

experimental study advanced very slowly, and was too dependent to the highly variable environmental conditions (i.e. cloud cover), we set to study the modification of the upper opening and its light shelf, with the use of photometric simulation tools: specifically the combination of analysis programs Autodesk Ecotect + LBNL Radiance. Four dimensioning possibilities for the upper opening were tested: the original 30 cm height, plus another three: 35, 40, and 45 cm. The four options provided a protection of 100% from solar direct radiation during the first three months of the overheated period (May, June, July), however the 45 cm opening considerably lost its protective effectiveness during the months of August and September, at a monthly rate slightly superior to 15 %. In a similar way, but during the underheated period, the 30 cm opening was too limiting on the required solar heat reception, as its shading coefficient didn't go under the 30 % value during any month of the year. A very similar behavior was appreciated with the 35 and 40 cm openings. Nonetheless, and although it was only by a small difference, the 40 cm opening performed 3 % better to the thermal requirements of the cold period. Taking into account the balance between solar heat profiting, and excess direct radiation shading, during the two annual periods with heating and cooling requirements, the analysis results are that the 40 cm opening performed better, hence, it has been proposed as the new dimension to use with the Optimized Modular window design. It has been demonstrated that the Optimized Modular window produces the best overall daylight conditions in the interior of the room, because it improves the illuminance levels on the deeper area (far from the window), contributes to a more uniform light distribution, and at the same time protects from overheating and potential glare effect.

References

[1] P. Oteiza; M. Pérez; C. Bedoya; J. Neila; Modular window daylighting performance vs. Conventional window, Lighting Research and Technology (in approval process).

[2] P. Oteiza; C. Pérez; M. Pérez; Modular window thermal performance vs. Conventional window, Energy and Buildings (in approval process).

[3] D. Phillips, Daylighting: Natural Light in Architecture, Architectural Press, London (2004).

[4] P. Poyce, C. Hunter, O. Howlett, The Benefits of Daylight through Windows, Rensselaer Polytechnic Institute, New York (2003)

[5] A. Soler, P. Oteiza, Lightshelf Performance in Madrid, Spain, Building and Environment 32 (1997) 87-93.

[6] Natural Frequency Online Community; wiki.naturalfrequency.com; archive site for autodesk ecotect analysis educational resources; consulted on August 2010.

[7] Grupo de Termotecnia de la Escuela Superior de Ingenieros de Sevilla; Agencia Estatal de Meteorología; Spanish Weather for Energy Calculations SWEC, Seville, Spain (2008)

[8] J. Neila, Arquitectura Bioclimática en un Entorno Sostenible, Editorial Munilla-Lería, Madrid 2004.

[9] A.J. Marsh, Square One research, University of Western Australia (2008).

Volumetric – Spatial design and daylight in apartment buildings. Study case: Havana City.

D. González Couret[1,*], D. F. Abreu de la Rosa[2]

[1, 2] *Faculty of Architecture, ISPJAE, Havana, Cuba*
** Tel: +53 7 2607242, E-mail: dania@arquitectura.cujae.edu.cu*

Abstract: The relationship between architectural shape and daylight is very well known. The geometry of the building and its context influence quantitatively and qualitatively indoor natural illumination. But this architectural feature highly determines also the thermal environment and sometimes these two requirements are contradictory.

The results presented in the paper are part of a wider research that intends to evaluate the influence of the transitional spaces (indoors – outdoors) on the interior spaces environment. In order to do that, measurements of temperature and humidity have been carried out in housing buildings in some urban areas in Habana City, and at the same time, daylight conditions in those buildings and spaces have been simulated. The results of this computer simulation and its discussion are presented in the paper, focused on the performance of the geometry of these transitional spaces.

A representative sample of apartment buildings typologies that are being studying in different urban areas was selected in order to simulate daylight performance indoors, using the professional software "DIALux". The better daylight conditions are got in spaces related to wide streets. On the contrary, small yards are not enough, depending on its proportions.

Keywords: *Daylight, Simulation, Architectural design, Apartment buildings.*

1. Introduction

Taking advantage of the urban land is an essential condition to a sustainable built environment. That's why many developed countries are intending to increase density in cities. On the other hand, conservation of traditional urban centers is another important requirement in order to pass to the future generations the historical legacy of each society.

Related to that, the National Institute of Physical Planning in Cuba is promoting the integral rehabilitation of traditional cities, and a departing point for what should be the insertion of new housing buildings in the available plots. But how should these new housing building be? What architectonic references should be taken?.

During the 60's and the 70's, mostly new urbanizations were developed out of the traditional urban grid, using block type building by repetitive projects in open urban areas. When no repetitive projects were built in the consolidated urban zones during the 80's in Havana, the mistakes committed [1] showed the lack of knowledge about the traditional repertory of apartment buildings preexisting in these urban contexts. Finally, the last two decades has been characterized by disperse low density urbanizations that generate a disproportioned and unsustainable urban growing.

Then, projecting and constructing new apartment buildings in traditional urban centers is unavoidable as part of their integral rehabilitation process and for that, it is necessary to know the wide precedent repertory of buildings integrated to the context and conforming the city, to take them as references of the good practices to be recovered and the mistakes to be avoided.

Several researches have been carried out in the Faculty of Architecture of Havana during the last ten years, driven to characterize the repertory of existing apartment buildings in the traditional urban centers and to evaluate their performance according to the quality of the thermal and luminous indoor environment, taking into account besides, the inhabitant's perception.

The results of the evaluation of the volumetric and spatial solution of apartment buildings existing in three different urban contexts of Havana City according to their influence on indoor daylight are specifically presented in this paper.

2. Methodology

In order to evaluate the influence of the building volumetric - spatial design on the indoor daylight levels, real spaces were selected from the study sample composed by 279 apartment buildings located in three different context in Havana City (Centro Habana, El Vedado y Miramar) [2], to simulate interior daylight. The selected spaces are related to outdoors in different ways, according to the volumetric – spatial solution of the building and the urban context.

Indoor daylight depends on several variables. The geometry of the transitional space between indoors and outdoors is the one to be evaluated in this work, which determines the exposition angle to the sky and to direct daylight (e_0), and also to the light reflected by the exterior elements in the context (e_e).

The interior daylight level is also influenced by the reflection coefficient of the surfaces (indoor or outdoor ones), the window area, its location, proportions and type of enclosure (the windows itself) and color, that determine the reduction coefficient for daylight incoming. In order to isolate the studied variable (the transitional space geometry), the rest of the variables were cancelled, assuming the same values or features in all the simulated cases.

The volumetric – spatial design solution was characterized by angles (horizontal and vertical) that determine the exterior geometry respect to the exposed façade of the indoor space to be evaluated. Each way of indoor – outdoor relationship was identified by the angles, the surface that they determine (closed or open) and one dimension, since having only one dimension and the proportions (angles), it is possible to get the characterization of the whole geometry
Indoor – outdoor relationship ways were classified in precedent researches [3]:

- To the streets: main streets (15m) and secondary ones (6m), considering longer dimensions as exceptional.
- To corridors, parallel or perpendicular to the street, belonging to the building itself, it means, inside its volume, as part of the architectural solution.
- To lateral, back and surrounding corridors: open spaces (without roof) annexed to the building as port of the urban context.
- To internal yard: open spaces (without roof) located to the interior of the plot, with width between 1.7m and 4.0m, and length between 4.0m and 26.0 m.
- To lateral yard: open spaces (without roof) located to the interior of the plot, but laterally, where one of the dimensions is considerably larger than the other, with width between 1.0m and 6.0m and length between 9.0m and 25.0m.
- To small yards ("patinejos" or wind boxes): open spaces (without roof), but closed in their four vertical surfaces, located to the interior of the plot, with smaller dimensions than the yards (width between 0.5m and 1.7m, and length between 1.2m and 4.0m).

- To "grecas": open space (without roof) similar to small yards, but also open by one of the vertical surfaces.

Departing from this detailed classification, only three general types of transitional spaces have been identified for the simulation, according to the geometric characterization: corridor (Figure 1), yard and "greca" (Figure 2).

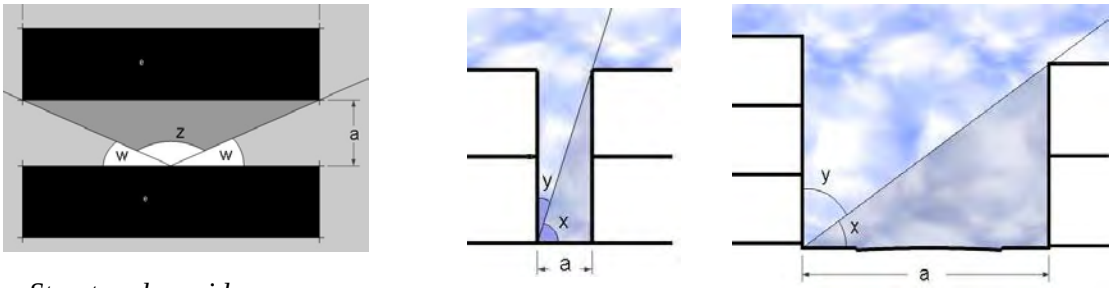

Street and corridor *Corridor section* *Street section*

Fig. 1. Corridor type spaces: closed in the front and open laterally (corridors and streets).

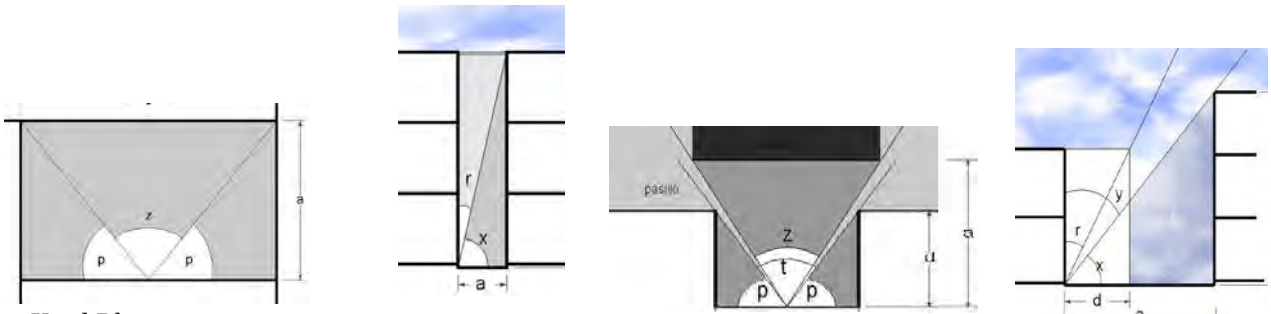

Yard Plan *Yard Section* *Greca Plan* *Greca Section*

Fig. 2. Yard and Greca type spaces

Where X: frontal obstruction angle in section; Y: angle of opening to the sky in section (x +y =90^o); Z: frontal obstruction angle in plan; W: lateral opening angle in plan (z +2w =180^o); r: lateral obstruction angle in section; t: frontal opening angle in plan; p: lateral obstruction angle in plan (t +2p =180^o); **a:** distance from the angle origin to the frontal obstruction surface.

2.1. Study cases

Taking into account this geometric characterization of the transitional in – out spaces, 44 spaces were selected from the repertory of apartment buildings studied in precedent researches, representatives of each of the three urban context considered (Centro Habana, El Vedado and Miramar), and of each transitional type, including diverse orientations.

Despite orientation was taken into account to select the study cases (because of its influence in the thermal environment studied in other parallel research), this variable was not considered in the simulation of daylight performance, since the used software departs from a uniform sky to determine the daylight factor.

The spaces selected in Centro Habana are related to outdoors by streets and yards, streets with different sections (proportions) and orientation, and yards with extreme proportions. In El Vedado and Miramar, the spaces selected are related to yards, corridors and "grecas". (Table 1)

Table 1. Study Cases, according to type of transitional space and urban context.

Urban Context	Corridor	Yard	Greca	Total
Centro Habana	6	8	-	14
El Vedado	8	8	1	17
Miramar	4	4	5	13
Total	18	20	6	44

2.2. Software

Four software were evaluated to simulate indoor daylight performance: DIALux 4.6 (2007), Ecotect (2007), Relux (2007), Adeline (1998), by comparing the results achieved with each of them to real values measured by De la Peña in 1986 [3] in a living room rectangular in plant (5.2m x3.6m) with unilateral daylight through a balcony, locating the luxometer in the center of the space. The daylight factor achieved in the measurement was 0.56.

In order to simulate daylight using Dialux 4.6 a transference coefficient for windows was considered as 0.90 (glass windows), reflection coefficients for ceiling, walls and floor as 0.70, 0.50 and 0.20 respectively, and the sky type was assumed as uniform, according to the model defined to Havana. The daylight factor (e) was simulated on a surface located 0.75m over the floor, and the point located in the middle of the space was used to compare to the real measurements. The coincidence between the values simulated and measured (e=0.56) confirms the possibility of using Dialux 4.6 for interior daylight simulation. Dialux 4.6, besides, allows making the model of the space easily, quickly and with high precision, and offers numerical and graphic results with high quality renders.

2.3. Simulation

The study cases were considered in extreme conditions, that's why the spaces were located on the ground floor, and the time assumed was December at 4.00 pm, the more critical for indoor daylight.

Dialux 4.6 considers an overcast sky that corresponds to the uniform sky as a theoretical model, with the same luminance in all directions. The model is appropriate to Havana's sky, defined as partially cloudy, with tendency to be overcast and not permeable to the solar rays, intermittent light and constant luminosity, as an isotropic model with the alternative presence of the sun [4]. Fort the latitude of Havana, in December at 4.00 pm Dialux 4.6 assume diffuse daylight values on an outdoor horizontal plane, equivalent to 10 163 lux.

In order to simulate indoor daylight in the selected study cases, a standard space (3.60m by 3.60m in area and 2.80m in height) was taken, with a louver wooden windows (1.40m wide by 1.20m height), white colored and located to the center of the wall, as traditionally used. The reflection coefficients considered to surfaces were: 0.2 to the floor, 0.5 to the ceiling and 0.7 to the walls, as well as 0.5 to the exterior ones, coincident to the values recommended by the software; the windows transmittance was assumed as 36% and reflectance as 79% (light color). The values of indoor daylight were considered on a gridded plane located at 0.75m height from the floor level.

The simulation process started with a space directly exposed to outdoors in an open context, which result was compared to the simulation of spaces related to outdoors by different types of transitional spaces with their particular geometry, in order to evaluate the influence of the volumetric – spatial solution on the indoor daylight.

3. Results

The results got in the simulation process were summarized in relation to the geometry of the transitional space and the percentage of reduction in comparison to a similar space connected to outdoors without obstruction, where "a" is infinite and "x" equivalent to 0^0.

The simulated spaces didn't compliment the required daylight level (daylight factor value=1.5 for kitchens), and only in one case, the minimum uniformity (0.3) is achieved. The higher daylight levels are got in spaces related to corridors (width streets and the more favorable urban context is Miramar, with lower land occupation. (Table 2)

Table 2. Daylight Factor and Uniformity indoors according to transitional space and context

Urban Context	Corridor		Yard		Greca	
	e_0	U	e_0	U	e_0	U
Centro Habana	0.32	0.09	0.03	0.18	-	-
	0.09	0.03	0.01	0.02	-	-
	0.46	0.15	0.02	1.00	-	-
	0.17	0.06	0.01	1.00	-	-
	0.20	0.09	0.00	0.00	-	-
	0.32	0.11	-	-	-	-
El Vedado	0.01	0.07	0.05	0.07	0.02	0.05
	0.01	0.07	0.05	0.07	-	-
	0.03	0.04	0.05	0.07	-	-
	0.03	0.04	0.05	0.07	-	-
	0.15	0.05	0.01	0.25	-	-
	0.02	0.05	0.05	1.00	-	-
	0.02	0.05	0.00	0.00	-	-
	0.02	0.05	0.00	0.00	-	-
Miramar	0.16	0.04	0.04	0.26	0.08	0.05
	0.14	0.05	0.04	0.26	0.06	0.31
	0.33	0.09	0.04	0.26	0.19	0.08
	0.14	0.04	0.04	0.26	0.19	0.08
	-	-	-	-	0.12	0.08

However, the influence of the geometry of the transitional space on the indoor daylight can be evaluated taking into account the reduction of daylight level (in %) respect to the reference space directly related to an open outdoors.

4. Discussion and Conclusions

There is a direct relationship between the type of transitional space and the reduction of indoor daylight. The corridors constitute spaces only closed on the front, but open to the top and laterals. Those spaces, as well as the "greca" type, opened by one of their vertical surfaces

(frontal or lateral ones) besides the top, are more favorable than yards from the daylight point of view. (Figure 3)

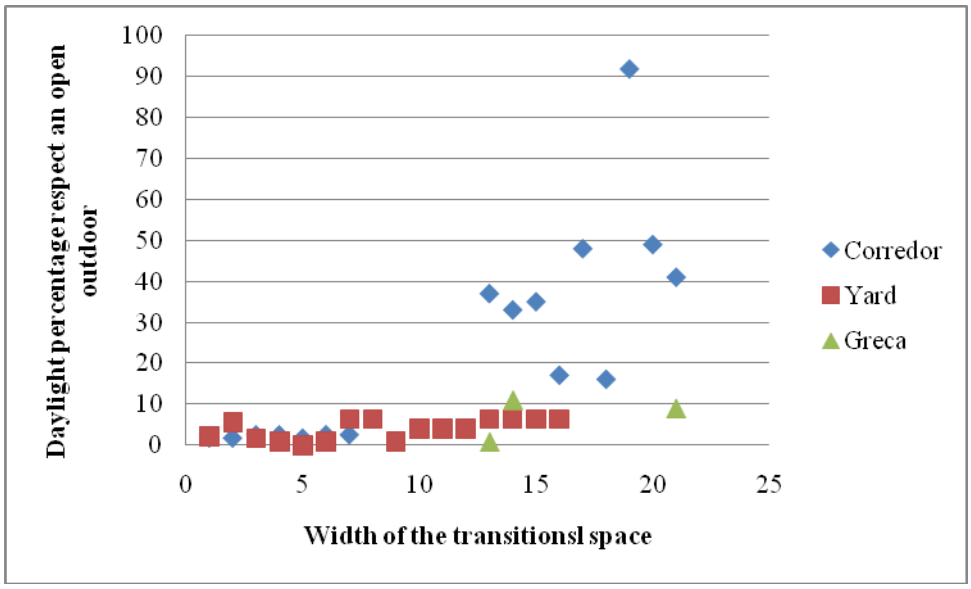

Fig.3. Percentage of daylight in spaces related to each transitional space, respect to a direct relationship to an open outdoors.

Of course, the dimensions and proportions of the transitional spaces also influence indoor daylight that decreases with the reduction of the separation between volumes, it means, with the dimension of the transitional space. In that sense, spaces with width minor than 10m reduce daylight levels in more than 50%. Something similar happen related to the building height that determines the vertical angle (x). With angles over 60^0, also indoor daylight decreases to less to the half of the value achieved in relation to an open context (x=0.0).
For the same height of building volume and distances between them, open corridors are better than closed yards respect to daylight.

These results reinforce some conclusions formerly achieved respect to the convenience of reducing land occupation in current compact urban areas and to avoid using small yards to provide daylight and natural ventilation in housing buildings. Next steps in the research requires an evaluation of this transitional spaces also from the thermal point of view, according to the Cuban climate, to get a balance about what could be really more appropriate form an integral point of view.

References

[1] R. Gómez Briñoles, Edificios multifamiliares en la ciudad de La Habana, Tesis de Maestría en Vivienda Social, Facultad de Arquitectura, ISPJAE, Havana, 2001.

[2] A. Zorrilla Rodriguez, Edificios de apartamentos en la ciudad de La Habana. Tipología de diseño volumétrico espacial, Tesis de Maestría en Vivienda Social, Facultad de Arquitectura, ISPJAE, Havana, 2008.

[3] A.M. De la Peña, Iluminación natural en la vivienda cubana, Revista Arquitectura y Urbanismo No. 3, ISPJAE, Havana, 1986, pp. 40 – 45.

[4] A.M. De la Peña, Iluminación natural en edificios bajo las condiciones de Cuba, Tesis de Doctorado, Facultad de Arquitectura, ISPJAE, Havana, 1992.

Modeling of Skylight on Dome Shaped Roof of Low Energy Adobe House Located in New Delhi (India)

Arvind Chel [1,*] and G.N.Tiwari[2]

[1,2] *Centre for Energy Studies, Indian Institute of Technology Delhi, New Delhi, India*
** Corresponding author. Tel: +91 9968144689 Fax: +91 26581121, E-mail: dr.arvindchel@gmail.com*

Abstract: The daylight factor model given by Charted Institute of Building Services Engineers (CIBSE) was modified in this paper to incorporate time variations with respect to zenith angle (θz) and vertical height (h) of working surface above ground surface which was normalized with central height (H) of skylight dome. The modified model contains constant exponents which are determined using linear regression analysis based on hourly experimental data of inside and outside illuminance for each month of the year 2007–2008. The prediction of modified model is found in good agreement with experimental observed inside illuminance data on the basis of values of root mean square percentage error (e) and correlation coefficient (r). The annual average daylight factor values for big and small dome skylight rooms are determined as 2.3% and 4.4% respectively. The energy saving potential of skylight rooms for selected climatic locations in India is also presented in this paper. This paper also investigates embodied energy of an existing eco-friendly and low embodied energy adobe house with dome shape roof located at Solar Energy Park inside IIT Delhi campus in New Delhi (India). Based on embodied energy analysis, the energy payback time for the adobe house was determined as 18 years. The embodied energy per unit floor area of reinforced cement concrete (R.C.C.) building (3702.3 MJ/m^2) is quiet higher as compared to adobe house embodied energy (2298.8 MJ/m^2).

Keywords: *Skylight, Dome shape roof, Daylight Factor, Illumination, Mud house*

Nomenclature

A_e	*effective area…….* m^2		H	*height of source*	*m*
A_f	*floor area…….* m^2		A_g	*total area of glazing*	m^2
A_s	*working surface area ……* $.m^2$		*At*	*total area of room-surface*	m^2
B_F	*ballast factor or efficiency…*	$0 \le BF \le 1$	*C*	*correction factor for glazing*	$0.5 \le C \le 0.9$
DF	*percentage daylight factor*	*%*	*h*	*vertical height above ground surface*	*m*
I_d	*diffuse solar radiation*	W/m^2	I_g	*global solar radiation*	W/m^2
L_i	*illuminance inside the room*	*lux or* lm/m^2	L_o	*outside diffuse illuminance*	*lux or* lm/m^2
M_F	*maintenance factor*	$0 \le MF \le 1$	*m*	*constant exponent*	…..
n	*constant exponent*	…….	O_F	*glazing orientation factor*	$0.97 \le OF \le 1.55$
R	*average reflectance of surface*	$0 \le R \le 1$	U_F	*utilization factor*	$0 \le UF \le 1$

Greek letters

ε	light source luminous efficacy *lm/W*	Ø	total luminous flux *lumen*
τ	transmittance of glazing $0 \le \tau \le 1$	θ	vertical angle of visible sky from horizon degrees
θ_Z	zenith angle degrees		

1. Introduction

Daylighting is an important issue in modern architecture affecting the functional arrangement of spaces, occupant comfort (visual and thermal), structure and energy use in building [1]. Daylight is considered as the best source of light for good color rendering and its quality is the one light source that most closely matches with human visual response. It gives a sense of cheeriness and brightness that can have a significant positive impact on the people. The amount of daylight penetrating a building is mainly through window openings which provide the dual function not only of admitting light for indoor environment with a more attractive

and pleasing atmosphere, but also allowing people to maintain visual contact with the outside world. People desire good natural lighting in their living environments [2,3].

The energy consumption of lighting in buildings is a major contributor to carbon emissions, often estimated as 20–40% of the total building energy consumption as reported by Building Research Establishment (BRE) energy consumption guide [4] and Chartered Institute of Building Services Engineers (CIBSE) [5]. Furthermore, the heat gains produced from artificial and natural lighting have an important influence upon he ating and cooling loads reported by Peacock et al. [6]. Using controls for demonstrating the optimized configuration for daylight supplemented electrical lights is well-documented by Greenup et al. [7], Reinhart [8] and Li and Lam [9], with particular interest on the effect of thermal loads reported by Franzetti et al. [10]. However, the more advanced and material-based solutions were reported by Lee et al. [11], Tong et al. [12] and Smith [13] for optimizing daylight. They provide innovative solutions for reducing lighting-energy consumptions.

With the project considering a large number of buildings, it is important that the approach should be as efficient as possible with regards to the available time as reported by Reinhart and Fitz [14]. While building-simulation packages and time-series techniques can be used for detailed predictions of lighting use [15]; they can be both time consuming and unnecessary for obtaining first-order estimate. The annual variation in daylight availability in UK can be represented using data reported by CIBSE [16] and Hunt [17,18]. The domestic lighting demand was determined using simple model developed by Stokes et al. [19]. The economics of lighting retrofits for emission reduction was reported by Mahlia et al. [20]. Daylighting is one of the basic components of passive solar building design and its estimation is essential. Laouadi et al. [21] had reported that the daylight factor of building depends upon position of light source with respect to the room orientation, the room geometry, the optical characteristics of the room indoor surfaces, any outdoor obstructions and the optical behaviour (transmission, reflection and light scattering) of the fenestration system through which light is admitted into the room space. Daylight coefficient is independent of sky luminance distribution as reported by Tregenza and Waters [22]. Recently, calculating indoor natural illuminance in overcast sky conditions was reported by Rosa et al. [23]. In India and many parts of the world, the availability of measured outside illuminance values are very few. The Indian climate is generally clear with overcast conditions prevailing through the months of June–September, which provides good potential to daylighting in buildings as reported by Joshi et al. [24]. This paper investigates a mathematical model for existing skylight integrated dome shaped mud-house to estimate daylight factor based on the modifications in the model developed by CIBSE [25]. The daylight factor model developed by CIBSE [25] was validated for ground surface illuminance by Chel et al. [2] using experimental data of the existing building. The model developed by CIBSE [25] does not include time variation in a day and vertical height (h) of the work plane above ground surface. Hence, there is need for the modification in the model developed by CIBSE [25] to incorporate vertical height (h) normalized with respect to central height (H) of the skylight room and time variations in terms of zenith angle (hz). This concept of modeling for skylight is rarely reported in the literature for New Delhi composite climate. The constant exponents in the modified model were determined on the basis of linear regression analysis which is explained in depth in this paper. The values of exponent were determined based on hourly inside and outside illuminance data for typical clear day in each month.

Using the modified model, the daylight factor is determined for three different work planes at different vertical heights (h) from ground surface, i.e. at h = 0 (or ground surface), 0.75 m and

1.5 m above ground surface. The study of work plane at ground level implicates to the students seating on floor and reading and writing in rural village schools in India. The vertical height of 0.75 m implicates to reading on work plane (or table) in modern schools and colleges in India while the 1.5 m vertical height implicates to standing posture of a working person like engineer in the factory (or teacher in school/conference room). The daylight factor values using modified model and experimental data were tabulated and presented in this paper. The energy saving potential of the skylight big and small domes for different selected climatic conditions is reported in this paper.

The annual average artificial lighting energy saving potential and corresponding CO2 emission mitigation were evaluated for the existing building by Chel et al. [2]. The research pertaining to energy savings due to existing experimental setup of mud-house integrated with an earth to air heat exchanger and embodied energy analysis of building were respectively reported by Chel and Tiwari [26,27]. The existing dome shape building is found to be a promising example of sustainable and low carbon building (or green building) integrated with stand-alone photovoltaic reported by Chel and Tiwari [28].

2. Pyramid shape skylight over dome shape roof of Mudhouse

Laouadi and Atif [29] and Chel et al. [2] had reported other different skylight shapes for daylighting in buildings. The existing mud-house has vault (or dome shape) roof structure integrated with pyramid shape skylight as shown by the pictorial view in Fig.1. The inside view of skylight circular aperture is also shown in Fig.1.

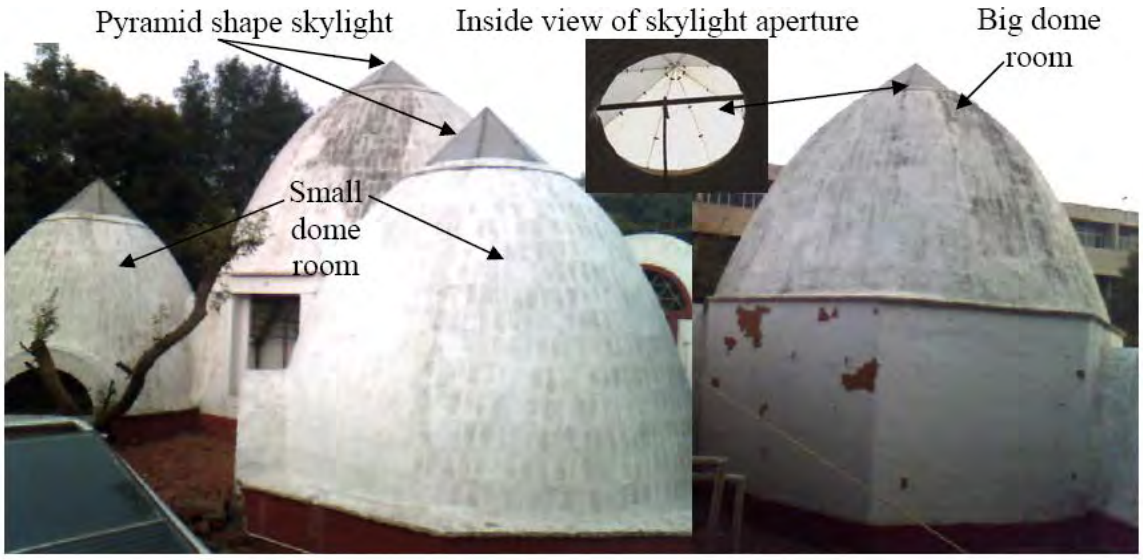

Fig. 1 Pyramid shape skylight over the dome shaped roof of Mudhouse

3. Percentage daylight factor, DF (%) for the naturally illuminated work plane

The percentage daylight factor, DF (%) is the percentage ratio of inside illuminance, Li (lux) on the horizontal work plane and outside diffuse illuminance, Lo (lux) on horizontal surface. The daylight factor for skylight integrated dome shape building at ground level is given by Eq.(1) developed by Chartered Institute of Building Services Engineers (CIBSE) [25] and validated by Chel et al. [2] as follows:

$$DF = \left[\frac{L_i}{L_o}\right] \times 100 = \left[\frac{\tau \times C \times A_g \times \theta \times O_F}{A_t \times (1 - R^2)}\right] \quad (1)$$

The various parameters in Eq. (1) are tabulated with their values considered in Table 1. The variation of daylight factor (%) with the time of the day and vertical height (h) above ground surface is developed by Chel et al.[30] and expressed in the Eq. (2) as follows:

$$DF = \left[\frac{L_i}{L_o}\right] \times 100 = \left[\frac{\tau \times C \times A_g \times \theta \times O_F}{A_t \times (1 - R^2)}\right] \times \left(1 + \frac{h}{H}\right)^m \left(\cos\theta_z\right)^n \quad (2)$$

Line equation can be easily written as follows:

$$Y' = M'\left[X'\right] + C' \quad (3)$$

This Eq.(3) of line is represented for following Eq.(3) as follows:

$$\ln\left[\frac{L_i}{L_o} \times 100\right] = \left[n \times \ln\left(\cos\theta_z\right)\right] + \left\{m \times \ln\left(1 + \frac{h}{H}\right) + \ln\left[\frac{\tau \times C \times A_g \times \theta \times O_F}{A_t \times (1 - R^2)}\right]\right\} \quad (4)$$

$$Y' = \ln\left[\frac{L_i}{L_o} \times 100\right] \text{ and } X' = \left[\ln\left(\cos\theta_z\right)\right] \quad (5)$$

$$m = \frac{\left\{C' - \ln\left[\frac{\tau \times C \times A_g \times \theta \times O_F}{A_t \times (1 - R^2)}\right]\right\}}{\ln\left(1 + \frac{h}{H}\right)} \quad (6)$$

Where, $n = M' =$ slope of line and $C' =$ intercept of line on Y'axis

The total power of lighting, P (W) can be determined by considering the artificial light source luminous efficacy, ε (lm/W) and efficiency of ballast, B_F (or ballast factor). The total power of artificial electrical lighting required for the measured amount of total luminous flux, Ø (lumen) from the existing skylight in building can be determined mathematically by Eq.(7) using Jenkins and Newborough [31] as follows:

$$P = \left[\frac{Ø}{B_F \times \varepsilon}\right] \quad (7)$$

$$Ø = \left[L_i \times A_s\right] \quad (8)$$

Where, L_i is measured illuminance level (lux or lumen/m^2) inside the skylight building on the horizontal working surface area, As (m^2).

The total lighting-energy consumption, E (W h/day) can be determined by multiplying total power of lighting, P (W) and required number of hours of operation per day, N (h/day). The total lighting-energy consumption can be expressed mathematically using Eq.(9) as follows:

$$E = \left[P \times N\right] \quad (9)$$

Table 1. Values of parameters considered for daylight factor estimation

No.	Parameter	Value	Parameter	Value
1	Total area of room surfaces in big dome (A_t, m^2)	80	Total area of room surfaces in small dome (A_t, m^2)	25
2	Floor area of big dome (A_f, m^2)	26	Floor area of small dome (A_f, m^2)	5
3	Transmittance of glazing (τ)	0.8	Vertical angle of visible sky from horizon (θ, degrees)	90
4	Correction factor for glazing due to poor maintenance/dust ($0.5 \leq C \leq 0.9$)	0.6	Vertical height of work plane above floor surface (h, m) [0, 0.75 m, 1.5 m]	0, 0.75, 1.5
5	Orientation factor for glazing ($0.97 \leq O_F \leq 1.55$)	1	Average reflectance of all room-surfaces ($0 \leq R \leq 1$)	0.3
6	Total area of glazing (A_g, m^2) for big dome	2.6	Total area of glazing (A_g, m^2) for small dome	1.5
7	Ballast factor (B_F)	0.9	Artificial light luminous efficacy (ε, lm/W) (CFL lamp)	40

4. Results and discussion:

Based on e xperimental data of inside and outside diffuse illuminance, the daily average experimental value of percentage daylight factor is determined and compared with daily average predicted value of daylight factor using modified model Eq.(2) for each month in Table 2 (DF- Daylight Factor (%), B- Big Dome, S-Small Dome with h= 0 cm, 75 cm, 150 cm).

Table 2. Experimental comparison of daylight factor with developed skylight model

Month	Model/ Experimental values	DF-0 B (%)	DF-75 B (%)	DF-150 B (%)	DF-0 S (%)	DF-75 S (%)	DF-150 S (%)
Jan	**Model**	1.54	1.99	2.41	2.85	3.23	3.97
	Experimental	1.58	1.90	2.35	2.80	3.37	4.15
Feb	**Model**	1.54	1.58	2.20	2.86	2.87	3.34
	Experimental	1.19	1.57	2.08	2.48	3.00	3.52
Mar	**Model**	1.51	2.05	2.89	2.86	5.39	6.30
	Experimental	1.52	2.11	2.99	4.02	5.49	7.07
Apr	**Model**	1.54	2.55	3.22	2.88	4.54	5.57
	Experimental	1.91	2.55	3.20	3.55	4.56	6.20
May	**Model**	1.54	2.59	2.97	2.81	4.51	6.30
	Experimental	1.78	2.41	2.91	3.78	4.80	6.07
Jun	**Model**	1.53	2.02	2.42	2.84	4.24	6.25
	Experimental	1.61	2.07	2.53	3.00	4.49	6.61
Jul	**Model**	1.51	2.09	2.75	2.85	4.50	5.60
	Experimental	1.95	2.40	2.86	3.74	5.14	6.10
Aug	**Model**	1.53	2.26	2.82	2.83	4.11	5.39
	Experimental	2.02	2.45	2.92	3.55	4.41	5.46
Sept	**Model**	1.50	2.22	2.94	2.81	3.95	5.16
	Experimental	2.03	2.47	2.95	2.69	3.87	5.31
Oct	**Model**	1.52	2.27	2.82	2.84	3.87	5.54
	Experimental	1.98	2.43	2.88	3.27	4.24	5.72
Nov	**Model**	1.52	1.87	2.37	2.83	3.72	4.58
	Experimental	1.83	2.20	2.59	3.05	4.12	5.30
Dec	**Model**	1.52	1.57	1.98	2.82	2.89	4.54

Experimental	1.18	1.69	2.12	2.22	2.87	3.64

The linear regression analysis was carried out as explained in section 3 and the results were potted for big dome for h= 0.75 m as follows in Fig.2.

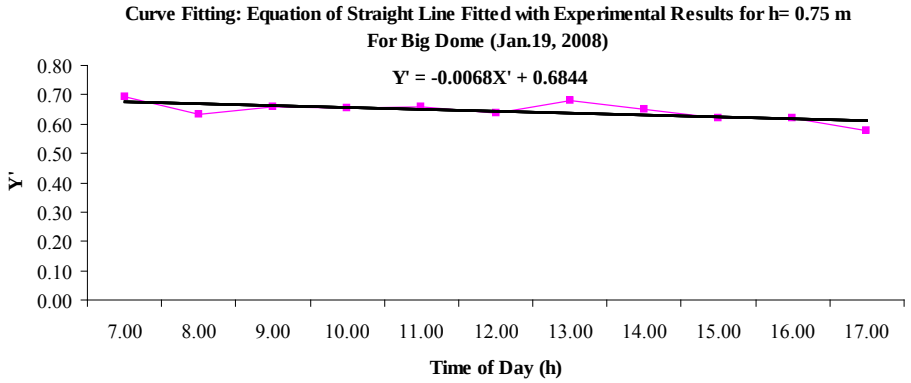

Fig.2. Linear regression of experimental results for big dome at h=0.75 m

The validation of daylight factor (DF) using experimental data of daylight factor for big and small domes at three different heights above floor surface were carried out for January and June based on the prediction of developed skylight model Eq.(2) and plotted as shown in Fig.3 (for January). The annual average energy saving potential for three heights for big and small domes were determined for selected locations in India and plotted as shown in Fig.4.

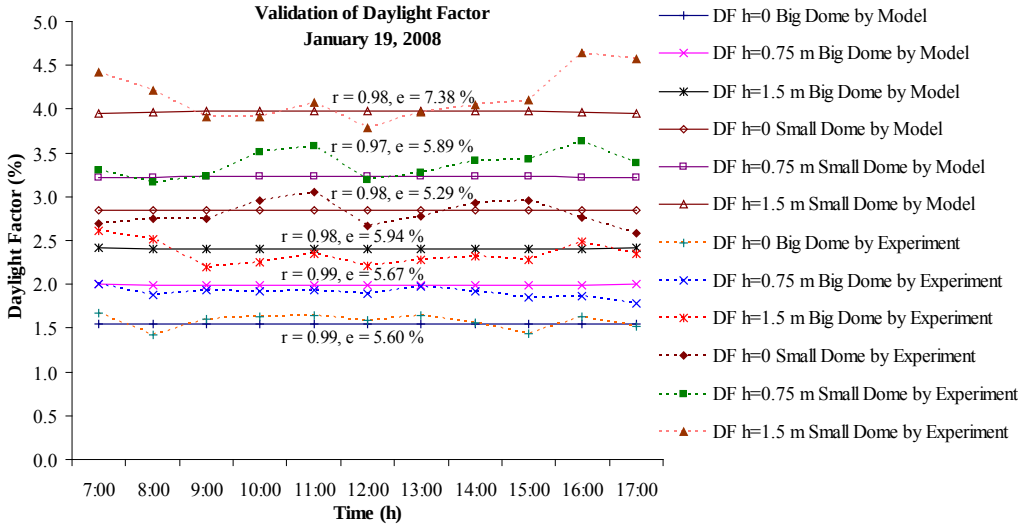

Fig.3. Validation of daylight factor model for big and small dome in January

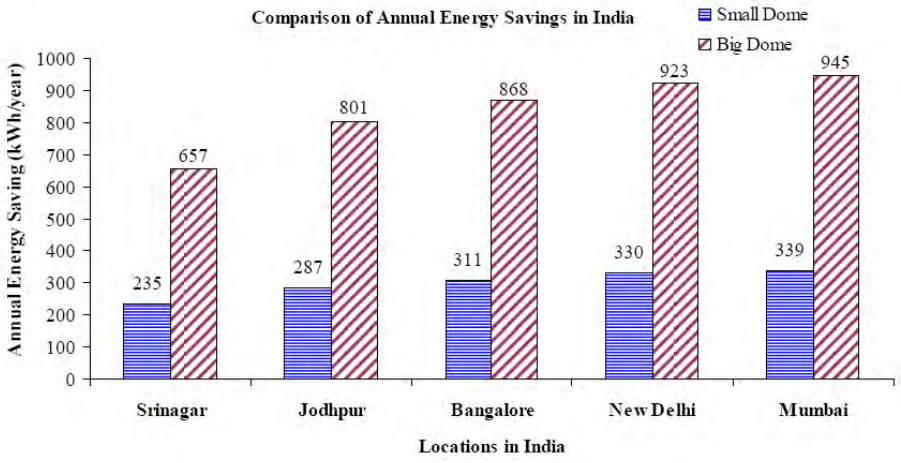

Fig.4. Annual energy saving potential of skylight for big dome room in India

5. Conclusions

The following key conclusions can be drawn from the study as follows:

1. It is found that the root mean square percentage error is small and varies in the range of 5–8% for the developed model Eq.(2). Hence, the proposed daylight factor model represented by Eq.(2) can be used to estimate the daylight factor (%) and corresponding inside illuminance at different vertical heights in skylight integrated dome shape roof mud-house which can be seen from Figs.5.
2. The illuminance level inside the mud-house was found sufficient for office work inside the room from 9 am to 5 pm. The small dome room has maximum illuminance value (for h = 0–1.5 m) in the range of 450–650 lux (in winter) and 800–1800 lux (in summer) while big dome room with maximum illuminance value (for h = 0–1.5 m) 250–400 (in winter) and 400–900 lux (in summer) in New Delhi (India).
3. The illuminance level was found 100 lux (minimum) inside both small dome and big dome rooms from 9 am to 4 pm in all months of the year in New Delhi composite climatic conditions.
4. The experimental daylight factor over the year for big dome room (for h = 0–1.5 m) are found in the range of 1.5–2.5% (January) and 1.5–3.5% (June) while for small dome rooms (for h = 0–1.5 m) it varies in the range of 2.5–4.5% (January) and 3–7.5 (June) based on skylight performance in both winter and summer. The annual average value of percentage daylight factor (for h = 0–1.5 m) is determined as 2.3% and 4.4% for big and small dome skylight rooms respectively. Hence, the skylight rooms are suitable for office building, e.g. state government offices in rural and urban areas of India, temple, church, mosque, etc.
5. The vertical height (h) of work plane above floor surface for the skylight room gets significantly different amount of illuminance. This effect shows that distance of work plane from skylight is directly proportional to amount of illuminance received on that work plane surface. This can be observed from different values of daylight factor (%) at different vertical height (h) above floor for working surfaces inside big and small dome rooms.

References

[1] Webb AR. Considerations for lighting in the built environment: non-visual effects of light. Energy Build 2006; 38(7):721–7.

[2] Chel A, Tiwari GN, Chandra A. A model for estimation of daylight factor for skylight: an experimental validation using pyramid shape skylight over vault roof mud-house in New Delhi (India). Appl Energy 2009; 86(11):2507–19.

[3] Aries MBC, Newsham GR. Effect of daylight saving time on lighting energy use: a literature review. Energy Policy 2008; 36(6):1858–66.

[4] Building Research Establishment (BRE). Energy consumption guide 19, Energy use in offices, energy efficiency best practice programme, BRECSU Enquiries Bureau, Garston, Watford; 1997.

[5] Guide F. Energy efficiency in buildings, Chartered Institute of Building Services Engineers (CIBSE); 1999.

[6] Peacock AD, Newborough M, Banfill PFG. Technology assessment for the existing built-asset base (TARBASE), WREC, Aberdeen; 22–27 May 2005.

[7] Greenup P, Bell JM, Moore I. The importance of interior daylight distribution in buildings on overall energy performance. Renew Energy 2001; 22(1–3):45–52.

[8] Reinhart CF. Lightswitch-2002: a model for manual and automated control of electric lighting a blinds. Solar Energy 2004; 77(1):15–28.

[9] Li DHW, Lam JC. An analysis of lighting energy-savings and switching frequency for a daylit corridor under various indoor design illuminance levels. Appl Energy 2003; 76(4):363–78.

[10] Franzetti C, Fraisse G, Achard G. Influence of the coupling between daylight and artificial lighting on thermal loads in the office buildings. Energy Build 2004;36(2):117–26.

[11] Lee ES, Bartolomeo DLD, Selkowitz SE. Daylighting-control performance of a thin-film ceramic electrochromic window: field study results. Energy Build 2006;38(1):30–44.

[12] Tong TDW, King Sing L, Cheung TM, Leung CS. Potential energy saving for a side-lit room using daylight-linked fluorescent lamp installations. Light Res Technol 2002;34(2):121–33.

[13] Smith GB. Materials and systems for efficient lighting and delivery of daylight. Solar Energy Mater Solar Cells 2004; 84(1–4):395–409.

[14] Reinhart C, Fitz A. Findings from a survey on the current use of daylight simulations in building design. Energy Build 2006; 38(7):824–35.

[15] ASHRAE, Fundamentals handbook; 2001 [chapter 29].

[16] Guide A. Environmental design, Chartered Institute of Building Services Engineers (CIBSE); 2006.

[17] Hunt DRG. Availability of daylight, Department of Environment, London, Building Research Establishment (BRE) Report, Garston, Watford; 1979.

[18] Hunt DRG. The use of artificial lighting in relation to daylight levels and occupancy. Build Environ 1979; 14(1):21–33.

[19] Stokes M, Rylatt M, Lomas K. A simple model of domestic-lighting demand. Energy Build 2004; 36(2):103–16.

[20] Mahlia T, Said M, Masjuki H, Tamjis M. Cost-benefit analysis and emission reduction of lighting retrofits in residential sector. Energy Build 2005;37(6):573–8.

[21] Laouadi A, Reinhart CF, Bourgeois D. Efficient calculation of daylight coefficients for rooms with dissimilar complex fenestration systems. J Build Perform Simulat 2008;1(1):3–15.

[22] Tregenza PR, Waters IM. Daylight coefficients. Light Res Technol 1983; 15(2):65–71.

[23] Rosa AD, Ferraro V, Kaliakatsos D, Marinelli V. Calculating indoor natural illuminance in overcast sky conditions. Appl Energy 2010; 87(3):806–13.

[24] Joshi M, Sawhney RL, Buddhi D. Estimation of luminous efficacy of daylight and exterior illuminance for composite climate of Indore city in Mid Western India. Renew Energy 2007; 32(8):1363–78.

[25] Chartered Institute of Building Services Engineers (CIBSE), Daylighting and window design, Lighting Guide 10; 1999.

[26] Chel A, Tiwari GN. Performance evaluation and life cycle cost analysis of earth to air heat exchanger integrated with adobe building for New Delhi composite climate. Energy Build 2009;41(1):56–66.

[27] Chel A, Tiwari GN. Thermal performance and embodied energy analysis of a passive house – case study of vault roof mud-house in India. Appl Energy 2009; 86(10):1956–69.

[28] Chel A, Tiwari GN. Stand-alone photovoltaic (PV) integrated with earth to air heat exchanger (EAHE) for space heating/cooling of adobe house in New Delhi (India). Energy Convers Manage 2010; 51(3):393–409.

[29] Laouadi A, Atif MR. Daylight availability in top-lit atria: prediction of skylight transmittance and daylight factor. Light Res Technol 2000; 32(4):175–86.

[30] Chel A., Tiwari G.N. and Singh H.N. A modified model for estimation of daylight factor for skylight integrated with dome roof structure of mud-house in New Delhi (India), Appl Energy 2010; 87(10): 3037-50.

[31] Jenkins D, Newborough M. An approach for estimating the carbon emissions associated with office lighting with a daylight contribution. Appl Energy 2007; 84(6):608–22.

Double layer glass façade in the refurbishment and architectural renewal of existing buildings in Italy

Silvia Brunoro[1*], Andrea Rinaldi[2]

[1] *University of Ferrara, Department of Architecture, Architettura>Energia Research Center, Ferrara, Italy*
[2] *University of Ferrara, Department of Architecture, Architettura>Energia Research Center, Ferrara, Italy*
** Corresponding author. Tel: +39 0532 293633, Fax: +39 0532 293647, E-mail: silvia.brunoro@unife.it*

Abstract: The aim of this paper is to assess the use of an intelligent glass envelope in the refurbishment of existing buildings in Italy in order to fit their energetic performance considering Mediterranean climate inputs. With the new European and Italian regulations on energy efficiency of buildings, envelopes are not only forced to respect heat transmission limits (e.g. U value) and to improve their thermal insulation, but also to use and receive benefits from environmental input such as passive solar gains. Comparing to the North European solutions, a glass envelope seems not to be the most suitable solution for a Mediterranean climate, mainly due to the great incidence of solar gains and the risks of overheating during summer season. Examples presented in this paper indicates how double skin glass façades, that are commonly used in new constructions where the concept starts from a low environmental impact, can be also employed in the refurbishment of existing buildings, which is the main challenge for the global reduction of CO_2. An overview on the main technical of intervention can indicate to architects and planners the weakness/strength points to take in consideration in the use of a double layer glass façade in a Mediterranean climate in order to reduce the overall energy balance.

Keywords: *Building envelope, Sustainable technologies, Energy retrofit, Double skin glass façades.*

1. Introduction

This paper purpose to remark the importance of the use of sustainable technologies, such as a double layer glass envelopes, in the renewal of existing buildings in order to fit their energetic performance to different climatic inputs. This solution is mainly used in public buildings (offices and productive buildings) where the potential of a new high-tech image may easily justify high costs of realization. Moreover, the use of double layer glass envelopes is heavily conditioned by the climatic factor. The main purpose of the double glass envelope is to balance the desire for daylight and outdoor view with the concerns for heat gain and loss. The air cavity can be heated by the sun to create a warm buffer zone that protects rooms in winter and can be configured to function as a thermal chimney in summer utilizing the stack effect to remove excess heat. Case studies presented in this paper indicates how double glass envelopes, that are commonly used in new constructions, can be also employed in the refurbishment of existing buildings, which is the main challenge for the global reduction of CO_2. An overview on the main technical of intervention can indicate to architects and planners the potentiality for the improvement of the existing buildings, in order to reduce the overall energy balance. The energy failure in existing building stock is mainly due to the poor insulating efficiency of the façades. Making use of hi-tech envelopes, not only the energetic balance, but also the architectural value of a building can be improved. A set of rules concerning energy efficiency in buildings has been acknowledged in Italy by enacting the Decree 311/2006, that states new standards for the energetic performance including also the existing building stock, except for cultural heritage. The experiences gained till now in other Countries suggest wide chances of interventions on building stock by promoting the use of "intelligent envelopes": dynamic and active bounding surfaces automatically able to gear their performance to the changes of the environmental conditions, as they integrates a great deal of working functional devices. Following these experiences it is possible, therefore, not only to introduce basic standard improvements but even proper architectural lifting on the building

façades, mainly considering post war building stock that is one of the most cause of energy consumption due to the poor building techniques and the heavy state of decay.
A sustainable upgrade should mainly provide active or passive energy from renewable sources in order to achieve the highest indoor comfort by restricting the use of HVAC (Heating Ventilation Air Cooling) units and artificial lights. The most efficient technical solutions that can be used to refurbish buildings are based on fundamental principles of the sustainable architecture such as: heat gaining by collecting and storing solar energy in winter, use of passive cooling and natural ventilation in summer, maximum natural day lighting, reduction of heat loss through the walls, use of systems with low environmental impact such as dry technologies.

1.1. Methodology

This study examines three case studies in Italy where the refurbishment of existing building envelopes was done using a double layer glass façade. The aim of this study is to assess which technical solution can improve the energy efficiency and the global quality of the building by considering some variables:
- The climatic conditions: in Italy climate is very different from Northern Europe, where the double layer glass envelopes are largely used. The main problem is the risk of overheating in spring/summer season as, in Mediterranean climate, the energy efficiency is based not only on the performance of thermal insulation such in Northern countries, but also on the necessity to reduce big solar gains and improve ventilation in summer;
- The composition of the technical solution: in the most cases of refurbishment the original inner façade is conserved and improved by insulation, so the "double layer glass" systems turns in "hybrid" system where opaque parts of parapets are present;
- The applicability of different solutions (full height façades, cell façades, natural or forced ventilation) to the existing façade by considering operations and costs/benefits.

The evaluation was done on the basis of the following steps:
- Energetic diagnosis of the building before the intervention (mainly considering energy consumptions in operational phase);
- Examination of the project/design/technical details;
- Visit in building site during the construction;
- Monitoring of the building for one year, by considering the grade of satisfaction/comfort of the occupants and energy consumption recording.

2. Double layer glass façades: the technical solution

A typical double glass envelope system includes a single glass layer and a double-glazing low emissive layer separated by an air space. An operable shading device is installed in the cavity to minimize the solar heat gain in summer. In addition to the energy savings, the double envelope system has other potential benefits such as: acoustic control, water penetration resistance and an enhanced office atmosphere because of the external view and the utilization of daylight. Double glass façades in the refurbishment are generally hybrid systems, formed by the existing wall and a new glass envelope. The external envelope is a glass façade: during the winter season it supports the solar gain that, by heating the air cavity, consequently improves the thermal capacity of the whole system. The use of high – performing glasses is fundamental to obtain solar reflection and to prevent overheating. If the refurbishment is oriented to the complete substitution of the existing envelope, also the internal wall is a glass façade, forming the conventional double-layer skin. In the most cases, it's more convenient to conserve the existing wall and, after the changeover of the windows, to add up insulating panels on the structure and on the parapets.

In winter, during the warmest hours, the heating of the air cavity is the fundamental factor that reduces the thermal losses and the air permeability through the wall. During the night, the air vents are closed, preventing the entrance of cold air. In summer, through the solar shadings, good levels of internal comfort can be obtained. Throughout the day, the cavity is closed to avoid the entrance of warm air, while during the night the natural air flue cools down the walls and the rooms.

The thermal performance of double façade systems depends on many factors, such as:
- The composition and performance of the layers (glass/glass or glass/wall, kind of glass used);
- The (height) extent of the air cavity (which can be continuous or divided in floor-height cells, in this case the ventilation is related to each cell);
- The thickness of the air cavity (which can range between 20 cm to 90, if it encloses maintenance routes);
- The type of ventilation in the cavity (natural or forced) that is strictly related to the height of the façade and to the climatic conditions;
- The relationships between air cavity and HVAC systems (possibility to utilize warmed air from the cavity and expel internal air. This is rare occurrence in the refurbishment).

2.1. Typologies of construction

Double layer glass façades can be realized in three main typologies of construction:
Full height: in this case the air cavity is continuous and comprehends the whole façade surface. The external glass layer is fixed on the existent envelope in a limited number of points (generally in correspondence of concrete border beams). Air cavity thickness ranges between 40 to 90 cm. Pipes: the external façade is fixed to the internal by means of a common frame or punctual anchorages. The cavity is sectioned in vertical or in horizontal: this means that the surface is divided in several ventilations chimney, instead of an unique air cavity area. Air cavity thickness ranges between 40 to 90 cm. Cells: The façade is formed by the aggregation of modular cells, independent each other, one floor height and generally not more than 30 cm thick. Each cell has his inlet airs. Table 1 analyzes the suitability of the typologies of construction in the refurbishment of existing buildings.

Table 1. Main typologies of construction and applicability in the refurbishment

Typology of façade	Scheme	Description	Applicability
Full Height		Air cavity is continuous. Anchorages are punctual Thickness ranges from 40 to 90 cm	high
Pipes		Air cavity is vertically sectioned. The thickness ranges from 20 to 50 cm	medium
Cells		The façade is formed by the aggregation of modular cells, independent each other. Each cell has his inlet airs. The thickness is 20 - 40 cm	medium

2.2. Air cavity ventilation

The cavity in double glass façades is either naturally or mechanically ventilated. In case of natural ventilation, the air in the cavity flows naturally: if properly designed, wind flowing over the façade can create pressure differences between the inlet and outlet inducing air movement. Air vents at the bottom and at the top of the façade allows the natural flowing in the cavity by the so called "chimney effect" of the warmest air that naturally rises up. In this configuration the internal layer is the layer with thermal performance (insulation on parapets, low-e glass windows) while the external layer is single glass. The temperature in the air cavity is closer to the external temperature. Internal windows can be opened or not. If internal windows can be opened, this allows the natural ventilation of the rooms, even it's necessary to carefully evaluate the right period of opening (winter day- summer night), otherwise the positive effect of the natural air could be neutralized. Natural ventilation is not without risk. It may create a door-opening problem due to pressurization. Besides, if the air path is not appropriately designed, the solar heat gain within the façade cavity will not be removed efficiently and will increase the cavity temperature. If windows can not be opened this helps in the air cavity control, but decreases the user requirements (necessity of fresh air). In the case of forced ventilation air is compressed into the cavity by mechanical devices. The mechanically assisted ventilation systems usually use an under floor or overhead ventilation system to supply or exhaust the cavity air to ensure good distribution of the fresh air. This air rises and removes heat from the cavity and continues upwards to be expelled or re-circulated. Because air is not pumped in directly from the outdoors, there is potentially less risk of condensation and pollution in the cavity. The internal façade is generally closed and single glass made while the external layer is the insulated and performing layer. The temperature in the air cavity is more similar to the air temperature in the rooms. In areas with severe weather conditions or poor air quality, the mechanically assisted ventilation system can keep conditions in the buffer zone nearly constant to reduce the influence of the outdoor air to the indoor environment. The relationship between type of ventilation and applicability in the refurbishment is synthesized in table 2.

Table 2. Main typologies of ventilation and applicability in the refurbishment

Typology of façade	Scheme	Description	Applicability
Natural ventilation	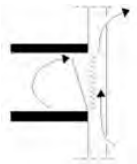	The air in the cavity flows naturally by chimney effect Internal layer= performing glass External layer= single glass	high
Forced ventilation		The air in the cavity flows by means of mechanical devices. air is utilized by HVAC systems. External layer= performing glass Internal layer=single glass	low

2.3. Case studies

2.3.1. Torno International Headquarter in Milan

Originally built in 1950, the building had many problems mainly related to: lack of thermal and noise insulation, overheating in summer season, lack of natural light into the offices. Big consumption was registered due to the necessity of heating in winter but most of all for the big air conditioning use in summer. An average consumption date was estimated in about 250

Kwh/m^2 per year. The strategy of intervention was to coat opaque parts of façade (e.g. concrete skeleton, ground floor) with a dry coat finished with gypsum panes. The south façade, made by single layer windows and thin brick wall parapets, was replaced with full height double low-e glass windows. Starting from the first floor, a full height glass facade was overlapped. The air cavity is 55 cm wide, air flows naturally: at the bottom the cavity is always open thanks to a metallic grid (also helpful for maintenance routes), at the top moveable glass louvers can control the air flow in the different climatic conditions (maximum ventilation in summer, minimum in winter). Solar shadings are in the air cavity: aluminum venetian blinds in front of the internal windows. Internal wall can not be opened, this helps in the control of the natural phenomenon of the chimney effect in the cavity. Main benefits with this intervention were obtained. For first, the reduction of thermal losses due to the air cavity that acts like a warm buffer zone in winter and improves solar gain: this caused the reduction of HVAC of about 35% in winter and 40% in summer. Moreover, the improvement of noise insulation (a reduction of 6 Db was registered). The cost of the intervention is about 1100 Euro/m^2.

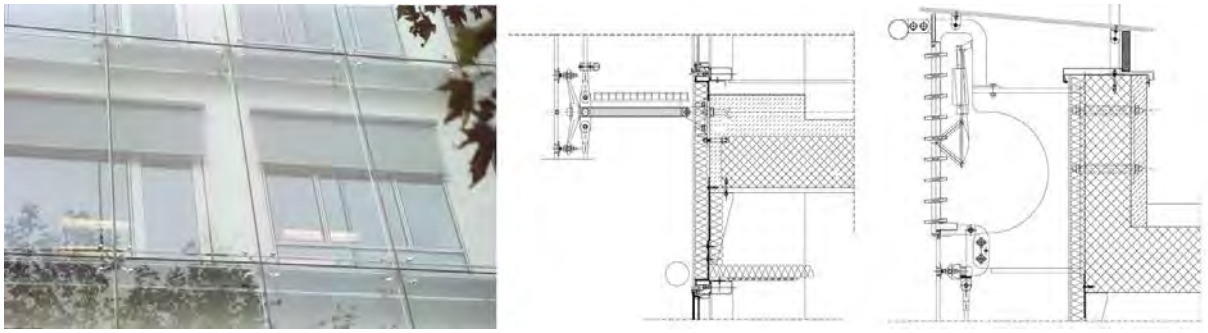

Fig. 1. Image and technical details (bottom – top) of the new façade

2.3.2. Johnson Wax Headquarter in Milan

The building, 20 m tall, was originally built in 1977 with a curtain wall façade. Main requirements that was asked to the designers were:
- to allow the natural ventilation that could be independently managed by the users of each office;
- to achieve high thresholds of natural light, even for environments located in the central part of the buildings, while avoiding the phenomena of glare and overheating of indoor air;
- to ensure adequate levels of sound insulation from noise coming from the adjoining highway;
- to carry out the remediation of asbestos cladding;
- to improve the quality of architecture.

The facade of the building was replaced with a double skin façade made by aluminum windows (internal layer) and 8 mm safety glass layer supported by a system of spiderglass and rotules (external layer). A full height natural ventilated façade was designed to meet users and owners' s requirements. In the cavity, 90 cm thick, air flows naturally but mechanical fan at the top of the façade were installed to provide to forced ventilation in case of low-pressure. The façade works as a dynamic filter for the regulation of energy exchange between inside and outside. In winter time the cavity acts as a "thermal buffer" by reducing heat loss and heat gain by allowing the greenhouse effect. Internal wall can be opened: three doors per side allows natural air exchange and the access to the corridors for maintenance routes. Aluminum blinds in the cavity allows to avoid summer overheating, moreover also 90 cm grilled corridors contributes to shield the solar radiation. Concerning the indoor comfort, an average temperature of the rooms was calculated, ranging between 18 ° and 20 ° C for opaque

surfaces, and between 16 ° and 17 ° C for glass panes. Indoor relative humidity is about 50/60%: this means that the temperature inside of the cavity can exclude any risk of condensation. Main technical data after the refurbishment are: the reduction of thermal losses of 30%, reduction of HVAC of 30% in winter and 40% in summer, noise insulation damping: 7 Db, The cost is about 1300 Euro/m^2 .

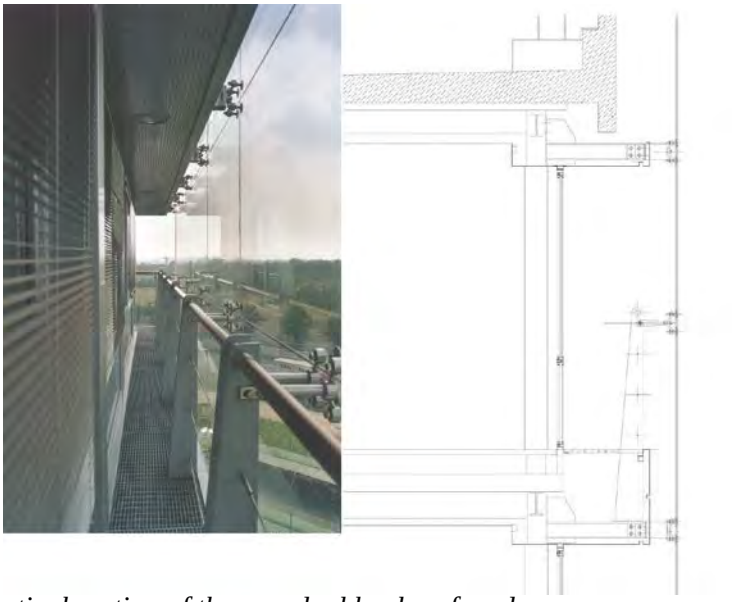

Fig. 2. Image and vertical section of the new double glass façade

2.3.3. Hines Headquarter in Milan

The building is a part of a commercial area, consisting of 4 buildings of the '60s. The project was organized around some architectural choices towards environmental design and energy conservation. Main design guidelines were: a new double skin glass façade on the main building, the partial covering of the internal courtyard, the creation of an indoor garden, the careful control of the natural day light. In particular, for the building towards via Bergognone, characterized by significant thermo-acoustic lacks (single-glazed windows and wooden panels as parapets without insulation) the energy retrofit was done by the removal of the existing façade that was replaced by a double skin façade on the south-west front. The air cavity is 75 cm thick, full height and natural ventilated. The inner envelope, made by low-e double glass, acts as thermal and acoustic insulation and solar control factor, while the external front (a system suspended by metal cables to fixed glass components), due to a special surface treatment with oxides of iron, is able to harness the positive effects of solar radiation in winter and to control the flow during the summer (solar factor g of 65%). Natural ventilation is ensured by the openings at the base and the top of the façade. Moreover joints between the glass panes are open: a distance of 10 cm, allows ventilation in the cavity during the summer to avoid overheating. For this reason, it was chosen not to govern the dynamic condition by systems of opening/closing of the inlet and outlet air vents. Main results after the refurbishment are: the reduction of reduction of HVAC of 35% in winter and 40% in summer.

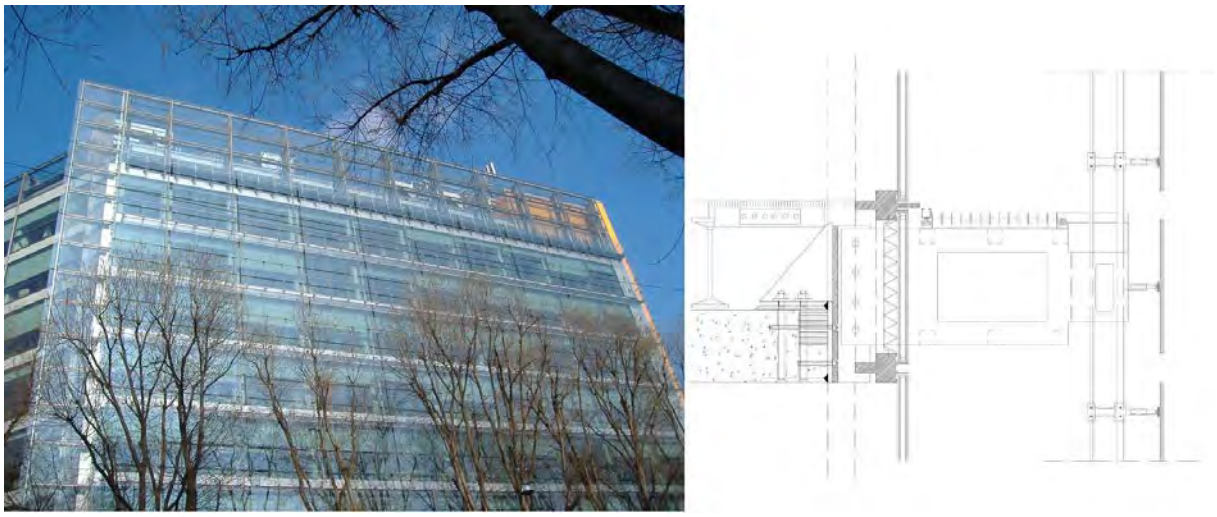

Fig. 3. Front of the building and vertical section of the new double glass façade

2.4. Results

By considering the case studies examined some conclusions can be made. The most useful typology in the refurbishment is the full height façade: generally the overlapping of a new glass layer doesn't greatly alter the whole system: in these cases, the original windows are replaced with double-glass windows and an insulating coating is applied on the opaque parts. The natural ventilation of the cavity doesn't involve big plant variations, this is the reason why the solution is the most suitable in case of refurbishment. The careful design of the air cavity (thickness, position and dimensions of air vents) is fundamental, so that the phenomenon of the natural draught can properly occur. The use of cells façade is the most convenient when the building is so high that the natural flow of air is impossible, even if it's not suitable for in each case. The operational route of the double skin façade in Mediterranean countries such as Italy remains unknown today. The climate conditions, warmer and wetter than in the North-European Countries, make very difficult to exploit a system of natural ventilation of the facade able to make use of its full potential performance. For this reason, the design strategies undertaken by the Italian projects have used the double-skin "buffering" system, that can reduce the heat load and meet the sound insulation and sealing requirements, rather than operate on the heat and energy recovery through installations. Because of the typical Mediterranean conditions, the natural ventilation of the rooms through the cavity was generally avoided in the most examined projects, keeping the skin closed and obtaining internal comfort through air conditioning systems. The decision to equip the inner shell with opening windows has a helpful effect on the psychological health of the people, but must be assessed in relation to the climatic conditions of the site. In the Italian context, the choice may not be appropriate since it does not provide guarantees on the benefits offered by the air present in the cavity. This choice also involves the reduction of the noise level of the system.
For the project of renovation of the Hines company in Milan, for example, the strategy of refurbishment has prioritized the issue relating to the control of the thermal load and the daylight through the use of high-performance glass rather than the use of natural ventilation in the offices. In the renovation of the Johnson Wax building, the possibility of opening the inner façade exist: this helps the comfort of users, who can enjoy natural ventilation in the workplace, even if, in the reality, the optimal conditions for opening the windows occur only during the summer night-time and the achievement of the comfort is largely delegated to the air conditioning. For the Torno International headquarters the internal façade can not be opened and an external skin made by laminated security glass was realized. The lower air vent is full open, the upper is electronically adjustable by made of moveable louvers. In tall

buildings, when the cavity is over 20 meters, an area of low pressure can occur: this can block the chimney effect and consequently, the need to move this critical area as high as possible. One solution should be to design the outlet air vent (at the top), according to a generalized average of 2 to 1 respect to the inlet air vent (at the bottom).

3. Conclusions

Double skin glass façades are in the most cases used in the refurbishment of office and public buildings where high investment costs can be justified with the architectural renovation of the building. In the summer season in Italy, the maximum performance obtainable from a naturally ventilated double skin glass façade is mainly to act as a "buffer space" to reduce overheating. This implies that the main result that could be obtained is the reduction of operating costs for cooling, due to the increased thermal performance of the envelope.
All of these case studies demonstrated that a reduction of energy consumption both in summer that in winter season is possible: the average consumption of the buildings before the interventions was about 250-270 Kwh/m^2 , that was reduced of about 30-40% thanks to the realization of the new envelope. The most suitable solution might be an integrated plant that regularly provide for a mechanical ventilation of the cavity and it should be operative when the outside conditions are extreme. An interesting way that might really enhance the management of the energy balance, should also include to support the system with integrated photovoltaic panels or solar collectors, combining the benefits offered by the double skin structure (in terms of ventilation, noise protection and control of the pressure exerted by the wind), with the possibility of an active exploitation of the solar energy.
The payback for incremental investment in energy efficiency using a double glass envelope has been estimated at 20-25 years. Investment costs could have a fast payback if the glass envelope integrates active solar energy devices (e.g. photovoltaic systems).

References

[1] A Compagno, Intelligent glass facades, Birkhauser, Berlin, 1999.

[2] C. Schittich, Building Skins. Concepts, layers, materials, Birkhauser, Berlin, 1999

[3] S. Brunoro, Efficienza energetica delle facciate, Maggioli, Rimini, 2006

[4] Brunoro Silvia, Technical improvement of housing envelopes in Italy, in: Bragança L., Wetzel C., Buhagiar V., Verhoef L.G.W. (edited by), COST C16 Improving the quality of existing urban building envelopes. Facades and roofs, Volume 5, IOS Press, Amsterdam, 2007, pp.69-82

[5] S. Brunoro, An assessment of energetic efficiency improvement of existing building envelopes in Italy, in: Management of Environmental Quality. An international Journal, Volume 19, Number 6, 2008

A model study of the daylight and energy performance of rooms adjoining an atrium well

Jiangtao Du[1,*], Steve Sharples[2], Neil Johnson[1]

[1] *School of Architecture, University of Sheffield, Sheffield, UK*
[2] *School of Architecture, University of Liverpool, Liverpool, UK*
** Corresponding author. Tel: +44 7892841534, Fax: +44 114 222 0315, E-mail: jiangtao.du@yahoo.co.uk*

Abstract: Daylight has been regarded as a significant environmental advantage of atrium buildings because the natural light can illuminate potentially dark core areas and decrease energy consumption. This study has investigated the average daylight factors (overcast sky conditions) and annual lighting energy load (real weather conditions of Sheffield, UK) in adjoining spaces to assess the fundamental daylight performance and energy performance in an atrium model. Radiance and Daysim (based on Radiance algorithm) were the tools to simulate the daylighting and lighting energy use. A comparison of the measurement and simulation showed the validation of the basic Radiance simulation in the model. In terms of the well façades (decided by the ratio of window area to solid wall area) and well surface reflectance, the variations of daylight level and annual electrical lighting use in the adjoining rooms have been analysed and some design strategies for supporting preliminary design decisions are presented. Only the square atrium model and relatively simple climate conditions have been considered in the investigation.

Keywords: *Atrium Building, Daylight Performance, Lighting Energy Saving, Simulation*

1. Introduction

Daylight use in an atrium is particularly beneficial as the atrium well can allow natural light to reach potentially dark core areas in adjoin rooms, decrease energy use by artificial lighting and improve the indoor environment on psychological and ergonomic grounds. In general, the daylight levels in the adjoining rooms are directly influenced by the vertical daylight levels on the well facade and the room properties (size and surface reflectances) [1, 2]. A linear relationship between the vertical daylight factor at the facade and the average daylight factor in the room with a specific dimension and reflectance can be given by a theoretical expression [3]. It has been found that well geometries and surface reflectances have a direct effect on the decay of vertical daylight levels across the well wall in atria [4]. Well geometry can be quantified in terms of the well index (WI) [1], equation (1) which is a function of well length (l), width (w) and height (h) (Fig. 1):

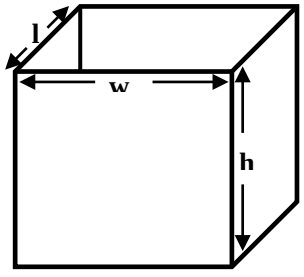

Fig. 1. Atrium geometry and WI definition [1].

$$WI = \frac{h(w+l)}{2wl} \qquad (1).$$

Two measurements using scale models [5, 6] pointed out that changing the proportion of glazing or opening areas between well and adjacent spaces could be a practical solution to the imbalance of light flux received at the top and bottom of the atrium walls and adjoining spaces. A common rule was suggested: small glazing areas on the top floor and the fully gazing areas on t he ground floor. Nevertheless, a recent study [7] based on Radiance simulation indicated that increasing well surface reflectances had little impact on the daylight level of full glazed rooms at ground floor because of the lack of solid reflecting surfaces. This demontrates the complexities of refleted light in atria. It is still essential to carry out more investigations on daylighting performance of rooms in atria with various facade systems. Moreover, the lighting enegy saving under the conditions of daylight use in atria is another significant toipc to be studied. A field measurement [8] in two large atria showed that daylighting illumination can displace 46% and around 15% of annual lighting consumptions through introducing two different lighting control systems respectively. By providing sufficient daylighting illumination, the daylight use in atria displaces the artificial lighting load in the adjacent spaces, which is regarded as one of the most important and hardest-to-achieve objectives of atrium environmental design [2].

This study investigated the daylight performance and energy performance (annual lighting use) of adjoining rooms in a five-story atrium model with various façade systems and well reflectances. Radiance and DaySim (Radiance-based package) were used in the calculations of daylight factor and annual lighting load respectively. Firstly, a comparison between model measurements and Radiance simulations was undertaken to validate the basic Radiance outputs. Next, more Radiance simulations were carried out to display the impact of façade configurations and well reflectances on t he average daylight factors in rooms. Thirdly, the lighting energy consumption of rooms in the atrium model was considered. Finally, some design strategies have also been suggested.

2. Comparisons of simulation and measurement

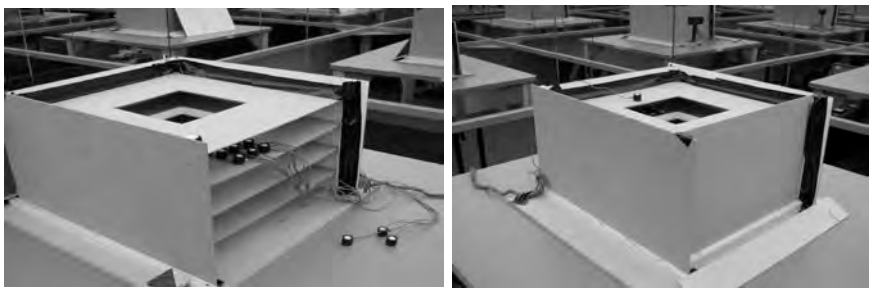

Fig. 2. Physical atrium model in a mirror box artificial sky.

A physical atrium building model was tested in a mirror box artificial sky that reproduced a CIE standard overcast sky (Fig.2). The measured data were compared with simulated data from Radiance. The scale building model had an atrium well and adjoining spaces. In the centre of the building, the well had a square plan of 200mm × 200mm whilst the whole building had a square plan of 500mm × 500mm. With a height of 350mm the atrium well had a WI value of 1.75, which represents a medium atrium. Four-storey adjoining spaces were set around the well and the height and the depth of each side room at each floor were 70mm and 150mm respectively. There were two different façade types: rooms with unobstructed windows and rooms with balconies on t he border of the well (balcony height = 1/3 room height). The well floor had been given three different surface reflectances: low (black), medium (grey) and high (white).

For models with balconies, the comparisons of measured and simulated average daylight factors (ADF) in rooms are indicated in Fig.3. It can be seen that, generally, the simulations are close to the measurements at the ground, 1st and 2nd floors. However, the measured data are underestimated by the simulations at the top floor, which is dominated by direct sky light. Taking the measurements as reference, the percentage differences of simulations are 18.5% (maximum), 0.06% (minimum) and 9.5% (average) respectively.

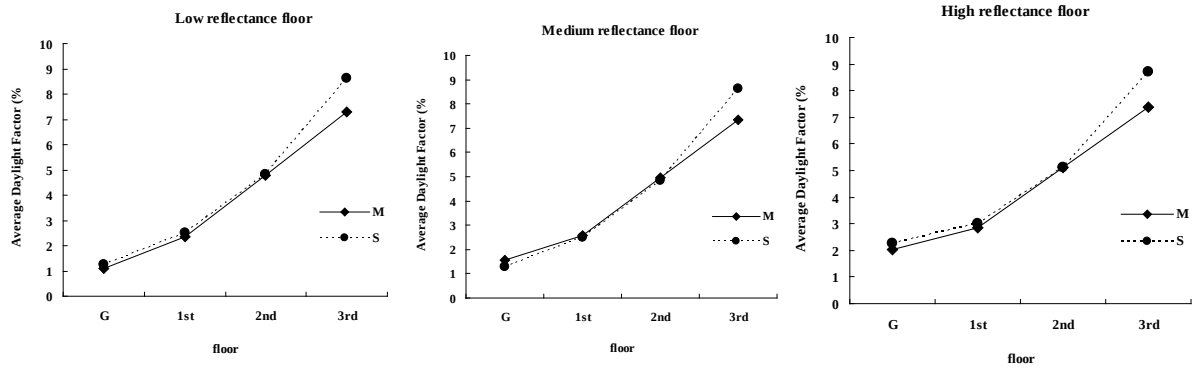

Fig. 3. Comparison of measured (M) and simulated (S) average daylight factors at each floor in a four-story atrium model with balconies.

For models with open facades, Fig.4 shows the comparisons of measured and simulated ADF in the adjoining rooms. The models without balconies have a very similar form of variation of average daylight level to the models with balconies: the top floor has a divergence between the two values; other floors have achieved a good agreement. Likewise, the three percentage divergence values are: 17.8% (maximum), 0.43% (minimum) and 8.6% (average).

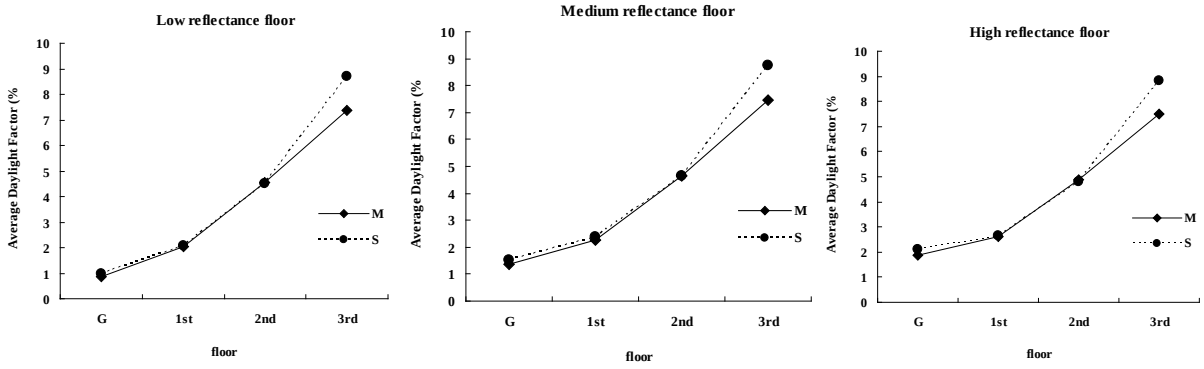

Fig. 4. Comparison of measured (M) and simulated (S) average daylight factors at each floor in a four-story atrium model without balconies.

Overall, the varying trends of the simulated data are similar to those of the measured data in the atrium models with various facades and well floor reflectances. The trends express an exponential form from the atrium base to the top. For all the models studied, the average percentage difference between simulation and measurement was less than 10% even though a few positions see a relatively larger divergence. The bigger disagreements between the measurement and simulation can be explained by the geometric and photometric deviations between the physical model and the Radiance model, which have been analysed in two earlier papers [9, 10]. In addition, the nature of some Radiance algorithms also contributed to the divergence brought by the reflected light from the lighter surfaces. In general, the Radiance simulations have been validated by the measurements in this study.

3. Daylighting performance in an atrium

Radiance was used in this section to calculate the average daylight factor in adjoining rooms of an atrium model. The ADF was used as an indicator of fundamental daylight performance in rooms of atria under CIE overcast sky conditions.

3.1. Atrium model

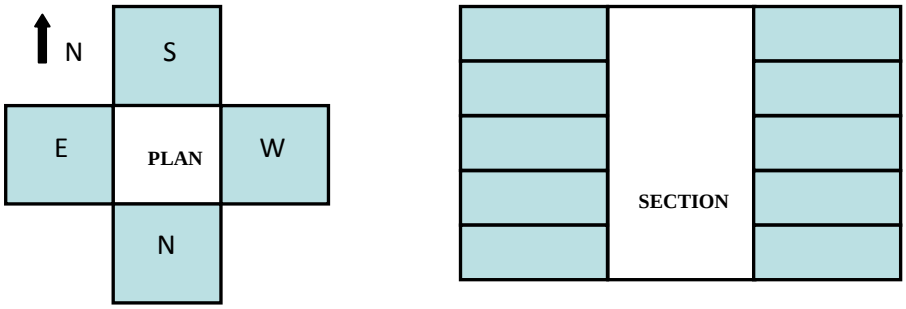

Fig. 5. Plan and section of a five-story atrium model (dark part: rooms; white part: well).

The atrium model studied consisted of a five-story building with a centre square well and four-sided rooms with the same size (Fig. 5), where N, E, S and W indicate the direction the well opening is facing. The WI value of the atrium model was 1.55, which means a medium atrium. The solid part of the well (including well floor and balcony) had reflectance values of 0, 0.2, 0.4, 0.6 and 0.8. The rooms had a fixed ceiling reflectance (0.8), wall reflectance (0.5) and floor reflectance (0.25). In addition, the models were divided into three groups in terms of the façade/balcony type - see Fig. 6 where (a) = window with no balcony (opening façade); (b) = 1/4 room height balcony; (c) =1/2 room height balcony.

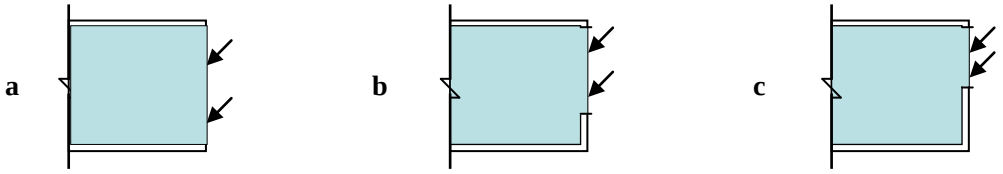

Fig. 6. Three different types of façade.

3.2. Average daylight factors in rooms

The rooms at the top floor (4th floor), middle floor (2nd floor) and ground floor were studied. Fig. 7 shows the variations of ADF in rooms at the three different heights in the atrium with various well reflectances and façade systems. Apparently, the higher balcony reduces the incident light for the rooms, giving a lower ADF. The 1/2 balcony room had the least daylight. At different floors, the daylight levels in the 1/4 balcony room are close to those in the room with no balcony, which are much larger than those of 1/2 balcony room. Interestingly, when the positions of room become lower, the differences between curves of the 1/2 balcony and the curves of the open window tended to be smaller. This implies that the impact of the balcony on ADF is decreasing near the base. On the top floor, the ADF values of rooms are not significantly influenced by the increasing well solid surface reflectances. The middle floor and ground floor, nevertheless, see that an increasing well surface increases the ADF in rooms. The lower are the floors then the slopes of the curves (reflectance as a function) are steeper. This means increased magnitudes of ADF by increasing reflectance tend to be larger at lower floors than those at upper floors, especially for the model with 1/2 balcony. For instance, the relative differences between refl0 and refl0.8 of the open window and 1/2 balcony on the top floor are 2% and 12% respectively, whilst the two values have greatly increased to 73% and

188% on the ground floor. This might be due to the fact that the main components of ADF consist of reflected light. For all models, the rooms on the top floor have the largest daylight level which decays in an exponential form toward the atrium ground (see the sub-figure at the right of the below part in Fig.7). This responds with the results of scale model measurement in section 2.

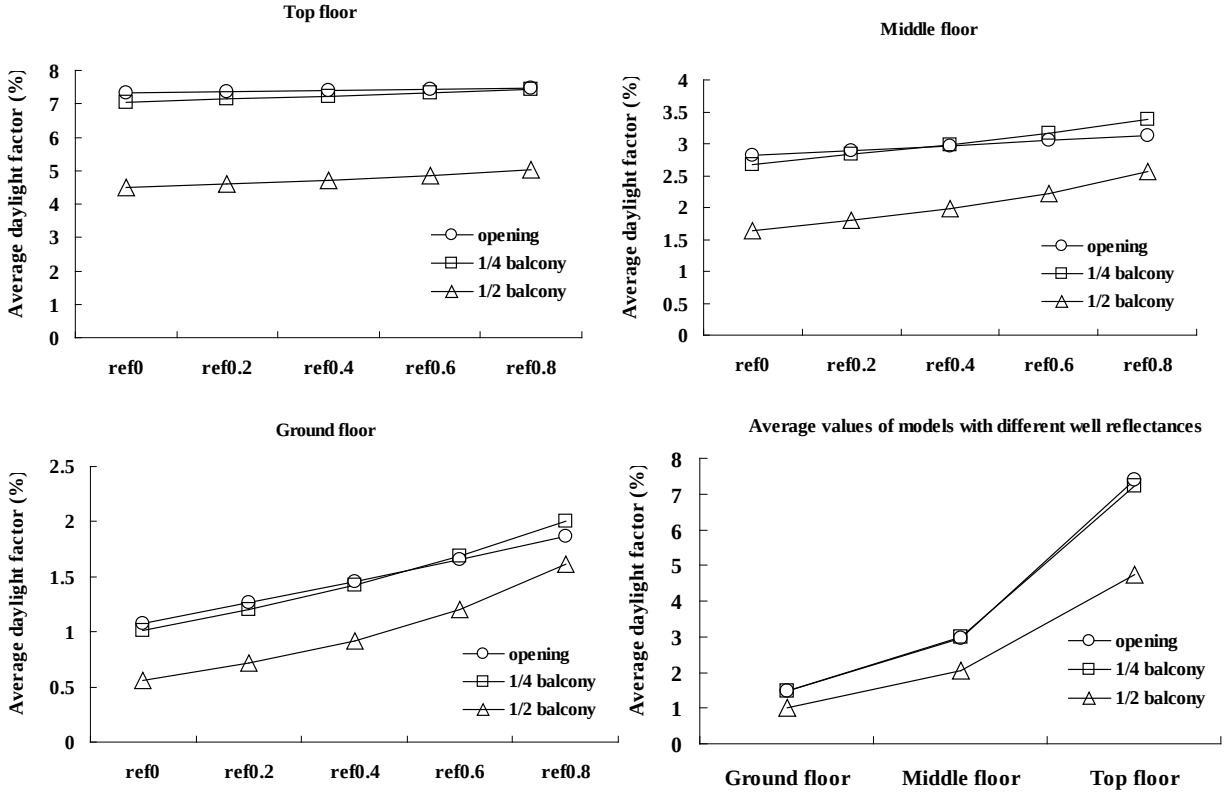

Fig. 7. Variations of ADF in rooms of different floors in an atrium with various façades and well surface reflectance.

4. Energy performance in an atrium

DaySim (using basic Radiance algorithm) [11, 12] was utilized here to predict the annual electrical lighting energy usage in adjoining rooms of the atrium model. The annual lighting consumption per unit area was used for the assessment of fundamental lighting energy performance in the daylit adjoining rooms. Based on the weather datasets, Daysim can derive the sky conditions include a large range of sky models like overcast sky, intermediate sky and clear sky [11].

4.1. Simulation preparations

The atrium model studied for energy analysis was the same as the model in section 3.1. The location of the atrium was in Sheffield, UK (Lat: 53.50′N; Lon: 1.00′E). According to Fig.5, the rooms at different sides can be named as: east-facing room (e), west-facing room (w), south-facing room (s) and north-facing room (n). The reflectances of room components were still kept the same while only a medium value 0.4 was adopted as the well solid surface reflectance. The facades followed the three types shown in Fig.6.

For lighting energy calculation, several fundamental aspects [12] were quoted as follows:
(1) Daylight savings time is from April 1st to October 31st; (2) The atrium is in an office building. All adjoining spaces are used as the working zone, which is occupied Monday through Friday from 8:00 AM to 17:00 PM; (3) A minimum illuminance level of 500 lux is

needed to support the working task of occupants; (4) The electric lighting system has been installed in the adjoining spaces with a typical lighting power density of 14.00 W/m^2; (5) The adjoining rooms do not use any dynamic shading device system and the lighting system is manually controlled with an on/off switch.

4.2. Lighting energy usage in rooms

Fig. 8 shows the annual electrical lighting energy consumptions (unit area) of rooms at the three different heights and four different sides in the atrium with various façade systems. It is obvious that generally the rooms on the higher floors have the lowest electricity load for the task illuminations in a whole year because the positions can receive the most incident daylight from the sky. The ground floor rooms are the ones which consume the most electrical lighting energy. Surprisingly, the lighting energy usage in rooms in the middle floor is just a little lower than the rooms on the ground floor while it is much larger than the top floor. Taking the east-facing side room as an example, the average annual lighting load at three different floors are 24.23 kWh/m^2 (top), 30.87 kWh/m^2 (middle) and 31.30 kWh/m^2 (ground) respectively. Considering the energy algorithm in Daysim [11], the orientations of the rooms also have some impact on the lighting energy usage. The rooms facing south or east apparently consume the less energy (28.76 kWh/m^2 or 28.8 kWh/m^2) whilst the rooms facing west and north need more electricity for task lighting (29.14 and 29.23 kWh/m^2). Interestingly, the differences between rooms with 'good' orientation and rooms with 'bad' orientation are not very large. This might be explained by a fact that the building location (Sheffield, UK) is dominated by overcast sky conditions, which has a radial symmetric sky luminance distribution [12].

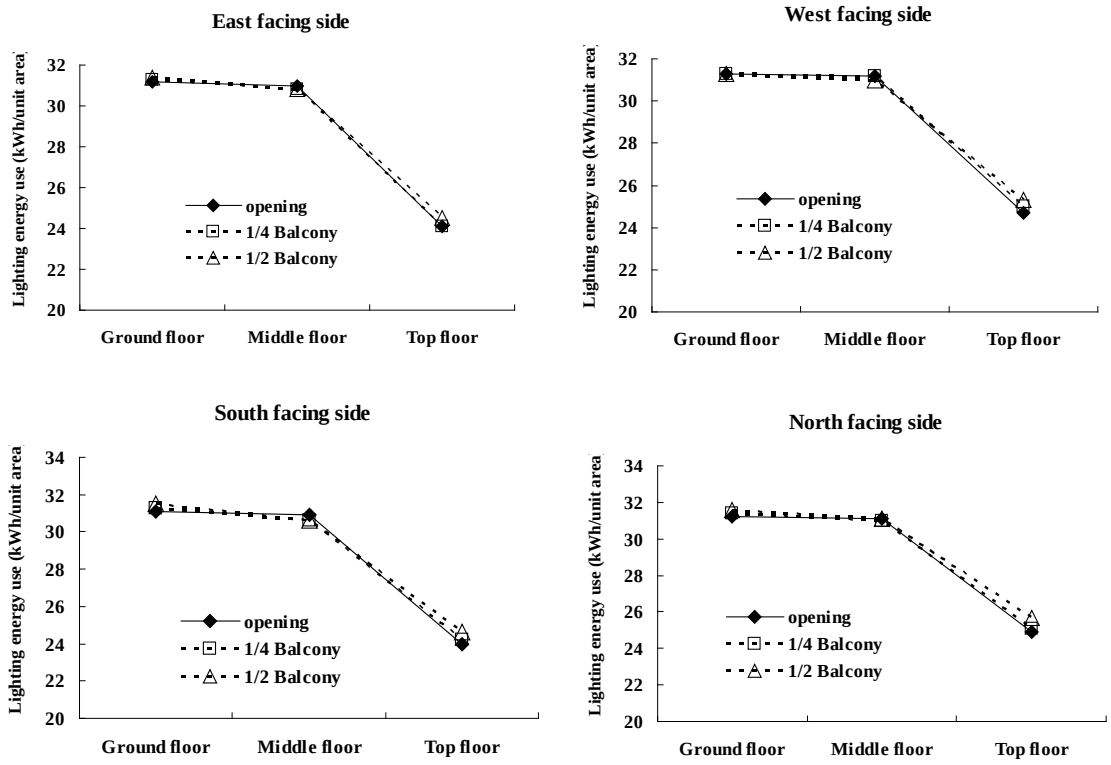

Fig. 8.Annual lighting energy consumptions (kWh/m^2) of adjoining rooms at different floors and different sides in an atrium.

Table.1 expresses the effect of façade systems on the annual lighting energy consumption in adjoining rooms. For the top floor and the ground floor, the higher is the balcony then the more is the lighting energy usage. This actually coincided with the basic daylight performance

(worst scenario: overcast sky) of rooms in section 3.2. However, the middle floor sees a different trend: the rooms with two different balconies have the same energy consumption which is less than the value of rooms with an open façade system. The trend displays a little difference from the variation of basic daylight performance (overcast sky) on this floor. It should be noted that the daylighting calculation used in the Daysim energy analysis is based on real weather dataset and the sunlight has also been included. Also, the daylight levels in the room of middle floor would be significantly influenced by the well wall, which can bring more reflected light into the rooms than other floors [3, 4]. But, the average lighting consumption in all rooms with opening façade is 28.88 kWh/m^2, while the values in all rooms with 1/4 balcony and 1/2 balcony are 28.94 and 29.12 kWh/m^2 respectively. So, increasing the balcony height generally increases energy consumption if all the rooms of in the atrium are considered.

Table 1. Annual lighting energy consumptions (kWh/m^2) and atria with various facade systems.

Floor	Side	Annual lighting consumption (kWh/m^2)		
		opening	1/4 balcony	1/2 balcony
Ground floor	E	31.2	31.3	31.4
	W	31.3	31.3	31.3
	S	31.1	31.3	31.5
	N	31.2	31.4	31.6
	4 sides average	31.2	31.3	31.5
Middle floor	E	31	30.8	30.8
	W	31.2	31.2	31
	S	30.9	30.6	30.6
	N	31.1	31	31.1
	4 sides average	31.0	30.9	30.9
Top floor	E	24.1	24.1	24.5
	W	24.7	25	25.3
	S	24	24.2	24.6
	N	24.9	25.1	25.7
	4 sides average	24.4	24.6	25.0

5. Conclusions

This study has given an assessment of daylight performance and artificial lighting consumption in adjoining spaces in an atrium model. Some findings can be drawn from the results and discussions above:

(1) There is an agreement between scale model measurements and Radiance simulations on average daylight levels of rooms in a medium height atrium. This enhances again the validation of basic Radiance algorithm in calculating atrium daylight levels.

(2) Under overcast sky conditions, the varying trend of average daylight levels in rooms expresses an exponential form along the vertical direction from the top to the base.

(3) Under overcast sky conditions, only the highest balcony can have a detrimental effect on the average daylight levels in rooms.

(4) The rooms on the top floor mainly receive direct sky light and are clearly not influenced by the variation of well reflectances; the rooms on the middle floor get both the direct

daylight and reflected daylight; the rooms at ground floor level are substantially dependent on reflected daylight.
(5) In an atrium with four-sided adjoining rooms, the rooms on the top floor need the least energy for electrical lighting; the lighting energy performances are similar for the rooms at the middle floor and ground floor, both of which are much worse than the top floor.
(6) In an atrium with four-sided adjoining rooms located in the northern hemisphere, the rooms facing east and south perform better than the rooms facing north and south in terms of the lighting energy saving through daylight usage.
(7) In a four-sided atrium with adjoining rooms, the well facade consisting of the higher balconies and open windows would generally have a more negative impact on lighting energy saving in rooms than the open facades or facades with lower balconies (façade types in fig. 6).
The limitations of the study are: (i) only the model with a square plan was analyzed, whose four sides were the same length; (ii) the façade configurations were relatively simple and no glazing has been considered in the models; (iii) the energy calculations are just focused on a site with a simple cloudy sky condition with little sunlight involved. Future work will focus on models with a broader range of geometries, more complicated well facades and a variety of sky luminance conditions at typical climate zones around the world.

References

[1] M. Aizlewood, The daylighting of atria: a critical review，ASHRAE Transactions 101，1995, pp. 841-857.

[2] S. Sharples and D. Lash, Daylight in atrium buildings: a critical review, Architectural Science Review 50, 2007, pp. 301-312.

[3] P. Littlefair, Daylight prediction in atrium buildings, Solar Energy 73, 2002, pp. 105-109.

[4] J. Du and S. Sharples, Computational simulations for predicting vertical daylight levels in atrium buildings, Proc. of International Building Performance Simulation Association Conference, 2009, pp. 272-279.

[5] R. J. Cole, The effect of the surfaces adjoining atria on the daylight in adjacent spaces, Building and Environment 25, 1990, pp. 37-42.

[6] Ø. Aschehoug, Daylight in glazed spaces, Building Research & Information 20, 1992, pp. 242-245.

[7] B. Calcagni and M. Paroncini, Daylight factor prediction in atria building designs, Solar Energy 76, 2004, pp. 669-682.

[8] M. R. Atif and A. D. Galasiu, Energy performance of daylight-linked automatic lighting control systems in large atrium spaces: report on two field-monitored case studies, Energy and Buildings 35, 2003, pp. 441-461.

[9] M. Aizlewood, K. Isaac, P. Littlefair, A scale model study of daylighting in atrium buildings, Proc. of the IESANZ, 1996.

[10] M. Aizlewood, J. Butt, K. Isaac, P. Littlefair, Daylight in atria: a comparison of measurement, theory and simulation, Proc. of Lux Europa, 1997.

[11] C. F. Reinhart, S. Herkel, The simulation of annual daylight illuminance distributions – a state-of-the-art comparison of six Radiance-based methods, Energy and Buildings 32, 2000, pp. 167-187.

[12] C. F. Reinhart, Tutorial on the use of Daysim simulations for sustainable design, IRC-NRCC, 2006.

Numerical analysis on daylight transmission and thermal comfort in the environments containing devices called "Double Light Pipes"

O. Boccia*, F. Chella, P. Zazzini

D.S.S.A.R.R., Faculty if Architecture University "G. D'Annunzio", Pescara , Italy
** Corresponding author. Tel: +39 854537291, Fax: +39 854537268 , E-mail:oreste.boccia@libero.it*

Abstract: In this paper the authors present the results of a numerical analysis concerning the study of daylight transmission and thermal comfort in underground areas and basements of a building without any direct openings toward the external environment. The study was carried out on a two-level building, illuminated by the "Double Light Pipe" (DLP), an innovative technological device developed in the Laboratory of Technical Physics, Faculty of Architecture, Pescara, Italy.

The DLP consists of two concentric pipes of different diameter, able to illuminate both the final room and the intermediate one and to allow the entry and the extraction of the air inside the environments of life.

In this first phase, the authors carried out a numerical analysis by the soft-wares RADIANCE and ECOTECT with the aim to define the illuminance distribution in the intermediate room illuminated by the DLP in standard conditions of sky; in addition the CFD code FLUENT/AIRPACK is employed with the aim to define the thermal comfort level considering external wind condition, air temperature and solar radiation. The indoor air temperature and velocity, mean age of air and the indexes PMV and PPD have been evaluated so verifying the indoor air quality.

Keywords: *Light pipe, Lighting, Daylight, Indoor air quality, Numerical analysis*

1. Introduction

Buildings use almost 40% of the world's energy [1] and artificial light is responsible of a significant part of the whole energy consumption of a building. A considerable reduction of energy consumption is achieved when natural light inlet is optimized and this can be achieved both by traditional sources, as windows or skylights, or by technological devices, as light pipes [2, 3]. The latter are particularly suitable in underground areas of buildings, in large commercial or industrial buildings, with windows placed on perimetral walls away from the centre of the room, or in exhibition rooms, museums or similar, where a particularly diffuse light with not too high illuminances on the work plane and a uniform luminance distribution of walls are preferred in order to guarantee a correct perception of the work of arts, particularly paintings on display. Moreover underground areas or rooms without any direct interface outwards need mechanical ventilation systems to make the necessary change of air in order to realize comfortable conditions for the occupants. In this paper the authors address the problem and propose a solution which is the Double Light Pipe (DLP), an innovative technological device recently developed in the laboratory of Technical Physics of Pescara [4, 5]. The DLP is an evolution of a traditional light pipe. The latter transport daylight from the collection point, commonly on the roof top of the building, trough the ceiling to the final rooms where it is distributed by a diffuser [6, 7]. When an intermediate area has to be crossed by the system, its encumbrance makes it a problem to position the device in the centre of the passage room. The idea is to give the system an illuminating function both for the destination room and the passage area. In this case it becomes acceptable indeed desirable, particularly in wide plant area rooms such as museums or exhibition areas, in which a high quality light, characterized by low illuminances on the work plane and quite a uniform distribution of luminances of the walls, is requested. In this paper the authors present the double light pipe modified in its geometric configuration in order to allow an efficacy circulation of air in the

passage room able to effect the necessary change of air requested for the comfort of the occupants. This is a ventilated double light pipe, whose performances have been analyzed in the Laboratory of Technical Physics of Pescara through a numerical analysis, by which the thermal and visual comfort level are realized in a large area room without any direct interface to outwards, by the ventilated double light pipe.

2. Methodology

A numerical analysis was carried out by the authors: the soft-wares RADIANCE and ECOTECT were used with the aim to calculate the illuminance distribution in the intermediate and final room illuminated by the DLP in various standard conditions of sky. The CFD code FLUENT/ AIRPAK [8] is employed to determine the values of the parameters by which the thermal comfort level for the occupants can be defined, depending on external wind condition, air temperature and solar radiation. In particular, by means of the numerical tool, the indoor air temperature, air velocity, mean age of air and the indexes PMV and PPD have been evaluated in order to verify the indoor air quality. [9]

2.1. Description of the test room

The test room modeled by the sw is a two levels square modular form. Each level consists of a 12x12 m plant area room, 4 m high, in which four ventilated double light pipes are installed, able to introduce daylight both in the passage and the final level, while natural ventilation is achieved in the passage room thanks to openings properly applied on the top and the bottom of the pipes. In Fig. 1 a three-dimensional representation and a cross section of the device are shown. The DLP described in [4, 5] is modified in order to allow the air circulation in the room. The inner pipe is narrow at the top and the outside is narrow at the bottom, so the air cavity between the two concentric pipes has a convergent section at the bottom for the introduction of air and the inner pipe has a convergent section at the top for the extraction of air. In the test-room four DLP are installed, two for the extraction and two for the introduction of air. At the top and the bottom of each DLP openings are properly realized in order to allow air introduction and extraction from the environment.

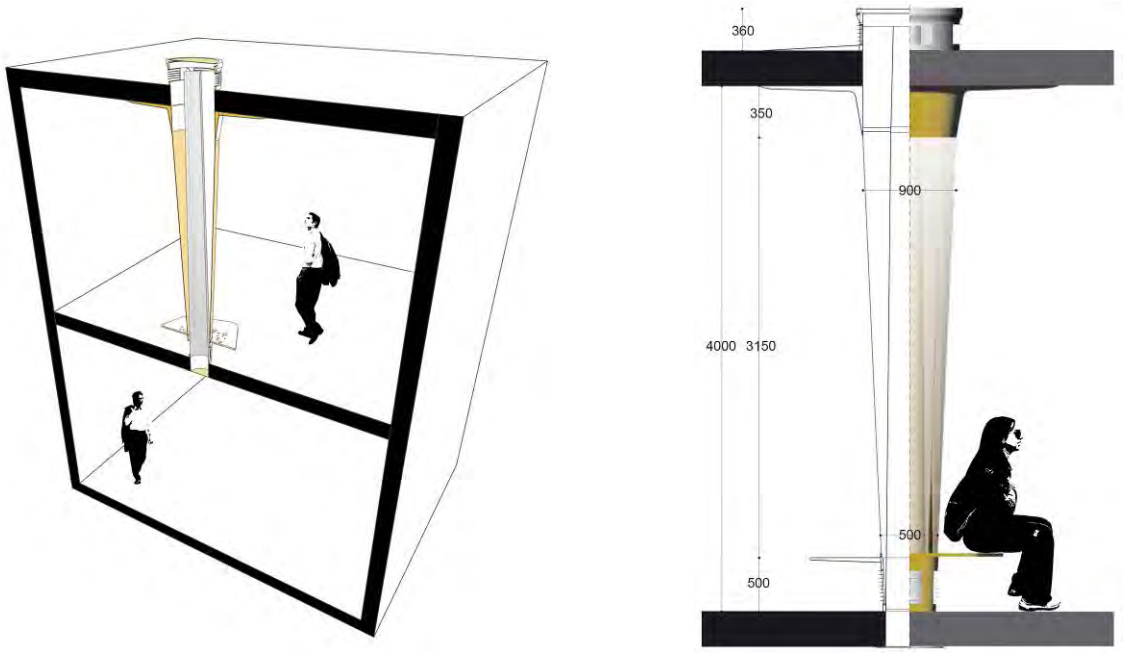

Fig. 1. A three-dimensional representation and a quoted section of the Double Light Pipe

3. Daylight results

In Fig. 2 the daylighting levels distribution on a 0,8 m high horizontal work plane by the sw Ecotect is illustrated on December the 21st under CIE Overcast sky (a) and on June the 21st under CIE Clear sky (b) .

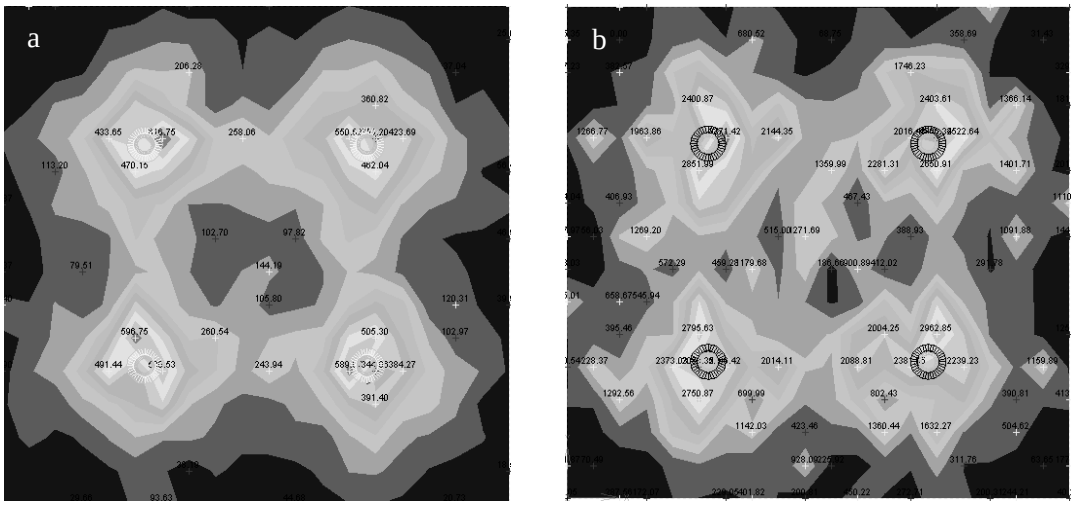

Fig. 2. Daylight Illuminance (lux) by Ecotect in Winter (a) and Summer (b) conditions

In Figg. 3 and 4 the luminance and illuminance data by Radiance are shown, respectively in winter and summer conditions. In the first case, the simulation is effected under Overcast sky on December the 21st , while, in the second, under Clear sky on June the 21st.

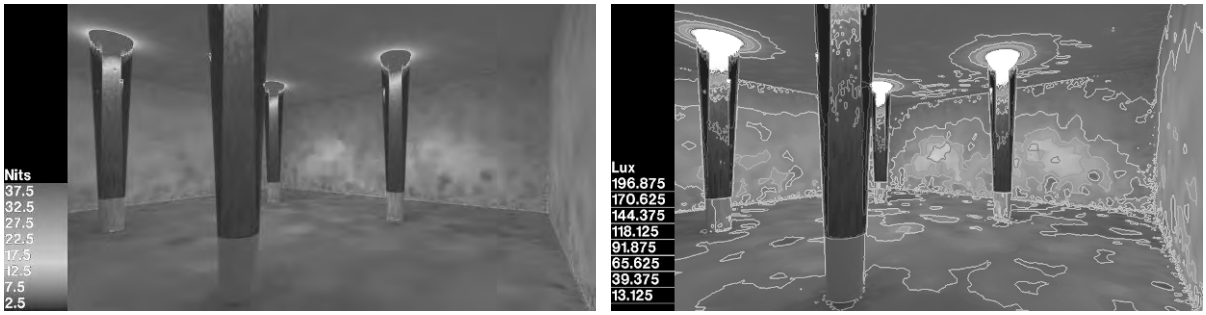

Fig. 3. Daylighting simulation by Radiance in Winter condition

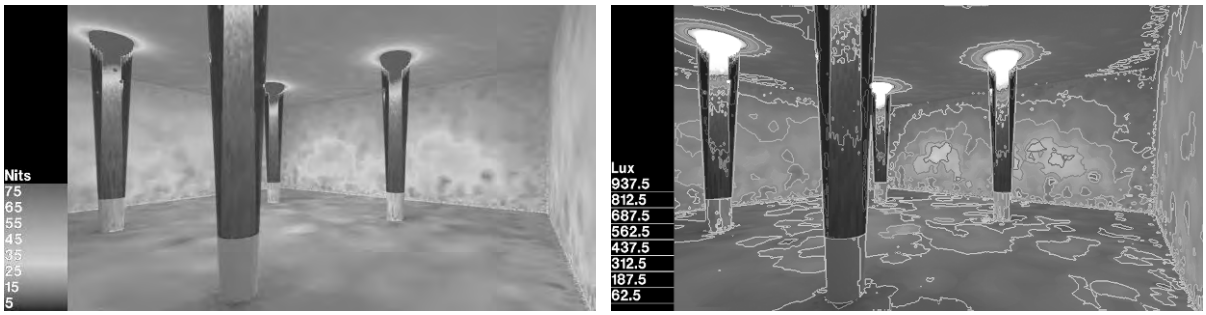

Fig. 4. Daylighting simulation by Radiance in Summer condition

4. Thermal comfort results

The numerical analysis was carried out by Fluent/Airpak in steady state summer and winter conditions. The following results regard the test on September the 16th at 13 a.m. with the following boundary conditions:

External air temperature: t_{ext} = 27°C;
Mean radiant temperature t_{mr} = 27°C;
Mean internal surface temperatures of floor, t_f = 25°C
Mean internal surface temperatures of walls t_w = 26°C
Mean internal surface temperatures of ceiling t_c = 26,5°C
Inlet air velocity close to the vent 1 and 2: v_{in} = 3 m/s;
Surface temperature on the polycarbonate collector: t_g = 36°C.
The external air temperature was experimentally measured at the same time, while a higher temperature of the collector was imposed to take into account the solar radiation heating.
In Fig. 5 a qualitative trend of air introduction and extraction by the device is shown. Each DLP can function as an extraction or introduction system. In the extraction pipe the inner tube is open at the top and the bottom, and the air cavity is closed, while in the introduction pipe the air cavity is open and the inner pipe is closed.

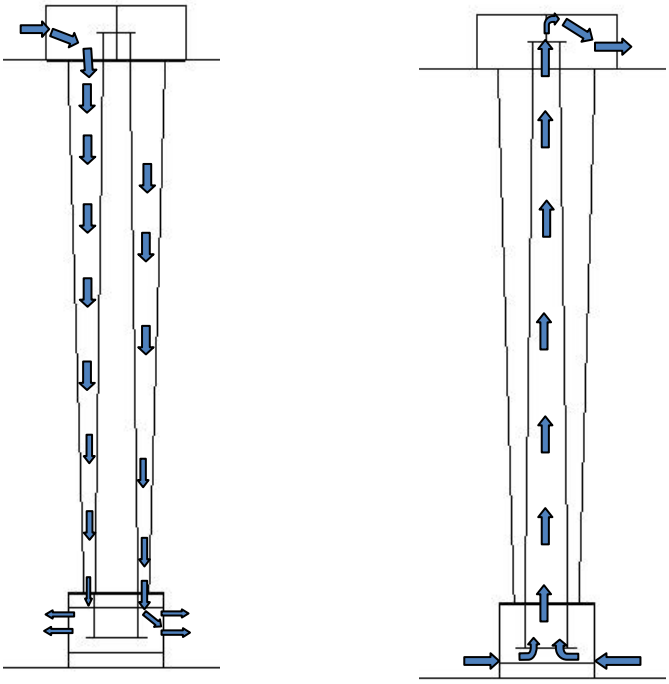

Fig 5. Qualitative Air circulation through the two DLP in the room

In Fig. 6 (a) the air speed distribution on a horizontal plane 1,6 m high on the floor is shown: a good uniformity is verified in the room. In Fig. 6 (b) the air speed distribution is calculated on a vertical cross section 1 m distant from to the extraction DLP. This last image underlines higher values of speed in correspondence to the openings used for the air circulation. However the air speed is comfortable in the whole environment, with very low values everywhere in the room as confirmed by Fig. 7 (a). The Fig. 7 (b) shows the air temperature on a vertical plane vs the height on the floor. It is evident that a low vertical gradient of temperature is obtained. Fig. 8 confirm this trend.

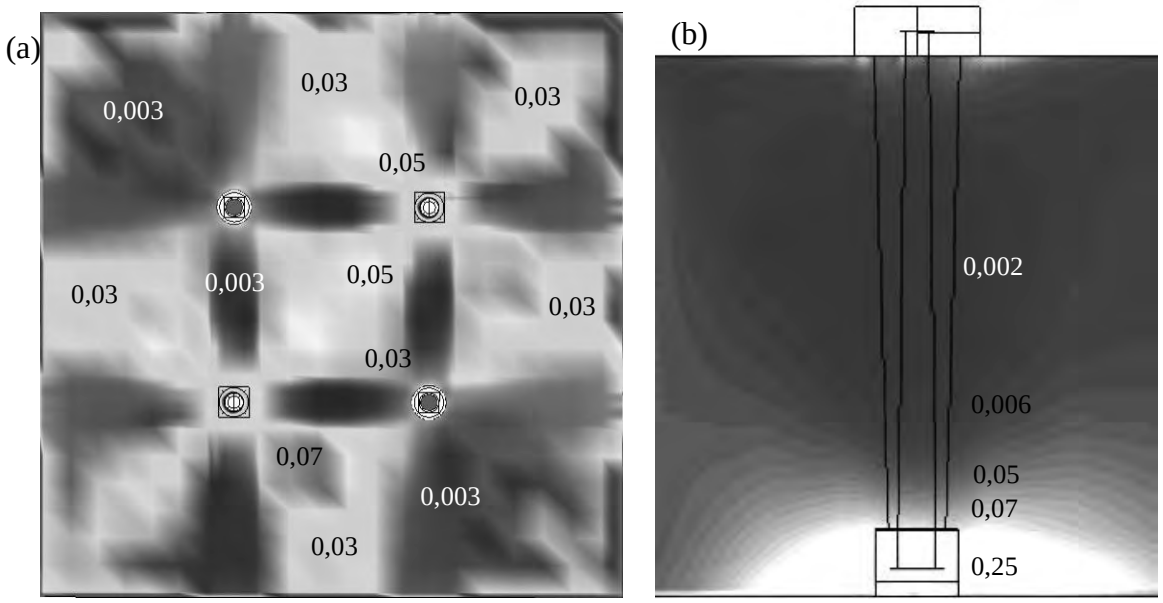

Fig 6. Air speed distribution (m/s) on a horizontal plane 1,6 m high on the floor (a) and on a vertical plane 1 m distant from the DLP (b)

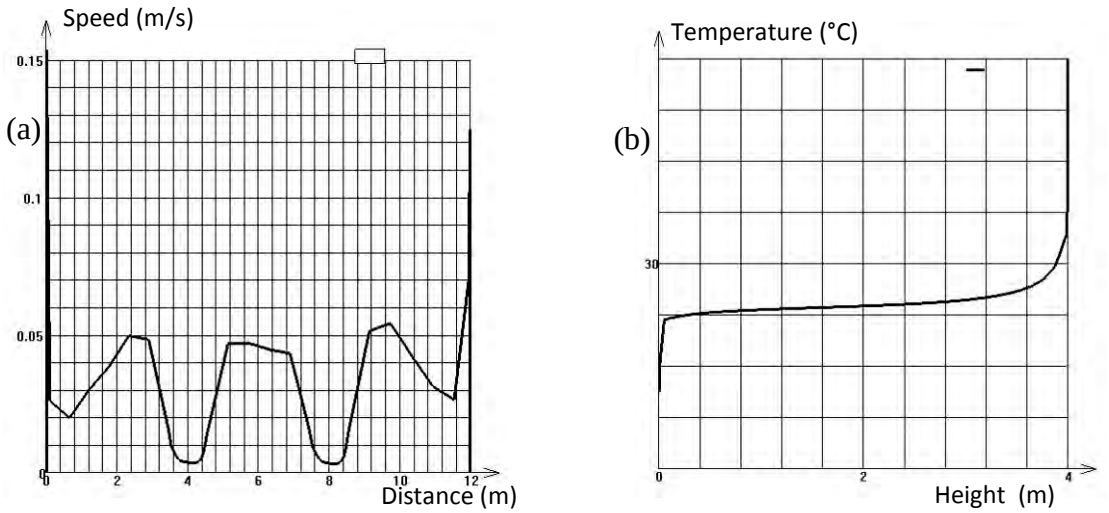

Fig 7. Air speed vs distance from wall to wall at the centre of the room on a horizontal plane 1,6 m high on the floor (a); air temperature vs height exactly at the centre of the room (b).

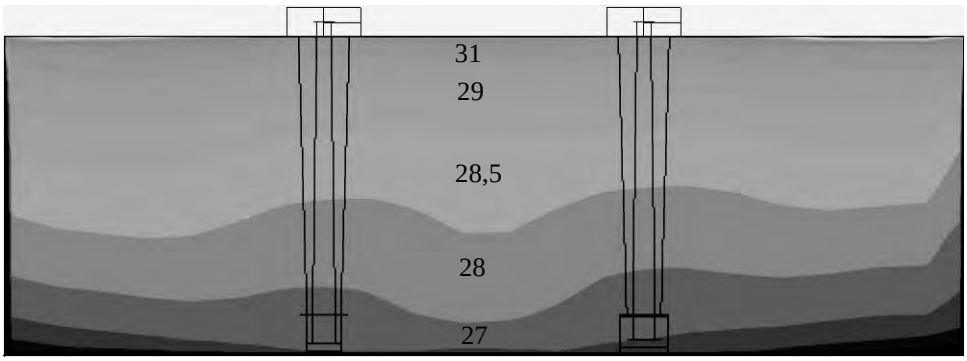

Fig. 8. Air temperature field (°C) on a vertical cross section at the centre of the room

The predicted mean vote (PMV) is commonly used as a measure of the average response about thermal comfort from a large group of people voting on a range included between -3 and +3. In this work the PMV has been calculated on a reference horizontal plan in the room and the results are shown in Fig. 9. A satisfactory condition is obtained considering that the PMV is very uniform and close to the optimum value 0. This is confirmed by the predicted proportion dissatisfied (PPD) index which provides a measure of the percentage of people who will complain of thermal discomfort in relation to the PMV. In this case it is about 13-14 % as shown in Fig. 10. The PMV and PPD are evaluated considering a metabolic rate level of 1,6 met and a clothing level of 0,9 clo.

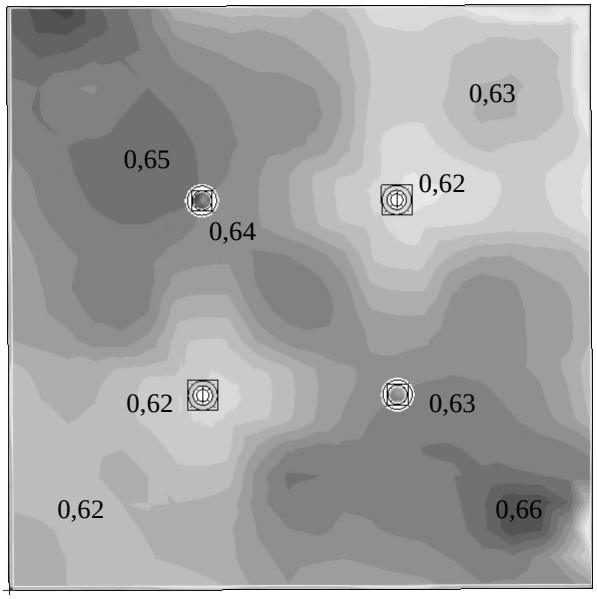

Fig. 9. PMV index distribution on a horizontal plane 1,6 m high on the floor

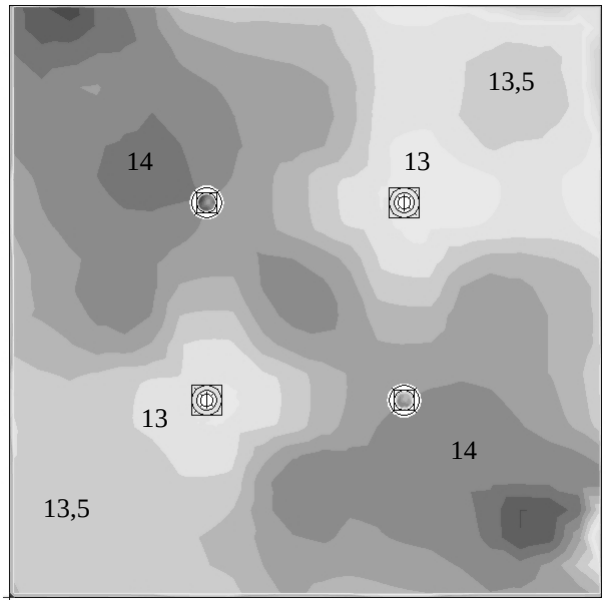

Fig. 10. PPD index distribution (%) on a horizontal plane 1,6 m high on the floor

In Fig. 11 the mean age of air distribution calculated by the numerical tool on a horizontal plane 1,6 m high on the floor is shown. It is obviously higher in the corners of the room and very low in correspondence of the DLP where the change of air is very efficacy, but in the whole environment the air change seems to be very comfortable.

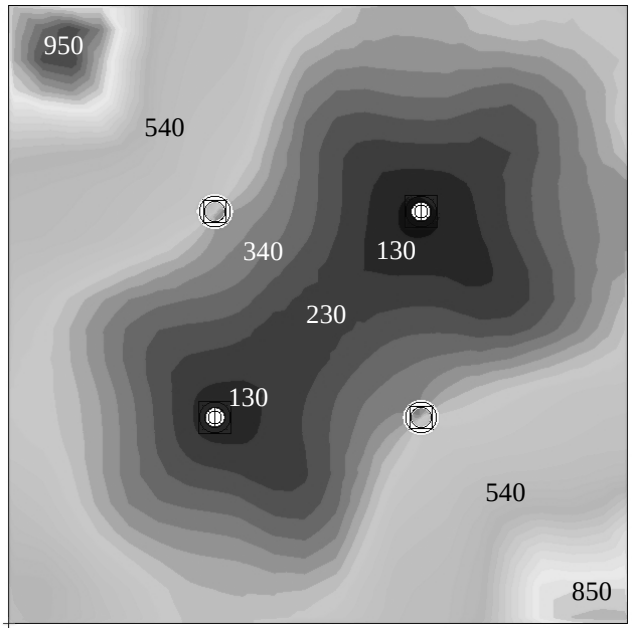

Fig 11. Mean age of air distribution (s) on a horizontal plane 1,6 m high on the floor

The results obtained in winter conditions are similar to the summer ones about the indoor air speed field, but with higher values. On the contrary the indoor temperatures are obviously very different, as shown in Fig. 12. In winter condition the thermal comfort is not assured due to the absence of a thermal plant.

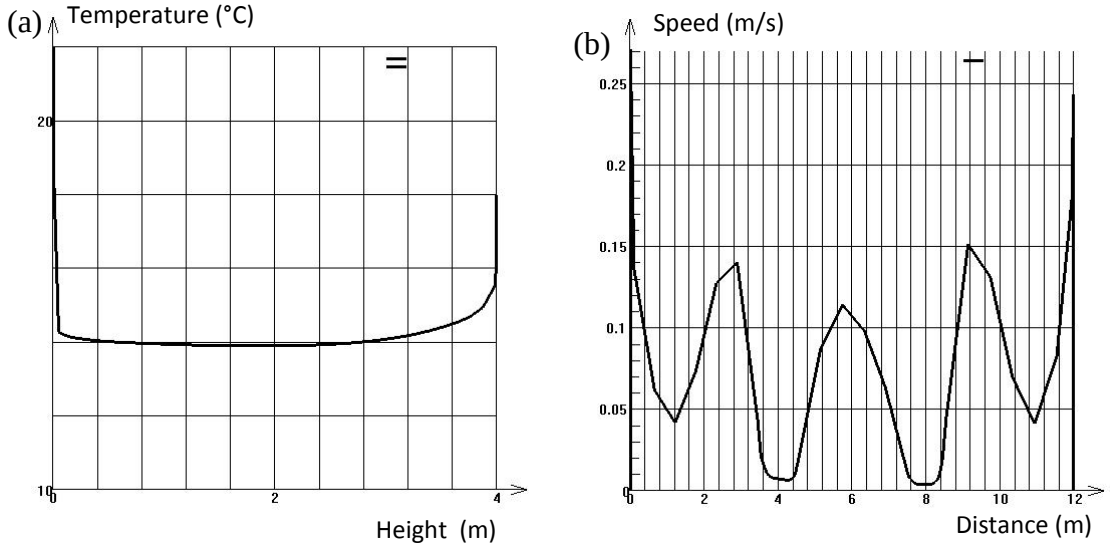

Fig 12. *Air temperature vs height exactly at the centre of the room (a); air speed vs distance from wall to wall at the centre of the room on a horizontal plane 1,6 m high on the floor (b) in winter conditions.*

5. Conclusions

The DLP previously developed by the authors with the aim to distribute daylight in a two/level underground building has been modified in order to allow the air circulation in the upper level necessary to ensure the thermal and hygienic comfort for the occupants. The first numerical results show how the Ventilated Double Light Pipe can be successfully used both to introduce daylight and to allow natural ventilation in the room. It is suitable for large area

exhibition rooms or museums due to its encumbrance and the features of daylight distribution in the environment. Quite uniform illuminace data with low luminances of the boundary walls of the room is realized, except for the higher portion of the system which is characterized by high luminances with the risk of glare. The authors are developing a solution for this problem, using a diffusing film applied on the upper portion of the system, but this work is chiefly devoted to demonstrate the capacity of the system to be employed as a tool for the air change of the room. The first results encourage the authors to carry on the work. Transient numerical analysis has to be carried out in order to simulate the behavior of the system with various external conditions of wind velocity and test its capacity of making an efficacy change of air of the room.

References

[1] M. Santamouris, Alternative cooling techniques for building (Keynote lecture), Proceedings of the 6th International Conference on Sustainable Energy Technologies SET 2007, Santiago de Chile, 2007, pp. 19-24.

[2] D. Jenkins, T. Muneer, Modelling light pipe performances-a natural daylight solution, Building and Environment 38, 2003, pp. 965-972.

[3] D. Jenkins, X. Zhang, T. Muneer, Formulation and semi-empirical models for predicting the illuminance of light pipes, Energy Conversion and Management 46, 2005, 2288-2300.

[4] C. Baroncini, F. Chella, P. Zazzini, Numerical and experimental analysis of the Double Light Pipe, a new system for daylight distribution in interior spaces, International Journal of Low Carbon Technologies, 3/2, 2008, pp.110-125.

[5] C. Baroncini, O. Boccia, F. Chella, P. Zazzini, Experimental analysis on a 1:2 scale model of the Double Light Pipe, an innovative technological device for daylight transmission, Solar Energy, 84, 2010, pp.296-307.

[6] Chella, F., Zazzini, P., Carta, G. 2006. Compared numerical and reduced scale experimental analysis on light pipes performances. 5th International Conference on Sustainable Energy Technologies SET 2006, Vicenza, Italy, pp. 263-268.

[7] Zazzini, P., Chella, F., Scarduzio, A. 2006. Numerical and experimental analysis of light pipes' performances: comparison of the obtained results. In Proceedings of PLEA 2006 – The 23th Conference on Passive and Low Energy Architecture, Geneva, Switzerland, vol. II, pp. 219-224.

[8] Airpak 2.1 User's Guid Fluent Inc. April 2002.

[9] ISO 7730:1994. Moderate thermal environments - Determination of the PMV and PPD indices and specification of the conditions for thermal comfort.

Ventilated Illuminating Wall (VIW): Natural ventilation and daylight experimental analysis on a 1:1 prototype scale model

O. Boccia*, F. Chella, P. Zazzini

D.S.S.A.R.R., Faculty of Architecture University "G. D'Annunzio", Pescara , Italy
** Corresponding author. Tel: +39 854537291, Fax: +39 854537268, E-mail:oreste.boccia@libero.it*

Abstract: In this paper the authors present the first experimental results about the natural ventilation obtained by a device called Ventilated Illuminating Wall (VIW), which carries out the function to introduce natural light in underground areas or that don't have facing outwards, contemporarily operating in the same areas a natural ventilation effective action necessary to guarantee thermal comfort and healthy conditions to the occupants.
The VIW is represented by a 1:1 prototype scale model, constituted by a precast removable manufactured product set to a window of a room. Such device is able both to transport the natural light, captured by the coverage, in underground areas and to introduce outside air for the required ventilation through the vents positioned both inside the room and in the retaining structure of the coverage.

Our study's objective is to verify experimentally, through air speed measurements in different points, if in every condition the indoor air quality is guaranteed.

The results about daylight performances of the system are satisfactory; besides they show that the VIW is able to assure a significant natural air ventilation, but the thermal analysis can be improved measuring the air mass flow rate and the comfort parameters for the occupants.

Keywords: *Ventilated illuminating wall, Natural ventilation, Energy efficiency, daylight, Experimental analysis.*

1. Introduction

Buildings are often equipped by underground areas in which the absence of natural light and ventilation create uncomfortable conditions for human activities. In many cases mechanical ventilation and artificial light are used to ensure comfortable conditions for the occupants. It is known that buildings use almost 40% of the world energy [1] and, obviously, a meaningful part of the whole energy consumption of an edifice is due to artificial light and mechanical ventilation of underground rooms.

Moreover, the case can be considered of buildings utilized as museums, exposition rooms or similar. These spaces need a particularly soft luminance distribution, avoiding direct solar radiations from windows or skylights or very intense reflections from shiny surfaces that may be present in the environment, which can generate the risk of glare. Besides, the paintings on display can be sensitive to light and deteriorate in the presence of high values of illuminance. Usually in museums or exhibition rooms low illuminances are preferred over the illuminated surfaces because, in this case, a favorable balance of luminances is more easily obtained between the visual task and its background.

For these reasons, in these cases any direct interface to outdoor environment through traditional windows or skylights is often avoided and artificial light is adopted all the time. The absence of windows and skylights makes it impossible natural lighting and ventilation. On the other hand it is known that the enjoyment of works of art is better in the presence of natural light than in the absence of it, and a significant energy saving can be achieved by using natural light instead of artificial light. Taking into account that every effort must be made in order to reduce energy consumption of buildings, many technological systems have been applied in architecture with the aim to ensure comfortable conditions for the occupants, concurrently providing a significant energy saving. In recent years many technical devices,

such as light pipes and similar, have been proposed with the aim to introduce natural light in areas without direct interface with outwards and many papers have been published in order to explain the way to design tubular light pipes or similar technological devices [2, 3, 4, 5] .

In some cases light pipes are equipped with technological systems able to ensure air extraction from the room in which they are installed [6]. In this work the authors present an innovative device able to capture daylight from a transparent horizontal surface on the top of the device and redirect it into the room, and simultaneously allow the introduction and extraction of air. This device, called Ventilated Illuminating Wall (VIW), was built in real scale and experimentally tested in order to verify its lighting and air circulation performances, in order to reduce the use of electric light and mechanical ventilation and so diminishing the energy request of the building.

2. Description of the V. I. W.

An innovative technological system was developed by the authors named "Ventilated Illuminating Wall (VIW)". Moving from the idea of building an apparatus able to introduce daylight in underground areas or rooms without direct interface to outdoor, simultaneously ensuring the necessary air circulation, the authors developed a multilayer boundary wall, equipped with a glass plate cover on the top able to capture daylight and a vertical interspace internally covered by a highly reflective film (3M Radiant Mirror Film) by which light is redirected to a transparent surface, like a window, and introduced into the room.

Thanks to a second exterior vertical air cavity, which allows the greenhouse effect in presence of thermal solar radiations in the case of not underground buildings, and fifteen openings with wire mesh properly practiced on the walls, air is allowed to circulate for extraction and introduction in the room so creating an effective air change able to ensure internal comfortable conditions for the occupants. The Ventilated Illuminating Wall is particularly suitable in large exposition areas, which don't have facing outwards and need diffuse light, avoiding glare phenomena which occur when intense direct light from windows comes towards the illuminated surfaces.

3. Methodology

An experimental analysis was carried out on a 1:1 prototype scale model of the V.I.W. The tests were carried out by measuring internal and external illuminance, wind velocity and direction, and internal air velocity in various positions of the room: near the air inlet and outlet vents and in the centre of the room.

3.1. Experimental apparatus

The test room is a 5x3 m plant area room, 2,7 m high. The V.I.W. is constituted by a precast removable manufactured product placed against the window in the north-west wall perimeter of the room. In Fig. 1 some pictures of the system are shown taken during successive stages of its construction: an iron frame was applied against the window on the perimeter wall of the laboratory (a, b); an air space was created between the window and the first opaque layer, which consists of a 4 cm black painted polystyrene panel which gives the necessary thermal insulation and improves the greenhouse effect in the second vertical hole. This last is a 10 cm air space between the polystyrene panel and the external 1 cm transparent polycarbonate panel applied on a second iron frame (c). On the top of the system a glass plate cover is applied which allows daylight entering the room (d).

Fifteen openings with wire mesh allow the natural air circulation necessary to ensure favorable hygienic conditions in the room. The internal ones are shown in Fig. 1 (e) and the external in Fig. 1 (f), where the final configuration of the apparatus is shown.

Fig. 1. Realization steps of the VIW.

The experimental line used to carry out the analysis consists of four CIE Lux-meters sensors, range 0-25 klux, accuracy 3% of the reading value, for the internal illuminance, a CIE sensor range 0-100 klux, tolerance 1.5 %, for the external illuminance, a data-logger with 20 inputs, by which data are registered and elaborated; three internal hot wire anemometers, range 0-20 m/s, accuracy 0,01 m/s, 1%; one tacho-gonioanemometer with direct output.
In Fig. 2 a section of the device with a description of the principal components of the V.I.W. and a quoted section of the system are shown.

3.2. Description of the experimental test conditions

The experimental tests were carried out positioning the sensors in the room as represented in Fig. 3, in which a plant and a section of the room are shown with the position of each sensor.
The tests were carried out in summer and autumn conditions. Air temperature was measured in positions 1, in the center of the room, and in positions 2 and 3, close to the wire mesh applied on the inferior and superior openings. In the same positions air velocity was measured, while illuminance was measured in positions 4, 5, 6 and 7 (Fig. 3).
On the roof top of the building, close to the transparent glass covering plate by which light is collected from the sky, the external lux-meter and the tacho-gonioanemometer dedicated to measure wind velocity and direction were positioned.

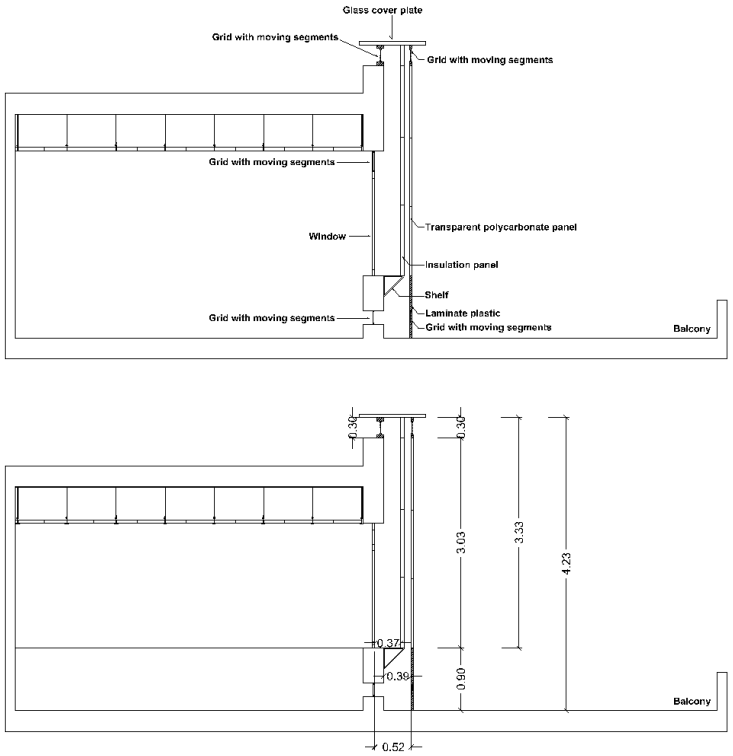

Fig. 2. Sections of the VIW.

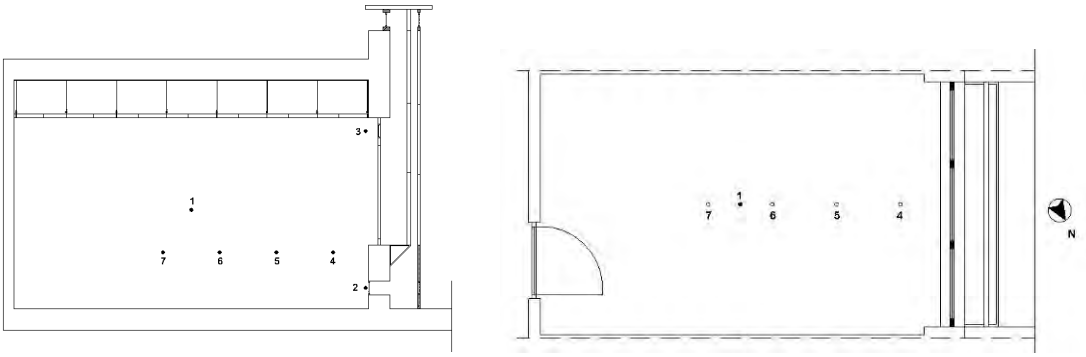

Fig. 3. Section and plant of the test room with the measure positions

4. Results

In Fig. 4 illuminance data measured on September the 16th are shown. External illuminance is referred to the right axis while the ratios between internal and external illuminance in the measure positions are referred to the left one. In this case, with a very regular trend of external illuminance, the influence of the V.I.W. on internal distribution of illuminance is significant up to quite 2 m from the system for a large range of daytime, but in the morning some very high pick values are verified in positions 4 and 5 close to the V.I.W and the influence of V.I.W. is meaningful also in positions 6, quite 3 m distant from the VIW, as shown in table 1, thanks to reflections directly coming from the Radiant Mirror Film.

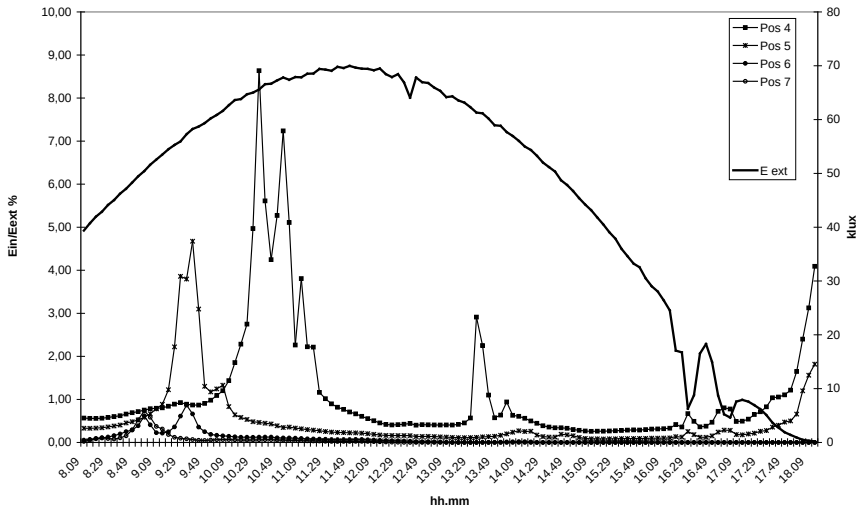

Fig. 4. Illuminance data in positions 4-7 on September the 16th

Table 1. Minimum, Medium and Maximum illuminance data in positions 4-7, on September the 16th

	Pos. 4	Pos. 5	Pos. 6	Pos. 7
Minimum (lux)	9	4	0	0
Medium (lux)	572	222	46	24
Maximum (lux)	5664	2722	497	372
Distance from V.I.W. (m)	0,5	1,3	2,1	2,9

In autumnal conditions, with lower and less regular external illuminance, in the measure positions a similar situation is verified, but pick values of illuminance in the morning are absent and the influence of the system to internal illuminance is significant up to 2 m from it, as shown in Fig. 5.

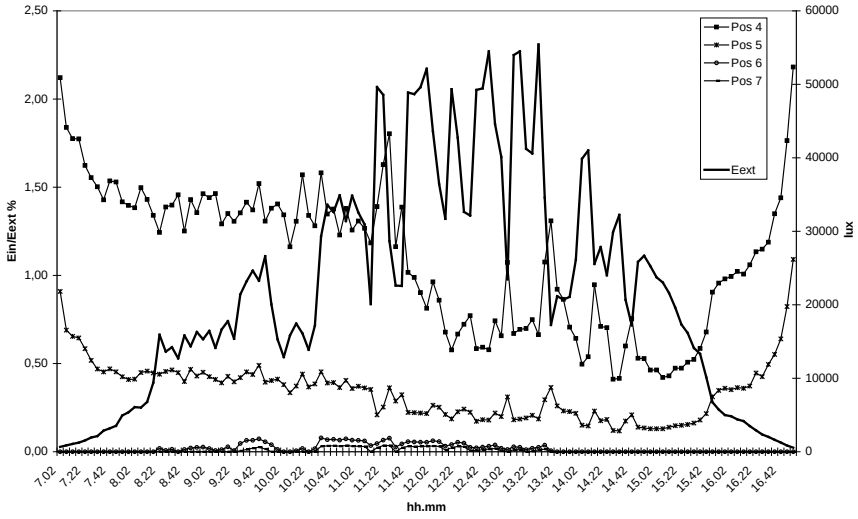

Fig. 5. Illuminance data in positions 4-7 on November the 5th

The natural ventilation allowed by the V.I.W. permits the necessary change of air in the room and different ways are traced in summer (night and day) and winter conditions. In the design phase the authors provided for the behavior of the system as shown in Fig. 6 in which a representation of expected natural ventilation in summer and winter is shown, obtained by

different configurations (close/open) of the openings. In particular, the Fig. 6 (a) shows the expected natural ventilation in daily summer condition, while Fig. 6 (b) the expected natural ventilation in night summer and in winter (night and day) conditions.

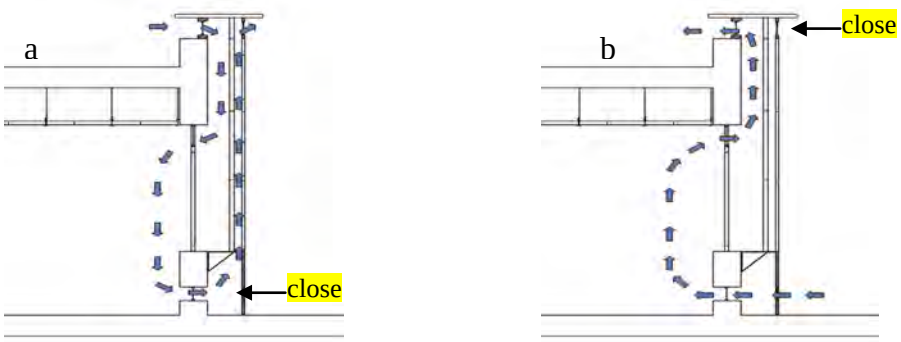

Fig. 6. Natural ventilation in daily summer conditions (a), night summer and winter conditions (b) .

In Fig. 7 data of wind direction and velocity on September the 17th are shown. Higher speeds are verified from 9 am to 5 pm with a medium wind direction angle from North of about 97°, while a medium value of about 158° is verified in night conditions, just favourable for a good air circulation. All the summer tests carried out confirm this trend, that can be considered representative of summer conditions.

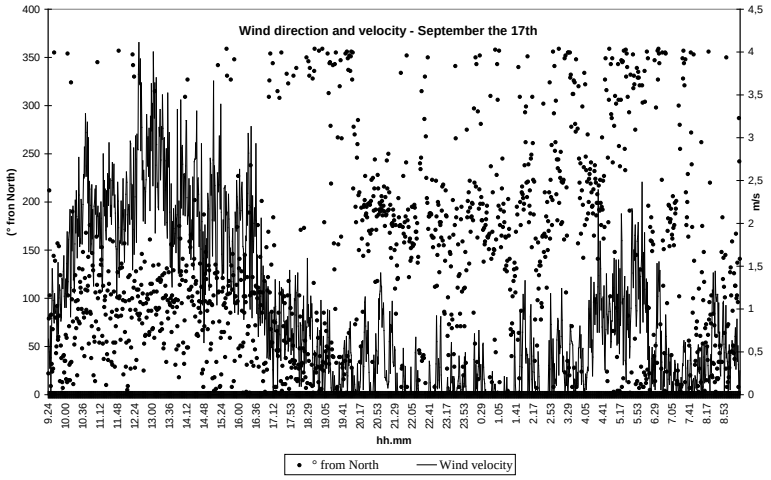

Fig.7. Wind direction and velocity on September the 17th

In Fig. 8 air speed is shown on September the 17th, measured in positions 2 and 3 close to the air inlet and outlet vents. Table 2 shows minimum, medium and maximum data. During the day the vent 2 is the outlet opening and the 3 is the inlet one, while at night the reverse situation occurs. In the centre of the room (position 1) air velocity is less than 0,03 m/s all the day with a mean value of about 0,005 m/s, while in night conditions the maximum value is the same with a lightly higher value of the mean velocity, of about 0,007 m/s.

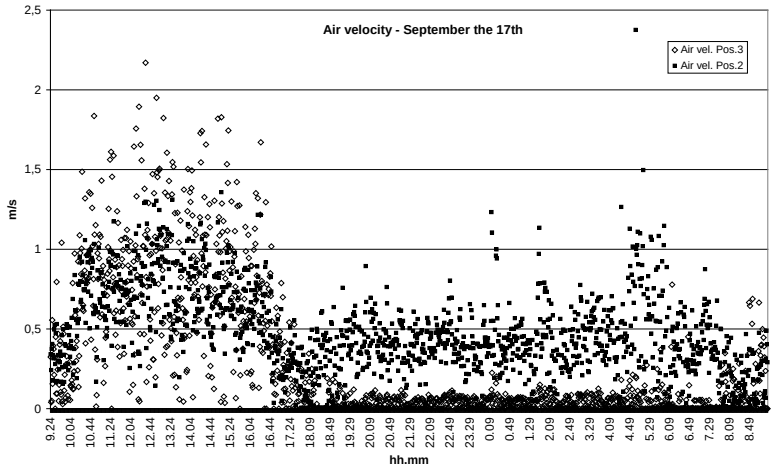

Fig. 8. Inlet and outlet air velocity on September the 17th

Table 2. Minimum, Medium and Maximum air velocity in positions 2 and 3 on September the 17th

	DAY		NIGHT	
	Pos 3 - inlet	Pos 2 - outlet	Pos 2 - inlet	Pos 3 - outlet
Min. air velocity (m/s)	0	0,021	0	0
Med. Air velocity (m/s)	0,7	0,64	0,39	0,05
Max. air velocity (m/s)	2,17	1,36	2,38	0,78

In Fig. 9 data about wind direction on November the 5th are shown. In daily conditions from 10.30 am and 6.30 pm the medium wind direction angle from North is 132°, while a medium value of about 195° is verified in night conditions. This is a less favourable situation than in summer, particularly in daily condition, nevertheless the VIW seems to assure acceptable performances also in this case, thanks to an efficacy stack effect.

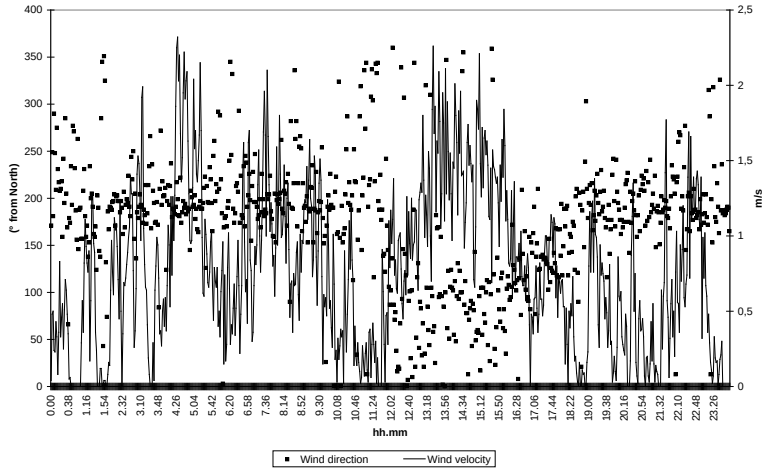

Fig. 9.Wind direction and velocity on November the 6th

In Fig 10 air speed in positions 2 and 3 are shown with winter configuration of openings. During the day the inlet and outlet air speeds are similar because they are only influenced by the difference of temperatures between internal and external environments, while during the night a more favourable wind direction allows to obtain higher values of inlet air velocity.

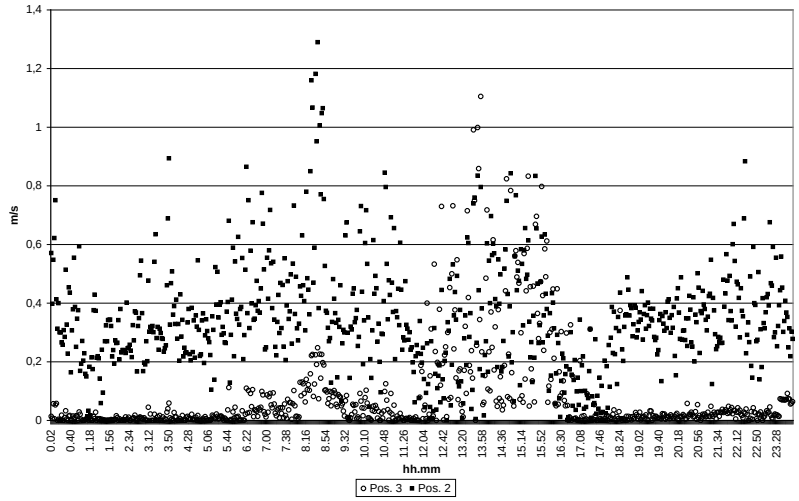

Fig. 10. Air velocity on November the 6th with winter configuration of openings

5. Conclusions

The V.I.W. is a new daylight technological device able to make also an efficacy natural ventilation in underground areas of buildings or rooms without direct outward interface. The building steps of the V.I.W. are described and the first experimental data of indoor illuminances and air speed are shown. The V.I.W. seems to allow an efficacy change of air of the test-room, although the mixing of air does not probably involve the whole environment. The daylighting efficacy is completely satisfactory in presence of high external illuminance, but must be improved with low external illuminance, by an efficient cleaning of the reflective film. The continuous monitoring the V.I.W may prove its efficacy in terms of energy saving and the spin-off uses of the system, particularly in museums or large exhibition rooms in which it may be used together with traditional or double light pipes.

References

[1] M. Santamouris, Alternative cooling techniques for building, 6th International Conference on Sustainable Energy Technologies SET 2007, Santiago de Chile, 2007, pp. 19-24.

[2] D. Jenkins, T. Muneer, Modelling light pipe performances-a natural daylight solution, Building and Environment 38, 2003, pp. 965-972.

[3] D. Jenkins, X. Zhang, T. Muneer, Formulation and semi-empirical models for predicting the illuminance of light pipes, Energy Conversion and Management 46, 2005, 2288-2300.

[4] C. Baroncini, F. Chella, P. Zazzini, Numerical and experimental analysis of the Double Light Pipe, a new system for daylight distribution in interior spaces, International Journal of Low Carbon Technologies, 3/2, 2008, pp.110-125.

[5] C. Baroncini, O. Boccia, F. Chella, P. Zazzini, Experimental analysis on a 1:2 scale model of the Double Light Pipe, an innovative technological device for daylight transmission, Solar Energy, 84, 2010, pp.296-307.

[6] S. Varga, A. C. Oliveira, Ventilation terminal for use with light pipes in buildings, Applied Thermal Engineering 20, 2000, 1743-1752.

Ventilated Illuminating Wall (VIW): Natural ventilation numerical analysis and comparison with experimental results

O. Boccia*, F. Chella, P. Zazzini

D.S.S.A.R.R., Faculty if Architecture University "G. D'Annunzio", Pescara, Italy
** Corresponding author. Tel: +39 854537291, Fax: +39 854537268 , E-mail:oreste.boccia@libero.it*

Abstract: The authors propose a comparison among the first experimental and numerical results of an analysis carried out about the theme of the natural ventilation and the energy efficiency relatively to a device called Ventilated Illuminating Wall (VIW). The VIW is represented by a 1:1 prototype scale model, constituted by a precast removable manufactured product set to a window of the room, able both to transport the natural light, captured by the coverage, in underground area, and to introduce outside air for the required indoor ventilation. The experimental data, object of a work previously carried out, are obtained from temperature and air speed measurements in different points inside the tested room.

Based on some meaningful environmental parameters, internal and external temperature of the building, direction and wind speed in different times of the year, the device performances are evaluated through the software Fluent/Airpak, able to make fluid dynamics modeling and simulations, with the aim to calculate the air flow rate distributions, air speed and temperature field inside the room. The numerical analysis is carried out in steady state condition and produces results that, sometimes, are overestimated with respect to experimental ones. The results may be improved by a transient analysis.

Keywords: *Ventilated illuminating wall, Natural ventilation, Energy efficiency, Thermal comfort, CFD.*

1. Introduction

The energy consumption of buildings takes a significant role in the energy question, because buildings are responsible of about 40 % of the whole world energy demand [1]. In buildings in which underground areas are present the energy consumption is increased because they need to be artificially enlighten and ventilated. Particularly mechanical ventilation is generally adopted in these cases. Moreover, when internal environments of buildings are used as museums or exhibition rooms, they need a particularly uniform luminance distribution of the walls with low illuminances all over the work plane in order to allow the correct perception of works of art on display, particularly in the case of paintings, with the right contrast of luminances between the visual task and the background, avoiding the risk of glare. Since this risk is often present when natural light is introduced in the room through traditional daylight sources, for the presence of intense direct solar radiations that can be reflected by shiny walls, in these cases it is better avoiding natural light entering through windows or skylights and technological daylight systems, as light pipes or double light pipes [2, 3], can be used in order to provide better conditions for visual comfort. The absence of windows makes it impossible the natural ventilation of the room. In some cases light pipes, used to introduce daylight in underground areas, are equipped with technological systems able to ensure air extraction from the room [4, 5]. The innovative system presented in this paper, named Ventilated Illuminating Wall (VIW), has been developed by the authors in order to simultaneously allow natural lighting and ventilation for the environment. So, when underground areas are used or rooms without any direct interface to outwards the VIW allows air ventilation and natural light inlet, giving the room a high quality of light and comfortable conditions of indoor air. It is a combination of a daylight transport system and a passive solar system set up in a real scale by the authors. In this paper a numerical analysis of the device is presented and the results are compared with some experimental data of air circulation parameters.

2. Methodology

Moving from the availability of some data obtained by the experimental analysis, such as internal and external temperatures, wind direction and speed in different times of the year, the authors carried out a numerical analysis with the aim to evaluate the performances obtainable by the VIW. In particular they analyzed the system in steady state conditions and compared the numerical results with experimental ones in order to test the used numerical code with the aim to be sure that it is a suitable tool of analyzing the performances of the VIW.

2.1. Numerical analysis

The numerical analysis was carried out by the software Fluent with the aim to calculate the air flow rate distributions, air speed and temperature field inside the room. Due to the complexity of the geometry and the 3D characteristics of the flow, only numerical methods, often referred to as CFD, can be used to solve the velocity, pressure and temperature field. The fundamental set of partial differential equations (PDEs) describing fluid flow, known as the Navier-Stokes equations [6], can be applied to the problem under consideration, assuming the hypothesis of incompressible flow.

The governing PDEs of fluid flow (conservation of mass, momentum and energy) can be written in a generic form as the following:

$$\frac{\partial(\rho\Phi)}{\partial t} + div(\rho\vec{v}\Phi) = div\left(\Gamma_\phi \overrightarrow{grad}\Phi\right) + S_\phi \qquad (1)$$

in which Φ represents the predicted variable, ρ the density of the fluid, Γ_Φ the diffusion coefficient and S_Φ the source term. If Φ =1 the continuity equation is obtained. The actual form of the variables in Eq. (1) is summarized in Table1.

Table 1 - Variables in eq. 1

Φ	Γ_Φ	S_Φ
v_x	μ_{eff}	$-\partial P/\partial x$
v_y	μ_{eff}	$-\partial P/\partial y - g$
v_z	μ_{eff}	$-\partial P/\partial z$
C_pT	$k+k_t$	Q

In order to simulate the turbulent behaviour of the flow, the RNG (“renormalization group") k-ε model was used, which requires the solution of two additional equations [6]. Details of turbulence model are referred in [7, 8, 9 and 10].

In this work, a commercial program package called Ansys/Fluent (Airpak) was used to simulate the airflow. It adopts a control-volume-based technique. The linearization of the discretized equations is accomplished using a first-order accuracy upwind scheme.
The pressure field is computed by the body-force-weighted scheme, which is good for high-Rayleigh-number natural convection flows. The problem domain was subdivided into 2.034.334 tetrahedral elements whit 352.215 nodes.

The linearized governing equations are written in an “implicit" form with respect to the dependent variable of interest. The calculated variables are used within the various

postprocessing with the aim of determining the volume flow rate, which is a derived scalar quantity computed from the velocity field.

2.2. Experimental analysis

The experimental analysis was carried out by measuring the environmental parameters (air temperature and speed, wind direction and speed) in a test room properly built in the Laboratory of Technical Physics of the Faculty of Architecture of Pescara, between September and November in various external climatic conditions.

2.3. Experimental apparatus

The experimental apparatus is constituted by a 5x3 m plant area room, 2,7 m high in which a 1:1 scale prototype of the Ventilated Illuminating Wall (VIW), is placed against the window in the north-west wall perimeter of the room. The VIW is a removable structure applied to the window able to introduce natural light and ventilation in the room. The daylight is captured by a horizontal glass plate cover applied on the top of the system and redirected in the room thanks to a multilayer highly reflecting film applied on the vertical internal closing panel of the device.

Fig. 1. External and internal views of the VIW.

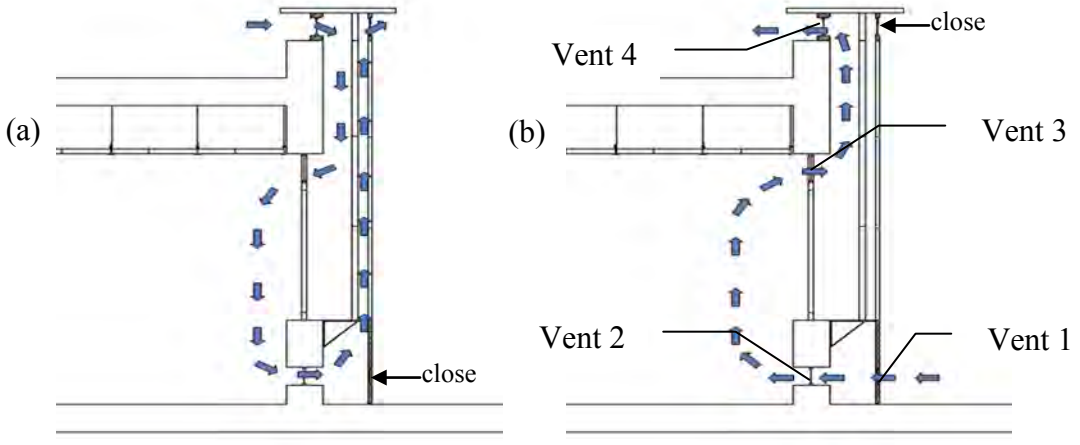

Fig. 2. Section of the VIW with qualitative air circulation and the positions of inlet and outlet vents

In Fig. 1 two external and internal views of the device are shown. The natural air circulation necessary to ensure favorable hygienic conditions in the room is guaranted by fifteen openings with wire mesh practiced on the internal and external closing panel of the system. In

Fig. 2 a qualitative representation of the expected air circulation is shown. In particular, the Fig. 2 (a) shows the expected natural ventilation in daily summer condition and Fig. 2 (b) in night summer and in winter (night and day) conditions.

The experimental line consists of a data-logger type LSI/BABUC-ABC, characterized by 20 inputs, by which data are registered and elaborated, three internal hot wire anemometers type BSV105#S-LSI, range 0-20 m/s, accuracy 0,01 m/s, four temperature probes PT 100, type LSI BST101#S – DIN IEC 751, class A; one tacho-gonioanemometer with direct output, model DNA021-LSI. The air temperature and speed are measured in three positions, in the centre of the room (1), near the opening at the bottom of the wall (2) and near the opening at the top of the wall (3), as indicated in Fig. 3.

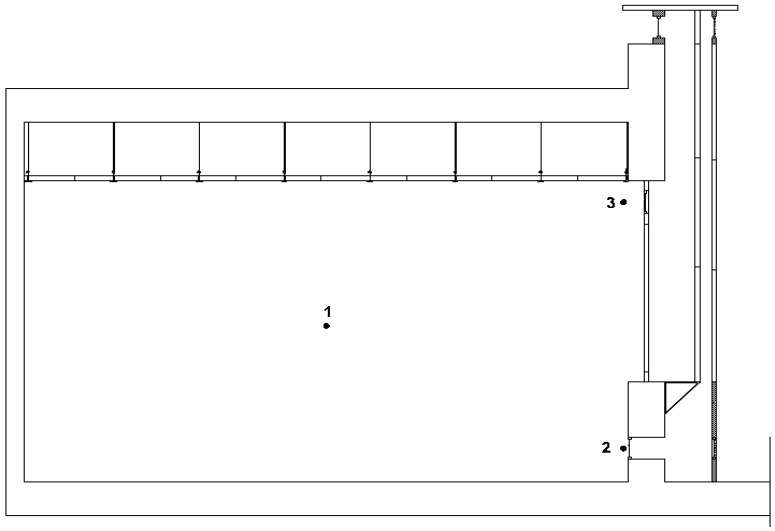

Fig 3. Air temperature and velocity sensors positions.

3. Numerical Results

The Figg. 4-8 show the steady numerical results by Fluent/Airpak in winter configuration, with the following boundary conditions, experimentally measured on November the 7th at 9 a.m.:
External air temperature: t_{ext} = 11°C;
Mean internal surface temperatures (floor, walls and ceiling): t_s = 22°C;
Inlet air velocity close to the vent 1: v_{in} = 0,6 m/s;
Wind direction: 210° from North;
Wind velocity: 2,8 m/s.
Surface temperature on the glass plate cover: t_g = 18°C;
Surface temperature on the external polycarbonate vertical panel: t_p = 15°C.
In Fig. 4 the air speed field and the flow lines in the room are shown while in Figg. 5 and 6 the air velocity distribution on two horizontal planes, 2,4 m high on the floor, close to the vent 3, and 0,3 m from the floor, close to the vent 2, are illustrated. The comparison between the two images highlights the different trend of the air speed distribution in correspondence of the two inlet and outlet vents of the wall. The inlet and outlet velocities involve a mass flow rate of =0,0854 m^3/s, which correspond to about 6,6 air changes per hour, considering that the volume of the room is equal to 46,1 m^3. A second test carried with data of the same day at 2 p.m. allowed to calculate a mass flow rate of 0,058 m^3/s, corresponding to 4,5 air changes per hour.

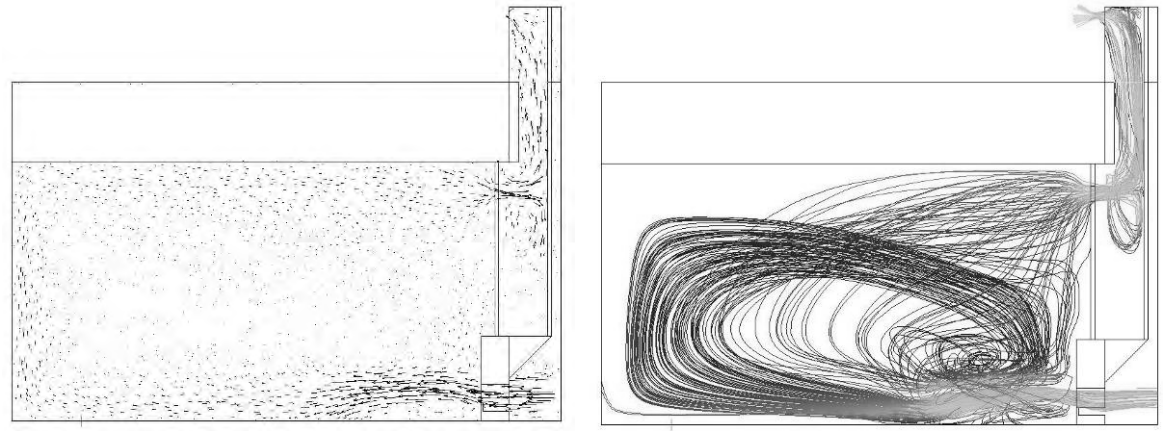

Fig 4. Air speed field and flow lines in the room.

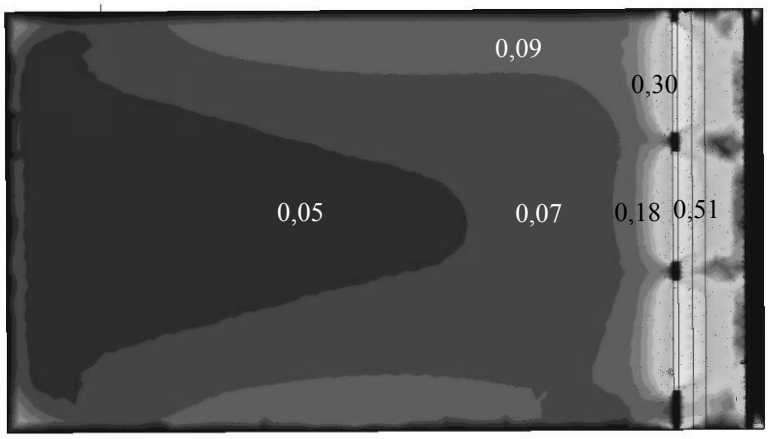

Fig 5. Air velocity (m/s) on a horizontal plane 2,4 m high on the floor, close to the outlet vents.

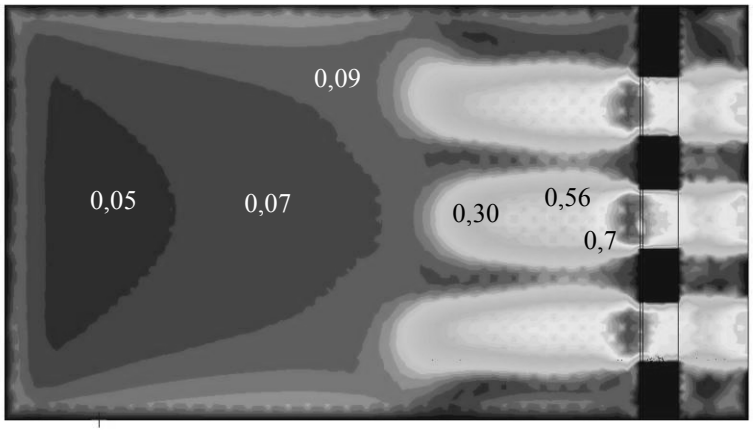

Fig 6. Air velocity (m/s) on a horizontal plane 0,3 m high on the floor, close to the inlet vents.

In Figg. 7 and 8 the temperature field in the room and the temperature vertical trend in the centre of the room and on a vertical plane containing the measure positions 2 and 3 close to the inlet and outlet vents are shown. It's evident how the temperature profile is influenced by the absence of any heating system and the introduction of low temperature air from the opening at the bottom of the wall, particularly close to the vents.

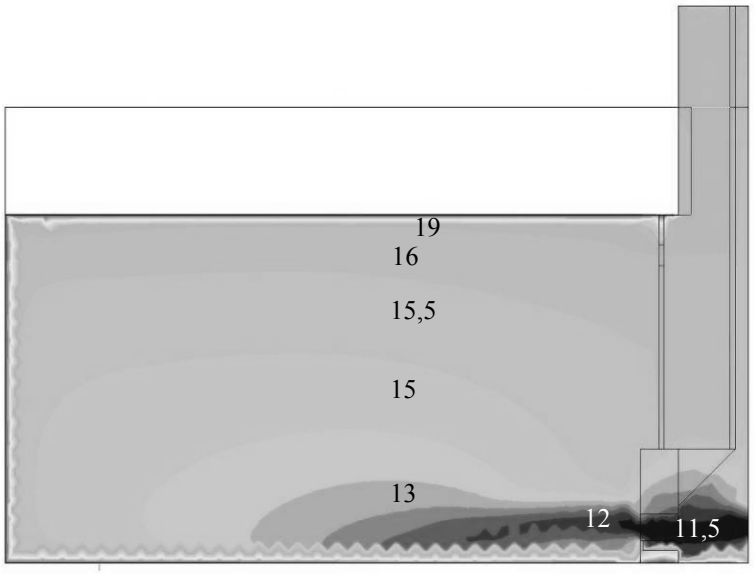

Fig 7. Air temperature field (°C) in the room.

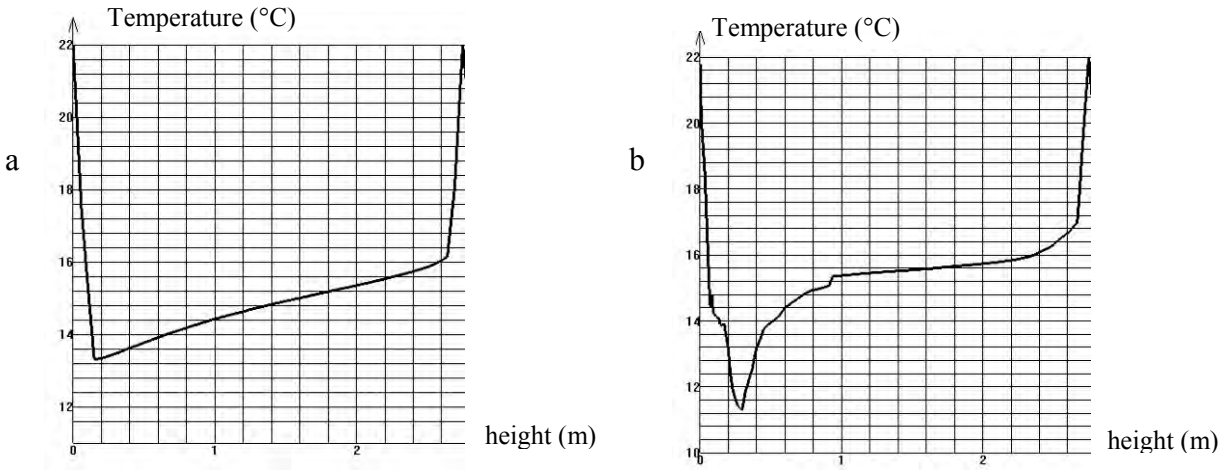

Fig 8. Air temperature vs height on the floor in the centre of the room (a) and close to the outlet and inlet vents (b).

4. Comparison between numerical and experimental results

A comparison was carried out between the numerical results by Fluent/Airpak and the experimental data in the measure positions 1, 2 and 3. The comparison was made with reference to the data of November the 7th at two different times: 9 a.m. with a wind velocity of about 2,8 m/s and a favourable direction (210° from North), and 2 p.m. with a very a lower wind velocity of about 0,9 m/s and a different wind direction (45° from North). This last does not give any contribution to air inlet, and in this case the only stack effect allows the air circulation.

As shown in table 2, a good agreement is obtained between numerical and experimental air temperatures both at 9 a.m. and at 2 p .m. On the contrary, the comparison between the numerical and experimental air velocities shows a good agreement in position 1, in the centre of the room, while a more significant discrepancy is verified in positions 2 and 3, close to the air inlet and outlet vents, partially due to the influence of the boundary conditions. This disagreement is verified in both the situations considered.

As an example, in Figg. 9 and 10 the air velocities comparison is shown between data at 9 a.m.

Table 2 – Comparison between numerical and experimental air temperature T_a

	Position 1		Position 2		Position 3	
	Exp.	Num.	Exp.	Num.	Exp.	Num.
T_a (°C) at 9 am	14,75	14.74	11,77	11.37	17,74	16.1
T_a (°C) at 2 pm	17,4	18,7	16,8	16,8	18,2	19,3

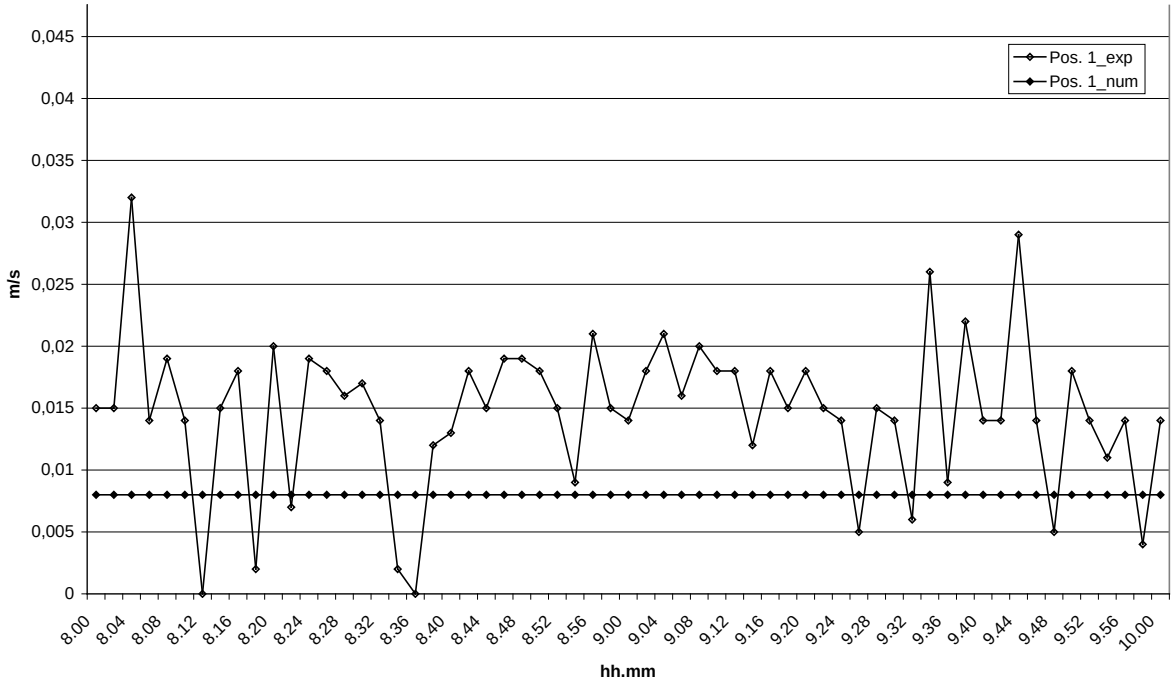

Fig 9. Experimental and numerical air velocity in position 1 in the centre of the room

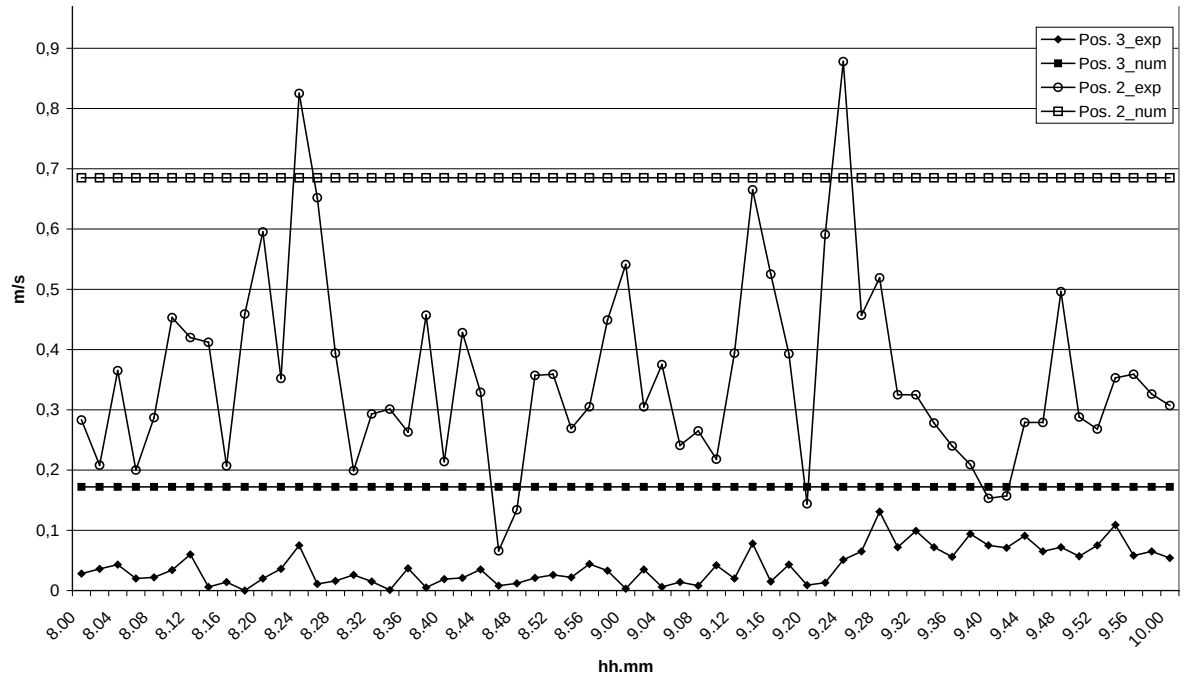

Fig 10. Experimental and numerical air velocity in positions 2 and 3, close to the inlet and outlet vents

5. Conclusions

The numerical analysis carried out by the sw Fluent/Airpak allows to determine the main features of the VIW in terms of its capacity of making an efficacy natural ventilation in rooms without direct interface to outwards. Data about the temperature field are satisfactory if compared with experimental ones, while the air velocities seems to be affected by a significant degree of error partially due to the steady state analysis and the boundary conditions. Even if overestimated, data of mass flow rate show how the VIW can assure an efficacy change of air only by natural ventilation. A transient analysis may certainly provide a more precise determination of the behavior of the system. The availability of a large quantity of experimental data will be a useful tool for the validation of the sw. In any case the first results encourage the authors to carry on the analysis, since the VIW seems to be an efficacy system of daylight transport and natural ventilation for underground areas of buildings or rooms without any direct interface to outwards. It seems particularly suitable for large exhibition rooms or museums where the absence of windows or skylight makes it impossible daylight and natural ventilation of the environment.

References

[1] M. Santamouris, Alternative cooling techniques for building (Keynote lecture), Proceedings of the 6th International Conference on Sustainable Energy Technologies SET 2007, Santiago de Chile, 2007, pp. 19-24.

[2] C. Baroncini, F. Chella, P. Zazzini, Numerical and experimental analysis of the Double Light Pipe, a new system for daylight distribution in interior spaces, International Journal of Low Carbon Technologies, 3/2, 2008, pp.110-125.

[3] C. Baroncini, O. Boccia, F. Chella, P. Zazzini, Experimental analysis on a 1 :2 scale model of the Double Light Pipe, an innovative technological device for daylight transmission, Sola Energy, 84, 2010, pp.296-307.

[4] S. Varga, A. C. Oliveira, Ventilation terminal for use with light pipes in buildings, Applied Thermal Engineering 20, 2000, 1743-1752.

[5] A. C. Oliveira, A. R. Silva, C. F. Afonso, S. Varga, Experimental and numerical analysis of natural ventilation with combined light-vent pipes, Applied Thermal Engineering 21, 2001, 1925-1936.

[6] F. M. White, Fluid Mechamics, 2nd ed. McGraw Hill, New York, 1986.

[7] S. V. Patankar. Numerical Heat Transfer and Fluid Flow. Hemisphere, Washington D.C., 1980

[8] Airpak 2.1 User's Guid Fluent Inc. April 2002.

[9] B.E. Launder, D.B. Spalding, The numerical computation of turbulent flows, Computational Method. Applied Mechanical Engineering, 3 (1974) 313.

[10] P.V. Nielsen, F. Allard, H.B. Awbi, L. Davidson, A. Schalin, Fluidodinamica computazionale applicata alla progettazione della ventilazione ed. D. Flaccovio 2009.

Experimental and numerical study on the performance of solar walls in Mediterranean climates

Francesca Stazi[1], Alessio Mastrucci[1,*], Costanzo Di Perna[2]

[1] *Dipartimento di architettura, costruzioni e strutture (DACS), Facoltà di Ingegneria, Università Politecnica delle Marche, Via Brecce Bianche, 60131 Ancona, Italy*
[2] *Dipartimento di energetica, Facoltà di Ingegneria, Università Politecnica delle Marche, Via Brecce Bianche, 60131 Ancona, Italy*
** Corresponding author. Tel: +39 3491604465, E-mail: alessiomastrucci@gmail.com*

Abstract: This article focuses on the behavior of an accommodation with Trombe walls in a Mediterranean climate, in terms of energy savings and comfort during wintertime and summertime.
The aims of this study are to identify experimentally temperatures and heat fluxes of the solar wall; compare the solar wall's behavior with a traditional wall from the point of view of consumptions and comfort; optimize the wall in relation to energy savings. In order to do that, various activities were carried out: a series of monitoring activities for several years in different seasons (in this paper only the results obtained for winter and autumn are reported); dynamic simulations with software EnergyPlus on a virtual model calibrated by comparison with experimental results; parametric analyses for the optimization of the wall.
The results demonstrated that solar wall is an efficient system in temperate climates, with an energy savings of 12,2% and summer comfort comparable to that provided by traditional housing. Finally it was possible to identify optimal design features (Thickness of the wall, absorbance, type of glass).

Keywords: *Trombe walls, Building envelope, Thermal comfort, Monitoring, Parametric analyses.*

Nomenclature

s	component thickness ..... cm	$T_{s,int}$	internal surface temperature ..... °C
U	thermal transmittance ..... W/m^2K	T_{room}	indoor air temperature °C
Y_{mn}	periodic thermal transmittance ..... W/m^2K	T_{op}	indoor operative temperature ..... °C
f_d	decrement factor ..... -	$F_{solar\ glob\ hor}$	horizontal global solar radiation ..... W/m^2
φ	time shift ..... h	F_{int}	internal surface heat flux density ..... W/m^2
T_{out}	outdoor air temperature ..... °C		
$T_{s,ext}$	external surface temperature ..... °C		

1. Introduction

The recent European Directives on the energy performance of buildings established a common direction for the reduction of buildings energy consumptions. Consequently the Member States set up a series of minimum requirements and made it necessary to achieve high building envelope performances. Solar passive systems can give a significant contribution to achieve these performances and they may help to save energy both for winter heating and for summer cooling. However there are still few studies in literature on the behavior of solar passive systems, especially on solar walls, in summer [1, 2], on design recommendations [3, 4, 5], on comfort conditions produced [6], in Mediterranean climates and in well-insulated envelopes required by national regulations.

Solar wall is a passive solar system used to store heat and transfer it inside the building. It is generally made of a concrete or masonry wall painted black, an air layer and glazing on the exterior. Trombe wall is a particular type of solar wall equipped with vents for the air circulation. Precedent studies [7, 8], focusing on the mode of use of Trombe walls, highlighted that recirculation vents determine consistent heat losses during the cold season and problems of powder rising. For this reason this study focuses on unvented solar walls.

The objectives of the study are: the assessment of solar walls' effects on energy consumptions and indoor comfort of residential buildings; the development of design recommendations for solar walls in a Mediterranean climate. The methodology used comprehends experimental and analytical activities: a series of monitoring activities on a case study to collect data related to the thermal behavior of solar walls; numerical simulations in dynamic conditions on a model calibrated by comparison with the experimental data; simulations and parametric analyses to extend the results.

2. Case study

The case study is a residential building in Ancona, central Italy, and it was built in 1983 to test many passive solar systems. The building includes nine flats on three floors, each equipped with a different passive solar system on the south-facing wall (Fig. 1). The house has a compact shape and it is oriented along the E-W axis in order to maximize solar supply.

The research focused on the accommodation with Trombe walls (Fig. 2), that resulted from precedent studies [7] the best solar system among the ones in the house. The system is made up of a 40 cm concrete wall painted black, a 10 cm air layer and glazing on the exterior. Adjustable vents are placed on the top and on the bottom of the wall and on the top of the external glazing to activate ventilation. Roller shutters and horizontal overhangs provide solar radiation control. The configuration of solar wall considered in this study is: ventilation not active (closed vents); movable shading open in winter and middle seasons, closed in summer.

Fig. 1. View of the case study.

Fig. 2. External view of Trombe wall.

3. Methodology

The research consisted of experimental activities in autumn and winter and analytical activities to extend the study to other periods.

3.1. Experimental activities

Monitoring activities in the case study were performed for several years in different seasons. In this paper we report only a part of the data measured, regarding these periods:

- Autumn monitoring: 12th October 2007 – 21st October 2007
- Winter monitoring: 20th December 2008 – 7th January 2009

Trombe walls were used with closed vents during experiments to reproduce unvented solar walls. Heating system was off during autumn monitoring, while it was switched on in winter with set point 20°C and program: 1:30-3:30, 7:30-9:30, 17:30-21:30.
Experimental set-up is described in Fig. 3 and Fig. 4. Data loggers and different types of probes were used to carry out the following investigations: survey of the outdoor climate conditions using an external weather station that included hydro-thermal probe, wind speed

and direction probe, solar radiation probes (Fig. 5); survey of indoor environmental conditions using indoor microclimate stations with hydro-thermal probe and black-globe temperature probe (Fig.6); detailed thermal survey of Trombe wall using a set of thermo-resistances to measure internal and external surface temperatures and heat flux sensors (Fig.7). External probes were screened from direct solar radiation to avoid values alteration.

Fig. 3. Experimental set-up: plan of the house

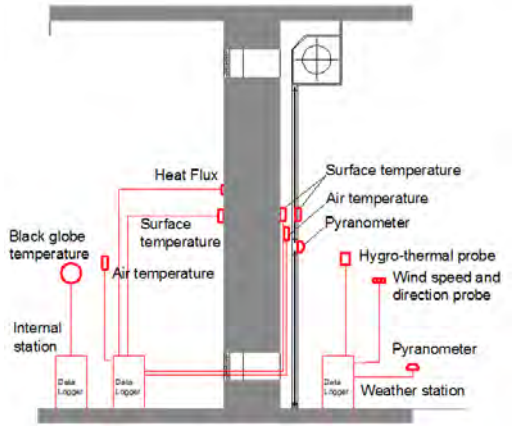

Fig. 4. Experimental set-up: vertical section of Trombe wall indicating the position of probes.

Fig. 5. View of weather station.

Fig. 6. View of indoor microclimate station.

Fig. 7. View of the probes on the outside face of Trombe wall.

3.2. Analytical activities

Numerical simulations were performed in dynamic state using software EnergyPlus. Trombe walls can be modeled in EnergyPlus using the algorithm *"TrombeWall"* validated BY ELLIS [9].

3.2.1. Model inputs and comparison with experimental data

Data collected during experimental activities were used as inputs for the model in order to reproduce the real conditions: we developed a climatic input file containing the outdoor conditions measured during experiments, then we defined programs regarding the real users profiles for the building (occupancy, air ventilation, heating system program and set point). The values obtained by calculations were compared with data collected during experimental activities in order to verify the reliability of the simulation tools in reproducing real situations. Indoor air temperatures, surface temperatures and the heat fluxes of the trombe wall were compared. Once the model had been calibrated, it w as possible to generalize the results running the calculation for a whole year and setting standard input data for the model, according to national reference UNI/TS 11300:2008.

3.2.2. Analytical studies on solar walls

Numerical simulations were performed all over the heating season (1st November to 15th April in Ancona, according to national requirements) in order to determine the thermal behavior of solar walls. Total energy contribution, defined as the difference between solar gains and heat losses through the wall, was used to evaluate the performance of solar wall compared to a traditional one, with the characteristics in Table 1.

Table 1. Thermal characteristics of solar wall and traditional wall according to ISO 13786:2007.

Type of wall	s (cm)	U (W/m^2K)	|Ymn| (W/m^2K)	fd (-)	φ (h)
Solar wall	51,4	2,267	0,12	0,10	12,48
Traditional wall	34,5	0,343	0,12	0,54	6,83

3.2.3. Analytical studies on building envelopes with solar walls

In order to assess how solar walls can contribute to the performances of a building complying with current energy regulations, the insulation level of envelope components of the case study (except solar walls) was varied to meet national requirements. Then the energy performance of the same accommodation was calculated varying the type of south-facing wall between solar wall and traditional wall, defined above, to assess the energy efficiency of solar wall in comparison with the traditional one.

Indoor thermal comfort analyses were performed to assess indoor quality. Thermal comfort conditions were estimated for the whole year with simulations. PMV method, according to UNI EN ISO 7730:2006 and UNI EN 15251:2008, was applied in winter when the heating system is on. PMVe method [10] was applied in summer (with coefficient e = 0,7) with the hypothesis that the cooling system is not present. Category II, according to UNI EN 15251:2008, was assumed in the assessment of comfort limits.

3.2.4. Parametric study on solar wall characteristics

A parametric study was performed using the *level factorial plan* technique [5]. With this technique it is possible to calculate the effect of variations of single parameters and combinations of parameters on a given phenomenon. The parameters listed in table 2 were chosen. For each of the eight combinations of parameters in Table 3 a simulation was run to determine the effects of variations on the seasonal energy needs for heating of the house.

Table 2. Parametric analyses on the solar wall system.

Parameters	Designation	Minimum value	Maximum value
Storage wall thickness (cm)	X1	30	40
Absorbance	X2	0,85	0,90
Type of glazing	X3	Single glass (SG)	Double glass (DG)

Table 3. Combinations of parameters.

Parameters	1	2	3	4	5	6	7	8
X1	30	40	30	40	30	40	30	40
X2	0,85	0,85	0,90	0,90	0,85	0,85	0,90	0,90
X3	SG	SG	SG	SG	DG	DG	DG	DG

4. Results

4.1. Results of experimental activities

Monitoring activities allowed the assessment of the thermal behavior of solar walls in different conditions and periods.

4.1.1. Autumn monitoring

Data measured during three typical sunny days in October are reported in Fig. 8 and Fig. 9. On sunny days the wall reaches temperatures over 50°C on the external surface. Internal surface reaches temperature peaks during nighttime, with a time shift of about 10 hours, and maintains an average temperature of 23,6°C. Internal surface temperature is higher than room temperature all time, consequently heat flux is directed from the wall to the room and determines a daily heat gain of 0,95 MJ/m^2. It can be noticed that heat flux is higher during nighttime, when the difference between surface and air temperature is higher. This contributes to maintain a constant temperature of about 20°C inside the room, with benefits for thermal comfort.

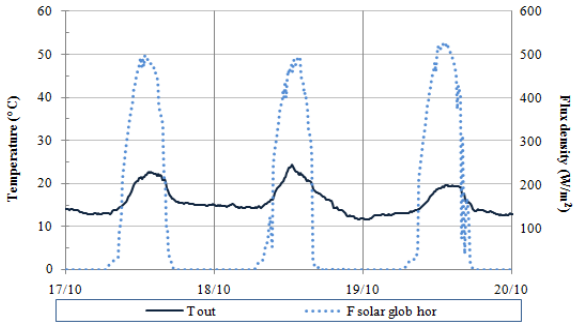

Fig. 8. Climatic data.

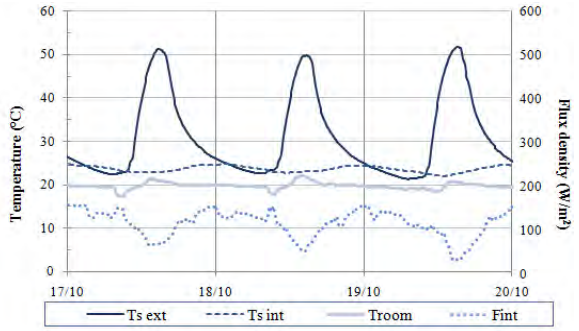

Fig. 9. Temperatures and heat fluxes of Trombe wall and temperature of the room.

4.1.2. Winter monitoring

Fig.10 and Fig.11 show the results of monitoring during three winter days, the first sunny, the second cloudy the third sunny again. On sunny days external surface temperatures can get up to 35-40°C, while on cloudy days the temperatures are not far from outside air temperature. After a sunny day, internal surface temperatures remain higher than room temperatures and heat flux is directed toward the room, with daily heat gains of 0,45 MJ/m^2. On cloudy days internal surface temperatures are lower than room temperatures and this fact causes the inversion of heat flux, from the room to the wall, and daily heat losses of 0,54 MJ m^2.

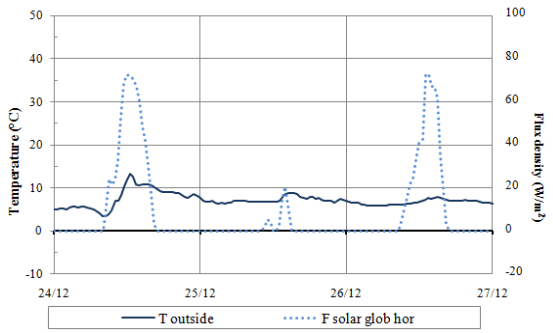

Fig 10. Climatic data.

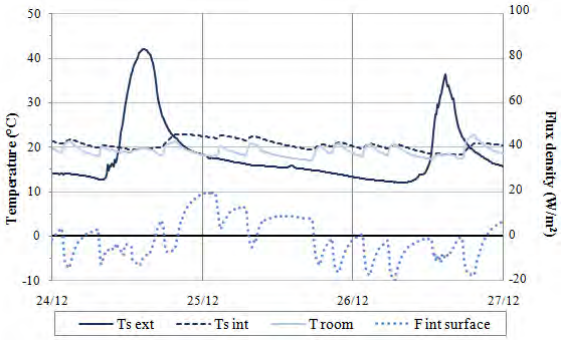

Fig. 11. Temperatures and heat fluxes of Trombe wall and temperature of the room.

4.2. Results of analytical activities

4.2.1. Comparison with experimental data

The comparison demonstrated a good agreement between experimental data and simulated data. Fig. 12 shows the results of surface temperatures comparison, the same analysis was performed for heat fluxes. Deviations for internal surface temperatures and heat flux densities are lower than 5%. Deviations for external surface temperatures are around 10%.

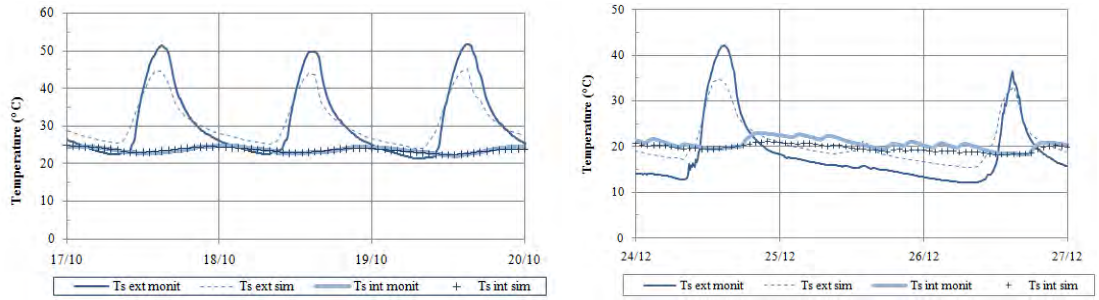

Fig. 12. Comparison of surface temperatures measured and calculated in autumn and winter.

4.2.2. Energy performance of solar walls

Total energy contribution was used to compare the performances of solar and traditional wall in winter (Fig. 13) and in summer (Fig. 14).

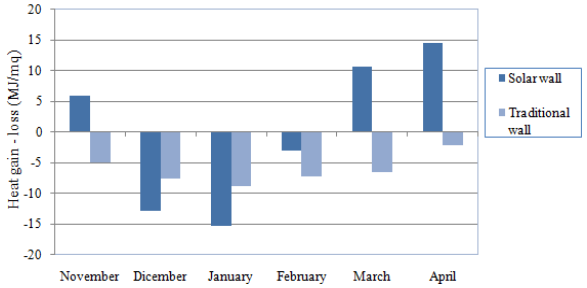

Fig. 13. Total energy contribution of solar wall and traditional wall in winter.

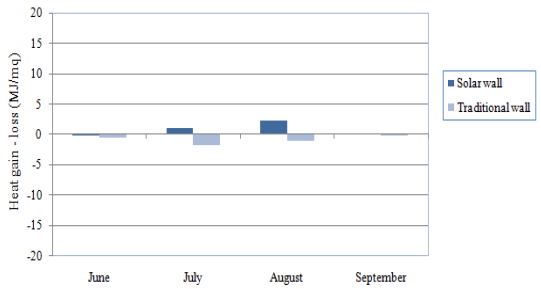

Fig. 14. Total energy contribution of solar wall and traditional wall in summer.

Solar wall's heat losses are higher in the coldest months, due to the high transmittance, but these losses are balanced in other months when solar gains are higher. Considering the whole heating season, traditional wall disperses 37,29 MJ/m^2 while solar wall disperses 0,20 MJ/m^2. In summer solar wall, even if shaded from solar radiation, behaves worse than traditional wall, because the high transmittance determines higher unwanted heat gains. Considering the whole summer season, solar wall produces heat gains equal to 3,21 MJ/m^2, while traditional wall determine heat losses equal to -3,47 MJ/ m^2.

4.2.3. Energy performance of building envelope with solar walls

Energy analysis confirmed that the house with solar walls has a saving of 12,2 % in heating energy needs compared to the house with traditional walls (Fig. 15). The energy saving is 0,46% for each square meter of surface of solar wall.

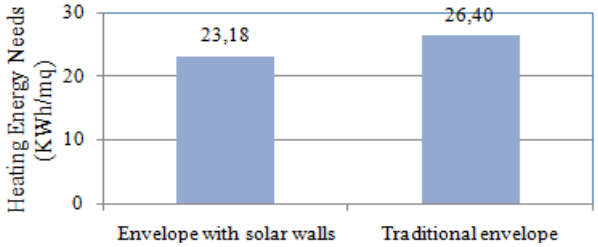

Fig. 15. Seasonal heating energy of building with different types of envelope.

The results of thermal comfort analysis in winter (Fig. 16) are very similar for the building with solar wall and with traditional wall because the influence of heating system is relevant in this season. However in the middle seasons solar walls' heat gains determine higher indoor air temperature and consequently higher PMV values. In these periods it could be necessary to shade solar walls to avoid overheating problems.

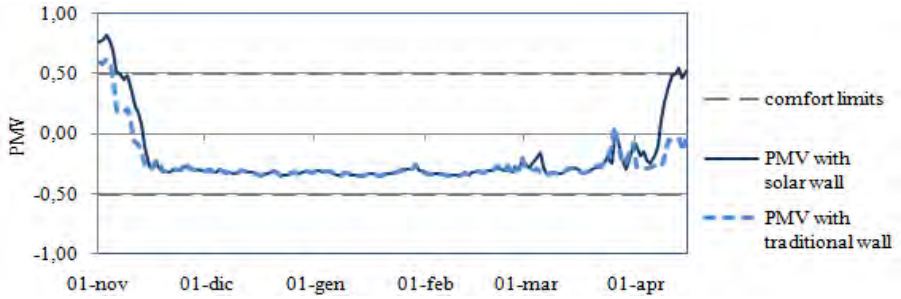

Fig. 16. Comfort analysis with PMV method in winter.

In summer the building with solar walls, shaded from solar radiation, has indoor comfort level comparable to the traditional one. The results of PMVe analysis for summer (Fig. 17) highlighted overheating problems for the hottest days, when PMVe exceeds the comfort superior limit of 0,5 for both the cases considered.

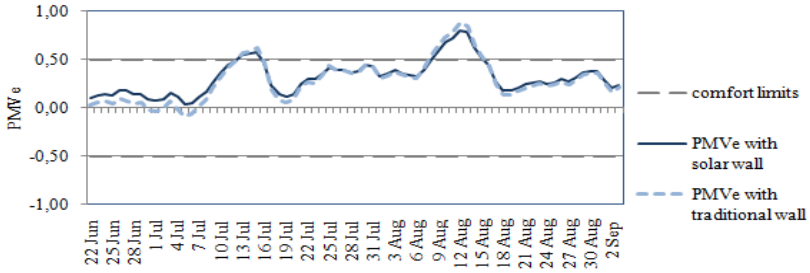

Fig. 17. Comfort analysis with PMVe method in summer.

4.2.4. Optimization of solar walls

Results of parametric analyses on the configuration of solar wall are in Fig. 18. The single variation of wall thickness from 40 cm to 30 c m (X1) increases energy needs; the single variations of external surface's absorbance (X2) or the type of glazing from single to double (X3) decrease energy needs. The type of glazing resulted to be the parameter with a greatest influence, with a reduction of -4,28 kWh/m^2 on energy needs.

The interactions between parameters are small, except the one between wall thickness and type of glazing. This implies that, even if the single effect of reducing wall thickness is disadvantageous, combining this variation with the variation of glazing from single to double

has a beneficial effect. The best performance as obtained with a wall thickness of 30 cm, absorbance 0,90 and double glasses.

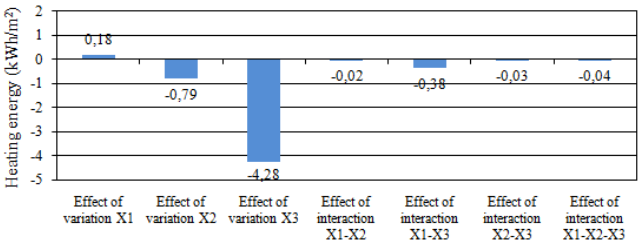

Fig. 18. Results of parametric analyses with level factorial plan.

5. Conclusions

An experimental and analytical study on the performances of solar walls in a residential building in central Italy was carried out. The study confirmed that solar wall is an efficient system in reducing energy needs for the heating season and assuring suitable comfort levels. Some problems of overheating emerged in summer in buildings with well-insulated envelope. This drawback can be reduced using adequate solar protections for solar walls; however we consider necessary further investigations on the behavior of the system in summer. Parametric analyses made it possible to compare different configurations of solar wall; the results may be used as design recommendation for solar walls.

References

[1] G. Gan, A parametric study of Trombe walls for passive cooling of buildings, Energy and buildings 27, 1998, pp. 37 - 43.

[2] G. Gan, S. B. Riffat, A numerical study of solar chimney for natural ventilation of buildings with heat recovery, Applied Thermal Engineering 18, 1998, pp.1171-1187.

[3] V. H. Hernandez Gomez, et al., Design recommendations for heat discharge systems in walls, Applied Thermal Engineering 30, 2010, pp.1616 - 1620.

[4] H. Chan, S. B. Riffat, J. Zhu, Review of passive solar heating and cooling technologies, Renewable and Sustainable Energy Reviews 14, 2010, 781-789.

[5] L. Zalewski, S. Lassue, B. Duthoit, M. Butez, Study of solar walls – validating a simulation model, Building and Environment 37, 2002, pp. 109-121.

[6] A. Fernandez-Gonzalez, Analysis of the thermal performance and comfort conditions produced by five different passive solar heating strategies in the United States Midwest, Solar Energy 81, 2007, pp.581-593.

[7] F. Stazi, A solar prototype in a Mediterranean climate: reflections on project, use, results of the monitoring activities, calculations, Proceedings World Renewable Energy Congress WREC, Aberdeen, 2005.

[8] F. Stazi, C. Di Perna, C. Filiaci, A. Stazi, The solar wall in Italian climates, International Journal of Mathematical, Physical and Engineering Sciences 2, 2008, pp.86-94.

[9] P. G. Ellis, Development and validation of the unvented Trombe wall model in EnergyPlus. Master's Thesis, University of Illinois at Urbana-Champaign, 2003.

[10] P. O. Fanger, J. Toftum, Extension of the PMV model to non-air-conditioned buildings in warm climates, Energy and Buildings 34, 2002, pp.533-536.

Thermal Performance Evaluation of Domed Roofs

Ahmadreza K. Faghih[1,*], Mehdi N. Bahadori[2]

[1] *Yazd University, Yazd, Iran*
[2] *Sharif University of Technology, Tehran, Iran*
** Corresponding author. Tel: +98 351 8122561, Fax: +98 351 8210699, E-mail: faghih@yazduni.ac.ir*

Abstract: Domed roofs (DRs) have been used in Iran and many other countries to cover large buildings such as mosques, shrines, churches, schools, etc. They have been also employed in other buildings like bazaars or market places in Iran due to their favorable thermal performance. The aim of this research is to study about DRs thermal performance in order to determine how they can be helpful in reducing the maximum air temperature of inside buildings during the warm seasons considering all parameters like air flow around them, solar radiation, radiation heat transfer with the sky and the ground as well as some openings on the building. The results of the study show that the thermal performance of the investigated DR is better than the building with flat roof (FR), particularly when the dome is covered with glazed tiles. In addition to their aesthetic values, domes covered with glazed tiles have thermal benefits of keeping the inside air of these buildings relatively cool during the summer. Moreover, openings cause passive air flow inside building, which is helpful for human comfort.

Keywords: *domed roof, thermal performance, air flow, solar radiation, numerical simulation, thermal network*

Nomenclature

C	*Specific heat* ..... $J.kg^{-1}K^{-1}$	l'	*Depth of ground* ..... m
C_D	*Discharge coefficient*	m	*Inside building air mass* ..... kg
C_p	*Pressure coefficient*	$\dot{m}$	*Air mass flow rate* ..... $kg.s^{-1}$
D	*Wall or roof thickness* ..... m	$\dot{q}$	*Heat transfer rate* ..... $w.m^{-2}$
F	*View factor*	t	*Time* ..... s
H,h	*Height* ..... m	β	*Slope* .....
R	*flow resistance* ..... $kg.m^{-4}.s^{-1}$	ε	*Surface emittance* .....
T	*Temperature* C	ε_s	*Sky emissivity* .....
$\dot{V}$	*Volumetric air flow rate* ..... $m^3.s^{-1}$	ρ	*Density* ..... $kg.m^{-3}$
V	*Velocity* ..... $m.s^{-1}$	σ	*Stefan-Boltzmann constant* ..... $w.m^{-2}.k$

Subscript

R	*Roof*	i	*Inner surface, Inside building, i opening*
W	*Wall, roof*	j	*j opening* .....
H	*Height*	m	*Maximum* .....
a	*Air*	n	*Minimum, Natural, North* .....
abs	*Absorbed*	o	*Outer surface, Ambient* .....
c	*Convection*	r	*Radiation* .....
dp	*Dew point*	rg	*Radiation with ground* .....
e	*East*	rs	*Radiation with sky* .....
f	*Floor*	s	*Absorbed solar radiation, Sky, South* .....
g	*Ground*	w	*West* .....

1. Introduction

DRs have traditionally been used throughout the world to cover large areas. Solar energy absorbed by a DR causes its temperature to rise above the ambient air temperature. Wind blowing over the dome increases the convection heat transfer to the ambient air. Furthermore, the heat loss from the roof is increased by thermal radiation to the sky. The rest of the heat absorbed by the dome is conducted through the dome material, and is finally transferred to the

inside air by convection, and to the interior walls by radiation. The geometry of these roofs causes the wind velocity to increase over them, resulting in an increase in the convection heat transfer coefficient. Furthermore, the heat transfer from these roofs is increased by the fact that their areas are greater than the comparable flat ones. In addition to their structural applications, DRs have been employed in Iran for natural ventilation and passive cooling of buildings. A cross section of a typical DR employed in such applications is shown in Fig. 1.

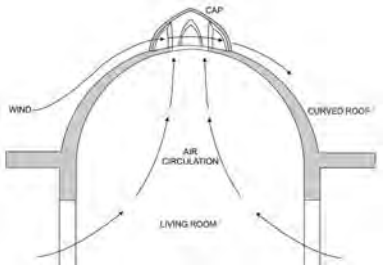

Fig. 1. Cross section of a typical DR, with air circulation in and over it [1]

In 1978, Bahadori introduced the important role of DRs in providing cold water in cistern as well as indoors air condition in warm and dry areas in Iran [1]. Konya [2] showed that the temperature of domed roof buildings (DRBs) is lower compared to flat ones. Mainstone [3] professed that the main reason of lower temperature of inside DRBs in comparison with FRs is the higher ground and sky reflected radiation heat loss. Olgyay [4] guessed that lower indoor air temperature in DRBs is due to the lower absorbed solar radiation in comparison with FRs. Tang [5] showed greater solar radiation and heat transfer through DRs and refused what Bahadori [1] had been asserted before. The aim of this research is to study about DRs thermal performance considering all parameters like air flow, solar radiation, radiation heat transfer with the sky and the ground as well as some openings on the building by using the thermal network method. Constant wind velocity and direction is assumed, and the IAT during a day is the comparison index.

We investigated air flow over domed and FRBs numerically [6] and experimentally [7] to find proper data for our own study. In these studies we consider the three-dimensional model of the dome of the School of Theology (the reference dome) shown in Fig. 2 which is located in Yazd, Iran (a city with very high solar radiation) with a specified boundary layer air flow. For this study, the absorbed solar radiation reported by the authors in [8] for the reference dome and the corresponding flat one with the same base area is used. In [8] it is found that DRs receive more solar radiation in comparison with flat ones.

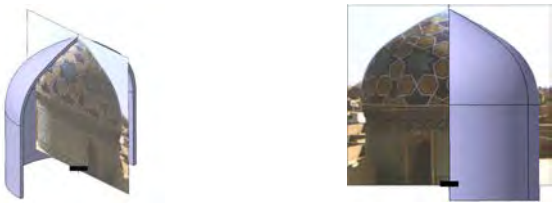

Fig. 2. Model of the reference DR

2. Absorbed Heat

In Eq. (1), solar radiation (Q_s) in each hour is assumed to be constant and is equal to its exact amount in the middle of the specified hour. The convection heat transfer between the ambient air and the outer surface of the building is defined in Eq. (2) [9].

$$Q_{abs} = Q_s + Q_c + Q_{rs} + Q_{rg} \quad (1)$$

$$Q_c = h_0 A(T_{ao} - T_W) \quad (2)$$

$$h_o = \sqrt{h_n^{\,2} + \left[2.38 V_W^{\,0.89}\right]^2} \quad (3)$$

V_W is the air flow velocity near the wall which is defined by the authors numerically and experimentally in [6, 7]. Boundary layer air velocity profile near the ground defined in Eq. (4) [10] is assumed in those studies. V_{400} is the wind velocity at height 400 m. h_n in Eq. (3) is the natural convection coefficient defined in Eq. (5) and (6) for upward and downward heat transfer respectively [11].

$$\frac{V_h}{V_{400}} = \left[\frac{h}{400}\right]^{0.28} \quad (4)$$

$$h_n = 9.482 \frac{\sqrt[3]{|\Delta T|}}{7.238 - |Cos\beta|} \quad (5)$$

$$h_n = 1.810 \frac{\sqrt[3]{|\Delta T|}}{1.382 + |Cos\beta|} \quad (6)$$

β is the slope of each surface and ΔT is the temperature difference between the ambient and each surface in the specified time. The ambient air temperature is defined using Eq. (7) [12].

$$T_{ao} = \left(\frac{T_m + T_n}{2}\right) + \left(\frac{T_m - T_n}{2}\right).Cos\left(180\left(\frac{t-15}{12}\right)\right) \quad (7)$$

The radiation heat transfer between the outer surface of the building and the sky and the ground is defined by Eq. (8) and (11). Note that ε is assumed to be 0.85, T_s is the sky temperature defined in Eq. (9) [13] and T_g is the ground temperature which is similar to the ambient temperature at each time.

$$Q_{rs} = \varepsilon\sigma(T_S^{\,4} - T_W^{\,4})\left(\frac{1 + Cos\beta}{2}\right) \quad (8)$$

$$T_S = \varepsilon_S^{\,0.25}(T_{ao} + 273.15) \quad (9)$$

$$\varepsilon_S = 0.74 + 0.006 T_{dp} \quad (10)$$

$$Q_{rg} = \varepsilon\sigma(T_g^{\,4} - T_W^{\,4})\left(\frac{1 - Cos\beta}{2}\right) \quad (11)$$

3. Boundary Conditions

The outer surface: This surface receives absorbed heat transfer which is discussed in Section 2. The absorbed coefficient of the ordinary material and the glazed tile are assumed to be 0.8 and 0.4 respectively. The FR and the wall are covered with the ordinary material, but both the ordinary material and the glazed tile are considered to cover the DR. wall thickness: Conduction heat transfer parameters are k=1.4 $w.m^{-1}.k^{-1}$, C=880 $J.kg^{-1}.K^{-1}$, and $\rho = 2300$

kg.m^{-3}. The inner surface and the floor: For simplification, constant convection heat transfer coefficient (3 w.m^{-2}.k^{-1}) is considered. The wall base: assumed to be insulated.

4. Initial Conditions

The initial temperature of the walls, roof, floor, and inside air are equal to the ambient air temperature at initial time, which is 6 A.M. lumped system is considered for the IAT and changing of this parameter can be determined by Eq. (12). Δt is time step, m is the inside building air mass, and C_v is assumed to be 717 J.kg^{-1}.K^{-1}. Deviations of the IAT during a specified day (6 August) in the city of Yazd, in the central desert region of Iran (31.54 N; 54.17 E; maximum air temperature: 37.9 ^{o}C; minimum air temperature: 21.7 ^{o}C; dew point: 8 ^{o}C), for the domed and the FRBs are compared.

$$\frac{\Delta T_{ai}}{\Delta t} = \frac{\sum h_i A(T_{Wi} - T_{ai})}{mC_v} \qquad (12)$$

5. Thermal Network

A cylinder with the height of 3m and diameter of 6m is assumed to be a building for both models (Fig. 2). The height of the dome and the wall thickness in both models are 3m and 15cm respectively. In the air flow study of these models V_{400} = 48.6 m/s, therefore according to Eq. (4) the air flow velocity on top of the DR (6 m) is 15 m/s (Re=5.8×10^5). In this method, the geometry of the building has been simplified to take the radiation heat transfer between inner surfaces of the building into account. Fig. 3 shows the simplified geometry. All view factors can be determined in this simplified geometry. In this geometry, the heights are similar to the actual model, but the dome is assumed as a triangular pyramid. Each surface of this pyramid faces to the north, south, east or west. To have similar base area, the base width and length are assumed to be 5.32m.

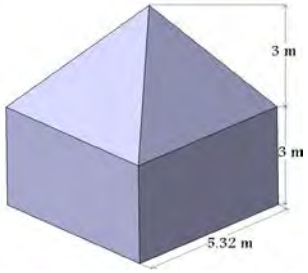

Fig. 3. The simplified model of the DRB used in the thermal network method

5.1. Heat Transfer Equations

The thermal network of the DRB used in this study consists of 18 nodes. 8 nodes are located on the outer surfaces (4 nodes on the roof surfaces and 4 nodes on the wall surfaces), 8 nodes are located on the inner surfaces, 1 node representing the inside building air and 1 node representing the floor. There are 12 nodes in the thermal network of the FR. Fig. 4 shows the thermal network of the southern roof in the simplified DRB. As shown in Fig. 4, the inner surface of the southern roof has radiation heat transfer with the three other inner surfaces of the roof (north, east and west) as well as four inner surfaces of the wall. There is a convection heat transfer with the inside building air as well. Eq. (13) and (14) show the energy balance of the inner and outer nodes of the southern roof.

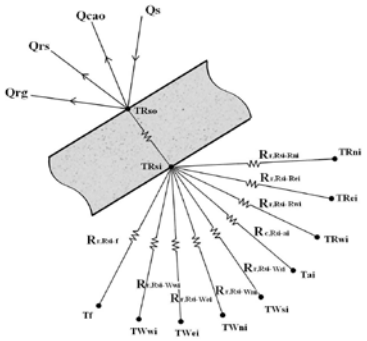

Fig. 4. The thermal network of the southern roof in the simplified DRB

$$(\dot{q}_s + \dot{q}_{cao} + \dot{q}_{rs} + \dot{q}_{rg}) + k\frac{T_{Rsi} - T_{Rso}}{D} = \rho_W \frac{D}{2} C \frac{T'_{Rso} - T_{Rso}}{\Delta t} \tag{13}$$

$$kA_{Rsi}\frac{T_{Rso} - T_{Rsi}}{D} + \frac{A_{Rni}\sigma({T_{Rni}}^4 - {T_{Rsi}}^4)}{\frac{1-\varepsilon_{Rni}}{\varepsilon_{Rni}} + \frac{1}{F_{Rni-Rsi}} + \frac{1-\varepsilon_{Rsi}}{\varepsilon_{Rsi}}\frac{A_{Rni}}{A_{Rsi}}} + \ldots + \frac{A_f\sigma({T_f}^4 - {T_{Rsi}}^4)}{\frac{1-\varepsilon_f}{\varepsilon_f} + \frac{1}{F_{f-Rsi}} + \frac{1-\varepsilon_{Rsi}}{\varepsilon_{Rsi}}\frac{A_f}{A_{Rsi}}} + h_{c,Rsi-ai}A_{Rsi}(T_{ai} - T_{Rsi}) = \rho_W A_{Rsi}\frac{D}{2}C\frac{T'_{Rsi} - T_{Rsi}}{\Delta t} \tag{14}$$

In Eq. (13), $\dot{q}_s$ is the averaged absorbed solar radiation of the quarter of the dome face to the south. $\dot{q}_{cao}$ is the convection heat transfer which is calculated based on Eq. (2) and (3). Air flow velocity is the average air velocity near the quarter of the dome face to the south. Energy balance equations for all nodes are derived similarly. Emittance of all surfaces is assumed to be 0.85 in this study. Fig. 5 shows the thermal network of the floor. As shown in Fig. 5, there is a conduction heat transfer between the floor and the depth of the ground (l'=5m) [14] with the annually averaged temperature ($\overline{T}$) of the under study area (Yazd) which is reported 18 ^{o}C. Eq. (15) shows the energy balance of the floor node.

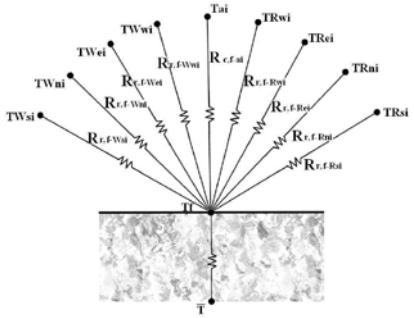

Fig. 5. The thermal network of the floor

$$k_f A_f \frac{\overline{T} - T_f}{l'} + \frac{A_{Rsi}\sigma({T_{Rsi}}^4 - {T_f}^4)}{\frac{1-\varepsilon_W}{\varepsilon_W} + \frac{1}{F_{Rsi-f}} + \frac{1-\varepsilon_f}{\varepsilon_f}\frac{A_{Rsi}}{A_f}} + \ldots + h_{c,f-ai}A_f(T_{ai} - T_f) = \rho_f A_f \frac{l'}{2} C_f \frac{T'_f - T_f}{\Delta t} \tag{15}$$

In this study ρ_f =1300 kg.m^{-3}, k_f=0.75 w.m^{-1}.K^{-1} and C_f=970 J.kg^{-1}.K^{-1}. Eq. (16) shows the energy balance of the inside building air. In this Eq. $\dot{m}$ is the air mass flow rate (kg.s^{-1}) which is equal to zero, when there is no opening on the building.

Energy balance equations define all temperatures for next time steps. This method is not sensitive to the time step. We consider the time step of 15 seconds for both the domed and the FRBs. The simulation starts from 6 A.M. and it continues until we get 0.1 ^{o}C difference between the IAT for the specified day (6 August) and a day after that at 6 A.M.

$$h_{c,ai-f} A_f (T_f - T_{ai}) + h_{c,ai-Rsi} A_{Rsi} (T_{Rsi} - T_{ai}) + ... + \dot{m} C_p (T_{ao} - T_{ai}) = \rho_a V C_v \frac{T'_{ai} - T_{ai}}{\Delta t} \quad (16)$$

5.2. Thermal Network Results

Fig. 6 shows the sky, the ambient, and the IAT for the DRB covered with the ordinary material, when the wind direction is south. There are similar figures for other cases, but they are not presented here for the sake of brevity. Table 1 compares the maximum IAT. The reference DRB has better thermal performance in comparison with the FRB with similar conditions. It can be also seen that using glazed tiles improves DRB thermal performance. Wind direction does not have considerable affect on the thermal performance of buildings.

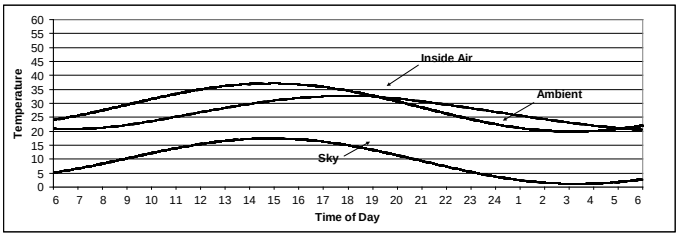

Fig. 6. The sky, the ambient, and the IAT for the DRB covered with the ordinary material

Table 1. Maximum air temperature, using the numerical simulation method

Time	Max. Temperature	Roof Absorb Coefficient	Type of Roof	Wind Direction
16:43	37.30	0.8	Flat	South
17:35	37.09	0.8	Dome	
17:35	36.04	0.4	Dome	

Fig. 7 shows the deviation of all heat transfer to the outer surface of the DRB covered with the ordinary material, when the wind direction is south. Convection heat transfer between the outer surface of the building and the ambient air is always negative except from 4.5 to 7 A.M., which shows that most of the time the walls and the roof are warmer than the ambient.

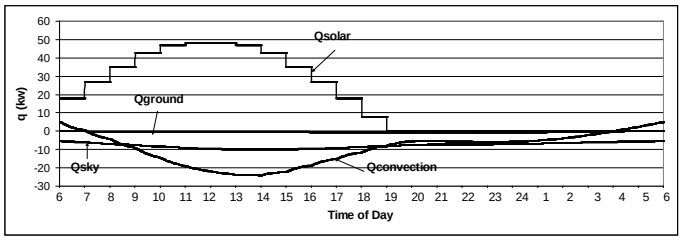

Fig. 7. The deviation of all kinds of heat transfer to the outer surface of the DRB

5.3. Openings

To investigate the effect of openings, we consider the model shown in Fig. 8. This Fig. depicts the locations and dimensions of two openings on the wall and one hole on its apex. One opening faces to the wind flow (windward) and the second one is behind (leeward). In the following, we study two scenarios which are "no wind flow" and "with wind flow".

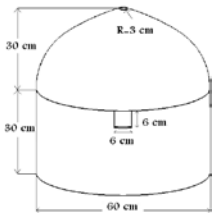

Fig. 8. The locations and dimensions of two openings on the wall and one hole on its apex

5.3.1. No Wind Flow

Air temperature difference causes air flow in this condition. Air flow rate can be defined by Eq. (17) or (18) [11]. C_D in these equations is opening discharge coefficient [11]. Considering Eq. (16), as well as the air flow rate we can define the IAT in the next time step (T'_{ai}). The convection heat transfer coefficient between the inner surface of the building and the IAT is assumed to be always 4 $w.m^{-2}.K^{-1}$.

$$\dot{V} = C_D A \sqrt{2g\Delta H \frac{(T_{ai} - T_{ao})}{T_{ai}}} \qquad T_{ao} > T_{ai} \qquad (17)$$

$$\dot{V} = C_D A \sqrt{2g\Delta H \frac{(T_{ao} - T_{ai})}{T_{ao}}} \qquad T_{ao} < T_{ai} \qquad (18)$$

$$C_D = 0.4 + 0.0045\left|T_{ai} - T_{ao}\right| \qquad (19)$$

The results show that the maximum IAT in this scenario is 42.95 which is at 16:27. In the same situation when the wind direction was south in section 5.2, the maximum IAT was 37.09. This means that without wind flow, openings cannot be helpful. Furthermore, we see that the convection heat transfer reduces in this situation. It is due to the reduction in the air flow velocity near the building's roof and wall. Increasing in radiation heat transfer with the sky is sensible because the temperature difference between walls and the sky increases.

5.3.2. With Wind Flow

In the wind flow scenario, both air temperature difference and air pressure difference between openings cause air flow inside the building. To define the air flow caused by pressure difference, flow network method is used in this study. In this method, air volumetric flow rate from each opening (j) is defined by Eq. (20). Where P_i is the inside air pressure and P_j is the air pressure on the related opening. P_j can be determined by Eq. (21). C_{pj} is defined in previous surveys [6, 7]. C_p is assumed to be -1.1, 1, and 0.3 for the hole on apex, windward opening, and leeward opening respectively. In this study all openings discharge coefficients are assumed to be 0.65. The inside air pressure coefficient (C_{pi}) is defined by using Eq. (21) with i as its index. Combining Eq. (20) to (22), the air flow rate of the opening can be found by Eq. (23).

$$\dot{V}_j = \frac{P_j - P_i}{R_{ij}} \qquad (20)$$

$$P_j = C_{pj} \frac{1}{2} \rho V_0^{\,2} \qquad (21)$$

$$R_{ij} = \frac{\sqrt{\frac{1}{2}\rho (P_j - P_i)}}{A_j C_{dj}} \qquad (22)$$

$$\dot{V}_j = A_j C_{dj} V_0 \left[\frac{C_{pj} - C_{pi}}{\sqrt{\left|C_{pj} - C_{pi}\right|}} \right] \qquad (23)$$

Using Eq. (21) with i as its index and (23) and try and error method, C_{pi} and $\dot{V}_j$ can be determined. For the wind velocity profile similar to (4), the network flow method leads to the value of 1.28 m^3/s. We use the reference velocity of 15 m/s. This amount is assumed to be constant during the day. The convection heat transfer coefficient between the inner surface of the building and the inside building air is assumed to be constant and equal to 6 $w.m^{-2}.K^{-1}$. This coefficient is the greatest one in comparison with the other cases (3 and 4 $w.m^{-2}.K^{-1}$) due to the higher air flow velocity near the inner surface of the building. Maximum air temperature in this condition is 37.46 occurred at 15:09. In similar conditions with no openings, maximum air temperature was 37.09. So again in the wind flow condition the thermal performance of the building with no opening is better, however the air flow inside the building caused by openings can be helpful for human comfort on warm days.

6. Conclusions

Based on the analysis carried out the following conclusion can be made: Thermal performance of the DRB under investigation is better than the building with FR on warm days, particularly when the dome is covered with glazed tiles. Wind flow direction is not an important parameter in decreasing room temperature of the DRB of the specified cases. For no wind flow condition, the FRB performs better than the DR one. The passive air flow inside the DRB caused by openings can be helpful for human comfort on warm days.

References

[1] M. N. Bahadori, Passive Cooling Systems in Iranian Architecture, Scientific American, Vol. 238, 1978, pp. 144-154.

[2] A. Konya, Design Primer for Hot Climate, the Architectural Press, 1980, pp. 3-42.

[3] R. J. Mainstone, Developments in Structural Form, M.L.T. Press, 1983, pp. 95-136.

[4] V. Olgyay, Design with Climate, Princeton University Press, Princeton, 1973, p. 7.

[5] R. Tang, I. Meir, Y. Etzion, Thermal Behavior of Buildings with Curved Roofs as Compared with Flat Roofs, Solar Energy, Vol. 74, 2003, pp. 273-286.

[6] A. K. Faghih, M. N. Bahadori, Three Dimensional Numerical Investigation of Air Flow over Domed Roofs, J Wind Eng Ind Aerod, Vol. 98, 2010, pp. 161-168.

[7] A. K. Faghih, M. N. Bahadori, Experimental Investigation of Air Flow over Domed Roofs, Iranian J of Science and Technology; Engineering, Vol. 33, 2009, pp. 207-216.

[8] A. K. Faghih, M. N. Bahadori, Solar Radiation on Domed Roofs, Energy and Buildings, Vol. 41 (B3), 2009, pp. 1238-1245.

[9] M. Yazdanian, J. Klems, Measurement of the Exterior Convective Film Coefficient for Windows in Low-rise Buildings, ASHRAE Transactions 100 (1), 1994, pp. 1087–1096.

[10] A. D. Penwarden, Wise, Wind Environment around Buildings, Bldg. Res. Estab., 1975.

[11] ASHRAE, ASHRAE Handbook-Fundamentals, American Society of Heating, Refrigerating, and Air-conditioning Engineers, Inc., Atlanta, 1997.

[12] M. N. Bahadori, Chamberlain, Simplification of Weather Data to Evaluate Daily and Monthly Energy Needs of Residential Buildings, Sol Energy, Vol. 36, 1986, pp. 499-507.

[13] Berdahl, Fromberg, the Thermal Radiance of Clear Skies, Solar Energy, Vol. 29, p. 299.

[14] E. Ahmadi, Heat Transfer Analysis in Ground, M.S. Thesis (in Persian), School of Mechanical Engineering, Sharif University of Technology, 1999.

A study of single-sided ventilation and provision of balconies in the context of high-rise residential buildings

Mohamed M. F.[1,2,*], King S.[2], Behnia M.[3], Prasad D.[2]

[1] *Faculty of Engineering and Built Environment, Universiti Kebangsaan Malaysia, Bangi, Malaysia*
[2] *Faculty of the Built Environment, The University of New South Wales, Sydney, Australia*
[3] *School of Mechanical Engineering, The University of Sydney, Sydney, Australia*
** Corresponding author. Tel: +614 24898387, E-mail: farid0906@yahoo.com*

Abstract: Passive design strategy is an important approach to reduce energy consumption of a building such as improving indoor thermal comfort through enhanced natural ventilation performance. This is crucial in achieving a more sustainable building especially for a tall high density residential development where energy consumption is huge. This paper looks into the potential of high-rise residential buildings to utilize abundant naturally available prevailing wind by mean of passive design strategy. Its objective is to investigate the potential to improve the ventilation performance of a single-sided ventilation strategy of high-rise residential buildings by introducing a series of balconies on their façades. Computational Fluid Dynamics (CFD) was used as a tool for investigation. Since CFD requires a validation process to investigate its reliability, existing wind tunnel experiments and empirical models were used in the validation process. This study found that an appropriate combination of balcony configurations and single-sided ventilation strategy could improve indoor ventilation performance of high-rise residential buildings; however, incorrect combination could further reduce the ventilation performance of an already inefficient ventilation strategy. Therefore, understanding the concept of single-sided ventilation strategy is crucial, and application of appropriate tools such as CFD is important to ensure ventilation performance optimization is achieved.

Keywords: *Single-sided ventilation, Balcony, High-rise residential building, CFD.*

Nomenclature

Q	*ventilation rate*..... $m^3 \cdot s^{-1}$	ΔP	*pressure difference*..... $N \cdot m^{-2}$
A	*inlet opening area*..... m^2	C_V	*opening effectiveness*..... *dimensionless*
C_D	*discharge coefficient of opening*..... *dimensionless*	V	*air velocity*..... $m \cdot s^{-1}$

1. Introduction

The only solution to solve the human's basic need for shelter in urban environment through vertically constructed high-density residential buildings leads to either favorable or unfavorable impacts to the environment as well as to its occupants. There are various opportunities associated with high-density tall residential buildings such as optimization of land with less floor plinth, greater control of water and energy usage through central management, reduced transportation distance to workplaces, opportunities to waste recycling, utilization of natural lighting and ventilation for indoor environmental quality, etc. Therefore, vertical construction such as high-density residential building is an option of sustainable building approach if properly designed and managed.

This study looks into the potential of high-rise residential buildings to utilize naturally available prevailing wind. Optimization of the outdoor wind environment for indoor air quality and thermal comfort by mean of passive design strategies can reduce dependency on mechanical ventilation and, subsequently, reduces the energy consumption of buildings. Optimization of the prevailing wind for ventilation requires micro and macro investigations to ensure the objective of enhanced indoor airflow is achieved. This includes better understanding on the relationship between local wind climate and indoor ventilation performance.

While cross ventilation strategy is a well accepted and recognized ventilation approach, the potential of single-sided ventilation strategy is always neglected by designers and policy-makers. Coupled with a common provision of balconies in high-rise residential buildings, this paper discusses the relationship between single-sided ventilation strategy and the provision of balconies in the context of high-rise residential buildings. Therefore, the outlined objective of this paper is to discuss and investigate the potential to improve the ventilation performance of single-sided ventilation strategy of high-rise residential buildings by introducing a series of balconies on the façades of the buildings.

2. Ventilation

2.1. Single-sided ventilation

Ventilation strategies for building are categorized into two: single-sided ventilation and cross ventilation. In the context of this study, single-sided ventilation is defined as a condition where one or more openings exist only at one façade of a closed room or building, whereas, for cross ventilation, two or more openings are exist at two or more façades. Existence of an opening at more than one building facades in cross ventilation strategy potentially creates a much higher pressure gradient encouraging better natural ventilation performance. Therefore, generally, cross ventilation has a greater potential to manipulate the pressure gradient developed around buildings. However this is not the case for single-sided ventilation where it is limited to pressure gradient developed only at a single façade. Thus, ventilation performance of cross ventilation is always assumed to be better than single-sided ventilation. Despite the disadvantage of single-sided ventilation strategy in ventilation performance, it is still commonly used as a ventilation solution for apartments. This is due to various factors such as site constraint and unit number optimization. Since there is a greater potential of single-sided ventilation to fail in ventilating indoor residential spaces, but still, it is widely adopted as ventilation strategy in many residential apartments, greater understanding of its potential and limitation shall be attained to ensure that the potential of single-sided ventilation strategy is optimized and to avoid failure in indoor ventilation performance.

The ventilation performance of a single-sided ventilated apartment can be enhanced through appropriate façade treatments. There are various façade treatments and detailed building configurations which may change the pressure distribution across the building façades. For examples, the provision of balconies on the façade of a building as well as protruding and sunken floor plan layout. Complex façade treatment and floor plan result in a more complicated pressure distribution across building's façades and, consequently, causes changes in indoor ventilation performance. Therefore, these changes, if positively utilized, can enhance indoor ventilation performance by optimizing the available prevailing wind.

2.2. Balcony as a passive design strategy

Balcony is defined as "a platform projecting either from an inside or an outside wall of a building" [1]. A balcony can provide various benefits from the aspects of social, economy and environmental, for examples, it provide private outdoor spaces, enhanced the monetary value of a building and provides protection from extreme outdoor climate, respectively [2,3]. There are many studies on the impact of balcony on airflow [3, 4, 5, 6]; however, none of researchers looking into the affect of the provision of balcony on the performance of single-sided ventilation strategy in the context of tall buildings. Since a provision of balconies could change the pressure distribution on the façades of a building [4, 6], it is seen as a potential

which can be utilized to induce indoor ventilation performance of single-sided ventilated buildings.

3. Methodology

Computational fluid dynamics (CFD) is the main tool for this study which has been widely used to predict indoor ventilation performance. However, CFD comes with two great setbacks: it requires huge computational effort and validation and verification process. With current advances in computer technology and greater affordability, CFD has been widely used by researchers such as van Hooff and Blocken [7] and Cheng et al. [8] to investigate ventilation performance of large buildings.

There are various approaches to predict indoor ventilation performance for tall buildings. The followings are commonly used approaches:

A. Combination of small-scale models and empirical models (Approach A).
B. Combination of CFD models with empirical models (Approach B).
C. Coupled CFD simulation (Approach C).
D. De-coupled CFD simulation (Approach D).

According to Jiru and Bitsuamlak [9], Approach C is a preferred approach compare to Approach D since the accuracy of Approach D can easily be compromised though it gives an advantage of lower computational effort. Among all the approaches, only Approach D was excluded in this study, while the others were used to predict ventilation rate. Empirical models used for the validation study were Equation 1 [10] and Equation 2 [11]. The value of discharge coefficient of opening, C_D, used for this study was 0.5 since the opening area was less than 10% of the area of the façade. In the case of single opening, the inlet area, A, was taken to be half of the opening, and the reference pressure is taken to be at the middle of the inlet. For Equation 2 the value of opening effectiveness, C_V, was 0.025.

$$Q = C_D \cdot A \cdot \sqrt{(2 \cdot \Delta P / \rho)} \quad (1)$$

$$Q = C_V \cdot A \cdot V \quad (2)$$

This study utilized existing wind tunnel experimental data [12] to validate its results with initial validation study for cross ventilation strategy with perpendicular wind direction which was completed earlier [13]. An additional validation study for single-sided ventilation strategy (wind angle 45° only) and cross ventilation strategy (0° and 45°) was completed, where Approach C was validated against Approach A and Approach B.

3.1. Computational Fluid Dynamics (CFD)

This study used commercial code CFD software which was Ansys CFX 12.0. The turbulence model used is standard k-epsilon turbulence model. The turbulence model was selected due to its robustness which was important in this complex and huge coupled outdoor and indoor simulation study though it may be less accurate in areas with vortex shedding [14, 15]. It was a steady-state CFD simulation simulated under isothermal condition where the effect of buoyancy force on ventilation was not included. Mesh independence study is an important procedure in CFD simulation to understand the simulation accuracy as well as to optimize computational effort. Since this paper is a subsequent study to the previous investigation [13] which uses similar overall building forms, mesh independence study and the setup of computational domain were not discussed in this paper. The maximum number of element

used in this study was around $2.4x10^7$ which consists of mainly tetrahedral mesh except at the ground of outdoor domain where prism shape was used. Tetrahedral mesh was selected due to its robustness where it can easily mesh all building configurations used in this study.

3.2. Simulation setup and model configurations

Table 1. A list of case studies tested.

Test case	Ventilation strategy	No. of opening	Façade treatment	Wind angle
Case 1	Cross	2	Flat	0°
Case 2	Single-sided	1	Flat	0°
Case 3	Single-sided	1	Balcony (1.5m)	0°
Case 4	Single-sided	2	Balcony (1.5m)	0°
Case 5	Cross	2	Flat	45°
Case 6	Single-sided	1	Flat	45°
Case 7	Single-sided	1	Balcony (1.5m)	45°
Case 8	Single-sided	2	Balcony (1.5m)	45°

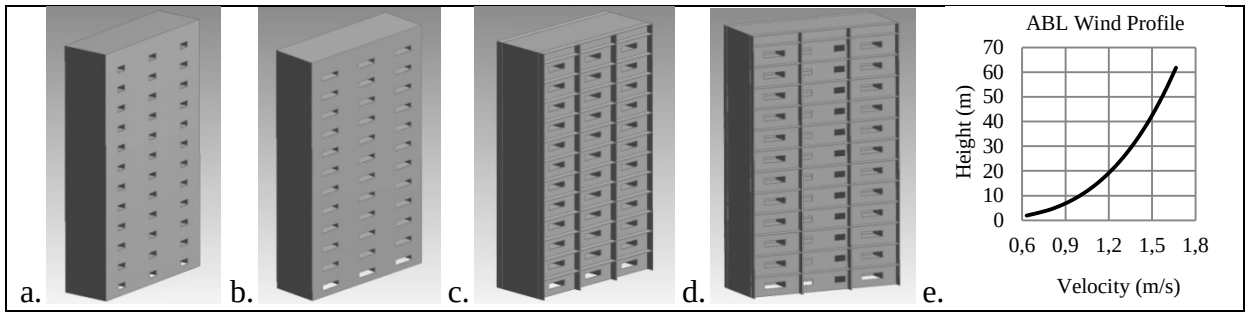

Fig. 1. The building configurations for Case 1and 5 (a), Case 2 and 6 (b), Case 3 and 7 (c) and Case 4 and 8 (d), together with ABL wind profile with mean speed exponent of 0.28 (e).

This study used the building configuration similar to the models used in wind tunnel experiment by Ismail. The overall dimension of the model was 30m (width) x 50m (height) x 10m (depth) to resemble 36 units apartment with 12-storey height. Three units were located at each floor with floor to floor height is 4m. While Ismail's models did not include opening an indoor space, this study provided a single or double openings (Fig. 1). The dimension of the opening was 4.4m (width) x 1.15m (height) for setup with single opening, and 2.2m (width) x 1.15m (height) each for double openings located at a single façade or at two opposite façades. The total opening area provided at each unit was $5.06m^2$, which was approximately 5% of the floor area. This study only focused on units located at the middle.

4. Analysis and Findings

4.1. Validation Study

Fig. 2 and Fig. 3 (see below) show that CFD predictions of wind pressure on facades of a building were inaccurate at areas located at the bottom leeward of the building where CFD over predicts the values of wind pressures. Therefore, if the wind pressure data were used in Approach B to predict indoor ventilation rate, it will result in under prediction on units located at the bottom of the building. The figures also suggest that if Approach C is used, it might also result in under prediction of indoor ventilation rate for lower units. Generally, the wind pressure distribution predicted by CFD was found to be acceptable.

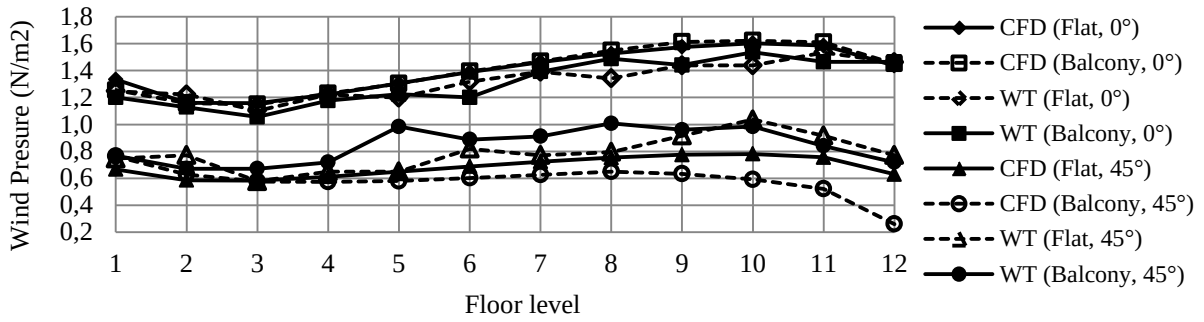

Fig. 2. Windward wind pressure distributions for flat façade and façades with balconies (opening is not provided).

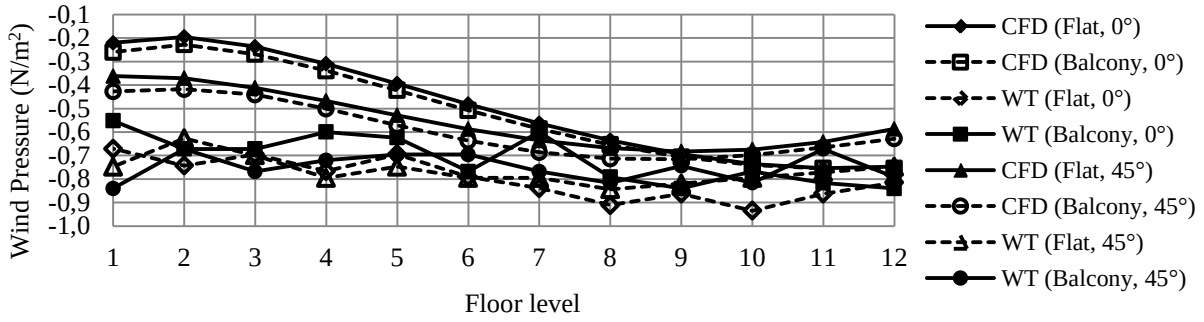

Fig. 3. Leeward wind pressure distributions for flat façade and façades with balconies (opening is not provided)

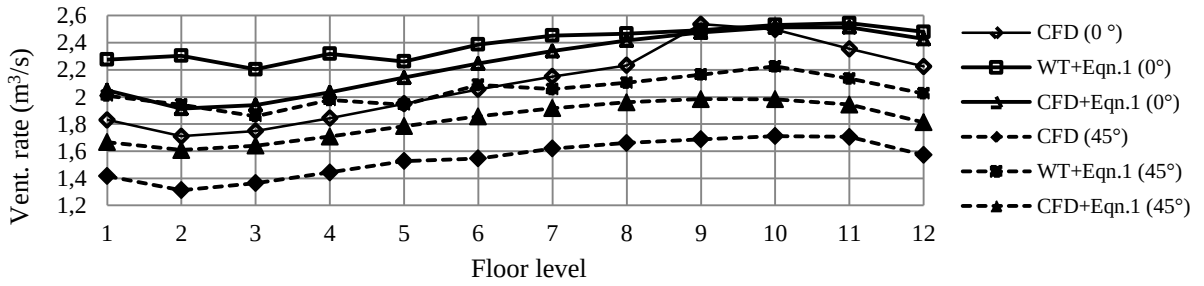

Fig. 4. Predicted ventilation rates for Case 1and Case 5 using Approach A, B and C.

For cross ventilation strategy (Fig. 4), it was found that Approach B and Approach C provided acceptable ventilation rate predictions for 0° wind angle with the worst prediction occurs at units located at lower floors. The average inaccuracies for Approach B and Approach C were found to be 6% and 12.5%, respectively. The inaccuracy at the lower level was expected due to the difficulty of the selected turbulence model to predict the recirculation zone at the bottom leeward side of the building.

For wind angle of 45°, it was found that Approach B and Approach C under predict indoor ventilation performance in comparison to Approach A, with the average inaccuracies of 24% and 11%, respectively. It was also found that the inaccuracies were relatively similar to all units. These greater inaccuracies can be due to the fact that the value of discharge coefficient of opening, C_D, used was 0.5 even though the wind direction close to the opening is travelling almost parallel to the facade of the building which shall suggests that the value may not be appropriate and shall be lower. This is supported by Equation 2 which suggests that the ventilation rate for wind angle of 45° shall be between 50 to 70 percent of the ventilation rate for 0° wind angle based on the suggested values of opening effectiveness, C_V, by ASHRAE

[11] (ASHRAE suggests the value to be 0.25-0.35 for 45° and 0.5-0.7 for 0°). This is also supported by an experiment completed by Larsen and Heiselberg [16] which found that the ventilation rate for a cross ventilated single cell building at 45° wind angle is reduced by around 55% in comparison to 0°.

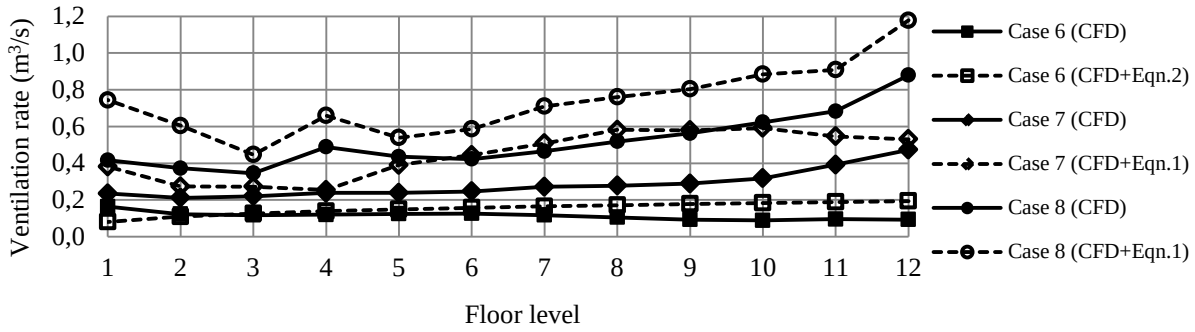

Fig. 5. Predicted ventilation rates for Case 6, 7 and 8 using Approach B and C.

In the case of single-sided ventilation strategy, only wind direction of 45° was used for validation study. For Case 6, Approach B with Equation 2 was used. Approach B with Equation 1 was used for Case 7 and Case 8 assuming that the CFD wind pressure difference across two reference point is acceptably describing the reality though it may come with some inaccuracies. Even though, both approaches might have not provided accurate predictions due to being applied to a difference building context, more or less, it shall give some idea on the ventilation rate. Fig. 5 shows that Approach C under predicted ventilation rate for all cases. The average percentage of difference between Approach C and Approach B for Case 6, 7 and 8 were 25%, 45% and 30%, respectively. Though the prediction differences for the values of ventilation rate were found to be high, Approach C was found to acceptably predict ventilation rate improvement due to changes on façade treatment.

Validation of single-sided ventilation strategy for building with 0° wind angle was not performed in this study. This is due to the limitation of Equation 1 and Equation 2 in predicting single-sided ventilation for the building configuration under the 0° wind angle. For example, in Equation 1, two reference pressures (if taken at a midpoint of each opening) are equal or almost equal, thus prediction of ventilation rate is zero or almost zero. In reality, this is not the case since there is a distinct pressure difference across each of the openings, thus inlet and outlet exist within the opening itself. On the other hand, Equation 2 is not appropriate due to the immediate outdoor air characteristic of airflow is different from low rise building where the equation is normally used and derived from. Thus, it was assumed that if Approach C was acceptably validated in earlier validation studies, the approach should also give an acceptable prediction under the 0° wind angle.

4.2. Ventilation Rate for Various Façade Treatments

Fig. 6 (see below) shows that cross ventilation strategy was far more effective in comparison to single-sided ventilation strategy. Cross ventilation strategy was also able to optimize the increased wind speed at upper floors. However, this was not the case for single-sided ventilation trategy with wind direction of 0° wind angle. This finding shows that under the circumstances, the ventilation performance of units located at upper units was relatively lower than units at the lower floor. This was due to the units being located within the stagnation zone, where the pressure difference across the facades was very low (see Fig. 2). Under 0° wind angle, the provision of balconies (Case 3) was also found to reduce indoor ventilation

performance of single-sided ventilated apartments, however, by splitting the opening into two (Case 4), it slightly increased the ventilation performance.

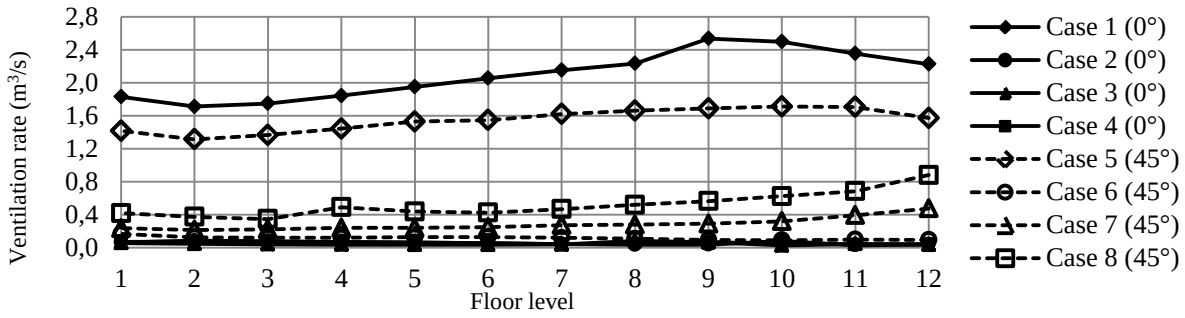

Fig. 6. Comparison between predicted ventilation rates for Case 1 to 8 using Approach C.

In the other hand, in the case of 45° wind angle, it was found that ventilation performance of single-sided ventilation strategy was improved in comparison to 0° wind angle, while for cross ventilation strategy, it was slightly reduced. For units with a balcony, their ventilation performances were higher than units with flat façade. This was due to external airflow travelling almost parallel to the openings at the building with flat façades, thus reducing its impact on ventilation performance. Additional to this, with a simple reconfiguration of opening from a single opening to double openings located close to protruding vertical walls of a balcony (Case 8), it has enhanced indoor ventilation rate by almost four times the ventilation performance of the model with a single opening with flat façade (Case 6).

5. Conclusions

Being a less effective ventilation strategy, single-sided ventilation strategy should be adopted in building design with clear understanding of its effectiveness and potential. This study found that cross ventilation strategy is a preferred option. However, if single-sided ventilation strategy is the only option, its ventilation performance effectiveness can be improved with appropriate façade reliefs such as a balcony. Below are the findings on the potential of balconies to enhance ventilation performance of single-sided ventilation strategy for tall buildings:

a. Perpendicular wind towards the façade of a tall building shall be avoided, where an introduction of a series of balconies could reduce indoor ventilation performance. This can be observed in Case 3. Under this wind condition, it is found that the balconies act as a buffer protecting the indoor spaces from direct penetration of wind.
b. For 45° wind angle, it was found that the provision of balconies, such as in Case 7 and Case 8, significantly improve indoor ventilation performance in comparison to a flat façade building (Case 6). However, the improvement shown in Case 7 and Case 8 was still much lower than Case 5, which adopt cross ventilation strategy.
c. Opening configuration plays an important role to improve an indoor ventilation performance. An appropriate combination of a balcony and opening configurations improves indoor ventilation performance (Case 8); otherwise, it reduces the indoor ventilation performance (Case 7).

References

[1] H. J. Cowan, & P. R. Smith, Dictionary of architectural and building technology. 4th ed. London: Spon Press (Taylor & Francis Group), 2004, p. 24.

[2] M. F. Mohamed, M. Mohd Tahir, & D. Prasad, A study on balcony and its potential as an element of ventilation control in naturally ventilated apartment in hot and humid climate. Proceedings of International Conference on Construction and Building Technology (ICCBT 2008), 2008, pp. 173 – 180.

[3] N. Papamanolis, An overview of the balcony's contribution to the environmental behaviour of buildings. Proceedings of The 21th Conference on Passive and Low Energy Architecture (PLEA2004), 2004.

[4] I. Chand, P. K. Bhargava, & N. L. V. Krishak, Effect of balconies on ventilation inducing aeromotive force on low-rise buildings. Building and Environment, 33**,** 1998, pp. 385-396.

[5] E. Prianto, & P. Depecker, Characteristic of airflow as the effect of balcony, opening design and internal division on indoor velocity: A case study of traditional dwelling in urban living quarter in tropical humid region. Energy and Buildings, 34**,** 2002, pp. 401-409.

[6] H. Kotani, & T. Yamanaka, Wind pressure coefficient and wind velocity along building wall of apartment building with balcony. 6th International Conference on Indoor Air Quality, Ventilation & Energy Conservation in Buildings - IAQVEC 2007, 2007.

[7] T. Van Hooff, & B. Blocken, Coupled urban wind flow and indoor natural ventilation modelling on a high-resolution grid: A case study for the Amsterdam Arena stadium. Environmental Modelling & Software, 25**,** 2010, pp.51-65.

[8] C. C. K. Cheng, K. M. Lam, R. K. K. Yuen, S. M. Lo & J. A. Liang, study of natural ventilation in a refuge floor. Building and Environment, 42**,** 2007, pp. 3322-3332

[9] T. E. Jiru, & T. Bitsuamlak, Advances in applications of CFD to natural ventilation. The Fifth International Symposium on Computational Wind Engineering (CWE2010). 2010.

[10] R. M. Aynsley, W. Melbourne & B. J. Vickery, Architectural aerodynamics, London, Applied Science Publisher Ltd, 1977, pp. 189 – 194.

[11] ASHRAE 1997. ASHRAE Handbook: Fundamentals, Atlanta, American Society of Heating, Refrigerating and Air-Conditioning Engineers, Inc. 1997, p. 25.13.

[12] A. M. Ismail, Wind-driven natural ventilation in high rise buildings with special reference to the hot humid climate of Malaysia. Phd Thesis, University of Wales College of Cardiff, 1996.

[13] M. F. Mohamed, S. King, M. Behnia, D. Prasad & J. Ling, Wind-driven natural ventilation study for multi-storey residential building using CFD. Proceedings of 44th Annual Conference of the Australian and New Zealand Architectural Science Association, 2010.

[14] R. Yoshie, A. Mochida, Y. Tominaga, H. Kataoka, K. Harimoto, T. Nozu & T. Shirasawa, Cooperative project for CFD prediction of pedestrian wind environment in the Architectural Institute of Japan. Journal of Wind Engineering and Industrial Aerodynamics, 95**,** 2007, pp. 1551-1578.

[15] S. H. L. Yim, J. C. H. Fung, A. K. H. Lau & S. C. Kot, Air ventilation impacts of the "wall effect" resulting from the alignment of high-rise buildings. Atmospheric Environment, 43**,** 2009, pp. 4982-4994.

[16] T. S. Larsen & P. Heiselberg, Single-sided natural ventilation driven by wind pressure and temperature difference. Energy and Buildings, 40**,** 2008, pp. 1031-1040.

Impact of ventilation heat recovery on primary energy use of apartment buildings built to conventional and passive house standard

Leif Gustavsson[1,2], Ambrose Dodoo[2,*], Roger Sathre[2]

[1]*Linnaeus University, 35195 Växjö, Sweden*
[2]*Mid Sweden University, 83125 Östersund, Sweden*
** Corresponding author. Tel: +46 63165383 , Fax: +46 63165500, E-mail: ambrose.dodoo@miun.se*

Abstract: In this study we analyze the primary energy implications of ventilation heat recovery (VHR) in residential buildings, considering the entire energy chains. We calculate the operation primary energy use of a case-study apartment building built to conventional and passive house standard, both with and without VHR, and heated with electric resistance heating, bedrock heat pump or district heating. VHR increases the electrical energy used for ventilation and reduces the heat energy used for space heating. The primary energy savings of VHR are greater for the passive building than for the conventional building. Significantly more primary energy is saved when VHR is used in resistance heated buildings than in district heated buildings. For district heated buildings the primary energy savings are small. VHR systems can give substantial final energy reduction, but the primary energy benefit depends strongly on the type of heat supply system, and also on the amount of electricity used for VHR and the airtightness of buildings. This study shows the importance of considering the interactions between heat supply systems, VHR systems, building thermal properties and its airtightness to reduce primary energy use in buildings.

Keywords: *Mechanical ventilation; Heat recovery; Heat supply systems; Electric resistance heating; Heat pumps; District heating; CHP plant; Primary energy.*

1. Introduction

Ventilation has a significant impact on the energy performance of buildings, accounting for 30 to 60% of the energy use in buildings [1, 2]. Energy is used to cover the heat losses due to the ventilation air and to move the ventilation air for mechanical ventilation. The ventilation system also influences the air infiltration through the building envelope.

Building regulations currently require high energy efficiency of buildings, and therefore considerable efforts have been made to improve airtightness and insulation of buildings. In such buildings mechanical ventilation with heat recovery (VHR) is often used to recover heat from exhaust air to reduce ventilation heat losses. Ventilation heat losses can be typically 35-40 kWh/m^2-year in residential buildings, and up to 90% of this can be recovered with VHR depending on airtightness and insulation of buildings [3]. VHR is therefore gaining increasing interest in low energy and retrofitted buildings. In very low energy buildings, such as passive house buildings, VHR units are often equipped with additional air heaters to cover the space heating demand.

Sweden has set targets to reduce the final energy use per heated building area by 20% and 50% by 2020 and 2050, respectively, using 1995 as the reference [4]. Heat recovery from exhaust ventilation air is considered an important means to reach this target, and increased attention is being placed on VHR. There is a technology procurement project to develop and promote VHR systems which can be adapted for existing Swedish apartment buildings [5].

Most studies on the energy impact of VHR have focused on final energy use [e.g. 6-8]. Primary energy use, in contrast to final energy use, largely determines the natural resource use and the environmental impact of end-use energy services. The concept of primary energy is used to denote the total energy needed in order to generate the final energy service, including

inputs and losses along the entire supply chains. Fewer studies have analyzed the primary energy implication of VHR in buildings. In this study, we analyze the impact of VHR on the operation primary energy use for residential buildings. We determine situations where mechanical ventilation with heat recovery can reduce primary energy use for building operation.

2. Methodology

This analysis is based on simulation modeling of a case-study apartment building with mechanical ventilation. We model the primary energy use for the original and improved level of energy efficiency of the building, both with and without VHR. Next we compare the primary energy use of the buildings and calculate the net primary energy savings achieved by the VHR, taking into account the changed electricity use due to VHR, as well as the changed heat demand due to VHR and changed air infiltration.

2.1. Building description

Our case-study building is a 4-storey multi-family wood-frame building with 16 apartments and a total heated floor area of 1190 m^2. Persson [9] describes the construction and thermal characteristics of the building in detail. A new building is then modeled with thermal properties of passive house but otherwise identical to the existing building. Table 1 shows the thermal characteristics of the existing, conventional building and the new, passive building. In addition to lower U-values, the passive building is assumed to have much better airtightness than the conventional building.

Table 1. Thermal properties of the building components

Building	*U-value (W/m^2K)*					*Air leakage*
	Ground floor	External walls	Windows	Doors	Roof	l /s m^2 at 50 Pa
Conventional	0.23	0.20	1.90	1.19	0.13	0.8
Passive	0.23	0.10	0.85	0.80	0.08	0.3

For both the conventional and passive buildings, we analyze the use of mechanical ventilation with and without VHR. The designed airflow rate for the building is 0.35 l/s m^2, based on Swedish regulations [10]. For the buildings without VHR, exhaust air is extracted from the kitchens, bathrooms and closets with fan and duct system, and fresh air is supplied through slot openings under windows in the bedrooms and living rooms. For the buildings with VHR, the ventilation system provides the same airflow rate as in the buildings without VHR. For the existing, conventional building the existing ventilation system is complemented with ventilation ducts for incoming air and a heat recovery unit [5].

2.2. Heat supply

We analyze cases where space heat is delivered by electric resistance heating, heat pump or district heating. For the electric resistance heating and heat pump we assume that the electricity is supplied from a stand-alone plant based on biomass steam turbine (BST) technology. We assume that the district heat is supplied from a combined heat and power (CHP) plant based on biomass steam turbines technology (CHP-BST). We consider scenarios where the CHP plant accounts for either *50%* or *90%* of the district heat production, with oil boilers accounting for the remainder. To show the impact of energy supply technology being developed, we also analyze a case where biomass integrated gasification combined cycle (BIGCC) technology is used instead of the BST technology for both CHP and stand-alone

power production. Furthermore, Gustavsson et al. [11] explored the structure of district heat production under different environmental taxation regimes. They found that the CHP production should be 80-83% of the total district-heat production when using BST technology and 76-78% when using BIGCC technology. The difference in share of district-heat production between the technologies varies because the BIGCC technology is more efficient and capital intensive than the BST technology. To explore the implications of this for VHR, we calculate the primary energy savings when district heating is based on s uch CHP production systems.

2.3. Final energy calculations

We simulate the annual final energy use of the conventional and the passive buildings, both with and without VHR, using the ENORM software [12]. This software calculates the space heating, ventilation, domestic hot water, and household and facility management electricity use of a building based on the building's physical characteristics, internal and solar heat gains, occupancy pattern, outdoor climate, indoor temperature, heating and ventilation systems, etc. We use climate data for the city of Växjö in southern Sweden, and assume an indoor temperature of 22°C. Table 2 shows principal values used to calculate the electricity use for ventilation. Other values including fan efficiency and operation mode of the ventilation systems are based on the default assumptions of the ENORM software.

Table 2. Major ventilation input values

Description	*Value*
Air change rate (l/s m^2)	0.35
Heat recovery efficiency (%)	85
Ventilated volume (m^3)	2861
Supply air flow rate (m^3/h)	1540

2.4. Primary energy calculations

We use the ENSYST software [13] to quantify the primary energy that is used to provide the final energy use in the different cases. The software calculates primary energy use considering the entire energy chain from natural resource extraction to final energy supply. We credit the electricity cogenerated by the CHP plant to the district heat system, assuming that it replaces electricity produced by a stand-alone plant with similar technology and fuel [14]. We assume the increased electricity use due to VHR is covered by stand-alone plant with similar technology and fuel as the heat supply system used.

3. Results

Table 3 compares the annual final energy use of the conventional and the passive buildings with and without VHR. The annual total final energy use of the passive building with VHR is about 21% lower than for the alternative without VHR. The corresponding value for the conventional building with VHR is 10%. VHR decreases the final energy for space heating, but increases the electricity used to operate the ventilation system. Overall, VHR reduces the final energy for space heating and ventilation by 55 a nd 22% for the passive and the conventional building, respectively, relative to the alternatives without VHR.

Table 3. Annual final operation energy use for the building scenarios

Building	*Final energy use (kWh/m^2-year)*				
	Space heating	Ventilation electricity	Tap water heating	Household and facility electricity	Total
Conventional building	70	4	40	52	166
Conventional building with VHR	50	8	40	52	150
Passive building	43	4	40	52	143
Passive building with VHR	13	8	40	52	113

Table 4 shows the annual operation primary energy use for the conventional and the passive buildings when using different end-use heating systems with energy supply based on BST technology. Ventilation accounts for 2-11% of the operation primary energy use. The primary energy for heating for the district heated buildings is low due to the high overall efficiency of district heating systems with CHP plants. The cogenerated electricity replaces electricity that otherwise would have been produced in a stand-alone plant with much lower efficiency.

Table 4. Annual operation primary energy use for the building with different end-use heating systems with energy supply based on BST technology

Description	*Primary energy use (kWh/m^2-year)*				
	Space heating	Ventilation electricity	Tap water heating	Household and facility electricity	Total
Resistance heating:					
Conventional building	209	12	119	155	496
Conventional building with VHR	149	24	119	155	448
Passive building	128	12	119	155	415
Passive building with VHR	39	24	119	155	337
Heat pump:					
Conventional building	78	12	45	155	290
Conventional building with VHR	55	24	45	155	280
Passive building	48	12	45	155	260
Passive building with VHR	14	24	45	155	239
District heating, 50% CHP:					
Conventional building	66	12	38	155	271
Conventional building with VHR	47	24	38	155	264
Passive building	41	12	38	155	246
Passive building with VHR	12	24	38	155	229
District heating, 90% CHP:					
Conventional building	42	12	24	155	233
Conventional building with VHR	30	24	24	155	233
Passive building	26	12	24	155	217
Passive building with VHR	8	24	24	155	211

Table 5 compares the percentage primary energy savings of VHR in relation to the primary energy use for space heating and ventilation, and to the total primary energy use for operation, including space heating, ventilation electricity, tap water heating and household and facility management electricity. The VHR primary energy savings ranges from 0-55% of space heating and ventilation primary energy use.

Table 5. Percentage primary energy savings of VHR, in relation to the primary energy used for space heating and ventilation for the different end-use heating systems with BST energy supply technology

Building	*Relative primary energy savings*			
	Resistance heating	Heat pump	District heating, 50% CHP	District heating, 90% CHP
Conventional	22%	12%	9%	0
Passive	55%	37%	32%	16%

The change in annual primary energy use for space heating and ventilation electricity when using VHR with different end-use heating system with BST or BIGCC energy supply are shown in Figure 1. The net savings are shown in Figure 2 for both BST and BIGCC technologies. The primary energy savings of VHR is significantly greater when using resistance heating, followed by heat pump and district heating with *50% CHP*. However, much smaller or no primary energy savings is achieved when using district heating with *90% CHP*. The savings of VHR are larger for the passive building than for the conventional building. The BIGCC technology gives similar results as the BST technology, but the net primary energy savings are lower compared to the case of BST.

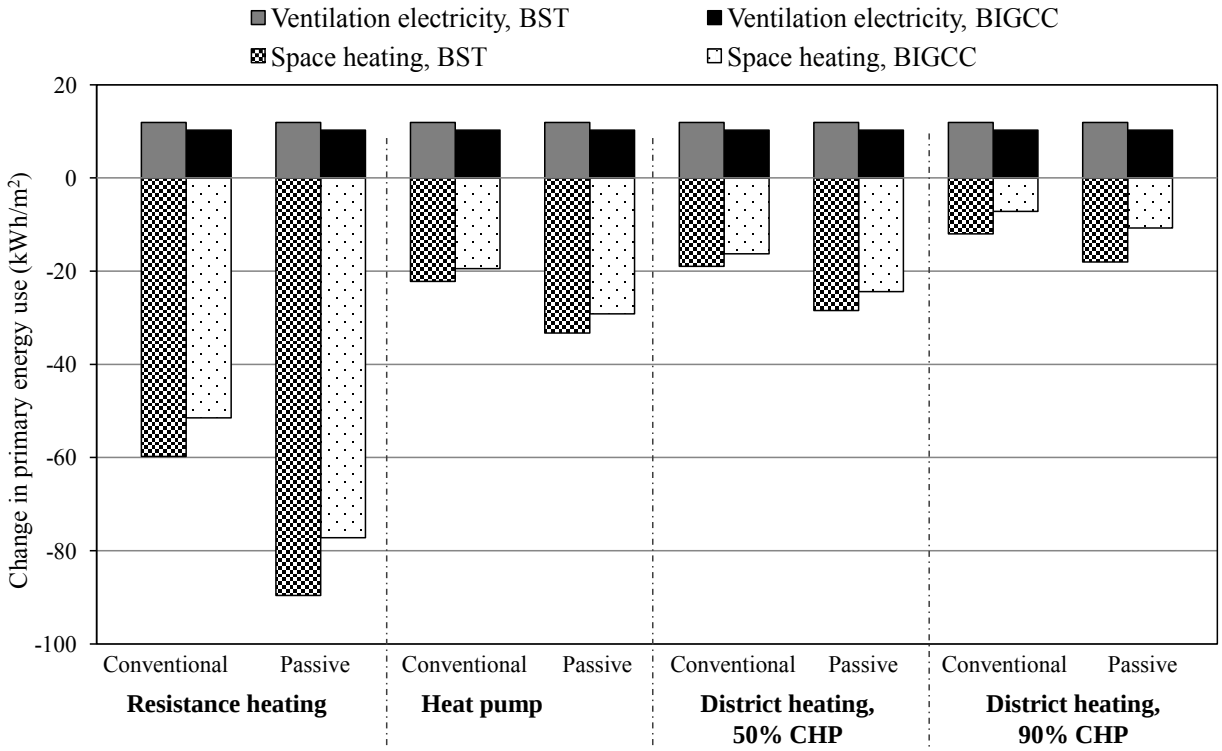

Figure 1. Change in annual primary energy use for space heating and ventilation electricity when using VHR with BST or BIG/CC energy supply

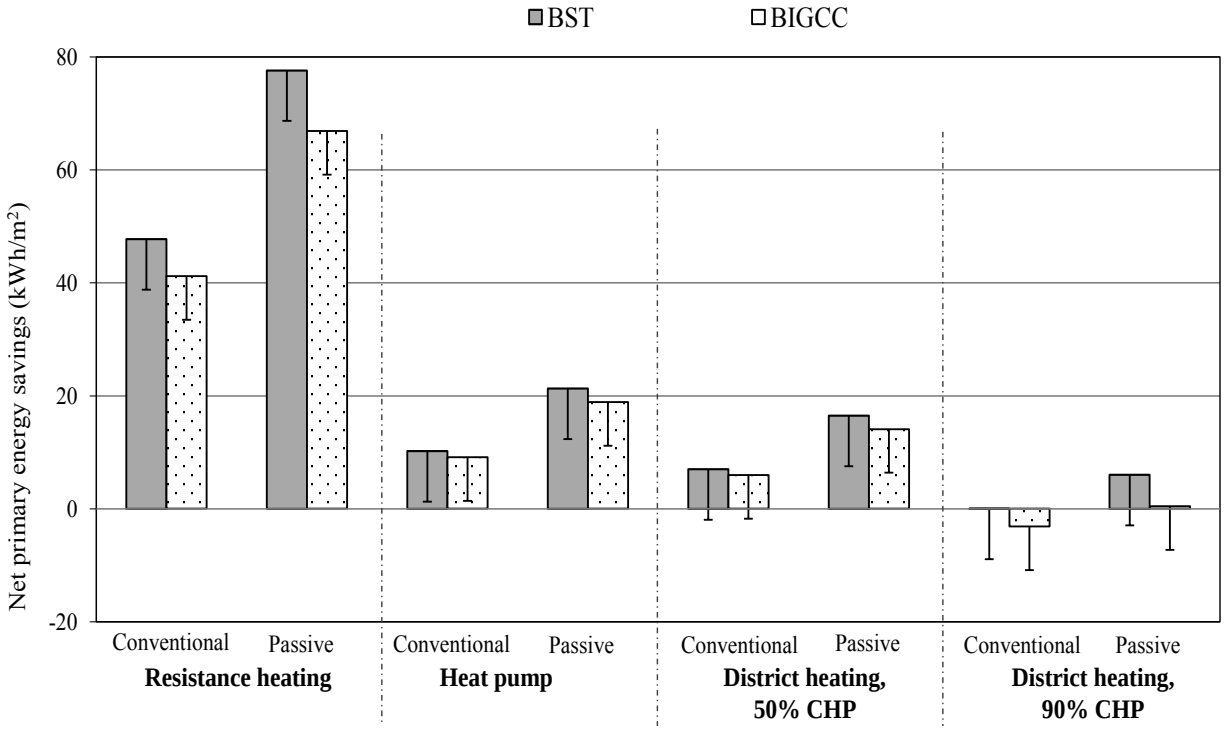

Figure 2. Net annual primary energy savings for VHR when using BST or BIGCC energy supply. The error bars show the savings when electricity use by the VHR is 7 kWh/m^2

In cold climatic regions VHR systems usually encounter frost during severe winters, and additional energy may be needed for defrosting. VHR systems may be fitted with additional preheating device to overcome this problem, increasing the electricity use for VHR [15]. Our base calculations are based on electricity use of 4 kWh/m^2 for the VHR and do not include electricity to defrost the system. Tommerup and Svendsen [3] reported that electricity use in VHR system of 80-90% efficiency is typically 7 kWh/m^2 under Danish conditions, and suggested this might be reduced to 3 kWh/m^2 with more efficient systems. In Figure 2 the error bars show the change in net primary energy savings for VHR, when the electricity use for VHR is 7 kWh/m^2 instead of 4 kWh/m^2. The higher electricity use for operating VHR reduces the net primary energy savings, in particular for the district heated buildings. In fact, a ventilation electricity use of 7 kWh/m^2 increases the net primary energy use for the buildings with district heating based on *90% CHP*. Hence low electricity use for VHR is important. For the conventional building with lower airtightness together with district heating based on a large share of CHP production, VHR may be counterproductive and increase primary energy use.

In our base case calculations, the CHP production accounts for 50 and 90% of the total district heat production [16]. In this section, we show the net primary energy savings for VHR when more optimally designed CHP production systems are used. Figure 3 shows the net primary energy savings for VHR when district heating is based on the lower and upper optimal CHP productions according to Gustavsson et al. [11]. VHR increases net primary energy use for all buildings when the electricity use for VHR is 7 kWh/m^2. The net savings is positive, but very low, for the conventional buildings with VHR systems using 4 kWh/m^2.

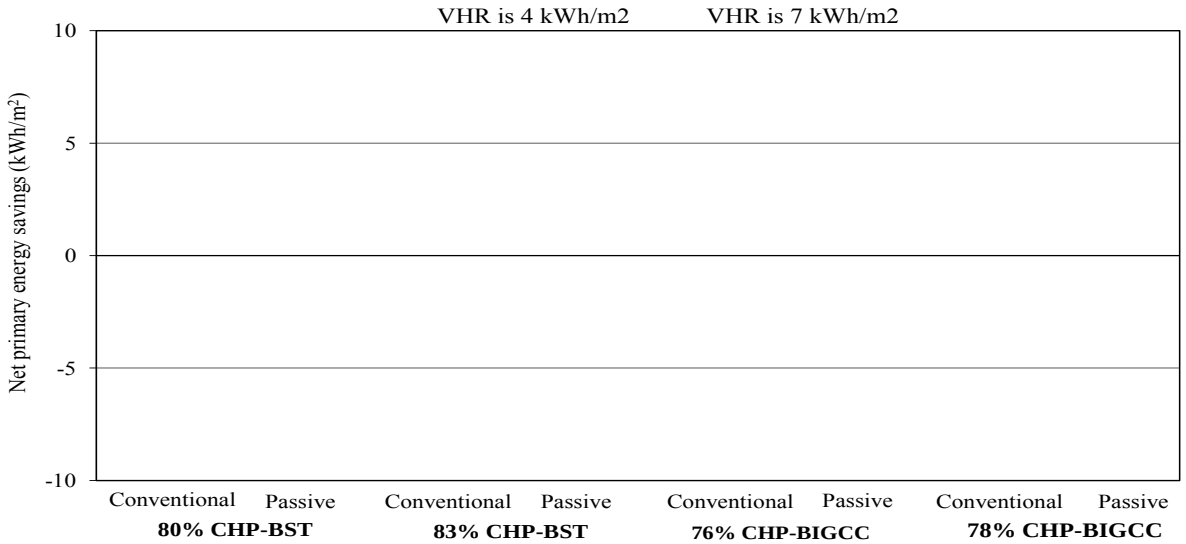

Figure 3. Net annual primary energy savings for VHR when more optimally designed CHP production systems are used

4. Discussion and conclusions

Our results show that primary energy savings of VHR can be very significant, depending on the type of heat supply system, the airtightness and thermal properties of buildings, and the amount of increased electricity used to operate the VHR system. The biggest savings is achieved when VHR is installed in a resistance heated building. However, small primary energy savings is achieved when the VHR is installed in CHP-based district heated buildings. VHR gives much smaller primary energy savings for the district heating with 90% CHP than with 50% CHP, supporting the findings of Dodoo et al. [16] and Gustavsson et al. [11]. For district heating systems mainly based on CHP, the reduced heat demand reduces the potential to cogenerate electricity, and is more significant if BIGCC technology is used instead BST technology.

The primary energy savings of VHR are greater for the passive building than for the conventional building, confirming that VHR systems perform better with improved airtightness [3, 6]. Hence, the air-tightness of buildings should be in the range as for newly constructed passive houses to minimize primary energy use when using VHR systems. We found that the greatest primary energy savings is achieved when VHR is incorporated in resistance heated passive building. The primary energy savings of VHR depend on the electricity use to operate the VHR system. Therefore the amount of electricity required to operate VHR system should be minimized.

Our results show that VHR may give low or negative primary energy savings in passive house buildings when combined with energy-efficient heat supply systems. For example, the case-study passive building with VHR in some cases uses greater primary energy than the same building without VHR. It is important to build houses with airtightness comparable to that of passive houses but such houses need to be ventilated using strategies that minimize primary energy use.

When deciding on installing VHR, attention should therefore be given to the interaction between the electricity use for VHR, the airtightness of the building and the type of heat supply system. This is particularly important when using district heating with a large share of

CHP production, as suggested by Dodoo et al. [16]. A primary energy analysis is necessary to evaluate the energy benefits of VHR in residential buildings.

References

[1] H.B. Awbi, Chapter 7-Ventilation, Renewable and Sustainable Energy Reviews, 2(1-2), 1998, pp. 157-188.

[2] M. Orme, Estimates of the energy impact of ventilation and associated financial expenditures, Energy and Buildings, 33 (3), 2001, pp. 199-205.

[3] H. Tommerup, and S. Svendsen, Energy savings in Danish residential building stock, Energy and Buildings, 38 (6), 2006, pp. 618-626.

[4] Swedish Government Bill 2005/06:145. A national programme for energy efficiency and energy smart construction. Web accessed at http://www.regeringen.se on April 20, 2009.

[5] Å. Wahlström, Å. Blomsterberg, and D. Olsson, Värmeåtervinningssystem för befintliga flerbostadshus, Förstudie inför teknikupphandling, 2009.

[6] D. Hekmat, H. E. Feustel, and M. P. Modera. Impacts of ventilation strategies on energy consumption and indoor air quality in single-family residences, Energy and Buildings, 9 (3), 1986, pp. 239-251.

[7] R. Lowe, and D. Johnston, Mechanical ventilation with heat recovery in Local Authority, low-rise housing: Final report on the Derwentside Field Trial. Leeds: Leeds Metropolitan University, 1997.

[8] TIP-Vent, Towards improved performances of mechanical ventilation systems, 2001. http://www.inive.org/Documents/Tip-Vent_Source_Book.pdf on March 1, 2010.

[9] S. Persson, Wälludden trähus i fem våningar: Erfarenheter och lärdomar, Report TVBK-3032, Department of Structural Engineering, Lund Institute of Technology, Sweden, 1998.

[10] Boverkets, Byggregler: Boverkets Författningssamling. Karlskrona: The National Board of Housing, Building and planning, 2009.

[11] L. Gustavsson, A. Dodoo, N.L. Truong, and I. Danielski, Primary energy implications of end-use energy efficiency measures in district heated buildings, Energy and Buildings, 43 (1), 2011, pp. 38-48.

[12] EQUA (Simulation AB), ENORM, Version 1000, Stockholm, Sweden, 2004.

[13] Å. Karlsson, ENSYST, Version 1.2, Lund University, Sweden, 2003.

[14] L. Gustavsson, and Å. Karlsson, CO2 mitigation: on methods and parameters for comparison of fossil-fuel and biofuel systems, Mitigation and Adaptation Strategies for Global Change, 11(5-6), 2006, pp. 935-959.

[15] J. Kragh, J. Rose, T.R. Nielsen, and S .Svendsen, New counter flow heat exchanger designed for ventilation systems in cold climates, Energy and Buildings, 39 (11), 2007, pp. 1151-1158.

[16] A. Dodoo, L. Gustavsson, and R. Sathre, Life cycle primary energy implication of retrofitting a Swedish apartment building to passive house standard, Resources, Conservation and Recycling, 54 (12), 2010, pp. 1152-1160.

Energy and comfort benefits of a cool roof application in a non-residential building belonging to Roma Tre University

E. Carnielo[1,*], A. Fanchiotti[1], M. Zinzi[2]

[1] *Roma Tre University, Rome, Italy*
[2] *ENEA Research Center, Rome, Italy*
** Corresponding author. Tel: +39 3493678683, Fax: +39 065593732, E-mail: emiliano.carnielo@gmail.com*

Abstract: The Mediterranean architecture was characterized by passive solutions able to ensure thermal comfort conditions in the built environment during the hot season. This cultural heritage is almost disappeared, delegating the comfort conditions to artificial systems. One of the above mentioned passive solutions concerns the use of light colors to redirect most of the incident solar radiation. Cool roofs are a mix of these old concepts and modern technologies. The paper reports the results of a cool roof application in a senior recreation center, belonging to Roma Tre University. The cool roof was applied on a part of the whole surface of the roof in order to assess the difference in thermal conditions obtained with this solution compared to the original case. The experiment was carried out in two phases. During the first phase the building was monitored with sensors of temperature, humidity and solar radiation. The second phase concerned the creation of a building model inputted in a dynamic simulation tool used to evaluate the building performances due to this cooling technique. This study demonstrate the positive impact of the technology in terms of cooling and total energy savings as well as on the indoor thermal conditions in Mediterranean buildings.

Keywords: *Cool roof, Passive cooling, Reflectance, Emissivity*

1. Introduction

Global warming is a planetary problem monitored depending on latitude and economic development but with completely different intensity and consequences in relation to these two influences. The Mediterranean area is particularly vulnerable, with a predicted temperatures increase of 2 °C by 2030, and with alarming expectations by 2100 (IPCC, 2007). This is the scenario in which lies the need for new energy-saving techniques for conserving nature and preserving public health in every area of development. This problem is present even in the civil sector and in particular it is mainly due to two factors: The emergence of the urban heat island phenomenon and the continuing growth in electricity consumption for summer air conditioning of buildings, not only for the tertiary but recently also for the residential sector. One of the techniques used to limit the dangers associated with the temperature rise is the passive cooling of buildings that includes the use of cool roof [1].

Cool materials are those materials that do not rise significantly their surface temperature under solar radiation. They are characterized by a high solar reflectance (high ability to reflect solar radiation incident on the material) and thermal emissivity (high ability to radiate heat in the infrared wavelengths). The high reflectivity is due to pigments characterized by a high reflectance in the infrared portion of the solar spectrum, maintaining the typical profile in the visible spectrum. This means that the material does not warm up significantly during daylight hours. High emissivity allows the material to stay cool during the night, radiating towards the sky the heat absorbed during the day. The employ of these materials is very useful for the construction of roofs, being the most used building materials characterized by high solar absorption (and therefore low reflectance). The application of cool roof technology can produce a surface temperature profile lower than a normal coating. This leads to a reduction of heat flow entering the building, contributing to an effective reduction in the average indoor air temperature or a reduction in consumption for cooling [2]. The large use of materials with these characteristics in an urban area also leads to indirect energy savings related to the high solar reflectance which reduces the temperature of the agglomerate of buildings. The decrease

of temperature induces a better energy balance in the areas involved and facilitates the mitigation of urban heat island effect [3]. Cool roofs are not necessarily realized with paints, in fact different technological solutions exist for the reflective cool coatings: Membranes, sheaths, asphalt, bitumen, paving bricks [4]. The most common construction materials for roofs have a reflectance between 20 and 30%, with a significant solar load for the rooms directly under the ceiling. Fig. 1 shows the trend of the reflectance as a function of wavelength for some cool materials and common materials.

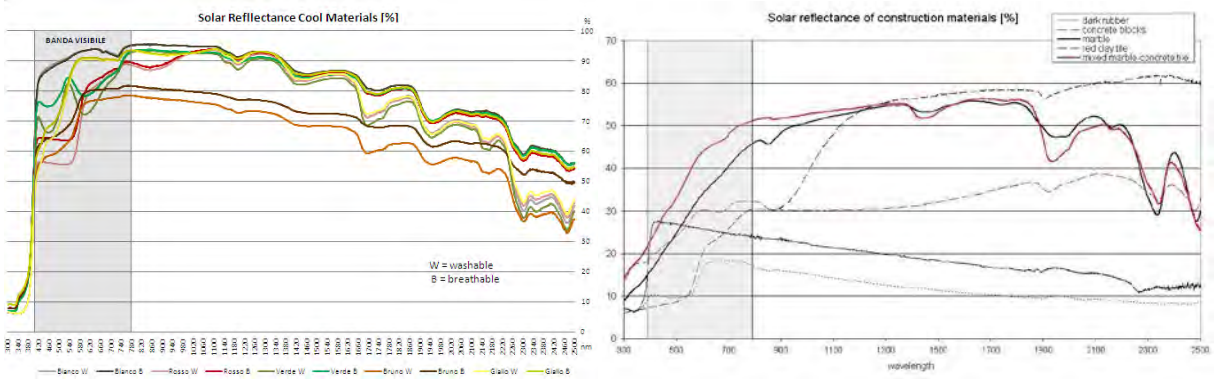

Fig. 1. Solar Reflectance [%] for Cool Materials and Typical Materials

The thermal emissivity of building materials is generally between 0.8 and 0.9. Only the metals have lower values of emissivity and this limits the radiant power towards the sky during night. For this reason, metal cool roofs shall be efficient only if they have extremely high values of solar reflectance (greater than 0.75-0.8). An unexplored aspect is related to the maintenance of the initial properties of the products. A rapid decrease in efficiency of material would render useless the economic investment.

2. Case Study: Social and cultural center "Vasca Navale"

The building examined in this work is situated in Rome close to San Paolo district. It is located on a plot belonging to Roma Tre University, and recently has been used as a senior recreation center.

The choice fell on this building because it has standard features for study to which it was submitted. Indeed it is an excellent test bench to verify the performances of a high reflectance roof. This is due to the extended horizontal surfaces that capture solar radiation. The plan of the structure extends mainly in length and has an area of 275 m^2. The layout of the rooms is very simple: There are five rooms arranged in a row and they are all characterized by a rectangular plan. The orientation of the longer sides is South-North. The entire structure has a low insulation level characterized by transmittance values significantly higher than those established by Italian reference standard for the climate zone of Rome [5]. The Table 1 shows the layers of vertical walls, ceiling, floor, internal walls, their thickness and transmittance.

Table 1. Wall Layers

	Ext.Wall	Ceiling	Floor	Int.Wall	WindowSingleGlazed
Thickness [m]	0.350	0.310	0.475	0.210	-
Transmitt. [W/m^2K]	1.23	0.96	0.91	1.6	2.8

The windows are single glazed (Table 1) equipped with a dark gray aluminum frame for which it was suggested an absorbance of solar radiation of 85%. The frame area occupies about 30% of the total area of a window.

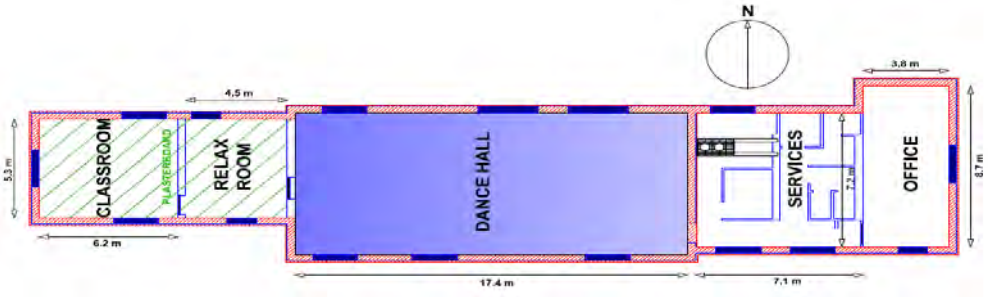

Fig. 2. Plan of Recreation Center

Inside, the ceiling has a height of 3.8 meters except in the classroom and in the relax room (Fig. 2) where there is a suspended ceiling made of plasterboard to 3.1 meters above the ground. In these two rooms the phenomena of heat exchange with the outdoor take on different characteristics compared to the other three rooms, due to the presence of an air gap in the ceiling of 70 centimeters. In blue (Fig. 2) it is shown a portion of the roof of 133 m^2 on which a cool roof was applied, corresponding to the "Dance Hall". The material used for the roof is a white mineral membrane based on milk and vinegar of Ecobios Laboratories. The original roof is a bituminous sheath. The superficial layer is made of slate. Samples of the two types of materials were analyzed with a double beam spectrophotometer from which the trend of the reflectance was obtained as a function of the wavelength of the incident beam between 300 and 2500 nanometers. The bituminous slated sheath does not have a uniform color. For this reason three tests were carried out in three different portions where the beam generated by the spectrophotometer affects the corresponding sample. An arithmetic average was carried out to obtain the trend of the reflectance. With the data obtained by the spectrophotometer, it was performed a weighted average of the reflectance values in the range considered (300 nm - 2500 nm) according to ISO 9050 2003 following the energy distribution of the solar spectrum [6]. The integrated reflectance for the slate is 13.7%. It is very low if compared to the one of the mineral membrane Ecobios which reaches a value of 86.4%. The Fig. 3 shows the comparison between the measured reflectance: In blue it is shown the cool material, the other three trends are the tests relating to slate, they have slight differences depending on the point of incidence of the light beam outgoing from the instrument on this surface. Regardless the expected behavior in the wavelength of visible (the membrane is white mineral, slate is dark gray), the cool material presents very interesting values of reflectance in the wavelength of near infrared. Indeed it has a value of more than 95% in a range that goes from 770 to 1100 nanometers. The reflectance of the slated sheath remains consistently below 20% throughout the measuring range. Both materials have a thermal emissivity of 0.88.

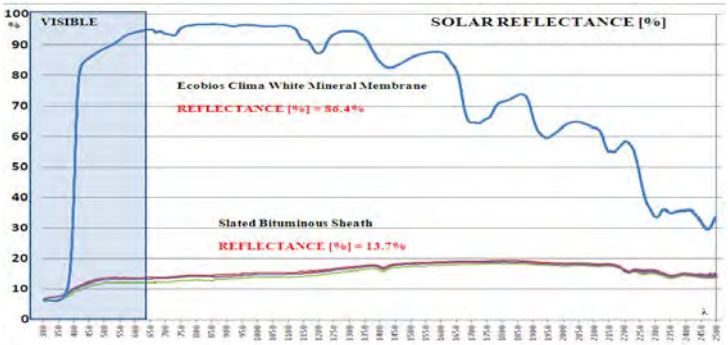

Fig. 3. Solar reflectance [%] of Ecobios Clima cool membrane and a slated sheath

3. Placement of Sensors

A pyranometer to measure the intensity of solar radiation and a sensor for measuring outdoor temperature and humidity were placed on the roof. In this way it was possible to collect data on the weather during the measurement campaign [7]. This data were also inserted into the TRNSYS processor radiation software to obtain more realistic simulation results. To compare the surface temperatures between the two different roofs, two heat-resistance were placed on the cool roof and two on the slated sheath. In order to monitor the temperature on each side of the roof two other heat-resistance were placed in the inner surfaces of it. Sensors for indoor air temperature and humidity were placed in the "Dance Hall" where the cool roof is applied, in "Services" and in "Office". In this way it was possible to verify the efficiency of a cool roof on the indoor temperature of a room in comparison to the other indoor temperatures. On 12th August, after a routine check on the conditions of the cool roof, a layer of dust and soil was found on its surface probably caused by the presence of a dockyard adjacent to the building in question. This incident has caused the depletion of the surface properties of the cool material, decreasing its efficiency. The TRNSYS simulation software was used to determine the new value of reflectance detected in the points most affected by the problem just mentioned. Indeed, after creating a model of roof to simulate the surface temperature, the reflectance of it was changed to obtain a temperature profile very similar to the one measured by the sensors. By performing the above procedure, the new solar reflectance value found is 68%.

4. Comparative analysis of measured data

4.1. Temperature profiles

Through the data stored by the surface temperature sensors, it was possible to produce the temperature profiles of the outer and inner surfaces of the roof slab. The profiles of the "Dance Hall" above which was applied the membrane with high reflectance (blue) were compared to the profiles of the area called "Office" characterized by the slated sheath (red). The comparisons, shown in Fig. 4, refers to two days of August. The temperature of the surface of the reflective membrane is significantly lower than the one of the slated sheath. The maximum of the difference between the two outer surfaces is in the middle of the day at the peak of solar radiation when cool roof has the highest efficiency.

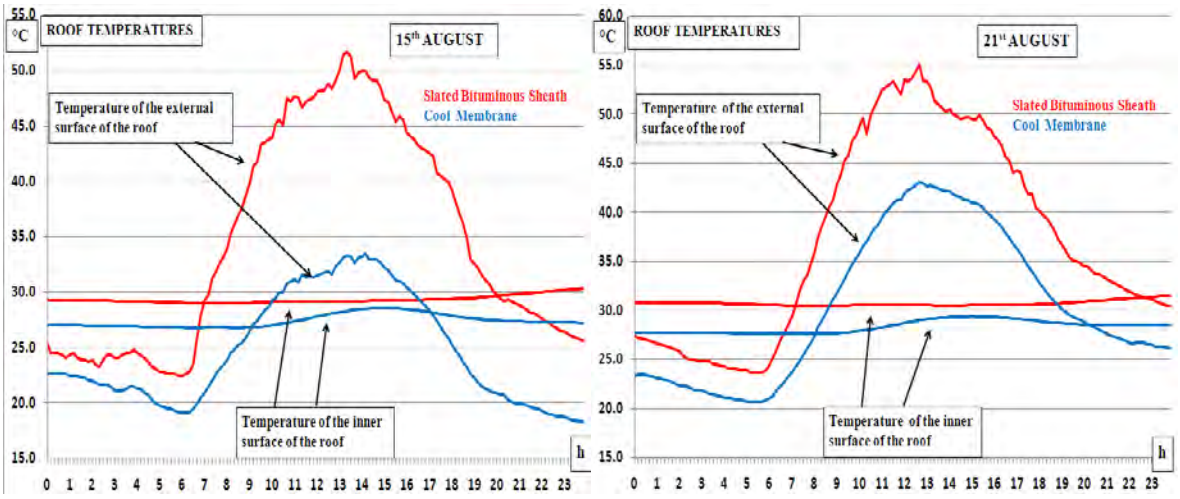

Fig. 4. Surface temperature profiles of the roof (Cool Membrane and slated roof)

The difference in temperature is above 20 °C. A lower surface temperature will decrease the heat flow through the roof changing the indoor temperature.

4.2. Comparison of internal temperatures

It was not possible to monitor simultaneously the difference in indoor air temperature due to the cool membrane and the original slate mantle in the same thermal zone. For this reason two periods of two days were chosen, corresponding to the beginning of two heat waves in July and August whit almost identical trends of solar radiation and outside temperature. In the first of these two periods the cool roof had not yet been applied to the area of interest. In this way it was possible to compare the values of indoor air temperature in a room equipped with and without a cool roof.

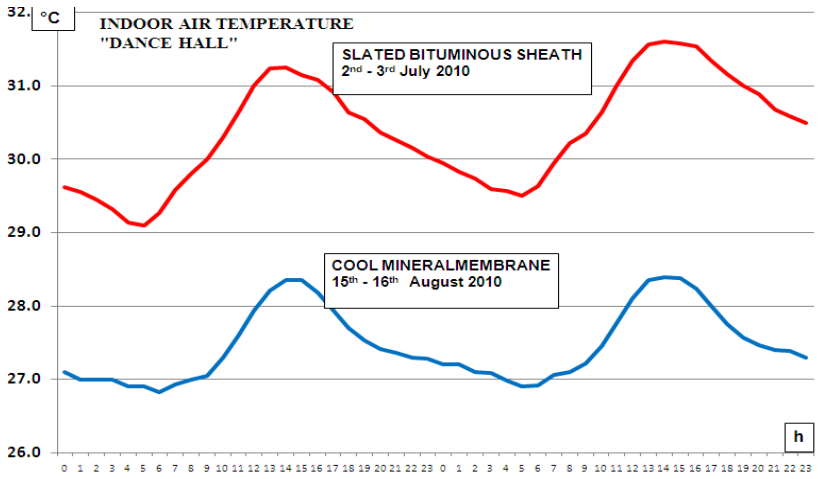

Fig. 5. Indoor air temperature of the "Dance hall"

In the Fig. 5 above, the trend in blue, typical of a cool roof, denotes the positive effect of this technology of passive cooling by limiting the maximum temperature below 28.5 °C. With the slated sheath the values are higher than 31 °C. It is important to remember that the performance measured are relative to a cool roof not at its maximum efficiency, but with limited performance due to dust and soil deposited on it.

5. Simulations Results

The model included in the simulation software TRNSYS was calibrated to the measured indoor temperature profile and to the external surface temperature of the roof. To achieve optimal calibration, the parameters of air infiltration and the values of internal and external shading of non-opaque surfaces were modified obtaining a maximum deviation between the real temperatures and those obtained with the simulator under three tenths of a degree. The first session of simulations is aimed at obtaining a comparison of results for the internal operative temperature with no cooling systems. The second part concerns the evaluation of air conditioning loads. Both sessions were conducted considering three reflectance values of the roof slab.

Three models were created, each one with a different value of insulation:

1. Real values of insulation of the building;
2. Real values of insulation of the building except the transmittance of the roof according to Italian standard reference;
3. Insulation according to Italian standard reference Zone D (vertical wall = 0.36 W/m^{2}K, ceiling = 0.32 W/m^{2}K, floor = 0.36 W/m^{2}K, window = 1.9 W/m^{2}K, window with frame including 2.4 W/m^{2}K) for the entire building.

5.1. Operative Temperatures

The operative temperature of a zone is the temperature which takes into account both the internal air temperature and the average temperature of the inner surfaces of the structure. From the simulations results was extracted the total number of hours in which the operative temperature of the "Dance Hall" exceeds some chosen values in the period from 17th June to 1st September. The values of solar reflectance used are: 16% to simulate the original coating, 86% for the mineral membrane and 68% to simulate mineral membrane with performances compromised by dust and soil. The following are histograms for the three chosen levels of insulation.

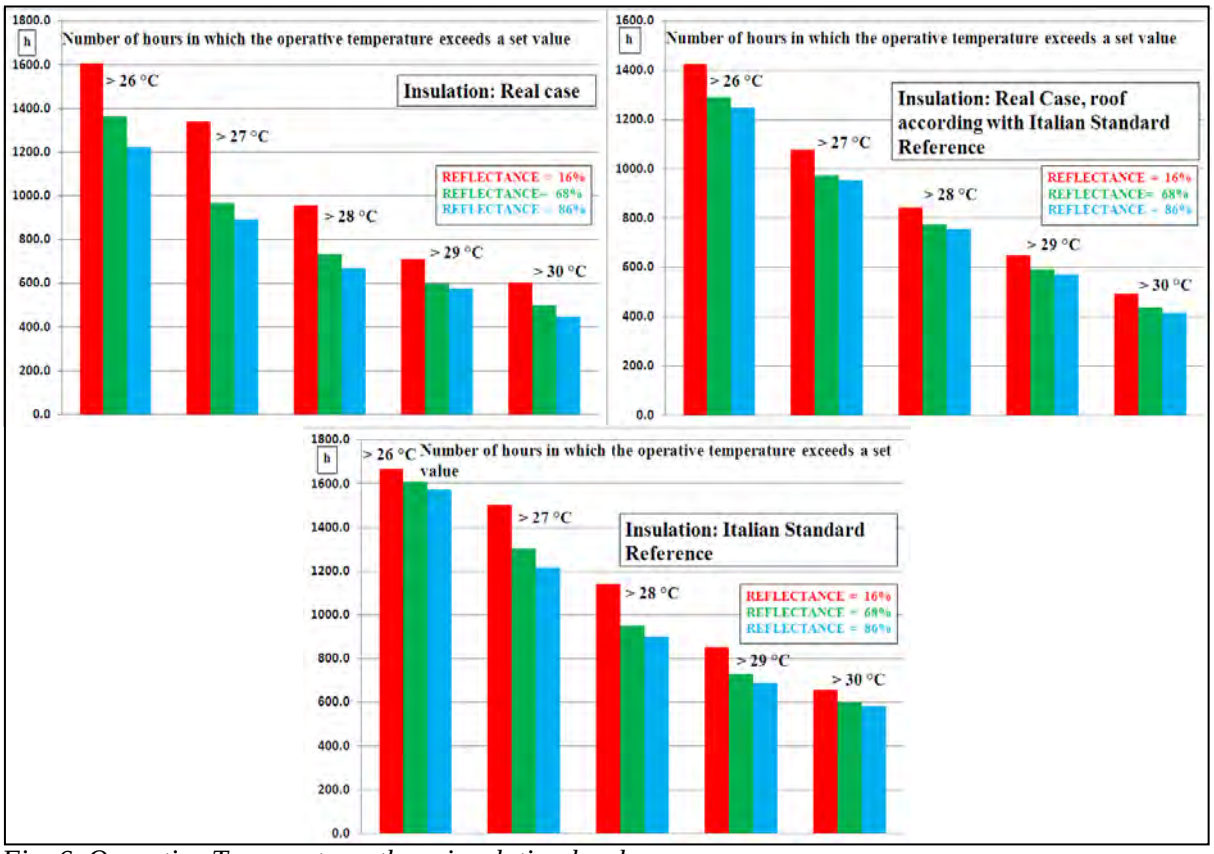

Fig. 6. Operative Temperature, three insulation levels

The use of a high reflectance material is a contributory factor to increase the number of hours in which there are thermal comfort conditions. On the other hand, increasing insulation level, the number of hours in which the temperature is greater than a specific value tends to increase. Indeed, being equal the reflectance, the configuration with insulation according to Italian standard reference has internal temperatures higher than the ones registered in the building with the real level of insulation. This phenomenon occurs in the climatic zone of middle Mediterranean in buildings characterized by high solar gains through non-opaque surfaces. The significant solar gains through windows increase the indoor air temperature. The value of the latter become very similar to the outdoor temperature during daylight. The low transmittance value determines a small outgoing heat flow which lasts even during the night. The heat is trapped inside, creating a sort of greenhouse effect. In warmer climates the gap between indoor and outdoor temperatures is generally high and the phenomenon described above is less evident.

5.2. Air conditioning loads

The simulations performed on the model equipped with an air conditioning system of unlimited power, conducted during summer (17th June - 1st September), are designed to assess the extent of energy savings depending on the reflectance of the roof. The reflectance of the roof of the "Dance Hall" assumes the three values previously used. From the results were extrapolated the net loads for the summer period necessary to maintain the temperature of the zone below the set-point of 26 °C for the three levels of insulation.

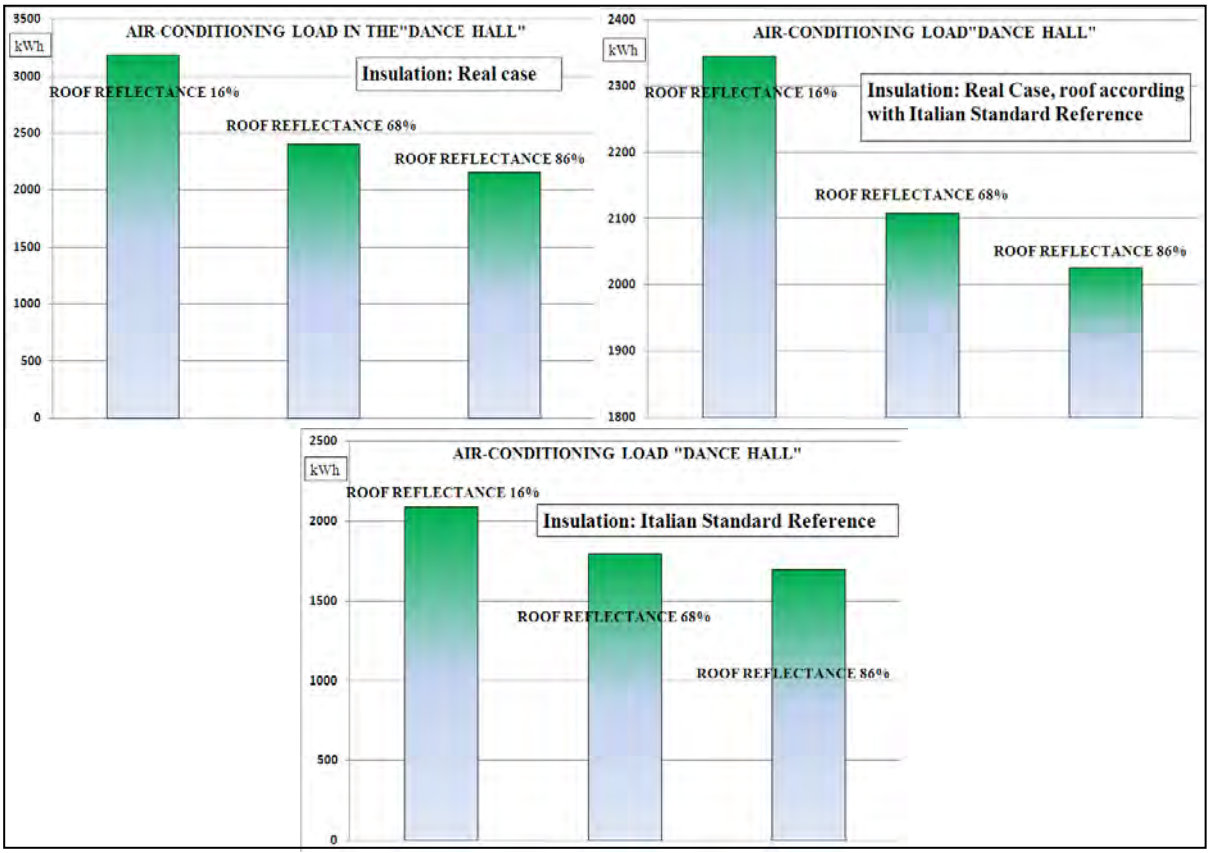

Fig. 7. Air conditioning loads, three insulation levels

Fig. 7 shows a decrease of load proportional to the increasing of reflectance. Again, as in the previous group of simulations, the more insulated building results less sensitive to changes in reflectance. Comparing building with real insulation and roof reflectance of 16% and building with roof insulation level established by Italian standard reference and roof reflectance 86%, the value of energy used to cool the "Dance Hall", decreases from 3200 kWh to 2050 kWh, with a saving of about 9 kWh per square meter. Considering the insulation level in accordance with Italian standard reference for the whole structure of the building, the consumption decreases from 3200 kWh to about 1700 kWh with an energy saving for air conditioning in the area of about 12 kWh per square meter. Considering the entire warm season, including the months of May and September, the savings would be greater, even more if a cool roof were applied over the entire roof surface.

6. Conclusions

The application of a cool roof reduces roof surface temperatures, limiting the incoming heat flow from it and, in any case, decreasing the temperature of the indoor environment. The case study examined in this report has demonstrated, through appropriate measurements of temperature, the potential of a cool roof. The Ecobios Clima reflective membrane has proved

to be an excellent material for this use. The ease of application on any surface is another quality of this product. The area of the building that received the benefits from the application of this membrane is affected by a large number of thermal factors that have tested the capabilities of the cool roof. The large glass surfaces exposed to the South are subjected to heavy solar gains and even if they were shielded from direct sunlight they influenced the indoor temperatures. Adding to this, the poor insulating level and low volume of air circulation make the Dance Hall the more thermally critical zone of the building. The cool roof decreased the indoor air temperatures by 2.5 °C in average. This is a very interesting result considering the fact that it did not work at its maximum value of reflectance because of external agents described above. It was possible to quantify the extent of energy saving on internal loads, noting in this case as it increases in direct proportion to the level of reflectance. Benefits relating to this passive technique of cooling are obtained even only increasing both levels of reflectance and insulation of a roof. From the observations made in this report, it is possible to note that the employ of a cool roof on existing buildings and on new buildings under construction with expected high insulation levels offers significant advantages in both cases.

References

[1] M. Zinzi for Earthscan/Aber, Advances in building energy research, vol.4, Cool materials and cool roofs: Potentialities in Mediterranean buildings, Earthscan, 2010, pp. 1 – 6.

[2] M. Zinzi for Earthscan/Aber, Advances in building energy research, vol.4, Cool materials and cool roofs: Potentialities in Mediterranean buildings, Earthscan, 2010, pp. 6 – 11.

[3] A. Christen, R. Vogt, Energy and radiation balance of a central European city, International Journal of Climatology 24, (2004), pp. 1395 – 1421.

[4] Cool Roofs - EU, Database of cool materials, www.coolroofs-eu.eu.

[5] DLgs 192 August 19th, Implementation of directive 2002/91/CE on energy efficiency in buildings (Italian standard reference), 2005, pp 16 – 17.

[6] ISO 9050, UV, visible and energetic characteristics of materials, 2003.

[7] A. Fanchiotti, E. Carnielo, (Data collection), Impatto di tecnologie Cool Roof sulle prestazioni energetiche degli edifici. Caso Studio (Cool Roof technology impact on energetic performances of buildings. Case Study), ENEA, 2010, pp. 27 – 58.

Solar reflectance performance of roof coverings in Istanbul, Turkey

Sinem Kultur[1,*], Nil Turkeri[2]

[1] *Bahcesehir University, Istanbul, Turkey*
[2] *Istanbul Technical University, Istanbul, Turkey*
** Corresponding author. Tel: +90 2123810515, Fax: +90 2123810500, E-mail: sinemkultur@gmail.com*

Abstract: Cooling energy load can be reduced by reflective roofs. The reflective roofs are recognized by Turkish architects, contractors and manufacturers, however, the solar reflectance performance of new and aged roof coverings produced in Turkey is still unknown. Purpose of this paper is to assess short-term and long-term solar reflectance performance of these roof coverings. In this context, solar reflectance measurements were conducted both in laboratory and in field. Firstly, solar reflectance performance of 13 unexposed test samples including clay, cement, bituminous and metal based was measured in laboratory. Then, 6 of these test samples were exposed to simulated solar radiation for a duration that is equivalent to 1-year exposure. The laboratory measurements indicated that white and shiny ceramic tile is the most reflective covering while black corrugated sheet is the most absorptive one. Secondly, two test specimens (red clay tile and bituminous shingle covered surfaces) with an automated weather observation system were set up in a field in order to measure the solar reflectance performance of the roof surfaces. The initial results demonstrated that the clay tile-covered roof surface had higher reflectance values. This paper will enable designers to choose the roof covering appropriate for reflective roofs that can be used to rehabilitate existing roof coverings or to design new roofs.

Keywords: *Solar reflectance performance, Roof covering, Reflective roof.*

1. Introduction

Future climate projections demonstrate that the western part of Turkey will experience temperature increases up to 6^0C notably in summer in addition to urban heat island effect, whereas the temperature increase for the entire country is estimated to be around 2-3^0C (The Ministry of Environment and Foresty, 2007). Increase in temperature will result in increase in summer cooling load, electricity consumption and amount of carbon dioxide in atmosphere. Survey of literature indicates that cooling energy load can be reduced by reflective roofs which comprise high-albedo roof coverings that have high solar reflectance and high infrared emittance and maintain these properties for the service life of the covering (Liu, 2005).

There are many researches that assess short-term and long-term solar reflectance performance of materials both in laboratory and in field. In one of these researches, a series of field measurements was conducted on 9 residential buildings in Florida, USA (Parker et.al., 1995) in order to determine the impact of reflective roof coatings on buildings' air-conditioning energy use. Results of the research indicated that application of white coloured reflective coatings can reduce cooling energy consumption in between 2% and 43%. In the same study, reflective coatings under actual conditions experience a reduction in their solar reflectance rates from 71% to 47% in value at the end of 1-year.

Another research (Prado and Ferreira, 2005) conducted in laboratory presents the long-term solar reflectance performance results of roofing materials commonly used in Brazil. In this study, long-term solar reflectance rates were calculated from a mathematical equation defined by California Energy Commission. The roofing materials' surface temperatures were calculated according to their emittance and reflectance rates. The results demonstrated that same coloured metallic and ceramic materials reached different surface temperatures according to their emittances.

Benefits of reflective roofs are recognized by Turkish architects, contractors, and manufacturers, however, the solar reflectance performance of new and aged roof coverings produced in Turkey is still unknown. Therefore, short-term and long-term solar reflectance performance of roof coverings that are produced and commonly used in Turkey were measured in laboratory and in field. Purpose of this paper is to describe methodology and to present results of the measurements.

2. Methodology

Solar reflectance measurements of the roof coverings were conducted both in laboratory and in field.

2.1. Laboratory measurement

2.1.1. Test specimens

Types of roof coverings were determined according to the research conducted by Çatıder (Association of roofing industrialists and businessmen in Turkey) which presented the market share distribution of roof coverings in Turkey for the year of 2007 (Ozturk, 2008). Clay, cement, metal and bitumen based 13 roof coverings were determined. 2 of them are commonly used in flat roofs while the remaining are the coverings having highest market shares defined at the list of the research. The selected roof coverings with their materials and colour/surface characteristics are given in Table 1.

Table 1. Test specimens.

Roof Coverings/Test specimens		**Colour / Surface Characteristics**	**Roof Slope**
Clay based	Tile	Red	Steep
	Ceramic tile	White	Low slope
	Ceramic tile	White-shiny	Low slope
Cement based	Concrete Tile	Red	Steep
Metal based	Tile	Red/natural granule covered	Steep
	Galvanised sheet	White	Low slope
	Aluminium sheet	Silver	Low slope
	Copper sheet	Bronze	Low slope
	Titanium-zinc sheet	Black	Low slope
	Titanium-zinc sheet	Silver	Low slope
Bitumen based	Membrane	Red/natural granule covered	Low slope
	Shingle	Red	Steep
	Sheet	Black/corrugated	Low slope

Red colour was held constant for a later comparison between some test specimens depending on the material composition and surface roughness since most of the roof coverings can be produced in red colour. Dimensions of the specimens range from 4x4-cm to 10x10-cm as

described in ASTM E 903-96 "Standard Test Method for Solar Absorptance, Reflectance and Transmittance of Materials Using Integrated Spheres".

2.1.2. Test instruments

Spectrophotometer; a radiation measuring device in a sensitivity range between 200 nm and 2500 nm was used for the solar reflectance measurements. It has a 150-mm diameter-integrating sphere attached at its center where the test specimens were placed. At the beginning of the measurements, the spectrophotometer was calibrated with a mirror (as a reference sample) for calculating the reflectances of other materials (ASTM E 903-96, 1996).
Accelerated weathering tester; a device was used for exposure of the specimens to xenon arch light (simulated solar radiation). It can run out at the spectral range of 300 to 800 nm. The environmental stresses on roofing; exposure to wind, moisture, atmospheric gases, pollutants and biological growth were not within the scope of this simulation.

2.1.3. Test protocol

The test method described in ASTM E 903-96 "Standard Test Method for Solar Absorptance, Reflectance and Transmittance of Materials Using Integrated Spheres" was followed for measuring reflection rates of new and aged roof coverings in laboratory.

Initially, the spectrophotometer was calibrated at 1 nm intervals and then a 12-minute measurement was performed for each test specimen. UV-WIN software was used to obtain test results and graphics. The test results and the graphic demonstrations were converted to Excel format, then, calculated and assessed as average reflectance rates at each spectral range (ultraviolet, visible and infrared). After that, 6 of these test samples excluding metallic ones were determined to be exposed to xenon arc light in accordance with the standard ASTM G155-05a "Standard Practice for Operating Xenon Arc Light Apparatus for Exposure of Non-Metallic Materials". The selected specimens were put into the accelerated weathering tester for 50 day-period which corresponds to 1-year exposure. One sample of each material was left as unexposed for making comparison between new and aged situations. Finally, a series of measurement was conducted using the spectrophotometer for aged test specimens.

2.2. Field measurement

Field measurements were performed at the campus of Istanbul Technical University in Ayazağa, Istanbul. For conducting the measurements, approximately 100-m² area was organized.

2.2.1. Test specimens

2 types of test specimens were specified as clay based tile and bitumen based shingle. Both of the roof coverings were in red colour and were applied in order to set up 4.00x4.00-m dimensioned two roof surfaces. The roof surfaces were sloped to provide drainage of rain water.

2.2.2. Test instruments

Automated weather observation system (AWOS) were set up for field measurements. It comprises a pyranometer, a data logger, a solar panel, a temperature sensor, wind direction sensor, a moisture sensor, a rain sensor and a sensor measuring earth's temperature. In addition to AWOS, a pyranometer and a portable data logger were placed in order to measure reflected solar radiation. Thus, incoming solar radiation data was obtained from the data

logger of the AWOS while reflected solar radiation data was obtained from the portable data logger.

Pyranometer; a radiation measuring device in a sensitivity range between 305 nm and 2800 nm was used for the solar reflectance measurements. 2 pyranometers were located back to back to build up an albedometer.

Data logger: Pyranometer's analog data was converted to and collected as digital data by the data logger.

2.2.3. Test setup and protocol

Test specimens were located facing the south direction. The automated weather observation system was erected on wheels to be driven over the two test specimens. Test setup is shown in Fig. 1. The measurements were conducted under the actual environmental conditions according to test method given in ASTM 1918-06 Standard Test Method for Measuring Solar Reflectance of Horizontal and Low Sloped Surfaces in the Field. The data obtained from the measurements in ASCII format was transferred to a PC computer and converted to Excel format. Then the averages of initial solar reflectances were calculated.

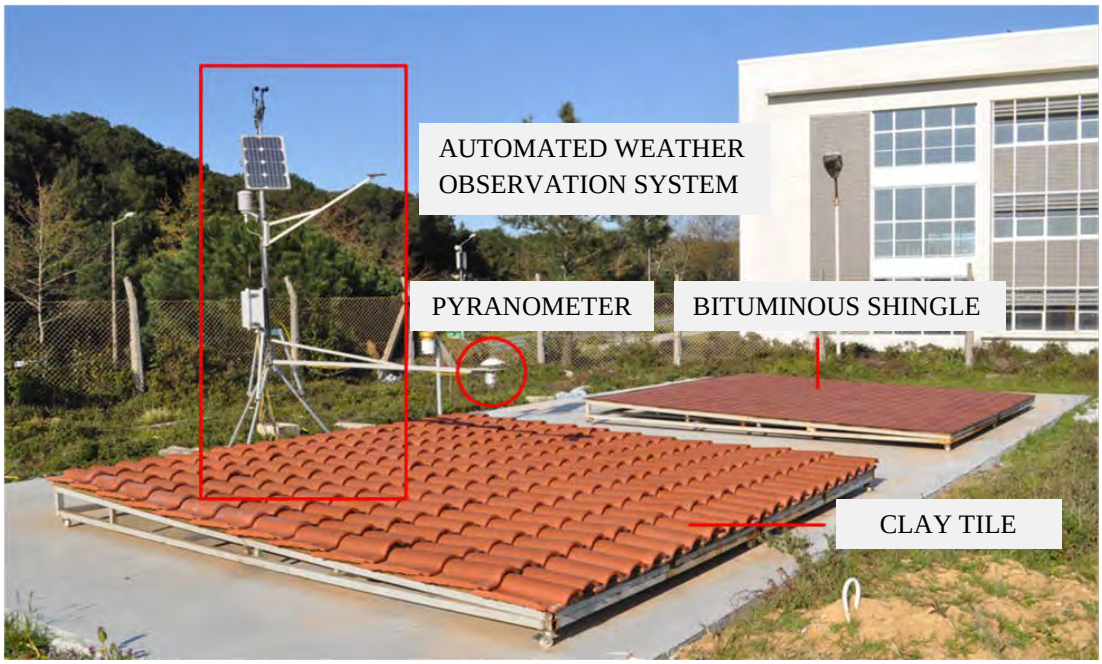

Fig. 1. Test setup.

3. Results

3.1. Laboratory measurement

The test results of new and 1-year aged test specimens are given in Table 2. Solar reflectance rates of each roofing material for each spectral range and situation (new-aged) are presented. Spectral ranges are stated in four sections as ultraviolet (UV), visible (VIS), infrared (IR) and total.

Table 2. Solar reflectance rates of new and 1-year aged roofing materials.

ROOFING MATERIALS / TEST SPECIMENS	SOLAR REFLECTANCE RATES % R							
	NEW (UNEXPOSED)				AGED (1-YEAR EXPOSED)			
	SPECTRUM (NM)				SPECTRUM (NM)			
	UV	VIS	IR	TOTAL	UV	VIS	IR	TOTAL
	200-380	380-780	780-2500	200-2500	200-380	380-780	780-2500	200-2500
CLAY BASED								
TILE-RED	6.05	21.28	73.46	**35.40**	7.10	22.42	73.60	**35.90**
CERAMIC TILE-WHITE	15.09	71.73	75.80	**70.40**	---	---	---	---
CERAMIC TILE-WHITE,SHINY	27.98	83.00	76.96	**77.80**	29.39	82.16	76.70	**78.10**
CEMENT BASED								
CONCRETE TILE-RED	6.98	24.71	43.20	**29.70**	7.16	25.10	43.59	**29.70**
METAL BASED								
TILE-RED, N. GRANULE COVERED	3.62	10.13	36.64	**17.20**	---	---	---	---
GALVANISED SHEET-WHITE	7.16	77.72	64.61	**70.70**	---	---	---	---
ALUMINIUM-SILVER	41.56	61.32	75.88	**64.00**	---	---	---	---
COPPER-BRONZE	7.25	22.97	63.32	**33.20**	---	---	---	---
TITANIUM ZINC-BLACK	6.75	6.03	9.58	**6.20**	---	---	---	---
TITANIUM ZINC-SILVER	43.30	55.10	72.61	**54.70**	---	---	---	---
BITUMINOUS BASED								
ROLL-RED, N. GRANULE COVERED	5.36	12.84	21.75	**14.80**	5.59	13.38	22.00	**15.20**
SHINGLE-RED	3.66	9.32	10.09	**9.30**	3.64	9.78	10.68	**9.70**
CORRUGATED SHEET-BLACK	4.33	4.03	3.99	**3.60**	4.64	4.66	8.43	**5.20**

3.2. Field measurement

Initial results of field measurements are demonstrated graphically for each roof surface in Fig 2. and Fig. 3.

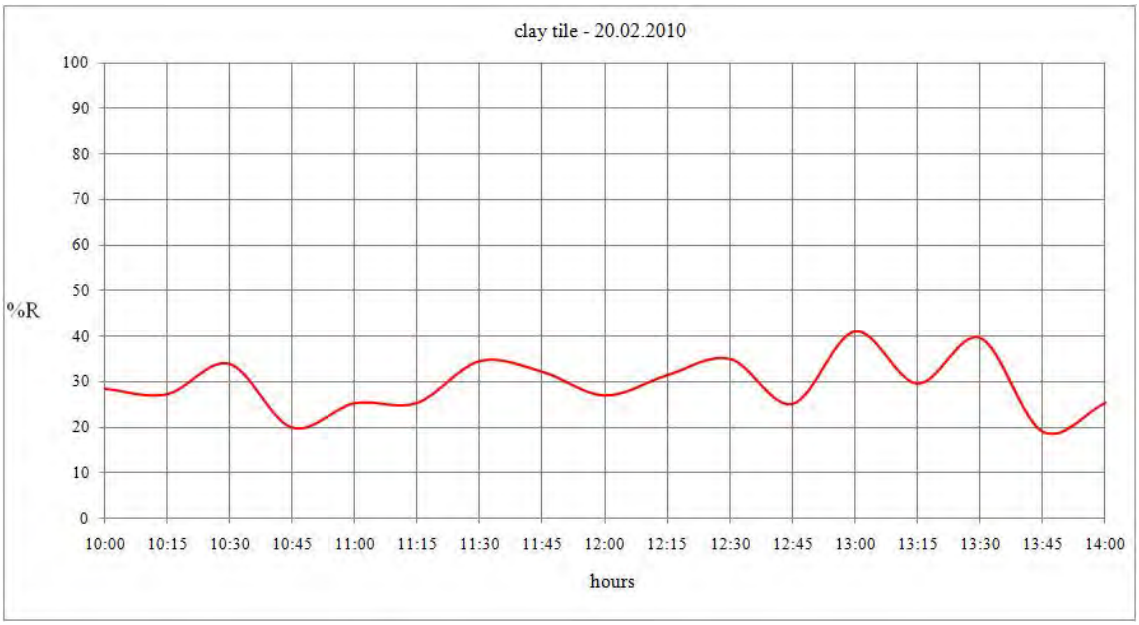

Fig. 2. The initial measurement results of clay tile covered roof surface for 20 February 2010.

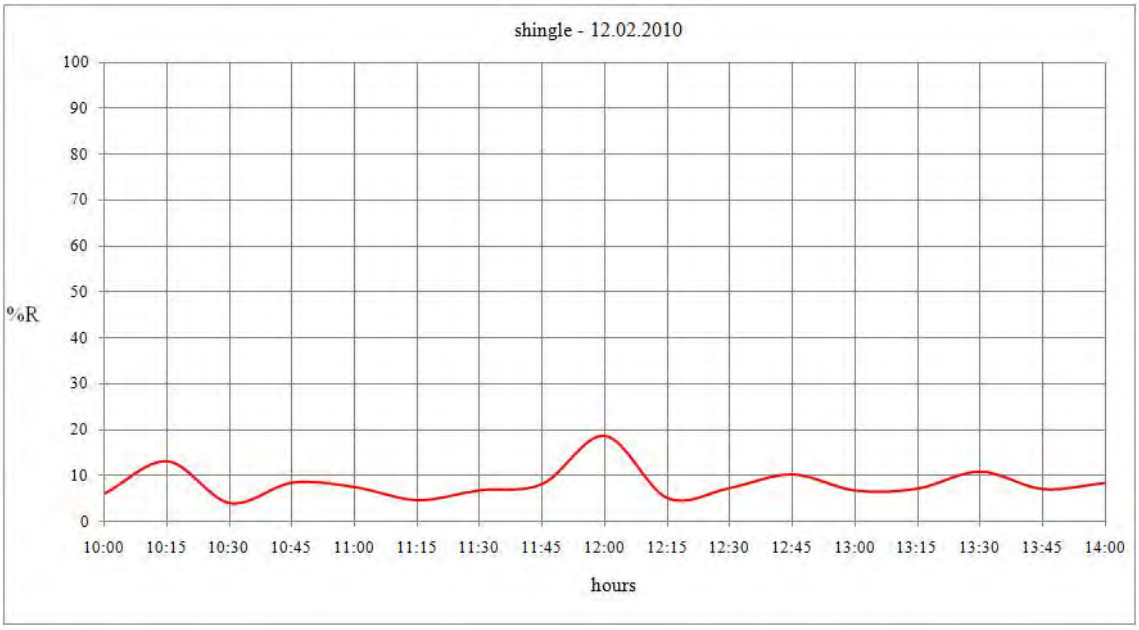

Fig. 3. The initial measurement results of bituminous shingle covered roof surface for 12 February.

The measurement results enable comparative assessment between the same colored and same sloped (3%) roof surfaces under actual weather conditions. The average solar reflectance performance of roof surfaces was calculated from the initial measurement results of the days without rain. Accordingly, the initial solar reflectance performance of clay tile covered roof surface is 29%, while bituminous shingle covered roof surface has an initial value of %8.

4. Discussion and Conclusions

This paper presents the solar reflectance performance of roof coverings used in Istanbul, Turkey. In accordance with this purpose, the laboratory and the field measurements were conducted.

The laboratory measurements' results can be assessed in two ways as short-term and long-term solar reflectance performance of roof coverings. For the short-term performance, the most reflective roofing material is the white and shiny clay based ceramic tiles while the black corrugated bituminous based sheet has the lowest solar reflectivity. On the other hand, only in the ultraviolet spectrum, the silver coloured titanium-zinc is the most reflective material. Reflectivity in the UV region indicates the sensitivity to UV radiation, hence material degradation. After accelerated 1-year exposure, all the materials had almost the same performance with their short-term performance and no change in appearance was observed (Table 2).

The field measurements' initial results enable the comparisons between 2 roof surfaces under the same conditions. The red coloured clay tile covered roof surface is more reflective than the same coloured shingle covering. The laboratory and the field measurements have approximately the same results when initial solar reflectance rates of red clay tile and red bitumen shingle are considered.

Environmental Protection Agency (EPA) had described the reflective roofing materials according to their application on low-sloped or steep roofs. Based on EPA, for instance, the red clay tile can be considered as reflective roof covering while red bitumen shingle as absorptive material.

Field measurements will be conducted for 1-year in order to evaluate effect of weathering on the solar reflectance performance. Then, the long-term solar reflectance performance results of laboratory and field measurements will be compared.

Results of this paper will enable designers to choose the roof covering appropriate for reflective roofs that can be used to rehabilitate existing roof coverings or to design new roofs, which in return will provide cooling energy savings and hence sustainable development of Turkey.

References

[1] American Society for Testing and Materials. (1996). Standard Test Method for Solar Absorptance, Reflectance and Transmittance of Materials Using Integrated Spheres. *ASTM Standards, E 903*. USA: ASTM International.

[2] American Society for Testing and Materials. (2001). Standard Practice for Operating Xenon Arc Light Apparatus for Exposure of Non-Metallic Materials, *ASTM Standards, G 155*, USA: ASTM International.

[3] American Society for Testing and Materials. (2006). Standard Test Method for Measuring Solar Reflectance of Horizontal and Low Sloped Surfaces in the Field. *ASTM Standards, E 1918*. USA: ASTM International.

[4] Liu, K. (2005). Towards Sustainable Roofing. Institute for Research in Construction. Canada, <http://irc.nrccnrc.gc.ca/pubs/fulltext/nrcc48173/nrcc48173.pdf>, accessed on 20.04.2009.

[5] Ozturk, M. (2008). Eğimli Çatılarda Nihai Çatı Kaplama Malzemeleri 2007 Yılı Sektör Büyüklüğü Araştırması. 4. Ulusal Çatı & Cephe Kaplamalarında Çağdaş Malzeme ve Teknolojiler Sempozyumu (s. 115-120). İstanbul: Altan Basım Ltd..

[6] Parker, D.S., Barkaszi, S., Chandra, S. and Beal, D.J. (1995). Measured cooling energy savings from reflective roofing systems in Florida: field and laboratory research results. Report No: FSEC-PF-293-95 Florida Solar Energy Center, FL.

[7] Prado, R. and Ferreira, F. (2005). Measurement of albedo and analysis of its influence the surface temperature of building roof materials. Energy and Buildings, 37, 295-300.

[8] The Ministry of Environment and Foresty. (2007). First National Communication on Climate Change. <http://www.cevreorman.gov.tr>, accessed on 15.03.2007.

Hydrogen Economy and the Built Environment

S. El Azzeh[1], M. Sarshar2[*], R. Fayaz[3]

[1] *Liverpool John MooresUniversity, Liverpool, UK*
[2] *Institute of Energy and Sustainable Development,De Montfort University, Leicester, UK*
[3] *Art University, Karaj, Iran*

** Marjan Sarshar Tel: +44 116 257 7961, Fax: +44 116 257 7977, E-mail:msarshar@dmu.ac.uk*

Abstract: The hydrogen economy is a proposition for the distribution of energy by using hydrogen, in order to potentially eliminate carbon emissions and end our reliance on fossil fuels. Some futuristic forecasters view the hydrogen economy as the ultimate carbon free economy. Hydrogen operated vehicles are on trial in many countries. The use of hydrogen as an energy source for buildings is in its infancy, but research and development is evolving. Hydrogen is generally fed into devices called fuel cells, to produce energy.
A fuel cell is an electrochemical device that produces electricity and heat from a fuel (often hydrogen) and oxygen. Fuel cells have a number of advantages over other technologies for power generation. When fed with clean hydrogen, they have the potential to use less fuel than competing technologies and to emit no pollution (the only bi-product being water).
However, hydrogen has to be produced and stored in the first instance. It is possible to generate hydrogen from renewable sources, but the technology is still immature and the transformation is wasteful. The creation of a clean hydrogen production and distribution economy, at a global level is very costly.
Proponents of a world-scale hydrogen economy argue that hydrogen can be an environmentally cleaner source of energy to end-users, particularly in transportation applications, without release of pollutants (such as particulate matter) or greenhouse gases at the point of end use. Critics of a hydrogen economy argue that for many planned applications of hydrogen, direct use of electricity, or production of liquid synthetic fuels from locally-produced hydrogen and CO2 (e.g. methanol economy), might accomplish many of the same net goals of a hydrogen economy while requiring only a small fraction of the investment in new infrastructure.
This paper reviews the hydrogen economy, how it is produced, and distributed. It then investigates the different types of fuel cells and identifies which types are relevant to the built environment, both in residential and non-residential sections. It concludes by examining what are the future plans in terms of implementing fuel cells in the built environment, and discussing some of the needs of built environment sector.

Keywords: *Hydrogen, Fuel cells, Hydrogen economy, PEM Fuel Cells*

1. Introduction- Hydrogen

1.1. The Hydrogen economy

A "Hydrogen Economy" is proposed as an ultimate solution for clean energy and the environment. Hydrogen communities have been formed for the promotion of this goal. They produce publications and organise meetings and exhibitions. The excitement is mainly about having a carbon free world. Electricity is considered one of the main CO2 emission sources relying on burning fossil fuels. A change in the production sources of energy is essential. Hydrogen is seen as a potential electricity carrier which is 100% clean and natural, but the challenge remains in its production, storage and distribution processes. Hydrogen is not found on its own in the globe, so it needs to be extracted from other elements that contain it. A key question is: is mass production of hydrogen physically possible? Similarly one needs to pose the question of: are the costs of producing, storing and distributing hydrogen affordable?

Hydrogen is not a natural fuel, but a synthetic energy carrier. It only carries energy generated by other processes. For example, hydrogen may be produced from electricity by electrolysis of water. In addition, high-grade electrical energy is also required to compress or liquefy it, and to transport, transfer, and store it [1]. Without question, the technology for a hydrogen economy exists or can be developed. In fact, vast amounts of hydrogen are generated,

handled, transported and used in the chemical industry today. But this hydrogen is used as a chemical substance, not an energy source. Hydrogen production and transportation costs are absorbed in the price of the synthesized chemicals. The cost of hydrogen remains irrelevant as long as the final products find markets. However, today's debate for the use of hydrogen as an energy source is governed by economic arguments and not merely theoretical considerations.

In the academic literature, the production and the use of hydrogen have attracted significant attention, while the practical aspects of a hydrogen economy are rarely addressed. Fig.1 below shows that like any other product, hydrogen must be packaged, transported, stored, and transferred to bring it from production to final use. These common market processes require energy [1]. Can we justify the transition to a hydrogen economy, based on practical and financial considerations? Some authors believe not!

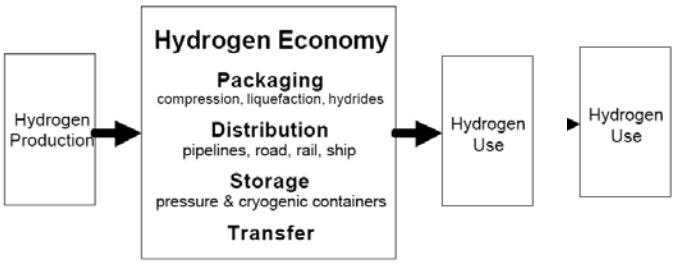

Figure 1: Schematic Representation of an elemental "Hydrogen Economy [1]

On the other hand, some scientists argue that novel energies need long, and sometimes very long periods of time; typically many decades to find their way onto the market. It may require up to half a century in order to establish of a novel energy regime in an irrevocable fashion. Hydrogen is no different. It is the right time to start the implementation of the hydrogen energy economy and see it through [2]. Winter [2] argues that Hydrogen is on track, because sustainable energy without the hydrogen economy is difficult to achieve, although there are still many milestones ahead.

Currently one needs to increase awareness amongst professionals and scientists around new technologies so that further development into realistic solutions becomes possible. "*It takes about 50 years for a new idea to break through and become vogue; no one likes an intruder, particularly when he is upsetting the commonplace*"[2].This paper provides some background to the hydrogen economy.

1.2. Sources of Hydrogen

Dunn [3] pointed that Hydrogen is hard to find on Earth as a separate element. Instead, it is primarily found in combination with oxygen in water, in combination with carbon in a range of hydrocarbon fuels, and in combination with carbon in plants, animals, and other forms of life. Once it is extracted, this colourless, odourless, and tasteless element becomes a useful "feedstock", or input, to a variety of industrial activities and a potentially ubiquitous fuel sufficient to energize virtually all aspects of society, from homes to electric utilities to business and industry to transportation. Therefore, hydrogen production means extracting and isolating hydrogen in the form of independent molecules, at the level of purity required for a given application [4].

Hydrogen is not widely used today in the Built environment sector, but has been tested on vehicles as exemplars and showcases. Winter [2] stated three main sources of Hydrogen, mentioning some of each source requirements and obstacles. He stated that Hydrogen can be produced from fossil fuels, renewable sources, or nuclear fission. (1) From fossil fuels via reformation or partial oxidation or gasification, preferably from natural gas, like today, or from coal, in the future, with capture and sequestration of coproduced carbon dioxide in order to prevent its release into the atmosphere. (2) From renewable electricity via electrolysis, but not before a number of further decades of development and in competition with the direct use of renewable electricity in the power market; or (3) From nuclear fission, if society accepts it.

Hydrogen production systems using renewable energy sources have been developed mostly in the United States (US) [5]. Example of that is the Telonicher Marine Lab in Trindad, California where they have installed the first solar hydrogen-Fuel cell system. The three major renewable hydrogen projects that have been completed in Europe are the Utsira hydrogen project, launched in July 2004 in Norway, the HARI project at West Beacon Farm, Leicestershire, UK, and PURE project in Unst (Shetland), opened in May 2005.

According to the DTI report Meeting, The Energy Challenge [6], Hydrogen and fuel cells are linked technologies with significant carbon-saving potential where the hydrogen is produced from renewable or low carbon sources. Furthermore, Hydrogen would facilitate the shift from limited non-renewable stocks of fossil fuels to unlimited flows of renewable sources, playing an important role in reducing and eliminating Carbon dioxide (decarbonisation) in the global energy system needed to avoid the most severe effects of climate change. Replacement of oil and other fossil fuels with hydrogen would achieve reductions in carbon emissions and avoid a doubling of pre-industrial carbon dioxide (CO_2) concentrations in the atmosphere [3].

Total's company publication [7] on hydrogen and fuel cells indicates that hydrogen can be produced through two broad process technologies:

1. By reforming or gasification of fossil fuels (e.g., natural gas, petroleum, coal) or products derived from the biomass (e.g., ethanol);

2. Alternatively, by electrolysis of water (using electricity generated by nuclear, wind, solar or other power).

According to Pant and Gupta [8], the current global hydrogen production is 48% from natural gas, 30% from petroleum, 18% from coal, and 4% from electrolysis.

1.3. Hydrogen Production in Reality

Hydrogen is a fascinating energy carrier. It can be produced from electricity and water. Its conversion to heat or power is simple and clean. Hydrogen forms water when combusted with oxygen. No pollutants are generated or emitted. The water is then returned to nature where it originally came from. But hydrogen, the most common chemical element on the planet, does not exist in nature in its pure form.

Hydrogen has to be separated from chemical compounds by electrolysis from water or by chemical processes from hydrocarbons or other hydrogen carriers. The electricity for the electrolysis may eventually come from clean renewable sources such as solar radiation, kinetic energy of wind and water or geothermal heat. Therefore, hydrogen may become an important link between renewable physical energy and chemical energy carriers [1].

Hydrogen is considered the "forever fuel", since, like electricity, it can be produced from any primary energy fuel: coal, oil, natural gas, nuclear, all sorts of renewable energies, and from grid electricity. Certainly, because of its environmental and climatic cleanness, hydrogen made from renewable energies is the ultimate aspiration. This is, however, not a pre-requisite for building a hydrogen energy economy.

Dunn [3], stated that about 99 % of the hydrogen produced today comes from fossil fuels. Over the long run, this proportion needs to be shifted towards renewable sources, for hydrogen production to be sustainable. Hydrogen, produced from renewable energy (e.g., Solar) sources, would result in a permanent energy system, which will not need to be changed [9].

Bossel [10] believes that electrolysis may be the only practical link between renewable energy and hydrogen. Although solar or nuclear heat can also be used for high-temperature cyclic processes, it is unlikely that a recognisable fraction of the global energy demand can be served with hydrogen from solar concentrators or high-temperature reactors. Local wind farms are likely to deliver energy at lower costs than distant solar or nuclear installations.

Winter [2] argues that the future of electrolytic hydrogen depends clearly on the price of electricity. If the price of the electrolysis process for the production of hydrogen is high, the production will become harder, and vice versa. He notes that in all likelihood the future average electricity price will increase rather than decrease (at least in industrialized countries), electrolytic hydrogen may get its market only where the electricity demand is temporarily low, e.g., at night, or where base load (nuclear) power station has been underused.

A case study by Bossel in 2006 [10] finds interesting questions and indicates major challenges. He states that if about 50 jumbo jets leave Frankfurt Airport every day, each loaded with 130 tons of kerosene, to replace the energy by hydrogen, 50 tons of liquid hydrogen are needed per plane. The daily needs would be 2500 tons or 36 000 m3 of the cryogenic liquid, enough to fill 18 Olympic-size swimming pools. Every day 22 500 tons of water would have to be electrolyzed. The continuous output of eight 1-GW power plants would be required for electrolysis, liquefaction, and transport of hydrogen. If all 50 planes leaving the airport were converted to hydrogen, the entire water consumption of Frankfurt and the output of 25 full-size power plants would be needed to meet the hydrogen demand of air planes leaving just one airport in Germany. This case study demonstrates that the hydrogen economy is not a panacea and more effort in understanding the cost and the effort is required.

This doesn't prove that hydrogen is not the ideal solution. It does indicate that electrolysis (depending on water and electricity) is not the right solution at least for now, and an alternative should be studied before rising the issue of producing hydrogen from renewable sources. This indicates that current studies could be seen as misleading, from the point of view that they are just seeing and arguing about the benefits of using hydrogen for energy generating, which is true. Yet, more studies about the real life possible applications with all disadvantages must be considered as well. As mentioned before, the development and storage costs of hydrogen are to be explored before committing to using it.

1.4. Storing and transporting Hydrogen

Hydrogen seems to have some difficulties in storing and transporting. Some researchers have made remarkable points about this subject as hydrogen molecules are extremely tiny and will leak from almost any container or pipe, meaning that it needs to be liquefied at temperatures near absolute zero. Compressed hydrogen, at very best, would take up at least 4 times as much

space in a tank as gasoline for the same amount of energy. Plus the storage tanks for compressed hydrogen cost 100 times the cost of a gas tank. Also, stronger materials, like steel, are more likely to react with hydrogen and become brittle. Combined with the high pressure, this makes the tanks susceptible to bursting [11].

Winter [2] added a few words on storage, he stated that: stationary hydrogen storage is at hand, both for gaseous and liquid hydrogen in high pressure steel flasks or cryogenic dewars*.

Large capacity underground storage for gaseous hydrogen in leached salt domes may build on what has been learned from operational underground air or natural gas storage, though special care needs to be taken to prevent leakage of the smallest element of the periodic table of elements: hydrogen! The most challenging venture is the tank onboard motor vehicles. For a usual vehicle range of, say, 500 km, the tank for gaseous hydrogen requires an inner pressure of 700 bar, which from a manufacturing and lifelong safety standpoint, is not at all trivial to achieve and maintain.

2. Fuel Cells

2.1. Main characteristics of Fuel Cells

Stambouli and Traversa [12] stated that, a Fuel Cell is an energy conversion device that produces electricity by electrochemically combining fuel (hydrogen) and oxidant (oxygen from the air) gases through electrodes and across an ion conducting electrolyte. According to the DTI report, Meeting the Energy Challenge [6], the fuel cell does not run down or require any recharging; unlike a battery, it will produce energy as long as fuel is supplied. The battery is an energy storage device where all energy available is stored within the battery itself [13]. According to the European commission summary report [14], because of fuel cells' low noise and high power quality, fuel cells systems are ideal for use in hospitals or IT-centres, or for mobile applications.

Fuel cells generally have a heat to power ratio of roughly 1:1 with overall efficiencies of around 80% when fired on hydrogen. Fuel cells powered with pure hydrogen have potential power efficiencies of up to 45% i.e. 45% of the hydrogen is converted into electrical energy. However, when we add a reformer to convert other fuels to hydrogen, this can drop significantly [15].

Neef [16] argues that hydrogen and fuel cells are technologies that still need to prove their capability in order to produce marketable products.

Three application areas for fuel cells are emerging: (1) In portable electronics fuelled with the help of hydrogen or methanol cartridges (e.g. laptops and mobile phones) (2) in stationary applications, (e.g. buildings) and (3) in the transportation sector in busses, passenger and light duty vehicles, later in heavy duty trucks, in aviation and at sea [2].

*Dewar: a double-walled flask of metal or silvered glass with a vacuum between the walls, used to hold liquids at well below ambient temperature.

2.2. Fuel Cells types for buildings

Stambouli and Traversa [12] explain that there are many types of fuel cells, which are normally sorted by either by their operating temperature or by their classification. The latter is generally done according to the nature of electrolyte. The basic differences in the different types of fuel cells are:

- The electrolytes used;
- The operating temperature of the device;
- The design, and their fields of applications, bearing in mind that each fuel cell type has specific fuel requirements [17].

Operating temperatures of fuel cells vary depending on their type. There are two main categories for classification:

Firstly, the low temperature fuel cells with operating temperatures as low as 80°C. These can be installed in private households, light commercial operations, and large industrial operations. An examples of this type is the Proton exchange membrane fuel cell (PAFC). In low-temperature fuel cells, all the fuel must be converted to hydrogen prior to entering the fuel cell.

Secondly, the high temperature fuel cells, such as molten carbonate (MCFC) and solid oxide (SOFC), may be adapted for larger industrial applications. With operating temperatures between 600-1100°C these high temperature cells can tolerate a contaminated source of hydrogen and hence can use unreformed natural gas, diesel or gasoline. Furthermore, the heat generated can be used to produce electricity by driving steam turbines.

Fuel cells in the stationary sector, i.e. for residential energy and for industrial application, will use different fuels and convert them into hydrogen as long as there is no hydrogen infrastructure in place. In the case of low temperature fuel cells, a reformer is used that converts natural gas into hydrogen and CO2, for example. High temperature fuel cells can convert the fuel, e.g. biogas, internally. Once again, the advantages of such stationary fuel cell systems compared to the competing condensing boilers or conventional heat and power plants consist of higher efficiencies and reduced emissions, but also of a contribution to the decentralised electricity production and to stability of the electric grid [16].

The most common fuel cells types found in the literature today and suitable for buildings are:

- Proton Electrolyte Membrane Fuel Cells (PEMF C),
- Alkaline Fuel Cells (AFC),
- Phosphoric Acid Fuel Cells (PAFC),
- Molten Carbonate Fuel Cells (MCFC) and
- Solid Oxide Fuel Cells (SOFC)

listed in the ascending order of their operating temperature, where the most electrical efficient of them is found to be the SOFC which has a high operating temperature. Lipman *et al*., [18], explain that low temperature PEM fuel cells are considered the leading contenders for automotive and small stationary applications. SOFC, PAFC, and MCFC operate at higher temperatures (from 2001C to 10001C) and are expected to be used for larger stationary applications. Regarding efficiency, generally fuel cells have high efficiency, where they convert up to 50–70% of available fuel to electricity (90% with heat recovery) [12].

Winter [2] stated that depending on the type of fuel cell, it provides the right temperature for heat applications in stationary use: 100 C for proton exchange membrane (PEM) fuel cells (FCs), around 200 C for high-temperature PEMs or phosphoric acid FCs (PAFCs), 600–650 _C for molten carbonate FCs (MCFCs), and 700–900 _C for solid oxide fuel cells (SOFCs).

Low to high temperature PEMs are exactly what is needed for homes or buildings or hospitals, depending under which climate and weather conditions they serve; MCFCs fit the exigencies of many small-to-medium size industries, hospitals and large laboratories, and SOFCs are an excellent topping technology for gas turbine/steam turbine combined cycles [2].

But to be more precise the types we are concerned with in this project, are the types that rely on hydrogen only as their fuel, and from the existing applications. Table 1 below shows that PEM and PAFC are the two fuel cells types that could generate electricity for buildings with the use of hydrogen as their fuel. According to Lidderdale and Jones [15] PAFC type is the most successful technology, in terms of numbers deployed above 200 kWe, where it is used primarily for large back-up and remote power applications in hospitals, schools, and other locations where an engine generator would traditionally be used. Increasingly being used in environments where high availability of either electrical or thermal power is a criterion.

T →					
	DMFC	**PEMFC**	**PAFC**	**MCFC**	**SOFC**
Electrolyte	Proton conducting membrane	Proton conducting membrane	Phosphoric acid	Molten carbonate	Ceramic
Temperature Range (°C)	< 100	< 100	ca. 200	ca. 650	800-1000
Fuel	methanol	hydrogen	hydrogen	Natural gas, coal gas, biogas	Natural gas, coal gas, biogas
Power Range	W / kW	W / kW	kW	kW / MW	kW / MW
Application (examples)	Vehicles, portables	Vehicles, house energy, CHP	CHP	Power plants	House energy, Power plants

DMFC
Direct Methanol FC
PEMFC
Proton Exchange Membrane FC
PAFC
Phosphor Acid FC
MCFC
Molten Carbonate FC
SOFC
Solid Oxide FC

Table 1: fuel cells types and main characteristics [16]

Realistically speaking and because the technology (Fuel cells) is still newly introduced to the built environment, a definite answer about the most appropriate type for buildings cannot be stated yet, it will take several years and many real life pilots to proove what is and what is not suitable for buildings.

2.3. Future plans for Fuel Cells implementations

Winter [2] stated that like any other energy, hydrogen energy has to meet a range of criteria before successfully entering the market. The two major, perhaps dominating criteria are costs and CO2 emissions. Of course, costs are the key for the entry of any energy into a competitive large scale market, and hydrogen energy is not different.

Same is applicable for fuel cells technology; cost, reliability and lack of experience are the major issues. To resolve these problems and to answer all unclear questions, implementing the technology in several projects is a necessity and this should be supported by the government and large private energy companies as a start, because like any other technology the cost of it at present is considerably high which makes it hard for the end users to even consider installing such technology in their houses or projects, especially that sustainable and clean hydrogen sources are not readily available as yet. Therefore, support is required at this stage to implement the technology for a small community and learn from the experiences.

According the Fuel cells handbook 2004 [13], for a fuel cell to compete with other generation sources, its price must be reduced dramatically and research and development is required to improve the performance and reduce the cost of renewables, storage, and fuel cell technologies. Technologies are needed that can produce hydrogen for the same price as gasoline. Storage technologies must be developed to allow cheap, safe hydrogen storage. Finally, fuel cell technology must advance to improve efficiency.

In addition, Safety is seen as a prime consideration for stationary fuel cells. As fuel cells come closer to the customer, codes must be written and building inspectors educated to allow the introduction of fuel cell power systems.

Another interesting point to be taken care of for moving forward with fuel cells technologies is obtaining insurance for hydrogen projects. This needs to be undertaken by the government to provide a layer of insurance coverage. In addition, insurance companies must be educated as to the proper handling of hydrogen and the associated risks. This would allow for property, liability, and efficacy insurance to be offered at reasonable rates.

3. Future directions and future research needs

Renewbles are one of the few rapidly growing business sectors, and developers are working hard to forge a link between renewable and fuel cell technology in order to put power generation on a sustainable basis. In the next five to ten years biogas fuel cells are supposed to operate worldwide, and active research will take place on wood and biomass gasifiers for hydrogen production. Wind power will be used to generate hydrogen in some locations, while solar hydrogen will be produced in others to power a small fleet vehicles [19].

The fuel cell industry itself is in its infancy. The early products have problems with reliability and affordability. It is as yet unclear which types of fuel cells will prove more appropriate for the different types of buildings and usage. Early piloting of the technology must be facilitated by government organisations and major corporations.

The construction industry is still not prepared for the introduction and maintenance of such eventual novel technologies. The design, implementation, and maintenance of them require specialist knowledge, which is still non-existent within the industry.

Future research needs to be collaborative, including stakeholders from the construction industry, the energy sector and the fuel cell technology sector (i.e. chemical engineers). Possible research areas include:

- Potential solutions for hydrogen production on site;
- Hydrogen harvesting, i.e. the best sustainable source for hydrogen production with the least cost;
- A critical analysis of the different types of fuel cells for different building types;
- Hydrogen onsite storage mechanism;
- Legislative barriers and enablers.

References

[1] Bossel U, Eliasson B (2003) Energy and the Hydrogen Economy,(available online http://www.methanol.org/pdfFrame.cfm?pdf=HydrogenEconomyReport2003.pdf [accessed on 20/08/2009])

[2] Winter C (2009) "Hydrogen energy d Abundant, efficient, clean: A debate over the energy-system-of-change". International Journal of hydrogen energy 34:1-52

[3] Dunn S (2002) "Hydrogen futures: toward a sustainable energy system". International Journal of Hydrogen Energy, 27, 235–264.

[4] Sorensen B (2005) "Hydrogen and Fuel Cells, Emerging technologies and applications, A volume in the "Sustainable World" series". ELSEVIER academic press. chapter 2, pages 5-110.

[5] Gazey R, Salman S, and Aklil-D'halluin D (2006) "A field application experience of integrating hydrogen with wind power in a remote island location". Power sources 157: 841-847

[6] DTI report, Meeting the Energy Challenge (2007) Energy white paper HMG CM 7124. Published by the stationary office (TSO).

[7] Total company publication (2007) hydrogen and fuel cells, (available online http://www.total.com/en/corporate-social-responsibility/Publications/ [accessed on 15/12/2008])

[8] Pant K, and Gupta R, Edited by Gupta, R (2009) "Hydrogen fuel: production, transport, and storage" chapter 1: Fundamentals and Use of Hydrogen as a Fuel, Published by: Taylor & Francis Group.

[9] Veziroglu T, and Sahin S (2008) "21st Century's energy: Hydrogen energy system". Energy conversion and management 49: 1820-1831.

[10] Bossel U (2006) "Does a Hydrogen Economy Make Sense?". Proceedings of the IEEE 94: No. 10, 1826-1837

[11] Energy justice fact sheet: Hydrogen and fuel cells (2007) (available online http://www.energyjustice.net/ [accessed on 25/09/2008])

[12] Stambouli A, Traversa E (2002) "Fuel cells, an alternative to standard sources of energy". Renewable and Sustainable Energy Reviews 6: 297–306

[13] Fuel cell handbook (2004) seventh edition, by U.S.Department of Energy, office of fossil energy.(available online http://www.brennstoffzellen.rwth-aachen.de/Links/FCHandbook7.pdf [accessed on [1/1/2009])

[14] European Commission (2007) Combating climate change, The EU leads the way. (available online http://ec.europa.eu/publications/booklets/move/70/en.pdf [accessed on 10/04/2009])

[15] Lidderdale J, and Jones P (2006) "Fuel cells CHP for buildings", proceeding of the CIBSE (The Chartered Institution of Building Services Engineers) national conference. (available online http://www.cibse.org/index.cfm?go=page.view&item=581[accessed on 10/04/2009])

[16] Neef H (2009) "International overview of hydrogen and fuel cell research".Energy 34: 327-333.

[17] Ibrahim H, Ilinca A, Perron J (2008) "Energy storage systems-Characteristics and comparisons". Renewable and Sustainable Energy Reviews 12: 1221–1250

[18] Lipman T, Edwards J, and Kammen D, (2004) "Fuel cell system economics: comparing the costs of generating power with stationary and motor vehicle PEM fuel cell systems". Energy Policy 32:101–125

[19] Fuel cell technology handbook (2002) edited by Gregor Hoogers, proceedings of the institution of mechanichal engineers, Automobile engineering 217: no.5.

Developing a probabilistic tool for assessing the risk of overheating in buildings for future climates

David P. Jenkins[1,*], Sandhya Patidar[2], Phil Banfill[1], Gavin Gibson[2]

[1] *Urban Energy Research Group, School of Built Environment, Heriot-Watt University, Edinburgh, UK*
[2] *School of Mathematical and Computer Sciences (address as above)*
** Corresponding author. Tel: +44 (0)1314514637, E-mail: D.P.Jenkins@hw.ac.uk*

Abstract: The effect of projected climate change on building performance is currently a growing research area. Building designers and architects are becoming more concerned that buildings designed for the current climate might not provide adequate working and living environments in the coming decades. Advice is needed to guide how existing buildings might be adapted to cope with this future climate, as well as guidance for new building design to reduce the chances of the building failing in the future. The Low Carbon Futures Project, as part of the Adaptation and Resilience to Climate Change (ARCC) programme in the UK, is looking at methods of integrating the latest climate projections from the UK Climate Impact Programme (UKCIP) into building simulation procedures. The main obstacle to this objective is that these projections are probabilistic in nature; potentially thousands of equally-probably climate-years can be constructed that describe just a single scenario. The project is therefore developing a surrogate procedure that will use regression techniques to assimilate this breadth of climate information into the building simulation process.

Keywords: *Climate change, Building simulation, Overheating*

Nomenclature

$T_o(t)$ *internal air temperature at hour t..... °C*
θ_0 *regression constants .....*
m_j *regression coefficients .....*
$\chi_j(t)$ *hourly climate parameter .....*

1. Introduction

In the UK, for both new build and building refurbishment sectors, legislation is currently being discussed to achieve low-carbon buildings through the use of new design and technologies [1]. It is therefore inevitable that a level of uncertainty exists with regards to the future energy performance of such buildings. In addition to this, with future climate warming being predicted over the coming decades for the UK, there is an uncertainty with regards to the comfort performance of such buildings – will future climate warming negate certain design assumptions for buildings designed or retrofitted for a current climate? For a naturally ventilated building this might mean internal temperatures exceeding design thresholds for significant periods of the year, whereas a mechanically cooled building might be operating with an under-sized cooling plant. This describes the problem that the concept of "adaptation" is trying to solve; what changes to our current approach should be taken now to ensure a building will maintain adequate levels of thermal comfort in the future? Such an analysis requires a suitable form of future climate projections, which themselves are inherently uncertain. Previous approaches to climate projections have been deterministic [2], in that they specify an estimated value of expected climate change for a specific scenario. The most recent UK Climate Projections (UKCP'09[3]) from the UK Climate Impact Programme (UKCIP) takes a different approach, with climate projections provided in a probabilistic form. These have been constructed from multiple iterations of climate models, which have undergone a degree of downscaling by geography and temporal resolution. The result of this can be many thousands of possible climate files describing just a single future scenario (see section 2). If such information is to be incorporated into building design approaches, it is clear that an

additional step is required which can either simplify this climate information or provide an algorithm which processes this data in a way that might be useful for a building designer. If this goal can be achieved, then the result will be a method for incorporating the uncertainty of climate projections into building design and allowing the designer to choose adaptation options (such as shading or ventilation techniques) which will give a high probability of adequate thermal comfort in that building for a future climate. This work forms part of the Low Carbon Futures project, sponsored by the Adaptation and Resilience in a Changing Climate (ARCC) Programme [4].

2. Methodology

The following section will describe the approach being taken by the Low Carbon Futures project, which includes obtaining weather data, carrying out extensive building simulation and then using the obtained relationships to construct a regression relationship between climate and internal temperatures of a building.

2.1. Weather Generator

The Low Carbon Futures project [5] obtains future climate projections from the UKCP'09 Weather Generator. This can provide a number of statistically equivalent 30-year time series projections which describe a specific future scenario (e.g. low-emission, 2020-2049) for a specific location (based on a grid map of the UK). The weather variables can be generated at monthly, daily or hourly scales and include: total hourly precipitation (mm), mean hourly temperature (ºC), vapour pressure (hPA), relative humidity (%), sunshine fraction (of an hour), downward diffuse radiation and direct radiation (both W/m^2). If the user is downloading 100 time-series (the maximum allowed for each iteration), each run will produce 3000 (30years x 100 files) equally probable climate years at an hourly resolution. The resulting climate information can therefore be vast in scale. If using building simulation, the options might be to either i) choose just one (or a small number) of these representative climate-years to simulate a building with or ii) provide a short-cut or emulation step to make the building simulation process itself, over many climates, more efficient. The Low Carbon Futures project is investigating the latter approach. The timelines looked at for this study will be 2020-2049, 2040-2069 and 2060-2089 (referred to as "2030s", "2050s" and "2080s" respectively). The Weather Generator provides three future emission scenarios, namely "low", "medium" and "high" (as defined by UKCP'09), all of which will be included in the analysis. With two locations currently being investigated by the project (Edinburgh and London), this provides a total of 20 climate scenarios, including a baseline "current" climate (from 1960-1990 data) in both locations.

2.2. Building Simulation

While the described approach could be used with any building simulation software, the project uses ESP-r, an open-source package. To adequately describe internal temperature profiles (and therefore provide useful information with regards to overheating metrics), it is important to carry out these simulations with dynamic simulation software and at a suitable temporal resolution (in this case hourly). Such software will allow for the thermal response of the building over time to be suitably expressed, as well as providing a method for defining various adaptation scenarios. A range of buildings are being simulated by the project, some taken from real case-studies while others are adopted from previous simulation studies such as the Tarbase project [6]. This paper overviews two of these buildings: a standard dwelling [7] and a primary school [8], both of which are naturally ventilated. Different buildings have different overheating definitions and might have specific adaptation options that are related to

the occupancy and construction characteristics. It is therefore important, when assessing overheating risks through simulation, to have a method that can be used for a range of buildings and a range of overheating metrics. The hypothesis of the project is that one initial simulation can identify the relationship between an hourly climate file and hourly internal temperatures of a building, summarised by an appropriate regression equation. This regression equation can then be used for a vast array of climates, without the designer having to resort back to full building simulations for all the other climates. This methodology is seen as an acceptable compromise between maintaining the detailed calculation of dynamic simulation software (as such a calculation will be required to start the process), while providing a means to achieving the equivalent of (up to) thousands of climate inputs through a given building model.

For validation purposes, each building in the project is simulated for a total of 2000 climate-years, encompassing the described range of emission scenarios, timelines and locations. A script has been developed for the project (by University of Strathclyde, who develop ESP-r) that allows many climates to be simulated in succession. While this is still a time-consuming process (and would not be practical for use in industry), it allows the project team to carry out a validation exercise across a large number of climates. For each iteration, the hourly internal temperature profile for the entire year is recorded for use in the regression exercise.

2.3. Validation of regression analysis

Following the building simulations, a large database of hourly climate metrics and hourly internal temperatures (by zone in the building, where the user may choose to focus on the area of the building that is most prone to overheating or has the highest occupancy) is created. The next step is to demonstrate a statistical relationship between the climate projections and the resulting building temperatures. A regression equation can be formulated describing this that is calibrated using just one climate, i.e. calculating the appropriate regression coefficients, and this same relationship can be used for all the other climates to investigate whether the same relationship will hold for that building. A simple regression equation will have a large number of terms; not only should the range of influential climate metrics be included (listed in section 2.1) for a given hour, but also the same metrics for previous hours, due to the dynamic thermal response of a building to such changes over time. It is found that the regression equation can emulate simulation results if climate information from the previous 72 hours is included. Taken across seven different climate metrics this potentially provides 504 terms in the regression equation (i.e. 72 x 7 = 504). However, using the established statistical technique of Principal Component Analysis (PCA), these terms can be reduced to just 33 (this is discussed in detail elsewhere [9]). The resulting regression equation is then of the form:

$$T_0(t) = \theta_0 + \sum_{j=1}^{33} m_j X_j(t) \qquad (1)$$

For adaptation scenarios (e.g. a physical change to the building that might combat overheating), Eqn. (1) can either be recalibrated following another simulation or a series of correction equations applied that are specific to those adaptation choices [9].

The results of the validation exercise, comparing hourly internal temperatures from the calibrated regression equation to that of ESP-r simulation, are demonstrated in Fig. 1. This is for the case of a domestic building, without any adaptation measures and with 100 climate-years representing a London 2030, medium emission scenario (though similar results have been obtained from other buildings and adaptation and climate scenarios).

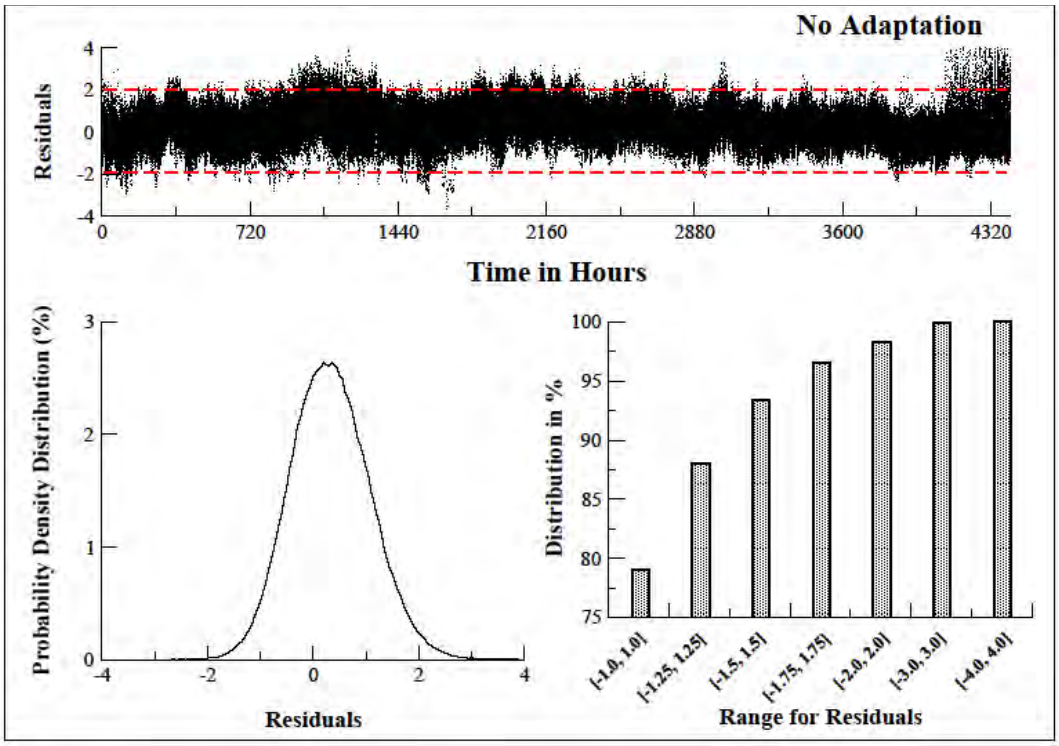

Fig. 1. Comparison of ESP-r and regression equation hourly temperatures scenarios for "no adaptation", London 2030 Medium emission scenario

In summary, Fig. 1 presents (top graph) over 400,000 data points between April and October for the specific scenario, where "residual" is the difference between the internal hourly temperature of ESP-r and the regression equation (in degrees). Due to the large amount of data, it is difficult to discern a typical error from this graph alone, hence the use of the left graph which shows that the majority of the "error" between ESP-r and the regression equation is ±1°C – deemed an acceptable error over such a vast amount of data and for an hourly resolution. The right graph demonstrates that almost 80% of the data is within this error. The validation exercise provides an indication that an appropriately calibrated regression equation can be used to emulate a dynamic simulation over a large number of climates, providing an initial simulation has been carried out to establish the relationship in the first place.

2.4. Design approach

The integration of any future-climate design tool into the building design process involves an understanding of existing design practices. To investigate this, the project is running several focus groups to obtain feedback from a wide range of design professionals in the UK. These focus groups will discuss how current overheating analyses are carried out for domestic and non-domestic buildings, and how low-energy buildings might be more susceptible to future overheating for certain scenarios.

In summary, it is imagined that the methodology discussed in sections 2.1 to 2.3 might be used as follows:

1. A building is designed to current building regulations with an overheating analysis based on dynamic simulation of, nominally, a current hourly climate file
2. The proposed regression tool, working in parallel with the simulation engine for step 1, generates a series of regression coefficients based on the documented principal component analysis framework (see section 2.3)

3. A random selection of 100 climate years for a specific future scenario can be selected from the UKCP'09 database (e.g. the user would choose: London, medium emission, 2020-2049) – this can be integrated into the tool so that the user would not need to access the climate information separately. These climates will not need to be simulated through the dynamic building software
4. The user chooses an overheating metric, such as the percentage of hours over 28°C or another defined threshold, that is suitable for that building type
5. The regression tool provides an overheating risk output, demonstrating the probability of different scales of overheating for that building in a future climate (see section 3 for examples)

If a building is designed to achieve adequate thermal comfort for a current climate, the above methodology can estimate whether that same building will meet thermal comfort criteria for chosen future climates.

3. Results

The project is looking at a selection of buildings, two of which will be used below to demonstrate the way that the analysis described in section 2 can be used to quantify the effect of adaptation scenarios to prevent overheating in a naturally ventilated building. The technique is also being applied to mechanically cooled buildings, with results forthcoming.

3.1. Domestic building

The domestic building case study is designed to represent a typical UK 3-bedroom dwelling, with infiltration rate of 0.7ac/h, with wall U-value of 0.37W/m^{2}K. Detail of the construction and internal activity can be found in previous publications [7]. Fig. 2 shows the simulation diagram used by ESP-r.

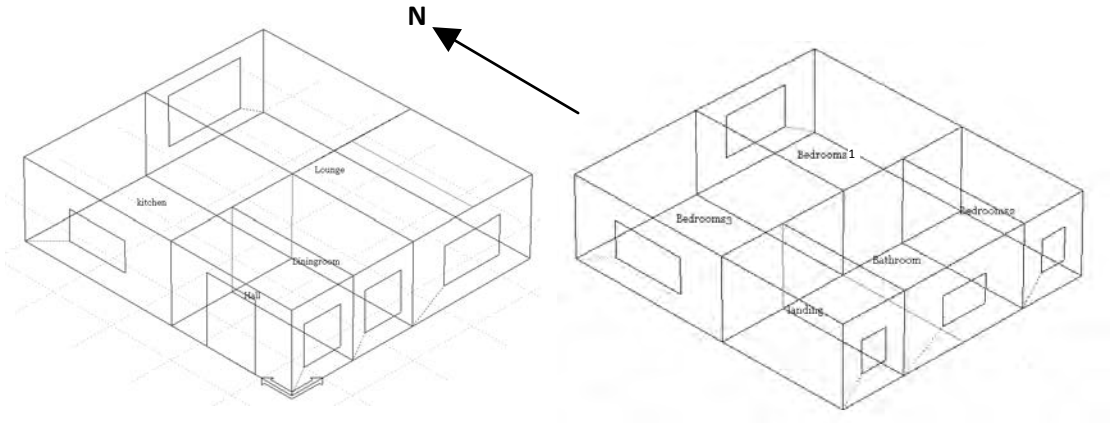

Fig. 2. ESP-r diagram of ground floor (left) and first floor (right) of modelled dwelling

While a large range of overheating criteria could be specified for this building type, the chosen metric for this paper is the number of hours in the bedroom that exceed 23.9°C at night. This definition, justified elsewhere [7], proposes that the lack of options to adapt to overheating at night may cause an occupant to take other measures (e.g. purchase a domestic air-conditioning unit) to provide an improved level of thermal comfort. The building is simulated for all the climate scenarios identified in section 2.1, and for three adaptation scenarios, applied cumulatively: i) "no adaptation", where the occupant does not react to overheating at all; ii) "window opening", where windows are opened in the bedroom zones if that zone exceeds 23.9°C (and closed if the temperature then drops below); iii) "external shading and reduced internal gains", where horizontal slats are placed above every window to

reduce solar gain, while internal heat gains (from appliances and lighting) are reduced by 25% to represent more efficient technologies. For simplicity, Fig. 3 only shows the results for the 2030s medium emission scenario for a London location, though the same format can be applied to any climate scenario. The x-axis of the graph shows relative change in the overheating metric (i.e. number of hours above the 23.9°C threshold at night) against a 1960-1990 baseline. With 100 equally probable climate-years used for this future climate scenario, it is possible to construct a cumulative frequency plot that suggests the probability of different levels of overheating occurring. The effect of the adaptation scenarios is clear, with the overheating risk curves being morphed in the negative direction on the x-axis – representing reduced overheating risk. Such a graph could be used to design a building to be sensitive to a future climate: for example, the "no adaptation" scenario estimates a 96% probability of more overheating (i.e. the part of the cumulative curve that is to the right of the "zero" dotted line representing no change) for the future climate used. Applying both adaptation scenarios reduces this to just 14%; i.e. the building now has just a 14% chance of being warmer in the future. This may be a suitably low future overheating risk, providing the client with the confidence that their building should provide adequate thermal comfort in the future.

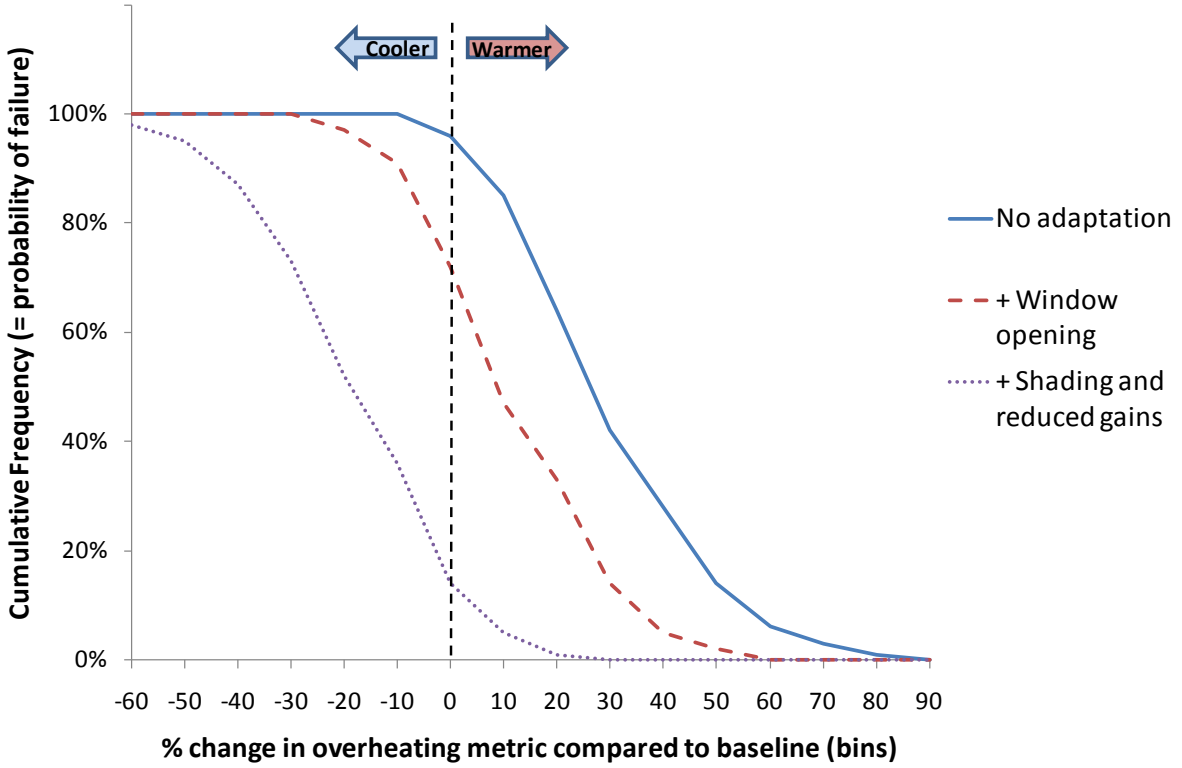

Fig. 3. Predicted increase in dwelling overheating for 100 random climates for London, Medium Emission, 2030 scenario

3.2. Primary School

The exercise is repeated for a primary school building, previously analysed with deterministic climates in the Tarbase project [8]. The construction and internal activity is specified in detail in this aforementioned reference and relates to UK Building Regulations for the assumed build date of 2000. The overheating criterion used for this building is the percentage of hours above 28°C in teaching areas, as suggested by UK building guides [10]. As with the previous case-study, the methodology of section 2 is carried out to assess future overheating risks. Fig.4 summarises the floor plan and building design.

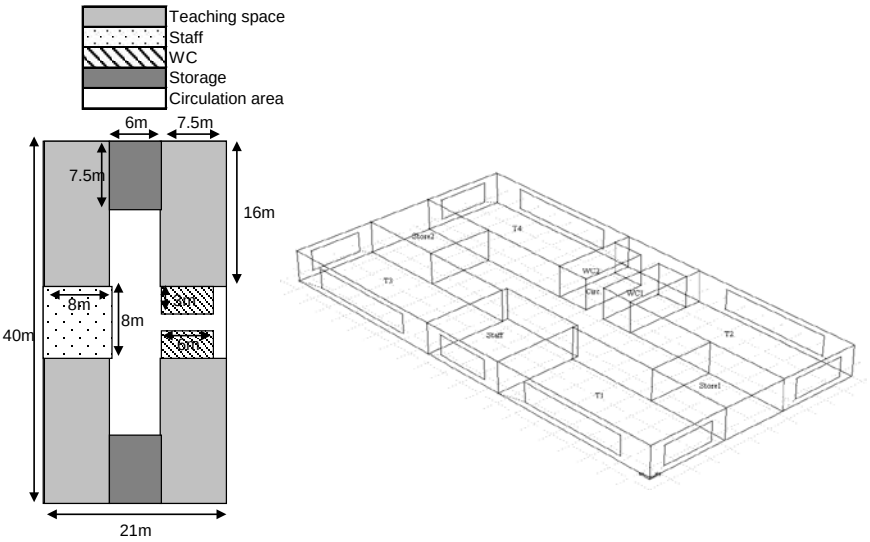

Fig. 4. Layout and plan of primary school case-study

Fig. 5 demonstrates the predicted overheating curves, again for the 2030s medium emission scenario for a London location. The adaptation scenarios are: i) "no adaptation"; ii) "Increase Vent", where maximum ventilation rates are increased from 8l/s/person to 12l/s/person; iii) "Reduced gains", for energy-efficient appliances and lighting that reduce internal heat gains (as quantified elsewhere [8]); iv) "External shading", with simple horizontal shades added above each window. As with the domestic case study (Fig. 3), a substantial improvement is made as a result of the adaptations – ranging from a 96% chance of increased overheating for "no adaptation" to a 0% chance once all adaptations have been applied.

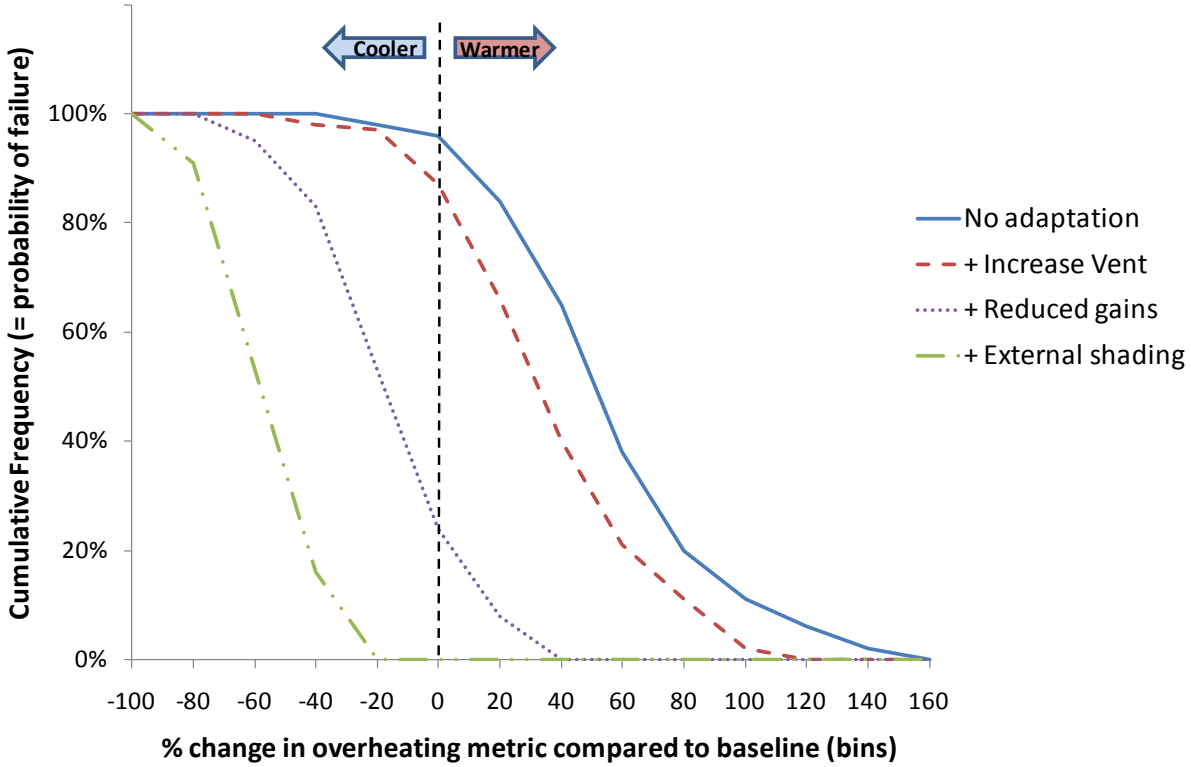

Fig. 5. Predicted increase in school overheating for 100 random climates for London, Medium Emission, 2030 scenario

4. Discussion and Conclusions

The Low Carbon Futures project aims to provide guidance for designing buildings, or retrofitting existing buildings, so that they will provide adequate thermal comfort for a future climate. There are essentially two problems to be addressed: i) how can designers be encouraged to design for a future climate, rather than just using existing climate definitions and ii) if future climates are presented in a probabilistic form (as with UKCP'09), can this be integrated into the design process in an efficient way? If this latter problem provides an additional barrier to building design, then it will not be adopted in practice. However, if this form of climate projection can be linked to an overheating "risk analysis", which might have parallels with existing risk assessments that the building industry are required to carry out, then the described method might be seen as attractive to both building professional and their client. The methodology described in this paper, which produces probabilistic overheating curves for a specific building once that building has undergone a single simulation, is suitable for use in a design tool that would not require a dramatic increase in building simulation time, despite the use of hundreds of climate-years from the UKCP'09 database. The results suggest that it should be possible to find a compromise between an efficient calculation method and a reliable output that maintains the detail from the probabilistic climate projections used, though it should be stressed that the proposed tool emulates building simulation output, not empirical data. The project will subsequently be testing this approach against a wider selection of buildings and adaptation scenarios to determine if the described methodology is truly universal for future overheating analyses of buildings in the UK.

References

[1] UK Government Department of Communities and Local Government, Proposals for amending Part L and Part F of the Building Regulations, April 2010

[2] M. Holmes and J.N. Hacker, Climate change, thermal comfort and energy: Meeting the design challenges of the 21st Century, Energy and Buildings 39, 2007, pp. 802-814

[3] P.D. Jones et al., UK Climate Projections science report: Projections of future daily climate for the UK from the Weather Generator, available from http://ukclimateprojections.defra.gov.uk

[4] Adaptation and Resilience in a Changing Climate Network (ACN), Programme website http://www.ukcip-arcc.org.uk/content/view/605/519/

[5] Low Carbon Futures project summary page, http://www.ukcip-arcc.org.uk/images/stories/pdfs/lowcarbon_future_leaflet.pdf

[6] Carbon Vision Buildings "Tarbase" project website, http://www.tarbase.com

[7] A.D. Peacock, D.P. Jenkins and D. Kane, Investigating the potential of overheating in UK dwellings as a consequence of extant climate change, Energy Policy 38, 2010, pp. 3277-3288

[8] D.P. Jenkins, A.D. Peacock and P.F.G. Banfill, Will future low-carbon schools in the UK have an overheating problem?, Building and Environment 44, 2009, pp. 490-501

[9] S. Patidar, D.P. Jenkins, G. Gibson, and P.F.G. Banfill, Statistical techniques to emulate dynamic building simulations for overheating analyses in future probabilistic climates, Journal of Building Performance Simulation, In Press, 2010

[10] Chartered Institution of Building Services Engineers (CIBSE), Environmental Design, CIBSE Guide A, 2006

Energy Efficient Buildings with Functional Steel Cladding

M. A. Joudi, M. Rönnelid, H. Svedung and E. Wäckelgård*

School of Technology and Business Studies, SERC, Dalarna University, SE-791 88 Falun, Sweden
** Corresponding author. Tel: +46 23778738, E-mail: ewc@du.se*

Abstract: The aim of the study is to develop a model for the energy balance of buildings that includes the effect from the radiation properties of interior and exterior surfaces of the building envelope. As a first step we have used ice arenas as case study objects to investigate the importance of interior low emissivity surfaces. Measurements have been done in two ice arenas in the north part of Sweden, one with lower and one with higher ceiling emissivity. The results show that the low emissivity ceiling gives a much lower radiation temperature interacting with the ice under similar conditions. The dynamic modelling of the roof in ice arenas shows a similar dependence of the roof-to-ice heat flux and the ceiling emissivity.
A second part of the study focus on how to realise paints with very low thermal emissivity to be used on interior building surfaces.

Keywords: *Energy balance, Low emissivity, Radiation properties*

1. Introduction

The need for buildings to be highly energy efficient requires that a building envelope must be air tight and well insulated. It is also important that both interior and exterior surfaces has appropriate optical functions. The exterior surfaces (roof and facades) should in a hot climate have high solar reflectance and high infrared emissivity in order to reduce space-cooling loads. Buildings in colder climates should have exterior surfaces with high solar absorptance and low thermal emissivity to reduce space-heating loads. Buildings in all types of climates should have interior walls and ceilings with low thermal emissivity which will reduce the radiation exchange between persons and interior surfaces and thereby the need for decrease/increase the air temperature in order to compensate for too high/low interior radiation temperature.

The research has been extensive in finding solutions for hot climates to prevent over heating and one concept here is the so called cool roof, works from Synnefa et al [1] and Levinson et al [2] shows that it is a large potential for reducing energy use for cooling by use of near infrared high reflectance exterior paints. There has not been as much focus on interior surfaces and how functional optical properties can influence the energy demand in hot or cold climates. Development in paint formulation has made it possible to produce coating with higher reflectance in the long wave radiation spectra. This kind of coatings has been found mainly useful for interior coatings where it is expected to act like a thermal barrier for the radiation energy potentially emitted or absorbed by the surface when the radiation temperature differs significantly from the panel surface temperature. For instance, Daoud et al [3] has shown that low emissive interior coatings can contribute to the energy savings in an in doors ice rink.

In a previous work by Joudi et al [4] introduces a model for calculating the effect of both interior and exterior optical properties of a horizontal roof sandwich panel in terms of net energy flux per unit area. Sandwich panels usually consist of two coil coated steel sheet profiles, which are tightly pressed and glued to an insulation core. They can be manufactured even without trans-sectional supports to avoid thermal bridges. The results from the study indicate potential energy saving by the smart choice of optical properties of interior and exterior surfaces. In the present report we introduce a model that includes a roof panel and a

floor and vertical heat exchange. The model is applied on indoor ice rinks as a case study where it has been performed measurements.

Due to the importance of having low thermal emissivity of the interior surfaces a part of the study was devoted to investigate the potential to further reduce the thermal emissivity in low emitting paints for interior use applied on coil coated stainless steel in sandwich panes. The main components of the paint counted from the steel surface are the primer, and the paint layer comprising the binder, pigment and aluminium flakes. The aluminium flakes are used for enhancing the infrared reflectance and by that reduce the thermal emissivity.

2. Methodology

As a first step we have used two ice rinks situated in the north of Sweden (Luleå) as case study objects to investigate the importance of the emissivity of the ceiling for the ice conditions. One of the ice-rinks has a highly emissive coil-coated steel sheet interior roof whereas the other ice-rink has a low emissive galvanized steel sheet interior roof. These buildings are of comparable design with similar roof heat transfer values. In order to study the dependence of the radiation heat flux on the interior surface thermal emissivity in building interior spaces with considerable surface temperature differences, continuous measurements of surface-, air-, and radiation temperatures in the two different indoor ice-rinks were made. Surface- and air temperatures were measured using T-type thermocouples and radiation temperatures were measured using pyrometers facing the ceiling and the ice floor respectively. The measurement data were collected using Intab loggers.

To investigate the flux of thermal radiation from the ceiling to the ice in indoor ice rinks with both low and high emissive interior roofs surfaces, the simulation environments IDA SE and IDA ICE 4.0 are used to solve a system of non-linear equations simultaneously, based on the work presented in [4]. In this model both interior and exterior surface temperatures, as well as discrete cell temperatures through the roof panel are simultaneously solved and coupled in an hourly dynamic simulation with varying outdoor conditions (i.e. solar irradiance, ambient and sky temperature) and different inside air and interior radiation temperatures (i.e. a radiation temperature as seen by the interior roof surface). Table 1 shows the model input parameters. Note that the location in the simulation is Stockholm, due to presently lack of data for Luleå.

Table 1. Model input parameters

Location		Stockholm	
Insulation	thickness	0.3	m
	Thermal conductivity	0.036	$Wm^{-1}K^{-1}$
	Density	20	Kgm^{-3}
	Specific heat	750	$Jkg^{-1}K^{-1}$
Exterior roof optical properties	Total Solar Reflectance	0.3	-
	Thermal Emittance	0.9	-
Ground reflectance		0.7	-
Air temperature under the ceiling		12	°C
Ice surface Temperature		-4	°C

Effective emittance, ε_{eff} with embodied view factor, f_{ci} are calculated from Eq. (1) where ε and A are long wavelength emittance and area in m^2 and subscript c and i represent ceiling and ice, respectively [5]

$$\varepsilon_{eff} = \left[\frac{1}{f_{ci}} + \left(\frac{1}{\varepsilon_c} - 1 \right) + \frac{A_c}{Ai} \left(\frac{1}{\varepsilon_i} - 1 \right) \right]^{-1} \quad (1)$$

The emittance of the low emissivity interior paint and its main components were determined from optical measurements of reflectance in the infrared wavelength range. For the primer, binder and the full paint formulation a Bruker Tensor 27 FTIR with gold-coated integrated sphere was used to measure in the wavelength range 2.5 to 20 µm. The flakes could be measured individually using a Hyperion microscope attached to the Technor FTIR. The thermal emissivity is calculated as an average emittance weighted by the black body radiation distribution for room temperature.

The binder was applied with a metal roll stick on optically smooth aluminium substrates. The thickness of the coatings was varied using different applicator rods. The primer was also applied on the same type of aluminium substrate and roll technique. The whole paint formulation was applied on stainless steel in a full-scale roll coating industrial process.

3. Results

Surface- and radiation temperatures measured in the two ice-rinks during a couple of warm summer days clearly indicate a reduced radiation heat flux from the ceiling to the ice floor in the low emissivity interior roof ice-rink compared to that in the ice-rink with the highly emissive interior roof surface. In Fig. 1a, it can be seen that the radiation temperature seen by the upwards looking pyrometer in the highly emissive interior roof surface ice-rink is very close to the interior roof surface temperature measured by a thermocouple mounted in contact with the surface. In contrast, as shown in Fig. 1b, in the ice-rink with the low emissive interior roof surface the corresponding radiation temperature is much lower and closer to the ice-temperature.

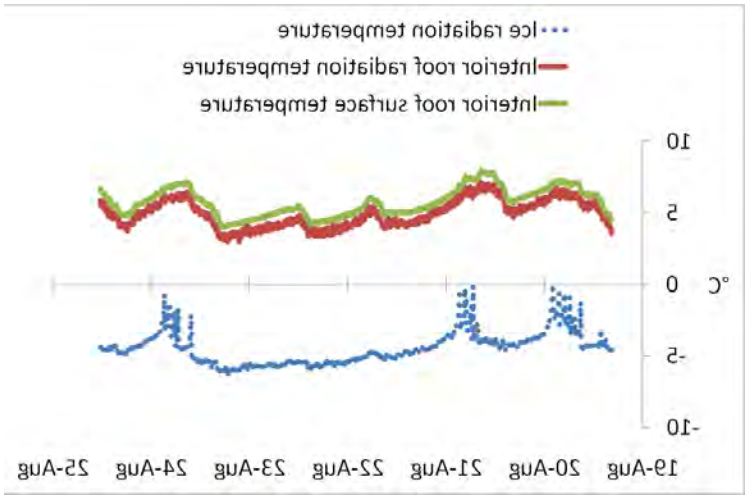

a)

Fig. 1. The interior roof surface temperature, the radiation temperature measured by the upwards viewing pyrometer facing the interior roof surface and the radiation temperature measured by the downwards viewing pyrometer facing the ice are given vs. time during a series of summer days in a) the highly emissive interior roof surface ice-rink.

b)

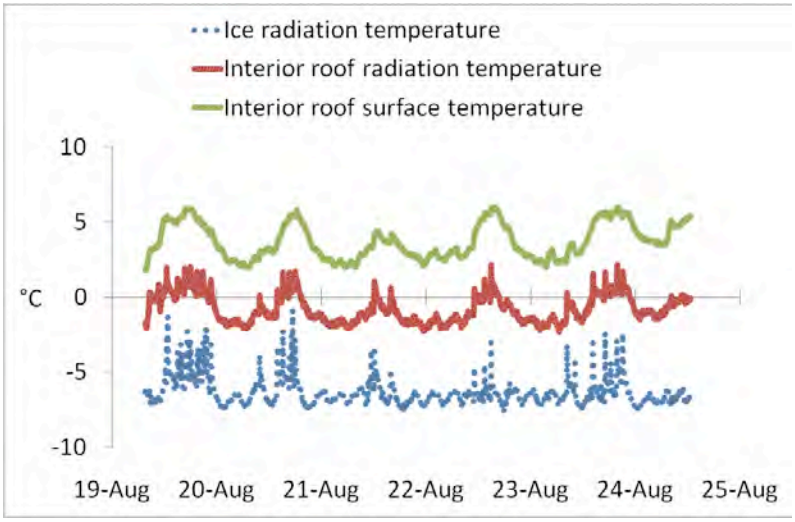

b) The low emissive interior roof surface ice-rink.

Calculations with the dynamic model show in Fig. 2 the thermal radiation to the ice surface, on monthly basis, for three different sets of effective emittance values of the ceiling. It shows that using low emissive coating on the roof interior decreases the radiative heat dissipation to the ice surface, resulting in less cooling load to maintain the ice surface at desired temperature. On the other hand, the monthly variation in the low emissive ceiling are almost negligible, arguably as the interior air temperature is maintained constant.

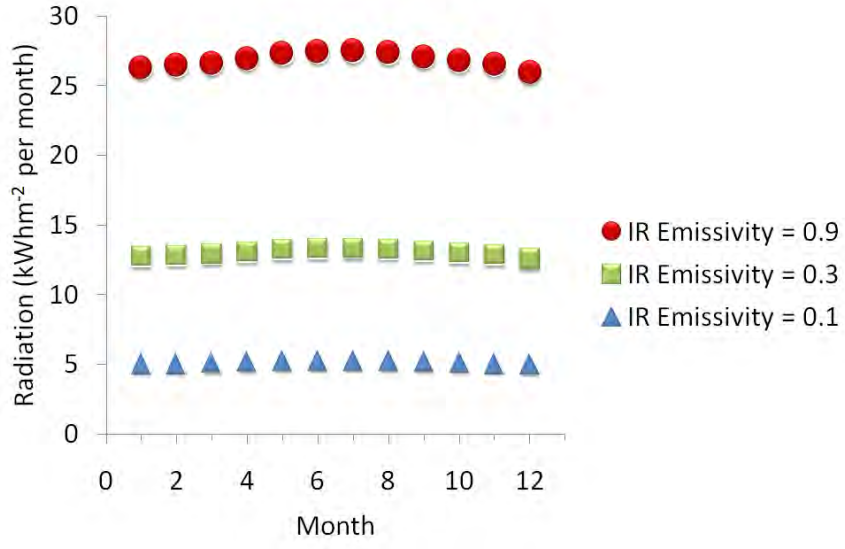

Fig. 2. Thermal radiation to the ice surface for each month for a ceiling for Stockholm climate.

Combining a high TSR (total solar reflectance) exterior roof coating and low emissive interior can reduce the total heat flux into the building; increasing the total solar reflection, TSR of the exterior coating reduces the solar gain, thus total heat flux into the building (heat surplus) will decrease. Further more, low emissive interior, reduces the radiation heat dissipation to the interior surfaces as demonstrated in the Fig 3.

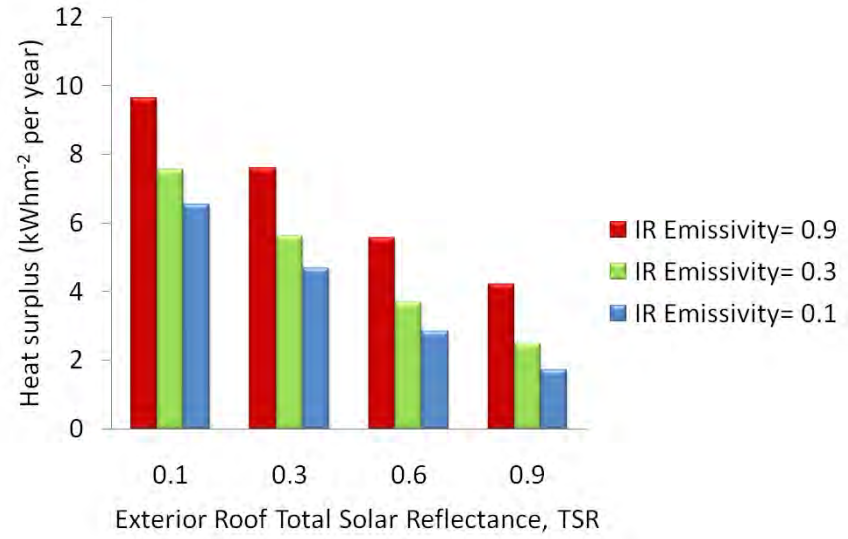

Fig. 3. The effect of combined different infrared emittance interior and high TSR exterior coatings on the heat surplus (cooling load) per roof area for Stockholm climate.

The reflectance measurements of the paint components are shown Fig. 4. The reflectance of the flakes cannot be measured for the longest recorded wavelengths due to the limited flake size (about 50 µm on average). It is notable that the flake reflectance is about 0.90 (emittance 0.10) as the best case for the shorter wavelength, which is considerable lower than for a smooth aluminium surface (0.05). It is seen by visible inspection in the FTIR-microscope that the flakes have surface defects that will cause a reduced reflectance. The binder, which is a 3-micrometer thick polyester shows a thermal emittance of 0.4. Results from optimization of the paint system shows an emittance of about 0.35 for an optimized paint layer. The optimised paint contains 25 % volume fraction of flakes and is about 7 µm thick. The quality of the aluminium flakes that are used in the paints as emissivity-reducing components has also been studied. It was found that the paint with non-leafing type of flakes had lower emissivity than paints with leafing type.

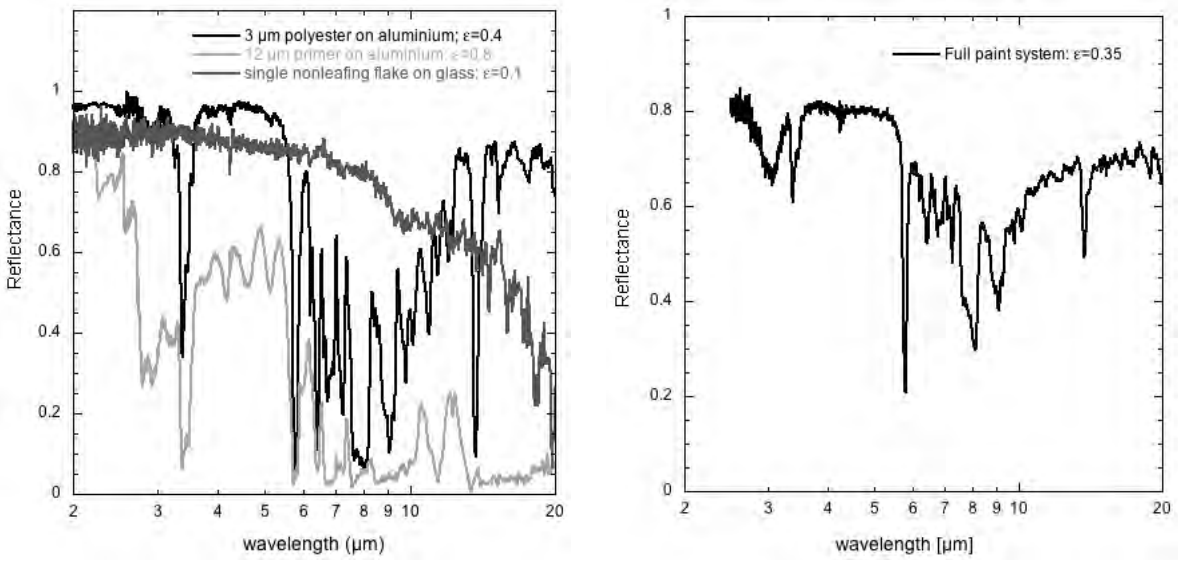

a) *b)*

Fig. 4. The reflectance measured on a) the main paint components: a single non-leafing aluminium flake, polyester binder on optical smooth aluminium and primer on the same substrate and b) a complete paint with the same types of components on galvanised steel.

4. Discussion and Conclusions

The results show the importance of using low-emitting interior surfaces in such applications as indoor ice-rinks. The ice-rink measurements have so far only been presented for a few summer days but are now continuously being measured in order to cover a whole year. The dynamic model of the roof for vertical heat transfer gives an estimate of the amount of energy involved in the radiant transfer from ceiling to ice and also the amount of saved energy on an annual basis. The model will be further developed in order to account for dynamic effects from the convection in the interior space and how it relates to the emissivity of the ceiling. There is obviously a potential to save energy in ice-rinks using low-emissivity paints instead of ordinary paints and it is therefore important to continue the work on paints to reach as low emissivity as possible. However the low-emissivity paints developed so far has about twice the emissivity of a pristine galvanised steel surface and work is needed to develop binders with weaker infrared absorption (especially in the range 8 to 10 µm) and flakes with higher reflectance.

References

[1] A. Synnefa, M. Santamouris, and H. Akbari, Estimating the effect of using cool coatings on energy loads and thermal comfort in residential buildings in various climatic conditions, Energy and Buildings 39, 2007, pp. 1167 – 1174

[2] L. Levinson, H. Akbari, and J. C. Reilly, Cooler tile-roofed buildings with near-infrared-reflective non-white coatings, Energy and Buildings 42, 2007, pp. 2591- 2605

[3] A. Daoud, N. Galanis, and O. Bellache, Calculation of refrigeration loads by convection, radiation and condensation in ice rinks using a transient 3D zonal model, Applied Thermal Engineering 28, 2008, pp. 1782-1790

[4] A. Joudi, H. Svedung, M. Rönnelid, Energy Efficient Surfaces on Building Sandwich Panels - A Dynamic Simulation Model, submitted to Building and Energy September 2010

[5] ASHRAE Handbook of Refrigeration - SI Edition 2006

Acknowledgement

The study has been funded by The Knowledge foundation in Sweden (KK-stiftelsen) and in cooperation with SSAB and Plannja AB. The authors would also like to thank Irina Tran at Akzo Nobel and **Thomas Forsberg** Luleå Technical University for contributions in the project.

Energy Efficiency in Historic Buildings: a Tool for Analysing the Compatibility, Integration and Reversibility of Renewable Energy Technologies

Elena Lucchi [1],*

[1] *Politecnico di Milano, Milano, Italy*
** Corresponding author. Tel: +39 0396085262, E-mail: elena.lucchi@polimi.it*

Abstract: The paper presents a tool for defining the most appropriate energy and environmental retrofit on cultural heritage, to enhance the historical value of a building, to preserve the surrounding landscape, to reduce energy consumption and to improve human comfort, health and safety. It allowed the evaluation of the conservation risks, energy consumption, spatial layout and maintenance procedures and also led to a proposal on the most appropriate energy actions. The tool examines the synergies and difficulties of integrating green practices with historic preservation, and offers recommendations for ways in which sustainable standards could be more accommodating for historic and bounded buildings. The approach was used in the Renaissance building of Sant'Alessandro University located in the centre of Milan (Italy).

Keywords: *Renewable energy, Cultural heritage, Compatibility, Integration, Reversibility*

1. Introduction

The architectural heritage is a capital of irreplaceable spiritual, cultural, social and economic value. Old buildings help to understand the past and the concerns of the society that created them. The interplay between historic buildings, energy efficiency and sustainability is a topic of great importance. Environmental sustainable and energy savings measurements can be considered as a means of protecting real estate, not necessarily in contrast with conservation policies. There are numerous compelling reasons to believe that preservation concerns with environmentally sustainable development. Historic buildings are often located in densely populated urban areas, where infrastructure and mass transit already exists, thereby eliminating the need for new infrastructure and encouraging alternative models of transportation. Historic buildings are also typically constructed with durable and local materials, and are often sited for having full advantage of their surrounding environment. Furthermore, there is high embodied energy in ancient patrimony, which is defined as the sum of energy required to extract or harvest a raw material, manufacture and fabricate that material into a useful form, and transport it to the place of use. Heritage conservation is also a key component for economic revitalization of cities' centre. Often, historic buildings serve as small business incubators. Finally, to increase the preservation of cultural heritage is an important component of social sustainability.

1.1. Energy efficiency policies

Energy efficiency is a central theme in the European policies. The Directive on energy performance (2002/91/EC) requires minimum energy standards for new and existing buildings that undergo major renovation. Despite the Directive admits a few exception for listed buildings, the International Energy Standards cannot be completely waived. Energy performance requirements can be excluded only "(…) where compliance with requirements would unacceptably alter their character or appearance" (Art. 43). At the same time, recent European policy officially introduces the concept of energy balance towards nearly zero-energy buildings and incentives the decreasing of 20% of environmental emissions and the increasing of 20% of renewable energy technologies within 2020 (2010/31/EU Directive). To achieve these goals, it is necessary to reduce user demand as well as to improve the efficiency

of energy systems and to use renewable sources. Heritage must adapt to changes, physical and intellectual, within its environment. The decision, inevitably, must be faced with the energy efficiency of existent buildings, independently by local bounds. Therefore we should develop techniques to maintain, refurbish and adapt the existing buildings to new requirements.

1.2. Environmental sustainability policies

Preservation-based sustainability is offered as a m ore comprehensive approach to development, as it takes into consideration environmental, economic, social, and cultural implications of buildings. These principles constitute the basis of the more important sustainable tools (1). These programs emphasize design, construction and operation for obtaining a "high green performance" building to reduce environmental impacts through energy efficiency, use of recycled materials, storm water management, and other innovations.

1.3. Sustainable conservation principles

High energy and environmental performances may lead the preservation of a building, but each action on historic and listed heritage gives attention to the matter of vulnerability, physical alteration, and decreasing of immaterial and material value. The most important principles for sustainable conservation regard:

- Compatibility: modern materials tend to be harder, less flexible, and less moisture permeable than traditional ones. For these reasons when are used in direct conjunction with historic fabric can greatly accelerate decay in the original work;
- Aesthetic integration: history and authenticity of historic building should be respected as essential to its significance;
- Reversibility: the unavoidable changes of the building should wherever possible be made to be fully reversible. Adopting this principle, the valuable historic fabric can be returned to its original state without damaging the building;
- Emphasis on e ffective maintenance: care, planned conservation, and management should include regular inspections so that defects can be discovered whilst still small and easily fixable. This permits to preserve historic fabric, minimize cost and disruption to the building's owners and users.

The retention of older buildings or the re-using of components in-situ and allowing for their energy upgrading in benign and sympathetic ways, can provide excellent finished results which are fully in accordance with the principles of building conservation and sustainability.

2. Methodology

Energy efficiency and environmental sustainable programs should be developed on the basis of a thorough knowledge of the property, blending technological and landscape requirements. This means understanding original construction, alterations, actual conditions, qualities, material and immaterial values, lacks, and retrofitting opportunities. The tool is structured in the following phases:

- Historical analysis of city, urban site and heritage building;
- Analysis of functions, performance and needs of users;
- Building energy audit;
- Evaluation of environmental performance;
- Individualization of energy and environmental lacks;
- Definition of possible retrofitting actions;
- Evaluation of the compatibility, the integration and the reversibility of each action.

1) See: U.S. Green Building Council's "Leadership in Energy and Environmental Design" (LEED), "Building Research Establishment Environmental Assessment Method" (BREAM), "Comprehensive Assessment System for Building Environmental Efficiency" (CASBEE), Green Star, Minergie and Ecolabe programs.

The tool allowed the evaluation of the conservation risks, energy consumption, spatial layout and maintenance procedures and led to propose the most appropriate actions (Fig. 1).

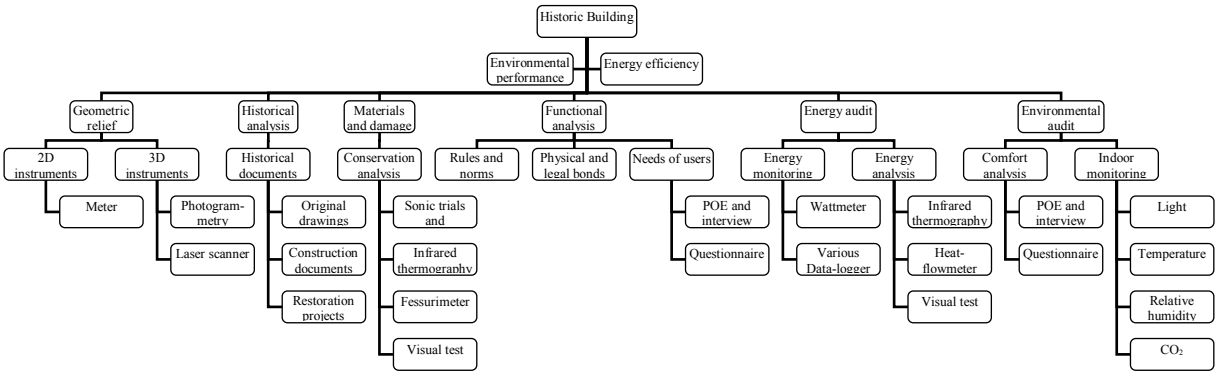

Fig. 1. Method for analyzing energy and environmental performance of historic building.

3. The case study: Sant'Alessandro University in Milan

The tool was used in the Renaissance building of Sant'Alessandro University located in the centre of Milan (Italy). The construction has been modified during the centuries. The most important projects regard the addition of a Baroque Church and the transformation into a Public University in XX^{TH} Century.

3.1. Historical analysis

Technical compatibility and aesthetical integrations are guarantee only by a deep knowledge of history, dimensions, structures, original and restoration materials, and management procedures. Also, it is important to comprehend how modern materials and technical approaches impact on ancient buildings. Failure to understand the nature of the building being inspected can have serious technical consequences, physical damage and possible legal claims. The historical analysis comprehend the physical relief, the study of traditional construction and local techniques, the instrumental tests of original and restoration materials. Cartographic map, land registry, cadastral map, historical and construction drawings permit to reconstruct the original form, the spatial relation and the history of the building. First of all, the original drawings, the construction documents and the restoration projects were collected. The geometric relief was made to verify dimensions, performances, and damage of structures. It was conducted using linear meter, photogrammetry and laser scanner, in order to reconstruct the morphology, the form, the dimensions, the spatial layout, the external and internal features. Final result after processing of the raw data produced drawings, CAD models, 3D surface models and video animations. Particularly, the analyses permitted to verify the reliability of historical documentation and to comprehend the constructive phases and the modifications realized in different ages.

3.2. Performance and functional analysis

First of all, it is important to define the meaning of "high performances" in historic building through the right balance with requirements, rules, norms, physical and legal bonds that condition the quality of life for occupancies. The international literature (ASHRAE, English Heritage) proposes to provide specific "classes of performance" for satisfying needs of access, comfort and security. For this purpose, all activities made by the users (students, teachers, staff, stakeholders) were investigated during different hours and periods of the year. In this way, a specific knowledge of the real requests was obtained.

3.3. Energy audit

Building audit is a process to evaluate the energy consumption of the building in order to identify the opportunities for retrofit actions (2). This means to effect inspection, analysis and survey of energy flow, for reducing energy inputs, improving comfort, health and safety. Energy performance of envelope, functioning of mechanical systems, and management data are necessary to realize the audit. Particularly, the following data was obtained:

- Location, urban planning, orientation and environmental context;
- Dimensions of the buildings;
- Construction features of building envelope;
- Efficiency, functioning and maintenance of mechanical and electric systems;
- Leakage rate or infiltration of air;
- Energy consumption.

3.4. Evaluation of environmental performance

Environmental evaluation considers the opposite exigencies for caring and valorizing the cultural heritage. The balance for conservation and human comfort was defined through the confront among environmental, caretaker and management standards. The evaluation regarded the following analyses:

- Microclimate monitoring of light (illumination level, luminance, UV and IR radiance), temperature (external and internal temperature, daily and seasonal gradient), relative humidity (external and internal relative humidity, daily and seasonal gradient) and air (air change rate, indoor air movement, CO_2 concentration, and pollutants dissemination);
- Thermal, visual and acoustic comfort of users;
- Maintenance procedures and operating data (opening times, operation hours, number and frequency of the visitors).

4. Results: energy and environmental performance

In Sant'Alessandro University was particularly difficult to find information about the technological characteristics because of the lack of original plans and of the alterations of the original asset. In order to individualize the original structure, destructive testing, such as coring or endoscope techniques, were excluded because the methods are not suitable for the architectonic values of the building. For this reason, technological data were estimated comparing handbooks, regulations, heat flowmeter measurements, infrared thermography and computations of energy performances.

4.1. Evaluation of energy performance

Non-destructive testing gave a precise recognition of constructive phases, authentic parts, original and restoration materials, constructive techniques, decay, durability and resistance of the structure. Particularly, infrared thermography verified the historical data and individualized the most important energy problems. IR inspection evidenced the presence of thermal bridges, low U-value of envelope, heat gradient through the walls, internal moisture, mould and air leakage at windows, joints and junctions of the building envelope. Sonic trial proved the presence of some mechanical anomalies and confirmed the real composition of the envelope realized by double masonry in bricks and rubble mix. Heat flowmeter measurement calculated the thermal conductance of the walls (Fig. 2).

2) The European Directive 2006/32/CE related to energy efficiency in final users defines energy audit as a «[…] systematic procedure to obtain adequate knowledge of the energy consumption profile of a building or group of buildings, an activity and/or industrial facility or public or private services, to identify and quantify energy saving opportunities from a cost-effectiveness profile and to report the results».

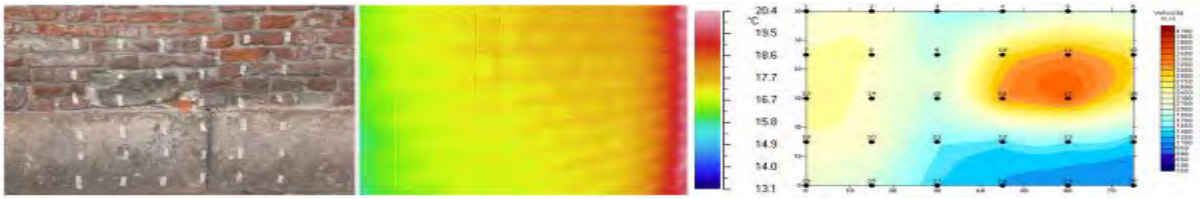

Fig. 2. Confront among visual test, infrared thermography and sonic trial of opaque envelope.

On plants, infrared thermography showed the high temperature of radiators (80°C) and of artificial lighting (60°C) and the functioning of plant in unused ambient. Visual test and environmental monitoring illustrated the low energy performance of HVAC, the incorrect energy management relating to the continual opening of windows and doors, the internal high temperature of air and ignition of lighting during all the day (Fig. 3).

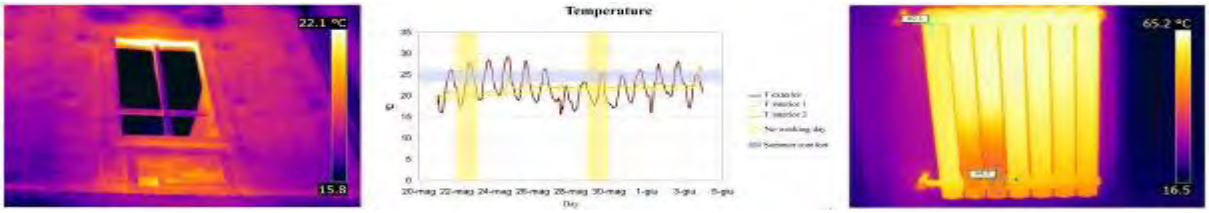

Fig. 3. Environmental monitoring and infrared thermography showed the high temperature of air.

Energy monitoring confirmed the low performance of HVAC and the high fuel bills of the last five years. Energy opportunities of the building regard the thermal mass of envelope, the breathable, and the natural moisture management. Energy performances were evaluated using static and dynamic simulations. The building was in the lower class of energy label with high annual energy consumption.

4.2. Evaluation of environmental performance

Environmental tests verified the presence of damage due to great flux of people and of incompatibility of the protecting policies. Users comfort was appraised with questionnaires and interviews conducted using the Post Occupancy Evaluation method. The analyses were realized on three categories of users: students, teachers and staff. The comparison between discomfort problems and environmental conditions showed the malfunctioning of mechanical systems and the use of incorrect management procedures. Particularly, environmental treats regarded high temperature and heat gain in the attics (mean temperature: 24°C in winter and 33°C in summer), high value of relative humidity in the laid undergrounds (60-65%), temperature fluctuation, low light level (200-300lux), discomfort glare and inadequate lighting (Fig. 4).

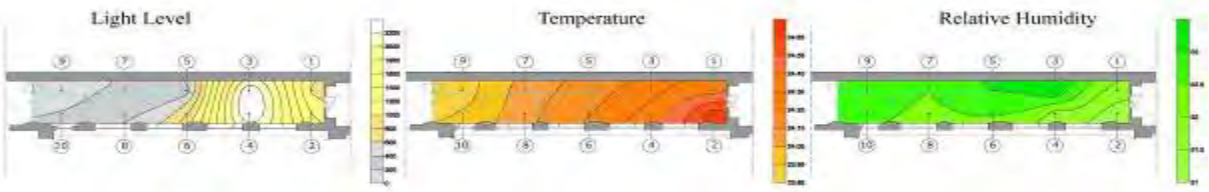

Fig. 4. Monitoring of light level, temperature and relative humidity of air in a room.

Comfort analysis demonstrated the abuse of artificial lighting and the use of wrong light sources (neon light). There is a direct relationship between environmental condition and surface decay. Damage regards cracks, surface breaking, moisture sources, water absorption, and percolation (Fig. 5).

Fig. 5. Decay problems are directly related to environmental condition and regard cracks, surface breaking, moisture sources, water absorption, and percolation.

5. Retrofit actions

The integration of conservation, design and operation is a radical approach to future-proofing historic buildings. Compatibility, integration and reversibility of retrofit actions are the principal items involved in the study of historic buildings. The lack of compatibility may cause serious long term problems of decay, such as bacteriological germination due to air permeability of windows or cracking in masonry due to low mechanical performance, water absorption, percolation and internal moisture. The lack of integration could have a negative effect on the physical composition and static resistance of the structure.

First of all, in Sant'Alessandro University was necessary to understand how traditional buildings behave as environmental systems. Non-destructive testing shows that the envelope didn't require insulation systems because the walls guarantee good thermal and hygrometric performances, both in winter and in summer. However, the invasiveness of internal or External Thermal Insulation Composite Systems (ETICS) or double façades may erase the historical traces and artistic value of the heritage. On the laid undergrounds it is possible to insulate with thermal plaster or internal rigid insulation in transpiring materials, because of the absence of historic traces. The basement and the roof have high energy losses due to the missing of insulation. To insulate the lower insole preserving the original floor, it is possible to add rigid or sprayed foam insulation on the internal surface. To insulate the roof could be installed underside insulation or insulated ceiling characterized by mechanical, chemical and physical compatibility with the original roof. Transparent envelope has high thermal losses and air infiltrations. For this reason, it is necessary to evaluate the replacement of existent glasses and frames with new windows (low-e glasses and wooden frames) having better performances of thermal insulation, air permeability, water resistance and UV protection. The PVC cover on the roof presents convection, air leakage, water adsorption and solar gain. It is necessary to study the replacement with Transparent Insulating Materials, solar control or selective glasses. For protecting the office from solar gain and discomfort glare can be installed internal shading devices and curtain (Table 1).

The main problem is caused by mechanical plants. The existent boilers have very low thermal performance. May be evaluated the replacement with an innovative heat pump, that balances heating and cooling needs. The low performance of radiators and fan-coil get worse by the absence of insulation on thermal distribution, climatic control and heat accounting systems. Furthermore, air-conditioning systems damages the artifacts and the buildings because the movement of air masses soils and dusts the walls, the frescoes, the inlays and the decorations. The intervention requires the evaluation of the insertion of radiant panels on existing floor (not characterized by particular historic value). Instead, it is necessary to insert thermostatic valves on existing radiators and heat accounting systems. The electric system not always is safety from risks. The lighting has discrete energy performances, guaranteed by the integration with daylight, halogen lamps and periodic maintenance on inefficient devices. To increase the level of light can be installed diffusers on existent glasses of the office and high efficiency sources. Solar energy technologies must be integrated within buildings and their

surrounding landscapes, in order to obtain financial support and to increase their efficiency. The use of photovoltaic panels is recommended for decreasing the high electric consumption (Table 2).

Table 1. Definition of possible retrofit actions for the building envelope.

Measurements	Compatibility	Integration	Reversibility
Roofs			
Add rigid insulation on the top surface	■	■■	■
Apply sprayed foam insulation to the top	■	■■	-
Install underside insulation	■	■	■
Install insulated ceiling	■■	■	■
Walls			
Insulate with thermal plaster or wall	■	■	-
Basement			
Install underside insulation	■	■	■
Windows and doors			
Install high-efficiency doors and windows	■	■	-
Install low-e glasses on existing frames	■	■■	-
Transparent Insulating Materials	■	■	-
Install selective materials	■	■	-
Install weather-stripping on windows	■	■■	■■
Shading devices			
Install internal shading devices	■	■	■
Day lighting systems			
Install diffusers on existent glasses	■	■	-
Install interior curtain	■■	■■	■

Incompatible actions: replace with insulated or green roof; insert ETICS or double façades; install storm windows, films or supplemental glazing; add veranda or solar greenhouse; maintain fit, closure and sealing of windows; install external shading devices, skylights, light pipes or light shelves; painting for minimizing the sunlight absorption

Note: ■■ = Yes - = No ■ = Specific project is required

Table 2. Definition of possible retrofitting actions for plants and renewable technologies.

Measurements	Compatibility	Integration	Reversibility
Boiler plants			
Test boiler efficiency	■■	■■	■■
Optimize the air-fuel ratio	■■	■■	■■
Install air conditioning units and heat pumps	■■	■	-
Install an exhaust air heat recovery system	■■	■	■
Clean and repair radiators and convectors	■■	■■	■■
Replace exiting systems with radiant panel	■	■	-
Install single-zone systems	■■	■	■
Install thermostatic controls	■■	■■	■
Optimize the operating temperatures	■■	■■	■■
Electric systems and artificial lighting			
Install the most efficient lamps and ballast	■	■	■■
Install dimmers	■■	■	■
Maintenance of lamps	■■	■■	■■
Solar energy technologies			
Install photovoltaic panels	■	■	■
Install solar heating panels	■	■	■

Incompatible actions: install mechanical ventilation pant; insulate the distribution system; insert wind technology systems

Note: ■■ = Yes - = No ■ = Specific project is required

A software simulation with Design Builder allowed to verify the energy benefit related to various retrofit actions. In this way, the proper interventions have been selected in order to improve energy and environmental efficiency of the building (Table 3).

Table 3. Retrofitting actions to be realized in Sant'Alessandro University .

	Measurements		Reduce of		
			Thermal loss	Thermal gain	Air infiltrations
A	Roofs	Add insulation on the top surface	70-80 %	-	-
		Install insulated ceiling	60-70 %	-	-
B	Walls	Insulate with thermal plaster	30 %	-	-
		Insulate with thermal wall	50 %	-	-
C	Basement	Install underside insulation	50-60 %	-	-
D	Doors	Install high-efficiency	10-20 %	-	70 %
E	Windows	Install high-efficiency windows	50-70 %	25-40 %	90 %
		Install low-e glasses on frames	30-40 %	25-40 %	60 %
		Install weather-stripping	-	-	40 %
F	Curtain Roof	Transparent Insulating Materials	50-80 %	30-40 %	50 %
		Install selective materials	50-60 %	50-60 %	50 %
		Install internal shading devices	-	20-30 %	-
G	Boiler plants	Test boiler efficiency	-	-	-
		Optimize the air-fuel ratio	20 %	-	-
H		Install thermostatic controls	30 %	-	-
I	Electric systems	Install the most efficient lamps	30 %	-	-
L		Maintenance	-	-	-

Note: ■ = Most efficiency action

The most important problem regards the education of staff and stakeholder to a correct thermal and light management of rooms, corridors and foyers. The building can save up to 35% energy, without compromising heritage value and occupancies comfort, by implementing the mentioned ECMs.

6. Conclusion

The objective of energy end environmental quality in historic building can only be achieved by combining a diversification of energy production from various renewable sources together with cutting greenhouse gas emissions. The goal may be obtained only by an integrate analysis of historic, dimensional, functional, energy and environmental matter. A deep knowledge of a real need permits to propose the most appropriate retrofit actions. On the contrary, non-critical application of energy standards and general models disadvantage the existing building or its parts, without getting a real advantage in the overall energy balance.

References

[1] American Society of Heating, Refrigerating and Air Conditioning Engineers, ASHRAE Handbook. Fundamentals, ASHRAE, Atlanta, 2009.

[2] English Heritage, Energy Conservation in Traditional Buildings, English Hertitage, London, 2008.

[3] E. Lucchi, Tutela e v alorizzazione. Diagnosi energetica e ambientale del patrimonio culturale, Maggioli Editore, Sant'Arcangelo di Romagna, 1st Edition 2009.

[4] A. Thumann, W. J. Younger, Handbook of Energy Audits, The Fairmont Press, Lilburn, 7th Edition, 2008.

Towards an objective assessment of energy efficiency in heritage buildings

V. Ingram[1,*], P.F.G.Banfill[1], C.Kennedy[2]

[1] *Heriot-Watt University, Edinburgh, UK*
[2] *Historic Scotland, Edinburgh, UK*
** Corresponding author. Tel: +44 1314514637, E-mail: vgi1@hw.ac.uk*

Abstract: All dwellings in the UK are required to have an Energy Performance Certificate (EPC) when sold or let, giving potential owners or tenants information on the cost and associated CO_2 emissions of heat and power. The Scottish traditional construction of solid stone walls tends to get unfavourable EPC ratings, leading to a perception that 'old is cold': this paper uses alternative calculation methods to question that perception.

The difference in results from steady-state and dynamic energy assessment methods is investigated for a dwelling with high thermal mass. The study focuses on modelled data and concludes that SAP 2009's monthly assessment estimates lower energy use and therefore gives a more favourable EPC rating than the annually based RdSAP 2005; and further that the application of dynamic simulation models may not be the optimum solution to further understanding energy efficiency of this type of dwelling.

Keywords: *Energy assessment, Behaviour, Thermal mass, Heritage, Dynamic simulation*

1. Purpose of the research

1.1. Introduction

In Scotland, nearly 20% of the housing stock was built pre-1919[1], and is considered to be of traditional construction. For the purpose of this research, traditional construction is defined as a dwelling with solid stone walls, although it is worth noting that other construction types were used in this pre-1919 era. For many people there is a perception that these types of dwellings are draughty, cold, and expensive to heat. The introduction of EPCs has tended to affirm that perception, with very low ratings for larger dwellings of this construction. However, work by Historic Scotland, the Government department responsible for the historic environment in Scotland, and others, is starting to question this perception. The perception of "old is cold" can be viewed from many angles, as different variables are important to different groups. For example, a government may look at statistics provided via EPCs, a homeowner may consider fuel bills, a tenant whose rent includes bills (and therefore has little concept of the cost of heating) may purely consider the temperature of surfaces (stone walls feel cooler to the touch) or the feel of draughts. If the relationship between thermal inertia, occupancy and energy use can be better understood, energy modelling can be instrumental in changing people's perceptions of energy use within dwellings, better educating them towards reducing energy use.

This research sets out to compare three energy assessment methods for a case study dwelling – a traditional mid-terrace, mid-floor, tenement flat in Edinburgh. It aimed to investigate how well the models predict energy demand, and how they assimilate the high levels of thermal mass seen in solid wall construction throughout the model, including feedbacks.

2. Approach and methodology

2.1. Dwelling types

The research aimed to be relevant to as many stakeholders as possible. Therefore, the most recent Scottish House Condition Survey (SHCS) report data from 2009 is used to assess the Scottish housing profile. Direct comparison can be made between just the pre-1919 dwellings

using detailed data - Table 1 shows the dwelling types and which are most prevalent within the age band, hence the choice of tenement flat as the case study dwelling, being a considerable proportion of the pre-1919 housing stock[1].

Table 1. Housing split across pre-1919 housing stock in Scotland[1].

House type	Number	Percentage of pre-1919 stock
Detached	109,000	24
Semi-detached	68,000	15
Mid-terrace	53,000	12
Tenement flat	180,000	40
Other flats	39,000	9
Total	*449,000*	*100*

2.2. Models

There are a number of building performance simulation models available globally and in the UK. To maintain relevance for the widest audience, the project uses models that are accredited in the UK to produce energy performance certificates and carry out Building Standards compliance checks.

Standard Assessment Procedure (SAP)[2] is used for new-build dwellings, Reduced Data SAP (RdSAP) is used for existing dwellings[3], and IES<VE> is a dynamic simulation software used for non-domestic buildings. The background to each model used is explained, with a summary of how the model was used and the assumptions made.

2.2.1. SAP 2009

The primary purpose of energy assessment in the UK is producing Energy Performance Certificates (EPCs) for both domestic and non-domestic buildings, at the point of sale or rent.

Standard Assessment Procedure (SAP) began in 1993, with a number of both major and minor alterations to the methodology since[2]. The largest overhaul was following the introduction of the Energy Performance of Buildings Directive (EPBD) in 2002: an update to SAP was needed to ensure it was consistent with energy assessment methods across the EU.

The latest update to SAP came in April 2010, as the Government released SAP 2009, v9.90, to be used from October 2010[2]. This new model has updated carbon emission factors, fuel prices, climate information, and also now includes space cooling. The biggest difference to v9.90 is that it has moved from an annual calculation to a monthly calculation. SAP uses a steady-state calculation, in that it assumes that variables are constant within each time step, implying that the method has become more detailed and aims to be more accurate, however, it does not include feedbacks within the system.

While the technical guide and calculation methodology for SAP are open to anyone to view and download, the majority of software providers allow access to their SAP programmes only to qualified assessors. A minority allow unlimited or academic access. The defined SAP methodology[2] has therefore been put into a bespoke spreadsheet model to enable detailed examination of the calculations and relationship between variables.

2.2.2. RdSAP 2005[3]

The most significant change to SAP has been the introduction of RdSAP in 2007, used solely for predicting the energy demand in existing dwellings. It does this by providing a database of information to be used in the calculation where an assessor finds information unobtainable (such as wall construction, thickness, U-values) as the dwelling is already built. For dwellings built in the 20th century the system is relatively fair, creating age bands of dwellings. For example all housing post-1984 will have the same characteristics. However for dwellings built prior to 1919, the focus of this research, there is a single age band, which may lead to unrepresentative information being used in the model, affecting the modelling result[4].

Figure 1 shows that the frequency of updates to SAP and RdSAP has increased, but also shows that the model used for RdSAP is consistently behind SAP which is used for new-builds. Since October 2010, new-build dwellings are required to use SAP 2009, v9.90, whilst existing buildings continue to use SAP 2005, v9.83, using the previous set of carbon factors and out of date fuel prices.

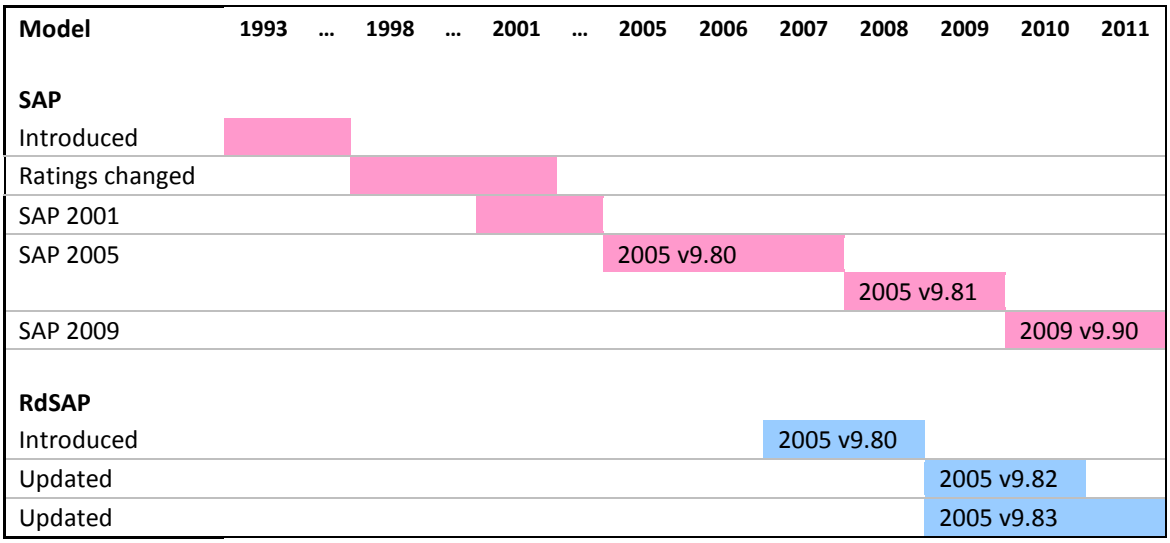

Fig 1. Changes to SAP since its introduction in 1993[2]

Similarly to the method used for SAP, the defined RdSAP methodology[3] has been put into a bespoke spreadsheet model, enabling in-depth examination of the calculations and relationships between variables. This method also allows direct comparison between entering known values and those from the construction database.

2.2.3. Dynamic Simulation Models

There may be scope for non-domestic models, their principles or methods to be included within domestic models, or to replace them. In addition to the standard domestic (SAP and RdSAP) and non-domestic methods, the UK National Calculation Methodology (NCM) includes Dynamic Simulation Models (DSMs). These DSMs look at both high spatial resolution as well as high temporal resolution to model the changes that occur over time using fundamental mathematics of the heat transfer processes that occur both inside and around a building.

As well as the basic heat gains and losses calculations, DSMs also include convection, heat transfer by air movement, thermal radiation transmitted by surfaces, solar transmission, and absorption and reflection by any glazing. The heat gains utilised are both sensible heat (the

temperature change in the air of the room) and latent heat (the change in humidity in the room). Dynamic models require the building to be divided into multiple zones, and use much more detailed weather data than in SAP and RdSAP, from the Chartered Institute of Building Services Engineers (CIBSE)[5].

In the UK, there are two DSMs accredited to produce EPCs for non-domestic buildings: this research uses IES<VE>, or Virtual Environment. IES originated from academic research, but became commercial in 1994 with a user-friendly interface[6], and by using the same user-interface as professionals in the construction sector it is believed that the conclusions of this research will be accessible to a larger number of readers.

2.3. Occupancy

The SHCS provides information on the demographics of occupants in dwelling types within the pre-1919 age band of housing[1]. Using this data three occupancy profiles were produced, summarised in Table 2. These are expanded upon using studies by the Energy Saving Trust and reasonable assumptions (by the authors), to provide a list of appliances used in each occupancy profile, and assumptions are made with respect to use of heating and behaviour towards ventilation and heating where possible within the models used.

Table 2. Summary of occupancy profiles to be assumed in the research.

	Occupancy Profile		
	1	2	3
Description	Single adult	Small family	Older smaller
Number of adults	1	2	2
Age of adults	16-34	45-54	70-80
Number of children	0	2	0
Age of children	-	14-17	-

To assess the effect of occupancy on energy use in dwellings of traditional construction, IES<VE> is used, as neither SAP or RdSAP include appliance use in energy consumption calculations. During the initial model runs when comparing IES<VE> and the two SAP methods, occupancy profiles from the NCM are used, to ensure that as many variables as possible are the same in the DSM as in SAP 2009 and RdSAP 2005. However, to assess occupancy effects, the profiles from Table 2 are used, with tailor-made equipment, lighting, appliances and occupant activity profiles defined within the DSM.

2.4. Data Collection

For any type of building performance simulation, certain basic details are required, such as dimensions, heating system information, and constructions. Depending on the model used and therefore level of information required, additional details are sometimes required. A complete data set for the Case Study dwelling was collected by the author, through consulting with architectural plans and discussions with the homeowner/occupant. Typically, however, assessments of existing dwellings are done by site visits and physical measurements made. For this case study, architectural plans were available following work carried out on the flat in 1992.

By collecting sufficient data for a DSM, certain variables are known in greater detail than are needed for SAP and certainly for RdSAP. The methodology within RdSAP requires that certain variables are entered as defaults, and others are entered in more detail.

3. Results

3.1. SAP 2009 vs RdSAP 2005

When comparing the two domestic energy assessment methods, the variables that differ greatly are solar gains, fuel for space heating, and CO_2 emissions from space heating (see Table 3). The factors contributing to these variables can be traced back through the calculation to further understand the differences.

3.1.1. Solar gains

The method used to calculate solar gains in RdSAP 2005 uses a UK average vertical solar flux for the year, applied to each area of glazing. The SAP 2009 method is far more detailed, doing a monthly calculation using the mean global solar radiation on the horizontal for latitude 53.4° (approximately Manchester, UK), then calculating the vertical solar flux from that using orientation, and then calculating solar gain, again applied to each area of glazing.

3.1.2. Fuel for space heating

The fuel used for space heating is a factor of the heating system *efficiency* (identical in both SAP 2009 and RdSAP 2005 and therefore negligible) and the heating *requirement* – the kWh/year needed to heat the dwelling to the required internal temperature. This heating requirement is where the difference between the methods lies.

In SAP 2009, the heating requirement is a factor of the Heat Loss Coefficient, the total internal gains, the average external temperature, and the average internal temperature. In RdSAP 2005 the heating requirement is a factor of just the internal gains and the Heat Loss Coefficient. The SAP 2009 calculation is therefore more detailed and is also monthly. In both methods, the solar gains are a direct factor towards calculating heating demand, so any errors or differences in calculating solar gains will feed through and enhance the differences in fuel used for space heating.

3.1.3. CO_2 emissions for space heating

These are a direct function of the fuel used for space heating, and will always be different between models where the fuel demand is different. Additionally, the CO_2 emissions are calculated using emission factors ($kgCO_2/kWh$) which were updated in 2009 and for mains gas are now 2% higher.

3.2. SAP 2009 vs IES<VE>

The results that can be analysed from IES<VE> are similar to those from SAP 2009, as they are both in monthly formats. However, IES<VE> allows the user to go into more detail down to hourly level, and view in graphical format the energy use, emissions, and internal variables such as temperature.

Table 3 compares the key variables from SAP 2009 with those from IES<VE>. IES includes equipment in its total electricity figures while SAP and RdSAP do not, therefore only electricity for lighting is shown here for more accurate comparison.

It is obvious from Table 3 that IES<VE> is the most onerous method of assessing energy and emissions from this tenement flat. Additional analysis may assess whether the reason is inaccuracies in the database's default values, the calculation method, or inconsistencies in data entry across all three models due to the inputs required.

Table 3. Summary of key variables across the three models.

Variable	Units	RdSAP 2005	SAP 2009	IES<VE>
Space heating demand	kWh/year	6813	3366	13,067
DHW demand	kWh/year	2791	2371	161
Lighting electricity demand	kWh/year	317	298	1457
Total energy demand	kWh/year	10,052	6165	15,900
Space heating emissions	$kgCO_2$/year	1322	666	} 2566
DHW emissions	$kgCO_2$/year	542	469	}
Lighting emissions	$kgCO_2$/year	134	154	615
Total emissions	$kgCO_2$/year	2052	1357	3674
SAP rating	n/a	78	87	*
EPC rating	n/a	C	B	*

Notes: * = Not calculated within IES<VE> for this dwelling.

3.3. Occupancy effects

Both SAP 2009 and RdSAP 2005 use a standard assumption of the number of occupants in a dwelling. The equations used differ but both are factors of the total floor area. In this case study the results are the same, assuming occupancy of 2.13 people, while in reality the flat is home to 2 adults. Consequently, in this case study it can be suggested that the energy requirements for domestic hot water, heating and lighting may not differ wildly when using the exact figure of 2 people. However, as mentioned in 3.2, SAP does not include the energy for equipment and appliances. By including these, it is suggested that the total energy demand and total emissions will both increase. This case study has two bedrooms, and could potentially also house two young children in the second bedroom, increasing the equipment use with additional televisions etc, but also increasing all other loads within the dwelling, as more showers are taken, more food is prepared, and more rooms require heating and lighting.

4. Discussion

Energy assessment in the domestic sector has one main purpose – the production of EPCs. With new-build dwellings, energy assessment methods can be used during the design phase to reach a particular level of design and CO_2 and energy savings as required by planning conditions, by suggesting constructions, insulation levels, and low or zero carbon technologies. For existing dwellings, energy assessment can also be used for this, but if the assessment is inaccurate, it may result in inadequate, deficient or inefficient retrofits.

While the EPC system is designed to be standardised across the UK, with standardised occupancy and location information used (in RdSAP at least), it only serves its purpose truly for sale and rentals, as it informs the new occupier of suggested costs. The methodology as it is cannot identify areas of high energy use or optimum areas for retrofit for a particular occupancy. For example, in a large house with occupancy profile 3, greater emissions savings may be made with retrofit options that favour reduced heating thereby reducing bills and raising quality of life as the occupants regain use of rooms previously cut off as ‘too cold’. In a small flat with occupancy profile 2 where appliance and equipment use is heavy, it may be wiser to reduce electrical demand through efficient appliances, or introduce renewable electricity supply.

In terms of the human impact on energy assessment and on the occupant's energy use the second biggest factor is the way the assessor carries out the data collection and RdSAP calculation. There are a number of areas within RdSAP where detailed information can be found if the assessor has the time or inclination to find it, but due to time constraints on a project they may use more default information from the database than is ideal. While assessors undergo training and examination, there is currently no quality control stipulated in the Building Standards for Scotland [7]. Only if an assessor is accredited through an English-based company will they undergo recurrent checks on their assessments. It is suggested that these assessor errors could be significant, and further research on this is in progress.

As outlined earlier, energy assessment needs to be as accurate as possible for informed decision making, but there are varying levels of complexity of models, and balance is needed between simplicity and complexity. DSMs use detailed input data and are time intensive, whereas simplified steady state methods use a less accurate approach in a faster time. It remains to be seen whether a single optimal method can be found that combines improved levels of detail with short timescales. To combine accuracy and speed, a statistical approach could be used to define polynomial functions from the DSM to provide statistical methods that in essence are a simplified dynamic approach [8,9]. Table 4 outlines the main differences between the types of model looked at within this research.

Table 4. Summary of main variables and differences between assessment methods

	SAP	**RdSAP**	**Dynamic**
UK Accredited for:	New-build Domestic	Existing Domestic	Non-domestic
Construction details	Exact, from plans	Database unless known	Database unless known
Thermal Mass	Limited	✗	✓
Include heat gains	✗	✗	✓
Overheating risk (as standard)	✗	✗	✓
Climate variables	Monthly	Annual	Hourly
Time to assess	1-2hrs	1-2hrs + site visit	1-2 days + site visit
Cost to assess	££	££	£££ upwards

RdSAP and SAP both require a number of simplifications in the data input. In both methods, a default database U-value for solid sandstone walls was used; however work is ongoing at Historic Scotland to measure U-values in-situ. It may be possible in future to use measured U-values to better represent a particular dwelling's heat loss.

The research in this paper could be compared to real energy bills in an attempt to validate the analysis, but there will still be inconsistencies, as so many aspects of the SAP and RdSAP methodologies are standardised and fail to include equipment and appliances. An energy assessment was carried out on this property in 2009, but comparisons between the assessment here and the EPC are difficult for three main reasons: the EPC assessor assumed no flats on the ground floor, substantially increasing the area of heat loss; the EPC assessor used a different floor area ($75m^2$ to the $65m^2$ used from plans); a new boiler was installed in 2010, improving the space and water heating efficiency and therefore energy demand. The first two points here are indicative of the human error aspect explored in Section 4.

Rapid changes within the construction industry and Building Standards equally past, present and future, combined with updates to the energy assessment methodology, mean that energy assessment stakeholders work in a rapidly changing arena. Updates to Building Standards are expected in 2013 and beyond, and changes in the EPBD cannot be ruled out. Future Standards may require different things of existing buildings, and energy assessment may have a different purpose. Therefore, while the outcomes of this research are relevant in 2011, their relevance in the future cannot be predicted.

5. Conclusions

It can be seen here that the models disagree on key variables. Where SAP 2009 and RdSAP agree quite well as to the energy required for DHW and lighting, IES predicts a far higher lighting demand, but a much lower DHW demand. Similarly to the lighting, IES predicts far higher space heating demand than the domestic models. If comparing just the domestic models, SAP 2009 predicts lower energy use for all variables than RdSAP 2005. Further work will be carried out into the variations in energy demand predicted by the models used.

This work shows there is still potential for improving energy assessment, and the complexity of *precise* energy assessment does not necessarily lead to *accurate* energy assessment.

References

[1] SHCS. 2010. Scottish House Condition Survey: Key findings for 2009. http://www.scotland.gov.uk/Topics/Statistics/SHCS/Downloads Accessed 14 December 2010

[2] BRE, 2010a. The Government's Standard Assessment Procedure for Energy Rating of Dwellings. 2009 Edition. Available at http://www.bre.co.uk/sap2009/page.jsp?id=1642 Accessed 3 May 2010

[3] BRE. 2009. Standard Assessment Procedure 2005 v9.83. Available at www.bre.co.uk/sap2005 Accessed 12 March 2010

[4] Barnham, B., Heath, N., Pearson, G. 2008. Energy modelling analysis of a traditionally built Scottish tenement flat. Edinburgh, Changeworks

[5] IES. 2009. ApacheSim Calculation Methods <Virtual Environment> 5.9. Integrated Environmental Solutions Limited

[6] IES. 2010. About Us [online content]. Available at http://www.iesve.com/About-us Accessed 14 December 2010

[7] Hughes, A.M. 2010. Discussion on QA/Audit process for Scottish energy assessments. [Telephone conversation] (Personal communication, 05 May 2010)

[8] Caldera, M., Corgnati, S.P., Filippi, M. 2008. Energy demand for space heating through a statistical approach: application to residential buildings. Energy & Buildings 40(11) pp1972-1983

[9] Jaffal, I., Inard, C., Ghiaus, C. 2009. Fast method to predict building heating demand based on the design of experiments. Energy & Buildings 41(6) pp669-677.

Climate control in historic buildings in Denmark

Poul Klenz Larsen[1,*], Tor Broström[2]

[1] *The National Museum, Department of Conservation, Copenhagen, Denmark*
[2] *Gotland University, Visby, Sweden*
** Corresponding author. Tel: +45 33473533, Fax: +45 33473327, E-mail: poul.klenz.larsen@natmus.dk*

Abstract: In many historic buildings, conservation heating has been used to control the RH in winter. Heat pumps are much more energy efficient than direct electric heating, so this technology may be adapted for climate control. Dehumidification has not been regarded as appropriate for historic buildings due to poor regulation, but recent development in electronic hygrostats makes this technology an attractive alternative. The annual energy consumption for both control strategies was calculated from statistical meteorological data for Denmark. The most energy efficient control strategy is determined by the U-value of the building, the air exchange rate and the volume. For large buildings conservation heating with heat pump technology seems to be the most energy efficient, unless the thermal insulation is very poor. For small buildings dehumidification is more efficient unless the building is very leaky. The two strategies for climate control were tested in historic houses owned by the National Museum in Denmark and used for exhibition only in the summer season. Kommandørgården has an uncontrolled climate in summer due to open doors in the opening hours. In winter the RH is controlled to 60-70% by hygrostatic heating. Liselund is an 18th century mansion located in a romantic garden on the island Møn at the Baltic Sea. The house is open only for guided tours in the summer, and the RH is controlled all year by dehumidification.

Keywords: *Dehumidification, conservation heating, air infiltration, historic building, climate control*

1. Introduction

Denmark has a mild and humid coastal climate due to the influence of the Atlantic Ocean and the Gulf Stream. The average relative humidity is high, and frequent rainfall and mist from the sea is a source of humidity to any building. An ordinary house usually has a moderate RH inside due to heating and ventilation. But a historic building, which is not used for living or working anymore, has a high RH even if there is no human activity. The humidity comes from the outside air and in some cases also from rising damp or rain penetrating the walls. A permanent high RH has dramatic consequences for preservation of the interiors. Woodworms may eat up the furniture and moth will feed on the textiles if nothing is done to reduce the RH. There are two options for a simple humidity control strategy in historic houses which are not permanently occupied by humans: Conservation heating or mechanical dehumidification. The question is which of the two strategies is the most energy efficient, and how to decide for the one or the other. In the present paper the question is dealt with through energy calculation of a generic building and a case study of two Danish buildings: Kommandørgården is a traditional farmhouse on the island Rømø, and Liselund is a mansion located on the island Møn.

Conservation heating is a well established practice to control the relative humidity for preservation purposes [Staniforth et al 1994]. It is a simple and robust method, but the stability of RH depends on the air infiltration rate and the temperature control. A leaky house with a thermostatic control will experience large variations in RH. Hygrostatic control is more flexible, but may suffer the problem of positive feedback due to evaporation from damp walls or floors. Another peculiar aspect of conservation heating is that heating is required also in summer to maintain a moderate RH. The summer heating may be avoided if the house has large south facing windows [Rademacher 2010]. As energy conservation becomes more and more important, heating all year is less attractive for climate control. The heat loss is much larger from historic buildings than from modern houses due to poor thermal insulation of

walls and ceilings. Leaky doors and windows further increase the heat loss. In a historic house, the potential to improve the thermal performance is limited. Instead, the source of energy must be efficient. Electric heaters are frequently used because they need little installation work. Heat pumps are much more energy efficient, so this technology might be adapted for use in historic buildings [Brostrom and Leijonhuvud, 2008].

Dehumidification has until recently not been regarded as an appropriate control method due to the risk of damage caused by too much drying. Surely old fashioned dehumidifiers without proper RH control used in buildings sites were not suitable for historic houses. But the development of electronic hygrostatic control has made dehumidifiers an attractive alternative for historic buildings, where heating is not needed for human comfort. There are two methods for dehumidification of atmospheric air; absorption and condensing. The condensing dehumidifier contains the same elements as a refrigerator, but in a different combination: A fan drags the air through the cooling unit to extract the moisture, which drips into a bucket or to a drain. The cooled air then passes through the heating unit and back into the room a little warmer than before. This method works well in heated buildings but is less efficient below 8˚C. The absorption dehumidifier passes the air through a desiccant, usually silica gel, which absorbs the water vapour from the air. When the desiccant is full, a supply of warm air removes the moisture to the outside. The advantage of this method is that it works at low temperatures, even below zero degrees. The humidity is not transformed into a liquid, so the device does not need a drain or a bucked to be emptied. However, the device requires ducts for the release of the warm humid air to the outside.

2. Theory

A model building with a total volume of 500 m^3 was used for the calculation of energy efficiency. The building had one level with a rectangular plan of 10 x 17 m^2 and 3 m to the ceiling. The U-value of the ceiling and the walls was 1.0 W/m^2K, which equals 50 cm solid brick masonry or 5 cm wood planks. The model did not take into account heat loss or gain from the floor. Solar radiation to the building and heat radiation to the open sky was not considered. The building was empty and had no internal sources of humidity. The only source of moisture into and out of the building was the outside air, which would enter at a constant rate. If nothing was done, the inside climate of the building would be almost the same as outside. But the RH was to be maintained constant at 60% all year, either by heating or by dehumidification. The calculation used the monthly averages of temperature and relative humidity in Denmark. For every month the appropriate temperature for conservation heating and the excess moisture to be removed by a dehumidifier was determined. These data are presented in table 1.

The energy needed for conservation heating and dehumidification as a function of the Air Exchange Rate (AER) is shown in Fig. 1. In the case of dehumidification (blue line) the energy demand depends only on the AER. It was assumed that an absorption dehumidifier would use 1 kWh to remove one kg of water from the air. The energy was used to heat up the air stream that evaporated the moisture from the adsorbent. In the case of conservation heating (red line) the energy needed to achieve the target RH depends on the temperature difference between inside and outside. It is assumed that the heat pump gives of 3 kWh of heat for each kWh of electric power (COP = 3). As for dehumidification, the energy demand increases proportional to the AER. But even an airtight structure needs heating due to the heat loss by transmission thought the walls and ceiling. This depends on the U-value and defines the intersection with the Y-axis. The crossing point of the two straight lines divides the diagram into two segments. Dehumidification is more energy efficient than heating with a heat pump if

the air exchange rate is lower than 1 per hour. At higher air exchange rates heating becomes more favorable. The heat loss from a highly insulated building (U = 0.1 W/m^{2}K) and a very lightly build house (U = 2.0 W/m^{2}K) is shown for comparison. A heat pump is more energy efficient for climate control in a well insulated building if the AER is higher than 0.1 per hour, whereas dehumidification is favorable in a building with little thermal insulation if the AER is below 2 times per hour.

Table 1. Monthly average for outside temperature (Out T), relative humidity (Out RH) and outside absolute humidity (Out AH) for Denmark. Estimated inside temperature (In T) and temperature difference (T dif) for conservation heating to a constant RH at 60%. Estimated inside absolute humidity (In AH) and difference in absolute humidity (AH dif) for dehumidification to a constant 60% RH.

	Meteorological data			Conservation heat		Dehumidification	
Month	Out T (°C)	Out RH (%)	Out AH (g/m^3)	In T (°C)	T dif (°C)	In AH (g/m^3)	AH dif (g/m^3)
Jan	0	87	4.2	5.5	5.5	2.9	1.3
Feb	0	85	4.1	5.0	5.0	2.9	1.2
Mar	2	83	4.6	7.0	5.0	3.4	1.2
Apr	7	76	5.9	10.5	3.5	4.7	1.2
May	12	68	7.2	14.0	2.0	6.4	0.8
Jun	16	68	9.2	18.0	2.0	8.2	1.0
Jul	18	71	10.8	21.0	3.0	9.1	1.7
Aug	17	74	12,0	22.5	5.5	8.7	3.3
Sep	14	78	9.4	18.5	4.5	7.2	2.2
Oct	9	83	7.3	14.0	5.0	5.3	2.0
Nov	5	87	5.9	11.0	6.0	4.1	1.8
Dec	3	88	5.2	9.0	6.0	3.6	1.6

For every U-value there is an AER, at which heating and dehumidification is equally efficient. The relation between AER and U-value is linear as shown in Fig. 2. If a building with 500 m^3 volume has a combination of AER and U-value above the blue line, then dehumidification is the most efficient way to control the RH to 60% over the year. This is typical for historic buildings which are not used for living or working. If the combination of AER and U-value is below the blue line, then a heat pump is more efficient for climate control. Modern buildings which are ventilated for human comfort are in this segment. Similar lines for equal energy efficiency is shown for a large building (2000 m^3) and a small building (100 m^3). Heating is favorable for most combinations in a large building, whereas dehumidification is more efficient in small buildings for most combinations of AER and U-value.

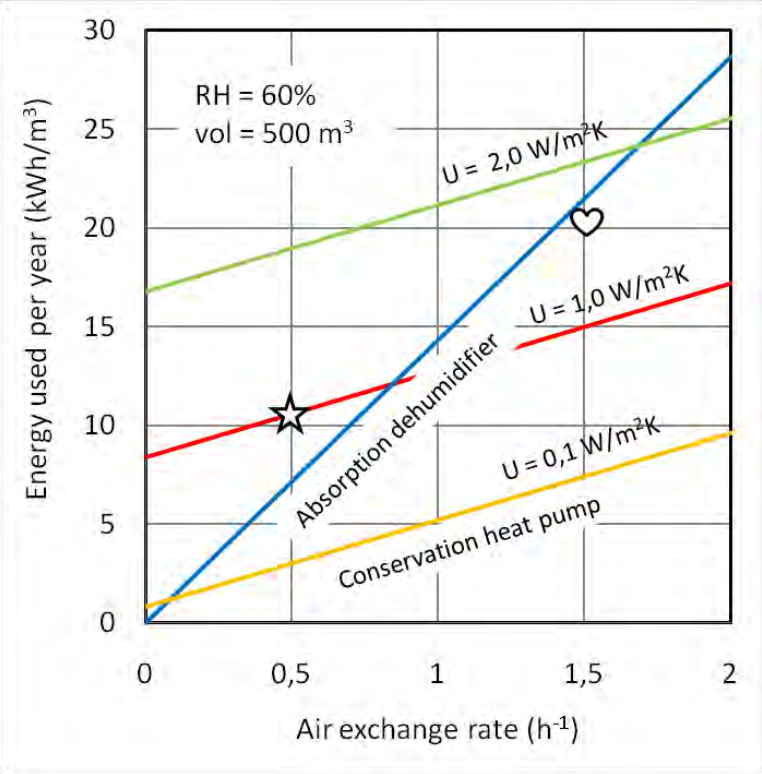

Fig. 1. The energy used per year by two different strategies to control the relative humidity to 60% in a 500m³ building. The calculations were based on monthly statistic data presented in tab. 1. The star represents Kommandørgården and the heart represents Liselund.

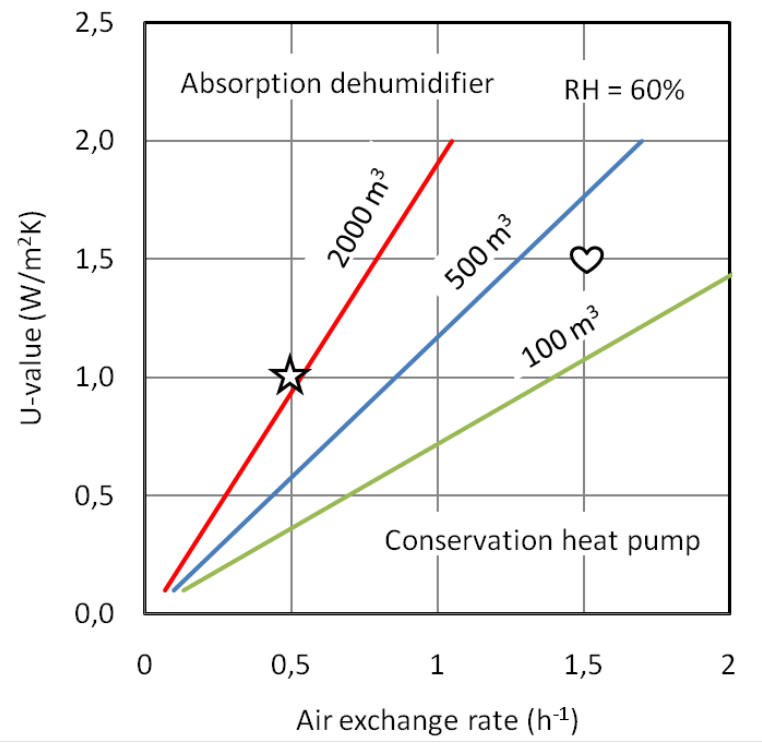

Fig. 2. Lines of equal energy efficiency with dehumidification and heating by a heat pump for controlling the RH to 60%. The size of the building is indicated for each line. The star represents Kommandørgården and the heart represents Liselund.

3. Conservation heating at Kommandørgården

The concept of conservation heating was implemented in Kommandørgården (Fig.3). The traditional farmhouse is located on the island Rømø at the west coast of Jylland, exposed to the strong winds from the North Sea. The building has solid walls of brick masonry with wooden panels or glazed tiles on the inside. The floors and ceilings are wooden planks and the roof is thatched. The average U-value of the walls and ceiling is 1.0 W/m^2K. The volume of the ground floor is 250 m^3. It is used as an open air museum in summer, and climate control is not possible due to the many visitors during the day. In the winter 2006 conservation heating was introduced with portable heating fans in the three main rooms. Each heater was controlled by a hygrostatic switch placed in some distance from the warm air stream. Climate records for 1 January to 1 July 2006 shows that the temperature was raised from 2-3 ˚C to 8-12 ˚C, and the RH dropped from 90% to 65 – 55 % (Fig. 4). The heating was stopped when the museum opened at the end of March, and the RH soon rose back above 80%. The RH dropped to 60-70% again in the two first weeks of May, when the house was heated due to conservation works. This episode shows that conservation heating would be feasible also in the spring.

The air exchange rate in winter was measured by the PerFlour-Tracergas method (PFT) in collaboration with the Building Research Institute (Bergsøe). An inert fluorcarbon gas was emitted at a constant rate to the interior from metal tubes distributed in the rooms. The gas was collected by glass tube samplers mounted in distance from the emission tubes. The amount of gas collected over a 4 weeks period was a measure of the average concentration, which depended on the infiltration of outside air. Usually the procedure should be repeated both in summer and winter to account for the different outside conditions, but in this case the measurement was done only in February, where the AER was 0.5 h^{-1}. This result is plotted with a star in the diagrams in Fig. 1 and 2. From Fig. 2 it seems that dehumidification would be more energy efficient for controlling the RH in winter, and perhaps also in summer if an air lock was installed at the entrance.

4. Dehumidification at Liselund Mansion

Dehumidification has been used for climate control in Liselund mansion, which dates back to 1800. The building is situated at a small pond in a romantic park on the island Møn at the Baltic Sea (Fig. 5). The walls are 50 cm solid masonry and the roof is thatched. The floors are wooden planks and the ceiling is gypsum plaster. The building has large single glazed windows and doors, which take up 25% of the wall surface area. The volume of the basement and the ground floor is 650 m^3 and the average U-value is 1.5 W/m^2K. In summer there are guided tours, but apart from that it remains closed all year.

The RH is controlled by an absorption dehumidifier (Munters) located in the basement. The dry air is distributed with ducts into each room through small grills in the floor. The air is returned though the staircase to the basement. The desiccant is embedded in a revolving unit, which enables the dehumidifier to work continuously. Absorption and evaporation takes place simultaneously from separate segments of the unit. The RH was 55-65% all year, whereas the temperature was drifting from around 0 ˚C in winter to 20 ˚C in summer (Fig. 6). The annual energy consumption for dehumidification was 13 MWH or 20 kWh per m^3 per year. The Air Exchange Rate was not measured, but can be estimated to 1.5 h^{-1} from Fig. 1. The doors and windows are indeed rather leaky, and much energy would be saved by improving the air tightness of these components.

Fig. 3. View of Kommandørgården from the southeast. The traditional farmhouse is located on the island Rømø at the West coast of Jylland close to the North Sea.

.

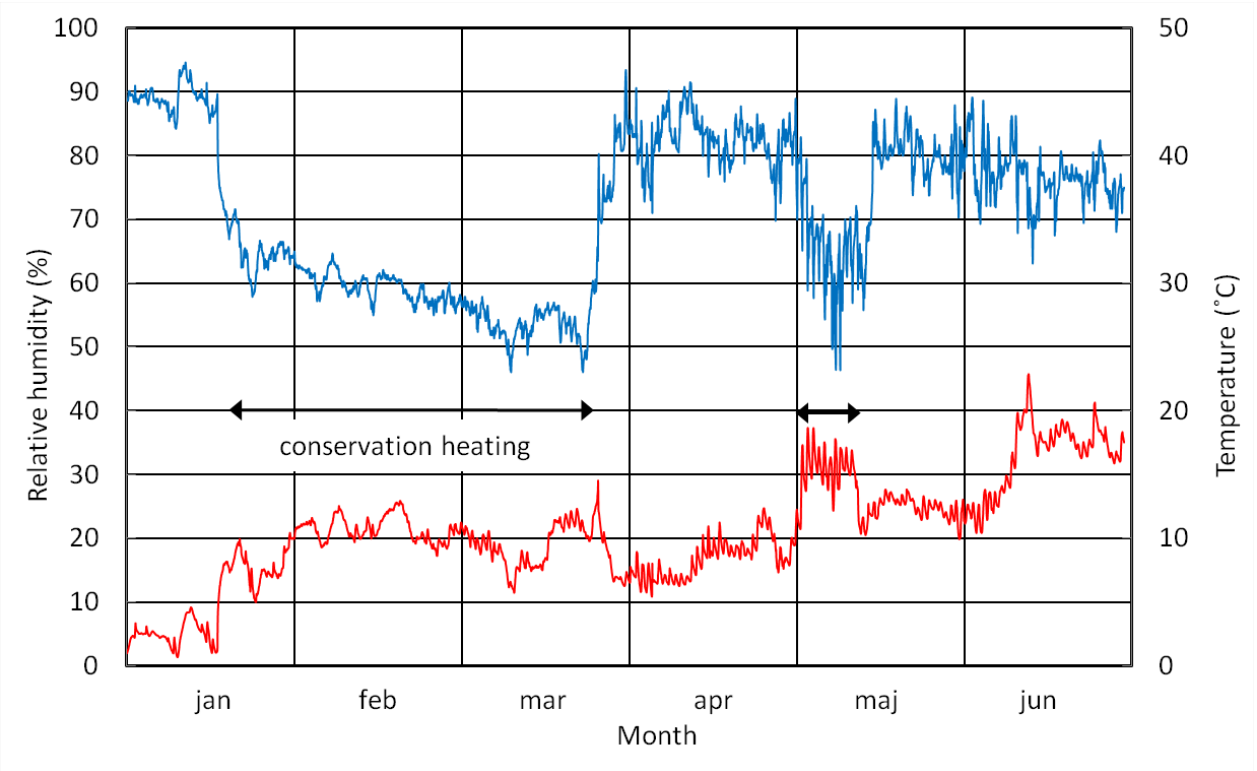

Fig. 4. Indoor climate records from Kommandørgården over six months in the winter and spring 2006. Conservation heating with hygrostatic control to 60% was started in mid January and terminated at the end of March when the museum opened for the Easter holidays.

Fig. 5. View of Liselund Mansion from the southwest. The building is located in a romantic garden on the island Møn close to the Baltic Sea.

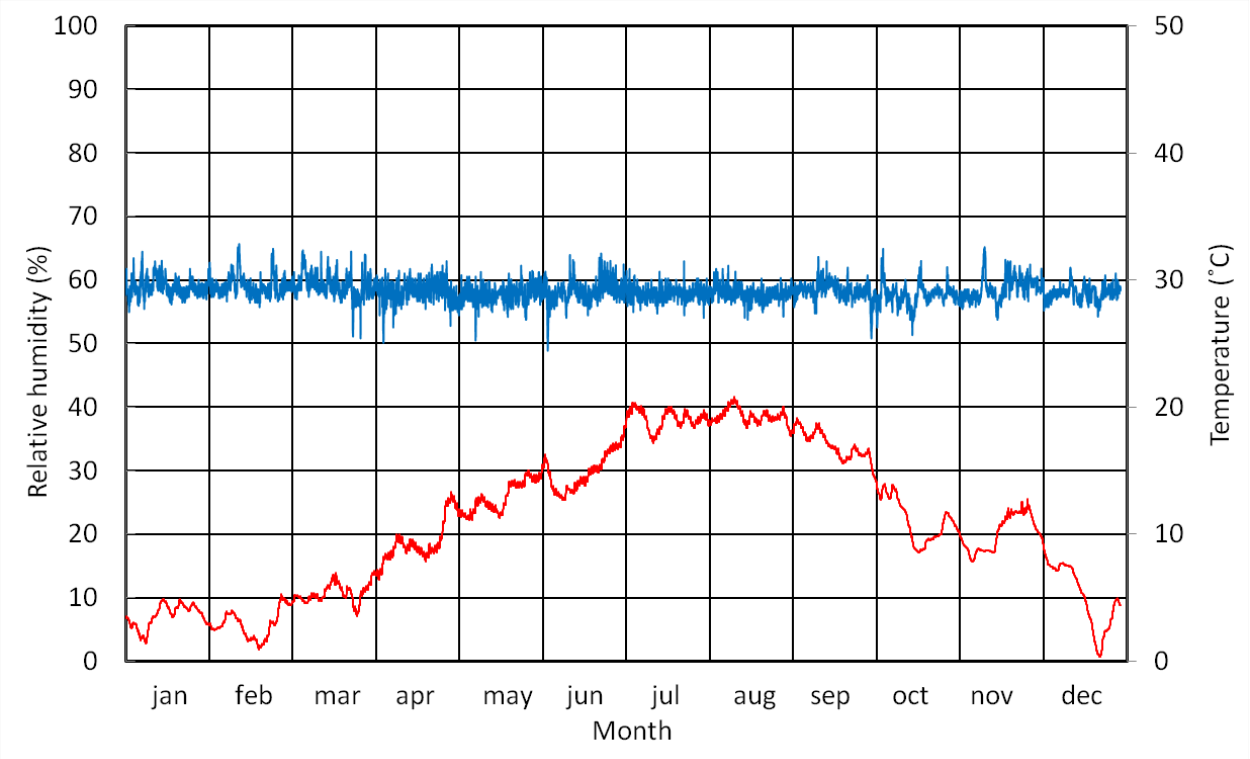

Fig. 6. Indoor climate records from Liselund Mansion in 2009. The relative humidity (RH) was controlled to 55- 65 %RH by dehumidification. The indoor natural temperature variation was 0 – 20 °C due to the influence of the outside temperature.

The combination of U-value and estimated AER is plotted in Fig. 2 with a heart. According to this, conservation heating with a heat pump would be more energy efficient if nothing is done to reduce air infiltration. Another reason for the high energy consumption could be evaporation of moisture from the ground. The basement floor is only slightly above the water level of the pond outside. Such external sources of moisture are not included in the calculations and are a potential source of error.

5. Conclusion

The strategy for climate control in historic buildings depends on whether the house is occupied by humans or not. In many historic buildings, conservation heating has been used to control the RH in winter. But the heat loss is usually large, because historic buildings are leaky and have poor thermal insulation. It is difficult to improve the performance of the building envelope, so the energy source must be efficient. Heat pumps are much more energy efficient than direct electric heating, so this technology may be adapted for climate control. Dehumidification has not been regarded as appropriate for historic building, but better regulation makes this technology an attractive alternative. The paper gives a general method to determine the most energy efficient strategy for humidity control in relation to buildings characteristics. The most energy efficient control strategy is determined by the U-value of the building, the air exchange rate (AER) and the volume. For large buildings, conservation heating with heat pump technology seems to be the most energy efficient, unless the thermal insulation is very poor. For small buildings dehumidification is more efficient unless the building is very leaky. The results are only valid for locations with natural climatic conditions similar to Denmark. Further research will generalize the method and also take into account internal moisture sources as well as other types of dehumidifiers.

References

[1] S. Staniforth, B. Haves and L. Bullock, Appropriate Technologies for Relative Humidity Control for Museum Collections Housed in Historic Buildings, Preventive Conservation: Practice, Theory and Research, Preprints of the contributions to the Ottowa Congress. London, The International Institute for Conservation of Historic and Artistic Works (IIC), 1994, pp. 123 – 128

[2] H. Rademacher, Feuchtegesteuerte Beheizung zur präventiven Konservierung einess Schlossmuseums, Klima und Klimastabilität in historichen Bauwerken, Wissenschaftlich-Techniche Arbeitsgemeinschaft für Bauwerkserhaltung e.V. Arbeitsgruppe 6.11., 2010, pp 77-88

[3] T. Brostrom, G. Leijonhufvud, Heat pumps for conservation heating, Nordic Symposium on Building Physics, Copenhagen, June 2008, pp

[4] N.C. Bergsøe, Passive tracer gas method for ventilation investigations. Description and analysis of the PFT-method, SBI report 227, Danish Building Research Institute, Hörsholm, 1992

Solar energy and cultural-heritage values

Tor Broström[1,*], Karin Svahnström[1]

[1] *Gotland University, Centre for Energy Efficiency in Historic Buildings, Visby, Sweden*
** Corresponding author. +46 498 299 922., E-mail: tor.brostrom@hgo.se*

Abstract: The use of solar energy in a building of cultural-heritage value is an issue that brings the trade-off between aspects of use and preservation to a head. A sustainable use and preservation of historic buildings requires broad and long term compromises between social, economic and environmental aspects. The objective of the present paper is to present and discuss a decision framework for such compromises regarding the use of solar energy in historic buildings.

Keywords: *Solar energy, Renewable energy, Historic buildings, Cultural heritage*

1. Introduction

The heavier demands that society now places on the efficient management of finite resources in general and energy in particular is bound to have consequences for our ability to use and thus preserve the built cultural heritage. When rising energy prices coincide with people's greater insistence on indoor comfort, all the more historically valuable buildings stand the risk of being insufficiently heated and, ultimately, either abandoned or vulnerable to damp, mould and vermin. Such a trend runs diametrically counter to the goal of long-term use and preservation of these buildings.

The use of solar energy in a building of cultural-heritage value is an issue that brings the trade-off between aspects of use and preservation to a head. On the one hand, solar energy facilitates long-term use as it makes it possible for buildings to be heated with renewable energy at a lower running cost; on the other hand, the visible installations – the solar collectors or solar cells – have a marked impact on their appearance and cultural heritage value. Conversely, while non-installation protects the buildings' cultural-heritage values, in the short term, there is a danger that such a decision will make them less attractive for long-term use and thus limit opportunities for their preservation. Economically and ecologically sustainable heating solutions must therefore be found that make it possible to use the buildings without jeopardising their cultural heritage value.

There is a general agreement that the use of solar energy in historic buildings must be considered carefully. The problem today is that decisions too often are based on relatively short term techno-economic and ecological considerations on one hand and considerations of vaguely defined cultural heritage values, with a focus on aesthetics, on the other hand.

A sustainable use and preservation of historic buildings requires broad and long term compromises between social, economic and environmental aspects. The decision context is multi-disciplinary and decisions are elaborated on the basis of both qualitative and quantitative data. There is therefore clearly a need for a structured approach to the decision-making which minimizes the risk for arbitrary and ad-hoc decisions which will have negative long-term impact on energy use, preservation or, in the worst case, both. The objective of the present paper is to present and discuss a simple decision framework for such compromises regarding the use of solar energy in historic buildings.

The cultural heritage can be seen as a cultural capital not unlike other forms of capital, with the important differences that it is possibly irreplaceable and its societal value is likely to be

higher than its market value[1]. Given this irreplacability, the cultural heritage should be considered a non-renewable national resource that demands efficient and careful management with a long time perspective.

A fundamental consideration when taking a decision on energy saving or energy transition, such as the introduction of solar energy, should thus be whether it will facilitate the sustainable management of the building, taking into account both long-term use and preservation. To achieve this, as with all other aspects of sustainable development, one must act from a perspective that aims to satisfy today's needs without it compromising the opportunities for future generations to satisfy theirs.

This fundamental tenet of the sustainability discourse is, not new. A similar philosophy was espoused by John Ruskin back in 1849 in his *The Seven Lamps of Architecture*, in which he describes older buildings thus: *"They are not ours. They belong partly to those who built them and partly to all the generations of mankind who are to follow us."*[2]

2. Sustainability in cultural heritage buildings

2.1. A model

The following is a development of Kohler's[3] model for sustainability in the built environment, based on the three general dimensions of sustainability. *Ecological values* comprise embedded energy and the resource use of the building. *Economic values* are market value, running costs and revenues. *Social values* are functional values and cultural values. Cultural values are referred to as *cultural heritage values* which in turn are divided into documentary values and experiential values. The objective is not to add to the scientific discussion of these value categories, but rather position them in the overall context of the present paper.

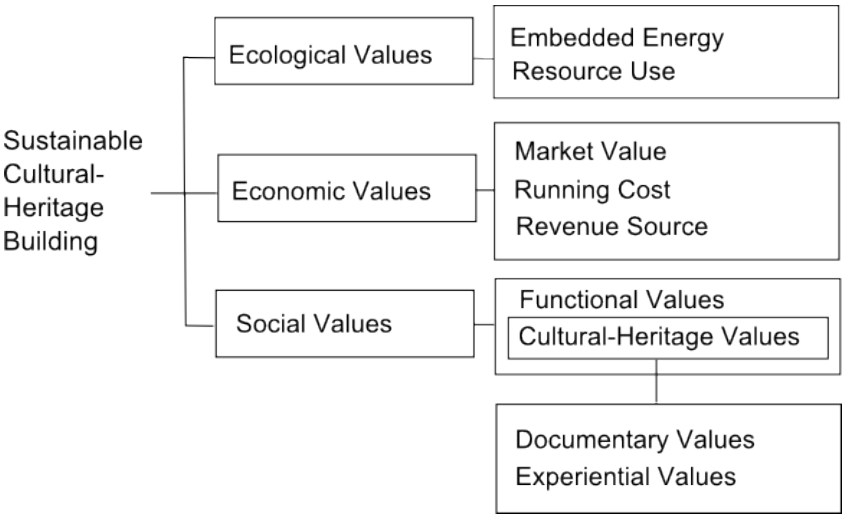

Fig 1: Conditions for sustainable cultural heritage buildings

If we are to achieve a truly sustainable management of buildings, we must take all three categories of values into account. A sustainable approach to the built heritage thus requires showing far-sighted consideration for all value categories, seeking balance between them, and understanding that they are mutually dependent rather than isolated quantities.[1] Such management demands the identification of the built environment's values in order to ascertain how they are affected by change. In the following section the three value categories are discussed in a generic way, with a focus on the dependency between cultural heritage values and the two other value categories.

2.2. Social values

Social values help to promote human wellbeing and can be broken down into functional and cultural-heritage values. All building types embody functional values, which is to say values that help to fulfil people's practical, aesthetic and symbolic needs.

The built heritage also contains cultural values, which, like their functional counterparts, contribute to human wellbeing. However, these latter values can also be of more overarching significance to sustainable development. The Faro Convention defines European cultural heritage as a resource for memory, understanding and identity.

The functional value of a building would generally increase with the use of solar energy. In some building where there are no viable options, for example unheated buildings with moisture problems, the use of solar energy can have a strong positive effect.

Cultural-heritage values can be divided into *documentary* and *experiential* values. The documentary value is associated with the building's function as source material – which on examination and analysis can yield information about the past – and chiefly comprises traditional value criteria based on historical knowledge (e.g. architectural-historical and personal-historical value). Estimating the documentary value of a building or built environment requires a degree of prior knowledge of the observer.

Experiential values are, by definition, more subjective than documentary values, and focus on the architectonic and aesthetic expression of a building or built environment. Experiential values are based mainly on immediately perceivable properties and qualities that thus require no prior knowledge to appreciate. Experiential values include architectonic value, artistic value, patina, environmental value and continuity value.

In the short term, the use of solar energy would have a negative effect on cultural heritage values. It is important to differentiate between irreversible effects on documentary values and reversible effects on experiential values. Ultimately, the fundamental cultural heritage values are dependent on the long term use and preservation of the building and thus on all other values.

2.3. Economic values

The economic aspects that are to be considered for a sustainable building management are market value, running cost and revenue. In addition to that we need to consider communal values related to the building in its context.

The market value of the building depends, of course, on running costs and revenues. Culture heritage values generally have a positive effect on the market value, even though this relation hardly lends itself to be quantified.

Revenue values, through direct utilisation (e.g. entrance fees) or indirect utilisation (restaurants, hotels and dwelling), are affected by culture heritage value in the same way as market values are.

Running costs are usually the main driving force when it comes to energy efficiency measures. High running costs can jeopardise the building's use or maintenance, which can lead to disrepair and dilapidation. This can reduce its value as a building as both its functional and market value are brought down, which, in the long run, will impact on its cultural-heritage value.

On being classified as "cultural heritage", a building undergoes a process of commoditisation to become a product, by which is meant an item or phenomenon possessing economic value. The "cultural capital" of a town or region has become an important resource in the scramble to attract desirable businesses and consumers with purchasing power, competition in which cultural heritage is exploited as a product around which the image and character of the area can be assembled. Such marketing also enables a property owner to use a building's cultural-heritage values in order to offer business and residential space that appear more attractive than offices and houses lacking such value.[4] Cultural-heritage values can thus be a factor that boosts the market value of a building, but if the building, by virtue of such a classification, is granted legal protection, the effect can be the opposite in that its market value drops.[5] It is not only the owner of such a building who can profit from its cultural heritage status; since property prices are location-bound and thus determined, for example, by the qualities of the cultural heritage environment, neighbouring buildings can also benefit. A change in the qualities that characterise an environment can thus impact upon the market value of other buildings in the vicinity.

That the market value of a built environment increases by virtue of the experiential values to which other buildings of cultural-heritage value give rise can therefore be seen as an externality, i.e. a side-effect that is of benefit to a third party. The built heritage can also generate other kinds of externalities, such as tourism, jobs and regional development[5], and in so doing contribute to national economic growth. In this way, the building, even if privately owned, can serve as a kind of collective utility and thus as something that benefits the wider community.[6]

2.4. Ecological values

Part of the ecological value is the embedded energy. The building is a non-renewable resource that, like other non-renewable resources, should be managed efficiently and carefully. Existing buildings can be seen as ecological capital comprising different type of construction materials, the consumption needs of which can be limited by their preservation, maintenance and continuing use. This also reduces the need for energy-demanding newbuilds.

The other part of the ecological values is related to the use of energy and other resources. Prudent energy efficiency measures can make this kind of building more energy efficient as well, and thus increase its value as a resource for sustainable development.

The use of non-renewable resources would in most cases decrease with use of solar energy, adding to the ecological value. More importantly, a sustained use of the building would make a continued use of the energy embedded in the building.

3. The impact of solar energy installations on a buildings values

A decision to introduce solar energy is usually motivated with an expected increase in the building's economical, ecological or functional value. At the same time, the installations risk damaging the cultural-heritage value of the building and/or its surroundings which in turn could have an effect on the other values.

A decision not to introduce solar energy has the least impact on the cultural heritage value, in the short term. However it will reduce the ecological values. More important is that a non-decision in the long term may reduce economic and functional values even to the point where it might eventually threaten the use and condition of the building and thus also more fundamental cultural-heritage value.

This line of reasoning sheds light on two aspects of the point at issue: firstly, the various value categories are, in different ways and to different degrees, interdependent, which means that the preservation or reinforcement of all value categories is a decisive factor in achieving the goal of long-term use and preservation of the built heritage. Secondly, it shows how vulnerable the value categories are to mutual conflict. The decision-making process therefore demands of the various actors involved an ability to take judicious decisions that can help to optimise the preservation of the different values of the building or the built environment. Looking solely to the cultural-heritage values in such a situation, for example, can ultimately damage opportunities for a building's long-term use and preservation, which can have a knock-back effect on its cultural-heritage value. Decisions on energy measures for buildings of cultural-heritage value therefore require a conscious and insightful balance of priorities between the various value categories of the building in question.

4. Risk assessment

Having identified the various values of a building, a risk analysis can be made in order to assess the short and long-term effects of a proposed change on all the value categories. A similar analysis should also be conducted on the basis of a no-installation scenario in which no change is made.

A simple risk-benefit matrix, see Fig 2, can be used to identify different types of problems. In cases with a low benefit or a high risk, marked in red, one should be restrictive. Low risk and high benefit, marked in green, is generally a win-win situation. Cases involving medium risk and medium to high benefit, marked in yellow, would probably need more attention.

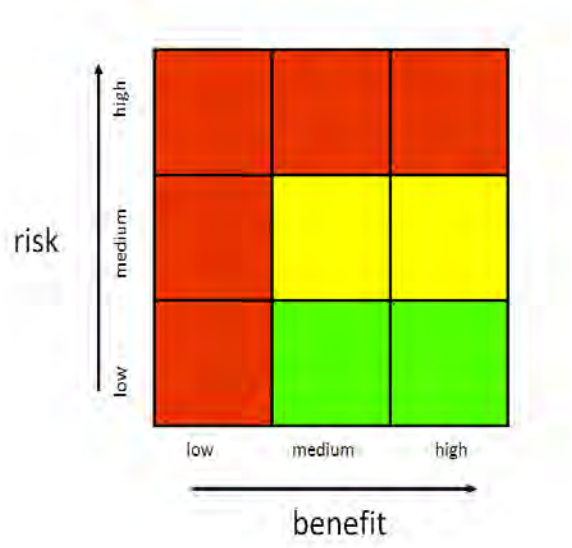

Fig 2: A matrix for a risk – benefit analysis

5. Two generic examples

5.1. A medieval church.

From a technical point of view, the steep and large south facing roof are a good place for solar collectors or solar cells, see fig 3. Depending in the alternatives, the use of solar energy adds to the ecological value in most cases. Depending on the investment, there might also be an economic value added in a lower energy cost. The visible impact would be considerable

and, for most people, have a negative effect on the experiential cultural heritage value of the church as well as its surroundings. The document value of the building need not necessarily be affected, if installations are made in a careful and reversible manner.

If solar cells are used to produce electricity for the grid, one should consider the option of producing electricity somewhere else. If this is an option, the only benefit of installing solar cells on the church roof would be an added symbolic value, allowing the church to make a green statement. Thus there is a low or medium risk and small benefit.

In the case of a church with moisture problems, mould is a common, solar panels could be used for conservation heating. This would add to, or at least secure, the functional value as mould may render a building unfit for use. In the long term, the use of the building is the most important factor for a sustained preservation of the building and it's cultural heritage values. Here, the use of solar heating would have a positive and maybe decisive effect on the functional and cultural heritage values of the building. Thus there would a high benefit, and a low to medium risk.

Fig 3 An illustration of the examples, a medieval church and the roofscape of Visby

5.2. A hotel in a World Heritage town.

The Hanseatic town of Visby on the island of Gotland is a world heritage site:

> "A former Viking site on the island of Gotland, Visby was the main centre of the Hanseatic League in the Baltic from the 12th to the 14th century. Its 13th-century ramparts and more than 200 warehouses and wealthy merchants' dwellings from the same period make it the best-preserved fortified commercial city in northern Europe."[7]

A small family hotel situated in the Visby wants to use solar energy to produce hot water in the tourist season. The main building has a large south facing roof well suited for solar collectors, but it is also well visible to the public. The use of solar energy would add to the ecological value in most cases. The added economic value is significant since any other option would give a high investment in relation to the short period of use. The building itself is ordinary, the risk is associated with the visible impact on the roofscape of the city, se fig 3. As the installation would be visible Visby has a lot of visitors, the overall effect on the experiential value would be high. In the long term, extensive solar energy installation could have a negative effect on tourism, thus reducing the economic viability of both the hotel and the city. Thus we have both a high risk and high benefit. A more depth investigation of this case should focus on optional solutions, either finding a less visible location for the solar collectors or another source of energy.

6. Closing discussion

The management of the built cultural heritage should strive to ensure its posterity to future generations. Since the value categories of buildings are mutually dependent, long-term use and preservation require a management process that takes their economic, ecological and social values into consideration.

It is thus impossible to provide a general answer to the question of whether the installation of solar energy technology should be considered a measure that contributes to the long-term use and preservation of a building of cultural-heritage value, or whether it constitutes a threat to the cultural-heritage values that make the building or the built environment worth preserving in the first place. This is a judgement call that must be made on a case-by-case basis by weighing the potential risks and benefits (fig. 4). Should the risks be deemed relatively high, installation should not proceed. Conversely, if the benefits are relatively high, installation can be considered appropriate. However, the most problematic cases arise when both the risks and benefits of solar energy are equally high. These cases require a thorough impact analysis to ascertain the best action to take in the interests of long-term use and preservation.

Much of the debate around solar energy and built heritage concerns individual cases. A challenge for the future is to seek a more coordinated, inter-sector planning and decision-making process based on a holistic view of the built environment. Such a process should take account of all the value categories represented in the building in question and the environment in which it stands. Involving all concerned parties at an early stage of the process and identifying all values makes it possible to create a planning and decision-making process with clear allocations of rights and responsibilities. This, in its turn, will enable an assessment of the positive and negative consequences an installation might have for the various value categories, and thus of which decision creates the most favourable opportunities for the sustained use and preservation of the building and the built environment.

References

[1] D. Throsby, “Culture, economics, sustainability”, *Journal of Cultural Economics*, 19 (3) (1995).

[2] J. Ruskin, *The seven lamps of architecture* (London: Allen & Unwin 1925).

[3] N. Kohler, “The relevance of green building challenge: an observer’s perspective”, *Building Research & Information*, 27 (4/5) (1999) pp 309-20.

[4] J. Grundberg, Kulturarvsförvaltningens samhällsuppdrag: en introduktion till kulturarvsförvaltningens teori och praktik (The Character of Cultural Heritage Management and its Public Agenda), Lic. Thesis, (Department of Archaeology, Gothenburg University, 1999).

[5] M. Hutter, “Economic Perspectives on Cultural Heritage: An Introduction”, *Economic perspectives on cultural heritage* (Basingstoke : Macmillan, 1997) p.16.

[6] K. Olsson, *Från bevarande till skapande av värde: kulturmiljövården i kunskapssamhället*, PhD thesis, (Royal Institute of Technology, Department of Urban Planning and Environment, Stockholm, 2003).

[7] UNESCO World Heritage List. http://whc.unesco.org/pg.cfm?cid=31&id_site=731

Exergy analysis of different solutions for humidity control in heritage buildings

M. Molinari[1,*], T. Broström[2],

[1] *KTH, Stockholm, Sweden*
[2] *Gotland University, Gotland, Sweden*
** Corresponding author. Tel: +46 87909026, E-mail: marco.molinari@byv.kth.se*

Abstract: Energy use in the building stock represents a major contribution to the total energy use in developed countries. Increasing limitations to the energy demand of the new buildings have been imposed by the building codes in the last decades, which resulted in improved building envelopes.
Yet, in many cases it is not either technically or economically feasible to improve the existing building shells. A typical example is represented by historical buildings, such churches and old buildings, which often may not be improved for aesthetical or economic reasons. Often poorly insulated, such buildings would require a high energy demand to keep them at the preferable hygro-thermal conditions. As a consequence they are often left unheated, which also affects the usability of these buildings. However, the risk of moisture damage often requires them to be slightly heated to a certain temperature.
As the energy demand is linked to the possibility of improving the building shell, for instance by adding insulation or making it more airtight, the exergy approach gives interesting insights on the problem. Exergy analysis emphasizes the thermodynamic valuable part of the energy demand in the building and straightforwardly defines the minimum energy demand for a certain process. The energy demand being equal, it is still possible to lower the exergy demand and consumption. A lower exergy demand paves the way to the exploitation of renewable sources, such as solar power.
Often the main task is to keep the RH humidity within a certain range. Aim of this paper is to perform a theoretical exergy analysis of three different solutions for lowering the RH in the building. The basic approach keeps the temperature of the indoor space at a constant level. A second approach-the so-called conservation heating- consists in letting the temperature vary according to the maximum allowed indoor relative humidity. In the third case the target is reached by means of a dehumidification process. Advantages and disadvantages of the different approaches are shown under the energy and exergy points of view.
The present research is done within the framework of the "Spara och bevara" project, which targets cost-efficient solutions for the conservation and the use of heritage buildings in Sweden and the IEA Annex49 and ESF COSTexergy projects, which aim at energy-efficient buildings and communities through the application of the low-exergy approach.

Keywords: *Exergy analysis, Energy efficient buildings, Heritage buildings, Renewable energy.*

Nomenclature

$Ex_{s,th}$	*thermal specific exergy* ..... *J/kg*	*RH*	*relative humidity* ..... -
$Ex_{s,th}$	*chemical specific exergy* ..... *J/kg*	ω_i	*room humidity ratio* ..... kg_w/kg_a
R_a	*ideal gas constant for air* ..... *J/(kgK)*	ω_o	*environment humidity ratio* ..... kg_w/kg_a
T_i	*room temperature* ..... *K*	Δv	*humidity added from the building structure* ..... g/m^3
T_0	*environment temperature* ..... *K*		

1. Introduction

In European countries, residential and commercial buildings are the sector with the largest share of primary energy use, 25% (1) and a relevant share of that is supplied by fossil fuels. The reduction of the energy demand and the exploitation of renewable energy sources has then become a priority in the EU political agenda. A widely used approach to reduce the energy demand in buildings is to improve their thermal insulation. While cost-effective during the construction phase of the building, this approach is expensive in existing buildings and alternative strategies should then be applied. The reduction of the quality of the energy supply in buildings is recognized as beneficial to reduce the environmental impact due to the energy use in buildings. An effective tool to quantify the quality of energy is exergy.

The IEA ECBCS Annex 37 (2) and the IEA ECBCS Annex 49 (3) showed that a great potential for improving the energy use in buildings resides in lowering the energy quality, i.e. the exergy, in buildings. A relevant share of the energy demand is represented by space heating and domestic hot water, (4) and (5), which is energy with low quality; buildings have a high energy demand but a low exergy demand. In contrast to this they are often supplied with valuable energy sources, such as direct electricity heating and gas. The exergy analysis applied to buildings explains how to use the energy in a more rational way by reducing the exergy losses, i.e. the energy quality mismatch between sources and end-use energy. This reduction can be obtained by supplying the building demand with degraded forms of energy, such as waste and low-temperature heat, that would be unsuitable for high-exergy processes, which occur for example in industry and transportation.

The application of the low exergy approach benefits also the exploitation of renewable sources. Renewable energy supplies have often low specific power. So-called low-exergy systems are systems with low temperatures and therefore low specific power. A floor heating, for instance, has low emission temperatures and lower emission power per unit area than radiators. It is therefore suitable for low supply temperatures, i.e. low exergy supply, such as energy from ground heat storages or from solar panels.

Optimized low-exergy systems need to be integrated and require a holistic approach. A prerequisite to an improved use of energy is to perform an exergy analysis of the system demand to highlight what is the potential for improving the overall system. In the present paper, exergy analysis was applied to the specific case of the historical buildings.

In such buildings the control of the relative humidity, RH, is important to decrease the risk of formation of mould and condensation. The lowering of RH can be obtained by heating, i.e. increasing the temperature of the air, or by dehumidifying, i.e. decreasing the water vapor contained in the unit mass of air. A common process in dehumidification consists in decreasing the air temperature needs below the dew-point, to condense the water vapor, and then to reheat it, thus making the process energy demanding.

Aim of this paper is to explore the potential for the reduction of the relative humidity. Three different approaches have been chosen and analyzed exergy-wise in two different Swedish locations.

2. Methodology

Exergy is defined as the maximum work that can theoretically be extracted by a device working between two states in non-equilibrium. When temperature, pressure and chemical composition are the same as the surroundings, thermodynamic equilibrium is reached and no more work can be extracted. These conditions are called dead-state. For buildings, the surroundings are represented by the environment and the dead-state conditions, often called reference conditions, are represented by environment temperature, pressure and chemical composition. In buildings exergy analysis the chemical composition regards the moisture content of the air, which some studies have shown to affect in a relevant way the exergy calculation, especially in warm and humid climates, (6) and(7).

In the present paper, exergy analysis has been applied to the three strategies for reducing the risks of condensation in historical buildings. An upper limit of 70% RH has been considered safe in this paper, following the approach used in (8). The building has been modeled into indoor room space and outdoor environment, whose conditions represent the so-called reference state.

To reach certain set-point conditions of the indoor air, a flow of exergy has to be supplied. The minimum flow needed is determined by the physical conditions of the unit air, i.e. the exergy content per unit mass. The minimization of the exergy content is the necessary prerequisite to the decrease of the exergy demand. The air exergy content resulting from the different strategies to lower the RH has then been compared. This approach allows to keep a general approach that can be applied to several types of buildings and also to benchmark the expected performance of the different strategies in terms of exergy.

Two different Swedish locations have been simulated, Gothenburg and Östersund. Gothenburg is located on the southwest coast of Sweden (latitude 57º43´) and it has a coastal climate with high RH most of the year. Östersund is located in the middle of Sweden (latitude 63º) and it has an inland climate, considerably colder than Gothenburg.

The first strategy is the background heating, which consists in keeping the indoor temperature at 12 ˚C by providing heat to the room. If the ambient temperature is higher than this set-point temperature, the building is left unheated.

The second strategy is the so-called conservation heating, which consists in the use of heating to keep the internal humidity under a certain level above which the risk of mould formation is considered to increase consistently. This target relative humidity, which in this paper is set to 70% (8), is kept by raising the indoor temperature. As the temperature increases, the saturation pressure of the water vapor decreases, i.e. the air is capable to dilute more vapor, and so does the relative humidity decreases. When the indoor RH was higher than the 70% set-point, then the indoor temperature was set to the value corresponding to this RH set-point, by calculating the saturation pressure of the vapor. When the RH was lower than the RH set-point, no change in the indoor temperature took place.

In the third case, the target relative humidity is kept to 70% by dehumidification. This process is usually done by decreasing the temperature of the air under the dew-point, condition at which the water contained in the air starts to condense. By removing it and post-reheating it the air becomes drier. The exergy content in an ideal dehumidification process (9) was calculated when the RH was higher than the 70% set-point.

In the second and the third strategy, indoor thermo-hygrometric conditions have also been investigated for two different levels of internal moisture generation, $\Delta v=1$ g/m^3 and $\Delta v=2$ g/m^3, with Δv (g_{vapor}/m^3_{air}) being the humidity added from the building structure.

In the Table 1 a summary of the set-points for RH and temperatures are shown for the different strategies.

Table 1: Summary of temperature and RH set-points in the different strategies. The temperature in the constant temperature heating is kept at 12˚C or higher in warmer seasons. In the conservation heating strategy, the values of the internal temperature depends on the relative humidity. In the dehumidification strategy, the temperature in the room is the same as the environment.

Strategy	Room set-point temperature [˚C]	Room set-point RH [%]
Constant temperature heating	12	-
Conservation heating	Dependent on RH	70
Dehumidification	-	70

The expressions for the calculations of the specific exergy have been derived from (7) and (9):

$$Ex_{s,th} = \left(c_{p_a} + \omega_i c_{pv}\right) T_0 \left(\frac{T_i}{T_0} - 1 - \ln\left(\frac{T_i}{T_0}\right)\right) \quad (1)$$

$$Ex_{s,ch} = R_a T_0 \left(\left(1 + 1.608\omega_i\right) \ln\left(\frac{1 + 1.608\omega_0}{1 + 1.608\omega_i}\right) + 1.608\omega_i \ln\left(\frac{\omega_i}{\omega_0}\right)\right) \quad (2)$$

In the equation (1) $Ex_{s,th}$ is the thermal specific exergy, T_i is the ambient temperature, T_0 is the environment temperature and c_p is the specific heat capacity of the air. In the equation (2) $Ex_{s,ch}$ is the chemical specific exergy, R_a is the ideal gas constant for air, T_0 is the environment temperature, 1.608 represents the molar mass of air to that of water vapor, ω_i is the humidity ratio of the room and ω_0 is the humidity ratio of the environment. The air exergy content of the three different strategies have been calculated with time-steps of 1 hour for a whole year. This simplified model doesn't take into account the moisture storage in the structure; the structure itself acts as a constant moisture generator (Δv=1 and Δv=2 g/m^3). The exergy calculated in each time-step is then the exergy needed to keep the air in conditions of temperature and humidity considered safe to avoid condensation and mould growth.

3. Results

In Figure 1, the average monthly values of the temperature and the relative humidity, derived from the hourly calculations, are displayed. The temperatures are plotted for all the analyzed cases; the simulations of the conservation heating strategy are shown for the different Δv (cases 2a, 2b and 2c). The RH is the same in all the simulations of the case 2 due to the RH control strategy. The environment RH is above the 70% limit for most of the year. The constant temperature heating strategy (Case 1) has an indoor temperature constantly set to 12 ˚C, except in summertime, when it is higher. This strategy decreases the moisture to very low levels in winter time, which is not a favorable condition for artworks possibly present in this type of buildings. In the conservation heating strategy (Case 2) and dehumidification (Case 3) the RH indoors is in the range between 60 and 70% during the whole year, due to the control of the humidity. The indoor temperature of the dehumidifying case is the same as the outdoor temperature, while the case of the conservation heating case it is slightly higher when a decrease of the RH is needed.

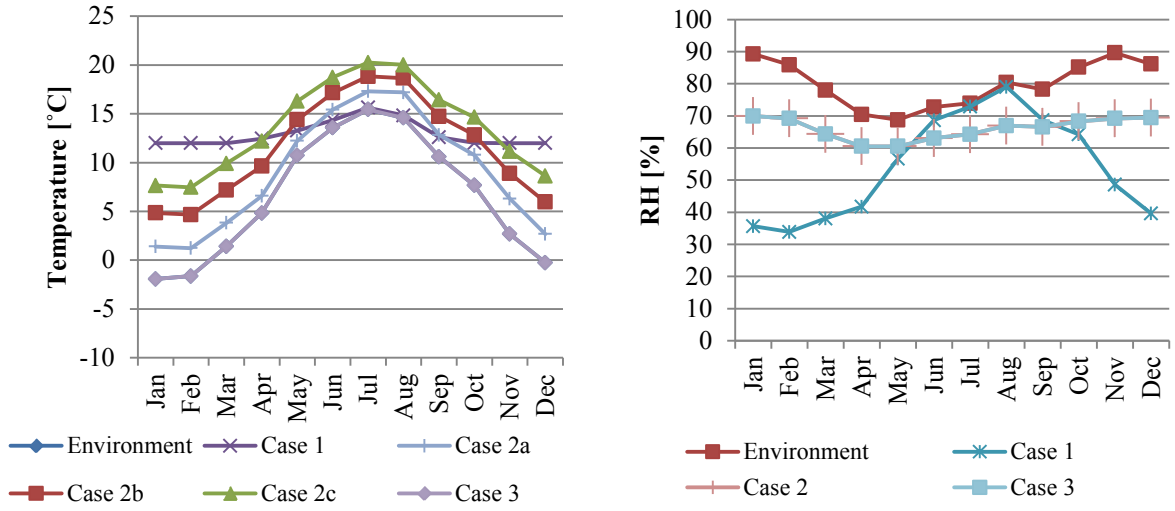

Figure 1: Monthly temperature distribution (left) and relative humidity RH (right) in the three cases in the Gothenburg simulations. Case 1 is the constant temperature heating, Case 2a is the conservation heating for Δv=0 g/m³, Case 2b for Δv=1 g/m³, Case 2c for Δv=2 g/m³ and Case 3 i s the dehumidification.

In the Figure 2 results from the calculations for Gothenburg are presented. The exergy content for three different cases, sum of the time-steps for εαch month, iσ σhown. For Δv=0 g/m^3, the exergy content in the air is significantly lower for the conservation heating and dehumidification strategies in the cold period of the year, when compared to the constant temperature strategy. In fact, in the January average conditions with an environment temperature of -1.9 ˚C and RH of 89 %, the temperature necessary to keep the RH under 70% is 1.5 ˚C. By hεαting up to 12 ˚C the RH falls to 34%, which is a low level of moisture in the air at the expense of a great exergy content.

The exergy content increases for both constant heating and dehumidification strategies αsΔv increases, due to the higher temperatures that must be reached in the room to decrease the relative humidity for the conservation heating and to the greater potential of chemical exergy in the dehumidification case. Yet, in the period between December and February the exergy content of the constant temperature heating is the double of the conservation heating with Δv=2 g/m^3.

In the warm season, i.e. from May until September, the exergy content of the constant heating gradually decreases, due to the increasing environment temperatures, but the relative humidity of the room in these conditions is higher than the limit value of 70%.

In the warm season the exergy content of the conservation heating and the dehumidification αpproach iσ comparαblε for the diffεrεnt valueσ of Δv. Howεver, the εxεrgy contεnt of the αir in the conservation heating cases becomes remarkably higher in the cold months, from December to March, when the environment relative humidity has the highest yearly peaks.

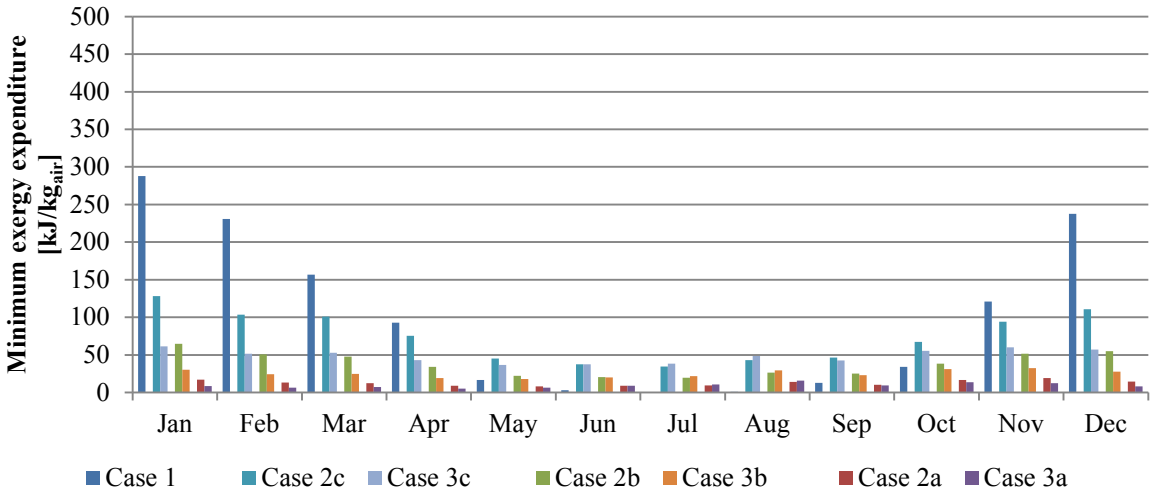

Figure 2: Comparison of the minimum exergy expenditure per kg of indoor air, in the Gothenburg climate. The air exergy content is the sum of the values calculated for each time-step. Case 1 is the constant temperature heating, Case 2a is the conservation heating for Δv=0 g/m^3, Case 2b for Δv=1 g/m^3, Case 2c for Δv=2 g/m^3, Case 3a is the dehumidification for Δv=0 g/m^3, Case 3b for Δv=1 g/m^3, and Case 3c for Δv=2 g/m^3.

In Figure 3, average monthly temperatures are shown for Östersund, together with the average values for the monthly temperatures for RH. The temperature patterns are similar to the ones obtained for the Gothenburg climate, but the minimum average temperature is lower (-5.9 in February) than in Gothenburg (-1.9 in January). The relative humidity is also lower: the yearly average RH in Östersund is 74.8% while in Gothenburg is 79.9%. This makes it possible that all the three approaches keep the average value of the RH under the 70% limit value. The temperature difference between environment and room in the cold period is greater than 15 ˚C in four months for the constant temperature heating case, causing the RH of the room to drop down to values in the range of 20-30%. The range of RH for the conservation heating and the dehumidification are within 60% and 70% during the whole year, which is an ideal condition.

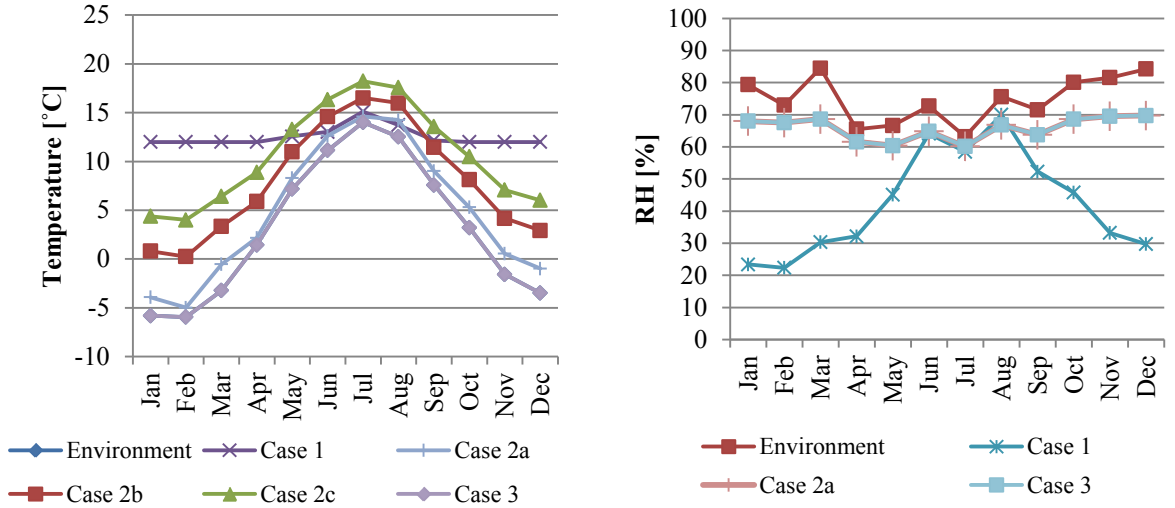

Figure 3: Monthly temperature distribution (left) and relative humidity RH (right) in the three cases in the Östersund simulations. Case 1 is the constant temperature heating, Case 2a is the conservation heating for Δv=0 g/m3, Case 2b for Δv=1 g/m3, Case 2c for Δv=2 g/m3 and Case 3 is the dehumidification.

In Figure 4, the exergy content of the room air in the different cases is shown for Östersund. In the cold season from October to March, the constant temperature heating approach has an exergy content three times higher than the conservation heating and ten times higher than the dehumidification with $\Delta v=2$ g/m^3. The increase of Δv has a relevant effect on the increment of exergy content both for the conservation heating and dehumidification strategies. Similarly to the Figure 2, the exergy content is significantly lower in the cold season in the dehumidification when compared to the conservation heating, while in warmer season there is little difference between the two strategies.

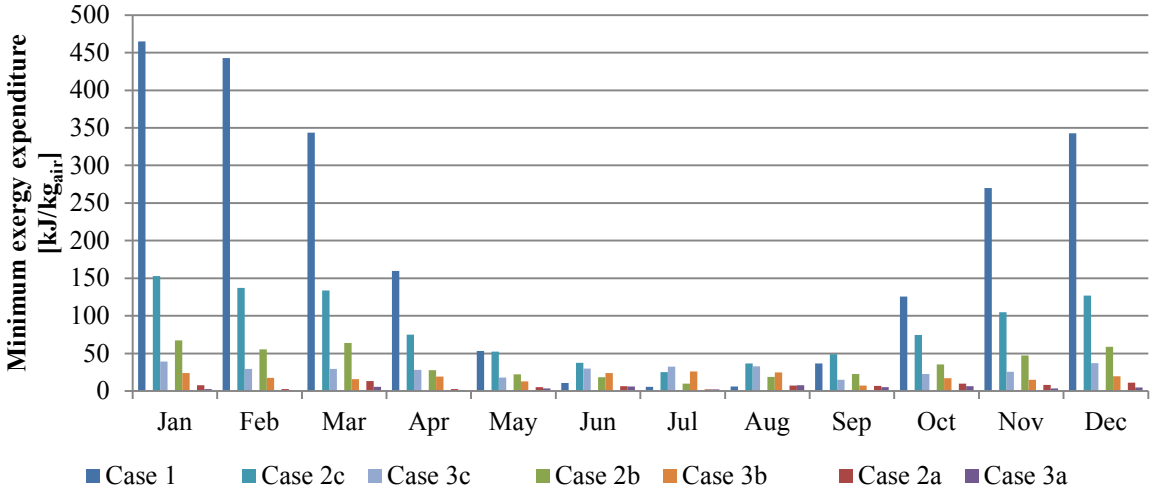

Figure 4: Comparison of the minimum exergy expenditure per kg of indoor air, in the Östersund climate simulation. The air exergy content is the sum of the values calculated for each time-step. Case 1 is the constant temperature heating, Case 2a is the conservation heating for $\Delta v=0$ g/m^3, Case 2b for $\Delta v=1$ g/m^3, Case 2c for $\Delta v=2$ g/m^3, Case 3a is the dehumidification for $\Delta v=0$ g/m^3, Case 3b for $\Delta v=1$ g/m^3, and Case 3c for $\Delta v=2$ g/m^3.

4. Discussion

For both Gothenburg and Östersund, some general trends can be highlighted.

- In the cold season the temperatures reached in the constant temperature approach are too high, causing both the RH to decrease too much, and at the same time the exergy content to increase significantly. In the warmer period it is ineffective in maintaining the RH under the 70% limit in one of the two cases analyzed (Gothenburg).

- The increase of the internal moisture generation Δv decreases the advantage of the conservation heating and dehumidification strategies on the constant temperature heating, due to the higher temperatures that must be reached in the room to decrease the RH and the higher moisture exergy content.

- The dehumidification approach has a significantly lower exergy content in the cold months, when compared to the constant temperature and the conservation heating approach.

- In warmer months, the difference of the exergy content between conservation heating and dehumidification is minimal

5. Conclusions

In the present paper the exergy concept has been applied to explore the potential energy savings to limit th e relative humidity of the air, which plays an important role in the preservation of historical buildings. Three different strategies have been simulated in two different locations in Sweden, Gothenburg and Östersund.

Constant temperature heating has proved to be inefficient and not efficacious at the same time. This strategy is not able to limit the RH under the target values and it consumes unnecessary exergy in cold periods due to the large temperature difference between the environment and the room.

In the conservation heating approach, the temperature differences between environment and room are approximately constant during the year, also with increasing Δv. This feature is very important when a heat pump is used. The coefficient of performance (COP) of a heat pump is highly dependent on the difference of temperature between condenser and evaporator, $\Delta T_{c\text{-}ev}$. The smaller the $\Delta T_{c\text{-}ev,}$ the higher is the COP of the heat pump, which makes this strategy attractive for the building heritage.

References

[1] Commission of the European Communities, Action Plan for Energy Efficiency: Realising the Potential, 2006.

[2] International Energy Agency ECBCS Annex 37, Heating and Cooling with Focus on Increased Energy Efficiency and Improved Comfort - Guidebook to IEA ECBCS Annex 37 Low Exergy Systems for Heating and Cooling of Buildings. VTT, Technical Research Centre of Finland, 2003.

[3] International Energy Agency. Low Exergy Systems for High Performance Buildings and Communities. [Online] 2005-2009, http://www.annex49.com.

[4] International Energy Agency ECBCS Annex 39, Vacuum insulation panels, study on VIP components and panel for service life prediction of VIP building applications, 2005.

[5] European Commission, Directorate General for Energy & Transport, The new Directive on the energy performance of buildings – Moving closer to Kyoto, 2003.

[6] P. Sakulpipatsin Exergy Efficient Building Design, Doctoral Thesis, Department of Building Technology, University of Delft, 2008.

[7] M. Shukuya, A. Hammache, Introduction to the concept of exergy - For a b etter understanding of low-temperature heating and high-temperature cooling systems, VTT Research Notes, 2002.

[8] T. Broström, G. Leijonhufvud, Heat pumps for conservation heating. Proceedings of the 8th Symposium on Building Physics in the Nordic Countries. 2008, pp. 1143-1150.

[9] M. Alhazmy, Minimum work requirement for water production in humidification-dehumidification desalination cycle, Desalination, 2007, pp 102-111.

[10] P. Sakulpipatsin et al., An Exergy Application for Analysis of Buildings and HVAC systems. Energy and Buildings, 42, 2009, pp 90-99.

[11] D. Camuffo, (editor). Church Heating and the Preservation of the Cultural Heritage. Guide to the Analysis of the Pros and Cons of Various Heating Systems. Electa, 2006.

[12] A. Bejan, Advanced Engineering Thermodynamics. John Wiley, New York, 1997.

New software for generation of typical meteorological year

Abdulsalam Ebrahimpour[1,*]

[1]*Departament of Mechanical Engineering, Islamic Azad University,Tabriz Branch, Tabriz, P.O.Box 51589, Iran*
[*] *Corresponding author. Tel.: 98 9123060463; fax: 98 411 3317146, E-mail addresses: Salam_ebr@yahoo.com*

Abstract: The correct selecting of typical meteorological year is an important factor for accurate building energy simulation. In this study, the Sandia method has been applied to prepare the new TmyCreator software for selecting the proper data as the typical meteorological year (Tmy2). Also, the results of this new software have been compared with the available Tmy2 weather data file for two cities. It is found that, the results of TmyCreator software have good agreement with the old created Tmy2 weather data file for these cities.

Keywords: Typical meteorological year; Building energy simulations; Finkelstein–Schafer statistics

1. Introduction

The weather data is the most important factor for building energy simulation software. The hourly data of meteorological parameters such as solar radiation, dry bulb temperature, relative humidity, wind speed, atmospheric pressure and etc are usually needed to simulate building energy.

Many methods have been suggested to provide the typical meteorological year. Typical meteorological year has been presented in different types for examples Tmy2 (NREL 1995) and WYEC2 (ASHRAE 1997) in the United States and Canada and TRY (CEC 1985) in the Europe. The Tmy2 and WYEC2 typical weather years contain more solar radiation and illumination data than older formats such as Tmy (NCDC 1983), WYEC (ASHRAE 1985) and TRY (NCDC 1981).

From 1970 to 1983, Ashrae commissioned three research projects to represent weather year data for energy calculations (WYEC), which used the TRY format but included solar data (measured data, if available or calculated based on cloud cover and type). In the early 1990s, Ashrae began to update the WYEC data set. New WYEC data sets were listed in Tmy format, and calculated hourly illuminance data, data quality as well as source flags, were included [1].

Typical meteorological year has been obtained in various types and for different cities in the earth's surface. Apple L.S. Chan [2] reviewed various types of typical weather data sets in a paper and then the Finkelstein–Schafer statistical method applied to analyze the hourly measured weather data of a 25-year period (1979–2003) in Hong Kong. A. Kalogirou [3] presented the generation of a type 2 typical meteorological year (Tmy2) for Nicosia, Cyprus. Also, Joseph. C. Lam [4], Zhang Qingyuan[5] and T. N. Anderson[6] in the different researches, provided the various typical meteorological years based on different year periods and in many places of the Earth's surface. The author (A. Ebrahimpour[7]) in previous research, created the typical meteorological year data from the measured weather data of a 14-year period (1992–2005) in Bandarabass using Sandia method [8].

In spite of this fact, the majority energy simulation softwares use typical Meteorological Year, so the exact values are necessary in order to correct estimation of the building energy consumption

at the year. In this study, the Sandia method [8] has been used to create the TmyCreator software. Using the TmyCreator software, the typical meteorological year can be select from the measured weather data of a available year period (such as 1961–2010) in a city. The result of TmyCreator software has been compared with the available Tmy2 weather data file for various cities such as Salt Lake City.

2. Sandia method

The Sandia method is an empirical approach that selects individual months from different years of the period of record. For example, in the case that contains 30 years of data, all 30 Januarys are examined and the one judged most typical is selected to be included in the Tmy. The other months of the year are treated in a similar manner, and then the 12 selected typical months are concatenated to form a complete year. Because adjacent months in the Tmy may be selected from different years, discontinuities at the month interfaces are smoothed for 6 hours on each side. The Sandia method selects a typical month based on nine daily indices consisting of the maximum, minimum, and means dry bulb and dew point temperatures; the maximum and mean wind velocity; and the total global horizontal solar radiation. For each month of the calendar year, five candidate months with cumulative distribution functions (CDFs) for the daily indices that are the closest to the long-term CDFs are selected. The CDF gives the proportion of values that are less than or equal to a specified value of an index. Candidate monthly CDFs are compared to the long-term CDFs by using the following Finkelstein-Schafer (FS) statistics for each index.

$$FS = (1/n)\sum_{i=1}^{n} \delta_i \qquad (1)$$

Where, δ_i is absolute difference between the long-term CDF and the candidate month CDF at xi and n is the number of daily readings in a month.

Because some of the indices are judged more important than others, a weighted sum (WS) of the FS statistics is used to select the 5 candidate months that have the lowest weighted sums. The weighting factors listed in Table 1 for Tmy type.

$$WS = \sum w_i FS_i \qquad (2)$$

Where, w_i is weighting for index and Fs_i is *FS* statistic for index.

All individual months are ranked in ascending order of the WS values. A typical month is then selected by choosing from among the five months with the lowest WS values the one with the smallest deviation from the long-term CDF. In Hall's original method, persistence structures characterized by frequency and run length of days are included. The persistence of mean dry bulb temperature and daily global horizontal radiation are evaluated by determining the frequency and run length above and below fixed long-term percentiles. For mean daily dry bulb temperature, the frequency and run length above the 67th percentile and below the 33rd percentile are determined. For global horizontal radiation, the frequency and run length below the 33rd percentile are also determined. The persistence data are used to select, from the five candidate months, the month to be used in the Tmy. The highest ranked candidate month in ascending order of the WS values that meet the persistence criterion is used in the TMY. Then, the 12 selected months were

concatenated to make a complete year and smooth discontinuities at the month interfaces for 6 hours each side using curve-fitting techniques. [9 & 10]

Table 1: The weighting factors in Sandia method

Wearher index	**weighting factor**
Maximum dry bulb temperature	1/24
Minimum dry bulb temperature	1/24
Mean dry bulb temperature	2/24
Maximum dew bulb temperature	1/24
Minimum dew bulb temperature	1/24
Mean dew bulb temperature	2/24
Maximum wind speed	2/24
Mean wind speed	2/24
Total horizontal solar radiation	12/24
Direct normal solar radiation	--

3. Tmy2 selection procedure in TmyCreator software

For using the TmyCreator software, The hourly measured weather data of Dry Bulb Temperature {C}, Dew Point Temperature {C}, Relative Humidity {%}, Atmospheric Pressure {Pa}, Wind Direction {deg}, Wind Speed {m/s}, Global Horizontal Radiation {Wh/m2},Direct Normal Radiation {Wh/m2} and Diffuse Horizontal Radiation {Wh/m2} have been prepared.

In Sandia method, the hourly measured data of dry bulb temperature, dew point temperature and wind speed have been used to select the Tmy2. So, calculating the maximum, minimum, and mean dry bulb and dew point temperatures and the maximum and mean wind velocity during a day and total global horizontal solar radiation during a day have been based on hourly measured data in TmyCreator software.

Other remained data in the Tmy2 weather file has not been calculated and the default values of Energyplus document software have been used [11].

4. The TmyCreator software

To use the TmyCreator software (Figure 1) the hourly measured weather data must be prepared for the desired period (such as 1990-2010). Also, the hourly measured weather data are the Dry Bulb Temperature {C},Dew Point Temperature{C}, Relative Humidity{%}, Atmospheric Pressure{Pa}, Wind Direction {deg},Wind Speed {m/s}, Global Horizontal Radiation{Wh/m2},Direct Normal Radiation{Wh/m2} and Diffuse Horizontal Radiation{Wh/m2}.

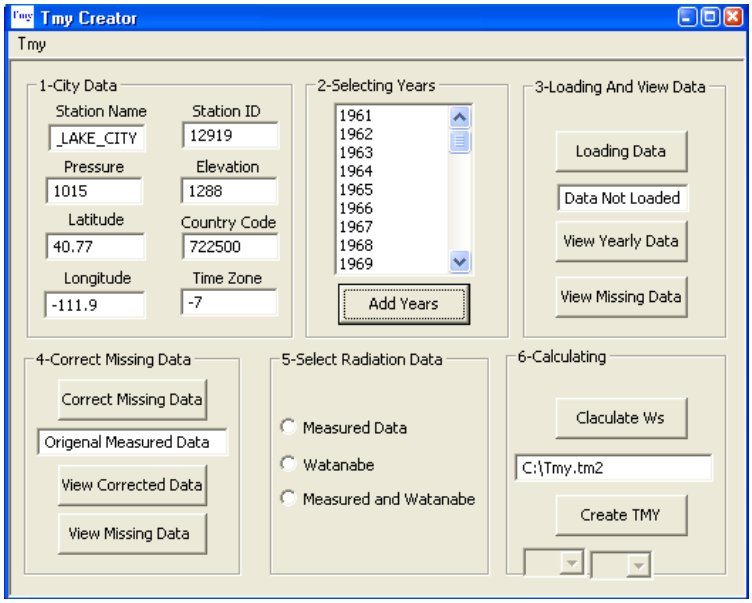

Figure 1: The TmyCreator software

4.1. Correct Missing Data

The TmyCreator software corrects the missing data using other available data as following method:

The missed data = (the amount of after three hour+ the amount of before three hour)/2

5. Validating the TmyCreator software

To validating of the TmyCreator software two methods have been used. In the first method, the Tmy2 weather data for the two city of the USA have been created by TmyCreator software from hourly weather data and the created Tmy2 file have been compared with the created Tmy2 weather data by NREL[1].

5.1. Comparing the Tmy2 Weather file

In the first stage, the 30 year period (1961-1990) hourly weather data for two city of the USA have been provided from the NCDC[2] and NSRDB[3] (for solar radiation data) and using this data the Tmy2 weather file have been created by TmyCreator software . Then the information about of selected year in the Tmy2 weather file created by TmyCreator software and NREL has been compared.

The Table 2 and 3 shows the number of not available hourly weather data for Abilene and Salt Lake City in USA in the year. It can be seen that the missing data for Abilene City is more than Salt Lake City.

The result of running the TmyCreator software using this hourly weather data for mentioned cities have been displayed in the Table 4 and 5.

[1] National Renewable Energy Laboratory
[2] http://www1.ncdc.noaa.gov
[3] http://rredc.nrel.gov

Table 2: number of not available hourly weather data for Abilene in the year

Year	Wind Direction{deg}	Wind Speed{m/s}	Dry Bulb Temperature{C}	Wet bulb Temparature{C}	Dew Point Temperature{C}	Relative Humidity{%}	Atmospheric Pressure{Pa}	Global Horizontal Radiation	Direct Normal Radiation	Diffuse Horizontal Radiation
1961	981	2	2	2	2	2				
1962	665	2	2	2	2	3				
1963	702			1	1	1				
1964	227	4	4	4	4	4				
1965	5883	5836	5836	5837	5837	5836				
1966	5914	5840	5840	5840	5840	5840				
1967	5888	5840	5840	5841	5841	5840				
1968	5880	5840	5840	5840	5840	5840				
1969	5864	5840	5840	5840	5840	5840				
1970	5854	5840	5840	5841	5841	5840				
1971	5854	5840	5840	5840	5840	5840				
1972	5845	5840	5840	5840	5840	5840				
1973	166	149	151	156	157	2501				
1974	156	92	97	99	100	601				
1975	286	209	203	216	219	246				
1976	280	208	210	222	225	703				
1977	240	165	159	165	168	179				
1978	245	203	197	205	206	213				
1979	308	205	205	204	206	229				
1980	224	147	146	150	150	159				
1981	217	99	106	107	108	113				
1982	92	2	2	2	2	2				
1983	263	1	1	1	1	1				
1984	84	1		1	1	1				
1985	108			1	1					
1986	186									
1987	233	1	1	1	1	2				
1988	209									
1989	140	1								
1990	171									

Table 3: number of not available hourly weather data for Salt Lake City in the year

Year	Wind Direction{deg}	Wind Speed{m/s}	Dry Bulb Temperature{C}	Wet bulb Temparature{C}	Dew Point Temperature{C}	Relative Humidity{%}	Atmospheric Pressure{Pa}	Global Horizontal Radiation	Direct Normal Radiation	Diffuse Horizontal Radiation
1961	387	1	1	1	1	1				
1962	322									
1963	296			2	5					
1964	363	1								
1965	320									
1966	190		1		1					
1967	186					1				
1968	421				8					
1969	318			1	3					
1970	301			12	12	12				
1971	159			1	1					
1972	201									
1973	210	1	1	1	1	1				
1974	195	1		1	2					
1975	309	1								
1976	350	6	2	2	7	1				
1977	301	91	78	75	91	80				
1978	285	13	7	3	14	6				
1979	269		1		2					
1980	359									
1981	258									
1982	193									
1983	217			1	1					
1984	284				2					
1985	323	1	1	1	1	1				
1986	323	2	2	3	3	2				
1987	216			1	1					
1988	179									
1989	274			1	1					
1990	409			1	1					

Table 4: Compared result of TmyCreator software and available Tmy2 data by NREL for Salt Lake City

	City Name	Salt Lake	
		Name of years used by NREL	Name of years used by TmyCreator software
1	JANUARY	1976	1976
2	FEBRUARY	1971	1973
3	MARCH	1967	1987
4	APRIL	1976	1976
5	MAY	1989	1988
6	JUNE	1968	1968
7	JULY	1976	1976
8	AUGUST	1973	1989
9	SEPTEMBER	1972	1972
10	OCTOBER	1967	1968
11	NOVEMBER	1962	1962
12	DECEMBER	1965	1965

Table 5: Compared result of TmyCreator software and available Tmy2 data by NREL for Abilene City

	City Name	Abilene TX	
		Name of years used by NREL	Name of years used by TmyCreator software
1	JANUARY	1974	1974
2	FEBRUARY	1980	1961
3	MARCH	1961	1961
4	APRIL	1969	1969
5	MAY	1981	1981
6	JUNE	1979	1979
7	JULY	1974	1988
8	AUGUST	1981	1970
9	SEPTEMBER	1962	1970
10	OCTOBER	1980	1980
11	NOVEMBER	1977	1971
12	DECEMBER	1967	1979

In these tables the selected year for each month of the year by TmyCreator software and NREL have been showed. It can be seen that the TmyCreator software selected the years for 7 month like as selected year in NREL weather data for Salt Lake City and also selected the years for 6 month like as selected year in NREL weather data for Abilene City. Complete dissimilarity years selected for each month in the NREL file and the file produced by TmyCreator software is the following reasons:

1- As shows in Table 2 and 3, the missing data for these cities is more and not known that NREL How corrected the missing data when created the Tmy2 weather data file. The TmyCreator software corrects the missing data using other available data as following method :

The missed data = (the amount of after three hour+ the amount of before three hour)/2

2- Because the solar radiation data have important role in selecting the year of the Sandia method, it not known that NREL used of hourly measured radiation data or predicted data.

So, we can say that the TmyCreator software is acceptable.

6. Conclusions

In this study, the Sandia method has been applied to prepare the new TmyCreator software for selecting the proper data as the typical meteorological year (Tmy2). Also, the results of this new

software have been compared and it is found that, the results of TmyCreator software have good agreement with the old created Tmy2 weather data file. Using this software the Tmy2 weather file can be prepared for anywhere of the earth. The Tmy2 weather data file have been prepared for 6 city of IRAN (Tehran, Tabriz, Esfahan, BandarAbass, Shiraz, Boshehr and Yazd).

References

[1] Crawley D, Hand J, Lawrie L. Improving the weather information available to simulation programs. Washington, DC: US Department of Energy.

[2] L.S. Chan, T.T. Chow, K.F. Fong and Z. Lin, Generation of a typical meteorological year for Hong Kong, Energy Conversion and management,47 (2006), pp. 87–96.

[3] A. Kalogirou, Generation of typical meteorological year (Tmy2) for Nicosia, Cyprus, Renewable Energy, 28 (2003), pp. 2317–2334.

[4] C. Lam, C.M. Hui and L.S. Chan, A statistical approach to the development of a typical meteorological year for Hong Kong, Architectural Science Review, 39 (1986), pp. 201–209.

[5] Zhang Qingyuan, Joe Huang, Lang Siwei. Development of Chinese weather data for building energy calculations. In: 4th International conference on indoor air quality, ventilation and energy conservation in buildings, Changsha, Hunan, China, 2–5 October, 2001. p. 1211.

[6] Anderson TN, Duke M, Carson JK. A typical meteorological year for energy simulations in Hamilton, New Zealand. IPENZ engineering treNz 2007-003, ISSN 1177-0422.

[7] A .Ebrahimpour, M. Maerefat, A method for generation of typical meteorological year, Energy Conversion and Management, 51(2010), pp. 410–417

[8] J.M. Finkelstein and R.E. Schafer, Improved goodness-of-fit tests, Biometrika 58 (3) (1971), pp. 641–645.

[9] Hall I, Prairie R, Anderson H, Boes E. Generation of typical meteorological years for 26 SOLMET stations, SAND78-1601. Albuquerque, NM: Sandia National Laboratories; 1978.

[10] Marrion William, Urban Ken. User's manual for Tmy2s typical meteorological years. National Renewable Energy Laboratory, US Department of Energy; 1995.

[11] EnergyPlus documentation, software. <http://apps1.eere.energy.gov/buildings/energyplus/>.

[12] J.A. Duffie and W.A. Beckman, Solar energy of thermal processes, John Wiley, New York (1980).

[13] The Climate Consultant [version 5] software [http://www.energy-design-tools.aud.ucla.edu]

[14] The HEED (Home Energy Efficient Design, http://www.energy-design-tools.aud.ucla.edu/heed/)

[15] The eQUEST (Quick Energy Simulation Tool, http://www.doe2.com) software

Use of stochastic weather generators in the projection of building energy demand in a changing climate

David R. S. Williams[1, 2,*], Lucia Elghali[1], Russel C. Wheeler[2]

[1] *Centre for Environmental Strategy, Faculty of Engineering and Physical Sciences, University of Surrey, Guildford, Surrey, GU2 7XH, UK*
[2] *Parsons Brinckerhoff, Westbrook Mills, Godalming, Surrey, GU7 2AZ, UK*
** Corresponding author. Tel: +44 (0)1483 528406, E-mail: williamsdav@pbworld.com*

Abstract: Compliance with building codes in many countries requires energy simulation of designs in local climate conditions. However, over a building's lifespan, weather conditions may alter considerably due to climate change. There is a risk therefore that a future climate may alter lifecycle heating and cooling demands from those experienced today. The development of 'stochastic weather generators' provides an opportunity to produce synthetic weather data representative of a future climate. These models are calibrated against observed data, before being refitted to the climate change projections of global circulation models. The generator's output is thousands of years of weather data for a particular future time period. Theoretically these outputs would be appropriate for building energy demand simulation, although analysis of such a high number of projected years would be impractical. This research has developed a method whereby a unique energy "fingerprint" is created for a building and used to estimate heating and cooling demands without the requirement for hours of computation. Energy demand estimates from the fingerprint have been crosschecked with dynamic simulation, indicating a high degree of correlation. The weather generator utilised in this study has been produced by the UK Climate Impact Programme (UKCIP) and is freely available on-line.

Keywords: *Climate change, building energy demand*

1. Introduction

The 2008 Climate Change Act commits the UK to a challenging 80% reduction in greenhouse gas (GHG) emissions from a 1990 baseline by 2050 [1]. With buildings responsible for almost half of UK emissions [2], the construction industry will play a significant role in achieving this aim.

To drive reductions in GHG emissions, many countries have adopted energy benchmarking processes that require calculation of building energy demand over a single year [3]. For example, the Energy Performance of Buildings Directive (EPBD) in Europe requires member states to develop calculation methodologies to allow building energy demand to be determined [4]. These calculations are required to account for the fabric and systems proposed within a design, as well as the outdoor climate conditions typically found at the location of the building.

Measures such as the EPBD may be effective in reducing GHG emissions assuming steady climate conditions. However, evidence suggests that significant changes to the climate in recent years have already altered the energy performance of buildings. Wright [5] was able to demonstrate changes in heating degree-days over the period 1976-2000 consistent with a warming climate. Similarly Jenkins *et al*. [6] indicated an 18% reduction in heating degree-days, along with a 32% increase in cooling degree-days in London over the period 1961-2006.

Given the long lifespan of many buildings, it is reasonable to assume the climate a building is exposed to over its life could be different to that assumed during the design stage. This could influence the heating and cooling loads of the building, and potentially increase the GHG emissions beyond those expected. To ensure GHG emissions resulting from energy demand

are limited across the lifecycle, a method of analysing the possible influences of climate change is required. This paper describes how hourly weather sequences representative of a range of possible future climate alternatives may be produced in a format suitable for routine building energy analysis. The following section outlines work previously completed by others in this field.

1.1. Background

Hundreds of software applications have been developed for the estimation of building energy demands [7]. The most advanced of these tools simulate the performance of designs against hourly (or even sub-hourly) inputs. Weather sequences representative of the proposed building site are therefore required at this hourly resolution. However, there is a lack of data at this level of detail that accounts of the influence of climate change in the future.

1.1.1. Building analysis and climate change

Cole and Kernan [8] first identified the need to consider the influence of a changing climate on building lifecycle energy demands in 1996. However, at the time no suitable weather data were available to undertake such a study. Since then various methods have been developed to address the problem. The most simplistic approach has been to substitute weather data local to the site for that of a remote location that may be representative of a changed future climate. Gatrell and McEvoy [9] used this approach by using weather data from Rome and Milan as an approximation of London's possible future climate. The drawback of this method is that the relative humidity and diurnal temperature range of the substitute location may be quite different to that of the present site, even if the temperatures are similar to those expected for the future. In addition, the hours of sunlight and solar inclination may be unrealistic and would clearly not be subject to variation, even considering climate change.

1.1.2. Morphed weather data

In an effort to produce more suitable weather data accounting for future climate change, Belcher [10] developed an approach whereby the weather conditions of a given site are "morphed" inline with the projections of large scale climate models. In this work, Belcher used the Global Circulation Models completed by the United Kingdom Meteorological Office Hadley Centre and presented by the UK Climate Impacts Programme (UKCIP) in 2002 [11]. The process provided an estimate of possible future conditions by "shifting and stretching" hourly recorded weather data. This created a new annual sequence with monthly average conditions equal to those projected by climate models. The morphed data produced by this process have been applied by many researchers [12] [13] [14], although it does suffer from two potential drawbacks. Firstly, only one year of data can be produced for a given time period in the future, so the uncertainty in the projection cannot be satisfactorily addressed. Secondly, the morphing technique relies on the baseline recorded weather being from the same time period as the baseline in the climate model. This is not always possible.

1.1.3. Weather generators

More recently a new method has been made generally available that offers an alternative form of 'future' hourly climate data – stochastic weather generators. In 2009 the UKCIP produced an on-line user interface that allows generation of hourly synthesised weather data for any decade up to 2080 at any location following a 5km grid [15]. A full technical description of the weather generator and reference to the underlying scientific papers is provided by Murphy and Jones [16] [17]. A simplified description of the workings of the weather generator is however now provided by way of introduction.

The main difference between the 2002 and 2009 projections presented by the UKCIP is that a spread of probabilistic climate change is presented rather than one prediction. UKCIP have achieved this by simulating a number of subtly different, but equally plausible, models that all represent the climate in a slightly different way. From each of these models, "change factors" are produced that provide an indication of possible variation in weather variables at a monthly time scale. The weather generator is then used to downscale the monthly projections into a synthesised daily, and finally hourly, time step. Jones *et al*. [17] describe that like most weather generators a stochastic rainfall model is used to synthesise other weather variables based on the rainfall state. To achieve this, the weather generator is first calibrated using observed rainfall data and other weather conditions to produce relationships between the variables. The monthly change factors from the probabilistic models are then used to produce a future rainfall condition, which in turn is used to generate other future weather variables including temperature, humidity and cloud cover. To ensure that a wide range of plausible climate models are applied, a minimum of 100 sequences of data are produced by the weather generator. In addition to this, to ensure that a future climate can be well defined from the synthesised weather, each sequence is 30 years in length. This means that the weather generator produces at least 3,000 years of possible future weather data for any future decade.

The challenge for building energy modelling is how to apply such a vast quantity of data to assess the probabilistic performance of buildings in the future. Some progress has been made by Smith *et al*. [18] in the application of the new data. However in this study all 3,000 years were applied to a specific case study requiring specialised batch simulation and advanced processor power. The work discussed here aims to simplify the process so that analysis can be completed quickly as a routine activity within building design.

2. Methodology

The objective of simulating building energy performance against future weather conditions is to determine the sensitivity of the design against a range of future scenarios. In doing so, the energy required over a lifecycle may be reduced. However, the energy required by one building in the future may be different to that of another. For example, a heated and naturally ventilated building may use less energy in a 'warm future', as no air-conditioning system is present. Conversely, a building with high casual heat gains and a full air-conditioning system may require much more energy in a warmer climate. Many buildings may fall between these extremes. The method adopted therefore first tests a building's response to different weather conditions to define a unique 'fingerprint'. The fingerprint is then used to estimate energy demand (in the form of equivalent carbon dioxide, CO_2eq, emissions) from all 3,000 years of data. The following sections outline how this has been achieved.

2.1. Selection of example weather years

To understand how a building responds to differing climate conditions, a range of example years are required to define a suitable profile. In this analysis, dry-bulb temperature is used to differentiate between the years and indicate the potential energy demand of the building. However, taking a simple average of annual temperature does not indicate how much energy a building may require for heating and cooling. This is because it is the variation of hour-by-hour temperature either side of the average that indicates energy demand. For example, if an annual average temperature is 14°C, it is not known if the temperature spends a long time around this value, therefore requiring little heating or cooling energy in the building, or if wide extremes are experienced over the course of the year leading to high energy loads. Therefore, to indicate the amount of time in a year when temperature is at a particular value, a Cumulative Distribution Function (CDF) is produced for each of the 3,000 years.

When these CDFs are plotted and overlaid, a complete 'envelope' is created. Fig. 1 shows a hypothetical example of CDF plots of temperature. Example years are then chosen from across the full range of the envelope to test the building against a wide range of conditions. These are selected by plotting percentile positions across the envelope, then selecting the year which has the closest fit to the percentile points. To achieve this, a "goodness of fit" test is applied in a similar way to that used in the development of Test Reference Years (TRYs) for the UK Chartered Institute of Building Services Engineers (CIBSE) [19] [20].

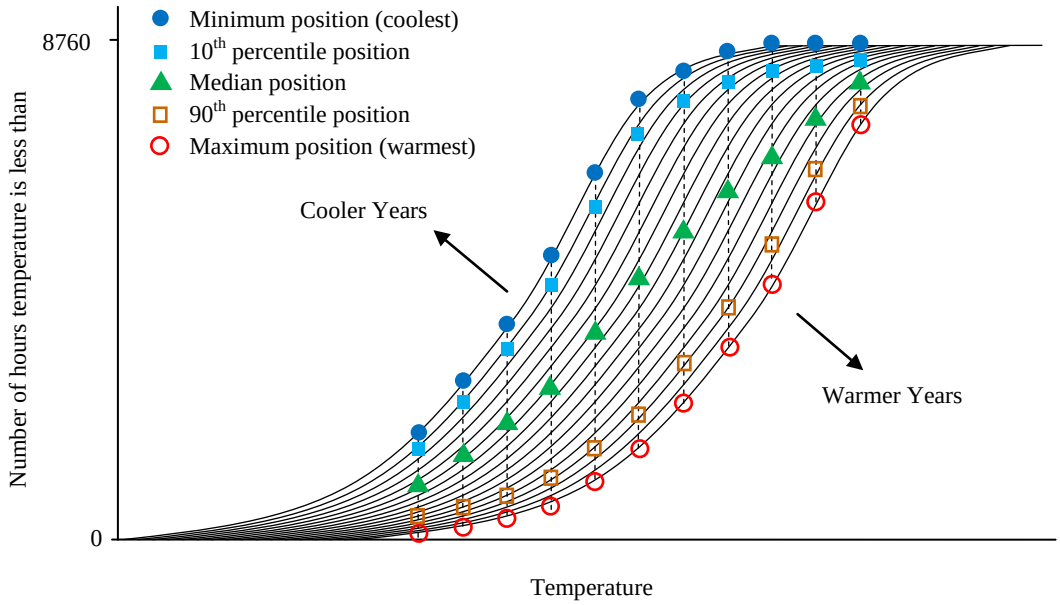

Fig. 1. Hypothetical example of Cumulative Distribution plots from UKCIP Weather Generator output. Each line represents a single synthesised year. In practice the generator would produce at least 3,000 years, each with equal probability of occurring.

In total, nine years are selected from the envelope at a spread of 10 percentile intervals. These years are then used as the external weather conditions in a thermal simulation of a building. To illustrate the process, an example building is described in the next section.

2.2. Testing of building performance

The building used to create an example fingerprint is a small Police Station in the south of the UK. It consists mainly of offices and meeting rooms, but also includes a relatively large computer server room. To complete the dynamic thermal simulation of the nine weather years, Integrated Environmental Solutions[1] (IES) v5.9 has been used. The outputs of heating and cooling energy demand are converted to CO_2eq values using a conversion factor typical to the UK [22] (0.198 kgCO_2eq/kWh for natural gas and 0.517 kgCO_2eq/kWh for grid supplied electricity). The hourly values are then aggregated into daily totals and a corresponding average daily temperature is calculated.

A binned frequency approach is then applied, where frequency of occurrence of daily average temperature in 1°C bins is determined. Using the same bins, the corresponding heating and

[1] The IES software determines annual building energy demands by modelling heat transfer processes at an hourly, or sub-hourly, time step. It is approved for use in building regulations compliance in the UK [21].

cooling energy demand (in CO_2eq) is summated. An example of the output of this process is shown in Fig. 2. Unsurprisingly, most building heating load occurs at low external temperatures and more cooling demand is found at higher temperatures. In addition to this, it is seen that of temperature frequency shows some correlation with the emissions, particularly cooling. This indicates some consistency between average daily dry bulb temperature and total heating and cooling load. The final stage is to use this profile to define a unique building energy fingerprint.

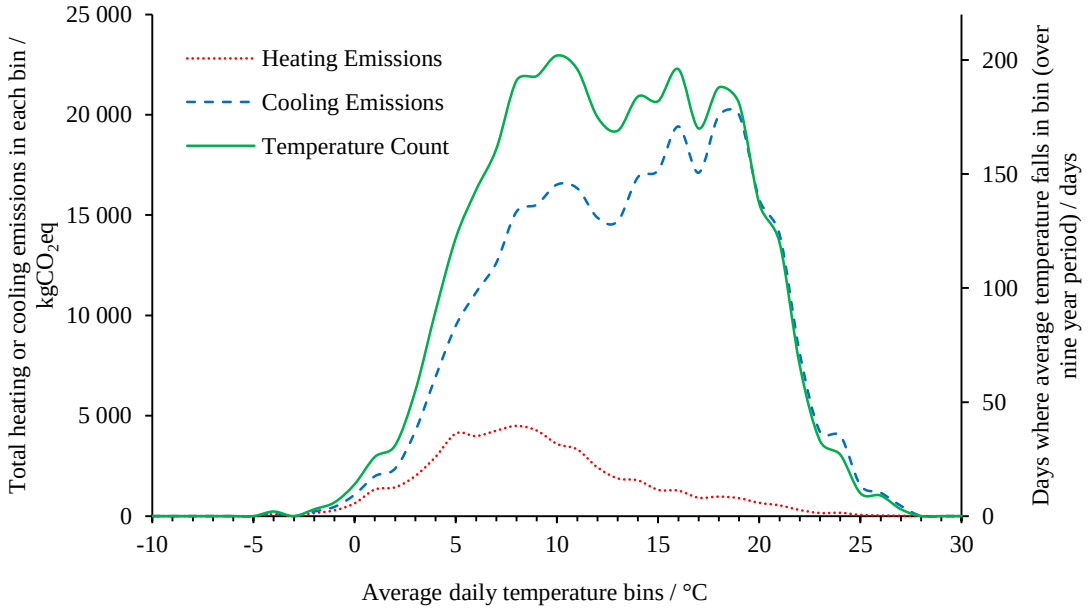

Fig. 2. Total CO_2eq emissions from example building heating and cooling demands and temperature frequency of occurrence in daily average temperature bins of 1°C

2.3. Production of unique fingerprint

To produce the fingerprint, the heating and cooling emissions are simply divided by the frequency of temperature occurrence. This gives a varying heating and cooling coefficient at each of the temperature bins with units of kgCO_2eq/day. Fig. 3 shows the unique fingerprint for the example police station building. In this particular case a minimal year round heating demand can be seen regardless of external temperature. This is due to a continual requirement for domestic hot water. Similarly a continual baseline load is also present for cooling as a result of the computer server room air conditioning equipment. In this case CO_2eq emissions are clearly dominated by cooling demand.

Once the fingerprint is created, annual CO_2eq emissions can be determined for any year with no need for further dynamic thermal simulation. This is achieved by simply multiplying the coefficient by the frequency of temperature occurrence for a given year, which can be readily achieved using a spreadsheet application.

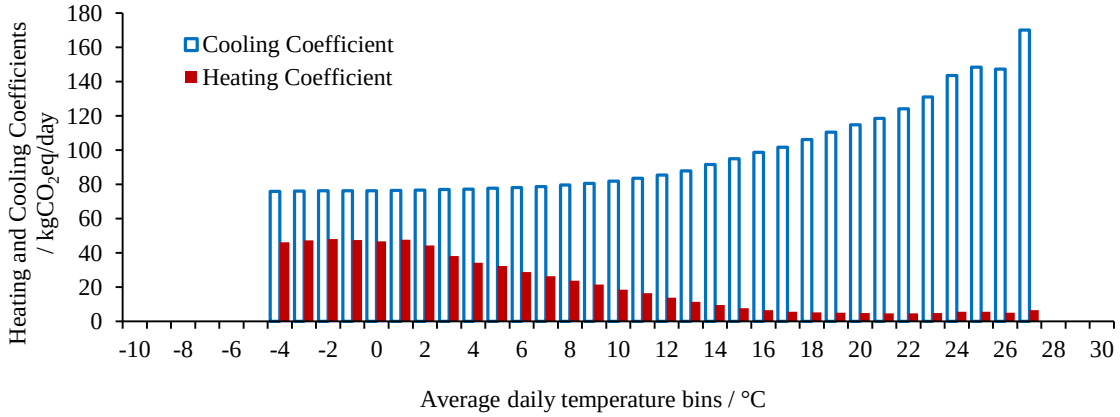

Fig. 3. Unique fingerprint of example building built from heating and cooling coefficients

3. Results of validation

To check the validity of the developed approach, the accuracy of the fingerprint at estimating building energy demand has been crosschecked using dynamic thermal simulation. To complete this, a number of years have been selected from the UKCIP weather generator and energy demand for heating and cooling has been determined in the example building using both methods. The years chosen for this process did not include those used to produce the fingerprint. Figure 4 shows the correlation between total (heating plus cooling) CO_2eq emissions for the example building against fourteen different years of weather.

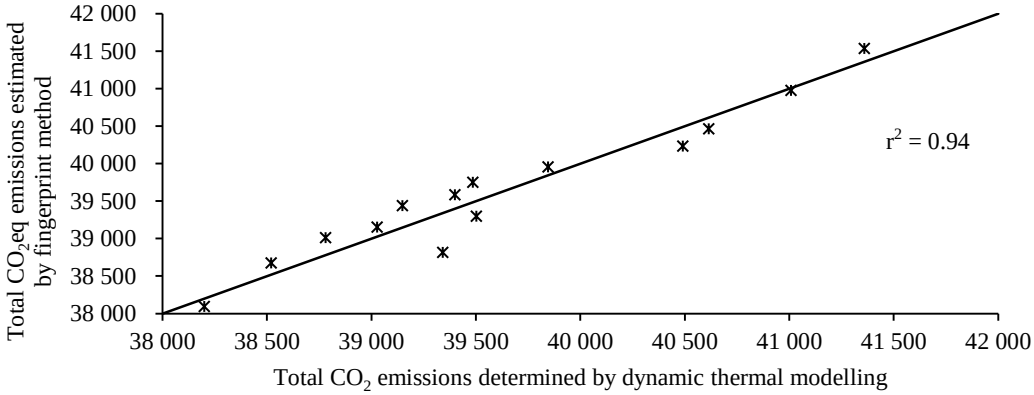

Fig. 4. Comparison of CO_2eq emissions between estimated figures using fingerprint method and dynamic thermal simulation

An r^2 value of 0.94 has been found between the two methods, indicating a high degree of correlation. This would suggest that for the case study examined, the fingerprint method is an acceptable way of estimating building energy demand for multiple years of data without requiring thermal simulation of each year.

4. Discussion and conclusions

The process developed here allows building CO_2eq emissions to be estimated directly from probabilistic climate change projections with minimal computation. The degree of correlation of the 'fingerprint' estimate to that determined by dynamic thermal simulation is very high, and greater than anticipated. It was previously assumed that a lower correlation may have been found, as the fingerprint method does not consider varying solar radiation and

(de)humidification requirements, focusing instead only on external dry-bulb temperature. It is however well known that these weather variables may affect building energy demand separately form dry-bulb temperature. It is assumed that as the weather data are produced by a 'generator', there may be a stronger link between the variables than experienced in reality. For example, in the generator it may be that warm days are generally also sunny and that cool days are frequently cloudy. This is not always true in reality. It may therefore be that the Weather Generator produces weather sequences where the variables are more correlated than reality (due to the known link to the stochastic rainfall state) and therefore particularly suitable for building energy estimation. However, as the method described in this paper is only applicable to generated weather sequences, this limitation is not a primary concern. Despite this, the issue is recommended for investigation in future work.

The method developed in this study allows any building design to be tested against possible future climate conditions. The advantage of using a weather generator as the basis of this work is that a wider range of climate conditions can be investigated than previous methods allowed. This will allow a design to be checked in multiple scenarios, allowing poor performing systems to be focused on for improvement. The main benefit of the approach is that a wide range of weather conditions can be explored without excessive levels of thermal simulation. It is hoped that this approach will be applicable to the routine thermal analysis of buildings. Further work is however required to investigate the accuracy of the fingerprint method in different building types in different locations to fully validate the method.

Ultimately, by investigating building energy demand performance over a range of possible weather conditions a better insight is provided into possible CO_2eq emissions that may be released as a result of heating and cooling a building over its operational lifecycle. The situation to be avoided is one where emissions in the future increase as a result of increases in cooling demand due to a warmer climate. This would be counterproductive to the UK achieving its target reduction of 80%.

5. Acknowledgements

The authors gratefully acknowledge the support of the UK Engineering and Physical Sciences Research Council (EPSRC) for this research, which forms part of the University of Surrey / Brunel University Engineering Doctorate Programme in Environmental Technology. They would also like to thank Parsons Brinckerhoff for their continued support of the programme.

References

[1] United Kingdom. Climate Change Act 2008 (c. 27). London: HMSO

[2] BERR (2008) Strategy for Sustainable Construction, Department for Business, Enterprise and Regulatory Reform (BERR) [online] Available at: http://www.berr.gov.uk/files/file46535.pdf (accessed December 2010)

[3] W. Lee and J. Burnett, Benchmarking energy use assessment of HK-Beam, BREEAM and LEED, Building and Environment, 43, 2008, pp. 1882-1891

[4] European Union, On the energy performance of buildings, Directive 2010/31/EU of the European parliament and of the council of 19 May 2020, Official Journal of the European Union, 2010, Brussels

[5] A. J. Wright, Evidence for climate change relevant to building design in the UK, 1976-2000, Building Services Engineering Research and Technology 23 (4), 2002, pp. 279-285

[6] G. J. Jenkins, M. C. Perry and M. J. Prior, The climate of the United Kingdom and recent trends, Met Office Hadley Centre, Exeter, UK

[7] D. Crawley, J. Hand, M. Kummert and B. Griffith, Contrasting the capabilities of building energy performance simulation programs, Building and Environment, 43, 2008, pp. 661-673

[8] R. Cole and P. Kennan, Life-Cycle Energy Use in Office Buildings, Building and Environment 31 (4), 1996, pp. 307-317

[9] M. Gaterell and M. McEvoy, The impact of climate change uncertainties on the performance of energy efficiency measures applied to dwellings, Energy and Buildings, 37, 2005, pp. 982-995

[10] S. Belcher, J. Hacker, S. Powell, Constructing design weather data for future climates, Building Services Engineering Research and Technology, 26 (1), 2005, pp. 49-61

[11] M. Hulme *et al*., Climate Change Scenarios for the United Kingdom: The UKCIP02 Scientific Report, Tyndall Centre for Climate Change Research, School of Environmental Sciences, University of East Anglia, 2002

[12] D. Coley and T. Kershaw, Changes in internal temperature within the built environment as a response to changing climate, Building and Environment, 45, 2010, pp. 89-93

[13] D. Jenkins, Y. Liu and A. Peacock, Climate and internal factors affecting future UK office heating and cooling energy consumptions, Energy and Buildings, 40 (5), 2008, pp. 874-881.

[14] M. Jentsch, A. Bahaj and P. James, Climate change future proofing of buildings – Generation and assessment of building simulation weather files, Energy and Buildings, 40, 2008, pp. 2148-2168

[15] UKCIP, UK Climate Projections: Login Page, [online] Available at: http://ukclimateprojections.defra.gov.uk/ (accessed December 2010)

[16] M. Murphy et al. UK Climate Projections Science Report: Climate change projections. Met Office Hadley Centre, 2009, Exeter

[17] P. Jones, C. Kilsby, C. Harpham, V. Glenis and A. Burton, UK Climate Projections science report: Projections of future daily climate for the UK from the Weather Generator. University of Newcastle, 2009, UK

[18] S. Smith, V. Hanby and C. Harpham, A probabilistic analysis of the future potential of evaporative cooling systems in a temperate climate, Energy and Buildings, 2010, in press. doi:10.1016/j.enbuild.2010.10.016

[19] J. Finkelstein and R. Schafer, Improved goodness-of-fit tests, Biometrika, 58 (3), 1971, pp. 641-645

[20] G. Levermore and J. Parkinson, Analysis and algorithms for new Test Reference Years and Design Summer Years for the UK, Building Services Engineering Research and Technology, 27 (4), 2006, pp. 311-325

[21] Integrated Environmental Solutions, Available at: http://www.iesve.com/ (accessed December 2010)

[22] The Government's Standard Assessment Procedure for Energy Rating of Dwellings, Building Research Establishment on behalf of the Department for Energy and Climate Change, Available at: http:// www.bre.co.uk/sap2009/ (accessed December 2010)

Daylighting, Daylight Simulation and Public Health: Low-Energy Lighting for Optimal Vision/Visual Acuity and Health/Wellbeing

E. V. Ellis[1*], N. B. Handly[1], D. L. McEachron[1],
A. Del Risco[2], M. Baynard[1]

[1] *Drexel University, Philadelphia, USA*
[2] *Florida State University, Tallahassee, USA*
** Corresponding author. Tel: +01 2153804276, Fax: +01 2157822226, E-mail: genaellis@drexel.edu*

Abstract: *Indoor Ecology* (IE) is an emerging research field that aims to develop new approaches and technologies which allow indoor environments and occupants to dynamically co-adapt to each other in order to enhance human wellbeing and productivity while simultaneously optimizing energy efficiency. The central idea in IE is that humans, building systems and the interior environment form a single, integrated complex 'ecosystem'. One way to IE optimization is though lighting, especially daylighting and daylight simulation. Current approaches to energy-efficient buildings emphasize only limited aspects of interior lighting, such as the carbon footprint, without regard to the multiple effects lighting has on human health, wellbeing and productivity which must be considered if truly sustainable interior spaces are to be designed. This paper documents five on-going investigations which study various aspects of the lighting-human interaction in a variety of circumstances. For example, students in the classroom setting are exposed to wide changes in lighting as well as inadequate light during early classes, likely affecting attention, retention and performance. Subjects displayed a marked preference for natural lighting when given the option; supporting a general hypothesis that daylighting might be a solution to the twin problems of promoting health and productivity while decreasing energy use.

Keywords: *Daylighting, Low-energy lighting, Visual acuity, Health, Wellbeing*

1. Introduction

The emerging discipline of Indoor Ecology seeks to develop the theories, methodologies and technologies needed to recast building design and architectural space in terms of flexible, sustainable and evolving human-building ecosystems. As part of this larger initiative, the effects of environmental lighting on human physiology and behavior must be investigated alongside the physical parameters of architectural space. The objective of the current research initiative into the effects of lighting on vision/visual acuity and health/wellbeing is to establish guidelines that can assist in the development of sustainable lighting solutions to promote the health and wellbeing of building occupants. This process-based research investigation looks to nature as a way of remodeling the built environment by considering the human-building relationship as a complex, evolving ecological network. Such an approach requires that environmental lighting be viewed from multiple perspectives – visual acuity, mood, chronobiology, health, energy efficiency, etc. – in order to inform the technological development of sustainable interior lighting systems [1]. Sustainable in this sense is broader that typically used in architectural design and includes the effects of light on human health and productivity as well as energy-efficient lighting design. The overall on-going research objective is to develop design criteria, guidelines and parameters to support the development of low-energy sustainable architecture at the nexus of health, energy and technology.

1.1. Background

Recent research indicates that lighting has increasingly become a public health issue [2]. These studies have shown that individuals working in natural sunlight are more productive, more effective, and happier than those who work under traditional artificial light. In addition, several studies have demonstrated a connection between environmental lighting levels and higher productivity and better performance from building occupants [6, 7]. Natural changes in

daylight balance the body's circadian rhythm, which determines sleeping and eating patterns, cognitive activity, heart rate, hormone levels – in fact, virtually all physiological and behavioral parameters. Circadian phase shift and transmeridian travel have been shown to contribute to jetlag, seasonal affective disorder (SAD), delayed sleep phase syndrome (DSPS), and is implicated in more various diseases and disorders, including cancer [3]. In industrialized nations it is estimated that up to 20% of the workforce are involved in some kind of shift work [4] which is associated with exposure to unusual or abnormal levels and/or patterns of light and dark. Studies have associated these unusual levels and patterns with higher incidences of breast cancer and colorectal cancers [1]. Thus, the sustainability of human productivity and well-being, even life itself, is directly tied to environmental lighting.

Lighting is also a sustainability issue in terms of energy use. Buildings consume 39% of the primary energy in the United States—on average 18% is used by lighting systems alone [5]. Also, the heat produced by a lighting system can generate up to 24% of the total building cooling load [6]. Proper lighting utilization using low-energy systems that generate little heat could result in significant cooling energy savings for buildings and a smaller carbon footprint.

The twin requirements of promoting human health and productivity and designing energy efficient lighting systems appear to be at odds. How can lighting be designed sufficiently bright enough to sustain human health and productivity while suitably energy efficient enough to sustain the planet? One possibility is the creative use of natural daylight. Daylight brings enough light to meet lighting needs of 50 to 70% of the occupancy period in the temperate zone of the earth while saving energy up to 50% of the gross full yearly use of light [8, 9].

For proper health and energy savings it is important to understand how light affects physiology and behavior. Ocular light, or light reaching the eye, serves two major functions: vision and control of circadian rhythm [10]. Daylighting provides the quality light necessary for maximum vision and visual acuity [11] and provides the full spectrum of light needed for health and wellbeing [3]. Circadian rhythm is regulated by changes in visible light from the sun throughout the day [12] and is controlled daily by the full spectrum of natural light together with darkness in the environment [10].

1.2. Physiology and Daylight

Natural daylight is crucial to promote productivity, health and wellbeing due to light's visual and non-visual effects. In addition to object recognition or visual information, light provides data on the timing and intensity of light and dark to synchronize the body's biological rhythms. Photonic information (non-visual effects of light) is transmitted from the eye to the suprachiasmatic nucleus (SCN) located in the hypothalamic region in the center of the brain, leading to a cascade of hormonal changes in the pituitary, pineal, adrenal and thyroid glands.

The SCN serves as master pacemaker or biological clock in humans, synchronizing the circadian rhythms that regulate and modify virtually every physiological and behavioral process in the human body. The human SCN displays a natural period slightly longer than 24 hours and must be reset by light of the appropriate spectrum and intensity, at the proper time, to provide a consistent temporal order. When this temporal order is significantly disrupted – through inappropriate interior lighting, for example – it can lead to damaging emotional and physiological effects such as those associated with seasonal affective disorder, jet lag, delayed sleep phase syndrome, and may exacerbate serious conditions such as cancer. These effects are especially evidenced by people involved in shift work [13, 14, 15], such as the doctors and staff working in the Emergency Department at Hahnemann who are part of this research.

The hominid ancestors of humans did not live in buildings and evolved their circadian system – which present humans have inherited – exposed to the natural day/night cycle. The full spectrum of light available in this cycle includes UVA, UVB and visible light: at noon there is high intensity in the *blue light* region, in the late afternoon blue light is preferentially scattered out of (removed from) incoming sunlight so that the late afternoon sun provides red and orange light, and when the sun sets it becomes dark. Circadian rhythms are controlled primarily by daily exposure to levels of light in the blue-green spectrum together with alternating darkness in the environment. Blue light triggers the production of serotonin in the body, which enhances alertness and cognitive performance, while red or amber light signals the onset of dusk; the absence of light encourages melatonin secretion [16, 17]. Returning buildings to a natural light environment through the use of daylighting or mimicking the full spectrum of natural light using energy-efficient artificial lighting would both conserve energy and promote the wellbeing of building occupants [18].

2. Methodology

There are five on-going investigations to determine the effects of a variety of lighting options in different architectural settings. These studies are designed to test environmental preference for natural light, artificial light effects on human health and productivity, different artificial light sources effects on vision and visual acuity with respect to energy use, and the effects of light shelves on indoor illumination levels. Preliminary results are documented in this paper.

3. Results

3.1. Hahnemann Hospital Emergency Department Waiting Room Daylighting Study

The waiting room of the Hahnemann Hospital Emergency Department is a poorly monitored space: patients suffering from an accident, illness or even fear, are also unsure as to how long they may be waiting or what will happen once they see the doctor. After the recent death of a Philadelphia man waiting for care, attention has been refocused to emergency department waiting rooms. While it is not clear what led to his death, the event does suggest that health care providers should know more about what is happening to patients, both in the short and long term, while they are in the waiting room of emergency departments.

Although the effects of the environmental lighting should influence designs for healthcare spaces, this is rarely the case. Light exposure of specific frequencies and intensities has been shown to affect mood and performance [20, 21, 22] and even treat certain aspects of depression [23]. Not known is whether lighting can affect a person's health and wellbeing over short and irregular time periods such as while waiting for care at emergency departments. Waiting durations vary from less than a minute to as much as 12 hours – longer wait times are associated with increasing levels of impatience and agitation.

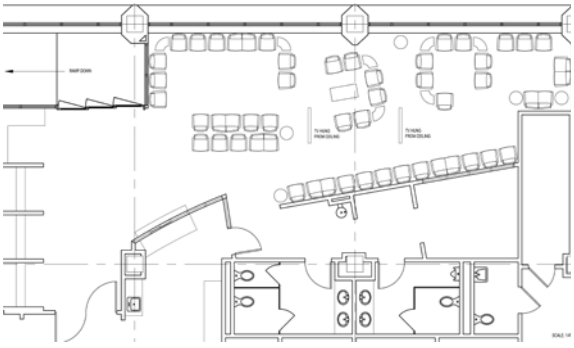

Fig. 1. Plan of the Hahnemann Emergency Department Waiting Room (north side top of drawing).

In addition to effects of lighting on patient attitude and mood, lighting may also affect the underlying health problem that brought the patient to the hospital in the first place. The current lighting of the Emergency Department waiting room at Hahnemann Medical Center was analyzed as a first step in assessing effects of lighting on waiting patients (Fig. 1).

The next step is to determine the effects of the current lighting on patients. The initial hypothesis is that patients will aggregate in areas of high light intensity or natural lighting. In the daytime, the seats adjacent to the north windows receive the most natural daylight. The prediction is there will be a natural gradient of persons within the waiting room tending to sit near the windows. However, at night there is little difference in lighting (all artificial lighting) and no gradient of persons is expected as a result of lighting conditions. The artificially-lit waiting room of the evening hours will be used as a control to determine if there is a preference to sit near the windows. Other factors must be considered such as location relative to televisions, where other persons have already occupied a seat or even proximity to bathrooms or vending machines. The lighting measurements will be correlated to seat positions in another series of measurements. Data is presently being gathered; initial results support the hypothesis suggesting a trend to prefer sitting near the windows in daylight hours.

3.2. Hahnemann Emergency Department Baseline Staff Productivity Study

Another aspect of patient care is the performance of the health care providers. Given the well known performance deficits associated with circadian disruption and sleep deprivation, is it possible for environmental lighting to act as a counter agent to these effects? Current practice for emergency room service delivery involves doctors participating in schedules that involve 8- or 10-hour shifts of two days of daytime, two days of afternoon/evening, two days of overnight and two days off. An initial staff productivity study will serve as a baseline inventory of sleep, self reported quality of wellbeing, burnout, sleepiness and preferred phase of circadian activity as well as the Emergency Department (ED) lighting environment. In this second ED study, resident physicians will wear light sensing wrist actigraphs that measure movement to assess objective sleep-wake activity patterns in different lighting conditions for one work cycle. Within the ED, lighting apparently varies little and there is no natural lighting once inside the patient treatment areas. However, lighting conditions may change based upon specific tasks being undertaken and/or the influence of lighting on performance may be task dependent. Lighting levels will be measured and correlated to tasks to assess how the Emergency Department lighting could be better designed to support ED staff performance.

3.3. Lighting and the Educational Environment

It is well known that time of day affects performance and learning. Sleep deprivation and fatigue are detrimental to an array of neurocognitive functions and, by extension, decrease learning. However, these observations have not been systematically applied to scheduling classes with the goal of enhancing a student's learning experience.

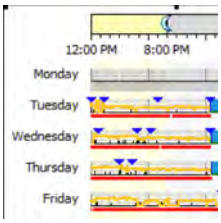

Fig. 2. Actogram from wrist actigraph demonstrating ambient light exposure, sleep, rest, and activity periods for an average subject over 21 days.

Lighting levels are being documented in several Drexel University classrooms and show significant variation from room to room and at different times of day in the same room. In fact, the lighting levels have been found to vary significantly from desk to desk within a single room even when the room is artificially illuminated. The discrepancy in lighting levels is even more pronounced when the room also has access to natural daylight, compounded with orientation to the sun (whether east, west, north or south orientation). To determine how these varying lighting conditions effect learning, students are being monitored for activity and light exposure using wrist actigraphy (Fig. 2). The data will be

cross-referenced with the student's performance to determine the effects of lighting and sleep/wake cycles on academic achievement. Further studies will evaluate classroom seating position with respect to lighting and effects of lighting on mood, sleepiness and performance.

Preliminary investigations consist of data collection using wrist actigraphy for 2 weeks during a school term. Weekdays were analyzed to determine the average light exposure students received during the day. Light was recorded in 60 second epochs. 180 epochs were averaged to create six, 3 hour bins from 06:00-24:00. Average light exposure (lux) was compared across the bins. While previous analysis failed to reveal a significant exposure to ambient light during the night (24:00-06:00), daytime exposure was shown to vary significantly by time of day. A one-way ANOVA was used to test for differences in average light exposure in 3 hour bins from 06:00-24:00. Exposure differed significantly across the six time bins, $F(5, 102) = 3.78$, $p = .003$. Also, a trend toward increasing light exposure was seen as a result of time of day with the hours of 12:00-14:00 showing the highest average lux per subject. Additionally, during students' earliest waking hours, from 06:00-09:00, analysis revealed significantly reduced light levels, equivalent to the sleeping environment, despite student's schedules and activity measurements correlating this time period as active class time.

3.4. Light Source, Vision and Visual Acuity

Not only are lighting levels, light with respect to time of day, and physiologically experiencing the full spectrum of natural daylight important for the work environment, but also the *quality* of the light can be crucial—especially in an emergency medicine situation when the attending physician may be tired and yet responsible for completing tasks that require precise visual acuity, such as making incisions and stitching wounds.

During the summer 2010, five lighting experiments were set up to compare and contrast five different light sources for visual acuity and comfort, which were cross-referenced with age, gender and whether or not corrective lenses were used. Each lighting experiment had an eye chart with verse from Ralph Waldo Emerson's *The Conduct of Life*, with point sizes varying from 1pt to 7pt, each illuminated by a different light source. The test subject looked through goggles to ensure the same focal distance from the eye chart and selected the smallest point size that could be read. The lighting level was been set at +/- 530-650 lux for each of the four artificial light sources: LED, Phillips incandescent, compact fluorescent and GE incandescent (Fig. 3). The fifth lighting experiment used available natural daylight and the test subject noted the lighting level at the time of the test; daylighting levels tended to vary within the range set up for the artificial lighting sources at +/- 530-650 lux. The test subject was requested to indicate which one of the light sources was the most comfortable (Fig. 4). Sixty-five people were surveyed with ages ranging from 9 to 77 years. While the use of corrective lenses did not seem to affect the study, the daylight source was overwhelmingly preferred. However, this was not the case during the spring when daylighting levels varied 200-500 lux.

Fig. 3. Light Boxes, from left to right: LED, Phillips incandescent, CFL, GE incandescent

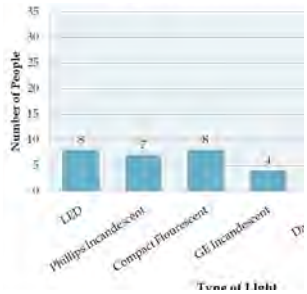

Fig. 4. Light Source Preference

Determining quality of light with respect to light source and energy consumption is critical to meet today's energy conservation needs. Daylighting is ideal because it consumes no energy and is cost-free. On the other hand, radiant energy from light results in heat gain; potentially in the winter a reduction in heating costs, while in the summer an increase in cooling loads. Indirect daylight is ideal because of lowered radiant heat gains. A comparison of the artificial light sources used in this experiment reveals that although users indicated little preference between the artificial light sources, while the LED (light emitting diode) light source is considerably more sustainable, it costs nearly double the CFL (compact Fluorescent); however, both use considerably less energy than either incandescent (Table 1). Additionally, while not measured in this study, both the LED and CFL also generate less heat.

Table 1. Artificial light sources.

LED: Pharox 40 Warm White Light	Incandescent: Philips Duramax R20	Compact Fluorescent: Ecosmart Soft White Cold Cathode	Incandescent: GE Soft White 25
230 lumens 5W 36K hours	205 lumens 30W 2.5K hours	200 lumens 5W 20K hours	210 lumens 25W 2.5K hours
No mercury, no UV, 100% recyclable	contains mercury		
cost over 36,500 hours = $76.38	Cost over 36,500 hours = $219.15	Cost over 36,500 hours = $39.35	Cost over 36,500 hours = $159.15

3.5. Natural Daylighting and Light Shelf Efficacy

Lighting energy accounts for a large portion (30-50%) of total energy consumption of typical commercial buildings [l9], and about 15% percent of residential consumption in the U.S. [5]. Daylight generates enough light to meet lighting requirements of 50 to 70% of the occupancy period in the temperate zone of the earth. Energy savings by using daylighting can be up to 50% of the gross full yearly use of light for interior conditions [8, 9]. For these reasons, techniques that can maximize daylight use in indoor spaces while minimizing heat gain would be useful to ensure both quality light and energy savings in buildings.

A south-facing room was used as a test site. It is a typical office plan illuminated by windows all along the south wall from about 42" above the floor to the ceiling at ten feet above the floor. The orientation is skewed from true south as indicated in the plan (Fig. 5). Light shelves were installed along the central horizontal dividing mullion at approximately six feet above the floor level. A 99.7% reflective coating provided by 3M Corporation was installed on the top surface of the light shelf and on the ceiling above to redirect the reflected sunlight back down into the room. Lighting levels were documented at one hour intervals from 10:00-15:00. It was noted whether or not it was Sunny (Clear Sky), Partly Cloudy, Cloudy, or Rainy. Three separate readings were taken each hour: no light shelf, light shelf horizontal to the floor, and light shelf inclined at 10^{o} below the horizontal. Readings were taken on twenty separate days over a period of six weeks at three locations as indicated on the plan (Fig. 6).

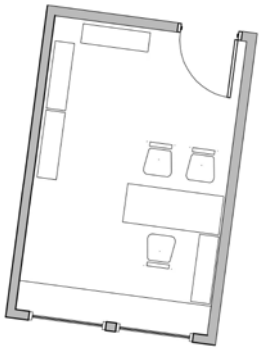

Fig. 5. Office (oriented north up).

Preliminary results suggest that light shelves help to evenly distribute interior lighting levels across the room when located on south-facing windows; glare is reduced at the window due to

the shelf shading adjacent work surfaces while lighting levels are increased at work surfaces within five to eight feet from the window (Fig. 7). Surfaces beyond eight feet receive much less benefit. Daylighting is most effective when the sun is perpendicular to the window, explaining why illumination levels for this test location were highest at 14:00 instead of noon.

4. Conclusions

While human behavior is occasionally considered in the design of low-energy architecture, energy use and efficiency can often take precedence over human comfort, performance and/or wellbeing. Buildings have been designed to efficiently use energy while illuminating building interiors. However, rarely is visual acuity a consideration in lighting design nor are the effects of lighting on physiology and behavior. As a result, lighting is often energy-efficient while building occupants have difficulty succeeding in tasks requiring keen vision, such as suturing a wound or reading fine-print text. Additionally, buildings with 24 hour illumination generally produce the same intensity and wavelengths throughout the period, increasing chances for circadian disruptions with consequent health and performance decrements. The quality and timing of light should be controlled to ensure the physical and mental wellbeing of building occupants. Future areas for research include: 1) evaluating the feasibility of artificially mimicking the full spectrum of light by phase-shifting the day of night-shift workers to reset their biological clocks to be in sync with their natural circadian rhythms; 2) optimizing the educational environment by coordinating course schedules with time of day and classroom lighting levels to enhance student academic performance and alertness; and 3) developing criteria for sustainable architectural design at the nexus of health, energy and technology.

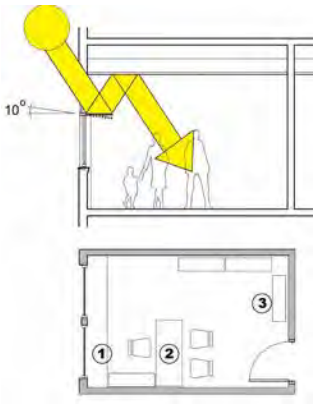

Fig. 6. Section through office showing light shelf and locations of daylight readings.

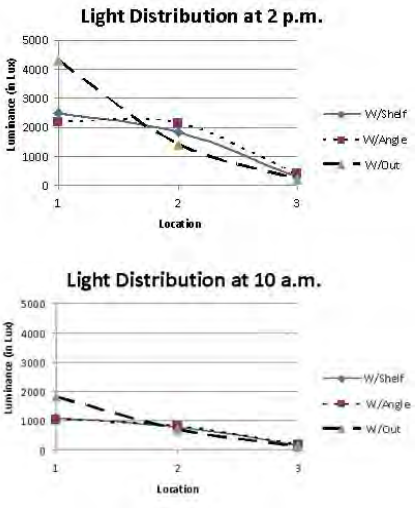

Fig. 7. Light distribution.

References

[1] J. Benyus, Biomimicry: Innovation Inspired by Nature, New York: Harper Collins, 1997.

[2] S.M. Pauley, Lighting for the human circadian clock: recent research indicates that lighting has become a public health issue, Medical Hypotheses 63, 2004, pp. 588-596.

[3] J.E. Roberts, Therapeutic Effects of Light in Humans, Photobiology for the 21st Century, edited by Thomas P. Coohill and Dennis P. Valenzeno, Overland Park, Kansas: Valdenmar Publishing Company, 2001, Chapter 2, pp. 17-29.

[4] A.R. Webb, Considerations for lighting in the built environment: Non-visual effects of light, Energy and Buildings 38, 2006, pp. 721-727.

[5] DOE, 2006 Buildings Energy Data Book, U.S. Department of Energy, http://buildingsdatabook.eren.doe.gov/.

[6] R. P. Leslie, Review: Capturing the Daylight Dividend in Buildings, Why and How?, Building and Environment 38, 2003, pp. 381-385.

[7] C. Fay, *Daylighting and Productivity A Literature Review*, Lighting Research Center, Rensselaer Polytechnic Institute, 2002, Report of Project "Cross-Cutting R&D on Adaptive Full-Spectrum Solar Energy Systems for More Efficient and Affordable Use of Solar Energy in Buildings and Hybrid Photo-Bioreactors" sponsored by U.S. Department of Energy.

[8] M. Fontoynont, Perceived Performance of Daylighting Systems: Lighting Efficacy and Agreeableness, Solar Energy 73:2, 2002, pp. 83-94.

[9] E. Ne'eman and D. Shrifteilig, Daylighting Buildings in a Hot Climate, Energy and Buildings 4, 1982, pp. 195-204.

[10] J.E. Roberts, Daylight as a Visual Stimulus, Light Congress 2008, presentation.

[11] A.F. Bliss, The Chemistry of Daylight Vision, Journal of General Physiology 1946, pp. 277-297.

[12] J. Aschoff, Response curves in circadian periodicity, Circadian Clocks (Edited by J. Aschoff), North-Holland, Amsterdam, 1965, pp 95-111.

[13] A. Aanonsen, Medical problems of shift work, Indust. Med. Surg. 28, 1959, pp. 422-427.

[14] T. Akestedt and M. Gillber, Sleep disturbances and shift work, Advances Biosciences 30, 1981, pp. 127-137.

[15] C. Czeisler, M. Johnson, J. Duffy, E. Brown, J. Ronda, and R. Kronauer, Exposure to bright light and darkness to treat physiologic maladaptation to night work, New England Journal of Medicine 322, 1990, pp. 1253-1259.

[16] S. Kaplan, The Restorative Benefits of Nature: Toward an Integrative Approach, *Journal of Environmental Psychology 1*5, 1995, pp. 169-182.

[17] V.Lubkin, P. Beizai and A. Sadun, The Eye as Metronome of the Body, Survey of Ophthalmology 47:1, 2002, pp. 17-26.

[18] P.R. Mills, S.C. Tomkins and L.J.M. Schlangen, The effect of high correlated colour temperature office lighting on employee wellbeing and work performance, Journal of Circadian Rhythms 5, 2007, p. 2.

[19] R. Bevington and A. H. Rosenfeld, Energy for Buildings and Homes, Energy for Planet Earth, Scientifc American, 1991.

[20] Daurat, A., Aquirre, A., Foret, J., Gonnet, P., Keromes, A., and Benoit, O. (1993). Bright light affects alertness and performance during a 24-h constant routine. Physiol. Behav. 53: 929-936.

[21] Dawson, D. and Campbell, S.C. (1991). Timed exposure to bright light improves sleep and alertness during simulated night shifts. Sleep 14: 511-516.

[22] Brainard, G.C., Sherry, D., Skewerer, R.G., Waxler, M., Kelly, K., Rosenthal, N.E. (1990). Effects of different wavelengths in seasonal affective disorder. J. Affective Disorders 20: 209-216.

[23] Kent, S., McClure, L., Crosson, W., Arnett, D., Wadley, V. and Sathiakumar, N. (2009). Effect of sunlight exposure on cognitive function among depressed and non-depressed participants: a REGARDS cross-sectional study. Environmental Health 8: 34 doi:10.1186/1476-069X-8-34.

Simulations of comfort cooling strategies in Passive Houses in a Swedish climate

J. Persson[1,*], M. Westermark[1]

[1] *Division of Energy Processes, Department of Chemical Engineering and Technology, Royal Institute of Technology, Stockholm, Sweden*
** Corresponding author. Tel: +46 87906223, E-mail: tjp@kth.se*

Abstract: Passive Houses have gained popularity the last ten years as a way of improving the energy efficiency in the housing stock. The challenge of avoiding external heating during the cold winter climate in Sweden has pushed the design of a Passive House in a direction where problems with excessive temperatures might occur summertime. The aim of this paper is to evaluate comfort cooling strategies for attaining good indoor climate summertime while maintaining good energy efficiency. Also, to add knowledge of comfort cooling strategies for Swedish conditions as the summer season is short and comfort cooling is normally not installed. The studied strategies include: airing, shading, increased ventilation, cooling machine and evaporative cooling. Additionally, combinations of these methods are studied. To evaluate the cooling strategies and their impact on the indoor temperature and the amount of electricity needed for their operation, computer simulations have been made using the simulation tool *IDA Indoor climate and energy*. The building model is based on an existing Passive House in the district Lambohov in Linköping, Sweden, where continuous logging of temperatures are available. Without comfort cooling the simulations show excessive temperatures summertime which is consistent with the field measurements from the real house. The overall judgement is that passive cooling strategies can provide sufficient cooling during the hottest part of the summer and that both shading and airing strategies should be used for a maximum cooling effect.

Keywords: *Building simulation, Comfort Cooling, Passive House*

1. Introduction

Passive Houses have gained popularity the last ten years as a way of improving the energy efficiency in the housing stock. A Passive House uses only the internal heat gains from lighting, equipment, humans and the incoming solar radiation to heat the building. This is possible through a combination of a highly insulated building envelope and a heat exchanger that heats the incoming air with the exhaust air. A Passive House has therefore no need for a traditional heating system, but occasionally, when the temperature drops fast during a cold period, there might still be a need for additional heating. The challenge of avoiding external heating during the cold winter climate in Sweden has pushed the design of a Passive House in a direction where problems with excessive temperatures might occur summertime.

The aim of this paper is to evaluate comfort cooling strategies in order to attain good indoor climate summertime while maintaining good energy efficiency. Can a clever use of shading, airing and ventilation provide enough cooling to avoid an installation of comfort cooling equipment. Moreover, the use of a cooling machine as well as evaporative cooling is also evaluated.

Socialstyrelsen (The Swedish National Board of Health and Welfare) recommends that the indoor temperature does not exceed 24 and 26 °C wintertime and summertime respectively (Socialstyrelsen 2005). Further, Boverket (The Swedish National Board of Housing Building and Planning) recommends an indoor temperature between 23 and 25 °C summertime (Boverket 2007) and FEBY(Forum for Energy Efficient Buildings) recommends that the indoor temperature does not exceed 26 °C more than 10 % of the time summertime in the hottest part of the building (FEBY 2009).

A study by SP (Technical Research Institute of Sweden) with temperature loggings from 20 terraced house apartments in 4 Passive Houses in Lindås, Sweden, show a mean indoor temperature of 25.2 °C summertime (Ruud and Lundin 2004). Some of these apartments have temperatures within good levels throughout the summer but others have periods with temperatures between 25 and 30 °C and there are occasions when the indoor temperature reaches 30 °C. Dwellers in Passive Houses in the districts of Oxtorget, Glumslöv and Frillesås responded to a questionnaire study about their indoor temperature summertime. The outcome of the questionnaire gave the result that in Oxtorget 31 %, in Glumslöv 56 % and in Frillesås 11 %, respectively, claimed it was too warm during this period (Samuelsson and Lüddeckens 2009). More reports of excessive temperatures summertime have been made from dwellers in a two-storey Passive House in Lidköping and from dwellers living on the top floor in a three-storey apartment building in Brogården, Alingsås (Janson 2010). In Lambohov, Linköping, temperature measurements from two Passive Houses also show excessive temperatures summertime. During the month of July 2010, the mean value of the exhaust air temperatures from these two apartments were 27.3 °C. Further, the exhaust air temperatures from these two apartments were 26 °C or higher during 60 % of this time (KTC 2010).

In contrast to warmer countries, comfort cooling equipment is normally not installed in Swedish dwellings. However, the combination of the isolating capacity of a Passive House and the large solar gains summertime could result in excessive temperatures even in this cold climate. Methods for comfort cooling in warmer countries are normally: shading, ventilation, cooling machines, evaporative cooling, solar chimneys, earth tubes, reflectors and night-time radiation cooling.

2. Methodology

With the use of computer simulations this paper investigates strategies for comfort cooling for a Passive House in a Swedish climate. The simulations have been carried out using the software *IDA Indoor climate and energy (ICE)*, a software that since its release in 1998 has grown to become one of the leading international tools (U.S. Department of Energy 2009). The input data representing the human presence, the use of electricity and domestic hot water are based on a collection of user related data from Boverket (2007). Applied to this household it results in the internal gains of 4.6 W/m^2. The building model in the IDA ICE-simulations is based on an existing Passive House apartment in Lambohov, Linköping, Sweden, where continuous logging of temperatures are available, see Fig. 1. It is one of two 4-room apartments in a Passive House building, both with two floors and an area of 105 m^2. The ground floor has a ceiling height of 2.5 meters and the second floor has a ceiling height of 2.4 meters. The apartment is equipped with an FTX-system that recovers the heat in the exhaust air to heat the incoming air and a constant air volume (CAV) ventilation system with two temperature meters controlling the ventilation. Further, a climate file from Meteonorm is used in IDA ICE to simulate the climate in Linköping. More details are presented in Appendix.

In order to evaluate the different comfort cooling strategies, the first ten days in the month of July, a period with excessive temperatures in the real Passive House are simulated. The reference case without different measures to cool the apartment is compared with implementations of different strategies for comfort cooling. Their individual cooling performances as well as the combinations of these are then evaluated.

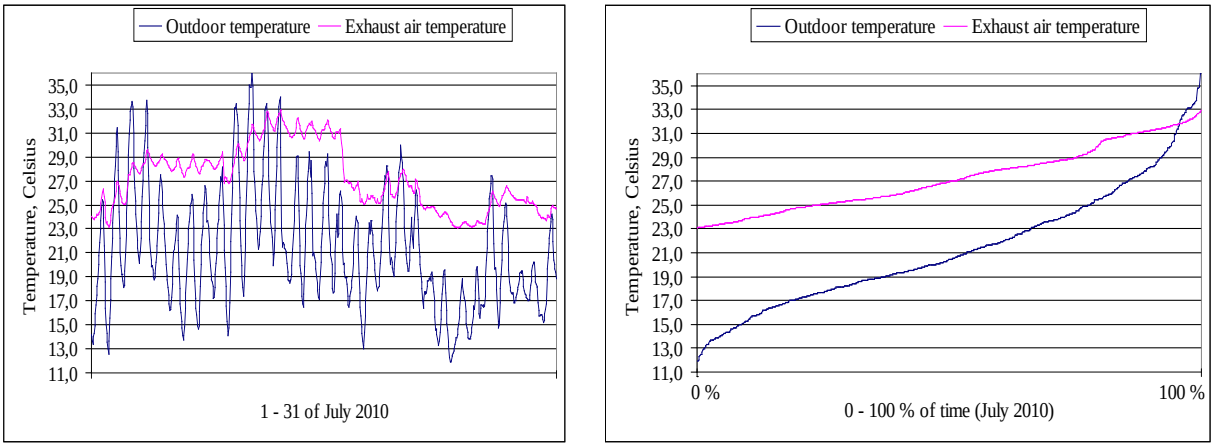

Fig. 1. Temperature loggings during July 2010 from the real Passive House in Lambohov, to the right presented in a duration diagram.

3. Comfort cooling strategies

The simulated comfort cooling strategies and their implementations in IDA ICE are here presented.

3.1. Integrated and external window shading

Integrated and external window shadings of separate types are used. In the simulations the integrated window shading is controlled by the solar radiation, the time of the day and the indoor temperature. It is activated if the direct normal radiation exceeds 100 W/m^2 and if the room temperature is higher than 22 °C. For the integrated shading the solar gains factor (g-value) equals 0.14, the short-wave shading coefficient (T-value) equals 0.09 and the U-value equals 1.0. Moreover, the integrated window shading is not used on the east façade since it could make the apartment too dark inside. This restriction is not made on the use of the external window shading, where an awning is implemented on every window at all times of the day.

3.2. Airing with windows

In contrast to shading, airing with windows is due to safety reasons only allowed certain hours of the day and only with the windows on the second floor. The hours for airing are set to 18:00-22:00 but only if the room temperature is higher than 22 °C and higher than the outdoor temperature. In that case the windows will be 25 % opened.

3.3. Increased ventilation

When the ventilation system is used as a mean to remove excess heat, the ground state of the CAV-ventilation and its airflow of 45 l/s is increased to 90 l/s.

3.4. Airing with a roof hatch

As an option for airing with windows which is only allowed daytime, a roof hatch is implemented in order to investigate how much night-time airing can lower the temperature. It is assumed that security measures are taken in order to keep it open night-time. The roof hatch has an area of 0.7 m^2 and is located in the upper hall. It is intended to be open between 18:00–08:00 but only if the indoor temperature in the room is higher than 22 °C and higher than the outdoor temperature.

3.5. Cooling machine

The cooling machine is connected to the FTX-system which distributes the cooling to the building. The set-point for the exhaust air temperature is 24 °C and the minimum allowed supply air temperature is set to 15 °C.

3.6. Evaporative cooling

Evaporative cooling is investigated as an alternative to the cooling machine. It is connected to the FTX-system and has an efficiency of 80 %. The set-point for the exhaust air temperature is 24 °C and the minimum allowed supply air temperature is set to 15 °C.

4. Results

The simulation results in Fig. 2 show that passive cooling can provide sufficient cooling during the hottest part of the summer. The best cooling result is obtained when both shading and airing strategies are used. Here, the most effective strategy is the combination of the external window shading and the roof hatch. The roof hatch proves to be the best single way to lower the temperature in the apartment. Fig. 3 shows that the combination of the increased ventilation with window shading also can provide a satisfactory cooling result. If the cooling machine or the evaporative cooling is used, the best combination are in both cases either with the external window shading or with the increased ventilation as can be seen in Fig. 4 and Fig. 5. The cooling machine has a better cooling performance than the evaporative cooling but with the standard ventilation airflow none of them can lower the temperature to a comfortable level. Higher ventilation or lower supply temperature than 15 °C is required.

The electricity use of the fans during the ten simulated days is 14.4 kWh/10 days with the standard flow of 45 l/s. The extra power demand for the doubled ventilation is 100 kWh/10 days. In comparison the power demand of the cooling machine for reducing the supply air temperature to 15 °C is about 30 kWh/10 days (cooling demand 100 kWh /10 days) but the temperature reduction is less.

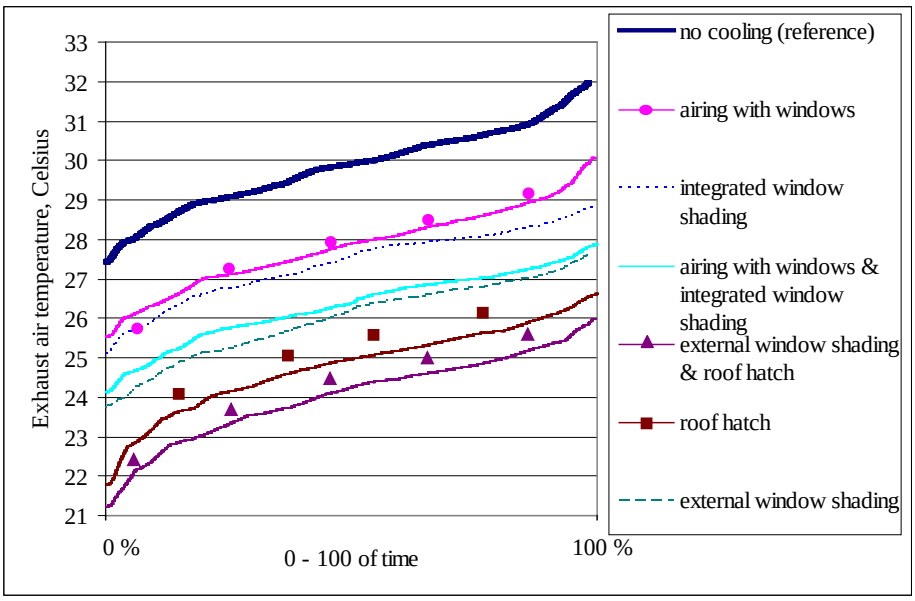

Fig. 2. Simulation results with passive cooling methods. The period is 1 – 10 of July.

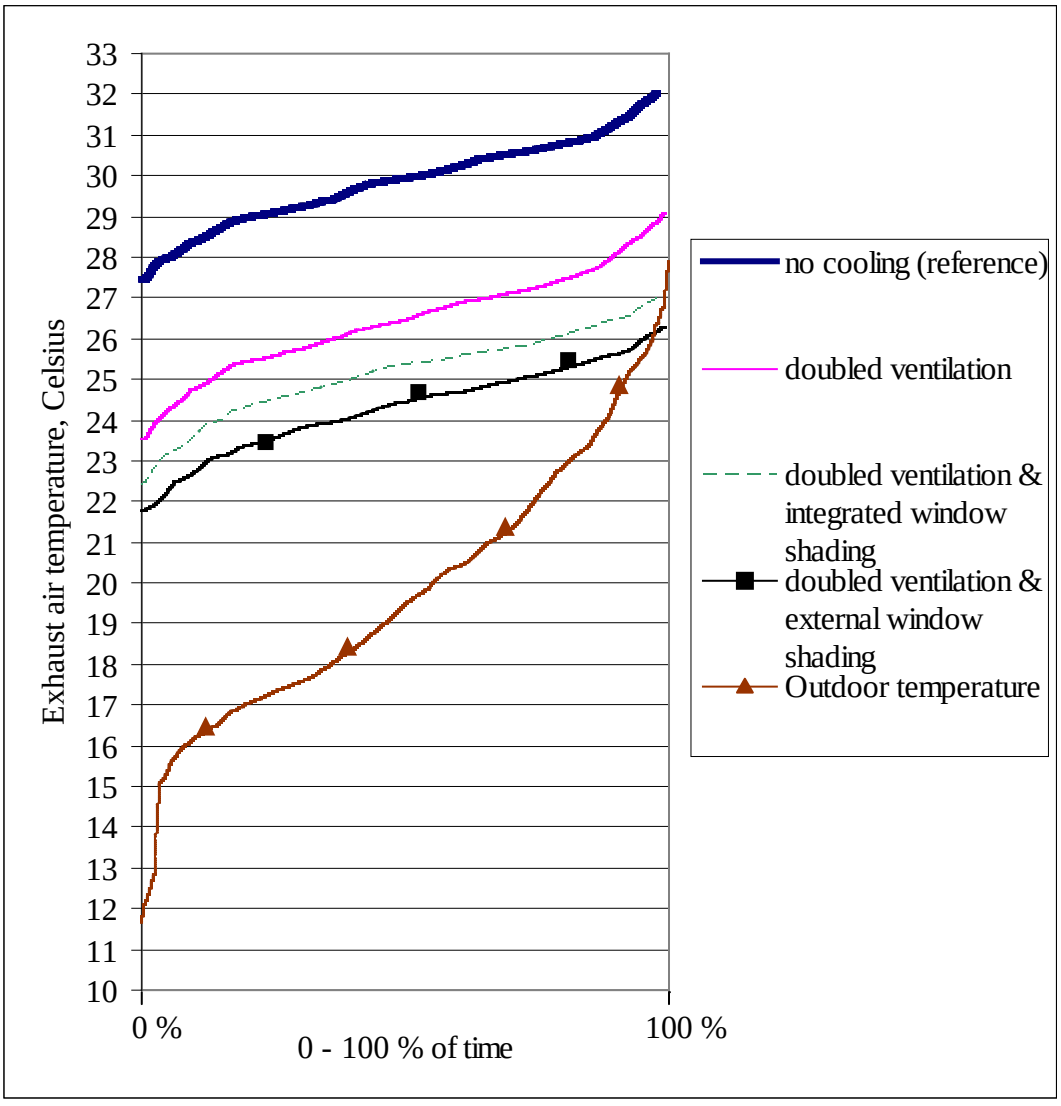

Fig. 3. Simulation results with an increased airflow in the ventilation system, with and without window shading. The period is 1 – 10 of July.

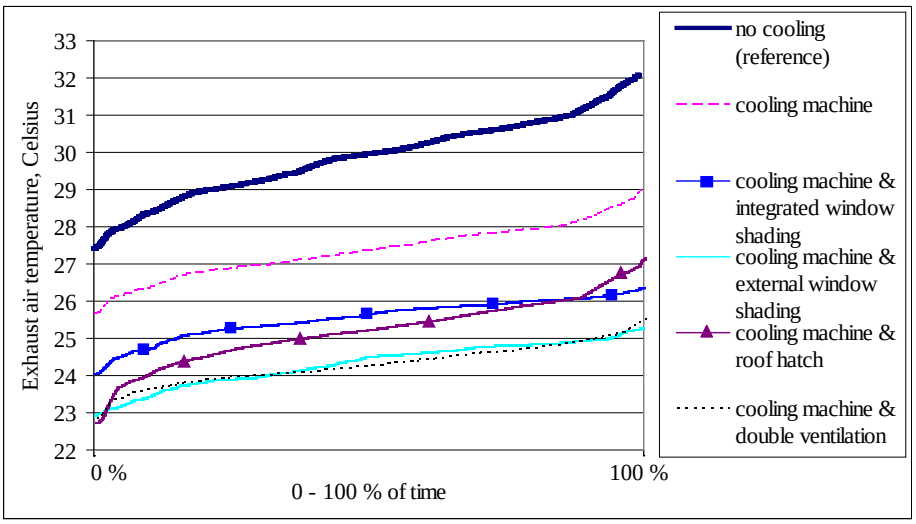

Fig. 4. Simulation results with the cooling machine, with and without passive cooling methods or an increased airflow in the ventilation system. The period is 1 – 10 of July.

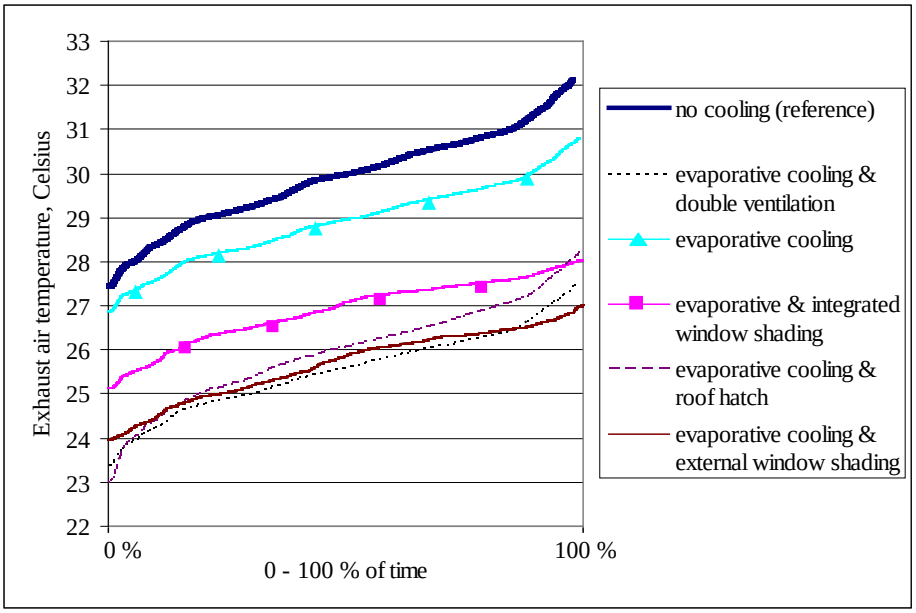

Fig. 5. Simulation results with evaporative cooling, with and without passive cooling methods or an increased airflow in the ventilation system. The period is 1 – 10 of July.

5. Conclusions

The simulation for the reference case agrees well with the practical experiences of excessive summer temperatures in Passive Houses. It seems likely that passive cooling strategies can provide sufficient cooling during the warmest part of the summer. A combination of shading and airing strategies should be used for the maximum cooling effect. However, in these simulations it is assumed that sophisticated devices are controlling the airing and shading based on the indoor and outdoor temperature and the solar radiation. Such devices are normally not yet installed in Passive Houses but nevertheless, the results demonstrate the potential with the use of passive cooling. On the other hand Fig. 2 illustrates that the best result of the passive cooling strategies is obtained with the roof hatch and the external window shading, two strategies that necessarily do not need any controlling devices. Instead of using a roof hatch, an already existing window could be kept open night-time, this would also require that security measures are taken but the installation of a roof hatch would

not be needed. In addition, since an increased airflow in the ventilation system appears as an effective tool for lowering the indoor temperature, it should be made possible for the dwellers to control the airflow after their needs. Neither the cooling machine nor the evaporative cooling can by itself lower the temperature to a comfortable level, it has to be combined with higher ventilation or the supply temperature must be allowed to be lower than 15 °C.

The outcome of these results shows that options for passive cooling should be applied before any cooling machine or such equipment is installed. Since Passive Houses can contribute to increased energy efficiency in the housing stock, it is of great importance that they are well adapted to the summer climate, ensuring a comfortable living.

The outcome of simulations of this sort is highly depending on the implementation of the internal gains and the compilation of user related data used for this in this paper only offers an indication of these amounts. Furthermore, the amount of solar gains summertime is responsible for the excessive temperatures and different simulation software will differ in this result (Lundh and Wäckelgård 2009). Other sources of error come from the software's limitation in computational accuracy. Additionally, a more exact study of the ventilating capacity of a single roof hatch or window could be made using CFD-tools (Computational Fluid Dynamics). In our case the simulated reference case agrees very well with the actual temperature loggings in the house as can be seen by comparing Fig. 1 and 2.

Acknowledgements

This work has been carried out under the auspices of The Energy Systems Programme, which is primarily financed by the Swedish Energy Agency.

References

[1] Socialstyrelsen, Temperaturer inomhus, ISBN: 91-7201-972-7, 2005.

[2] Boverket, Indata för energiberäkningar I kontor och småhus, 2007.

[3] FEBY, Kravspecifikation för minienergihus, 2009.

[4] Ruud, S. and Lundin, L., Bostadshus utan traditionellt uppvärmningssystem – resultat från två års mätningar, 2004.

[5] Samuelsson, M. and Lüddeckens, T., Passivhus ur en brukares perspektiv, 2009.

[6] Janson, U., Passive houses in Sweden – From design to evaluation of four demonstation projects.

[7] KTC, www.ktc.se, 2010.

[8] U.S. Department of Energy, http://apps1.eere.energy.gov/buildings/tools_directory/pdfs/contrasting_the_capabilities_of_building_energy_performance_simulation_programs_v1.0.pdf, 2009.

[9] Lundh, M., Wäckelgård, E., Evaluation of the solar heating model in a building simulation tool, 2009.

Appendix

Simulation input data

Building envelope	m^2	W/m^2K
Apartment area	105	
External wall		0.1073
Internal wall		0.6162
Internal floors		0.2259
Roof		0.08735
External floor		0.1289
Glazing		0.8800
Outer door, front		0.7500
Outer door, back		0.9000

Thermal bridges	m	W/mK
Edge beam	54	0.094
Wall corner	45	0.027
Windows & Doors	120	0.041
Wall/Joists	63	0.025

Ventilation		
Air leakage (at +/- 50 Pa)	0.24	$l/s,m^2$
Mechanical ventilation	45	l/s
Fan pressure	488	Pa
Fan power	60	W
Efficiency of ventilation fan	73	%
Efficiency of heat exchanger*	87	%

* During the cooling season the heat exchanger is only used if the outdoor temperature exceeds the indoor temperature

Ground reflection	20	%
Internal gains	4.6	W/m^2

Theory versus practice of energy and comfort in 4 low energy houses in Belgium

Griet Verbeeck[1,*], Werner Carmans[1], Veerle Martens[1]

[1] *PHL University College, Diepenbeek, Belgium*
** Tel: +32 11249207, Fax: +32 11249201, E-mail:gverbeeck@mail.phl.be*

Abstract: Climate change made governments introduce energy performance regulations like the Energy Performance of Buildings Directive (EPBD) and these regulations will be tightened in the future. However, the real performance of current low energy dwellings does not always match the theoretical expected performance and therefore lessons can be learned from the real performance of these houses for future low energy houses.
For four low energy houses, energy consumption and indoor climate have been analyzed through calculations, monitoring and occupant surveys. All houses appeared to be more energy saving in theory and practice than the current Flemish building standard, but with large differences between the houses and with still a large potential for improvement, especially the heating systems. Also the measured CO_2 concentrations in winter strongly differed between the houses and the occupants' perception of indoor air quality did not always match the measured quality. The weakest point according to the surveys was summer comfort, especially in the sleeping rooms, but this was not always confirmed by measurements and calculations. This shows that common comfort theories are not adapted to dwellings and that summer comfort should be evaluated in detail during design. These lessons should be taken into account when designing and evaluating future low energy houses.

Keywords: *Post-occupancy evaluation, Energy, Thermal comfort, Indoor air quality, Occupant behavior*

1. Introduction

The challenges of climate change and the exhaustibility of natural resources made governments all over the world introduce energy performance regulations in order to avoid the construction of energy devouring buildings. These regulations will be tightened in the future, as is already the case with the recent recast of the EU EPBD. Architects and building occupants however do not wait for the tightening to build dwellings that performa better than the legal standard. In Flanders, Belgium, in 2006 at the introduction of the Flemish EPBD version (called EPB), only 2.5% of all new dwellings performed at least 40% better than the legal standard (according to the theoretical calculated energy performance level) whereas in 2009 already 11% of all new dwellings performed at least 40% better than the legal standard [1]. Weak point is that these are theoretical performances and that there often is a discrepancy between theory and practice [2,3]. In order to improve the real performance of future low energy houses, the knowledge of real energy and comfort performance of present low energy houses should be increased. In this research the post-occupancy performance of four low energy houses has been analyzed for the aspects of energy consumption and indoor climate (thermal comfort and relative humidity (RH) in winter and summer, and indoor air quality (IAQ) in winter). Underlying to the analysis were following questions: (1) are these houses as energy saving in practice as calculated in theory? and (2) is the indoor climate satisfactory in these houses, both in winter and summer? In this paper, first, the methodology is presented with a description of the four houses and the calculation method for energy consumption and summer comfort. Also the monitoring campaign is described as well as the survey and the evaluation criteria for energy and indoor climate. Then, the main results of this evaluation are presented and discussed. Finally conclusions are formulated on lessons to learn from this post-occupancy evaluation for the design of future low energy houses.

2. Methodology

2.1. Description of the low energy houses

The dwellings are all located in the province of Limburg, Flanders, near the border with The Netherlands and Germany. Three dwellings are newly constructed and one old dwelling is thoroughly renovated. House 1, 2 and 3 are designed (or renovated) by the same architect, chosen by the occupants for her expertise with energy saving dwellings, whereas for the architect of house 4, it was his first low energy house and also the occupants were not familiar with low energy concepts. The main characteristics of the dwellings are given in Table 1.

Table 1. Characteristics of the dwellings

	House 1	House 2	House 3	House 4
				
Construction year	2005	2004	1830, renovated in 2002	2007
Typology	Detached	Detached	Detached	Semi-detached
# occupants	6	5	5	3
Volume	687 m³	952 m³	770 m³	629 m³
Floor area	294 m²	333 m²	278 m²	252 m²
Heat loss area	549 m²	549 m²	530 m²	419 m²
U_{mean}	0.30 W/m²K	0.28 W/m²K	0.50 W/m²K	0.30 W/m²K
Glass to floor ratio	24%	18%	28%	14%
Heat production system	Soapstone wood stove + backup boiler on gas	Condensing boiler on gas + wood stove	Soapstone wood stove + electrical heater in bathroom	Condensing boiler on gas
Domestic hot water system	Storage tank connected to wood stove + boiler backup	Storage tank connected to boiler on gas	Storage tank connected to wood stove + electrical backup	Storage tank connected to boiler on gas
Heat emission system	Floor and wall heating	Floor heating and radiators	Stove	Floor heating
Ventilation system	Balanced ventilation with ground pipe and heat recovery, summer bypass	Balanced ventilation with ground pipe and heat recovery, no summer bypass	Mechanical supply, connected to ground pipe, natural exhaust	Balanced ventilation with ground pipe (not yet installed)
Renewable solar energy	10m² thermal collectors	4.7m² thermal collectors	4.14m² thermal collectors	4.8m² thermal collectors

2.2. Calculation of energy consumption and summer comfort

Both the calculation method for energy consumption and the assessment method for summer comfort, applied in this research, form part of the Flemish version of the EPBD (further called EPB). The main principles of these calculation procedures are described below.

2.2.1. Calculated energy consumption

The end energy and primary energy consumption for heating and domestic hot water are calculated with the calculation procedure for the EPB. The procedure is mainly based on the EN ISO 13790(2004). It is a steady state monthly based one-zone model, taking into account the insulation quality of the building envelope, useful internal and solar heat gains, performance of ventilation system and heating system and presence of renewable energy systems. Despite the simplifications, the energy consumption calculated with a monthly based steady state one-zone model is very comparable with the energy consumption calculated with a dynamic multi-zone model [5]. The average indoor temperature is 18°C for heating. The outdoor climate is the Test Reference Year of Brussels, Belgium. In the calculation procedure, the volume of domestic hot water used depends on the building volume and the energy consumption for domestic hot water depends on the performance of the heat production system, presence of a storage tank and a solar collector and length of pipes. Also the auxiliary electricity consumption for pumps and fans is calculated. The EPB considers a primary energy conversion factor for electricity of 2.5.

2.2.2. Calculated risk for summery overheating

In the EPB for dwellings, also the risk for summery overheating is assessed, through the overheating indicator. The indicator is calculated based on the yearly surplus heat gains compared to the set point temperature of 18°C. The surplus gains depend on the overall monthly heat gains (internal and solar), the thermal capacity of the building and the proportion of heat losses to heat gains. For the overheating indicator a threshold value of 8000Kh and a maximum value of 17500Kh is set. Below the threshold value, no risk for summery overheating is expected, above the maximum value the summer comfort is totally unacceptable and the designer is obliged to take measures to improve the summer comfort. Between threshold and maximum value, a real risk for summery overheating is assumed, linearly depending on the distance to the threshold value. This means that it is assumed that in practice, there is a real risk that the occupant will install an active cooling system after the house is built, thus increasing his energy consumption significantly. Weakness of this steady state one-zone model is that summer comfort is evaluated at the level of the overall building, whereas overheating typically is a local and dynamic problem that not necessarily occurs in all rooms of a dwelling. But since this method, as part of the EPB method, is used in Flanders to enhance the awareness of architects for summery overheating, it also has been used within this research to roughly assess the summer comfort.

2.3. Monitoring of energy consumption and indoor climate

In the dwellings, indoor climate and energy consumption are monitored from March 2009 until February 2010. The indoor temperature and RH are measured every 15 minutes with an ONSET HOBO H8 logger in the living room and in a north oriented and a south oriented sleeping room. During the winter (November 2009 till January 2010) also the CO_2 concentration in the living room is measured every 5 minutes with a Telaire 7001, coupled with a HOBO H8 logger. With a maximum distance of 30km between the dwellings, the outdoor temperature and RH are only measured at one location. The energy consumption of natural gas, electricity and wood have been noted by the occupants on at least a weekly basis.

2.4. Survey of the building occupants

Apart from calculations and monitoring, also the occupants are surveyed. Their behavior as well as their perception of the indoor climate is analyzed through a survey on the winter and summer situation. Questions are asked on their presence in the house during daytime, on their

habits of opening windows, setting off the heating system during absence and taking measures against summery overheating during absence. Also occupants have to evaluate their perception of thermal comfort, draft and IAQ through a scale of [-3,-2,-1,0,1,2,3] for thermal comfort, a scale of [0,1,2,3] for draft and [-3,-2,-1,0] for IAQ, for winter and summer for the rooms that are monitored. Also questions are asked on the adaptation of the heating system to fluctuating indoor temperatures (eg. due to change in solar irradiation) and whether any room is uncomfortably warm or cold at a certain time of the day.

2.5. Evaluation criteria for energy consumption and indoor climate

To assess the real performance of the low energy houses and to compare the theoretical performance with the real performance, the following evaluation criteria have been used.

For energy consumption, the monitored consumption of all energy carriers (gas, electricity, wood) in each house is normalized into an end energy consumption in kWh/year per m² floor area and a primary energy consumption in kWh/(m².year). Gas and wood consumption are first normalized for a standard year by means of the degree day method (1800 degree days during monitoring and 2087 degree days in a standard year in Brussels). This is compared with the theoretical energy consumption according to the EPB. Since electricity for household appliances and lighting is included in the monitored electricity consumption, but not in the EPB, both the primary energy consumption with and without electricity is given as a result. However, by excluding the electricity consumption, also the electricity for pumps, fans and eventually electrical backup for domestic hot water is excluded. As the results will show, this makes it difficult to mutually compare the houses.

For thermal comfort, the mean indoor temperature and standard deviation are calculated from the monitored data for winter and summer for the different rooms. Also the percentage of time, the temperature in the different rooms is below, in or above the comfort zone is calculated. For the winter situation a comfort zone of 20°C - 24°C is set for the living room and 18°C - 22°C for the sleeping rooms; for the summer a comfort zone of 23°C - 26°C is set for all rooms. This is based on ISO 7730:1994 [4] for a maximum PPD (Predicted percentage of dissatisfied) of 20%. Weak point is that this comfort theory is developed for office buildings. In fact, none of the current comfort theories (Fanger, adaptive model, weighted temperature exceedings,…) is adapted to assess thermal comfort in dwellings and certainly not in sleeping rooms. The measured results for thermal comfort are compared with the perceived thermal comfort by the occupants and with the calculated overheating indicator.

The IAQ is assessed by means of the RH and the CO_2 concentration. The comfort zone for RH is 30-70%. For CO_2 concentration, four IAQ-levels are considered: IDA1 (< 400ppm above outdoor level), IDA2 (400-600ppm above outdoor level), IDA3 (600-1000ppm above outdoor level) and IDA4 (> 1000ppm above outdoor level). An outdoor level of 400ppm is assumed. For a good IAQ normally at least an IDA2 level has to be aimed for. The results are compared with the perceived IAQ by the occupants.

3. Results

3.1. Energy consumption

Table 2 presents the monitored energy consumption for the four houses, with a distinction between yearly consumption of gas and wood for space heating and domestic hot water (row 1 and 2) and yearly electricity consumption for household, lighting, fans and pumps (row 3). In case of house 3, this includes also backup heating for domestic hot water.

Table 2. Monitored yearly energy consumption in all four houses, normalized for outdoor climate

	House 1	House 2	House 3	House 4
Gas [kWh/yr]	3.201	5.577	-	9.301
Wood [kWh/yr]	16.036	1.053	8.992	-
Electricity [kWh/yr]	3.881	5.768	10.188	2.970
Total end energy [kWh/yr]	23.118	12.398	19.180	12.271

Based on these data, the total end energy consumption per year and per m² floor area is calculated, as well as the total primary energy consumption, including and excluding the electricity consumption. Also the energy consumption according to the EPB is calculated, representing the energy consumption for space heating, domestic hot water and auxiliary electrical energy for pumps and fans. Also here the total end energy consumption per year and per m² floor area is calculated, as well as the total primary energy consumption, including and excluding the electricity consumption (here for fans and pumps). These results are shown in figure 1, with the light grey bars representing the monitoring results and the dark grey bars the theoretical consumption. The black bar represents the maximum allowable energy consumption for these houses (in kWh/m²) according to the current Flemish regulation for new dwellings. Although house 3 is renovated and not obliged to meet the regulation for new dwellings, here it is treated as if it were a new dwelling. Results are discussed in section 4.

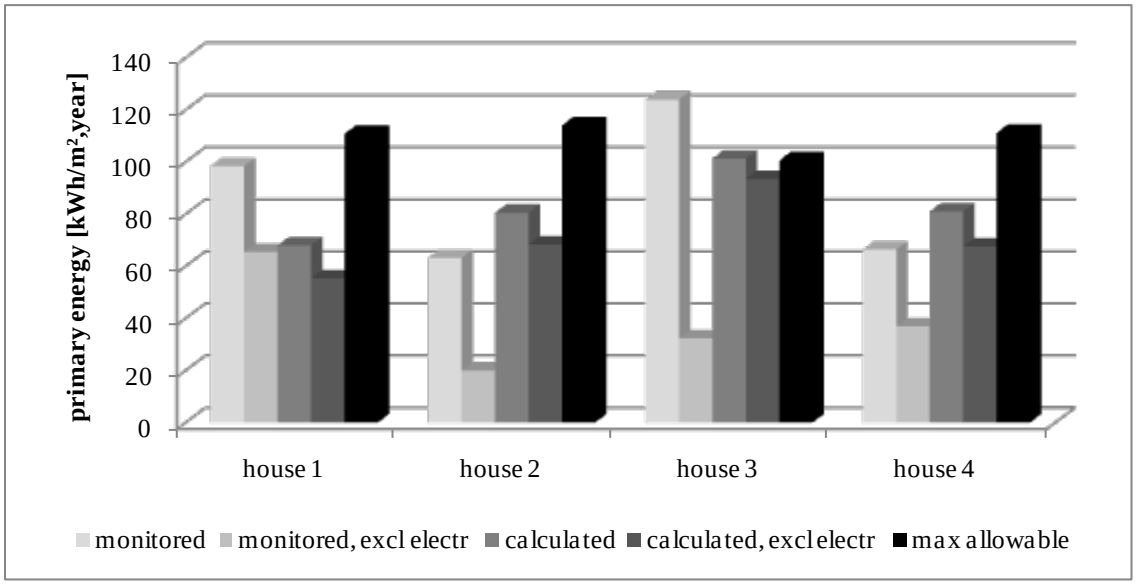

Fig. 1. Comparison of monitored and calculated primary energy consumption (in kWh/m²,year) for all four houses, with distinction between energy consumption with and without electricity consumption.

3.2. Indoor temperature and thermal comfort

Table 3 gives for each house the mean temperature ± standard deviation in the three monitored rooms during the months November 2009 till January 2010 and during the months June till August 2009. For each room also the percentage of time that the indoor temperature lies in the comfort zone is given. For the remaining time in winter, the temperature is nearly always below the comfort zone. For the summer also the percentage of time the temperature is above the comfort zone is presented, as it is an indication for summery overheating.

Table 4 presents the overheating indicator for all houses, calculated as described in section 2.2.2. Based on the threshold and maximum allowable value also the risk that an active cooling installation will be installed afterwards is calculated and presented in table 4.

Table 3. Indoor temperature in winter and summer in living room, sleeping room north and south in all houses

November 2009 – January 2010	House 1	House 2	House 3	House 4
Living room				
Mean temp ± stand.deviation [°C]	22,2 ± 0,7	21,4 ± 0,6	20,2 ± 2,1	20,7 ± 0,5
% time in comfort zone	100%	98%	72%	91%
Sleeping room north				
Mean temp ± stand.deviation [°C]	18,0 ± 1,3	14,8 ± 2,0	18,6 ± 1,7	19,3 ± 0,6
% time in comfort zone	41%	13%	68%	99%
Sleeping room south				
Mean temp ± stand.deviation [°C]	17,3 ± 1,3	15,7 ± 1,7	17,7 ± 1,6	20,3 ± 0,5
% time in comfort zone	25%	8%	31%	100%
June 2009 – August 2009	House 1	House 2	House 3	House 4
Living room				
Mean temp ± stand.deviation [°C]	24,9 ± 1,0	24,0 ± 1,0	24,3 ± 1,8	24,1 ± 1,1
% time in comfort zone	88%	78%	80%	81%
% time above comfort zone	11%	1%	5%	6%
Sleeping room north				
Mean temp ± stand.deviation [°C]	24,6 ± 1,2	23,9 ± 1,2	24,4 ± 1,1	24,5 ± 1,0
% time in comfort zone	81%	72%	82%	87%
% time above comfort zone	10%	3%	4%	8%
Sleeping room south				
Mean temp ± stand.deviation [°C]	24,3 ± 1,4	24,1 ± 1,1	24,8 ± 1,6	24,8 ± 1,3
% time in comfort zone	70%	77%	63%	78%
% time above comfort zone	15%	2%	22%	16%

Table 4.Overheating indicator and risk for active cooling for all houses

	House 1	House 2	House 3	House 4
Overheating indicator [Kh]	13.494	11.548	6.118	8.945
Risk for active cooling system [%]	58%	37%	0%	10%

3.3. Relative humidity, CO_2 concentration and indoor air quality

The RH was within the comfort zone of 30-70% for most of the time. In winter in house 1 and 3, the RH was below 30% during 1% of the time and in house 2 during 5% of the time, but only 0,5% of the time below 25%. In summer only in house 3, the RH was above 70% during 1% of the time. Since human beings are very insensitive for RH and problems with RH are more related to high RH levels (due to risk for moisture damage), these results are very satisfactory, there will be no further discussion on the RH.

Figure 2 shows for each house the percentage of time the different IAQ levels were reached in the living room during the months November 2009 till January 2010.

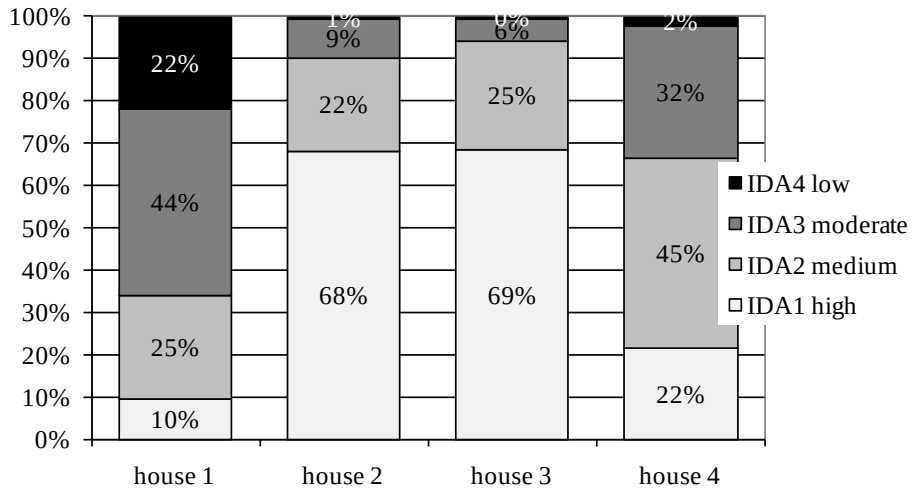

Fig. 2. Percentage of time IAQ levels are reached in each living room during Nov. 2009 till Jan. 2010.

4. Discussion

4.1. Energy consumption

As figure 1 shows, the monitored primary energy consumption is lower than the maximum allowable for all houses, except for the renovated house 3. However, the monitored consumption includes also the electricity for household and lighting, which is not included in the maximum allowable value. Furthermore, the calculated energy consumption assumes a mean indoor temperature of 18°C, whereas the monitored rooms in house 1, 3 and 4 have an overall mean indoor temperature higher than 18°C, except for house 2. This way, it can be concluded that all houses perform better than the current legal standard. The results also show that the houses with condensing boiler (house 2 and 4) perform best and better than calculated in theory. In house 1 the wood consumption is very high, with an energy consumption for heating, higher than the calculated energy consumption (bar 2 vs. bar 4 in figure 1), whereas in house 3 the electricity consumption is very high. For house 1 this might be explained by the higher indoor temperature in the living room, and for house 3 by the electrical backup heating of domestic hot water and the electrical heater in the bathroom. Remarkably, none of the houses has temperature setback during night or absence, probably due to the high inertia of the installed system (soapstone wood stoves and/or floor heating). The occupants with soapstone stove slightly complain about the fact that the massive heating system is not easily adaptable to changing temperatures, thus causing overheating in winter at some moments.

4.2. Thermal comfort

The measured temperature in winter in the living room remains in the comfort zone for all houses, except for house 3, where the temperature slightly decreases during cold days. However, for the occupants the indoor temperature is never too cold, only sometimes slightly too warm. For the sleeping rooms, only the occupants of house 2 complain about the cold temperature in the north oriented sleeping room, but they never choose to put on the radiators in this room. For the other sleeping rooms of all houses, there were no complaints, although the measurements showed lower mean temperatures. This is probably due to the fact that these rooms are only used for sleeping and not for studying.

For the summer, the calculations showed a risk for overheating in house 1 and 2, but hardly any risk for house 3 and 4. However, in house 1, despite temperatures > 26°C during 10-15% of the time in all rooms, the occupants only had small complaints of overheating in the living

room and the south oriented sleeping room. In house 2, the monitoring did not show any overheating, although the occupants complained of overheating in the living room and the south oriented sleeping room and the overheating indicator indicates a 37% change that active cooling will be installed. The occupants of house 3 and 4 strongly complained of overheating in the south oriented sleeping room, which was confirmed by the measurements, but not predicted by the overheating indicator, that only assesses the overall thermal comfort.

4.3. Indoor air quality

Concerning IAQ, the monitoring showed a satisfactory IAQ in the living room of house 2 and 3 during more than 90% of the time. However, the occupants of house 3 were not totally satisfied with the IAQ and also had complaints about draft. The occupants of house 2 had no complaints on the IAQ. The IAQ was worst in house 1 and this was also confirmed by the occupants. In despite of the presence of a balanced ventilation system, they ventilate the sleeping rooms by opening windows and the living room by opening the door between sun porch and living room. They also confessed to adapt their behavior depending on the CO_2 value on the monitoring equipment. In house 4, the moderate IAQ can be explained by the fact that the balanced ventilation system was not yet installed. The occupants only ventilated by opening windows in the north oriented sleeping room in the morning.

5. Conclusions

This research shows that although the four houses are performing better than the current legal standard, there still is quite some potential for improvement. Especially the choice and use of the heating system can be improved. The soapstone wood stove has been chosen for its environmental friendliness, but practice shows that control of the system is very difficult. A robust and simple system like the condensing boiler shows to be a more energy saving solution. Furthermore, it can be concluded that there is no adequate comfort theory to assess the thermal comfort in dwellings, as the existing theories are developed for office buildings. Finally, design of low energy houses should not only focus on low energy consumption during winter, but also on good summer comfort to avoid installation of cooling afterwards by less environmentally conscious occupants. To assess the summer performance of a dwelling, summer comfort should be evaluated in detail during design and on room or zone level, based on an appropriate comfort theory.

References

[1] VEA, Press release of the Minister of Energy and Housing, Flemish new houses much more energy saving than 4 years ago!, 5 March 2010, www.energiesparen.be/node/1869.

[2] Guerra Santin O. (2010) Actual energy consumption in dwellings (PhD Dissertation T.U.DELFT). Series Sustainable Urban Areas 33, 252 pages, Amsterdam (IOS Press).

[3] van den Ham E.R., Leyten J.L. et al. (2009) Robust climate design as a concept for comfortable, healthy and energy efficient indoor spaces. Proceedings of the 4th International Building Physics Conference. Energy Efficiency and New Approaches. Bayazit, Manioglu, Oral & Yilmaz (eds.) June 15-18 2009, Istanbul, Turkey.

[4] ISO 7730:1994 Moderate thermal environments – Determination of the PMV and PPD indices and specification of the conditions for thermal comfort.

[5] Van der Veken J., Saelens D. et al. (2004) Comparison of steady-state and dynamic building energy simulation programs. Proceedings of the International Buildings IX ASHREA Conference, Clearwater Beach, Florida.

Energy simulations on switchable mirrors - comparisons between three simulation tools

Andreas Jonsson[1,*], Arne Roos[1], Yamada Yasusei[2]

[1] *Uppsala University, Uppsala, Sweden*
[2] *National Institute of Advanced Industrial Science and Technology, Nagoya, Japan*
** Corresponding author. Tel: +46 184901215, Fax: +46 184713270, E-mail: andreas.jonsson@angstrom.uu.se*

Abstract: In a research collaboration between the National Institute of Advanced Industrial Science and Technology (AIST) in Japan and Uppsala University switchable mirrors have been evaluated from an energy perspective using energy simulations for smart windows based on gasochromic switchable mirrors. Optical properties and U values for the transparent and reflectivestates are used as input for the energy simulations. A test room has been built and is located in Nagoya, Japan. Simulations on energy use for smart windows based on switchable mirrors have been compared between three energy simulation tools. The simulations show good agreement and the simulation results also address the importance of a good control strategy for the smart windows.

Keywords: *Switchable Mirrors, Smart Windows, Energy Simulations, Gasochromic windows*

1. Introduction

A step towards a society not based on fossil fuels might be to use more renewable energy. Another step is energy conservation. Smart or switchable mirrors can be one way to conserve energy within buildings. They can reduce cooling needs in warm and/or varying climates since the transmittance of light and hence the solar heat gain factor can be reduced. This reduction can be achieved when people are present to give a comfortable level of daylight and when people are not present adapted to a level which leads to the lowest energy need for the building. The control strategy of such windows is important for their energy performance [1, 2].

In this study the focus has been on smart windows based on gasochromic switchable mirrors based on metal hydrides [3]. The state of the window is changed using a gas mixture with argon and hydrogen to turn the window to a transparent state and using a gas mixture with oxygen to revert the window back to a reflective state. This means that it is necessary to combine a switchable glass in a window of at least two panes and control the window by letting in either gas mixture in between the panes.

2. Methodology

2.1. Energy simulations

Proper energy simulations on smart windows require that the simulation tool can handle building components with varied properties over time. In this project three simulation tools were used. WinSel is a static window simulation tool developed at Uppsala University, VIP Energy [4] is a commercial dynamic building simulation tool and eQuest [5], which is also a dynamic building simulation tool developed by Lawrence Berkeley National Laboratory. Meteorological input data have been obtained from the software tool Meteonorm [6].

2.1.1. WinSel

WinSel is a software tool for evaluating and comparing windows. The software calculates the energy for heating and cooling caused by the windows as a building component. The purpose

is to be a simple tool for selecting windows. Using the window properties solar gain and U value, different windows can be compared for a building located in a specific climate using just balance temperature and a climate data file as input. The WinSel simulation parameters can be found in table 1. Due to the simplicity of the program, it is suitable as a tool for selecting the right type of window for a certain building. The result achieved from the program is the energy balance for the heating season and the cooling season. The energy balance is calculated per square meter glazing area from the equation:
Energy balance = Solar heat gain - Thermal losses

Table 1. WinSel simulation parameters.

Parameter	Value
Climate (from Meteonorm 5.0):	Nagoya
Ground reflection	20%
Building balance temperature	12°C
Allowed temperatures	20-26°C
U value, transparent state	2,40 W/m^{2}K
g-value, transparent state	50%
T_vis, transparent state	35%
U value, reflective state	1,67 W/m^{2}K
g-value, reflective state	6%
T_vis, reflective state	5%

WinSel can simulate smart windows with variable solar gain, g-value, and variable thermal performance, U value. In the software the g-value and the U value can be time dependent and are regulated using different control strategies. Six different control strategies have been developed to exemplify different approaches for controlling smart windows:

EO – "Energy optimization" means that the windows are always kept in the state which is best from an energy perspective. In the simulations the windows are kept in mirror state whenever there is a cooling need and in a transparent state whenever there is a heating need.

DO – "Daylight optimization" means that the windows are in a state which is optimized from a daylight perspective. The perpendicular component of the transmitted direct solar radiation was thus regulated by the switchable mirror in the window to a maximum of 200W/m2. This mode of the control mechanism reduces annoying glare when the sun is low in the sky and when the solar irradiation is close to perpendicular to the window. Solar radiation at glancing incidence angles does not turn the window into a reflective state.

O1 – "Office 1" mode corresponds to having the window in "daylight optimization" mode between 7:00 a.m. and 6:00 p.m. and otherwise in "energy optimization" mode.

O2 – "Office 2" mode corresponds to having the window in "daylight optimization" mode during half of the time between 7:00 a.m. and 6:00 p.m. and otherwise in "energy optimization" mode. This is a simplified way of simulating that the office is occupied only during half of the time.

R1 – "Residential 1" mode corresponds to having the window in "daylight optimization" mode between 6:00 a.m. and 8:00 a.m. and also between 4:00 p.m. and 10:00 p.m. and otherwise in "energy optimization" mode.

R2 – "Residential 2" mode corresponds to having the window in "daylight optimization" mode during half of the time between 6:00 a.m. and 8:00 a.m. and also between 4:00 p.m. and 10:00 p.m. and otherwise in "energy optimization" mode. This is a simplified way of simulating that rooms in the building are only occupied during half of the time.

The different control strategies can easily be modified. Over a year the time resolution of an hour is assumed to be averaged and the simplifications of the strategies is a way to make the results more comprehendible. Switchable windows can then be evaluated and compared to static windows at different locations and in different buildings.

2.1.2. VIP Energy and eQuest

VIP Energy is a commercial software simulation tool for whole building simulations and eQuest has been developed by the Lawrence Berkeley National Laboratory and is based on DOE2.2. These software tools are based on dynamic simulation models and thus take the heat storage in the building structure into account. They also take the air flows in the ventilation system and leakage in other building components into account.

Since user precence is assumed to be time dependent and this controls the window state, it is desirable if the software tool can handle time dependent building components. Unfortunately this is not the case for VIP Energy. Instead separate simulations were made for transparent and reflecting states and the energy needs were summarized hour by hour manually. To be able to do this we had to set the indoor temperature to a constant 22°C for the whole year. For eQuest the indoor temperature were allowed to vary between 20-26°C. Other simulation parameters were kept as similar as possible and a list of the most important can be found in table 2.

Table 2. Common building parameters used in VIP Energy and in eQuest.

Parameter	Value
Climate (from Meteonorm 5.0):	Nagoya
Ground reflection	20%
Ventilation volume	14 m^2
Floor area	5.75 m^2
U value, roof	0.49 W/m^2K
U value, south/west wall	0.33 W/m^2K
U value, window	2.40/1.67 W/m^2K

3. Results and Discussion

3.1. WinSel

The results from the WinSel simulations show the importance of the control strategy. For a south facing window for example the energy balance of the window switches from negative to positive with more advanced control strategies for the Nagoya climate as can be seen in figure 1. The energy balance results are presented per square meter window area.

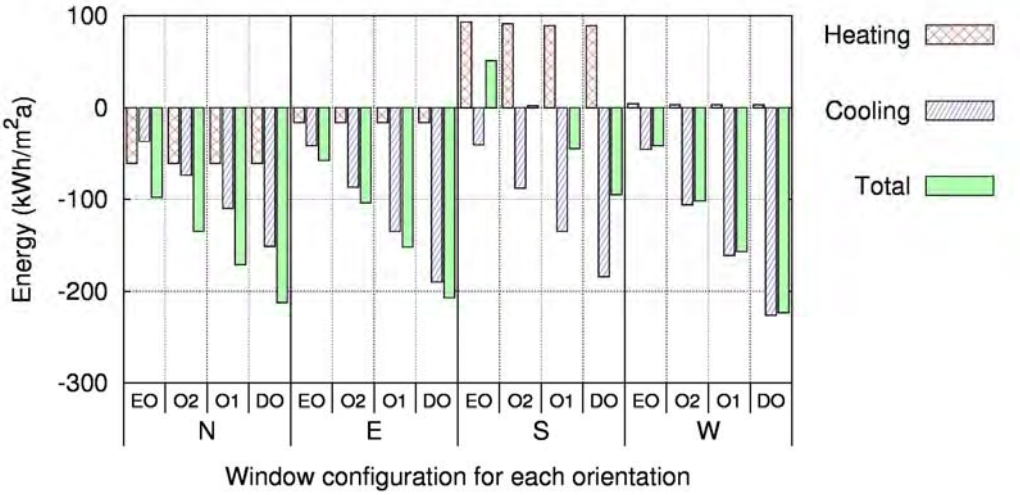

Fig. 1. Simulated energy balance for the test building located in Nagoya using WinSel.

3.2. VIP Energy

The whole building simulations made in VIP energy show similar results, found in figure 2, but are presented as energy use per square meter floor area. Comparisons are also made with static windows having g values equal to 30 and 70 % respectively showing that the switchable windows outperform the static windows if using control strategies "O2" (office with presence detectors) or "EO" (switchable window always controlled for a low heating and cooling need.)

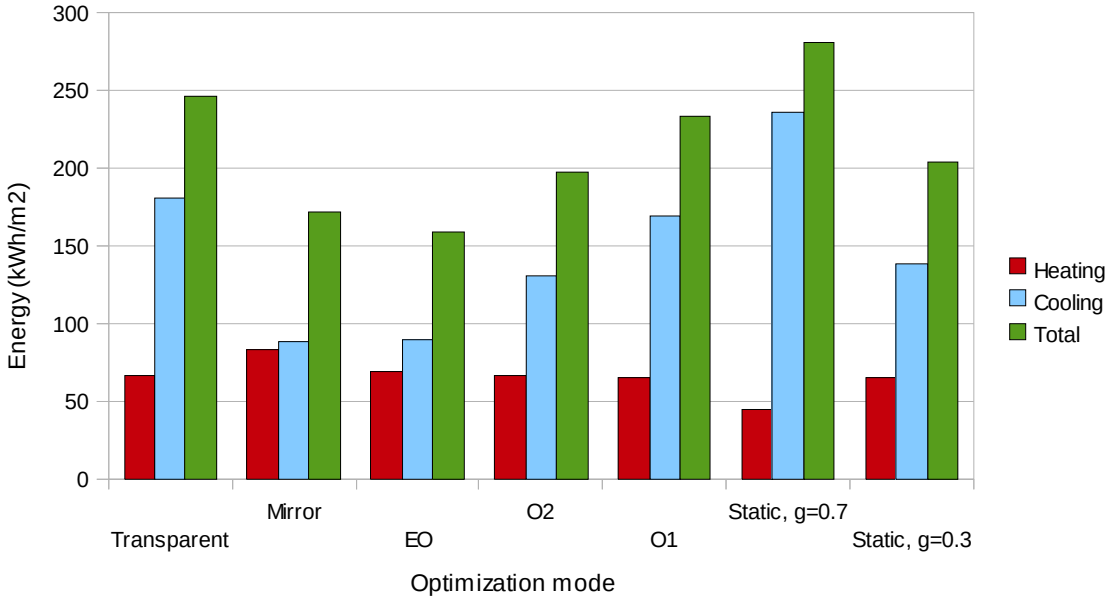

Fig. 2. Simulated energy balance for the test building located in Nagoya using VIP Energy.

3.3. Comparisons between three simulation softwares

Comparisons between simulations made in VIP Energy, eQuest and WinSel show differences of about 20% for the total energy need. Unfortunately the building models in the simulation softwares cannot be set up in exactly the same way. In VIP Energy there is no built in support for time dependent components. Therefore the indoor temperature had to be set to a constant value at 22°C and two separate simulations for transparent and reflective state were made and the results from these simulations were summed up manually. It is reasonable that this leads to a higher than expected energy need, as also can be seen in figure 3.

The results for WinSel and eQuest are lower but an explanation to the somewhat higher energy need given by the WinSel simulation software might be that the balance temperature is assumed constant over the entire year. One should also remember that this is a static simulation tool and has a very simplified way of handling heat storage within the building.

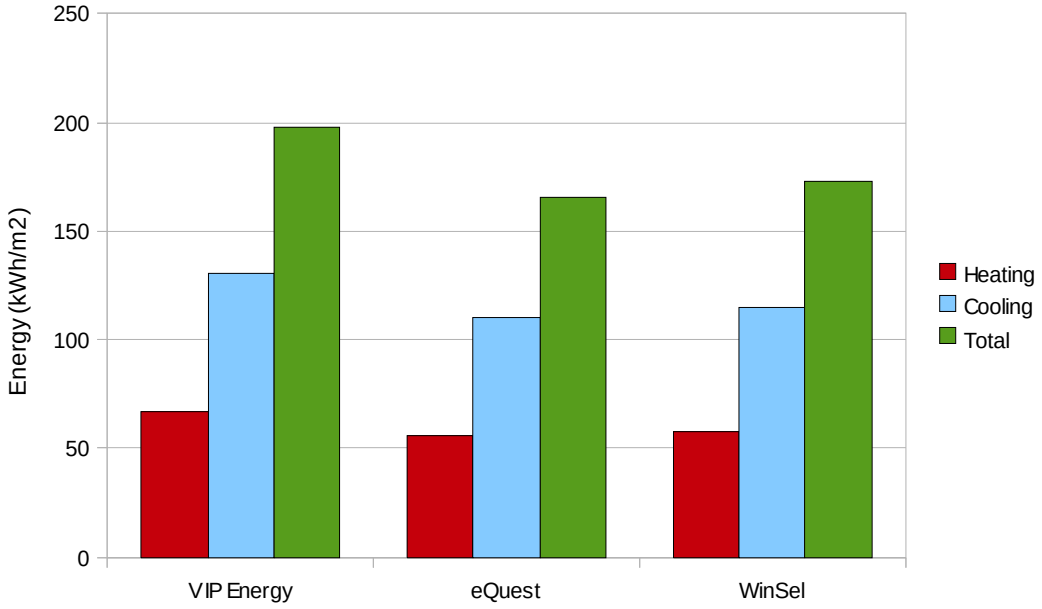

Fig. 3. Simulated energy balances for "O2" optimization mode (office with presence detectors) for three different simulation software tools for the test room located in Nagoya.

4. Acknowledgement

This work was supported by the New Energy and Industrial Technology Development Organization program (NEDO).

References

[1] A. Jonsson, A. Roos, Evaluation of control strategies for different smart window combinations using computer simulations, Solar Energy, 2010, pp. 1 – 9.

[2] A. Jonsson, Optical Characterization and Energy Simulation of Glazing for High-Performance Windows, Thesis, Uppsala University, 2010.

[3] K. Yoshimura, Y. Yamada, M. Okada, Optical switching of Mg-rich Mg–Ni alloy thin films, Applied Physics Letters 81, 4709, 2002.

[4] VIP Energy software homepage: http://www.strusoft.com/index.php/en/products/vip-energy

[5] eQuest software homepage: http://doe2.com/equest/

[6] Meteonorm software homepage: http://www.meteonorm.com

Rice-straw based cement brick microclimatic thermal impact assessment in Cairo, Egypt

Tamer Akmal[1], Mohammad Fahmy[2,*], Abdul-Wahab El-Kadi[3]

[1] *Department of Architecture, Faculty of Engineering, Misr International University, Cairo, Egypt*
[2] *Department of Architecture, Military Technical Collage, Cairo, Egypt*
[3] *Department of Architecture, Al-Skerouk Higher Institute of Engineering, Al-Sherouk Academy, Cairo, Egypt*
** Corresponding author. Tel: + (202)2 40 29 382, Fax: + (202)2 26 21 908, E-mail: md.fahmy@live.com*

Abstract: The population and urbanization growth will lead to more dependency on mechanical cooling which is not a long term sustainable strategy. Therefore, it is important to ensure all elements involved in urban sustainable developments are well performing. Of these elements, building materials have an essential role to adjusting outdoor heat environment transfer to the indoors. As part of the research society work in Cairo towards minimizing the "black cloud" generated due to burning rice roots and straw after cultivation, this paper studies the thermal performance of a novel manufactured brick using rice straw fibbers on a cement-aggregate mixture basis. It has been designed to provide a recycled constructional biomaterial, to help healthy urban environment and reduce cooling energy demands. ENVI-met BETA5 numerical simulations were held for an existing microclimatic area to assess the impact of this brick on outdoor comfort in terms of Predicted Mean Vote, PMV, as well as for indoor conditions in terms of ambient air temperature. Among the many mixtures to produce the least bricks number suitable for transportation (1000 bricks), only two were optimum for cost, mechanical and thermal properties. In comparison with normal cement brick, PMV records showed fixed values using the selected rice-straw based cement brick mixture. In evening, it recorded less mean outdoor air temperature as different wall heat interaction occurred due to the new brick k-value. This suggests that the new brick balances between indoor and outdoor needs and contributes to further investigations in terms of energy conscious urban planning.

Keywords: *Rice-straw cement brick, thermal impact assessment.*

1. Introduction

Cooling energy consumption increase due to climate change [1-5] and due to unsustainable urban developments [6-8] has motivated research society in Egypt towards urban planning applied solutions by urban form design [9-12]. And despite the initiative building construction energy code [13] to legislate energy saving conscious materials for single building, there still no consideration for the recycled materials and biomaterials specially with regard to the large urban development movements around major cities of Egypt. From this standing point, rice crop is considered one of the major agriculture products in the world and in Egypt as a food supplementary as well as many by-products using its remnants and residuals after cultivation. Agriculture by-products are acknowledged as biomass energy source [14], as low cost building materials [15] and as reinforcing materials [16], whereas all these approaches stand as recycling strategies to reduce environmental impacts such as increase of CO_2 emissions [15, 17].

Rice-straw based brick is one of the agriculture by-products internationally acknowledged such as through the development of either clay sand or cement mixtures with rice-straw [18]. In India, [19] presented the rice-straw based cement panel but didn't consider the commercial sizes of brick, or its thermal properties on a neighborhood scale which is considered a local scale from a climatology point of view.

In Egypt what is so called a black cloud is basically attributed to two reasons; burning the remnants of rice straw and the brick industrial pollution. Rice straw residuals per year is around 3.5 million tons, of which about 1.5 million tons is used in production of organic

fertilizers, to be used with storage of some crops (onions - potatoes), plantation of non-traditional crops (mushrooms) and to feed farm animals instead of hay [20].

A wasted amount 2: 2.5 tons per year of rice straw are disposed of burning which has a big share in the formation of the black cloud specially in southern delta governorates and almost whole Greater Cairo specially in winter when humidity settles the suspended smog [19] which causes a serious health problem. The ministry of state for environmental affairs, MSEA, in cooperation with many sectors started establishing factories in delta for composting and converting rice-straw to other forms such as untraditional fertilizers, thermal gas and bio fuels but a recycling towards involvement in construction industry such as low-cost housing materials hasn't been approached yet [17].

2. Methodology

The main objective of the research is to preserve the environment benefit from rice straw recycling so that a low cost building material is produced and sustainable implications on a neighborhood scale can be achieved in terms of energy saving and thermal comfort. The Egyptian standards for the concrete work was the base of the brick sample and then some differentiations in the components were done [21, 22].

2.1. Field work

The starting blend idea was the addition ratio of rice straw to mix the concrete bricks to replace the aggregates (Haswa) part as filler and for non-loaded bearing brick to achieve less dense as possible to save the cost of the structure of the building, less cost as possible to achieve an economic retrofit, and enough coherent brick for the trading and handling with minimum damage. Research was conducted with more than 250 different mixtures divided into three main groups based on the ratios of sand to aggregates of 2:1, 4:3 and 1:1 with varying amounts of rice straw and cement in kilograms with each ratio as fiber filler, fig. 1. A mixture without using aggregates to reduce the weight and increase the amount of straw was also prepared. The parameters of the density-price were initially compared with its corresponding normal cement bricks (1880:1720 Kg/m^3) manufactured by the National Company of Cement and then on a local scale thermal performance basis to assess their impacts on the pedestrian comfort as well as on the ambient air temperature which is associated with specific indoor climate conditions, comfort, cooling energy demand and green house gases emissions.

Fig. 1: Instrumentations used to prepare the different mixtures' samples.

2.2. Measuring brick properties

In order to assure the strength of each brick sample from each mixture, solid and hollow bricks were produced for the common size 25 × 12 × 13cm, fig. 2. The first set of samples were manufactured on the basis of 4 cm3 aggregate + 4 cm3 Sand + straw + Cement. By gradually increasing the amount of straw to a range of mixtures ranging from 2 kg to 7 kg straw for the same mixture with the change in the percentage of cement added to the mixture from 10: 30 kilograms cement as the volume of the mixture increases with the amount of straw added. Samples with the first increase in the proportion of straw had been inconsistent, even with the increase in the proportion of cement; therefore, according to the mechanical pressure test, other groups of samples have been fixed of sand to aggregate to be 4: 3, 2: 1 and new 15 samples designed to produce only solid brick with a size of 25 × 12 × 6 cm. The most successful mixtures with respect to cost were of the brick blend no.1 and no.4 as fig. 2 and table 1 indicate. Measures were done for samples in the Housing and Building Research Centre in Cairo and in the main laboratories of Major Projects Corp of the Egyptian Armed forces. Results of measure show that all samples of both solid and hollow bricks don't have any color change due to chemical salts' residuals from hydration process. Water absorption factor varied from 4-21% of the brick weight for 25 × 12 × 13cm, 25 × 12 × 6cm and 25 × 12 × 13cm solid, solid, hollow bricks respectively. Adding coloring powders didn't affect any of the mechanical or physical properties of any sample. The most important factor was the brick breaking stress which was best for the mixtures no. 1 and 4 as highlighted in table 1. Samples of each brick mixture have been produces for measurements and analysis purposes with ratios of sand : aggregates and by increasing the amounts of cement and rice-straw in 15 steps, table 1. To produce (1000) bricks of both these two bricks, unlike the samples components amounts produced just for measurements, amount of materials of the brick mixture were for mix. no. 1; 8.5cm^3 sand, 8.5cm^3 aggregate, 42kg straw, 180kg cement and its properties for the less cost of 46.8EGP were 1545kg/m3 density, and 18.7kg/m^2 stress. Mix. no. 4 was 8.0cm^3 sand, no aggregate, 100kg straw, 350kg cement and its properties for the less cost of 48.4EGP were 884kg/m^3 density, and 4.4kg/m^2 stress. The later mixture had to have a compression of about 15% of its height due to the more straw. Cost (on 2005) was calculated according to about 270EGP/tone cement, 10EGP/m^3 of Sand, 25EGP/m^3 of aggregate 50 EGP/tone of rice straw and 80 EGP/tone of stone powder. Despite brick stress varied between 4-20 kg/m^2 which is not compared with the stress of the brick used as bearing walls, but this brick is designed for non-loaded walls usage.

Fig. 2: Unsuccessful hollow and successful solid rice-straw based brick.

Table 1: samples of the designed mixtures, the mark (--) means that sample was inconsistent.

			mix. no. 1 (ratio in volume)			mix. no. 2			mix. no. 3			mix. no. 4		
		1 sand: 0 aggregate				4 sand : 3 aggregate			2 sand : 1 aggregate			1 sand : 1 aggregate		
No.	Cement Kg	Straw Kg	Stress Kg/cm^2	Cost EGP	Density Kg/m^3	Stress Kg/cm^2	Cost EGP	Density Kg/m^3	Stress Kg/cm^2	Cost EGP	Density Kg/m^3	Stress Kg/cm^2	Cost EGP	Density Kg/m^3
1	2	10	18.7	46.8	1545	7.2	50.3	1571	--	53.5	1606	--	--	--
2	2	15	24.1	61.4	1603	--	--	--	--	--	--	--	--	--
3	3	10	--	--	--	--	--	--	13.2	47.6	1384	--	--	--
4	3	15	12.8	57.2	1488	12.2	60.4	1472	13.5	64.4	1451	--	--	--
5	3	20	14.3	70.6	1542	--	--	--	12.5	81.2	1519	--	--	--
6	4	15	--	--	--	11	52.99	1288	6.6	54.4	1226	8.8	58.4	1065
7	4	20	9.6	62.6	1366	9.2	65.9	1340	9.5	68.5	1282	--	--	--
8	4	25	15.07	74.4	1413	--	--	--	--	--	--	9.6	91.9	1199
9	5	15	--	--	--	8.9	46.4	1128	--	47.3	1063	4.4	48.4	884
10	5	20	8.4	56.3	1227	8.5	57.7	1173	--	59.3	1112	8.9	62.2	939
11	5	25	11.8	66.9	1269	9.4	69.0	1218	8.5	71.4	1160	--	--	--
12	5	30	--	--	--	--	--	--	10	83.5	1208	--	--	--
13	6	20	--	50.5	1100	8.2	51.4	1045	9.2	52.5	983	--	--	--
14	6	25	9.75	59.9	1138	10.5	61.4	1085	--	63.0	1026	3.3	64.8	852
15	6	30	--	69.3	1375	--	71.3	1125	10.2	73.6	1068	11.2	76.4	899

2.3. Numerical simulation:

As the main idea of this paper is to study how biomaterial such as rice-straw based cement brick can modify outdoor-indoor climate in terms of pedestrian comfort and outdoor air temperature T_a, ENVI-met BETA5 urban climate numerical package has been used. Numerical simulations were held to easily simulate neighborhood complexities to help providing design and planning decision support [23]. ENVI-met [24] is a three-dimensional numerical model that can simulate the surface-plant-air interactions of urban environments with a typical resolution of 0.5 to 10m in space from a single building up to neighborhood. It is CFD based but with much improvements than only a package for fluid dynamics' simulations [25]. Simulations using the k-value of the rice-straw based cement brick in comparison with normal cement brick were applied on the 1st of July which is the extreme summer hot day analyzed by ECOTECT2010 [26].

Table 2 show the data input for simulations for brick mixture no. 4 which has the less density and hence the less k-value. Nevertheless, first parameter assessed is the PMV at 1.2m above ground level to represent outdoor conditions modifications in terms of pedestrian comfort. Second is the ambient temperature T_a also at 1.2m above ground level to represent the site air temperature modified after the new brick which gives impression about reductions of indoor cooling demand in comparison of that of using normal cement brick. For these purposes, a case study in Cairo, latitude of 30° 7'N and longitude of 31° 23'E, is a semi-arid mid-latitude climate zone [27], is examined. The case study is part of the Fifth community which is built in late 20th century, as one of New Cairo communities. It lies to the east of the 1st Greater Cairo's ring road, fig. 3.

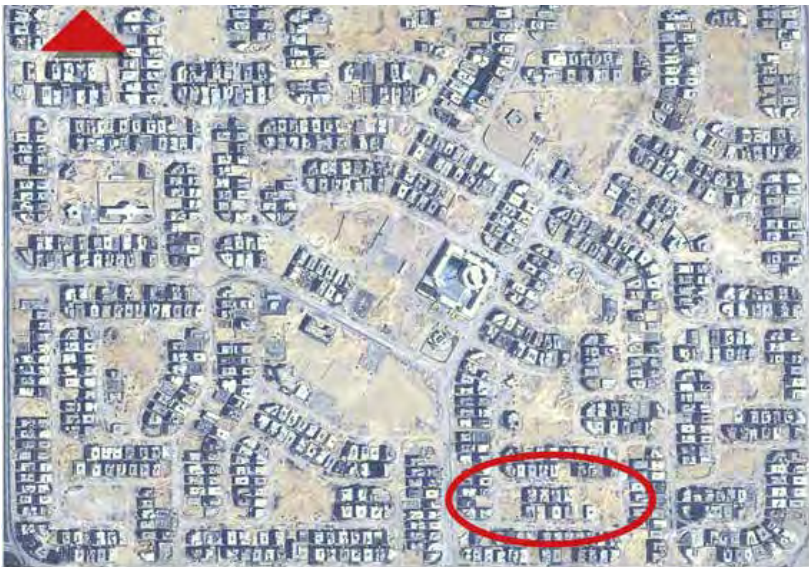

Fig. 3: Location of the case study area on the layout of the neighbourhood located in New Cairo.

Table.2: Inputs used in simulations for both rice-straw and normal cement brick [13, 24, 28].

No.	Parameter	Value
1	*Ta*	301.95˚ K
2	*RH*	59%
3	*V*	3.5 m/s at 10m height
4	k-value Walls	0.41 and 1.25 watt/m.K for rice-straw and normal cement brick respectively
6	Albedo Walls	0.25
8	Human walking speed	1.1 m/s
9	Pedestrian Clo.	0.50

3. Results implications

Basically, as ENVI-met model considers the fabric as heat sink for the outdoor environment, a heat exchange should have generated the shift in air temperature as shown if fig. 4. A ir temperature using the normal cement brick T_n is less than its corresponding of the Rice-Straw based brick by about 0.1 ˚C early simulation time and the opposite at evening time.

Outdoor temperature was less than indoors attributed to the less k-value of the Rice-straw brick of 0.41 which intercept more outdoor heat compared with 1.25 k-value for the normal cement brick. This clarifies why pedestrian comfort in terms of PMV hasn't any change in its values which can be attributed to the holistic nature of PMV as it considers all environmental and personal aspects which haven't been changed except the air temperature, therefore there was no need to add PMV figure. Just to mention not to list these factors affecting PMV; the outdoor radiation environment and the walls reflectivity factor stayed fixed in both simulations and in turn PMV stayed as it is using both the thermal conductivity k-values for of both brick types.

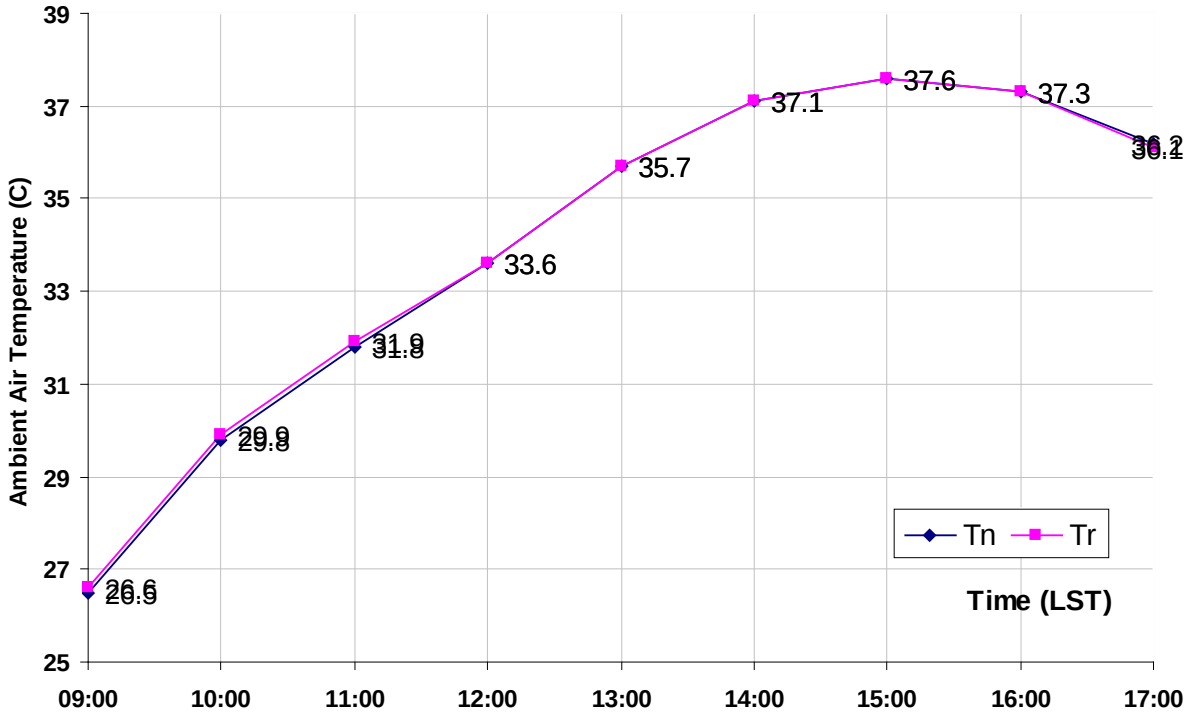

Fig. 4.

4. Discussion and conclusion

Studied in this paper, a new brick type based on the recycled rice-straw was innovated. The rice-straw has replaced part of the aggregates used in the normal cement brick by the try and error to generate a stable blend after which mechanical and thermal experiments have been conducted. Among the many mixtures examined, both mixtures highlighted in table 1 were only the stable but the mixture of 1 sand: 0 aggregate with 2kg cement and 10 straw and a pressure of 0.15 from the brick height, was the most efficient in terms of cost. Eventually, to examine its environmental thermal impact, ENVI-met BETA5 numerical simulations were held to generate pedestrian comfort levels and ambient air temperature.

The fist parameter hasn't been changed due to the fixation of the many environmental and personal factors affecting PMV. The later parameter showed promising changes and in turn a

promising energy savings in the cooling demand especially with respect to the time simulations were held in at which electricity used in mechanical cooling in Egypt suffers many cut off. Moreover, this recycled bio-brick not only helps in decreasing air pollution, but also reduces construction cost and indicate a maximized cost reductions if added to energy reductions. However, further simulations can be on larger scales and different cases' climate conditions to ensure quantitevily such numerical simulation findings in this work.

References

[1] Radhi, H., A comparison of the accuracy of building energy analysis in Bahrain using data from different weather periods. Renewable Energy, 2009. 34(3): p. 869-875.

[2] McEVOY, D., Climate Change and Cities. Built Environment, 2007. 33(1): p. 5-9.

[3] Rosenfeld, A.H., H. Akbari, S. Bretz, B.L. Fishman, D.M. Kurn, D. Sailor, and H. Taha, Mitigation of urban heat islands: materials, utility programs, updates. Energy and Buildings, 1995. 22(3): p. 255-265.

[4] Wilby, R.L., A Review of Climate Change Impacts on t he Built Environment. Built Environment, 2007. 33(1): p. 31-45.

[5] Levermore, G.J., A review of the IPCC Assessment Report Four, Part 1: the IPCC process and greenhouse gas emission trends from buildings worldwide. Building Service Engineering, 2008. 29(4): p. 349-361.

[6] El Araby, M., Urban growth and environmental degradation. The case of Cairo, Egypt. Cities, 2002. 18(3): p. 135-149.

[7] Fahmi, W. and K. Sutton, Greater Cairo's housing crisis: Contested spaces from inner city areas to new communities. Cities, 2008. 25(5): p. 277-297.

[8] Sutton, K. and W. Fahmi, Cairo's urban growth and strategic master plans in the light of Egypt's 1996 population census results. Cities, 2001. 18(3): p. 135-149.

[9] Fahmy, M., Interactive urban form design of local climate scale in hot semi-arid zone, in School of Architecture. 2010, University of Sheffield: Sheffield.

[10] Fahmy, M. and S. Sharples, On the development of an urban passive thermal comfort system in Cairo, Egypt. Building and Environment, 2009a. 44(9): p. 1907-1916.

[11] Fahmy, M., Urban form adaptation towards minimizing climate change effects in Cairo, Egypt., in Accepted abstract and submitted Manuscript to Building Sustainability in the Arabic Region. 2010, HBRC, Housing and Building Research Centre: Cairo.

[12] Fahmy, M., A. Trabolsi, and S. Sharples, Dual stage simulations to study microclimate thermal effect on comfort levels in a multi family residential building., in 11th International Building Performance Simulation Association Conference 2009: University of Strathclyde in Glasgow, 27-30 July.

[13] HBRC, Energy Efficiency Residentail Building Draft Code (EERBC) for New Residentail Buildings, Additions and Retrofits. 2003, E gyptian Ministry of Housing, Utilities and Urban Communities; Housing and Building Research Centre.: Cairo.

[14] Shyam, M., Agro-residue-based renewable energy technologies for rural development. Energy for Sustainable Development, 2002. 6(2): p. 37-42.

[15] Pappu, A., M. Saxena, and S.R. Asolekar, Solid wastes generation in India and their recycling potential in building materials. Building and Environment, 2007. 42(6): p. 2311-2320.

[16] Brandt, A.M., Fibre reinforced cement-based (FRC) composites after over 40 years of development in building and civil engineering. Composite Structures, 2008. 86(1-3): p. 3-9.

[17] EEAA, Egyptian Environemnt Report. 2008, E gyptian Environmental Affairs Agency, Ministry of State of Environmental Affairs: Cairo.

[18] Rahman, M.A., Properties of clay-sand-rice husk ash mixed bricks. International Journal of Cement Composites and Lightweight Concrete, 1987. 9(2): p. 105-108.

[19] Mansour, A., J. Srebric, and B.J. Burley, Development of Straw-cement Composite Sustainable Building Material for Low-cost Housing in Egypt. Journal of Applied Sciences Research, 2007. 3(11): p. 1571-1580.

[20] 20. Akmal, T., Recycling Rice-Straw for the manufacure of construction brick, in Arabic. 2005.

[21] ES1991, Egyptian standards 1292/1991 for concrete construction 1991, E gyptian Ministry of Housing, Utilities and urban Communities; Housing and Building Research Centre.: Cairo.

[22] HBRC, Egyptian Code of the basics of the design and implementation of the requirements of building works. 1995, Ministry of Housing, Utilities Research Center of Housing and Construction and Urban Planning: Cairo.

[23] Bruse, M. and H. Fleer, Simulating surface-plant-air interactions inside urban environments with a three dimensional numerical model. Environmental Modelling and Software, 1998. 13(3-4): p. 373-384.

[24] Bruse, M., ENVI-met V3.1, a m icroscale urban climate model, [Online], Available: www.envi-met.com. Accessed 18/3/2009. 2008.

[25] Ali-Toudert, F. and H. Mayer, Numerical study on the effects of aspect ratio and orientation of an urban street canyon on outdoor thermal comfort in hot and dry climate. Building and Environment, 2006. 41(2): p. 94-108.

[26] AutoDesk. ECOTECT2010, [Online], Available at: http://www.autodesk.co.uk/adsk/servlet/mform?validate=no&siteID=452932&id=14205163. Accessed 19/4/2010. 2010 [cited.

[27] ASHRAE, ASHRAE Hand Book of Fundamentals (SI Edition). 2005, Atlanta: American Society of Heating, refrigerating, and Air-Conditioning Engineers Inc.

[28] Oke, T.R., Boundary layer climates. 1987, London: Methuen.

Comparative survey on using two passive cooling systems, solar chimney-earth to air heat exchanger and solar chimney-evaporative cooling cavity

Amin Haghighi Poshtiri[1,*], Neda Gilani[2], Farshad Zamiri[3]

[1] *Guilan University, Rasht, Iran*
[2] *Tarbiat modares University, Tehran, Iran*
[3] *Mapna Company, Tehran, Iran*
** Corresponding author. Tel: +98 1316690273, Fax: +98 1316690271, E-mail: aminhaghighi_p@yahoo.com*

Abstract: In this study using two low-energy systems to enhance passive cooling and natural ventilation in a solar room have been compared. First system consists of a Solar Chimney (SC) and an Evaporative Cooling Cavity (ECC) and the second one includes a Solar Chimney (SC) and an Earth-to-Air Heat exchanger (EAHE). To determine the heat and mass transfer characteristics of the systems, a mathematical model based on conservation equations of mass and energy has been developed and solved by an iterative method. The findings show that when the cooling demand of the room is 116W and the relative humidity is lower than 50%, the SC-ECC system can make acceptable indoor air conditioning even at ambient 40°C, with weak solar intensity of 200 W/m^2. It is also found that, the proposed system can provide thermal comfort conditions even during the night with zero solar radiation. The results about SC-EAHE system show that when the ambient temperature and cooling demand are high (1500W), proper configurations could provide good indoor condition even at poor solar intensity of 100 W/m^2 and high ambient air temperature of 50°C. Comparative survey shows the SC-EAHE system is the best choice for buildings with poor insulation at day time, but SC-ECC system is better for night ventilation and cooling purposes especially in arid climates.

Keywords: *Comparative survey, Passive cooling, SC-EAHE, SC-ECC.*

Nomenclature

A	area	m^2
ACH	air change per hour	h^{-1}
b	width of cooling cavity	m
C	specific heat of air	J/kgK
c	pressure loss coefficient of fittings	-
d	air gap depth, diameter	m
f	wettability percent	%
fre	frequency of temperature oscillation	rad/s
g	gravitational constant	m/s^2
H	distance	m
h	convective heat transfer coefficient	$W/m^2.K$
hr	radiative heat transfer coefficient	$W/m^2.K$
k	thermal conductivity	$W/m.K$
L	length	m
m	mass flow rate of air	kg/s
Q	heat transfer to air stream	W/m^2
R	thermal resistance	$m^2.K/W$
RH	relative humidity	%
r	radius	m
S	solar radiation absorbed by plate	W/m^2
T	temperature	K
t	thickness	m
U	overall heat transfer coefficient	$W/m^2.K$
u	air velocity	m/s
V	volume of room	m^3
x	coordinate system	m

Greek symbols

γ	constant in Eq.(2)	-
δ	heat penetration depth	m
λ	thermal diffusivity	m^2/s
ξ	friction factor	-
ρ	density	kg/m^3
ω	humidity ratio	kg_{water}/kg_{air}

Subscripts

a	ambient
abs	absorber wall
cc	cooling cavity
f	air flow
g	glass
hyd	hydraulic
i	internal
in	inlet
r	room
su	undisturbed soil
s	soil
t	pipe
o	outlet
w	water

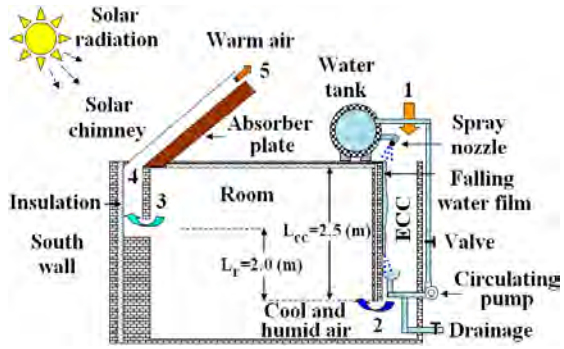

Fig. 1. Schematic diagram of SC-ECC system.

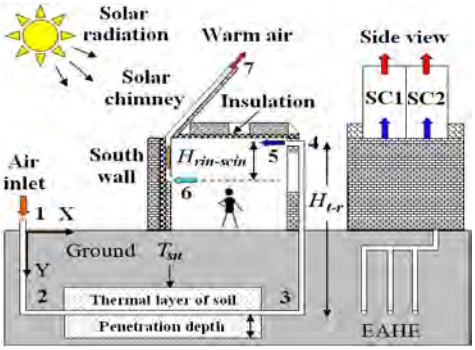

Fig. 2. Schematic diagram of SC-EAHE system.

1. Introduction

In order to reduce global warming and to reduce electricity peak demands during summer time low or zero energy cooling systems are required. passive cooling applications shall offer great advantage and it is growing at an increasing rate worldwide. These systems had attracted much attention of investigators and researchers. Giabaklou and Ballinger [1] presented a method of passive cooling in low-rise multi-storey buildings through a simple water cascade associated with openings and balconies of individual. This system applies the evaporative cooling technique to reduce ambient air temperature by passing air over the water falling film. Manzan and Saro [2] studied a system consisting of a ventilated roof with a wet lower surface of the cavity which flows the external air. They investigated thermal performance of the system by numerical modeling of evaporative cooling process through the chimney. Dai et al. [3] presented a new passive cooling system for humid climate using the solar chimney and adsorption cooling system. They showed that the system increases the rate of ventilation and provides the cooling without increasing humidity of the room. Chungloo and Limmeechokchai [4] experimentally investigated the performance of a system consisting of a solar chimney and water spraying system that was placed on the roof under hot and humid climate. They reported that the system performed well in high ambient temperature. Maerefat and Haghighi [5] presented another technique, using a system consisting of a SC and an ECC. The capability of the system to meet the required thermal needs of individuals, the effects of main geometric parameters on the system performance and the dependence of the system performance on outdoor air temperature was also studied. Maerefat and Haghighi [6] introduced and investigated integrated EAHE-SC system. They showed that the SC can be perfectly used to power the underground cooling system during the daytime, without any need for electricity.

Here, using SC-ECC and SC-EAHE systems to enhance passive cooling and natural ventilation in a solar room have been compared together. Figs.1 and 2 illustrates a schematic plan of the two systems. The SC consists of a glass-made surface faced to the south and an absorber wall. EAHE consists of horizontal long pipe placed underground. The air gets warmed in SC, and by natural convection mechanism, the outside air is sucked-in through the pipe or ECC. It will be shown that these systems can provide good indoor condition in accordance with the Adapted Comfort Standard (ACS) (Fig. 3). ACS does not recommend the ventilation rate. Therefore, the minimum ventilation rate is set around 3 ACH [7].

2. Problem formulation

The modeling includes models of SC (Fig. 4), ECC (Fig. 5) and EAHE (Fig. 6). The following assumptions are made in this analysis.
1. The air temperature at the room is uniform.

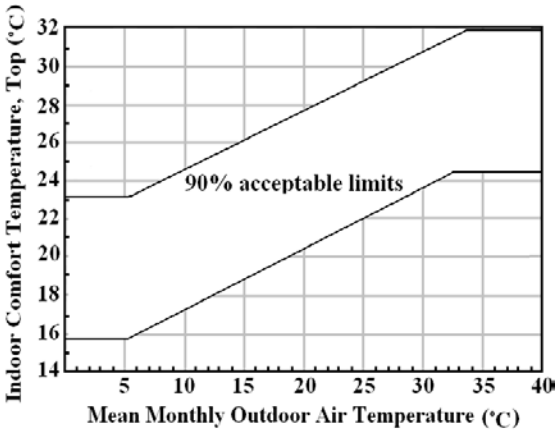

Fig. 3. Adaptive Comfort standard.

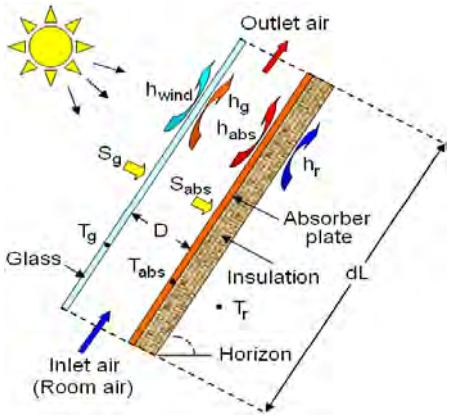

Fig. 4. Diagram of the heat transfer in the SC.

2. Only buoyancy force is considered and wind induced natural ventilation is not included.
3. The flows in the channels are laminar and hydro dynamically and thermally fully developed.
4. The glass cover is opaque for infrared radiation.
5. Thermal capacities of glass and wall are negligible.
6. The air flow in the channel is radiative non-participating medium.
7. The soil is homogeneous and the soil type does not change along the channel.
8. Thermal resistance of water film is negligible.
9. The spray enthalpy is negligible.
10. The air enthalpy is expressed as linear function of wet bulb temperature.
11. The Lewis number correlating heat and mass transfer is 1.0.
12. All thermo physical properties are all evaluated at average temperature.
13. The system is at steady-state condition.

2.1. Mathematical modeling of SC-ECC

An element of the model for SC is shown in Fig. 4. In principle and based on the energy conservation law, a set of differential equations are obtained along the length of SC [5].

$$S_g A_g + hr_{abs-g} A_{abs}\left(T_{abs} - T_g\right) = h_g A_g\left(T_g - T_{fsc}\right) + U_{g-a} A_g\left(T_g - T_{fsc}\right) \quad (1)$$

$$h_{abs} A_{abs}\left(T_{abs} - T_{fsc}\right) + h_g A_g\left(T_g - T_{fsc}\right) = -mC_{fsc}\left(T_{fsc} - T_r\right)/\gamma \quad (2)$$

$$S_{abs} A_{abs} = h_{abs} A_{abs}\left(T_{abs} - T_{fsc}\right) + hr_{abs-g} A_{abs}\left(T_{abs} - T_g\right) + U_{abs-a} A_{abs}\left(T_{abs} - T_a\right) \quad (3)$$

All of coefficients and the overall heat transfer coefficients are obtained from Ref. [5].

An element of the model for ECC is shown in Fig. 5. For the energy and mass conservation law a set of differential equations are to be considered along the length of the cooling cavity.

$$\frac{d\omega_{fcc}}{dx} = -h_m fb\left(\omega_{fcc(T_w)} - \omega_{fcc}\right)/m \quad (4)$$

$$\frac{dT_{fcc}}{dx} = \frac{bh_{fcc} f\left(T_w - T_{fcc}\right)}{mC_{fcc}} + \frac{H_{fcc(T_w)} - H_{fcc}}{C_{fcc}} \frac{d\omega_{fcc}}{dx} + \frac{bU_{a-fcc}\left(T_a - T_{fcc}\right)}{mC_{fcc}} \quad (5)$$

$$\frac{dT_w}{dx} = \left[m\frac{dH_{fcc}}{dx} + b\left(U_{r-w} f\left(T_r - T_w\right) - mC_{pw} T_w \frac{d\omega_{fcc}}{dx} \right) \right] / m_w C_{pw} \quad (6)$$

The required boundary conditions for solving Eq. 4-6 in a cocurrent type air flow configuration are:

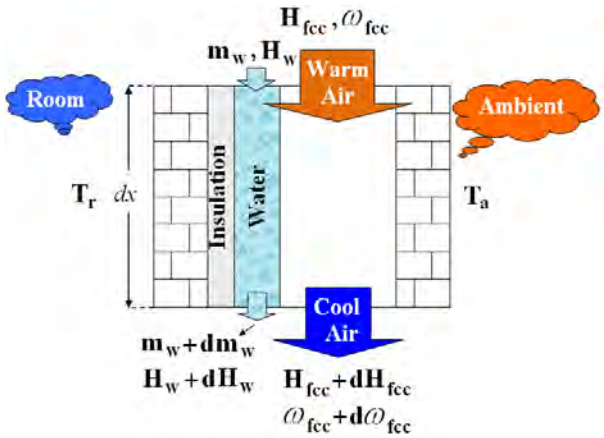

Fig. 5. Diagram of heat and mass transfer in the ECC.

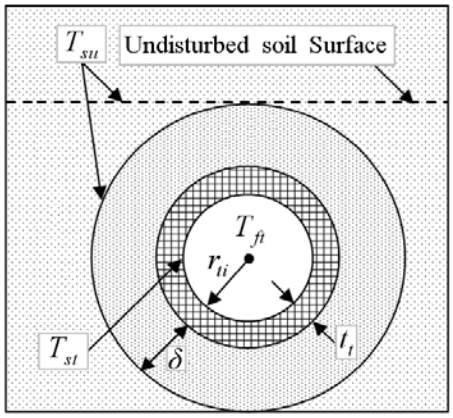

Fig. 6. Cross section of an EAHE.

$$T_{fcc}(0.0) = T_a,\ T_w(L) = T_w(0.0) \tag{7}$$

$$RH_{fcc}(0.0) = RH_a \tag{8}$$

A mathematical model based on *Bernoulli's* equation is used to estimate the system flow rate. The air velocity in the SC can be obtained as [5]:

$$u_{fsc} = \sqrt{\frac{Bouyancy\ \ Terms}{Friction\ \ Terms}} \tag{9}$$

$$Bouyancy\ \ Terms = 2\left\{\left(\rho_{fa} - \rho_{fsco}\right)gL_{sc}\mathrm{Sin}(\theta) - \left(\rho_{fcco} - \rho_{fr}\right)gL_r + \left(\rho_{fcco} - \rho_{fa}\right)gL_{cc}\right\} \tag{10}$$

$$\begin{aligned} Friction\ \ Terms = {} & \left\{c_5 + \xi_{sc}\frac{L_{sc}}{\left(d_{hyd}\right)_{sc}}\right\}\rho_{fsco} + c_4\left(\frac{\rho_{fsco}A_{sco}}{\rho_r A_{sco}}\right)^2\rho_{fr} + c_3\left(\frac{\rho_{fsco}A_{sco}}{\rho_r A_{scin}}\right)^2\rho_{fr} \\ & + c_2\left(\frac{\rho_{fsco}A_{sco}}{\rho_{fcco}A_{cc}}\right)^2\rho_{fcco} + c_1\left(\frac{\rho_{fsco}A_{sco}}{\rho_{fa}A_{cc}}\right)^2\rho_{fa} + \xi_{cc}\frac{L_{cc}}{\left(d_{hyd}\right)_{cc}}\left(\frac{\rho_{fsco}A_{sco}}{\rho_{fcco}A_{cc}}\right)^2\rho_{fcc} \end{aligned} \tag{11}$$

The coupled governing equations (1)-(3), (4)-(6) and (9) are the full description of the system. The governing equations have to be solved iteratively until convergence of the results.
The ACH is calculated under steady-state conditions by the following equation:

$$ACH = 3600m/\left(\rho_{fsc}V\right) \tag{12}$$

The room air temperature which depends on room heat gain (Q_r) is given by:

$$T_r = T_{fscout} - Q_r/\left(mC_{fr}\right) \tag{13}$$

2.2. Mathematical modeling of SC-EAHE

The cross section of EAHE used in the model is shown in Fig. 6. In order to impose the ground thermal loads as boundary conditions at the EAHE wall, the undisturbed soil temperature (T_{su}) has been applied in the equations as well. The soil temperature is nearly constant at the penetration depth. It is defined when the surface of the soil is subject to periodic temperature [6].

$$\delta = \sqrt{2\lambda_s / fre} \tag{14}$$

The air temperature through the EAHE is calculated by the following equation [6].

$$T_{ft}(x) = T_{su} + \left(T_a - T_{su}\right)\exp\left(-x/\left(m_{ft}C_{ft}R_{total}\right)\right) \tag{15}$$

Where R_{total} represents the overall thermal resistance and is given by [6]:

Table 1. Thermophysical properties.

Parameter	Value
Absorptivity of the glass	0.06
Emissivity of the glass	0.90
Transmissivity of the glass	0.84
Absorptivity of the absorber wall	0.95
Emissivity of the absorber wall	0.95
Thermal conductivity of the break wall	0.72 (Wm^{-1} K^{-1})
Thickness of break wall	0.10 (m)
Thermal conductivity of SC and ECC insulation	0.16 (Wm^{-1} K^{-1})
Thickness of SC and ECC insulation	0.002 (m)
Thermal conductivity of the pipe (PVC)	0.23 (Wm^{-1} K^{-1})
Soil density	2050 (kg m^{-3})
Thermal conductivity of the Soil	0.52 (Wm^{-1} K^{-1})
Specific heat of soil	1840 (J kg^{-1} K^{-1})

$$R_{total} = \frac{1}{2\pi L_t}\left(1/h_{ft} + \ln(\frac{r_{ti}+t_t}{r_{ti}})/k_t + \ln\left(1+\frac{\delta}{r_{ti}+t_t}+\sqrt{\left(1+\frac{\delta}{r_{ti}+t_t}\right)^2-1}\right)/k_s\right) \quad (16)$$

The air velocity in the SC based on *Bernoulli's* equation can be obtained by the Eq.9 [6].

$$Bouyancy\ \ Terms = 2\begin{Bmatrix}\left(\rho_{fa}-\rho_{fsco}\right)gL_{sc}\mathrm{Sin}(\theta)-\left(\rho_{fscin}-\rho_{fr}\right)gH_{rin-scin}\\-\left(\rho_{ft}-\rho_{fr}\right)gH_{t-r}\end{Bmatrix} \quad (17)$$

$$Friction\ \ Terms = c_6\left(\frac{\rho_{fsco}A_{sco}}{\rho_{fr}A_{scin}}\right)^2\rho_{fr}+\left\{c_7+\xi_{sc}\frac{L_{sc}}{\left(d_{hyd}\right)_{sc}}\right\}\rho_{fsco} + \left\{\left(\sum_{j=1}^{5}c_j+\xi_t\frac{L_t+H_{t-r}+Burried\ \ depth\ \ of\ \ EAHE}{d_t}\right)\left(\frac{\rho_{fsco}A_{sco}}{\rho_{ft}A_t}\right)^2\right\}\rho_{ft} \quad (18)$$

All of coefficients and the overall heat transfer coefficients are obtained from Ref. [6]. The coupled governing equations have to be solved iteratively until convergence of the results.

3. Methodology

Two systems are located in Tehran, having 35.44°N latitude position. A south-facing solar chimney with the length of 4.0 m, air gap depth of 0.2 m and inlet dimensions of 0.4 ×0.4 m is assumed for analysis. The outlet dimensions of SC and room are 0.2 m×1.0 m and 0.1 m×4.0 m respectively. A detailed study on solar chimney found the optimum angle of 50° to capture more radiation [5].

The ECC is a Cubic channel with the height of 2.0 m and 2.0 m×0.05 m inside cross section. The wettability percent of wetted wall is 0.7. The calculations are carried out for a room, having a size of 4.0 m×4.0 m× 3.125 m without air infiltration. The ECC outlet is lowered 2.0 m below the SC inlet (Fig.1).

The cooling pipe of EAHE is a PVC pipe with 25.0 m length, 0.002 m thickness, and inside diameter of 0.5 m and is buried 3.0 m below the soil surface. The initial soil temperature at surrounding is approximated to be 19°C and it is considered to be the heat source temperature. It should be noted that the SC inlet is lowered 0.5 m below the EAHE outlet (Fig.2). The cooling demand is assumed to change within the range of 0.0-1000W in the calculations.

Table 2. Performance of the SC-ECC system at different indoor and outdoor conditions.

Cooling demand (W)	Ambient air RH. (%)	Ambient air temp. (^oC)	Solar radiation (W/m^2)	ACH (h^{-1})	Room air temp. (^oC)
		40	100	2.12	31.18
	30	42	500	3.76	31.34
		43	900	4.76	31.92
		40	200	2.23	31.45
116	50	41	500	3.78	31.58
		42	900	4.85	32.00
		35	300	3.10	31.28
	70	36	500	3.82	31.57
		37	900	4.83	31.92
		34	300	3.55	32.00
	30	35	500	4.23	31.57
		37	900	5.13	31.88
		31	400	4.00	31.40
500	50	32	500	4.28	31.70
		34	900	5.18	32.00
		28	400	4.00	31.35
	70	29	500	4.34	31.67
		31	900	5.23	32.00
1000	Thermal comfort cannot be provided.				

The indoor room air temperature is kept in the thermal comfort range (Fig. 3) to secure the desired condition inside the room space. The ambient air temperature, relative humidity and wind velocity are 34oC, 30% and 1.0 m/s, respectively. The thermo physical properties of the materials included in the modeling are given in Table 1. The values of the properties specified in the table are kept constant in the computation unless specifically noted otherwise.

4. Result and discussion

4.1. Effects of environmental conditions on the performance of SC-ECC system

The influence of solar radiation and humidity on ACH and room air temperature is investigated herein. The ACH depends on the density difference between ambient air and SC outlet air. This difference is more highlighted when the solar radiation rises therefore leading to higher ACH as shown in Table 2. Comparison of the results which are obtained for one SC and ECC shows that the variation of ACH due to the variation of ambient RH is not significant. However, the applicability of system to provide thermal comfort conditions is reduced at higher ambient air RH. At low ambient air temperatures, good indoor condition can be achieved in a wide range of the ambient air humidity. The results also shows that when ambient R.H. and temperature are less or equal to 50% and 40^{o}C, respectively, room air temperature and ACH would remain in the desired range of thermal comfort. It means that when air temperature rises, thermal comfort can be achieved in lower humidity. It is found that the proposed system can provide thermal comfort conditions even during the night with zero solar radiation (Table 3). It is due to the buoyancy effect in the cooling cavity which can

draw the cooled air into the room. At night, the chimney effect is non-existant. Therefore, the buoyancy effect of the ECC will be the dominant. Anyhow, to reduce the pressure losses of the air flow during the night, the discharged air may leave the room through an opened window.

Table 3. Performance of the system at zero solar radiation (cocurrent type)

Cooling demand (W)	Ambient air temp. (^oC)	Ambient air RH. (%)	ACH (h^{-1})	Room air temp. (^oC)	Number of SC & ECC
116	35	30	1.71	28.80	1
		50	1.63	31.77	1
		70	Thermal comfort cannot be provided.		
	40	30	2.21	31.72	1
		50	Thermal comfort cannot be provided.		
		70			

Table 4. Performance of the SC-EAHE system at different indoor and outdoor conditions.

Cooling demand (W)	Ambient air temp. (^oC)	Solar radiation (W/m^2)	ACH (h^{-1})	Room air temp. (^oC)	Number of SC	Number of EAHE
500	40	100	3.28	29.61	5	3
		500	5.16	31.13	3	3
		900	4.14	28.06	1	1
	45	100	3.01	30.92	6	4
		500	4.30	31.12	3	4
		900	4.02	31.27	2	4
	50	100	3.05	31.02	6	6
		500	3.45	31.62	3	5
		900	3.06	31.52	2	5
1000	40	100	4.98	30.51	8	6
		500	4.10	31.95	2	2
		900	3.63	30.69	2	4
	45	100	4.15	30.00	8	6
		500	3.27	31.15	3	5
		900	3.00	30.90	2	5
	50	100	4.18	31.95	8	7
		500	3.05	31.98	3	6
		900	3.15	31.53	3	12
1500	40	100	5.20	31.36	8	4
		500	3.29	30.61	3	5
		900	3.00	30.35	2	5
	45	100	3.95	31.00	9	9
		500	3.62	31.70	4	9
		900	3.17	31.60	3	12
	50	100	Thermal comfort cannot be provided.			
		500				
		900				

4.2. Effects of environmental conditions on the performance of SC-EAHE system

In the present study, the environmental conditions are referred to as solar radiation and outdoor ambient temperature. Table 4 shows the summary of results pertinent to theoretical calculations for different environmental conditions related to SC-EAHE system. The

buoyancy driving force increases directly with increment of solar intensity and it causes higher ACH. Thus, less number of SCs are required to drive the cool and heavy air through the EAHEs and to compensate the pressure drops. The results of calculations also show that the required number of EAHEs should be increased to retain the thermal comfort condition when the number of ACH and indoor air temperature are increased at high solar radiation. The effect of ambient air temperature on stack effect of SC is vice versa. The stack effect decreases when the ambient outdoor temperature rises. Under these conditions, more number of SCs will be required to suitably ventilate the room. The results show that the system can provide the required indoor temperature and ACH number even at harsh environmental conditions i.e. high temperature of 45^{o}C and low solar radiation of 100 W/m^{2}. If the temperature is higher than 45^{o}C, the SC won't be able to provide the stack effect and the use of a small fan can help the cool air to flow from EAHE into the room in order to provide thermal comfort conditions.

5. Conclusions

In this paper using two solar systems (SC-EAHE and SC-ECC) to meet the cooling load of buildings and thermal needs of inhabitants were compared. The numerical experiments showed that, although the performance strongly depends on the indoor air heat gain and ambient air conditions; the SC-ECC system can prepare good indoor thermal conditions when both cooling demand of the room and the relative humidity of ambient air are low. It was also revealed that, this system can provide thermal comfort conditions even during the night with zero solar radiation. The results about SC-EAHE system show that when both the ambient temperature and cooling demand are high, proper configurations could provide good indoor condition even at poor solar intensity and high ambient air temperature. It should be noted that proper insulation is useful for reducing the number of required SCs and buried pipes and consequently the total initial cost. Comparative survey shows that the SC-EAHE system is the best choice for buildings with poor insulation, but SC-ECC system is better for well insulated building, especially in dry and arid climates and also for low cost night ventilation.

References

[1] Z. Giabaklou, JA. Ballinger, A passive evaporative cooling system by natural ventilation, Building and Environment 31(6), 1996, pp. 503-507.

[2] M. Manzan, O. Saro, Numerical analysis of heat and mass transfer in passive building component cooled by water evaporation, Energy and Building 34, 2002, 369-375.

[3] YJ. Dai, K. Sumathy, RZ. Wang, YG. Li, Enhancement of natural ventilation in a solar house with a solar chimney and adsorption cooling cavity, Solar Energy 74, 2003, pp. 65-75.

[4] S. Chungloo, B. Limmeechokchai, Application of passive cooling system in the hot and humid climate: the case study of solar chimney and wetted roof in Thailand, Building and Environment 42, 2007, pp. 3341-3351.

[5] M. Maerefat, AP. Haghighi, Natural cooling of stand-alone houses using solar chimney and evaporative cooling cavity, Renewable Energy 35, 2010, pp. 2040-2052.

[6] M. Maerefat, AP. Haghighi, Passive cooling of building by using integrated earth to air heat exchanger and solar chimney, Renewable Energy 35, 2010, pp. 2316-2324.

[7] GS. Brager, RJ. De dear, A standard for natural ventilation, ASHRAE Journal 42(10), 2000, pp. 21-28.

Experimental Study of Long-Wave Night Sky Radiation in Owerri, Nigeria for Passive Cooling Application

N. V. Ogueke[1,*], C. C. Onwuachu[1] and E. E. Anyanwu[1]

[1] *Mechanical Engineering Department, Federal University of Technology, P.M.B. 1526, Owerri, Nigeria.*
** Corresponding author. Tel: +234 802 540 5757, E-mail: nvogueke@yahoo.co.uk*

Abstract: An experimental study to determine the net flux of long wave radiation from the earth's surface to the atmosphere in Owerri, south east Nigeria for passive cooling applications is presented. The values of the effective sky temperatures are also determined. The experimental rig which is a thermal radiator consists of a flat mild steel plate of dimensions 152.2cm x 38.1cm x 0.3cm coated with high emissivity black paint. A copper tube was used to form five turns and then soldered to the steel plate. Water from a well insulated tank placed at about 0.8 m above the surface of the thermal radiator flowed through the radiator. Thermocouples were strategically inserted on the radiator assembly to measure the plate temperature and water temperature as it flowed along the copper tube. The tests were conducted under the meteorological conditions of Federal University of Technology, Owerri for the period covering March to May; a period often free from the harmattan dust haze. The results revealed that a net long-wave nocturnal cooling power of 66.1 W/m^2 is possible. These results are in the same order of magnitude with those obtained elsewhere with similar climatic condition as Owerri, Nigeria.

Keywords*: Nocturnal cooling, Experimental, Long wave, Passive cooling, Radiation*

Nomenclature

A_p	*Plate area ……..m^2*
c_{water}	*Specific heat capacity of water…J/kgK*
F_p	*Plate view factor*
h	*Convection heat transfer coefficient between air and plate ……..W/m^{2}K*
$\dot{m}_{water}$	*Mass flow rate of water ……kg/s*
q_{net}	*Net outgoing radiation ……..W/m^2*
Q_{cond}	*Heat transferred by conduction……W*
Q_{conv}	*Heat transferred by natural convection ……..W*
Q_{net}	*Net thermal radiation from plate …..W*
Q_{water}	*Heat transferred from water ……W*
T_{amb}	*Ambient temperature ……K*
T_{in}	*Water inlet temperature……K*
T_{out}	*Outlet water temperature.....K*
T_p	*Plate temperature ……..K*
T_{pwb}	*Temperature of the underside of plywood ……...K*
T_{sky}	*Sky temperature ……K*
U_{ins}	*Overall heat transfer coefficient of the combined plywood and cotton wool ……..W/m^2*
φ_d	*Downwards radiation ……...W/m^2*
φ_u	*Upward radiation ……...W/m^2*
ε_p	*Emissivity of plate*
σ	*Stefan-Boltzmann constant ….W/m^{2}K^4*

1. Introduction

There is a growing demand for space cooling in hot climates resulting from increasingly harsher climatic conditions as a result of global warming and climate change. This has resulted to an increase in demand for grid connected electrical energy, hence reducing the available energy for other services. Countries with such climates like Nigeria therefore face serious peak energy demand problems. Interestingly, the sky is known to be very cold and as such it can be used as a heat sink for radiating bodies on the earth's surface. This is because the atmospheric temperature decreases with elevation and the atmosphere is partly transparent to some radiation within the infrared region of the spectrum. This concept, which requires a good knowledge of atmospheric radiation flux at the earth's surface, if effectively harnessed could be used significantly to reduce the demand placed on grid connected electricity from air conditioning as well as reduce the energy bills resulting from it. Apart from air condition for comfort, it can also be used for agricultural studies and solar collector analysis [1].

Ordinarily if the emitted radiation from a surface exceeds its absorbed radiation, cooling will result. Thus it is possible to cool hotter surfaces and objects on the ground by radiation to the night sky; a concept called nocturnal (night sky) radiation. The cooling resulting from it is called radiative cooling. Rate and degree of radiative cooling achieved depend on the intensity of the nocturnal radiation. Many factor affect nocturnal radiation intensity; they include weather condition as well as the nature of the radiating surface. Some works have been reported on efforts to measure nocturnal radiation intensity in different locations. Angstrom [2] and Maurer [3] investigated the nocturnal cooling of bodies exposed to the sky, Ezekwe [1] carried out nocturnal radiation measurements in Nsukka, Nigeria while Armenta-Déu et al [4] carried out a thermal analysis of a prototype to determine radiative cooling thermal balance. More recently, knowledge of availability of nocturnal radiation in some regions have been used to design and construct nocturnal radiators for space cooling. These include the works of Cheikh and Bouchair [5], Khedari et al [6], Bagiorgas and Mihalakakou [7] and Dimoudi and Androutsopoulos [8]. Results obtained from these indicate the possibility of significant space cooling by effectively harnessing the nocturnal radiation available in a particular locality.

This work therefore deals with an experimental investigation of the nocturnal radiation intensity in Owerri, a tropical south eastern town in Nigeria. It has three major seasons in a year (rainy, dry and harmattan seasons) with an average day time temperature for all the seasons being in the range of 31 – 35^{o}C. At night these temperatures scarcely come down, especially during the dry seasons, thus there is the need to artificially drop them to fairly comfortable values, particularly within a building envelope.

2. Description of the Thermal Radiator.

The experimental rig is a thermal radiator consisting of an unglazed mild steel plate of dimensions 152.20 cm x 38.10 cm x 3.30 cm. Copper tube of outer diameter 12.20 cm was curled into five equal turns covering the plate area and then soldered to the mild steel plate such that a perfect thermal contact was achieved between the plate and the tube. The radiator assembly was mounted on a ply wood base 1 cm thick with an insulation material (cotton wool) 1 cm thick placed between the thermal radiator and the ply wood base to further reduce heat transfer by conduction. The mild steel plate of the radiator assembly was painted black to increase its emissivity. Water is made to flow through the radiator by gravity by connecting it to a water tank (using an insulated flexible hose) placed on a wooden stand higher than the height of the thermal radiator. Water was continuously circulated through the array of copper tubing. The tank is made of galvanized steel drum and perfectly insulated using fibre glass insulation. The insulation was subsequently wrapped in an aluminium foil; all to reduce heat transfer to the ambient air. Two manual valves were installed on the tank; a wedge valve (inner valve) which was used to start up or stop the process and a parallel gate valve (outer valve) used to control the mass flow rate of water through the thermal radiator assembly. The tank was kept about three metres away from the thermal radiator assembly to avoid obstruction of long-wave radiation. Five K-type thermocouples were inserted at equal distances each on the thermal radiator to measure the temperature of water along the various points on the mild steel plate and hence, determine the average temperature of the radiator. Other parameters monitored are the water tank temperature, ambient temperature and exit water temperature from the thermal radiator. Figs 1a and 1b show the schematic diagram of the thermal radiator and a picture of the experimental rig used for the experiment while Fig. 2 shows the sectional view of the radiator assembly.

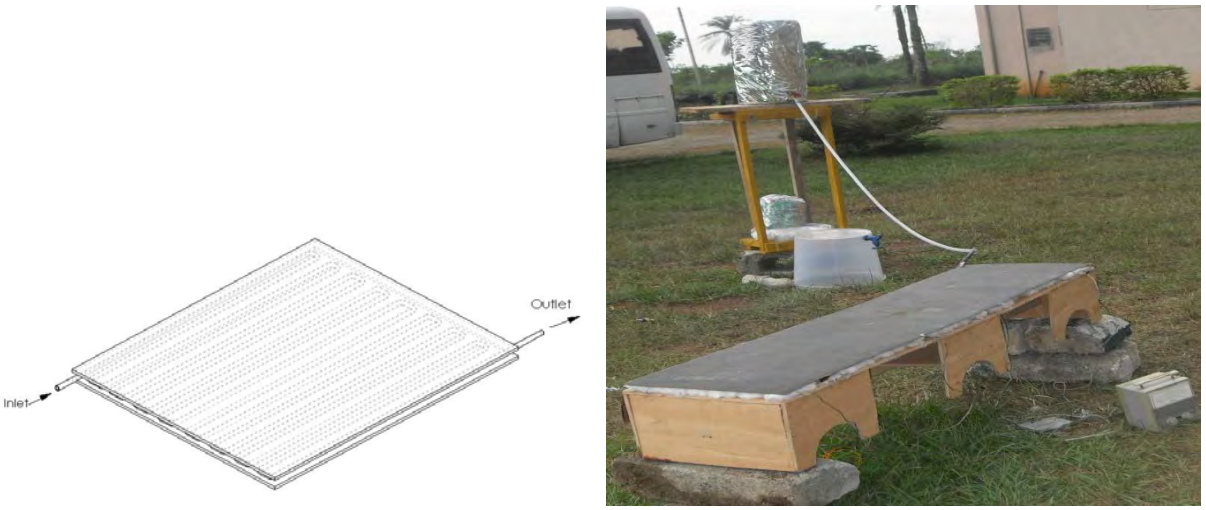

(a) (b)

Fig 1 (a): Schematic diagram of the thermal radiator and (b): the pictorial diagram of the experimental rig.

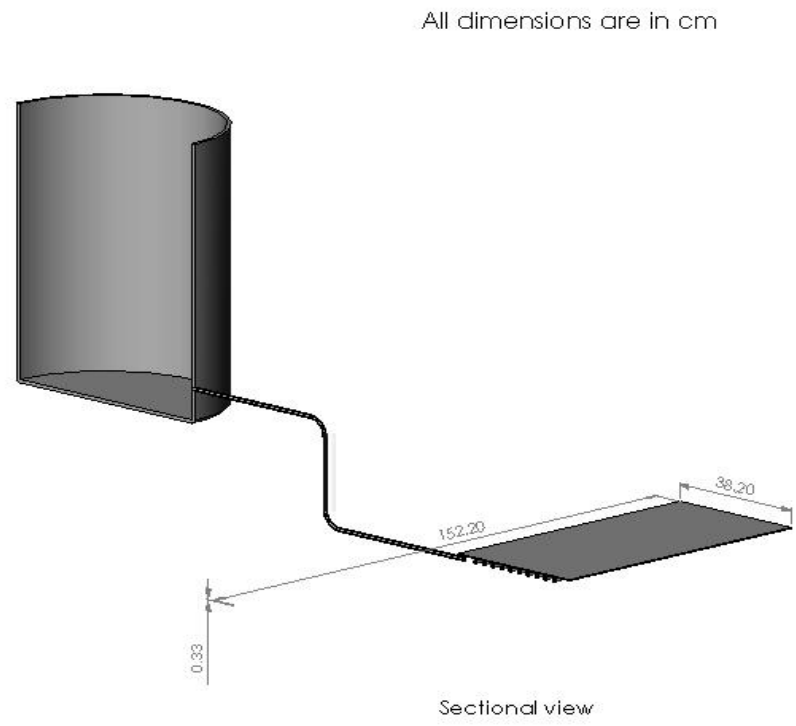

Fig. 2 Sectional view of the radiator assembly

3. Experimental Tests and Analysis

Experiments using the thermal radiator were conducted in Owerri, a city in south eastern Nigeria with three major climatic conditions namely; wet, dry and harmattan seasons. During the experimentation, the following parameters were measured: temperature of water at five different points on the mild steel plate, plate temperature, water tank temperature, ambient temperature and exit water temperature from the thermal radiator. The readings were taken at intervals of 30 mins, beginning from 19:00 hrs to 06:00 hrs the following day. These

temperatures were determined with a K-type thermocouple connected to a 10 – channel Comark electronic thermometer with an accuracy of ±0.1^{o}C. Data collected were analysed as given below.

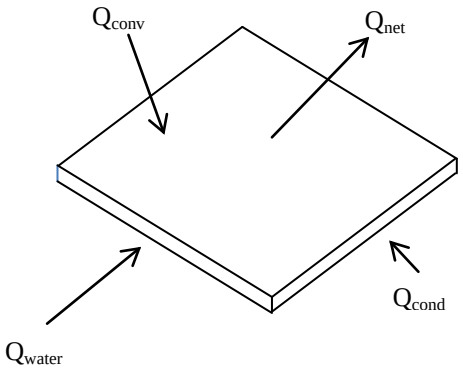

Fig. 3 An energy balance on the nocturnal radiator.

Considering an energy balance on the nocturnal radiator as shown above, the following eqn. (1) results, which enables the determination of the effective sky temperature as well as the downward atmospheric radiation and hence the net outgoing radiation from the plate to the night sky.

$$Q_{water} + Q_{conv} + Q_{cond} = Q_{net} \tag{1}$$

Q_{net} is the net thermal radiation from the plate to the sky and it is obtained from

$$Q_{net} = \sigma \varepsilon_p A_p F_p \left(T_p^4 - T_{sky}^4\right) \tag{2}$$

The heat transferred from the water flowing through the tubes to the plate, Q_{water} is obtained from eqn. (3) below

$$Q_{water} = \dot{m}_{water} c_{water} \left(T_{in} - T_{out}\right) \tag{3}$$

while the natural convection heat transfer to the plate is obtained from

$$Q_{conv} = hA_p \left(T_{amb} - T_p\right) \tag{4}$$

The heat transfer by conduction through the plywood and insulation to the plate, Q_{cond} is obtained from the relation;

$$Q_{cond} = A_p U_{ins} \left(T_{pwb} - T_p\right) \tag{5}$$

Eqn. (1) was solved using the data collected from various experimental measurements to obtain the only unknown parameter, the effective sky temperature. Assuming the sky to be a black body at an effective temperature T_{sky}, the downward long-wave sky radiation was computed with the Stefan-Boltzmann law using the sky temperature. This is given as eqn. (6).

$$\varphi_d = \sigma T_{sky}^4 \tag{6}$$

Similarly, the upward long-wave sky radiation flux was obtained from eqn. (7) by using the ambient air temperature.

$$\varphi_u = \sigma T_{amb}^4 \tag{7}$$

Consequently the net outgoing radiation flux from the earth's surface was obtained using eqn. (8) below.

$$q_{net} = \varphi_u - \varphi_d \tag{8}$$

4. Results and Discussion

Readings were taken between March and May, a period often free from the harmattan dust haze and enough to give considerable insight into the night sky radiation pattern during the dry season. The month of May however, marks the outset of rainy season. Based on data collected, values of the night sky temperature, downward long wave sky radiation, upward long wave sky radiation and the net long wave sky radiation were determined using eqns. 1, 6 – 8. Figs. 4 and 5 show the hourly variation of the night sky temperature and its depression below that of the ambient for the dry and rainy seasons while Figs. 6 and 7 show the hourly variation of the upward and downward long wave radiation as well as their net long wave radiation.

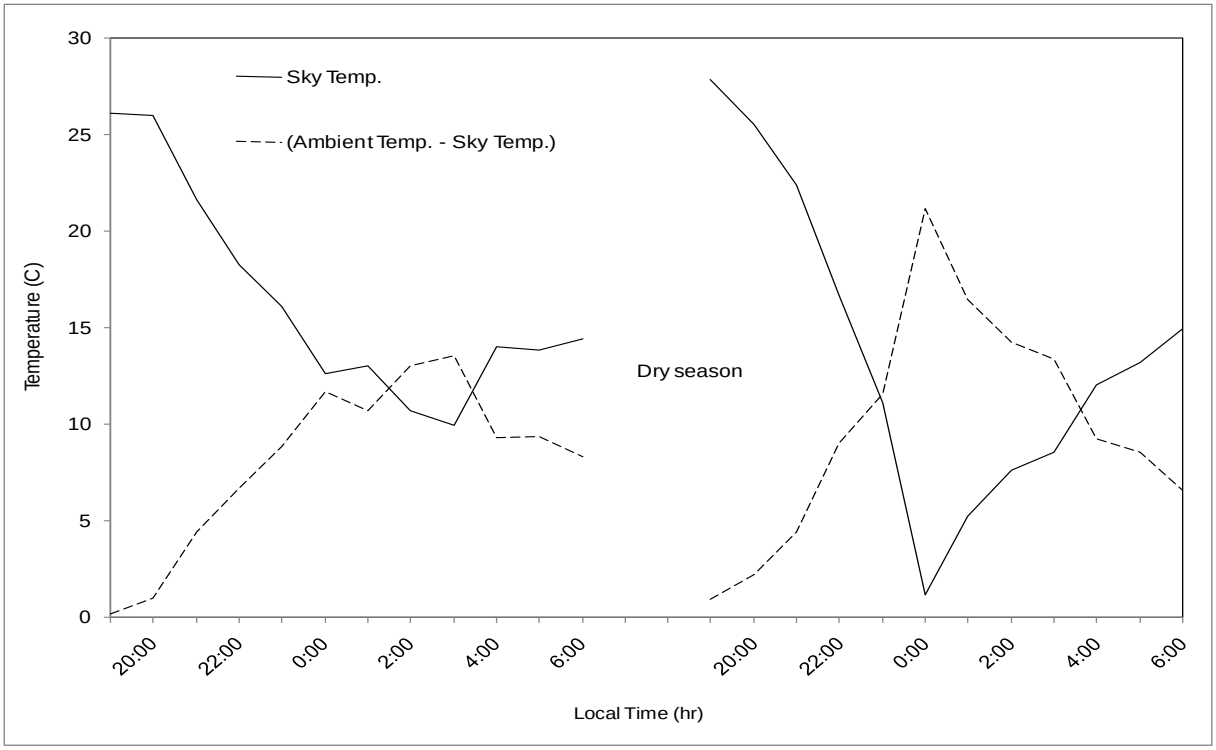

Fig. 4 The night sky temperature and its depression below ambient temperature during the dry season.

It can be seen from these figures that the dry season (characterized by high dry bulb temperature and sometimes a low relative humidity) has lower sky temperatures and higher net long wave radiation than the rainy (wet) season though the variation pattern showed more strong dependence on time of day. The rainy season, with much lower dry bulb temperature and high relative humidity, on the other hand, has more steady sky temperature with a minimum value of about 12^{o}C. Its net long wave radiation was mostly below 70 W/m^2. These results show that net log wave radiation is higher during the dry than in the rainy season. This may be as a result of a combination of the following factors; clear night sky and lower relative humidity than the rainy season. The rainy season is characterized by overcast sky and high

relative humidity, hence the lower values recorded. However ambient temperatures are generally lower within this period, thus less cooling is required in order to achieve comfort. In general the net long wave radiation is highest between 22:00 hours – 5:00 hours of the following day with the values ranging between 50 – 130 W/m^2. These values are well in the same order of magnitude with those obtained for similar climatic conditions and if properly harnessed could provide cooling; enough to provide reasonable comfort during the night times, especially during the dry season when high ambient temperatures make sleeping difficult.

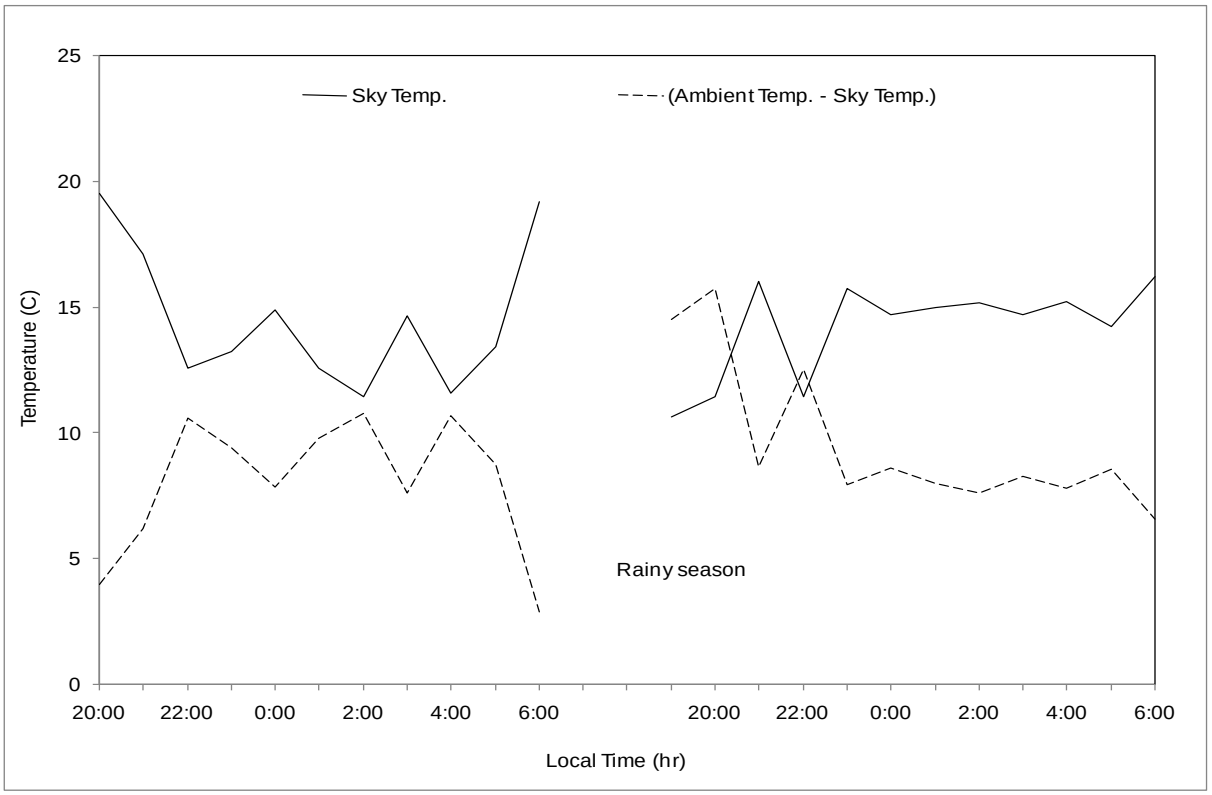

Fig. 5 The night sky temperature and its depression below ambient temperature during the rainy season.

5. Conclusion

Measurements to experimentally determine the long wave night sky radiation in Owerri, a tropical south eastern city in Nigeria, have been conducted. Measurements were taken at periods of the year representative of the three major climatic conditions of this city. Based on the results obtained after analysis of data collected, the following conclusions may be drawn.

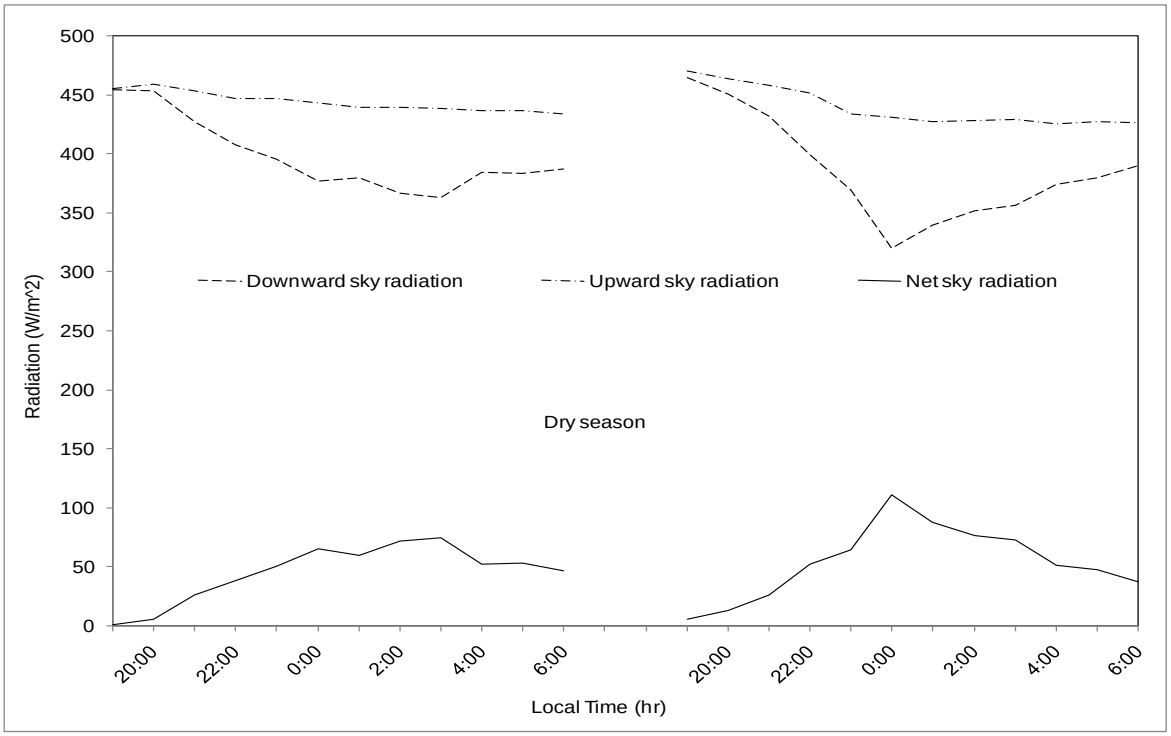

Fig. 6 The night sky radiation at the location during the dry season.

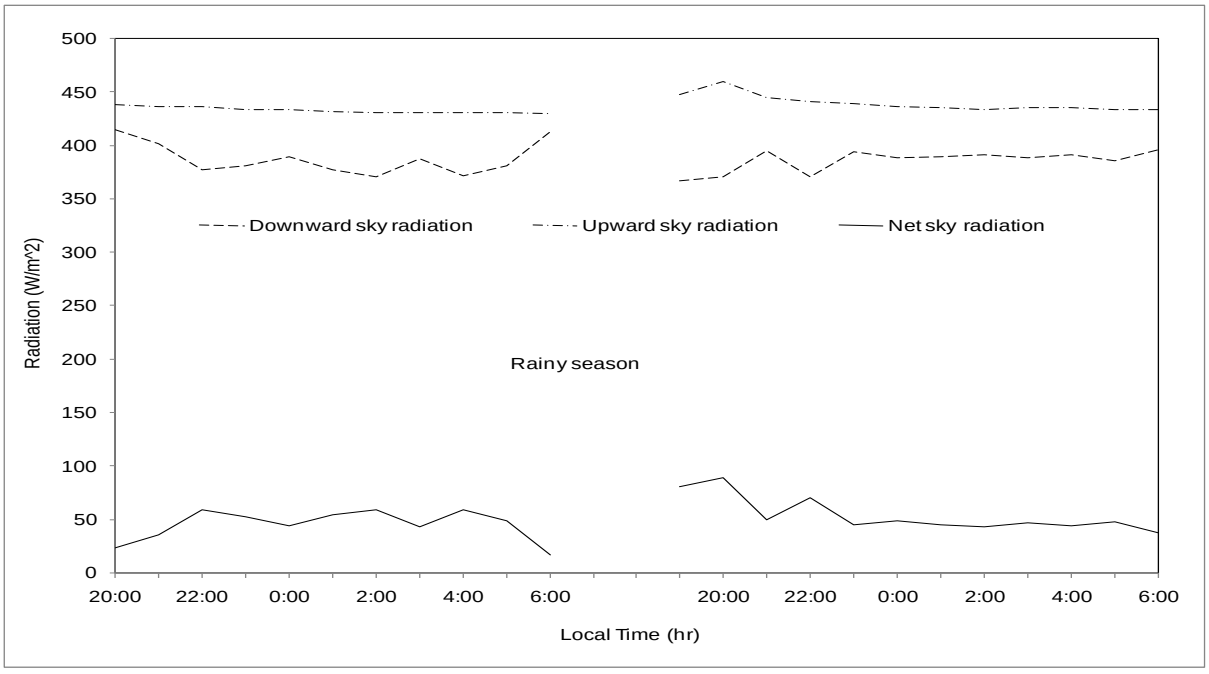

Fig. 7 The night sky radiation at the location during the rainy season.

i.) The net radiation to sky of up to 130 W/m^2 is possible depending on time of day and period of the year. Overall, an average value of about 66 W/m^2 is possible.

ii.) The dry season presented better potential for space cooling using the night sky radiation. Fortunately, this is the period of year when comfort is desired most.

References

[1] Ezekwe, C.I. (1986). Nocturnal radiation measurements in Nigeria. Solar Energy 37(1), pp.1 – 6.

[2] Angstrom, A. (1913). An International Review of Spectroscopy and Astronomical Physics.The Astrophysical Journal, Vol. 37, pp305-317.

[3] Maurer, J. (1887). Measurement of Nocturnal Radiation. Annales de Chime at de Physique, Vol. 20, pp 204-220.

[4] Armenta-Déu, C., Donaire, T. and Hernando, J. (2003). Thermal analysis of a prototype to determine radiative cooling thermal balance. Renewable Energy 28, pp. 1105 – 1120.

[5] Cheikh, H.B. and Bouchair, A. (2004). Passive cooling by evapo-reflective roof for hot dry climates. Renewable Energy 29, pp. 1877 – 1886.

[6] Khedari, J., Waewsak, J., Thepa, S. and Hirunlabh, J. (2000). Field investigation of night radiation cooling under tropical climate. Renewable Energy 20, pp. 183 – 193.

[7] Bagiorgas, H.S. and Mihalakakou, G. (2008). Experimental and theoretical investigation of a nocturnal radiator for space cooling. Renewable Energy 33, pp. 1220 – 1227.

[8] Dimoudi, A. and Androutsopoulos, A. (2006). The cooling performance of a radiator based roof component. Solar Energy 80, pp. 1039 – 1047.

Acknowledgement

The authors gracefully acknowledge the financial support of the World Bank under its STEP-B research grant for renewable energy research in the Federal University of Technology, Owerri, Nigeria.

Design of a sustainable house including the requisites of the Spanish Regulation

Luis Abades Martínez, Erika Martínez Pérez, Laura Cristóbal Andrade, Pastora M. Bello Bugallo*

Department of Chemical Engineering and Seminar of Renewable Energy (Aula de Energías Renovables), University of Santiago de Compostela, Spain
** Corresponding author. Tel: +34 881816757, Fax: +34981528050, E-mail: pastora.bello.bugallo@usc.es*

Abstract: Green Building is a philosophy aiming to maintain a high quality of the built environment while optimizing the use of resources, both materials and energy. Related to green building, sustainable construction consists in the creation and operation of a healthy built environment giving rise to high-performance green buildings.
These building concepts have already been taken into account by the European Union (EU) that has promoted the use of alternative energies, thermal insulation and responsible consumption programs, among others. The Directive 2002/91/EC came into force to regulate energy efficiency in new buildings. Member States transposed this text to their legal systems, considering the particularities of to their territories, geography, economy and society. In Spain, the Spanish Technical Building Code (*CTE- Código Técnico de Edificación*) promotes sustainable building. Other regulations regarding energy buildings certification, energy efficiency or renewable energy promotion have already been adopted.
This work presents a house designed taking into account some aspects of the sustainable house design, and compares it with a reference house. These aspects include the thermal requirements of the house following a simplified option established in the basic documents HE1 (Limitation of the energetic demand) and HE4 (Minimal solar contribution for heating domestic water) of the Spanish Building Technical Code

Keywords: *Sustainable construction, Thermal insulation, CTE, Energetic demand*

1. Introduction

Almost 30% of world's energy is used in housing (40% in Europe [1]) and the 50% of this energy is used in building for the weather conditioning systems [2] (heating or cooling), and lighting. Energy consumption for housing and services was 371.4 Mtoe (millions tons of oil equivalent) in 2000 [3], which is higher than for other sectors such as transport and industry.

Due to the figures of the increased CO_2 emission levels associated with this energy production, the EU has decided to harden the standards for building and their heating and hot water systems in order to reduce the amount of energy consumed [4]. Simultaneously to these new standards a new philosophy, Green Building, has emerged, with the aim of maintaining high quality of the built environment while optimizing the use of resources, both materials and energy. On the topic of green building, sustainable construction is about the creation and operation of a healthy built environment based on ecological principles and resource efficiency [5], giving rise to "high-performance green buildings". The main characteristics of these constructions are [6]: significantly less energy, materials and water consumption; healthy living and working atmosphere; and great improvements on the quality of the built environment. The control of natural lighting and ventilation as well as better insulation also help, not only reducing energy consumption but also increasing safety and security, promoting welfare and helping assisted living [7].

Housing energy use has been a concern for the European institutions, which have promoted the application of alternative energies, thermal insulation and responsible energy usage campaigns by developing a specific legal framework. Accordingly, the European building

sector has provided itself with the Directive 2002/91/EC [1], which aims to control the energy efficiency in buildings, and the Directive 2006/32/EC [8], whose purpose is to enhance the cost-effective improvement of energy end-use efficiency. Several Member States have transposed these European directives to their own legal systems, trying to adapt them to their geographic, economic and social characteristics. That is the case of Spain, where the European directives have been adapted to the national legal framework by Royal Decree 1027/2007 [9], on Thermal Installations in Buildings (*RITE –Reglamento de Instalaciones Térmicas en los Edificios*), that controls heating systems and hot sanitary water in buildings in order to reach a good comfort level and an optimal energy use, and Royal Decree 1675/2008 [10], the Spanish Technical Building Code (*CTE – Código Técnico de Edificación*), that came into force to promote sustainable building.

This work presents the energy-related considerations taken into account during the design of a sustainable house intended to be energy efficient, including the requisites of the Spanish Building Technical Code (*CTE*). The energy parameters of this house will be compared with a reference house designed under conventional criteria.

2. Methodology

This work compares energetic parameters of two houses intended to be in the same location and with the same space distribution, but that have been designed under different building criteria. The first one is the "reference house" (RH), designed using conventional building criteria. The second house, the "sustainable" one, is the so called "insulated house" (IH), which applies the *CTE*, specifically the simplified option established in the basic document HE1 about *Limitation of the energetic demand*, as well as the guidelines set by the basic document HE4 about *Minimal solar contribution for heating domestic water*. This calculation option is based on the indirect control of the building energetic demand, limited by the characteristic parameters of the internal and external walls (thermal envelope). Accordingly, the methodology includes the following steps:

- Definition of the climatic area.
- Classification of the spaces of the building.
- Thermal isolation.
- Analysis of the thermal requirements of the house.
- Air infiltrations.
- Underfloor heating system.
- Boiler selection.
- Solar collectors for hot water production.
- Materials selection.

Finally the energetic parameters proposed in the *CTE* are compared for both houses, showing the benefits of the "sustainable" design.

3. Characterization of the houses

3.1. Definition of the climatic area

The proposed houses will be located in Lugo (Galicia), in the northwest of Spain. Lugo is classified by the *CTE* climate severity criteria as a D1 region, which means that the Winter Climate Severity (WSC) is high (D in a scale from A to E), and the Summer Climate Severity (SCS) is low (1 in a scale from 1 to 4).

3.2. Classification of the spaces of the building

Both the RH and the IH are intended to be located in a North-South oriented rectangular parcel with a 20% slope, which is not affected by any shadowing element in its environment. The houses will have four levels: the underground level, where the garage is located; the ground floor, with the kitchen, living-room, one bedroom and the access to the house; the first level, which is the dormitories area; and finally the top floor, which is really a terrace where the collectors and control devices will be located.

3.3. Thermal isolation

In the RH the external walls will be conformed by external plasterwork (25 mm), a double brick layer and an internal layer of plasterwork (25mm). The 290 mm width structure will be protected by both internal and external painting.

In the IH external walls are conformed by external plasterwork of 25 mm, a layer of light thermo-clay of 190 mm followed by another concrete layer. Insulation is provided by two layers: 20 mm of expanded polystyrene and an air chamber of 20 mm. Finally it is an internal brick layer covered by plasterwork. The 370 mm width structured is protected both internally and externally by painting. The formation of thermal bridges has also been considered, owing to the energy losses they involve.

3.4. Thermal requirements

The study of the thermal requirements will be based in the indirect control of heat demand as required in the *CTE*. This estimation method uses the characteristic parameters of the thermal envelop or U-values. Thermal transmittance U ($W/m^2 \cdot K$) is defined by Eq. (1), where R_T is the total thermal resistance for the constructive component.

In the case of associations of materials in homogeneous thermal layers, total resistance could be calculated by Eq. (2), where R_1, R_2 are the thermal resistances of the n layer conforming the wall, and R_{si}, R_{se} are the superficial thermal resistances corresponding to the internal and external air, considering the wall situation in the building and the direction of the heat flow.

The last consideration is the calculation of the thermal resistance in a thermal homogeneous layer provided by Eq. (3), where e is the thickness of the layer (m) and k the thermal conductivity of the material ($W/m \cdot K$).

Global transmission coefficient for the building also has been calculated, Eq. (4), in order to collect the previous parameters in a more representative figure, where sub-index w, s, r and h refer to walls, soil, roofing and holes respectively, and A is the area of each layer.

$$U = \frac{1}{R_T} \quad (1) \qquad R_T = R_{si} + R_1 + R_2 + ... + R_n + R_{se} \quad (2)$$

$$R = \frac{e}{k} \quad (3) \qquad U_G = \frac{(U_W \cdot A_W) + (U_S \cdot A_S) + (U_R \cdot A_R) + (U_H \cdot A_H)}{A_W + A_S + A_R + A_H} \quad (4)$$

3.5. Air infiltrations

Air renewal by infiltrations is an important parameter affecting both the hygienic conditions and the overall heating demand, as the incoming air must be conditioned. Air renewal takes place by infiltration through carpentries and by ventilation. Infiltration can be quantified by

permeability, defined by Eq. (5), where C_v is the window coefficient (specific for the woodwork, dimensionless), ΔP is the pressure difference between indoors and outdoors (mm H_2O) and S_h is the total surface of the hollow (m^2). Ventilation is mainly controlled by the inhabitants except for the kitchen and the bathrooms, both having independent mechanical ventilation systems.

$$\rho = C_v \cdot \Delta p \cdot S_h \qquad (5)$$

3.6. Heating System Design

Aiming to determine the heating requirements of the building, specific studies of every single space of the house have been carried out, considering heat losses by transmission and air renewal in each one of the spaces. Heating system, by underfloor heating, was designed considering that indoor temperature is set at 20 ºC and that the system must face up minimal temperatures of -5 °C during winter time.

Heating system design is based on the results obtained for the heat losses. Design parameters considered were water flow and water temperature, which can be calculated by Eq. (6) since Q is the known total heat losses, where T_{ma} is the average water temperature (ºC), T_{obj} is the objective temperature set in 20 ºC and U is the global thermal transmission coefficient, considering heat flow will occur by conduction and convection.

Water flow for heating system is calculated by Eq. (7), where C is the mass flow rate (kg/h), Cp is specific heat of the water (kJ/kg·K) and ΔT is the difference between inlet and outlet water in the system, considered to be 10 ºC.

$$Q = U \cdot \left(T_{ma} - T_{obj}\right) \qquad (6) \qquad\qquad Q = C \cdot C_p \cdot \Delta T \qquad (7)$$

3.7. Boiler Selection

The installation of efficient boilers is promoted by the *RITE* to reduce pollutant emissions and improve energy savings. In this case study a condensation boiler has been selected because it can be adapted to the thermal needs of an underfloor heating, providing hot water at 60 ºC. Moreover a 30% energy saving and a 70% NO_x y CO_2 emissions reduction is expected.

3.8. Sanitary Hot Water Installation

The sustainable design also includes a solar thermal installation able to provide a great percentage of the total hot water demand for the house, exceeding the 30 percent required by the *CTE* for this kind of houses.

Initial data needed for the design and calculation of this installation, will be the use conditions of the Sanitary Hot Water (SHW) and weather specifications of local region. Energetic demand is determined by the monthly hot water consumption rate and the temperature set for the SHW, while climatic specifications are obtained by the global radiation in the collecting field, average day temperature and network water temperature.

Calculation method was the f-chart method. This method allows the assessment of the solar device coverage as well as its average performance in an amount of time.

3.9. Fuel consumption

It is nearly impossible to estimate fuel consumption in heating systems, since it heavily depends in variable conditions such as weather, user needs or control systems. However, it is possible to perform yearly estimations by using a method that can be found in UNE 100002 [11] regulations. It can be done by using Eq. (8), where G stands for HDD (ºC), P for consumed power (kcal/h), U is the use coefficient (dimensionless), I is the intermittence coefficient (dimensionless), η is the boiler performance, LCP is the Lower Calorific Power of the natural gas (kcal/m^3N), (T_i-T_e) relates to the difference of temperatures between the inside and outside of the house. For this case, T_i is set as 20 ºC and T_e as 2 ºC.

$$C = \frac{G \cdot 24 \cdot P \cdot I \cdot U}{\eta \cdot LCP \cdot (T_i - T_e)} \qquad (8)$$

4. Results

This section presents the results obtained after applying the aforementioned equations to the proposed case studies. The limit values set by the *CTE* for the proper design of the IH are: 20 ºC indoors temperature, 55% indoors relative humidity, 273 $m^3/h \cdot m^2$ woodwork permeability for a D1 zone, and 30% of annual minimal solar contribution for fossil energy source at 60 ºC.

According to Eq. (1-3) and following the layer schema described in the previous section, calculations of the U-values have been done. The results obtained are presented in Tables 1 and 2, where sub-index W, S, R and H refer to walls, soil, roofing and holes respectively. Next sub-index are: IH: Insulated House, LV: Limit value set by the *CTE*, RH: Reference House.

Table 1. U-values comparison for the insulated house and the reference house with the limit values established by CTE.

Orientation	U_{WIH} (W/m^2 K)	U_{WLV} (W/m^2 K)	U_{WRH} (W/m^2 K)	U_{HIH} (W/m^2 K)	U_{HLV} (W/m^2 K)	U_{HRH} (W/m^2 K)
N	0.46	0.66	1.57	2.23	2.50	3.8
E	0.49	0.66	1.69	2.10	2.90	3.68
O	0.48	0.66	1.57	2.18	2.90	3.25
S	0.52	0.66	1.63	2.18	3.50	3.68

Table 2. U-values comparison between the insulated house and the reference one with the limit values established by CTE.

U_{SIH} (W/m^2 K)	U_{SLV} (W/m^2 K)	U_{SRH} (W/m^2 K)	U_{RIH} (W/m^2 K)	U_{RLV} (W/m^2 K)	U_{RRH} (W/m^2 K)
0.33	0.49	1.70	0.33	0.38	0.62

Fig. 1 represents the comparison of the U-values for the considered elements (walls, soil, roofing and holes) for the IH, LV and RH. The U-values selected for walls and holes correspond to the north orientation.

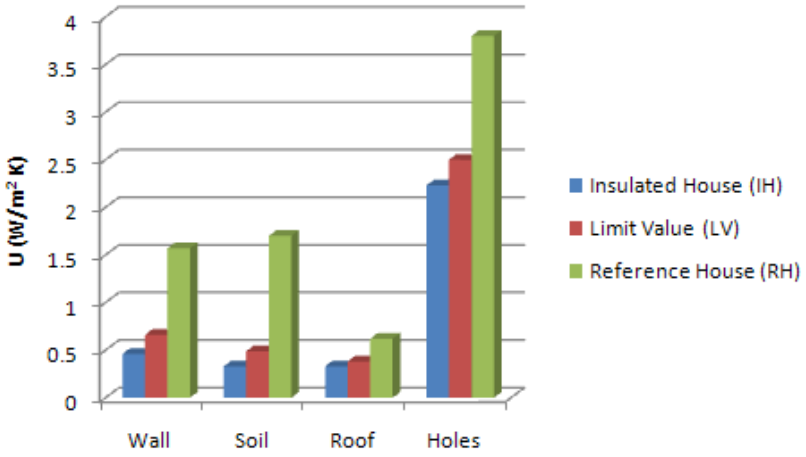

Fig. 1. Comparison of U-values for the walls, soil, roof and holes in the IH and the RH regarding the limit values set by the CTE.

The air renewal parameters have resulted in the data displayed in Table 3, whereas Table 4 shows the results obtained after calculating the thermal requirements for both houses. Heating system design results are included in Table 5.

Table 3. Calculations to establish the total ventilation of the buildings.

Air renewal	Reference house	Insulated house
Permeability (m^3/h)	1263,14	248,14
Mechanical Ventilation (m^3/h)	114,55	114,55
Natural ventilation (m^3/h)	97,52	97,52
TOTAL (m^3/h)	1475,21	460,21

Table 4. Thermal Requirements in the building.

	Reference House	Insulated House
Total Area (m^2)	204.91	204.91
Heat losses by transmission (W)	16,528.30	6,378.13
Heat losses by air renewal (W)	11,956.38	5,640.01
Total Heat losses (W)	28,484.68	12,018.14

Table 5. Resulting heating system parameters.

	Water temperature (ºC)	Flow rate (l/s)
Insulated House	30	0,267
Reference House	47	0,658

To calculate the SHW installation it is necessary to consider some additional factors. Hot water consumption is estimated to be 30 liters/inhabitant each day at 60 ºC. Concerning weather conditions, Lugo is located 465 meters high and in 43 º latitude. The house is placed in a flat ground with little vegetation, and atmosphere is considered clean since the house location is within a rural zone.

A Buderus Logasol SKN 3.0 is chosen as the collector. This device has an open surface of 2.25 m^2 and its efficiency slope parameters are η_0=0.775, k_1=3.599 W/m^2·K and k_2=0.008 W/m^2·K^2. Table 6 contains the results obtained for an installation comprising 3 collectors and an accumulator of 400 liters.

Table 6. Results for SHW installation calculations.

Parameter	Value
Total thermal load (MJ)	13,658.0
Net energy collected (MJ)	10,413.1
Yearly Solar Coverage (%)	76.2
Yearly Average Performance (%)	33.7

Finally, fuel consumption and CO_2 emissions were calculated to complete the analysis and comparison between both houses (Table 7).

Table 7. Fuel consumption estimation for each house and related economic costs and CO_2 emissions.

	Fuel consumption (m^3/year)	Economic costs (€/year)	CO_2 emissions (ton/year)
Insulated house	1,759	1372.20	4.00
Reference house	4,169	3252.17	9.60

5. Discussion

The comparison of both houses, RH and IH, leads to some obvious conclusions. First of all, when selecting building materials the priority has been their insulating capacity, but keeping also in mind their environmental impact and life-cycle. In fact, thermo-clay is a recyclable ceramic material with really good chemical, mechanical, thermal and acoustic properties. Expanded polystyrene is an excellent insulating material, also recyclable, and the woodwork employed is made of PVC with thermal break, with a Climalit glass of 9 mm thickness. Besides, aiming to reduce thermal gains through the windows in summer, eaves have been installed to reduce solar radiation penetration in the south faced windows and the balcony. This measure is expected to cause a 50% reduction in radiation depth for these rooms.

Concerning U-values for the thermal envelope (Tables 1 and 2), it is observed that the insulating measures used in the design of the IH make it possible to comply with the *CTE* requirements. More detailed analysis of these data reveals that U-values for the IH are about 24% lower than the limit values whereas the results for the RH are much higher in each part of the thermal envelope. For the global transmission coefficient, results are U_{GIH}=0.51 W/m^2·K and U_{GRH}=1.61 W/m^2·K. Coefficient value for the RH is about 3 times the insulated coefficient value.

The results obtained for air renewal show that, in the IH, the total air renovation is roughly the same as the volume of the house, as demanded in the *CTE* (Table 3). Concerning the RH, air renovation is 3 times the volume of the house, which is excessive and will lead to extra fuel consumption.

According to results shown in Table 4 for thermal requirements, it is possible to assess that total heat losses for the IH are only the third part of the RH. This fact leads to the reduction of the fuel oil consumption, and therefore the reduction of CO_2 emissions to the atmosphere.

Regarding the heating system design, results show that for the same heating system, water temperature and flow rate are lower in a well insulated house (Table 5). Consequently both the energy needed for water heating and electrical energy to drive the pump will be lower.
The fulfilling of the conditions of the *CTE* is proved, since the SHW installation provides a solar contribution of 76% of the total energetic needs in the house with a yearly average performance above 30%, as requested in the *CTE* (Table 6).

Finally, the application of constructive solutions in the IH project means saving around 5.5 ton CO_2/year emissions (Table 7).

Therefore it can be concluded that taking into account energy efficiency criteria during building design can result in important savings in energy consumptions, as heat losses are highly reduced (even three times shorter in the IH than in the RH) and hot water requirements are much lower than in a typical house. The application of the *CTE* not only limits the energy demand in buildings on the basis of U-values for thermal envelope, but it also avoids surface condensations inside the enclosure or the woodwork, limits energy loses by air infiltrations and minimizes solar contribution for sanitary hot water.

References

[1] European Union, Directive 2002/91/EC on the energy performance of buildings, Official Journal of the European Communities L1, 2002, pp. 65- 71.

[2] D. M. Roodman, N. Lenssen, A building revolution: how ecology and health concerns are transforming construction, Worldwatch Institute, 124, 1995.

[3] Eurostat, Annual Report, 2000, available at http://ec.europa.eu/index_en.htm.

[4] European Union, Combating climate change - The EU leads the way, European Communities, 2007, available at http://ec.europa.eu/publications.

[5] C. J. Kibert, Principles of sustainable construction, Proceedings of 1st International Conference on Sustainable Construction, 1994, pp. 1-9.

[6] C. J. Kibert, The next generation of sustainable construction, Building Research & Information 35 (6), 2007, pp. 595-601.

[7] European Union, Summaries of the European Legislation. http://europa.eu/legislation_summaries/index_en.htm

[8] European Union, Directive 2006/32/EC on energy end-use efficiency and energy services and repealing Council Directive 93/76/EEC, Official Journal of the European Communities L114, 2006, pp. 64-85.

[9] Spanish Government, Royal Decree 1027/2007 approving the Regulation of Thermal Installations in Buildings, Official Gazette 207, 2007, pp. 35931- 35984.

[10] Spanish Government, Royal Decree 1675/2008 amending the Royal Decree 1371/2007, which approves the document DB-HR Protection against noise of the Technical Building Code and amending the Royal Decree 314/2006 approving the Technical Building Code, Official Gazette 252, 2008, pp. 41655- 41656.

[11] Spanish Association for Standardization and Certification (*Asociación Española de Normalización y Certificación – AENOR*), http:// www.aenor.es

Carbon footprint of a 100-year old house: Case-study of improvements and implications for the UK housing stock.

Arthur A. Williams[1*], Mark Gillott[2]

[1] *Dept. Electrical & Electronic Engineering, University of Nottingham, Nottingham, UK.*
[2] *Dept. Architecture & Built Environment, University of Nottingham, Nottingham, UK.*
** Corresponding author. Tel: +44 115 8468484, Fax: +44 115 9515616, E-mail: arthur.williams@nottingham.ac.uk*

Abstract: Before 1930, most houses in the UK were built with solid brick walls, which have high heat losses and are difficult to insulate. These homes represent nearly one-quarter of the UK housing stock. This paper covers a case-study that shows some of the difficulties to meet the UK government's target to reduce carbon emissions by 80% by 2050. Such a target can only be met with refurbishment of all older properties and even then, energy-savings initiatives are probably not sufficient; integration of renewable energy sources is also necessary. Comparison with refurbishment initiatives in Germany demonstrates the massive investment that needs to take place, and some of the practical limitations. Strategies to limit increasing demand for energy use will be required in order to meet these ambitious targets. The case-study demonstrates the types of practical problems likely to be encountered, but also shows the importance of disseminating the experience gained by pioneers of refurbishing older homes in the UK.

Keywords: *Energy Efficiency, Refurbishment, Carbon Saving*

1 Introduction

In northern Europe, the energy use in residential buildings is largely associated with space heating and hot water provision as well as lights and appliances. Reducing energy consumption in residential buildings has the potential to help countries meet their targets to reduce carbon emissions. Approximately 30% of carbon emissions in the European Union are due to energy use in residential buildings, of which around 50% is used for space heating [1]. Significant reduction in these carbon emissions can be made by three methods – firstly, demolishing old homes and replacing them with new "low-carbon" dwellings; secondly, switching to energy sources that do not rely on fossil fuels; thirdly, making existing homes more energy efficient. In many parts of Europe, including the UK, the demand for new homes is high because the number of households is increasing. Apart from energy use, older houses have many attractive features, so demolition occurs at a very slow rate [2]. The second of these options requires investment in alternative energy infrastructure, which is occurring, but not fast enough to impact significantly yet on carbon emissions. The third of these options, i.e. refurbishment of existing buildings for improved energy efficiency, has other public benefits such as employment opportunities, increasing the aesthetic quality of existing housing stock and reducing the number of families suffering from fuel poverty. For the occupants, energy efficiency measures can lead to improved indoor comfort, lower running costs and a healthier indoor environment.

Government housing data shows approximately 23% of the UK housing stock is comprised of houses built between 1800 and 1930, of which over 70% are owner occupied. These houses are highly inefficient in their use of heating energy, contributing a disproportionate fraction of UK carbon emissions. It is logical that these should be a prime focus of energy efficiency improvements but there are significant barriers to implementing such changes. Before 1930, most UK houses were built without cavity walls and with other design features that make their energy performance difficult to improve. Much of the heat loss is through the walls of the house, which can only be reduced by applying internal or external insulation. External

insulation has the advantage of retaining the thermal mass of the building within the insulated envelope. It has been applied within a number of social housing projects in the UK, but so far has been rarely used in owner occupied houses, which is the focus of this paper.

The case-study energy use data has been analysed to find the contribution of the energy improvements to a reduced carbon footprint. Data from other examples has also been compared in order to identify the practical limitations to reducing the carbon footprint of older residential buildings. Carbon emissions for the UK have been calculated using data for 2007 published by the Carbon Trust: electricity: 0.544 kg CO_2/kWh; gas: 0.184 kg CO_2/kWh.

2 Refurbishment Case-study

The study analyses energy savings in a detached family house of 98 m^2 built in 1910 using 225 mm solid brick walls, some of which were rendered on the outside. This house is of typical construction for its era, with slated roof and originally with single-glazed windows. It is heated by a gas-fired central heating system and also had an open gas heater in the living room. The house has been refurbished since 2001 in two phases. In the first phase, improvements were made through installation of double glazing, replacement of an inefficient gas boiler by a Worcester Greenstar combi condensing boiler, which has a SEDBUK efficiency of 90.3% (previously water was heated by an electric immersion heater). The loft insulation was topped up to 200 mm using Warmcel recycled paper insulation. Energy efficient lighting, mainly compact fluorescent, was installed throughout the property. Draught-proofing was carried out and both external doors were replaced, as the original doors were ill-fitting. The energy savings from these improvements have been estimated using values from similar properties given by Lomas [3], which suggest that the energy use for space heating was reduced by 30% and energy use for lighting by 65%. Using the figures above, the resulting CO_2 emissions reduced from 7.8 to 4.4 tonne/year. One problem that was made worse by these initial improvements (apparently common in houses of similar construction, after fitting draught-proofing and double glazing [4]) was the incidence of mildew growth in poorly ventilated areas of external wall, due to condensation.

Figure 1. View of house from south side, before and after external insulation.

In the second phase, insulation has been applied to the walls of the house, internally where limited by the architecture of the building, but mainly externally. This has the advantage (in winter) that internal temperatures drop less when the heating is off during the night time. The external insulation is 60 mm of phenolic board with a protective cement render, which achieves a total U-value of 0.32 W/m^{2}K [5]. This is very close to current UK standard for new dwellings of 0.30 W/m^{2}K. Equivalent internal insulation would also have had the disadvantage of reducing the usable floor area by around 2%. The appearance of the property was not significantly altered by the application of the insulation, as seen in Figure 1. A line of "brick slips" was applied to replicate the original features of the house.

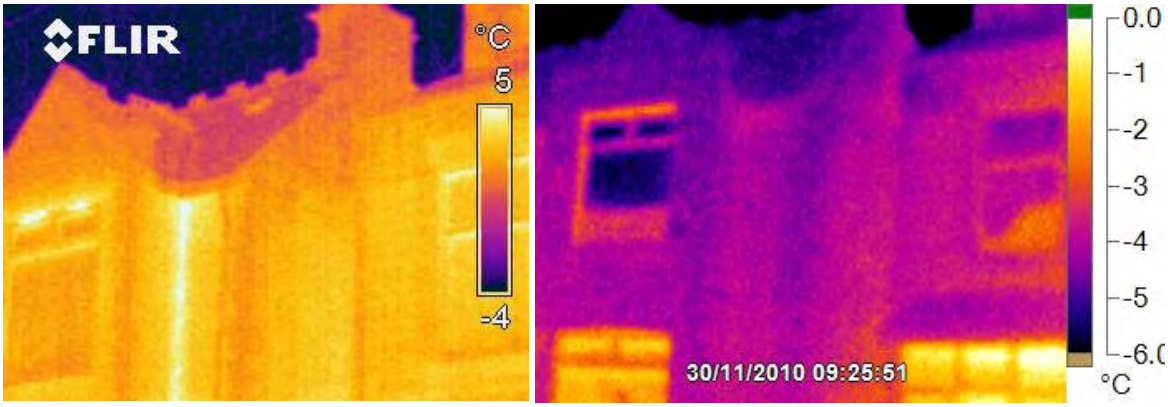

Figure 2. Thermal images of NW corner before and after insulation (and part of neighbouring house).

Thermal images of the house were taken before and after insulation, as seen in Figure 2. Both images were taken on a cold day, with the house heated to 18C, but the quantitative results are not directly comparable. Unfortunately, it was not possible to match the temperature scales exactly as a different camera was used for the second image. However, a qualitative comparison shows how the leakage of heat from the corners of the frontage has been reduced. On the end wall, no significant temperature difference now exists between the heated part of the house and the unheated loft (above the loft insulation, where the internal temperature is below +5 C). Where possible, at the top of the first floor the external insulation was brought above the level of the loft insulation in order to reduce thermal bridging.

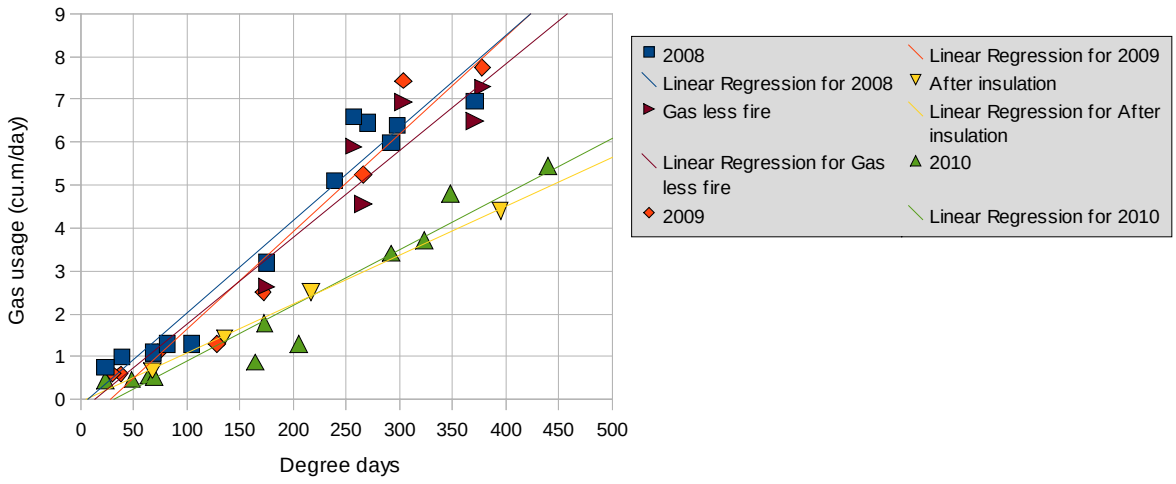

Figure 3. Mean daily gas usage plotted against heating degree-days on a monthly basis.

Evidence of the effectiveness of the insulation is shown better by looking at data for gas usage. Figure 3 shows the correlation between gas usage and degree-day values (taken on a monthly basis using values from Vesma [6]). An open gas heater in the living room was removed and replaced by a wood-burning stove. Although this was only used for supplementary heating (as there is a radiator in the room) it made up about 8% of the original gas use. Since applying external insulation, the appearance of mildew has been significantly reduced as internal wall temperatures are generally above the dew point.

Electricity use in the house is significantly below the national average. This is partly due to reduced use of electrical appliances – e.g. a kettle is used on the gas hob in preference to an electrical kettle and there is no TV, video recorder, etc. Plotting electricity use against day length shows a clear correlation due to lighting use (see Figure 4) which is estimated to be 750 kWh per year, 25% of the total. The increase in electricity consumption shown at the time of insulating the property is due to the installation of a dishwasher at around the same time. The graph shows a reduction in the minimum gas usage per day, due to less use for heating washing-up water. This contributes around 4% to the saving in gas. When this and the change to wood-burning in the living room is taken into account, the reduction in gas usage due to the insulation is 35 %, representing a carbon saving of almost 1 tonne/year based on the 20-year average temperature. The overall reduction in CO_2 emissions relative to the unimproved state of the house is approximately 60 %.

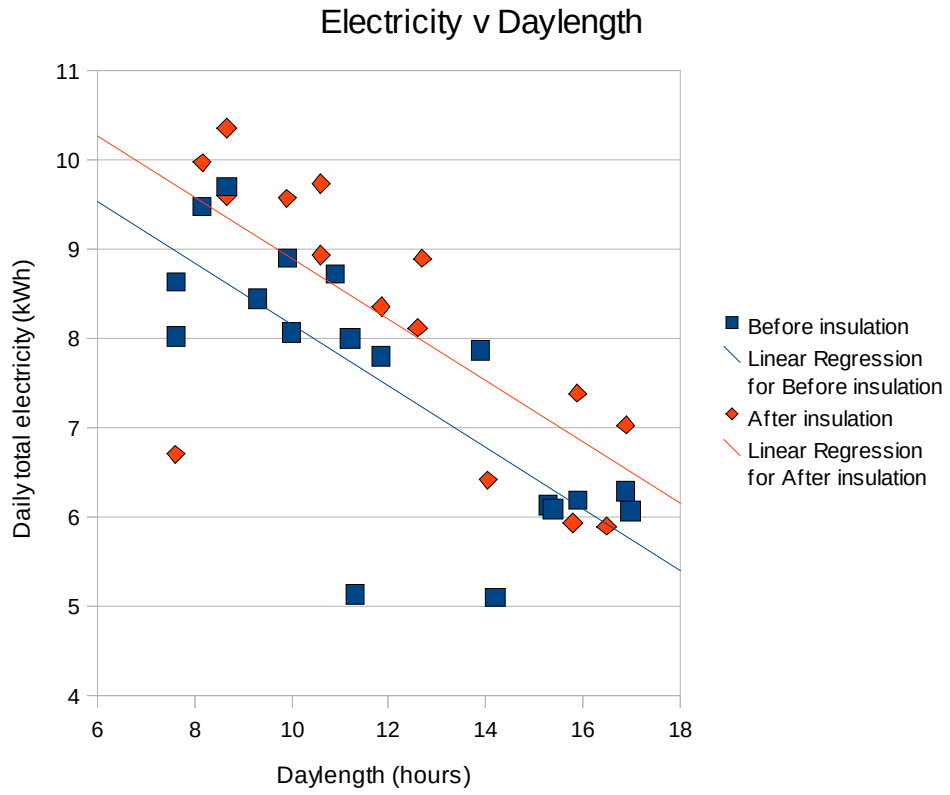

Figure 4. Electricity usage, showing the changing lighting load.

The amount of energy used for the wood-burning stove is difficult to assess, but is reckoned to be 200 kg of wood with an average energy content of 12 MJ/kg. This represents 6% of the total energy use in the home. This not only reduces carbon emissions, but so far has also reduced costs, as the wood used has been obtained free of charge. It is possible to extrapolate

the number of households that could use such free sources of wood – much of it from builders' skips. According to the UK Government department Defra, the amount of waste wood from construction industry is 5 million tonne/year [7]. Just 10% of this would be enough for 1 million homes to provide a similar level of wood heating.

The overall energy use after refurbishment, corrected to average 2203 degree-days per year, is 125 kWh/m^2 of which 71% is from gas and 23% electric.

3 Comparison with other data

3.1 Scottish case-study

A refurbishment case-study of three types of dwelling in Scotland by Jenkins [8] includes a stone-built house of a similar age. The comparison is useful because the house is also detached and occupied by a family of four, with the same floor area of 98 m^2. However, in the Scottish house the window area is approximately 30% less, and the walls are much thicker. Without wall insulation but with other energy-saving interventions, Jenkins predicted a reduction from 327 kWh/m^2 to around 200 kWh/m^2 after refurbishment. Further Carbon savings (down to 4 tonne CO_2 per year) could be achieved using solar thermal, solar PV and wind energy.

The figures can be usefully compared with figures for different house types and ages given in another report on Scottish Housing [9]. Although similar data for England was not easily available, the Scottish data gives a useful comparison. Degree-day data for Scotland shows that energy demand for heating is likely to be 10 – 15% higher than in Nottingham. The Scottish data show mean CO_2 emissions of 17.5 tonne/year for pre-1919 detached houses.

3.2 Data from Germany

Most of the technologies for external insulation available in the UK are adapted from a system developed in Germany, known as *Wärmedämmverbundsystem* (WDVS). In general, German residential buildings are much more energy efficient than those in the UK. They use, on average, less energy per unit floor area, despite colder winter temperatures. Energy efficiency standards have been stringent since 1977 (similar to UK 2001 standards) and current minimum standards are still higher than in the UK. When houses are refurbished, they tend to be fitted with higher levels of insulation - 160 mm is the current recommendation for external insulation on solid walls in Germany.

In 2009, the German "Bank for Reconstruction" *(KfW)* provided loans of €8.9 bn toward the energy refurbishment of 620,000 homes, estimated to reduce carbon emissions by an average of 2.4 tonne/year/dwelling. Germany has fewer older houses than the UK – about 75% were built after 1945. A study [10] of multiple flats in larger houses in Germany *(Mehrfamilienhäuser)* – comparable in format to Scottish tenement housing - shows how older buildings have little capacity for energy improvement and predicted energy savings are often not achieved. In Figure 5 the data has been converted from kWh/m^2 using German emissions data (from *UmweltBundesAmt*) and taking an average floor area of 90 m^2.

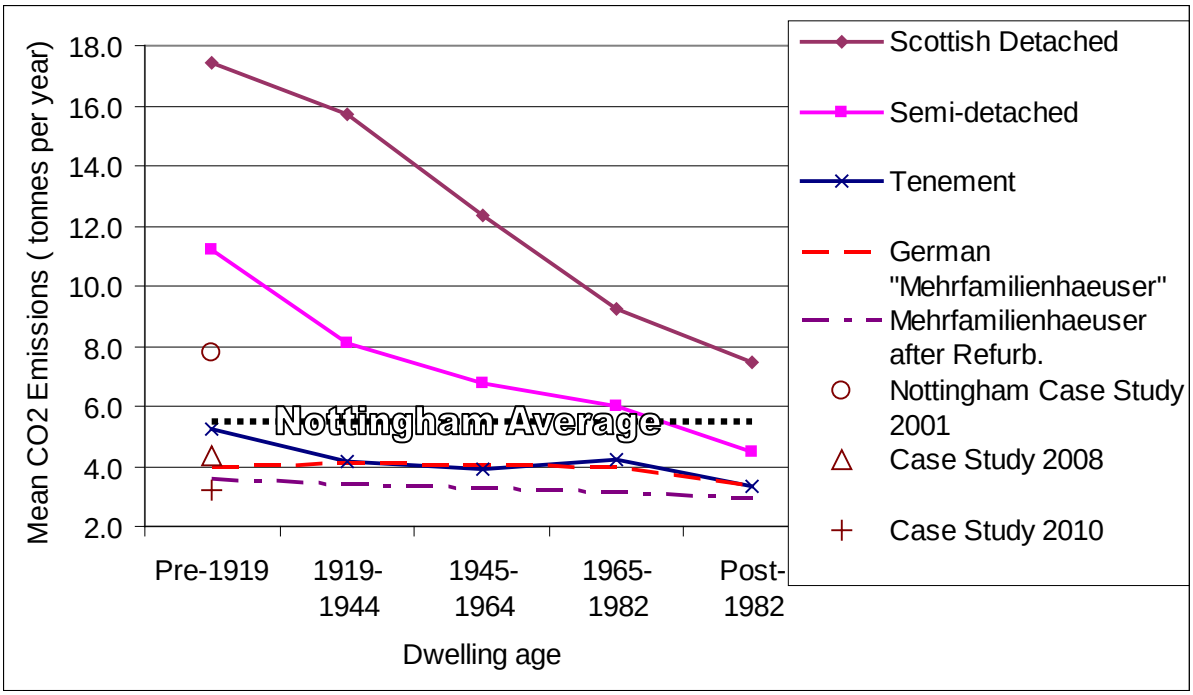

Figure 5. Comparison of CO_2 emissions per dwelling for different ages of houses and flats.

3.3 Other UK data

The previous UK government's main domestic energy efficiency programme was CERT (Carbon Emissions Reduction Target) which has been implemented through Energy Supply Companies. In contrast to the German investment, in 2009 around £400m (€0.45 bn) was invested, mostly in loft insulation (616,000 homes) and cavity wall insulation (500,000 homes); only 17,700 homes were fitted with solid wall insulation. A recent study published by the Department of Energy and Climate Change suggests that even homes in the UK with cavity walls cannot all be insulated easily. Although there are now around 5 million homes with unfilled cavities, most of these will be "hard to fill" because of the nature of the cavity walls and the materials used [11].

A portfolio of houses that have been refurbished to achieve at least 60% carbon reduction is presented by the Sustainable Energy Academy [12] under the slogan "Old Home, Superhome". This includes 39 case studies of houses built between 1800 and 1930, of which 22 were treated mainly with internal insulation and 17 with external insulation. To achieve this level of carbon reduction, very few houses rely on insulation alone: 36 of the 39 cases have at least one renewable energy source. The most common is solar thermal, but 40% have solar PV, 45% have wood stoves/boilers and 10% have ground source heat pumps. More than half have some form of underfloor insulation in addition to solid wall insulation. For the case study house, installation of 3.8 kW of PV is planned for 2011 at a cost of £13,700, with a predicted further saving of 1.7 tonnes of CO_2, approximately half of the 2010 emissions.

Lectures about existing local examples of refurbished homes gave information and inspiration before implementing the case study described in section 2. Among these were a Nottingham "Eco-home" included in the Sustainable Energy Academy portfolio and a refurbished home owned by a local Member of Parliament described in [13]. The importance of occupier behaviour is also critical to the success of such energy improvement schemes. Hence, the E-On house project at University of Nottingham, which will demonstrate the process of

converting a typical 1930's house to a zero-carbon home, incorporates a sophisticated array of monitoring equipment to learn more about this aspect [13].

4 Conclusions

The energy-saving measures in the Case Study have been effective in reducing the carbon footprint of the house. However, it is clear that the main reduction in carbon emissions was made by the first stage of improvements, which were more cost-effective. The greatest contribution to carbon reduction probably came from two changes which did not affect heat loss from the house: (i) installation of a condensing boiler; (ii) changing from electricity to gas for domestic hot water. Changes in carbon emissions are highly dependent on fuel choice because currently CO_2 emissions per unit of energy are three times higher for electricity than for gas. However, the combination of energy-saving measures employed in the case study make internal temperatures much more even, reduce condensation and contribute significantly to reduction in use of fuel for heating. Nevertheless, it is clear that one reason for the low final carbon footprint is the behaviour of the house occupants. Typical room temperature in living areas is 18 C, 3.5 degrees less than the temperatures considered as normal by the Tarbase study [8].

The external insulation cost £9000, which at current gas prices will take more than 20 years to payback financially. However, it has probably enhanced the overall property value, particularly with the current requirement for Energy Performance Certificates. Nevertheless, depending on interest rates, this length of payback could mean that such improvement would not meet the requirements of the new UK government's proposed Green Deal, as costs might be greater than current fuel savings. Also, if Energy Performance Certificates are dropped, as some sources have indicated, the property value incentive would reduce.

From this case study, it is possible to extrapolate that 60% carbon savings could be made by implementing similar improvements throughout the 5 m older housing stock and 5 m "hard-to-fill" cavity homes. However, to reach this target by 2040, the number of homes treated needs to increase (from the current level of approx. 18,000) at a rate of 20% per year until 2027, by which time the level of refurbishment would be 600,000 homes per year (as currently in Germany). This level of growth cannot be envisaged without a coherent policy for incentives and appropriate dissemination of information to home owners. Some of the likely policies are set out by Boardman in [2].

References

[1] R. Bowie and A. Jahn, European Union – The New Directive on the energy performance of buildings – Moving closer to Kyoto, Société Royale Belge des Electriciens, April 2003. Available at: www.managenergy.net (accessed Dec, 2010).

[2] B. Boardman "Home Truths: a low-carbon strategy to reduce UK housing emissions by 80% by 2050", University of Oxford Environmental Change Institute – research report, Nov. 2007.

[3] K. Lomas, "Energy Use in dwellings: decarbonising the stock and people" in ESRC Seminar Series How people use and 'misuse' buildings, 26 Jan, 2009.

[4] C. Pearson, The Complete Guide to External Wall Insulation, York Publishing Services, 2006.

[5] Energy Savings Trust, "External insulation for dwellings" Good Practice Guide 293 (2006).

[6] V. Vesma, Degree Day Data available at www.vesma.com/ddd/ (accessed Dec, 2010).

[7] Department of Environment, Food and Rural Affairs, "Waste Wood as a Biomass Fuel", April 2008, p8.

[8] D. Jenkins, "Energy Modelling In Traditional Scottish Houses: Heriot-Watt University analysis of potential CO2 savings of building variants", Tarbase Group report for Historic Scotland, 2008.

[9] S. Walker et al, "Scottish House Condition Survey: Key Findings for 2009" Published by the Scottish Government, 25th November 2010.

[10] C. Michelsen, S. Müller-Michelsen, "Energieeffizienz im Altbau: Werden die Sanierungspotenziale überschätzt? Ergebnisse auf Grundlage des ista-IWH-Energieeffizienzindex", Wirtschaft im Wandel, Institut für Wirtschaftsforschung Halle, Issue 9 (2010) 22 Sept. 2010.

[11] Inbuilt Ltd & Davis Langdon, "Study on hard to fill cavity walls in domestic dwellings in Great Britain", Report for UK Dept. for Energy & Climate Change, October, 2010.

[12] www.sustainable-energyacademy.org.uk (Accessed December 2010)

[13] M. Gillott and C. Spataru, "Materials for energy efficiency and thermal comfort in the refurbishment of existing buildings", in "Materials for energy efficiency and thermal comfort in buildings", Edited by M Hall, Woodhead Publishing, April 2010.

Effect of Condenser Air Flow on the Performance of Split Air Conditioner

Amr O. Elsayed[1,*], Abdulrahman S. Hariri[1]

[1]*College of Engineering, University of Dammam, Saudi Arabia*
** Corresponding author. Tel: +966551885676, Fax:* +966 3 8584331*, E-mail:amro9992000@yahoo.com*

Abstract: Split air conditioning units are usually used for small and medium scale residential buildings. Therefore, more energy efficiency and lower cost are needed along with reliable control for the air conditioning units. An experimental investigation has been carried out to study the performance of a direct expansion air conditioning (A/C) unit having a variable speed condenser fan. The modulation of heat rejection airflow has been controlled with the outdoor air temperature via a Proportional Integral Differential (PID) controller. The control algorithm allows increasing the speed of condenser fan with the increase of outdoor air temperature and vice verse. The maximum rated air flow of the fan is 0.43 m3/s at 42ºC outdoor air temperature and the minimum is 0.28m3/s. To facilitate variation of refrigerant flow rate according to the evaporator load, the traditional capillary tube was replaced with a suitable thermostatic expansion valve and liquid refrigerant reserve. The influence of condenser airflow and its temperature on the A/C unit performance and compressor power consumption has been investigated and presented at different evaporator cooling load. It has been found that a 10 % reduction in compressor power consumption is achieved by increasing the condenser air flow by about 50%.

Keywords: *Split air conditioners, A/C unit performance, Variable speed condenser fan.*

Nomenclature

COP	*coefficient of performance*	T_{cond}	*condensation temperature.....°C*
h	*refrigerant enthalpy…..…..kJ.kg^{-1}*	Q_{ev}	*evaporator cooling capacity..... kW*
m_{ref}	*refrigerant flow rate…….. kg.s^{-1}*	W_{comp}	*compressor power consumption...kW*
P	*pressure……..kPa*	W_{Fan}	*condenser fan power……..kW*
T_{ev}	*evaporation temperature…… °C*		

1. Introduction

Energy saving is the practice of decreasing the quantity of energy used. It may be achieved through efficient energy use or by reducing the consumption of energy services [e.g. 1-3]. Air conditioning units are usually used for small and medium scale residential buildings. The amount of energy consumed by air conditioners, refrigerators and water heaters is increasing rapidly, since the consumed power by air conditioners occupies about 20% of the total power consumption. The improvement of refrigeration cycle performance can be done by lowering the compressor power consumption, increasing the condenser heat rejection capacity or reducing the difference between condenser and evaporator pressures.

A. Benamer and D. Clodic [4] offered a method for the comparison of energy consumption of variable and fixed speed scroll compressor in a refrigeration system. They showed that the lower the heat load, the higher the energy savings associated with variable speed. Also, variable speed compressor generates up to 40% savings in power consumption. S. Hu and B. Huang [5] presented a high efficiency split residential water-cooled air conditioner that utilizes cellulose pads as a filling material of the cooling tower. They showed that the water cooled condenser results in decreasing the compressor power consumption from 1.189 to 1.02 kW and the cycle COP is improved from 2.96 to 3.45. S. Wang et al. [6] presented a split air conditioner with a hybrid equipment of energy storage and water heater all year around. In summer, ice storage coils work as evaporator. In winter, energy storage tank absorbs the condenser heat to store heat during the heating process. They obtained around 28% increase in cooling capacity and 21.5% improvement in the COP. F. Yu and K. Chan [7] showed how the COP of air-cooled chillers can be improved by modulating heat rejection airflow via variable speed condenser fans. They introduced an algorithm that makes use of a set point of

condensing temperature to determine the number and speed of condenser fans staged to provide the airflow required for any given heat rejection. Also, in order to achieve maximum COP under condensing temperature control with variable speed condenser fans, the set point of condensing temperature should be adjusted based on the chiller load together with the outdoor temperature. Potential energy saving for using water cooled air conditioner in residential building has been illustrated by H. Chen et al. [8]. A split air conditioner with air and water cooled options was set up for experimental study at different indoor and outdoor conditions. The overall energy saving were estimated to be around 8.7% of the total electricity consumption.

Recently, T. Mahlia and R. Saidur [9] reviewed requirements and specifications of various international test standards for testing and rating of room air conditioners and refrigerators sacking for efficiency improvement of these appliances. Also, M. Jiang et al [10] evaluated the influence of condensing heat recovery on the dynamic behavior and performance of air conditioners. They showed that the condensing heat recovery has a negative effect on the cooling capacity at the start of the heat recovery process, while the average COP of the system is improved.

As shown in the previous literature, variable speed condenser fans have been handled for a large scale (i.e. chiller). The main objective of this study is to investigate the effect of condenser heat rejection modulation, via a variable speed fan, on the energy consumption and on the performance of a residential air conditioner. The speed of condenser fan is simultaneously controlled with the outdoor air temperature. The characteristics of refrigeration cycle that served by a thermostatic expansion valve will be presented at different indoor and outdoor temperatures at the steady state operation condition.

2. Experimental apparatus and procedure

A split type, 2.64 kW nominal capacity, air conditioner using R-22 was employed to exam the modulation of condenser heat rejection and its effect on the conditioner performance. The conditioner contains the basic components of a vapor compression system: a compressor, a condenser, a capillary tube, an evaporator and such attachments as filter/dryer and fans. The indoor unit includes a DX evaporator with copper tubes and aluminum fins, a fan and a capillary tube. The outdoor unit includes a constant speed rotary compressor and an aluminum finned-plate condenser that is provided with a constant speed propeller fan. The cooling output has ON/OFF control in accordance with the indoor set point temperature.

The normal method of adjusting the refrigerant mass flow in the evaporator is to add an expansion valve and an accumulator to the system. Therefore, a thermostatic expansion valve (with 0-1 orifice) and 1 kg liquid refrigerant accumulator have been installed in the refrigeration cycle. The condenser fan was employed to extract the room air through a foam duct and discharge it outside the room as shown in Photo 1, where Photo 2 shows the evaporating unit. Electric heaters were installed in the path of entering air to evaporator and condenser. Each heater was connected with a variable capacity transformer to control the heater power.

The refrigeration cycle of the conditioner was provided with controlling and measuring devices at the key locations of cycle. A schematic diagram of the experimental apparatus is shown in Fig. 1.

Photo 1: Condensing unit

Photo 2: Evaporating unit

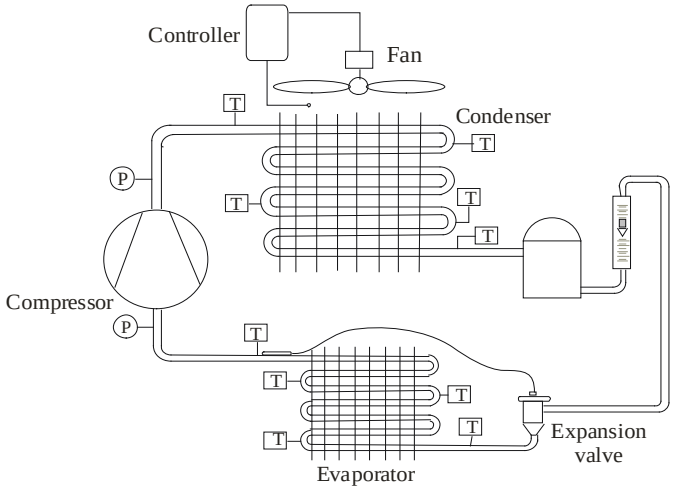

Fig. 1 A schematic view of the experimental apparatus

The temperature was measured via a type-T thermocouple with a maximum uncertainty of ± 0.2ºC. Thermocouples were placed at the inlet and outlet of the evaporator and condenser. Also, thermocouples were installed along the tube length of the evaporator and condenser to determine the condensation and evaporation temperatures. The thermocouple junctions were soldered at the outer surface of the tubes and the thermocouple wires were connected to a digital thermometer. The condition of air at the inlet and outlet of each of evaporator and condenser was measured by means of a digital humidity/temperature meter with 1% accuracy of relative humidity and ±0.1 accuracy of dry bulb temperature. The liquid refrigerant mass flow rate was measured by a calibrated flowmeter with a maximum uncertainty of ±0.5 kg/hr. A digital wattmeter with ±1% reading uncertainty was provided to measure the compressor power consumption.

A Proportional Integral Derivative (PID) controller was used to control the speed of condenser fan. The controller had been connected with a temperature sensor, thermistor (LM35), which was positioned inside the foam duct at the front of condenser. When the condenser inlet air temperature is increased above the desired set point, the condenser fan speed is increased and vice verse. The velocity of air at the inlet condenser coil was measured via a digital vane anemometer with 0.1 m/s accuracy, where the air velocity inside the condenser duct was ranged from 1.25 to 1.9 m/s.

It is worth mentioning that the room temperature was maintained at 24-26 ºC during the experiments. All test runs were performed in an identical manner and at the steady state condition.

3. Data reduction

As mentioned, the air velocity (m/s) inside the condenser duct is measured via a vane anemometer and the rate of air flow (m^3/s) is calculated by multiplying the duct cross section into the average air velocity. The evaporator cooling capacity, Q_{ev}, can be calculated as:

$$Q_{ev} = m_{ref} (h_1 - h_4) \quad (1)$$

Where: h_1, h_4 are enthalpies of the refrigerant at evaporator inlet and outlet, respectively (kJ/kg). The common approach in determining the refrigeration cycle performance is to use the coefficient of performance, COP, depending on the compressor power consumption as;

$$COP = Q_{ev} / W_{comp} \quad (2)$$

4. Results and discussion

The performance of the refrigeration cycle is a result of the balance between the four essential cycle components. When the outside ambient temperature varies, it affects the performance of the condenser, which in turn, affects the performance of the evaporator, expansion device and the compressor. The affecting parameters that influence the conditioner performance have been considered for illustration. Also, the modulation of condenser heat rejection airflow and its effect on the conditioner performance has been presented.

4.1. Effect of evaporator inlet air temperature

The refrigeration load of indoor unit may vary due to several reasons, such as the variation of ambient temperature. The influence of evaporator entering air temperature (return air temperature) on the evaporating temperature and evaporator cooling capacity, Q_{ev}, is presented in Fig. 2. It is observed in this figure that higher cooling capacity is achieved at 26ºC which is the design operation condition recommended by manufacturers. As the inlet air temperature increases the evaporating temperature increases and the cooling capacity decrease.

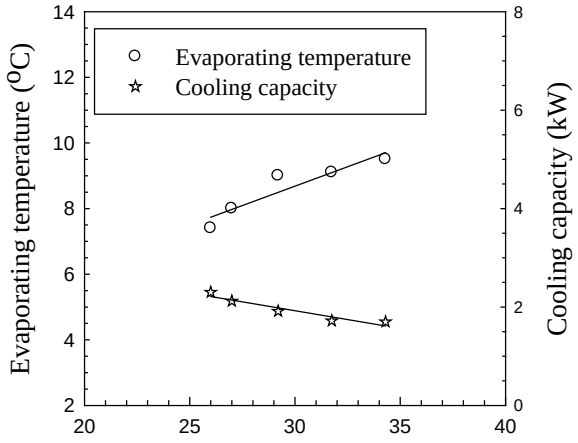

Fig.2 Variation of evaporator entering air temperature with evaporating temperature and evaporator cooling capacity

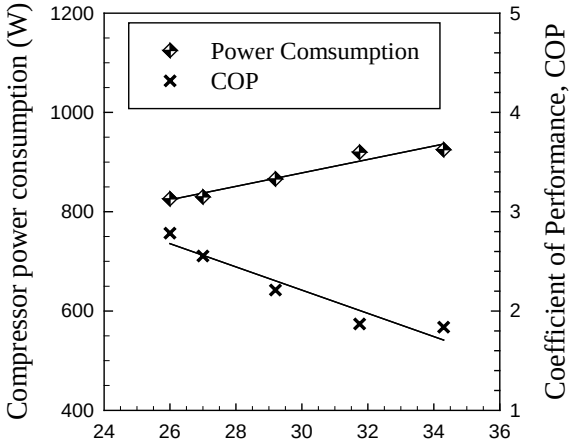

Fig.3 Effect of evaporator inlet air temperature on compressor power consumption and cycle COP

The reduction of Q_{ev} is about 25%, when the inlet air temperature increased from 26 to 35ºC. This reduction in Q_{ev} is referred to the evaporator starving which reduces the heat transfer coefficient in evaporator, since there is no sufficient refrigerant to accommodate the heat load. Here, it should be mentioned that the degree of superheating was varying from 5 to 9 ºC and the corresponding mass flow rate of the refrigerant varied from 0.0106 to 0.0133 kg/s. Also, the degree of subcooling was varying from 2 to 3 ºC. Fig. 3 reveals that when the inlet air temperature increases the compressor power consumption increases causing a reduction in the coefficient of performance of the cycle. The increase of power consumption is about 12%, while the reduction of COP is about 35%.

4.2. Effect of condenser inlet air temperature

The effect of condenser inlet air temperature on the cycle performance is shown in figures 4 and 5.The temperature of air entering the condenser was varied by heating the supply air to the desired temperature. During these experiments, the ambient temperature was kept constant at 26 ºC and the speed of condenser fan was constant which gives 0.28m^3/s of air. It is seen from Fig. 4 that the condensation temperature increases as the inlet air temperature increases,

as expected, and the cooling capacity decreases with the increase of condenser temperature. This reduction in cooling capacity is due to the increase of evaporation temperature which is accompanied with the condenser temperature, since the compressor has a constant speed. The reduction of cooling capacity is about 32% as the condensing temperature increased by 17%. Fig.5 shows the variation of compressor power consumption and the cycle COP with the condensation temperature. The increase in condensing temperature, so thus the condenser pressure and the pressure ratio, leads to an increase in power consumption and a decrease in the cycle COP. The power consumption is increased by 36% and the reduction in COP is about 45% as shown in the figure.

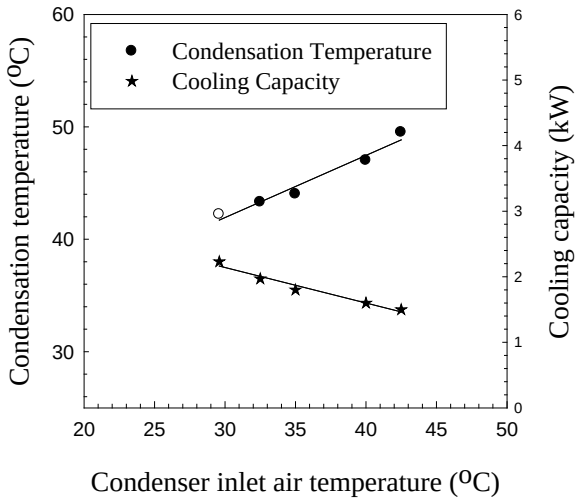

Fig.4 Variation of condenser entering air temperature with condensing temperature and evaporator cooling capacity

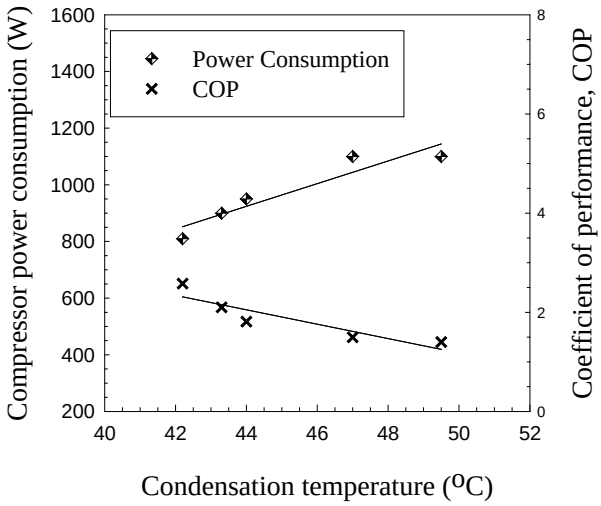

Fig.5 Effect of condensation temperature on compressor power consumption and cycle COP

4.3. Modulation of condenser air flow at constant inlet air temperature

During these experiments, the temperature of air, which cools the condenser, was kept constant at 36ºC and the airflow through the condenser was varied by controlling the speed of fan manually. Although the increased heat rejection airflow causes the additional fan electric demand, the decreased condensing temperature results in a considerable reduction in compressor electric demand. This is shown in Fig.6, as the rate of air flow increases from 0.28 to 0.43 m^3/s the condensing temperature decreased by about 8% and the corresponding reduction in compressor power consumption is about 10%. These findings indicate that the compressor power depends on how condenser fan is controlled to provide the heat rejection airflow required for any given cooling capacity.

4.4. Modulation of condenser air flow at different inlet air temperature

The condensing temperature can be controlled at a minimum point by modulating the heat rejection airflow continuously. During these experiments, the condenser fan speed was varied according to the condenser inlet air temperature that represents outdoor air temperature. To show the effect of variable air flow for improving condenser heat rejection, a comparison between constant and variable fan speed has been presented in Figs. 7-9. Fig.7 illustrates the variation of condensing temperature with the inlet air temperature for constant and variable airflow.

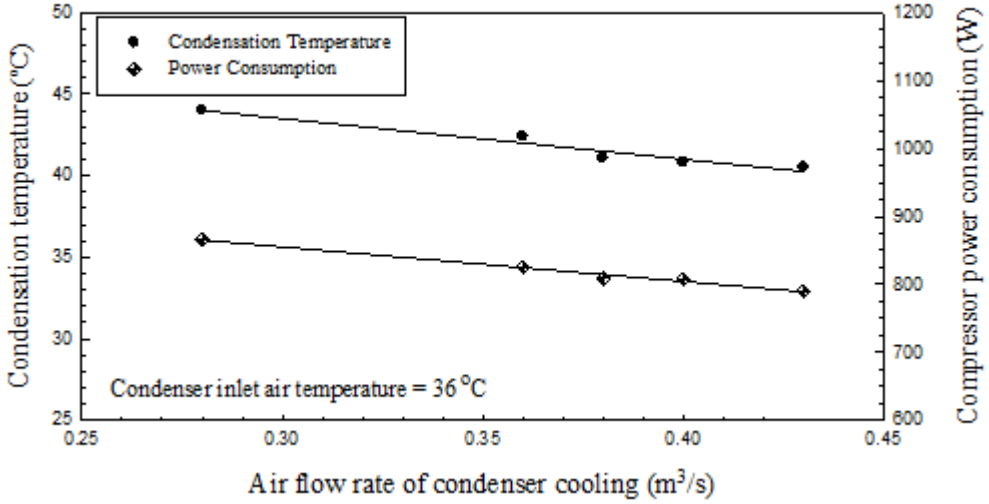

Fig.6 Variation of condenser airflow with condensation temperature and compressor power consumptic

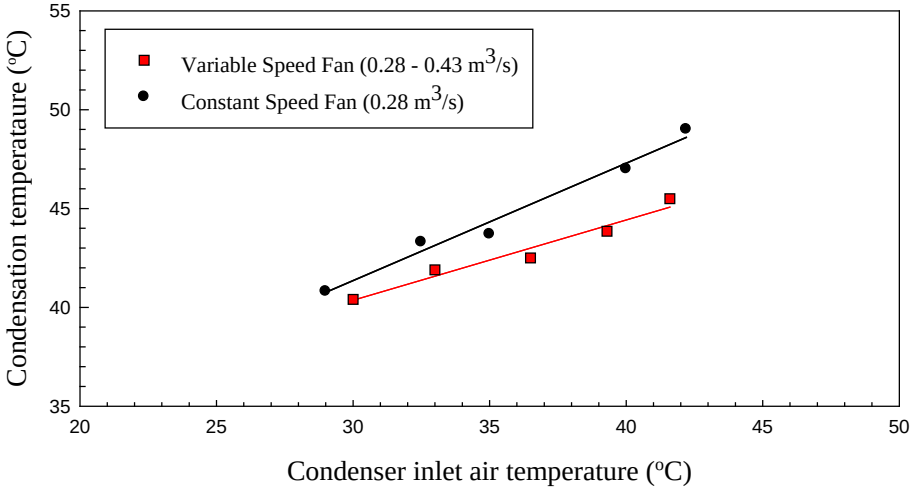

Fig.7 Variation of condensing temperature with condenser inlet air temperature for constant and variable airflow

As expected, by increasing the rate of airflow an improvement in condenser heat rejection is observed during which the condensing temperature has been reduced by 7% at 42ºC inlet air temperature as shown in figure. The corresponding reduction in compressor power consumption is recorded in Fig.8. It is seen from this figure that at 42ºC inlet air temperature the power consumption has been reduced by about 15%, while at 36ºC inlet air temperature the reduction is about 9%. As mentioned earlier, the increase of heat rejection airflow needs an additional fan electric demand; however, this demand is small compared with the energy saved by the compressor. In addition, the max power required for condenser fan is only used at the peak of outdoor air.

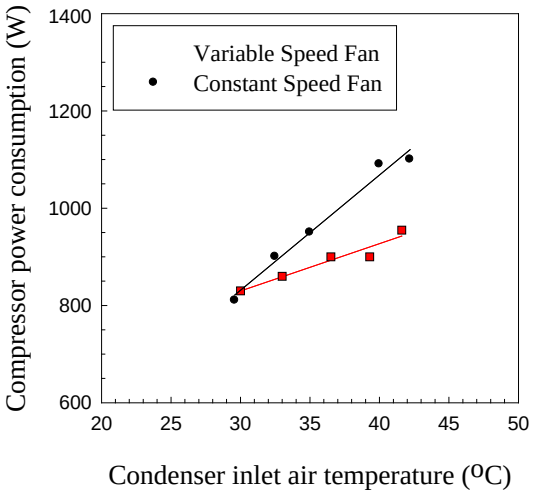

Fig.8 Variation of compressor power consumption with condenser inlet air temperature for constant and variable airflow

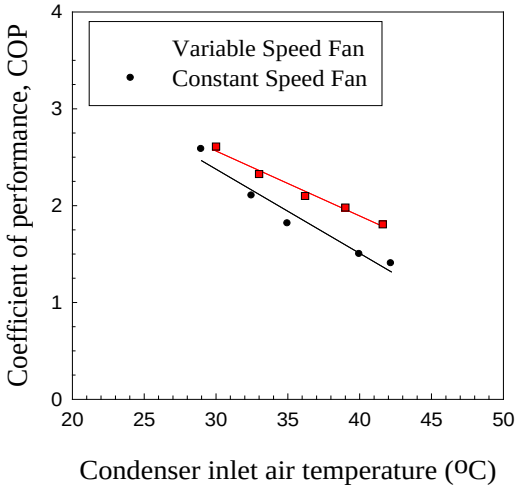

Fig.9 Variation of cycle COP with condenser inlet air temperature for constant and variable airflow

Fig.9 reveals the coefficient of performance of the conditioner during constant and variable airflow for condenser cooling. It is seen in this figure that, the COP of the cycle decreases as the condenser inlet air temperature increases for both constant and variable airflow. Since the increase in compressor power consumption is higher than the increase of the evaporator cooling capacity, so the COP of the cycle decreases. On the other hand, an improvement, about 28%, in the cycle COP is observed for variable condenser airflow due to the lower compressor power consumption.

To evaluate the energy saving due to the improvement of COP, shown in Fig. 9, the unit coefficient of performance is presented in Fig. 10. This performance coefficient includes the power consumption of the condenser fan and is defined as:

$$COP_U = Q_{ev} / (W_{comp} + W_{Fan}) \quad (3)$$

As Fig. 10 shows, the unit COP_U for variable condenser fan is greater than that for constant speed fan. The profit payback of the present energy saving method can be calculated by the economic analysis. The retrofitting of the present conditioner will be handled in a future work

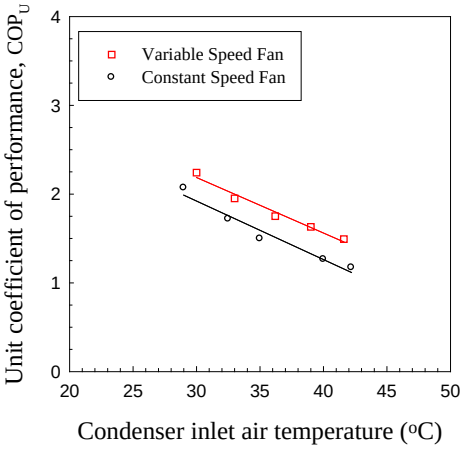

Fig.10 Variation of unit COP with condenser inlet air temperature

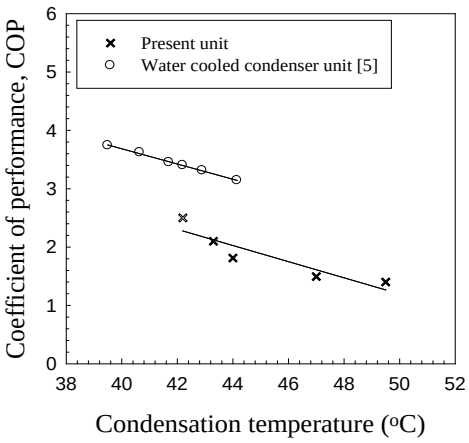

Fig.11 Comparison between the COP of the present conditioner and water cooled high performance conditioner in Ref [5]

The study is conducted to compare the present conditioner performance with the performance of water-cooled air conditioner in Ref [5]. As shown in Fig. 11, the COP of the water-cooled

air conditioner is higher by about 35% than that for the present conditioner. This is due to the high heat capacity of water compared with the air.

5. Conclusions

From the above findings, it can be concluded that:

- The power consumption of the compressor was increased by 12% and the cooling capacity was decreased by 25%, when rising the evaporator inlet air temperature from 26 to 35 ºC.
- The cooling capacity of the evaporator was decreased by 32% when rising the condenser entering air temperature from 30 to 42ºC, while the compressor power consumption was increased by about 36 %.
- At constant inlet air temperature, a 10 % reduction in compressor power consumption has been obtained when increasing the condenser cooling air flow by about 1.5 times.
- For variable speed condenser fan, it is found that the compressor power requirement has been reduced by 15% at 42ºC condenser entering air temperature; while at 36ºC the reduction is about 9%.
- The use of variable speed condenser fan causes an increase in the COP of the conditioner by 28% at 42ºC condenser entering air temperature.

Variable speed motor is recommended for the condenser fan with advanced control to accommodate the variation of outdoor air temperature for tracking and adjusting the condensing temperature.

References

[1] C.F. Gao, W.L. Lee, and Hua Chen, Locating Room Air-Conditioners at Floor Level for Energy Saving in Residential Buildings, Applied Thermal Engineering, 29, issues 2-3, 2009, pp. 310-316.

[2] E. Hajidavalloo, H. Eghtedari, Performance Improvement of Air-Cooled Refrigeration System by Using Evaporatively Cooled Air Condenser, Int. Journal of Refrigeration, 33, issue 5, 2010, pp. 982-988.

[3] Zhenjun Xu, Huaizhi Wu, Meiling Wu, Energy Performance and Consumption for Biogas Heat Pump Air Conditioner, Energy, 35, issue 12, 2010, pp. 5497-5502.

[4] A. Benamer, D. Clodic, Comparison of Energy Efficiency Between Variable and Fixed Speed Scroll Compressors in Refrigeration System, Proceedings of technological innovations in refrigeration in air conditioning and in the food industry into third millennium, 8th-9 June, 1999, pp.1-8.

[5] S.S. Hu, B.J. Huang, Study of a High Efficiency Residential Split Water-Cooled Air Conditioner, Applied Thermal Engineering, 25, 2005, pp. 1599–1613.

[6] S. Wang, Z. Liu, Y. Li, K. Zhao and Z. Wang, Experimental Study on Split Air Conditioner with New Hybrid Equipment of Energy Storage and Water Heater All Year Round, Energy Conversion and Management, 46, 2005, pp. 3047–3059.

[7] F.W. Yu and K.T. Chan, Advanced Control of Heat Rejection Airflow for Improving the Coefficient of Performance of Air Cooled Chillers, Applied Thermal Engineering, 26, 2006, pp. 97–110.

[8] H. Chen, W.L. Lee and F.W. Yik, Applying Water Cooled Air Conditioners in Residential Buildings in Hong Kong, Energy Conversion and Management, 49, 2008, pp. 1416–1423.

[9] T. Mahlia and R. Saidur, A Review on Test Procedure Energy Efficiency Standards and Energy Labels for Room Air Conditioners and Refrigerator-Freezers, Renewable and Sustainable Energy Reviews, 14, Issue 7, 2010, pp. 1888-1900.

[10] M. L. Jiang, J. Yi Wu, Y. X. Xu and R. Z. Wang, Transient Characteristics and Performance Analysis of a Vapor Compression Air Conditioning System with Condensing Heat Recovery, Energy and Buildings, 42, Issue 11, 2010, pp. 2251-2257.

Volume 9

Marine and Ocean Technology

Assessment of a multi-cell fabric structure as an attenuating wave energy converter

M.R.Hann[1,*], J.R.Chaplin[1], F.J.M. Farley[1]

[1] *University of Southampton, UK*
** Corresponding author. Tel: +44 23 8059 4656, E-mail: mrh1g08@soton.ac.uk*

Abstract: Fabriconda is an attenuating wave energy device constructed from inelastic fabric. It is a flooded distensible tube constructed from a series of smaller flooded tubes, called cells, joined longitudinally. This paper presents a theory to predict the shape a Fabriconda forms at different tube and cell pressures and shows it successfully predicts the shape of a model Fabriconda. A 1D linear finite difference simulation based on the conservation of fluid momentum and mass in both the central tube and cells provides a prediction of the free bulge wave speed along the device. Experiments using a piston to artificially generate a bulge wave within the central tube of a model Fabriconda have produced bulge speeds that demonstrate good agreement with these predictions.

Keywords: *Wave energy, Wave power device, Finite difference model*

Nomenclature

θ	*half-vertex angle*	x	*cell horizontal chord length* ..... *m*
n	*number of cells*	R	*central tube radius* ..... *m*
s	*cell arc-length* ..... *m*	A_t	*central tube cross-sectional area*……. m^2
p_t	*tube pressure* ..... *Pa*	A_c	*cell cross-sectional area*…… m^2
p_c	*cell pressure*..... *Pa*	A_0	*initial, static cross-sectional area* …… m^2
r	*radius of curvature of cell* ..... *m*	ρ_o	*density*..... $kg \cdot m^{-3}$
T_1	*fabric tension of cell – external interface*. *N*		
T_2	*fabric tension of cell – tube interface* ..... *N*		

1. Introduction

The Anaconda wave energy converter [1], [2] consists of a submerged and flooded rubber distensible tube lying perpendicular to incoming wave fronts. As the waves pass over, they induce a series of travelling bulges in the tube, and an internal oscillatory flow. If the speed of free bulge waves is close to that of the external water waves, energy is progressively transferred to the flow inside the tube, terminating in a power take-off system.

The purpose of this paper is to outline initial work on a fabric version of the Anaconda, named the Fabriconda [3], [4]. In the Fabriconda, distensibility is provided not by the elasticity of the walls (as in the Anaconda), but by the form of construction of the tube. A number of tubes (or 'cells') made of inelastic fabric are joined together longitudinally to form a larger central tube (Fig.1). The tube and the cells are separately flooded. Local changes in the cross-sectional area of the tube are facilitated by changes in the shapes of the surrounding cells. When the cells are circular, the tube area is at a minimum; when the cells are flat it is at a maximum. The tube's distensibility and the speed of free bulge waves in it depend on the ratio of the pressure in the tube to that in the cells.

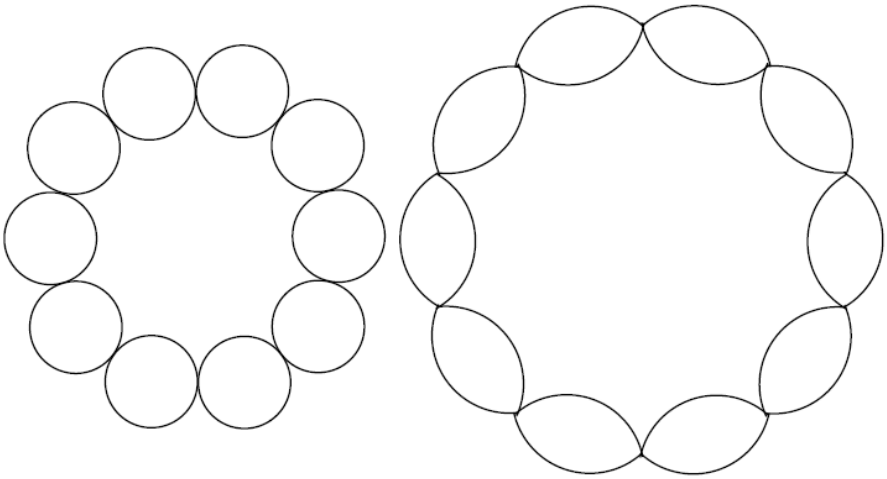

Fig. 1. Example cross-section of a Fabriconda with 10 cells, showing the structure at its minimum cross-section and at its medium point [3].

The potential advantages of this construction are that it removes the danger of aneurysm that can occur in rubber tubes. It also substantially reduces energy losses through hysteresis and construction may be cheaper. This paper presents the static shape theory of the Fabriconda and compares this with experimental results. A 1D finite difference model of the tube is introduced and used to predict the Fabriconda's free bulge speed. A comparison with measurements of free bulge speed is made.

2. Methodology

2.1. Static shape

The cells are lenticular in shape and are formed by the intersection of two circular arcs (fig. 2.). The geometry of a Fabriconda with *n* cells can be defined via the half vertex angle, θ. The half vertex angle depends on the fluid pressures p_t and p_c within the tube and cells and the arc length s, the width of fabric from which half a Fabriconda cell is constructed.

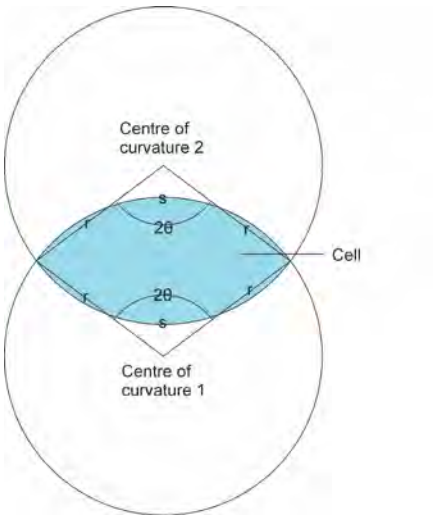

Fig. 2. – The formation of a lenticular shaped cell by two circular arcs.

By comparing the ratio that arc length s represents of the circle circumference to the ratio that 2θ represents of the whole circle equation 1 for circle radius is found:

$$r = \frac{s}{2\theta} \tag{1}$$

Simple geometry now gives *x*, the cell chord length and *R* the central tube radius (fig. 3.).

$$x = \frac{s\sin(\theta)}{\theta} \tag{2}$$

$$R = \frac{s\sin(\theta)}{2\theta\sin\left(\frac{\pi}{n}\right)} \tag{3}$$

Finally cell and tube areas can be defined, again in terms of the variable θ.

$$A_c = 2\left(\frac{s^2}{4\theta} - \frac{s^2 \sin(2\theta)}{8\theta^2}\right) \tag{4}$$

$$A_t = n\left(\frac{s^2 \sin^2(\theta)}{4\theta^2 \tan\left(\frac{\pi}{n}\right)} - \frac{s^2}{4\theta} + \frac{s^2 \sin(2\theta)}{8\theta^2}\right) \tag{5}$$

Each cell has two boundaries, the first between the cell and the external environment and the second between the cell and the tube. The pressure difference across these two boundaries generates separate tensions in the fabric defining the boundary, T_1 and T_2 (fig. 3).

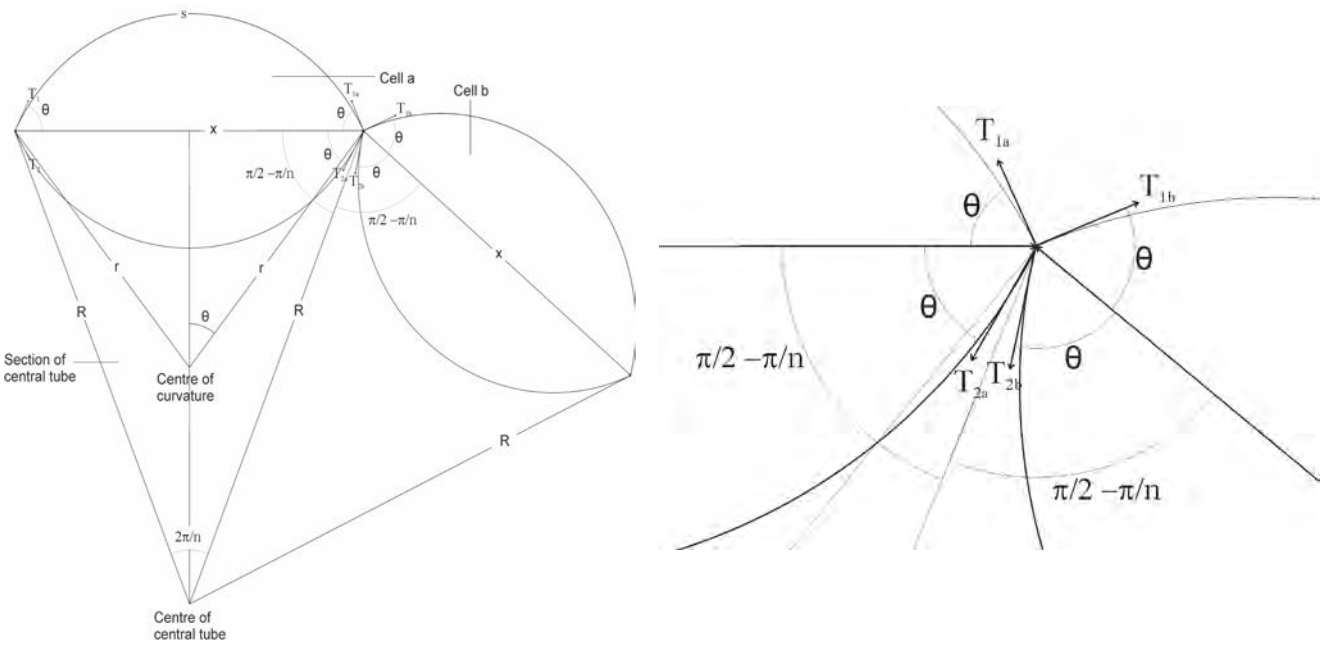

Fig. 3. Geometry of two Fabriconda cells

At the joint between cells the two tensions from each cell must balance. Using this condition a relationship between θ and T_2 and T_1 can be found:

$$\tan(\theta) = \frac{T_2 + T_1}{T_1 - T_2} \tan\left(\frac{\pi}{n}\right) \tag{6}$$

The two tensions are given by the pressure differences across the two boundaries and the cell radius of curvature. Applying this half vertex angle, and hence Fabriconda geometry, is defined in terms of cell and tube pressure:

$$\tan(\theta) = \frac{2p_c - p_t}{p_t} \tan\left(\frac{\pi}{n}\right). \quad (7)$$

2.2. 1D finite difference model

Predictions of how free bulge speed varies with the fluid pressure within the tube and cell have been made using a 1D finite difference model of the Fabriconda. The fabric is assumed to act as an inelastic membrane. Linear conservation of momentum (equation 8) and continuity (equation 9) are applied to the flow in a single cell and the 1/*n*th segment of central tube defined by that cell.

$$\rho_0 \frac{\partial u}{\partial t} = -\frac{\partial p}{\partial x} \quad (8)$$

$$\frac{\partial A}{\partial t} = -A_0 \frac{\partial u}{\partial x} \quad (9)$$

By differentiating equation 8 with respect to position and equation 9 with respect to time, velocity is eliminated from the problem, giving equation 10 to describe flow in the tube segment and equation 11 describing the flow in the cell.

$$\frac{\partial^2 A_t}{\partial t^2} = \frac{A_{to}}{\rho} \frac{\partial^2 p_t}{\partial x^2} \quad (10)$$

$$\frac{\partial^2 A_c}{\partial t^2} = \frac{A_{co}}{\rho} \frac{\partial^2 p_c}{\partial x^2} \quad (11)$$

Equations 4 and 5 are substituted into 10 and 11 to give two equations describing the dynamic properties of the device in terms of both tube and cell pressure. A Du Fort-Frankel finite difference scheme is applied to give two quadratic equations (equations 12 and 13) in terms of tube and cell pressure. The two pressures are solved at each time step using a Newton iteration method:

$$F = z p_{t\,i,j+1}^{\,2} + y p_{t\,i,j+1} + m p_{t\,i,j+1} p_{c\,i,j+1} + w p_{c\,i,j+1} + v p_{c\,i,j+1}^{\,2} + q = 0 \quad (12)$$

$$G = z_1 p_{t\,i,j+1}^{\,2} + y_1 p_{t\,i,j+1} + m_1 p_{t\,i,j+1} p_{c\,i,j+1} + w_1 p_{c\,i,j+1} + v_1 p_{c\,i,j+1}^{\,2} + q_1 = 0 \quad (13)$$

A sinusoidal fluctuation is applied to the bow boundary condition and the speed at which the resulting pressure bulge propagates along the Fabriconda tube is measured.

2.3. Experimental set-up and measurements

A 7.0m long, 10 cell, model Fabriconda with a cell arc length of 0.121 ± 0.003m was constructed to verify the static shape theory as well as to provide measurements of free bulge speed. The experimental set-up is shown in figure 4. The model was constructed from 450 decitex woven Nylon and each cell and the central tube had a 0.16mm latex inner tube

inserted to make the device water tight. The central tube was connected to a 250mm diameter piston cylinder at one end and a 250mm diameter pipe with a 90^o bend at the other. This pipe was the first part of a power take off system not relevant to these measurements. The cells were closed at the piston cylinder end and connected to a cell reservoir via 1.4m long, 25mm diameter pipes at the other. The top of central tube was 100mm below the water surface.

Fig. 4. Experimental set-up with piston in the main tube to artificially generate bulge waves.

Pressures within the model were measured simply using manometers connected to each cell and the central tube. To verify the static shape theory the model was inflated to various cell and tube pressure combinations and cell chord length (x) of the top cell measured using callipers.

Free bulge speed was measured by artificially generating bulge-waves using an actuator driven piston [5] producing a single sinusoidal oscillation. Nine pairs of 50mm long strain gauges were attached to a single cell, spaced evenly along the device with a separation of 75.0cm. These gauges recorded the curvature of the cell and hence the passage of the bulge produced by the piston oscillation. The time difference between the bulge arriving at each gauge allowed the bulge speed to be calculated.

3. Results

3.1. Static inflation shape

For various tube and cell pressures, figure 5 compares measured cell chord lengths with those obtained from the static theory above. Values of θ are calculated using equation 7 from the measured inflation pressures.

Agreement is seen to be satisfactory; the coefficient of determination (R^2) value between experimental values and theory is 0.97.

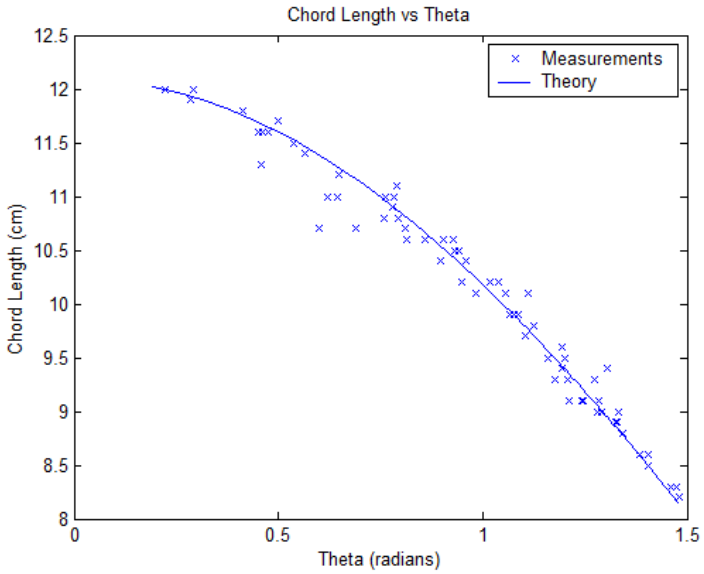

Fig. 5. Chord length measured from modelled during the inflation of a model Fabriconda compared to the value predicted by theory.

3.2. Bulge speed simulations and measurements

Figure 6 shows an example output from the strain gauge pairs attached to a cell of the model Fabriconda as a bulge wave generated by a piston oscillation propagates along the tube. Two speeds were measured by identifying the time difference between the two sets of equivalent points indicated in figure 6, the trough and the peak of the pressure bulge. The outputs used are from the 1st and 7th gauges as these provided the data sets that covered the longest available interval, 4.5m. Specific measurement points for the 9th gauge could often not be obtained owing to strong reflections from the tube end.

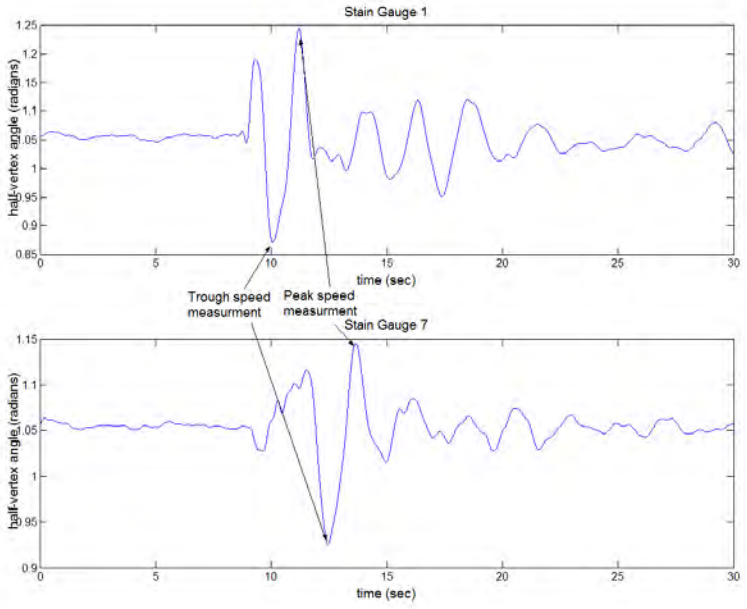

Fig. 6. Example gauge output showing free bulge propagation when p_t = 25.7m and p_c = 82.7m

Measurements of bulge speeds were made for a constant cell pressure at a head of 82.7cm, with tube pressures between a head of 4.2 cm and 39.0cm. The 1D finite difference model was used to provide predictions of how the speed of the free bulge propagation changed in this pressure regime. Figure 7 shows the results of these simulations and the experimental results found from the two pairs of points indicated in figure 6.

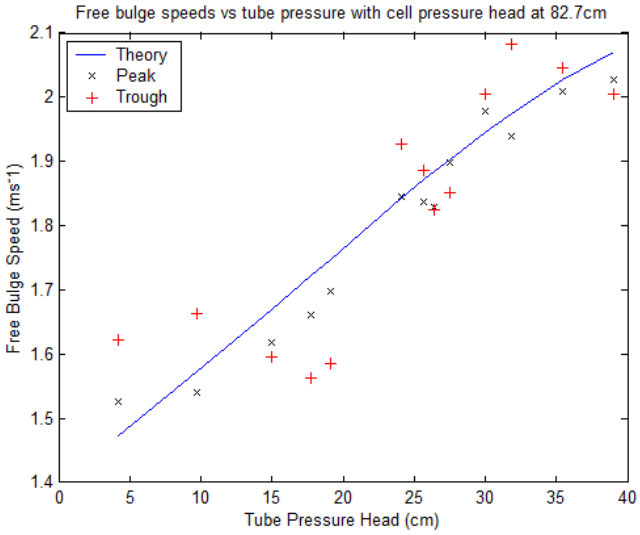

Fig. 7. Simulated and measured free bulge speed vs. tube pressure at a constant cell pressure.

4. Discussion

The results of the stationary inflation experiments (fig. 4) show good agreement between measured values and those predicted by theory. The theory assumes that the Fabriconda is fully submerged, which was the case during experimental measurements. An actual Fabriconda will actually be partially floating on the surface and bending in the vertical plane, potentially leading to distortions away from the symmetrical shape assumed in a similar fashion to that reported for floating cylindrical containers [6]. However the impact of this is likely to be small since changes in elevation along the device would be much less than the internal pressure head.

Measurements of the speed of bulge waves generated by an externally driven piston at one end of the tube show a good correlation with those predicted from numerical simulations, especially with respect to the propagation of the peaks in the strain gauge signals. These correspond to peaks in the half-vertex angle of the cell and correspondingly a trough in the bulge wave as the overall Fabriconda cross-section area reaches a minimum. The bulge speeds predicted by simulation in the tube pressure region investigated ranged from 1.47 ms^{-1} to 2.07 ms^{-1}. It is predicted that greater tube pressures should result in higher bulge speeds. Further experimentation is planned for these higher pressures.

5. Conclusion

This paper has introduced the concept of the Fabriconda, a distensible tube attenuating wave energy converter made from inelastic fabric. A theory for the static shape of the device has been presented along with experimental confirmation of its predictions. One-dimensional linear finite difference modelling suggests that the Fabriconda can be tuned to a wide range of different bulge speeds, and experimental results seem to confirm these predictions over a

limited pressure range. Future work will measure experimentally the propagation speed of a free bulge wave versus both tube and cell pressure at higher pressure combinations before numerical and experimental measurements are made of Fabriconda capture width and bandwidth.

References

[1] Chaplin, J.R., Farley, F.J.M., Prentice, M.E., Rainey, R.C.T., Rimmer, S.J., Roach, A.T. Development of the anaconda all-rubber WEC, Proceeding of the 7th European Wave and Tidal Energy Conference, Lisbon 2007

[2] Farley, F.J.M., Rainey, R.C.T. Anaconda - The bulge wave sea energy converter. Technical Note 5 Nov 2006, online www.bulgewave.com, 2006

[3] Farley, F.J.M. All fabric Anaconda . Marine Energy Devices Ltd. Confidential memo paper, 2008.

[4] Farley, F.J.M. Fabriconda design and power take-off. Marine Energy Devices Ltd. Confidential memo paper, 2008.

[5] Heller, V., Chaplin, J. R., Farley, F. J. M, Hann, M. R. and Hearn, G. E. Physical model tests of the anaconda wave energy converter. In*,* First European Congress of the IAHR*,* Edinburgh, Scotland 2010

[6] Hawthorne, W. The early development of the dracone flexible barge, Proceedings of the institution of mechanical engineers 175, 1961, pp 52-83

The WaveCat© – Development of a new Wave Energy Converter

Gregorio Iglesias[1,*], Hernán Fernández[1], Rodrigo Carballo[1], Alberte Castro[1], Francisco Taveira-Pinto[2]

[1]*University of Santiago de Compostela, Spain*
[2]*Faculty of Engineering, University of Porto, Portugal*
** Corresponding author. Tel: +34 982823650, Fax: +34 982285926, E-mail: gregorio.iglesias@usc.es*

Abstract: The development of efficient, reliable Wave Energy Converters (WECs) is a fundamental prerequisite for wave energy to become a commercially viable energy source. Intensive research is currently under way on various technologies, among which WaveCat©—a new WEC recently patented by the University of Santiago de Compostela. The purpose of this paper is to present the WaveCat concept and the ongoing work toward its development. WaveCat is a floating offshore WEC whose principle of operation is wave overtopping. It consists of two hulls, like a catamaran (hence its name). Unlike a catamaran, however, the hulls are not parallel but convergent—they are joined at the stern, forming a wedge in plan view. The methodology adopted to develop this patent is based on physical model tests which are described in the paper. A 1:30 model was tested in a wave tank under regular and irregular waves; waves and overtopping rates were measured, as were the model displacements—the latter using an advanced motion capture system. The data thus obtained will be used to validate a 3D numerical model currently under development, which in turn will be used to optimize the design of WaveCat for best performance.

Keywords: *Wave energy converter, Overtopping, Physical modelling, Numerical modelling, CFD.*

Nomenclature

α	*wedge angle* ..... [–]	T	*wave period (regular waves)* ..... *s*
H	*wave height (regular waves)* ..... *m*	T_p	*peak wave period (irreg. waves)* ..... *s*
H_s	*significant wave height (irreg. waves)* ..... *m*		

1. Introduction

In order to reduce the emissions of greenhouse gases it is crucial to work along two lines. The first is to develop the already operational renewable energy sources, such as wind or photovoltaic energy. The second is to research and develop new energy sources [1]. Among these, marine renewable energy has a great potential for development in Europe. The European Science Foundation estimates that "by 2050 Europe could source up to 50% of its electricity needs from Marine Renewable Energy" [2]. Although Marine Renewable Energy comprises many different energy sources (offshore wind, wave energy, tidal currents, ocean currents, salinity gradient, thermal gradient and marine biomass), those with the highest potential are arguably wave energy, offshore wind and tidal energy. Two main issues must be resolved, however, for wave energy to become a fully established, commercially viable energy source. First, the wave resource along the coastline must be assessed; it presents significant spatial and temporal variations (e.g. [1, 3-4]), as is the case of other renewables. Second, efficient, reliable and low-impact Energy Converters (WECs) must be developed. This paper deals with WaveCat, a recently patented WEC. Its objectives are: (i) to present the WaveCat concept; and (ii) to describe the methodology used for its development, centred around physical model tests conducted in a 3D wave tank.

2. The WaveCat concept

WaveCat is a floating WEC intended for offshore deployment (water depths of 50-100 m), which has the advantage of a higher wave energy potential relative to onshore or nearshore

locations (wave energy decreases as waves approach the shoreline). Another advantage of WaveCat is its low visual impact. The name WaveCat alludes to the fact that it is composed of two hulls, like a catamaran. Unlike a catamaran, however, these hulls are not parallel but convergent. The single-point mooring to a catenary-buoy allows the device to swing as the wave direction changes, thereby ensuring that the wedge opening always faces the waves (Figure 1). As waves propagate into the wedge, their height is enhanced by the convergence of the lateral boundaries (the hulls) until, eventually, they overtop the inner hull sides. Overtopping water is temporarily collected in on-deck tanks. The higher water level in these tanks relative to the sea level is taken advantage of to propel ultra-low head turbines as the water is drained back to sea. A fundamental issue in designing a WEC—especially an offshore WEC—is its survivability, i.e. its ability to sustain heavy storm conditions. The design of WaveCat includes a number of elements aimed at survivability, most notably the possibility of varying the angle formed by the hulls (hereafter referred to as wedge angle) between 120º and 0º according to the sea state. When a storm approaches, the angle is reduced to 0º, i.e. the wedge is closed, thereby transforming WaveCat into a monohull—similar to a conventional ship from the standpoint of seakeeping. Freeboard and draft are also variable: in the model they were varied by means of solid ballast; in the prototype, ballast tanks filled with water will be used (as in ships). The prototype hull length is 90 m.

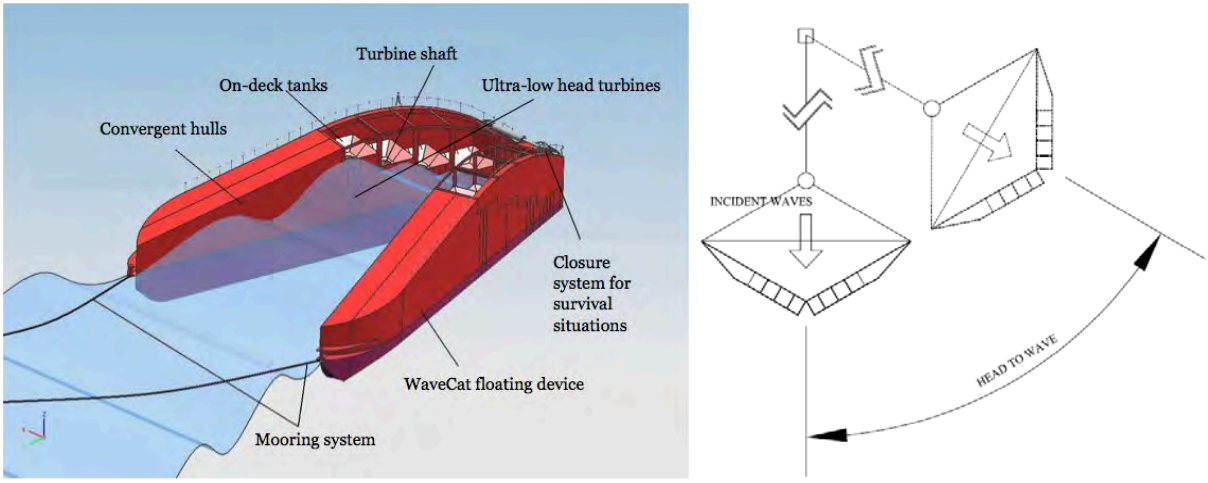

Fig. 1. The WaveCat concept (left) and a plan view of the single-point mooring system (right).

3. Methodology

The research and development of WaveCat combines physical and numerical modeling. So far, physical model tests in a wave tank have been completed. The methodology of these tests is the focus of this section (subsections 3.1 to 3.3). The numerical model, which is currently under development, is briefly presented in subsection 3.4.

3.1. Physical model

The 3D model, constructed of marine board, represented the WaveCat at a 1:30 scale (Figure 2). Tests were conducted at the wave tank of the University of Porto, with dimensions of 28 × 12 × 1.25 m; at its centre was a pit with dimensions of 4.5 × 2 × 1.5 m (Figure 3). The catenary-buoy mooring system was anchored at the front end of the pit (Figure 4). Wave generation was carried out with a directional (multielement) piston-type wavemaker. The experimental setup included six wave gauges aligned with the centreline of the tank, and four other on the model (one for each water tank). The quiescent water depth in the tank was set to 0.90 m (or 2.40 m in the central pit) for all tests.

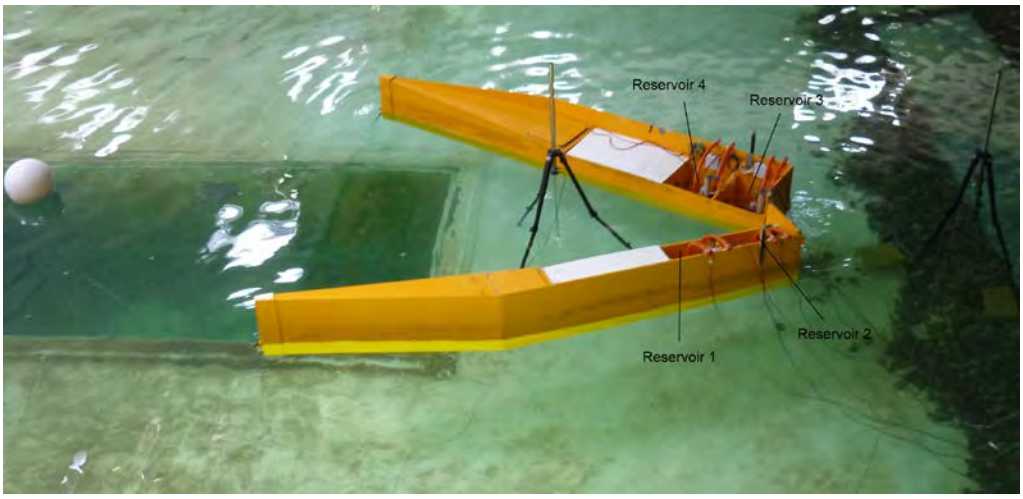

Fig. 2. The physical model in the wave tank with its four reservoirs for collecting overtopping water.

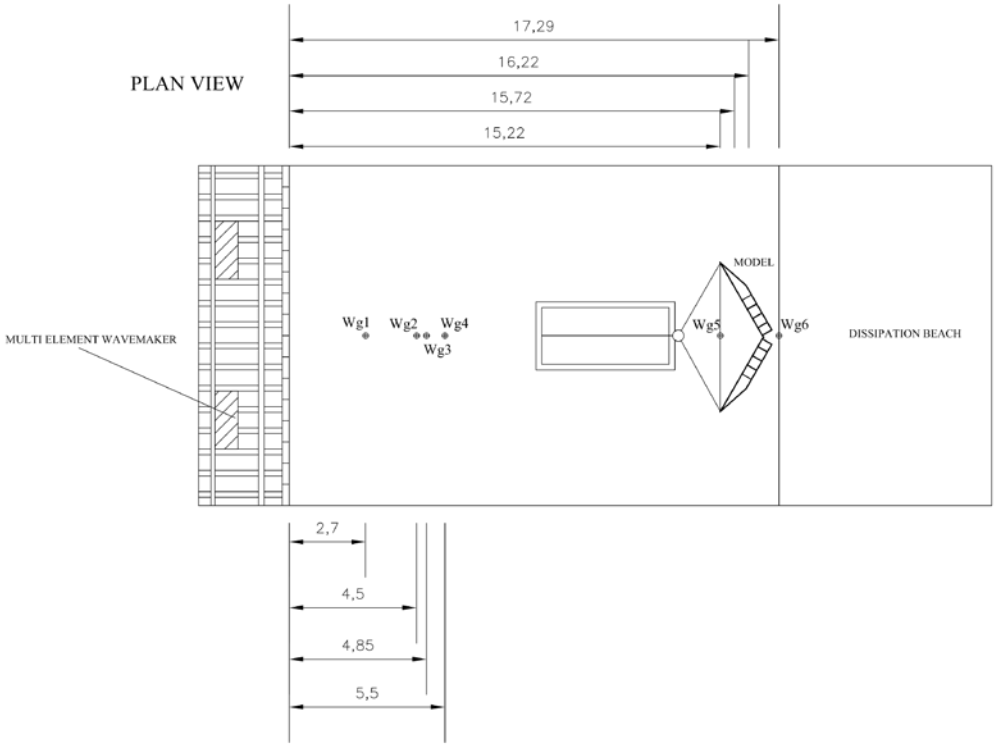

Fig. 3. Wave tank layout and experimental setup, showing the WaveCat model and the location of the wave gauges outside the model (Wg1 to Wg6). [Dimensions in *m*].

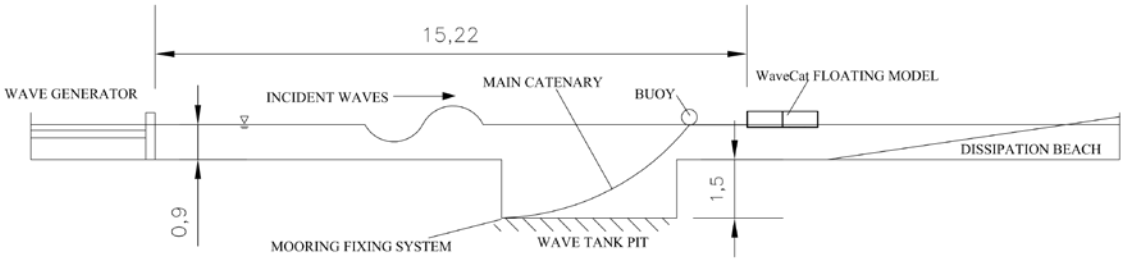

Fig. 4. Longitudinal section of the wave tank showing the model and the catenary-buoy mooring system. [Dimensions in *m*].

3.2. Experimental campaign

In total, the experimental campaign comprised 43 tests, 25 of which with regular waves and 18 with irregular waves. The wedge angle (α) was varied between four values: 30º, 45º, 60º and 90º. Three quiescent freeboard values (F_b) were used: 0.04 m, 0.09 m and 0.10 m. Regular waves were in the ranges H = 0.07 – 0.10 m and T = 1.65 – 2.20 s. Irregular waves varied in the ranges H_s = 0.067 – 0.100 m and T_p = 1.83 – 2.20 s. For illustration the parameters in some of the tests (the irregular wave tests with the lowest freeboard) are shown in Table 1.

Table 1. Parameters in the irregular wave tests with a quiescent freeboard F_b = 0.04 m.

Test case	α (°)	H_s (m)	T_p (s)
AA07_I3	60	0.083	2.013
AA07_I5	60	0.100	2.196
AB07_I3	90	0.083	2.013
AB07_I5	90	0.100	2.196
AD07_I3	45	0.083	2.013
AD07_I5	45	0.100	2.196
AE07_I3	30	0.083	2.013
AE07_I5	30	0.100	2.196

Each of the four water reservoirs (two per hull) in the WaveCat model is equipped with a pump and a control system (Figure 5). The control system operates based on the water level in the reservoir as measured by a capacitance-type gauge. The pump begins to function when the water reaches a certain (maximum) level, and stops when it has gone down to a minimum value. The water level in two reservoirs, #3 and 4, during the test AD07_I5 is shown in Figure 6; the intervals of pump operation correspond to the near vertical lines of the graph. A typical record of the free surface level during the same test is shown in Figure 7.

In the model, for simplicity, the pumps worked with a constant flowrate, and during (generally short) intervals of time. It is important to mention that this pumping system in the model is not intended to replicate the functioning of the turbines in the prototype, but merely to allow a longer test duration. Instead, the control system in the prototype will aim for continuous operation of the turbines, with the tanks acting as buffers to provide continuous outflow toward the turbines in spite of the discontinuous nature of the overtopping events. The outflow rate in the prototype will be set by its own control system so as to maintain the continuous turbine operation, taking into account the overtopping rate (which depends on the sea state) and the turbine-generator characteristics.

3.3. Measurement of model displacements

During the tests, the displacements of the model under wave action were recorded by means of a motion capture system consisting of three infrared video cameras, reflective elements on the model, a dedicated computer and *ad hoc* software. The cameras detected the positions of a number of small reflective spheres installed at different points on the model (Figure 8). Their motions were then converted by the system software into model displacements along the three coordinate axis (heave, surge, sway) and rotations around them (roll, pitch, yaw). For illustration, the pitch and roll of the model during test AD07_I5 are shown in Figure 9.

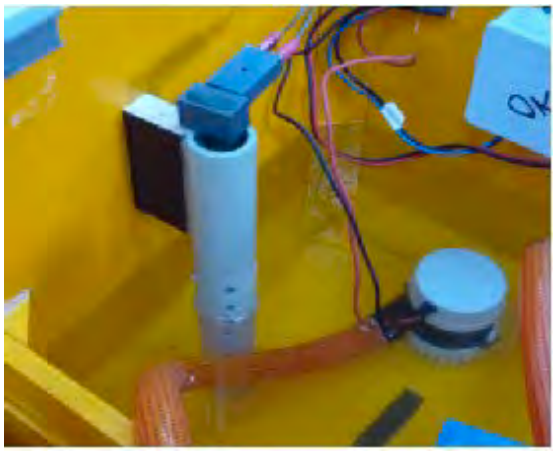

Fig. 5. Pump and control system in one of the water reservoirs of the model.

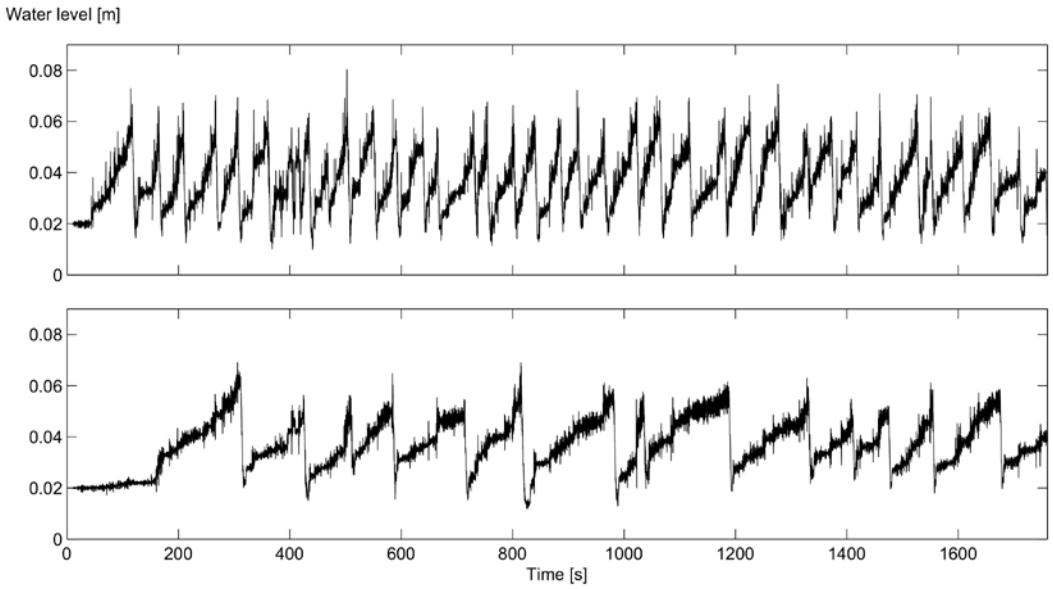

Fig. 6. Water level in reservoirs #3 (aft reservoir, above) and #4 (fore reservoir, below) during test AD07_I5. [Refer to Figure 3 for the location of the reservoirs in the model].

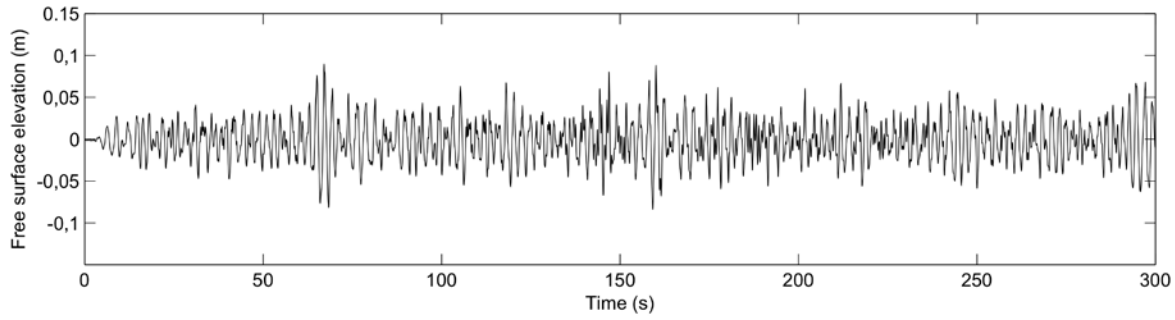

Fig. 7. Free surface elevation signal at the wave gauge in front of the model (Wg4) during test AD07_I5. [For clarity, only the first 5 min of the test are shown].

3.4. Numerical model

The development of a numerical model for WaveCat started with a 2D RANS-VOF model. This model was successfully validated using results from 2D physical model tests carried out

in the wave flume of the University of Santiago de Compostela. Currently a 3D numerical model is being implemented; the model solves the RANS (Reynolds-Averaged Navier-Stokes) equations with a volume-of-fluid approach, using a state-of-the-art parallel code (Star-CCM+). The model simulates the WaveCat response as a floating body interacting with waves. It is expected that this model will be validated in the (hopefully near) future based on the results of the physical model tests presented above. A preliminary image from a simulation is shown in Figure 10.

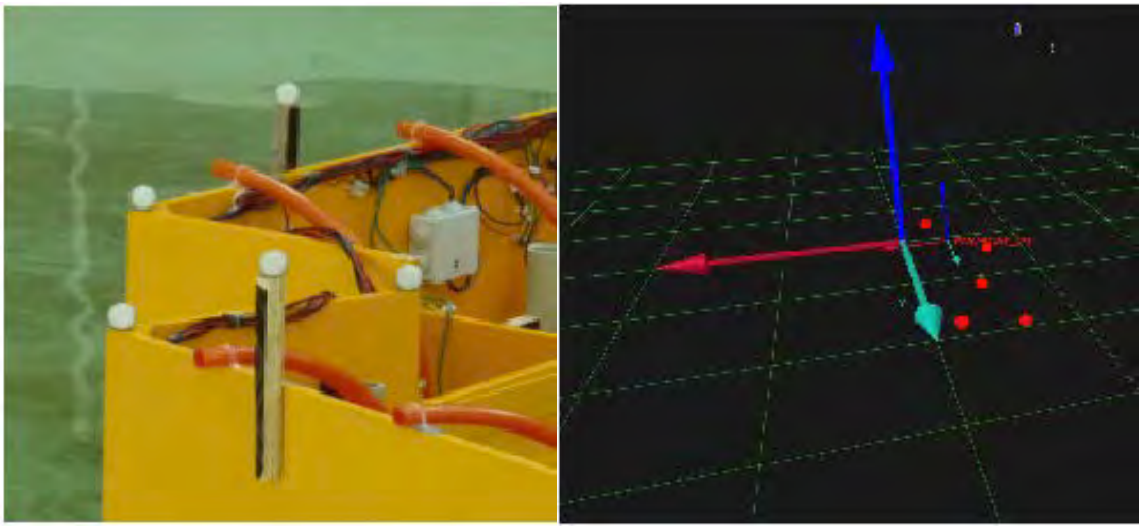

Fig. 8. White reflective spheres on the model (left) and detected by the motion capture system (right).

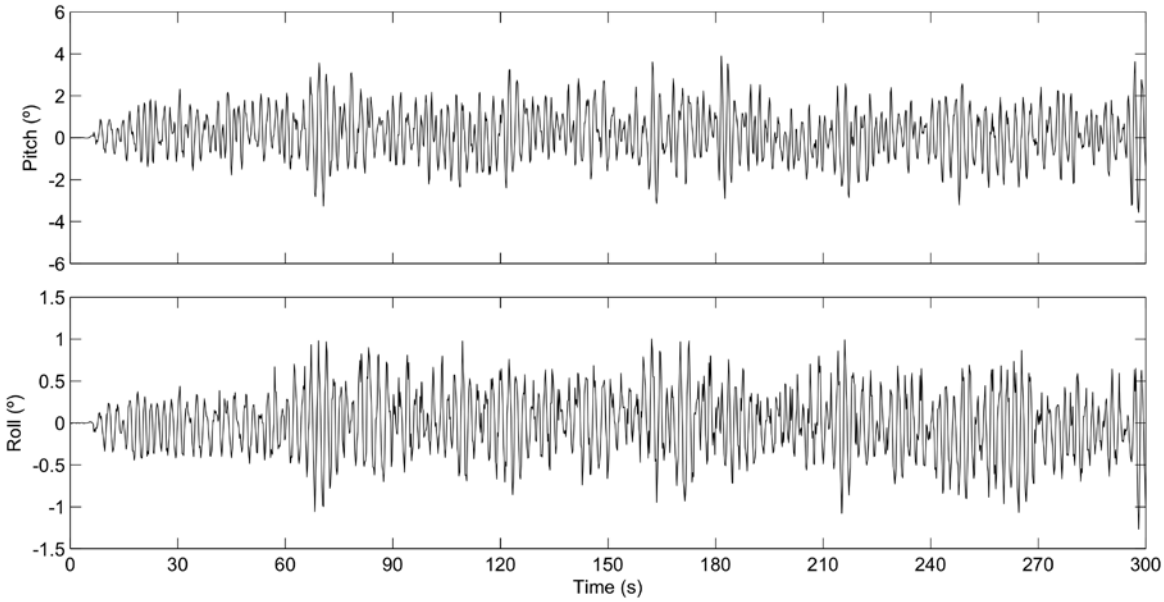

Fig. 9. Pitch and roll during test AD07_I5. [For clarity, only the first 5 min of the test are shown].

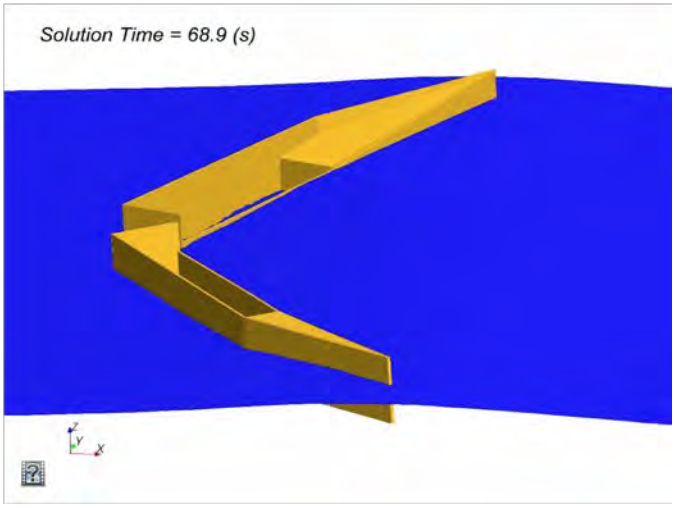

Fig. 10. One of the video frames of a simulation with the 3D numerical model under development.

4. Results and Discussion

The present paper presents the WaveCat, a recently patented WEC, and the ongoing work to develop it as a commercially viable system. A 1:30 model was constructed and tested in a large wave tank. In total 43 tests were carried out, both with regular and irregular waves. In addition to the wave parameters (wave height and period in the case of regular waves, significant wave height and peak period in the case of irregular waves), two fundamental model parameters were varied in the tests: wedge angle and freeboard. The motions of the model during the tests were measured by means of a motion capture system which included three infrared video cameras.

The results of the tests may be classified into three different levels or categories. First, on a conceptual level, the tests enabled to verify the WaveCat as a valid concept for wave energy conversion. The second level concerns the design of WaveCat and, in particular, of the water reservoirs. In the tested model the two reservoirs in each hull have the same volume and occupy the same length along the hull side. In Figure 6 it is apparent that the aft reservoir (#3) experiences significantly heavier overtopping than the fore reservoir (#4) during test AD07_I5. This imbalance was consistently observed throughout the experimental campaign, the aft reservoir collecting larger volumes of water than the fore reservoir. If the turbine-generator configuration in the prototype is the same for both reservoirs, this consistent difference in overtopping rates is clearly suboptimal. One method to overcome this problem is to increase the volume of the fore reservoir by extending its length along the hull side at the expense of the aft reservoir, to the extent necessary to balance the overtopping rates. The other is to maintain the same volume and length along the hull side for both reservoirs, as in the tested model, but to use different turbine-generator configurations in the prototype—the aft reservoir would have a turbine-generator with greater rated power than the fore reservoir, in accordance with its larger overtopping rate. Although the first option would appear to be more attractive, no definitive decision has been taken so far. Finally, the third level of results comprises the time series of overtopping rates and model displacements and rotations gathered during the tests, which will be used to validate the 3D numerical model currently under development. Once validated, the model will be used to optimize the design of WaveCat for best efficiency under a given set of wave conditions, which will be chosen according to the wave climate of the deployment area. Thus, the physical model tests presented in this paper are a crucial step in the development process of this new WEC.

The WaveCat concept (Section 2) presents four main advantages with respect to other WECs. In the first place, its design with two converging hulls and, in particular, the fact that the angle between them can be varied according to the sea state constitute a significant asset for survivability; in effect, under extreme (storm) conditions the wedge can be closed, thereby transforming WaveCat into a monohull vessel. In the full size WaveCat, a "locking system" will be provided to keep both hulls together during a storm without creating excessive stresses on the bow hinge. The freeboard on the outer hull sides is considerably larger than that on the inner hull sides. With no waves overtopping the inner hull sides, the survivability of WaveCat is greatly enhanced. The second advantage of the WaveCat design is that the wedge angle can be varied during normal operation to optimize the efficiency—the smaller the waves, the larger the wedge angle. Third, the moving parts activated by the waves are only the turbine-generators; there are no complex joints moving with the passage of each wave, as is the case of other WECs. This may be expected to result in better reliability—and reliability is a key aspect of economic viability. Finally, the water tanks are placed along the hulls, rather than at the back of the wedge; therefore, the motions of WaveCat in waves may be expected to affect the overtopping rate less, merely causing a displacement along the hull of the point where overtopping begins. If the wave tanks along the hulls were substituted by a single tank at the back of the wedge, the motions of the WEC—in particular, its heave—could significantly reduce the overtopping rates under resonant conditions.

5. Conclusions

The development of a new Wave Energy Converter is a long process. At the current stage of development of WaveCat, wave tank tests of a 1:30 model were successfully completed, with an experimental setup that included an advanced motion capture system. With these physical model tests, involving many different sea states and model configurations (different wedge angles and freeboards), the WaveCat concept as a wave energy conversion system was verified. A second conclusion refers to the design of the water reservoirs. In view of the consistent imbalance in overtopping rates that was found during the experimental campaign there are two main options. Either the design of the tested model is kept in the prototype, in which case the turbine-generator configuration in the aft reservoirs must be different from that in the fore reservoirs (with greater rated power in the aft reservoirs), or the volume of the fore reservoir is increased at the expense of the aft reservoir, in which case the same turbine-generator configuration can then be used for both reservoirs. Finally, the data on model motions (displacements and rotations) and overtopping rates obtained in the experimental campaign presented in this paper will be the basis on which the 3D numerical model currently under development will be validated. This model will enable to optimize the design of WaveCat for best performance under specified wave conditions. Upon optimization, the next step will be the construction of a full-size demonstrator and its sea trial.

References

[1] G. Iglesias, M. López, R. Carballo, A. Castro, J.A. Fraguela, P. Frigaard, Wave energy potential in Galicia (NW Spain), Renewable Energy 34, 2009, pp. 2323-2333.

[2] European Science Foundation, Marine Board Vision Document 2, 2010.

[3] G. Iglesias, R. Carballo, Wave energy potential along the Death Coast (Spain), Energy 34, 2009, pp. 1963-1975.

[4] G. Iglesias, R. Carballo, Wave energy resource in the Estaca de Bares area (Spain), Renewable Energy 35, 2010, pp. 1574-1584.

Extreme Loads on the Mooring Lines and Survivability Mode for the Wave Dragon Wave Energy Converter

S. Parmeggiani[1,*], J. P. Kofoed[2], E. Friis-Madsen[3]

[1] *Wave Dragon Ltd., London, United Kingdom*
[2] *Aalborg University, Aalborg, Denmark*
[3] *Wave Dragon Aps, Copenhagen, Denmark*
** Corresponding author. E-mail: stefano@wavedragon.net*

Abstract: One of the main challenges Wave Energy Converters have to face on the road towards commercialization is to ensure survivability in extreme condition at a reasonable capital costs. For a floating device like the Wave Dragon, a reliable mooring system is essential. The control strategy of the Wave Dragon aims at optimizing the power production by adapting the floating level to the incoming waves and by activating the hydro-turbines and regulating their working speed. In extreme conditions though, the control strategy could be changed in order to reduce the forces in the mooring system, lowering the design requirements with almost no added cost. The paper presents the result of the tank testing of a 1:51.8 scale model of a North Sea Wave Dragon in extreme wave conditions of up to 100 years of return period. The results show that the extreme loads in the main mooring line can be reduced by approximately 20-30% by lowering the crest level and balancing the device to lean a little towards the front.

Keywords: *Wave Dragon, Wave Energy Converter, Survivability, Mooring system, Control strategy*

1. Introduction

Wave Energy Converters (WECs) have to withstand extreme events that put very high standards on their design requirements, increasing capital costs. From an economical point of view, such expenditure can be justified only by high performance in the often mild operational conditions where these devices operate for the main part of their lifetimes. One of the challenges the industry has to face in this early phase to help commercialization is therefore to jointly reduce the capital expenditures due to the survivability in extreme conditions and increase the performance in operational conditions. An efficient control strategy can help to meet both requirements with very low added cost.

1.1. The Wave Dragon WEC – Mooring system and control strategy

The Wave Dragon (WD) is a floating, slack-moored WEC of the overtopping type. Incoming waves are focused by two wing reflectors towards a ramp where they surge up and overtop into a reservoir placed at a higher level than the Mean Water Level (MWL). Energy is extracted as the stored water is led back to the sea through a set of low head hydro-turbines.

For an off-shore floating device like the WD the mooring system represents one of the main components ensuring the survivability. The mooring system of the WD consists of slack mooring chains of equal length distributed in circular spread, see Fig. 1. These are connected to a Catenary Anchor Leg Mooring (CALM) buoy, which again is connected to the WD platform and wings. An additional single mooring line can be connected to the rear of the platform to limit the excursions of the device.

The control strategy of the WD has three components: in a time scale of hours, the first one is aimed at optimizing the floating level of the device according to the incoming wave height in order to maximize the overtopping flow; in the time scale of minutes, the second one is the on/off regulation of the propeller turbines, which ensures a high storage efficiency of the

reservoir; finally, in the time scale of seconds, the third one is the speed control of the turbines to ensure a constant high efficiency of the turbine-generators.

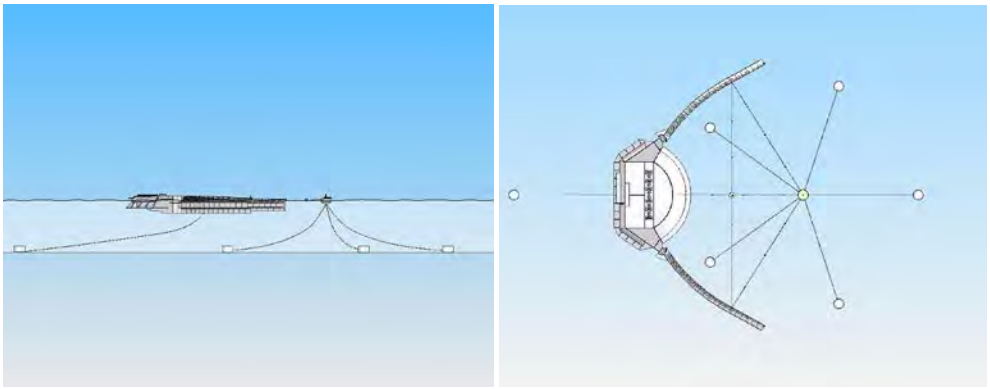

Fig. 1. Conceptual mooring system of the Wave Dragon WEC.

In extreme conditions the goal of the control strategy should no longer be to optimize the performance, but to limit the forces in the mooring system and in the structure in general. In this sense by keeping the floating level low the forces in the mooring line connecting the device to the CALM buoy, also called the main mooring line, can be decreased. This kind of control, which is hereafter referred to as the *survivability mode* of the WD, can help reducing the design requirements on the mooring system.

The paper presents the results of an experimental investigation conducted on the 1:51.8 scale model of a North Sea WD to assess the efficiency of the mentioned control strategy. Different wave and setup conditions have been tested and their influences on the forces in the main mooring line and on the dynamic response of the device have been established.

In the following the tests and data analysis procedure used are presented. From the results the efficiency of the survivability mode is assessed and important considerations regarding the stability of the device are drawn. Finally, the main conclusions and future work required are presented.

2. Method

The study has been conducted through the wave tank testing of a scale model of the WD at the deep water basin of the Hydraulic and Coastal Laboratories of Aalborg University during October 2010.

2.1. Test setup

The model tested is at 1:51.8 length scale of a North Sea WD, which has a rated power of 4 MW in a wave climate of 24 kW/m. The proposed mooring system was schematically reproduced, connecting the model to an anchor at the front through the main mooring line, the stiffness of which was modeled by means of a spring to deliver the horizontal compliance. Two mooring lines at the back have been used with the only purpose of keeping the device in position.

The forces in the main mooring line (F), as well as the movements of the device in surge (S), heave (H) and pitch (P), have been recorded during the tests.

2.2. Tested conditions

The wave states considered are extreme waves with return period of 10, 50 and 100 years typical of the Danish part of the North Sea. The number of wave states tested has been increased by considering for each of them three different values of peak wave steepness $S_p = H_s/L_p$ (-), being H_s (m) the significant wave height and L_p (m) the peak wave length. All waves have been generated as irregular according to a JONSWAP spectrum with peak enhancement factor 3.3. The water depth considered corresponds to 33.7 m in full scale.

The influence of the height of the crest freeboard above the mean water level (R_c) and of the directionality of the waves, expressed through the *s* parameter of the Cos^{2s} spreading function, have been investigated leading to a total of 42 tests. The values of the parameters considered in the study are resumed in Table 1, where the wave states are described by their H_s and peak period T_p.

Table 1. Summary of the parameters considered in the study (values are given in full scale).

Parameter name	Description	Values
T_{r10}	Wave with return period of 10 years	H_s = 8 m, T_p = 13.1 s
T_{r50}	Wave with return period of 50 years	H_s = 9 m, T_p = 13.8 s
T_{r100}	Wave with return period of 100 years	H_s = 10 m, T_p = 14.5 s
S_p (-)	Peak wave steepness	S_{p0}: standard wave state S_{p+1}: *Hs* increase of 0.5 m S_{p-1} = *Tp* increase of 1 s
s (-)	Spreading coefficient	s_1 = 20 (2D waves) s_2 = 2 (3D waves) s_3 = 10 (mildly 3D waves)
R_c (m)	Crest level above MWL	R_{c1} = 4 m R_{c2} = 3 m R_{c3} = 2 m R_{c4} = 1 m

2.3. Floating stability

During the tests it has been observed that the model had a natural tendency to trim backwards. This behavior was found to affect the recorded forces too, as the less stable the device was, the higher were the forces. Its influence was found to be comparable to the one due to the R_c modifications and was therefore also investigated. Following this, some modifications to the model lead to consider one setup with high stability for each R_c, as the floating level was well maintained horizontally in average, and one with low stability.

2.4. Data analysis

For both forces and movements the extreme values are estimated as the average of the $1/250^{\text{th}}$ of the highest values recorded for each time series, denoted $X_{1/250,}$ X being the variable considered. Other statistical values such as the mean value X_m and standard deviation X_{stdev} have been used in the data analysis. As these quantities have been evaluated on records of 30 min, corresponding in average to 1000 waves, their reliability is considered good.

In each of the cases tested the R_c has been derived from the mean heave by applying a vertical offset according to the model geometry. The waves have been recorded by a 2D rig of 7 wave gauges. The analysis of the wave records allowed to separate the incident and reflected components according to the Mansard–Funke method. The first one has been the only considered in the data analysis, characterized by the values of H_s, T_p and s.

3. Results

In the following the most significant results of the tests are shown in a non-dimensional form. The extreme forces are presented as

$$F_{nd} = \frac{F_{1/250}}{\rho \cdot g \cdot H_{m0} \cdot A_c}(-) \qquad (1)$$

where H_{m0} (m) is the significant wave height derived from the frequency domain analysis and A_c (m^2) is the cross sectional area of the ramp of the WD, calculated as the product of average ramp width and total height (from crest to draft).

The non-dimensional heave and surge are calculated respectively as $H_{nd} = H_{1/250}/H_{m0}$ (-) and $S_{nd} = S_{1/250}/H_{m0}$ (-), while the pitch is directly considered as $P_{1/250}$ (deg).
In order to consider both the dependency on R_c and on L_p the independent variable chosen is the non-dimensional product of $S_p \cdot R = R_c/L_p$ (-). $R = R_c/H_s$ (-) is the non-dimensional crest level, a parameter usually considered when dealing with overtopping.

The reference system has been chosen so that displacements in surge are positive in the direction of the wave propagation, those in heave upwards and the rotations in pitch as they lower the back of the device.

The R_c tested have been grouped in High (R_{c1}, R_{c2}), Mid (R_{c3}) and Low (R_{c4}). As for both High and Low R_c no significant difference was observed in the results between low and high stability, all the tests have been grouped into a total of 4 dataset for the data analysis: High R_c, Mid R_c-low stability, Mid R_c-high stability and Low R_c.

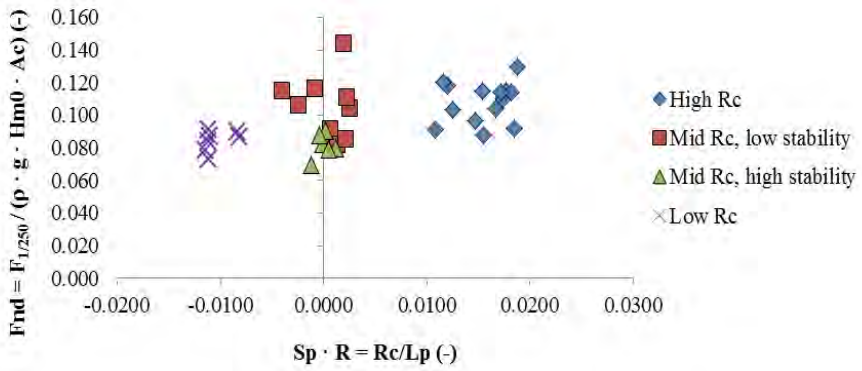

Fig. 2. Non-dimensional extreme forces in the main mooring line for 2D waves (s_1).

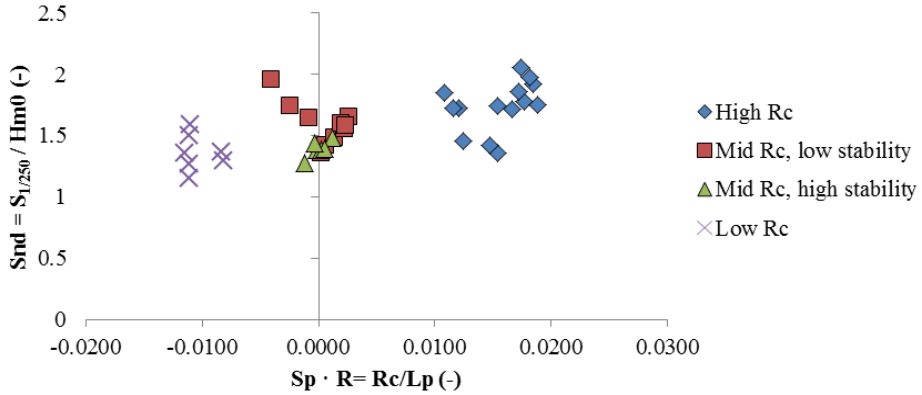

Fig. 3. Non dimensional extreme response in surge for 2D waves (s_1).

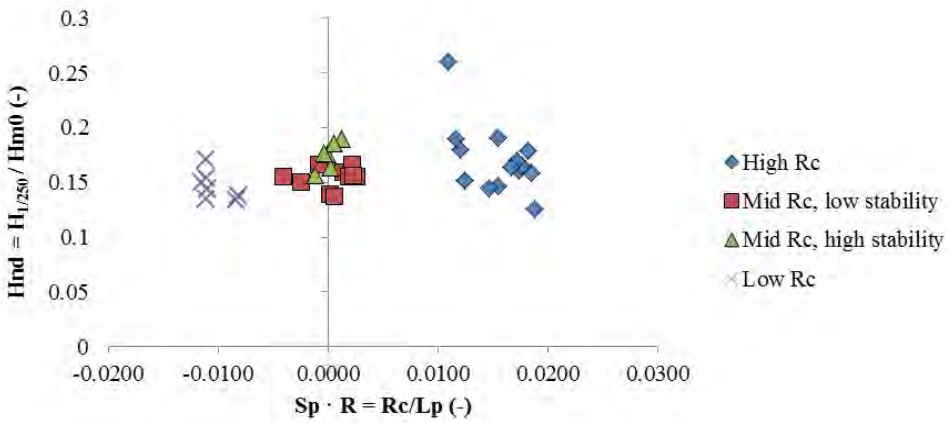

Fig. 4. Non dimensional extreme response in heave for 2D waves (s_1).

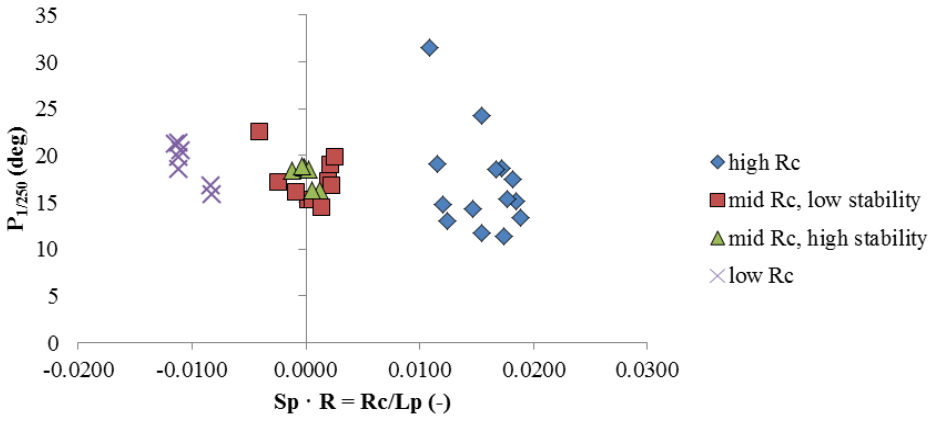

Fig. 5. Extreme response in pitch (deg) for 2D waves (s_1).

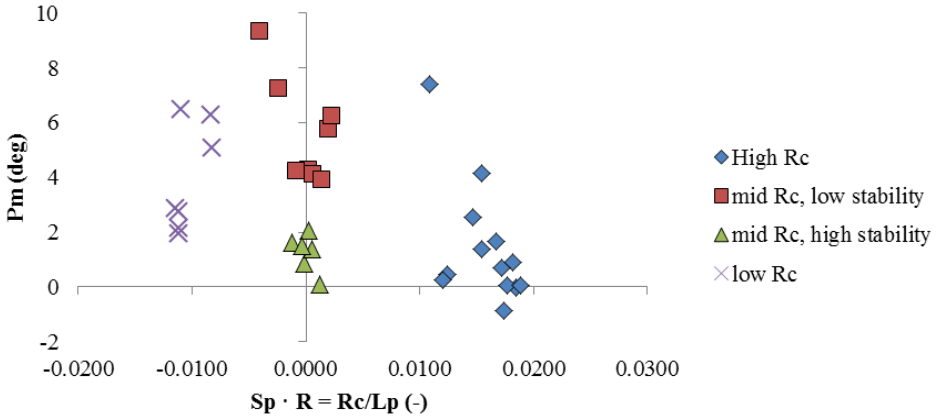

Fig. 6. Mean pitch position, or trim (deg) for 2D waves (s_1).

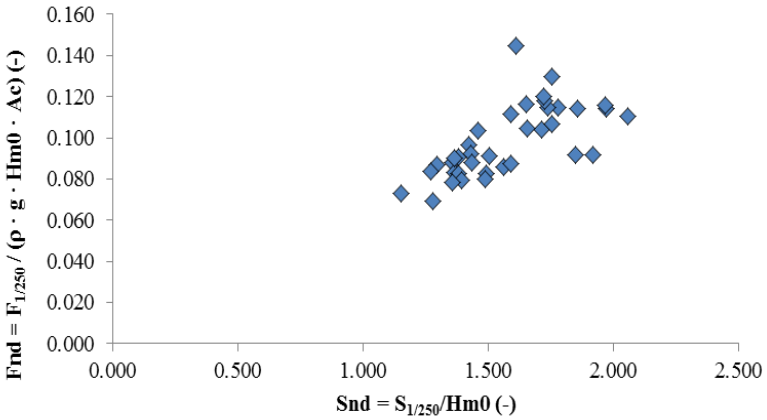

Fig. 7. Direct proportionality between non-dimensional extreme response in surge and non-dimensional extreme forces in the main mooring line, for 2D waves (s_1).

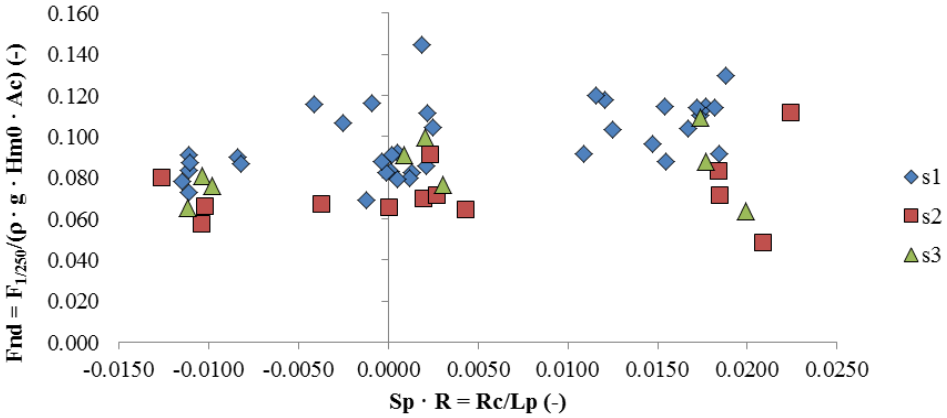

Fig. 8. Difference in the non-dimensional extreme forces in the main mooring line due to variation in the wave directionality.

4. Discussion

Fig. 2 shows two very important facts. First of all the forces in the main mooring line are reduced at lower crest levels, confirming the assumption behind the proposed survivability mode. This gets to the point where it could be considered to lower the crest level even down to negative mean values, which would not make sense in terms of power production, highlighting once more how the control strategy differs switching from operational to extreme conditions.

The floating of the device at negative values of the R_c can be explained by considering the hydrodynamics of the model during the tests: at very low floating levels the waves are completely overpassing the model, which determines a negative mean value R_c over the test duration. Nonetheless the buoyancy of the model is still higher than its weight. Therefore as the waves stop, the R_c is raised up again to the target (positive) floating level.

Fig. 2 also shows how the mooring forces are highly influenced by the floating stability. The forces in the Mid R_c dataset is are fact in the order of the ones recorded at High R_c when the stability of the device is low, while they become comparable to the ones recorded at Low R_c as the stability is increased.

Fig. 6 shows how this behavior can be well described in terms of mean pitch, the mean position around which the device oscillates, also known as trim. Focusing on the Mid R_c dataset, at low stability the values of P_m are much larger than at high stability. When the mean pitch increase, the device is tilted backwards and it also increases the surface against which the waves can exert pressure on the lower part of the device; as P_m approaches zero instead (or even as it becomes negative) proportionally more waves are hitting the ramp and as they surge it up the forces on the structure are reduced.

From a comparison of Fig. 2 and Fig. 3 it can be seen how the extreme forces in the main mooring line follow very much the extreme response in surge. This is confirmed also in Fig. 7, where a direct proportionality between the extreme response in surge and extreme forces can be seen.

The extreme response in heave (Fig. 4) is quite constant and independent on the R_c, while the pitch shows a tendency to increase within each dataset as the R_c lowered (Fig. 5).

Fig. 8 shows how the directionality of the waves has a significant influence on the forces. In all the cases tested the forces are reduced as the waves become 3D, due to the balancing of the components with opposite directions of the forces exerted by the waves on the device, which are not transmitted to the mooring system.

5. Conclusions and further work

The efficiency of the proposed survivability mode is assessed. As the floating level is lowered the extreme forces in the main mooring line can be reduced in the order of 20-30%.
For the Wave Dragon this can be achieved simply by emptying the air chambers as a storm is foreseen. With no further control this condition can maintained even in the case of loss of the grid connection: a “fool-proof” passive system ensuring a high survivability.

The pitch stability of the device also plays an important role in the determination of the mooring forces, especially at intermediate R_c. In this study the stability has been described in

average, by considering the mean value of the pitch. A reduction in this reduces the extreme forces recorded. Nevertheless it is here suggested that a more sensible parameter, possibly able to describe also the instant stability of the device, is found and used for further analysis of this behavior.

Acknowledgement

The first author acknowledges the support from the FP7 Marie Curie Actions of the European Commission, via the Initial Training Network wavetrain2 (contract-Nº MCITN-215414).

References

[1] J. P. Kofoed, P. Frigaard, Development of Wave Energy Devices: the Danish case, Journal of Ocean Technology, Vol. 4, No 2, 2009.

[2] NIRAS, Wave Dragon 1:4.5: up-scaling of mooring system, EU contract ENK5-CT-2002-00603, Work package 2.6, deliverable 33, 36& 43, September 2006.

[3] J. Tedd et al., Model Testing of Forces in the Reflector Joint and Mooring Forces on Wave Dragon, DCE Technical Report No. 27, Aalborg University, Department of Civil Engineering, 2005.

[4] T. Hald, J. Lynggaard, Hydraulic Model Tests on Modified Wave Dragon, Technical Report, Project No. ENS-51191/00-0067, Aalborg University, Department of Civil Engineering, 2001.

[5] J. W. Kamphuis, Introduction to coastal engineering and management, World Scientific, Advanced series on Ocean Engineering, Volume 16, 2000

Design of a 100 GWh wave energy plant

Jayashankar.V[1,*], Mala.K[1], Kedarnath.S[1], Jayaraj.J[1], Omezhilan.U[2], Krishna.V[1]

[1] *IIT Madras, Chennai, India*
[2] *Kings College of Engg., Pudukottai, India*
** Corresponding author. Tel: +91-44-22574427, Fax: +914422574427, E-mail:jshankar@ee.iitm.ac.in*

Abstract: The near shore Oscillating Water Column (OWC) based wave energy plant shows enormous promise for the commercialization of wave energy. The design details of such a plant, with an average incident energy of 24 kW/m and capable of producing 100 GWh over a two year period are described. The caisson, which could be a part of a breakwater, is constructed in a modular fashion in widths of 20 m. The power module is built around a 4.5 m diameter twin unidirectional impulse turbine with a rating of 900 kW. A key feature of the design is to combine the output from several OWCs into a single power module. Simulations show that the efficiency of the turbine can exceed 60 % from 10 to 100 % of the rated power. It is shown that a breakwater length of about 660 m with 11 such turbine generators is sufficient to meet the design requirement, with an overall wave to wire efficiency of about 36 %. The power electronics interface to the grid could be implemented with doubly fed induction generators or variable speed synchronous generators directly obtainable from the wind power industry. Laboratory experiments on a model turbine are used to validate the main claims.

Keywords: *OWC, twin unidirectional turbine topology, doubly fed induction machine*

Nomenclature

C_a	*input coefficient*	*DP*	*differential pressure*..... *Pa*
C_t	*torque coefficient*	*J*	*moment of inertia* .....kgm^2
phi	*flow coefficient*	*T*	*torque* .....*Nm*
η	*efficiency*	*w*	*angular velocity*..... $rad \cdot s^{-1}$
		Q	*volumetric flow rate*.....$m^3 \cdot s^{-1}$

1. Introduction

The Oscillating Water Column (OWC) based wave energy plant is probably the most researched approach in the conversion of wave energy to electrical energy. Several documented demonstration plants around the world, in places such as Japan [1], India [2], UK [3] and Portugal [4], attest to the allure of the concept. In this approach, the energy conversion occurs in three steps. The variations in sea surface elevation (ocean waves) are converted to pressure fluctuations in the OWC. A turbine converts this pneumatic power into mechanical shaft power and an electrical generator coupled to the turbine gives electrical power. The overall efficiency of the conversion from wave to wire is given by

$$\eta = \eta_a * \eta_t * \eta_g \qquad (1)$$

where η_a is the efficiency of the OWC
η_t is the efficiency of the turbine, and
η_g is the efficiency of the generator

The hydro dynamic efficiency of the plant can exceed 60% as reported in [1]. Table1 shows a summary of the reported experience with the OWC based wave energy plants mentioned above. The two different configurations of the Indian wave energy plant are shown in Fig. 1. The vertical axis 2 m Wells turbine power module is shown in Fig. 1a, while Fig. 1b shows the horizontal axis twin 1 m Wells turbine power module.

Table 1. Design details and performance of OWC plants

Plant	OWC effective area (dimension)	η_{OWC}	Power module		Comment
			Turbine	Generator	
Sakata port	115 m^2 (6 x 20)	> 60%	Twin 1.337m Wells'	60 kW 1800 - 2000 rpm	Variable speed
Vizhinjam	67.5 m^2 (6.75 x 10)	> 60%	2 m Wells	110 kW 1000 rpm	Fixed speed
Pico	144 m^2 (12 x 12)	> 50%	2.3 m Wells	440 kW 750 - 1500 rpm	Variable speed
LIMPET	126m^2 6x 21	> 60%	2.6 m Wells	2 x 250 kW 1050 rpm	Fixed speed

Fig. 1a. The Indian wave energy plant, 1991

Fig. 2b. The Indian wave energy plant, 1996

A recent study by the Carbon Trust [5] also describes the features of possible designs of near shore OWC plants. A generic OWC is assumed to perform with hydrodynamic efficiency of 42 %, utilizing a turbine operating with 65 % efficiency and a generator having 91 % efficiency, yielding an overall efficiency (wave to wire) of 24.8 %. In this work we consider the design of a plant which could yield a wave to wire efficiency of 36 % based on a new power module design. The proposed design satisfies the requirement for a plant producing 100 GWh over a two year period [6].

2. The twin unidirectional impulse turbine topology

An impulse turbine for use with unidirectional flow was proposed in [7]. The characteristics of the turbine under steady flow are shown in Fig. 2. The efficiency of the turbine is also illustrated in Fig. 2. It is seen that the turbine is capable of operating with efficiency better than 60%, for flow coefficients ranging from 0.317 to 0.948. A new power module incorporating two such turbines was proposed in [8] and the experimental results were shown in [9]. Conceptually, the topology uses two unidirectional turbines in conjunction with fluidic diodes as shown in Fig. 3. The fluidic diode assists in ensuring unidirectional airflow across the turbines, allowing only negligible flow in the reverse direction. The guide vane/ rotor blade profile also provides a significant contribution towards the higher impedance in the reverse direction. A consequence of this fact is the high efficiency in each cycle.

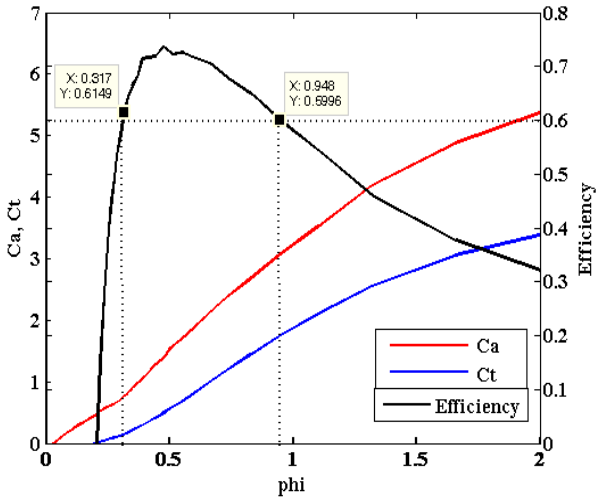

Fig. 2. Characteristics of unidirectional impulse turbine

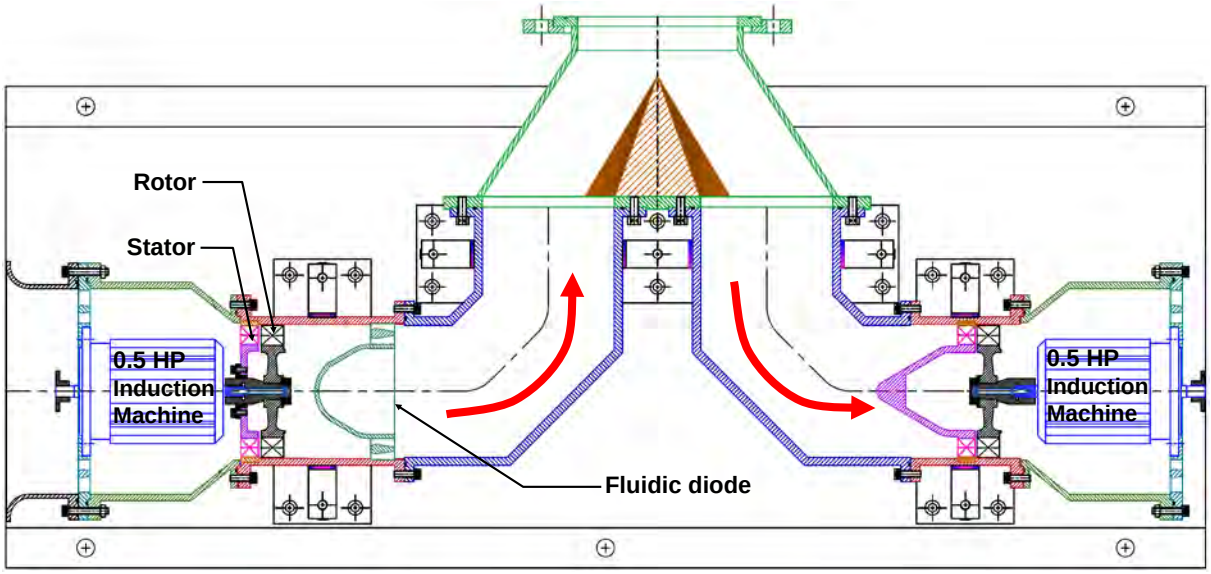

Fig. 3. Sectional view of the laboratory model of twin unidirectional turbine topology

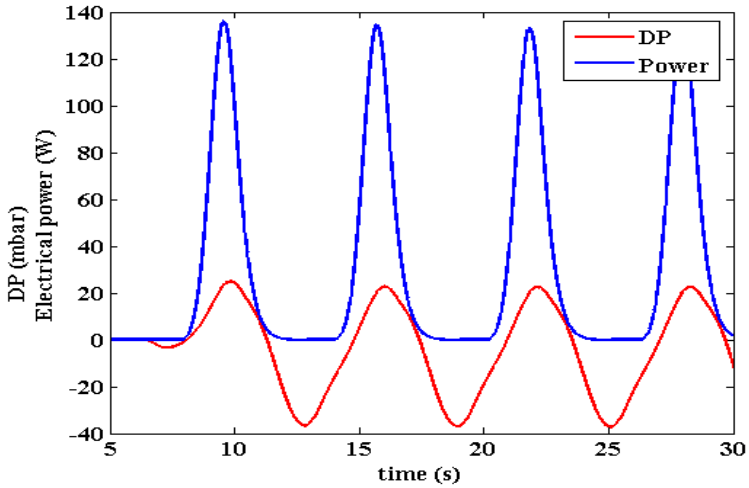

Fig. 4 . Measured parameters of single 165 mm turbine, coupled to a 375 W dc generator

The laboratory results on a 165 mm turbine with induction generator [9] showed that the concept was valid. In order to characterize the forward and reverse flow characteristic of the unidirectional turbine, an experiment was performed with a single turbine subjected to oscillating flow in a facility described in [9]. The turbine was coupled to a 180 V, 375 W, 3000 rpm dc generator with a fixed resistive load. As seen in Fig. 4, the positive stroke produces a power of 135 W with a differential pressure of 2.2 kPa. In the reverse flow the differential pressure is 3.7 kPa, thus clearly highlighting the differing impedances. In this experiment the generator was. A further realisation was the notion that the unidirectional turbine topology permits the summing of pneumatic outputs from different OWCs with a single turbine of a large diameter.

3. Design of a power module for a 20 m OWC

The incident yearly wave power input is assumed to be 24 kW/m. Thus the average wave power for an OWC with 20 m opening is 480 kW. With an OWC efficiency of 0.6, the average pneumatic power is 288 kW. This would give an average mechanical output of 184.3 kW with 64% turbine efficiency with turbine diameter of 2.6 m. Assuming that the plant should have the capability to withstand incident wave energy as high as 40 kW/m occasionally, the mechanical output will be 307 kW. With three OWCs feeding a single turbine the rating is 922 kW. The turbine diameter is now 4.5 m. It may be remembered that the average mechanical output of this combination would be 553 kW, corresponding to 24 kW/m of incident wave power.

We now consider the simulation of a turbine of diameter 4.5m when connected to an induction generator. Fig. 5 shows the basic block diagram of the simulation and has been extensively described and validated in [10]. The input to the program is the differential pressure time series obtained from a typical recording in the Indian wave energy plant. The record is scaled in order to cater to the overall range that will be encountered in the proposed design.

The program evaluates the expression

$$J\frac{dw}{dt} = T_t - T_g - T_l \qquad (2)$$

where J is the moment of inertia of the system
T_t and T_g are the turbine and generator torques
T_l is the term accounting for losses

The operation of the power module is highlighted in Fig.6, which illustrates the time variation of the relevant parameters of the power module. The differential pressure (DP) across the turbine, the pneumatic power (P_a), the mechanical power (P_m) and the flow coefficient (Phi), are all illustrated in Fig.6. In this run of 8 minutes, the average mechanical power from the turbine was approximately 500 kW which is close to the yearly average power. It may also be noted that the peak mechanical power obtained was around 3.4 MW, which is very similar to the power ratings in wind energy industry as well. By allowing summation of the pneumatic outputs of multiple OWCs with a larger diameter turbine, the twin turbine topology reaches power ratings similar to those seen in the wind power industry. This would enable the direct utilization of wind power modules in OWC based wave energy plants as well.

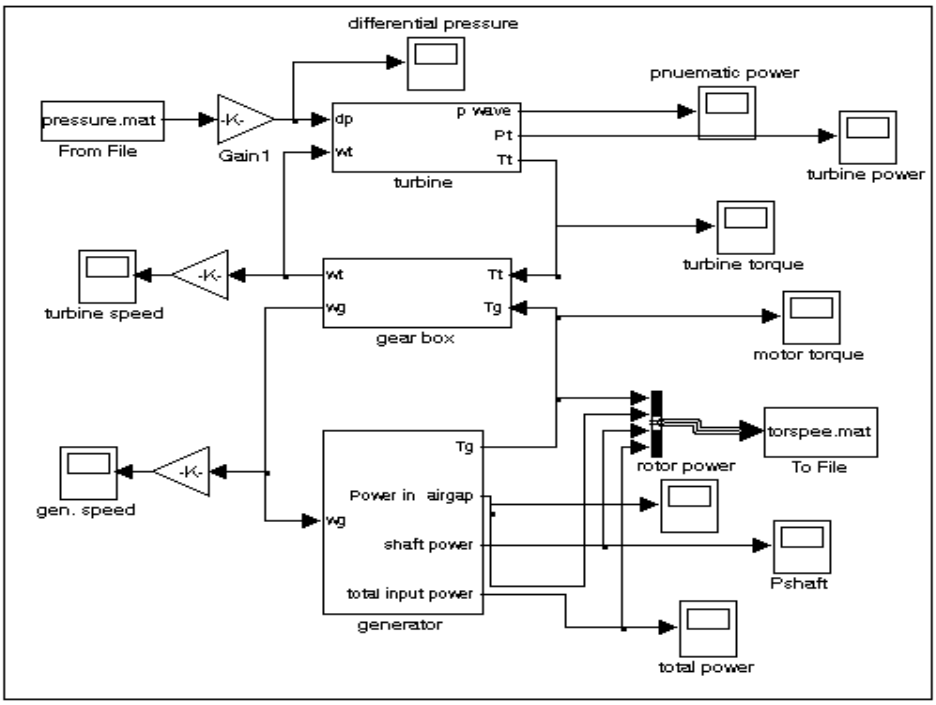

Fig. 5. Block diagram of simulation of 4.5 m diameter turbine coupled to an induction generator

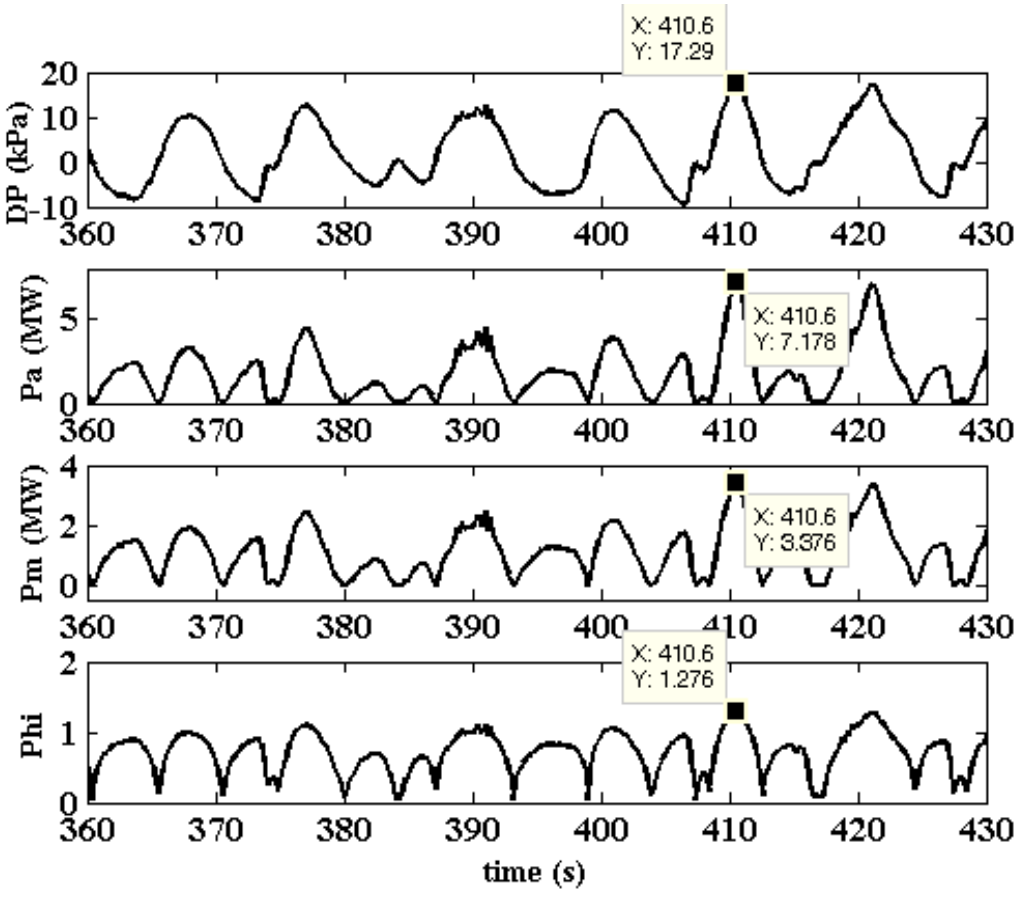

Fig. 6. Simulated plots highlighting the operation of 4.5 m, 200 rpm turbine

The simulation is repeated for several values of pneumatic incident energy. Fig. 7 shows the mechanical power over the range of incident pneumatic power for speeds of 150 rpm, 200 rpm and 375 rpm. The upper axis corresponds to the incident wave power with an assumed hydrodynamic efficiency of 0.6 for the OWC. It can be seen from Fig. 7 that higher speeds of operation tend to give better efficiency at increased power levels, while lower speeds tend to give better efficiency at reduced wave power levels. This point is clearly delineated in Fig. 8, which shows the average efficiency. It is evident from the graph that efficiency can be significantly improved over a wide range of input wave power, if the turbine speed is made to vary, as opposed to a fixed speed operation It is very important to note that high efficiency can be obtained by operating over a range of speeds varying by nearly a factor of 2. Variable speed power modules from the wind power industry may be easily adapted for this purpose.

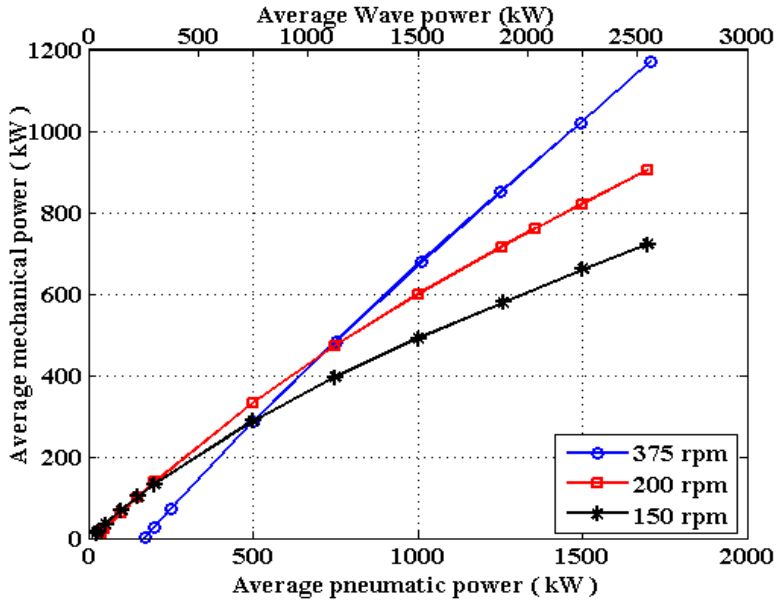

Fig. 7. Average mechanical powers for the variable speed operation of the 4.5 m turbine

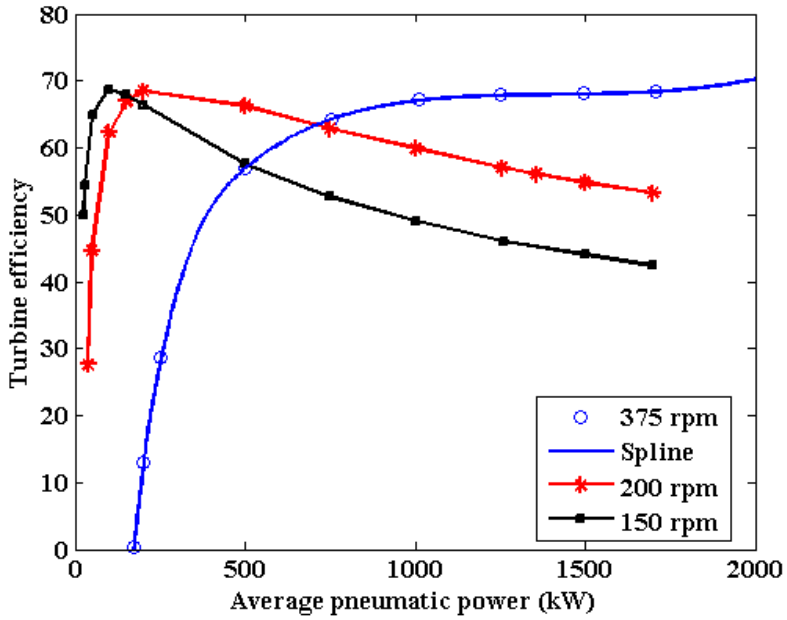

Fig. 8. Average turbine efficiency for the variable speed operation of the 4.5 m turbine

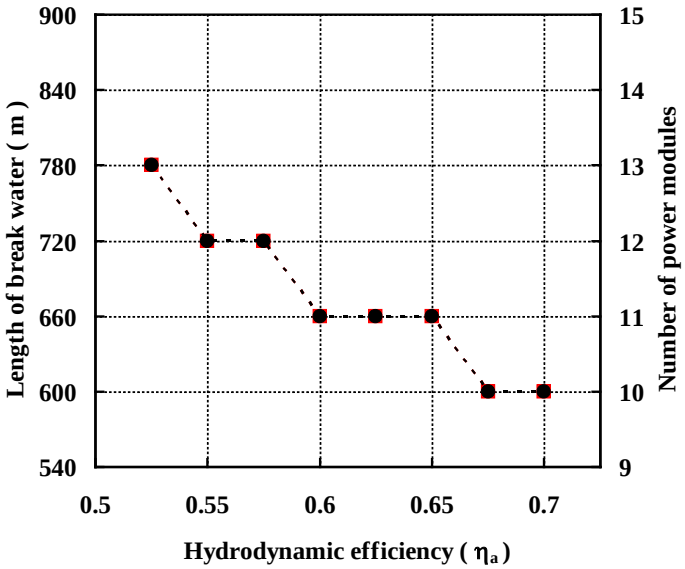

Fig. 9. Influence of the hydrodynamic efficiency on the modular design of the 100 GWh wave energy plant

4. Implications for a 100 GWh plant

It was shown in the previous section that a single 4.5 m diameter turbine could be designed for an average power of 553 kW. Taking a generator efficiency of 94%, each turbine generator set (i.e. the power module) would now be capable of generating 519 kW of electrical power on average. A requirement of 100 GWh over two years implies a 5707 kW plant with 100 % availability. Thus 11 turbine generators will be sufficient to produce the requirement of 100 G Wh. A breakwater integrated design of such a plant would cover a length of 660 m, operating at 60 % hydrodynamic efficiency. The modular design is not significantly altered even if the efficiency of wave capture is different. Fig. 9 indicates the number of power modules required to cater to the requirement of 100 GWh, over the expected range of hydrodynamic efficiencies. The size of the corresponding break water is also indicated in Fig.9.

The important features are that the power electronics interface is directly obtainable from the wind industry. This implies that a doubly fed machine which can cater to such a speed variation of 200 to 375 rpm will be adequate for this purpose. With a peak rating of 922 kW doubly fed machines as well as permanent magnet synchronous machines with converters are available. These correspond to the Type C and Type D types of power modules in the wind industry [11].

5. Conclusions

A twin unidirectional turbine power module in an OWC plant can produce an average efficiency of above 60% over a wide range of input excitation. The twin unidirectional turbine topology allows a single turbine generator set, to capture the pneumatic outputs of multiple OWCs. Eleven turbine generator sets of 4.5 m diameter, spread over a 660 m breakwater integrated OWC plant, are sufficient to produce 100 G Wh over a period of two years. Variable speed operation is suggested to maintain high efficiency over a wide range of expected incident wave power. Doubly fed induction machines as well as the synchronous machines, commonly used in wind power industry, can be used for the power module in the wave energy plant.

Annexure

The equivalent circuit parameters of the 6 kV , 12.5 kW induction generator used in the simulation of the 4.5 m unidirectional turbine were taken from [12]. They are as follows.

$R_1 = R_2 = 0.018\ \Omega$
$X_1 = X_2 = 0.18\ \Omega$
$X_m = 14.4\ \Omega$

Acknowledgement

The authors wish to express their heart felt gratitude to Dr. T.Setoguchi, Saga University, Japan for all his help over the years. The authors would also like to thank the NIOT, India for their support in developing the necessary experimental facility required for this research.

References

[1] Ohno H., Funakoshi T., Saito K., Oikawa K., and Takahashi S., Interim report on the Second Stage of Field Experiments on a Wave Power Extracting Caisson In Sakata Port, *ODEC*, 1993, pp. 173-182.

[2] Ravindran M., Jayashankar V., Jalihal P. and Pathak A.G., The Indian Wave Energy Program – an overview, Teri Information Digest on Energy 7(3), 1997, pp.173-188.

[3] Heath, T., Whittaker, T.J.T and Boake, C.B., The design, construction and operation of the LIMPET wave energy converter, Proceedings of the 4th European Wave Energy Conference, 2000, pp. 49-55.

[4] Le Crom, Brito-Melo A.,Neumann F., Sarmento A.J.N.A., Portuguese grid connected OWC power plant: Monitoring Report, Proceedings of the 20th International Offshore and Polar Engineering Conference, 2010.

[5] Marine Energy Challenge: Oscillating Water Column wave energy converter evaluation report, © The Carbon Trust, 2005.

[6] The Saltire prize challenge. Available online: http://www.scotland.gov.uk/Topics/Business-Industry/Energy/Action/leading/saltire-prize; April 1, 2003 [accessed13.09.09].

[7] Takao M., Setoguchi T., Kaneko K., Kim TH, Maeda H. and Inoue M., Impulse turbine for Wave power conversion with Air flow rectification system, International Journal of Offshore and Polar Engineering 12(2), 2002, pp.142 – 146.

[8] Jayashankar V., Anand S., Geetha T et al., A twin unidirectional topology for OWC based wave energy plants, Renewable Energy 34, 2009, pp. 692-698.

[9] Mala K., Jayaraj J., Jayashankar V. et al., A twin unidirectional impulse turbine topology for OWC based wave energy plants - Experimental validation and scaling, Renewable Energy 36, 2011, pp. 307-314.

[10] Anand S, Jayashankar V, Nagata S, Toyota K, Takao M, Setoguchi T., Performance estimation of bi-directional turbines for wave energy plants, International Journal of Thermal Science 15(4), 2007, pp.346 -52.

[11] Michalke G., "Benefits for the development of wave and tidal energy conversion from the lessons learned in wind energy", 3rd International Conference on Ocean Energy, 2010.

[12] Ion Boldea, Variable speed generators, CRC press, 2006, pp.1-16.

The Wave Excitation Forces on a Floating Vertical Cylinder in Water of Infinite Depth

William Finnegan[1], Martin Meere[2], Jamie Goggins[3,*]

[1] *College of Engineering and Informatics, National University of Ireland, Galway, Ireland*
[2] *School of Mathematics, Statistics and Applied Mathematics, National University of Ireland, Galway, Ireland*
[3] *Ryan Institute for Environmental, Marine and Energy Research, National University of Ireland, Galway, Ireland*
** Tel: +35391492609, E-mail: jamie.goggins@nuigalway.ie*

Abstract: When carrying out any numerical modeling it is vital to have an analytical approximation to insure that realistic results are obtained. The numerical modeling of wave energy converters is an efficient and inexpensive method of undertaking initial optimisation and experimentation. Therefore, the main objective of this paper is to determine an analytical solution for the heave, surge and pitch wave excitation forces on a floating cylinder in water of infinite depth. The boundary value problem technique, using the method of separation of variables, is employed to derive the velocity potentials throughout the fluid domain. A Fourier transform is used to represent infinite depth. Additionally, Havelock's expansion theorem is used to invert the complicated combined Fourier sine/cosine transform. An asymptotic approximation is taken for low frequency incident waves in order to create an analytical solution to the problem. Graphical representations of the wave excitation forces with respect to incident wave frequencies for various draft to radius ratios are presented, which can easily be used in the design of wave energy converters.

Keywords: *Infinite depth, Wave energy, Wave structure interaction, Wave water problem*

Nomenclature

a	radius of cylinder	m	
A	amplitude of incident wave	m	
b	draft of cylinder	m	
F	force	N	
F_c	Fourier cosine transform		
$F_{1,ext}$	surge excitation force	N	
$F_{3,ext}$	heave excitation force	N	
G	gravity	$m \cdot s^{-2}$	
k_0	wavenumber	m^{-1}	
m	integer		
n_j	j-component of the normal		
$p_m(\xi)$	coefficient		
q_{m0}	coefficient		
$q_m(\xi)$	coefficient		
r	radius	m	
S_B	wetted surface		
t	time		
v	flow velocity	$m \cdot s^{-1}$	
x	horizontal coordinate	m	
z	vertical coordinate	m	
ε_m	Neumann symbol		
θ	polar coordinate	rads	
ξ	separation constant		
ρ	density	$kg \cdot m^3$	
φ	frequency domain velocity potential	$m \cdot s^{-1}$	
φ_I	incident wave velocity potential	$m \cdot s^{-1}$	
φ_s^i	interior scattering velocity potential	$m \cdot s^{-1}$	
φ_d^e	exterior diffraction velocity potential	$m \cdot s^{-1}$	
φ_s^e	exterior scattering velocity potential	$m \cdot s^{-1}$	
Φ	time domain velocity potential	$m \cdot s^{-1}$	
ω	wave angular frequency	s^{-1}	

1. Introduction

One of the main stages in the design of wave energy converters (WECs) is the numerical modelling of a given converter. In this paper, an analytical solution for the wave excitation forces on a floating cylinder in water of infinite depth is provided. The solution will act as a method of validating the results from numerical models of WECs, as it provides an estimation of forces on a cylinder representation of an arbitrary shaped axisymmetric WEC.

The solution of the scattering and radiation problem for floating bodies, in finite or infinite depth water, has being explored for decades for a various shapes of bodies. In 1948, Fritz Ursell[1] explored the forces on an infinitely long horizontal floating cylinder in infinitely deep water and, in 1955, Sir Thomas Havelock[2] solved the radiation problem for a floating half-immersed sphere in infinitely deep water. In 1971, Garrett[3] solved the scattering problem by determining the vertical force, horizontal force and torque for a circular dock in water of finite depth. In 1975, Black[4] looked at the wave forces on bodies which are vertically axisymmetric using an integral equation formulation in water of finite depth. In 1981, Yeung[5] presented a set of theoretical added mass and damping coefficient for a floating cylinder in finite depth, which he also truncated for the infinite depth problem. In 2003, Bhatta and Rahman[6] used a similar technique as Havelock to solve, although using a semi-analytic solution, the scattering and radiation problem for a floating vertical cylinder in water of finite depth. Previously, an analytical solution for wave excitation forces on a floating cylinder in water of infinite depth has not been derived. Therefore, the solution derived in this paper is for a semi-submerged vertical cylinder in infinite depth water. A boundary value problem is used to derive an analytic solution, from the scattering problem, for the heave, surge and pitch excitation forces.

2. Methodology

The problem considers a vertical cylinder, of radius, *a*, and with a draft, *b*, which can move in surge, heave or pitch motion, and an incident wave of amplitude, *A*, and angular frequency, ω, as depicted in Fig. 1. The wave progresses in the positive x-direction with the origin at the still water level (SWL) and the positive z-direction is vertically downwards. In the formulation of the solution, a number of assumptions are used:

- The water is both incompressible, as frequencies are low, and effectively viscid.
- As the air has such a small density, pressure change is negligible and, thus, is at constant pressure.
- The surface tension at air-water interface is negligible.
- The water is at constant density and temperature.
- The Reynolds' number for the flow is sufficiently small for the flow to remain laminar.
- The waves are progressive and only travel in one direction and the wave motion is irrotational.

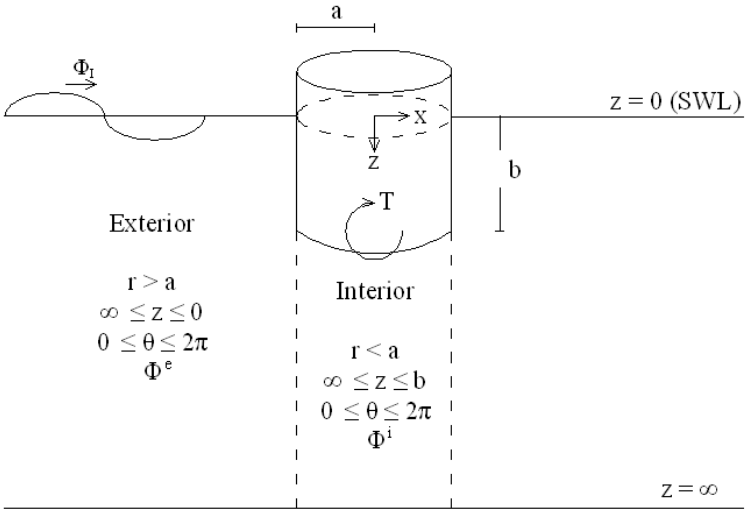

Fig. 1 Graphical set-up of the Boundary Value Problem for a Vertical Cylinder

Yeung[5] and Bhatta and Rahman[6] employed the technique of dividing the domain into two regions, which is used in this paper. The two regions are the interior region, which is the area underneath the cylinder, and the exterior region, which is the remaining area of the fluid (Fig. 1). The problem is solved in the frequency domain. Therefore, the velocity potential, φ, to be solved is transformed to the frequency domain, as follows:

$$\Phi(r,\theta,z,t) = \mathrm{Re}\{\varphi(r,z,\theta)e^{-i\omega t}\} \quad (1)$$

where Φ is the time domain velocity potential, r is radius, θ is the angle, i is the standard imaginary unit, ω is the wave angular frequency of the wave, and φ is the frequency domain velocity potential. The force is then calculated by integrating the velocity potential over the wetted surface area of the cylinder, S_B, using the following equation:

$$\hat{F} = i\rho\omega\int_{SB}\oint n_j \, dS \quad (2)$$

where ρ is water density, n_j is the j-component of the normal, S is surface and F is the force, where $F = \mathrm{Re}\{\hat{F}e^{-i\omega t}\}$. The equations and boundary conditions that need to be satisfied throughout the problem are: the Laplace's equation, the deep water condition, the free surface equation and the radiation condition, respectively[7]:

$$\nabla^2\varphi = \frac{1}{r}\frac{\partial\varphi}{\partial r} + \frac{\partial^2\varphi}{\partial r^2} + \frac{1}{r^2}\frac{\partial^2\varphi}{\partial\theta^2} + \frac{\partial^2\varphi}{\partial z^2} = 0 \quad (3)$$

$$|\nabla\varphi| \to 0 \text{ as } z \to \infty \quad (4)$$

$$\omega^2\varphi - g\frac{\partial\varphi}{\partial z} = 0 \text{ on } z = 0,\ r \geq a \quad (5)$$

$$\lim_{r\to\infty}\sqrt{r}\left(\frac{\partial\varphi}{\partial r} - ik_0\varphi\right) = 0 \quad (6)$$

where k_0 is the wavenumber ($k_0 = \omega^2/g$). Since the motion is irrotational and incompressible, the Laplace's equation was arrived at by substituting $v = \nabla\varphi$ into $\nabla \cdot v = 0$, where v is the flow velocity. The solution being developed is for infinitely deep water. Thus, the deep water condition defines the flow velocity near the sea bed. The free surface equation defines the velocity potential at the free surface away from the floating body. The radiation condition defines the velocity potential of the wave at the distance from the body when the effect of the body on the wave has dissipated. The scattering problem deals with the excitation force on a fixed body and, therefore, the following structural boundary conditions must be imposed:

$$\frac{\partial\varphi_S^i}{\partial\bar{z}} = 0 \text{ on } \bar{z} = 0, \quad \text{where } \bar{z} = z - b \quad (7)$$

$$\frac{\partial\varphi_S^e}{\partial r} = 0 \text{ at } r = a \quad (8)$$

where φ_S^i and φ_S^e are the interior and exterior scattering velocity potentials, respectively. Since we are dealing with infinite depth, a Fourier sine/cosine transform is employed when dealing with the vertical or z-component. For the interior region, in order to satisfy the structural equation (Eq. (7)) a Fourier cosine transform is required. Therefore, introducing a constant, ξ, yields:

$$F_C\left(\varphi_S^i(r,\theta,\bar{z})\right) = \sqrt{\frac{2}{\pi}}\int_0^\infty \varphi_S^i(r,\theta,\bar{z})\cos\xi\bar{z}\,d\bar{z} \tag{9}$$

$$\square\ \varphi_S^i(r,\theta,\bar{z}) = \sqrt{\frac{2}{\pi}}\int_0^\infty F_c\left(\varphi_S^i(r,\theta,\bar{z})\right)\cos\xi\bar{z}\,d\xi \tag{10}$$

where F_c is the Fourier cosine transform. The method of separation of variables is used to solve the Laplace's equation (Eq. (3)) in order to formulate an expression for the interior scattering velocity potential φ_S^i, as follows:

$$\varphi_S^i(r,\theta,\bar{z}) = \sum_{m=0}^{\infty}\sqrt{\frac{2}{\pi}}\int_0^\infty p_m(\xi)\frac{I_m(\xi r)}{I_m(\xi a)}\cos\xi\bar{z}\,d\xi\cos m\theta \tag{11}$$

where I_m is the modified first Bessel function of order m and $p_m(\xi)$ is an unknown coefficient.

Kim[8] gives the incident wave velocity potential, φ_I, in the frequency domain for deep water in oblique sea as:

$$\varphi_I(r,\theta,z) = -\frac{gA}{\omega}e^{-k_0 z}\sum_{m=0}^{\infty}\varepsilon_m i^{m+1}J_m(k_0 r)\cos m\theta \tag{12}$$

where J_m is the first Bessel function of order m, ε_m is the Neumann symbol, defined by $\varepsilon_0 = 1$ and $\varepsilon_m = 2$ for $m \geq 1$. Similarly, for the exterior region, when dealing with infinite depth in the method of separation of variables, a Fourier sine/cosine transform is used. In order to satisfy the free surface equation (Eq. (5)), a combination of the Fourier sine and Fourier cosine transform is required. Again, introducing a constant ξ, the following is obtained:

$$F\left(\varphi_d^e(r,\theta,z)\right) = \sqrt{\frac{2}{\pi}}\int_0^\infty \varphi_d^e(r,\theta,z)\left[\xi\cos\xi z - k_0\sin\xi z\right]\cos\xi z\,dz \tag{13}$$

where φ_d^e is the exterior diffraction velocity potential. The Havelock's expansion theorem [9] is used to obtain the inverse Fourier transform. Similarly, the method of separation of variables is used to solve the Laplace's equation (Eq. (3)) in order to formulate an expression for the exterior diffraction velocity potential, which is given as:

$$\begin{aligned}\varphi_d^e(r,\theta,z) = \sum_{m=0}^{\infty}\Bigg[&q_{m,0}\frac{H_m^{(1)}(k_0 r)}{H_m^{(1)}(k_0 a)}e^{-k_0 z}\\ &+\sqrt{\frac{2}{\pi}}\int_0^\infty\frac{q_m(\xi)}{\xi^2+k_0^{\,2}}\frac{K_m(\xi r)}{K_m(\xi a)}\left[\xi\cos\xi z - k_0\sin\xi z\right]d\xi\Bigg]\cos m\theta\end{aligned} \tag{14}$$

Therefore, since the scattering velocity potential is the sum of the incident and diffraction velocity potentials (i.e. $\varphi_S = \varphi_{I+}\varphi_d$) and incorporating $-gA\omega^{-1}\varepsilon_m i^{m+1}$ into the $\varphi_d^e(r,\theta,z)$ term in Eq. (14), the scattering velocity potential for the exterior problem is given as:

$$\varphi_S^e(r,\theta,z) = \sum_{m=0}^{\infty} -\frac{gA}{\omega}\varepsilon_m i^{m+1}\left[\left\{J_m(k_0 r) + q_{m,0}\frac{H_m^{(1)}(k_0 r)}{H_m^{(1)}(k_0 a)}\right\}e^{-k_0 z} + \sqrt{\frac{2}{\pi}}\int_0^{\infty}\frac{q_m(\xi)}{\xi^2 + k_0^{\,2}}\frac{K_m(\xi r)}{K_m(\xi a)}\left[\xi\cos\xi z - k_0\sin\xi z\right]d\xi\right]\cos m\theta \quad (15)$$

where $H_m^{(1)}$ is the first Hankel function of order m and K_m is the modified second Bessel function of order m. The unknown coefficients of $p_m(\xi)$ in Eq. (11), and $q_{m,0}$ and $q_m(\xi)$ in Eq. (15), are found by matching the velocity potentials across the boundary at $r = a$. The conditions which are to be satisfied at the boundary are:

$$\varphi_S^e(r,\theta,z) = \varphi_S^i(r,\theta,\bar{z}), \text{ if } b \le z \le \infty \quad (16)$$

$$\frac{\partial\varphi_S^e(r,\theta,z)}{\partial r} = \frac{\partial\varphi_S^i(r,\theta,\bar{z})}{\partial r}, \text{ if } b \le z \le \infty \quad (17)$$

$$\frac{\partial\varphi_S^e(r,\theta,z)}{\partial r} = 0, \text{ if } 0 \le z \le b \quad (18)$$

3. Results

In order to create an analytical solution, asymptotic approximations for the excitation forces are derived for low frequency waves or, in other terms, when the wavenumber, k_0, tends towards zero. Therefore, in addition to Eq. (16)-(18), the approximation that k_0 tends towards zero is imposed when matching the interior scattering velocity potential, given in Eq. (11), and the exterior scattering velocity potential, given in Eq. (15), across the boundary $r = a$ in order to solve for the unknown coefficients $p_m(\xi)$, $q_{m,0}$ and $q_m(\xi)$,. Using this additional approximation, it was found that $q_m(\xi)$ tends to zero and the coefficient, $q_{m,0}$, is approximated as:

$$q_{m,0} = -J_m'(k_0 a)\frac{H_m^{(1)}(k_0 a)}{H_m^{(1)\prime}(k_0 a)} \quad (19)$$

and the coefficient, $p_m(\xi)$, is given as:

$$p_m(\xi) = -\frac{gA}{\omega}\varepsilon_m i^{m+1}\sqrt{\frac{2}{\pi}}\left\{J_m(k_0 a) + J_m'(k_0 a)\frac{H_m^{(1)}(k_0 a)}{H_m^{(1)\prime}(k_0 a)}\right\}\frac{e^{-k_0 b}k_0}{\xi^2 + k_0^{\,2}} \quad (20)$$

where prime is the derivative. Therefore, an analytical approximation is created and shown graphically for various draft, b, to radius, a, ratios in Fig. 2-4.

When calculating the surge, or horizontal, excitation force the only non-zero solution is when $m = 1$, as this is the only non-zero solution to the integral $\int cosm\theta\ cos\theta\ d\theta$, which arises in the force calculation. Furthermore, when integrating the velocity potential over the surface area,

the integration is performed only over the curved surface of the cylinder and, hence, the exterior velocity potential at $r = a$ is used. Therefore, the surge excitation force, $\hat{F}_{1,ext}$, is given as:

$$\begin{aligned}\hat{F}_{1,ext} &= i\rho\omega\int_{SB}\phi_S^e(r,\theta,z)n_1\,dS = i\rho\omega\int_0^{2\pi}\int_0^b\varphi_S^e(a,\theta,z)n_1\,a\,dz\,d\theta \\ &= -\frac{\rho g A a}{k_0}\sum_{m=0}^{\infty}\varepsilon_m i^m\{J_m(k_0a) - J_m'(k_0a)\frac{H_m^{(1)}(k_0a)}{H_m^{(1)\prime}(k_0a)}\}(1-e^{-k_0b})\int_0^{2\pi}\cos m\theta\cos\theta\,d\theta \qquad (21)\\ &= -\frac{2\pi i\rho g A a}{k_0}\{J_1(k_0a) - J_1'(k_0a)\frac{H_1^{(1)}(k_0a)}{H_1^{(1)\prime}(k_0a)}\}(1-e^{-k_0b})\end{aligned}$$

where $n_1 = -\cos\theta$. Graphical representations of surge excitation forces with respect to incident wave frequencies for various draft to radius ratios of devices are shown in Fig. 2.

When calculating the heave, or vertical, excitation force from the velocity potential, the only non-zero solution is when m is equal to zero due to the integral $\int\cos m\theta\,d\theta$. Furthermore, when integrating the velocity potential over the surface area, the integration is performed only over the base of the cylinder and, hence, the interior velocity potential, at $\bar{z} = 0$, is used. Therefore, the heave excitation force, $\hat{F}_{3,ext}$, is given as:

$$\begin{aligned}\hat{F}_{3,ext} &= i\rho\omega\int_{SB}\phi_S^i(r,\theta,\bar{z})n_3\,dS = i\rho\omega\int_0^{2\pi}\int_0^a\varphi_S^i(r,\theta,0)n_3\,r\,dr\,d\theta \\ &= -i\rho\omega\sqrt{\frac{2}{\pi}}\int_0^{2\pi}\int_0^a\int_0^{\infty}p_m(\xi)\frac{I_m(\xi r)}{I_m(\xi a)}d\xi\,r\,dr\cos m\theta\,d\theta \qquad (22)\\ &= -2\pi i\rho\omega a\sqrt{\frac{2}{\pi}}\int_0^{\infty}p_0(\xi)\frac{I_1(\xi r)}{\xi I_0(\xi a)}d\xi\end{aligned}$$

where $n_3 = -1$. Graphical representations of heave excitation forces with respect to incident wave frequencies for various draft to radius ratios of devices are shown in Fig. 3.

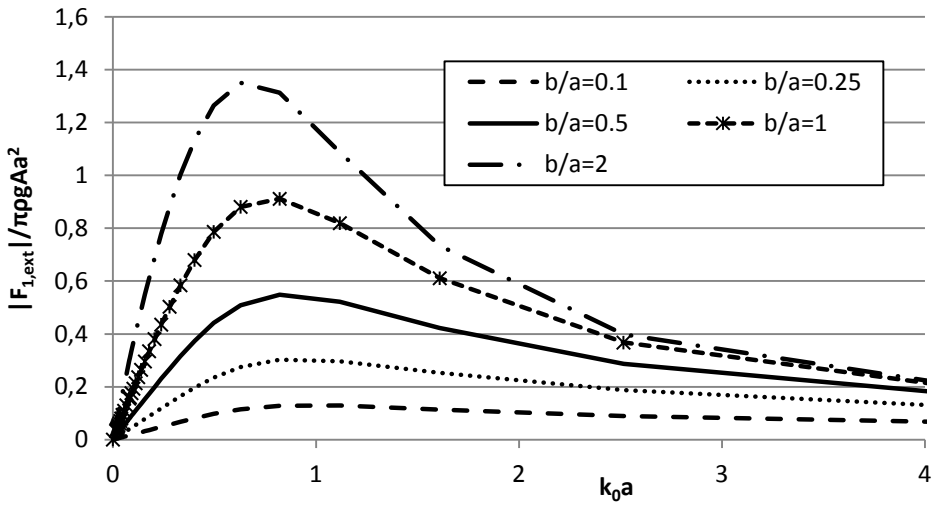

Fig. 2 The normalised surge (or horizontal) excitation force, in the frequency domain, as a function of k_0a for various radius to draft ratios.

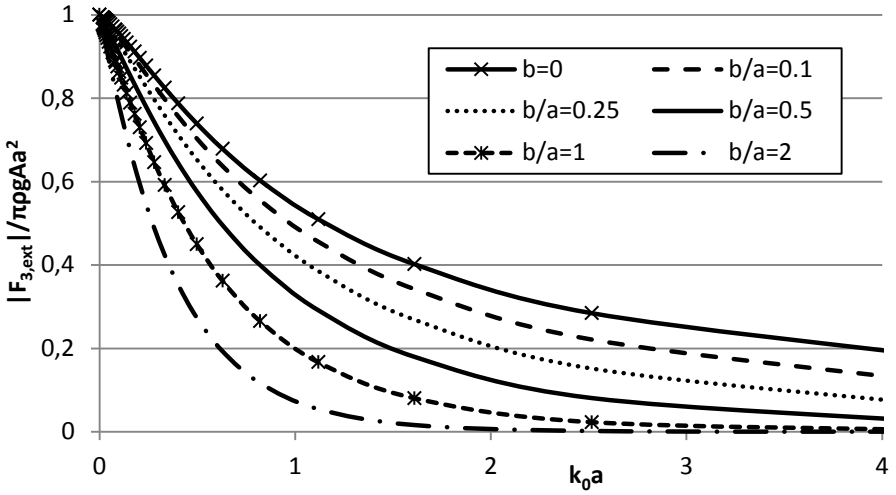

Fig. 3 The normalised heave (or vertical) excitation force, in the frequency domain, as a function of k_0a for various draft to radius ratios.

The pitch, or torque, excitation force arises from the surge and heave forces on the wetted surface of the cylinder. The pitch is taken about the axis which is transverse to the incident wave at the centre of the base, as shown by *T* in Fig. 1. When calculating the pitch the only non-zero solution, similar to surge, is when *m = 1*. Therefore, the pitch excitation force, $\hat{F}_{5,ext}$, is given as:

$$\begin{aligned}
\hat{F}_{5,ext} &= i\rho\omega \int_{SB} \oint_S (r,\theta,z) n_5 \, dS \\
&= -i\rho\omega \int_0^{2\pi} \int_0^b \varphi_S^e(a,\theta,z)(z-b)\cos\theta \, a \, dz \, d\theta + i\rho\omega \int_0^{2\pi} \int_0^a \varphi_S^i(r,\theta,0) r^2 \cos\theta \, dr \, d\theta \\
&= -2\pi i\rho g A a \{J_m(k_0 a) - J_m'(k_0 a) \frac{H_m^{(1)}(k_0 a)}{H_m^{(1)\prime}(k_0 a)}\} \int_0^b (z-b) e^{-k_0 z} \, dz \\
&+ \pi i\rho\omega a^2 \sqrt{\frac{2}{\pi}} \int_0^\infty p_1(\xi) \frac{I_2(\xi r)}{\xi I_1(\xi a)} d\xi
\end{aligned} \tag{28}$$

Graphical representations of pitch excitation forces with respect to incident wave frequencies for various draft to radius ratios of devices are shown in Fig. 4.

4. Discussion and Conclusions

An analytical solution to determine the heave, surge and pitch wave excitation forces on a floating cylinder in water of infinite depth has been presented in this paper. For ease of use in the design of wave energy converters, a graphical representation of the wave excitation forces with respect to the incident wave frequencies for various draft to radius ratios of devices are given. In particular, the heave, surge and pitch excitation forces, which are the only three forces on an axisymmetric device, were derived. The analytical solutions were obtained using an asymptotic approximation for low frequency incident waves.

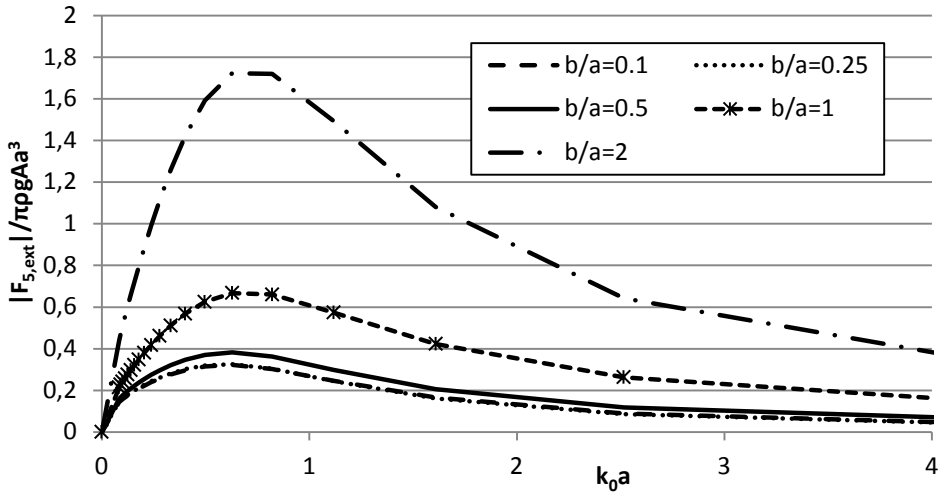

Fig. 4 The normalised pitch (or torque) excitation force, in the frequency domain, as a function of k_0a for various draft to radius ratios.

Acknowledgements

The first author would like to acknowledge the financial support from the National University of Ireland under the College of Engineering & Informatics Postgraduate Fellowship.

References

[1] F. Ursell, On The Heaving Motion of a Circular Cylinder on the Surface of a Fluid, The Quarterly Journal of Mechanics and Applied Mathematics, 2(2), 1949, pp. 218-231.

[2] T. Havelock, Waves due to a Floating Sphere Making Periodic Heaving Oscillations. Proceedings of the Royal Society of London, Series A, Mathematical and Physical Sciences, 231(1184), 1955, pp. 1-7.

[3] C.J.R. Garrett, Wave forces on a circular dock, Journal of Fluid Mechanics, 46(01), 1971, pp. 129-139.

[4] J.L. Black, Wave forces on vertical axisymmetric bodies, Journal of Fluid Mechanics, 67(02), 1975, pp. 369-376.

[5] R.W. Yeung, Added mass and damping of a vertical cylinder in finite-depth waters, Applied Ocean Research, 3(3), 1981, pp. 119-133.

[6] D.D. Bhatta and M. Rahman, On scattering and radiation problem for a cylinder in water of finite depth, International Journal of Engineering Science, 41(9), 2003, pp. 931-967.

[7] C.M. Linton and P.McIver, Handbook of Mathematical Techniques for Wave/Structure Interactions, Chapman & Hall/CRC, 2001.

[8] C.H. Kim, Nonlinear Waves and Offshore Structures, Advanced Series on Ocean Engineering, World Scientific Publishing Co. Pte. Ltd, 2008.

[9] A. Chakrabarti, On the Solution of the Problem of Scattering of Surface-Water Waves by the Edge of an Ice Cover, Proceedings: Mathematical, Physical and Engineering Sciences, 456(1997), 2000 pp. 1087-1099.

2D numerical simulation of ocean waves

Qingjie. Du*, Y.C. Dennis. Leung

Department of Mechanical Engineering, The University of Hong Kong, Hong Kong, China
** Corresponding author. Tel: +852 51743593, E-mail: qingjie.du@gmail.com*

Abstract: As fossil energy is depleting and global warming effect is worsening rapidly, developing renewable energies become the top priority on most developed and some developing countries. Among different kinds of renewable energies, wave energy attracts more and more attention in recent years due to its high energy density and enormous global amount. However, some technical difficulties still need to be overcome for extracting wave power. In designing a wave energy converter, it is important to develop an efficient method to determine the wave load and predict its response. In this paper, a numerical investigation of ocean waves is presented. Commercial software code FLUENT is used as a computational platform in this study. Based on the Navier-Stokes equations for viscous, incompressible fluid and Volume of fluid (VOF) method, a two dimensional numerical wave tank is established. Dynamic meshing method is used to simulate the wave maker, and Geo-Reconstruct scheme is used to capture the free surface. A wave-absorbing method employing porous media model is proposed, which can absorb the wave energy efficiently. Moving boundary, wall boundary and pressure-inlet boundary are used to construct the computational domain. Linear regular waves are simulated accurately using the proposed numerical model. The numerical results matched with the theoretical calculation.

Keywords: *Numerical wave flume, FLUENT, VOF method, Dynamic meshing*

Nomenclature

u	velocity component (x-direction)	$m \cdot s^{-1}$	
v	velocity component (y-direction)	$m \cdot s^{-1}$	
ρ	density	$kg \cdot m^{-3}$	
μ	dynamic viscosity	$kg \cdot m \cdot s^{-1}$	
p	static pressure	Pa	
g_x	body force (x-direction)	$N \cdot Kg^{-1}$	
g_x	body force (x-direction)	$N \cdot Kg^{-1}$	
S	paddle stroke	m	
T	wave period	s	
k	wave number	m^{-1}	
h	wave free surface	m	
ω	angular frequency	s^{-1}	
f	body forces	N	

1. Introduction

The World Energy Council (1999) reported that the total globally extractable wave energy is about 2 Terawatts [1], which is the same order of magnitude as the world's total electricity consumption. How to harness this huge energy has attracted more and more scientists' attention. In the design of wave energy converter, predicting wave loads and the structure responses have become increasingly important. In the past, the study of wave-structure interaction is mainly based on physical model experiment, which is both time consuming and money costly. Nowadays, following the rapid development in computational method and computer hardware, numerical simulation of the wave-structure interaction has attracted more and more attention.

The computation of unsteady free-surface flow is a key point in two-phase flow. Hirt and Nichols [2] developed the Volume of fluid (VOF) method to solve the two-phase problem, which uses a geometrical reconstruction scheme to capture the free surface. Wang et al [3] employed a numerical method to simulate the wave group development in long tanks. Zou [4] and Liu [5] used a moving boundary to simulate the piston-type wave maker, and successfully generated regular waves. Wei et al [6] and Chawla [7] implemented a source function method to generate ocean waves, based on Boussinesq model. Based on the 2D form of Navier-Stokes

equations, Dong and Huang [8] established a 2 D numerical wave tank to simulate small-amplitude waves and solitary waves. Lu et al [9] numerically simulated wave overtopping against seawalls in regular wave case.

During the last two decades, numerous scientists have developed their numerical methods to simulate ocean waves that are nonlinear and unsteady free-surface flows. In this paper, the research is focused on the simulation of a two-dimensional numerical wave flume. FLUENT is used as the main computational platform. Some User-Define-Function (UDF) has been implemented to simulate the wave maker and wave absorbing bench. Dynamic meshing technique is used to simulate a piston-type wave maker, which can generate both regular and irregular waves. VOF model is used to capture the free surface between water and air. Porous media model acts as the wave absorbing bench to absorb the wave energy. Both linear and nonlinear waves are simulated and compared with theoretical result.

2. Governing equation

In fluid dynamic research, there are several important assumptions. F irst, the fluid being studied is assumed to be a continuum; second, all field involved are differentiable, such as velocity field, pressure field. Moreover, for the water fluid dynamic field, some other sound assumptions are also established. Water is assumed to be Newtonian fluids, and it is incompressible and its density will not change with time. Based on the above assumptions, the Navier–Stokes equation and continuity equation are used to describe the fluid motion, which are also the governing equations in this study.

2.1. Navier–Stokes equation

Equation 1 shows the Navier-Ssokes equation in vector form:

$$\rho\left(\frac{\partial V}{\partial t} + V \cdot \nabla V\right) = -\nabla p + \mu \nabla^2 V + f \tag{1}$$

Rewriting the vector equation explicitly in 2D Cartesian coordinates:

$$\rho\left(\frac{\partial u}{\partial t} + u\frac{\partial u}{\partial x} + v\frac{\partial u}{\partial y}\right) = -\frac{\partial p}{\partial x} + \mu\left(\frac{\partial^2 u}{\partial x^2} + \frac{\partial^2 u}{\partial y^2}\right) + \rho g_x \tag{2.a}$$

$$\rho\left(\frac{\partial v}{\partial t} + u\frac{\partial v}{\partial x} + v\frac{\partial v}{\partial y}\right) = -\frac{\partial p}{\partial y} + \mu\left(\frac{\partial^2 v}{\partial x^2} + \frac{\partial^2 v}{\partial y^2}\right) + \rho g_y \tag{2.b}$$

2.2. Continuity Equation

Equation 3 shows the continuity equation in 2D Cartesian coordinates

$$\frac{\partial u}{\partial x} + \frac{\partial v}{\partial y} = 0 \tag{3}$$

3. Numerical method

3.1. Boundary condition

Given proper boundary condition and initial condition, the above equations can be solved computationally. For a 2D case, given the velocity potential Φ, the boundary conditions are as follows:

(a) dynamic free-surface condition:

$$\frac{\partial \phi}{\partial t} = -g\eta - \frac{1}{2}|\nabla \phi|^2 - \frac{P_0}{\rho} \quad (4)$$

where P_0 is the pressure on the free surface.

(b) kinematic free-surface condition:

$$\frac{\partial \eta}{\partial t} = -\nabla \phi \cdot \nabla \eta + \frac{\partial \phi}{\partial y} \quad (5)$$

(c) No normal-flux condition:

$$\frac{\partial \phi}{\partial n} = 0 \quad (6)$$

applied on the rigid bottom, and at the vertical end-wall of the numerical flume.

In FLUENT, boundary condition (a) and (b) is satisfied by using the VOF scheme, and boundary condition (c) is satisfied by using wall condition.

3.2. Free surface--VOF model

The main goal of the present research is to study the characteristics of ocean waves under different scenarios. In this research, the key problem is how to accurately describe the free surface between the two different phases. In this paper, since all the calculation is based on FLUENT, VOF model is used to simulate the free surface between water and air. The method is based on the idea of so called fraction function α_q. It is defined as the integral of fluid's characteristic function in the control volume (namely volume of a computational grid cell). Basically, when the cell is empty, $\alpha_q = 0$; if the cell is full, $\alpha_q = 1$; if $0 < \alpha_q < 1$, then the volume is the interface between the two phases. For this study, it is a two-phase problem, so q=1,2, representing air and water respectively. q is tracked by solving the continuity equation below for q^{th} fluid.

$$\frac{\partial \alpha_q}{\partial t} + \frac{\partial (u\alpha_q)}{\partial t} + \frac{\partial (v\alpha_q)}{\partial t} = 0 \quad (7)$$

$$\sum_{q=1}^{2} \alpha_q = 1 \quad (8)$$

3.3. Wave maker--dynamic mesh

A piston-type wave maker is simulated using the dynamic mesh technology in this study. Moving boundary is used to model the oscillating paddle in the physical wave maker. A user-defined function (UDF) is used to describe the motion of the oscillating paddle. In order to make the simulation more smoothly, the velocity of the paddle is described as follows:

$$U = \frac{t}{2T}\frac{S}{2}\omega \cos(\omega t) \qquad t \leqq 2T \quad (9.a)$$

$$U = \frac{S}{2}\omega \cos(\omega t) \qquad t > 2T \quad (9.b)$$

where S is the stroke of the paddle, t is the run time, T is the wave period, ω ($\omega = 2\pi/T$)is the angular frequency.

3.4. Wave absorbing bench--Porous media

The mathematic model of the porous medium is defined as:

$$S_i = -\left(\frac{\mu}{\alpha}v_i + C_2\frac{1}{2}\rho|v|v_i\right) \quad (10)$$

where i represents x, y, z; $\frac{1}{\alpha}$ & C_2 are the coefficients of viscous resistance & inertial resistance respectively.

In this 2D model, only $\frac{1}{\alpha}$ is considered. How to decide the value of $\frac{1}{\alpha}$ is very important. If $\frac{1}{\alpha}$ is too small, the wave energy cannot be absorbed completely and when waves reach the right boundary, it will reflect. If $\frac{1}{\alpha}$ is too large, the fluid property will change dramatically in the interface between the water and porous medium, so the wave will reflect too. In this simulation, the coefficient is defined as a function of the position, which is described by a UDF, in order to make the resistance of the porous medium change smoothly.

3.5. Computational model

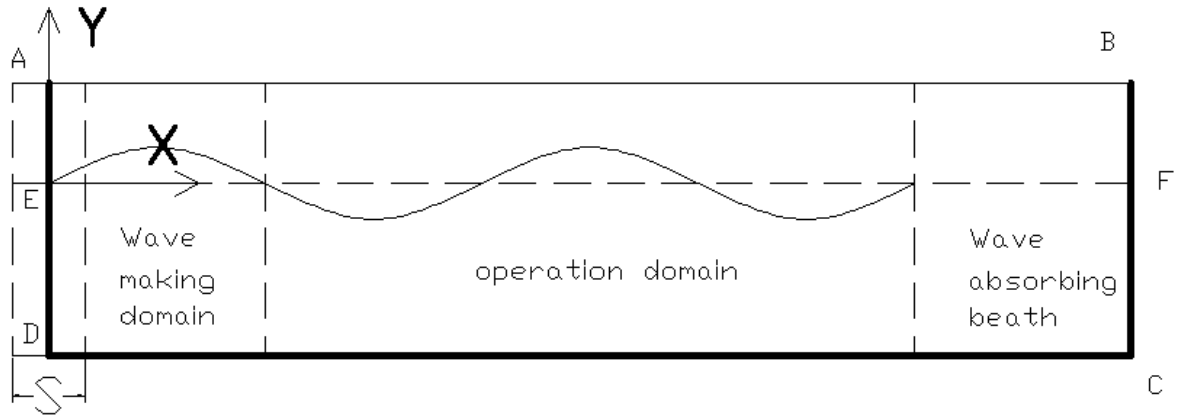

Fig.1 computational model scheme

Fig.1 shows a computation scheme of this study. Boundary AD represents the oscillating paddle; Boundary DC represents the wave flume bottom; Boundary BC represents the end of the wave flume; Boundary AB represents the top of the flume. The Volume of Fluid model is used to describe the free surface between the air and water.

4. Results and discussion

In this study, the numerical model is based on the dimension of a physical wave flume in the laboratory, with a dimension of 9m long and 0.45m high. In this simulation, the initial water depth is 0.3m. A linear regular wave with a wave height at 0.05m and wave period at 1.8s will be simulated by the numerical model. The theoretical analysis will be performed too. The wave form in the whole tank is monitored at certain times. Also the surface elevation history at point x=4.5m, which is the center point of the physical wave tank, is monitored too. These data will be compared with the theoretical result.

Under the assumption of both small amplitude paddle motion and small wave height, linear wavemaker theory has been developed by Dean and Dalrymple [10]. Assuming the original place of the paddle is at x=0, and the wavemaker stroke is S, the angular frequency of the paddle is ω, the wave elevation on the free surface η in the wave tank with water height d is shown as follows:

$$\eta = \frac{S}{2}\left[\frac{4\sinh^2(kd)}{2kd+\sinh(2kd)}\cos(kx-\omega t)\right] \tag{11}$$

$$\omega^2 = gk\tanh(kd) \tag{12}$$

Fig.2 shows the water elevation history at x=4.5m from the time of 40s to 50s. 40s, which is about 20 wave periods, is thought to be long enough for the wave to be fully developed. The black line with stars represents for the numerical result, and the green dotted line represents for the theoretical result.

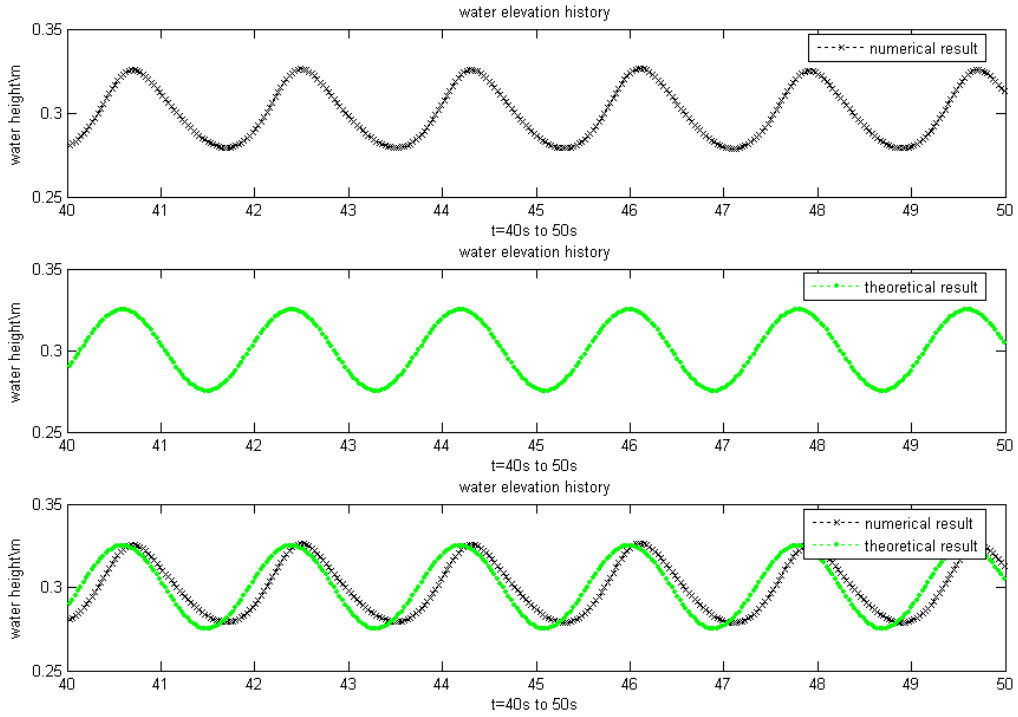

Fig.2 surface elevation history at point x=4.5

Though there is a slight shift in the phase, the numerical result matches the theoretical result well. The phase shift is due to the first 2 periods. In the simulation, during first 2 periods, all the parameters were dividing by 2T for smoothing issue.

Fig.3 shows the water free surface at t=40s, 45s and 50s. The water surface is sinusoidal, which matches the theoretical analysis.

Fig.3 wave surface at t=40s, 45s, 50s

Noted that for the wave absorbing model, the waves are absorbed completely by the porous media in the right part. Otherwise, the waves will reflect since the right boundary condition is wall.

5. Conclusion

In this study, the wave simulation model is developed based on a commercial software FLUENT for modeling fluid flow. Linear regular waves and wave absorbing bench are simulated well with a self-developed numerical model. The simulation of a wave with a wave height of 0.05m and period of 1.8s is conducted successfully. Comparison between the numerical and theoretical results shows that the numerical method works well.

Compared with the physical model experiments, this numerical model is more adaptable. The wave tank dimension can be changed according to the specific situation. The use of this numerical model is costless and is very convenient.

Based on this model, the wave-structure interaction can be studied. What's more important is that it can serve as a platform to predict the hydrodynamic response of wave energy convertors (WECs) in waves, and the result can be used to optimize the WECs.

Acknowledgement

The authors wish to acknowledge the IEEE of the University of Hong Kong for supporting the project.

References

[1] Thorpe, T.W., A brief review of wave energy. ETSU Report Number R-120 for the DTI, 1999.

[2] Hirt, C.W. and B.D. Nichols, Volume of fluid (VOF) method for the dynamics of free boundaries. Journal of Computational Physics, 1981. 39(1): pp. 201-225.

[3] Wang, P., Y. Yao, and M.P. Tulin, Wave group evolution, wave deformation, and breaking: simulations using LONGTANK, a numerical wave tank. International Journal of Offshore and Polar Engineering, 1994. 4(3): pp. 200-205.

[4] Zou, Z., Numerical simulation of nonlinear wave generated in wave flume by VOF technique. Journal of Hydrodynamics, 1996. 11(1): pp. 93-103.

[5] LIU, J.H., Making waves in 2-d numerical flume and feature analysis of the numerical waves. Journal of Sichuan University, 2004. 36(6): pp. 28-31.

[6] Wei, G., J.T. Kirby, and A. Sinha, Generation of waves in Boussinesq models using a source function method. Coastal Engineering, 1999. 36(4): pp. 271-299.

[7] Chawla, A. and J.T. Kirby, A source function method for generation of waves on currents in Boussinesq models. Applied Ocean Research, 2000. 22(2): pp. 75-83.

[8] Dong, C.M. and C.J. Huang, Generation and propagation of water waves in a two-dimensional numerical viscous wave flume. Journal of Waterway, Port, Coastal and Ocean Engineering, 2004. 130(3): pp. 143-153.

[9] Lu, Y.j., et al., Numerical simulation of two-dimensional overtopping against seawalls armored with artificial units in regular waves. Journal of Hydrodynamics, 2007. 19(3): pp. 322-329.

[10] Dean, R.G. and R.A. Dalrymple, Water wave mechanics for engineers and scientists. 1984.

The potential of chemical-osmotic energy for renewable power generation

Adel O. Sharif*, Ali. A. Merdaw, Mohammed. I. Sanduk, Sami. M. Al-Aibi, Zena Rahal

Centre for Osmosis Research & Applications, Chemical & Process Engineering Department, University of Surrey, UK
** Corresponding author. T:+44(0)1483686584; F: +44(0)1483686584 email: a.sharif@surrey.ac.uk*

Abstract: This paper presents a study on the potential of osmotic energy for power production. The study includes both pilot plant testing and theoretical modelling including cost estimation. A projected cost of 30 $/MWh of clean electricity could be achieved by using a Hydro-Osmotic Power (HOP) plant if a suitable membrane is used and the osmotic potential difference between the two solutions is greater than 25 bar; a condition that can be achieved in a number of ways.
Results have shown that the membrane system account for 50% - 80% of the HOP plant cost depending on the osmotic pressure difference level. Thus, further development in membrane technology and identifying suitable membranes would have significant impact on the feasibility of the process and the route to market. The results have shown the strong dependency of the produeced power cost on the membrane permeability. The results have also shown that a substantial reduction in the membrane area requirment for a given power output can be acheived as the osmotic pressure differnece between the two solutions increases beyoned 50 bar.

Keywords: *Osmotic Power, Salinity Gradient, Osmotic Energy, Renewable Energy*

1. Introduction

The world's searching for cost-effective renewable energy (RE) sources is continuous and has taken many dimensions and directions. This has become more so, given the current urgency of climate change, dwindling world supplies of conventional fossil fuels, and increased oil prices. Alternative energy sources, including solar, wind, tidal wave, and biomass, have been used to provide secure, sustainable and adequate energy sources. However, expensive equipment and high installation costs of these technologies, coupled with the uneven availability distribution, have prevented them, so far, from being used widely. Affordable, clean, secure, and adequate energy sources remain one of the world's biggest challenges. Similarly, we have the great challenge of sufficient world freshwater availability.

Recent R&D activities at the Centre for Osmosis Research and Applications (CORA) at the University Surrey, and in collaboration with Modern Water plc, have investigated the potential of a relatively unexplored, renewable clean energy source with little or no environmental impacts, namely the Osmotic Energy (OE), or the power of osmosis [1,2]. Osmotic Energy is produced by the osmotic pressure difference between two miscible solutions of different potential energy due to, e.g., the concentration gradient. It is released in the process of mixing a low concentration solution and a high concentration solution, such as in the mixing of freshwater, which is relatively of low osmotic pressure, and seawater, which normally has higher osmotic pressure, through a semi-permeable membrane. The membrane retains the solute movement between the two solutions and only allows pure water. In an osmotic power plant, a large percentage of the osmotic potential difference, or the chemical energy of fresh water is converted into hydraulic pressure.

Theoretically, most of the consumed mechanical energy in the Reverse Osmosis (RO) process is stored in the concentrated solution in the forms of kinetic energy (hydraulic pressure) and osmotic or chemical energy (chemical potential). However, some of the energy dissipates in a form of heat at the high pressure pumps or in the frictional losses through and along the membrane. Up to 50% of this osmotic energy or chemical energy stored in the concentrated solution (brine), which is otherwise wasted, can be converted into mechanical energy through

a Pressure Retarded Osmosis (PRO) process and recovered into hydropower [3-5]. This recovered pressure can be used to generate electricity using a hydro-turbine and generator in a similar way to conventional hydropower plants.

For example, each cubic meter of freshwater that runs into the sea with a salinity of about 35 g/*l* has, in theory, a chemical potential difference of about 0.7 kWh of energy [6]. This is because the osmotic pressure difference between seawater and freshwater is around 27 bars, which is theoretically equivalent to a 270 m waterfall. Therefore, each cubic meter of freshwater that runs into the sea could produce 0.7 kW of electricity (based on water flow through the membrane of 1 m^3/h). However, for higher salinity solutions, such as the Dead Sea or other salty lakes (e.g. salinity is higher than 20%), the chemical potential difference is higher and the produced power would be higher. The power production potential, is a function of the solutes concentration difference between two solutions, and does not require one to be freshwater, and the other to be salty water.

The generated hydraulic pressure can be utilised for the production of electricity by utilising the concept of the PRO by using a hydro-turbine and a generator in a form of land based Hydro-Osmotic Power (HOP) plant [7-9], or sub-sea or seabed-anchored plant, termed a Submarine Hydro Electric Osmotic Power Plant (SHEOPP) [10]. The generated hydraulic pressure can also be directly used through PES for pumping or other purposes [11].

The potential of osmotic energy is huge. According to Statkraft, the Norwegian power company, an osmosis-power plant could produce eco-electricity for $50-100 per MWh [12]. Its potential can be increased by combination with other renewable energy sources, such as solar, wind, tidal wave, biomass, and low-grade excess heat to further concentrate salty solutions. The global resource has been estimated at 2.6 TW [13]. The technical potential has been estimated at 2000 TWh/a [14]. Bearing in mind that these figures were derived, based purely on operation between the osmotic potentials of fresh and seawater. Additional opportunities are offered, as briefly mentioned in the introduction, by discharges from the desalination industry.

An economic assessment of a 48 MWe power plant, using the brine from an RO-concentrated seawater plant, estimated the cost of produced electricity at about 28 $/MWh [15,16]. This figure compares to about 29, 22, 12, and 5 $/MWh to produce electricity from nuclear, coal, natural gas and hydropower plants, respectively.

1.1. Open and Closed Cycle HOP Processes

There are a number of ways to recover the osmotic or the chemical energy of concentrated and salty solutions.. For the case of seawater and freshwater, e.g. up to 50% of the OE can be recovered across a semi-permeable membrane in an open cycle system. The low salinity water, Feed Water (FW), is fed at low osmotic and hydraulic pressures to one side of an Osmotic Membrane Unit (OMU), while a Draw Solution (DS), e.g. seawater or brine, is fed to the other side at higher osmotic and hydraulic pressures, where the hydraulic pressure of the DS is normally lower than the osmotic pressure. The discharged concentrated FW is circulated to the freshwater source, while the diluted DS is used to operate a turbine in order to generate power. A more efficient process can be achieved by recycling some of the pressurised solution, leaving the OMU and through a PES to assist in pumping the brine to the OMU. This process is applied when there is a continuous supply of freshwater and seawater, e.g., at a river run-off point to a sea or to a salty lake [12].

Alternatively, a closed cycle HOP plant has also been proposed [1, 10], where a DS can replace the seawater. The draw agent is retained in the system by using a Regeneration Unit (RU), which may be another separation technique, such as evaporation, crystallization, or membrane separation. In the closed cycle HOP plant, the generated hydraulic pressure can be used to produce electricity in a similar way to the open cycle system or could be transferred to other liquids through a PES for pumping processes. The efficiency of the closed HOP system depends on the availability of a low-grade energy source and/or renewable energy sources for the regeneration of the osmotic agents. Examples of renewable energy sources include, solar, geothermal, and wind for evaporation in hot and dry climates or cold temperature for crystallisation in cold climates, and/or waste heat from power and chemical plants anywhere. Recent development has been carried out to the closed-cycle process by usimg ammonia-carbon dioxide solution as DS, which is regenerated by thermal separation [17].

2. Commercial Potential and Cost Estimation

Research and development activities at CORA, and in collaboration with Modern Water plc, have shown that the potential of the hydro-osmotic power (HOP) is far greater than what had been previously assessed by other workers in this field [3,12,18]. CORA activities have involved both pilot plant testing and theoretical studies to investigate the potential of osmotic energy. For a closed-cycle HOP plant, several design and economic parameters have been assumed to carry out the calculations.

For two different, but constant, system permeabilities (A_w), 0.1 and 1 l/m^2.h.bar , Fig. 5 shows the total capital cost, the cost of the produced electricity, and the total required membrane area by using a closed cycle plant for 25 MW net electricity production. The resutls are obtianed for a rnage of osmotic pressure differences, $\Delta\Pi_f$, between the inlet concentrated, DS, and the inlet dilute, FW, to the osmotic membreane unit, OMU. The regenration unit has been assumed to be as another osmotic (FO) unit with similar membrane permeability.

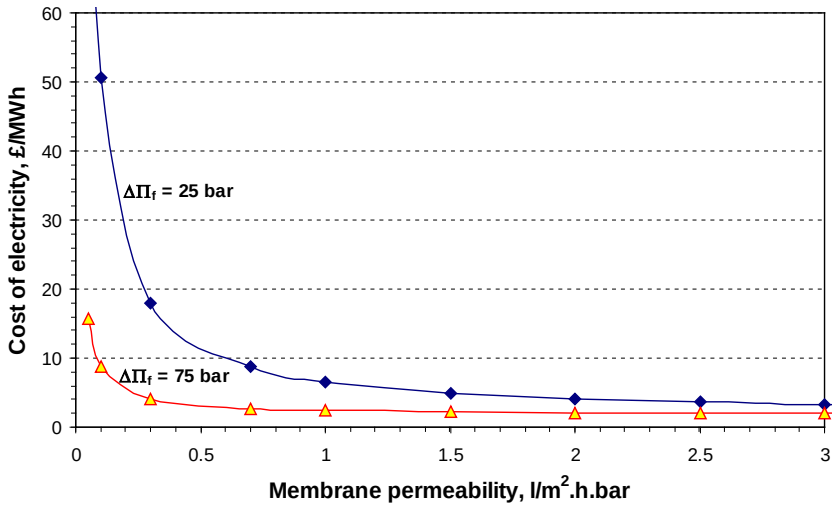

Fig. 5. The estimated cost of electricity of the proposed closed cycle HOP plant for 25 MW net power production at two osmotic pressure differnces $\Delta\Pi_f$) at the FO unit, 25 and 75 bars, by utilising 15 bars hydraulic pressure at the DS side, as a function of the membrane permeability.

It can be clearly noted the high effect of the membrane permeability on the total capital cost due to membrane contribution. The results also show that a substantial reduction in the membrane area requirment for a given power output can be acheived as the osmotic pressure differnece increases beyoned 50 bar. The cost breakdown for such a plant is calculated. More

clearly, Fig. 5 shows the cost of electricity as a function of the membrane permeability for two cases of $\Delta\Pi_f$, e.g. 25 and 75 bar, respectively.

The results suggest that for osmotic pressure difference higher than 50 bar, increasing the membrane permeability beyoned 0.3 l/m^2.h.bar has little or no effect on the overall cost of the produced electricity.

3. Experimental Setup

Several pilot plant runs have been carried out with variable DS inlet hydraulic pressure at constant temperature (25^{o}C) and feed flow rates using an OMU module having high surface area (more than 100 m^2). The pilot plant setup is schematically shown in Fig. 2. A controllable needle valve was used to replace the turbine generator assembly. The DS and FW used were aqueous solutions of NaCl salt at different concentrations to simulate fresh water (280 ppm), brackish water (6,900 ppm), seawater (~35,000 ppm), and high salinity water (145,000 ppm).

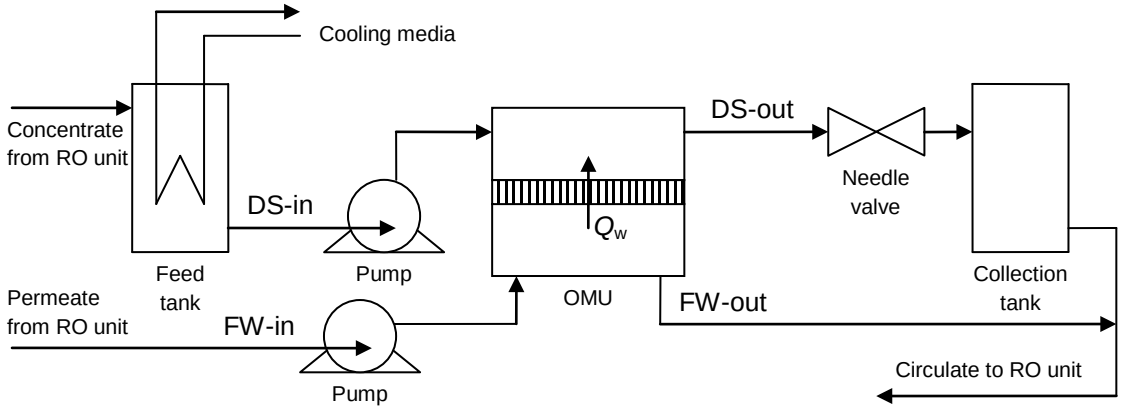

Fig. 2. Schematic diagram for the pilot plant setup.

Table 1 shows the main operational conditions of these three experiments. The discharges from the OMU were circulated to an RO unit to regenerate the concentrated DS as well as the diluted FW. A cooling for the feed tank has been used to control the increase of temperature during operation.

Table 1. The operational conditions for the pilot plant runs

Experiment no.	FW-in		DS-in		$\Delta\Pi_f$, bar
	Concentration, ppm	Flow rate*, l/min	Concentration, ppm	Flow rate, l/min	
1	240	11.1	34560	9.8	27.4
2	6900	10.9	145000	5.5	125.3
3	6900	9.5	34690	5.5	22.1

* Average value

The inlet FW is fed to the module at constant hydraulic pressure, though its flowrate was variable depending on the rate of membrane flux. The concentration measurements at the different locations of the process were obtained by using a portable conductivity meter, while

flowrate and pressure measurements were taken from online digital flow meters and pressure gauges, respectively.

4. Results and Discussion

Firstly, the pure water permeability has been measured for the membrane (A_{wm}) by using pure water as feed (into the DS side) at 25°C. The test has been carried out by modifying the OMU to an RO setup. The A_{wm} found to be decreasing with ΔP within the experimental range of 5 to 30 bars, according to the following relationship:

$$A_{wm} = 0.3265 - 0.0045 \ln(\Delta P) \quad (1)$$

The system permeability (A_w) has then been experimentally determined in a PRO setup as the product from dividing the measured water flux by the net driving pressure ($\Delta\Pi$-ΔP). Each experiment has been referred to by its number as indicated in Table 1. The A_{wm} is also shown in this figure for comparison. The A_{wm} is the upper limit for the A_w; it departs from A_{wm} as the entered solutions become more concentrated or as the ΔP increases. This indicates the effect of the A_{ws}, which is estimated by using Equations (1) and plotted in Fig. 3 as a function of the DS inlet hydraulic pressure.

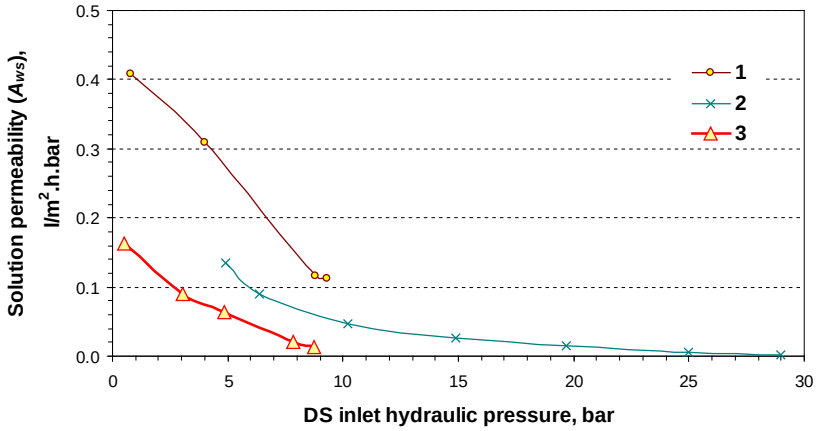

Fig. 3. The solution permeability coefficient (A_{ws}) as a function of the DS inlet hydraulic pressure.

From a comparison between the obtained values for A_{wm} and A_{ws}, the controlling phase for water transfer can be predicted. It can be noted from the case of experiment 1, where freshwater was used as FW and seawater as DS, that the membrane phase controls water transfer at low hydraulic pressures, as A_{wm} value is lower than that of A_{ws}, while at higher hydraulic pressures, the solution phase appear to be the controlling one. In the other two cases of experiments 2 and 3, where higher concentration solutions were used on both sides of the membrane, the A_{ws} was always lower than A_{wm}, which refer to the higher effect of the solution.

The following figures illustrate the calculated P_G, ρ_E, E_S, and W, (The gross power production, energy density, specific energy production and the power obtained from the PRO process respectively) as a function of the hydraulic pressure of the inlet DS. Results shown in Fig. 5 that the produced gross power, P_G, increases as the osmotic pressure (or the solute concentration) difference between the inlet FW and the inlet DS increases. Values of up to 90 watts were obtained when using freshwater as FW and seawater as DS.

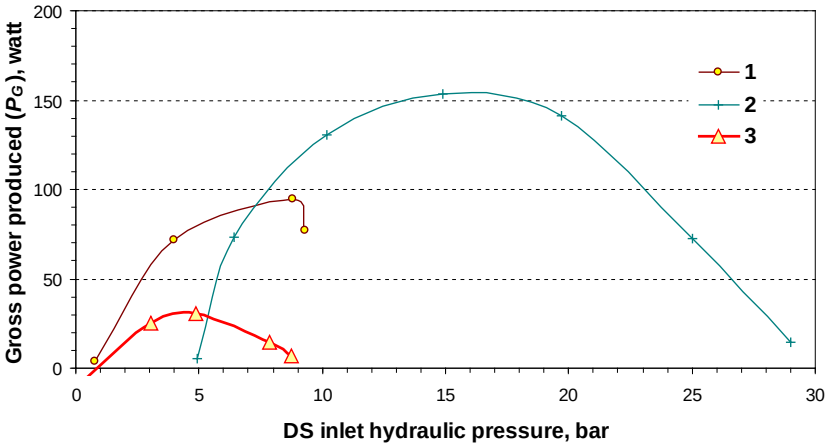

Fig. 4. Gross power produced (P_G) as a function of the DS inlet hydraulic pressure.

By using brackish water as FW with the same DS, less P_G was produced with maximum obtained values of up to 30 watts, while by utilising brackish water as FW and high salinity water as DS, the maximum P_G produced was more than 150 watts.

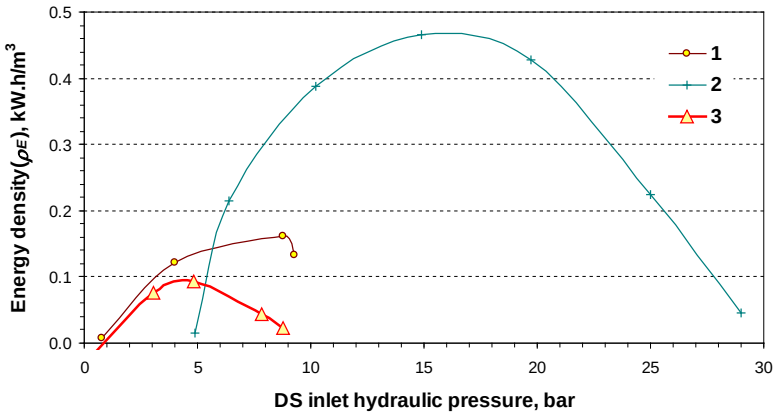

Fig.5. Energy Density (ρ_E) of the Ds as a function of its inlet hydraulic pressure for different osmotic-systems.

The effect of the hydraulic pressure at the DS side on P_G has been found to be dependant on the DS and the FW inlet concentrations, i.e. $\Delta\Pi_f$. However, different results are expected to be obtained with different membrane modules even if similar solutions and operational conditions are utilised. Practically, it has been found that the maximum value of the P_G is achieved when the hydraulic pressure drop at the DS side ($P_{DS\text{-}in}$-$P_{DS\text{-}out}$) becomes at minimum.

Fig. 5 shows the energy density (ρ_E) (in kWh/m^3 or J/m^3) of the input DS as a function of its inlet hydraulic pressure. Results show that the ρ_E, similarly to P_G, increases as the osmotic pressure difference between the FW and the DS increases. Fig. 6 shows the specific power production (E_S) of the system, based on the permeate rate, as a function of the DS feed hydraulic pressure. Results show that the E_S increases as the feed hydraulic pressure of the DS increases; however, it decreases when P_G becomes low and by increasing $\Delta\Pi_f$.

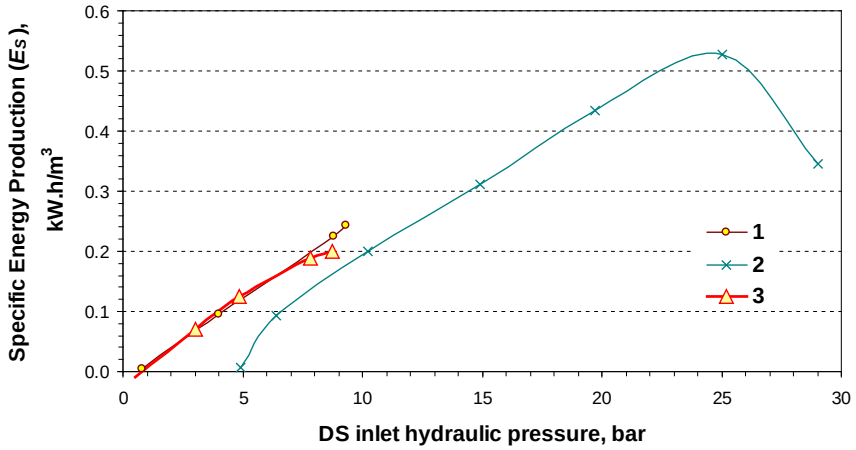

Fig. 6. Specific Energy Production (E_S) as a function of the DS inlet hydraulic pressure for different osmotic systems.

5. Conclusions

In this study both theoretical and experimental investigations of the potential of the osmotic energy (salinity gradient) for power generation have been carried out. The results indicate a high potential of the osmotic energy for power generation using the Hydro Osmotic Process. Several theoretical calculations have been presented, which show e.g. that a clean electricity could be produced using the HOP process at a projected cost of 30 $/MWh, if a suitable membrane is used, and the osmotic potential difference between the two solutions is greater than 25 bar; a condition that can be readily achieved in many sites around the world. The results also illustrate the effect of the membrane permeability and the osmotic pressure difference across the membrane in the osmotic membrane unit (OMU) on the HOP plant cost and productivity.

This study further presents the pilot plant results under different operational conditions. The experiments show the effect of the physical properties of the FW and the DS solutions on the water permeability across the semi-permeable membrane in PRO processes. The permeability of the membrane is a critical issue when the HOP process feasibility is being evaluated. Increasing of the membrane permeability decreases the capital cost and increases the productivity. The interaction between the fluid properties and the membrane properties need to be considered when these processes are to be developed in future.

It has been experimentally found that the gross power produced is obtained when the hydraulic pressure drop at the draw solution side of the OMU becomes minimal.

Acknowledgements

The financial supports of Modern Water plc and the UK Royal Society Brain Mercer Award for Innovation to undertake this work are gratefully acknowledged. The authors would like to sincerely thank Mr Cliff Crossley of Modern Water for his useful feedback and comments.

References

[1] A. Al-Mayahi, and A.O. Sharif, Energy Generation Method (Osmotic Energy), European Patent number, EP1660772

[2] A.O. Sharif, Separation Method, UK Patent Appl. No. GB0621247.

[3] S. Loeb, Large-scale power production by pressure-retarded osmosis, using river water and seawater passing through spiral modules, Desalination 143 (2002) 115-l 22.

[4] S. Loeb, Method and apparatus for generating power utilizing pressure-retarded-osmosis, US patent, US3906250, Sep 1975.

[5] S. Loeb, Method and apparatus for generating power utilizing pressure-retarded-osmosis, US patent, US4193267, Mar 1980.

[6] K.S. Spliegler, and Y.M. E1-Sayed, The energetics of desalination processes, Desalination 134 (2001) 109-128.

[7] A. Achilli, T.Y. Cath, and A.E. Childress, Power generation with pressure retarded osmosis: An experimental and theoretical investigation, Journal of Membrane Science 343 (2009) 42–52.

[8] A.O. Sharif, Z. Rahal, and A.A. Merdaw, Power from salt water- is water going to be the World's new oil?, Arab Water World XXXIV (2) (2010) 6-9.

[9] S. Loeb, T. Honda, and M. Reali, Comparative mechanical efficiency of several plant configurations using a pressure-retarded osmosis energy converter, Journal of Membrane Science 51 (1990) 323-335.

[10] T. Harrysson, D. Lönn, and J. Svensson, http://exergy.se/goran/cng/alten/proj/97/o/

[11] A.A. Merdaw, A.O. Sharif, and G.A.W. Derwish, Water permeability in polymeric membranes, Desalination 257 (2010) 184-194.

[12] S.E. Skilhagen, J.E. Dugstad, and R.J. Aaberg, Osmotic power - power production based on the osmotic pressure difference between waters with varying salt gradients, Desalination 220 (2008) 476-482.

[13] United Nations Atlas of the Oceans (2004) http://www.oceansatlas.com/unatlas/uses/EnergyResources/Background/Salinity/sp1.html

[14] A.T. Jones, and W. Finley, Recent Developments in Salinity Gradient Power, OCEANS 2003 Proceedings 4 (2003) 2284-2287.

[15] R. J. Aaberg, Ocean energy proposal Salinity Power 2, Statkraft Energi AS, Norway, 2004.

[16] S. Loeb, Energy production at the Dead Sea by pressure-retarded osmosis: challenge or chimera?, Desalination 120 (1998) 247-262.

[17] R.L. McGinnis, J.R. McCutcheon, and M. Elimelech, A Novel Ammonia-Carbon Dioxide Osmotic Heat Engine for Power Generation, Journal of Membrane Science 305 (2007) 13-19.

[18] L. Panyor, Renewable energy from dilution of salt water with freshwater: pressure retarded osmosis, Desalination 199 (2006) 408-410.

Ocean power conversion for electricity generation and desalinated water production

Rafael Ferreira[1,*], Segen Estefen[1]

[1] *COPPE/ Federal University of Rio de Janeiro, Rio de Janeiro, Brazil*
** Corresponding author. Tel: +55 2125627789, Fax: +55 2125627790, E-mail: rafael@lts.coppe.ufrj.br*

Abstract: Ocean power is a promising source of renewable and alternative energy used to fuel human activities. Generated energy from ocean power devices can be converted into electrical or mechanical energy, which can in turn be used as a driving force together with the desalination and water treatment by reverse osmosis processes. In this article, applications of high pressure wave energy converters (WEC) and hydrokinetic turbine for current energy conversion (TEC), described in Estefen et al [1], are presented. Due to its conceptual design, these ocean energy converters (OEC) are able to transform the hydraulic energy available from the sea into mechanical energy and then in turn into electricity generation, reverse osmosis desalination or as the driving force for hydraulic machines. A theoretical production estimation of wave and currents devices was conducted, which considered their performance from laboratorial tests associated to ocean parameters. Results are promising and indicate that it is indeed possible to supply domestic, industrial and agricultural demands of electricity and/or water, respecting the corresponding standards required.

Keywords: *Ocean power, Wave power, Current power, Desalination, Isolated communities.*

1. Introduction

In recent years, several kinds of ocean power converter prototypes have been developed, according to the expertise of each inventing team and/or specific issues from the local sea where it was planned for. This amount of prototypes indicate that the most suitable technology is not defined yet, i.e., which amongst will be applied to commercial purposes. The conversion technology from ocean power has been developed or adjusted from experience and knowledge in hydraulic and wind projects, besides from the activities performed in the offshore oil industry. According to the classification of Brooke [2] and Pontes & Falcão [3], Wave Energy Converters (WEC) can be sorted by the location in shoreline, near shore and offshore devices or by technology in Oscillating water column systems, Overtopping Systems, Point absorbers systems, Surging devices and other devices.

Tidal energy converters (TEC) can be classified into three main groups: horizontal axis turbines (axial flow), vertical axis turbines (cross flow) and oscillating hydrofoil. The former is based on hydrofoils impulsion from lift force caused by tidal current flow. In the sequence, hydraulic cylinders are driven, which in turn causes the electricity generation. Furthermore, the classification proposed by Bryden and Couch [4] includes Venturi systems, based on turbines endowed with a diffuser to increase the pressure difference.

The concept of high pressure wave power converter, described in Estefen et al [1], is based on the use of an hyperbaric chamber, which stores wave power converted from highly pressurized water. The first version, denominated onshore, works as a bi-supported beam with one beam fixed deep down into the soil and the other on a buoy, which follows the waves´ movement. Once a wave passes by the buoy, it causes beam displacement, which is joined with a hydraulic pump and then pressurizes the water. This pressurized water is stored in a high pressure system, consisting of a hydro-pneumatic accumulator and hyperbaric chamber.

The chamber works as a hydraulic accumulator. When the pressure inside the accumulator reaches its operational level, the water is delivered, through a valve to a hydraulic turbine, which is linked to an electrical generator in order to produce electricity.

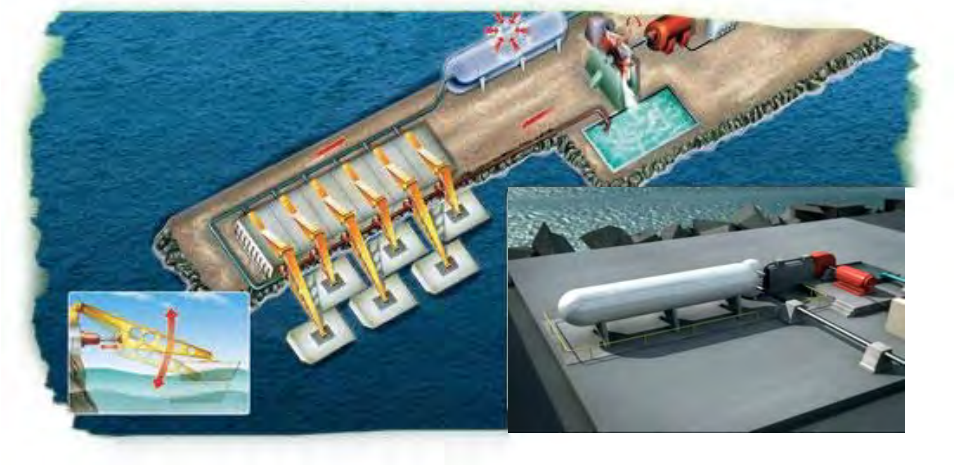

Figure 1: Wave power plant using high pressure system as described in Estefen et al [1]
In detail the high pressure system including hyperbaric chamber and accumulator

Power harnessed by ocean devices can be converted into electrical or mechanic energy, and applied as a driving force for engines or even, in the desalination and water treatment from the reverse osmosis process. The produced drinking water can supply households, industries and agricultural irrigation. For domestic use, salt concentration around 300 mg/L is required, including other quality parameters which can be achieved through the reverse osmosis conventional process, pre and post-treatment. Power consumed to pressurize water could be totally supplied by the ocean energy converter system. In industrial processes, e.g. thermo electrical plants, salinity standards similar to humans, around 300 mg/L is required in order to avoid the corrosion of equipment. Finally, in agricultural use, it is possible that large amounts of desalinated water can be produced, allowing irrigation of between 1 to 3 hectares per unit, at severe conditions of hydric demand typical in semi-arid regions.

Power supply is considered to be one of the main issues for economic and social development, since it is applied during the whole process of production and services, providing the basics necessities of modern life. For example, according to Pereira et al [5], Brazilian households without access to electricity stands at 2.8%, the majority of which are from isolated communities and rural areas, limiting electrical supply under conventional means. Such restrictions lead to a large expense of these families incoming in fossil fuels or to employment of old and inefficient techniques to generate power [5]. On the other hand, the same regions which lack electricity beholds a significant amount of alternative and renewable energy sources, for example, solar, wind, hydraulic, tidal and biomass energy. In regard to tidal current power, there are feasible possibilities of supply for isolated communities spread throughout Brazilian and South American territories.

2. Methodology

In order to estimate the amount of power extracted by an Ocean Power Converter (OEC), uneven wave or tide conditions must be considered, but also the device characteristics, the power take-off system, and the control strategy to name a few [6]. The power comprised in the wave incident to a device, according to EPRI [7], is based on two parameters: the significant wave height and its peak period, see Eq. (1).

$$E_u = 0.42 \times (H_S)^2 \times T_P \quad (1)$$

where E_u is the power of each meter of wavefront in kW/m
H_S is the significant wave height in meters
T_P is the peak period in seconds, being the inverse of frequency where spectra reached its maximum value
The coefficient 0.42 varies according to the wave spectra considered for a specific sea state.

The Eq. (1) can be employed to estimate the amount of power incident from a wave with H_S and T_P known. On the other hand, each device will be able to convert a fraction of wave incident power. In order to estimate the production of each device, a table must be created in which the cell represents the amount of power converted by the device for specific conditions of wave height and peak period. Generally, these results have been obtained through laboratorial or field tests, therefore it reflects only their performance on a small scale.

The wave parameters used as a reference for the calculations below have a significant wave height of 1.6 m and peak period of 6 seconds. The performance of the wave energy converter was obtained in tests with a reduced model, and these conditions reached a level of 18 kW of converted hydropower. The average energy absorbed in each conversion cycle, equivalent to the work done by the piston pump with each passing wave period, is calculated in Eq. (2).

$$\Delta W = \int_0^T P(t)dt = \int_0^T F_P(t)y(t)dt \quad (2)$$

where F_P is the periodic force exerted on the piston;
y is the piston displacement, consisting of a term of steady state and another transient.

Similarly, the generation of electricity through the power of tidal currents, the potential energy is calculated from Eq. (3).

$$\Delta W = \int_0^T \frac{1}{2} C_P \rho A_{turb} v^3(t)dt \quad (3)$$

Where C_P is the power coefficient;
A_{turb} is the transversal area of the turbine;
v is the speed sinusoidal of the current.

An energy converter of currents around 7 meters in diameter working in a tidal current speed with a sine wave amplitude of 1.8 m / s and power co-efficiency of 35%, will absorb an amount close to the energy converted by the WEC in the wave conditions presented, equivalent to an average of 18 kW. This amount of energy is absorbed primarily by the drive which is available in the oceans. From this point on, this energy is stored in the form of pressure and can be directed to the generation of electricity in a Pelton turbine or a module of reverse osmosis to produce desalinated water.

The desalination and water treatment for drinking can be accomplished through the process of reverse osmosis coupled with the energy converters of the sea. Reverse osmosis is a water

treatment process that uses synthetic semi-permeable membranes to intercept components of water, especially salt particles. Unlike the phenomenological natural osmosis, in reverse osmosis the goal is to produce water with low salt concentration obtained from the introduction of energy in the system. This energy is transformed into a driving force for pumping the water of higher salt concentration through a semi-permeable membrane, thus producing potable water.

In this sense, the pressure reached by the system must be sufficiently greater than the osmotic pressure between the two different salt concentrations before and after the membrane, not only to reach the balance in osmotic pressure, but also to produce a reasonable flow of water permeated, reversing the flow. In the case of converting energy from the high sea pressure [1] these pressure levels are easily achieved through the sizing of pumps attached to the primary conversion module, which provides power to the system.

The salty sea water with salinity levels of 33‰ and temperature of 24ºC has an osmotic pressure equivalent to 27.5 bar. According to marketing literature, working pressure levels of about 55 bar are required to obtain significant flow of desalinated water in the reverse osmosis process. The flow of desalinated sea water, depending on the energy converted from the sea and made to the system can be estimated by integrating the van't Hoff formula for the osmotic pressure, described in Eq. (4). This energy converted by the converter device serves as a driving force, allowing the seawater admission and pumping it to a reverse osmosis module.

$$\Delta W = -\int_{V_1}^{V_2} \pi dV = N \cdot R \cdot T \cdot \ln(V_1 / V_2) \qquad (4)$$

where ΔW is the required energy per pump cycle
N is the number of moles of salt in seawater
R is the universal gas constant
T is the temperature in Kelvin
V_1 e V_2 are the initial and final volumes of the pump piston, their difference represents the volume of water actually pumped.

The energy required to pump a volume through a semi-permeable membrane can be calculated by Eq. (5). The liquid pressure achieved by the system must be greater than the osmotic pressure between the concentrations before and after the membrane, coupled with a pressure associated with the flow of permeated water.

$$W = \int_{V_1}^{V_2} (P_S + \Delta P) dV = \left[\frac{P_{sea} \cdot (1 - \alpha / 2)}{(1 - \alpha)} + \Delta P \right] \cdot \Delta V \qquad (5)$$

where α is the recovery rate of the desalination system.

For the recovery rate of 45%, the energy required to desalinate a liter of water would be 6.5 kJ/L. Taking the energy available in the system to the conditions of wave and current previously calculated as 18 kJ per second and the complete cycle of pumping of 6 seconds, can be obtained from the flow pumped by each cycle in Eq (6).

$$\Delta Q = \Delta V \cdot (1 / cycle) = 235 m^3 / day \qquad (6)$$

The reverse osmosis modules available on the market specifically for the desalination of sea water have recovery rates of 40 to 50%. The number of modules to be used for each energy converter device of the sea was estimated from information of a type widely sold for this purpose. Table 1 shows the main parameters of this model.

Table 1. Parameters of the module of reverse osmosis desalination for seawater

Membrane area	35 m²
Unit permeated flow	14 L/hour/m²
Number of elements per pressure vessel	Up to 7
Recovery rate	45%

The production of each element will be 490 L/h and the number of elements required will be obtained by the ratio between the flow obtained by Eq. (4) and this unit flow, resulting in 20 elements. Pressure vessels can include up to seven elements of desalination in the series, which represents the need to install at least three pressure vessels coupled with each module of ocean power converter device. Whereas the recovery rate to feed flow rate will be 521 m³/day of seawater from the sea.

On the other hand, in the reverse osmosis process, as well as in other processes of desalination, wastewater is produced with higher concentrations of salt than the average salinity of the sea. The final disposal of these effluents should be studied carefully to avoid causing damage to the immediate environment, especially marine biota. Studies using models of hydrodynamic circulation and transport of water constituents are desirable for evaluation of local impact. In any case, the use of sea energy for desalination by reverse osmosis is configured as a viable cost effective alternative, especially for locations where there is a scarcity of drinking water, such as on islands and coastal areas which are far from large sources of freshwater.

3. Results

3.1. General applications for the OEC devices

Possible applications for tidal and waves energy are similar to any other energy source, which can be to provide for the electrical system, the seasonality of supply and daily peak time consumption. It can also serve as a complement to thermal energy to replace pollutants in places where few options for energy supply exist. Remote markets and isolated spots, such as villages on islands, coastal and riverside population, units of offshore oil, scientific research and the military, marine farms and fisheries.

3.2. Applications for electricity

In the case of electricity production, each high-pressure ocean power convertor, e.g. described at [1], is able to supply the demand of an average 36 households, considering the wave or current conditions described above with an average residential consumption of 12 kWh/day. Electricity produced from the sea energy converters can be used in a variety of projects, either as a principal supply, or as a supplement to other sources. The first application is domestic supply, especially in residences near marine resources located on the coast where waves or tidal estuaries are present. In South America, there is sparse population along the coast and inland waters, poor supply of electricity can benefit from these types of project. Other applications include the use of electricity in scientific and military bases located on islands and remote locations, hotels and resorts in exploiting the tourist appeal of the device itself and also drive the production of clean and renewable energy.

3.3. Applications for desalinated water

The applications of water treated by reverse osmosis from sea power converters include residential, industrial and agricultural processes through irrigation. The production capacity of treated water per converter module of wave energy or currents has a power equivalent to 18 kW and an average of 235 cubic meters per day, as shown in Eq. (6), which allows for the supply of approximately 940 people.

As an example of industrial use, the water process in power plants must meet very stringent standards for salinity in order to prevent corrosion of equipment. The salinities suitable for this purpose is 300 mg/L, similar to that required for human consumption. The unit consumption of treated water per megawatt hour produced in power plants varies from 180 to 720 U.S. gallons or 0.68 to 2.72 m³, depending on the fuel coal, gas or nuclear power and technology of the cooling tower [7] as shown in Fig. 2.

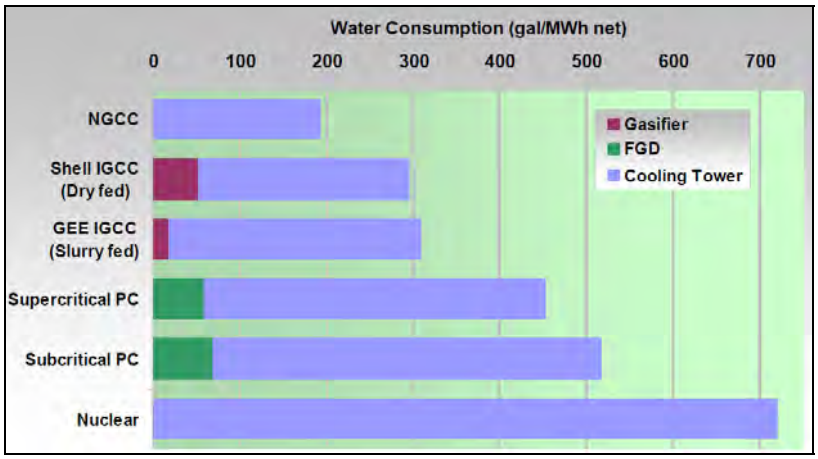

Fig. 2. Water consumption in the processes of coal-fired, gas and nuclear applications. Source: Gerdes and Nichols [7]

Considering the average production of treated water for ocean energy converters of 235 cubic meters per day, you can meet the thermoelectric consumption for the values shown in Table 2.

Table 2. Production of OEC to supply the thermoelectric water consumption

	Combined cycle (dry Tower)	Simple steam cycle (dry tower)
Water consumption	0,11 L/s	0,27 L/s
Power attained for No. of OEC modules	24 MW/Module	10 MW/module

Another application of desalinated water from OEC's is for the service of irrigated crops. Agricultural irrigation is water consumptive, due to the fact high water demand from the crops throughout the growth phase and the planting and irrigation techniques have low levels of efficiency in water management. The quality of irrigation water is usually based on the total content of dissolved salts, measured by the electrical conductivity and sodium adsorption ratio (SAR), assessing the risk of sodicity in soil [8]. The required concentration of dissolved salts in irrigation water is limited to the potential impact on soil structure, corresponding in terms of electrical conductivity to between 250-750 micromhos/cm and, in some cases, 2,250 micromhos/cm. In terms of salt concentration, the values are between 160 and 480 mg/L.

To illustrate this application, the water requirements for cultivation of cane sugar in a Brazilian region characterized by lack of rainfall during summer in the Southern Hemisphere

will be described below, along with the possibilities that this demand can be met by OEC modules. The observed rainfall in the Alagoas region during 2008 is presented in Table 3.

Table 3: Average monthly rainfall (mm) in the region of Alagoas (Brazil)

JAN	*FEB*	*MAR*	*APR*	*MAY*	*JUN*	*JUL*	*AUG*	*SEP*	*OCT*	*NOV*	*DEC*
41	206	214	257	256	261	276	238	76	48	12	41

The months of November, December and January show a significant drop of rainfall, resulting in severe consequences for water users in this region. In Fig. 3 (a), the curve shows the agrometeorological cane ratoon, the evolution of the crop water demand throughout its growth in the months of the planting period, August through to July, the harvest season.

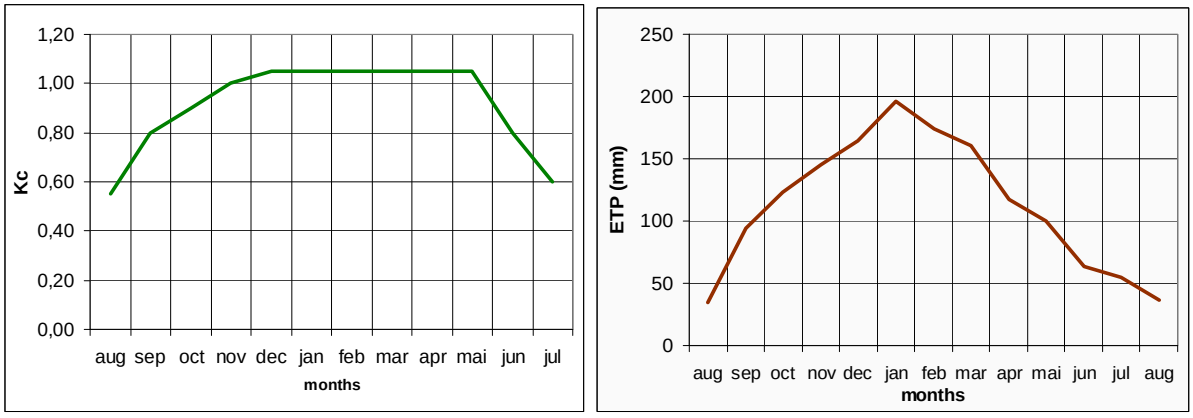

Fig. 3. (a) Agrometeorological curve (Kc) and (b) Evapotranspiration of the sugarcane ratoon (mm)

Thus, the water demand in each month of sugarcane ratoon crop irrigation can be calculated by the difference between the amount of water precipitated and crop evapotranspiration. The amount of irrigation water demand is presented in Table 4.

Table 4: Monthly water demand for irrigation of sugarcane ratoon (in mm)

Month	*AUG*	*SEP*	*OCT*	*NOV*	*DES*	*JAN*	*FEB*	*MAR*	*APR*	*MAY*	*JUN*	*JUL*
Lamina (mm)	85,1	-18,25	-74,8	-133,2	-123	-155,1	32,1	53,6	139,8	156,2	197,2	221,9
Daily irrigation flow (m^3/day/ha)	0	6,1	24,9	44,4	41,0	51,7	0	0	0	0	0	0

As shown in Table 4, negative values mean that there was a demand for irrigation in the corresponding months. The daily flow irrigation during the critical months was calculated taking into account the water depth required. Based on a water salinity content of 300 mg/L and the flow of irrigation in the most critical month of January, it shows that the production of water from ocean energy converter of 18 kW is capable of supplying irrigation in 4.5 hectares of cultivation.

4. Conclusions

An estimation of wave and tidal current power converter production was conducted, which focused on a high pressure system concept [1] developed by Submarine Technology Laboratory at UFRJ (Brazil). The WEC is an oscillating body type, which pumps water to the hyperbaric chamber and uses conventional Pelton turbine coupled with an electrical generator. Also, the hydrokinetic turbine is connected to a hydraulic pump and from this stage it is similar to the architecture described above. Due to its conceptual design, these ocean energy

converters (OEC) are able to transform the hydraulic energy available at sea into mechanical energy and then into electricity generation, reverse osmosis desalination or as a driving force for hydraulic machines. As a reference, the energy amount converted by this WEC in a typical wave condition was used for the following calculations, and it was compared to the similar amount generated by the TEC. The estimate indicated that for a significant wave height of 1.6 meters, the WEC can generate 18 kW or 235 m³/day of desalinated water and the same production can be obtained by the hydrokinetic turbine at a current speed of 1.8 m/s.

Electricity, fresh water and driving force resulting from OEC can be employed in domestic, industrial and irrigation uses, especially in regions which lack these natural resources, *e.g*. islands, coastal and riverside isolated communities. Additionally, industries and agricultural irrigation settled near to the coast can be potential users of treated water and electricity generated by the mentioned OEC. The water supply for each case is simulated herein. For domestic use, each module of WEC or hydrokinetic turbine can supply 940 people. The industrial application was illustrated by the water demand of a thermoelectric plant, providing values of each 10 MW in the Combined Cycle can be supplied by one OEC module, and in the Simple, each 5 MW. The irrigation use was demonstrated through the water consumption of sugarcane cultivation during a critical month associated with low precipitation. In this case, up to 5 hectares of cultivation can be irrigated by the production of one module. Harnessing ocean power is a way to provide decentralized electricity generation which could supply remote sites, promoting the diversification of energy matrix and becoming an economical development vector, especially in coastal communities of developing countries.

Acknowledgements
The authors would like to thank CNPq (*Conselho Nacional de Desenvolvimento Científico e Tecnológico*), Brazilian research agency, for supporting the conference attendance.

References

[1] S. F. Estefen, P. R. Costa, E. Ricarte, and M. M. Pinheiro, Wave energy hyperbaric device for electricity production, in OMAE-2007, San Diego (CA), United States, June 2007.

[2] J. Brooke, Wave Energy Conversion. Elsevier Ocean Engineering, New York, US, 2003.

[3] M. T. Pontes, A. Falcão, Ocean Energies: Resources and Utilization, 18th Congress World Energy Congress, Buenos Aires, Argentina, 2001.

[4] I. G. Bryden, S. J. Couch, ME1—marine energy extraction: tidal resource analysis, Renewable Energy, Volume 31, 2006, pp. 133-139.

[5] A. O. Pereira Jr., J. Soares, R. G. Oliveira, R. P. Queiroz, Energy in Brazil: Toward sustainable development?, Energy Policy, Volume 36, Issue 1, January 2008, pp. 73-83.

[6] G. Hagerman, R. Bedard, Guidelines for preliminary estimation of power production by offshore wave energy conversion devices, Rep. E21 EPRI-WP-US-001, Dec. 2003, pp. 3-10.

[7] K. Gerdes, C. Nichols, Water requirements for existing and emerging thermoelectric plants technologies, Report from DOE/NETL, United States, August 2008, pp. 5-9.

[8] L. A. Richards, (Editor), Agriculture Handbook 60, US Department of Agriculture, United States, 1954, pp.69-82.

Physical Investigation into an array of onshore OWCPs designed for water delivery

Davide Magagna[1,*], Dimitris Stagonas[1], Gerald Muller[1]

[1] *Sustainable Energy Research Group, University of Southampton, Southampton, United Kingdom*
** Corresponding author. Tel: +44(0) 238059465, Fax: +44 (0)23 8067 7519, E-mail:d.magagna@soton.ac.uk*

Abstract: An OWC Wave Pump (OWCP) for seawater desalination is under development at University of Southampton. The paper presents experimental results for work carried out on an array of OCWPs at a scale of 1:40. The interaction between singles components of the array is determined in order to assess the layout which gives the maximum power output from an array of 3 OWCPs. The results provide a benchmark for comparison against the data available in literature obtained from BEM simulation. Results show that amplification of the wave signal up to 4.8 times can be achieved within the array. Increasing the distance between devices by two times the width of the chamber resulted in a reduction of the magnification factor up to 30%.

Keywords: *Arrays, Oscillating Water Column, Separation Distance, Capture width*

Nomenclature

MWL	*Mean Water Level*	P_a	*Power output of Array* ..... *kW*
N	*Number of devices in array*	P_s	*Power output of a Single device* ..... *kW*
OWC	*Oscillating Water Column*	P_{out}	*Power output* ..... *kW*
OWCP	*Oscillating Water Column Wave Pump*	Q	*Flow rate* ..... $m^3 \cdot s$
WEC	*Wave Energy Converter*	s_d	*Submersion depth* ..... *m*
q	*Array Factor*	T_N	*Natural period of Oscillation* ..... *s*
A	*Section of duct* ..... m^2	T_W	*Incoming wave period* ..... *s T*
d_s	*Separating distance* ..... *m*	z_r	*Removal height* ..... *m*
g	*Gravitational constat* ..... $m \cdot s^{-2}$	α	*Angle of inclination of output duct* ..... *rad*
H	*Wave height* ..... *m*	ρ	*density* ..... $kg \cdot m^{-3}$
h	*Water depth* ..... *m*	ω_D	*Wave Frequency* ..... $rad \cdot s^{-1}$
l	*Output duct length* ..... *m*	ω_N	*Natural Frequency Oscillation* ..... $rad \cdot s^{-1}$
l_1	*Input duct length* ..... *m*		

1. Introduction

Recent progresses made on the development of Wave Energy Converters (WECs) have encouraged researchers to evaluate the deployment of arrays of WECs in order to maximize the power-output. Whereas it would seem straightforward that the output obtained from an array of WECs is higher than the power generated by multiple items working separately, the interferences between devices and waves could have a negative effect reducing the overall power output. The effects generated by the geometrical disposition of the device are measured by the q factor, as presented by Babarit in [1]. q represents the ratio between the power output P_a generated by N devices deployed in array configuration, against the power of N devices working autonomously P_s, e.g without interaction.

$$q = \frac{P_a}{N \cdot P_s} \tag{1}$$

When q≥1 positive effects are obtained by the array disposition of multiple WECs. One of the determining factors in the evaluation of q is the separation distance, d_s, which indicates the

space between two devices in the array. The practical role of d_s is to influence the interaction between the radiated waves generated by the oscillation of each single device.

The determination of q, thus far, has been predominantly conducted using numerical phase resolving Models. Mathematical models are used to simulate the wave-device dynamics and to assess the performances of the array. They allow for a faster evaluation of the problem, but present limitations due to the formulation of the problem. Linearization of the equations involved, and assessment of infinitely long arrays being the main case. Alexandre et al [2] investigated the changes in the performances of point absorbers WEC disposed in array by assessing changes in the wave field due to the radiation of each components. Falcao presented the case of power extraction by a periodic linear array OWC (Oscillating Water Column) [3]. Other examples of mathematical model for the evaluation of WECs working in array can be found in [4-6] . The use of physical tests to evaluate the performances of arrays is, however, limited mostly due scaling problems and to the availability of appropriate facilities.

Current research at University of Southampton is focusing on the development of an Oscillating Water Column Wave Pump (OWCP) for water delivery. The device is designed to operate in arrays in order to maximize water delivery and increase the frequency response spectrum. This paper presents the results obtained from physical model tests carried on array of 3 OWCPs.

2. The OWCP and Array Configuration

The OWCP is a resonant type WEC, based on the more common Oscillating Water Column (OWC). The OWCP is designed to exploits the resonant conditions obtained during the oscillatory motion of the water contained in the chamber to deliver water to a fixed height. The OWCP can be considered as an overtopping type of WEC; however it differs from the standard overtopping devices such as the Wave Dragon [7] or the Composite Sea Wall [8], since they exploit the run-up of the water over an inclined ramp to deliver water to a reservoir.

The device is composed of two-part duct; with a horizontal underwater section (input duct), and an inclined pumping section extending above Mean Water Level (MWL) (Figure 1). The OWCP acts as a resonator with natural period of oscillation equal to T_N. To maximize performances the device has to be tuned with the incoming wave period T_W. It is possible to implement resonance control by varying the angle α of inclination of the output duct, e.g. changing the mass of water contained within the OWCP.

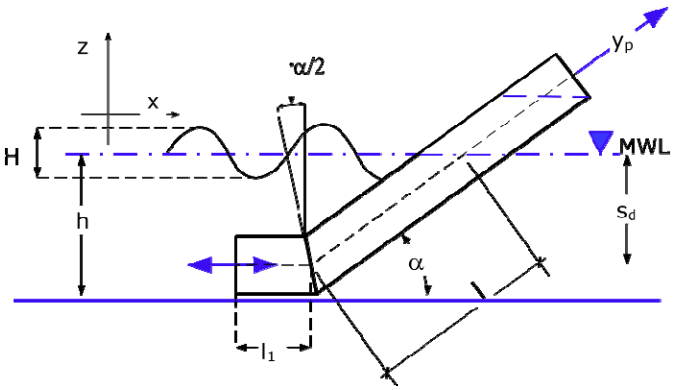

Figure 1. Schematic definition of the OWCP WEC. Where l is the length of the output duct, l_1 is the input duct, y_p the delivery height of water, h water depth, H is the wave height, s_d the submersion depth and α is the angle of inclination.

In order to maximize the delivery of water, the deployment of arrays of multiple OWCPs has been considered. Arrays of 3 OWCPs are considered in this paper. In particular, a close investigation focuses on the deployment of 3 differently tuned OWCPs devices in order to maximize performances and broaden the array response under different wave conditions. The concept of using differently tuned devices is justified by the need to provide a simple resonance control system for the array, and to phase out the destructive radiation waves generated by the downward motion of the column of water exiting the device. Initial results on the response of an array of multiple OWCPs have shown that the deployment of multiple devices broadens the frequency response of the array [9]. The role of the separation distance over the performance is therefore assessed.

3. Methodology

Experimental tests were carried in order to assess the performance of the different configuration of the arrays. The tests were carried in a 4m long, 1.7 m wide and 0.4m deep wave basin. Froude scale was employed with a scale factor Λ=40. Linear waves were generated by a piston type wave maker, with the wave heights ranging between H = 1 - 4.5 cm and period T_W between 0.8 and 2 s. The water depth in the basin was kept at 14 cm, with submersion depth s_d of 7 cm. 7 models of the OWCP were built out of transparent acrylic (3 mm thick). Their characteristics are presented in Table 1.

Table 1. Specifications of the models of the OWCP built for 1:40 scale tests.

Model	Inlet shape	Dimension (mm)	α	l_1 (mm)	T_N (s_d=7cm)
OWCPS1	Square	24×20	30º	40	0.851 s
OWCPS2	Square	24×20	30º	40	0.851 s
OWCPS3	Square	24×20	30º	40	0.851 s
OWCP20	Circle	24 ∅	20º	55	1.022 s
OWCP25	Circle	24 ∅	25º	50	0.935 s
OWCP30	Circle	24 ∅	30º	40	0.851 s
OWCP35	Circle	24 ∅	35º	35	0.795 s

The configurations of the array tested are presented in Table 2, along with the separation distances between the devices.

*Table 2. Configurations of the type of arrays tested. The * indicates the device located in the centre of the array. The Square array employs 3 similarly tuned devices.*

Array name	Models used	Separation distances (mm)
Square	OWCPS1- OWCPS2*- OWCPS3	0 – 15– 30 mm
20-25-30	OWCP20- OWCP25*- OWCP30	0 – 30 – 60 mm
20-25-30W	OWCP20- OWCP25*- OWCP30	0 – 30 – 60 mm with reflective wall
25-30-35	OWCP25- OWCP30*- OWCP35	0 – 15 – 30 mm

The arrays are located in the centre of the wave basin, with an absorbing beach installed on the back to reduce the reflection of waves from the walls (Figure 2). Resistance type wave gauges are employed to monitor the wave conditions. Wave Gauges are also installed within each device in the array to determine the lift of water (Figure 3).
The performances of the array and of each device are assessed with the magnification factor, M, given by equation (2).

$$M = \frac{y_p}{H} \tag{2}$$

Where y_p represents the lift of water within each OWCP. By using M to assess the performances of the arrays, the case of no Power Take Off (PTO) installed is evaluated. The power output, P_{out}, of each device can be estimated in relation with to M or y_p, once the delivery height z_r is defined, as shown in equation(3). This relates to the crest Power determined by Margheritini et al. [10] for the assessment of the efficiency of the SSG wave energy device.

$$P_{out} = Qz_r rg \tag{3}$$

Where Q represents the flow rate of the delivered water, ρ the water density and g the gravitational constant. For each incoming wave Q can be determined by

$$Q = \left(y_p \sin a - z_r\right)' \frac{A}{T_W} \tag{4}$$

Where A represents the cross-sectional area of the OWCP duct. For the study presented in this paper the value of Q can be estimated over a wave cycle. For irregular waves, the average Q has to be determined. It has to be noted that both Q and A are both frequency dependent, therefore maximum values of P_{out} can only be achieved close to resonance conditions.

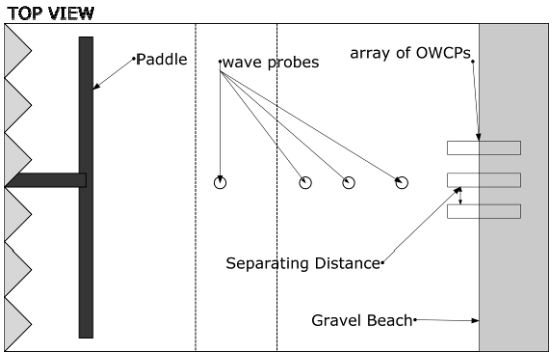

Figure 2. Experimental Setup

Figure 3. Array of 3 OWCP devices

4. Results

The response of each component of the arrays is assessed, and the values of M for different wave conditions is then determined. These are compared in order to determine the effects of the separation distance on the single and overall performance. Figure 4 presents the changes in M with d_s, for the 25-30-35, Square and 20-25-30 arrays configuration. It can be noticed that positive effects towards the delivery in the central pipe are achieved in each array configuration. It can be seen that for the cases when the devices are differently tuned higher values of M are achieved. With increasing separating distances, the values of M drop. On average a reduction in M of 14% is seen by increasing the d_s from 0 to 15 mm, with a further reduction of 12% moving from 15 to 30 mm d_s. Only the OWCP25 (Figure 4.a.) and OWCP20 (Figure 4.b) devices are subject to an increase in M with d_s. In Figure 5 the changes of M for different d_s are assessed along with the changes in the non-dimensional frequency

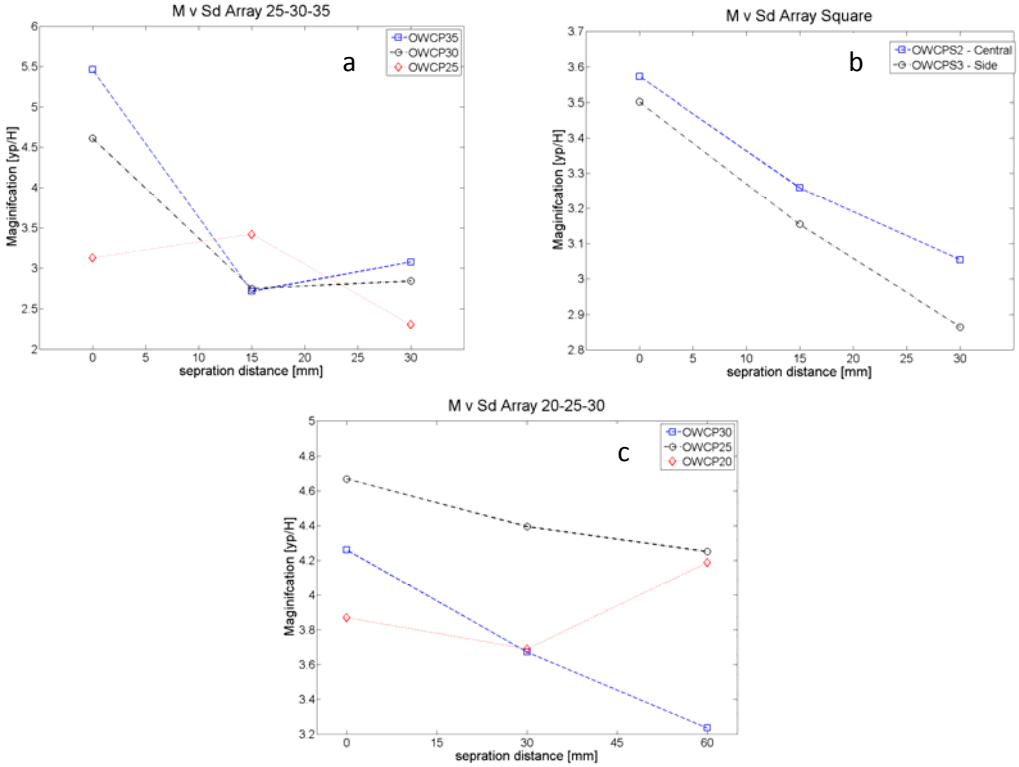

Figure 4.a) Changes in M with d_s for the 25-30-35 Array configuration. b) Changes in M with d_s for the Square Array configuration. c). Changes in M with d_s for the 20-25-30 Array configuration.

a

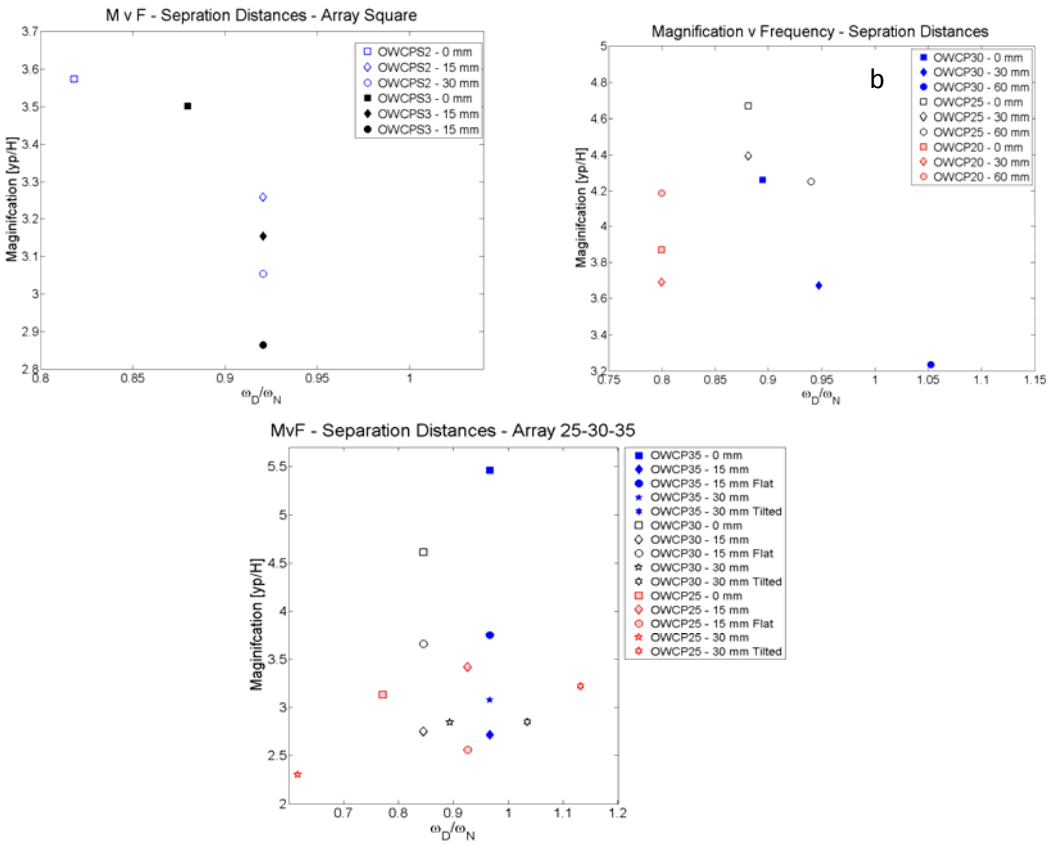

Figure 5. Maximum M against the non dimensional frequency ω_D/ω_N, for different d_s. a) Square Array. b) 20-25-30 Array. c) 25-30-35 Array. The Flat configuration considers the mouth of the device being leveled, whilst Tilted indicates the central pipe being pushed forward compared to side devices.

ω_D/ω_N . The non-dimensional frequency represents the ratio between the angular wave frequency ω_D and the natural frequency of oscillation of the device ω_N. When the ratio is close to 1, each device is operating as a stand-alone and no interferences are affecting the performances of the device. It can be seen that, with the increase in d_s, all devices tend to operate as stand alone, with maximum M achieved when ω_D/ω_N=1.

Maximum delivery however are achieved for d_s = 0 mm with $\omega_D/\omega_N \cong 0.8$. It is believed that strong arrays interference affects the damping of the devices, causing as a result a stronger response, hence higher M are obtained. Even for the cases presented in Figure 5.b and Figure 5.c different behaviors are observed in the OWCP20 and OWCP25 device. In the first case changes in M and d_s do not reflect changes in ω_D/ω_N, whilst for the OWCP25 a wider spectrum of frequencies is obtained.

Figure 6 and Figure 7 present the responses, expressed in terms of M, of the central and side device for the Square Array and for the 20-25-30 Array respectively. In both cases it can be seen how higher M, 3.57 and 4.67 respectively, are achieved in the central OWCP. Figure 6 and Figure 7 show the effect of ω_D/ω_N and of the wave steepness on M, it can be noticed that the area of response of the devices broadens with minimum separating distance. In Figure 6, where results for a Square Array are presented, one can notice that both devices present a similar response, however the central device presents a broader amplification area compared to the OWCPS3 located on the side. In Figure 7, it is possible to notice how the bandwidth response reduces for both the OWCP30 and OCWP25 with increasing d_s. Furthermore, a steady decrease of M can be noticed in both devices, indicating negative interaction between

devices.

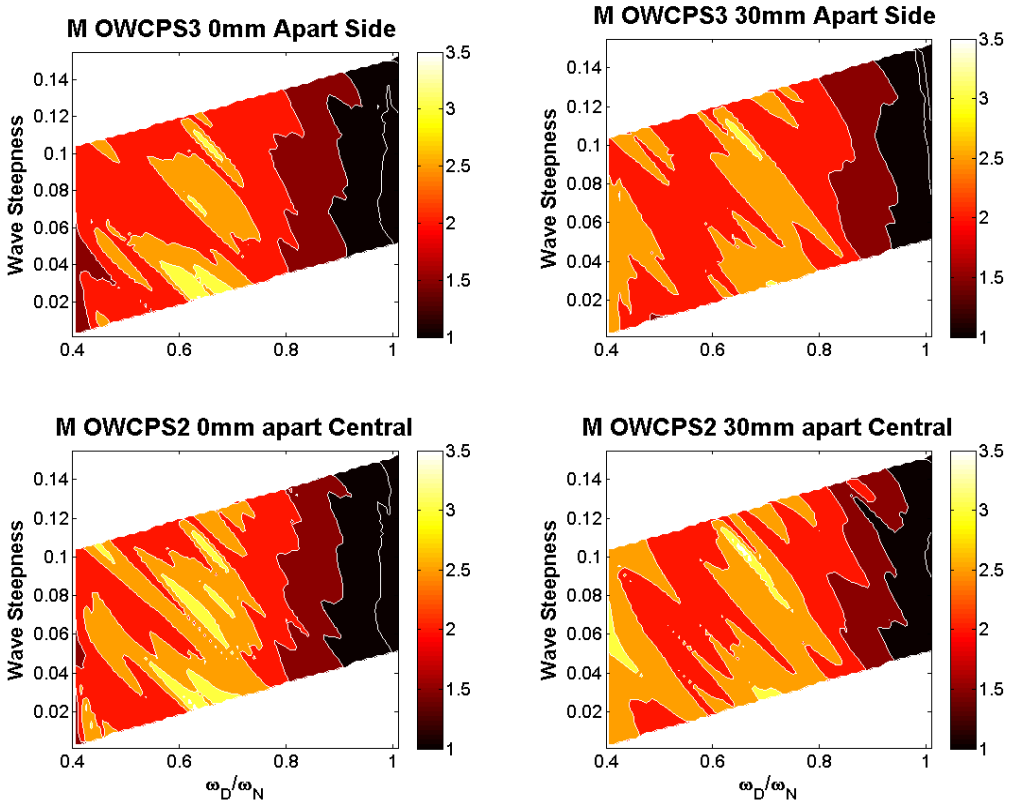

Figure 6. Magnification Factor for the components of the Square Array. Focus in given at the behavior of the side pipe (OWCPS3, top) and at the central pipe (OWCPS2, bottom) for values of s_d=0 and 30 mm (left and right).

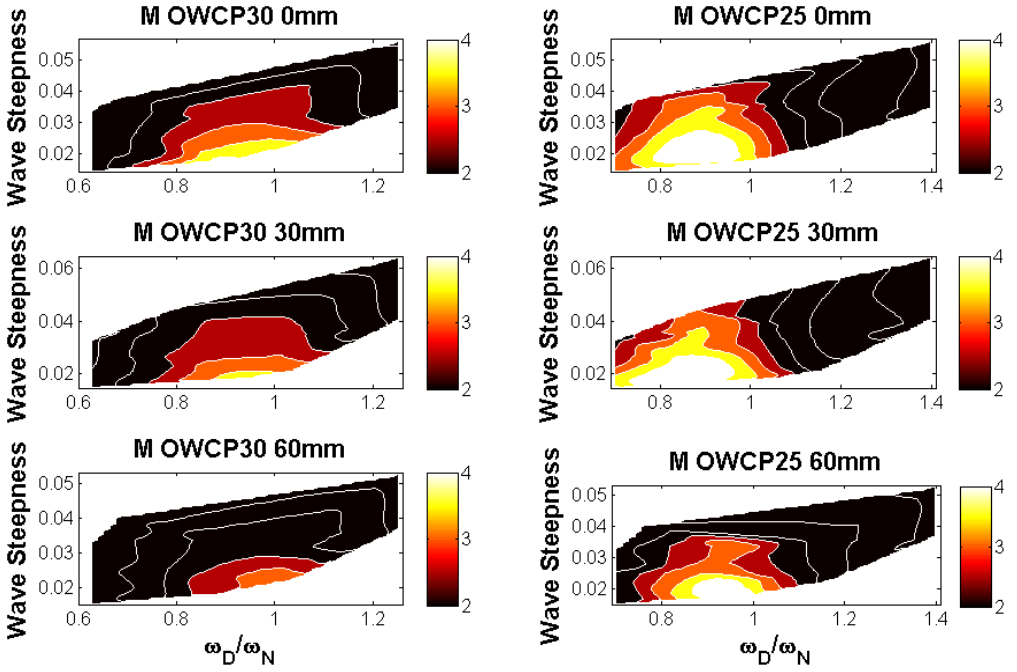

Figure 7 Magnification Factor for the components of the 20-25-30 Array. Focus in given at the behavior of the side pipe (OWCP30, left) and at the central pipe (OWCP25,right) for values of s_d= 0, 30 and 60 mm (top to bottom.).

5. Conclusions

In this paper physical experiments on arrays of onshore OWCP devices have been presented. The main aim was to investigate the role of the separating distances between devices, and how it affected the overall performance of the device and the one of the array. Array installations for WECs have been considered in order to amplify the power output of a single device.

In this paper arrays of similarly tuned devices, as well as differently tuned devices have been investigated. From experimental testing it has been highlighted that when the devices are operating with a minimum separating distance, better performances. In particular, the device located in the centre is positively affected in all the cases investigated.

The results presented show better performances by the arrays with differently tuned devices. Maximum values of M were obtained for the cases when d_s = 0. The values of M varied according to the array configuration with M =5.46 for the 25-30-35 array, M = 4.669 for the 20-25-30 array and M = 3.573 for the square array. Reduction in M of 14% can be expected by increasing s_d of 15 mm, however the reduction is dependent on the configuration. Decrease in M varied between 30% for the 25-30-25 array to 6% for the 20-25-30 for a 30mm increase in the separating distance. The results obtained show that s_d and configuration of the device play a strong role on affecting the performances of the arrays.

This is believed to be due to the different phase responses by the water column exiting the device in the downward motion. In the downward motion the mass of water generates a radiated wave that contrasts the incoming wave train interfering with the energy conversion process in the OWCP. When the devices in the array are phased out, the radiation is minimized and higher M can be achieved. The same can be assumed for 15-30 mm d_s, when the devices are separated the radiated waves affects the operation of the nearer devices.
The work here presented shows that it is possible to increase the bandwidth response of multiple devices by arranging them in array configurations. The overall performances, however, are dependent on the separation distance between the devices and their natural period of oscillation. It has been shown that by reducing to a minimum the distance between the devices, maximum performances can be achieved.

Acknowledgements

The research leading to these results has received funding from the European Community's Seventh Framework Programme (FP7/2007-2013) under grant agreement n°212423.

References

[1] A. Babarit, *Impact of long separating distances on the energy production of two interacting wave energy converters.* Ocean Engineering, 2010. **37**(8-9): p. 718-729.

[2] A. Alexandre, T. Stallard, and P.K. Stansby. *Wave field modification due to a WEC array*. in *Coastlab - Third International Conference on the Application of Physical Modelling to Port and Coastal Protection*. 2010. Barcelona, Spain: Grupo Pacifico.

[3] A.F. Falcão, *Wave-power absorption by a periodic linear array of oscillating water columns.* Ocean Engineering, 2002. **29**(10): p. 1163-1186.

[4] M. Folley and T.J.T. Whittaker, *The effect of sub-optimal control and the spectral wave climate on the performance of wave energy converter arrays.* Applied Ocean Research, 2009. **31**(4): p. 260-266.

[5] P. McIver, *Wave interaction with arrays of structures.* Applied Ocean Research, 2002. **24**(3): p. 121-126.

[6] P.C. Vicente, et al., *Dynamics of arrays of floating point-absorber wave energy converters with inter-body and bottom slack-mooring connections.* Applied Ocean Research, 2009. **31**(4): p. 267-281.

[7] J.P. Kofoed, et al., *Prototype testing of the wave energy converter wave dragon.* Renewable Energy, 2006. **31**(2): p. 181-189.

[8] G. Muller, et al. *Composite Seawalls for Wave Energy Conversion*. in *Coasts, Marine Structures and Breakwaters 2009* 2009. Edinburgh, Scotland, United Kingdom: ICE.

[9] D. Magagna, et al. *Physical investigations into the capture width of an array of OWC Wave Pumps for maximum efficiency*. in *3rd International Conference on Ocean Energy*. 2010. Bilbao, Spain: ICOE

[10] L. Margheritini, D. Vicinanza, and P. Frigaard, *SSG wave energy converter: Design, reliability and hydraulic performance of an innovative overtopping device.* Renewable Energy, 2009. **34**(5): p. 1371-1380.

Preliminary design of the OWEL wave energy converter commercial demonstrator

M. Leybourne[1,2*], W. Batten[1], A.S. Bahaj[1], N. Minns[2] and J. O'Nians[2]

[1] *Sustainable Energy Research Group, University of Southampton, UK*
[2] *IT Power Ltd, Bristol, UK*
** Tel: +44 1172140517, Fax: +441172140511, E-mail: mark.leybourne@soton.ac.uk*

Abstract: The consortium responsible for the next stage of development of the OWEL wave energy converter will construct and test a large scale, pre-commercial demonstrator. It is expected that this will be installed at Wave Hub during 2013 and grid connected for a testing period lasting around 12 months. This paper reports on the preliminary design work being undertaken in the development of the marine demonstration device. This concentrates primarily on producing a fully costed design by detailing the hydraulic design and aspects of stability as well as providing insight into various design features such as the power take-off, naval architecture, moorings and control. The design is being largely informed by the results of a 12 month research project funded by the South West Regional Development Agency (SWRDA) in which a detailed techno-economic model for a large scale OWEL device was generated.

Keywords: *Wave Energy, Pre-commercial Demonstrator Design, Wave Hub*

1. Introduction

The OWEL (Offshore Wave Energy Limited) wave energy converter is a floating, moored device that uses incident, deep water waves to compress air and drive an air turbine. It is designed to be deployed offshore in energetic deep water locations.

The device concept has been in development for a number of years and has successfully undergone a number of phases of research. The first proved the concept at small scale for a number of different arrangements. A much larger scale device was tested in the second phase in order to demonstrate the ability of the concept to be scaled up. The latest phase of development was funded by the South West Regional Development Agency (SWRDA) and has recently been completed. This incorporated a number of experimental and computational studies to optimise the design and inform the design of the large scale, marine demonstrator. The results from these three phases of testing are reported in detail in [1-4]. A level of confidence has been achieved through the wide variety of results and studies conducted. This has led to the progression of the device and its potential to be developed for commercial deployment.

A pre-commercial, marine demonstration unit is being currently designed for ocean deployment at the Wave Hub facility in the south west of England. This phase of development is intended to demonstrate the performance of a large scale OWEL unit and its ability to be deployed at sea and grid connected, with the overall goal of generating a costed, DNV accredited, full scale, commercial design. This work will represent a critical stage in the commercial route to market. The 3 year £5M project is being funded through a £2.5m award by the UK's Technology Strategy Board (TSB). Private investment will fulfil the remaining half of the required project funds.

This paper presents the initial design of the demonstrator based on the findings from the SWRDA research programme. The design process that will be used to generate the final design is discussed with the associated challenges for such a project and the plans for the future development of OWEL.

2. Principle of Operation

The OWEL converter is a floating duct which is open at one end to capture incident waves. The sides and floor are angled inward to induce a rise in wave height within the duct. As a wave enters the device, it creates a seal with the roof creating a trapped pocket of air ahead of the wave front. As the wave progresses, the air is compressed and passes through an exit pipe to the power take-off system. A schematic of this process is shown in Fig. 1. This proposed method will generate uni-directional air flow meaning standard air turbines can be used instead of the less efficient bi-directional turbines used in oscillating water columns.

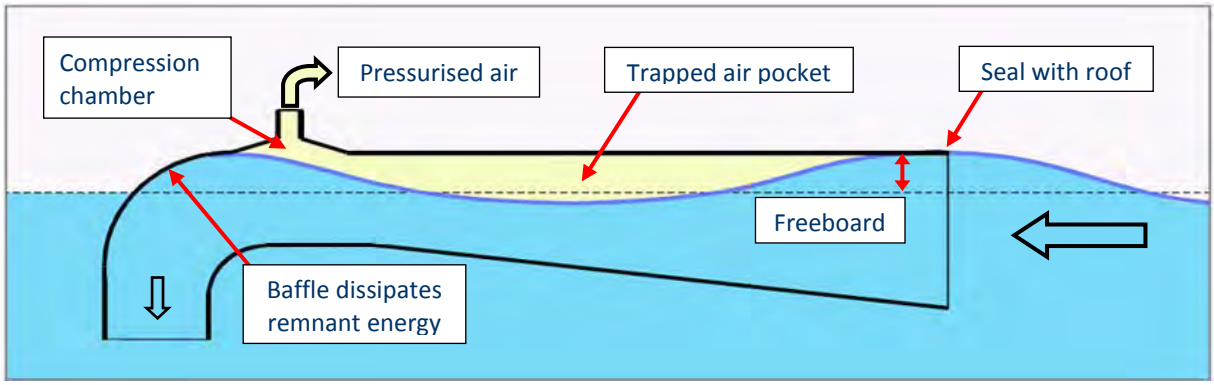

Fig. 1, Schematic of the device operation.

3. Project Overview

The design presented in this paper is considered the initial, baseline design that has been based purely on the results from the previous phases of testing. It is expected that the design will evolve and transform through the course of the project as the various demands from each subsystem are met and compromises made. A significant portion of this project will be spent generating a d etailed, engineering design for the demonstration and commercial devices. £2.5m is available to the project through the TSB funding grant with a further £2.5m of co-financing being sought in order to complete the 3 year project from design to decommissioning.

A further aim of the project is to demonstrate the ability of the device to meet the criteria of the successor to the Marine Renewables Development Fund (MRDF). It is therefore intended to keep the device on s tation for about a year as part of this project in order to verify the consistency of power output, sea-keeping properties and demonstrate reliability and survivability. In addition to the at-sea testing activity, techno-economic modelling will be used to optimise the design so as to minimise the cost of delivered energy.

Effort has been made to progress the OWEL development programme in systematic and methodical order, in line with EMEC standards [5]. By following a logical progression through ever increasing scales, more knowledge has been assimilated and the risk of failure or mistakes, reduced. The results from the previous development phases have provided enough confidence in the device design to progress to a much larger scale. It is anticipated that many lessons will be learnt from testing in an oceanic environment as there are limitations to what can be realised in a laboratory. That being said, the testing to date has identified many key design variables, device characteristics and results that have been fundamental in creating an initial design for the demonstrator.

4. Design Implications from Experimental Results

4.1. 2D Wave Flume Experiments

The 2D testing of a ~1:80 scale model of an OWEL duct, at the University of Southampton showed two regions of peak performance, as shown in Fig 2a. All of the tests were run for a fixed model with mono-chromatic waves. Although these were idealised conditions, a large amount of knowledge was gained from the results of these tests. By running over 200 wave cases for each design configuration it became straight forward to build a detailed picture of the performance and how design changes altered this.

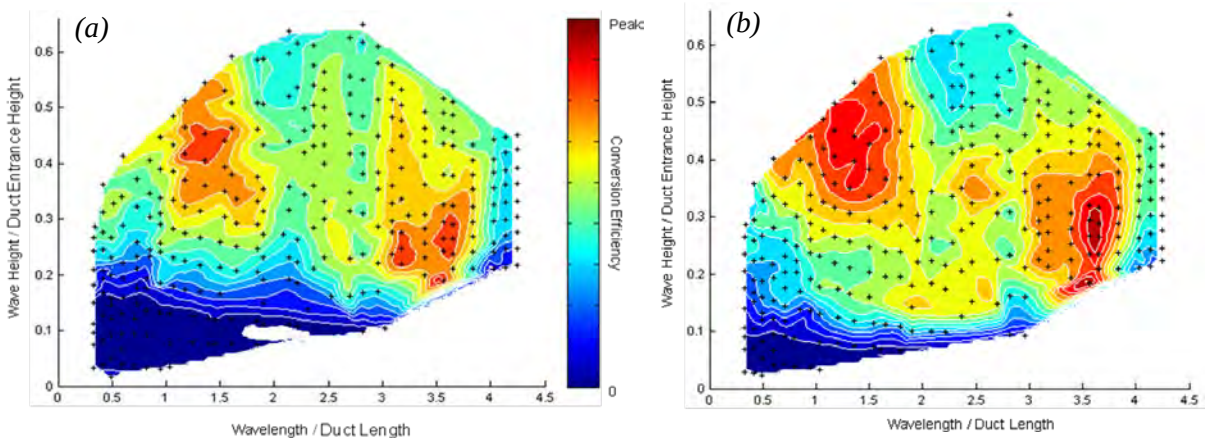

Fig. 2, Non-dimensional performance contour plots for a 2D scale model, in baseline configuration (a) and improved configuration (b).

The experiments resulted in an improved design that featured a re-designed rear duct and also demonstrated that the orientation of the duct is critical to increase performance over a wider range of wave heights. Fig. 2 compares the performance, contour plots as functions of non-dimensionalised wavelength and height, for the original design (a) and the improved design configuration (b). The improved configuration had better performance and wider bandwidths of peak efficiency and was used as the design for the model in the subsequent testing phase.

4.2. 3D Wave Basin Experiments

A series of testing at the wave basin in HMRC, Cork during 2009 generated many results and insights into previously un-investigated aspects of the device. A multi-duct, small scale model (fig. 7) was tested over a range of idealised and realistic conditions with both floating and fixed configurations. A fundamental and detailed understanding of OWEL was gained, including performance, motion and loading characteristics. The non-dimensional, performance contour plot for a floating model, tested in short crested, Bretschneider sea states is shown in Fig. 3. This compares well to the performance shown in Fig. 2, and peak performance was similar. It was found that the bandwidth performance peak widened for a floating model in comparison to a fixed model with mono-chromatic waves.

These results gave confidence in the ability of OWEL to be designed for a particular wave climate, as the peak performance can be shifted to different wavelengths by altering the duct length. Fig. 4 shows the average wave power available at Wave Hub [6], where the peak energy is at T_z=7.5s, H_s=4m, which corresponds to a wavelength/Duct length (λ/DL) ratio of just less than 2. The length of the demonstrator has been dictated by the results of the small scale testing in order to position the peak performance in Fig. 3 at the conditions of maximum energy in Fig. 4.

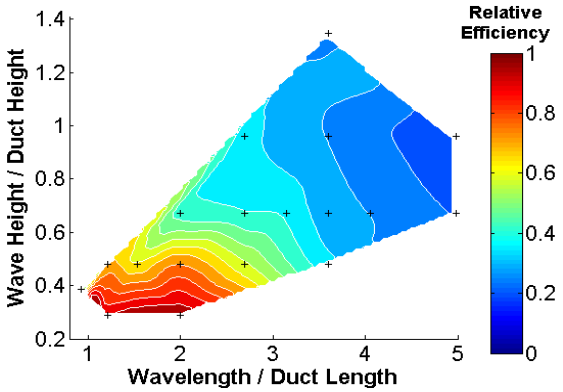

Fig. 3, Performance contour plot, with efficiencies relative to maximum, for a floating 3D model in directional sea states.

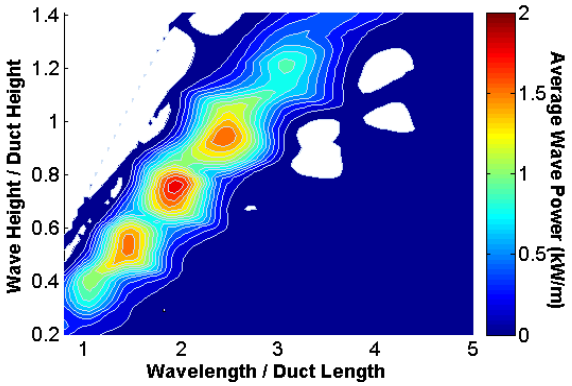

Fig. 4, Average wave power available at Wave Hub

The motions of the small scale, multi-duct OWEL model were measured in realistic, scaled sea states and their effect on performance was investigated. The tests showed that the motions of the duct helped to improve performance for certain sea states. This broadened bandwidth and led to better performance for most sea states and in particular at λ/DL ratios of 2-3. This was because the phase relationship between the incident wave and pitch and surge was such that the model pitched bow down and surged forward into the incident wave. The pulse of power occurred at around a 90° phase lag to the pitch which is thought to be optimum. At the design wave, the motions resulted in a 20% increase in performance over the fixed configuration. This ideal response improves the capture performance of each duct through better wave sealing and air compression within it. This relationship can be seen in the time series motions and power plot in Fig. 5. The RAO (Response Amplitude Operator) plot in Fig. 6 clearly shows the increased pitch and surge motions occurring between 2-3 λ/DL and these are the motions that are beneficial to the power capture. It is therefore important to consider these motions when specifying the naval architecture of the demonstrator. Motions of the design will be assessed using a w ave diffraction code such as ANSYS AQWA to ensure that similar behaviour is exhibited in order to benefit performance.

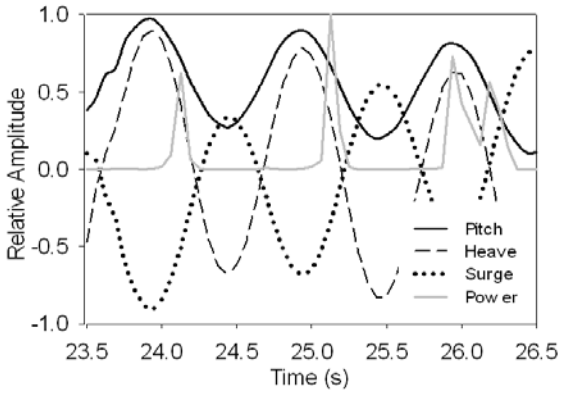

Fig. 5, Time series of motions and power output for a small scale, multi duct model.

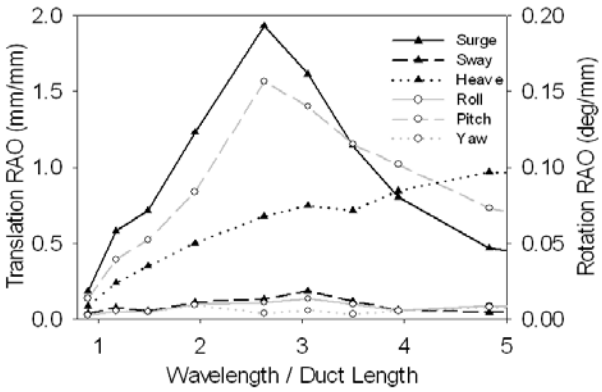

Fig. 6, RAOs for a small scale, multi duct, model of OWEL.

An orifice was used to provide damping to the exiting airflow and the pressure differential across it was measured to determine flowrate and power in order to calculate the conversion efficiency. Fig. 8 shows a typical, time-series pressure trace measuring the pressure drop across the orifice. The dashed line shows the average pressure of the time span which demonstrates that the peak pressures are significantly greater than the average. This type of flow regime is similar to that of an OWC however, unlike an OWC the airflow exhibits very little return flow. Therefore, air flow rectification or self rectifying turbines are not required

and so a more conventional air turbine is well suited. A number of orifice sizes were tested in the previous experimental studies to find the optimum applied damping. It is expected that the damping of the air turbine will be variable and so can be controlled to best suit the incident wave climate. This along with the flow rates and pressure data will help to specify the requirements of the turbine characteristics.

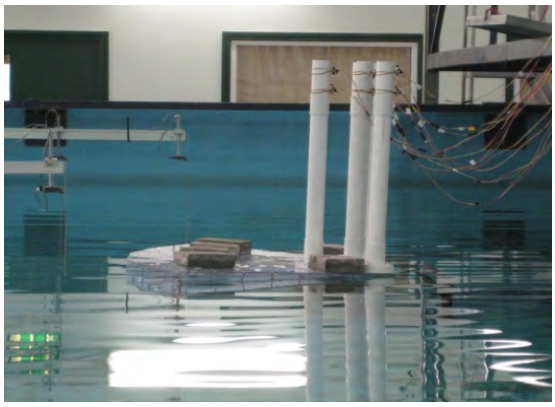

Fig. 7, Experimental testing of a multi- duct, 3D model at HMRC, Cork.

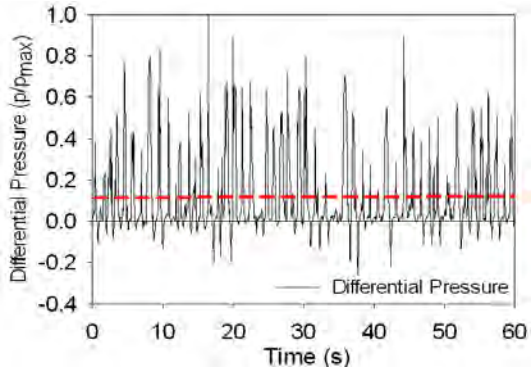

Fig. 8, Plot of normalised, orifice pressure drop for a typical sea state.

Various mooring configurations were also trialled during the wave basin testing and it was seen that different designs have clear effect on the motions of the device as well as the peak and average loads. These small scale moorings, were intended as simple models of a full scale mooring system to provide initial data on the order of the loads that can be expected. As the waves at Wave Hub have low directionality [6], the full scale mooring system will be designed to keep the device on station and orientated towards the predominant wave direction. Computational analysis of the motions and moorings, using a commercial diffraction code, will be undertaken to assess loading and support the final design.

5. Initial Design

5.1. Overview

The Wave Hub, marine demonstrator has been designated the D500 as it is expected to be rated at 500kW. The unit will be a scaled down version of the full scale, commercial design and comprise a single floating duct rather than a large, multi-duct, floating platform as has been previously suggested. This means that a smaller duct can be tested and used as a development platform before a full scale commercial device is designed. An artist's impression and a selection of key figures are given in Fig. 9, whilst the drawings of the initial design are shown in Fig. 10 with the key dimensions and components labelled.

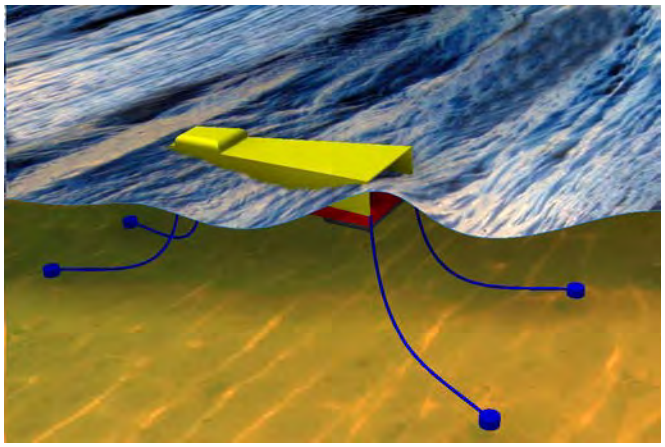

D500 Key Figures

LOA ca.	42m
Beam ca.	18m
Draft ca.	8m
Lightship ca.	650t
Ballast ca.	300t
Total ca.	900t

Fig. 9, An artist's impression and key figures of the D500 demonstrator.

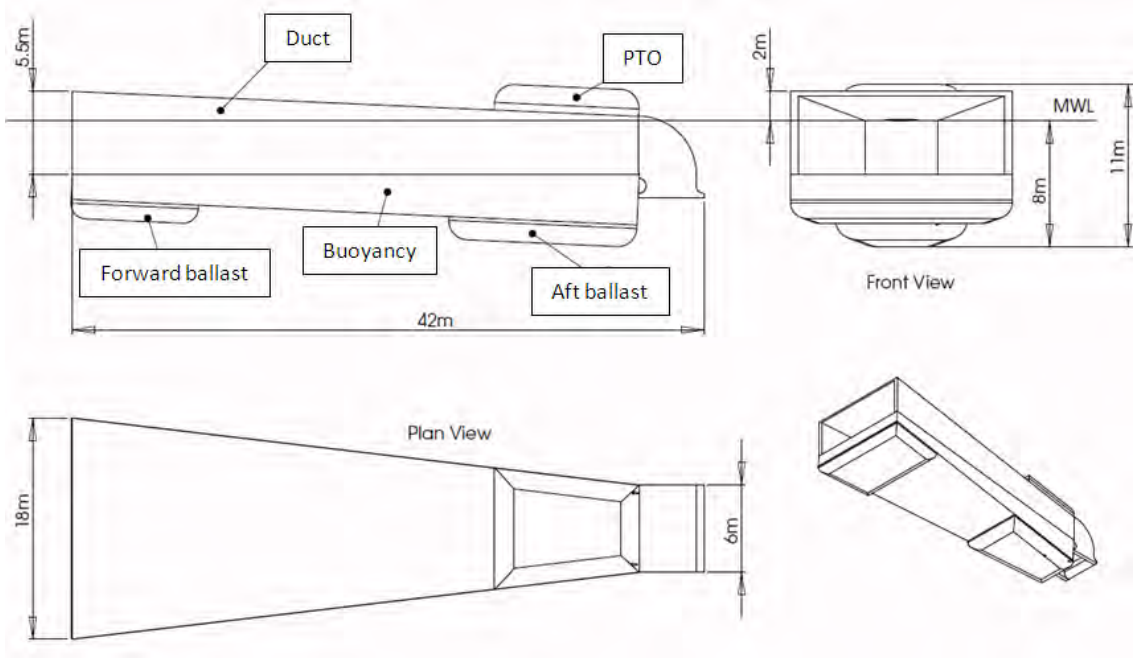

Fig. 10, The general assembly drawings of the initial design of the OWEL demonstrator.

The main duct is likely to be made of steel however concrete is being considered as an alternative material depending on structural loading requirements and costs. The power take-off unit, a turbine and generator set, will be located in a watertight housing at the rear of the duct, above the waterline. Below the main duct will be the main volumes of ballast and buoyancy required to correctly trim the device and determine the motion responses.

A control system to alter the freeboard and natural pitch frequency is being considered. This will involve controlling the volume of air or water in tanks below the duct. By altering the buoyancy, the freeboard can be varied to match the incident wave climate. This also forms a part of the survival strategy in that during storm conditions the freeboard can be reduced to lessen the impact of incident waves on the device. Controlling the position of the ballast about the centre of buoyancy will allow the natural pitch period to be tuned to the optimum value. This will ensure that the phase difference between pitch and wave front is beneficial to the performance as described by the results discussed in the previous section.

5.2. Project Organisation

The demonstrator will be developed by a consortium of organisations that, between them, bring together the wealth of experience needed to successfully deliver a project of this nature. IT Power and OWEL will lead the project whilst the DNV will monitor the design process in order to provide confidence and certify it to DNV standards [7]. In order to best demonstrate the responsibilities of each consortium member, the device can be broken down into its main constituent parts and subsystems, as shown in Fig. 11.

Involving a number of organisations is beneficial to a large and complex project such as the development of a wave energy converter. It brings a wide variety of knowledge into the design process and also clearly demonstrates that third-parties have confidence in the project. Ensuring that the design progresses as planned will be challenging, given the level of communication required between the various consortium partners. A robust design method will be used to facilitate the process, meaning that the design requirements and expectations will be clear.

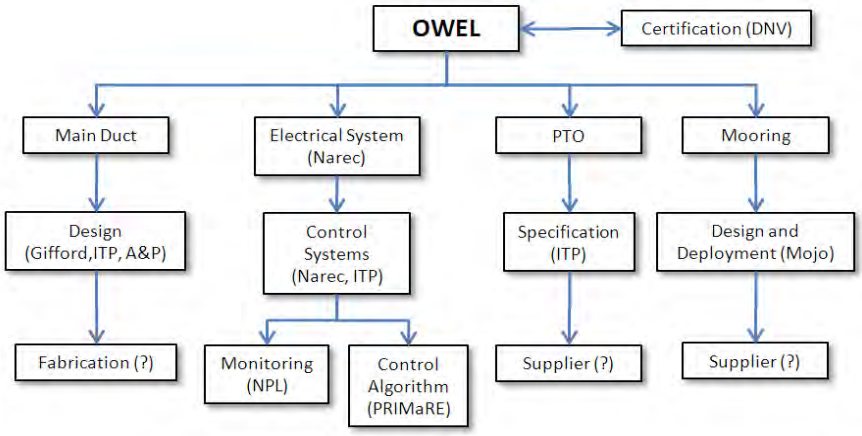

Fig. 11, A chart showing the breakdown of the main subsystems of the OWEL demonstrator and the consortium members responsible.

5.3. Design Framework

The design framework that will be used in the process, works by formulating a "Problem Definition" and "Design Solution" for each major subsection or component in the system. The problem definition is a document created to identify the requirements and constraints on the design, which includes stakeholder expectations, design constraints and assumptions, problem boundaries and interfaces. This also includes functional analysis to determine what the design needs to achieve and a validation to check that the problem that has been defined is actually that which requires a solution. A design solution is then generated to meet the requirements of the problem definition. This begins by assessing and recording all possible ideas and alternative designs. A final design is chosen through modelling, life-cycle cost analysis and risk analysis. The solution is then validated against the problem definition to ensure that the design solution fulfils the problem definition, stakeholder expectations and functional requirements.

Consortium members will likely resort to their own design methods to devise design solutions, however, the problem definitions will be created for all necessary design points. This will unify the group as it will be clear what the problem is and the requirements of the solution. It is then the responsibility of the organisation involved with each design point to generate a suitable design solution. This process mitigates any potential confusion over the design requirements and also clearly sets out responsibilities.

6. Future Development

The forthcoming decade is likely to bring about large advances in wave energy device development. In order for a device to have commercial promise, it has to be successfully demonstrated in a marine environment. The industry is therefore gearing itself towards providing proving and development sites for device teams. Once a machine has been proven at an ocean site at large scale, it will most likely be deployed in small arrays of 3-5MW. In order to attract interest from utilities, device deployment of this magnitude will be required, along with demonstrated reliability. OWEL is therefore aiming to develop its converter to meet these capability requirements.

6.1. Single Duct Commercial unit

Following on from the Wave Hub demonstrator, a first generation commercial OWEL D1000 will be developed as a refinement of the single duct design. It will incorporate advances made following the lessons learned through the D500, meaning that the output for a single duct

should rise. It is envisaged that the first commercial scale deployment of OWEL will feature a number of these single ducts in small array. Deployed in a higher energy wave climate, such as that at the Portuguese Pilot Zone, the improved design will likely be rated at about 1MW per device.

6.2. Multi Duct Commercial unit

A second generation commercial OWEL device could comprise a number of ducts combined to form a large floating platform with a multi-megawatt output. This concept is shown in the artist's impression in Fig. 12. By combining a number of ducts the device could benefit from shared costs of subsystems such as mooring, grid connection, control systems and power take-off. Multiple ducts could also help to smooth power output if the compressed air pulses from each duct were designed to arrive at the turbine of out of phase at staggered times.

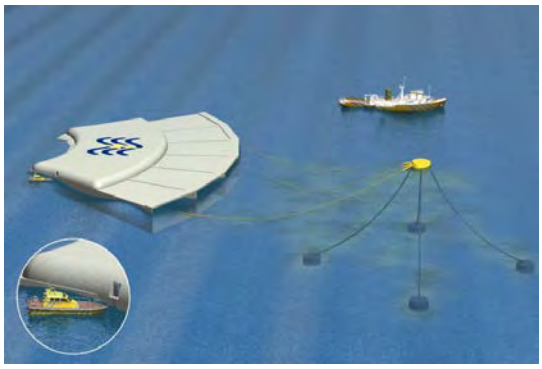

Fig. 12, An artist's impression of a second generation OWEL MD3000 3MW unit

Acknowledgements

The authors gratefully acknowledge IT Power Ltd. Offshore Wave Energy Ltd and the Engineering and Physical Sciences Research Council (EPSRC) for funding this research as part of an Engineering Doctorate study. The Technology Strategy Board (TSB) and the South West Regional Development Agency (SWRDA) are also thanked for funding these phases of the development of OWEL.

References

[1] J. Kemp, A. Derrick, J. O'Nians, and D. Upadhyay. 'The OWEL Wave Energy Converter as a Platform for Combined Wave and Wind Power Generation'. 6th European Wave and Tidal Energy Conference, Glasgow, UK, 2005.

[2] M. Leybourne, W.M.J. Batten, A.S. Bahaj, J. O'Nians and H. Traylor, Preliminary findings from a laboratory scale model of a ducted wave energy converter, 10th World Renewable Energy Congress, Glasgow, UK. 2008.

[3] M. Leybourne, W.M.J. Batten, A.S. Bahaj, J. O'Nians and N. Minns, A Parametric Experimental Study of the 2D Performance of a Ducted Wave Energy Converter. 8th European Wave and Tidal Energy Conference, Uppsala, Sweden. 2009.

[4] M. Leybourne, W.M.J. Batten, A.S. Bahaj, J. O'Nians and N. Minns, Experimental and Computational Modelling of the OWEL Wave Energy Converter. 3rd International Conference on Ocean Energy, Bilbao, Spain. 2010.

[5] B. Holmes, Tank Testing of Wave Energy Conversion Systems. EMEC Standards. European Marine Energy Centre. Orkney, UK. 2009.

[6] Halcrow, Wave Hub Technical Feasibility Study, 2005, Appendix A – Coastal Processes

[7] Det Norske Veritas (DNV), Certification of Tidal and Wave Energy Converters, Offshore ServiceSpecification DNV-OSS-312, 2008.

Investigation of Wave Farm Electrical Network Configurations

Mr. Fergus Sharkey[1,*], Dr. Michael Conlon[2], Mr. Kevin Gaughan[2]

[1] *Dublin Institute of Technology, Dublin, Ireland; ESB International, Dublin, Ireland*
[2] *Dublin Institute of Technology, Dublin, Ireland*
** Corresponding author: Tel: +353 1 7038000, E-mail: fergus.sharkey@esbi.ie*

Abstract: Wave Energy Converters (WECs) have been in development for a number of decades and some devices are now close to becoming a commercial reality. As such, pilot projects are being developed, particularly in the UK and Ireland, to deploy WECs on a pre-commercial array scale. There is little experience in the wave energy or utility industry of designing and installing electrical networks for WEC arrays with the closest comparison being offshore wind farms. There are some key features of WECs which will ultimately dictate that the electrical configuration differs from that of offshore wind farms.

This paper investigates the potential representative electrical network configurations for small (10MW), medium (40MW) and large scale (150MW) 'wave farms' in order to establish a development path for such projects. The configurations are evaluated for efficiency (power loss), redundancy and short circuit levels. Key interfaces in the electrical infrastructure are identified and discussed. This paper also identifies the key differences between offshore wind farm electrical networks.

Keywords: *Wave Energy, Electrical Network, Array*

1. Introduction

Many countries have ambitious targets by 2020-2030 for ocean energy [1], [2] and there are several ocean energy test facilities with grid connection such as EMEC and Wavehub. Collaborative projects have also explored the area of WEC electrical arrays such as the Equimar Project [3] and these have also been investigated in [4]-[10]. The ultimate ambition is to have large wave farms installed in a similar fashion to offshore wind.

Offshore wind energy projects have been developed up to 300MW installed capacity and it is acknowledged that the industry can serve as a useful source of knowledge for the wave energy sector. Investigating the state of the art in offshore wind farms and also looking at all the information available within the wave energy sector will enable a feasible assessment of wave farms to be studied.

2. Offshore Wind Electrical Systems

A survey of the 25 largest offshore wind farms (as of December 2010) shows that the majority are installed less than 15km from shore and in less than 30m depth. As the installed capacity and distance from shore increased offshore, platform based, substations were required in order to step up the voltage to HVAC (>100kV) for transmission to shore. The requirement for an offshore substation is typically above 100MW capacity or 10km distance from shore.

HVDC transmission will be used in larger offshore wind farms located far from shore such as the BARD Offshore Wind Farm (400MW, 100km from shore) which is expected to be commissioned by 2011. There are also development projects on deepwater wind farms and floating wind turbines [11].

All offshore wind farms have a MVAC infield network, typically 20-36kV, with the majority >30kV. The infield network configuration of offshore wind farms is typically a series of radial circuits containing 7-8 turbines connected back to a central location (either onshore or offshore), as illustrated in Fig. 1. The radial circuit is protected using switchgear in the wind

turbines and the substation. The cables in each radial are tapered in size towards the radial extents and this is viewed as the best way to minimise cable costs [12]

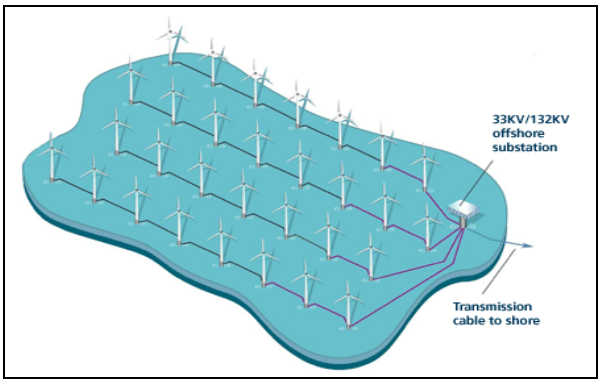

Fig. 1 Typical electrical layout of offshore wind farm [Source: Barrow Wind Farm]

Redundancy and Sectionalising have been proposed in [13] & [14] and have been shown to offer advantages in increasing availability. To date, however, these are rarely utilised due to the inherent additional up front costs.

The average capital expenditure (Capex) for offshore wind in 2009 was €2.3m/MW [15]. From [15] we can also see that for Horns Rev and Nysted offshore wind farms the infield and transmission systems represent ~21% of the total Capex. The electrical system is a significant proportion of the overall investment in a wind farm and, assuming that capacity factors and costs per MW for WECs approach those achieved by offshore wind, then it is expected that the same will hold true for wave energy.

3. Wave Energy Device and Site

The Wave Energy Converter (WEC) used in this study is the Wavebob device [16], which is a point absorber type WEC. The site used for this study is Belmullet, located off the west coast of Ireland, where a test site is currently under development. Using the Wavebob frequency domain model with an electrical rating of 1MW, and a scatter diagram from the test site, the energy yield distribution histogram can be established for a Wavebob device on the site. Fig. 2 shows the energy yield distribution on the site over the course of a year. This demonstrates that almost 20% of energy yield is from >90% output of the device. This information is used in establishing the energy yield efficiency of the electrical network in later sections.

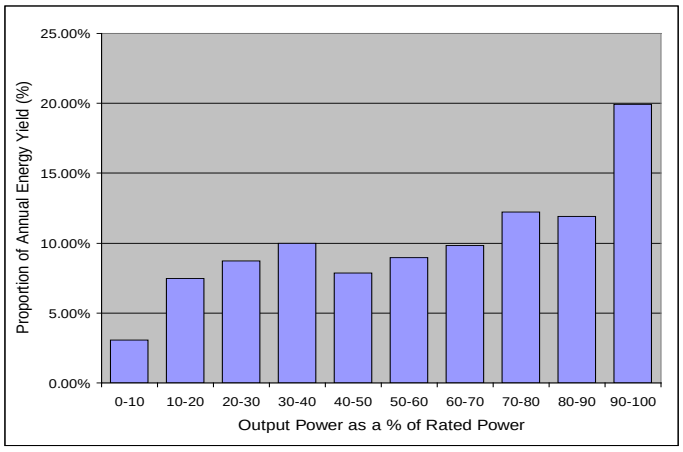

Fig. 2 Energy yield distribution histogram of the Wavebob device at Belmullet

The Wavebob device is designed for 100m+ water depth and is typical of floating WECs. Fitzgerald indicates in [17] that such compliantly moored wave energy converters are likely to be moored close to 100m in general for survivability reasons. The 100m depth contour off the west coast of Ireland lies between 10 and 25km from the shoreline therefore the transmission distance will be selected within this range.

Ultimately the device spacing will be selected based on a variety of factors, namely resource capture and interference [18], [19] mooring footprint [17], marine operation requirements, and minimising cable costs and losses. Therefore 200, 300 and 400 metres device spacings have been selected for this paper. No hydrodynamic interference or directional effects are considered in this paper, however it must be noted that this will limit the maximum rows permissible in an array.

As with offshore wind there will be three types of connection concepts, namely single MV transmission, multiple MV transmission and HV transmission from an offshore substation. As such three candidate wave farms are outlined in Table 1 which will be analysed in this paper.

Table 1 Wave Farms under analysis in this paper.

Wave Farm	Capacity	Distance to Shore	Transmission Voltage	# Transmission Lines
1	10MW	12km	MVAC	1
2	40MW	15km	MVAC	2+
3	150MW	20km	HVAC	1

4. Methodology

The wave farm electrical network will be arranged in radial circuits as this has proven the most cost effective option for offshore wind. For larger arrays a 'forked' radial is utilised as this further reduces cable cross sectional area (CSA) in the radials. The effect of additional redundancy is discussed later. All cables will be three-core XLPE with copper conductors. The methodology is as follows;

- Cables (infield and transmission) are sized for maximum continuous current at 10kV, 20kV & 33kV and, for Wave Farm 3, 132kV. Practical limitations are observed.
- Active Power losses (using lumped parameters) are assessed for the range of 0-100% wave farm output for each case.
- Using the site/device information given in Section 3 the energy yield efficiency for the wave farm is obtained, i.e. the percentage electrical energy delivered in a year.
- If an energy yield efficiency of 96% is not achieved initially then an iterative approach is taken to increase the cable CSA to achieve this target.

For practical limitations a minimum cable CSA of 35mm^2 for 10kV & 20kV and 50mm^2 for 33kV are assumed. A maximum cable CSA of 500mm^2 is assumed as this is one of the largest dynamic cables installed to date in the Maari Oil Field. 10-15 WECs will be connected in each radial depending on the voltage and the total installed capacity. ABB present the practical limitations for transmission at various voltages in [20] which are replicated below in Table 2. These do not account for maximum distances which are of importance when considering very long lines (i.e. >50km) which we are not considering here.

Table 2 - Recommended maximum transmission capacities given in [20]

Voltage	10kV	20kV	30kV	66kV	132kV
Maximum Power	15MW	30MW	50MW	100MW	200MW

For initial wave farms the voltage rating may initially be limited by certain components, notably cable connectors and submarine power equipment. Given sufficient demand it is likely that these components would become available at higher voltages.

Cable parameters for the study are obtained from [21], Nexans and ABB. No sheath or armour losses are considered, however dielectric losses are calculated in all cases. Infield voltage regulation and switching transients are also not considered, but are naturally important considerations for future work.

For larger arrays the short circuit contribution of the grid and generators must be calculated as the short circuit requirements for the cables may result in a larger CSA cable than dictated by the current carrying requirements. Generator selection is critical here as certain generator types will contribute less fault current than others. In [22] fault currents for synchronous and asynchronous generators are given as 15 p.u. and 8 p.u. respectively, whereas double-fed induction generators and power converter interfaced generators contribute approx 1-2 p.u.

5. Results

The layouts of the proposed wave farms illustrated in Fig. 3 are based on a radial approach and within the limitations outlined in Section 4. These are electrical circuit layouts and the physical layout could differ without affecting the cable lengths. These will be analysed according to optimum voltage levels, efficiency and redundancy. The methodology shown in Section 4 will be used to size the cables to achieve 96% energy yield efficiency, i.e. the annual efficiency of exporting MWhrs.

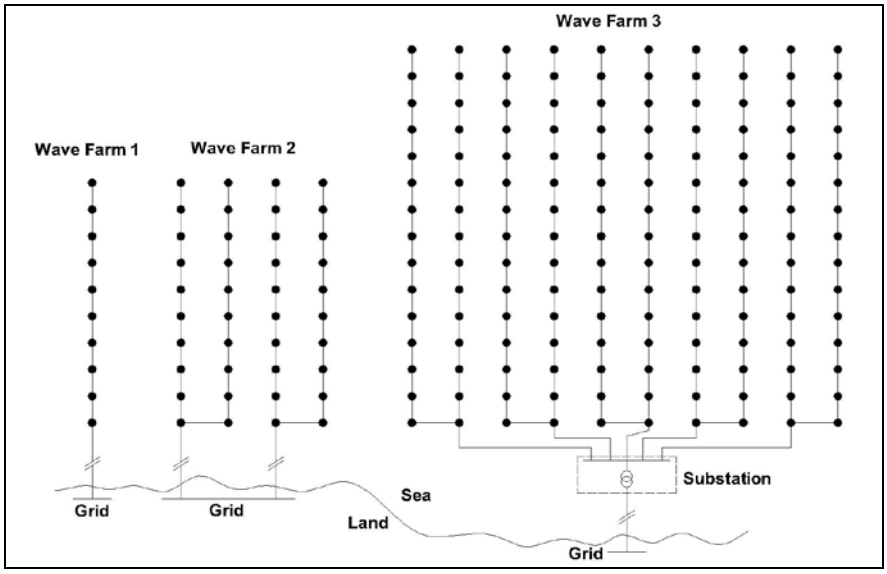

Fig. 3 Selected Wave Farms for Investigation

As mentioned previously this is an iterative process; initially sizing based on maximum continuous current, and then refining based on efficiency. The resultant achievable energy yield efficiencies are illustrated in Fig. 4. >96% energy yield efficiency is achievable in almost all cases, however up to almost 99% is possible for larger wave farms with HVAC connection to shore. Table 3 outlines the cable CSAs required to achieve these figures.

The device spacing has a negligible effect on energy yield efficiency; particularly for larger arrays. Increased spacing will, however, also increase infield cable lengths. The effect of this becomes more pronounced for larger arrays as shown in Fig. 5. Up to 38% increase in cable length is required for larger wave farms when the spacing is doubled.

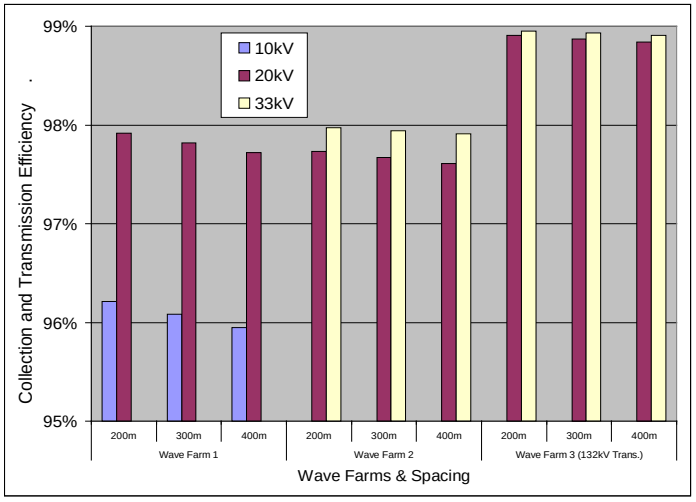

Fig. 4 Achievable Energy Yield Efficiency for Case Study Wave Farms

Table 3 Cable CSA (mm^2) required to achieve efficiencies shown in Fig. 4.

	Wavefarm 1 (10MW)		Wavefarm 2 (40MW)		Wavefarm 3 (150MW)	
	Infield	Transmission	Infield	Transmission	Infield	Transmission
10kV	35-300	400	N/A	N/A	N/A	N/A
20kV	35-95	185	35-95	400	35-500	500*
33kV	N/A	N/A	50*	150	50-300	500*

** Minimum or Maximum limits apply*

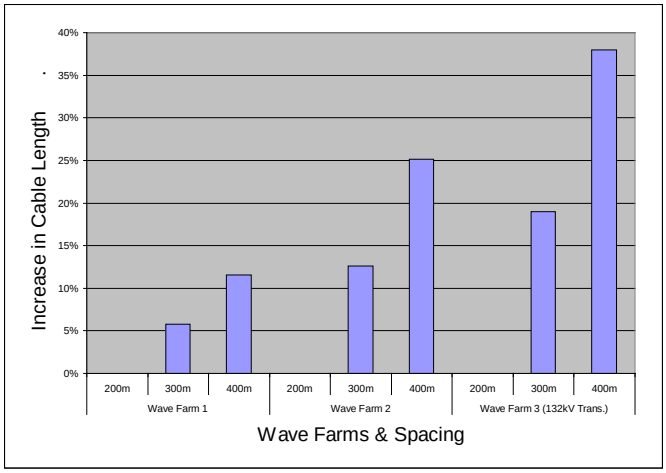

Fig. 5 Percentage Increase in overall farm cable length for spacing increase from 200m.

Redundancy can be added to the network in a variety of ways and has been proven to increase availability while naturally increase cost. Nevertheless, redundancy could have a dual purpose for wave farms as the WEC devices will have to be routinely removed and brought to port facilities for maintenance. Redundant circuits could provide an alternative route for the power during this maintenance period. Fig. 6 shows some possible redundant circuits for Wave Farm 2, which would involve either increasing CSA of cables within the radial or addition of secondary cables running the length of the radial.

Alternatives to redundancy that could be utilised for wave farm maintenance regimes are;

- The availability of ‘standby’ or ‘dummy’ WECs to ‘slot’ into place.
- A system for temporarily ‘bridging’ the gap left by the WEC in the electrical circuit.
- Submarine switchgear allowing continued operation of the infield circuit.

These could prove a more cost effective alternative than additional redundancy.

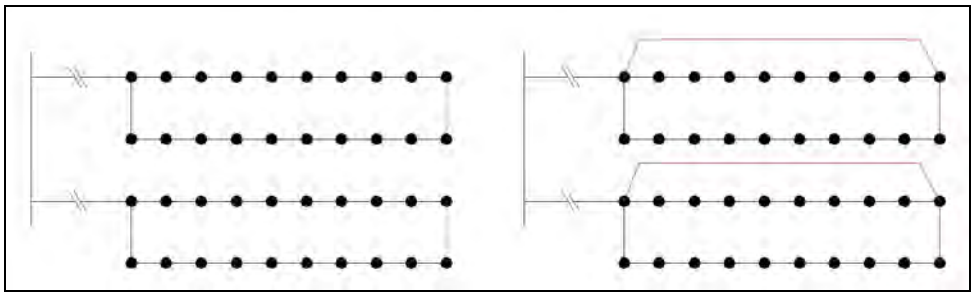

Fig. 6 Wave Farm 2 redundant circuit options

6. Key Interfaces

The studied wavefarms are presented in single line diagrams only. There are a number of key interfaces identified which are a functional part of the wave farm. The key interfaces are;

1. Dynamic Cable to WEC interface
2. Dynamic Cable to Static Cable interface
3. MV Switchgear interface (onboard WEC or seabed installation)
4. Offshore Substation (when applicable)

Interfaces 1, 2 & 3 are of particular interest as they can provide critical functionality in the wave farm system. Some of this functionality overlaps as outlined in Table 4 below. As each of these three key interfaces overlap, each WEC developer must establish the exact functionality and components required for each of these interfaces

.

Table 4 Possible functionality of key interfaces

Functionality of Key Interfaces						
	Connection/Disconnection of WEC	Isolation	Protection	Cable Installation	Deck/Hull Penetration	Maintain Radial Circuit
1	Y	Y**	N	Y	Y	N
2	Y	Y**	N	Y	Y	N
3	Y*	Y	Y	N	N	Y

(with integrated connectors for submarine switchgear; ** with strict control procedures)*

Interface 3 (WEC MV switchgear) is significant to the electrical network as it is a necessary protection function but can also be used for redundancy. Most importantly is its function as part of a safety and isolation system. Submarine switchgear systems have been developed mostly for use in the oil and gas industry.

From [23]; for systems above LV in wind farms (on and offshore), the UK HV safety rules apply [24]. [24] states that in order to work on or near HV power systems the equipment should be isolated and earthed with isolation points and earth points locked where practicable. It would be impractical to expect that submarine switchgear, where required for isolation and earthing, could be locked in this position. The safe control of work would be extremely difficult to undertake given submarine switchgear units.

For interface 4, as is the case in offshore wind, an offshore substation would typically be required for wave farms larger than 100MW. As the wave farm in question will be located in 100m water depth, although the onboard equipment will be identical, the type of foundations typically used in offshore wind farm substations, i.e. monopile, tripod and gravity base, will be impractical. Jacket structures have been used for ‘deepwater’ sites such as in [11]; however this is only 45m depth. The choices for an offshore substation in 100m water depth would be;

- Strategically locating the wave farm in proximity to a <50m water depth location and locating the offshore substation at an midpoint between the wave farm and the shore

- Building a jacket or compliant tower type structure such as those in use for oil platforms
- Building the substation on a floating platform such as the semi-submersible, tension leg or spar type structures in use for oil platforms
- Locating the offshore substation on the seabed

This key interface requires further study to establish the most cost effective option available.

7. Conclusions

This paper explored the technical issues surrounding a development path for electrical networks for future offshore wave farms. The paper concludes that key issues for offshore wind farm electrical networks are cost and efficiency. Following the same configurations as wind farms electrical networks are developed for small, medium and large wave farms which should provide a high level of efficiency. The characteristics of the Wave Energy converter and the site must be taken into account for establishing the 'true' energy yield efficiency.

It will be possible to establish small wave farms (<15MW) using 10kV infrastructure, however this will lead to large cable sizes within the array and particularly to shore. More suitable voltages are 20kV and 33kV within the array and for transmission up to 100MW with offshore substation and 132kV transmission required for transmission for large scale wave farms (>100MW)

Increasing the device spacing within the wave farm has a negligible effect on energy yield efficiency, particularly for larger arrays and does not require increasing cable CSA. There will, however, be a cost impact from having longer infield cables. Doubling the device spacing could add an additional 38% to the overall cable length of the infield and transmission system.

Redundancy can be introduced to the electrical networks, however at a financial cost. Redundancy may prove more important due to larger numbers of devices per radial in wave farms. Redundancy in the electrical network could form an integral part of the maintenance strategy also, however other solutions could be developed to overcome this.

There are a number of key interfaces which a WEC developer must consider at the early stages of device design. If these key interfaces are managed correctly the WEC can lend itself to a flexible, cost effective, and much standardised electrical network, which will make it attractive for deployment on an array scale.

The key differences between offshore wind and wave farms have been identified;

- WECs have lower MW ratings than wind turbines allowing more devices per radial
- Devices will require removal for maintenance having impact on circuit integrity
- Depth at the site is significantly deeper than any offshore wind farm and distance from shore could be further.
- Devices are not fixed structures making cable installation potentially complicated

References

[1] Offshore Renewable Energy Development Plan 2010 - http://www.dcenr.gov.ie/

[2] UK Renewable Energy Strategy 2009 – www.decc.gov.uk

[3] Equimar Deliverable 5.1 2009 – http://www.equimar.org/

[4] M. Kenny. Electrical Connection Issues for Wave Energy Arrays. Masters Thesis, University College Cork, 2010.

[5] A. Kiprakis, A Nambiar, D. Forehand, A Wallace. Modelling Arrays of Wave Energy Converters Connected to Weak Rural Electrical Networks. International Conference on Sustainable Power Generation and Supply, 2009

[6] Czech, B.; Bauer, P.; Polinder, H.; Korondi, P. Modeling and simulating an Archimedes Wave Swing park in steady state conditions. 13th European Conference on Power Electronics and Applications, 2009.

[7] M. Molinas, O. Skjervheim, B. Sorby, P. Andreasen, S. Lundberg, T. Undeland. Power Smoothing by Aggregation of Wave Energy Converters for Minimizing Electrical Energy Storage Requirements. 7th European Wave and Tidal Energy Conference, 2007.

[8] T. Ahmed, A. Zobaa. Offshore power conditioning system connecting arrays of wave energy converters to the electric power grid. 8th International Conference on Advances in Power System Control, Operation and Management, 2009.

[9] M. Santos, D. Ben Haim, F. Salcedo, J. Villate, Y. Torre-Enciso. Grid Integration of Wave Energy Farms: Basque Country Study. 3rd International Conference on Ocean Energy, 2010

[10] D. O'Sullivan, G. Dalton. Challenges in the Grid Connection of Wave Energy Devices. 8th European Wave and Tidal Energy Conference, Uppsala, Sweden, 2009

[11] S. Breton, G. Moe. Status, Plans and Technologies for Offshore Wind Turbines in Europe and North America. Renewable Energy, 2009. Pg. 646-654

[12] J. Twidell and G. Gaudiosi – Offshore Wind Power. Multi Science Publishing, 2007

[13] H. Landsverk, O. Granhuag, P. Skryten, S. Rafoss. 36kV Vacuum Circuit Breaker Panel - The Perfect Switchgear for Wind. 20th International Conference on Electricity Distribution, Prague, Cezch Republic 2009

[14] J. Yang, J. O'Reilly, J. Fletcher. Redundancy Analysis of Offshore Wind Farm Collection and Transmission Systems. International Conference on Sustainable Power Generation and Supply 2009

[15] R. Green, N. Vasilakos. Economics of Offshore Wind. Energy Policy, 2010. Pg. 1-7

[16] W. Dick. 'Wave Energy Converter'. U.S. Patent Number 6857266

[17] J. Fitzgerald. Position Mooring of Wave Energy Converters. PhD Thesis, Chalmers University, Sweden. 2009 – pp 36

[18] C Fitzgerald, G. Thomas. A Preliminary Study on the Optimal Performance of an Array of Wave Power Devices. 7th European Wave and Tidal Energy Conference, 2007.

[19] P. Ricci, J-B Saulnier, A. Falcao. Point Absorber Arrays: A Configuration Study off the Portuguese West Coast. 7th European Wave and Tidal Energy Conference, 2007.

[20] ABB – Cables for Offshore Wind Farms. www.abb.com

[21] C. Moore. BICC Electrical Cables Handbook 3rd Edition. Blackwell 1997.

[22] P. Karaliolios, A. Ishchenko, E. Coster, J. Myrzik, W. Kling. Overview of Short-Circuit Contribution of Various Distributed Generators on the Distribution Network.

[23] Renewable UK – Wind Turbine Safety Rules. http://www.bwea.com/safety/safety_rules.html

[24] UK National Grid – The Electricity Transmission Safety Rules 3rd Edition. http://www.nationalgrid.com/

Performance analysis of a floating power plant with a unidirectional turbine based power module

Prasad Dudhgaonkar[1], Kedarnath S.[2], Biren Pattanaik[1], Purnima Jalihal[1], Jayashankar V.[2,*]

[1] *National Institute of Ocean Technology, Chennai, India*
[2] *Indian Institute of Technology Madras, Chennai, India*

** Corresponding author. Tel: + Tel: +91 4422574427, Fax: +91 4422570509, E-mail: jshankar@ee.iitm.ac.in*

Abstract: A major attraction of a floating wave power plant as opposed to a fixed Oscillating water column (OWC) plant is in the cost of construction. The price paid is in the lower efficiency of conversion in the hydrodynamic stage. This puts onus on the subsequent power module stage in achieving an efficiency that is necessary for a commercial plant. A new backward bent ducted buoy (BBDB) was designed in which the power module is a twin unidirectional turbine. Basic experimentation on the power module is done on a turbine with 165 mm diameter and characterized with bidirectional flow with widely varying flow rates. The efficiency is shown to be better than 68% over the expected working range. The details of a plant producing 50 kW for Indian conditions is described. The range of powers over which a BBDB structure compares with a fixed OWC is highlighted.

Keywords: *Wave energy, floating power plant, backward bent ducted buoy.*

1. Introduction

The oscillating water column (OWC) principle is an attractive approach to convert wave energy into electrical energy as exemplified by operational plants in several countries [1]. As of today it is reasonable to expect a wave to wire efficiency of about 24 % with a fixed OWC device [2]. Of this, the OWC efficiency would be about 60 %, and the power module (comprising bidirectional turbine and generator) would be about 40 %. One aspect of the fixed OWC is that the structural cost could lie between 70 to 85 % of the overall cost [3]. This has motivated the development of floating OWCs which promise reduced cost with an accompanying reduction in efficiency in the hydrodynamic stage. The largest of such structures was the Japanese Mighty Whale [4]. While laboratory results predicted a best efficiency of 50 % in the hydrodynamic stage, practical measurements showed that the best efficiency was about 30 %. Hence the overall wave to wire efficiency was closer to 15 %. There have been continuous attempts to improve the efficiency of floating OWCs and the backward bent ducted buoy (BBDB) is one such attempt [5]. In this work we show that an improved power module for the BBDB with variable speed twin unidirectional turbines can achieve 65 % efficiency and thus make the floating structure attractive in spite of the lower hydrodynamic efficiency.

2. The Backward Bent Ducted Buoy (BBDB)

The Backward Bent Ducted Buoy (BBDB) has been conceived as a relatively low cost wave energy device to convert wave energy into electricity. The BBDB has a backwardly inclined oscillation water column, which has been proved to be more effective than a forwardly inclined one. It uses an oscillating column of water in reverse L shaped chamber or duct, such that the open mouth of the duct is away from the incident waves. The horizontal limb has an opening to the sea and is submerged under water. The vertical limb traps a column of air at the upper region of the duct and a regulated vent allows air to pass in and out under cyclic pressure and partial evacuation of air due to oscillating water surface. The enclosed water column is, not influenced by the wave movements around the buoy, whereby it oscillates

relative to the wave motion moving the buoy itself. The air current, which arises, drives an air turbine installed above the water column. This airflow becomes a means to produce power. Fig. 1 shows a BBDB which was initially deployed for testing without a power module. It had an equivalent orifice in order to simulate a turbine. The dimensions of the model were determined after model studies as reported in [6]. The Indian conditions require a zero crossing period of about 8 seconds and a significant wave height of 1.2 m yielding average incident energy of 6.3 kW/m. The overall design is based on an improvement in the power module in the work reported in [7].

Fig.1. The BBDB being deployed with an orifice for charactering hydrodynamic performance

3. Basic simulations on fixed guide vane and unidirectional impulse turbines

The design of the BBDB described in [7] was based on a fixed guide vane impulse turbine. It was concluded that an optimum turbine diameter of 1.5m would yield a power output of 30 kW with H_s = 2.25 m and T_z = 8.5 s where H_s and T_z are the significant wave height and zero crossing period respectively. We show that an equivalent power module with a twin unidirectional turbine topology [8] would substantially improve the efficiency of the power module and thus the overall power conversion. In order to validate the concept, studies are done in a turbine of diameter 165 mm coupled to a 375W, 3000 rpm dc generator. An oscillatory flow rig is used to characterize the performance. The diameter was based on two criteria: The oscillatory flow rig is sufficient for characterizing its performance over the entire flow regime and more importantly the damping offered by the turbine matches that of the orifice used in the BBDB hydrodynamic test. This is shown in Fig. 2 which portrays the pressure- flow behavior of the 165mm unidirectional turbine (UDI), a 165 mm fixed guide vane impulse turbine (FGV) and orifices ranging from 52.5 mm to 77.9 mm in diameter. As is known the best hydrodynamic efficiency occurs when the area ratio between the orifice and the OWC water plane lies in the 1/100 to 1/150 range. The 165 mm turbine meets this requirement. Fig. 3 shows a comparison of the performances of FGV turbines and UDI turbines estimated from steady state tests. The comparison is in terms of the efficiency, output shaft powers and the operating flow coefficient ϕ. Both machines operate at 3000 rpm. A fixed speed of operation is initially considered with an induction generator as an option. It is seen that the UDI turbine has a higher efficiency than the FGV turbine. A more important result is established based on a careful study of Fig. 3. It can be seen that the efficiency of the UDI turbine drops when the pneumatic power increases. One solution to remedy this aspect is to consider a variable speed generator as opposed to a fixed speed one. Accordingly Fig. 4

shows the performance of the UDI for various speeds from 1500 rpm to 3500 rpm. The remarkable result that emerges is that with a variable speed machine, the efficiency can be made to remain at about 0.7 over the entire range of operation from 4 W to 160 W. Further the variation in speed is within the range feasible with doubly fed induction machines or permanent magnet synchronous machines.

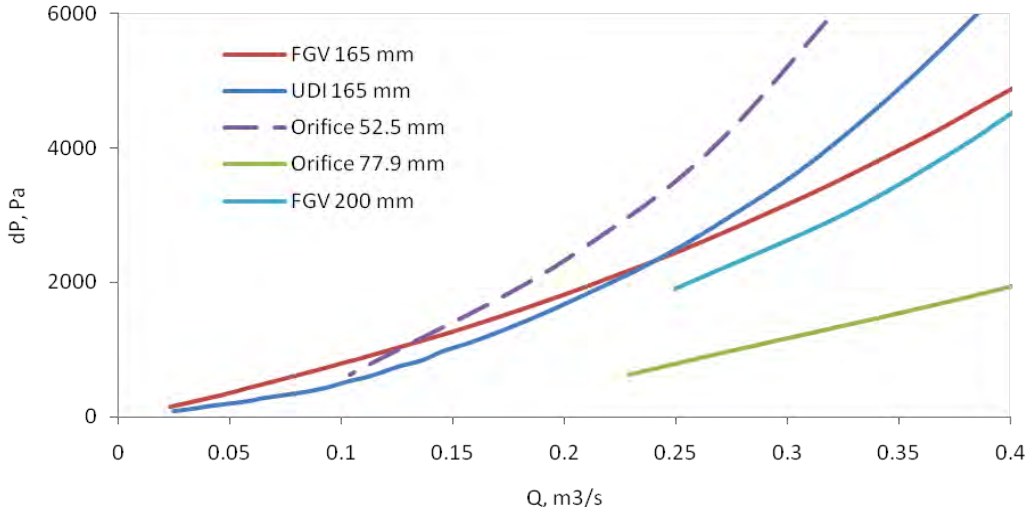

Fig.2: Differential pressure across fixed guide vane impulse turbine and unidirectional impulse turbine for diameter 165 mm for different flow rates (3000 rpm)

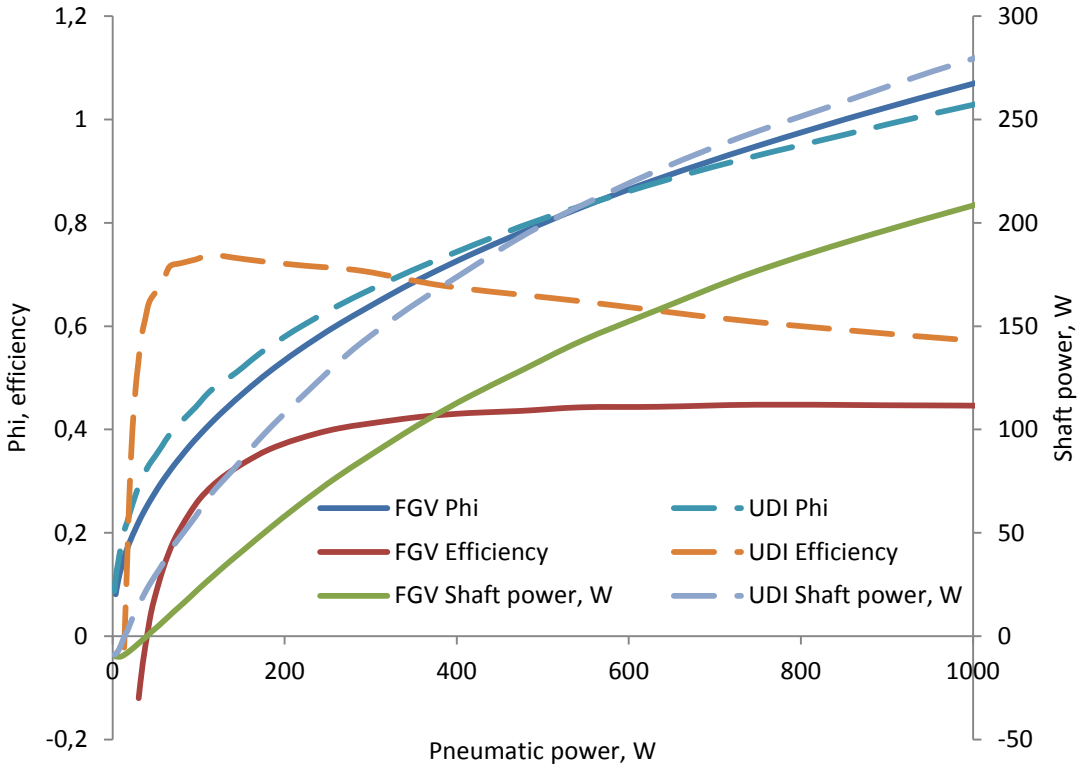

Fig. 3: Comparison of performance of fixed guide vane impulse turbine and unidirectional impulse turbine for diameter 165 mm (3000 rpm)

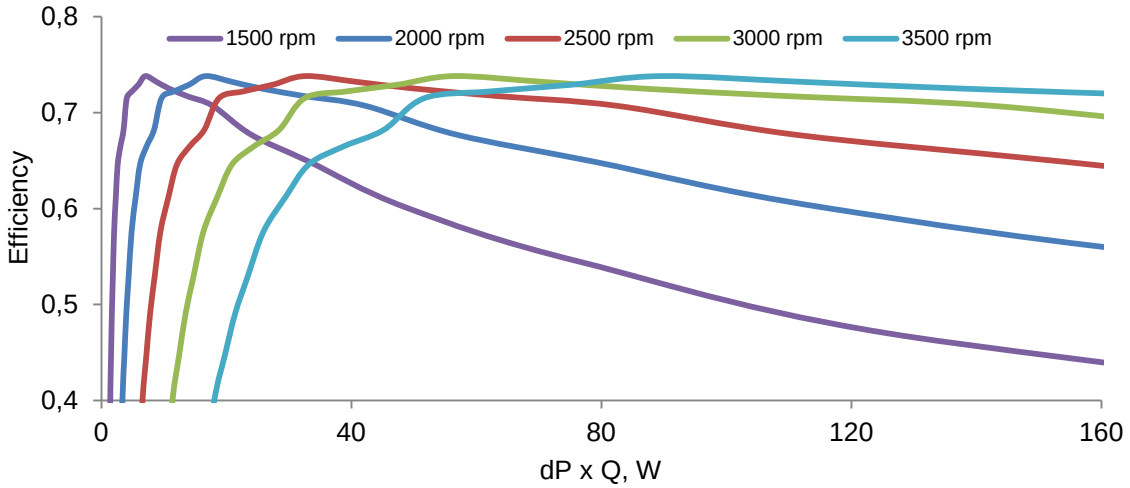

Fig. 4. Estimated performance characteristics for unidirectional impulse turbine of 165 mm diameter over a range of speeds

4. The power module for the BBDB

The prototype BBDB recently made for experiments in Japan had a length of 25 m, breadth of 5.25 m and a draft of 10 m [7]. It could produce a peak output of 30 kW at Hs = 2.25m with a 1.5 m FGV turbine. We now consider the use of a 1.5 m UDI turbine for the same purpose. Fig. 5 shows the comparison. Fig. 5 a compares the shaft output from the two classes of turbines with speeds of 300 rpm and 600 rpm with input powers up to 400 kW. The corresponding efficiencies are shown in Fig 5 b. Fig. 5 b again highlights the importance of variable speed operation for the UDI turbine.

The next section concerns the experimental validation of the UDI concept.

5. Experimental setup for validation of the UDI turbine

The basic experimental setup for oscillatory flow studies was described in [8] wherein it was also shown that induction generators could be used for the power module. In this work a slightly different approach was used. Two pipe sections were independently coupled to the common oscillatory flow rig. One of them housed a 165 mm UDI turbine with a 3000 rpm, 180 V, 375 W dc generator. The other housed an orifice in conjunction with a fluidic diode (bluff body) as shown in Fig. 6. This was to ensure the matching of the turbine damping to that of an appropriate orifice and also to ensure that the intake stroke provides flow to the orifice and the exhaust stroke vents air through the turbine. It can be appreciated that several basic experiments on the performance of various shapes of fluidic diodes could also be tested with this arrangement. In effect it tests the ability of passive fluidic diodes in controlling flow.

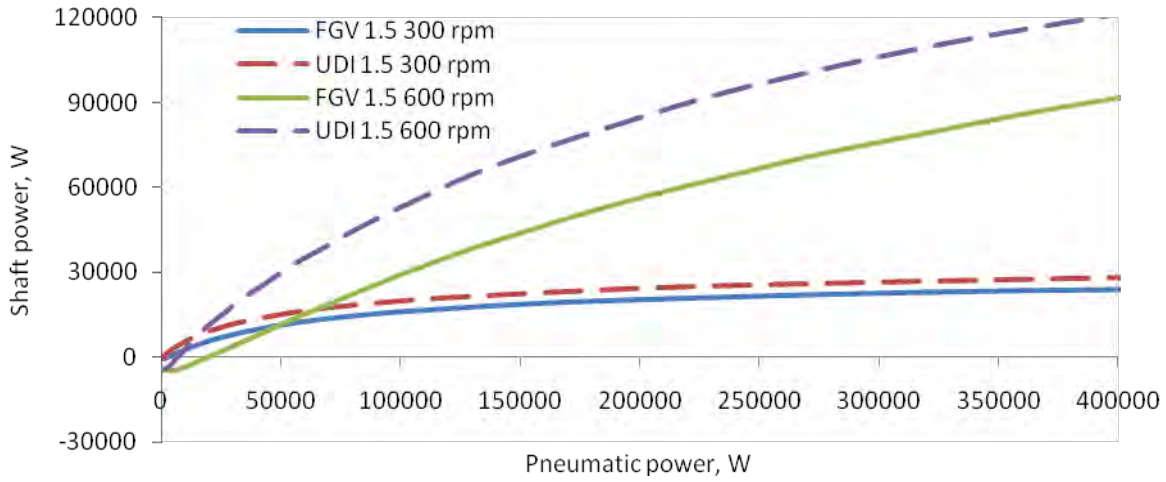

(a)

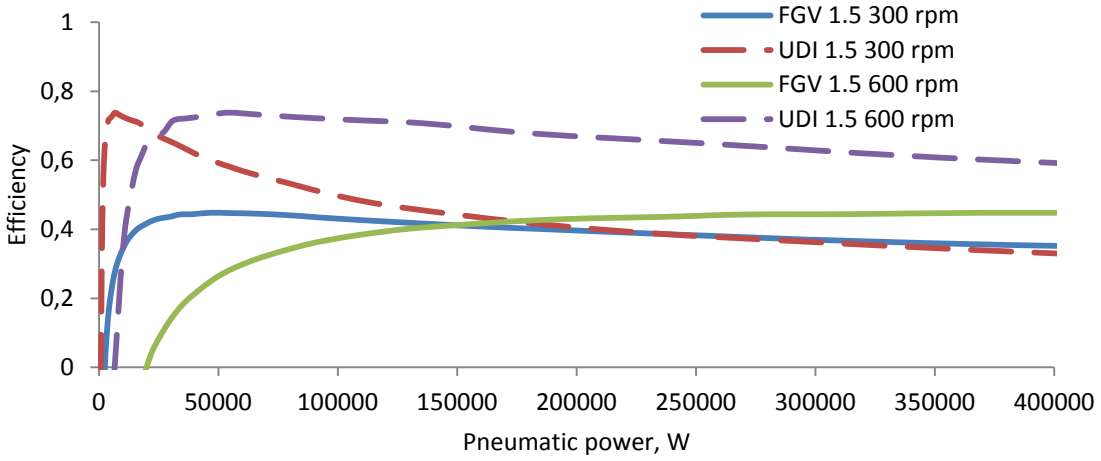

(b)

Fig.5: Comparison of performance of fixed guide vane turbine and unidirectional flow turbine for diameter = 1.5 m for different speeds

Figure 6 presents the comparison of the performance of a FGV turbine of diameter 1.5 m presented in [7] with the estimated performance of a UDI turbine of the same diameter. It can be noted that the variable speed UDI turbine can deliver up to 20 to 30 % more power over FGV turbine. Also the overall wave to wire efficiency of the BBDB with UDI turbine is higher for the entire range of operation.

The quantities measured were pressure across the impulse turbine and the orifice, the turbine inlet duct pressure, the turbine speed, the generator voltage, load current.

Pressure measurements

The differential pressure across the turbine and orifice were measured using calibrated differential pressure transmitters (STD 120) made by M/s. Honeywell.

Voltage and Current measurements

The generator terminal voltage was measured using voltage transducers made by M/s. LEM. The load current was measured using current sensors by M/s. LEM, USA. All of these devices were calibrated before use, with accuracies better than 1%.

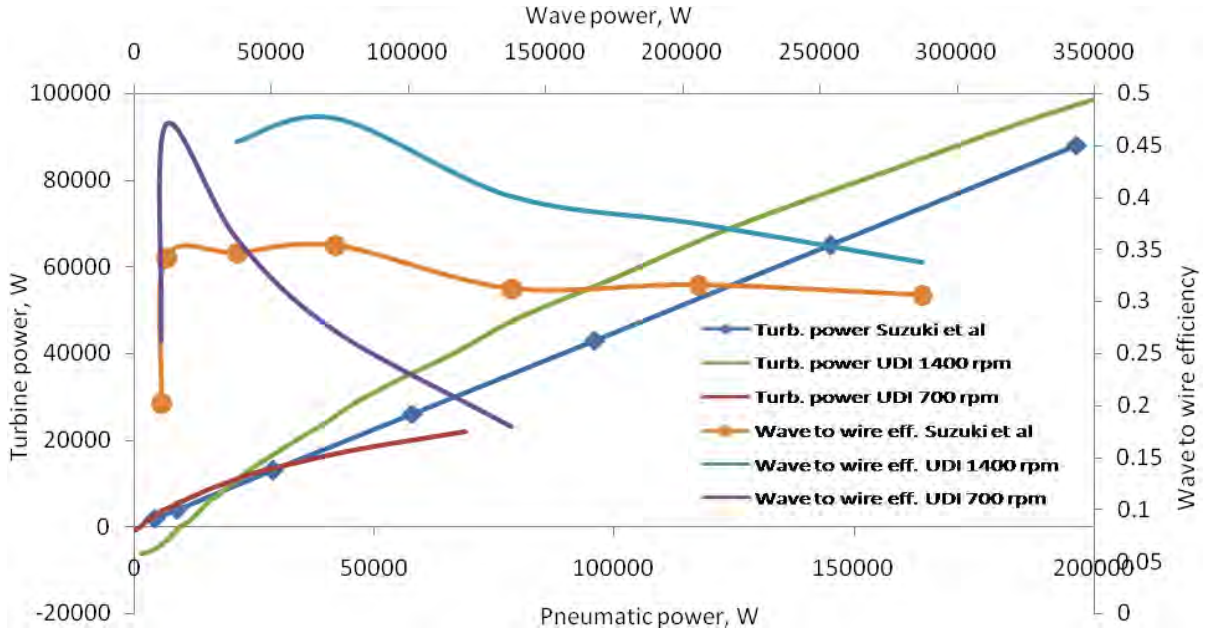

Fig. 6: Estimated power output of a 1.5 m diameter unidirectional impulse turbine

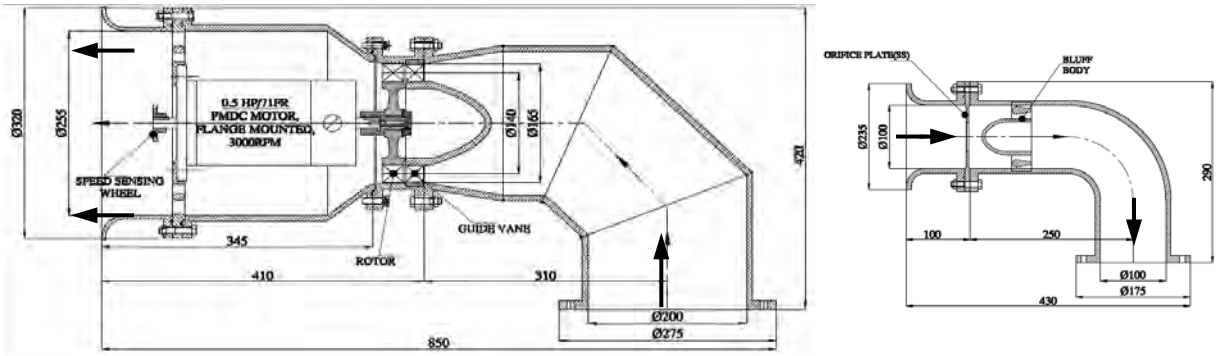

(a) (b)

Fig.7 : 165 diameter unidirectional flow turbine for exhaust and air vent with bluff body for intake

Power and speed

The electrical power was estimated from the generator terminal voltage and load current. The turbine speed was estimated from the generator terminal voltage to within 2% error.

Data acquisition

All the data pertinent to the evaluation were logged by a data acquisition system (DAQ, USB 6215, National Instruments) at 1 kS/s. Low pass filters were employed to remove noise in the signals.

Fig. 8 shows one typical result. It primarily validates the notion of using twin UDI turbines by ensuring appropriate intake and exhaust flow though the turbine and orifice respectively and also quantitatively establishes the efficiency of the turbine. Fig. 8 shows the output from the generator for various stroke lengths of the piston that drives the oscillatory flow. The peak pressure drop observed on the test rig across a 30 mm diameter orifice matched with the peak pressure drop across the turbine.

In effect the experiments and simulation confirm the likely improvements in BBDB performance by replacing the FGV turbine with a UDI turbine.

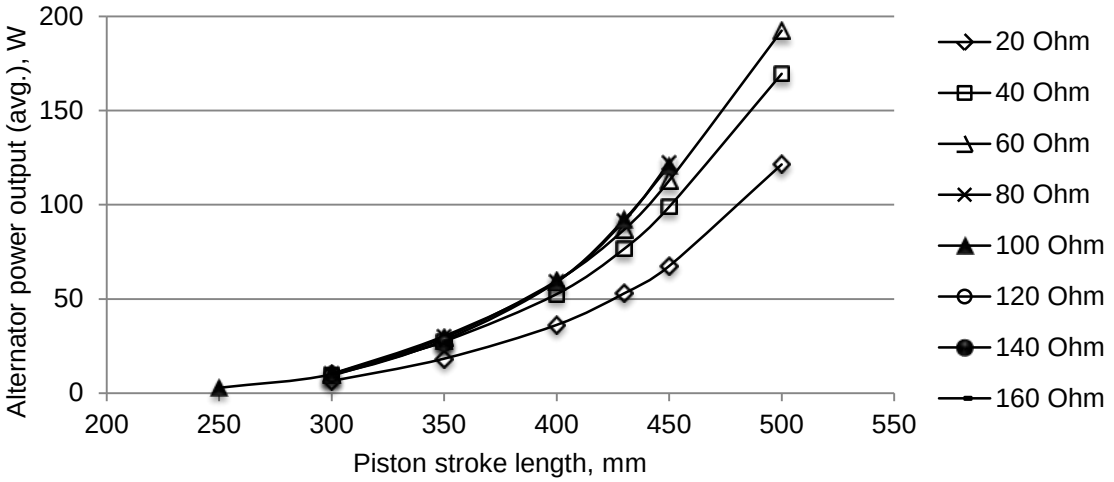

Fig. 8. Average power output of alternator vs. piston stroke length vis-à-vis electrical resistance

6. Conclusions

A power module based on the twin unidirectional impulse turbine topology can substantially improve the efficiency of a BBDB. Experiments on a 165 mm turbine validate the claims of improved efficiency. A 1.5 m turbine can produce about 50 kW in comparison with 30 kW from a fixed guide impulse turbine for the same wave excitation. Variable speed operation is a must in order to retain the high efficiency over the range of operation. There exists a strong case for floating OWCs in several applications involving powers in the tens of kW range.

References

[1] Heath, T., Whittaker, T.J.T & Boake, C.B.; The design, construction and operation of the LIMPET wave energy converter, Wave Energy 2000, 2000

[2] Ohno H., Funakoshi T., Saito K., Oikawa K., and Takahashi S., "Interim report on the Second Stage of Field Experiments on a Wave Power Extracting Caisson In Sakata Port," *ODEC*, 1993, pp. 173-182.

[3] Marine Energy Challenge: Oscillating Water Column wave energy converter evaluation report, © The Carbon Trust 2005.

[4] Research and development of technology on wave energy utilisation, Jamstec 2004

[5] Masuda Y *et al* "The BBDB an improved floating type wave power device", Proceedings Ocean 88, pp 1067-1072.

[6] A.G. Pathak, A. Subramaniam, " Performance studies on a scaled model BBDB under regular and random waves ", Proceedings ISOPE, 1999 pp 139-141.

[7] Suzuki *et al* "Performance of OWC type floating wave power plant employing impulse turbine" 3rd International conference on ocean energy, Bilbao, 2010.

[8] Mala K., Jayaraj J., Jayashankar V. et al., "A twin unidirectional impulse turbine topology for OWC based wave energy plants – Experimental validation and scaling," Renewable energy 36, 2011, pp. 307-314.

Impact of tidal stream turbines on sand bank dynamics

Simon P. Neill[1,*], James R. Jordan[1], Scott J. Couch[2]

[1] *School of Ocean Sciences, Bangor University, Menai Bridge, UK*
[2] *Institute for Energy Systems, The University of Edinburgh, Edinburgh, UK*
** Corresponding author. Tel: +44 1248 713808, E-mail: s.p.neill@bangor.ac.uk*

Abstract: Previous results from one-dimensional model studies have demonstrated that large-scale exploitation of the tidal stream resource could have a significant impact on large-scale sediment dynamics. In this research, we model the impact which such exploitation would have on the dynamics of offshore sand banks. Such banks have an important role in natural coastal protection, since they cause waves to refract and induce wave breaking. As a case study, we examine the Alderney Race, a strait of water between the island of Alderney (Channel Islands) and Cap de la Hague (France). A morphological model is developed, incorporating tidal energy converter (TEC) device operation as a momentum sink in the three-dimensional hydrodynamic module. Through a series of model experiments, we demonstrate the impact which a full-scale (300 MW) TEC array would have on sediment dynamics when sited in the vicinity of headlands and islands. It is important to understand this aspect of the environmental impact of full-scale TEC operation, since headland and island sand banks comprise of readily mobile sediment grain sizes. Therefore, small changes to the tidal regime can have a large effect on the residual sediment transport pathways, and hence sand bank evolution, over the life cycle of a TEC device.

Keywords: *Tidal stream turbines, Tidal energy converter devices, Sediment dynamics, Sand banks, Alderney Race*

1. Introduction

Tidal energy converter (TEC) devices operate by intercepting the kinetic energy in strong tidal currents (typically through a turbine unit). This intercepted energy is then converted to electrical energy through a power take-off system (e.g. an induction generator) and conditioned for dispatch to the electricity network. Theoretically, this is similar to the operation of a typical wind energy device. However, what is significantly different from the wind energy analogy is the environment that TEC devices operate in [1], and the potential for TEC devices to interact with their environment [2]. Given the proliferation of at-sea demonstration devices, the environmental impacts of TEC device operation is a timely issue to consider. The major research questions in the tidal energy context have already been identified [3]. However, progress to-date has been limited in addressing these research issues. The impact of TEC operation on sediment dynamics has yet to be explored in the scientific literature beyond an idealised one-dimensional (1D) model pilot study [4], stimulating the present study.

Extracting energy from a tidal system will lead to an overall reduction in current speed over the larger area domain [2]. This reduction in current speed, even for relatively large TEC array extraction scenarios, is generally quite small. For example, in a tidal channel the impact of energy extraction on current speed U becomes noticeable only when the energy extracted reaches around 10% of the available kinetic energy flux [5], a considerably large amount of energy to extract from a channel. More realistic extraction scenarios (typically 1% of the available kinetic energy) could therefore be perceived to have very little environmental impact. However, bed shear stress is a function of U^2. Therefore, small changes in the tidal currents could potentially lead to large changes in the resulting bed shear stress. Further, the transport of sediments is proportional to an even higher power of velocity than bed shear stress, e.g. total load transport by currents (bedload and suspended load) is a function of $U^{2.4}$

[6]. Therefore, relatively small changes to the residual flow field due to exploitation of the tidal stream resource could have a significant effect on the transport of sediments. This has been reported in a 1 D idealised study of the Bristol Channel (UK), where the morphodynamics were significantly impacted 50 km from the site of energy extraction [4]. In the case of a simple tidal channel or an estuary, much insight can be gained from such 1D model studies, since much of the flow is similarly 1D. However, for more complex situations such as flow past islands and headlands, two- or three-dimensional (2D or 3D) models are required to predict and understand the complexity of the flow field and estimate the impacts of energy extraction.

Strong tidal flow past headlands and islands leads to the generation of large eddy systems, with an opposite sense of vorticity between the flood and ebb phases of the tide [7]. Sand banks form either side of such headlands due to a b alance between the outward-directed centrifugal force and the inward-directed pressure gradient within the eddies [8], leading to a convergence of relatively coarse sand as a function of the instantaneous tidal currents (Fig. 1). The sand banks which form as a result of this convergence can be up to 10 km in length, and have an important role in coastal defence (since offshore banks affect both wave refraction and breaking), and can be a strategic source of marine aggregates. Regions of strong tidal flow past headlands and islands have been listed as potential sites for the exploitation of the tidal stream resource, such as Portland Bill in the English Channel [9], and flow past the island of Alderney in the Channel Islands [10]. The aim of this study is to determine how such exploitation in the vicinity of headlands and islands would affect the maintenance of the associated sand banks. This is addressed through the investigation of a modelling case study: the Alderney Race.

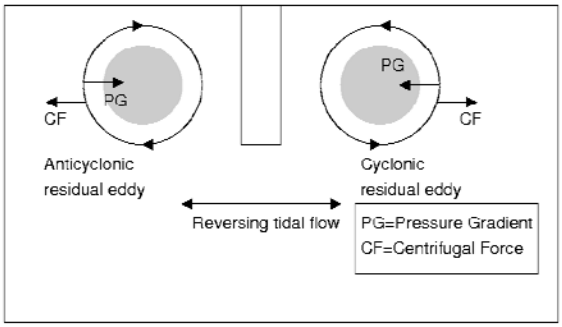

Fig. 1. Headland or island sand bank formation. Reversing tidal flow past the headland or island leads to the generation of eddy systems with an opposite sense of vorticity between the flood and ebb phases of the tide. The outward-directed centrifugal force within each eddy is balanced by an inward-directed pressure gradient. This leads to the inward movement of relatively coarse sediment near the bed (where the centrifugal force is weaker due to bed friction), and the formation of headland or island sand banks. Grey shading indicates the location of sand banks.

2. The Alderney Race

The Alderney Race is a 15 km strait of water separating the island of Alderney (Channel Islands) and Cap de la Hague in France (Fig. 2). With a mean spring tidal range of around 6 m and mean spring tidal currents exceeding 2.5 m/s [11], the Alderney Race presents one of the most hostile environments within the northwest European shelf seas. However, over 20 km^2 of the Race has a w ater depth in the range of 25-45 m, the typical depth range suitable for practical TEC device operation [1] which, in conjunction with consistently high current speeds, represents one of the best opportunities in the world for large-scale exploitation of the tidal stream resource. This opportunity has been recognized by the formation of the Alderney

Commission for Renewable Energy (ACRE), with powers to regulate the operation of marine energy in the territorial waters of Alderney (www.acre.gov.gg). Using current technology, the practical exploitable annual energy output for the Alderney Race has been estimated as 1340 GW h at a rated turbine array capacity of 1.5 GW [10], and a large portion of this energy is contained within the three nautical mile territorial limit of Alderney.

To the south of Alderney there are a series of sand banks known as the South Banks (Fig. 2). The scale of these banks is substantial, 4 km in length and covering an area of seabed around 3 km^2. Hence, the sand banks are important to the economy of Alderney in terms of offering natural coastal protection, as a potential strategic source of marine aggregates, and as a hazard to navigation. The South Banks are maintained by recirculating tidal flows in the lee of Alderney during the ebb phase of the tide (as described in Section 1) and, despite some degree of interannual variability (primarily due to the stochastic nature of waves and wind-driven currents), have persisted in more-or-less their current configuration for several thousand years.

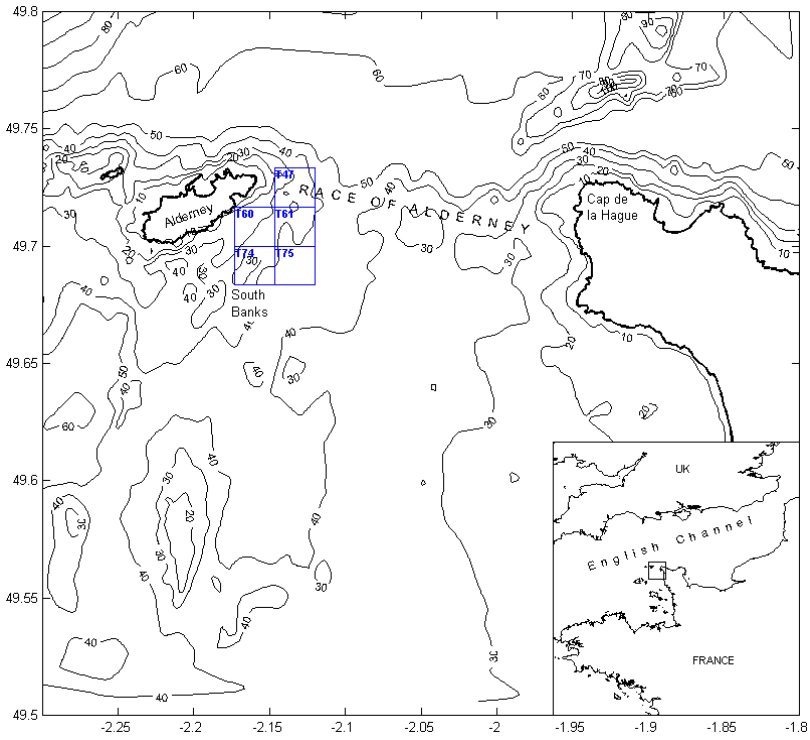

Fig. 2. Bathymetry of the Alderney Race and surrounding waters. Contours are water depths (in metres) relative to mean sea level and squares (labeled T47, T60, T61, T74 and T75) are regions (or blocks) identified by the Alderney Commission for Renewable Energy for exploitation of the tidal stream resource. For scale, the side length of each block is 1 nautical mile (1.85 km). The inset shows the location of the Alderney Race relative to the UK and France.

The ACRE has sub-divided the territorial waters of Alderney into 96 regions, or blocks. Detailed hydrographic and geophysical surveys have been carried out for blocks T60, T61, T74 and T75 (Fig. 2), and it is therefore assumed that these blocks would be developed first if the proposed tidal energy project were to proceed. However, block T47 is of particular interest to the present study since (a) it contains the highest velocities in the western part of the Alderney Race (Section 3), and (b) this location is close to the point of maximum vorticity due to tidal flow past the island. Hence, tidal currents in block T47 have a major controlling influence on the maintenance of the South Banks.

3. The Numerical Model and Baseline Results

Bathymetry for the study region was digitised from Admiralty Charts and interpolated onto a model grid with a horizontal resolution of approximately 150 m, and with 6 terrain-following (sigma) layers in the vertical. The boundary conditions were extracted from a larger area model of the northwest European shelf seas which had a resolution of 1/6° longitude × 1/9° latitude. The 3D POLCOMS model [12] was applied to the Alderney model configuration over a spring-neap cycle, using the dominant semi-diurnal tidal constituents, M_2 and S_2, as boundary conditions. The model of the Alderney region was successfully validated in terms of the magnitude and phase of the M_2 (lunar) and S_2 (solar) elevations at three stations taken from the Admiralty tide tables, and for the magnitude and phase of tidal currents at the location of four tidal diamonds taken from the Admiralty Chart of the region.

3.1. Baseline Results

The model was applied initially to a natural baseline case, in order to understand the residual currents and sediment transport pathways in the absence of artificial energy extraction. The residual currents for a spring-neap cycle are plotted in Fig. 3. Clearly, there are two large residual eddies in the vicinity of Alderney: one due to the ebb currents and one due to the flood currents. The former eddy (to the south of Alderney) is approximately centered over the South Banks, confirming the convergent process which maintains this sand bank (Section 1). Taking a median sediment grain size of 300 μm (medium sand) as representative of the region, the residual sediment transport over a spring-neap cycle is shown in Fig. 4, based on calculations of the total load transport [6]. Although the residual sediment transport vectors are similar to the residual flow field (Fig. 3), there are distinct differences. In particular, the residual sediment transport to the east of Alderney is predominantly directed southwards, partially explaining why the dominant sand bank of the region forms to the south of Alderney, with no corresponding sand bank associated with the residual eddy to the north[1].

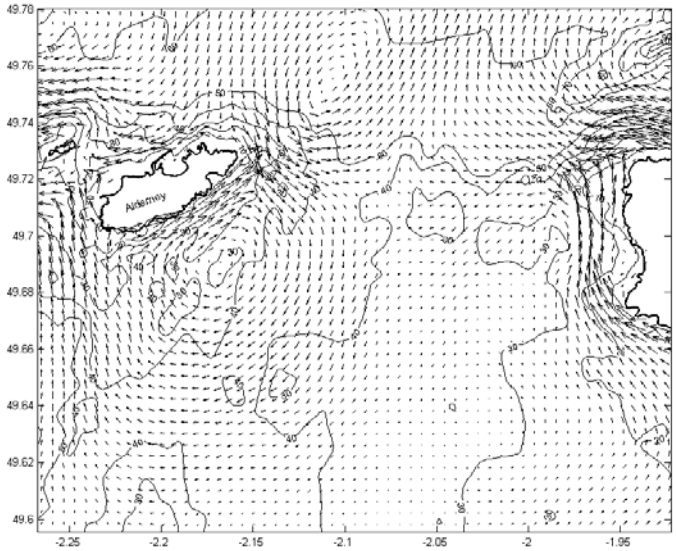

Fig. 3. Modelled residual tidal currents in the Alderney Race for baseline case (no artificial energy extraction). Contours are water depths (in metres) relative to mean sea level. For clarity, every third modelled vector has been plotted in both the x- and y-directions.

[1] In addition, there is a distinct asymmetry in the ambient water depths to the north and south of Alderney.

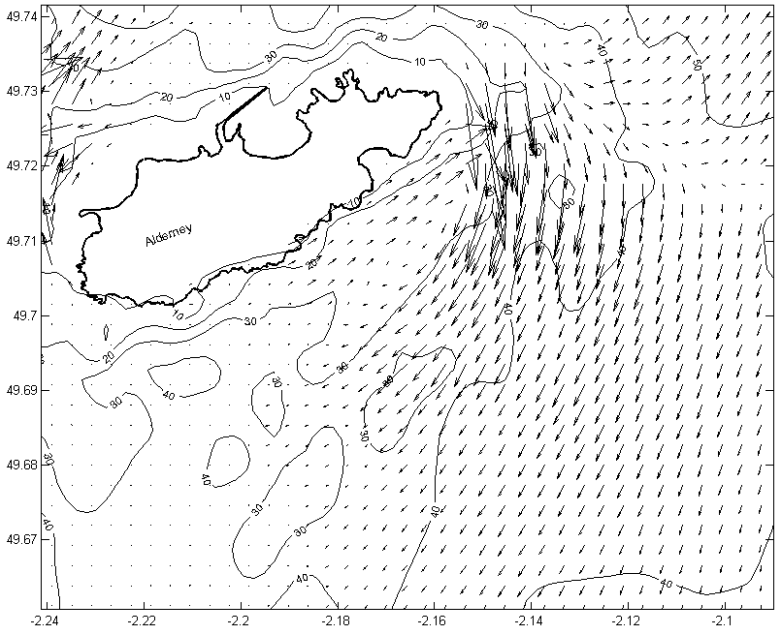

Fig. 4. Residual sediment transport around Alderney for baseline case (no artificial energy extraction). Contours are water depths (in metres) relative to mean sea level. For clarity, every second modelled vector has been plotted in both the x- and y-directions.

4. Energy Extraction

A momentum sink was incorporated in the 3D POLCOMS model code, with turbine characteristics parameterised from an OpenHydro turbine (with a 15 m diameter), the preferred technology supplier for Alderney Renewable Energy (ARE) (http://www.are.gb.com/technology-developers.php). Details of the OpenHydro power curve were taken from Bedard et al. [13], with a cut-in speed of 0.7 m/s, a rated power of 1.5 MW (at 2.57 m/s), and an assumed efficiency (at the point of extraction) of a constant 35%. Applying a minimum lateral spacing of 3 turbine widths and a minimum downstream spacing of 15 turbine widths to eliminate lateral and wake effects, respectively (e.g. [10]), a simple rectangular array of 200 OpenHydro devices (i.e. a 300 MW array) can easily be accommodated by each of the 1.85 × 1.85 km development blocks marked in Fig. 2. In this study, simulations were performed only for blocks T47 and T60.

4.1. Energy Extraction Results

The results are presented in this section as difference plots, i.e. the difference between each of the artificial energy extraction simulations *minus* the baseline simulation. In the region of energy extraction, the magnitude of mean velocity was reduced by around 0.05 m/s for each of the energy extraction scenarios (T47 and T60) (Fig. 5). The reduction in velocity was not localised to the turbine array, but extended a distance of up to 10 km from the array. Despite local reductions in the magnitude of velocity, the far-field velocity was increased by a similar magnitude (0.05 m/s), particularly to the northwest of Alderney. Changes to the sediment transport followed a similar pattern to velocity (Fig. 6). The instantaneous predictions of sediment transport were applied to a 2D continuity equation to predict the change in bed level over the 30 year life-cycle of a TEC device (Fig. 7). Again, the morphodynamic impact was non-localised, with bed level changes of about a metre occurring over a 30 year period. However, the most important result in terms of the main aim of this study is that a 300 MW TEC array would have a negligible impact on the morphodynamics of the South Banks,

maintained by recirculating tidal flows in the lee of the island. However, the morphodynamics of the region will be significantly altered by such large-scale exploitation of the tidal stream resource, and this effect will be evident up to 10 km from the point of extraction.

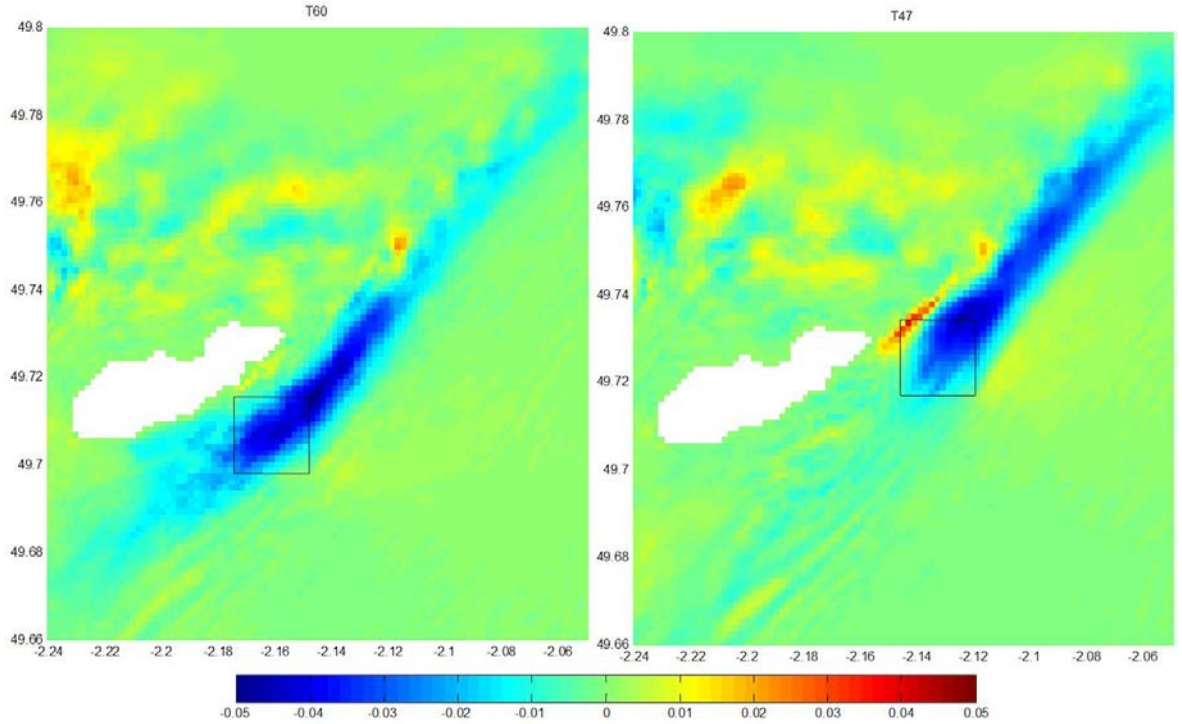

Fig. 5. Change in the magnitude of velocity (in m/s) due to energy extraction, averaged over a spring-neap cycle. Boxes show the limits of the TEC array for each case (T60 and T47).

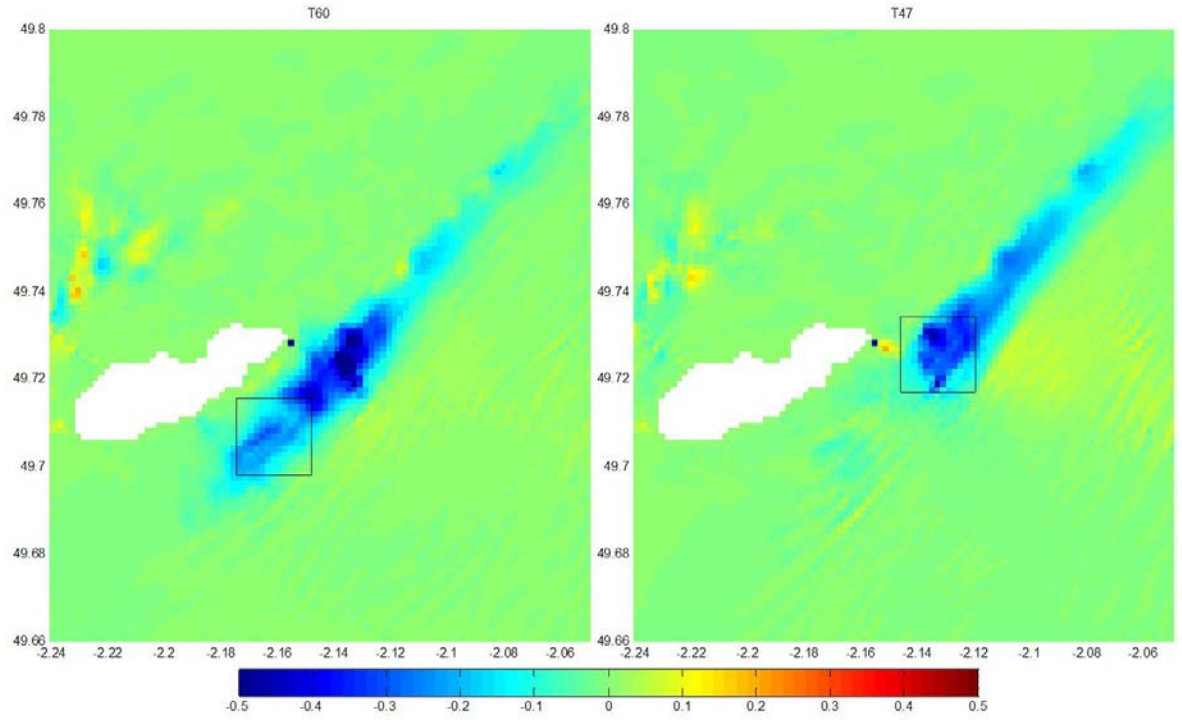

Fig. 6. Change in the magnitude of sediment transport for medium sand due to energy extraction, averaged over a spring-neap cycle. Boxes show the limits of the TEC array for each case (T60 and T47).

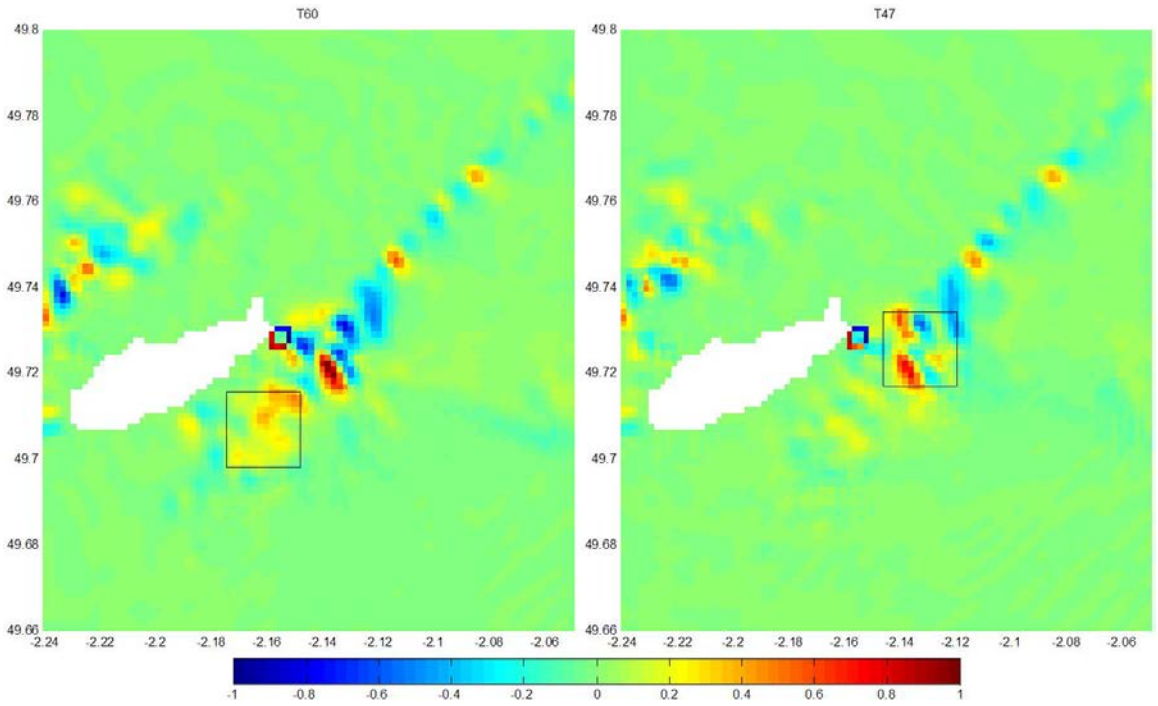

Fig. 7. Change in bed level (in metres) due to energy extraction, extrapolated to the 30-year life-cycle of a TEC device. Boxes show the limits of the TEC array for each case (T60 and T47).

5. Discussion and Conclusions

Strong tidal flow past islands and headlands leads to the generation of island wakes and headland eddies, and the formation of associated sand banks. Such strong tidal flows past islands and headlands are attractive regions in which to exploit the tidal stream resource. This study has demonstrated that despite extracting a relatively large amount of energy from the tidal streams in the vicinity of an island (a rated 300 MW TEC array), little change to the morphodynamics of the sand bank (formed by recirculating tidal currents in the lee of the island) occurs. This result is insensitive to the location of the TEC array in relation to the island. However, over the 30 year life-cycle of a TEC device, the morphodynamics of the surrounding region will change by up to a metre with such large-scale exploitation of the tidal stream resource.

References

[1] S.J. Couch and I.G. Bryden, Tidal current energy extraction: hydrodynamic resource characteristics, Proceedings of the Institution of Mechanical Engineers, Part M: Journal of Engineering for the Maritime Environment 220, 2006, pp. 185-194.

[2] S.J. Couch and I.G. Bryden, Large-scale physical response of the tidal system to energy extraction and its significance for informing environmental and ecological impact assessment, In: Proceedings Oceans 2007-Europe International Conference; 2007. p p. 912–916.

[3] The Robert Gordon University, A scoping study for an environmental impact field programme in tidal current energy, DTI Publication URN 02/882, 2002.

[4] S.P. Neill, E.J. Litt, S.J. Couch and A.G. Davies, The impact of tidal stream turbines on large-scale sediment dynamics, Renewable Energy 34, 2009, pp. 2803-2812.

[5] S.J. Couch and I.G. Bryden, ME1 - marine energy extraction: tidal resource analysis, Renewable Energy 31, 2006, pp. 133-139.

[6] R. Soulsby, Dynamics of marine sands, Thomas Telford, 1997, pp. 176.

[7] I.S. Robinson, Tidal vorticity and residual circulation, Deep-Sea Research 28, 1981, pp. 195-212.

[8] R.D. Pingree, The formation of the Shambles and other banks by tidal stirring of the seas, Journal of the Marine Biological Association of the United Kingdom 58, 1978, pp. 211-226.

[9] W.M.J. Batten, A.S. Bahaj, A.F. Molland, J.R. Chaplin and Sustainable Energy Research Group, Experimentally validated numerical method for the hydrodynamic design of horizontal axis tidal turbines, Ocean Engineering 34, 2007, pp. 1013-1020.

[10] L. Myers and A.S. Bahaj, Simulated electrical power potential harnessed by marine current turbine arrays in the Alderney Race, Renewable Energy 30, 2005, pp. 1713-1731.

[11] H.M. Pantin, The sea-bed sediments around the United Kingdom: their bathymetric and physical environment, grain size, mineral composition and associated bedforms, British Geological Survey Report SB/90/1, 1991, 47 pp.

[12] J.T. Holt and I.D. James, An s coordinate density evolving model of the northwest European continental shelf: 1 m odel description and density structure, Journal of Geophysical Research 106, 2001, pp. 14,015-14,034.

[13] R. Bedard, M. Previsic, O. Siddiqui, G. Hagerman and M. Robinson, Survey and Characterization of TISEC Devices, report number TP-004-NA, EPRI, pp. 56-64.

Experimental and numerical results of rotor power and thrust of a tidal turbine operating at yaw and in waves

Pascal W. Galloway[1,*], Luke E. Myers[1], AbuBakr S. Bahaj[1]

[1] *Sustainable Energy Research Group, School of Civil Engineering and the Environment, University of Southampton, Southampton, SO17 1BJ, UK.*
**Corresponding Author Tel +44(0)23 80595458, E-mail: P.W.Galloway@soton.ac.uk*

Abstract: Little has been done to investigate the behaviour of Marine Current Energy Converters (MCECs) in unsteady flow caused by wave motion and yaw. The additional loading applied to the rotor through the action of waves and whilst operating at yaw could dictate the structural design of blades as well as the proximity to the water surface. The strongly bi-directional nature of the flow encountered at many tidal energy sites may lead to devices employing zero rotor yaw control. Subsequent reductions in device capital cost may outweigh reduced power production and increased dynamic loading for a rotor operating at yaw. The experiments presented in this paper were conducted using a 1/20th scale 3-bladed horizontal axis MCEC at a large towing tank facility. The turbine had the capability to measure thrust and torque via a custom waterproof dynamometer. A BEM (Blade Element Momentum) code developed within the university was modified to include wave and yaw, with a view to further understanding the primary loading upon the rotor and individual blades.

Keywords: *marine current energy converter, wave-current interaction, strain gauge, loading*

1. Introduction

One of the enduring topics of interest in the field of coastal and offshore engineering is that of wave-current interactions and their effect on static and dynamic structures. The co-existence of waves and currents is a common feature in the marine environment [1]. Waves are strained and refracted by currents, causing exchanges of mass, momentum and energy to occur between the waves and mean flow [2]. The main energy in the coastal region can be attributed to tides, surges and wind waves. Interactions occur between these different 'waves' because the tides and surges change the mean water depth and current field experienced by the waves [3]. The usual approach to the interaction problem has been to ignore the interaction between waves and currents and simply add the two together (using their particle velocity vectors) so as to calculate the forces on a body [4].

Marine Current Energy Converter (MCEC) technology is currently at the prototype stage where unique devices are being deployed at specific sites or marine energy testing centers. There is little detailed knowledge of the flow field properties at highly energetic tidal energy sites [5]. Generally peak flow speeds are measured but the effect of wave and bed generated turbulence is neglected. The effect this will have on MCECs is unclear, which may lead to prototype devices being installed at sheltered locations where these effects are minimised [5]. If this becomes a trend with developers it may result in reduced energy capture as blade diameters are constrained and potentially higher energy flows are not utilised. MCECs of a given rated power typically experience four times the thrust of a wind turbine of the same rated power, even though the MCEC will be significantly smaller in diameter. Thus it is expected that rotor loading and general structural integrity could be significant for MCEC devices. Therefore the need to quantitatively assess the blade/rotor loading caused by wave-current interaction is clear. At present, few experimental wave-current studies have been conducted in the presence of MCECs. One particular study combined Blade Element Momentum (BEM) theory for wind turbines and linear wave theory to predict rotor torque and thrust and to assess the influence of waves on the dynamic properties of bending moments at the root of rotor blades [6]. The outcomes were limited, particularly those for the

blade loading. In the field, research carried out at the European Marine Energy Centre showed that in a water depth of 45m, wave effects penetrated as far down as 15m whilst turbulence from the bottom boundary layer penetrated up as much as 17m. This resulted in approximately a third of the water column remaining relatively tranquil [7]. If blade loading in the more turbulent regions could be quantified then this may allow for greater energy capture from larger diameter rotors.

2. Methodology

2.1. Towing Tank Experiment

The experiments presented in this paper were conducted in a wave/towing tank (60m long x 3.7m wide x 1.8m deep). A $1/20^{th}$ - scale tidal turbine model (see Fig.1) was equipped with the capability to measure rotor thrust and torque (utilising a waterproof dynamometer) and rate of rotation (via optical sensors). The parameters varied included: TSR (tip-speed-ratio), turbine yaw and turbine submergence depth. The blades utilised a NACA 48XX profile with varying thickness and twist along the chord length. The waves used had a height of 0.1m and a 1.34s intrinsic period; current speed was $0.9ms^{-1}$.

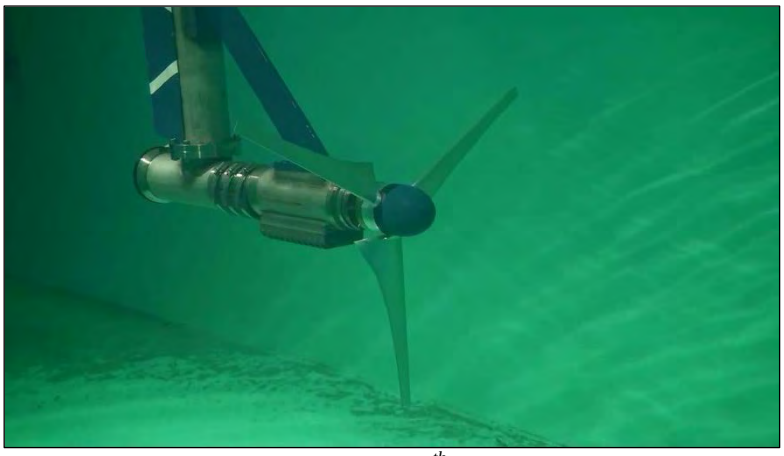

Fig. 1. Underwater photo of $1/20^{th}$ scale tidal turbine model

The design of the thrust-torque dynamometer utilised for this work is discussed previously [8] and was based on the extensive work carried out by Molland and Turnock [9] for their research on ship propellers. A wireless telemetry system located inside the turbine nacelle collected filtered and amplified signals from the strain gauges before data was conveyed above the waterline via a sealed umbilical cable. The model turbine is a Froude scaled representation of a 16m diameter MCEC. The maximum scaled current speed would be 4m/s, which is significant for a suitable MCEC location; however it is significantly lower than the maximum current speed of 8.55m/s used in the experiments conducted by Barltrop [6]. High velocities tend to be used in turbine experiments because a low Reynolds number can degrade the dynamical properties of the airfoil and can be a source of irregularity between the experimental data and simulation data [6]. Laboratory experiments are useful for approximating these wave-current phenomena since little detailed knowledge exists for tidal energy sites since there has never before been the need for such data [5]. The problem is that the use of a towing tank results in no actual Doppler shift in the waves because there is no real current present (see section 2.2). More complex facilities such as a circulating water channel with wave-making facilities would be more representative; however depths would need to be at least 2m with the ability to generate waves from a range of directions relative to the current.

2.2. Numerical Model

Numerical modelling has shown that the influence of waves complicates the flow with its influence being more than just adding turbulence. The dynamic part of the waves causes significant oscillations in the power and thrust, which in-turn influence the 'quality' of the electrical power production. High frequency oscillations (known as flicker) occur. It is thought that this flicker is caused by variations of the angle of attack under the influence of wave motion [10]. The nature of wave-current interaction is complex: If a current encounters a wave in the same flow direction, the wave height decreases with an increase in wavelength, whilst the current speed increases. The opposite is true if the current encounters a wave in the opposite flow direction [3].

A Doppler shift is observed when surface waves and current velocities interact. The primary effect of a current is to change the frequency of the waves due to a Doppler shift. The observed angular frequency, ω, of the ωaves in a frame of reference moving ωith the current, σ, the intrinsic angular frequency and the wave number, k, is given by:

$$\omega = \sigma + kU \tag{1}$$

This relationship describes how the observed wave frequency reduces or increases based on current velocity. A Doppler shift is valid in the case of a constant current, but a more complex effect is noted in the case of sheared currents. Use of linear wave theory superimposed on a uniform current does not give a strictly accurate representation of wave-current interaction effects. It is however a straightforward approach and may yield adequate results for a MCEC. Linear wave theory has been found to be a fairly accurate representation of wave-current interaction in depths of water greater than 12.5m and with significant wave heights lower than 5m for the purposes of dispersion [3].

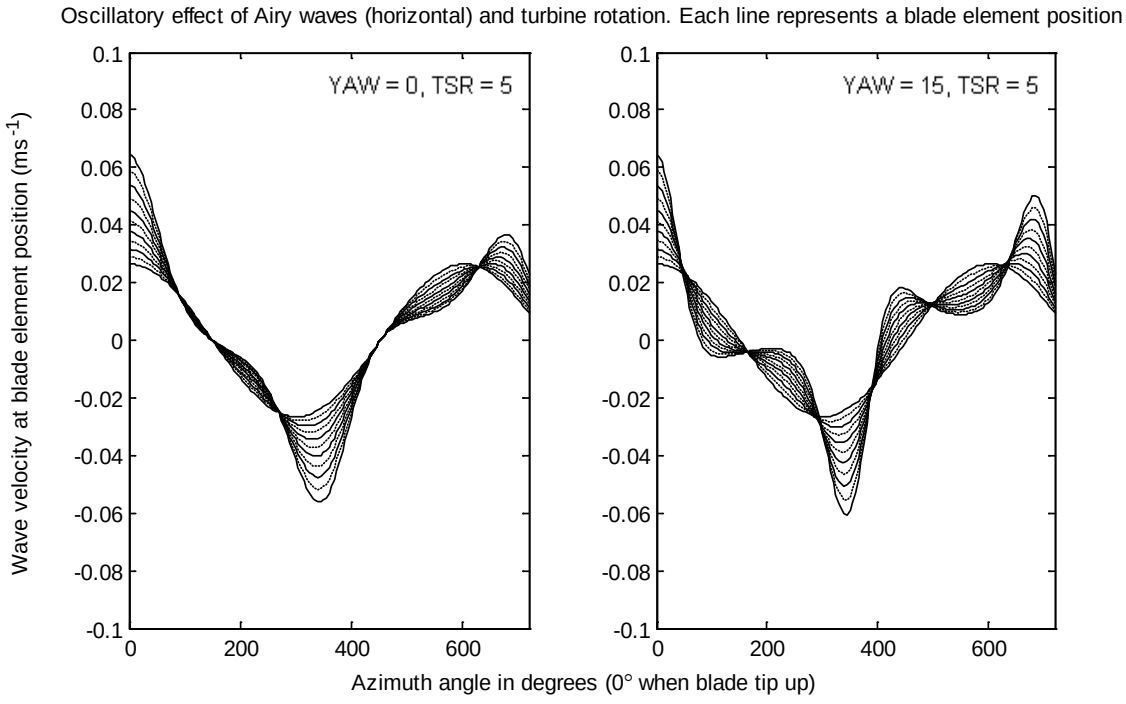

Fig. 2. 1st order wave-current interaction velocities as seen at individual blade elements over two revolutions. The left figure is for zero yaw, the right figure is for 15° yaw. The largest oscillations can be observed at the outer element i.e. at X=1, the tip of the blade (X = elemental radius/blade radius)

It is well known that BEM theory is commonly used by wind turbine designers for predicting loads and power outputs for wind turbines. Although this theory is readily applicable to MCECs there are some differences. Wind for example does not have a characteristic property that resembles wave-current interaction; therefore this must be taken into account when designing prototype MCECs. A BEM code has been modified to include the effect of monochromatic waves on a uniform current with the inclusion of yawed flow if desired. The model assumes that there is no distortion to the incoming flow field or lateral velocity variation and that rotor speed is constant. An example of the wave velocities observed at a single blade can be seen in Fig.2. These velocities are calculated using linear wave theory with a D oppler shift. Based on BEM geometry, these velocities are then calculated instantaneously at each blade element for a given TSR and yaw angle. This output then feeds directly into the BEM code (see Fig.3 for an outline of the numerical model).

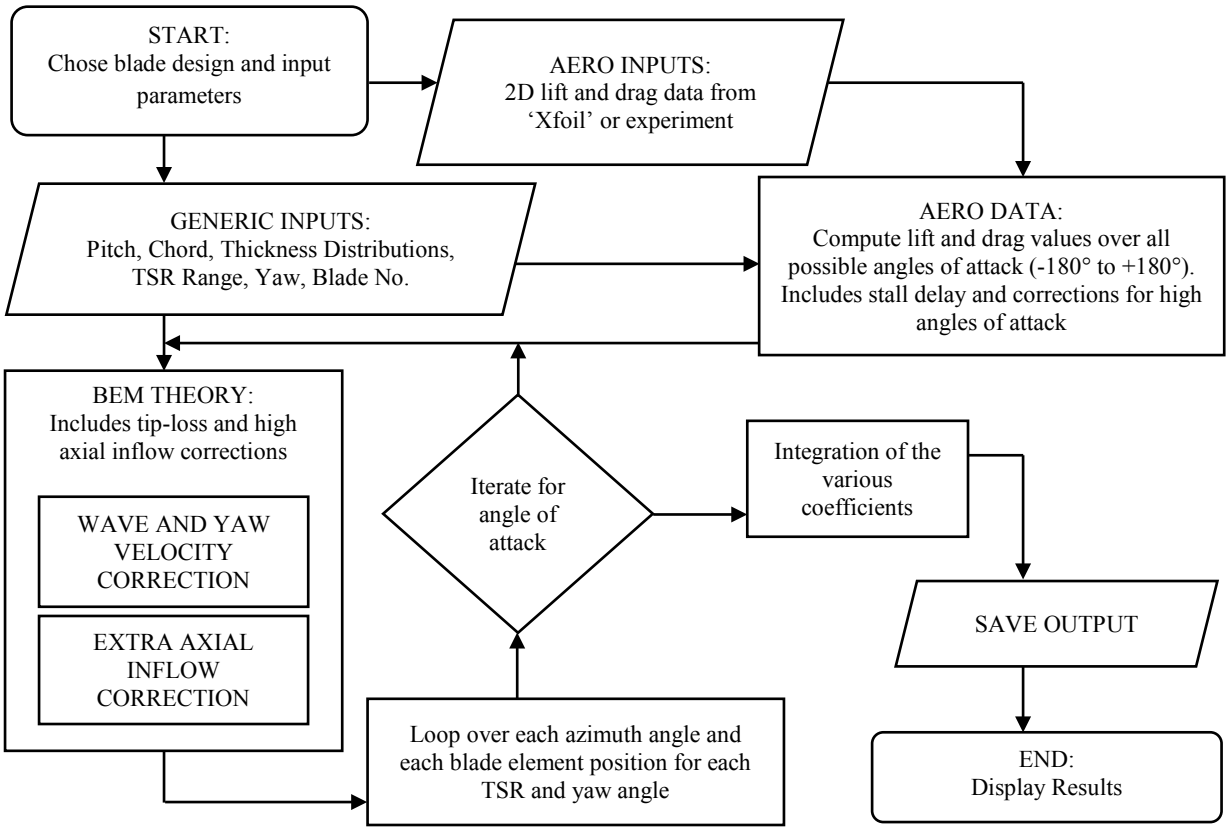

Fig. 3. Flow diagram for BEM numerical model showing the processes involved

3. Results and Discussion

The model MCEC (Fig.1) was used to acquire measurements of thrust, torque and rotor speed for both yawed and wave environments. Fig.4 shows the comparison between experimental data and numerical model for a yawed and un-yawed case. Blockage corrections by Barnsley and Wellicome [11] have been applied to the data. This is a requirement since measurements tend to be over predicted in relatively narrow channels (blockage is ~7%). Figures 5-8 are for a NACA 63-8XX blade, used for comparison with Bahaj et al. [12]. Results show good agreement, which when viewed alongside Fig.4, gives some confidence that the numerical model is valid. No figure is included to show the effect of waves on mean C_P and C_T because the resulting mean wave velocity at the rotor is approximately zero.

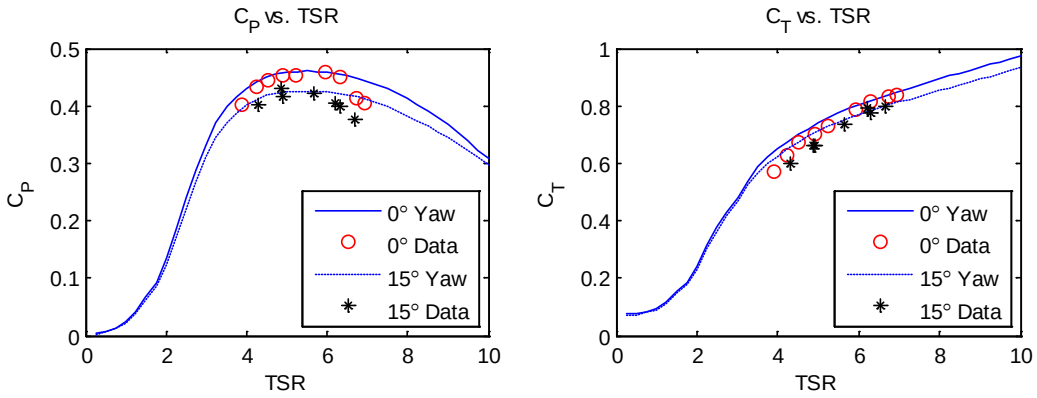

Fig. 4. Left: Power coefficient (CP) vs. TSR for 0° yaw and 15° yaw with experimental data included for comparison. Right: Thrust coefficient (CT) vs. TSR for respective yaw angles

The effect of waves is pronounced when investigating the azimuthal variation of C_P and C_T however, and has serious implications for the fatigue loading of blades as shown in Figures 5 and 6. A few of the parameters used in BEM are shown in these figures and the range over which they vary is represented by the plot line thickness. In Fig.5, the gradient of C_P is calculated using several of the other variables shown in the figure, amongst others. At zero gradient, C_{P_MAX} occurs at 85% blade radius, which is also the region of maximum power variation. This model assumes constant rotor speed which is unlikely to occur in reality. The variations seen in the angle of attack are likely to cause acceleration and deceleration of the rotor which may lead to a greater range of C_P.

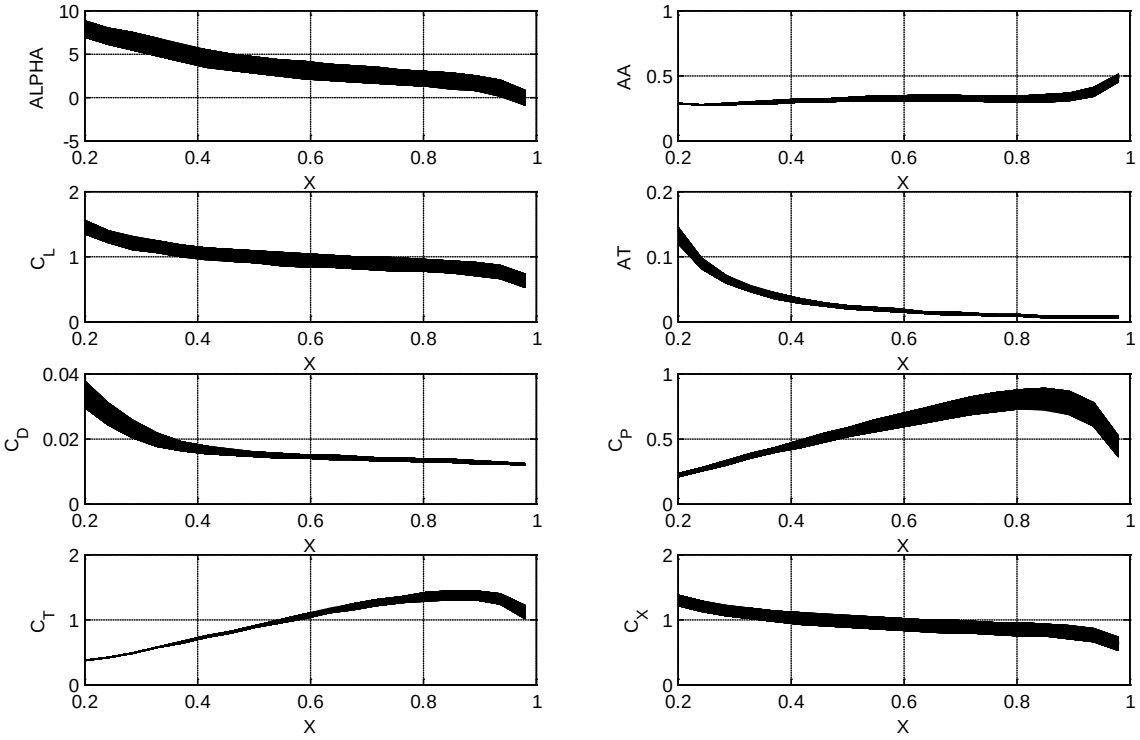

Fig. 4. Plots showing change in Alpha (angle of attack), C_L (lift coeff'), C_D (drag coeff'), AA (axial inflow factor), AT (tangential inflow factor), C_P (power coeff'), C_T (thrust coeff'), C_X (axial force coeff') across the blade span. Line thickness in each plot shows the effect of azimuthal variation. Only small waves are shown here. TSR = 6, Yaw = 0°

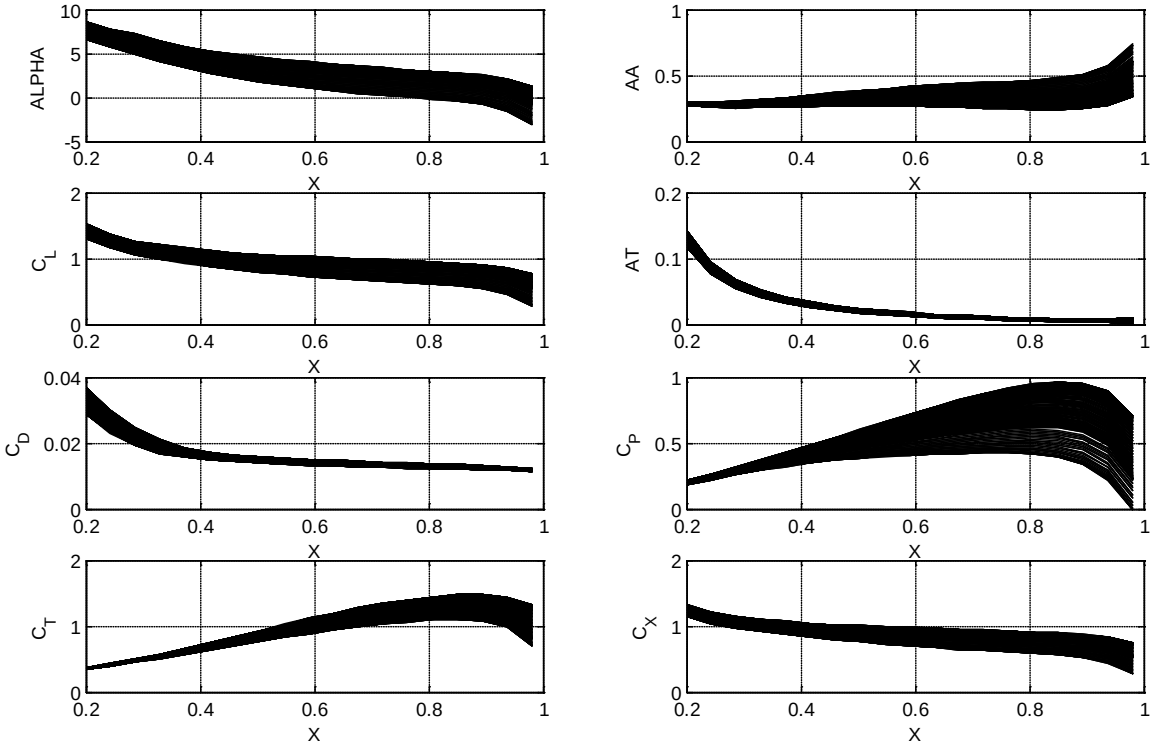

Fig. 5. See Fig.5 for description. Small waves and 15° yaw are shown here. TSR = 6, Yaw = 15°

This vindicates the concerns of flicker due to varying angle of attack (see section 2.2); since high frequency oscillations in voltage, caused by rapid changes in rotor speed, can lead to flicker in the power.

When a turbine is yawed to the flow, both power and thrust are reduced (see Fig.4). This is only apparent above 7.5° yaw with an approximate 20% power reduction at 22.5° yaw [8]. This is a noticeable difference and is likely to be higher than the 20% suggested because the rotor experiences a reduced effective velocity in yawed flow, hence reduced TSR.

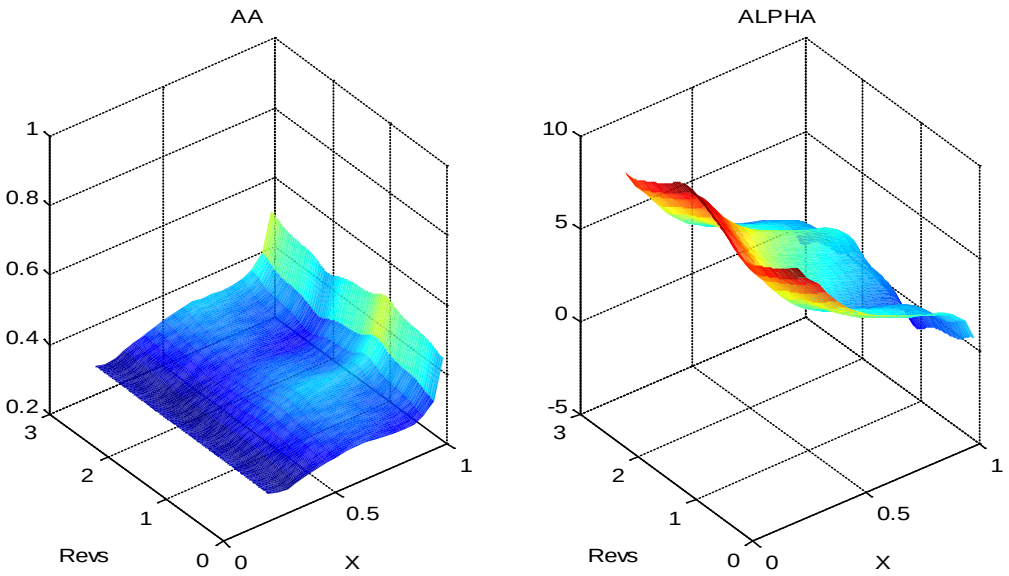

Fig. 6. Surface plots showing axial inflow factor and angle of attack from Fig.5 varying with blade radius and azimuth (3 revolutions)

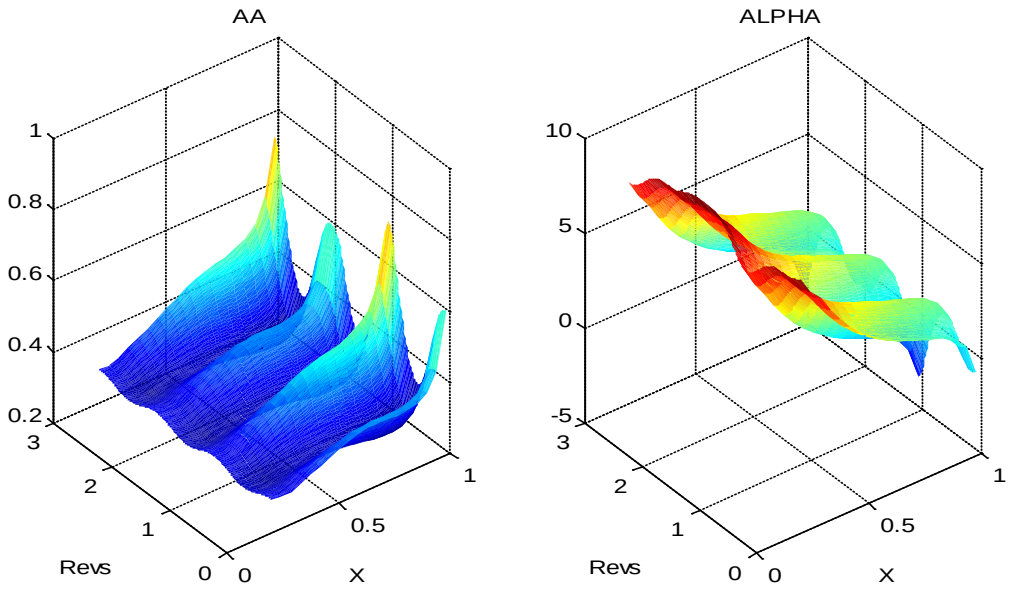

Fig. 7. Surface plots showing axial inflow factor and angle of attack from Fig.6 varying with blade radius and azimuth (3 revolutions)

The inclusion of yaw dramatically increases the range over which some of the parameters vary (see Fig.6). CP in particular varies ~3 times more at 85% blade radius for 15° of yaw. Surface plots in Figures 7 and 8 have been included to show how the axial inflow factor and the angle of attack vary over 3 blade revolutions, with and without yaw (15°). It should be noted that in Fig.8, the waves have less influence than yaw in the power producing region of the blade. This is an important point because the yaw effect can easily be avoided with the use of a yaw drive.

4. Further Work

This research is ongoing and further work will include more detailed experiments including additional testing at yaw into waves and measurement of individual blade loading. When the effects of linear theory have been properly evaluated, the next phase of testing will be to verify findings using waves on a non-uniform current. Barltrop [6] showed that the bending moments at roots of MCEC blades were found to fluctuate significantly; 50% of the mean value for out-of-plane bending moments and 100% of the mean value for in-plane bending moments. This justifies the need for individual blade loading experiments. In addition, steeper waves were found to impose lower bending moments in both directions about the roots of the rotor blade. It should also be noted that the in-plane bending moment is affected by the gravity bending moment component, so a neutrally buoyant blade would be desirable, if not impractical for a small model.

The BEM code will be expanded to describe the loading effects on a turbine blade in more detail. Further work will include modelling of blade acceleration, gravity effects and added mass, with a view to providing a model for fatigue analysis. This model could then be used for the design of optimised MCEC blades for tidal environments.

5. Conclusions

It has been demonstrated that waves are likely to have a detrimental impact on MCECs. This is not a significant problem in terms of power output, other than to further complicate the

power electronics required for smoothing the power/flicker. The main issue with wave-current interaction around a MCEC is the cyclic loading, which will likely result in accelerated fatigue to the rotor and blades. This is particularly evident in the axial flow direction. Another important consideration is whether a rotor yaw drive is required at any specific tidal site. Large amounts of directional swing will occur around headlands and can cause a significant reduction in power and increase in dynamic loading if a yaw drive is omitted. The continuing work presented in this paper will eventually assist in the structural design of MCEC rotor blades, quantify the loading effects caused by waves and maximise rotor diameter to achieve a robust, high energy yield device.

References

[1] C. Swan, R. L. James, A simple analytical model for surface water waves on a depth-varying current, Applied Ocean Research, Vol. 22, 2001, pp. 331-347.

[2] J. A. Smith, Wave-Current Interaction in Finite Depth. Journal of Physical Oceanography, Vol.36, 2006, pp. 1403-1419.

[3] J. Wolf, D. Prandle, Some observations of wave-current interaction, Coastal Engineering, Vol. 37, (1999), pp. 471-485.

[4] M. A. Srokosz, Models of Wave-Current Interaction, Advances in Underwater Technology, Ocean Engineering, Vol.12, 1987, pp. 313-325.

[5] L. E. Myers, A. S. Bahaj, Scale reproduction of the flow field for tidal energy converters, Proc. 10th World Renewable Energy Congress, Glasgow, UK, 2008.

[6] N. Barltrop, et al. Wave-current interactions in marine current turbines, Proc. 6th European Wave and Tidal Conference, Glasgow, UK, 2005, pp. 33-38.

[7] J. V. Norris, E. Droniou, Update on E MEC activities, resource description, and characterisation of wave-induced velocities in a tidal flow, Proc. 7th European Wave and Tidal Energy Conference, Porto, Portugal, 2007.

[8] P. W. Galloway, L. E., Myers, A. S. Bahaj, Studies of a scale tidal turbine in close proximity to waves, Proc. 3rd International Conference on Ocean Energy, Bilbao, Spain, 2010.

[9] A. F. Molland, The design, construction and calibration of a five-component strain gauge wind tunnel dynamometer, University of Southampton, Ship Science Report, 1/77, ISSN 0140-3818, 1976.

[10] C. Abonnel, et al. Some aspects of EDF modelling and testing activities, within its marine current energy research and development project, Proc. 6th European Wave and Tidal Conference, Glasgow, UK, 2005, pp. 1-10.

[11] Barnsley and Wellicome, Final report on the 2nd phase of development and testing of a horizontal axis wind turbine test rig for the investigation of stall regulation aerodynamics, carried out under ETSU agreement E.5A/CON5103/1746, 1990.

[12] A. S. Bahaj, et al. Experimental Investigation into the Hydrodynamic Performance of Marine Current Turbines, Sustainable Energy Series, Report 3, 2005.

Hydro-environmental Impact Assessment of the Significance of the Shape of Arrays of Tidal Stream Turbines

Reza Ahmadian[1,*], Roger Falconer[1] and BettinaBockelmann-Evans[1]

[1] *Hydro-environmental Research Centre, Cardiff School of Engineering, Cardiff University, UK*
** Corresponding author. Tel: +44 29208 75713, Fax: +44 29208 74939, E-mail: AhmadianR@cardiff.ac.uk*

Abstract: This study focuses on far-field hydro-environmental impacts of turbine arrays, with different shapes located in the Severn Estuary and Bristol Channel, UK, using a dynamically linked 1-D/2-D hydro-environmental model. The estuary, including the Bristol Channel, is approximately 200 km long and has the third highest rise and fall of tide in the world, with typical spring tidal range of over 14 m, whilst the spring tidal currents in the estuary are well in excess of 2 m/s. There are a number of tidal renewable energy options being considered around the Severn Estuary, including but not limited to: tidal stream turbines, offshore tidal impoundments and a barrage - at various locations. The model was used to predict the hydrodynamic, sediment transport and water quality processes as well as power output predictions. In order to simulate the impact of the tidal stream turbines, the model was refined and the turbines were included as momentum sinks in the momentum equation.

This study shows that the impact of the arrays on the water levels was negligible. However, the impact on velocities was more significant and the flow was retarded both upstream and downstream of the arrays, whilst it was faster on the side of the arrays. It was found that changes in the suspended sediment concentrations did not follow a simple pattern and that more detailed model studies are required to achieve a better understanding of this process. Finally, it was found that the power generated was dependent on the array layouts with the power output of different arrays used in this study varied by up to 20%.

Keywords: *Marine renewable energy, Hydro-environmental modelling, Tidal stream turbines, Severn Estuary and Bristol Channel.*

1. Introduction

The European Union have introduced targets among member states to increase the share of renewable energy in the overall energy consumption to 20% of total energy budget by 2020, this is almost three times the levels of 2008. Amongst the different types of renewable energy, marine renewable energy is an emerging energy sector with a bright future. Tidal devices and, in particular, tidal stream turbines have attracted considerable interest in recent years, due to the vast resources available in parts of the EU, modularity, minimal visual impact and their predictable energy generation.

As for many other emerging renewable schemes, the environmental impacts of tidal stream turbines are not clear and therefore need to be investigated before considering any site for deployment of such turbines. Although every single tidal stream device has a small footprint, the overall impact of an array of turbines can only be investigated by considering the scale of the array.

This study focuses on hydro-environmental modelling of different arrays of turbines and investigating the impact of the shape and density of the arrays on the flow, water levels, sediment transport and faecal bacteria concentrations as well as the energy output. The site selected for this study is the Severn Estuary and Bristol Channel, UK (shown in Fig. 1), which has the third largest tidal range in the world with typical spring and neap tidal ranges peaking at over 14 m and 7 m respectively, and the spring tidal currents are well in the excess of 2m/s. The site is one of the most attractive sites for marine renewable energy schemes and a number

of schemes, including several barrages sites, lagoons and stream turbines have been proposed for the area.

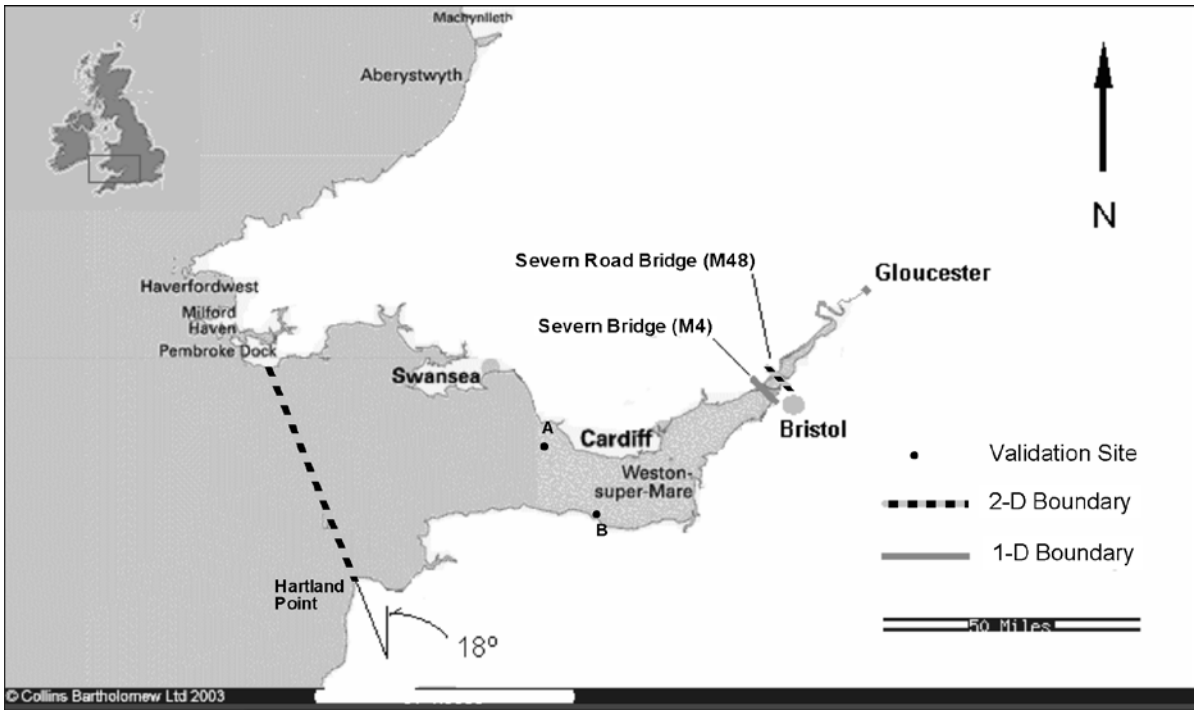

Fig 1. The model domain extent and validation sites. Site A: Southerndown Site, B: Minehead Site (Source: Yang et al. [1])

2. Hydro-Environmental Modelling Methodology

The dynamically linked DIVAST (Depth Integrated Velocities And Solute Transport) and FASTER (Flow And Solute Transport in Estuaries and Rivers) models were implemented to model the hydro-environmental impacts of the stream turbines. The modelling domain was extended from the outer Bristol Channel, close to Lundy Island (where an imaginary line between Milford Haven and Hartland Head can be drawn) at the western end of the domain to Gloucester at the eastern extremity (Fig. 1). Both, DIVAST and FASTER models are based on a finite difference alternating direction implicit solution of the Reynolds Averaged Navier-Stokes equations and the solute transport equation in 2D and 1D, for the hydrodynamic, sediment transport and water quality process predictions respectively[2]. The solute/sediment concentrations were calculated considering the effects of dispersion, diffusion, decay, adsorption and desorption as well as deposition and erosion.

The 2D downstream boundary was a water level boundary and the water level values for the simulation period at this location were obtained from the Proudman Oceanographic Laboratory (POL) Irish Sea model. Since this boundary was so far seawards of the region of interest, the concentrations of faecal indicator organisms were set to zero along the downstream boundary. The 2D upstream boundary was a flow boundary, flow and all the water quality indicators were dynamically transferred through the 1D-2D link. A flow rate varying between 60m^3/s and 106 m^3/s was used as a 1-D upstream model boundary condition, at Gloucester. The downstream boundary of the 1D model, located close to the Severn Bridge, was specified as a water level boundary and the values of the water levels were acquired from the 2D model. A structured 200×200 m^2 grid was used for the 2D model while the 1D model

was consisted of four reaches and two junctions with an average distance between the two consecutive cross-sections being approximately 240 m.

2.1. Governing Equation

Only the 2D model governing equations are briefly explained in this section, for more information on the 2D and 1D models refer to: Falconer[3] and Kashfipour[4]. The 2D hydrodynamic equations used in this model are based on the depth-integrated three-dimensional Reynolds equations for incompressible and unsteady turbulent flows. Also, the effects of the bottom friction, wind shear and the earth's rotation are included to give for the x-direction[5]:

$$\frac{\partial \xi}{\partial t} + \frac{\partial q_x}{\partial x} + \frac{\partial q_y}{\partial x} = 0 \qquad (1)$$

$$\frac{\partial q_x}{\partial t} + \beta\left[\frac{\partial u q_x}{\partial x} + \frac{\partial v q_x}{\partial y}\right] = f q_y - gH\frac{\partial \xi}{\partial x} + \frac{\tau_{xw}}{\rho} - \frac{\tau_{xb}}{\rho} + \varepsilon\left[2\frac{\partial^2 q_x}{\partial x^2} + \frac{\partial^2 q_x}{\partial y^2} + \frac{\partial^2 q_y}{\partial x \partial y}\right] \qquad (2)$$

where q_x, q_y = discharges per unit width in the x, y directions ($m^2\ s^{-1}$), ζ = water surface elevation above datum (m), H = total water depth (m), β = momentum correction factor for non-uniform vertical velocity profile, f = Coriolis parameter (rad s^{-1}), g = gravitational acceleration (ms^{-2}), τ_{xw}, τ_{xb} = surface and bed shear stress components respectively in the x-direction ($N\ m^{-2}$), and ε = depth averaged eddy viscosity. The equation for the y-direction can be written similarly to that given for the x-direction (i.e. equation (2)).

The 2D advective-diffusion equation for predicting solute transport is acquired by integrating the 3D solute mass balance equation over the depth, giving:

$$\frac{\partial \phi H}{\partial t} + \frac{\partial \phi q_x}{\partial x} + \frac{\partial \phi q_x}{\partial y} - \frac{\partial}{\partial x}\left[HD_{xx}\frac{\partial \phi}{\partial x} + HD_{xy}\frac{\partial \phi}{\partial y}\right] - \frac{\partial}{\partial y}\left[HD_{yx}\frac{\partial \phi}{\partial x} + HD_{yy}\frac{\partial \phi}{\partial y}\right] = H\sum \Phi \qquad (3)$$

where ϕ = depth averaged concentration (unit/volume) or temperature (°C), H = total water depth (m) and $\Sigma\Phi$ = total depth average concentration of the source or sink solute. The bacteria decay can be modelled using a first order decay formulation according to Chick's Law[6] and given as:

$$\frac{dC}{dt} = -KC \qquad (4)$$

where K = decay coefficient, generally expressed in units of day^{-1}; t = time (s^{-1}) and C = bacterial concentration, expressed herein as Colony-Forming Units (CFU) per 100ml.

Some researches have shown that the concentration of Faecal Indicator Bacteria (FIB) on bed sediments can be 100-2000 times higher than the concentrations within the water column[7, 8, 9]. This suggests that the sediment re-suspension or deposition can increase or decrease the

bacteria levels, respectively. This emphasises the importance of including the interaction of sediment and bacteria while predicting the bacteria concentration. Hence, to model the bacteria processes more realistically, the interaction of the sediment and bacteria has been included in the model as outlined in: Stapleton et al.[10, 11], Yang et al.[1] and Ahmadian et al.[12].

2.2. Model Calibration and Validation

The model predictions were initially calibrated using Admiralty Chart data and finally the field data collected by Stapleton et al. [10, 11] at two locations at two sites (shown in Fig. 1) were used to validate the model predictions. The model predictions showed good agreement with the validation data, more information regarding the model validation can be found in Ahmadian et al.[12]. Typical comparisons between the measured and predicted water elevations, current speeds, sediment fluxes and faecal bacteria concentrations are shown in Fig. 2 and Fig. 3 respectively.

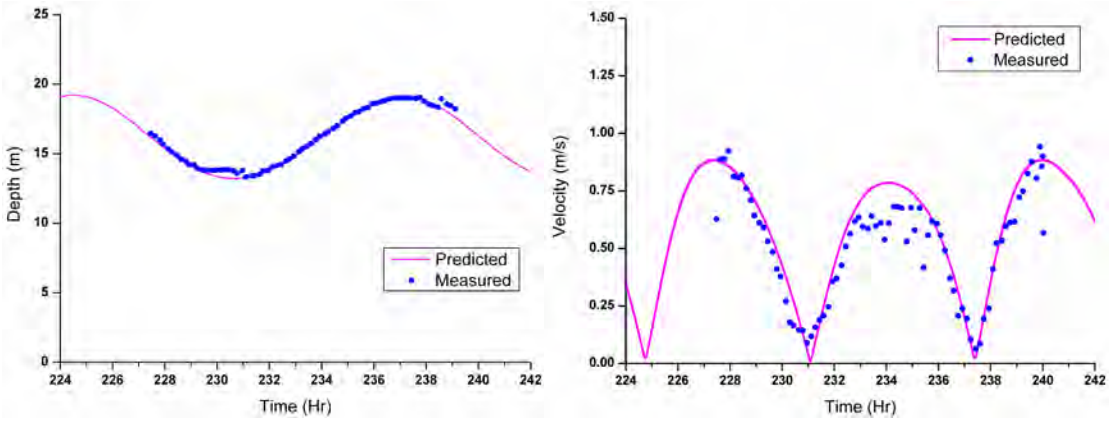

Fig 2. Comparison of predicted and measured water elevations (left) and current speeds (right) at Minehead (site B)

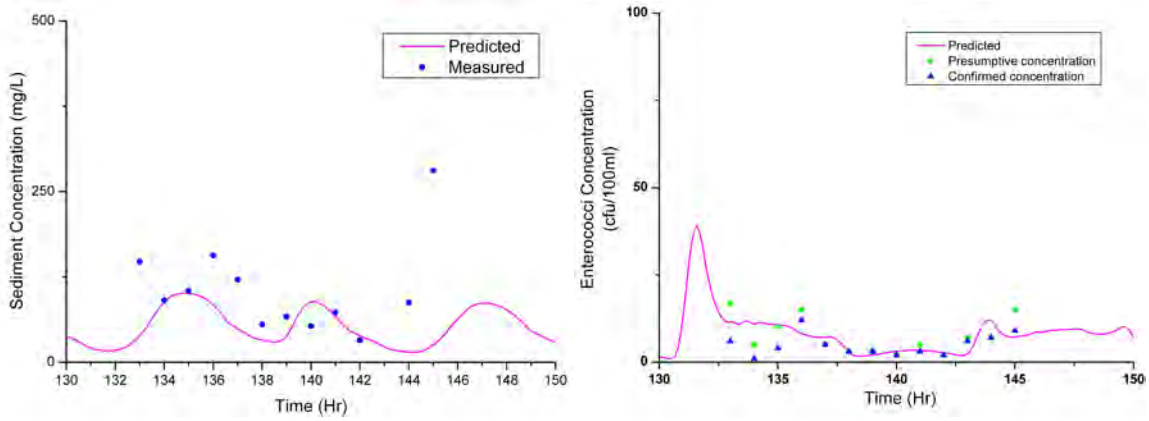

Fig 3. Comparison of predicted and measured suspended sediment concentrations (left) and enterococci concentrations (right) at Southerndown (Site A)

2.3. Turbines Modelling

Using the same analogy as used for wind turbines, the energy flux available for a turbine is [13]:

$$P = \frac{1}{2} C_p \rho A U^3 \quad (5)$$

where P = energy flux (W m^{-2}), ρ = water density (kg m^{-3}), A = area of the control volume (m^2), U = component of the water flow velocity perpendicular to the cross-section of the channel (ms^{-1}) and C_p = power coefficient. Energy extraction by turbines, consequently, causes a thrust force (T) induced on the turbine in the direction of flow and can be calculated as [13]:

$$T = \frac{1}{2} C_T \rho A U^2 \quad (6)$$

where C_T = thrust coefficient. It is shown that both the power and thrust coefficients are related to the hub pitch and varies with the Tip Speed Ratio (TSR)[13]. In this study, the momentum equation (Eq. 2) was modified to include the impact of the turbines.

3. Modelling Results

The model was then applied to three imaginary arrays of turbines in the Severn Estuary and Bristol Channel (illustrated in Fig. 4), and the impacts of the arrays on water levels, current speed, sediment transport and faecal bacteria levels were investigated. These arrays are arbitrary and were chosen purely for the model demonstration purposes and none of the protocols required for a site selected for deployment of turbines[14] have been taken into account in selecting these sites. It was assumed that the same number of turbineswere deployed in each formation. Formations a and b occupied the same area and consequently, have the same number of turbines per unit area, which will be referred to as the array density in this paper, while the density of the formation c is more than 10 times less than the formations a and b.

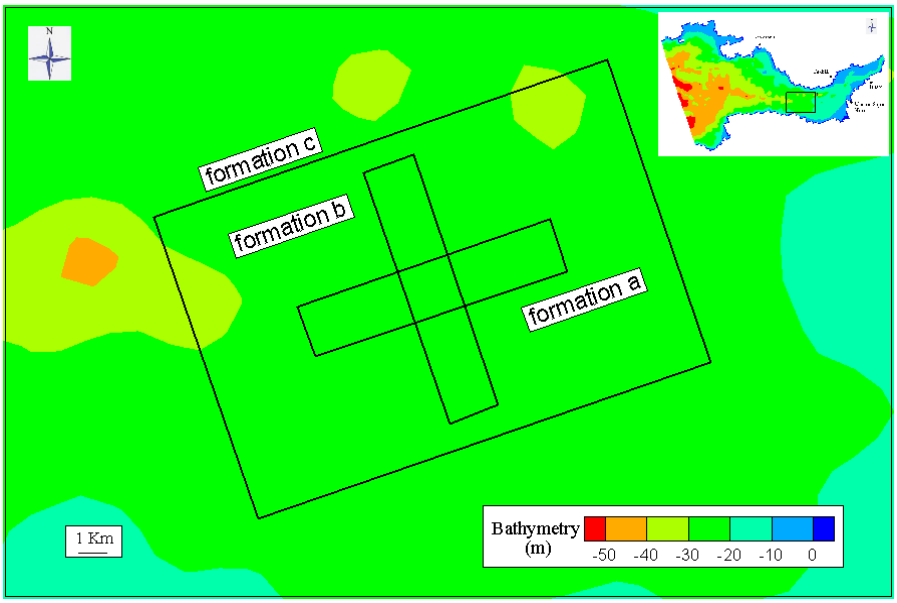

Figure 4: Array Formations

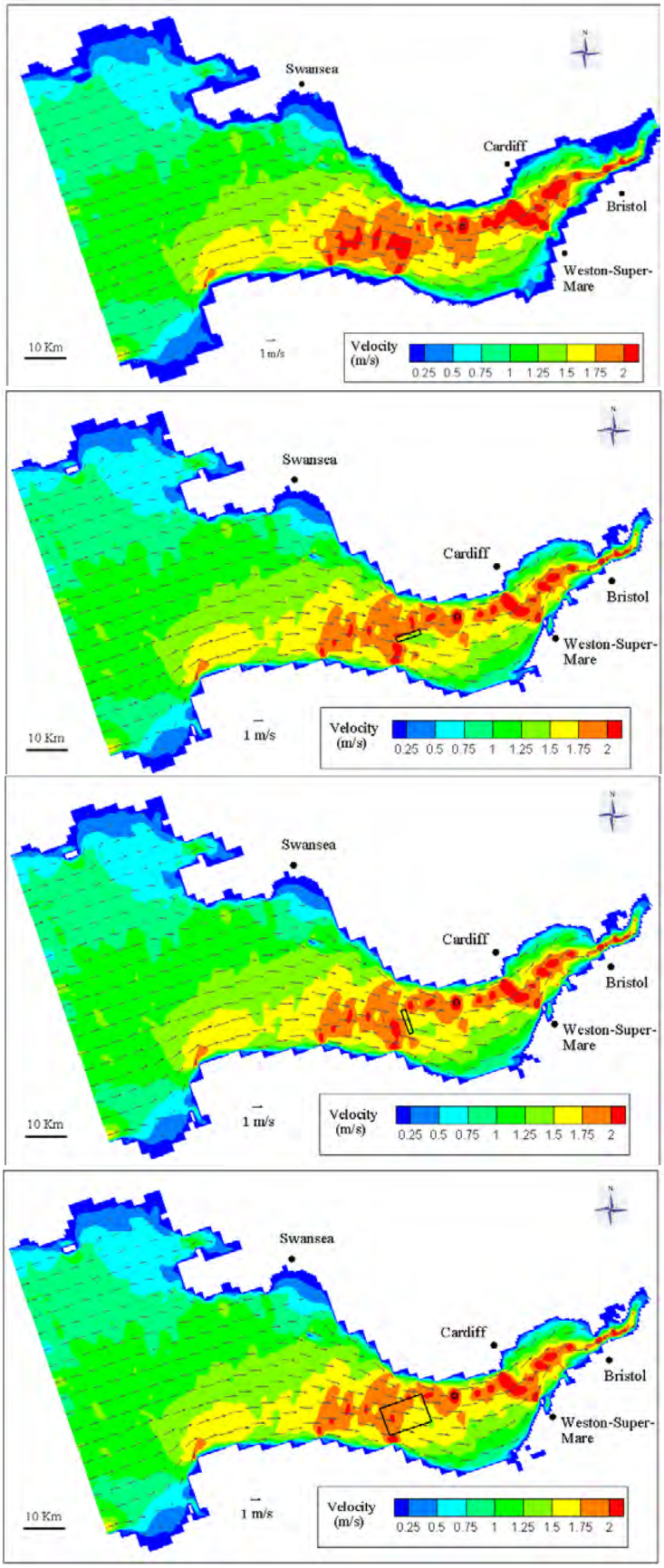

Figure5: Comparison of the velocities across the estuary without (i) and w ith different array formations; "formation a"(ii), "formation b"(iii) and "formation c"(iv) at mean flood at Barry (red dot)

The current speeds in the estuary at mean flood at Barry (red dot) before including the arrays and with the different arrays are shown in Fig. 5. Although, in this study it was assumed that the turbines can rotate to face the flow and subsequently the flow speed is equal to the effective velocity on the turbine, it can be seen that arrays with the same density but different orientations can impact the flow differently. It can also be seen that the arrays with a smaller density would change the currents to a much lesser extent while the average electricity generated by each turbine in this array can be up to 50% more than the average electricity generated by the turbines in the denser arrays. It was also found that the arrays would not change the water levels noticeably, however, as a result of changes in the currents sediment transport the faecal bacteria levels would be altered. These results are not shown here in the interest of space, however, publication of results will follow.

4. Conclusions

The dynamically linked 1-D/2-D hydro-environmental model of the Severn Estuary and Bristol Channel has been refined to assess the hydro-environmental impacts of an arbitrary array of tidal stream turbines by including the turbines as momentum sinks in the momentum equation. The model without the turbines was first calibrated and then was validated against field data.

The model was used to study the hydro-environmental far-field impacts of different shapes of an array of tidal turbines and the electricity generated. It was found that the impact of any formation of the arrays on the water levels were negligible. However, the impacts on velocities were more significant and the flow was retarded both upstream and downstream of the arrays, while it was faster on the side of the arrays. Although, this pattern was consistent for all the arrays, the extent of changes in the velocity was different regarding to the array formation. These changes were less significant for a less dense array (formation c), however, the average electricity generated by each turbine in this array was up to 50% more than the average electricity generated by the turbines in the denser arrays. Finally it was also found that the changes in the sediment and faecal bacteria levels were higher in the denser arrays.

5. Acknowledgements

The study is carried out as a part of MAREN project which is part funded by the European Regional Development Fund (ERDF) through the Atlantic Area Transnational Programme (INTERREG IV).

References

[1] Yang, L., Lin, B. and Falconer, R. A., 2008. Modelling enteric bacteria levels in coastal and estuarine waters. Proceedings of Institution of Civil Engineers, Engineering and Computational Mechanics, 161(4), 179-186.

[2] Kashefipour, S. M., Lin, B., Harris, E. L. and Falconer, R. A., 2002. Hydro-environmental modelling for bathing water compliance of an estuarine basin. Water Research, 36(7), 1854-1868.

[3] Falconer, R. A., (1992). Flow and water quality modelling in coastal and inland waters. Journal of Hydraulic Research, IAHR, 30(4), 437-452.

[4] Kashefipour, S.M., Falconer, R.A., Lin, B., Harris, E.L. (2000). FASTER Model Reference Manual. Hydro-environmental Research Centre Report, Cardiff University.

[5] Falconer, R.A. (1993). An introduction to nearly horizontal flows. In: Abbott, M.B. and Price, W.A., Coastal, Estuarial and Harbour Engineers' Reference Book. London: E & FN Spon Ltd., pp. 27-36.

[6] Chick, H. (1910). The Process Of Disinfection By Chemical Agencies And Hot Water. Journal of Hygiene. 10 (2), pp. 237-286.

[7] Marshall, K.C. (1978). The effects of surfaces on microbial activity. Water Pollution Microbiology. vol. 2, pp. 51–70.

[8] Burton, G.A., Gunnison, D. and Lanza, G.R. (1987). Survival of Pathogenic Bacteria in Various Freshwater Sediments. Applied and Environmental Microbiology, 53(4), pp. 633-638.

[9] Obiri-Danso, K. and Johns, K. (2000). Intertidal sediments as reservoirs for hippurate negative campylobacters, salmonellae and faecal indicators in three EU recognised bathing waters in North West England. Water Research. 34(2), pp. 519-527.

[10] Stapleton, C.M., Wyer, M.D., Kay, D., Bradford, M., Humphrey, N., Wilkinson, J., Lin, B., Yang, Y., Falconer, R.A., Watkins, J., Francis, C.A., Crowther, J., Paul, N.D., Jones, K. and McDonald, A.T., 2007a. Fate and Transport of Particles in Estuaries, Volume II: Estimation of Enterococci Inputs to the Severn Estuary from Point and Diffuse Sources. Environment Agency Science Report SC000002/SR2, Bristol: Environment Agency.

[11] Stapleton, C.M., Wyer, M.D., Kay, D., Bradford, M., Humphrey, N., Wilkinson, J., Lin, B., Yang, Y., Falconer, R.A., Watkins, J., Francis, C.A., Crowther, J., Paul, N.D., Jones, K. and McDonald, A.T., 2007b. Fate and Transport of Particles in Estuaries, Volume IV: Numerical Modelling for Bathing Water Enterococci Estimation in the Severn Estuary. Environment Agency Science Report SC000002/SR4, Bristol: Environment Agency.

[12] Ahmadian, R., Falconer, R.A. and Lin, B.L. (2010). Hydro-environmental modelling of proposed Severn barrage, UK. Proceedings of the Institution of Civil Engineers, Energy, 163(EN3), pp 107–117.

[13] Bahaja, A.S., Mollandb, A.F., Chaplina, J.R. and Batten, W.M.J., 2007. Power and thrust coefficients of marine current turbines operating under various hydrodynamic conditions of flow in cavitation tunnels and towing tanks. Renewable Energy, 32, pp. 407–426.

[14] Willis, M., Masters, I., Thomas, S., Gallie, R., Loman, J., Cook, A., Ahmadian , A., Falconer, R., Lin, D., Gao, G., Cross, M., Croft, N., Williams, A., Muhasilovic, M., Horsfall, I., Fidler, R., Wooldridge, C., Fryett, I., Evans, P., O'Doherty, T., O'Doherty, D., and Mason-Jones, A., 2010. Tidal Turbine Deployment in the Bristol Channel – A Case Study, Proceeding of Institution of Civil Engineers- Journal of Energy, 163(3), pp. 107–117.

Experimental investigation of the effects of the presence and operation of tidal turbine arrays in a split tidal channel

Tim Daly[1*], Luke. E. Myers[1], AbuBakr S. Bahaj[1]

[1] *Sustainable Energy Research Group, University of Southampton, Southampton, United Kingdom*
** Corresponding author. Tel: +44 2380592134, E-mail: td2e09@soton.ac.uk*

Abstract: The installation of arrays and farms is the next major step in the development of tidal energy converters. Many tidal farms are currently in the process of development. A number of studies have also identified potentially lucrative sites for future farm and array development elsewhere. In some of these sites, the flow velocities can at least in part be attributed to the presence of constraining landmasses and the resultant splitting of channels into two or more sub channels. Given the cubic relationship between flow velocity and kinetic energy flux, even modest acceleration in these areas can cause a considerable increase the potential power available.
The analysis in this paper investigates flow acceleration effects in a split tidal channel due to the presence of tidal turbine arrays. As well as their presence, the effect of changing lateral and longitudinal position of the array and number of turbines in the array was also examined. Results show that flow acceleration of up to 14% can occur in an empty channel due to the presence of tidal arrays. This could potentially have major implications for tidal farm design in areas where channels branch into multiple sub channels.

Keywords: *Split tidal channel, Obstruction, Actuator fences, Flow acceleration, Acoustic Doppler velocimeter.*

1. Introduction

Studies have shown that the presence of tidal turbine arrays in any channel has the potential to have a significant effect of the surrounding flow environment [1]. They will also impact human activities such as shipping and sensitive environmental processes such as sediment transport, shore erosion and fish migration. Many areas worldwide in which split tidal channels are present have been identified as having high potential tidal energy resources. Examples include the Sound of Islay, Scotland, UK [2], Bay of Fundy, Canada [3] and Puget Sound, Washington, USA [4]. In areas such as these, aforementioned effects are likely to be greater, as placing turbines in one sub channel may alter the flow in some or all other sub channels. While many of these effects will obviously depend on the bathymetry of the site in question, there will undoubtedly be many generic effects which will be common to all sites of this kind.

This paper outlines the methods and results of experimentation carried out to examine some of the effects of tidal turbine arrays located in split tidal channels. Experimentation was carried out in the University of Southampton Chilworth hydraulics laboratory using a circulating water channel, actuator fences and acoustic Doppler velocimeters (ADV). The hypothetical site investigated was a simple channel which splits into two equally sized sub channels due to the presence of an impenetrable landmass between them. One of the sub channels had a tidal array installed, while the other was left empty. The resultant flow velocity in the empty sub channel was compared to the natural flow velocity to determine the percentage increase which resulted due to energy extraction.

2. Review of previous studies

Despite the high velocity magnitudes present in areas of split tidal channels, there is considerable variability in the bathymetry and hydrodynamic environment from site to site. This makes these areas much more complex to analyse from a resource assessment and environmental impact point of view. Also unlike single channel areas, it can be very difficult

to determine theoretical expressions which will be applicable to all sites. One study which aimed to develop such theoretical expressions is outlined in [5]. The paper presents the case of a simple channel connected to two infinite oceans, and divided into two equal sub channels by an island in the centre. One sub channel has energy extracted by tidal energy converters, while the other is left empty. The authors derive expressions for power extracted by turbines and total fluid power as functions of head drop across the turbines and head drop across the entire channel between the two oceans respectively. The authors conclude that a maximum of 38.49% of total fluid power can be extracted, a figure which agrees with estimates for efficiency developed from single channel extraction theory developed by Garrett and Cummins in [6].

A site specific analysis of an area known as Johnstone Strait was carried out in [7]. The Johnstone Strait region consists of a number of sub channels, and the authors used both analytical methods developed by Garrett and Cummins [6] and a numerical model to examine the maximum power extracted by turbines in a total of four different sub channels. The authors found that their numerical model agreed reasonably well with the analytical theory developed in [8] for two particular cases. However for the other two investigated instances, theory was not valid, as the theory developed is only valid for instances where the flow of water cannot be diverted away from the sub channels where tidal turbines are installed [7]. Further analysis also examined some effects to the hydrodynamic environment by comparing natural tidal heights and amplitudes with those observed following energy extraction.

These studies use different methods of accounting for the presence of turbines, with [5] using head loss coefficients to calculate head drops and resultant power values, and [7] increasing natural bottom friction coefficient to include the effects of turbines presence. However undoubtedly the biggest difference is that [7] acknowledges the effects of energy extraction in different areas on the surrounding area, and attempts to quantify it briefly by examining changes to tidal amplitude and height. While [5] estimates high possible extractable power for an area of Johnstone Strait, there is no way for a potential developer to determine whether the changes to the surrounding hydrodynamic environment will render extraction of this energy unacceptable from an environmental point of view.

In contrast to both of these studies, the far field effects of tidal energy extraction was the sole subject of investigation in an analysis of four different tidal site configurations carried out in [8]. The four types of channel networks investigated were:
(a): A single constriction, which is a simple narrowing of a tidal channel.
(b): A multiply connected network, where flow is diverted from one channel into two sub channels, each of which contains a single constriction, and which meet again later in the flow.
(c): A branching network, where flow is diverted from one channel into two sub channels each of which contains a constriction. However these sub channels do not meet later in the flow.
(d): Serial constrictions, where a single channel contains a number of areas where constrictions are present.

Analytical methods were used to examine far field effects included shallow water equations, the conservation of mass and the conservation of energy. Results found that the largest tidal amplitude changes occur in the Branching network, biggest changes in kinetic power density occurring in the multiply connected network and changes to transport amplitude and frictional power dissipation approximately equal in all cases.

These three investigations all contain elements of resource assessment which are crucial to the process of designing and installing a tidal turbine farm. However all rely solely on analytical and numerical models and no experimental results are present in these analyses. Section 3 outlines the methodology and reasoning for experimentation carried out to examine the changes to the hydrodynamic environment of a network of channels due to the presence of tidal energy converters. It is hoped that this analysis will further aid in the exploitation of the maximum potential energy in these sites with minimal and justifiable environmental effects.

3. Experimental method

3.1. Flume setup

The experimentation for this investigation was carried out in the indoor flume of the University of Southampton Chilworth hydraulics laboratory. The flume is a conventional gravity fed flume, with water pumped from sumps and through a flow channel, and mass flow rate, depth and flow velocity magnitude controlled via valves and a tail gate. The working section is 21m in length, 1.37m wide with a maximum flow depth of 0.5m. A 100mm wide dividing wall was placed along the streamwise centerline of the flume over a length of 4m (Fig. 1). The wall was placed between 8.5m and 12.5m from the inlet of the 21m channel. This split the flow into two hypothetical sub channels in a similar fashion to an impenetrable landmass in a real tidal channel.

3.2. Turbine array simulation

Tidal turbine arrays were represented in the Chilworth flume using porous actuator fences. The porous actuator fence is a convenient alternative to rotating turbines in the analysis of tidal farms and arrays. The main difference between fences and turbines is opposed to extracting kinetic energy from a fluid, actuator fences convert this energy to small scale turbulence in their wake. Other differences include the inability of fences to induce swirl effects in the flow and the differences in the structure of vortices shed from both. These factors mean that actuator fences are unsuitable for examining farm or array power output or the structure of the near wake of tidal arrays.

However analysis in [9] has shown that they are highly accurate in predicting the far wake effects of tidal turbine farms, which are likely to impact on farm layout and surrounding flow environment. Actuator fences also have the advantage of being easier and cheaper to construct than turbines. They are also advantageous for numerical modeling, as CFD simulations with actuator fences can be run in steady state as opposed to unsteady state for rotating turbines, and also require much less complex meshes.
Two actuator fences were used in this analysis. They were created from 300mm wide and 100mm high sheets of PVC with a thickness of 4mm. Holes were drilled in the sheets to achieve the desired open to total area ratio's (porosities).

3.3. Flow velocity magnitude measurements

All flow velocity measurements were taken using an acoustic Doppler velocimeter (ADV). The instrument used for this work was set to sample at 50Hz, just below the noise floor. The sample volume is cylindrical with a fixed diameter of 6mm. the volume height is user-defined and was chosen to be 3mm. Larger sample volumes will intercept more suspended matter in the water leading to stronger acoustic return signals and greater accuracy. However this can be negated as velocity shear between the top and bottom of the sample volume can lead to inaccuracies. Due to the high levels of suspended matter in the Chilworth flume, no doubt arising from being located in a hard water area, the signal strengths were found to be very

strong. With the water depth set to 0.3m the sample height represented 1% of the depth thus ensuring that velocity shear was minimal across measurement volume. To eliminate any errors which may have occurred due to random velocity fluctuations, the data were filtered subsequent to experimentation. The method used in this instance was the velocity correlation filter outlined in [10]. Other filtering methods determine the criteria upon whether a measurement is invalid on the basis of the relationship between successive measurements. These methods would be unsuitable for this analysis, as groups of random fluctuations are likely to exist due to the turbulent nature of the flow downstream of the actuator fences. The velocity correlation filter is more suitable to the present study as the criteria for determining the validity of a measurement is calculated based on its relationship to all velocity measurements in the sample.

Fig.1. Front and rear of split mechanism in Chilworth channel.

3.4. Base flow map and actuator fence positioning

3.4.1. Analysis of natural flow environment

Initial flow mapping work was conducted in the absence of actuator fences in order to quantify the baseline flow environment with the split present. The depth was set to 0.3m and the depth-averaged flow velocity was approximately 0.3m/s. Comprehensive flow velocity measurements were taken laterally (cross-flume) and throughout the depth upstream of the wall split, and also in the sub channels on both sides of the wall. This velocity deficit would be able to give a measure of the extent to which the flow slowed down or accelerated due to the presence and various positions of actuator fences and is given by the expression:

$$U_{deficit} = 1 - \frac{U_w}{U_o} \qquad (1)$$

Where $U_{deficit}$ is the velocity deficit, U_w is the velocity at a specific point in the wake of the disk and U_o is the natural freestream flow velocity at this specific point.

3.4.2. Wake mapping of actuator fences

An actuator fence with porosity (ratio of open to total area) of 0.38 was placed in the centre of one of the sub channels at a distance of 0.4m downstream of the front of the split, which was also 8.9m from the inlet of the flume. This setup is displayed graphically in Fig. 2. Flow velocity measurements were then taken in both sub channels. The first position to be measured was 3 fence diameters downstream of the fence and up to 21 diameters downstream of it in increments of 3 diameters. For each downstream position, several lateral positions

were taken, while for each lateral position, 8 flow depths in increments of 30mm depth were taken. A similar analysis was carried out for the case of two actuator fences being present in a single sub channel. In this case two fences of porosity 0.38 and 0.4 were placed alongside each other. This case represented a very high blockage ratio, as the total width of the sub channel was approximately 635mm and the width of the two fences combined was 600mm. Once again the wake was examined by taking flow velocity measurements at several positions downstream of the fences, in both channels, using the ADV.

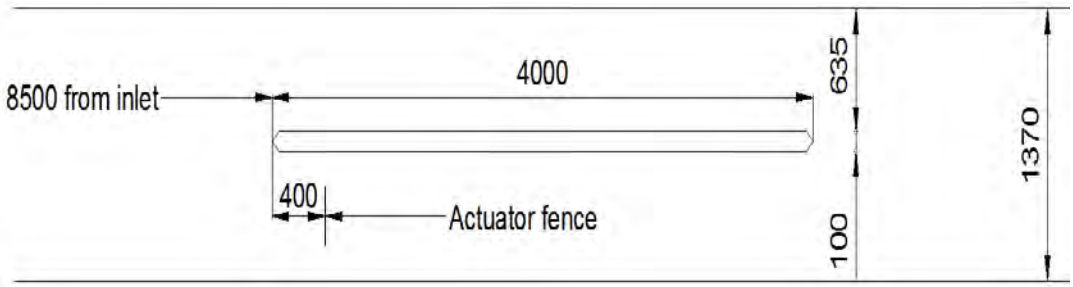

Fig.2. Plan view of Chilworth channel with porous actuator fence and split present (all dimensions in mm)

3.4.3. Flow acceleration analysis

As well as wake mapping in both channels, flow acceleration effects in the empty sub channel were examined. ADV's were positioned at two lateral points in the empty channel at a distance of 0.4m from the front of the wall split, or 8.9m from the inlet to the channel (Fig. 3). In the case of a sub channel with a single fence, a fence of porosity 0.4 was used. The fence was placed in 3 lateral positions, with the centre of the fence being positioned 180mm, 320mm and 460mm from the sidewall of the flume. For each of these lateral positions, the fence was also placed in the same downstream position as the front of the split, and was then moved gradually back in 100mm increments to 500mm downstream of the front of the split, then in 200mm increments up to 2000mm downstream. For each of these fence positions, the ADV recorded the flow velocity magnitude at the aforementioned points in the empty sub channel. Similar analysis was carried out for the case of a sub channel with two actuator fences present. Due to the fences occupying the vast majority of the width of the channel, changes to lateral position were not examined. Instead only the changes to the downstream positions were examined exactly as described for the case of a single fence. The high blockage ratio also meant that flow acceleration effects were anticipated.

Fig.3: Diagram of Chilworth flume setup indicating location of split, measurement points in empty channel (indicated in red) and points where fence centre is located (indicated in green).

4. Results and discussion

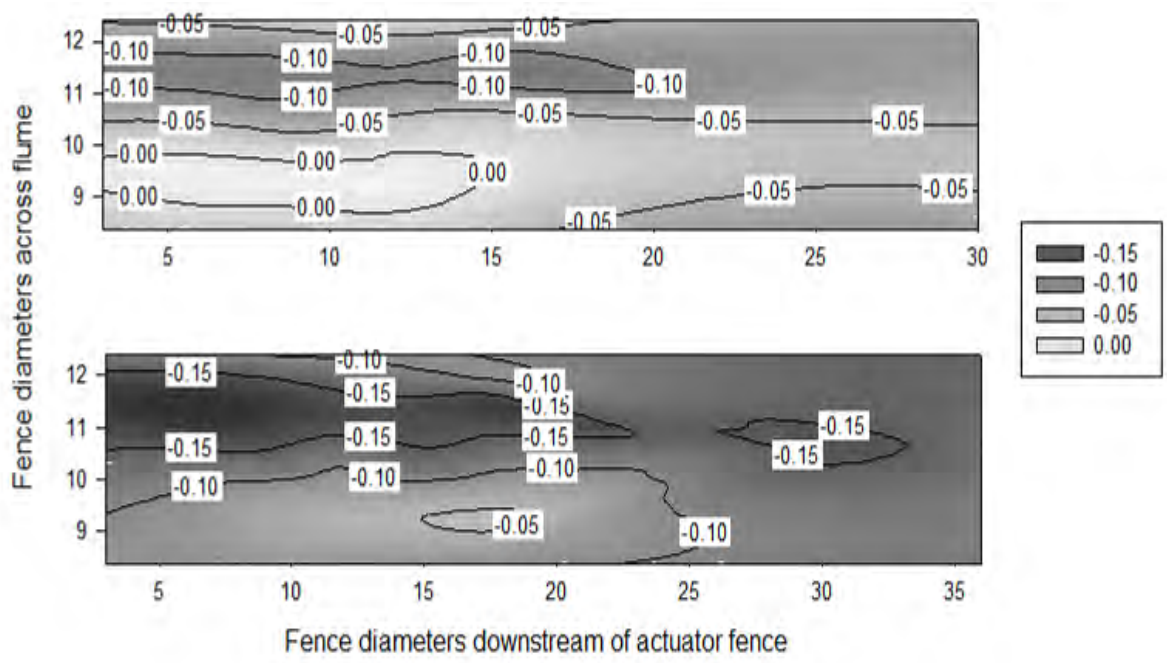

Fig.4. Contour plots showing velocity deficit variations in empty sub channel downstream of single 0.38 porosity fence (top) and downstream of 0.38 and 0.4 porosity fence (bottom).

Figure 4 shows the results of the wake mapping analysis of the areas downstream of both the single fence (top figure) and two fences (bottom figure), as discussed in section 3.4.2. These plots show that some flow acceleration is present in both cases, but also that it is much greater when two fences are present in the opposite channel. Velocity deficit values are zero or very close to zero in the top figure, while they approach values of -0.15 in the bottom figure.

Figures 5 and 6 show the results of the flow acceleration analysis outlined in section 3.4.3. These also demonstrate the presence of flow acceleration due to the presence of fences in the opposite channel. In the case of a single fence in figure 5, there is no immediately apparent definite pattern or relationship between fence position, both laterally and in the downstream direction, and the percentage increase in freestream velocity magnitude. There is only a small difference between the readings given by the ADV positioned at 870mm from the sidewall (left) and that positioned 1100mm from the sidewall (right). Despite this lack of any definite relationship, it should be noted that the flow acceleration is quite small in itself, being 7% or less. Also the Chilworth flume has a variation in flow velocity at any point of approximately between 1% and 2% for any flow rate. For such small changes to flow, a lack of any definite relationship between the investigated parameters is not an unexpected result.

Much higher flow acceleration is observed from the results for the case of two actuator fences as displayed in figure 6. The scatter plot shows flow acceleration of between 8% and 14%. 14% flow acceleration is a potentially significant result from a tidal farm perspective. If the installation of more tidal converters in this empty channel could be justified both economically and environmentally, there is potential for up to 48% more power to be

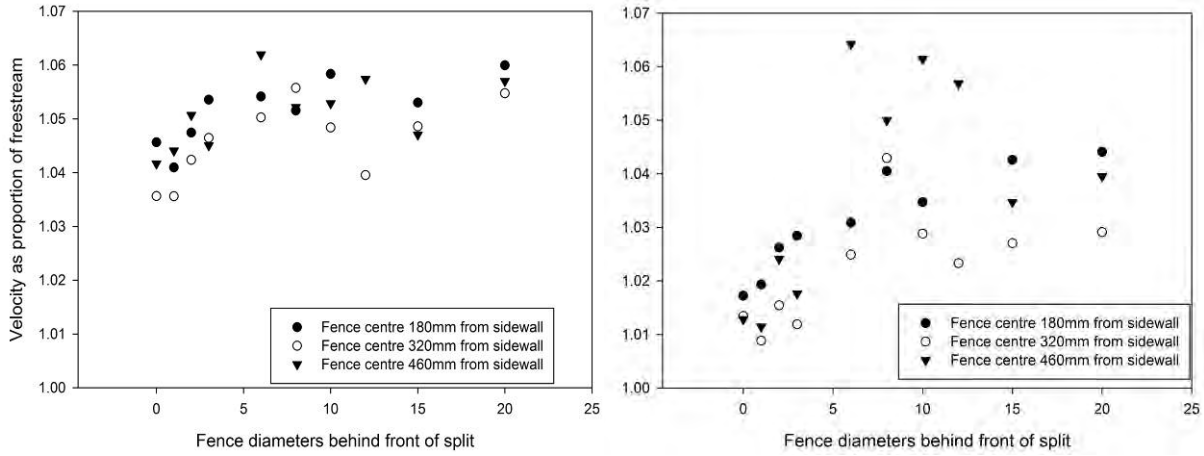

Fig.5. Flow acceleration in empty sub channel at lateral positions of 870mm (left) and 1120mm (right) due to movement of single actuator fence in opposite channel.

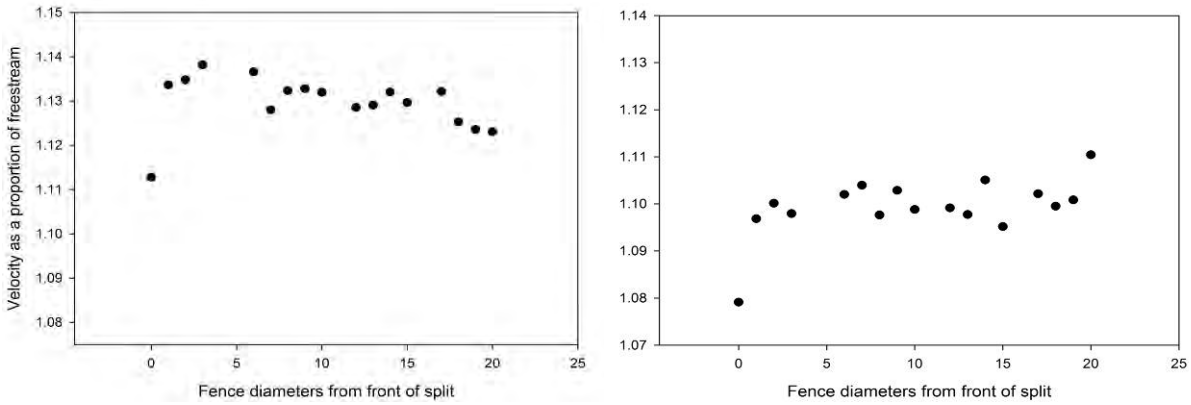

Fig.6. Flow acceleration in empty sub channel at lateral positions of 870mm (left) and 1120mm (right) due to movement of two side by side actuator fences in opposite channel.

extracted than without arrays in the other sub channel. However this would obviously be dependent on other factors such as internal turbine efficiency. It is also interesting to note from the scatter plots that the percentage acceleration is higher closer to the split than further laterally along the channel. This only occurs for the case of two fences. This might suggest that the presence of a greater number of turbines in an array may cause the flow to diverge further upstream than smaller arrays. Nearer to the split, there is also some reduction in flow acceleration as the array is moved further back from the split. This is another result which does not appear to happen further laterally across the channel. This may suggest that the flow is steadier and developed further away from the split, and that changes to longitudinal positioning of the array may only affect flow velocities in certain regions of the empty sub channel.

5. Conclusions and future work

The single actuator fence in this analysis occupied approximately 1/6th of the total area of one sub channel (1/3rd of the depth and ½ of the width), and resulted in relatively low flow acceleration. There was also no obvious relationship between acceleration and either longitudinal or lateral position. In contrast, two actuator fences occupying 1/3rd of the total area resulted in much higher acceleration, in some cases up to 14%, with some dependence on longitudinal position apparent. These results suggest that total area blocked by turbines in a sub channel has implications for flow acceleration effects. Future work will examine this

relationship between acceleration and blockage by using different sized actuator fences in one sub channel.

Higher flow acceleration in the region closer to the split also suggests that the initiation of flow divergence between the two sub channels may be dependent on the area blocked in one sub channel. Future work will examine the area upstream of the front of the tidal split in an attempt to determine at what point flow divergence begins and how dependent is the point of flow divergence on the area occupied by turbines. Results also show that high flow acceleration still occurs even when the actuator fences are a relatively large distance downstream of the front of the split. Future experimentation will attempt to determine at what array position downstream of the split flow acceleration will no longer exist.

References

[1] T. Daly, L.E. Myers, A.S. Bahaj, Experimental analysis of the local flow effects around single row tidal turbine arrays, Proceedings of the 3rd International Conference on Ocean Energy, 2010.

[2] A. Mortimer, Tidal power with Hammerfest Strom technology: Towards commercialisation, Proceedings of 3rd International Conference on Ocean Energy, 2010.

[3] R.H. Karsten, J.M. McMillan, M.J. Lickley, R.D. Haynes, Assessment of the tidal current energy in the Minas Passage, Bay of Fundy, Proceedings of the Institution of Mechanical Engineers, Part A: Journal of Power and Energy 222, 5, pp. 493- 507

[4] B.L. Polagye, M. Kawase, P. Malte, In-stream tidal energy potential of Puget sound, Washington, Proceedings of the Institution of Mechanical Engineers, Part A: Journal of Power and Energy 223, 5, pp. 571- 587

[5] J.F. Atwater, G.A. Lawrence, Power potential of a split tidal channel, Renewable energy 35, 2, pp. 329-332.

[6] C. Garrett, P. Cummins, The power potential of tidal currents in channels, Proceedings of the Royal Society A: Mathematical, Physical and Engineering Sciences, 461, 2060, pp. 2563-2572.

[7] G. Sutherland, M. Foreman, C. Garrett, Tidal current energy assessment for Johnstone Strait, Vancouver Island, Proceedings of the Institution of Mechanical Engineers, Part A: Journal of Power and Energy 221, 2, pp. 147- 157

[8] B.L. Polagye, P.C. Malte, Far field dynamics of tidal energy extraction in channel networks, Renewable energy, 36, 1, 222-234.

[9] L.E. Myers, A.S. Bahaj, Experimental analysis of the flow field around horizontal axis tidal turbines by use of scale mesh disk rotor simulators, Ocean engineering, 37, 2-3, 218-227.

[10] L. Cea, J. Puertas, L. Pena, Velocity measurements on highly turbulent free surface flow using ADV, Experiments in fluids 42, 3, pp. 333-348.

The downstream wake response of marine current energy converters operating in shallow tidal flows

Jack Giles[1,2*], Luke Myers[1], AbuBakr Bahaj[1], Bob Shelmerdine[2]

[1]*University of Southampton, Southampton, UK*
[2] *IT Power Ltd., Bristol, UK*
** Corresponding author. Tel: +44 7855037885, E-mail: jack.giles@soton.ac.uk*

Abstract: This paper presents findings from an experimental study investigating the downstream wake response from marine current energy convertors operating in various degrees of vertical flow constraint. The paper investigates deep vertically unconstrained sites, mid-depth sites and there is a particular emphasis on shallow tidal stream sites. Shallow tidal resources could be utilised for the deployment of first generation farms. The nature of the downstream wake flow will be a critical factor when determining the farm layout and the wake length is heavily influenced by the flow depth or ratio of rotor diameter to flow depth. A porous actuator disk is used to model the marine current energy convertor and an Acoustic Doppler Velocimeter is used to map the downstream wake. Linear scaling of length ratios suggests mid depth sites of 30-50m will produce the shortest wake lengths and for deeper and shallower sites the wake length increases. It is hoped that these relationships between vertical flow constraint and wake length will help with the layout design of tidal stream farms.

Keywords: *wake, vertical flow constraint, shallow tidal flows, farms.*

Nomenclature

C_t	*thrust coefficient*	$\overline{U}$	*Mean velocity of sample* ..... $m \cdot s^{-1}$
U_{def}	*velocity deficit* ..... $m \cdot s^{-1}$	D	*actuator disk diameter* ..... m
U_w	*wake velocity* ..... $m \cdot s^{-1}$	u	*downstream velocity component* ..... $m \cdot s^{-1}$
U_o	*free-stream velocity at hub height* ..... $m \cdot s^{-1}$	v	*lateral velocity component* ..... $m \cdot s^{-1}$
I	*turbulence intensity* ..... %	w	*vertical velocity component* ..... $m \cdot s^{-1}$

1. Introduction

Shallow tidal flows hold a number of advantages for first generation tidal stream farms. Shallow flows, of depths less than 20m, often have a reduced cross-sectional area suitable for energy extraction compared with deeper channels, but they also have other benefits including close proximity to the shore with many sites situated away from shipping channels. This could make construction and grid connection both easier and more economically feasible. Fig. 1 presents results showing potential sites for device deployments in shallow tidal flows in the UK. The data for bathymetry and mean spring peak velocities was obtained from the BWEA "Marine Energy Resource Atlas" [1] and the layers were manipulated using geographic information system (GIS) software. The highlighted areas show sites with depths between 10-20m and spring peak velocities of greater than 1.5m/s.

When deploying a farm of Marine Current Energy Converters (MCECs), the nature of the downstream wake flow will be a critical factor when determining the farm layout and packing density. It is known that the wake length is heavily influenced by the flow depth or the degree of vertical flow constraint. This paper presents experimental findings of the flow fields around scale MCEC simulators operating in a circulating flume at varying depths to represent the range of depths present at the many sites suitable for MCEC deployment. Examples of shallow tidal sites include; the Bristol Channel, the Humber Estuary and areas around the Channel Islands (see Fig. 1). Deeper flows exist in the Pentland Firth and in various locations around the West of Scotland.

Previous work presented by Myers et al. [2] concluded that MCECs operating in shallow fast-moving flow regimes will see a difference in the downstream flow field compared with devices installed in deeper water. It was stated that the effects of sea bed proximity have shown that wake recovery is not as favourable when the flow field is very deep beneath the rotor disk. This is due to reduced shear forces and lack of accelerated flow generated by the close proximity of the sea bed and surface that serve to drive wake dissipation. This paper presents work developed from the previous study [2] to further investigate the effects of vertical flow confinement on the downstream wake development of MCECs. A thorough understanding of wake development is critical for the optimisation of the downstream device spacing in tidal stream farms. Minimising the downstream spacing will enable a higher farm device density and hence higher yields from a specific site.

For a multiple-row MCEC array, longitudinal spacing of devices is expected to be great enough to ensure that downstream devices have an incoming flow regime (and hence power production) that is comparable to devices located upstream. However, at spatially constrained sites this approach to spacing may be tightened in order to increase energy capture per surface area of the site and to reduce electrical connection costs. It is postulated that there may be an optimum device height to flow depth ratio that will lead to the minimisation of downstream wake length. For sites that are deeper or shallower than this optimum depth range, the downstream wake length is expected to increase. Whilst an explanation has been provided for deeper flows [2] it is expected that in a very shallow flow vertical blockage is high and flow acceleration above and below the MCEC will be restricted. Both of these factors are expected to result in reduced mixing between the wake and ambient flow thus increasing wake length.

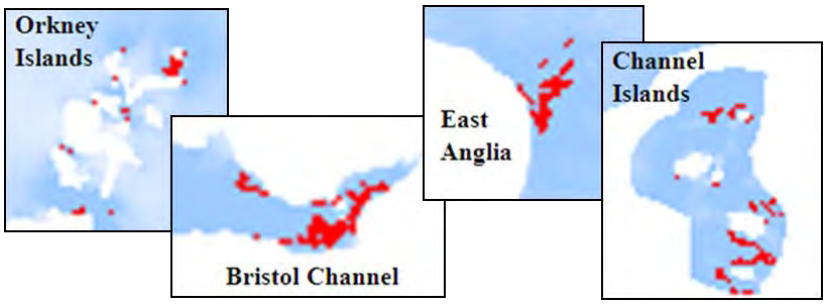

Fig. 1 Potential UK first generation shallow tidal flow sites, not to scale.

2. Methodology

In order to conduct the testing at a reasonable scale a porous mesh disk was used to model a horizontal axis turbine (often referred to as actuator disks). Actuators are now an accepted method for modelling MCECs and have been extensively used for horizontal axis turbines, but the method could equally be used to model vertical axis and oscillating hydrofoil devices. Actuator and momentum theory is discussed extensively by Burton et al. [3]. Work concerning the use of small scale actuator disks for the representation of far wake conditions has been addressed by a number of authors for both wind and tidal energy applications [4,5] . The principle difference between flow fields around actuators and full scale MCECs is the representation of the near wake and these differences are generally known to dissipate in less than four rotor diameters downstream [6,7].

For this work the principle parameters that require replication from large to small scale are [2]:

a) Device thrust force controlled through the level of actuator disk porosity (ratio of open to closed area).
b) Linear scaling of length ratios such as disk diameter to water depth and channel width.
c) Replication of ambient flow field conditions such as Froude number, vertical velocity profile and turbulence intensities. Full-scale and model Reynolds numbers cannot achieve parity at small scale but should lie within the turbulent classification.

Testing was conducted at a scale of 1:100 using actuator disks of 0.1m diameter. The porous actuator's impedance was specified using an empirical relationship between thrust coefficient (C_t) and plate porosity. This relationship was developed from a combination of experimental findings from the University of Southampton and from equations presented by Whelan et al. [8]. The actuator disk used is of the same porosity as that used in Myers et al. [2].

The actuator disk was mounted on a thin stainless steel support arm which made up part of a pivot arrangement to magnify the small thrust forces on the actuator disk. The rig can be seen in Fig. 2, a 10N button load cell was used to measure the total thrust force.

Shallow-depth experiments were conducted in the tilting flume at the Chilworth hydraulics laboratory, University of Southampton, UK. The working section of this flume is 21m in length, 1.37m wide and a maximum depth of 0.4m for steady operation.

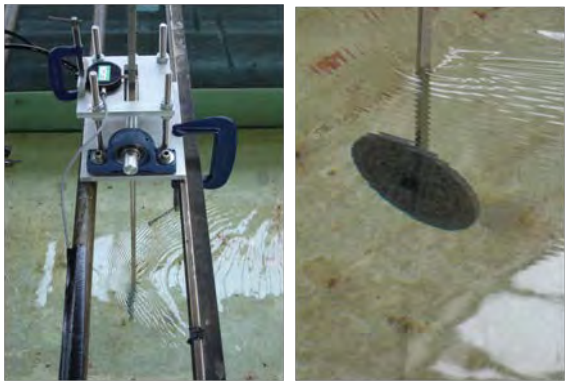

Fig. 2 Actuator lever arm rig (left) actuator disk mounted on lever arm (right)

The vertically unconstrained results which were used to compare with the constrained tests were presented by Myers et al. [2] and were conducted in the IFERMER circulating channel, Boulogne sur Mer, France. The channel has a working section of 18m in length, 4m wide and 2m deep. The downstream wake was mapped using a high frequency Acoustic Doppler Velocimeter (ADV). Operational issues and the accuracy of ADVs have been addressed at length in many publications [9-11]. The ADV was set to sample at 50Hz. For each data point 7500 readings were taken over a 150 second period.

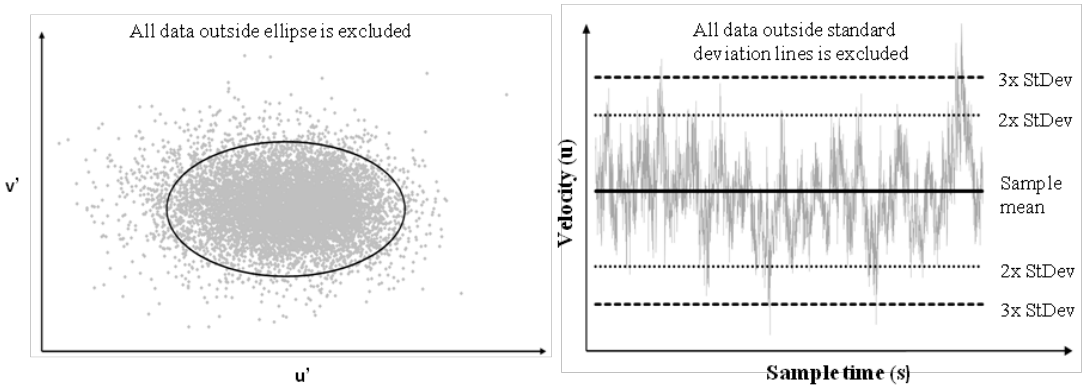

Fig. 3 Velocity correlation filtering method (left) and minimum/maximum filter (right).

Data was filtered to remove noise and spurious points (Fig. 3, shows data spikes) although the large quantity of suspended particles in the Chilworth channel minimised sample errors. Filtering is required to improve measurements of higher order flow effects such as turbulence intensity and shear stresses as spikes in the data give the impression of increasing energy within the flow. However filtering has a very small effect for mean flow velocities as spikes are generally equally positive and negative. All samples were filtered using a velocity cross-correlation filter ultimately chosen due to ease of use and effectiveness after a single pass [12]. This method plots the varying components of velocity against each other and constructs an ellipsoid in 3-dimensional space to exclude any data points that deviate significantly from the sample mean (Fig. 3, left). Similar filters can be set up to remove statistically or physically improbable values. Table 1 compares the velocity cross-correlation filter to a minimum-maximum filter (Fig. 3, right) that removes time-series values ±3 standard deviations from the sample mean. The effectiveness of the cross-correlation filter for the turbulence data is apparent.

Table 1 Minimum/maximum and velocity correlation filter comparison.

Sample	u-plane velocity ($m.s^{-1}$)				u-plane turbulence intensity (%)			
	Raw	Min/ max	Vel. Cor.	% Change from raw	Raw	Min/ max	Vel. Cor.	% Change from raw
1	0.245	0.245	0.246	+0.54	9.80	9.56	7.43	-24.18
2	0.295	0.295	0.291	-1.29	18.86	18.86	15.17	-19.54
3	0.286	0.286	0.286	-0.11	11.30	10.59	8.91	-21.14
4	0.287	0.286	0.284	-0.93	13.47	11.55	10.05	-25.41
5	0.246	0.246	0.247	+0.56	9.31	9.26	7.31	-21.45

The recovery of the wake is defined in terms of velocity deficit; this is a non-dimensional number relative to the free-stream flow speed at hub height and the wake velocity, defined by Eq. (1).

$$U_{def} = 1 - U_w / U_o \tag{1}$$

The ambient turbulence intensities in the circulating channel used during this study were approximately 6-8% and were calculated in all three planes (u,v,w). Turbulence intensity is commonly defined as the root-mean-squared of the turbulent velocity fluctuations divided by the mean velocity of the sample. Table 2 details the parameters of the constrained flow tests conducted as part of this work and the previously conducted unconstrained flow tests conducted at the IFERMER facility. Dimensions are detailed in disk diameters (D).

Table 2 experimental test parameters.

Test	Water depth	Channel width	Actuator centre from surface	Depth-averaged Froude No.	Depth-averaged Reynolds No.	Disk height/depth ratio
1	4.0	13	2.00	0.15	$1.2x10^5$	0.25
2	3.0	13	1.50	0.15	$7.8x10^4$	0.33
3	2.5	13	1.25	0.15	$5.7x10^4$	0.40
4	2.0	13	1.00	0.15	$4.2x10^4$	0.50
5	1.5	13	0.75	0.15	$2.7x10^4$	0.66
6*	20	40	2.00	0.113	$9.9x10^5$	0.05

*unconstrained test conducted at IFERMER, France.

Myers et al. [2] showed experimentally for a constant depth the wake velocity deficit is independent of velocity (for a representative range of Froude numbers).

3. Results and Discussion

Three cases from Table 2 will be addressed herein; A deep-unconstrained tidal site (test #6), a mid-depth tidal site (test #1) and a shallow-depth tidal site (test #4).

3.1. Free-stream results

Fig. 4 (left) shows the normalised vertical velocity profiles for the three cases, these are the free-stream results from the Chilworth and IFREMER facilities. Depth is expressed in terms of disk (or rotor, full scale) diameters (D). The velocity profile at Chilworth is well developed but the close proximity of the bed induces a more pronounced gradient that leads to disparate mass flow rates above and below the disk, this is most noticeable in the shallow-depth scenario. Flow speed in the deep site case is similar above and below the disk.

Fig. 4 (right) shows the ambient turbulence intensities in all three planes (u,v,w) for the deep-unconstrained and mid-depth scenarios (IFERMER and Chilworth channels, respectively). At the Chilworth facility the presence of the flume bed 2-diameters below the disk causes an increase in turbulence intensity immediately above the bed. u and v components are of a similar magnitude at 6-7% whilst turbulence intensity in the vertical plane is slightly greater. The IFERMER channel turbulence intensity is more constant with depth close to the disk. The turbulence intensity in the vertical plane is much lower than at Chilworth. The difference occurs due to the nature with which water is delivered to the upstream end of the working section.

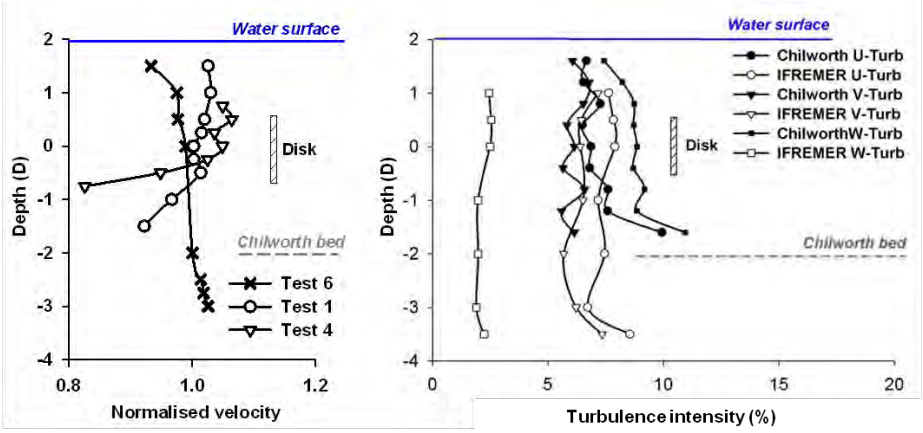

Fig. 4 Normalised vertical velocity profiles at the Chilworth and IFERMER water channels (left) and Turbulence intensities (right).

3.2. Wake length

Fig. 5 shows the longitudinal centre plane velocity deficits for the three depth cases. It is clear that in the mid-depth case the wake is broken down in a significantly shorter downstream distance than in the deeper and shallower cases (approximately 6D). This results from flow acceleration above and below the actuator disk that acts to break the wake down through greater lateral turbulent mixing. This effect was postulated by Myers et al. [2] and is reinforced following analysis of these results.

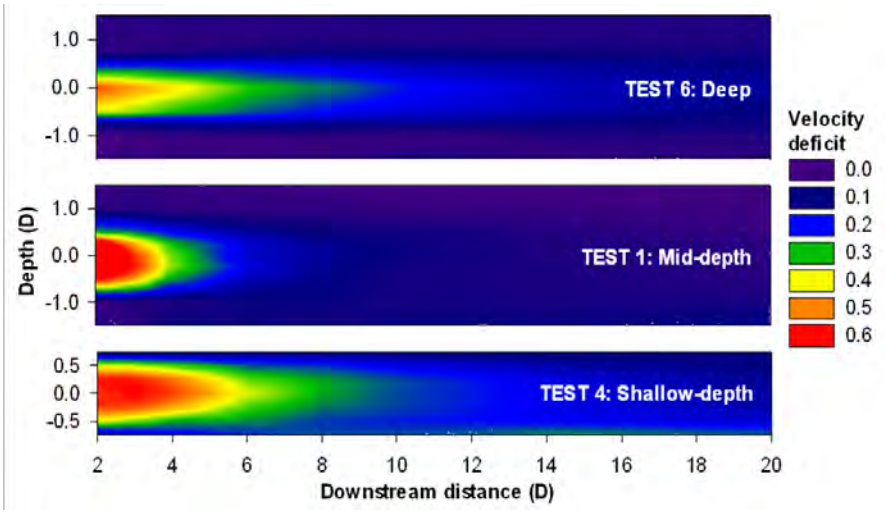

Fig. 5 Centre plane velocity deficit profiles; deep-site, mid-depth site & shallow-depth site.

The wake persists much further downstream in the deep-unconstrained and shallow depth cases (10-12D downstream), this results from restrictions in flow acceleration around the MCEC. In the deep-unconstrained case vertical blockage is low and hence flow acceleration is reduced, thus allowing the wake to persist further downstream. In the shallow flow scenario vertical blockage is high and hence local flow acceleration above and below the MCEC is restricted, again allowing wake to persist further downstream.

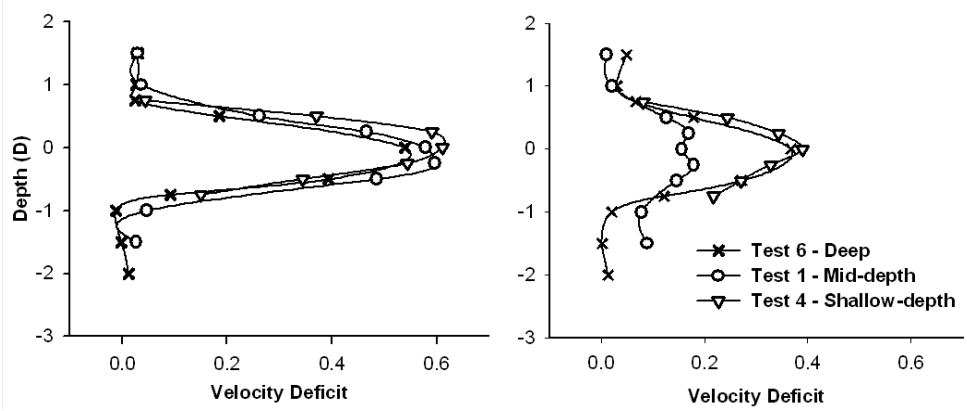

Fig. 6 Vertical velocity deficits at 3 diameters downstream (left) and 6 diameters (right)

Fig. 6 shows vertical line plots of velocity deficit at two downstream locations for all three depth cases. Looking at the 3D downstream graph it is clear that the initial velocity deficits directly behind a MCEC are similar irrespective of the vertical flow constraint; this is because wake is re-energised by turbulent mixing from the surrounding flow and in the near wake this effect is less pronounced. Further downstream e.g. 6D, the effects of varying degrees of vertical blockage can be seen. The deep and shallow cases give similar profiles, whereas the velocity deficits for the mid-depth case are reduced considerably because of increased turbulent mixing between the wake and accelerated surrounding flow. The effects of flow acceleration in the mid-depth case can be observed.

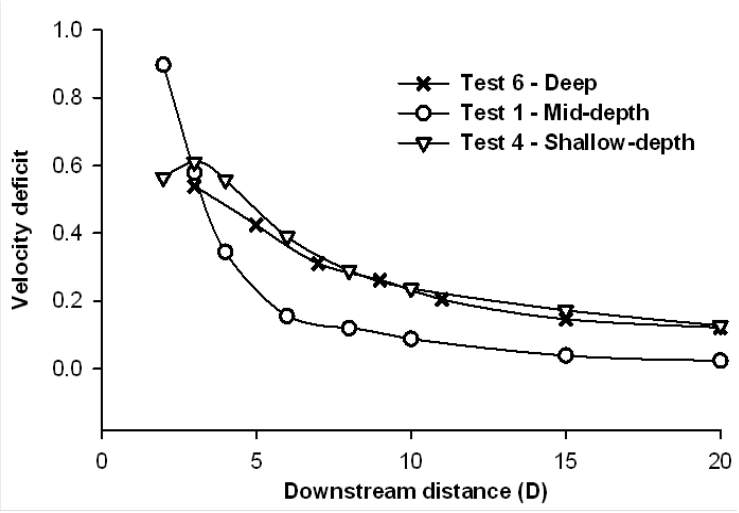

Fig. 7 Disk centreline velocity deficit comparison.

Fig. 7 shows the downstream centreline deficits. As suggested by Fig. 5 the wake recovers much more quickly in the mid-depth case. Again the principal mechanism for this is flow acceleration around the disk which serves to break up the wake more rapidly. In Fig. 7 the similarities in terms of downstream velocity deficits between the shallow and deep cases are clearly illustrated.

3.3. Farm row optimisation

This section highlights the significance and importance of this work to tidal stream farm design and optimisation. Fig. 8 shows there is an optimum rotor diameter/flow depth ratio in terms of wake recovery and minimising downstream wake length. Three different downstream location cases are compared for all the tests detailed in Table 2. It appears that 0.25 is the optimum rotor diameter/flow depth ratio for minimising downstream spacing. At full scale this might equate to a site with a depth range of 30-50m depending on the rotor diameter.

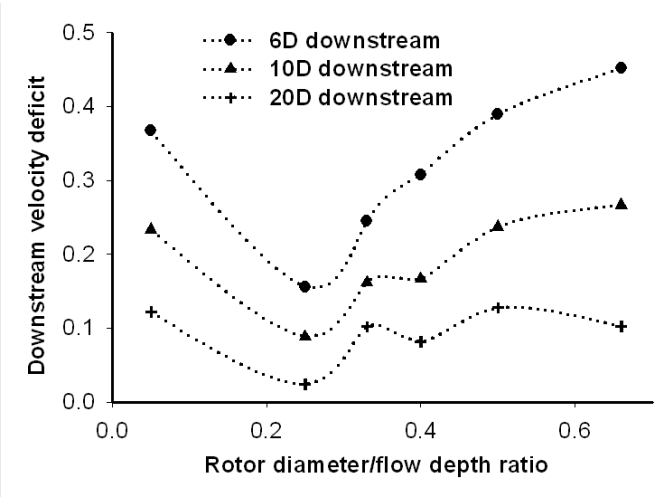

Fig. 8 Optimum rotor diameter/flow depth ratio in terms of wake recovery

4. Conclusions

From the results presented in this paper, it is critical that tidal stream farms or arrays are optimised in terms of downstream spacing and packing density, it will thus be important to tune the downstream device spacing to the local flow depth. Although at spatially constrained sites the spacing may be tightened in order to increase energy capture per surface area of the site and to reduce electricity connection costs. It is anticipated that many first generation sites will be located in shallow tidal flows and hence the longer wake lengths compared with mid-depth sites must be factored into the design process. In terms of the full scale significance and to reduce wake length, the optimum rotor diameter/flow depth ratio is 0.25. This would equate to a flow depth range of 30-50m depending on the rotor diameter.

The wake length is controlled by the degree of lateral flow mixing between the retarded wake flow and the surrounded accelerated free-stream flow. Increased wake length in very deep and very shallow flows result from vertical blockage, in a deep flow vertical blockage is minimal and hence local flow acceleration around the wake is reduced. In a very shallow flow vertical blockage is high and flow acceleration above and below the MCEC is restricted. Both these

factors result in less lateral flow mixing and thus increased wake length. It is hoped that the relationship between vertical flow constraint and wake length will help with the layout design of future tidal stream farms.

Acknowledgements

This work has been conducted as part of an Engineering Doctorate study and has been jointly funded by the European and Physical Sciences Research Council (EPSRC) and IT Power Ltd. Work at IFERMER was funded by the Marine Environment Tests and Research Infrastructure (METRI II) programme and the UK Technology Strategy Board. "Performance characteristics and optimisation of marine current energy converter arrays", project number T/06/00241/00/00.

References

[1] ABP, 'Atlas of UK Marine Renewable Energy Resources: Technical Report', ABP Marine Environmental Research Ltd, Department for Business, Enterprise & Regulatory Reform, 2008.

[2] L. Myers, A.S. Bahaj, G. Germain, J. Giles, 'Flow boundary interaction effects for marine current energy conversion devices', World Renewable Energy Congress X, Glasgow, 2008.

[3] T. Burton, D. Sharpe, N. Jenkins, E. Bossanyi, 'Wind Energy Handbook', Wiley, 2001

[4] A.S. Bahaj, L. Myers, M.D. Thomson, N. Jorge, 'Characterising the wake of horizontal axis marine current turbines', 7th European Wave and Tidal Energy Conference, Porto, Portugal, 2007.

[5] L. Myers, A.S. Bahaj, R.I. Rawlinson-Smith, M.D. Thomson, 'The effect of boundary proximity upon the wake structure of horizontal axis marine current turbines', 27th International Conference on Offshore Mechanics and Arctic Engineering, Estoril, Portugal, 2008.

[6] P. J. Connel, R.L. George, 'The wake of the MOD-0A1 wind turbine at two rotor diameters downwind on 3 December 1981', Pacific Northwest Laboratory, Battelle, U.S., 1982.

[7] P.E.J. Vermuelen, 'Mixing of simulated wind turbine wakes in turbulent shear flow', TNO Rep. 79-09974, Apeldoorn, Holland, 1979.

[8] J. Whelan, M. Thomson, J.M.R. Graham, J. Peiro, 'Modelling of free surface proximity and wave induced velocities around a horizontal axis tidal stream turbine', 7th European Wave and Tidal Energy Conference, Porto, Portugal, 2007.

[9] A. Lohrmann, R. Cabrera, N. Kraus, M. ASCE, 'Acoustic-Doppler Velocimeter (ADV) for Laboratory Use', Fundamentals and Advancements in Hydraulic Measurements and Experimentation, New York, USA, 1994.

[10] G. Voulgaris, J.H. Trowbridge, 'Evaluation of the Acoustic Doppler Velocimeter (ADV) for Turbulence Measurements', Journal of Atmospheric and Oceanic Technology, 1998, 15, pp. 272 – 289.

[11] P.J. Rusello, A. Lohrmann, E. Siegel, T. Maddux, 'Improvements in Acoustic Doppler Velocimetery', The 7th Int. Conf. on Hydroscience and Engineering, Philadelphia, USA, 2006.

[12] L. Cea, J. Puertas, L. Pena, 'Velocity measurements on highly turbulent free surface flow using ADV', Experiments in Fluids, 2007, 42, pp. 333 – 348.

Development of a Low Cost Point Absorber Wave Energy Converter for Electric Mobility

Jacob W. Foster[1], Reza Ghorbani[1], Pierre Garambois[2], Emma Jonson[3], Sten Karlsson[3]

[1]*University of Hawai`i at Manoa, Honolulu,USA;*
[2]*INSA, Lyon,France;*
[3]*Chalmers Univ. of Technology, Gothenburg, Sweden*
**Corresponding author: Tel 713-419-666; E-mail: fosterja@hawaii.edu*

Abstract: This paper presents a developing concept of a low cost "point absorber" Wave Energy Converter (WEC). The WEC is unique in that instead of operating with one buoy, two are used to optimize the hydrodynamic response and energy output. This makes the design a three-part system: the surface buoy provides the vertical translation and hosts the primary interface for energy absorption, the power take-off (PTO) device which is a direct drive permanent magnet AC generator, and lastly the tension buoy that feeds through the PTO to the surface buoy. The total cost of the 2 KW WEC is less than $2000 USD including the PMAC generator, power converter and cable to charge the batteries for electric vehicles. The integrated dynamics of the WEC and the PTO are presented using a simplified model of a heaving buoy. The wave energy resource of a test location is analyzed and presented based on data from a global Wave Watch III model surrounding Oahu. The characteristics and distributions of the movement patterns of individual vehicles are measured. It was shown that regenerative braking power has the major role in reducing the total energy consumption and decreasing the size of the required battery to be charged externally by the WEC. In addition the power used by vehicle follows the Rayleigh distribution. Thus, the batteries for individual driver are customizable. This significantly reduces the amount of energy required by distributed WEC generators.

Keywords: *Wave energy conversion, point absorber, electric vehicle*

1. Introduction

Throughout the development of Wave Energy Conversion devices theoretical solutions have been produced for various methods of energy extraction for both point absorbing buoys and oscillating water column devices. Analytical solutions are formulated from the hydrodynamic interaction between the device interfaces with incoming waves (see Evans 1981, Newman 1979; McCormick 1980, Cruz 2008, Garnaud and Mei 2010).

As WEC technologies have evolved some commercial entities have taken the stage in pursuing industrial development of these devices for large scale energy production (Clément et al. 2002). Care is taken into selecting design criteria based on hydrodynamic and power-take-off (PTO) parameters. It is of use to identify these criteria so as to perform a wave climate-wise optimization. This paper presents the design of a wave-energy conversion device and a brief overview of the wave-climate at the location where the device is to be tested. The characteristics and distributions of the movement patterns of individual vehicles are measured. It was shown that regenerative braking power has the major role in reducing the total energy consumption and decreasing the size of the required battery to be charged externally by the WEC. In addition the power used by vehicle follows the Rayleigh distribution. Thus, the batteries for individual driver are customizable. This significantly reduces the amount of energy required by distributed WEC generators.

2. Methodology

To develop a general equation for the power capture capability of this device the analytical solution of a small point absorber, as presented by Garnaud and Mei (2010), is discussed and extended for the WEC device in this section. A wave climate analysis is provided to present

base climate criteria of which control variables must be optimized for WEC. The site selected is located off the North East coast of the Island of Oahu where trade-wind seas are predominant.

2.1. Power extraction concept:

The premise for the WEC device is the uniqueness of the power-take-off system. The PTO unit is sealed and anchored to the sea-floor. Housed within are the motor/generator and inertial wheel which are driven via an external capstan (see Fig.1). The design is based on a dry PTO unit. In this setup the PTO is not sealed watertight to be submerged and anchored to the sea-floor (see Fig. 2.). Rather, it is suspended safely above the sea-surface via a column fastened to the concrete anchor-base.

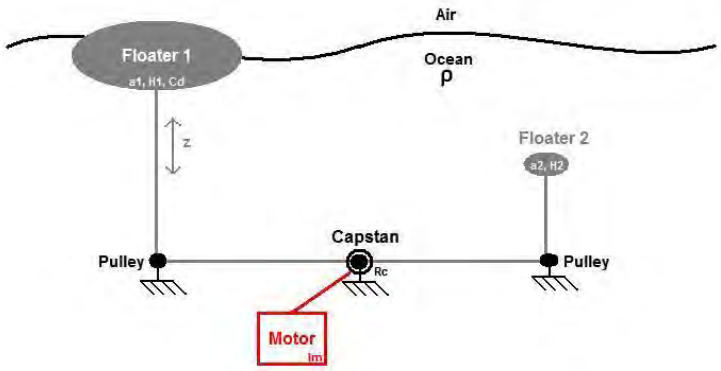

Fig. 1. Schematic of the three-part WEC device

The PTO capstan is the primary interface between the two buoys. Through it, the vertical buoy motion due to forcing from incoming waves is transferred to rotational motion to be resisted by the motor/generator and inertial wheel. While the larger-floating buoy acts as a *point absorber* with incoming waves the smaller submerged buoy provides the required tension to resist slipping between the tension line and the capstan. The tension relationship is defined as:

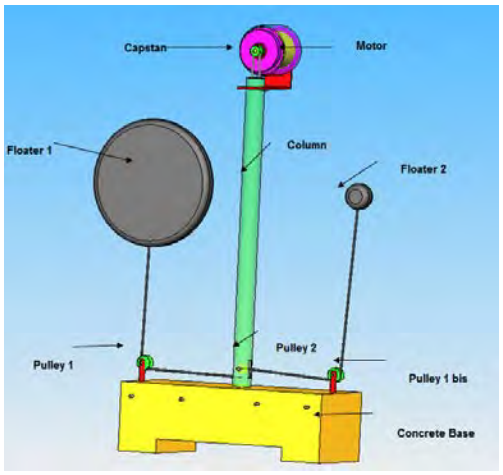

Fig. 2. Dry PTO WEC design

$$T_2 = T_1 e^{\mu * \theta round}, \quad (1)$$

where, $\mu = 0.4$ (the friction coefficient between rope and steel) and T_1; T_2 are the tension on the line approaching the point-absorber and the tension buoy respectively.

Through investigation we find that the required size of tension buoy is significantly smaller than that of the point-absorber. With this in mind we begin to develop the general equation for the average power extraction of the three-part WEC device.

The following formulation for such a solution is an extension of the analytical solution presented by Garnaud and Mei (2010) for a single-small point absorber. To demonstrate the performance of a single degree of freedom system, a buoy responding due to the vertical heave forcing of a wave (with angular frequency ω and amplitude A) is considered. Incoming wave potential is defined as

$$\Phi_I = \varphi_I e^{-i\omega t} \tag{2}$$

with

$$\varphi_I = \frac{Ag}{i\omega}\frac{\cosh(k(z+h))}{\cosh(kh)}e^{ikx} \tag{3}$$

where ω and k are related by the dispersion relation

$$\omega^2 = gk\tanh(kh)\,. \tag{4}$$

At this point Garnaud and Mei (2010) make a simplification based on the small size of the surface buoy relative to incoming wave length, in that the scattered and radiated waves are negligible. This is from the Froude-Krylov approximation where the hydrodynamic pressure on the buoy is dominated by the undisturbed incoming wave (Newman 1979). The vertical excitation force on a buoy of radius, a, and draft, H, becomes

$$i\rho\omega\int\int(0,0,0),dS = \rho gA\pi a^2\,. \tag{5}$$

We now include the power-take-off influence of the 3-part device to the general WEC equation by assuming the PTO exerts a load of $\omega^2\lambda_g\zeta$ where λ_g is the extraction rate, and ζ is the buoy displacement. The force due to the inertial wheel can be included as $\frac{I * \ddot{\zeta}}{R_c}$, where I is the inertia the drive system, and R_c is the radius of the capstan. The added buoyancy force on the floating buoy, due to heave is $\pi a_1^2\rho g\zeta$ then by Newton's law

$$(M_1\zeta + M_2\zeta + \frac{I\zeta}{R^2{}_c})\omega^2 + \lambda_g\zeta i\omega + \pi\rho g a_1{}^2\zeta = \pi\rho g a_1{}^2 A\,, \tag{6}$$

where M_1 and M_2 can be defined from Archimedes principle as:

$$M_1 = \rho\pi a_1{}^2 H_1 \tag{7}$$

and

$$M_2 = \rho\pi a_2{}^2 H_2 / 2\,. \tag{8}$$

From this we can define a transfer function for amplitude of response as

$$\frac{\zeta}{A} = \frac{1}{\{\frac{H_1}{g} + \frac{H_2}{2g}(\frac{a_1}{a_2})^2 + \frac{I}{R_c^2\rho\pi a_1^2}\}\omega^2 + \frac{\lambda_g}{\rho\pi a_1^2 g}i\omega + 1} \tag{9}$$

This lets us define the time average rate of energy extraction at a single frequency as

$$P_{buoy} = \overline{\lambda_g [\ \ e(\varsigma e^{\ i\omega t})]^2} = \frac{1}{2}\omega^2 \lambda_g |\varsigma|^2 \tag{10}$$

or, for an irregular time series of multiple frequencies

$$P_{buoy} = \frac{1}{2}\lambda_g |\dot{\varsigma}|^2 . \tag{11}$$

2.2. Wave climate and optimization schemes

The data for the climate-wise optimization was provided by (Arinaga and Cheung 2011 and Stopa and Cheung 2011). Ten years of wave hindcast parametric spectral data based on significant wave height, H_s, and peak period, T_P, were generated using a global Wave Watch III simulation with a nested output for the Hawaiian Islands. (An explanation of wave power spectrum can be found in Cruz, 2008). Fig. 2 depicts this data in a multivariate histogram displaying the frequency of occurrence in color of a sea-state with parameters $H_{s,}$, T_P along the vertical and horizontal axis.

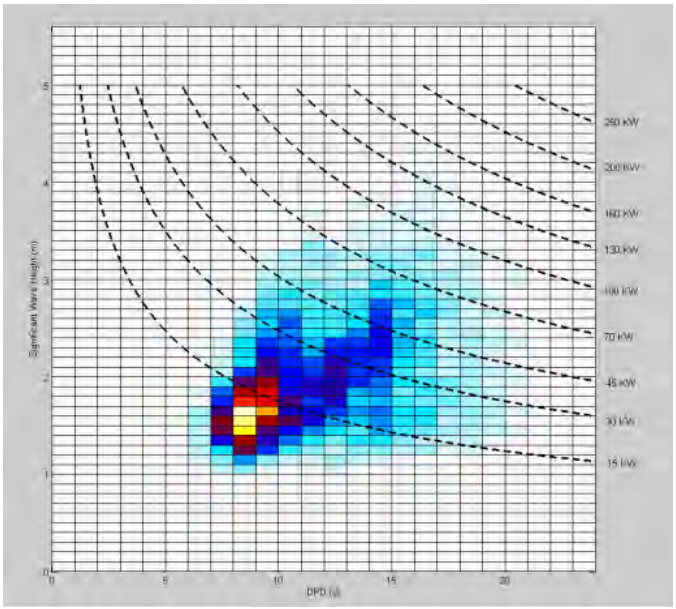

Fig 2. Multivariate histogram of sea-state occurrence with incident wave power contour lines. The horizontal and vertical axis relate to the peak period and significant wave height of a six-hour sea-state respectively. The frequency of occurrence is shown in color, and contour lines depict wave power per sea-state at the associated Tp and Hs per the Bretschneider spectrum approximation.

The contour lines represent the *average power per energy period* within a sea-state at the associated $H_{s,}$, T_P value and are given by:

$$P_o = \rho g^2 \frac{H_s^2 T_e}{64\pi} . \tag{12}$$

This formulation is derived from the statistical moments of a wave power spectrum. For a Bretschneider spectrum

$$S(\omega) = \frac{5}{16} H_s^{\,2} \frac{\omega_p^{\,4}}{\omega^5} e^{-5/4(\frac{\omega_p}{\omega})^4} \tag{13}$$

the following relationship can be defined:

$$T_e = 2\pi \frac{m_{-1}}{m_o} = 0.857 * T_P \,. \tag{14}$$

Where m_{-1}, m_o are spectral moments of the curve, $S(\omega)$. The wave amplitude for any given angular frequency can be found from

$$A = \sqrt{2 * S(\omega) * \omega} \,. \tag{15}$$

The *Capture Width* of a device is used evaluate a WEC's performance at any given frequency. This is the ratio of the *total mean power* absorbed by the WEC to the *mean power per unit wave crest width* of the incident wave train;

$$l(\omega) = \frac{P_{buoy}}{P_o} \,. \tag{16}$$

Since the incident wave power is per unit wave crest width, the absorption width is length dimensional (and ideally greater than the width of the device itself). The total incident wave power in a single sea-state, $S(\omega)$, is given as

$$P_T = \rho g \int_0^\infty S(\omega) c_g(\omega) d\omega \tag{17}$$

where

$$c_g(\omega) = g / 2\omega \tag{18}$$

for deep water, as derived from the dispersion relationship. The power absorption capability in a sea-state can be computed by multiplying the capture width of a WEC at each frequency in the above integral to obtain the total absorbed power. This is defined as

$$P_T = \rho g \int_0^\infty S(\omega) c_g(\omega) l(\omega) \, d\omega \tag{19}$$

Since $P_T = f(H_s, T_P)$ for each sea-state, a long-term analysis for a single site requires the use of the multivariate histogram to compute the probability of occurrence of sea-states, $S(\omega)$, which may occur during the operational lifetime of the WEC. With this knowledge in hand one can begin to identify variable design parameters to be optimized for device operation. We allow λ_g to be the free variable for power extraction optimization since the extraction rate can be controlled by power delivery mechanisms. If the desire is to optimize the WEC system in a "robust" manner (i.e. that it is suited for a range of sea-states which may occur over the lifetime of the device) this variable is optimized for maximum average power extraction

according to Eq. (19) where the capture width $l(\omega)$, by definition, carries λ_g from Eq. (10) and Eq (16).

However, in the interest of fine-tuning the device response for individual incoming sea-states, which may be predicted by meteorological and wave forecast methods, the optimization will be performed on Eq. (11) alone, such that an optimum value of λ_g can be found at each frequency (ω) of a wave power spectrum Eq. (13). To illustrate the latter optimization scheme the generator extraction rate, λ_g, was set to values of 1000, 5000 and 10000 kg/s respectively.

3. Results

3.1. Wave Buoy Response Simulation

The buoy response was computed in the time domain utilizing the time series simulation platform Simulink from MATLAB. The response transfer function, Eq. (9), was directly applied to a simulated 200 second time series wave-record which was generated by discretizing a Bretschneider Spectrum Eq. (13). The numerical spectrum was formed with a significant wave height was 1.5 meters and peak period of 9 seconds to agree with the typical sea-states at the selected site. Following Eq. (11) the average power extraction of the device is computed, and then by simple integration the energy is calculated and presented. As expected the buoys response experiences a lag of the incoming wave motion and varies significantly based on the selected extraction rate as shown in Fig. 4.

3.2. Electric Vehicle Power Study

A Swedish car movement data project started in June 2010 in the Västra Götaland county, going on until June 2011. The aim is to gather a larger amount of data on the characteristic and distribution of the movement patterns of individual, privately driven cars in Sweden by measurement with gps equipment.

We use data from six cars in the Swedish car movement data project, each driving one day, to investigate the probability distribution of the momentary power consumption. The propulsion is equal to the sum of the aerodynamic drag, frictional forces and the acceleration force. The potential energy from regenerative braking, i.e. the integral of negative power, is, based on this statistics data, greater than 50% of the propulsion energy (53 MJ compared to 100 MJ). Regenerative braking therefore has good potential for reducing energy use per km driven. The power could be approximated by a Rayleigh probability density function as shown in Fig. 5. The performance of electric vehicles can be improved by modifying the type of the batteries to be a combination of high-power and high-energy batteries. The high-power batteries improve the gas mileage through regenerative braking and the high-energy batteries can be charged by WEC during opportunity charging. This reduces the required number of charging stations and perhaps the total infrastructural cost associated with electric mobility using distributed energy sources.

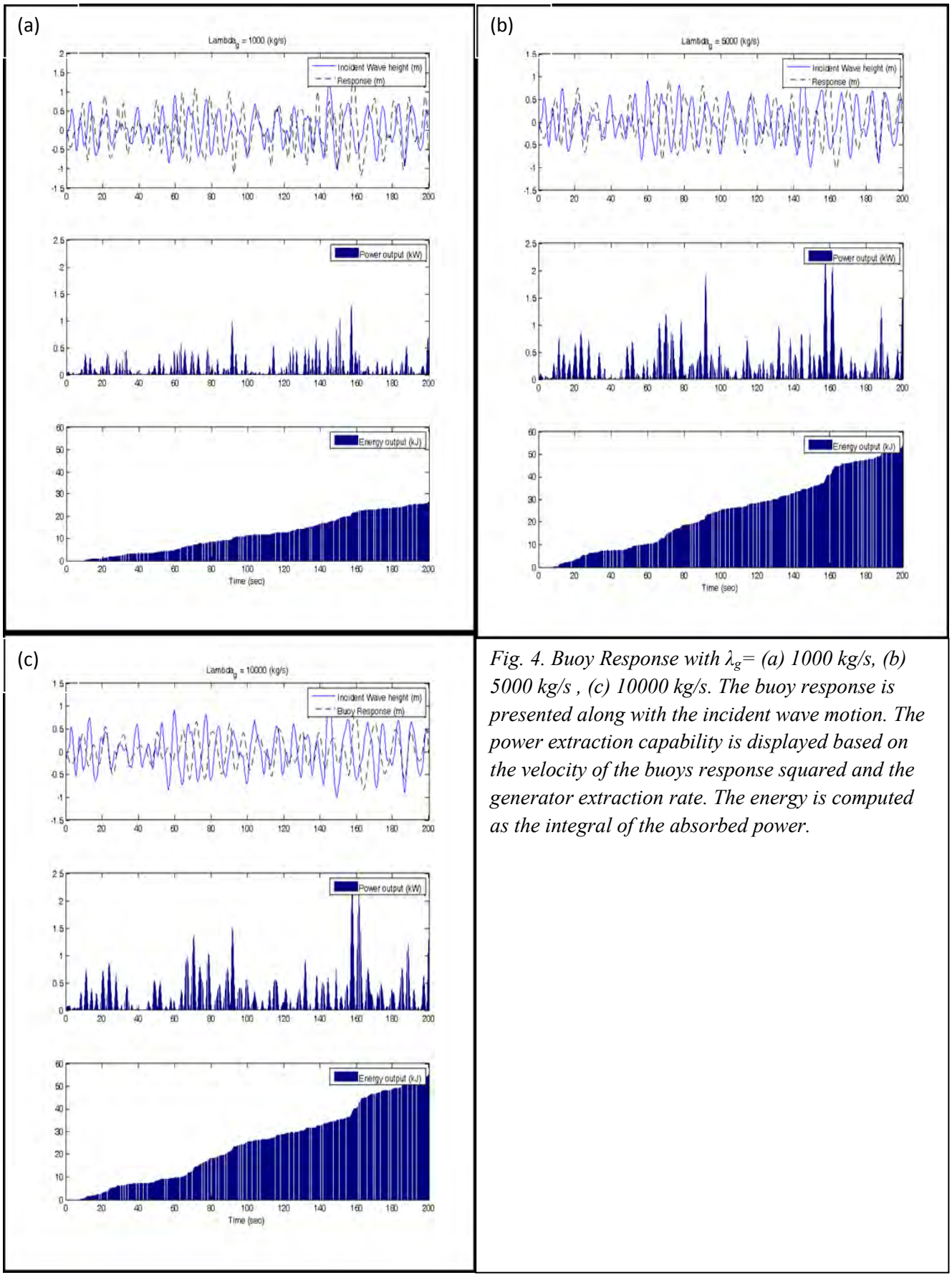

Fig. 4. Buoy Response with λ_g= (a) 1000 kg/s, (b) 5000 kg/s , (c) 10000 kg/s. The buoy response is presented along with the incident wave motion. The power extraction capability is displayed based on the velocity of the buoys response squared and the generator extraction rate. The energy is computed as the integral of the absorbed power.

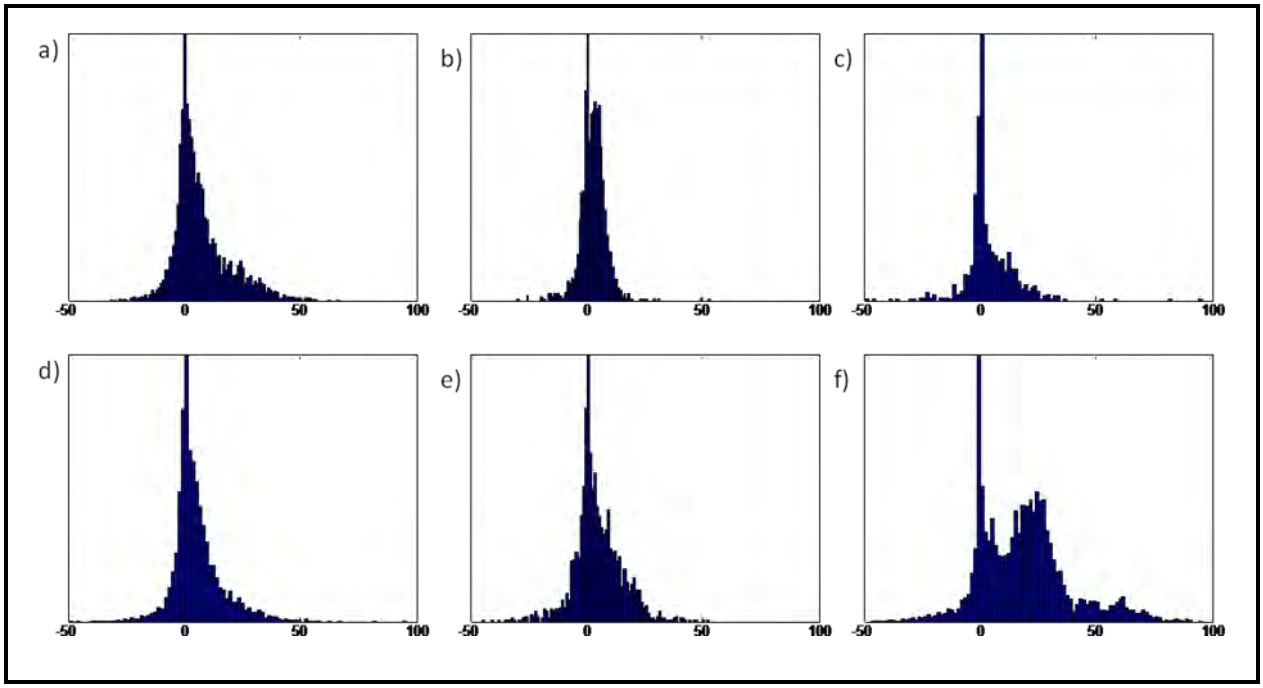

Fig. 5. Probability Histograms

References

[1] Evans, D. V. "Wave-power Absorption by Systems of Oscillating Surface Pressure Distributions." Journal of Fluid Mechanics 114.-1 (1982): 481-99. Print.

[2] Newman, J. "Absorption of Wave Energy by Elongated Bodies." Applied Ocean Research 1.4 (1979): 189-96. Print.

[3] MacCormick, Michael E. Ocean Wave Energy Conversion. 1981. Print.

[4] Cruz, João. Ocean Wave Energy. Berlin: Springer, 2008. Print.

[5] Garnaud, Xavier, and Chiang C. Mei. "Bragg Scattering and Wave-power Extraction by an Array of Small Buoys." Proceedings of the Royal Society 466.2113 (2010): 79-106. Print.

[6] Cle´ment,, Alain, Pat McCullen,, Antonio Falca˜o, Antonio Fiorentino, Fred Gardner, Karin Hammarlund, George Lemonis, Tony Lewis, Kim Nielsen, Simona Petroncini, Teresa Pontes, Phillippe Schild, Bengt-Olov Sjo¨stro¨m, Hans Christian Sørensen, and Tom Thorpe. "Wave Energy in Europe: Current Status and Perspectives." Renewable and Sustainable Energy Reviews 6 (2002): 405-31. Print.

[7] Arinaga, R.A. and Cheung, K.F. Atlas of global wave energy from 10 years of reanalysis and hindcast data. Renewable Energy, in review

[8] Stopa, J.E., Cheung, K.F., and Chen, Y.-L. (2011). Assessment of wave energy resources in Hawaii. Renewable Energy, 36(2), 554-567.

Volume 10

Policy Issues

Technical feasibility of integration of renewable energies in the EU

Marta Szabo[*1]

Renewable Energies Unit - Institute for Energy (IE)
European Commission - Joint Research Centre (JRC), Ispra, Italy
** Corresponding author. Tel: +39 0332 78 3882, E-mail: marta.szabo@ec.europa.eu*

Abstract: According to the Article 4(3) of Directive 2009/28/EC on the promotion of the use of energy from renewable energy sources the EU Member States submitted their forecast documents. The analysis of the forecast documents resulted that the EU will exceed the 20 % renewable energy consumption target with 0,3 % in 2020. The paper gives an overview about the technical feasibility of the integration of the renewable energy sources in the energy systems in the EU and analyze the critical factors and possible solutions.

Keywords: *EU Renewable Energy, Integration, National Renewable Energy Action Plan*

1. Introduction

In accordance with Article 4(3) of Directive 2009/28/EC and of the Council of 23 April 2009 on the promotion of the use of energy from renewable sources each Member States shall adopt a National Renewable Energy Action Plan. The MS-s had to submit them to the Commission by 30 June 2010 using a template according to the Commission Decision of 30 June 2009.

In the national renewable energy action plans each member state has to set the national targets for the share of energy coming from renewable energy sources consumed in electricity, heating and cooling, and transport sector as well in every second year up to 2020; taking into account the effect of energy efficiency related measures on final consumption of energy compared to the indicative trajectory. The member states announce the excess or deficit production which can be used in the cooperation mechanism or in the statistical transfer.

However, each member state has its own different technical, environmental, economic and political situation to consider in meeting its commitments. Cost competitive production of renewable energy and the system by which it reaches are key issues in establishing a viable market. Besides competitiveness, another important issue is security of supply, and a mechanism should be created for resource adjustment at a European level. This could be achieved through international partnerships and contracts, and possibly by establishing adequate storage capacity.

On the subject of environmental protection, emissions trading might prove helpful. Whether competitiveness, environmental protection or security is perceived as having the greatest priority will depend on the circumstances of the specific state. Programs in most of the EU Member States promote a reduction in energy consumption and increase energy efficiency. With a move away from traditional energy sources, the demand for power can only be met by a corresponding increase in energy generation from renewable sources. The main questions are: how realistic are the goals and what potential domestic energy resources can be exploited? What are the main drivers and barriers – mainly from technical point of view - of the integration of renewable energy sources in the energy systems?

2. Methodology

The Directive 2009/28/EC on the promotion of the use of energy from renewable energy sources requires Member States to adopt a National Renewable Energy Action Plan (NREAP) and to submit to the European Commission by 30 June 2010 using a template in accordance with Article 4 of the Directive [1]. Previously all Member States have prepared their forecast documents [2] and submitted them in accordance with the Article 4(3) of the Directive.

The forecast documents indicated the estimated excess production from renewable energy sources compared to the indicative trajectory which could be transferred to the other Member States and the estimated demand for energies from renewables to be covered by means other than domestic production until 2020. It had to be stated also how big is the estimated potential for joint projects until 2020.

Comparative and summary analysis has been executed in order to see the size and the ability of the contribution of the Member States from the forecast documents and national and European project reports [3, 4].

3. Results

Most of the EU Member states are optimistic on the way to meet their target from only domestic action and resources. The forecast documents of the Member States resulted that the EU in 2020 will exceed the 20 % Renewable Energy consumption target with 0,3 %. From the forecast analysis it can be expected also that the EU will reach a net surplus also in the interim period until 2020 probably each year as it is presented in the Figure 1.

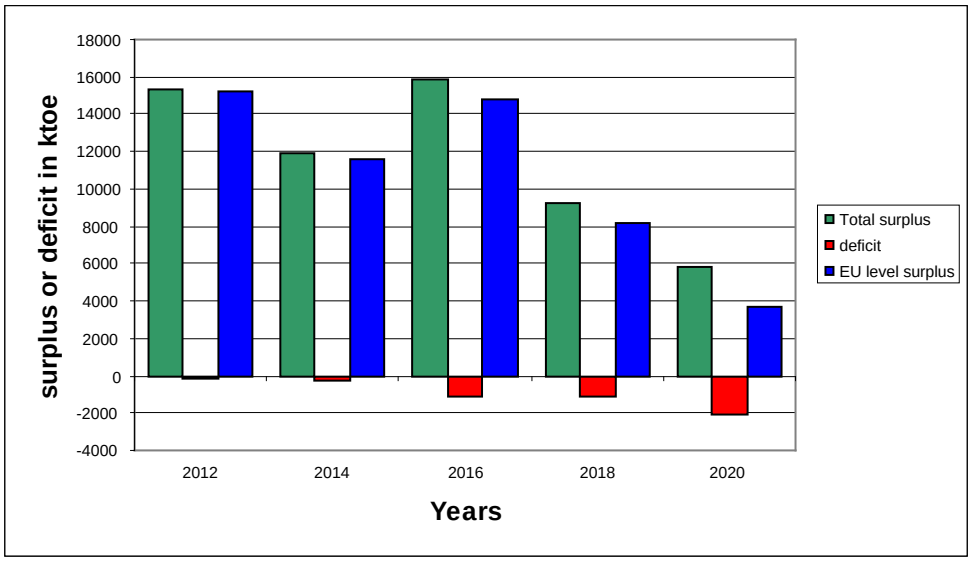

Fig. 1. The RES surplus or deficit between 2010 an 2020 in the EU27 .

3.1. Energy consumption Scenarios

The Member States prepared their forecast taking into account the Additional energy efficiency scenario and many Member States emphasized that the projected targets can be reached only applying the energy efficiency measures.

The main renewable energy resources are biomass, hydro and wind. The majority of the Member States announced biomass as the main renewable energy resource, some of them emphasized also hydro energy and wind energy.

9 Member states announced **surplus** by the year 2020 as it is presented in Figure 2. The highest surplus in absolute term has Germany and Spain with 1387 and 2700 ktoe respectively.

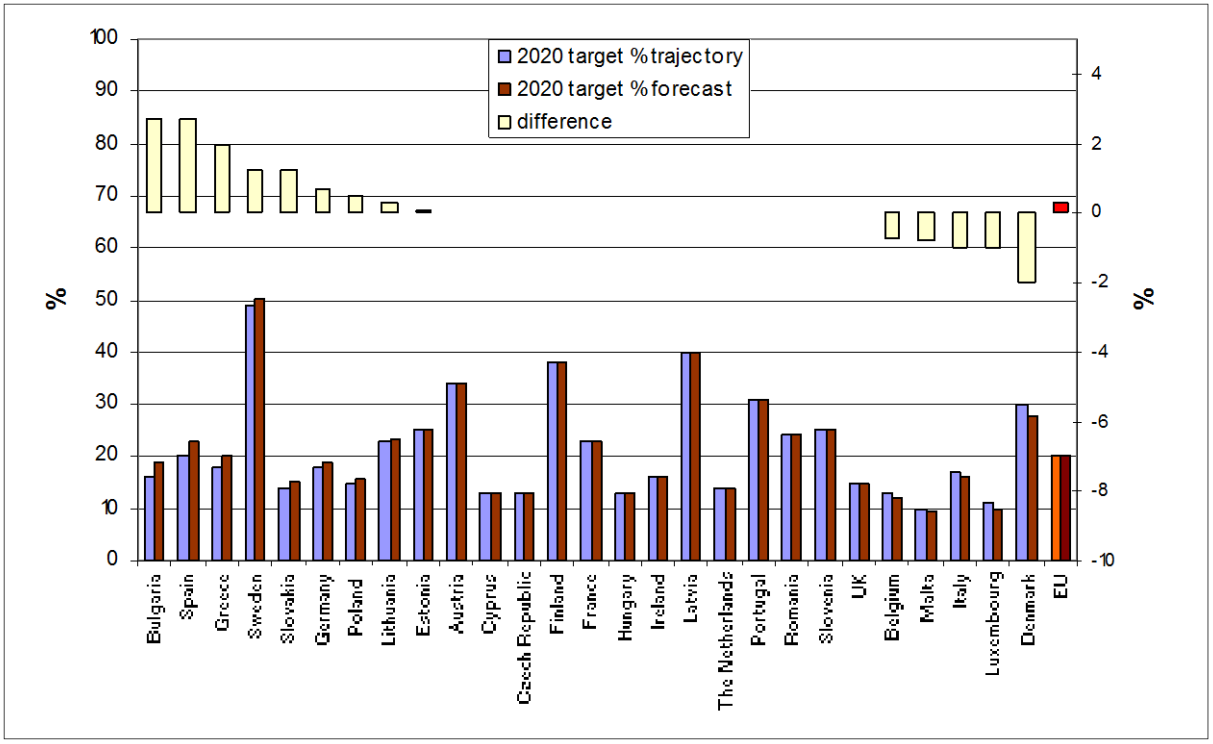

Fig. 2. The indicative and forecasted share of the Renewable Energies in the EU 27 by 2020

5 Member states forecasted **deficit** in 2020, Italy has the highest absolute deficit with a -1170 ktoe (-1 %).

The member states can use cooperation mechanisms to help with their surplus or meet their deficit. 13 member states are willing to use the **Joint projects**, and 8 to use the **statistical transfer**. Wind and biomass are the most involved resource in the joint projects in power generation using the existing electricity links in the Balkan area.

3.2. Sectorial use break down

Some Member States already provided forecast on the sectorial breakdown of the RES development until 2020. Among these countries the highest share had the renewable electricity and also heating and cooling represented a big proportion, as it is demonstrated in the Figure 3.

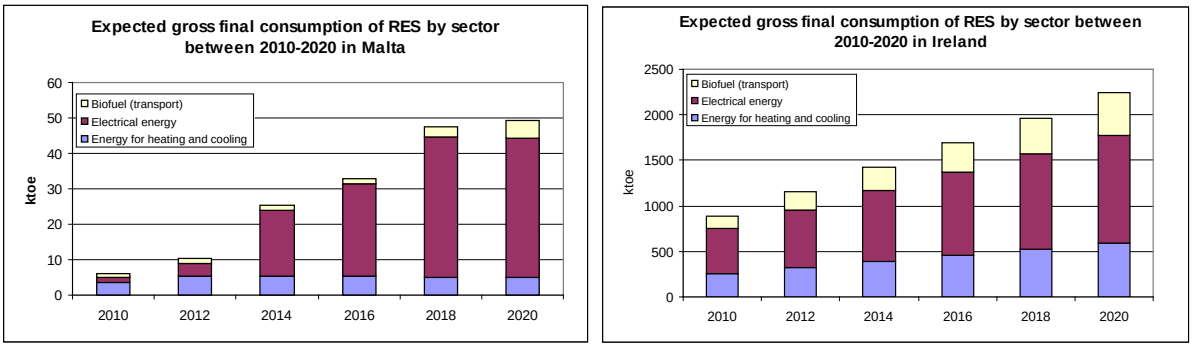

Fig. 3. Forecasted sectorial breakdown of RES final consumption in some member states

Many of the Member States raised critical factors which are barriers in reaching the targets or which need development in order to achieve a better performance of the targets. Among the obstacles countries mentioned their isolated geographical situation and restrictions in interconnection capacity; thus they expressed the need of development in interconnections.

Regional differences appear from the recourse aspects and also in the energy use. Countries like Italy and Greece have a high PV potential, high air conditioning penetration but have high summer peaks, and countries like France or Bulgaria have high level of electrical heating and lower PV potential but low summer peaks.

However it is a good potential of offshore wind resource, the implementation depends mainly on the development of infrastructure for integration wind energy to the grid.

Solar energy has the highest potential in terms of availability, with daily and seasonal variation in different geographical location. There is an expressed need for flexibility of grid management and of generation mix. The advantages of PV are that it can provide peak power and can be used in the decentralized electricity; this means reduction of network losses. Grid electricity losses are proportional to the distance between the points of generation and use, so as PV is a distributed and decentralized source it needs shorter transmission route.

The integration of wind and biomass could help increase the predictability, in the storage and in the simultaneity aspects, although wind and PV require the same measures in the grid development. PV is easier to forecast and less impacted by local topography, wind has higher energy density and its integration into the grid is more similar to that of conventional concentrated generation.

General need is the modernization of electrical grids, the reinforcement of grid infrastructure and electricity interconnection and also the offshore wind development. As the share of RES electricity from renewable is around 35 % in the EU there is a general need to improve the stability of the European electricity grid which requires new infrastructure. There is no harmonized method for transmission planning over the EU Countries and there is a lack of harmonization of the grid connection rules of wind plans

There are inconsistencies in regulations of the transmission planning, i.e. there are different policies in different countries; RES has not the same priority in all countries, the related grid expansion costs are shared differently and not always in transparent way. There is inconsistency in the technical requirements and the separation of generation, transmission and retail services complicates the process.

4. Conclusions

The system integration challenges are dependent of several factors like the energy resource (location, potential, technical development), technology and the technological development of the system components (from the production through the transformation, storage, distribution system, interconnection capacities, etc.).

The biggest challenges appear in the electricity as the main form of the energy integration. The penetration of PV, wind and bioelectricity is highly dependent on the system flexibility. In the different EU member states the different transmission and distribution grids means a kind of barrier, and as it was formulated already in the forecast documents the grid infrastructure needs to be reinforced and requires new infrastructure at generation, at transmission and also at distribution level. An integrated European grid needs harmonized codes, policies, regulations and technical standards; as well an improvement in the transmission planning method. With these measures the indicative targets can be achieved.

References

[1] European Commission 2009 Directive 2009/28/EC on the promotion of the use of energy from renewable energy sources. Official Journal of the European Communities/L 140/16/.

[2] Renewable energy forecast documents. Available online on the Commission Transparency Platform, established in conformity with Article 24 of the Directive. 2010: http://ec.europa.eu/energy/renewables/transparency_platform/forecast_documents_en.htm

[3] EUROSTAT, 2010. statistic Database: Energy

[4] Szabó, M. 2009. Perspectives on Renewable Energy Sources in Hungary. Renewable Energy 2009. Global regional Outlook. Sovereign Publications, London. p. 129-131.

[1]The views expressed in this paper are those of the authors and do not necessarily represent European Commission policy.

Development of the Sustainable Technology Balance Sheet (STBS) - A generic method to assess the sustainability of renewable energy technologies

Alan C Brent[1,*], Wildri D Peach[2, 3], William Stafford[2]

[1] *Centre for Renewable and Sustainable Energy Studies, School of Public Leadership, Stellenbosch University, Stellenbosch, South Africa*
[2] *Sustainable Energy Futures, Natural Resources and the Environment, Council for Scientific and Industrial Research, Pretoria, South Africa*
[3] *Graduate School of Technology Management, University of Pretoria, Pretoria, South Africa*
** Corresponding author. Tel: +27 21 881 3952, Fax: +27 21 881 3294, E-mail: acb@sun.ac.za*

Abstract: The impacts of technologies on sustainability have to be assessed through structured approaches to provide decision-makers with strategic information. Traditional technology assessment methods can be complex and highly resource intensive with long lead times; consequently, the applications of these methods are limited, especially in Africa. Where these methods have been applied, the conclusions that are generated are also not always effectively communicated, which leads to limited buy-in from stakeholders. The paper therefore proposes a generic rapid technology assessment framework and implementation process that utilises a popular method that has been modified to include sustainability factors and a systems approach, while remaining simple and intuitive: the Sustainable Technology Balance Sheet (STBS). The method addresses technology assessment from a qualitative view by including sustainability criteria developed through stakeholder engagement and technical factors through expert opinion, while inducing a life cycle approach to ensure system awareness. A case study approach, using a bioenergy value chain, is used to demonstrate the developed STBS method.

Keywords: *Sustainability assessment, technology assessment, Africa.*

1. Introduction

Energy is closely linked to the sustainable development paradigm. The impact of energy technologies can include climate change, which is associated with excess use of energy, and poverty, due to a lack of access to energy. Solutions to these sustainability problems may be achieved by using new technologies, such as renewable energy technologies (RETs), that reduce pollution and, in some instances, provide development opportunities. Such solutions can, however, only be achieved if the correct technology strategies are followed by effectively assessing and communicating viable options to policy makers.

A key issue for sustainable development is the various implications of the extraction, generation and use of energy that must be evaluated in a comprehensive manner. As the worldwide demand for energy resources increases so too does the diverse range of impacts that occur over the respective energy value chains relating to the various acquisition and operational activities as well as from the utilised technologies.

In attempting to address the sustainable development challenges that technology presents, structured approaches and firm methodologies must be developed and implemented as a prerequisite to ensure the comprehension and coordination to reach intended outcomes. Technology assessment methods can provide the basis for this development [1].

2. Development of the Sustainable Technology Balance Sheet (STBS) method

The conventional Technology Balance Sheet (TBS) is one technology assessment method that has been utilised effectively [2]. It is a graphical representation of the interrelationships, inter-dependence and reliance between the factors of technologies, processes, products, and markets. The foundation for the TBS is the relative relationship between these four factors.

Originally the relationship was based on economics and how the factors met each other's demands [3].

The simplistic logic of the framework, which is indicative of the relationship between the factors considered, makes use of a simple matrix to relate two specific factors. This is then augmented by other matrices to enhance the relationship or connection between factors while still retaining the straightforward logic behind each matrix (see Fig. 1).

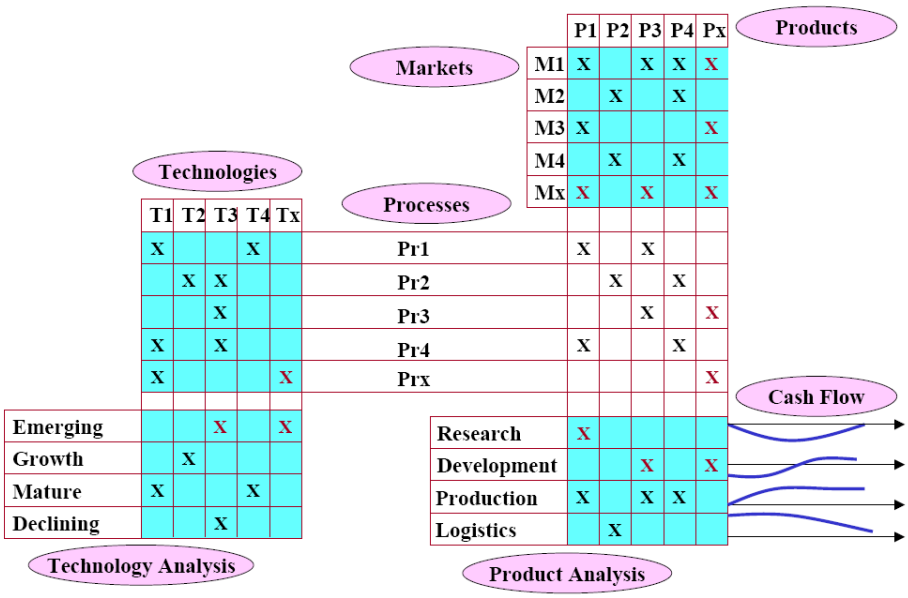

Fig. 1. The conventional Technology Balance Sheet method [3].

Within this framework, when a new technology is incorporated into an existing or new process to produce a product, which meets an established market demand, or creating a whole new market niche. The technology thus acts as a driver for new products and processes due to its enabling characteristics needed for existing products and process. This defines the connection between the four factors through the interconnected nature of the factors [4].

The TBS is a business-orientated tool designed to aid managers in the technology decision making process. The tool intends to facilitate and guide an enterprise through a technology assessment process towards a clearer understanding of the conclusions ultimately produced by the framework. The enlightenment generated by the process is often more valuable than the outcome obtained. This would include a better understanding of how organisational structures relate to each other and how operational flows affect the business, both by means of a greater internal and external awareness. Nevertheless, the TBS will still be a communication tool, to effectively communicate the outcomes to those not involved in the process, as well as non-technical stakeholders who will be able to draw logical conclusions and intrinsically generate the correct answer, which is so important for personal buy in and ultimate project success [4].

The TBS answers the questions of "where we are" as a business looking at technology and provides strategic direction by answering "where to go" as well as "where to get out" by making use of technology s-curves and analysing where a technology is located in the technology life cycle [3]. The TBS indicates the forces at work within the techno-economic system. These forces manifest themselves within the organisation as opposing directional force, simply as a push or a pull [3]; they are produced by different elements within the factors. A market force can be described as a pulling force pulling business output towards the

market demand, be it though desired products, which occur only once the force has been transmitted to the processes to generate the capabilities within the business. However to produce the products and develop these processes only occurs once the pull force has been transferred to the technology factor to grow, develop and provide the methodologies required to generate the processes required to create the products to meet the market need. If one considers technology as a push force we can experience a force from a new technological invention or development pushing along new capabilities and new processes, which can lead to new or advanced products and through their existence create new markets or change the dynamics of existing ones. These two forces can have a feedback effect on the entire system as the process and capabilities continue to grow and so a type of causal loop system has been created.

The TBS provides organisational value by highlighting the drivers at work within the organisation and how these can be manipulated to be successful in meeting the business goals. As one becomes more aware of how each factor relates to the others, one is more able to grasp their impact. This would not only be unique to being economically successful, as is the traditional intent of the TBS, but by reviewing the intent, aligning the point of view and reassessing the goals we will be able to use the simple TBS framework to meet any desired outcomes; for the problem at hand, to address sustainability while critically assessing different energy technologies. Therefore, sustainability can be introduced in the TBS by making use of the principles or criteria used for the assessment of environmental, social and economic sustainability and would include those applied in the broad sustainability body of knowledge [5] and refined through a needs analysis that comprises stakeholder engagement.

2.1. STBS framework and Implementation Process

A sustainable technology assessment tool has subsequently been developed [6] and consists of two parts: first, the Sustainable Technology Balance Sheet (STBS) which is a rapid technology assessment and communication framework; and second, an integral part that is referred to as the Implementation Process, which is a structured method through which the relevant stakeholders can be engaged and qualitative data can be obtained. Each part consists of specific methodologies and underlying logic, which can be summarised as shown in Fig. 2.

The Implementation Process consists of four steps initiated by a facilitator during stakeholder engagement workshops to generate the information needed to populate the STBS, create system awareness and project enlightenment among these stakeholders [6]:

- Step 1a: Value Chain Generation: through a life cycle analysis and by the investigation of the product/process life cycle to generate, firstly a generic value chain and secondly, once the components of the value chain are validated, a case specific process value chain is generated.
- Step 1b: Sustainability Criteria Development: Sustainability aspects addressed by stakeholder engagement and literature review, which is done concurrently during the initial engagement stages. Once systems-thinking has been instilled, discussions surrounding the creation of specific Sustainability Criteria may be fulfilled. This would reaffirm the stakeholders' intentions toward sustainability.
- Step 2: Technology and Process Awareness: Achieved through the creation of input-process-output diagrams, which indicate process linkages known as Technology Super Structures. This is done for each one of the value chain components indicated by the dashed rings of Fig. 2. A short discussion surrounding the grouping or indexing of Sustainability Criteria into sectors may also be accomplished.

- Step 3: STBS Development: The utilisation of the generated information and understanding to populate the STBS so as to formalise the information and to communicate conclusions accurately.
- Step 4: Strategic Direction and Conclusion Analysis the presentation of STBS outcomes to relevant stakeholders is of vital importance. This new impetus, created by the indicated strategic direction, needs to be subscribed to and further investigations can be made in an enlightened and qualified direction. These investigations can include, amongst others, multi-criteria decision analysis (MCDA) trees and life cycle analysis (LCA) studies to add more rigour to the indicated outcomes and strategic conclusions.

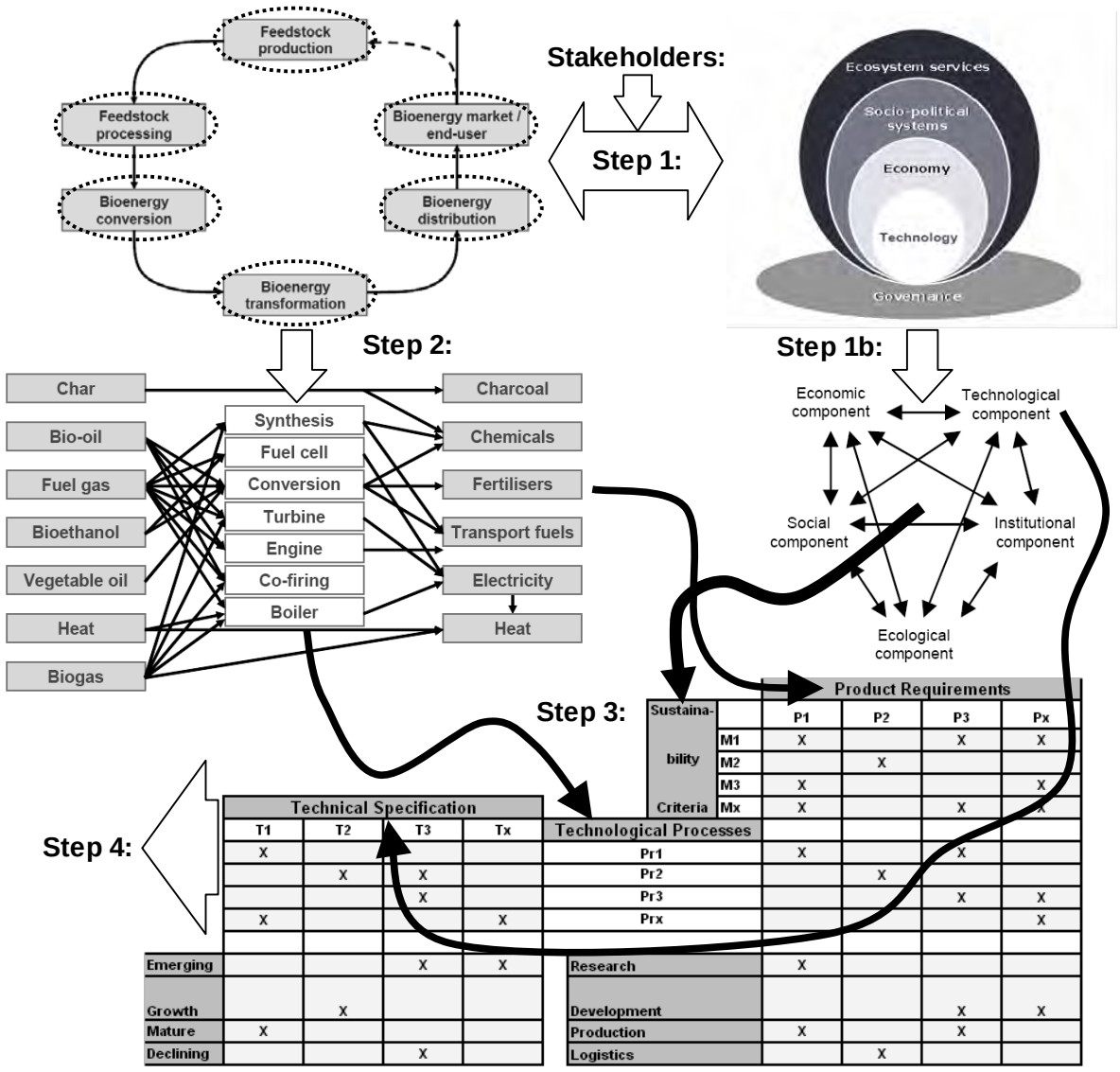

Fig. 2. The Implementation Process of the Sustainable Technology Balance Sheet (STBS).

3. A case study to investigate the STBS method

A case study approach was used to understand and test the developed STBS method. The case is of the Working for Energy (WfE) programme, which is an initiative of the South African Department of Water Affairs and Forestry (DWAF) to utilise waste invasive alien biomass as an energy source effectively adding value such as job creation and energy resources to the Working for Water projects through new Public Private Partnerships (PPPs). The need to

assess suitable technologies for these PPPs was identified and the STBS tool was deemed as a suitable option.

The STBS was firstly discussed informally among a group of energy technology analysis experts to generate relevant information and determine the key stakeholders, which can be utilised during the development of the tool. These meetings then became provided feedback of developments and obstacles to the various experts and stakeholders.

Finally, a formal presentation of the proposed STBS tool was made during a workshop to experts, which included members of the national DWAF and other stakeholders at which time further inputs could be given. The consequence was a process of conceptualisation of a modified TBS, making use of a reiterative approach to generate constant learning.

4. Results

Step one of the STBS involves the creation of the value chain (see Fig. 2). These are useful to identify specific components for the value chains and by providing the relevant technologies to be assessed. Consequently, the first step in the STBS process is to investigate the project life cycle so that a generic project value chain can be formulated. In this case, the value chain would initially take the form of a generic bioenergy value chain, which can then be evaluated and expanded to add specific information pertaining directly to the specific case under evaluation. These value chains are an efficient way to generate system- and complexity-understanding and to communicate this knowledge easily to non-technical individuals.

Within a 'Call for Expression of Interest (EOI)' document, the WfE programme clearly indicated their understanding of the relevant components that form the project value chain. This provided the WfE group with insights relating to the relevant technologies and the four interrelated factors that influence each other:

- Technological Process indicates the conversion processes and the intrinsic technology used. These two factors, process and technology, are inseparable and are thus assessed as a functional unit. The linkage between the technological process and products created is also undeniable as the one determines the other, which must thus also remain within consideration. These factors are easily generated by expert opinion, as they are the available processes required to meet the desired outputs and the project goals. For the Primary Energy Conversion component, four main technological processes were identified due to the overwhelming relevance of these technologies within literature as well as within the market place especially within the EOI. The Technologies proposed were combustion, slow pyrolysis, fast pyrolysis and gasification.
- Technical Specifications are technical aspects that pertain to the technology for only this specific point in the product life cycle or specific value chain component. From an operational point of view, these factors are invaluable to more technical stakeholders as they pertain directly to constraints and challenges, which will be faced. These factors include: complexity of operations, feedstock requirement, residence time and capital cost. Technical Specification focuses on the operational aspects of the Technological Process and may be general or specific.
- Product Requirements creates a linkage between the technological process, its products and their specifications, as required by stakeholders or subsequent processes. This is done to improve the assessment of the technology, as one cannot generate conclusions from the technological process if one does not take aspects and requirements of its products into account. These include the meeting of the stakeholder requirements as well as indicating the various process/product strategies and their affects on sustainability thus the close link

between the technology, the process, and the product is required to assess performance in relation to the Sustainability Criteria. In this specific case the Product Requirements are difficult to quantify as most of these products are merely subsidiaries and do not directly meet the needs of stakeholders. It is, however, imperative that the stakeholders' needs are considered at this stage so that the correct process/product strategies may be implemented at this early stage to ensure customer satisfaction and ultimately ensure a true reflection of sustainability. The process/product strategy becomes especially important when multiple products and undesirable wastes are produced thus highlighting product benefit trade-offs, as the product number and specifications can be manipulated by changing the process and technical specification. In this case study example it was not deemed necessary to investigate all the various process/product strategies nor all of the products, which could be generated by each general Technological Process. The EOI documents were used as a guide and only products specified within these were assessed, so as to limit the assessment scope as indicated by the stakeholders.

- Sustainability Criteria are key areas that need to be considered for sustainability. Stakeholder engagement and expert opinion is utilised to develop areas for the assessment of the technology in terms of its sustainability. This is the key factor to the STBS and the technology assessment body of knowledge in addressing sustainability. By considering the Sustainability Criteria with the Product Requirements (representing the Product/Process/ Technology complex) matrix in Fig. 3, the clear influence of technology assessment, such as the Multi Criteria Decision Analysis (MCDA) methodologies can be seen. This has been implemented in a simplistic fashion along with the understanding that the Sustainability Criteria and the outcomes generated are likely to form part of an MCDA study to be done after the initial STBS study indicating a strategic direction. The synergies between the STBS and the MCDA are apparent as the STBS facilitates the initial stages of the MCDA cutting down on the time and engagement required by the MCDA but as a rapid assessment tool lacks its quantitative rigour. The STBS focuses qualitative data providing a strategic standpoint through the ranking of factors. Further investigations using strong quantitative data can vindicate the STBS strategic direction and provide further insights. STBS proves valuable in reducing time and costs of a blind MCDA by providing rapid direction and limiting the possibilities assessed by the MCDA, thus limiting the expense of such a time-consuming study. Life Cycle Analysis (LCA) was also investigated and regarded as an excellent tool to further guide decision makers once the STBS had indicated general strategic directions. The LCA decision trees are invaluable to assess process/product strategies that were initially identified by the STBS, quantified by the MCDA and then synthesised by the LCA.

These factors are compared in three assessment matrices to provide insights to the viability and sustainability of the technologies; Fig. 3 provides an example:

- The Technological Process vs. Technical Specification Matrix - evaluates the Technological Process using Technical Specifications to indicate the viability of the various projects and technologies.
- The Technical Process vs. Product Requirement Matrix - evaluates the product aspect pertaining to the ability of the process to provide products that can meet the demands of the market.
- The Technical Process and Product Requirement vs. Sustainability Criteria Matrix- evaluates the products that are integral to the Technological Process and the Sustainability Criteria pertaining to the sustainability of the Product/Process.

Sustainability criteria	Product Specification and Requirements												
		Charcoal from Slow pyrolysis	Electricity from Combustion plant	Charcoal and briquettes from Slow pyrolysis	Electricity from Gasification	Weighting per sustainability group	Comments	Specific Energy Supply and Need: Heat	Specific Energy Supply and Need: Steam	Specific Energy Supply and Need: Bio-char	Specific Energy Supply and Need: Bio-Oil	Specific Energy Supply and Need: Gas	Specific Energy Supply and Need: Syngas
	Efficiency (1)	2	2	3	5	3					x	x	x
	Maturity (2)	3	5	3	5	3		x	x	x			
	Modularity (3)	3	1	3	2	3				x			
	Size capacity and distribution	2	1	2	3	3				x			
	Local capacity (5)	2	1	2	1	3		x	x	x	x	x	x
	Lifespan (6)	2	2	2	2	3		x		x			
	Product(s) (7)	2	3	2	4	2					x	x	x
	Unit cost EROI (8)	3	5	3	4	2						x	x
	CAPEX (9)	3	5	3	2	2				x			
	OPEX (10)	4	3	4	2	2				x			
	Energy balance, EROEI (11)	3	3	3	4	4		x	x			x	x
	GHG footprint (12)	4	4	4	4	4		x	x	x	x	x	x
	Water footprint (13)	5	3	5	4	4		x	x	x	x	x	x
	Biodiversity (14)	5	4	5	4	4		x	x	x	x	x	x
	Waste (15)	3	3	3	5	4					x	x	x
	Job creation (16)	2	2	2	3	5		x	x	x	x	x	x
	Skills development (17)	2	1	2	2	5		x	x	x	x	x	x
	Poverty reduction (18)	2	2	2	2	5		x	x	x	x	x	x
	Welfare benefits (19)	2	4	2	4	5		x		x	x		
	Change in land-usage and	4	4	4	4	5		x		x	x	x	x
	Energy security (21)	4	5	4	5	5			x	x	x	x	x
	Energy sovereignty (22)	1	1	1	1	5				x			
	Community acceptance (23)	3	4	3	4	5		x		x			
	Race (24)	5	3	5	3	5				x			
	Gender (25)	5	3	5	3	5				x			
	Income group (26)	4	3	4	3	5				x			
	REFIT (27)	2	4	2	4	1		x	x	x	x	x	x
	CDM/CER (28)	4	2	4	5	1		x	x	x	x	x	x
	Other (29)					1							
	Total	5.1875	4.59125	4.9375	5.34875								

Fig. 3. The Technical Process and Product Requirement vs. Sustainability Criteria Matrix [6].

5. Conclusions and recommendations

The recommendations of the WfE stakeholders and experts were diverse, including simple suggestions on framework structure to improve legibility and complex discussions surrounding the communication of STBS factors, driving forces, and the underlying logic of the method. The outcomes included:

- Unambiguous understanding of the conceptual framework and underlying logic, even if the process would still require a facilitation aspect in order to retain integrity.
- A clear buy-in of all the assessment factors in general was communicated and special attention was given to the Sustainability Criteria factor, the formulation of which was deemed to be of critical importance.
- The effectiveness at which the data surrounding the factors where communicated was commended especially the awareness of the Technical Specification factors.
- The strategic intent and direction was intrinsically communicated by the framework.
- The concern surrounding the trade-off between the rapid assessment and the rigour of the assessment was highlighted and it was concluded that the rigour was dependent on the quality of the data used and rate at which the assessment was required. Both factors can be adjusted within the STBS tool to meet the stakeholder requirements.

Thus, the framework itself provides an accurate communication tool aimed at non-technical stakeholders and political decision-makers at various stages in the project life cycle. It provides them with a simple-to-understand strategic direction, a better understanding of the complex system under review using the implementation process insights, which systems thinking provide. This ensures a much improved stakeholder buy-in as well as general “trust brokering”. The framework acts as a high-level cognitive decision tool making use of stakeholders’ priorities, and together with the implementation process it is designed to

compliment and integrate with other tools such as the MCDA and LCA, from which it draws heavily and where the STBS act as a precursor.

The STBS also utilises information generated by other preceding stakeholder engagement tools, thus acting as a truly integrative tool creating a link between other tools and methodologies, which is invaluable to both stakeholders and practitioners alike. In general, expert opinions had been positive in regards to the STBS addressing sustainability, its rapid flexibility and its ease of communication.

As a way forward, the STBS needs further refinement and active development by further case study analyses. The case study requirement is based on specifically utilising the STBS from an early project stage and providing focus for the STBS as the main strategic assessment tool. This would, however, be done in relation to and in close conjunction with other integrative tools developed so as to add value to the STBS and other tools utilised.

References

[1] H. Bossel, Indicators for sustainable development: Theory, method, applications, A Report to the Balaton Group, IISD, Canada, 1999.

[2] M.W. Pretorius, G. de Wet, A model for the assessment of new technology for the manufacturing enterprise, Technovation 20(1), 2000, pp. 3-10.

[3] G. de Wet, Corporate strategy and technology management: Creating the interface, Graduate School of Technology Management, University of Pretoria, 1992.

[4] H.K. Grover, H.K., M.W. Pretorius, The technology assessment of demand side bidding in the South African context, South African Journal of Industrial Engineering 19(2), 2008, pp. 93-108.

[5] R.K. Singh, H.R. Murty, S.K. Gupta, A.K. Dikshit, An overview of sustainability assessment methodologies, Ecological Indicators 9, 2008, pp. 189–212.

[6] W.D. Peach, The development of the Sustainable Technology Balance Sheet: A generic technology assessment tool to assess the sustainability of renewable energy technologies, Masters dissertation, Graduate School of Technology Management, University of Pretoria, 2010.

The SIMPLE methodology for supporting innovations in the field of renewable energy and energy efficiency

Olof Hjelm*

Environmental Technology and Management, Department of Management and Engineering, Linköping University, 581 83 Linköping, Sweden
**Corresponding author. Tel: +46 13285647, Fax: +46 13281100, E-mail: olof.hjelm@liu.se*

Abstract: In this article, I present my experiences stimulating development of new products and services in small companies in the environmental arena. The focus on small companies is justified since many new innovations originate from such companies and they often have special needs compared to larger companies. In the region of Östergötland Sweden, we have developed a model called SIMPLE (Successful implementation of eco-design in small enterprises) to support small companies' environmental innovations. SIMPLE uses the Triple Helix approach. Triple Helix is often used to describe the interaction between university, government, and industry to promote innovation by building on active participation and interaction between regional actors. In short, the SIMPLE methodology uses coaching, network activities and education, and financial support to encourage development of new ideas. Three cases are presented to illustrate the diversity of innovations that can be supported using the SIMPLE methodology. Observations suggest that individual company's needs must be the main concern of any methodology and networks can significantly stimulate individuals and organizations to speed up the development process and time to market.

Keywords: *Innovation, Small Companies, Renewable energy, Energy efficiency.*

1. Introduction

A rapidly growing demand for renewable energy solutions and energy efficient products calls for innovations. New products and services are realized in a large diversity of organizations including companies of various size and character. This paper focuses on the small company. Product and service development is strategically important for the development of a company, yet Gibb and Scott [1] noted the absence of formal planning models in small companies. Even when the development is strategically important, much of the planning is iterative and not formalized. This is rather far from the linear and structured product and business development models often presented in student textbooks (see Ulrich and Eppinger [2]). Gibb and Scott [1] also noted the importance of strategic awareness and personal commitment. One of the recommendations the authors give to policy makers is to encourage "the development of the strategic awareness and personal commitment of the owner manager".

To stimulate environmentally driven development of small companies, several national and regional initiatives are currently on going in Sweden and Europe. Different approaches and methods can be used and the aim of this paper is to present a methodology, the SIMPLE methodology, developed in the region of Östergötland, SE Sweden. The paper starts with a general description of the methodology followed by three cases of small companies developing new products and services. Special focus is on innovations in the field of renewable energy and energy efficiency. The experiences using the methodology are discussed and conclusions are drawn on the general applicability of the presented methodology.

2. Methodology

The approach used in this study can be referred to as action research. The description of the SIMPLE methodology and all findings in this paper primarily are based on my observations,

as a researcher, actively taking part in the general management of the project. The SIMPLE methodology has been developed and tested in three different business development projects involving approximately 50 SMEs in Östergötland, Sweden between 2002 and 2010. The findings presented in this article are from the latest project lasting from May 2008 to December 2010. Earlier descriptions of the methodology can be found in Hjelm [3] and Rennie et al. [4]. My tasks in the current project were to arrange network meetings and to coach actively the companies. However, I did not take part in the individual development projects at the companies. At the end of the project (September-October 2010), I performed semi-structured interviews with company representatives. During these interviews, the respondents were asked to describe their product development and their experiences with the project. I also had continual contact with the companies during the project and collected documentation such as consultancy reports and marketing material produced by the companies. All companies made project plans for the development projects and wrote a short report after finalizing their projects.

In total, 26 companies took part in the latest project including furniture producers, creativity consultants, and heat pump producers. For this paper, I have made a selection of three companies based on the character of their business activities and development. All three are active in the field of renewable energy and energy efficiency, but I tried to select companies having differing characteristics to demonstrate the diversity of companies/innovations that can be supported using the SIMPLE methodology. General facts about the case study companies are found in Table 1.

Table 1. General facts regarding case study companies.

Company	Size (employees)	Main competence area	Development project
Rydell & Lembke, Kyl och Värmeteknik AB	11	Construction and production of cooling and heating equipment	New generation of cooling and heat pump
Pencraft Services AB	3	Renewable energy solutions for generation of electricity and hot water	Energy efficient heater (biogas driven)
Biototal AB	8	Waste product management. Nutrient recycling	Harvesting of biomass for removal of nutrients and substrate for biogas production

3. Description of the SIMPLE methodology

The SIMPLE-model builds on formal and informal networks between companies, the project team, and external resources. This can be visualized as a triangle as described in Figure 1.

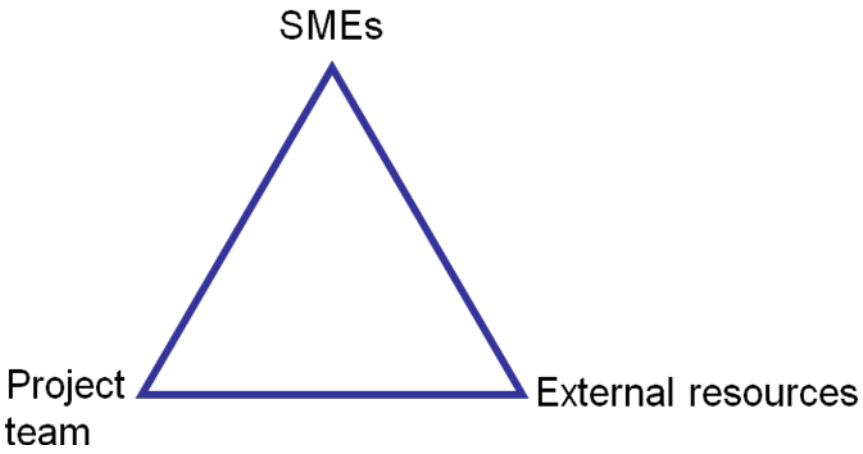

Fig 1. The SIMPLE Model. Each corner represents a different type of network that together constitute the project members. Interactions between the different networks are further described in the text. SMEs=Small and Medium Sized Enterprises.

To explain the different components and structure of the model, it is beneficial to know the underlying goals for the different development projects using the methodology. The main aim has been to create economic growth by stimulating product and business development in small companies and simultaneously solving environmental problems. A secondary aim has been capacity building among regional actors for regional sustainable development and building up a strong network of companies, authorities, and business support organizations in this field. The model is inspired by the Triple Helix approach. Triple Helix is a model used to describe the interaction between university, government, and industry to promote innovation in a region. The triple spiral symbolises the dynamic cooperation between the three actors and the model builds on active participation and interaction between regional actors. A common vision is developed and resources for development are coordinated to increase the capacity for innovations and produce a higher yield as related to the resources spent.

3.1. Small and medium sized enterprises (SMEs)

Two types of companies have participated in the projects. One group includes companies which have products that aim to reduce environmental problems (sometimes labelled as Cleantech companies), while the other group involves companies developing ordinary products that take into consideration environmental concerns (environmentally conscious design). The companies included had been established for at least a couple of years (no start ups were allowed) and had the financial and personal resources to start and finalize a development project. Company size varied between 2 and 75 employees.

Three types of development projects were conducted. The first type included projects that aimed to reduce use of material and energy, to increase conscious choices of material, to substitute toxic materials or chemicals, and to improve recyclability, etc. The second ype of development projects included products or services that solve an environmental problem. The

third type included products or services that provide the same customer value but with significantly lower environmental impact compared to established products or services.

3.2. Project team

From the beginning, the project team was designed to comprise individuals and organizations with complementary skills. During all three projects, the organizations represented in the project team have been the County Administrative Board of Östergötland, Linköping University, and the business support organization ALMI företagspartner AB. All actors were members of a larger regional partnership for stimulating regional development and had agreed on a set of regional development strategies that included stimulation of environmentally driven business.

The County Administrative Board is the national government representative office in the county of Östergötland. The Administrative Board has many responsibilities and those of special relevance for this study are development of business and trade as well as protection of the environment. Although these activities are normally managed by different offices, both offices were included in the project reported in this article. The County Administrative Board had the role as project owner and provided administration duties and co-financing.

ALMI företagspartner AB is a state-owned company that provides financing and business development. Each region has a local ALMI-company working together with other actors to improve regional development. It has daily contacts with companies and helps support innovation, a focus of particular interest in this article. As a consequence, ALMI has a very broad network of consultants and other business developers. Before the start of environmental development projects, they had little experience with environmental considerations in business development. Therefore, one ambition has been to develop skills and experience among ALMI-officers in this type of business support.

The local university, Linköping University, added the knowledge of environmental technology and management skills to the project team. The university joined the project to become more involved in direct business development and interact more with the society, acting as a bridge between the academy and business. Zilahy et al. [5] discussed the role of academia in fostering sustainable regional development and give several examples of roles universities can take as first movers and as a resource that offers competent staff and knowledge of the complex issue of sustainable development, goals all in line with the role Linköping University has had in these projects. Furthermore, the university acted as a change agent [6] together with the other organizations in the project team trying to accelerate the region's transition towards sustainability.

3.3. External resources

The external resources are a very loose and informal network of consultants, researchers, students, industrial designers, research institutes, etc. who were found to have the skills needed for in the development projects. This group was not determined beforehand; however, depending on the needs of each individual company in the project, these resource organizations were identified by the project team or the individual company. This is further described below.

3.4. Way of working

The different steps in the model are presented and explained below.

3.4.1. Start up

After deciding to start a new project (often after securing financing), one of the first tasks for the project team was to find companies willing to enter the project so as to develop the network. The process of finding companies was started by compiling a long list of potential companies. This list was shortened (about 20-30 companies) by scrutinizing each company's line of business, financial status, etc. Companies also were identified if they already had approached one of the project team organizations seeking cooperation. In selecting companies, no special line of business was favoured; instead we sought diversity. A first individual visit was done to present the project and learn more about the company's activities and its ambitions and ideas for development. If the company was judged as suitable, it was offered a place in the project. Finally, an agreement was signed between the company and the project. After a suitable number of companies (7-10) had joined the project, the network was closed and all companies met for a first network meeting.

3.4.2. Network meetings

Network meetings can have many purposes. In the SIMPLE model, we used four to six meetings for education, exchange of experiences, and stimulation of individual meetings between the companies. Experts from academia and business were invited to present lectures and workshops on subjects decided by the group members jointly. These forums included information about eco-design methodologies, intellectual property rights, marketing, and sales. Each network meeting also had a designated time for the companies to present their recent development activities and experiences gained during the process. These sharing of experiences induced further discussion and also inspired the other companies in their development projects.

3.4.3. Individual development project

As indicated above, all companies worked on an individual development project. Typically, this involved development of a new customer's offer. The aim and activities of the development project were described in a simple project plan, and based on this plan a decision was made for financial support. This support (a consultancy check) could be used to cover 50% of the costs incurred by the company for hiring of external resource organizations. The companies did not participate in the exact same activities, so each company decided what activities to support using this financial aid. Typical activities were pre-studies, design, prototype construction, testing, and verification.

3.4.4. Coaching activities

Members of the project team had regular contact with each company via telephone and face-to-face meetings. At these contacts, the development projects were discussed, and eventual changes or extra need of support (such as longer discussions with the project team or meetings with other experts) were discussed.

3.4.5. Completion

Each group worked for approximately 18 months. When completing a group, the results in new products and services and knowledge gained were collected via interviews and written reports. To strengthen the benefits of reporting, a publication for each project was produced and a public exhibition and seminar was arranged to market the participating companies and their projects. These seminars also intended to stimulate further development both in the participating companies and among other actors attending these events.

4. Cases

To illustrate the diversity of development projects that can be supported, the following section contains a description of three small companies that participated in the project. For each company, a short general presentation is given followed by their development project.

4.1. Rydell & Lembke Kyl och Värmeteknik AB

This company (11 employees) builds cooling and heating equipment. Within the project, they developed a new generation of a combined refrigeration machine and heat pump, a combination that has many applications. The method is based on refrigerants encapsulated in small, sealed systems and is built on a different technical platform compared to conventional cooling machines.

4.2. Pencraft Services AB

Pencraft Services (three employees) mainly works with new product development. Its main business area is renewable energy solutions for generation of electricity and hot water. In the current development project, they have been developing energy efficient heating solutions for tap hot water and heating in family houses or small apartment buildings. The system is built on an accumulator for heat storage combined with an air/water heat pump, solar panels, and an extra facility for peak heat demands. All parts of the system are built on existing technologies except the extra device for peak heat demands. The company wanted to solve the peak heat demand by using a burner driven by biofuels. In the project, several options were evaluated and finally biogas was chosen as the fuel for the burner. Consequently, the company developed such a burner to complete the energy system for hot tap water and heating.

4.3. Biototal AB

Biototal (eight employees) is active in nutrient recycling and their general business idea is to recycle nutrients from different wastes. Recycling is achieved by quality assurance of wastes, nutrient balance calculations, and mediation of different nutrient-rich waste products. For example, mediation of by-products from biogas production can produce fertilizer in agriculture. The development project run in this project was a feasibility study for harvesting of biomass from highly eutrophicated waters. This harvested biomass could then be used as a substrate for biogas production and the by-products formed could be used as fertilizer in agriculture. By creating this eco-cycle, several environmental benefits are achieved including substitution of fossil fuels via biogas production and replacement of energy demanding production of commercial fertilizers, removal of nutrients from the water environments, replacement of non-renewable fertilizer with bio-fertilizers in agriculture, and finally increased biodiversity in water environments as a result of the harvesting. The feasibility study highlighted several opportunities and Biototal is currently conducting the first large-scale field tests to verify the results of the feasibility study.

5. Discussion and conclusions

Two of the cases presented above resulted in new products introduced on the market (Rydell & Lembke and Pencraft Services). Biototal is still performing field experiments needed before going to market. This subsample illustrated fairly well the general results of the project. Out of 26 companies, only three did not develop any new products or services. The reasons for this were market problems or that pre-studies identified already existing technologies available. At the end of the project, company leaders from the participating

companies were asked about their experiences of being part of the project. The experiences were generally positive. More specifically, they mentioned three major benefits of being part of the project: creation of networks, development of contacts with the university and other support organizations, and receiving extra funding for financing the development projects.

As mentioned in the introduction, Gibb and Scott [1] noted the absence of formal planning models in small companies; hence they recommended that policy makers encourage strategic awareness and personal commitment. In the SIMPLE model, we have addresses Gibb and Scott's concerns in several intertwined ways: networking, education, financial support, and direct coaching. The SIMPLE-methodology is based on the assumption that networks can significantly stimulate business development. It can be argued that small companies always work in networks since they cannot do everything themselves because of their small size [7]. There are many different forms of networks. In this model, we use strategic formalized networks as well as informal networks. Strategic networks can be defined as a cooperative relationship between two or more companies that i) have made an active choice to cooperate and ii) provide some sort of representative for the strategic network [8].

The experience with this project indicates that trust issues are important for well-functioning networks. Since all companies developed new products or services, intellectual property rights (IPR) and patents were important. In the SIMPLE-model, we tried to achieve a balance between openness to present and share new ideas and the protection of these ideas (secrecy). Such issues were thoroughly discussed at the first network meeting and a contract governing secrecy was presented. However, no group signed any contract but instead a verbal agreement was reached. In short, that agreement regulated openness between participants and active participation with the awareness to not mention issues that might hinder such things as patent applications. A general agreement also was concluded not to mention details to people outside the network. These "gentlemen's agreements" proved to be sufficient and we have not experienced any problems with IPR. The oral agreement was sufficient and an open atmosphere contributed to sharing of experiences and mutual learning in the networks.

One important learning outcome from conducting the project is that company perspectives must come first. This can be discouraging for the researcher or business developer who has developed a tool or an approach that the companies are supposed to follow. We tried to minimize the formal procedures and document writing by focusing on the development project as such. The coaching was mainly in the form of discussions with the business leaders so as to help them find the right competencies for their needs. Here the extra funding via the consultancy checks was very useful for companies seeking help from consultants, researchers, etc.

Most likely, the method described in this article can be applied in any type of project trying to stimulate small businesses development of products and services. Important building stones are strong networks, access to a broad group of resource organizations, and some extra money to stimulate the companies to seek help from outside their own organizations.

Acknowledgements

This project was financed by European Regional Development Fund.

References

[1] A. Gibb and M. Scott. Understanding small firms growth, in: Small firms growth and development, M. Scott, A. Gibb, J. Lewis and T. Faulkner. Blackmore Press. Dorset. 1986.

[2] K.T. Ulrich and S. D. Eppinger. Product design and development, Second edition. Irwin McGraw-Hill, Boston. 2000.

[3] O. Hjelm. ”Advantage Eco-design”: A partnership for promoting eco-design activities in small companies. Proceedings: Partnership for Sustainable Development. November 7-10, 2004. 12th International Conference of Greening of Industry Network, Hong Kong.

[4] A.E.W. Rennie. C.G. Lambert. N.J. Baker and O. Hjelm. A transnational approach to the implementation of eco-design methodologies in SMEs. Presented at the 5th International Conference on Design and Manufacture for Sustainable Development, Loughboroug, UK 10-11 July 2007.

[5] G, Zilahy, D. Huisingh, M. Melanen, V.D. Phillip, and J. Sheffy, Roles of academia in regional sustainability initiatives: outreach for a more sustainable future. Journal of Cleaner Production 17, 2009, pp 1053–1056

[6] J.C. Stephens, M.E. Hernandez, M . Román, A.C. Graham, and R.W. Scholz. Higher education as a change agent for sustainability in different cultures and contexts. International Journal of Sustainability in Higher Education 9, 2008, pp 317–338.

[7] Nutek 2004:10. Tio frågor och svar om samverkan i småföretag. In Swedish.

[8] K. Elmhester. Små företag i strategiska nätverk – hur påverkas det enskilda företagets utveckling? Linköping Studies in Science and Technology Dissertations, No.1217. 2008. In Swedish

Tools and mechanisms fostering EU GCC cooperation on Energy Efficiency

A. Papadopoulou[1*], H. Doukas[1], C. Karakosta[1], I. Makarouni[1], R. Ferroukhi[2], G. Luciani[3], J. Psarras[1]

[1] *Management & Decision Support Systems Laboratory, Department of Electrical and Computer Engineering, National Technical University of Athens, Athens, Greece*
[2] *Masdar A Mubadala Company, Abu Dhabi, UAE*
[3] *Gulf Research Center Foundation, Geneva, Switzerland*
** Corresponding author. Tel: +30 210 7722083, Fax: +30 2107723550, E-mail: alexpapa@epu.ntua.gr*

Abstract: In order to respond to the need for European Union (EU) - Gulf Cooperation Council (GCC) clean energy cooperation and provide a practical instrument fostering such activities, the EC External Relations Directorate General has launched the project "Creation and Operation of an EU-GCC Clean Energy Network". To the best of our knowledge, there are no practical tools and instruments to guide structured discussion on EU-GCC clean energy cooperation avenues, acting as catalyst and element of coordination.

Aim of this paper is to present the first outcomes of the Discussion Group "Energy Demand Side Management (DSM) and Energy Efficiency (ENEF)" of the Network. Indeed, there exist a significant potential for promoting cooperation EU-GCC on ENEF & DSM and specific areas of cooperation of mutual benefit, which are identified and discussed in this paper. The key message is the importance of taking action over discussion for promoting cooperation on ENEF & DSM, in the sharing of related expertise and knowledge and in raising general public awareness and collaborating in the framework of common project activities.

Keywords: *Gulf Cooperation Council, European Union, Clean Energy, Network, Cooperation*

1. Introduction

The Gulf Cooperation Council (GCC) is a regional organization created in May 1981, to promote stability and economic cooperation among the Arab States of the Gulf, namely Bahrain, Kuwait, Oman, Qatar, Saudi Arabia and United Arab Emirates (UAE). The GCC countries are among the world leading oil and gas producing and exporting countries, and constitute prominent members of the Organization of the Petroleum Exporting Countries (OPEC). Indeed, in the GCC countries all power generation is oil and gas based. Especially, the quantities of proved reserves of crude oil and natural gas were estimated to represent about 39.5 per cent and 22.9 per cent of the world's total reserves respectively in 2008 [1].

These countries are also among the highest energy consumers worldwide; especially domestic energy consumption continues to increase fast. Based on International Energy Agency (IEA) data, the GHG emissions have increased by more than approximately 50 per cent in the last decade [2]. Furthermore, electricity demand is increasing particularly fast, at average growth rates of 7 per cent, which implies a doubling of the needed power generation capacity every 10 years. The electricity load curve in the GCC countries shows very high summer loads - in general and in particular during peak hours. At the same time approximately 45 per cent of domestic electricity consumption is linked to these appliances [3]. This strong electricity demand growth is also driven by artificially low prices.

Despite the high exploitable potential, till now, only pilot, research and some small scale activities related to the renewable energy and energy efficiency were conducted in the Arab States of the Gulf and as a result, some small and medium capacity projects were installed and tested [4]. However, the current situation has been changing as the government, the financial organizations, the academics, the general public and the private sector start realizing the inevitability of putting climate change issues on the top of the priorities' list in the process of sustainable development [5]. Furthermore, the price fluctuations, the rapid population growth

and the increasing energy demand contribute to the increased necessity of sustainable energy solutions, as the region cannot depend on conventional fuels forever. As also depicted in recent studies, the GCC countries have recently adopted a more pro-active approach toward ecological modernization. This reorientation has not yet resulted in the development of consistent strategies and policies. However, pioneering projects such as Masdar City, the Energy City Qatar and innovative regulation like the green building code in Dubai will spread within the GCC [6-8].

The European Union (EU) has a well founded interest to cooperate with the GCC countries and support them in addressing and successfully tackling clean energy issues. This is particularly true taking into consideration that on one hand EU is the leading world proponent of climate change prevention and on the other hand is one of the world's major importers of hydrocarbons. Indeed, the global warning poses certain constraints to energy usage with direct impacts to the international economic activity and the producer-consumer dialogue is currently focused on the identification of prospects and opportunities for the development of a sustainable energy economy in order to pass from the current carbon constrained economy to new and prosperous sustainable development paths.

To the best of our knowledge, there are no practical tools and instruments to guide structured discussion on EU-GCC clean energy cooperation avenues, acting as catalyst and element of coordination. Aim of this paper is to present the first outcomes of the Discussion Group "Energy Demand Side Management (DSM) and Energy Efficiency (ENEF)" of the Network. Indeed, there exist a significant potential for promoting cooperation EU-GCC on ENEF & DSM and specific areas of cooperation of mutual benefit, which are identified and discussed in this paper.

The paper, apart from this first introductory section, is structured along the following sections. Section 2 is focused on a short description of the EU-GCC Clean Energy Network initiative. Section 3 provides, in a concise way, the activities and methodological procedures followed within the D/G of the Network. Section 4, which is the main part of the study, focuses on the first outputs within the Energy Demand Side Management and Energy Efficiency D/G, providing areas for EU-GCC cooperation under this D/G. Section 5 presents the main conclusions drawn from work carried out so far under the Energy Demand Side Management and Energy Efficiency D/G.

2. The EU GCC Clean Energy Network

The EU-GCC partnership started officially in 1988, when the EU and the GCC signed a Cooperation Agreement, which put into place a regular high level framework of dialogue. The Cooperation Agreement established two important bodies:

- On the strategic level, an annual Joint Council and Ministerial Meeting between the EU and the GCC foreign ministers and between senior officials at a Joint Cooperation Committee.
- On the operational level, an Energy Experts Group that started its work at the beginning of 1990's.

The EU – GCC on the 17th GCC-EC Joint Co-operation Committee (March 2006) outlined the need for policy support towards the promotion of renewable and energy efficiency options in the Arab States of the Gulf. In the EU – GCC expert meeting on climate change on the 22nd of January 2007 in Brussels, all participants underlined the importance of Clean Development Mechanism (CDM) projects for GCC countries and especially in the areas of Carbon Capture

and Storage (CCS) technology, energy production, energy efficiency and conservation, petroleum refining and petrochemical industries. Respectively, the EU – GCC meeting on climate change on the 11th of February 2008 in Brussels focused on the need for better technology cooperation frameworks and technology transfer progress. The Workshop "Enhancing the EU-GCC Relations within the New Climate Regime: Prospects and Opportunities for Cooperation", on the 26th of February 2009 underlined the importance of EU-GCC co-operation issues related to energy and the environment [9].

In this context, the European Commission (EC), External Relations Directorate General has commissioned the project "Creation and Operation of an EU-GCC Clean Energy Network". The specific objective of this project, aimed to create and facilitate the operation of an EU-GCC Clean Energy Network. This network aims to act as a catalyst and element of coordination for development of cooperation on clean energy, including the related policy and technology aspects, among various stakeholders in the EU and GCC countries. The 20th EU-GCC Joint Council and Ministerial Meeting, Luxembourg, 14 June 2010, welcomed the EC-GCC Clean Energy Network.

In light of the above facts, an integrated procedure for the identification of appropriate renewable and energy efficiency solutions could stimulate the interest of donors (GCC funds, EU funds, International donors' funds, National Funds) and foster joint activities and deployment of technologies in the area of clean energy. It is also noted that the Network will support the identified project ideas, by the:

- Identification and mobilisation of available sources of financing for joint EU-GCC projects and activities;
- Identification, preparation & submission of applications and implementation of research projects under FP7 funding and other R&D financing programmes;
- Assistance in development of project fiches and submission to international donors and other financing institutions.

This Network's scope and operation aims to identify the huge potential for EU-GCC cooperation, as well as to strengthen the cooperation ties between these two regions.

3. Discussion Groups' Structure and Methodological Procedures

To achieve these results, the network (EU-GCC Clean Energy Network) is designed in a way that allows robust operation, efficiency and flexibility, so as to provide the wide variety of services necessary to achieve the expected results. Essential features of the project are the Discussion Groups (D/G) that focus on areas of common interest.

The thematic Discussion Groups (D/Gs) contribute to the Network's strategic objectives for enhancing EU-GCC clean energy cooperation. The five key thematic areas on which the D/Gs' work is focused are:

- D/G 1: Renewable Energy Sources
- D/G 2: Energy Demand Side Management and Energy Efficiency
- D/G 3: Clean Natural Gas and Related Clean Technologies
- D/G 4: Electricity Interconnections and Market Integration
- D/G 5: Carbon Capture and Storage (CCS).

The Discussion Groups (D/G) are structured in a simple way, so as to allow ease of operation and flexibility. The proposed organisational structure of a D/G is presented in the following Figure 1.

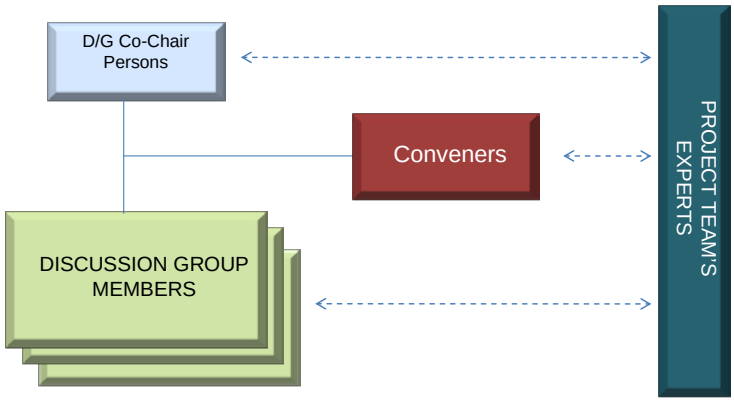

Fig. 1. Structure of a Discussion Group.

The D/Gs work in a continuous "collaboration mode", by communicating mainly through the Network's Communication- Collaboration- Dissemination Platform (NCCDP). There is a specific "area" within the NCCDP for each D/G, where D/G members have full access. The D/Gs works under an agreed yearly Work-Plan with clearly identified working directions regarding analysis and advice on:

- Best practice technologies.
- EU and GCC Policies.
- Cooperation opportunities- projects among EU and GCC entities.
- Exchange of ideas/know-how for the specific D/G clean energy topics.

Communication and collaboration within the D/G members is supported by the NCCDP "D/G area" that provides tools for: discussion on topics, exchange of documents and information, collaborative work on documents, web-meetings (convened by the D/GC or D/G Co-Chair Persons), Training Webinars, etc. The D/GC assisted by the D/G co-chair persons mobilize, coordinate and facilitate communication and collaboration. Discussion Group members are registered in the D/G Mailing List to receive important D/G notifications from the D/GC, the D/G Co-Chair Persons and the Network Administration.

4. First Outputs within the Energy Demand Side Management and Energy Efficiency D/G

In the following parts, the main points drawn up from the background report elaborated within the D/G are presented. It is noted that this background report is a collaborative work/contribution among D/G experts, which is aimed to be further enhanced so as to constitute a "Thematic EU-GCC Co-operation Roadmap" on DSM and ENEF.

4.1. EU & GCC State of Play

4.1.1. EU State of Play

The EU region is a frontrunner in tackling climate change and energy efficiency issues. The 20-20-20 target set for 2020 has placed very ambitious goals for the reduction by 20% of GHG emissions and primary energy consumption.

According to a WEC report [10], EU has one of the lowest primary energy intensities in purchasing power parities in the world, and significantly lower than the world average. Figure 2 below depicts this favorable EU standing in the world as far as the primary energy intensity levels in 2008 are concerned.

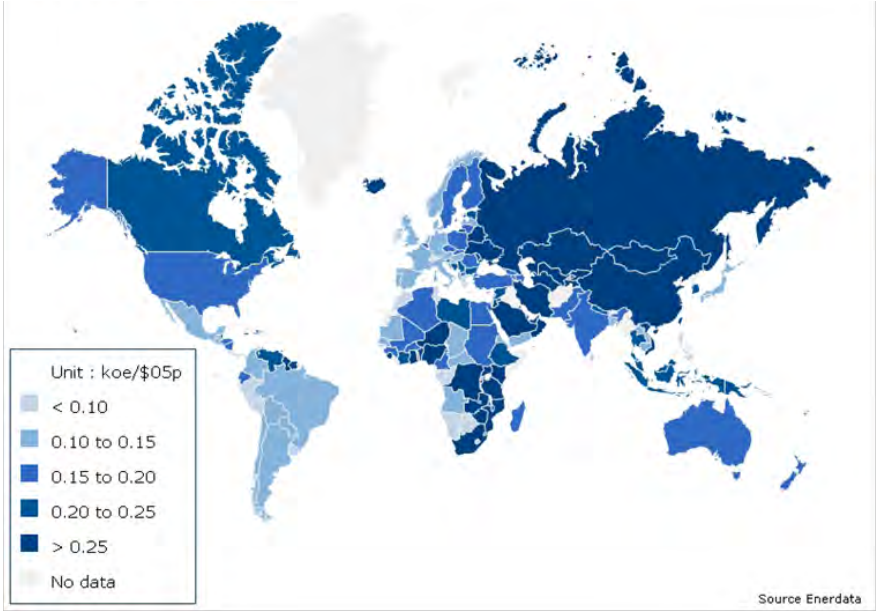

Fig. 2. Primary energy intensity levels by country (2008).

Source: WEC 2010

EU has taken significant legislative action so as to further enhance energy efficiency in the region. Although tackling energy consumption through demand side management activities in the national level remains a very challenging task, EU central policy developed is a key driver towards the achievement of the 20-20-20 target.

4.1.2. GCC State of Play

While no harmonized policy on DSM exists in the GCC states, recent developments show some changes in individual GCC countries. In the following paragraphs, an outline of the prevailing situation in these countries is presented.

- **UAE:**
  - Urban master Plan Abu Dhabi 2030 addresses sustainability as a core principle. Estidama, which is the Arabic word for sustainability, is an initiative developed and promoted by the Abu Dhabi Urban Planning Council (UPC), while the early aspirations of Estidama are incorporated into Plan 2030 and other UPC policies.
  - The Pearl Rating System for Estidama is one of the key tools for driving and determining the core principles of sustainable development. It is a framework for sustainable design, construction and operation of communities, buildings and villas, specifically tailored to the hot climate and arid environment of Abu Dhabi.
  - The Economic Affairs Unit of Abu Dhabi is currently working with other government and non-government entities to develop a comprehensive Demand Side Management strategy for electricity and water consumption within the Emirate.
  - As regards Dubai, the government adopted a sustainable development policy ("Dubai Strategic Plan 2015"), covering all aspects of society. In the energy branch, green building standards, and water and energy conservation and management are

relevant aspects. The Green Building Regulation came into effect in April 2010 and aimed at reducing energy demands of new buildings by up to 40%.
    - Moreover, the Emirates Authority for Standardisation and Metrology (ESMA) has launched a new energy efficiency label and standard scheme in a bid to reduce country's environmental impact. The new certification will be placed on electronic goods - in particular air-conditioning units - and will be based on an international standards template while being specifically designed for the UAE market.
- **Kuwait:** The Ministry of Electricity and Water has developed a code of practice for energy conservation in buildings, placing emphasis on HVAC, since 1983. A revised version of the code was issued in 2010.
- **Saudi Arabia:**
    - Ministry of Water and Electricity systematically promotes DSM, by founding the Energy Conservation and Awareness Department, imposing limits to the maximum power that can be delivered to electricity consumers, establishing DSM actions, and rationalizing the use of electricity.
    - Saudi Arabian Standards Organization adopted several standards aiming to limit the penetration of in-efficient electrical appliances, without however having the effective power to enforce these standards.
- **Qatar:**
    - Qatar Green Building Council (QGBC) with mission to educate and increase awareness and develop a set of green building best practice guidelines.
    - Qatar Sustainable Energy and Water Utilisation Initiative is a project to improve desalination technologies, and promote public awareness of sustainable use of energy.
    - National Vision 2030 on sustainable development is supported by Dohaland, introducing edge urban living concepts, aimed at delivering a sustainable development that is energy-efficient, high in performance and low in wastage.
- **Oman:** Electricity companies trying to implement certain DSM programmes are facing difficulties, such as large subsidies offered for tertiary sectors' tariffs.
- ***Bahrain:*** A number of activities promoting energy conservation and DSM measures have been realized. These programmes are targeted towards thermal insulation, energy audit, power factor, CFLs, labels and energy standards, load control and awareness raising.

4.2. EU & GCC main technology and policy fields of interest

Main technological focus till now from the GCC side has been placed upon Combined Heat and Power Generation, as well as the development of cross-cutting technologies in the industrial sector (compressed air pumps, electric motors, ventilation and air conditioning, steam generation, cooling etc.). Nevertheless, the significant progress being made on the implementation of RUE technologies in the tertiary sector cannot be neglected.

Some potential technology and policy fields of interest for EU/GCC cooperation include:
- Application of efficient labels and standards for energy household appliances;
- Redesign of subsidies offered for tertiary sector tariffs;
- Use of bioclimatic architecture;
- Promotion of energy efficiency awareness campaigns;
- Promotion of energy audits in all sectors (industries, tertiary sector buildings, households);
- Realization of RUE technologies in public buildings, as demonstration projects;
- Common efforts of government/electricity companies to promote DSM measures;

- Introduction of smart meters not only for the large consumers, but for the household sector as well.

4.3. Promoting co-operation on Energy Efficiency & Demand Side Management

Particular emphasis was laid on the discussion for the identification of a few concrete examples of areas on which the EU and the GCC could cooperate. These areas are the following:

- Air Conditioning (AC) maintenance and AC technicians' certification,
- Replacement of incandescent lamps, further introduction of solar water heaters, reverse osmosis.
- To support legislation and infrastructures e.g. through information platforms and the development of standards

In addition, fruitful discussions were elaborated on financing measures that could foster related cooperation activities, such as:

- Lower than market cost tariffs halter the significant promotion of energy efficiency. However, raising prices to more cost reflecting tariffs is already happening.
- District cooling is a promising option for GCC. However, currently the district cooling pricing is double than the cost of using AC units.

5. Conclusions

The main points drawn from the discussion group on "Energy Demand Side Management and Energy Efficiency", as also discussed within the 1st Meeting of the Network's Discussion Groups, 30th November - 1st December 2010, Dubai, UAE, include the following:

- The GCC region is facing increasing energy demand and high environmental concerns. Especially as concerns the electricity consumption, the increasing rates in the GCC region have more than doubled within a ten years period, while the load curve shows very high summer loads in general and in particular during peak hours.
- Implementation of Demand Side Management (DSM) schemes is gaining ground in the region. More specifically, Abu Dhabi has incorporated their utilization in the energy policy 2030, while efforts are being made for their implementation also in Bahrain, Oman and Saudi Arabia. In addition, KSA and UAE have already started pilot projects on smart energy meters, while activities such as the Abu Dhabi Masdar City, the Qatar Energy City, the Bahrain World Trade Center and the KAUST Sustainable Campus, show the GCC interest in these fields.
- The EU has placed significant emphasis on promoting energy efficiency through the adoption of the 20-20-20 target. In addition to the EU common policy measures, the EU member states possess significant experience in the promotion of energy efficiency measures and technologies.
- GCC countries can benefit, through the exchange of experiences and know how in the field of policies and measures, based on the EU related efforts and activities. The FP7 Programme could also provide opportunities for related collaborations of EU/GCC entities.

Indeed, the Discussion Group outcomes in terms of exploration of possibilities for joint projects (both technological research and pilot industrial scale projects) are of significant importance for enhancing EU-GCC Clean Energy Cooperation in fields of mutual interest.

The future direction is to make this Network a forum of action and not just discussion. The discussion and networking opportunities this platform provides the potential users/

beneficiaries with should be a means to deliver projects which could push forward the GCC region on the global scene in the field of clean energy. These potential users/ beneficiaries, including donors (GCC funds, EU funds, International donors' funds, National Funds), other financing institutions and energy actors, should work together for preparation & submission of applications as well as implementation of research projects under FP7 funding and other R&D financing programmes.

Acknowledgements

This paper was elaborated within the framework of the project "Creation and Operation of an EU-GCC Clean Energy Network – http://www.eugcc-cleanenergy.net" (Contract Number SI2.551874), European Commission, Directorate General External Relations. The content of the paper is the sole responsibility of its authors and does not necessarily reflect the views of the EC.

References

[1] BP - Beyond Petroleum, BP Statistical Review of World Energy, BP, London, June 2009.

[2] International Energy Agency (IEA), Key world energy statistics 2010, IEA, Paris, 2010.

[3] M. Al-Sulami, Poor-quality electrical appliances banned, Arab News, 2010, April 26. Retrieved from: http://arabnews.com/saudiarabia/article47257.ece.

[4] H. Doukas, K.D. Patlitzianas, A.G. Kagiannas, J. Psarras, Renewable Energy Sources and Rationale Use of Energy Development in the GCC Region: Myth or Reality?, Renewable Energy, 31(6), 2006, pp. 755-770.

[5] United Nations Framework Conversion on Climate Change (UNFCCC), Kyoto Protocol Status of Ratification, UNFCCC, Bonn, Germany, 2009. Retrieved from: http://unfccc.int/files/kyoto_ protocol/status_of_ratification/application/pdf/kp_ratification_20090826corr.pdf.

[6] D. Reiche, Energy Policies of Gulf Cooperation Council (GCC) countries – possibilities and limitations of ecological modernization in rentier states, Energy Policy, 38(5), 2010, pp.2395-2403.

[7] D. Reiche, Renewable Energy Policies in the Gulf countries: A case study of the carbon-neutral "Masdar City" in Abu Dhabi, Energy Policy, 38(1), 2010, pp.378-382.

[8] H.M. Taleb, A.C Pitts, The potential to exploit use of building-integrated photovoltaics in countries of the Gulf Cooperation Council, Renewable Energy, 34(4), 2009, pp.1092-1099.

[9] J. Psarras, A. Flamos, K. Patlitzianas, Background Paper of the Workshop "Enhancing the EU-GCC Relations within the New Climate Regime: Prospects and Opportunities for Cooperation", Brussels, Belgium, 26th of February 2009, Al Jisr project on "Public Diplomacy and Outreach Devoted to the European Union and EU-GCC Relations", February 2009.

[10] World Energy Council, Energy Efficiency: A recipe for success, 2010.

The emerging bio-economy in Europe: Exploring the key governance challenges

K. McCormick[1*]

[1] *International Institute for Industrial Environmental Economics (IIIEE) at Lund University, Lund, Sweden*
** Corresponding author. Tel: +46 46 222 0256, E-mail: kes.mccormick@iiiee.lu.se*

Abstract: The purpose of this paper is to identify, analyse and discuss the key governance challenges for the emerging Knowledge-Based Bio-Economy (KBBE) in Europe focusing on bioenergy, particularly biofuels for transport and the biorefinery concept. This paper is based on a literature review, discussions with European researchers and practitioners, and questionnaires of bioenergy industry associations. The growing bio-economy and bioenergy in Europe face a host of socio-technical issues that comprise a mix of technological, economic, social, political, environmental, regulatory and cultural aspects. More specifically, this research work highlights three key governance challenges of increasing relevance for the bio-economy, including: the important role of public-private networks; city-regions as drivers for the KBBE, especially through climate governance; and consumer-citizens and NGOs as key players in the development of the bio-economy.

Keywords: *Bio-economy, Bioenergy, Governance, Socio-technical, Sustainability*

1. Introduction

The emerging Knowledge-Based Bio-Economy (KBBE) in Europe represents a significant transformation from economic, social and environmental perspectives. In short, the concept of the KBBE can be understood as an economy where the basic building blocks for materials, chemicals and energy are derived from renewable biological resources, such as plant and animal sources [1]. Worth nearly €2 trillion, the existing bio-economy in Europe currently employs around 22 million people across sectors as diverse as agriculture, forestry, fisheries, food, and bioenergy [2]. The increased attention on the bio-economy is being driven by the recent surge in scientific knowledge and technical competences that can be used to harness biological processes for practical applications as well as efforts to reduce greenhouse emissions and dependency on oil and fossil fuels.

Within the KBBE, the focus of this paper is on bioenergy – particularly biofuels for transport and the biorefinery concept (see Box 1). The purpose of this paper is to identify, analyse and discuss the key governance challenges for the emerging bio-economy in Europe. There are two underlying objectives. The first is to investigate different perspectives and understanding of the bio-economy and its key components. The second is to consider the bio-economy in terms of positive and negative impacts as well as drivers and constraints. Overall, this paper begins to explore the complexity of the socio-technical issues (covering technological, economic, social, political, environmental, regulatory and cultural aspects) that surround the bio-economy. It is timely to investigate the role of governance for the bio-economy as a European KBBE strategy is expected to be launched in 2011 [3].

2. Approach

The emerging bio-economy in Europe is attracting the attention of a diversity of actors (with different interests and values) since it affects a range of sectors and activities. Furthermore, biofuels for transport (and the biorefinery concept) are under intense debate regarding sustainability issues. In this paper, governance is considered as encompassing complex processes, which involve multiple actors in decision-making and policy-making [4]. This

paper further defines governance in two ways. First, it refers to the different tiers at which governance takes place and the interactions between the tiers, which for Europe is local municipalities, national governments and the EU. Second, it refers to the myriad of networks between public and private actors that shape governance activities.

Box 1: Bioenergy

Humans exploit biomass (plant and animal matter) for many purposes. When it is utilized to produce heat, electricity or fuels for transport it is commonly called ***bioenergy***. Biomass can be considered as 'stored' solar energy because the process of photosynthesis 'captures' energy from the sun in growing plants. Utilizing biomass for energy purposes is in fact tapping into the vast energy available from the sun. Bioenergy systems comprise both technical aspects, such as conversion technologies, and non-technical aspects, such as government policies.

Biofuels for transport are commonly categorised as follows: first generation biofuels made from food crops, such as wheat and sugar beet; second generation biofuels from non-food biomass, such as lignocellulosic materials; and third generation biofuels from algae. At present only first generation biofuels can be produced on a large-scale. However, the commercialisation of second generation biofuels is expected over the coming decades. The third generation biofuels are in a research and development phase.

The ***biorefinery concept*** offers exciting potential to better manage and capture value from biomass resources. Similar to petroleum refineries, which produce multiple fuels and products from petroleum, biorefineries imply the integrated production of energy, fuels and chemicals from biomass. Biorefineries have been identified as one of the most promising routes towards the KBBE. While partial biorefineries exist today, considerable research, development, demonstration and commercialisation is required to make advanced biorefineries a reality.

Source: [5]

This research work utilised different research methods to meet the requirements of 'method' triangulation, including a literature review, discussions with European researchers and practitioners, and questionnaires of bioenergy industry associations. The World Bioenergy Association (WBA), the European Biomass Association (AEBIOM), the Swedish Bioenergy Association (SVEBIO), the Spanish Bioenergy Association (AVEBIOM), and the Renewable Energy Association (REA) in the UK, which represents bioenergy interests, completed questionnaires. The discussions with informants from a range of sectors and different backgrounds also ensure 'informant' triangulation.

3. Analysis

3.1. What is the bio-economy? What are the key components of the bio-economy in Europe?

Bioenergy industry associations show some diversity in perspectives on the bio-economy. Heinz Kopetz (questionnaire, 18 June 2010) of AEBIOM states: "The bio-economy is a rather new word. It is that part of the economy that relies on energy and raw materials originating from green plants." Tricia Wiley (questionnaire, 3 September 2010) of the REA points out the UK Biomass Strategy provides a definition of the bio-economy as "economic activities which capture the latent value in biological processes and renewable bioresources to produce improved health and sustainable growth and development". The UK Biomass Strategy is based on the definition of the OECD [6]. Furthermore, the OECD [6] highlights the important role of biotechnology in the emerging bio-economy (see Box 2).

Box 2: Biotechnology

Biotechnology can be understood as the science of using living things to produce goods and services. It therefore involves manipulating and modifying organisms to create new and practical applications. ***Industrial biotechnology*** or ***white biotechnology*** uses enzymes and micro-organisms to make bio-based products in a diverse range of sectors, including chemicals, food and feed, bioenergy, paper and pulp, and textiles. ***Green biotechnology*** is biotechnology applied to agricultural processes. ***Blue biotechnology*** is a term that has been used to describe the marine and aquatic applications of biotechnology. And finally, ***modern biotechnology*** is used to distinguish newer applications of biotechnology, such as genetic engineering and cell fusion, from more conventional methods, such as breeding or fermentation.

Source: [6]

Kjell Andersson (questionnaire, 14 June 2010) of SVEBIO states: "I was not aware that there is a concept of an 'emerging bio-economy'. I think we have a very strong move towards a more sustainable energy system, with more energy efficiency and more renewable energy, which bioenergy is an important component." Francisco Gonzalez (questionnaire, 4 August 2010) of AVEBIOM states that bioenergy is at the core of the bio-economy. Overall, Kent Nyström (questionnaire, 20 August 2010) of the WBA highlights that the key components of the bio-economy are sustainability in a broader sense including fair competition between energy, food and feed as well as fair competition for water supply and land use. This highlights that sustainability is central to the KBBE but also the challenges of designing and managing the bio-economy.

The concept of the bio-economy has generated considerable 'excitement' in Europe and around the world. However, it is immediately apparent that the bio-economy means very different things to different people. A better understanding of the bio-economy and its key components remains a vital foundation for the growth of the KBBE in Europe. Interestingly, the bio-economy is one of the oldest sectors (including all industries and economic activities that produce, manage and exploit biological resources, such as agriculture, food, forestry, fisheries and bioenergy), but it is being transformed into one of the newest sectors. The key components of the bio-economy include biotechnology and the biorefinery concept. Biofuels for transport are a key product and agriculture is the primary source of raw materials.

3.2. Why promote the bio-economy in Europe? What are the main positive and negative impacts of the bio-economy?

Not surprisingly, bioenergy industry associations in Europe are largely optimistic about bioenergy. However, there is a strong awareness that supportive policy schemes need to stimulate well-designed bioenergy systems that incorporate strict sustainability standards. Heinz Kopetz (questionnaire, 18 June 2010) of AEBIOM believes that negative impacts will occur if a sustainable production of biomass is not achieved, which includes the fertility of soils and the availability of water, or if more biomass is used than annually produced, and a competition between food and non-food use of biomass takes place. Kent Nyström (questionnaire, 20 August 2010) of the WBA is confident the expanding bio-economy can avoid substantial negative impacts. However, there are challenges ahead for the expanding bio-economy to meet stricter sustainability requirements.

Kjell Andersson (questionnaire, 18 June 2010) of SVEBIO states that the main positive outcomes of the bio-economy are "a more sustainable energy and material system, based on

solar energy and natural processes, instead of depleting finite resources." Tricia Wiley (questionnaire, 3 September 2010) of the REA suggests there are a number of economic, security and environmental benefits associated with the bio-economy, including job creation as well as investments in industry and deprived areas and communities. Francisco Gonzalez (questionnaire, 4 August 2010) of AVEBIOM argues that the generation of employment opportunities in rural areas and new incomes streams for farmers will be some of the major positive results of the growing bio-economy.

When looking at the positive and negative impacts of the bio-economy a distinction needs to be made between the near-future as opposed to the long-term perspective based on visions. There are diverging visions of the bio-economy from wildly optimistic about an industrial revolution in the coming decades [7] to 'real' concern about significant negative impacts, especially related to increasing biofuels for transport [8]. Additionally, the current status of the bio-economy remains unclear, despite studies to define the scale and attributes of the existing bio-economy. Finally, there is growing knowledge related to the biorefinery concept and efforts to speed up the development and implementation of biorefineries in Europe, but there is still great uncertainty about the potentials and impacts associated with biorefineries.

3.3. How can the bio-economy expand in Europe in a sustainable and competitive way? What are the main drivers and constraints for the bio-economy?

The marginal understanding of the bio-economy and the 'missing' carbon taxes in many European countries are considered key constraints by some bioenergy industry associations. Heinz Kopetz (questionnaire, 18 June 2010) of AEBIOM states: "The basic principle of the bio-economy lies in the fact that the carbon comes via photosynthesis from the atmosphere and not from the earth's crust. As long as the depletion of the earth's crust brings more profit than the use of carbon via photosynthesis the development of the bio-economy will be held back." There are in fact discussions about carbon taxes across the EU, especially based on the positive experiences from Sweden. In addition to expanding bioenergy, Sweden has also made significant progress on biofuels for transport, especially bioethanol (see Box 3).

Box 3: Bioenergy and Bioethanol in Sweden

In 2009, ***bioenergy*** overtook oil as the largest source of energy in Sweden. Oil accounted for 30.8% while bioenergy provided 31.7% of the total energy use. A major reason for the growth of bioenergy in Sweden has been the carbon tax established in 1991. It is based on the 'polluter pays principle' in that emitters of CO2 pay for the costs of CO2 emissions. The carbon tax makes it profitable to use fossil fuels efficiently and switch to renewable energy. The carbon tax has transformed the energy system in Sweden towards bioenergy.

Over 1,400 of Sweden's 4,000 service stations offer fuels from renewable energy sources, predominantly ***bioethanol***. In addition to economic incentives, service stations (of certain sizes) are mandated by law to provide a renewable alternative. Presently, there are some 4.2 million cars on Sweden's roads and almost 200,000 are flexi-fuel cars (that can operate on bioethanol, petrol or varying blends). There are economic incentives to purchase flexi-fuel cars, and subsidies and tax reforms make bioethanol competitive with regular petrol.

Source: [9,10]

Kjell Andersson (questionnaire, 18 June 2010) of SVEBIO states: "Strong traditional industries lobbying to preserve their dominance (oil, coal, gas, nuclear) and big 'sunk costs' in the existing energy systems make it hard for new alternatives to compete. The fossil energy

systems also do not, in most countries, pay for their full external costs, like damage on the economy, climate costs, and safety and security costs (nuclear)." Francisco Gonzalez (questionnaire, 4 August 2010) of AVEBIOM concurs that the main obstacles for the KBBE arise from the capacity of the oil and gas sectors to lobby political and business leaders. For the UK, Tricia Wiley (questionnaire, 3 September 2010) of the REA suggests that complex and inconsistent regulations, and the perceived risks of policy changes, are constraints for the bio-economy.

The drivers and constraints for the bio-economy are mixed together with challenges (and opportunities). There is also a difference between global and European issues and trends, and more 'concrete' drivers or constraints at the national and local levels. Supportive policy schemes and social acceptance by a broad range of stakeholders appear to be key ingredients for the growing bio-economy. A more integrated and strategic policy approach is required to stimulate the KBBE in Europe, which is combined with a strong emphasis on engagement with the general public and key stakeholders. While there is an increased effort on research and development, it is imperative to also fund demonstrations and implementation. There are also many difficult policy decisions to make, especially regarding the sustainable supply of raw materials for the bio-economy [11].

4. Discussion

4.1. The importance of public-private networks

The bio-economy is critically dependent on policy 'intervention' that creates a favourable environment for investment. The type of governance that is shaping the bio-economy in the EU is not liberal or market-based or coordinated and state-led, but it is rather characterised by public-private networks. There is a pattern of combined public and private investments in various parts of the bio-economy, which involves a complex interplay between publicly funded science and business firms, regulated markets, emerging professional groups, attempts to integrate activities across government authorities, and efforts to create positive public attitudes to the KBBE [12]. The development of public-private networks appears to be an essential characteristic of the emerging bio-economy, particularly for the biorefinery concept, which requires significant support and investment.

EuropaBio [13] states that the main challenges in Europe are that a more integrated and strategic approach is needed for the EU to develop a globally competitive bio-economy within the next decade. This paper suggests that such an integrated approach should be focused on long-term opportunities and open to partnerships between public and private actors within the EU (and around the world). For EuropaBio [13] it should involve five key aims, including: improving and securing access to renewable raw materials; supporting targeted research, training and innovation; developing technologies and systems, and bridging the gap between research and markets; stimulating demands for bio-based products; and improving awareness of the bio-economy through communication and educational activities.

4.2. The role of city-regions

In a European context, many of the policies and strategies that are implemented by local municipalities were formulated by the EU and filtered through national governments. Silvestrini et al. [14] examine the implementation of the Biofuels Directive in Germany, the UK, Italy and Finland by looking at the role of city-regions, namely Berlin, London, Milan and Helsinki. Interestingly, and extremely relevant for the emerging bio-economy, is that networking between city-regions is allowing an exchange of knowledge and experiences, and

contributing to practical and policy learning around the Biofuels Directive [14]. This paper argues that city-regions and local municipalities are well-positioned to play an important role in the KBBE, especially in relation to biofuels for transport.

The scope for action by local municipalities is defined by their jurisdiction and responsibilities, and their financial independence. However, Gupta et al. [15] suggest that local municipalities are often able to establish more ambitious goals and policies than national governments, which is particularly evident in regards to climate governance. Furthermore, the goals and policies of city-regions related to the bio-economy can be framed through climate governance, which can help to mobilise actors and coordinate diverse interests. For the bio-economy, climate governance by local municipalities and city-regions can be an important mechanism to translate abstract visions of the KBBE (often framed by national or international actors) into concrete agendas based on local and regional contexts.

4.3. The engagement of consumer-citizens

Creating awareness amongst the general public and key stakeholders about the KBBE appears to be a vital foundation for expanding the bio-economy in Europe. This paper argues that an EU strategy for communication and stakeholder involvement is necessary, which is combined with actions across countries and city-regions. However, it is clear that increased information and communication do not directly translate into public acceptance. On the contrary, the success of the bio-economy will likely depend on active public and stakeholder engagement both in policy formulation and specific projects. Demonstrating the benefits of expanding the bio-economy in parallel with trade-offs to consumer-citizens will be required to create the foundations for the KBBE in Europe [16].

The concept of consumer-citizens can be utilised to shape communication strategies. On the one hand, the bio-economy needs to be marketed to ‘consumers’, and on the other hand, proponents of the bio-economy need to also actively engage ‘citizens’ in planning and implementation processes. Additionally, there is a need to identify and positively engage with target audiences, particularly opinion-formers, such as NGOs, that can influence the general public. NGOs are currently establishing their positions on the KBBE. It can be expected that NGOs will become further engaged as the bio-economy grows. NGOs are likely to be important opinion-formers for the implementation of the biorefinery concept and they are already deeply engaged in debates on biofuels for transport.

5. Reflections

This paper concludes with two reflections. First, serious concerns have been raised about the sustainability of biofuels for transport, which are an integral part of the KBBE. The underlying message is that biofuels only make sense if the raw materials are based on truly renewable and sustainable sources. The European Commission has decided to establish binding sustainability criteria for biofuels, which will become stricter over time. The efforts by the European Commission all point towards increased emphasis on the sustainability for bioenergy generally and biofuels for transport specifically. Furthermore, the biorefinery concept offers the potential to move towards more sustainable production of biofuels combined with other bio-based products.

Second, while sustainability appears to be on the top of the political agenda, it is impossible to measure the sustainability of biofuels, the biorefinery concept or the bio-economy, without taking into consideration the scale and pace of growth. This challenges current thinking and

ideas about the economy. Put simply, the bio-economy cannot replace the fossil-based economy as it is set-up today. On the contrary, the emerging bio-economy demands attention on consumption issues as much as the production side. For example, biofuels for transport must be integrated into broader mobility strategies that encompass more than the introduction of 'new' fuels. Ultimately, the move towards a sustainable KBBE is directly connected to achieving sustainable development on a 'grand' scale.

References

[1] European Commission, En Route to the Knowledge-Based Bio-Economy, 2007. URL: http://ec.europa.eu/

[2] European Commission, The Knowledge-Based Bio-Economy: Achievements and Challenges, 2010. URL: http://ec.europa.eu/

[3] M. Geoghegan-Quinn, The Bio-economy for a Better Life, 2010. URL: http://europa.eu/

[4] A. Duit, V. Galaz, Governance and Complexity: Emerging Issues for Governance Theory, Governance, 2008, 21(3): 311-335.

[5] International Energy Agency (IEA) Bioenergy, An International Collaboration in Bioenergy, 2010. URL: http://www.ieabioenergy.com/

[6] Organisation for Economic Cooperation and Development (OECD), The Bio-economy to 2030: Designing a Policy Agenda, 2009. URL: http://www.oecd.org/

[7] European Commission, Plants for the Future, 2004. URL: http://ec.europa.eu/

[8] R. Smolker, The New Bio-economy and the Future of Agriculture, Development, 2009, 51(4): 519-526.

[9] Swedish Bioenergy Association (SVEBIO), The Beauty of Carbon Tax, 2010. URL: http://www.svebio.se/

[10] Swedish Energy Agency (STEM), Energy in Sweden, 2009. URL: http://www.energimyndigheten.se/

[11] H. Langeveld, J. Sanders, M, Meeusen, The Bio-based Economy: Biofuels, Materials and Chemicals in the Post-oil Era, 2010. London: Earthscan.

[12] M. Benner, H. Löfgren, The Bio-economy and the Competition State: Transcending the Dichotomy between Coordinated and Liberal Market Economies, New Political Science, 2007, 29(1): 77-95.

[13] European Association for Bio-industries (EuropaBio), Building a Bio-based Economy for Europe, 2010. URL: http://www.europabio.org/

[14] A. Silvestrini, S. Monni, M. Pregernig, A. Barbato, J. Dallermand, E. Croci, F. Raes, The Role of Cities in Achieving the EU Targets on Biofuels for Transportation: The Cases of Berlin, London, Milan and Helsinki, Transportation Research, 2010, 44: 403-417.

[15] J. Gupta, K. Van der Leeuw, H. de Moel, Climate Change: A 'Glocal' Problem Requiring 'Glocal' Action, Environmental Sciences, 2007, 4(3): 138-148.

[16] K. McCormick, Communicating Bioenergy: A Growing Challenge, Biofuels, Bioproducts and Biorefining, 2010, 4:494-502.

Tools for Sustainable Energy Engineering

Göran Wall

Department of Culture, Energy and Environment, Gotland University, Visby, Sweden
Tel: +46(0)498299131, Fax: +46(0)498299962

Abstract: Exergy concepts and exergy based methods offer an insight to the understanding of sustainable energy engineering. The utilization of energy and other resources by applying physical concept as exergy and exergy based methods and the value of these tools in the design and optimization are presented, in particular Life Cycle Exergy Analysis (LCEA). Optimization methods incorporating both exergy and economic conditions are also presented. This brings a new approach and insight to the engineering conditions for a sustainable development that is further elaborated. The importance of introducing this new knowledge into present engineering education and practices is argued for.

Keywords: *Renewable energy, Energy Policy, Energy engineering, Sustainable development, Education.*

Nomenclature

E	exergy ..... J	t	time ..... s
E_{indirect}	exergy indirect input ..... J	t_0	time when a project starts, e.g. the first steps to build a power plant ..... s
E_{in}	exergy input ..... J	t_{close}	time when an operation closes, e.g. a power plant close down ..... s
$\dot{E}_{\text{in}}$	exergy power input ..... W	t_{life}	time when a project finally closes, i.e. after complete restoration to original state ..... s
E_{out}	exergy output ..... J	t_{payback}	time when a payback situation is reached ..... s
$E_{\text{net,pr}}$	exergy net of product ..... J	t_{start}	time when an operation starts ..... s
E_{pr}	exergy of product ..... J	T	temperature ..... K
$\dot{E}_{\text{pr}}$	exergy power of product ..... W	T_0	temperature of the environment ..... K
E^{tot}	total exergy ..... J	U	internal energy ..... J
E_{tr}	transit exergy ..... J	V	volume ..... m^3
E_{waste}	exergy of waste ..... J	μ_{i0}	chemical potential of substance i in its environmental state ..... J mol^{-1}
H	enthalpy ..... J		
i, j, k, l	unit, 1, 2,….....		
P_0	pressure of the environment ..... Pa		
Q	heat (thermal energy in transit) ..... J		
S	entropy ..... J K^{-1}		
S^{tot}	entropy of the total system, i.e. the system and the environment ..... J K^{-1}		

1. Introduction

Exergy is a well established scientific concept suitable in the work towards sustainable development. Exergy accounting of the use of energy and material resources provides unique knowledge on how effective a process is in utilizing physical resources. This knowledge can identify areas in which technical and other improvements should be undertaken, and indicate the priorities, which should be assigned to conservation measures, efficiency improvements and optimizations. Thus, exergy concept and tools are essential to the creation of a new engineering paradigm towards sustainable development.

2. Exergy

The exergy concept originates from works of Carnot [1], Gibbs [2], Rant [3] and Tribus [4] and the history is well documented [5]. Exergy of a system is [6], [7]

$$E = U + P_0 V - T_0 S - \sum_i \mu_{i0} n_i \quad (1)$$

where U, V, S, and n_i denote extensive parameters of the system (energy, volume, entropy, and the number of moles of different chemical materials i) and P_0, T_0, and μ_{i0} are intensive parameters of the environment (pressure, temperature, and chemical potential). Analogously, the exergy of a flow can be written as:

$$E = H - T_0 S - \sum_i \mu_{i0} n_i \quad (2)$$

where H is the enthalpy.

All processes involve the conversion and spending of exergy, thus high efficiency is of utmost importance. This implies that the exergy use is well managed and that effective tools are applied. Presently, an excellent online web tool for calculating exergy of chemical substance is also available [8].

Energy is always in balance, however, for real processes exergy is never in balance due to irreversibilities, i.e. exergy destruction that is related to the entropy production by

$$E_{\text{in}}^{\text{tot}} - E_{\text{out}}^{\text{tot}} = T_0 \Delta S^{\text{tot}} = \sum_i \left(E_{\text{in}} - E_{\text{out}} \right)_i > 0 \quad (3)$$

where ΔS^{tot} is the total entropy increase, $E_{\text{in}}^{\text{tot}}$ is the total exergy input, $E_{\text{out}}^{\text{tot}}$ is the total exergy output, and $(E_{\text{in}} - E_{\text{out}})_i$ is the exergy destruction in sub process i.

The exergy loss, i.e. destruction and waste, indicates possible process improvements. In general “tackle the biggest loss first” approach is not always appropriate since every part of the system depends on each other, so that an improvement in one part may cause increased losses in other parts. As such, the total losses in the modified process may in fact be equal or even larger, than in the original process configuration. Also, the use of renewable and non-renewable resources must be considered. Therefore, the problem needs a more careful approach.

3. Exergy diagrams

In engineering, flow diagrams are often used to describe the energy or exergy flows through a process. Fig. 1 shows a typical thermal power station, its main components and roughly the main energy and exergy flows of the plant. This diagram shows where the main energy and exergy losses occur in the process, and also whether exergy is destroyed from irreversibilities or whether it is emitted as waste to the environment. In the energy flow diagram energy is always conserved, the waste heat carries the largest amount of energy into the environment, far more than is carried by the exhaust gases. However, in the exergy flow diagram the temperature of the waste heat is close to ambient so the exergy becomes much less. The exergy of the exhaust gas and the waste heat are comparable.

Fig. 2 illustrates the energy and exergy flows of an oil furnace, an electric heater, an electric heat pump and a combined power and heat plant, i.e. a cogeneration plant. The produced heat is used for space heating. In the oil furnace the energy efficiency is assumed to be typically about 85%, losses being due mainly to the hot exhaust gases. The exergy efficiency is very

low, about 4%, because the temperature difference is not utilized when the temperature is decreased, to a low of about 20°C, as a comfortable indoor climate.

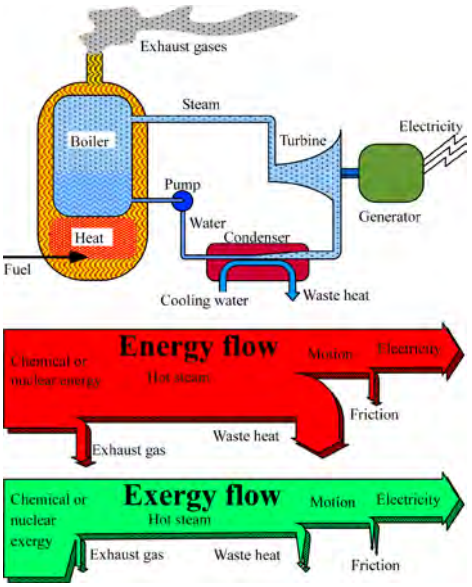

Fig. 1. Energy and exergy flow of a thermal power plant.

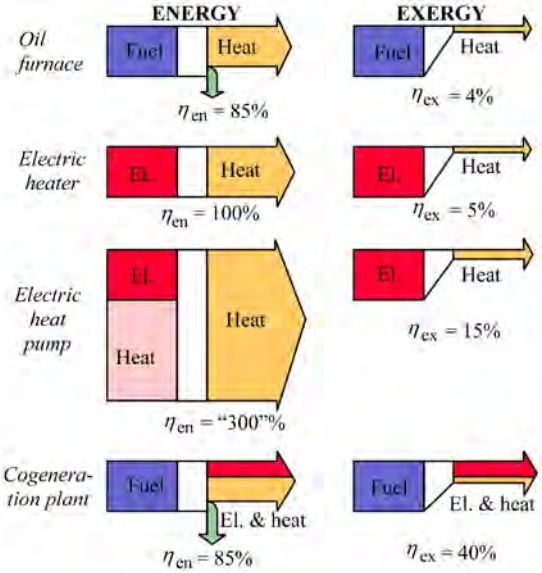

Fig. 2. Energy and exergy flows through typical some energy systems.

Electric heating by short-circuiting in electric resistors has an energy efficiency of 100%, by definition of energy conservation. The energy efficiency of an electric heat pump is not limited to 100%. If the heat originating from the environment is ignored in the calculation of the efficiency, the conversion of electrical energy into indoor heat can be well over 100%, e.g. 300% as in Fig. 2. The exergy flow diagram of the heat pump looks quite different. The exergy efficiency for an electric heater is about 5% and for the heat pump, 15%.

In Fig. 1 the energy and exergy efficiencies are the same since both energy and exergy is almost equal for the inflow of fuels and the outflow of electricity. For a combined power and heat plant, i.e. a cogeneration plant (Fig. 2) the exergy efficiency is about the same as for a thermal power plant (Fig. 1). The main exergy loss occurs in the conversion of fuel into heat in the boiler. Since this conversion is practically the same in both the condensing and the combined power plants, the total exergy efficiency will be the same, i.e. about 40%. However, it may be noted that the power that is instead converted into heat corresponds to a heat pump with a coefficient of performance (COP) of about 10. Thus, if there is a heating need a cogeneration plant is far superior to a condensing power plant. The maximum energy efficiency of an ideal conversion process may be over 100%, depending on the definition of efficiency. The exergy efficiency, however, can never exceed 100%.

4. Exergy analysis

To estimate the total exergy input that is used in a production process it is necessary to take all the different inflows of exergy to the process into account. This type of budgeting is often termed Exergy Analysis [6] & [7], Exergy Process Analysis, see Fig. 3, or Cumulative Exergy Consumption [9], and focuses on a particular process or sequence of processes for making a specific final commodity or service. It evaluates the total exergy use by summing the contributions from all the individual inputs, in a more or less detailed description of the production chain.

Environmentally oriented Life Cycle Analysis or Assessment (LCA) are common to analyze environmental problems associated with the production, use and disposal or recycling of products or product systems, see Fig. 4. Every product is assumed to be divided into these three "life processes", or as it is sometimes named "from cradle to grave".

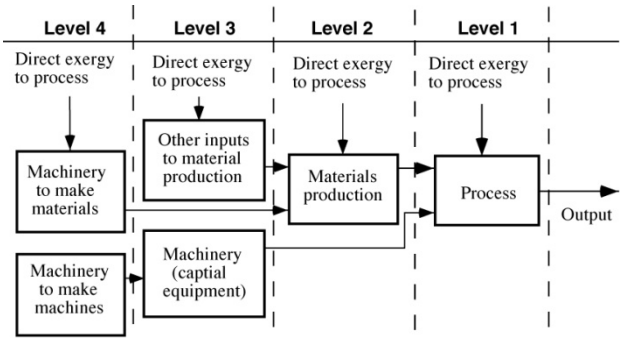

Fig. 3. Levels of an exergy process analysis.

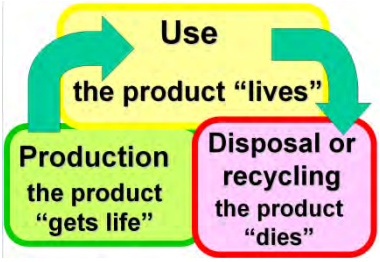

Fig. 4. The life cycle "from cradle to grave".

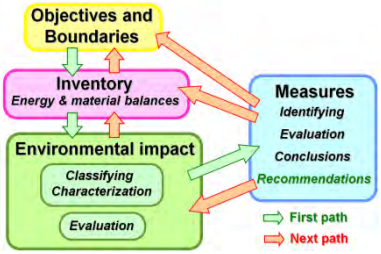

Fig. 5. Main steps of a LCA.

For every "life process" the total inflow and outflow of energy and material is computed, thus, LCA is similar to Exergy Analysis. In general Exergy Analysis and LCA have been developed separately even though they are strongly linked. This inventory of energy and material balances is then put into a framework as described in Fig. 5. Four stages in the LCA can be distinguished: (1) Objectives and boundaries, (2) Inventory, (3) Environmental impact, and (4) Measures. These four main parts of an LCA are indicated by boxes, and the procedure is shown by arrows. Green arrows show the basic steps and red arrows indicate suitable next steps, in order to further improve the analysis.

In LCA the environmental burdens are associated with a product, process, or activity by identifying and quantifying energy and materials used, and wastes released to the environment. Secondly one must assess the impact on the environment, of those energy and material uses and releases. Thus it is divided into several steps (Fig. 5).

The multidimensional approach of LCA causes large problems when it comes to comparing different substances, and general agreements are crucial. This problem is avoided if exergy is used as a common quantity, which is done in Life Cycle Exergy Analysis (LCEA) [10].

In this method we distinguish between renewable and non renewable resources. The total exergy use over time is also considered. These kinds of analyses are of importance in order to develop sustainable exergy supply systems in society. The exergy flow through a supply system, such as a power plant, usually consists of three separate stages over time (Fig. 6). At first, we have the construction stage where exergy is used to build a plant and put it into operation. During this time, $0 \leq t \leq t_{start}$, exergy is spent of which some is accumulated or stored in materials, e.g. in metals etc. Secondly we have the maintenance of the system during time

of operation, and finally the clean up or destruction stage. These time periods are analogous to the three steps of the life cycle of a product in an LCA. The exergy input originating from non renewable resources used for construction, maintenance and clean up we call indirect exergy E_{indirect}. Indirect exergy input originating from renewable recourses are not accounted for. When a power plant is put into operation, it starts to deliver a product, e.g. electricity with exergy power $\dot{E}_{\text{pr}}$, by converting the direct exergy power input $\dot{E}_{\text{in}}$. In Fig. 6 the direct exergy is a non-renewable resource, e.g. fossil fuel and in Fig. 7 the direct exergy is a renewable resource, e.g. wind.

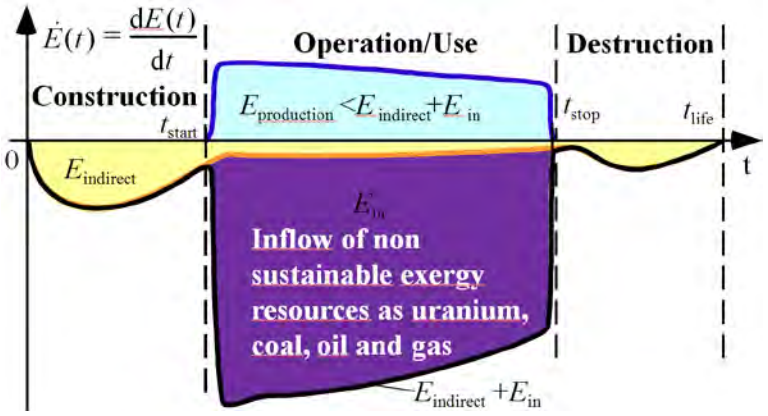

Fig. 6. LCEA of a fossil fueled power plant.

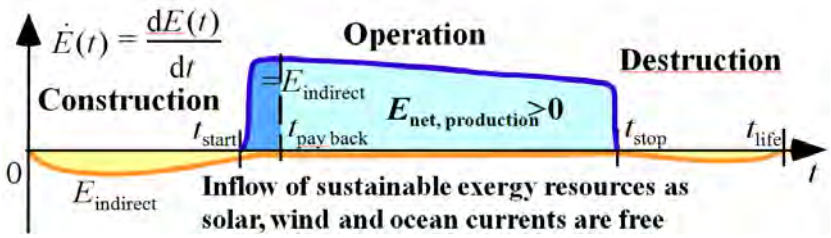

Fig. 7. LCEA of a wind power plant.

In the first case, the system is not sustainable, since we use exergy originating from a non-sustainable resource. We will never reach a situation where the total exergy input will be paid back, simply because the situation is powered by a depletion of resources, we have $E_{\text{pr}}<E_{\text{in}}+E_{\text{indirect}}$. In the second case, instead, at time $t=t_{\text{payback}}$ the produced exergy that originates from a natural flow has compensated for the indirect exergy input, see Fig. 7, i.e.

$$\int_{t_{\text{start}}}^{t_{\text{pay back}}} \dot{E}_{\text{pr}}(t)dt = \int_{0}^{t_{\text{life}}} \dot{E}_{\text{indirect}}(t)dt = E_{\text{indirect}} \tag{4}$$

Since the exergy input originates from a renewable resource we may not account for it. By regarding renewable resources as free then after $t=t_{\text{payback}}$ there will be a net exergy output from the plant, which will continue until it is closed down, at $t=t_{\text{close}}$. Then, exergy has to be used to clean up and restore the environment, which accounts for the last part of the indirect exergy input, i.e., E_{indirect}, which is already accounted for (Eq. 4). By considering the total life cycle of the plant the net produced exergy becomes $E_{\text{net,pr}}=E_{\text{pr}}-E_{\text{indirect}}$. These areas representing exergies are indicated in Fig. 7. For modern wind power plants this time is less than one year [11]. Then the system has a net output of exergy until it is closed down, which for a wind power station may last for decades. Thus, these diagrams could be used to show if a power supply system is sustainable.

LCEA is very important in the design of sustainable systems, especially in the design of renewable energy systems. Assume a solar panel, made of mainly aluminum and glass that is used for the production of hot water for household use, i.e. about 60°C. Then, it is not obvious that the exergy being spent in the production of this unit ever will be paid back during its use, i.e., it might be a misuse of resources rather than a sustainable resource use. The production of aluminum and glass require a lot of exergy as electricity and high temperature heat or several hundred degrees Celsius, whereas the solar panel delivers small amounts of exergy as low temperature heat. LCEA must therefore be carried out as a natural part of the design of renewable energy systems in order to certify a sustainable resource use. Another case to investigate is the production of biofuels in order to replace fossil fuels in the transport sector. This may not necessarily be sustainable since the production process uses a large amount of fossil fuels, directly for machinery or indirectly as fertilizers, irrigation and pesticides. Thus, it may well turn out to be better to use the fossil fuels in the transport sector directly instead. This will be well described by a LCEA.

Sustainable engineering could be defined as the use of renewable resources in such a way that the input of non-renewable resources will be paid back during its life time, i.e. $E_{\mathrm{pr}} > E_{\mathrm{in}} + E_{\mathrm{indirect}}$. In order to be truly sustainable the used non-renewable resources must also be completely restored or, even better, not used at all. Thus, by using LCEA and distinguishing between renewable and non-renewable resources we have an operational method to define sustainable engineering.

LCEA diagrams are of particular importance in the planning of large scale renewable energy systems of multiple plants. Initially, this system will consume most of its supply within its own constructions phase. However, some time after completion it will deliver at full capacity. Thus, the energy supply over time is heavily affected by internal system dynamics.

5. Exergy and economics

Exergy measures the physical value of an energy resource. Thus, it relates to the economic value, which reflects its usefulness. This makes exergy a valuable energy policy tool.

In order to encourage the use of sustainable resources and to improve resource use, an exergy tax could be introduced. The use of non-renewable resources and its waste should be taxed by the amount of exergy it accounts for, since this is related to depletion of resources and an environmental impact. In addition to this, toxicity and other indirect environmental effects must also be considered. In the case of irreversible environmental damage, a tax is not suitable, instead restrictions must be considered. Eventually, this should also be the case for the depletion of assets from future generations. At least it indicates a moral dilemma.

A system could be regarded as a part of two different environments, the physical and the economic environment. The physical environment is described by pressure P_0, temperature T_0, and a set of chemical potentials μ_{i0} of the appropriate substances i, and the economic environment by a set of reference prices of goods and interest rates. These two environments are connected by cost relations, i.e. cost as a function of physical quantities (Fig. 8).

With the system embedded in the physical environment, for each component there are mass and energy balances needed to define the performance of the system. In addition, these balances describe the physical behavior of the system.

If the cost relations are known, then the physical and economic environments could be linked. The cost equations can sometimes be simplified to a scale effect, times a penalty of intensity. Then the system of lowest cost, which is physically feasible, can be found. Usually the maintenance and capital costs of the equipment are not linear functions, so in many cases these costs have more complex forms. If, by some reason, it is not possible to optimize the system, then at least cost could be linked to exergy by assuming a price of exergy. This method is called Exergy Economy Accounting (EEA).

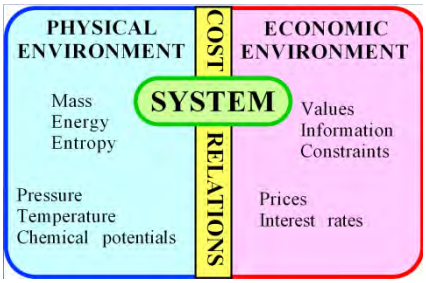

Fig. 8. The system surrounded by the physical and the economical environments, which are linked through cost relations.

Since exergy measures the physical value, and costs should only be assigned to commodities of value, exergy is thus a rational basis for assigning costs, both to the interactions that a physical system experiences with its surroundings and to the sources of inefficiency within it. The exergy input is shared between the product, and the losses, i.e. destruction and waste.

EEA simply means determining the exergy flows and assigning economic value to them. Thus, EEA does not include consideration of internal system effects. It does not describe how the capital investments in one part on the system affect exergy losses in other parts of the system. In the EEA method the exergy losses are numbers and not functions. However, this simple type of analysis sometimes gives ideas for, otherwise, not obvious improvements, and a good start of an optimization procedure, in which the exergy losses would be functions.

When constructing a system, the goal is often to attain the highest possible technical efficiency at the lowest cost, within the existing technical, economical and legal constrains. The analysis also includes different operating points (temperatures, pressures, etc.), configurations (components, flow charts, etc.), purpose (dual purpose, use of waste streams, etc.), and environments (global or local environment, new prices, etc.). Usually, the design and operation of systems have many solutions, sometimes an infinite number. By optimizing the total system, the best system under the given conditions is found. Some of the general engineering optimization methods could be applied, in order to optimize specific design and operation aspects of a system. However, selecting the best solution among the entire set requires engineering judgment, intuition and critical analysis. Exergy Economy Optimization (EEO) is a method that considers how the capital investments in one part of the system affect other parts of the system, thus optimizing the objective function. The marginal cost of exergy for all parts of the system may also be calculated to find where exergy improvements are best paid off.

6. Final words

These tools must be incorporated with energy engineering and policy to develop sustainable energy systems. My own experience from education is a strong positive feedback from the students and parts of the educational establishment, e.g., the UNESCO project *Encyclopedia*

of Life Support Systems (EOLSS) [12]. However, sometimes there is also a strong skepticism among the academic establishment for this that also has to be dealt with. Thus, traditional boarders between different disciplines must be removed and more of interdisciplinary studies and activities must be applied at both high school and university levels. More problem oriented approaches and a focus on sustainable development issues are also to be encouraged.

7. Conclusions

Exergy based tools are excellent to describe the utilization of renewable energy resources and important within sustainable energy engineering. A system that consumes the exergy resources at a faster rate than they are renewed is not sustainable. The educational system has a crucial role to play to introduce these tools in order to promote education for sustainable development. This education must be based on a true understanding of our physical conditions. Exergy is a concept that offers a physical description of the life support systems as well as a better understanding of the use of energy and other resources in society. Thus, exergy and descriptions based on exergy are essential for our knowledge towards sustainable development.

8. Acknowledgements

The permission to use my work for the UNESCO's Encyclopedia of Life Support Systems [12] for this paper is hereby gratefully acknowledged.

References

[1] S. Carnot, Réflections sur la puisance motrice du feu et sur les machines propres a développer cette puissance, 1824, R. Fox, Paris, Bachelier, 1978.

[2] J.W. Gibbs, A Method of Geometrical Representation of the Thermodynamic Properties of Substances by Means of Surfaces, Trans. Conn. Acad, vol. II, 1873, pp. 382-404.

[3] Z. Rant, Exergie, ein neues Wort für 'technische Arbeitsfähigkeit'. (Exergy, a New Word for Technical Available Work), Forschungen im Ingenieurwesen, vol. 22, 1956, pp. 36-37.

[4] M. Tribus, Thermostatics and Thermodynamics. New York: Van Nostrand, 1961.

[5] E. Sciubba, and G. Wall, A Brief Commented History of Exergy from the Beginnings to 2004, Int. J. of Thermodynamics, vol. 10, 2007, pp. 1-26.

[6] G. Wall, "Exergy — a Useful Concept within Resource Accounting", Report No. 77-42, Institute of Theoretical Physics, Göteborg, 1977. http://www.exergy.se/ftp/paper1.pdf.

[7] G. Wall, "Exergy — a Useful Concept" Ph.D. thesis, Chalmers University of Technology, Göteborg, Sweden, 1986. http://www.exergy.se/ftp/thesis.pdf.

[8] The Exergoecological Portal, http://www.exergoecology.com.

[9] Szargut J, Morris D. Cumulative exergy consumption. Energy Research, vol. 11, 1987, pp. 245–61.

[10] M. Gong and G. Wall, "On Exergy and Sustainable Development − Part 2: Indicators and methods", Exergy, an International Journal, vol. 1, 2001, pp. 217-233.

[11] Schleisner L. Life cycle assessment of a wind farm and related externalities. Renewable Energy, vol. 20, 2000, pp. 279–88.

[12] EOLSS, Encyclopedia of Life Support Systems. www.eolss.net.

Policy intervention and technical change in mature industry: The Swedish pulp and paper industry and the biorefinery

Kersti Karltorp[1,*], Björn A Sandén[1]

[1] *Chalmers University of Technology, Department of Energy and Environment, Gothenburg, Sweden*
**Corresponding author. Phone:+46 317724907, E-mail: kersti.karltorp@chalmers.se*

Abstract: Energy technologies based on biomass conversion are put forward as major means to curb climate change and enable a transition to a carbon neutral society. Many policies at international and national level are set up to support this transition. The pulp and paper industry is strongly linked to the conversion of biomass in Sweden and have a decisive role for the future of these technologies. This study aims to describe and explain the Swedish pulp and paper industry's reaction to policy with regard to the development of biorefineries. It turns out that firms are developing along two technological trajectories; 1) gasification for fuel production with a business model similar to the current one and 2) separation and refining for production of high value products, which requires a modified business model. Firms are also repositioning themselves within the regime and across regime borders. We conclude that the regime is in a phase of fragmentation. The policy implications from this analysis are that effective policy intervention needs to consider that multiple signals that are affecting the regime and policies should be designed depending on what degree of regime fragmentation that is desirable.

Keywords: *Energy policy, Biorefinery, Pulp and paper industry, Multilevel perspective, Incumbent firm strategy*

1. Introduction

A transition to a carbon neutral society will require extensive efforts to curb climate change. This involves large-scale changes in the energy system, switching from fossil to renewable energy sources. In Sweden increased use of biomass is considered as one step along this path, since the country has large biomass resources. Policies at international and national level, e.g. EU's directive on promotion of use of energy from renewable sources and the green certificates in Sweden, put forward energy technologies based on biomass conversion as major means to enable this transition. The pulp and paper industry in Sweden is strongly linked to the development of energy technologies based on biomass conversion, since the industry are in control of a large proportion of the biomass flow and have extensive knowledge of technologies based on biomass feedstock. Thus the industry can effectively hinder or induce the development of these technologies and consequently the transition that large-scale diffusion of these technologies could permit. Implementation of this type of technologies in the pulp and paper industry is often referred to as conversion of pulp and paper mills to biorefineries, i.e. a plant that efficiently use the incoming biomass to produce chemicals and energy simultaneously or instead of conventional fibers for paper products (definition inspired by [1]). Moreover, the pulp and paper industry is a large actor in the Swedish society, employing around 23,000 people in the country and contributing to 11% of Swedish exports [2]. Due to the strong link to biomass conversion and the size of the industry, it is an important actor for the development of biorefineries in Sweden. Policies' strong incentive for development of these technologies and the pulp and paper industries central role for biomass conversion make it important to understand the industry's reaction to policy. This study aims to describe and explain the Swedish pulp and paper industry's reaction to policy with regard to the development of biorefineries. In order to describe how the regime, that constitutes the Swedish pulp and paper industry, is reacting this article combines literature on transition and strategy.

2. Methodology

This section describes how data was collected and the theoretical framework used for the analysis.

2.1. Data collection

For this study data was collected 2009-2010, through semi-structured interviews with representatives (often technical directors) from the Swedish pulp and paper industry. Other stakeholders, e.g. Universities and research companies, were also interviewed. The companies interviewed for this study represents more than 75% of the pulp and paper production in Sweden. The study is mainly focusing on the companies' operations in Sweden, even though it can be difficult to isolate international companies' strategies and actions to one country.

2.2. Theoretical framework

What policy that is viewed as effective in the steering of technical change processes depends on what model that is used to understand the system. A simple model could be that policy is seen as a signal going into the system urging the system to react. In contrast to this model, empirical evidence suggests that the adoption and wide diffusion of novel technologies tends to take many decades [3] and that incumbent firms are unwilling to make radical changes but tend to focus on incremental change along a trajectory within the prevailing technological paradigm [4, 5]. Nevertheless, over longer time frames the economy is characterised by the emergence, development and decline of different industries [6, 7]. Rip and Kemp [8] suggested a three layer model of technical change, further developed by Shot and Geels [9, 10] to explain the dynamics of such technological transitions. The intermediate layer, called the 'regime level', is constituted by a well-established socio-technical system that provides a function or a set of products. This includes the incumbent firms in an industry, consumers and other involved actors as well as technical infrastructures and production systems and the regulatory, normative and cognitive rules deciding what is allowed, desirable and sensible. At a micro level new technological options grow in 'niches'. Over time these may challenge the existing regime and form new systems. It is argued that such change is made possible by changes at a higher society wide macro level, the 'socio-technical landscape', which put pressure on the regime and destabilizes it and thereby opens windows of opportunities for niche technologies [9].

In the multi-level perspective (MLP) tradition it is recognised that regime change can take many pathways [10]. Additionally, as has been recognised before in the literature on economics of innovation [e.g. 7], incumbent actors may have critical roles also in radical change processes [10]. New biomass conversion technologies need to be linked up to biomass flows already governed by mature industries. This may indicate that biorefineries are more likely associated with a 'transformation path' [10], rather than more disruptive transition patterns. If such a transformation path is to be guided by policy, we believe it is crucial to develop more refined descriptions of regime dynamics. In the MLP literature 'the regime' tends to be treated at a highly aggregated level. To trace the emergence of regime fragmentation and transformation processes we see a need to decompose this aggregate. More specifically, we believe that much could be gained if the implications of the diversity among incumbent firms were studied more closely. To this end the literature on firm strategy can contribute.

According to Porter [11], a firm should strive to create a unique and valuable position. There are two strategies to achieve this. Either the firm should try to perform different activities

compared to its rivals or it should perform the same activities as its rivals, but perform them differently. In addition, the strategy should protect the industry structure, rather than threaten it since this could result in decreased industry profitability. Thus from Porter's perspective incumbent firm gain the most by diversifying its activities, but only so much that they still reinforce the prevailing industry regime. Porter also stresses the importance of clusters for driving direction and pace of innovation [12]. Another perspective is offered by the resource based view, in which e.g. Grant [13] claims that a competitive position is best explained by the firm's resources and capabilities. Firms should identify its internal resources and skills and match these against the opportunities and risks created by its external environment. However, incumbent firms often find it difficult to adapt to changes at the landscape level if it requires strategies that are not aligned with its core capabilities, which then can become core rigidities [14]. Additionally, firms are not acting in accordance with some universal rationality. Instead, they are guided by mental models, which are used as a filter to simplify reality and enable decision making [15]. These models are based on successes and failures of previous actions, but are seldom explicit. Yet, these models are only valid as long as the variables and circumstances they are based on are not changed [15]. Thus changes at the landscape level could imply that a new mental model must be developed in order to make better decisions.

In combination these views on firm strategy suggest that if we want to understand regime response to multiple landscape pressures and new technological opportunities we need to take into account the relative positioning of firms in industries, geographical clusters, the firms' capabilities and their individual historical experiences of success and failure.

3. A multilevel perspective on the Swedish pulp and paper industry

This chapter describes the Swedish pulp and paper industry from a multilevel perspective, including the industry structure at a regime level, changes at a landscape level and finally technological developments at a niche level.

3.1. Industry structure at regime level

The companies within the Swedish pulp and paper industry have different characteristics and prerequisites for development and implementation of biorefinery options. From a technical perspective, the type of mill is important. Most mills are integrated mills, which mean that they have both pulp and paper production at the same site [16]. Integration of biorefinery options is of interest in pulp mills, which can be divided into two categories mainly mechanical, i.e. the raw material is grinded mechanically, or mainly chemical, i.e. the raw material is treated with chemicals and heat to degrade and dissolve the lignin from the cellulose and hemicelluloses [16]. Due to the large flow of by-products in chemical processes there are many opportunities for integration of biorefinery solutions in chemical pulp mills.

Within the industry, there are large variations in firm size and extent of vertical integration, ranging from firms operating one single mill, e.g. Domsjö Fabriker, to large multinational companies, e.g. Stora Enso. The diversity in the industry is illustrated in Fig. 1, in which the extent of vertical integration and difference in size are shown for six Swedish pulp and paper firms.

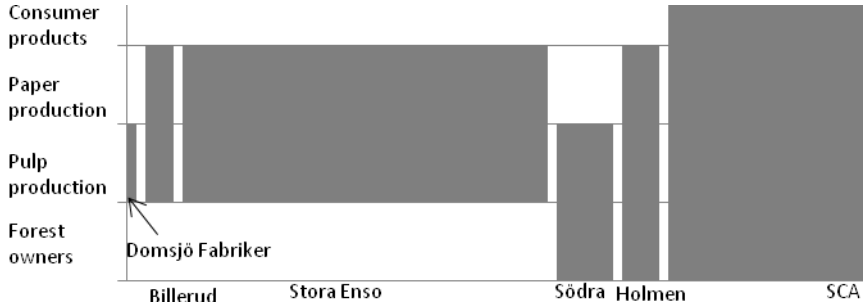

Fig. 1 The diversity in vertical integration and firm size for six Swedish pulp and paper firms. The value chain is characterised by four segment; forest ownership (ownership of 50% or more of raw material requirements), pulp production, paper production and production of consumer products. The size is indicated by relating the number of employees to the size of the bar that represent each firm.

Firms' actions are also governed by the mental models. One example of two different mental models of company leaders could be seen when Domsjö Fabriker was created in 2000, as a result of a small group of people buying the pulp mill from the corporation MoDo. In contrast to the former owner the new owners were convinced that the unprofitable pulp mill could be transformed into a modern biorefinery [17].

3.2. Landscape changes

We can identify three main trends at the landscape level that are influencing the industry: changing patterns of demand for paper, economic and industrial development in South America and Asia and increased political attention to energy and environmental issues. While none of these have unambiguous effects, all of them create tension at the regime level.

During the last decades the printed media has experienced competition from electronic media, the industry has experienced decreasing demand, particularly for news print [18]. On the other hand, demand for personal care products is increasing as living standards are raised in many countries. The same applies for packaging products, probably as a result of the debate on climate change that has emphasised the importance of renewable materials [19].

The European market is the main market for most Swedish pulp and paper companies and Sweden's part of the supply has increased at the same modest pace as the European consumption [18]. The rapid economic growth in other parts of the world opens potential new markets. However, increased production capacity in South America and Asia reduces the possibility for European companies to take advantage of these emerging markets. Instead, these companies face competition from firms outside Europe with lower production and feedstock costs.

The debate on climate change and security of energy supply has resulted in raised prices on electricity and fuels, which has increased the production cost for the European pulp and paper industry. European mills have become more energy efficient, less fuel oil and other fossil fuels are used and the fraction of biomass in total fuel consumption has increased [20]. These trends are also valid for the Swedish pulp and paper industry, which produces more electricity with back-pressure power and deliver more heat to nearby communities [18].

3.3. Technological developments at niche level

The technological development of biorefineries has been going on for decades and can be divided into two main technological fields; 1) gasification and 2) separation and refining. In Sweden, the development of the gasification started in the 1970s with an emphasis on production of methanol, mainly through gasification of coal and peat, but biomass was also considered as a possible fuel [21]. As the focus shifted to ethanol produced by enzymatic hydrolysis in the 1980s, gasification was no longer prioritized. Despite this the competence about the technology lived on in the electricity sector [21]. In the mid 1990s to early 2000s the gasification technology re-emerged in three parallel tracks; biomass gasification for production of dimethyl ether (DME) or Fisher Tropsch (FT) diesel and finally gasification of black liquor to produce methanol [21]. The future development of both gasification and enzymatic hydrolysis for ethanol production is now dependent of successful pilot and demonstration plants. Some technologies have, however, reached a commercialisation state for example LignoBoost, which is a process for lignin extraction and an example of a separation technology. Södra is today working on a plant in commercial scale and research for future applications of lignin is going on in parallel [22].

4. Regime response

The result of changes at landscape level and technological niche developments can be seen in the regime, as the first signs of a fragmentation becomes visible. We identify restructuring along two different technological trajectories. We also observe repositioning within existing value chains and more radical repositioning, i.e. repositioning that transcends traditional industry boundaries.

4.1. New technological trajectories

Biorefinery concepts offer new business opportunities for an industry regime under pressure from landscape changes. However, while fuel production from the large biomass resource of the Swedish forests has been a primary target for Swedish Energy Authorities since the end of the 1970s, the Swedish pulp and paper industry has demonstrated little interest [21]. With the increased pressure over the last couple of years this is now slowly changing. While few companies have gone so far that they have actually started to implement biorefinery technologies many are now becoming engaged in research and investigations of options that can convert their mills into biorefineries. In different ways, the companies try to match the new technological options with their existing processes and business models. At this point we can distinguish two main technological trajectories.

4.1.1. Gasification and fuel production

The first trajectory is centred on gasification technologies. Biomass or black liquor can be used as raw material for this process. The product is syngas, which can be used for the production of a spectrum of refined products for example methanol, methane, DME, FT diesel and hydrogen. Companies that are interested in gasification of biomass or black liquor tend to focus on production of bio fuels rather than chemicals, which equally well could be produced. In most cases the companies are interested in gasifying low grade biomass in parallel to continued production of pulp or paper. The business model behind this strategy seems to rely on the possibility to sell large volume of fuel, in a similar way as pulp or paper are sold today. However, additional biomass will be needed for implementation of these technologies.

Stora Enso motivates its preference for biomass gasification technology with the argument that it is flexible in the choice of end product and in the choice of raw material, thus different

raw materials could be used at different geographical locations [19]. The preference for transportation fuels is driven by the competences their partner, Neste Oil, has in this field and the belief that the production of fuels can contribute more to prevent climate change than production of materials [19]. The arguments for this option reflect the present business model's focus on efficient production of bulk products. While implying major investments in new technology, the change in business model is minor and the core business of producing pulp and paper is not questioned.

4.1.2. Separation and refining to high value products

The processes employed in the second trajectory are typically enzymatic processes, hydrolysis and fermentation. Compared to gasification technology the choice of process is linked more directly to a specific product. Companies in this trajectory have a broader perspective on the kind of products they could produce in the future; chemicals, materials or possibly fuels. The business model linked to these products focuses on the possibility to sell small quantities of these products at a high price. One key argument for this strategy is to use the full potential of the fiber in biomass. The industry has traditionally done a lot of research on cellulose fiber. Consequently, utilising knowledge about cellulose fibers for production of materials and chemicals relates to one of the industry's core competences.

Södra with their implementation of the LignoBoost technology and Domsjö Fabriker's production of specialty cellulose for production of viscose clothes are both examples of development along this trajectory. These firms have in common that they operate (non-integrated) chemical pulp mills. Södra has investigated many different technological options, driven by the will to extend capacity at its mills and the need to find new energy carries to increase the export of energy from the mills [22]. The outspoken argument for production of specialty cellulose, for the clothes market, at Domsjö is that cotton is claimed to be less environmentally friendly due to the large quantities of chemicals and water that is used for its production. Hence, materials produced from forest products, like viscose, could offer a more environmentally friendly solution [23]. Since the amount of raw material needed for realization of options along this trajectory could be small, the original process could be affected to a minor extent and additional biomass is not necessarily needed. In this way companies can create more value from the same input. There are, however, technological options along this trajectory that would include the entire raw material flow, such as production of ethanol from cellulose, but none of the interviewed companies show any signs of interest in restructuring its processes entirely for this process.

4.2. Repositioning within a regime and across regime borders

Vertical integration is a strategy that could be used to achieve a competitive position within an industry. For SCA, which has a high degree of vertical integration (see Fig. 1), it seems to have been a successful choice to keep its forests and at the same time pursue a vertical integration towards personal care products [24]. Billerud is another example of a firm that shows a tendency to extend its vertical integration as they have initiated a co-operation with a well-pap packaging company, which contributes to increase Billerud's access to the market for transportation of fruit and vegetables [25].

One example of a more radical repositioning, i.e. repositioning beyond current value chains or across regime borders, is the joint venture between Stora Enso and Neste Oil for development of gasification technology and transport fuels [19]. Smaller firms seek collaboration in local clusters, e.g. in the area around Örnsköldsvik a cluster involving research company,

universities, municipalities and the pulp producing company Domsjö Fabriker are working together to develop 'the biorefinery of the future'. In southern Sweden, Södra has been operating closely with the research organisation Innventia and Chalmers University of Technology. Within this cluster there is a shared belief in the development of high value products that can be produced in parallel to the existing pulp process. The repositioning between regimes indicates that a radical form of regime fragmentation involving several industry regimes may wait around the corner. The growing use of biomass for energy has made utility firms interested in biomass as a source of energy. The development of different types of biorefinery concepts for production of chemicals or fuels also attracts the chemical industry, the oil and gas industry and the car industry.

5. Conclusions

Political attention to energy and environmental issues has resulted in policies aiming at increased implementation of biorefinery concepts. However, this is not the only signal urging the industry to react. The Swedish pulp and paper industry regime is affected by several landscape changes and technological niche developments. Furthermore within the regime the firms have different prerequisites to react to policy and other external signals. The industry's reaction is characterised by technological development along two technological trajectories and a third trajectory of repositioning (partially overlapping the technological trajectories) within the regime and across regime borders, see Fig. 2. This can be regarded as a phase of fragmentation of the Swedish pulp and paper industry regime, but it is by no means clear where this regime fragmentation will end.

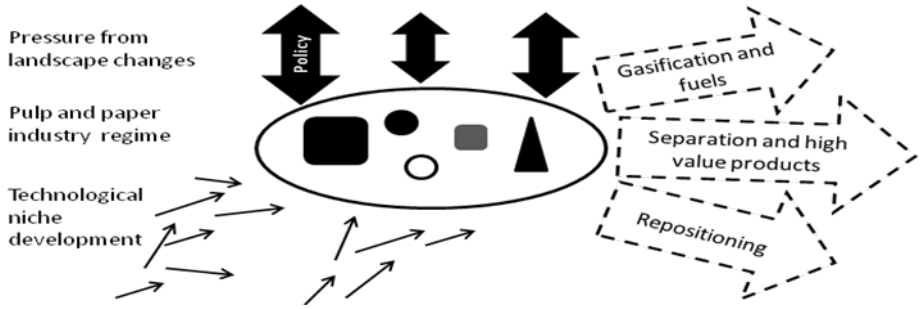

Fig. 2 The Swedish pulp and paper industry is affected by pressure from landscape changes, including policies, and technological niche developments. Furthermore within the regime the firms have different prerequisites for their reactions. The Swedish pulp and paper industry regime is restructuring itself along several trajectories initiating a phase of fragmentation.

In this context, policy makers need to consider how much fragmentation that is desirable. Strong policies will guide the industries towards a more uniform response, which could be attractive for achieving a rapid diffusion of novel technologies. A less forceful policy might encourage several trajectories to be followed in parallel, which could be desirable if policy makers have doubt about which technologies to diffuse and therefore would like several technologies to be developed and diffused.

References

[1] Ö. Larsson and B. Ståhl, More refined products – Wood based biorefineries increase the prices per kilo on wood (in Swedish), Vinnova, 2009.

[2] Pappers – Swedish Paper Workers Union, 2010, accessed 2010-08-26 at www.pappers.se.

[3] A. Grübler, Time for a change: On the patterns of diffusion of innovation, Daedalus 125 (3), 1996, pp 19-42.

[4] R.R. Nelson and S.G. Winter, An evolutionary theory of economic change, Belknap Press of Harward University Press, 1982.

[5] G. Dosi, Technical paradigms and technological trajectories, Research Policy 11, 1982, pp 147-162.

[6] C. Freeman and F. Loucã, As Time Goes By: From the Industrial Revolutions to the Information Revolution, Oxford University Press, 2002.

[7] F. Malerba and L. Orsenigo, The dynamics and evolution of industries, Industrial and Corporate change 5(1), 1996, pp 51-87.

[8] A. Rip and R. Kemp, Technological Change in Human Choice and Climate Change, S. Rayner and E.L. Malone Editors, Battelle Press, 1998, pp 327-399.

[9] F.W. Geels, Technological transitions as evolutionary reconfigurations processes: a multi-level perspective and a case-study, Research Policy 31, 2002, pp1257-1274.

[10] F.W. Geels and J. Schot, Typology of sociotechnical transitions pathways, Research Policy 36(3), 2007, pp 399-417.

[11] M.E. Porter, What is strategy, Harvard Business Review November-December, 1996, pp 61-78.

[12] M.E. Porter, Clusters and the new economics of competition, Harvard Business Review November-December, 1998, pp 77-90.

[13] R.M. Grant, The Resource-Based Theory of Competitive Advantage: Implications for Strategy Formulation, California management Review 33, 1991, pp 114-135.

[14] D. Leonard-Barton, Core Capabilities and Core rigidities: A Paradox in Managing New Product Development, Strategic Management Journal13, 1992, pp 111-125.

[15] R. Foster and S. Kaplan, Creative Destruction - Why companies that are built to last underpreform the market and how to successfully transform them, Doubleday, 2001.

[16] G.A. Smook, Handbook for pulp and paper technologists, Angus Wilde Publications Inc, 2002.

[17] M. Norlin, Interview with Director at the board at Domsjö Fabriker, 2010.

[18] Swedish Forest Industries, Facts and Figures 2009, 2009 (electronic format can be found at http://www.skogsindustrierna.org).

[19] A. Jääskeläinen, Interview with SVP Biorefining and Bioenergy at Stora Enso, 2009.

[20] CEPI, Key Statistics 2009 – European Pulp and Paper Industry, 2010.

[21] B. A. Sandén and K. M. Jonasson, Variety Creation, Growth and Selection Dynamics in the Early Phases of a Technological Transition -The Development of Alternative Transport Fuels in Sweden 1974-2004, Chalmers University of Technology, 2005.

[22] A. Andersson, Interview with Energy Coordinator at Södra Cell, 2009.

[23] P. Blomqvist, Interview with Manager of DomInnova at Domsjö Fabriker, 2010.

[24] A. Andersson, Interview with Director Technical Development at SCA Forest Products, 2010.

[25] M. Wikström, Interview with Technical Director at Billerud AB, 2009.

Incentive regulation of CHP performance

Aviel Verbruggen

University of Antwerp, Antwerp, Belgium
Tel:+32 476 888 239; E-mail: aviel.verbruggen@ua.ac.be

Abstract: Main contentious issues of public regulation to support CHP as an efficient thermal power cycle are discussed. First the merit of CHP is defined as the transformation of residual heat in conventional power plants into useful heat; this merit suffices to rank CHP activity prior to standard thermal power generation wasting the heat. Second, the main metrics of CHP performance is the amount of co-generated electricity requiring uncontested identification when CHP activity is mixed with condensing power generation (mainly in extraction-condensing steam turbines). The proper method is based on design characteristics of CHP processes, not on arbitrary averages as CEN proposes. Therefore, the novel concept of "bliss point" of a CHP activity is developed. Third it is argued why co-generated power – clearly measured – is a sufficient performance indicator. Additional qualifications based on external benchmarks (as the EU-Directive allows) may imply perverse incentives in impeding CHP development qualitatively and quantitatively. The difference between perverse and benign regulations explains the wavering position of the EU-2004 Directive on the promotion of CHP.

Keywords: *CHP quality, Power-to-heat ratio, EU Directive, Incentive Regulation, Benchmarking*

Nomenclature

E	*Electricity or power ..... MWh or MW*	β	*power loss factor .....*
F	*Fuel energy or fuel flow..... MWh or MW*	σ	*power-to-heat ratio.....*
Q	*Heat energy or heat flow ..... MWh or MW*	η	*efficiency.....*

Acronyms for activities CHP = Cogeneration; Cond = Condensing; Plant = both activities

1. Introduction

Cogeneration or Combined Heat & Power (CHP) is as old as its natural cradle, the thermal power plant that after power extraction dumps all residual heat in the environment. Diverse CHP technologies are applied in plants ranging from a few kW to a few hundreds MW. CHP diffusion in countries with similar economies is uneven, due to diverging energy policies and according regulations. CHP is in principle more energy efficient than its counterpart that dumps the residual heat. Public policy in favor of efficient fuel use also supports CHP. This was intended by EU-Directive 2004/8/EC [1], but not confirmed by effective and efficient regulation. This section introduces the subject. Section 2 highlights different visions on the merit of CHP, determining the acceptability of proposed policies. Quality of CHP is shown to equal quality of standard thermal power generation, and "CHP-specific" qualification is not needed. Section 3 covers the issue of defining and measuring CHP activity in a transparent and accurate way. Section 4 shows how external benchmarking of CHP plants can be the source of very perverse incentives for the development of CHP. A brief conclusion follows.

1.1. CHP support

Why should the EU support CHP in itself? Many argue that support is only warranted when CHP delivers a reduction in CO_2 emissions and/or reduction in fuel combustion because high efficiency separate heat and power generation might be better in reducing CO_2 than a low efficiency CHP facility. The latter argument points to the core issues of what about CHP is why supported. During the 2004 EU Directive's preparation phase proposals abounded to evaluate along CHP other aspects like the type of fuel used or the amount of reduced CO_2 emissions. However well intended, this debate created confusion and obliterated the attention for the core duty: what attributes or results of CHP are eligible for support? Poorly answering

this question backfires on the good regulatory intentions when biased methods of CHP qualification are applied (section 4).

The core task is accurately identifying what CHP activity means, in particular in plants that simultaneously mix CHP and condensing power generation. Once CHP activities are fully characterized it is possible to discuss what aspects of that activities may be promoted and supported, and how this can be done in the most transparent and effective way.

1.2. Incentive regulation

Incentive regulation sets the factors right that improve the economics of CHP activities. It obeys the overall standards of proper regulation such as: identify precisely what is the object of regulation; select the appropriate variables to monitor and measure the object; preclude arbitrary values or averages; specify specific but similar rules for similar cases to minimize discrimination; promote stated goals by appropriate rules and incentives. The promotion of CHP as a competitive power generation practice needs consideration of salient aspects like: optimize technical characteristics and select high power-to-heat ratios; stimulate economies of scale and high capacity factors by opening a large market for both outputs of CHP plants; guarantee fair terms for exchanges of power (as surplus, make-up, or back-up flows) with the grid. The latter terms significantly impact the development of any independent and decentralized power generator. But for CHP the complexity increases because the joint outputs power and heat are delivered to separate markets. When regulations truncate CHP's freedom of operation on the power market the economics of CHP deteriorate.

One peculiar aspect of the EU CHP Directive is the adoption of external benchmarking as the basic method for qualifying the outputs of CHP plants. Generally benchmarking is '*the continuous, systematic process of comparing the current level of own performance against a predefined point of reference, the benchmark, in order to evaluate and improve the own performance*' [2]. The choice of benchmark is crucial because the own performance is measured as a 'distance-to-targets' with the benchmark characteristics as targets, and because the own activity is changed to resemble the benchmark as much as possible. When benchmarking is applied in a private context, the actor controls the selection of targets and the degree and pace of approaching the targets. The actor can accommodate fuzzy aspects in definitions, data availability and methods applied. In a public regulatory context the definitions must be based on argued, transparent and robust methods requiring indicators that are measured in an uncontested way. The first issue is whether the benchmarking framework as such makes sense, i.e.: are the benchmarks valid references for improving the regulated subject's performance? (e.g. do they belong to comparable categories?). When diversity is too high, it is problematic to screen and evaluate diverse participants (competitors) on a particular performance, in particular when followed by remunerations or penalties.

1.3. CHP performance

What variables can express CHP performance? Using the recovered heat $\mathbf{Q_{CHP}}$ as indicator is not recommended because investors and operators are not stimulated towards high-quality cogeneration activity. Also as an additional indicator there are few arguments to include the heat output variable, neither when taking the quality of the useful heat into account [3]. While heat at higher temperature corresponds to a higher availability (quality) of the energy flows, rewarding this in CHP activities counteracts the incentives to reduce the applied temperatures of heat end-uses in buildings and processes. The lower the useful end-use temperatures of heating applications can be set, the more "nearby waste" heat flows can be recuperated, the more ambient heat sources can be included (solar heating, heat pumps) and the more efficient

cogeneration systems can be inserted (in particular Rankine cycles). The necessary and sufficient CHP performance indicator is the amount of co-generated electricity $\mathbf{E_{CHP}}$ when measured accurately. Because $\mathbf{E_{CHP}} = \boldsymbol{\sigma}.\ \mathbf{Q_{CHP}}$ maximizing $\mathbf{E_{CHP}}$ includes incentives to maximize heat recovery ($\mathbf{Q_{CHP}}$) and quality (power to heat ratio $\boldsymbol{\sigma}$) of the CHP activities.

2. CHP Merit and Quality

Opposite visions on the merit of CHP in the energy economy create diverging propositions about CHP's role with impact on its valuation (2.1). There is much fuss about quality of CHP processes, but does quality differ for CHP and non-CHP thermal power processes? (2.2).

2.1. Opposite visions on the merit and role of CHP

Policy starts with a vision on the subject of regulation. Visions on the merit and the role of CHP range from Promoting to Blocking CHP development (Table 1). One favors the development of CHP when taking the position that the merit of CHP is in recovering all or part of the heat being otherwise discarded to the environment in a thermal power plant. Adding additional tests upon this basic merit leads to fencing in the application of the CHP principle. For example one can require that CHP plants perform a factor X better in generating power and heat jointly than the best available references of separate generation technologies (power condensing plants and heat only facilities). External benchmarks provide valuable information to a would-be investor in CHP capacity and to the operator of existing CHP facilities, but must be handled more carefully in a regulatory context (see section 1.2).

Table 1: Promoting and blocking views on the merit and role of CHP

	Promoting CHP	Blocking CHP
CHP Merit	Use of – all or part of – the discarded fatal heat at thermal power plants	CHP has but merit when it excels above the best separate power and heat benchmarks
CHP Role: who first?	CHP dominates the condensing only thermal power generation cycle, and therefore is, ceteris paribus, preferred. Valid is also part recovery of fatal heat.	Limit CHP to full heat loading operations. As a corollary: obstruct CHP plants operating in part/full condensing mode

When the basic merit of CHP is recognized it is logical to attribute priority to the CHP mode above the condensing only mode for investing in thermal power plants[1]. The blocking vision sees the role of CHP very restrictive to particular joint power-heat load conditions where a full heat load can be guaranteed 'all the time'. This attitude also fences the entry to the power market by setting particular tariffs for power exchanged between the CHP facility and the interconnected grid. Unfair conditions for exchanging power with the grid are main barriers to a balanced development of CHP in both the heat and the power markets [4].

2.2. The quality of thermal power and of CHP

CHP is always based on some thermal power generation cycle. The latter is its natural cradle and determinant of the performance, economics and quality of the CHP process. Every thermal power process rejects residual heat in the environment. The merit of CHP is to

[1] In Denmark the 1979 Heat Supply Act has made this principle reality.

recover part or all of this heat and transform it into 'useful' heat. Some CHP processes (steam turbines) occasion a loss of power output when condenser heat is upgraded to useful heat. The power loss **β** is almost proportional to the temperature of the extracted heat (steam) from the turbines, and therefore it is important to minimize the required temperature of the heat applications that are supplied by CHP processes. Gas turbines, internal combustion engines, some fuel cells, do not occasion significant power loss because generally the temperature of the rejected heat is sufficiently high for the heat end-use purposes.

The quality of CHP processes is recorded by the power-to-heat ratio **σ**. There is no generally approved definition of this ratio. The metamorphosis of a condensing power process into CHP is happening by transforming residual heat into useful heat. Therefore the high (low) quality CHP process is embedded in a thermal power plant of high (low) electricity conversion efficiency (the linkage is further discussed in section 3.3).

3. Identifying and measuring CHP activity

The valid indicator of CHP activity is the amount of co-generated electricity $\mathbf{E_{CHP}}$ (section 1.3). For a thermal power plant without residual heat rejection, no $\mathbf{E_{CHP}}$ identification problem exists because all activity of the plant is combined and all electricity is co-generated. Defining this variable and measuring it when co-generation takes place *joined to* condensing power generation, is the problem to solve. In addition, but fully overlooked in the EU regulation, is it necessary to identify and measure the share of fuel consumed for the combined activity $\mathbf{F_{CHP}}$. The bottleneck holding up effective regulation by the EU Directive is identification, and so reliable measurement, of what precisely is CHP *activity*.

3.1. The EU CHP Directive [1] on measuring CHP activity

Annex II "Calculation of electricity from cogeneration" of the Directive opens with "Values used for calculation of electricity from cogeneration shall be determined on the basis of the expected or actual operation of the unit under normal conditions of use." Then it splits the approach in two cases. First, when the overall thermal efficiency of the operations exceeds 75% for steam back-pressure turbines, gas turbines with heat recovery, internal combustion engines, micro turbines, Stirling engines and fuel cells, all power generated is accepted to be co-generated. Analogously, an 80% efficiency threshold applies for CCGT with heat recovery and for steam condensing extraction turbines. Second, when overall efficiency falls short of the stated thresholds of 75/80 %, co-generated electricity $\mathbf{E_{CHP}}$ should be calculated according to the formula $\mathbf{E_{CHP} = \sigma . Q_{CHP}}$ with **σ** the power-to-heat ratio. Article 3(k) states "'power to heat ratio' shall mean the ratio between electricity from cogeneration and useful heat when operating in *full cogeneration mode* using *operational* data of the specific unit". The latter expression is not specified, although most CHP units cannot operate in full cogeneration mode. Hence the Directive's method is incomplete in identifying and measuring $\mathbf{E_{CHP}}$. By lacking the correct method, Annex II offers average default values by technology group, but this is "*notably for statistical purposes*".

The wrong answer to the difficulties in quantifying $\mathbf{E_{CHP}}$ is to negate the question, and proceed without solution. The EU does this by Annex III forgetting Annex II and qualifying cogeneration performance on the basis of mixed values with perverse effects for the development of CHP (section 4). The EU skips identification of fuel consumption $\mathbf{F_{CHP}}$, necessary to assess the efficiency $\boldsymbol{\eta_{CHP}}$ of the cogeneration activity of a thermal power plant. Simplifying estimations of $\mathbf{E_{CHP}}$ by splitting CHP activities in two groups, as Annex II does, increases the workability, but average 75/80% default efficiencies are arbitrary, not promoting "high efficiency CHP". Field data [5] document CHP efficiency ranges between 60 and 94%.

The Directive (Art.12) does not impose its immature methods, allowing member states the use of "Alternative calculations". Unsolved identification of CHP activity is not increasing harmonization, stated as a "general objective of the Directive" (Whereas n° 15). For overcoming the identification problem the novel concept of "bliss point" of a CHP process is developed in section 3.3.

3.2 The CEN manual [6] for Measuring CHP activity

The objective of the CEN Manual is "to present a set of transparent and accurate formulae and definitions for determination of CHP (cogeneration) energy products and the referring energy inputs. The CEN/CENELEC Workshop Agreement shall simply formulate the procedure for quantifying CHP output and inputs." CEN adopts the Directive Annex II proxy of splitting CHP plant outputs in above and below 75/80% average efficiency operations, the "above ones" seen as full CHP. For the "below ones", CEN addresses the disentangling of CHP from the *mixed* activity and searches to quantify both $\mathbf{E_{CHP}}$ and $\mathbf{F_{CHP}}$ values. CEN hereby distinguishes cogeneration processes *with* power output loss when recovering residual heat at the thermal power process from the ones *without* power output loss when heat is recovered. CEN focuses on extraction-condensing steam turbines[2] where mixed activity and power loss are prominent, with the added complexity that useful heat extraction may occur at several pressures (temperatures). For this most important and most complex CHP case CEN elaborates a seven-step approach [6, p.38-40], but steps 3 and 4 contain a "circular reference": $\mathbf{E_{CHP}}$ is calculated in step 4, but step 3 includes $\boldsymbol{\eta_{CHP}}$ whose assessment requires $\mathbf{E_{CHP}}$ (next to $\mathbf{Q_{CHP}}$ and $\mathbf{F_{CHP}}$). CEN escapes from its circular reference by applying "the CHP overall efficiency according to Annex II of the CHP Directive" [6, p.38], or more clearly: CEN adopts a fixed value of 75/80% for $\boldsymbol{\eta_{CHP}}$. Adopting averages does not cover the reality of CHP technologies and applications and ripples the CEN stated objective of "transparent and accurate formulae".

3.3. Closing the CHP identification and measuring gap: find the "bliss point"

A consistent regulation has no need for arbitrarily fixed parameters [7]. The first law of thermodynamics applied on a thermal power plant states: Fuel input = Electricity output + (Recoverable) Heat output + (Non-recoverable) Losses. For a CHP plant showing the split between CHP and condensing activities the law applies as (table 2):

$$\mathbf{F_{CHP} + F_{Cond} = E_{CHP} + E_{Cond} + Q_{CHP} + Q_{Cond} + Non\text{-}recoverable\ Losses}$$

Table 2: Energy flows in a CHP plant obey the First Law of Thermodynamics

	CHP	+ Condensing	= Plant
Fuel F =	F_{CHP}	F_{Cond}	F_{plant}
Electricity E	E_{CHP}	E_{Cond}	E_{plant}
+ Heat Q	Q_{CHP}	Q_{Cond}	Q_{plant}
+ Losses non-recoverable	-	-	L_{plant}

[2] CEN/CENELEC [6, p.14] considers backpressure steam turbines as units *without* power loss, based on the argument of complementary power and heat outputs. However, power loss in steam turbines is due to heat extraction at above ambient condensing regimes.

When $\mathbf{Q_{Cond}} = 0$, it follows $\mathbf{E_{Cond}} = 0$; $\mathbf{F_{Cond}} = 0$, and $\mathbf{E_{CHP}} = \mathbf{E_{plant}}$; $\mathbf{F_{CHP}} = \mathbf{F_{plant}}$. Rather than by adopting arbitrary 75/80% efficiency thresholds, all electricity is $\mathbf{E_{CHP}}$ when the plant does not deliberately reject heat. There may be peculiar conditions why the overall efficiency of a CHP plant falls short of the 75/80% thresholds, e.g. when the plant is combusting waste fuels. The distinguishing property among "mixed" and "pure" CHP plants is whether they reject – yes or no – recoverable heat. If "no" ("pure" CHP activity) the $\mathbf{E_{CHP}}$ identification problem vanishes because all power relates to cogeneration and the 75%/80% thresholds are of no use.

When cogeneration and condensing activities take place jointly none of the variables in table 2 equals zero, but directly observed are only: $\mathbf{Q_{CHP}}$, and the total plant flows $\mathbf{F_{plant}}$, $\mathbf{E_{plant}}$, $\mathbf{Q_{plant}}$, $\mathbf{L_{plant}}$. In order to split the fuel and electricity quantities in their CHP and condensing shares, two additional process characteristics are needed: $\boldsymbol{\eta_{cond}}$ or the condensing power efficiency when no cogeneration occurs, and the power loss factor[3] $\boldsymbol{\beta}$ of the transformation of $\mathbf{Q_{Cond}}$ into $\mathbf{Q_{CHP}}$ ($\boldsymbol{\beta}$ may be zero when no power is lost during that transformation, e.g. at gas turbine plants). Then all information is available to find the *bliss point* ***S*** and the *design* power-to-heat ratio $\boldsymbol{\sigma}$ of the CHP plant. The bliss points can be multiple and virtual, so also the ratio's $\boldsymbol{\sigma}$ can be multiple, but the $\boldsymbol{\sigma}$ are always real [7]. Fig. 1 shows the method graphically with efficiency units on both axes. The line AB assumes 100% efficiency with all fuel converted in electricity or recoverable heat (representing the fictive case of non-recoverable losses being zero). The parallel line XY subtracts from AB the non-recoverable losses, i.e. compared to line AB, XY represents $\boldsymbol{\eta_{CHP}}$ (the CEN proposal fixes XY = 0.75AB or = 0.80AB).

*Figure 1: Finding the bliss point **S** and power-to-heat ratio $\boldsymbol{\sigma}$ of a CHP activity*

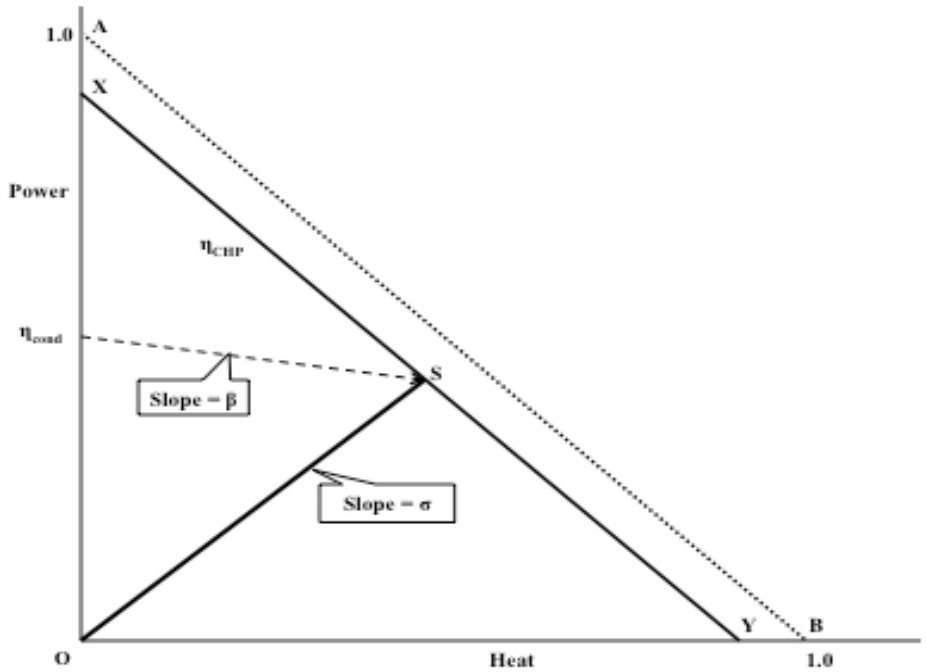

n the ordinate and follows the slope of the power loss factor $\boldsymbol{\beta}$. The two data define the dashed

[3] Power loss is discussed widely in the technical CHP literature but generic statistics are published rarely because the loss factors are application specific. See however figure 1 in [8].

downward sloping line $\eta_{Cond} - S$, and the crossing with XY fixes point **S**. The design power-to-heat ratio σ is the then found as the slope of **OS**. The production possibility set of the CHP activity is given by the triangular area $O - \eta_{Cond} - S$. While CEN is compatible with the method of fig. 1, avoiding the insertion of arbitrary efficiency numbers is more accurate and transparent (see [7] for further detail).

4. External Benchmarking and the EU Directive Qualification

The EU CHP Directive benchmarks the outputs of CHP plants on the efficiencies of separate generation processes of power and of heat. The imposed power reference is the high efficient CCGT process and at the heat side it is a high-efficiency boiler. Next to the difficulties in pointing down the "right" efficiency values, the assumption that CHP power and CCGT power are perfectly comparable and exchangeable all time of the year[4] weakens the case for applying external benchmarking [9]. Some countries have based their regulation on external benchmarking: acceptance or exclusion of CHP plants from support depends on their performance on the *quality norm*. This *norm* links the outputs of a CHP ***plant*** to the efficiencies of reference separate heat and power generation processes. It is shown [10] that the *quality norm* entails little incentive to improve the real quality of the CHP process. This is a crucial shortcoming because the future of CHP depends on its competitive position and this in turn is dependent on the quality of the processes. The more electricity a CHP plant can generate the better for the competitiveness of CHP. The *quality norm* is not effective in stimulating CHP quality and is perverse in truncating the production possibilities of CHP plants. Investment in well-scaled and flexible CHP capacity is choked by the qualification procedure. In existing plants CHP operators are driven to produce smaller quantities of power either by partly loading or by shutting down capacities. Most of the negative effects are due to the amalgamation[5] of the cogeneration and condensing activities in the CHP plants into plant quantities, and by omitting separate identification and measurement of the actual CHP activity within such plant (see table 2).

Conclusion

Public regulation obeys a number of quality standards to reach its stated objectives. Incentive regulation of CHP sets the factors right that improve the economics of investing and operating high quality processes. External benchmarking of CHP plants on separate high-efficient power and heat production processes implies perverse effects. A good CHP regulation starts at clearly stating the merit of CHP as the transformation of all or part of the residual heat of thermal power processes into useful heat. This merit assigns, ceteris paribus, to CHP activity

[4] In actual power systems, CCGT is not a marginal power supplier (high efficiency CCGT requires constant full load conditions). A common CHP plant of 35~40 percent power efficiency is of higher merit than a peak-load unit of 25~30 percent efficiency, but CHP activity will be constrained by imposing the 50~55 percent benchmark efficiency. This shows how external benchmarking becomes perverse. It obliterates the regulatory roles. Comparing power generation performance of CHP with grid power is to be done by a clear regulation of grid access pricing. Promoting CHP (as the EU wants) is to be done on the basis of the own merit of CHP.

[5] A metaphor of wrong amalgamation: a city board wants to promote cycling in the city by rewarding bike use (assumed: in the city perimeter). Some lobby imposes that bikes only get support when faster than motorized traffic. Bikes are equipped with a meter registering distance and running time. Within the city perimeter most bikers are faster than motorized traffic. However the biker's performance is the sum of all km and time (within and beyond the city perimeter) compared with the external benchmark. This obviously will not stimulate a good deployment of bike use in and around the city.

a priority ranking above standard thermal power. The performance of CHP is fully gauged by the quantity of cogenerated electricity when identified and measured in the proper way. The latter task is tricky when the CHP activity is mingled with condensing power generation. The article offers a solid methodology based on the first law of thermodynamics; new is the definition of the "bliss point" of a CHP activity, being the crossing of the lines with as slopes respectively the power-loss and power-to-heat parameters. Bliss points are virtual in most condensing-extraction cycles and multiple when heat is recovered at various pressures. This finding is the basis for assigning the proper power-to-heat characteristic to various CHP activities, sidelining the inaccurate use of average efficiencies as proposed by CEN [6]. Using arbitrary averages for efficiencies does not provide the right incentives to maximize real efficiencies when investment in CHP plants takes place.

References

[1] European Parliament and Council, Directive 2004/8/EC of the European Parliament and of the Council of 11 February 2004 on the promotion of cogeneration based on a useful heat demand in the internal energy market and amending Directive 92/42/EEC, Official Journal of the European Union, 21.2.2004, L52/50-60.

[2] J. Couder, A. Verbruggen, Technical Efficiency measures as a tool for energy benchmarking in industry?, Energy & Environment 14, 2003, pp. 705-724

[3] G. Schauman, Energy Efficiency in Industry, keynote lecture at 4th European Congress on Economics and Management of Energy in Industry, Porto, 27-30 November 2007.

[4] D. Toke, A. Fragaki, Do liberalized electricity markets help or hinder CHP and district heating? The case of the UK, Energy Policy 36, 2008, pp.1448-1456

[5] EDUCOGEN, An educational tool for cogeneration, SAVE EU programme, 2001, pp. 199

[6] CEN Workshop Agreement, Manual for Determination of Combined Heat and Power (CHP), CWA 45547, CEN/CENELEC, Brussels, 2004, pp. 78

[7] A. Verbruggen, The merit of cogeneration: Measuring and rewarding performance, Energy Policy 36, 2008, pp. 3059-3066

[8] D. Harvey, Clean Building Feature, Cogeneration and On-Site Power Production, 2006, pp.107-115

[9] U. Franke, Die Thermodynamik der KWK aus systematischer Sicht Euroheat & Power 33, 2004, pp. 28-33

[10] A. Verbruggen, Qualifying Combined Heat and Power (CHP) Activity, Int. J. Energy Technology and Policy 5, 2007, pp. 36-52

An optimization model for the integration of renewable technologies in power generation systems

Andreas Poullikkas [1,*]

[1] *Electricity Authority of Cyprus, P.O. Box 24506, 1399 Nicosia, Cyprus*
** Corresponding author. Tel: +357 22 201810, Fax: +357 22 201809, E-mail: mspoul@ucy.ac.cy*

Abstract: In view of the expanding Renewable Energy Sources (RES) generation worldwide and in particular in European Union, it is crucial for every country to consider the cost of integrating the necessary mixture of RES-E technologies in their existing and future generation systems. In this work, an optimization model for the integration of RES electricity (RES-E) technologies in power generation systems is developed. The purpose of the optimization procedure is to assess the unavoidable increase in the cost of electricity of a given power generation system at different RES-E penetration levels. The optimization model developed uses a genetic algorithm (GA) technique for the calculation of both the additional cost of electricity due to the large penetration of RES-E technologies as well as the required RES-E levy in the electricity bills in order to fund this RES-E penetration. The above GA procedure enables the estimation of the level of the adequate (or eligible) feed-in-tariff (FiT) to be offered to future RES-E systems. The overall cost increase in the electricity sector for the promotion of RES-E technologies, for a given period, is analyzed taking into account factors, such as, the fuel avoidance cost, the carbon dioxide emissions avoidance cost, the conventional power system increased operation cost, etc. The applicability of the developed optimization model is applied to the small isolated power generation system of the island of Cyprus. The results indicated that in the case of 15% RES-E penetration by providing FiTs with a 10% internal rate of return the required level of RES-E levy in the electricity bills will be 0.53€c/kWh.

Keywords: *Power generation, renewable energy sources, genetic algorithm, optimization*

1. Introduction

The European Union (EU) has already tuned its energy policy into achieving maximum carbon dioxide (CO_2) emissions reduction from power generation plants. In this context, it has already set out a strategic objective of achieving at least a 20% reduction of greenhouse gases by 2020 compared to 1990 levels [1]. This strategic objective represents the core of the new European energy policy. Recognizing the positive effects of renewable energy sources (RES) technologies towards achieving this goal, the EU has taken a range of specific actions in the direction of enhancing the integration of RES in the existing European power generation system as a major step towards the reduction of global warming and climate change phenomena. Specifically, an action plan in the form of an EU Directive on the promotion of the use of energy from renewable sources [4] has been introduced by the EU whereby a target of RES share of 20% out of the gross final energy consumption of the EU has been set to be reached by the year 2020. The RES Directive [4] establishes a common framework for the promotion of energy from RES. It sets mandatory national targets for each Member State for the overall share of energy from RES in gross final consumption of energy and for the share of energy from RES in transport. Also, it lays down rules relating to statistical transfers between Member States, joint projects between Member States and with third countries, guarantees of origin, administrative procedures, information and training, and access to the electricity grid for energy from RES.

In line with the EU RES policy, each Member State must adopt a national RES action plan. The national RES action plans are expected to set out Member States' national targets for the share of energy from RES consumed in transport, electricity and heating and cooling in 2020, taking into account the effects of other policy measures relating to energy efficiency on final

consumption of energy, and adequate measures to be taken to achieve those national overall targets. In view of the expanding RES generation in EU, it is crucial for Member States to consider the cost of integrating the necessary mixture of RES-E technologies in their existing and future generation systems up to the year 2020. For such an investigation, it is fundamental to perform an analysis of the new technical, economic and environmental status that the integration of such technologies will affect in the current and long term strategic planning of the EU generation systems expansion. The available existing software can only provide an estimate of the cost increase based on predetermined capacity factors or energy production of RES-E technologies. However, in order to perform more detail analysis and more accurate cost estimates there is a need for the implementation of an optimization model implementing unit commitment algorithms

In this work, an optimization model for the integration of RES electricity (RES-E) technologies in power generation systems on a unit commitment basis is developed. The purpose of the optimization procedure is to assess the unavoidable increase in the cost of electricity of a given power generation system at different RES-E penetration levels. The optimization model developed uses a genetic algorithm (GA) technique for the calculation of both the additional cost of electricity due to the large penetration of RES-E technologies as well as the required RES-E levy in the electricity bills in order to fund this RES-E penetration. The algorithm combines the WASP IV software [11], for optimal expansion plan for a given power generating system and the IPP v2.1 software [7] for the optimum cost of electricity produced from both conventional and RES technologies. Also, this GA procedure enables the estimation of the level of the adequate (or eligible) feed-in-tariff to be offered to future RES-E systems. The applicability of the developed optimization model is applied to the small isolated power generation system of the island of Cyprus.

In section 2, the simulation methodology and the optimization GA developed are described. In section 3, the methodology is demonstrated for the integration of RES-E technologies in the Cyprus power generation system. The conclusions are summarized in section 4.

2. Optimization model

The optimization model developed uses a GA technique for the calculation of both the additional cost of electricity due to the large penetration of RES technologies as well as the required RES-E levy in the electricity bills in order to promote such penetration. A schematic diagram of the optimization flow chart is shown in *Figure 1*. The algorithm combines the WASP IV software [11], for optimal expansion plan for a given power generating system and the IPP v2.1 software [7] for the optimum cost of electricity produced from both conventional and RES technologies. Both have been used extensively during the past years for similar studies (e.g., [8], [10]). A brief description of simulation software follows.

2.1. WASP IV software

The future generation system is simulated using the Wien Automatic System Planning IV (WASP IV) software package [11], which is widely used for automatic generation planning. The WASP IV software package finds the optimal expansion plan for a given power generating system over a period of up to 30 years. The foreseen seasonal load duration curves, the efficiency, the maintenance period and the forced outage rate of each generating plant are taken into account. The objective function, which shows the overall cost of the generation system (existing and candidate generating plants), is composed of several components. The components, related to the candidate generating units, are the capital cost and the salvage capital cost. The components, which are related to both the existing and candidate generating

units are the fuel cost, the fixed operation and maintenance costs, such as, staff cost, insurance charges, rates and fixed maintenance, the variable operation and maintenance costs, such as, spare parts, chemicals, oils, consumables, town water and sewage.

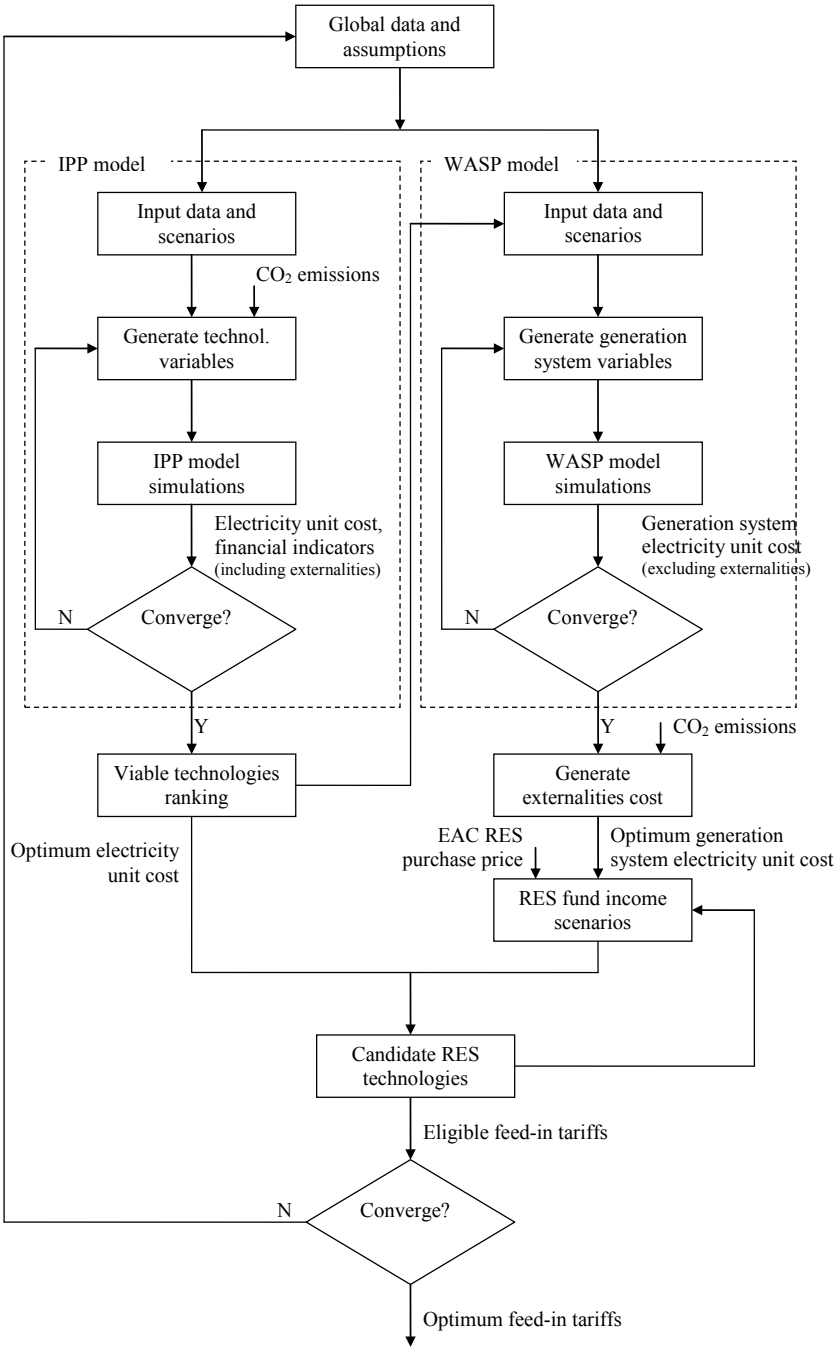

Figure 1: Flow chart of the optimization model

The cost to the national economy of the energy not served (ENS) because of shortage of capacity or interruptions is, also, taken into consideration. In the production simulation of WASP, a one-year period is divided into, at most, 12 s ub-periods for each of which probabilistic simulation is applied. Equivalent load duration curves in the probabilistic simulation are approximated using Fourier series. The Fourier expansion makes it computationally simple to convolve and deconvolve generating units in the probabilistic simulation. The decision of the optimum expansion plan is made by the use of forward

dynamic programming. The number of units for each candidate plant type that may be selected each year, in addition to other practical factors that may constrain the solution is specified. If the solution is limited by any such constraints, the input parameters can be adjusted and the model re-run. The dynamic programming optimization is repeated until the optimum solution is found. Each possible sequence of power units added to the system (expansion plan) meeting the constraints is evaluated by means of a cost function (the objective function), which is composed of (a) capital investment costs, I, (b) salvage value of investment costs, S, (c) fuel costs, F, (d) non-fuel operation and maintenance costs, M, and (e) cost of energy not served, Φ. Thus,

$$B_j = \sum_{t=1}^{T} \left[I_{jt} - S_{jt} + F_{jt} + M_{jt} + \Phi_{jt} \right], \quad (1)$$

where, B_j is the objective function attached to the expansion plan j, t is the time in years (1, 2, …., T) and T is the length of the study period (total number of years). All costs are discounted to a reference date at a given discount rate. The optimum expansion plan is the $minB_j$ among all j. Details of the optimization algorithm implementing the above mathematical formulation can be found in [11].

2.2. IPP v2.1 software

In order to calculate the cost of electricity from the various RES candidate technologies each plant operation is simulated using the IPP v2.1 software [7]. The software emerged from a continued research and development in the field of software development for the needs of power industry. This user-friendly software tool can be used for the selection of an appropriate least cost power generation technology in competitive electricity markets. The software takes into account the capital cost, the fuel consumption and cost, the operation cost, the maintenance cost, the plant load factor, etc. All costs are discounted to a reference date at a given discount rate. Each run can handle 50 different candidate schemes simultaneously. Based on the above input parameters for each candidate technology the algorithm calculates the least cost power generation configuration in real prices and the ranking order of the candidate schemes. A brief description of the optimization procedure is given below. The technical and economic parameters of each candidate power generation technology are taken into account based on the cost function:

$$\min\left(\frac{\partial c}{\partial k}\right) = \min\left\{ \frac{\sum_{j=0}^{N} \left[\frac{\frac{\partial C_{Cj}}{\partial k} + \frac{\partial C_{Fj}}{\partial k} + \frac{\partial C_{OMFj}}{\partial k} + \frac{\partial C_{OMVj}}{\partial k}}{(1+i)^j} \right]}{\sum_{j=0}^{N} \left[\frac{\frac{\partial P_j}{\partial k}}{(1+i)^j} \right]} \right\}, \quad (2)$$

where c is the final cost of electricity in €/kWh, in real prices, for the candidate technology k, C_{Cj} is the capital cost function in €, C_{Fj} is the fuel cost function in €, C_{OMFj} is the fixed O&M cost function in €, C_{OMVj} is the variable O&M cost function in €, P_j is the total electricity production in kWh, j=1,2,…N is the periods (e.g., years) of installation and operation of the

power generation technology and i is the discount rate. The least cost solution is calculated by:

$$least\ cost\ solution = \min\left[\frac{\partial c}{\partial k}\right] . \quad (3)$$

During the simulations procedure the following financial feasibility indicators are calculated (a) electricity unit cost or benefit before tax (in €/kWh), (b) after tax cash flow (in €), (c) after tax NPV (net present value: the value of all future cash flows, discounted at the discount rate, in today's currency), (d) after tax IRR (internal rate of return: the discount rate that causes the NPV of the project to be zero and is calculated using the after tax cash flows. Note that the IRR is undefined in certain cases, notably if the project yields immediate positive cash flow in year zero) and (e) after tax PBP (payback period: the number of years it takes for the cash flow, excluding debt payments, to equal the total investment which is equal to the sum of the debt and equity). Details of the optimization algorithm implementing the above mathematical formulation can be found in [5], [7].

3. RES-E integration analysis

In this section, the above model is tested for the assessment of the cost increase of electricity by the integration of the necessary RES-E technologies mixture by 2020 in the case of the island of Cyprus. The optimization model used is based on a GA technique, for the calculation of both the additional cost of electricity due to the large penetration of RES technologies as well as the required RES-E levy in the electricity bills, in order to promote and fund such penetration.

3.1. RES-E penetration scenarios

Over the study horizon, the analysis examines 4 levels of RES-E penetration in the electricity sector of 10%, 15%, 20% and 25%. Based on the above levels of penetration a total of 5 scenarios, regarding the future power generation expansion of the Cyprus generation system are examined. The first scenario considers the expansion of the Cyprus generation system without any RES-E technologies but only with natural gas combined cycle technologies of 220MWe capacity, which is considered as the BAU expansion scenario. The remaining four scenarios consider expansion with RES-E technologies. This is done in order to assess the additional electricity unit cost (compared to the BAU scenario) of the future Cyprus generation system with the expected integration of the necessary RES-E technologies mixture by the year 2020.

In all four RES-E scenarios, the natural gas combined cycle plants of 220MWe capacity remain a candidate option for the system expansion, with the addition of four RES-E candidate technologies, namely wind, PV, biomass and CSP with 6 hour thermal storage [9], in different capacity mixtures per scenario based on (a) satisfaction of the minimum indicative trajectories for the penetration of RES-E technologies in the Cyprus power generation system as set out in [3] and [4], (b) available potential of each individual RES-E technology, (c) level of penetration of each individual RES-E technology into the grid without any technical problems, (d) RES-E capacity installation priority and (e) RES-E contribution to the power generation system capacity reserve margin. Real data have been used in the case of conventional power generation technologies and RES-E technologies technical, economic and environmental parameters. In the case of fuel prices as well as CO_2 EU ETS trading cost, projections have been used in line with recent EU estimates.

3.2. Simulations results and discussion

One of the measures for the promotion of the use of RES-E technologies is the feed-in tariff (FiT) measure. FiT sets a guaranteed premium price to the RES-E producer and puts an obligation on the grid operators to purchase the output. The FiT price is typically guaranteed for a long period in order to encourage investments in new RES-E plants. Therefore, in order for the FiTs, corresponding to various RES-E technologies, to become attractive, a satisfactory IRR to the RES-E producer is necessary. The optimum results concerning FiTs, with an acceptable level of IRR to the RES-E producers, of 10% are illustrated in Figure 2.

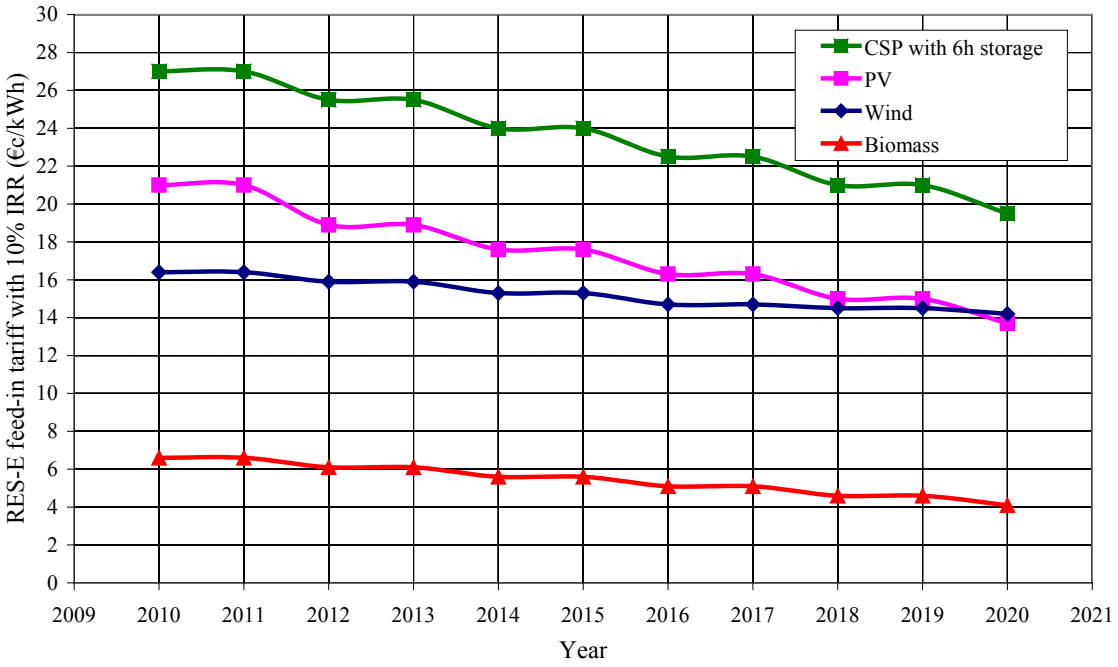

Figure 2: Optimum RES-E FiTs for 10% IRR

The results concerning the estimated overall cost increase in the electricity sector for the promotion of RES-E technologies, for the period 2010-2020 are illustrated in *Figure 3*. This is a differential cost increase compared of each RES-E scenario to the results obtained with the BAU scenario and takes into account the following factors: (a) fuel consumption since by increasing RES-E penetration fuel consumption is reduced, (b) CO_2 emissions since by increasing RES-E penetration CO_2 EU ETS trading cost is reduced and (c) conventional power system since by increasing RES-E penetration the conventional power system operating cost is increased due to the increased requirements of conventional reserve capacity and due to the operation of conventional plants at lower capacity factors.

The overall cost increase in the electricity sector is expected to be recoverable through the electricity bills partly as a direct cost (RES-E levy) and partly as an indirect cost (utility RES-E purchasing price and/or CO_2 trading auctioning). For comparison purposes the following two cases are examined: (a) RES-E investments with no profit (i.e., IRR at 0%) and (b) RES-E investments with profit (i.e., IRR at 10%). The overall results concerning the differential electricity unit cost from BAU scenario (no RES-E penetration) for the different RES-E penetration scenarios investigated are illustrated in Figure 3. For example, for 15% RES-E penetration, in the case of investments with no profit (i.e., IRR at 0%) the overall additional cost will be 0.79€c/kWh (in real prices), however, in the case of investments with FiTs with

IRR at 10% the overall additional cost will be 1.28€c/kWh (in real prices). For the latter the required level of RES-E levy in the electricity bills need to increase from the current level of 0.44€c/kWh to 0.53€c/kWh.

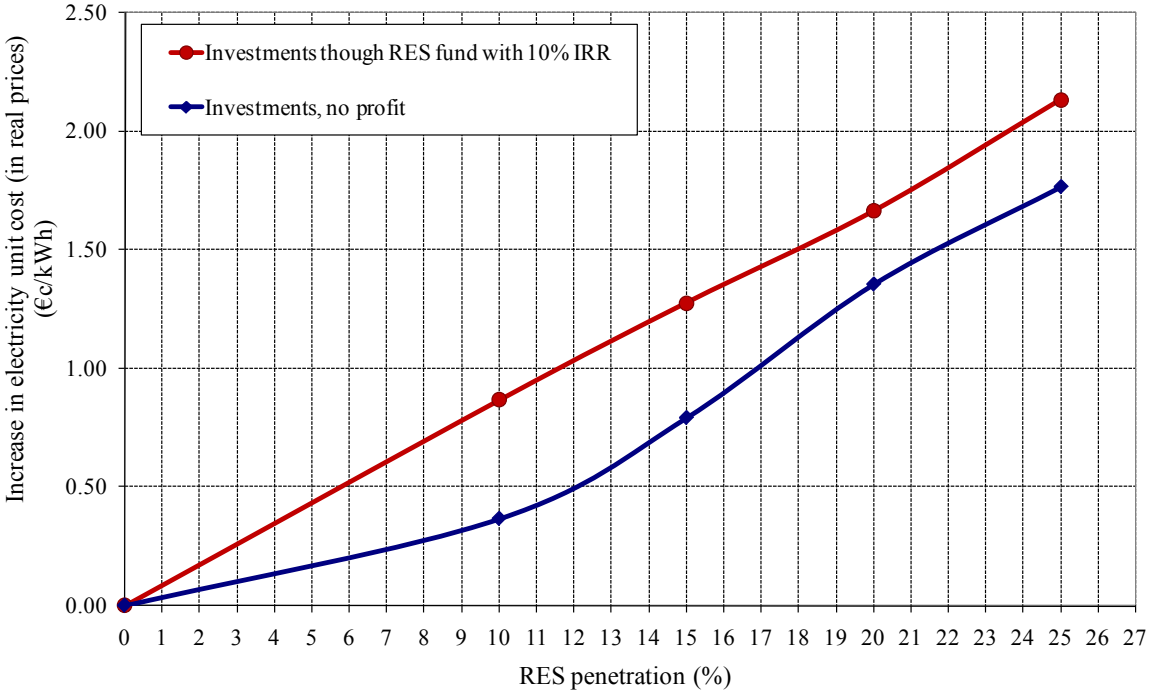

Figure 3: Overall results for the differential electricity unit cost from BAU for RES-E promotion (in real prices)

4. Conclusions

The main purpose of this work was to assess the unavoidable increase in the cost of electricity of a generation system by the integration of the necessary RES-E technologies for the EU Member States to achieve their national RES energy target. The optimization model developed uses a GA technique for the calculation of both the additional cost of electricity due to the penetration of RES-E technologies as well as the required RES-E levy in the electricity bills in order to fund this RES-E penetration. Also, the procedure enables the estimation of the level of the optimum FiT to be offered to future RES-E systems. Such decision support methodology for the optimum RES-E penetration cost level is of high importance not only from an economic point of view, but also from a political prespective since it can be used to help politicians to decide on the least cost RES-E penetration scenarios.

The applicability of the developed optimization model was applied to the small isolated power generation system of the island of Cyprus. The overall cost increase in the electricity sector for the promotion of RES-E technologies, for the period 2010-2020, was analyzed. This is a differential cost increase compared of each RES-E scenario to the results obtained with the BAU scenario and takes into account factors, such as, the fuel avoidance cost, the CO_2 emissions avoidance cost, the conventional power system increased operation cost, etc. The overall results indicated that in the case of RES-E investments with IRR of 10% the cost of integration is higher compared to RES-E investments with no profit (i.e., IRR at 0%) by 0.3€c/kWh – 0.5€c/kWh (in real prices), depending on the RES-E penetration level.

References

[1] European Commission, Renewable Energy Road Map - Renewable energies in the 21st century: building a more sustainable future, 2006, COM(2006) 248.

[2] European Commission, Barcelona Process: Union for the Mediterranean, 2008, COM(2008) 319.

[3] European Commission, Commission Decision of 30 June 2009 establishing a template for National Renewable Energy Action Plans under Directive 2009/28/EC of the European Parliament and of the Council, 2009, 2009/548/EC.

[4] European Commission, Directive 2009/28/EC of the European Parliament and of the Council 23 April 2009 on the promotion of the use of energy from renewable sources and amending and subsequently repealing Directives 2001/77/EC and 2003/30/EC, 2009.

[5] Poullikkas A., I.P.P. ALGORITHM v2.1, S oftware for power technology selection in competitive electricity markets, 2006, © 2000 – 2006, User Manual.

[6] Poullikkas A., "Implementation of distributed generation technologies in isolated power systems", Renewable and Sustainable Energy Reviews, 2007, 11, pp. 30-56.

[7] Poullikkas A., "A decouple optimization method for power technology selection in competitive markets", Energy Sources, 2009, Part B, 4, pp. 199-211.

[8] Poullikkas A., 2009, "Economic analysis of power generation from parabolic trough solar thermal plants for the Mediterranean region – A case study for the island of Cyprus", Renewable and Sustainable Energy Reviews, 13, pp. 2474-2484.

[9] Poullikkas A., 2009, Introduction to Power Generation Technologies, NOVA Science Publishers, Inc., New York, ISBN: 978-1-60876-472-3.

[10] Poullikkas A., Hadjipaschalis I., Kourtis G., 2010, "The cost of integration of parabolic trough CSP plants in isolated Mediterranean power systems", Renewable and Sustainable Energy Reviews, 14, pp. 1469–1476.

[11] Wien Automatic System Planning (WASP) Package: A Computer Code for Power Generating System Expansion Planning Version WASP-IV with User Interface User's Manual, 2006, International Atomic Energy Agency, Vienna.

U.S. Climate and Energy Policy: *What Went Wrong, and What it Means for Global Renewable Energy Technology Development*

Elias Hinckley

Kilpatrick Townsend & Stockton LLP, Washington, DC, USA
Georgetown University, Washington, DC, USA
Tel: +202.824.1444, Fax: +202.585.0015, E-mail: eh@georgetown.edu

Abstract: This paper examines the breakdown in discussion and the legislative process in the U.S. Government that led to the surprising failure to enact meaningful energy or climate legislation during the first two years of the Obama Presidency, while his Democratic party held control over the Government, including factors like opposition, the legislative process, the Gulf oil spill, and lack of understanding. From this critical understanding the paper will examine where U.S. policy stands today, and what the likely path forward for U.S. energy and climate policy may be and how those policy decisions absent climate legislation will effect renewable energy technology development and deployment in the U.S. and global marketplace over the coming years.

Keywords: *Policy, Renewable energy, Climate, U.S., Greenhouse gases*

1. Introduction

While reports have the U.S. slipping behind China as the now second largest consumer of energy on the globe, [1] U.S. action on climate and energy remains one of the critical pieces of the global policy discussion about the future of renewable energy.

Proponents of climate change legislation in the U.S., were dealt a stunning defeat when the U.S. Senate failed to reach a consensus and pass a climate and energy law. In November of 2008 the Democrats won a 'supermajority' in Congress and took control of the White House—seemingly the only question was how quickly the U.S. would take a global leadership role on climate change. More than 2 years into the Obama Presidency, no significant law on climate change or energy policy has been enacted, and the path forward for a changed energy and emission policy in the U.S. remains strikingly opaque.

2. Methodology

Following several inquiries about the process and explanations for the failure of the U.S. congress to pass comprehensive climate legislation during 2010 the author began to compile information on the process through major media coverage, direct interviews with members of the U.S. congress and their respective staffs. In combination with available information on U.S. and global energy markets, this collected information was analyzed to determine why legislation was not passed, and what the near-term future of U.S. energy and climate policy will likely be.

3. What Went Wrong

That the U.S. Government did not pass a comprehensive carbon cap and trade law during 2009 or 2010 was surprising to many observers both inside and outside of the U.S. The consensus government, with Democrats controlling the White House, House of Representatives and with a super majority in the Senate, appeared perfectly positioned to act on the campaign promises of Barack Obama that the U.S. would act in a meaningful way on climate change by signing greenhouse gas limits into law, would take a leading role in

managing greenhouse gases globally, and accelerate the development of a clean energy economy. For proponents of renewable energy this inaction by the U.S. government, while Democratic supporters were so well positioned to take decisive steps on both climate and energy, was seen as significant failure.

The first hint that the passage of sweeping legislation related to climate change might face substantial headwinds despite the Democratic control of the government came in the weeks leading up to the Conference of Parties in Copenhagen in December of 2009. Despite Obama's publically expressed desire to go to Copenhagen with a new U.S. law as a base for negotiations there was little compromise in the month leading up to the COP on what that platform would be and effectively no legislative action. [2] With results from the Copenhagen meeting providing less clarity on the future plan for global climate change action than supporters had hoped (and with many pointing to the U.S.'s unwillingness to commit as a key reason why there was not more progress during the Copenhagen talks), the President returned to the U.S. again pledging action on new laws in the U.S. [3]

Throughout the winter and spring following Copenhagen, the debate over U.S. climate and energy policy circled around two proposals which were both based on cap and trade programs similar to the EU's cap and trade scheme designed to reduce greenhouse gas emissions. The American Clean Energy and Security Act of 2009 (also known as the Waxman-Markey Bill) was passed by the House of Representatives in June of 2009.[4] Several members of the U.S. Senate worked to pass a companion bill which could be reconciled with Waxman-Markey and then sent to the President to be signed into law. Of the many ideas and positions that were raised, the leading option that eventually took center stage in the Senate was a proposed collaboration by Sen. John Kerry, a Democrat, Sen. Joe Lieberman, an Independent and Sen. Lindsay Graham, a Republican. This bill, nicknamed KGL, was eventually drafted and formally introduced in the Senate, but not before Sen. Graham had splintered from the group citing concerns over Democratic action over immigration policy, growing concerns about the potential negative economic impact of cap and trade and tremendous pressure from some of his Republican colleagues.

The resulting bill, the American Power Act [5] was introduced late in the Spring of 2010. Timing, increased partisanship over energy and climate, lingering economic concerns, and a strong lobbying presence by fossil fuel companies, all combined to limit substantive discourse on this bill. By the time the bill was actually introduced on May 12th the Senate was nearly through its Spring session leaving only a light Summer schedule, which ended at the start of August under the 111th Congress [6] to debate and vote on legislation that was both divisive and complex on an unprecedented scale. Republicans pulled together in an increasingly tight anti-climate block during this period, pointing to potential economic damage to a still weak U.S. economy. Similarly, fractures in the Democratic majority over those economic concerns and tremendous uncertainty about broader energy policy questions as the Deepwater Horizon spill in the Gulf of Mexico continued unabated though the summer eroded support and slowed the debate process. During this period the fossil fuel industry waged a coordinated lobbying effort to erode the support of both Democrats and Republicans for the bill by highlighting the potential increases in energy costs and job losses. The result was that Democratic leadership in the Senate never managed to even get the bill brought up for a full vote by the Senate.

During this period a number of alternative proposals designed to directly support the renewable energy industry had been developed and introduced in both Houses of Congress. Bills ranging from national renewable energy standards to expanded renewable energy research and development funding to energy efficiency and building use targets all gained

substantial support. Leadership kept the Climate Bill as effectively the first order of business, with the only other focus of the session being related to rules governing offshore drilling—and there was even a movement to combine these two efforts into a sweeping climate and offshore drilling package. The result was that these two high-profile, but extremely divisive issues stayed in front of every other clean energy proposal and the Senate's summer session closed without even targeted energy legislation moving forward.

There is little doubt that the results of the recent congressional elections in the U.S. will mean less support for incentives or new regulation that benefit the manufacture or deployment of renewable energy facilities. Republicans now control the House of Representatives. The party has, broadly, been less supportive of renewable energy integration or of restrictions on CO_2 emissions. This lack of support has found very specific backing by several members who are attacking the science underlying the connections between fossil fuel use and climate change, as well as the widely held belief that the integration of energy resources, which are viewed as more expensive than traditional energy mix, will cause irreparable damage to an already struggling economy. This includes very open attacks by the members who vied for control of the House Energy and Commerce Committee, which was eventually won by Rep. Fred Upton. [7]

4. Where U.S. Policy Stands

The current make-up of the U.S. government makes it difficult for either party to pass a new law. Democrats control the Senate and the White House while Republicans hold a strong majority in the House of Representatives. In order for a new law to be enacted, it must pass both the House and the Senate (and because of procedural rules, the minority party can prevent a proposed law or bill from passing by using a minority block of 41 votes to prevent a bill from being debated or voted upon. [8] Only after passage in both chambers of Congress is the bill sent to the President, who would then sign the bill into law or exercise his power of veto to reject the bill.

Given the divide that has been growing between Democrats and Republicans over energy and climate, the current split in the control of Congress means that finding areas of compromise on energy or climate issues will be difficult, if not impossible over the next two years.

A national cap and trade bill is very clearly not a viable near-term option. The next presumed Speaker of the House, Rep. John Boehner, commented before the election that “This election is going to be a referendum on [Democrats’] job-killing policies, one of which is cap and trade,” Boehner said. “There will be no tax increases; there'll be no cap and trade bill,” he added. [9] The failure of Democratic leadership to consolidate support this past summer to pass comprehensive climate legislation, combined with an increase of climate-science denial rhetoric by the Tea Party and the far-right of the Republican party means that there is simply no path to legislate a national price on greenhouse gases over the next two years (unless there is some very significant exigent event that dramatically focuses public perception on climate change).

It seems very clear that natural gas, and possibly nuclear power, will play a meaningful role as lower-carbon options in the policy focus for both the power and transportation sectors over the next few years. Natural gas, as an expandable source of electric generation (and as a potential power source to meet increased demand from the electrification of the transportation sector, which has broad support of both Democrats and Republicans) and as a direct use fuel in the transportation fleet, appears to be the most likely near term area of policy compromise.

There is substantial and inexpensive domestic supply of natural gas supported by the rapid growth in recoverable unconventional or shale gas made available by advances in hydrological fracturing technology. As this is domestically sourced fuel, this new expansion of natural gas supply is seen to address energy security and trade imbalance concerns. Additionally, on a relative basis natural gas has a much lower carbon output than the current energy supply mix in the U.S., so a shift to natural gas is seen as a step towards cutting greenhouse gas emissions. When speaking at a press conference following the election, President Obama indicated his support of natural gas development, "We've got, I think, broad agreement that we've got terrific natural gas resources in this country," Obama said. "Are we doing everything we can to develop those?" [10]

A rapid expansion (relative to the typical pace of energy infrastructure development) of natural gas use and demand is likely if part of an energy bill includes incentives to switch from coal to natural gas fired electric generation. The scale and pace of the demand expansion is unclear, and it will be limited by the available economically-competitive excess natural gas supply (and the real cost of new nuclear development as that becomes better understood). It is not clear at this early stage whether the election results will dramatically change the landscape with respect to environmental regulations related to non-conventional gas extraction (specifically for shale gas and the issues associated with hydraulic fracturing), as there is effectively no Federal oversight of these activities currently in place, though there are rules enforced at by state governments. A meaningful set of environmental controls could eventually act to slow available low-cost gas supplies and limit the role of natural gas as the driver of U.S. energy policy. In any event, the use of natural gas will likely be the lead approach in all energy and climate policy platforms developed in the U.S. over at least the next two years.

Another dynamic at play in the national policy debate around greenhouse gas limitations is that there are a series of rules being drafted by the EPA under its authority to manage greenhouse gas emissions under the Clean Air Act.[11] The Clean Air Act, however, does not include any specific language with respect to greenhouse gases, and whether and how the Act should be applied to carbon emissions is a point of considerable acrimony. Republicans in the House have already pledged to attack the EPA directly as well as through funding cuts to slow this rulemaking process.

This attack the EPA regulation of greenhouse gases will be a priority for Republicans, and the initial reaction from the Obama Administration is that it will work to find a compromise on the scope and pace of EPA regulation of greenhouse gases in exchange for other policy platforms that will act as alternative carbon mitigation tools, such as expanded use of renewables power and natural gas as a coal replacement. President Obama reinforced the idea this week, stating that "the EPA is under a court order that says greenhouse gases are a pollutant that fall under their jurisdiction. . . Cap and trade was just one way of skinning the cat; it was not the only way. . . And I'm going to be looking for other means to address this problem. . . I think EPA wants help from the legislature on this. I don't think that the desire is to somehow be protective of their powers here. I think what they want to do is make sure that the issue is being dealt with."[12]

5. Where Does the U.S. Go From Here

As things currently stand it appears that any action on energy (or climate) by the U.S. Government will be cautious and targeted. Given the failures of several attempts at comprehensive policy changes, the safer and therefore more likely near-term approach will be

small, targeted initiatives. These targeted policy platforms tend be directed at specific industries and have historically been incentive based. Some of these platforms can actually be contradictory, as constituencies push for support of their own areas of focus without regard for the broader energy or climate policy landscape. The result is that short term market distortions and the lack of long term certainty of price signals reduces investor appetite in all segments of industry development. Even when considered in concert with the broad concerns over the lack of a developed approach to national energy and climate challenges, these problems will almost certainly not be an adequate incentive to revisit a more sweeping approach to energy or climate policy for at least the next two years.

The most likely program platform will be direct incentive based programs have historically proven complex and challenging. Especially for non-U.S. based companies, requiring a U.S. tax base or deep understanding of the U.S. tax system. Some programs require compliance with rules such as U.S. sourced materials and labor. The most significant support mechanism for renewable energy has been tax credits for the development or operation of renewable energy facilities. Most of these credits are in place through the term of the new Congress, with two notable exceptions. The credit for wind power generation is set to expire at the end of 2011 and will require legislative action in order to be extended. Also, the popular 1603 Grant program, which provides a direct payment in lieu of the tax credits is currently set to expire at the end of 2010, though this may be extended by a year through last minute dealings in the final days of the current "lame duck" Congress. These two programs, along with other popular programs like funding for energy research and development are a very real risk, despite widespread conceptual support, as the focus of government programs is turned to balancing the budget and deficit reduction. Extending or re-funding these programs may require matching offsets to produce the savings or revenue increases necessary to make the net cost to the government zero, which is an extremely contentious process.

Another popular program, at least from the Government's perspective is the Federal Loan Guarantee Program, which is administered by the U.S. Department of Energy and supports, among other things, the deployment of renewable energy technologies and manufacturing capacity. As with many of the direct incentive programs these guarantees have been complex and challenging to secure, which has been a source of substantial criticism from the industry and investors. Further, the potential default of some early guarantees may also bring potential program costs into sharp focus as further program funding is contemplated, leaving the future of these programs in some doubt.

Enactment of a national clean energy standard is one broad platform possibility in the coming months (and a program may be enacted by the time of the World Renewable Energy Congress). Renewable Energy Standards have been a popular state government tool, but despite several attempts the program has never been enacted at the national level. These programs are generally structured so that the local distribution company is required to hold Renewable Energy Certificates (RECs) commensurate with a set percentage of power that is required to be produced from identified renewable resources. Production of renewable power creates a REC for every unit of power that is produced, which can be sold along with the power or separately. Due to its regulatory requirements to hold some number of RECs, the local distribution company sets overall demand (possibly in combination with some voluntary buyers) based its need to meet the target for renewable power purchases.

It appears likely that in the near term states and regional programs will take the lead on climate specific rule-making (and possibly more aggressive renewable power targets). As many states as many as 33 states have some form of renewable portfolio standard in

operation. A handful of states have begun to experiment with feed-in-tariff programs similar to those used in Germany and Spain to drive rapid growth in solar and wind development. Several northeastern states are part of the Regional Green House Gas Initiative, which is a low-cost carbon cap and trade program for electric production facilities within member states, and in the Western US, the Western Climate Initiative as well as aggressive targets for California are both driving the development of regional markets. These state based programs have generally been embraced by the public and local politicians, at least sufficiently to see programs enacted and expanded. During the mid-term elections that saw historic Republican victories, California voters rejected a challenge to that state's cap and trade law, and New Mexico simultaneously enacted its own cap and trade program.

6. Impact of Inaction by the U.S. on Global Energy and Climate Developments

The slow pace with which the U.S. is embracing clean energy and climate policies will mean that deployment opportunities in the U.S. market will remain limited. The U.S. accounts for as much as 25% of global energy resource consumption, and the lack of U.S. commitment will create friction against the pace of a global energy transition. Given the scale of the U.S. energy economy, its pool of available energy investors, and the fact that the lack of clearly defined market for much of the new technology due to the lack of policy clarity will lead to less talent being engaged in the development of clean energy technology and business than would otherwise be engaged in the U.S., this resistance will be a drag on the pace of global growth for renewable power.

Despite the absence of the U.S. as a fully engaged stakeholder in this global energy and climate transformation, the absolute scale of the global opportunity will keep some U.S. companies and investors engaged in the new energy economy and continue to drive some U.S. investment into these industries. This limited role by the U.S. market will lead to better opportunities in both those developed nations where policy is better defined and in developing nations where sharp demand growth in fuelling investment. Development of renewable energy in Europe has matured more quickly than in in the U.S., as it has been supported by the EU ETS and targeted renewable energy programs like feed-in-tariffs combined with higher energy prices. In China aggressive government driven development programs have accelerated the maturity of the clean energy industry there, and by some accounts China has overtaken the U.S. in clean energy investments.[13]

7. Conclusion

Inaction by the U.S. Congress on climate and energy policy has created a great deal of uncertainty in the both the U.S. and global energy marketplace. Short-term relief for companies with exposure to greenhouse gas emission limitations will quickly give way to challenges planning for mid- and long-term investment choices. This uncertainty is intensified when combined with a likely increase in volatility in the global oil market. The one point of confidence that all stakeholders can work from is that the fall-out from this legislative push for climate legislation all but guarantees that for the next few years (notwithstanding a significant disruptive event), the path forward in the U.S. will be driven locally, or in very measured steps nationally. As arguably the most important energy market in the world, the lack of clear long-term market signals in the U.S. will continue to impair the real value of many new energy and emission mitigation technologies.

References

[1] *China Tops U.S. in Energy Use*, Spencer Swartz and Shai Oster, Wall Street Journal, July 18, 2010.

[2] John M. Broder, *As Time Runs Short for Global Climate Treaty, Nations May Settle for Interim Steps*, N.Y.Times, October 20, 2009.

[3] Barack Obama, *Remarks by the President on the Economy at Carnegie Mellon University*, http://www.whitehouse.gov/the-press-office/remarks-president-economy-carnegie-mellon-university (Last visited Dec. 15, 2010).

[4] H.R. 2454, American Clean Energy and Security Act of 2009.

[5] American Power Act Unreleased Draft, http://climateprogress.org/wp-content/uploads/2010/05/PowerActDraft_051110.pdf (last visited Dec. 15, 2010).

[6] Congress was in session for September and October prior to the election, but doe to the extended campaign period leading into the election there was no reasonable expectation of action during this period; similarly the lame duck period following the election carries additional procedural hurdles that made action impossible.

[7] Office of Congressman Joe Barton, *Climate Change and Policy Implications*, http://joebarton.house.gov/Issues.aspx?Section=52 (last visited Dec. 15, 2010).

[8] This process, the filibuster, is a procedural peculiarity of the Senate and provides a great deal of power to the minority party to block legislation.

[9] Elana Schor, *Election a Rreferendum on Democrats' Support for Cap and Trade – Boehner*, GreenWire, October 5, 2010, http://www.eenews.net/Greenwire/2010/10/05/archive/5?terms=boehner.

[10] Press Conference by the President (November 3, 2010), *available at:* http://www.whitehouse.gov/the-press-office/2010/11/03/press-conference-president.

[11] 40 CFR Part 51, 52, 70, 71, Prevention of Significant Deterioration and Title V Greenhouse Gas Tailoring Rule, June 3, 2010 *and* 40 CFR Part 52, Action to Ensure Authority to Issue Permits Under the Prevention of Significant Deterioration Program to Sources of Greenhouse Gas Emissions: Federal Implementation Plan, August 23, 2010; *et al*.

[12] *Id*.

[13] The PEW Charitable Trusts, Who's Winning the Clean Energy Race? Growth, Competition and Opportunity in the World's Largest Economies, http://www.pewglobalwarming.org/cleanenergyeconomy/pdf/PewG-20Report.pdf (last visited Dec. 15, 2010).

Follow-up of local energy and climate strategies – A study of six small Swedish municipalities

Jenny Ivner[1,*], Sara Gustafsson[1]

[1] *Linköping University, Linköping, Sweden*
** Corresponding author. Tel: +46 13282754, Fax: +46 13281101, E-mail: jenny.ivner@liu.se*

Abstract: Local authorities are important actors in the transition of energy systems towards renewable energy resources and efficient energy use. One mean to manage and develop local energy systems is using energy and climate strategies. Sweden has a long history of energy-planning, which effectiveness has been debated. However, in the light of climate change, many Swedish local authorities have adopted energy and/or climate strategies in recent years. These strategies are intended to clarify, prioritize and suggest measures for achieving energy and climate related goals. To be able to assess the strategies' effectiveness it is important to identify progress and goal achievement. There is little knowledge whether and how local authorities do this kind of follow-up.

The aim of this paper is to explore approaches to energy strategy follow-up in six small and medium-sized local authorities in Sweden. Based on interviews with representatives from six Swedish municipalities, this paper discusses prerequisites for energy and climate strategy follow-up. Challenges for the follow-up, such as methodological descriptions, organization and lack of high quality data are identified and discussed. A conceptual model for a systematic approach to follow-up is presented. Conclusions on how a systematic approach to follow-up could facilitate organizational learning and a more strategic approach to energy issues are drawn. It is also discussed how a developed practice could be beneficial in terms of common methodologies and possibilities to request better statistical data from the national level.

Keywords: *Energy and climate strategies, local authorities, evaluation, follow-up*

1. Introduction

The local level is important when it comes to developing sustainable energy systems. Arguments for this is for example the proximity to citizens, but also the diverse roles of local authorities such as responsibilities for planning, maintenance of infrastructure and as educators are important when it comes to forming and implementing energy strategies [1, 2]. Another important role of the local level is that there is greater emphasis on hands-on projects and what can actually be affected [3]. This means that local authorities have an important role in the transition of energy systems towards renewable energy resources and energy efficiency. To support local authorities in these issues there are a number of initiatives to provide networks, information sharing and knowledge transfer. For example, in the EU a large number of cities and communities participate in initiatives such as ManagEnergy Programme and the Covenant of Mayors. In Sweden there are several programs supporting local authorities in their work with energy and climate related issues, for example Sustainable Municipalities initialized by the Swedish Energy Agency and the Climate Municipalities funded by the Swedish Environmental Protection Agency. One important component in all of these programmes is the formulation of local energy and/or climate strategies or plans [4-7]. Such strategic documents are used to clarify, prioritise and suggest measures connected to the local authority's fields of responsibility and activity within the energy system. There is also a legal requirement in Sweden that all municipalities should adopt a municipal energy-plan.

The potential of local energy strategies have been highlighted in a number of studies [8-10]. Historically there have however been debates about the effectiveness of producing such documents, for example because many of the factors influencing the energy system lie beyond the reach of local authorities [11, 12]. To what extent energy strategies have been

implemented is however not known, partly because follow-up has been paid little attention. Follow-up is central to long-term overall effectiveness of a plan or an effort as it facilitates continuity and taking experiences from the past into the present. There is no formal requirement for follow-up of energy-plans in Swedish legislation and follow-up is often neglected in planning practice [13].

However, energy-plans should be subject for environmental assessments and environmental assessment of programs and plans according to the EU directive 2001/42 should include follow-up [14]. Follow-up in environmental assessments is advocated in literature for example as a means for controlling plan implementation and, if necessary, formulating adaptive management actions. Follow-up may also and enhance organizational learning and process development [15]. This means that there is a powerful potential for improved energy-planning practice as follow-up processes generate information that can be used in different ways for improving the actual environmental situation and for improving working procedures and processes [16].

1.1. Aim of this paper

The aim of this paper is to explore approaches to energy strategy follow-up in six small and medium-sized local authorities in Sweden and discuss the possibilities for developed practice.

2. Methodology

Initially it was decided to choose municipalities for this study based on two criteria: they should be small in a Swedish context, which means less than 25,000 inhabitants and the energy-plan should be recently adopted. The first criterion was chosen because two thirds (192 of 290) of Swedish municipalities have 25,000 inhabitants or less [17]. The latter criterion, that the energy-plan should be recently adopted, was chosen as it was regarded more likely that the persons involved during the energy-planning process would still be working at the local authority and thus available to answer questions about how the issue of follow-up was treated in the planning process. These criteria however proved hard to fulfill as only six small in municipalities that possess such recent energy-plans were identified. Three of these declined to take part of the study for different reasons, for example since the person who had been responsible for the planning process changed jobs. In order to get a more information on how follow-up of energy plans is undertaken additionally three (in a Swedish context, 30,000-45,000 inhabitants) medium-sized municipalities were chosen. The final set of municipalities in the study is presented in, table 1.

Table 1. Empirical basis in the study: six small (<25,000 inhabitants) and medium sized (<45,000 inhabitants) Swedish municipalities.

Municipality	Size	Energy-plan adopted	Responsible for planning process	Follow-up	No of Respondents
A	Small	2008	Workgroup and external support	Yes	2 (Public official, energy advisor)
B	Small	2009	Workgroup and external support	No	2 (Public official, energy advisor)
C	Small	2003	Workgroup	Yes	1 (Energy advisor)
D	Medium	2008	Consultant	No	2 (Public official, consultant)
E	Medium	2010	Workgroup	Yes	2 (Public officials)
F	Medium	2003	Consultant	No	1 (Public official)

For all municipalities the energy-plan was analyzed regarding how follow-up were supposed to be handled. In those cases where a person was stated as responsible he or she was interviewed about how follow-up had been conducted in practice. The named authors of the energy plan were interviewed about whether follow-up was regarded during the planning process. All interviews were conducted by telephone in a semi-structured form.

3. Results

This section presents the intentions for follow-up in the energy-planning process, how this was manifested in the energy-plans, and how follow-up has been conducted in practice in the six studied municipalities.

3.1. Municipality A

According to the energy-plan the progress should be monitored yearly in an annual "energy account". Regional monitoring of environmental goals by the County Administrative Board will also be used as indicators of goal effectiveness. The municipal government is utmost responsible for this account, which is then presented to the municipal parliament. Two persons are involved in the practical work compiling the energy account. One was part of the planning process and one is new in the organisation. This new person has experienced difficulties in interpreting how the baseline values were calculated. This means that some parts of the energy-plan have not been followed up. This respondent also comments that the indicators chosen for goal achievement are not necessarily suitable for the purpose. For example, whether district heating leads to less emission depends on the fuel mix in the incinerator and what is substituted. An experienced obstacle for the follow-up is the quality of the available national statistics. The respondent means that local data is preferable to national statistics but in practice a mix is used. However the mix of different data sources is a problem since methodology descriptions from the baseline calculations during the planning process are missing.

3.2. Municipality B

Two persons are working with strategic energy issues in municipality B. One person has the main administrative responsibility and functions as contact person to the politicians. The other person's main responsibility is to make sure that actions proposed by the energy-plan are implemented. The intended methodology for follow-up is to produce an environmental account where progress in implementing actions from the energy-plan is described. Focus in the follow-up will thus be on actions and whether they are implemented or not. The next step is to analyse to what extent this action has contributed to fulfilling goals in terms of decreased energy use and lowered emissions. This analysis is regarded as important since it sends a distinct message to the politicians. Exactly how the follow-up will be performed is not yet decided. However, the respondents emphasise the importance of this follow-up to become part of ordinary working procedures to avoid that the work becomes yet another burden for the public officials. Also in this case the low quality of available statistics is regarded as an obstacle to follow-up; therefore indicators based on local data will be used instead.

3.3. Municipality C

The energy and climate plan does not include any description on follow-up. The respondent in Municipality C has a supportive and advisory role in the energy-planning process; however he/she has not been involved in the follow-up. The energy-plan was followed up annually between 2004 and 2006, but since then no follow-ups have been performed. The respondent experiences that there has been a lack of continuity in the follow-up process during the last

few years and that the work with the energy and climate plan has been very dependent on one specific person. According to the respondent, there are no clear directives on how to proceed with the energy-plan. Follow-up was not an issue during the energy-planning process. Few of the goals stated in the energy-plan are quantifiable, which would complicate the follow-up process. Some follow-up has however been performed since the implementation of actions suggested in the energy-plan has been monitored.

3.4. Municipality D

According to the energy-plan, follow-up will be part of the local authority's annual economical account. The energy-plan presents a follow-up system based on forms to be filled out by each part of the municipal administration and that compilation of the results will be made by the environmental coordinator. In addition to this, the energy-plan states that a number of indicators to monitor progress towards local environmental goals shall be designed.

The environmental coordinator has the overall responsibility for the follow-up. This person was not employed at the local authority during the energy-planning process and the energy-plan for the municipality was produced by a consultant. This consultant means that they did not only produce an energy-plan for the municipality, they also designed a strategic and continuous energy-planning process for the local authority to "inherit". Even though the process was meant to be easily adopted into the local authority's organisation, the environmental coordinator has experienced difficulties in understanding methods used and origins of data. Since a method description is missing, also the consultant has difficulties in explaining how data was obtained and how calculations were made in retrospect. The environmental coordinator does not think that there will be any problems in following up whether actions are accomplished or not, since they are very "hands-on". But when it comes to evaluating whether actions lead to any actual decrease of carbon dioxide emissions this person thinks there will be difficulties. In the energy-planning process there was little attention paid to how to follow-up whether measures contribute to the overall goal for the plan. Instead efforts were laid on how to monitor whether actions are implemented. Also in this case the low quality of available statistics is mentioned as an obstacle to the follow-up.

3.5. Municipality E

Municipality E has a long tradition of producing and monitoring energy-plans and follow-up is a part of the administrative routines in the local authority. Results from the annual follow-up are presented in the municipality's annual environmental account. All goals stated in the energy-plan are connected to indicators for monitoring whether goals are fulfilled or not. Also actions will be followed up in the environmental account as they are implemented in the environmental action program. The environmental coordinator has main responsibility for this and leads a group of public officials that work with the follow-up.

As the last energy-plan was produced an extra human resource was employed. Both this official and the environmental coordinator tell that the goals and indicators for the energy-plan were carefully chosen to suit available data and the (poor) quality of the national statistics. Describing the baseline year and methods for calculations have also been important parts of the work. Feasibility for follow-up has therefore been a precondition in the energy-planning process. When it comes to actions in the energy-plan, focus is to follow-up their implementation. To what extent different actions contribute to overall goals are currently not followed up as it proved complicated to perform such calculations.

3.6. Municipality F

In municipality F the local climate strategy also functions as energy-plan. According to this climate strategy follow-up should be conducted annually by monitoring the development in the energy field. If there are any significant changes in practice compared to what is stated in the plan, the plan should be revised. However, there are no concrete instructions for follow-up in the climate strategy, nor are there any time plans or responsibilities designated for implementing proposed actions.

The respondent in Municipality F has no formal role in the follow-up of the climate strategy. However, this person was active in the design process since one of the local environmental goals is connected to energy issues. According to the strategy a steering group and a reference group should be formed to take responsibility for energy issues. Also a local energy group with stakeholders should be initialized. However, none of these supportive structures have been formed. The goals in the climate strategy have instead been integrated in the local environmental goals where they also are followed up. The respondent means that one reason for the lack of follow-up of the climate strategy is that there is no organization for this task and that this work would have been facilitated if follow-up had been regarded during the climate strategy design.

4. Analysis

The results from this study indicate that follow-up has not been particularly prioritized in the energy-planning process, at least when it comes to defining working procedures for this follow-up. In one of the six studied municipalities with recent energy-plans follow-up is not mentioned in the energy-plan at all. Some kind of Follow-up activities have been undertaken in three of the six. Only in one case are there both structured documentation and organization for energy-planning follow-up (municipality 4). This municipality has long traditions and continuity in their strategic energy work and also resources allocated for these tasks.

One reason for not doing follow-ups is, according to the respondents, lack of resources. Another reason is that there were no thought about follow-up in the active planning phase and that it has taken time to build up structures for the follow up. When follow-up is conducted these activities are limited to monitoring whether or not actions are implemented. To follow-up whether these actions lead towards desired goals is however regarded too complicated. One of the obstacles towards calculating contribution to overall goals is lack of high quality data. Several of the respondents are frustrated with the low usefulness of the statistics produced at the national level. Since this data is unreliable there is a need to complement with local data. This in turn leads to methodological challenges as data origin from different years and sources. If the methods for data collection and baseline calculations are not very carefully reported follow-up will be almost impossible. In one case where the energy-plan was produced by consultants (municipality 2) this situation is evident. There were no methodological descriptions for calculating baseline values in the energy-plan, which has lead to that the public official needs to recalculate everything and invent own indicators for follow-up.

5. Discussion - How may follow-up be facilitated?

Municipalities produce a wide range of plans, programs and policies and what is common for all, is that that in order to be effective, follow-up and evaluation is needed. Planning is often seen as a linear process where follow-up is little discussed [16]. Evaluating the plan's implementation by analyzing the development after the adoption is of course important not

only in order to decide whether revision is needed but also to explore the effectiveness of the plan and to learn from that; If the plan did not lead to the desired changes, how should the plan and planning process be designed to be more effective?
When adopting such continuous approach to energy-planning it is important to remember that municipal plans exist in a context. This context includes various institutional aspects and practices. Experience has shown that a success factor for energy-planning is taking the existing working procedures into account [18, 19]. Many local authorities have implemented environmental management systems [20] and in these, making use of the already implemented systematic approach and continual improvements may be a way forward to improving follow-up practice in energy-planning [16, 21]. Standardized Environmental management systems (EMS) approach is organizational oriented and aims at continual improvements. This means that follow-up has a key role [22]. Adopting the systematic approach and continuity of EMS to planning could help overcoming the shortcomings in energy-planning follow-up, for example by providing annual follow-ups of goals and actions. Opportunities of connecting environmental management systems (EMS) to the planning processes have been discussed by for example Hjelm et al [16], where it is argued that EMS could contribute with continuity, routines and improvements of plans and planning. Connecting EMS processes and knowledge to energy-planning could also lead to other benefits as professionals from traditionally different fields meet and exchange knowledge and ideas. Figure 1 presents a conceptual model for the connections between energy-planning and EMS in the local authority.

However, EMSs are more often used in larger local authorities so in the case of the municipalities in this study such an approach may be overkill. Several of the municipalities in this study have instead related their energy-plans to either their environmental account or budget system. This is to some extent analog to the EMS connection to the planning, since it implies continuity. The annual reports in accounts or budget systems could contribute to a systematic gathering of information for follow-up and revision of energy-plans.

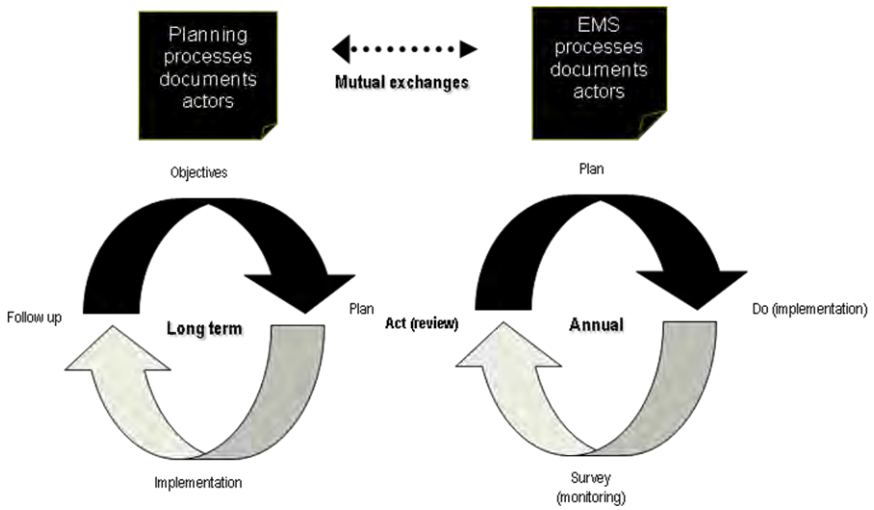

Figure 1**.** Conceptual framework for a continuous approach to planning and to link planning activities to organizational management such as EMS. The picture is inspired by Hjelm et al [16].

Based on the findings in this study, the municipalities seem to mainly follow-up whether or not actions have been taken rather than evaluating if the actions have led to e.g. reduced emissions of greenhouse gases. There is a challenge to find a methodology or approach, including this latter type of follow-up or evaluation. Also in this case a systematic approach

with a clear organizational setting with settled responsibilities could facilitate to make the energy-plan integrated in the daily work. Only when energy issues are a natural part of the daily work will it be possible to take the step further to strategic goals rather than implementing separate actions. If an EMS-approach is adopted, several advantages would be achieved: there are existing guidelines and vast practical experience from the EMS-field. The guidance in ISO 14004 stresses the importance of planning for the follow-up in terms of methods, indicators for activities and processes that give the most useful information [23]. The guidance also points out the importance of documented routines for follow-up. It would also be natural to lead experiences from implementation and monitoring back into the policy and planning processes for organizational learning and to formulate new actions as implied by for example Partidàrio [15].

Another aspect on the adaption of an EMS-inspired approach to energy-planning follow-up related to the identified obstacles identified in this study is that it can facilitate the development of a common working practice and methodology. This would not only benefit the public officials who would recognize working procedures even if they change working places. Also, if many local authorities (and also consultants) adopt a similar working approach it would be easier to enquire better quality on specific statistical data from the Swedish Energy Agency.

6. Conclusions and recommendations

The aim of this paper was to explore approaches to energy strategy follow-up in six small and medium-sized local authorities in Sweden and discuss the possibilities for developed practice. It was found that in these cases follow-up is limited. Sometimes follow-up is neglected already in the planning phase and sometimes it is limited due to of lack of resources. Those who manage to conduct their follow-up have related their energy-plans to either their environmental account or budget system. This is one way to include the follow-up in a continuous process.

If energy-planning follow-up is included in processes of continual improvement there are several possible gains: the working procedures in EMS are well-known and can facilitate the development of working practice and also the standardization of data use and methodology. This systematic work could also lead to well-defined organizational settings for energy issues which can both contribute to putting strategic energy issues on the municipal agenda and to organizational learning and adaptive local energy policies.

References

[1] J. Ivner, Municipal Energy Planning: Scope and Method Development. 2009, Doctoral Thesis. Linköping University: Linköping.

[2] Joanneum Research. Handbuch für kommunale und regionale Energieplanung, 2000.

[3] B. Rydén, Energy Planning as Part of Public Planning, in Energy and the Built Environment in Sweden, B. Johansson, et al., Editors., Formas, 2006.

[4] Klimatkommunerna. Klimatstrategi - Processguide, 2008.

[5] Swedish Energy Agency. Handbok Uthållig Kommun, 2008.

[6] Covenant of Mayors, How to Develop a Sustainable Energy Action Plan (SEAP) - a Guidebook. 2010.

[7] European Commission. ManagEnergy. What Can Local Actors Do?, 2011.

[8] T. Anderson and A. Doig, Community Planning and Management of Energy Supplies - International Experience, Renewable energy (19), 2000, pp. 325-331.

[9] F.M. Butera, Moving Towards Municipal Energy Planning - the Case of Palermo: The Importance of Non-Technical Issues, Renewable Energy (15), 1998, pp. 349-355.

[10] M. Jaccard, L. Failing, and T. Berry, From Equipment to Infrastructure: Community Energy Management and Greenhouse Gas Emission Reduction, Energy Policy 25(13), 1997, pp. 1065-1074.

[11] S. Guy and S. Marvin, Disconnected Policy: The Shaping of Local Energy Management, Environment and Planning C, Government and Policy 14, 1996, pp. 145-158.

[12] B. Olerup, Scale and Scope in Municipal Energy Planning in Sweden, Journal of Environmental Planning & Management 43(2), 2000, pp. 205-221.

[13] A. Cherp, S. Emilsson, and O. Hjelm, Seamless - Strategic Environmental Assessment in Local Authorities in Sweden, in Effective Environmental Assessment Tools - Critical Reflexions on Concepts and Practice, L. Emmelin, Editor., Blekinge Institute of Technology . 2006.

[14] 2001/42/EC, Directive 2001/42/EC of the European Parliament and of the Council of 27 June 2001 on the Assessment of the Effects of Certain Plans and Programmes on the Environment. 2001, European Parliament and the Council: Official Journal of the European Communities. p. 0030 - 0037.

[15] M.R. Partidario and J. Arts, Exploring the Concept of Strategic Environmental Assessment Follow-Up, Impact Assessment and Project Appraisal 23(3), 2005, pp. 246-257.

[16] O. Hjelm, S. Gustafsson, and A. Cherp, From Tool Technique to Tool Practice. Experiences from the Project Seamless: Strategic Environmental Assessment and Management in Local Authorities in Sweden. 2011, Blekinge Tekniska Högskola: Karlskrona.

[17] Statistics Sweden. Folkmängd i riket, län och kommuner 31 December 2009 Och Befolkningsförändringar 2009-2010, 2010.

[18] J. Ivner, Energy Planning with Decision-Making Tools: Experiences from an Energy-Planning Project, Local Environment 14(9), 2009, pp. 833-850.

[19] R. Jank, ed. Advanced Local Energy Planning (Alep) - a Guidebook. Energy Conservation in Buildings and Community Systems Program. 2000, International Energy Agency.

[20] S. Emilsson and O. Hjelm, Mapping Environmental Management System Initiatives in Swedish Local Authorities - a National Survey, Corporate social responsibility and environmental management 9, 2002, pp. 107-115.

[21] S. Emilsson, S. Tyskeng, and A. Carlsson, Potential Benefits of Combining Environmental Management Tools in a Local Authority Context, Journal of Environmental Policy and Management 6(2), 2004, pp. 131-151.

[22] ISO, ISO 14001:2004. Environmental Management Systems- Requirements with Guidance for Use. 2004, Swedish Standards Institute.

[23] ISO, ISO 14004: 2004, Idt. Environmental Management Systems- General Guidelines on Principles, Systems and Supporting Techniques. 2004.

Green Jobs? Economic impacts of renewable energy in Germany

Ulrike Lehr[1,*], Christian Lutz[1]

[1] *Gesellschaft für Wirtschaftliche Strukturforschung mbH, Osnabrück, Germany*
** Corresponding author. Tel: +4954140933280, Fax: +4954140933110, E-mail: lehr@gws-os.com*

Abstract: The labor market implications of large investment into renewable energy (RE) are analyzed in this text. Although a growing RE industry can be observed in Germany the overall effect of large increases of expensive electricity and heat generating technologies on the German economy require a careful model based analysis. The paper shows the overall effects under different assumptions for fossil fuel prices, domestic installations and international trade. Most of these scenarios exhibit positive effects.

Keywords: *Renewable Energy, Germany, Economic Effects*

1. Introduction

The positive impacts of an increasing share of renewable energy (RE) on the mitigation of climate change as well as on the decrease of the dependence of energy imports are indisputable. However, such are currently still the additional costs of heat and electricity generation from most renewable energy sources (RES). For a stable economic development, the overall balance of positive and negative effects under different possible future development pathways of fossil fuel prices, global climate policies and global trade is of interest. To account for all effects in a consistent framework, a macroeconometric model is employed. Economic development is measured via the comparison of economic indicators such as GDP and employment from different simulation runs. Overall net positive effects can be seen for instance as higher employment in one simulation run compared with the other.

Additionally, the sectoral disaggregation of our model leads to a wide array of interesting results in terms of winners and losers of policies to support renewable energy. This contribution is organized as follows: This introduction is followed by section 2 on the methodology applied. The modeling framework is explained and the scenarios are described. Section 3 presents modeling results followed by a discussion. Section 4 concludes.

2. Methodology

2.1. Net economic effects

The discussion about employment effects of the increase of renewable energy often centers on so-called net employment. The rising installation of renewable energy systems in some European countries such as Germany, Denmark and Spain has intensified the discussion of costs and benefits of renewable energy systems. One suggestion is that price increases from increasing shares of renewable energy lead to job losses somewhere else in the economy and the net effects will be negative.

Production, installation, operation and maintenance of windmills, solar modules, biomass power plants or heating systems as well as biogas and solar thermal applications have a positive investment effect on the respective industries (Figure 1). Employment in these sectors increased steadily in Germany over the last years (cf. [1]) and is often referred to as gross employment. International demand for RE technologies increases employment in these sectors. The wind industry, for instance, makes up to 70% of its 2009 turnover from exports. Hydro energy and solar modules also exhibit high export shares in their respective turnover.

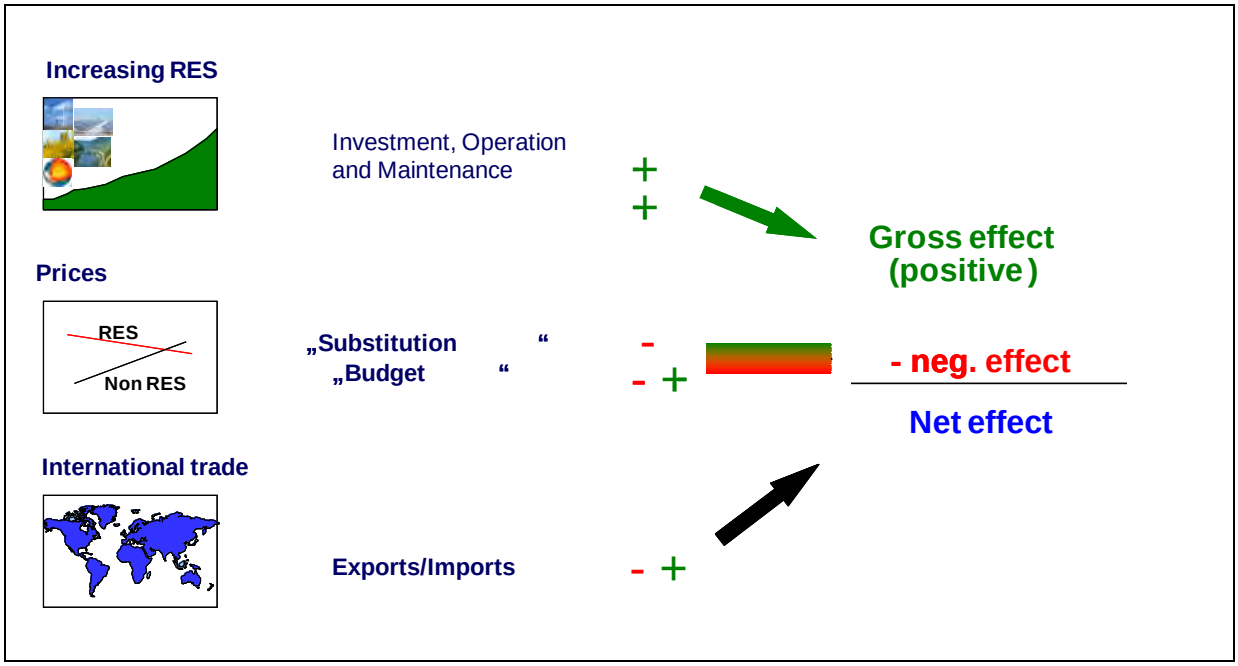

Figure 1: Economic effects of an RE increase on the labor market (cf. Staiß et al. 2006)

Negative impacts on the economy stem from 2 different sources: firstly, investment in renewable energy technologies crowds out investment in fossil fuel technologies such as coal fired power plants, oil fired heating systems and maybe at some future point gasoline driven cars. This substitution effect leads to profit losses in the respective economic sectors.

The second negative effect is larger than the substitution effect and comes from the additional costs of RE systems. Germany supports RE electricity with a feed-in tariff, which leads to electricity price increases for households and firms. This so-called budget effect (Figure 1) reduces the budget for other expenditures resulting in job losses in the respective sectors. Positive and negative impacts are multiplied and distributed through the economic system: additional employment results in additional expenditure on consumption and additional jobs in the respective sectors as well as additional taxes and therefore increases in the governmental budget. Negative impacts affect the economy through the same channels. For information on the net effects one has to employ a model of the total economy.

2.2. Model

The environmental macroeconometric model PANTA RHEI is at the core of our methodological approach. PANTA RHEI is an environmentally extended version (cf. [2], [3], [4], [5]) of the macro-econometric simulation and forecasting model INFORGE. It is based on official statistics and consistently describes inter-industry flows between 59 sectors. It includes consumption, government, investment, construction, inventory and exports as well as prices, wages, labor compensation, profits, taxes, etc. on the sectoral and macroeconomic level [6],[7].

The behavioral equations reflect bounded rationality rather than optimizing behavior of agents. All parameters are estimated econometrically from time series data (1991 – 2008). Producer prices are the result of mark-up calculations of firms. Output decisions follow observable historic developments, including observed inefficiencies rather than optimal choices.

The energy module captures the dependence between economic development, energy input and CO_2 emissions. It contains the full energy balance with primary energy input, transformation and final energy consumption for 20 energy consumption sectors, 27 fossil energy carriers and the satellite balance for renewable energy [8]. The energy module is fully integrated into the economic part of the model.

To examine the economic effects of increasing shares of renewable energy in Germany our analysis applies PANTA RHEI to a set of scenarios and compares the resulting economic quantities.

2.3. Scenarios

Scenarios, in contrast to forecasts, present consistently derived different possible future developments. They enable a "what-if" analysis. For Germany, we apply the official scenario for the development of new RE installations, the so-called "Lead Scenario [9]. This scenario includes bottom-up modeled cost-structures of RE technologies, based on the learning curves for 10 RE technologies. It is a target oriented scenario, in which 84.7 percent RE will be reached in electricity generation, 49.4 percent in heat generation and 49.5 percent in primary energy supply. A scenario with zero investment in RE since 2000 serves as the respective (hypothetical) reference development.

The scenario technique is often applied when future development hinges on the development of some crucial quantities, whose development is highly uncertain. Future employment effects from increasing renewable energy, for instance, critically depend on the relative costs of renewable energy compared to fossil fuels, on national policies for the support of renewable energy and on international climate regimes and RE strategies.

Thus we constructed the following scenarios for the development of each of these decisive factors (cf. Table 1):

1. two different price paths for international energy prices
2. three different scenarios for the domestic investment
3. four different export scenarios, which vary by the share of imports and domestic production in 10 world regions and 10 technologies and with respect to the trade shares of Germany.

2.3.1. International energy prices

International energy prices determine the reference price for the additional costs of renewable energy systems in Germany, because large shares of fossil fuels are imported. The future development path of import prices for fossil fuels is highly uncertain considering the large fluctuations in the past couple of years. Therefore we implement a lower price scenario and a higher price scenario with the respective consequences for renewable energy diffusion. The price scenarios follow essentially the projections of the IEA. The higher price level coincides with the projections in the World Energy Outlook (WEO) 2009 [10]. The lower price level is lower than the more recent projections in WEO 2010, [11], but the upper price level exceeds the assumptions there. Since our analysis tries to stay on the conservative side of things, in the following we report the findings for the lower price level.

2.3.2. Domestic investment

Germany has experienced a boom in the installation of photovoltaic panels in 2010. While the German government annually updates its "Lead Scenario" [12] for the future development of

electricity and heat from renewable energy, the latest update in 2009 did not include this rapid increase. Therefore, we included two more scenarios in our analysis, taking the likely PV developments into account. It turned out that the higher path of this set will even be overachieved in 2010, so that only the results of the original scenario and the highest sensitivity will be reported here.

2.3.3. International development and exports

Export is a major driver of the economic performance in Germany. This holds for the economy as such as well as for the sector of the production of facilities for the use of renewable energy. Earlier studies have shown [2] that net employment strongly depends on export levels. Therefore, RE technology exports have been modeled in great detail. Our analysis follows an idea developed by [13] for "green" goods. They analyze the world market for green goods and derive German export quantities from shares of traded goods in this market and shares of German producers in world trade. We follow a similar logic and determine the trade volume of renewable energy technologies for as a calibration for the projections. For this year, the trade shares of German producers can be estimated from statistical data and additional structural knowledge. For the future we develop four scenarios, all of them based on the Energy [r]evolution scenario for global installations [14].

Table 1: An overview of the most important scenario assumptions (highlighted scenarios are reported further), real prices (2005)

	2009			2020			2030		
1. import prices	Oil	Gas	Coal	Oil	Gas	Coal	Oil	Gas	Coal
	$/bbl	€/TJ	€/t	$/bbl	€/TJ	€/t	$/bbl	€/TJ	€/t
a. high	58	5,794	79	96	10,700	155	118	13,800	202
b. Low	58	5,794	79	79	8,400	123	94	10,000	147
2. domestic investment	billion €[5]								
a. lead scenario	20.4			15.4			15.1		
b. higher PV	20.4			16.0			14.1		
c. high PV	20.4			16.6			14.0		
3. export	billion €								
a. minimum	8.6			7,1			7,1		
b. slow	8.6			19.9			32.7		
c. optimistic	8.6			32.9			47.8		
d. maximum	8.6			41.3			59.1		
BMU (2010)									

The minimum case for exports is defined by holding the volume of exports constant until 2030. This translates into a high loss of German trade shares. The maximum case is determined by holding the trade shares constant on a rapidly expanding market, which can be seen as an almost tenfold increase of export volumes. Both scenarios serve as an upper and lower boundary to the more likely developments. The optimistic scenario assumes that Germany maintains significant shares in global trade. The slower scenario can either be seen as a slowdown in German competitiveness or as a tendency to wall off markets in the future. Table 1 gives an overview of the main scenario settings.

Instead of a business-as-usual reference run, which in many studies describes a development under which no further measures are taken [15], this study uses a zero scenario (for the same approach [16]). It describes a consistent hypothetical development in energy generation without renewable energy from 2000 onwards and includes the additional fossil power plants and heat generation plants that would then be necessary along with the associated investment. In this scenario, renewable energy makes only a very limited contribution to the heat and electricity supply, for the latter predominantly from large-scale hydropower, which was already competitive even before the Renewable Energy Sources Act came into force.

In the following analysis results will be reported for the low price path and the high domestic investment path. All export scenarios will be included in the reported results.

3. Results

The economic impact of an activity such as the expansion of renewable energy is assessed by comparing a simulation without the activity or economic policy measure with a simulation that includes the activity.
The zero scenario based on the low price path is now compared to a development with differing degrees of domestic investment in RE and differing export trends based on the same price path. The comparison of simulation results shows macroeconomic effects such as net employment effects which can be traced back to the different scenario assumptions.

3.1. Net employment

To gain an overview of selected results in all the simulation runs, the charts below show the results for net employment over time. Absolute deviations from the zero scenario with the low price path are shown. Positive values should be seen as positive net employment by comparison with a development without expansion of renewable energy. Negative values indicate that employment lags behind the value it would have had without the expansion of renewable energy.

The increase of renewable energy leads in most of the scenarios studied to positive net employment, rising steadily, particularly from 2020 onwards. The net effects are negative in the scenarios with minimal exports (i.e. remaining constant at today's level), although this should be seen here more as a notional lower limit. In this case, for the two expansion paths (Lead Scenario 2009 and PV2) lower values for employment are observed by comparison with the zero scenario. However, at the end of the observation period there is a reversal in these cases: the net employment effects become slightly positive or are neutral. The influence of exports on the domestic employment level also becomes very evident in the scenarios studied: using the optimistic expectations, the positive net employment effect rises by 2030 to values in excess of 150,000. In combination with cautious export expectations, there are less positive deviations from the zero scenario up to 2015. After that the positive employment effects of exports become apparent.

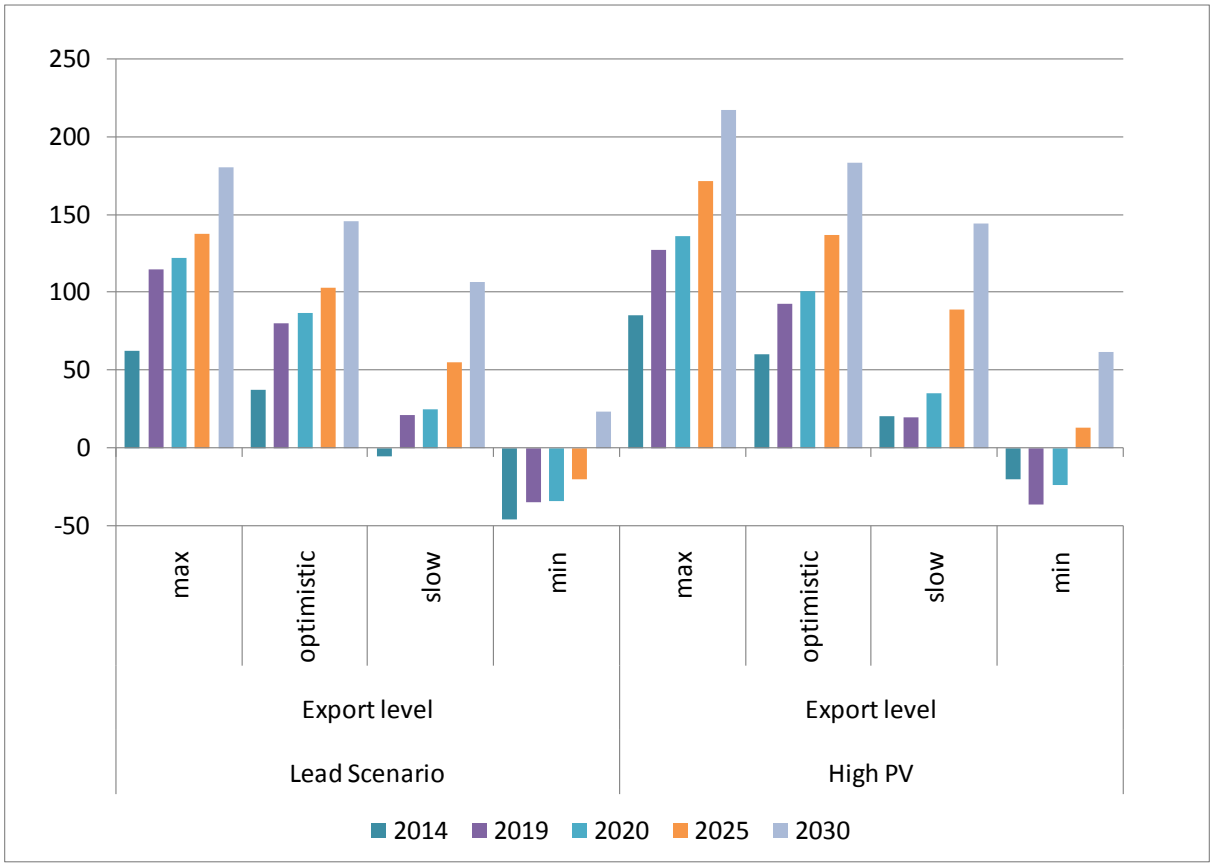

Figure 2: Employment in absolute differences to the zero scenario, in 1000 persons.

Since we are demonstrating only the low price path here, the higher additional costs, brought about by low prices for fossil energy sources, attenuate the positive net employment effects. Overall, the highest net employment stems from maximal export in combination with high PV expansion. Here net employment in 2030 is a little in excess of 200,000 people higher than it would have been without expansion of renewable energy in Germany.

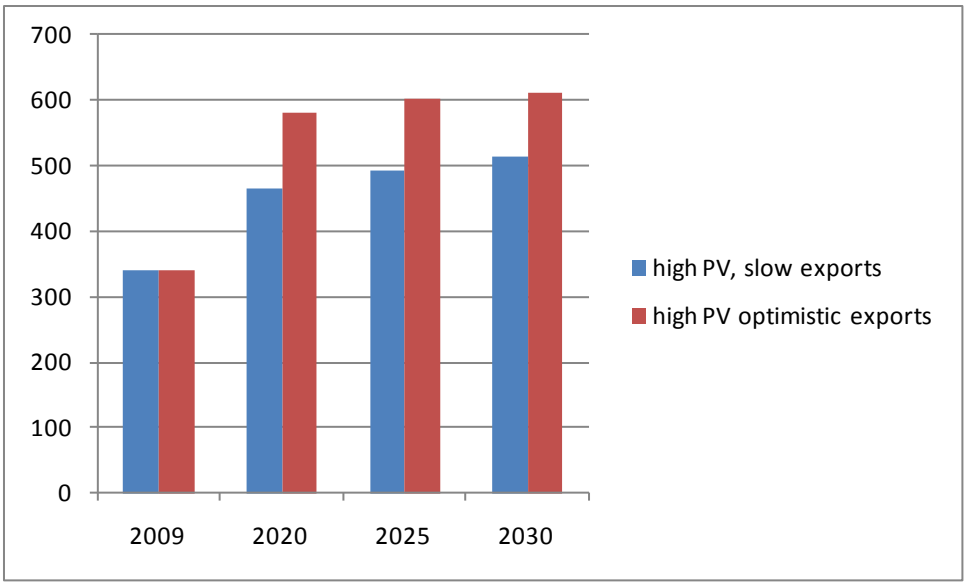

Figure 3: Gross employment in 1000 for two selected scenarios based on high domestic photovoltaic increase combined with slow (blue) or optimistic (red) exports.

The RE industries will employ 500-600.00 people. The figure rises with firms continue to be successful on international markets. The importance of global markets can be read from Figure 3. The different assumptions about exports lead to 100.000 jobs more in the RE industry in the optimistic export scenario.

The future increases in gross employment will not be as fast as they have been in the past. In Germany, the industry doubled its employment between 2004 and 2009 [17]. 2009 339,500 people worked in the production, operation and maintenance, fuel production and input production of RE systems. Our results show a little less than twice this number by 2025.

4. Discussion and Conclusions

Our analysis shows possible positive impacts of the expansion of renewable energy in Germany – and the conditions and policy implication for a positive development. The literature also provides analysis with the prediction of negative impacts – for Germany and other countries. Frondel [18] calculates the additional costs of a projected increase with a national focus and claims that especially the costs of photovoltaic systems cannot be balanced. For Spain, Alvarez [19] showed negative economic impacts, only focusing on the domestic market. However, the main wind energy systems producer, Gamesa, realizes more than 90% of its turnover abroad. A sensible consideration of exports and global markets helps to understand the dynamics of countries which developed a RE industry sector.

For the EU27, the EMPLOY-RES project [20] showed slightly positive effects. The two models used in this study are either more rigid in their price adaptation or they assume perfect substitution of all factors. The PANTA RHEI approach is less rigid but does include adaptation costs as opposed to perfect substitution.

The issue of economic impacts of the expansion of renewable energy will be part of the sustainability discussion for the time to come. On the one hand, increasing installation brings down the specific costs through learning curves and scale effects. On the other hand, parity of electricity generation costs from renewables will only be reached within the next 10-15 years. The German example shows how a large domestic market leads to the development of a successful industry. However, these successes are vulnerable to abrupt policy changes, as experiences with the US industry or the Spanish market show.

5. Acknowledgements

This research has been supported by the German Federal Ministry for the Environment, Nature Conservation and Nuclear Safety. The full analysis includes more aspects and Dietmar Edler, Marlene O'Sullivan, Peter Bickel, Barbara Breitschopf and Joachim Nitsch contributed.

References

[1] O'Sullivan, M., Edler, D., Ottmüller, M, Lehr, U., Gross employment from renewable energy in Germany in 2009 - a first estimate, Federal Minister of the Environment, 2010.

[2] Lehr, U., Nitsch, J., Kratzat, M., Lutz, C. & Edler, D., Renewable Energy and Employment in Germany. Energy Policy, 36, 2008, pp. 108-117.

[3] Meyer, B., Lutz, C., Schnur, P., Zika, G., Economic Policy Simulations with Global Interdependencies: A sensitivity analysis for Germany. Economic Systems Research, 19(1), 2007, p. 37-55.

[4] Lutz, C., Meyer, B., Nathani, C., Schleich, J., Endogenous innovation, economy and environment: impacts of a technology based modelling approach for energy-intensive industries in Germany. Energy Studies Review, 15(1), 200, pp. 72-18.

[5] Lutz, C., Meyer, B., Nathani, C., Schleich, J., Endogenous technological change and emissions: The case of the German steel industry. Energy Policy, 33 (9), 2005, pp. 1143-1154.

[6] Meyer, B., Distelkamp, M., Wolter, M.I., Material Efficiency and Economic-Environmental Sustainability. Results of Simulations for Germany with the Model PANTA RHEI, Ecological Economics, 63(1), 2007, pp. 192-200.

[7] Ahlert, G., Distelkamp, M., Lutz, C., Meyer, B., Mönnig, A. & Wolter, M.I.,. Das IAB/INFORGE-Modell. In: Schnur, P. & Zika, G. [Eds.]: Das IAB/INFORGE-Modell. Ein sektorales makroökonometrisches Projektions- und Simulationsmodell zur Vorausschätzung des längerfristigen Arbeitskräftebedarfs. IAB-Bibliothek 318, Nürnberg, 2009, pp. 15-175.

[8] Arbeitsgemeinschaft Energiebilanzen, Energiebilanzen für die Bundesrepublik Deutschland, Satellitenbilanz „Erneuerbare Energien“ 2010.

[9] Nitsch, J. and Wenzel, B., Entwicklung der EEG-Vergütungen, EEG-Differenzkosten und der EEG–Umlage bis zum Jahr 2030 auf Basis des Leitszenario 2010, Federal Minister for the Environment, 2010.

[10] IEA (2009): International Energy Agency. World Energy Outlook 2009. Paris.

[11] IEA (2010): International Energy Agency. Energy Technology Perspectives 2010. Paris.

[12] Nitsch, J. and Wenzel, B., Lead Study 2009, Federal Minister for the Environment, 2009

[13] Edler, D. And Blazejczak, Wirtschaftsfaktor Umweltschutz, 2007.

[14] Krewitt (2008): Krewitt, W., Teske, S., Pregger, T., Naegler, T., Simon, S., Graus, W., Blomen, E. et al. “Energy (R)evolution – a Sustainable World Energy Outlook.” Study commissioned by Greenpeace Int. and the European Renewable Energy Council (EREC); DLR Stuttgart, Ecofys Utrecht, 2nd edition 2008.

[15] Prognos/EWI/GWS, Energieszenarien für ein Energiekonzept der Bundesregierung. Study commissioned by the Federal Ministry of Economics and Technology (BMWi), 2010.

[16] Kratzat, M., Lehr, U., Nitsch, J., Edler, D., Lutz, C., Erneuerbare Energien: Arbeitsplatzeffekte 2006, Final report, Federal Minister for the Environment, 2007.

[17] O’Sullivan, M., Edler, D., Ottmüller, M, Lehr, U., Nienhaus, K., Breitschopf, B., Bickel, P., Khoroshun, O., Renewable employed!, Federal Minister of the Environment, 2010

[18] Frondel (2010): Frondel, M., Ritter, N., Schmidt, C. and Vance., C. Economic Impacts from the Promotion of Renewable Energy Technologies: The German Experience, study supported by Institute for Energy-Research

[19] Alvarez, G. 2009, Study of the effects on employment of public aid to renewable energy sources, Study supported by Institute for Energy-Research.

[20] ISI (2009): ISI, Ecofys, EEG, Rütter + Partner Socioeconomic Research + Consulting, LEI, SEURECO. EMPLOY-RES - Employment and growth impacts of sustainable energies in the European Union, Karlsruhe.

Cost and benefit of renewable energy in europe

Yoram Krozer

University Twente/Sustainable Innovations Academy, Enschede/Amsterdam, the Netherlands
Corresponding author. Tel: +31 6 51 23 13 71, Fax: +31 20 663 19 63, E-mail: krozer@xs4all.nl

Abstract: Costs and benefits of renewable energy use in electricity generation in the EU are assessed during low oil prices 1998-2002 and high oil prices 2003-2009. The EU statistical data is used. The renewable energy use in the EU was about 21% of the total energy inputs in 2008 and it was growing by 5% annual average during 2003-2008 compared to nearly nil growth of the fossil fuel input. During high and fast increasing oil prices, the correlations between the changes of consumers' electricity prices and the growth of renewable energy use indicates that the large and growing use did not increase the prices but decreased the consumers' electricity prices in several EU countries. An explanation is that the renewable energy enabled input diversification in electricity generation, which has reduced the costs. Consumers' electricity prices are simulated in case these had followed the fossil fuel input costs and compared with the observed prices. It is found that high oil prices invoked substantial efficiency-increase and that the renewable energy input has been net beneficial to the EU citizens even when the periods of low and high fossil fuel prices are taken together.

Keywords: *Renewable energy, Electricity prices, Cost-benefit, Feed-in tariffs*

1. Introduction

The European Union (EU) policy aims at a shift in electricity generation away from fossil fuels (coal, oil, gas and nuclear) towards renewable energy resources, which are biomass and waste, hydro-, geothermal-, solar-, and wind power; co-generation heat plants (CHP) is sometimes included (EU, 2005). This shift, however, is not evident because energy policies of the twenty seven EU member countries differ (Blok, 2006) and because renewable energy use for electricity generation is considered costly (Steger et al., 2005; EU, 2008). However, the cost-reducing technological progress (Gross et al, 2008) in combination with increasing oil prices after the year 2003 till 2008 created a competitive edge for renewable energy use in electricity generation called grid parity and global investments in renewable energy expanded from USD 29 billion in 2004 to USD 151 billion in 2008, out of it more than a third in the EU (UNEP, SEFI, New Energy Finance, 2010). Oil prices fluctuate cyclically, they fell down after 2008, and the renewable energy use became costly. A challenge in the EU policymaking is how to foster the shift regarding the oil price cycle.

The EU policy could act anti-cyclic. It could support renewable energy during low oil prices. This support would maintain high investments entailing the cost-reducing technological progress and thereby, anticipate high oil price when no or little support is needed. Such an anticipation policy, however, causes social costs because it drives up electricity prices above the prices that would be based on the lower input prices on international markets. A higher input price also provides social benefits because it invokes efficiency-increase and reduces pollution, especially greenhouse gas emission due to lower combustion of fossil fuels (Sensfuß et al, 2007). A few available cost-benefit studies are inconclusive. For example, a study commissioned by the German government suggests that the German support of renewable energy in 2006, if scaled up to the EU level, would provide net benefit of 9.4 billion euro in the EU, out of it 5 billion euro efficiency increase, 1 billion lower imports and 3.4 billion euro due to lower pollution (Böhme and Dürrschmidt, 2007:29), but another German study, one into a fossil fuel tax in electricity generation, indicates net costs of this policy, albeit the benefits of lower pollution and innovations in energy saving are unaccounted (Walz and Schleich, 2009). Studies in the US suggest that some technical and social benefits of the renewable energy use are often omitted, such as lower thermal, transport

and conversion losses in electricity generation, transmission and use (NREL, 1997; Sawin and Moomaw, 2008), respectively self-reliance and local job creation (Bird et. al., 2008).

2. Methodology

The starting point in this paper is that supporting renewable energy during low oil prices to anticipate high oil prices is a costly policy. It is justifiable only if the renewable energy use would be net beneficial during the whole cycle of low and high oil prices, which means when the costs of renewable energy use during low oil prices would be outweighed by the benefits during high oil prices. This paper looks back at the last oil price cycle from the year 1998 when the annual average price was at the lowest point in the last half century to 2008 when the price was at the highest point (www.inflationdata.com). Question is if renewable energy in electricity generation in the EU was net beneficial during the price cycle. The price cycle is divided into a period of low oil prices 1998 – 2002 when prices have fluctuated around the price in 2002 and the period of high oil prices 2003 – 2008 when the prices have annually increased. In the calculations, all fossil fuels prices are annual averages in constant (year 2000) FOB prices using the US Energy Information Administration (EIA) data (www.eia.doe.gov). All EU data is based on the EUROSTAT (the EU statistical bureau), which is data on energy and electricity generation and consumption. The consumers' electricity prices are excluding taxes in constant (2005) Euro (www.statline.eu). The assessment covers only the statistically observable prices.

The uses and prices of energy inputs in electricity generation are presented in Section 2. The impact of the renewable energy use on consumers' electricity prices during high fuel prices is discussed in Section 3. The costs and benefits of the renewable energy use in electricity generation are covered Section 4. The conclusions are drafted in Section 5.

3. Results

3.1. Energy inputs

The question addressed in this section is if renewable energy has substituted fossil fuels. The following data is compiled for the periods 1998 – 2002 (low oil prices) and 2003 – 2008 (high oil prices): the shares of energy inputs in electricity generation in 2008, the average annual volume growth, the annual average international market prices of fossil fuels and the prices of fossil fuel mix in electricity generation (weighed for volume). The prices of nuclear power and renewable energy are not found. Table 1 shows the data.

The energy inputs in electricity generation have changed during the prices cycle 1998-2008 alongside with 2% annual electricity generation growth. During high oil prices, coal and oil inputs decreased, even though the coal price is below the oil price, nuclear somewhat decreased, and the gas use has increased albeit its price follows neatly the oil price. The renewable energy has grown by 5% during the high oil prices compared to 1% in the period of low oil prices. In result, the share of renewable energy in total energy inputs increased from 18% in 1998 (not shown in the table) to 21% in 2008. In addition, the CHP share in energy input increased from nearly nil in 1998 to 11% in 2008. Hydropower and biomass & waste are the largest renewable energy uses, whereas solar- and wind energy uses grow very fast though the volumes were nearly nil in 1998. Renewable energy use has substituted fossil fuels. The substitution cannot be attributed to the public support of renewable energy because the support of fossil fuels in the EU was much larger (EEA, 2004). The renewable energy use in electricity generation has, apparently, advantages during high oil prices.

Table 1 Energy inputs for electricity generation, excluding CHP and geothermal energy

*Volume data from Eurosta *), prices data from EIA(**)*	*Input in total*	*Average annual volume growth*			*Average annual prices €/t.o.e.*		
	2008	*1998-2008*	*1998-2002*	*2003-2008*	*1998-2008*	*1998-2002*	*2003-2008*
Coal	18%	-0.1%	1%	-1%	85	62	104
Oil	3%	-6%	-3%	-9%	230	161	288
Gas	26%	7%	8%	7%	194	159	223
Nuclear	31%	0.0%	1%	-0.9%	N.A.		
Fossil fuels mix (volume weigh)	79%	1%	2%	0.6%	149	115	177
Biomass & waste	5%	5%	2%	8%	N.A.		
Hydropower	12%	0.3%	-0.1%	0.6%			
Solar	0.2%	61%	47%	73%			
Wind	4%	29%	38%	22%			
Renewable energy	21%	3%	1%	5%			

*(*) No Eurostat data for the biomass & waste use; here assumed 80% of all production is for electricity generation with 15% conversion efficiency. (**).Price converted into €/t.o.e.: Euro/USD with the www.inflationdata.com*42.2 €/GJ * EIA inputs prices, which are for coal USD/metric ton*24GJ, for oil USD/b.o.e*6.1 GJ, for gas USD/1000m^{3}feet*35.5*39GJ*

3.2. Consumers' electricity prices

In this section we discuss whether renewable energy growth caused higher consumers' electricity prices in the EU. If renewable energy would be costly compared to fossil fuels, its growing use would drive up consumers' electricity prices, this predicts theory, and this impact on prices would be significant because the renewable energy use has a substantial share in the total energy inputs. To assess this impact, the countries' annual volume growth of renewable energy in electricity consumption is rank correlated with the annual changes of consumers' electricity price. A positive rank correlation of the volume growth with the price change indicates that the renewable energy use causes higher price, and vice versa a negative rank correlation indicates that the use causes lower prices. A rank correlation (R^2) 0.8 and higher, or – 0.8 and lower is assumed to indicate a significant impact. The assessment covers the period 2003 - 2008 and within this period the timeframe 2005 – 2008 when the oil prices almost doubled. Table 2 shows: countries' share of the renewable energy use in electricity consumption, energy growth, prices changes and the rank correlations during 2003 - 2008 and 2005 – 2008.

Table 2 Growth of the renewable energy use in gross electricity consumption and changes of the consumers' electricity prices (without taxes). Bold: significant negative correlation, italic: average consumers electricity prices above the EU average price (2005-2008), Minus: net importers of electricity

Eurostat data for the volume and prices	*2008(*) Renewable energy use electricity consump.*	*2003-2008 Volume growth*	*Prices*	*Correlat. Volume: prices*	*2005-2008 Volume growth*	*Price*	*Correlat. Volume: prices*
EU(**)	17%	3%	6%	(0.2)	6%	5%	0.0
Belgium -	5%	19%	1%	0.4	26%	7%	(0.4)
Bulgaria	7%	13%	3%	(0.5)	4%	5%	(0.3)
Czech R. -	5%	8%	2%	0.7	18%	13%	(0.6)
Denmark	29%	10%	-3%	(0.5)	7%	7%	(0.9)
Germany -	15%	16%	1%	(0.4)	17%	1%	(0.8)
Estonia -	2%	53%	5%	0.9	33%	4%	0.8
Ireland	12%	20%	7%	0.4	25%	10%	0.2
Greece	8%	13%	9%	(0.8)	-2%	13%	(0.9)
Spain	21%	8%	4%	0.1	3%	6%	0.7
France -	14%	-2%	-5%	0.1	2%	0%	0.4
Italy -	17%	-1%	19%	(0.1)	2%	5%	(0.9)
Cyprus	N.A.						
Latvia -	41%	4%	11%	0.8	9%	16%	0.8
Lithuania -	5%	14%	5%	0.6	20%	8%	0.5
Luxemb.	4%	7%	-4%	0.5	17%	5%	0.1
Hungary	6%	48%	7%	(0.0)	68%	13%	(0.7)
Malta	N.A.						
Netherland	9%	13%	-3%	0.6	15%	6%	0.5
Austria	62%	0%	5%	0.2	5%	7%	(0.2)
Poland -	4%	14%	1%	0.9	26%	9%	0.8
Portugal	27%	13%	-2%	0.1	8%	-4%	0.2
Romania -	28%	2%	10%	0.8	6%	15%	1.00
Slovenia	29%	-1%	-4%	0.2	4%	2%	0.3
Slovakia	16%	1%	1%	0.6	10%	3%	0.6
Finland	31%	3%	2%	(0.4)	7%	3%	(0.8)
Sweden -	56%	0%	-2%	0.1	8%	5%	(0.9)
Un.King -	6%	14%	0%	0.4	17%	14%	(0.8)

(*) Renewable energy use is excluding CHP
(**) The EU average price is total EU value of sales divided by the volume of sales.

In the period 2003 - 2008 the significant positive rank correlations between the renewable energy growth and the changes of consumers' electricity prices are found for Estonia, Latvia, Poland and Romania but all these countries hardly use renewable energy, which is largely imported. The high negative correlation is found for Greece that is a large user of renewable energy. The findings in the period of the fast increasing oil prices 2005 – 2008 provide more insight. Next to the significant positive correlations for the countries that hardly use renewable energy, significant negative correlations are found for Denmark, Germany, Greece, Italy, Finland, Sweden and United Kingdom. All these countries except United Kingdom are large users. These significant negative correlations cannot be explained by

cheap domestic and imported hydropower because it has decreased in all EU countries except Bulgaria and Romania. Cheap imports of other renewable energy inputs can be somewhat relevant for Germany, Italy, Sweden and United Kingdom but not for Greece, Denmark and Finland that are net exporters of renewable energy. It could be that the countries in which the significant negative impact is found already experience higher consumers' electricity prices than the EU average, which holds for Germany, Italy and United Kingdom but not for Greece, Denmark, Finland and Sweden.

The growing renewable energy use had low impact on the consumers' electricity prices during 2003-2008 and it has contributed to the lower electricity prices during 2005-2008 (when fossil fuel prices increased very fast) particularly in the countries that are large users of renewable energy. A plausible explanation is that the electricity generators that start with using renewable energy face higher input costs, which are reflected in the higher electricity prices. The generators that use much renewable energy learn to benefit from this input diversification with positive effects on the production costs, which are reflected in the lower consumers' electricity prices

3.3. Cost and benefits of renewable energy

Regarding the positive impact of renewable energy use on the consumers' electricity prices question is whether its use is costly throughout the oil price cycle. Therefore, the observed annual consumers' electricity prices are compared to a hypothetical situation in which electricity prices would have follow the fossil fuel mix prices (see Table 1). The social benefits are in case of lower consumers' electricity prices than if the prices had shadowed the fossil fuel mix prices, and vice versa the social costs are in case of higher consumers' electricity prices than had they shadowed the fossil fuel mix prices.

In the assessment, the year 2002 is taken as the reference because thereafter the oil prices have annually increased and the renewable energy use has grown. Since the electricity prices during 1998 - 2002 are not available for all EU countries it is assumed that they equal to the price of 2002, which is acceptable for this assessment because the annual fossil fuel mix prices fluctuated around the 2002 price. The total social costs and benefits are assessed and the costs and benefits that can be attributed to the renewable energy use, which is based on the additional renewable energy use compared to the reference year 2002. Table 3 shows the energy inputs and outputs in electricity generation, the renewable energy use and its additional use after the reference year, costs of energy outputs and electricity prices, social costs and benefits.

Table 3 Social costs and benefits of renewable energy use in electricity production.

	Reference 2000	*Average a year 1998-2002*	*2003-2008*	*Year 2008*
Energy inputs and electricity generation in GWh				
Total energy inputs	2,753,671	2,667,958	2,930,344	2,987,611
Renewable energy use	474,417	482,221	550,345	628,069
Additional use compared to 2002	-	7,804	75,928	153,652
Electricity consumption	2,599,739	2,510,120	2,779,549	2,855,561
Price of energy inputs and electricity in €/GWh				
Fossil fuels prices	9,826	9,849	15,207	18,784
Electricity price (‘98-‘01 equal 2002)	83,019	83,019	102,632	115,033
Index energy input cost	100.0	100.2	155	191
Index electricity price	100.0	100.0	124	139
Social costs and benefits of electricity consumption in € billion				
Had electricity followed fossil fuel price	216	210	358	453
Observed electricity prices	216	208	286	328
Total net social benefit	-	1.88	72	125
Benefit additional renewable energy use	-	0.65	8	18

During low oil prices (1998 – 2002), the consumers’ electricity prices closely shadowed the fossil fuel prices, but during high oil prices (2003 – 2008) the consumers’ electricity prices were well below the fossil fuel mix prices. The improvements created a net social benefit on average 72 billion euro a year, which is equivalent of 20% efficiency increase. Out of this benefit on average 8 billion euro a year should be attributed to the additional use of renewable energy. Note that in 2008 the total net social benefit has peaked to 152 billion euro, out of it 18 billion euro attributable to the renewable energy use. Throughout the whole oil price cycle 1998 - 2008 the total net benefit attributable to the renewable energy use approached 49 billion euro. When looking back, support of the renewable energy with the incentives of this order of magnitude would be justifiable because it would create cost-neutral renewable energy capacity that would enable to anticipate increase of fossil fuel prices.

4. Conclusions

With reference to the EU policy that aims to shift from fossil fuels to renewable energy in electricity generation, the question is discussed whether it is socially beneficial to support renewable energy during the low oil prices in order to anticipate high oil prices. An answer is given using statistical data for the periods of low oil prices (1998-2002) and high ones (2003-2008). The fossil fuel mix prices in electricity generation have shadowed oil prices though coal at lower prices. During high oil prices 3% of the fossil fuels use is substituted by renewable energy because the latter has grown much faster and within fossil fuels the coal and oil use is substituted by gas. The growing use of renewable energy in the EU did not increase the consumers’ electricity prices except in the countries that hardly use it but had a significant calming effect on the prices in the countries that are large user of renewable energy. A plausible explanation of this finding is that the renewable energy diversifies energy inputs and thereby creates opportunities for efficiency increase in inputs allocation. The cost - benefit assessment for the whole oil prices cycle 1998 – 2008 confirms it. The observed electricity prices are compared with the electricity prices had they shadowed the fossil fuel prices and it is assessed whether the additional renewable energy use has caused higher costs or benefits. It is found that 72 billion euro net social benefits are attained in the EU (about 20% efficiency increase). About 11% these net benefits are attributable to the additional

energy use. For the whole oil price cycle 1998 - 2008 the total net benefit attributable to the renewable energy use is estimated at 49 billion euro. The renewable energy, though it is uncompetitive during low oil prices, becomes a viable option during high fossil fuel prices. The policy that anticipates the high prices through incentives for renewable energy has a calming effect on consumers' electricity prices and is socially beneficial.

References

[1] European Commission, *Communication from the Commission - The support of electricity from renewable energy sources*, 2005.

[2] Blok, C. Renewable energy policy in the European Union. Energy Policy, 2006, 34:251-255.

[3] Steger, U, W. Achterberg, K. Blok, H. Bode, W. Frenz, C. Gather, G. Hanekamp, D. Imboden, M. Jahnke, M. Kost, R. Kurz, H.G.Nutzinger, T. Ziesemer, *Sustainable Development and Innovation in the Energy Sector*, 2005, Springer, Berlin-Heidelberg, pp. 211-222.

[4] EU, Commission Staff Working Document, *Energy Sources, Production Costs and Performance of Technologies for Power Generation, Heating and Transport*, 2008, Commission of European Communities, Brussels.

[5] Gross, R., M.Leach, A.Bauen, 2003, Progress in Renewable Energy, *Environment International*, 29, 2003, 105– 122.

[6] UNEP, SEFI, New Energy Finance, *Global Trends in Sustainable Energy Finance 2008*, 2008, United Nations Environment Program

[7] Sensfuß, F., M. Ragwitz, M. Genoese, *The Merit-order effect: A detailed analysis of the price effect of renewable electricity generation on spot market prices in Germany*. Working Paper Sustainability and Innovation, No. S 7, 2007, Fraunhofer Institute Institute Systems and Innovation Research, Karlsruhe.

[8] Böhme D., W. Dürsschmidt, Renewable Energy Resources in figures – national and international development, 2008, Federal Ministry for Environment, Nature Conservation and Nuclear Safety, Berlin.

[9] Walz, R., J. Schleich, *The Economics of Climate Change Policies*, 2009 A Springer Company, Heidelberg, pp. 33-51.

[10] NREL - National Renewable Energy Laboratory, 1997,. Benefits of Renewable Energy, US Department of Energy.

[11] Sawin, L.J., W.R. Moomaw, *Renewable Revolution: Low Carbon Energy by 2030*, Worldwatch Institute, 2009, Danvers, US.

[12] Bird, L.A., K.S. Cory, B.G. Swezey, *Renewable Energy Price-Stability Benefits in Utility Green Power Programs*, National Renewable Energy Laboratory, Technical Report NREL/TP-670-43532, 2008, Battelle.

[13] http://www.inflationdata.com/inflation/Inflation_Rate/Historical_Oil_Prices_Table.asp

[14] EIA, Annual Review 2009, DOE/EIA – 0384, 2009 www.eia.gov/aer

[15] EEA, European Environmental Agency, *Energy Subsidies in European Union, A brief overview*. Technical Report 1, 2004, Copenhagen.

Utilities' Business Models for Renewable Energy: Evidence from Germany

Mario Richter

Centre for Sustainability Management (CSM), Leuphana University of Lüneburg, Lüneburg, Germany
Tel: +49 17626392486, Fax: +49 41316772186, E-mail: Mario.Richter@uni.leuphana.de

Abstract: This study on German utilities' business models for renewable energies provides new insights into the thinking of Germany's leading utilities about future business models. Two generic business models are derived from the literature and are subsequently analyzed based on a series of in-depth interviews. A core result is that utilities clearly favor large scale projects over small scale projects on the customer-side. This result can be explained with the return potential and renewable energy portfolio standards. Contradictory to the existing literature, German utilities do not see electricity generation on the customer-side as threat to their business model. Instead, they develop very different approaches for large scale projects. It can be concluded that utility engagement in customer-side business models will remain limited in Germany, whereas large scale projects are seen as a promising future business model. The analysis from a business model perspective also shows that both business models, for small scale as well as for large scale projects, still offer room for innovation. Hence, business model innovation can help utilities to create and capture more value in the energy transition.

Keywords: *Renewable Energy, Business Model, Utility, Energy Transition*

1. Introduction

About 82% of the world's electric energy supply is either based on fossil fuels like coal, gas, and oil, or nuclear energy [1]. A key measure to fight climate change and resource depletion is the transformation of the electric power sector towards a more sustainable form of energy production based on renewable energies [2]. It is expected that the transformation will change the structure of the industry and the electric utilities as its largest actors. Several studies on this issue indicate that there will be little room for the utilities' business model in its present form [3][4][5].

The present study contributes to the discussion about utilities' business models for renewable energies by providing insight into the thinking of Germany's leading utilities. The traditional utility business model is delivery of electricity generated from large centralized power plants to the end customer. Since renewable energies are more decentralized, some authors argue that the increasing share of renewable energy generation by customers is a threat to the traditional utility business model, because it leads to decreasing electricity demand and, consequently, erosion of revenues [3][4][6][7]. Following this argument, finding new approaches to serve customers with less and cleaner energy requires a fundamental rethinking of how utilities produce, transmit, and sell electricity. Therefore the research question of this work is: *How do German utilities shape their business models for renewable energies?*

Two generic business models are derived from the literature and are subsequently analyzed on the basis of in-depth interviews with managers of German utilities. The preliminary results show that utilities clearly favor large scale projects and do not expect small scale renewable energy projects on the customer-side to be of great importance. This preference can be explained with transaction costs, economies of scale, and ambitious renewable portfolio standards.

The study is organized as follows. Section 2 introduces the business model concept and provides a literature review on utilities' business models for renewable energies. Section 3 describes the methodology, section 4 displays the results. The essay finishes with a discussion in section 5 and a conclusion in section 6.

2. Literature Review

2.1. The Business Model as a Tool for Analysis and Management

The business model is a valuable new tool for analysis and management in research and practice [8]. In terms of analysis, the concept enables the examination and comparison of companies and markets in a structured way. Using the business model as a classifying device helps to expand the understanding of business phenomena by building generic categories and the development of ideal types [9]. As a management tool, the business model helps managers to design, implement, operate, change, and control their business [10]. In this context, business models can function as "recipes" or "blueprints" that are ready for copying or variation and innovation [9]. Furthermore, thinking in business model terms also enable managers to react to external factors and influences quicker and more appropriately.

Despite the increasing importance of the business model concept in the academic literature there is no generally accepted definition. A review of the literature shows that many business model definitions are comprised of *four basic elements* [11][12][13]. The *value proposition* describes the products and services that are offered to the customers [11][14]. The *customer interface* describes the overall interaction with the customer [15]. The *infrastructure* comprises the companies' activities and assets required to create the value proposition, thus the internal organization of the value creation process [11]. The *revenue model* represents all revenues and costs associated with selling the value proposition [13][14][15].

Table 1. The Business Model Conceptualization [12][15]

Business Model Pillar	Description
Value Proposition	The value proposition describes the bundle of products and services that create value for the customer and allows the company to earn revenues.
Customer Interface	Customer interface comprises the whole contact with the customer.
Infrastructure	The infrastructure describes the architecture of the company's value creation.
Revenue Model	The revenue model describes the relationship between costs to produce the value proposition and the revenues that are generated by offering the value proposition the customers.

The conceptualization of the business model displayed above refers to the terminology of Alexander Osterwalder and Yves Pigneur [12][15]. The authors define: *"a business model describes the rationale of how an organization creates, delivers, and captures value"* [15]. This conceptualization offers some advantages: first, it is easy to apply and has been extensively tested in practice. Second, the terminology is widely used and accepted, and third, it has already been successfully applied to the field of renewable energies [16].

2.2. Utilities' Business Models for Renewable Energy

The renewable energy business model currently most widespread in Germany (as well as in the United States and Europe) functions as follows: the customer or a private investor owns and controls a renewable energy system, while the utility provides grid connection and is obliged to purchase the electricity. The costs for these services can be passed on to the consumer, but no return may be earned from this service [6]. The utility remains passive and just complies with the regulation. In this model, an increasing share of renewable energies is a threat to utilities, because utilities lose market share and revenues.

Many studies on utilities' business models have focused on this threat from customer-side renewable energy systems. Authors of these studies argue that an increasing share of renewable energy systems owned and operated by customers leads to decreasing electricity demand and consequently erosion of revenues [3][4][5][6][7]. Hence, the question for utilities is how to benefit from increasing customer-side generation. The literature provides different ideas on how an utility business model for customer-side renewable energy could look like [6][7]. For example, Frantzis et al. observed that the most promising approach for utilities is to own and operate the renewable energy system, because a return on the assets can be earned [3][6]. Referring to these studies a generic business model for customer-side renewable energy can be characterized as follows:

> *Customer-side renewable energy business model:* In this business model the renewable energy systems is located on the property of the customer. Possible technologies are photovoltaic, solar thermal hot water, CHP micro power, geothermal heat pumps, and micro wind turbines. The size of the systems usually ranges between a few kilowatts and about 1 MW. The value proposition offered by the utility can range from simple consulting services to a full-services package including financing, ownership and operation of the asset [3][4][5]. Utility financing and ownership of customer-side assets intensifies the customer relationship and can provide access to new customer segments, of customers who otherwise could not afford installation of renewable energy systems [4]. As far as the utilities' architecture of value creation is concerned, a management approach for small scale projects is needed [7]. The revenues for the utility come from return on the assets and charge for services, while costs arise from administration, installation and operation of the systems [6].

Another option for utilities is to invest in large scale renewable energy projects. This approach is represented by the second generic business model:

> *Utility-side renewable energy business model:* The projects are larger than customer-side projects and range from one to some hundred megawatts. Typical technologies are on- and offshore wind farms, large scale photovoltaic projects, biomass power plants, and solar thermal power plants [4][6][7]. The value proposition in this business model is bulk generation of electricity that is fed into the grid [6]. Therefore, the customer interface consists of power purchase agreements on a business to business level, rather than a relationship to the end-customer. As far as the infrastructure is concerned, these projects are much more similar to traditional centralized power plants than the customer-side business model. They are much closer to the utilities' core competency of asset management and operation [6][7]. Costs arise from construction and operation of the

energy project, while revenues come from regulated feed-in tariffs for electricity or tax- or investment credits.

The two generic business models are “ideal types” and represent the two sides of a spectrum [9]. Of course variations are possible. Both business models will be subsequently analyzed in the context of the German utility sector to identify challenges and potential and eventually derive evidence for future trends.

3. Methodology

The present study is based on an explorative qualitative research design, because there is no empirical evidence on this issue from the German market yet. The data is derived from a series of semi-structured interviews with managers of German utilities. The sample selection focuses on Germany, because the country is considered one of the world's leading markets for renewable energies. Of some 800 utilities of very different size and scope of activity four categories were identified by theoretical sampling [18]. Since the selected qualitative approach does not allow to derive statistically relevant information, the innovation leaders in every of the four category were selected - following the idea of extreme cases by Yin [19]. The selected companies were identified through internet research and consultation of industry experts from utilities, industry associations, and consulting.

Table 2. Categories of German Utilities

Category	Revenues in million €	Size of Category
1. Multinational utilities	>10.000	4
2. Regional utilities	10.000-1.000	10
3. Large Local Utilities	999-100	~ 80
4. Small Local Utilities	100-0	~700

To date, 15 interviews have been conducted, with managers from 11 utilities. In some cases two interviews per utility were helpful when the responsibility for customer-side and utility-side business models lay in different departments. It is planned to conduct 9 more interviews in the coming weeks. Therefore, the results of this essay are preliminary. So far, the following utilities are included in this study: E.on, Vattenfall, EnbW, RWE, Stadtwerke München, EWE, Mainova, HEAG Südhessische Energie, Stadtwerke Aachen, Stadtwerke Karlsruhe, and Hamburg Energie. The interviewees are directors or managers, mainly from business development departments. The interviews are partly conducted in person and partly via telephone. Length of the conversations varies between 45 and 90 minutes. The interviews are recorded on tape and subsequently transferred into a written protocol. The protocols were analyzed following the conceptual business model components presented above.

4. Preliminary Results

The results show that the interviewed utilities have very different opinions on the future role of customer-side renewable energies. Whereas the future development in this market is not at all clear today, the business model for utility-side projects is clear and plays a significant role in utilities current activities. The reasons for this result can be explained by analyzing the two generic business models following the four pillar structure (see section 2.1).

4.1. Customer-Side Renewable Energy Generation

The interviews show that contrary to the argumentation in the literature, 9 out of 11 interviewed utility managers do not see customer-side generation as a threat to the current utility business model. They mainly see customer-side renewable energy as a niche market without much revenue potential for utilities.

4.1.1. Value Proposition

Five of the 11 interviewed companies offer customer-side renewable energy products or services. For example they support their customers to install solar PV systems or micro CHP systems. But in practice, none of them is actively promoting these offers, because none of the offerings is actually profitable. In practice, it is far from clear what utilities intend to offer to their customer. Only 2 out of 15 interviewees expect customer generation to become a severe threat to the current value proposition. The rest does not see a profitable market and thus no urgent need to develop new value propositions in this field. The utilities that actively try to develop new value propositions admit that they severely struggle to find economically sustainable business models.

4.1.2. Customer Interface

Renewable energy is considered to have positive effects on the customer relationship by all interviewees. The existing products and services for end-customers are designed to increase the individual customer relationship and secure long term gas and electricity delivery. Projects like installation of solar systems on schools or public buildings are used to demonstrate community involvement.

4.1.3. Infrastructure

Infrastructure for customer-side business models exists on a very small scale, because the projects are not profitable yet. Activities are seen as “pilot project” and are organized in separate firms to have better control over costs and revenues. The main purpose is testing the market. New infrastructure is hardly built up before the value proposition and revenue model are clear. One approach to be active without the need to build up own infrastructure is to establish partnerships with local companies that provide installation and other services.

4.1.4. Revenue Model

All interviewed utilities’ that have some sort of some customer-side renewable energy business model struggle to earn sufficient returns. There is no economic sustainable revenue model in the market yet. Customer-side projects are too small and too fragmented to be able to contribute significantly to the earnings of the company. An economically sustainable revenue model is the key to unlock the market of customer-side renewable energies for utilities.

4.2. Utility-side Renewable Energy Generation

The interviewed utilities are currently investing billions of Euros into utility-side renewable energy projects. Most attractive technologies are on- and offshore wind energy as well as biomass and biogas. Solar energy only plays a minor role in investment budgets, since this technology only contributes a small share to the electricity generation capacity.

4.2.1. Value Proposition

The interviewees do not see the traditional value proposition under pressure by increasing shares of large scale renewable energy projects. On the contrary, most managers see an additional value that can be offered to the customer in the form of green electricity tariffs.

4.2.2. Customer Interface

The interviewees perceive customers as increasingly critical towards utilities. In this context utilities try to strengthen their customer relationship by positioning themselves as environmentally friendly. In addition, the regional and local utilities use renewable energies to demonstrate community involvement. On the other hand, utilities face stakeholder opposition towards new large scale renewable energy projects. One approach to ease such a conflict is offering participation in the project. This way utilities and customer become joint investors. Overall, the utilities see the customer interface positively affected by renewable energies.

4.2.3. Infrastructure

Utilities are currently investing massively in projects to create their own renewable generation infrastructure. In this context they also develop the corporate infrastructure to operate and manage the renewable energy assets. The main question in this context is in which steps of the renewable energy project value chain the utility should become active. Larger utilities tend towards integration of project development and maintenance services into their business model. This way they enhance the value creation in the project and are able to earn a higher overall return with the energy project. Smaller utilities rely much more on external service providers for project development and maintenance service, because it is too costly to hire skilled personnel for a small generation infrastructure. While “blueprints” for utility-side revenue models are available in the market, it seems as if the project value chain offers room for business model innovation for all types of utilities.

4.2.4. Revenue Model

Investment decisions for utility-side renewable energy projects are usually based on well defined return expectations. Therefore, the revenue model is the key to the decision whether a renewable energy project is realized or not. Although renewable energy projects provide lower returns than conventional power projects, they include less risk which makes them attractive to utilities from a financial viewpoint as well. While the interviewed multinational utilities point out the role of business model innovation to increase revenues and decrease costs, the interviewed regional and local utilities emphasize the need to also include community aspects in their decisions. The optimization of the value chain according to the utilities competencies offers large potential to increase earnings.

5. Discussion

The present study shows that the interviewed utilities mainly do not perceive revenue erosion by customer-side electricity generation as a threat to their current business model. Only two interviewees speak of a severe threat. The utilities clearly favor large scale utility-side projects over customer-side projects, as the former offer more attractive returns and allow to reach renewable portfolio standards more quickly. The higher returns were identified to be mainly a consequence of transaction costs, which e.g. comprise project development cost, such as costs for planning, permission, and administration. These costs account for a significant portion of the overall costs and do not rise in proportion with the size of the

project. Also larger projects allow favorable cost structures for asset management as well as operation and maintenance. Therefore, larger projects have comparatively lower project development costs [20]. Besides, for the same reason larger projects make reaching a certain renewable portfolio ratio in a given time easier and cheaper. Furthermore, the analysis from the business model perspective revealed that utility-side projects offer a series of advantages: they do not make new value propositions necessary, the customer interface is positively affected, and revenue potential is clearer than is seen with customer-side projects. Customer-side renewable energy was not considered an interesting future market by most interviewed utilities. Some of the utilities have undertaken first steps to build customer-side business models, but activities are at a very early stage and budgets are small. The analysis reveals that many questions about the value proposition, the infrastructure, and the revenue model are unanswered. The main challenge is to reach profitability of the revenue model.

Many authors on utilities' business models for renewable energy argue that customer-side electricity generation from renewable energies requires utilities to develop new value propositions to combat loss of market share and revenue erosion [3][4][7]. The analysis in this study shows that most utilities focus on large scale projects and do not see customer-side renewable energy as a threat to their business. From a business model perspective it makes sense to invest in large scale projects, because business model templates are available and returns are higher. Furthermore, large scale projects make it easier to reach the renewable portfolio standards. From these findings it can be concluded, that utility engagement in customer-side business model for renewable energy will remain limited in Germany, whereas large scale renewable energy projects are a promising future business model for utilities.

The findings are subject to some limitations. The method of conducting qualitative semi-structured interviews has proven well suited to gain a first insight into utility thinking, but it does not allow drawing any rigorous generalizations. Furthermore, the high level approach in the interviews creates the danger of over-simplification. The same is true for the approach to analyze two generic business models, which cannot cover all details of real world utility business models. Furthermore, business models are highly dependent on the regulatory framework, so the results might not easily be transferred to other markets [6]. Also, the data collection is not fully completed yet, therefore, the results of this article are preliminary.

The research raises a series of new questions on how utilities can improve their business models. Further research should focus on both utility-side business models as well as customer-side business models in more detail. The former still offer room for revenue improvement when further steps in the value chain are integrated or suitable collaborations are installed. The latter represents a market which is mainly untapped by utilities to date, due to comparably low return expectations. Research on new business model designs might help to overcome this hurdle and open a large new market for utilities.

6. Conclusion

The present study shows that utilities focus on large scale utility-side project rather than on customer-side projects. The analysis showed that both business models offer much room for innovation. Consequently, utilities should intensify their thinking about business models to increase their potential to create and capture value from the energy transformation. Furthermore, policy-makers should pay close attention to the developments in this field in order to shape the framework for a truly sustainable energy future.

References

[1] International Energy Agency (IEA), Key World Energy Statistics, 2009.

[2] Intergovernmental Panel on Climate Change (IPCC), IPPC fourth Assessment Synthesis Report, Cambridge University Press, 2007.

[3] L. Frantzis, S. Graham, R. Katofsky, H. Sawyer, Photovoltaic Business Models, National Renewable Energy Laboratory, 2008.

[4] R. Duncan, Renewable Energy and the Utility: The Next 20 Years, Renewable Energy World 2 (3), 2010.

[5] F. Klose, M. Kofluk, S. Lehrke, H. Rubner, Toward a Distributed-Power World, The Boston Consulting Group Report, 2010.

[6] J. Nimmons, M. Taylor, Utility Solar Business Models: Emerging Utility Strategies & Innovation, SEPA Report, 2008.

[7] J. Schoettl, L. Lehmann-Ortega, Photovoltaic Business Models: Threat or Opportunity for Utilities?, R. Wüstenhagen, R. Wuebker (Eds.), Handbook of Research on Energy Entrepreneurship, Edward Elgar Publishing Ltd., 2010.

[8] C. Zott, R. Amit, The Fit between Product Market Strategy and Business Model: Implications for Firm Performance, Strategic Management Journal 29, 2008, pp. 1-26.

[9] C. Baden-Fuller, M. Morgan, Business Models as Models, Long Range Planning 43, 2010, pp. 156–171.

[10] B.W. Wirtz, O. Schilke, S. Ulrich, Strategic Development of Business Models, Long Range Planning 43, 2010, pp. 272–290.

[11] M. Johnson, Seizing the white space. Business model innovation for growth and renewal, Harvard Business Press, 2010.

[12] A. Osterwalder, The Business Model Ontology, Diss. at University of Lausanne, 2004.

[13] P. Stähler, Geschäftsmodelle in der digitalen Ökonomie, Josef Eul Verlag, 2001.

[14] R. Wüstenhagen, J. Boehnke, Business models for sustainable energy, A. Tukker, M. Charter, C. Vezzoli, E. Sto, M.M. Andersen, System Innovation for Sustainability 1. Perspectives on Radical Changes to Sustainable, 2008, pp. 85–94.

[15] A. Osterwalder, Y. Pigneur, Business Model Generation, Modderman Druckwerk, 2009.

[16] L. Okkonen, N. Suhonen, Business models of heat entrepreneurship in Finland, Energy Policy 38, 2010, pp. 3443-3452.

[17] Gordijn, J. & Akkermans, H. (2007): Business Models for distributed generation in a liberalized market environment. Electric Power Systems Research Vol. 77, Issue 9, July 2007, 1178-1188.

[18] K. M. Eisenhardt, M. E. Graebner, Theory Building from Cases: Opportunities and Challenges, Academy of Management Journal 50, 2007 (1), pp. 25-32.

[19] R. K. Yin, Applications of case study research, Sage Publications, 2003

[20] O. E. Williamson, Transaction-Cost Economics: The Governance of Contractual Relations, Journal of Law and Economics 22 (2), 1979, pp. 233-261.

Energy Security Centres in support of the development of a comprehensive EU Energy Policy

K. Nagy[1,*], K. Körmendi[2]

[1] *Special Advisor, Triones Institute of Technology, Budapest, Hungary*
[2] *Phd student, Zrínyi Miklós National Defense University, Budapest, Hungary*
** Corresponding author. Tel: +36 305350951, E-mail: knagy794@t-email.hu*

Abstract: There are paradoxes and contradictions in the interpretation of the concept of energy security among the micro sphere (the level of business organizations and individual users), the macro sphere and the global level. For example, in the global interpretation it is no longer sufficient to focus on meeting objective social needs for energy alone. We should also take into consideration the environmental impacts of meeting these needs (global warming, climate change etc.) as well as sustainability. We need to adopt a comprehensive approach at the level of our energy security policy as well. This may be effectively supported by Energy Security Centers (ESC), which are virtual energy security knowledge centers. The essay analyses the issues for consideration listed in the "Stock taking document - Towards a new Energy Strategy for Europe 2011-2020" from the aspect of the possible application of ESCs to the solution and support of these issues and proposes the EU level establishment of ESCs. Based on the analysis of the stock taking document, the aim of the study is to highlight the advantages resulting from the institution of an European network of knowledge centres (Energy Security Centres) for the implementation of the European Energy Policy.

Keywords: *Energy policy, Energy Security Centres, European Union*

1. Introduction

The authors' research in the field of energy security has revealed the necessity of the establishment of energy security centres to facilitate the knowledge management support of the solution of energy security problems. Regarding their basic nature, energy security centres function as virtual energy security centres. In a legal sense, they are autonomous public administration institutions. By autonomous public administration institutions we mean institutions like agencies of various profile in the United States, directly subordinated to Congress. This legal status along with normative financing ensures the independence of these institutions, which is a prerequisite for authentic operation. According to our concept [1], the main role of such an Energy Security Centre (ESC) is to provide authentic information to aid the solution of energy security problems and to create the conditions required for decision makers to use this authentic information effectively in practice. With the help of knowledge centres it also becomes possible to place the knowledge transfer supporting energy security on qualitatively new foundations. The authors hold that the establishment of knowledge centres and the development of a knowledge centre network open up new opportunities in the interactive development and implementation of the comprehensive energy policy of the European Union.

The study points out the issues for consideration listed in the Stock taking document towards EU Energy Strategy for the period 2011 – 2020 [2] where the application of knowledge centres is of outmost importance. Based on a background analysis, the study considers the most important advantages resulting from the functionality of ESCs, points out the most important aspects of developing an ESC network, and makes specific recommendations regarding its establishment.

2. The Role of Energy Security Centres: A Comprehensive Approach

2.1. The Functionality of Energy Security Centres

Former inquiries regarding the concept of energy security reveal that there are paradoxical contradictions among micro level, macro level and global interpretations. [3] As a result, certain statements which may be true using a given approach, for example at the level of the micro sphere, will not hold if we apply a macro level or global approach. It is becoming more and more typical that even the management of relatively simple, local problems requires a global approach.

With reference to the above study we should mention that the interpretation belonging to the micro sphere, in other words to the world of companies and organization, starts out from a threat to the satisfaction of our demands for energy and applies a supply security centred approach. The macro level interpretation of energy security focuses on issues related to the satisfaction of the objective energy needs of a given society. The global interpretation examines the question of need satisfaction in close connection with the results of the satisfaction of needs. It takes into consideration that the method of need satisfaction will have an impact on the possibility of the satisfaction of future needs.

Accordingly, the complete satisfaction of energy demands in a given country by no means guarantees that objective energy needs in that country are also completely satisfied, or saturated. The recognition of needs and their transformation into demand is influenced by a number of distorting factors. The most important of such factors are related to our shortcomings in recognizing these needs and the impact of various interests on demands. The recognition of needs is a task for science, while the transformation of these needs into goals is a political task, and the determination of specific demands belongs to the realm of the market and the economic interests in play. These three areas are characterized by close interaction and a contradictory relationship with each other. What they all have in common is that none of them can exist without authentic factual information. The importance of the need for factual information is well illustrated by an EU Commission Staff Working Document [4], which states the following:

“The problem that requires action is the lack of consistent data and information on investment projects (in their different phases) and the related shortcomings. ..... EU institutions lack relevant/consistent data on the development of energy infrastructure in the EU to assess the strategic supply/demand balance. Industry is potentially affected by insufficient transparency on the likely evolution of the EU energy system.” [4]

The solution of energy security problems through the application of a global approach may be effectively supported by energy security centres. [1] Regarding their basic nature, energy security centres are virtual energy security centres with the following functionality:

A) Fast and efficient output of new knowledge and information required for competent energy-related policy-making, energy-related developments, environment statutes, etc.

B) Acceleration of the acquisition of practical knowledge required for competent energy related policy-making, implementation of policy guidelines and for the identification of specific problems arising in connection with energy security.

C) Creation, maintenance and continuous improvement of a platform designed for the efficient transfer of knowledge; establishment of foundations with completely new

characteristics, to be used in addressing energy security issues in order to provide best practice methodology.

The application of modern ICT solutions and knowledge management to support the implementation of energy policies and the solution of energy security problems is not a unique idea. For example, we should mention the book edited by M. Bazilian and F. Roques [5] and the work of K. Metaxiotis [6] The concept of ESCs is different from the approaches appearing in these works and various other publications in a sense that it treats the creation of the authentic spatial information required for problem solving, the development of the capacities required for the effective use of information, and knowledge transfer as part of the same system.

The realization of the basic functions of energy security centres in accordance with the above is relevant not only to the solution of specific energy security problems but the implementation of energy policies as well. A network of energy security centres covering EU member states would be able to provide effective support to the implementation of a comprehensive EU Energy Policy. In the following we will discuss the role of a network of energy security centers in the implementation of the Stock Taking Document [2].

2.2. The basic concept of the " Stock Taking Document"

An analysis of the Stock Taking Document reveals that the approach used at its drafting reflects what we have referred to as a global approach. The document addresses the following issue:

"Completing the internal energy market, achieving energy savings and promoting lowcarbon innovation are the main vectors to reach the objectives of competitiveness, sustainability and security of supply. A well functioning internal market, based on regional and pan-European interconnections, will serve all consumers, ensure energy security and allow the transition towards a low-carbon electricity system. There remains large scope for cost-efficient energy saving measures in order to reduce greenhouse gas emissions; energy savings also lower the energy bill and reduce dependence on energy imports. Finally innovation will be essential to make our energy system sustainable and to renew Europe's manufacturing base and create green jobs." [2]

In other words, the Stock Taking Document aims to resolve the contradictions between supply objectives based on demand and objective needs, and states that there is a need for the recognition and exploitation of the connections between existing needs and the consequences of the satisfaction of these needs.

The Stock Taking Document lists the key issues of Energy Strategy for Europe 2011-2020 as well as the priority areas for the future strategy. They are the following [2]:

- Modern integrated grids
- Making progress towards a low-carbon energy system
- Leadership in technological innovation
- A strong and coordinated external energy policy
- Protecting EU citizens against the lack of supply and/or unaffordable energy prices

The document summarizes the issues for consideration for the short-term as well as the issues for consideration for the longer-term with regard to each priority area, the following of which

may be effectively supported through the realization of the basic functions of energy security centres:

a) Strengthening cooperation and coordination at EU-level of energy networks to build a pan-European integrated, interoperable, secure and modern grid.
b) Strengthening the role of ACER (Agency for Cooperation of Energy Regulators) & ENTSOs (European Network of Transmission System Operators) to develop a more integrated regional and European energy market.
c) Using consumer-centred tools (e.g. labels, information campaigns and long-term education initiatives) to promote energy savings, smart use of energy and fuel switching by energy users.
d) Using market-based instruments to give the right price signals and incentives for energy savings, smart use of energy and fuel switching by energy users, through the emissions trading scheme (ETS), energy taxation and phasing-out of fossil fuel subsidies.
e) Developing a more coordinated European approach towards the licensing and design certification framework for nuclear investments.
f) Implementing the European Strategic Energy Technology Plan (SET-Plan)
g) Launching a dedicated set of large industrial innovation programmes of strategic importance for European energy future.
h) Intensifying efforts in the global energy organisations and initiatives (e.g. IEA, G20, WTO) to promote well-functioning, open, transparent and competitive energy markets, good governance and comprehensive energy policies.
i) Deepening cooperation with consumer countries, including emerging economies, to promote adoption of sustainable energy policies and a shared view on energy security.
j) Increasing transparency. Improving market transparency on network operation and supply which guarantees equal access to information, making pricing more transparent, increasing trust in the market and helping to avoid market manipulation.
k) Providing with guidance on the appropriate tools to facilitate consumer participation in the energy markets through transparency and clarity of information and comparability. [2]

Specific support may be characterized by the following:

- By ensuring the authenticity of the information used, ESCs make an effective contribution to the development of coordination and collaboration. This is particularly important in case of the tasks listed in points a), b), e), f), g), h), i) since authentic information is a basic requirement for good collaboration and successful coordination. Authentic information can be provided through the realization of the first basic function of ESCs. The second basic function, which is the acceleration of the acquisition of practical knowledge, also has a fundamental role in the support of coordination and collaboration. Coordination and collaboration are not only a question of intent: Their implementation requires a considerable amount of expertise. ESCs can support the fast and effective acquisition of this special knowledge with their simulation services.
- The implementation of objectives c), d), j) and k) also requires access to authentic information. This is important not only with regard to the direct use of information. The authentic information provided by ESCs also makes it possible to control the authenticity of the information published by market players, governments and various other institutions, and the existence of such a control will force data providers to adopt an ethical behaviour.
- While the main aim of the second function (the function based on simulation) is to support the preparation and work of decision makers and developers (for example in objectives f), g), h), i)), transparency, information provision and the strengthening of conscious consumer attitudes are ensured through the realization of the third (knowledge transfer)

function. Access to authentic information has a crucial importance regarding the above objectives, especially the ones listed in point j) such as "helping to avoid market manipulation", as well. The realization of effective knowledge transfer has primary importance in strengthening the role of ACER & ENTSOs in accordance with point b). It must be emphasized that our first priority is not the knowledge transfer development between ACER & ENTSOs and national (member state) institutions collaborating with them. Rather, we point out the importance of the knowledge transfer taking place between and among member state institutions and market players. This knowledge transfer will ensure the development of a unified view at the EU level and the recognition of the significance of collaboration with ACER & ENTSOs.

- The implementation of the SET-Plan and launching a dedicated set of large industrial innovation programmes require the coordinated realization of the three basic functions.
- Basically, all the issues for consideration listed in the Stock Taking Document [2] could be supported by knowledge centres one way or another. The objectives set in a)-k) and highlighted above specifically require and cannot lack such support. The matrix below illustrates the strongest connections between the different functions and the issues for consideration.

Table 1. Connections between ESC functions and issues for consideration

	Functions of ESC		
Issues for consideration	A)	B)	C)
a)	X	X	
b)	X	X	X
c)	X		
d)	X		
e)	X	X	
f)	X	X	X
g)	X	X	X
h)	X	X	
i)	X	X	
j)	X		X
k)	X		

Besides the support resulting from the realization of the basic functions, the implementation of issue j) also depends on the way ESCs are applied and the regulations in force. Member state and EU level regulations should ensure access to authentic factual information provided by knowledge centres free of charge. Access to simulation and knowledge transfer services should also be made available with one condition: namely, that in the case of certain services users may have to pay a charge.

Apparently, the income resulting from the provision of the above services is not sufficient to finance the operation of knowledge centres. Member state and EU level support are both needed, and the form of support should ensure the independence of knowledge centres. The essay previously referred to [1] discusses in detail the possible forms of financing; here we will only note that it would make sense to develop a normative financing method, where the sums of support are determined in proportion with the income and expenditure of individual member states and the European Union. The independence of knowledge centres, which is a guarantee for their authenticity, should be strengthened with legal regulations. At the nation state level, these institutions should be set up and operated as autonomous public administration institutions. In other words, they should be subordinated only to legislative

bodies such as Parliament or Congress. In this regard, we should consider the practice applied in the United States concerning the establishment of agencies subordinated to Congress alone. We should note that, as a result of developments in political power relations, in certain member states not even such measures will be sufficient to guarantee independence. In that case we can still count on the authenticating function of the ESC network, through which the not authentically functioning ESC may be excluded from cooperation.

3. A Few Questions Regarding the Application of Energy Security Centers

The application of energy security centres to solve the issues raised in the Stock Taking Document has the following guidelines: The energy security centres should be set up in the member states (possibly one in every member state) so that they enjoy autonomy and operate independently from the central government. This is a basic requirement in order to ensure authentic and credible operation. [1] EU level recommendations should also be made to promote the standardization of the legal status of energy security centres.

The authorization of energy security centres for cooperation and information exchange should constitute an integral part of legal regulation. It should be a commonly applied principle that energy security centres may obtain information only from open sources such as the internet, journals, books, conferences, governmental and market data provision etc. The situation is similar regarding the classification of the confidentiality of output information as well: Information provided by energy security centres may not be classified. This rule will no doubt create considerable problems at the level of individual nation states, but desired levels of efficiency cannot be attained otherwise and the missing, or zero information created as a result of classification could create serious problems in simulation procedures supporting the realization of the second basic function.

The virtual solution, according to which the operation of the centres is based primarily on rented ICT capacities, makes possible the application of an exceptionally cost effective solution due to network level cooperation. For example, one or more European super computer centres would be able to serve the entire network of European energy security centres. It is already apparent that there is sufficient band-width available at the level of the entire European Union. What should be concentrated due to the costs involved in interfaces is the simulation capacity required. Therefore, an European energy security simulation centre should be established after the model of The National Exercise Simulation Center (NESC) of Federal Emergency Management Agency (FEMA) of US Department of Homeland Security [7]. As it has been discussed in detail in the essay published in Energy [1], the functionality of FEMA NESC is very close to the second function of energy security centres, which is placing the acquisition of empirical knowledge on qualitatively new foundations. This does not mean that simulation cannot be of divided parameter at the same time. In this regard applications such as IBM Serious Games could play an important role. All the above could be realized on the basis of cloud computing as well. In the case of individual ESCs the goal was the creation of the conditions required for virtual simulation. However, an ESC network would be able to create such an interface and other conditions which would make it possible to employ a mix of live, virtual and constructive simulations.

As the example of the 2009 gas crisis shows, the failure of gas supply can seriously affect electricity supply, domestic heating and industrial heating. The lack of gas supply could also lead to shutting down factories and plants, resulting in serious economic consequences. One of the tasks of the simulation centre may be the modelling and analysis of the impacts of the disruption of gas supply and the exploration of the possible consequences of unexpected

events. The other task of simulation is the analysis of the effectiveness of measures aiming to reduce or avoid negative impacts. This analysis could provide a basis for the further development of common EU energy policy tools as well.

The interactive conference centre module can also be virtualized or set up as a divided parameter network of accredited conference criteria. In this regard, the application of standardized video conferencing systems is of primary importance. A new element compared to the former concept of energy security centres is the institutionalization of the application of IBM Jam. It means that the European Union could organize EU level IBM Jams on a regular basis to promote the solution of problems emerging during the implementation of the energy strategy and to support innovation. The usefulness of the application of the IBM Jam in this field is supported by a number of references. [1]

4. Conclusions

A network of ESCs, outlined only briefly due to the scope of the present paper but discussed in more depth in earlier publications, is capable of satisfying "ripe" objective needs. We should add that these needs do not appear only at the level of the European Union, but at a global level as well. The reason for that is that energy security is a global problem, which can only be solved through global cooperation. Knowledge centres of a different specialization created after the model of the ESC Network will create the background for the qualitative changes envisioned by Manuel Castells [8], according to which the present, oversized national state institutions trembling under the burden of hopeless problem solving will be transformed into development states focusing on planning a desirable future.

We have pointed out that the significance of the creation of an EU level ESC network goes beyond the question of the solution of direct energy security problems and it would create qualitatively new conditions for the implementation of the new energy policy of the European Union. The establishment and development of an ESC network is an EU institutional development task. Its realization requires the support and cooperation of the member states and the creation of an EU level legal regulatory framework.

It must be emphasized that the ESCs should by no means be regarded as research institutions or think-thanks. The task of the latter is to add value information to authentic factual information, while ESCs focus solely on supplying authentic factual information. While it is not possible to support the above argument in more detail in the present paper, the authors hold that there are no significant functional overlaps with regard to other EU or nation state institutions either.

The virtual solution proposed with regard to the establishment of ESCs would create a background for the cost effective development of an EU level ESC network. The European Energy Security Simulation Centre would be the only component of the network tied to specific geographic coordinates, the creation of which could be based on various other, similar EU institutions. The simulation centre should be set up at a location where the critical mass of intellectual and technological potential required for interactive development is already available.

[1] http://www.globalpulse2010.gov/index.html , http://www.prnewswire.com/news-releases/security-experts-cite-need-for-major-policy-changes-to-protect-global-security-in-report-to-nato-and-the-european-union-93254954.html , http://www.ibm.com/ibm/responsibility/minijam/overview.html

Based on the above, we recommend the following:

I. The initiation of the development of a European ESC network and its global extension by the EU Presidency.
II. The inclusion of the creation of an ESC network in EU strategies and plans, with special focus on EU Energy Policy and the SET-PLAN.
III. The development and financing of research and development programs and projects required for the creation of an ESC Network.
IV. The simulation of the development of the ICT infrastructure required for the operation and collaboration of ESCs.

As a form of support to the realization of the above, we offer the results of the eSCIT'09 (Global IT Infrastructure of Energy Security Centres) organized on 5-6 October 2009 in Veszprém, Hungary and the expected results of the eSCIT'11 conference, the organization of which is taking place currently.

References

[1] K. Nagy, "The additional benefits of setting up an energy security centre", Energy 34, 2009, pp. 1715-1720.

[2] Stock taking document Towards a new Energy Strategy for Europe 2011-2020 http://ec.europa.eu/energy/strategies/consultations/doc/2010_07_02/2010_07_02_energy_strategy.pdf (downloaded 14 December 2010.)

[3] K. Nagy, "The concept of energy security in the light of global security", Chemical Engineering Transactions 18, 2009, pp. 297-302. (Published by AIDC, Roma, 2009., ISBN 978-88 95608-04-4, ISSN 1974-9791)

[4] Commission of the European Communities. Commission staff working document. Accompanying document to the Draft Council Regulation (EC) concerning the notification to the Commission of investment projects into energy infrastructure within the European Community and Repealing Council Regulation (EC) n°736/96 Executive Summary of the Draft Impact Assessment{COM(2009) xxx final}{SEC(2009) xxxx} http://ec.europa.eu/energy/strategies/2009/doc/sec_2009_executive_summary.pdf (downloaded 14 December 2010.)

[5] Analytical Methods for Energy Diversity & Security, Edited by: Morgan Bazilian and Fabien Roques, Elsevier Global Energy Policy and Economics Series 2009. Elsevier Ltd. ISBN: 978-0-08-056887-4

[6] K. Metaxiotis: Intelligent Information Systems and Knowledge Management for Energy: Applications for Decision Support, Usage, and Environmental Protection. Information Science Reference. 1st edition. 2009.

[7] US Department of Homeland Security, Federal Emergency Management Agency (FEMA) The National Exercise Simulation Center (NESC) http://www.fema.gov/news/newsrelease.fema?id=47280 (downloaded 14 December 2010.)

[8] M. Castells, The Information Age – Economy, Society and Culture, Volume III. End of Millennium, Blackwell Publishers, 2nd Edition, 2000, pp. 282-283.

Diversity, security, and adaptability in energy systems: a comparative analysis of four countries in Asia

Liang-huey Lo[1,*]

[1] *Science & Technology Policy Research and Information Center, National Applied Research Laboratories, Taipei, Taiwan*
** Corresponding author. +886 227377692, Fax: +886 27377448, E-mail: lhlo@stpi.narl.org.tw*

Abstract: In ecology study, numerous ecologists have been concerned with the concept of diversity in studying the structure and functions of ecosystems for a very long time. Diversification can be seen as a long-term survival strategy of ecosystems by allowing high flexibility and adaptability. Similarly, diversity is also seen as an important characteristic of a stable socio-economic system. In energy policy, diversity plays important roles in energy supply security, efficiency of energy use, and adaptability of energy system. Many of the trends reflect the increasing significance of renewable energy relative to conventional energy sources, and it will increase diversity of energy supply. It is also beneficial for a system both through extending choice and increasing competition. However, changing the structure of energy sources and increase energy diversity for strategic system security can be difficult for the countries which highly depend on the imported energy. This paper considers that the diverse distributions of energy flows in a system can open up more possibilities and channels for cooperation and interdependency in energy utilization. Not only diversity of supply side, but also diversity of demand side is critical for an energy system because increasing variance and balance of the energy consumers enhances efficiency and adaptability. In this paper, we develop a quantitative analysis method to explore both of supply and demand sides of energy system structure for four Asian countries, Japan, Korea, Taiwan and Indonesia based on the OECD data set from 1987 to 2006. The tremendous growth Asian countries have seen in recent decades required a huge amount of energy. Energy systems of Japan, Korea, and Taiwan are short of indigenous energy sources and highly dependent on imported energy sources except Indonesia. Indonesia's indigenous energy source reserves support national economy as a source of energy, industrial raw material and export goods. And then Indonesia's renewable energy also can be as a source of energy to support energy use. Furthermore, we are not only to compare the diversity temporal patterns of national energy supply and use, but also to compare the industry sector diversity temporal patterns of energy use of these countries.

Keywords: *Energy system, Diversity, Security, Adaptability*

1. Introduction

In recent years, there have been many interests in energy security due to the high oil prices and the geopolitical supply tensions. Security of energy supply can be defined as a system's ability to provide a flow of energy to meet demand in an economy in a manner and price that does not disrupt the course of the economy [1]. Many of the trends reflect the increasing significance of energy sources, including renewable energy, relative to conventional energy sources (including coal, oil, natural gas, and nuclear). Measuring security of energy supply is therefore becoming an important topic on the studies of energy policy. Diversity in energy (fuel) type and geographic sources is thought to be an important means of hedge against supply risks [2,3] and is used frequently as a key indicator to assess energy security. For example, Stirling's application of the Shannon-Wiener diversity index to electricity resources provides some useful insights into how government and electric utilities can objectively measure diversity and thereby gauge the effectiveness of their own investments in alternative resources [4].

Stirling (1999)[5] argues that an index of energy diversity should consider three key elements: Variety (the number of categories into which the quantity in question is partitioned), Balance (the pattern in the apportionment (spread) of that quantity across the relevant categories), and Disparity (the nature and degree to which the categories themselves are different from each

other). Both through extending choice and increasing competition, energy diversity is thought as an important characteristic in energy supply security, financial risk, efficiency of energy use, and the environment [4,6]. Increasing diversity of energy supply is beneficial for a system both through extending choice and increasing competition. It is traditionally argued that diversity is best achieved by a mix of fuel sources and by a preference for domestic over imported energy supplies [7].Grubb et al. (2006) [1] calculated diversity of fuel source mix to represent one dimension of security-robustness against interruptions of any one source and applied diversity indices to electricity system scenarios. Furthermore, diversity is considered as an important property of energy system which provides resilience against physical supply disruptions. Global energy disruptions are more and more translated into price shocks, which can spill over from one market to another [3].

In ecological researches, however, measuring diversity is not a new method for studying ecosystem properties. Numerous ecologists have been concerned ecological diversity in studying the structure and functions of ecosystems [8,9,10,11,12]. From a systematic perspective, diversity of interacting components builds feedback loops and these loops regulate materials absorption, storage and release and landscape structure construction[13,14]. Webs of connections and feed-back information are the basis of system's self-regulation. Following a succession adjustment period, feedbacks regulate absorption, storage and release of materials, and construction of landscape structures [13]. A diversified ecosystem system is therefore considered as a more resilient and stable system. By allowing high flexibility and adaptability, the existence of diversity can be seen as a long-term survival strategy for systems as a consequence of permanently changing environmental condition [15]. Ecosystems either adapt to their internal scarcity by optimizing the use of the scarce resources or are flexible and able to changing environmental conditions [15,16].

Additionally, one can transfer the knowledge and the understanding from biological sciences to social sciences based on the analogies between biological and socioeconomic evolution [17]. Matutinović (2001) [17]argued that the functional properties of diversity in socioeconomic system are analogous to that of biological evolution: (1) adaptation to different environment, (2) avoidance of head-to-head competition, (3) efficient use of energy and resources and (4) providing a range of responses to new selective pressures. Socioeconomic system diversity is therefore expected to generally increase during development and to improve efficiency, productivity and output of the system [18,19]. In order to studying the relationships between diversity and socioeconomic development, Templet (1999) [19] defined diversity of economic system as the number of sectors by using energy and the equitability of the energy flows among them. He adopted an energy flow network method and development capacity formula [18] to investigate the relationships among economic diversity, output and development policy. His conclusion is that economic system is generally capable for making more efficient use of energy and reducing energy intensity as the diversity rises.

Based on ecological theory of diversity and the analogies between ecological and energy systems, diversity of interacting components in energy systems is thought as an important property to build feedback loops regulating energy use, storage, and release. Diversity of energy system can enhance the energy efficiency and open up the channels for the cooperation of energy use. A diversified energy system is therefore considered as a more resilient and adaptable system to cope with disturbances. However, most of recent studies on energy diversity are generally focused on the issues of energy supply. The importance for diversifying systemic components and building feedback loops in energy systems were gotten fewer attentions in energy policy studies. Moreover, for the countries which highly depend on

the imported energy, changing the structure of energy sources to increase energy diversity for strategic system security is relatively difficult. This paper therefore considered that not only the diversity of energy sources (supply side) but also the diversity of energy use (demand side) is critical for an energy system because increasing variance and balance of the energy consumers enhances efficiency and adaptability. In this paper, we develop a quantitative analysis of diversity to explore both of supply and demand sides of energy systems for four Asian countries, Japan, Korea, Indonesia and Taiwan based on the data sets from 1987 to 2006. Furthermore, we are not only to compare the diversity temporal patterns of national energy supply and use, but also to compare the industry sector diversity temporal patterns of energy use of these countries.

2. Methodology

2.1. Diversity indicators

The index mostly used to measure diversity is the Shannon–Wiener index:

$$H = -\sum_i p_i \ln p_i$$

with p_i representing the share of fuel i in the energy mix or the market share of supplier i. The higher the value of H, the more (dual concept) diverse the system is. This index rises monotonically with increasing variety and balance.Ecologists frequently apply diversity as an index of ecosystem stability [14]. Templet (1999) [19] use the Shannon and Weaver (1949) equation to capture how many deferent types of economic activities exit within the system and how equitably energy is distributed between them. The Shannon-Weiner index was considered to be the most satisfactory measure of energy diversity because it incorporates the concepts of variety and balance [4].

In this study, we also use the Shannon–Wiener index to calculate the diversity of energy consumption and industry sector. We consider that the diverse distributions of energy flows in a system can open up more possibilities and channels for cooperation and interdependency in energy utilization. Not only diversity of supply side but also diversity of demand side is critical for an energy system because increasing variance and balance of the energy consumers enhances efficiency and adaptability.

2.2. Data sets of four countries in Asia

Our quantitative analysis method primarily based on the OECD data sets: Energy balances of OECD and non-OECD countries, from 1987 to 2006 [20,21]. Year presented the energy balances in various sources of energy and different origins and uses. In energy supply side, six types of energy supply source data (see Fig.1.) are analyzed diversity index in these four countries by year (see Fig.2.). In energy consumption side, energy demand data of these four countries is collected into five categories labeled industrial, transport, residential, commerce and public services, and agriculture sector. Then, we calculate energy demand data by economic sectors (see Table.1.) and analyzed diversity index in these four countries by year (see Fig.3.). Energy demand data of industry sector are also collected into 13 categories labeled iron and steel, chemical and petrochemical, non-ferrous metals, non-metallic minerals, transport equipment, machinery, mining and quarrying, food and tobacco, paper, pulp and printing, wood and wood products, construction, textile and leather, and non-specified. To analysis diversity index trend in these three countries highly depend on imported energy, we calculate these data sets and draw the lines of result by year (see Fig.4.).

Japan is the world's second largest economy after the United States in 2009 [22]. Gross domestic product (GDP) per capita of Japan increases almost two fold between 1987 (i.e. $20,025) and 2009 (i.e. $39,372) [23]. Because of low self-sufficiency index (0.1788 in 2008), Japan is the first-largest net importer of coal (114.19 Mtoe) in 2008, and increases coal use for power generation; Japan is also the second-largest net importer of oil (224.82 Mtoe) in the world [20], and most all the oil is imported from the Middle East. Above all, the aim of Japan's energy policy will achieve the 3E's goal-energy security, economic growth and environmental protection-in an integrated manner [24].

Korea has experienced tremendous economic growth over the last three decades. GDP per capita of Korea increases over six fold between 1987 (i.e. $3,366) and 2009 (i.e. $22,055) [23]. As low self-sufficiency index (0.1971 in 2008) like Japan, Korea's energy policies currently promote a stable energy supply, market efficiency through competition, and implementation of an environmentally friendly energy system with the end-goal of sustainable development [20,25].

Taiwan is one of the most densely populated areas in the world, and GDP per capita of Taiwan increases over three fold between 1987 (i.e. $5,276) and 2009 (i.e. $18,867) [23]. There are no oil or coal reserves in Taiwan, but gas reserves are around 8.4 billion cubic meters [24]. Here, Taiwan has very limited domestic energy resources and relies on imports for most energy requirements. According to IEA's indicator, Taiwan's total energy self–sufficiency index is 0.12 in 2008 [21]. In 2009, Taiwan draw up the "Master Plan on Energy Conservation and GHG Emission Reduction" [26] and set up the national reduction targets as energy efficiency, emission reduction and low carbon energy. One of these targets is reducing energy intensity by 2% per annum and totally reducing 25% in 2015. Further reduce energy intensity by 50% in 2025 with technological breakthrough and administrative measures.

Indonesia's GDP per capita of Indonesia is $511 in 1987; it is $2,323 in 2009[23](IMF estimated). Indigenous oil, gas and coal reserves have played an important role in Indonesia's economy as a source of energy, industrial raw material and foreign exchange. In 2008, oil and gas exports contributed the largest share (21.1%) of Indonesia's total exports of USD 136.76 billion, followed by minerals (including coal) at 18.8% [24]. According to IEA's indicator, Indonesia's total energy self–sufficiency index is 1.75 in 2008 [21].

3. Results of energy analysis

3.1. Diversity index of energy supply side

Total primary energy supply (TPES) of four countries respectively increases rate of 41.24% (Japan), 224.29% (Korea), 176.79% (Taiwan), and 136.88% (Indonesia) between 1987 and 2006. Comparing to four countries' supply fuel shares in 1987 and 2006 (see Fig. 1.), TPES in Japan, Korea and Taiwan is dominated by oil and coal, through the portion of natural gas has increased rapidly in recent year. Japan and Korea both increase nuclear energy supply, however, Taiwan decreases the nuclear supply and Indonesia does not have the energy supply in TPES. Relative to conventional energy supply, the renewable energy supply share (including hydro, geothermal, solar, wind, etc.) of Indonesia's TPES is much higher than Japan, Korea and Taiwan. The renewable energy supply shares of Indonesia's TPES in 2006 are 33%, but other three countries' are below 3%.

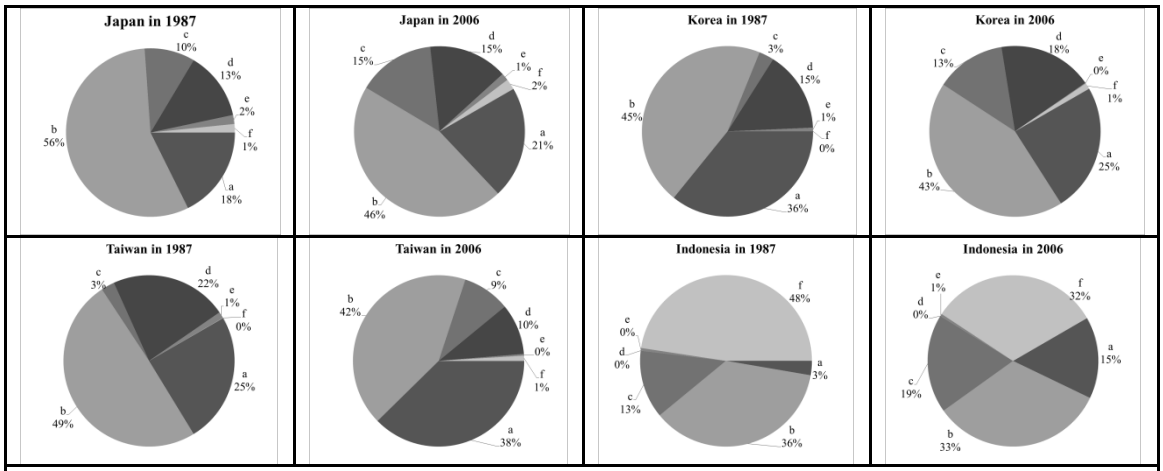

a. Coal and coal products / b. Oil and products / c. Natural gas / d. Nuclear / e. Hydro / f. Geothermal, solar, wind, etc.

Fig.1. Fuel shares in these four Asia countries (source: IEA, 2010).

A representative set of country's supply diversities are shown in Fig 2 over time. Comparing to diversity of four countries' energy supply, Japan's diversity index trend is the highest and it is going steadily. Indonesia's diversity trend is going up continuously, and in 2006 its diversity index is the highest of the four countries. Before 1994, Taiwan's diversity trend is going down and it reaches the lowest point in 2002. After 2002, it goes up quickly, but in 2006 its diversity index is the lowest of the four countries. Korea's diversity number is lowest in 1992, but it has a peak in 1994, then, after 1997 it is going up straightly.

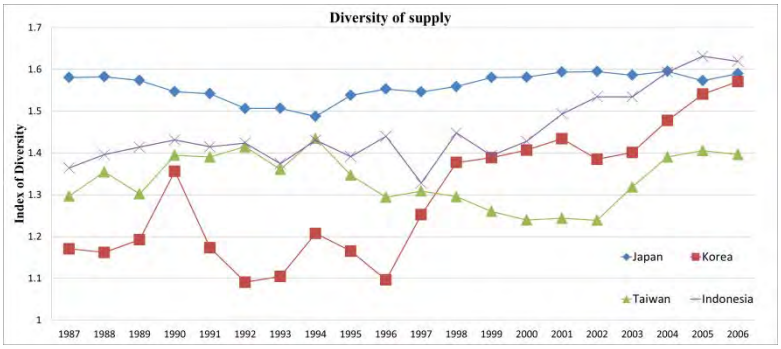

Fig.2. Country diversity of energy supply by year.

3.2. Diversity index of energy consumption side

Total final energy consumption (TFC) of four countries respectively increase rate of 39.40% (Japan), 170.99% (Korea), 128.72% (Taiwan), and 120.36% (Indonesia) between 1987 and 2006. By sector of energy use, industry sector are the large share of energy consumption, accounting for almost or over 30% of total demand, and the industry sector of Indonesia has the distinct growth rate of energy use(see Table 1). By energy source, oil products are the most important one of energy consumption, accounting for over 50% of total energy demand in Japan, Korea and Taiwan. Oil products and bio-energy are accounting separately for 34.2% and 35.44% of total energy demand in Indonesia.

A representative set of country's demand diversities are shown in Fig 3 over time. Comparing to diversity of four countries' energy consumption, the diversity index in Korea is the highest of the four countries. The diversity index trends of Korea and Japan are similar, and these lines go down gently. Taiwan's diversity index trend climbs up gently, and Indonesia's diversity index climbs up obviously.

Table 1. Sector of energy use. (Source: IEA, 2010)

Sector of Energy Use	Japan		Korea		Taiwan		Indonesia	
	1987	2006	1987	2006	1987	2006	1987	2006
Industry sector (%)	40%	33%	31%	36%	51%	44%	13%	28%
Transport sector (%)	28%	29%	23%	28%	25%	30%	15%	21%
Residential sector (%)	16%	15%	32%	17%	11%	11%	70%	46%
Commerce and public services sector (%)	12%	22%	10%	16%	6%	8%	1%	3%
Agriculture sector (%)	4%	1%	4%	3%	7%	7%	1%	2%
Total final consumption (only energy use) (Mtoe)	224.89	313.50	41.78	113.22	21.76	49.77	55.45	122.19

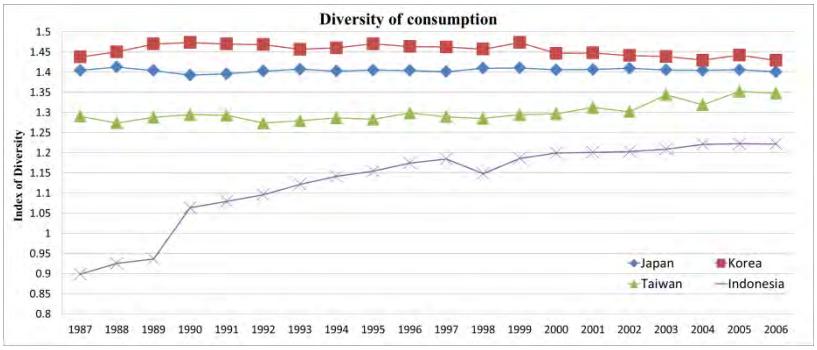

Fig.3 Diversity of national energy consumption

Due to Japan, Korea and Taiwan highly depend on the imported energy, except Indonesia. And all three countries face rapidly economic development and their energy supply and demand rate increase significantly. In the same way, industry sector of three countries is the primary energy consumer (see Table.1.) Therefore, we focus on industry sector diversity index trend in three countries, and analysis the meaning of them. As shown in Fig 4 over time, Korea's line climbs up continuously, but Japan and Taiwan go down steadily.

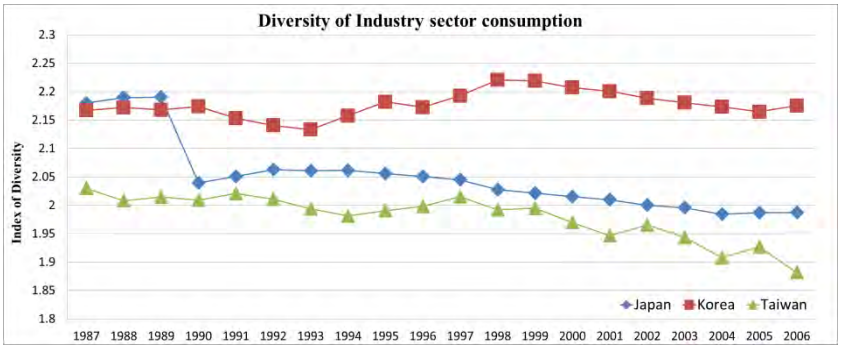

Fig.4. Country industry sector diversity of energy consumption by year.

4. Discussion and conclusion

4.1. Discussion and Conclusion

The fuel shares of these four Asia countries are shown in Figure 1 in this paper, and our quantitative analysis method primarily based on the OECD data sets from 1987 to 2006. Energy systems of Japan, Korea, and Taiwan are short of indigenous energy sources and highly dependent on imported energy sources except Indonesia. Indonesia's indigenous

energy source reserves have played an important role in national economy as a source of energy, industrial raw material and export goods. And then Indonesia's renewable energy also can be as a source of energy to support energy use. These three countries are usually other-directed for the imported energy types, price, and geographic sources and are sensitive to the fluctuations of international fuel supply. Therefore, it is difficult for them to change the structures of energy sources to increase diversity for their strategic energy security. The restricted variation of fuel-type diversity of energy supply of Japan, Korea, and Taiwan are revealed in Figure 2. However, the diversity index pattern of an indigenous energy system as Indonesia reveals a more flexible characteristic.

Recent years, all the total energy consumptions of these four countries were dramatically increased. Industrial sectors are the main energy consumers in Japan, Korea, and Taiwan. The energy consumption of commerce and public services sectors in these countries increase a little bit (see table 1). In Indonesia the residential sector is the main energy consumer. This study calculated the diversity index for national energy consumption (demand side) and the results showed that the temporal patterns of energy diversity in demand side of Japan, Korea, and Taiwan remained steady over two decades. However, energy diversity of Indonesia rose due to the significant decrease of residential sector and the raise of the energy consumption in industrial and transportation sectors (see Fig. 3).

Furthermore, this study also investigates diversity of energy use in the industrial sectors because the industrial sector of Japan, Korea, and Taiwan is the main energy consumer. The results show that energy diversity of Taiwanese industrial sector was going down due to the concentration of energy use in the iron and steel sector as well as the chemical and petrochemical sector (see Fig. 4). The energy diversity of Japanese industrial sector was also going down because several industrial production sectors were shrinking in past two decades. Relatively, diversity of Korean industrial sector was remained steady. The decreasing diversity of Industrial sector indicates a centralization of energy flow in the dominated industrial production.

Based on the analyses of energy diversity of fuel types, the results show that changing the structure of energy sources and increase energy diversity for energy security is difficult for the countries which are highly dependent on imported energy source. However, from the analogies of the concept of diversity between ecological and socioeconomic systems we argue that the diversified distributions of energy flows in an energy system can open up more possibilities and channels for cooperation and interdependency in energy utilization. The diversity of energy distribution in demand side is critical for an energy system. Diversity can increase variance and balance of the energy consumers and enhances energy efficiency. Moreover, diversity also improves the internal adaptability for coping with energy scarcity and external disturbances.

References

[1] M. Grubb, L. Butler, P. Twomey, Diversity and security in UK electricity generation: The influence of low-carbon objectives, Energy Policy 34, 2006, pp.4050-4062.

[2] J.C. Jansen, W.G. vanArkel, M.G. Boots, Designing indicators of long-term energy supply security, ECN-C–04-007, 2004, pp. 35.

[3] B. Kruyt, D.P. vanVuuren, H.J.M. deVries, H. Groenenberg, Indicators for energy security, Energy Policy 7, 2009, pp.2166-2181.

[4] A. Stirling, Diversity and ignorance in electricity supply investment, Energy Policy 22, 1994, pp.195-216.

[5] A. Stirling, On the economics and analysis of diversity. SPUR Electronic Working Paper Series. 1999, Paper No. 28.

[6] R. Ghanadan, J. G. Koomey, Using scenarios to explore alternative energy pathways in California, Energy Policy 33, 2005, pp.1117-1142.

[7] D. Helm, Energy policy: security of supply, sustainability and competition, Energy Policy 30, 2002, pp. 173-184.

[8] R. M. May, Will a large complex system be stable? Nature 238, 1972, pp.413-414.

[9] E. C. Pielou, Ecological Diversity, Wiley-Interscience, 1975.

[10] S. L. Pimm, The complexity and stability of ecosystems. Nature 307, 1984, 321-326.

[11] D. Tilman, J. A. Downing, Biodiversity and stability in grassland. Nature 367, 1994 , pp.363-365.

[12] D. Tilman, D. Wedln, J. Knops, Productivity and sustainability influenced by biodiversity in grassland ecosystems. Nature 379, 1996, pp.718-720.

[13] E. P. Odum, Fundamentals of Ecology, 3rd edn, Saunders, 1971.

[14] H. T. Odum, Systems Ecology, An Introduction, Wiley, 1983.

[15] I. Ring, Evolutionary strategies in environmental policy. Ecological Economics 23, 1997, pp.237-249.

[16] J. Korhonen, J.-P. Snäkin, Analyzing the evolution of industrial ecosystems: concept and application, Ecological Economics 52, 2005, pp.169-186.

[17] I. Matutinović, The aspects and role of diversity in socioeconomic systems: an evolutionary perspective, Ecological Economics 39, 2001, pp.239-256.

[18] R.E. Ulanowicz, Growth and Development. Ecosystem Phenomenology, Springer-Verlag, 1986.

[19] P.H. Templet, Energy, diversity and development in economic systems; an empirical analysis, Ecological Economics 30, 1999, 223-233.

[20] International Energy Agency (IEA), Energy balances of OECD countries, CD type 2010 Edition, 2010.

[21] International Energy Agency (IEA), Energy balances of non-OECD countries, CD type 2010 Edition, 2010.

[22] International Monetary Fund (IMF), World Economic Outlook Database, 2008.

[23] International Institute for Management Development (IMD), IMD World competitiveness online 1995-2010, 2010.

[24] Asia-Pacific Economic Cooperation (APEC), APEC energy overview 2009, APEC Secretariat, 2010, pp.61-94, pp.178-185.

[25] E. Jun, W. Kim, S.H. Chang, The analysis of security cost for different energy source, Applied Energy86, 2009, pp.1894-1901.

[26] Ministry of Economic Affairs (MOEA), Taiwan's Masterplan on Energy Conservation and GHGs Emission Reduction, What next? International Practical Experience of Carbon Management, 2010, pp.3-4.

Applications of energy security assessment in Strategic Environmental Assessment

Chi-Feng Chen[1,*]

[1] *Department of Natural Resources, Chinese Culture University, Taipei, Taiwan R.O.C.*
** Corresponding author. Tel: +886-2-28610511 ext 31432, E-mail: cqf2@faculty.pccu.edu.tw*

Abstract: Energy security is crucial for an energy policy but so far is not included in the current Strategic Environmental Assessment (SEA) program in Taiwan. The SEA report of energy policy prepared by the Bureau of Energy, Ministry of Economic Affairs, also demonstrated the same need. However, a feasible and quantifiable indicator has been missing. For the reason, this study is aimed to establish a practical assessment tool to assess energy security. Two indexes are suggested, which are the energy mix diversification (EMD) and energy import diversification (EID). The former one considers the national energy structures and expressed as Shannon index. The later is to assess the dependency on imported sources. The both indexes result in low energy security in Taiwan because of too high percentage of imported coal and oil in energy structure. The example of SEA policy is according to the Taiwan's Sustainable Energy Policy Framework, in which the energy efficiency is set to increase 2% annually in the future eight years. The increasing energy efficiency does not contribute significantly to improve energy security. The indexes used in this study can assess diversity of the whole energy structure and the imported energy sources, should benefit to SEA quality and energy security assessment.

Keywords: Strategic Environmental Assessment, Energy Security, Diversity.

1. Introduction

Strategic Environmental Assessment (SEA) is aimed to pre-assess the likely integrated environmental impacts from a policy, plan, or program (PPPs). Unlike a project with specific development content, the assessment scopes of SEA are vague and uncertain. In Taiwan, SEA is included in the Environmental Impact Assessment Act and the SEA Regulation is announced as the basic guideline. Energy policy is one of the listed policies which ought to carry out SEA under the Regulations. Several assessment items are appointed; however, these items cannot reflect the core issue of an energy policy, which is energy security. Energy security equals to national security and should be considered in SEA. Although energy security does not induce direct impacts on natural environment, it does impact significantly on the whole environment.

The SEA Regulation was announced in 2000 but only five cases completed to date. Sustainable Energy Development Framework was proposed by the Bureau of Energy. According to the requirement of SEA Regulations, the Bureau initiated the SEA in 2006 and the draft was completed in 2009. The SEA draft pointed out that the assessment items should be adjusted to specifics of policies to strengthen the relations between assessment items and policies. Thus, additional assessment factors, such as stability, efficiency, and clean of energy policy were suggested to be added.

Energy security is a complex issue and comprises diverse components, such as supply security, consumption security, production security, transportation security, ecological security, environmental security, and so on. Unfortunately, the definition of energy security is not received consensus (Loschel, et al., 2009). Due to the complicated definition, it is hardly to quantify its security level. Some definitions can be found in Bohi and Toman (1996), IEA (2007), Lin (2008), Commonwealth of Australia (2009), and Kruyt et al. (2009). In addition to the Taiwanese experiences, the assessment of energy security for SEA of energy policies is weak and obscure (Noble, 2002; Jay, 2010; Josimovic and Pucar, 2010).

Therefore, the objective of this study is to establish feasible tools to address the impacts of PPPs on energy security. Energy security consists of three important respects, which are adequacy, reliability, and affordability (Commonwealth of Australia, 2009). Due to economic analysis is necessary to examine the affordability of energy policies and more monetary information are required, this study excludes the considerations of affordability and is focus on diversity or dispersion of energy policies as energy security assessment.

2. Material and Method

2.1. Energy Security in Taiwan

Taiwan depends on extremely high imported energy. The dependence on imported energy is up to 99.23% in 2008, in which the dependence on oil is 49.5% and 83.62% of imported oil is from middle-east counties. The heavily high dependence on particular imported regions is a big challenge to conserve energy security. Besides, the imported value of oil occupies 19.35% of the whole imported value due to the increased oil price. It is the first time that the imported value of oil is larger than 10% of GDP in Taiwan. Not only the high dependence on imported energy, but also the high energy consumption is opposite to the international trend which decreases fossil fuel usage. Chang (2004) compared oil supply of six Asia countries with Shannon-Weiner Index and concluded that high risk happened in Taiwan and Philippines. In these two countries, mostly oil is imported from west Africa where politics is unstable. Lin (2008) assessed Taiwanese energy security with economic model and demonstrated the decreased trend of energy security since 2000, because of the high energy intensive business structure. The official annual report addressed energy security with five indicators, including energy dependency on imports, energy dependency on oil, values of energy imports/total imports, oil imports dependency on the middle east, and oil dependency on imports. The major causes to low energy security in Taiwan are the high dependency on imported energy and imported oil.

2.2. Strategic Environmental Assessment in Taiwan

The implementation of SEA in Taiwan is based on the article 26 in Environmental Impact Assessment Act, in which the PPPs with significant environmental impacts should be assessed. The SEA Regulations was announced in 2000 and amended in 2005 and 2006. In the Regulations, ten policies are required to implement SEA. Until December, 2009, only five SEA cases were finished. Many arguments have been discussed, such the listed policies, assessment scope, and assessment tools. Basically, the policy proponent checks whether the proposed policy is listed in the Regulations. If yes, the proponent cooperates with professional agency to produce the SEA report and submit it to official administration. A consult committee under administration will do the final examination and feedback to the policy proponent. The SEA report is the supplement document provided to decision maker. Eight impact aspects are assigned in the Regulations, i.e., environmental capacity, natural ecology and landscape, public health and safety, land resources, water resources, cultural property, international environmental regulations, and society and economy. In each impact aspects, several sub-factors are listed. The final assessment results are expressed as qualitative symbols, ++, +, 0, -, --. The symbols indicate significant positive effect, positive effect, none effect, negative effect, and significant negative effect, respectively.

2.1. Energy Security Indicators

The quantitative indicators for assessing energy security can be divided into two types. One is focus on particular aspect and uses individual indicator, such as the dependency on imported

energy or imported oil, the percentage of imported energy, the concentration of energy supply, and so on. The other is integrated index, which combines several concerned aspects of energy security into one integrated index. for example, the energy security market concentration (ESMC) and energy security index (ESI) by International Energy Agency (IEA, 2007), and the Energy Indicators for Sustainable Development developed by International Atomic Energy Agency, which are to assess energy security with considerations of economic, social, and environmental impacts (IAEA, 2005; Vera and Langlois, 2007). Some indicators are incorporated with risk evaluations, such as geopolitical market concentration risk (Blyth and Lefévre, 2004) and risk weight in energy security (Wu et al, 2006).

The energy security should satisfy stable supply and affordable price (IEA, 2007). In this study, the stable supply is particularly considered in SEA and the economic impact on energy price is excluded at this stage. While considering the physical characteristic of energy security, the more vulnerable to physical disturbance means the less energy security. The vulnerability usually comes from less energy sources in energy structure or high dependency on particular sources. The diversification of energy policy is used to demonstrate the physical disturbance. Two commonly indices are developed for assessing diversity, i.e., Shannon-Wiener index and Herfindhal-Hirschman index. The shannon-wiener index is orginially served as a biodiversity measure, combinding the number of species and the proportion of each species. A value of shannon-wiener near to zero means that almost the sample is the same species, implying very low diversity. on the contrary, the great value indicates the species distribute more equally and the diversity is high. the herfindhal-hirschman index is a common meaure of market concentration. it is calculated by summng the squares of the maket share of each firm.

In Taiwan situation, the most important issue on energy security is to increase energy diversification because more than 99% of energy in Taiwan is depended on imported energy. Therefore, indicators to assess energy diversity in energy policy is focused and two indicators are used in this study. Regarding to energy diversity, diversity in national energy structure, diversity in imported energy, and diversity in different energy sources are concerned. Two indicators are able to express the concerned diversity with simple calculation. They are Energy Mix Diversification (EMD) and Energy Imported Diversification (EID). The EMD mimics Shannon Index, considering the number and distributions of energy sources, to evaluate the national energy diversification. The EID further assesses the imported countries of the same energy source and the percentage of energy quantity from each imported country. The EID is able to reveal the imported distributions of particular energy source, such as oil, coal, or natural gas. Due to this indicator is focus on imported energy, high imported percentage of the overall national energy will decrease this indicator significantly. The two indicators share similar concept with Shannon index and ARE easily to use. The required information can be found in public annual statistic report and not necessary on complex computations. Although the core concept is similar, the highlights of the two indices are different. The EMD index focus on diversity of the whole energy structure and the EID underlines diversity of imported energy and diversity of each energy source as well.

The equations of the two indicators are as follows.

$$EMD = -\sum_i p_i \times \ln p_i \qquad (1)$$

$$EID = (1 - \sum_i p_i)(\frac{\sum_i p_i \times I_i}{\sum_i p_i}) \quad (2)$$

where p_i is the percentage of energy type i in the overall energy (%), I_i is the imported diversity of energy type i and calculated by $I_i = -\sum(w_{i,j} \times \ln w_{i,j})$. $w_{i,j}$ is the percentage of energy type i imported from country j.

3. Results and Discussion

3.1. Energy security of the current policy

The energy security indicators, EMD and EID, are used to demonstrate the past and current situation in Taiwan. The energy data is from official statistic report.

(1) EMD analysis

The energy sources in Taiwan are classified as seven types, i.e., coal, oil, natural gas, hydropower, nuclear energy, solar and wind power, and thermal energy. The highest diversity occurs when average distribution among the seven energy types, which is 1.95. However, more than 80% of energy is coal and oil. The EMD is ranged at 1.13 ~ 1.18, depicted as Fig. 1(A). There is no significant change in the past 15 years, implying that the energy supply structure does not change, or, not improved.

(2) EID analysis

Except renewable energy, the fossil fuel and nuclear energy are almost imported. In 2008, the coal is imported from five countries and more than 90% is from Australia and Canada. The oil is imported from seven countries and 55% is concentrated in Saudi Arabia and Kuwait. The natural gas is also from seven countries and 65% is from Indonesia and Malaysia. Therefore, the imported diversity of the different energy sources is 0.77, 1.69, and 1.52 for coal, oil, and natural gas, respectively. The performance of diversity of energy type shows that the diversity of oil is better because of the more imported countries and higher distributions. In addition, the percentage of the three energy types to the overall energy is 32.42%, 49.46%, and 9.42% in 2008. Thus, the EID in 2008 is 0.117. The EID trend is as Fig. 1(B). Due to the dependency on imported energy is too high, the EID value is very low.

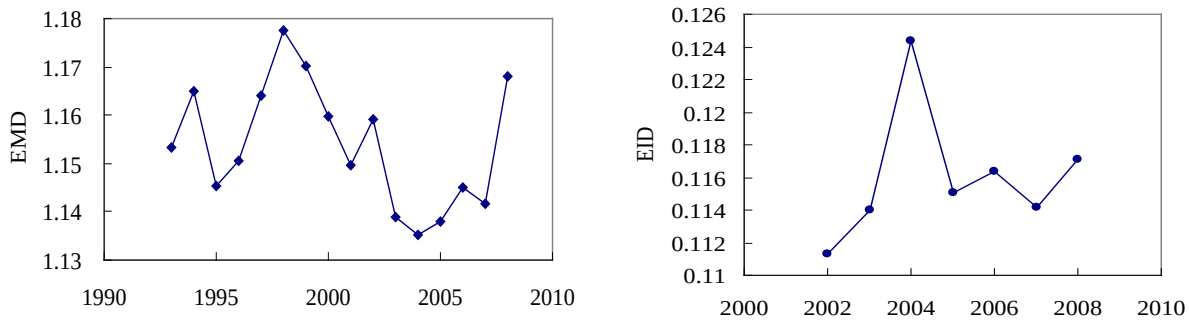

(A) (B)

Figure 1 The results of (A) EMD index and (B) EID index in Taiwan.

3.2. Energy security of Sustainable Energy Development Framework

(1) scenario of energy policy

The lately announced energy policy in Taiwan is the Sustainable Energy Development Framework. In this study, one of the strategies listed in the framework is used to demonstrate the energy security assessment. Many objectives are set in this Framework and one of them is to increase energy efficiency. In this study the objective of energy efficiency is used as energy policy scenario, in which the energy efficiency is increased 2% annually in future eight years and the energy intensity (or energy consumption) is decreased 20% of the level of 2005 by 2015.

The energy efficiency is the ratio of energy production to input, expressed as NT$/ LOE (New Taiwanese Dollar/ litter of equivalent oil). In 2009, the energy efficiency is 113 NT$/LOE and the value will become 133 NT$/LOE in 2017 under the policy scenario. If the production is 1000 NT$, the 8.85 litter of oil is required in 2009; however, only 7.52 litter of oil is required in 2017 according to its higher energy efficiency. Therefore, the 15% of energy will be saved in 2017 if assuming other impact factors are maintained. This means primary energy consumption of 121,333 thousand kLOE in 2009 will decrease to 103,557 kLOE in 2017. The total saved oil is 17,776 thousand kLOE in 2017. The assumed trend of energy efficiency and primary energy is showed in Fig. 2. After translating the policy objective into the detailed energy change information, the information is used to assess the impact of energy security incurred by the policy.

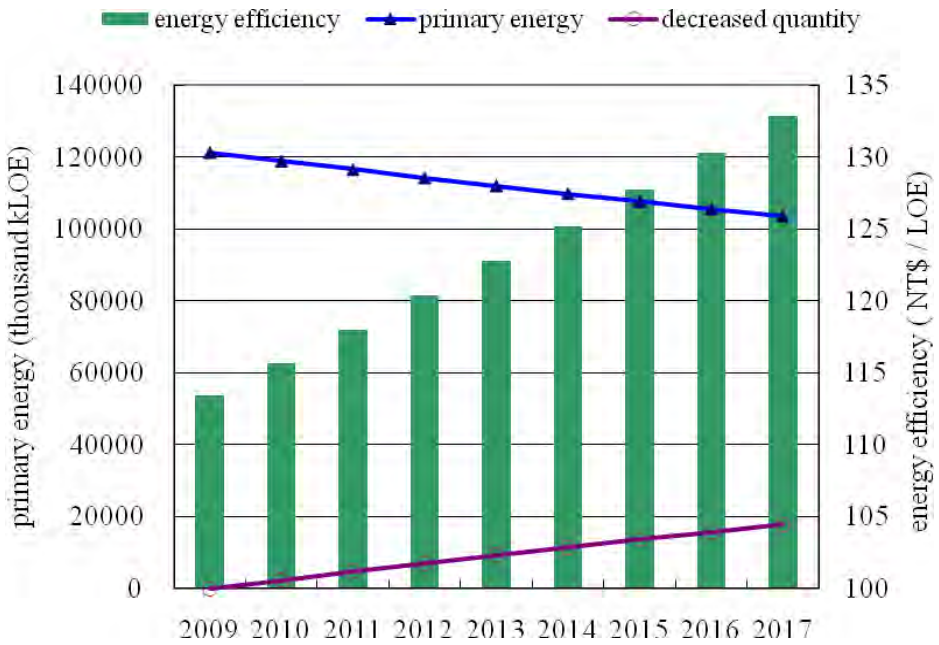

Figure 2 The simulated trend of energy efficiency and primary energy under the scenario of increased 2% of energy efficiency annually in eight years (base year 2009).

(2) EMD analysis

Due to the increased energy efficiency, the total of 17,776 thousand kLOE can be saved in 2017. If the saved energy is contributed to coal and oil savings and the other energy maintains as the same quantity in 2009. The energy structure is then changed as Fig. 3. The percentage

of coal is from 34.6% in 2009 decreased to 31.9% in 2017 and the oil is from 45.2% to 44.4%.

The performance of EMD is 1.167 in 2009 and 1.254 in 2017 because of the decreasing percentage of coal and oil. Although the distribution of energy sources is slightly raised because of the improved energy efficiency, the EMD value is still less than Japan and Korea, which is 1.38. The big difference is caused by the high percentage of coal and oil. Even in 2017 scenario, the percentage of coal and oil is summed up to 76.3%. However, this value in Japan and Korea is less than 70%, which implies that the improvement of energy efficiency seems not contribute significantly to energy security and the developments of the other energy are important as well.

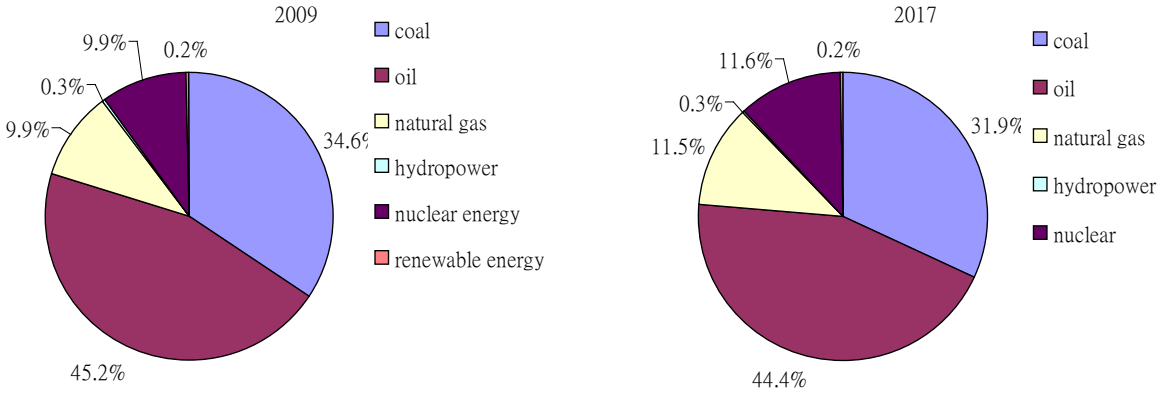

Figure 3 The energy structure in 2009 and 2017

(3) EID analysis
There is no detailed information about the change of energy imported countries under the scenario of improved energy efficiency. Assuming the number and distribution of energy imported countries is the same with that in 2009, i.e., 0.77 for coal, 1.69 for oil, and 1.52 for natural gas. But the percentage of coal, oil, and natural gas to the overall energy is changed, the final EID is therefore from 0.117 in 2009 to 0.164 in 2017. The more diversity energy structure in 2017 results a better consequent EID value as well.

4. Conclusions

Energy security is the core issue of energy policy and should be included in SEA. However, assessing energy security is difficult due to its indistinct definition and no indicators can reflect the complete energy security. The need of a quantitative tool of energy security is obvious in Taiwan; especially applying it in SEA. This study clarifies the physical characteristics of energy security and suggests that diversification can represent the energy security. Two indicators are proper to quantify the diversification, which are energy mix diversification (EMD) and energy imported diversification (EID). The EMD reveals the diversification of the national energy structure. When disperse the dependency on particular energy sources, the EMD will sequentially increase. The EID is an advanced indicator and is able to reflect the imported diversity of a particular energy type.

In Taiwan, the domestic energy production is very low and almost 99% of energy depends on imported energy. The results of EMD and EID show the consistent low energy security. The current energy structure is heavily relied on coal and oil and results in low EMD value. The high percentage of imported energy causes low EID value. Even increasing energy efficiency

according to the objective of a newly energy policy, the improvement on energy structure is limited. Unless the dependency on coal and oil is decreased to less than 70%, the energy security would not promote dramatically in Taiwan.

Reference

[1] Loschel, A., Moslener, U., Rubbelke, D., 2009, Indicators of energy security in industrialized countires. Energy Policy doi:10.1016/j.enpol.2009.03.061.

[2] Bohi, D. R. and M. A. Toman, 1996, The Economics of Energy Security, Norwell,

Massachusetts： Kluwer Academic Publishers.

[3] International Energy Agency (IEA), 2007, Energy Security and Climate Policy-Assessing Interactions, p. 150.

[4] Lin, S.M., and Fon, C.C., 2008, Energy security assessment in Taiwan, 2008 Annual conference of Taiwan Economy Association, Taiwan.

[5] Commonwealth of Australia, 2009, National Energy Security Assessment.

[6] Kruyt, B., van Vuuren, D.P., de Vries, H.J.M, Groenenberg, H., 2009, Indicators for energy security. Energy Policy 37: 2166-2181.

[7] [7] Noble, B.F., 2002, Strategic environmental assessment of Canadian energy policy, Impact Assessment and Project Appraisal, 20 (3), pp. 177-188, Beech Tree Publish, UK.

[8] [8] Jay, S. 2010, Strategic environmental assessment for energy production, Energy Policy, 38, pp. 3489-3497.

[9] Josimovic, B., and Pucar, M., 2010, The strategic environmental impact assessment of electric wind energy plants: Case study ‘Bavaniste’ (Serbia), 35, pp. 1509-1519.

[10] Chang, S.L., 2005, Feasibility analysis of energy supply security and oil dispersion policy, International Conference on Sustainable Energy Development and GHGs Mitigation, Taipei, Taiwan.

[11] International Atomic Energy Agency (IAEA), 2005, Energy indicators for sustainable development: guidelines and methodologies, p.171.

[12] Vera, I., Langlois, L., 2007, Energy indicators for sustainable development. Energy 32: 875-882.

[13] Blyth, W. and N. Lefévre, 2004, Energy Security and Climate Change Policy Interactions: An assessment framework, Paris: IEA.

[14] Wu, G., Liu, C.C., Fang, I., Wei, I.M., 2006, Analysis of risk on imported oil with HHA method, Cross Conference on Energy Economy and Policy, Beijing, China.

Have to Re-examine Renewable Energy

Chen Yong[1, *], Yuan Haoran[2]

[1] *Guangzhou Branch of Chinese Academy of Sciences, Guangzhou 510070, China,*
[2] *Guangzhou Institute of Energy Conversion, Chinese Academy of Sciences, Guangzhou 510640, China*
** Corresponding author. Tel: +8620 87057622, Fax: +8620 87683787, E-mail: chenyong@ms.giec.ac.cn*

Abstract: In this paper, it was emphasized that the conversion process of renewable energy resource was non-renewable, and energy resources were re-classified as self-consumption-based energy resource which mainly consumed itself and carrier-consumption-based energy resource which mainly consumed carriers. This classification avails to improve energy conversion efficiency and utilization efficiency based on their respective disciplines and mechanisms.
Conventional energy system is established on the basis of self-consumption-based energy resource. And its theoretical, academic and technical contents have been unable to meet the needs of carrier-consumption-based energy resource for technological innovation. Therefore, in the era of vigorously promoting renewable energy resource, the energy theory and technology system corresponding with carrier-consumption-based energy resource must be established and new ways to use energy must be explored corresponding with carrier-consumption-based energy resource conversion mechanism.
We emphasized that it was necessary to set up the new theoretical and technical system of energy to adapt to renewable energy development, which was the key to solve energy problems.
Although the new theory deviates from the conventional view, it's crucial for establishment of new energy science and technology innovation system, and would play a significant role on sustainable development of human society and low carbon technology innovation.

Key words: *Renewable energy, Self-consumption-based, Carrier-consumption-based.*

Nomenclature

E_A *Available energy* ..... *j*
E_S *Self energy* .....*j*
η_c *Conversion efficiency*
η_{cc} *Carrier consumption efficiency*
e_{PE} *Index of unit energy environment* ..... $ppm \cdot j^{-1}$
P_{ep} *Pollution in equipment production process*.....*ppm*
P_{EP} *Pollution in energy production process*.....*ppm*
E_P *Energy production* .....*j*

1. Introduction—Energy resource and energy

Energy resource has always been a hot debate since the outbreak of oil crises. There are about twenty definitions of energy resource up to now. In The Encyclopedia of Science and Technology, energy resource is defined as the resources from which energy, such as heat, light, electricity and so on, can be obtained. In Encycopedia Britannica, energy resource is a union of all fuels, water, solar, wind, and can be converted into required energy by the appropriate means. Thus energy resource is not equal to energy. Energy resource can be considered as the resources which can be converted into energy. And these resources can't be utilized directly, but be utilized in the form of energy after corresponding conversion. So energy is the outcome of energy resource conversion and not equal to energy resource.

This paper clarified the difference between energy and energy resource through the systematic expatiation and proposed corresponding solution for the deficiency existing in the present energy research. And methods to improve the energy utilization efficiency were proposed through a clear classification of different types of energy utilization in order to clarify each

bottleneck of energy utilization efficiency. Therefore, the current low energy utilization efficiency could be improved fundamentally, and the new energy was promoted to become the leading energy resource.

2. Analysis of non-renewability for "renewable energy resource"

The history of human civilization is a history of human utilization of energy resource, and creation of any substance is inseparable from energy resource utilization. The development of human society has experienced three stages [1]: a stage that mainly utilize "renewable energy resource" such as solar, wind, geothermal, water and so forth; a stage that mainly utilize fossil fuels such as petroleum, natural gas, coal, and so on, which are not renewable; and a stage devoting major efforts towards development of renewable energy resource. At the first stage, human used natural energy sources intuitively to do simple work, provide heat and keep warm etc. At the second stage, the invention of steam engine promoted development of industrialization marked as fossil fuels (petroleum, natural gas and coal). Theory and technology system corresponding with energy resource generated gradually. But lack of theory and technology system corresponding with renewable energy resource constrained the development of energy resource. At the third stage, serious environmental problems and energy resource supply issues emerged constantly due to the large-scale utilization of fossil fuels at the second stage. Human is once again faced with the necessity to strongly emphasize the development of renewable energy resource.

In order to meet the demand of industrialized society, the emerging energy resources should be developed in a high efficiency, low consumption, high energy density, sustainable and little environmental impact direction. Therefore the renewable energy resources should be converted into stable energy such as electric power. With respect to high energy-density energy resources, such as oil and coal, most of renewable energy resources are low energy-density energy resources, such as wind, solar, tidal energy resources, they will consume more equipments (also carriers) in conversion process. The conversion efficiency, life, cost, and resources of carriers will determine the utilizing efficiency and the development of renewable energy resource. This is the reason why the renewable energy resource was substituted by fossil fuels at the second stage and couldn't be utilized on a large scale at the third stage [2].
To solve this problem, we proceeded with the substrate of renewable energy resource and explored ways to improve its efficiency through the technological analysis of renewable energy resource.

3. Energy system methodology

3.1. Classification of energy resource by dichotomy

Currently energy resource is classified into fossil energy, renewable energy, nuclear energy and hydropower, etc. in the form of energy resource, rather than in the form of energy resource utilization and conversion. From an objective point of view, some energy resources including fossil energy, nuclear energy and biomass energy are all available through their own consumption, while other energy resources, such as solar, wind, geothermal, ocean energy, etc. are available through carrier consumption. And these two forms of energy utilization and conversion have their own rules and theoretical basis.

When wind energy and solar energy included in renewable energy resource are converted from resource into energy, carriers are needed during the conversion process and the conversion efficiency depends on the adoptive carriers. Herein it can't simply be thought that energy resource is renewable so that the whole process of energy resource utilization is

renewable. Because the energy resource utilization efficiency doesn't depend on energy resource itself but depend on the adoptive carriers attributed to the low energy-density. Although this type of renewable energy resource are considered to be renewable but its renewability during the conversion process accompanied by carriers' consumption is untenable. So this type of renewable energy resource can't be entitled as "renewable energy resource". Here we focused on the different determinants in the energy resource utilization process and reclassified energy resource, which conduced to the development of new energy resource and acceptance of new energy resource as the mainstream in this society.

Here we focused on the different determinants in the energy resource utilization process, abandoned the existing classification of energy into renewable energy and non-renewable energy, reclassified the overall energy system, cleared the direction of the new energy development, which could conduced to effective solution of the new energy efficiency bottleneck issues, and acceptance of new energy as the mainstream in this society.

According to the determinant of energy efficiency, energy resource is re-classified as self-consumption-based energy resource which mainly consumes itself and carrier-consumption-based energy resource which mainly consumes carrier. According to the energy resource utilization ways, energy resource is re-classified as fuel type energy resource and non-fuel type energy resource. From the perspective of energy efficiency, the energy efficiencies of self-consumption-based energy resource and fuel type energy resource mainly depend on the substance itself, while the energy efficiencies of carrier-consumption-based energy resource and non-fuel type energy resource low energy-density are mainly determined by carrier ascribed to low energy-density. This classification is conducive to improve energy efficiency more effectively when studying laws and mechanisms, respectively, and to clear the relationship between different types of energy resources, finally clear the development direction of renewable energy resource.

At present, all of the energy resource theories are built on the basis of traditional energy resources. However, these theories have been established before the emergence of new energy resource. And new energy resource here mainly means carrier-consumption based energy resource and non-fuel-based energy resource proposed above.

In other words, these theories can't meet the demand of the existing energy resource technology innovation. And traditional production and living style, and traditional energy resource utilization ways can't pull birth of more rational, more scientific, more efficient, low-cost, new energy resource technologies. Therefore, in this era vigorously advocating the development of renewable energy resource, energy theories and technical systems corresponding with new energy resource should be build up, new energy resource utilization ways consistent with new energy resource conversion mechanism should be explored, and a revolutionary energy resource technology innovation should be developed, finally a new industrial revolution which is different from the previous industrial revolution marked as the steam engine should be activated.

3.2. Life circle analysis of energy technologies

We demonstrated the above view through life cycle analysis (LCA) of the energy utilization. LCA [3, 4] is an approach in which all energy and material inputs and outputs are accounted for in a technology system, and compilation and evaluation of the potential environmental impacts. The assessing object of LCA method is environmental impacts and material conversions caused by the product system or service system. LCA can identify and quantify

the energy consumption and waste discharge associated with the assessing object, and it also can assess the caused environmental burden correspondingly. Assessment of the environmental impacts caused by energy consumption and waste discharge can help provide an overview interaction between the product system and environment as complete as possible. It avails to find the timing and means to improve energy utilization efficiency and protect the environment, and provides products and technology criteria. Therefore, LCA can determine the non-renewability of energy utilization process and demonstrate bottlenecks of energy utilization efficiency through energy consumption, which not only proved the correctness of our classification, but also point out how to improve the energy utilization efficiency from the point of an overall view.

Therefore, human must re-examine the "renewable energy resource" problem. Carrier-consumption-based energy resource and non-fuel type energy resource are inexhaustible, clean and pollution- free as the existing substance in nature. They need to be converted into energy in the application process. And carriers must be used in the conversion process. Once these energy resources are converted into energy through carriers, the utilization process will consume carrier materials and give rise to pollution of the production process, coat, efficiency and waste proposal issues, which are critical issues of this energy resource utilization. In order to clarify the impact factors and developing direction of energy resource, the corresponding LCA-type formulas are established shown as below:

$$E_A = E_S \times \eta_C \times \eta_{CC} \tag{1}$$

$$e_{PE} = (P_{ep} + P_{EP}) \div E_P \tag{2}$$

The energy production and costs of energy production in the utilization process can be clarified according to above formulas. Solar and wind energy are chosen as an example. Since solar and wind energy can be greatly influenced by the natural environment and climatic conditions, with instability and uncertainty, in order to improve power quality, new energy storage devices must be set in new energy power generation system so that excess energy is stored when the external energy is sufficient, and lacked energy is complemented when the external energy is insufficient. For example wind generator can store the wind energy through inductive energy storage device and improve the quality of power supply. In addition to the traditional batteries and energy storage inductor, modern energy storage devices have been developed such as super-capacitors and flywheels, etc., but the exploitation of these materials and preparation process has huge energy consumption.

Amorphous silicon cells in solar photovoltaic industry provide an example [5, 6]. The photovoltaic industry chain consists of four parts: silicon material, silicon chips, solar cells, solar energy battery components. Preparation of silicon materials have gone through silicon ore mining, preparation of industrial silicon, the process of preparation of crystalline silicon and so on. Investigation of energy storage systems and examination of issues associated with waste disposal of expired batteries and development of energy storage devices for long-term use must be carried out in order to achieve stability in the independent power generation. At present, solar power plant construction requires an investment which is approximately 7-8 times that of coal [7], the power generation cost of solar electricity is about 8-9 times of coal, and requires much more land area than coal-fired electricity. By this token, the solar power generation technology presents not only high-cost problem but also the problem of consumption of resources, the process of pollution, waste disposal and other issues.

Take wind energy as an example [8], the world's wind power calculation is based on the standard of power generated by the largest wind of annual local detection, known as peak power. However, the maximal wind power of the year couldn't be maintained every day. In fact wind power unit effective power only reach to 20% of peak power, which makes wind energy cost of unit power very high; brings about large quantity of consumption of resources such as converting equipment, fan blades, transmission, generator; causes equipment maintenance and waste disposal problem latterly [9]. Without exception, the utilization efficiency of above energy in the utilization process mainly depends on the energy conversion means, which is the carrier consumption we mentioned above. In other words, this type energy converts through the carrier consumption. So we named this type energy carrier-consumption-based energy.

Here we propose the existing problems of new types of energy, don't oppose vigorously the development of new energy resources, and don't deny classifying energy into the renewable energy resource and non-renewable energy resource, but understand energy resource from another point of view. At the same time due to the shortage of fossil energy, we need to develop new energy resources vigorously. Raising these issues is only for pointing out that the new energy resource developing road is a materials innovation road, technological innovation road, process optimization road.

Through the re-classification of energy resource, developing directions of different types of energy resources can be clarified, e.g. the developing directions of self-consumption based energy resource and fuel type energy resource are the deployment of process and the implementation of energy saving measures; the developing directions of carrier-consumption-based energy resource and non-fuel type energy resource are choose of materials, study of technical principles. Here selection of materials for carrier-consumption-based energy resource mainly includes new materials for energy efficiency improvement and cost reduction etc.

3.3. New energy resource theory and technology system

There is another reason for the difficulty of existing new energy resource technologies to break through. It is that so far no scientific research institutions or scholars could propose a systematic concept and planning for energy science and energy systems, so the real energy discipline has not been established. The so-called discipline has two meanings: the disciplines and branches of knowledge; teaching, research and other functional units, which is relative definition on the teaching and research activities. Here "discipline" partially refers to the latter meaning, but are also relevant with the first meaning. While there are quite a bit researches on the branches of energy resource in the world and there are quite adequate research methods for all kinds of energy resources, the researches on energy system and energy discipline are relatively less, which causes the division between the disciplines, non-shared resources, over-specialization of talent education, narrow range of knowledge, narrow direction of research, overall low benefit and relatively decentralized scientific research especially individual research.

The re-classification on energy resource can't make changes on the nature of energy resource, but is very helpful for the improvement of energy efficiency, the establishment of energy discipline and talent education. For example, for the self-consumption-based energy, the establishment of discipline should be interdisciplinary-based on chemical engineering, energy chemistry, thermal engineering and so on; for carrier-consumption-based energy, the

establishment of discipline should be interdisciplinary-based on mechanical engineering, material science, energy biology, energy physics and so on.

Construction of a discipline possesses multiple functions, such as talent education, scientific research, social services, etc. Discipline set up under the right guidance of academic philosophy could develop the discipline of various functions of discipline much better. The establishment of energy discipline is in line with this standard. From the view point of energy classification, it can be analyzed that energy discipline is the intersection of parts of materials science, chemical technology, physics and mechanical engineering etc.

From now on, the systematic energy discipline hasn't been established, which causes a serious split within the disciplines. So, logical relationships between different types of disciplines, discipline characteristics and patterns of development can't be reflected accurately. This situation not only seriously affect the interaction between the cross discipline, integration, resulting in blind comparisons and vicious competition between different disciplines, impeding the normal development of energy disciplines, but also affect the energy talent education. Rational energy talent education is more conducive to the development of energy resource disciplines and the correct development path for energy can properly guide the efficient development and utilization of energy resource. Therefore, we must create the right energy system, adjust the energy disciplines reasonably, and establish the corresponding theoretical basis in order to study its regularity and mechanism. E.g. theoretical system for carrier-consumption-based energy resource may include energy ecology, energy transfer study, energy materials, energy bionics, energy chemical, biological energy, energy physics etc., and its technology system should include collection technology, conversion technology, energy storage technology, using technology and so on.

Discipline construction can promote the development of scientific research and industry and then stimulate the improvement of scientific research level and overall strength. With the social development and technological progress, the discipline construction has been the crucial factor to strengthen internal discipline, enhance the overall academic level of scientific research and promote talent education. In the beginning of establishing a new energy discipline system, the direction of development may not be stable. Therefore, it need to go through a period of adjustment, differentiation, and eventually evolved into a purposeful, organized common action. When this action is recognized by the society, a new discipline comes into being.

4. Conclusions

In this paper, starting from the energy resource, the non-renewability of energy utilization process was proposed on the basis of the exploration of the energy resource and it was pointed out that the existing energy utilization theory could not meet the existing demand for energy technology innovation. Therefore, new energy theory and technology system should be established corresponding with the new energy system and new energy utilization ways should be explored corresponding with the new energy conversion mechanism. So classification of energy resource by dichotomy was proposed and energy was re-classified as self-consumption-based energy and carrier-consumption-based energy. And this viewpoint was demonstrated by the LCA. In conclusion, after effectively addressing these problems, the corresponding energy systems should be established through discipline construction to promote scientific research and industrial development.

Today is accelerating development new energy resources. We must start from the origin of energy utilization and promote new energy resource into the mainstream of energy resources through exploring the origin of energy, principle inquiry, technological innovation, discipline construction and other means, so as to establish a new industrial revolution different from that marked as steam engine.

References

[1] Bent Sørensen, A history of renewable energy technology, Energy Policy 19, 1991, pp. 8-12.

[2] Veit Bürger, Stefan Klinski, Ulrike Lehr, Uwe Leprich, Michael Nast, Mario Ragwitz, Policies to support renewable energies in the heat market, Energy Policy 36, 2008, pp. 3150-3159.

[3] Margaret K.Mann, Pamela L.Spath, Life Cycle Assessment of a Biomass Gasification Combined-Cycle Power System, Beijing: China Environmental Science Press, Edition, 2000.

[4] Shujuan Wang, Huiling Tong, Life Cycle Assessment On CO2 Emissions From Coal-Fired Power Plant In China[C], 1st US-China Symposium on CO2 Emission Control Science&Technology, 2001.

[5] Adolf Goetzberger, Christopher Hebling, Hans-Werner Schock, Photovoltaic materials, history, status and outlook, Materials Science and Engineering: R: Reports 40, 2003, pp. 1-46.

[6] Michael Mauk, Paul Sims, James Rand, Allen Barnett, Thin Silicon Solar Cells Practical Handbook of Photovoltaics 2003, pp. 185-225.

[7] M. EL-Shimy, Viability analysis of PV power plants in Egypt, Renewable Energy 34, 2009, pp. 2187-2196.

[8] G.M. Joselin Herbert, S. Iniyan, E. Sreevalsan, S. Rajapandian, A review of wind energy technologies, Renewable and Sustainable Energy Reviews 11, 2007, pp. 1117-1145.

[9] Ryan H. Wiser, energy finance and project ownership: The impact of alter native development structures on the cost of wind power, Energy Policy, 25, 1997, pp. 15-27.

Evaluation and Analysis of Renewable Energy Sources Potential in Slovenia and its Compatibility Examination with Slovenian National Renewable Energy Action Plan

Matevž Obrecht[1,*], Matjaž Denac[1], Patricija Furjan[1], Milena Delčnjak[2]

[1] *University of Maribor, Faculty of Economics and Business, Maribor, Slovenia*
[2] *SODO d.o.o., Electricity distribution system operator, Maribor, Slovenia*
[*] *Matevž Obrecht, Tel: +386 40565128, Fax: +386 22296571, E-mail: matevz.obrecht@uni-mb.si*

Abstract: Environmental problems and high import dependency from fossil fuels are core problems of the energy policy of the European Union (EU), therefore the EU has committed to increase the share of renewable energy sources (RES) in final energy consumption to 20% by 2020. Individual targets for each EU member must be incorporated in National Renewable Energy Action Plan (NREAP). To evaluate the possibilities for development of sustainable energy industry and for preparation of NREAP, evaluation of future energy needs must be made, national RES potentials must be examined and increase of RES share must be planed. In this paper the energy balance and the consumption structure of energy sources in Slovenia, EU and the World is analyzed. The share and growth of RES in Slovenian energy balance is compared with the average values of EU and the World, with emphasis on examining RES potential in Slovenia. Compatibility of RES potentials with the planed utilization for individual RES potentials in Slovenia is analyzed from economic and technological point of view with environmental considerations taken into account. The purpose is to examine which RES potentials have not been fully exploited and compatibility of measures provided in Slovenian NREAP with the estimated potential of RES.

Keywords: *Energy, Renewable energy sources, Energy Policy, Slovenia, Potentials*

1. Introduction

In the 20th century, dramatic 20 fold increase of energy consumption has been noticed [1]. It is expected that the energy consumption will also rise in the future. The forecast of International Energy Agency (IEA) in its reference scenario estimate, that world energy demand from 2005 to 2030 will rise for approximately 52% [2], while predictions of World energy council estimate double energy demand by 2050 what is comparable to IEA. Other recent estimates suggest that energy demand over the next five years will rise 2.5% annually and after that for 1.5% annually by 2030. Fossil fuels will remain the major energy source, which will cover approximately three quarters of elevated energy needs.

The amount of fossil fuels consumed annually (about 80% of the total energy consumption) is about 7.5 billion tons when converted to carbon units (toe). Because the current world population is more than 6.86 billion people, the average consumption of fossil fuel energy by the people of the world at the turn of the century was just a little more than one ton per person. World average in annual energy consumption in 2008 was approximately 1.44 toe per capita. Calculation based on the data in national energy balance [3] shows, that the average consumption of fossil fuels in Slovenia is about 50% higher than the world average while average annual energy consumption in Slovenia is 2.38 toe, which is 65% more than world average what, on this criteria, range Slovenia among developed countries. Energy mixes of the members of EU-27 typically include approximately 60% of fossil fuels. IEA noted that predicted increase of energy demand in the next twenty years will have a simultaneous influence on increased prices of energy sources and increased green house gas (GHG) emissions. That is why IEA is drawing attention to the problems of fossil fuels consumption and calls for international climate agreement to cut GHG emissions. Continuous increase of

energy consumption in Slovenia in the past and the future expectations are not sustainable and energy related emissions are already around 80% of all GHG emissions in Slovenia [4].

Pollution, GHG emissions, rising energy demand and high import dependency of energy are the core of energy problems in EU as well as in Slovenia. That is why RES are seen as a long-term solution and a short-term reduction of the above stated problems. The EU is aware of the issues related to conventional energy sources (CES) and supports the development of RES and sustainable energy. Sustainable energy comprises two key components: energy efficiency (EE) and RES. The investments in EE and RES are highly important since RES causes less or no pollution, enables use of local resources, lowers import dependency and increases EU competitiveness at the same time.

First ambitious goal set in EU in 2001 for the EU Member States, was 12% share of RES in 2010, which is unlikely to be reached. Second goal is represented in 20/20/20 objectives that require 20% of RES in EU by 2020. Specific target for Slovenia is 25% of RES. Achieving this objective is encouraged also with renewable energy Directive (2009/28/EC) that requires Member States to submit NREAP by 30th June of 2010. These plans had to be prepared in accordance with the template published by the Commission, provided detailed roadmaps of how each Member State expected to reach its legally binding 2020 target for the share of RES in their final energy consumption. Member States had to set out the sectoral targets, the technology mix they expected to use, the trajectory they would follow and the measures and reforms they would undertake.

The ever-growing worldwide consumption of fossil fuels and the concomitant emissions as well as the limited availability of fossil fuels, have led to a growing interest in the application of RES, therefore RES potentials must be examined. The increased general awareness of the negative environmental impact of the use of fossil fuels demands sustainable alternative energy sources. To enable further growth of sustainable energy sector, energy consumption and RES share must be examined, that is why we are analyzing and comparing energy consumption and RES share between 2000 and 2010 in Slovenia, EU and the World. We are also examining and evaluating individual RES potential. Total, technical and economic potentials of individual RES and plans of Slovenian energy policy are analyzed and additionally evaluated with our own recognitions and calculations. Our thesis is that potentials of RES are certainly not taken appropriately into account in the Slovenian NREAP that is why we have also tested compliance of RES potentials in Slovenia with NREAP.

2. Methodology

Statistical data presented in the study are gathered on the base of compilation method. Different independent sources (statistical offices, national, international and private studies and analysis, scientific papers and national energy balances) were used. Data of energy consumption, RES share, total, technical and economic RES potentials (exploited and unexploited), barriers of RES exploitation and all others data are statistically analyzed, evaluated and cross-compared.

Comparison energy production and RES share in Slovenia, EU and the world presents situation analysis. Our contribution is identification and combination of data, since individual data from different sources are not comparable because they were obtained by different methodologies. On this basis actual similarities and differences of energy statistics of Slovenia, EU and the world were than examined and cross-compared. In the second part RES potentials of Slovenia are examined. We examined and critically evaluated many existing studies, evaluations and documents. Where the deviations of RES potential between

individual studies were large, comparison with our own calculations of RES potentials that was based on characteristics of Slovenia (natural and physical characteristic, theoretical energy conversions) was made. In case of solar potential, our estimation is calculated on the base of average annual solar radiation and multiplied with the total surface of Slovenia and in case of wood biomass potential, our calculation is based on annual natural forest increase and annual forest cut down and supported with the average heat of combustion. Our calculations and synthesis of many different data from different sources and characteristics of Slovenia presents the basis on which we made a comparison and compliance testing with the data and measures about RES potentials and measures written in Slovenian NREAP and national energy program (NEP).

The survey and analysis of Slovenian RES potentials is held on t he basis of currently established economical, technological and environmental acceptability. We assume that technological and economic RES potential will increase in the future due to technological development, internalized external costs and increased prices of fossil fuel but the environmental potential will be reduced because of stricter environmental requirements. Although the study relates to NREAP that also includes calculations and forecasts about heat pumps, whose potentials are not yet fully discovered and liquid biomass that is mostly going to be imported in Slovenia, these two categories are not included in this study.

3. Results and discussion

3.1. Energy consumption in Slovenia, EU and the World

In order to achieve the development of sustainable energy policy all over the world, an international agreement, similar to 20/20/20 objectives, that are obligatory for EU members, is necessary. Gross inland consumption of primary energy in Slovenia compared to EU and World in 2000 to 2009 is presented in Table 1. From table 1 it is also visible that in EU RES share and the production of energy from RES increases more successfully than in Slovenia. Calculation of trend, based on data from table 1, for years 2005 to 2009 has shown that EU-27 is reaching its target of renewable energy sources much faster than Slovenia itself.

Share of RES in Slovenian gross primary consumption is more or less constant from 2000 to 2009. The biggest share of RES in Slovenia belongs to wood and hydroelectric energy. Minor changes in RES share between 2000 and 2009 are mostly a result of hydrological conditions in Slovenia. RES share and energy production from RES is growing slowly; only from 2007, meanwhile RES share in EU-15, EU-25 and EU-27 is growing constantly from 2002. We have also compare Slovenia with the world energy statistic because we surprisingly found some similarities of Slovenia and the world, like later mentioned peak energy consumption or share of RES in world primary energy consumption that is like in Slovenia also more or less constant from 2000 to 2008. These pattern similarities are sometimes even stronger and more visible than similarities with EU pattern, although Slovenia is more similar to EU because it is a developed country above the world average from the energy use, GDP and standard of living point of view. However the world energy production from RES is growing. The cause is that the world growth of energy production from RES is the same as the growth of world primary energy consumption. Energy intensity in Slovenia slightly rose in 2008 and in 2009 it fall back to the level of 2007. Meanwhile EU energy intensity is continually declining since 2003 [5, 6]. Peak of gross primary consumption in Slovenia was in 2008, while EU-15 reached peak consumption in 2005, EU-25 in 2005, EU-27 in 2006 and the world in 2007 [2, 5, 6]. A giant decline in energy production in 2009 can be seen in all analysed objects. This data among others also suggested cooling of economy, especially in most developed countries in EU and could be used as a forecast of economic trends in the near future.

Energy demand in Slovenia exceeds Slovenian production capacity that is why Slovenia is going to import around 50.6% of its energy and energy sources in 2010. S lovenian dependency on energy imports (49% in 2009) is very close to the EU-25 average (51%). Both data shows that Slovenia and EU are highly dependent on energy imports. This dependency that causes economical, political and social vulnerability of EU members must be seen as a challenge and opportunity for sustainable energy policy. Slovenia is going to import 100% of hard coal, anthracite, coke and oil products along with 99.7% of natural gas. Domestic supply in year 2010 is based on lignite, brown coal, hydro energy, wood biomass and electric energy from nuclear power plant Krško [3]. Oil products will cover the biggest share, approximately 47.6%, of imported energy sources [4]. Oil also remains the dominant fuel in the primary energy mix of EU-27 till 2035 [2].

Table 1. Total primary energy supply - TPES (2000-2009) [1, 2, 5, 6, 7].

Slovenia	**2000**	**2001**	**2002**	**2003**	**2004**	**2005**	**2006**	**2007**	**2008**	**2009**
TPES (ktoe)	6360	6749	6820	6931	7129	7307	7318	7336	7749	6990
RES (ktoe)	761	776	716	714	822	774	768	735	845	874
RES share (%)	12.0	11.5	10.5	10.3	11.5	10.6	10.5	10.0	10.9	12.5
EU-15										
TPES (Mtoe)	1454	1469	1502	1497	1530	1552	1552	1544	1527	n.a.
RES (Mtoe)	85	88	85	92	99	103	110	124	130	n.a.
RES share (%)	5.8	6.0	5.7	6.2	6.5	6.6	7.1	8.0	8.5	n.a.
EU-25										
TPES (Mtoe)	1655	1668	1706	1702	1743	1766	1766	1764	1747	n.a.
RES (Mtoe)	90	93	97	95	103	111	115	123	137	n.a.
RES share (%)	5.4	5.6	5.7	5.6	5.9	6.3	6.5	7.0	7.9	n.a.
EU-27										
TPES (Mtoe)	1724	1763	1759	1803	1825	1825	1826	1808	1799	1681
RES (Mtoe)	98	101	100	108	116	121	129	143	151	151
RES share (%)	5.7	5.8	5.7	6.0	6.4	6.6	7.1	7.9	8.4	9.0
World										
TPES (Gtoe)	10.02	10.17	10.23	10.58	11.04	11.44	11.60	12.06	12.00	n.a.
RES (Gtoe)	1.29	1.29	1.31	1.33	1.37	1.41	1.44	1.50	1.47	n.a.
RES share (%)	12.9	12.7	12.8	12.6	12.4	12.3	12.4	12.4	12.3	n.a.

From the energy mix analysis it is clear, that if we can not place our expectations on intensification of nuclear energy, we will need to focus our efforts into the development of renewable energy. Slovenia will have to restrict its attention to those technologies that could be introduced at a significant scale in the near future.

3.2. Estimation, analysis and examination of RES potentials in Slovenia

Because RES are the key element of sustainable energetics, we analysed and examined data about RES potentials in Slovenia. RES potentials are presented in table 2. Presented data and calculations from table 2 are not fully comparable, because they are combined from many different sources and studies of RES potentials in Slovenia that were or at least should be considered in preparing NREAP and NEP and compared with our own calculations. Differences also occur because forecasting RES potentials can not be totally reliable. Indicative prices for RES energy plants are a s ubject of investments in electricity (cogeneration) power plants only. Investments in heating power plants are much lower.

A hydro energy potential (HE) of Slovenia, a high efficiency of hydro electric power plants (HEPP), a very long life (over 100 years) and non-emission operation together with obtained cheap energy should make HEPPs the priority of the Slovenian energy industry. We estimate that the investments in large and small HE should be a priority of Slovenian electricity sector, because HEPP can significantly impact on mid-term replacement of CES. HE in Slovenia allows construction of small HE with additional 100 MW installed power [8, 9]. Small HEPPs also have positive impact on t he decentralization of energy industry and are over 90 % efficient. Technical and economical potential of large HEPP is much higher than small HEPP potential but the construction of large HEPP causes a large local environmental impacts. Meanwhile small HEPPs cause much less environmental strain, can be built in many locations and require relatively small total investments, that is why small HEPPs are attractive also for private capital. Small HEPPs must also be encouraged in rural regions because they present social and economic benefits for rural development. Despite efficiency of HE exploitation can be improved also with renewing and upgrading existing HEPPs, Slovenia is not giving enough emphasis on this measure.

Table 2. RES potentials in Slovenia at the end of 2010 [5, 8, 9, 10, 11, 12].

RES	Total potential (TWh/a)	Technical potential (TWh/a)	Economical potential by 2020 (GWh/a)	NREAP 2020 goal (GWh/a)	Price (million EUR/MW)	Installed (MW)
Hydro	19.4	9.1	6370	923		819
large HEPP		8.6-8.0	6070	837	1.5-2.6	
small HEPP		0.5-1.1	300	86	1.3-3.0	90
Solar	25835.4	8.6-2777.8	139-1300	343	3.0-5.0	17
Wind	15.6	3.1	226-1000	191	1.0-1.4	0
Wood biomass	19.6	2.9-10.1	300-4305	1249	2.0-4.5	115.4
Biogas	47.3	2.8-4.3	265-927	255	3.6	20.5
Geothermal	>5.4	0.6	44.4 - 150	38	4.6	0

Total potential of solar energy potential is approximately 25.84 PWh/year. As we can see from table 2, technical potential is estimated approximately from 0.01 to 2.77 PWh/year [11]. If we would like to achieve the maximum value of technical potential which is 10.8% of total potential, we should cover 10.8% of Slovenia's surface that is why we estimate this as an unrealistic value. However we have been witnessed 300% growth of photovoltaic in year 2009 [12]. High growth is expected also in 2010. The reasons are the current level of operating support and guaranteed purchase price. However reference costs will be 20% lower in 2011 and 30% lower in 2012 therefore moderate growth can be expected in the future.

Wind energy potential in Slovenia is currently totally unexploited. Total installed capacity of wind power plants (WPP) in Slovenia is 0 MW [12] despite the fact that wind is one of the cleanest and fastest growing RES on the world and especially in EU. The usage of WPP is limited due to lack of appropriate geographic locations, as well as the fact that almost 36% of Slovenia is included into NATURA 2000 network. Although construction of WPP represents significant intervention in the environment, we can achieve synergy with nature by thoughtful and sustainable positioning of WPPs, especially in degraded areas near roads. We propose the installation of a few pilot WPPs and the examination of their functioning. The results obtained would facilitate the decisions about new investments in WPPs and critics of environmental organizations which do not support WPPs in Slovenia. We have witnessed some unsuccessful investments in installations of WPP, therefore Slovenia is going to study and analyse proper areas for WPP. Because of the trends of WPP in EU, Slovenia's department for energy is

going to make a list of environmentally undisputed areas with sufficient wind that would attract potential investors. This measure will enable faster commercialization of wind energy.

Maximal technical potential of wood biomass estimated in NREAP and NEP seems excessively high. Technical potential is indeed estimated from 2,875 to 10,108 GWh/year [11]. However estimation 2,875 GWh/year covers only wood biomass that can be exploited only in minor energy plants and households, while maximum estimation covers also wood biomass that can be exploited in major energy plants and as co-incineration in thermal power plants. In spite of that, differences in wood biomass potential estimations are significant and very different from our calculation. Annual natural forest increase in Slovenia is 8 million cubic meters and average energy potential calculated from average heat of combustion of eleven different types of domestic Slovenian wood is 2,440GWh per million cubic meters of wood [11, 13]. That means that for achieving maximal technical potential Slovenia should exploit approximately one half of annual forest increase what is almost impossible, because of wood processing industry and current annual cut down that is approximately 3 million cubic meters of wood. Because of that we believe that this estimation is overestimated. Although NREAP goal for wood biomass is ambitiously set, wood biomass increase will have to be well supported for achieving the objective.

Relatively high biogas potential of Slovenia also seems to be overestimated. In similar studies which were not included in the preparation of NREAP and NEP (like the study of BigEast), estimated technical and total potential is much smaller. However, the NREAP goal is not so ambitiously set, because the study made by Agricultural and forestry chamber, that was not included in the preparation of NREAP and NEP, estimates that biogas potential by 2020 is 927 GWh/year [13] which is almost four times more than the NREAP goal is for 2020.

Slovenia currently exports a lot of biological waste to Austria [4]. Instead of this we believe that Slovenia should search for options for bigger domestic exploitation of biological waste. Important emphasis also must be made on cogeneration of heat and electricity and more extended use of landfill gas. Especially problematic is the use of heat from biogas plants, because they are mainly in the areas where not many heat consumers live. Slovenia should also support the cooperation between local farmers and local communities that should become partners in biogas plant investments. This kind of partnership is very appropriate for rural development and for preserving jobs in rural areas that means that positive effects of biogas as a RES are not just a matter of energy policy. Future measures are appropriate, because exploitation of biogas has strong growth. Growth from 2008 to 2009 was considerable 117%. Despite the enshrined measures, the main problem of biomass exploitation, whether to exploit rural areas for food or for energy corps supply remains the same.

Estimated geothermal energy potential of Slovenia differs greatly in different sources and studies. Geothermal energy potential data are collected every 5 years. Last available data are from year 2005, therefore Slovenian geothermal potential can not be accurately estimated. Nevertheless we can say the annual potential is at least 5443 GWh [11].

As it is evident in table 2 comments, NREAP has both good and bad sides and does not only deal with RES potentials but is also a plan for the future state of Slovenian energy sector.

3.3. Key factors for forecasting and planning future energy policy in Slovenia

Whereas the preparation of NREAP is a challenging project, only four members of EU have managed to submit NREAP in time (until 30.6.2010) and six members still did not submit it

until the end of 2010. Slovenian NREAP was submitted to EC with minor delay (8.7.2010) which is a result of completion and improvement of the NREAP content. Slovenian energy consumption forecasts and goals are presented in table 3. Calculation of future energy use in Slovenia for 2016, directed with 2006/32/EC, is based on 2006/32/EC directive methodology.

Table3. Forecasting and planning final energy consumption (FEC) for achieving 20/20/20 or 25 objectives [3, 10, 11]

category	**2007**	**2008**	**2009**	**2009** evaluation	**2010** forecast	**2012** forecast (Kyoto)	**2016** objective **(-** 9%)	**2020** objective (20/20/20)
FEC in Slovenia (ktoe)	4867	5232	4891	4960-5176	4744/ 4927*	5031*	4267 (9%) / 5214*	5232* or "*x*"
RES in FEC in Slovenia (ktoe)	745	780	787	813-849	840/ 872*	941*	1137*	1324* or 0.25 "*x*"
RES share in Slovenia (%)	15.3	14.9	16.1	16.4	17.7	18.7	21.8	25.3
RES share in EU-27 (%)	9.7	10.3	11.0	n.a.	12.0	n.a.	n.a.	20.0

* - NREAP forecast 9% - goal of directive 2006/32/EC

In the table 3 we can see that NREAP plan shows 20/20/20 objectives are achievable at Slovenian and EU level. Because 2020 goals do not prescribe future energy consumption but only the share of RES, we marked energy consumption in 2020 with "*x*". For 20/20/20 objectives future energy consumption is not so important but it is essential that RES share advocates 25% of "*x*". Especially important and problematic for achieving 25% of RES in Slovenia is raising share of transport [10] that is becoming the biggest problem in meeting Kyoto GHG emission targets as well. The lack of implementation of past objectives can also be seen in NREAP planning. Objective 33.6% of electricity from RES, set for 2010 for example, is planned to be reached (exceeded) only by 2015. In table 3 we can also see that NREAP objective is not planning to lower final energy consumption but to lower its growth. Because smaller and energy efficient use is also the goal of EU and because energy use declined in 2009 [5], mainly because of the economic crisis, we only have to retain it on the current level, what is more favorable than reducing it. That is why this is not a very ambitious goal. NREAP is actually planning to breach 2006/32/EC directive, which directs Slovenia to achieve 9% energy savings relative to the annual average energy consumption of 2001-2005 by 2016. We believe that increased EE and gradual change of consumer habits should be fully included in NREAP, because this brings the best long-term opportunity for smaller and efficient energy use. However it is realistic to expect a smaller growth of energy consumption by 2015 due to economic recovery but this trend must be limited already in the present.

Disregarding Kyoto targets can also be seen. Planed closure of inefficient blocks of thermal power plant could be made in 2012 instead of 2014 [8]. With this measure Slovenia would significantly reduce possible penalty for failing Kyoto targets and improve the basis for the South Africa agreement as a successor to the Kyoto.

4. Conclusions

In the study we have proven that studies and data about RES potentials differ significantly. That makes the estimates about RES potentials and future energy policy goals planning partly inaccurate. We discovered that our calculations about RES potentials are not exactly the same as in NREAP and NEP therefore we are not totally sure about appropriateness of goals and

measures set by Slovenian energy policy. Possible cause of differentiation of different studies about RES potential could be inaccurate data, different databases or different methodology of some studies. It is also possible that data presented in NREAP and NEP could be more accurate if more studies and researches about RES potentials would be made. However, all the studies had shown that Slovenia has many unexploited RES potentials, especially hydro, solar and wood biomass potentials, which are appropriate for future exploitation from technological, economical and environmental point of view, therefore they must be particularly stimulated. NREAP goals are ambitiously set and high growth of RES in all four sectors of NREAP is planned. Wood biomass and hydro potential will be increased most of all. Our opinion is that achieving these goals will be the most problematic. We have also noticed the lack of ambitious measures for smaller and energy efficient use, based on cogeneration or threegeneration, that could also be based on the 2006/32/EC directive.

We believe that reduced and efficient energy use is the only solution that leads to the sustainable energetics. Most important is that efficient technologies will be used regardless of the RES and that measures regarding RES and EE will be combined and implemented.

References

[1] H. Komiyama, S. Kraines, Vision 2050: Roadmap for a Sustainable Earth, Springer, 2008.

[2] *International Energy Agency (IEA), WORLD ENERGY OUTLOOK 2010* FACTSHEET, IEA, 2010.

[3] Ministry for Economy, Energy balance for the Republic of Slovenia for the year 2010, 2010, (in the Slovenian language).

[4] Environmental Agency of the Republic of Slovenia, Environmental indicators of Slovenia, available on: http://kazalci.arso.gov.si/, [10.12.2010], 2010, (in the Slovenian language).

[5] SURS Statistical Office of Republic of Slovenia. Annual Energy Statistic 2009 - final data, 2010, (in the Slovenian language).

[6] EUROSTAT, Energy statistics – main indicators and quantities, EUROSTAT, 2010.

[7] Federal Ministry for the Environment, Nature Conservation and Nuclear Safety, Renewable Energy Sources in Figures – National and International Development, 2010.

[8] M. Obrecht, M. Denac, Evaluation of potential and options of renewables for development of sustainable energy in Slovenia, Facing the Challenges of the Future: Excellence in Business and Commodity Science, 17th IGWT Symposium and 2010 International Conference on Commerce, 2010.

[9] Holding Slovenske elektrarne, HSE and RES in Slovenia, 2010, (in the Slovenian language).

[10] NREAP, National Renewable Energy Action Plan, Ministry of the Economy, 2010.

[11] Jožef Štefan Institute, National energy program (NEP) 2010 Long-term energy balance 2010 to 2030, Ministry of the Economy, 2010, (in the Slovenian language).

[12] Energy Agency of the Republic of Slovenia, Register of declarations for the production facilities of electricity from renewable sources and high-efficiency cogeneration, 2010, (in the Slovenian language).

[13] Agricultural and forestry chamber, Data about wood biomass and biogas in Slovenia, available on: http://www.kgzs.si/gv/gozd/les-in-biomasa.aspx, [25.11.2010], 2010.

Regulation for Renewable Energy Development: Lessons from Sri Lanka Experience

Priyantha D C Wijayatunga

Asian Development Bank, Manila, Philippines
** Corresponding author. Tel: +6326326131, Fax: +6326362338, E-mail: pwijayatunga@adb.org*

Abstract: The paper examines the key features of the small hydropower development environment in Sri Lanka which led to sector's rapid expansion. The recent development framework of the small hydropower sector was based on the importance of using indigenous resources, recognizing the positive environmental impacts and the avoidance of high cost alternative thermal generation. This framework also recognized the pioneering effort of the developers in site identification by giving rights to develop on a first-come first-served basis. The policy framework was later extended with a renewable energy portfolio standard to achieve 10% of power generation through renewable energy. The standard power purchase arrangements reduced the transaction costs. The feeding tariffs originally based on avoided costs later shifted to cost based, technology specific tariffs encouraging diversification of the renewable energy portfolio. The introduction of net-metering for renewable energy based distributed generation and the limited interventions in the form of green tariffs also assisted the renewable energy development. The paper concludes that the policy and regulatory frameworks and different approaches to implementing them have been mostly successful experiences in Sri Lanka and they would provide useful lessons for similar countries when formulating and implementing related polices, regulations and legal frameworks.

Keywords: *Renewable energy, regulation, feed-in-tariff, avoided cost, net-metering*

1. Introduction

Sri Lanka has a long history of using renewable energy for its power generation dating back to early 20th century when most of the tea plantation companies installed small hydropower plants to provide their electricity needs. Since then, the country's power generation system gradually developed into a large hydropower dominated system until early 1990s when almost 100% of its supplies came from hydropower. With the exponentially increasing demand for electricity and due to limited large hydro resources the country turned to oil based thermal power plants to supply its base-load requirements. The small hydropower development, though impeded until 1980s due to penetration of the national grid and large hydropower domination, became an attraction, with the increasing fuel costs for thermal power generation.

The paper examines the key features of the framework for grid connected renewable energy and in particular small hydropower development in Sri Lanka and how the policy and regulatory interventions assisted the sector's rapid expansion.

2. Policy Environment

2.1. Renewable Energy Development Policy

In the mid 1990s there was a resurgence of the interest in small hydropower development, particularly on the grid connected power plants. The policy environment was developed by the government with the assistance of the Ceylon Electricity Board (CEB) which was the sole purchaser of power generated by outside its own generation system. This process involved, assigning sites for development, licensing and power purchase agreement. Later with the rapid development of the small hydropower sector, the need to facilitate expansion into other renewable energy sources led the government to specifically address these aspects in the energy policy being drafted in 2006/07. From the beginning, the government policy has been to allow the private sector to develop all grid-connected plants up to 10MW.

The Energy Policy and Strategies of Sri Lanka has given due emphasis to the development of both the conventional and non-conventional renewable energy based generation (NCRE) [1]. One of the key policy elements is the promotion of indigenous resources in energy supplies. The relevant strategies have been identified in order to achieve this objective. They are the following

- The use of economically viable, environmentally friendly, non-conventional renewable energy sources to be promoted by providing a level playing field in generation sector development
- Concessionary financing to be sought to implement hydroelectric projects which are not viable under normal commercial terms
- Necessary incentives to be provided to other non-economic non-conventional renewable energy resources where appropriate to ensure their contribution to the energy supply
- A separate facilitation centre dedicated to the systematic planning and promotion of non-conventional renewable energy sources will be established.
- Appropriate steps to be taken to ensure the development and efficient use of non-commercial energy supplies such as biomass.
- Research and development on adopting new technologies and practices to be promoted

The policy has identified small hydropower, biomass power and wind energy as the three leading non-conventional forms of renewable energy sources to be promoted in Sri Lanka for grid connected electricity generation. The Government would endeavour to reach a level of 10% of grid electricity generated to be produced using NCRE by 2015. Though this policy has not yet been formally translated into a renewable energy portfolio standard issued by the regulator, the government and the regulator are taking necessary measures to reach this target.

The government has recognized the principle that the natural resources are public goods and hence the associated benefits need to be passed on to all the citizens in the country. But in the interest of expanding the NCRE technology penetration no resource cost is charged for a period of 12 years from the date of commercial operation. The resource charges will be used to finance incentives for further NCRE development through the Energy Fund. Therefore this recent development framework for renewable energy sources within which the small hydropower sector operates was based on the importance of using indigenous resources while recognizing the positive environmental impacts and the avoidance of high cost alternative thermal generation.

2.2. Institutional Framework

During the initial development phase of the small hydropower sector, CEB was the main institution involved as the sole purchaser of electricity generated by these plants. Central government agencies and provincial and local authorities have been involved in the areas such as land acquisition, environmental clearance and water rights. Once after commissioning the plant, apart from licensing and notifying the annual power purchase tariff determined by CEB, the central government's role in the sector was minimal.

With the expansion of the small hydropower sector and the interest of the private sector in developing other renewable energy sources, the government strongly felt the need to have a dedicated agency with adequate authority for NCRE resource development. Not only this agency needed to be able to facilitate the process of NCRE development but also it was to have the statutory powers to intervene and overcome barriers. Addressing this requirement the Government passed a new legislation to establish the Sustainable Energy Authority (SEA)

in 2007 [2]. The board of directors of SEA has the representation from all important stakeholder state agencies and the private sector. This has enabled SEA to address many of the critical issues within their board meetings.

2.3. Site Selection and Development

The CEB developed the hydropower master plan in 1989 which identified many of the hydropower development sites greater than 1MW capacity [3]. In addition, independent investigations by prospective developers and interested individuals and groups also have led to identification of many sites for small hydropower development including those below 1 MW capacity. The government policy has been to allow private sector to be the sole developer of all the sites below 10MW capacity connected to the national grid. The right to develop each of the sites has been awarded on a first-come first-served basis through a letter-of-intent offered by the CEB, recognizing the pioneering effort of the developers in site identification. Later, in order to avoid excessive delays in developing sites for which the letters-of-intent have been issued, the government decided to impose a time limit for development activities to start and progress. If no progress is made within the timeframe provided the letter-of-intent for the relevant site is withdrawn.

During the development of the grid-connected small hydropower sites, the developers usually respond to the needs of the local population partly advocated by the local government bodies in order to ensure smooth implementation. Such interventions by the developers include those such as construction of paved access roads and bridges in the surrounding rural areas which improve transport facilities for the rural communities. In addition, local manpower and other resources are used to the maximum during construction and operation of the plants.

The off-grid micro-hydropower sites often identified by rural communities have been developed by the community organizations themselves, with the assistance of some non-governmental organizations. The community contributes both in-kind through manpower and material for construction and operation of the plants and in cash. These micro-hydro plants have varying capacities ranging from 5kW to 25kW each serving 25- 200 village households depending on the capacity.

3. Regulatory Environment

The regulatory environment for small-hydropower involves licensing, power purchase agreements and feed-in tariffs. In the initial stages of development the institutions involved in this regard were the Ministry of Power and Energy and the CEB. With the establishment of the Public Utilities Commission of Sri Lanka (PUCSL) in 2003 and the enactment of the Sri Lanka Electricity Act of 2009, the regulatory authority over the small-hydropower sector fell within the purview of the PUCSL.

3.1. Standardized Power Purchase Agreement

In 1997 CEB introduced a standardized power purchase agreement (SPPA) for small grid-connected renewable energy based electricity generating plants less than 10MW. SPPA binds the CEB to purchase power generated by these plants without a limitation at a tariff declared every year. Further, the generator was assured a minimum tariff of 90% of tariff in the first year of its commissioning, throughout the SPPA duration.

3.2. Feed-in Tariffs

3.2.1. Avoided Cost Based

In 1997/98 the government declared that the SPPA tariff would be based on the "avoided cost" principle. The tariff calculated as the three year moving average was published at the beginning of each year. Initially the avoided cost was determined using the long term generation planning model which derives the generation expansion plan for the country for the following 20 years. It is a rolling plan and the calculation methodology captured the long term impact of the addition of renewable energy based small power plants in the overall long term generation plan. Later with the understanding between the CEB and developers the methodology was shifted to the operational planning model used in the system control centre where the short term operational costs provided the key inputs to the calculation process [4].

3.2.2. Project Cost based

In 2007/08 the government took a decision to reexamine the feed-in tariff regime as a part of the new energy policy where specific renewable energy targets are to be achieved by 2015. This process led to the introduction of the technology specific cost based feed-in tariffs for all types of renewable energy based plants which would be developed. Initially these renewable energy sources were limited to small-hydropower, wind and biomass. The tariff is designed to make sure that the developer would always have positive cash flow during the SPPA period. The tariff is revised periodically to ensure gradual penetration of different technologies. This new tariff is expected to encourage wind and biomass based plants which tend to have costs higher than those can be recovered through avoided cost based tariff. The plants already in operation or those in which SPPAs had been signed were given the option to remain in the previous tariff regime or to switch to the new regime.

3.2.3. Green-Power Tariff

In 2008 PUCSL initiated action on the allowing interested consumers to purchase power from identified NCRE based power plants. Though direct power wheeling from the generators to the users has not been legally permitted under the electricity act, PUCSL could encourage green-power consumers to enter into agreements with the generators to pay an additional charge directly for the power delivered while paying the standard consumer tariff to the CEB. PUCSL annually verifies whether the energy delivered to the consumers by such generators would satisfy their annual consumption expectation of green-power as agreed in advance. Accordingly, the final payments are reconciled.

3.3. Net-metering

On the advice of SEA, government and the CEB agreed for net-metering of premises with NCRE based systems connected to the grid in 2009. Though the feed-in tariff is not offered to these systems unless they have an SPPA, these premises can still use the grid as an energy storage. If systems are properly designed, net-metering now opens the door for such premises to be carbon neutral in their power consumption.

3.4. Exemptions from generation license

In the initial stages of development, off-grid generators never used to obtain generation (and distribution) license which is required under the law. The authorities ignored this situation considering that the requirements to fulfill for generation license are too cumbersome for the community operated small off-grid systems to fulfill, though operating these systems without a license was in contravention to the Electricity Act. When the PUCSL became empowered

with regulatory authority over the power sector in 2009, under the provisions of the Sri Lanka Electricity Act it has been taking steps to exempt off-grid generators from licensing.

4. Analysis and Discussion

4.1. Policy

The government policy of working towards an NCRE development target by 2015 has helped the SEA, CEB and the PUCSL to justify incentives for NCRE development. This can be in the form of direct government subsidies or cross-subsidies in the sector.

The policy of allowing private sector to develop all grid-connected power plants below 10MW and offer of an standardized power purchase agreement with guaranteed unlimited power purchase at a predictable price have encouraged both local and foreign investors to enter into the small hydropower sector. The sector was further attracted by the investors due to the policy of offering sites on a first-come first-served basis which incentivized rapid site identification, investigation and development. The resulting exponential development since 1998 can be seen in figures 1 and 2 where NCRE development up to 2008 has been totally dominated by small hydropower.

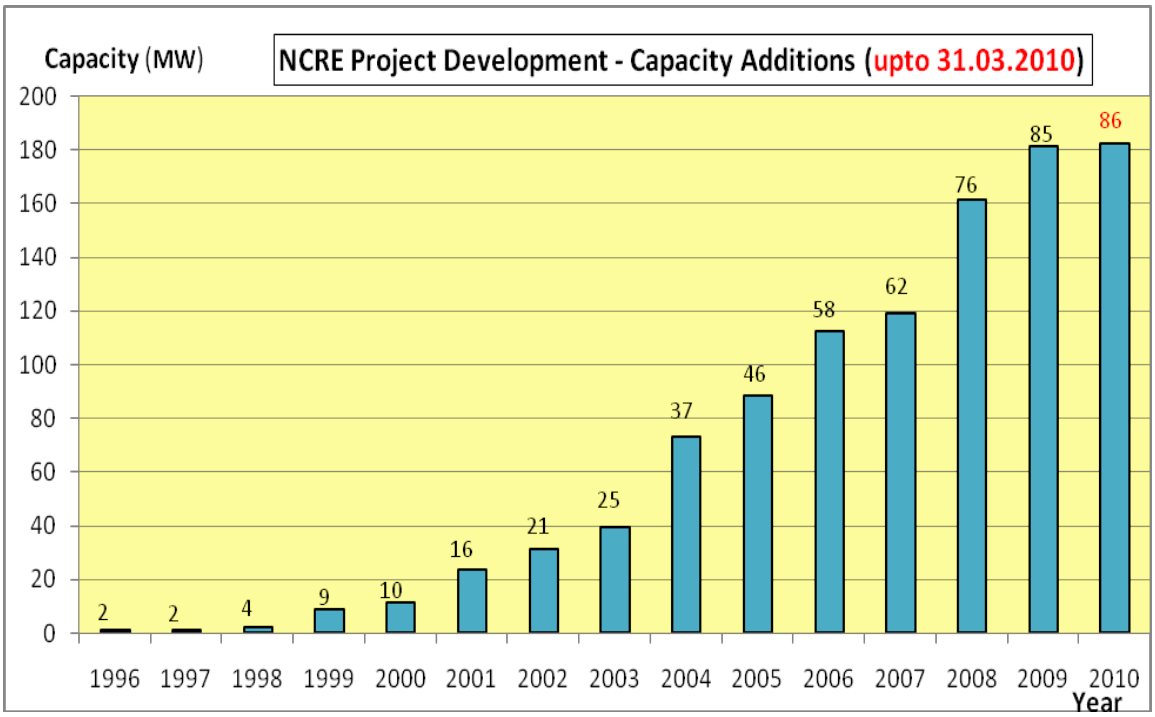

Source: Ceylon Electricity Board

Fig. 1. Total Capacity Additions of Non-Conventional Renewable Energy Based Generation

During the initial stages, the rights to develop the sites were obtained by those who actually wanted to invest in the projects. As the sector development gathered momentum, interested parties used the prevailing policy of site allocation to obtain the right to develop the site and sell the rights to other investors. This created an unhealthy market for letters-of-intent for small hydropower sites which eventually increased the effective project costs and delayed development. This situation was arrested to a certain extent with the introduction of a time limit for development where the investment needed to be in place within a specific time frame.

The optimal capacity of the power plant to be constructed at given site is a function of the investment and the returns it brings based on the hydrological conditions. As a result of the investors being allowed to choose the capacity of the plants to be constructed, the plant capacity became a function of available financing. This has resulted in under-sizing of plant capacity in certain sites leading to an economic loss. This situation could have been avoided if the utility or the SEA carried out an independent assessment and incentivized the developers to construct the plants to their optimal capacity.

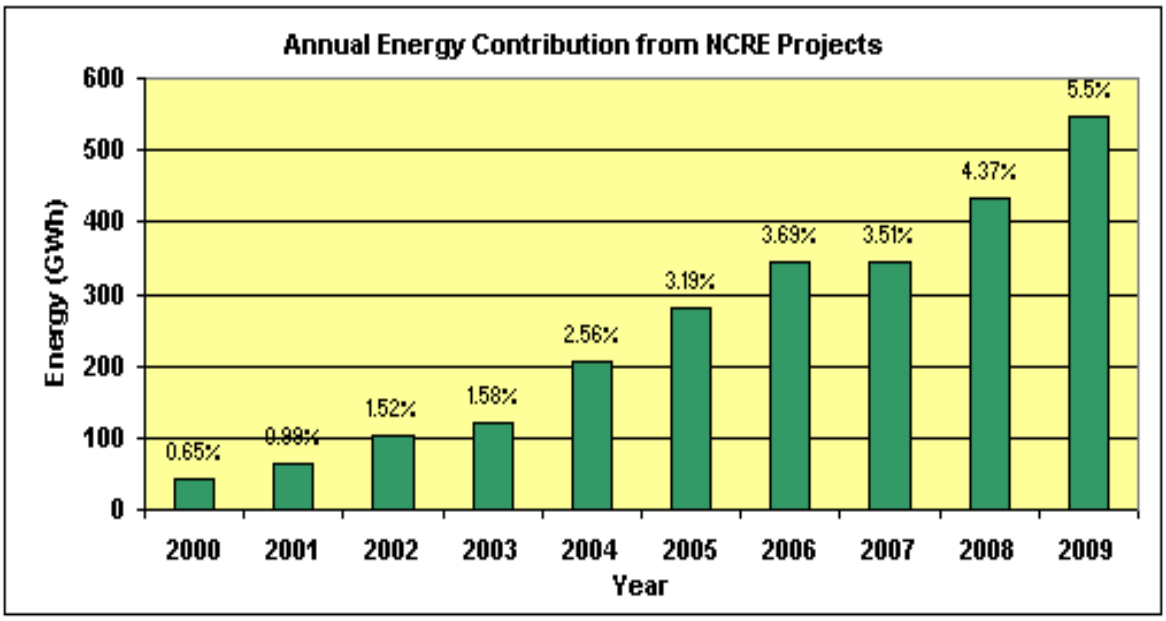

Source: Ceylon Electricity Board

Fig. 2. Total Energy Supply from Non-Conventional Renewable Energy Based Generation

4.2. Regulation

The feed-in tariff based on the avoided cost of generation provided significant returns to the investors of small hydropower plants, in the initial phase of development where most of the better sites had been developed. Since during this initial period the avoided cost calculation was based on the long term generation plan, the feed-in-tariff was linked to the most economical generation expansion in the country. But this hardly reflected the actual situation on the ground where the CEB could not follow this plan due to external interventions. This led to the avoided cost calculation being shifted to the operational plan where short term generation schedule was the key input to the calculation. Since the generation system has been suboptimal the avoided cost determined in this manner provided even a higher feed-in-tariff. This environment attracted more investors to the small hydropower sector since even less economically efficient sites could be now developed while the more economically efficient sites led to significantly large returns to the investors. With this approach to feed-in-tariff, the benefit of low cost hydropower was never passed on the final electricity consumer nor it did not assist development of other NCRE sources such as wind and biomass.

With the introduction of the cost based feed-in-tariff the small hydropower sector provided savings which could be used to subsidize other more expensive technologies such as wind and biomass while still providing adequate returns to the investors in small hydropower sector. Also it reduced the financial burden on the government and the final electricity consumers due to addition of these expensive plants.

Green-power transactions facilitated by the PUCSL opened a new approach to supplying green-power to the interested consumers within the existing legal framework where power "wheeling" is not allowed. This enables, particularly green manufacturing which is fast becoming an important export oriented sector, to expand. Net-metering arrangements can further enhance these opportunities for the green-power generation and consumption.

5. Conclusions

The paper discussed the experience in the policy and regulatory environment in the Sri Lanka renewable energy sector. This included the areas such as renewable energy targets, institutional mechanisms, renewable energy site selection and allocation, feed-in tariffs and green-tariffs.

The paper concludes that the policy and regulatory frameworks and different approaches to implementing them have been mostly successful experiences in Sri Lanka. These along with less successful experiences would provide useful lessons for similar power systems in other countries when formulating and implementing related polices, regulations and legal frameworks leading to accelerated development of the renewable energy industry.

References

[1] Energy Policy and Strategies of Sri Lanka, Ministry of Power and Energy, 2009

[2] The Priyantha D.C. Wijayatunga, Darshana Prasad, Clean energy technology and regulatory interventions for Greenhouse Gas emission mitigation: Sri Lankan power sector, Energy Conservation and Management, 50, 2009, pp 1595–1603

[3] Master Plan for the Electricity Supply of Sri Lanka, Ceylon Electricity Board Sri Lanka, 1989

[4] Resource Management Associates (Pvt.) Ltd. Study on grid connected small power tariff in Sri Lanka. Final Report, Resource Management Associates (Pvt.) Ltd., No. 3, Charles Terrace, Colombo 3, Sri Lanka, 2001.

.

Policy and Strategy aspects for Renewable Energy Sources use in Latvia

Peteris Shipkovs[1,*], Uldis Pelite[2], Galina Kashkarova[1], Kristina Lebedeva[1], Lana Migla[2], Janis Shipkovs[1]

[1] *Institute of Physical Energetics, Energy Resources Laboratory, Riga, Latvia*
[2] *Riga Technical University, Riga, Latvia*
** Corresponding author. Tel: +371 67553537, Fax: +371 67553537, E-mail: shipkovs@edi.lv*

Abstract: Existing Policy & Strategy as well as new tendency in renewable energy sources (RES) use in Latvia will be presented in the paper. The main directions of the energy policy are aimed at improving the security of energy supply of the country by encouraging diversification of supplies of primary energy resources. Creation of competition conditions, promotion of use of renewable and local energy resources and environmental protection also play a substantial role.
In accordance with the Latvian "Law on the Energy Performance of Buildings" environmental and economic considerations, as well as binding regulations of the local government and other regulatory enactments, shall be taken into account in designing buildings, in order to evaluate the possibility to use as an alternative solution in these buildings systems, in which RES are used.
Paper will describe good experience and practice of this Policy and Strategy.
Papers will describe the geothermal energy and solar energy using opportunities in Latvian conditions. Recommendations for new legislation on RES effective and rational use will be presented.
The main directions of the energy policy are aimed at improving the security of energy supply of the country by encouraging diversification of supplies of primary energy resources. Creation of competition conditions, promotion of use of renewable and local energy resources and environmental protection also play a substantial role.
The main objectives of the energy policy are to ensure sustainable accessibility to necessary energy resources and security of supply in order to foster economic growth and improve quality of life; to ensure environmental quality retention and meet the objectives set in the Kyoto protocol of UN FCCC and Latvian Climate Change Program on GHG emissions reduction for years 2005 – 2010.

Keywords: *policy, renewable energy sources*

1. Introduction

The main directions of the energy policy are aimed at improving the security of energy supply of the country by encouraging diversification of supplies of primary energy resources. Creation of competitive conditions, promotion of the use of renewable and local energy resources and environmental protection also play a substantial role.

The main objectives of the energy policy are to ensure sustainable accessibility to the necessary energy resources and security of supply in order to foster economic growth and improve quality of life; to ensure environmental quality retention and meet the objectives set in the Kyoto protocol of UN FCCC and Latvian Climate Change Program on GHG emissions reduction for years 2005 – 2010.

Latvia's total final energy consumption is secured from local energy resources and the flow of primary resources from Russia, the CIS countries, the Baltic countries, EU and other countries. Currently, three types of energy resource making up approximately equal proportions dominate in the delivery of Latvia's primary resources – oil products (mainly petrol and diesel), natural gas and wood-fuel. Like many other European Union (hereinafter – EU) countries, Latvia is dependent on imports of primary resources. Having regard to the reduction of economic activity in Latvia, although consumption fell during 2008.

The share of RES has traditionally been significant in Latvia's energy supply and in 2008 it comprised 29.9% of the total final energy consumption. Rapid growth in final energy consumption and the slow development of RES projects has reduced the RES proportion by 2.6% compared with 2005. In the consumption structure for electricity, the RES segment is made up of hydropower plants, wind power plants, biogas power plants and biomass power plants, as well as cogeneration stations utilising RES. In 2008, RES made up 39.6% of the total final consumption of electricity, with the majority of this, a little over 97%, supplied by large hydropower plants, with the remainder coming from wind power plants, biomass cogeneration power plants and small hydropower plants. RES makes up the largest proportion in the final consumption of heat energy, including district heating, at 42.7%. [6]

The import of fossil energy resources is characterised by large price fluctuations, which does not facilitate the sustainable development of the economy. Latvia's natural gas is supplied by only one country – Russia – Latvia, having regard to the potential of RES available in its territory and the significant position RES already takes in Latvia's current primary energy resource balance compared with other European Union Member States, must attain national energy independence both through promoting measures to increase energy efficiency and increasing the share of local RES in energy, diversifying energy resources and energy supply sources and reducing energy imports. [6]

2. Policy and Strategy for the RES use

2.1. *Energy policy framework documents:*

2.1.1. Guidelines for Energy Sector Development for 2007-2016

The main bases for Energy policy are: The guidelines to ensure security of supply in the country as the main goal of energy Policy. The increasing of self-sufficiency and greater diversification of energy resources supply are the next very important subjects of Energy sector development. Latvia has to search for its own fossil fuels and to increase effective use of renewable sources of energy and energy production in cogeneration (CHP) processes;

2.1.2. Guidelines for Use of Renewable Sources of Energy for 2006-2013

Setting targets for the use of RES are:

- 49.3 % share of RES-E by 2010;
- 8 % share of electricity produced in highly efficient CHP using biomass by 2016;
- 5.75 % share of biofuels in total consumption by 2010;
- 10 % share of biofuels by 2016 (in comparison to less than 2 % in 2006).
- 35 % share of RES in the Energy Balance (in comparison to 28 % in 2007).

2.2. Legal Framework

2.2.1. EU Directives:

- Directive 2001/77/EC on electricity production from RES;
- Directive 2004/8/EC on the promotion of cogeneration based on a useful heat demand in the internal energy market.
- Directive 2009/28/EC on the promotion of RES usage

2.2.2. National laws:

- Energy Law;
- RES Energy Law (project);
- Electricity market Law;

- Law on the Energy Performance of Buildings;
- Regulations No. 262 on Production of Electricity from Renewable Sources of Energy;
- Regulations No. 221 on Electricity Production in Cogeneration Regime.

2.3. Main support instruments

2.3.1. Mandatory procurement of electricity produced from RES on basis of fixed purchase price formulas

- Regulations No. 262 on Production of Electricity from RES (in force since March 2010);

These Regulations (No. 262) indicated criteria's of produced electricity as compulsory purchase trades. If electricity produced of biomass or biogas in power station with installed capacity over 1 MW, it is possible to get guaranteed fee of set up power.

- Regulations No. 221 on Production of Electricity in Cogeneration Regime (in force since March 2009).

2.3.2. EU Structural Funds

In accordance with the Latvian "*Law on the Energy Performance of Buildings*" environmental and economic considerations, as well as binding regulations of the local government and other regulatory enactments, shall be taken into account in designing buildings, in order to evaluate the possibility to use as an alternative solution in these buildings systems, in which RES are used.

2.3.3. Investments in the energy sector

State support in the energy sector is only given to Projects linked to adjustment of heat supply system. The priorities for the use of EU Structural Funds are listed in the Development Plan; these priorities are sub-divided into measures, which in turn are sub-divided into activities. It is planned to allocate approximately EUR 140 million in the energy sector from the Cohesion Fund in the next Structural Funds utilization period of 2007-2013. This amount will be distributed to measures for increase of efficiency of district heating systems, for development of cogeneration plants that use biomass and development of wind farms in Latvia.

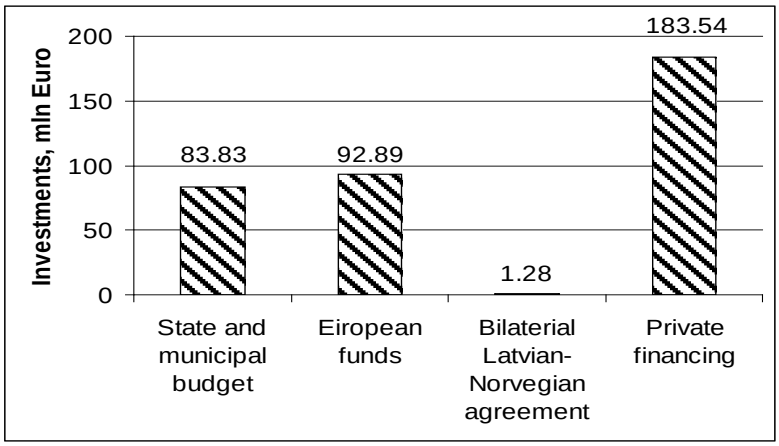

Fig. 1. Potential financial sources for development of RES use (2006-2013)

2.3.4. A feed-in tariff (FiT)

A feed-in tariff involves the obligation on the part of a utility to purchase electricity generated by renewable energy producers in its service area at a tariff determined by public authorities and guaranteed for a specific period of time (generally 20 years). A FiT's value represents the

full price per kWh received by an independent producer of renewable energy, i.e. including a premium above or additional to the market price, but excluding tax rebates or other production subsidies paid by the government.

Different tariffs can be defined for different technologies (wind, solar, biomass, etc.) or different countries depending on resource conditions (e.g. solar irradiation). The rate of a FiT is furthermore reduced each year for new installations in order to stimulate decrease in production costs. Feed-in laws have been the primary mechanism used to support RES development in Europe and the US. They have a track record of some two decades and are well established throughout the European Union. At present, they are being applied in 21 EU member countries. While many countries in Europe have introduced a FiT on different levels, only some of them (e.g. Germany) have adopted appropriate rates specifically for PV. Others used inadequate FiT parameters (for instance Austria – too low a ceiling on total installed PV capacity) and thus failed to stimulate significant investor interest.

The feed-in tariff (the mandatory procurement of the energy produced from renewables), a method of support Latvia has chosen, is a straightforward and effective way to reach the renewable targets. This approach is widely used in other member states, too. However, it also bears a number of risks, namely: the procurement price and support timeline is tied to the moment when the energy production equipment becomes operational; and the pricing formula relies on electricity prices and fossil fuel prices. A thorough and unbiased analysis of conditions needs to be carried out as well as a calculation of reasonable return on assets. The pace and direction of technological progress needs to be estimated, a hard task. Misjudgements in setting the procurement price and the length of support could go both ways. Truly effective, market-based mechanisms are yet to be found. In Latvia, a quick analysis of the procurement price for the energy produced from biogas or in established hydro-electric power plants reveals overestimates. The quota system favours a closed circle of businesses, whose ties to the political parties are apparent. No wonder the Ruling Coalition Council had to agree on the pricing principles and quota volumes before the decision was made by the Cabinet of Ministers. Unreasonable procurement pricing undermines the principles of renewable energy use for sustainable development. [7]

2.3.5. Other support mechanisms

In EU countries exist significant variety of support mechanisms. Their main goal is to introduce renewable energy sources into the market and to make them as a common source for gaining electricity. It is commonly admitted that activity of scientific circles and informational campaigns connected with demonstration projects play an important role in the RES development. In case of photovoltaic FiT Tariff is the most important and most effective way in creating development in that branch provided that correct designing of FiT law is submitted.

Investment based support mainly depends on providing investment subsidies, tax credits, and bank loans with beneficial interest rates. Supports mentioned above are significant due to their impact on initial market development. Investment based support has importance in case of expensive technologies and currently it is used in many European countries.

Quota schemes (also called Renewable Portfolio Standard - RPS) oblige the producers of electricity and retail provider to attain a specified minimum level of shares RES in its mix. RPS is commonly combined with the Tradable Green Certificates system (TGC). TGC relies

on market competition and therefore is unstable in the matter of price. These certificates being the subject of trade contain additional profit for the renewable user of energy. Tradable Green Certificates system does not favor the most future-orientated and ecological technologies of producing green electricity such as photovoltaic and off-shore wind turbine.

Tendering or Competitive Bidding is a transitional mechanism between FiT and RPS. Under a tendering scheme developer of project submits his own proposal and indicates the wholesale price he would like to get for the produced electricity. The one, who offers the lowest production costs of every kWh, will be able to sell electricity for the lower price and will enter a contract which guarantees that electricity will be bought over a defined period of time.

2.4. New Energy Policy

The first proposals are submitted to the Ministry of Economy of Latvia. Some recommendations for the new legislation on effective and rational use of the RES:

- there is a well-established national support scheme for production of electricity from RES – mandatory procurement applicable to electricity production in wind-, hydro-, biomass- and biogas PP;
- with regard to the RES, we convinced to reach a balance between electricity demand and supply potential from local Power Plants by years 2011 – 2012;
- to further develop and implement support schemes for highly efficient cogeneration and use of renewable energy resources in the power generation;
- to improve facilitation activities for bio-fuel production and consumption;
- to implement energy efficiency measures;
- to actively participate in EU and other international R&D projects;
- as a major challenge we regard the upcoming renewable energy policy development on the EU level and the ambitious individual target for Latvia – 42 % by 2020;
- to develop pilot projects and implementation.

2.4.1. New Latvian Policy on RES

Overall, the national renewable energy policy is to promote their use, respecting environment and achieving CO_2 emission reduction. The main renewable energy policy objectives to be achieved is as follows

- Electricity production of RES is 49,3% of all produced electricity in 2010;
- Renewable energy must be at least 37% in total energy balance;
- The share of biofuels of all marketed transport fuel should be 5,75% in 2010.

The aim of the Government policy is to achieve the balance between electricity demand and supply potential from Power Plants by years 2011-2012;
The goal is to promote maximum energy efficiency measures and supply of the power plants that use local fuels and renewable sources of energy in the high-efficiency co-generation cycle.

The remaining part of the required supply capacity will be diversified to other fossil fuels, to prevent over-dominance of natural gas.
During the development of cogeneration plants, energy from renewables will increase power capacity potential of transmission and distribution systems. Two support tools have been selected for this purpose:

- compulsory purchase at a specified price, whether in terms of all Latvian electricity consumer payment in proportion of consumption;

- Renewable sources of energy promote the development of cogeneration power plants earmarked for investment in the power structure, the purpose of EU structural funds.

For improvement of RES use and promotion of the development of biomass cogeneration, it is expected to attract the means of EU Structural Funds and support of Cohesion Fund. Till the year 2016 it is expected to attract 8,1 million LVL from the State Budget and 27 million LVL from EU Structural Funds.

RES exploitation strategy is closely connected with the introduction measures of energy efficiency. RES policy includes an integrated approach to energy efficiency issues.

2.4.2. RES Law (project)

Aims and Objectives

Aims of the Law:

- to promote local RES production, use and export;
- to determine stable long term investment environment for production, usage and export of local RES support;
- to contribute reducing technologies of the greenhouse effect and gas emission;

Law challenges to achieve goals:

- Till the year 2020 increase the RES usage in gross final consumption up to 40% and continue to gradually increase it;
- to promote openness and accessibility of information on energy scope;
- to establish administrative procedures in RES production and usage;
- to determine the support measures for local RES production and usage.

2.4.3. National goals of RES use

Law enforcement is a specific period till the year 2020 to achieve the following percentage of gross in RES usage:

- till year 2012 not less than 34,08%;
- till year 2014 not less than 34,82%;
- till year 2016 not less than 35,93%;
- till year 2018 not less than 37,04%;
- till year 2020 not less than 40%.

2.4.4. Republic of Latvia National Renewable Energy Action Plan for implementing Directive 2009/28/EC of the European Parliament and of the Council of 23 April 2009 on the promotion of the use of energy from renewable sources and amending and subsequently repealing Directives 2001/77/EC and 2003/30/EC by 2020.

The action plan 'Latvia's national renewable energy action plan' stipulates indicative targets for the share of RES in each type of final energy consumption, to foster the fulfillment of the common objective pursuant to Directive 2009/28/EC, taking into account the potential RES available and usable in Latvia. Having regard to the potential of economically usable RES available in Latvia, the main types of usable RES will continue to be solid biomass, mainly wood, as well as biogas, wind power and hydro power. [6]

2.6. North Vidzeme Biosphere Reserve as a good practical experience

The administration of the North Vidzeme Biosphere Reserve (NVBR) has completed erection of the Environmental Education and Information Centre with a potential area of 675m^2 in the town of Salacgriva. This centre is expected to provide local residents, businesses, municipalities and state institutions with information about the natural assets of the reserve as well as about protection of natural resources and the use of innovative solutions in the regional development. By now, a project of the environment-friendly building in the Biosphere Reservation (BR) on the north of Latvia (Vidzeme) has been accomplished. The BR covers the area of Salacas River − a temperate forest zone characteristic of the Baltic Sea coastal ecosystems. Its land area is 4577km^2, with the population of about 80 000 people. Half its area is covered by forests and 15% by wetlands. The reservation includes 167.5 km^2 of the Gulf of Riga coastal aquatorium. The Environmental Education and Information Centre building were completed in 2009. The relevant project was funded by the European Economic Area and Norwegian Government Financial Mechanism. The Centre will serve as a model for the use of environment-friendly renewable energy. According to the project, the heating-and-cooling equipment was installed for geothermal energy use and solar collectors – for preparing hot water. Energy savings through compression modular equipment were used in the reverse cycle heating of the building and solar collectors − for hot water production up to 90 MWh/ year. As a result, the following was achieved:

- CO_2 reduction (taking fossil fuel use as the basis) − 56.6 tonnes / year.
- Number of holes drilled for space heating and cooling − 11;
- Solar collector's area for production of 500 l hot water − 18 m^2.

Such systems are highly efficient, therefore they were selected with the aim to reduce the management costs of Environmental, Education and Information Centre. Although there are some Backlogs, however system works and functions in full.

3. Conclusions

Recommendations for RES effective use were prepared upon the realized projects and analyses of the National RES Policy and Strategy.
Within the frame of the State Research Program's Project ''Research and development of the renewable energy resources production and consumption technologies for climate changes generated by energy sector mitigation'' suggestions were worked up also for rational RES use.

The action plan provides for guidance towards the more extensive use of local RES in Latvia, noting the measures to be taken to attain the target prescribed in Directive 2009/28/EC, implementing sustainable development, conserving environmental quality and contributing to the reduction of greenhouse gas emissions, increasing Latvia's energy self-sufficiency, ensuring the sustainable utilisation of Latvia's natural resources and the socio-economic benefits of their utilisation. Support mechanisms for generating energy from RES that operate more successfully than previous ones must be established, not only for electricity but also for heating and transport fuel. [6]

The EU has stepped up efforts to harmonize policies on the promotion of the use of energy from renewables in all member states by defining legally binding policy principles for the renewable energy promotion measures and setting individual renewable energy targets for each of the countries. Despite that, Latvia's renewable energy support policy, particularly the mandatory procurement scheme for the energy produced in power plants using renewables, is an area with an unstable legal framework, susceptible to frequent fluctuations in political

opinions and interests, which often are not based in the country's economic and welfare considerations. The New RES Law is prepared to approval. The Law will improve the current situation of RES in total, as well as will prevent confusion.

In the recent years, Latvia's energy policy practice was marked by inconsistencies and the lack of socio-economic reasoning, which allows, in some cases, to suspect influence of lobbyists on the development of legal framework. Examples of that trend are the aforementioned frequent changes in the mandatory procurement regulation and the feed-in pricing formula, which is politically motivated rather than based in thorough economic reasoning. In the energy sector, is the lack of flexibility in the mandatory procurement scheme, which is meant to promote the use of renewable energy resources. The inflexibility may lead to situations when support schemes follow the letter of the EU directives, but not the spirit. The quota system supports the renewable energy target (49.3%) on paper, but the structure of the system does not prevent the situation when the businesses with the procurement rights do not set up the planned renewable energy plants whilst the businesses that would be willing to do so have no access to the quotas.

The Environmental Education and Information Centre fulfilled its function as to promoting the state's comprehension of the importance of the RES use. Investments involved in the project were an economically viable option; besides, the realized project helps to reduce the yearly maintenance costs. As a result of the project it has become clear that the energy independence of Salacgriva from imported energy resources is an invaluable and nationally important issue, which could be as a model to several European Union countries. The project also includes informational events that promote the advantages of using renewable energy for heating; this especially concerns heat pumps in combination with solar collectors.

As one more example of good experience, must be mention Institute of Physical Energetics (IPE). It is leader for solar energy research and development in Latvia. Achieved solar energy is used for IPE hot water supply. Solar energy polygon could be used not only as auxiliary heat supplier for IPE, but also as an education and training polygon for new specialists - students, PhD students, etc.

References

[1] Latvian Energy Law (03.09.1998).

[2] P.Shipkovs, G. Kashkarova, I. Purina, K. Lebedeva, M.Jirgens, A.Zigurs, A.Cers, Financing schemes for biomass in Latvia, World Sustainable Energy Days, Wels, Austria, 5.3.-7.3.2008., CD proceedings, 9 pp.

[3] P.Shipkovs, RES in Latvia policy and strategy, Workshop „Data Gathering on Renewable Energies for New Member States and Candidate Countries", 13-15 November 2007, Istanbul, Turkey. Book of proceedings, EUR 23558 EN-2008, 300-319 pp.

[4] Regulations No. 262 on Production of Electricity from RES (March 2010);

[5] Energy Efficiency Law (18.04.2007.).

[6] Republic of Latvia National Renewable Energy Action Plan;

[7] Dr. A. Sprūds, Latvian energy policy: towards a sustainable and transparent energy sector, Soros Foundation - Latvia, 2010

New and Renewable Energy Policies of Jeju Island in Korea

Youn Cheol Park[1,*], Dong Seung Kim[2], Jong-Chul Huh[1], Young Gil Kim[3]

[1] *Department of Mechanical Engineering, Jeju National University, Jeju, Korea*
[2] *Clean Energy Research Center, Jeju National University, Jeju, Korea*
[3] *Future Strategic Industry Section, Jeju Special Self-Governing Province, Jeju, Korea*
** Corresponding author. Tel: +82 647543626, Fax: +82 647563886, E-mail:ycpark@jejunu.ac.kr*

Abstract: This study provides information on the energy status of Jeju Island in Korea (located at south of the Korean Peninsula), including general demographics, primary energy consumption and energy consumption by source, energy consumption by sector, power generation, and new and renewable energy.
The purpose of this study is to establish a regional sustainable energy supply system and to promote new and renewable energy industries throughout Jeju. Although Jeju, and Korea in general, already have some renewable energy development, there is strong demand and desire to greatly expand the level of renewable energy adoption. Jeju will not only expand the solar and wind industries, but also pursue bioenergy, geothermal power, hydropower, stationary and mobile fuel cells, ocean energy, and waste energy.
Jeju's regional energy planning is based on the *Energy Basic Law* established in 2006. Specifically, these programs have included policies supporting loans for purchase of renewable energy infrastructure, subsidies for renewable-based facilities, the 100 thousand green homes program, subsidies for solar thermal development, subsidies for local government investment in green technology, certificate programs, training programs, feed-in-tariffs, the formulation of new companies specialized in new and renewable energy, and regulations for mandatory use of new and renewable energy in new public buildings.

Keywords: *Jeju Island, Renewable Energy, Energy Policy*

1. Introduction

Energy use is a primary component of daily life. It is the basic to economic development and modernization. Energy consumption is also related to physical comfort and military strength. This fossil fuel-based lifestyle triggers some problems, such as economic instability, environmental pollution and hazards, and global warming. For economic instability, if the economic system of a country is based upon fossil fuels, the amount and price of fossil fuels, especially oil, will directly influence economic development and stability.

Regional energy planning is an extremely important component of any future development goal. Not only is it important for regions to know how development will unfold in their own jurisdiction, but also understand how development will unfold in nearby jurisdictions that are inherently linked to their own. Many times regional energy planning can capture specific development goals that are not achievable through national- or international-level policy. It is because of the localized framework in which regional energy plans are developed that they are able to focus on region-specific goals and accomplish tasks that are sometimes overlooked at the national level. In many areas of the world, regional energy plans have been under development for many decades and have become increasingly utilized since the 1990s.

The purpose of this study is to discuss the establishment of a regional sustainable energy supply system and to promote new and renewable energy industries throughout Jeju. Renewable energy development is an integral part of energy sustainability. Various forms of renewable energy can be exploited for electricity generation, with hydro and wind power currently dominating the renewable energy economy. Wind power is already competitive compared to fossil fuels in terms of cost of generation, and it has been shown that risk assessments favor this type of energy.

2. Basic Information

2.1. Overview of Energy Status in Jeju

This section provides information on the energy status of the Province of Jeju, including general demographics, primary energy consumption and energy consumption by source, energy consumption by sector, power generation, and new and renewable energy as shown in Tables 1 to 6. This information will be used at a later point in this paper to assist the analysis of the energy, environmental, economic, and social components of Jeju's energy framework.

Table 1. Area, population and gross regional domestic product (2006)

	Area (km^2)	Population (1,000)	Population Density (persons/km^2)	GRDP (2005, current price, billion Won)
Korea	99,678	49,268	497.8	817,811.9
Jeju	1,848	560	303.9	7,663.9

Table 2. Primary energy consumption (2006) (Unit: 1,000TOE(Tonnage of equivalent energy))

	Total	Coal	Petroleum	LNG	Hydro	Nuclear	Others
Korea	233,372	56,687	101,831	32,004	1,305	37,187	4,358
Jeju	1,149	-	1,120	-	-	-	29

Table 3. Total energy consumption by source (2006) (Unit: 1,000TOE)

	Total	Coal	Petroleum	City gas	Electricity	Heat energy	Others
Korea (%)	173,584	22,660 (13.1)	97,037 (55.9)	18,379 (10.6)	29,990 (17.3)	1,425 (0.8)	4,092 (2.4)
Jeju (%)	924	0	653 (70.7)	3 (0.3)	249 (27)	0	19 (2.0)

Table 4. Energy consumption by sector in Jeju (Unit: 1,000 TOE)

Criteria	Total	Coal	Petroleum	City Gas	Electricity	Heat energy	Others
Total	924	0	653	3	249	0	19
Industry	209	0	130	0	78	0	2
Transportation	359	0	359	0		0	
Residential/ Commercial	302	0	151	3	146	0	2
Public & others	54	0	14	0	25	0	15

The purpose of Jeju's mid- and long-term Roadmap is to establish a regional sustainable energy supply system and to promote new and renewable energy industries throughout Jeju. Korea already has some experience with renewable energy; as of June 2008, 100 thousand homes have adopted solar power systems, accounting for almost 22 MW of photovoltaic power and an additional 8.4 MW is planned for power generation. Solar thermal water heating systems have also been in use since the 1970s, but have experienced technical setbacks. Wind power has also experienced some development with 192 MW of wind power installed by 2007 in Korea.

Table 5. Power generation (2006)

	Generation Facilities (MW)	Generation (MWh)
Korea	65,514	381,180,710
Jeju	631	2,073,144

Table 6. New & renewable energy (2006)

		Korea		Jeju	
		Capacity	Production(TOE)	Capacity	Production(TOE)
Total		-	1,249,920	-	16,012
Wind		78,941kW	59,728	3,210kW	9,196
Solar Power		22,322kW	7,756	427kW	296
Solar thermal		24,314m^2	33,018	269m^2	770
Geothermal		10,007RT	6,208	70RT	28
Bio	Total	-	274,482	-	2,861
	Biofuel	141,597t/y	53,346	-	--
	Biogas	30t/h	77,390	-	--
	Others	-	143,746	4,133t (RDF)	2,861(LFG, RDF)
Fuel cells		270kW	1,670		-

2.2. Energy Development at a National Level

Much of Jeju's positive attitude towards renewable energy comes from the overall Korean desire to achieve sustainability. In Korea's 2008 *National Energy Basic Plan,* goals were set to achieve a 46 percent energy efficiency improvement for newly installed energy and nearly fivefold increase in new and renewable energy by 2030. It is planned to expand photovoltaic power by 44 times, from 80 to 3,504 MW; wind 37 times from 199 to 7,301 MW; bioenergy 19 times from 1,874 to 36,487 G cal; and geothermal 51 times from 110 to 5,606 G cal. Further, there are plans to introduce a renewable portfolio standard (RPS) with mandatory obligation for public buildings, and a *1 Million Green Homes* program supporting wind, ocean, and bioenergy sources of energy. Lastly, the plan seeks to increase investment in research and development (R&D) for wind, fuel cells, and solar power.

Achieving Korea's goals will require an investment of 111.5 trillion won ($93.3 billion USD) by 2030. A large portion of this funding will go towards basic R&D, including the development of specific technologies such as Si PV (Silicon based Potovolatics) by 2015, thin Si PV and CIGS(Copper-Indium-Gallium-Selenide based Potovoltaics) by 2015, and organic PV by 2020. For wind power, goals are to develop 2 MW by 2010 and 5 MW by 2016 with a strong emphasis on wind turbines in urban areas, deploying by 2010. Solar thermal goals are the most aggressive, vying for 10 kW of generation by 2012 and 200 kW by 2013.

Specific policy initiatives include market- and private-driven plans such as a RPS by 2012 including new and renewable energy for public and private buildings; and a major increase in the role of local government. Further, Korea seeks a large increase in private investment through policies including removal of market barriers, an increase in flow of public information, development of new industrial codes, and development of human resources.

3. Regional New and Renewable Energy Pane

Jeju's regional energy planning is based on the *Energy Basic Law* established in 2006, which consists of: (1) energy demand projections; (2) measures to provide reliable energy supply; (3) the new and renewable energy plan; (4) measures relating to carbon emission reductions; (5) district heating development; (6) development of new energy resources; and (7) other energy issues necessary for the region. Specifically, these programs have included policies

supporting loans for purchase of renewable energy infrastructure, subsidies for renewable-based facilities, the 100 thousand green homes program, subsidies for solar thermal development, subsidies for local government investment in green technology, certificate programs, training programs, feed-in-tariffs, the formulation of new companies specialized in new and renewable energy, and regulations for mandatory use of new and renewable energy in new public buildings.

Although the development of the 10 MW wind farm in Haengwon(located in Jeju Island) is a noteworthy accomplishment, the wind farm accounts for only 1 percent of Jeju's electricity demand. Another project, the *Green Village Project*, includes 57 households powered by PV electricity, producing 160 thousand kWh/year and accounting for 75 percent of the households' loads. Excess peak electricity is sold back to the grid, thus turning some profit for the homeowners in wind Green Village. However, these projects account for a very small portion of total energy consumption and thus renewable energy development is needed to a much greater degree.

The prospects for new and renewable energy development in Jeju are promising, since 60 percent of the national wind potential is concentrated in Jeju Island if its offshore areas are included. As such, Jeju plans to build 500 MW of wind generating facilities by 2020, accounting for 20 percent of Jeju's total electricity demand at that time. Jeju plans to achieve this level of growth by concentrating on self-generating facilities located close to the end-users and limiting the development of large-scale facilities. Jeju will also consider the development of transmission lines between the mainland and the island, allowing for transmission of excess generation or sale of generation at a competitive rate.

Geothermal development will face barriers of high cost, but is applicable for large-scale projects. Comprehensively, Jeju hopes that the 20 percent target for wind power can be achieved sooner than planned. In the meantime, Jeju will deploy large geothermal generation plants to complement the intermittency of wind and solar power. Landfill gas plants will also provide additional renewable energy. Hydrogen power is a longer-term prospect, but a hydrogen refueling station is already being considered at the site of the Haengwon wind farm for the purpose of introducing a hydrogen car by the end of 2009.

3.1. Wind Power

Jeju has outlined basic goals to foster increased wind power development in the province by maximizing its wind potential for future energy resources. In 2050 produce 440.8 thousand TOE (936.2 MW) potential energy by wind power, accounting for 30 percent of renewable energy supply.

Jeju's public and private investment projects for wind power seek to develop 936MW of wind capacity by 2050 according to the following schedule: 289MW in 2013, 565 MW in 2020, 809MW in 2030, and 936MW in 2050. Out of 809 MW in 2030, 609 MW is scheduled to come from the off-shore wind development. As of 2007 the installed wind capacity in Jeju was only 34MW. As of the end 2008, the installed capacity of wind power in all of South Korea was 236MW.

Jeju Island's first demonstration project for wind power generation was planned by the Korean Government's Ministry of Trade, Industry and Energy and the Korea Institute of Energy Research (KIER), and started operating in February 1995 (CADDET, 1998). In 2003 the first major wind farm was installed in the island. Local government administration has enjoyed broad autonomy while the public support for environmental conservation increases.

For these reasons, Jeju has good prospects to develop renewable energy sources, including wind power.

Jeju has outlined goals to meet 30 percent of its renewable energy with wind power by 2050. The above global trends in wind power development combined with Jeju's excellent wind potential suggest that Jeju could have more than 30 percent of renewable energy supply from wind power. According to the Roadmap, 60 percent of Korea's national wind potential is concentrated at Jeju Island including its offshore areas. This potential should be exploited to the furthest degree possible. In most applications, wind power is least expensive form of renewable energy and Jeju should pursue this technology as its flagship renewable technology.

3.2. Geothermal Power

Jeju has outlined basic goals to foster increased geothermal energy development in the province, especially through building geothermal facilities located close to the industrial sites. In 2050 produce 220.5 thousand TOE (130.1 MW) of energy by geothermal power, accounting for 15 percent of total renewable supply.

This project involves a trial development of geothermal electricity and heating and cooling services for large-scale industrial parks in Jeju. This project will involve the attraction of private capital as well as a feasibility study on a 10MW geothermal plant. The benefits of this project include the development of a true fossil fuel-free city which relies entirely on renewable energy. This will likely prove to have environmental and economic benefits for the businesses located in the industrial park.

In Korea, hydrogen fuel cells, PV, and wind power have been selected as the main areas of development (IEA, 2004). For geothermal energy, Korea has just begun to develop its geothermal resources, and the technology has not been implemented on a large scale. Compared with other countries it is evident that geothermal use in Korea is considerably less than other similar regions. As such, the government should devote greater resources to developing advanced geothermal resources, especially in geographically-promising areas like Jeju.

Geological conditions and economic costs are two crucial limitations for geothermal energy development. Jeju island has abundant geothermal potential and has annual investment plan from year 2008 to 2011. Therefore, geothermal energy could play a significant role in Jeju's renewable energy future.

3.3. Solar Power

Jeju has outlined basic goals to foster increased solar power development in the province. Solar power, especially PV, is currently being heavily researched both in academia and in the industrial sector. Solar power is a broad term that covers many different types of energy production. Among these are photovoltaics (PV) and different types of solar thermal such as solar hot water and large scale solar thermal power. Jeju could build solar power plants by using surplus property within wind farms. A summary of the goals, as discussed in Jeju's Roadmap, is provided here. In 2050 produce 110.1 thousand TOE (449.7 MW) of energy by solar PV power, accounting for 7.5 percent of total energy supply. In 2050 produce 36.8 thousand TOE (681,482 square meters) of energy by solar thermal power, accounting for 2.5 percent of renewable energy supply.

By 2030, the target of Jeju's renewable resources in total will account for 30 percent of the energy supply. Since Jeju island has a high degree of solar insolation, it is projected that solar PV will account for 8 percent and concentrated solar thermal plants will account for 2 percent.

The use of solar power technologies in South Korea is becoming increasingly important to meet the growing needs of energy and address the shortage of energy resources. In addition, electricity generated through renewable energy sources has been aggressively promoted because energy prices are soaring and awareness of environmental issues is increasing. To facilitate more extensive adoption of solar power electric generation, Jeju launched programs and incentive policies aimed at increasing solar energy supply, such as direct funding of solar installations, the green home project, and the construction of the solar power plant. Further, Jeju will create a desalination plant using solar energy, which in effect advances both desalination and solar technologies.

3.4. Biomass and Biofuels

Jeju has outlined basic goals to foster increased biomass development in the province. R&D will be conducted to develop vehicle technology in order to accommodate biogas industry. By 2030, 25 percent of diesel consumption will be replaced with biodiesel (BD20 blend). In 2050 produce a total of 10 thousand TOE (9,479 net cubic meters) of energy by biogas. In 2050 produce a total of 136.9 thousand TOE (161,000 kiloliters) of energy by biofuels. In total, biomass will account for 10 percent of renewable energy supply.

The biofuel projects involve the construction of biodiesel production and supply facilities from 2007 to 2010 and secondly, bioethanol production and supply facilities from 2010 to 2012. The biodiesel(feedstock is Rapeseed Oil) project will have an installed production capacity of 3.4 million gallons (13,000 kiloliters) per year. The bioethanol project will have an installed capacity of 22.1 million gallons (76,000 kiloliters) per year and will produce and supply bioethanol by using discarded citrus for processing.

The biogas projects involve the creation of a biogas facility using livestock manure and other organic waste sources. The goals are to treat organic waste at a rate of 100t/day and produce biogas at 11,000 m^3/day and organic fertilizer at 20t/day. The project will have a total investment of US$362 million (420 billion Won).

3.5. Hydrogen and Fuel Cells

Jeju has outlined basic goals to foster increased hydrogen development in the province. The goal is to provide a hydrogen economy through a focus on hydrogen technology. In 2050 produce 514.4 thousand TOE (455 MW) of energy by fuel cells, accounting for 35 percent of renewable energy supply.

This project involves the construction of a test and evaluation research center for hydrogen and fuel cells. Construction of the research center will have a total budget of US$31.9 million (37 billion Won) (from the Central Government) and had been constructed from 2005-2008 by the Korea Institute of Energy Research. Secondly, the project involves a monitoring project for commercialization of the hydrogen fuel cell vehicle supply. The monitoring project will have a total budget of US$82.8 million (96 billion Won) and will be undertaken from 2008-2010 by the Central Government and Hyundai Motors. This project will include the construction of two hydrogen stations and operation of four hydrogen-electric vehicles (three sedans and one bus). The primary benefit of this project is the development of an integrated system of fuel cells and hydrogen which is produced from domestic renewable energy resources.

The hydrogen source in Jeju could be electrolysis. The electricity of the power needed to electrolysis is wind power. As mentioned before, Jeju has a large potential of the wind power even the electricity consumption of the province is small. The idea to using hydrogen in Jeju is based on surplus wind power which cannot be used due to quality of electricity when it connected to the grid line.

3.6. Specific Development Targets

The Korean central government aims to increase the share of new and renewable energy in electricity generation to 11 percent of total energy demand by 2030 (National Energy Basic Plan in 2008). In response to these goals, Jeju pursues the development of six leading new and renewable projects, including projects for wind, geothermal, solar, biodiesel, bioethanol, biogas, and hydrogen.

Mid- and long-term projections of electricity demand show an annual growth rate of 2.5 percent for Korea and 2.4 percent for Jeju to 2020. The annual growth rate of primary energy in Jeju will be 2.2 percent during 2007-2016; then 1.5 percent during 2017 to 2030; and then 0.7 percent during 2031-2050. Wind power generation will experience rapid growth, accounting for 9 percent of electricity demand in 2011, 17 percent in 2015, and 28 percent in 2020. Renewable energy in total will account for 10 percent in 2013, 20 percent in 2020, 30 percent in 2030, and 50 percent in 2050. By 2030, wind energy will account for 50 percent of total renewable generation, solar will account for 8 percent, concentrated solar thermal plants will account for 2 percent, geothermal 15 percent, bioenergy 10 percent, and fuel cells 15 percent as shown in Table 7.

Table 7. New and renewable energy supply targets by energy source(Unit: 1,000TOE)

Year	2007	2013	2020	2030	2050
Wind	16.0(90.4%) 34 MW	136.2(70%) 289 MW	266.4(60%) 565.8 MW	380.8(50%) 808.8 MW	440.8(30%) 936.2 MW
Solar Power	0.34(1.9%) 1.36 MW	17.4(8.9%) 71.1 MW	56.6(12.7%) 231.2 MW	60.9(8.0`%) 248.7 MW	110.1(7.5%) 449.7 MW
Solar thermal	0.046(0.2%) 848m^2	2.1(0.1%) 38,889m^2	10.0(2.3%) 185,185m^2	15.2(2.0%) 281,482m^2	36.8(2.5%) 681,482m^2
Geothermal	0	7.7(4.0%) 4.5 MW	44.4(10%) 26.2 MW	114.3(15%) 67.4 MW	220.5(15%) 130.1 MW
Bio energy	1.3(7.3%)	30.2(15.5%)	44.4(10%)	76.1(10%)	146.9(10%)
Fuel cells	0	1.0(0.5%) 0.88 MW	22.2 (5%) 19.6 MW	114.3(15%) 101.1 MW	514.4(35%) 455 MW
Total	17.7	194.6	444.0	761.7	1,469.5

3.7. Annual Investment Plan('09-'13 1st step Project)

The Annual Investment Plan for 2009 to 2013 is the first step in a larger scheme. The plan has a total budget of US$718.8 million (833 billion Won). Details on the allocation of the budget are provided in Table 8.

Table 8. Jeju's annual investment plan (Unit : Million Won)

	Total	'08	'09	'10	'11	'12	'13
Total	833,100	101,610	207,527	57,028	178,855	149,040	139,040
Central Government	53,067	5,700	27,767	4,800	4,800	5,000	5,000
Jeju	44,153	7,800	22,953	3,200	3,200	3,500	3,500
Private Investment	627,255	30,500	143,820	41,000	160,855	130,540	120,540
Research Institute	108,625	57,610	12,987	8,028	10,000	10,000	10,000

4. Conclusions

The Roadmap has clearly identified the energy demand and supply up to the target year (2050). The target year of choice is an important component of the regional energy plan. The Roadmap's proposed rates of the development of new and renewable energy sources correlate to each decade and are interestingly proportional as shown in Table 9. Jeju aims for 20 percent new and renewable energy share in 2020; 30 percent in 2030; and 50 percent in 2050. Achieving a 50 percent renewable energy contribution will require aggressive and smartly-crafted policy intervention.

Table 9. Overview of new and renewable energy supply targets in Jeju(Unit : 1,000TOE)

	2007	2013	2020	2030	2050
Primary energy demand	1,708	1,946	2,220	2,539	2,939
Renewable energy	17.7	194.6	444.0	761.7	1,469.5
Renewable share (%)	1%	10%	20%	30%	50%

References

[1] CADDET, Wind power generation at Jeju island, Korea. 2009

[2] IPCC, Climate Change 2007: The Physical Science Basis, Contribution of Working Group I to the Fourth Assessment Report of the Intergovernmental Panel on Climate Change, Summary for Policymakers, 2009.

[3] IEA, Energy Efficiency; Policies and Measures. Retrieved November 20, 2009.

[4] Korea Energy Economic Institute, Economic Analysis in Renewable Energy, 2008.

[5] EWEA, Global 2008 Wind Energy Statistics, 2009.

Renewable energy policy in Turkey

S.Kucukali[1,*], K.Baris[2]

[1] *Cankaya University, Department of Civil Engineering, Balgat, 06530 Ankara, Turkey*
[2] *Zonguldak Karaelmas University, Zonguldak, Turkey*
* *Corresponding author. E-mail: kucukali78@hotmail.com*

Abstract: This study aims to explore the availability and potential of renewable energy sources in Turkey and discuss the government policies and economic aspects. Turkey is a country which has the highest hydropower and wind energy potential among European countries. Current energy policy of Turkey primarily aims to maximize geothermal, wind and hydropower potential of the country in next 15 years. In Several incentives were developed for electricity generation from renewable energy sources by the publication of Law No. 5346 in 2005. The most important ones are: ease of land acquisition and feed-in-tariffs which promises purchasing of electricity generated by legal entities with a price of 5-5.5 €c/kWh. Since Turkey is a European Union (EU) candidate its laws and regulations must be compatible with EU. As the legislation in EU member states is investigated it is apparent that Law No. 5346 should be restructured. This should include: (i) redetermination of feed-in-tariff amount according to type and capacity of renewable energy source, (ii) taking installed capacity into account instead of reservoir area for hydroelectric power plants as renewable energy source, (iii) making detailed Environmental Impact Assessment (EIA) report obligatory for renewable energy plants. The emphasis has been given on hydropower and wind energy. The renewable energy policy of Turkey has been compared with the advanced economies in Europe like Germany and Norway

Keywords: *Renewable energy, EU policy, Turkey.*

1. Introduction

Energy is one of Turkey's most important development priorities. Hence, utilization of domestic renewable energy sources is of vital importance for Turkey to reduce its dependence on foreign energy supplies, provide supply security and prevent the increase in greenhouse gas emission. Turkey's energy policy targets to increase the current share of renewable energy which is 20% to 30% in coming years. Turkey has quite miscellaneous energy resources including hard coal, lignite, oil, hydropower, natural gas, geothermal, wood, animal and plant wastes and solar. However, utilization of these resources is not adequate to meet the demand of the country. The energy demand of Turkey has been growing more rapidly than the energy production since it is a socially and economically developing country (Fig. 1).

Insufficient government efforts have forced Turkey to increase its dependence on foreign energy supplies. Instead of sufficiently promoting the usage of domestic energy resources and taking necessary precautions governments has relied highly on foreign energy supplies.

Thus, for example, the share of natural gas by the year 2005 as a thermal power plant fuel reached to 60% though Turkey has insufficient natural gas reserves [1]. It was reported that 74% of Turkey's total energy demand was met by imported energy in 2007. In Turkey, natural gas and electricity prices for residential and industrial use have increased by almost 8 and 7 times, respectively between 1999 and 2010. Thus, renewable energy sources have become a challenging alternative to fossil fuels for the country. In this study, current situation of renewable energy sources was investigated in detail and energy policies applied in Turkey was scrutinized by taking EU policy into account. The promotion of electricity from renewable energy sources (RES) is a high European Union (EU) priority.

The RES Directive (2009/28/EC) concerns electricity produced from non-fossil renewable energy sources and it states that the share of renewable energy in the total energy consumption of the EU must increase to %20.

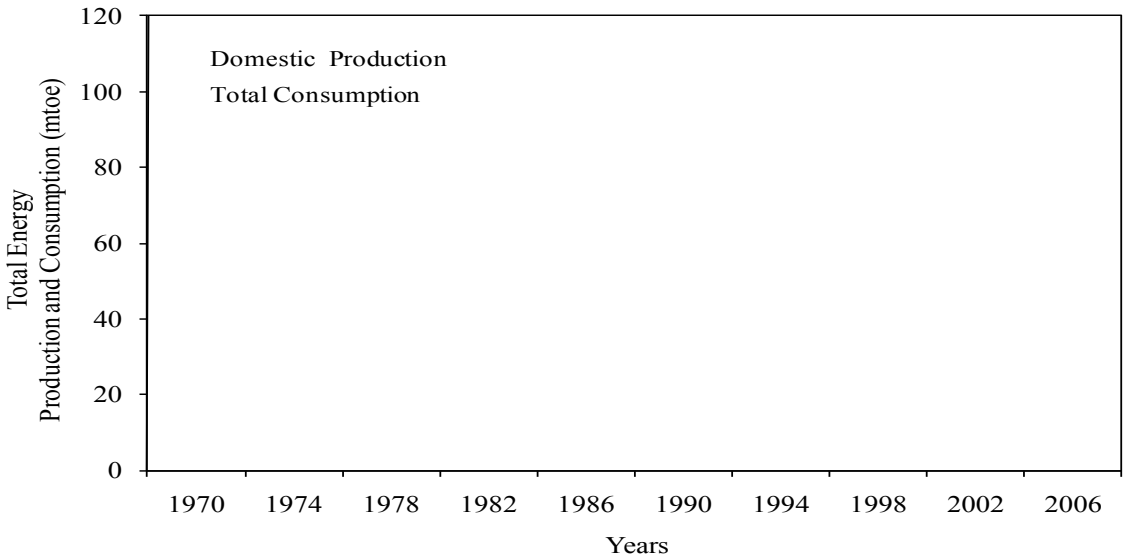

Fig. 1. Trends in total energy production and consumption of Turkey between 1970 and 2006 (data source: [1]).

2. Current Energy Trends and Economic Profile of Turkey

Monopoly of public sector was finished in 1982 in Turkey and private sector was allowed to build power plants and sell the electricity generated to Turkish Electricity Administration. The first law (Law No. 3096) that formed the frame for the participation of private sector in electricity industry was published in 1984. This law constituted the legal basis for private entrepreneurs to build new generation plants by means of Build-Operate-Transfer (BOT) contracts. Law No. 4283 (Law on Building and Operating of Electricity Generation Plants by BOT Model and Regulation of Energy Marketing) which provided the participation of private sector in building and operating of energy plants inured in 1997.

Turkey has become one of the biggest economies around Europe and the world within last 30 years with rapid increase in population and industrialization. According to International Monetary Fund (IMF), by the year 2008, Turkey was 15th biggest economy of the world and 6th biggest economy of Europe with a GDP (based on purchasing power parity) of 915.4 billion USD. In addition, average annual growth of GDP (based on current prices) is 4.3% in last 20 years [2]. Economic growth and increase in population, of course, has brought more energy demand. Annual growth rate and population increase projections show that this trend will continue in coming years. In addition to a number of forecast models developed for Turkey, current authors also proposed a model based on fuzzy logic methodology to forecast gross electricity demand of Turkey [3]. In the model proposed gross electricity demand was predicted only using GDP data. The fuzzy logic model proposed has showed that there is a direct relationship between GDP and gross electricity demand. This finding is also consistent with the literature. Mahadevan and Asafu-Adjaye (2007) stated that for electricity importing countries there is a mutual causality between GDP and energy consumption.

3. Renewable Energy Potential of Turkey and Current Situation

Turkey is quite a rich country in terms of renewable energy potential. Turkey has a significant hydropower and wind energy potential with its coastal line of 7200 km and an average

elevation of 1132 m . Turkey's wind energy potential is primarily focused in Aegean, Marmara and Mediterranean regions from higher to lower, respectively. Since Turkey's geological structure has volcanic origin the existence of more than 600 hot water sources whose temperature reach almost 100°C makes the country very rich in terms of geothermal energy. By the year 2009, hydropower, wind, geothermal and wastes (biogas +biomass) is used in electricity production (Table 1).

Table 1. Potential of renewable energy sources in Turkey and current situation in 2009.

Type of Energy	Technical Potential (MW)	Economical Potential (MW)	Installed Capacity (MW)[a]
Hydropower	54,000	42,000	14,553
Wind	114,000	20,000	802.8
Geothermal	1,500	600	77.2
Wastes (Biogas +Biomass)	-	-	81.2
Solar	56,000	-	-

[a]Data source: [5]

Although Turkey has the highest technical hydro and wind power potential in Europe, only very small portion of this potential is used when compared to those countries (Table 2). It can be easily seen that Germany, Spain and Austria is leader countries in developing their wind power potential. This is mainly due to incentive policies that government of these countries implement towards promoting the utilization of renewable energy sources.

Table 2. Comparison of wind and hydropower potential of Turkey to some European countries.

Country	Land Area ($x10^3$ km^2)	Technical Hydropower Potential (TWh/yıl)[a]	Technical Wind Power Potential (TWh/yıl)[b]	Developed Hydropower Potential by 2006 (%)[c]	Developed Wind Power Potential by 2006 (%)[c]
Turkey	781	216	166	20.5%	0.1%
Norway	324	200	76	59.7%	0.9%
Sweden	450	100	41	72.8%	2.4%
France	547	100	85	56.3%	2.5%
Italy	301	105	69	35.2%	4.3%
Austria	84	75	3	46.5%	57.4%
Switzerland	41	43	1	71.9%	1.5%
Spain	505	66	24	38.8%	95.9%
Germany	357	25	24	79.6%	128.0%
England	244	3	114	153.3%	3.7%

Data sources: [a][6], [b][7], [c][8]

4. Assessment of Renewable Energy Policies in Turkey in EU Policy Perspective

Renewable energy sources have gained importance in last decades due to growing energy demand. It can clearly be seen that policies applied by governments towards the utilization of renewable energy sources have a pronounced importance on the promotion of the utilization of these resources. Thus, though their financial and environmental disadvantages, incentive policies and privileges foster the utilization of renewable energy sources. In this context, it is

considered that the increase of the utilization of renewable energy sources strongly depends on government policies.

A total of 64 countries are supporting electricity generation from renewable energy sources and 45 countries are offering purchase guarantee by feed-in-tariffs for electricity generated from renewables in the world by the year 2009 [9]. As a result of these policies installed capacities of solar battery and wind power plants increased by 6 and 2.5 times, respectively. For example, after the publication of Renewable Energy Law in Germany in 2000 electricity generation from wind and solar energy in 2007 increased by 5 and 50 times, respectively.

Turkish government primarily targets to increase the share of renewable energy sources in electricity generation to at least 30% while decreasing the share of natural gas below 30%. In this context, Turkish government has planned to make the required changes in Law No. 5346 in 2010 to (i) utilize the whole economically feasible hydropower potential in electricity generation, (ii) utilize the whole economically feasible wind energy potential in electricity generation, (iii) provide full utilization of economically feasible geothermal energy potential of 600 MW, (iv) encourage and expand the utilization of solar energy for electricity generation until 2023. In order to achieve these targets Turkey needs to increase the installed capacities of hydropower and wind power plants to 20000 MW and 19200 MW, respectively within the next 15 years [10].

Since Turkey is an EU candidate its laws and policies are expected to be consistent with those of EU. In terms of energy production EU is promoting electricity production from renewable energy sources to decrease energy import and reduce greenhouse gas emissions throughout the union. Main instruments used in promoting renewable energy in EU are; purchase guarantees by feed-in-tariffs, quota applications and energy tax exemptions. In Turkey first promotion instrument towards electricity generation from renewable energy sources was the publication of Electricity Market Law (Law. No. 4628) in March 2001. In the context of this law, individual and corporate entities built electricity generation facilities from renewable energy sources having maximum installed capacity of 500 kW were exempted from licensing obligations and setting up a company. Moreover, by this law Energy Market Regulatory Authority (EMRA) was founded and private sector entrepreneurs were allowed to build and operate power plants by taking out a license from EMRA. In May 2005, Law on the Utilization of Renewable Energy Sources for Electricity Generation (Law No. 5346) was published in official gazette in Turkey. Renewable energy sources included in the context of this law were; wind, solar, geothermal, biomass, biogas, wave, stream energy and tide, channel, SHP or hydropower production facilities having a reservoir area less than 15 km^2. Some incentive mechanisms were introduced to Turkish market for electricity generation from renewable energy sources by Law No. 4628 and 5346. These mechanisms can be classified as licensing, land appropriation and purchase guarantee by a constant feed-in tariff. Table 3 presents the details of these mechanisms developed in Turkey. Even though these mechanisms were introduced in Turkey markets they are still inadequate when compared to EU countries leading the utilization of renewable energy sources. For example, Germany offers different feed-in tariff amounts for different energy sources specified in German Renewable Energy Law (Table 4). Nevertheless, in Turkey, a feed-in tariff of 5.5 €c/kWh is applied without taking energy source into account and any installed capacity limitations. This issue is considered to cause a serious confliction to EU.

Table 3. Incentive mechanisms offered to individuals and corporate entities by Law No. 4628 and 5346.

Incentive Mechanism	Incentives
1) Licensing	a) Installed capacity of 500 kW are exempted from licensing and setting up a company b) Only 1% of the licensing cost is paid by corporate entities applied to get a license and these entities do not pay annual licensing cost for the first eight years. c) Priority is given for system connection.
2) Land Appropriation	a) Real properties which are either regarded as forest or the private property of Treasury are leased or right of easement or usage permits are given to such properties. b) 85% discount is applied to rent, right of easement and usage permits and Forest Villagers Development Revenue, Forestation and Erosion Control Revenues are not demanded during the first 10 years.
3) Purchase Guarantee	a) Government guarantees to buy electricity generated for 10 years offering a feed-in tariff amount of 5-5.5 €cent/kWh.

Table 4. Feed-in tariff amounts specified in German Renewable Energy Act 2009.

Type of Energy	Feed-in Tariff Amount
Hydropower	12.67 €c/kWh, P<500 kW; 8.65 €c/kWh, 500 kW<*P*<2 MW 7.65 €c/kWh, 2 MW<*P*<5 MW
Wind Energy	9.2 €c/kW, in the first five years after the installation 5.02 €c/kW
Solar Radiation	43.01 €c/kWh, P<30 kW; 40.91 €c/kWh, 30 kW<*P*<100 kW 39.58 €c/kWh, 100 kW<*P*<1 MW 33 €c/kWh, *P*>1 MW

Publication of Renewable Energy Law in Turkey had a clear effect on hydropower development (Table 5) as well as on the installed capacity of wind power which increased from 20 MW to 802 MW between 2005 and 2009 (Fig. 2). Hydropower potential increased by 15% in 2007 as compared to 2006 and planned plants increased by 4 times in the same year. Furthermore, planned installed capacity increased by 7% in 2007 as compared to 2006 and most of the projects at that year was composed of SHPs [11]. Fig.3 presents the status of hydropower energy in Norway and in Turkey. Norway is a country nearly produced its total electric energy from hydropower. But 22.2% of its hydropower potential is not used in order to preserve protected areas [12]. On the other hand in Turkey, the hydropower policy is based on to develop its all hydropower potential which is not complying with the EU Water Framework Directive. However in the country, ecologically sensitive sites should be preserved like the example of Norway.

Table 5. Progress in hydropower plants after the publication of Renewable Energy Law in Turkey ([13], [14]).

	In Operation (2006)	In Operation (2007)	Under Construction (2006)	Under Construction (2007)	Planned (2006)	Planned (2007)
Number of projects	142	148	40	158	573	977
Installed Capacity (MW)	12788	13306	3197	6564	20765	22260
Energy (GWh/yıl)	45930	47590	10518	23620	73851	79177

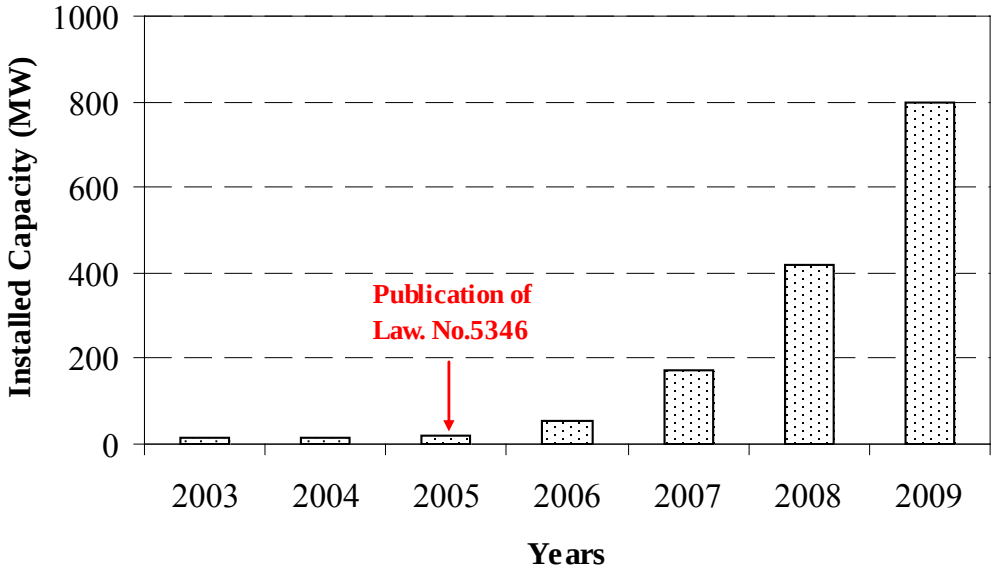

Fig. 2. Progress in installed capacity of wind energy in Turkey between 2003 and 2009.

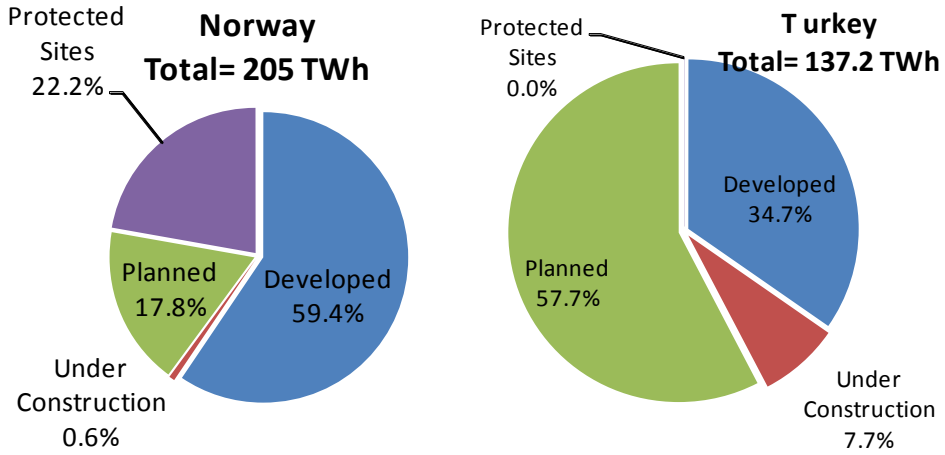

Fig.3 The total hydropower production in Norway and Turkey at the end of 2007 (Data sources: for Norway; [12] and for Turkey; [11]).

5. Conclusions

In this study, availability and potentials of renewable energy sources in Turkey was evaluated as well as the effectiveness of government policies focused particularly on Renewable Energy Law (Law No. 5346) and its compatibility to EU policy. Even though Law No. 5346 contradicts with EU legislations, its effect can be clearly seen immediately after it w as

published. Nevertheless, conflictions of Renewable Energy Law (Law No. 5346) published to increase the utilization of renewable energy sources with EU policies creates serious obstacles to achieve this target. First confliction is, on the contrary to EU, the constant feed-in tariff amount offered in Turkey without taking capital investments of specific energy sources into account. Second issue considered as a confliction is that hydropower plants with a reservoir area less than 15 km^2 are considered within the definition of renewable energy defined by Law No. 5346, thus shifting private sector interest from SHPs to big hydropower plants. This issue is handled differently in EU in a way that governments take installed capacity of power plants into account and plants with lower installed capacities get higher amount of incentive. The last issue considered as another contradiction to EU legislation is that no detailed Environmental Impact Assessment (EIA) report is required in the construction of power plants utilizing renewable energy sources in Turkey. However, in EU, the organizations such as Europe Investment Bank investigate the probable harms of a project to the environment while considering financing it [15]. This is a serious confliction as more and more attention is being paid to environmental issues in EU as well as the world.

References

[1] EUAS, Electricity Generation Company of Turkey, http://www.euas.gov.tr , accessed October 2010.

[2] IMF, World Economic Outlook Database. International Monetary Fund, (www.imf.org), accessed October 2010.

[3] Kucukali, S. and Baris, K., Turkey's short-term gross electricity demand forecast by fuzzy logic approach, *Energy Policy*, 38(5), 2010, 2438-2445.

[4] Mahadevan, R. and Asafu-Adjaye, J., Energy consumption, economic growth and prices: A reassessment using panel VECM for developed and developing countries, *Energy Policy*, 35, 2007, 2481-2490.

[5] MENR, Ministry of Energy and Natural Resources , Policy and Legal View in Wind Energy, Workshop: Development of Wind Energy in Turkey, Ankara, Turkey, 2010.

[6] Hydropower & Dams World Atlas, Aqua-Media International, UK, 2006.

[7] Erdogdu, E., On the wind energy in Turkey, *Renewable Energy and Sustainable Energy Revie ws*, 13, 2009, 1361-1371.

[8] ECD-European Commission Directorate, 2009. EU Energy and Transport in Figures. Statistical Pocketbook 2009.

[9] WEC, World Energy Council, Survey of Energy Resources, 2007.

[10] MENR, Ministry of Energy and Natural Resources, Document on E lectricity Energy Market and Supply Security Strategy, Ankara, Turkey, 2008.

[11] Kucukali, S. and B aris, K., Assessment of small hydropower (SHP) development in Turkey: Laws, regulations and EU policy perspective, *Energy Policy,* 37, 2009**,** 3872-3879.

[12] Brekke, H. Design and performance of small hydro. *Proc., Hydro* 2010 Conf., Lisbon, Portugal, 2010.

[13] Tutus, A., 2008. Hydropower Plants and Dams, Symposium on Today and Tomorrow of Energy Sector in Turkey and the World, METU, Ankara, Turkey.

[14] DSI, General Directorate of State Hydropower Works, Statistics of Turkey HydropowerPlants, Ankara, 2006.

[15] Kucukali, S., Comments on a quadratic helix approach to evaluate Turkish renewable energy, *Energy Policy*, 38(4), 2010, 2064-2065.

Energy and sustainability: public perspectives on what are the issues, who should address them and how

Olga Di Ruggero[1*]

[1] *Delft University of Technology, Delft, the Netherlands*
** Corresponding author. Tel: +31 15, E-mail: o.diruggero@tudelft.nl*

Abstract: In this work we present the results of a Q -study aimed to systematically represent lay-people's perspective on energy and sustainability issues. Especially we explored lay-people' perspectives on what are the overriding issues related to energy, (e.g. energy security and environmental crisis) as well as which actors are responsible to address these issues. In this context we elicited people's opinions on contested alternative technologies (e.g. nuclear power, wind energy, hydrogen). We were able to identify tree different environmental perspectives and a non-environmental one. Despite interesting common points (e.g. mistrust in the government) the data show dissimilarities in the perception of how the future energy system might look like. The main divergences turn around the employment of nuclear energy and in general of large scale decentralized system vs. small scale one. Although the presence and the distribution of the results in the larger population it is still to further enquire we retain the results useful for policy makers and practitioners involved in the designing, the decision making or implementation phase of new technologies to achieve energy sustainability as well as in the communication activity with the large public.

Keywords: *Lay-people's perspectives, Energy, Sustainability, Q-methodology,*

1. Introduction

Challenges like climate change, energy security or air pollution require a long-term strategic decision making where different policies are designed and implemented today to develop the sustainable energy system of tomorrow. These strategies will change the shape of the current system by supporting certain technologies and promoting certain behaviors (e.g. less car use, more solar panel installations in households).

Ideally these strategies result from the negotiation of the different actors' perspectives in the policy arena. We can define a perspective (or frame [1]) as a constellation of values, beliefs, assumptions and interests, which determines not only the problem that matter but also the boundaries of the solution space. Given that no perfect solution is possible, these strategies reflect the negotiated priorities, values, the issues that should be solved (e.g. energy independence or carbon emission) and how (e.g. biomass, nuclear energy or bicycles).

However this negotiation process is not isolated within the boundaries of the policy arena, but is affected by more or less stable exogenous factors like cultural or technological innovation. A relatively unstable and influential exogenous factor is public opinion, which can affect the process by determining the discussion agenda or by giving more power to certain actors in the arena [2].

In this context we aimed to explore people's opinion on energy related issues, controversial technologies (e.g. biomass, hydrogen or nuclear energy) and other non technical solutions. Especially we aimed to explore how people look at the issue, if and how they construct the problem boundaries and thus define the solution space (perspective thus as a combination of beliefs on what are the problems, who is responsible to solve them and how).

The research aims are resumed in the following research questions: *What are the lay people's perspectives on energy related issues? How are these perspectives agreeing and/or conflicting?*

We expected that divergences in the acknowledgement of the issues and responsibilities by the public would have led to the preferences towards different technologies. Moreover we expected to find other perspectives beside the largely explored environmentalism. Similarly to the environmentalism we expected these other perspectives to lead to the preference (or rejection) towards the different technologies but for different reasons.

Aiming to understand the line of reasoning behind the preferences we opted for a qualitative research method, rather then a quantitative one. After a brief description of the chosen method (section 2) we will present the results of the study (section 3) and discuss them in section 4. We reserved some considerations in the conclusive section (section 5).The study, which is an ongoing research, has been designed to be an intercultural project in two countries: the Netherlands and Italy. For the sake of clarity, in this paper we will be presenting and discussing only the results from the Italian work.

2. Methodology

To pursuit our research scope we chose for the Q-Methodology, which combines qualitative and quantitative techniques to make explicit the different perspectives on a certain topic [3] [4] [5]. The Q-methodology was thought to be particularly suitable to overcome the possible lack of knowledge on the technical aspects of the topic or the absence of a preexisting opinion in the respondents. In fact in a Q-study the subjects are asked to assess a set of sentences through a *likert* scale (for example agree vs. disagree) but in the context of an interview. We thought the sentences, formulated as opinions, would have facilitated people to give reactions at least on the sentences themselves. Moreover, unlike conventional R-surveys in a Q-sort the sentences are not considered singularly but rather ranked and put in relation one to each other. The respondents are asked to distribute the sentences written on small cards in a predefined grid accordingly to how much they agree or disagree with them. The task of ranking is enriched by comments and explanations on the different choices. In this way through a Q-sort (a particular disposition of the cards) it is possible to build up and organize in a structure the personal point of view, even if it was not present before. In other words, the Q-method can either elicit an existing perspective or help in constructing one.

In a second quantitative phase all Q-sorts are statistically related and grouped in shared perspectives. Given the nature of the statistics used, the q-methodology doesn't require big samples, as far as the sample guarantees a sufficient variety of perspectives. This technique hence does not aim to give a representatives distribution of the opinions among the population (such an opinion pool) rather to disclose the variety of perspective on a certain topic and dig into them [4]. The "extreme" positions are frozen as cardinal points between which everybody will than distribute their opinions.

The use of statistic helps the researcher to process more information at the same time and can reveal unexpected results when combining the subjects' profiles. The comments collected during the interviews are used to reconstruct the narratives. Contrarily to a conventional quantitative analysis, the perspectives are enriched with useful qualitative data about the "how" and the "why" certain variables are related. The interpretation of the links among variables derives directly from the point of view of the interviewees and not from the free interpretation of the researcher.

A Q-study entails different steps. Firstly it is necessary to record and resume all the variety of opinions and beliefs that represent the *flow of communication* object of the study. In our case we organized 7 focus groups[1] for a total of 49 people interviewed covering different age and

background. We asked people to discuss about what are the main problems related to energy production and consumption and which actors are responsible to do something about it. The entire flow of communication has been reduced into 40 sentences (a sample of them is showed in table 2), which have been chosen to represent the variety of perspectives rather than for their frequency or relevance.

In the second step of a Q-study the respondents (the P-set) are asked, in the context of a single interview, to dispose the sentences written on 40 small cards in a predefined grid, with the shape of a quasi normal distribution. As in qualitative studies the P-set is selected so to represent the maximum variety of perspectives. In our case, we started by collecting the environmentalist's perspectives by interviewing people belonging to association or companies working in the sustainability field but also people living in the countryside and having solar or photovoltaic panels. Starting from few of these people we continued contacting people by snowballing: each interviewee was asked to put us in contact with somebody who thought similarly and someone who thought very differently. With the snowball method we contacted up to the 5th level of interconnection. As a further control variable we looked for people with very different political preference. In this way we got to a P-set of 36 subjects whose characteristics are resumed in table 1. Together with the task of disposing the cards into the grid the subjects were asked to comment the cards and explain the reasons behind their disposition.

Table 1 Socio-demographic characteristics of the Italian P-set. The subjects are all living in the province of Ancona, in the center of Italy. We organized the data dividing the P-set in subgroups according to the political preference. We show the average age (∏) and its standard deviation (Δ); gender (M=male; F=female) and the education level measured in years (high-school degree or less =13y; bachelor degree=16y; master degree or more+18y)

Socio-demographics →	Age		Gender		Education (in years)		
↓ Political preference	∏	Δ	M	F	≤13y	16y	≥18y
Left (PC, 5Stelle,SeL)	29	11	5	2	1	2	4
Center-Left (PD)	46	14	3	4	-	-	7
Center (non specified)	41	10	1	3	-	1	3
Center-Right (PDL-UDC)	40	11	3	2	1	-	4
Right (FN, exAN, LN)	39	13	6	1	3	1	3
No preference	39	13	3	3	3	1	2
TOTAL	39	14	21	15	8	6	22

The last step of a Q-study is the data analysis. With the PQMethod program, we performed a centroid factor analysis and we ortognally rotated the 7 resulting factors through the varimax. To perform the Q analysis we selected four of the seven the factors, which had the Eigenvalues higher than 1.4 of and at least four subjects loading purely (subjects highly correlating only with one of the four factors). The selected factors explained alone the 55% of cumulated variance and are presented in section 3.

3. Results

Through statistic analysis we identified four different factors representing four shared perspective on the matter of energy related issues. Recalling the qualitative information collected during the interviews we reconstructed the narratives of the factors. We also labeled each factor with a title resuming the core of the perspective.

In the following sections (3.1 to 3.4) we resume in few lines the main points of the logics behind the different factors.

3.1. Factor 1 the hopeless environmentalist.

Whatever problem there is with energy (like climate change, pollution or overconsumption) the point is that nobody cares about. People don't care, the newspapers don't talk about these things, the Government does nothing, the technologies are ready but there is a powerful lobby that is blocking their venue in the market. The only way out is that future generation will become more responsible in energy consumption. Therefore education since the primary school is the key solution. Nuclear should not be implemented, because of the waste, because it's dangerous, because it is hold. The decentralization of the energy production is a good idea, so to avoid the transport energy and to keep multinational's hands off the energy. Off-grid houses, usage of urban waste or biomass to produce energy, small-scale renewable energy plants, this is how the future should look like.

Table 2 Example of the 40 sentences composing the set of cards that people have been asked to q-sort in a scale from -5 to +5. On the right side of the table we can see the ranking value of each sentence per each of the 4 factors identified.

	Factors			
Sentences	1	2	3	4
I am a climate-skeptical. I don't think climate change is an issue. There are even scientists that say that it is a normal process and that it has nothing to do with our energy consumption.	-3	-1	0	-5
Humans are more important than nature, we are on top. We should satisfy our needs, but not completely disregard the nature.	-1	-4	3	-2
The majority of oil comes from political unstable countries. We would have a serious problem if the Middle East would close the tap of oil. We should not depend on them.	2	4	5	1
I wish it would be possible to completely independent from the electric grid. I would prefer producing the energy at home on my own.	3	-3	3	2
Maybe we could come back in doing things locally, also energy. It would be nice to produce energy locally and not to transport it	4	-2	2	4
Nuclear energy is good way to solve the issues related to energy.	-4	2	2	-4

3.2. Factor 2, the practical environmentalist

This factor underlines the socio-political aspects of the issue. The real problem is the uncontrolled consumerism: the overconsumption is an issue in itself. This overconsumption is also bringing issue with the energy like the environmental problems: human being is part of the nature and we have to respect it since everything we do against nature will backfire on us anyway. Noteworthy in this perspective the environment is intended as the landscape, the air-quality thus the local natural resources rather than the global issues like climate change. The overconsumption may also lead to less availability of energy and in anyway it is unacceptable to depend on other countries for our energetic needs, especially if they are politically unstable, totalitarian and culturally outdated like the Middle East.

From this perspective the government is incapable of handling this situation, although it should have only a marginal role. The mistrust in the government is compensated by the trust in the liberal market: the change will come from down-up, when the people consume less and better, new sustainable products will diffuse in the liberal market. The Government should support this chain through education, which makes of people responsible consumers.

Concerning the solutions, decentralization is not the future, nor the local production and certainly not the independent houses. Decentralizations means too much responsibility on people and it would be impossible for them to mange all this. Centralized production and the use of existing infrastructure: that is the key. Nuclear is a good compromise: it can increase our energy independence in an economically viable way without harming too much the environment. Using urban waste to produce energy is indeed a good idea, since it solves two problems in one (i.e. where putting the waste and energy availability) while using potential food might be an issue (table x.4.3).

3.3. Factor 3 No to no - Yes to progress, the futuristic citizen

This is the economic and technical focused perspective. The real issue is not the environment: climate change is a natural process and the human activity is too small to have any effect on it. Pollution? We are much more aware of our environment now than in the past and definitively air was more polluted during the industrial revolution than nowadays.The reality is that we need energy for everything we do. We cannot come back to stone-age and consume less: the progress lead us to an increase in the quality of life, we cannot go back! We are at the top of the chain, therefore we have to find a way to have enough energy to satisfy our needs, of course without completely disregard nature. Developing countries are their energy consumption, but in the end energy availability is not a problem: we don't know which technological surprise science holds for us in the future.

The focus of the issue with energy is at the geo-political level. The worries are not for the increasing consumption of developing countries, which means more people pulling the corner of the same blanket, but rather the energy dependence issue. Particularly it is not seen favorably the dependence from Middle East countries (but also from Russia) for our energy supply. For these issues people cannot do a lot. The government should take instead a key role, not only by giving the guidelines, but also giving clear directives to people on what to do. In this discourse technology has a central role. For example if hydrogen is the future, we should go for it. What ever change in the system or in people behavior is needed to realize the future it should have to be pushed top-down, promoted or even imposed if necessary. An example is the smoking-ban. People might be not so open-minded or lack of long-term vision and therefore block the progress.

Progress and technology will give us the solution and it is not possible to say always no to any new technology, like the incinerators or hydrogen. Why not having hydrogen at home or in a car?! What is scaring of new technologies? Terrorism? Why no to nuclear energy? Why no to Methane? Say yes to progress.

3.4. Factor 4 the liberal environmentalist.

From this perspective the current (over)consuming model is leading our society nowhere. We should consume less and better. For instance we should consume locally. This doesn't hold only for seasonal-local food but also for the energy sources. Although technology can help us no technical fix is possible: we need to change our behavior, that is why education to sustainability is so important.

The responsibility of making our world more responsible is equally divided among the different actors: it is true that industry consume and pollute a lot, but we buy their products. We should stop to blame the industry or China for pollution. Also the Government has limited power, since it is a complex international issue, with delicates geopolitical balance.

The government can help with taxation or monetary incentives and especially with education, since a real change cannot come without a deep awareness. The change should be realized bottom-up: the responsible and aware consumers will pull the market, the companies will invest in research and better technologies will be developed. Decentralization is definitively the way to go, so using waste or biomass to produce energy? OK, but these are buffering solutions not the future. In the future we should produce less waste rather than count on them for our energy supply! Nuclear is a 30 years old question, and the answer is NO! (x.4.5)

4. Discussion

In the previous section we described the narratives resuming the four identified perspectives on energy issues and sustainability. The Eigenvalues of the factors are higher than 1.4 and they explain alone the 55% of cumulated variance, both values indicating rather strong results.

The Hopeless, the Practical and the Liberal environmentalist (factors 1, 2 and 4) substantially share an environmental position especially if compared with the Futuristic citizen (factor 4) that instead focuses on the geo-political and technical aspects of the issue minimizing the environmental crises. The three perspectives sharing the environmental focus however, give different meanings the word "environment": from the global aspects of climate change (the *liberal* and the *hopeless environmentalist*) to the aesthetic view of the natural surroundings (the *practical environmentalist*). The fourth perspective (the *futuristic citizen*) claims also the need of a change but in the name of progress rather than a supposed environmental crisis.

The responsibilities of this change are distributed in a different way in the four perspectives: some see the need of a top-down change, with clear indication of what to do, since citizens do not have a long-term view nor enough knowledge. From another perspectives, sustainability can come out of the liberal market as far as people want it: through a bottom-up change the citizens/consumers pull the market by changing their consuming behavior.

As we hypothesized, the four lines of reasoning drive to different vision of the future energy system. It is noticeable the clear-cut anti-nuclear position of environmentalists (the *liberal* and the *hopeless*) as well as the pro-nuclear position of the other two perspectives: the practical environmentalists see nuclear energy as an inevitable necessary compromise, while the futuristic citizen welcome it as any other alternative technology. Although everybody seems to be in favor of the diffusion of the renewable and alternative energy sources, in different measure wind, solar, biomass but also urban waste there is a clear distinction of their role in the future energy system. The decentralization of the energy production, i.e. communities and single individuals producing energy, is seen as a key change from the environmentalists (the *liberal* and the *hopeless*). At the opposite side is the other environmentalist sub-group, the *practical environmentalist,* which sees decentralization as an excess of responsibility on lay-people, while centralized production system should guarantee lower cost of energy and security of supply. The *futuristic citizen* instead seems to give a different meaning to the (de)centralization: the production of energy will be with but not limited to local/individual systems because this is the direction that technology is taking.

Last, we would like to underline an interesting pattern observed in our data: an apparent coherence (but not statistically proven) between the perspective and the political preference. In our sample the *futuristic citizen* seems to be consistent with a *rightist* political perspective; the *liberal environmentalist* compatible with a *leftish* one; the *centrists* (center left and center right) divided themselves among the *hopeless* and the *practical* environmentalist.

5. Conclusion

We started this work asking two questions, formulated in section 1 of this paper as: What are the lay people's perspectives on energy related issues? How are these perspectives agreeing and/or conflicting? We hypothesized that differences in looking at the issue would have led to a divergence in defining the solution space and thus what is acceptable or not from the lay-people's point of view.

We performed a Q-methodology study, which combines qualitative and quantitative techniques to identify the different perspectives and the agreeing/conflicting points. Through this methodology we were able to identify the nuances among the three identified environmental point of views, i.e. the difference meanings given to the word "environment" and the different attitudes towards the issue, i.e. hopeless. Remarkably we identified a fourth non-environmental perspective, which is, to the best of our knowledge, still unexplored in the literature.

According to our results these different frames correspond to different solution space demarcation, e.g. different ways of looking at the future. The hopeless and the liberal environmentalist, these who look at the global environmental issues, claim for a deep societal change. This change is expressed also in a revolution in the current energy system, where the energy is locally produced and managed by people's organization. The same deep change is claimed as well by the other environmental group but it is expressed in a completely opposite way: a business as usual but clean. At the implementation level, the futuristic citizen surprisingly comes in the middle: for different reasons they envisage a combination of the two. If the data result to be externally valid, a special attention should be given in the communication, firstly distinguishing which kind of environmentalist are addressed and secondly by taking into account that other frames are in audience that would also step onboard but for different reasons.

Interestingly but not surprisingly, the data suggest a possible political conflict around the energy issue. Notably political preference and solutions space seem to be strongly related a priori, since few political parties in the Italian political arena have a clear program on the topic energy and sustainability.

However, being a qualitative study we are careful in claiming a systematic relationship among frames, solution space and political preference. These aspects could find a (dis)confirmation in a quantitative study. Concerning the external validity of the data, many authors [3] [4] claim that the Q-methodology is capable of disclosing the variety of perspective by means of small samples provided that the latter offers a sufficient variety of way of thinking. However, given the difficulties in our work to identify a priory the "sufficiency" of the variety, it would be interesting to verify how stable are the data and if and how these perspectives are distributed in the larger population.

In conclusion we underlie that according to our results, other frames beyond environmentalism justify the shift towards a new energy system in lay-people perspective; in addition, different frames seam to lead to the preference towards different kind of future energy system (especially concerning the implementation of centralized vs. decentralized systems and the employment of the primary energy sources, like nuclear power.), this aspect deserve further research to be (dis)confirmed. Future research will address the definition and the distribution in the larger population of the above-described frames and solution spaces

(i.e. technology preference and policy acceptance). We think that the results can be used by policy makers and practitioners both in the designing and decision making process as well as in the communication phase.

References

[1] D.A. Schön and M. Rein, Frame Reflection: Towards the resolution of intractable policy controversies, New york, Basic books, 1994

[2] P.A. Sabatier, An advocacy coalition framework of policy change and the role of policy oriented learning therein, Policy Sciences 21, 2, 1988 p. 129-168.

[3] Stephenson W., The Study of Behavior: Q Technique and its Methodology, University of Chicago Press, Chicago, 1953

[4] Brown S., Political Subjectivity: Applications of Q-Methodology in Political Science, Yale University Press, 1980

[5] NJA van Exel, G de Graaf. Q-methodology: A sneak preview [www.qmethodology.net]. 2005E.

[i] Six focus groups were conducted with Dutch participants, while one was conducted with Italians (living in the Netherlands from less than 4 years). It might be argued that organizing the focus groups in the Netherlands might have led to overlooked some important issues from the perspective of the Italians. However, during the interviews, we asked to the Italians interviewee if some important aspects were missing. Only one over 36 remarked that a sentence about the "future threat of a war among nations because of energy depletion" was missing. The same topic raised up during the Italian focus group and during the coding was classified under the geo-political topic and thus included in the sentence "The majority of oil comes from political unstable countries. We would have a serious problem if the Middle East would close the tap of oil. We should not depend on them". In this light we think that the 40 selected sentences are indeed representing the main points of the energy related issues including a sufficient variety of point of views.

Performance of Jatropha biodiesel production and its environmental and socio-economic impacts - A case study in Southern India

Lisa Axelsson[1], Maria Franzén[1], Madelene Ostwald[1, 2,*], Göran Berndes[1], N.H. Ravindranath[3]

[1]*Physical Resource Theory, Department of Energy and Environment, Chalmers University of Technology, Göteborg, Sweden*
[2]*Centre for Climate Science and Policy Research, Department of Water and Environmental Studies, Linköping University, Norrköping, Sweden*
[3]*Centre for Sustainable Technologies & Centre for Ecological Science, Indian Institute of Science, Bangalore, India*
** Corresponding author. Tel: +46 11363292, Fax: +46 11363292, Email: madelene.ostwald@liu.se*

Abstract: In India expectations have been high on production of biodiesel from the oil-crop Jatropha. Jatropha is promoted as a drought- and pest-resistant crop, with the potential to grow on degraded soil with a low amount of inputs. These characteristics encourage hope for positive environmental and socio-economic impacts from Jatropha biodiesel production. The purpose of this study was to explore the performance of Jatropha biodiesel production in Southern India, to identify motivational factors for continued Jatropha cultivation, and to assess environmental and socio-economic impacts of the Jatropha biodiesel production. 106 farmers who have or have had Jatropha plantations were visited and interviewed regarding their opinion of Jatropha cultivation. The result indicates that 85 percent of the farmers have discontinued cultivation of Jatropha. The main barriers to continued cultivation derive from ecological problems, economic losses, and problems in the development and execution of the governmental implementation of the Jatropha programme. The Jatropha characteristics were overrated, and the plantations failed to provide income to the farmer. A common factor for the farmers who continued Jatropha cultivation was that they had the economic means to maintain non-profitable plantations. As the Jatropha programme was not as successful as expected, the expected positive environmental and socio-economic impacts have not been realized.

Keywords: *Household interviews, Drivers and barriers, Land use, Rural development.*

1. Introduction

Jatropha Curcas (Jatropha) has been regarded as one of the most promising crops for securing energy supply and for socio-economic development in developing countries. Jatropha is a small tree or large bush that develops fruits containing seeds with an oil content of 32 to 40 percent, which can be transformed into biodiesel [1]. Promoters of Jatropha argue that the biodiesel from Jatropha does not compete directly with food production since the whole plant is toxic and hence non-edible. More importantly, the potential of Jatropha to grow on degraded soil and its resistance to drought and pests enable cultivation on land that is not suitable for food production [2]. The characteristics of Jatropha have raised expectations for positive environmental and socio-economic impacts from biodiesel production.

India is one of the countries that have had high expectations on production of biofuels for secured energy supply and sustainable environmental and socio-economic development. In 2003 the Indian government declared a National Mission on Biofuels, to drive large-scale implementation of biofuel production. The National Mission on Biofuels stated a five percent blending target of biodiesel in conventional diesel, with a 20-percent blending target for 2012 [2]. The Planning Commission for the National Mission on Biofuels announced that Jatropha was found to be the most suitable biodiesel crop for the stated energy, environmental, and socio-economic purpose, and initiated a programme for Jatropha implementation [3]. The Planning Commission estimated land areas needed to achieve the blending target and identified land areas available and suitable for Jatropha cultivation.

2. Description of the study and methodology

This study was performed during the spring of 2010 with the purpose to explore the performance of Jatropha biodiesel production under prevailing energy and agricultural conditions in Southern India. The focus was to identify motivational factors for continuation and termination of Jatropha cultivation and to assess environmental and socio-economic impacts of the Jatropha biodiesel production.

To address the purpose, semi-structured interviews with farmers in the states Andhra Pradesh and Tamil Nadu who have or have had Jatropha plantations were performed with the aid of a translator. Questions regarding the socio-economic situation of the farmers, the performance of their Jatropha plantations, and their reasons for continuing/discontinuing cultivation were asked. Farmers targeted for participation in this study were respondents from a field study performed in 2005-06 by researchers from the Indian Institute of Science in Bangalore which focused on gaining knowledge on the performance of Jatropha plantations in Southern India and the socio-economic status of the Jatropha farmers. Additional farmers were added to the sample during the process to get a more complete picture of Jatropha cultivation within the two states.

The total number of respondents was 106 (77 in Andhra Pradesh, 29 in Tamil Nadu), where 54 were a part of the previous study. A distinction was made between the respondents depending on the ownership of their land, dividing them into three groups; private farmers, community land, and industry/research land. The majority of the respondents were private farmers, having ownership rights to their land or having land assigned specifically to them by the government to sustain their livelihood. Apart from the interview respondents government officials, scientific researchers, and other concerned actors contributed to understanding of the subject through informal discussions.

Three limitations made within the study need to be acknowledged. Geographically the field study was limited to the two states Andhra Pradesh and Tamil Nadu. Regarding the exploration of the performance of Jatropha biodiesel production the study mainly focused on the cultivation stage, since the production process in the studied districts had often not reached further stages. When analysing the results private farmers have been in focus due to that one of the objectives of the study was to assess the socio-economic impacts of Jatropha cultivation.

3. Results

The results of the field study provide information on the performance of Jatropha cultivation, and information on socio-economic status of Jatropha farmers was needed for understanding and further interpretation of the results. For knowledge on socio-economic status the private farmers were asked basic questions regarding landholdings, size of household, occupation and education level. The results indicate that Jatropha farmers commonly have small landholdings and low level of education, and that the economic situation is stronger among Jatropha farmers in Tamil Nadu than in Andhra Pradesh.

3.1. Implementation of Jatropha

The initiation of large-scale Jatropha cultivation was driven by the government through national and state government agencies, and within the states the different district governments were encouraged to design and initiate implementation programmes for Jatropha plantation. The National Mission on Biofuels stated that investments in the implementation of

biodiesel production should have been made by the government, for example by using already existing poverty alleviation programmes.

The implementation in the studied districts was driven mainly by agricultural and rural departments of the government, but in some cases also by local NGOs and private companies. A majority of the respondents, 74 percent in Andhra Pradesh (57 of 77 respondents) and 90 percent in Tamil Nadu (26 of 29 respondents), state that the idea of initiating Jatropha plantations came from a government agency.

To promote plantation of Jatropha to farmers the local governments announced incentives in the form of free Jatropha seedlings, financial subsidies, subsidised agricultural facilities, bank loans and promises of future income from the plantations. The involved farmers were also promised information and training in cultivation practices.

3.2. Continuation and termination

The field study shows that a majority of the interviewed farmers discontinued cultivation of Jatropha; 85 percent of the farmers (90 of 106 respondents) discontinued cultivation and 15 percent (16 of 106 respondents) continued, with or without maintenance of the plantations (see Fig. 1).

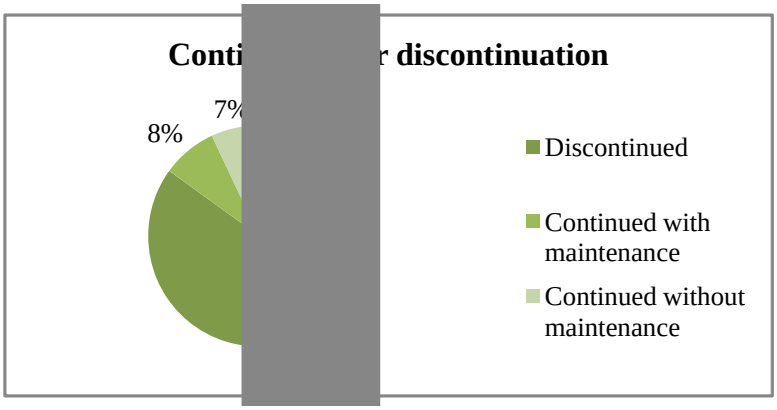

Fig. 1. Percentage of the total number of respondents who have discontinued or continued (with or without maintenance) cultivation of Jatropha.

3.3. Drivers

The field study shows that only 15 percent of the interviewed farmers (16 of 106 respondents) have continued cultivation of Jatropha. Of the continuing 16 respondents nine have continued with maintenance of their plantations and the other seven respondents have stopped maintaining their plantations but have not removed the plants in order to use the land for other purposes. Reasons mentioned for keeping plantations or parts of plantations without maintenance and with no expectation on outcome are costs for removal of the plants and not having any plans for alternative uses for the land.

Drivers to continued Jatropha cultivation mentioned by the farmers were divided into three categories: economic, ecological and implementation (see Fig. 2). Drivers mentioned were hope for future economic possibilities, that the Jatropha plants have a positive effect on other plants, that the plants have survived even if the plantations are not maintained and that the plantations were implemented and kept for demonstration purposes. Each farmer could mention more than one driver.

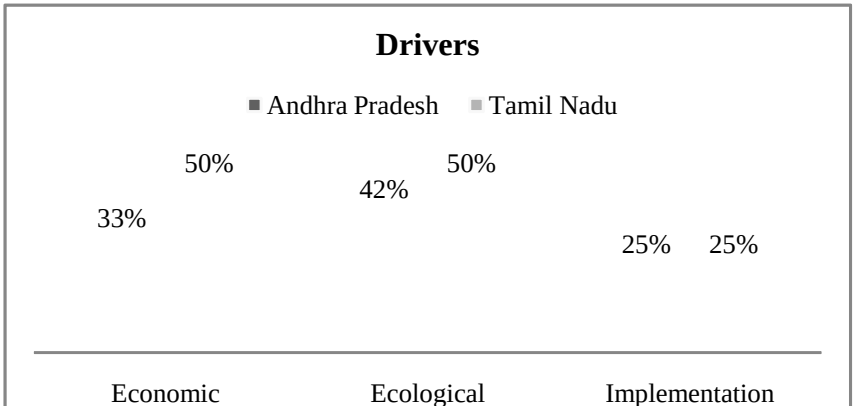

Fig. 2. Percentage of the respondents from both states who mentioned drivers within each of the three categories.

The number of continuing farmers is small, they work under different agricultural and economic conditions and have a variety of reasons for keeping their plantations, and there are no clear differences between drivers mentioned by farmers in Andhra Pradesh and farmers in Tamil Nadu. Hence it is difficult to draw any general conclusions on the drivers for continued cultivation of Jatropha. What can be noted is that all farmers who have kept and maintained their plantations have the economic means to maintain non-profitable plantations. In the case of private farmers or companies who have continued they all have other sources of income and incomes from Jatropha are considered additional. Where non-private actors have continued cultivation, the plantations are undertaken and continued for the purpose of demonstration or research and are not privately funded.

3.4. Barriers

The main reason for choosing Jatropha for the large-scale programme for biofuel production was its agricultural characteristics: the suitability for cultivation on barren and fallow land, the low demand for inputs, and the resistance to pests and drought. Experiences from plantations clearly show that Jatropha production has not been able to meet the high expectations, 85 percent of the interviewed farmers (90 of 106 respondents) have discontinued cultivation of Jatropha.

The farmers were asked about their reasons for not continuing cultivation of Jatropha and mentioned a wide range of barriers to cultivation. These barriers were divided into five main categories: economic, ecological, market, knowledge, and implementation, where barriers within the ecological category were most frequently mentioned (see Fig. 3). The main barriers within the ecological category are connected to problems for Jatropha to grow and yield under poor conditions; 54 percent of the respondents (57 of 106 respondents) state water scarcity and climatic problems as barriers, and 11 percent (12 of 106 respondents) mention insufficient yields. In the economic category the most mentioned barriers are insufficient income from the plantations and cost for labour. The respondents also experienced barriers derived from the implementation of the Jatropha programme; the most mentioned barriers within the

implementation category are lack of support from the government or other actor that initiated Jatropha cultivation, and that promises made in the initial stage had not been fulfilled. Some of the reasons mentioned are closely connected, sometimes it is difficult to distinguish one single barrier since one problem mentioned may be the root of another. For example, if low or no income is mentioned as a barrier to continued cultivation, this lack of income may be due to low yields caused by water scarcity.

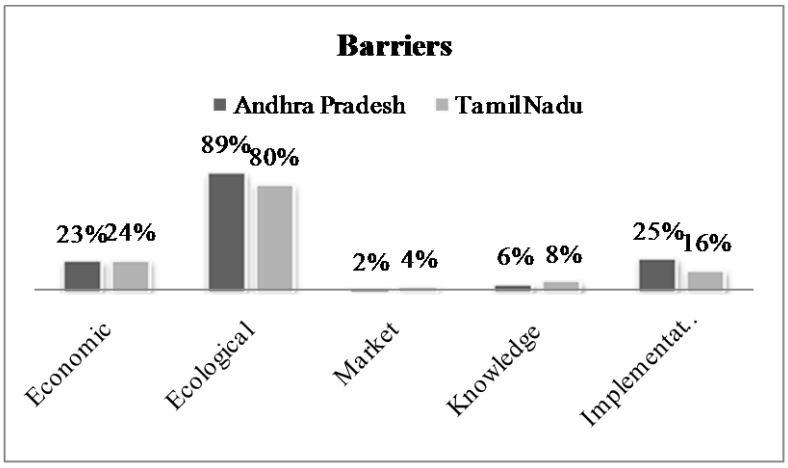

Fig. 3. Percentage of respondents from both states who mentioned barriers within each of the five categories.

3.5. Inputs

Jatropha was promoted as a crop that could survive and yield on barren land without inputs of water and fertilizers. Jatropha's drought resistance provided an opportunity for farmers on rainfed lands, who had been suffering from drought and had not been able to gain yields from their land. But under harsh rainfed conditions Jatropha plantations failed to yield and could often not even survive. The single largest barrier to continued cultivation of Jatropha mentioned by the interviewed farmers was water scarcity. It seems that inputs of both water and fertilizers are needed for survival of the plantations on poor soils. 70 percent of the interviewed farmers (74 of 106 respondents) mentioned that they have been using some kind of irrigation system, and 25 and 32 percent used chemical and biological fertilizers, respectively. Note that these figures do not take amount and frequency into consideration. However, even with inputs Jatropha failed to give satisfying yields.

3.6. Insufficient yields and incomes

One of the most important barriers to continued cultivation of Jatropha was the low or non-existing economic returns from the plantations. In most cases there was no or very low yield, and hence no incomes from harvests to cover the cost for the plantation. 6 percent (5 of 77 respondents) in Andhra Pradesh and 55 percent of the respondents (16 of 29 respondents) in Tamil Nadu harvested seeds from their plantations. The resulting amount of dry seeds from these 21 respondents who harvested ranged from 2.5 to 2470 kgs/ha/year, where only two of the respondents reached more than 370 kgs/ha/year, while the yield suggested by district initiators ranged from 2470 to 12355 kgs/ha/year [4]. Adding to the financial problems many farmers substituted Jatropha for other crops and experienced loss of income from these crops.

3.7. Jatropha plantation details

Jatropha was promoted as a plant that could be cultivated on wasteland, not suitable for cultivation of other crops, to avoid competition with food production. In Andhra Pradesh, 78 percent of the land used for Jatropha was regarded by the respondent as cropland, 17 percent was wasteland or barren land, four percent of the land was used for grazing, and one percent was considered forest land. In Tamil Nadu 93 percent of the land used for Jatropha was cropland, three percent wasteland/barren land, and three percent was used for grazing. In total, 82 percent of the interviewed farmers in the two states planted Jatropha on cropland, which was previously used to grow a variety of food crops that were removed for plantation of Jatropha. However, to consider land as cropland does not necessarily mean that the land is high-quality arable land since there are often discrepancies in what is regarded as cropland depending on who defines it.

In general the Jatropha plantations in both states were kept for a short period of time. Out of the farmers who have discontinued Jatropha cultivation no respondent have kept their plantation for more than 5 years, a majority discontinued within three years, and 33 percent already within one year. The results indicate that the respondents in Andhra Pradesh in general kept their plantations for a shorter period of time than the respondents in Tamil Nadu.

4. Discussion

The results from the field study have provided a picture of the performance of Jatropha cultivation and the experiences of the Jatropha farmers. However, the interviews did not always provide a clear picture of the reasons to problems experienced in the field, and further discussion is needed for understanding of these problems.

4.1. Insufficient yields

One of the main problems encountered during Jatropha cultivation is the failure to reach satisfying yields. To some extent the explanation can be that the expectations on Jatropha characteristics, such as drought resistance and ability to grow on degraded soils, have been too high and that cultivation under poor conditions has failed. But experiences in the studied districts show that even if inputs are applied and plantations are properly maintained the yields have not reached expected levels. The field study has failed to provide any explanation to this problem. When questioned about reasons for yields failing, neither farmers, researchers, nor government officials were able to provide clear answers. They have mentioned reasons such as unsuitability of soil and climate or poor maintenance. One theory, provided during an informal discussion with a representative of an institute involved in Jatropha research, is that cross-pollination by air has created hybrids of different Jatropha varieties that do not possess the agricultural characteristics of *Jatropha Curcas*. This would mean that what the farmers actually grow on their fields is not *Jatropha Curcas* but a variety that is not as resistant and high-yielding as the intended crop.

4.2. Plantation life time

When discussing failing yields, one important aspect to consider is the life time of the Jatropha plantations. Jatropha is not producing any economic yield the first three years, but most farmers have removed their plantations within three years after planting, hence before the time when economic yield could be expected. Furthermore, 33 percent of the farmers removed their Jatropha plantations within one year after planting. This may affect the total perception of yield failure, since the plantations could possibly have yielded if maintained for a longer time. However, most of these farmers cultivated Jatropha under poor conditions and

as plantations on similar lands in the area have failed, it is uncertain if this aspect has a significant effect overall.

One explanation for the early removal is that farmers could not afford to maintain plantations without any additional sources of income. Without maintenance, the plantations were in bad condition, which made it hard to expect that a good yield would ever be reached. Another explanation may be in the guidelines for implementation of the Jatropha programme. These guidelines provided the opportunity to implement plantations under already existing poverty alleviation programmes. As a consequence, a large part of the targeted actors were poor and marginal farmers. People living in poverty are constantly in acute need of cash to sustain their livelihood, and many farmers accepted to start Jatropha plantations just to get access to the financial subsidies and loans promised in the implementation programme. The farmers received seedlings to start their plantations, but in most cases other subsidies failed to reach the farmers. Without income, poor farmers could not afford to maintain their Jatropha plantations. With government subsidies or loans it could have been possible for farmers to keep their plantations until the time economic yields could be expected. A prerequisite for this is that the farmers are aware of details regarding yield expectations and the stages of the plantation development.

4.3. Effects of the planning and implementation of the Jatropha programme

Many of the problems seem to root in poor planning and implementation of the national Jatropha programme. It is common practice in the studied districts to make a technical assessment and present a scientific protocol before the release of new crops to ensure compatibility with prevailing conditions. In the case of Jatropha no trials were made, instead district level authorities trusted information from the national and state level, and provided this to the farmers. If studies under prevailing conditions had been made prior to implementation, the inability to meet the expectations on Jatropha´s agricultural characteristics could have been discovered and the government departments could have avoided promotion of an unsuccessful crop to the local farmers. Pre-studies could also have allowed for better-performing varieties to be developed. Better information on Jatropha and its characteristics would have enabled better extension services to the farmers, and the farmers need not have been insufficiently knowledgeable about maintenance and use.

Another problem rooting in poor implementation is lack of government support to Jatropha farmers. The National Mission on Biofuels stated that investments in the implementation of Jatropha production should be made by the government. This would be ensured by subsidies and loans to the farmers. From the interviews it is clear that the incentives promised during the implementation programme often did not reach the farmers. The majority of the farmers received free seedlings as promised. Only 39 percent of the private farmers (37 of 96 respondents) received some kind of support apart from free seedlings. Many farmers mentioned lack of government support or unfulfilled promises as barriers to continued cultivation of Jatropha.

4.4. Land use and competition with food production

One of the main reasons Jatropha was chosen for the biofuel programme was that it would not compete with food production. The Planning Commission identified land areas available and suitable for Jatropha plantation. The identified land areas were on land classified as wasteland, not suitable for cultivation of other crops, to avoid competition with food production. Still, 82 percent of the farmers (87 of 106 respondents) removed plantations of food crops for Jatropha, or planted it on land which is suitable for other crops. One reason for

this could be a gap in perception of what is considered wasteland; the government targeted farmers on land they classified as wasteland, while the farmers viewed it as cropland. The reason could also be that economic incentives, promises of higher incomes and pressure from the district authorities pushed farmers to substitute Jatropha for their food crops. The district authorities may have been influenced to implement Jatropha on cropland due to lack of information on the National Mission on Biofuels and pressure for fast implementation from national and state governments. In 2008, the Indian government announced a new biofuel policy that further emphasized some of the issues that were criticised in the National Mission on Biofuels, among these the competition with food production.

5. Conclusions

85 percent of the interviewed farmers have discontinued cultivation of Jatropha due to poor performance. Jatropha biodiesel production was advocated based on the idea that Jatropha could be cultivated on degraded or barren land, that demand for inputs was low, and that the crop was resistant to drought and pests. Experiences in the field show that Jatropha has failed to survive and/or grow on poor soils and that a majority of the farmers planted Jatropha on cropland. The plantations have not been able to tolerate drought as well as expected, and pest attacks have occurred in several cases. Farmers have experienced that the crop requires inputs for survival and growth and have used irrigation, fertilizers, manure, and pesticides. Even when planted on fertile land and provided inputs, Jatropha did not produce a sufficient yield. Problems experienced in the field can be related to the planning and implementation of the Jatropha programme where a major problem is that the implementation was not preceded by studies of cultivation under prevailing conditions. A major problem experienced by the farmers is that they have not received subsidies and other support that was promised during the implementation process.

The Jatropha programme was expected to have positive socio-economic and environmental impacts. However, 82 percent of the farmers planted Jatropha on cropland, which entailed competition with food production. Instead of gaining additional income from Jatropha plantations, farmers experienced financial losses and reduced income. Further, as only small amounts of Jatropha biodiesel was produced, the positive impacts on environment and energy security was not realized.

In Southern India there is still on-going research on Jatropha and hope for Jatropha biodiesel production, but more scientific knowledge on Jatropha characteristics is needed, and development of high-yielding and resistant varieties is required, for Jatropha to become a successful biodiesel crop.

References

[1] W. M. J. Achten, L.Verchot, E. Franken, Y. J. Mathijs, V. P Singh, R. Aerts, B. Muys, Jatropha bio-diesel production and use, Biomass and Bioenergy 32, 2008, pp. 1063-1084

[2] P. K. Biswas, S. Pohit, R. Kumar, Biodiesel from jatropha: Can India meet the 20% blending target? Energy Policy, article in press.

[3] Ministry of New & Renewable Energy, Government of India, National Policy on Biofuels, 2008 (http://www.svlele.com/nbp.pdf)

[4] DWMA – District Water Management Agency (2005) *Annual Action Plans 2005-06.* http://www.rd.ap.gov.in/CRDAction%20plans/actionplans/Kadapa.htm (2010.05.21)

PURE - Public Understanding of Renewable Energy

Lars Broman[1,*], Tara C. Kandpal[1,2]

[1]*Strömstad Academy, SE-45280 Strömstad, Sweden*
[2]*Centre for Energy Studies, Indian Institute of Technology IIT-Delhi, Delhi 11001, India*
** Corresponding author. Tel: +46 708 810 178, E-mail: lars.broman@stromstadakademi.se*

Abstract: Public understanding of science PUS is a central concept among science communicators. Public understanding of renewable energy PURE is proposed as an important sub-concept of PUS. The aim of our paper is to interest and invite renewable energy scientists to join a PURE research project. Four separate important questions for a PURE research project can be identified: (A) Is PURE important? (B) Which issues of PURE are the most important ones, according to renewable energy scientists? (C) What understanding of renewable energy has the general public today, worldwide? (D) How to achieve PURE?

Keywords: *Public understanding of science, PURE, Renewable energy, science communication, science centre.*

1. Introduction and Definitions

Public Understanding of Science is today an established concept. There is even since 1992 a scientific journal with this name. The concept is usually referred to as *PUS*. Bauer [1] has given a 3-fold definition of PUS: (1) "Debunking of superstitions, half-knowledge, complete and utter ignorance, misunderstanding and mumbo-jumbo, and virulent memes that give rise to anti-science." (2) PUS is to "improve science literacy, to mobilize favourable attitudes in support of science and new technology, to increase interest in science among young people and other segments of society, and to intensify public's engagement with science in general and for the greater good of society." (3) "PUS considers common sense as an asset" and PUS research should "chart out the public controversies arising from new developments and in different regions of the world" exemplified by "the impact of the climate of opinion on knowledge production."

During the planning of Sweden's first science centre The Futures' Museum, one of the authors (Broman) gave seven reasons for creating a science centre [2], slightly revised [3]: (1) Give an insight that science is understandable. (2) Awaken curiosity. (3) Give people the courage to experiment. (4) Facilitate public understanding of science. (5) Provide preparedness to withstand superstition and pseudoscience. (6)Amuse and entertain. (7) Provide aesthetic experiences. The reasons have been described in some detail in English elsewhere [4]. Reason (4) is in line with Bauer's definitions (2) and (3), and reason (5) coincides with Bauer's definition (1).

Underlying the statements is the notion that PUS is important, which scientists happily believe, and we of course agree, but it is not as simple as that. There are e.g. so many different sciences (which in turn are divided into many disciplines). A rather popular notion is that "science" is that same as "natural sciences", but that is not the case. Again citing Bauer, science also "includes engineering and medicine, the social sciences and humanities, old and new disciplines with clear boundaries, but also ... fuzzy transdisciplinary techno-sciences." But maybe all different disciplines are not equally important that the public understands?

It is also vital to identify target groups, since some may be more important than other. Loosely defined target groups frequently mentioned are young people (in the world of science centres often restricted to the "7-eleven group" of elementary school children), voting adults,

and decision makers. Other interesting groups may include teenagers, refugees, religious fundamentalists, senior citizens, people living in villages as well as cities, just to name a few.

It is also important to identify groups of science communicators. As an example, The European Science Communication Network ESCOnet, 2005-8 developed and conducted a series of workshops on science communication training aimed at young post-doc researchers [5].

Since renewable energy is our main interest, the authors have decided to investigate a sub-set of PUS, namely public understanding of renewable energy PURE. The remainder of this article attempts to give a starting point of a potential research project on PURE. The main questions are "is PURE important?" and, if the answer is *yes*, "how could PURE be achieved, and which means of achieving PURE are potentially useful?"

2. On the Importance of Public Understanding of Renewable Energy

There are several reasons why public understanding of renewable energy might be important. Four of them are these:

(1) The earth is a lonely planet in a vast space, not as crowded as the impression one gets from science fiction movies. For humans to move from a destroyed earth to another hospitable planet is just impossible.

(2) The earth is a planet alive with a dead sister and a dead brother. Venus is too hot for life due (also) to too much greenhouse gas, while Mars is too cold due (also) to too little greenhouse gas.

(3) Anthropogenic influence on the world's climate, in particular climate warming due to release of greenhouse gasses like carbon dioxide CO_2 and methane CH_4 is generally agreed upon among [6].

(4) One major source of greenhouse gases is combustion of fossil fuels, which has to be replaced by increased energy efficiency and large-scale worldwide dissemination of appropriate technologies for harnessing renewable sources of energy.

A reasonable conclusion is that public understanding of renewable energy is important. An important task of a research project on PURE would be to identify pros and cons in this respect. There are also several attendant questions: What do professionals - researchers, planetarians, teachers - say? How interested is the public - and different target groups - in renewable energy, and what do they already know? Which disciplines in renewable energy science are more important than others? A very crucial role exists of common people in the success of this objective of large scale harnessing of renewable sources of energy, since as adoption as well as design, developing, manufacturing etc, would require their participation.

3. How Could Public Understanding of Renewable Energy be Achieved, and which Means are Potentially Useful?

There are of course several different channels that can be and are used in conveying attitudes towards and knowledge of renewable energy subjects: Newspapers, TV programs, books, interactive exhibits in science centres, lessons in the school. Different media certainly attract different target groups. One of the tasks for the project to find out is of course how science

centres with interactive exhibits can be used for the envisaged purpose i.e. PURE. It is even not possible to judge all centres the same - it is of course a great difference between large science centres (like Nehru Science Centre in Bombay, Cité de Science and Technologie in Paris or Exploratorium in San Francisco) and small ones (like Ekohuset in Strömstad and Molekylverkstan in Stenungsund; both Sweden).

As has been shown by several authors, among them Franck Pettersen in a master thesis [7], is that a combination of watching a planetarium show and doing experiments related to the show is very useful. (Planetariums used to be devoted basically to astronomy using a classical opto-mechanical star projector. Increasingly, planetariums today concentrate on edutainment shows with astronomic content, using all-dome video technique. Shows related to climate change and its solutions would be easily produced using modern planetarium projectors and would fit nicely under the planetarium dome.) Here are two other voices on interactivity:

Michael Spock, former Director of *Boston Children's Museum,* borrowed the Chinese philosopher Confucius' proverb as a motto for the museum: I hear and I forget, I see and I remember, I do and I understand (cited in [8]).

William Glasser wrote [9]: We learn 10% of what we read, 20% of what we hear, 30% of what we see, 50% of what we both see and hear, 70% of what is discussed with others, 80% of what we experience, and 95% of what we teach.

An important component of achieving PURE is likely to be interactivity and hands-on experience, and useful environments for this are science centres. Some examples of this are shown elsewhere [10] in photographs from the Teknoland outdoor science centre 2000-2001: Yourself a Sundial, Toddlers' Teknoland, Solar Energy Surfaces, The Greenhouse, and The Solar Heated Chess Board.

3.1. Popular Education of Renewable Energy through IASEE and ISREE

International Association of Solar Energy Education IASEE started in December 1989. In September 1990, IASEE became the International Solar Energy Society ISES Working Group on education (see e.g. [11]). Also since 1991, IASEE has arranged a series of symposiums, International Symposium on Renewable Energy Education ISREE, held every or every second year, sometimes as part of the biennial ISES Solar World Congress. At each symposium, between 10 and 30 papers were presented. Most papers have dealt with education in schools and at university level, and certainly school children and university students are important target groups, but here we will concentrate ourselves on the general public.

One of the 1991 ISREE papers presented was *On the Need for Solar Energy Education* [12]. In this paper, elementary and secondary school education, vocational training, university courses, educating decision makers, and educating the general public are treated. An excerpt from the paper reads (slightly edited):

> EDUCATING THE GENERAL PUBLIC
>
> Ordinary people are the ultimate utilizers of energy from the sun and accordingly need basic knowledge in how to make use of this new technology and be motivated to use it. A number of ways to educate large populations are readily available. Some proven examples:

Mass media. This includes newspapers, weekly magazines, radio, and TV. You address professional journalists, and if you manage to teach them some basic facts, they will frequently make o good job in popularizing what they have learned.

Exhibitions. We have built both Science Centre exhibitions (1986 and 1990 on solar measurements for the Futures' Museum in Borlänge, Sweden) and travelling exhibitions (Alternative Energy 1976, Solar Energy Exhibition 1989 [13]). The educational value of an exhibition is greatly improved if it provides hands-on experiences.

Another kind of exhibition is the trade fair with commercial and institutional exhibitors. Such fairs can range in size from the one hundred m^2 or so of exhibits that accompany SERC's Solar Energy Days to the multi-acre exhibition of the UN Conference on New and Renewable Energy Sources of Energy in Nairobi 1981. Such fairs contain up-to-date technological information for many categories of visitors and should be made available both to professionals and to the general public.

Lectures, etc. General admission popular lectures sometimes attract good-size crowds, especially if arranged as debates or panel discussions, or if a well-known speaker is featured. Lectures can also be video-taped, and can, with appropriate solar powered equipment, be shown just about anywhere (see [14]).

Community college courses. These are excellent in giving interested individuals more-than-basic knowledge. The aim of such courses can even be that every participant builds his own solar collector (see [15]).

Another paper at ISREE'91 dealt with renewable energy education and training in an Egyptian village with a programme consisting of public presentations, group discussions, simple solar kits, children competitions, technical training workshops, exhibits with working models, working systems, video-training systems, and a communal library [14].

A regional training workshop was held in Libya in December 1990 with the objective of familiarizing women in developing countries with renewable energy development and technology; the workshop was presented at ISREE'92 [16].

A community college type of educating people that is popular in Sweden is called study circles. A typical study circle consists of a circle leader - the teacher - and 5-10 participants. Especially during the 1990ies, knowledge about solar heating was spread in many locations in Sweden in this form, where each study group built a solar heating system at one of the participants' house, using a popular build-yourself solar collector kit; this was presented at ISREE'93 [15]. A thorough investigation of this kind of education is a case study done by Henning [17].

The importance of public understanding of renewable energy was dealt with at ISREE'02 [18]. In this paper, a result from SAS [19] was cited:

> The study *Science and Scientists* (SAS) asked ten thousand (10 000) 13-year old pupils in 21 countries:
>
> *"What do you want to learn about?"*

"New sources of energy - sun, wind"
was among the 25% least popular answers, and it was much less popular among girls than among boys.
* Why is it so?
* Should we do something about it?
* If so, how?

* Why is it so?
Pupils - and adults - are interested in scientific and technological subjects for a number of reasons:
* Economical reasons
* Usefulness
* Interesting, fun
* Relevant

Renewable energy obviously does not meet these requirements! At ISREE'02, the rhetorical question *Should we do something about it*" was answered with a *Yes*! followed by *If so, how?* and a try to answer [18]:
* Visibility of renewable energy is important
* The school is important
* Media are important
* Exhibitions, Science Centres and Science Parks could be used to meet people of all ages.

Experiences from using science centre exhibits in educating the general public on renewable energy were presented at ISREE'03 [10].

3.2. Renewable Energy Dissemination at Village Level

A large proportion of the Earth's population is rural, and their quality of life could be improved at the same time as their impact affection on climate is decreased by introduction of renewable energy utilization at village level: "Low carbon technology for low-purchasing power people." This includes a multitude of technologies and education of users is therefore critically important. A good example is dissemination of family size biogas plants in India - to date 4 million units and the aim to increase the number of plants to 12 million.

Another example: Electricity for light has quickly become affordable by the development of low-cost white high-intensity low-energy light emitting diodes (LED). Mobile phones are spreading rapidly also among rural people in developing countries, and these are effectively charged using the same small not-so-expensive photovoltaic (PV) modules used for powering LED lamps.

When educating rural people, it should be understood that many people live below the poverty line and that illiteracy is common. It is not always easy as the following example may illustrate [20]. Egyptian authorities wanted in the early 1980ies to implement solar collectors for water heating in a rural area. The farmers however refused to use them for from their point of view good reasons. In an earlier campaign in the same area, authorities had tried to introduce family planning, and the local people suspected that this new technology was just another attempt to decrease their fertility.

4. A PURE Research Project Proposal

As obvious from the preceding chapters, we have for several years been interested in public understanding of renewable energy. We believe however that presently this concept is more important than ever. An interdisciplinary and international science communication project on public understanding of renewable energy is proposed with the hub at Strömstad Academy (www.stromstadakademi.se) in Sweden. It should include both research on the importance of PURE and on the impact of different methods to achieve PURE including determining which methods are best adapted for different target groups.

This means that different target groups have to be approached from renewable energy specialists and energy policy makers to school teachers [21], engineering students [22] and different kinds of end-users. A variety of methods, such as questionnaire studies, interviews and focus groups, should be considered.

We have made a start by supervising Science Communication master students and teacher students at Dalarna University during the last decade. Some of them have written their theses on the impact of experimenting with renewable energy at science centres on school pupils in ages 6 to 18. One example is the thesis of Harahsheh [23], indicating a measurable impact on 15-yr. old pupils on their attitude towards renewable energy.

There is however much more that need to be done. A possible start could be a questionnaire distributed world-wide to a well-defined target group (such as visitors to science centres) aiming at finding out the present level of public understanding renewable energy. We would also like to know how renewable energy scientist grade different topics in PURE.

Please contact us if you would like to participate in the PURE project. The corresponding author's email address is found at the top of the article.

References

[1] M.W. Bauer, Editorial, Public Understanding of Science 18, 2009, pp.378-382.

[2] L. Broman, Populärvetenskapliga centra växer fram i Sverige (Science Centres are Growing Up in Sweden), Svenska Museer 1/1984, pp. 7-12. (In Swedish.)

[3] L. Broman, Kommunicera vetenskap och extramuralt lärande (Communicating Science and Extramural Learning), in E. K. Henriksen and M. Ødegaard, editors, Naturfagenes didaktikk - en disiplin i forandring?, Norwegian Academic Press, pp. 503-513 (in Swedish).

[4] L. Broman, Multiple Interests - a Hypothesis with Possible Implications for Science Centers, in C. Michelsen, editor. NNORSC-2005 Proceedings Report from Odense University, Denmark, 6 pp.

[5] S. Miller, D. Fahy, and The ESConet Team, Can Science Communication Workshops Train Scientists for Reflexive Public Engagement? Science Communication 31, 2009, pp.116-126.

[6] IPCC Intergovernmental Panel on Climate Change IPCC Climate Change 2007: Fourth Assessment Report. www.ipcc.ch.

[7] F. Pettersen, Master thesis on informal learning at University of Oslo (unpublished). Results were presented at the 12th Nordic Planetarium Association Conference, Oslo 6-8 October 1995.

[8] A. Ott, Forum för lärande (Forum for learning), compendium from Göteborg University 2001 (in Swedish, unpublished).

[9] W. Glasser, The Quality School, Harper & Row, 1990.

[10] L. Broman, Solar Energy Studies and Extramural Learning. Proc. ISES Solar World Congress, https://shop.ises.org/bookshop/pages/displayBook.xsp?id=16.

[11] K. Blum, L. Broman, and S. Niwong, This is IASEE, ISES' Working Group on Education, Progress in Solar Energy Education 3, 1994, pp. 1-2.

[12] L. Broman and A. Ott, On the Need for Solar Energy Education, Progress in Solar Energy Education 1, 1992, pp. 23-25.

[13] L. Broman and K Gustafsson, An Educational Travelling Exhibition on Solar Energy, Proc. ISES Solar World Congress, Denver, USA, 1991, pp 3849-3852.

[14] S. Arafa, Renewable Energy Education and Training at the Village Level, Progress in Solar Energy Education 1, 1992, pp. 1-4.

[15] K. Börjesson, K. Gustafsson, and K. Lorenz, The Spreading of Solar Energy Now-How Through Educating Homebuilders, Progress in Solar Energy Education 3, 1994, pp. 19-20.L. Broman and A. Ott, On the Need for Solar Energy Education, Progress in Solar Energy Education 1, 1992, pp. 23-25.

[16] M.F. Bara, and M. A. Muntasser, Renewable Energy Education and Training for Women in Developing Countries, Progress in Solar Energy Education 2, 1993, pp. 1-2.

[17] A. Henning, Ambiguous Artefacts. Solar Collectors in Swedish Contexts. On processes of Cultural Modification, pp 177-232. Stockholm Studies in Social Anthropology 44, Almqvist & Wiksell International. ISBN 9172650346, 2000.

[18] L. Broman, On the Importance of Public Education and Public Understanding of Renewable Energy. Luncheon presentation at the 8th International Symposium on Renewable Energy Education, Orlando, Florida, 2002.

[19] S. Sjøberg, Naturvetenskap som allmänbildning (Science as General Knowledge). Studentlitteratur. ISBN 9144009992, 2000.

[20] I. Sakr, Private communication at 1st International Conference on Solar Energy Optics in Kromeric, Czechoslovakia, 1984.

[21] T.C. Kandpal and S.S. Mathur, Solar Energy Experiments for School Level Students. Proc. Indian National Solar EnergyConvention. Allied Publishers Ltd., New Delhi, 1982.

[22] H.P. Garg and T.C. Kandpal, Renewable Energy Engineering Education. Omega Scientific Publishers, New Delhi, 1996.

[23] S.S. Harahsheh, (Lars Broman, supervisor), How the Energy-Hunting Project Affected the Intention of Eight Grade Pupils towards their Future Education and Career in Natural Science and Technology in Compulsory Schools of Borlänge, Sweden. Thesis HDa-SciCom-38, 2007.

Potential Renewable Bioenergy Production from Canadian Agriculture

Tingting Liu[1,2], Brian McConkey[1,*], Stephen Smith[3], Bob MacGregor[3], Ted Huffman[3], Suren Kulshreshtha[4], Hong Wang[1]

[1] *Agriculture and Agri-Food Canada, Swift Current, Canada*
[2] *Renmin University of China, Beijing, China*
[3] *Agriculture and Agri-Food Canada, Ottawa, Canada*
[4] *University of Saskatchewan, Saskatoon, Canada*
** Corresponding author. Tel: +1 3067787281, Fax: +1 3067783188, E-mail: brian.mcconkey@agr.gc.ca*

Abstract: Agriculture has the potential to supply large amounts of biomass for renewable energy production from residues from traditional crop production and from dedicated energy crops. This renewable energy production has significant potential to contribute to the reduction of GHG emissions in the energy sector by using ethanol and biodiesel to displace petroleum based liquid fuels and direct burning of biomass to displace coal for generating electricity. To quantify this biomass potential, we used the Canadian Economic and Emissions Model for Agriculture to estimate renewable energy production from biomass and the impact on agricultural production. We used two scenarios: the first scenario that looks at a combination of market incentives and mandates, and a second scenario that looks at only market incentives. The results show that: in the markets and mandates scenario, biomass production is higher, both ethanol and electricity are required to take place and land use change occurs. Agriculture has significant potential to generate biomass for energy under different scenarios, the incentive mix can have a large impact on the type of bioenergy produced, there is significant potential for GHG emission reductions and there is potential for unintended GHG effects, such as the increased clearing of land for crop production.

Keywords: *Bioenergy, Policy, Agriculture, Greenhouse gas emissions, Land use change*

1. Introduction

For several years, countries have been expanding their production of renewable energy from biomass [1-3]. To date in Canada, most renewable energy has come from grains and oilseeds to supply first generation biofuels. In Canada and elsewhere, significant research is underway on the uses of cellulosic biomass, such as residues and dedicated energy crops to expand the biomass supply available for renewable energy production [4-6].

Climate change is an important issue to governments around the world [7-8]. The effort to reduce net emissions of GHG in Canada could have major implications for Canadian agriculture. Renewable energy production has the potential to contribute to GHG emission reductions by displacing GHG intensive sources of energy. Based on previous analysis [9], the largest potential for agriculture to contribute to reduced GHG emissions is to provide bioenergy feedstocks that would substitute for fossil fuels. However, the use of biomass for renewable energy can have unintended consequences, such as land use change, which could increase GHG emissions from agriculture. Further, the use of biomass for renewal energy has implications for food availability.

Increasing renewable energy production from biomass can be accomplished by mandates that require their use or market incentives, such as a carbon price that rewards emission reductions and is technology neutral. There has been extensive work done at Agriculture and Agri-food Canada (AAFC) on the implications of using biomass for renewable energy. This paper will present results from two illustrative forward looking scenarios that will allow us to examine the impacts of using a combination of market incentives and mandates on biomass production

and renewable energy production compared to using only a market based incentive. It will conclude with a discussion of results and highlight areas for future areas of research.

2. Methodology

We used two scenarios that represent possible outcomes for market and policy conditions that could be present in 2017. We then used the Canadian Economic and Emission Model for Agriculture (CEEMA) to estimate how different policy scenarios will affect resource utilization, GHG emissions and bioenergy production.

2.1. Canadian Economic and Emissions Model for Agriculture (CEEMA)

CEEMA is composed of two models – the Canadian Regional Agriculture Model (CRAM) which assesses the regional resource use implications and the Greenhouse Gas Emissions Module (GHGEM) which assesses the GHG emissions associated with these resource changes (Figure 1). The CRAM component of CEEMA was also enhanced to have a limited ability to clear land based on land availability estimates from a mapping and remote sensing overlay exercise.

2.1.1. The Canadian Regional Agricultural Model (CRAM)

CRAM is the main analytical tool used to assess the economic impacts and resource utilization patterns resulting from the scenarios examined. CRAM is a static partial equilibrium model of the Canadian agriculture sector. While CRAM does not give information on the growth of the sector over time, it can provide a very detailed before (baseline) and after (scenario) snapshot of the agriculture sector. CRAM incorporates all of the primary production for both crops and livestock, and also includes some processing activities, such as oilseed crushing, production of biofuels form grains and oilseeds, dairy and livestock slaughter. CRAM is spatially disaggregated across 55 regions in Canada.

For the purpose of this analysis, CRAM used AAFC's 2008 Medium Term Outlook to generate a baseline for the agriculture sector in 2017. This 2017 baseline already includes expectations about the state of the domestic and international biofuels market and assumes that Canada has met its existing target that ethanol replace 5% of gasoline and biodiesel replace 2% of diesel fuel and heating oils [10].

2.1.2. The Greenhouse Gas Emissions Module (GHGEM)

The GHGEM is a spreadsheet based accounting model that translates changes in resource utilization, as determined by CRAM, to GHG emission estimates. It contains modules to estimate direct and indirect GHG emissions from production of crops and livestock. The three greenhouse gases that the model provides estimates for are carbon dioxide (CO_2), methane (CH_4) and nitrous oxide (N_2O) [11]. The emissions can be broadly grouped into the following categories: emissions from farm level activities, emissions that are indirectly related to the farm level activities, emissions from induced economic activities, and emissions from other agro-ecosystem related land use [12].

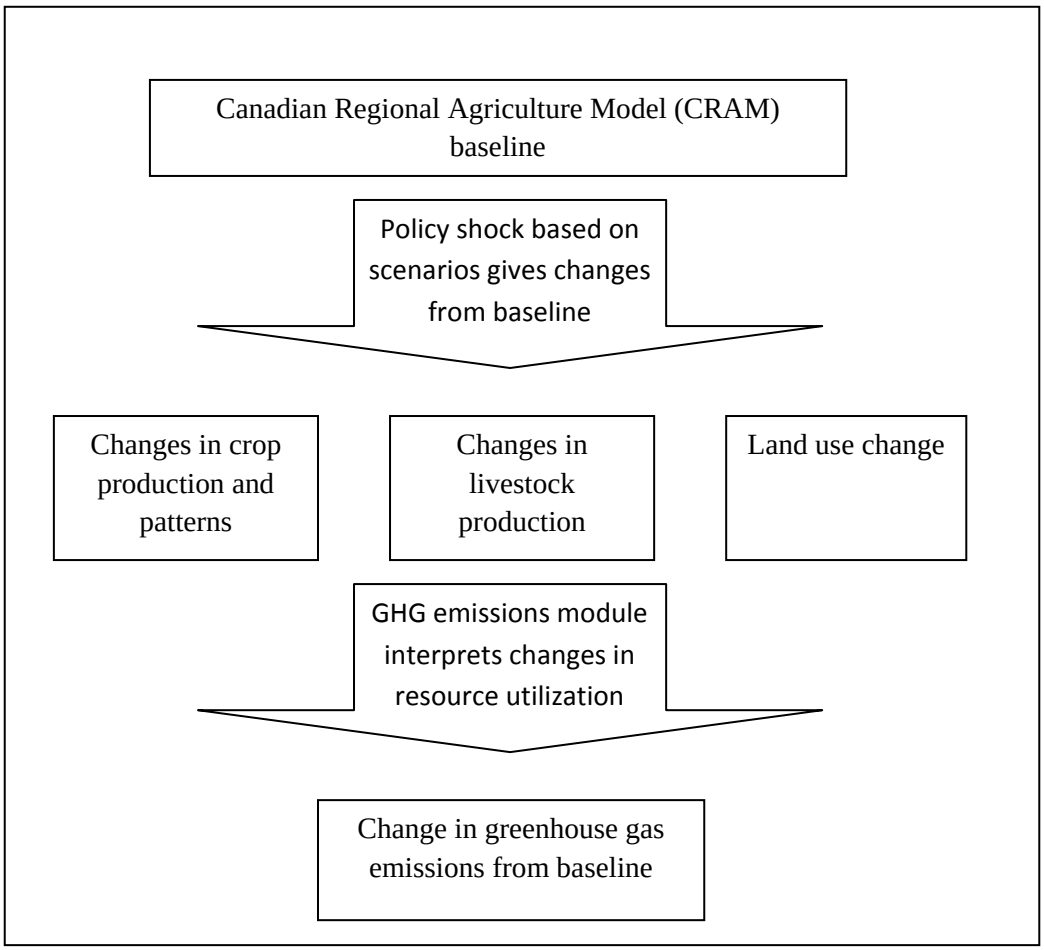

Figure 1. Structure of CEEMA

2.1.3. Land availability estimation

We also enhanced CRAM to have ability to clear land for new agricultural production based on land availability estimates. We estimated the area of non-agricultural land on soils with agricultural potential by examining the intersection of soil capability maps and land cover maps. Soil capability for agriculture maps for most of the southern parts of Canada were created through interpretation of detailed soil maps and aerial photographs under the Canada Land Inventory program (Department of Regional Economic Expansion, 1969) and are available in digital format (Natural Resources Canada, 2008). These maps were intersected with land cover maps derived through classification of 30-metre Landsat satellite imagery by Agriculture and Agri-Food Canada (2008). This data was then used to populate CRAM with information on which regions had land that could be cleared of forest or shrub cover for crop production [13].

2.2. Scenarios

Two scenarios were used. Each scenario is drawn from a family of scenarios that were used for previous analysis. Each scenario allows for the use of corn stover, cereal straw, hybrid poplar and perennial grass for renewable energy production. These scenarios were intended to be illustrative as opposed to prescriptive, given the uncertainty related to what will be the actual policy and market environment in 2017 [14].

2.2.1. Scenario I: "Markets and mandates" scenario

The "Markets and Mandates" scenario is drawn from a family of scenarios that were originally developed to examine the effects of various future renewable energy targets and market conditions on the Canadian agriculture sector. The scenarios consisted of a combination of market drivers and mandates that impact the production of renewable energy. The main renewable energy options in the scenarios are liquid fuels for transport and electricity for the displacement of coal power. Although we considered a range of oil prices, carbon prices, and mandated renewable energy targets, for this paper we are drawing on the scenario with the following characteristics:

Table 1.Policies assumptions in "Markets and mandates" scenario

Market incentives		Mandates		
Oil price ($/bbl)	Carbon price ($/Mg CO_2 eq.)	Ethanol (% of gasoline)	Biodiesel (% of petroleum diesel)	Electricity (% of coal based energy substituted)
120	50	20	8	20

This scenario contains the highest oil price, carbon price, and mandated renewable fuel use. We also required that 50% of ethanol must come from cellulosic biomass.

2.2.2. Scenario II: "Markets only" scenario

The markets only scenario is drawn from a family of scenarios that were developed to look at the impact of a technology neutral carbon price to provide an incentive for renewable energy production. The scenarios looked at the impact of a $10, $30 and $50 CO2e price on the agriculture sector. This scenario did not assume a specific oil price but it is built into the scenario that implementing a carbon price will put some upward pressure on the overall price of energy from fossil fuels. This results in an oil price of roughly $80/bbl. For the purpose of this paper, we will be drawing on only the results from the $50 carbon price scenario.

3. Results

3.1. Biomass production

Biomass production is higher in the markets and mandates scenario. The mandates require that a minimum amount of renewable energy be produced that, in turn, requires the production of large amounts of biomass for various source (Figure 2). Total biomass production in the markets and mandates scenario is 37.3 MT compared with 20.6MT in the markets only scenario.

In both cases the biomass supply is dominated by residues, and the distribution of biomass production among the various types of biomass is relatively similar.

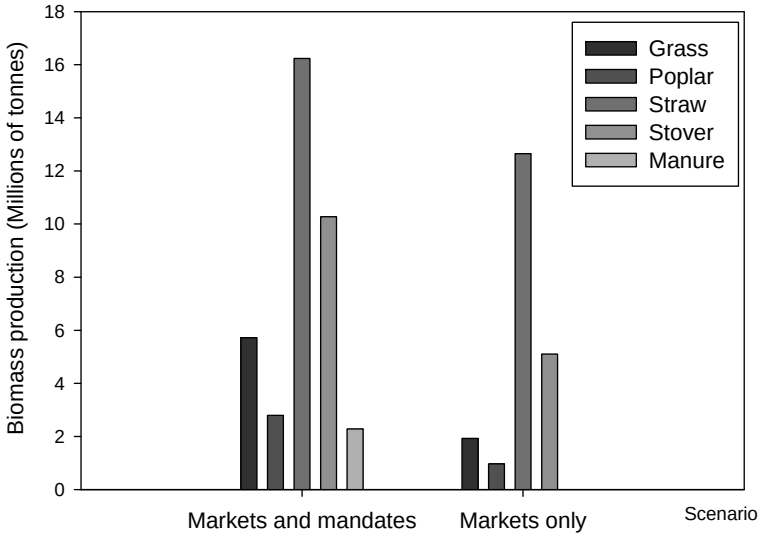

Figure 2. National biomass production by scenarios

3.2. Bioenergy production

In the markets and mandates scenario the production of both ethanol and electricity are required to take place. Production of electricity only takes place due to the mandates, as the higher oil price for ethanol out-competed the effect of the carbon price on electricity production for biomass. In the markets only scenario where the only driver is the carbon price, nearly all of the biomass produced is used to offset coal based electricity as there is far greater emission reduction potential associated with reducing use of coal compared to gasoline.

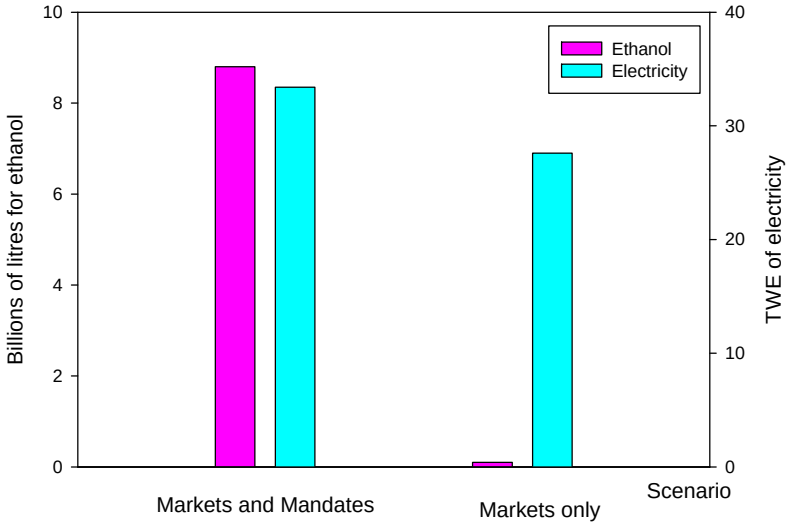

Figure 3. Renewable energy production by scenarios

3.3. Land use change

Land use change occurs only in the markets and mandates scenario. Because this scenario places very high pressure on the agricultural land base to supply biomass, additional land

comes into production. Overall 319 kHa would be cleared in 2017 for agricultural production, representing a 1% increase in land available for cropping. There is no land use change observed in the markets only scenario.

3.4. Greenhouse gas emissions

Emissions reductions in the energy sector are much greater than the emissions savings in the agriculture sector (Figure 4). Almost all the emissions reductions in the energy sector are accomplished from the use of biomass to offset coal. Very little emissions reductions are associated with ethanol use.

It should be noted that because of the land use change in the markets and mandates scenario overall emissions can significantly increase. Emissions from land use change could reach 181 MT CO_2e (lower if biomass removed during clearing is used), overriding any initial positive benefit associated with bioenergy production. Over time continued emission reductions from bioenergy production can potentially offset the initial release of carbon, but this will only take place after several years and these future emission reductions are not reflected in the results presented above.

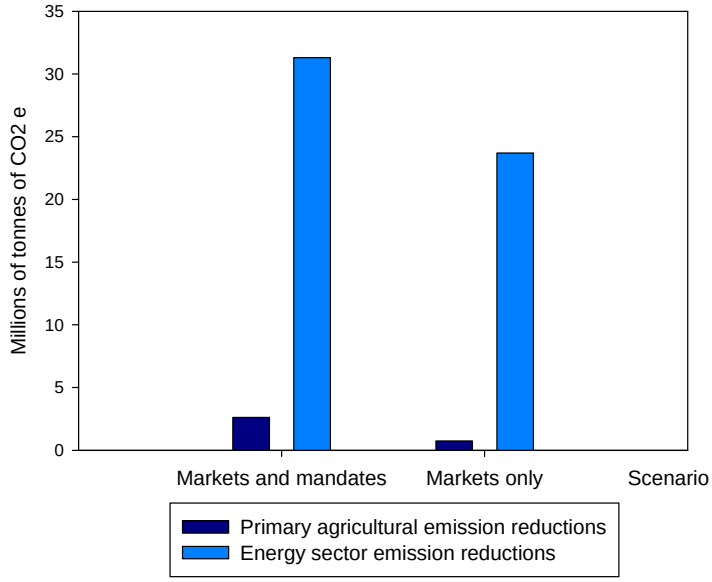

Figure 4. Emission reductions related to bioenergy production

4. Discussion and conclusions

4.1. Biomass production and impact on agricultural commodity production

In both scenarios, the majority of the biomass production comes from the use of residues. Residues generally outperform dedicated energy crops due to the fact that they are a by-product of crop production only require harvesting, nutrient replacement, and transportation costs. As residues come from existing land already under the production of traditional crops they do not have to compete for land the way dedicated energy crops do, and since residues already come from existing land, their use requires less land be used exclusively used for renewable energy production. To meet Canada's current bioenergy target of 5% ethanol and 2% biodiesel that is expected to come from grains and oilseeds, 5% of cropland would be required to provide the necessary feedstock. In the markets and mandates scenario with 20% ethanol, 8% biodiesel and 20% coal displacement this would increase to 16% of cropland

used exclusively for bioenergy, not including the impact of increased corn imports from the US. In the markets only scenario, because electricity accounted for almost all the bioenergy produced there was no increase in the use of grains for first generation biofuels. There was some expansion in the production of dedicated energy crops but this amounted to only 7% of cropland as most feedstock came from residues and did not impact traditionally commodity production. Through the diversion of land from traditional commodity production can place additional pressure on the overall system's ability to supply agricultural commodities; the shifts in Canadian production are not expected to impact world commodity prices.

4.2. Renewable energy production

While the distribution of biomass production in the two scenarios is relatively close, the production of renewable energy is not. When incorporating the effects of mandates and a higher oil price, there is a much stronger tendency to produce ethanol from biomass. When looking at the impact of only a carbon price and no mandates, the results show that biomass production is used mainly to displace coal electricity. Mandates require specific renewable energy outputs to be met while the use of market based instruments allows the market to allocate resources.

4.3. GHG reductions

In our modeling framework, GHG-reducing activities will benefit from the carbon market. For example, producing liquid biofuels from grains and biomass, as well as electricity from biomass are assumed to generate GHG reductions that add value to the production activity relative to the strength of their emission reductions. In this analysis using one unit of biomass for coal electricity displacement generated roughly 10 times the benefit of using that same unit for ethanol to displace gasoline. The impact on soil organic carbon with the production of additional perennial crops was also incorporated but it had a relatively small impact compared to the downstream benefits from renewable energy production.

Canada has about 10 million ha of land that has potential for agriculture that is currently and predominantly under shrubs or forest. If the scope of GHG considered in the policy does not include emissions from this clearing this land and land use change occurs, then the emission from that clearing could result in a large initial increase in emissions and it would time for emission reductions from bioenergy to drive the system to being a net contributor to GHG reductions.

4.4. Other considerations and future areas of research

There are other items that are not addressed in this paper such as the longer term impact of residue removal on soil erosion and the broader interaction with the forestry sector. These are important items for future research that will need to be carefully considered related to the large scale production of biomass from residues and dedicated energy crops.

References

[1] E.S. Lora, R.V. Amdrade, Biomass as energy source in Brazil, Renewable and Sustainable Energy reviews (13), 2009, pp.777-788.

[2] J.Goldemberg. Ethanol for a sustainable energy future, Science (315), 2007, pp.808-810.

[3] M.F. Demirbas, M. Balat, H. Balat, Potential contribution of biomass to the sustainable energy development, Energy Conversion and Management (50), 2009, pp.1746-1760.

[4] L.R. Lynd, Overview and evaluation of fuel ethanol from cellulosic biomass: technology, economics, the environment, Annual Review of Energy and Environment, 1996(21), pp.403-465.

[5] Y. Lin, S. Tanaka, Ethanol fermentation from biomass resources: current and prospects, Applied Microbiology and biotechnology (69), 2005, pp.627-642.

[6] R.H. Sims, A. Hastings, B. Schlamadinger et al., Energy crop: current sataus and future prospects, Global Change Biology (12), 2006, pp.2054-2076.

[7] N.H. Stern, The economics of climate change: the Stern review, Cambridge University Press, 2007, pp. 118-315.

[8] IPCC, Climate Change 2007: Synthesis Report, Contribution of Working Groups I, II and III to the Fourth Assessment Report of the Intergovernmental Panel on Climate Change Core Writing Team, Pachauri, R.K. and Reisinger, A. (Eds.) IPCC, Geneva, Switzerland. pp.1-104.

[9] R. Gill, G. Achuo, GHG Abatement Cost Curves for the Agriculture Sector: Potential to Reduce Emissions

[10] S. Smith, B. MacGregor, GHG mitigation potential for the agriculture sector, Agriculture and Agri-Food Canada, 2010.

[11] S.N. Kulshreshtha, B. Junkins, R. Desjardins, Prioritizing greenhouse gas emission mitigation measures for agriculture, Agricultural Systems(66), 2000, pp.145-166.

[12] S. Kulshreshtha, C. Nagy, E. Knopf, Greenhouse and Energy Use Implications under Seleted Biofuel Scenarios, University of Saskatchewan, 2009.

[13] S. Smith, B. MacGregor, Quantifying biomass availability and land use change in the agriculture sector from renewable energy production: Implications for Sustainable Resource Use, Agriculture and Agri-Food Canada, 2009.

[14] B. McConkey, S. Kulshreshtha, S. Smith, et al., Maximizing Environmental Benefits of the Bioeconomy using Agricultural Feedstock, Report to the PERD-CBIN Bio-energy project, Agriculture and Agri-Food Canada, 2008, pp.21-96.

Drivers and barriers to rural electrification in Tanzania and Mozambique – grid extension, off-grid and renewable energy sources

Helene Ahlborg[1*], Linus Hammar[2]

[1,2]*Environmental Systems Analysis, Chalmers University of Technology, Göteborg, Sweden*
**Corresponding author. Tel: +46 31 7728601, E-mail: helene.ahlborg@chalmers.se*

Abstract: Mozambique and Tanzania are countries with very low rural electrification rates – far below 5 % percent of the rural population use electricity. The pace of rural grid electrification is slow and for most remote areas access to the national electricity grids will not occur within a foreseeable future. Off-grid (decentralized) electricity grids are seen as a complement and fore-runner to the national grid, making electricity available many years in advance and creating demand and a customer base. Most off-grid systems are supplied by diesel generators which entail unreliable and costly electricity. Alternative off-grid energy sources exist in the region, such as biofuels, wind, micro-hydro and solar PV; but there are significant barriers to adoption, adaptation and diffusion of such RE-based technologies. In this study, the specific drivers and barriers for rural electrification and off-grid solutions in both countries are explored across a stakeholder spectrum. It is part of a larger research effort, undertaken in collaboration between Swedish and African researchers from natural, engineering and social sciences, aiming at an interdisciplinary assessment of the potential for an enhanced utilization of available renewable sources in off-grid solutions. By qualitative methodology, data was collected in semi-structured stakeholder interviews carried out with ten national level energy sector actors. Findings illustrate country-specific institutional, financial and poverty-related drivers and barriers to grid and off-grid electrification, as perceived by different energy sector stakeholders.

Keywords: *Rural Electrification, Off-grid Systems, Renewable Energy, Africa, Drivers and Barriers*

1. Introduction

There is little doubt that access to and use of electricity is a benefit to people, not only in the current electricity-dependent world but also in developing rural areas. While electricity may not bring development on its own it is a highly desired commodity and a prerequisite to rural development in long term perspective [1] [2]. In the first industrial countries massive electrification was initiated in the 1880's, to be completed only decades after the World War II; a huge effort backed by powerful institutions. The challenge is now to spread the same technologies in emerging economies with often very different institutional, cultural and financial conditions. One such region is sub-Saharan Africa where the electrification level is minute – especially in rural areas.

In this study, the current and future prospects for rural electrification (RE) in Mozambique and Tanzania are assessed in terms of drivers and barriers for RE through grid extension and off-grid solutions; based on interviews with key stakeholders from government, international donors, private sector and civil society in both countries carried out during 2010. The aim is to conduct a cross-sector analysis of country specific drivers and barriers to successful RE and use of renewable energy sources (RES) in off-grid systems, as perceived by stakeholders influencing the development in each country. Both countries have very low RE levels and there is a long history of Swedish bilateral partnership within the energy sectors. The analysis reveals important drivers and barriers at national and local level, some of which are not addressed in literature reviewed. The paper starts with a description of current conditions for RE in sub-Saharan Africa. Thereafter, the electricity sub-sectors of Tanzania and Mozambique are outlined followed by a section on method. The results for each country are presented and discussed, followed by conclusions.

1.1. Prerequisites for rural electrification in sub-Saharan Africa

In any country the construction of electric grids to distribute power in rural areas is an infrastructure assignment carrying huge expenses, not less so in most African countries where existing infrastructure is rudimentary. In Africa and elsewhere, RE has largely been the responsibility of the public sector, which in the African context generally implies a large influence from donors. In comparison with industrial countries and own ambitions, RE in Africa has been progressing at a slow pace. In order to speed up the process and involve the private sector as encouraged by the World Bank, many African countries have in later years taken on energy sector reforms, strategies which have yet not shown intended results [3]. The large distances and low incomes make distribution expensive and rural customers financially unattractive to private sector investors.

Expenses associated with vast distance could be met by decentralized grids in wait of full grid coverage. Such off-grid approaches for supplying electricity in remote areas are frequently powered by diesel generators which are dependent on fuel transports for operation, and generate a comparatively higher running cost. An alternative to diesel powered off-grid are available renewable energy sources (RES). In sub-Saharan Africa the potential of RES is high [4] and particularly micro hydro power and solar photovoltaic (PV) have been utilized so far. Due to the low population density and geographical distances, RES are often the least-cost alternative and financing instruments like the Clean Development Mechanism can become an important driver for RES in both countries [4, 5].The extensive pan-African literature covers progress and constraints of such RES based off-grid implementations [6] [7] [8]. Moreover, development programs have addressed the use of PV systems, solar home systems (SHS), in rural households which have resulted in an internal market for these technologies in some countries. The SHS trend is accompanied by a substantial impact assessment literature. Rural area energy transition is not unproblematic and several barriers have been identified – both regarding RE in general and regarding the use of RES in off-grid in particular. An earlier literature review [9] identified barriers within the following areas: institutions and stakeholders performance; economy- and finance; social dimensions; technical system and its management; technology diffusion and adaption; and rural infrastructure.

1.2. Rural electrification in Tanzania

Tanzania's current electricity generation relies heavily on hydropower; secondary sources are domestic natural gas and imported oil. In 2008 the total power generation capacity was 1100 MW. The transmission grid covers a minor part of the country leaving out most areas, particularly western and southern regions. District capitals and other important centers are supplied by diesel generators. The RE level is currently 2% (2009). There is an outspoken intention to utilize the prominent availability of RES, in particular for enhancing RE [10]. Still, there is little use of RES for electricity generation and only 13 % of the disbursed budget 2008/2009 was used for RE and RES altogether (corresponding to 1/3 of what was used for the gas and petroleum sector).

The Tanzanian power subsector, under the Ministry of Energy and Minerals, is dominated by the public agency Tanesco (Tanzania Electric Supply Company). An energy sector reform has taken place during the last decade, leading to the enactment of the Electricity Act in 2008 [10]; private sector is now encouraged to take an active role within the sector and a regulatory oversight of the tariff system is ensured by the EWURA (Energy and Water Utilities Regulatory Authority), established in 2006. The responsibility of RE has been transferred from TANESCO to the Rural Energy Agency, REA, which became operational in 2007. REA is responsible for facilitating RE which is done by supporting applicants (public, NGO or

private) with grants for organizational learning and for capital investment (normally covering up to 30% of the project). Other important actors are donors, who provide major parts of the energy budget, NGO's (primarily TaTEDO) and international consultants.

1.3. Rural electrification in Mozambique

In Mozambique the electricity generation is heavily dominated by the 2075 MW hydro power station Cahora Bassa, situated in the north western part of the country. Cahora Bassa, a few smaller hydropower stations and a back-up coal power station supply all electricity to the national grid. The lion share of electricity from Cahora Bassa is exported to neighboring countries but transmission lines reach the largest cities and some towns. Since the country is stretching over enormous distances transmission losses are significant and the power supply becomes fragile in the outskirts of the grid. Numerous diesel generators have been allocated to supply smaller and remote districts. In difference to Tanzania the country has endured a long lasting civil war, ended in 1992. Since then the efforts in grid extension have been significant; still the RE level was below 2% in 2007.

EdM (Electricidade de Moçambique) is the governmental utility responsible for electrification (generation, transmission and distribution) in Mozambique, but a restructure is considered. EdM buys most of its distributed electricity from the Cahora Bassa dam to low costs which somewhat complicates competition and introduction of other energy sources. The private sector, however, are free to contribute. EdM carries out RE by extending the national grid and the tariff is regulated by the Ministry of Energy. Another public institution is FUNAE (National Fund for Rural Electrification), founded in 1997 and strongly supported by donors, in practice responsible for rural off-grid electrification mainly using diesel generators and solar PV systems. Like in Tanzania, foreign consultants play an important role both in development of national strategies and project specific planning. In Mozambique very few NGO's are involved in RE.

2. Method

The study was conducted during eight weeks of field work in Tanzania and Mozambique in January-March 2010. By qualitative methodology data were collected through interviews with stakeholders. The interviews addressed six themes: (1) current state of the electricity infrastructure in rural areas; (2) institutional and socioeconomic drivers and barriers to RE; (3) productive uses of electricity; (4) potential for off-grid and renewable energy systems; (5) local participation in electrification processes; and (6) impact from electricity on people's lives. The themes were based on a review [9] of mostly African-related peer-reviewed literature (results presented in Table 2 alongside interview results). The interviews were recorded (unless circumstances made this impossible) as sound files. The interviews were semi-structured, i.e. asking open-ended questions, using an interview guide, and considering the professional experience of the respondent [11]. This paper presents the findings from 17 interviews carried out with government staff, donors, consultants and NGOs. The respondents were selected based on their influence in and experience of RE processes. Some interviews are with two or three respondents at the time. Our analytical strategy is based on theoretical propositions [12] and the concepts of 'drivers' and 'barriers', which are commonly found in the management literature, but are also commonly used by stakeholders in the field, as to signify factors that enhance or hinder the wished-for development.

The interviews have been transcribed and then analysed using the Atlas.ti software for qualitative data analysis. Each interview is read through and then all meaning units

(quotations) are sorted into subcategories (e.g. "communication problems"), that are part of categories (e.g. "barriers for RE") which are in turn related to the themes. This type of analysis combines a deductive analysis (categories are based on the themes of interest) with inductive analysis (subcategories emerge from the material) in an iterative process [11]. The software then allows for analysis of e.g. specific categories, subcategories and Boolean queries. The result is a cross-sector mapping allowing for comparison between various perspectives, organizations and between countries.

Some methodological weaknesses should be pointed out. First and foremost, the analysis is limited in scope both in terms of number of respondents and time allocated in each interview. The respondents are in general very knowledgeable in their area and much more can be learnt from each stakeholder. For practical reasons, only one interview was held with each respondent, implying that the analysis reflects what stakeholders found relevant at a specific point in time. However, the format of semi-structured interviews allows for respondents to reflect on their own answers and bring up additional aspects even if not asked for. Second, there is always a risk of misunderstandings, due to lacking language skills. Interviews were held in English and translated by local interpreter when necessary. Further, information given must be assessed critically as respondents may lack knowledge or hold subjective perceptions that are inaccurate in some areas. Such weaknesses are addressed through triangulation of findings. It also matters if there are sensitive issues to which respondents are unwilling to answer. The question of biases in interviews, the concepts of reliability and validity (coming from quantitative science) are discussed in length in literature and take on a slightly different meaning for this type of analysis [11]. In this study, trustworthiness of results is sought by two researchers searching for inconsistencies and comparing findings to existing literature.

3. Results

3.1. Indicated drivers and barriers for rural electrification

Results of identified barriers and drivers are shown in Table 1 and 2 respectively, and discussed in section 4. The respondents' reflections regarding the potential for renewable energies are not included in the tables but presented in the following section (3.2.).

3.2. Respondents' reflections regarding the potential of renewable energy sources

Among the renewable energy sources known to be available in the region micro/pico hydro power were evidently the source most appreciated among respondents. In Mozambique most respondents and in particular the EdM were very enthusiastic about the potential of micro scale hydro for off-grid applications (notably, no larger expansion of hydro power have been undertaken since colonial time in the country). Apart from hydro power EdM showed little interest for renewable sources. In Tanzania the potential exploitation of new hydro power resources, including micro scale, was greatly advocated by Consultant A who also stated that hydro power expansion in Tanzania are being successfully counteracted by the gas lobby. Hydro power has the strong benefit of higher capacity than e.g. solar PV while the flipside of the coin are the seasonal droughts that in particular have affected Tanzania. Regarding wind power there were little support in both countries, with skepticism related to costs and fluctuations. However, wind power got some support from Tanesco's research division. Solar PV is used for off-grid electrification in both countries still it was referred to as generally expensive and of low productive use. Regarding geothermal energy conversion Consultant A reported that a previous assessment has indicated good resources but low political interest.

Table 1. Identified barriers or constraints to successful RE in general (B) and to off-grid electrification in particular (b) extracted from stakeholder interviews and Africa-related literature (L). Tanzania: 1=Tanesco, 2=REA, 3=TaTEDO, 4=Donor, 5=Consultant A. Mozambique: 6=EdM, 7=FUNAE, 8=Donor, 9=Consultant B, 10=Consultant C. Number of interviews: i-iii.

Identified barrier	Source										
	L	**1** *iii*	**2** *ii*	**3** *i*	**4** *ii*	**5** *i*	**6** *iii*	**7** *ii*	**8** *i*	**9** *i*	**10** *i*
Institutions and stakeholder performance											
Low institutional quality	B				B	B	B				B
Inadequate planning capacity	B	B			B	B			B		
Organizational structure and strategies	B					B					
Lack of co-investments (rural develop.)	B					B					
Lack of private sector involvement	B		b		B						
Incompatible donor policies						b					
Top-down management in energy sector				b	B	B	B				
Economy and finance											
Tariff system and connection fees	B		b		B	B					
Subsidies	B		b		B						
Insufficient rural financial institutions	B		b		B						
Poor rural market and low productive use	B	B	b		b		B		B	B	B
Admin. costs in small off-grid systems	B									B	
Compensation (in land acquisition)		B									
Lack of consistency between RE projects		B									
High costs of diesel		B		b			b	b		B	b
Donor dependency					B	B	B		B	B	
Social dimensions											
Poverty and low household affordability	B	b	b	b	b	B	B				
Gender issues	B			b							
Problems in local participation and theft	B								B		B
Lack of local engagement						b		b			
Change of mind among costumers								b	B	B	
Technical system and local management											
Lack of access to skilled personnel	B		b							B	b
Weak maintenance culture	B			b		B				B	b
Low capacity of solar PV systems	B					b		b			
Low access to required components	B	B					B	b			
Low generation capacity						B	B		B		B
Technology diffusion and adaption											
Unwillingness of behavioral change	B		b	b							
Users' low awareness of techn. potential	B										
Lack of local entrepreneurship						B	B				
Rural infrastructure											
Scattered population	B	B				B	B	b	B		
Limited rural infrastructure (roads etc.)	B					B					
Long distance transmission							B				B
Traditional houses (electricity prohibited)					b	B					
Devastating cyclones										B	
Nature reserves and national parks					B	B	B				

Table 2. Identified drivers to RE in general (D) and to off-grid electrification in particular (d) extracted from stakeholder interviews. Tanzania: 1=Tanesco, 2=REA, 3=TaTEDO, 4=Donor, 5=Consultant A. Mozambique: 6=EdM, 7=FUNAE, 8=Donor, 9=Consultant B, 10=Consultant C. Number of interviews with each organization: i-iii.

Identified driver	Source									
	1 *iii*	**2** *ii*	**3** *i*	**4** *ii*	**5** *i*	**6** *iii*	**7** *ii*	**8** *i*	**9** *i*	**10** *i*
Policy and poverty mitigation ambitions										
Governmental policies and subsidies	D	d	d	D	D	D	d	D		D
Political campaigning	D					D			D	
Donor push / support			d	D	D			D	D	
Pushing from individuals in gov. agencies					D					D
Private sector involvement										
Market incentives	D	d							D	
Churches		d			d					
Social responsibility in private sector						D				
Niche market for certain energy systems								D		
Local demand										
Increasing demand (industry, households)	D	d	d			D	d	D		D
Grass-root organizing				D		D	d			
Off-grid RE creates demand for grid ext.					D					D
Other										
Need of increased sustainability in grid						D		D		
Promotion of renewable energy / CDM				d					d	

4. Discussion and conclusions

According to stakeholders, the main drivers for RE in Tanzania are political priorities. Tanzania confronts challenges both at the national and local levels, while no references are made to important actors at the intermediate level. Tanesco is considered the main actor but with major financial and organizational problems. According to donors and consultants, lack a of planning at government level is a main issue, causing inefficient implementation and financing problems – in fact only a minor part (14%) of available funds for energy projects in 2008-2009 were disbursed on time. The opening up for private sector involvement is considered a driver but so far little private investment is taking place in RE. Low return rates, political setting of tariffs and a weak customer base in rural areas makes RE unattractive. Tanesco and REA both use economical potential and productive energy use as indicators for RE planning, still, much would be gained if RE projects would also be accompanied with complementary infrastructural investments according to experienced consultants. Among local barriers, most stakeholders mention poverty and low population density – the latter having huge impact on both distribution and transmission costs. Despite low tariffs (that are financially unviable), rural customers find it difficult to afford connection and subsidies are often used to overcome this barrier. To find a level appropriate both for satisfying consumers and encouraging private sector incentives in the energy sector is difficult. For off-grid, all stakeholders agree that diesel generators are costly and unreliable, but where grid extension is not economically feasible, off-grid solutions are necessary for political goals to be attained.

Also in Mozambique, political ambitions are considered the main driver for RE, for social and economical reasons. EdM regard RE as means to slow urbanization, providing better health care and education, and lower birth rates in rural areas. The lack of industry poses a barrier as

RE is not commercially viable and in comparison to Tanzanian agencies the emphasis on prevalent economical potential and productive use are seemingly not used as a strong indicator of where to direct RE. New generation is needed; Mozambique is depending on the large hydro plant Cahora Bassa and long distances leave most of the country without power. Another recognized barrier is that private actors find it hard to compete with Cahora Bassa's cheap electricity. The energy sector is top-down oriented and donor dependency creates problems in budgeting; the budget becomes more of a wish-list than a planning instrument. Diesel generators are very common for small-town electrification and rural off-grid systems but very costly and unappreciated. There is a good hydro potential but virtually no expansion have been implemented since colonial times. FUNAE has a major mission carrying out off-grid throughout the country but is still a rather limited and new organization. Off-grid barriers are high costs of diesel, logistics (incl. spare-parts), and communication with costumers due to bad infrastructure. For sustainable off-grid solutions, a technical support system is needed to facilitate maintenance, and most probably there are huge benefits waiting in micro hydro power. Local people's engagement is important but variable, according to FUNAE, impacting off-grid system sustainability. Along the coast, the occurrence of cyclones destroys infrastructure and impedes investments.

In comparison, the two countries face similar challenges with low population densities, weak customer bases, large distances and inadequate infrastructure. While domestic actors regard social demand as an important driver for RE this view is less pronounced by the foreign actors who rather regard the (lack of) economic demand as a barrier. At the national level, both countries rely on external funding for RE, but low institutional capacity and quality – both countries suffer from corruption and politically motivated but economically unviable plans– hinder efficient implementation and use of funds. There is political recognition that grid extension needs to be complemented by off-grid solutions, but the responsible agencies are yet to become fully operational.

The drivers and barriers identified in this study are largely corresponding to those in the literature, as can be seen in Table 2. However, the problems associated with donor dependency and how this impacts budgeting and implementation comes out as important constraints for both countries, which is not discussed in any detail in the RE literature. Institutional weaknesses are often discussed in terms of bad governance, but in Tanzania the lack of correspondence between local realities and donor criteria for RE projects also create institutional barriers. In this study it further found that traditional building techniques (using mud and grass) in rural areas slow down connection rates; a barrier not previously emphasized. All stakeholders turned out to share a view on diesel generators as expensive and unreliable. Here, appropriate RES could assist but the interest among stakeholders is weak. A barrier with certain relevance for the region is the reported lack of complementary services and co-investments to accompany RE. Here, Tanzania seems to have taken more account of recognizing other rural development when carrying out RE. In sum, our results support earlier findings but complement with country-specific drivers and barriers. To be remembered, importantly, RE takes decades to implement even in the wealthiest country; due to strong political ambitions, donor support and an accumulating experience among stakeholders the rate of electrification is keeping up in both studied counties.

The methodological weaknesses are primarily due to time constraints and a follow up on sector development over the coming years would improve credibility of finding. This study provides an assessment of drivers and barriers to RE that is broader in scope and more detailed than earlier writings, and provides an excellent basis for cross-country comparison

and in-depth studies for each country. It is also valuable for stakeholders, such as donors, consultants and policy makers, to gain overview of challenges to address.

References

[1] G. Foley, Rural electrification. The institutional dimension, Utilities Policy, 1992, pp. 283-289

[2] R. Holland, et al., Decentralised rural electrification : Critical success factors and experiences of an NGO, Refocus 2(6), 2001, pp. 28-31

[3] N. Wamukonya, Power sector reform in developing countries: mismatched agendas, Energy Policy 31(12), 2003, pp. 1273-1289

[4] S. Karekezi, Renewables in Africa-meeting the energy needs of the poor, Energy Policy 30(11-12), 2002, pp. 1059-1069

[5] A.K. Akella, R.P. Saini, and M.P. Sharma, Social, economical and environmental impacts of renewable energy systems, Renewable Energy 34(2), 2009, pp. 390-396

[6] G.J. Jones and G. Thompson, Renewable energy for African development, Solar Energy 58(1-3), 1996, pp. 103-109

[7] J.T. Murphy, Making the energy transition in rural east Africa: Is leapfrogging an alternative? Technological Forecasting and Social Change, 68(2), 2001, pp. 173-193

[8] M. Pigaht and R.J.v.d. Plas, Innovative private micro-hydro power development in Rwanda, Energy Policy 37, 2009, pp. 4753-4760

[9] H. Ahlborg, et al., A background on social context and renewable energy sources in Mozambique and Tanzania: an initial report from the STEEP-RES project, Chalmers University of Technology, in ESA Report 2008:21, 2008, Göteborg

[10] MEM, Final report on Joint Energy Sector Reveiw for 2009, Ministry of Energy and Minerals, United republic of Tanzania, 2009, Dar es Salaam

[11] B. Mikkelsen, Methods for development work and research. A new guide for practitioners, Sage Publications, second edition, 2005, New Dehli/Thousand Oaks/London

[12] R.K. Yin, Case study research. Design and methods, SAGE Publications, 4 ed., Applied social research methods series, Vol. 5, 2009, Los Angeles

Renewable energy policies implementation drivers and barriers for Abu Dhabi

Toufic Mezher[1,*], Gihan Dawelbait[1], Zeina Abbas[1]

[1] *Masdar Institute, Abu Dhabi, UAE*
** Corresponding author. Tel: +971 2 6988173, Fax: +971 2 6988121, E-mail: tmezher@masdar.ac.ae*

Abstract: Climate change and fossil fuel depletion are the main drivers for the recent focus on finding alternative energy resources. Renewable energy (RE) is an obvious choice to reduce carbon dioxide and other pollutants contributing to global warming. However, the high cost of RE technologies is the main obstacle facing the diffusion of RE power generation, therefore economical and political intervention is inevitable. In the United Arab Emirate (UAE) population and economic growth are the main reason of a fast increase of energy demand, leading to two problems, first the UAE has one of the highest carbon footprint in the world and second, the fast depletion of its main energy generation resource – fossil fuel, which highlights the need to establish a RE sector. In this study, literature reviews are conducted covering 61 countries focusing on their efforts to adopt RE resources in the power generation sector as well as policies implemented by their respective governments and decision makers. Furthermore, we investigated the applicability of the main RE policies implemented worldwide in the Abu Dhabi - the capital of the UAE- context. As a result of our analysis, we recommend to apply a mixed policy of Feed-in-Tariff (FIT) and the Quota system for RE electricity generation in order for the UAE to meet its 7% target by 2020.

Keywords: *Renewable Energy, Renewable Energy Policy, Masdar Initiative*

1. Introduction

Climate change and fossil fuel depletion are the main drivers for the recent focus on finding alternative energy resources. Renewable energy (RE) is an obvious choice to reduce carbon dioxide and other pollutants contributing to global warming. However, the high cost of RE technologies is the main obstacle facing the diffusion of RE power generation, therefore economical and political intervention is inevitable. These interventions usually include legislation, incentives to investment, energy generation targets, guidelines for energy conservation, strategies to stimulate the energy industry, and taxation [1]. Economic support policies that encourage investments in new technologies that promote the adoption of RE have been implemented in many countries. In particular, a variety of economic support policies for RE has been developed and implemented mainly in Europe and the USA. These policies include: Quotas, Feed in Tariffs (FITs), Bidding or Tendering, Tax incentives, and Subsidies.

In the Unite Arab Emirate (UAE), population and economic growth are the main reason for the fast increase of energy demand, leading to two problems, first the UAE has one of the highest carbon footprint in the world [2] and second, the fast depletion of its main energy generation resource – fossil fuel, which highlights the need to establish a RE sector. To address these issues, in this work we study the fundamental requirements to introduce relevant RE polices as a first approach to promote RE use in the UAE. In 2008, the first RE policy set by UAE government -at least seven percent of the emirate's power generation capacity will come from RE sources by 2020- provided a critical missing piece of the UAE‘s overall strategy in energy and sustainability. This policy marks the start of new energy era in the UAE; nevertheless, this policy does not state the mechanism of how to achieve this target.

This paper will first introduce the key features of the different (RE) policy options. Second, it will present a comparative analysis of the RE policies mechanisms as well as summarizing the requirements for their successful implementation. Third, the findings from the 61 surveyed countries focusing on RE technologies, capacities and policies are presented. Finally, the challenges and existing constraints for the development of RE Policy in Abu Dhabi are presented and discussed. The paper concludes with summary and recommendations.

2. Background

Even though it is widely agreed that support schemes need to be put in place to promote the use of RE, there is almost no consensus as to what are the best RE policies to use. In the following we introduce the different policy options including their respective advantages, disadvantages and recommendations for successful implementation.

Feed-in Tariffs (FITs), are performance-based regulation incentives aimed at increasing the adoption of RE sources. The term "feed-in tariff" derives from the German Stromeinspeisungsgesetz of 1990, which literally translated means "electricity feeding-in law." Germany implemented the Electricity Feed-in Law (1991) in order to create a market for renewable electricity by offering providers a fixed but attractive price for the recovery of generation costs and since then it stands as the paradigmatic example of effective FIT regulation [3].

Renewable Portfolio Standard (RPS), Renewables Obligation (RO), Mandatory Market Share (MMS) policy or Quotas are the different names given to a similar set of incentives for RE in various countries, RPS in USA, RO in UK, MMS in China and renewable quotas in European countries [4]. The shared theme of all these incentives is that the government sets a percentage of electricity to be generated by renewable sources, assigns an actor, such as electricity users, suppliers or generators, to meet the specific percentage and penalizes those who fail to meet their goals. These mechanisms are essentially market based and they are designed to achieve a cost-efficient generation of RE [5]. Quotas are presently applied in a number of countries around the world. The RPS in Texas has been very effective due to good local resource, presence of tax credits and strong penalties for non-compliance [6]. Although they have resulted in a growth of renewables in most countries, they have not achieved the same success as the FITs in Germany and Denmark [7].

Centralized Bidding or Tendering systems are one of the major policies for promotion of RE in the electric power sector. These mechanisms have been applied in the early stages of RE development in UK and are presently employed for wind power in China under the name of concession program [8]. As the name implies, the policy mechanism works by calling for bids from investors for RE projects. It is essentially a market-based policy, which strives to develop RE projects at the least possible cost. The policy of bidding for RE contracts was first started by UK in the form of Non Fossil Fuel Obligation (NFFO) in 1990. This policy was then discontinued in 1998 when it was realized that NFFO was not able to achieve required implementation of RE. In 2002, it was replaced by Renewables Obligation (RO). The other major example of a bidding system is the Chinese Concession System for wind power development. The system was started in 2003, and fifth bidding round was completed in December of 2007 [8]. Chinese RE Law of 2005 makes provisions for implementation of FITs, quotas and bidding systems [4].

Tax Credits is one way to lower the costs of RE through market compensation. The main types include investment, and production tax credits. They are largely used in Europe, USA, Japan, and India as well. Investment Tax Credits can cover the cost of the RE system itself, or even the total cost of the installation. Investment Tax Credits can prove to be useful at the early stages of the technology, where there are high costs, or at times when utilities are being deployed on remote areas. They aid lowering the level of risk involved and the costs of investing in RE technologies [9]. In the United States, businesses receive a 10 percent tax credit for purchases of solar and geothermal RE property, subject to certain limitations. Some U.S. states have Investment Tax Credits of up to 35% [10].

The high upfront investment cost of renewable makes them unattractive choices for investors. Removing this barrier by reduction in the initial capital outlay by consumers for RE systems is accomplished through direct ***subsidies or rebates***. These subsidies are used to share the initial capital cost of the system, so that the consumer sees a lower price [10]. Subsidies have been used by many countries for stimulating growth in RE sector. A combination of investment subsidies, low-interest loans, net metering and public education has resulted in an early success of PV in Japan [9]. Similar subsidies have been employed in many countries for RE development. In most cases, they are used in combination with other RE support mechanisms. This is in stark contrast with investment tax credits, which tend to favor large companies with greater tax liabilities [6].

In general, RE policies can be grouped into two categories, *Investment Focused Policies,* e.g., Rebates/Subsidies, Investment Tax Incentives and Bidding/Tendering, *and Generation Based Policies*, e.g., FITs, Quotas and Green Credits [11].

3. Current state of Renwable Energy and lessons learned.

When put in an international comparative perspective the UAE is found to be far behind the world's leaders in RE. Yet, the recent move of introducing an RE sector is an unprecedented initiative in the region that might play an important role in setting the stage for similar decisions by other comparable countries. We conducted a comprehensive analysis of the current state of RE in order to identify RE policy trends to help inform potential adaptation of RE initiatives in new projects or countries. The analysis was performed by reviewing RE data of 61 countries mainly focusing on RE technologies, capacities and policies implemented by the different countries. For demonstration purposes, Table 1. summarizes a selection of 7 countries out of the 61 studied as geographical representations to their regions; the table covers the following categories: RE policies, targets, projects, produced electricity and installed capacities.

As a result of this study, here, we highlight the main finding of the analysis based on the data from the 61 countries analyzed as follows: Europe is dominating the RE scene, since more than 50% of all countries that uses RE projects are European followed by Asia, America and finally Africa. Furthermore, most of the European countries use hydroelectric and wind power and very few use geothermal energy. This can be explained by the fact that hydro and wind are the most abundant energy source in Europe and geothermal energy is the least used energy source and this is due to the immaturity of most of the state of the art geothermal technology solutions.

Table 1 summurizes the RE policies, targets, RE sources used and their installed capacity of 7 countries

			RE Target		*RE Projects*			
Country	*RE Policy*	*RE mechanism*	*Primary energy*	*Electricity*	*Type*	*Electricity Produced*	*Installed Capacity*	*Reference*
China	FIT since 2005		15.4% by 2020	21% by 2020	Small hydro		60 (GW) as of 08	[12, 18, 20, 21, 23]
	Public investment	A total of USD731 million is allocated to support biogas			Wind	0.20%	26.01 (GW) as of 2009	
	Capital subsidies and grants	A subsidy of (USD2.93)/W to support the BIPV system installation.			Solar PV		0.3 (GW) as of 2009	
	Quotas, Energy tax, PCB, Tax credits							
Germany	FIT since 1990	Investment support for solar PV	18% by 2020	12.5% by 2010	Small hydro		1.4 (GW) as of 2008	[7,13, 14,15, 16, 17,20]
	Investment tax credit	Parts of the revenue of energy taxes finance RES			Wind	6.40%	25.78 (GW) as of 2009	
	PCB				Solar PV	1%	9.83 (GW) as of 2009	
	Net metering				Geothermal		0.006 (GW) as of 2008	
	Capital subsidies and grants	Only in exceptional cases 30% of invest.			Biomass	4.40%	4 (GW) as of 2008	
	Energy tax	Eco-tax on conventional electricity			Concentrated Solar Power		1.5 (MW) as of 2009	
	Public investment and Loans	R&D support			Hydropower	3.30%	4.7 (GW) as of 2008	
India	FIT since 1993		20% by 2020	12% by 2012	Small hydro		2 (GW) as of 2008	[12, 14, 18, 20, 24, 25]
	Quota system			15% by 2020	Wind	1.60%	10.93 (GW) as of 2009	
	Energy Investment Tax	Wind Power: per good. Biomass: total exemption			Solar PV		0.12 (GW) as of 2009	
	Capital subsidies and grants	For small hydro up to 25 (MW).			Biomass	0.20%	2.1 (GW) as of 2009	
					Hydropower	15%	32.892 (GW) as of 2009	
Japan	FIT	FIT for Solar PV		1.63% by 2014	Small hydro		3.5 (GW) as of 2008	[14,18,20, 21,22,]
	Capital subsidies and grants	Solar PV household subsidy			Wind	0.20%	2.21 (GW) as of 2009	
	Public investment and loans	National stimulus Package of 22 billion USD			Solar PV	0.20%	2.6 (GW) as of 2009	
	Green Certificate Trading				Geothermal	0.30%	0.54 (GW) as of 2008	

			RE Target		*RE Projects*			
Country	*RE Policy*	*RE mechanism*	*Primary energy*	*Electricity*	*Type*	*Electricity Produced*	*Installed Capacity*	*Reference*
	Quotas				Hydropower	7.50%	27.759 (GW) as of 2009	
UAE	Quotas, Bidding and Subsidies			7% by 2020	Solar PV		10 (MW)	[26]
					Solar thermal		100 (MW)	
UK	RO since 2002	TGC as part of RO scheme	15% by 2020	10.4% by 2010/2011	Small hydro		0.173 (GW) as of 2008	[7, 13, 14, 17, 19, 20]
	Public investment and Loans	R&D and offshore wind support. A total 10.4 billion GBP for low carbon economy.		15.4% by 2015/2016	Wind	1.30%	4.05 (GW) as of 2009	
	Energy Tax	Tax exemption for electricity from RE.			Solar PV		0.032 (GW) as of 2009	
	FIT, Quotas and NFFO				Biomass	2.80%	1.368 (GW)	
					Hydropower	2.30%	1.513 (GW)	
US	RO			20% by 2030	Small hydro		3 (GW) as of 2008	[13, 14, 18, 20, 21, 22]
	FIT since 1978				Wind		35.159 (GW) as of 2009	
	Energy Tax	Production of Tax Credit-extension			Solar PV		0.824 (GW) as of 2010	
	Public investment and Loans	30 billion $ in loan guarantee for RE projects as of 2009			Geothermal	0.40%	3.10 (GW) as of 2009	
	Tax credits	Payment in lieu of tax credits for investment on RE			Biomass		8 (GW)	
	Capital sudsides and grants				Concentrated Solar Power		188 (MW) as of 2009	
					Hydropower	6.30%	95.0 (GW) as of 2009	

Among all the RE projects in the studied countries, wind, hydro and biomass were found to constitute the biggest share of RE installed capacity, where Wind installed capacity ranges between 35-10 GW in the US, China, Germany and India, Hydropower ranges between 95-27 GW in the US, Russia, Brazil, China, India and Japan, and finally Biomass reaches up to 70GW in Costa Rica"

On the policy front, approximately 70% of the 61 countries are applying feed-in tariff policy which portrays it as an effective policy to encourage the use of RE sources. This wide use of FIT is due to its several advantages that include: offering investment security and market stability as well as it being very effective in increasing the amount of electricity generated from RE sources such as wind and solar.

As a whole, the most used RE source is hydroelectric energy. This suggests that, in general, hydro energy is the most abundant energy in comparison to the other projects such as geothermal, solar PV, solar thermal and biogas. All the countries that have more than 30% RE targets to be fulfilled between 2020 and 2050, has mainly wind and hydro projects where the hydro projects have the highest installed capacity.

An example of a successful RE implementation story, Costa Rica is already producing 99% of its electricity from renewable sources which makes it the first carbon-neutral country in the world.

4. Renewable Energy Policy in Abu Dhabi

The only operating RE solar PV plant in Abu Dhabi is the 10 MW plant in Masdar City which is also registered as a CDM project for carbon credit purposes. The 10 MW plant, consisting of 87,777 panels (50% thin film and 50% crystalline silicon) is projected to generate 17,500 MWh of clean energy each year (with a single kWh of clean energy being the carbon-offset equivalent of 0.8 kg depending on an area's network and its energy-producing source). The cost of kwh produced in the 10 MW PV plant is 48 US cents (2009).

4.1. Existing Barriers for the Development of RE

In [27], Patlitzianas made an overall review of the existing barriers that can impede the development of RE in the Gulf countries and including the UAE. The barriers of the UAE are grouped into three main categories: market technology, policy legislation, and cost. All of these categories are related to infrastructure and institutions. As a conclusion, the authors argue that the barriers that unfairly discriminate against RE are mainly the lack of commercial skills and information, the absence of relative legal and policy framework, the high initial capital costs coupled with lack of fuel-price risk assessment, as well as the exclusion of environmental externalities in the cost.

4.2. Toward a Comprehensive RE Policy for Abu Dhabi

Currently Abu Dhabi Government has set a target that 7% of its electricity generation to come from renewable sources. Solar power is the most favorable source of RE for Abu Dhabi. The 10-MW PV solar plant is already installed and operating, and supplying power to Masdar City operations and connected to the existing Grid. It is a small amount of electricity generated but its success opens the market to have individuals, private builders and property owners to consider RE technologies.

As a result of our analysis, we recommend to have a mix policy between Fee-in-Tariff (FIT) and Quota system in order to share the RE electricity generation. Currently, the Abu Dhabi government through the Abu Dhabi Executive Affairs Authority (ADEAA) is reviewing the energy policy in general and electricity generation in particular in conjunction with all the actors. In order to ensure that this policy is effective we need to take many things into considerations:

1. There has to be continues political support to encourage the adoption of RE.
2. Through the Masdar Initiative, the main RE technologies that can comply with the policy mechanism are Solar and Wind (mainly off-shore). The market has to develop the most effective options.

3. Must ensure that the electricity provider, ADWEC, buys the electricity generated from RE sources. Transco, the power transmission company, provides the grid connection of all RE sources.
4. Develop a trading mechanism between RE generators and ADWEC.
5. Using a Guarantee of origin certificates is a good example to use as a proof of generation and compliance under a more controlled environment.

5. Conclusion and recommendations

Abu Dhabi, with the Masdar Initiative, is regarded as a pioneer in its efforts to promote RE in the Middle East region especially in Gulf States that share similar characteristics such as abundance of solar resources and oil rich economies that can support such an initiative. The paper listed the RE policies and mechanisms for many countries in addition to their different RE technologies and installed capacities. One thing to notice is that UAE (Abu Dhabi) has a policy target of 7% RE share of electricity generation by 2020 but there are no additional legislations or mechanisms to promote power generation such as feed-in tariffs, renewable portfolio standards, capital subsidies or grants, investment tax credits, sales tax or VAT exemptions, green certificate trading, direct energy production payments or tax credits, net metering, direct public investment or financing, and public competitive bidding.

References

[1] R. Saidur, M.R. Islam, N.A Rahim, and K.H Solangi, A review on global wind energy policy. Renewable and Sustainable Energy Reviews, 14 (7), 2010, pp. 1744-1762.

[2] B. Ewing, S. Goldfinger, A. Oursler, A. Reed, D. Moore, and M. Wackernagel, Ecological Footprint Atlas. Global Footprint Network, 2009.

[3] B.K. Sovacool, The Dirty Energy Dilemma: What's Blocking Clean Power in the United States. Praeger Publishers, 2008, ISBN: 978-0-313-35540-0.

[4] J.A. Cherni, and J. Kentish, Renewable energy policy and electricity market reforms in China. Energy Policy, 2007, pp. 3616-3629.

[5] P. Komor, Renewable Energy Policy. New York: Diebold Institute for Public Policy Studies, 2004.

[6] K. Mallon, Renewable Energy Policy and Politics: A Handbook for Decision-Making. Earthscan Publications Ltd, 2006.

[7] J. Lipp, Lessons for effective renewable electricity policy from Denmark, Germany and the United Kingdom. Energy Policy, 2007,pp. 5481-5495.

[8] J. Han, A.P.J. Mol, Y. Lu, and L. Zhang, Onshore wind power development in China: Challenges behind a successful story. Energy Policy, 37(8) , 2009, pp. 2941-2951.

[9] D. Aßmann, U. Laumanns, and D. Uh, Renewable Energy: A Global Review of Technologies, Policies and Markets. Earthscan Publications Ltd, 2006.

[10] F. Beck, and E. Martinot, Renewable Energy Policies and Barriers. Encyclopedia of Energy, 2004.

[11] R. Haas, W. Eichhammer, C. Huber, O. Langniss, A. Lorenzoni, R. Madlener, P. Menanteau, P.-E . Morthorst, A. Martins, A. Oniszk, J. Schleich, A. Smith, Z. Vass, and A. Verbruggen, How to promote renewable energy systems successfully and effectively. Energy Policy, 32(6), 2004, pp. 833-839.

[12] World Future Council (WFC) Feed-In Tariffs- Boosting Energy for our Future. 2007.

[13] D. Toke, The EU Renewables Directive- What is the fuss about trading? Energy Policy, 36(8), 2008, pp. 3001-3008.

[14] International Energy Agency (IEA). Statistics. Renewables. . [Online] 2010. [Cited: 5 30, 2010. http://www.iea.org/stats/prodresult.asp?PRODUCT=Renewables.

[15] M. Frondel, N. Ritter, and C.M. Schmidt, Germany's solar cell promotion: Dark clouds on the horizon". Energy Policy, 36(11), 2008, pp. 4198-4204.

[16] B. Hillebrand, H.G. Buttermann, J.M. Behringer, and M. Bleuel, The expansion of renewable energies and employment effects in Germany. Energy Policy, 34(18), 2006, pp. 3484-3494.

[17] D. Reiche, and M. Bechberger, Policy differences in the promotion of renewable energies in the EU member states. Energy Policy, 32(7), 2004, pp. 843-849.

[18] International Energy Egency. Global Renewable energy: Policies and measures. [Online] [Cited: February 5, 2010.] http://www.iea.org/textbase/pm/grindex.aspx.

[19] D. Fouquet, and T. Johansson, European renewable energy policy at crossroads-Focus on electricity support mechanisms. Energy Policy, 36(11), 2008, pp. 4079-4092.

[20] Renewable Energy Policy Network for the 21st Century (REN21). Renewables International Action Programme. [Online] http://www.ren21.net/pledges/pledges.asp.

[21] A. Sayigh, Renewable energy- the way forward. Applied Energy . 64(1-4), 1999, pp. 15-30.

[22] P.H. Kobos, J.D. Erickson, and T.E Drennen, Technological learning and renewable energy costs: implications for US renewable energy policy. Energy Policy , 34(13), 2006, pp. 1645-1658.

[23] Q. Hang, J. Zhao, Y. Xiao, and C. Junku, Prospect of concentrating solar power in China-the sustainable future. Renewable and Sustainable Energy Reviews, 12(9), 2008, pp. 2505-2514.

[24] Ramachandra, T.V and Shruthi, B.V. (2007). Spatial mapping of renewable energy potential. Renewable and Sustainable Energy Reviews, 11(7), pp. 1460-1480.

[25] C.H. Narenda, Renewable Energy Act: To meet India's future needs. Merinews Power to People. [Online] February 2, 2007. http://www.merinews.com/article/renewable-energy-act-to-meet-indias-future-needs/126343.shtml.

[26] The renewables market in MENA – opportunities and challenges. A report by Freshfields Bruckhaus Deringer LLP. [Online] February 2010. http://www.freshfields.com/publications/pdfs/2010/-feb10/27386.pdf

[27] K.D. Patlitzianas, Enhancing renewable energy in the Arab States of the Gulf: Constraints & efforts. Energy Policy, 34(18), 2006,pp. 3719–3726.

Barriers to and Drivers of the Adoption of Energy Crops by Swedish Farmers: An Empirical Study

Anna C. Jonsson[1,*], Madelene Ostwald[1, 2], Therese Asplund[1], Victoria Wibeck[1]

[1] *Centre for Climate Science and Policy Research, Linköping University, Norrköping, Sweden*
[2] *Physical Resource Theory, Department of Energy and Environment, Chalmers University of Technology, Göteborg, Sweden*
** Corresponding author. Tel: +46 11 36 32 34, Fax: +46 1336 32 92, E-mail: anna.c.jonsson@liu.se*

Abstract: Since the Swedish government and the EU intend to encourage farmers to expand energy crop production, knowledge of the factors motivating adoption decisions is vital to policy success. Earlier studies have demonstrated that important barriers to farmer adoption of energy crops include converting from annual to perennial crops and from traditional crops or production systems to new ones. Economic motivations for changing production systems are strong, but factors such as values (e.g., aesthetics), knowledge (e.g., habits and knowledge of production methods), and legal conditions (e.g., cultivation licenses) are crucial for the change to energy crops. This paper helps fill gaps in the literature regarding why farmers decide to keep or change a production system. Based on a series of focus group interviews with Swedish farmers, the paper explores how farmers frame crop change decisions and what factors they consider most important. The main drivers of and barriers to growing energy crops, according to interviewees, are grouped and discussed in relation to four broad groups of motivational factors identified in the literature, i.e., values, legal conditions, knowledge, and economic factors. The paper ends by discussing whether some barriers could be overcome by policy changes at the national and European levels.

Keywords: *Climate change, Energy crops, Farmers' incentives, Drivers, Barriers*

1. Introduction

The national goal of converting the Swedish energy supply from fossil fuel to renewable energy has been made more urgent by the climate change debate and a general emphasis on the sustainable development concept. As a member of the European Union (EU), since 2007 Sweden has been subject to an overall binding target of making its energy supply 20% renewable by 2020 [1]. Reducing total national emissions by producing more energy-related products or energy crops on traditionally agricultural land, i.e., "energy farming" [2], is one of the highlighted changes. At present, approximately 2% of Sweden's arable land is used for energy production [3]. Several studies indicate that energy crop production from the agricultural sector will play a more important role in the future [4,5]. The Swedish agricultural sector produced 1–1.5 terrawatt hours (TWh) of energy in 2006 [5, 6]. It has been calculated [7] that the agricultural sector could produce 15–30 TWh, depending on economic and political measures, and the Federation of Swedish Farmers (LRF) has committed to increasing energy production to at least 5 TWh in the near future [8]. A high potential for increased energy crop cultivation has also been identified at the European level [2,9]. At the same time, the problematique inherent in using limited land resources to produce renewable energy in a situation of high commodity prices and continuously growing world population should not be underestimated.

Currently, 13 energy crops are available to Swedish farmers [10], each with particular cultivation opportunities and restrictions and sets of drivers and barriers. The three most extensive energy crops currently produced in Sweden are straw (a by-product), oil crops, and wheat, each covering 15,000–25,000 ha [10]. Earlier studies of conditions for land use change at the Swedish and international levels have demonstrated the importance of economic incentives in encouraging individual actors to change production or land use [11,12]. In the Swedish case, economic evaluations of investment in energy crop production produce

contradictory results. Despite the potential profit, existing subsidies, and considerable farmer interest in energy crop cultivation [11], the extent of energy crop production in Swedish agriculture is limited [13,14]. Earlier studies have likely been too focused on purely economic incentives, which alone cannot explain farmer behaviour concerning the conversion to energy crop production. This leaves a knowledge gap regarding the involved social, cultural, institutional, and environmental issues, and how they are seen from the perspective of society and individual actors [9].

To address this knowledge gap, we had previously reviewed the scientific and gray literature dealing with *why* farmers decide to stay with or change a production system, and what motivational factors serve as drivers of or barriers to specific crops [10]. The review indicated that, although economic incentives to change the production system are strong, factors such as values (e.g., aesthetics), knowledge (e.g., habits and knowledge of production methods), and legal conditions (e.g., property rights and cultivation licensing) may also be crucial for production system change [10]. However, no empirical, explorative study of this matter has yet been carried out.

This paper builds on our earlier analysis of motivational factors as described in the literature, adding the findings of an empirical study of the conditions necessary for farmers to engage in energy crop production, which can serve both climate change mitigation and adaptation purposes. The specific research questions are: i) What drivers of and barriers to energy crop production, from the farmers' perspective, can be empirically identified? ii) How do these relate to the factors identified in the literature? The results will enhance our knowledge of *why* farmers choose to change their land use, including motivational factors. In terms of increasing energy crop production – a Swedish government goal – our analysis can provide a basis for policy decisions regarding enhancing drivers and removing barriers.

2. Motivational factors as drivers and barriers

Studies of the public understanding of environmental issues have identified a frequent gap between peoples' opinions and their actions – an "attitude–behaviour divide" (see, e.g., [15,16]). Even though actors may be knowledgeable regarding environmental issues, they may not always act in ways that contribute to environmental sustainability [17]. The reasons for this vary, but one possible explanation is that many environmental problems are characterized by complexity and uncertainty; they are often global in nature and their effects may be distant in time and space [16, 18].

Many studies focus on a single crop [19,20] or a particular aspect of energy farming [21]. Very few studies take a more integrated view of a wider range of crop alternatives and motivational factors relevant to the farmer considering energy farming. Rosenqvist et al. [19], for example, statistically analysed the characteristics of individual farmers who have adopted salix cultivation, and compared this group with a strategic sample of farmers who have not. The only more holistic study we found in the surveyed literature was that of Paulrud and Laitila [11], who use a methodologically strict and quantitative approach (i.e., a choice experiment) to investigate a limited number of motivational factors affecting a limited number of crops. Building a more comprehensive understanding of what affects farmers' adoption of energy crops calls for a more explorative and qualitative approach. Hence, it is important to contextualize attitudes, i.e., to analyze not only actors' stated opinions, but also the barriers preventing people from acting and the drivers encouraging them to do so [16,17].

To understand the contextual factors that restrain and enable farmers' actions, it might be useful to distinguish between *proximate causes* and *underlying driving forces* of individual land use change decisions [12,22]. Proximate causes are the motivational factors directly experienced by land users, such as an available market's increased demand for a product driving a change in land use or decreased dependence on subsistence farming due to off-farm income-generating activities. Underlying driving forces are indirect and more process oriented, such as climate change or expanding national/regional markets.

Our previous review of the literature dealing with the motivational factors guiding farmer decisions to engage in energy crop production identified four broad groups of motivations relating to values, legal conditions, knowledge, and economic factors [10]. Along with these, a variety of more specific factors was found that may serve as drivers of or barriers to individual farmers considering the adoption of certain energy crops. The analysis indicated that, although several studies have been undertaken, we still lack knowledge of the various groups of motivational factors and how they are assessed by individual farmers. More specifically, we lack knowledge of the direction of the motivational factors associated with various crops, the relative strengths of these factors, whether different strata of farmers assess motivational factors differently, and the precise identity of the proximate causes and underlying forces.

This paper represents a preliminary attempt to fill this knowledge gap. We aim to identify a wide variety of barriers and drivers discussed by Swedish farmers during four focus group interviews, dealing not with the adoption of specific crops, but with the motivational factors affecting whether or not one engages in "energy farming". These barriers and drivers will be discussed in relation to the four broad groups of motivational factors mentioned above, i.e., values, legal conditions, knowledge, and economic factors [10].

3. Methodology

This study builds on four focus group interviews involving 21 Swedish farmers, 20–70 years old, in 2010. A focus group is a group interview in which a small number of participants is brought together to discuss a specified issue under the guidance of a moderator who preferably assumes a low-key position [23]. The comparatively free form of discussion occurring in focus groups enables the researcher to uncover aspects of the chosen topic that were not anticipated but were spontaneously raised in the discussions and thereby proven to be important to the participants. Focus groups were chosen for this study since they offer a research method well suited to generating a rich understanding of participants' beliefs and experiences [24]. Moreover, focus group methodology enables analyses of what participants bring to the group; focus groups constitute "thinking societies in miniature" [25], in which the process of joint meaning-making may be studied in action [26]. Focus group methodology is well suited to studying socially shared knowledge as it is constructed, expressed, and negotiated in a group [27]. Nevertheless, like all research methods, focus groups have their limitations. Their purpose is not to draw statistical conclusions that are generalizable to a general population [28]. Instead, focus groups provide in-depth insight into particular topics, insight that can productively be combined, for example, with survey research.

Each interview started with a discussion of climate change and of the information sources used by the participating farmers to learn about this issue. This part of the interview is not analyzed here, but will be used for other purposes in the K3 project. The last 30–45 minutes of the focus group interview were designed as a participatory exercise in which farmers were asked to mention factors that they saw as facilitating or impeding their adoption of a certain

energy crop (one annual and one perennial). The factors were written down on cards, and participants were then asked to rank them in order of importance [29]. In the discussions, we used four example crops: wheat for energy production, hemp, salix, and hybrid aspen, of which two are annual (wheat and hemp) and two have a turnover time of more than 20 years (salix and hybrid aspen). Despite the use of specific example crops, the discussions were framed in general terms as dealing with the drivers of and barriers to energy farming.

4. Results

As shown in Table 3, the four groups of motivational factors mentioned by farmers during the focus group discussions include numerous aspects and conditions affecting decisions to begin growing energy crops. In Table 3, these are grouped into the four categories of motivational factors identified by Ostwald et al. [10]. In several cases, the same factor may serve as a driver of adopting an annual crop and a barrier to adopting a perennial crop, or vice versa.

5. Discussion, conclusions, and ideas for further research

Table 3 indicates that many of the factors identified in the literature review were mentioned in the focus groups. Legal factors, however, were not mentioned by the participating farmers as having any motivational impact. Knowledge factors, which were not mentioned that often, served mainly as barriers.

Value-driven motivational factors include environmental concerns, which seem to serve mostly as drivers of the adoption of both annual and perennial energy crops. The food versus energy antithesis and the heritage aspect served as very strong barriers to adopting perennial energy crops. This was particularly so in Group 1, comprising farmers in a forest area, who described adopting such crops as a “crossroads” choice that would undo the work of generations of ancestors who have striven to keep the fields clear to enable food production. To some extent, the food versus energy antithesis also served as a barrier to annual crop adoption, as it was seen as unethical to “burn food”. From this perspective, annual energy crops were slightly less bad than perennial crops, as they at least kept open the option of growing food crops in the near future. Moreover, lifestyle issues such as workload and curiosity served as drivers of the adoption of perennial energy crops.

Economic factors were, together with the value-related factors, those most often mentioned in the groups. In particular, the issue of flexibility was discussed thoroughly by all groups, mostly as a barrier to the adoption of perennial energy crops and a driver of annual crops. The inflexibility of the “crossroads” choice of perennial crops focused on the long turnover time of these crops as well as the difficulty of reconverting to annual crops after harvesting the perennial crop. The potential for better risk management by applying a portfolio perspective to the farm’s “crop basket” (identified by Berg et al. [4]) was also mentioned. Moreover, issues of profitability, subsidies, output value in relation to input costs, and other more straightforward economic aspects were also mentioned, particularly by Group 4, which consisted of relatively young farmers in an intensive farming area.

Table 3. Empirically identified barriers, B, and drivers, D, for farmers adopting energy crop production. Each B or D indicates that a factor was mentioned at least once in each focus group.

Identified factors	<1 year turnover	>20 years turnover	Typology of factors
VALUES			
responsibility for nearby environment	D	B	environmental concerns
destroying nice views	D	B	
wildlife refuge (in open landscapes)		D	
preserve cultural landscape	D	B[2]	
environmentally friendly		D	
low negative environmental impact		D	
grow food for the world	BB	B[2]	food vs. energy
potential food becomes energy	B		
producing either food or energy	D		
not usable for other purposes (food)	B		
honour/dishonour ancestors	D	B	tradition/ heritage
"culture" = cultivation	D	B	
fun to try something new		D	fun, curiosity
curiosity		D[2]	
less work, more leisure time		DDD[2]	work load
good timing with other crops		D	
KNOWLEDGE			
too little knowledge		BB	knowledge
well-known crop	D		
not the optimal energy crop (input/input ratio)	B		
ECONOMY			
flexibility	D	BBB	flexibility
destroys field drainage, etc.	DD	BBB[2]	
"crossroads" choice	D	B	
market flexibility (many buyers)	D	BD	
contract (if food wheat price goes up, you lose)	B	D	
unclear political ambitions + long-term perspective	D	B[2]	
lack of flexibility + too little knowledge	D	B	
not such a long turnover time		D	
global wheat trade reduces the risk of unexplainable price price fluctuations	D		
short term – easier to plan	D		
if land is available/marginal land	B[1]D	DD	available land
no available land	BB[1]	B[2]	
unsuitable for soil type/intensive farming region		B	
profitability	BB[1]DD	DD[2]	other factors
subsidies	D	D	
soil degradation	B	B[2]	
(no) need for special equipment	D	B	
rational production		D	
low inputs (labour and agrochemicals)	B	D	
lower quality specifications compared with those of food wheat	D		

[1] Hemp
[2] Hybrid aspen

Moreover, our results have implications for policy formulation in general and for climate change communication and extension service to farmers in particular. In terms of the time and energy spent discussing the different types of motivational factors, value and economic factors were clearly regarded as the most important by participating farmers. In fact, value-related issues seemed to constitute the basis of individual identity – "what it is to be a farmer" – functioning as a filter or background for other factors, including economic ones, which were always assessed in relation to this identity. Hence, in discussing the potential for energy crop production, advisors and authorities must understand farmers' interpretative frames, i.e., what determines how they interpret and understand such messages, and in which agricultural setting they conduct there trade. There is also a clear divide between how various motivational factors serve as either drivers or barriers when annual or perennial energy crops are discussed. New policies to promote energy farming must take this into account, and design specific policy components for specific types of crop so that the overall policy package is coherent in terms of its motivational effects on farmers' decisions.

This paper has presented the results of a preliminary analysis of four focus group interviews of a planned sequence of eight. The following issues will be explored in an upcoming analysis of the present material, complemented by four additional focus groups to be held in 2011:

Firstly, the motivational factors identified here are mainly analyzed with regard to their direction, i.e., whether they serve as drivers of or barriers to the adoption of annual and perennial energy crops. Analyzing the ranking of the identified factors and any correlations between them to establish a hierarchy of importance would improve our qualitative understanding of what affects farmers' adoption of energy crops. Preliminary results indicate that value-related factors are at least as important as economic factors.

Secondly, the motivational factors discussed here were identified from the perspective of individual farmers and the decision contexts that face them when considering converting to energy crop cultivation. The factors all directly influence the outcome, but often they stem from trends and developments on a national or even global scale. The distinction between proximate and underlying forces [12] may sharpen the analysis considerably.

Finally, the increased cultivation of energy crops can be seen as a way society can adapt to climate change by reducing greenhouse gas emissions. Clearly, the opportunities created by increased national and global demand for energy crops enhance risk management and portfolio thinking for farmers, who can benefit from a wider choice of crops when deciding whether to stay in traditional food production or convert to energy crops. These and other adaptation possibilities for individual farmers also merit investigation.

Future quantitative studies, i.e. surveys, could productively explore the relative and absolute importance of various motivational factors to different strata of farmers (e.g., depending on age, type of land tenure, and location).

Acknowledgements

The paper is part of the research project K3Jordbruk (www.cspr.se) funded by the Swedish Farmers' Foundation for Agricultural Research. The authors would like to thank the participants of the focus groups for their generosity, time, and willing participation. We are also grateful for the comments from two anonymous reviewers.

References

[1] European Commission. Renewable Energy Road Map Renewable energies in the 21st century: Building a more sustainable future. Communication from the Commission to the Council and the European Parliament. 2007;10.1.2007. COM(2006) 848 final.

[2] Faaij APC. Bio-energy in Europe: changing technology choices. Energy Policy 2006;34(3):322–342.

[3] Government of Sweden. Bioenergy from agriculture and forestry. 2008:Fact Sheet Ministry of Agriculture.

[4] Berg M, Bubholz M, Forsberg M, Myringer Å, Palm O, Rönnbäck M, et al. Förstudie-sammanställning och syntes av kunskap och erfarenheter om grödor från åker till energiproduktion. Värmeforsk, rapport 2007;1009.

[5] Swedish Government Official Reports. Bioenergi från jordbruket – en växande resurs. 2007;SOU 2007:36.

[6] Berndes G, Magnusson L. The future of bioenergy in Sweden. Background and summary of outstanding issues. 2006;2006:30.

[7] Swedish Government Official Reports. Sverige inför klimatförändringarna – hot och möjligheter. 2007;SOU 2007:60.

[8] The Federation of Swedish Farmers (LRF). De gröna näringarnas klimatlöfte. Available at: http://www.lrf.se/Miljo/Klimat/LRFs-klimatlofte/. Accessed 01/12, 2011.

[9] Domac J, Richards K, Risovic S. Socio–economic drivers in implementing bioenergy projects. Biomass Bioenergy 2005;28(2):97–106.

[10] Ostwald M, Jonsson A, Wibeck V, Asplund T. *Mapping energy crop cultivation and identifying motivational factors among Swedish farmers.*. Conditionally accepted in Biomass and Bioenergy .

[11] Paulrud S, Laitila T. Lantbrukarnas attityder till odling av energigrödor. Värderingsstudie med choice experiment. 2007;Miljöinstitutet, I.V.L.

[12] Ostwald M, Wibeck V, Stridbeck P. Proximate causes and underlying driving forces of land-use change among small-scale farmers–illustrations from the Loess Plateau, China. Journal of Land Use Science 2009;4(3):157–171.

[13] Swedish Board of Agriculture. Bioenergi- ny energi för jordbruket. 2006;2006:1.

[14] Lantz M, Svensson M, Björnsson L, Börjesson P. The prospects for an expansion of biogas systems in Sweden--Incentives, barriers and potentials. Energy Policy 2007;35(3):1830–1843.

[15] Grob A. A structural model of environmental attitudes and behaviour. J Environ Psychol 1995;15(3):209–220.

[16] Nicholson-Cole SA. Representing climate change futures: a critique on the use of images for visual communication. Comput , Environ Urban Syst 2005;29(3):255–273.

[17] Kollmuss A, Agyeman J. Mind the gap: why do people act environmentally and what are the barriers to pro-environmental behavior? Environmental Education Research 2002;8(3):239–260.

[18] Moser SC, Dilling L. Making climate hot. Environment: Science and Policy for Sustainable Development 2004;46(10):32–46.

[19] Rosenqvist H, Roos A, Ling E, Hektor B. Willow growers in Sweden. Biomass Bioenergy 2000;18(2):137–145.

[20] Hillring B. Rural development and bioenergy--experiences from 20 years of development in Sweden. Biomass Bioenergy 2002;23(6):443–451.

[21] Skärbäck E, Becht P. Landscape perspective on energy forests. Biomass Bioenergy 2005;28(2):151–159.

[22] Geist HJ, Lambin EF. Proximate causes and underlying driving forces of tropical deforestation. Bioscience 2002;52(2):143–150.

[23] Litosseliti L. Using focus groups in research. London: Continuum Intl Pub Group; 2003.

[24] Morgan DL. The focus group guidebook. Thousand Oaks, Calif.; London: SAGE; 1998.

[25] Jovchelovitch S. *Contextualising focus groups: understanding groups and cultures*. 2001;Paper prepared for the V Meeting of the Group 'Conversation et language', Laboratoire Européen de Psychologie Social, Paris.

[26] Wibeck V, Dahlgren MA, Öberg G. Learning in focus groups. Qualitative Research 2007;7(2):249.

[27] Marková I, Linell P, Grossen M, Salazar Orvig A. Dialogue in focus groups : exploring socially shared knowledge. London: Equinox; 2007.

[28] Bauer MW, Gaskell G. Towards a paradigm for research on social representations. Journal for the Theory of Social Behaviour 1999 JUN;29(2):163.

[29] Jonsson A, Andersson L, Alkan-Olsson J, Johansson M. (accepted). Defining goals in participatory water management: merging local visions and expert judgements. Journal of Environmental Planning and Management 2011;September 54((6)):xx--yy.

The Chinese Grain for Green Program – assessing the sequestered carbon from the land reform

Madelene Ostwald[1,2,*], Jesper Moberg[2], Martin Persson[2], Jintao Xu[3]

[1]*Centre for Climate Science and Policy Research, Department of Water and Environmental Studies, Linköping University, Norrköping, Sweden*
[2] *Physical Resource Theory, Department of Energy and Environment, Chalmers University of Technology, Göteborg, Sweden*
[3]*College of Environmental Science and Engineering, Peking Universit, Beijing, China*
**Corresponding author. Tel: +46 11363292, Fax: +46 11363292, Email: madelene.ostwald@liu.se*

Abstract: Grain for Green Program was launched in China as a national measure to control erosion and increase vegetation cover in 1999. With a budget of 40 billion US dollar, the program that targets cropland and barren land has today converted over 20 million hectares of land into primarily tree-based plantations. Even though the design of the program includes a category of energy forest only a negligible part is planted as such (0.61%). The majority of the land converted is for protection (78%). The use of these plantations in the future is however unclear and a hypothesis of energy substitution is valid.
In this paper, we try to estimate the overall carbon that has been sequestered due to the program by using official statistics from the program and by calculating it according to mainly three different approaches; calculations made on I) net primary production, II) figures from IPCC's greenhouse gas inventory guidelines, and III) mean annual increment. We also highlight several of the uncertainties that are associated with the program and the estimations.
The result shows that conversion of cropland and barren land generated carbon sequestration over its 10 first years ranging from 222 to 468 million tonnes of carbon, with the IPCC approach yielding the highest estimate whereas the other two approaches had more similar outcome (around 250 million tonnes of carbon). Uncertainties associated with the assessment lies within the use of growth curves not designed for the particular species and their different locations, actual survival rate of the plantations, and discrepancies in figures concerning the program (e.g. area, type, survival rates) at different levels of authority (from national to local). The carbon sequestered in the biomass (above and below ground) from this program is equivalent to 14% (based on median of all three approaches) of China's yearly carbon dioxide emissions due to fossil fuel use and cement production.

Keywords: *Land-use change, Mitigations impact, Plantations, Carbon sink, Bioenergy.*

1. Introduction

As China continues its rapid rate of development, dealing with the massive and growing emissions of greenhouse gases (GHG) (6.5 mega tones of carbon dioxide (tCO2) in 2007 corresponding to 22% of the global total) the country will be vital in the context of global climate change [1]. Afforestation and reforestation have become important measures in China to slow down the wind and water erosion. In 1999 the Chinese government introduced the Grain for Green Program (GGP) also known as Slope Land Conversion Program [2] or The Conversion of Cropland to Forest and Grassland Program [3]. The large-scale afforestation under the GGP will result in a large amount of new forest and hence enhance the carbon sequestration capacity in the terrestrial ecosystems. With this quick background setting the objectives of the paper are to i) estimate how much carbon the program has sequestered, ii) how a national assessment can be conducted and the potential strengths and weaknesses it holds, and finally iii) what the potentials are to use the biomass produced as an energy substitute for fossil-fuel.

2. The program and the setting

The GGP feature the conversion of steep-sloped and degraded cropland and barren land to forest and grassland by millions of small landholders in 25 provinces, municipalities and

autonomous regions (Fig. 1). The primary targeted area of the GGP was the basins of the Yellow and Yangtze River. The Loess plateau located in the upper and middle reaches of the Yellow River is a part of this area. It is well known for severe soil erosion and degraded land. Over 60% of the land suffers from various degrees of soil erosion as a consequence of unsustainable use and degraded vegetation cover, as well as the presence of deep, loose yellow soils [4]. The GGP mainly focuses on steep slopes that seriously threaten to degrade the water quality in the rivers.

Figure 1.Grain for Green Program coverage in China (yellow) indicating the sensitive areas around the Yellow River and Yangtze River.

3. Methods and materials

To estimate the carbon in the trees planted under the GGP information on area, location of plantation and the locations physical characteristics, species, increment per year and survival rate were needed and collected from forestry statistics and national and province level and scientific literature. To estimate the carbon sequestration performance of the programme we assumed a baseline of what plausible would happen in the absence of the implementation. Due to the targeted soils' degraded character with high erosion and unsustainable agriculture we assume the carbon sequestration would be equal to zero of negative. The carbon pools included in the calculation was above and below ground biomass with the latter as a ratio of 0.26 of the former [5].

The total carbon stock for the different regions, i.e. provinces, is calculated according to equation 1:

$$C_{Total} = \sum_{j}\left[\sum_{i}(A_{i,j} \times C_{j} \times (Y - i))\right] \qquad \text{Equation 1}$$

where $A_{i,j}$ (ha) is the converted cropland for region *j* in year *i*. *Y* is the year the study was conducted, i.e. 2009. This means that the trees planted in year i=2008 has been growing for 1 year. C_j (tonnes carbon (ha yr)$^{-1}$) is the carbon increment per hectare and year fitted for the climate conditions of each for region *j*. The time frame used is from 1999 to 2008/2009. The amount of land converted is presented in Fig. 2.

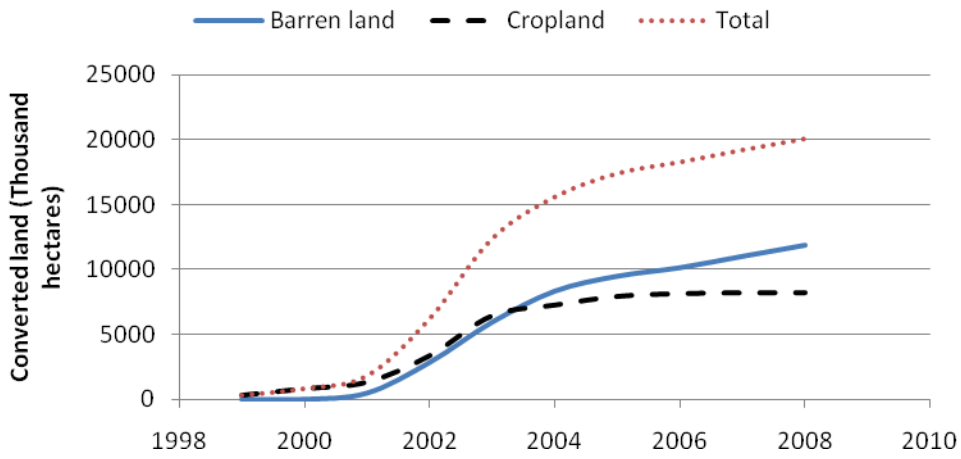

Fig 2. Total accumulated converted cropland and barrenland area 1999-2008, data missing for barren land 1999-2000 (Administration 1999-2008).

Three different values were used to assess the carbon in the terrestrial vegetation in GGP. 1) Net Primary Productivity (NPP), 2) Intergovernmental panel on climate change (IPCC) Guidelines for National Greenhouse Gas Inventories (GNGGI) and, 3) mean annual increment (MAI). Two of the NPP values were derived from China specific studies [6], [7] and one on global average [8]. IPCC default values i.e. in the lower accuracy level Tier 1, were used for natural and managed forest [9]. MAI values are primarily derived from a national assessment [10] or when missing a global value of 1.6 tC/ha/yr [11] was used.

4. Results

4.1. Carbon sequestered under GGP

The total area of barren land converted is larger than the area of cropland converted. Because of this the result of carbon sequestrated by barren land conversion is also larger as can be seen in Fig. 3. The highest value for cropland and barren land conversion is 468 million tonnes carbon (MtC) and the lowest value is 222 MtC. There is a large difference, 246 MtC, between the highest and the lowest values.

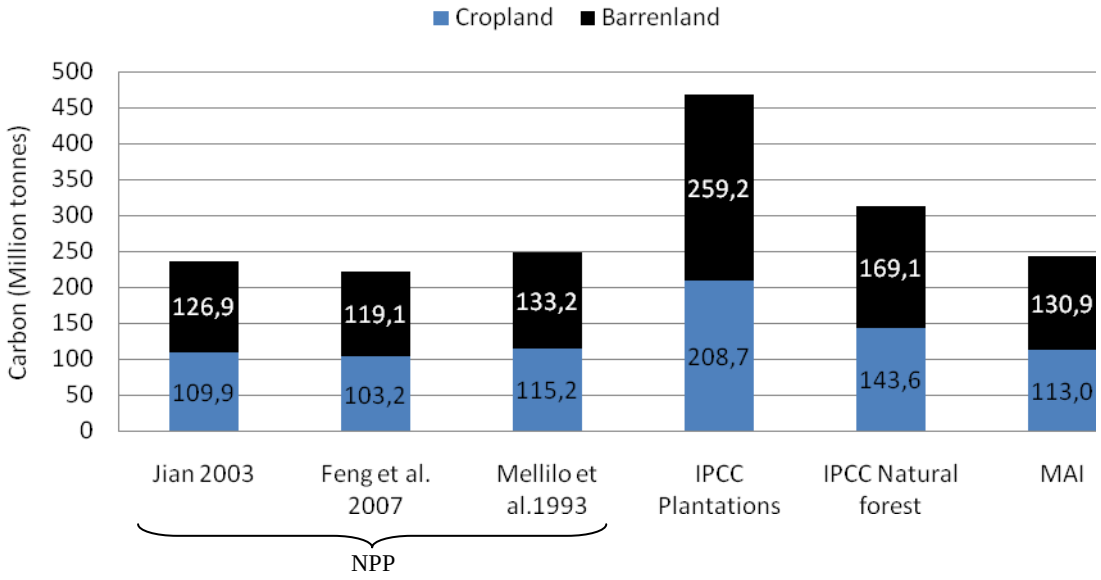

Fig 3. Total amount of carbon sequestrated by conversion of cropland under the GGP 1999-2008 (tonnes).

The reason behind the high value of the IPCC plantation figure can be that the default values are assessed for heavily managed systems including rotation.

4.2. Saptial differences in carbon from GGP

In most provinces the carbon sequestration under barren land and cropland is almost equally large, barren land being a little larger (Fig. 4). Only Xinjiang, Qinghai, Shaanxi, Sichuan and Jilin have larger carbon sequestration through cropland conversion than through barren land. Sichuan has the largest value, 31.7 MtC while Tibet has the lowest, 209 thousand tC.

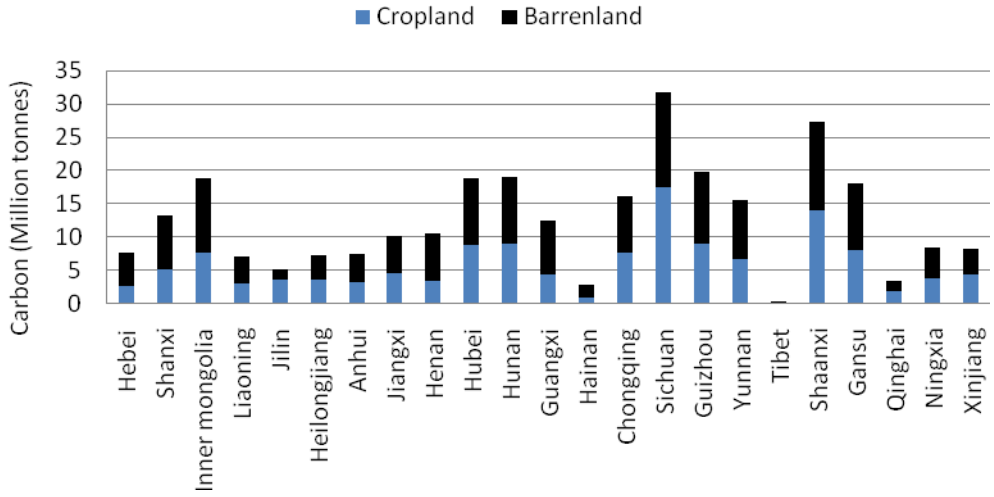

Fig 4. Average amount of carbon sequestrated by conversion of cropland 46.4% and barren land 53.6% under the GGP 1999-2008 per province (Million tonnes).

4.3. Sequestration level and potential impacts

From this 20 Mha plantation program the sequestering rate has been ranging from 222 to 470 MtC with a median on 246 MtC. This would mean that the annual sequestration range from 22-47 MtC/yr with a median on 25 MtC. Or if taken on a hectare basis, a carbon content of

11-23 tC/ha, which indicates a low productivity. Taking the median of 246 MtC it corresponds to 14% of the carbon emitted only in the year of 2009.

5. Discussion

There are large differences in figures depending on the biomass growth used in the model; differing up to 103%. This is due to assumptions on regional differences, species growth patterns and management impacts. Further, the different species and place of planting is crucial for the outcome. Also, the actual area that has been converted differs between sources ranging from 20 to 32 Mha, where we have chosen the lower value from the China forestry yearbook.

Since the legislation behind the GGP states that the forest planted may not be harvested until over-matured there are low potential to grow fast rotational energy forests on the land converted by the GGP. Further, the legislations defines only 0.61% of the forest planted as 'energy forest' whereas as much as 78% of the forest planted are for protection and most of these species are not suitable for usage as bio-energy. Hence, the potential for bio.energy for the forest planted within GGP is low. This is further evident when looking at the amount sequestered carbon that is fairly low, ranging from 11-23 tC/ha .

In order to make the estimation more accurate it would be interesting to collect province specific data regarding the species used and province specific biomass growth rate for all provinces. This would make the estimation more accurate since biomass growth is strongly dependent on local factors such as soil quality, thinning, irrigation and fertilization.

Another way to obtain more accurate results would be to divide the converted land into smaller areas that has a homogenous climate. By doing so better approximations of the biomass growth rates could be obtained by relating the growth rate to the climate.

6. Conclusion

- The carbon sequestrated by the conversion of cropland and barren land under the GGP ranges between 222.3 and 467.9 MtC. The median is 246 MtC while the mean is 289 MtC. With IPCC's approach for natural forests the amount of carbon sequestrated by the conversion of cropland and barren land between 1999-2009 is 312 MtC.

- 246 MtC sequestrated between 1999-2009 corresponds to 14% of the total carbon emitted from Chinas carbon emitted in one year (2009).

- The potential for bio-energy from the forest planted due to the Grain for Green program is low since the part of trees planted that are suitable for bio-energy is low and since the legislations prevents harvesting of the forest until over mature.

References

[1] Caldwell, I. M., V. W. Maclaren, et al. (2007). An integrated assessment model of carbon sequestration benefits: A case study of Liping county, China. Journal of Environmental Management 85(3): 757-773.

[2] Ostwald, M., E. Simelton, et al. (2007). Relation between vegetation changes, climate variables and land-use policy in Shaanxi Province, China. Geografiska Annaler: Series A, Physical Geography 89: 223-236.

[3] Bennet, J., X. Wang, et al., Eds. (2008). Environmental Protection in China Land-Use Management. Cheltenham, UK ; Northampton, MA Edward Elgar.

[4] Li, X., Y. Huang, et al. (2009). A study of the development of bio-energy resources and the status of eco-society in China. Energy In Press, Corrected Proof.

[5] Cairns, A. M, et al. (1997). Root biomass allocation in the world's upland forests. Berlin, Allemagne, Springer

[6] Jian, N. (2003). Net primary productivity in forests of China: scaling-up of national inventory data and comparison with model predictions." Forest Ecology and Management 176: 485-495.

[7] Fang, J., G. Liu, et al. (2007). Carbon budgets of three temperate forest ecosystems in Dongling Mt., Beijing, China. Science in China Series D: Earth Sciences 50: 92-101.

[8] Melillo, J. M., A. D. McGuire, et al. (1993). "Global climate change and terrestrial net primary production." Nature 363: 234-240.

[9] IPCC (2007). Climate Change 2007: Synthesis Report.

[10] Xu, D., X.-Q. Zhang, et al. (2001). Mitigation Potential for Carbon Sequestration Through Forestry Activities in Southern and Eastern China. Mitigation and Adaptation Strategies for Global Change 6: 213-232.

[11] Sathaye, J. A., W. R. Makundi, et al. (2001). Carbon mitigation potential and costs of forestry options in Brazil, China, India, Indonesia, Mexico, the Philippines and Tanzania. Mitigation and Adaptation Strategies for Global Change 6: 185-211.

How would renewables fair if a return to planned electricity markets was introduced?

Stephen Thomas[1,*]

[1] *University of Greenwich, London, UK*
** Corresponding author. Tel: +44 2083319056, E-mail: stephen.thomas@gre.ac.uk*

Abstract: For nearly all their history, modern renewables have had to fit into electricity systems that otherwise operate using the model of competitive wholesale markets and retail competition for consumers. Renewables' costs are generally too high for utilities to choose them in preference to other generation technologies. However, there is wide agreement that fossil fuel generation has to be phased out in favour of technologies that produce low levels of greenhouse gas emissions. There have always been question marks about whether the free market model for electricity would be sustainable but doubts are now beginning to emerge from an unexpected quarter and much more influential quarter, the pioneers of liberalised electricity markets, Britain. In December 2010, the British government published a White Paper on its proposed reforms to the electricity market that are widely expected to see foresee a much more interventionist approach. However, the British government also has a strong policy to promote new orders for nuclear generation and concerns have been expressed that the market reforms will be designed to favour nuclear power at the expense of renewables. This paper reviews previous policies in Britain to promote renewables and examines options available in a more planned electricity system.

Keywords: *Electricity liberalisation, renewable obligation, feed-in tariff, carbon market, capacity auction.*

1. Introduction

For nearly all their history, modern renewable generation technologies have had to fit into electricity systems operated using the liberalised model of competitive wholesale markets and retail competition for consumers. Their costs are too high and, for some options, the technologies are not mature enough for utilities to choose them in preference to other generation technologies. However, there is wide agreement that fossil fuel generation has to be phased out in favour of technologies that produce much lower levels of greenhouse gas emissions. As a result, it has been necessary for governments to override the markets in various ways to stimulate investment in renewable.

In Britain, there is now recognition that there are fundamental problems with the electricity market that will require a return to a more planned approach. In December 2010, the British government published a White Paper that set out its initial thoughts on market reforms. The situation in Britain is complicated by the strong policy, supported by all three major parties, to promote nuclear power, overtly as a way to reduce greenhouse gas emissions.

2. Why have electricity markets failed?

In February 2010 when the British government and the energy regulator both reported major problems with competitive electricity markets, they implied there were two main problems: that the market would not build sufficient new renewable capacity; and that the market could not be relied on to ensure there was enough overall capacity to ensure demand would be securely met.

The British Energy Minister, Ed Miliband, told the Times[1]:

[1] The Times 'Labour prepares to tear up 12 years of energy policy' February 1, 2010, p 37

> The Neta system [the British wholesale market], in which electricity is traded via contracts between buyers and sellers or power exchanges, does not give sufficient guarantees to developers of wind turbines and nuclear plants. He said that one alternative would be a return to "capacity payments" - in which power station operators would be paid for the electricity they generate and also for capacity made available. The idea of such payments is to give greater certainty to investors in renewables and nuclear energy.

A day later, Ofgem stated[2]:

> 'The unprecedented combination of the global financial crisis, tough environmental targets, increasing gas import dependency and the closure of ageing power stations has combined to cast reasonable doubt over whether the current energy arrangements will deliver secure and sustainable energy supplies.'

And

> 'There is an increasing consensus that leaving the present system of market arrangements and other incentives unchanged is not an option.'

Neither argument is convincing. The mechanisms to get renewables built inevitably took them out of the main market and if these mechanisms did not work, it was not the fault of the market, it was in the design of these policies, as is argued below. On the more general point of supply security, it is hard to know why this has come up as an issue now. The market model has always relied on the wholesale market price being high enough that sufficient capacity will remain on-line to ensure supply security and that market signals would be seen early enough to stimulate sufficient new capacity to meet demand growth and replace old plant. So far this has proved the case in Britain and supply security has been maintained although it is arguable this has been the result of market imperfections rather than the efficiency of the market [1]. There are a large number of new power plant projects that could be on-line within five years, albeit mostly gas-fired, so there would seem to be no reason as to why doubts on supply security should arise now.

Thomas [1] argues that the faults are more fundamental and would apply even if there was no need to replace fossil fuel plants with low-carbon generation. He argues that: if wholesale markets became truly competitive, investment in new capacity would be intolerably risky; retail competition inevitably disadvantaged small consumers and within small consumers, the poorest consumers; and the costs of competition are bound to outweigh any conceivable benefits.

3. Renewables in competitive markets

In Britain, renewables have been supported through two separate mechanisms, a capacity auction system from 1990-98 financed by the Fossil Fuel Levy (FFL) through the Non-Fossil Fuel Obligation (NFFO) and from 2002 onwards a Renewables Obligation (RO) system. A Feed-In Tariff system was introduced in 2010 but only for much smaller sources than are covered in, for example, Spain and Germany. Each of these mechanisms has had its

[2] Ofgem (2010)'Action needed to ensure Britain's energy supplies remain secure' Press release R5, February 2010.
http://www.ofgem.gov.uk/Media/PressRel/Documents1/Ofgem%20-%20Discovery%20phase%20II%20Draft%20v15.pdf

advantages and disadvantages. In principle, all could be used in a more planned system so it is important to examine their record.

3.1. The NFFO

The NFFO was an accident born of the failure to privatise the nuclear power sector in 1990. The nuclear power plants were placed in a new publicly owned company, Nuclear Electric. The operating costs of the existing nuclear plants were found to be about double the expected market price for electricity so to allow the company to continue trading, a subsidy had to be introduced. 10 per cent of all consumer bills, the Fossil Fuel Levy (FFL) was allocated to this subsidy raising about £1m per year. The European Commission judged this an unfair state aid to nuclear power and required that it be phased out by 1998.

Nearly all of the FFL was paid to Nuclear Electric. For political reasons, a small proportion of this, rising from 0.5 per cent of the subsidy in 1990/91 to 8 per cent in 1994/95 was allocated to renewables and this was disbursed through capacity auctions [2]. A total of five auctions were held. Typically, the auctions would specify the amount of capacity that would receive subsidies and could also be targeted at particular technologies, for example, waste-to-energy. In terms of prices, the results were impressive with the last auction in 1998 producing an average successful bid of £27/MWh compared to £75/MWh in 1990.

However, the completion rate on the successful bids was very poor. This was partly because of difficulties in obtaining finance and planning consents, and problems of equipment supply. The time limit on the FFL imposed by the European Commission meant also that projects could only receive subsidies for a short period of time up to 1998 when the FFL had to be phased out. In 1996, the FFL for nuclear was abolished and remained at a much lower level until 1998 specifically to subsidise renewables. Because subsidies for renewables were allowable under European Union law, it was possible to extend to 15 years the period for which subsidies could be given and this meant that for the final auction, much longer contracts of 15 years could be awarded to successful bidders rather than the contracts up to 1998 that had applied previously.

3.2. The Renewables Obligation

There was a hiatus from 1998 to 2002 while the government considered how to replace the NFFO. In April 2002, the British government announced that a Renewable Obligation (RO) on electricity retailers would be introduced. This effectively requires them to source a given percentage of their electricity from renewable sources. The level was set at 3 per cent in 2003, rising to about 10 per cent in 2010 [3]. Companies that fell short of their target percentage are required to ‘buy out’ their obligation at 3p/kWh (rising annually with inflation). The funds raised are redistributed to the suppliers that complied with the obligation using certificates. The RO was expected to force electricity retail companies to meet their obligation as cheaply as possible to ensure their tariffs remained competitive.

There have been a number of problems with the RO [4]. First, the design of the penalties means that if all the companies fall short of the target, none of them is financially or competitively disadvantaged. The cost of the buy-out may be judged preferable to the risk and extra cost of building new renewable facilities. Given the structure of the British electricity market, under which all the major electricity retailers are owned by the six large generation companies, the RO is also a barrier to entry for new generators. The retail arms of the ‘big six’ companies will generally have a strong incentive to either own or control the resources they contract and will be able to prevent entry by new renewable generation companies.

3.3. Feed-in tariffs

Feed-in tariffs (FITs) have been highly effective, for example, in Spain and Germany, at rapidly expanding renewable capacity and, given the poor rate of installation of renewables in the UK, this has led to pressure to adopt FITs in the UK. In 2008, the UK Energy Act [6] introduced provisions for FITs and in April 2010, FITs were introduced, but only for installations with a capacity of 5MW or less. This scheme can clearly only have a limited impact and seems focused mainly on households. It is too early to assess how successful it will be yet. Elsewhere, experience suggests that the key to successful use of FITs is to set the fixed tariffs at a level that is high enough to stimulate investment but not so high as to lead to wasteful over-investment with larger than necessary public subsidies.

3.4. Review of experience to date

While Britain has probably the best renewable resource base in Europe, at least with current technology, it has one of the poorest rates of installation and costs have been high [4]. The evidence that costs are high is particularly damning given the emphasis with the two main policies, the NFFO and the RO, on market mechanisms as a means to minimise the cost to consumers.

4. The Future

In the next decade, the requirements for installing renewable generation will be massively increased. Under the RO, British electricity retailers are required to source about 10 per cent of their *electricity* from renewables. Under the European Commission's '20-20-20' targets, Member States would need to source 20 per cent of their *energy* from renewable sources. Given that in the UK, electricity makes up less than 20 per cent of final energy consumption, meeting this target would require a massive increase in installation rates. Even if we assume that half of these renewables would not be used for electricity generation (e.g., bio-fuels), this would require that renewable generation capacity would have to increase more than 5-fold in less than a decade.

It would seem that cost-minimisation can no longer be the dominant policy force. Clearly, electricity needs to remain affordable, especially if we are going to require that it substitutes for direct use of fossil fuels, for example, in space-heating and transport, so cost has to remain an important consideration. However, future generations will not be impressed if we fall well short of the '20-20-20' target no matter how cheap the renewables we do build are.

The major unknown is the attitude of the British government to nuclear power. Nuclear proponents claim that nuclear power is the only feasible way to meet such ambitious targets as the '20-20-20' policy. Nuclear is claimed to be a proven, low-carbon, base-load source that can be deployed in large numbers with no resource constraints that cannot be overcome.

Its detractors, apart from the well-rehearsed arguments on safety, proliferation and waste disposal, dispute that it is as low-carbon as it is portrayed and they are concerned about the extent of uranium reserves. The designs now available for order have yet to be demonstrated. They also claim that nuclear's costs are far higher than governments promoting it acknowledge and that rates of installation for nuclear programmes worldwide have almost invariably fallen far short of the rates forecast. To illustrate the two latter points, they note that estimated construction costs of the latest generation of plants has increased from US$1000/kW less than a decade ago to US$6000/kW and if history is a good guide, outturn costs will be even higher. On installation rates, when President Bush launched the US Nuclear

2010 programme in 2002, the assumption was that one or two new reactors would be in service by 2010. It seems likely that the first reactor under this programme will not be finished much before 2020 and many of the utilities that expressed interest in the programme are now dropping out. Nevertheless, the British government is convinced that a rapid expansion of nuclear power will be the main tool for Britain to reduce its fossil fuel usage.

A number of mechanisms have been mooted in Britain to encourage renewables (and nuclear) development.

4.1. Capacity payments

These were mentioned by the Energy Minister in his February 2010 announcement so it seems likely they are in the mind of officials at the energy ministry (now the Department of Energy and Climate Change, DECC). Capacity payments would be paid to generation sources simply for being available to generate and would clearly be an advantage to potentially base-load sources, but would be of little or no value to intermittent sources such as wind, wave or solar. They would be a particular advantage to nuclear power however, which because of its rigid cost structure is vulnerable to market price variations.

However, the logic of capacity payments would seem to be that they should be targeted at peaking capacity. The annual loading of such plant is highly variable depending on weather and demand, and, for several years, a peaking plant whose availability is needed for supply security might earn little or no income from sale of electricity. A capacity payment sufficient to cover its fixed costs would give plant owners a strong incentive to keep such plant on-line. If a base-load source is not earning enough money to cover its costs from sale of electricity this suggests either that there are market defects or that that source is simply uncompetitive.

It should also be noted that from 1990-2002, the British electricity market design included a type of capacity payment. However, this was continually manipulated by the generators to increase, unfairly, the level of payment they received.

4.2. Fixing the Carbon price

The idea of fixing the carbon price came up in the context of the 2008 UK White Paper on nuclear power [5]. According to this, for nuclear power to be economic, using even the government's highly optimistic figures, the carbon price would have to be at least €36/tCO_2. It may have been that this was simply the easiest way for the British government to maintain the illusion that nuclear power was an economic option that companies would choose unprompted if some enabling measures were introduced. A centre piece of the British policy since then has been that no public subsidies would be offered to induce the construction of new nuclear capacity. However, the discussion of the Carbon price was seen by many as an indication that the British government was considering putting a floor on the Carbon price at a level that would make nuclear power economically viable. A Carbon price floor would also provide a more secure income stream for all renewable options, but whether it would be sufficient by itself to ensure that renewable capacity was built is far from clear. The same reservation applies equally to nuclear power.

In practice, the Carbon price is set in the European Union's Emissions Trading Scheme (EU ETS). Britain cannot choose arbitrarily to fix the Carbon price unless it exited the EU ETS and set a floor Carbon price for a new British Carbon market, which does not seem likely to be politically viable. Alternatively the Carbon price could be fixed if the EU ETS was substantially changed to include a floor price for the whole of Europe.

Few would argue that the EU ETS has worked well and the Carbon price has remained low, far below the levels seen by the British government as being necessary to make nuclear power viable. Whether simply giving up on the market entirely to creatively find ways of reducing greenhouse gas emissions by fixing the Carbon price is necessary is far from clear.

4.3. Energy efficiency

Clearly, reducing demand substantially would make the 20 per cent target much easier to achieve. An aggressive programme of energy efficiency measures would also have other policy pay-offs. Britain now has a serious problem of 'energy poverty', a condition under which a household is required to spend more than 10 per cent of their household disposable income on buying energy for the house. This has risen, as energy prices have increased from about 7 per cent of households in 2002 to more than 20 per cent in 2010. A programme of energy efficiency measures targeted at low income households would have major welfare benefits, would be likely to create large numbers of new jobs in the construction sector. It might also allow existing welfare payments, such as the winter fuels allowance under which all pensioners receive a sum of the order of £300 every December as a contribution to their energy bills.

5. Conclusions

5.1. Political considerations

It is arguable that it was always an illusion that a free market for electricity was feasible except in the few years around the turn of the century when fossil fuel markets were over-supplied and the extent of the challenge posed by climate change had not been fully assimilated at the highest policy level. Renewables are, in general, some way, in terms of cost and technological maturity from the position in which it can be left to the market to order them.

If this is the case, the announcements from the British government of concerns about the electricity market should not have been a shock not because of what was said but because Britain is seen as the pioneer, advocate and most successful implementer of electricity markets.

The European Union is in an even more difficult position than the UK. It bought into the rhetoric of electricity markets fully and has spent more than 15 years trying to impose essentially a copy of the 'British Model' on Member States. In the process it irreversibly dismantled structures and companies which, while far from perfect, had delivered reliable affordable electricity for many decades. For the Commission to admit that this effort was all misconceived will be politically difficult. However, the Commission cannot escape the reality that a free market electricity system is not feasible. A likely outcome is that what will emerge is a 'Frankinstein's Monster' of a system with a veneer of competition, but which in reality is subject to strong centralized planning with inadequate regulation.

5.2. Practical options

The capacity auction mechanism under the NFFO, and the Renewables Obligation and the European Union Emissions Trading Scheme have all suffered from serious design issues that meant that none worked as planned. It is hard to say whether, with better design, these could have been effective or whether it is the fate of all market mechanisms, no matter how attractive in principle, to fail in practice, often through manipulation by the companies.

However, if the '20-20-20' targets are a necessary and viable target, we may not have the time for more experiments with market mechanisms. We will also not have the luxury of cherry-picking only cheap renewable options, such as on-shore wind, we will have to pursue more expensive renewable options.

Feed-in tariffs remain the option with the best track-record of bringing large quantities of renewables on-line. They can also be tailored for a variety of sources with different prices on offer for different technologies.

References

[1] S Thomas, The British Model in Britain: failing slowly, Energy Policy 34, 2006, 583-600.

[2] P Connor, UK renewable energy policy: a review, Renewable and sustainable energy reviews, 7, 2003 65–82.

[3] C Mitchell & P Connor, Renewable energy policy in the UK 1990–2003, 32, 2004, 1935–1947

[4] R Gross & P Heptonstall, Time to stop experimenting with UK renewable energy policy, ICEPT Working Paper, October 2010, ICEPT/WP/2010/003.

[5] Department for Business, Enterprise and Regulatory Reform, Meeting the energy challenge: a white paper on nuclear power, HMSO, 2008.

[6] Department for Business, Enterprise and Regulatory Reform, Energy Act, HMSO. 2008.

Investment in Wind Power & Pumped Storage in a Real Options Model – A Policy Analysis

Wolf-Heinrich Reuter[1,2], Sabine Fuss[1,*], Jana Szolgayová[1,3], Michael Obersteiner[1]

[1] *International Institute for Applied Systems Analysis, Laxenburg, Austria*
[2] *Institute for International Economics, Vienna University of Economics and Business, Austria*
[3] *Department of Applied Mathematics and Statistics, Faculty of Mathematics, Physics and Informatics, Comenius University, Bratislava, Slovakia*
** Corresponding author. Tel: +43 2236 807 550, Fax: +43 2236 807599, E-mail: fuss@iiasa.ac.at*

Abstract: Promoting renewable energy has been a key ingredient in energy policy seeking to de-carbonize the energy mix and will continue to do so in the future given the European Union's high ambitions to further curb carbon emissions. A wide range of instruments has been suggested and implemented in various countries of the EU. A prominent policy promoting investment in renewable technologies is the use of feed-in tariffs, which has worked well at large scale in e.g. Germany, but which has only been implemented in a very limited way in countries such as the UK. Being subject to environmental uncertainties, however, renewables cannot be seen in isolation: while renewables-based technologies such as wind and solar energy, for example, suffer from uncertain loads depending on environmental conditions, hydropower allows for the storage of water for release at peak prices, which can be treated as a premium (partially) offsetting higher upfront investment costs. In addition, electricity prices will respond to changes in electric capacity in the market, which is often neglected in standard investment models of the electricity sector. This paper contributes to the existing literature of real options approaches to electricity investment by investigating the specific characteristics of renewables and their associated uncertainties in a stylized setting taking explicitly into account market effects of investment decisions. The prices of the model are determined endogenously by the supply of electricity in the market and by exogenous electricity price uncertainty. The inclusion of market effects allows us to capture the full impact of public incentives for companies to invest into particular technologies.

Keywords: *Real Options, Energy policy, Renewables, Market effects.*

1. Introduction

According to the International Energy Agency (e.g. [1]), Norway's electricity production is almost exclusively based on hydropower. However, the potentials for large-scale hydropower has been almost exhausted over the past and in the pursuit of meeting emission reduction goals without compromising the security of energy supply, the Norwegian government has been promoting other renewable energy sources such as hydro- and wind power. The latter is particularly attractive for Norway, as it enjoys both high wind speeds and a long coast line.

Within the European Union the most common policy to encourage the installation of renewable capacity has been feed-in tariffs to date. This works such that producers receive a fixed price for the supplied electricity, which exceeds expected market prices. Often these tariffs decrease over time. The policy for the promotion of Norwegian wind power has been an investment subsidy before the project has started. Even though it had been planned to – jointly with Sweden - introduce a market arrangement for electricity certificates to substitute for these investment subsidies from 2007 on, these plans had to be postponed until after 2010. Under this arrangement, as outlined in [2] consumers will have to buy a certain amount of certificates for their electricity bought and eligible power plants will yield certificates for the electricity producers which can be sold. Policymakers then decide upon the type of electricity production, which should be eligible, and on the respective amount of certificates. This way the countries can exploit the renewable resources and distribute the burden on the producers in the most efficient way and the aggregate quota will thus be attained at a lower total cost compared to feed-in tariffs or quotas.

[3] use a real options approach taking into account the uncertainty from certificate price fluctuations to estimate the amount of new renewable capacity coming online under such a joint Swedish-Norwegian electricity certificate scheme. In this study, we want to focus on the current policy of investment subsidies. In addition to the policy context, another factor that we want to take into account in our analysis is the intermittency of wind power, which has tended to make it an unattractive option next to fossil-fuel-fired generation options [4]. In a related study, [5] explored how the integration of energy storage with individual wind turbines could smooth out the wind speed fluctuations. Their results for different types of wind conditions illustrated that short-term wind power fluctuations could be substantially reduced.

Several studies over the past few years have further looked into technologies to realize such benefits and pumped-storage wind-hydro plants, which use reservoirs to store water previously pumped up with wind power, have been found to be profitable under particular circumstances [6]. Especially on islands, where wind potentials are high, pumped-storage wind-hydro plants have been found to be a promising option, with larger islands offering potential for even more profitable investments, where wind-hydro could even serve as base-load (e.g. [7], [8]).[1] Finally, a number of ancillary benefits add to the attractiveness of the technology. These include, inter alia, that the stored water can in emergency cases be used for consumption, irrigation, and to fight fires, etc. Also, wind-hydro plants are almost carbon-free in terms of emissions. Finally, the wind-hydro plant can contribute substantially to grid stabilization by acting as a swing producer (consuming in off-peak times to pump up the water and generating during peak times). Most of the studies reviewed above have found that pumped-storage wind-hydro plants generally only become profitable at high electricity prices or significantly improved design and efficiency combined with high wind speeds. In this paper we want to explore the profitability of such a system both in Norway, but also in Germany considering the impact of uncertainty on investment decisions. Uncertainty emanates from two sources in our study: the development of the electricity price, which can additionally also be influenced by new capacity additions, and the intermittency of wind, which leads to a fluctuating load and thus uncertainty in profits. We therefore want to explore pumped-storage wind-hydro plants to stabilize profits from wind. While this might appear like an attractive solution for particular demonstration cases, it has to be kept in mind that such equipment is extremely costly and it is questionable whether the premium from profit stabilization would make up for this deficiency and whether therefore public funding should rather be directed at R&D targeted at cost reductions in the first place.

We adapt the real options model presented in [9] in order to capture all these elements to answer the research questions outlined above and apply it to the German and Norwegian market situations to get a picture of the profitability of pumped-storage wind-hydro plants in the respective countries. The model focuses on the plant and its operation and abstracts from problems of integrating wind power into the grid, which is why the results have to be interpreted with caution.

2. A Real Options Model for Wind Power Investment with Pumped Storage

2.1. Model formulation

In this section we formulate the model that will be used for the analysis in section 3. We study the profitability of the wind technology combined with pumped storage when compared

[1] This is attractive for small and isolated electricity production systems, which does not apply to Norway.

to the standard wind farms. The investor tries to find the investment strategy that maximizes expected profits during the planning period. He can decide whether and when to construct new electricity generating capacities. There are two possible technologies available: a standard wind farm (referred to as wind) and wind combined with pumped storage (referred to as wind + hydro). The assumptions underlying the model formulation can be summarized as follows:

1. The decisions can be made only once a year, the planning period is finite (*T* years).
2. The total number of power plants that can be built is limited to *n*, where only one power plant can be built during one year.
3. The load factor of both technologies is assumed to be uncertain, which leads to the annual electricity production being uncertain. Therefore, the annual electricity supply of both technologies is assumed to be equal and is denoted by q_t^w, which is modeled in each year as an independent random variable with known distribution.
4. The supply of the investor is given by the maximum quantity as $q_t^w(n_t^w + n_t^h)$, where n_t^w, n_t^h denote the number of wind and wind + hydro power plants built by the investor prior to year *t* respectively. The aggregate supply Q_t in year *t* is given by
$$Q_t = Q_0 + Nq_t^w(n_t^w + n_t^h), \quad (1)$$
where Q_0 is the quantity supplied by firms that do not invest during the planning period and the quantity produced by plants outside the planning period, i.e. which already existed in t=0. *N* is the multiplier of the new investment. This represents the assumption that the new investment in the market is of the same structure as the one chosen by the investor.
5. The electricity price in year *t* (P_t^e) is assumed to depend both on income and demand in the current year and is subject to exogenous shocks, i.e.
$$P_t^e(Q_t, X_t) = Y_t^{-\varepsilon_i/\varepsilon_p} Q_t^{1/\varepsilon_p} X_t \quad (2)$$
where Y_t is the disposable income in year *t* and $\varepsilon_i, \varepsilon_p$ denotes the income and price elasticity respectively. X_t is the exogenous shock, which is assumed to be an independent random variable with known distribution for each *t*.
6. As has been already explained in section 2.1, wind when combined with pumped storage is able to affect the timing of supply and thus to benefit from the price fluctuations within a year. Thus the average price of electricity per kWh sold by a wind + hydro combination is higher than that of a standard wind. This is represented in the model by the price premium *p*, which denotes the price increment in percentage of the yearly electricity average price at the market.
7. The capital costs are annualized, representing a situation where the overnight construction costs are covered by a loan with the annualized capital costs being the yearly installments of such a loan. The O&M costs depend not only on the number of the power plants of the individual technologies, but also on the electricity supply in the given year, Therefore the yearly costs $c(n_t^w, n_t^h, q_t^w)$ of the investor are a function of n_t^w, n_t^h and q_t^w. The yearly income of the investor can be calculated as
$$\pi(n_t^w, n_t^h, q_t^w, X_t) = P_t^e(Q_t, X_t) q_t^w (n_t^w + (1+p) n_t^h) - c(n_t^h, n_t^w, q_t^w). \quad (4)$$

Under these assumptions the investor's problem can be formulated as

$$
\begin{aligned}
\max_{u_t^w, u_t^h} \quad & E[\sum_{t=0}^{T-1} \frac{1}{(1+r)^t} \pi(n_t^w, n_t^h, q_t^w, X_t)] \\
& n_{t+1}^w = n_t^w + u_t^w && t = 0,\ldots,T-1 \\
& n_{t+1}^h = n_t^h + u_t^h && t = 0,\ldots,T-1 \\
& n_0^w = 0, \quad n_0^h = 0 && \\
& n_t^w + n_t^h \le n, \quad u_t^w + u_t^h \le 1, && t = 0,\ldots,T-1 \\
& u_t^w \in \{0,1\}, \quad u_t^h \in \{0,1\} && t = 0,\ldots,T-1 \\
& q_t^w, X_t - \text{random variables with known distribution} && t = 0,\ldots,T-1
\end{aligned} \tag{5}
$$

where r is the subjective discount rate, n_t^w, n_t^h are the state variables, u_t^w, u_t^h the control variables that are binary and represent the decision of the investor to invest in year t into a wind/wind + hydro power plant respectively.

The resulting problem is a stochastic optimal control problem in discrete time with all the underlying variables being discrete in each time step. Thus it can be solved by recursive dynamic programming. The solution is then the optimal control in terms of feedback control telling the investor the optimal action for each time step and each possible state in that time.

To analyze the impact of the individual features of the model (impact of climate policy, wind load uncertainty), this output is further processed. In the results section, two indicators of the optimal control are usually reported: the mean amount of wind + hydro farms that are built within the planning period, and the value of the firm. The mean value of the firm is directly given by the value function in the first year that is derived by the dynamic programming. For the average number of wind + hydro plants, Monte Carlo simulations are used. Future load and price shocks are simulated and for each simulation the feedback optimal control is used to extract the decision realized in that simulation. These decisions are then used for the calculation of the average investment into wind. In addition, these can be used to calculate the sum of the discounted profits over the planning period in each simulation, which gives us a distribution of the value of the firm as well. For the application, the values of the individual parameters have to be estimated, the functional forms and the remaining data still have to be specified. This is explained more in detail in section 2.3.

2.2. Data

In our paper the investment decisions of the producers are exemplarily surveyed in the countries Germany and Norway. The producers can choose between a farm of wind power plants and a farm of wind power plants in combination with a hydro pump storage plant. Both investment opportunities are adjusted so that the maximum output per year is the same. Furthermore the ratio of the size of the wind farm respectively the combination of wind farm and hydro pump storage in Norway and Germany is equal to the ratio of the size of the two electricity markets (Q_0). [9] calculate the optimal size of the pump storage plant in relation to the wind farm and derive the ratio of 1:3. We use this ratio together with their estimate for the electricity loss caused by the pump process in the hydro pump storage plant of 0.1128 to calculate the setting of the combination. The cost estimates we use are taken from the 2010 [10] and summarized in Table 2. To derive the costs in € rather than US$, we used the exchange rate given in the IEA report [10] of 0.68 and the same measure (average exchange rate of 2008) for the translation of € into Norwegian Kroner at 8.22 (OECD, 2010 [11]).

Table 1 Cost Data

		Yearly production	Ann. Capital Costs / Plant	Variable Costs (O&M + Fuel + Permit expenses)
Wind	Germany	25,916.9 GWh/a	275.9 Mio. €/a	24.90 €/a
	Norway	6,120.5 GWh/a	535.8 Mio. NK/a	204.78 NK/a
Wind + Hydro Pump Storage	Germany	25,916.9 GWh/a	543.1 Mio. €/a	32.08 €/a
	Norway	6,120.5 GWh/a	1,054 Mio. NK/a	263.78 NK/a

Source: calculated from [10] IEA, 2010.

The load factor of the wind plants is assumed to be normally distributed around a mean of 23% (according to [11]) with a standard deviation of 6% (as estimated for Europe in [12]). There is a huge amount of literature estimating the demand and its elasticity for electricity. Two often cited survey articles in this stream are Dahl (1993, [13]) and Espey and Espey (2004, [14]). Together they analyze some 84 articles with estimations of the elasticity for electricity. For modelling our price process, we rely on the basic model to keep the analysis transparent. The elasticities are thus estimated as follows:

$$\ln Q_t = \varepsilon_p \ln P_t^e + \varepsilon_i \ln Y_t + x_t \tag{6}$$

with x_t denoting the error term. The articles also calculate mean values of the estimates found in the analyzed articles for equation (6). The authors report an interval with the mean price elasticity of demand ε_p at -0.80 and the mean income elasticity ε_i at 0.93. The estimations using the form in (6) exactly estimate the price process used in our model described given by equation (2). For the stochastic shock (error term in (6)) we assume a normal distribution with mean 1 and standard deviation of 0.2 (which is approximately the size of the variance of the error term when estimating equation (6) with our underlying data). We model the disposable income using a starting value Y_0 from 2009 and the average annual growth rate y of the last 20 years (1990 – 2009). As the firm has no investments at time $t=0$ we take the actual total gross electricity generation of 2009 as the original supply in the market Q_0 and assume that respectively the big electricity producers of a country simultaneously take the same decisions. The data is summarized in Table 2.

Table 2 Price Process Data

	Y_0	y	Q_0	N
Germany	2,445.5 Bio. €	0.0288	577,380 GWh	4
Norway	2,264.3 Bio. NK	0.0389	136,353 GWh	5

Source: EUROSTAT (2010), OECD (2010) [11].

The considered planning period T is chosen as 30 years and following the standard assumptions in this stream of literature, we assume a discount rate r of 0.05. Each firm is allowed to invest a maximum of four times. Note from the data that the difference between the "Germany case" and the "Norway case" lies in two characteristics: the size of the market and the electricity price process (and the underlying parameters).

3. Model Results and Policy Analysis

3.1. Price Premium

An investment into the combination of a wind farm and a hydro pump storage plant conveys the following characteristics: a) the (uncertain) output of the wind farm is the same as without the hydro pump storage, but b) the producer now has the opportunity to save some output if

the prices are low and sell the output plus the saved electricity if prices are high. Thus c) on average the producer earns a higher price per unit of output, i.e. he receives a price premium for having the opportunity to postpone the selling of current production. This premium has to outweigh the d) investment costs for the hydro plant, the variable (O&M) costs of running the hydro pump storage plant and the (small) loss of output through the storage process. Figure 1 shows the average number of investments into the combination at the end of the planning period for different levels of price premia. One can see that only with a price premium as high as 70% in Germany and 75% in Norway the combination gets relatively profitable and the producers invest into it at least once. To get the maximum average number of investments a premium of at least 115% would be needed in Germany and 150% in Norway. Such high differences in the average price per output unit cannot be realistic. E.g. [15] calculated the optimal operation and size of a wind-hydro power plant combination. They found the yearly average per unit profits of the combination to be 20.12% higher than the per unit profits of an equally sized wind farm. Thus, we can conclude that today the investment into a combination of a wind farm and a hydro pump storage plant without public support is not profitable for a producer compared to only investing into a wind farm.

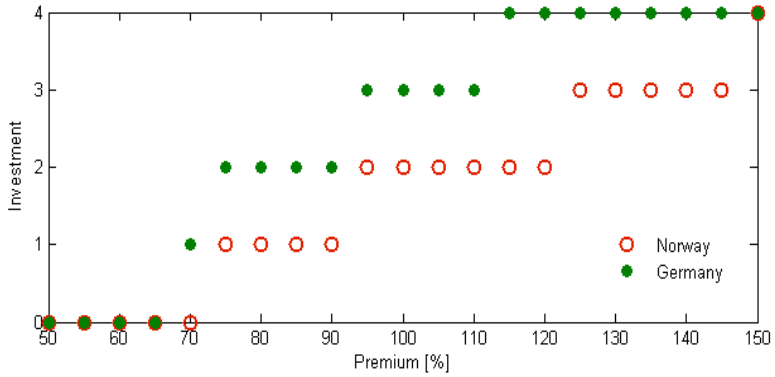

Figure 1: Average investments into wind-hydro at the end of the planning period for different levels of price premia

Two factors we do not consider in our study are grids and economies of scale. One can think of the additional costs surrounding the transmission of the electricity from the wind farm to the pump storage plant and back into the system as an increase in the variable costs of each produced unit. These costs are higher the farther the wind farm is away from the pump storage plant or in the periods (high-peak vs. low-peak) during which the electricity is transported. Thus, a large fraction of the literature shows that the combination is most profitable on small islands and could even serve as base-load on larger islands (see e.g. literature review in Anagnostopoulos and Papantonis (2007) [6]). In our framework, taking into account the costs grid adjustments would increase the threshold premium needed to make the combination relatively profitable. Economies of scale work in the other direction. So a bigger wind farm or e.g. an already existing bigger hydro pumped storage plant can produce the electricity at lower per unit costs, which will result in a lower threshold premium.

3.2. Investment Subsidy

Due to the positive externalities of the combination, i.e. for example stored water can in emergency cases be used for consumption and irrigation, etc, it makes sense for a country to support the investment into these combinations. E.g. Norway supports the investment into the combination by paying a subsidy on the investment costs before the project starts. This subsidy would need to be high enough to make up for the difference in the premium needed (as seen in the chapter before) and a realistic premium.

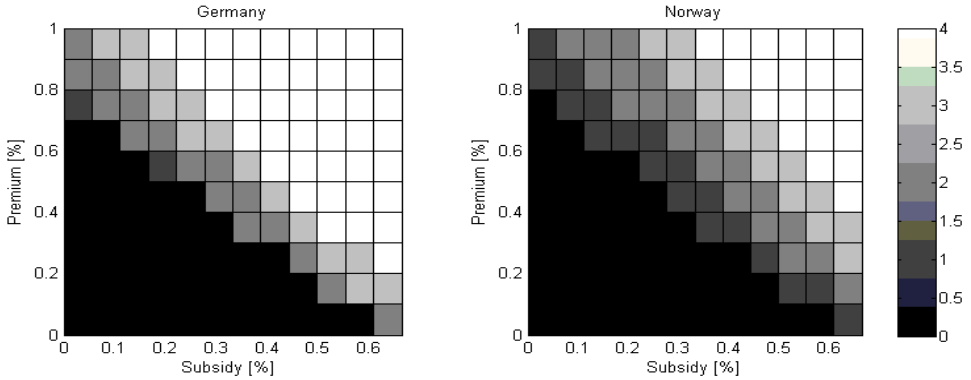

Figure 2: Average investments into wind-hydro at the end of the planning period for different levels of capital cost subsidies.

Figure 2 shows the average number of investments into the combination at the end of the planning period for different levels of capital cost subsidies. The different areas are shown for a variation of price premia between 0% and 100%. For realistic premia values (i.e. between 10% and 30%) the threshold subsidy to trigger at least one investment into the combination in Germany and Norway lies between 35% and 50%. To get the maximum average number of investments a subsidy of up to 70% in Germany and 90% in Norway would be needed. In general, one can see that the investment activity of the producers is much more sensitive to an increase in the subsidy in Germany than in Norway. This can be explained by the relatively higher threshold level needed to trigger investments in the Norwegian market, i.e. prices start relatively lower in Norway due to the relatively higher already installed capacity in t=0 in Norway. Afterwards the follow-up investments happen later due to the higher number of big firms investing at the same time and the higher (in absolute terms) price level. Since in our framework we compared the investments into wind farms and the investments in a combination of wind power with hydro pump storage plants, the introduction of a likely Swedish-Norwegian tradable green certificates system, which would affect both types of plants symmetrically, would in general not change our results. The results would only change if policy makers would allocate different amounts of certificates to units of electricity produced by wind or water plants and categorize the electricity produced by the hydro pump storage plant as electricity generated by water rather than by wind. In that case the result in our framework would be a decreased (if the allocation is in favor of water; increased otherwise) threshold premia. Producers will earn an uncertain but positive additional amount per unit produced.

4. Conclusion

This paper has presented a model for the economic evaluation of the adoption of a hybrid technology combing wind power and hydro pumped storage. We have chosen the market situation in Germany and Norway as case studies and explicitly accounted for uncertainty about the development of the electricity price and the market effects of new capacity additions, the intermittency of wind leading to a volatile load and the policy of an investment subsidy. While the stabilization of profits and its raise by a premium from being able to sell at peak prices might appear attractive, our study shows that without substantial public support the technology is not profitable and will not be adopted for realistic premia. If grid stabilization, CO_2 mitigation and other objectives than profit-maximization enter the objective, there is thus a case of intervention to promote this type of technology.
Apart from the conventional policy measures ranging from feed-in tariffs to investment subsidies, another important dimension recommended to policy makers for consideration is

the investment into R&D to decrease the costs and increase the efficiency of the technology in general. Rather than supporting investments today with relatively high costs compared to other green technologies, this can prove to lead to a faster diffusion of the technology at lower cost. Further research should also try and include factors that have not been considered explicitly in this analysis: grids, economies of scale and – in the case of Norway – the planned green certificate system.

Acknowledgements

This work has been conducted in the frame of the Norwegian PURELEC Project. The authors want to thank the partners of the PURELEC consortium for their advice and help.

References

[1] International Energy Agency. Energy Policies of IEA Countries Norway: 2005 Review, SourceOECD Energy, vol. 2005, no. 28, 2005 [ISBN 9264109358].

[2] Soederholm, P. The political economy of international green certificate markets. Energy Policy 36, 2008, 2051– 2062.

[3] Fleten, S.E. and Ringen, G. New renewable electricity capacity under uncertainty: the potential in Norway. The Journal of Energy Markets, 2009, 71–88.

[4] Lund, P.D. and Paatero, J.V. Energy storage options for improving wind power quality. Nordic Wind Power Conference, 22-23 May, 2006, ESPOO, Finland.

[5] Paatero, J.V., Lund, P.D. Effect of energy storage on variations in wind power. Wind Energy, 2005, 424-441.

[6] Anagnostopoulos, J.S. and Papantonis, D.E. Pumping station design for a pumped-storage wind-hydro power plant. Energy Conversion and Management, 2007, 3009-3017.

[7] Bakos, G.C. Feasibility study of a hybrid wind/hydro power-system for low-cost electricity production, Applied Energy, 2002, 599-608.

[8] Bueno, C. and Carta, J.A. Wind powered pumped hydro storage systems, a means of increasing the penetration of renewable energy in the Canary Islands. Renewable and Sustainable Energy Reviews, 2006, 312-340

[9] Reuter, W., Szolgayova, J., Fuss, S., Obersteiner, M. Renewable Energy Investment: Policy and Market Impacts. Int. Conference on Applied Energy - 16-18 May 2011 - Italy.

[10] IEA, 2010, "Projected Costs of Generating Electricity". IEA/OECD.

[11] SourceOECD, 2010, National Accounts Data & Main Economic Indicators, OECD.

[12] Atkinson, N., Harman, K., Lynn, M., Schwarz, A., Tindal, A., 2006, "Long-term wind speed trends in north-western Europe", BWEA 28, Glasgow.

[13] Dahl, C. A Survey of Energy Demand Elasticities in Support of the Development of the NEMS (1993) Contract De-AP01-93EI23499, U.S. Department of Energy.

[14] Espey, J.A., Espey, M. Turning on the Lights: A Meta-analysis of Residential Electricity Demand Elasticities. Journal of Agricultural and Applied Economics, 2004, 36, 65-81.

[15] Castronuovo, E., Lopez, J., 2004. Optimal operation and hydro storage sizing of a wind–hydro power plant. Electrical Power and Energy Systems 26, 2004, 771–778.

Grid-Connected Renewable Energy in China: Policies and Institutions in a Socialist Market Economy

Clara García[1*]

[1] *Complutense University, Madrid, Spain*
** Corresponding author. Tel: +34 633504758, E-mail: clara.garcia@ccee.ucm.es*

Abstract: Chinese policies and institutions for the deployment of renewable electricity are only partially compliant with what is internationally recognized as "best practice"; and divergences from the optimal policy and institutional model are frequently interpreted as obstacles to renewables in China. Much as a political economy perspective has aided understanding of why Chinese economic reforms were partial and unique, the contextualization of Chinese policies and institutions for renewables in the broader picture of China's political economy (said contextualization being the purpose of this paper) might help explain why those policies and institutions diverge from best practice. Further, given that China proved successful in promoting its economic growth with partial and unique reforms, the partiality and uniqueness of its renewable policy and institutions need not impede the rapid development of renewable electricity. Our analysis combines a review of specialized literature and the business press with semi-structured interviews held with relevant actors in policy, business, and research related to renewable energies.

Keywords: *Renewable energy, Policies, Institutions, Political Economy, China.*

1. Introduction and methodology[1]

There is an extensive literature that describes the particularities of China's political economy, as well as, in many cases, the impact of said political economy on socio-economic performance. These are usually studies that deal with quite broad views of political economy as well as with broad outcomes (such as economic growth). Nevertheless, one observes less emphasis in trying to relate the features and performance of more specific economic sectors (e.g. renewable energy) to the particularities of the Chinese political economy. Instead, when looking into concrete economic sectors, it is not uncommon for specialists to analyze China by applying concepts and theoretical models developed for other realities. Also not uncommonly, the fact that Chinese regulations do not fit nicely into such concepts and models leads observers to pessimistic expectations on Chinese performance.

In this paper, we look into the Chinese grid-connected renewable energy (GCRE) sector as an exercise in overcoming the mainstream de-contextualization of the analysis of Chinese policies and institutions when it comes to specific economic sectors. To be more concrete, we attempt to explain why Chinese policies and institutions do not nicely fit into the "best practice" model, in view of China's principles for decision-making. Whereas such model could be portrayed as a sector-specific description of a Liberal Market Economy (LME), Chinese policies and institutions for GCRE more resemble the sector-specification of what could be termed a Socialist Market Economy (SME); more concretely, policies and institutions are informed by three principles of decision-making particular to the Chinese political economy: gradualism, developmentalism, and socialism.

Our analysis combines a review of specialized literature and the business press with semi-structured interviews held with relevant actors in policy, business, and research related to renewable energies. Interviews were conducted at: departments of the Government of Spain;

[1] The author would like to acknowledge the financial support of a Becas Complutense-Del Amo grant, as well as the insights provided by John Zysman and Steven Vogel, and various doctoral students at University of California, Berkeley.

Chinese public research centers; institutions for international cooperation in energy and the environment; and multinational companies operating in China.

2. Policies and institutions for GCRE: "best practice" and the case of China

There is an extensive literature describing sets of policies and institutions[2] that foster the deployment of renewable energy (and GRCE in particular). Such collections of prescriptions are scattered, appearing mostly in professional reports and policy handbooks published by energy organizations or associations (see for example GWEC, 2005; IEA, 2007 and 2008; IREC, 2004; World Bank, 2008; WEC, 2004).

In a previous paper (García, 2010), we assembled a systematic collection of the policy and institutional prescriptions posited in these reports as "best practice"; also characterizing such prescriptions as a sector-specific description of a particular kind of capitalism, sometimes termed LME, as in Hall and Soskice (2001). In particular, the model consists in: (1) policies that eliminate economic barriers to renewables (barriers to investment related to insufficient revenue or excessive cost) by leveling the playing field of renewables vis-à-vis fossil fuels, as well as by implementing support mechanisms that compensate for high costs, limited access to finance, and insufficient demand; and (2) institutions that eliminate non-economic barriers (barriers to investment related with institutions) by ensuring good governance on the part of the State and corporate competition. In other words – in terms closer to those describing LMEs – policies consist in regulations that intend to facilitate private investment via the perfection of market mechanisms; and institutions consist in liberal-market institutions, which would also facilitate investment. See a detailed summary of the "best practice" model in Table 1.

Also, the aforementioned paper (García, 2010) discussed the extent to which China's policies and institutions for GCRE fit into the "best practice" model, concluding that they do so only partially and imperfectly. China's policies diverge from best practice insofar as: negative externalities of fossil fuels are not compensated for (as with a coal tax); regulations do not incentivate feeding power into the grid, but instead focus on installing capacity (China's renewable portfolio standard does not refer to actual power fed into the grid but to installed capacity; and the tender system for wind that prevailed until 2009 had no provisions to ensure generation and transmission); remuneration levels are low and duration of tariffs is short (be they tariffs set in tenders, in local licenses, or through FITs); regulations do not include enough provisions for the reduction of tariffs over time, necessary for the promotion of cost-reducing innovations; and PPAs do not ensure connection. Meanwhile, concrete divergences in institutions include the following: general legal insecurity; complex and lengthy red-tape; unpredictable policy instruments (insufficient stability and transparency); insufficient competition in generation due to market concentration, a high market share remaining in public hands, and limits to foreign presence; and restrictions to innovation in manufacturing brought about by barriers to external trade and to foreign investment. See Table 1.

[2] Policies here refer to those rules offered by public authorities as the preferred course of action toward a desired outcome; and institutions refer to structures of economic actors (governmental or corporate) and the mechanisms that influence those actors and relations between them.

Table 1. Summary of "best practice" for the deployment of renewables, and the Chinese divergence from "best practice"

	Policies and institutions for renewables in the "best practice" model	Elements typical of a liberal market economy	Chinese divergences with "best practice"
Policies to overcome economic barriers	Elimination of coal subsidies	Perfection of markets: role of government is to, with an arm's length approach, eliminate market distortions and compensate for market failures	Negative externalities not fully compensated for
	Compensation for the negative externalities of fossil fuels (pollution…)		
	Remuneration for the positive externalities of renewables		
	Compensation for high initial costs (mandated market policies): quantity-based and price-based schemes		Regulations focus on installed capacity rather than power generation Remuneration levels are low, and duration of tariffs is short
	Increased access to capital: fiscal and financial aids		Regulations do not include enough provisions for reduction of tariffs
	Ensuring sufficient demand (PPAs)		PPAs do not ensure connection
Institutions to overcome non-economic barriers	General legal security	Liberal-market institutions: role of government is to set formal and predictable (stable, non-discretionary, and transparent) rules that are effectively enforced; and to ensure low barriers of entry and competition	General insecurity and uncertainties
	Capable bureacracy: coordination and cutting of red-tape		Incomplete coordination, and complex and lengthy red-tape
	Quality of regulations in renewables: specific, legally binding targets, and predictable instruments		Targets not compulsory, and instruments lacking stability and transparency
	Competition and technology-friendly policies in generation: unbundling, absence of oligopolies, openness to FDI		Limits to competition in generation (market concentration, public ownership, and barriers to foreign entry)
	Competition and technology-friendly policies in manufacturing: openness to external trade and FDI		Limits to innovation (barriers to foreign trade and entry)

Source: Author's design.

3. China's policies and institutions for GCRE in light of principles of policymaking

We contend that singularities in Chinese policies and institutions for GCRE are better understood in light of the overall framework of the Chinese political economy or, more specifically, of the general principles of decision-making in China[3]. We use authoritative secondary sources, as well as insights obtained in interviews, to identify those factors that might help understand the partiality and uniqueness of the Chinese fit into "best practice". In doing so, we stress the importance of gradualism of reforms, developmentalism, and socialism in explaining most particularities of Chinese GCRE's policies and institutions.

Gradualism in Chinese economic reforms has been widely documented[4], with reforms being implemented incrementally and also experimentally. Addressing electric sector reform in particular, Ma and He (2008) and Chen (2010) describe how the transformation of policies and institutions has moved gradually and incompletely toward those of a market system. Various interviewees for the present study described Chinese policies in renewables as being implemented slowly, and through experimentation and trial-and-error (author's interviews). Indeed, many of the aforementioned divergences from "best practice" in the promotion of renewable electricity can be explained in light of gradualism, such as for instance: increasing but still insufficient taxation of coal; the focus on promoting installed capacity before focusing on efficiency as the goal of either mandated market policies or financial incentives; the increasing but still insufficient remuneration and duration of mandated market policies (whether tenders, independent projects, or even FITs); and increasing but incomplete regulation and enforcement of PPAs[5]. Also, institution building is clearly underway, and the following institutional barriers could be seen as the result of gradualism: general legal insecurity; fragmentation of the bureaucracy; targets that remain non-binding; insufficient regulatory details in the REL and its provisions; increasing albeit insufficient wholesale competition, or the preeminence of public ownership in generation. Finally, experimentation can be seen in the wide range of policies implemented: China uses (or has used) most of the policies in the toolbox, also experimenting with institutions – for instance, frequent modifications of incentives to foreign participation in generation or manufacturing.

Nevertheless, interpreting obstacles to renewables in view of gradualism might suggest that there is but one single path for policy- and institution-making for GCRE, which China is following, however slowly. But – as Naughton (1996) and Rawski (1999) indicated – gradualism implies not only that China crosses the river by groping for stones, but that it might be unclear what is on the other side (what the regulatory goals are). If so, the fit of Chinese GCRE policies and institutions with "best practice" might remain forever partial. Also, because other institutional forces, beyond transition, shape Chinese policies and institutions for GCRE, divergences from what is considered an optimal framework for investment could perpetuate[6]. From among such forces, we highlight developmentalism and socialism[7].

[3] For a comparison of how political economy factors (in particular, principles and power structures informing policymaking) explain differences between China, India, and Brazil in reforming electric utilities, see Rufín et al. (2003).
[4] See, for instance, McMillan and Naughton (1992), and Naughton (1996).
[5] Although the amendment to REL introduced in December 2009 specifies the fine to be payed by non-compliant grids, some analyses contest that rather than making connection requirements simpler and stronger, the amendment barely modifies REL, or even complicates its directives (see http://www.chinaenvironmentallaw.com/2009/12/28/chinas-renewable-energy-law-amendments; last accessed 12 December 2010).
[6] That there is no convergence into a single policy and institutional model, even when countries might share the same discourse and general pro-market trends, is stressed in Rufín et al. (2003) for reforms in the electric sector.
[7] Together with Chinese traditional culture, development and socialism are identified by Ogden (1989) as the three core values informing decisionmaking in China.

We contend that the Chinese State exhibits elements of developmentalism that help explain some of the uniqueness of China's policies and institutions for GCRE. As in the paradigmatic cases of Japan or South Korea[8], in China: (1) economic policy has developmental goals; (2) development is deemed as necessary for political legitimacy and stability; and (3) development is to be achieved by means of the State's involvement in the mobilization and allocation of resources. On similar grounds, McNally and Chu (2006) argue that China is another case of a developmental state, although a "diffuse" one, insofar as the central government merely sets the overall incentive and policy framework.

First, the Chinese government is widely recognized to have developmental goals, in the present century with an emphasis on equitable and sustainable growth – an emphasis embedded in the idea of Scientific Development. We should also stress that China shares with prototypical developmental states an emphasis on development goals attached to a somewhat lesser emphasis on rules: concreteness and transparency of regulations are not necessary for development[9]; and ideology can be set aside when deciding regulation, opening the door to pragmatism, flexibility, and eclecticism in the choice of policies and institutions.

Bringing the developmental state to electricity and renewables, there are very diverse non-renewable-energy goals embedded in China's decisions regarding renewables. Goals include energy security (limiting oil imports, avoiding black-outs), socio-economic development (developing local industry, providing employment, lessening rural-urban inequalities and consequent migration…); and environmental protection (diminishing local pollution, as well as emissions of greenhouse gases) (Martinot and Li, 2007; author's interviews). In fact, the delay in using feed-in-tariffs and the early favoring of tenders might reflect the growth imperative insofar as the latter instrument kept prices lower than the FIT system would (Lema and Ruby, 2007).

We have also found an emphasis on goals vs. regulations in Chinese policies and institutions for GCRE. Several interviewees noted the relevance of REL, not for the (few) regulatory details included in that law, but for the signal it sent of Beijing's commitment to pursuing renewable-related goals. In regard to pragmatism, and referring to reforms in the electricity sector, Rufín et al., 2003, see this as an element of Chinese ideology informing the particularities of such reforms.

Second, China's developmentalism is frequently seen as the means to preserve its political regime. Changes in policies and institutions are not in conflict with the preservation of the political system, but reforms are instead conducive to development, and therefore necessary to such preservation. For the case of electricity and GCRE, Yeh and Lewis (2004) argue that the electric sector reform was not an embrace of competitive market models, but the "creative, dynamic response to a set of technical and economic constraints on the one hand, and the political imperative to stay in power on the other. This logic of reform motivates the strategic decision to increase electricity production in order to meet current demand and fuel future economic growth. Such growth, in turn, is part of a larger effort by the party-state to maintain legitimacy by channeling potential citizenship demands into consumption and thus pacifying newly middle-class consumers" (Yeh and Lewis, 2004: 464). Similarly, it is arguable that if Chinese policies and institutions for GCRE do not fit into "best practice", it is because these are not an advancement toward the perfection of electricity markets and the creation of

[8] Frequently cited references on the Developmental State in Japan or South Korea are Johnson (1982) and Amsden (1989).
[9] See Johnson (1982) for a portrayal of the importance of the executive vs. the legislative in the Japanese developmental state.

market-friendly institutions. Rather, they are the necessary response to diverse development needs that, if unattended, could lead to a loss of legitimacy of China's political regime.

Third, the policy and institutional instruments to achieve developmental goals are not strictly those of a liberal market economy, but closer to those of developmental East Asia (World Bank, 1993). Essentially, these include a wide array of non-market-distorting instruments, as well as instruments that do distort resource allocation. In other words, the role of the State in China is not one of creating and perfecting markets, or of ensuring that the proper market institutions are in place, but rather to control these in search of the aforementioned developmental goals (Huang, 2008; McNally, 2008[10]). Involvement of the State in the allocation of resources is exerted via a range of mechanisms that extend from indicative planning to industrial policy and direct ownership of companies. Indicative planning can be seen, in general, in China's Five Year Plans; and, in the case of GCRE, in documents such as the National Medium and Long-Term Development Plan for Renewable Energy in China. Also, the corporatization of state owned enterprises (SOEs) was not simply a gradual move toward privatization, but an attempt to create national-scale holding companies where "state ownership was in a controlling position, to develop large-scale enterprises across territorial and product sector lines, introduce advanced technology, create new products, and work toward achieving international competitiveness. Although it was unstated, this was essentially the model of the huge Korean enterprise groups" (Yabuki and Harner, 1999: 42). In other words, the most recent advancements in industrial reforms demonstrate mixed elements of industrial policy (an effort to nurture certain industrial sectors) and public ownership as means to achieve developmental goals. The tender system for wind (delays in implementing FITs), low remuneration, and other aforementioned limits to foreign competition in power generation (not to mention in distribution) are better understood in light of China's intentions to preserve and nurture public control and even ownership over strategic sectors.

Finally, socialism also informs policymaking and institution-building in China. Some even see gradualism and experimentation as the result of the inherited socialism: in particular, of "communist ideology, nationalistic ambitions, (…), and less opposition from interest groups" (Ma and He, 2008: 1699). And the ongoing prevalence of socialism, even after thirty years of reform, is observable in the official branding of China's economic regime as Socialism with Chinese Characteristics, or in the endorsement, since 1993, of a SME. This system, simply put, entails public ownership (dominating in key sectors) while at the same time having all entities participate within a market system. Also, the SME includes a desire for self-reliance, no longer understood as autarchy but via strategic integration in the global economy (Liu, 2007). Under Mao's Socialism, the State combined government and business roles, and that was also the case for the electricity sector (Ma and He, 2008). Under current Socialism, the government and business roles have been split into different government agencies, to the point where (starting in 2003 according to Ma and He, 2008) public entities in charge of the electricity business have been "corporatized", but not privatized. Also, as already stated, the desire to preserve public ownership might explain many of the policies and institutions described for China's GCRE: delays in implementing FITs, the possibility of keeping remuneration low and tariff duration short, uncertainties in law implementation, and all other difficulties for private and/or foreign competitors in electricity generation.

[10] McNally (2008), who indicates that "China's industrial capitalism remains heavily shaped by the hand of the state" (McNally, 2008: 116).

4. Conclusions

This work has looked into China's grid-connected renewable energy (GCRE) as an exercise in overcoming the mainstream de-contextualization of the analysis of Chinese policies and institutions when it comes to specific economic sectors. To be more concrete, we have reviewed how Chinese policies and institutions do not nicely fit into a "best practice" model; and we have tried to explain such imperfect fit by virtue of China's principles for decision-making: gradualism, developmentalism, and socialism.

We have found that gradualism helps understand most of China's particularities in policies and institutions for GCRE, such as, among others, negative externalities that are not fully compensated for, remuneration levels and tariff durations that grow gradually, increasingly secure PPAs, gradual specifications and predictability of regulations, or a paced opening to competition. Developmentalism, in turn, explains, for instance, the multi-faceted goals of GCRE policies and institutions (these including energy security, environmental, and socio-economic goals); the lack of details and unpredictability of regulations; and all limitations to competition – insofar as competition could endanger industrial policy or public ownership. Finally, socialism also helps understand any measures favoring public corporations (from the delay in using FITs to regulatory uncertainties).

Further research would be necessary to determine: (1) whether there are more elements of the Chinese political economy that should be taken into account in order to better understand the departure of China's policies and institutions for GCRE from "best practice" (certain procedures of decision-making, such as fragmented authoritarianism, decentralization, and government-business coordination, may deserve special attention); and (2) whether the fact that gradualism and partiality of overall economic reforms have not been obstacles to China's economic growth and development should lead us to consider the gradualism and partiality around the application of "best practice" in GCRE as more of an opportunity than an obstacle.

References

[1] GWEC, Wind Force 12. A Blueprint to Achieve 12% of the World's Electricity from Wind Power by 2020, Report, GWEC and Greenpeace, 2005.

[2] IEA, Global Best Practice in Renewable Energy Policy Making Expert Meeting, Workshop Proceedings, IEA, 2007.

[3] IEA, Deploying Renewables. Principles for Effective Policies, IEA, 2008.

[4] IREC, Policy Recommendations for Renewable Energies, document produced at the International Renewable Energy Conference, 2004.

[5] World Bank, REToolkit: A Resource for Renewable Energy Development, Issues Note of the REToolkit, World Bank, 2008.

[6] WEC, Renewable Energy Projects Handbook, WEC, 2004.

[7] C. García, Policies and Institutions for Grid-Connected Renewable Energy: 'Best Practice' vs. the Case of China, proceedings of the XII World Economy Meeting, World Economy Society, 2010.

[8] P. Hall and D. Soskice, An Introduction to Varieties of Capitalism, in P. Hall and D. Soskice, Varieties of Capitalism, Oxford University Press, 2001.

[9] J. McMillan and B. Naughton, How to Reform a Planned Economy: Lessons from China", Oxford Review of Economic Policy, 8: 1, 130-143, 1992.

[10] B. Naughton, Growing out of the Plan. Chinese Economic Reform 1978-1993, Cambridge University Press, 1996.

[11] C. Ma and L. He, From State Monopoly to Renewable Portfolio: Restructuring China's Electric Utility, Energy Policy, 36, 1697-1711, 2008.

[12] L. Chen, Playing the Market Reform Card: the Changing Patterns of Political Struggle in China's Electric Power Sector, The China Journal, 64, 69-96, 2010.

[13] T.G. Rawski, Reforming China's Economy. What have We Learned?, The China Journal, 41, 139-156, 1999.

[14] C.A. McNally and Y.W. Chu, Exploring Capitalist Development in Greater China: A Synthesis, Asian Perspective, 30:2, 31-64, 2006.

[15] E. Martinot and J. Li, Powering China's Development. The Role of Renewable Energy, Special Report, WorldWatch, 2007.

[16] A. Lema and K. Ruby, Between Fragmented Authoritarianism and Policy Coordination: Creating Chinese Market for Wind Energy, Energy Policy, 35, 3879–3890, 2007.

[17] C. Rufín, U.S. Rangan, and R. Kumar, The Changing Role of the State in the Electricity Industry in Brazil, China, and India: Differences and Explanations, American Journal of Economics and Sociology, 62:4, 649-675, 2003.

[18] S. Ogden, China's Unresolved Issues: Politics, Development and Culture, Prentice-Hall, 1989.

[19] C. Johnson, MITI and the Japanese Miracle: The Growth of Industrial Policy, 1925-1975, Stanford University Press, 1982.

[20] A. Amsden, Asia's Next Giant: South Korea and Late Industrialization, Oxford University Press, 1989.

[21] E.T. Yeh and J.I. Lewis, State Power and the Logic of Reform in China's Electricity Sector, Pacific Affairs, 77:3, 437-465, 2004.

[22] World Bank, The East Asian Miracle: Economic Growth and Public Policy, Oxford University Press, 1993.

[23] Y. Huang, Capitalism with Chinese Characteristics. Entrepreneurship and the State, Cambridge University Press, 2008.

[24] C.A. McNally, The Institutional Contours of China's Emergent Capitalism, in C. A. McNally (ed.): China's Emergent Political Economy. Capitalism in the Dragon's Liar, Routledge, 2008.

[25] S. Yabuki and S.M. Harner, China's New Political Economy, Westview Press, 1999.

[26] J. Liu, What is Socialism with Chinese Characteristics, document presented at the Congrès Marx International V, 2007.

Policies and Institutions for Grid-Connected Renewable Energy: "Best Practice" vs. the Case of China

Clara García[1*]

[1] *Complutense University, Madrid, Spain*
** Corresponding author. Tel: +34 633504758, E-mail: clara.garcia@ccee.ucm.es*

Abstract: A consensus seems to have emerged around what constitutes "best practice" in policymaking and institution-building for the deployment of grid-connected renewable energy (GCRE). However, this consensus, found scattered throughout reports and policy papers, or in the discourse of policymakers and businesspeople, has yet to be systematized. And still, an implicit "best practice" model does seem to exist, against which national cases are frequently assessed, being portrayed as "good" or "bad" for the deployment of renewables in view of, respectively, convergences and divergences from the model. In this paper, we attempt to systematize what are frequently considered the best policies and institutions for renewable electricity. We also seek to portray the prevailing model as a sector-specific description of the policies and institutions present in liberal market economies. Subsequently, we explore the case of China, arguably not a liberal market economy, where policies and institutions coincide with "best practice" only partially and imperfectly, even following enactment of the nation's Renewable Energy Law (REL) in 2006.

Keywords: *Renewable energy, Best practice, Policies, Institutions, China.*

1. Introduction and methodology[1]

There is an extensive literature describing policies and institutions that foster the deployment of renewable energy. To our knowledge, there has been no academic effort to systematically collect the policy and institutional prescriptions posited in diverse sources as "best practice"; such is our current intent. Furthermore, given the diversity of national economic systems, even within market economies, we aim to compile those policies and institutions that constitute a "best practice" model in a way that reveals this model as a sector-specific description of a particular kind of capitalism, sometimes termed "liberal market economy" (LME, as in Hall and Soskice, 2001).

Next, we present China as our case study, whose policies and institutions fit the "best practice" model only partially and imperfectly, even following enactment of a Renewable Energy Law (REL)[2] in 2006. When judged against the model, Chinese particularities appear to be imperfections, or even obstacles to the deployment of renewables. Since the overall Chinese economic system arguably does not fit the definition of an LME, this case study shows: (1) the need for further research in order to determine whether Chinese particularities are indeed imperfections, or simply the sector-specific manifestation of an alternative variety of capitalism; and (2) the need to question the "best practice" model, insofar its prescriptions might be valid only for certain political economies (those of LMEs).

Our analysis combines a review of specialized literature and the business press with semi-structured interviews held with relevant actors in policy, business, and research related to renewable energies. Interviews were conducted at: departments of the Government of Spain; Chinese public research centers (Chinese Academy of Social Sciences, Energy Research

[1] The author would like to acknowledge the financial support of a *Becas Complutense-Del Amo* grant, as well as the insights provided by John Zysman and Steven Vogel, and various doctoral students at University of California, Berkeley.
[2] See the REL at: http://www.ccchina.gov.cn/en/NewsInfo.asp?NewsId=5371 (last accessed November 23, 2009).

Institute, and Pekin University); institutions for international cooperation in energy and the environment; and multinational companies operating in China.

2. Common views on the policies and institutions needed for GCRE[3]

2.1. Overcoming economic barriers to GCRE: policies for the creation of markets

Economic barriers are those high costs and/or insufficient revenues that prevent greater investment in the deployment of renewable technologies. The purpose of policy, according to the guidelines published by relevant international actors (cited below), should therefore be to remove, or compensate for, such obstacles, thus making renewable technologies competitive vis-à-vis traditional alternatives. As we shall see, the economic barriers identified in the specialized literature are basically obstacles that derive from market distortions or failures that, once removed, allow renewable technologies to move towards market competitiveness.

In particular, governments should aim at: (1) "leveling the playing field for renewables" (IEA, 2007:9); and (2) introducing support instruments for an increasingly cost-effective deployment of renewable technologies. Leveling the field entails the elimination of market distortions that favor traditional sources over GCRE: elimination of subsidies to conventional fuels, plus internalization of negative and/or positive externalities. But even if the playing field is leveled, the deployment of GCRE encounters other economic obstacles which "continue to be financially costlier for the investors in renewable power plants than conventional generation" (World Bank, 2008:47). The most cited include: the higher initial cost of installing generating capacity in GCRE; more restricted access to capital; and insufficient demand. Overcoming these obstacles would be achieved by mandated market policies (World Bank, 2008; REN21[4]), financial incentives, and actions to ensure demand.

Regarding mandated market policies, the usual classification establishes that schemes are either quantity-based (basically renewable portfolio standards, RPS, and tender procedures) or price-based (feed-in tariffs, FITs[5], and feed-in premiums). Meanwhile, financial incentives for deployment would aim to promote investment by lowering the costs of such investment, via financial and fiscal aids (grants, loans and loan guarantees, tax credits, etc.). Finally, and regarding demand for GCRE, the clearest recommendations are to ensure grid access and to institute Power Purchase Agreements (PPAs). Although there has been much debate over instrument effectiveness – especially between price-based and quantity-based mechanisms – the latest recommendations (IEA, 2008; World Bank, 2008) underline the importance, not so much of the choice of a particular instrument, but of how an instrument is implemented. In particular: (1) these schemes should be fine-tuned for each renewable technology; (2) remuneration for each technology should be sufficient to ensure profitability – IEA sets minimum levels of remuneration at USD 0.070/kWh for wind, and at USD 0.080/kWh for biomass; (3) the schemes should be of long enough duration to recover investment and ensure profitability; (4) any financial support to renewables should be designed to ensure that both investment and efficiency are achieved, in order to "move technologies quickly towards market competitiveness" (IEA, 2008:23); and (5) production-based supports are preferable to supports to investment, or to installed capacity, since they reward the desired outcome.

[3] This discussion is mostly based on IEA, 2008; GWEC, 2005; IREC, 2004; WEC, 2004; World Bank, 2008; and author's interviews (mostly Western interviewees, since these agreed upon most of what constitutes "best practice").
[4] See: http://www.ren21.net/RenewablesPolicy/PolicyInstruments/RegulatoryPolicies/tabid/5623/Default.aspx (last viewed November 23, 2010).
[5] We understand feed-in tariffs as tariffs that are fixed and equal for any generating company.

2.2. Overcoming non-economic barriers: developing market-friendly institutions

Guidelines on how to promote the use of renewables also focus on the need to eliminate non-economic barriers, which some studies identify as particularly damaging to the development of renewables. Non-economic barriers, at the risk of simplification, consist of features of the institutional framework that prevent greater investment in an increasingly cost-effective deployment of renewable technologies. The purpose of policy, therefore, should be to remove institutional barriers that impede the good functioning of markets.

In systematizing the diverse lessons in this arena, we find that: (1) Regarding government-related institutions, it is proposed that "good governance" prevails by way of general legal security, a capable bureaucracy, and predictable regulations for renewables; and (2) regarding corporate-related institutions, prescriptions include low barriers of entry and competition, as well as a technology-friendly corporate structure. It is proposed that State institutions should first tend towards the development of an overall (not only in energy) regulatory framework that is conducive to market transactions. WEC (2004) refers to the non-observance of property rights as a barrier to renewables; and IREC (2004) identifies as detrimental the absence of "transparent and enforced (…) anti-corruption policies and regulations" (IREC, 2004:7). Second, there are calls for a capable, coordinated bureaucracy; even for "joint policy-making and priority setting between energy ministries and rural development, health, education, water, environmental, and other ministries" (IREC, 2004:11). A capable bureaucracy also entails well-trained officials, and fewer administrative hurdles. Third, regulations around renewables should have specific institutional features: goals should be concrete, formally specified, and binding; policies should be long-term and stable, follow pre-established rules, and be simple and transparent. In sum, rules should be predictable: policy effectiveness for deployment "is more affected by the perceived investment risk on renewables projects than on their potential profits and/or costs" (IEA, 2007:11).

Regarding corporate structure, the "best practice" lessons proposed by the literature relate closely to electricity sector reforms. First, production and transmission should be unbundled in order to avoid oligopolies and achieve wholesale competition. Sometimes implicit in the pro-competition rationale, and clearly stated by most Western interviewees, is the need for room for foreign participation, as this could bring about technology and skill upgrades.

2.3. The "best practice" model as a sector-specific description of an LME

Here we show how the "best practice" model fits into a broader set of policies and institutions present in an LME. Beginning with policies to overcome economic barriers, the very goal of fostering (private) investment through market-incentives presumes the existence of an LME, where investors are atomized companies making decisions in view of costs and revenues. Note that both major sets of prescribed policies restrict a government's role to perfecting the functioning of markets: leveling the playing field explicitly entails the need to eliminate market distortions and compensate for market failures; and support mechanisms are not meant to be part of industrial policy, but should compensate for economic disadvantages of GCRE vis-à-vis fossil fuels arising from market distortions. Regarding institutions to overcome non-economic barriers, the goal is an institutional environment that motivates (private) investment. The prescribed institutions basically reflect those of an LME: the role of government is to set and enforce formal and predictable "rules of the game", so that corporations may freely "play" in the market with no major uncertainties and/or discrimination. Thus do prescriptions include legal security, a capable bureaucracy, and predictable regulations, plus low barriers of entry to both domestic and foreign participation.

The perfecting of markets through arm's length policies and the setting of formal, predictable regulations both fit well into the standard role of a State within an LME. In such a system the State plays an arm's length role while setting competition requirements that prevent coordination between companies. Also, corporate competition in an LME entails that technology transfers occur through market mechanisms, such as hiring or joint ventures (Hall and Soskice, 2001). In similar fashion, the "best practice" model calls for competition or foreign participation as a source of innovation or technology transfer (assuming that these will not be coordinated). Also, LMEs include financial systems with short-term horizons, like those in the "best practice" model (a financial system delinked from the State and non-financial corporations, and unwilling to take long-term risks).

3. Chinese policies and institutions for GCRE[6]: divergences from "best practice"[7]

3.1. Policies for the creation of markets?

As for leveling the playing field for renewables vis-à-vis traditional technologies, Cherni and Kentish (2007) describe how the usual market distortions favoring traditional technologies apply to China. The fact that the average tariff paid to coal-fired power generators is at 0.050 USD/kWh[8] somehow reflects the low cost of producing electricity with coal (for comparison, see below for tariffs paid for renewable sources). A revamped tax on coal is being discussed, but the uncertainties around such tax reform are still many[9]. However, China does implement all the aforementioned support-to-deployment instruments: mandated market policies, financial incentives, and support for demand. But as we shall detail, imperfections in implementation (with respect to "best practice") are significant.

Within quantity-based mandated market policies, China has implemented a renewable electricity standard: all generating companies with installed capacity above 5MW are required to have an installed capacity of renewable energy of at least 3% of total by 2010. Note that this obligation refers not to actual power fed into the grid, but merely installed capacity, which, as some interviewees indicated, results in around 30% of the installed capacity for renewable electricity remaining dormant. Another quantity-based system for GCRE is a tendering system, which prevailed in the case of on-shore wind between 2003 and 2009 and has recently begun to operate for solar. During this period, five national tenders for wind concessions were carried out by the National Development and Reform Commission (NDRC). Winning prices fell between 0.055 and 0.080 USD/kWh; and concessions were for 25 years, but the fixed tariff was guaranteed for the first 30,000 full load hours of operation (GWEC, 2005). Because low remuneration levels and the short duration of fixed tariffs proved insufficient for profitability (Lema and Ruby, 2007; author's interviews), foreign investors were barred from winning these tenders. Remuneration was either below or scarcely above what IEA (2008) identifies as a threshold for deployment of wind power (0.070 USD/kWh), and even below the price set for wind in China before the tender system (Lema and Ruby, 2007); also below what some studies have cited as the threshold for profitability (0.082-0.102 USD/kWh, according to Li et al., 2006). Moreover, the 30,000-hour duration of the tariff corresponds to about half of a wind park's life (author's interviews). Finally, the winning of a concession does not necessarily imply that the project will generate and feed

[6] Many particular policies and institutions will refer only to onshore wind power, given the lag in regulation for other renewable electricity sources, as well as their still-marginal presence in the Chinese installed capacity mix.
[7] Here we use "author's interviews" as a reference to interviewees, be they Western or Chinese, as long as there was a major coincidence in opinions. Otherwise we make disagreements explicit.
[8] All data will be provided in USD. Conversions are made at an exchange rate of 6.8 RMB per 1 USD (December 2009).
[9] Author's interviews and press articles: http://uk.reuters.com/article/idUKTOE62O02R20100325; http://www.eeo.com.cn/ens/Politics/2010/03/29/166354.shtml (last accessed November 23, 2010).

electricity into the grid (REN21, 2009). Apart from national tenders, all wind projects below 50MW are to be approved at the provincial level[10], with specific licensing criteria set locally. According to REN21 (2009), tariffs set for provincial development projects have been between 0.075 and 0.099 USD/kWh, close to what IEA (2008) considers a minimum for deployment and below the estimated threshold for profitability (Li et al., 2006).

Regarding price-based mandated market policies, there is a FIT for biomass, set at the price of coal plus 0.036 USD/kWh for 15 years (RELaw Assist, 2007); and a FIT for wind was established in July 2009, ranging from 0.075 USD/kWh to 0.089 USD/kWh. There are expectations that a FIT for solar will follow, to be set between 0.160 and 0.220 USD/kWh[11]. Given an average coal price of 0.050 USD/kWh, the premium set for biomass raises its FIT to an average of 0.086 USD/kWh, scarcely above what IEA (2008) considers the minimum tariff for policy effectiveness. The FIT for wind also falls very close to the IEA's minimum tariff[12]. Furthermore, although the FIT does set prices slightly above most tariffs resulting from national concessions, it departs little from the average remuneration of independent projects negotiated locally. As with tendering or the independent project systems, the fixed tariffs for wind apply to 30,000 hours of operation, or about half the life of a park. Finally, provisions for the reduction of tariffs over time have been thus far specified only for biomass.

As for financial incentives, we find in China both financial support and fiscal aids. A very recent example of financial support is that solar PV generation projects above 500MW have been eligible, since July 2009, for the enhanced "Golden Sun" project, which includes a 50% subsidy for all investment[13]. The REL itself, in Article 25, dictates that "financial institutions may offer preferential loan with financial interest subsidy" to projects in renewables. On the fiscal side, there are tax reductions, the most relevant being the 50% cut in the VAT tax rate for electricity generated by wind (Lema and Ruby, 2007). Article 26 of the REL also includes tax benefits to renewables. In any case, financial support is frequently given to the manufacturing and development of installed capacity, but with scarce incentives to production, efficient use of resources, or quality improvements and cost reductions (Cherni and Kentish, 2007). Finally, China implements certain demand-enhancing schemes. Transmission companies are obliged to provide each facility with connection to the grid, at the connection point closest to the generator; and, under PPAs, they are obliged to purchase all renewable electricity. Nevertheless, grid companies may prove reluctant to comply with rules: grid companies suffer losses from the purchase of renewable power at fixed tariffs (Cherni and Kentish, 2007). Also, even when generators are provided with connection points, these may be too far from the point of generation[14]. Finally, the grid simply lacks the technical requirements for connecting increasing volumes of renewable electricity (author's interviews). In 2008, as a result of difficulties in connection, and coupled with the fact that the RPS applies to installed capacity and not dispatched power, a significant portion of installed wind capacity remains unconnected to the grid (author's interviews).

[10] See China's "Administrative Provisions for Renewable Energy Power Generation" (http://www.martinot.info/China_RE_Law_Guidelines_2_NonAuth.pdf; last accessed November 23, 20010).
[11] Press article: http://www.renewableenergyworld.com/rea/news/article/2009/08/ldk-solar-signs-500-mw-pv-project-deal (last accessed November 23, 2010).
[12] IEA (2008) notes that even remunerations well above the minimum might not be effective, if not coupled with the removal of non-economic barriers.
[13] Press article: http://solarglobalgreen.com/pg/blog/justin/read/1278/china-golden-sun-project-aims-to-speed-construction-of-solar-farms (last accessed April 28, 2010).
[14] China's "Administrative Provisions for Renewable Energy Power Generation" (http://www.martinot.info/China_RE_Law_Guidelines_2_NonAuth.pdf; last accessed November 23, 2010) indicates that "the connection system should be built by the power grid enterprises at their own costs", which according to business interviewees does not imply that this is the case over the entire length of the line.

3.2. Market-friendly institutions for renewables?

Concerning institutions related to the State, and general legal security, empirical studies, together with our own interviews, show that foreign companies are discouraged by general regulatory uncertainty in China. As for the capability of the bureaucracy to design, implement, and enforce goals and instruments for the promotion of renewables, coordination has increased since the centralization of energy regulation into new public entities (Lema and Ruby, 2007), such as the National Energy Administration (NEA) or the State Electricity Regulatory Commission (SERC). But a multiplicity of stakeholders continues to prevail, posing at least three problems. First, it brings uncertainty to the degree that the *de iure* or *de facto* responsibilities of each government organism are unclear[15]. Second, even under the umbrella of Beijing's determination, fragmentation assists the designs of public players disinterested in the development of renewable electricity. For example, Ma and He (2008) explain how Chinese local officials have been historically evaluated according to economic growth, de-prioritizing compliance with environmental regulations. Third, in relation to the multiplicity of stakeholders, there exists in China a multiplication of bureaucratic procedures. As to the quality of policies around renewables, we find that the Chinese government does indeed have specific targets for renewable electricity, as demanded by the "best practice" literature (see for instance NDRC's National Medium- and Long-Term Development Plan for Renewable Energy in China, 2006-2020). Nevertheless, according to Ma and He (2008), those targets are weak insofar as they are not compulsory. Also, China seems not to rank particularly high regarding predictability of policy (resulting mostly from regulation being stable, rules-based, and transparent). For instance, when it comes to clarity and transparency of rules, we see that REL includes very few regulatory details; and other renewable energy legislation in China also lacks specificity (Cherni and Kentish, 2007; IEA, 2007; author's interviews). In particular, there are critiques to the uncertainties around tariffs, connectivity and PPAs (negotiated case-by-case), grid upgrades, and enforcement measures.

We now turn to the corporate structure for renewable electricity. Electrical sector reform included the separation between government and business operations, as well as the unbundling of generation and transmission. Also, an independent regulatory and supervisory agency (the SERC) was established. In any case, reforms in the sector are widely perceived as unfinished, mostly in that free entry and competition are restricted, both in terms of transmission/distribution and generation. Regarding transmission, the State Grid and the Southern State Grid are essentially monopolies, as well as monopsonies, in their respective regions. Also, regulations regarding connection and PPAs are not rigorously enforced, probably because of the limited regulatory capacity of SERC vs. NDRC, and SERC's limited authority over the transmission companies, given the administrative ranks of SOE managers, which parallel those of the government officials at SERC.

In the area of generation, public and private companies are allowed to compete with the "big five" state corporations that resulted from the 2002 unbundling of the State Power Corporation (SPC). But competition is hindered by industry concentration, public ownership and control, and barriers to foreign competition. The latter not only restrict overall competition but also limit the technology and know-how utilized in development and generation. The five big holding companies own nearly 40% of total generation assets[16] and produce about half of China's electricity[17]. Much of the remaining assets belong to other

[15] See Cherni and Kentish, 2007; Lema and Ruby, 2007; Ma and He, 2008, about the limited authority of SERC vs. NDRC.
[16] Information on asset ownership is as of 2006, and according to Ma and He (2008).
[17] Information on production is from the Energy Information Administration of the United States, at http://www.eia.doe.gov/cabs/China/Electricity.html (last accessed November 23, 2010).

companies administered by the central government (10%) or by local governments (45%). The "big five" power companies, which traditionally generate electricity with coal, also dominate the renewable power sector. For instance, under the national tender system for wind development, all winners but one have been "big five" subsidiaries (Lema and Ruby, 2007). And seven wind mega-projects planned for construction will be led by China's "big five"[18]. Moreover, the "big five" are SOEs, and since most other generation assets are controlled by central or local governments, any semblance of market-like competition is hindered further. At the same time, foreign competition in development and generation remains marginal: foreign companies (including joint ventures) produce about 6% of total electricity in China; and out of the 12GW installed in wind in 2008, about 95% belonged to Chinese capital, with most of the remaining 5% belonging to joint-ventures, and only a marginal share being wholly foreign-owned (author's interviews). The scant presence of foreign developers and generators might be explained by policies already reviewed, which deter foreign investment (author's interviews; RELaw Assist, 2007): (1) the fact that foreign companies could not win concessions through national tendering; (2) low remuneration and short duration for all incentive schemes; and (3) the fact that foreign projects are allowed a debt-financing percentage below the 80% permitted for domestic projects. Other policies and institutions also reviewed could conceivably deter the entry of any company, but foreign competitors especially: grid access and PPAs that are time-consuming and difficult to negotiate; the general departure of the Chinese legal and contractual framework from Rule of Law principles; administrative hurdles in licensing procedures; institutional weaknesses of the policies for renewables; etc. (Cherni and Kentish, 2007; author's interviews).

In manufacturing, both industry concentration and the market share of Chinese companies are lower than in power generation. In wind, prior to 2004 there were fewer than five manufacturers of wind-power components. By the end of 2008, wind turbine manufacturers numbered 70 (REN21, 2009). Nevertheless, the three biggest manufacturers dominate, with over half the market[19]. Among those 70 companies making turbines in China, more than 50 are Chinese-owned, eight are joint ventures, and nine are foreign-owned. But the presence of foreign capital in manufacturing has decreased over time: in 2004 the domestic market share for wind turbines was 18% (GWEC, 2005); the 2008 share for domestic and joint-venture companies was 75% (REN21, 2009). And in view of certain recent government incentives, it is likely that Chinese companies will continue to increase their market share. For instance, all majority Chinese-owned domestic manufacturers will be awarded up to $88 per kW for their first 50 wind turbines certified and connected to the grid; also, Chinese companies will apparently benefit most from the aforementioned mega-wind farms project[20]. Foreign production of equipment faces some difficulties. Frequently mentioned policies include the 70%-local-content standard for wind turbines, and the turbines' import duties structure: in 2000, a 12% tariff for turbines (3% for components) was re-introduced. Also, compared to domestic companies, foreign manufacturers face restrictions (some related to policies and institutions described). Examples of discriminatory policies include: the tendering system for wind, which favors turbine price over quality; subsidies for Chinese companies only; and the very recent "buy Chinese" policy wherein projects financed by the economic stimulus package must seek government permission before buying foreign goods and services.

[18] Press article: http://www.chinadaily.com.cn/cndy/2009-07/07/content_8385497.htm (last accessed December 10, 2009).
[19] Press article: http://rightsite.asia/en/article/tapping-chinas-wind-turbine-market (last accessed April 26, 2010).
[20] Press article: http://english.peopledaily.com.cn/90001/90778/90857/90860/6694805.html (last accessed April 26, 2010).

4. Conclusions

A consensus seems to have emerged, among Western organisms and practitioners, around which policies and institutions are best for GCRE. We find that the "best practice" model basically amounts to a sector-specific description of an LME: policies should consist in regulations that facilitate private investment via the perfection of market mechanisms; and institutions should be market-friendly, also to facilitate investment. In China, arguably not an LME, we have encountered policies and institutions for GCRE that have moved toward the described prescriptions, but gradually and only partially. Although the accuracy of the details presented in this paper may suffer from the rapid pace at which Chinese regulations evolve, general imperfections here mentioned will likely prevail in the medium term.

As stated, when measured against the "best practice" model, China's particularities appear to be obstacles to the deployment of renewable technologies. But, seen in a wider perspective – that of China not fitting into the definition of an LME – further research would be necessary to determine whether Chinese particularities are indeed imperfections, or simply the sector-specific manifestation of an alternative (non-LME) variety of capitalism. Moreover, the fact that China has proven quite successful in GCRE should lead us to question the "best practice" model, insofar its prescriptions might be valid only for certain political economies.

References

[1] P. Hall and D. Soskice, An Introduction to Varieties of Capitalism, in P. Hall and D. Soskice, Varieties of Capitalism, Oxford University Press, 2001.

[2] IEA, Global Best Practice in Renewable Energy Policy Making Expert Meeting, Workshop Proceedings, IEA, 2007.

[3] IEA, Deploying Renewables. Principles for Effective Policies, IEA, 2008.

[4] GWEC, Wind Force 12. A Blueprint to Achieve 12% of the World's Electricity from Wind Power by 2020, Report, GWEC and Greenpeace, 2005.

[5] IREC, Policy Recommendations for Renewable Energies, document produced at the International Renewable Energy Conference, 2004.

[6] World Bank, REToolkit: A Resource for Renewable Energy Development, Issues Note of the REToolkit, World Bank, 2008.

[7] WEC, Renewable Energy Projects Handbook, WEC, 2004.

[8] J.A. Cherni and J. Kentish, Renewable Energy Policy and Electricity Market Reforms in China, Energy Policy, 35, 2007, 3616-3629.

[9] A. Lema and K. Ruby, Between Fragmented Authoritarianism and Policy Coordination: Creating Chinese Market for Wind Energy, Energy Policy, 35, 2007, 3879-3890.

[10] J. Li, J. Shi, H. Xie, Y. Song and P. Shi, A Study on the Pricing Policy of Wind Power in China, Chinese Renewable Energy Industries Association and GWEC, 2006.

[11] REN21, Background Paper: Chinese Renewables Status Report, Background Paper, Renewable Energy Policy Network for the 21st Century, 2009.

[12] RELaw Assist, Renewable Energy Law in China. Issues Paper, Australia-China Bilateral Partnership on Climate Change and REEEP, 2007.

[13] C. Ma and L. He, From State Monopoly to Renewable Portfolio: Restructuring China's Electric Utility, Energy Policy, 36, 2008, 1697-1711.

Expansion of the Swedish Elcert certificates system to the Netherlands: a cost-benefit analysis

Jaap C. Jansen[1,*], Sander M. Lensink[1], Adriaan J. van der Welle[1]

[1] *Energy research Centre of the Netherlands , Petten, the Netherlands*
** Corresponding author. Tel: +31 224564437, Fax: +31 224568338, E-mail: j.jansen@ecn.nl*

Abstract: This paper investigates the net benefits of adjusting the Dutch renewable electricity support system from a feed-in premium (FIP) scheme into a hybrid renewable portfolio standard (RPS), i.e. an RPS on top of, and well-integrated with, the existing FIP. The alternative scenario envisages, moreover, the establishment of a joint support scheme with Sweden on the basis of the existing Swedish Elcert certificates system. The paper benchmarks the costs of the alternative renewable electricity support scenario against the baseline FIP scenario. A major limitation is the exclusion of network impacts. Moreover, the analysis of the economic impacts in Sweden is limited to distributional effects. The aggregate welfare impact for the Netherlands is robustly positive. In both countries major winners and losers are identified.

Keywords: *Hybrid RPS schemes, Joint support schemes, Bottom-up harmonisation of national support schemes*

1. Introduction

The paper draws on an ongoing study by the Energy research Centre of the Netherlands, ECN, into the social costs and benefits of readjustment of Dutch renewable electricity support from a feed-in premium system (FIP) into a FIP in combination with a renewable portfolio standard system (RPS), hereafter referred to as *a hybrid RPS system*. The RPS is endorsed by certificates (Elcerts), issued on behalf of qualifying renewable generators. The latter sell their certificates to electricity suppliers and certain end-users, who have to prove compliance with the mandatory RPS target with Elcerts. The RPS target implies that a certain calendar-year-specific minimum % of electricity deliveries (suppliers) or consumption (end-users) has to be sourced from qualifying renewable generation technologies. Some of these technologies need more support to become competitive on the electricity market. The FIP regulations may provide additional technology-specific support to the latter technologies, contingent on government decisions. The hybrid RPS system concept as a basis for EU support harmonization was introduced at meetings of a CEPS/ECN Task Force [1].

This paper focuses on a two-country hybrid RPS as an example of bottom-up harmonization of the (envisaged) national support schemes for RES-E (renewable electricity). The Netherlands and Sweden are considered to launch a joint hybrid RPS on the basis of the existing Swedish Elcert certificates system. The EU Renewable Energy Directive (RED), 2009/28/EU allows such bottom-up harmonization subject to certain conditions. It is to be an application of 'joint support schemes', i.e. one the 'cooperation mechanisms' in the RED.

The key driver towards potential market-based joint support schemes is to achieve higher cost-effectiveness in target compliance by capitalizing on the gains from trade. Expanding the domain of a well-designed joint support scheme may lead to a reduction of total RES-E generation costs to achieve the sum of the national RES-E targets[1] of the participating countries [2],[3].

[1] *The RED sets mandatory national targets for the share of renewables in final energy consumption.*

The goal of this paper is to evaluate the economics of a Dutch-Swedish joint hybrid RPS support scheme from a Dutch societal perspective. Towards that aim, it compares the latter support scheme as the alternative scenario with the existing Dutch FIP system as baseline. In the alternative scenario, the existing Dutch FIP system, henceforth referred to with the Dutch acronym SDE, is retained in the Netherlands in a fully compatible way with the joint hybrid RPS support scheme.

The baseline scenario consists of a continuation of the existing national support schemes: the Dutch SDE scheme and the Swedish Elcert certificates scheme respectively. The alternative joint hybrid RPS on suppliers is presumed to be launched as from the start of year 2014. Part of the additional RES-E consumed in the Netherlands might be produced by qualifying Swedish RES-E generators.

The analysis considers primarily the vantage point of Dutch society. Even so, it investigates distributional effects on major stakeholder categories in both the Netherlands and Sweden.

This paper is structured as follows. First the methodology is succinctly explained (Section 2). Research results are shown in Section 3. Section 5 winds up with conclusions.

2. Methodology

2.1. Baseline scenario background

2.1.1. Baseline scenario

To date, the SDE is the Dutch government's main subsidy instrument in support of the deployment of renewable electricity. It is a feed-in premium system, granting technology-specific production subsidies for renewable generators. It is attempted to set the SDE premium for an installation of a certain SDE category commissioned in a certain calendar at such a level to cover the so-called 'financial gap' without overcompensation.

The so-called *base rate* for an installation's SDE premium is determined by the installation's anticipated RES-E generation cost with some *adjustment factors*. Part of the anticipated premium is paid at regular intervals on the basis of actual production. After each calendar year settlement of last year's SDE subsidy is based on the difference between the base rate and last year's average baseload price. However, an electricity *price floor* and a corresponding maximum SDE subsidy rate is determined upon closure of the SDE subsidy contract.

Adjustment factors relate to:

- Insurance costs: to provide some hedge against the risk for the RES-E operator that the electricity price drops through the set electricity price floor.
- Transaction costs: anticipated transaction costs to sell electricity (especially for SDE categories with many small-scale RES-E operators).
- System imbalance charges: applicable for wind power, and PV.
- Profile costs: applicable to intermittent sources assuming a non-negligible share in the electricity fuel mix (relate to the downward 'merit order' effect on the power price and to the technology-specific time profile of electricity production which may yield below-average or above-average baseload prices).

The electricity price floor implies a non-negligible risk to the investor and his financers. If the electricity price is to drop below the set electricity price floor, the SDE subsidy rate will not

suffice to provide full coverage of the 'financial gap' that needs to be bridged to render the RES-E power plants concerned financially viable. In practice, the adjustment rate for insurance against this risk does not give complete solace.

2.2. Baseline scenario design

The baseline scenario is taken from [4], a study also used for the design of the Dutch Renewable Energy Action Plan. The baseline scenario assumes an intensified continuation of the SDE feed-in premium scheme, so that a 35% in gross energy consumption will be achieved by 2020 completely based on (45 TWh) inlands renewable energy generation. Furthermore, the SDE is supposed to become financed through a surcharge on the electricity bill instead of being paid by government finances. As such, the SDE forms the basis for a stable investment climate, where energy companies can plan new renewable energy investments years in advance. This stable investment climate is a necessity for reaching high levels of renewable electricity in the short time period up to 2020.

The wind power capacity grows to 6000 MW onshore in 2020 and 6000 MW offshore slightly thereafter. Co-firing of biomass in coal fired power plants is supported through subsidies, and is projected to reach on average up to 20% co-firing, on energy basis, for all coal fired power plants in operation. The economic co-firing potential in 2020 is foreseen to be around 10 TWh. The baseline scenario includes a significant rise in electricity production from stand-alone biomass installation, up to 7 TWh in 2020. No options are limited by budget ceilings, except for solar PV. Figure 1 below indicates the total RES-E production, differentiated by technology, for the period 2012-2020.

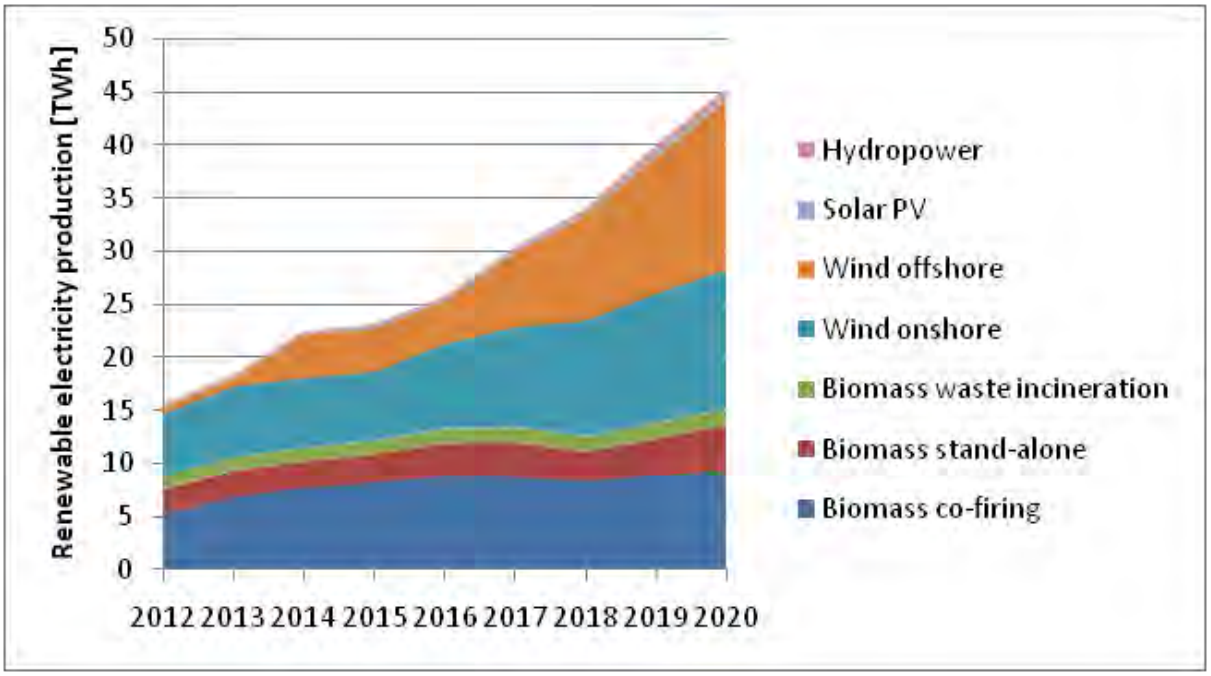

Fig. 1 Baseline scenario: Dutch RES-E production [TWh].

For reasons of containing the modeling complexity, we have refrained from accounting for the (in practice very small) negative impact of changes in the SDE surcharges on power demand.[2]

2.3. Alternative scenario background

The alternative RES-E stimulation scenario is predicated on the presumed realization of a joint support scheme with Sweden as per 1 January 2014. The basic idea behind such a scheme is that within a certificates-based joint RPS support scheme, in principle, each of the participating countries has the right to introduce additionally at the national level supplementary support measures. (Changes in) supplementary support measures can be adopted in close bilateral government-to-government consultation and in a way that is supportive to the well-functioning of the joint Elcert certificates market. In the case of the Netherlands this will be the existing SDE support scheme. The joint support scheme will be integrated into the SDE regulations.

In the absence of the SDE high-cost marginal Dutch RES-E generation options, notably offshore wind, would determine the – in that case potentially very high – Elcert price. Hence, given the steeply rising Dutch RES-E supply curve, supplementary Dutch support to high-cost renewable generation options is warranted to contain windfall profits in both the Netherlands and Sweden. Moreover, it provides an additional instrument to limit the net import volume of Elcerts from Sweden, should the joint Elcert market and the Swedish RES-E sector show signs to become overstretched.

The Swedish RPS, called "the electricity certificate system", requires all electricity suppliers and certain electricity users to purchase Elcert certificates equivalent to a pre-set target proportion of their respective electricity demand, set for each calendar year of the Swedish RPS scheme. The scheme became operational as per 1 May 2003 and is scheduled by law to last until the end of year 2030. Its main stated purposes are to help increase the production of renewable electricity and reduce emissions of greenhouse gases.

Information from the Swedish Energy Agency ([5], [6]) suggests that from both an effectiveness and a cost efficiency criterion, the Swedish RES-E support scheme appears to function well. The Swedish support scheme is well on track to meet its pre-set RES-E deployment objectives. RES-E support cost hover around €ct 3 / kWh of qualifying RES-E.
In a previous ECN study Sweden has been identified as the best fit for a joint hybrid RPS support scheme with the Netherlands [7]. Besides the well functioning of the Swedish support scheme, major reasons include:

- The quite diverse portfolios of RES-E resources between Sweden and the Netherlands, making for a large *gains from trade* potential.
- The scope for additional RES-E production in Sweden at relatively moderate cost on top of complying with Sweden's RES target in 2020 as laid down in the Renewable Energy Directive. In contrast, the Netherlands is only to meet its 2020 RES target completely inlands at quite high cost. This further strengthens the potential for win-win trade.

[2] *For the same reason, the (small) negative impact of (changes in) the cost of Elcert certificates to be borne by suppliers/end-users on power demand has been disregarded likewise.*

2.4. Alternative scenario design

We assume that differences in market conditions facing RES-E project developers under the baseline and alternative scenario respectively, small differences in technology-specific generation costs will occur. Because of space restrictions, we refer to [8] for specific production costs for different production categories for both the SDE and RPS systems and further explanation of underlying cost factors.

It is assumed that the launching date will be beginning of 2014.[3] As explained in [8] certain regulatory costs have been assumed for the Dutch public sector, CertiQ as the Dutch Elcerts issuing and tracking agency as well as RES-E generators and suppliers. We note that the in practice important benefits of improved Elcert market functioning as a result of market domain expansion [3] have not been captured in our modeling exercises.

Our main modeling assumption regarding the evolution of the Dutch RES-E generation are the following ones. As a result of net import of Elcerts from Sweden corresponding to about 9 TWh in 2020, Dutch RES-E generation is projected correspondingly less than under the baseline scenario. This refers especially to high cost options wind offshore and (in the Netherlands) biomass stand-alone. In Sweden the extra 9 TWh are projected to be generated by primarily wind onshore.

3. Results

The cost-benefit analysis results are succinctly explained below. Once more we refer to [8] for more details.

3.1. The Dutch societal perspective

The annual cashflows of (positive or negative) net benefits to the Dutch economy of the alternative scenario over and above the baseline scenario are shown in Table 1. Positive (negative) figures indicate lower (higher) costs for the alternative support scheme than the corresponding baseline cost. The overriding factor determining the overall impact for the Dutch economy are the strongly positive net savings on differential RES-E cost to the Dutch economy. The savings on lower production by high-cost marginal RES-E generators in the Netherlands are dominating the extra costs of net import of Elcert certificates from Sweden. Also the projected slightly lower per unit technology-specific generation cost are relatively modestly explain these results.

Table 1. Shift to Alternative III: RPS SE - Annual incremental net benefits to the Netherlands [€$_{2010}$ million].

	2013	2014	2015	2016	2017	2018	2019	2020
Savings on differential RES-E cost		217	234	275	281	459	633	805
Savings on imbalance cost of wind power		0	0	0	0	6	14	21
Regulation cost public sector	-20	-0.7	-0.7	-0.7	-0.7	-0.7	-0.7	-0.7
Regulation cost CertIQ	-1	-0.5	-0.5	-0.5	-0.5	-0.5	-0.5	-0.5
Regulation cost suppliers and RES-E generators	0	-1	-1	-1	-1	-1	-1	-1
Total (€ million)	**-21**	**214**	**232**	**272**	**278**	**464**	**645**	**824**

[3] *In practice, even in a smooth preparation process it might not be earlier than in 2015 or 2016.*

Table 1 (cont.)

2021	2022	2023	2024	2025	2026	2027	2028	2029	2030	2031	2032	2033	2034	2035
757	698	629	612	629	568	522	497	329	280	275	198	55	-50	-153
21	21	21	21	21	21	21	21	21	21	21	21	21	21	21
-0.7	-0.7	-0.7	-0.7	-0.7	-0.7	-0.7	-0.7	-0.7	-0.7	-0.7	-0.7	-0.7	-0.7	-0.7
-0.5	-0.5	-0.5	-0.5	-0.5	-0.5	-0.5	-0.5	-0.5	-0.5	-0.5	-0.5	-0.5	-0.5	-0.5
-1	-1	-1	-1	-1	-1	-1	-1	-1	-1	-1	-1	-1	-1	-1
776	**718**	**648**	**631**	**648**	**587**	**541**	**516**	**348**	**299**	**294**	**217**	**74**	**-30**	**-134**

To bring out the more near-term impact of a change from the baseline scenario to the alternative scenario, we calculated the projected NPV of differential cash-flows for the period 2013-2020. More structural trends can be observed from the projected NPV pertaining to the period 2013-2035 and its difference with the one pertaining to 2013-2020. For the purposes of this study application of a *real* discount rate[4] of 2.5% would seem appropriate. Reasons are the relatively modest size of non-diversifiable project risks, whilst the cost risks of RES-E tend to be counter-cyclical with respect to macro-economic business cycles. In showing the sensitivity of the results to the discount rate applied, we have applied a 0% and 5% discount rate as well.

The resulting NPV values are shown in Table 3. Applying the recommended 2.5% discount rate, our projections indicate that a shift in 2014 from the baseline support scheme to the alternative one would reduce, in the period 2013-2020, the costs of RES-E support to the Dutch society by 2.4 billion Euros (at prices of year 2010). The resulting cost reductions for Dutch RES-E market stimulation as measured against the baseline benchmark are set to continue after 2020 reaching an aggregate level of 4.2 billion Euros in the period 2021-2035, whilst the projected upshot for the total analysis period 2013-2035 is 6.6 billion Euros saved on RES-E market stimulation. These results are insensitive in nature to the choice of discount rate within the (rather wide) 0-5%/a interval.

Table 3. Net benefits from a Dutch socio-economic perspective of a shift in year 2014 from the prevailing SDE support scheme to a joint hybrid Renewable Portfolio Standard support scheme with Sweden (RPS SE).

Net present value in 2010 ($€_{2010}$ billion)							
Period		2013 - 2020			2013-2035		
Discount rate		0 %/a	2.5 %/a	5 %/a	0 %/a	2.5 %/a	5 %/a
Alt.Scen.	RPS SE	2.9	2.4	2.0	9.0	6.6	4.9

Source: authors' projections

3.2. Distributional effects upon Dutch stakeholders

Apart from the relatively limited cost to the *public sector* for introducing and supervising the demand-side RPS system, the shift to such a support scheme is budget-neutral. The distributional effect for CertiQ is slightly positive as this agency will be charged with the task of operating the Elcert certificates tracking system in the Netherlands, in close association with its Swedish counterpart. High-cost RES-E generators are set to be strongly adversely

[4] *A real discount rate is roughly equal to the projected nominal discount rate applicable to projected cashflows in current prices minus the projected rate of general price inflation. Our cashflow analysis is based on cashflows at a constant general price level of year 2010, i.e. "at prices of to-day". The recommended nominal discount rate with a projected rate of inflation of 2% would be for the present study: ≈ 2.5% + 2% , i.e. ≈ 4.5%.*

affected, whilst biomass co-firing thermal power plants will gain to a lesser extent. Also other non-RES generators stand to gain: they may fill part of the gap resulting from lower RES-E production volumes and benefit from a according to our modeling results very small upward power price effect as well. Power consumers are poised to lose initially but are indicated to win as from year 2019 to an increasing extent with savings on SDE cost surcharge on their electricity bill as the dominating underlying factor.

3.3. Distributional effects upon Swedish stakeholders

Exercises with the COMPETES model suggest that net Dutch imports of Elcerts up to a level of about 9 TWh is to lead to a maximum upward effect of the Elcert price of €ct 1.1/kWh to a level of €ct 3.49/kWh in 2020, after which year this upward effect will gradually dissipate. Remarkably the resulting extra RES-E production in Sweden is poised to have a much stronger downward effect on the average baseload price in Sweden, than the corresponding reduction in the RES-E production expansion in the Netherlands will have on the average Dutch baseload price in opposite (upward) direction. Differences in network topology, robustness and flexibility (also on the demand side) of the respective power network systems and the size of interconnections to evacuate surpluses and import national power deficits might be undercurrents of this result.

A strong winner will be the *Swedish RES-E sector* at large, most strongly the Swedish onshore wind sub-sector. The drop in baseload power prices in Sweden is good news for power users and bad news for notably *power generators that do not qualify for Elcerts* (including operators of pre-2003 hydro power plants). On average, qualifying generators will be more than compensated by extra revenues from Elcert sales. Assuming a zero price elasticity of power demand exercised by unprivileged consumers, the overall effect of the Alternative III scenario on Swedish power consumers can be disaggregated into the following underlying effects:

- A negative effect on account of the at least initially significantly upward reacting Elcert price. Contingent on company market strategy and competition circumstances on the Swedish retail market, Swedish suppliers will pass through their costs of acquiring Elcerts to comply with the Elcert system target more or less completely to their customers on a *pro rata* basis. The size of the effect depends on the Elcert price reaction and on the system target.
- A positive effect on account of the reaction of the wholesale market and its knock-on effect on the power price on retail market. This combi-effect regards all final power users.
- With a strong caveat for the crudeness of our modeling simulations of the Swedish distributional effects – our modeling outcomes suggest that the second effect is the dominant one. If this result can be confirmed indeed by more profound research, this will be good news for Swedish electricity consumers.

4. Conclusions

The main conclusion is that the Dutch economy would gain in a robustly positive way from the introduction of a joint hybrid RPS support scheme with Sweden. In the Netherlands, the largest distributional effects fall upon RES-E generators, other generators, and power consumers. On aggregate, Swedish renewable generators applying qualifying technologies for participation in the Elcert system are set to be clear winners and other Swedish generators clear losers. Less robust indications suggest that Swedish consumers may benefit.

Our quantitative analysis has focused on those effects that can be quantified with a fair amount of robustness. For example, in our quantitative analysis we have refrained from taking recourse to sweeping, speculative assumptions on the nature and volume of external effects of specific 'innovation pathways', the innovation dynamics of inter-technology competition, the strategic value of bottom-up harmonisation of national support schemes, etc. A major limitation is the exclusion of network impacts. Moreover, more elaborated research is needed to analyse the impacts of the joint Dutch-Swedish support scheme considered here on the Swedish economy.

References

[1] Jansen, J.C, K. Gialoglou and C. Egenhofer, 2005, Market Stimulation of Renewable Electricity in the EU: What Degree of Harmonisation of Support Mechanisms if Required?, CEPS Task Force Report No. 56: CEPS, Brussels; http://www.ceps.eu/book/market-stimulation-renewable-electricity-eu-what-degree-harmonisation-support-mechanisms-requir.

[2] Swedish Energy Agency (SEA), 2005, The consequences of an expanded electricity certificate market, Stockholm.

[3] Swedish Energy Agency (SEA), 2010, Gemensamt elcertifikatsystem med Norge, 2010, Stockholm.

[4] Daniëls, B, S. Kruitwagen (ed.), 2010, Referentieraming energie en emissies 2010-2020, ECN/PBL, report ECN-E--10-004, PBL 500161001, Petten/Bilthoven. April 2010.

[5] Swedish Energy Agency (SEA), 2008, The electricity certificate system, 2008, Stockholm.

[6] Swedish Energy Agency (SEA), 2009, The electricity certificate system, Stockholm.

[7] Jansen, J.C., 2010, Preliminary qualitative assessment of proposed measures to foster renewable and low carbon sources in the Dutch electricity mix, ECN report ECN-E--10-012, February 2010.

[8] Jansen, J.C., S.M. Lensink, Ö. Özdemir, J. van Stralen, A.J. van der Welle (forthcoming), Cost-benefit analysis of alternative support schemes for renewable electricity in the Netherlands, ECN report, Petten.

Proposal of a framework for the selection of renewable energy technology systems in Africa

Marie-Louise Barry[1,*], Herman Steyn[1], Alan Brent[2]

[1] *University of Pretoria, Pretoria, South Africa*
[2] *University of Stellenbosch, Stellenbosch, South Africa*
** Corresponding author. Tel: +27 82 901 7569, Fax: +27 12 362 5307, E-mail: mlb@up.ac.za*

Abstract: Energy is essential for economic development in Africa. The current electrification figures show that countries in sub-Saharan Africa are facing major challenges in reaching positive economic growth and supplying basic energy services to rural communities. Prior to this study a comprehensive framework of factors to select renewable energy technologies did not exist. The purpose of this research was to develop such a framework and to validate it by means of empirical analyses. A triangulation of methodologies including a literature analysis, focus group, Delphi study and case study was used to determine the framework of factors. This paper presents the final framework that includes both the thirteen criteria and measures to be used for the selection of renewable energy technologies in Africa. The paper further recommends the critical documentation that must be created for each competing technology.

Keywords: *Renewable energy technology selection, Developing countries, Sustainable energy, Selection criteria, Framework of factors*

1. Introduction

Energy is essential for economic development in Africa [1]. The current electrification figures show that countries in sub-Saharan Africa are facing major challenges in reaching positive economic growth and supplying basic energy services to rural communities [2]. Sustainable energy technologies are available and can be used to great effect in Africa to alleviate this problem [3]. Sustainable energy technologies can also contribute to job creation [4]. The implementation of renewable energy technologies in sub-Saharan Africa to date, however, has not always been successful due to both technical and non-technical factors [4-9]. Prior to this study a comprehensive framework of factors to select renewable energy technologies did not exist. The purpose of this research was to develop such a framework and to validate it by means of empirical analyses.

2. Methodology

A triangulation of methodologies was used to determine the framework of factors [10]. The analysis of the literature investigated renewable energy technologies and their application, the challenges in renewable energy technologies for implementation in Africa, and the selection methods in the fields of project, portfolio, programme and technology management. This was followed by a focus group [11, 12] with three experts,[13] in which thirty eight factors that need to be taken into account during the selection of renewable energy technologies in Africa were identified [13]. The factors identified by the focus group were confirmed and the eleven most applicable factors were selected through a two-round Delphi study [14-16]. Finally, case studies on the implementation of renewable energy technologies were undertaken in three countries [17, 18]. These case studies confirmed the eleven factors identified during the Delphi study and identified a further two factors that were added to the framework [19].

3. Results

The final list of factors, factors identified during the focus group, the Delphi study definition of each factor as well as the important issues for each factor identified in the case studies, is shown in Table 1.

Table 1. Framework of thirteen final factors to consider for sustainable, renewable energy technology selection in Africa

Factor description	Focus group identification	Delphi study definition	Important issues for each factor from case studies
Technology factors			
Ease of maintenance and support over the life cycle of the technology	Maintenance/ support	Security of supply is enhanced. It also implies that spares are affordable and can be easily acquired.	Quality of the installations, the maintenance plans, the training of technicians, maintenance training for users, keeping maintenance simple and adapting the technology to the specific environment
Ease of transfer of knowledge and skills to relevant people in Africa	Transfer of knowledge and skills	Transfer of knowledge and skills to the community involved. Dedicated personnel to run the facility are required.	Identification of stakeholders to train; methods of skills transfer applicable to the environment; quality of training; and formalization of skills transfer.
Site selection factors			
Local champion to continue after implementation	Local hero – champion to continue after implementation	Facilitators of the technology exist which will ensure that the facility will continue after implementation.	Local champions must be identified during technology selection, their responsibilities must be clearly defined and they must be aware of the long term implications of their role
Adoption by community	Passion/ ownership/ buy-in/ adoption by community, responsibility	Community adopting the technology, accepting ownership, demonstrating buy-in and taking responsibility	A determination must be done of the capacity of the population to adopt the new technology, the benefits of the new technology must be determined and communicated to the community and that measures must be in place to ensure client satisfaction
Suitable sites ready for pilot studies	Pilot study site selection issues	Pilot studies are necessary to demonstrate technology to decision makers	Selection of pilot sites is very important and valuable; pilot sites must be selected in such a way that they will be accessible for demonstration purposes to the community
Access to suitable sites can be secured	Not applicable	Access for implementers to sites where the technology can be implemented must be secured up front	Determine priorities of population; set implementation targets; identify site criteria; and identify site
Economic/ financial factors			
Economic development	Economic development (community eventually able to pay), economic	Economic development translates into (a) the community being able to pay for services and (b) economic sustainability	Income generation, cost and time saving and national income and savings all contribute to economic development

Factor description	Focus group identification	Delphi study definition	Important issues for each factor from case studies
	sustainability		
Availability of finance	Available budget – the finances to support a project	The determination of the required budget and the availability of finance for this budget are addressed here. The type of finance whether debt, equity or grant must also be taken into account.	Finance can be facilitated by implementing payment methods which are applicable for the households, as for example, bartering and that finance methods must be in place before the technology can be implemented on a large scale
Achievability by performing organization			
Business management	Proper project management	The performing organization having the business management capacity and procedures in place to ensure that the implementation of technology can be done successfully	Which business management skills should be transferred, how the skills are to be transferred and what to do in the short term when the skills of the organization are lacking
Financial capacity	Financial capacity	Both the administrative capacity to manage finances and the ability to deliver, given the payment conditions.	Financial capacity for performing organizations can be problematic at the outset but that various methods can be used to alleviate the financial capacity required by the performing organization.
Technological capacity	Capacity	The performing organization has the correct technology necessary for implementation of the project at their disposal.	Technological capacity is directly related to quality. Quality assurance must be enforced; regulation of performing organizations and the dictating of standards also contribute to quality installations.
Other factors			
Government support	Regulatory financial incentive, tax regimes must be supportive" and does it fit under national priorities	Governmental support has been obtained for the technology	In the first place, the government must be aware of the new technology and support its implementation. If the government is also prepared to assist in the implementation, success of implementation is further enhanced.
Environmental benefits	Environmental impact assessment	The implementation of the technology will have a positive impact on the environment	Environmental benefits may include: decrease in the release of greenhouse gasses; protection of fragile ecosystems; halting soil erosion; halting desertification; prevention of fresh water pollution.

The focus group used the nominal group technique to identify 38 factors that need to be taken into account for the selection of renewable energy technologies in Africa and classified these factors into six categories.

The Delphi study was conducted over two rounds with the purpose of confirming and prioritising the factors identified during the focus group. The Delphi questionnaires were sent to experts (both academics and practitioners) in the field of renewable energy, with the emphasis on Africa.

In the first round, respondents were presented with the factors identified during the focus group and then asked to: comment on the classification of factors; comment on the description of factors; provide additional factors that were overlooked during the focus group; and provide a preliminary rating of the factors identified during the focus group in terms of feasibility, desirability and importance of considering these factors during the selection of renewable energy technologies in Africa. At the end of the first round Delphi the factors were regrouped into four categories.

In the second round of the Delphi study, the respondents were presented with a summary of the comments and ratings supplied in the first round and were then asked to supply new ratings in terms of feasibility, desirability and importance. The results were analysed. Eleven of the factors were rated by the experts to be feasible, highly desirable and highly important when selecting renewable energy technologies in Africa.

The eleven factors identified in the Delphi study were then used to generate the framework for the eight case studies which were conducted in the following three African countries: Rwanda; Tanzania and Malawi. The sources of evidence used included interviews, documentation and observation. The case studies confirmed that the eleven factors identified during the Delphi study are important for the selection of renewable energy technologies in Africa. Two additional factors were also found to be important and the wording of one of the factors was changed.

In conclusion, the thirteen most important factors that need to be considered for the selection of renewable energy technologies in Africa have been collated into a framework.

4. Discussion and/or Conclusions

The critical documentation that must be generated before renewable energy technologies are selected in Africa is shown in Table 2. The issues that have been identified in this study that must be addressed for each of the factors are also shown.

Table 2. Critical documentation for selection of renewable energy technologies in Africa

Description	Quality plan	Maintenance plan	Technology plan	Human resource plan	Financing plan
Technology factors					
Ease of maintenance and support over the life cycle of the technology	Standards, monitoring, evaluation, corrective action, responsibility, warranty	Operator maintenance, technical maintenance, spares	Adaption of technology	Responsibility for maintenance	Maintenance funding model
Ease of transfer of knowledge and skills to relevant people in Africa				Local skills levels, operator training and manuals, technical training and manuals, responsibility, quality, stakeholders, skills transfer	Skills transfer funding model
Site selection factors					
Local champion to continue after implementation				Identification of local champions	
Adoption by community			Capacity determination, benefits determination, information distribution, adoption probability		
Suitable sites ready for pilot studies			Selection of pilot sites		Pilot site funding model
Access to suitable sites can be secured			Priorities of population, implementation targets, site criteria identification		
Economic/ financial factors					
Economic development					Income generation, domestic cost and time

Description	Quality plan	Maintenance plan	Technology plan	Human resource plan	Financing plan
					savings, national income saving
Availability of finance					Initial investment donor funding, loan availability and rates, government support
Achievability by performing organization					
Business management				Capabilities of current organizations, business skills training, interim measures	
Financial capacity				Administrative capacity of performing organizations	Capital outlay requirements, capital outlay funding
Technological capacity	Quality assurance responsibility; technical guarantees	After sales service	Technological capacity of performing organization, regulation of standards for technology	Manufacturing training, installation training, maintenance training, refresher courses, quality training, technical backstopping	Financial incentive for quality
Other factors					
Government support			Government acceptance and support; energy policies, legislation and standards		Relief on taxes or duties; funding or subsidies; licensing
Environmental benefits			Environmental benefits of technology		

The critical documentation can be used at various levels and by various organizations to select the most appropriate renewable energy technologies for implementation in Africa. The critical documentation must be completed for each competing technology. The technology that performs the best in terms of addressing all the issues for all of the factors can then be selected. By using the framework proposed in this study, selection of renewable energy technologies can be done with the assurance that the most important factors for the successful implementation of these technologies have been taken into account.

The successful implementation of renewable energy technologies in Africa will lead to the improvement of the lives of the population in Africa, will increase their productivity and quality of life, and will contribute towards the alleviation of poverty and the empowerment of women and children. African children who have sustainable access to energy will be better educated and thus be better future leaders.

Further work is required to implement the factors into a selection method for example the analytical hierarchy process or analytical network process.

References

[1] International energy agency, "Renewables in Global Energy Supply: An IEA Fact Sheet," vol. 2008, Not stated, 2007.

[2] Energy sector management assistance program, "Technical paper: energy sector reform and pattern of poor: Energy use and supply a four country study: Botswana, Ghana, Honduras and Senegal," vol. 2008, 2006.

[3] United Nations Energy Agency, "Energy for sustainable development: Policy options for Africa," vol. 2008, 2007.

[4] G. Prasad and E. Visagie, "Renewable energy technologies for poverty alleviation. Initial assessment report: South Africa," vol. 2007, 2005.

[5] I. Dunmade, "Indicators of sustainability: assessing the suitability of a foreign technology for a developing economy," *Technology in Society*, vol. 24, pp. 461-471, 2002.

[6] K. A. Ruder, M. W. Pretorius and B. T. Maharaj, "A technology selection framework for the telecommunications industry in developing countries," in *ICC 2008 Proceedings*, 2008, pp. 5490.

[7] S. Teitel, "On the concept of appropriate technology for less industrialised countries," *Technological Forecasting and Social Change*, vol. 11, pp. 349-369, 1978.

[8] O. J. Ebohon, B. G. Field and R. Ford, "Institutional deficiencies and capacity building constraints: the dilemma for environmentally sustainable development in Africa," *International Journal of Sustainable Development & World*, vol. 4, pp. 204-213, 1997.

[9] B. T. Jimenez, A. Alvear, A. AlYabes and A. Olaoye, "Technology assessment and selection of renewable energy sources in the galapagos islands - ecuador," in *PICMET 2007 Proceedings*, 2007, pp. 2509.

[10] T. A. Scandura and E. A. Williams, "Research methodology in management: Current practices, trends and implications for future research," *Academy of Management Journal*, vol. 43, pp. 1248-1264, 2000.

[11] R. Blackburn, "Breaking down the barriers: Using focus groups to research small and medium-sized enterprises," *International Small Business Journal*, vol. 19, pp. 44-63, 2000.

[12] A. Gibbs, "Focus Groups," *Social Research Update,* vol. 19, pp. 1-7, 1997.

[13] M. Barry, H. Steyn and A. C. Brent, "The use of the focus group technique in management research: the example of renewable energy technology selection in Africa," *Journal of Contemporary Management,* vol. 6, pp. 229-240, 2009.

[14] F. Hasson, S. Keeney and H. McKenna, "Research guidelines for the Delphi survey technique," *Journal of Advanced Nursing,* vol. 32, pp. 1008-1015, 2000.

[15] A. L. Delbecq, A. H. ven de Ven and D. H. Gustafson, *Group Techniques for Program Planning: A Guide to Nominal Group and Delphi Processes.* Glenview, IL: Scott, Foresman and Company, 1975.

[16] M. L. Barry, H. Steyn and A. C. Brent, "Determining the most important factors for sustainable energy technology selection in Africa," *South African Journal of Industrial Engineering,* vol. 20, pp. 33-51, Nov, 2009.

[17] M. Barry, A. C. Brent and H. Steyn, "Selection of renewable energy technologies in africa: The case of efficient stoves in malawi," in *Second International Conference on Energy and Sustainability, 2009,* 2009, .

[18] M. Barry, A. C. Brent and H. Steyn, "Selection of renewable energy technologies in africa: The case of bio-gas in rwanda," in *18Th International Conference on the Management of Technology (IAMOT 2009),* 2009, .

[19] M. Barry, "Contributions to the Theory and Practice of Technology Selection: The Case of Projects to Ensure a Sustainable Energy Base for Africa," 2010.

Biofuel sustainability: relationships between the directive 2009/28/EC and scientific research

Luca Spreafico[1,*], Massimo Peri[2]

[1, 2] *Department of Agricultural, Food and Environmental Economics*
Università degli Studi di Milano, Milan, Italy
** Corresponding author. Tel: +39 50316469, Fax: +39 50316486, E-mail: luca.spreafico3@studenti.unimi.it*

Abstract: With the aim to reinforce the sustainability of biofuel production the EU directive 2009/28/EC has recently introduced a set of criteria aiming to reduce environmental effects of uncontrolled biofuel production. The criteria introduced by the directive define a procedure to compute the Green House Gases (GHG) emission of biofuel production based on the Life Cycle Analysis (LCA) approach. Nevertheless, although this approach is quite consolidated in some production systems, it represents a novelty in the biofuel sector. Using the Strengths, Weaknesses, Opportunities and Threats (SWOT) analysis in this paper it is compared the approach introduced by the directive with the main results emerged from a selection of papers, on the same subject, published in international journals in the last five years. The main results show as the new approach and the calculation method adopted could be a positive guideline for a better assessment of GHG emission at European level. However, some aspect could improve the efficiency of the new directive. Indirect land use change, functional unit and the involvement of other environmental impacts are some of the aspects that should be considered in order to refine the directive calculation method. Moreover, the paper highlights how it is fundamental to establish a right trade-off between LCA application and bureaucratic constraints for economic agents operating in biofuel production chain.

Keywords: *Biofuel sustainability, Life Cycle Analysis, Directive 2009/28/EC*

1. Introduction

Biofuels are considered one of the best alternatives to mineral oil derivatives in the transport sector, so their production and consumption are highly supported by the political framework, especially in Europe and in the United States. Although biofuels cover a small part of total energy requirement, the increasing demand could make doubtful their real sustainability, especially considering that feedstock production takes place in different countries around the world. In this regard there is a broad debate from which emerge several opinions: sceptical positions on the usefulness of biofuels (e.g.: Koonin, 2006; Odling, 2007; Righelato and Spracklen, 2007); judgements and criticisms (e.g.: Fargione *et al*., 2008; Melillo *et al*., 2009); encouraging considerations on future prevision related to the develop of the second-generation biofuels (e.g. Tilman *et al*. 2006; Fargione *et al*., 2008). The debate still remain open and the opinions on the effectiveness of a biofuel policy are not always in agreement (e.g. Kennedy, 2007; Robertson *et al*., 2008; Fargione, *et al*., 2008). From a conceptual point of view reasoning on biofuel sustainability pass through the definition of what basis utilize to discriminate which of them are sustainable and then identify the sustainable policy framework for biofuel development. In this regard it could be useful to decompose the question into two elements: the first, technical, seeks to understand whether biofuels are sustainable products, while the second, institutional, it is dedicated to understand whether the implemented policy framework to promote biofuels is sustainable.

These two aspects support each other: it is politically correct to promote the biofuels use only if they prove to be technically sustainable (in particular if the goal of the political action is precisely the sustainability), on the other hand, not having the absolute certainty that such products are sustainable, or that the production methods are sustainable, the policy action can

orient economic operators to those supply chains able to demonstrate their sustainability by using rules, certifications system or other effective evaluation methods.

In line with the existing implemented policy framework for biofuel development and with the aim to reinforce the sustainability of EU biofuel production the directive 2009/28/EC has recently introduced a set of criteria aiming to reduce environmental effects of uncontrolled biofuel productions incorporating technical patterns into institutional framework. The criteria introduced by the directive define a procedure to compute the Green House Gases (GHG) emission of biofuel production based on the Life Cycle Analysis (LCA) cradle-to-grave approach. Nevertheless, although LCA approach is quite consolidated in some production systems, it represents a novelty in the biofuel sector. Using the Strengths, Weaknesses, Opportunities and Threats (SWOT) analysis in this paper it is compared the approach introduced by the directive with the main results emerged from a selection of papers, on the same subject, published within international journals during the last five years.

2. The SWOT analysis applied to the LCA approach of the directive 2009/28/EC

From a theoretical point of view the SWOT analysis is an evaluation methodology that assess the possibility for a subject to achieve a goal highlighting strengths and weaknesses of the subject and the opportunities and threats that can occur from his setting, in respect to the goal. In order to analyse possible benefits, problems, opportunities and limits that can occur in the application of the LCA in the biofuel sector as regulated form the recent directive 2009/28/EC on the promotion of the use of energy from renewable sources, in this paper strengths and weaknesses are pointed out by comparing the directive with the institutional framework, while opportunities and threats are highlighted examining the technical aspect emerged from a literature review concerning the LCA methodology applied to biofuel sector.

2.1. Strengths and Weaknesses

Strengths and weaknesses of the application of the directive are deduced from the analysis of the relationship between the content of the directive and the political objectives that European Union aim to achieve through a sustainable development of biofuels sector. From a conceptual point of view to identify strengths and weaknesses the paper analyse the three major objectives of the EU biofuel policy (energy security, climate change mitigation and rural development) in respect to the principal sector involved by the application of the directive such as biofuel sector, energy sector, agricultural and food sector, environment and rural development. Within this contest strengths and weaknesses are presented considering that what in the directive can be helpful to reach these objectives has been considered strengths, while problems about biofuels development that the directive can not solve has been treated as weaknesses.

2.1.1. Strengths

Before declining the different aspects that could be classified as strengths it is important to highlight some general concepts having a positive impact on the institutional framework. Before the adoption of the directive the EU political framework in support of biofuel developments were only related to production incentives both on the supply and demand side. Among the different policies implemented in the EU to stimulate biofuel supply, we recall the directive 2003/96/EC on energy taxation, the energy crop premium and the non-food set-aside payment. While on the demand side, we recall the directive 2003/30/EC on the promotion of biofuel use, which fixed a share of biofuel blends equal to 2% of the overall consumption of gasoline and diesel in transport for the end of 2005, rising to 5.75% in 2010. Moreover, the

directive here examined (2009/28/EC), has increased the European biofuel target to 10% by 2020. This political framework has had a great impact on production: from 2005, the first biofuel target year of the directive 2003/30/EC, to 2009, the EU-25 biodiesel production rose to 184%. In the same period biodiesel production capacity increased from 4.2 to 20.9 million tons, the equivalent of an increment of 395% (EBB, 2010).

Considering the uncontrolled development of biofuel production, the adoption of the directive with sustainable constrain for biofuel production and use can be viewed as the only way for the prosecution of the European biofuel policy. In this regard, one of the more significant strengths of the directive is that it is highly innovative and in line with the European political action, that is largely based on the enhancement of sustainability goals. Moreover the new framework imposed by the directive forces Member States to monitoring the environmental, economical and political problems related to biofuels production and consumption, providing new basis for consciously decisions.

In respect to the biofuel sector the new target fixed by the directive, equal to 10% of renewable energy in transport sector by 2020, is set up in a more clear framework able to demonstrate and communicate the real sustainability of biofuel products. This new scenario could stimulate institutional investors that could be attracted by the ethic aspect of sustainable biofuel and in the same time also new investors can look at biofuel sector with a growing interest in relation to the reduced risk related to a more controlled supply chains, as a consequence of the application of the LCA approach.

Also the agricultural and food sector is indirectly involved by the directive, indeed it allows a double counting of energy produced by waste, residues and lingo-cellulosic biomass. Trough this mechanism the second generation of biofuels are promoted and then, the so criticized conflict between food and non food use of feedstock, should be attenuated.

From the environmental point of view two related aspects can be considered as strengths. First, the directive fixes a minimum level of GHG reduction, so the environmental benefit can be assured, second the calculation method for the GHG emission is fixed and equal for all EU Member States, reducing technical disagreement in emissions assessment and consequently market asymmetry and trade distortions.

2.1.2. Weaknesses

As for the strengths patterns, also for the weaknesses can be formulated some general considerations related to the adoption of the directive. If the innovative character of the directive is analysed as a strengths pattern, from a conceptual point of view it could be also viewed as a limitation, indeed it is possible that it can be incomplete and inexact.

Monitoring of environmental, economic and political aspect imposed to Member State is not sufficient to control these problems, in the directive there are not specific interventions able to manage indirect land use change, fluctuation in commodities prices and food insecurity. However, it is admitted that these problems are very complex and their management required more knowledge. Through the National Action Plan the directive encourages the processing sector and the biofuel consumption, but does not highlight any specific intervention in support of farmers. The sustainable standard introduced with the adoption of the directive could be viewed as a constrain in the commercial relation, European imports restriction imposed on non sustainable biomass and biofuels could stimulate international trade partners to introduce non tariff barriers on other relevant products for European community. Another general

weaknesses is related to the methodology adopted for the calculation of the GHG reduction, indeed the directive suggests two different approaches, analytic and concise, that could produce different results.

In respect to the implication related to the biofuel sector the introduction of the mass balance system, as a method for the traceability of the products, does not appear completely clear. This unsettled contest opens the interpretation and application of the directive liable to a lobby activity from processing and trader agents reducing the efficiency of all the system.

With reference to agricultural and food sector it is possible to underline that no specific and direct interventions are considered to reduce food no food conflict, so the promotion of sustainable biofuels could not be enough to reduce this conflict. Moreover within the directive there are not specific actions devoted to promote biofuels supply chains in rural areas. Finally, with regard to energy sector, although the contribute of biofuel development to energy security is, at the moment, in absolute value limited, their development do not contribute to energy security. Indeed the feedstock necessary for biofuels production in the next future will continue to be imported from extra EU country, making null the contribute of biofuel sector to the energy independency goal, simply the question shifts from fossil fuel to food commodity. Indeed, the Commission itself expects an increasing flow of imports of biomass for biofuel use. Moreover, these latter questions appear in contrast with the recent publication of the proposal reform of the Common Agricultural Policy for the period past 2013, where one of the three main objectives is directed to revaluate the European food security.

2.2. Opportunities and Threats

In this article the opportunities and threats related to the adoption of the directive are investigated in respect to the technical pattern, looking up weather biofuels are sustainable products in respect to their GHG emission within the contest of LCA approach. In order to highlight the most widespread problems the paper has compared the methodology proposed by the directive with the main results, on the same topics, emerged from a literature review. The paper has considered fourteen articles relative to the LCA application in biofuels sector published on international journals during the period 2004 to 2010.

The articles considered span from general reports where authors compare several LCA with the aim to underline the origin of the variability in the results obtained to very critical articles that explain conceptual mistakes in LCA structure and proposing new methods to assess biofuels sustainability.

In the following it is itemized the main criticisms of LCA application to biofuel sector emerged from literature review:

- definition of the system boundaries of LCA analysis; system boundaries should be consistent with the goal of analysis, because outputs are greatly affected by the numbers of steps considered in supply chain examined (Feng *et al.*, 2008; Gnansounou *et al.*, 2009; Quirin *et al.*, 2004; Rowe, 2009; Singh *et al.*, 2009).
- definition of the reference systems; to obtain reliable results of GHG reduction, it is relevant to have clearly defined reference systems as regards fossil fuels, alternative uses of biomass, uses of co-products substitutes (Cherubini *et al.*, 2009; Gnansounou *et al.*, 2009; Quirin *et al.*, 2004).
- choice of functional unit; functional unit should be consistent with the system boundaries considered. The same biofuel can appear sustainable using one functional

unit and not sustainable using another (Cherubini *et al.*, 2009; Gnanosunou *et al.*, 2009; Quirin *et al.*, 2004; Singh *et al.*, 2009).

- choice of input considered; when the inputs considered are different, biofuel sustainability could appear different within the same system boundaries (Rowe, 2009).
- data quality and representativeness; data used in LCA could be *out-of-date* or little representative, a particular phenomenon could be difficult to measure, so data could not be reliable. Moreover the data used could be significant only for local condition considered and then not replicable in different context (Cherubini *et al.*, 2009; Chiaramonti and Recchia, 2010; Larson, 2006; Menichette and Otto, 2008; Quirin *et al.*, 2004; Rowe, 2009).
- assessment of another environmental impacts; CO_2 emissions are always assessed, but other GHG are also important, besides other possible impacts, like acidification or eutrophication, could occur during biofuels production (Delucchi, 2004; Larson, 2006; Menichette and Otto, 2008; Quirin *et al.*, 2004).
- efficiency of energy conversion; it is important to consider the energy efficiency of engines and conversion plants. Indeed, with high engine efficiency emissions are lower (Delucchi, 2004; Larson, 2006; Menichette and Otto 2008; Rowe, 2009).
- consideration of fuels/biofuels mixtures; technical features of mixtures affects emission levels (Croezen and Kampman, 2009; Gnansounou *et al.*, 2009)
- effects of agricultural residues removal; the removal of agricultural residues for producing biofuels could affects the level of CO_2 emissions, so this effect should be assessed and considered (Cherubini *et al.*, 2009).
- choice of allocation method; different allocation methods of GHG emissions between biofuels and co-products cause different results (Chiaramonti and Recchia, 2010; Gnansounou *et al.*, 2009, Larson, 2006; Luo *et al.*, 2009, Menichette and Otto 2008; Quirin *et al.*, 2004; Rowe, 2009; Singh *et al.*, 2009; Wang *et al.*, 2010).
- consideration of direct land use change; this phenomenon is highly relevant because it can cause CO_2 emissions or savings, so LCAs should consider it (Cherubini *et al.*, 2009; Delucchi, 2004, Gnansounou *et al.*, 2009; Larson, 2006; Menichette and Otto, 2008).
- consideration of indirect land use change; like the preceding point (Cherubini *et al.*, 2009; de Gorter and Tsur, 2009; Feng *et al.*, 2008; Gnansounou *et al.*, 2009; Menichette and Otto, 2008).
- conceptual mistake of LCA; (de Gorter and Tsur, 2009; Delucchi 2004; Feng *et al.*, 2008).

In the following the LCA calculation methodology proposed by the directive has been compared with the main aspect emerged by the literature review just detailed. Where there is consistency there is an opportunity, while where the directive shows a lack of precision there is a threat.

2.2.1. Opportunities

- Within the directive the system boundaries is defined by the cultivation of biomass and by the use of biofuels in cars, this approach is in line with the well-to-wheel approach recommended in literature for LCAs of biofuels for transportation;
- the directive fixees which inputs must be considered in calculation of GHG emissions, while in the literature there is not an agreement about this choice;

- the directive provides default values of GHG emissions, this data are representative of the typical European supply chains and, furthermore, they are conservative; in this way it should be an agreement in assessments at European level, while in literature the approach is not univocal;
- allocation method adopted in the directive is energy allocation; in the literature this approach does not appear as the best method, but is admitted that is almost exact; besides, energy allocation is more easy to perform;
- direct land use change is considered in the calculation methodology proposed by the directive, indeed it provides an equation to assess consequent GHG emissions or savings.

2.2.2. Threats

- the calculation methodology of the directive regards only a reference system relative to fossil fuels, while there is not a reference system for co-products and alternative uses of biomass;
- the functional unit fixed by the directive is mega joule of energy content, while it should be kilometre driven by cars in order to be consistent with the system boundaries;
- the directive does not consider other environmental impacts like acidification or eutrophication;
- the directive calculation method for GHG emission considers only energy efficiency of biomass processing, while does not consider the cogeneration processes;
- features of fossil fuels/biofuels mixtures are not considered in the directive;
- indirect land use change is not considered in the directive calculation method.

3. Conclusions

In this paper the directive 2009/28/EC has been analysed with the aim to find possible benefits and complications that his application could involve. Directive has been studied using the SWOT analysis conceptual structure, that identifies Strengths, Weaknesses in relation to the institutional framework and Opportunities and Threats in respect to literature review on LCA application to biofuel sector. The main result of the analysis allow to highlight the innovative feature of the directive and how its implementation could facilitate policy maker to reach the main goal of the European biofuel policy, promoting production and consumption of really sustainable biofuels. This scenario could stimulate the entry into the market of new ethical investors attracted by a real sustainable sector. However, some relevant aspects are not completely resolved like the relationship between biofuel development and fluctuation in commodity prices or the definition of the role played by rural area. On the other hand, from a technical point of view, some positive aspects with a certain importance are emerged too like, for example, the definition of default value for GHG emissions for all the EU, reaching an agreement in assessments at European level or the definition of the inputs to be considered in the calculation method. On the contrary the directive uses a functional unit that does not appear in line with the literature examine and, moreover, does not consider indirect land use change. Overall, considering that the directive is highly innovative, the presence of some weaknesses and threats can be considered normal. A deeper investigation would be useful to improve the efficiency of the EU biofuel policy.

References

[1] S. E. Koonin, Getting serious about biofuels, Science 311, 2006, p. 435

[2] L. Odling, Biofuels bandwagon hits a rut, Nature 446, 2007, p. 483

[3] R. Righelato, D. V. Spracklen, Carbon mitigation by biofuels or by saving and restoring forests?, Science 317, 2007, p. 902

[4] J. Fargione, D. Tilman, Land clearing and the biofuel carbon debt, Science 319, 2008, pp. 1235-1237

[5] J. M. Melillo, J. M. Reilly, D. W. Kicklighter, A. C. Gurgel, T. W. Cronin, S. Paltsev, B. S. Felzer, X. Wang, A. P. Sokolov, C. A. Schlosser, Indirect emissions from biofuels: how important?, Science 326, 2009, pp. 1397-1399

[6] D. Tilman, J. Hill, C. Lehman, Carbon-Negative biofuels from Low-Input High-Diversity Grassland Biomass, Science 314, 2006, pp. 1598-1600

[7] D. Kennedy, The biofuels conundrum, Science 316, 2007, p. 515

[8] G. P. Robertson, V. H. Dale, O. C. Doering, S. P. Hamburg, J. M. Melillo, M. M. Wander, W. J. Parton, P. R. Adler, J. N. Barney, R. M. Cruse, C. S. Duke, P. M. Fearnside, R. F. Follet, H. K. Gibbs, J. Goldenberg, D. J. Mladenoff, D. Ojima, M. W. Palmer, A. Sharpley, L. Wallace, K. C. Weathers, J. A. Wiens, W. W. Wilehlm, Sustainable biofuels redux, Science 322, 2008, pp. 49-50

[9] EBB (European Biodiesel Board), 2010. EBB Publishes Annual Biodiesel Production Statistics, Press Release, July.

[10] H. Feng, O. D. Rubin, B. A. Babcock, Greenhouse Gas Impact of Ethanol from Iowa Corn: Life Cycle Analysis versus System-Wide Accounting, American Agricultural Economics Association Annual Meeting, 2008, selected paper

[11] E. Gnansounou, A. Dauriat, J. Villegas, L. Panichelli, Life cycle assessment of biofuels: Energy and greenhouse gas balances, Bioresource Technology 100, 2009, pp. 4919-4930

[12] M. Quirin, M. Pehnt, G. A. Reinhardt, CO2 mitigation through Biofuels in the Transport Sector Status and Perspectives, IFEU- Institut fùp Enepgie- und Umweltforschung Heidelberg Gmbh, 2004, Main report

[13] R. Rowe, Sustainable bioenergy and biofuels. Can life cycle analysis provide the answer?, Bioenergy news Issue 9, 2009,, pp. 2-4

[14] A. Singh, D. Pant, N. E. Korres, A. S. Nizami, S. Prasad, J. D. Murphy, Key issues in life cycle assessment of ethanol production from lignocellulosic biomass: Challenges and perspective, Bioresource Technology 101, 2009, pp. 5003- 5012

[15] F. Cherubini, N. D. Bird, A. Cowie, G. Jungmeier, B. Schlamadinger, S. Woess-Gallasch, Energy- and green house gas-based LCA of biofuel and bioenergy systems: key issues, ranges and recommendations, Resources, Conservation and Reiclling 53, 2009, pp. 434-447

[16] D. Chiaramonti, L. Recchia, Is life cycle assessment (LCA) a suitable method for quantitative CO_2 saving estimations? The impact of field input on the LCA results for a pure vegetable oil chain, Biomass and Bioenergy 34, 2010, pp. 787- 797

[17] E. D. Larson, A review of life-cycle analysis studies on liquid biofuel systems for the transport sector, Energy for Sustainable Development Vol. X No. 2, 2006, pp. 109-126

[18] E. Menichette, M. Otto, Energy Balance & Greenhouse Gas Emission of Biofuels on a Life-Cylce Perspective, Proceednings of the Scientific Committee on Problems of the Environment (SCOPE) International Biofuels Project Rapid Assessment, 2008

[19] M. A. Delucchi, Conceptual and methodological issues in lifecycle analyses of transportation fuels, U.S. Environmental Protection Agency Office of Transportation and Air Quality, 2004

[20] H. Croezen, B. Kampman, The impact of ethanol and ETBE blending on refinery operations and GHG- emissions, Energy Policy 37, 2009, pp. 5226- 5238

[21] L. Luo, E. van der Voet, G. Huppes, H. A Udo de Haes, Allocation issues in LCA methodology: a case study of corn stover-based fuel ethanol, International Journal of Life Cycle Assessment 14, 2009, pp. 529- 539

[22] M. Wang, H. Huo, S. Arora, Methods of dealing with co-products of biofuels in life-cycle analysis and consequent results within the U.S. context, Energy Policy (2010), doi:10.1016/j.enpol.2010.03.052.

[23] H. de Gorter, Y. Tsur, Towards a Genuine Sustainability Standard for Biofuel Production, Cornell University- Department of Applied Economics and Management New York, 2009, working paper.

Which factors affect the willingness of tourists to pay for renewable energy?

I. Kostakis[1], E. Sardianou[2,*]

[1]*Harokopio University, Athens, Greece*
[2]*Harokopio University, Athens, Greece*
** Corresponding author. Tel: +30 2109549266, Fax: +30 2109577050 E-mail: esardianou@hua.gr*

Abstract: This study presents insights into the determinants of tourists' intention to pay a premium for accommodation in a hotel with renewable energy sources. The empirical analysis is based on the estimation of binary logistic regression models. Four subsets of independent variables were used in this empirical analysis, namely: (*i*) demographic factors, (*ii*) economic variables, (*iii*) past experience with regard to renewable energy sources and (*iv*) variables regarding environmental awareness and information dissemination. Empirical results suggest that middle-aged people are probably more willing to pay for their stay in a hotel using renewable energy. In general, men are more likely than women to pay extra money for accommodation in a "green" hotel. However, the results suggest that marital status and educational level are not statistically significant factors in the willingness to pay more. Rather, environmentally-conscious and adequately informed tourists are more willing to pay for renewable energy than others. Our analysis is focused on intention because we expect that those people willing to pay for staying in a green hotel are a potentially relevant market segment for developing sustainable tourism in Greece.

Keywords: *Tourists, WTP, Renewable energy*

1. Introduction

Contrary to fossil fuels, the intensive use of renewable energy is inextricably linked to zero greenhouse gas emissions. Thus, the penetration and implementation of renewable energy projects is one of the major goals of European countries in their quest for achieving sustainable development. However, the use of renewable energy sources is strongly related to public acceptance.

Previous studies have focused on attitudes towards green energy and on acceptance of renewable energy sources (Ek, 2005; Roe et al, 2001; Mallett, 2007; Jodert et al., 2007 Zoellner et al., 2008). Others have examined the intention of hotel customers to stay at a green hotel employing the theory of planned behaviour (Han et al., 2010; Han and Kim, 2010). In general, consumers who are more receptive to environmental products, and choose to purchase them, are willing to pay more for environmental benefits. Empirical studies have also focused on the amount that consumers are willing to pay by way of premium for renewable energy investments and the role of socio-demographic determinants in the case of Italy (Bollino, 2009) and Korea (Ku and Yoo, 2010).

Several studies have been conducted on the issue of renewable energy penetration in Crete (NTUA, 1992; Vamvuka and Tsoutsos, 2002). Crete hosts one-fifth of all tourists visiting Greece. More than 50% of all renewable energy projects in the Greek islands are implemented in Crete (Michalena and Angeon, 2009). The willingness of Crete's residents to pay for renewable energy sources was investigated by Zografakis et al. (2010).

The aim of this study is to examine the determinants that affect tourists' intention to pay more for their stay in a hotel using renewable energy sources. For this purpose, we employ cross-section data from the largest Greek island, Crete. Unlike previous studies, we chose tourists

because we expect tourists willing to pay for a stay in a green hotel to be a potential market segment important for the development of sustainable tourism on the island.

The paper proceeds as follows: Section 2 presents the methodological issues and the data used in the empirical analysis. Section 3 presents the empirical results, while the conclusions of the analysis and policy implications are discussed in Section 4.

2. Methodology

The research provides some insights into the determinants that affect tourists' positive attitude towards renewable energy. The empirical analysis is based on a cross-section data set. We carried out an extensive survey of 400 tourists during their summer holidays in Crete in 2009, using the random stratified sampling method. In particular, we distributed 100 questionnaires in each of the fourth prefectures of the island (Chania, Rethymno, Heraklion and Lasithi). The survey was conducted using a structured questionnaire and personal interviews. Given the purpose of our study, we interviewed tourists at hotels (Veal, 2006). We chose hotels at random taking into account the official hotel directory. The response rate was 80% and the survey resulted in a data set of 320 tourists. As a prerequisite, the respondents were above 18 years of age and income-earners.

Empirical results are based on the estimation of logistic regression models. Logistic regression (sometimes called the logit model) is used for predicting the probability of an event occurring by fitting data to a logit function. Logistic regression is a useful way of describing the relationship between one or more independent variables (e.g. age, gender, etc.) and a binary response variable, expressed as a probability, that has only two possible values (such as willingness or unwillingness).

In our case, under the binary logistic model, the estimated value of the dependent variable is interpreted as the probability that a tourist will pay more for accommodation in a "green hotel", as identified by the values of the explanatory independent variables. Thus, binary logistic analysis enables us to measure the impact of each variable on a tourist's intention to stay in a hotel using renewable energy sources. Four subsets of independent variables were used in this empirical analysis, namely: demographic factors, economic variables, past experience with regard to renewable energy sources, and variables regarding environmental awareness and information dissemination. Therefore, in the empirical study, we employed the following expanded specification for a tourist's willingness to pay more for accommodation in a "green" hotel:

$$W_i = b_o + b_1 A_i + b_2 TA2_i + b_3 M P g_i + b_4 K_i + b_5 D_i + b_6 I r d e_i + b_7 D_i + b_8 E_i + b_9 R h x e_i + b_1 S \rho_{i0} + b_1 R i a e n_1 + b_1 n E t_{i2} + u_i \quad (1)$$

where WTPi is a binary variable indicating whether the tourist *i* is willing to pay extra for hotel accommodation using renewable energy sources or not; specifically, the variable takes the value 1 when the tourist is willing and zero otherwise[1]. $Gender_i$ is a dummy variable accounting for 1 if the respondent is male and zero if female; Age is the respondent's age;

[1] To be more precise, we asked "Are you willing to pay extra for hotel accommodation with RES?" (Yes/No). A similar question format was followed by (Dalton et al., 2008) in Australia. Jun et al. (2010) had also performed contingent valuation methodology employing dichotomous choice questions.

$Age2_i$ is the square of the respondent's age; $Married_i$ is a dummy variable taking the value 1 if the respondent is married and zero otherwise; Kid_i is a dummy variable accounting for 1 if the respondent has children and zero otherwise; $Degree_i$ is a dummy variable accounting for 1 if the respondent has completed undergraduate studies and zero otherwise; $Income_i$ is the respondent's monthly private income in euros; $Days_i$ is a quantitative variable indicating the average duration of a hotel stay while on holidays; $Expense_i$ is a quantitative variable expressing the average holiday cost per person; $Rhome_i$ is a dummy variable accounting for 1 if the consumer has already implemented an energy conservation system at home and zero otherwise; $Satisf_i$ is a dummy variable expressing the tourist's satisfaction with a previous stay in an energy-conserving hotel (yes: 1, 0: otherwise); $Rinf_i$ is a quantitative variable expressing awareness of renewable energy sources; $Envin_i$ is a dummy variable accounting for 1 if the respondent is aware of global environmental problems and zero otherwise; and u is an error term. The empirical results from the estimation of Eq. (1) are presented in Section 3 of this study.

Table 1 summarizes the expected sign for bi coefficients of Eq. (1). In particular, it is assumed that the people most likely to pay more for accommodation in a hotel with RES are those with a positive previous experience with the implementation of energy-conserving practices. Therefore, the expected sign for variables "Rhome" and "Satisf" is positive. We also assumed that adequately informed consumers are more likely to participate in eco-friendly actions. Thus, a positive relationship should be expected between "Rinf" or "Envin" and willingness to pay. In addition, previous studies reported that higher income groups are more willing than others. Higher income groups tend to spend more money on vacations. Thus, we also expected a positive sign for "Expense". On the other hand, it may be difficult for these groups, who have longer vacation periods, to pay a premium for environmental purposes. In this case, the expected sign for the variable "Days" is negative. Although, it is difficult to predict the impact of demographic characteristics on the decision to pay more for accommodation in a hotel with RES, it is expected that highly educated consumers are more prone to support energy-conserving actions. Thus, a positive sign is expected for the variable "Degree".

Table 1. Expected sign of the variables specified in the empirical binary logistic regression

Designation	Expected sign	Designation	Expected sign
Gender	+/-	Days	-
Age	+/-	Expense	+
Age2	+/-	Rhome	+
Married	+/-	Satisf	+
Kid	+/-	Rinf	+
Degree	+	Envin	+
Income	+		

3. Results

In this section we present the results of the statistical and econometric analyses to estimate the profile of 'green' tourists. As 'green' tourists we define those consumers willing to pay extra for accommodation in a hotel using renewable energy sources.

3.1. Descriptive Statistics

From the sample of 400 tourists in question, 53.1% were women and 46.9% men. Most respondents were between the ages of 31 and 50 years (36.9%); 18.1% were between 25 and

37 years, 12.8% between 51 and 71 years and 29.7% between 18 and 24 years. As regards the educational level, 60.9% were university-educated. The majority were employees with 40% working in the private and 21.9% in the public sector, whereas 14.1% were freelancers. The tourists' average monthly private, non property-related, income was €1,400, with a large percentage of monthly incomes being no higher than €500 (17.5%). The income of 3.4% of tourists varied between €800 and €1,100 and 22.2% declared having an income above €2,000. 34.4% of tourists were married. The majority (32.8%) reported holiday expenses between €251 and €500; 25.3% between €751 and €1000 and 7.8% over €1,500. As shown in figure 1, 45% of tourists were willing to pay more for accommodation in a hotel with renewable energy sources. As to the vacation's purpose, the vast majority of respondents (92.2%) reported recreation and the rest professional reasons. Next, interviewees were asked about their past experience with renewable energy sources. In particular, 71.3% of tourists had previously implemented an energy conservation project at home, and only 25% were satisfied with their past accommodation at an energy-conserving hotel.

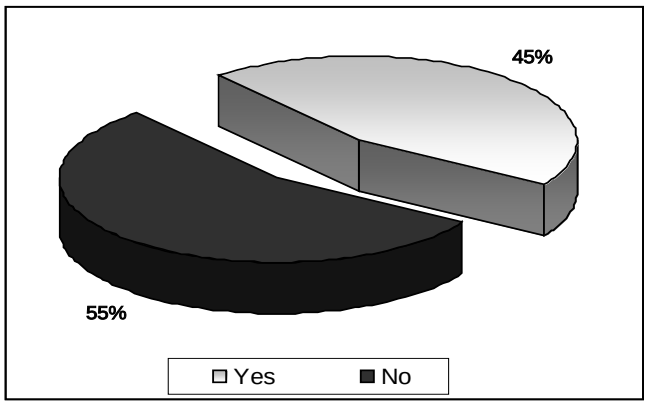

Fig. 1. Willingness to pay for accommodation in a hotel with RES

3.2. Logistic Regression Analysis

Several interesting results were obtained from the empirical estimation of Eq. (1). Table 2 summarizes the empirical results of the logit equation's estimated coefficients with respect to the willingness to pay extra for accommodation in a hotel using renewable energy sources. Statistically non-significant variables were omitted from model II. The final results for explanatory variables of tourists' willingness to pay are set out in the last column of Table 1, Model III. All the estimated coefficients of the explanatory variables presented in the final model have the expected sign and are statistically significant at a level of 5% or 1%. Estimated standard errors are corrected using White Heteroskedasticity. The Hosmer and Lemeshow statistic is one of the most reliable tests of model fit for binary logistic regression. The overall percentage of correct predictions for the final estimated model (model III) is 72.8%. The p-value 0.721 uses the Hosmer and Lemeshow Goodness-of-Fit Test with n-2 degrees of freedom. We are not able to reject the null hypothesis that there is no difference between the observed and predicted values of the dependent, implying that the model's estimates adequately fit the data. A p-value less than 0.05 indicates a good fit for a binary logistic regression model.

As follows from Table 2, men are more willing to pay extra than women, at a 10% level of significance (Model I & II). However, we didn't find any statistically significant relation between family status ("Married" and "Kid") and willingness to pay more for staying in a "green" hotel.

Age is a statistically significant factor in the willingness to pay more for accommodation in a hotel with renewable energy sources, at a 5% level of significance. Indeed, it is estimated that younger tourists are less willing to pay extra than middle-aged tourists. However, the negative sign of the estimated coefficient for the variable 'Age2' implies that age positively affects the dependent variable, but at a decreasing rate - reaching a maximum at 53 years of age

$$\frac{\partial(b_1 \text{"}A\text{"} + b_2 \text{"}AGE\text{"})}{\partial \text{"}AGE\text{"}} = b_1 + 2b_2 \text{"}A\text{"} \quad \text{"=0.106+2*(-0.001)*"AGE"=0.}$$

In particular, for all tourists under the age of 53, an increase in age will positively affect the probability of paying more to stay in a green hotel. The importance of age on willingness to pay for RES was also reported by Dalton et al. (2008), who performed a frequency statistics analysis.

Table 2. Estimated binary logistic regressions of tourists' willingness to pay more to stay in a hotel with renewable energy sources (yes: 1 no: 0)

Independent variables	Model I	Model II	Model III
Constant	-2.910***	-2.967***	-1.269**
	(4.460)	(6.146)	(4.032)
Gender	0.279*	0.308*	
	(1.715)	(1.656)	
Age	0.106**	0.104**	0.020**
	(2.619)	(3.361)	(4.136)
Age2	-0.001**	-0.001*	-0.001**
	(2.266)	(2.390)	(2.481)
Married	0.154		
	(1.204)		
Kid	-0.017		
	(0.002)		
Degree	0.090		
	(0.103)		
Income	0.135		
	(1.230)		
Days	-0.045*	-0.065**	-0.070**
	(1.839)	(3.938)	(4.500)
Expense	0.001		
	(1.577)		
Rhome	0.796***	0.796***	0.703***
	(8.085)	(8.187)	(6.691)
Satisf	0.074**	0.069**	0.075**
	(4.076)	(3.669)	(4.443)
Rinf	0.273***	0.273***	0.288***
	(4.715)	(5.018)	(5.758)
Envin	0.662**	0.635**	0.610**
	(3.033)	(2.980)	(2.873)
- 2 Log likelihood	393.541	395.512	399.677
Nagelkerke R Square	0.282	0.325	0.360

Note: ***, *, represent levels of significance at 1% and 10%, respectively. Wald statistics are presented in parentheses. Standard errors are corrected using White Heteroskedasticity.

As expected, the longest-staying respondents were also the least willing to pay more, at a 5% level of significance (Model I & II). Educational level is also included in the first model, indicating that there is a positive, but statistically insignificant relation, between higher education and willingness to pay. Generally, tourists with a positive past experience at an energy-saving hotel are more likely to be willing to pay extra for their accommodation in a hotel implementing renewable energy projects, at a 5% level of significance. Accordingly, those tourists who have not previously adopted an energy conservation project at home are less likely to pay more for staying in a "green" hotel than others, at a 1% level of significance. As Bollino (2009) mentioned, those consumers who have a positive attitude to renewable energy technologies, will be prone to pay a surplus.

As far as economic parameters are concerned, the estimated coefficients for income and holiday expenditure are (as expected) positive, but not statistically significant. These results may explained by the following three parameters: (i) the economic uncertainty that influences consumers' decision making process (ii) the fact that consumers stated preferences vary over time depending on their experience or knowledge and (iii) the hypothetical nature of the contingent valuation question and the fact that and consumer may value different public goods (Wang and Whittington, 2005). In contrast to the above-mentioned conclusion, the empirical results indicate that there is a positive, statistically significant, relation between information dissemination on renewable energy sources and willingness to pay, at a 1% level of significance. This result is in line with Roe et al. (2001) study for U.S. electricity consumers. Accordingly, environmental awareness about global environmental problems positively affects the probability of paying more, at a 5% level of significance. Zografakis et al. (2010), had also pointed out that high awareness levels or energy saving behavior resulted in a positive attitude for renewable energy sources.

4. Discussion and Conclusions

This paper has focused on providing insights into which factors affect tourists' willingness to pay for renewable energy sources in Greece. The empirical results suggest that middle-aged people and men are more likely than others to pay a premium for accommodation in a hotel with renewable energy practices. This study also shows the importance of information dissemination and environmental awareness in the willingness to pay for renewable energy sources. In particular, past experience, environmental awareness and information dissemination are strong, statistically significant, factors that positively affect tourists' willingness to pay for accommodation in a green hotel. Bearing in mind that tourism is considered to be Greece's "heavy" industry, it is important for enhancing sustainable development that hotels embrace renewable energy technologies. Accordingly, policies aimed at increasing consumer acceptance of green hotels can contribute to the adoption of sustainable lifestyles. As tourists become more sustainable consumers, the impact of tourism on the environment is limited. In this context, investigating the socioeconomic profile of tourists willing to pay a premium would have multiple useful policy implications. In particular, in the business sector, green hotel managers could expand their market share by focusing their advertising campaigns on those less willing to pay for renewable energy sources. Thus, green advertising can enhance a hotel's economic viability by increasing tourist demand. On the social level, renewable energy projects in hotels can contribute to environmental protection. However, further research is needed to achieve this goal in the tourism sector. Specifically, more analysis is needed on how information feedback can influence a tourist's actual choice in favour of a green hotel, rather than relying solely on self-reported intentions to pay more for one. More importantly, there must be an emphasis on the various barriers that tourists report when it comes to accepting to pay more for renewable

energy sources. In the case of willing tourists, research is needed on economic or other incentives for paying more and achieving sustainable behavioral consumption patterns.

References

[1] K. Ek. Public and private attitudes towards ‘‘green’’ electricity: the case of Swedish wind power. Energy Policy 33. 2005. pp. 1677–1689.

[2] B. Roe. M. F. Teisl. A. Levy. M. Russell. US consumers' willingness to pay for green electricity. Energy Policy 29. 2001. pp. 917- 925.

[3] A. Mallett. Social acceptance of renewable energy innovations: The role of technology cooperation in urban Mexico. Energy Policy 3. 2007. pp. 2790-2798.

[4] A. Jobert. P. Laborgne. S. Mimler. Local acceptance of wind energy: Factors of success identified in French and German case studies. Energy Policy 35. 2007. pp. 2751-2760.

[5] J. Zoellner., P. Schweizer-Ries. C. Wemheuer. Public acceptance of renewable energies: Results from case studies in Germany. Energy Policy 36. 2008. pp. 4136–4141.

[6] H. Han. L. T. J. Hsu. C. Sheu Application of the Theory of Planned Behavior to green hotel choice: Testing the effect of environmental friendly activities. Tourism Management 31. 2010. pp. 325–334.

[7] H. Han. Y. Kim. An investigation of green hotel customers’ decision formation: Developing an extended model of the Theory of Planned Behaviour. International Journal of Hospitality Management 29. 2010. pp. 659–668.

[8] C. A. Bollino. The Willingness to Pay for Renewable Energy Sources: The Case of Italy with Socio-demographic Determinants. The Energy Journal 30. 2009. pp. 81-96.

[9] S.-J. Ku. S.-H. Yoo. Willingness to pay for renewable energy investment in Korea: A choice experiment study. Renewable and Sustainable Energy Review 14. 2010. pp. 2196-2201.

[10] National Technical University of Athens (NTUA), 1992. Feasibility study for the hydropower exploitation of Crete. Final Report of the research project No. XVII/4.1040/92-22 carried out within the framework of program JOULE II of EU, Athens.

[11] D. Vamvuka. T.D. Tsoutsos. Energy exploitation of agricultural residues in Crete. Energy Exploration and Exploitation 20. 2002. pp. 113-121.

[12] E. Michalena, V. Angeon. Local challenges in the promotion of renewable energy sources: The case of Crete. Energy Policy 37. 2009. pp. 2018 – 2026.

[13] N. Zografakis. E. Sifaki. M. Pagalou. G. Nikitaki. V. Psarakis. Konstantinos P. Tsagarakis. Assessment of public acceptance and willingness to pay for renewable energy sources in Crete. Renewable and Sustainable Energy Reviews 14. 2010. pp. 1088–1095.

[14] A. J. Veal, 2006. Research methods for leisure and tourism: a practical guide. 3rd Edition, Prentice Hall, United Kingdom.

[15] G.J. Dalton. D.A. Lockington. T.E. Baldock. A survey of tourist attitudes to renewable energy supply in Australia hotel accommodation. Renewable Energy 33. 2008. pp. 2174-2185.

[16] E. Jun. W.J. Kim. Y.H. Jeong. S.H. Chang. Measuring the social value of nuclear energy using contingent valuation methodology. Energy Policy 38. 2010. pp. 1470-1476.

[17] H. Wang. D. Whittington. Measuring individuals' valuation distribution using stochastic payment card approach. Ecological Economics 55. 2005. pp. 143-154.

A dynamic hypothesis for developing energy-efficiency technologies in housing industry

Ibrahim A. Motawa*, Phil F. Banfill

School of the Built Environment, Heriot-Watt University, Edinburgh, EH14 4AS, UK
** Corresponding author. Tel: +44 1314514620, Fax: +44 1314513161, E-mail: i.a.motawa@hw.ac.uk*

Abstract: The UK target to significantly reduce CO_2 emissions from housing has been challenged by the fact that 80% of the UK housing stock existing in 2030 has already been built. Energy-efficiency technologies for existing housing are developed in attempt to meet this target, e.g. fabric upgrades, ventilation systems, etc, but the interrelationship between the technical and social aspects of using these technologies is not fully understood. From the household perspective, a clear financial case in addition to other intangible benefits should exist to create high demand for these technologies. On the other hand, many technological interventions are still in the development stage and according to the technology diffusion theory there will be a delay in adopting these technologies on the expected scale. This study will use system dynamics modelling to investigate the relationship between the supply and demand of energy-efficiency technologies for existing housing. A dynamic hypothesis will be set to analyse the interrelationships among the controlling variables of technologies development over a period of time. This paper introduces the main structure of the study and discusses the technique adopted to model the identified dynamic hypothesis.

Keywords: *Energy-efficiency technologies, System dynamics*

1. Introduction

The housing industry in the UK is experiencing its transition period from traditional to energy efficient. The call for energy efficient houses has been intensified in the light of the high demand for energy. The growth of energy prices increases the pressure on householders to find solutions to the energy bills, and on the industry to develop more energy efficient technologies for houses. The introduction of UK targets to reduce CO_2 emissions has also a great effect on both the householders and developers. In the UK, approximately 26% of CO_2 emissions are attributable to the domestic sector[1]. At least 70% of the UK housing stock that will be present in 2050 have been already constructed before year 2005[2]. Therefore, modifications to the existing housing are essential to meet the targets of the UK Climate Change Bill. However, it is not only energy efficiency technologies that will achieve the CO_2 emissions target, but the changes to occupants' behaviour will also have a great influence to accommodate these modifications.

Despite the growing development in Energy Efficiency technological interventions, the uptake of these technologies is not great enough to show that there is a significant reduction in energy consumption and CO_2 emissions. Among the reasons for this market failure might be that the costs and benefits of refurbishment options are often complex to determine[3]. Achieving the target of CO_2 emissions will require large investments in the stages of energy generation, transmission, conversion and end-use, together with measures to control demand. Oreszczyn and Lowe[4] indicated that this necessitates the need for research to help formulate and evaluate policy, to measure progress, and to help industry to deliver.

2. Methodology

A previous study, 'TARBASE'[5], investigated a number of technologies in the field of end use technology, building fabric and energy supply technologies to achieve reductions in CO_2 emissions. Three intervention sets were identified with their effect on CO_2 emissions

attributable to two selected dwelling types, namely; 'comprehensive', 'complete', and 'limited' intervention sets. A Whole Life Cost (WLC) approach has been conducted to investigate the cost implications for the uptake of these intervention sets by householders. The study concluded that there is no clear financial case over a 25 year horizon for householders to invest in the proposed interventions. The results also revealed the need for new policy approaches to overcome the financial and non-financial hurdles for a mass uptake of Energy efficiency technologies[6]. This paper builds on the results of TARBASE and investigates in a wider context the development and diffusion of energy efficiency technologies for housing. Variables affecting different policies to reduce CO_2 emissions such as subsidy, rising energy price, R&D investment from the industry, etc. are considered. Technology diffusion theory reveals that technological development and implementation includes a long delay to be fully diffused. In addition, effective implementation of technological innovations requires an understanding of the complexity underpinning the process and the inherent uncertainty about the actual performance of low energy housing[4]. The adoption of innovative technologies also requires reliable performance indicators to be employed to ascertain the condition of such processes. Models that simulate the implementation of new technologies need to consider the effect of experimentation, iteration and refinement of activities that are reliant on volatile information[7, 8]. These models should consider that many variables are time dependent and/or carry a high level of uncertainty. It is understood for example that the efficiency of new technologies is expected to rise by further development and experience in use. In addition, it must be stressed that the emissions savings are only realized when behavioural change accompanies the technological deployment.

Different motivational frames might alter the appraisal of costs and benefits related to a specific pro-environmental behaviour. Understanding the needs satisfied by the purchase of an energy efficient technology would allow their costs to be compared to the cost of other purchases satisfying other needs[9]. It is more likely that only a part of the family budget currently allocated for household improvements would actually be spent on energy efficiency improvements, even for those informed individuals with strong pro-environmental attitudes. Additionally, there is no financial incentive associated with the investment if reduction in utility expenditure (at current energy process) is taken as the sole benefit. The deployment of deep cut intervention sets are likely to result in other benefits, such as improved comfort and increased asset value of the property. It is feasible that when all benefits are aggregated, financial incentives will appear for householders and this needs to be explored further[5, 9].

In conclusion, the emissions reduction targets required to address the climate change agenda are only likely to be met through a combination of demand and supply side interventions. Identifying technological solutions for achieving a reduction in UK domestic dwellings is complex. Assumptions have to be made regarding for instance construction, occupancy and occupant behaviour in order to define the baseline for assessment of technological interventions which themselves are often interdependent. This would suggest that stressing the ethical or environmental appeal of an energy saving technology will only have limited effect if the technology is perceived by the consumer as having a high capital cost. In response to the challenge posed by this complexity, a System Dynamics (SD) based model is proposed in this research. It can investigate policies that affect the development and diffusion of energy efficiency technologies related to the housing industry during its transition period, considering both the demand and supply sides. SD modelling can identify the causal structure underlying the behaviour of complex systems, simulate the behaviour of time dependent variables and assess the usefulness of different energy policies such as energy tax and R&D subsidy for diffusing energy efficiency technologies.

SD modelling involves the following steps[10]:

1. Articulating the problem to be addressed
2. Formulating a dynamic hypothesis or theory about the causes of the problem
3. Formulating a simulation model to test the dynamic hypothesis
4. Testing the model output to satisfy the purpose
5. Designing and evaluating policies for improvement

Based on the relevant literature and data available from TARBASE, the proposed SD model was developed as a hypothetical model. This paper discusses the first two steps of the model development. Further development, requiring additional data, will build a comprehensive SD model.

2.1. Problem Articulation

The problem in hand is not only about the typical process of technology diffusion, but also about the effect of the pressure to reduce CO_2 emissions and the social and economical implications of using these technologies. Therefore, this step in modelling will identify the major controlling variables of technology diffusion and the effect of using these technologies on CO_2 emissions. In addition, the reference mode of the system behaviour will be identified. Reference mode is the graphical representation of the system behaviour over a period of time. This can be based on historical or pre-defined/required behaviour. The optimum behaviour of the system occurs if the pattern of the demand for house upgrading follows the same pattern of the diffusion of the technological intervention sets. Therefore, the technology diffusion theory will help identifying the reference mode of the demand for house upgrading. The time period assumed for the study is to 2050, when the CO_2 emissions reduction target is set.

2.1.1. Technology Diffusion Theory

Diffusion process is the methodology of adopting an innovation by members of a certain community. Rogers[11] categorizes the five stages of the diffusion of innovations as: knowledge (awareness), persuasion (interest), decision (evaluation), implementation (trial), and confirmation (adoption). Over the time of the diffusion process, new individuals adopt the innovation while others might reject it. Four factors were identified that influence adoption of an innovation, namely: 1) the type and need for innovation, 2) the communication channels used to spread information, 3) time period of diffusion, and 4) the nature of the community to whom innovation is introduced. Technology adoption rate always follows an S-curve that represents the length of time required for a certain percentage of community members to adopt the technology[11], as shown in Fig. 1. There are categories of adopters: innovators, early adopters, early majority, late majority, and laggards. This pattern of technology adoption will be used for the purpose of modelling as "reference mode of diffusion", which for this research will be the reference mode of "demand for house upgrading". The demand for house upgrading will be investigated from the perspective of householders, industry, and government. Individuals usually adopt an innovation if it has some attributes, namely: (1) the innovation has some relative advantage over an existing one, (2) the innovation is compatible with existing values and practices, (3) the innovation is not too complex, (4) the innovation has trialability (i.e. can be tested for a limited time without adoption), (5) the innovation offers observable results.

Various models have been developed in order to simulate the typical diffusion of technological innovations. For example, Veneris[12] developed a SD model which takes into account various diffusion patterns modelled via differential equations. The model did not consider that technology development is dynamic as there is always development or

improvement over the time of diffusion all along the S-curve. Therefore, the S-curve is actually made up of a series of S-curves of different sections of a population adopting different versions of technologies. It did not also simulate the effect of the pressure to reduce CO_2 emissions and the social and economical implications of using these technologies

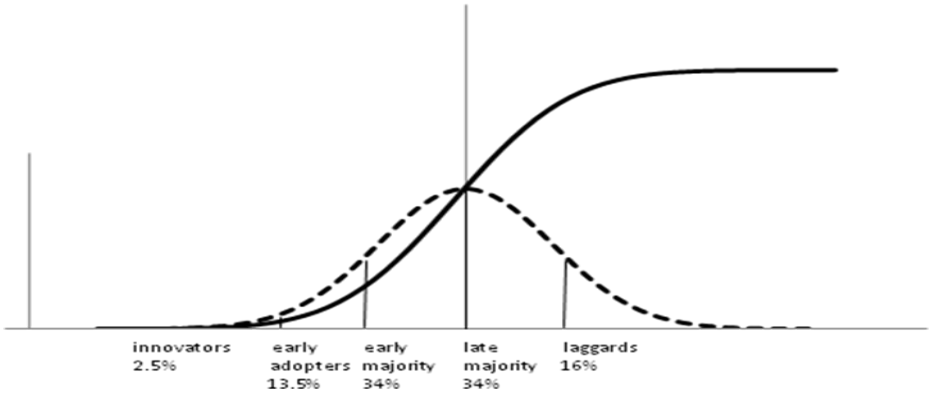

Fig. 1. Innovation adoption rate (Rogers[11])

The other main reference mode required for this model is for the rate of CO_2 emissions reduction. The target set for the year 2050 will be used as a guidance reference mode in this model (further data is required to refine this mode in a more accurate rate). Fig. 2 suggests that the linear emissions reduction rate since 1970 was 7.5 M t(CO_2)/decade. This would achieve a 60% reduction in CO_2 emissions from UK buildings by 2050. To achieve the 80% reduction adopted by the UK government in 2009, a faster rate of reduction (around 10 Mt(CO_2)/decade) might be needed[4].

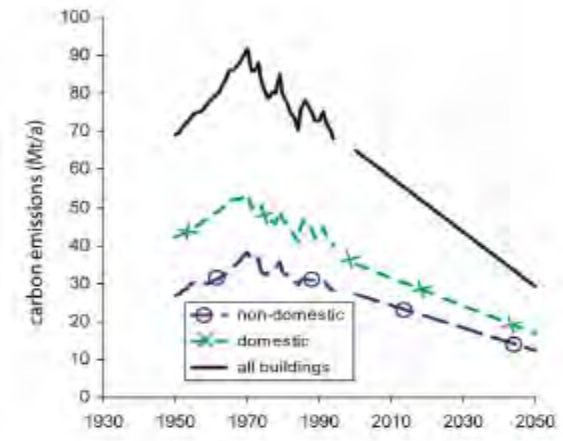

Fig. 2. Domestic and non-domestic carbon emissions to 1994 with trajectories to 40% of 1990 emissions in 2050 (reported in Oreszczyn and Lowe [4])

2.2. Formulation of the dynamic hypothesis

A dynamic hypothesis is set to explain the behaviour of the system and the relationships among its variables that develop its reference mode. Four mapping tools were used to develop this hypothesis, which are: Subsystem diagram, Model boundary chart, Causal loop diagrams, and Stock and flow maps. As this paper aims only to introduce the hypothetical model, the Stock and flow maps will not be presented.

2.2.1. Subsystem diagram

Fig. 3 classifies the architecture of the studied system into a number of subsystems. Each subsystem is mainly controlled by a certain variable, as illustrated by the variable name in each box of Fig. 3. The main control variables of each subsystem and the interactions between each other will be identified on the causal loop diagrams. For example, the actual proportion of dwellings using the intervention sets is used to measure technology diffusion. The other identified variables influence this measurement, namely; Rate of technology change, Unit energy consumption, R&D Investment, and CO_2 emissions. A number of feedback loops have been identified that control the subsystems behaviour, namely; Technology change loop, R & D loop, Consumption loop, and Emission loop. These loops will be studied and simulated to show how the system behaves under different conditions and policies.

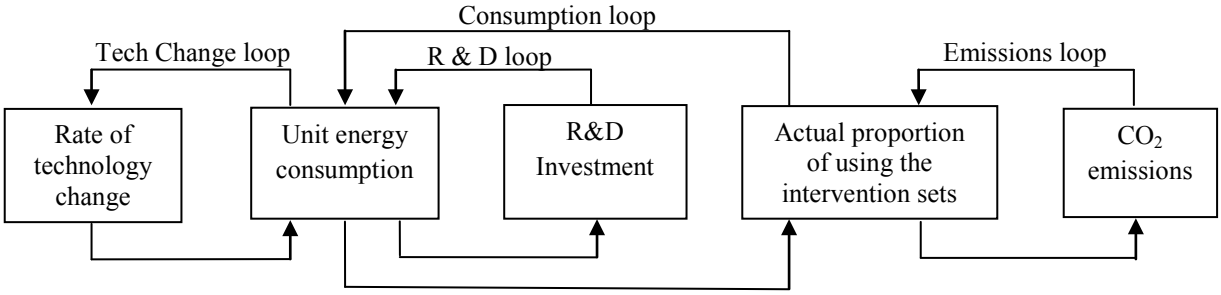

Fig. 3. Model sub-systems

2.2.2. Model boundary chart

The chart identifies the scope of the model by classifying the variables into endogenous, exogenous, and excluded variables, as shown in Table 1. This classification is essential to identify the model boundary in terms of the type of each variable and the relationships among variables.

The current version of the model excludes the interest rate on saving/investing the cost of house upgrade assuming that they will balance the effect of inflation on all expenses. The variables considered for the selection of intervention sets are: energy price (economical factor) and CO_2 emission (environmental factor) and R&D investment as financial support. Other variables influencing technological developments such as market impact or other new ways of house upgrading are excluded. The exogenous variables have great impact on the endogenous structure but their behaviour will be included from one single relationship for the purpose of this model.

2.2.3. Main Causal Loop Diagram (CLD)

For each of the above subsystems, a CLD is developed. The main CLD for the adopted model (Fig. 4) shows how the variables are related to each other. The resulting reinforcing loops and balancing loops will be discussed next.

Table 1. Model boundary chart

Endogenous	Exogenous	Excluded
• Actual use of intervention sets • Average CO_2 generation rate per until energy need • Effect of technology on unit energy consumption • Average energy production price • Average unit energy consumption • Indicated house upgrade demand • Average energy demand • R& D investment • Effect of cost on house upgrade • Indicated unit energy cost • House value • Industry revenue • Technology change rate • Actual energy consumption • CO_2 emissions	• Energy tax • Other cost of house upgrade • Reference energy price • Government subsidy • Intangible effects	• Inflation rate • Interest rate • Other factors to influence selection of sets • Effect of competition on technology change rate

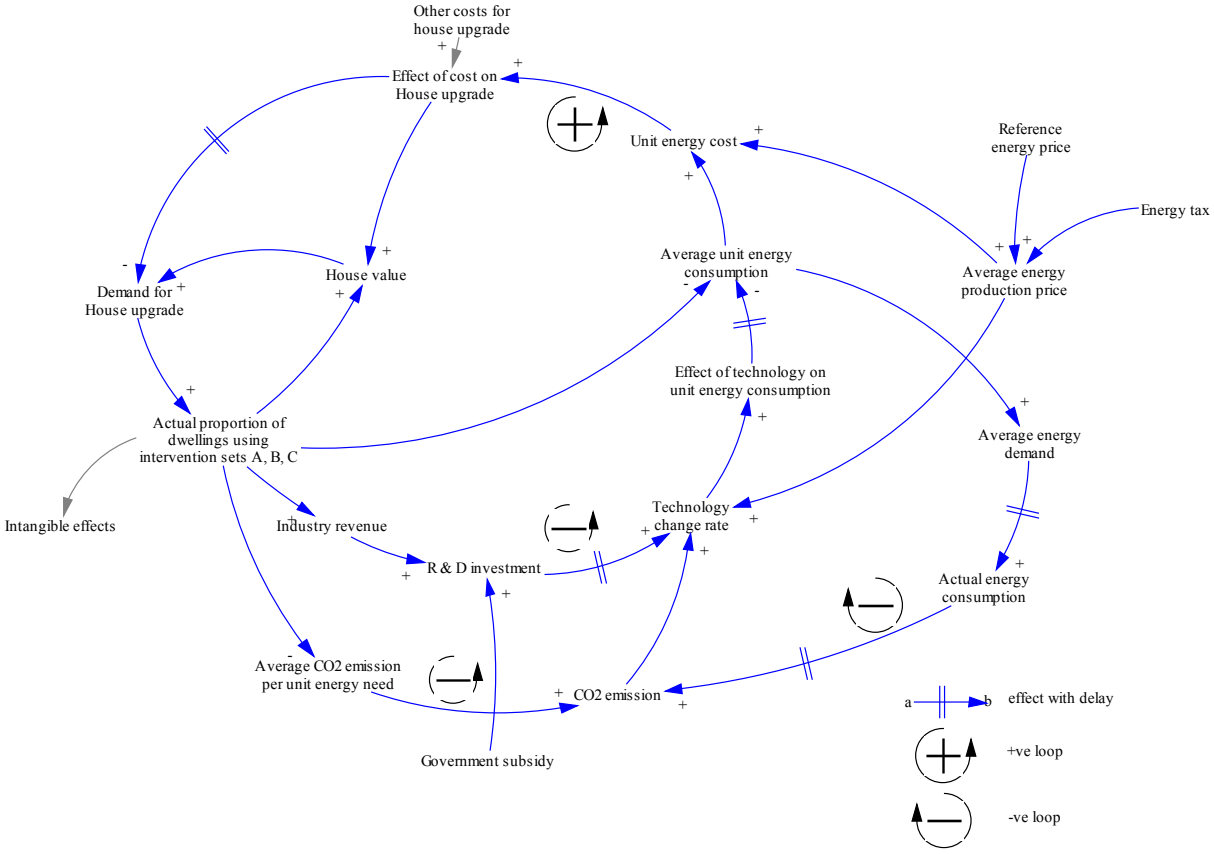

Fig. 4. Main Causal Loop Diagram

3. Results

The model variables and the causal relationships among them are defined. Positive signs are given to parallel relationships, while negative signs are for inverse relationships. The structure

of system variables and relationships may create feedback loops. The polarity of a feedback loop (i.e., positive or negative) is identified by summing the polarities of the relationships among its variables. Loops with an odd number of negative relationships are negative. Loops with an even number of negative relationships are positive. Variables within positive loops will continue to increase indefinitely, therefore positive loops are self-reinforcing. Variables within negative loops will stabilize over time, therefore negative loops are self-balancing. Feedback loop structures, once identified, are translated into stock-flow diagrams to enable the SD simulation. The simulation part is beyond the scope of this paper. Clearly, the degree of details at which a CLD is defined strongly influences the success of this approach, and considerable care should be taken to develop it right.

3.1. Consumption loop (+ve loop)

Improving average unit energy consumption by increasing the actual proportion of using intervention sets; [Average unit energy consumption – unit energy cost – Effect of cost on house upgrade – Demand for house upgrade – Actual proportion of using intervention sets A,B,C - Average unit energy consumption]. Energy efficiency improvement can be measured by the reduction in the Average unit energy consumption, which reduces the unit energy cost and subsequently the effect of cost on house upgrade, which leads to an increase in the demand for house upgrade. High demand for house upgrading will increase the use of intervention sets, which in turn decreases the average unit energy consumption.

3.2. R&D loop (-ve loop)

R&D Investment results in reducing the unit energy consumption; [Average unit energy consumption – unit energy cost – Effect of cost on house upgrade – House value – Demand for house upgrade - Actual proportion of using intervention sets A,B,C - Industry revenue – R & D investment – Technology change rate – Effect of technology on unit energy consumption - Average unit energy consumption]. R&D investment is increased by input from industry and government sources. The higher ratio of industry revenue from selling more intervention sets, the higher dedicated funds for R&D. This will lead to more advanced technologies that reduce the average unit consumption.

3.3. Emissions loop (-ve loop)

The increasing use of the technology intervention sets will reduce CO_2 emissions; [Average unit energy consumption – unit energy cost – Effect of cost on house upgrade – Demand for house upgrade – Actual proportion of using intervention sets A,B,C – average CO_2 emissions per unit energy need – CO_2 emissions - Technology change rate – Effect of technology on unit energy consumption - Average unit energy consumption].

3.4. Technology change loop (-ve loop)

While the increase in the Average unit energy consumption might increase the actual energy consumption and the CO_2 emissions, but this in turn will accelerate the rate of technology change; [Average unit energy consumption – Average energy demand – Actual energy consumption – CO_2 emissions - Technology change rate – Effect of technology on unit energy consumption - Average unit energy consumption].

The double lines shown on some links indicate the expected delays in realising a significant effect of one variable on the other, such as effect of technology development on application (the average unit energy consumption). These delay relationships are important to understand the behaviour of the system and the estimated time to measure the effect of the technological intervention sets during the transition period. There are a number of variables (on the gray

arrows) which are modelled as exogenous inputs or policy variables based either on data series of reality or using some reasonable assumptions. By definition, these exogenous variables may influence the model behaviour but are not part of the main causal loops.

4. Conclusions

The diffusion of energy efficiency technologies for housing, considering both the demand and supply sides, has been investigated in this paper. Modelling the diffusion process using SD principles shows that various relationships within the process are developed that can help achieving the target of CO_2 emissions. The developed CLD with negative feedback loop will have a systemic resistance to undesirable outcomes within the system. However, a positive feedback loop will cause instability to the system performance. Therefore, when implementing changes for variables in a positive feedback loop, all other variables should be monitored to ensure that undesirable outcomes are controlled. Further analysis is required to validate the system behaviour against the identified reference modes.

References

[1] DEFRA, e-Digest of Environmental Statistics, online available from (http:// www.defra.gov.uk/environment/statistics /index.htm), 2009.

[2] Z. Zavody, Pathway to zero-carbon homes. In, European Council for an Energy Efficient Economy (eceee) 2007 Summer Study, Côte d‟Azur, France, 4-9 June 2007.

[3] Sustainable Construction Task Force, Making the most of our built environment, DTI, 2004.

[4] T. Oreszczyn and R. Lowe, Challenges for energy and buildings research: objectives, methods and funding mechanisms, Journal of Building Research & Information, Volume 38 (1), 2010, pages 107 – 122

[5] A. Peacock, P. Banfill, M. Newborough, D. Kane, S. Turan, D. Jenkins, M. Ahadzi, G. Bowles, P. Eames, H. Singh, T. Jackson, and A. Berry, Reducing CO_2 emissions through refurbishment of UK housing. In, European Council for an Energy Efficient Economy (eceee) 2007 Summer Study, Côte d‟Azur, France 4-9 June 2007.

[6] G. Pellegrini-Masini, G. Bowles, A. Peacock, M. Ahadzi, P. Banfil, Whole life costing of domestic energy demand reduction technologies: householder perspectives. Construction Management and Economics, Vol 28 (3), 2010, pages 217 – 229

[7] I. Motawa, A. Price, and W. Sher, A Fuzzy approach for evaluating the iterated implementation of innovations in construction, International Journal of IT in Architecture, Engineering and Construction, Vol. 1(2), 2003, pp 105-118.

[8] I. Motawa, A. Price, and W. Sher, Modelling the implementation of technological innovations in construction, International Journal of Computer Applications in Technology: Special Issue on Interoperability for SME-based environments, Vol. 20 (3), 2004, pp 78-89**.**

[9] G. Pellegrini-Masini, The carbon-saving behaviour of residential households. In: Futures of Cities 51st IFHP World Congress, Copenhagen, 2007.

[10] J. Sterman, Business dynamics: systems thinking and modelling for a complex world. McGraw-Hill, 2000.

[11] E. Rogers, Diffusion of innovations. New York: Free Press ISBN 0029266505, 1995.

[12] Y. Veneris, Modelling the transition from the Industrial to the Informational Revolution, Environment and Planning, 22 (3), 1990, pp. 399-416.

Swedish building policy and the manufacturers of single-family houses in the county of Dalarna. A collaboration for the future goal of the improvement of energy efficiency?

K. Perman

Solar Energy Research Centre (SERC), Dalarna University Falun Sweden
Tel: +46 23778727, Fax: +46 23778050, E-mail: kpm@du.se

Abstract: Sweden's goal is to reduce the use of energy per heated unit area in dwellings by 20 percent by 2020, and by 50 percent by 2050. To fulfil these goals, Sweden's dependency on electricity and, in particular, the large use of electricity for heating must be taken into account. The aim of this article is to study the effects of the Swedish building regulations from 1 January 2010, with regard to improving energy efficiency. The article follows the energy policy revision through policy documents and interviews.

The political goal of reducing both the annual electrical energy and the maximum instant power for heating is, on the whole, fulfilled by more efficient heat pumps. The study also shows that, in spite of the stricter building regulations for electrically heated houses, the standard of insulation required for the building to fulfil the building regulations is dependent on the heating and ventilation systems installed in the house. These changes towards more stringent requirements are also counteracted by there not being the same requirements for the existing housing stock.

Keywords: *Building policy, Energy efficiency, Manufacturers of single-family houses, Electrically heated houses.*

Nomenclature

A_{temp} *the temperate area of the building* ……..m^2	*HRV exhaust and supply air ventilation with heat recovery*.....….*dimensionless*

1. Introduction

The energy used in the built environment constitutes 40 percent of the total energy use in Sweden. Consequently, a more efficient use of energy within the built environment is one of the most important means of achieving sustainable community development and fulfilling the environmental and climate goals. [see also 1, 2].

Sweden's goal is to reduce the demand of energy per heated unit area in dwellings by 20 percent by 2020 and by 50 percent by 2050 [3]. To fulfil these goals, Sweden's dependency on electricity and, in particular, the large demand of electricity for heating must be taken into account. Sweden has the largest number of heat pumps of the member countries of the E U. In 2008, almost 40 percent of single family houses in Sweden were heated completely or partially by heat pumps. [4, 5]. But the Swedish building regulations for electrically heated houses became stricter in 1 January 2010. The new building regulations concern the use of energy and power demand for new construction. The focus is partly on the supplied energy, i.e. purchased energy per m^2 floor area, and partly on limiting the maximum power demand of electrically heated houses [6].

The aim of this article is to study the effects of the Swedish building regulations from 1 January 2010, with regard to improving energy efficiency. The research question is if the revised building regulations from 2010, regarding energy use and power demand for new

buildings, have resulted in changed building construction and/or a choice of alternative heating systems.

2. Theory and Methodology

Evert Vedung considers that different outcomes follow an intervention by the government, for example taxation laws or state subsidies. By outcomes he means what happens when the specific intervention reaches those who Vedung calls final recipients– that is the individuals or groups which are the goal for the intervention – and the final recipients' action caused by the public intervention. Three different types of intervention can be distinguished: the immediate, the intermediate and the final result [7]. We use a model which focuses on goals and fulfilment of goals, called a side effect evaluation. The evaluation focuses on the goals, and if the interventions have resulted in the fulfilment of the set goals [7]. According to Evert Vedung, two questions have to be asked in order to study this. These are: do the results correspond to the agreed goals for the interventions? And, if so, does this depend on the intervention?

A qualitative method makes it possible to reach an understanding of people's behaviour in relation to the surrounding environment (Merriam 1994:46). The housing companies' accounts have been followed during a three year period from when the building regulations were being framed until they were in force. During the autumn 2009 and the spring 2010, 10 representatives from manufacturers of prefabricated, single-family houses[1] were interviewed. They have their head offices and production in the county of Dalarna. The interviews focused on the house manufacturers' reasoning and how they acted during the period of transition from 1 February 2009 until 1 January 2010. After the building regulations came into force, follow-up interviews were carried out with the house manufacturers during the spring 2010 [see also 8]. Further analysed material is from group discussions from 2007, when researchers from Dalarna University and house manufacturers discussed heating systems which the companies could consider [see also 9].

3. The building regulations after 2010: u-values, power and energy use.

During the last 30 years there has been a change in households' choice of heating systems in Sweden. Owners of single-family houses have changed from using oil fired boilers to using more district heating, heat pumps and bio-fuels [10]. But the energy use per m^2 heated area for new built premises and dwellings has, on the other hand, been constant from 1993 to 2005. An explanation which was given before the revision of the building regulations in 2006 was the lack of a requirement for improvement of energy efficiency [11].

The building regulations on energy management from 1 Jan 2010 concern permanent residences, and not vacation homes. The regulations imply, above all, a tightening up of the requirements for newbuilt, electrically heated houses with both an energy requirement and a power requirement. Even houses with waterborne electric heating and heat pumps are now classified as electrically heated if the installed power demand exceeds 10 W/m^2. For buildings

[1] The definition prefabricated, single-family housing companies includes three different groups: 1) companies which manufacture houses according to the client's requirements (customer adapted houses), 2) housing companies which produce standard houses, and houses according to the client's requirements, and also 3) housing companies which only manufacture standard houses (Fredling & Sellin 2003).

with other methods of heating there are no tightening up of the requirements[2]. There are even somewhat less stringent requirements in the north of Sweden because there are three different zones instead of the previous two climate zones (see table 1). An electric immersion heater or electric boiler is, however, almost always used as a temporary reserve in single-family houses, which is true, for example, for houses with solid fuel boilers. This means that, in principle, all houses would be classed as electrically heated, and only houses with district heating would be omitted. For this reason there is an exception in the building regulations which says that "the electric power in a solid fuel appliance, which is installed to be a temporary reserve, is not counted if the solid fuel appliance is constructed for permanent operation" [6]. During this period the importance of flexible heating systems is also emphasised and the opportunity for flexibility in new building encouraged [12].

The three climate zones are: the most northerly, climate zone I (the counties of Norrbotten, Västerbotten and Jämtland), with an alleviation in the requirements for houses which are not heated by electricity, compared with earlier requirements. Climate zone II consists of the central parts of Sweden, including the county of Dalarna, the region which is in focus in this article[3]. Climate zone III comprises of the southern parts of the country.

The building regulations are based on the building's specific energy demand (see table 1) which is the energy use of the building divided by A_{temp}[4]. The energy use of the building is the energy which is used for heating and domestic hot water, and also that part of the electricity supplied to the property which is related to the requirements of the building. This means all permanently installed equipment within, under, or on the outside of the building. Pumps, fans, cooling machinery and heating cables are included if they supply the building[5]. When fuel is used, the amount of fuel and its calorific value is used to calculate the energy demand. Energy from solar collectors and solar panels, and also free cooling which is taken directly from the ground is not included in the energy use of the building [6].

[2] According to The Swedish Board of Housing, Building and Planning's instructions all buildings shall be classified as electrically heated if the installed electric power demand for heating is greater than10 W/m^2.

[3] Climate zone II includes the counties of Västernorrland, Gävleborg, Dalarna and Värmland

[4] A_{temp} is the area of all the floors, including stairs and shafts, for the spaces which shall be heated to over 10ºC. A garage within the building may not be included in $A_{temp,}$ but its heating requirements shall be included in the energy use of the building (Boverket 2008,p.35).

[5] Fixed lighting in common areas shall be included but not lighting in gardens and on external footpaths. Neither shall electricity for other uses, for example as engine pre-heaters and car coupé heaters, be included. Electricity which is used for comfort cooling shall be adjusted upwards by a factor of three for houses which are not electrically heated (Boverket 2008).

Table 1: Requirements for specific energy use and power demand for buildings from 1 January 2010 [6]

Climate zone	Form of heating	Maximal specific energy use [kWh/m^2·year]	Maximal installed electric power [kW]	Overall heat transfer coefficient [W/m^{2}K]
I	Electricity, addition when A_{temp}>130 m^2	95	6 +0,035(A_{temp}-130)	0,40
	Other	150	-	0,50
II	Electricity, addition when A_{temp}>130 m^2	75	5 +0,030(A_{temp}-130)	0,40
	Other	130	-	0,50
III	Electricity, addition when A_{temp}>130 m^2	55	4,5 +0,025(A_{temp}-130)	0,40
	Other	110	-	0,50

4. The building regulations; problems and opportunities

When researchers from Dalarna University talked to different housing companies during the summer and autumn of 2007, it was evident that there was concern and speculation on how the building regulations on the improvement of energy efficiency would finally be framed and what this would mean to them. One of the people interviewed said that ”there is a proposal, which is being circulated for comments, and which has been postponed a number of times, which says that heat pumps will be classified as electric resistance heating. It has been circulated time and time again and no-one knows when it will be introduced”. But it is clear, the informant said, that the government and the Swedish Board of Housing, Building and Planning want to tighten up the requirements and reduce the use of energy in newbuilt houses (housing manufacturers, group discussion 1).

The housing manufacturers were interviewed during the autumn 2009, which is during the period of transition which started in January 2009. Therefore they had access to the revised wording and the opportunity to digest the changes presented and form a strategy to allow their production to fulfil the requirements for the improvement of energy efficiency. But as 2009 was a period of transition and the regulations did not come into force until 1 January 2010, some housing manufacturers were still ambivalent on how they would deal with the new regulations, and what change would materialise in the end. During 2010, the questions on how they should fulfil the Board of Housing, Building and Planning’s requirements have ceased.

4.1. Insulation thicknesses and tightness

One change which the interviewees presented was additional insulation in walls and roofs. There are companies which increase insulation from 195 mm to 240 mm, but there are also companies which keep the thinner insulation and change from air source heat pumps to ground source (rock) heat pumps instead. Most of the interviewees said that a relatively easy measure for improving energy efficiency was thicker walls. One of them said that their manufacturing process was constructed so that further insulation could be added without much trouble and therefore it is not expensive (interview 2)

One of the interviewees emphasised that more insulation and a thicker wall is less a question of saving energy than of a psychological effect. He said ”the saving in energy by constructing a thicker wall is not as great as you think (interview nr 1). He also considered that there was a limit to wall thicknesses as they take up far too much of the floor area if they are too thick. The floor area is limited in prefabricated single-family houses because the transport from the factory to the building owner is by lorry, and they want to limit the number of lorries. A larger house means more lorries, which in turn leads to higher house prices (e.g. in interview 3).

There is a requirement for a limited average heat transfer coefficient in the Swedish Board of Housing, Building and Planning's building regulations (BBR) 2010. This is that the house shall not have a higher average heat transfer coefficient than 0,4 W/m^2K for electrically heated houses and 0,5 W/m^2K if the house has other methods of heating [13]. However, according to Persson and Heier (2010), the requirement for the average heat transfer coefficient is so low that it does not have any practical significance. It is principally the energy and power requirements which set the limits for the insulation standard of the house [14]. There is no specific requirement in BBR on the tightness of the building envelope, only that it shall be sufficiently tight to fulfil the energy and power requirements. The house companies pointed out that if the house purchaser chose to buy the house from them, but selected another company to erect the house, it is the house purchaser, in his role as commissioner of a building project, who is responsible for the building envelope having the required tightness to fulfil the energy requirements. This is an obligation which the interviewees thought could be neglected because the house purchaser was not aware of his/her responsibility (interview nos 7).

4.2. Choice of heating systems

There are many different parameters to be considered when choosing a heating system[6]; living area, size of supplementary areas, ventilation, acceptable noise level, economy etc. [9]. The choices open to house manufacturers and house purchasers in Sweden are different types of heat pumps, district heating and bio-fuel boilers or bio-fuel stoves. Solar collectors can be included in all these systems.

In the autumn 2009, the companies were very confident that the air and ground source heat pump manufacturers would improve their products and the products' energy generation, and thereby simplify the work with energy management and the possibility of fulfilling the requirements of the Swedish Board of Housing, Building and Planning (interviews 1, 2, 5 among others). One of the interviewees expected a great change in the production of heat pump products and, according to him, the heat pump suppliers have done ”a really good job” (interview 1). During the interviews it was pointed out that one air source heat pump company has become more interesting to the market because of its technology, an improved exhaust air heat pump, and because of the changed building regulations (interviews 6, 4). It is a company which has existed for almost 10 years and has increase its sales from about 30 heat pumps per year to 600 per year (Henning 2009).

The house manufacturers' customers seldom or never choose pellet boilers or pellet stoves Solar heating is also often rejected. The house manufacturers emphasise that bio-fuels are troublesome because they take a lot of space and need a lot of work. They say that the people who are interested in the environment install solar heating (interview 4,5,7). To make the

[6] A heating system is not always included in the house sale; if this is not the case the customer can be responsible for the installation him/herself.

disadvantages of pellets and solar heating clear the house manufacturers often emphasise the advantages of air source heat pumps and ground source (rock) heat pumps, for example that they are economical and easy to handle (interviews nr 5,2).

In this study it seems as though the changeover from the traditional exhaust air heat pump, which has the lowest investment cost but the highest total cost, to the improved exhaust air heat pump [7] took place because the requirements were changed, not because it was, in fact, also financially profitable [15]. The product has existed for a number of years, but the company increased its sales substantially after the revision of BBR in 2010. The new regulations originate in an aim to reduce electrical heating and increase the use of bio-fuels [3, 11] However, Persson and Heier (2010) show that the revised building regulations mean that the choice of a bio-fuel, in this case pellets, needs the supplement of an exhaust and supply air ventilation with heat recovery (hereafter called HRV system). On the other hand ground source (rock) heat pumps fulfil the Swedish Board of Housing, Building and Planning's energy requirements without HRV. Ground source (rock) heat pumps also have an advantage, as the possibility of omitting HRV means a lower investment cost. The interviews show that a low investment cost is an advantage when choosing a heating system for the new house.

4.3. Current and future changes

The companies could see opportunities in this energy political goal and in current, as well as in possible future, changes in the building regulations. An example of this is one of the companies which has bought a company which produces low energy houses. They want to take part in, and at the same time follow, a new market with low energy. Therefore, the company has invested in a show house where the building envelope and heating system with heat storage is different from their other standard houses. The show house has extra well insulated walls, solar collectors and district heating and also three storage tanks (total of 750 litres) [16].

However, according to the interviewees, these changes towards more stringent requirements are counteracted by there not being the same requirements for the existing housing stock. There are not the same constraints in spite of the fact that the heating of the existing housing stock requires more energy (interviews nos 2,4,7). One of the interviewees makes the effect of these unequal requirements clear when he says that the stringent requirements for newconstructed dwellings can lead to too high prices for some of the prospective house owners. They choose to buy an older house instead (interview 1).

The interviewed manufacturers that produce vacation homes sold within the region of Dalarna, also have to adjust to the requirements specified for permanent homes. This is because even thought the vacation homes are not affected by the energy requirements in the government building regulations, Malung –Sälen municipality has started to insist the vacation homes follow the same requirements as permanent homes. This is because new buildings in Malung – Sälen municipality is manly of vacation houses which have similar designs to permanent houses and therefore similar energy demands. If these do not follow the more stringent energy regulations, the energy demand will increase and may require an increase in the capacity of the power distribution net. (interview 4,5 and a politician from Malung-Sälen).

[7] An improved exhaust air heat pump is an electrically driven heat pump which cools the exhaust air to approximately -15º C, and also makes use of heat from condensation of the humidity in the air.

5. Conclusions

If we use Evert Vedung's concepts and model, this study shows that the immediate outcome of the Swedish Board of Housing, Building and Planning's building regulations from 2010 regarding the improvement of energy efficiency is, in some cases, an improvement of the building envelope, in particular supplementary insulation of the walls, but above all a changeover from an exhaust air heat pump to either an improved exhaust air heat pump or a ground source (rock) heat pump.

The intermediate outcome is that prospective house owners choose to buy an older house with a high energy consumption instead of a new with less energy demand. The changes towards more stringent requirements are counteracted by there not being the same requirements for the existing housing stock. Prospective house owners choose to buy an older house instead of a new one, because of higher prices caused of the stringent requirements for new constructed dwellings. To make it attractive for a prospective house owner to build a house it is also important to focus on regulations concerning the existing building stock and energy use.

The intermediate outcome is also a question of increased performance of exhaust air heat pumps and the effects of this. Increasing insulation was not always a result of the Swedish Board of Housing, Building and Planning's energy requirements. The requirements could be fulfilled with the help of a more efficient air source heat pump instead. A parallel can be drawn between this study and a Norwegian study on state intervention and house manufacture. The Norwegian study shows that state regulations are regarded as an indication of the least which should be done and the smallest possible changes are carried out [17]. It is interesting, though, that in contrast to the manufacturers, Malung-Sälen municipality requests more than what is defined in the building regulations. The vacation houses are being used mainly during the winter and are the same size as permanent houses[8] the interviewed emphasized the importance of having the same requirements for all the new built houses. That is to prevent for instance the need to expand the power distribution grid.

The final outcome of this study is that the new building regulations do not automatically lead to better insulated houses. The conclusion is that it is sufficient to change from an ordinary exhaust air heat pump to an improved exhaust air heat pump or a ground source heat pump. A trend, where heat pumps and (electrically heated) passive houses continue to dominate Swedish house production means that the housing stock is becoming more and more based on electric heating. It is true that the houses fulfil the requirements in the building regulations, but, at the same time, they increase the problem of high power loads during the winter which demand great flexibility in production capacity.

The building regulations focus on reducing the households' bought energy instead of climate impact. From a regional and vacation houses perspective this is interesting, because the log house industry feels that its work and normally bio-fuel heated houses are threatened**.** From a climate perspective it can be discussed if a log house built and heated with wood from the region is not preferable to a low energy house built in concrete and heated with a ground source heat pump [see also 18].

[8] For example, the average size of the houses produced by one of the manufacturers was 120 $m^{2.}$ (interview 6)

Acknowledgements
This work was financed within the project SWX-Energi, financed by the European Union, Region Dalarna, Region Gävleborg and Högskolan Dalarna.

References

[1] Proposition 2004/05:150, Svenska miljömål: ett gemensamt uppdrag.

[2] Proposition 2008/09:163, Energi. En sammanhållen klimat- och energipolitik.

[3] SOU 2008:110, Energieffektiviseringsutredningen. Vägen till ett energieffektivare Sverige.

[4] SCB, Energistatistik för småhus 2008.

[5] EU, Färdplan för förnybar energi. Meddelande från kommissionen till rådet och EU-parlamentet, 2008.

[6] Boverket, Regelsamling för byggande, BBR 2008: supplement februari 2009, 9 Energihushållning, 2009.

[7] Vedung, E., Utvärdering i politik och förvaltning. Studentlitteratur: Lund, 1 ed., 2002.

[8] Perman, K., Byggregler och småhustillverkare i Dalarna, in Klimatsmart villavärme? Solvärm, nya byggregler och möjligheten att förändra, Henning A. (ed), Falun: Centrum för solenergicentrum (SERC), Högskolan Dalarna, 2010.

[9] Henning, A., Vem fattar beslut om värmesystemen i monteringsfärdiga småhus?, in Klimatsmart villavärme? Solvärme, nya byggregler och möjligheten att förändra, Henning A. (ed). Falun: Centrum för solenergicentrum (SERC), Högskolan Dalarna. 2010.

10] Perman, K, Från el till värme : en diskursanalytisk policystudie av energiomställning på statlig, kommunal och hushållsnivå. Örebro: Örebro universitet. Örebro Studies in Political Science 23, 2008.

[11] Proposition 2005/06:145, Nationellt program för energieffektivisering och energismart byggande.

[12] SFS 2008:51, Förordning om ändring i förordningen (1994:1215) om tekniska egenskapskrav på byggnadsverk, m.m.

[13] Boverket, Regelsamling för byggande, BBR 2008; supplement februari 2009, 9 Energihushållning, 2009.

[14] Persson, T. and J. Heier, Småhusens framtida utformning - Hur påverkar Boverkets nya byggregler? Falun: Centrum för solenergiforskning (SERC), Högskolan Dalarna, 2010.

[15] Henning, A. (ed), Klimatsmart villavärme? Solvärme, nya byggregler och möjligheter, Falun: Centrum för solenergiforskning (SERC), Högskolan Dalarna, 2010.

[16] Lorentz, K., Möten med husföretag, in Klimatsmart villavärme? Solvärme, nya byggregler och möjligheten att förändra, Henning A. (ed), Falun: Centrum för solenergiforskning, Högskolan Dalarna, 2010.

[17] Ryghaug, M. and K.H. Sørensen, How energy efficiency fails in the building industry. Energy Policy 37, 2009, p. 984-991.

[18] Janols, H., F. Lindberg, and I. Nygren, Uppgradering av traditionellt byggsystem. Delprojekt 1: Produktutveckling- timmerhus och energihushållning, Falun: Akademin Industri och samhälle, Högskolan Dalarna, 2010.

Promoting renewable energy and energy efficiency in Central Africa: Cameroon case study

Joseph Kenfack[1,*], Médard Fogue[1], Oumarou Hamandjoda[1], Thomas Tamo Tatietse[1]

1. National Advanced School of Engineering, Yaounde, Cameroon
** Corresponding author. Tel: +23799416002, Fax: +23722229116, E-mail: joskenfack@yahoo.fr*

Abstract: Central Africa owns important renewable energy potential. This important potential is still suffering from poor development. The main cause of the poor use of renewable energy is the poor commitment and dedication of governments who have not taken the necessary measures to boost the sector. Thermal plants are hence among other solutions planned or under construction. The purpose of this paper is among other things aiming at ensuring that the renewable energy resources of Central Africa are known and are subject to be used optimally. The work also shows availability of renewable energy sources and suggests actions to promote and sustain its development. Based on the knowledge of the Central African energy sector, this paper will identify actions for improved access to sustainable, friendly, affordable energy services to users as well as a significant improvement of energy infrastructure in Central Africa and the promotion of renewable energy and energy efficiency. The work will show the potential for solar, biomass and hydro while showing where available the level of development. Then identified obstacles for the promotion of clean energy will be targeted. Finally, suggestions will be made to help the countries develop a vision aiming at developing good clean energy policy to increase the status of renewable energy and better contribute to fight against climate change. Cameroon case study will be examined as illustration. We will use several documents from institutions in the region and abroad, and maps when available.

Keywords: *Renewable energy, Potential, Central Africa, energy policy, Cameroon*

1. Introduction

Central Africa owns important renewable energy potential, namely hydro, solar and biomass. This important potential is still suffering from poor development up to the point where the sub region is still abundantly using the fossil energy as main power source. The main cause of the poor use of renewable energy is the poor commitment and dedication of governments who have not taken the necessary measures to boost the sector. This issue will also be addressed. Since the region is experiencing power shortage, thermal plants are among other solutions planned or under construction. This solution currently under implementation in Cameroon and other countries in the region, is not environment friendly and hence is not a long term solution.

2. Methodology

The work shows availability of renewable energy sources and suggests actions to promote and sustain its development. Based on the knowledge of the Central African energy sector, this paper will identify actions for improved access to sustainable, friendly, affordable energy services to users as well as a significant improvement of energy infrastructure in Central Africa and the promotion of renewable energy and energy efficiency.

The work will show at first the potential for the three primary energy sources which are solar, biomass and hydro while showing where available the level of development. Then identified obstacles for the promotion of clean energy will be targeted. Finally, suggestions will be made to help the countries develop a vision aiming at developing good clean energy policy to increase the status of renewable energy and better contribute to fight against climate change. Cameroon case study is very interesting because the country has a great renewable energy potential and can develop and export energy to neighboring countries.

The state of art in energy sector in Cameroon will be made. Based on ongoing projects and strategic documents adopted by the country, directions towards which actions will be made will be suggested. From the overview of institutional structure reform of the Cameroon power sector and assessments, specific suggestions based on the weaknesses of the institutions will be made for the enhancement of the renewable energy and hence sustain energy access and security in general and in remote areas in particular, where the fight against poverty is more difficult. We will use several documents from institutions in the region and abroad, and maps when available.

3. General information on Central Africa

Central Africa (Cameroon, Central African republic, Gabon, Republic of Congo, Chad, Equatorial Guinea, Democratic republic of Congo) is situated between latitude 13° south and latitude 22° north, longitude 8° East and longitude 22 East.

Central Africa is endowed with an abundance of renewable energy resources but the region is still looking forward to facing the challenge of harnessing its resources effectively and efficiently. There is still a vast dependence on fossil fuels and biomass. The use of fuel wood for lighting and cooking is still very familiar in the region given the poor income of populations. This negatively impacts the environment and causes infant mortality from acute respiratory illness associated with the inhalation of wood smoke. Approximately 1.6 million people die every year because of indoor air pollution - that's one death every 20 seconds [1]. This indicates that there is a need to develop efficient, sustainable and safe technologies to relieve population from such a burden.

4. Renewable energy potential in central Africa

4.1. Hydro potential

These countries own important hydro potential. Although 3.4 GW has already been developed, above 100 more GW of hydro power still remain untapped with an economically feasible hydropower potential above 900 TWh. Given the importance of the hydrographic network, tidal energy can also be envisaged, as well as ocean energy along the guinea golf.

Table 1 Thermal power, hydropower potential and development in Central Africa: source: [2] and [3]

COUNTRY	Gross theoretical hydropower potential (TWh/year)	Under operation in 1999 (MW)	Technically feasible (TWh)	Thermal plants
CAMEROON	294	725	115	300
GABON	80	170.2	32	210
DEMOCRATIC REPUBLIC OF CONGO	1397	2440	774	NA
CONGO	50	89	NA	
CENTRAL AFRICA REPUBLIC	NA	19	3	24
EQUATORIAL GUINEA	NA	1	NA	28
CHAD		0	0	37

4.2. Wind potential

According to GEOS-1 satellite measures from NASA [**Error! Bookmark not defined.**] from july 1983 to june 1993, the wind potential of the region is poor within the equator. Chad is the only country with an average speed above 5 m/s throughout the country, allowing the possibility for wind development.

4.3. Geothermal potential

Some hot water sources are identified in the region, but detail study for the assessment of the geothermal potential have not yet been done so far in Central Africa, although one important volcano (mount Cameroon) is still in activity. The eastern part of the Democratic Republic of Congo might have important geothermal potential since it is part of the Indian Ocean ring of fire.

4.4. Solar Potential

Africa is situated from one side to another at the Equator level, hence making this continent one of the sunniest in the world. Based on the data from Solar Radiation project (SoDa) [4], the lowest daily mean radiation ranges from around 4 kWh/day/m² (wet forest) to above 8kWh (dry desert in Chad). The modified map below from SoDa shows the average solar radiation of the region. It appears that Central Africa has a great solar potential.

4.5. Biomass Potential

Central Africa holds up to one-quarter of the world's tropical forests. This forest is the second largest tropical forest in the world after the Amazon forest. Its mosaic of ecosystems regulates local climate and the flow of water. The forest covers an important area, from the Albertine Rift (Rwanda, Burundi, Uganda) to the Gulf of Guinea (Equatorial Guinea, Gabon, Cameroon) and harbors a variety of forest. It's one of the place where wild dense forests can still be found in the world with an area around 500 million acres, spanning the boundaries of Cameroon, the Central African Republic, the Democratic Republic of Congo, Equatorial Guinea, Gabon and the Republic of Congo.

Inadequate and improper forest management practices is a threat to the long-term viability of these forests, significantly reducing their economic potential and resulting in negative social and environmental impacts. Over 50 percent [5] of the Congo Basin's forests are under commercial logging leases. Despite several sustainable forest management programs, Central Africa tropical forests are disappearing at an alarming rate.

5. The energy sector in the region

The energy sector differs from one country to another, depending on the available potential. Some countries have liberalized the sector and others are still on the way to doing it. Each country has its own energy sector management and regulations. The countries are still looking forward to having transborder regulations. This will for instance facilitate grid interconnection and sustainable management of energy sources. All the countries have developed important thermal plants.

6. Energy efficiency

The issue of energy efficiency is suffering from poor information and dissemination on energy efficiency technologies. The contributions in Central Africa should mainly be oriented towards building capacities and information dissemination on energy efficiency technologies. The grand objective of this initiative is to lighten the economical burdens of the countries in

the region thereby improving the life quality. Due to the reason of affordable prices, most of the countries are using, less efficient equipment notably in their industry, transportation or household sectors (generator, wood, petrol…). Most of such equipment, which can be second-handed (from developed countries), obsolete or of inefficient technology (non efficient stoves, incandescent light bulb…), is less efficient than the latest models being used to date and thus consumes more energy. These inefficient apparatuses often produce more air pollutants that can cause environmental destruction and threat of contracting serious diseases for people.

Many countries in Central Africa are oil producers. The availability of fossil fuels is hence not an important issue. The energy efficiency technology could help reducing the negative environmental impact of human activities by decreasing the consumption of fossil fuels, and thereby yielding the same results as the renewable energies. Actions should be undertaken to ameliorate and sustain the Energy Intensity, defined here as the ratio of the total energy consumption to the Gross Domestic Production (GDP), to a level below 0.5 (developed countries between 0.2 and 0.3).

Introducing high efficiency technologies into Central Africa will be foreseen to lighten their economical burden by reducing the total conventional fuel consumption, electricity bills and the high deforestation level, and thus improving their productivity. Given the high level of biomass consumption (80% household energy in Cameroon [6]), energy efficiency will be foreseen to lighten the desert encroachment and thus climate change.

The issue of implementing hybrid renewable energy system can also be envisaged, namely solar/hydro/biomass/wind.

7. Barriers to renewable energy and efficient energy implementation

There are significant barriers to the further implementation of renewable energy that need to be addressed. The key issues include the following:

- Biomass, hydro, solar and wind energy technologies remain expensive (high capital costs), compared to firewood, charcoal, petrol and gas energy supplies,
- Poor long period support of renewable energy projects (till reaching profitability)
- Lack of consumer awareness on benefits and opportunities of renewable energy solutions.
- Poor decentralized solutions for energy services (generation, distribution…)
- Financial, legal, regulatory and organizational barriers need to be overcome in order to implement renewable energy technologies and develop markets.
- Lack of specific access to key energy infrastructure such as the national electricity grid,
- Poor availability of funds for development of renewable energy
- Poor organization and sector institutions

8. Suggestions

8.1. Vision

The region needs to develop a vision leading to strategies and programs. This should be politically sustained in order to mitigate the poor leadership and poor renewable energy and energy efficiency policy formulation in the sector. In order to sustainably fight against climate change, strategic action plans should be developed or reviewed where available to fit with clean development mechanism. This should be done through capacity building and capacity enhancement of stakeholders in the region.

Central Africa in general is suffering from a poor vision on the issue of renewable energy and energy efficiency. Very few countries have developed a vision on this issue and other are still looking forward to doing it. The strategies and programs exist in some countries. They should match the vision and meet the targets.The region should identify the long term perspective action on the issue of promoting renewable energy and energy efficiency. Where there is no vision on this issue, it is important to focus on stakeholder's capacity to define and adopt a long-term perspective on renewable energy and energy efficiency. If need be, capacity building and/or capacity enhancement should be prior to the formulation of the vision.

In order to meet the renewable energy and energy efficiency targets, effective leadership is a key issue for the attainment of the targets within Central Africa. At national and regional levels, political authorities should be involved and support the action. This would lead to the generation of champions.

Other important points are:

- enforce energy policy at the regional level,
- promote and develop power trade and ancillary services,
- increase access to clean energy to populations and reduce poverty,
- create a free regional energy market and improve energy system reliability and quality of supply in the whole region.
- initiate pilot projects funded to help develop the market for sustainable energy,
- create favorable regulatory and policy frameworks,
- Promote innovative finance and business models to activate the private sector,
- develop and support policy-maker networks at regional level with initiatives in the field of energy efficiency, sustainable energy regulation, renewable energy and regional regulatory board
- disseminate mirroring of well-reasoned input

8.2. Enabling environment

Given the purchase power of the population and the economic constraints, renewable energy requires an enabling environment for its promotion. As mentioned above, the renewable energy initial capital cost is high compared to conventional energy sources. This can only lead to making them commercially uncompetitive in the short to medium-term. To overcome this situation, specific actions need to be taken at several levels, namely fiscal, financial, social and legislative levels. This includes commitment and dedication of actors for a good leadership and encouragement of champions. National and international bodies hosting development agencies based in each country should also work together to attain the promotion of renewable energy and energy efficiency targets. Full implementation of free trade within Economic Community of Central African States (ECCAS) will facilitate regional programs and collaboration among states.
Addressing the human resource issue is a key point for attaining the objectives. The region experiences poor human resources in the field of designing, evaluating and implementing renewable energy and energy efficiency projects. Good governance and good regulation in the sector are also very important for promoting and enabling environment for scaling up investments and mobilizing public and private initiatives.

The real potential and benefits of all renewable energy sources is still to be assessed. Because some studies are not done or not fully done, the costs for developing renewable energy tend to

be very high and there is a reluctance to invest in what are sometimes considered to be risky investments.

8.3. Role of financial instruments

The profitability of renewable energy is subject to discussion in a market driven energy economy. To address this issue, many countries in Europe have adopted different specific renewable power generation approaches (feed in tariff, certificates, fixed tariff). In order to achieve the target, the introduction of renewable energy technologies into a market driven energy economy will require the allocation of funding to assist in overcoming the initial high capital cost. It could be done through government bodies, private institutions sustained by government or simply through dedicated funds (budgetary allocation, subsidies, incentives...). The process should be stopped as soon as the renewable energy technologies become competitive and are driven by market forces alone.

Other actions to be undertaken are:

- Establishment of a good organizational framework and robust energy policy and strategy
- Public sensitization
- Promotion of efficient techniques and marketing strategies (4Ps)
- Knowledge management and networking with other partners and projects, governmental and private sector partnership

9. Cameroon case study

Cameroon power sector heavily relies on hydropower with 721 MW of Hydro schemes over the total installed capacity of above 1000MW. According to the World Bank Investment Climate Assessment, limited access to reliable electricity is among the 5 top obstacles to doing business in Cameroon. It is estimated that the lack of reliable energy services is costing Cameroon close to 2% of the gross domestic product growth. In order to rehabilitate existing power station, as well as transmission and distribution networks, the electricity utility AES SONEL recently secure a EURO 260 million loan financing for its five year investment program. In order to secure energy supply for the country, the Government of Cameroon commissioned a least cost power sector development plan (PDSE 2030) which is on the way to being updated. Given the time needed for the studies, development and funding of hydro plants, the country has been obliged to take emergency measures based on thermal solutions to cover current and foreseen energy shortages in the short term. If the funding doesn't follow, emergency measures taken for electricity production might become permanent, producing more than one million tons of carbon dioxide per year.

9.1. Main current and future thermal plants

From 2004 to 2011, thermal plants capacity from fossil energy has been multiply by four. Several thermal plants are permanently under operation. The most important are the Limbe thermal plant and the Yassa thermal plant with an installed capacity of 85 MW each. The construction of Kribi thermal plant (gas) with a capacity of up to 300 MW is ongoing. To meet energy shortage foreseen in the country in the short term, the Government plants plans to develop up to 100 MW additional thermal capacity in the cities of Bamenda (20 MW), Ebolowa (10 MW), Mbalmayo (30 MW) and the capital city Yaounde (40 MW). To face the growth of the demand estimated above 50 MW per year, important reforms and midterm development plans have been done. As demonstrated above, renewable energy is far from being the first solution for addressing energy shortage issues in Cameroon.

9.2. Institutional reform

Prior to the current status, electricity was supplied in Cameroon by a single vertically integrated company that had the responsibility for production, transmission, distribution and retail sales. The country established a sector regulator (ARSEL), a rural electrification Agency (AER) and also created the Electricity Development Corporation (EDC) which, as Government of Cameroon's asset holding company, is responsible for the management of public sector assets in the power sector, in particular hydropower assets, as well as the regulation of power flows. Nowadays, more than 20 texts govern the sector which is liberalized since 1998. The aim of liberalization was to attract private sector investments to help the country develop its power sector. The generation, transmission, distribution and sales of power are submitted to concession agreement, license or authorization, declaration regime, free regime and the special regime for rural electrification.

9.3. Renewable energy promotion

No specific action dedicated to the promotion of renewable energy has been undertaken so far. Programs for efficient stoves are ongoing for energy efficiency but many other issues still to be addressed. The country also has a rural electricity fund for the promotion of rural electricity. The formulation of strategic actions to boost the energy sector in all parts of the country is still ongoing in the Ministry of Energy and Water. The promotion of renewable energy and energy efficiency is among these actions. But given the poor experience of the stakeholders, pilot projects should be initiated and disseminated.

9.4. Identified regulatory barriers to renewable energy

Challenges (regulatory and others) to sustainable energy in Cameroun include:

- The restructuring of the electricity utility AES-SONEL mission;
- The establishment of connection charges and tariffs from renewable sources;
- The update and implementation of low cost solutions and safety standards for rural electrification;
- The encouragement of the ongoing policy for entrepreneurs willing to enter the electrical service contracting business;
- The consolidation of the provision of incentives to encourage entry of new electricity retailers in cities and rural areas through rural electrification fund;
- The promotion of energy efficiency
- The dissemination of bests practices.

The mission of the electricity utility should be restructured to encourage energy from renewable sources, through attractive connection charges and feed in tariffs. In order to boost the sector, the rural electricity fund should promote the development of hydro and solar plants where need be and disseminate information about champions.

9.5. Weaknesses of the institutions

The country will be experiencing in the future for the first time a true management of new operators, for only two licenses are granted so far. All the projects are currently facing poor visibility on the issue of feed-in, transport and tariffs. The electricity regulatory agency (ARSEL) created in the framework of liberalization hence has limited experience.

For each of the ongoing projects, there will be specific negotiations if necessary measures concerning regulations are not taken in time. The sector is also suffering from a lack of

transborder regulation for interconnection among countries, because Cameroon can be a net electricity exporter. Options for encouraging decentralized solutions in remote areas are currently ongoing through rural electricity fund, but the experience is still limited. To address these issues, Cameroon is developing several strategic action plans. The promotion of renewable energy and energy efficiency hence still has a long way to go.

10. Conclusion

Central Africa is a region with great renewable energy potential, a place were almost all renewable energy sources can be found. The region owns the first hydro potential of the continent, the second tropical forest in the world and an important solar radiation all year long. Despite the great renewable energy potential, the region is experiencing very poor renewable energy and energy efficiency promotion. Although some actions are ongoing, more specific actions in the region are needed at several levels. Suggestions have been made to help the region develop a good vision to address the issue and take the necessary measures at all levels for promoting renewable energy and energy efficiency.

References

[1] WHO, Fact sheet N°292, June 2005

[2] Aqua~Media International, Word Atlas and Industry guide, The International journal on Hydropower&Dams, 2009, pp 64-68

[3] Conseil mondial de l'énergie, Potentiel de développement intégré de l'énergie au plan régional en Afrique : Document de Travail, 2003

[4] http://www.soda-is.com

[5] http://www.tropicalforestfoundation.org/projects/gabon

[6] Ministère de l'énergie et de l'eau, Système d'information énergétique du Cameroun, rapport 2007

[7] Hanchery, overview of the National Hydropower Study: the Value, Potential, and Role of Hydropower as a Future Energy Source", Proceedings Waterpower '79: An International Conference on Small Scale Hydropower, U.S. Army Corps of Engineers and U.S. Department on Energy, 1979, pp.675-680,

[8] P. Maher, N.P.A. Smith, A.A Williams, Pico hydro power for rural electrification in developing countries, International Journal of Ambient Energy, Vol 19 Number 3, July 1998

[9] Société Nationale d'Electricité du Cameroun, Atlas du Potentiel hydroélectrique du Cameroun, Sine loco, 1983.

The impact of the GB Feed-in Tariffs and Renewable Heat Incentive to the economics of various microgeneration technologies at the street level

A.Papafragkou*, P.A.B James, A.S.Bahaj

School of Civil Engineering and the Environment, University of Southampton, UK
** Tel: 00 44 2380 59394, E-mail: ap1004@soton.ac.uk*

Abstract: England, Scotland and Wales planning regulations require zero carbon homes by 2016. This can be expected to accelerate the uptake of microgeneration technologies. To incentivise small low-carbon generators the UK Department of Energy and Climate Change (DECC) proposed two new systems: the Feed-in Tariffs (FIT) and the Renewable Heat Incentive (RHI). This paper investigates the impact of these two systems on the carbon performance and the economics of various microgeneration technologies under two scenarios: (a) at the single dwelling level and (b) a local microgrid at the street level. The economic implications of combining a number of houses to form a local microgrid are assessed and expressed in terms of percentage of capital investment outstanding. The paper concludes that the current structure of the FIT and RHI does not incentivise microgeneration technologies according to their carbon performance and does not favour street-level schemes such as the one investigated in this paper. However it is sufficient to drive the market forward.

Keywords: Microgeneration, Microgrid, FIT, RHI, Residential, Renewables, Economics

1. Introduction

England, Scotland and Wales planning regulations require zero carbon homes by 2016 [1]. For large-scale residential developments, this implies the use of biomass combined heat and power (CHP) systems with potential contributions from photovoltaics or solar thermal systems. Micro wind power is unlikely to be suitable for the majority of developments due to the poor wind resource in the urban environment [2]. Smaller-scale developments and notably individual houses will be dependent on a combination of microgeneration technologies to meet their demand in heat and electricity. Undoubtedly the main barrier to the microgeneration technologies to date has been the high capital costs. In order to support and incentivise small low-carbon generators, the Department of Energy and Climate Change (DECC) in the UK proposed two new systems: The Feed-in Tariff (FIT) and the Renewable Heat Incentive (RHI).

A zero carbon home as defined in the "Code for Sustainable Homes", takes into account energy efficiency usage within the boundaries of the house. However, Department of Communities and Local Government (DCLG) recognise that there may be cases where it is not reasonable to expect zero carbon to be achieved through on site measures alone [3]. This means that policies will set out a series of solutions that can deal with the emissions that cannot be dealt with on the site of the development ('allowable solutions').

This paper considers a slightly less restrictive definition of the "zero carbon home" where various microgeneration technologies are directly connected to and operating for small-scale developments of fewer houses than would be typical for a developer-driven housing development (Figure 1). The impact of linking a number of houses at the street-level to the economics of various microgeneration technologies is investigated and compared with the economics for the single house case.

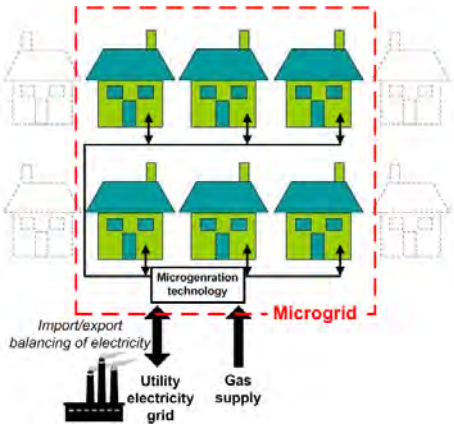

Fig.1 Conceptual combined thermal and electrical microgrid at the street level

2. Assessing the thermal and electrical demand of a residential housing cluster

For the prediction of the thermal heating demand (space heating and domestic hot water) the dynamic simulation package *TRNYS* [4] was used. Figure 2 illustrates the relationship between the main parameters used in *TRNSYS* to predict the thermal demand.

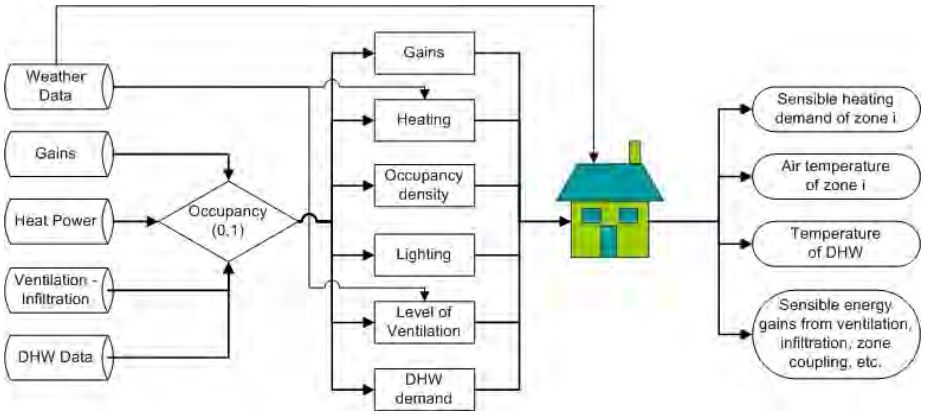

Fig. 2 Schematic illustration of the main signal flows used in TRNSYS for predicting the thermal demand

2.1. Space heating demand

The study considered a notional detached house constructed post-1965, which essentially represents ~17% of the total UK building stock [5]. Three user occupancy profiles were used: (a).Retired couple, (b).Professional working couple and (c).Family with 2 children.

2.2. Domestic hot water demand

Load profiles developed by Ulrike and Klaus [6] were used for the domestic hot water demand. Domestic hot water data and occupancy profiles were synchronised with a Fortran routine developed within *TRNSYS*, effectively operating as a load buffer [7].

2.3. Electrical demand

For this study real data was used for the generation of the electrical demand profiles; this had the form of five-minute interval data from an eco-home development of 9 low energy houses in Havant, near Portsmooth, UK [8]. Three datasets were chosen from the Havant trial to represent

the three occupancy profiles in this study. Table 1 summarises the demand levels for the three occupancy profiles and the cluster of 10 houses.

Table 1. Demand profiles in kWh for the 3 occupancy profiles and the cluster [7]

	Retired couple	Working couple	Family	10 house cluster
Space heating	12,178	8,161	10,287	118,008
DHW	3,006	3,002	5,230	36,706
Electrical	2,800	3,500	4,000	33,700

3. Clustering approach - Microgrids

The energy consumption of ten detached houses was modelled. Detached houses were chosen as they are a common house type of the UK building stock, accounting for more than 20% of the total UK building stock [5] and they are more likely to adopt any of the technologies considered in this study due to the availability of space as required by some technologies.

The clustering of ten houses at the street level to form a local microgrid was chosen as the basis of this study to assess any potential financial benefits. The reasons for adopting such an approach are:
(*a*) Smoother demand profile with less distinctive peaks, for both heat and electricity, maximizing the local use of the energy generated. More continuous thermal demand is expected to result in fewer losses from the thermal storage and buffer tanks and less volatile electrical demand is expected to result in lower levels of electricity export.
(*b*) Increased thermal load, allowing CHP technologies to operate under better regime.
(*c*) Proportionally smaller peak demand of a cluster compared to a single dwelling, which translates to smaller total installed capacity for the microgeneration technologies.
(*d*) Lower capital and maintenance costs for the microgrid compared to the single house.

The short proximity of the houses within the residential cluster implies a small electrical network, where distribution losses may be ignored. The heat network was assumed to be equally small and highly insulated, therefore heat losses were also considered to be negligible.

4. Microgeneration technologies

Four types of microgeneration technologies were considered and modelled in *TRNSYS* at the single house level and the street-level microgrid [7]: Solar thermal, Photovoltaics (PV), Ground Source Heat Pumps (GSHP) and Combined Heat and Power (CHP).

4.1. Solar thermal

A typical active, indirect, flat plate solar thermal system of 4.4kW$_p$ capacity was modelled for the single house and the street cluster (x10). A 300 litre stratified thermal storage tank was assumed per house. For the street-level cluster the same thermal storage tanks were assumed to be linked, essentially operating as a common thermal storage.

4.2. Photovoltaics (PV)

A monocrystalline PV module of 1.8 kW$_p$ manufactured by Suntech Power [9] was modelled for each house, requiring 13m^2 total roof area [7]. The main limiting factor for sizing the PV system

was the available roof space with right orientation and the minimum shading. This size is of a typical domestic application which may vary from 1.5kW$_p$ to 2kW$_p$ [10]. For the 10 house cluster the PV arrays were linked to form a local microgrid. Each house within the cluster was connected to a local distribution grid, allowing electricity to be transferred from one house to another and excess generated electricity to be exported to the utility grid.

4.3. Ground Source Heat Pumps (GSHP)

A single ground source heat pump system per dwelling was modelled to meet the space heating demand. To maximise the heat pump's thermal performance, heat storage was also considered. For intervals where heating demand could not be met by the heat pump, a backup boiler delivered any heat shortfall. GSHPs were modelled for 45°C output temperature, essentially modelling high temperature underfloor heating and low temperature radiators. For the single house a GSHP of 6.4kW$_p$ rated heating output was modelled, whilst for the cluster at the street-level two large heat pumps of 32.6kW$_p$ rated output each operating in series were considered [11].

4.4. Combined Heat and Power (CHP)

In terms of using fuel more efficiently, the concept of a CHP system was considered. Small CHP systems are commonly high heat:electricity ratio systems (>3:1) and as stated in the government's standard assessment procedure (SAP) [12], are assumed to be heat-led, meaning that they are allowed to operate only when there is demand for heat. On the grounds of economics, the installation of a CHP unit with a secondary back-up boiler would be unattractive. CHP units were therefore examined as an alternative to condensing gas-fired boilers.

For the single house a stirling engine micro-CHP system from Whispergen [13] was modelled, whilst for the residential cluster two options were investigated:

(a). a mini CHP operating as common facility for the microgrid and;
(b). three CHP units of different capacities (7kW$_{th}$/1kW$_e$, 14kW$_{th}$/5.5kW$_e$, 30kW$_{th}$/15kW$_e$) operating in series to provide the same peak thermal and electrical output as the single mini-CHP (51kW$_{th}$/21.5kW$_e$).

A thermal storage tank of 150 litres per dwelling was considered. Multi-stage operation involves the problem of scheduling the CHP devices operating in series. For this reason a heuristic, greedy construction algorithm was designed and incorporated in the CHP model.

5. Feed-in-Tariffs (FIT) and Renewable Heat Incentive (RHI)

In order to support and incentivise small, low-carbon generators and also make low carbon generation more cost effective to communities and householders, the UK Department of Energy and Climate Change (DECC) proposed two new support systems: the FIT and the RHI. With the FIT and RHI the UK Government introduces clean energy cash-back for renewable electricity and heat. Table 2 presents the tariffs for generated electricity and heat as proposed by DECC.

For electricity generation technologies, electricity exported to the national grid will be incentivised by an extra 3p/kWh$_e$.

Table 2. FIT and RHI generation tariffs for the UK, as proposed by DECC in February 2010

	FIT or RHI tariff (p/kWh)	
	Single house	**Cluster**
Solar thermal (kW_{th})	18.0	17.0
PV (retrofit) (kW_{el})	41.3	31.4
GSHP (kW_{th})	7.0	5.5
CHP (kWh_{el})	10.0	0

6. Results

At the first step, the carbon emissions from the 10-house cluster were estimated for the business as usual scenario (BaU) of a 90% efficient condensing boiler and electricity from the national grid. The BaU carbon footprint was then compared with the carbon footprint after deploying the microgeneration technology at (A) the individual house level and (B) the microgrid level. Results are summarised in Table 3 and clearly illustrate the improved carbon performance of the microgrid. It should be noted that micro-CHP for the single dwelling was the only technology with poorer carbon performance than the BaU scenario. PV system for the microgrid achieved a higher utilisation factor of the generated electricity, with 6% lower import and 15% lower export. However, in terms of carbon performance, the two schemes were equivalent as the system effectively displaces electricity with the same carbon intensity as the electricity imported. CHP's improved carbon performance for the microgrid was mainly due to lower electricity import from the national grid (13% for the mini-CHP unit and 24% for the 3 CHPs in series). For the carbon emission analysis a carbon intensity factor of 0.19kgCO_2/kWh was used for natural gas and 0.43kgCO_2/kWh was used for electricity imported from the UK national grid [12].

Table 3. Estimated tnCO_2 savings per annum compared with the BaU scenario

Tones CO_2 saved compared with BaU	**Solar thermal**	**PV**	**GSHP**	**micro-CHP**	**1 mini-CHP**	**3 CHPs in series**
10 non linked houses (A)	3.8 (48%)	8.0 (54%)	10.3 (41%)	-2.2 (-4.7%)	-	-
Microgrid (B)	4.3 (55%)	8.0 (54%)	11.5 (46%)	-	7.0 (15%)	7.8 (17%)
Difference (A-B)	0.5	0	1.2	-	-	-

The costs of the generated energy from each technology were estimated for a 15-year period, for the 10 non-linked houses and for the microgrid. The impact of the FIT and RHI schemes was assessed for each technology. For each case, both 0% and 3% interest rate was investigated for the capital investment. The prices used for gas and electricity were: 5p/kWh for gas and 16p/kWh for electricity (£1=100p) assuming a 3% annual increase over the 15 year period. Figure 3 illustrates the predicted cost of ownership for all the microgeneration technologies assessed in this paper.

For solar thermal the single house system was priced at £3,000 with maintenance cost £50 per annum to cover engineering inspections. For the microgrid the total investment, including the piping to connect the houses, was priced at £36,000. Without the RHI support the savings achieved by the system were negated by the interest rate and the system's economics diverged. Taking into account the RHI tariffs, the system achieved a financial break-even after 10 years of operation. Financially the microgrid scheme performed better, achieving 10% greater savings on energy bills compared to the 10 non-linked houses.

The main benefit of forming a microgrid when considering PV, was the increase of local utilisation of the electricity generated by the system. With the current FIT structure, the PV microgrid scenario was predicted to have worse performance than the standard single-house installations. Due to the very high tariff for generation and the additional export tariff, savings from the avoided import were insignificant compared to the savings due to generation. Assuming 3% interest rate, the financial payback period was predicted to be ~10.5 years for the 10 non-linked houses and ~13 years for the microgrid. Assuming no FIT the microgrid performed marginally better than the single-house case. The capital cost used for the analysis was

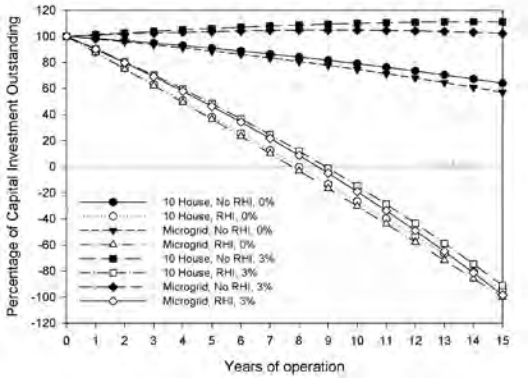

a. Solar thermal

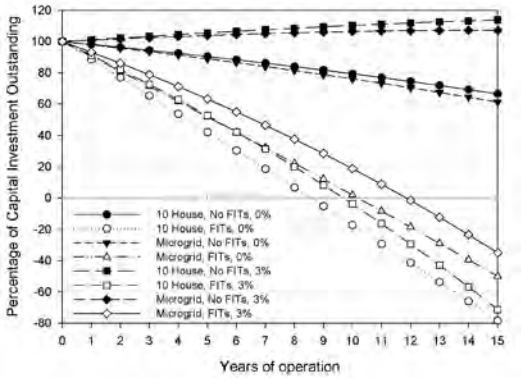

b. Photovoltaics (PV)

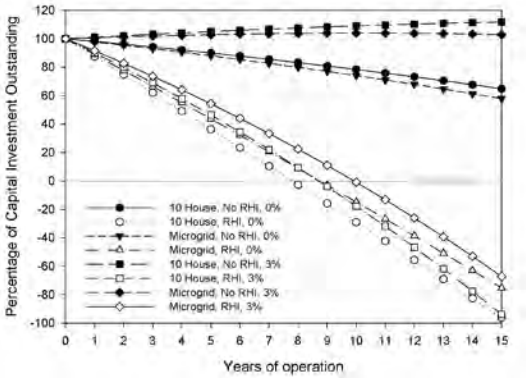

c. Ground Source Heat Pumps (GSHP)

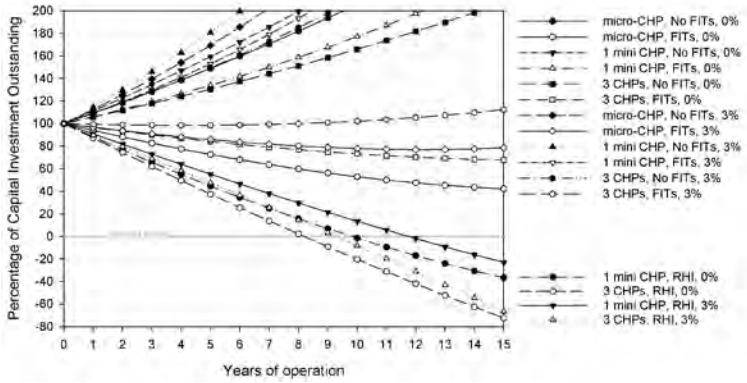

d. Combined Heat and Power (CHP)

Fig. 3 Cost of ownership profile for all microgeneration technologies considered in this study, assuming a 3% annual increase in the energy prices.

£4,500 per kWp installed and an annual OPEX of 2% of the initial capital cost was assumed for maintenance and the replacement of the system's inverter.

The improved carbon performance of the microgrid with GSHP systems was also followed by improved financial performance. With the current RHI tariffs microgrid was estimated to perform better than the 10 non-linked houses, with payback periods of ~9.5 and ~11 years respectively, despite the lower tariff offered for larger systems. Without the RHI support, all systems were far from the financial breakeven point. The capital cost assumed for the GSHP system was £1,000 per kWp [14] installed and a 1% maintenance cost was allowed for an annual inspection.

CHP units were examined as an alternative to boilers; hence the economics were calculated against the BaU scenario of a 90% efficiency condensing boiler, priced at £900 per unit with an annual maintenance cost of £50. Capital costs used were £26,000, £45,000 and £50,600 for the micro-CHP scheme, the mini-CHP scheme and the 3 CHPs in series respectively, including the heat piping network. A 2% of the capital cost was allowed for annual maintenance. As seen in Figure 3d, none of the three CHP schemes modelled reached the financial breakeven point within 15 years of operation, even when taking into account the current FIT. It should be noticed that despite its poor carbon performance, micro-CHP performed financially better, followed by the 3 CHP units in series and then the mini-CHP operating for the microgrid. The lower part of Fig. 3d illustrates a hypothetical scenario where the communal CHP units are supported through the RHI scheme. A price of 3.5p/kWh$_{th}$ would be required for these systems to reach the financial break-even point after 8-10 years of operation assuming 0% interest rate, whereas when a 3% interest rate was assumed breakeven took an additional 2 years.

Figure 4 shows a summary of the financial performance of all the microgeneration technologies considered for the residential cluster at the street level, with the current FIT and RHI tariffs, assuming 3% annual increase in energy prices and a 3% interest rate for the capital investment. It is shown that CHP technologies can not be economically viable if not incentivised. Current support for solar thermal, GSHP and PV proved to be sufficient to drive the market forward, even for the case of a 3% interest rate for the capital investment.

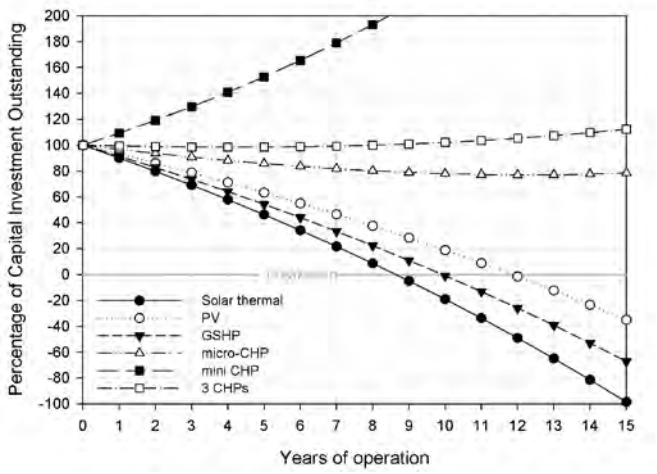

Fig. 4 Cost of ownership profile for all microgeneration technologies for the residential cluster, under the current FIT and RHI structure, assuming a 3% annual increase in the energy prices and 3% interest rate for the capital investment.

7. Conclusions

This paper investigated the impact of the UK FIT and RHI tariffs on the economics of various microgeneration technologies when they operate as common facilities for a cluster of houses at street level. It was shown that the carbon performance of these technologies was not followed by similar financial performance. A comparison between the individual house level and the cluster of 10 linked houses showed that there are potential carbon benefits and better matching of the generation-consumption profile. In some cases, however, the benefits are almost negated by the current FIT and RHI structure, due to the lower tariffs offered for larger installations and because of the high tariff offered for generation which overshadows the financial benefits from local consumption/avoided import. For this work, linked microgeneration technologies have been regarded as one larger installation, but financial benefits could further increase if each unit could be incentivised individually. The clustering approach proved to benefit CHP technologies more than any other, delivering 7-8tnCO_2/year per cluster. With no support from the Government such schemes were not predicted to reach the financial breakeven point within their lifetime. As heat-led processes they could be supported through the RHI scheme. With a generation tariff of 3.5p/kWh_{th}, CHP technologies could breakeven financially after 8-12 years and proliferate in the residential sector.

References

[1] CLG (2009), Sustainable New Homes – The Road to Zero Carbon, Consultation, 2009.

[2] James, P.A.B., Sissons, M.F., Bradford, J., Myers, L.E., Bahaj, A.S., Anwar, A. and Green, S. (2010). Implications of the UK field trial of building mounted horizontal axis micro-wind turbines, Energy Policy 38: 6130–6144.

[3] DCLG (2008). Definition of zero carbon homes and non-domestic buildings, Consultation.

[4] TRNSYS (2005). TRNSYS 16, Solar Energy Laboratory, University of Wisconsin-Madison

[5] CLG (2009). English house condition survey 2007, Annual report.

[6] Ulrike, J. and Klaus, V. (2001). Realistic Domestic Hot-Water Profiles in Different Time Scales, 2.0 edn, University of Marburg.

[7] Papafragkou, A. (2010). Urban Carbon and Energy Analysis: Calculation of energy flows and emissions from residential housing clusters and assessment of sustainable energy solutions, PhD Thesis, University of Southampton, UK.

[8] Bahaj, A.S. & James, P.A.B. (2007). Urban energy generation: The added value of photovoltaics in social housing, Renewable & Sustainable Energy Reviews 11(9).

[9] Suntech (2009). http://eu.suntech-power.com/en/products/residential.html

[10] EST (2005a). Photovoltaic (PV) - solar electricity, Factsheet.

[11] Viessman (2010). http://www.viessmann.co.uk/prod-vitocal300.php, March 2010.

[12] DEFRA (2008). The Government's Standard Assessment Procedure for energy rating of dwellings (SAP 2005), Technical Report Revision 2, Watford.

[13] WhisperGen (2010). www.whispergen.com, March 2010.

[14] EST (2005). Ground source heat pump, Factsheet.

The Parameters used in Multiple Criteria Decision Making Methodologies for Drafting out Renewable Energy Sources Support Schemes

Savvas C. Theodorou[1]*, Georgios Florides[2], Savvas A. Tassou[1]

[1]*Brunel University, Uxbridge, United Kingdom*
[2]*Cyprus University of Technology, Lemesos, Cyprus*
**Corresponding author. Tel: +357 99563234, Fax: +357 22380535, E-mail: first.author@institution.org*

Abstract: The increasing environmental concerns and energy issues required for a sound design of decision patterns increased the parameters to be considered in deciding and developing an efficient energy strategy through the optimisation of support schemes for renewable energy technology. The correct identification and evaluation of the decision making parameters leads amongst others to correct political decisions for maximising the benefit of investment cost, social and environmental gains and improvement of technologies. The paper is focussed in analysing the parameters to be used in a Multiple Criteria Decision Making method and in suggesting a ranking scale for the parameters to be ued in drafting their weights. Fourteen parameters were selected and analysed. The analysis is contacted through literature review, personal communication with key personnel and through questionnaires.

Keywords: *Renewable Energy Parameters; MCDM Methods; Renewable Energy Policy.*

1. Introduction

Energy planning and support methodologies have been developing through the years for supporting decision makers to evaluate conflicting alternatives and derive a way to come to a compromise in a transparent process. Very common methods used in energy planning are the Analytic Hierarchy Process (AHP), PROMETHEE, ELECTRE, Multi Attribute Utility Theory (MAUT) and in order to validate a result more than one of the methods can be used.

During the70's and 80's, the increasing environmental concerns and energy issues changed the design of decision patterns so as to include the environmental and social implications in energy planning. This caused an increase in the parameters to be considered in deciding and developing an energy strategy. The paper discusses the parameters used in decision making for drafting out Renewable Energy Systems (RES) support schemes and through the outcome of questionnaires suggests the parameters' rankings to be used in further developing their weights. The first part lists a number of indicative parameters briefly explaining them and the second part deals with the questionnaires results.

2. Methodology

A literature review has been conducted in identifying the most commonly used parameters. The study in ranking the parameters and identifying their weights is carried out through literature review, personal communication with key personnel and the fulfillment of questionnaires. The outcome of this paper draws out conclusions regarding the major parameters to be used along with indicative suggested weights. The correct identification and evaluation of the decision making parameters leads amongst others to correct political decisions for maximising the benefit of investment cost, social and environmental gains and improvement of technologies.

3. Indicative Parameters

The parameter evaluation has to provide tools of judgment for decision makers (DM), which must verify the consistence of choices with the expectations of the DM and with the needs of the other involved actors. A number of criteria can be developed to best suit the alternatives and decision makers' familiarity with the alternatives and the criteria. In this chapter, criteria that could be used in deciding the best mix of RES subsidy scheme are examined.

Generally, the parameters used in each country and for each RES technology may vary, however, in general the parameters to be used should be:

- compatible with political, legislative and administrative situation (willingness, level of cooperation of governmental departments and political parties);
- consistent with the local technical and economic condition, which depends on the local capacity of managing the innovation both at technical and financial levels (availability of technology, cost factors, maturity);
- consistent with energy demand predictions (projection of final energy consumption may affect greatly the decision outcome since it will affect the aggressiveness of the support schemes);
- compatible with the existing environmental and ecological constraints (International agreements can shape the final classification of the alternatives).

The parameters to be used should be agreed on and accepted by all the actors involved in the decisional process. A list of potential parameters is presented below:

3.1. Maturity / reliability

A mature technology can be defined as a technology that has been in use for long enough and most of its initial faults and inherent problems have been removed or reduced by further development [1]. Another key indicator of a mature technology is the ease of use for both non-experts and professionals. The judgment is expressed within the range of 1-4. A rank order is applied, with increasing preference from 1 to 4, as follows: (1) technologies that are only tested in laboratory; (2) technologies that are only performed in pilot plants; (3) technologies that could be still improved; (4) mature technologies, close to reaching the theoretical limits of efficiency [2]. Popp, et al. 2010 expressed the necessity in evaluating the maturity of renewable energy technologies for drafting future energy policy and developing efficient support schemes.

3.2. Market maturity

This criterion is an estimation of the market availability and the status in the penetration process of a given technology and the materials and services associated with the considered action [3]. A Judgment scale provided by Becalli et.al. 2003 is the following: (1) not present on the market at least in a experimental stage; (2) pilot plants; (3) start of market availability; (4) market availability of the technology for less than 10 years; (5) market availability of the technology for more than 10 years.

3.3. Consistence of installation and maintenance requirements with local technical know-how

The evaluation of this criterion is oriented to a qualitative comparison between the complexity of the considered technology, and the capacity of local actors of ensuring an appropriate installation and operating support. The technology maturity and market maturity are highly correlated with this criterion since the market availability for installation and maintenance requirements depends on them. The following qualitative scale of ranking is used: (1) insufficient technical background for installation/maintenance; (2) middle technical background for installation/maintenance; (3) great technical background for installation/maintenance [2].

3.4. potential / Climatic conditions

Unlike fossil fuel technologies, the efficiency of renewable technologies is generally very site specific. Thus, it would be expected that photovoltaics in the UK would incur a higher cost per kWh than countries located at lower latitudes such as Cyprus. In general, the geographical potential can be considered as the energy flux theoretically extractable in areas that are considered suitable and available for energy production i.e. in areas which are not excluded by other incompatible land cover/use and/or by constraints set on local characteristics such as elevation and other land characteristics [4]. This criterion is only concerned with the geographical potential of a certain region. The scale to be used is not in the form of energy output but a use of a more general linguistic scale is more appropriate. The scale proposed considering the available renewable energy technology, is as follows: (1) Almost no potential; (2) Very low potential; (3) Low potential; (4) Medium potential; (5) High potential; (6) Very high potential.

3.5. Continuity and predictability of performance

In assessing renewable energy it is important to know the conditions of continuous operational patterns. This condition is often a characteristic of a given technology and does not indicate a factor of unreliability. For example the output performance of photovoltaic is more predictable than the one of windpower. As of 2008, Germany produces between 1500 and 7700 GW h/month depending on wind conditions. This makes traditional scheduling of power generation for the day ahead very unsure [5]. The judgment of this parameter can be expressed according to the following scale: (1) unpredictable and not continuous operation; (2) predictable but not continuous operation; (3) predictable and continuous operation.

3.6. Value of energy output

Possible future revenues from investments in RETs are crucial for facilitating an economically viable period of heavy installations that is needed to fulfill the new environmental goals. The costs are the initial investment and the operational and maintenance (O&M) costs [6]. To evaluate the profits of renewable energy projects without including any of the policy support mechanisms, the following equation can be used for the value of energy output (VEO).

$$VEO = E[XsmPsm + XcmPcm] \qquad (1)$$

where E is the monthly energy output by the renewable system, Xsm is the percentage of energy sold in the spot market, Xcm is the percentage of energy sold in the contract market, Pcm is the contract market price and Psm is the spot market price.

3.7. Value of environmental benefits (VEB)

Renewable energy sources, which are often (but not always) carbon-free, are among the technology options available to reduce carbon emissions in the electricity sector [7]. Governmental policies regarding environmental protection and emission reductions are amongst others mainly based on the promotion of RET. The VEB can be calculated using two scenarios, the renewable energy certificates and the certified emission reductions scenario.

3.7.1. *Renewable energy certificates (REC)*

In REC, the benefits can be defined as the value of the energy output and the RECs revenue. One REC represents the environmental attributes associated with one MWh of electricity from renewable energy technologies.

3.7.2. Certified emission reductions (CER)

The CER is based on the Clean Development Mechanism of the Kyoto Protocol. The registered CDM project obtains one CER for each 1 ton of CO_2 reduced by the project. Besides, the sale of CERs represents an additional source of project income. However, the development of a CDM project generated extra costs for the project developer, also known as transaction costs. These costs are related to the formalization and validation of the CDM project, as well as the monitoring and verification of the emission reductions.

3.8. Environmental benefits of the reduction of pollutant emissions

With a direct price for emissions—via either an emissions tax or a tradable emissions permit system—the fossil fuel sector has an incentive to lower its emissions rate until the marginal cost of reduction equals the emissions price [8]. In order to have a synthetic index, the score can be expressed through the following qualitative scale of values: (1) very high emissions, when each category is relevant; (2) high emissions, when at least two of the categories are relevant; (3) middle emissions, when at least one category is relevant; (4) low emissions, when all the emissions category are insignificant or do not exist.

3.9. Land requirement

This criterion represents one of the most critical factors for the intervention site, especially where the human activities are relevant factors of environmental pressure. A strong demand for land can also determine economic losses, which are proportional to the specific value of the site and the possible attendant alternative needs. An approximate scale can be as follows: (1) high land requirements and significant landscape alternation that can limit future growth of the area; (2) high land requirements and significant landscape alternation that has no affect on future growth of the area; (3) middle land requirements and landscape alternation; (4) low land requirements and landscape alternation; (5) no land requirements and landscape alternation [9].

3.10. Sustainability according to other environmental impacts

Landscape impact, acoustic emissions, electro-magnetic interferences, bad smells, and microclimatic changes are evaluated. A synthetic judgment can be expressed through the following scale: (1) very high intensity impacts; (2) high intensity impacts; (3) middle intensity impacts; (4) low intensity impacts; (5) not existing impacts. This parameter can be considered highly subjective since it includes impacts such as landscape changes. While large dams and

wind farms change the landscape significantly, people might argue whether the change is positive or negative.

3.11. Labor impact

An estimation of labor potentials due to employment of RET can be used. Additional direct and indirect employment and the possible indirect creation of new employment must also be assessed. The following linguistic scale can be used: (1) low employment occurring only at the installation process; (2) low employment that will provide further jobs during the maintenance of the RET; (3) medium employment during installation and maintenance; (4) high employment during installation however low during the maintenance of the RET; (5) high employment both during installation and maintenance.

3.12. The net present value (NPV)

At present, for most of the RET, the investment costs, along with the risks of renewable energy, remain high [10]. The NPV calculation relies on the initial investment, the total accumulated cash-flow and the discount rate. The cash-flows are the costs and the benefits associated to the project. The benefits taken into account are the value of the energy output (VEO) and the value of the environmental benefits (VEB). The following scale is an indication of the investment's profitability. (1) NPV < 0 not a profitable investment; (2) NPV = 0 not gain and not loss; (3) NPV > 0 added value [11].

3.13. Distribution cost

Modern small scale generation plants with standardized modular design are competitive, less capital intensive, more efficient, quicker to build and have more sophisticated control technologies for operation and transmission networks. [12]. However, this parameter is highly location correlated and each project case should be examined accordingly. A general linguistic scale can be used: (1) High cost for connection to the grid lowering significantly the NPV; (2) Medium cost for connection to the grid with impact on the NPV; (3) Low cost for connection to the grid with minimal impact on the NPV.

3.14. Compatibility with political, legislative and administrative framework

It is of high importance for governments to realize that RETs with high fixed but low variable costs can provide price stability and a good hedge against the risk of fuel price volatility [13]. Many countries are pursuing greater use of renewables. However, there is little agreement on what policies are most effective in promoting renewables, or even in what it means for a policy to be 'effective.' The goal of RE policy appears simple: to get more renewables in place. However, a closer look reveals that there are in fact many goals that renewables are intended to accomplish. Renewables can be seen as a way to reduce carbon emissions, to promote industrial development, to decrease fossil fuel imports, and meet other policy goals. Each of these goals leads to a different set of programs and technologies. [14]. The examined criterion assesses the qualitative relevance of the above considerations, with regard to government support, the tendency of institutional actors, and the policy of public information. The overall value judgment is expressed in the following way: (1) absent; (2) middle; (3) high.

4. Sampling of Parameter weights using questionnaires

Questionnaires were used in finding an approximation of the weight for each parameter. The questionnaires asked the responders to rate the importance of each parameter from a scale of one to ten. Moreover, the following information was collected from each responder: (a) Educational background; (b) Occupation and position; (c) Familiarity with renewable energy sources. The questionnaires were given to a range of professionals consisting of university lecturers, business consultants, mechanical and electrical engineers, environmental scientists, civil engineers, IT consultants and engineers, researchers, accountants and economists. Questionnaires were not handed to a specific group of responders but rather to a wide range of professionals employed in a wide spectrum of the Cypriot economy. As expected the range of answers varied considerably according to the responders' educational background and familiarity with RET.

4.1. Familiarity of the responders

The familiarity of each responder for RET was also recorded (Fig. 1). The responders were asked to give their subjective judgment on how familiar they are with RET using a scale of one to ten (legend of Fig. 1) where 1 is representing "not familiar at all" and 10 representing "an expert". About 28% of the responders answered that they are somewhat familiar (number six), and only about 1% answered that they considered themselves experts.

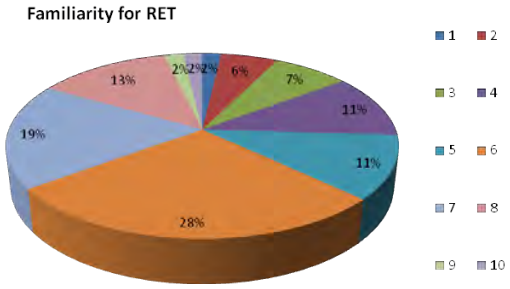

Fig 1. Familiarity of responders for RET

4.2. Responders view

An analysis has been conducted using the responders' view without taking into consideration their knowledge and familiarity as regards the RET. The results (Fig 2) reveal that the highest ranked parameter and in turn the most important one that should carry the highest weight in a multiple criteria decision making model is the "Potential/climatic conditions".

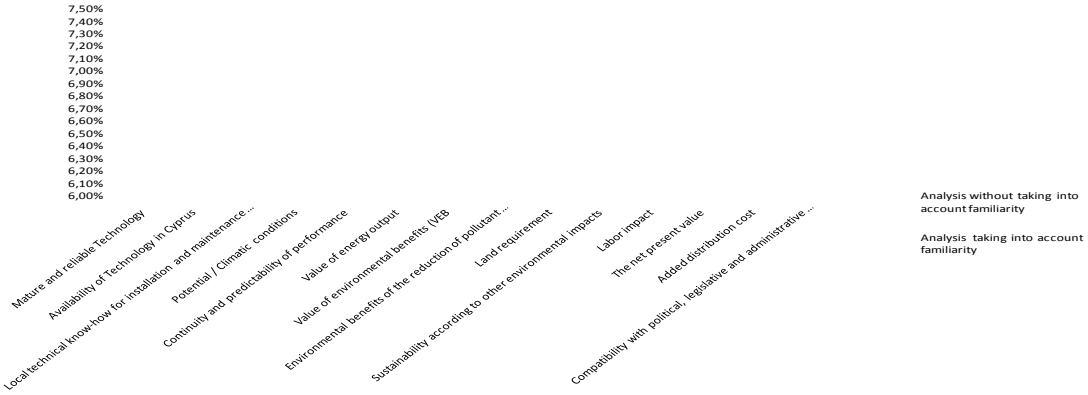

Fig 2. Responders' view

Using the above rankings incorporating the responders' answers for each parameter, we can deduct the weight of each parameter. It is suggested to use the percentage values since it will give a more precise indication of the closeness of each parameter's weight.

Responders' high rank for the "Potential / Climatic conditions" parameter reveals the relation this parameter has on all the other parameters in question. We can say that the effect of this parameter reflects on other parameters such as the value of energy output and in return the "net present value" and the "Value of environmental benefits (VEB)", the market maturity and in return to the local technical know-how for installation and maintenance requirements, the continuity and predictability of performance, land requirement and the compatibility with political, legislative and administrative framework. Though the "Environmental benefits of the reduction of pollutant emissions" is ranked second, parameters that address other environmental issues such as "Sustainability according to other environmental impacts" and "waste treatment" are ranked in much lower positions. The "Value of environmental benefits (VEB)" parameter is ranked third which can be contributed to the fact that the parameter is expressed in monetary terms which is easily translated to direct benefits of the individual investor.

Using the weighted sum method and then multiplying by each rating according to the responder's answer, the final results are better adapted to suit the familiarity with the ratings given. The parameter regarding "Potential / Climatic conditions" is still ranked first indicating its importance in drafting an energy policy regarding the promotion of renewable energy sources. Thus, if we were going to use this parameter in a decision matrix then it should have one of the highest weights. The "Environmental benefits of the reduction of pollutant emissions" is still ranked second and the "Value of environmental benefits" is still on the third position. The change is noticed when accessing the "Continuity and predictability of performance" which is now ranked seventh while VOE is sixth showing a higher importance. The "Local technical know-how for installation and maintenance requirements" is ranked one place higher; this might be due to the fact that the responders with higher familiarity give more emphasis on the technological aspect of RET

5. Conclusions

When assessing the parameters to be used in a Multiple Criteria Decision Making problem, one should define the problem as thoroughly as possible and examine the parameters in detail. In deciding the optimum mix of renewable energy sources to be implemented, a multidimensional approach should be used. Most of the parameters concerning this decision are correlated and an advantage of one alternative in a specific parameter will result in a higher ranking for other alternatives too.

The outcomes rely on a great degree on responder's answers which may lead to misleading results since the answers are subjective. When analyzing the results and viewing the outcomes we can note that the parameters concerned with environmental issues were amongst the higher ranked parameters. However, recycling and reusing in Cyprus is still in its infancy as a practice of the Cypriot citizen. The social desirability bias can lead to wrong rankings of the parameters and to misleading outcomes. The above results however, are a good indication of the parameters rankings and even if we consider that the results are highly affected by the social desirability bias we can view them as an indication of society's point of view on the parameters.

The responders' views reveal great similarities on drafting the weights for the parameters. The differences occur mainly to each responder's familiarity. Familiarity combined with the educational background and occupation can give a more precise inside into each parameter's weight. However, in order to be more precise in the determination of the final weights, the input of all high level officials taking part in the decision making process should be taken into consideration.

References

[1] Huang, L, The global trend of green procurement. QualityMagazine 44 (8), 2008, pp. 36–40.

[2] M. Beccali, M. Cellura M. Mistretta, 2003,. Decision-making in energy planning. Application of the Electre method at regional level for the diffusion of renewable energy technology, Renewable Energy 28, 2003, pp. 2063–2087

[3] Peter Lund, Market penetration rates of new energy technologies, Energy Policy 34, 2006 pp. 3317–3326

[4] Bert J.M. de Vriesa,_, Detlef P. van Vuurenb, Monique M. Hoogwijka, Renewable energy sources: Their global potential for the first-half of the 21st century at a global level: An integrated approach, Energy Policy 35, 2007, pp. 2590–2610

[5] T.J. Hammons, Integrading Renewable Energy sources into European grids. Electrical Power and Energy Systems 20, 2008, pp. 462-475

[6] Skoglund, M. Leijon, A. Rehn, M. Lindahl, R. Waters, On the physics of power, energy and economics of renewable electric energy sources - Part II Renewable Energy 35, 2010, pp. 1735–1740

[7] D. Popp, I. Hascic N. Medhi, Technology and the diffusion of renewable energy, Energy Economics, 2010, Article in Press.

[8] C. Fischer and R. Newell, Environmental and Technology Policies for Climate Change and Renewable Energy Discussion Paper 04-05, resource for the future, 2004

[9] F. Evrendilek, C. Ertekin, Assessing the potential of renewable energy sources in Turkey Renewable Energy 28, 2003, pp. 2303–2315

[10] Y-C Shen, T.R. Grace, K-P Li, J.C. Yuan, An assessment of exploiting renewable energy sources with concerns of policy and technology Energy Policy 38, 2010, pp. 4604–4616

[11] I. Falconett, K. Nagasaka, Comparative analysis of support mechanisms for renewable energy technologies using probability distributions, Renewable Energy 35, 2010, pp. 1135–1144

[12] D. Weisser, Renewable and Sustainable Energy Reviews 8, 2004, pp. 101–127

[13] K. Venetsanos, P. Angelopoulou, T. Tsoutsos, Renewable energy sources project appraisal under uncertainty: the case of wind energy exploitation within a changing energy market environment,. Energy Policy 30, 2002, pp. 293–307.

[14] P. Komor, M. Bazilian, Renewable energy policy goals, programs, and technologies, Energy Policy 33, 2005, pp. 1873–1881

Windpower contribution to sustainable development in Brazil

Moana Simas[1,*], Sergio Pacca[2]

[1, 2] *University of São Paulo, São Paulo, Brazil*
** Corresponding author. Tel: +55 11 9236-4152, E-mail: moana@usp.br*

Abstract: Global electricity consumption rose exponentially over the last decades powered by fossil fueled thermal power plants. In comparison, Brazil relies on large hydroelectric plants to generate most of its electricity. Nevertheless, the share of thermal electricity generation in Brazil has increased because thermal power can balance the seasonality of the hydroelectric based system and is cost competitive. Regardless its great wind potential, the use of this technology in Brazil is still timid. The country had only 835 MW of installed windpower capacity until November 2010, or 0.75% of its total. An aggressive wind power deployment has been constrained by its cost until recently. However, windpower has potential to act as a complementary energy source to hydropower during dry seasons, and its development could displace thermal power plants. This paper aims to quantify potential greenhouse gas (GHG) emission reductions and jobs creation in three different scenarios of wind energy development up to 2019. In the baseline scenario, windpower will create over 93,000 jobs and reduce up to 96 million tones of CO_2 by 2019. In comparison, a massive windpower deployment scenario, , foresees the reduction of up to 176 million tones of CO2 and the generation of more than 225,000 jobs, most of them in the manufacturing sector. Therefore, wind power is an important alternative for promoting sustainable development in Brazil because it reduces GHG emissions and creates green jobs.

Keywords: *Wind power, Wind industry, Jobs, Sustainable development, Brazil*

1. Introduction

Over the past years concerns on climate change left the scientific and environmental spheres and got strong social and political engagement. The establishment of carbon markets, coupled with international oil price volatility, stimulated a rapid development of renewable energy (RE) generation technologies [1]. RE generation systems are free of harmful emissions and their energy sources are ubiquitous. In comparison to other RE windpower stands out because despite its small share in the global electricity market, it was subject to a rapid growth in recent years [2].

A turning point for windpower development in Brazil was the renewable energy incentive program (Proinfa) of the Ministry of Mines and Energy, established in 2002. However, the high energy costs for wind projects compared to traditional and other renewable energy sources precluded a massive deployment of this energy technology. The realization of dedicated windpower auctions in 2009 and 2010 attracted more projects, making windpower more competitive with traditional fossil fueled power plants.

The Brazilian electricity mix encloses a significant share of hydropower. In 2009, this energy source was responsible for 85% of the total domestic electricity supply [3]. Windpower development in Brazil is unique because in the Northeast region, which contains approximately 50% of the Brazilian wind resource, besides high average wind speeds, its availability complements the hydrologic cycle [4]. Therefore, windpower can be used to match the power loss during the hydropower offseason displacing thermal power plants that are currently balancing the electricity supply [5].

Windpower could contribute in various ways for sustainable development (SD). Developing a clean RE source helps maintaining the low greenhouse gas (GHG) emission factor of the Brazilian grid. Moreover, the establishment of a domestic industry brings in innovation and the development of new indigenous technologies, in addition to new job positions [6], which

become relevant as a response to economic crisis and sensible investments in RE must be evaluated according to this yardstick [7].

Nevertheless, the exploitation of the windpower potential depends on long term policies that facilitate the deployment of this RE source. Despite the recent success, the existing medium and long term official energy supply scenarios do not foresee a significant increase in the share of this energy source [8].

The current work aims to evaluate potential benefits and quantify the avoided emissions and the employment generation potential of windpower development in Brazil. Initially we carry on a brief review of the present state-of-the-art of windpower in Latin America (LA) and Brazil. Next, we assess the potential of this RE source in Brazil and we evaluate its contribution to SD and energy security in the country. Finally we compare different scenarios, which are based on official data and a massive windpower development vision.

2. Windpower in Brazil

Forecasts prepared by the Global Wind Energy Council (GWEC) consider LA as a promising windpower market due to its sizeable wind potential and increasing energy needs in the region [2]. In fact, since the beginning of the century, various countries in the region have implemented policies to support the development of RE, including windpower [9]. Over the last years, a timid growth was observed in the share of windpower in LA in comparison to Europe, North America, and Asia. In 2009, the installed capacity in LA doubled from 653 MW to 1,274 MW. However, until August 2010, only two countries were responsible for a significant share of windpower in LA. Brazil and Mexico were responsible for 44% and 29% of the total installed power in the region, respectively [10].

According to a recent GWEC assessment, Brazil has the largest windpower market potential in LA due to its large remaining wind resources, the ability to complement hydropower generation, and the possibility of hosting wind equipment manufacturing plants. Moreover, the country is considered as a future equipment supplier to the region [2].

Although the first wind turbine was installed in Brazil in 1992, in Fernando de Noronha Island [11] the share of windpower in the Brazilian matrix became noticeable only after 2006 with the first Proinfa results. A total of 54 wind projects totaling 1.4 GW of installed capacity were supported by the Program [12], which was instrumental to the expansion of windpower in Brazil. Presently, Proinfa supported facilities are responsible for 95% of the installed windpower capacity in Brazil, or 835 MW up to December 2010 and yet, its contribution corresponds to less than 1% of the total power capacity of the country.

Other milestone that has contributed to the installation of the wind manufacturing industry in the country was the 60% minimum requirement share of domestic equipments in wind projects [13].

Until 2009, the cost of the windpower based electricity was still a barrier to its expansion. The average electricity price of Proinfa projects in 2007 was in the range of $119 to $135 per MWh, depending on the individual capacity factor of each one [14]. Up to this point, windpower was considered unfeasible and not competitive despite the considerable potential that was revealed in the first national assessment at 143 GW [15].

The turning point was due to a conjunction of good policies and global market conditions. In 2009, the first auction fully dedicated to windpower was commissioned. Possibly due to great availability of wind resources in areas with low population density, the variation of the exchange rate, and the economic crisis in 2008-2009, a significant supply of equipment was available and both domestic and international companies were led to invest in the Brazilian market. In August 2010, a second windpower auction took place, along with other RE sources in which, wind energy competed with small hydroelectric plants (SHP) and biomass cogeneration projects. For the first time wind energy prices ($73/MWh) were below other RE prices [16]. Additional 6 GW of windpower projects were enabled to participate in the auction [17], and certainly most of these will be hired in future.

Considering the projects assisted by Proinfa and by the latest auctions, more than 5 GW of windpower will be added to the Brazilian grid by the end of 2013. It is more than the current 0.8 GW but still far away from the total indigenous potential. Currently the country uses around 0.5% of its potential. If windpower electricity trade in dedicated auctions persists, the expansion trend continues and costs decrease over time. In the future windpower could occupy a significant share of electricity generation and complement the current hydro-thermal system.

In comparison to major future hydroelectric projects in the Brazilian Amazon, windpower resources are closer to energy load areas along the coast line (figure 1), and major transmission lines of the national grid [18]. Therefore, transmission costs and losses associated with windpower are smaller than the ones associated with large expected hydroelectric projects.

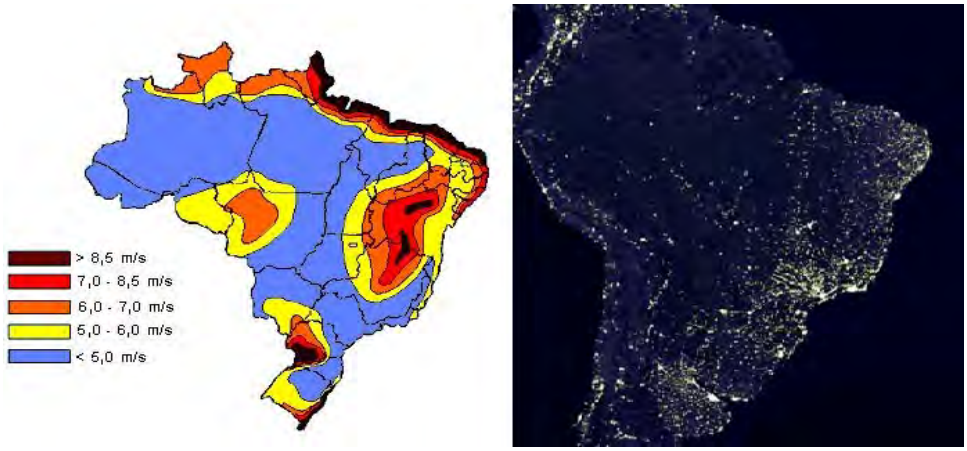

Fig. 1. Wind resources at a 50m height in Brazil [19] and its correlation to urban areas [20]

In summary, windpower that was considered unfeasible just one year ago is nowadays, not only competitive with other alternative energy sources, but also with traditional fossil fueled based electricity generation technologies. The turning point in Brazil was due to a conjunction of good policies and global market conditions. As a result, low impact windpower projects are a real supply option to meet power needs.

2.1. Complementarity between wind energy and hydroelectricity

RE face various difficulties such as high cost and resource intermittency. To increase the performance of RE, diversified complementary sources should be spatially and seasonally

combined. Traditionally, thermal generation plants are used to support systems based on renewable sources. In recent years, alternative energy sources have been contemplated for this role [21]. This phenomenon can be observed in Brazil.

The share of renewable sources in the Brazilian energy matrix corresponded to 47% in 2009, well above the world average. Moreover, hydropower comprises 85% of all electricity supply in the country, and additional 5% comes from other RE sources [3]. The hydroelectric system encloses several large reservoirs, capable of multi-year regulation.

Nevertheless, due to environmental concerns, most of the future dams in Amazonia will be run-of-river hydroelectric plants, with lower dams [8], leading to further reliance on climatic conditions. Thus, because wind resource availability in the Northeast of Brazil complements hydrologic regimes, it could lead to optimal use of reservoirs [4]. Indeed, windpower might displace part of the fossil fuel based electricity generation, reducing pollution and maintaining the high share of RE in the Brazilian matrix.

2.2. Economic benefits of windpower deployment

Both climate and RE policies will change the way economies are currently structured. Climate change consequences may negatively affect the economy in most countries, especially the ones in which the contribution of vulnerable sectors, such as agriculture, plays an important role [22].

Investing in a low-carbon economy creates risks and opportunities. On the one hand, a few studies show that in the long run subsides in RE in Germany have led to high costs with few or no benefits to the economy [23,24,25]; on the other hand, most economy-wide studies show positive economic outcomes from investing in low-carbon technologies [7,26,27].

According to Fankhauser et al (2008) [28], the most important benefit from climate and RE policies is innovation, which demands technical change adapted to a new market structure. The quest for new technologies and processes increases the demand for skilled labor, and countries that position themselves as leaders in low-carbon technologies might become key exporters. Over the past few years, Brazil has attracted various wind turbine manufacturers (e.g. Enercon, Impsa, GE), and due to the fast growing market, might become an exporter to other LA countries.

In periods of low economic growth, as the one seen in the financial crisis in 2008-2009, unemployment rates tend to grow, and so does the concern about job loss related to large amount of subsides invested in RE [7]. In fact, employment generation driven by RE promotion has been disputed, especially in the United States [28].

2.2.1. Green Jobs

According to the United Nations Environmental Programme (UNEP), green jobs are work in various activities that contribute to preserving or restoring environmental quality. Most studies reveal that RE is more labor-intensive than fossil fuel-based power generation [27,29,30]. Hence, the substitution of RE for fossil fuels leads to a positive net effect on employment. In Brazil, the creation of new jobs, due to windpower development, should be compared with the creation of jobs due to the development of concurrent alternatives such as hydro.

Nevertheless, based on the available information about green jobs generation, global employment in the RE sector was above 2.3 million in 2006. Brazil is one of the most significant RE employer, with 500,000 jobs on the biomass sector. In contrast, globally, wind energy generated 300,000 jobs up to 2006, and it is expected that employment in this sector will reach 2.1 million in 2030 [22]. Most of these jobs are located in manufacturing, according to the level of domestic production of equipments [30].

3. Methodology

To quantify GHG emissions reductions and job generation in the wind sector, we used a baseline scenario up to 2019, developed by the Ministry of Mines and Energy. Based on that scenario, and the recent growth of the wind energy market in Brazil, we developed two alternative scenarios, one moderate and one optimistic. The scenarios have the following characteristics (Figure 2):

a) Scenario A, or Baseline Scenario, foresees an installed wind capacity of 6 GW by the end of 2019 [8];
b) Scenario B, or Moderate Scenario, estimates a raise of 50% in the installed capacity up to the end of the period, resulting in 9 GW, based on expectations of the Brazilian Wind Energy Association (ABEEolica) of 10 GW in 2020 [31];
c) Scenario C, or Optimistic Scenario, predicts annual hiring of 1.5 GW in exclusive windpower auctions, to be installed from 2013 onwards. By the end of the period, 14 GW of windpower capacity will be commissioned.

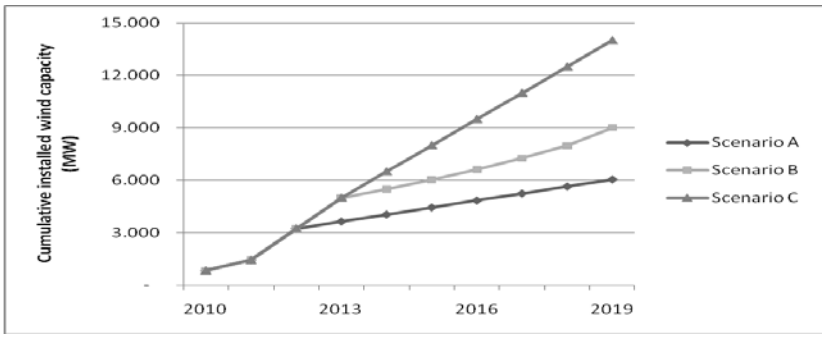

Fig. 2. Installed capacity in the years 2010-2019 in the three proposed scenarios

For estimating job creation, a multiplier provided by the Economical and Social Development Bank (BNDES) which estimates in 15 jobs/MW in manufacturing and construction and 0.4 jobs/MW in operation and maintenance of wind turbines [32]. These figures refer to total jobs, accounting direct and indirect employment over the supply chain.

For estimating potential GHG emission reduction, we considered that windpower displaces fossil fired power plants using natural gas and coal, the main thermal sources foreseen in the long-term national energy plan. Emission factors were taken from the International Energy Agency report, published in 2009 [33]. Emission reductions were estimated over the period between 2011 and 2020.

4. Results

Scenario A results in up to 96 million tons of CO_2 reductions between 2011 and 2020 and yields 93,850 jobs, out of which, 83% are in the manufacturing and installation of wind farms.

Scenario B emission reductions are 34% greater than scenario A, which mitigates up to 129 million tons of CO_2 and generates over 143,000 jobs, 85% in manufacturing and installation.

The most optimistic scenario foresees a reduction up to 176 million tons of CO_2 - 83% higher than in scenario A - and the employment of more than 225,000 people, 87% of them in manufacturing and installation.

According to the Brazilian Inventory of Anthropogenic Emissions and Removals of Greenhouse Gases, published in 2010 by the Ministry of Science and Technology, in 2005 the electricity generation, transmission and distribution emitted about 52 million tons of CO_2 [34]. Scenario A suppressed 28% of the baseline emissions, while the scenario C reduces annual emissions by 65% in 2020.

5. Conclusions

Wind energy is a source experiencing rapid growth worldwide. Following the trend, although timid, windpower market has rapidly developed in Brazil after Proinfa and mainly after the wind dedicated auctions of 2009 and 2010. Further expansion of the industry depends on continued support for RE in the country e.g. frequently auctions plus the inclusion of RE in medium and long term energy expansion plans.

This study shows the potential contributions that a significant expansion of wind capacity during this decade could bring to the country's sustainable development. The use of wind energy as a substitute for fossil-fuel power plants reduces up to 28% GHG annual emissions in the electricity sector in the year 2020, based on the year 2005, in the scenario proposed by the government, while a scenario of intense deployment displaces up to 65% of these emissions.

The development of the wind industry brings several benefits such as innovation and technology transfer, and possibly the emergence of Brazil as a production center for wind equipment in Latin America. Nevertheless the more significant effect is the creation of 93,000 to 226,000 green jobs by 2019.

References

[1] L. Bird, M. Bolinger, T. Gagliano, R. Wiser, M. Brown, B. Parsons, Policies and market factors driving wind power development in the United States, Energy Policy, 33, 2005, pp. 1397-1407.

[2] Global Wind Energy Council [GWEC], Global Wind 2009 Report, 2010.

[3] Empresa de Pesquisa Energética [EPE], Balanço Energético Nacional 2010 – Ano-base 2009 – Resultados preliminares, 2010. Available from <https://ben.epe.gov.br/>.

[4] R. M. Dutra, A. S. Szklo, Incentive policies for promoting Wind Power production in Brazil: Scenarios for the Alternative Energy Sources Incentive Program (PROINFA) under the New Brazilian electric power sector regulation, Renewable Energy, 33, 2008, pp. 65-76.

[5] A. Filgueiras, T. M. V. Silva, Wind energy in Brazil – present and future, Renewable and Sustainable Energy Reviews, 7, 2003, pp. 439-451.

[6] M. I. Blanco, G. Rodrigues, Direct employment in the Wind energy sector: An EU study, Energy Policy, 37, 2009, pp. 2847-2857.

[7] U. Lehr, J. Nitsch, M. Kratzat, C. Lutz, D. Edler, Renewable energy and employment in Germany, Energy Policy, 36, 2008, pp. 108-117.

[8] Empresa de Pesquisa Energética [EPE], Plano Decenal de Energia 2019, 2010. Available from <http://epe.gov.br/PDEE/Forms/EPEEstudo.aspx>.

[9] S. Arango, E. R. Larsen, The environmental paradox in generation: How South America is gradually becoming more dependent on thermal generation, Renewable and Sustainable Energy Reviews, 14, 2010, pp. 2956-2965.

[10] Global Wind Energy Council [GWEC], 2010 *apud* Windpower Monthly, Special Report: Windpower in Latin America, August 2010, p. 9.

[11] M. S. M. Araújo, M. A. V. de Freitas, Acceptance of renewable energy innovation in Brazil – case study of wind energy, Renewable and Sustainable Energy Reviews, 12, 2008, pp. 584-591.

[12] Eletrobrás, Programa de Incentivos às Fontes Alternativas de Energia — PROINFA: Relação de Empreendimentos Contratados, 2010. Available from <www.eletrobras.com>.

[13] Ministério de Minas e Energia [MME], Programa de Incentivo às Fontes Alternativas de Energia – PROINFA, 2010. Available from http://www.mme.gov.br/programas/proinfa.

[14] L. A. Lima, C. R. Bezerra Filho, Wind energy assessment and Wind farm simulation in Triunfo – Pernambuco, Brazil, Renewable Energy, 35, 2010, pp. 2705-2713.

[15] Centro de Pesquisas de Energia Elétrica [CEPEL], Atlas do Potencial Eólico Brasileiro, 2001, p. 43. Available from <www.cresesb.cepel.br>.

[16] Empresa de Pesquisa Energética [EPE], Leilões de Fontes Alternativas 2010, published on August 26, 2010. Available from <http://www.epe.gov.br/imprensa/PressReleases/20100826_1.pdf>.

[17] Empresa de Pesquisa Energética [EPE], EPE conclui habilitação técnica para Leilões de Fontes Alternativas, published on August 11, 2010. Available from <http://www.epe.gov.br/imprensa/PressReleases/20100811_1.pdf>.

[18] N. F. da Silva, L. P. Rosa, M. R. Araújo, The utilization of Wind energy in the Brazilian electric sector's expansion, Renewable and Sustainable Energy Reviews, 9, 2005, pp. 289-309.

[19] Centro Brasileiro de Energia Eólica [CBEE], Atlas Eólico do Brasil – Resultados preliminares, 1998.

[20] National Aeronautics and Space Administration [NASA], Astronomy picture of the day: Earth at night, published on November 27, 2000. Available from http://apod.nasa.gov/apod/ap001127.html.

[21] H. H. Chen, H. Kang, A. H. I. Lee, Strategic selection of suitable projects for hybrid solar-wind power generation systems, Renewable and Sustainable Energy Reviews, 14, 2010, pp. 413-421.

[22] UNEP/ILO/IOE/ITUC, Green Jobs: Towards Decent Work in a Sustainable, Low-Carbon World, 2008

[23] R. Küster, I. R. Ellersdorfer, U. Fahl, A CGE-analysis of energy policies considering labor market imperfections and technology specifications, Fondazione Eni Enrico Mattei, Working Paper 73, 2007.

[24] B. Hillebrand, H. G. Buttermann, J. M. Behringer, M. Bleuel, The expansion of renewable energies and employment effects in Germany, Energy Policy, 34, 2006, pp. 3484-3494.

[25] M. Fondel, N. Ritter, C. M. Schmidt, C. Vance, Economic impacts from the promotion of renewable energy technologies: The German experience, Energy Policy, 38, 2010, pp. 4048-4056.

[26] E. Jochem, R. Madlener, The forgotten benefits of climate change mitigation: Innovation, technological leapfrogging, employment and sustainable development, Working Paper OECD Working Party on Global and Structural Policy, 2003.

[27] M. Wei, S. Patadia, D. M. Kammen, Putting renewables and energy efficiency to work: How many jobs can the clean energy industry generate in the US? Energy Policy, 38, 2010, pp. 919-931.

[28] S. Fankhauser, F. Sehlleier, N. Stern, Climate change, innovation and jobs, Climate Policy, 8, 2008, pp. 421-429.

[39] J. Goldemberg, The case of renewable energies, Thematic Background Paper, International Conference for Renewable Energies, 2004.

[30] J. Rutovitz, A. Atherton, Energy sector jobs to 2030: A global analysis, Institute for Sustainable Futures, 2009. Available from <www.isf.uts.edu.au/>.

[31] Tony Danby, Interview with Brazilian wind industry vice president Lauro Fiuza, Windpower Monthly, published on August 13, 2010. Available from <http://www.windpowermonthly.com/news/1022252>.

[32] Banco Nacional de Desenvolvimento Econômico e Social [BNDES], Um panorama da indústria de bens de capital relacionados à energia eólica, BNDES Setorial, Rio de Janeiro, 29, 2009, pp. 229-278.

[33] International Energy Agency [IEA], CO_2 emissions from fuel combustion – Highlights, 2009, p. 14.

[34] Ministério de Ciência e Tecnologia [MCT], Inventário Brasileiro de Emissões Antrópicas por Fontes e Remoções por Sumidouros de Gases de Efeito Estufa não Controlados pelo Protocolo de Montreal – Parte 2, 2010. Available from <http://www.mct.gov.br/upd_blob/0214/214061.pdf>.

Wind Electricity Generation in Three States of India: Policies and Status

Sridhar Thyageswaran

Coimbatore Institute of Technology, Coimbatore-641014, India
**corresponding author: E-mail: t.sridhar@cit.edu.in*

Abstract: Many state governments in India rely on wind energy generation (WEG) to overcome chronic electricity shortages. This paper provides a citizen's view of WEG in India, in the backdrop of (a) the ever-rising national demand for primary energy, (b) the national electricity policy, and (c) wind energy policies in its three highly industrialized states – Tamil Nadu, Maharashtra, and Gujarat. Data from public domain such as the web-sites of government departments is used. Each state has increased its share of WEG with incentives for investment in this sector. The remarkable increase in installed capacity for WEG over the past years has not led to a proportionate increase in the kWh of wind power generated. The unbridled growth in this sector has pitted farmer activists against wind energy companies. A stampede for commissioning large wind farms can potentially destroy local ecosystems through changes in land use patterns. Few studies have been made in India to address such socio-economic concerns. Policies of doling out excessive incentives for MW-scale under-utilized wind farms that feed inefficient grids must be reconsidered. The people of India must receive direct tangible benefits from WEG for it to be a truly clean option of green energy for them.

Keywords: *Government, Policy, Status, Capacity, Utilization*

1. Introduction

Energy-starved India faces many challenges to sustain the remarkable growth in its GDP witnessed over the past decade. The consumption of manufactured products and services has sharply increased with a rise in disposable incomes, and its people expect better living conditions. Ambitious projects are underway to upgrade the nation's infrastructure, to transform India into another economic superpower. To meet these expectations, India's electricity generation capacity must be significantly increased from its current gross value of 164.8 GW [1]. Demand for primary commercial energy, which grew at an average annual rate of 6% during 1981-2001, is expected to grow more rapidly in the future [2].

1.1. Background

Energy policies world-wide are giving an increasing importance to clean sources of energy. A UN-panel has recommended an 85% cut in global greenhouse gas emissions (GHGE) from year-2000 levels to prevent the ill-effects of global warming. India currently produces about $1/4^{th}$ of the world's annual per capita emissions of 4.48 $t{\cdot}CO_2e$ (tonnes of CO_2 equivalent). During the last G-8 Summit, India agreed to work with other major economies in identifying a global goal for reducing GHGE [3]. Critics opine that India has compromised its policy of rejecting legally binding limits on its GHGE, and any caps would affect its future developmental plans. An 85% cut may force India to lower its emissions to < 0.2 $t{\cdot}CO_2e$.

1.1.1. India's energy and electricity demand scenario

With only 0.4% of the globe's proven reserves of crude, India accounts for 2.8% of the world's total oil consumption. To fuel a booming transport sector, 70% of its oil requirements are imported at huge costs to the exchequer. Large imports of LNG too are required to supplement indigenous production. As the numbers of vehicles in India grow, oil and LNG imports will follow suit. Food items and essential commodities became pricier when oil prices peaked in 2008. Unprecedented high inflation levels, attributed by policy makers to oil market economics and India's growth story, have stretched the budgets of many families.

Global petroleum price increases will pose concerns for India as she copes with her apparently insatiable demand for crude oil. Another facet of India's energy concerns is that growing numbers of new vehicle buyers are opting for compact electric vehicles (EV) which can be re-charged easily using a domestic electrical socket, and several manufacturers are catering to this new demand. The road use policy currently requires no license, registration, or taxes for such EV. With improved affordability, many Indians are buying air-conditioners and electrical appliances that were, not long ago, considered items of luxury. As the numbers of EV, TV-sets and washing machines in use grow, enormous demands are placed on India's already scarce power supply. Several Indian cities experience daily power outages, inconveniencing its citizens and many small and medium business enterprises.

1.1.2. National electricity policy (NEP)

India aims to augment its power generation capacity by 100 GW during the 10^{th} (2002-07) and 11^{th} Plan periods (2007-12), besides improving the annual per capita energy availability to 1 MWh [1]. In 2005, a national program was launched to electrify all villages and make electricity accessible to all households by 2012, through a mix of grid-connected, standalone systems and isolated lighting technologies. The NEP also aims to overcome chronic shortages in meeting peak electricity demand, besides ensuring efficient and reliable supply of power of specified standards at affordable prices.

1.1.3. The way forward with renewable energy

India has a large under-exploited potential for hydro-power generation, confined to certain geographical locations. She currently produces limited amounts of atomic energy for civilian use, due to her foreign policy leanings towards nuclear fuel exporting nations. Although the recent (and controversial) Indo-US nuclear agreement assures fuel supplies and reactor equipment, India has far to go before nuclear power overtakes fossil fuel power generation. To eradicate chronic electricity shortages, and compete in a carbon-sensitive global economy, India must go in for decentralized renewable energy (RE) technologies. Decentralization is essential for reducing transmission and distribution (T&D) losses in the existing grid networks. In the present centralized set-up, maintenance shut-downs, grid failures, and strikes impact vast areas of densely-populated India. Decentralization would also promote power production using locally available resources; such as biomass and wind [4].

1.2. Purpose of the study

Several policies have been formulated by successive governments that offer fiscal incentives to the users of RE. Over 25 years ago, India launched a national program for the assessment of her wind resources to promote WEG. As one outcome, 233 sites with an annual average wind power density (WPD) > 200 W/m^2 have been identified thus far. Many such sites are in the industrialized states of Tamil Nadu (TN), Maharashtra (MH) and Gujarat (GJ). Estimates suggest a gross potential of 48.6 GW of wind power for the entire country, with TN (5.5 GW), MH (4.6 GW), and GJ (10.6 GW) among other front-runners in this category [5].

There are many functional, and many more upcoming, WEG projects within India. This study attempts to assess (a) whether the current policies that aggressively promote WEG have yielded any significant addition to the overall power generation scenario, and (b) whether there has been any alleviation in chronic electricity shortages as a consequence. This study is limited to ascertaining the policies for, and status of, WEG in the states of TN, MH, and GJ, which have witnessed a boom in wind energy installations in the past few years. When

juxtaposed with other concurrent policies relating to power production and supply, it is hoped that a more holistic view of WEG within India would emerge.

1.3. Methodology of the study

Data has been sourced from the web-sites of central and state agencies involved in WEG, which in most cases tended to be in fair consonance. Reports on electricity shortages, energy policy and WEG in the print media (e.g. national-level newspapers), and reports by reputed non-governmental agencies, have been utilized. Data obtained from web-sites is referenced by mentioning the date of access (DoA).

2. State-wise electricity scenario and wind energy generation

2.1. In Tamil Nadu

Located in peninsular India, TN experiences both the monsoons: south-west and north-east. The state's annual per capita power consumption is nearly 1 MWh. Its major WEG sites are near the *Western Ghats* and (to a small extent) along its coastline. From 1986-93, 120 WEG units totaling 19.4 MW were installed. By 2009, the total installed capacity (IC) for WEG was 4.288 GW, against a gross power generation capacity of 10.214 GW [5, 6].

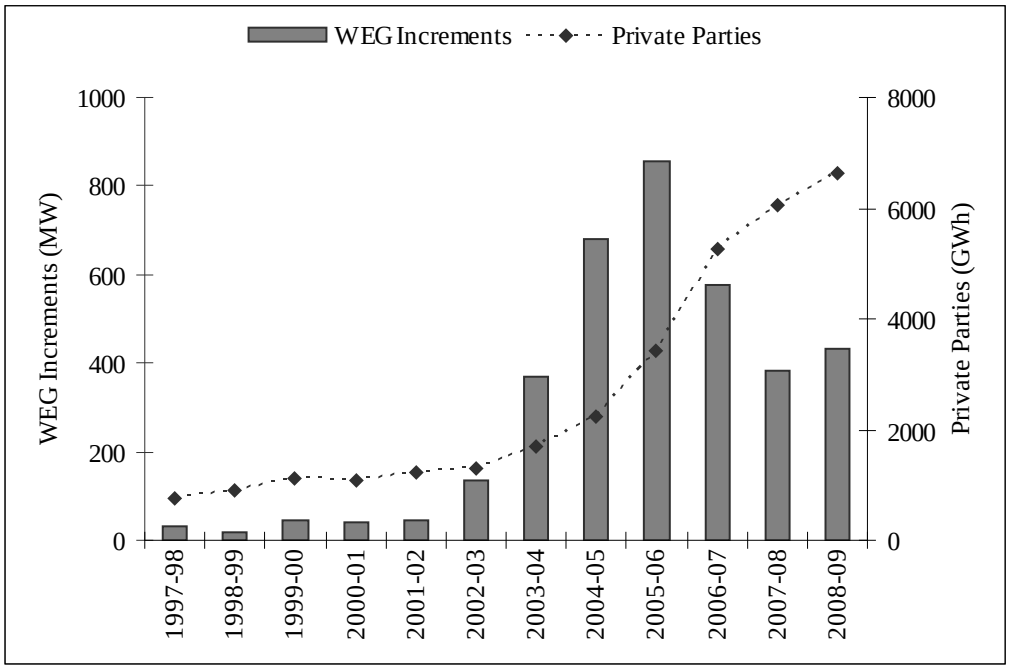

Fig. 1. Increments to WEG, and contributions to WEG by privately-owned units, in Tamil Nadu [6].

The state inducts independent power producers (IPP) into its WEG program. The state electricity board (TNEB) charges the IPP a fee of Rs. 2.575mn (million) per MW installed, plus more if creation and maintenance of T&D facilities by the TNEB is opted for. The IPP have to execute a 15-year power purchase agreement with the TNEB. In 1995-96, the IPP were paid Rs.2.25 per kWh by the state, with a 5% annual increment. Currently, Rs.3.39 is offered based on the recommendations of the state electricity regulatory commission (SERC), in view of the rising capital, interest and maintenance costs. Contributions to WEG from private parties are shown in Fig. 1. In recent years, there is a decline in the augmentation of TN's WEG capacity (see Fig. 1). Saturation of existing sites may be one reason. Investors have also shifted to MH and GJ which offer competitive prices (refer Table 1).

Table 1. State-wise wind electricity generation policies [7].

Policy Item	Tamil Nadu	Maharashtra	Gujarat
(a) Captive use of WEG	Allowed	Allowed	Allowed
(b) Wheeling charge rate	5%	2% + 5% for T&D losses	4%
(c) Buy-back (Rs./kWh)	3.39 (fixed)	Levelized tariff (refer [7])	3.56 (fixed)
(d) Third party sale	Allowed	Allowed	Allowed
(e) Other incentives	None	Off-take facilities, road, loans	Excise exemption

2.1.1. Electricity crisis in Tamil Nadu

Since late-2007, serious electricity shortages plague TN. Over the past decade, the state has pro-actively sanctioned investments into its information technology, automobile and manufacturing sectors, all clustered around its capital city Chennai. Spurred by such policy, demand for electricity has grown every year. It is reported that while the peak demand touched 9.5 GW on some days, the generation was only 6.7 GW [8]. According to industry experts the electricity crisis would continue for another 3-4 years [9]. To tide over shortages, the TNEB formulated policy changes to curtail consumption. A 40% cut imposed in the permitted power consumption by industries effectively crippled operations in many automobile ancillaries, farming and fishing industries all over TN. Textile industries are reportedly worst-hit, with machines requiring a 2-2.5 hour interval after restart to attain their full capacity, each time they are tripped by the erratic power supply. Automobile manufacturers are reported to have diverted their orders elsewhere, instead of sourcing products from within the state [10].

2.1.2. Status of wind electricity generation in Tamil Nadu

Plots of IC and "workable" (available) capacity (WC) for WEG on the 15th day of each month are shown in Fig. 2, based on daily TNEB reports [11].

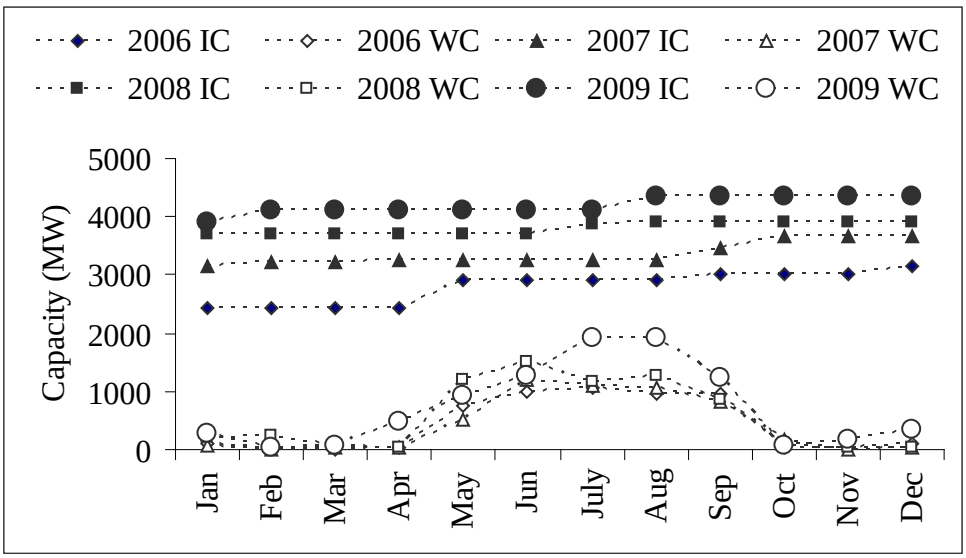

Fig. 2. WEG in Tamil Nadu: Monthly variations in installed and workable capacities [11].

Only one day's data was chosen as being representative for an entire month because several electronic reports were missing or were corrupted. Besides, the number of figures and data

being presented here had to be limited. The following can be observed from Fig. 2: (a) From Jan. 2006 to Dec. 2009, there has been an 80% increase in the IC for WEG, and (b) WEG is significantly more during May to Sep., compared to the other months of each year. The May-Sep. averaged generation was 950 MW (in 2006), 942 MW (2007), 1204 MW (2008), and 1451 MW (in 2009). When the above seasonal averages are normalized by the corresponding IC for WEG, the figures reveal that the capacity utilization factor (CUF) was 0.33 (in 2006), 0.29 (2007), 0.32 (2008), and 0.36 (in 2009). Although the IC has substantially increased during 2006-09, the available capacity has remained steady at roughly 33% of the IC, and that too during these five months in a year. During the remaining months, the CUF of the WEG units are extremely small numbers.

One reason for the low utilization could be the wind patterns: if monsoons fail during a particular year, it is the wind conditions that are blamed. But WEG in TN has suffered not just because the winds play truant. Even with favorable winds, only 5.25bn (billion) kWh could be generated, as against a possible 8.25bn kWh. It is claimed that due to inadequate evacuation facilities for wind electricity, losses to the tune of 0.8-0.9 GW arise, and that the TNEB prefers to shed load. In southern TN, out of the IC of 2.21 GW for WEG, only 1.2 GW are generated [12]. Due to the poor off-take policies, wind power producers in TN claim they have lost close to Rs.9bn, and Rs.45bn worth of their investments lie idle. The TNEB counters that the IPP install a unit every six months, but it takes nearly 12 months to build new transmission lines. Connecting remote wind farms to the grid is not easy when the lines have to pass over private lands.

2.2. In Maharashtra and Gujarat

2.2.1. Maharashtra

Within MH, thermal and hydro-power plants having a total IC of almost 10 GW are owned and operated by the state. Nearly 1.8 GW of power is produced by IPP. During the 1990s, the state was embroiled in a dispute over the Enron-Dabhol power project which was supposed to provide nearly 2 GW of gas-based power. That project did not take-off as expected. More recently, MH has faced acute shortages to the extent of 5-6 GW in meeting peak demands. The state has generally had a poor record of managing T&D losses in its electricity networks.

In an effort to showcase the viability of WEG, the state has installed demonstration projects totaling 11.09 MW. These and other favorable policies of the state towards WEG have attracted investments close to Rs.105bn. From a mere 190 MW in 2000-01, nearly 2.1 GW of wind power projects had been set up by 2010 [13]. Many older units of 250 kW operating at 30 m above ground (250 kW, 30 m) were replaced with 1 MW, 50 m units to exploit the higher WPD and realize lower investment costs per MW. Yearly increments to WEG capacity have been declining, though. The state added 545 MW in 2005-06, 485 MW in 2006-07, and 268 MW in 2007-08. It has targeted to add 600 MW to its WEG capacity each year from 2008-09, to achieve a cumulative capacity > 4.1 GW by 2012. A 1 GW wind farm, the largest of its kind, is currently under erection in the state.

To promote wind farm development, the govt. allows the use of state-owned wastelands which are leased out to private developers for 30 years at market rates. For other incentives offered, refer Table 1. But all is not well with wind power projects in MH, as revealed in a status paper which claims that though 1.76 GW of WEG units were installed by 2008, their combined annual generation was only 1.8bn kWh [14]. CUF increased from a mere 8.6% in 2000-01 to 11.7% in 2007-08, after touching 19.2% in 2003-04. That article also points out that investors are not interested in WEG and have merely invested in these facilities to gain

from the accelerated depreciation and tax benefits offered by the govt. There have been other independent reports of developers clashing with locals, over issues of land acquisition.

2.2.2. Gujarat

Thermal and hydro-power, are the mainstays for electricity generation in this state. The IC for power generation is 9.6 GW, with nearly 1.5 GW in projects under development. IPP provide close to 3.7 GW. The demand for power is expected to grow to 14 GW by 2011-12. This was one state that was comfortably placed as regards electricity supply [15], but the situation has changed due to coal and LNG shortages [16]. Endowed with a long coastline, GJ receives the south-west monsoon winds almost head-on. The state set up its first WEG demo unit in 1986. Later, more units were installed totaling 16.3 MW. In 1993 the state govt. declared an incentive program inviting private-sector participation, and from 1993-98 investments in WEG boosted the IC to 150 MW. In 2002, the govt. revealed a new policy, and WEG capacity grew by 220 MW till Nov. 2006, reaching 570 MW by Mar. 2007. It is reported that these units generated close to 455mn kWh in 2006-07. In 2007-08, new capacity additions of 616 MW were made and the total IC for WEG rose to 1.2 GW [17]. For the 11th Plan period, the state proposes to add nearly 4 GW of capacity to WEG. The Indian Railways plans to invest Rs.700mn for a 10.5 MW wind farm in the state. Power so generated is proposed to be wheeled away for railway electric traction – an unlikely prospect. Although the state now ranks next only to TN and MH in terms of the IC for WEG, the CUF of the units in operation are a measly 8% [18].

3. Discussion

On one hand, it may be said that the rapid growth in India's WEG sector has been facilitated by several incentive-laden policies which make investments into WEG very attractive for investors. On the other hand, it may be said that when incentives are geared to attract investments rather than improve the utilization of existing WEG units, such projects could become conduits to launder money. A study has alleged a nexus between monopolistic wind turbine makers and cash-rich investors, to avail of the huge (80%) depreciation benefits offered to WEG units during their first year of operation besides tax holidays and a slew of other duty cuts [14]. If this were the case, investors would care less whether the installations have poor CUF, or whether they remain idle. The same report also claims that business dealings in wind energy are opaque, and that the true costs of capital are unclear. Instead of reducing, based on economies of scale, costs of WEG units have reportedly gone up from Rs.40mn to Rs.60mn per MW over the years. Agreements exist to sell wind electricity to grids, third parties, or use for own consumption. Very few records are available in the public domain on how much wind power is actually delivered to the grid. Rules prescribe a certain percentage of wind electricity produced to be supplied to a grid, but enforcement is lax and the miniscule quotas are usually exhausted by other sources of green energy. The SERCs must make daily reporting of WEG mandatory for all IPP and state electricity boards.

Land acquisition for wind farming has affected many vulnerable farmers reeling under repeated crop failures and loans from usurers, and families coping with farmer suicides. There are reports of coercive methods being adopted for land grabbing by middle-men representing wind farm developers [19]. Villagers are promised monetary compensation and other benefits in return, but most promises never materialize and the sellers find their position a lot worse afterwards. Govt. policies must insure that land, instead of being sold, is leased out to wind farm companies and fair market rents are paid to the lessors. Large-scale removal of trees and forest cover to erect wind farms affects the livelihood of villagers dependent on

these natural resources. They languish in poverty and darkness with noisy wind turbines for company, and whatever little power the units generate is wheeled away to the cities.

Besides rapid industrialization, other factors contribute significantly to the India's widening electricity deficit. Many political parties in India, at the centre and in the states, have used provision of free electricity for farming as a poll plank. Income from agriculture qualifies for federal income-tax relief too. Such policies have led to write-offs of huge debts owed by farmers to the state electricity boards. The provision of free power for farming has an adverse cascading effect. During droughts, farmers use electricity to pump out ground-water for irrigation. These pumps run endlessly, deplete the ground-water table and increase soil salinity. With power available for free, shortages notwithstanding, farmers neither conserve the precious ground-water nor the electricity. Illegal connections, faulty meters, lax monitoring, and T&D losses allow for gross under-recoveries of electricity consumed. Revenue losses stifle genuine investments in the power sector and promote an indifference towards electricity conservation. In many instances, power is simply wasted when consumers deliberately choose not to switch off. Extravagant lighting for political gatherings, cine-artiste shows, mega-bucks night-time cricket tournaments, etc. has become a routine affair.

Instead of viewing WEG as a panacea for their ailing power sector, Governments could frame policies to award discounts on electricity bills to consumers who (a) reduce their electricity usage, and (b) maintain it thereafter within a certain threshold. Such incentives can be offered with ease since billing is nowadays computerized, allowing for the processing of long-term electricity usage patterns. Governments must implement policies that offer cash discounts for the purchase of CFLs and LEDs for domestic lighting. Such products continue to be prohibitively expensive for many, who opt instead for inefficient incandescent bulbs.

4. Conclusions

Policies for, and status of, wind electricity generation (WEG) in three major states of India are explored. The policies of the various state governments to promote WEG have led to a spree of investments in this sector. But the spectacular increase witnessed in the recent past in the installed capacity for WEG has not necessarily translated into a mitigation of electricity shortages in these states. Existing units face problems relating to under-evacuation and grid integration, and operate with poor capacity utilization factors. Very little credible information exists in the public domain on the actual power delivered by wind farms to the electricity grids, the true costs incurred, and the incomes generated. The liberal incentives offered are possibly being misused by investors for pecuniary benefit. In order to change this situation for the better, governments must revise their relevant wind energy policies to remove loop-holes. Instead of promoting a headlong rush into WEG projects with further sops, govt. policies must reward generation and optimum utilization of the existing units. One way would be to increase and strictly regulate the percentage of wind power supplied to the grids by the IPP, and not to yield to demands for more concessions from the wind energy lobby. Novel applications of wind electricity to suit Indian requirements must be thought of. Instead of MW-scale grid-connected units, smaller-scale solar-assisted decentralized WEG units that can be installed at community levels must be promoted. Electricity so produced can be used to provide metered back-up for residential use, street lighting, or water supply. The use of wind electricity for decentralized applications such as battery-charging, water treatment and purification, and production of compressed air must be explored. WEG must be matched properly with demands of an appropriate kind, in order to maximize the benefits.

References

[1] Ministry of Power, Govt. of India, (DoA: Oct. 20, 2010) at www.powermin.nic.in/indian_electricity_scenario/introduction.htm, www.powermin.nic.in/whats_new/national_electricity_policy.htm.

[2] Planning Commission, Govt. of India, (DoA: Oct. 20, 2010) at www.planningcommission.gov.in/plans/planrel/fiveyr/10th/volume2/v2_ch7_3.pdf, www.planningcommission.gov.in/plans/planrel/fiveyr/11th/11_v3/11th_vol3.pdf, www.planningcommission.gov.in/reports/genrep/rep_intengy.pdf.

[3] R. Ramachandran, Climate change and the Indian stand, The Hindu, Jul. 28, 2009.

[4] P. Purohit, and A. Michaelowa, Potential of wind power projects under the Clean Development Mechanism in India, Carbon Balance and Management, 2(8) (doi: 10.1186/1750-0680-2-8).

[5] Centre for Wind Energy Technology, (DoA: Oct. 21, 2010) at www.cwet.tn.nic.in.

[6] Tamil Nadu Electricity Board, (DoA: Oct. 21, 2010) at www.tneb.in.

[7] Wind Power India, (DoA: Oct. 20, 2010) at www.windpowerindia.com/govtinc.html.

[8] V. P. Abhir, South India reeling under a power crisis, IBN-Live, Nov. 26, 2008.

[9] R. Ashok, Power crisis to continue for 3-4 years: CII study, Business Line, Sep. 27, 2008.

[10] Power Crisis has hit farming, industry hard, The Hindu, Sep. 01, 2008.

[11] TNEB Reports, Daily online reports, at http://tnebldc.org/tnercreports.htm.

[12] M. Allirajan, Gone with the wind, Business World, Feb. 01, 2008.

[13] Maharashtra Energy Development Authority, (DoA: Oct. 26, 2010) at http://www.mahaurja.com.

[14] N. Jamwal, and S. Lakhanpal, Fanning an alternative, Down To Earth, Centre for Science and Environment, New Delhi, 17(6), 2008.

[15] V. Pandit, Gujarat: Energizing the nation with power, natural gas, Business Line, Oct. 09, 2007.

[16] C. H. Hansen, Bottom-up electricity reform using industrial captive generation: A case study of Gujarat, India, Oxford Institute for Energy Studies, Mar. 2008, pp. 9.

[17] Gujarat Energy Development Agency, (DoA: Oct. 26, 2010) at www.geda.org.in (for wind related articles refer to www.geda.org.in/wind/wind_power.htm).

[18] Govt. fumbles for ‘power’ as wind energy is left untapped, Express News Service, Sep. 16, 2008.

[19] M. Suchitra, Windmills on tribal land, Down to Earth, Centre for Science and Environment, New Delhi, 19(7), 2010.

Managing the diffusion and adoption of renewable energy technologies in Nigeria

Hakeem A. Bada*

University of Vaasa, Vaasa, Finland
** Corresponding author. Tel: +358445517141, E-mail:hakeem.bada@uwasa.fi*

Abstract: Increments in the price of oil in 1970s have brought many countries in search of alternative energy sources which will not cause harm to their entire environment as like fossil fuel does. The only available energy source that is capable of providing perhaps without harm to the environment is renewable energy. Renewable energies are important to an energy supply portfolio as they contribute to the world energy supply security, as well as to reducing dependency on the use of fossil fuel. They also contribute to mitigating greenhouse gases. The diffusion and adoption of a new technology such as renewable energy technologies needs the proper understanding of the environment as well as the existing sources of energy in the area. This paper investigates the current status of energy production and the potential of renewable resources in Nigeria. These investigations were carried out by analyzing the available policies and barriers toward the promotion of using renewable energy technologies in Nigeria. These barriers include political issues, environmental issues, technical issues, as well as economic and social issues.

Keywords: *Innovation, Renewable energy, Diffusion and adoption.*

1. Introduction

Nigeria is one of the countries with high potential in energy resources; the country is blessed with both fossil energy resources such as natural gas, coal and crude oil, and renewable energy resources such as biogas, biomass, solar energy and many more.

Energy is claimed to be one of the essential inputs for socio-economic development (Brew-Hammond, 2010). It is then clear that the connection between energy and the millennium development goals (Parcaco and Takada, 2004) make it more necessary to address the issue of energy problem in Nigeria, most especially electricity generation and distribution (Brew-Hammond, 2010; Karekezi, and Majoro, 2002; Modi, 2004; Porcaro and Takada, 2004). Therefore, the provision of a constant power supply is the sign of a developed economy. A nation with unstable power supply risks keeps losing potential investors and development (Okoro and Chikuni, 2007). Nigeria is blessed with natural resources; therefore every Nigerian should have access to electricity. For this to materialize there is only one question which needs a quick answer: how can it become reality? The inability of the Power holding of Nigeria to supply Nigerians with adequate electricity has severely affected many sectors of the economy such as manufacturing industries, mining, agricultural production, and households.

This paper will be looking at (1) the current status of energy production in Nigeria, most especially electricity. The policies promulgated by the energy commission of Nigeria will be reviewed, to see which of these policies are in support of the diffusion and adoption of renewable energy in Nigeria. (2) Potential of renewable energy resources in Nigeria will also be reviewed. Nigeria is a country which is blessed with abundant natural resources which includes renewable energy resources such as biomass, solar, biogas, etc. With all these resources in place, Nigerian still depends heavily on the use of fossil fuel for electricity generation.

2. Genesis of electricity production in Nigeria

Electricity generation in Nigeria dates back to 1896, which was the first time of generating electricity in the city of Lagos with a capacity of 60KW. After the first generation, an arm of the then government was established under the jurisdiction of the public works department (PWD) with the responsibility of electricity supply in Lagos. Later, 1950 a central body called the Electricity Corporation of Nigeria (ECN) was established in order to integrate electricity power development and make it more effective (Okoro and Chikuni, 2007).

In complement the work of Electricity Corporation of Nigeria, a new body called Niger Dam Authority (NDA) in charge of dam construction and maintenance, both on the river Niger and in other places within the country. In 1972, both ECN and NDA were merged to become an entity called National Electric Power Authority (NEPA) (Okoro and Chikuni, 2007). The two organizations were merged in the hope that their merger would result in the improvement of production and distribution of electricity power supply throughout the whole country, which would reduce excessive spending on both organizations; and that it would result in the utilization of available resources such as human, financial and other to the electricity supply throughout the country (Okoro and Chikuni, 2007:52).

The above two bodies then metamorphosed into the National Electric Power Authority (NEPA) which then later transformed into the Power Holding Company of Nigeria (PHCN). The Power Sector Reform Bill was signed into law in March 2005 to enable private companies' participation in electricity generation, transmission, and distribution (Okoro and Chikuni, 2007:52). The bill split PHCN into eleven distribution firms, six generating companies, and a transmission company, all of which will be privatized. The bill is yet to become operational due to opposition from the labour unions.

The Energy Commission of Nigeria (ECN) is the only apex government organ empowered to carry out overall energy sector planning and policy implementation, as well as to promote the diversification of energy resources through the development and optimal utilization of all, including the introduction of new and alternative energy resources like solar, wind, biomass and nuclear energy (The Energy Commission of Nigeria, 2010).

2.1. Position of energy in Nigeria

Nigeria is an energy rich country as stated above, also rich in human resources with a total population of 140.4 million by the 2006 population census, with an annual population growth rate of about 2.8% (Akinbami, Ilori, Oyebisi, Akinwunmi, and Adeoti, 2001). Logically, with all of these abundant energy resources, it is expected that Nigerians should have sufficient and sustainable energy, but the reverse is the case. The national energy use trend reveals a dichotomy between urban and rural households, due to the nature of energy forms consumed in Nigeria, specifically commercial energy such as petroleum products, natural gas, coal, and electricity, and non-commercial or traditional energy, like fuelwood and other biomass.

The Manufacturer Association of Nigeria (MAN) claims that about 60 million Nigerians now own power generating sets for their electricity, using generators of varying sizes with diesel as their sources of fuel, which is not environmentally friendly. The same numbers of people spend a staggering N1.56 trillion ($13.35million) to fuel their generators annually (The Energy Commission of Nigeria, 2010). In his own contribution, Mr. Steven Dimitryer a senior private specialist at the World Bank notes that 'Nigeria experiences the worst electricity crisis among its contemporaries, which underscores the nightmarish generation, distribution and supply in the country' (The Energy Commission of Nigeria, 2010). Electricity is the most

important infrastructure bottleneck in Nigeria, most of the industries in Nigeria experience power outage and about 85% of these industries own generators as an alternative source of power generation (ECN, 2010). Presently, about 10% of rural households and 40% of the country's total population have access to electricity in Nigeria (Mbendi.com, 2011).

3. Renewable energy resources in Nigeria

With respect to this paper, the renewable energy sources in Nigeria that will be considered are hydropower, solar energy, wind, and biomass energy.

3.1. Hydropower

Like every other renewable energy source, hydropower has tremendously contributed to the world energy supplies. The current world capacity of hydropower in 2004 was 2810 TWh and is projected to be 4903 TWh by 2030 with growth of 1.8% per year, although the share will still remain at 2% of the world energy supplied (IEA, 2007).

There is high potential for hydroelectricity generation in Nigeria: the current hydropower plants contributed about 29% of electricity generation to the nation total power supply (Aliu and Elegba, 1990; Sambo, 2005), while all the rest is coming from fossil fuels. The resources for hydroelectricity, unlike other types of renewable energy resources, require only a flow of power over a period of time added up to an annual energy (Boyle, 2004). The availability of rivers and natural falls mean that Nigeria has the potential to provide the needed amount of electricity to revitalize the economy. Total hydropower resources potential exploitable in Nigeria is estimated to be 11,000MW (Sambo, 2005).

3.2. Small hydropower

Small hydropower in Nigeria refers to small hydropower generation with a capacity of 1-10 MW. Nigeria is blessed with large rivers along with some natural falls. Nigeria's rivers have the capacity to generate about 11,000 MW of electricity, of which 19% are currently being developed. Existing hydropower plants in the country need rehabilitation due to lack of adequate maintenance (Aliyu and Elegba, 1990; ECN, 2010). There is no standard definition which size of hydropower is small or large, but Table 1 shows classification of ranges of hydropower along with their capacity.

Table 1. Classification of Hydropower Range (adopted from Aliyu and Elegba,1990) .

Range of Hydropower	Capacity of Range (MW)
Large	>100
Medium	15-100
Small	1-15
Mini	0.5-1
Micro	<.05

3.3. Solar energy

Nigeria is a country with abundant solar resources with an annual average daily sunshine of 6.26 hours, ranging between 3.5 hours along the coastal area and about 9.0 hours on the far northern border (Bala, Ojosu, and Umar, 2000). Approximately 5.08 x 1012 KWh of energy can be received in Nigeria per day from the sun with an efficiency of 5%. This amount of energy is able to produce 2.54 x 106 MWh of electricity from solar energy (Sambo, 2005). Solar energy can be utilized in every part of the country, most especially for rural domestic use and for power supply to remote areas where electricity is still not provided.

3.4. Wind energy

Wind is another free gift to the nation. Its intensity depends on the location of the country. Nigeria is situated within a low to moderate wind zone. Windmills were successfully used in the 1960s, especially in the northern part of Nigeria such as Dundaye village in Sokoto State for pumping water from the borehole. They were also used in Garo, near Kano, for supplying water to notable places such as a school, dispensary and to some houses (Anyanwu and Iwuagwu, 1994). All of these old windmills still exist in their different locations, but they are not working any more due to poor maintenance.

3.5. Biomass energy

Resources for biomass in Nigeria can be found in wood, animal waste obtained from agriculture, forestry, municipal and industrial activities and also from aquatic biomass, forage grasses and shrubs. Fuelwood constitutes 37% of the total energy demand in Nigeria. 95% of this fuelwood is consumed by households (Energy Commission of Nigeria, 2005). Figure 1 below indicates the share of fuelwood compared with other types of energy sources.

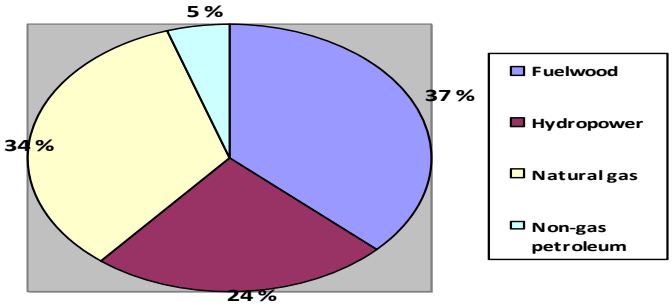

Figure 1. Share of fuelwood compared with other types of energy sources. Data source (ECN, 2005).

3.5.1. Biogas

The amount of waste generated in urban areas alone is capable of generating substantial electricity for the populace within the environment. This waste can be transformed into biogas. Biogas is a mixture of about 60 to 70% methane (CH_4), 23 to 38% carbon dioxide (CO_2), about 2% hydrogen (H_2) and some traces of hydrogen sulphide (H_2S). Biogas is produced by a process known as anaerobic digestion in the absent of oxygen. This gas can be used in cooking and lighting, as well as for agricultural and industrial production.

The use of biogas is fast spreading all over developing nations, particularly in countries like China, Indian, Taiwan, and Philippines (Akinbami et al., 2001). Biogas production units do exist in the sub-Saharan Africa, with a capacity ranging from less than 100 cubic metres to a larger digester of production capacity of greater than 100 cubic metres (Akinbami, et al., 2001).

The use of biogas is not yet pronounced in Nigeria, but some notable work on it is in progress, which is still at the research stage. The current capacity of digesters in Nigeria ranges between 10-20 cubic metres. These are produced by the Sokoto Energy Research Centre (SERC) and use cow dung, human excreta and piggery waste for biogas production (ECN, 2005; Akinbami, 2001).

4. Managing renewable energy technology in Nigeria

The development of a nation's economy is said to be an indication of how well energy is utilized along with the conversion of available energy resources to useful energy technologies

(Sambo, 2005). In order to ensure optimal, adequate, reliable and secure supply of energy to, and its efficient utilization in the country, it is important to put in place a harmonized, articulate and comprehensive energy policy to support the appropriate energy technologies for the country.

Before now, existing policies in the energy sector have been those of the separate energy sub-sector, that is, electricity, oil and gas and solid minerals. There have also been energy-connected policies developed in sub-sectors whose activities are strongly dependent on those in the energy sector. These include transportation, agriculture, science and technology and environment, among others. The sub-sectoral policies, however, reflect the individual sub-sectoral perspectives. ECN, (2003) realized that there is a need to have an integrated energy policy which will guide future energy related sub-sectoral policy developments, in order to avoid policy conflicts which may otherwise arise.

4.1. Nigeria's energy policy and objectives

The overall driving force of the energy policy objectives in Nigeria has been the optimal utilization of the nation's energy resources for sustainable development. These policy objectives and implementation have been carefully defined with the notion that energy is crucial to developmental goals and that government has a prime role in meeting the energy challenges facing the nation, most especially the electricity stumbling block. In addition, the nation's dependence on oil can be reduced through the diversification of the nation's other energy sources, aggressive research, development and demonstration (RD & D), human resources development and many more. Each of the energy sources in Nigeria has its own policy which forms the overall policy of the nation.

4.2. National Policy position toward the diffusion and adoption of renewable energy in Nigeria

Stated below are some of the significant elements in national policy toward diffusion and adoption of renewable energy in Nigeria (ECN, 2003).

i. Harnessing hydropower potential available in country for electricity generation, also paying attention to the development of the mini and micro hydropower schemes.

ii. Exploitation of the hydropower resources in an environmentally sustainable manner and encouraging private sectors and indigenous participation in hydropower development.

iii. Promoting the use of alternative energy sources to fuelwood by developing an appropriate technology to use wood chips rather than the direct use of wood.

iv. Aggressive use and integration of solar energy into the nation's energy will be done, by developing the nation's capability in the utilization of solar energy as well as monitoring worldwide development of solar energy technology. To enable the use of solar energy as complementary energy resources in the rural and urban areas.

v. Developing wind energy resources and integrating them with other energy resources to form a balanced energy mix. It will as well involve taking necessary measures to ensure that wind energy is harnessed at a sustainable cost to both suppliers and consumers in the rural areas.

vi. Developing local capability in wind energy technology and applying it in areas where it is technically and economically feasible.

vii. Harnessing non-fuelwood biomass energy resources and integrating them with other energy resources. Also promoting efficient methods in the use of biomass energy resources.

Increasing the percentage of the contribution of hydro electricity to the total energy mix is yet to be achieved in the country; the survey carried out in harnessing hydropower is yet to be put into effect. Most of the rural areas in the country are still experiencing blackout due to the absence of electricity, while the current hydropower has in one way or the other contributed to ecosystem damage preventing fishermen from getting their daily bread. Furthermore, the maintenance of those available hydro electricity generating plants in the country is far below standard as a result of poor management of the whole system.

About 60% of Nigeria's population is highly dependent on fuelwood for cooking and other domestic uses. The use of fuelwood arises as a result of lack of appropriate cooking methods. This is not limited to the rural environment alone: even people in the urban area use it as well. It is discerned that the rate of fuelwood consumption far exceeds the replenishing rate, which has resulted in environmental setback. Therefore, the use of innovative ways of cooking is urgently needed both in the rural areas and the urban areas in order to curb the results of global warming.

Rogers, (1995:5) defined diffusion as the process by which an innovation is communicated through certain channels over time among the members of a social system. The rate of diffusion and adoption of renewable energy is very low in Nigeria, as a result of heavy dependence on the use of fossil fuel, since the nation's economy solely depends on the exportation of crude oil and gas. Innovation in the Nigeria energy system needs foreign investors to boost her energy sector: Nigeria's position as one of the lowest consumers of electric power per capita in Africa remains a big issue. Figure 2 shows Nigeria consumption of electric power per capita ranking among some selected countries in Africa.

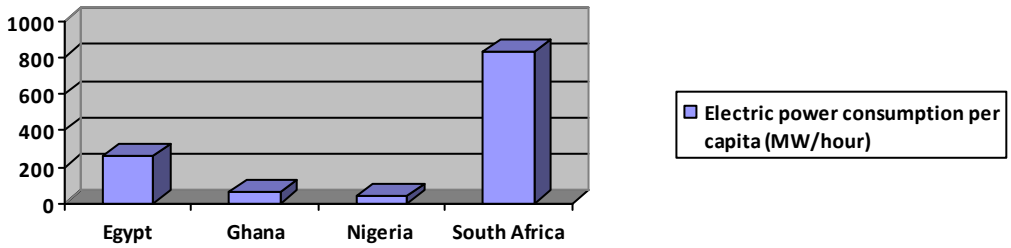

Figure 2. Per capita electric power consumption of some selected countries

4.3. Barriers to diffusion of renewable energy technologies (RETs)

Painuly, (2001:75) argues that there are many barriers 'that have prevented penetration of RETs'; some are discuss below.

4.3.1. Political issues

First and foremost, there should be stability and transparency in the political environment of Nigeria, with the notion of creating a country of a stable political atmosphere which will attract investors. Complete reform of the current policy on electricity generation and distribution should be overhauled to create a fair way for the whole group of stakeholders in

the emerging power sectors within and outside Nigeria. Right now, there are some parts of the country which urgently need attention when it comes to investment, such as the Niger Delta area. Establishing viable projects within these areas will not be an easy task, since this region is somehow controlled by the rebels. Other parts of the country with similar political instability issues should be addressed in order to give ways to investors.

4.3.2. Environmental issues

When planning for the type of innovation for diffusion and adoption, the government should consider the environmental impacts of the technology before adoption. Also the area where it will be used should be taken into consideration: for example a community with less people should not be allowed to have a gigantic project unless the community is a supply power for other areas. More so, a city with high level of industrial waste should be denied of having similar project to avoid polluting the city together with the inhabitants. Also the use of heavy duty generator fuel with diesel should be discouraged.

4.3.3. Technical issues

The worst problems facing most of the power plants in Nigeria at present are technical issues. Inadequate maintenance of existing power plants has led to an insufficient electricity supply. There is a lack of standards, codes, and certification. The educational system of the country is too broad and the curriculums are not tailored to the need of the environment at large.

4.3.4. Economic and social issues

It is very appropriate to provide substantial capital for the promotion of renewable energy systems in Nigeria, if the government really wants consumers to have access to electricity that is affordable and available. This capital should have a defined time frame to ensure efficiency improvement in renewable energy technology and the enhancement of the nation's power industries. Therefore, in order to make electricity available to consumer, it will require utilization of the renewable energy resources in the country.

5. Conclusion

Energy is as an essential commodity for nation building, Nigerians deserve a constant supply of electricity. This paper has highlighted the genesis of electricity in Nigeria, as well as the potential of renewable energy in the country. It was identified that about N1.56 trillion ($13.35million) were spent on the fueling of generators as a result of lack of available sustainable electric power to both private and corporate users. Dependence on the use of fossil fuel couple with low per capita consumption of electricity and barriers have a contributed greatly to the low rate of diffusion and adoption of renewable energy technologies in Nigeria

References

[1] U. O. Aliyu and S. B. Elegba, Prospect for small hydropower development for rural applications in Nigeria. Nigeria Journal of Renewable Energy, 1990, vol.1, pp.74 – 86.

[2] E.E. Anyanwu and C.J. Iwuagwu, Wind Characteristics and Energy Potentials for Owerri, Nigeria. Renewable energy, 1994, vol. 6. No. 2, pp. 125-128.

[3] J-F. K. Akinbami, M. O. Ilori, T. O. Oyebisi,, I. O.Akinwunmi, and O. Adeoti, Biogas Energy Use in Nigeria Current Status, Future Prospect and Policy Implications. Renewable and Sustainable Energy Reviews, 2001, vol. 5, pp.97-112.

[4] E.J. Bala, O.J. Ojosu and I.H. Umar Government Policy and Programmes on the Deveolopment of Solar-PV Sub-sector in Nigeria, 2000.

[5] G. Boyle, Renewable Energy: power for sustainable future, 2004.

[6] A. Brew-Hammond, Energy access in Africa: Challenges ahead. Energy Policy, 2010, vol.88 pp. 2291–230.

[7] Energy commission of Nigeria, National Energy policy, Federal Government of Nigeria, April 2003.

[8] Energy commission of Nigeria, Renewable Energy Master Plan, 2005, November.

[9] S. Karekezi, and L. Majoro, (2002). Improving modern energy strategies for rural Africa's urban poor. Energy Policy 30 (11-12), 1059-1069.

[10] O.I. Okoro, and E. Chikuni, Power sector reforms in Nigeria: Opportunities and challenges. Journal of Energy Southern Africa, 2007, vol. 18 No 3.

[11] Z. Peidong, Y. Yanli, S. Jin, Z. Yonghong, W. lisheng, and L. Xinrong, Opportunities and challenges for renewable energy policy in China. Renewable and Sustainable Energy Reviews, 2007, 13 pp. 439-449.

[12] J. Porcaco, M. Takada, In: Archiving the Millennium Development Goals: The Role of Energy Services- Case studies from Brazil, Mali and the Philippines, UNDP, 2004, New York.

[13] J.P. Painuly, Barriers to renewable energy penetration; a framework for analysis. Renewable Energy 24 (2001) 73-89.

[14] E.M. Rogers, Diffusion of innovations, The Free Press, NY, Fourth edition, 1995, ISBN 0-02-926671-8.

[15] A.U. Sambo, Renewable Energy for Rural Development: The Nigerian Perspective, ISESCO Science and Technology Vision, 2005, Vol. 1, pp. 12-22.

[16] V. Modi, In: Energy Service for the poor, Commercial paper for the millennium project Task Force 1. Mimeo, Columbia University, 2004, New York.

[17] Mbendi.com, http://www.mbendi.com/indy/powr/af/ng/p0005.htm, 2011.

Shifting the policy paradigm of solar photovoltaic and other renewable energy technologies supply in rural Ghana

Simon Bawakyillenuo[1,*]

[1] *Institute of Statistical, Social and Economic Research, University of Ghana, Accra, Ghana*
** Corresponding author. Tel: +233275224939, E-mail: bawasius@hotmail.com*

Abstract: Energy, inter alia, other structures, have been sine qua non to socio-economic development, enhancement of rural production and food security, improvements in healthcare and standards of living in human societies. Currently, while energy can help extricate rural societies in the developing world from poverty and augment development, they can only be realised through the implementation of effective energy policy approaches. Employing instruments from both qualitative and quantitative methods to analyse data gathered from two solar PV projects' sites in Ghana as case studies, the paper explores the interface between the policy approaches that have been used for the supply of electricity to rural Ghana, and the energy needs of these rural communities. The paper concludes that, due to the prevalence of poverty among rural societies in Ghana and other parts of the developing world, energisation and not electrification, is the optimal policy paradigm that will underpin rural socio-economic development and the adoption of renewable energy technologies (RETs).

Keywords: *Rural Electrification, Renewable Policy, Energisation*

1. Introduction

The positive interconnectivity between energy and the plenary human development dates back to the beginning of human existence. Energy, inter alia, other structures, have been *sine qua non* to socio-economic development, enhancement of rural production and food security, improvements in healthcare and standards of living in human societies. Unequivocally, therefore, energy has a pivotal role to play in the attainment of the goals of the twined global development paradigms: *sustainable development* and the 'Millennium Development Goals' (MDGs), despite the non-explicit mention of energy in any of the MDGs. The argument is that, communities, both rural and urban, will be well placed to achieve both social and economic prosperity and poverty alleviation once they have access to effective, reliable and affordable modern energy services (The EU Energy Initiative, 2006; Bawakyillenuo, 2009). Conversely, the upshot in the absence of adequate, affordable, reliable and safe modern energy services is stunted socio-economic development - a manifestation of poverty (Department for International Development, 2002). The International Energy Agency (IEA) (2002), corroborated the importance of energy in the socio-economic fabric of rural areas, by outlining the adverse effects of its non-existence: "[the] lack of electricity exacerbates poverty and contributes to its perpetuation, as it precludes most industrial activities and the jobs they create" (p.33). It has been estimated that an additional 700 million people worldwide will need to be provided with reliable and affordable modern energy services by 2015, in order to meet the MDG poverty reduction target (Flavin and Aeck, 2004).

Notwithstanding the importance of energy in fostering development, globally, about 1.6 billion people are without access to modern forms of energy especially, electricity, while 2.4 billion people rely on traditional biomass fuels for their energy needs (DFID, 2002; Flavin and Aeck, 2004; Niez, 2010). Predominantly, these people are found within the rural areas of developing countries especially, Sub-Saharan Africa and South Asia (Duke et al, 2002; Niez, 2010). For instance, more than 83% of Africa's rural population is without electricity, with an incremental figure of 92% in Sub-Saharan Africa (Bawakyillenuo, 2009). In a similar vein,

traditional biomass fuels account for about 70-90% of primary energy supply and up to 95% of the total consumption in some African countries (Karekezi, 2002).

The original approach, and still, the dominant in the supply of electricity to rural areas in the developing world, is centralisation, which involves the distribution of power from the grid (Bawakyillenuo, 2009). Almost all Sub-Saharan African countries follow this centralised grid-based strategy in rural electricity supply. An alternative approach, which has been favoured by many individuals, nations and organisations, is the decentralised approach: the usage of decentralised sources of energy generation technologies particularly, 'new' renewables (micro hydropower, solar PV, wind, biofuel, solar thermal electric and geothermal), diesel-engine generator set or hybridisation of any of these energy technologies. The hyper support for the latter approach notably, the utilisation of 'new' renewables, emanates from their environmental benignity, modularity, least-cost advantage on a life-cycle basis compared with grid and diesel generators. Using life-cycle accounting and externalities associated with energy systems as the yardsticks, renewable energy technologies are cost-competitive as well as reliability-competitive with conventional energy sources in many applications including, off-grid electrification with solar photovoltaic (PV), solar photovoltaic pumping (PVP) irrigation systems etc., (IEA-PVPS T9-07, 2003; Flavin and Aeck, 2004).'New' renewables also have the potentials to offset the vulnerability of developing countries to oil price spikes, reduction in both import dependence burden on foreign exchange (Radulovic, 2005; Flavin and Aeck, 2004). However, it is still quite elusive with respect to whether the use of both approaches (centralised and decentralised) in the supply of electricity to rural populations, always have the desired effects on them.

Predicating the argument on analysed data from two solar PV projects' sites in Ghana as case studies, this paper explores the interrelationship between the policy approaches that have been used to supply electricity to rural Ghana, and the energy needs of these rural communities. In particular, it examines the extent to which these policy approaches have helped serve the energy needs of these communities after solar PV and other RETs were incorporated in the Rural Electrification Programme (REP). It concludes with recommendations for the energy policy approaches that could be the panacea to poor rural communities' needs in Ghana and other developing countries.

2. Rural electrification versus energisation – a contextual account

Energy encompasses light, heat, mechanical power and electricity from various sources of fuels - fossil fuels and renewable energy sources (DFID, 2002). The need or desire for energy, therefore, is a 'derived demand' from the demand for varied energy services – cooking, water heating, lighting, refrigeration, water pumping for productivity, transport, communications, etc. Rural electrification and energisation are two different sources providing these energy services.

Rural electrification has been defined diversely. However, the points of divergence are centred on the approaches (centralised, decentralised or both) used in the supply of the electricity. For instance, some observe rural electrification to be the extension of the central grid to rural areas. Conversely, rural electrification has been viewed as the process by which access to electricity is provided to households or villages in isolated or remote parts of a country irrespective of the approach (Niez, 2010). Characteristic of rural electrification in the developing world is the emphasis on lighting service to the exclusion of cardinal services especially, productivity (DFID, 2002). Although lighting enhances off-farm productive

activities, on the whole, rural electrification programmes are usually devoid of responding holistically to the energy needs of the rural poor. Many rural electrification programmes are top-down in approach. Often, huge sums of money are spent to extend grid to selected rural areas without any consideration to the availability of adequate generation capacity (Ramakumar, 2007).

The concept of energisation on the hand is very holistic. It embraces electrification, and emphasises on the provision of the composite varied energy services, based on the needs of the rural beneficiary communities. Unlike rural electrification, the central theme of energisation focuses on matching the needs of end-users of energy services with available resources (Ramakumar, 2007). Therefore, notwithstanding the approaches (centralised, decentralised, or both) used to supply energy services to beneficiary communities, the existence of such services are usually fulfilling the expressed energy needs of the communities, hence, will have more support from them. In other words, the delivery of energy services through energisation programme follows the bottom-up approach.

3. Geography, energy perspectives and socio-economic issues of Ghana

Surrounded by Cote D'Ivoire, Burkina Faso, Togo and the Atlantic Ocean, Ghana is between 4^0 and 12^0 degrees north latitude, and longitude 30^0W and 1^0E. The climatic conditions range from warm and relatively dry along the southeast coast, hot and humid in the southwest, and hot and dry in the north. With an approximate population of 22.4 million, coupled with an estimated annual growth rate of 2.7%, 54 and 46 percent are rural and urban respectively (Bawakyillenuo, 2009).

Ghana, abounds with renewable energy resources (hydro, solar, wind, biomass, etc), and has a considerable amount of oil deposit in the off-shore. The country's energy consumption is estimated at 6.6 million tonnes of oil equivalents (TOE) with an estimated per capita consumption at 360 kilograms of oil equivalent (KOE). Traditional fuels constitute 59% of the total consumption, whilst petroleum products and electricity account for 32% and 9% respectively. Though with majority of the population in the rural areas, an inverse relationship exists concerning access to modern sources of energy between the urban and rural areas. About 17% of the total rural population, and only 5% in the rural population of the northern part of the country, have access to electricity, juxtaposing with 77% access in the urban area (Bawakyillenuo, 2009). The lighting and cooking energy services' needs of the rest of 83% are derived from traditional fuels - kerosene, candles, dry cell batteries, oil lamp, etc (ibid). Modern energy services for productive activities especially, cottage industries, irrigation farming, etc., are either non-existent or negligible in these rural areas (Bawakyillenuo, 2007).

In response to the Economic Recovery Programme (ERP) of the 1980s, the Government of Ghana instituted the National Electrification Scheme (NES) in 1989 principally, as the tool for the extension of the grid to the nooks and cranny of the country, especially all district capitals, towns and villages exceeding 500 inhabitants, over a thirty-year period (1990-2020) (Abavana, 2004). The Self-Help Electrification Project (SHEP) was later initiated to complement NES: it makes provisions for communities within 20km radius of existing 33 KV or 11 KV sub-transmission line to speed up their electrification projects, once they secure all poles for the low voltage network with 30% of houses wired. In 2001, the Government of Ghana mainstreamed solar PV and other renewable energy technologies in the REP.

With respect to the economy, Ghana has approximately twice the per capita output of poorer West African countries, with an estimated per capita GDP at $2,600 in 2006 (CIA World Factbook - Ghana, 2007). Agriculture (farming, rearing and fishing) is the mainstay of the economy, accounting for 37.3% of GDP (2006) and 60% workforce; followed by the service sector with 25% workforce; and industry – 15% percent (ibid). The rural economies within the three belts of the country (coastal, middle and northern) are fundamentally based on rain-fed agriculture, 90% of which is peasant-based. In the coastal belt, fishing is the main occupation followed by livestock rearing; in the middle belt with bimodal rainfall regime, crop farming predominates, followed by livestock rearing and fishing; and in the northern belt with a unimodal rainfall regime, crop farming and livestock rearing are the main economic activities. The northern belt (the two solar projects' zone) is frequently subjected to poor yields and food shortages, because of the single rainfall regime, climate variability and lack of facilities to undertake complementary farming activities in the dry season. Though richer than other poorer West African nations, poverty is still pervasive in the rural areas of Ghana, since rain-fed agriculture is the main occupation. Incidence of poverty is quite acute in the rural areas, accounting for 84% of Ghana's poor – the northern belt ranks the highest in poverty.

4. Wechiau and Bunkpurugu/Yunyoo's PV solar household system (SHS) projects

The two case studies were carried out through field survey in 2005 by the author as part of his PhD thesis' fieldwork. The projects are the Government of Ghana/Spanish Government off-grid solar PV rural electrification project in Wechiau in Wa West District (1998) and the UNDP/GEF/Ghana Government Renewable Energy Service Project (RESPRO) in Bunkpurugu/Yunyoo District in 1999. The goal of the Wechiau project was to assess the social, economic and technical performance of solar PV as an instrument for rural electrification in off-grid communities. The project comprised of a battery centre and PV/SHSs, with the implementing body being the Ministry of Energy (MOE). The financing mechanism used to supply the PV/SHSs to customers was the fee-for service. While customers paid a flat installation fee of ¢100,000 cedis (US$ 13.92), users of both the 50Wp and 100Wp modules paid ¢15,000 (US$2.09) and ¢25,000 (US$3.48) monthly tariffs respectively. The Wechiau project was managed by two formal indigenous groups after its implementation (i.e. operators of the battery charging centre and a solar committee) with different responsibilities. Operators of the battery charging centre were tasked with charging of batteries commercially, passing the fees charged onto the solar committee, and undertaking basic servicing of the installed PV/SHS. The solar committee on the other hand, was to collect the monthly tariff from the users on behalf of the MOE and deposit it at the bank.

Implemented from 1999 to 2004, the main aim of RESPRO was to initiate the development of a commercial market for renewable-based electricity services in rural Ghana, with an initial emphasis on PV/SHS. An individual customer could apply for one of two PV/SHSs, 50Wp and 100Wp. Because the main market model was the fee-for-service, customers paid a ¢250,000 (US$34.86) installation fee and ¢90,000 (US$12.55) six months advanced tariff for 50Wp SHSs before installation was carried out. On the other hand, customers wanting 100Wp SHSs paid a ¢500,000 (US$69.72) installation fee and 150,000 (US$20.91) six months advanced tariff. Six months after installation, customers began paying monthly tariffs - ¢15,000 (US$2.09) for a 50Wp system and ¢25,000 (US$3.48) for a 100Wp system. A default in paying the tariff for three months resulted in the removal of the system. RESPRO was implemented by a subsidiary unit of the MOE, which was formed through the secondment of some of its personnel. Personnel included a national co-ordinator in Accra, two engineers and

six field technicians, who were responsible for the installation and maintenance of the solar PV systems.

5. Methodology

Data for this paper were gathered using, documentary gathering of energy policy literature of Ghana; formal and informal interviews with three PV technicians who worked on the two PV/SHS projects, three officials at the Ghana's energy ministry; the administering of households questionnaires to twenty PV/SHS users, twenty non-PV/SHS users and four cottage industrialists. Of particular importance were the incorporation of the Likert scale of measurement and a weighting system based on ranked choices, in the questionnaires. In the application of the Likert scale, respondents indicated the strength of agreement or disagreement on series of statements. In the case of the weighting system, a defined ranking scale (1, being the least, and 10, the maximum) was used, and respondents were asked to indicate their preferences/choices on a set of energy related issues having recourse to this scale. As a result, the total responses for a particular choice are multiplied by its position in a descending order, and the weights are then summed up to reveal the relativity in choices. The various themes addressed in the questionnaires were: the socio-economic features of PV/SHS adopters and non-adopters, sources of the various energy services in the rural areas, factors underpinning the adoption and non-adoption of PV/SHS, knowledge on energy policy, etc. Content analysis, Statistical Package for Social Scientists (SPSS) and Excel were the analytical tools. A limitation of this paper is the small sample size. However, this is catered for, as emphasis is on policy analysis and not statistical significance or econometric analysis.

6. Results

Results of the processed data are presented in the below figure and tables. Also, manifest in the results are the following associated features of the two PV/SHS projects: most of the rural dwellers did not adopt the PV/SHSs; withdrawal of qualified technicians after the projects' implementation phases; malfunction of majority of the installed PV/SHSs; lack of maintenance services after the projects' implementation phases.

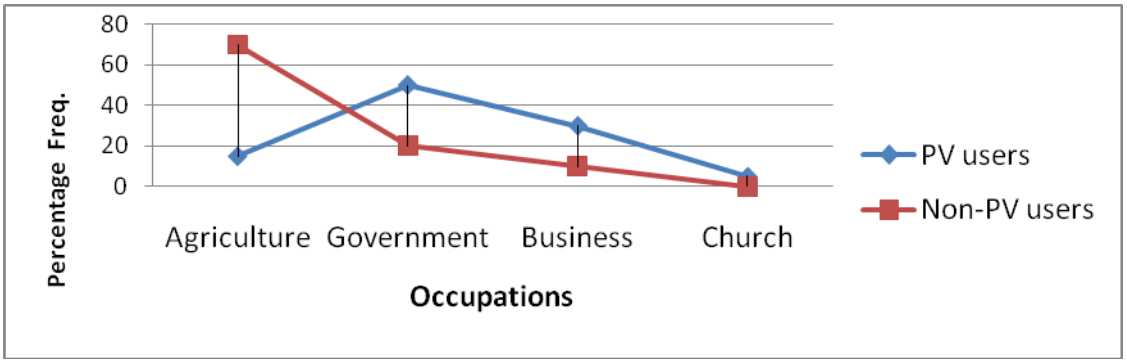

Fig. 1. Occupations of respondents (40) with and without PV/SHS at the two case study areas

Table 1. Main uses of PV/SHS by beneficiaries (20) in the two case study areas

Uses	Frequency	Percent
Lighting	20	100
Entertainment	15	75
Business	4	20
Cooking	0	0
Education	7	35
Agriculture	0	0

Table 2. Reasons for the non-adoption of PV/SHS by non-users (20) in the two case study areas

Reasons	Number	Percent
Expensive	20	100
Prefers grid	12	60
Inaccessible	10	50
Lack of PV know-how	9	45
Unreliable	8	40

Table 3. Relative importance of various energy services to PV/SHS users and non-users

	Lighting		Agriculture (irrigation)		Cooking		Entertainment		Cottage industry	
Ranking (1...5)	PV users	Non users	PV users	Non users	PV users	Non users	PV users	Non users	PV users	Non users
Very important	9	2	2	10	5	5	7	2	2	6
Important	6	4	2	6	5	7	5	2	3	4
Somewhat important	3	5	3	3	4	5	5	0	4	4
Less important	2	5	4	1	3	1	3	6	6	4
Least important	0	4	9	0	3	2	0	10	5	2
Weighted score	82	55	44	84	66	72	76	40	51	68

Succinct explanation to the survey results in the figure and tables above is advanced. Figure 1, reveals the lopsidedness of the occupational characteristics between PV/SHS adopters and non-adopters: agriculture forming the main occupation of majority of non-adopters of PV/SHS and vice versa; and government work (civil service), the main occupation of majority of PV/SHS adopters and vice versa. The most important services from PV/SHS according to beneficiaries are lighting and entertainment (Table 1), while uses for agriculture are non-existent. Non-adopters of PV/SHS see cost, preference for grid and inaccessibility to PV/SHS as the main reasons for their non-adoption of PV/SHS (Table 2). Table 3, also depicts a very disparate rankings between users and non-users of PV/SHS. Lighting, followed by entertainment, dominate the weighted scores by PV/SHS users, with agriculture the least. Inversely, agriculture, followed by cooking and cottage industry are the highest weighted scores by non-adopters of PV/SHS, with entertainment the least.

7. Discussion and conclusion

Critical analysis of the survey results, the socio-economic attributes of the rural people in Ghana and the energy perspectives of the country in tandem, raise key interrelated issues: accessibility to, and affordability of modern energy services by rural people; and the congruity/incongruity of Ghana's energy policy direction with the needs of the rural people.

7.1 Accessibility and affordability

Conjointly, accessibility and affordability are some of the key issues that emerged from the analysis of data for this paper. As indicated in the results section, a key feature of the case studies is that, most inhabitants in the PV/SHS projects' communities did not adopt the

technology - a phenomenon that intertwines with accessibility and affordability etc. Accessibility dimension is particularly depicted in Table 2, whereby 10 out of the 20 non-users of PV indicated inaccessibility as one of the reasons for their non-adoption of the technology. Six people out of the 10 that indicated inaccessibility were civil servants and business people, who could not adopt the solar PV/SHS before the projects ended. Notwithstanding the social group that pointed out inaccessibility as the hindrance, poor access to modern energy services is profound in rural Ghana as well as most rural societies in the developing world (Bawakyillenuo, 2009). With respect to the affordability trajectory, Table 2 reveals that cost (expensiveness) is a key factor to the non-use of PV/SHS, while Figure 1 depicts the occupation of majority of these non-users to be agriculture. The lack of affordability of PV/SHS by these non-users is highly correlated with the features of their occupation – rain-fed agriculture, which creates abject poverty among them (see section 3). Enhancing their affordability level can only be made possible by an increase in their incomes, hence, the need for concrete policies on productivity as well as financing. For example, it has been noted that 50 percent of rural households in the developing world will still be unable to afford solar PV even with the use of credit and fee-for-service financing models (Bawakyillenuo, 2007, citing Jacobson, 2004).

7.2 Ghana's energy policy direction vis-à-vis the needs of rural communities

Analysis of the energy policy documents and survey results reveal the unidirectional nature of the energy policy of Ghana in general, as well as on 'new' renewables. Emphasis on these technologies, especially PV (the only renewable technology in application in Ghana), is electrification. The onset of PV utilisation was premised on the fact it was virtually impossible to electrify certain islands on the Volta Lake and remote areas via the grid (Abavana, 2004). The uni-focus nature of policy towards these 'new' renewables is buttressed by the main uses of PV/SHS by beneficiaries in the two study areas (Table 1). While lighting and entertainment services predominate the uses, direct application of motive power from PV for agricultural purposes are non-existent. This policy slant on 'new' renewables on the one hand, and the survey results in Table 3 on the other hand, bring out the incongruity between the policy and the energy needs of rural dwellers. The non-users of PV/SHS, who are predominantly peasant farmers, and riddled with poverty, place more value on energy services that will boost agriculture, cooking and cottage industry. Arguably, such energy services have the overall impact of increasing income levels. The choices by PV/SHS users (who are the middle class and the minority in the rural areas), however, contrast with those of the non-users. The choices of PV/SHS users are not far-fetched because, their occupations can afford them certain amount of disposable incomes, which are enough to propel them up the rungs of the energy ladder (i.e. the desertion of the application of kerosene and dry cells to the utilisation of electricity from modern energy technologies). It is an established fact that, higher incomes enhance the ability to afford more energy (DFID, 2002).

The flagship outcome of this paper is that, the focus of energy policy in Ghana, even with the incorporation of RETs is that of electrification (lighting) – a faltered policy strategy, because it does not address the composite and core energy services needs of poor rural communities. Electricity is not always the most appropriate form of energy services to the poor (DFID, 2002). Irrespective of numerous solutions advanced by scholars and organisations for the expansive dissemination of RETs especially, PV in rural areas of developing countries, findings of this paper affirm that their slow adoption process and sustainability boil down to the disregard for appropriate policies measures. Effective policy structures act as stimulants to PV/SHS dissemination (Bawakyillenuo, 2009).

As a result of the prevalence of poverty among rural societies in Ghana, and for that matter the developing world, energisation is the optimal policy trajectory for these areas. Through this policy approach, energy services needs of various social and income groups are met via the conduction of needs assessment in a 'bottom-up'' approach, rather than a 'top-down' (a common element with electrification). Thus, two alternatives for parties interested in clean lighting services will be available – PV/SHS and solar lantern; the former, more costly than the latter. But, also available is PVP or hybrid of wind pump/PVP for productivity (irrigation agriculture, cottage enterprises, etc), to individuals and groups wanting to augment their production. These energy services that are geared towards productivity are the bedrock to extricating rural people from poverty. The reasoning is that, the application of such productive energy services can create a virtuous growth cycle among poor rural societies; and this cycle will in turn motivate them to crave for other energy services such as lighting, entertainment, education, etc. In other words, the application of energy services for production (irrigation and other cottage industries) can increase incomes, and the ripple effect of such an increase is the ability to afford other modern energy services.

References

[1] The EU Initiative, Increasing access to energy for poverty eradication and sustainable development, 2006, pp. 1-11.

[2] S. Bawakyillenuo, Policy and institutional failures: the bane of photovoltaic solar household system (PV/SHS), Energy and Environment Journal, No. 6, 2009, pp. 927-947.

[3] DFID, Energy for the poor. Underpinning the Millennium Development Goals, 2002, pp. 1-32.

[4] IEA, World Energy Outlook 2002, second edition, 2002.

[5] C. Flavin and M. Aeck, Energy for development. The potential role of renewable energy in meeting the millennium development goals, 2004, pp. 1-45.

[6] A. Niez, 2010, Comparative study on electrification policies in emerging economies, 2010, pp. 1-116.

[7] R. Duke, D. Jacobson, A. Kammen, Photovoltaic module quality in the Kenyan solar home systems market, Energy Policy Journal, Vol. 30, Issue 6, 2002, pp. 477-499.

[8] S. Karekezi, Poverty and energy in Africa – a brief review, Energy Policy Journal, Vol. 30, Issues 11-12, 2002, pp. 915-919.

[9] IEA-PVPS T9-07, 16 case studies on the deployment of PV technologies in developing countries, 2003, pp. 1-115.

[10] V. Radulovic, Are new institutional economies enough? Promoting PV in India's agricultural sector, Energy Policy Journal, Vol. 33, pp. 1883-1899.

[11] Ramakumar, Renewable energy utilisation scenarios: a case for IRES in developing countries, Proceedings of ISES Solar World Congress, 2007, pp. 2917-2921.

[12] S. Bawakyillenuo, Rural electrification in Ghana: issues of photovoltaic utilisation, Unpublished Ph.D. thesis, University of Hull, pp. 1-379.

[13] C. Abavana, Ghana: energy and poverty reduction strategy. EU energy initiative's facilitation workshop and policy dialogue, Ouagadougou, Burkina Faso, 2004.

[14] CIA World Factbook–Ghana, 2007.

Measures to Promote Adoption of Residential Photovoltaic Systems

Yoshihiro Yamamoto*

Department of Economics, Takasaki City University of Economics, Takasaki, Japan
** Corresponding author. Tel: +81 273447538, Fax: +81 273434840, E-mail: ysyama@tcue.ac.jp*

Abstract: The purpose of this paper is to clarify the effects of a combination of electricity rates, the price of the electricity generated with a photovoltaic (PV) system, and a subsidy when a government aims at achieving a certain level of PV-system adoption. A microeconomic model based on classical demand theory is made. The case is mainly analyzed where the amount of PV-generated electricity is different from household to household while the amounts of electricity consumption and budget as well as utility functions are identical. Other cases are also mentioned. It is shown that a household prefers a higher PV-generated electricity price with a higher electricity rate to a higher subsidy if any one of the following conditions is satisfied with other things being equal: (1) it will have a relatively large amount of PV-generated electricity if it installs; (2) it has a relatively large amount of budget; or (3) it has a relatively small amount of electricity consumption. Furthermore, other things being equal, the difference in utility functions has no effect on the preference. This suggests, though the mixed effects of these conditions are not examined, that a combination optimal for a household does not always optimal for another.

Keywords: *Residential Photovoltaic System, Feed-in tariff, Subsidy*

1. Introduction

There will be several measures to promote adoption of residential photovoltaic (PV) systems. One is that a government subsidizes a household to install the system. Another one is that the electricity generated by a PV system is purchased by an electric utility. Moreover, the retail rate of electricity will influence a household's economic situation and affect the decision to install the system. Accordingly, three parameters, an electricity rate, a price at which the PV-generated electricity is purchased by a utility, and a subsidy for installation, play a role in increasing the number of system-installed households. A government generally has control over these parameters. The purpose of this study is to obtain information available when a government sets them.

Most of existing studies addressing relevant issues are empirical or simulation ones calculating the value of PV systems or a break-even point, a combination of the parameters that makes it pay a household to install the system. For example, Mills et al. (2008) examine empirically the impact of electricity rate design on the economic value of PV systems for commercial customers in California. Carley (2009) shows using a two-part probit model that interconnection standards and RPS policies significantly increase the likelihood that a customer will adopt distributed generation capacity in the U.S. Rigter et al. (2010) determine the cost of PV system and obtain the optimal feed-in tariff by net present value analysis with Chinese data. Black (2004) shows that PV system installation is financially feasible under government incentives, net metering, high electricity rates, and other conditions in terms of rate of return, increase in property value, and cash flow.

These studies show the three parameters play an important role but do not deal with interrelations among them explicitly. This paper aims at filling this gap. I employ a different approach based on classical demand theory, in which consumers make decisions about purchases of goods by maximizing utility subject to budget constraints. Interestingly, to the best of my knowledge, the problem has not been investigated this way. I make a microeconomic model, examine efficient combinations of the parameters when a government

intends to make a given number of households install the system, and analyze the payoffs of the relevant parties such as system-installed households, no-system households, and an electric utility.

I identify the locus of an electricity rate, a PV-generated electricity price, and a subsidy on which a government can make a given number of households install the system. The utility levels of a system-installed household and a no-system household are calculated and the utility maximization point for each household is identified. This will make some contribution to the discussion on how the electricity rate, the PV-generated electricity price, and the subsidy should be set from an equity point of view.

2. Methodology

A microeconomic model is set up. Since rational consumers will optimize decisions on purchasing PV systems based on their usual lifespan of 10-20 years, all quantities and monetary values employed in the model are set forth in terms of a fixed system lifespan.

Consider *N* households with a market consisting of three goods: electricity, PV systems, and a composite of conventional goods. *N* is sufficiently large. The government has a target of installed systems in *n* of *N* households.

Since the price elasticity of demand for electricity may be very low, we assume that if electricity rates change, household electricity consumption, *x*, will remain constant. Each installed PV system produces *e* units of electricity. It is assumed that $x > e$.

All monetary value is normalized without loss of generality such that the price of the composite good is 1. The price of a PV system, which includes the prices of PV generation equipment and installation, is denoted by *K* and is constant.

In the model, a single electric utility, a government-regulated monopoly, supplies electricity to all households. Electricity rates may therefore be understood to be set by the government. For analytical simplicity, we assume the electricity rate to be a single, variable rate. Let *c* represent the cost of generating a unit of electricity for the electric utility. Suppose the conventional electricity rate is set at *c*.

Let *y* represent the budget of a household. The sum of the budgets of all households is denoted by *Y*. Funds for the subsidy are raised by taxation. It is assumed that a household must pay a tax according to its income, that is, the budget. Let *S* be a subsidy for a household with an installed system. Then the tax rate for each household should be nS/Y.

Let the quantities of PV systems and composite goods purchased by a household be denoted by q_1 and q_2, respectively, with q_1 taking one of two values, 0 (no PV system installed) or 1 (PV system installed). Let the utility function be denoted by $u(q_1, q_2)$. We exclude utility obtained from electricity consumption. A household can do without a PV system since it can purchase all the electricity it consumes from the electric utility. Hence, it is plausible that the installation of a PV system can be valued in terms of finite quantities of the composite good. Thus, we define a function $v(q_2)$ such that the utility level at point $(0, q_2)$ is equal to that at point $(1, q_2 - v(q_2))$ on the *r-p* plane, i.e., $u(0, q_2) = u(1, q_2 - v(q_2))$. In other words, function $v(q_2)$ indicates the opportunity cost of installing the system in terms of the quantity of the composite good. It is reasonable to assume that $v(q_2)$ should satisfy $0 \le v(q_2) \le q_2$. $v(q_2)$ is

twice differentiable and that it holds that $0 < v'(q_2) < 1$ and $v''(q_2) < 0$. This implies that the larger the budget of a household, the higher the value of a PV system to that household, but the smaller the incremental value.

3. Results

There are many variables to be considered, *e*, *x* and *y* as well as $u(q_1, q_2)$ and $v(q_2)$. It is difficult to deal with them simultaneously, so we focus on *e* in subsection 3.1 and then mention how to deal with the other variables in subsection 3.2.

3.1. Different amounts of PV-generated electricity

Suppose that household *i*'s amount of PV-generated electricity is e_i. It is assumed that $e_i > e_j$ for all *i* and *j* such that $i < j$. It holds $N > \sum_n e_i / e_n$ since *N* is sufficiently large. It is assumed that for any household *i*, $v(y - cx) < K - ce_i$ and $v(y - r_0 x) \geq K - r_0 e_i$ for some sufficiently large r_0. The meaning of this assumption, as shall become clear, is that if the electricity rate and PV-generated electricity price are both *c* when $S = 0$, no household will install PV systems, and that if both are r_0, all households will install systems.

The budget of household *i* increases practically from $(1 - nS/Y)y - rx$ to $(1 - nS/Y)y - rx + S + pe_i$ if it installs a PV system. This is equivalent to the situation in which the budget remains at the same level $(1 - nS/Y)y - rx$ while the price of PV systems decreases by $S + pe_i$. Hence, the budget constraint of household *i* is $(K - S - pe_i)q_1 + q_2 \leq (1 - nS/Y)y - rx$.

Since households maximize utility subject to the budget constraint, household *i* installs the system if $v((1 - nS/Y)y - rx) \geq K - S - pe_i$ and does not if $v((1 - nS/Y)y - rx) < K - S - pe_i$. Therefore, the necessary and sufficient condition for exactly *n* households to install the system is that the two inequalities $v((1 - nS/Y)y - rx) \geq K - S - pe_n$ and $v((1 - nS/Y)y - rx) < K - S - pe_{n+1}$ hold simultaneously. It will be shown step by step that there exists a combination (r, p, S) that satisfies the following equation:

$$v\left(\left(1 - \frac{nS}{Y}\right)y - rx\right) = K - S - pe_n. \quad (1)$$

Eq. (1) guarantees that exactly *n* households install the system.

3.1.1. Controls of price and rates

We first analyze a special case, where $S = 0$. Let us make the arguable assumption that as the electricity rate rises, it becomes more favorable for a household to install a system and generate electricity itself, rather than purchase it if the PV-generated electricity is purchased at the electricity rate. In other words, it holds that $v(y - rx) - (K - re_i)$ is increasing in *r*, i.e., $xv'(y - rx) < e_i$.

Lemma 1. There exist r_1 and p_1 that uniquely satisfy Eqs. (2) and (3), respectively.

$$v(y - r_1 x) = K - r_1 e_n, \quad (2)$$

$$v(y - cx) = K - p_1 e_n. \quad (3)$$

Proof. These are shown from the assumptions $v(y-cx) < K - ce_i$, $xv'(y-rx) < e_i$, and $v(y-r_0x) \geq K - r_0e_i$.

Suppose the government chooses the lowest *r* for any *p* or the lowest *p* for any *r* to make exactly *n* households install systems.

Lemma 2. The *r* and *p* set by the government must satisfy the following equation:

$$v(y-rx) = K - pe_n . \tag{4}$$

Proof. The curve defined by Eq. (4) on the *r-p* plane connects points (c, p_1) and (r_1, r_1), and is strictly upward-sloping (Fig. 1). Hence, there exists a unique solution *r* for any *p* that satisfies Eq. (4), and vice versa. A point on the curve represents the lowest *r* for any *p* or the lowest *p* for any *r* that satisfies the two inequalities.

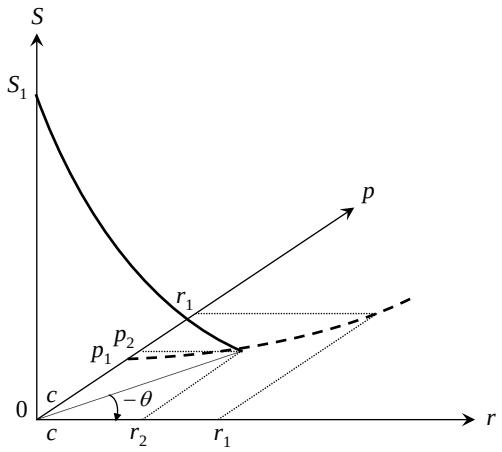

Fig. 1. The curves guaranteeing that exactly n households install the PV system in the r-p-S space. The dashed curve corresponds to the case where there is no subsidy. The solid curve corresponds to the case where a subsidy is introduced with the electric utility being compensated for the costs of purchasing PV-generated electricity.

The utility levels of system-installed household *i* and a no-system household, and the profit of the electric utility, are as follows, respectively:

$$u\left(1, y - rx - (K - pe_i)\right) \ \left(i = 1, \cdots, n\right), \tag{5}$$

$$u(0, y - rx), \tag{6}$$

$$\left(r - c\right)Nx - \left(p - c\right)\textstyle\sum_n e_i . \tag{7}$$

The government may make its decisions in determining *r* and *p* that the electric utility should be compensated for the costs of purchasing PV-generated electricity. Namely, the profit of the utility (7) is set at zero:

$$\left(r - c\right)Nx - \left(p - c\right)\textstyle\sum_n e_i = 0 . \tag{8}$$

This forms a straight line containing point (c,c) on the *r*-*p* plane. Solving simultaneous equations (4) and (8) for *r* and *p* we obtain the solution (r_2, p_2) shown in Fig. 1.

3.1.2. Controls of subsidy for households

Next we analyze another special case, where $r = p = c$.

Lemma 4. There exists a unique solution, S_1, that satisfies Eq. (1) when $r = p = c$. The government chooses S_1.

Proof. $v((1-nS/Y)y - cx) - (K - S - ce_n)$ is strictly increasing in *S*, and negative if $S = 0$ and positive if $S = (r_0 - c)Yx/(ny_n)$. Therefore, there exists a unique solution S_1.

3.1.3. Controls of price, rates, and subsidy

Now we return to a general case. Suppose that the electric utility is compensated for the costs of purchasing PV-generated electricity, that is, Eq. (8) holds.

Proposition 1. The curve defined by simultaneous Eqs. (1) and (8) is convex and connects points $(r_2, p_2, 0)$ and (c, c, S_1) in the *r*-*p*-*S* space (Fig. 1). The government chooses the *r*, *p*, and *S* on the curve.

Proof. See Appendix 1.

The utility levels of system-installed household *i* and a no-system household are as follows, respectively:

$$u\left(1, \left(1 - \frac{nS}{Y}\right)y - rx - (K - S - pe_i)\right) \quad (i = 1, \cdots, n), \tag{9}$$

$$u\left(0, \left(1 - \frac{nS}{Y}\right)y - rx\right). \tag{10}$$

The combination (r, p, S) that maximizes the utility of each household is obtained by maximizing the quantity of q_2 subject to simultaneous Eqs. (1) and (8). Let us investigate such a combination.

Proposition 2. For system-installed household *i*, the optimal combination is $(r_2, p_2, 0)$ if $e_i \geq \sum_n e_i / n$. Specifically, the optimal combination is $(r_2, p_2, 0)$ for household 1. On the other hand, for system-installed household *n* and no-system households, the optimal combination is (c, c, S_1).

Proof. See Appendix 2.

Proposition 2 implies that if a household will have a relatively large amount of PV-generated electricity with a PV system, it prefers $(r_2, p_2, 0)$, while if it will have a relatively small amount of PV-generated electricity, it prefers (c, c, S_1).

3.2. Modeling differences in budgets, electricity consumption, or utility functions

First, suppose the amount of budget of household i is y_i while x and e are constant. To take into account that as a budget increases, installing a PV system becomes easier, we assume that $y_i > y_j$ for all i and j such that $i < j$. We can then do an analysis similar to the case considered above and show if a household has a relatively large budget, it prefers $(r_2, p_2, 0)$, while if it has a relatively small budget, it prefers (c, c, S_1).

Next, suppose the amount of electricity consumed in household i is x_i, where $x_i > e$, while e and y are constant. As the amount of electricity consumption increases, the budget for purchasing a PV system and the composite good decreases, and therefore installing a system becomes more difficult; to take this into account, we assume that $x_i < x_j$ for all i and j such that $i < j$. Then a similar analysis can be done and it is shown if a household has a relatively small amount of electricity consumption, it prefers $(r_2, p_2, 0)$, while if it has a relatively large amount of electricity consumption, it prefers (c, c, S_1).

Lastly, we consider the case in which utility functions are different from household to household. Suppose household i has a utility function $u_i(q_1, q_2)$, while e, x, and y are constant. Assume $u_i(q_1, q_2) > u_j(q_1, q_2)$ for all i and j such that $i < j$ for any (q_1, q_2) and define a function $v_i(q_2)$ such that $u_i(0, q_2) = u_i(1, q_2 - v_i(q_2))$ and $v_i(q_2) > v_j(q_2)$. The analysis in this case can also be done in the same way. In this case, it is shown that any combination (r, p, S) guaranteeing exactly n households install the PV system bring about the same level of utility to each household regardless of PV system installation.

4. Conclusions

In this paper, I have analyzed the relationship between an electricity rate, a PV-generated electricity price, and a subsidy to achieve a certain level of PV system installation, and examined the impact on the utility of households.

I found that a household prefers a higher PV-generated electricity price with a higher electricity rate to a higher subsidy if any one of the following conditions is satisfied with other things being equal: (1) it will have a relatively large amount of PV-generated electricity if it installs a PV system; (2) it has a relatively large amount of budget; or (3) it has a relatively small amount of electricity consumption. Furthermore, other things being equal, the difference in utility functions of households has no effect on the preference.

The results imply that welfare distribution varies depending on the parameter settings even if a fixed number of households install PV systems. This is because each household has its own amounts of PV-generated electricity, budget, and electricity consumption and utility function. Hence, it will be difficult to set parameters with which every household is satisfied. It then may be a policy option that a menu consisting of a combination of an electricity rate, a PV-generated electricity price, and a subsidy for installation is offered to households. This may relieve unfairness to some extent.

In the model, each effect of the amounts of PV-generated electricity, budget, and electricity consumption and utility functions was investigated separately but the mixed effect of them was not. Investigating the mixed effects is very important particularly when a government practically determines the value of each parameter. An analytical approach used in this paper

may be difficult to apply directly but the formulation can be used if, for example, a simulation method is used.

References

[1] A. Mills, R. Wiser, G. Barbose, and W. Golove, The impact of retail rate structures on the economics of commercial photovoltaic systems in California, Energy Policy 36, 2008, pp. 3266-3277

[2] S. Carley, Distributed generation: An empirical analysis of primary motivators, Energy Policy 37, 2009, pp. 1648-1659

[3] J. Rigter and G. Vidican, Cost and optimal feed-in tariff for small scale photovoltaic systems in China, Energy Policy 38, 2010, pp. 6989-7000

[4] A.J. Black, Financial payback on California residential solar electric systems, Solar Energy 77, 2004, pp. 381-388

Appendix 1: Proof of Proposition 1

The curve defined by simultaneous equations (1) and (8) connects $(r_2, p_2, 0)$ and (c, c, S_1) in the *r*-*p*-*S* space. First, we show the curve is strictly downward-sloping. Define θ as the angle formed by the line (8) and the *r*-axis on the *r*-*p* plane (Fig. 1). Then it follows that $\cos\theta = \sum_n e_i / A$ and $\sin\theta = Nx/A$, where $A = \sqrt{(\sum_n e_i)^2 + (Nx)^2}$. We are allowed to show the proposition with respect to the curve obtained by rotating the original curve define by (1) and (8) around the *S*-axis by $-\theta$. The obtained curve is on the *r*-*S* plane:

$$v\left(\left(1-\frac{nS}{Y}\right)y-\left[c+(r-c)\frac{\sum_n e_i}{A}\right]x\right)=K-S-\left[c+\frac{Nx}{A}(r-c)\right]e_n. \qquad \text{(A1)}$$

The slope of the tangent is as follows:

$$\frac{dS}{dr}=-\frac{\left[Ne_n-v'(r,S)\sum_n e_i\right]x/A}{1-(n/N)v'(r,S)}, \qquad \text{(A2)}$$

where $v'(r,S) \equiv v'((1-nS/Y)y-[c+(r-c)\sum_n e_i/A]x)$.

This is strictly negative due to the assumption $Ne_n > \sum_n e_i$, and thus the curve is strictly downward-sloping. Hence, there exists a unique solution *r* for *S* and vice versa that satisfies simultaneous equations (1) and (8). The government will choose a point on the curve since points on the curve represent the lowest *r* for *S* or the lowest *S* for *r* that satisfies the two inequalities.

It can be verified that the second-order differential d^2S/dr^2 is always positive since $v''(q_2) < 0$. Hence, the curve is convex in the *r*-*p*-*S* space.

Appendix 2: Proof of Proposition 2

We are allowed to prove Proposition 2 with respect to the rotated curve around the *S*-axis by $-\theta$. First, I deal with system-installed household *i*. The quantity of q_2 when $q_1 = 1$ is as follows:

$$\left(1-\frac{n}{N}\right)S+\frac{\left(Ne_i-\sum_n e_i\right)x}{A}(r-c)+y-K-(x-e_i)c \quad (i=1,\cdots,n). \tag{A3}$$

The points giving a fixed amount of q_2 form a straight line on the *r*-*S* plane. The quantity of q_2 is always increasing in *r* due to the assumption $Ne_n > \sum_n e_i$ and in *S*, too. The slope of the line giving a fixed amount of q_2 is obtained from (A3).

$$\frac{dS}{dr}=-\frac{\left(Ne_i-\sum_n e_i\right)x/A}{1-n/N} \quad (i=1,\cdots,n). \tag{A4}$$

This is strictly negative due to the assumption $Ne_n > \sum_n e_i$. The difference of the absolute values of slopes (A4) and (A2), which is denoted by $F_i(r,S)$, follows:

$$\begin{aligned} F_i(r,S) &\equiv \left[\frac{\left(Ne_i-\sum_n e_i\right)x/A}{1-n/N}\right]-\left[\frac{\left(Ne_n-v'(r,S)\sum_n e_i\right)x/A}{1-(n/N)v'(r,S)}\right] \\ &= \frac{x}{A}\cdot\frac{Ne_i-\sum_n e_i-(N-n)e_n-(ne_i-\sum_n e_i)v'(r,S)}{(1-n/N)\left[1-(n/N)v'(r,S)\right]} \end{aligned}. \tag{A5}$$

The sign of $F_i(r,S)$ is positive if $e_i \geq \sum_n e_i/n$. Then, the optimal point is $(r_2, p_2, 0)$ for household *i* since the utility is increasing both in *r* and *S*. For household *n*, the optimal point is (c,c,S_1) since $F_n(r,S)<0$. Note that if $i<j$, i.e., $e_i > e_j$, the absolute value of dS/dr of household *i* is larger than that of household *j* from Eq. (4).

The proof for a no-system household is done similarly. We obtain the quantity of q_2 when $q_1=0$ as a function of *r* and *S*:

$$-\frac{x\sum_n e_i}{A}(r-c)-\frac{n}{N}S+y-cx. \tag{A6}$$

This is always decreasing both in *r* and *S*. The slope of the line giving a fixed amount of q_2 for a no-system household is obtained from (A6):

$$\frac{ds}{dr}=-\frac{x\sum_n e_i/A}{n/N}. \tag{A7}$$

This is negative. The difference of the absolute values of slopes (A7) and (A2), which is denoted by $G(r,S)$, is as follows:

$$\begin{aligned} G(r,s) &\equiv \left[\frac{x\sum_n e_i/A}{n/N}\right]-\left[\frac{\left(Ne_n-v'(r,S)\sum_n e_i\right)x/A}{1-(n/N)v'(r,S)}\right] \\ &= \frac{x}{A}\cdot\frac{\sum_n e_i-ne_n}{(n/N)\left[1-(n/N)v'(r,S)\right]} \end{aligned}. \tag{A8}$$

This is always positive. Therefore, the optimal point is (c,c,S_1) since the utility is decreasing both in *r* and *S*.

The new course of FITs mechanism for PV systems in Italy: novelties, strong points and criticalities

Salvatore Favuzza, Gaetano Zizzo*

Dipartimento di Ingegneria Elettrica, Elettronica e delle Telecomunicazioni - Università di Palermo Palermo, Italy
** Corresponding author. Tel: +39 0916615205, Fax: +39 091488452, E-mail: zizzo@dieet.unipa.it*

Abstract: The paper deals with the new course of the Feed-in Tariffs mechanism for photovoltaic systems that will start from January 1, 2011 in Italy with the actuation of the Government Decree DM 06/08/2010. After a short introduction on Feed-in Tariffs and Net-metering in Italy, the paper focuses the attention on an economical comparison between the incentives established by the Government Decree DM 19/02/07, ended on December 31, 2010 and those introduced by the DM 06/08/2010. The economical comparison is based on three indexes: the Pay Back Period, the Net Present Value and the Internal Rate of Return, characterizing the investments done for the realization of the photovoltaic systems. In particular, simulations show how the new Decree significantly penalizes the architectural integration, that represents a strongly criticism of the new incentive policy.

Keywords: *Renewable Energy Resources, PV systems, Feed-in Tariffs, PBP, NPV, IRR*

Nomenclature

F	*FIT value* ..... €/kWh	N	*lifetime of the investment* ..... *year*
$c_{kWh,t}$	*the electricity price at the* t^{th} *year* ... €/kWh	*NPV*	*Net Present Value* .....€
u	*percentage of maintenance cost* ..... %	*IRR*	*Internal Rate of Return* ..... %
C_0	*initial investment cost*..... €	*PBP*	*Pay Back Period*..... *year*
C_{add}	*yearly insurance cost* ..... €	E_t	*Energy produced at the* t^{th} *year* ..... *kWh*
i	*Weighted Average Cost of Capital (WACC)*..... %		

1. Introduction

In 2001 [1], the EU has officially recognized the need of promoting Renewable Energy Sources (RES) as a priority measure since their exploitation contributes to environmental protection and sustainable development and makes it possible to meet Kyoto [2] targets more quickly. The latest evidence of the diligence of the European countries in promoting the use of RES is the European Council Directive 2009/28/EC [3], targeting an objective of 20% as contribution of the RES on the total European energetic consumption in 2020. Such a bond represents, without doubts, a challenging goal, that will be able to be reached only with an effective RES incentive policy and with a concrete effort towards the improvement of the energetic efficiency of these sources.

Photovoltaic (PV) had a higher grow rate in the last decade with respect to the other RES-based systems. The data reported by Nomisma Energia [4] show how, among all the RES-based technologies, PV expected to contribute a major share of renewable energies in the coming decades.

PV technology is still very expensive and its development is strongly connected to incentive policies promoted by national governments and encouraged by the EU, which is striving to ensure the PV industry remains competitive on the worldwide market.

The most common incentive mechanism in Europe, adopted by 15 countries, is represented by Feed-in Tariffs (FITs) [5]. It involves the obligation on the part of an electric utility to

purchase electricity generated by renewable energy producers in its service area paying a tariff determined by Public Authorities and guaranteed for a specific time period.

In Italy FITs mechanism has been introduced in 2005 with a Government Decree [6] and has been changed during the years through another Government Decree in 2007 [7] and arriving today, with the Decree of the Ministry of the Economical Development 06/08/2010 [8], at its third version.

The purpose of this work is to highlight the novelties of the last Decree, and the differences with the previous one and to examine the effects of this new course on the diffusion of photovoltaic in Italy.

2. Feed-in Tariffs in Italy

FITs mechanism obligates an utility to purchase electricity generated by PV systems in its service area, paying a tariff determined by the public authorities and guaranteed for a specific time period. The value of a FIT represents the full price received by an independent producer for any kWh of electric energy produced by a PV system.

Different tariffs are defined for different countries, depending on resource conditions and socio-political situation. In Italy, since 2005 various Government Decrees have defined a support system that allows the producers to have recourse contemporary to FIT and Net-metering for PV installations with rated power not over 200 kWp [6,7,8].

Net-metering is a support strategy that allows the customers to offset their electricity consumption with small-scale RES over an entire billing period using it at a different time than it is produced, without considering when the power is consumed or generated and storing their energy in the Utility's grid. With Net-metering the energy produced and injected in the grid has the same economical value of the energy sold by the Utility to the customers.

Over 200 kWp, the customer could choose if selling the whole electric energy produced by the PV system to the local Utility or if using part of this energy for its own consumptions.

In this case the support system is composed by two terms:

- a FIT for the whole electricity produced by the PV system;
- a value for the electricity produced by the PV system which can be used for the own consumption (with a saving in the electricity cost) or partially or totally sold to the local Utility at a price established by the Italian Authority for Electric Energy and Gas.

Therefore, while in the other countries the FIT is paid only for the energy effectively sold to the Utility, in Italy, for 20 years, the producer receives a FIT for the whole produced electric energy and a payment for the part of electric energy sold to the Utility.

A new Decree of the Ministry for Economical Development in 2007 (DM 19/03/2007) simplified the procedure to obtain the incentive and changed the FITs values distinguishing among Field installed or not integrated in building, Partially Integrated in Building and Building Integrated PV Systems [7].

Today, thanks to the success and to the experience done with the DM 19/03/2007, the Italian Government has emitted the DM 06/08/2010, that replaces the previous one, introducing new rules and new tariffs for PV systems in Italy starting from January 1, 2011 [8].

The main differences introduced by the new Decree deal with the classification of the PV systems and the values of the related FITs. The new classification is the following:

- in buildings PV systems;
- building integrated PV systems with innovative characteristics;
- concentration PV systems (CPV);
- PV systems with technological innovation;
- other PV systems.

The characteristics of the PV systems with technological innovation and the related FITs will be established with a further Decree.

Tables 1 and 2 report the FITs values, respectively, for building integrated PV systems with innovative characteristics and for CPV (categories not contemplated by the previous Decree).

Table 1. FITs in DM 06/08/2010 for PV systems integrated with innovative features.

Rated power range (kW)	FIT (€/kWh)
$1 \leq P \leq 20$	0.440
$20 < P \leq 200$	0.400
$20 < P \leq 5000$	0.370

Table 2. FITs in DM 06/08/2010 for PV concentration systems.

Rated power range (kW)	FIT (€/kWh)
$1 \leq P \leq 200$	0.370
$200 < P \leq 1000$	0.320
$1000 < P \leq 5000$	0.280

Table 3 reports the values of the FITs stated by the 2007 and by the 2010 Decrees in the period may-august 2011.

Table 3. FITs in DM 19/02/07 and DM 06/08/10.

Rated power range (kW)	DM 19/03/2007			DM 06/08/2010	
	Not integrated (€/kWh)	Partially Integrated (€/kWh)	Totally Integrated (€/kWh)	PV in buildings (€/kWh)	Other PVs (€/kWh)
$1 \leq P \leq 3$	0.384	0.422	0.470	0.391	0.347
$3 < P \leq 20$	0.364	0.404	0.442	0.360	0.322
$20 < P \leq 200$	0.346	0.384	0.422	0.341	0.309
$200 < P \leq 1000$	0.346	0.384	0.422	0.335	0.303
$1000 < P \leq 5000$	0.346	0.384	0.422	0.327	0.289
$P > 5000$	0.346	0.384	0.422	0.311	0.275

PV systems are considered in the category “PV systems in buildings” if they are installed according with particular modalities proposed by the DM 06/08/10; if the PV systems do not fulfill these modalities, they must be included in the category “Other PV systems”.

With reference to the previous classification, inside the category “PV in buildings” are, therefore, included some totally integrated PV systems and almost the totality of the partially integrated PV systems; in the category “other PVs” are included field PV systems, not

integrated PV systems and some of the partially integrated PV systems.

Only with reference to the PV systems typologies of the previous classification and belonging to the new ones, in Table 4 the FITs percentage variation between the old and the new decree are reported.

Table 4. FITs percentage variations.

Rated power range (kW)	Not integrated (other PVs) (%)	Partially Integrated (other PVs) (%)	Partially Integrated (PV in buildings) (%)	Totally Integrated (PV in buildings) (%)
$1 \leq P \leq 3$	- 9.64	- 17.77	- 7.35	- 16.81
$3 < P \leq 20$	- 11.54	- 20.30	- 10.89	- 18.55
$20 < P \leq 200$	- 10.69	- 19.53	- 11.20	- 19.19
$200 < P \leq 1000$	- 12.43	- 21.09	- 12.76	- 20.62
$1000 < P \leq 5000$	- 16.47	- 24.74	- 14.84	- 22.51
$P > 5000$	- 20.52	- 28.39	- 19.01	- 26.30

The analysis of the percentage variations puts into evidence that the new FITs mainly penalize totally integrated PV systems with respect to the not integrated ones.

3. Methodology

In the following the previous Decree and the new one are compared, simulating different characteristics of the sample PV systems, in order to explore the possible situations in which the two Decrees give place to different values of the economical indexes.

The economical analysis is performed by calculating, the cash flow, the PBP, the NPV and the IRR of the investment done for realizing the PV systems.

The cash flows depend on several factors such as the equivalent hours produced, the FITs value, the gain for the avoided bill cost, the maintenance and management costs, etc.

All these factors can be translated into cash flows C_t^* by means of the following equation obtained by adding algebraically all the costs C_i and all the profits P_i related to the generic i^{th} year:

$$C_t^* = \sum_i P_{i,t} - \sum_i C_{i,t} = F \cdot E_t + c_{kWh,t} \cdot E_t - u \cdot C_0 - C_{add} \quad (1)$$

In order to carry out a realistic analysis, the cash flows are annualized using the classical expression according to [9]:

$$C_t = \frac{C_t^*}{(1+i)^t} \quad (2)$$

Equation (2) allows to obtain the equivalent present value of the cash flow of the t^{th} year, knowing its nominal value[1].

[1] For example, in the case of i=5%, a cash flow C_t*=1000€ produced at the 10^{th} year is equivalent to 614€ at year 0.

The NPV and the IRR indices are defined by the following expressions [9]:

$$NPV = \sum_{t=1}^{N} \frac{C_t^*}{(1+i)^t} - C_0 \quad ; \quad C_0 - \sum_{t=1}^{N} \frac{C_t}{(1+IRR)^t} = 0 \qquad (3)$$

4. Results

General data:
Yearly reduction of the photovoltaic production: 1%; Electricity price at year 0: 0.15 €/kWh;
Coefficient evaluating the maintenance and management cost: 1%; WACC: 3%

First case: 10 kW PV system
Classification according to DM 19/02/07: Not integrated – FIT Value: 0.364 €/kWh
Classification according to DM 06/08/10: Other PVs – FIT Value: 0.322 €/kWh
Initial investment cost: 45000 € - Yearly production at year 0: 14730 kWh

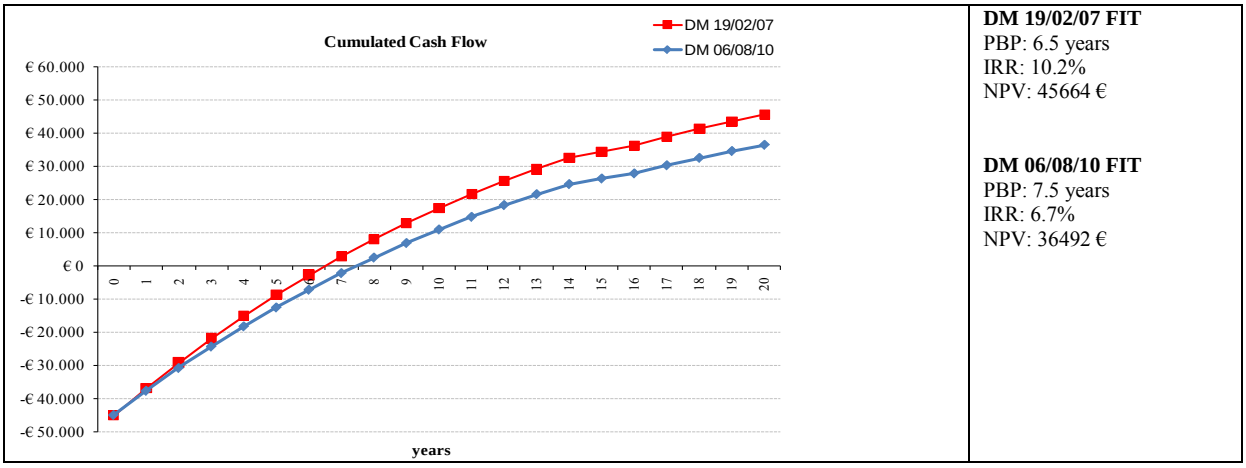

Fig. 1. Cumulative cash flow – Case 1: 10 kW Not integrated-Other PV system.

Second case: 10 kW PV system
Classification according to DM 19/02/07: Partially integrated – FIT Value: 0.404 €/kWh
Classification according to DM 06/08/10: PV in buildings – FIT Value: 0.360 €/kWh
Initial investment cost: 45000 € - Yearly production at year 0: 14730 kWh

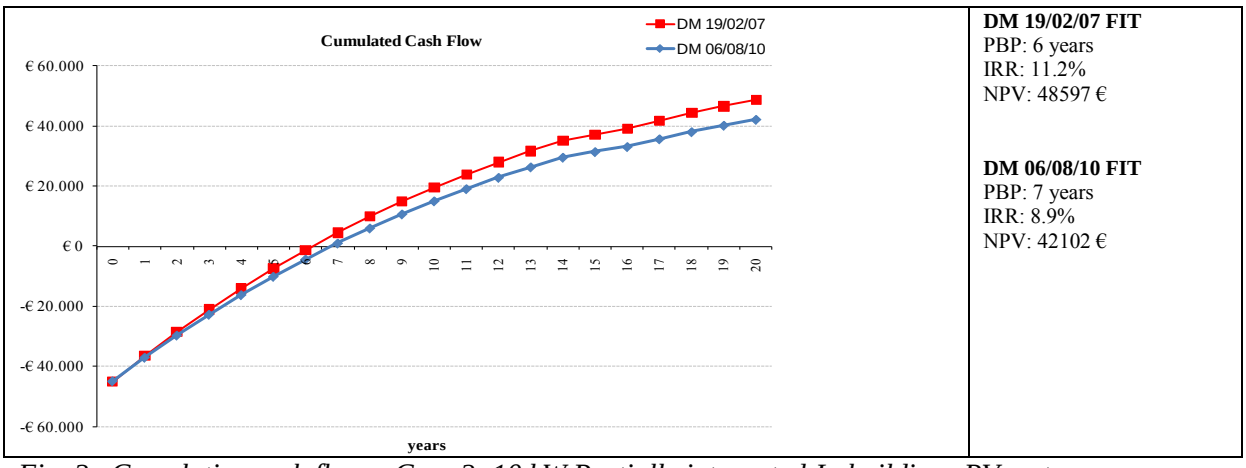

Fig. 2. Cumulative cash flow – Case 2: 10 kW Partially integrated-In buildings PV system.

Third case: 10 kW PV system
Classification according to DM 19/02/07: Totally integrated – FIT Value: 0.442 €/kWh
Classification according to DM 06/08/10: PV in buildings – FIT Value: 0.360 €/kWh
Initial investment cost: 45000 € - Yearly production at year 0: 14730 kWh

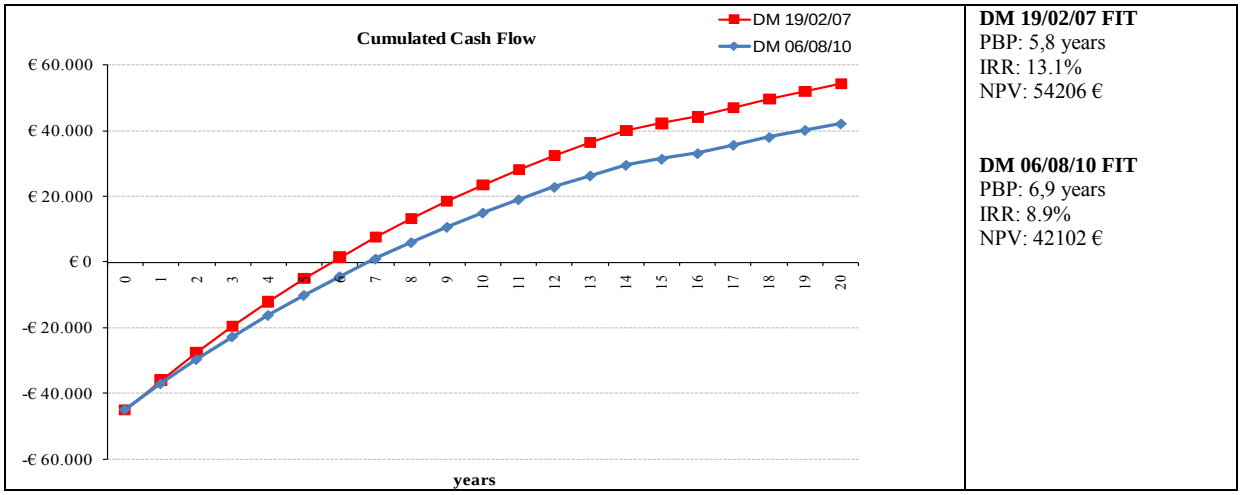

Fig. 3. Cumulative cash flow – Case 2: 10 kW Totally integrated-In buildings PV system.

Fourth case: 250 kW PV system
Classification according to DM 19/02/07: Not integrated – FIT Value: 0.346 €/kWh
Classification according to DM 06/08/10: Other PVs – FIT Value: 0.303 €/kWh
Initial investment cost: 1000000 € - Yearly production at year 0: 268250 kWh

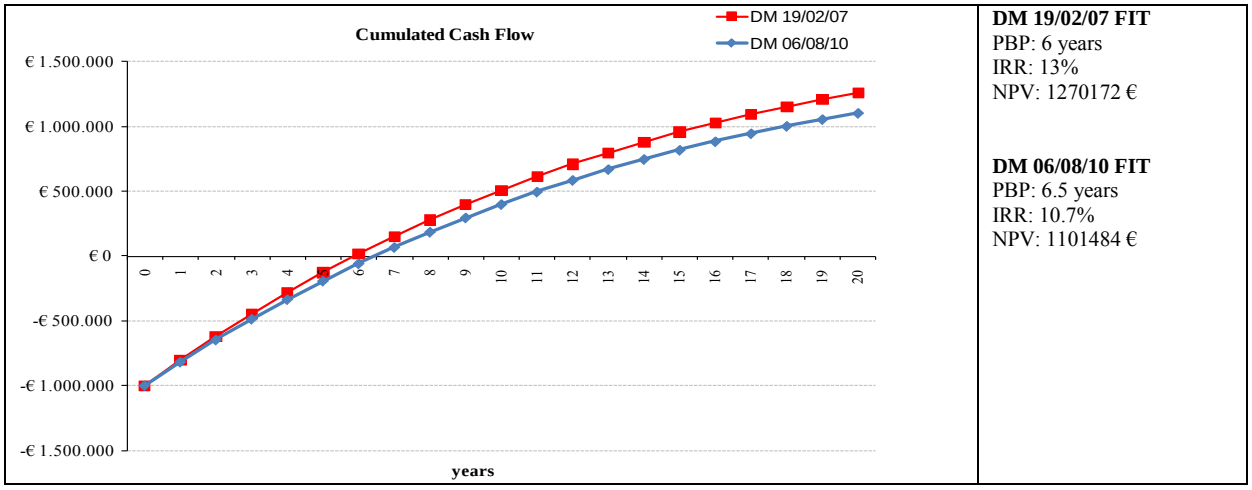

Fig. 4. Cumulative cash flow – Case 1: 250 kW Not integrated-Other PV system.

Fifth case: 250 kW PV system
Classification according to DM 19/02/07: Partially integrated – FIT Value: 0.384 €/kWh
Classification according to DM 06/08/10: PV in buildings – FIT Value: 0.335 €/kWh
Initial investment cost: 1000000 € - Yearly production at year 0: 268250 kWh

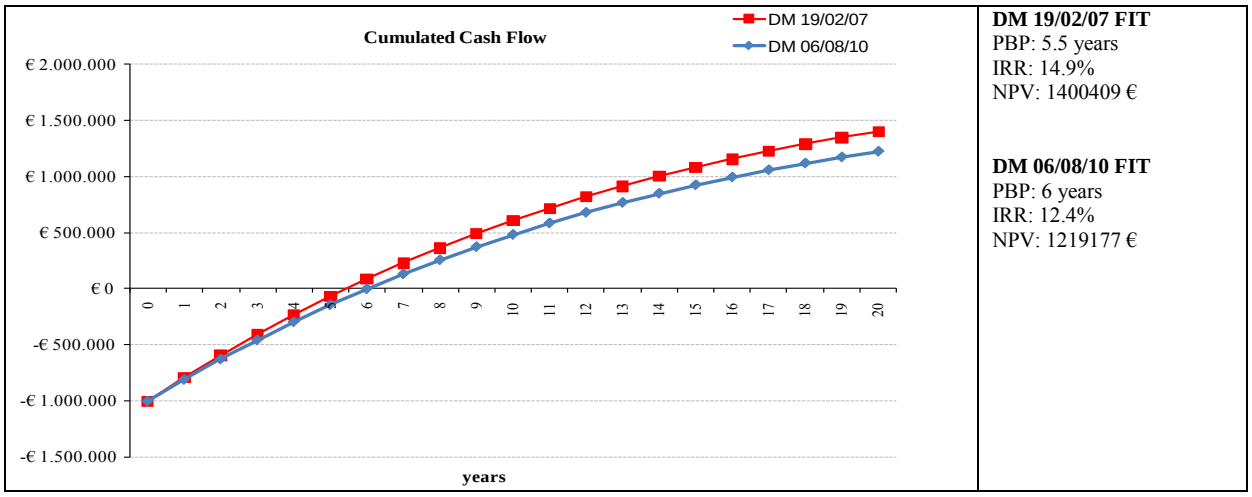

Fig. 5. Cumulative cash flow – Case 2: 250 kW Partially integrated-In buildings PV system.

Sixth case: 250 kW PV system
Classification according to DM 19/02/07: Totally integrated – FIT Value: 0.422 €/kWh
Classification according to DM 06/08/10: PV in buildings – FIT Value: 0.335 €/kWh
Initial investment cost: 1000000 € - Yearly production at year 0: 268250 kWh

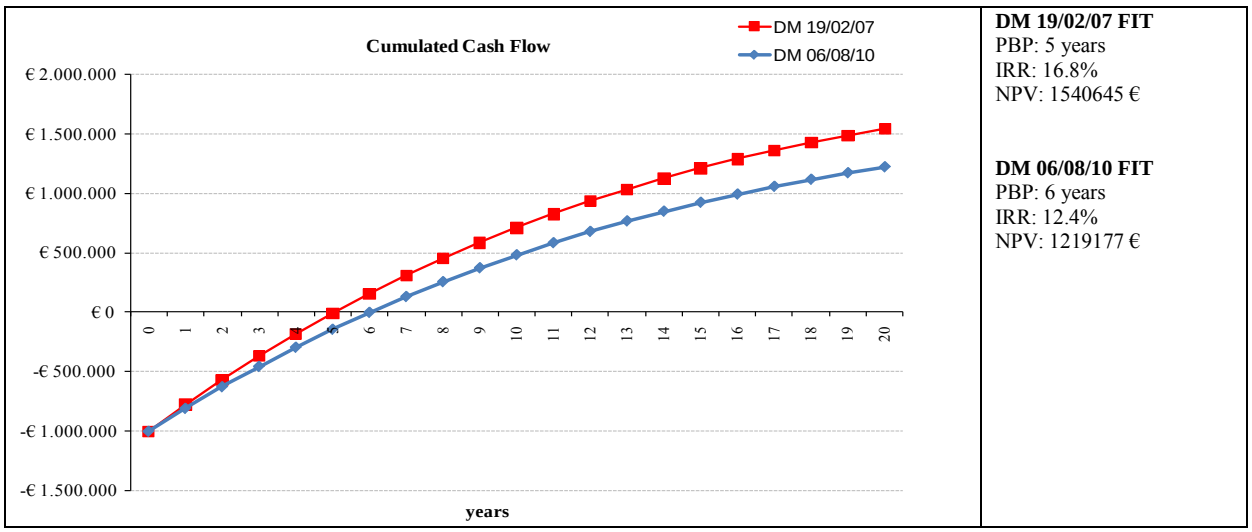

Fig. 6. Cumulative cash flow – Case 2: 250 kW Totally integrated-In buildings PV system.

5. Discussion and Conclusions

Simulations show that in the transition from the DM 19/02/07 to the DM 06/08/10:

- PBP increases and IRR and the NPV indexes decreases of about one year in all cases;
- The most significant variations are in the case of Totally integrated PV systems that, with the new Decree, are considered PV systems in building as the major part of Partially integrated PV Systems;
- The differences between economical indexes evaluated are higher for PV systems with lower rated power.

This last consideration, together with the fact that the new FITs have been decreased mainly for totally integrated PV systems, puts into evidence that the new Decree significantly penalizes the architectural PV integration.

This items represents a strongly criticism of the new incentive policy, because it seems to not adequately promote the reduction of the visual impact of PV systems with traditional components.

Really, the new Decree also considers, as above mentioned, PV systems with innovative components for total building integration, for which higher FITs values are established; in the present work these PV typologies have not been analyzed due to the fact that precise indications for their characterization are still lacking. A possibility of improvement, leading to higher incentives for building integrated PV system, can come from the definition of these characteristics, operated so as to include the higher number of situations of architectural integration accepted by the DM 19/02/07.

References

[1] European Council, Directive 2001/77/EC of the Council on the promotion of electricity produced from renewable energy sources in the internal electricity market, 2001.

[2] Kyoto Protocol to the United Nations Framework Convention on Climate Change, 1997.

[3] European Council, Directive 2009/28/EC April 23, 2009.

[4] Nomisma Energia, Le nuove fonti rinnovabili per l'energia elettrica in Europa, Arti Grafiche Tilligraf Srl, 2007.

[5] A. Campoccia, L. Dusonchet, E. Telaretti, G. Zizzo, Comparative analysis of different supporting measures for the production of electrical energy by solar PV and Wind systems: Four representative European cases, Solar Energy Vol. 83 Issue 3, 2009, pp. 287-297.

[6] Italian Ministry for Productive Activities Decree, Criteri per l'incentivazione della produzione di energia elettrica mediante conversione fotovoltaica della fonte solare (D.M. 28/06/2005), 2005.

[7] Italian Ministry for Economical Development Decree, Criteri e modalità per incentivare la produzione di energia elettrica mediante conversione fotovoltaica della fonte solare in attuazione dell'articolo 7 de l decreto legislativo 29 di cembre 2003 n. 387 (D.M. 19/02/2007), 2007.

[8] Italian Ministry for Economical Development Decree, Incentivazione della produzione di energia elettrica mediante conversione fotovoltaica della fonte solare (D.M. 06/08/2010), 2010.

[9] B. J. Feibel, Investment Performance Measurement. Wiley Interscience, 2003.

Channelling Norwegian hydropower towards greener currents: The challenge of conflicting environmental concerns?

Audun Ruud[1,*] Helene Egeland[1], Gerd B. Jacobsen[1], Jørgen K. Knudsen[1,*], William M. Lafferty[1]

[1] *SINTEF Energy Research, Norway*
** Corresponding author. Tel: +47 22965971, Fax: +47 22965980, E-mail: audun.ruud@sintef.no*

Abstract: Nearly 100 percent of electricity used in Norway stems from hydropower, but no further large-scale production is politically viable. There is however increased interest in hydropower as both a supplement to the national energy supply and as provider of balance within the European energy system. Interest focuses on: (1) increased pumping and storage; (2) upgrading of existing hydropower installations; and (3) small-scale hydro production. Such measures are also considered as climate-change mitigation. As a fourth developmental path there are also alternative processes aiming at reinforcing environmental concerns in existing hydropower, not least by revising granted licenses. These processes coincide with a reinforced focus on biodiversity. This dual environmental challenge is also enhanced by Norway's follow-up of the EU Directive on renewable energy (RES) and the EU Water Framework Directive (WFD). In this context, we here assess current political and regulatory practice in Norway, focusing on the status of environmental concerns, and the challenges Norwegian hydropower policy faces by the implementation of the EU Directives. The policy challenge is manifest as 'trade-offs' among hydropower priorities at both the strategic and project-specific levels; and is further enhanced by lack of clarity as to the ultimate impact of the relevant EU Directives.

Keywords: *EU, Renewable Energy Directive, Water Framework Directive, Norwegian hydropower, policy, governance, Environmental Policy Integration (EPI), trade-off*

1. Introduction

Nearly 100 % of electricity consumption in Norway stems from hydropower. Since 2001 it has been politically stated that the 'era of new large-scale hydropower constructions is over' **[1]**. At the same time, there is an increased interest for hydropower as a way of meeting national climate change commitments and to sustain the national power balance. Furthermore, there is an increased interest for extending the export potential of hydropower 'balance' to Europe, given the increased intermittent renewable (wind) power production in the EU. In parallel, there is growing concern over the environmental status of Norwegian water courses. Norway is committed by the former and current EU Directives on renewable electricity and energy (RES) (adopted in 2001 and 2008, respectively), as well as the EU Water Framework Directive (WFD; adopted in 2000) **[2] [3].** [1] The directives clearly involve 'trade-offs' among competing concerns for security of energy supply; climate change; biodiversity; and improved water quality.

In this light, there are *in principle* three major options for further development of hydropower in Norway: (1) extend the potential for pumping and storage to increase capacity for balancing; (2) refurbish and/or upgrade existing power production; and (3) promote small-scale hydropower. The third option can also be related to the first, since upgrading can entail increased storage capacity. Furthermore, with respect to environmental concerns for the water courses, there is a fourth 'path' which implies a stronger regard for environmental concerns in

[1] While not assuming the full responsibilities of EU membership Norway participates fully in the EU internal market, as well as being involved in related EU policy areas. This is since 1994 regulated through the Agreement on the European Economic Area (EEA).

the formal processes for revising licenses for existing facilities – with possible modifications and reductions in the production volume.

Referring to these four *developmental paths*, the present paper begins by assessing current political and regulatory practice for hydropower in Norway, focusing on the status of environmental concerns, and the emerging challenge of trade-offs between climate-change and biodiversity. The paper then goes on to discuss the challenges met by the implementation of the EU WFD and RES Directives. The empirical data are based on an ongoing research project on the political and regulatory framework for hydropower, and the related follow-up at the project level. This includes insights from four recent case studies **[4] [5] [6]**.[2]

As a conceptual approach to the analysis, we employ the notion of *Environmental Policy Integration* (EPI), which is an increasingly valuable tool for dealing with the potential synergies and trade-offs related to the goal of sustainable development. As indicated, any further development of hydropower in Norway involves competing economic, social and environmental concerns. Article 11 of the 'Principles' of the treaty of the European Union states that: 'Environmental protection requirements must be integrated into the definition and implementation of the Union's policies and activities, in particular with a view to promoting sustainable development'**[7]**. Our analysis is guided by the meaning of this stricture within the context of the academic discourse on EPI **[8]**.

In the following section, we present the analytical and methodological approach. Section 3 presents the main features of the current Norwegian political and regulatory framework, as well as the challenges raised by the EU RES and WFD Directives. In section 4 we discuss how these challenges have been met – and can be assumed to be met in near future, given the established national framework. And in section 5 we provide our conclusions.

2. Analytical framework

The challenge of integrating environmental concerns into economic and social policies is a key focus of the EPI approach. De-coupling economic drivers from environmental degradation is particularly crucial to achieve 'sustainable development' **[9]**. According to a principal interpretation of EPI, environmental concerns should be accorded 'principled priority' in order to reduce the degradation of the life-sustaining capacities of affected ecosystems **[8] [9]**. In the present context, EPI provides a basis for analysing trade-offs between environmental and other concerns relevant for hydropower, from policy strategies down to specific projects. Several mechanisms for applying EPI principles have been explored and analysed in Europe during the last twenty years **[10] [11]**.

Applying EPI principles to the further development of hydropower in Norway, we begin by identifying the *trade-off processes*- and *arenas* where different actors pursue different interests and concerns. A trade-off process in this context is understood as the decision-making procedures in place for resolving conflicts of interest in specific hydropower arenas at both the strategic and project-specific levels.

[2] The research project *Governance for Renewable Electricity Production* (GOVREP; 2009-12) focuses on policies and regulations for renewable electricity in Norway and Sweden. The project is part of the Norwegian Centre for Environmental Design of Renewable Energy (CEDREN), and is co-funded by the Norwegian Research Council, Statkraft and Agder Energy Production.

Such conflicts generally arise when hydro power production is assessed vis-à-vis measures to improve the environment, particularly since strong environmental measures often imply changes in the discharge of water, often affecting established energy production. The challenge of integrating environmental concerns also depends on the perspective employed. Are the concerns addressed at the European, national or local level of analysis? The underlying assumption here is that a European perspective will imply a stronger priority of climate-change mitigation over more local environmental concerns, including biodiversity. However, biodiversity is also a global challenge and entails international commitments.

It is in this light that we aim to identify and assess factors that condition the prioritization and application of environmental concerns. Context-specific studies of this kind are also decisive in order to supplement the traditional techno-economic approach of understanding the phase-in of new energy production **[12]**.

3. The political-regulatory framework for integrating environmental concerns in Norwegian hydropower production

Given its dominant role, hydropower is a crucial part of the general energy policy strategy in Norway. The public management of water courses began as early as 1887 with legislation which is still valid, though frequently revised and amended. The first Protection Plan for Watercourses was adopted in 1973, followed by three additional plans plus a supplement (1980, 1986, 1993 and 2005). In 1981 the Parliament adopted a Master Plan for Water Resources which ranks watercourses according to economic and environmental dimensions as well as the degree of expected political controversy. The Plan has since become the central reference for hydropower development.

Licenses for hydropower production are granted on the basis of both a general Energy Act (covering all forms of energy production and distribution) and more specific legislation on water regulations and water resources (two legal acts)**[6]**. In addition, there are several laws pertaining to the protection of water course environment directly relevant for hydropower.[3] Although these laws do not imply unalterable environmental requirements, they do provide important factors that must be considered in relation to licensing, and changes in licenses.

The four developmental paths for hydropower in Norway (as stipulated above), must, therefore, be based on the general strategic framework put forth in the Master Plan and protection plans, as well as more specific legislative requirements. With respect to *pumping and storage*, however, a more substantial exploitation of this potential in a European perspective is still not accounted for in any existing plan. The existing legislative framework applies, though questions can be raised as to whether this is sufficient given new challenges as to the need for stronger coordination between different licenses within the same watercourse system, most particularly with regard to affected environmental concerns.

The *refurbishment and upgrading* (R/U) of existing installations has been encouraged by political signals, being perceived as environmentally sound as it contributes to increased hydropower with lower environmental impacts than traditional hydropower production since

[3] Although the environmental focus in the water legislation traditionally is related to the local environmental context, there is an increasing focus on biodiversity following from international commitments. In particular, a Biodiversity Law was adopted in 2009, and there is also a specific protection regime for the salmon: The Law on Salmons and freshwater fish, together with regulations for protected salmon rivers and fjords. This also constitutes the Norwegian follow-up of international commitments for the preservation of salmons.

new physical interventions are not required. No overall target for R/U (or for any other aspect of hydropower generation for that matter) has been set at the national level. Licenses for R/U are granted within the legislative framework referred to above.

Small-scale hydropower (up to 10 MW installed capacity) has also been increasingly encouraged by both national and regional authorities, not least as a way of providing new economic activity and income for rural areas. Although guidelines for the planning and impact assessment of small-scale hydro projects at the county level were adopted in 2006, there is no overall national plan. Licenses for small-scale hydro projects are granted directly from the NVE, without additional approval from the MoPE. Another important development in the regulatory framework is a parliamentary decision from 2005 which allows the construction of small-scale projects below 1 MW to be constructed within protected water courses.

Efforts to improve the environmental standard of existing hydropower projects in regulated water courses constitute an important means for improving the water course environment in Norway.[4] Processes where trade-offs are being practiced include: (1) The *revision of licenses* – where the main objective is to rectify earlier regulatory initiatives which mainly emphasized the provision of electricity as a welfare benefit with little concern for environmental impacts. (2) The *revision of regulations affecting water discharge.* This includes licenses containing specific conditions and requirements, such as the protection of salmon. In such cases the particular condition stipulated has more leverage than other concerns, but is still weighted in relation to the consequences of restricting the hydropower production. (3) Finally, with direct relevance for newer licenses (after 1973), it is also possible to reinforce environmental measures applying more general standards, as long as the net energy output is not reduced.

In all of these processes the Norwegian licensing authority (the NVE), is authorized to coordinate related assessments and trade-off processes. The actual importance of the affected concerns will, however, vary from case to case as a consequence of the character of the process itself, as well as the case-specific context. Important aspects of these processes also involve actors at the regional and local levels. The management of hydropower is, however, characterised by sectoral fragmentation, as reflected by the different laws and plans mentioned above. The NVE, together with the Ministry of Petroleum and Energy (MoPE), manage and administer the laws concerning hydropower resources and the related licensing procedures. The Protection Plans, the Master Plan and the laws concerning nature protection and land use planning are, on the other hand, managed by the Ministry of the Environment (MoE) and the Directorate for Nature Conservation (DN).

Furthermore, in a number of cases related to hydropower development, particularly large-scale hydropower plants, the NVE provides only recommendations, whereas the MoPE makes the final decision, which in some cases must also be approved by the Parliament. In the course of these processes, divergences between the 'MoPE'- and 'MoE-segments' often materialise, based on their different mandates.

[4] The four case studies conducted as part of the GOVREP project, focus on different processes of changing the conditions in already granted licenses; the opportunities for integration of environmental concerns, and the trade-offs being made at different levels of governance[4] [5]: (1) Iveland: Upgrading of an existing hydropower plant; (2) Laudal: Revision of regulation of water currents concerning a special condition requiring protection of the salmon stock; (3) Suldalslågen: Revision of regulation of water currents in order to balance the hydro power production and the protection of the salmon stock in a more optimal manner, and (4) Aura: General revision of conditions in a granted license.

3.1. Follow-up of the EU Directives

It is within this general 'policy landscape' that new international commitments – on both climate-change and biodiversity – must be adapted and reconciled. The *EU Directive on the promotion of renewable energy (RES),* adopted in 2008, sets national, binding targets covering electricity, heating/cooling as well as biofuels, and is part of the EU's climate policy strategy **[2]**. The EU RES Directive is, however, still not (as of December 2010) formally adopted by Norway. Due to the extent of Norway's renewable energy resources (both hydropower and wind power), one expects that the EU will require an ambitious national target for Norway (through the EEA Agreement) **[13]**. Related to this process, Norway is currently negotiating with Sweden in order to establish a common scheme for tradable certificates for renewable electricity, and a protocol stipulating the principles of the system was signed by the two countries in December 2010. These efforts build on similar, but failed, negotiations in 2006 **[14]**.

A major objective of the *EU Water Framework Directive (WFD*) is to identify water courses where constructions or operations have affected the ecological status **[2]**. In such cases, one speaks of 'highly modified water courses'; for which the objective is to achieve 'good ecological potential' (as distinguished from a 'good ecological status' for 'purer' water courses) **[2]**. In principle, all water courses affected by larger hydropower activities are considered to be highly modified. The WFD was adopted in 2000, but the inclusion in the EEA Agreement was delayed and Norway did not start implementation before 2006. By focusing on 29 pilot areas Norwegian authorities aimed at coordinating their initial follow-up with the common EU implementation. The EU WFD Directive has stimulated a debate on the future usage of water resources, and the implementation of the Directive has evoked conflicts of interest between energy production and nature conservation in Norway.

The 'complete' Norwegian follow-up is to be coordinated with the second phase of the EU implementation plan, that is 2010-15. This will provide a more complete picture of the effect of the WFD in Norway. The River Basin Management Plans and Programmes of measures (as stipulated by the Directive) related to the first phase were approved by the Government in June 2010 **[15]**. An important part of the Norwegian follow-up is the general principle that concrete measures must be based on sectoral legislation. In general, this means that the NVE continues to coordinate the license processes for hydropower as before, only now being 'informed' of the regional water management plans. The environmental goals of the plans are, therefore, only to be considered along with other existing laws regulating water courses.

4. What is the role of environmental concerns?

As indicated in section 3, Norway's hydropower policy has traditionally been based on a strategic framework which can be characterised as a 'trade-off arena' at the national level. In recent years, the Master Plan's ranking of potential projects based on specific criteria can also be associated with Norway's ambitions on sustainable development (SD). The issue of trade-offs among the three dimensions of SD – economic, social and environmental – is thus increasingly difficult to resolve at both the political-strategic level and in relation to individual projects. Given a general lack of specificity in the Master Plan for hydropower, however, the actual assessments of trade-offs are primarily taking place at the local-regional project level. This has been confirmed by the four case studies of the GOVREP project **[4] [5]**.

Another important finding from these case studies is that environmental concerns must be viewed as compatible with economic interests if they are to be accommodated at all **[4] [5]**. In

particular, in relation to revision of regulation of water discharges (Suldalslågen, Laudal) economic interests related to the salmon stock (fishing, tourism) entailed protection measures, including restrictions of the hydropower power production **[4] [5]**. At the same time, in other cases, the focus on economic interests has led to the priority of increased hydropower production, whereas biodiversity-related environmental concerns have been offered only limited attention **[4] [5]**. Hence, although environmental concerns constitute the point of departure for many revisions of existing licenses and installations, pro-environment trade-off's are not stipulated in advance.

Economic concerns also seem to be decisive for small-scale hydropower: The main driver here is clearly a general concern for sustained economic development in rural areas **[6]**. Small-scale hydropower is, however, mentioned as a relevant factor in Norway's most recent climate-change policy strategy **[16]**. Small-scale hydro is also promoted as environmentally benign because no reservoirs are needed, in contrast to large-scale hydro projects. Small-scale initiatives do not, therefore, represent an option for an increased RES balancing of the European energy market. Further, small-scale installations have a number of potentially negative impacts on water course environments, not least due to the high and increasing number of installations. Again, we see no evidence in our studies of overall trade-offs among these partly contradictory objectives **[6]**.

The potential effects and impacts of increased pumping and storage in relation to European energy production has not yet been assessed, nor included in the climate-change policy strategy. Norwegian politicians increasingly refer to this option, however, as a climate-policy measure. Pumping and storage is also seen as an alternative way of fulfilling Norway's impending target under the EU RES Directive. Thus far, however, no public figures have been supplied as to the potential of these and other 'new RES' sources for Norway's obligations under the EU Directive.

R/U initiatives have, however, been framed as a climate-change mitigation option, although not specifically in relation to the overall national climate-change policy strategy. In an R/U project studied within GOVREP (Iveland) the 'climate-argument' was employed to justify the upgrading of the installation **[4]**. This reflects a perception of R/U cases as contributing to an overall reduction of greenhouse gas emissions by hydropower supply. Once again, however, no overall target for R/U has yet been stipulated.

The most relevant SD trade-off processes are thus conducted at a project level within the framework of an outdated Master Plan. More recent national policy targets for climate change, biodiversity and improved water management have thus far not been substantially affected by the national-strategic trade-off decisions. This is most clearly illustrated by the implementation of the WFD Directive. The follow-up here has thus far not resulted in – or been directed by – any overall national objectives, although the process has contributed to a strengthened focus on environmental concerns in water course management and development. In the years to come, the WFD will, nevertheless, require a broader environmental input to the assessment of hydropower projects. As shown in the GOVREP case studies, however, the eventual effect of this input will probably vary from case to case, and from process to process **[4] [5]**.

Finally we can mention that, by examining the regional management plans conducted during the first phase of the WFD follow-up, one is struck by the comprehensive mapping and assessment of the different factors leading to highly modified water courses **[6]**. At the same

time, however, no clear provisions as to the further development of hydropower – with eventual direct impact on specific projects – are stipulated by the plans. The main approach is to delegate the responsibility for the formulation of mitigating measures to the energy-sector authorities. Together with the Government's decision to treat environmental concerns primarily in relation to the licensing of hydropower projects – and to only 'be informed' as to the implications of the regional water management plans – the situation clearly reinforces an impression of a relatively passive and incremental Norwegian follow-up of the WFD.

5. Conclusion: The overall status of environmental concerns

The traditional project-specific approach to trade-offs in relation to Norwegian hydropower development reflects a generally 'robust' approach. The environmental dimension is, however, of more recent and increasing importance as a crucial factor in hydropower licensing and development. In addition, both climate-change mitigation and biodiversity are increasingly important national concerns; but, at the same time, concerns that increasingly will conflict with each other. Whereas climate-change will figure more prominently at the strategic level, biodiversity concerns will generally be activated more strongly at the local level and related to specific projects. No overall assessment or specific guidelines exist at to the management of these complex 'trade-off' challenges. The challenge is manifest in growing confrontations between protagonists for stronger environmental concerns and protagonists of more hydropower; and is being directly incorporated into the different mandates of environmental and energy authorities. A stronger focus on biodiversity, and new efforts of establishing a more sector-encompassing water management through the implementation of the WFD, has not altered the relative positions of the responsible agencies thus far. The setting of a new EU-related national RES target, has the potential to induce changes which can reinforce the need to develop hydropower, and thereby lead to even stronger conflicts with biodiversity. The final act in the shaping of Norway's water management system, as well as the future of Norwegian hydropower in an EU energy context, is thus strongly dependent on the follow-up of both the RES and WFD Directives. Whether at the level of national energy-climate strategy, or specific regional-local waterpower projects, the issue of 'trade-offs' is the name of the Norwegian sustainable-development game.

References

[1] White Paper 37, 2000-01, On hydropower and the power balance (in Norwegian), Oslo: Ministry of Petroleum and Energy (MoPE).

[2] OJEC, Directive 2000/60/EC of the European Parliament and of the Council of 23 October 2000 establishing a framework for Community action in the field of water policy. In *Official Journal of the European Communities (OJEC), 22 Dec. 2000, L 327/1.*

[3] OJEU, Directive 2009/28/EC of the European Parliament and of the Council of 23 April 2009 on the promotion of the use of energy from renewable sources and amending and subsequently repealing Directives 2001/77/EC and 2003/30/EC. In Official Journal of the European Union, 5 June 2009, L 140/16.

[4] H. Egeland & G.B. Jacobsen, On the case studies of Laudal and Iveland (in Norwegian), Technical Report, Trondheim: SINTEF Energy Research, 2011a, forthcoming.

[5] H. Egeland, H. & G.B. Jacobsen, On the case studies of Suldalslågen and Aura (in Norwegian), Technical Report, Trondheim: SINTEF Energy Research, 2011b, forthcoming.

[6] J.K. Knudsen, Norwegian hydropower management and the integration of environmental concerns, Technical Report, Trondheim: SINTEF Energy Research, 2011, forthcoming.

[7] CEC, Consolidated Version on the Treaty of the Functioning of the European Union, in Official Journal of the European Union, C 115/47, 9 May 2009. Brussels: The European Communities.

[8] J.K. Knudsen, Environmental Policy Integration: Conceptual clarification and comparative analysis of standards and mechanisms, Dissertation submitted to obtain the degree of Doctor. Enschede: University of Twente, 2009.

[9] W.M. Lafferty & E. Hovden, Environmental Policy Integration: Towards an Analytical Framework, Environmental Politics, Volume 12, Issue 3, 2003, pp. 1 – 22.

[10] A.J. Jordan & A. Lenschow (eds), Innovation in Environmental Policy? Integrating the Environment for Sustainability, Cheltenham UK: Edward Elgar, 2008.

[11] W.M. Lafferty (ed.), Governance for Sustainable Development, Cheltenham UK: Edward Elgar, 2004.

[12] W.M. Lafferty & A. Ruud A. (eds), Promoting Sustainable Electricity in Europe: Challenging the Path Dependency of Dominant Energy Systems, Cheltenham UK: Edward Elgar, 2008.

[13] A. Ruud & J.K. Knudsen, Renewable energy policy making in the EU: What has been the role of Norwegian stakeholders?, Teknisk Rapport TR A6860, Trondheim: SINTEF Energy Research AS, 2009.

[14] J. Knudsen, A. Ruud & O.M. Larsen, Norway: Promoting new renewables in a hydro-based petroleum economy', in W.M. Lafferty and A. Ruud (eds): Promoting Sustainable Electricity in Europe: Challenging the Path Dependency of Dominant Energy Systems. Cheltenham UK: Edward Elgar, 2008, pp. 250-278.

[15] Ministry of the Environment, Royal decree approving regional management plans according to the WFD Directive (in Norwegian), Oslo: Ministry of the Environment, 2009.

[16] Committee Recommendations 145, Innstilling fra energi- og miljøkomiteen om norsk klimapolitikk (in Norwegian). Oslo: Parliament, 2008.

Small Hydropower Development and Legal Limitations in Thailand

Thanaporn Supriyasilp [1,*], Kobkiat Pongput [2], Challenge Robkob[3]

[1] *Department of Civil Engineering, Faculty of Engineering, Chiang Mai University. Thailand. 50200.*
Science and Technology Research Institute, Chiang Mai University. Thailand. 50200.
[2] *Water Resources Engineering Department of Kasetsart University, Bangkhen, Bangkok, Thailand. 10900.*
[3] *Biodiversity-based Economy Development Office (Public Organization), Laksi, Bangkok, Thailand. 10210.*
** Corresponding author. Tel: +66 53942461, Fax: +66 53942478, E-mail: thanaporn@eng.cmu.ac.th, istdir@chiangmai.ac.th*

Abstract: The northern region of Thailand which consists of the Ping, Wang, Yom, and Nan river basins has potential for small hydropower development. The Ping and Wang River Basins are used as case studies. Apart from technical aspects such as electricity generation, engineering and economic aspects, the socio-economics, environment, law and regulation, and stakeholder involvement aspects are also taking into consideration. There are 64 potential projects in the Ping River Basin. The overall electricity potential is about 211 MW with annual power generation of about 720 GWh. For the Wang River Basin, there are 19 potential projects with about 6 MW and an annual power generation of about 30 GWh. However, most of these potential projects are located in forested areas with legal limitations. The various types of forests can result in different levels of legal obstacles. Therefore, the procedure required for permission is varied and is dependent on both the desired development and the forest in question. The laws and regulations related to project development in forested areas are reviewed and are summarized on a case by case basis in a way that is easily understood and accessible for others to use as a reference for other areas. The suggestions for policy adjustments with environmental friendly consideration are also discussed.

Keywords: *Hydropower development, legal limitations, forested area*

1. Introduction

Hydropower is one of the few renewable and clean energy sources. According to the Thailand 15 year power development plan for 2008 to 2022 (Power Policy Bureau, 2010), the total hydropower potential from every region in Thailand is about 328 MW.

This power is generated from 3 different categories of hydropower plants: the Royal Irrigation Department (RID)'s water resources project about 168 MW, small hydropower contributes about 154 MW, and from very small hydropower plants, about 6 MW of power. Among the regions in Thailand, the northern part of Thailand has a very high potential for small hydropower development due to its steep slope topography. However, the suitable sites for small hydropower development are usually in forested areas with legal limitations. Various types of forests present different levels of legal obstacles. There are many laws and regulations that prohibit project development such as the B.E. 2484 (1941) Forest Act, the Ministerial Regulations Number 16, B.E. 2498 (1955), the B.E. 2504 (1961) National Park Act, the B.E. 2535 (1992) Wildlife Reservation and Protection Act, and the B.E. 2507 (1964) National Reserved Forest Act. Therefore, the procedure required for permission is varied and is dependent on both the desired development and the forest in question. In the past, no one has summarized or categorized the means to develop projects in forested areas, especially for the case of hydropower and the case when project sites involve more than one type of forested regions.

The objectives of this research are to analyze the laws and regulations related to project development in forested areas and to summarize on a case by case basis in a way that is easily understood and accessible for others to use as a reference for other areas. The suggestions for policy adjustments with environmental friendly considerations are also discussed. The small

hydropower development sites in the Ping and Wang river basins which are the two main river basins in the northern part of Thailand are used as case studies.

2. Methodology

Supriyasilp et al.(2009a) have reviewed laws and regulations related to project development in forested area and have classified the forested areas into three groups based on type of regulations. Each law and regulation has a specific procedure.

The first type are those forests which are protected by law, such as state forests, national parks, wildlife conservation areas, no-hunting areas, national reserved forests, and environmental protection areas. The laws related to the forest in this type are 1) the B.E. 2484 Forest Act, 2) the Ministerial Regulations Number 16, B.E. 2498, 3) the B.E. 2504 National Park Act, 4) the B.E. 2535 Wildlife Reservation and Protection Act, 5) the B.E. 2507 National Reserved Forest Act. If the area involves the B.E. 2484 Forest Act or the Ministerial Regulations Number 16, B.E. 2498, then the project can be developed. If the area involves the other laws, then the project development in the area is prohibited. However, there is exception for the B.E. 2504 National Park Act and the B.E. 2507 National Reserved Forest Act. Under the article 19 of the B.E. 2504 National Park Act, the project or any activities can be done within the area if it is done under the cooperation with the national park. However, the benefit of the project should be used for the purpose of the national park only. For the areas which fall under the B.E. 2507 National Reserved Forest Act, the project can be done by the government agencies using the procedure under article 13.

The second type of forests is those provided by Cabinet Resolutions. This type of forest involves various laws and regulations regarding catchment quality and land use prohibition**.** By status, cabinet resolutions are not laws. But it is the government's policy that all governmental units abide by the cabinet resolutions. According to the Cabinet Resolution of 28 May B.E. 2528 (1985) which concerns the criteria for judging the quality of catchment and measures for land use (along the Ping and Wang Rivers), the area announced as the catchment quality class 1A and 1B is prohibited for all types of project development. This area is reserved as the source of the river. Regarding the Cabinet Resolution of 15 May B.E. 2533 (1990), which concerns permission to use land in the forest areas, the area defined as the conservation area (zone c) cannot be used by a private agency. A government agency can implement a project in the area but must do an environmental impact assessment first.

The third type of area include areas such as parks, arboretums, and state forestry plantations of all kinds including those commemorating the members of the royal family, areas in preparation to be national parks, wildlife breeding and protection areas and areas where hunting is prohibited.

The principles that should be kept in mind when considering the forested area with legal limitation can be summarized as follows.
1) If it is prohibited by law, with no provision for exception, go by the law. When time is needed in the process of annulling/invalidating the law, avoid using the disputed area altogether.
2) If the law has provision for exception, but there is cabinet resolution prohibiting permission, a move to make changes to the resolution must be done first.

3. Case studies and application

3.1. Study areas

The Ping and Wang river basins are selected as case studies. The Ping river basin covers about five provinces namely Chiang Mai, Lamphun, Tak, Kamphaeng Phet, and Nakhon Sawan. It originates in the Pee Pan Nam mountain range in the Chiang Dao district, Chiang Mai province. After passing the town of Chiang Mai, it flows through the provinces of Lamphun, Tak, and Kamphaeng Phet. At the confluence with the Nan River at Nakhon Sawan (also named Paknam Pho in Thai) it forms the Chao Phraya River. The area of the Ping River Basin is approximately 34,856 km^2. The total length is 740 km. The Wang river basin is smaller than the Ping river basin. It covers most areas of the Lampang province. The watershed area is about 10,793.57 km^2 with the total river length of 460 km. The Wang River flows through Lampang province and meets the Ping River at Tak province.

3.2. Potential hydropower development projects

The National Research Council of Thailand (NRCT) has provided funding for the study of potential hydropower development in Thailand. According to the recent research on the study of potential sites for hydropower development in the Ping and Wang river basin (Supriyasilp et al., 2009b; Supriyasilp et al., 2010), there are 64 and 19 potential projects in Ping and Wang river basin, respectively. The Ping river basin has a much steeper slope than the Wang river basin and therefore, it has more potential projects than the Wang River Basin. Moreover, the very small projects which provide installed capacity less than 100 kW are neglected for the hydropower potential analysis in the Ping River Basin. For the Ping river basin, the overall electricity potential is about 211 MW with annual power generation about 720 GWh. For the Wang River Basin, the electricity potential is about 6 MW and the annual power generation is about 30 GWh.

The hydropower schemes in the studies of hydropower development in the Ping and Wang river basins are classified into three types: low head Q based (LHQB), waterway (WW), and dam with storage (DwS) or reservoir type. When analyzing the power capacity, amount of water flow and head of water are two major factors to be considered. The Q in LHQB type stands for discharge or amount of flow per unit of time. The head is a vertical change in elevation between the headwater level and the tail water level excluding loss. The LHQB type is usually applied when the head is low and the amount of flow is large such as in the lower reach and major tributary. The WW type is also called the diversion type or run-of-river type, which part of water is diverted from the main stream to the facilitated channel through the penstock to the turbine. In DwS type, a dam is built to store river water as a reservoir. Following a specific operation rule, water may be released either to meet electricity needs or to maintain an appropriate reservoir level.

Supriyasilp et al. (2009b) has classified the potential sites for the analysis into 6 categories based on the available data and development practices in power generation evaluation. The details of each group are as described as follow.

Group I: The new sites in main river.
For the Ping River, there are many sub watershed and several tributaries. The major tributary usually gives large amount of flow with low head. Thus, the hydropower scheme in this group is the LHQB type. However, the hydropower development in this group is limited since Thai communities are usually situated along the river because the main occupation of the Thai people is agriculture. Even though, nowadays the way of life has changed to be more

industrialized, the preference of a place for living is still near the river. Therefore, there are a lot of communities along the way of the Ping River. Only two potential sites were found in this group to avoid the serious impact on the communities. For the Wang River, there is no project under this group.

Group II: The existing reservoirs
There are several existing reservoirs in Thailand. Most of them are the responsibility of the Royal Irrigation Department (RID). These reservoirs are mainly used for irrigation. They are also considered for hydropower potential development in order to increase the value added of the water in the reservoir. There are three potential sites in each river basin that fall within this category. The hydropower scheme in this category is considered as DwS type.

Group III: The sites in previous studies
Several organizations related to the development of energy such as Electricity Generating Authority of Thailand (EGAT) have studied on the potential sites to develop hydropower projects. In the past, the large dam construction was usually obstructed by the people in the area and the non-government organizations (NGOs). The sites found in the previous studies are also considered in the study of Supriyasilp et al. (2009 and 2010) but need to be reanalyzed on the amount of flow and cost of construction in the engineering and economic aspects. The hydropower scheme in this group is DwS type. There are four sites in this category in the Ping river basin.

Group IV: The sites studied by the Department of Alternative Energy Development and Efficiency (DEDE)
There are 12 sites for the Ping river basin and no sites for the Wang river basin found in the study of the DEDE. Most sites in this group were located in minor tributaries which had a steep topography. All of them are WW type.

Group V: The sites in water organization's development plan.
The sites in this group are from the development plans of relevant water organizations such as the RID and the Department of Water Resources (DWR). The water resource development projects in these plans mainly aim for irrigation purposes. Thus, the analysis has been done under the concept of adding the power capacity to the projects and generating electricity as a by-product. This introduces the value added of the projects and makes the projects more feasible to develop. The hydropower scheme in this group is DwS type. There are 23 sites for the Ping river basin.

Group VI: The new sites from major tributaries
Apart from the sites in group I, the sites in this group have just explored and examined other than previous studies. The study process was started from the site selection. There are 9 WW sites and 11 DwS sites found for Ping river basin, while there are 7 WW sites and 9 DwS sites for Wang river basin.

4. Discussion

Table 1 shows the legal limitations for each potential site in the Ping and Wang river basin based on forested area type. For both river basins, none of the sites is within the forested area type 3. Most of the sites involve more than one type of forested area and more than one law in each forest type. The procedures are summarized in 6 categories as follows. Even though

the categories are illustrated based on the Ping and Wang cases, they can be applied as the references for other project development in forested areas.

Category I: the site involves the area announced by the Cabinet Resolution concerning the catchment quality class 1A and 1B. The resolution for that area has to be removed first before one can follow the steps to request use of that area for other laws.

Category II: the site involves the area announced by the Cabinet Resolution as zone C. The environmental impact assessment has to be done for the project development at that site. The process usually takes time.

Category III: the site involves the National Park Act. Under article 19 of the B.E. 2504 National Park Act, the project or any activities can be done within the area if it is done under the cooperation with the national park. However, the benefit of the project should be used for the purpose of the national park only.

Category IV: the site involves the Wildlife Protection Act. Project development in this area is prohibited.

Category V: the site involves the Reserved Forest Act. The project can be done by the government agencies using the procedure following article 13 of the Act.

Category VI: the site involves the Forest Act. The project can be done following the Ministerial Regulations Number 16, B.E. 2498. Therefore, if the project is in category VI only, the procedure is easiest among all categories.

Even though the technical aspects such as electricity generation is important, engineering and economics aspects, the socio-economics, environment, law and regulation, and stakeholder involvement aspects should also be taken into consideration. The sites in group 3 can provide the most installed capacity. However, large dams have to be constructed. This can cause a lot more impacts to the environment comparing to the DwS in other groups, which dam's size is much smaller. The sites in group 1 have low interest rate of return (IRR) and high electricity generating cost (Supriyasilp et al., 2009b). Therefore, the sites in group 1 and 3 are not preferred.

Among the groups, the sites in group 2 seem to be the most preferable due to less legal limitations. Also their environmental impacts are less than the other groups since they already have a reservoir. Group 5 involves less laws and regulation than group 4 and 6. Therefore, they are more preferable. The sites in group 4 and 6 involve more than one type of forested area. There are two sites in the Ping river basin in Category IV, which is prohibited. Most of the sites involve with the Cabinet Resolution 1A (category I) and zone C (category II) together with either the National Park Act (category III) or the Reserved Forest Act (category V).

Table 1. Laws and regulations related to each potential site.

Site no.	Group	HP scheme	Installed capacity (kW)	Annual energy production (GWh)	Forest by laws				Cabinet resolution	
					F. A.	NP. A.	WP. A.	RF. A.	1A/ 1B	Zone C
P1	1	LHQB	100	0.6				●		
P2	1	LHQB	700	4.3	●					
P3	2	DwS	2,000	6.1	●					
P4	2	DwS	110	0.8				●		
P5	2	DwS	257	2.1				●		
P6	3	DwS	77,000	104.5				●	●	●
P7	3	DwS	26,000	55.1				●	●	●
P8	3	DwS	8,000	58.6				●	●	●
P9	3	DwS	8,000	25.9	●					
P10	4	WW	13,600	49.6		●		●	●	●
P11	4	WW	628	3.6				●		
P12	4	WW	930	4.1				●	●	●
P13	4	WW	1,600	7.8				●	●	●
P14	4	WW	90	3.8				●		●
P15	4	WW	1,051	5.3				●	●	●
P16	4	WW	1,447	7.1		●		●	●	●
P17	4	WW	1,450	6.8				●		●
P18	4	WW	1,322	7.0		●		●		●
P19	4	WW	164	0.8		●		●	●	●
P20	4	WW	760	3.8		●		●	●	●
P21	4	WW	417	2.1				●	●	●
P22	5	Plan DwS	1,043	7.1		●		●	●	●
P23	5	Plan DwS	11,058	59.3				●	●	●
P24	5	Plan DwS	2,218	9.3				●		
P25	5	Plan DwS	883	1.4	●					
P26	5	Plan DwS	1,413	2.0				●		
P27	5	Plan DwS	142	0.3				●		
P28	5	Plan DwS	1,457	2.0	●					
P29	5	Plan DwS	761	1.4				●		
P30	5	Plan DwS	674	1.3				●		
P31	5	Plan DwS	721	1.1				●		
P32	5	Plan DwS	333	1.2				●		
P33	5	Plan DwS	113	0.5	●					
P34	5	Plan DwS	982	8.6		●		●		
P35	5	Plan DwS	129	0.9		●				●
P36	5	Plan DwS	2,495	8.2	●					
P37	5	Plan DwS	107	0.4	●					
P38	5	Plan DwS	169	0.5	●					
P39	5	Plan DwS	812	6.7				●		
P40	5	Plan DwS	99	0.4		●		●		
P41	5	Plan DwS	429	1.5				●		
P42	5	Plan DwS	2,052	8.2				●		
P43	5	Plan DwS	5,026	43.8		●		●		●
P44	5	Plan DwS	114	0.9				●		

Table 2. Laws and regulations related to each potential site (con't).

Site no.	Group	HP scheme	Installed capacity (kW)	Annual energy production (GWh)	Forest by laws				Cabinet resolution	
					F. A.	NP. A.	WP. A.	RF. A.	1A/ 1B	Zone C
P45	6	DwS	2,000	12.4				●	●	●
P46	6	DwS	1,500	9.3		●		●	●	●
P47	6	WW	300	1.9		●		●		●
P48	6	DwS	1,000	6.1				●	●	●
P49	6	WW	600	3.6				●	●	●
P50	6	WW	300	1.8				●		●
P51	6	DwS	1,100	6.7				●	●	●
P52	6	WW	600	3.6				●	●	●
P53	6	WW	300	1.8				●	●	●
P54	6	DwS	1,000	6.1				●	●	●
P55	6	DwS	5,300	32.2				●	●	●
P56	6	DwS	300	1.8				●		
P57	6	WW	200	1.2				●		●
P58	6	DwS	1,800	10.8				●	●	●
P59	6	WW	1,600	9.6				●	●	●
P60	6	DwS	3,200	19.2				●	●	●
P61	6	WW	2,500	15.0				●	●	●
P62	6	WW	3,300	19.8				●	●	●
P63	6	DwS	2,800	16.8			●		●	●
P64	6	DwS	2,200	13.2			●			●
W1	6	WW	20	0.12	●				●	
W2	6	WW	20	0.12		●		●	●	●
W3	6	WW	230	1.38		●		●	●	●
W4	6	WW	30	0.18		●		●	●	●
W5	6	DwS	200	1.19		●		●	●	●
W6	6	DwS	370	2.21		●		●	●	●
W7	6	DwS	170	1.01		●		●	●	●
W8	6	DwS	140	0.83		●		●	●	●
W9	6	DwS	10	0.06		●		●	●	●
W10	6	DwS	20	0.12		●		●	●	●
W11	6	DwS	20	0.12		●		●	●	
W12	6	WW	10	0.06				●	●	●
W13	6	DwS	10	0.06				●	●	●
W14	6	WW	50	0.3				●	●	●
W15	6	WW	30	0.18				●		●
W16	6	DwS	10	0.06		●		●	●	●
W17	2	DwS	2,300	6.22				●		●
W18	2	DwS	2,200	15.92	●					
W19	2	DwS	50	0.07				●		

F.A= Forest Act; NP.A.= National Park Act; WP.A.= Wildlife Protection Act;
RF.A= Reserved Forest Act; P1= site no. 1 in Ping river basin; W1=site no.1 in Wang river basin

5. Conclusion

Legal matters present the main obstacle for small hydropower project development in the Northern Region of Thailand. The preferable site usually involves more than one type of forested areas. This paper has summarized the laws and regulations related to hydropower development in forested areas and has suggested the means to develop potential hydropower sites by classifying them into 6 categories. It is recommended that to promote the hydropower development, three issues have to be taken into consideration. First, the laws and regulations have to be systematically reformed so that they are consistent with each other and up to the country's present situation. Second, the issue about project ownership stated in the law has to be reconsidered. The community and private sector should be able to take part in the investment and receive benefits from selling electricity. Regarding the community's investment, people in the community would feel that they are the owner of the resources and as a result would have an incentive to take proper care of the resources. However, the regulation reform for this issue has to be done carefully by considering the concept of balancing the benefits of energy and the detriment to the environment. Lastly, the regulation limiting the use of electricity within the park area should be revised. The excess electricity from the park can then be used to support the national grid.

Acknowledgement

The authors would like to acknowledge the important support given by the National Research Council of Thailand (NRCT).

References

[1] Power Policy Bureau, Energy Policy and Planning Office, Ministry of Energy, Thailand. 25 Mar 2010.

[2] Forest Act B.E. 2484, Royal Thai Government Gazette 58, 73, 1941.

[3] Ministerial Regulations Number 16, B.E. 2498, Ministry of Natural Resources and Environment, Thailand, 1955.

[4] National Park Act B.E. 2504, Royal Thai Government Gazette 78, 80, 1961.

[5] Wildlife Reservation and Protection Act B.E. 2535, Royal Thai Government Gazette 109, 15, 1992.

[6] National Reserved Forest Act B.E. 2507, Royal Thai Government Gazette 81, 38, 1964.

[7] T. Supriyasilp, K. Pongput, C. Robkob, J. Ruangvichathorn, T. Boonyasirikul, and S. Boonyanupong, Law and Hydropower Project Development in Forested Areas, National Research Council Journal, the Special Edition for Renewable Energy, 2009a, pp. 28-39.

[8] Cabinet Resolution of 28 May B.E. 2528, 1985.

[9] Cabinet Resolution of 15 May B.E. 2533, 1990.

[10] T. Supriyasilp, K. Pongput, and T. Boonyasirikul, Hydropower Development Priority Using MCDM Method. Energy Policy 37, 5, 2009b, pp. 1866 -1875.

[11] T. Supriyasilp, K. Pongput, T. Boonyasirikul, S. Boonyanupong, C. Tuksaudom, and R. Yongprayun, the Study of Potential and Regulation Issues for Hydropower Development in Wang River Basin, NRCT report, 2010.

Reducing our emissions while achieving good status of our water bodies – is it possible? Swedish hydropower in the limelight

Peter M. Rudberg[1*], Måns Nilsson[1]

[1] *Stockholm Environment Institute; Kräftriket 2B; SE 106 91; Sweden*
** Corresponding author. Tel: +46 732-400 251, E-mail:peter.rudberg@sei.se*

Abstract: The conflict between climate change mitigation and ecosystems functions is highlighted in the implementation of two EU directives; the renewable energy directive (RES) and the water framework directive (WFD). This paper examines the Swedish implementation of the RES and WFD and possible outcomes in light of the setup and functioning of the present concession system of hydropower in Sweden. The paper discusses the degree of policy coherence of the present and foreseeable outcomes of the directives and suggests some possible policy alternatives to increase coherence in the implementation of the twin objectives.

Keywords: *Renewable Energy Directive, Water Framework Directive, Sweden, hydropower, coherence*

1. Introduction

"In reality we are talking about two goal conflicts. On one hand the renewable energy directive and the water framework directive where demands on increased minimum flow and bypass channels for fish could lead to decreased production of renewable energy. It is also a conflict between two environmental issues, local biodiversity conservation and [global] climate change."

This view regarding the conflict between renewable hydropower production – which is seen as a crucial step in reduced emissions of greenhouse gases – and biodiversity conservation of the river and its surroundings appears in one or another way among various stakeholders connected to the hydropower sector in Sweden today. This twin objective of reducing the emission of greenhouse gases and halting biodiversity loss was already addressed in a formalized way by the adoption of the Swedish Environmental Quality Objectives in 1999. The implementation of the Renewable Energy Directive (RES) and the Water Framework Directive (WFD) has increased the pressure for action to reach these objectives which for many stakeholders appears to be contradictory.

The RES and WFD are EU directives that have to be implemented in the member states of the EU. The RES sets the target of 49% renewable energy of gross final consumption in Sweden by 2020 from a level of 39.8% in 2005. This important level of renewable energy production is to a large extent possible thanks to the high level of hydropower production in Sweden which in 2008 ascended to 69 TWh [1]. The installed capacity has been relatively stable over the past decade, although production fluctuates with precipitation patterns. The WFD has the overarching goal that no water body is to experience a decrease in water quality and that all water bodies should reach good status or good potential by 2015 with the possibility of extension until 2027. A number of quality elements – including biological, hydromorphological and flow regime – have to be fulfilled in order to achieve the required status of the water bodies in a member state. The significant level of hydropower production in Sweden is one important factor leading to many rivers in Sweden at present not reaching the level good status or potential required by the WFD. The high level of hydropower production in Sweden which is positive for the fulfillment of the RES therefore simultaneously makes it harder to reach the requirements of the WFD.

In light of this potential conflict the present paper is focused on the Swedish implementation of the RES and WFD and possible outcomes in light of the setup and functioning of the present concession system of hydropower in Sweden. The paper will in the final part discuss the degree of policy coherence of the present and foreseeable outcomes of the directives and suggest some possible policy alternatives to increase the synergy and coherence in the implementation of the twin objectives.

2. Methodology

The methodology that has been used is document analysis as a first step to identify important issues and possible contradictions that could come from the implementation of the RES and WFD and the functioning of the Swedish governance system of hydropower. The primary data for analysis has been gathered from review and analysis of management and policy documents and literature on the subject. Insights from this step informed the questions that were brought up during semi-structured interviews with relevant stakeholders engaged in the hydropower governance system. Interviews have been conducted with representatives from the four largest hydropower producing companies and representatives from the main authorities dealing with the implementation of WFD and RES in Sweden such as the Swedish Energy Agency and River Basin District Authorities. The lack of centralized and accessible data has limited the analysis of outcomes of actual hydropower concession reviews which would have strengthened the analysis.

Literature on policy coherence has been used to provide a frame with which to analyze arguments raised by the actors and possible outcomes of the implementation of the directives and to what extent they are coherent. Policy coherence is focused on the outputs, implementation and outcomes of different policies and the way they interact. Policy coherence can be viewed as two or more sets of policy objectives that have objectives, instruments and implementation practices that are free from contradictions and have a logical order and clarity [2].

3. Results

The passing of the Energy and Climate bill in 2009 the government can be seen as a major step towards the fulfillment of the RES since it aims at creating a third leg of electricity production from wind and combined heat and power production largely run on biofuels [3]. To achieve this the same bill sets a national planning frame of 30 TWh for wind power and a production goal level of the renewable energy certificates to 25 TWh for 2020. Apart from wind, solar and biofuel production certain types of hydropower production do receive renewable electricity certificate such as production from new plants, plants with an installed capacity not exceeding 1.5 MW and increased production from existing plants. In 2008 production from hydropower plants receiving certificates amounted to 2.6 TWh out of a total of 14.2 TWh [4]. Although hydropower is not identified as an area of priority for expansion to reach the RES goals it is clear that in practice hydropower production does contribute a fair bit in the quota fulfillment partially as a result of the design of the renewable electricity certificates. Due to the old age of the existing hydropower stations there is also quite some potential for efficiency increases from refurbishments that will take place in the coming years. There are calculations pointing towards a potential of 3 TWh increased production simply by replacing existing turbines and generators and modifying the water intake of the stations [5].

As part of the implementation of the WFD water bodies affected by hydropower stations in Sweden are being classified as Natural, Heavily Modified (HMW) or Artificial depending

upon the extent of alteration of the water body or if it has been created for the purpose of electricity production. Natural water bodies are required to reach the environmental quality standards Good Ecological Status (GES) while heavily modified and artificial water bodies need to reach the less strict quality standard Good Ecological Potential (GEP). All water bodies in connection to hydropower stations with more than 10 MW potential have in the initial management round been given the status HMW. This adds up to roughly 200 dams in connection to hydropower stations that together represent 10% of the total number of hydropower stations that produce about 97% of the total of hydropower electricity [6]. These same water bodies have been given the general status moderate ecological potential which means that improvement measures should be required to reach GEP [7]. The extent and type of improvement measures needed to reach GEP is still not decided by the responsible River Basin District Authorities (RBDA). There are however indications that physical changes, such as construction of bypass channels, and changes to the flow regimes might be necessary. Bottenhavet RBDA have for example specified that they expect at least 55 new bypass channels to be constructed in hydropower and lake regulation dams in the coming years [7]. The changes required to reach GEP are specified in the program of measures that are created by the RBDA every six years. These programs of measures are targeted at public authorities who have the same tools – mainly supervision and review of concession and general regulation – as before the implementation of the WFD. The purpose is to make sure that the environmental quality norms are met in the water bodies adjacent to the hydropower stations [8].

The final step of implementation of both efficiency increasing measures of hydropower stations and changes required to reach GEP or GES in adjacent water bodies will normally go through the existing concession system of hydropower in Sweden. Hydropower concessions – which specify the conditions and restrictions of operations – are granted in a court of law, have legal force and unrestricted validity in time. This means that general regulations cannot limit the original freedom given in a concession while the operator has to stay within the restrictions of the same. No significant changes are allowed without a corresponding change to the concession which requires a new judicial process. Extended refurbishments which for example increase the water intake capacity of the turbines or increase the drop of the water require a change to the original concession. The vast majority - 88% - of hydropower concessions in force today have been given according to the 1918 Water Law or older [9]. An important number of these concessions allow full appropriation of the water flow for power production. In the case of stations with more than 10 MW potential this is allowed in the majority of cases while it is less common in smaller hydropower stations. Supervision of a given concession by the authorities will therefore often not lead to improved water quality of the adjacent water bodies.

The option that is left for significant changes to the hydropower stations with the current concession system is therefore a judicial trial of the change or a judicial review of the original concession. A judicial trial of a change to the hydropower station is a limited process where only the proposed change is examined by the court while the original concession stays largely unchanged. A judicial review is a more thorough process where the original concession is examined in light of the current Environmental Code and often leads to requirements of minimum environmental flow and in some cases bypass channels. When an old concession is up for review the operator has to tolerate a loss of up to 5% of the water flow for fish and environmental interests without compensation. The initiator of a judicial trial process has to pay the costs of all involved parties, the court process and the necessary investigations that form the basis of a ruling. When a review is initiated by public authorities in favor of general

interests the same rules apply except that the operator pays its own costs for participating in the process. A judicial process to change or review a concession is a very complex process where many stakeholders participate and where the nature of the process opens up many possibilities to protract the process if it is in the interest of either of the involved actors. A court ruling can for example be appealed to a Court of Appeal and in the final instance the Supreme Court. A single case can therefore take many years to solve if there is disagreement between the involved actors. One of the most protracted litigation processes in Sweden relates to the Stornorrfors hydropower station where it took 46 years for the parts to agree on appropriate compensatory measures for the damage caused to the fish stocks. For the court process to be effective and lead to a satisfactory result at a reasonable cost it is therefore vital with prior agreement between the involved actors [10]

At present the possibility of reaching prior agreement is limited since the main actors involved have very divergent interests. Hydropower operators risk losing energy production and up to 5% revenue from a concession review since the old concession in most cases allows for more generous appropriation of the water than a reviewed concession would. It is therefore in the economic interest of operators to try to limit the amount of reviews that are initiated and carried through. At the same time the authorities responsible for environmental issues have an interest in trying to maximize the amount of reviews that are carried out to update as many concessions as possible to be in line with the demands of the Environmental Code of Sweden. Currently the main authority responsible for environmental interests in hydropower concession trials is trying to create court practice that a petition from an operator for a judicial trial due to a change for an extended refurbishment requires a review of the original concession. The issue is not that the extended refurbishment will cause an unacceptable impact in itself but rather if the hydropower stations should have a modern concession or be allowed to continue with old concession that are not in line with the demands of the Environmental Code. With such a practice the operator would also have to shoulder the costs of the process as the initiator. Currently there are various ongoing concession trial processes where this issue is being deliberated.

As a result of the functioning and incentives in the concession system and operators and authorities following lines of action that are logical in light of their interests the Swedish concession system is currently working rather slowly and ineffectively. About 2/3 of the resources invested for restoration of water bodies are required for the process and only 1/3 goes to actual physical changes and improvements [10]. Between 1999 and 2009 a total of 73 hydropower concessions out of 3727 have been reviewed which amounts to about 2% of the total [9]. From interviews with operators it is also clear that the full efficiency gains from refurbishments of hydropower stations is not always reached since operators at times opt for a more limited refurbishment to avoid a protracted judicial process that could lead to a review of the original concession. The actions in court from both sides seem to have led to a rather antagonistic situation which became obvious from comments by a representative from one of the responsible authorities. “They [one of the studied energy companies] have stated that they do not intend to spill a single drop of water for environmental causes. I do not see why we should enter into negotiations with them”. In interview, at a different time, the responsible hydropower manager of the concerned company also had strong feelings on the subject “My opinion is that what they [the responsible authority] is doing…appears to be some sort of vendetta against the energy companies in cooperation with the Swedish sport fishing association”

The current functioning of the hydropower concession system therefore leads to results where the full efficiency gains from hydropower refurbishments are not always reached. This limits hydropower's share of the fulfillment of the RES objectives in Sweden. At the same time the slow functioning of the concession system makes it highly unlikely that it will be able to implement necessary changes emanating from the implementation of the WFD if the requirements for reaching GEP and GES require significant changes to a large part of existing hydropower stations.

4. Discussion and conclusions

At the strategic policy level there is a relatively high coherence between the implementation of the RES and WFD since the focus in Sweden lies almost exclusively on expansion of wind power and biofuel production to reach the mandatory level of renewable energy production. The integration of up to 30 TWh of intermittent wind power also seems to be possible to balance with 80% of the existing hydropower capacity which indicates that balance capacity in the Swedish electricity grid is not a limiting factor in the selected path to reach the RES targets [11]. The renewable energy certificate is however constructed in such a way that it gives a push for hydropower production as well and we have seen that around 18% of the increase in renewable electricity production to date comes from hydropower production increases.

At the level of implementation, that is at the project level, there is however a risk of some policy contradiction in the implementation of the WFD and RES since measures to improve the water quality could require a certain amount of water flow for bypass channels and minimum environmental flow in the rivers. There is however an important potential to increase the coherence by combining the measures for improved status of the water with extended refurbishments which would allow for higher production of renewable electricity despite of using a smaller share of the water. There is therefore a potential for win-win solutions where the increased efficiency of the hydropower stations could allow for both measures to improve the water quality and increased hydropower production or at least limit the production loss from measures to improve the status of the water. The results in this paper however clearly indicate that the current concession system and the behavior of the main actors involved in it makes it highly unlikely that such synergetic fulfillment of both the RES and WFD will take place.

One of the main barriers for the effective functioning of the system is the economic risk that operators face when engaging in a concession trial or review process since such a process could lead to a 5% loss of energy production and revenue. A possible policy alternative to remove this barrier could be to create a general insurance scheme from which resources could be taken to fully compensated operators from changes emanating from a concession review. By creating a general insurance scheme that all operators are required to participate in a common source of finance would be created that can be used to fully compensate concerned operators from changes to their concessions in a review process. Operators would in this case not have an incentive to protract review processes nor limit the amount of concession reviews that are carried out. Such an insurance scheme could be obligatory for all hydropower producers and consist of a sum of up to 5% of the production value of hydropower in Sweden which is the established limit in the Environmental Code of production loss that operators are required to bear.

With a more effective functioning of the concession system – and with the operators fully compensated for any energy losses in reviews – operators would be more inclined to realize

extended refurbishments, requiring concession reviews, which would yield higher efficiency gains in the refurbished hydropower plants and increased renewable electricity production than today. An important part of the energy loss that could results from diverting water for biodiversity requirements if it is necessary to achieve GEP could in this case be compensated for by increased efficiency gains from extended refurbishments of the hydropower stations. The total loss of potential renewable energy production in Sweden would with such a solution be significantly less and it is even probable that the net result would be an overall increase in hydropower production if the space for water improving measures is restricted to up to 5% for hydropower stations that have concessions according to the 1918 water law or older.

There is also an additional source of finance possible for the costs that the operators have to shoulder from review of concessions which comes from the renewable energy certificates. The overarching goal of the renewable electricity certificate is to "establish a more ecologically sustainable energy system in Sweden" [4]. At present this is focused solely on increased production of renewable electricity but with only slight changes it could also work in favor of improving the status of water bodies in Sweden. This would be possible by introducing a requirement that hydropower plants need to possess a reviewed concession according to the Environmental Code and WFD to be entitled support from the renewable electricity certificates scheme. Such a modification would increase the coordination between the WFD and RES and work towards the fulfillment of the twin environmental objectives of CO2 reduction and biodiversity conservation necessary for a more ecologically sustainable energy system.

Research on a global scale is pointing towards the increasing urgency of action both in terms of CO2 reduction and biodiversity conservation which leaves us little option than to tackle the two issues simultaneously [12]. The policy suggestions made in this paper are therefore aimed at improving the ability of the Swedish concession system of reaching synergetic and effective solutions in the hydropower sector that can provide solutions to both environmental challenges.

5. References

[1] IEA, *Key World Energy Statistics*. 2010, International Energy Agency.

[2] Nilsson, M., et al., *Policy Coherence - Discussion Note*. 2010, Stockholm Environmental Institute, Milieu and Collingwood environmental planning.

[3] Prop, *En sammanhållen klimat- och energipolitik - Energi [A combined climate and energy policy - Energy]*, Regeringskansliet, Editor. 2008/09:163.

[4] Energimyndigheten, *Elcertificatsystemet 2009 [The electricity certificate system 2009]*. 2009: Swedish Energy Agency.

[5] Bernhoff, H., et al., *Vattenkraftens utvecklingspotential i befintliga anläggningar [The development potential in existing hydropower facilities]*. *Rapport till Statens Energimyndighet*. 2003.

[6] nergimyndigheten, *Vattenkraften och energisystemet [Hydropower and the energysystem]*. *ER 2008:24*. 2008: Swedish Energy Agency.

[7] Vattenmyndigheten, *Förvaltningsplan Bottenhavets vattendistrikt 2009-2015 [Management plan Bottenhavets river basin 2009-2015]*. 2009.

[8] Naturvårdsverket, *Introduktion till miljökvalitetsnormer och åtgärdsprogram för vatten och deras tillämpning [Introduction to environmental quality norms and program of measures for water and their application] Dnr 190-2850-10 Rv*. 2010.

[9] SOU, *Vattenverksamhet [water activities]*, S.O. Utredningar, Editor. 2009:42.

[10] Bottenhavet, V., *Fria Vandringsvägar: Redovisning av regeringsuppdrag 51a [Open passage. Account of the government commission 51a]*. *ISSN 1403-624X*. 2008:16.

[11] Amelin, M., C. Englund, and A. Fagerberg, *Balansering av vindkraft och vattenkraft i norra Sverige [Balansing of wind power and hydropower in northern Sweden]*. Elforsk rapport 09:88, ed. Elforsk. 2009.

[12] Rockstrom, J., et al., *A safe operating space for humanity.* Nature, 2009. **461**(7263): p. 472-475.

Volume 11

Photovoltaic Technology

Impacts of CO_2 emission constraints on penetration of solar PV in the Bangladesh power sector

Md. Alam Hossain Mondal[1,*]

[1] *Energy Institute, Atomic Energy Research Establishment (AERE),Ganakbari, Dhaka-1349, Bangladesh*
** Corresponding author. Tel: +88027790009, Fax: +88027789337, E-mail: alam_90119@yahoo.com*

Abstract: This paper examines the impacts of CO_2 emission reduction targets and carbon tax on future technologies selection especially solar PV and energy use in Bangladesh power sector during 2005-2035. It also examines the co-benefits of energy security of the country. The analyses are based on a long-term energy system optimization model of Bangladesh using the MARKAL framework. The results of the study show that on a base **scenario**, power generated from solar PV is not yet competitive with that of fossil fuel-based power plants. Alternative **policy scenarios** on CO_2 emission constraints reduce the burden of imported fuel, improve energy security and reduce environmental impacts. The results show that the introduction of the CO_2 emission reduction targets and carbon tax directly affect the shift of technologies from high carbon content fossil-based to low carbon content fossil-based and clean solar PV technologies compared to the base scenario. The cumulative net energy imports during 2005-2035 would be reduced in the range of 33-61% compared to the base scenario. The total primary energy requirement would be reduced in the range of 4.5-22.37% and the primary energy supply system would be diversified. Solar PV plays an important role in achieving reasonable energy security.

Keywords: *Solar PV, CO_2 emission, MARKAL Model, Bangladesh Power Sector*

1. Introduction

The future economic development of Bangladesh is likely to result in a rapid growth in the demand for energy with accompanying shortages and problems. The country has been facing a severe power crisis for about a decade. Known reserves (e.g., natural gas and coal) of commercial primary energy sources in Bangladesh are limited in comparison to the development needs of the country [1]. Power generation in the country is almost entirely dependent on fossil fuels, mainly natural gas that accounted for 81% of the total installed electricity generation capacity (5,719 MW) in 2009 [2]. Only about 42% of total population has been connected to electricity [3], with vast majority being deprived of a power supply. The government of Bangladesh has declared that it aims to provide electricity for all by the year 2020, although at present there is high unsatisfied demand for energy, which is growing by more than 8% annually [4, 5]. Coal is expected to be the main fuel for electricity generation. The government of Bangladesh has planned to generate 2,900 MW power from coal in the next 5 years [1], although coal power has adverse environmental effects and coal reserves are limited. The government has also focused on furnace-oil-based peaking power plants. As a result, the share of CO_2 emissions coming from fossil-fuel-based power plants in the national CO_2 inventory is expected to grow, and there is a growing dependency on imported fossil fuels for power generation. On the other hand, technical potential of grid-commented renewable energy technologies specifically solar PV to generate electricity is relatively very high in Bangladesh that is 10 times higher than present generation capacity [3]. Increasing the use of fossil fuels to meet the growing worldwide electricity demand, especially in developing countries, not only counteracts the need to prevent climate change globally but also has negative environmental effects locally. In Bangladesh, the power sector alone contributes 40% of the total CO_2 emissions [6, 7]. CO_2 is the principal greenhouse gas (GHG), produced mainly from the combustion of fossil fuels. Improved efficiency in the use of fossil fuels and increased use of renewable energy sources are among the most promising options for reducing CO_2 emission [8]. In this case, it is necessary to develop and promote alternative energy sources that ensure energy security of Bangladesh without increasing

environmental impacts. Since developing countries are not obliged to reduce GHG emissions, studies in evaluating the impacts or co-benefits of GHG mitigation policies in developing countries are lacking [9]. For a developing country like Bangladesh, the evaluation of the impacts of GHG mitigation policies in the power sector would provide a basis for more comprehensive technological choice, and economic and environmental analysis. Such an evaluation would also support climate change mitigation policies aimed on sustainable power-sector development as part of the efforts to address the climate change issues identified in the United Nations Framework Convention on Climate Change (UNFCCC) which Bangladesh has already ratified.

This study examines the future technologies selection applying CO_2 emission reduction targets and carbon tax in the Bangladesh power sector during 2005-2035. This study also analyzes the co-benefits on energy security of the country from the CO_2 emission constraints. A bottom-up least cost energy system optimization model of Bangladesh was developed on the market allocation (MARKAL) modeling framework and the following scenarios were considered:

1) Base scenario: It presumes a continuation of current energy and economic dynamics and provides a reference for comparing impacts of future policies.
2) 10% CO_2 emission reduction scenario (hereafter referred as "CO210"): It evaluates the effects of CO_2 emission reduction in the entire energy-supply system. The CO210 is the 'what if' scenario, in which a cumulative reduction of not less than 10% of the cumulative CO_2 emission during the planning horizon in the base scenario is desired, all other things remaining the same as in the base scenario.
3) 20% CO_2 emission reduction scenario (hereafter referred as "CO220"): The CO220 scenario is defined similarly for cumulative reduction in CO_2 emission of not less than 20% from the base scenario.
4) 2500 Taka/ton (1 USD = 70 Bangladeshi Taka) carbon tax scenario (hereafter referred as "CT2500"): The CT2500 is the 'what if' scenario, in which a carbon tax of 2500 Taka/ton is applied during the planning horizon in the base scenario.

2. MARKAL methodology

The MARKAL model mainly consists of the description of a large set of energy technologies, linked together by energy flows, jointly forming a reference energy system. The reference energy system is the structural backbone of MARKAL for any particular energy system and its great advantage is that it gives a graphic idea of the nature of the system. Another important characteristic of MARKAL is that it is driven by a set of demands for energy services. The feasible solutions are obtained only if all specified end-use demands for energy for all the periods are satisfied. The user exogenously supplies these demands in the model. Once the reference energy system has been specified, the model generates a set of equations that hold the system together. In addition, the MARKAL model possesses a clearly defined objective, which is usually chosen to be the long-term discounted cost of the energy system. The objective is optimized by running the model, which means that configuration of the reference energy system, is dynamically adjusted by MARKAL in such a way that all MARKAL equations are satisfied and the long-term discounted system cost is minimized. In this process the model computes a partial equilibrium of the energy system at all intermediate stages in all aspects e.g. flow conservation, demand satisfaction, capacity transfer, capacity utilization, source capacity, growth constraints, emission and other constraints.

3. The MARKAL Bangladesh model

3.1. Reference energy system of Bangladesh power sector

For the purpose of this study, MARKAL-Bangladesh was developed. A major part of the work was to develop input parameter values. In MARKAL, the reference energy system is the first step towards building a model of the Bangladesh power sector (Fig. 1). The reference energy system represents the activities and technologies of an energy system, depicting energy demands, energy conversion technologies, fuel mixes, and the resources required to satisfy energy service demands [10]. The reference energy system is able to allocate energy sources for a given sectoral demand depending upon the efficiencies and other losses from the energy conversion device. The system does not provide any information about economics of a solution neither about the cost to the national economy for providing the energy supply. An optimized energy system can be obtained from the MARKAL model.

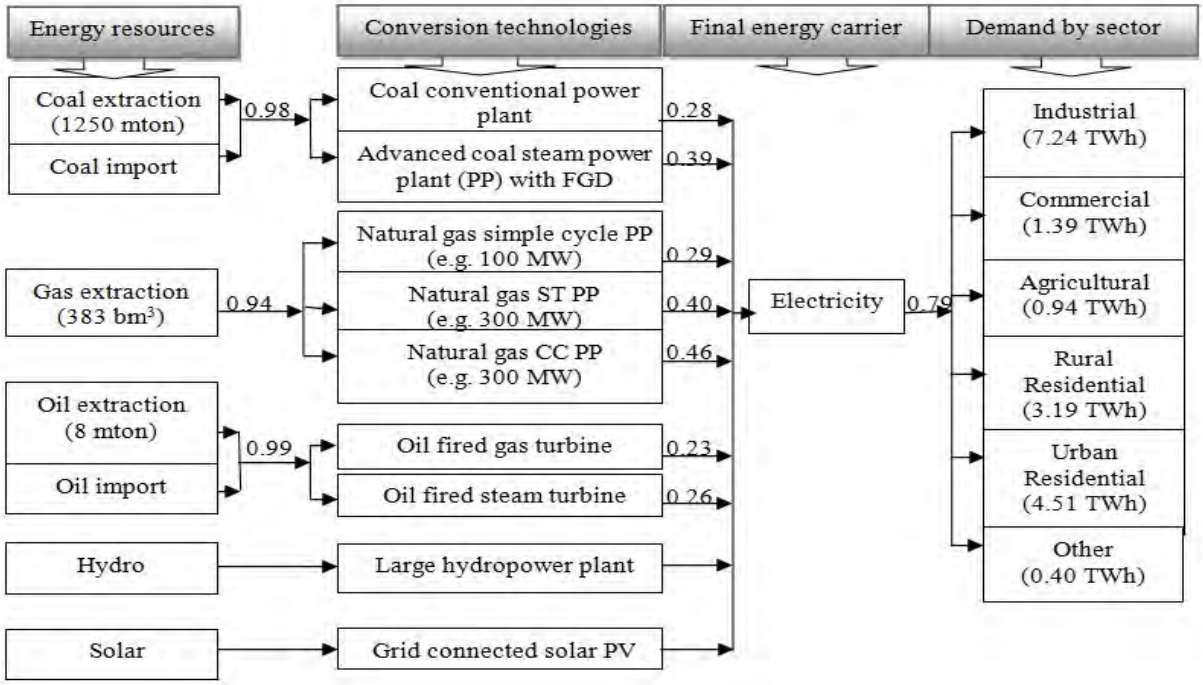

Fig 1. Simplified reference energy system of Bangladesh power sector
(Values shown indicate proven reserves, conversion & transmission efficiency, and demand in 2005)
(CC refers combined cycle, FGD refers flue gas desulphurization, mton refers million ton and bm^3 refers billion m^3)

3.2. Energy resources and emissions

The model requires that the cost of all primary energy sources be defined along with constraints on their availability. It is provided supply cost estimates and upper bounds on resource availability for fossil fuels and the maximum rates of introduction of solar PV and hydro are given in [1]. A limit on imported coal is not considered here. In mined coal, the average sulfur content is 0.57% and carbon 46.2% [11]. These values form the basis of the calculated emission coefficients used in this study. The IPCC (1996a) database is used for the CO_2 emission of imported coal. Due to different carbon content percentages in different gas fields in Bangladesh, the IPCC (1996a) emission factor is used in the model. CO_2 and SO_2 emission factors are calculated separately for diesel, kerosene and fuel oil products based on the IPCC workbook [12] and IPCC reference manual [13].

3.3. Energy demand

In 1994, the total electrical energy demand was 9.63 TWh and had increased to 17.64 TWh in 2005 [14]. The Long-range Energy Alternatives Planning (LEAP) tool was examined to form demand scenarios according to the trend of gross domestic product (GDP) growth rates (5.5%, 6.8% and 8%) and the nature of the energy sector itself, and taking into consideration broader factors, e.g., population, households, urbanization and other influencing factors for the time span 2005 to 2035. It is worth mentioning here that the actual GDP growth rate in Bangladesh is neither low nor high and therefore, in this study, the demand projection is based on a GDP growth rate of 6.8% is given in [15].

3.4. Conversion technologies[1]

The characteristics of all technologies must be provided to the model. Conversion technologies convert primary energy into final energy carriers. The model requires users to create detailed profiles for two sets of energy conversion technologies: one for converting primary into final energy carriers, and one for converting final energy carriers into energy services. A reasonably representative set of conversion technologies is developed, which includes a total of 9 distinct conversion technology types (coal steam conventional, advanced coal flue gas desulphurization (FGD) 300 M W, fuel oil-based steam, fuel oil-based gas turbine, gas-based simple cycle (SC) and steam turbine (ST), gas-based combined cycle (CC, hydro and solar PV). Other renewable energy technologies are not considered due to their limited technical potential to generate electricity [3]. For each of the technology types, values are specified for energy input per unit energy output (efficiency), capital cost, fixed and variable operation and maintenance costs, NO_2 and SO_2 emissions per unit of energy output, and the first year in which the technology was introduced**.** All costs are in Bangladesh Taka (1 USD = 70 Taka). The characteristics are performance and cost level inputs to the model for 2005-2035. For most of the technologies, the performance and cost levels are assumed to be constant over the whole analysis period except for solar PV, where the investment cost is expected to decrease by 3% annually [16] due to technological learning effects on solar PV cost after introduction in 2010. The model determines the capacity level for any technology. In this modeling, the most reliable studies are selected and evaluated to yield as consistent a set of cost data as possible.

3.5. Generic details

Besides the technical and financial parameters related to different stages of reference energy system of the Bangladesh power sector, the other parameters, assumptions and boundaries are also required by MARKAL which are discussed in [1].

4. Results

Under the base scenario, the total generation capacity is expected to increase from 5.56 GW in 2005 to 50.85 GW in 2035, i.e., at an average growth rate of 7.6 %. At the same time, the generation structure changes significantly. The share of gas-fired power plants reduces from 86% (4.83 GW) in 2005 to 37.4% (19.04 GW) in 2035 in total capacity, whereas the increase in the capacity of coal-based power plants 0.25 GW in 2010 to 30.75 GW in 2035 (60.4% of total capacity) is extremely high. It is observed that coal is the dominant electricity generation technology in base scenario. In the base scenario, the advanced coal flue gas desulphurization (FGD) produces 32% of electricity in 2015 and 91% in 2035, due to unused capacity of oil-

[1] Cost data, technology selection and technology specification data mainly based on Bangladesh Power Sector Master Plan, Bangladesh Power Development Board and Ministry of Power, Energy and Mineral Resources.

based power plants and limited gas is mainly used in the early period (2005-2025). Hydro capacity reaches its allowed upper limit in the base scenario. Solar photovoltaic (PV) is not selected in the base scenario due to its high investment cost and low efficiency.

The switch from gas- to coal-based power plants leads to a strong increase in coal consumption (178 PJ in 2015 to 1913 PJ in 2035), i.e., at an average growth rate of 26%. This rate is higher than the domestic availability. Thus, the country would need to import energy resources such as coal from 2025 onwards to meet the required demand. The proportion of imported coal in the total fossil fuel consumption would increase substantially from 16% (187 PJ) in 2025 to 57% (1178 PJ) in 2035. This deficiency would have adverse impacts on the country's balance of payments and the availability of foreign currency resources.

The introduction of the CO_2 emission reduction targets and carbon tax scenarios (the CO_2 emission reduction of 10%, 20% and carbon tax 2500 Taka/ton are referred to hereafter as CO210, CO220 and CT2500, respectively) directly affects the shift of technologies from high carbon content fossil-based to low carbon content fossil-based and clean renewable energy-based solar PV technologies. As a result of emission constraints, power generation based on solar PV is introduced and its generation capacity gradually increases during 2010–2035. Compared to the base scenario, 15.12 GW, 34.92 GW and 40.62 GW solar PV-based generation capacities are additionally selected in 2035 in the CO210, CO220 and CT2500 scenarios, respectively. Solar PV generation starts with a capacity of 0.02 GW, 0.05 GW and 0.06 GW in 2010 in the CO210, CO220 and CT2500 scenarios, respectively and grows at a rate of 29.5% per year. The total generation capacity is expected to increase from 5.56 GW in 2005 to 65.72 GW, 86.15 GW and 91.23 GW in 2035 in the CO210, CO220 and CT2500 scenarios, respectively (Fig. 2). The generation capacity is relatively higher in the CO_2 emission constraint scenarios than in the base scenario due to implementation of a higher solar PV capacity, which generates electricity only during the day.

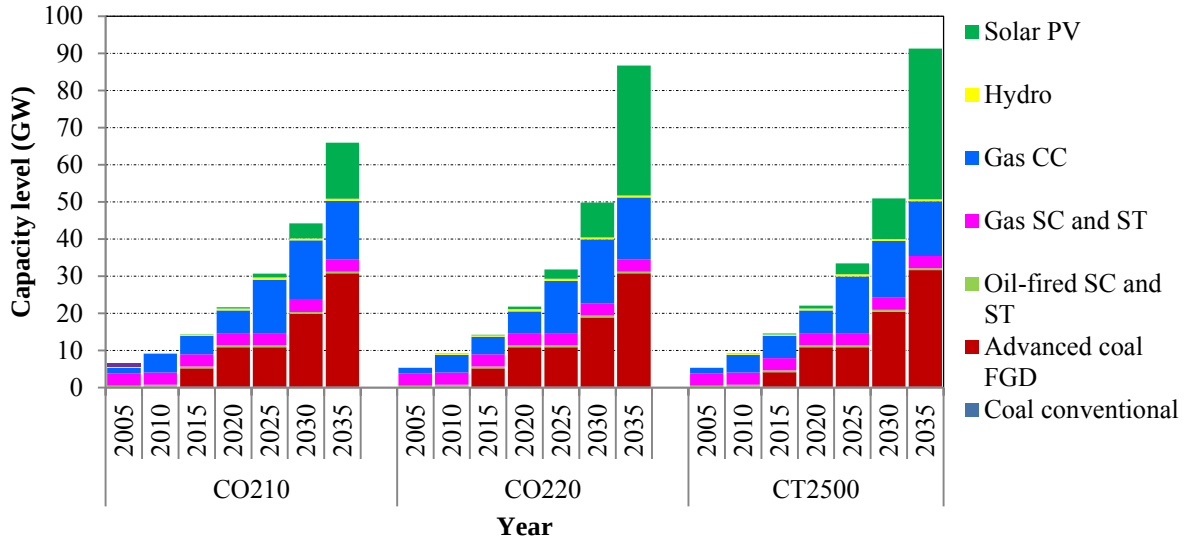

Fig 2. Technology capacity level in all CO_2 constraint scenarios

Gas-based combined cycle (CC) power plant capacity increases significantly in the later period (2020-2030) in all alternate scenarios compared to the base scenario. The model reveals that the least-cost solution is to use the limited gas reserves in the mid-term period, although the gas-based CC plants are mostly unused in the end period (2035). That is why the

power generation capacity based on coal FGD decreases significantly in the later period (2025-2030) in the CO_2 emission constraint scenarios compared to the base scenario. Due to high oil prices, oil-based power plants do not receive higher allocation in the CO_2 emission reduction targets and carbon tax scenarios. Gas-based simple cycle (SC) and steam turbine (ST) plants, coal conventional also do not get more allocation in the alternate scenarios. The capacity levels of hydro are the same in all scenarios. Coal FGD maintains the almost same capacity level in 2035 in all scenarios as gas resource is limited. Fossil fuel-based technologies would be required, as solar PV technology cannot cater for the entire future energy demand. The learning cost for solar PV enhances competitiveness of the technologies and leads to a higher rate of implementation of this technology in the analysis period.

To summarize the extensive results generated for each of the CO_2 emission reduction target and carbon tax scenarios by the MARKAL-Bangladesh model, the primary energy mix in 2035 is selected as the principal metric (Fig. 3). This provides a good indication of the types of choices made by the model to meet the various CO_2 emission constraints applied. The colored bars (except yellow in the middle) provide the breakdown of primary energy use for the base scenario in 2005 and all scenarios in 2035. The numbers above each bar indicate the total and percentage of the cumulative imported coal and the total cumulative and percentage of CO_2 emission reduction compared to the base scenario during the study period. Oil is not indicated, as it is not selected for power generation during the study period. The center yellow bar in the three scenarios on the right in this figure shows the change in cumulative total system cost relative to the base scenario. Due to the large uncertainties in this kind of analysis, the percentage change in system cost between the various scenarios as the measure of the cost impact of the changes imposed by each scenario is applied. The system cost for the base scenario is the reference cost in all cost comparisons.

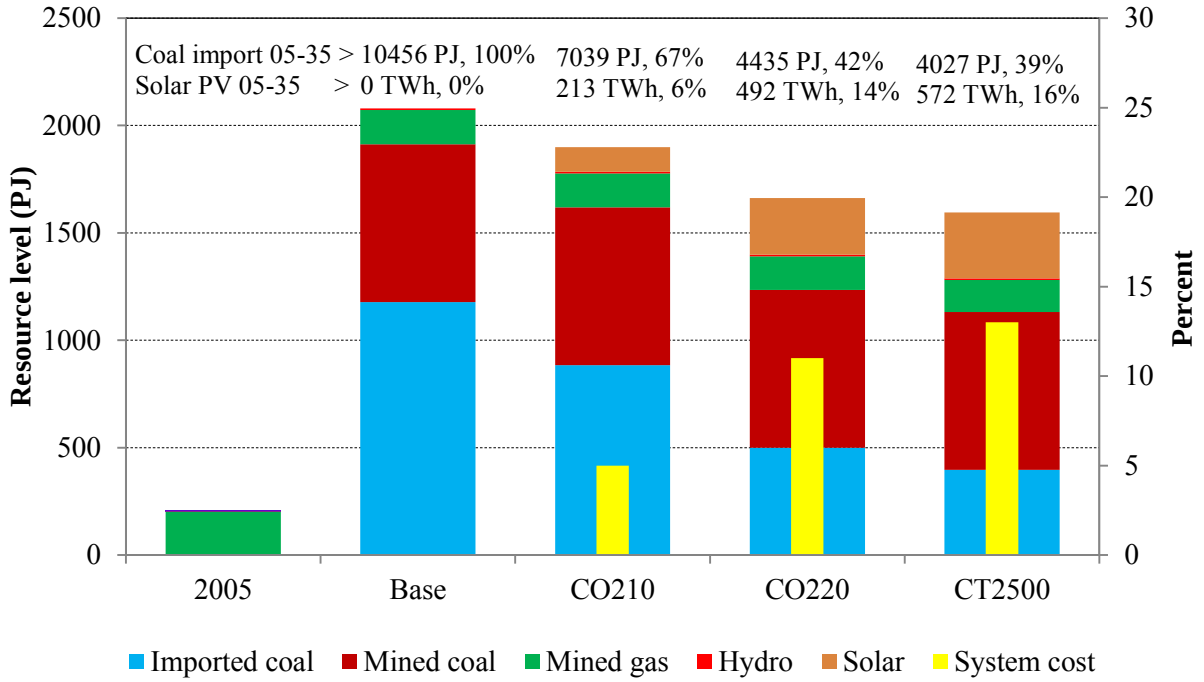

Fig 3. Primary energy mix in 2035 in all scenarios and percentage change in cumulative (2005-2035) system cost. Also indicated are the energy mix in 2005, the cumulative total and percentage of total imported coal, and the total electricity generation from solar PV.

CO_2 emission constraints have positive impacts on the energy security of the country. The energy security issue is analyzed in terms of changes in net energy import dependency and diversification of energy resources resulting from the selected CO_2 emission reduction targets and carbon tax. The CO210 scenario allowed a reduction in imported coal use of about 33% contributing an only 5% increase in system cost during 2005-2035. Import dependency reduces by 58%, and 61% in CO220 and CT2500 scenarios, respectively, compared to the base scenario during the study period, but led to an increase in the total system cost of 11% and 13%. Alternatively, import dependency based on the base scenario value 100%, drops to 67%, 42%, and 39% in the CO210, CO220 and CT2500 scenarios, respectively.

A reduction in the total primary energy requirement is another co-benefit of the CO_2 emission constraints. It is revealed that the total primary energy supply reduces by about 4.6%, 9.4% and 10.8% in the CO210, CO220 and CT2500 scenarios, respectively, during 2005-2035 as compared to the total primary energy supply in the base scenario due to efficient technology selection by the model. In the base scenario, primary energy use in 2035 is expected to be 2079 PJ, and reduces to 1595 PJ in the CT2500 scenario. Gas is the dominant energy source in 2005, and coal is dominant in all scenarios in 2035. Coal imports decrease from 1178 PJ in the base scenario to 884, 499 a nd 396 PJ (25%, 58% and 65%) in the CO210, CO220 and CT2500 scenarios in 2035, respectively. Solar energy use increases by 114 PJ, 263 PJ and 306 PJ in 2035 in the CO210, CO220 and CT2500 scenarios, respectively. In the base scenario, the expected electricity generation from solar PV is 0 TWh between 2005 and 2035; it is expected to increase by 213 TWh, 492 TWh and 572 TWh in the CO210, CO220 and CT2500 scenarios, respectively, during the study period.

5. Conclusions

This paper has analyzed the effects of selected CO_2 emission reduction targets and carbon tax on environmental emissions as well as energy technology and resource mix using the MARKAL model for Bangladesh power sector. It is observed that coal is the dominant electricity generation technology in all scenarios in the later period (2020-2035). In the later period, advanced coal FGD trends to be the first choice for Bangladesh. The introduction of the CO_2 emission constraints directly affects the shift of technologies from high carbon content fossil-based to low carbon content efficient fossil-based and clean solar PV-based technologies. Solar PV is an attractive technology in almost all alternate scenarios. It becomes more and more attractive with introduction of higher carbon tax and higher CO_2 emission reduction target.

The analysis results show that the degree of diversification in the total energy requirement would increase with the applied CO_2 emission constraints. The primary energy supply system would diversify from the one dominated by coal in the later period (2020-2035) to that involving a greater use of solar energy and gas under the selected emission reduction targets and carbon tax scenarios. The analysis results show that the primary energy requirement would decrease in the alternate scenarios. This would enhance the country's energy security.

Furthermore, the results show that the increase in total system cost for reduction of cumulative CO_2 emissions over the study period is around 543 Taka/ton, 603 Taka/ton and 615 Taka/ton in the CO210, CO220 and CT2500 scenarios, respectively. These costs are much lower than those in developed countries, as the solar-PV-based power generation is relatively much cheaper in Bangladesh. It could thus be attractive for developed countries to invest in solar PV to generate electricity in Bangladesh to reduce their committed CO_2 emissions defined in the Kyoto Protocol through the "clean development mechanism (CDM)".

References

[1] M. A. H. Mondal, M. Denich, and P. L. G. Vlek, "The future choice of technologies and co-benefits of CO2 emission reduction in Bangladesh power sector," Energy, vol. 35, pp. 4902-4909, 2010.

[2] BPDB, "BPDB Annual Report 2008-09, Bangladesh Power Development Board, Dhaka - 1000, Bangladesh," 2009.

[3] M. A. H. Mondal and M. Denich, "Assessment of renewable energy resources potential for electricity generation in Bangladesh," Renewable & Sustainable Energy Reviews, vol. 14, pp. 2401-2413, 2010.

[4] A. H. Mondal and M. Denich, "Hybrid systems for decentralized power generation in Bangladesh," Energy for Sustainable Development, vol. 14, pp. 48-55, 2010.

[5] M. A. H. Mondal, L. M. Kamp, and N. I. Pachova, "Drivers, barriers, and strategies for implementation of renewable energy technologies in rural areas in Bangladesh-An innovation system analysis," Energy Policy, vol. 38, pp. 4626-4634, Aug 2010.

[6] ADB, "Asia Least-cost Greenhouse Gas Abatement Strategy (ALGAS) Bangladesh, Asian Development Bank," Manila, Philippines, p 1871998.

[7] R. M. Shrestha, G. Anandarajah, and M. H. Liyanage, "Factors affecting CO2 emission from the power sector of selected countries in Asia and the Pacific," Energy Policy, vol. 37, pp. 2375-2384, Jun 2009.

[8] G. Dutt and F. Glioli, "Coping with Climate Change," in Economic and Political Weekly, October 20, 2007 2007, pp. 4239-4250.

[9] R. M. Shrestha and S. Pradhan, "Co-benefits of CO2 emission reduction in a developing country," Energy Policy, vol. 38, pp. 2586-2597, 2010.

[10] J. Mathur, N. K. Bansal, and H. J. Wagner, "Investigation of greenhouse gas reduction potential and change in technological selection in Indian power sector," Energy Policy, vol. 31, pp. 1235-1244, Sep 2003.

[11] B. Imam, Energy Resources of Bangladesh. Dhaka: University Grants Commission of Bangladesh, 2005.

[12] IPCC, "Revised 1996 IPCC Guidelines for National Greenhouse Gas Inventories: Workbook (Volume 2), Intergovernmental Panel on Climate Change," 1996a.

[13] IPCC, "Revised 1996 IPCC Guidelines for National Greenhouse Gas Inventories: Reference Manual, Intergovernmental Panel on Climate Change," 1996b.

[14] PSMP, "Power Sector Master Plan Update, Power Cell, Power Division, Ministry of Power, Energy and Mineral Resources, Dhaka, Bangladesh, p 180," 2005.

[15] M. A. H. Mondal, W. Boie, and M. Denich, "Future demand scenarios of Bangladesh power sector," Energy Policy, vol. 38, pp. 7416-7426, 2010.

[16] S. Messner, "Endogenized technological learning in an energy systems model," Journal of Evolutionary Economics, vol. 7, pp. 291-313, Sep 1997.

Comparing push and pull measures for PV and wind in Europe

Ruben Laleman[1*], Johan Albrecht[1]

1 Ghent University, Faculty of Economics and Business administration, Ghent, Belgium
**corresponding author. Tel: +32 92644209, E-mail: ruben.laleman@ugent.be*

Abstract: Successful technological innovation frameworks are based on synergistic packages of technology-push and demand-pull measures. As the massive deployment of premature renewable energy technologies risks becoming very expensive, the debate on the optimal trajectory of renewable technologies should explicitly consider the balance between deployment incentives and R&D efforts.

This paper explores this balance regarding wind and PV technology support in Europe. Based on rather conservative estimates, we calculate future deployment costs and compare these figures to the current public investments in PV and wind R&D. We find that, today, for each Euro spent on R&D to develop future technologies, 35 to 41 Euros are spent on the deployment of existing technologies. Furthermore, private PV and wind technology companies tend to underinvest in R&D for various reasons. In an alternative scenario, we assess the optimal R&D efforts for the PV and wind sectors based on a 7% R&D-to-sales benchmark that is typical for engineering sectors. If public R&D efforts would increase according to this benchmark, and hence compensate for the private underinvestments in R&D, pull/push ratios between 6 and 8 could be achieved. This leads us to conclude that the current balance between deployment and R&D is far from optimal.

Keywords: *Wind energy, PV-systems, Energy policy, Research and Development, Deployment subsidies*

1. Introduction

Climate and energy policies need to address at least two well-known market failures (1). Without a direct price on negative externalities such as CO_2 emissions, welfare losses will persist because economic agents lack incentives to invest in CO_2 abatement. In addition, private companies tend to underinvest in low carbon energy R&D. For both market failures, economists often advocate appropriate government interventions such as carbon pricing and comprehensive public R&D programs. This is essential in successful technological innovation frameworks, based on synergistic packages of technology-push and demand-pull measures (2) (3) (4) (5) (6). The high deployment cost of renewable technologies - especially of PV - attracts more and more attention in the largest European economies (7), also, RD&D efforts are generally considered to be insufficient (8) (9). We argue that the debate on the optimal deployment trajectory for renewables should explicitly consider the balance between deployment incentives and R&D support. This paper aims to provide insight in the balance between wind and PV deployment and R&D efforts in Europe.

2. Methodology

2.1. Expected growth in wind and PV electricity production

In order to estimate future costs we used two conservative scenarios (a moderate scenario and a policy driven scenario) on wind and PV electricity production up until 2020. These scenarios are based on reports by the European Photovoltaic Industry Association (EPIA) (10) and Tradewind (11) (Appendix, table 1-A). In the latter report we found projections of wind capacity growth (MW) which we then multiplied with full load hour data (FLH; [MWh/MW/y]) to estimate yearly wind electricity production. FLH data were calculated based on real production data for 2007 and 2008 by Eurobserv'er (12). We would like to point out that our FLH assumptions based on Eurobserv'er data are slightly lower than those based on EWEA (European Wind Energy Association) data (13). With respect to PV, the data on installed capacity (10) was multiplied with data on the yearly energy output [kWh/kWp/y]

obtained from PV-GIS Europe (Photovoltaic Geographical Information System) (14) to obtain estimates of total annual PV electricity production.

2.2. Current and future deployment costs

Current deployment costs in Euro/MWh are based on data by the European Renewable Energies Federation (EREF) (15). To estimate the further evolution of deployment costs, we follow the IEA (16) and assume that support schemes will be gradually phased out by 2020. Thus, we assume that PV-systems or wind turbines installed after December 31st 2019 no longer receive subsidies. For PV this assumption is a challenge, on-shore wind however is already competitive under optimal conditions. We are fully aware that the fading out of support schemes should not necessarily become a reality. This assumption however keeps the total deployment costs within a reasonable range. As a result, our calculations of the total deployment costs should be interpreted as very conservative. Based on existing schemes of Green Certificates or Feed-in Tariffs, the average production subsidies in the EU for PV and wind are estimated at respectively 326 €/MWh and 56 €/MWh in 2010. In practice, deployment subsidies vary significantly across Member States (15). We assumed that these support levels will decline steadily to be phased out by 2020 (Figure 1).

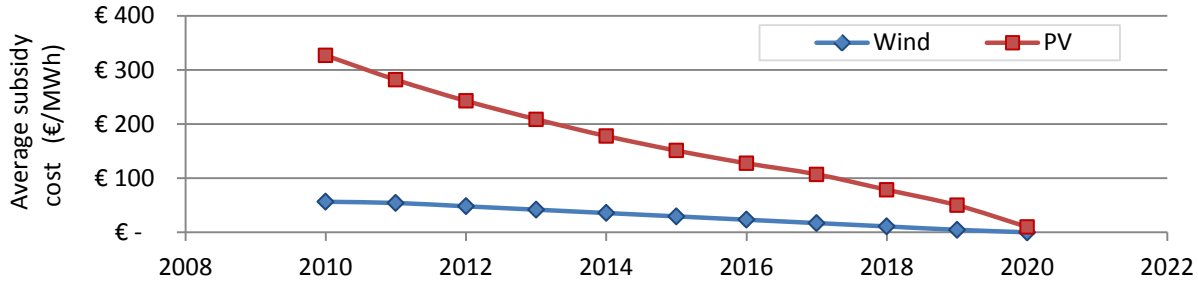

Fig. 1: Decline of average subsidies (€/MWh) for PV and wind electricity in the EU (based on(15))

In order to obtain total PV and wind deployment costs for each EU Member State, the estimated electricity production in a given year was multiplied with the corresponding production subsidy. In most countries the subsidies for PV electricity are guaranteed for 20-25 years, starting when the first MWh of electricity is produced. In this paper, a support period of 20 years was assumed for PV. Wind subsidies were assumed to be guaranteed for only 15 years. Note that these conservative assumptions on the duration of the guaranteed support have a huge impact on the total cumulative cost.

2.3. Research, development and demonstration

Public RD&D investment data from EU Member States were retrieved from the IEA RD&D database (17). Missing data from 2009 or 2008 were replaced by the most recent data available for a given Member State. For the alternative R&D scenario, R&D/sales ratios for PV and wind technology companies are compared to relevant benchmark values in competitive engineering sectors. As PV and wind technology companies have low R&D/sales ratios, an R&D-investment gap based on projected total sales for both technologies and the 7% R&D/sales benchmark of engineering sectors was calculated. As a matter of reference, we compare our investment gap estimates to investment needs obtained from recent IEA reports (8) (9). The methodology of the IEA is however fundamentally different since it uses a partial equilibrium model to find the cost-effective technology portfolios to halve global emissions by 2050. Nevertheless we believe it to be a good reference point in this framework.

3. Results and Discussion

3.1. Expected growth in wind and PV electricity production

From our conservative scenarios we find that, by 2020, 102-159 TWh is estimated to be produced by PV-systems and 311-399 TWh by wind turbines, in the EU-27. Table 1 shows that our estimates of future electricity production are quite conservative when compared to the standard scenarios from EREC (18), EPIA (19), EWEA (13) and the EU (20). We opted for this approach to ensure that the cost estimates resulting from our scenarios (see below) are within reasonable range. Furthermore, the wide range of projections given in Table 1 illustrate that estimating future electricity production comes with great uncertainty.

Table 1: Estimated wind and PV electricity production and share in total demand in the EU by 2020

Technology		This Paper	EPIA (19)	EWEA (13)	EREC (18)	EU (20)
PV	Prod (TWh)	102-159	140-420		180	
	Share (%)	*2.7-4.2*	*3.7-11.1*		*4.7*	
Wind	Prod (TWh)	311-399		580-681	477	399-525
	Share (%)	*8.2-10.5*		*15.3-17.9*	*12.6*	*10.5-13.8*

Sources: (13) (20) (18) *and* (19)*; total electricity demand in 2020 is estimated to be 3795 TWh* (20)

3.2. Current and future deployment costs

Figure 2 shows the evolution of annual and cumulative PV and wind electricity subsidy costs in the EU-27 from 2007 until 2040 in a moderate (Mod) and a policy driven (PD) scenario. It is clear that PV subsidy costs will be much higher than wind subsidy costs, and (given the above mentioned assumptions) also last for a longer period. We find that annual subsidy costs for PV in the period 2020-2026 will be € 18-26 Bio. Annual wind subsidy costs will rise up to € 6-9 Bio by 2020 and fade out by 2034. Total annual subsidy costs (PV + wind) will probably peak in 2020 and, depending on the scenario, could amount to € 25-35 Bio in that year. The total nominal cumulative cost of wind and PV subsidies are estimated to reach around € 471-661 Bio by 2040 for the whole of the EU-27.

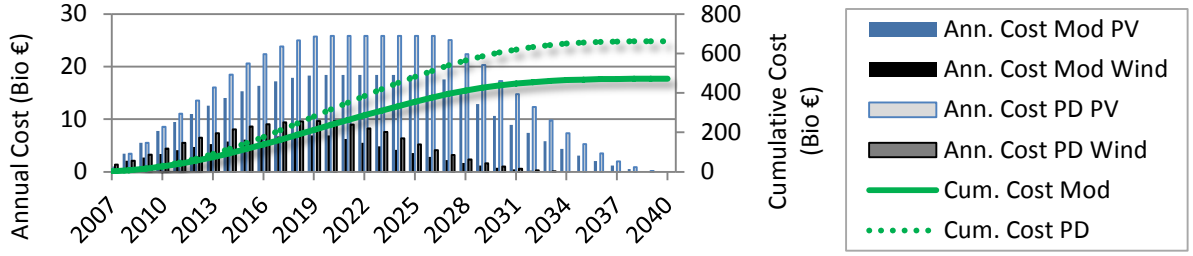

Fig. 2: Annual and cumulative deployment costs for PV and wind (based on (10), (11) and (15))

Table 2 illustrates that in 2020 the total average annual deployment cost per person (ADCPP) in Germany could reach € 156 in the policy driven scenario. These high costs are caused mainly by the high PV FIT's granted in Germany in the period 2007-2010, resulting in annual costs of € 4-5 Bio by 2010 already. By 2020, annual PV deployment costs in Germany are estimated at € 9-11 Bio, which is almost 50% of the total of EU-27 PV subsidy costs, and more than total annual wind subsidy costs for the whole of the EU. The data in Table 2 also indicates that countries that rely more on wind energy and invest little in PV will have fewer problems facing the subsidy costs. To illustrate this we compare the U.K. and the Czech Republic. Both are estimated to have a similar combined share of wind and PV in total electricity supply by 2020 (Wind and PV together account for 6-9% of total supply). The U.K.

will reach this primarily through the deployment of wind energy (wind shares of 5.2-8.5%), the Czech Republic, on the other hand will invest heavily in PV. Table 2 shows that this has major consequences for electricity consumers, with ADCPP by 2020 for the Czech electricity consumer of 72-115 €, compared to only 13-22 € for the U.K. consumer.

Table 2: Average annual deployment cost per person (ADCPP) across member states in the year 2020

ADCPP (€)		DE	EL	CZ	BE	ES	IT	PT	BU	FR	UK
PV	Mod	105	36	71	48	76	43	22	18	16	4
(€)	PD	132	91	121	56	92	62	47	44	28	7
Wind	Mod	18	11	2	12	22	18	45	3	15	10
(€)	PD	24	18	7	19	27	25	48	4	20	15
Total	Mod	123	46	72	60	98	61	67	21	31	13
(€)	PD	156	109	128	75	119	88	94	48	48	22
PV/wind	Mod	5,95	3,30	42,61	3,91	3,54	2,44	0,49	6,91	1,05	0,41
	PD	5,56	5,18	16,46	2,92	3,39	2,44	0,97	10,9	1,38	0,48

(Based on data from (10), (11) *and* (15)*)*

These figures do not reflect the net-cost for society since the production of renewable electricity avoids the production of fossil or nuclear electricity. More intermittent renewable electricity production will however imply significant additional grid investments. It is at this stage very speculative to derive the net-cost from the deployment cost between now and 2040. We can nevertheless assume that the cost increase to the average electricity consumer will be significant. Keep in mind that our calculations are restricted to PV and wind while most countries have regimes to support other renewable energy technologies as well. Adding for instance biomass or geothermal FIT's will further increase these costs.

3.3. Investments in Research, Development and Demonstration

3.3.1. RD&D needs according to the IEA

The IEA (8) (9) (17) claims that global annual public RD&D budgets for wind and solar (PV + concentrated solar power + solar boilers) should be around USD 1800-3600 Mio, which is about a fivefold increase compared to current PV public RD&D investments and a tenfold increase in wind public RD&D. In line with these recommendations, we assume that current public RD&D budgets in the EU-27 should be 5 times higher in the case of PV and 10 times higher in the case wind. Given current EU-27 RD&D budgets for wind and PV of respectively € 136 Mio and € 184 Mio, the above mentioned assumption resulted in estimated annual RD&D needs for wind and PV in the EU-27 of € 1360 Mio and € 920 Mio respectively.

3.3.2. Estimating optimal R&D expenditures

It is difficult to define the optimal R&D efforts for PV and wind technologies since these sectors are still in transformation and operate in an artificially protected and fully subsidized environment with production targets up to 2020. If the sectors would collectively agree not to innovate, they can continue to sell current technologies. Nemet (3), for example, has pointed out that demand-pull measures might negatively impact non-incremental technological change. In general, manufacturing firms in Korea and Canada spend about 5-6% of their turnover on R&D (21). Major consumer electronics firms that operate in competitive markets like Siemens, Samsung, Nokia, Sony and Robert Bosch spend about 6-10% of their sales on R&D (22). Based on the annual reports of the major international PV and wind companies however, we find that these companies invest on average only 2% of their sales in R&D. As

renewable energy companies are less R&D-intensive compared to comparable mature industries, we have strong indications of private underinvestment in renewable energy R&D.

To quantify this investment gap, we assume that the PV and wind industry should invest at least 7% of sales in R&D to replicate the average innovation dynamics of the engineering sectors. For this purpose we estimated total sales in the wind and PV sector between now and 2020. This was achieved by multiplying annual installed capacities with the cost per Watt. We assumed that wind energy investment costs would decline from 1.3 €/W in 2005 to 1 €/W in 2020. For PV we assumed a decline from 4 €/Wp in 2007 to 3.5 €/Wp in 2010 and 2 €/Wp in 2020 (cost estimates based on (11), (23), (24) and (25)). This resulted in fairly constant annual sales in the wind and PV industry between 2010 and 2020 (Fig. 3). Sales in wind are about 9 Bio/y in a moderate scenario and 14 Bio/y in a policy driven scenario. PV sales are higher, reaching around 30 Bio/y in a policy driven scenario and 18 Bio/y in a moderate scenario. If the public sector were to support the industry by funding R&D to obtain the 7% ratio, they would have to spend a complementary amount equal to 5% of sales (7% in total minus 2% private). Using this method we obtained "5% of sales" R&D estimates, which are much higher than current public RD&D investments in PV and wind (Table 3).

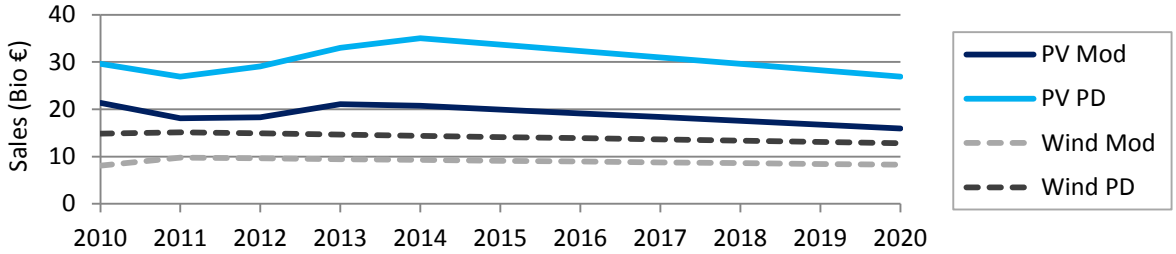

Fig. 3: Estimated annual sales for PV and wind in the EU-27 (based on (10) (11) (23) (24) & (25))

Table 3: Annual R&D gap as 5% of sales in the EU in the period 2010-2020

	Current EU public RD&D (€ Mio)	Annual sales (€ Mio)		R&D gap as 5% of sales (€ Mio)	
		Mod	PD	Mod	PD
PV	184	18000	30000	900	1500
Wind	136	9000	14000	450	700

(Based on data from (17) *and annual reports from the solar and wind industry)*

3.4. Balancing push and pull measures

3.4.1. Results

EU Member States have invested - and are likely to continue to invest - huge sums in demand-pull measures to stimulate the deployment of renewable technologies like PV and wind. When comparing these high costs to the low investments in RD&D supply-push measures, it appears that the budgets are not in balance. To obtain better insight in the imbalance between demand-pull and supply-push measures, we calculated a pull/push ratio under difference scenarios. Table 4 shows that the pull/push ratio would increase from 35-41 today to about 79-111 by 2020 if current RD&D budgets were to remain unchanged (baseline scenario). Such that by 2020, in a policy driven scenario, for every euro going to wind or PV RD&D, there are 111 euro's going to deployment subsidies. Wind and PV industries currently invest on average 2% of sales in R&D. Therefore, we believe that governments could support the industry by investing an amount equal to 5% of annual sales, such that a 7% sales/R&D ratio - common in engineering and electronics industry - would be achieved. This would result

in a significant decrease of the pull/push ratio from 35-41 (Baseline scenario) to 6-8 ("5% of sales" scenario) in 2010. Since in the "5% of sales" scenario R&D budgets evolve in line with annual sales, pull/push ratios are more flexible to changing market circumstances. Notice for example that the "5% of sales" pull/push ratio does not differ that much when comparing wind and PV, this in contrast to the other scenarios. The estimates of needed RD&D investments based on IEA suggestions result in pull/push ratios that are quite similar to the "5% of sales" ratio. However, the differences between the pull/push ratio for wind and PV are much bigger. Despite this fact, we are convinced that following the IEA's advice would certainly be a step in the right direction.

Table 4: Comparison of Push and Pull measures for wind and PV in the EU in 2010 and 2020

		PV (€ Bio/year)		Wind (€ Bio/year)		Total (€ Bio/year)	
		Mod	PD	Mod	PD	Mod	PD
Push	Baseline	0.184	0.184	0.136	0.136	0.32	0.32
	R&D 5% of annual sales	0.90	1.50	0.45	0.70	1.35	2.20
	IEA Annual RD&D needs	0.92	0.92	1.36	1.36	2.28	2.28
Pull	2010	7.77	8.57	3.37	4.43	11.1	13.0
	2020	18.4	25.6	6.95	9.67	25.4	35.5
Pull	Push	pull/push		pull/push		pull/push	
2010	Baseline	42	47	25	33	35	41
	R&D 5% of annual sales	9	6	7	6	8	6
	IEA Annual RD&D needs	8	9	2	3	5	6
2020	Baseline	100	141	51	71	79	111
	R&D 5% of annual sales	20	17	15	14	19	16
	IEA Annual RD&D needs	20	28	5	7	11	16

(Based on (8), (9), (10), (11), (15), (17) *and annual reports of solar and wind companies)*

3.4.2. Sensitivity analysis and remarks

Many authors agree that governments should invest more in renewable R&D; however the "optimal" amount of R&D efforts is difficult to estimate. Fischer and Newell (26) search for optimal R&D subsidy levels using a theoretical model that optimizes renewable policies. They find that the optimal R&D subsidy should be equal to 6%, which is remarkably close to our empirically estimated value of 5%. Furthermore, the optimal public R&D estimates by the IEA are also quite comparable to our estimates. From this we can conclude that our estimated "5% of sales" public RD&D budget is in line with recent findings. Nevertheless, it is interesting to evaluate the effect of the "5% of sales" assumption on the overall results. Table 5 shows that adapting this assumption does have significant effects on the pull/push ratio. However, even the very conservative estimate of 2.5% results in pull push ratios that are smaller than currently found in the EU (namely 25-33 for wind and 42-47 for PV). The ratios rise by 2020 due to rising deployment costs, however not as dramatic as compared to the status quo scenario (see Table 4).

When interpreting these results one should keep in mind that, throughout this paper, we have always opted for the more conservative approach. For example, the growth of wind and PV electricity production is assumed to be moderate compared to other scenario's (see Table 1). Also, the assumption that subsidies will gradually fade out by 2020 is a tentative one. To our knowledge, only a few governments have presented such decreasing policy schemes (for example Greece (15) and the region of Flanders). It remains to be seen whether or not this practice becomes widespread in Europe. Governments that do not reduce renewables support

over time will experience higher costs than the estimates mentioned above. If PV and wind electricity production were to grow at rates mentioned by the EWEA's 'high' scenario (13) or the EPIA's 'paradigm shift' scenario (19) costs will be much higher, resulting in even higher burdens on electricity consumers.

Table 5: Pull Push ratio under different assumptions on optimal public R&D budgets

Pull/Push		PV		Wind		Total	
year	R&D/Sales ratio	Mod	PD	Mod	PD	Mod	PD
2010	2.5% of annual sales	17	11	15	13	17	12
	7.5% of annual sales	6	4	5	4	6	4
2020	2.5% of annual sales	41	34	31	28	38	32
	7.5% of annual sales	14	11	10	9	13	11

4. Conclusion

Despite the uncertainties surrounding the mechanisms behind technology support measures, it seems that a pull/push ratio of 40, estimated here, does not seem optimal. This ratio could increase up to 79-111 by 2020 if current policies were to remain in place. Overall, we can safely say that European governments should critically evaluate current renewables subsidy schemes, especially for PV systems, and raise public RD&D investments. These higher RD&D budgets could drive down production costs, which will result in a decreasing need for demand-pull measures in the longer run. Further efforts should be made to obtain more reliable and complete data on public and private RD&D expenditure and to improve our understanding on the interactions between demand-pull and supply-push policy measures, such that policy makers have the knowledge and the tools to bring new, promising technologies to the market in an effective and efficient manner.

References

[1] R. G. Newell, The role of markets and policies in delivering innovation for climate change mitigation, Oxford Review of Economic Policy 26, 2010, pp. 253-269.

[2] V. Norberg-Bohm, The role of government in energy technology innovation: insights for government policy in the energy sector, Harvard University, Belfer Center for Science and International Affairs, 2002.

[3] G. F. Nemet, Demand-pull, technology-push, and government-led incentives for non-incremental technical change, Research Policy 38, 2009, pp. 700-709.

[4] T. Jamasb, W. J. Nuttal, and M. Pollit, The case for a new energy research, development and promotion policy for the UK, Energy Policy 36, 2008, pp. 4610-4614.

[5] P. H. Kobos, J. D. Erickson and T. E. Drennen, Technological learning and renewable energy costs: implications for US renewable energy policy, Energy Policy 34, 2006, pp. 1645-1658.

[6] G. F. Nemet and E. Baker, Demand subsidies versus R&D: Comparing the uncertain impacts of policy on a pre-commercial low-carbon energy technology, The Energy Journal 30, 2009, pp. 49-80.

[7] M. Frondel, N. Ritter and C. M. Schmidt, Germany's solar cell promotion: Dark clouds on the horizon, Energy Policy 36, 2008, pp. 4198–4204.

[8] IEA, Global gaps in clean energy R&D, International Energy Agency, 2010.

[9] IEA, Global gaps in clean energy research, development and demonstration, International Energy Agency, 2009.

[10] EPIA, Global Market outlook for photovoltaics until 2014, European Photovoltaic Industry Association, 2010.

[11] Tradewind, Integrating Wind, 2009.

[12] Eurobserv'er, State of renewable energy in Europe, 2009.

[13] EWEA, Pure power, wind energy targets up to 2020 and 2030, 2009.

[14] M. Šúri, T. A. Huld, E. D. Dunlop and H. A. Ossenbrink, Potential of solar electricity generation in the European Union member states and candidate countries, Solar Energy 81, 2007, pp. 1295-1305.

[15] EREF, Prices of renewable energies in Europe, European Renewable Energies Federation, 2009.

[16] IEA, Energy Technology Perspectives 2010, International Energy Agency, 2010.

[17] IEA, RD&D statistics [accessed 28 October 2010] <http://www.iea.org/stats/rd.asp.>

[18] European Commission, EU energy trends to 2030, 2010.

[19] EREC, RE-thinking 2050, European Renewable Energy Council, 2010.

[20] EPIA, Set for 2020, European Photovoltaic Industry Association, 2010.

[21] OECD, Measuring Innovation: a new perspective, 2010.

[22] National Science Board, Science and engineering indicators 2010, 2010. [accessed 25 November 2010] <http://www.nsf.gov/statistics/seind10/c/cs1.htm.>

[23] EWEA, Wind energy the facts, 2010. [accessed 5 December 2010] <http://www.wind-energy-the-facts.org/documents/download/Chapter3.pdf.>

[24] EPIA, Solar Generation 6, 2010. [accessed 25 November 2010] <http://www.epia.org/publications/epia-publications.html.>

[25] IEA, Technology Roadmap: Solar Photovoltaic Technology, 2010. [accessed 5 December 2010] <http://www.iea.org/papers/2010/pv_roadmap.pdf.>

[26] R.G. Newell and C. Fischer, Environmental and technology policies for climate mitigation, Journal of Environmental Economics and Management 55, 2008, pp. 142-162

Combined solar power and TPV

Erik Dahlquist [1,*], Björn Karlsson [1], Eva Lindberg [2],

[1] *Malardalen University, Box 883, 721 23 Vasteras, Sweden,* [2] *Dalarna University College, Borlänge, Sweden.*
Corresponding author: tel + 46-21-151768, fax +46-21-101370, erik.dahlquist@mdh.se,

Abstract: In this paper design for a combined TPV and solar power system for local heat and power production is discussed. PV cells are producing electricity when there is light, while TPV cells are used when it is dark. Biomass is combusted and the heat is generating photons for the TPV system. Higher combustion temperature will give higher electric output, but also faster deterioration of the materials in the combustor, where the temperature of the emitter is 1050-1250 ^{o}C. By combining PV-cells generating electric power summer time with TPV-cells generating electric power winter time, we can achieve a flexible local heat and power system all year round. As both systems generate DC-power, we also can see a potential to use the same DC components for e.g for charging batteries for electrical vehicles, DC-pumps, LED-lamps etc. Design criteria for the systems are discussed in this paper for a house that is principally self sufficient on energy. Both theoretical and practical obstacles are discussed, as there are a number of issues to solve before the technique can be used in ”real life”. The TPV system is not yet commercially available, but is tested in pilot scale.

Keywords: *Solar power, TPV, combination, heat, electricity*

1. Introduction

There will be a shortage of fossil fuels in the future and thus renewable energy like solar power and biomass will be interesting alternatives. One type of solar power is PV-cells, although there are other alternatives like Stirling engines, organic ranking cycles and even steam turbines when the sunshine is concentrated to heat an organic solvent or water/steam to high temperatures.

In this paper we are concentrating on the combination of PV-cells and TPV-cells, where the principles are to convert photons into electric power directly. In the PV-cells the photons are in the range 0.4- 0.8 um mostly, while in TPV cells we extend the wave lengths up to approximately 1.9 um. The advantage with a combination of PV and TPV cells is that we will consume no fuel during spring to autumn periods, but still can produce both heat and power when there is no or little light. At the same time we can use the same infrastructure with respect to DC-current and lower voltage than the normal 220 V in Europe. In this way we can be both self-producing all electric power needed without having to store electricity in batteries. The cost to store biomass is radically lower than the cost for storage in the batteries, and thus makes sense.

2. Conversion of biomass to heat and electric power using TPV

The combustion unit can be a conventional boiler extended with a TPV-unit where heat and electricity are produced simultaneously. The principles for a TPV unit developed by Malardalen University together with Dalarna university college in Borlange is principally making use of photons produced by combustion flames heating a steel plate, the emitter [1],[2],[3] and [4]. The photons produced are then filtered in an energy glass, and thereby only the energy rich ones hit a PV-cell, but with a slightly lower band gap than normal PV-cells. The cut off wave length and correspondingly band gap are seen in table 1 for different materials. Silica (Si) with a cut off at 1.1 um is good for visible light but not for longer wave length. GaSb and InGaAs are better giving cut offs suitable for TPV cells.

Table 1. Cut off and threshold energy for different materials

	Cut off wave length	Band gap
Si:	1.1µm	1.12eV
GaSb:	1.7µm	0.72eV
InGaAs	2.3µm	0.55eV
InGaAsSb	2.4µm	0.53eV

The cut-off here means that photons with a wave length higher than the cut-off are filtered off, while those with short wave lengths are passing through the glass to the PV-cell. The data are from [5]. By this the same amount of electricity can be produced with a surface area 100 times smaller than for conventional PV-cells. This means that the power output could be around 10 kW per m^2, compared to some 0,1 kW/m^2 for typical solar PV cells. As the TPV system can operate whenever you have a need, it can be used even when it is dark and in that way be acting as a back-up system for ”normal” PV cells.

Biomass can have many different origins. It can be biogas produced from household waste or crop waste like straw. The gas then will be mainly methane, which is the same fuel as if we use fossil “natural gas”. The biomass could also be produced from different algae specie, where the production will depend on the actual sun intensity, nutrients and temperature. Of course the technology can also be used for fossil fuels like oil, but that is from our perspective not interesting long term. Typical values of solar intensity at different places in Europe are seen in figure 1 below.

As can be seen the irradiation is approximately 8 kWh/m^2,day summertime at all sites, while only less than 1 kWh/m^2,day during December- January. We can assume that the growth rate for biomass is in the range 0.5 % to at best 5 % of the incoming sun light, which means 0.04-0.4 kWh/m^2,day summer time and 0.005 – 0.05 kWh/m^2,day winter time. The heat demand winter time would be some 0.5 – 240 kWh_{th}/d in single houses depending on the house type, and to this we can add an electricity demand for the house hold use of approximately 5 kWh_{el}/d for low consumers up to 40-50 kWh_{el}/d for high consumers. [6]. The lower heat demand is for modern “passive” houses while the higher values are for houses older than some 40 years and not retrofitted to modern standard.

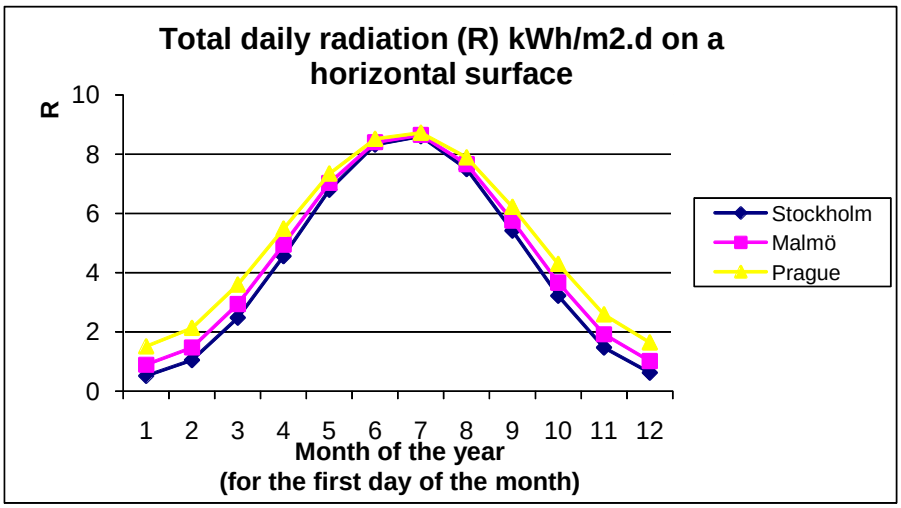

Figure 1 The total daily radiation by the sun on a horizontal surface in Stockholm, Malmo and Prague

The cells in the small pilot plant we have developed consist of 21 cells in three lines with 7 cells in each. The total surface area is 40 cm^2. The cells are from JX Crystals. The cells are mounted on a surface with water cooling, to keep the cell temperature below 50 ^oC. Different emitter materials were tested, but normal black iron actually turned out to be as efficient as more advanced materials. The reflectors were made of vacuum formed aluminium that was electro polished to get good reflectance properties. We had different type of edge filters. There was one specially designed glass surface, but it turned out that a normal energy glass was good enough. This simple pilot module thus was used in the tests performed and described below.

The heat source was an electrical furnace from Kanthal. This was a stable heat source which was easy to control. The experiments were made as seen in figure 2 below.

At the bottom we have the electric furnace, above the emitter and the reflecting cones. The glass edge filter was mounted between the two Aluminium cones as seen in figure 2. At the top are the cooled TPV-cells. The actual experimental set up is seen at the photo to the right, where also two of the authors (Eva Lindberg and Erik Dahlquist) are seen aside of Svante Nordlander.

Figure 2. The experiment set up with the pilot TPV unit.

The efficiency calculations were made using the following formulas:

For the first experiment the efficiency was calculated according to equation (1)

$\eta_1 = (P_c / A_c) / G$ (1)
P_c = Electric power of the TPV cells [W]
A_c =Cell area [m^2]
G =Irradiation intensity at the plane of the cells [W/m^2]

For the second experiment equation (2) was used for the efficiency calculation:

$\eta_2 = (P_c /Ac) / E_u$ (2)

E_u [W/m^2] is the irradiation power per area unit from the emitter and is calculated from equation (3).

$$E_u = \varepsilon \sigma T_e^4 \quad (3)$$

ε =emissivity [-]
σ =Stefan-Boltzmanns constant = 5,66697 10^{-8} [W/(m^{2}K^4)]
T_e =Emitter temperature [K]

Equation (3) also was used for the efficiency calculation in experiment 3. In figure 3 we see the results from experiment 1, where the effect of water cooling of the TPV cells was studied. As seen the water cooling of the cells gives a very strong impact on the cell performance. The efficiency calculations according to equation (1) was 4,8 % at 1950 W/m^2 and 8,7 % at 3000 W/m^2.

$$\eta_3 = (P_c / Ac) / (\gamma E_u)$$

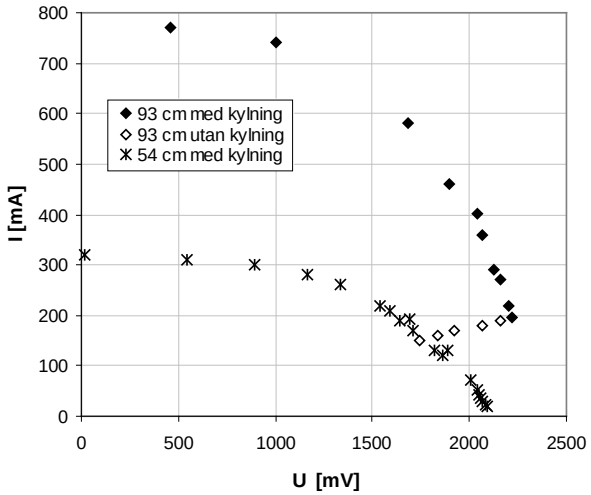

Figure 3. Results from experiment 1. Current – voltage curve for water cooled GaSb-cells irradiated with a halogen lamp at 1950 W/m^2 (93 cm) and ca 3000 W/m^2 (54 cm). The black prisms are with water cooling at 93 cm distance, the uncoloured prisms the same without cooling and the crosses at 54 cm distance with cooling.

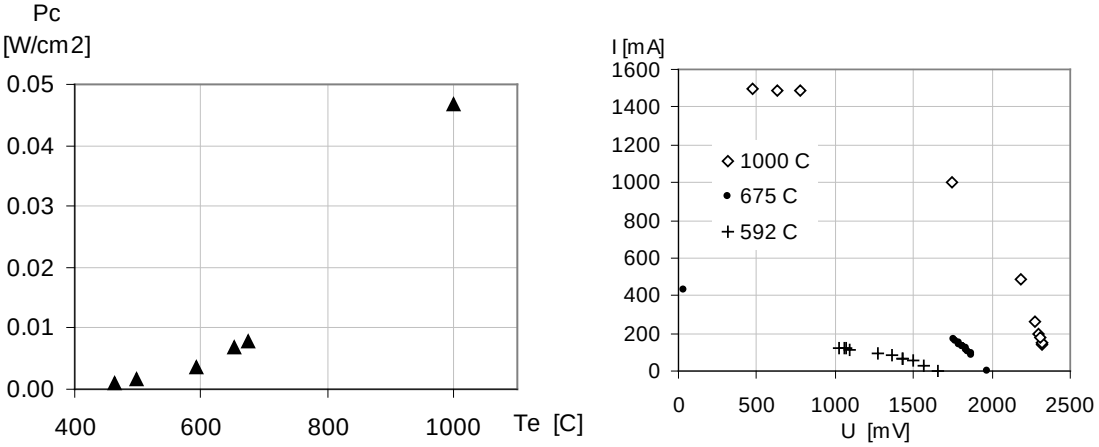

Figure 4. Power output as a function of the emitter temperature and current – voltage plot for different emitter temperatures.

In figure 4 we see the power output as a function of the emitter temperature. The average fill factor for the experiments was 0.6 calculated by the formula Fill factor = MPP/(I_{SC} x U_{OC}). Still, the spreading was relatively high as it was a bit difficult to measure the short cut current I_{SC} and the voltage at open circuit U_{OC} as well as the maximum power point MPP.

In figure 5 we see the current- voltage plots for emitter temperatures up to 1200 °C.

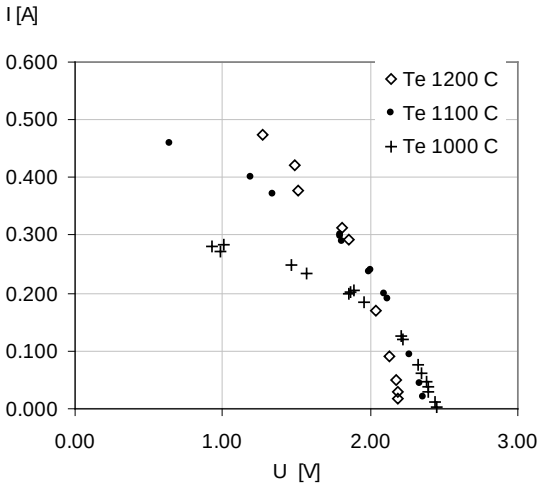

Figure 5. Current – emitter plot for higher emitter temperatures.

These higher emitter temperatures were tested in a special high temperature electric furnace from Kanthal which could be kept at constant temperatures up to 1700 °C. Still, it was not that easy to perform the actual measurements at the very high temperatures, so in practice we stopped at 1200 °C. These were the experiment 3 tests. In this last experiment we also tested the impact of the cones and the energy glass. The outcome can be seen in figure 6 below.

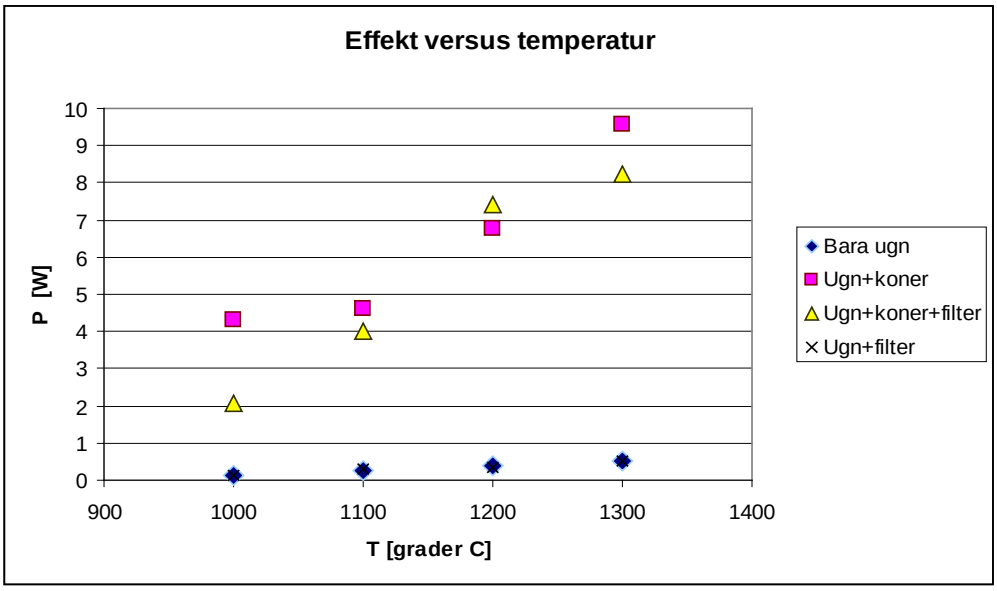

Figure 6. The power output from the TPV cells. At bottom (dark prisma) with radiation from furnace directly towards the TPV cell, (pink squares) furnace + reflecting cones and (yellow triangles) furnace, reflecting cones and edge filter using a standard energy glass.

At the bottom in figure 6 we see the power output when we only had the irradiation directly towards the cells placed at a distance corresponding to one cone. The squares are for furnace plus one reflector cone, but with no edge filter. Finally the triangles are for the two reflector cones with an energy glass in-between as seen in figure 2. The electric efficiency from fuel heating value to electricity production is going from around 0.5 % to 4- 5 % in the <1 kW $_{thermal}$ pilot plant tested. As we can see the reflector cones give a strong impact, and the two cones + an edge filter glass does not give significantly lower power output than with only one cone. Still, with two cones plus the glass we can have a long term good performance, which would not be possible without the energy glass, as the TPV cell would become too hot and deteriorate. The temperature drop in the combustion gases due to the TPV was negligible. By having a larger emitter and TPV area the electric output in relation to the heating value of the fuel can be increased. By this the efficiency as electricity divided by fuel heating value could be up towards 20%. Still, this also mean an increased cost for the TPV module. It should also be noticed that the remaining heat can be used to both heating water or drive an absorption cooling machine.

3. System aspects considering the demand and production capability of energy in detached houses.

The lowest heating demand is in so called passive houses that only utilize the heat from appliances and human bodies (approximately 100 W per person). If we should produce all electricity by TPV cells (5% efficiency) this means a fuel demand around (5 kWh/d) /(0,05) = 100 kWh fuel/day. For a four times larger TPV area the demand would be 25 kWh fuel per day. We assume that the electricity demand is only during 3 of 12 months, while the production is during 12 month, with an average of 5 kWh/m^2,day.

This means a demand of 100 kW h/d * 90 da ys = 9 000 kWh/year and assuming a net efficiency from the sun of 1% the biomass production will be 5 kWh/m^2,day*0.01 * 360 days = 18 kWh/m^2, year with respect to biomass. This means a need for 9 000/18= 500 m^2, if all the fuel should be produced in this way and all electricity come from the TPV-cells. For the four time larger TPV area the demand would be 25 kWh/d and the area for growing biomass would be 125 m^2 instead. With an efficiency from incoming sun to biomass of 5% would mean 100 m^2 instead of 500 m^2 , which might be economically feasible, but still on the high side. If we reduce the electricity consumption significantly by using low energy lamps, low energy refrigeration, using hot water instead of electricity in the washing machine and stay with low consuming TV and computers, it might be possible to reach perhaps even 50 m^2 solar heating surface area, and then also we could have PV-cells covering the rest of the need for the summer, autumn and spring time. With 5 kWh/ m^2, d, sunshine and 10-15 % net solar power efficiency, an average electric power output of 0.5 – 0.75 kWh/m^2,day could be achieved. We then would need some 5 m^2 for the house hold electricity for a single house. During summer there can be a net production that could be passed on to the power grid, while there might be a deficiency in October-November and February – March. A small battery would be good to have to give power also in the evening when it is dark, if there is enough PV-area to charge it during the day. Typical hot water and electricity demand for households have been presented in [6] and [7].

Summer time hot water production can be produced by solar heating panels. With a design with a t ank above the solar heaters a s elf circulation can be achieved, but the technical installation and the need to insulate the tank may make it le ss cost effective than using a circulation pump and a tank in the building..

4. Combination of PV cells and TPV cells

In figure 1 we can see that the sun can give a significant energy contribution from March to October. We already said earlier that TPV-cells can be used during the dark period November - February to produce both heat and electric power. Still, during the more sunny part of the year, we can utilize a combination of PV-cells and solar collectors described above. The good thing with a combination of PV and TPV cells is that all the electrical equipments for DC/AC conversion could be the same for TPV and PV-cells. The TPV system also is an alternative to investing in a large battery.

5. Energy utilization in a household in relation to local production

From a design perspective a single household would need some 0.4 kW base load electricity as an average over the year. The need for hot water production will be significant. If we assume that every person take a 4 minute shower three times a week, and the water used has an average temperature of 15 ^{o}C and is heated to 40^{o}C, the heat consumption per shower will be at 10 l/min: 0.17 kg/s *4.2 *(40-15) = 17.5 kW. During 4 minutes this means 1.17 kWh. For five persons taking three showers per week this will mean 1.17*5*3*52 = 910 kWh/year. Teen agers often take 10 minute showers and seven times a week, which would mean 2.9 kWh/shower*3*7 times/w*52 = 3 200 kWh/y + two grown-ups 1.17*2*3*52= 365 kW h/y with a total amount 3 565 kWh/y.

To this we should add hot water for washing cloths and porcelain, which will add up another 500 kWh/y at least. A total of some 4 000 kWh hot water then is needed. If we distribute this per day, it means some 11 kWh/day.

With the assumption that the incoming sun light is 3-4 kWh/m2,day in April a solar panel will produce some 35 l iter per m^2, day in April at the longitude of Vasteras/Stockholm with a temperature lift of 35 ^{o}C. This corresponds to 35*4.2*35/3600= 1.43 kWh/m^2,day. 11 kWh/day then mean 7.7 m2 solar panel. In March we only will get 15 l iter/m^2,day, which would mean a need for 18 m^2 to cover all.

6. Use of DC in households

As both PV and TPV systems generate DC-power, we also can see a potential to use DC components generally, e.g for charging batteries for electrical vehicles, DC-pumps, LED-lamps etc. The advantage with this would be that normally lower voltages could be used for many applications. This is important as the voltage normally is quite low in PV-systems, typically 12, 24 or 48 Volt. The draw-back is that it is causing more losses to transport energy as low voltage, and thus the distance has to be optimized between the production units and the appliances. It is not clear where the economic limits are for using DC on a larger scale in the buildings, but worth to investigate more in the future. Normal distances within a single house of average size will be no problem.

7. Discussion

To sum up: We assume a house-hold electricity demand of 3600- 5400 kWh/year = 10-15 kWh/day. To this a hot water demand of the same amount 10 kW h/d is assumed. The heat demand will vary over the year with a demand around 70-120 kWh/day in November-February, some 30- 50 during March-April and in September- October. The rest of the year there will be no de mand for heating. With a TPV system giving 10 kWh/d electricity we would produce also 50- 200 kWh/ heat and hot water, which would be enough to cover the

demand during November – February. During the rest of the year a 18 m2 solar panel + 20 m2 PV cells would be enough to cover all energy demands.

Adding some 5-10 m^2 PV-cells will give a house producing more energy than it consumes (emitting < 20 W/ m^2 building area when the outdoor temperature is – 15 ^oC - the definition used in Sweden for so called "low energy houses"). If the roof area is some 170 m^2 the solar panel units will cover less than 50% of the roof area, which is quite feasible.

For the case with the TPV system and production of biomass as such it would be primarily the TPV that is an issue, as the unit only exists as a pilot plant today, and not a full commercial product. Still, the prize tag is estimated to be relatively low (1000 – 3000 €/kW_{el}).

8. Conclusions

The conclusions are that the alternatives discussed can be motivated economically if we can achieve high efficiencies for all technologies and steps. It is difficult to judge which technology is the economically best comparing different systems that are not yet commercial. Still, the alternative with biomass production followed by TPV for heat and power production locally has a relatively short distance to being realized commercially, and the potential to be economically competitive is reasonably high.

Acknowledgements

We would like to thank Swedish energy agency for supporting the work with especially the development of the TPV technology.

References

[1] Lindberg, E. och Broman, L. (2003a) An animation tool for demonstrating the importance of edge filters in thermo photovoltaic applications. *Renewable Energy* 28(2003)1305-1315.

[2] Lindberg, E. och Broman, L. (2003b) Fabergé optics and edge filter for a wood powder fuelled thermo photo voltaic system. *Renewable Energy* 28(2003)373-384.

[3] Lindberg, E. och Broman, L. (2003c) Non-imaging optics in a thermo photovoltaic generator. *Fifth NREL Conf. on Thermo photovoltaic Generation of Electricity*, AIP Conference Proceedings 653, pp 222 -231. *Sixth NREL Conf. on Thermo photovoltaic Generation of Electricity*, AIP Conference Proceedings 738, pp 114-1223

[4] Dahlquist E. , Karim A., Bard G., Lindberg E., Broman L. and Nordlander S.: Modeling of a T hermo-photovoltaic System (TPV). Proceedings IIIrd International green energy conference in Vasteras, June 16-20, 2007.

[5] Qiu Kuanrong: Low Band gap TPV Cells and TPV Power Generation Systems, Proceedings IV th International green energy conference in Beijing, October 20-22, 2008

[6] Vassileva I., Lundh M., Dahlquist E. : Efficiency of interactive information on e nergy consumption in households in Sweden. Proceedings of the first International Conference on Applied Energy in Hong-Kong Jan 5-8, 2009.

[7] Widen J., : System studies and Simulations of Distributed Photovoltaic. PhD thesis 10 December, 2010, Uppsala University Press.

Comparative Performance of Various PV Technologies in Different Italian Locations

A. Colli[1,*], M. Marzoli[2], W. Zaaiman[3], S. Guastella[2], W. Sparber [1]

[1] *EURAC Research, Institute for Renewable Energy, Bolzano, Italy.*
[2] *Ricerca sul Sistema Energetico - RSE S.p.A., Milano, Italy.*
[3] *EC Joint Research Centre, Institute for Energy, Renewable Energy Unit, Ispra (VA), Italy.*
** Corresponding author. Tel: +39 0471 055630, Fax: +39 0471 055699, E-mail: alessandra.colli@eurac.edu*

Abstract: With the increasing number of photovoltaic (PV) installations on a worldwide scale, an outdoor performance analysis of various types of modules is needed. The purpose to assess and compare the performance of different types of modules in specific geographical locations, under various climatic conditions and to identify benefits/losses given by a specific surrounding context, is very important to evaluate the energetic behavior of future installations and direct them toward the most suitable technology to apply. The installations taken into consideration are located in Bolzano, Milan, and Catania, allowing comparison among three different Italian climate conditions and irradiance levels: the Alpine region, the upper Padana valley, and the see-side area in Sicily. In Bolzano, a multi-technology ground-mounted PV field is taken into analysis. For Milan and Catania, two multi-section PV power plants are monitored. The monitoring activities are done taking the international norm IEC 61724 as reference document, together with the best practice already existing in the field. The PV modules are evaluated in relation to ambient conditions, installation characteristics, module-specific behavior and state. Results are provided in a comparative way among the three considered geographical locations. Results are validated and an uncertainty estimation is shown. As instrumentation and environmental conditions are not the same, uncertainties for the locations might be different. Possible issues related to monitoring activities, as well as the performance of different PV technologies, will be highlighted.

Keywords: *Monitoring, PV System Performance, Energy Rating, Site-Dependent Performance Ratio.*

1. Introduction

The number of photovoltaic (PV) installations in Italy is quickly increasing, thanks to the national "Conto Energia" programme. An increasing trend has been also registered at European level, as well as worldwide. In this context, a detailed monitoring of selected PV plants and the analysis of operational data of these plants is needed to support a realistic outdoor performance analysis of various types of modules in specific geographical environments. This action supports both the scientific community and the different actors in the PV environment, such as developers, producers, installers, financing institutions, as well as decision-makers and customers.

2. The PV installations

The installations taken into consideration in this work are located in Bolzano, Milan, and Catania, allowing comparison among three different Italian climate conditions and irradiance levels: the Alpine region, the upper Padana valley, and the see-side area in Sicily. The evaluation has been limited to two months (September and October 2010) due to the recent operation activity of the installation located in Bolzano. From the different locations, four PV technologies are analyzed and evaluated: back-contact monocrystalline silicon cells (BC m-Si), heterojunction cells with intrinsic thin layer (HIT), copper indium gallium selenide (CIGS) and cadmium telluride (CdTe). All groups are mounted on 30°-tilted supports.

It must be stressed that the monitoring systems are, at the moment, different for Bolzano (supervised by EURAC Research and reading electrical data through the inverter system, with an SMA amorphous silicon reference device) in comparison with the installations of Milan and Catania (supervised by RSE and adopting a dedicated electrical monitoring system, using

a crystalline silicon reference device from the type EstiSensor [1]). This leads to differences in the acquired data, which are visible in their representation, but are also discussed and justified along the paper to make the comparison possible and valuable. A validation of the results of the performance ratio (PR) among the different groups, locations and monitoring systems is done in Section 4.

2.1. Airport of Bolzano Dolomiti (ABD) PV field

The multitechnology ground-mounted grid-connected PV field at the Airport of Bolzano Dolomiti (ABD), in the North-East of Italy, is in operation since August 10, 2010 and has a total peak power of 724 kWp. It is divided into two main parts: a 662 kWp commercial installation, mounting 8538 CdTe modules, and a 62 kWp experimental installation, mounting 24 different types of modules, divided into groups ranging between 1 and 2 kW each. The groups selected for the analysis are listed in Table 1. Results for two CIGS and two BC m-Si groups are shown, to highlight possible differences among the same product. For the commercial field using CdTe modules the monitoring results for a single inverter has been considered, connecting a total of 120 modules divided into 20 strings of 6 modules each. Figure 1 and 2 show the instantaneous PR for the four PV technologies calculated on a 15-minute base for each day of the month, respectively for September and October 2010.

Table 1. Groups and characteristics from ABD PV field in Bolzano.

Group	Type	kWp	Inverter	Overview
E2	HIT	3.87	SB4000TL-20	
E10	CIGS	1.12	SB1100	
E11	CIGS	1.12	SB1100	
E14-A	BC m-Si	1.2	SB1100	
E14-B	BC m-Si	1.2	SB1100	
Commercial	CdTe	9.3	SMC9000TL-10	

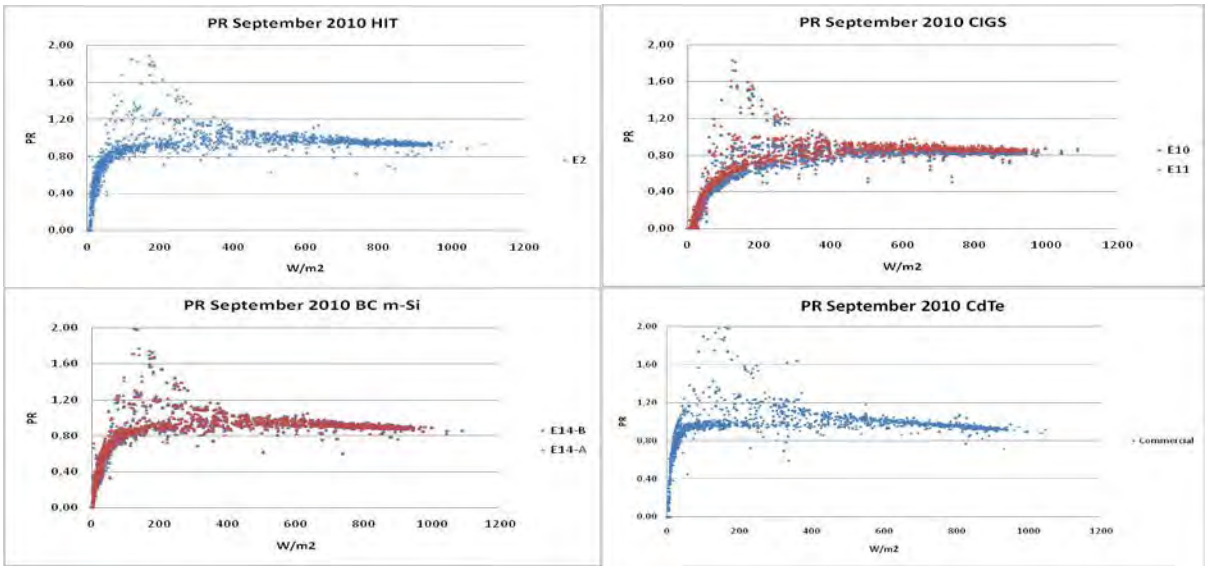

*Fig. 1. PR ($P_{AC}/(P_p$*Irrad.)) evaluated every 15 minutes for each day of September 2010 in Bolzano.*

The graphs highlight clouds of data at low irradiance levels (mainly between 100 and 200 W/m^2), due to the fact that the efficiency of the inverter is not stable for values of irradiance lower than 200 W/m^2. A general high performance and differences in behavior for the same

technology (as for CIGS, where differences in the trends are visible, especially clear in the month of October) can also be noticed.

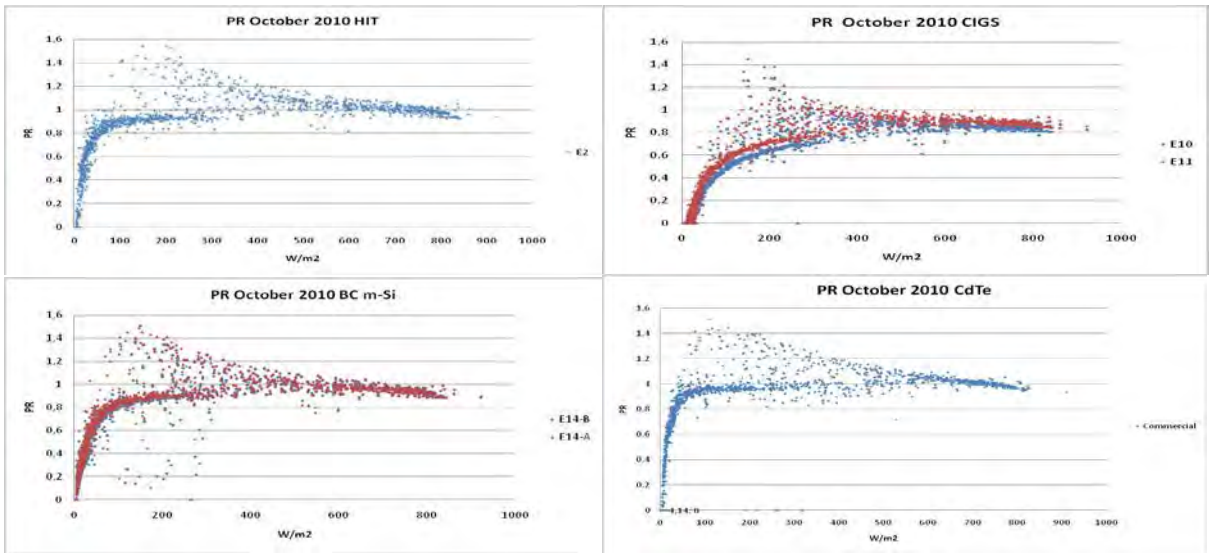

*Fig. 2. PR ($P_{AC}/(P_p$*Irrad.)) evaluated every 15 minutes for each day of October 2010 in Bolzano.*

2.2. PV test installation in Milan

The RSE test installation in Milan has a peak power around 8 kWp and consists of 6 groups of different technologies (polycrystalline silicon, two high-performance monocrystalline silicon, CIS, CdTe and amorphous silicon). The power production is monitored with a custom-made system to evaluate the current and voltage on both DC and AC sides of the inverter.

Table 2. Groups and characteristics in Milan.

Group	Type	kWp	Inverter	Overview
GFV11	HIT	1.05	SB1100	
GFV14	CIGS	1.2	SB1100	
GFV15	CdTe	1.16	SB1100	
GFV16	BC m-Si	1.2	SB1100	

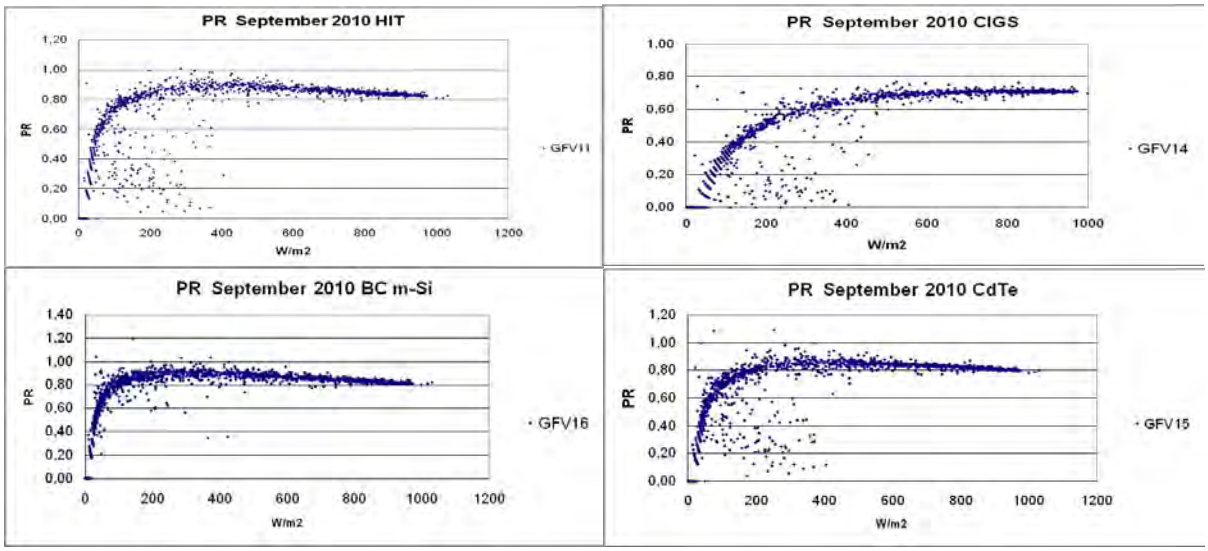

*Fig. 3. PR ($P_{AC}/(P_p$*Irrad.)) evaluated every 15 minutes for each day of September 2010 in Milan.*

The groups taken into consideration are listed in Table 2. Figure 3 and 4 show the instantaneous PR for the four PV technologies calculated on a 15-minute base for each day of the month, respectively for September and October 2010.

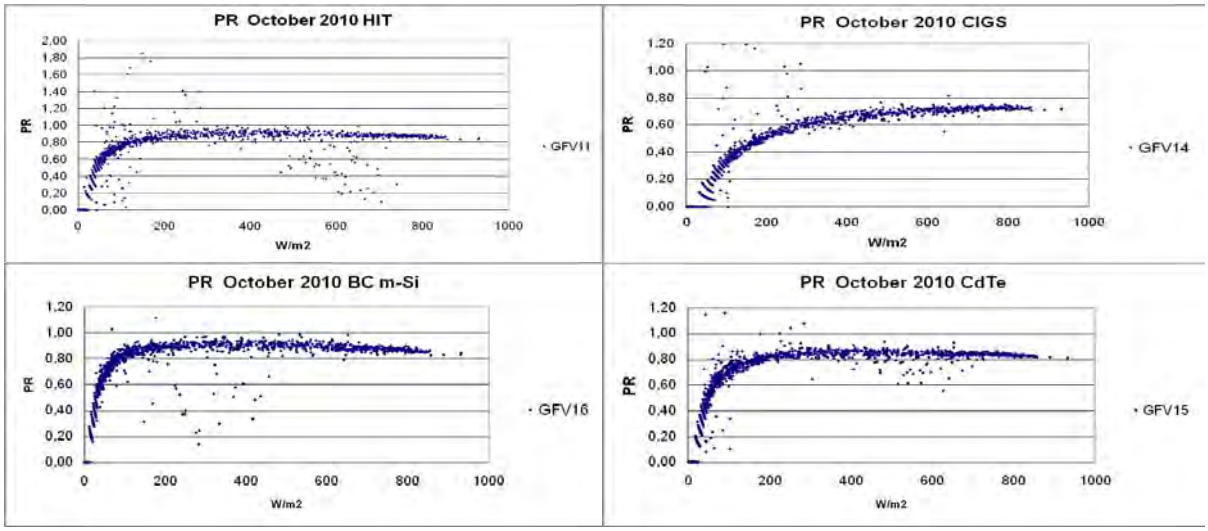

*Fig. 4. PR (P_{AC}/(P_p*Irrad.)) evaluated every 15 minutes for each day of October 2010 in Milan.*

2.3. PV test installation in Catania

The RSE test installation in Catania replicates the installation previously described for Milan in all its characteristics. The groups taken into consideration are listed in Table 3. Figure 5 and 6 show the instantaneous PR for the four PV technologies calculated on a 15-minute base for each day of the month, respectively for September and October 2010.

Table 3. Groups and characteristics in Catania.

Group	Type	kWp	Inverter	Overview
GFV1	HIT	1.05	SB1100	
GFV4	CIGS	1.2	SB1100	
GFV5	CdTe	1.16	SB1100	
GFV6	BC m-Si	1.2	SB1100	

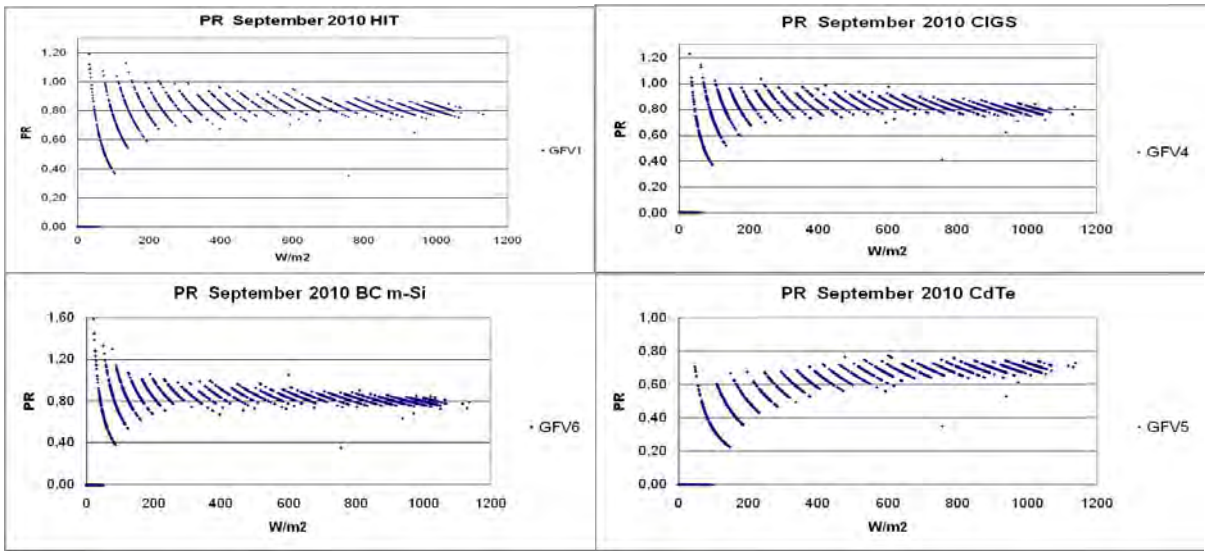

*Fig. 5. PR (P_{AC}/(P_p*Irrad.)) evaluated every 15 minutes for each day of September 2010 in Catania.*

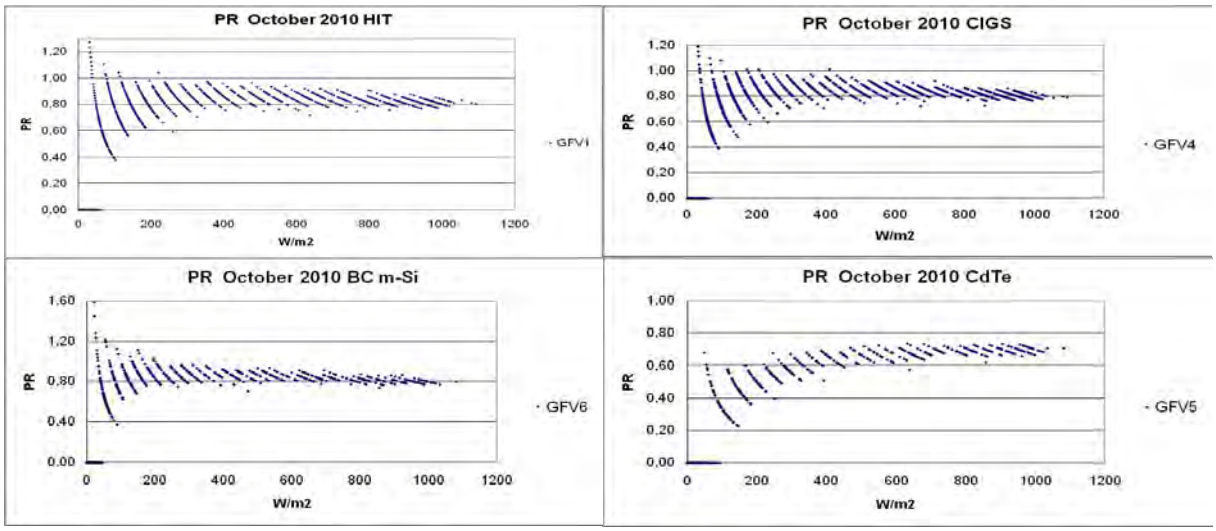

*Fig. 6. PR (P_{AC}/(P_p*Irrad.)) evaluated every 15 minutes for each day of October 2010 in Catania.*

The shape of the plots PR vs Irradiance in Catania is different from the previous considered cases. This is due to different settings of the resolution of the data acquired by the monitoring system, which takes into consideration only two decimal digits in the recorded AC power. The trend of the PR is, for higher irradiances, in line with the previous graphs.

3. Comparison

The comparison is conducted according to two indicators: the energy production per kWp of installed power and the PR, both processed for each month taken into consideration. Moreover, geographical environments and technology-specific behaviors are taken into account while evaluating the results.

3.1. Methodology

The calculation of the energy production in kWh/kWp is the main element of comparison among the various PV technologies; in fact, using this indicator the irradiance value is omitted as element in the calculation, avoiding the problem rising from mismatch and the difference in the reference devices among the sites. All inverters are from SMA, and each PV technology refers to the same module producer in all cases; anyhow, the issue of accuracy of the data acquisition system, as well as the accuracy in the kWp value by label, has to be considered. Following the indications of the international standard IEC 61724 [2], the performance of a PV system can be expressed by the PR, that shows the overall effect of losses (due to module temperature, irradiance usage, low components efficiency, faults) on the power output of the plant. The PR is calculated on a monthly base, according to the following ratio:

$$PR = \frac{Y_f}{Y_r} \qquad (1)$$

Where Yf = E/P_0 and Yr = H/G, and respectively E is the energy produced by the PV system, P_0 the installed peak power, H is the in-plane insolation (in kWh/m^2), and G is the irradiance at STC (1 kW/m^2).

3.2. Results

The energy production in kWh reported to the kWp of installed power (specific yield) allows a comparison among groups in the same location, but for different locations the energy

production has to be always seen in perspective of the irradiance value for the considered period. The values of the monthly global irradiance on 30° angle, respectively for September and October 2010, in the three considered locations are: Bolzano: 139.60 kWh/m^2 and 92.96 kWh/m^2; Milan: 144.01kWh/m^2 and 88.32 kWh/m^2; Catania: 169.94 kWh/m^2 and 126.54 kWh/m^2. Among c-Si technologies, HIT are performing better in Bolzano, while BC m-Si are dominant in Milan and Catania (see Table 4). CdTe modules compete with c-Si mainly in Bolzano and Catania, where the diffuse component of the irradiance is higher for the location characteristics. The production level (in terms of specific yield) of CIGS generally remains lower, with the exception of Milan, where production from CIGS is comparable to HIT. The PR can be compared only by taking into account the correction coefficient from Table 6.

Table 4. kWh of energy production per kWp of installed power per month, location and technology.

Date	Type	Bolzano	Bolzano	Milan	Catania
Sep-10	BC-mSi	127.7 (E14-A)	127.5 (E14-B)	121.8	139.4
Oct-10		88.7 (E14-A)	87.3 (E14-B)	76.5	105.5
Sep-10	HIT	134.0		118.6	138.5
Oct-10		93.2		73.9	103.7
Sep-10	CIGS	112.5 (E10)	118.9 (E11)	115.5	112.6
Oct-10		74.3 (E10)	79.4 (E11)	72.1	80.3
Sep-10	CdTe	135.6		93.3	138.6
Oct-10		90.9		56.4	103.6

Table 5. PR per month, location and technology.

Date	Type	Bolzano	Bolzano	Milan	Catania
Sep-10	BC-mSi	0.91 (E14-A)	0.91 (E14-B)	0.85	0.82
Oct-10		0.95 (E14-A)	0.95 (E14-B)	0.87	0.83
Sep-10	HIT	0.96		0.82	0.81
Oct-10		1.00		0.84	0.82
Sep-10	CIGS	0.81 (E10)	0.85 (E11)	0.65	0.66
Oct-10		0.80 (E10)	0.85 (E11)	0.64	0.63
Sep-10	CdTe	0.98		0.80	0.82
Oct-10		1.00		0.82	0.81

4. Validation of the measurement systems

In order to validate the results of the performance ratio, an attempt is made to compare the DC output power of the various groups with reference to the calculated installed power (kWp). Data sets with an average irradiance level (on 15 minutes) of 900 W/m^2 or higher, and available module temperatures are used to extrapolate the output power to standard reporting conditions of 25°C and 1000 W/m^2 irradiance level (excluding correction to airmass 1.5 global spectral irradiance). The values of the temperature coefficients for P_{max} used for the different PV technologies are as from [3] and are listed in Table 6. Concerning Bolzano, remarkable is the difference between two identical CIGS groups. The difference of 4% is also noted in Fig. 1 and 2. This is caused partially by the inverter data acquisition. Both BC m-Si groups show an overestimation in power of nearly 10%, but the difference between the two systems is negligible (< 0.5%). Also HIT technology shows an overestimation in power, which can be attributed to the mismatch in the spectral responsivity between the reference detector and the modules. This is valid for both silicon-based technologies.

Table 6. Correction coefficient for PR values.

Technology	BC m-Si	BC m-Si	HIT	CIGS	CIGS	CdTe
TC_Pm [%/°C]	-0.45	-0.45	-0.50	-0.36	-0.36	-0.21
Location	Bolzano					
Average DC_STC [kWp]	1.30	1.30	4.16	1.10	1.15	9.28
Standard deviation DC_STC [kWp]	0.03	0.03	0.12	0.03	0.02	0.13
Difference [%]	**7.9** (E14-A)	**8.3** (E14-B)	**7.6**	**-1.5** (E10)	**2.5** (E11)	**-0.2**
Location	Milan					
Average DC_STC [kWp]	1.16		1.03	1.01		1.17
Standard deviation DC_STC [kWp]	0.01		0.01	0.01		0.01
Difference [%]	**-3.2**		**-1.9**	**-16.0**		**0.5**
Location	Catania					
Average DC_STC [kWp]	1.14		1.00	1.10		1.05
Standard deviation DC_STC [kWp]	0.02		0.02	0.03		0.02
Difference [%]	**-5.0**		**-4.7**	**-8.7**		**-9.3**

For Milan, the difference between calculated power at 1000W/m^2 and 25°C and the measured DC power for the CIGS is very large, and cannot be justified by the spectral mismatch between c-Si reference detector and the spectral responsivity of the CIGS material. The differences of the BC m-Si and HIT materials can be attributed to spectral mismatch. The very small difference of the CdTe is also remarkable, as the spectral mismatch between c-Si and CdTe is normally around 8-10%. In Catania, it must be considered that the module temperatures are higher than for the two northern locations. The -8.7% difference for CIGS can be attributed to spectral mismatch, as well as the -9.3 for CdTe. The values for BC m-Si and HIT can originate from the temperature (as correction for T is more dominant than for the locations of Milan and Bolzano), as well as being influenced by the spectral mismatch.

As general remarks for the reference detector, guidelines are given in IEC 61724 [2] and require an irradiance reference detector with an accuracy better than 5%. As for the technologies CIGS, HIT, BC m-Si, a c-Si reference detector (as used by RSE in Milan and Catania) would reduce the effect of spectral mismatch. A rough estimation of ± 7% spectral mismatch for the above mentioned technologies should be taken in consideration for the Bolzano data (as an a-Si reference detector is used). For CdTe the spectral mismatch is estimated around ± 3%. These data will be used in the uncertainty calculation table. Some assumptions are made to estimate the overall uncertainty of the final PR value. For all uncertainty components, a “B” type standard uncertainty and a “R” (rectangular) distribution is assumed. Therefore the reduction factor is $\sqrt{3}$. The total index of uncertainty that is reported is calculated as the square root of the sum of the squares of the individual contributions. The uncertainties given in Table 7 are with a coverage factor (k) of 2. With a Gaussian probability distribution, this gives a confidence level of 95 %.

Table 7. Uncertainty values for the different PV technologies in the three considered locations.

	Location				Estimated Uncertainty	
	Bolzano		Milan&Catania		TF [%]	Si [%]
Standard uncertainty component	TF	Si	TF	Si		
Stability of Reference Device	1.73	1.73	0.58	0.58	3	1
Calibration of reference device	4.62	4.62	1.44	1.44	8	2.5
Spectral Mismatch	1.73	4.04	4.04	1.73	3	7
Irradiance DAS	0.00	0.00	0.58	0.58	0	1
Inverter / DAS	0.58	0.58	0.58	0.58	1	1
Installed power	2.31	1.15	2.31	1.15	4	2
Combined standard uncertainty	**5.7**	**6.5**	**5.0**	**2.7**		
Expanded standard uncertainty k=2	**11.5**	**13.0**	**9.9**	**5.4**		

5. Conclusions

The analysis shows a relevant impact of the geographical location (temperature, irradiance components) on the performance of selected PV technologies. In facts it clearly appears that certain technologies have a better energy production compared to others in the same location. Nevertheless, the importance of the monitoring devices and system components results clear while evaluating the performance. Commercial-type monitoring systems need improvements in quality and reference devices need regular maintenance activity. It is also important to match the module technology with an appropriate reference device. This issue becomes relevant when evaluating the PR. The monitoring system in Bolzano is under way to be improved to reduce data uncertainty and a collaboration with RSE is set to install additional monitoring devices on the DC and AC sides of the inverters for selected groups.

Acknoledgements

The Authors from EURAC Research would like to thank the European Regional Development Fund (ERDF) for co-financing the PV ABD project.
The Authors from RSE would like to acknowledge that their work has been financed by the Research Fund for the Italian Electrical System under the Contract Agreement between RSE (formerly known as ERSE) and the Ministry of Economic Development - General Directorate for Nuclear Energy, Renewable Energy and Energy Efficiency stipulated on July 29, 2009 in compliance with the Decree of March 19, 2009.

References

[1] H. Ossenbrink, K.A. Münzer, “The ESTIsensor – A New Reference Cell for Monitoring of PV Plant Performance”, 11th European Photovoltaic Solar Energy Conference and Exhibition, Montreux, Switzerland, 1992.

[2] International standard IEC 61724:1998 “Photovoltaic System Performance Monitoring - Guidelines for Measurement, Data Exchange and Analysis”.

[3] A.Virtuani, D. Pavanello, G. Friesen, “Overview of Temperature Coefficients of Different Thin Film Photovoltaic Technologies”, 25th EU PV SEC, 6-10 September 2010, Valencia, Spain.

An investigation of the impact of time of generation on carbon savings from PV systems in Great Britain.

P. A. Burgess[1,*], M.M. Vahdati [2], D. Davies [3]

[1] *Technologies for Sustainable Built Environments, University of Reading, United Kingdom*
[2] *School of Construction Management and Engineering, University of Reading, United Kingdom*
[3] *Solarcentury, London, United Kingdom*
** Corresponding author. Tel: +44 (0)7977 255 964, E-mail: p.a.burgess@pgr.reading.ac.uk*

Abstract: PV only generates electricity during daylight hours and primarily generates over summer. In the UK, the carbon intensity of grid electricity is higher during the daytime and over winter. This work investigates whether the grid electricity displaced by PV is high or low carbon compared to the annual mean carbon intensity using carbon factors at higher temporal resolutions (half-hourly and daily).

UK policy for carbon reporting requires savings to be calculated using the annual mean carbon intensity of grid electricity. This work offers an insight into whether this technique is appropriate.
Using half hourly data on the generating plant supplying the grid from November 2008 to May 2010, carbon factors for grid electricity at half-hourly and daily resolution have been derived using technology specific generation emission factors.

Applying these factors to generation data from PV systems installed on schools, it is possible to assess the variation in the carbon savings from displacing grid electricity with PV generation using carbon factors with different time resolutions.

The data has been analyzed for a period of 363 to 370 days and so cannot account for inter-year variations in the relationship between PV generation and carbon intensity of the electricity grid. This analysis suggests that PV displaces more carbon intensive electricity using half-hourly carbon factors than using daily factors but less compared with annual ones.

A similar methodology could provide useful insights on other variable renewable and demand-side technologies and in other countries where PV performance and grid behavior are different.

Keywords: *Renewable Energy, Photovoltaics, Carbon accounting*

1. Introduction

The carbon intensity of grid electricity varies with the seasons and also with the time of day. Similarly the production of electricity from PV is strongly dependent on the time of year and time of day. In the case of the variation in carbon intensity of the electricity grid, this is a function of the way that overall energy demand varies and the economics of the different electricity production methods. As the UK has a diverse mix of generation technologies, the variation in carbon intensity of the grid can be quite large. At times of low demand when nuclear makes up a relatively large proportion of the active generating plant, the carbon intensity tends to be relatively low; at times of the highest demand, the grid has all available nuclear and renewable power and a roughly equal mix of coal and gas supplying the remaining demand, leading to an intermediate carbon intensity figure. The times of highest carbon intensity occur when there is moderate to high demand and the cost of producing electricity from coal is lower than the cost of producing electricity using gas.

In the UK, company carbon reporting of the energy exported from microgeneration must be reported using the annual grid average carbon emissions factor [1] which may not be truly reflective of the grid mix at the time of generation.

This paper seeks to determine the relationship between the variation of the carbon intensity of the mixture of sources feeding the grid and the variation in the time of PV.

2. Methodology

There are three sources of data that or central to this work. Firstly, the half-hourly generation by fuel type data for the UK national grid [2]. This provides gross electricity production from eleven sources (including interconnectors and pumped storage hydro) for Great Britain. Data has been collated from November 2008 to June 2010. These figures do not make any allowance for parasitic loads within power stations which are considered in the second set of data, the average emissions factor for each fuel type in the half hourly generation by fuel type data. These generation emission factors (GEFs) are taken from AMEE [3] based on data in DUKES [4]. The GEFs provided by AMEE are for gross generation with a generated to supplied gross factor to allow for conversion from carbon intensity of gross electricity generation to the carbon intensity of the electricity fed into the grid. To convert these from grid supplied factors to the carbon intensity of electricity at the point of use, the losses in transmission and distribution (T&D) must be considered. We have used a flat figure for T&D losses of 9% [5].

Table 1 End use CO_2 emissions factors for each generation technology.

Fuel Type	Generated To Supplied Gross Factor	Mass CO_2 Produced per Energy Unit (kg/kWh)	Derived Supplied Net Factor (kg/kWh)	Derived End-use Factor allowing for T&D losses
CCGT	0.984	0.385	0.391	0.430
Coal	0.949	0.861	0.907	0.997
INTFR	1	0.082	0.082	0.090
INTIRL	1	0.549	0.549	0.603
NPSHYD	0.997	0	0	0
Nuclear	0.908	0	0	0
OCGT	0.944	0.525	0.556	0.611
Oil	0.828	0.737	0.889	0.977
Other	1	0	0	0
PS	0.997	0	0	0
Wind	1	0	0	0

Applying the resulting end-use GEFs (Table 1) to the generation by fuel type data gives the total CO_2 emissions from each fuel type for every half hour. Once this is completed, the task of deriving grid mix carbon intensity for any given time frame is achieved by dividing the total carbon emissions over the time by the electricity generated over that time. For this work, the time intervals considered are half hourly, daily and total period which varies slightly from system to system but all start between the 13th and 26th May 2009 and all run for between 363 and 370 days and can be thought of as an annual grid average carbon factor.

No account has been made for non-CO_2 GHG emissions from generation, for upstream emissions, for the embodied emissions associated with the generation infrastructure or end-of life disposal. The official methodology published by the UK Government [1] has only recently started including non-CO_2 GHGs in their electricity factors and these were not included for simplicity. The remaining omissions from this study are categories that are not consistent with the GHG reporting guidelines prevalent in the UK at the time of writing.

The final dataset used for this work was the generation from seven PV systems in the North of England provided by Solarcentury. All systems are 4 kW_p crystalline silicon systems oriented due south with a tilt of 30°. All data was for a period from a point in May 2009 to a point in May 2010 in 15-minute time steps. These were converted to half-hourly generation data.
In 32 half hourly periods across the generation by fuel type dataset only interconnector data had been recorded. In this study these half hours have been excluded from the analysis.
The carbon savings from PV generation were calculated using half hourly, daily and overall period emissions factors and the results compared.
All calculations were done using MS Excel 2007.

3. Results

The analysis of the variation in time of generation and carbon intensity of the grid presented in this section gives a clear indication of the main findings of the study. For systems with a similar generation profile, the differences between carbon savings from the annual average and from half-hourly carbon emissions factors are very similar.

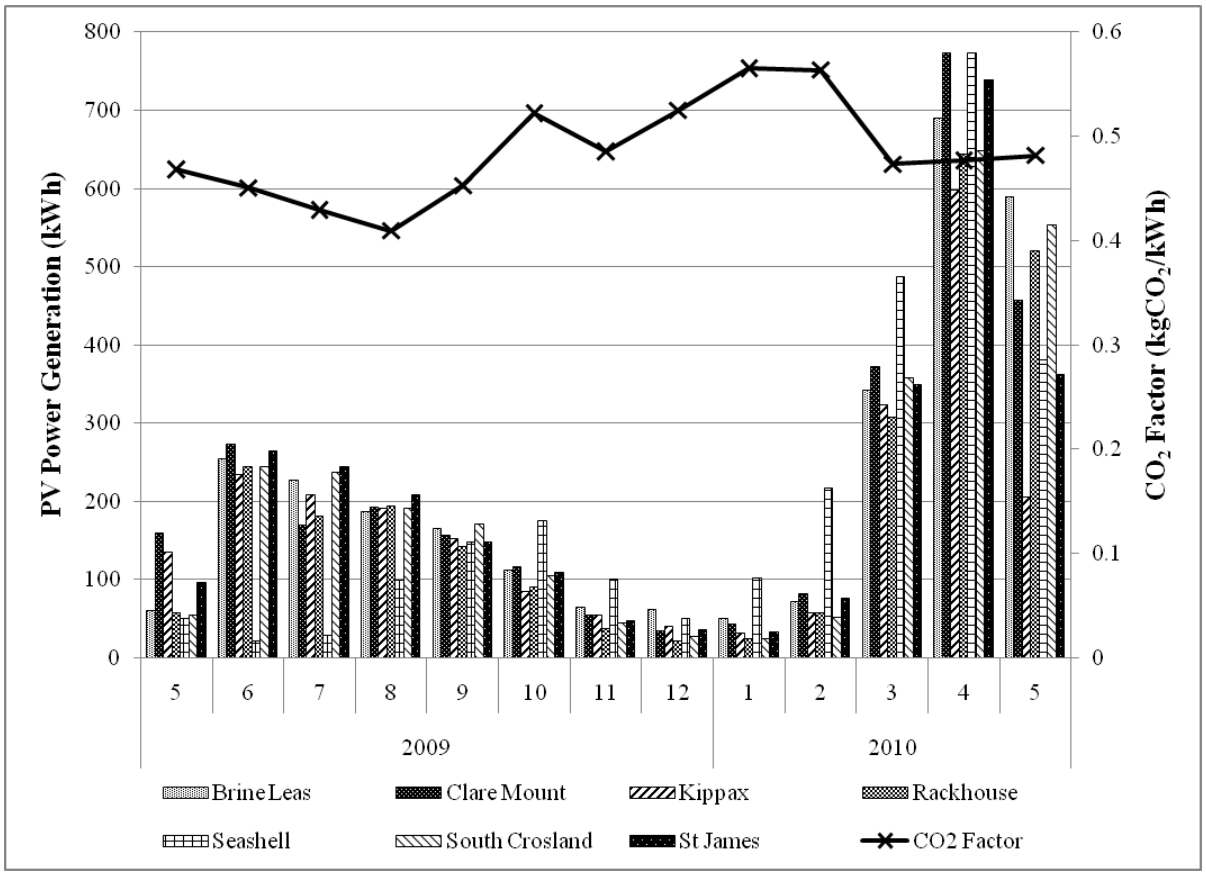

Figure 1 Monthly generation by each system (kWh) and Monthly average grid mix CO_2 emissions factor

Figure 1 shows a similar generation profile for all seven systems over the monitoring period with the exception of Seashell which has significantly lower generation in 2009 relative to the other systems. In all cases the generation in March to May 2010 is significantly higher than summer 2009 indicating that conditions for solar generation were more favorable in 2010 than 2009.

Figure 1 also gives a clear indication of the seasonal variation in CO_2 intensity with the highest monthly emissions factors being over the winter months (note the graph shows a year from May to May so winter is in the middle).

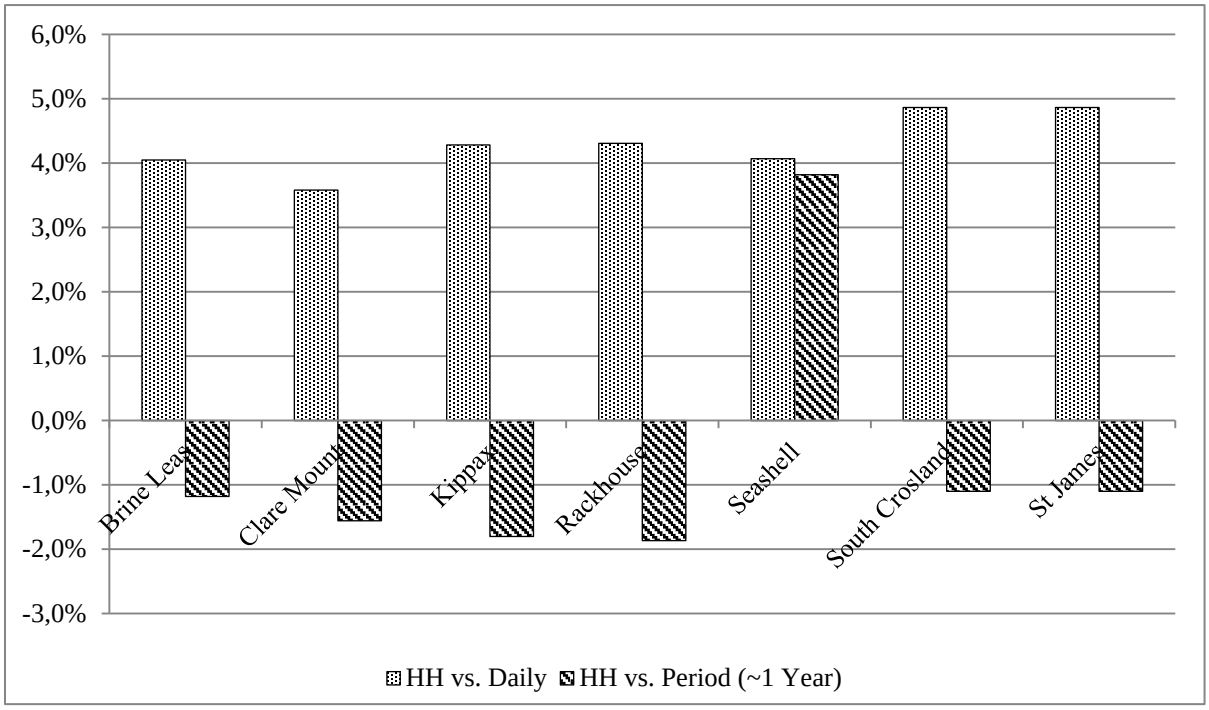

Figure 2 The difference between carbon savings using carbon factors with different time resolutions.

Figure 2 shows a clear trend across six of the seven systems analyzed with CO_2 savings assessed using half hourly emissions factors for the time of generation outperforming the average daily factor for the day of generation by between 3.5 and 5 percent. Comparing the half hourly performance against the period average grid mix emissions factor, carbon savings were 1 to 2 percent lower using the half hourly emissions factors. The clear exception to this is the comparison between the period average and half hourly figure for Seashell. This is likely to be a consequence of the different pattern of generation for Seashell seen in Figure 1 with a much smaller proportion of the system's generation in 2009 than in the other six cases.

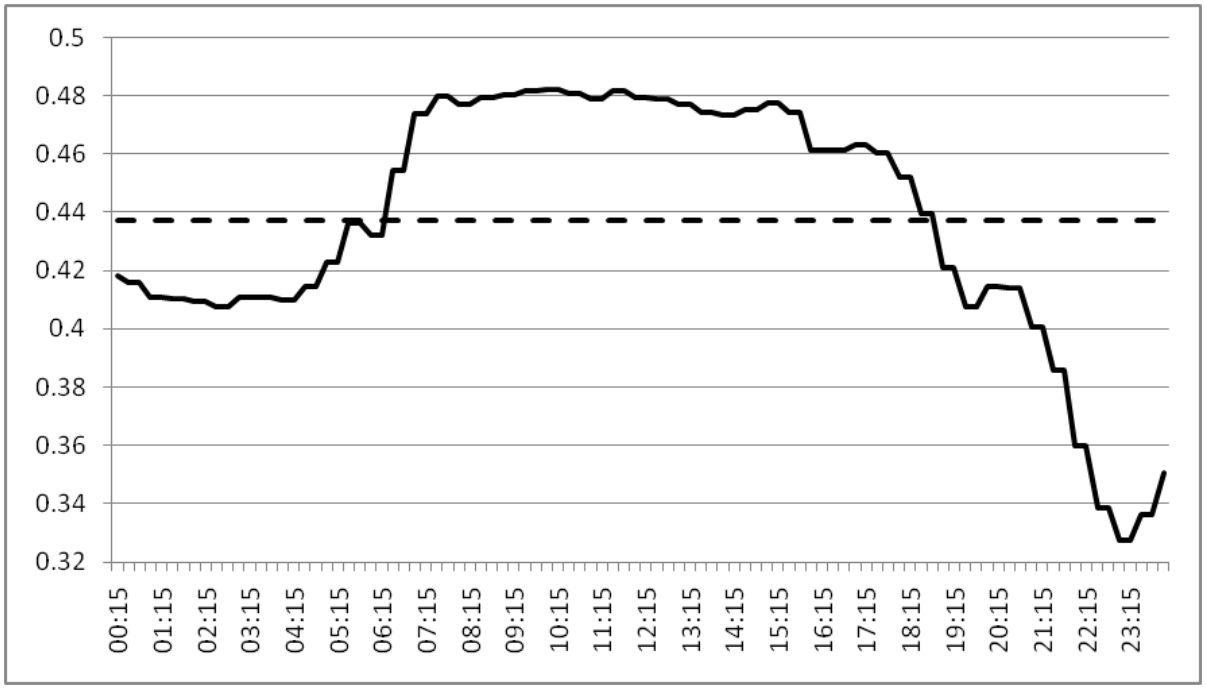

Figure 3 CO_2 factor variation for 17 July 2009 (typical summer day). Solid line is half hourly variation, dashed line is daily average.

The difference in carbon savings between half hourly and daily emissions factors can be easily understood by observing figure 3 which shows the variation in grid CO_2 for a typical summer's day. The profile is essentially a step function with lower carbon generation overnight and higher carbon generation over the daytime when PV will be generating. The typical winter profile is similar but with a still higher level in the evening corresponding to high demand for electricity for lighting, electric heating etc.

4. Discussion and Conclusions

4.1. Previous work

Previous studies have considered the carbon intensity of grid energy as it relates to PV generation for the purpose of life cycle analysis [6],[7] however these typically model emissions the typical conditions for an 'average' year rather than real data used for a historical analysis as in this work. Studies have also modeled the impact of PV at times of peak demand [8] but not the type of full year, short time-step analysis presented in this paper; the average relationship between time of generation and marginal emissions of CO_2 [9] and evaluated marginal emissions factors over a number of years [10].

Molin et al. [11] presented a study on the financial impacts of net metering for PV based on variable time intervals; hourly, monthly and yearly. This study suggested that net metering is most beneficial for PV using a full year for the time interval. This held true when assessed against data for Sweden, Germany and Spain using a 13-year long dataset. There are interesting parallels between this work which deals with financial performance at different time steps and our work which deals with carbon accounting at different time-steps. The key result of this study which applies to our own work is the suggestion that year-to year variation is relatively modest. It also highlights that an international version of our study would be of great value, particularly as the grid carbon intensity profile can be very different from country to country. As a caveat to this point, electricity markets where a single fuel dominates such as

France (nuclear) and hence only have limited variation in carbon intensity, a repeat of our study would not be worthwhile.

This work has as its basis the variation in average grid mix emissions factor on a half hourly basis without any consideration of inter-year variability. The aim of this work was to assess the validity of using annual average grid mix electricity emissions factors for calculating the carbon savings resulting from exported renewable microgeneration. Current company carbon reporting guidelines use overall grid mix carbon factors rather than marginal factors (which on the existing UK grid will almost always be higher than the average grid mix) on the basis that all consumers have a shared responsibility for electricity emissions rather than different consumers taking electricity from different sources, this work maintains this philosophy of shared responsibility at any given time but with variability introduced depending on the time of PV generation. The authors consider that there is merit to the use of a time-varying emissions factor as an incentive to businesses to engage in more active demand-side management, Gyamfi et al [12] found that the reduction of CO_2 emissions would be as significant motivation for consumers to initiate demand side management as price signals and second only to avoiding blackouts.

4.2. Sources of error

The results of this work are based on PV generation for a single year. As can be seen from the clear difference between the results for Seashell and for the other six systems, PV generation data gathered over a longer timescale would allow for more authoritative findings. It is clear that for systems with similar generation profiles, the resulting carbon savings are closely related.

The gaps in the half hourly generation by fuel type tables were explicitly omitted from the remainder of the study on the basis that they accounted for an extremely small proportion of the dataset. A more thorough treatment would entail the generation of synthetic data to fill these gaps based on a logical process which may include some combination of activity either side of the data gaps, prevailing conditions and additional datasets such as those for overall electricity demand.

The emissions factors for the grid used in this study are exclusively for direct carbon emissions from electricity generation and do not take account of any emissions upstream of the power station. Including these indirect emissions would result in a truer picture of the emissions associated with electricity generation at the cost of increased uncertainty about the exact level of GEFs depending on which indirect emissions are included and the assumptions made when calculating indirect emissions.

4.3. Simplifications and assumptions

In this study, PV generation is treated as a negative load on the grid. In Great Britain where there is only a small amount of PV on the grid, this approach is adequate however with a significant amount of PV generation on the grid the low carbon electricity produced by PV will be rolled into the overall grid mix emissions factor. In this scenario, a negative demand approach would lead to double counting of the carbon emissions reductions from PV.

4.4. Future & applications

The results of this work clearly show that for PV, the carbon emissions saved by the renewable electricity generated are different from that which is estimated using the annual average grid mix emissions factor. If similar work for other technologies including other

renewables and energy efficiency technologies which have a time-varying behavior can also be shown to differ from the annual average grid mix emissions factor, there may be a case for altering the reliance on the annual average for company reporting of carbon emissions. With the arrival of improved metering technology allowing for measurement of electricity use at high time resolution, this kind of temporally sensitive reporting would become genuinely feasible.

This study has shown that carbon savings from PV appear to be lower based on emissions factors for the time of generation than with annual average emissions factors in Great Britain where the grid is higher in carbon over the winter where demand peaks. The situation may well be reversed in a region where peak electricity demand and carbon intensity are over summer as a result of cooling loads.

The authors intend to develop a system for including real time carbon savings in PV system monitoring. The study presented here will be widened to cover a larger number of PV systems and a longer timeframe, given the similarity of the results across PV systems it may be possible to reliably estimate the percentage difference between half hourly and annual emissions factors for systems where this kind of analysis is not undertaken. An investigation of how real time carbon savings against marginal grid carbon emissions can be reliably calculated may also prove to be a valuable exercise.

Acknowledgements

The authors would like to thank the EPSRC for funding this work.

References

[1] DEFRA, Guidance on how to measure and report your greenhouse gas emissions, 2009, pp. 49 - 53

[2] Elexon Portal, Historic Generation By Fuel Type Data Files, https://elexonexchange.bsccentralservices.com/page_object_view.php?uid=76, Accessed online August 2010 (login required)

[3] AMEE, Fuel Emission Factors, http://explorer.amee.com/categories/Electricity_Generation_Emission_Factors/data, accessed online August 2010 (login required)

[4] DECC, Digest of United Kingdom Energy Statistics, 2009

[5] DTI, Future Network Technologies, 2006, pp. 4-5

[6] S. Krauter, Greenhouse Gas Reduction by PV, Proceedings of 3rd World Conference on Photovoltaic Energy Conversion, 2003, pp. 2610 - 2613

[7] R. Laleman et al, Life Cycle Analysis to estimate the environmental impact of residential photovoltaic systems in regions with a low solar irradiation, Renewable and Sustainable Energy Reviews Vol 15, 2011, pp. 267-281

[8] R. Spiegel et al, Demonstration of the Environmental and Demand-Side Management Benefits of Grid-Connected Photovoltaic Power Systems, Solar Energy Vol. 62, No. 5, 1998, pp. 345–358

[9] G. Keolian and G. Lewis, Modeling the life cycle energy and environmental performance of amorphous silicon BIPV roofing in the US, Renewable Energy 28, 2003, pp. 271–293

[10] A.D. Hawkes, Estimating marginal CO_2 emissions rates for national electricity systems, Energy Policy 38, 2010, pp. 5977–5987

[11] A. Molin et al, Positive power market value for grid-connected roof-top solar power in Sweden, in Proceedings of the 11th World Renewable Energy Congress (WREC XI), Abu Dhabi, UAE, 25-30 September 2010

[12] S. Gyamfi et al. Demand Response in the Residential Sector: A Critical Feature of Sustainable Electricity Supply in New Zealand, 3rd International Conference on Sustainability Engineering and Science, Auckland, NZ, 2008

Concentrator photovoltaic technologies and market: a critical review

Alaeddine Mokri, Mahieddine Emziane

Solar Energy Materials and Devices Lab,
Masdar Institute of Science and Technology,
Masdar City, PO Box 54224, Abu Dhabi, UAE
E-mailS: amokri@masdar.ac.ae, memziane@masdar.ac.ae

Abstract: This paper offers an overview about the current status of the concentrator photovoltaic technologies and market. It highlights the potential of this technology to bring the cost of electricity to competitive levels with fossil-fuel based resources. It starts with an overview about the photovoltaic market and then it narrows its scope to describe the concentrator photovoltaic technology (CPV). Then, it goes on quantifying the world CPV capacity based on the latest industry reports released in 2010. In this paper, we estimate the current world operational CPV capacity to be 21 MW. This paper also reports a minimum installation cost as low as 3.05 $/W and a levelised cost of electricity as low as 0.14 $/kWh. Those are the minimum costs announced in 2010. One interesting conclusion of this study is that CPV systems with high concentration have a higher economic potential comparatively with low concentration CPV systems.

Keywords: *solar energy, photovoltaic, concentrator photovoltaics, LCOE, grid parity.*

1. Introduction

Past and current trends in energy generation, supply and consumption have shown their unsustainability at the economic, social, and more importantly, environment levels. These trends led to the following [1]:

- The current GHG emission levels have not been seen for at least 800 000 years.
- By the year 2050, CO_2 concentration in the atmosphere will reach 380 part per million which is higher than the upper safe limit (i.e. 350 part per million) for avoiding severe climate change effects [2].
- In the past century, temperature of the planet increased by 0.7^{o} C and the sea levels by 20 cm.
- Ice caps are disappearing.
- The International Energy Agency (IEA) expects an increase of 50% in energy demand by 2030.
- Half of the CO_2 emissions from burning fossil fuels over the last 200 years were emitted in the last 30 years.

Without a decisive action, on the top of the facts listed above, increasing energy demand will raise concerns over energy security because of the continuous growth of the world population and economy [3].

The solution to this issue is to use clean renewable energy sources like solar, wind, geothermal, etc. Although these energy sources are abundant and free, their conversion to useful power comes at a higher cost than power from non-renewable sources and makes them less advantageous. Therefore, the main condition for the transition to a renewable energy era is to generate power from renewable sources at competitive costs with power from fossil-fuel based resources.

Since 2000, global photovoltaic (PV) capacity has been growing at an average rate of 40% per year to reach 14 Giga Watt in 2008 [3]. Expectedly, the annual photovoltaic capacity will represent 11% of the global electricity capacity by the year 2050 [3]. This will cancel 2.3 Giga tons of CO_2 emissions from the atmosphere [3].

PV energy encompasses a wide range of technologies: silicon, thin films and concentrator photovoltaics (CPV). While silicon modules represent 85-90% of the global annual market and thin film modules represent 10-15%, CPV modules represent less than 1% of the global annual market [3]. However, CPV is still emerging and has the highest potential of bringing the LCOE (Levelized Cost of Electricity) down to values that make solar power cost-competitive with conventional sources of electricity [4].

This article offers an overview of the current status of the CPV market and discusses the potential to achieve low LCOE.

2. Concentrator photovoltaic technology

A CPV system consists simply of a small solar cell and an optical component to concentrate light on it. Using low-cost optical components with small solar cells instead of large expensive solar cells is a key feature to achieve a low LCOE [5].

By doing some simple math, one can conclude that to generate a 1W of electricity, a 25% efficient solar cell under a 1000 concentration ratio requires 1775 less cell surface than a 14% efficient cell under no concentration. In the real world, CPV modules using 27%-36% efficient multi-junction solar cells are 25% efficient [4]. This is higher than the efficiency of converting power by using any of the other PV technologies. Comparatively with the other PV technologies, high CPV systems efficiency means that less land is needed to generate a given amount of power; or alternatively, more power can be generated if the same land area is used.

The claims above all depend to a large extent on the solar resource available. For instance, high-concentration CPV modules are economically viable in areas with more than 2200 kW/m^2 year of direct normal irradiance (DNI). Humid regions, areas with cloudy weather, windy areas and spots with an inappropriate topography all may not be suitable places for installing CPV power plants [4].

Based on their concentration ratio and the type of solar cells used, CPV technologies can be classified into three categories:

2.1. Low-Concentration Photovoltaic (LCPV):

Systems with a concentration lower than 40 suns fit in this category. These systems use Si solar cells and require passive cooling only to maintain their performance. Due to their large acceptance angle, high-precision tracking might not be required. Today, more than 20 companies are known for supplying LCPV modules.

2.2. Mid-Concentration Photovoltaic (MCPV):

This applies to systems with concentration ratios in the range 40-300 suns. These systems use multi-junction cells and may require active cooling. Active cooling is a requirement because typically when the temperature of the solar cells increases, their conversion efficiency goes down. High-precision tracking is also required to convert the maximum of the incident

sunlight. Based on the CPV Today Industry Report, 3 companies only supply MCPV modules [4].

2.3. High-Concentration Photovoltaic (HCPV):

These are systems with concentration ratios in the range 300-2000 suns. These systems require a high capacity heat sink, high-precision tracking and high-performance multi-junction solar cells; hence, their high cost. The potential of this technology relies on the very high-efficient multi-junction cells used. The 41.6 % efficiency recorded on a multi-junction cell under concentration in August 2009 by Spectrolab and the 35.6 % efficiency recorded on a solar cell under no concentration by Sharp, both highlight the potential of these CPV systems to achieve high efficiencies [4, 6]. Theoretically, the efficiency of multi-junction solar cells can reach 87 %. By using these high-performance cells, module efficiencies above 30% have been recorded [7]. About 33 companies do supply HCPV modules.

3. CPV installations worldwide

The total CPV capacity grew up from few kilowatts installed in 2006, to 1 MW in 2007, to 13 MW in 2008, and unexpectedly to 4 MW only in 2009 because of the world financial crisis. 50 MW capacity was expected to be installed worldwide in 2009 [8]. Nevertheless, 2009 witnessed the announcement of a 60 MW CPV power plant in Taiwan by Ya-Fei Green Energy and Guascor Foton.

Those numbers are much below the potential CPV capacity that can be provided. Today, the world manufacturing capacity of CPV is 1.23 GW and it is expected to reach 2.65 GW by 2012-2013.

Currently, the total operational HCPV capacity is estimated at 20.15 MW distributed among 48 installations worldwide. As for the pre-operational HCPV capacity, it is predicted that 23 installations will be operational to produce 247 MW.

For LCPV, the total operational capacity is 0.81 MW and it is distributed among 19 installations worldwide. Fig. 1 lists the CPV companies worldwide and the operational and the preoperational capacity of each one.

4. Current costs of electricity from CPV systems

The installed cost is a common criterion for ranking and comparing solar installations. It is the cost of the entire installation divided by the peak-power rating. The installed cost of CPV systems varies from one installation to the other; therefore, many values have been reported in the literature. Based on the CPV today Industry Report 2010, the overall installed cost of HCPV systems in 2010 ranges from 3.05 $/W to 7.25 $/W; however, for LCPV systems, the installed cost is 5.05 $/W [4].

The LCOE is also another useful measure for comparing and ranking solar installations. It is the cost of 1 kWh of energy from the system during its life time. For HCPV systems, the LCOE has been reported to vary between 0.14 $/kWh and 0.50 $/kWh. For LCPV systems, the LCOE has been reported to be 0.24 $/kWh.
These costs can be brought down by improving the efficiency of the cells, improving their reliability and also lowering the cost of the solar cells [4].

5. Conclusions

In this paper, we discussed the potential of CPV as a choice for generating clean energy at a low LCOE. The most up-to-date data indicate that the total installed CPV capacity in the world does not exceed 300 MW. We have also shown that this is much below the 1.23 GW manufacturing capacity available today.

For HCPV, installation costs as low as 3.05 $/W and LCOE as low as 0.14 $/kWh have been reported in 2010 based on real data. For LCPV, an installed cost of 5.05 $/W and LCOE of 0.24 $ have been reported. These numbers show that CPV systems with high concentration have a high economic potential comparatively with low concentration CPV systems.

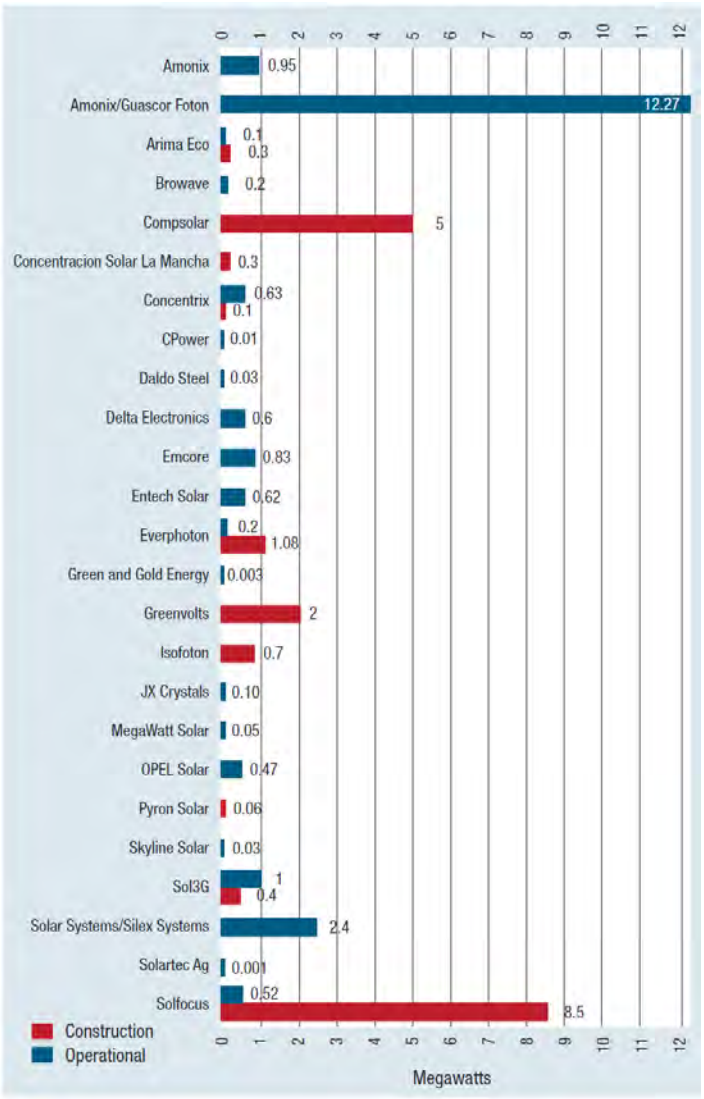

Fig. 1. Pre-operational and operational CPV power generation capacity by company (from reference [4]).

References

[1] Trevor M. Letcher, "Future Energy: Improved, sustainable and clean options for our planet." Elsevier, 2008.
[2] K. Rajeshwar, R. McConnell, S. Licht “Solar hydrogen generation toward a renewable energy future”, Springer, 2008.
[3] “Technology roadmap: solar photovoltaic energy,” International Energy Agency, 2010.
[4] A. Extance, C. Marquez, “The Concentrated Photovoltaics Industry Report 2010,” CPV Today, 2010.
[5] R. A. Sherif, N. H. Karam, R. R. King, D. R. Lillington, "The Path to 1 GW of Concentrator Photovoltaics Using multi-junction Solar Cells," 31 IEEE PVSC pp17-22, 2005; "multi-junction Solar Cells," Nature Photonics 2008.
[6] M. A. Green, K. Emery, Y. Hishikawa and W. Warta, Progress in Photovoltaics: Research and Applications, 2010; 18:346–352.
[7] R. Gordon, G. Kinsey, A. Nayaak, V. Garboushian, “30% CPV module milestone,” in proceedings of the 6th International Conference on Photovoltaic Systems (CPV-6), pp171, 2010.
[8] S. Kurtz, “Opportunities and Challenges for Development of a Mature Concentrating Photovoltaic Power Industry”, Technical Report NREL/TP-520-43208, Revised November 2009.
[9] D. Friedman, “National solar technology roadmap: concentrator PV”, Management Report NREL/MP-520-41735, June 2007.

Environmental impacts of large-scale grid-connected ground-mounted PV installations

Antoine Beylot[1,*], Jérôme Payet[1], Clément Puech[2], Nadine Adra[2], Philippe Jacquin[3], Isabelle Blanc[4], Didier Beloin-Saint-Pierre[4]

[1] *CYCLECO, Ambérieu-en-Bugey, France*
[2] *Transénergie, Ecully, France*
[3] *PHK consultants, Ecully, France*
[4] *MINES ParisTech Sophia Antipolis, France*
** Corresponding author. Tel: +33 437860712, E-mail: antoine.beylot@cycleco.eu*

Abstract: This study characterizes the environmental performances of large-scale ground-mounted PV installations by considering a life-cycle approach. The methodology is based on the application of the existing international standards of Life Cycle Assessment (LCA). Four scenarios are compared, considering fixed-mounting structures with (1) primary aluminum supports or (2) wood supports, and mobile structures with (3) single-axis trackers or (4) dual-axis trackers. Life cycle inventories are based on manufacturers' data combined with additional calculations and assumptions. Fixed-mounting installations with primary aluminum supports show the largest environmental impact potential with respect to human health, climate change and energy consumption. The climate change impact potential ranges between 37.5 and 53.5 gCO_2eq/kWh depending on the scenario, assuming 1700 kWh/m².yr of irradiation on an inclined plane (30°), and multi-crystalline silicon modules with 14% of energy production performance. Mobile PV installations with dual-axis trackers show the largest impact potential on ecosystem quality, with more than a factor 2 of difference with other considered installations. Supports mass and composition, power density (in MW_p/acre of land) and energy production performances appear as key design parameters with respect to large-scale ground mounted PV installations environmental performances, in addition to modules manufacturing process energy inputs.

Keywords: *Environmental impacts, LCA, PV installations*

1. Introduction

PV systems deployment and solar energy use are developing rapidly in Europe. In particular, Austria, Switzerland, Germany, France, Italy and the Netherlands experienced a two to four-fold increase in their annual installed photovoltaic power in 2009 [1]. Large scale PV systems (> 500 kWp) represent a lower share of the photovoltaic power production compared to small scale systems (< 3 kWp). However, their market is showing a dramatic increase in number of installations. In France a 90% increase was observed between the 2nd and 1st trimesters 2010 for installations of power superior to 500 kWp, compared to a 38% increase for small scale installations [2].

In this context of rapid development, the issue of PV systems environmental impacts characterization has been intensively addressed and discussed. While several initial publications underlined the higher external environmental costs of PV compared to those of nuclear energy and natural-gas-fuel power plants [3,4], new LCA databases have been built to comply with the improvements in PV systems [5,6]. They highlighted the photovoltaic potential for a low carbon energy supply and the environmental benefits of PV as opposed to fossil-fuel based energy [7, 8]. LCA data currently consider solar cells, panels and installation equipments production in the supply chain of different technologies. Up to now, most studies have focused on module technologies and small-scale installations. They exposed the key parameters for environmental performances of PV installations, when focusing on greenhouse gas emissions and primary energy use as environmental indicators: irradiation intensity received by PV installations, modules manufacturing electricity use and its corresponding fuel

mix and PV technology [9, 12]. However, only few evaluations of large-scale PV installations can be found in the literature [13, 14].

This study aims at characterizing the environmental impacts of large-scale grid-connected ground-mounted PV installations (5MWp), considering one module technology (mc-Si) with different structures and types of supports (fixed-mounting or mobile). The results highlight key parameters related to large scale PV systems environmental performances on a life cycle perspective. Impacts on climate change and energy consumption are considered as indicators for the environmental assessment together with human health and ecosystem quality indicators. Recommendations are finally given to enable stakeholders in the field of large scale PV systems to minimize the environmental impacts of future installations.

2. Methodology

This Life Cycle Assessment (LCA) study was performed in compliance with the ISO standards 14040 and 14044 [15, 16] and followed the provisions of the ILCD handbook [17].

2.1. Scope of the study

The Functional Unit is defined as the kWh of electricity produced by a large-scale grid-connected ground-mounted PV installation (5MWp), considering 1700 kWh/m².yr of irradiation on an inclined plane (30°) and 30 years of life expectancy.

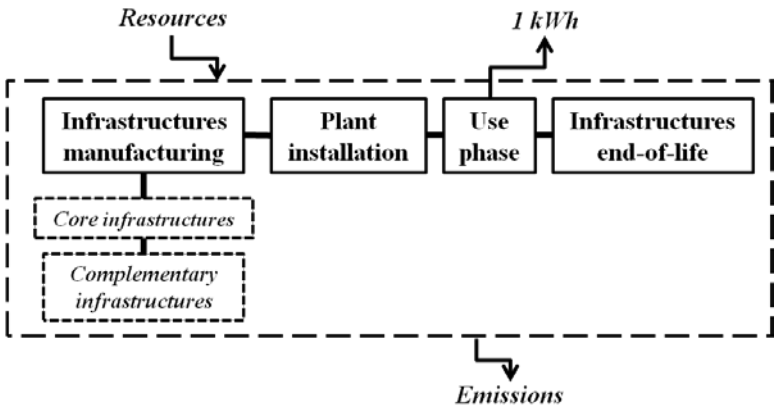

Fig. 1. Scheme of system boundaries

The system boundaries are described in Fig. 1. They include the manufacturing of core infrastructures (modules, mounting system, cabling, inverters, transformers), the manufacturing of complementary infrastructures (wire fences, control centers and road to access the plant), the plant installation (excavation and track construction), the use phase and the decommissioning (excavation, modules and structures end-of-life). Recycled waste material is assumed to substitute for primary produced material, without considering any correction factor.

Four grid-connected ground-mounted PV installations are compared in the study. Their differentiating key features are detailed in Tables 1 and 2. The multi-crystalline silicon (mc-Si) PV technology is chosen for every scenario. Consequently, only the type of structure and its related system energy production differentiate the scenarios.

Life cycle impact assessment is performed with the use of the IMPACT 2002+ method (v2.04) [18]. The results focus on four damage impact categories: climate change, resources, human health and ecosystem quality. The temporary carbon storage in bio-based goods (wood supports in one scenario) is taken into account in compliance with ILCD provisions, i.e. by considering "-0.01 kg CO_2-equivalents" per 1 kg carbon dioxide and 1 year of storage/delayed emissions.

Table 1. Scenarios key features

Scenarios	1	2	3	4
Module Technology	mc-Si	mc-Si	mc-Si	mc-Si
Structure key features	Fixed mounting Primary aluminum supports	Fixed mounting Wood-based supports	Mobile Single-axis trackers	Mobile Dual-axis trackers

2.2. Inventory

The inventory distinguishes between:

- foreground processes, corresponding to PV systems parameters, land occupation and electricity use and generation, for which specific data have been used.
- upstream and downstream processes, corresponding to materials extraction and transformation, PV modules fabrication, materials and products transport, electricity production mix, infrastructures end-of-life, for which semi-specific or generic data have been used. Ecoinvent v2.0 [19] was used as the reference database for semi-specific data.

2.2.1. PV installations electricity production

Energy efficiency of the PV modules is set at 14%, with an average performance ratio of 0.855 for the system. The increase in production thanks to mobility is respectively set to 5% for Scenario 3 considering single-axis trackers and to 32.5% for Scenario 4 considering dual-axis trackers, based on average manufacturers' data. The corresponding electricity generated over the 30 years installation life-time is given in Table 2 for the 4 scenarios.

Table 2. Energy production in scenarios

Scenarios	1	2	3	4
Increase in production due to mobility	-	-	5% (Average data from a Spanish supports manufacturer)	32.5% (Average data from an Italian supports manufacturer)
Electricity production over 30 years (in GWh)	218.0	218.0	228.9	288.9

2.2.2. Infrastructures

Data on infrastructures of large-scale PV installations have been either directly collected or calculated from manufacturers data, as detailed in Table 3. Ten 500 kW inverters are necessary for each PV installation, assuming 10 years of life expectancy (i.e. 30 inverters over each installation life-time), and five 1MW transformers, considering 30 years of life expectancy.

2.2.3. Key additional assumptions

In the absence of specific or semi-specific data for plant building operations (excavation, track construction), for engines composition (used in mobile installations) and for waste structures management (waste modules and supports), the model is based on hypothesis gathered in a Supporting information sheet. In particular, the necessary road to access the installation is assumed to be 3 km long. Moreover, multi-crystalline modules are assumed to be entirely recycled at the end of the installation life, by use of a thermal/chemical treatment. The life cycle inventory corresponding to modules recycling is partly based on literature data [20] completed with additional assumptions.

Table 3. Data collection for infrastructures in scenarios

	Scenario 1	Scenario 2	Scenario 3	Scenario 4
Modules	35714 m² - value based on calculations from energy production performances			
Area	92 888 m²(*)	92 888 m²(*)	96 922 m²(*)	418 770 m²(*)
Supports	Primary aluminum – Mass values from technical sheets from a German manufacturer	Wood, primary aluminum and iron – Mass values from data from a multi-MWp installation in France	Galvanized steel – Mass values from technical sheets from a Spanish manufacturer	Galvanized steel – Mass values from technical sheets from an Italian manufacturer
Foundations	Cast iron stakes - approximation based on technical sheets from an Austrian manufacturer	Concrete – Mass values from data from a multi-MWp installation in France	Concrete - Mass values from implementation schemes (*)	Concrete - Mass values from implementation schemes (*)
Cabling	Copper, aluminum and PVC – Mass values from implementation schemes (*)			
Transformers	Reference flows data compiled from a French manufacturer			
Complementary infrastructures	Control center building made of steel reinforced concrete + steel wire fences - Reference flows data compiled from a German manufacturer for one installation			

(*) computed from the experience of the consulting and engineering partner (Transénergie)

3. Results

3.1. Scenarios comparison

The Life Cycle Impact Assessment results are shown in Figure 2 and Table 4. Negative values represent the environmental benefits of recycling. Those environmental benefits are not taken into account in the global results since they could be applied in another production chain where recycled aluminum is used. Scenario 1, considering fixed-mounting virgin aluminum supports, shows the largest environmental impacts in terms of human health, global warming and resources, while Scenario 4 (dual-axis tracker systems) generates the largest impacts on ecosystem quality. Scenarios 2 and 3 (fixed-mounting wood-based and single-axis trackers) globally show the best environmental performances, with gaps between their potential damage impacts ranging from 1 to 3% depending on the considered category.

3.2. Detailed environmental performances

3.2.1. Climate change

Modules manufacturing represents the largest share of climate change impact for all scenarios (38 - 56% of the total impact). Moreover, virgin aluminum supports manufacturing stands for a large proportion of the total impact of scenario 1 (36%, if including environmental benefits due to aluminum recycling), contrarily to wood-based fixed-mounting supports (Scenario 2, 21% of the total impact) and galvanized steel mobile supports (Scenarios 3 and 4, respectively 5 and 12%). The climate change impact due to supports is 2 to 10 times larger in scenario 1 than in scenarios 2, 3 and 4. As a consequence, the total climate change impact is 28% larger in scenario 1 than in scenario 2, whereas the climate change impact due to modules is equal for both scenarios (21.4 g. CO_2 eq/kWh, a relatively low value to be related with the assumed use of the French electricity mix for modules manufacturing in scenarios).

Depending on the considered scenario, electric equipments (inverters, transformers and engines in case of mobile structures), complementary infrastructures (road, control centers) and foundations may represent a significant share of the total impact. For example, for

scenario 4, these elements represent up to 50% of the total climate change burden. This large share is partly due to the increase in electricity production, generating the decrease in environmental impacts of modules (16.1 g. CO_2eq/kWh), combined with an increase of the impacts of these balance of system (BOS) components.

Table 4. Damage impact assessment results for the four scenarios (Impact 2002+method v2.04)

Study case	*Human health (DALY/kWh)*	*Ecosystem quality (PDF.m².yr/kWh)*	*Climate change (g. CO_2eq./kWh)*	*Resources (MJ primary/kWh)*
Scenario 1	4.65E-08	2.46E-02	53.5	1.10
Scenario 2	3.24E-08	2.35E-02	38.0	0.88
Scenario 3	3.34E-08	2.32E-02	37.5	0.90
Scenario 4	4.12E-08	5.15E-02	42.8	0.88

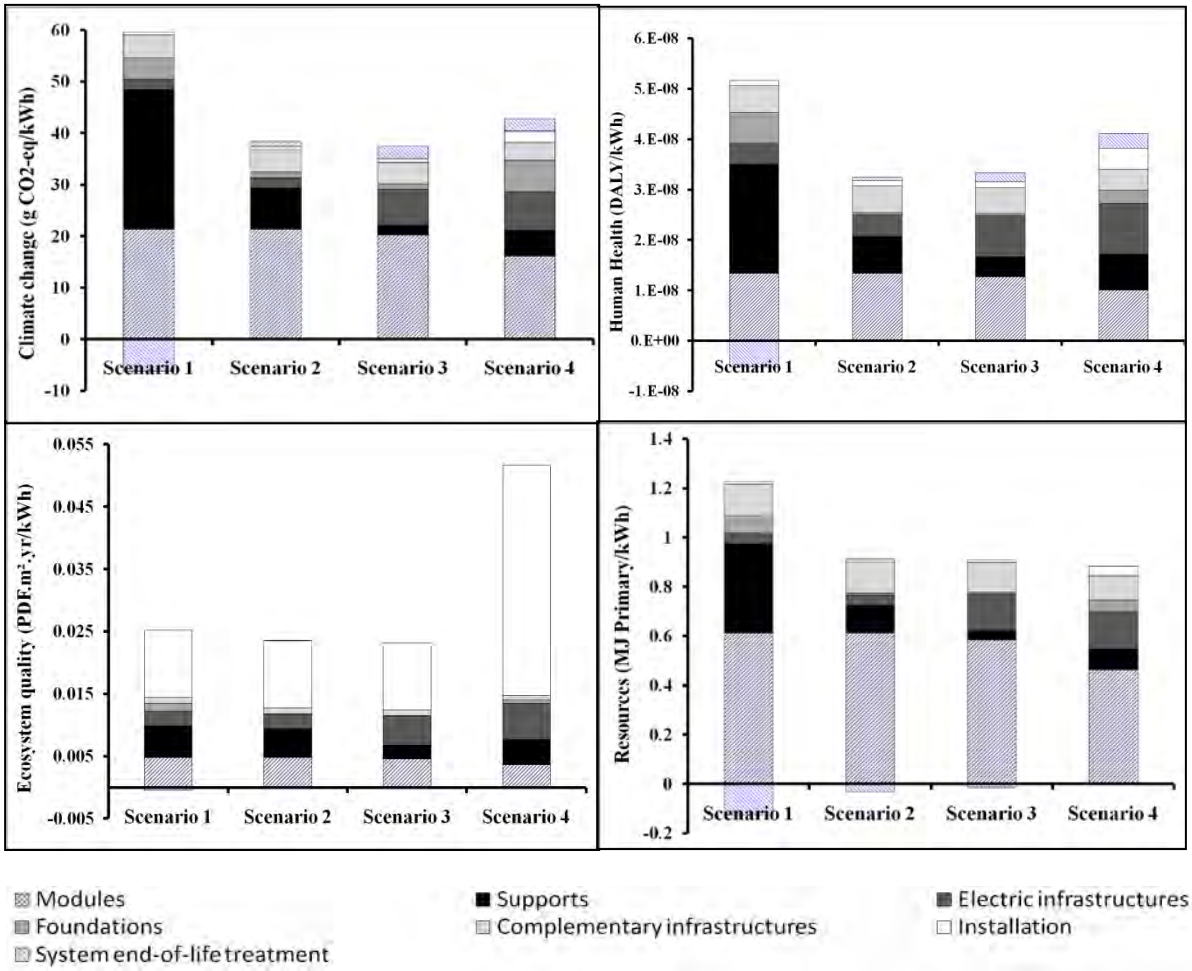

Fig. 2. Detailed environmental impacts of the 4 scenarios (considering 1700 kWh/m².yr of irradiation on an inclined plane, mc-Si modules with 14% of energy production performance and IMPACT2002+ v2.04 damage indicators)

3.2.2. Human health

Impacts on human health show a similar trend with the impacts on climate change, both in terms of overall impact comparison and predominant Life Cycle phases. Modules manufacturing generates the largest environmental burden for scenarios 2, 3 and 4 (from 29 to 41% of the total impact depending on the scenario), while virgin aluminum supports manufacturing represents the largest share for scenario 1 (33% if including benefits due to

recycling). Small particulates, NO_x and SO_2 air emissions related to aluminum production (due in particular to electricity requirements and mostly emitted in the aluminum country of origin) represent 22% of the total impact on human health for scenario 1. On the other hand, the human health impact of wood (scenario 2) and galvanized steel supports (scenarios 3 and 4) is lower in absolute value and also stands for a lower share of the total impact.

3.2.3. Resources

Modules manufacturing contribution to the total burden on resources amounts to 53 to 70% depending on the scenario. The environmental benefit gained from the increase in electricity production in case of mobile installations, which is directly reflected in terms of modules impacts, is counterbalanced by different requirements in infrastructures (e.g. electric equipments). As a consequence, whereas scenarios 3 and 4 consider larger electricity production from 5 to 32.5% compared to scenario 2, the gap in impacts on resources between these 3 scenarios is lower than 2%.

Impact on resources of virgin aluminum supports accounts for 24% of scenario 1 total impact (if including benefits from aluminum recycling). This impact is 2 to 6 times larger than impacts of wood-based and galvanized steel supports of scenarios 2, 3 and 4.

3.2.4. Ecosystem quality

The impact on ecosystem quality is mainly influenced by land occupation, which represents 44 to 47% of the impact in case of scenarios 1 to 3 and up to 72% of the impact in case of scenario 4. The difference in impacts on ecosystem quality amounts to a factor 2.1-2.2 between mobile scenario 4 (dual-axis trackers) and scenarios 1 to 3, to compare with a 4.5 ratio between scenario 4 and scenarios 1-3 occupied surfaces. Indeed, power plants with dual-axes trackers require expanding the distances between each element of the PV field, because the shades induced by the moving PV planes are more important: the “power density” in terms of MWp/acre of land used is therefore much lower than for fixed-mounting systems.

4. Discussion

4.1. Key environmental parameters

Irradiation intensity received by PV installations, modules manufacturing electricity use and its corresponding fuel mix and solar radiation conversion efficiency were shown to be key environmental parameters of PV installations in several studies [9, 12]. Similarly, this study highlights the large influence of modules production, and to a lower extent of electricity production increase in mobile conditions, on the environmental performances of large-scale grid-connected ground-mounted PV installations. In addition, two other critical parameters arise: structure supports and occupied surfaces.

4.1.1. Metal/Wood supports

The environmental impact of supports production is predominant considering climate change, resources consumption and impacts on human health, and is responsible for the environmental gap between scenarios in several cases (e.g. between Scenarios 1 and 2). The impact of supports is firstly related with their weight: as observed by Mason *et al.* [15], decreasing the quantity of metal supports in large-scale installations results in significant environmental improvements. However, materials nature appears as an even more critical environmental parameter. For example, the galvanized steel supports mass is 8% larger in scenario 4 than the primary aluminum supports mass in scenario 1 (considering mass per produced kWh), whereas the corresponding impact on e.g. climate change is 81% larger for supports of

scenario 1. Moreover, a sensitivity analysis has been conducted on aluminum supports, by considering secondary material (from old scrap) instead of virgin material. The use of secondary material generates significant decreases in environmental impacts of scenario 1: 42% for climate change, 39% for human health and 25% for resources, in compliance with the predominance of supports composition on the impacts of a large-scale PV installation.

4.1.2. Occupied surface

The occupied surface mainly determines the impact of large-scale PV installations on ecosystem quality. Consequently, land consuming alternatives such as mobile installations with dual-axis trackers will show relatively large impacts on ecosystem quality compared to fixed-mounting solutions, if considering the same modules technology.

4.2. Comparing large-scale grid-connected ground-mounted PV installations

The ranking of alternatives and their associated key parameters may differ from one environmental indicator to another, as observed when putting in perspective large-scale PV installations impacts on climate change and ecosystem quality. This study therefore enhances the need for a multi-criteria impact assessment method when comparing large-scale grid-connected ground-mounted PV installations. In addition, the results underline the multiplicity of parameters which may affect large-scale PV installations environmental performances. The environmental impacts of large-scale PV installations are the result of the interplay between a number of distinct parameters (e.g. energy production, supports mass and nature, electric equipments, etc.), whose related influence may counterbalance each other.

5. Conclusions, recommendations and perspectives

The impact assessment of large-scale ground mounted PV installations therefore gives a detailed picture of their related environmental performances. Key installations design parameters arise in an environmental perspective: supports mass and composition, power density (in MWp/acre of land) and energy production performances, in addition to key parameters related to modules manufacturing (in particular electricity consumption and electricity production mix).

The environmental performances of large-scale PV installations are not in linear correlation with a unique quantified plant parameter. In that sense, for example, increasing the electricity production thanks to mobile technologies does not necessarily bring environmental benefits if combined with an increase in requirements in materials. A multi-criteria perspective - with respect to environmental indicators and installations key design parameters - should be undertaken with a view to optimizing PV large-scale installations environmental performances in a near future.

Acknowledgements

ADEME is co-financing this project which brings together different French specialists from the PV industry and LCA fields.

References

[1] IEA. Trends in photovoltaic applications: Survey report of selected IEA countries between 1992 and 2006, Report IEA-PVPS T1-16:2007

[2] Syndicat des énergies renouvelables (SER), SOLER. Etat des lieux du parc photovoltaïque français au 30 juin 2010. 2010.

[3] European Commission, Directorate-General for Research. External Costs. Research results on socio-environmental damages due to electricity and transport. Office for Official Publications of the European Communities, Luxembourg. 2003.

[4] Australian Coal Industry Association, ACARP. Coal in a sustainable society. 2004.

[5] V.M. Fthenakis, E.A. Alsema, M.J. de Wild-Scholten. Life Cycle Assessment of Photovoltaics: perceptions, needs and challenges. 31st IEEE Photovoltaic Specialists Conference. 2005.

[6] N. Jungbluth, M. Tuchschmid, R. Dones. Photovoltaics: ecoinvent report N° 6-XII. Swiss Center for Life Cycle Inventories, Dübendorf, CH. 2007.

[7] E.A. Alsema, M.J. de Wild-Scholten, V.M. Fthenakis. Environmental impacts of PV electricity generation - A critical comparison of energy supply options. 2006.

[8] IEA. Analysis of PV system's values beyond energy – by country and stakeholder. Report IEA-PVPS 10-02:2008

[9] S. Pacca, D. Sivaraman, G. A. Keolian. Parameters affecting the life cycle performance of PV technologies and systems, Energy Policy, 2007, vol. 35, n°6, pp. 3316-3326

[10] R. Kannan, K.C. Leong, R. Osman, H.K. Ho, C.P. Tso. Life cycle assessment study of solar PV systems: An example of a 2.7 kW(p) distributed solar PV system in Singapore, Solar Energy, 2006, vol. 80, n°5, pp. 555-563

[11] I. Blanc, D. Beloin-Saint-Pierre, J. Payet, P. Jacquin, N. Adra, D. Mayer. Espace-PV: key sensitive parameters for environmental impacts of grid-connected PV systems with LCA. 23rd European Photovoltaic Energy Conference. 2008.

[12] D. Beloin-Saint-Pierre, I. Blanc, J. Payet, P. Jacquin, N. Adra, D. Mayer. Environmental impact of PV systems: effects of energy sources used in production of solar panels. 24th European Photovoltaic Energy Conference. 2009.

[13] K. Komoto, H. Uchida, M. Ito, K. Kurokawa, A.Inaba. Estimation of Energy Payback Time and CO_2 Emission of Various Kinds of PV Systems, 23rd European Photovoltaic Energy Conference. 2008.

[14] J.M. Mason, V.M. Fthenakis, T. Hansen and H.C. Kim. Energy Pay-Back and Life Cycle CO_2 Emissions of the BOS in an Optimized 3.5 MW PV Installation. 2006.

[15] International Standard Organization. ISO 14040. Environmental management – Life Cycle Assessment – principles and framework. 2006.

[16] International Standard Organization. ISO 14044. Environmental management – Life Cycle Assessment – requirements and guidelines. 2006.

[17] Institute for Environment and Sustainability. Joint Research Centre. European Commission. International Reference Life Cycle Data System handbook. 2010

[18] O. Jolliet, M. Margni, R. Charles, S. Humbert, J. Payet, G. Rebitzer, R. Rosenbaum. Impact 2002+: A new life cycle impact assessment methodology, International Journal of Life Cycle Assessment. 2003. Volume**:** 8, Issue: 6, Pages: 324-330.

[19] Swiss Center for Life Cycle Inventories. The life cycle inventory data version 2.0. http://www.ecoinvent.ch. 2008.

[20] A. Müller, K. Wambach, E. Alsema. Life Cycle Analysis of solar module recycling process. 20th European Photovoltaic Solar Energy Conference. 2005.

Progress in Luminescent Solar Concentrator Research: Solar Energy for the Built Environment

Paul P. C. Verbunt[1], Michael G. Debije[1]*,

[1] *Eindhoven University of Technology, Eindhoven, The Netherlands*
** Corresponding author: Tel: +31 40 2475881, Fax: +31 40 2436999, E-mail: mgdebije@tue.nl*

Abstract: This paper presents a concise review of recent research on the luminescent solar concentrator (LSC). The topics covered will include studies of novel luminophores and attempts to limit the losses in the devices, both surface and internal. These efforts include application of organic and inorganic-based selective mirrors which allow sunlight in but reflect emitted light, luminophores alignment to manipulate the emitted light path, and patterning of the dye layer. Finally, the paper will offer some possible 'glimpses to the future', and offer some additional research paths that could result in a device that could make solar energy a ubiquitous part of the built environment as sound barriers, bus stop roofs, awnings or siding tiles. Considering the reported efficiencies of the LSC are comparable to those reported for organic PVs, which are also being considered for use in the built environment, the results of the research on the LSC to date warrants more widespread attention.

Keywords: *Solar energy, Luminescent solar concentrator, Building integrated photovoltaics, Review*

1. Introduction

The European Committee wants all newly built buildings to be near-zero energy by 2020[1]. This demands architects integrate energy saving and energy generation into their designs. To give architects more freedom, the devices saving and/or generating energy must be easily adaptable. A readily available energy source in a built environment is the sun, which is clean, safe, inexhaustible and reliable but generation of electricity with conventional photovoltaic (PV) cells has several disadvantages in this environment: the cells remain costly, modules are heavy, and limited in coloration (black and dark blue). Furthermore, PV cells respond optimally to direct sunlight, while in the built environment much of the sunlight is diffuse due to scattering and reflections by other objects, such as trees, buildings, and even clouds.

An alternative solar energy harvester was proposed in the 1970's, the luminescent solar concentrator (LSC)[2]. In the LSC, sunlight penetrates the top surface of an inexpensive plastic or glass waveguide. This light is absorbed by luminescent molecules which are either embedded in the waveguide or applied in a separate layer on top or bottom of the waveguide. The luminescent molecules can be organic fluorescent dyes, or inorganic phosphors or quantum dots. The absorbed light is re-emitted at longer wavelengths, and a fraction of the re-emitted light is trapped in the waveguide by total internal reflection and becomes concentrated along the edges of the plate. Small PV cells attached to edges of the waveguide collect the emission light and convert it to electricity.

The LSC has potential advantages over silicon-based PV panels, especially in the built environment. For one, they can reduce the size of the PV cells more than 90% and the materials for making LSCs are inexpensive, reducing module prices. The plastic waveguide is lighter than the silicon PV panels, leading to a reduction in weight, which makes LSCs more viable for mounting to the sides of buildings. Sunlight can better penetrate the surface of the LSC waveguide from all angles, making them more appropriate for collecting non-direct sunlight. Lastly, LSCs have a great flexibility in design, which make them attractive for architects: they may be made thin and can be cut in any desired shape, cast in almost any color and may be transparent. Since LSCs can be thin, it becomes possible to make curved device. If the photon in/ photon out efficiency is high enough, the cost of electricity generated by the LSC could be competitive[3]. These combined features make

LSCs interesting devices for increasing public acceptance of solar energy: while the efficiency of an LSC will be lower than an equivalent area of a silicon PV, the reduced cost and flexibility in design could make LSCs viable for the urban area. The LSC hasn't yet been commercialized owing to several drawbacks which limit their efficiency[4]. Loss mechanisms for LSCs are shown in **Figure 1**.

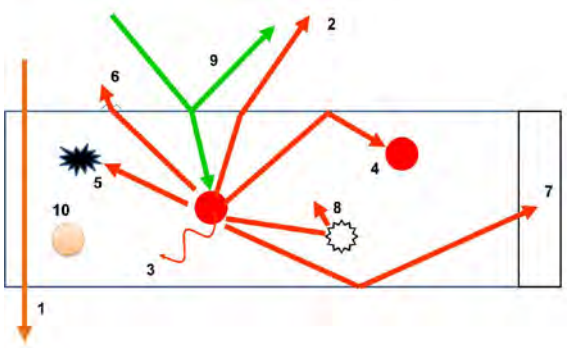

Figure 1*. Loss mechanisms in LSCs: 1) Input light not absorbed by the dye molecules, 2) Light emitted outside capture cone, 3) Quantum efficiency of the dye molecules <1, 4) Re-absorption of emitted light by another dye molecule, 5) Absorption of emitted light by the waveguide, 6) Surface scattering, 7) Solar cell losses, 8) Internal waveguide scattering, 9) Reflection from the e surface, 10) Limited dye stability.*

The first loss is sunlight not absorbed by the dye molecules: this light is lost through the bottom surface. The second is light emitted by dye molecules under an angle which is refracted out of the waveguide instead of reflected internally- (> 40% of all absorbed energy may be lost through the top and bottom surfaces of the LSC[5]). The third loss is absorbed photons not re-emitted by the dye molecules, but instead lost as heat and vibrations. Re-absorption of emitted photons by subsequent dye molecules via overlap of emission and absorption bands is a fourth loss. Waveguides can exhibit parasitic absorption, especially in the near infrared, and is the fifth loss cited. Sixth, imperfections of the waveguide surface can cause photons in the waveguide mode to leave the surface. Seventh, the PV cell at the waveguide edge has a non-uniform spectral response, with a fraction of incident photons being lost due to the finite conversion efficiency. Imperfections in the waveguide bulk lead to the eighth loss, scattered waveguided photons. In addition, a small part of the input light is reflected from the surface of the waveguide, shown as the ninth loss. Finally, there is loss caused by degradation of the dye molecules, primarily due to UV absorption.

2. Losses and Proposed Solutions

2.1. Surface Loss

Dye-emitted photons emitted inside the escape cone will be lost through the surfaces, and measurements suggest that 40-55% of all absorbed energy is lost in this way (this translates into a 50-70% loss of photons)[5]: these results were confirmed by simulation[6] . This surface loss is a key one for LSCs, and in the last couple of years multiple groups have done research on minimizing them by two processes: aligning the luminophores and applying selective mirrors.

Aligned luminophores: Organic luminophores are often dichroic in absorption and transmission[7], opening new possibilities in controlling the spatial distribution of emitted light, provided that the physical ordering of the dyes is macroscopically controlled. The alignment of dichroic dyes in liquid crystalline (nematic) materials has been previously investigated[8] and it was shown that the macroscopic alignment of the dyes in the liquid crystalline host resulted in anisotropy and dichroism in both absorption and emission. Aligning the dye luminophores perpendicular to the waveguide surface leads to an emission primarily in the direction of the waveguide, resulting in a sharp decrease of surface loss to less than 10%[9],confirmed by simulations using collimated light[6].

However, in this configuration the luminophores have low absorption, and concurrent low edge emission: trapping efficiency of emitted photons increases from ~65% to over 80% when vertically aligned luminophores in LSCs are excited by an isotropic light source[10].

Luminophores can also be aligned planarly, or parallel to the waveguide surface. This configuration can direct light so that 60% more energy is emitted from two edges of the LSC compared to the other two edges[11]: in this way the LSC can be used as a energy harvesting polarizer[12] which could be used in displays, for example. Additionally, if light is emitted primarily towards just two edges, the number of PV cells on the LSC can be reduced to two or even one, further reducing LSC cost.

Selective mirrors: A second way to reduce surface loss is by applying wavelength-selective mirrors [7, 21-31]. These mirrors are placed on top the LSC-waveguide with the goal that the reflectors not interfere with incoming sunlight that can be absorbed by the luminophores, but reflect only the luminophore-emitted light, which has a longer wavelength. Wavelength selective mirrors, made from chiral nematic (cholesteric) liquid crystals[13] or inorganics[13b,15], have both been applied to the LSC. Up to 30% of the light that had previously escaped the surface was turned into edge emission, translating into a 12% LSC output improvement using the organic reflectors[14f]. Similar enhancements were determined using the inorganic reflectors[4b]. Organic reflectors are cast from solution and spontaneously form the reflective layer: this is generally a much simpler and less expensive process than application of multilayer inorganic Bragg reflectors.

2.2. Re-absorption of emitted photons by other dye molecules

Most organic luminophores used in LSCs have small Stokes-shifts, leading to relatively large overlaps between the absorption and the emission spectrum [15]. As a consequence, luminophores-emitted photons can be re-absorbed by another luminophore molecule during transportation through the waveguide. Re-absorptions are not losses by themselves, but the limited quantum efficiency of the luminophores and re-emission into the escape cone do result in losses[16].

To reduce re-absorption events, researchers have experimented with luminophores with large Stokes-shift, like lanthanides[17] and quantum dots[18] ,but these classes of luminophore bring other challenges to the production of LSCs. Inorganics tend to suffer from low solubility in organic matrices, and often also suffer from a low absorption. To reduce the amount of reabsorptions Taleb et al.[19] doped a dye with a polar and highly mobile material, like thionin. The dopant increased the separation of the absorption and fluorescence bands of the dye molecules, increasing the Stokes-shift and reducing (but not eliminating) the overlap in absorption and emission spectrum.

An option to reduce encounters of emitted light with the dyes is to only attach the dyes in a thin layer at the surface of the waveguide rather than filling the luminophore within the bulk of the waveguide. In this way, emission light may be transported predominantly in the clear host material, and only encounter the dye layer again every second internal reflection. These layers have been made of acrylates, via sol-gel techniques[20], and polymerized liquid crystals[11].

Using spatially-separated patterns of luminophores on top of a waveguide, the number of re-encounters emitted light could have with other dye molecules was reduced [21]. The transport efficiency of the photons through the LSC increased with decreasing dye coverage. However, due to reduction in absorption, the total system output decreased. A lens system on top of the LSC is being developed that would increase absorption and thus the system output[22].

2.3. Dyes: Limited absorption, stability and fluorescence efficiency

The spectral breadth of the dye absorption is an important factors determining the potential efficiency of the LSC waveguide. There are a number of luminescent materials being studied for possible inclusion in the LSC. The workhorse of the organic dyes are based on perylenes or perylene derivatives[23]. The limitation of the organic dyes are often their lifetimes of operation in sunlight. Numerous studies are somewhat inconclusive as to the photostability of these materials: much depends on the processing conditions and polymeric environment of the fluorophore[24]. Organo-metallic molecules with good photostability (such as porphyrins) have also been proposed[25]. Inorganics such as lanthanides[17] hold promise as long-lasting replacements for organics, possibly with extended Stokes shifts. However, they tend to suffer from decreased absorption, and solubility becomes a definite issue. There is a large research effort directed at using quantum dots in the LSC[18], but they have not yet reached their promise as they continue to generally display small Stokes-shifts with limited photostability. A possible future research direction is into the use of surface plasmonics to enhance the emission of the dye materials, allowing the use of potentially lower quantum efficiency luminophores[26].

To aid in luminophore absorption, it is standard practice to apply a rear layer to an LSC to act as a reflector. The reflecting back layer effectively doubles the path length of incident light through the dye layer for enhanced absorption. Some of the initial experiments used a silver mirror[2b], but such a mirror is absorbing in the visible range. To avoid absorptive losses, most recent work has employed a white scatterer[4, 27]. When separated from the waveguide by a small air gap, the rear scatterer can provide additional light for waveguides least 35 cm long[28]. The scatterer also may direct that fraction of incident light that cannot be absorbed by the dye directly at the PV cell, allowing it to generate electricity. The separation of the scatterer from the waveguide by a low refractive index layer is important to maintain waveguided light in the trapping modes of the waveguide: every encounter with the attached scattering layer re-distributes the light, and a significant fraction of this re-directed light will be outside the waveguide modes of the system.

Another option is to allow the LSCs to be transparent. In this form, the device could be used as a window while generating electrical current. An alternative design uses, rather than a waveguide with embedded, inflexible dyes, two glass plates coated with a conductor, the space between being filled by a liquid crystal containing a dye molecule[29]. The liquid crystal can be continually switched between orientations, from planar to homeotropic through application of a voltage across the plates. In the former state, the dye molecules follow the alignment of the LC host, and into a position of maximal absorption. The dye may then emit light which is partially trapped in the glass panes making up the 'window', and generate electrical current. By switching from planar to a tilt configuration, the output of the window necessarily drops due to reduced light absorption, but still produces a current, and the efficiency of edge output is actually increased. This design, while still needing considerable work to get transmissive properties correct with acceptable coloration, has advantages over other 'smart' windows. Photo- and thermochromics[30]or standard blinds[31] can, for example, be automatically switched between light and dark states, but generate no electricity. Thin-film PV modules can generate electricity[32], but cannot have their transparency switched.

2.4. Photovoltaic losses

The standard silicon-based PV has a band gap corresponding to a photon of around 1100 nm (~1.1eV). Photons with energies above this threshold may still be processed by the solar cell, of course, but the excess energy of the photon is wasted, and converted most often into heat, and there is a reduction in the response of the cell for these shorter wavelengths. However, the LSC does not emit a spectrum remotely similar to the solar spectrum. Rather, it emits a narrow range of wavelengths, most-often centered at red and near-infrared wavelengths (630-720 nm at the

maximum). To better exploit the spectrum of the LSC, researchers have used type III-V PV cells based on GaAs and InGaP cells[4a] and obtained record-setting efficiencies. If these cells could be produced economically, it could hold great promise for widespread adoption of the LSC in future. Another option could be the use of organic-based PV cells, which often have a 'sweet spot' in the spectral range where the LSC emits[33].

2.5. Waveguide losses

Around 4% of incoming light is reflected from the waveguide surface (the refractive indexes of polymethylmethacrylate (PMMA) and polycarbonate (PC) being between about 1.49 and 1.59) and never enter the waveguide, and could thus be considered a loss. While anti-reflection coatings are very common in PV cells, they have not yet been applied to LSCs. As the LSC relies on total internal reflection from two smooth surfaces, textured systems as used in many antireflective coatings[34] are not a viable option. Rather, coatings utilizing differences refractive indices can reduce these reflective losses and can be applied to polymeric materials[35].

One challenge to produce luminophores with emissions approaching 800 nm for use in LSCs is that the waveguides, which are predominantly made of PMMA or PC, become parasitic, and absorb strongly at these wavelengths[36]. Additionally, additives made for improvement of various characteristics of the host matrix (such as altering UV stability or hardness) can have large impact on the device's capability of transporting light. For example, an additive that only shows a small absorption when measured through the width of the waveguide can have a severe impact on the edge output of the same object, for the pathlength is magnified many tenfold[37]. As waveguides age, UV-generated damage creates light 'traps' within the polymer. Research into co-polymer systems has demonstrated enhanced photostability over the single component[38]. Non-uniform edge emission from waveguides also causes additional losses, as illumination of the attached PV at anything less than uniformity results in decreased performance. Thus, the shape of the waveguide also influences the emitted light distribution[39].

3. Future directions

There are a great number of improvements that can and need to be made on the LSC to make it a more viable option for use in the urban environment. One aspect we find particularly intriguing is to provide an opportunity for the use of organic-based photovoltaics (OPV). One of the greatest challenges for OPV has been the inability of utilizing the ultraviolet portion of the UV spectrum, as well as survive the high energies of the UV light which causes premature degradation of the OPVs through destruction of the dye materials. However, the LSC does not illuminate the attached solar cell with a solar spectrum, but a much more narrow-band of light, generally in the near infrared, the range of wavelengths where OPVs perform their best. Coupled with the lack of exposure to UV light, this could provide the OPV with the first real niche application where they could excel.

A second largely unexploited research area is in the field of plasmonics. Many research publications show when a fluorescent molecule is brought close to a small metallic nanoparticle there is an enhancement of the fluorescence[40]. There has been application of surface plasmonics in PVs[41], but to our knowledge, no extensive work in the field of LSCs.

It is the opinion of the authors that the rôle of the LSC in future urban renewable energy plan should be re-defined. Given the decrease in the costs associated with traditional silicon-based PV, it would seem folly to attempt to compete directly with the well-established, traditional PV panel on a rooftop. Rather, the LSC could best be used as a complement to silicon PV rather than a competitor, positioning itself in areas not normally accessible, such as areas with increased fractions of diffuse

light. The LSC is to be brought directly into public view, not 'hidden away' as most silicon PV panels. Applications could include sound barriers, telephone poles, and bus stop roofing.

References

[1] Directive 2010/31/EU of the European parliament and of the council of 19 May 2010 on the energy performance of buildings, Vol. 2010.

[2] a) W. H. Weber and J. Lambe, Luminescent greenhouse collector for solar radiation Applied Optics 15, 1976, 2299, b) A. Goetzberger and W. Greube, Solar energy conversion with fluorescent collectors, Applied Physics A: Materials Science & Processing 14, 1977, 123.

[3] E. Bende et al., Proc. of the 23rd European PV and Solar Energy Conference 2008, 461.

[4] a) L. H. Slooff, et al., A luminescent solar concentrator with 7.1% power conversion efficiency Physica Status Solidi (RRL) - Rapid Research Letters 2, 2008, 257.

[5] M. G. Debije et al., Measured surface loss from luminescent solar concentrator waveguides, Applied Optics 47, 2008, 6763.

[6] S. McDowall, et al., Simulations of luminescent solar concentrators: Effects of polarization and fluorophore alignment, Journal of Applied Physics 108, 2010, 053508.

[7] a) M. van Gurp and Y. K. Levine, Determination of transition moment directions in molecules of low symmetry using polarized fluorescence. I. Theory, The Journal of Chemical Physics 90, 1989, 4095, b) C. Sanchez et al., Polarized photoluminescence and order parameters of *in situ* photopolymerized liquid crystal films, Journal of Applied Physics 87, 2000, 274.

[8] a) G. H. Heilmeier and L. A. Zanoni, Guest-host interactions in nematic liquid crystals. A new electro-optic effect Applied Physics Letters 13, 1968, 91, b) R. L. van Ewyk et al., Anisotropic fluorophores for liquid crystal displays Displays 7, 1986, 155, c) H.-W. Schinidt, Dichroic dyes, and liquid crystalline side chain polymers Advanced Materials 1, 1989, 218.

[9] P. P. C. Verbunt, D. J. Broer, C. W. M. Bastiaansen and M. G. Debije, The effect of dyes aligned by liquid crystals on luminescent solar concentrator performance, Proc. of the 24th European PV Solar Energy Conference 2009, 381.

[10] C. L. Mulder et al., Dye alignment in luminescent solar concentrators: I. Vertical alignment for improved waveguide coupling, Optics Express 18, 2010, A79.

[11] P. P. C. Verbunt et al., Controlling Light Emission in luminescent solar concentrators through use of dye molecules aligned in a planar manner by liquid crystals, Advanced Functional Materials 19, 2009, 2714.

[12] C. L. Mulder et al., Dye alignment in luminescent solar concentrators: II. Horizontal alignment for energy harvesting in linear polarizers, Optics Express 18, 2010, A91.

[13] a) M. G. Debije, et al., Using selectively-reflecting organic mirrors to improve light output from a luminescent solar concentrator, Proc. of the WREC IX 2006, b) J. C. Goldschmidt et al., Theoretical and experimental analysis of photonic structures for fluorescent concentrators with increased efficiencies, Physica Status Solidi (a) 205, 2008, 2811, c) M. G. Debije et al., Effect on the output of a luminescent solar concentrator on application of organic wavelength-selective mirrors, Applied Optics 49, 2010, 745.

[14] B. S. Richards, A. Shalav and R. P. Corkish., A low escape-cone-loss luminescent solar concentrator, Proc. of the 19th European PV Solar Energy Conference, 2004.

[15] S. A. El-Daly and S. Hirayama, Re-absorption and excitation energy transfer of N,N'-bis(2,5-di-tert-butylphenyl)-3,4:9,10-perylenebis(dicarboximide) (DBPI) laser dye, Journal of Photochemistry and Photobiology A: Chemistry 110, 1997, 59.

[16] a) R. W. Olson, et al., Luminescent solar concentrators and the reabsorption problem, Applied Optics 20, 1981, 2934, b) R. Sóti et al., Photon transport in luminescent solar concentrators, Journal of Luminescence 68, 1996, 105, c) L. R. Wilson et al., Characterization and reduction of reabsorption losses in luminescent solar concentrators, Applied Optics 49, 2010, 1651.

[17] B. C. Rowan, et al., Visible and near-infrared emitting lanthanide complexes for luminescent solar concentrators, Proc. of the 24th European PV Conference 2009, 346.

[18] a) A. J. Chatten et al., A new approach to modelling quantum dot concentrators, Solar Energy Materials and Solar Cells 75, 2003, 363, b) S. J. Gallagher, et al., Quantum dot solar concentrators: Electrical conversion efficiencies and comparative concentrating factors of fabricated devices, Solar Energy 81, 2007, 813, c) V. Sholin, et al., Semiconducting polymers and quantum dots in luminescent solar concentrators for solar energy harvesting, Journal of Applied Physics 101, 2007, 123114, d) G. V. Shcherbatyuk et al., Viability of using near infrared PbS quantum dots as active materials in luminescent solar concentrators, Applied Physics Letters 96, 2010, 191901.

[19] A. M. Taleb, Self absorption treatment for the luminescent solar concentrators, Renewable Energy 26, 2002, 137.

[20] R. Reisfeld, Fluorescent Dyes in Sol-Gel Glasses, Journal of Fluorescence 12, 2002, 317.

[21] S. Tsoi, et al., Patterned dye structures limit reabsorption in luminescent solar concentrators, Optics Express 18, 2010, A536.

[22] S. Tsoi, C. W. M. Bastiaansen and M. G. Debije, Enhancing light output of fluorescent waveguides with a microlens system, Proc. of the 24th European PV and Solar Energy Conference 2009, 377.

[23] a) R. Reisfeld, et al., Photostable solar concentrators based on fluorescent glass films, Solar Energy Materials and Solar Cells 33, 1994, 417, b) G. Seybold and G. Wagenblast, New perylene and violanthrone dyestuffs for fluorescent collectors, Dyes and Pigments 11, 1989, 303, c) M. G. Debije et al., A promising fluorescent dye for solar energy conversion based on a perylene perinone, Applied Optics 50, 2011, 163.

[24] a) I. Baumberg, et al., Effect of polymer matrix on photo-stability of photo-luminescent dyes in multi-layer polymeric structures, Polymer Degradation and Stability 73, 2001, 403, b) R. Kinderman et al., Performance and stability study of dyes for luminescent plate concentrators, Journal of Solar Energy Engineering 129, 2007, 277.

[25] M. J. Currie et al., High-efficiency organic solar concentrators for photovoltaics, Science 321, 2008, 226.

[26] a) W. R. Holland and D. G. Hall, Waveguide mode enhancement of molecular fluorescence, Optics Letters 10, 1985, 414, b) H. R. Wilson, Fluorescent dyes interacting with small silver particles; a system extending the spectral range of fluorescent solar concentrators, Solar Energy Materials 16, 1987, 223, c) K. Aslan, et al., Metal-enhanced fluorescence from plastic substrates, Journal of Fluorescence 15, 2005, 99.

[27]a) K. Heidler, Efficiency and concentration ratio measurements of fluorescent solar concentrators using a xenon measurement system, Applied Optics 20, 1981, 773, b) J. Roncali and F. Garnier, New luminescent back reflectors for the improvement of the spectral response and efficiency of luminescent solar concentrators, Solar Cells 13, 1984, 133.

[28] M. G. Debije et al., The effect of a scattering layer on the edge output of a luminescent solar concentrator, Solar Energy Materials and Solar Cells 93, 2009, 1345.

[29] M. G. Debije, Solar energy collectors with tunable transmission, Advanced Functional Materials 20, 2010, 1498.

[30] a) C. G. Granqvist, Oxide electrochromics: Why, how, and whither Solar Energy Materials and Solar Cells: Selected Papers from the Seventh International Meeting on Electrochromism (IME-7), 92, 2008, pp. 203, b) C. Bechinger and B. A. Gregg, Development of a new self-powered electrochromic device for light modulation without external power supply, Solar Energy Materials and Solar Cells 54, 1998, 405.

[31] M.-C. Dubois, Solar Shading and Building Energy Use, Ph.D. Thesis, Lund Institute of Technology, Lund, Sweden, 1997, pp. 1-100.

[32] a) J. Yoon et al., Ultrathin silicon solar microcells for semitransparent, mechanically flexible and microconcentrator module designs, Nature Materials 7, 2008, 907, b) P. Fath, H. Nussbaumer and R. Burkhardt, Industrial manufacturing of semitransparent crystalline silicon POWER solar cells, Solar Energy Materials and Solar Cells 74, 2002, 127.

[33] A. W. Hains, et al., Molecular semiconductors in organic photovoltaic cells, Chemical Reviews 110, 2010, 6689.

[34] S. Chattopadhyay et al., Anti-reflecting and photonic nanostructures, Materials Science and Engineering: R: Reports 69, 2010, 1.

[35] U. Schulz, Review of modern techniques to generate antireflective properties on thermoplastic polymers, Applied Optics 45, 2006, 1608.

[36] a) G. W. Chantry et al., Far infrared and millimetre-wave absorption spectra of some low-loss polymers, Chemical Physics Letters 10, 1971, 473, b) H. Ma, et al., Polymer-based optical waveguides: materials, processing, and devices, Advanced Materials 14, 2002, 1339.

[37] M. J. Kastelijn, et al., Influence of waveguide material on light emission in luminescent solar concentrators, Optical Materials 31, 2009, 1720.

[38] A. F. Mansour, Photostability and optical parameters of copolymer styrene/MMA as a matrix for the dyes used in fluorescent solar collectors, Polymer Testing 23, 2004, 247.

[39] a) M. Sidrach de Cardona et al., Edge effect on luminescent solar concentrators, Solar Cells 15, 1985, 225.

[40] T. K. Sau et al., Properties and applications of colloidal nonspherical noble metal nanoparticles, Advanced Materials 22, 2010, 1805.

[41] V. E. Ferry, et al., Design considerations for plasmonic photovoltaics Advanced Materials 22, 2010, 4794.

Design and simulation of a PV and a PV-Wind standalone energy system: A case study for a household application in Nicosia, Cyprus

Gregoris Panayiotou[1,2], Soteris Kalogirou[1,*] and Savvas Tassou[2]

[1] *Department of Mechanical Engineering and Materials Science and Engineering, Cyprus University of Technology, P. O. Box 50329, 3603 Limassol, Cyprus*
[2] *School of Engineering and Design, Brunel University, Uxbridge, Middlesex UB8 3PH, UK*
** Tel: +357 25 002621, Fax: +357 25 002637, E-mail: soteris.kalogirou@cut.ac.cy*

Abstract: In this work the design and simulation of two stand-alone renewable energy sources (RES) based systems for application in a household in Cyprus is presented. More specifically, the household is located in Nicosia and is used as the residence of a typical Cypriot family for which a baseline scenario of energy consumption is specified in order to define the annual load profile of the house. The first system is based on photovoltaic (PV) modules for the generation of electricity by harvesting the very high solar potential of Cyprus while the second one is a hybrid system combining PVs with a domestic wind turbine in order to take advantage of the wind potential especially during winter. Since both systems are stand alone the energy produced is stored in a battery bank. The software used for the modeling and simulation processes is TRNSYS. A comparison of the two systems in terms of both technical and economical aspects is presented in this study where it is concluded that the wind potential of the specific location of the house, which generally applies on the entire island, cannot substitute and compete in any way with the very high solar potential.

Keywords: *Stand-alone system, baseline scenario, Cyprus, hybrid, wind potential, solar potential*

1. Baseline Scenario Characteristics

In order to design the domestic standalone energy systems a typical house is considered for which a baseline scenario concerning several parameters is defined. It is very important to note that the baseline scenario concerns a future situation where all energy for the household is supplied by a RES system and the system is isolated from the grid. The characteristics of the baseline scenario concern the structure, location, occupancy and energy systems installed in the house examined. The data used to define these characteristics were based on the statistical analysis conducted by Panayiotou et al. [1] which concerned the characteristics and the energy behavior of the residential building stock of Cyprus in view of Directive 2002/91/EC.

The house examined in the baseline scenario is a single ground floor house with an area of 160 m^2 which was built in year 2000 and is located in Nicosia, Cyprus where the climatic conditions are those for lowland inland Mediterranean areas. The house has 3 bedrooms and it does not have pilotis, sofitta or a basement while it has a flat concrete roof with 140 m^2 of free space for any systems such as solar thermal or PVs to be installed. The house has a 5 cm polyurethane wall insulation and double glazing. The heating and cooling is covered with split type air conditioning units and the number of units installed are two 9,000 BTU (2.6 kW) in two of three bedrooms and one 12,000 BTU (3.5 kW) unit in the living room. For the production of domestic hot water (DHW) a solar water heating system is used while an immersed electric element is installed for backup.

2. Typical annual load profile definition

The typical annual load profile definition was also based on the statistical analysis conducted by Panayiotou et al. [1]. In this statistical analysis a sample of 500 houses along with analytical data given by the Electricity Authority of Cyprus were used and it was concluded that there are two peaks observed on the consumption of electricity in the domestic sector

annually; one in summer, which is the highest, and one in winter. On the other hand, autumn and spring periods have more or less the same consumption of electricity which is lower compared to that of summer and winter. Also, another very important thing to notice is that the daily average electricity consumption of a house is around 24 kWh during summer, 21 kWh during winter and 15 kWh during autumn and spring.

To be more precise on the definition of the typical annual load profile this was split into weekdays and weekends for each of the four seasons. The months contained in each season are as follows; Winter: December, January and February; Spring: March, April and May; Summer: June, July and August; and Autumn: September, October and November. Additionally, it should be noted that holiday periods are not considered in the examined typical annual load profile. The typical load profiles for weekdays of spring, autumn and winter are shown in Figs. 1-3 respectively.

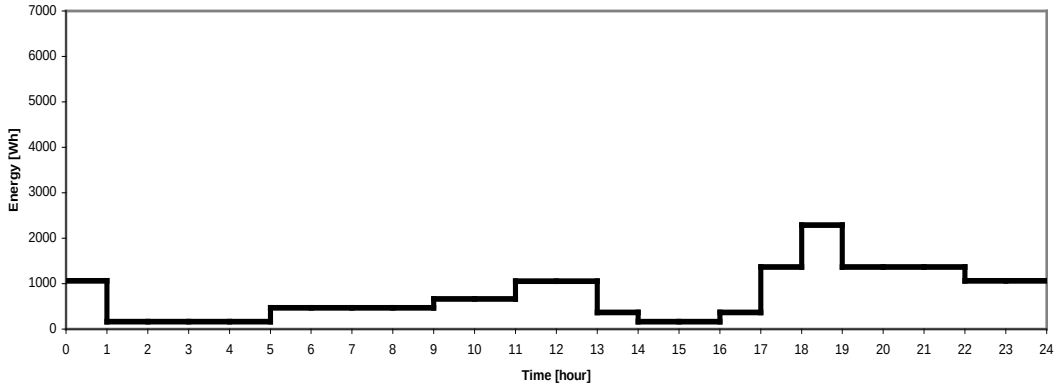

Fig. 1 Load profile for a typical spring/autumn weekday

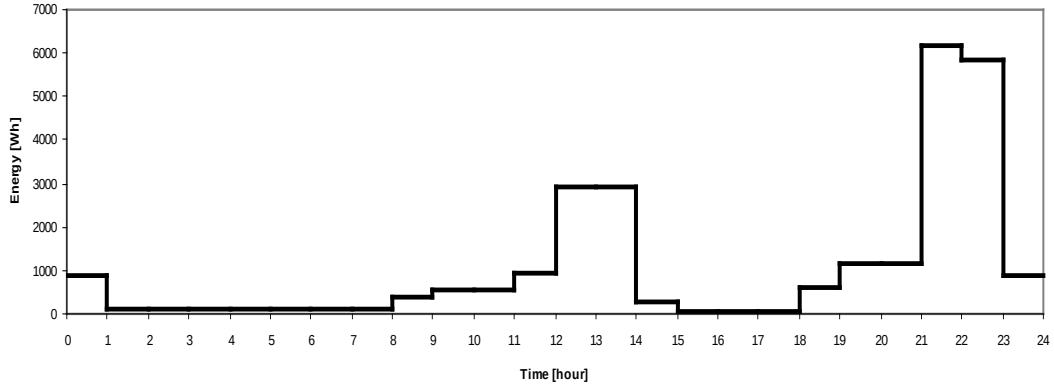

Fig. 2 Load profile for a typical winter weekday

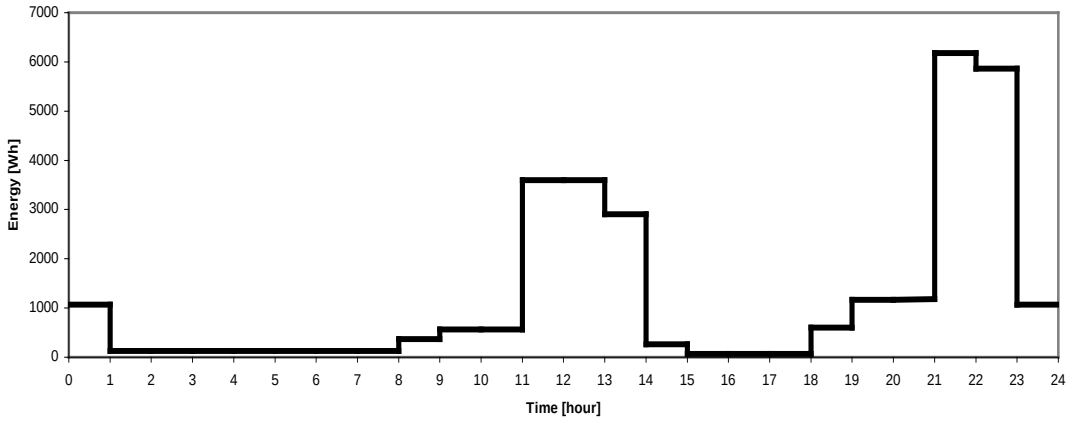

Fig. 3 Load profile for a typical summer weekday

3. Model design for standalone PV system

The model design process was carried out in the TRNSYS environment [2] which is considered to be a complete and extensible simulation environment for the transient simulation of solar and other energy systems.

The model of the standalone PV system includes the following components:

- Weather data processor model (Type 109)
- PV model (Type 180e)
- Inverter/Regulator model (Type 48b)
- Battery model (Type 47a)
- Load Profile model (Type 9a)

A very important parameter to consider when designing a standalone PV system is the nominal voltage of the battery bank which can be 12, 24 or 48 VDC. The parameters affecting the determination of the suitable nominal voltage for a system are the nominal voltage of the PVs, the size of the system and the input requirements of the inverter. For example, inverters which have a power of 6 to 12 kW require nominal voltage to be 48 V while inverters with a power of 2 to 5 kW require the nominal voltage to be 24 V. Since the system examined is neither a large system nor a small one, it was decided that the nominal system voltage is considered initially to be 24 V. The main reason for this decision is that since with a rough estimation the system will not exceed 10-13 kW of PV power it is much better to use three inverters of 4 kW instead of one inverter of 10-13 kW in order to secure basic load coverage in the case of a failure of one inverter.

It is also essential to know the slope of the PVs. A rule of thumb followed by the PV technicians in Cyprus is that the slope of the PVs should be somewhere between 27-31°. In order to define the optimum slope to be used in the modelling process a small model consisting of a typical meteorological year (TMY) and a single PV was developed and a series of simulations were carried out for slopes between 27-33°. The energy production for each slope is recorded and presented in Table 1.

Table 1 PV characteristics on standard testing conditions

Slope of the PV	Energy Produced [Wh/yr]
27°	89,516
28°	89,650
29°	89,748
30°	89,810
31°	**89,835**
32°	89,823
33°	89,775

According to the results of Table 1 the maximum energy production occurs for a slope of 31° (shown with bold on Table 1) and thus this is the optimum angle for the location examined and consequently for the island of Cyprus.

3.1. Simulation and economic analysis of standalone PV system

After the proper setting up of the complete model for the standalone PV system a series of simulations were carried out in order to specify the required storage capacity and PV array

power needed to cover the load over the time period of a typical year. Before running the simulations it is essential to decide the acceptable loss of load probability (LOLP) of the specific system which defines the required battery autonomy in days. For example, if a 1% acceptable LOLP is chosen it means that during the time period of a year there is probability to have 3.65 days where the load will not be covered. Thus, if we want to design a system where we will have a 100% annual load coverage, in order not to compromise the occupants' quality of living, then a first estimate for the required battery autonomy should be that of 4 days. It should be noted that the batteries capacity must be larger than that calculated for the 4 days of autonomy due to the fact that it is impossible to start the 4 days of autonomy with the batteries fully charged as these always supply electricity to the system during nighttime. Thus, in the system examined, it is predefined that one of the most important parameters to consider for the selection of the PV array size and the required storage capacity is to have 100% annual load coverage.

Since the nominal voltage of the battery bank is decided to be at 24 V and the nominal voltage of each battery cell is 2 V then the configurations of the battery bank used during the simulation consisted of 1, 2, 3 or 4 strings of 12 batteries connected in series.

The results of the simulation process were recorded in a data file and subsequently processed to evaluate the load coverage achieved by each configuration. The most important results estimated during the simulation are presented in Table 2.

Table 2 Results of the simulation process for the standalone PV system

Configuration No	No of PVs	PV array power	No of batteries	Battery capacity	Annual energy deficiency	Annual period of energy deficiency
	[-]	[kW]	[-]	[kWh]	[kWh]	[hrs]
1	40	7.2	36	108	566	607
2	45	8.1	36	108	381	451
3	50	9.0	36	108	228	220
4	60	10.8	36	108	25	33
5	63	11.34	36	108	12	2
6	65	11.7	36	108	2	10
7	40	7.2	48	144	496	503
8	45	8.1	48	144	320	365
9	50	9.0	48	144	193	186
10	55	9.9	48	144	80	97
11	58	10.44	48	144	13	29
12	59	10.62	48	144	0	0

From the results of Table 2 it can be seen that the systems that achieve 100% annual load coverage over a typical year are those of Configurations 6 and 12. Additionally, it is observed that the system of Configuration 5 is rather acceptable since it has a very low energy deficiency of 12 kWh or 2 hrs per year. Configuration 11 gives also a low energy deficiency of 13 kWh but it is not considered due to its high annual period of energy deficiency which is 29 hrs per year. It should be noted that two different approaches are considered for these systems with the difference between them being that Configuration 12 has larger energy storage capacity and lower PV array power (smaller size) while Configurations 5 and 6 have larger PV array power (larger size) and lower energy storage capacity. This is a very

important fact to consider when deciding which is the optimum configuration for the system to be designed. To do so, Configurations 5, 6 and 12 are evaluated in terms of economic viability for a total system life of 25 years. During this process the lifetime of each component is taken into consideration along with its current cost and is recorded in Table 3. The results of this analysis are presented in Table 4.

Table 3 Equipment prices used in the economic analysis

	Equipment Description	Price
1	Photovoltaic panels	€3.2 per W
2	Batteries	€640 per pc
3	Inverter (2.5 kW, 12 V)	€2069
4	Mounting system (for flat roof)	€200/kW
5	Electrical equipment (cables etc.)	€210/kW

Table 4 Economic analysis results for the systems of Configurations 5, 6 and 12

	Configuration 5					
	Equipment	Number	Power	Lifetime	Price	Price overall
1	PV	63	180	25	€36,288	€36,288
2	Inverter/Controller	3	4500	15	€7,977	€15,954
3	Elec. Equip.	-	-	25	€2,381	€2,381
4	Mounting	-	-	25	€2,268	€2,268
5	Batteries	36	1500 Ah	18	€23,040	€46,080
					TOTAL	€102,971
	Configuration 6					
	Equipment	Number	Power	Lifetime	Price	Price overall
1	PV	65	180	25	€37,440	€37,440
2	Inverter/Controller	3	4500	15	€7,977	€15,954
3	Elec. Equip.	-	-	25	€2,457	€2,457
4	Mounting	-	-	25	€2,340	€2,340
5	Batteries	36	1500 Ah	18	€23,040	€46,080
					TOTAL	€104,271
	Configuration 12					
	Equipment	Number	Power	Lifetime	Price	Price overall
1	PV	59	180	25	€33,984	€33,984
2	Inverter/Controller	3	4500	15	€7,977	€15,954
3	Elec. Equip.	-	-	25	€2,230	€2,230
4	Mounting	-	-	25	€2,124	€2,124
5	Batteries	48	1500 Ah	18	€30,720	€61,440
					TOTAL	€115,732

By evaluating the results of the economic analysis it is concluded that the optimum system is Configuration 5 which consists of 63 PVs (11.34 kW) and 36 batteries. The cost of such a system is €102,971. It is very important to notice that in all cases examined the main part of the cost, around 50%, concerns the batteries. Since the optimum configuration estimated has 36 batteries it is concluded that the decision for the nominal voltage of the battery bank to be at 24 V was correct due to the fact that if 48 V was chosen then the battery bank configuration

should have been either 1 or 2 strings of 24 batteries and it is obvious that the option of 24 batteries (1 string) would be undersized and thus insufficient while the option of 48 batteries (2 strings) would be oversized with a consequent increase of the overall cost of the system.

4. Model design for hybrid standalone PV-Wind system

The model for the hybrid standalone PV-Wind is based on the previously developed model for the standalone PV system. The difference between the two models relies on the addition of a small domestic wind turbine (Type 90). In this system, as in all hybrid power systems, more than one source of energy is used in order to diversify the sources and achieve load coverage under various climatic conditions during the entire 24 hours period. Furthermore, it is very important to note that the operation of this system differs from that of the PV system due to the fact that the power produced by the wind turbine is directly supplied to the load through a power conditioner and the rest of the load is covered by the PV subsystem. For the design of this model two wind turbines were chosen to be considered a 1.5 kW and a 2 kW. The reason for choosing these two low power domestic wind turbines is due to the fact that the wind potential in the area examined is rather low as it is illustrated in Fig. 4 where it can be seen that more than 86% of the time the wind velocity is between 0-6 m/s and the average wind velocity is 4 m/s. The curves of power against wind velocity for the wind turbines considered are presented in Fig. 5.

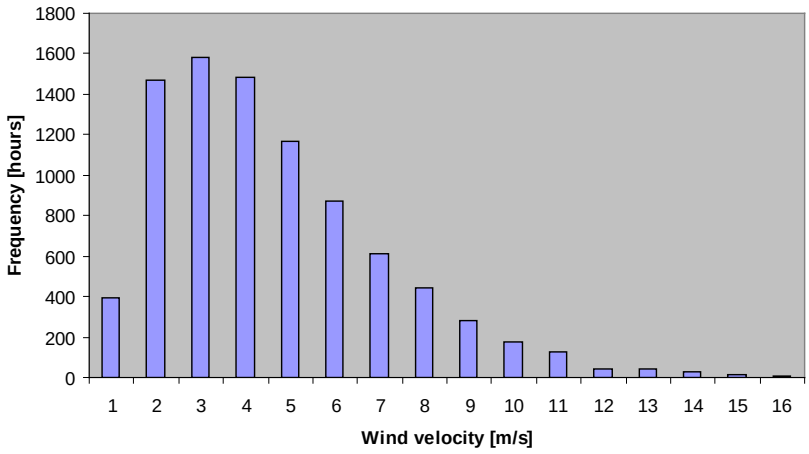

Fig.4 The wind profile of the examined location

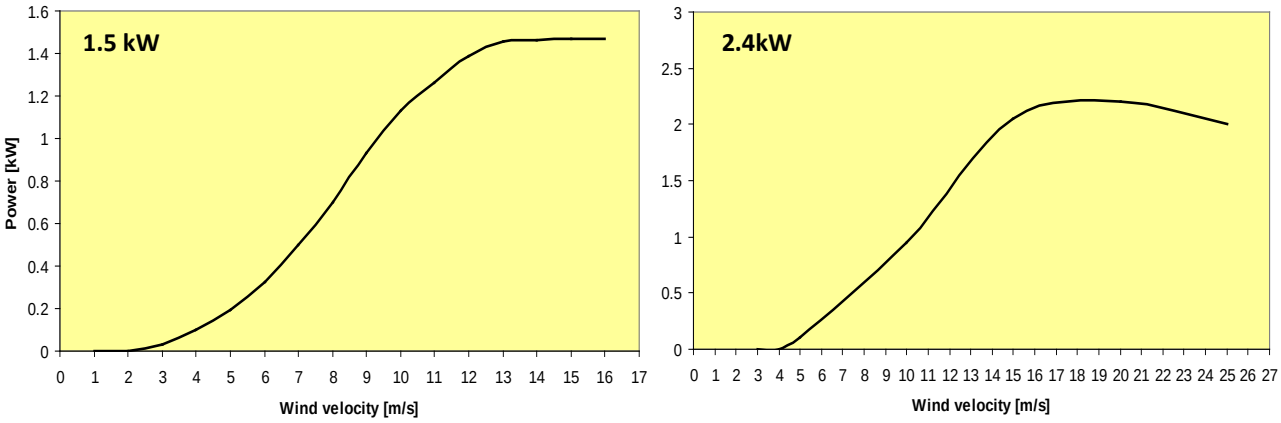

Fig. 5 Characteristic power curves for both wind turbines considered

By carefully analyzing the power curves of each wind turbine in conjunction with the wind profile of the examined location it is hypothesized that the most suitable wind turbine to be used in the system designed is the 1.5 kW one. This of course is only a hypothesis and in order to be validated a series of simulations using a simple model consisting of a TMY and a wind turbine were carried out. The results obtained are presented in Table 5. From these results it is concluded that the hypothesis was correct since the 1.5 kW wind turbine generates more energy than the 2.4 kW one. This is caused by the fact that the 1.5 kW wind turbine operates with higher efficiency at low wind velocity which prevail at the location examined.

Table 5 Simulation results for both wind turbines examined

Energy Produced [Wh]	1.5 kW-Wind turbine	2.4 kW-Wind turbine
Maximum	1,500	2,274
Average	146	145
Annual	1,279,346	1,271,074

4.1. Simulation and economic analysis of standalone PV-Wind system

The simulation process followed for this system was similar to the one carried out for the PV system. From the results concerning the two wind turbines it is clear that the wind turbine that should be used in the system designed is that of 1.5 kW.

Since the optimum capacity of the batteries to cover the load over a typical year was calculated during the simulation process for the PV system and found to be 108 kWh it is decided that this capacity should also be the same for the case of the PV-Wind system as the energy provided by the wind turbine is very small.

The results of the simulation process were recorded and processed to evaluate the load coverage achieved by each configuration. The most important of the results calculated during the simulation process are presented in Table 6. From these results it can be seen that the system that achieve 100% annual load coverage over a typical year is that of Configuration F. On the other hand the systems of Configurations B, C, D and E also gave rather acceptable results since the annual energy deficiency varied between 1-15 kWh while the annual period of energy deficiency varied between 7-22 hrs per year. Since all systems have the same battery capacity it is decided that the configuration to be compared with the PV system in the following section is that of Configuration C in order to have the same energy deficiency so as to be comparable.

Table 6 Results of the simulation process for the standalone PV-Wind system

Configura-tion Number	No of PVs [-]	PV array power [kW]	No of batteries [-]	Battery capacity [kWh]	Energy deficiency [kWh/yr]	Period of energy deficiency [hrs/yr]
A	55	9.90	36	108	24	33
B	57	10.26	36	108	15	22
C	58	10.44	36	108	11	7
D	59	10.62	36	108	7	10
E	60	10.80	36	108	1	10
F	61	10.98	36	108	0	0

5. Comparison and Conclusions

The comparison is carried out for a lifetime of 25 years for both systems and the results are recorded in Table 7. From the results of the economic analysis it can be seen that the two systems have the same lifecycle cost with a slight decrease in favor of the PV-Wind system. Nevertheless, the difference in cost is very small (€1000) and it is judged to be insignificant for the cost range of the systems examined.

Table 7 Economic analysis results for PV and PV-Wind systems

PV system						
	Equipment	Number	Power	Lifetime	Price	Price overall
1	PV	63	180	25	€36,288	€36,288
2	Inverter/Controller	3	4500	15	€7,977	€15,954
3	Elec. Equip.	-	-	25	€2,381	€2,381
4	Mounting system	-	-	25	€2,268	€2,268
5	Batteries	36	1500 Ah	18	€23,040	€46,080
					TOTAL	€102,971
PV-Wind system						
	Equipment	Number	Power	Lifetime	Price	Price overall
1	PV	58	180	25	€33,408	€33,408
2	Windturbine	1	1500	20	€2,250	€2,250
3	Inverter/Controller	3	4500	15	€7,977	€15,954
4	Elec. Equip.	-	-	25	€2,192	€2,192
5	Mounting system	-	-	25	€2,088	€2,088
6	Batteries	36	1500 Ah	18	€23,040	€46,080
					TOTAL	€101,972

From the results presented in this paper it is concluded that in spite of the fact that due to their ability to diversify the energy sources, hybrid systems are generally considered to be a better option for standalone applications, in the case of the location examined, the PV-only system is a better option. This lies on the fact that the PV system is based fully on the very high solar potential of Cyprus in contradiction to the PV-Wind system which is based on the very low wind potential observed in the area examined, which is also typical for the whole island.

It should also be noted that by not using the wind turbine in a domestic area several other possible negative aspects are avoided such as noise caused from the operation of the wind turbine, optical pollution and maintenance requirements which are not considered in the above analysis. By observing the cost analysis of both systems it can be seen that batteries represent over 50% of the overall systems' cost.

References

[1] G.P. Panayiotou, S.A. Kalogirou, G.A. Florides, C.N. Maxoulis, A.M. Papadopoulos, M. Neophytou, P. Fokaides, G. Georgiou, A. Symeou, G. Georgakis, The characteristics and the energy behaviour of the residential building stock of Cyprus in view of Directive 2002/91/EC, Energy and Buildings, 42, 2010, pp. 2083-2089.

[2] TRNSYS program manual.

High Efficiency Multijunction Tandem Solar Cells with Embedded Short-Period Superlattices

Argyrios C. Varonides[1,*]

[1]*University of Scranton, 800 Linden Street, Scranton Pennsylvania 18510, USA*
** Corresponding author. Tel: +1(570)941-6290, Fax: +1(570) 941-4015, E-mail: varonides@scranton.edu*

Abstract: We propose a 1cm^2 tandem solar cell with different lattice-matched materials based on a 2eV/1.42eV/0.66eV energy gap sequence. The top unit is a p-n-n AlAs/GaAs cell, connected in series with a bottom cell which is a bulk GaAs/Ge p-n-n cell; a narrow GaAs/Ge superlattice region embedded in the middle region. Transition of carriers between the two units is possible via a tunnel junction connecting the two units. More specifically, the upper cell is a 20 μm bulk p-n-n cell tuned to the visible range of the solar spectrum, producing short circuit currents near 30mA/cm^2, and open-circuit voltage (OC) of 1.04V; the bottom cell is an 80 μm bulk p-n-n GaAs/Ge with an embedded GaAs/Ge superlattice tuned at 1eV. The bottom cell produces short circuit current density at18.5 mA/cm^2 in the bulk; however a 20-period GaAs/Ge embedded short superlattice provides an additional 10 mA/cm^2 thermionic current density, so that total bottom current reach 28.5mA/cm^2, in close matching (5%) with the top currents, and an OC voltage of 0.968V. The tandem cell's basic parameters are (a) average fill factor of (FF) 85% (b) short circuit current 28.5 mA/cm^2 and (c) OC voltage 2.008V (due to the series connection); for 100mW/cm^2 standard solar radiation, collection efficiency of such a device is depicted in excess of 47% under one sun. Such small area cells are useful for CPV for their minimized size and material requirements.

Keywords: *Solar cells, Superlattices, Tuned quantum wells, High efficiency photovoltaics*

Nomenclature

J_{TH} *thermionic current density …....mA/cm^2*
J_{sc} *short-circuit current.…..…..…....mA/cm^2*
V_{oc} *open-circuit voltage.……..…..…..Volts*
L_w *quantum well width.…..……..…..…nm*
n_{ph} *photo-excited carriers ……..…..…..…...cm^{-3}*
g_o, *g(E) density of states.……..…..…...eV^{-1}cm^{-2}*
g_o, *g(E) density of states.…..…..…...eV^{-1}cm^{-2}*

1. Introduction

The field of high efficiency photovoltaics (HEPV) is maturing steadily; already the threshold of 40% efficiency has been reached and exceeded to 42.2 % [1, 2, 3, 4, 5, 6]. It is common place in the PV community that the 50% limit for crystalline solar cells will be within reach in the next five years. The common denominator of high efficiency cells is the idea of two to three different band gaps that absorb in different wavelengths, preferably in a successive fashion along with the visible and the infrared parts of the solar spectrum. A typical cell of such geometry contains three major layers of lattice-matched or suitably metamorphic semiconductor layers joined (in series) by means of tunnel junctions. The latter are needed to ensure current matching. The obvious advantage of such structures is the series connection of two p-n junctions essentially, with increased overall open circuit voltage (due to the series connection). In this communication we are proposing an ostensibly high efficiency structure based on the series connection idea, as mentioned above, but with a different design, especially in the area of long wavelength absorption. The latter is a process that can be realized by means of two dimensional geometry selections (or one dimensional option as well). The device is described in brief as follows: a top p-n or p-i-n bulk GaAs/AlAs/Alloy cell is proposed for short wavelength absorption (mainly visible). The unit is then grown on top of a tunnel junction (guaranteeing the series connection) and the bottom cell follows with a similar topography, namely, a p-i-n cell matched with the layers above it. The intrinsic region of this cell is replaced by a GaAs/Ge superlattice with reduced tunneling. The latter

selection is adopted for two reasons (a) Ge is lattice-matched with GaAs and (b) we want to ensure thermal current generation from the mid- (intrinsic/low-doped) to the n-region of the device, as shown in Figure 1 below:

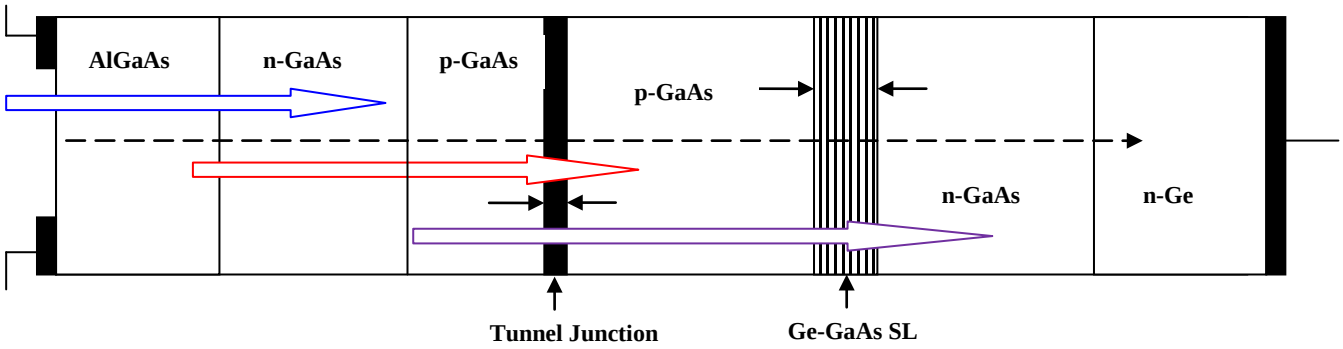

Fig. 1 Proposed tandem (1cm^2) p-n-n$^+$/p-n (Superlattice (SL))-n$^+$ multijunction solar cell, for high efficiency. Two cells in series through a tunnel junction. Maximum current density depicted at 28.5mA/cm^2; Open-circuit voltage values 1.04 and 0.968V respectively. Total V_{oc} = 2.008V, J_{sc} = 30mA/cm^2.

The structure promotes the series connection of two cells, with current matching. As seen from the figure above, the goal is to produce a composite cell where both short and long wavelengths are absorbed simultaneously; in this context, this can be succeeded via the two layers shown. Visible and near infrared absorption is guaranteed by the two cells respectively, while the MQW geometry is tuned to longer wavelengths via pre-selected eigen-state resonance. Therefore, analysis and simulation of the device will have to include both regions as depicted through (a) the top and (b) bottom cells and (c) through the tunnel junction (TJ). The latter is basically selected to be a double barrier heterostructure of p^{++} and n^{++} highly doped GaAs layers (TJ modeling for this purpose will be reported elsewhere). Fundamentally, photoelectrons induced from the top, tunnel through the mid-junction to join carriers from the lower cell. Ultimately, due to the series connection, matching will dictate the final current, in other words, the lowest current will keep the connection at the ON state. On the other hand, the series connection is expected to provide enhanced voltage (ideally the sum of the two OC voltages as they come from the two sub-cells). It is imperative therefore to model all regions for optimum current and voltage generation. In the following sections, modeling and simulations for two of the three mentioned regions is provided as a tool for optimization in design.

2. Top Cell for the visible solar spectrum

It is desirable to obtain a top layer suitable for visible spectrum absorption. Graded AlGaAs layers of variable aluminum fractional content is proposed according to the following table:

Table 1: Bandgap and wavelength at different Aluminum percentage content for AlGaAs

Al content (%)	Band-gap (eV)	Wavelength λ(μm)
0.98 (AlAs)	2.16	0.574
0.90	2.11	0.582
0.80	2.07	0.592
0.70	2.05	0.602
0.60	2.02	0.612
0.50	1.998	0.620

As seen from the table above, a feasible succession of lattice-matched AlAs-AlGaAs graded layer ensures visible spectrum absorption. Modeling of a 0.5 to 1.0μm p-AlAs/AlGaAs layer on top of an n-n^+ GaAs arrangement (upper part of Figure 1) leads to short circuit current at 30.50 mA/cm^2, and open-circuit (*OC*) voltage at 1.04V, with max power 28.30 mW [temperature 300 ^oK; one-sun exposure and power input of 100mW/cm^2; 10% internal reflection]. Figure 2 shows the J-V characteristics of the top cell, where both current-voltage and power-current curves are depicted. This is a high current solar cell and can stand alone. Note also that with an 88 to 90% fill factor (*FF*), this is a 27.9 % cell. Note also that a second junction could be used as the bottom cell, with exactly the same characteristics; in such a case, one (provided the tunnel junction can sustain 30mA/area) may end up with a double junction cell with 2V and 30mA/unit area, which would lead to a double-junction cell (area 1square centimeter) with collection efficiency with collection efficiency n(%) = (2x30mA/cm^2) x (FF)/(100mW/cm^2). For a collective fill factor near 80%, this leads to 48% collection efficiencies. Figure-2 below depicts a simulated J-V characteristic (extrapolation to the horizontal axis leads to 1.04V):

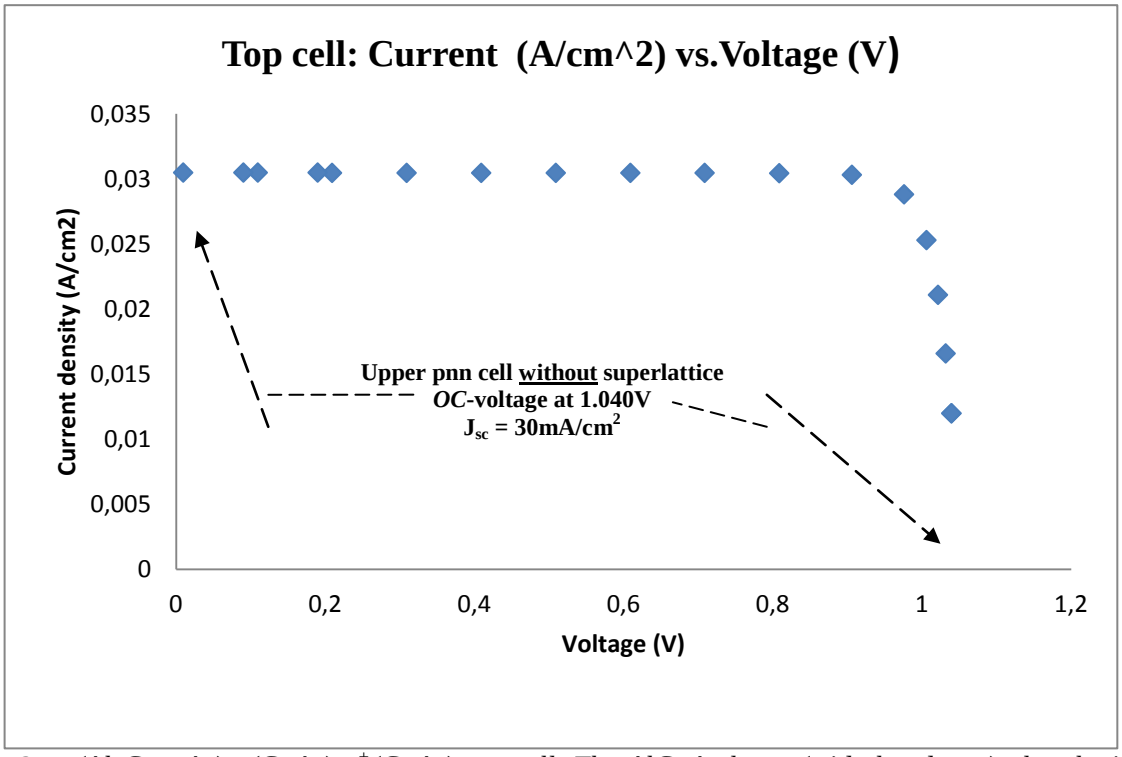

Fig.2. p ($Al_xGa_{1-x}As$)-n(GaAs)-n^+(GaAs) top cell. The AlGaAs layer (wide band gap) absorbs in the visible (see Table 1). Max current and OC-voltage extrapolated at 30.5mA/cm^2 and 1.04V respectively.

3. Bottom Cell

Out of several options for a double junction cell, we select a p-n-n *1.82eV/1.42eV/0.66eV* cell in order to demonstrate two points (a) to include long wavelength absorption and (b) to introduce the idea of tuning layers in the mid-regions to desired wavelengths. In this paper we are proposing a quantum well structure embedded in the mid-region of the bottom cell and tuned to 1eV solar photons. Regarding the 0.66 eV material (for long wavelengths: 1.24/0.66 = 1.878 μm) include in the bottom cell design, simulations lead to short circuit current density at J_{sc} = 18.50 mA/cm^2 and *OC*-voltage V_{oc} = 0.968V. Simulation and modeling of the bottom unit is basically in a structure depicted by lower portion of Figure-1, *without* the mqw region. The mqw region is a 20-period GaAs/Ge superlattice (no tunneling) with thin Ge-quantum

wells tuned at 1eV or with a 19.6 nm width. Potential barriers are selected at 100nm (in order to minimize tunneling). The total thickness of the reduced dimensionality superlattice is 20 x (200+19.6) = 4,392 nm = 4.392 μm; the latter is just 5.3% of the total lower cell, which is essentially a pnn GaAs/Ge solar cell with its J-V graph shown by figure-3:

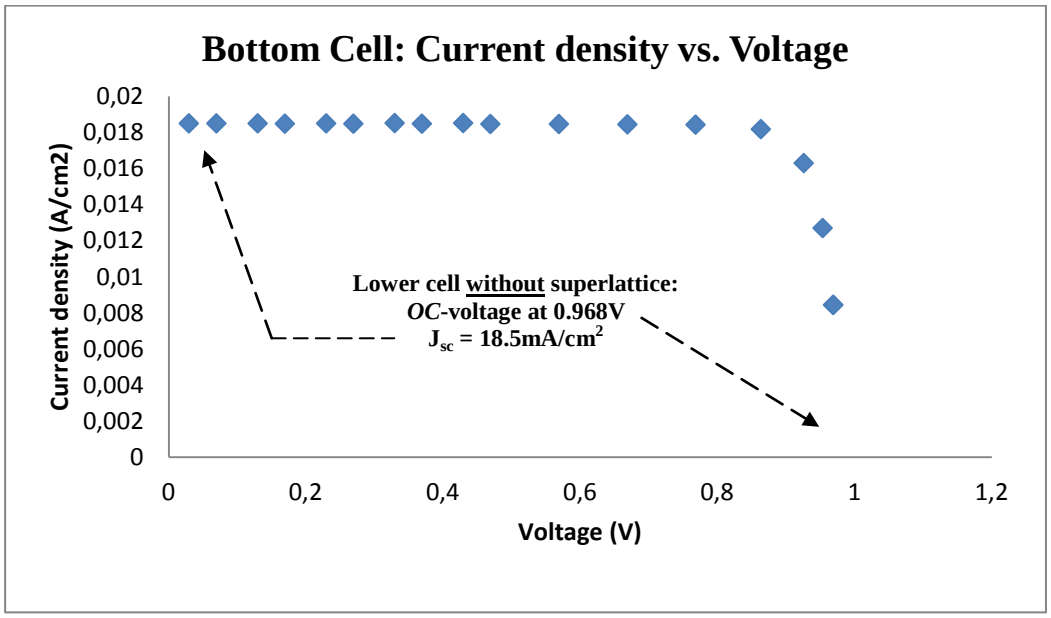

Fig. 3: Bottom cell J-V characteristics: a bulk pnn GaAs/Ge cell with 0.968V and 18.5mA/cm^2 (OC and SC) parameters respectively.

By proposing a superlattice in the mid region of the lower cell (in future designs this could be proposed for both cells as well!) we actually introduce a second channel of carrier current per unit area, such that the current in the lower part of the device might go increase as well. In the next section, we develop a formalism of thermionic current escape that contributes to the main bulk current of the bulk device as depicted in Figure-4 below:

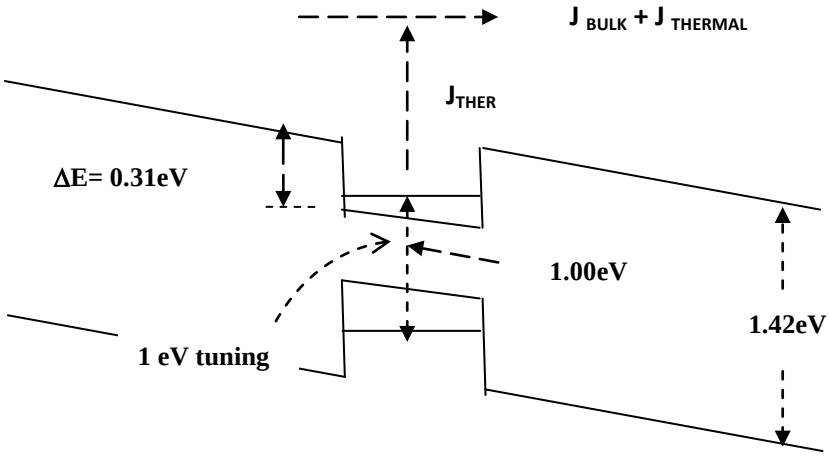

Fig. 4: Fine tuning at specific wavelengths can be achieved through quantum size effects in the traps of the intrinsic region. Electrons' thermionic conduction, from 20nm quantum wells, is schematically shown at the conduction band. Note the Fermi and intrinsic Fermi levels, and the addition of the two current components: bulk and thermal current components respectively.

Final current from the quantum traps adds constructively to the bulk current generated by the GaAs/Ge cell (18 mA/unit area, see Figure-3 above). Due to current matching, overall *SC*-current output is going to be based on the lowest current off the two cells. Thus, thermal escape generation becomes essential: simultaneous high current and voltage generation may lead to higher "ground" collection efficiency (one sun conditions). In the next section, modeling is geared towards thermionic current generation and current matching near $30mA/cm^2$.

4. Modeling of Thermionic current

As mentioned above and discussed elsewhere, photo-excitation forces excess carriers in quantum wells and an increase of total carrier population near 10^{12} cm^{-2}, per well [6]. Trapped photocarriers recombine and thermionically escape from the quantum traps. With recombination losses includes [8,9] and given that there is a non-zero probability for thermal escape, we model escaping carriers as thermionic currents over ΔE_C barriers. Once this is established, we consider the two current components as two current sources (in the bottom cell always), and we are adding these two components to find the total lower-cell current. In all probability, this result is not necessarily expected to match the top component, however, by imposing required conditions, selective doping and superlattice geometry; we expect total lower current to reach (as close as possible) the top one.

In the following, we briefly discuss this process. Thermionic emission from wells of depth ΔE_C leads to current density values of the type [8]:

$$j = q\int dxdEg(E)\,f(E)v(E)\delta n(x) \qquad (1)$$

Where q is the electronic charge, g(E) is the density of states (DOS) of the quantum trap (here quantum wells or quantum dots etc), f(E) is the Fermi level position in the gap of the semiconductor layer, v(E) is the "velocity" of the carriers at energy E and where δn(x) is the net carrier population in the traps of length/width L_W and after recombination. For an average excess carrier density $<\delta(x)> = \delta N = 10^{12}cm^{-2}$ per well, the above integral simplifies as follows:

$$j = q(\delta N)(L_W)g_o\int dEf(E)v(E) \qquad (2)$$

Thermionic currents can be calculated from the latter expression, where DOS represents the quantum system involved. In the present case we adopt quantum wells (faster and less cumbersome compared to quantum dots fabrication), where DOS is a constant function: (2-d DOS of quantum wells, $eV^{-1}cm^{-2}$). Based on the above and on the fact that the Fermi level is near (and above) 3(kT)'s below the conduction band of the low gap layer (E_C - E_F) (Fermi-Dirac approaches the Maxwell-Boltzmann distribution), the current relation yields the following explicit expression (by replacing for g(E) with g_o and relating the speed of the carriers with energy barrier ΔE_C of the heterojunction discontinuity):

$$j = q\times n_{ph}\times g_o\times L_W\times\sqrt{\frac{2}{m^*}}\times\int_E^\infty dE\sqrt{E-E_1}\times\exp(-\frac{E_1-E_F}{kT}) \qquad (3)$$

Where the difference $E-E_F$ is the activation energy relative to the Fermi level, E_1 is the lowest eigen-energy in the germanium quantum wells (near 10meV from the bottom of the wells, for

~20 nm width (L)). Note also that the excess carrier per unit area available per well is n_{ph}, and m* is the effective mass in germanium layers. Taking the lowest limit to be the ground eigen-state, the last expression leads to the following result:

$$j = q \times n_{ph} \times L_W \left(\frac{\sqrt{2\pi m^* k^3}}{\pi \hbar^2} \right) \times T^{3/2} \times \exp(-\frac{E_1 - E_F}{kT}) \quad (4)$$

Note from the above the dependence of the current on the activation energy through the exponential. For undoped germanium layers, activation energy values are the sum of eigen-energy value plus the $E_C - E_F$. The latter (for germanium) can be quickly computed [ ]:

$$\Delta E_{CF} = E_C - E_F = kT \ln(\frac{N_C^{Ge}}{n_i}) = 0.338eV \quad (5)$$

Where the factors in the fraction above are (a) the conduction band density and (b) the intrinsic concentration for Ge, and the 0.33 eV is essentially the intrinsic Fermi level. For such a result, our derived formula provides negligible thermal current (fraction of μA). For moderate doping levels near $10^{16}cm^{-3}$, we compute thermal currents 0.0429 mA/cm^2, which, for desired $10mA/cm^2$, would require a long superlattice (large number of periods, about 240). On the other hand, selecting doping levels near 10^{18} cm^{-3}, however, leads to current density near $0.4mA/cm^2$/well, which translates into 25 superlattice periods in all. Based on this, we propose an n-Ge/GaAs multi-junction layer in the middle region of the pnn GaAs/GaAs/Ge bulk lower cell, where total current will essentially reach the top-cell current and hence current matching will be succeeded within ~5% (note: top cell current $30mA/cm^2$, bottom cell currents: $18.5mA/cm^2$ plus $10mA/cm^2$ = $28.5mA/cm^2$). Based on this current matching and on the computed data (see short circuit currents, Figures 2 and 3), we estimate the following for the composite cell of Fig.-1: short circuit current of $28.5mA/cm^2$, and open circuit voltage $V_{oc1} + V_{oc2} = 1.04V + 0.968V = 2.008V$. This means that the composite cell (as long as the tunnel junction sustains normal operation) is expected to provide two volts at *OC* conditions and at least $28mA/cm^2$ at *SC* conditions. Both units of the tandem structure have fill factor values of 85 and 85.5 % respectively, as it can be found from the open-circuit voltages of each [12].Under one sun (AM 1.5), such a one-square centimeter tandem PV-device exhibits collection efficiency of [0.85x28.5x2]/100 = 48.45%. Obvious advantages in such a design are (a) minimal material usage (small area, and narrow superlattice layers; the latter suitable for growth technique selection (chemical vapor deposition or molecular epitaxy) (b) simultaneous short and long wavelength absorption (c) short-period tuned superlattice (d) high carrier mobility due to GaAs/Alloy major components (in contrast to mismatched cells with low mobility) (e) extension of design to include more than one superlattice tuned at desired wavelengths.

5. Conclusion

High efficiency solar cells are becoming a reality while collection efficiency levels near 40% have been achieved. It has been realized in recent years that more than one layer may lead to higher photon absorption due to varying energy band gaps involved. Indeed, this is the case for hetero-junction cells that include two or more materials in one unit; however, recently proposed tandems do not utilize superlattice components [5, 8]. In this paper we explore efficiency enhancement via (matched) current and voltage increase, with a 1eV-tuned superlattice embedded in one of the cells. Thus, a multijunction cell is proposed, with visible

and IR wavelength absorption capabilities. The proposed structured is a $1cm^2$ cell and is composed of two sub-cells: the bottom unit is a 20-period GaAs-Ge superlattice embedded in a pnn GaAs-Ge bulk solar cell. On top of this cell an AlAs-AlGaAs-GaAs cell is proposed, suitable for short wavelengths. The two units are connected in series via a standard tunnel junction, modeling of which is not discussed in this paper. Assuming ideality factors near one, modeling and simulation of the two devices shows a total voltage near 2 Volts and minimum current density 28.5 mA/cm^2. Collection efficiency is expected to exceed the 42% current threshold (one sun conditions). The cell structures involved, could individually perform well on their own at different wavelengths and with appreciable efficiencies respectively. Our proposed structure involves tuning of the lower device at desired photon energy input (1 eV). Under the same token, optimum tuning can be pre-arranged via specific superlattice geometry selections, while more than one superlattice in tandems seems to open the way for higher efficiencies. To probe further, two part-tandem cells, with a tuned superlattice in each region, should lead to collection efficiency in excess of 45% in the immediate future.

References

[1] M Yamaguchi et al, Super high-efficiency multijunction and concentrator solar cells, Solar Energy Materials & Solar Cells 90 (2006) 3068–3077

[2] AC Varonides, High Efficiency Lattice-Matched Multijunction Solar Cells via Tuned GaAs/Ge Quantum Wells25th European PVSEC, 2010

[3] M Yamaguchi et al, Novel materials for high-efficiency III–V multi-junction solarcells, Solar Energy 82, 173 (2008).

[4] R. King, et al, High Concentration PV Using III-V Solar Cells, 20th European PVSEC, 2005.

[5] Richard R. King, Daniel C. Law, Kenneth M. Edmondson, ChristopherM. Fetzer, Geoffrey S. Kinsey, Hojun Yoon, Dimitri D. Krut, James H. Ermer, Raed A. Sherif, and Nasser H. Karam, Advances in High-Efficiency III-V Multijunction Solar Cells, Hindawi Publishing Corporation, Advances in OptoElectronics, Volume 2007, Article ID 29523

[6] R Jones, J Ermer, P Pien, O Al Taher, R King, Spectrolab Progress in Multi-Junction Cell Performance and Cost, April 28-29, Toledo, Spain

[7] R.S. Miller, T.I. Kamins, Device Electronics for Integrated Circuits, J Wiley & Sons, 2nd Ed, 1986, pp 16-25

[8] C Algora, 2nd CPV Summit, April 28-29, Toledo, Spain.

[9] JF Geisz, S Kurz, MW Wanlass, JS Ward, A Duda, DJ Friedman, JM Olson, WE McMahon, TE Moriarty, and JT Kiehl, 40.8% efficient inverted triple-junction solar cell with two independently metamorphic junctions, Applied Phys. Letters 91, 023502 (2007).

[10] AC Varonides and RA Spalletta, Hopping currents in the intrinsic region of III-N-V quantum well structures in the tight binding approximation, Physica Stat. Sol. 5, No. 2 441 (2008)

[11] AC Varonides, Tunneling vs. Thermionic Currents in Multi-Quantum Well Photovoltaic, Structures, Physics E 14, 142 (2002)

[12] E. Lorenzo, Solar Electricity, Engineering of Photovoltaic Systems, Protomora General de Estudios, SA, 1994, Sevilla, Spain, p. 77

Simulations of Implantation Temperature Impact on Three-dimensional Texturing in Silicon Solar Cells

F.Jahanshah[1,*], K. Sopian[2], S. H. Zaidi[3], E.Gholipour[1]

[1] *Isfahan High Educations and Research Institute, I.R. Iran*
[2] *Solar Energy Research Institute, Universiti Kebangsaan Malaysia, Malaysia*
[3] *Gratings, Incorporated, USA*

** Corresponding author. Tel: +98 3114436396, Fax: +98 3113802061, E-mail: f.jahanshah@ieht.ac.ir*

Abstract: Recently new advance texturing is one of the candidates for enchaining optical absorption in mono crystalline thin film solar cells and making low cost solar cell. Silicon has relatively large reflection in UV-visible spectral region, also absorbs strongly in this region; however, its near IR absorption is weak. The absorption enhancement can occur through diffractive scattering from surface with feature dimension larger than λ/n, where n is silicon refractive index. For surface feature with size smaller than λ/n, surface is behaving like a gradient index film. By creating three-dimensional surface with sub wavelength textures on front and sidewalls, it may be possible to enhance absorption beyond the $4n^2$ statistical limit. There is an idea that says implantation process during fabrication process affect solar cell efficiency because of p-n junction dependence to temperature. This maybe complicated the efficiency prediction. Since Because of difficulty of laboratory test and fabrication the simulation of implantation temperature method is considered for a well know three dimensional texturing at first. Simulations in first step are done for an ideal three dimensional surface texturing with 21μm depth and an ideal p-n junction below 1μm under frontal surface. In this simulation the p-n junction has a constant depth all over the solar cell. Then by using implantation modeling tries to predict the p-n junction place by varying the temperature all over the surface. It is shown that the p-n junction position and its shape completely depend on the temperature that causes a variety of efficiency for a well known advanced texture. In this case the p-n junction shows a discontinuity at 700 ºC that case an efficiency drop for 21% to 10%. These simulations confirm the impact of implantation temperature on optical simulation. Results are shown to find out the best design for advance three-dimensional texturing need to predict discontinuity temperature in fabrication process. Simulations also show the dependence of efficiency with geometrical surface features and how discontinuity temperature change by shape and size of the periodic texture pattern. Results show there is a limitation in final performance of mono-crystalline solar cell with periodic texture pattern.

Keywords: *Renewable energy, solar cells, thin film, surface texturing.*

Nomenclature

d	*grating period* ..... *μm*	$\theta_{m,i}$	*diffraction order angle* .....
n	*refractive index*	Φ	*ion dose per square centimeter* ..... cm^{-2}
λ	*wavelength* ..... *nm*	$\eta_{i,j}$	*coupling efficiency* .....
θ_c	*critical angle*	Rp	*projected range* ..... *cm*

1. Introduction

Silicon has relatively high reflectance in UV-Visible spectral region, however it also absorbs strongly in this region [1] . In near IR (800-1100 nm) spectral region, particularly near the band edge, absorption is weak, i.e., absorption depth is ~ 100 μm at λ ~ 1 μm. This weak absorption fundamentally limits the efficiency of Si solar cells: in thin films due to incomplete optical absorption, and in thick films due to bulk recombination losses. Light trapping schemes based on geometrical optics considerations have been extensively investigated in conventional [2] . Maskless, random, pyramidal texturing with feature sizes >> λ on the front surface not only helps randomize scattering within the substrate, but also takes advantage of

the high refractive index of Si leading to total internal reflection of light rays outside the narrow cone defined by the critical angle ($\theta_c=\sin^{-1}(1/n)$).

In reducing reflection using sub-wavelength structures, defined either by lithography or random masking methods, light incident on the Si substrates generates no diffraction orders, and preferably only obliquely propagating orders inside the Si substrate [3-5]. For lithographically-defined surface, the period is chosen such that there are no diffraction orders in air, i.e., $\lambda/d > 1$. Inside the semiconductor, first and second diffraction orders are propagating due to its higher refractive index n, i.e., $2^* \lambda/(n^*d) < 1$. For the case of a randomly textured surface, incident light will support a large number of diffraction orders since it is a composite of several periodic structures[6]. The total optical path length neglecting back surface reflection for sake of simplicity is give by

$$optical - path - length = \sum_{i,j} \eta_{i,j} T_{i,j},$$

where the summation index i corresponds to grating period d_i of the random surface, and the summation index j corresponds to diffraction orders of the period d_i, and $\eta_{i,j}$ represents the coupling efficiency of the transmitted intensity $T_{i,j}$. The optical paths of each of the diffraction order is enhanced by $1/\cos(\theta_{m,i})$, where $\theta_{m,i}$ is the diffraction order angle with surface normal defined earlier. In this manner, frequency space inside the Si substrate can be effectively populated. Finally, for the third case, where features are smaller than the wavelength inside Si, no diffraction orders are propagate inside the Si substrate, which is similar to a gradient-index anti-reflection film, and is not conductive to enhanced solar cell performance.

In case of three-dimensional texturing, the trench sidewalls are also randomly textured with sub-wavelength features as described in Fig. 1.d. In such a case, each transmitted diffraction order on incidence at sidewalls, generates multiple beams, therefore, creating several more light paths than would have existed within textured/planar sheet [7]. Such an approach can potentially exceed $4n^2$ optical enhancement limit predicted by Yablonovitch [8].

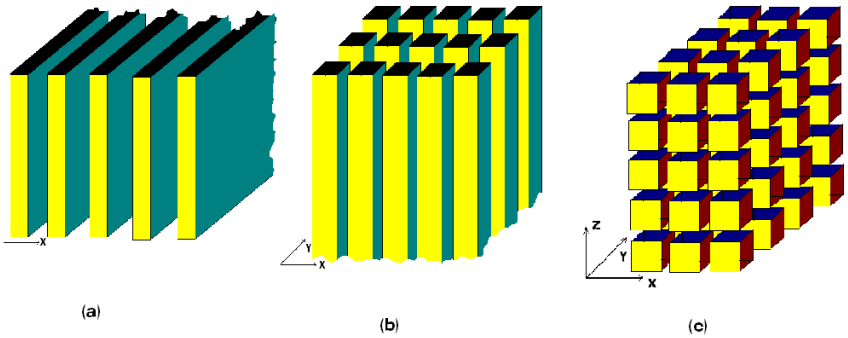

Fig. 1. Grating texture with (a) one dimension repetition (b) two dimension repetition (c) three dimension repetition. One dimension and two dimension use for solar cell application.

2. Mathematical implantation models

2.1. Gaussian Implant Model

There are several ways to construct 1D profile. The simplest way is using the Gaussian

distribution, which is specified by:

$$C(x) = \frac{\phi}{\sqrt{2\pi}\Delta R_{\rho}} \exp \frac{-(x - R_p)^2}{2\Delta R_p^2} \quad (1)$$

where Φ is the ion dose per square centimeter specified by the dose parameter. *Rp* is the projected range. *Rp* is the projected range straggling or standard deviation .

2.2. Pearson Implant Model

Generally, the Gaussian distribution is inadequate because real profiles are asymmetrical in most cases. The simplest and most widely approved method for calculation of asymmetrical ion-implantation profiles is the Pearson distribution.The Pearson function refers to a family of distribution curves that result as a consequence of solving the following differential equation:

$$\frac{df(x)}{dx} = \frac{(x-a)f(x)}{b_0 + b_1 x + b_2 x^2} \quad (2)$$

in which *f(x)* is the frequency function. The constants *a, b0, b1* and *b2* are related to the moments of *f(x)* by:

$$a = -\frac{\Delta R_p \gamma(\beta + 3)}{A} \quad (3)$$

$$b_0 = -\frac{\Delta R_p^2 (4\beta - 3\gamma^2)}{A} \quad (4)$$

$$b_1 = a \quad (5)$$

$$b_2 = -\frac{2\beta - \gamma^2 - 6}{A} \quad (6)$$

where $A = 10\beta - 12\gamma^2 - 18$; γ and β are the skew-ness and kurtosis respectively.

2.3. Dual Pearson Model

To extend the applicability of the analytical approach toward profiles heavily affected by channeling, the dual (or Double) Pearson was suggested Method. With this method, the implant concentration is calculated as a linear combination of two Pearson functions:

$$C(x) = \Phi_1 f_1(x) + \Phi_2 f_2(x) \quad (7)$$

where the dose is represented by each Pearson function *f1,2(x). f1(x)* and *f2(x)* are both normalized, each with its own set of moments. The first Pearson function represents the random scattering part (around the peak of the profile) and the second function represents the channeling tail region. Equation (7) can be restated as:

$$C(x) = \Phi[\Re f_1(x) + (1-\Re) f_2(x)] \qquad (8)$$

where $\Phi = \Phi_1 + \Phi_2$ is the total implantation dose and $\Re = \Phi_1 / \Phi$.

3. Simulation

Changing the period and depth of groove would affect efficiency. The goal is to find the best design with maximum efficiency. In modeling, physically-based process simulation predicts the structures that result from specified process sequences. In a complete simulation usually we need doing three stages; 1- process simulation 2- device simulation and 3- circuit simulation. SILVACO International provides an opto-electronic software product that models the behavior of semiconductor materials, devices, and circuits using finite element techniques. In fact it is "Virtual Wafer Fab" which can determine electrical characteristics of that device based conditions are inputted. There are different models that must take into account based on; drift and diffusion current, position dependent doping, optical carrier generation, and so on. The most important tools for solar cell simulation are ATLAS, ATHENA and Luminous which have been recently used [7]. Fig.2. shows typical solar cell simulations to find implantation impact on texturing effect.

By using etching process in different time it is possible to make rectangular texture in various depths and periods. In this investigation we consider phosphorous atom to implantation on a p-type Si substrate which heat up to 900K. By using Dual Pearson model we find there are some discontinuities in p-n junction which it appears in deep groove. Fig. 3 shows simulation results in some period and depths.

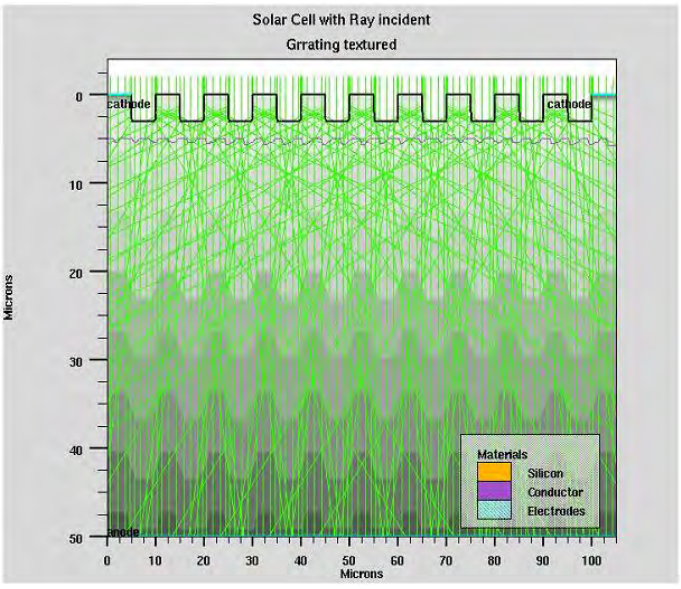

Fig. 2 Simulation of solar cell by using SILVACO software's, 1D grating structure with 10-μm period and 3-μm depth

4. Results

Table (1) and its related graphs (Fig. 4) shows output efficiency for different rectangular 2-D texturing. In all of those cases the temperature and time of doping consider constant with

700K and 30 minute respectively. The data shown in actual fabrication there is another limitation for efficiency boosting by implantation process. It is found out beside optimization of grove depth and period according to optical absorption by using wave optics, p-n junction discontinuity due to fabrication process might be considered as another parameter.

Table 1. Modeling results for solar cell efficiency due to variation in period and depth groove in 3D texturing

Depth (µm)	η(%) period 5 (µm)	η(%) period 10 (µm)	η(%) period 20 (µm)
50	0.76	6.17	9.4
40	1.24	8.21	9.44
30	2.45	9.5	9.47
20	9.5	9.54	9.2
10	9.6	9.56	9.52
5	9.6	9.5	9.53

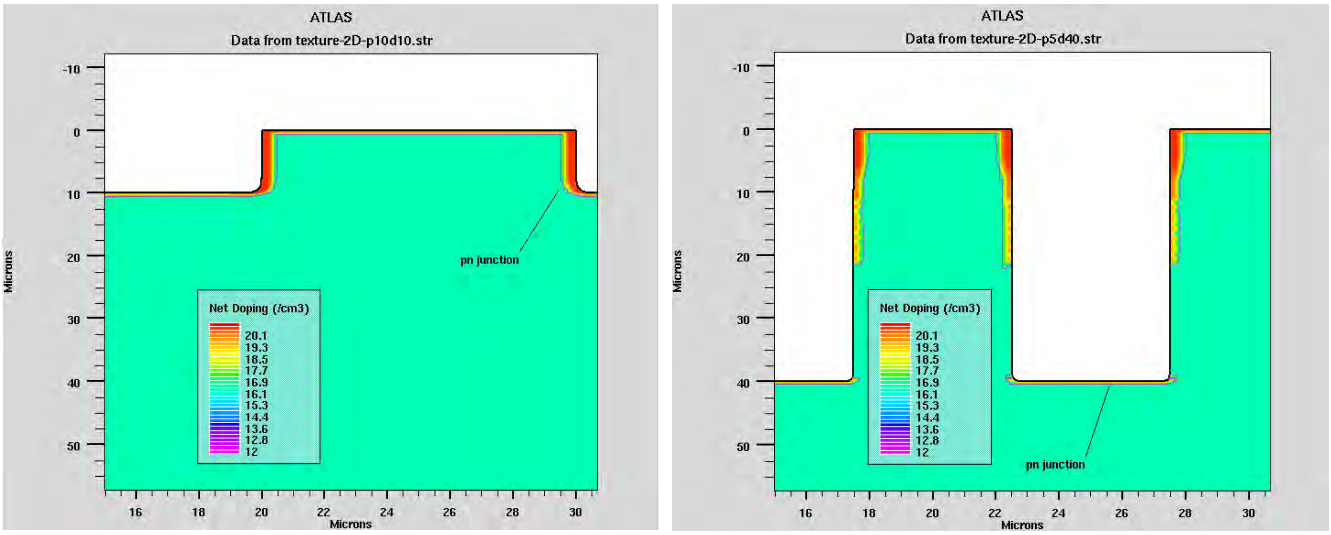

(a) *(b)*

Fig. 3 Simulation of solar cell by using SILVACO software's,(a) 2D grating structure with 20-µm period and 10-µm depth, and (b) 2D grating structure with 20-µm period and 40-µm depth. The discontinuity happened for the last at 20-µm.

5. Conclusion

Although rectangular grating on solar cell increase the efficiency but implantation impact during fabrication could affect on efficiency boosting. P-N junction discontinuing make a lost in thin monocrystalline solar cell. Simulation shows maximum relative efficiency is in the period range of 10-15 micrometer and 10-20 groove depth for phosphorus doping with 900K in 30 minutes. This result helps to design optimum configuration for solar cell texturing. It is shown that the p-n junction position and its shape completely depend on the temperatures that cause a variety of efficiency for a well known advanced texture. In this case the p-n junction shows a discontinuity at 700 ºC that case an efficiency drop for 21% to 10% (figure 4).

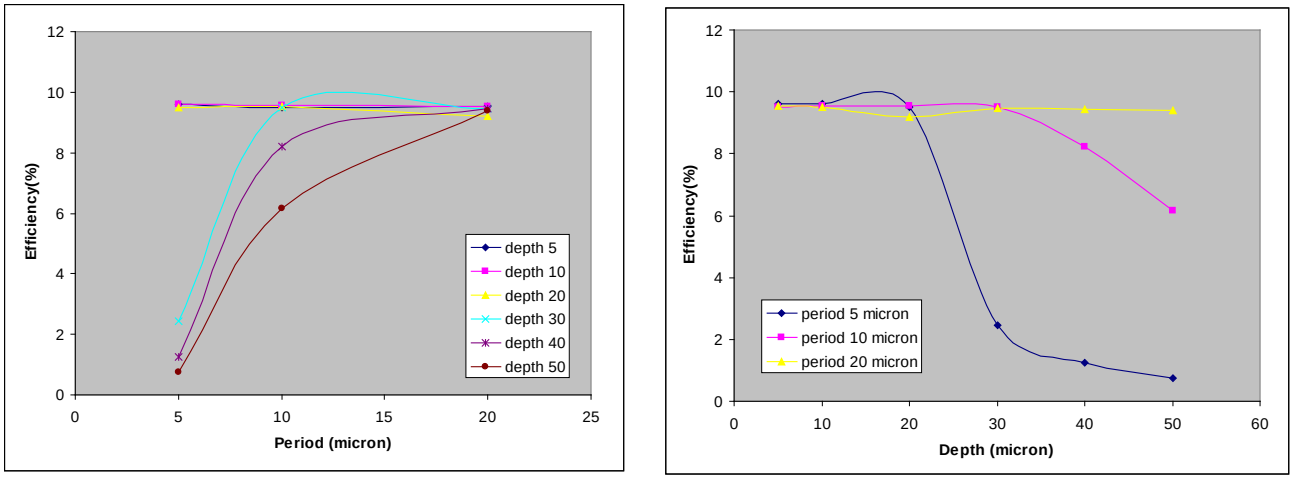

Fig. 4. Implantation period impact on solar cell efficiency. (a) Maximum relative efficiency was happened in 10-15 micrometer period.(b) Maximum relative efficiency was happened in 10-20 micrometer grove depth

Acknowledgment

The authors would like to express their thanks to Prof. I. Ahmad, VLSI Micro-fabrication and packaging of UKM.

References

[1] A. A. Munzer, K T. Holdermann, R. E. Schlosser, and S. Sterk, "Thin Monocrystalline Silicon Solar Cells", *IEEE ,1999*, vol. 46, p. 2055-2061.

[2] T. Tiedje , E. Yablonovitch,G. D. Cody,B. G. Brooks,, "Limiting Efficiency of Silicon Solar Cells," *IEEE,1984*, p. 711-716.

[3] K. Yamamoto, M. Yoshini, T. Suzuki, T. Nakata, T.Swada and K. Hagashi, "Large-Area and High Efficiency a-Si/poly-Si Stacked Solar Cell Submodule,"2000, *28Ih IEEE PVSC*, p. 1428-1432.

[4] K. Yamamoto, "Very Thin Film Crystalline Silicon Solar Cells on Glass Substrate Fabricated at Low Temperature,"1999, *IEEE*, vol. 46, p. 2041.

[5] M. A. Green, and M. J. Keevers, *Photovoltaics: Research and Applications*, vol. 3,1995, p. 189-230.

[6] S. H. Zadi,R. Marquadt,B.Minhas,J.W.Tringe," Deeply Etched Grating Structure For Enhanced Absorption in Thin C-Si Solar Cells",*IEEE* 2002, p1290-1293

[7] F.Jahanshah,K.Sopian,Y.Othman,H.R.Fallah," pn Junction depth impact on short circuit current of solar cell", *Solar Energy*,2009,p.1629-1633.

[8] E. Yablonovtch, G. D. Cody,, "Intensity Enhancement in Textured Optical Sheets for Solar Cells," *IEEE* vol. ED-29,1982, p. 300-305.

Development and new application of single-crystal silicon solar cells

G.S. Khrypunov*, V.R. Kopach, M.V. Kirichenko, R.V. Zaitsev

National Technical University «Kharkiv Polytechnical Institute», 21, Frunze Str., 61002, Kharkiv, Ukraine
Tel: +38-057-731-5691, E-mail: khrip@ukr.net

Abstract: The aim of research was development of the improved designs of high-efficiency single-crystal Si solar cells (Si-SC), intended for work in the conditions of ordinary and high-concentrated sun radiation, and also finding out of possibility to use of such devices as energy independent and enough sensitive sensors in the optical location systems. It was shown that for increase of the efficiency at cost reduction and production manufacturability of single-crystal Si-SC with base crystals (BC) thickness $180 \le t_{BC} \le 200$ μm having a polished light receiving surface (LRS) and back surface reflector (BSR) consisting of a transparent oxide and Al layers, a conductive transparent indium-tin oxide (ITO) layer of $t_{ITO} = 0.25$ μm interference thickness without of perforation is to be used. In case of Si-SC with inverted pyramid type texture of LRS at which the specificity of light distribution in the BC causes essentially total internal reflection of radiation from Si/ITO interface, the t_{ITO} value should be optimized in the 1÷2 μm range independently of t_{BC}. For efficiency increase of vertical multi-junction (VMJ) Si-SC by a factor of 1.2 approximately the modernization of in series connected unit diode structures (UDS) by the introduction along their vertical Si-boundaries single-layer ITO reflectors by thickness more than 1 μm is promising too. Accordingly to results of numerical simulation the character of open circuit voltage U_{OC} dependence on α angle value of light incidence onto LRS of VMJ Si-SC considerable depends on the minority charge carriers lifetime τ value in the BC of VMJ Si-SC, while light reflection coefficient R value for UDS Si/ITO boundaries effects on absolute U_{OC} value. It has been shown that purposeful decrease of τ value and providing of $95 < R < 100$ % should allowed to create the VMJ Si-SC with practically linear and easily registered $U_{OC}(\alpha)$ dependence for use the VMJ Si-SC as energy independent and enough sensitive sensors in the optical location systems.

Keywords: *High-Efficiency, Silicon Solar Cells, ITO Reflectors, New Application*

1. Introduction

Efficiency increasing at cost reduction as well as expansion of single-crystal silicon solar cells (Si-SC) application fields continue to remain the actual research and development tasks. Therefore the research purposes were development of the improved designs of high-efficiency single-crystal Si-SC, intended for work in the conditions of ordinary and high-concentrated sun radiation, and also finding out of possibility to use of such devices as energy independent and enough sensitive sensors in the optical location systems.

2. Results and discussion

2.1. *Single-junction solar cells*

One of the known methods to increase the efficiency of single junction (SJ) Si-SC is creation of back surface reflector (BSR) consisting of perforated SiO_2 and continuous Al films deposited layer-by-layer onto surface of Si base crystal (BC) from the side opposite to SJ Si-SC light receiving surface [1]. Such construction of BSR is used, for example, in most high-efficiency SJ Si-SC with PERL (Passivated Emitter, Rear Locally-diffused) and PERT (Passivated Emitter, Rear Totally-diffused) structures. At the same time the electrical contact of Al layer with Si- BC is realized via numerous through holes in SiO_2 the total area thereof making less than 1 % of the total Si-BC back surface area. Such multipoint contact character results in somewhat increased SJ Si-SC series resistance that compensates in part the efficiency gain attained due to reduction of solar radiation power losses resulting from using the double-layer BSR with dielectric oxide. Therefore, and also from the necessity to decrease the cost of such devices, when manufacturing SJ Si-SC with PERT-structure, it seems to be

reasonable to replace the BSR perforated dielectric oxide layer by a continuous layer of transparent conductive material. Accordingly to the results of this problem analysis, it can be solved by using the transparent indium-tin oxide (ITO) in double-layer BSR structure instead of SiO_2. In this connection, one of the research targets was to determine the most optimum thicknesses $l_{OX}^{opt.max}$ of conducting oxide providing a highest integral reflection coefficient R of solar radiation within the required wavelength λ range and to decrease the series resistance for SJ Si-SC of PERT-types both with smooth and with textured light receiving surfaces. As shown in [2], the required λ range depends on thickness t of Si-BC and at $180 \le t_{BC} \le 200$ μm (typical values of serial SJ Si-SC) is $0.88 \le \lambda \le 1.11$ μm.

In case of SJ Si-SC with smooth light receiving surfaces the $l_{OX}^{opt.max}$ determination method for ITO layer was similar to that used in [2] to find interference thicknesses $l_{OX}^{opt.max}$ for SiO_2/Al BSR and TiO_2/Al BSR oxide layers. Conceptually this method consisted of the following. Accordingly to [3], the optimum thicknesses $l_{OX}^{opt}(\lambda)$ of oxide providing the maximum R values for λ values from the above-mentioned λ range were determined first of all. Further, from the obtained $l_{OX}^{opt}(\lambda)$ dependence, the l_{OX}^{opt} values were selected corresponding to $\lambda_1 = 0.8$ μm, $\lambda_2 = 0.9$ μm, $\lambda_3 = 1.0$ μm and $\lambda_4 = 1.1$ μm, being $l_{OX1}^{opt} = 0.18$ μm, $l_{OX2}^{opt} = 0.21$ μm, $l_{OX3}^{opt} = 0.25$ μm and $l_{OX4}^{opt} = 0.28$ μm, respectively. For these l_{OX}^{opt} values, the dependences $R\left[\lambda, l_{OX}^{opt}(\lambda), n_0\right]$ in the $0.88 \le \lambda \le 1.11$ μm range according to [3] were calculated using appropriate relations in cases when light receiving surface of SJ Si-SC is protected by glass ($n_0 = 1.5$) and when it is not protected ($n_0 = 1.0$). The analysis of all the $R\left[\lambda, l_{OX}^{opt}(\lambda), n_0\right]$ dependences set shows that optimal oxide thickness $l_{OX}^{opt.max}$ providing the maximum integral reflectivity of ITO/Al BSR in the specified λ range is 0.25 μm at both n_0 values. Dependences $R(\lambda, n_0)$ for $l_{OX}^{opt.max} = 0.25$ μm are presented in Fig. 1.

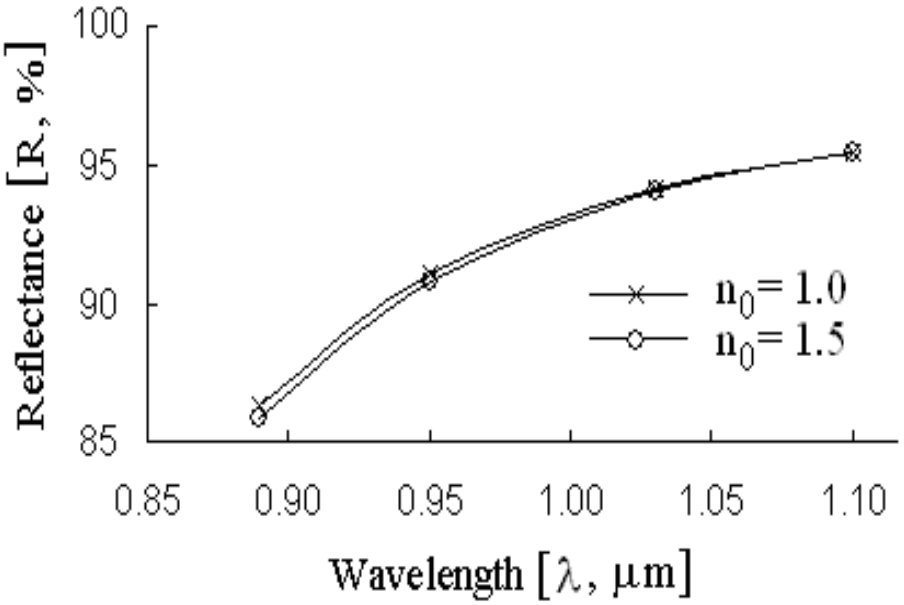

Figure 1: Dependences of R on λ and on n_0 for ITO/Al back surface reflector with $l_{OX}^{opt.max} = 0.25$ μm

In case of textured light receiving surface with the pyramids faceted by (111) type planes, the optimal oxide thickness for ITO/Al BSR is not so critical. This is due to the specificity of light ray trajectory inside Si-BC shown in Fig. 2 according to [4].

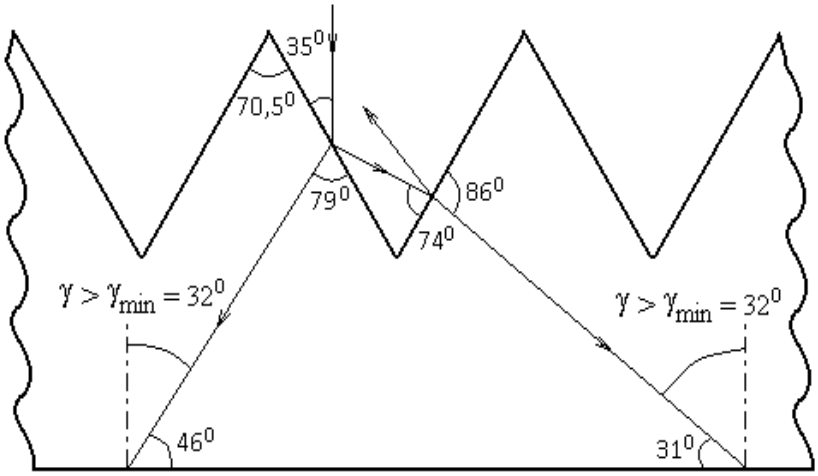

Figure 2: Light rays trajectory inside the Si-BC of the SJ Si-SC with textured frontal surface and smooth back surface

The angles γ of light incidence on a smooth back surface of such SJ Si-SC exceed 40°. It is a more than limit angle γ_{min} of light complete internal reflection from the Si/ITO interface because $\gamma_{\min} = \arcsin\left(n_{ITO}/n_{Si}\right) \approx 32^{o}$ [5], where $n_{ITO} \approx 1.9$ [6] and $n_{Si} \approx 3.6$ [7] are refractive indexes of ITO and of Si correspondingly at $0.88 \le \lambda \le 1.11$ μm. Thus, the above mentioned texture on the light receiving surface makes it possible to use a quite other approach to $l_{OX}^{opt.max}$ determination based on the account for light total reflection from the Si/ITO interface. In this case, to suppress the possible partial radiation power losses in the metal [8] being in contact with ITO and also to minimize the series resistance for SJ Si-SC the ITO layer thickness should be experimentally optimized in the $1 < l_{OX}^{opt.max} < 2$ μm range.

2.2. *Vertical multi-junction solar cells*

Use Si-SC of the special construction in the conditions of high concentrated radiation is perspective direction for the increase of efficiency and cost decreasing of solar energy photovoltaic conversion [9]. Such Si-SC include, in particular [10], vertical multi-junction (VMJ) Si-SC consisting of a monolithic set (more than 10) of single-crystal silicon plane-parallel vertical unit diode structures (UDS) with p-n junctions oriented perpendicular to the light receiving surface and connected in series by the metal interlayers between the appropriate planes of adjacent UDS. Let's notice, that at the unitary light reflection coefficient R = 0,89 in case of double light reflection the effective reflection coefficient $R_{EFF} \approx R^2 \approx 0.79$ and it corresponds to losses more than 20 % of solar radiation energy on absorption. From this follows, that elimination of such losses would allow increasing the efficiency of considered type VMJ Si-SC approximately at 1.2 times.

The analysis, carried out by us, indicate a capability of such efficiency increase for VMJ Si-SC with UDS at the expense of maximum approximation to 1 the reflection coefficient of solar radiation with $0.95 < \lambda < 1.11$ μm by vertical boundaries of these cells inside VMJ Si-SC. However, on reasons, to analogical indicated before, highly reflecting SiO_2/Al and TiO_2/Al double-layer reflectors with calculated in [2] optimum thickness of SiO_2 and TiO_2 dielectric layers, contacting with a silicon crystal, concerning to considered type VMJ Si-SC

are unacceptable. The above mentioned multipoint character of SC back electrode with a SI-BC contact leads to certain increase of SJ Si-SC series resistance, what partially compensates a benefits in efficiency achieved at the expense of solar radiation energy losses decrease at use of dielectric oxide/metal two-layer reflector. It is natural, that in case of VMJ Si-SC the multidot contact influence effect on the device series resistance should grow in direct proportion to amount of UDS in-series, and therefore reflectors from side of UDS vertical borders should provide a good electrical contact between the next UDS on all area of the mentioned borders.

For efficiency increase of the VMJ Si-SC the modernization of in series connected UDS by the introduction along their vertical Si-boundaries single-layer ITO reflectors by thickness more than 1 μm is promising too. The VMJ Si-SC of new design is shown schematically in Fig. 3. The new VMJ Si-SC design gives possibility to exclude the photoactive radiation losses depended on partial light absorption by metal interlayers between UDS in case of VMJ Si-SC using for photovoltaic conversion of high concentrated solar radiation the main part of which always incidence onto VMJ Si-SC light receiving surface at the angles $0 < \alpha < 90^o$. Thus taking into account that the highest angle of refraction $\beta_{max} = arcsin(1/n_{Si})$ [5] it is easy obtain $0 \le \beta \le 16.1^o$, that for $0.88 \le \lambda \le 1.11$ μm gives $73.9 \le \gamma \le 90^o$, and consequently $\gamma > \gamma_{min} \approx 32^o$ at $0 < \alpha < 90^o$.

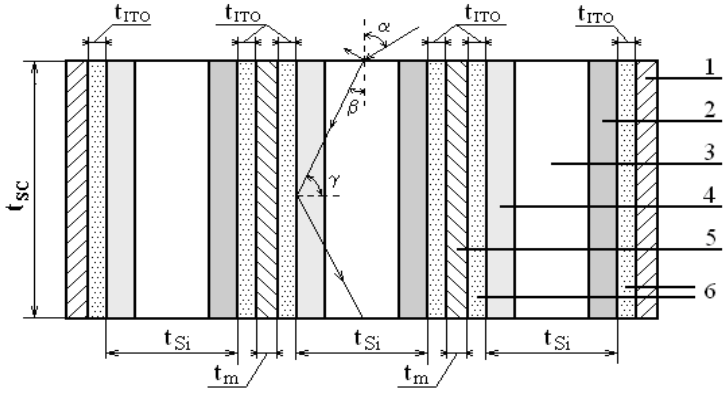

Figure 3: Cross-section of new VMJ Si-SC of $t_{SC} \approx 850$ μm thickness with ITO reflectors belonging to UDS of n^+-p-p^+ type (schematic image): 1 – metal electrode; 2 – p^+-Si layer of less than 1 μm thickness; 3 – p-Si layer of $t_{Si} \approx 160$ μm thickness; 4 – n^+-Si layer of less than 1 μm thickness; 5 - metal interlayer of $t_m \approx 10$ μm thickness; 6 – ITO reflectors of $1 < t_{ITO} < 2$ μm thickness

Therefore, at all actual values of light incidence angle α on the VMJ Si-SC external surface, hitting inside the UDS of such Si-SC, light with $0.9 \le \lambda \le 1.1$ μm should experience practically full internal reflection from considered reflectors that should essential approach the optical reflection coefficient from ITO/Si boundaries to unity. Obviously, that this effect will be result in to previously stated increase of VMJ Si-SC efficiency approximately in 1.2 times. Since according to [8] effect of full internal reflection is caused by wave processes in ITO layer by thickness no more wavelength of light, it, on the one hand, for suppression of radiation energy losses, which can be connected to penetration of radiation energy part into metal, contacting with ITO, and on the other hand, with the purpose of ITO layer resistance minimization to the current carrying through it, the thickness t_{ITO} of this layer should be experimentally optimized in the range of values 1 μm < t_{ITO} < 2 μm.

Besides as is known [6], the modern methods of ITO films with submicron and micron thicknesses deposition, inclusive of pulverization with following pyrolyze, allow to realize the

appropriate process at temperatures below 450 ^{o}C. It is well agree with the concept of single-crystal silicon SC manufacturing technology, according to which the most of high-temperature technological process operation should be the operation of submicron and highly-doped n^{+}-Si and p^{+}-Si layers manufacturing realized, as a rule, at 900÷1000 ^{o}C.

Accordingly to results of numerical simulation the character of open circuit voltage U_{OC} dependence upon α value considerable depends on t he minority charge carriers lifetime τ value in the VMJ Si-SC base crystals, while R value for vertical UDS Si/ITO boundaries effects on a bsolute U_{OC} value. It has been shown that purposeful decrease of τ value and providing of 95 < R < 100 % should allowed to create the VMJ Si-SC with practically linear and easily registered $U_{OC}(\alpha)$ dependence for use the VMJ Si-SC as energy independent and enough sensitive sensors in the optical location systems. The numerical dependence $U_{OC}^{norm}\left(\alpha, R, \Delta\xi\right)$, got as the result of indicated simulation using early resulted in [11] relation

$$U_{OC}^{norm}\left(\alpha, R, \Delta\xi\right) = \frac{U_{OC}\left(\alpha, R, \Delta\xi\right)}{U_{OC}\left(\alpha = 0, R, \Delta\xi\right)} = 1 + \frac{\ln\left[f\left(\alpha, R\right)\cos\alpha\right]}{2.3\left(\xi_2 - \xi_1\right)} \qquad (1)$$

where

$$f\left(\alpha, R\right) = R\frac{t_{Si}}{t_{SC}}\sqrt{\frac{n_{Si}^2 - 1 + \cos^2\alpha}{1 - \cos^2\alpha}} + R^2\left(1 - \frac{t_{Si}}{t_{SC}}\sqrt{\frac{n_{Si}^2 - 1 + \cos^2\alpha}{1 - \cos^2\alpha}}\right) \qquad (2)$$

and $\xi_1 < \xi_2$ are absolute values of indexes in degrees of short circuit current J_{SC} and diode saturation current J_0 densities accordingly, is presented in Fig. 4.

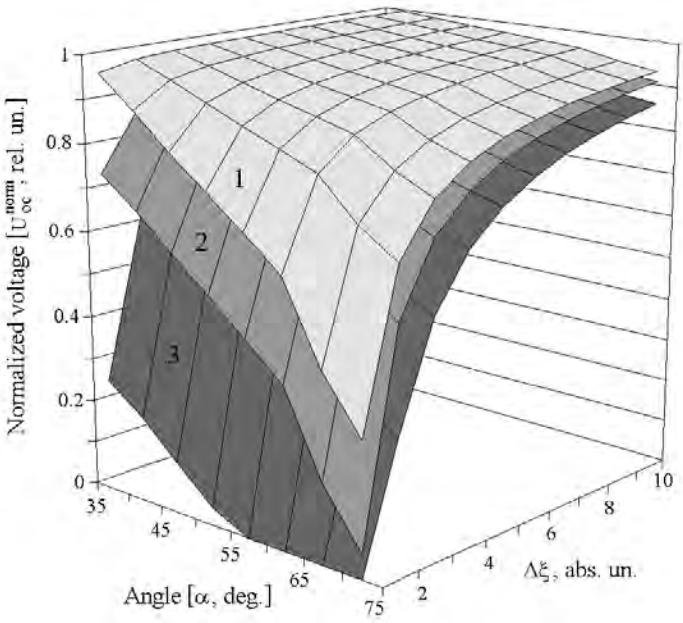

Figure 4: Dependence U_{OC}^{norm} values versus α and $\Delta\xi$ for considered VMJ Si-SC at the light reflection coefficients from vertical UDS boundaries: 1 - R = 100 %, 2 – R = 60 %, 3 - R = 20 %

It is well known [4] that values of J_{SC} and J_0, and consequently $\Delta\xi$, substantially depends from τ value in SC base crystals. Therefore at the use VMJ Si-SC as sensors the required

value of $\Delta\xi$ possibly to attain by a purposeful decrease of τ value in Si-BC. In accordance to numerical simulation results for using VMJ Si-SC as sensors in the optical location systems the optimal combination of parameters influencing on $U_{OC}(\alpha)$ dependence are $1 \le \Delta\xi \le 2$ and $95 < R < 100$ %.

3. Conclusions

It was shown that for increase of the efficiency at cost reduction and production manufacturability of single-crystal Si-SC with base crystals thickness $180 \le t_{BC} \le 200$ μm having a polished light receiving surface and back surface reflector consisting of a transparent oxide and Al layers, a conductive transparent ITO layer of t_{ITO} = 0.25 μm interference thickness without of perforation is to be used. In case of Si-SC with inverted pyramid type texture of light receiving surface at which the specificity of light distribution in the base crystals causes essentially total internal reflection of radiation from Si/ITO interface, the t_{ITO} value should be optimized in the 1÷2 μm range independently of t_{BC}. For efficiency increase of vertical multi-junction Si-SC by a factor of 1.2 approximately the modernization of in series connected unit diode structures by the introduction along their vertical Si-boundaries single-layer ITO reflectors by thickness more than 1 μm is promising too. Accordingly to results of numerical simulation the character of open circuit voltage U_{OC} dependence on α angle value of light incidence onto light receiving surface of vertical multi-junction Si-SC considerable depends on the minority charge carriers lifetime τ value in the base crystals of vertical multi-junction Si-SC, while light reflection coefficient R value for unit diode structures Si/ITO boundaries effects on absolute U_{OC} value. It has been shown that purposeful decrease of τ value and providing of $95 < R < 100$ % should allowed to create the vertical multi-junction Si-SC with practically linear and easily registered $U_{OC}(\alpha)$ dependence for use the vertical multi-junction Si-SC as energy independent and enough sensitive sensors in the optical location systems.

Acknowledgment

The work was supported by STCU under Project 4301.

References

[1] M.A. Green, J. Zhao, A. Wang and S.R. Wenham, “Progress and outlook for high-efficiency crystalline silicon solar cells”, Solar Energy Materials and Solar Cells, 65, 2001, pp. 9-16.

[2] V.R. Kopach, M.V. Kirichenko, S.V. Shramko, R.V. Zaitsev, I.T. Tymchuk, V.A. Antonova, A.M. Listratenko, “Back surface reflector optimization for thin single crystalline silicon solar cells”, Functional Materials, 14, 2007, pp. 555-561.

[3] M.M. Koltun, “Selective optical surfaces of solar energy converters”, Nauka, Moscow, 1979 (in Russian).

[4] A.L. Fahrenbruch, R.H. Bube, “Fundamentals of solar cells. Photovoltaic solar energy conversion”, Academic Press, New York, 1983.

[5] G. S. Landsberg, “Optics”, Nauka, Moscow, 1976 (in Russian).

[6] D.E. Morton, A. Dinca, “Ion-assisted deposition of E-gun evaporated ITO films at low substrate temperatures”, http://www.dentonvacuum.com/n-paper.

[7] H.R. Philipp, E.A. Taft, "Optical constants of silicon in the region 1 to 10 eV", Phys. Rev., 120, 1960, pp. 37-38.

[8] V.A. Kizel, "Light refraction" (Series "Physics and technology of spectral analysis"), Nauka, Moscow, 1973 (in Russian).

[9] P.J. Verlinden, "High–efficiency concentrator silicon solar cells", in: "Practical Handbook of Photovoltaics: Fundamentals and Applications", edited by T. Markvart and L. Castaner, Elsevier Science Ltd., Kidlington, Oxford, 2003 pp. 436–455.

[10] B.L. Sater, N.D. Sater, "High voltage silicon VMJ solar cells for up to 1000 suns intensities", Proceedings of the 29th IEEE Photovoltaic Specialists Conference, New Orleans , USA, 2002 pp. 1019–1022.

[11] V.R. Kopach, M.V. Kirichenko, S.V. Shramko, R.V. Zaitsev, S.A. Bondarenko, "New approach to the efficiency increase problem for multi-junction silicon photovoltaic converters with vertical diode cells", Functional Materials, 15, 2008 pp. 253-258.

Improvement of solar cells efficiency and radiation stability by deposition of diamond-like carbon films

Nickolai I. Klyui[1*], Anatoliy N. Lukyanov[1], Anatoliy V. Makarov[1], Volodymyr B. Lozinskii[1], Gennadiy S. Khrypunov[2], Andriy N. Klyui[3]

[1] *V. Lashkarev Institute of Semiconductor Physics National Academy of Sciences of Ukraine, Kiev, Ukraine*
[2] *National Technical University "Kharkiv Polytechnic Institute", Kharkiv, Ukraine*
[3] *Taras Shevchenko Kyiv National University, Kiev, Kiev, Ukraine*
** Corresponding author. Tel: +38044 5256202, Fax: +38044 5256202, E-mail:klyui@isp.kiev.ua*

Abstract: Diamond-like carbon films (DLC) deposited by PE-CVD technique were used as antireflection and protective coatings for Si and $A^{II}B^{VI}$ based solar cells (SC). Application of the DLC films as single- or double-layer antireflection coatings allows us to improve the Si-based solar cells efficiency up to 1.4-1.5 times (from ~10% to ~15%). It has been shown that optical bandgaps of DLC films were increased after UV irradiation. The films with greater amount of nitrogen show better irradiation resistance. It was also established that Si (both mono- and multicrystalline) and $A^{II}B^{VI}$ based SCs with even thin antireflection DLC film demonstrate higher stability against action of gamma-irradiation up to dose of 10^8 rad. The effect is connected with hydrogen atoms those are released from the film as a result of broken of carbon-hydrogen bonds by γ- or UV-quanta, diffuse to the SC, and passivate dangling bonds in the SC volume. It has been also shown that due to application of the DLC antireflection films with low refractive index the transparency of front ITO or ZnO (Al) contacts in $A^{II}B^{VI}$ based SCs may be substantially improved integrally to 10% in spectral range of 430-850 nm. As a result, short circuit current and efficiency of thin film SCs may be also improved.

Keywords: *Solar Cells, Antireflection Coatings, Radiation Stability*

1. Introduction

At present diamond-like carbon (DLC) films are rather widely used as very promising antireflection (AR) and protective coatings for silicon solar cells (SCs) [1-3]. The main advantages of DLC films are high hardness, chemical and radiation stability, and the possibility to change their optical properties under the variation of deposition conditions. The last one allows formation of multi-layer antireflection and protective coatings for SCs just during the same technological process. Thus, it enables to avoid deposition of different antireflection layers, such as, for example, SiO2, Si3N4, SiN:H, ZnO, ZnS, MgF2 etc. As a result the technological procedure of antireflection layers formation becomes simpler and cheaper. Moreover, it was also shown that hydrogen containing DLC films may be successfully used as protective coatings for SCs against action of radiation. The improvement of radiation resistance of the SCs is still of great importance. One of the factors for space SC efficiency degradation is the action of proton and electron irradiation of "solar wind". It leads to reduction in carrier concentration of the base region and decreasing the minority carrier lifetime. One more part of "solar wind" is γ-irradiation. It is less dangerous but more penetrating than proton and electron particles. So, space SCs should have resistivity to penetrating irradiation like γ-quanta. So, the protective coatings must protect from radiation, improve the SC's optical properties and be radiation stable themselves. To achieve simultaneously the aim of protection, passivation and antireflection the diamond-like carbon thin films may be used both for space and terrestrial SCs.

In this paper antireflection and protective properties of the DLC films and their applications for improvement of SC efficiency and radiation stability were investigated.

2. Methodology

The a-C:H:N films were deposited by the plasma-enhanced chemical vapor deposition method from the plasma of the RF discharge (13.56 MHz) at various RF discharge powers (100-250 Wt) and nitrogen contents in the gas mixture (10-45%). The gas mixture CH_4:N_2:H_2 was used, and the nitrogen content in it was varied by the gradual replacement of hydrogen by nitrogen. The gas pressure in a chamber was varied within the limits of 25–105 Pa. The film deposition was carried out onto substrates maintained at room temperature. The deposition time was 15 min.

The thicknesses of DLC films were measured with a Dektak profilometer (the instrumental error was ±5 nm) and an LEF-3G laser ellipsometer (λ=632.8 nm). The film topography was studied making use of a Digital Instruments scanning atomic force microscope (AFM) Nanoscope IV. Optical constants of the films were measured by using spectral ellipsometer. Measurements of the DLC film's transmission were conducted on the Fourier spectrometer firm "Perkin Elmer" Spectrum BX-II in the range (400 ÷ 2000) cm^{-1}. The transmission spectra of the films deposited onto glass substrates were measured by an S2000 spectrometer (Ocean Optics, USA) in the range 300— 800 nm.

Solar cell samples were fabricated on single- or multi-crystallite p-silicon, according to the technological routine which included diffusion of the doping impurity (phosphorus) from a $POCl_3$ source, formation of the front contacts by the screen printing method (multi-Si) or the photolithography method (mono-Si), formation of the Al back contacts. Some of the fabricated specimens of solar cells were irradiated by γ-quanta from a Co^{60} source to the exposure doses of 10^5, 10^6, 5×10^6, 10^7, 5×10^7, and 10^8 rad. The SCs with and without thick DLC films were subjected to proton implantation (E=50-150 keV, D=1.10^{14} – 1.10^{16} cm^{-2}). The proton depth distribution was calculated by Monte-Carlo simulation using TRIM-98 program. Some of DLC films and DLC – Si SCs structures were subjected to ultraviolet (UV) and focused UV (by 350 times) irradiation using light of Hg-lamp during 2 hours.

The solar cell samples were used to study the spectral dependences of the short circuit photocurrent and the light current-voltage load characteristics (LCVLCs). For this purpose, a special original certified setup was used [4]. The LCVLCs were used to determine the density of the short circuit current J_{sc}, the open-circuit voltage V_{oc}, the fill factor FF of the current-voltage characteristic, and the SC efficiency η. The spectral dependences were measured in the wavelength range 400-1200 nm. The spectral characteristics that had been obtained were used to determine the effective diffusion length L of minority charge carriers in the base region of SCs.

3. Results and Discussion

3.1. Application of DLC films as antireflection coatings for silicon solar cells

It is well-known that for optimal antireflection effect when single-layer antireflection coating is used refractive index of an antireflection coating must meet completely the equation

$$n_{film} = (n_{substrate})^{1/2} \qquad (1)$$

where n_{film} and $n_{\text{substrate}}$ are refractive indexes for substrate and antireflection film, respectively.

Refractive index of Si in spectral range where Si-SCs are photosensitive changes from 3.7 to

5.5. It means that for Si-based SCs the n value must be ~1.92-2.3, and on the average must be close to 2.0. As we can see from Fig. 1 so-called "hard" film satisfied this conditions very good in rather wide spectral range.

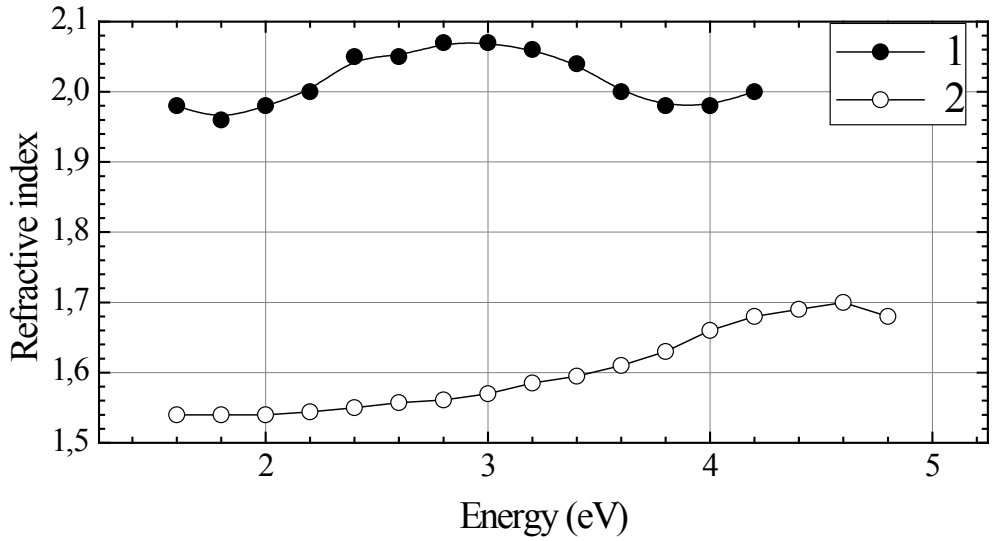

Fig. 1. Spectra of refractive index n(E) of "hard"(1) and "soft" (2) DLC films. Nitrogen content in gas mixture is 1 – 0 %, 2 – 45%.

Indeed, as its seen from Table 1, after deposition of single layer (SL) or double layer (DL) DLC films significant increasing of the SC efficiency (up to 1.5 times) is observed due to not only simple antireflection effect (short circuit current density J_{sc} increasing) but due to passivation of recombination active centers by hydrogen (fill factor FF and open circuit voltage V_{oc} increasing) as well [2]. It was also established that the FF and V_{oc} improvement effect is more pronounced for low quality SCs with high concentration of recombination active centers. On the whole, hydrogenation is very effective method for modification of defect recombination activity in Si, especially in multicrystalline-Si where high concentration of defects at grain boundaries exist. It should be noted that hard and stable DLC films also acts as a barrier against hydrogen diffusion from the SCs.

The SCs parameters were measured under AM 1.5 spectral conditions.

Table 1. Parameters of SCs with and without DLC antireflection coatings.

Sample number	I_{sc} (mA)	J_{sc} (mA/cm^2)	V_{oc} (V)	Fill factor	Efficiency (%)
Initial 1	59.5±0.93	25.54±0.40	0.598±0.001	0.722±0.001	11.03±0.51
Initial 1 covered by SL-DLC* coating	80.3±0.93	34.4±0.40	0.607±0.001	0.754±0.001	15.74±0.62
Initial 2	66.4±0.25	24.3±0.11	0.600±0.001	0.677±0.001	9.88±0.43
Initial 2 covered by DL-DLC* coating	91.4±0.93	34.3±0.40	0.613±0.001	0.707±0.001	14.87±0.53

**The refractive index and thickness for the coatings 1 and 2 are: 2.03, 71 nm ; 2.03/1.6, 71/108 nm, respectively. The films parameters were measured by laser ellipsometer at λ=632.8 nm.*

On the other hand, in case that the DLC films are used as antireflection coatings for materials with rather low refractive index value the films with as low as possible n_{film} value must be

deposited. We can satisfied this requirement by changing the DLC film deposition conditions. For example, we can decrease the rf discharge power, increase the gas pressure in plasma reactor during film deposition and add nitrogen and oxygen to gas mixture [5]. As a result, the film with rather low n_{film} value in wide spectral range may be obtained (so-called "soft" film) (Fig. 1).

It should be also noted that deposition rate of the DLC film may be rather high. For example, the SL-DLC film with refractive index ~2.0 and thickness of 71 nm may be deposited at 200 Wt discharge power during 3.5 minutes (Fig. 2). The deposition rate depends on rf discharge power and nitrogen content in gas mixture (Fig. 2).

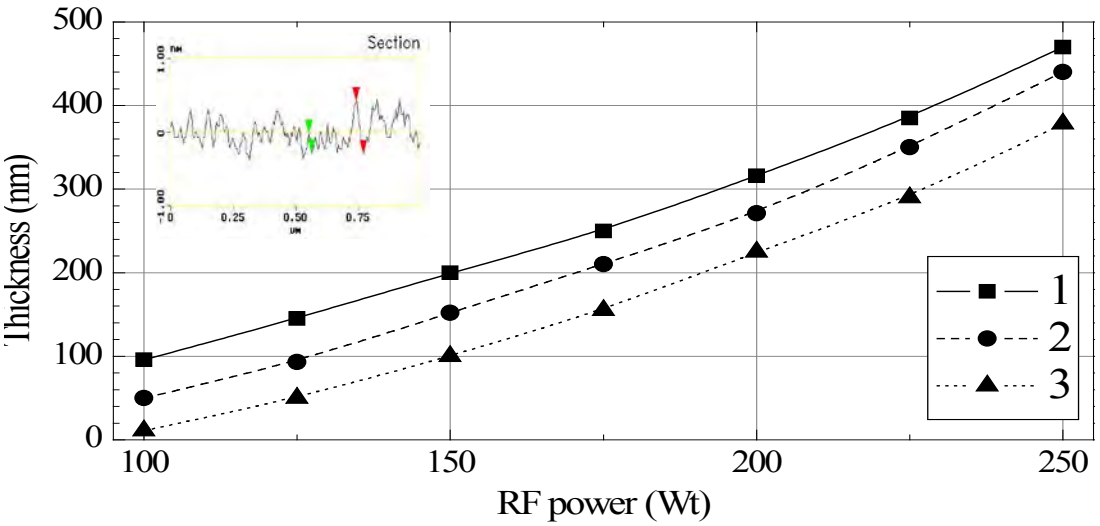

Fig. 2. Dependencies of the DLC (a-C:H:N) film thickness on RF power discharge. Deposition time is 15 minutes and nitrogen content in gas mixture is equal: 1 –20%; 2 – 30%; 3 –45%. Inset shows roughness of the DLC films measured by AFM.

Investigations of the DLC film surface by atomic force microscope show that the films have high surface homogeneity with the average roughness less than 0.65 nm (see insert to Fig. 2).

3.2. Application of thick DLC films as protective coatings

For application of DLC films as protective coatings for SCs of space application as thick as possible films should be deposited to prevent degradation of SCs under action of so-called "solar wind". The films must possess proper optical properties, namely high transparency to decrease absorption losses in the film. It was earlier shown that nitrogen containing DLC films have low level of internal mechanical strains [6]. It allows us to deposit rather thick films. We studied SC-DLC film structures with the film thickness of 1300 nm. Test SC without any protective film was also studied.

The SCs were subjected to implantation of protons of different energies (50-150 keV) and doses (10^{14} – 10^{16} cm^{-2}). Fig. 3 shows dose dependencies of efficiency (η) for the test SC and the SCs covered by DLC (a-C:H:N) protective film. In order to calculate depth distribution we used Monte-Carlo simulation (TRIM-98 program). It was established that for ion energies 50 and 100 keV protons do not penetrate into Si SC and stopped in DLC films (Fig. 3). As we can see from Fig. 4 in this case decreasing of efficiency for the irradiated SCs is not observed up to high implantation dose (10^{16} cm^{-2}). And only in case that proton energy is 150 keV marked decreasing of the SC efficiency takes place at doses higher than 10^{15} cm^{-2}. The degradation of the SC efficiency is caused by penetration of proton into the SC volume,

generation of defects and reduction minority carrier lifetime in the SC [3]. The conclusion is confirmed by calculations and in this case proton mean projective range is close to DLC film – Si SC interface (Fig. 3).At the same time, unprotected SC become dramatically degraded at this dose and proton energy of 100 keV (Fig. 3).

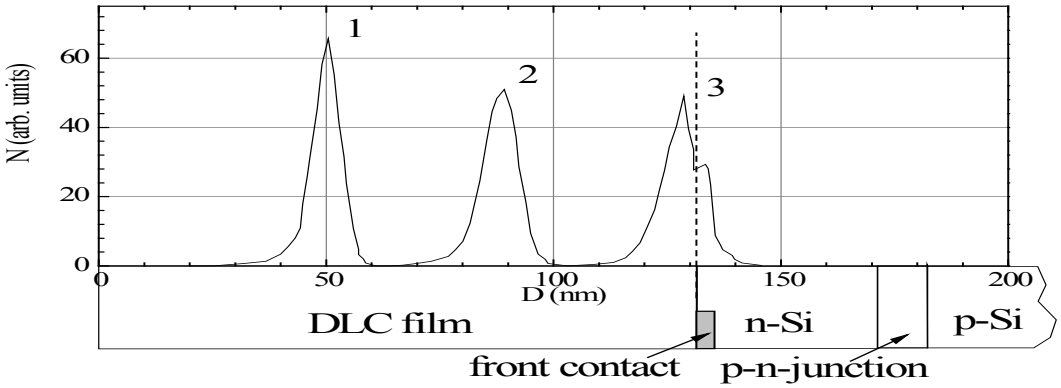

Fig. 3. Proton depth distribution of different energy in DLC film/Si-solar cell structure: 1 – 50 keV; 2 – 100 – kEv; 3 – 150 keV.

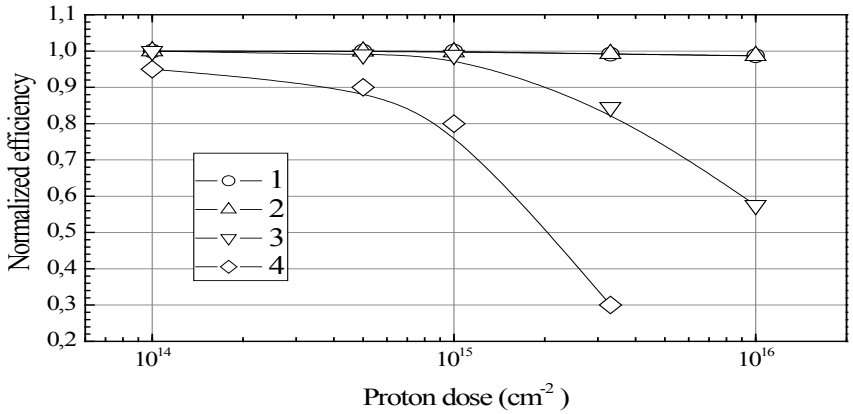

Fig. 4. Dependencies of normalized efficiency of solar cells from proton doses of different energy: 1 – 50 keV; 2 – 100 – kEv; 3 – 150 keV; 4 – 100 keV, solar cell without DLC coating.

3.3. Application of thin DLC films as protective coatings

Figs 5 and 6 present results of investigations of Si SCs subjected to γ-irradiation. It is seen from Fig. 4, that radiation resistance of the SCs covered by DLC films (curves 2, 4 in Fig. 5) is higher compared to unprotected SCs (curves 1, 2 in Fig. 5).

It should be pointed out that in this case we used thin (71 nm) DLC antireflection coatings. The statistical significance of the variation in Fig. 5 did not exceed ±0.01. Thus, for majority of points it is substantially lower than observed changes in normalized efficiency values. It should be noted that no marked changes of results presented in figs 5, 6 were observed in one year after γ-irradiation of the samples. So, the degradation stability of the SCs covered by DLC films is higher than that without any coatings. The effect is observed both for SCs produced from mono-crystalline silicon and from multi-crystallite one. We proposed the following mechanism of γ-radiation effect on Si SCs properties. The effect is connected with hydrogen atoms those are released from the film as a result of broken of carbon-hydrogen bonds by gamma-quanta, diffuse to the SC, and passivate silicon dangling bonds at grain boundaries and in the SC volume. As a result, lifetime and, consequently, diffusion length of minor charge carriers in the SCs degrade slower in the SCs covered by the DLC films (Fig. 6)

[7]. Effect of silicon dangling bonds passivation in the SCs volume is confirmed by appearance of absorption band near 580 c m^{-1} in infrared spectrum of irradiated DLC-SC structures (Fig. 7) those correspond to Si-H bonds.

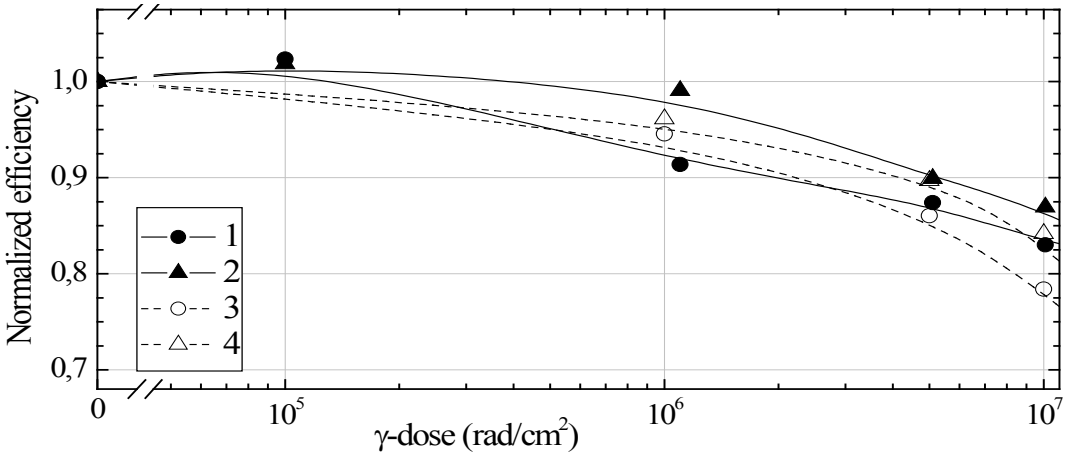

Fig. 5 Dependencies of normalized by initial value efficiency of solar cells from dose of γ-irradiation: 1 – mono-Si SC; 2 - mono-Si SC with DLC cover; 3 – multi-Si SC; 4 – multi-Si SC with DLC cover.

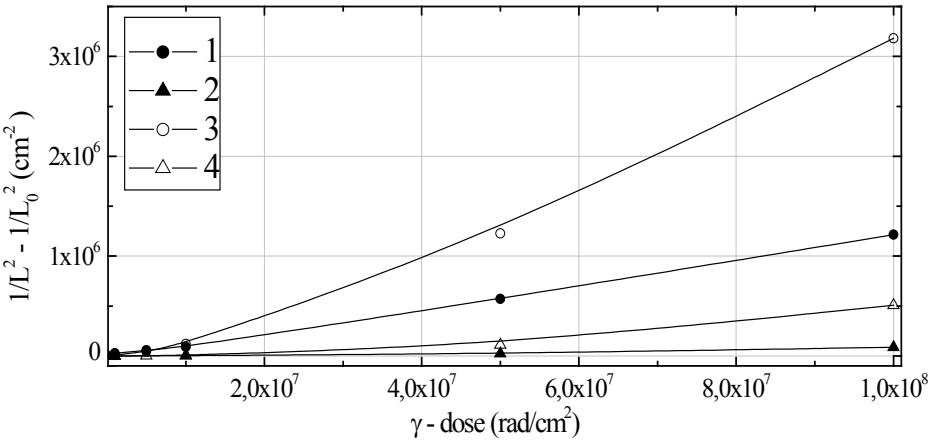

Fig. 6. Dependencies of $(1/L^2-1/L_0^2)$ of solar cells on dose of γ-radiation: 1 – mono-Si SC; 2 – mono-Si SC with DLC cover; 3 – multi-Si SC; 2 – multi -Si SC with DLC cover; Here L_0 and L are diffusion length of minor charge carrier of initial and irradiated SC, respectively.

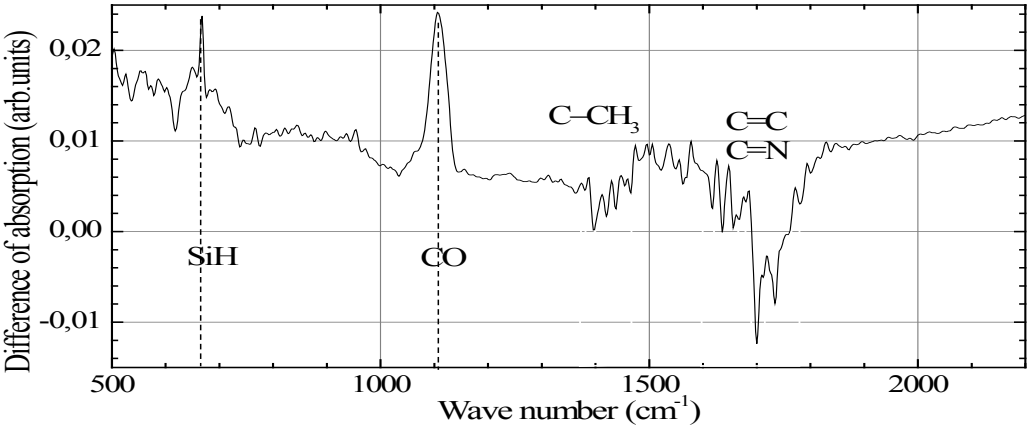

Fig. 7. Absorption difference between spectra of irradiated (γ-irradiation dose 10^6 rad/cm^2) and initial DLC film deposited from precursor gar with 45% of N_2.

3.4. Application of DLC films as antireflection coatings for materials with low refractive index

CdS, CdTe, CIS, and CIGS films are widely used for production of thin film or even flexible solar cells (SC). Because of low diffusion length of non-equilibrium carriers for the films it is especially important for such SCs to obtain highly conductive and transparent continuous front contact. As usual, for such contact indium-tin oxide (ITO) or ZnO doped with Al films are used. Refractive index of such films is higher than 2.0 [8] in the spectral region where the SCs are sensitive, therefore, rather significant reflection losses take place. In order to decrease the losses we propose to use diamond-like carbon (DLC) films with low refractive index to meet requirement for optimal antireflection effect. The DLC films were deposited by PE-CVD technique from gas mixture of nitrogen, methane and hydrogen. In some cases oxygen was also added to the gas mixture. As it was mentioned above we can deposit the DLC film with low refractive index (see Fig. 1). Theoretical modelling of optical properties for such multi-layered structures was also carried out to determine the required parameters of the antireflection DLC films. It has been shown that due to application of the DLC films transparency of front ITO or ZnO (Al) contacts may be substantially improved (Fig. 8). Further optimization of the DLC film deposition process allowed us to increase integral transmission of ZnO(Al) in spectral region 400-830 nm up to 1.1. times.. As a result short circuit current and efficiency of thin film SCs may be also improved.

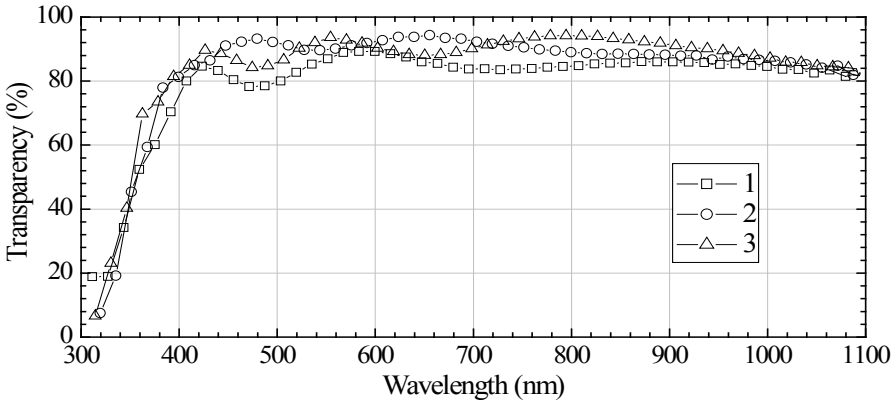

Fig. 8. Transparency of ZnO films (30 Ohm/cm^2): 1 – initial; 2 – covered by DLC film of 67 nm thickness; 3 – covered by DLC film of 100 nm thickness.

3.5. Effect of ultraviolet irradiation on DLC films properties

Diamond-like carbon films (a-C:H:N) were deposited by PE-CVD technique from gas mixture of nitrogen, methane and hydrogen. The films were irradiated by UV and focused UV (by 350 times) light of Hg-lamp during 2 hours.

Transparency in visible and IR range and Raman spectra were measured. It has been shown that optical bandgap of the DLC films was increased after UV irradiation (Fig. 9). It was connected with oxygen incorporation into the DLC films, changing of carbon-nitrogen bonds concentration and graphite-like clusters size. The films with greater amount of nitrogen show better irradiation resistance. Because of increasing of the films optical bandgap after UV irradiation no c hanges of parameters for Si SCs covered by the DLC coatings after UV irradiation was observed.

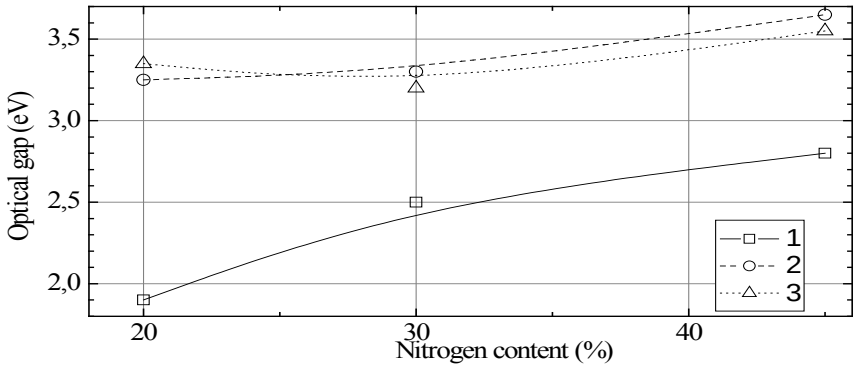

Fig. 9. Dependencies of DLC film optical energy gap on nitrogen content in gas mixture: 1 – initial DLC films; 2 – UV-irradiated DLC films; 3 –DLC films irradiated by concentrated UV light.

4. Conclusions

Finally, we may conclude that diamond-like carbon films are very prospective antireflection coatings not only for solar cells based on materials with high refractive index (like silicon) but for SCs produsedon the base of materials with low refractive index (like $A^{II}B^{VI}$ materials). In particular, efficiency of Si-based SCs may be improved up to 1.5 times due to deposition of the antireflection and passivative DLC films. It has been shown for the first time that even thin antireflection films (d=70 nm) allows us to substantially improve radiation resistance of silicon based solar cells against action of γ-radiation with the dose up to 10^8 rad. In its turn, thick DLC film (d=1300 nm) enable to protect SCs against action of intermediate energy protons (50-100 keV).

Acknowledgements

The work was supported by Science and Technology Center in Ukraine (project #4301) and by the Ukrainian governmental scientific-technical program "Creation of chemical-metallurgical branch for production of pure silicon in 2009-2012" (project #4.2).

References

[1] M.Allon-Alaluf, The influence of diamond-like carbon films on the properties of silicon solar cells, Thin Sol. Films 303, No. 8, 1997, pp. 273-276.

[2] N.I. Klyui, Silicon solar cells with antireflection diamond-like carbon and silicon carbide films, Solar Energy Materials & Solar Cells 72, 2002, pp. 597-603.

[3] V.G.Litovchenko, Solar Cells Based on DLC Film – Si Structures for Space Application, Solar Energy Materials & Solar Cells 68, No.1, 2001, pp. 55-70.

[4] Certificate of accreditation for center of photoelectric converters and batteries testing. Given to V.Lashkaryov ISP NASU by Ukrainian governmental centers of standardization, metrology, and certification. Date of issue – 29.04.2003.

[5] G. Adamopoulosa, Electron cyclotron resonance deposition, structure, and properties of oxygen incorporated hydrogenated diamondlike amorphous carbon films Journal of Applied Physics 96, No. 10, 2004, pp. 5456-5461.

[6] D. F. Franceschini, Structural modifications in a-C:H films doped and implanted with nitrogen, Diamond and Related Materials 3, 1993, pp. 88-93.

[7] N.I. Klyui, Influence of γ-irradiation on the parameters of silicon-based solar cells, Ukrainian Physical Journal 52, No. 3, 2007, pp. 245-250.

[8] D.R. Sahu, Development of ZnO-based transparent conductive coatings, Solar Energy Materials & Solar Cells 93, 2009, pp.1923–1927.

Formation of transparent and ohmic nanostructure thin films of fluorine-doped indium oxide prepared by spray

S.M. Rozati*, Z. Bargbidi

Department of Physics, University of Guilan, Rasht 42335, Iran
** Corresponding author. Tel: +981313220912, Fax: +981313220066 , E-mail: smrozati@guilan.ac. ir*

Abstract: In this research, indium oxide nanostructure undoped and doped with F were prepared on glass substrates using spray pyrolysis technique. Various parameters such as dopant concentration, deposition temperatures, amount of indium oxide powder were discussed. Structural properties of these films were investigated by XRD & SEM. Electrical and optical properties have been studied by Hall Effect and UV-Visible spectrophotometer respectively. The thickness of the films is determined by PUMA software. The variation in refractive index, extension coefficient and band gap of these films also were investigated.

Keywords: *Indium oxide,Indium doped oxide,Spray pyrolysis*

1. Introduction

Transparent conducting oxide (TCO) such as In_2O_3, ZnO, SnO_2 and In_2O_3:Sn (ITO) and In_2O_3:F (IFO) because of their high optical transparency in the visible region, good electrical conductivity are important. These characteristics are required in various applications research fields dealing with transparent heating elements for air craft and car windows [1], photovoltaic devices [2], solar cell [3], gas sensors [4]. A variety of deposition techniques such as vacuum evaporation [5], sputtering [6], spray pyrolysis [7], sol-gel [8], etc. have been used. All of these methods have advantages and disadvantage, but spray pyrolysis has a noticeable advantage, it is a low-cost and non-vacuum technique for large area applications. In_2O_3 transparent conducting thin films are n-type semiconductors with wide energy band gap equal to 3.6 eV. The structure of In_2O_3 in its crystalline form is body centred cubic with lattice constant a=10.118 Å .Doping indium oxide with fluorine, zinc, tin etc. as donor impurities yields films with low sheet resistance [1].This paper describes the results of our study in an attempt to correlate the electrical conduction with the optical and structural properties of prepared In_2O_3:F thin films.

2. Experimental Details

The chemical spray pyrolysis technique is one of the most commonly used techniques for preparation of transparent and conducting oxides owning to its simplicity, non-vacuum system of deposition and hence inexpensive method. The spray pyrolysis apparatus used in this work consists of a home made spraying unit, substrate holder with heater, and enclosure. The glass substrate is kept on a stainless steel (ss) plate. The heater is capable of heating the substrate up to a temperature of 700°C. The carrier gas used in all the experiments was air, which is supplied from an air compressor. The air produced by the compressor was first filtered and then connected to the glass spray-gun (atomizer) through a flow meter for controlling its flow. The custom glass spray gun having a nozzle diameter of 0.2 mm was positioned at a distance of 30cm above the substrate. The whole assembly is kept in an enclosure connected to an exhaust.

In this research, In_2O_3:F thin films were prepared by spraying a water solution containing indium chloride (0.2gr $InCl_3$) and NH_4F used as dopant onto glass substrates heated at

different substrate temperatures. The structural, electrical, and optical properties of TCOs are strongly affected by the temperature of substrate.

Deposition of parameters conclude: distance between the spray nozzle an substrates 25cm, the carrier gas using filtered compressed air, the spray rate 19 l it/min, volume of solution is 40 ml. All the above mentioned parameters were kept constant and only the concentration of NH_4F (0-15wt%) and substrate temperature (400-600 °C) were changed.

In this work we first optimize the concentration of F wt% using electrical resistivity and optical transparency and secondly focused on the effect of substrate temperature on structural, electrical, optical properties of the samples with a constant fluorine concentration of 2wt%.
X-ray diffraction (XRD) (Philips-pw-1830) was used to characterize the crystal structure of the films. Morphology of the films was examined by Cambridge scanning electron microscopy (SEM). The optical measurements of the In_2O_3:F thin films were carried out at room temperature using UV-Visible spectrophotometer(Cary 100 Scan Version).The electrical properties of thin films measured by Hall effect and Vander-Pauw set-up(RH 2010 PhysTech system).

3. Results and Discussion

Concentration of F in these films have been varied from 0-15wt%. As a result, the resistivity decreased quickly with increasing F concentration reaching a minimum of $\rho=1.35x10^{-3}$ Ωcm for an F concentration of 1wt% which demonstrate a good ohmic contact for electrode applications. For higher dopant content, the resistivity increased (Table 1). The higher transmittance observed in the films for 2wt% of F doped. Since we were looking for a layer with both high transparent and good resistevity, we used figure of merit (FOM). Thus the optimized layer with 2wt% of F concentration was selected according to the most FOM [9].
The X-ray diffraction result of IFO films in various concentrations are shown that, films are polycrystalline and crystallize in a cubic structure with preferential orientation along (222) and (400). Note also that no characteristic peaks of impurity and dopant phases have been observed.

Substrate temperature is an important parameter for spray pyrolysis deposition. It is observed that at lower substrate temperature (less than 250 °C), the growth rate is controlled by activated processes. At higher substrate temperature (greater than 550 °C), the size of the droplet decreases appreciably due to the evaporation of water molecule, resulting In a homogeneous reaction, the reaction may be completed above the substrate, leading to powder formation. Hence very low and very high temperatures are not suitable for preparation of these TCOs. For investigation of temperature effect on the growth mode, we fixed the doping concentration at 2wt% F and studied the effect of the substrate temperature on t he transparency. Figure shows the variation of substrate temperature of IFO films with change in transmission. Films deposited at substrate temperatures of 400 to 450 °C exhibited less transmission in visible region, while by increasing the substrate temperature we get better transparency (Fig. 1).

Table 1. The variation of electrical properties of IFO films as a function of dopant concentration deposited at 575 °C.

F wt%	R_{sh}(Ω/□)	ρ(×10^{-3} Ω cm)	n(×10^{20} cm^{-3})	μ (cm^2/V.s)	T% λ=550 nm	FOM (×10^{-5})
0	5850	147	0.06	6.71	77	1.25
0.5	335	6.36	0.26	37.4	77	21.9
1	96.5	1.35	2.53	18.2	68.2	22.6
2	140	1.92	1.13	28.6	87.6	190
10	333	8.73	0.99	7.23	77	7.79
15	527	15.30	0.72	5.63	81	23.07

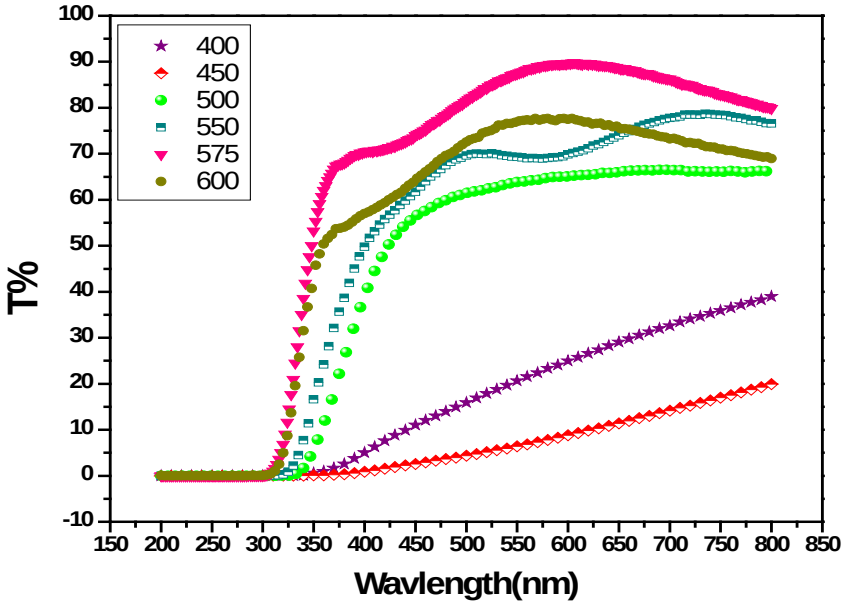

Fig. 1:Optical transmission of IFO films prepared at 2wt% F various substrate temperature

The XRD results (Fig.2) show that, films deposited at substrate temperature of 4 00 and 450 °C, in addition to (222), (400) peaks have (211), (411), (341), (440), (622) peaks with high intensity. The presence and intensity of peaks decreased with increasing substrate temperature; as a result crystallinity improves leading to well-transmission and resistivity.

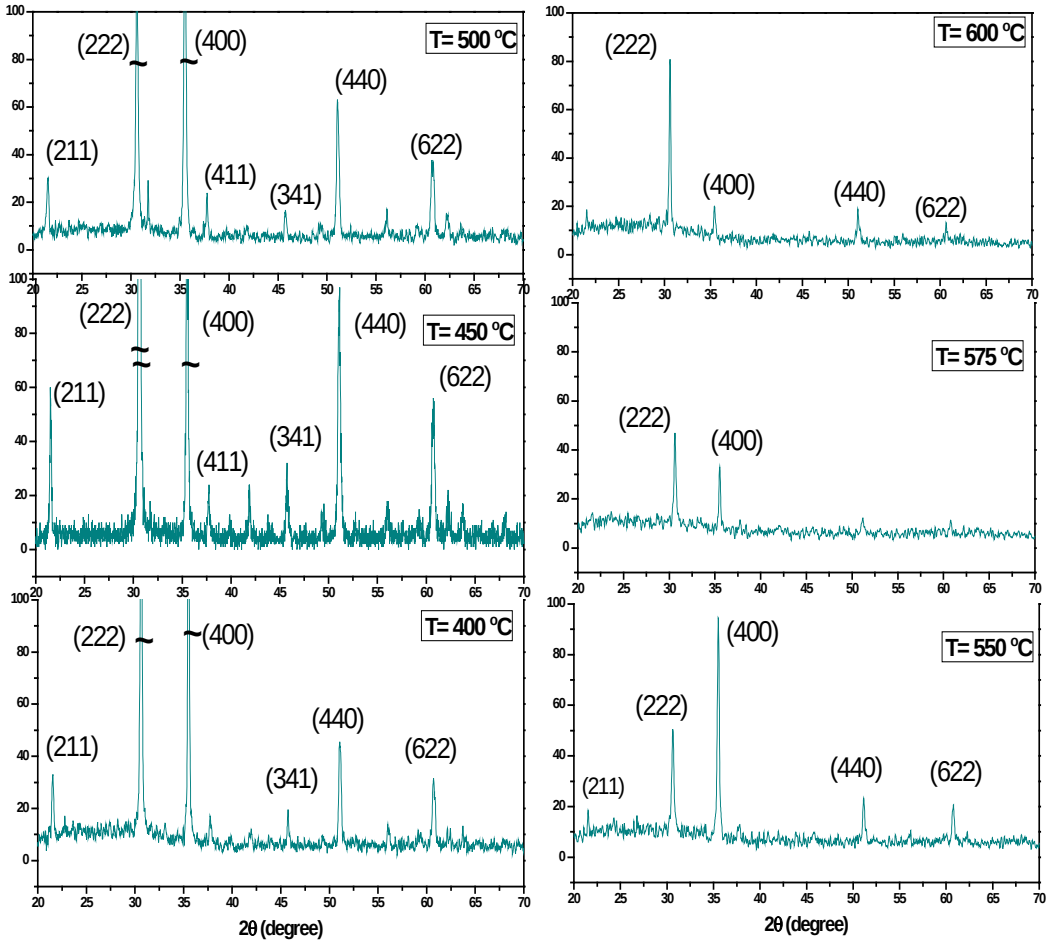

Fig. 2: XRD patterns of IFO films prepared at various substrate temperatures

The SEM results show that the size of crystals is in the range on nanometer. The size of particles changing with respect to deposition parameters. Fig. 3 shows that, the crystalline improved with increasing substrate temperature. Furthermore, the density of grain boundaries and dislocation therefore decreases, leading to the improvement of conductivity and transparency of IFO films.

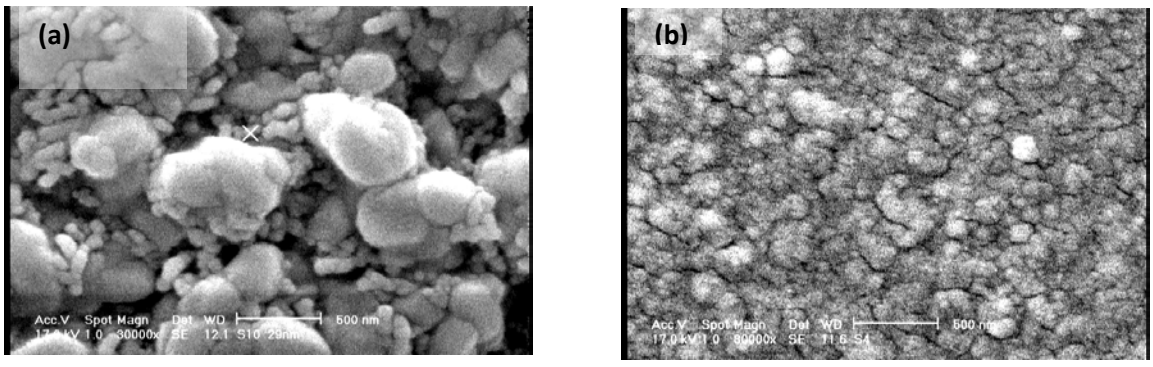

Fig.3 SEM images of IFO films prepared at different substrate temperature: a) 450 °C and b) 575 °C.

Subsequently the amount of indium powder also was investigated for the prepared films. Result show that the resistivity is decreased by increasing of indium powder but transparency is decreased. Besides, the thickness of the films is determined by PUMA software [10].

4. Conclusions

In this research, fluorine doped indium oxide (IFO) nanostructure were prepared at different F concentration, substrate temperature and $InCl_3$ concentration using spray pyrolysis technique. Then effects of above parameters on structural, electrical and optical properties of nanostructure thin films of IFO were investigated. The SEM results show that the size of crystals is in the range on nanometer. The size of particles changing with respect to deposition parameters. The presence and intensity of XRD peaks decreased with increasing substrate temperature; as a result crystallinity improves leading to well-transmission and resistivity.In conclusion, the optimum IFO films were prepared using 0.2 gr $InCl_3$ with F concentration of 2wt% at substrate temperature of 575 ° C. With this condition sheet resistance was 140 Ω/□ and the optical transmission in visible region was 87.6%.

Acknowledgment

This work was supported by the department of research of the University of Guilan.

References

[1] K.I. Chopra, S. Major, D.K. Pandya, *Thin Solid Films*, **102**, (1983), 1.

[2] C.V.R. Vasant Kumar, A.A. Mansingh, *J. Appl. Phys.*, **65**, (1989), 1270.

[3] J.A. Anna Selvan, A.E. Delahoy, S. Guo, Y. Li, A new light trapping TCO for nc-Si:H solar cells, *Solar Energy Mater. Solar Cells*, **90**, (2006), 3371–3376.

[4] G. Korotcenkov, V. Brinzari, A. Cerneavschi, *Sensors and Actuators B*, **98**, (2004), 122–129.

[5] S.M. Rozati, S. Mirzapour, M.G. Takwale,B.R. M arathe, V.G. Bhide, *Materials Chemistry and Physics*, **34**, (1993), 119.

[6] S. Boycheva, A.K. Sytchkova, M.L. Grilli, A. Piegari, *Thin Solid Films*, **515**, (2007), 8469.

[7] S. Golshahi, S.M. Rozati, R. Martins, E. Fortunato, *Thin Solid Films*, **518**, (2009), 1149-1152.

[8] R.B.H. Tahar, T. Ban, Y. Ohya, Y. Takahashi, *J. Appl. Phys.*, **82**, (1997), 865.

[9] G. Haacke, *J. Appl. Phys.*, 47 (1976) 4086.

[10] E.J. Biring, I. Chambouleyron, J.M. Martinez, Estimation of the optical constants and the thickness of thin films using unconstrained optimization, Journal of Computational Physics, 155 (1999) 862-880.

Research and development of dye-sensitized solar cells in the Center for Molecular Devices: from molecules to modules

Gerrit Boschloo[1,*], Anders Hagfeldt[1], Håkan Rensmo[1], Lars Kloo[2], Licheng Sun[2], Henrik Pettersson[3]

[1] *Uppsala University, Uppsala, Sweden*
[2] *Royal Institute of Technology, Stockholm, Sweden*
[3] *Swerea IVF, Mölndal, Sweden*
* *Corresponding author. Tel: +46 18 4713303 , E-mail: gerrit.boschloo@fki.uu.se*

Abstract: Dye-sensitized solar cells (DSCs) represent a relatively new photovoltaic technology with great potential: investment costs for initiating production are low and manufacturing costs below 0.5 US$/$W_{peak}$ are predicted. Furthermore, DSC offers the possibility of various colors and attractive designs, such as semitransparent modules. Record solar cell efficiencies are 11% for DSCs containing liquid redox electrolyte and 6% for DSCs with solid hole conductors. Promising stability data suggesting more than 20 years lifetime has been achieved. This paper presents the Center for Molecular Devices (CMD) in Sweden, which has as its objective to investigate and develop DSCs. Using a multi-disciplinary approach, significant advances in the scientific understanding of DSCs have been made, such as the demonstration of the presence of an internal electric field at the semiconductor / dye / electrolyte interface. Furthermore, novel components, such as triphenylamine-based dyes and cobalt-based mediator have been successfully tested. Finally, a monolithic DSC module technology with good performance is presented.

Keywords: *Dye-sensitized solar cell, PV modules.*

1. Introduction

Dye-sensitized solar cells (DSCs) represent a relatively new photovoltaic technology with great potential.[1] Certified record solar cell efficiencies are 11% for DSCs containing liquid redox electrolyte and 6% for DSCs with solid hole conductors. It is believed that this technology has the potential to reach production costs as low as 0.5 US$/$W_{peak}$,[2] which would make solar electricity generation competitive with conventional (fossil fuel based) electricity generation. Module efficiencies of 10% and lifetimes of 15 year were assumed for this calculation. More recent calculations, based on actual DSC devices and current material costs, give a manufacturing cost of 2.5 Euro/W_{peak}, which may decrease to less than 1 Euro/ W_{peak} taking the expected decrease in material cost into account.[3]

Dye-sensitized solar cells differ much from conventional solid state semiconductor based solar cells.[1] Dye molecules, rather than an inorganic semiconductor material, are responsible for light absorption. Furthermore, the functions of light absorption, electron transport and hole transport are separated into different materials. Electron transport takes place in a porous TiO_2 structure, while hole transport occurs in a liquid redox electrolyte.
In its standard form the DSC consists of the following components (see Figure 1a):

- The working electrode: a mesoporous film of TiO_2 nanoparticles (size ~20 nm) with a thickness of about 10 μm, on a fluorine-doped tinoxide (FTO) coated glass substrate. Dye-molecules are adsorbed at the surface of TiO_2. The TiO_2 framework acts as electron acceptor and transport medium.

- A redox electrolyte: solution containing a suitable redox couple in a high concentration, as well as some additives that improve solar cell performance. The most common redox couple used in DSC is iodide / triiodide.
- A counter electrode: an electrode with good catalytic activity for electron transfer to the redox electrolyte. The most common counter electrode in DSCs is platinum-coated FTO-glass. This electrode has the advantage that it can be transparent, as a very low loading of Pt is needed.
- Sealing. Hermetic sealing is very important in order to obtain stable solar cells with good long term stability. The most common DSC sealing material is thermoplastic. A thermoplastic frame is used to connect the WE and CE together, which ensures a fixed separation between the two electrodes.

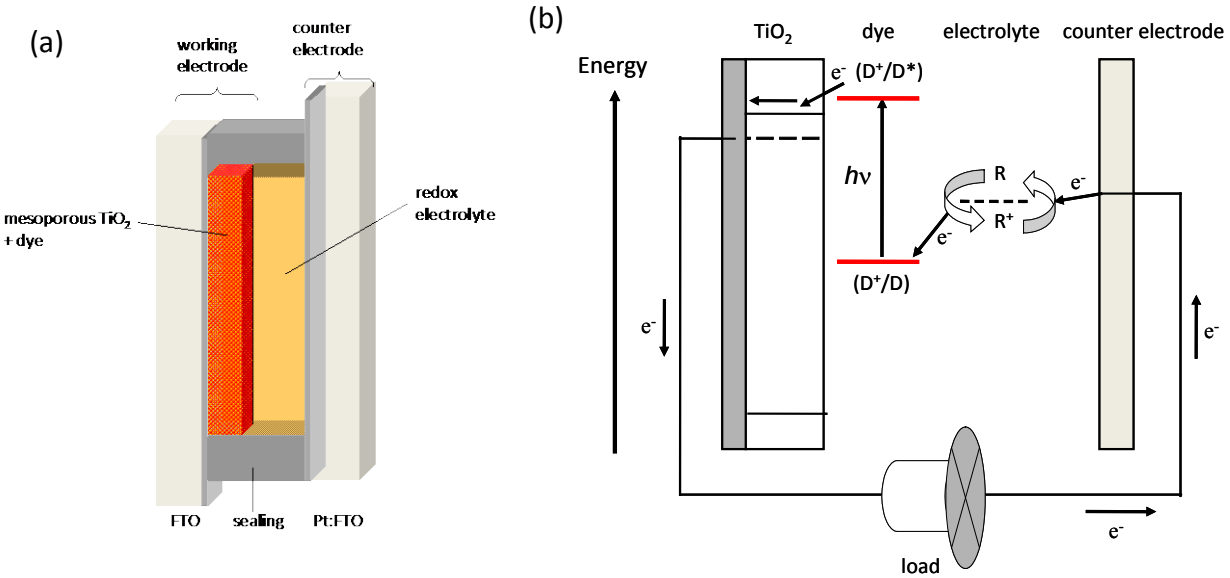

Figure 1. (a) Schematic structure of a dye-sensitized solar cell (sandwich design). FTO stands for fluorine-doped tinoxide-coated glass. (b) Energy scheme of a dye-sensitized solar cell. The arrows indicate electron transfer reactions.

The working mechanism of the dye-sensitized solar cell is displayed in Figure 1b. Light is absorbed by the dye molecules D resulting in excited dye molecules (D*). Ultrafast electron injection takes place from the excited dye into the conduction band of TiO_2. Regeneration of the oxidized dye by the redox mediator R. Electrons are collected at the conducting substrates and can perform electrical work in an external circuit. At the counter electrode, electrons reduce R^+, the oxidized form of mediator.

Despite intense research in the field of dye-sensitized solar cells, many fundamental aspects are still unclear. The Center for Molecular Devices (CMD) in Sweden has as its objective to investigate and develop DSCs. Using a multi-disciplinary approach, significant advances in the scientific understanding of DSCs, development of low-cost DSC components, and DSC module manufacturing have been made, as will be discussed here in this paper.

2. Methodology

We refer to our research papers (ref. 4-17) for details on mesoporous TiO_2 electrode preparation, dye synthesis, electrolyte preparation, solar cell assembly and solar cell characterization.

3. Results and Discussion

3.1. Design, synthesis and characterization of dye molecules for DSC

Research on dyes within CMD has been mainly focused on organic dyes with the general structure: donor - conjugated bridge – acceptor (D-π-A). Upon excitation, electron density will be displaced from the electron rich donor moiety towards the electron withdrawing acceptor moiety. The acceptor moiety is also equipped with suitable binding groups for attachment of the molecules onto the TiO_2 surface. The general structure of D-π-A dyes favors electron injection into TiO_2 upon excitation, while the remaining positive charge will be located on the donor part, positioned relatively far away from the TiO_2 surface. This will decrease the rate for direct geminate recombination. A very suitable donor group for D-π-A dyes is the triphenylamine (TPA) unit, while a suitable acceptor / binding unit is cyanoacrylic acid.

In 2005 the D5 dye was developed within CMD as the first in a series of D-π-A dyes (see Figure 2a).[4] Although the absorption spectrum has a maximum at about 480 nm and does not extend significantly beyond 600 nm, promising solar cell efficiencies of 6% were obtained in combination with the iodide / triiodide electrolyte. Other interesting results obtained with D5 are its suitability in solid-state DSCs, and its capacity for hole conduction when it is adsorbed on TiO_2 as a monolayer.[5]

Several modifications of the D5 base structure have been synthesized and tested. One of the most promising dyes developed within CMD to date is the D35 dye (see Figure 2). The most prominent alteration is the addition of two *o,p*-dibutoxyphenyl groups on the TPA unit. This provides the dye with suitable steric properties, making the dye very suited to be used in combination with cobalt-based redox electrolytes [6] or in solid-state DSC.

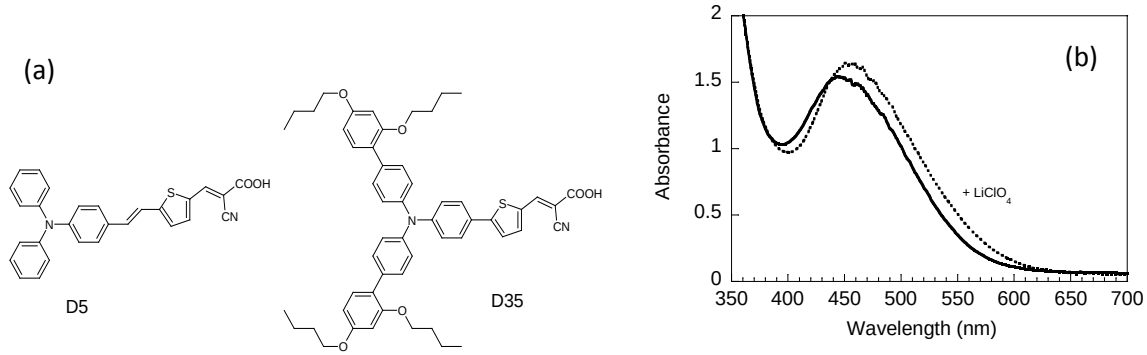

Figure 2. (a) Chemical structure of two efficient organic sensitizing dyes developed at CMD: D5 and D35. (b) UV-visible spectra of a D35-sensitized TiO_2 film in air (drawn line) and in contact with $LiClO_4$ in ethanol (dotted line).

3.2. Redox electrolytes and hole conductors

The standard redox electrolyte for DSC comprises of the iodide / triiodide (I^-/I_3^-) redox couple in an organic solvent. It is used in best performing DSCs to date, both in terms of efficiency and stability. It has good solubility, absorbs not too much visible light, it has a suitable redox potential, and provides rapid dye regeneration. But what I^-/I_3^- makes particularly successful is the very slow recombination kinetics between electrons in TiO_2 and the oxidized part of the redox couple, triiodide. A serious disadvantage of this redox mediator is that a significant part of the potential is lost due to intermediate reactions.[7] After electron injection, the oxidized dye (D^+) is reduced by iodide in the following way:

$$D^+ + I^- \rightarrow (D\text{--}I) \quad (1)$$

$$(D\text{--}I) + I^- \rightarrow D + I_2^{-\bullet} \quad (2)$$

$$2\ I_2^{-\bullet} \rightarrow I_3^- + I^- \quad (3)$$

The diiodide radical ($I_2^{-\bullet}$) is produced as an intermediate in this process (reaction 2). We estimate that the disproportionation reaction 3 corresponds to an internal loss of potential of as much as 400 mV. We believe that it is this internal loss that is largely responsible for the observed 'stagnation' in record efficiencies obtained for DSCs.

In order to obtained efficiencies larger than 12 %, it may be necessary to using one-electron redox couples or hole conductors instead of I^-/I_3^-, so that the losses due to internal conversion are avoided. Unfortunately, the use of one-electron mediators in DSC nearly always leads to strongly increased recombination between electrons in TiO_2 and the oxidized part of the redox couple, which seriously limits the solar cell efficiency. Recently, however, we obtained a breakthrough with cobalt polypyridine-based mediators in combination with D35 dye.[6] Careful matching of the steric bulk of the mediator and the dye molecules minimizes the recombination between electrons in TiO_2 and Co(III) species in the electrolyte and avoids mass transport limitations of the redox mediator. The organic sensitizer D35, equipped with bulky alkoxy groups, efficiently suppresses recombination, allowing the use of cobalt redox mediators with relatively small steric bulk. Its high extinction coefficient allows for making DSCs with thin TiO_2 films, which is favorable with respect to charge recombination and mass transport of redox mediator in the porous structure. The best efficiency obtained for a DSC sensitized with D35 and employing a $[Co(bpy)_3]^{3+/2+}$-based electrolyte was 6.7 % at full sunlight (1000 W m^{-2} AM1.5G illumination), which is more than a doubling of previously published record efficiencies using similar Co-based mediators. Notably, similar efficiencies with the D35 dye are obtained with I^-/I_3^- as a redox couple.

The use of a solid-state hole conductors in DSCs is very attractive, but also very challenging. Besides the above mentioned problem of enhance recombination, an additional problem is to fill the pores of the dye-modified mesoporous TiO_2 electrodes completely with the solid hole conductor. A possible solution investigated within CMD is melting infiltration of the hole conductor into the pores of the dye-sensitized TiO_2 electrode.[8] The rather high temperatures required for melting is damaging for the organic dye molecules and so far is limiting the efficiencies of the resulting solar cells.
The most well-tested hole conductor in solid-state DSCs is 2,2′,7,7′-tetrakis(*N*,*N*-di-*p*-methoxyphenylamine)-9,9′-spirobifluorene (spiro-MeOTAD). With the help of photoinduced absorption spectroscopy it was be shown that in principle all dye molecules appeared to be in contact with the hole conductor for a 6 μm thick TiO_2 film, even though pores are not filled to

100%.[9] A compelling result obtained within CMD research is that some perylene-based dyes performed much better in solid-state DSCs using spiro-MeOTAD than in standard iodide / triiodide electrolyte-based DSCs.[10] This can be attributed to the much faster regeneration kinetics observed in solid-state DSCs.

3.3. Advanced characterization of DSC components and complete devices

The dye-sensitized solar cell is a complex system with many interactions between its individual components. We have performed detailed characterization of dye-sensitized TiO_2 films using advanced techniques such as X-ray photoelectron spectroscopy [11] and scanning tunneling microscopy,[12] giving valuable information of the binding morphology of the dyes and energy levels.

Investigations on complete DSC devices have been particularly fruitful, as the interactions between different components can be studied. For instance, we have studied the effect of the DSC electrolyte additive 4-*tert* butylpyridine in detail and found that it was responsible for a band edge shift of the TiO_2 as well as for a reduction in the electron recombination rate constant.[13] More recently, we found that the additives guanidinium thiocyanate and *N*-methylbenzimidazole have a synergistic effect on the solar cell performance of DSCs with ionic liquid (I^-/I_3^-) electrolytes.[14]

Recently, we discovered that the Stark effect plays an important role in the transient absorption spectroscopy of DSCs.[15] The occurrence of the Stark effects implies that the electric field across the adsorbed dye molecules changes. The effect of electric fields can be even observed under steady-state conditions. Figure 2b shows the absorption spectrum of D35 adsorbed on mesoporous TiO_2. In the presence of lithium ions, a significant red shift of the spectrum is observed. This shift can be attributed to the Li^+ ions that adsorb onto the TiO_2 surface, thus changing its surface charge. This in turn affects the electric field across the dye monolayer, giving rise to a Stark shift. The occurrence of this shift implies that the dyes are, at least partially, located within the Helmholtz double layer at the metal oxides / electrolyte interface. The effect of the electric field is that the donor-acceptor character of the dye is enhanced, resulting in a red-shift of the absorption spectrum.

3.4. Monolithic DSC Modules

Screen printing as is low cost, scalable method to prepare thin films. Within CMD, a monolithic design is used in the development of DSC modules, see Figure 3a.[16, 17] The monolithic design has several advantages: it can give significant cost reduction as only one FTO-coated glass plate is needed, compared to two in other (sandwich) designs. FTO substrates are responsible for up to 25% of the total manufacturing costs in a sandwich design DSC. Furthermore, problems with alignment and glass bending encountered for large sandwich-design modules are avoided.

In Figure 3b some typical photocurrent density - voltage (*J-V*) curves of a 13.5 cm^2 sized DSC module are shown. The module consists of 4 cells connected in parallel. The solar to electrical power conversion efficiency depends on incident light intensity and ranges from 4.0% (1000 W m^{-2}) to 6.6% (56 W m^{-2}). This dependency is caused by internal resistance losses, of which the origin is currently under investigation. Stability tests as well as outdoor tests are ongoing. When the components in the DSC modules are well chosen (dye, electrolyte), the modules are completely stable after 2000 h in an accelerated aging test (1000 W m^{-2} simulated sunlight, 50ºC), with an efficiency of 5.0% at 200 W m^{-2} illumination.[17] Significant degradation is, however, observed under storage in the dark at 80ºC. These tests

were performed with the ruthenium-based complex K77 as the sensitizer and an iodide/ triiodide electrolyte with 3-methoxyproprionitrile as solvent.

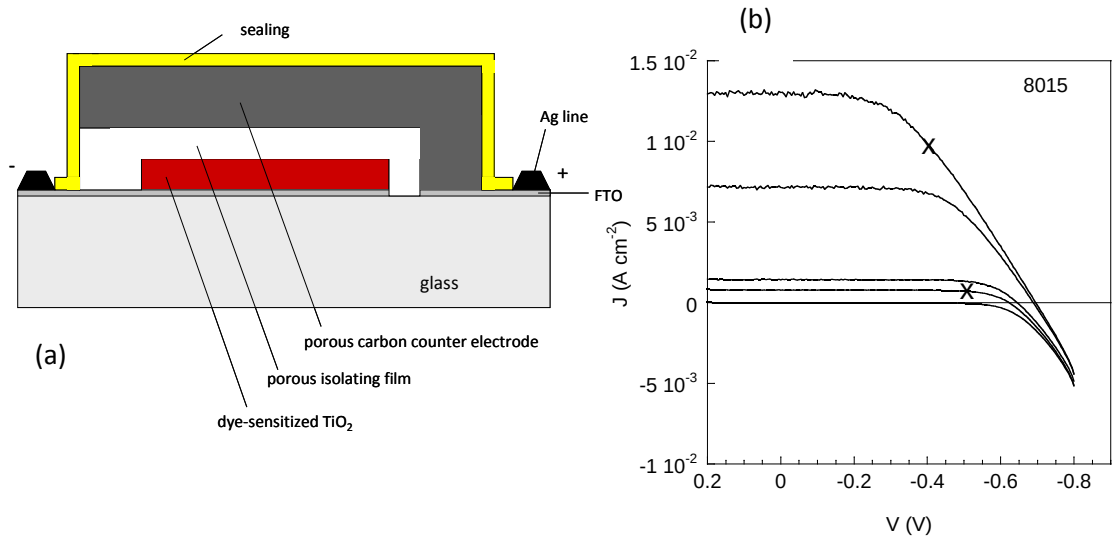

Figure 3. (a) Schematic structure of the monolithic design of the dye-sensitized solar cell.(b) J-V characteristics of a monolithic DSC module (active area: 13.5 cm^2).Light intensities: 1000; 534; 105; 56 and 0 W m^{-2}.

4. Conclusions

The work performed at the Center for Molecular Devices in Sweden has significantly contributed to the research field of dye-sensitized solar cells. CMD was among the first to develop organic sensitizer dyes equipped with triphenylamine donor groups, which are currently among the most efficient sensitizers in DSC. Cobalt-based redox couples were shown to be viable alternatives to the standard iodide / triiodide system, provided that a dye with suitable steric properties is used. Detailed in-situ studies of DSCs have revealed the occurrence of a Stark-effect, where an internal electric field changes the absorption of the dye. This effect can be used to provide fundamental understanding of the DSC. In development work, CMD has shown that monolithic DSC is a viable PV technology, although further development and testing is required.

Acknowledgement

We thank the Swedish Energy Agency, the Swedish Research Council, Vinnova, BASF SE and the Knut and Alice Wallenberg foundation for financial support.

References

[1] A. Hagfeldt, G. Boschloo, L. Sun, L. Kloo, H. Pettersson, Chem. Rev. 110 (2010) 6595.

[2] G. Smestad, C. Bignozzi, R. Argazzi, Sol. Energy Mater. Sol. Cells 33 (1994) 253.

[3] J. M. Kroon, N. J. Bakker, H. J. P. Smit, P. Liska, K. R. Thampi, P. Wang, S. M. Zakeeruddin, M. Grätzel, A. Hinsch, S. Hore, U. Würfel, R. Sastrawan, J. R. Durrant, E. Palomares, H. Pettersson, T. Gruszecki, J. Walter, K. Skupien, G. E. Tulloch, Prog. Photovolt.: Res. Appl. 15 (2007) 1.

[4] D. P. Hagberg, T. Edvinsson, T. Marinado, G. Boschloo, A. Hagfeldt, L. Sun, Chem. Commun. (2006) 2245.

[5] G. Boschloo, T. Marinado, K. Nonomura, T. Edvinsson, A. G. Agrios, D. P. Hagberg, L. Sun, M. Quintana, C. S. Karthikeyan, M. Thelakkat, A. Hagfeldt, Thin Solid Films 516 (2008) 7214–7217.

[6] S. M. Feldt, E. A. Gibson, E. Gabrielsson, L. Sun, G. Boschloo, A. Hagfeldt, J. Am. Chem. Soc. 132 (2010) 16714.

[7] G. Boschloo, A. Hagfeldt, Acc. Chem. Res. 42 (2009) 1819.

[8] K. Fredin, E. M. J. Johansson, T. Blom, M. Hedlund, S. Plogmaker, H. Siegbahn, K. Leifer, H. Rensmo, Synth. Metals 159 (2009) 166.

[9] U. B. Cappel, E. A. Gibson, A. Hagfeldt, G. Boschloo, J. Phys. Chem. C 113 (2009) 6275.

[10] U. B. Cappel, M. H. Karlsson, N. G. Pschirer, F. Eickemeyer, J. Schöneboom, P. Erk, G. Boschloo, A. Hagfeldt, J. Phys. Chem. C 113 (2009) 14595.

[11] M. Hahlin, E. M. J. Johansson, S. Plogmaker, M. Odelius, D. P. Hagberg, L. Sun, H. Siegbahn, H. Rensmo, Phys. Chem. Chem. Phys. 12 1507.

[12] M. Zuleta, S. Yu, S. Ahmadi, G. Boschloo, M. Göthelid, A. Hagfeldt, Langmuir 26 (2010) 13236.

[13] G. Boschloo, L. Häggman, A. Hagfeldt, J. Phys. Chem. B 110 (2006) 13144.

[14] Z. Yu, M. Gorlov, G. Boschloo, L. Kloo, J. Phys. Chem. C ASAP.

[15] U. B. Cappel, S. M. Feldt, J. Schoneboom, A. Hagfeldt, G. Boschloo, J. Am. Chem. Soc. 132 (2010) 9096.

[16] H. Pettersson, T. Gruszecki, R. Bernhard, L. Häggman, M. Gorlov, G. Boschloo, T. Edvinsson, L. Kloo, A. Hagfeldt, Prog. Photovolt: Res. Appl. 15 (2007) 113–121.

[17] H. Pettersson, T. Gruszecki, C. Schnetz, M. Streit, Y. Xu, L. Sun, M. Gorlov, L. Kloo, G. Boschloo, L. Häggman, A. Hagfeldt, Prog. Photovolt.: Res. Appl. 18 (2010) 340.

Studies of the anionic micelles effect on photogalvanic cells for solar energy conversion and storage in Sodium lauryl sulphate-Safranine-D-Xylose system

Prem Prakash Solanki[1*], K M Gangotri[2]

[1] *Department of Chemistry, Faculty of Science, Banaras Hindu University, Varanasi-221005, INDIA*
[2] *Solar Energy Laboratory, Department of Chemistry, Jai Narain Vyas University, Jodhpur-342005, INDIA*
** Corresponding author. Tel: +542 6702469, Fax: +291 2614162, E-mail: ppsolankibhu@gmail.com*

Abstract: The Sodium lauryl sulphate (NaLS) has been used as anionic micelle species, Safranine as photosensitizer and D-Xylose as electron donor for the enhancement of the electrical output and performance (storage capacity) of the photogalvanic cell with reduce the cost of construction for commercial viability. The photopotential and photocurrent generated were 893.0 mV and 207.0 μA, respectively. The observed conversion efficiency and the fill factor were 0.6800% and 0.3233, respectively at the power point of the cell. The photogalvanic cell can be used for 98.0 minutes in the dark.The effect of different parameters like concentration of micelles; photosensitizer and electron donor, variation of pH, light intensity and diffusion path length were observed. A current – voltage (i-V) characteristics of the photogalvanic cell was studied experimentally and a mechanism has also been proposed for the generation of the photocurrent. All observed results of the system were lower in absence of the micelles species.

Keywords: *Photogalvanic cell, Micelles effect, Safranine, D-Xylose, Conversion efficiency*

Nomenclature

i_{eq}	*photocurrent at equilibrium*.....μA	M	*Concentration in molarity*.....*mol/L*
i_{max}	*maximum photocurrent*.....μA	$t_{1/2}$	*performance (storage capacity)* .....*min*
i_{pp}	*photocurrent at power point*.....μA	V_{oc}	*open circuit voltage*..... *mV*
i_{sc}	*short circuit current*.....μA	V_{pp}	*photopotential at power point* ..... *mV*
pp	*power point*.....μW	η	*Fill fact*

1. Introduction

The flow of current between two unsymmetrical illuminated metal electrodes in sunlight was first observed by Becquerel[1] in 1839 and photogalvanic effect was first reported by Rideal and Williams[2] in 1925 but, it was systematically investigated by Rabinowitch[3] for iron–thionine system.

The photogalvanic and photovoltaic effects with anodized zirconium and niobium electrodes were observed by Graven et al. [4] while the photogalvanic effect with semiconductor anode was reported by Hall et al.[5].

Electron transfer via organic dye molecule and photo-induced electron transfer between micelle and thionine dye through a charge transfer interaction have observed by Alfredo et al.[6] and Mukhopadhyay and Bhowmik[7].

Bisquert et al.[8] have reported the physical–chemical principle of dye–sensitized solar cells, and Mayer[9] has presented the molecular approaches to solar energy conversion with coordination compounds.

Ameta et al.[10] Khamesara et al.[11] Pramila and Gangotri[12], Gangotri and Gangotri[13], and Genwa and genwa[14] have used miceller species with different photosensitizer and reductant in photogalvanic system for solar energy conversion and storage.

Jana and Bhowmik[15], Gangotri and Lal[16] and Lal[17] have used mixed dyes while Dube[18] and Gangotri and Indora[19] have used mixed reductant with different photosentizer in the photogalvanic systems.

Recently Genwa et al[20] Gangotri and Gangotri[21], Yadav and Lal[22], Gangotri and Bhimwal[23], Gangotri et al.[24] and Gangotri and Solanki[25] have developed some intrested photogalvanic cells with reasonable electrical output for solar energy conversion and storage.

They have used different photosensitizes, reductant and surfactants in photogalvanic cells but no attention has been paid to use Sodium lauryl sulphate-Safranine-D-Xylose system to enhance the electrical output and storage capacity of the cell. Our study reveals that a system of Sodium lauryl sulphate-Safranine-D-Xylose gives higher electrical output with better storage capacity, in addition, the cell is cost effective which makes it suitable for commercialization in near future, therefore, the present work was undertaken.

2. Methodology

All the solutions were prepared in doubly distilled water and the stock solutions of all the chemicals were prepared by direct weighing and were kept in coloured container to protect them from light. A mixture of known amounts of solution of Safranine, D-Xylose, Sodium lauryl sulphate and Sodium hydroxide were taken in an H-shaped glass tube. The total volume of the mixture was always kept at 25.0 mL with make up by doubly distilled water. A platinum electrode (1.0 X 1.0 cm^2) was immersed in one limb of the H-tube having a window and a saturated calomel electrode was immersed in the other limb. The terminals of the electrodes were connected to a digital pH meter (Systronics -335) and a microammeter as shown in Fig. 1.

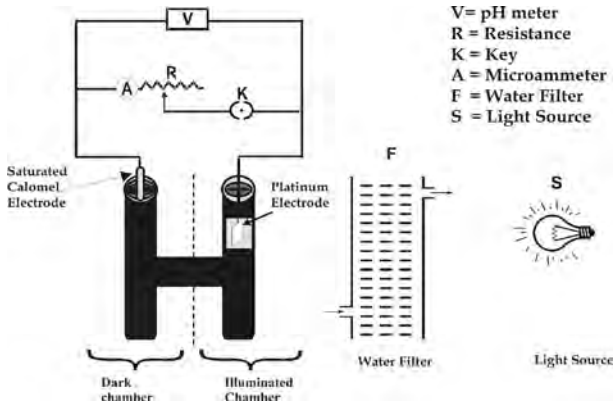

Fig.1. Experimental set up of photogalvanic cell

The whole system was first placed in the dark till a stable potential was obtained. Then, the limb having platinum electrode (whole platinum electrode area) was exposed to a 200 W tungsten bulb (Sylvania) while other limb having the saturated calomel electrode was kept in dark. A water filter was used to avoid thermal radiations. On illumination, the photochemical bleaching of photosensitizer was studied potentiometrically. The current-voltage (i-V) characteristics of the cell were studied by using an external load with the help of a carbon pot (log 470 K) connected in the circuit.

3. Results and discussions

3.1. Effect of variation of photosensitizer and reductant concentration

The electrical output of the cell was affected by variation of photosensitizer (Safranine) and reductant (D-Xylose) concentration. The results are summarized in Table 1.It was observed that on increasing the concentration of safranine, electrical parameters photopotential (ΔV) and photocurrent (i_{sc}) increases, which reaches a maximum value at a concentration 4.60 X 10^{-5} M, above which both parameters decrease. A lower concentration of safranine ([Safranine] < 4.60 X 10^{-5} M) resulted into a decrease in electrical parameters because limited number of photosensitizer molecule were available for the excitation and consecutive donation of the electrons to the platinum electrode whereas a higher concentration of safranine ([Safranine] > 4.60 X 10^{-5} M) again resulted into a decrease into electrical output as the intensity of light reaching the photosensitizer molecule near the electrode decreased due to absorption of the major portion of the light by photosensitizer molecules present in the path.

Table 1: Effect of variation of various parameters concentrations on the electrical output

Parameters	Photopotential(mV)	Photocurrent (μA)	Power (μW)
[NaLS] X 10^{3}			
5.56	791.0	170.0	134.47
5.60	827.0	189.0	156.30
5.64	893.0	207.0	184.85
5.68	837.0	186.0	155.68
6.72	796.0	164.0	130.54
[Safranine]X10^{5}M			
4.48	803.0	177.0	142.13
4.54	843.0	192.0	161.86
4.60	893.0	207.0	184.85
4.66	837.0	189.0	158.19
4.72	800.0	169.0	135.20
[D-Xylose]X10^{3}M			
1.34	767.0	161.0	123.48
1.38	817.0	185.0	151.15
1.42	893.0	207.0	184.85
1.46	820.0	180.0	147.60
1.50	777.0	157.0	121.98
pH			
12.66	817.0	179.0	146.24
12.68	849.0	195.0	165.55
12.70	893.0	207.0	184.85
12.72	840.0	192.0	161.28
12.74	812.0	176.0	142.91

A simillar result was observed for variation of the concentration of reductant. A lower concentration of reducing agent ([D-Xylose] < 1.42 X 10^{-3} M) resulted into a fall in electrical output because fewer reducing agent molecule were available for electron donation to the photosensitizer molecules whereas a higher concentration of reducing agent ([D-Xylose] > 1.42 X 10^{-3} M) again resulted in a fall in a electrical output because the larger number of reducing agent molecule hinder the photosensitizer molecule from reaching the electrode in the desired time limit.

3.2. Effect of variation of micelles concentration

The electrical output of the cell was found to increase on increasing the concentration of NaLS, reaching a maximum value at the concentration 5.64 X 10^{-3} M, and then, further increase in their concentration a decrease in electrical output of the cell was observed. The observed results are summarized in Table 1

It was observed that maximum electrical output obtain from the cell around their critical micelle concentration (CMC) of the surfactant. It indicates the presence of the some charge transfer interaction between the dye-surfactant and the photoejection of electron from dye-surfactant depends on the charge on micelle. The surfactant has not only solublized the dye molecules to a maximum extent and their cmc value but have stabilizes also the system. In present work, the photogalvanic cell containing micelles system was compared with the cell containing photosensitizer and reductant sysem only (without micelles). The results are summerized in the Table 2.

Table 2: A comparative study of electrical parameters of the photogalvanic systems (With & without micelles)

S. No.	Electrical parameters	Observed Values	
		With Micelles[1]	Without micelles[2]
1.	Open circuit potential (V_{OC})	1057.0 mV	917.0 mV
2.	Short circuit current (i_{sc})	207.0 μA	167.0 μA
3.	Photopotential (ΔV)	893.0 mV	743.0 mV
4.	Maximum photocurrent (i_{max})	337.0 μA	247.0 μA
5.	Charging time	110.0 min.	150.0 min.
6	Rate of fall in photopotential	15.26mV $min.^{-1}$	15.20mV $min.^{-1}$
7.	Rate of initial generation of photocurrent	19.92μA $min.^{-1}$	16.26μA $min.^{-1}$
8.	Power at power point (pp)	70.74 μA	54.54 μA
9.	Fill factor	0.3233	0.2478
10.	Conversion efficiency	0.6800 %	0.4426 %
11.	Performance of the cell, $t_{1/2}$	98.0 min.	87.0 min.

3.3. Effect of variation of pH

It was observed that there is an increase in the electrical output of the cell with increase in pH values and maximum value reaches at a particular pH value (pH=12.70). On further increasing in the pH value, a decrease in the electrical output of the cell was observed. The results are summarized in the Table 1

It is quite interesting to observe that the pH at the optimum condition for the reductant has a relation with its pKa value, i.e. the desired pH value should be slightly higher then their pKa value (pH > pKa), this may be due to the availability of the reductant in an anionic form, which is a better electron donor then its unionized form.

[1] [NaLS] = 5.64 X 10^{-3} M, [Safranine] =4.60 X 10^{-5} M; [D-Xylose] = 1.42 X 10^{-3} M; pH = 12.70; Light intensity = 10.4 mW cm^{-2}; Temperature = 303 K
[2]; [Safranine] =4.32 X 10^{-5} M; [D-Xylose] = 1.40 X 10^{-3} M; pH = 12.92; Light intensity = 10.4 mW cm^{-2}; Temperature = 303 K

3.4. Effect of diffusion path length

The effect of variation of diffusion path length on the electrical output and initial rate of generation of different photocurrent of the cell was studied by using H-shaped cell of different dimensions. The results are summerized in Table 3.

Table 3: Effect of diffusion path length

Diffusion path length D_L (mm)	Maximum photocurrent i_{max} (μA)	Equilibrium photocurrent i_{eq} (μA)	Rate of initial generation of current (μA $min.^{-1}$)
35.0	329.0	213.0	17.25
40.0	333.0	210.0	18.82
45.0	337.0	207.0	19.12
50.0	340.0	205.0	19.92
55.0	342.0	202.0	20.24

It was observed that in first few minutes of illumination there was a sharp increase in photocurrent and there was a gradual decrease to a stable value of photocurrent. This photocurrent at equilibrium state is known as equilibrium photocurrent (i_{eq}). This kind of photocurrent behaviour is due to an initial rapid reaction followed by a slow rate-determining step at later stage. On the basis of effect of diffusion path length on the current parameters, it may be concluded that the leuco or semi reduced form of dyes and dyes itself are the main electroactive species at the illuminated and the dark electrodes, respectively. However, the reducing agent and their oxidized products behave as the electron carriers in the cell diffusing through the path.

3.5. Current-voltage (i-V) characteristics of the cell

The open circuit voltage (V_{oc}) and short circuit current (i_{sc}) of the cell were measured with the help of a digital pH meter (keeping the circuit open) and with a micrometer (keeping the circuit closed), respectively. The potential and current values in between these two extreme values (V_{oc} and i_{sc}) were recorded with the help of a carbon pot (log 470K) that was in the circuit of the microammeter and through which an external load was applied. The current voltage (i-V) characteristic of the cell is shown in Fig. 2.

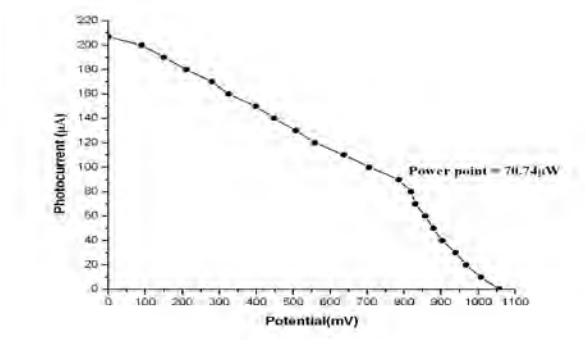

Fig. 2. Current-voltage (i-V) curve of the photogalvanic cell

It was observed that i-V curve for the cell deviated from their regular rectangular shape. A point in the i-V curve, known as power point (pp), was determined where the product of potential and current was maximum. With the help of the curve; fill factor (η) value 0.3233 was calculated using the following formula:

$$\text{Fill factor } (\eta) = \frac{V_{pp} \times i_{pp}}{V_{oc} \times i_{sc}} \quad (1)$$

Where V_{pp} and i_{pp} represent the value of potential and the current at the power point, respectively, and V_{oc} and i_{sc} represents open circuit voltage and short circuit current, respectively.

The conversion efficiency of cell was determined with help of photocurrent and photopotential values at power point (pp) and the power of incident radiation (light intensity 10.4 mW cm^{-2} which is measured by Solarimeter,CEL model SM 203), and it was 0.6800 % obtained by using the following formula:

$$\text{Conversion efficiency} = \frac{V_{pp} \times i_{pp}}{10.4\,\text{mW cm}^{-2} \times \text{Electrode area (cm}^2)} \times 100\% \quad (2)$$

3.6. Performance of the cell

The performance of the cell was studied by applying the desired external load ie resistance (carbon pot log 470 K) used as rheostate to vary the resistance, necessary to have the potential and current corresponding to the power point, after removing the light source of illumination till the output (power) was reduced to half its value (power = 70.74μW) at the power point in the dark. The performance was determined in terms of $t_{1/2}$ and it was observed that the cell can be used in the dark for 98.0 minutes, which directly indicates the storage capacity of the photogalvanic cell. The observed results are graphically shown in Fig.3.

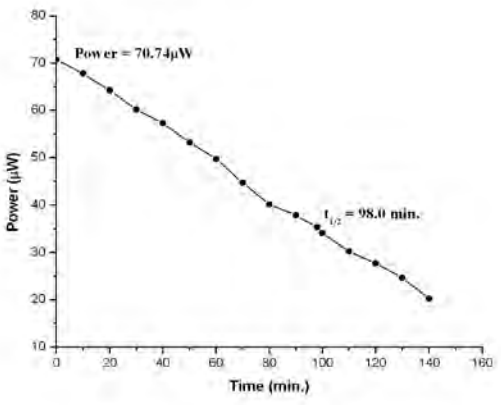

Fig. 3 Performance of the cell

4. Mechanism

On the basis of above observations, a tentative mechanism has been proposed for the generation of photocurrent in the cell as follows:

In illuminated chamber

$$\text{Safranine} \xrightarrow{h\nu} \text{Safranine}^* \quad (3)$$

$$\text{Safranine}^* + \text{D} - \text{Xylose} \rightarrow \text{D} - \text{Xylose}^+ + \text{Safranine}^- \text{ (Semi or leuco)} \quad (4)$$

At platinum electrode

$$\text{Safranine}^- \rightarrow \text{Safranine} + e^- \quad (5)$$

In dark chamber

At counter (SCE) electrode

$$\text{Safranine} + e^- \rightarrow \text{Safranine}^- \text{ (Semi or leuco)} \quad (6)$$

$$\text{Safranine}^- + \text{D} - \text{Xylose}^+ \rightarrow \text{Safranine} + \text{D} - \text{Xylose} \quad (7)$$

Where safranine* and D-xylose$^+$ are excited form of dye and oxidized form of reductant, respectively.

5. Conclusions

On the basis of the observed results of the photogalvanic cell containing NaLS, safranine and D-xylose system, we have observed that the micelles have not only enhanced the conversion efficiency but the performance of the cell also. Exhaustive efforts still have the scope to enhance the electrical output as well as performance of the photogalvanic cells alongwith reduction in their cost to make commercial viability.

References

[1] K. Becquerel, on electric effects under the influence of solar radiation, C. R. Acad. Sci., 9, 1839, 561

[2] E. K. Rideal, and E. G. Williams, The action of light on the ferrous iodine iodide equilibrium, J. Chem. Soc.,127, 1925, 258-269

[3] E. Rabinowitch, The photogalvanic effect I: The photochemical properties of the thionine-iron system. J. Chem. Phy., 8, 1940, 551-559

[4] Wendell M. Graven, Robert E. Salomon, and George B. Adams, Photogalvanic and photovoltaic effects with anodized zirconium and niobium electrodes, At. Energy Comm. TID-6514, 1960, 45-45

[5] D. E. Hall, William D. K. Clark, J. A Eckert, N. N Lichtin and P. D.Wildes, A photogalvanic cell with semiconductor anode, Ame. Ceramic. Soc. Bull., 56(4), 1977, 408

[6] O. Alfredo, P. Georgina and P. J. Sebasteian, Electron transfer via organic dye for solar energy conversion, Solar Energy Materials & Solar Cells, 59, 1990, 137-143

[7] M. Mukhopadhyay and B. B. Bhowmik, Kinetics of photoinduced electron transfer in a phptoelectrochemical cell consisting of thiazine dyes and Triton X-100 surfactant, J. Photochem. Photobiol. A: Chem., 69, 1992, 223-227

[8] J. Bisquert, D. Cahen, G. Hodes, S. Riihle and A. Zaban, Physical chemical principles of photovoltaic conversion with nanoparticles, mesoporous dye-sensitized solar cells, J. physical chemistry B, 108, 2004, 8106-8118

[9] G. J. Meyer, Molecular appraaches to solar energy conversion with coordination compounds anchored to semiconductor surfaces, Inorganic Chemistry, 44, 2005, 6852-6864

[10] S. C. Ameta, S. Khamesra, M. Bala and K. M. Gangotri, Use of micelles in photogalvanic cell for solar energy conversion and storage, Phill. J Sc., 119(4) 1990, 371-373

[11] S. Khamesra, S. Lodha, N. K. Jain and S. C. Ameta, Use of micelles in photogalvanic cell for solar energy conversion and storage: azur C-glucose system, Polish Journal of Chemistry, 65(2-3), 1991, 473-448

[12] S. Pramila and K. M. Gangotri, Use of anionic micelles in photogalvanic cells for solar energy conversion and storage: Dioctylsulfosuccinate–Mannitol–Safranine system, Energy Sources, Part A., 29, 2007, 1253-1257

[13] K. M. Gangotri and P. Gangotri, Studies of the micellar effect on photogalvanics: Solar energy conversion and storage–EDTA–Safranine O-Tween-80 system, Energy & Fuels, 23, 2009, 2767-2772

[14] K. R. Genwa and Mahaveer, Photogalvanic cell: A new approach for green and sustainable chemistry, Solar Energy Mat. & Solar Cells, 92(5) 2008, 522-529

[15] A. K. Jana and B. B. Bhowmik, Enhancement in power output of solar cell consisting of mixed dye, J. Photochem. and Photobio. A, 110, 1997, 41-46

[16] K. M. Gangotri and C. Lal, Studies in photogalvanic effect and mixed dye system: EDTA-Methylene blue-Toluidine blue system, Int. J. Energy Res., 24, 2000, 365-371

[17] C. Lal, Use of mixed dyes in a photogalvanic cell for solar energy conversion and storage: EDTA – thionine – Azur B system, J. Power Sources, 164(2), 2007, 926–930

[18] S. Dube, Simultaneous use of two reductants in a photogalvanic cell for solar-energy conversion and storage, Int. J. Energy Res., 17(4), 1993, 311-314

[19] K. M. Gangotri and V. Indora, Studies in the photogalvanic effect in mixed reductants system for solar energy conversion and storage: Dextrose and EDTA-Azur A System, Solar Energy, 84, 2010, 271-276

[20] K. R. Genwa, Arun Kumar and Abhilasha Sonel, Photogalvanic solar energy conversion: study with photosensitizers Toluidine Blue and Malachite Green in presence of NaLS, Applied Energy, 86, 2009, 1431-1436

[21] K. M. Gangotri and P. Gangotri, Studies of the micellar effect on photogalvanics: Solar energy conversion and storage–EDTA–Safranine O-CTAB system, The Arabian Journal for Science and Engineering, 35(1A), 2010, 19-28

[22] S. Yadav and C. Lal, Photogalvanic cells as a device for solar energy conversion and storage: An EDTA-New Methylene blue and Safranine O system, Energy Sources, Part A, 32, 2010, 1028-1039

[23] K. M. Gangotri and M. K. Bhimwal, Study the performance of photogalvanic cells for solar energy conversion and storage: Rose Bengal-D Xylose-NaLS system, Solar Energy, 84(7), 2010, 1294-1300

[24] K. M. Gangotri P. P. Solanki and M. K. Bhimwal, Use of anionic micelles in photogalvanic cells for solar energy conversion and storage storage: Sodium lauryl sulphate-Mannose-Brilliant cresyl blue system, Energy Sources: Party A, 2010, **accepted**.

[25] K. M. Gangotri and P. P. Solanki, Use of Sodium lauryl sulphate as a surfactant in photogalvanic cell for solar energy conversion and storage: Sodium lauryl sulphate-Methylene blue-Mannose system, Energy Sources: Party A, 2010, **accepted**.

New cadmium sulfide nanomaterial for heterogeneous organic photovoltaic cells

Jan Rohovec[1,*], Jana Touskova[2], Jiri Tousek[2], Frantisek Schauer[3], Ivo Kuritka[3]

[1] *Institute of Geology AS CR v.v.i, Prague, Czech Republic*
[2] *Department of Macromolecular Physics, Charles University in Prague, Prague, Czech Republic*
[3]*Polymer Centre, Tomas Bata University, Zlin, Czech Republic*
** Corresponding author. Tel: +420 233 087 258, Fax: +420 220 922 670, E-mail: rohovec@gli.cas.cz*

Abstract: Nanocrystalline cadmium sulfide particles were prepared by a new bench-top mild temperature procedure starting from cadmium ethylxanthate and using alkanolamines DEA, TEA as reaction media. The role of DEA, TEA in the whole reaction-nanocrystallization process is discussed. Basic spectroscopical properties of the new nano-CdS material formed were studied in order to characterize it as a material for the construction of photovoltaic solar cells.

Keywords: *Nanocrystalline Cadmium Sulfide, Preparation, Photovoltaic Solar Cells, Triethanolamine, Diethanolamine*

1. Introduction

Nanocrystalline cadmium sulfide is one of the most widely discussed and used material in the construction of photovoltaic solar cells. Several procedures for its preparation have been suggested. First synthetic approach to the nano-CdS is based on reactions in oleic acid or hexadecylamine at comparatively high temperatures (e.g., 160 °C), which results in the formation of nanoparticles covered by a surface shell of long, hydrophobic alkyl chains.[1] The prepared material is easy-to-handle, easily soluble in organic solvents, stable over a long shelf life, but the protective hydrophobic shell covering the nanoparticles hampered good performance of the material in solar cells. Some disadvantage of this approach is represented by the need of two different sources of cadmium and sulfur, e.g., $Cd(oleate)_2$ and S_8.

Another similar CdS synthesis based on the use of a trioctylphosphine oxide TOPO /trioctylphosphine TOP protective shell has been used for relatively long time, despite of the high toxicity and air sensitivity of the precursors.[2] It supplied cadmium sulfide nanomaterial of improved quality, but the photovoltaic properties were still not optimum.

A similar approach leading to CdS nanoparticles covered by long-chain alkylamine protective shell was designed, overcoming the need of two different educts bearing Cd and S for the product formation. As a starting compound bearing cadmium and sulfur in one molecule, various cadmium–sulfur containing precursors, like Cd-xanthates, thiocarbonates, thiophosphates etc. in alkylamine media (e.g., hexadecylamine HDA) were used in thermal decomposition techniques. In the reaction, the alkylamine molecule acts as a solvent and as a protective shell-forming agent at the same time.[3-6]

Experimental effort was then concentrated on the synthesis of protective shell-free nanoparticles. This was accomplished by the synthesis of CdS covered by HDA. The HDA protective shell was finally removed from the nanoparticle surface by extensive washing with pyridine.[7,8]

A more elegant method, directly leading to shell-free nano-CdS, is based on a template-free/shell-free formation of the target material by precipitation of Cd^{2+} salt in the medium of

in situ formed sulfide anion in aqueous media.[9] Sulfide is formed by hydrolytic reaction of thiosulfate anion $S_2O_3^{2-}$, thiourea, thioacetamide etc., possibly catalyzed by thioglycerol. The shell-free particles formed are less stable and much more difficult to handle, easily forming a coagulate, which is hardly re-dispersed. This type of nano-CdS is insoluble in organic solvents. On the other hand, improved material properties were demonstrated, such as electron exchange favorable for the construction of photovoltaic cells.

The optimized synthetic method of the nanocrystalline CdS formation should be a bench-top technique starting from well-defined, low-cost, stable and accessible educts, employing mild conditions, and not necessitating special precautions like inert atmosphere. Of course, a steady attention is given to the size, shape, homogeneity and size distribution of the nanoparticles formed.

In this paper, we report a synthesis of nano-CdS particles using a single-precursor, mild-temperature decomposition procedure. Cadmium ethylxanthate was used as a precursor. The key role in the procedure is played by the reaction medium used, namely diethanolamine DEA or triethanolamine TEA. The influence of alkanolamine on the material properties of the nano-CdS formed is discussed.

2. Methods

All chemicals used were supplied by the Sigma-Aldrich company. The alkanolamines diethanolamine DEA, triethanolamine TEA, and cadmium chloride hydrate were used as supplied without any further purification step, while potassium ethylxanthate was purified by dissolving in water and filtering through the 0.45 um RC filtration disc (Merck) in order to remove insoluble impurities. The potassium xanthate solution was reacted immediately after filtration.

UV VIS spectra were measured on the Cintra 303 spectrometer (GBC) in H_2O, DEA or TEA as a medium, in the range of 300–600 nm with a resolution of 2 nm. The course of nanocrystalline CdS formation was followed either by taking a sample of the reaction mixture and diluting it by H_2O or by a direct use of the reaction mixture.

Elemental analysis of the CdS product was performed on liquid samples formed by dissolution of sample in mixture of conc. nitric acid hydrogen peroxide in a closed vessel to ensure complete oxidation of the hydrogen sulfide released into the sulfate ion state. The samples were analyzed with the Intrepid DUO II ICP EOS instrument (Thermo Electron Corp.), using standard plasma conditions recommended by the manufacturer. In the same analytical run, trace impurities were checked as well.

Organic carbon content of the separated CdS nanoparticles was quantified in aqueous suspensions of the products by the Shimadzu analyzer, operated at 600 °C (catalytic oven temperature) with a run cycle of 10 min.

Samples for physical measurements were prepared by spin coating technique on either ITO glass substrates or p-silicon substrates. Approximately 100 µl of the DEA/TEA solutions of CdS were spread on the substrate at a rotation speed of 30–70 rps. The covered substrates were freeze-dried in the Alpha 1-2 (Christ) freeze-drying unit at 1E-4 kPa/-50 °C on a cooling system. The dried samples were handled in air at room temperature, being submitted for physical measurements as soon as possible.

Cadmium ethylxanthogenate (cadmium ethylxanthate) preparation and purification:

Cadmium ethylxanthate [$Cd(S_2C\text{-}OC_2H_5)_2$] was prepared basically according to the literature procedure, combining well stirred aqueous solutions of potassium ethylxanthate $KS_2C\text{-}OC_2H_5$ and cadmium chloride in a stoichiometric ratio.[3] The immediately formed white precipitate of cadmium ethylxanthate was filtered off and carefully washed with water to ensure removal of potassium and chlorides. After purification by re-crystallization, the product was dried overnight *in vacuo* and stored in a freezer at -20 °C. Elem. anal.: 31.9 % Cd, 36.26 % S, (ICP EOS).

Nanocrystalline cadmium sulfide was prepared using the following bench-top procedure:

Cadmium ethylxanthate (5–50 mg) was dissolved at a room temperature in alkanolamine (3 ml) without air exclusion. The dissolution was quite slow and was facilitated by intensive stirring by a glass rod. The yellowish solution obtained after a complete dissolution of the solid was heated in an air bath to 75–80 °C. The course of the reaction was followed by UV-VIS spectroscopy. After the formation of the target product, the reaction was interrupted by cooling of the reaction solution to a room temperature. The nanocrystals of the cadmium sulfide formed were either isolated by precipitation with copious amount of acetone and centrifugation, and purified by re-precipitation with acetone, or the reaction solution was used directly for the preparation of samples for physical measurements.

3. Results and Discussion

The procedure described above offers a preparative bench-top technique for the synthesis of CdS nanoparticles without the need of any special precautions like protection against air or moisture. It is based generically on literature reports, where the use of hexadecylamine HDA, oleylamine OA etc. as Lewis bases/reaction media, as well as shell-forming protective molecules is widely employed.[3-6] Similarly to the previous procedures, also the procedure described in this paper starts from easily accessible cadmium ethylxanthate, commonly used as a single-compound precursor for CdS formation. The mechanism of the cadmium ethylxanthate decomposition reaction used for CdS formation was proposed quite early and is generally accepted.[4]

We observed that the purity of the starting cadmium ethylxanthate is an important factor influencing the reproducibility of the crystallization of CdS. Older samples of cadmium ethylxanthate generally turn yellow due to decomposition, leading in our experience to a more rapid formation of CdS in the course of preparation.

The principal difference from the art known is based on the application of alkanolamines as reaction media for cadmium ethylxanthate decomposition. Alkanolamines, namely diethanolamine DEA $NH(CH_2CH_2OH)_2$ and triethanolamine TEA $N(CH_2CH_2OH)_3$, are commercially accessible, low-cost compounds with a good dissolution ability. We found that the above mentioned compounds can be successfully applied as solvents for cadmium ethylxanthate.

In the reaction course, they clearly play several roles. They act as:

i) high-boiling solvents with favorable viscosity characteristics,

ii) a weak base, catalysing the thermal decomposition of the Cd ethylxanthate precursor,
iii) a weakly coordinating medium for Cd ions,
iv) a shell-forming molecule.

The influence of the base on the thermal decomposition reactions of xanthates leading to the formation of metal sulfides was described in the literature. Similarly to the previous observation, the choice of solvent with appropriate basicity is essential also in the procedure discussed. In highly basic solvents, the decomposition of a xanthate precursor proceeds too fast upon the crystallization of sulfide of insufficient quality for photovoltaics, while in media of low basicity the thermal decomposition does not proceed at all. We had tried about 25 solvents before we concentrated on DEA/TEA. Aniline and its derivatives, pyridines or heterocycles, typically act as low basicity solvents. In contrast, short-chain primary amines were found to be too basic for the discussed application. The choice of over-basic medium leads to the decomposition of cadmium ethylxanthate already during the dissolution, thus the formation of CdS proceeds in a heterogeneous medium with serious consequences on the quality of the product formed.

There has been no discussion conducted yet as for the effect of coordination properties of the solvent used for nano-crystallization of cadmium sulfide. On the other hand, the coordination ability of the solvent during the thermal decomposition reaction governs the concentration of cadmium in the solution and can therefore strongly influence the crystallization process of CdS. The ability of DEA, TEA to coordinate cadmium ions in aqueous solutions is well documented, as well as the use of TEA as a masking agent in various analytical applications. In our case we expect that the nano-crystallization can be influenced by the formation of a complex between cadmium ions present in the reaction medium and DEA/TEA solvent. This complex consequently drives the crystallization process in the direction of the formation of CdS nanocrystals.

The reaction was followed by means of UV-VIS spectroscopy. In order to get a better insight into the time course of the reaction, lower temperatures and lower precursor concentrations were used than in the preparative procedure.

The evolution of UV-VIS spectra of the reaction system cadmium ethylxanthate/TEA *vs.* the reaction time is shown in Fig. 1. Absorption spectra obtained in the course of the nano-CdS formation show a gradual increase in the intensity of the excitonic transition as well as a shift of the signal toward higher wavelengths. The intensity of the transition reaches a plateau approximately after 60 min. as a result of the completion of the decomposition reaction. The shift of the signal reflects a gradual particle size increase. At the same time, the transition becomes broader, pointing to an increasing polydispersity of the product formed. This interpretation of UV-VIS spectral characteristics is in line with the previous works.[3,5] The particle size depends on the reaction time applied, thus the choice of the reaction time is a parameter useful for controlling the CdS particle size.

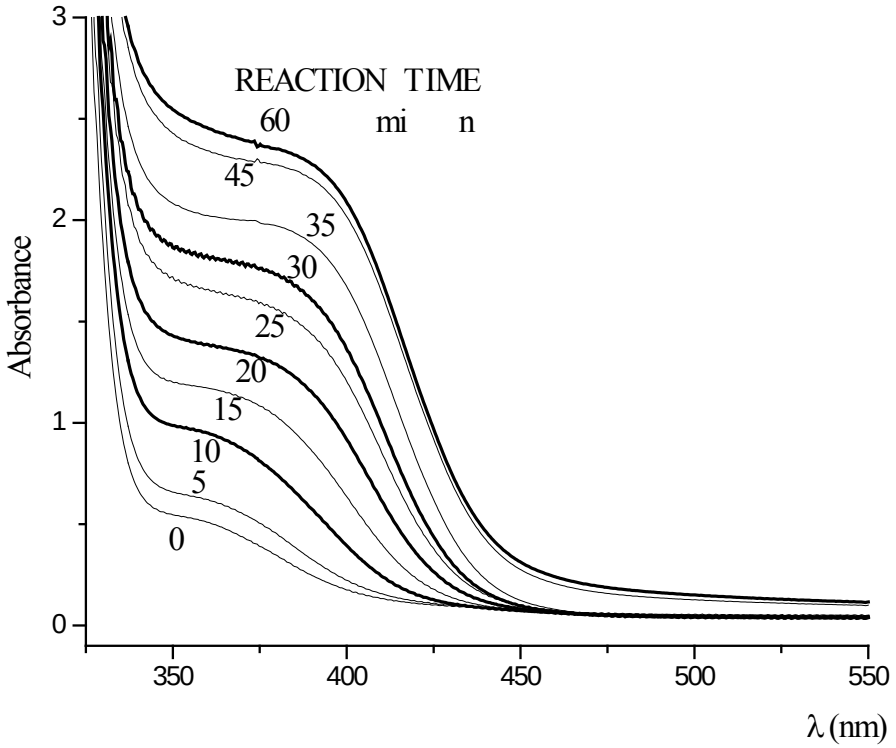

. Fig. 1. UV-VIS spectral study of the reaction course. Concentration of cadmium ethylxanthate 0.5 mg in 5 ml of TEA, reaction temperature 75 °C.

Another established parameter governing the growth and particle size is the concentration of the precursor in the reaction medium. In our case, we fixed the concentration of cadmium ethylxanthate at an appropriate value of 10 mg/ml given by the solubility of the precursor in all alkanolamines, without attempting to study this parameter in detail.

Reaction temperature critically influences the reaction course, reaction rate, size and the quality of the product formed. Alkanolamines are high-boiling compounds, so the reaction temperature can be chosen over a r elatively wide range. Typical UV-VIS spectra in a preparation run at several temperatures are demonstrated in Fig. 2.

In our experience, the decomposition reactions proceeds too fast at high temperatures, leading to smaller particles of insufficient quality. Therefore, the temperature area of 80 °C applied in the procedure described in the experimental section seems to be the optimum one, as the course of the reaction can be easily followed and the quality of the material produced is acceptable.

The nano-CdS particles can be easily isolated from the reaction medium by precipitation with an organic solvent, like ethanol or acetone. As the alkanolamines used as reaction media are freely miscible with common precipitation solvents, the choice of precipitants is not restricted to EtOH or acetone. After the synthesis, the alkanolamine molecule remains in touch with the nano-CdS particle, permitting the following manipulations, stabilizing the particle against coagulation, but can be easily removed as well.

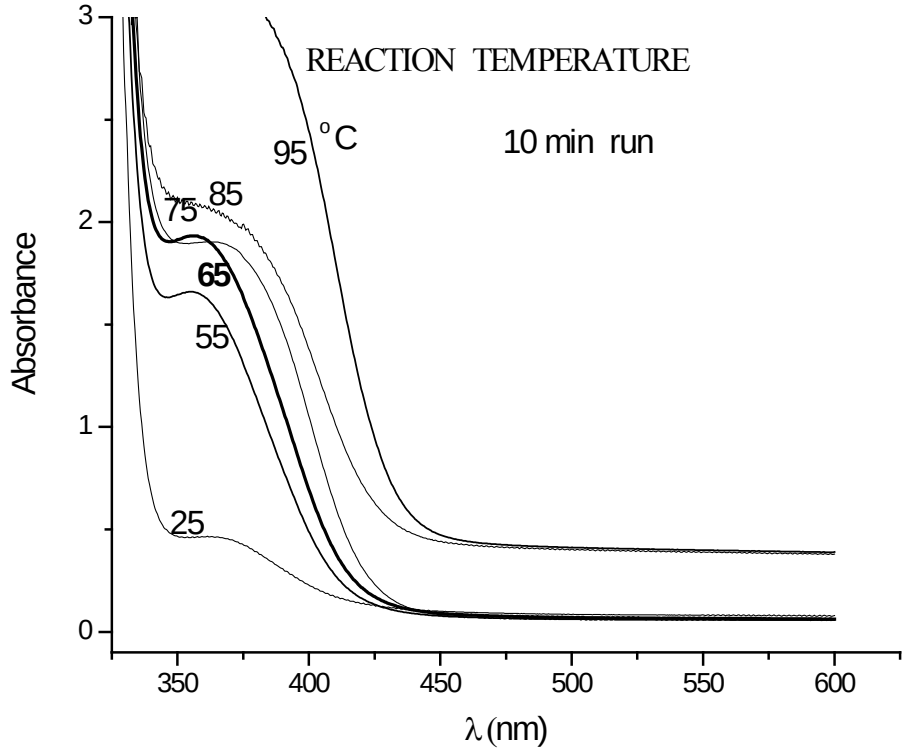

Fig. 2. UV-VIS spectral study of the reaction course. Concentration of cadmium ethylxanthate 0.5 mg in 5 ml of TEA, reaction time 10 min.

The presence of the alkanolamine protective shell on the surface of the CdS nanocrystals formed is another important point to be discussed. We tried to prove the presence of a DEA/TEA shell on the nano-CdS isolating the nanocrystals from the reaction medium by the precipitation procedure, washing the isolated material ten times with water and repeating the precipitation. The absence of free DEA in the final washings was proved by ninhydrine reaction, which is a sensitive color test for primary and secondary amine groups. After drying the preparation in a freeze drier, an elemental analysis was performed. Carbon content found in the preparation was 18 % C, which we explain by the presence of bonded/coordinated DEA/TEA on the surface of nano-CdS.

Indirect evidence also exists of the presence of the protective alkanolamine shell on the surface of the CdS nanocrystals. The nanocrystals formed are hydrophilic and can be easily re-dispersed in water. It should be empasized that the short alkyl-OH chains present in the alkanolamine molecules should not interfere in the electron transfer between CdS nanocrystals as strongly as the previously used long alkyl chains (HDA).

The elemental analysis of nano-CdS samples formed by the procedure under discussion proved the expected stoichiometric ratio Cd:S 1:1. The content of other metallic contaminants (Al, Ca, Fe, K, Mg, Mn, Na) in the sample was found to be negligible.

Spectral properties of the nano-CdS prepared were further studied by photoluminescence and Raman spectroscopy. In the PL spectrum, the peaks near 410 and 435 nm (excitation) are visible. In the Raman spectra of CdS nanoparticles isolated from the solutions in DEA and TEA, signals of DEA, resp. TEA are visible. This is in accordance with the results of

elemental analysis proving the presence of DEA/TEA in the final product. It is highly probable that the organic molecules form a protective shell on the nanoparticle surface. Besides the DEA/TEA signals, also spectral signals with Raman shifts of 300, 600 and 872 cm^{-1} (nano-CdS-DEA spectrum) and of 301, 602, 687 and 909 cm^{-1} (nano-CdS-TEA spectrum) were observed. The product was further studied by the TEM technique. The samples of nano-CdS taken from the reaction solution in DEA after a 20min. reaction at 85 °C (sample A), as well as in TEA after 20 min. and 120 min., respectively (samples B and C) were spin-coated. A successful observation of the nanocrystals was performed on silicon substrates. The TEM study was complicated by a very difficult removal of DEA, TEA from the samples.

4. Conclusions

We herein described the preparation of a new nanocrystalline CdS material, covered with a protective shell composed of triethanolamine or diethanolamine molecules. Due to the presence of the protective shell, the particles are highly hydrophilic. The new material is prepared from an accessible single precursor using a bench-top procedure and applying very mild reaction conditions. The factors controlling the reaction and nanocrystal formation are discussed. The preparation of the nano-CdS can be illustrated on the scheme below:

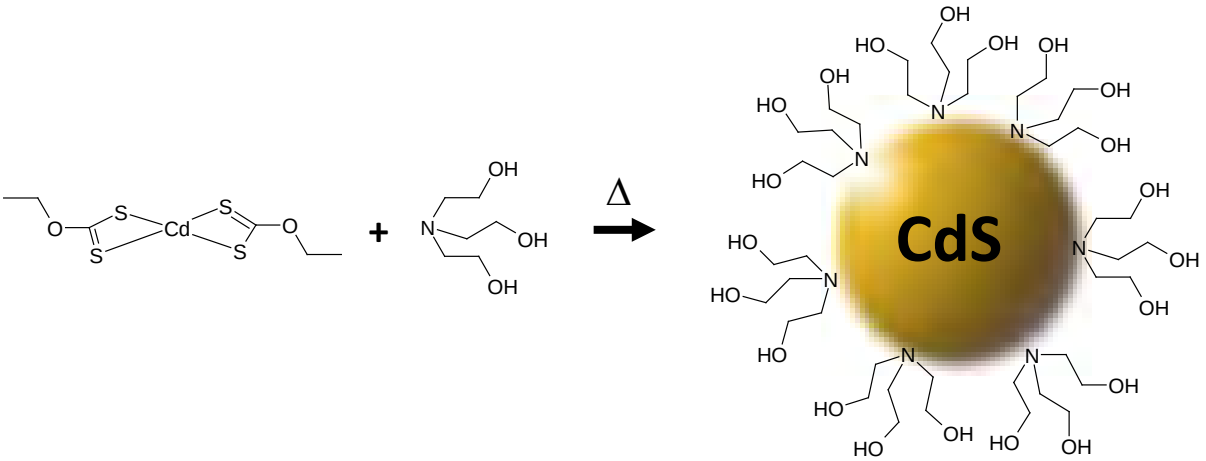

Acknowledgements

The project was funded by the Czech Science Foundation (GACR 202/09/1206) and Institutional Research Plan AV0Z30130516.

References

[1] Jin Joo, Hyon Bin Na, Taekung Yu, Jung Ho Yu, Young Woon Kim, Fanxin Wu, Jin Z. Zhang, Taeghwan Hyeon, Generalized and facile synthesis of semiconducting metal sulfide nanocrystals, J. Am. Chem. Soc. 125, 2003, pp. 11100 – 11105.

[2] Yongan Yang, Ou Chen, A. Angerhofer, C. Y. Cao, Radial-position-controlled doping in CdS/ZnS core/shell nanocrystals, J. Am. Chem. Soc. 128, 2006, pp.12428 – 12429.

[3] P. Sreekumari Nair, Thottaqckad Radhakrishnan, Neerish Revaprasadu, Gabriel Kolawole, Paul O'Brien, Cadmium ethylxanthate: A novel single-source precursor for the preparation of CdS nanoparticles, J. Mater. Chem. 12, 2002, pp. 2722 – 2725.

[4] Narayan Pradhan, Beni Katz, Shlomo Efrima, Synthesis of high-quality metal sulfide nanoparticles from alkyl xanthate single precursors in alkylamine solvents, J. Phys. Chem., 107 , 2003, pp. 13843 – 13854.

[5] Narayen Pradhan, Shlomo Efrima, Single-precursor, one-pot versatile synthesis under near ambient conditions of tunable, single and dual band florescing metal sulfide nanoparticles, J. Am. Chem. Soc. 125, 2003, pp. 2050 – 2051.

[6] Yunchao Li, Xiaohong Li, Chunhe Yang, Yongfang Li, Controlled synthesis of CdS nanorods and hexagonal nanocrystals, J. Mater. Chem. 13, pp. 2003, 2641 – 2648.

[7] Li Wang, YanShan Liu, Xi Jiang, DongHuan Qin, Yong Cao, Enhancement of Photovoltaic Characteristics Using a Suitable Solvent in Hybrid Polymer/Multiarmed CdS nanorod Solar Cells, J. Phys. Chem. C 111, 2007, pp. 9538 – 9542.

[8] Yan-Shan Liu, Wang Li, Dong-Huan Qin, Yong Cao, Photovoltaic devices from Multi-armed CdS nanorods and conjugated polymer composites, Chin. Phys. Lett. 23(12), 2006, pp. 3345 – 3348.

[9] C. Unni, Daizy Philip, S. L. Smitha, K. M. Nissamudeen, K. G. Gopchandran, Aqueous synthesis and characterization of CdS, CdS:Zn^{2+} and CdS:Cu^{2+} quantum dots, Spectrochimica Acta Part A 72, 2009, pp. 827 – 832.

CdS nanoparticles surfactant removal transport study by transient charge measurements

F. Schauer[1,3*], V. Nadáždy[2], Š. Lányi[2], J. Rohovec[4], I. Kuřitka[5], J. Toušková[6] and J. Toušek[6]

[1] *Department of Electronics and measurement, Tomas Bata University, Zlin, Czech Republic*
[2]*Institute of Physics, Slovak Academy of Sciences, Bratislava, Slovak Republic*
[3]*Department of Physics, Trnava University in Trnava, Trnava, Slovak Republic*
[4] *Institute of Geology, Academy of Sciences of the Czech Republic, Prague, Czech Republic*
[5]*Polymer centre, Tomas Bata University, Zlin, Czech Republic*
[6]*Department of Macromolecular Physics, Charles University in Prague, Prague, Czech Republic*
** Corresponding author. Tel: +420 605876867, E-mail: fschauer@fai.utb.cz*

Abstract: The electronic transport of CdS nanoparticles (nano-CdS) covered by hydrophilic alkanolamine molecules as surfactants was studied. The nanomaterial was prepared by low-temperature decomposition of cadmium ethylxanthate in hydrophilic solvents like mono-, di- or triethanolamine. The nanoparticles were isolated by precipitation procedures in solid state and they are easy to re-disperse in water systems. Films with nanoparticles were exposed to UV radiation, with the exposure varying in time interval 10 – 60 min.
The goal of the work was to study the electronic transport in the array of nanoparticles. The experimental techniques used was the Isothermal charge transient spectroscopy (IQTS) working with the a unique charge transient processor in the sampling range 2 μs – 900 ms with resolving power of about several hundreds of electrons. The second method was the surface photovoltaic method (SPV). Two basic novel phenomena were observed on the film formed by nano-CdS provided with tu surfactant, in *I-V* characteristics the increase of current was observed with a strong nonlinearity, marking the increased transport via nanoparticles, and the occurrence of charging–discharging phenomena with strong maximum described by the distribution of relaxation times and/or trapping states occurrence. The photoconductivity action spectra agree with the absorption edge of size distributed nanoparticles.

Keywords: *CdS nanoparticles, Alkanolamine surfactants, Isothermal charge transient spectrum, Hybrid solar cells.*

1. Introduction

The organic/inorganic hybrid solar cells work on the concept of bulk heterojunction, where excitons created upon photoexcitation are separated into free charge carriers at interfaces between two semiconductors-inorganic nanoparticle and bulk organic polymer forming a composite thin film[1][2][3]. Electrons will be then accepted by the inorganic nanomaterial with the higher electron affinity (electron acceptor, here the inorganic nanoparticle) and the hole by the polymer with the lower ionization potential (electron donor, here the polymer matrix). Both types of carriers are then transported by independent mechanisms to corresponding electrodes. The contemporary problems with the hybrid solar cells are the choice of suitable components for hybrid solar cells to match the solar spectrum, the solubility of both components and the transport of holes on the array of nanoparticles[4][5].

The aim of the paper is to elucidate the influence of the surfactant in the core – shell model on the transport of carriers (holes) by the process of diffusion on the array of nanoparticles. The main idea is to change the medium distance of nanoparticles by the surfactant length and thus changing the hopping probability of charge carriers resulting in the change of the average mobility and diffusion coefficient. For this purpose a new, extremely sensitive method for the study of transport and traps distribution, isothermal charge transient spectroscopy (IQTS) and surface photovoltaic method (SPV) for the diffusion study was used. For this purpose we examine one component of the hybrid organic/inorganic system MEH – PPV/nano-CdS nanoparticles covered by alkanolamine molecules as surfactant produced by a new technique.

2. Methodology

2.1. Sample preparation

The preparation of nano-CdS was described in detail elsewhere [6] so we will mention only few facts here. A new nano-CdS covered by hydrophilic alkanolamine molecules was prepared by low-temperature decomposition of cadmium ethylxanthate in hydrophilic solvents of mono-, di- or triethanolamine. By appropriate choice of reaction time, temperature and xanthate concentration, it was possible to tune the size and physical properties of resulting nanoparticles. The samples were deposited from ethanolamine solution by spincoating or drop casting on Au film evaporated on p-Si substrate or on borosilicate glass provided with ITO film and dried under the vacuum (rotary pump 10 Pa annealed at 80 ^{o}C and turbomolecular 10^{-4} Pa annealed at 100^{o}C) to remove the solvent. For the characterization of nanoparticles the UV-VIS absorption, photoluminescence and Raman spectroscopy was used [6].

2.2. Isothermal charge transient spectroscopy (IQTS)and Surface photovoltaic method (SPV)

Electronic transport measurements were performed with charge transient processor (CTP) in local mode [7], when the usual evaporated top electrode is replaced by the tip of the scanning probe in form of a sharpened 80-μm-tungsten wire oriented perpendicularly to the surface. The charge to voltage converter has the resolution of hundreds of electrons and time resolved transients from 2 μs to hundreds of ms can be recorded. The input converter integrates the current transients following the voltage pulses periodically applied to the sample. The duration of excitation pulses was set from 1 to 100 ms, their amplitude from 0.5 to 5 V, and the period from 147 to 547 ms. The isothermal charge transient spectrum (IQTS) is created by combining samples from charge transients at particular times using the formula $\Delta Q(t_1) = Q(t_1) - 1.5Q(2t_1) - 0.5Q(4t_1)$ [8] with t_1 swept with 2 μs step starting at the trailing edge of the pulse up to the maximal point for which $4t_1$ fits before start of the next pulse. This way of transient processing acts as a filter of measured relaxation times, i.e., IQTS signal is detected when the time constant of the relaxation process is comparable to t_1. In addition, this formula eliminates the linear component of the response, which is caused by the integration of dc current. The peak maximum corresponds to 0.174 of the total charge Q_0 responsible for the peak. To reduce the noise usually 50 transients were summed. The charge transient processor allows to evaluate in one special mode also the dc current by measurements of charge without application of excitation pulses using the formula: $I_{DC} = \Delta Q(t_2) - Q(t_1)) / (t_2\text{-}t_1)$, and to obtain the current voltage characteristic by sweeping the bias voltage.

2.2.1. Surface photovoltaic method (SPV) [9] [10]

Electrical field of space charge region (SCR) of the thickness d (Fig.1). drives the photogenerated charge carriers leading to the photovoltage. The photovoltage was measured in a sandwich structure between the substrate silicon and the top glass / ITO with a Mylar sheet serving as a separating dielectric layer The scanning microscope view of the film is in Fig.1. A capacitive couple is formed in this way. Illumination was performed through the top electrode into the bulk. The samples were irradiated by low-intensity monochromatic light chopped with a low frequency of 11 Hz generating an alternating voltage which was measured by lock-in amplifier Stanford SR 830. In our experiment the chopper frequency was sufficiently low to obtain saturated pulses not influenced by relaxations. The spectra were taken at room temperature and in air.

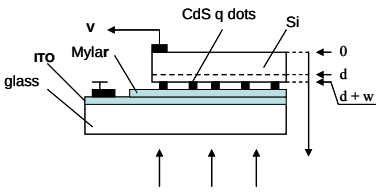

Fig.1. Arrangement of the SPV experiment. The polymer is illuminated with a chopped monochromatic light through transparent conductive electrode. As the second electrode serves the Si substrate.

3. Results

The SEM picture of the nano-CdS is in Fig.2 with the nanoparticles in the range of 20-30 nm. The representative I –V characteristics of Au / ano-CdS nanoparticles film / W probe (prepared in the standard way, i.e. annealed at 80 ^{o}C in the rotary pump 10 Pa vacuum) taken by IQTS for as deposited and UV irradiated sample (for 20, 40 and 60min are in Fig.3). We adjusted the filling and waiting time to ensure near to the steady-state characteristics. Corresponding IQTS signals are in Fig.4. The enormous increase of the *I-V* characteristics for positive applied voltage on ITO is recorded for degradation time 20 min, which gradually disappears with progressive degradation (40, 60 min). IQTS signals show for both polarities of the applied excitation pulses and do not depend on injection as the ability of both contacts (ITO and W) contacts are quite different as obvious from I–V transient characteristics. If we take into consideration the fact that the IQTS is stripped of the dc current, we then may conclude the observation is a bulk (contrary to contact) effect and most probably enhanced due to the decreased average distance among particles in the nano-CdS array.

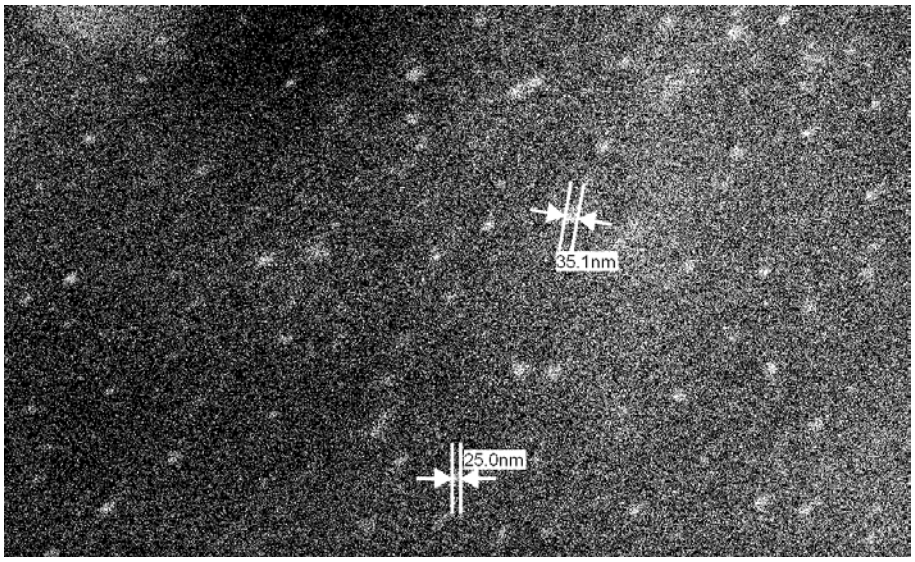

Fig.2. SEM photograph of nano-CdS on silicon substrate.

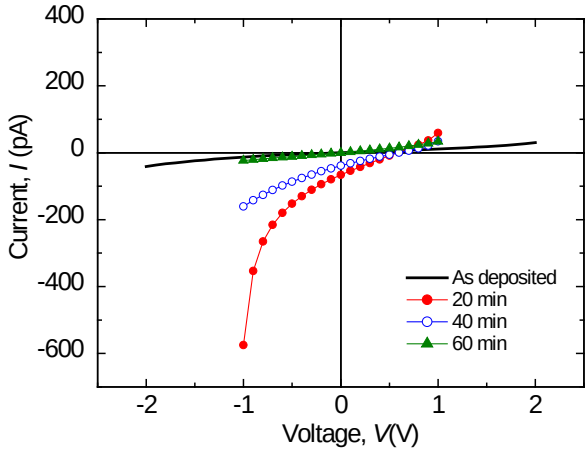

Fig. 3. Evolution of I-V characteristics (voltage is taken with respect to W probe) of the structure Au / nano-CdS nanoparticles film / W probe with exposure time to UV irradiation.

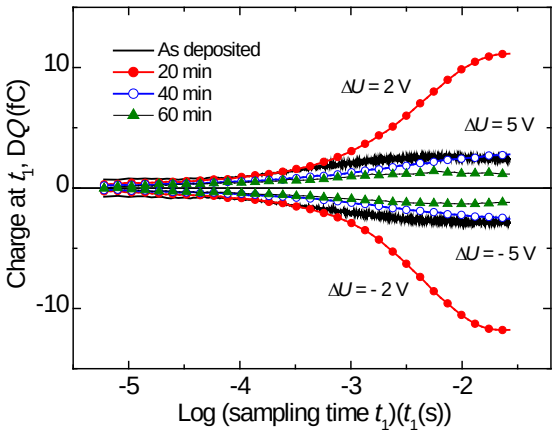

Fig. 4. Evolution of IQTS spectra of Au/nano-CdS /W.The parameter was the UV irradiation time and the polarity with respect to W tip. Bias voltage, U_b = 0, U_{ex}= 5 V for as deposited and 60 min exposed states, 2 V for 20 and 40 min exposed states. The period and duration of excitation pulses were set to 147 ms and 10 ms, respectively.

As the next step we measured we took the measurements on the identical sample degraded by 60 min UV (see Fig. 3 and Fig. 4) and carried out the anneal in vacuum 10^{-4} Pa at 100°C for 10 min. The I –V characteristics taken by CTP for annealed at 100°C and corresponding IQTS signals nearly returned to their original shapes (in Fig.3 and Fig.4). UV irradiation (for 20, 40 min) caused the same changes in I – V characteristics (Fig. 5) and corresponding IQTS signals in Fig. 6. The surprising recovery tendency and susceptibility to UV degradation changes are evident both in I - V and IQTS signals. The degradation for 20 min creates the bulk relaxation, similar to that in Fig.3 and Fig. 4.This observation may be due to the metastable degradation – recovery steps.

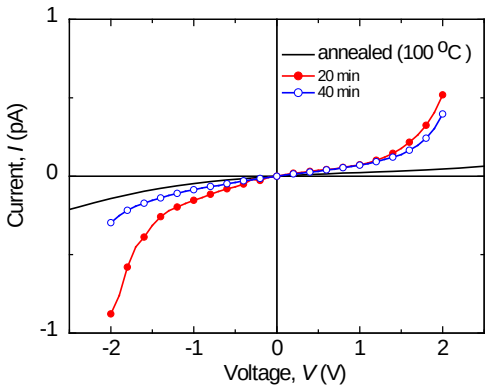

Fig. 5. Influence of annealing (100 °C for 10 min) on I-V characteristics (voltage is taken with respect to W probe) of the structure Au / nano-CdS nanoparticle film / W probe.

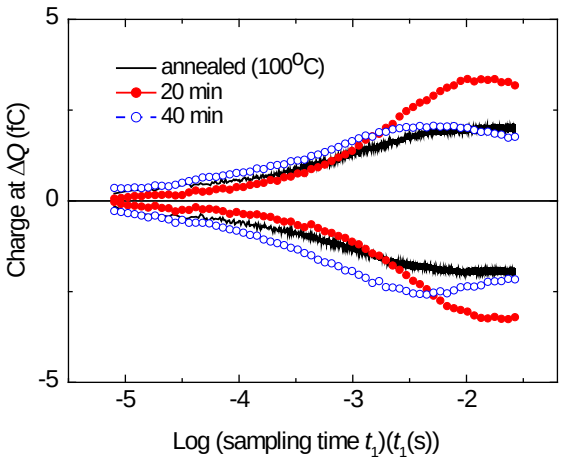

Fig.6. Influence of annealing (100 °C for 10 min on IQTS, all parameters identical to those in Fig.4.

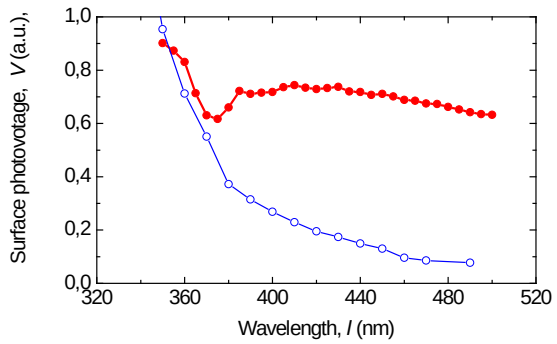

Fig.7. SPV spectrum of p-type silicon with nano-CdS (solid circles). The quantum size effect in the nanoparticles influences the spectrum from the 375 nm to 500 nm. SPV spectrum of the wafer is shown for comparison (open circles).

The SPV signals of nano-CdS on p-Si substrate isvisible in Fig. 7. The composed signal results both from photoconductivity of nano-CdS and from the Si substrate, as it is obvious from the signal on the bare Si substrate. The measurements of the diffusion coefficient in CdS due to the hopping transport diffusion is under way.

4. Discussion and Conclusions

The idea behind this experimental activity presented here was the obvious knowledge about the limiting ill influence of the hole transport in hybrid solar cells by hopping transport, where the average distance and coupling among particles was given by the shell (surfactant in this case) [4][5]. With this on mind and realizing our recent results on UV degradation of σ conjugated polymers resulting in weak bonds concept and metastability of PMPSi that may be recovered by alloying[11] we attempted to modify the interaction of nano-CdS provided with alkanolamine molecules as surfactant by UV radiation.

The results are encouraging. On the UV degradation considerable changes in relaxation processes of the fresh prepared sample (dried under vacuum 10 Pa and annealed at 80 ^{o}C) to irradiated (for 20 min), where relaxation process is emerging – subsequently disappearing (for 40 and 60 min) (Fig. 3 and Fig. 4). The same ordering of observations is visible when the same sample of nano-CdS is subjected to anneal at the turbomolecular vycuum 10^{-4} Pa and annealed at 100^{o}C (Fig. 5 and Fig. 6). No traps connected with the nano-CdS were visible on these experiments .

The detailed explanation is not obvious at the moment, there are following possibilities for explaining the observed phenomea. One is the decrease of the average distance among nanoparticles due to the decreased lengths of alkanolamine molecules due to their scissoring, or the stripping of the part of the alkanolamine molecules from CdS surface. Both these phenomena should posses the metastability in reconstruction of the original state by anneal.
The conclusions drawn from the presented results may be formulated:
- both applied highly sensitive methods of isothermal charge transient spectroscopy and surface photovoltaic method turned out to be very sutable methods for characterizing the transport processes in nanomaterials due to their sensitivity and spectroscopical character,

- the changes in surfactant on U V radiation cause the changes in collective relaxation processes and may positively influence the transport of hole charge carriers after their injection or charge-transfer processes. This may positively influence the efficiency of conversion of hybrid solar cells.

Acknowledgements

The work in Czech Republic was supported by the Grant agency of the Czech Republic under the project 202/09/1206.The work in Slovak Republic was supported by the ASFEU project Applied research of advanced photovoltaic cells, Activity 4.2, ITMS code 26240220047, supported by the Research & Development Operational Programme funded by the ERDF and by Slovak grant agency VEGA 2/0041/11.

References

[1] S. Gűnes, N. S. Sariciftci, Hybrid solar cells, Inorganica Chimica Acta 361, 2008, pp.581–588, D. J.Milliron, I. Gur, A. P. Alivisatos, Hybrid organic - Nanocrystal solar cells. Mrs Bulletin, 30, 2005, pp. 41-44.

[2] W. U. Huynh, J. J. Dittmer, A. P. Alivisatos, Hybrid nanorod-polymer solar cells, Science 295, 2002, pp. 2425-2427.

[3] W. U. Huynh, J. J. Dittmer, N. Teclemariam, D. J. Milliron, A. P. Alivisatos, K. W. J. Barnham, Charge transport in hybrid nanorod-polymer composite photovoltaic cells, Physical Review B 67, 2003, (11) 115326.

[4] I. Gur, N. A. Fromer, C. P. Chen, A. G. Kanaras, A. P. Alivisatos, Hybrid solar cells with prescribed nanoscale morphologies based on hyperbranched semiconductor nanocrystals. Nano Letters 2007, 7, pp. 409 -414,J.Rohovec, J.Touskova, J.Tousek, F.Schauer, I.Kuritka New cadmium sulfide nanomaterial for heterogenic organic photovoltaic cells, this conference.

[5] Š. Lányi, V. Nádaždy, Ultramicroscopy 110, 2010, p. 685.

[6] I.Thurzo, K. Gmucová, Rev. Sci. Instrum. 65, 1994, p.2244.

[7] J.Toušek, J.Toušková, Sol. Energy Mater. Solar. Cells, 92, 2008, p. 1020.

[8] J.Toušek, J.Toušková., I.Křivka, P.Pavlačková, D.Výprachtický,V.Cimrová,Org. Electronics 11, 2010, 50.

[9] F. Schauer, P. Schauer, I.Kuřitka, H. Bao,, Conjugated Silicon–Based Polymer Resists for Nanotechnologies: EB and UV Meditated Degradation Processes in Polysilanes. Materials Transactions, Special Issue on D evelopment and Fabrication of Advanced Materials Assisted by Nanotechnology and Microanalysis, 51, 2010, pp.197-201.

Charge transient and electrochemical measurements as a tool for characterization and degradation study of organic semiconductors - PMPSis and MEH-PPV

V. Nadáždy[*,1], K. Gmucová[1], Š. Lányi[1], F. Schauer[2,*], and I. Kuřitka[2]

[1]*Institute of Physics, Slovak Academy of Sciences, Bratislava, Slovak Republic*
[2]*Department of Electronics and measurement, Tomas Bata University, Zlin, Czech Republic*
** Corresponding author. Tel: +421 220910761, E-mail:vojtech.nadazdy@savba.sk*

Abstract: This contribution deals with application of several techniques based on charge transient contactless measurements (isothermal charge transient spectroscopy - IQTS), and by electrochemical methods of double step voltcoulometry and cyclic voltammetry, two complementary methods, which are potentially suitable for obtaining information about bulk relaxation and transport processes and the structure of electronic localized states and their basic parameters. Both methods were tested by two well known polymers, the first, Poly[methylphenylsilylene] and the second Poly(p-phenylene vinylene. The results were explained both in terms of bulk relaxation ant transport processes, trap parameters and the influence of UV degradation. The metastability in reconstruction of dangling bonds ensuing after the UV degradation due to the Si-Si σ conjugated bond scission and its ability to reconstruct after the thermal anneal was again found in accord with the previous results.

Keywords: *Organic semiconductors characterization, Electron structure, Transient charge method, Electrochemical method.*

1. Introduction

The material research in organic semiconductors is moving towards the applications. When optimizing the properties of devices one has to start from the correct microphysical parameters of materials in question. The complicating factors in this direction is weak (molecular) coupling and the disordered structure, which both make the spectroscopic methods known from disordered inorganic semiconductors difficult and sometimes impossible to apply. So the need for new methods is acute and the new methods have been developed for organic material characterization.

It was shown that suitable techniques to electrical characterization of organic materials are space charge limited currents [1] and thermally stimulated currents [2]. As a favorable approach turns out capacitance or charge transient measurements which are processed by properly combined values of measured transients taken at specified time instants originally applied in deep-level transient spectroscopy of defect states in inorganic semiconductors. This transient processing allows to determine salient features of the transport states distribution [3] and charge traps induced by structural or chemical defects [4-6]. Electron transport based on hopping is important in polymers and localized molecular traps serve as redox sites. These facts authorize the application of solid-state electrochemical measurements. Some issues related to the principles and analytical aspects of electrochemical techniques were discussed in review by P.J. Kulesza and J.A. Cox [7].

Here we present two new methods with expressed advantages for the application in the field of molecular materials, isothermal charge transient spectroscopy and double state voltcoulometry. Both methods are based on the injection (extraction) contacts and the resulting signals in the time domain, which is analyzed for the capacitance and diffusion currents, respectively. Thus, we obtain information about capacitive (displacement) and

diffusive (reduction-oxidation) phenomena that are quite complementary for the defects elucidation.

In the presented paper, we starting from the well known prototypical polymer - Poly[methylphenylsilylene] (PMPSi), intend to test both the methods by comparison with previous results and then to apply it on quite important in the field of organic photovoltaics - Poly(p-phenylene vinylene) (PPV).

2. Methodology

2.1. Sample preparation

Poly[methylphenylsilylene] (PMPSi) was purchased from Flurochem. PMPSi thin films were spin-coated from solution in toluene on the UV-ozone treated ITO substrates with a spin rate of 1500 rpm for 30 s and dried in vacuum of $3x10^3$ Pa at 60 ^oC for 4 hrs. Poly[2-methoxy-5-(2'-ethyl-hexyloxy)-1,4-phenylene vinylene] (MEH-PPV) was supplied by Aldrich and solved in tetrahydrofuran. The MEH-PPV films were also spin-coated on the UV-ozone treated ITO substrates with a spin rate of 4800 rpm for 30 s and dried in vacuum of 10^4 Pa at 100 ^oC for 12 hrs. Exposition to UV irradiation + ozone of thin films under investigation were done with low-pressure mercury lamp with the total UV intensity at the sample surface of 2 mW/cm^2 and the ozone concentration was 150 mg/m^3.

2.2. Isothermal charge transient spectroscopy - IQTS

The principle of the method IQTS is based on the time representation of the charge, induced in the external circuit by the driving pulse applied to the sample. This charge may be either due to the bulk relaxation processes, charge redistribution or release of charges from localized centres (traps). In this respect it is very similar to the method of post-transit extraction spectroscopy, where charges released from traps are time resolved collected and evaluated spectroscopically [1]. The IQTS spectrum is created by combining samples from charge transients at particular times using the formula $\Delta Q(t_1) = Q(t_1) - 1.5Q(t_2 = 2t_1) - 0.5Q(t_3 = 4t_1)$ [8] (see Fig. 1). The rate window τ defined by this filter is $1/t_1$ and it removes the linear component of the response, which is caused by the integration of direct current. The peak maximum corresponds to 0.174 of the total collected charge Q_0 responsible for the peak. Omitting the excitation pulse and the charge processing using the filter formula $I_{DC} = (Q(t_2) - Q(t_1)) / (t_2 - t_1)$ (see Fig.1) allows to evaluate direct current which flows through the sample. The measurement of current-voltage (I-V) characteristic is obtained by sweeping the bias voltage applied to the sample.

Electronic transport measurements were performed with charge transient processor (CTP) in local mode [9] when the usual evaporated top electrode is replaced by the tip of the scanning probe in form of a sharpened 80-μm-tungsten wire oriented perpendicularly to the surface. The charge to voltage converter has the resolution of hundreds of electrons and time resolved transients from 2 μs to hundreds of ms can be recorded. The duration of excitation pulses was set from 1 to 100 ms, their amplitude from 2 to 5 V, and the period from 147 to 547 ms. To reduce the noise usually 50 transients were collected and averaged. The I-V characteristics were measured with the sweeping rate of 100 mV/s. All IQTS and I-V measuremen were done at room temperature.

2.3. Double step voltcoulometry - DSVCM

The double step voltcoulometry (DSVCM) is a complementary method for studying the electrochemical processes in investigated material. While with the help of the electrical

methods the concentration of the active species and their energies either for the capture or for the emission from a defect/deep trap is measured, electrochemical methods yield the potential at which either reduction or oxidation of species under consideration take place. Realizing that oxidation describes the loss of electrons, while the reduction describes the gain of electrons, the emission from electron traps can be regarded as an oxidation process, the capture of electrons in electron traps as a reduction process. On the contrary, for hole traps the emission of holes from hole traps can be regarded as a reduction process, the capture of holes in hole traps as an oxidation process. Thereby the electrochemical methods can serve as a complementary and powerful tool for the study of the defect states formation or removing in organic semiconductors. Recently, we have reported the electrochemical observation of the formation of hydrogen- and hydroxyl-related defects in pentacene thin films [10].

The electrochemical analyser used in this work, developed in our laboratory, is similar in function to CTP [11]. During the single potential scan both the ramp voltage (voltammetric wave) and the incremental charge (voltcoulometric signal) are obtained. The excitation pulse is switched on and the transient current flowing in external circuit is integrated and processed by the time-domain filter $\Delta Q(t_1) = Q(t_1) - 2Q(t_2 = 5t_1) - Q(t_3 = 9t_1)$. This filtering scheme analogous to filter for IQTS eliminates both the constant and linear components of the signal, i.e. suppression of both the steady-state and capacitive contributions of the transient current with respect to the diffusion current contribution. The amplitude of measured signal reflects not only the concentration of measured species, but also the kinetics of the measured charge transfer. A peak present only at the recorded voltcoulometric signal, which is not accompanied with a voltammetric wave, originates in the charging of an electrical double layer only.

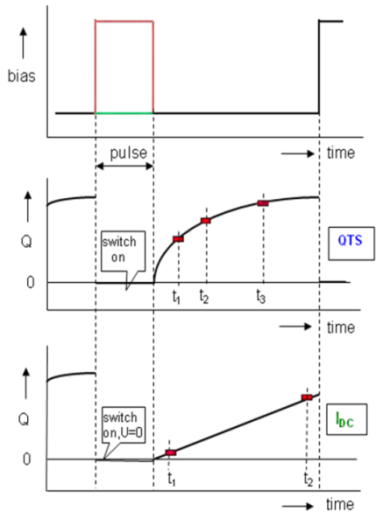

$$\Delta Q = Q(t_1) + aQ(t_2) + bQ(t_3),$$

$$I_{DC} = \left[\frac{Q(t_2) - Q(t_1)}{t_2 - t_1}\right].$$

Fig. 1. Timing chart of the applied voltage and measured charge transients used for isothermal charge transient spectroscopy (IQTS), direct current, I_{DC}, measurement, and double step voltcoulometry (DSVCM). The coefficients a, b, t_2, and t_3 are set as follows a = - 1.5, b = 0.5, $t_2 = 2t_1$, $t_3 = 4t_1$ for IQTS and a = - 2, b = 1, $t_2 = 5t_1$, $t_3 = 9t_1$ for DSVCM.

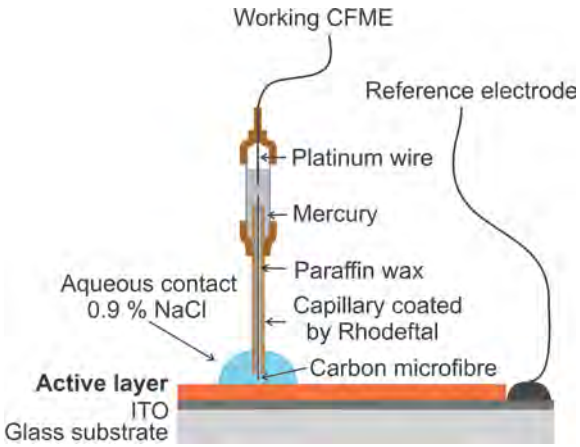

Fig. 2. Setup of electrochemical experiments.

The electrochemical experiments were carried out by the apparatus depicted in Fig. 2. The working carbon fiber microelectrode (CFME) was formed of a glass micropipette with up to eight carbon fibers (diameter of each fiber being approximately 7 - 8 μm). The pipette tip (diameter 100 - 150 μm) was filled with paraffin wax to prevent liquid from seeping inside around the carbon fibers. The exposed surfaces of the filaments were treated electrochemically before starting the experiments. First, a cathodic potential of - 0.8 V was applied for 40 s, followed by a triangular waveform of 0 to + 3 V for 10 s; finally, an anodic potential of + 1.5 V was applied for 10 s. The reported results correspond to the measurements made for the sweeping rate of 33.3 mVs^{-1}, the potential step amplitude for the voltcoulometric period of measurement was set to - 0.1 V and to 0.1 V for the anodic and cathodic scans, respectively.

3. Results

The representative signals measured on the PMPSi samples are in Figs. 3, 4, 5 for the fresh sample and subsequently degraded by the UV in time steps 2, 5 and 10 min. The remarkable increase in hole injection ability of the ITO contact was recorded (Fig.3a). The IQTS signal (Fig. 3b) measured on identical spots shows first neither the bulk relaxation processes or trapping states, on UV degradation gradual development of the hole trap states is observed, with the most expressed signal at t_1= 1.5 ms for degradation time 10 min. To examine the time dependence of the emitted carriers from the traps, the influence of the extraction voltage (U_b), keeping the injecting charge constant (given by U_b - ΔU) were measured (see Fig. 4). The signal shifts to shorter times t_1 with increasing U_b as expected due to the shorter extraction. On the contrary when applying the injecting voltage on tungsten electrode, it results in virtually no filling of the trapping states and only small IQTS signal is detected.

The steady-state voltammetry and DSVCM signals on identical samples of PMPSi are in Fig. 5a for anodic scans (ramp voltage is going from -1.5V to 1.5V) and in Fig. 5b for cathodic scans (from 1.5 V to -1.5 V). Steady-state voltammetry offers potential – current characteristics, where the presence of electrically active centre (defect) is detected by the presence of voltammetric wave, whose amplitude is proportional to the concentration of this centre. Therefore, the increasing current wave near the potential of + 0.8 V depicted in Fig. 5a corresponds to evolution of a defect in PMPSi, which is caused by the exposure of the PMPSi

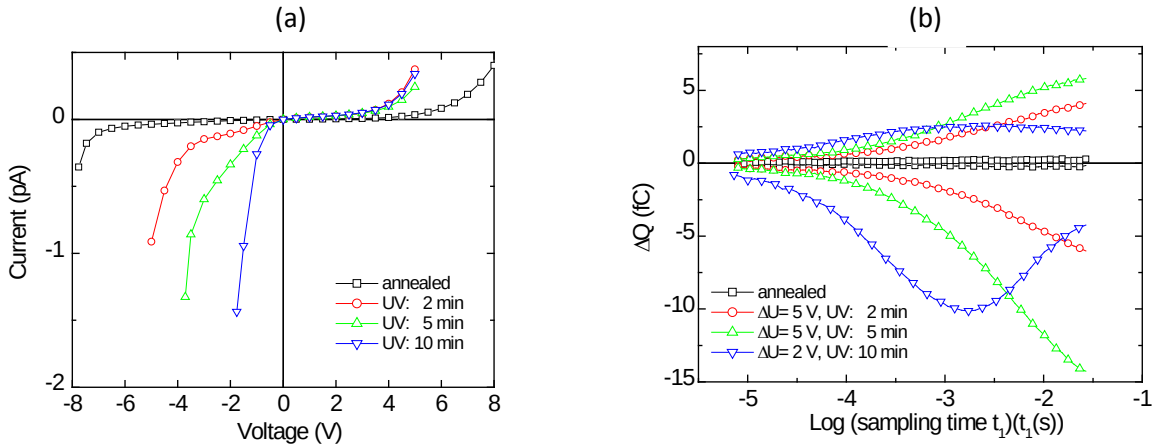

Fig. 3. Evolution of current – voltage characteristics (a) and IQTS spectra (b) of the structure ITO /PMPSi/ W probe with exposition time to UV irradiation. IQTS spectra in upper and lower parts correspond to excitation with positive and negative pulses. Bias voltage, U_b = 0, the height of excitation pulses takes into account the electrical conductivity of the PMPSi film: 5 V for annealed, 2, and 5 min for irradiated samples, 2 V for 10 min irradiated sample. The period and duration of excitation pulses were set to 147 ms and 10 ms, respectively.

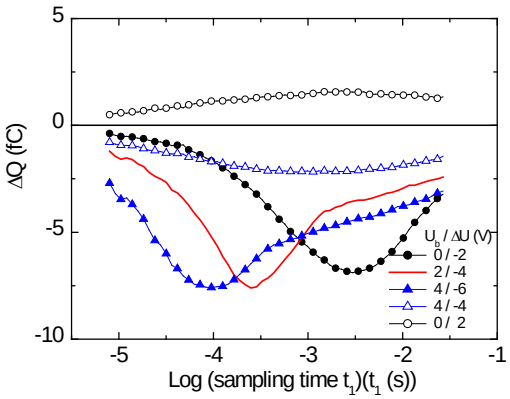

Fig. 4. Effect of bias voltage and the height of excitation pulses on the IQTS peak observed on ITO / PMPSi / tungsten probe structure after 10 min of exposure to UV irradiation. The period and duration of excitation pulses were set to 147 ms and 10 ms, respectively.

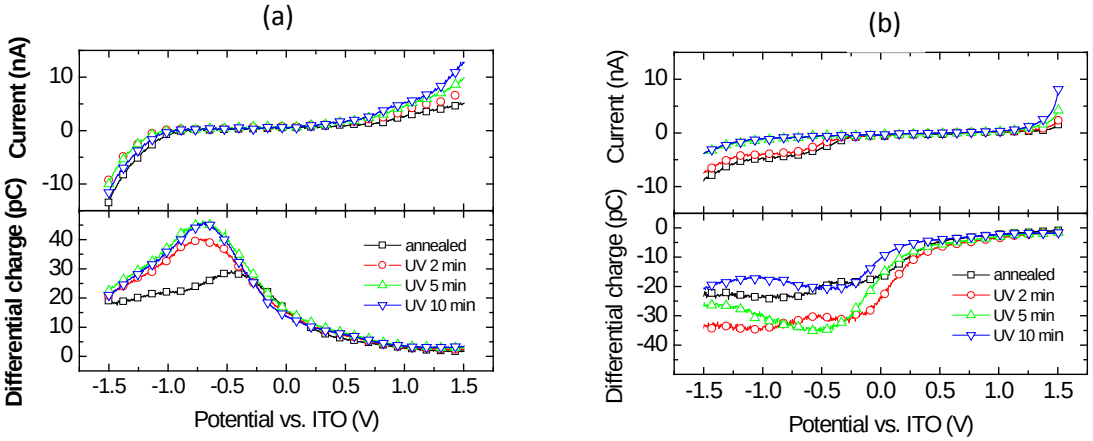

*Fig. 5. Voltammetric (upper part) and voltcoulometric (lower part) signals obtained for PMPSi thin film during (a) **anodic scans**, i.e, for the potential swept from -1.5 V to 1.5 V and (b) **cathodic scan**, i.e., for potential swept from 1.5 V to -1.5 V. Individual data sets have been obtained for various exposition times to UV irradiation.*

to UV irradiation. The position of voltcoulometric peak does not in general match the position of voltammetric wave on the I-V characteristic; the difference depends on the ratio of the apparent diffusion coefficients for the measured charge transfer of capture and emission of electrons or holes. Therefore, the tiny increase of voltcoulometric signal observed at potential + 0.5 V (Fig. 5a, lower part) can be related to the voltammetric wave at + 0.8 V.

While the voltammetric wave (anodic scan) in Fig. 5a is caused by the capture of holes by trap or the emission of electrons from trap, voltammetric wave in Fig. 5b (cathodic scan) represents measurement of electron capture or hole emission from the trap. Thus, the discharge of the process at about – 0.5 V (observed on both the voltammetric and voltcoulometric signals) can be regarded as drop-out of the ability of the PMPSi to capture electrons or emit holes from a PMPSi matrix after 5-minute exposure to UV irradiation. It should be noted that I-V characteristic and IQTS spectrum of anneled state was recovered by annealing the sample in vacuum at 80°C for 1 hour.

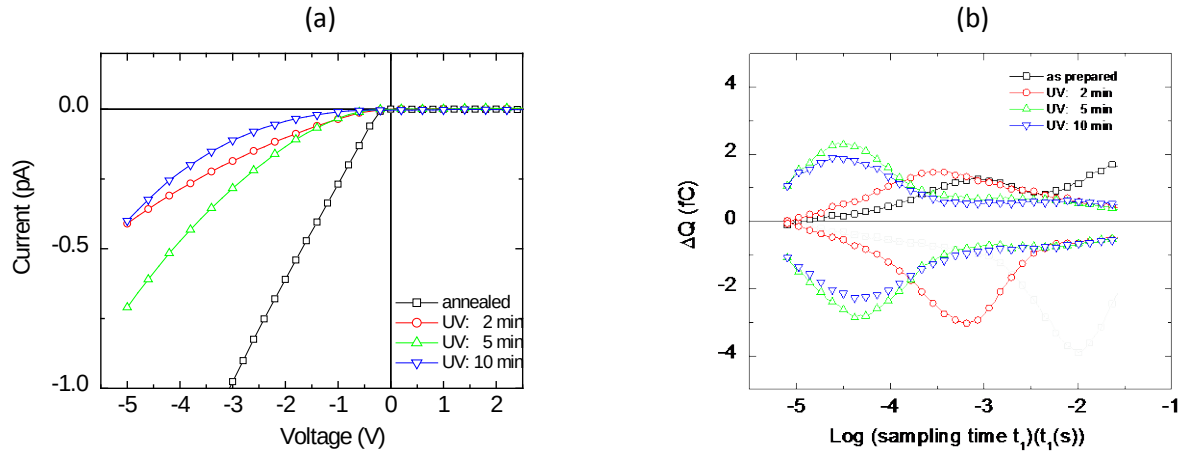

Fig. 6. Evolution of current – voltage characteristics (a) and IQTS spectra (b) of the structure ITO / MEH-PPV / tungsten probe with exposition time to UV irradiation. IQTS spectra in upper and lower parts correspond to excitation with positive and negative pulses. Bias voltage, U_b = 0, the height of excitation pulses was set to 5 V for annealed and exposed states. The period and duration of excitation pulses were set to 147 ms and 10 ms, respectively.

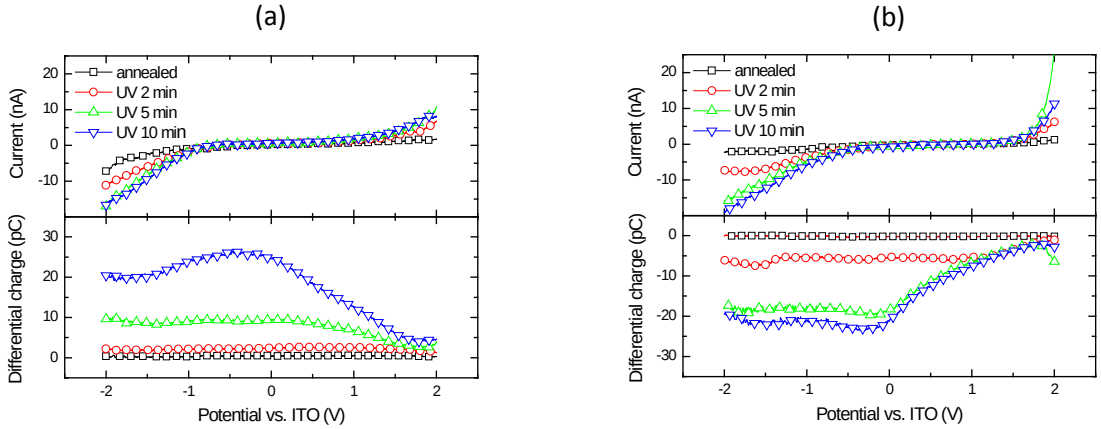

*Fig. 7. Voltammetric (upper part) and voltcoulometric (lower part) signals obtained on MEH-PPV thin film during (a) **anodic scan**, i.e, for potential swept from -1.5 V to 1.5 V and (b) **cathodic scan**, i.e, for potential swept from 1.5 V to -1.5 V. Individual data sets have been obtained for various exposition times to UV irradiation.*

Similarly, the signals in MEH PPV are visible in Fig. 6a (I-V) and Fig. 6b (IQTS). The behavior is quite different, as the injecting properties with UV irradiation decrease, contrary to PMPSi. The IQTS signals depict no trapping, but only bulk relaxation effects, testified by symmetrical signals for both polarities, independent on injection. Also, the DSVCM signals in Fig. 7a (anodic scan) and in Fig. 7b (cathodic scan) give evidence of the evolution of a charge transfer process caused by UV at about – 1.5 V.

4. Discussion and conclusions

In Fig. 8 there are the results of post-transit spectroscopy on PMPSi achieved by large signal transient SCLC [1]. The extreme filling of the traps was achieved by laser injection. On UV degradation the Si-Si σ bond breaking leads to the metastable states at about 0.55 eV, which are fully reconstructed on annealed [1]. The method is identical to IQTS with much less influence on the sample (UV laser used) due to its extreme sensitivity.

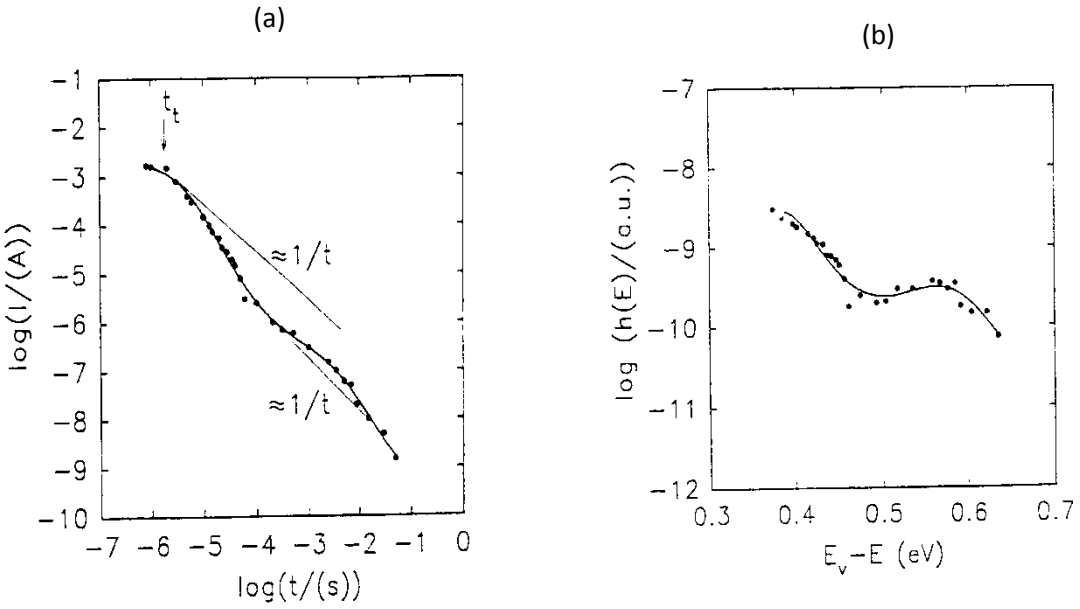

Fig. 8 The post-transit current in large signal SCLC on P MPSi (a), the corresponding DOS distribution (b).

UV irradiation causes bulk modification of both PMPSi and MEH-PPV films under investigation. It is remarkable that the same degradation treatment leads to opposite effect on I-V characteristics. The hole injection in the metal insulator metal (MIM) structure with PMPSi increases but that with MEH-PPV shows decrease of hole injection with degradation. The evolution of corresponding IQTS spectra (Fig. 3b and 6b), voltammetric, and voltcoulometric signals (Figs. 5 and 7) with time exposition to UV irradiation are rather complex. However, some common trends in their behavior can be inferred from the comparison with the evolution of I-V characteristics. Improvement of the hole injection for PMPSi leads to asymmetry of IQTS spectra for negative and positive polarity of excitation pulses. In voltamogram, decay of the current wave at negative potential of – 0.5 V is observed and the voltammetric wave at + 0.8 V is simultaneously developed. Deterioration of the injection for the structure with MEH-PPV is correlated with the development of symmetric

IQTS peak located at about 50 μs and voltammetric wave at about -1.5V. There is a clear two-step increase of this wave and shift in the IQTS peak position.

Steady-state voltammetry offers I-V characteristics, where the presence of electrically active centre (defect) is detected by the presence of voltammetric wave, which amplitude is proportional to the concentration of this centre. Voltammetric wave definitely reveals the presence of redox centers, i.e. electrically active traps. It means that in PMPSi some deep centers (continuum, corresponding to tail of IQTS spectra) decays and a shallower one arises. The increasing current wave near the potential of + 0.8 V depicted in Fig. 3 corresponds to evolution of a defect center in PMPSi caused by the exposure of the PMPSi to UV irradiation, which mediates charge transfer through redox reaction. On the other hand, the process at about – 0.5 V (observed on both the voltammetric and voltcoulometric signals) can be regarded as drop-out of other redox centre in PMPSi matrix after 5-minute exposition to UV irradiation + ozone. This process is accompanied with more effective hole injection. In the case of MEH-PPV, voltammetric wave at -1.5 V indicates a redox centre (trap). The IQTS peak position at 50 μs supposes relatively shallow trap. The determination of the activation will require IQTS measurements at several temperatures.

Acknowledgements

The work in Slovak Republic was supported by the ASFEU project Effective control of production and consumption of energy from renewable resources, Activity 4.2, ITMS code 26240220028, supported by the Research & Development Operational Programme funded by the ERDF and by Slovak grant agency VEGA, projects 2/0093/10 and 2/0063/11.

References

[1] F. Schauer, Space-charge-limited photoconductivity in polymers, Czech. J. Phys. 49, 1999, p. 871.

[2] J. Steiger, R. Schmechel, H. von Seggern, Synthet. Metals 129, 2002, p. 1.

[3] A.J. Campbell, D.D.C. Bradley, E. Werner, W. Brutting, Organic Electr. 1, 2000, p. 21.

[4] Y.S. Yang, S.H. Kim, J. Lee, H.Y. Chu, L. Do, H. Lee, J. Oh, T. Zyung, Appl. Phys. Lett. 80, 2002, p. 1595.

[5] C. Renaud, T.P. Nguyen, J. Appl. Phys. 107, 2010, p. 124505.

[6] I. Thurzo, H. Mendez, D.R.T. Zahn, phys. stat. sol (a) 202, 2005, p. 1994.

[7] P.J. Kulesza, J.M. Cox, Electroanalysis 10, 1998, p. 73.

[8] I. Thurzo, K. Gmucová, Rev. Sci. Instrum. 65, 1994, p. 2244.

[9] Š. Lányi, V. Nádaždy, Ultramicroscopy 110, 2010, p. 685.

[10] K. Gmucová, M. Weis, M. Della Pirriera, J. Puigdollers, phys. stat. sol. (a) 206, 2009, p. 1404.

[11] I. Thurzo, K. Gmucová, J. Orlický, J. Pavlásek, Rev. Sci. Instrum. 70, 1999, p. 3723.

Fabrication of Annealing-Free High Efficiency and Large Area Polymer Solar Cells by Roller Painting Process

Jae Woong Jung, Won Ho Jo*

Department of Materials Science and Engineering, Seoul National University, Seoul, Korea
** Corresponding author. Tel: +8228807192, Fax: +8228766086, E-mail:whjpoly@snu.ac.kr*

Abstract: The polymer solar cells were fabricated by a novel solution coating process, the roller painting. The roller painted film composed of poly(3-hexylthiophene) (P3HT) and [6,6]-phenyl-C61-butyric acid methyl ester (PCBM) has smoother surface than the spin coated film. Since the roller painting is accompanied with shear and normal stresses and is also a slow drying process, the process induces effectively crystallization of P3HT and PCBM. Both crystalline P3HT and PCBM in the roller painted active layer contribute to enhanced and balanced charge carrier mobility. Consequently, the roller painting process results in higher power conversion efficiency (PCE) of 4.6% as compared to that of the spin coating (3.9%). Furthermore, the annealing-free polymer solar cell (PSC) with high PCE were fabricated by the roller painting process with addition of a small amount of 1,8-octanedithiol. Since the addition of 1,8-octanedithiol induces phase separation between P3HT and PCBM and the roller painting process induces crystallization of P3HT and PCBM, the PCE of roller painted PSC is achieved up to 3.8% without post-annealing.

Keywords: *Roller Painting, Thin Films, Polymer Solar Cells, Device Performance*

1. Introduction

Polymer solar cells (PSCs) provide special opportunities for low cost, printable, light-weight, flexible, and portable energy source [1]. Over the last decade, these advantages of the PSCs have encouraged intensive research on PSCs, and as a result remarkable improvement has been achieved by molecular engineering, morphology control, and device optimization [2-6]. To date, the power conversion efficiency (PCE) over 5% has been obtained by using poly(3-hexylthiophene) (P3HT) or various low-bandgap polymers as a donor and [6,6]-phenyl-C_{60}-butyric acid methyl ester (PCBM) as an acceptor [7-10]. Therefore, the P3HT/PCBM combination is one of very promising candidates for commercialization of PSCs.

For commercialization, however, the fabrication process for mass production must be developed [11,12]. Most of the PSCs are manufactured through the spin coating process. Although the spin coating is very useful for fabricating very thin and homogeneous film and for controlling the film thickness [13], the spin coating process has several detrimental problems with mass production. First, the spin coating is not only difficult to scale up but also impossible to fabricate flexible devices. Second, the cost of the process is high, because the spin coating process causes inevitably waste of materials, and furthermore the cost of process increases exponentially as the substrate size increases. Third, as the spin coating is not a continuous process, this process has serious limitation for industrial production.

To overcome these problems, various methods for fabrication of PSCs have been proposed including doctor blading [14,15], ink-jet printing [16], spray coating [17-20], screen printing [21] and brush painting [22]. Although these processes have an advantage for fabrication of large area films and exhibit comparable performance to the spin coating, the thickenss control and inhomogeneity of the film still remain unsolved. In spray coating and brush painting, the film uniformity is not satisfactory. Particularly, the quality of thin film in large area cannot be guaranteed through these processes. Therefore, the development of alternative solution process which is low-cost, easy-to-use and continuous is strongly

demanded.
The roller painting process is easy-to-use, high throughput and the most widely used method for conventional painting. The substrate size for the roller painting is limitless, and the process cost is also low since the roller painting is a continuous process. Especially, an advantage of the roller painting compared to other coating processes is easiness to control film thickness and uniformity. Since the roller painting is very promising process for the industry of thin film fabrication, it can be used for fabrication of organic electronics including PSCs. In this work, we report the PSCs fabricated by the roller painting, primarily based on our previous report [23].

Furthermore, the roller painting process has another advantage in development of active layer morphology in PSCs, because the process is accompanied with shear and normal stresses. It is well known that the crystalline polymer such as P3HT can be effectively crystallized when the shear or normal stress such as nano rubbing, molecular reflow and nano imprinting is applied [24]. Particularly, Kim et al. [22] have reported that high efficiency PSCs are fabricated by using the brush painting because the shear stress during the brush painting induces the ordering of P3HT chains. Therfore, it is easily expected that the roller painting process which accompanies both the shear and normal stresses induces effectively the crystallization of P3HT and PCBM, and consequently yields enhanced solar cell performance.

2. Experimental

2.1. Materials

P3HT (Rieke Metals, 90-93% regioregular) and PCBM (Nano-C, 99.5%) were used as received. Poly(3,4-ethylenedioxy thiophene):poly(styrene sulfonate) (PEDOT:PSS) (Baytron P VP AI 4083) was purchased from H. C. Stark. For the roller painting process, rubber roller (Hwa Hong) was wrapped with thin PET film to give smooth surface.

2.2. Fabrication of polymer solar cells

ITO-coated glass (15 Ω/□) was cleaned with acetone and isopropyl alcohol, and then dried at 200 °C for 30 min. After complete drying, the ITO-coated glass was treated with UV-ozone for 15 min, and then PEDOT:PSS was spin coated with 40 nm in thickness, and the PEDOT:PSS film was annealed at 120 °C for 30 min in a N_2-filled glove box. P3HT and PCBM (1:1 by weight) were dissolved in o-dichlorobenzene (DCB) with several different concentrations (2-8 wt%) to control the thickness of the roller painted thin film. These solutions were stirred for at least 24 h at room temperature and then were passed through a 0.45 μm PES syringe filter before roller painting. The roller painting was processed at room temperature in N_2-filled glove box with the roller painting speed of 1 cm/s, and the roller painting was repeated 5 times. The spin coated PSCs were fabricated at 2500 rpm by using the solution with the same concentration as the roller painting. After complete drying of the active layer, Al (100 nm) were thermally evaporated on the top of the active layer under vacuum lower than 10^{-6} Torr. The PSC devices were then thermally annealed at 150 °C inside the glove box. The annealing-free PSC devices were fabricated at room temperature by addition of 5 wt% 1,8-octanedithiol as an additive in the solution of active layer materials. LiF (0.7 nm) was thermally evaporated before the evaporation of Al.

2.3. Measurement and Characterization

The UV-visible absorption spectra of roller painted or spin coated P3HT:PCBM films were measured by UV-visible spectrophotometer (HP 8452A). The morphology of the active layer films were observed by TEM (JEOL, JEM-1010 and Tecnai F20). The thickness of thin film was measured by AFM. The crystallinity of active layer was investigated by X-ray

diffractometer (M18XHF-SRA). The photovoltaic performance was measured under nitrogen atmosphere inside a glove box. The current density-voltage (J-V) characteristics were measured with a Keithley 4200 source-meter under AM 1.5 G (100 mW/cm^2) simulated by a Newport-Oriel solar simulator. The light intensity was calibrated using a NREL certified photodiode and light source meter prior to each measurement. The IPCE was measured using a lock-in amplifier with a current preamplifier under short circuit current state with illumination of monochromatic light.

3. Results and Discussion

To examine the effect of the coating process on the crystallization of P3HT, we compared the XRD pattern of the film fabricated by the roller painting with the film fabricated by the spin coating. The pristine P3HT film fabricated by the roller painting shows very sharp and intense peak at 2θ = 5.6° while the spin coated P3HT film exhibits relatively broad and lower peak intensity (see Fig. 1a). Also, the (200) and (300) peaks of as-roller painted P3HT film are more discernible than those of spin coated film, implying that the roller painting process induces higher crystallinity of P3HT than the spin coating process. The P3HT:PCBM blend film prepared by the roller painting also shows stronger and sharper peak than the spin coated films before thermal annealing, as shown in Figure 1b, indicating that P3HT in the blend film is more crystallized in the roller painted film than in the spin coated film. After thermal annealing, the intensity of (100) peak of the spin coated blend film is increased while the (100) peak of the roller painted blend film is nearly unchanged, indicating that P3HT in as-roller painted film is sufficiently crystallized during roller painting and thus the crystallization does not take place significantly during thermal annealing.

Since the diffraction angle at 2θ = 5.5° corresponds to the (100) packing which is associated with the interdigitation of the alkyl chians of P3HT as shown in Figure 1b [26], the exact interchain spacing between P3HT chains can be determined from the diffraction angle of (100) peak. When the interspacing was calculated by using the Bragg law, the interchain spacings of the roller painted P3HT:PCBM film and the spin coated film are 1.6 nm and 1.7 nm, respectively. One of reasons for higher crystallinity and closer packing of roller painted film is that the normal and shear stress accompanied with the roller painting induces effectively alignment of P3HT chains which inducess crystallization. Another reason for higher crystallinity of roller painted P3HT is slower drying of P3HT as compared to the spin coating process, which provides more time for P3HT to crystallize. These closely packed P3HT crystals would have an advantage in hopping and transport of hole carrier.

The effect of roller painting on the chain packing of P3HT was also observed by UV-Vis absoprtion spectroscopy (see Fig. 2a). Compared to the spin coated P3HT film, the absorption of the roller painted P3HT film is larger in the range of 520−640 nm wavelength. Since the thicknesses of both P3TH films are controlled the same, the larger absorption of the roller paintied film is origniated from close packing of the roller painted P3HT film [8]. The close packing of the roller painted P3HT is further evidenced by the distinct vibronic shoulder at 600 nm which has been assigned to highly delocalized excitation [26].

The absorption difference between the roller painted film and the spin coated film becomes more prominent in the P3HT/PCBM blend film, as shown in Figure 2b. The roller painted blend film exhibits the maximum absorption at 556 nm with a remarkable vibronic shoulder at 600 nm while the spin coated film does the maximum absorption at 522 nm with a weak vibronic shoulder. Moreover, the absorption intensity of the roller painted blend film is stronger than that of the spin coated film.

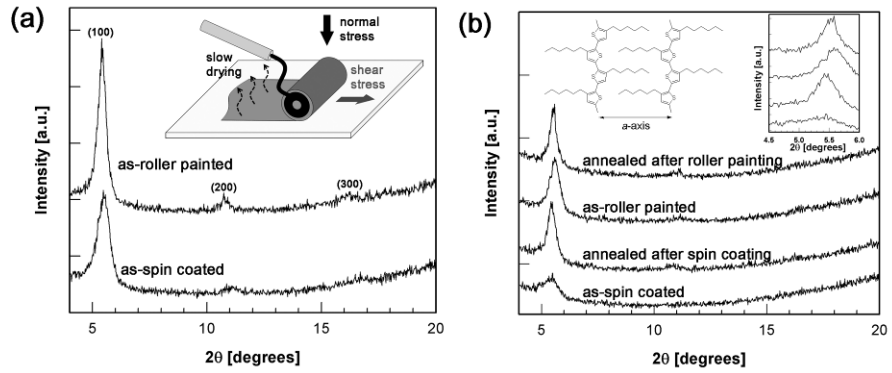

Fig. 1. XRD patterns of (a) P3HT films and (b) P3HT:PCBM films fabricated by the roller painting and the spin coating. Inset of Figure 2b clearly shows the shift of the (100) peak of the roller painted film compared to that of the spin coated film. Schematic illustration in Figure 2b shows the chain packing of regioregular P3HT in crystallite.

When the samples are annealed at 150 °C for 15 min, the absorption intensity of the spin coated film is increased, indicating that thermal annealing induces crystallization of P3HT in the blend film, whereas the absorption spectrum of the roller painted film does not increase significantly after thermal annealing. This result is consistent with the XRD measurement which exhibits almost the same crystallinity before and after annealing in the roller painted blend film (Fig. 1b). This high crystallization arising from the roller painting process without thermal annealing provides a very promising feature for the development of annealing-free PSCs for commercialization.

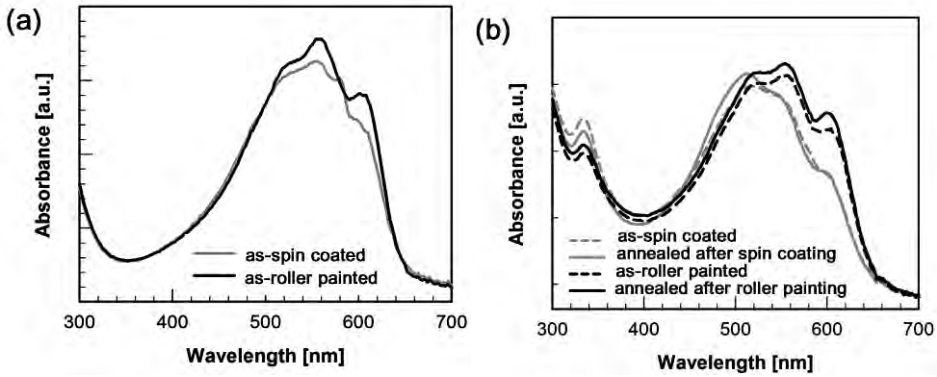

Fig. 2. UV-Vis absorption spectra of (a) pristine P3HT film and (b) P3HT:PCBM blend film fabricated by the roller painting and the spin coating.

The PCEs of the PSCs fabricated by the roller painting process are compared with those of the spin coating process in Table 1, and the corresponding current density-voltage (J-V) curves are shown in Figure 3a. To rationalize the measured values of the short circuit current density (J_{SC}), we also calculated J_{SC} from the incident photon-to-current efficiency (IPCE) measured by using the same device (Fig. 3b). When the J_{SC} values from IPCE were compared with those of device values of J_{SC}, it reveaed that two values were nearly equal within experimental errors. For the optimization of PCE, the samples are annealed after deposition of Al. The spin coated PSCs show the maximum PCE after thermal annealing for 15-20 min, while the roller painted PSCs show the maximum efficiency after annealing for 6-8 min at 150 °C. The maximum PCE of the roller painted solar cell is 4.6% which is 20% higher than the maximum PCE (3.9%) of the spin coated PSC. Since J_{SC} is nearly equal to that of the spin coated PSC under the optimum device condition, the main reason for higher PCE of the roller

painted PSC is slightly increased V_{OC}, and higher fill factor (FF) as compared with that of the spin coated PSC. Although the factors affecting FF are not completely identified yet [27], it has generally been accepted that FF is influenced by the morphology of the active layer, the balance between hole and electron mobility, and the interface of layers in PSC. Since we focused on the balance between hole and electron mobility in this study, we measured the charge transport from the dark current in a single-carrier device.

Table 1. Optimized performance of PSCs fabricated by roller painting or spin coating process. The thickness of the roller painted device and spin coated device are 245 nm and 230 nm, respectively.

Process	Annealing [min]	V_{OC} [V]	J_{SC} [mA/cm]	FF [%]	PCE [%]	μ_h [cm^2/Vs]	μ_e [cm^2/Vs]
Roller painting	0	0.57	7.5	0.56	2.4	5.07×10^{-5}	1.75×10^{-4}
	8	0.63	11.3	0.64	4.6	1.56×10^{-4}	3.90×10^{-4}
Spin coating	0	0.56	6.6	0.52	1.9	6.52×10^{-6}	4.50×10^{-5}
	15	0.61	11.1	0.58	3.9	4.94×10^{-5}	1.84×10^{-4}

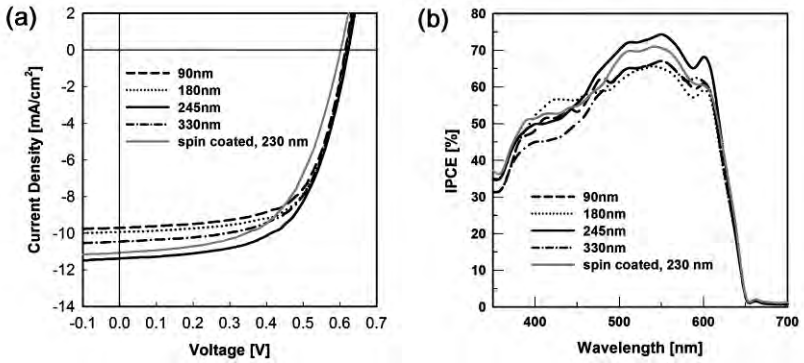

Fig. 3. (a) J-V curves of PSCs (100 mW/cm², AM 1.5G) fabricated by the roller painting with different thickness of active layer and the spin coating process, and (b) the corresponding IPCE spectra. All the devices are thermally annealed at 150 °C.

The hole and electron single-carrier mobilities were measured by the standard methods. In the roller painted device, the values of μ_h and μ_e are 5.07×10^{-5} cm^2 V^{-1} s^{-1} and 1.75×10^{-4} cm^2 V^{-1} s^{-1}, respectively, before thermal annealing. These values are comparable to those of the spin coated device after thermal annealing. As shown in Figures 1 and 2, the crystallinity of P3HT in the as-roller painted film is almost the same as that of the spin coated film after thermal annealing. Therefore, it is expected that the holes are transported effectively through the network of P3HT crystals in the roller painted film without thermal annealing. After the thermal annealing, the μ_e/μ_h ratio of the roller painted device is decreased from 3.5 to 2.5. As a result, the mobility mismatch between hole and electron transport becomes smaller and thus the space charge effect becomes diminished in the roller painted device. Due to enhanced and balanced charge conduction in the roller painted P3HT:PCBM film, the high FF of 0.64 was achieved in the roller painted device.

When the nanoscale morphology of the active layer is examined by TEM, the as-roller painted film exhibits interesting morphology, as shown in Figure 4a: very dark, cilia-like nanocrystals (width ~20 nm and length ~100 nm) are clearly observed. It is more interesting to observe that these nanocrystals are well packed and aligned normal to the rolling direction. This morphological characteristic is more pronounced after thermal annealing (see Fig. 4b). These nanocrystals must be grown from PCBM molecules, because PCBM phase is darker

compared to that of P3HT in bright-field TEM image. The selected area electron diffraction (SAED) pattern also indentifies clearly the PCBM nanocrystal [29], as shown in the inset of Fig. 4b. The fact that PCBM nanocrystals can be developed through simple roller painting is remarkable. These well developed PCBM crystals are expected to contribute to the enhancement of electron mobility in the roller painted device. Although the reason for the morphology difference between the roller painted device and the spin coated one is not clear, it is probably because the shear and normal stresses during the roller painting induces the molecular ordering of PCBM along the direction of the roller painting (Fig. 4a).

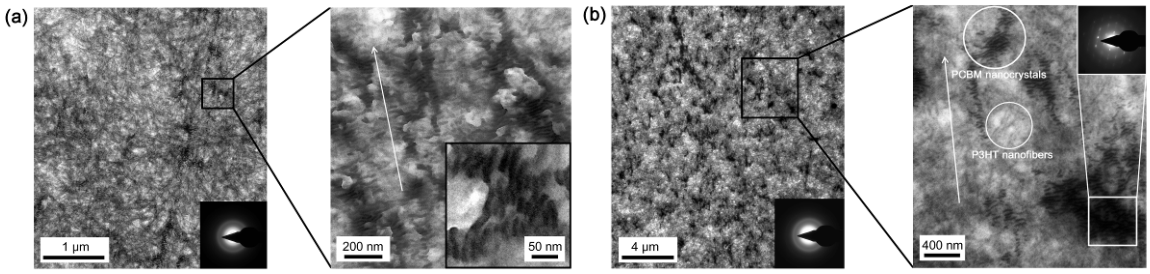

Fig. 4. Bright-field TEM images and the SAED patterns of P3HT:PCBM film fabricated by the roller painting (a) before and (b) after thermal annealing.

Achievement of highly efficient PSC without additional post-treatment is indispensable for industrialzation of PSC. However, most of efficient PSCs based on P3HT and PCBM require an additional treatment such as thermal or solvent annealing which induces phase separation and enhances the crystallinity. Since the additional process increases the fabrication cost of PSCs, development of annealing-free PSC is strongly demanded. Furthermore, high temperature for thermal annealing may not be suitable for preparation of flexible PSCs. Recently, the method of simple blending with an additive, which has lower solubility to PCBM than o-dichlorobenzene and therefore accelerates phase separation of the blend of P3HT and PCBM, has been reported for achievement of high efficiency without thermal annealing. Although the method has achieved around 3% PCE without thermal or solvent annealing, the PCE value is still lower than the optimized device with annealing process.

We have fabricated the annealing-free large area (5 cm^2) PSC device by combining the roller painting process with addition of 5 w t% 1,8−octanedithiol. When the performances of annealing-free devices fabficated by the roller painting are compared with those of spin coated device, the J_{SC} and FF of the roller painted PSC are higher than those of the spin coated PSC while V_{OC}s of both processes are almost the same. The PCE of annealing-free device is 3.8% at the active area of 0.04 cm^2. To the best of our knowledge, this value is the higest performance of annealing-free PSCs based on P3HT and PCBM.

4. Conclusions

We have fabricated high efficiency PSCs by the roller painting process. Since the roller printing is accompanied with normal and shear stresses and is a slow drying process, it induces effective crystallization of P3HT and PCBM. As a result, the roller painted PSC of P3HT/PCBM has achieved 4.6% PCE, which is 20% higher than that of the device fabricated by the conventional spin coating process (3.9%). This higher efficiency is originated from higher FF and J_{SC} of the roller painted active layer. By addition of small amount of 1,8-octanedithiol as an additive, annealing-free PSCs were also fabricated by the roller painting. By combining the roller painting and incorporation of additive, the PCE of 3.8% was achieved without any post-treatment. This is because the roller painting process enhances the

crystallization of P3HT and PCBM, and the additive induces phase separation effectively. To the best of our knowledge, this value (3.8%) is the best performance of annealing-free PSC based on P3HT and PCBM. Since the PCE of over 2.7% can be achieved at 5 cm^2 active area by the roller painting without post-treatment, it is concluded that the roller painting process is a very promising method for fabrication of large area solar cells. In short, since the roller painting process follows the basic process of the roll-to-roll processing, this research provides a model study for preparation of roll-to-roll processed organic electronics.

References

[1] C. J. Brabec, N. S. Sariciftci, J. C. Hummelen, Plastic Solar Cells, Adv. Funct. Mater. 11, 2001, pp. 15-26.

[2] G. Yu, A. J. Heeger, Charge separation and photovoltaic conversion in polymer composites with internal donor/acceptor heterojunctions, J. Appl. Phys. 78, 1995, pp. 4510-4515.

[3] P. Schilinsky, U. Asawapirom, U. Scherf, M. Biele, C. J. Brabec, Influence of the Molecular Weight of Poly(3-hexylthiophene) on the Performance of Bulk Heterojunction Solar Cells, Chem. Mater. 17, 2005, pp. 2175-2180.

[4] Y. K. Kim, S. Cook, S. M. Tuladhar, S. A. Choulis, J. Nelson, J. R. Durrant, D. D. C. Bradley, M. Giles, I. McCulloch, C. S. Ha, M. H. Ree, A strong regioregularity effect in self-organizing conjugated polymer films and high-efficiency polythiophene:fullerene solar cells, Nat. Mater. 5, 2006, pp. 197-203.

[5] P. W. M. Blom, V. D. Mihailetchi, L. J. A. Koster, D. E. Markov, Device Physics of Polymer:Fullerene Bulk Heterojunction Solar Cells, Adv. Mater. 19, 2007, pp. 1551-1566.

[6] G. Dennler, M. C. Scharber, C. J. Brabec, Polymer-Fullerene Bulk-Heterojunction Solar Cells, Adv. Mater. 21, 2009, pp. 1323-1338.

[7] J. W. Jung, J. U. Lee, W. H. Jo, High-Efficiency Polymer Solar Cells with Water-Soluble and Self-Doped Conducting Polyaniline Graft Copolymer as Hole Transport Layer, J. Phys. Chem. C 114, 2010, pp. 633-637.

[8] G. Li, V. Shrotriya, J. Huang, Y. Yao, T. Moriarty, K. Emery, Y. Yang, . High-efficiency solution processable polymer photovoltaic cells by self-organization of polymer blends, Nat. Mater. 4, 2005, pp. 864-868.

[9] Ma, C. Yang, X. Gong, K. Lee, A. J. Heeger, Thermally Stable, Efficient Polymer Solar Cells with Nanoscale Control of the Interpenetrating Network Morphology, Adv. Funct. Mater. 15, 2005, pp. 1617-1622.

[10] M. Campoy-Quiles, T. Ferenczi, T. Agostinelli, P. G. Etchegoin,Y. Kim, T. D. Anthopoulos, P. N. Stavrinou, D. D. C. Bradley, J. Nelson, Morphology evolution via self-organization and lateral and vertical diffusion in polymer:fullerene solar cell blends, Nat. Mater. 7, 2008, pp. 158-164.

[11] F. C. Krebs, Processing and preparation of polymer and organic solar cells, Sol. Energy Mater. Sol. Cells 93, 2009, pp. 394-412.

[12] F. C. Krebs, Roll-to-roll fabrication of monolithic large-area polymer solar cells free from indium-tin-oxide, Sol. Energy Mater. Sol. Cells 93, 2009, pp. 1636-1641.

[13] Gunes, H. Neugebauer, N. S. Sariciftci, Conjugated Polymer-Based Organic Solar Cells Chem. Rev. 107, 2007, pp. 1324-1338.

[14] C. J. Brabec, F. Padinger, J. C. Hummelen, R. A. Janssen, N. S. Sariciftci, Realization of large area flexible fullerene - conjugated polymer photocells: A route to plastic solar cells, Synth. Met. 102, 1999, pp. 861-864.

[15] P. Schilinsky, C. Waldauf, C. J. Brabec, Performance Analysis of Printed Bulk Heterojunction Solar Cells, Adv. Funct. Mater. 16, 2006, pp. 1669-1672.

[16] C. N. Hoth, S. A. Choulis, P, Schilinsky, C. J. Brabec, . On the effect of poly(3-hexylthiophene) regioregularity on inkjet printed organic solar cells, J. Mater. Chem. 19, 2009, pp. 5398-5404.

[17] D. Vak, S. Kim, J. Jo, S. Oh, S. Na, J. Kim, D. Kim, Fabrication of organic bulk heterojunction solar cells by a spray deposition method for low-cost power generation, Appl. Phys. Lett. 91, 2007, 081102.

[18] C. N. Hoth, R. Steim, P. Schilinsky, S. A Choulis, S. F. Tedde, O. Hayden, C. J. Brabec, Topographical and morphological aspects of spray coated organic photovoltaics , Organ. Electron. 10, 2009, pp. 587-593.

[19] R. Green, A. Morpha, A. J. Ferguson, N. Kopidakis, G. Rumbles, S. E. Shaheen, Performance of bulk heterojunction photovoltaic devices prepared by airbrush spray deposition, Appl. Phys. Lett. 92, 2008, 33301.

[20] K. X. Steirer, M. O. Reese, B. L. Rupert, N. Kopidakis, D. C. Olson, R. T. Collins, D. S. Ginley, Ultrasonic spray deposition for production of organic solar cells, Sol. Energy Mater. Sol. Cells 93, 2009, pp. 447-453.

[21] F. C. Krebs, M. Jorgensen, K. Norrman, O. Hagemann, J. Alstrup, T. D. Nielsen, J. Fyenbo, K. Larsen, J. Kristensen, A complete process for production of flexible large area polymer solar cells entirely using screen printing—First public demonstration, Sol. Energy Mater. Sol. Cells 93, 2009, pp. 422-441.

[22] S. Kim, S. Na, J. Jo, G. Tae, D. Kim, Efficient Polymer Solar Cells Fabricated by Simple Brush Painting, Adv.Mater. 19, 2007, pp. 4410-4415.

[23] J. W. Jung, W. H. Jo, . Annealing-Free High Efficiency and Large Area Polymer Solar Cells Fabricated by a Roller Painting Process, Adv. Funct. Mater. 20, 2010, pp. 2355-2363.

[24] G. Derue, S. Coppee, S. Gabriele, M. Surin, V. Geskin, F, Monteverde, P. Leclere, R. Lazzaroni, P. Damman, Nanorubbing of Polythiophene Surfaces, J. Am. Chem. Soc. 127, 2005, pp. 8018-8019.

[25] H. Sirringhaus, P. J. Brown, R. H. Friend, M. M. Nielsen, K. Bechgaard, B. M. W. Langeveld-Voss, A. J. H. Spiering, R. A. J. Janssen, E. W. Meijer, P. Herwig, D. M. De Leeuw, Two-dimensional charge transport in self-organized, high-mobility conjugated polymers, Nature 401, 1999, pp. 685-688.

[26] R. Osterbacka, C. P. An, X. M. Jiang, Z. V. Vardeny, Two-Dimensional Electronic Excitations in Self-Assembled Conjugated Polymer Nanocrystals, Science 287, 2000, pp. 839-842.

[27] M. Kim, B. Kim, J. Kim, Effective Variables To Control the Fill Factor of Organic Photovoltaic Cells, ACS Appl. Mater. & Interfaces 1, 2009, pp. 1264-1269.

[28] G. Lu, L. Li, X. Yang, Creating a Uniform Distribution of Fullerene C_{60} Nanorods in a Polymer Matrix and its Photovoltaic Applications, Small 4, 2008, pp. 601-606.

Bi-layer GaOHPc:PCBM/P3HT:PCBM organic solar cell

I.Kaulachs*, I.Muzikante[2], L.Gerca[2], G.Shlihta[1], P.Shipkovs[1], G. Kashkarova[1], M.Roze[3], J.Kalnachs[1], A.Murashov[1], G.Rozite[1]

[1] 1Institute of Physical Energetics, Aizkraukles 21, Riga, Latvia;
[2]Institute of Solid State Physics, University of Latvia, Kengaraga str.8, Riga, Latvia;
[3]Riga Technical University, Azenes 14, Riga, Latvia.
corresponding author : tel. +371 67558666, e-mail kaulacs@edi.lv

Abstract:. For production organic bulk heterojunction polymer solar cell one of the best materials is regioregular poly-3-hexylthiophene (P3HT), which is widely used as a donor molecule and a hole transporter, with soluble fullerene derivative (PCBM) as acceptor and electron transporter. The main drawback of this highly efficient blend is its limited spectral range, covering only 350-650 nm spectral interval. So main aim of present work was to extend the spectral range of the cell up to 850 nm by adding second bulk heterojunction layer of complementary absorption spectrum to P3HT:PCBM layer. For this purpose hydroxygallium phthalocyanine (GaOHPc) and PCBM blend was used as additional layer because GaOHPc has strong and wide intermolecular charge transfer (CT) absorption band around 830-850 nm. Thus novel organic bi-layer bulk heterojunction system (GaOHPc:PCBM/P3HT:PCBM) has been built by spin coating technique having high charge carrier photogeneration efficiency in 350 – 850 nm spectral range. It was found that thermal annealing in vacuum at 100C increases short circuit photocurrent external quantum efficiency (EQE) values more than 2 – 3 times, and these values reach more than 45% at P3HT absorption band (525 nm) and 25% at GaOHPc band (845 nm) for low light intensities (10^{12} photon/(cm^2*s)).

Keywords: *Full polymer film, heterojunction, organic solar cell.*

1. Introduction

At present, crystalline Si solar cells are by far most dominant PVs used, occupying more than 95% of the market [1]. But the main obstacle for the market implementation of these cells is the large production cost of Si-based technologies [2]. A promising approach towards low-cost photovoltaic devices is fabrication of solar cells based on organic materials [3-6]. The bulk heterojunction approach appears to be one of the most promising concepts of creating efficient, low-cost and easily producible solar cells [7,8]. For this purpose one of the best materials is regioregular poly-3-hexylthiophene (P3HT) [8-11], which is widely used as a donor molecule and a hole transporter, with soluble fullerene derivatives as acceptors and electron transporters. Blends of these molecules in PV cells exhibit the efficiency of light power conversion up to 5% [9-11]. Still, it is not sufficient to meet realistic requirements for commercialization. The main drawback of this highly efficient blend is its limited spectral range [7-9], which covers 350–650 nm interval, allowing only ~ 35% of the full solar spectrum energy to be used. In the present work, we tried to extend the spectral range of the cell by additional bulk heterojunction layer of hydroxygallium phthalocyanine (GaOHPc), which has a strong and wide intermolecular charge transfer (CT) band around 830 nm [12,13] and soluble fullerene PCBM. The choice of GaOHPc was dictated by the following reasons: 1) high thermal and chemical stability of phthalocyanines as compared with the most of molecular materials; 2) the NIR absorption providing the possibility to extend the photosensitivity spectral range (up to the NIR region) of the blend; 3) the CT character of the IR absorption band, which promises high efficiency of charge carrier photogeneration [13,14]; 4) the solubility in chloroform, which allows its processing by spin coating [12]. In this work we show, that by adding second bulk heterojunction layer of GaOHPc:PCBM to P3HT:PCBM cell we obtain bi-layer system GaOHPc:PCBM/ P3HT:PCBM which photosensitivity spectrum covers vide spectral range from 350 to 850 nm. It was found that

thermal annealing of cells in vacuum 10^{-5} - 10^{-6} mbar at 100C increases short circuit photocurrent external quantum efficiency (EQE) more than 2-3 times.

2. Methodology

For the electron donor and hole transporter in main bulk heterojunction layer we chose regioregular poly 3-hexylthiophene (P3HT) with an average molecular weight of 87000 (Sigma Aldrich) and for acceptor and electron transporter – [6,6]-Phenyl-C61 – butyric acid methyl ester (PCBM) with purity better than 99,5 % (from American Dye Source). The additional bulk heterojunction layer was composed from hydroxygallium phthalocyanine (GaOHPc) as electron donor and PCBM as electron acceptor. The molecules used and cell arrangement is shown in Figure 1.

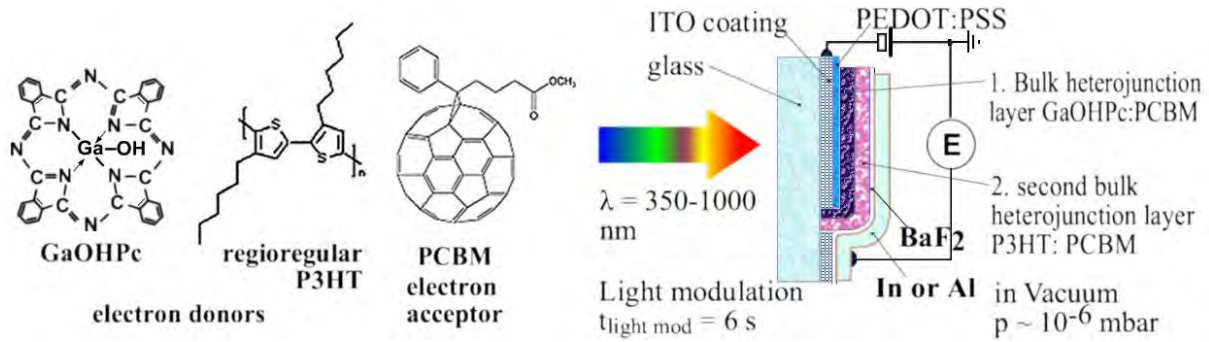

Fig. 1. Molecules used and cell arrangement.

As the sample substrate ITO – covered glass with Rsu = 4~10 Ohm/Sq was used. The ITO electrode after cleaning and etching anode configuration was covered with a 30 nm thick PEDOT:PSS (Clevios 1000) plus 5% DMSo +5% isopropanol to increase its conductivity [15] by spin coating at 9000 rpm, and dried for 30 min. at 140C in vacuum 10^{-5} mbar. This electrode was covered by GaOHPc:PCBM blend from the solution in chloroform and chlobenzene mixture by spin coating. This procedure was repeated till optical density of GaOHPc:PCBM layer reaches 0.5 – 0.6 at 840 nm. After drying in vacuum 10^{-5} mbar at 85C this layer was covered by second bulk heterojunction layer of P3HT:PCBM (1:1 by weight) by spin coating from the solution in chlorbenzene. As top electrode the In or Al was evaporated in vacuum of 10^{-5} – 10^{-6} mbar with surface resistance Rsu ~ 10 Ohm/Sq. In the case of In electrode, the 0.5 – 0.7 nm thick BaF_2 layer was incorporated under In by evaporation in vacuum. The thickness of BaF_2 layer during evaporation process in vacuum was controlled by 20 Mhz crystal oscillator and frequency meter. The photocurrent measurements were carried out at RT and 100C in vacuum of 10^{-6} – 10^{-5} mbar. The samples were illuminated using grating monochromator by chopper modulated monochromatic light through the ITO electrode in the 350 – 1000 nm spectral region with intensity 10^{9} – 10^{16} photon/(cm^2*s) (see Fig.1). Light modulation period was chosen as 6 s long and intensity was controlled by calibrated Si photodiode. The synchro-detection technique with the use of PC controlled data storage equipment [16] was employed for measuring the spectral dependences of photocurrent quantum efficiency: EQE = I_{photo}/Φ (where I_{photo} is the photocurrent (electrons/s) and Φ is photon flux (photons/s) incident upon the active area of sample)

3. Results and discussion

The spectral dependences of the external quantum efficiency (EQE) of short circuit photocurrent for low incident light intensities 10^{11} – 10^{12} photon/ (cm^2*s) and the optical

properties of novel bi-layer bulk heterojunction system GaOHPc:PCBM/P3HT:PCBM are shown in Fig.2 for top Al electrode and Fig.3 for top BaF_2/In electrode.

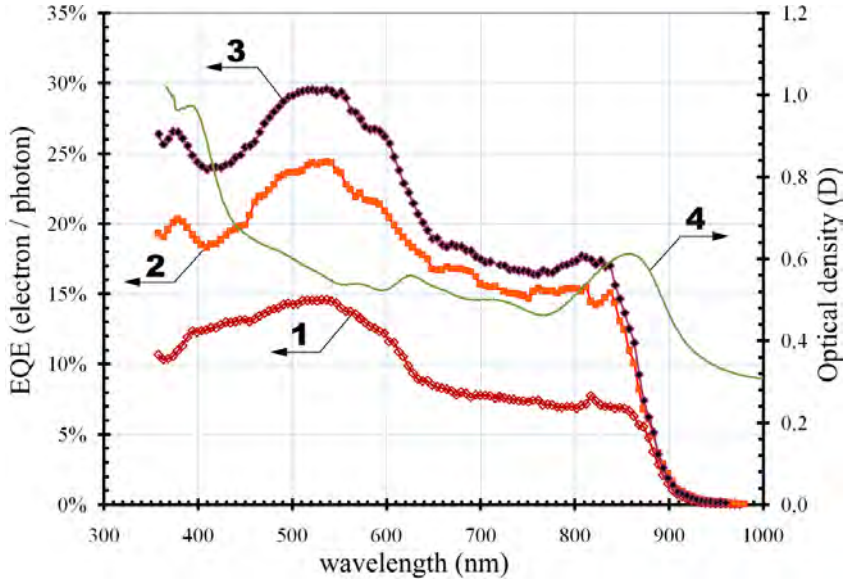

*Fig. 2. Spectral dependences of external quantum efficiency (EQE) of short circuit photocurrent at light intensity 10^{11} photon/(cm^2*s) and optical density for ITO/PEDOT:PSS/ GaOHPc: PCBM/P3HT:PCBM/Al cell:*
1 - EQE at room temperature (RT) for unheated sample;
2 - EQE at T = 100C;
3 - EQE at RT after sample therm. annealing in vacuum at T = 100C;
4 - Optical density of bi-layer system GaOHPc:PCBM/P3HT: PCBM.

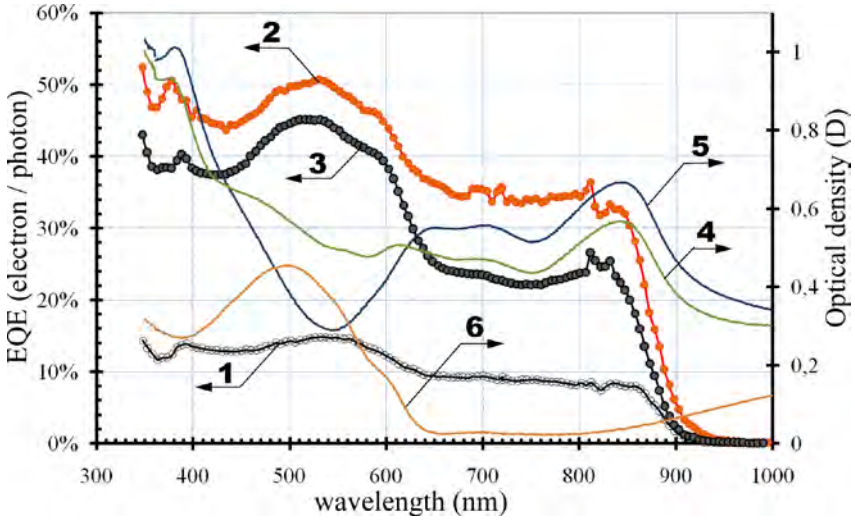

*Fig. 3. Spectral dependences of external quantum efficiency (EQE) of short circuit photocurrent at light intensity 10^{12} photon/(cm^2*s) and optical density for ITO/PEDOT:PSS/GaOHPc:PCBM/P3HT:PCBM /BaF_2/In cell:*
1 - EQE at room temperature (RT) for unheated sample;
2 - EQE at T=100C;
3 - EQE at RT after sample annealing in vacuum at T=100C;
4 - Optical density of bi-layer system GaOHPc:PCBM/P3HT:PCBM;
5 - Optical density of GaOHPc:PCBM layer;
6 – Optical density of P3HT:PCBM layer.

It is seen that absorption spectrum of GaOHPc:PCBM layer (curve 5 in Fig. 3) supplements well the P3HT:PCBM spectrum (curve 6 in Fig.3) enabling practically uniform absorption in 350 – 900 nm region of bi-layer bulk heterojunction system GaOHPc:PCBM/P3HT:PCBM (curves 4 in Fig.2 and Fig.3). Introducing GaOHPc:PCBM layer in the cell extends its photosensitivity spectrum beyond 850 nm (see curves 1 – 3 in Fig.2 and 3), but short circuit photocurrent EQE value for illumination in GaOHPc CT absorption band is 1.7 – 2 times less than for that in the P3HT absorption band possibly due to lower hole polaron mobility in GaOHPc fractal structure than in P3HT. The cell thermal annealing at 100C in vacuum for 48 hours after top electrode deposition significantly increases EQE values for all cells (compare curves 3 and 1 in Fig.2 and 3) due to change of morphology of used organic layers leading to increase of hole, and electron polaron mobilities and also probably by better contact with top electrode [10].

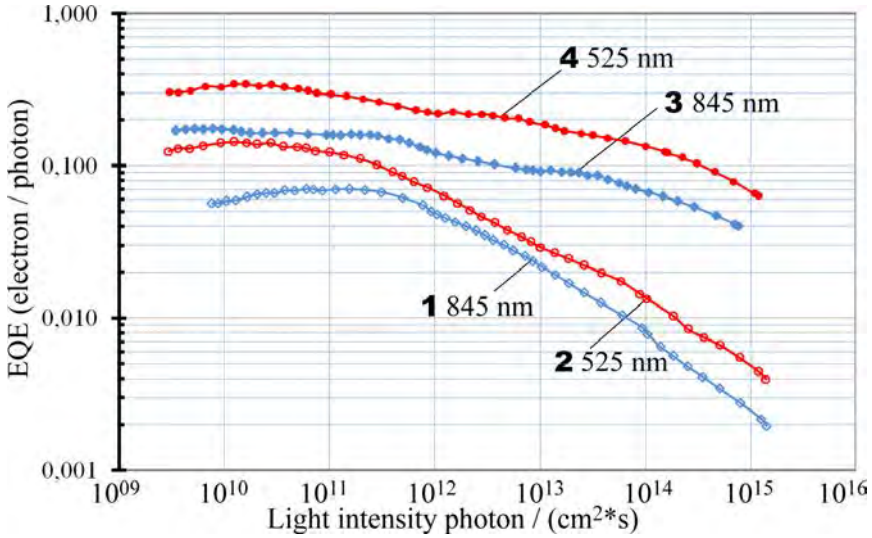

Fig. 4. Short circuit photocurrent external quantum efficiency (EQE) dependence on incident light intensity at room temperature for Al top electrode before annealing (curves 1,2) and after thermal annealing at 100C in vacuum (curves 3,4).

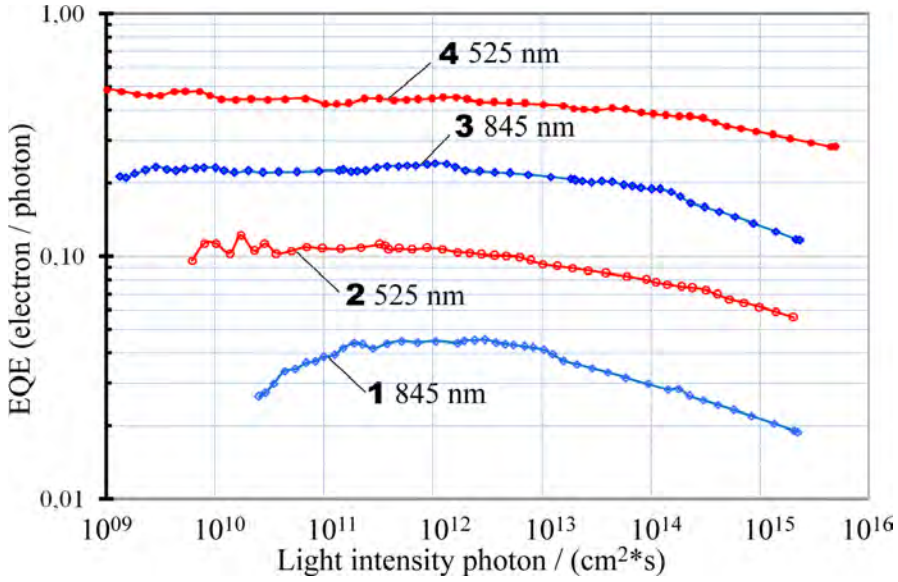

Fig. 5. Short circuit photocurrent external quantum efficiency (EQE) dependence on incident light intensity at room temperature for samples with In/BaF_2 electrode before annealing (curves 1,2) and after thermal annealing at 100C in vacuum (curves 3,4).

Highest EQE values were achieved for cells with top BaF_2/In electrode which after annealing reached values more than 45% (electron/photon) at P3HT absorption band (525 nm) and 25% (electron/photon) at GaOHPc charge transfer absorption band (845 nm) (curve 3 Fig.3), at room temperature and light intensity10^{12} photon/(cm^2*s). By increasing light intensities, EQE values decrease as shown in Fig.4 and Fig.5 probably due to low charge carrier mobilities. This photocurrent sublinear dependence on light intensity diminishes after thermal annealing (compare curves 3,4 with 1,2 in Figs 4 and 5) supporting idea, that improvements by thermal annealing at least partly can be explained by increase of charge carriers mobilities. Comparing curves in Fig.4 and Fig.5, we see that cells with top BaF_2/In electrodes has more linear photocurrent dependence on light intensity than cell with top Al electrode. Also fill factors (FF) are higher for cells with top BaF_2/In electrode than Al electrode (compare photocurrent efficiency dependences on applied external voltage in Fig.7 and Fig.6). It possibly can be explained by too thick Al_2O_3 formation under Al electrode, as spin coating procedure was performed in air and not in glove box with N_2 or argon atmosphere. So prepared organic layers would contain some O_2 in their volume which was not removed in vacuum camera before Al thermal deposition. This O_2 could slowly diffused out towards Al electrode during sample measuring procedure and form isolating Al_2O_3 layer, as it was discovered by Fan and Faulkner in 1978 [17] even for samples prepared in vacuum by thermal deposition.

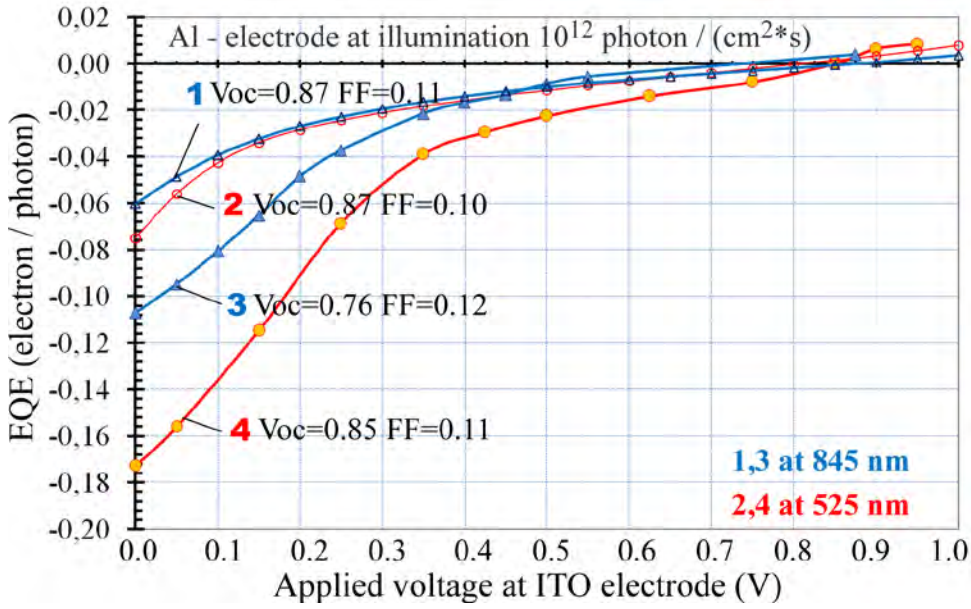

*Fig. 6. Photocurrent EQE dependences on applied external voltage for cells with Al electrode at room temperature before annealing (curves 1,2) and after annealing at 100C (curves 3,4), at light intensity 10^{12} photon/(cm2*s). Also open circuit voltages (Voc) and fill factors (FF) are shown.*

This could be the main reason for extremely low fill factor values (0.10 – 0.12) and high open circuit voltages Voc= 0.76 – 0.85 V for cells with top Al electrode (Fig.6). The cells with top BaF_2/In electrode exhibit higher fill factor values: 0.21 - before annealing and 0.22 – 0.29 after annealing, but low open circuit voltages: 0.42 V - before annealing and 0.43 – 0.48 V after annealing (see Fig.7). These low FF values could be explained by high electric resistance of GaOHPc:PCBM layer which could be diminished in future by appropriate doping.

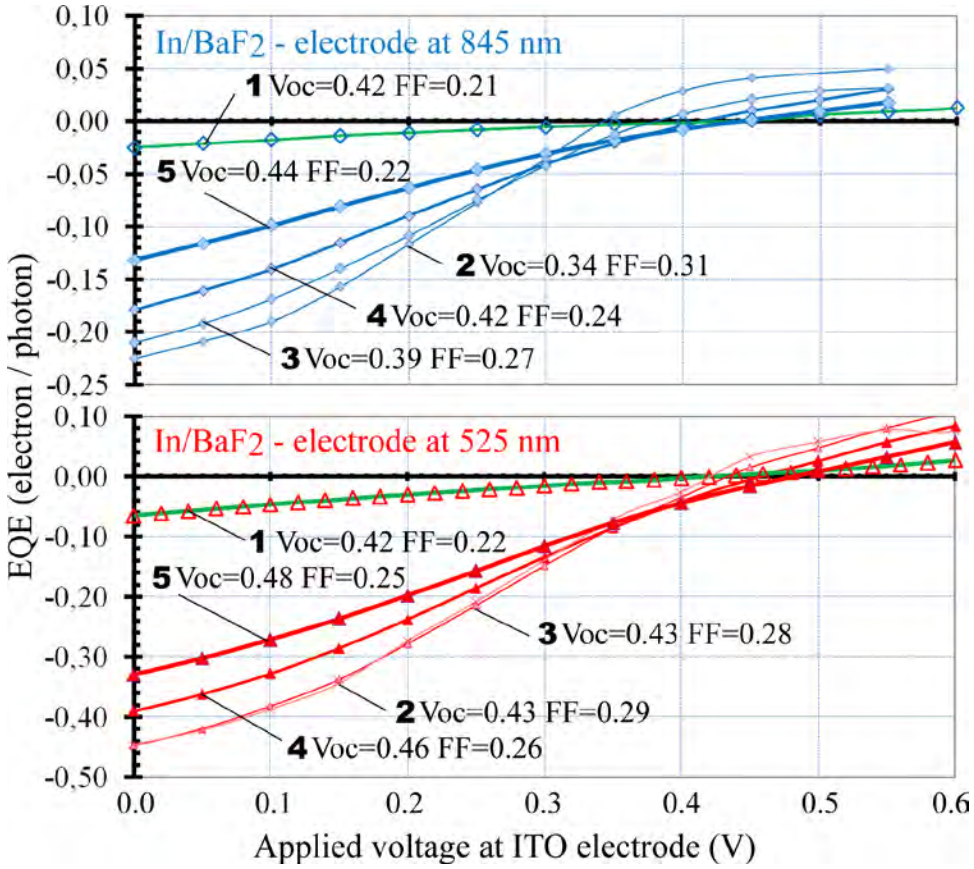

*Fig. 7. Photocurrent EQE dependences on applied external voltage for cells with In/BaF_2 electrode at room temperature before annealing at light intensity 10^{15} photon/(cm^2*s). (curves 1) and after annealing at 100C (curves 2-5), at following light intensities:*
*2 - 10^{12} photon/(cm^2*s); 3 - 10^{13} photon/(cm^2*s); 4 - 10^{14} photon/(cm^2*s); 5 - 10^{15} photon/(cm^2*s).*
Also open circuit voltages (Voc) and fill factors (FF) are shown.

4. Conclusions

1) The novel organic bi-layer bulk heterojunction system is built having high charge carrier photogeneration efficiency in 350-850 nm spectral range at low light intensities.
2) Thermal annealing significantly increases EQE values for all cells.
3) Thermal annealing significantly increases linearity of photocurrent dependences from light intensity.
4) Cells with In/BaF_2 electrode have higher EQE values and fill factors, than cells with top Al electrode.

5. Acknowledgments

The authors gratefully acknowledge the kind help of doctor V.Parra for synthesis of GaOHPc.

References

[1] Portman J., and Arkhipov V, Thin Film Solar Cells: Fabrication, Characterization and Applications, John Willey & Sons Ltd, 2006, pp. 471.

[2] Lewerenz H. J., and Jungblut H, Photovoltaic – Grandlagen und Anwendungen Berlin, Heidelberg: Springer, 1995.

[3] Shaheen S.E., Brabec C.J., Saricftci N.S. Padinger F., Fromherz T., Humalen J.C, 2.5% Efficient Organic Solar Cells Appl. Phys. Lett., 78, 2001, pp. 841–843

[4] Yu G., Gao J., Hummelen J.C., Wudl F., Heeger A.J, Polymer Photovoltaic Cells: enhanced efficiencies via a network of internal donor-acceptor heterojunctions, Science, 270, 1995, pp. 1789–1791

[5] Peumans P., Forrest S.R, Very-high-efficiency double hetero-structure copper-phthalocyanine /C60 photovoltaic cells, Appl. Phys. Lett., 80 (2), 2002, pp. 338–338

[6] Shaheen S.E., Radspinner R., Peyghambrian N., Jabbor G.E, Fabrication of bulk heterojunction plastic solar cells by screen printing, Appl. Phys. Lett. 79(18), 2001, pp. 2996–2998

[7] Winder C., Sariciftci N.S, Low band gap polymers for photon harvesting in bulk heterojunction solar cells, J. of Materials Chemistry, 14, 2004, pp. 1077–1085

[8] Al-Ibrahim M., Roth H.K., Zhokhavets U., Gobsch G., Sensfuss S, Flexible large area polymer solar cells based on poly(3-hexylthiophene)/fullerene, Solar Energy Materials & Solar Cell, 85, 2005, pp. 13–20

[9] Kim J.Y., Kim S.H., Lee H., Lee. K., Ma W., Gong X., Heeger A.J, New architecture for high-efficiency polymer photovoltaic cells using solution-based titanium oxide as an optical spacer, Adv. Mater., 18, 2006, pp. 572–576

[10] Ma W., Yang C., Gong X., Lee K., Heeger A.J, Thermally stable, efficient polymer solar cells with nanoscale control of the interpenetrating network morphology, Adv. Funct. Mater., 15, 2005, pp. 1617–1622

[11] M.Lenes, A.H.Wetzelaer, F.B.Kooistra, S.C.Veenstra, J.C.Hummelen, W.M.Blom, Fullerene Bisadducts for Enhanced Open –Circuit Voltages and Efficiencies in Polymer Solar Cells, Adv.Mater, 20, 2008, pp. 2116-2119

[12] Parra V., Vilar M.R, Battaglini N., Ferraria A.M., Botelho do Rego A.M., Boufi S., Rodríguez-Méndez M.L., Fonavs E., Muzikante I., Bouvet M, New Hybrid Films Based on Cellulose and Hydroxygallium Phthalocyanine: Synergetic Effects in the Structure and Properties, Langmuir 23 7, 2007, pp. 3712–3722

[13] Yamasaki K., Okada O., Inami K., Oka K., Kotani M., Yamada H, Gallium Phthalocyanines: Structure Analysis and Electroabsorption Study, J. Phys. Chem., 101, 1997, pp. 13–19

[14] Saito T., Sisk W., Kobaysashi T., Suzuki S., Iwayanagi T., Photocarrier Generation Processes of Phthalocyanines Studied by Photocurrent and Electroabsorption Measurements, J. Phys. Chem., 97, 1993, pp. 8026–8031

[15] H.Do, M.Reinhard, H.Vogeler, A.Puetz, F.G.Klein, W.Schabel, A.Colsmann, U.Lemmer, Polymeric anodes from poly(3,4-ethylenedioxythiopene):poly (styrenesulfonate) for 3,5% efficient organic solar cells, Thin Solid Films, 517, 2009, pp. 5900-5902.

[16] I.Kaulach., E.Silinsh. Molecular Triplet Exciton Generation via Optical Charge Transfer States in α – Metal Free Phthalocyanine, Studied by Magnetic Field Effect, Latv. J. Phys. Tech. Sci., **5,** 1994, pp. 12–22.

[17] F.R.Fan, L.R.Faulkner, Photovoltaic effects of metal-free and zinc phthalocyanines, J.Chem.Phys. 69 (7), 1978, pp. 3334-3349.

Pulse and direct current electrodeposition of zinc oxide layers for solar cells with extra thin absorbers

G. Khrypunov [1,*], N. Klochko [1], N. Volkova [2], V. Kopach [1], V. Lyubov [1], K. Klepikova [1]

[1] *National Technical University "Kharkiv Polytechnic Institute", Kharkiv, Ukraine*
[2] *National Aerospace University "Kharkiv Aviation Institute", Kharkiv, Ukraine*
**Corresponding author. Tel: +380-572-971928, E-mail: khrip@ukr.net*

Abstract: The feasibility of one-dimensional (1D) nanostructured zinc oxide array pulse plating has been presented. An effect of the electrolyte composition, deposition regime and subsequent annealing on structure and optical properties of the electrodeposited ZnO layers has been approved by X-ray diffraction and spectrophotometric analysis. We have determined that for obtaining of ZnO arrays with strong (002) preferable growth orientation in the c-axis direction it is necessary to diminish adsorption of hydrogen and Cl^--ions. It has been shown that such conditions are created in electrolyte that contains 0.05 M $Zn(NO_3)_2$ and 0.1 M $NaNO_3$ during electrodeposition on FTO-coated glass substrates in pulse plating regime with rectangular impulses of cathode potential (20 ms on-time at U_{on} = -1.4 V and 30 ms off-time at U_{off} = -0.8 V). Therefore, in this work we for the first time have demonstrated the successful growth of 1D ZnO nanostructures by pulse plating without using of templates. The novel electrodeposition technique gives possibilities for the manufacture of the ZnO arrays suitable for solar cells with extra thin absorbers.

Keywords: *Electrodeposition, Zinc oxide, Pulse plating*

1. Introduction

Zinc oxide (ZnO) has attracted a lot of research interest in recent years due to its unique optical and electronic properties and low cost of materials and fabrication. A wide variety of ZnO crystallite morphologies are observed for both precipitates and thin films including columnar grains, rods, stars and spherical habits [1-4]. Now highly transparent conducting ZnO windows are important components of photovoltaic devices and displays. Recently, solar cells with extra thin absorbers (ETA SC) have shown high potential of ZnO arrays as semiconductor covered electrodes and dye-sensitized photoanodes, particularly, ZnO nanorods proved to be suitable for application in organic photovoltaic devices [5, 6]. An assortment of ZnO nanostructures, such as whiskers, nanowires, nanorods, nanotubes, nanorings and nano-tetrapods have been successfully grown via a variety of methods including chemical vapor deposition, thermal evaporation, and electrodeposition. But despite numerous studies, there is little understanding of the mechanisms and factors that govern the observed morphology [1]. Among other deposition techniques electrodeposition has various advantages, viz. low processing cost, large scale, no vacuum system need, high deposition speed and no use of toxic gases. Effects of electrolyte formula, namely anionic composition [4] and presence of the different organic additives [6], deposition temperature and deposition time [7] and even gravitational level effects [9] on structure and properties of the electrodeposited ZnO nanowire arrays are studied extensively. Nevertheless, there are only rare attempts to employ a pulsed potential technique for ZnO electrodeposition [10]. On the same time, the use of pulse plating is well-known promising way to perfect properties of the electrodeposited layers. That's why purpose of this work is a comparative study of influence of direct current and pulse plating conditions, electrolyte composition and subsequent air annealing on ZnO film structure and optical properties in order to reveal means for obtaining of one-dimensional (1D) zinc oxide nanostructured layers applicable for ETA SC.

2. Methodology

ZnO arrays were electrodeposited on transparent indium tin oxide (ITO) or fluorine doped tin oxide (FTO) covered glass (Pilkington) cathodes in aqueous electrolytes contained $ZnSO_4$ or $Zn(NO_3)_2$, KCl and $NaNO_3$ (Table 1) in three-electrode cell with platinum counter-electrode and saturated Ag/AgCl reference electrode. Electrodeposition of each ZnO layer sample was carried out during 1 hour at 70 ^oC under potentiostatic conditions (at constant cathode potential U) or under pulse plating regimes with rectangular impulses of cathode potential (20 ms on-time at U_{on} and 30 ms off-time at U_{off}). All potential values in Table 1 are given versus saturated Ag/AgCl reference electrode. In some experiments electrolyte was magnetically stirred (marked + in Table 1). A following treatment of some ZnO layers was fulfilled by air annealing at 200 ^oC, 300 ^oC and 400 ^oC for 1 hour each.

Phase composition and structure of the deposited films were determined by XRD-method using an X-ray diffractometer DRON-4M with CoK_α radiation according to θ-2θ- scheme. Preferable orientations of the films were researched by analytical treatment of the X-ray diffractions by means of obtaining of texture factor P_i [11]:

$$P_i = \frac{(I_i / I_{0i}) \cdot N}{\sum_1^N I_i / I_{0i}} \qquad (1)$$

where I_i – experimental intensity of maximum; I_{0i} – intensity of this line in accordance with JCPDS card; N – total number of X-ray reflections.

Angles φ between texture axis and surface normal for all reflection planes and P_i values have been calculated according to relation [11]:

$$\cos\varphi = \frac{hh_i + kk_i + \frac{1}{2}(hk_i + h_ik) + \frac{3}{4}\frac{a^2}{c^2}l_il}{\sqrt{h^2 + k^2 + hk + \frac{3}{4}\frac{a^2}{c^2}l^2}\sqrt{h_i^2 + k_i^2 + h_ik_i + \frac{3}{4}\frac{a^2}{c^2}l_i^2}} \qquad (2)$$

A shape of function P = f(φ) allow [11] to distinguish degree of texture perfection: the texture is perfect if P decreases rapidly. When the function P = f(φ) has two or more vertexes, then the structure has two or some texture axes. Average crystalline sizes t (i. e. X-ray domains defined as volumes that diffract coherently) and lattice strains Δd/d of the electrodeposited ZnO arrays were determined by the Williamson-Hall formula for adherent deposits [12]. ZnO lattice characteristics a and c were calculated using the formula [11]:

$$\frac{1}{d^2} = \frac{4}{3}\frac{h^2 + hk + k^2}{a^2} + \frac{l^2}{c^2} \qquad (3)$$

Table 1. Electrolytes and electrolysis regimes used for deposition of ZnO.

Sample number	Electrolyte	Deposition regime	Cathode potential (V)			Magnetic stirring	Current density j (mA/cm^2)	Charge-area ratio q (C/cm^2)
			U	U_{off}	U_{on}			
1	$7 \cdot 10^{-4}$ M $ZnSO_4$	Potentiostatic	-1.3	−		−	+	2→1.4
6.1								
2	0.1 M KCl	Pulse	−	-0.9	-1.5	+	1.3→0.5	3.1
3	0.05 M $NaNO_3$	Pulse	−	-1.0	-1.6	+	2.6→1.5	5.4
4	$7 \cdot 10^{-4}$ M $ZnSO_4$ 0.1 M KCl 0.001 M $NaNO_3$	Pulse	−	-0.9	-1.5	+	0.6→0.4	1.4
5	0.05 M $Zn(NO_3)_2$	Potentiostatic	-1.1	−	−	−	1.1	4.0
6	0.1 M $NaNO_3$	Pulse		−	-0.8	-1.4	−	0.5→0.8
2.3								

The transmittance spectra of ZnO layers were measured by double beam spectrophotometer SF-46 in the spectral range 0.4 − 0.9 μm, when the sample ZnO/FTO/glass was put into working canal and FTO/glass or ITO/glass one was placed in reference canal.

3. Results

As-electrodeposited films were high adherent, semitransparent and scattered visible light. Samples 1 and 2 were grayish in color, but others were white. Figure 1 shows the transmittance spectra (T vs. wavelength λ) for the as-grown and air annealed ZnO layers. As it can be seen, from the one side, the grayish layers increase their transmittance after the annealing (they became white, probably owing to oxidation of Zn traces). From the other side, according to transmittance data, irrespective of electrolyte stirring, sample 3 offers the thinnest near transparent film, samples 1, 2 and 4 were thicker, samples 5 and 6 (not presented in Fig. 1) were the thickest. Assuming ZnO to be typical direct band gap semiconductor, the corresponding optical band gap has been estimated by the zero-crossing of the rising edge of the $[(-\ln T) \times h\nu]^2$ vs. hν curve [8] (Fig. 1, inset). All obtained band gap values as before such as after annealing correspond to ZnO (E_g near 3.2 - 3.3 eV) [2, 3, 9].

Investigation of structure of zinc oxide arrays electrodeposited in electrolytes and regimes presented in Table 1 has shown (Fig. 2) that all diffraction peaks match the hexagonal structure of wurtzite ZnO (with the exception of reflections assigned to FTO-glass or ITO-glass substrates). Comparative analysis of XRD patterns of the electrodeposited ZnO layers has revealed that, from the one side, the intensity of ZnO diffraction peaks is in direct proportion to concentration of NO_3^--ions in the electrolyte that allows us to conclude that thicknesses of ZnO layers grow when amounts of nitrates increase.

From the other side, a deviation of cathode potential towards more negative values (U = -1.3 V for electrodeposited in potentiostatic regime sample 1 and 20 ms on-time at U_{on} = -1.6 V and 30 ms off-time at U_{off} = -1.0 V for pulse plated sample 3) result in the obtaining of very thin near amorphous ZnO layers, in spite of their large current densities and charge-area ratios of the electrodeposition processes. To our opinion, the reason for that is a most probable intense additive cathode reaction of hydrogen generation in aqueous electrolytes for ZnO deposition that fulfilled at comparatively negative potentials according to relation [13]:

$2H_2O + 2\bar{e} \rightarrow H_2\uparrow + 2OH^-$ E^o = -1.05 V vs. saturated Ag/AgCl (4)

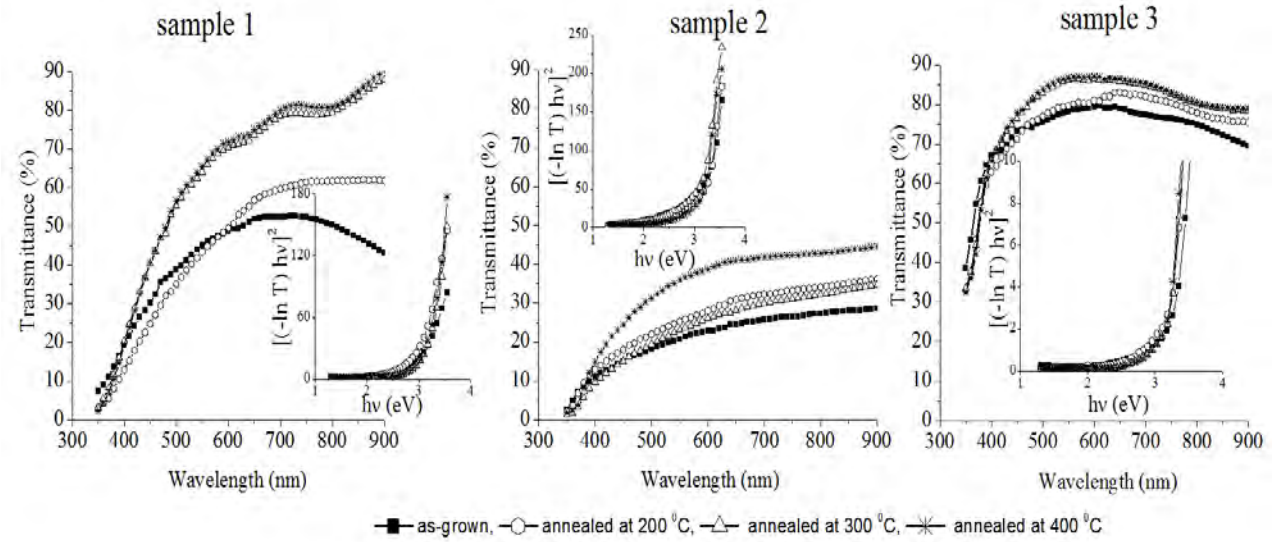

Fig. 1. Optical transmittance spectra and the corresponding band gap spectra (insets) of as-electrodeposited and air annealed ZnO arrays.

Probably, hydrogen beads adsorbed on the surfaces of substrates or on the growing ZnO crystals suppress adsorption of Zn^{2+} and OH^--ions and therefore inhibit growth of zinc oxide arrays, which could be carried out as follows:

$$Zn^{2+} + 2OH^- \rightarrow Zn(OH)_2 \rightarrow ZnO + H_2O \quad (5)$$

At less negative cathode potentials (U = -1.1 V for electrodeposited in potentiostatic regime sample 5 and U_{on} = -1.5 V and U_{off} = -0.9 V for pulse plated sample 2 and more clearly for sample 6 deposited in the pulse regime at U_{on} = -1.4 V and U_{off} = -0.8 V) current efficiency of the ZnO electrodeposition process increases, that can be seen from comparison of overall intensities of ZnO diffraction peaks for this samples (Fig. 2) and their current densities and charge-area ratios (Table 1).

Required for acceleration of ZnO synthesis cathode reductions of nitrate-ions with creation of OH^-- groups can be realized according to [13] as follows:

$NO_3^- + H_2O + 2\bar{e} \rightarrow NO_2^- + 2OH^-$ E^o = -0.21 V vs. saturated Ag/AgCl (6)

$NO_3^- + H_2O + \bar{e} \rightarrow NO_2\uparrow + 2OH^-$ E^o = -1.08 V vs. saturated Ag/AgCl (7)

$NO_3^- + 2H_2O + 3\bar{e} \rightarrow NO\uparrow + 4OH^-$ E^o = -0.36 V vs. saturated Ag/AgCl (8)

$NO_3^- + 7H_2O + 8\bar{e} \rightarrow NH_4OH + 9OH^-$ E^o = -0.34 V vs. saturated Ag/AgCl (9)

To our opinion, the most useful for ZnO deposition is cathode reaction Eq. (6), because processes Eq. (7) and Eq. (8) produce gaseous compounds whose adsorption can suppress

growth of ZnO, and reaction Eq. (9) is undoubtedly sophisticated multistage process as such as it consumes eight electrons. Therefore, high amount of NO_3^--ions is a cause of the elevated thicknesses of samples 5 and 6. Enhanced structure of sample 2 as compared with sample 1 is evidently a result of such advantage of pulse electrolysis as suppression of additive cathode reaction Eq. (4), because it is impossible at U_{off}, but during off-time ions NO_3^- and Zn^{2+} can diffuse to the cathode and can be realized processes Eq. (6), Eq. (8) and Eq. (9) which are useful for creation of ZnO.

Moreover, at on-time electrochemical reaction Eq. (7) and reduction of Zn^{2+} are doubtless:

$$Zn^{2+} + 2\bar{e} \rightarrow Zn \qquad E^o = -0.98 \text{ V vs. saturated Ag/AgCl} \qquad (10)$$

So, during off-time internal electrolysis is additive possible way for creation of ZnO arrays through following heterogeneous chemical reaction:

$$Zn + NO_3^- + H_2O \rightarrow NO_2^- + Zn(OH)_2 \qquad (11)$$

Table 2 shows structure characteristics of thicker ZnO layers. All ZnO arrays are nanostructured and characterized by little compressive stress (samples 2 and 5) or tension (sample 6). Lattice constants a are near value for single crystal ZnO of hexagonal modification, but the electrodeposited ZnO grains were elongated along c axis (according to JCPDS 36-1451, a = 3.250, b = 5.207).

Table 2. Structure characteristics of the electrodeposited ZnO arrays.

Sample number	Lattice constant (Å)		Average crystalline size t (nm)	Lattice strain $\Delta d/d \times 10^4$
	a	c		
2	3.251	5.228	27	14.5
5	3.249	5.226	54	3.5
6	3.253	5.220	16	-36.8

Comparison of preferable orientations has revealed (Fig. 3) that ZnO layer prepared in electrolyte with low concentration of nitrates (sample 2) has crystallites with random orientation. There seems to be main reason for such structure that the polar (002) crystal plane of the ZnO is capped by Cl^--ions (from the KCl supporting electrolyte), which [1, 4] redirect the growth of ZnO. Sample 5 plated at direct current in NO_3^--enriched electrolyte has two preferable orientations (002) and (103), probably because of influence of cathode reaction of hydrogen evolution by Eq. (4). Only sample 6 electrodeposited in electrolyte, which contains large concentration of NO_3^--ions at pulse plating conditions has strong (002) preferable growth orientation in the c-axis direction. According to [1], increase of (002) reflection in relative intensity is consistent with formation of ZnO rod crystallites along c-axis. In [2-4, 6] judgment, such preferential growth in the (001) plane results in 1D nanostructure of ZnO arrays, e.g. nanowires, nanorods or nanopillars, that grow along the direction perpendicular to the substrate.

4. Discussion and Conclusions

We have determined that for obtaining by electrodeposition of ZnO arrays preferential grown in the (001) plane it is necessary to diminish adsorption of Cl^--ions and hydrogen beads on this plane.

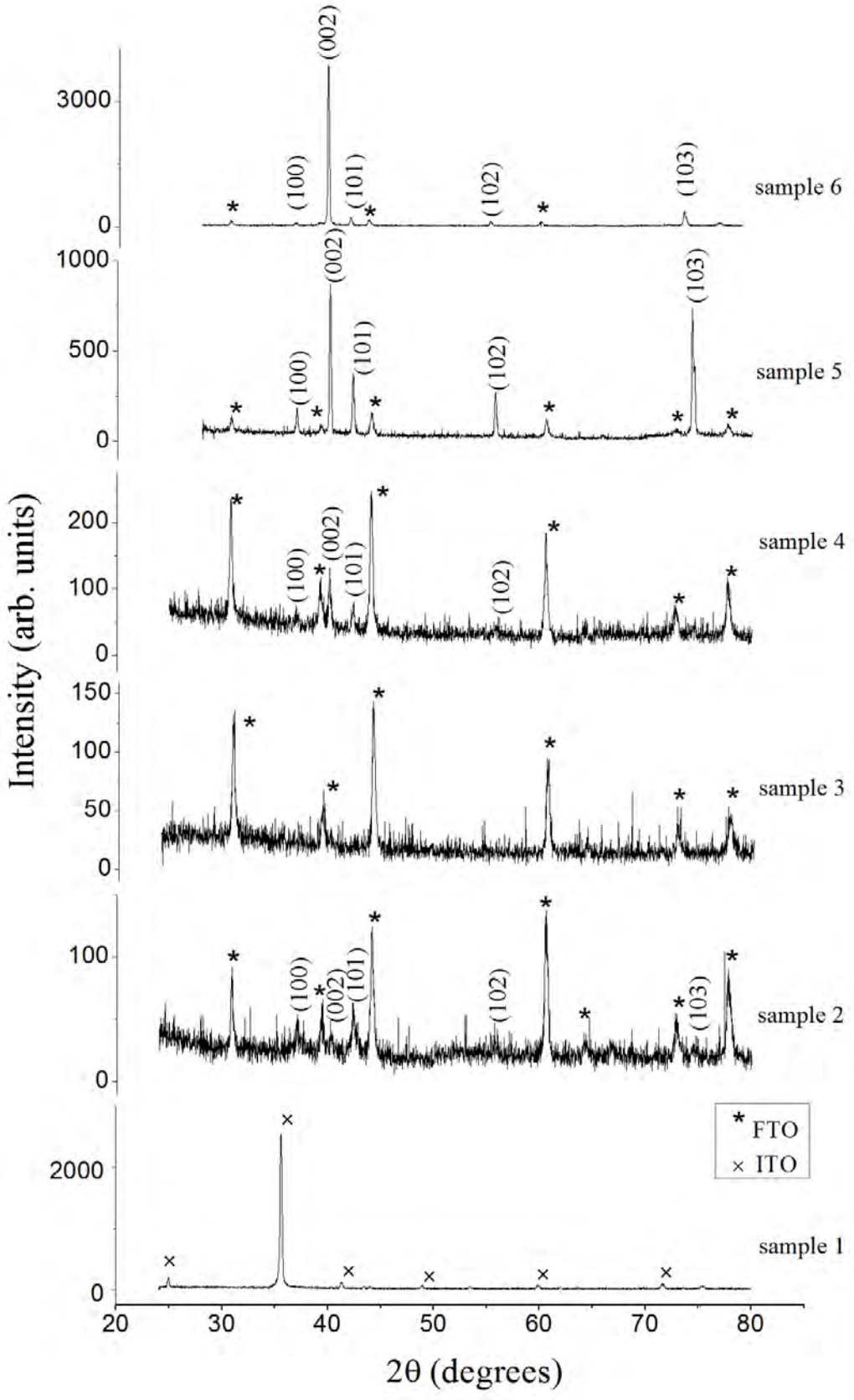

Fig. 2. XRD patterns of ZnO layers electrodeposited onto transparent conducting oxide coating glass substrates (− FTO, × − ITO).*

It has been shown that such conditions are created in electrolyte that contains 0.05 M $Zn(NO_3)_2$ and 0.1 M $NaNO_3$ during electrodeposition in pulse plating regime with rectangular impulses of cathode potential (20 ms on-time at U_{on} = -1.4 V and 30 ms off-time at U_{off} = -0.8 V) on FTO-coated glass substrates. Therefore, in this work we for the first time have demonstrated the successful growth of 1D ZnO nanostructures by pulse plating without using of templates. The obtained ZnO arrays have to be the suitable layers for solar cells with extra thin absorbers.

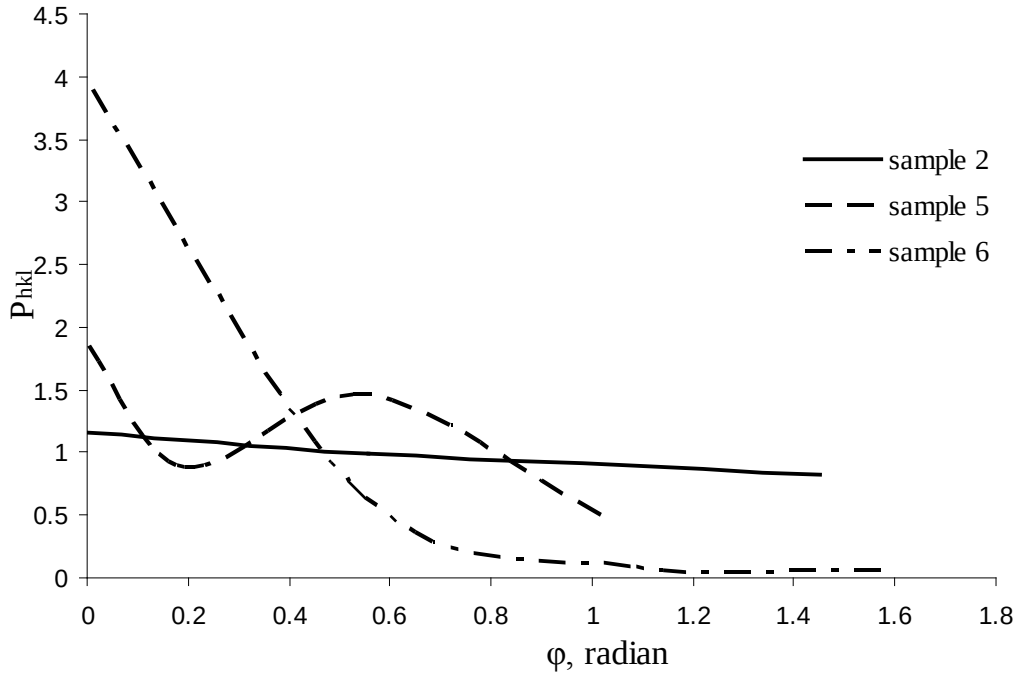

Fig. 3. Degree of texture perfection of electrodeposited ZnO arrays.

Acknowledgments

The work was supported by STCU under Project 4301.

References

[1] K. Govender, D. S. Boyle, P. B. Kenway. P. O'Brein, J. Mater. Chem. 14, 2004, pp. 2575-2591.

[2] C. X. Xu, X. W. Sun, Z. L. Dong, G. P. Zhu, Y. P. Cui, Appl. Phys. Lett. 88, 2006, pp. 093101.

[3] X. Hu, Y. Masuda, T. Ohji, K. Kato, Journal of the Ceramic Society of Japan 116 (3), 2008, pp. 384-388.

[4] D. Pradhan, M. Kumar, Y Ando, K. T. Leung, J. Phys. Chem. C 112, 2008, pp. 7093-7096.

[5] A.M. Peró, P. Ravirajan, K. Govender, D.S. Boule, P. O'Brein, D. D. C. Bradley, J. Nelson, J. R. Durrant, J. Mater. Chem. 16, 2006, pp. 2088-2096.

[6] X. Ju, W. Feng, X. Zhang, V. Kittichungchit, T. Hori, H. Moritou, A. Fujii, M. Ozaki, Solar Energy Materials and Solar Cells 93, 2009, pp.1562-1567.

[7] E. Michaelis, D. Wöhrle, J. Rathousky, M. Wark, Thin Solid Films 497, 2006, pp.163-169.

[8] D. Pradhan, K. T. Leung, J. Phys. Chem. C 112, 2008, pp. 1357-1374.

[9] Y. Fukunaka, K. Kuribauashi, Space Utiliz. Res. 24, 2008, pp. 27-30.

[10] M. Gupta, D. Pinisetty, J.C. Flake, J. J. Spivey, Journal of the Electrochemical Society 157, 2010, pp. D473-D478.

[11] Structura i phizicheskie svojstva tverdogo tela /edited by L.S. Palatnik, Kiev, Visshaja shkola, 1983, p.284 [in Russian].

[12] A. Malik, B.C. Ray, Thin Solid Films 517, 2009, pp. 6612-6616.

[13] Y. Y. Lurje, Spravochnik po analiticheskoy himiji, Moscow, Himija, 1989, p.448 [in Russian].

Rope-pump System Modelling using Renewable Power Combinations

Cai Williams[1], Andrew Beattie[1], Tim Parker[1], Jo Read[1], Julian D. Booker[1*]

[1]*University of Bristol, Bristol, UK*
[*]*Corresponding author. Tel: +44 117 331 5905, Fax: +44 117 929 4423, E-mail: j.d.booker@bristol.ac.uk*

Abstract: Rope-pumps are a highly successful method of lifting water by hand in developing countries. The primary aim of this work was to develop a validated methodology to decide the most cost effective renewable power sources in order to fully automate the operation of the rope-pump for given well depth, volume of water required and environmental conditions in the proposed installation location. The renewable energy sources considered were a 150W photovoltaic (PV) panel and a 100W wind turbine, either used in isolation or in combination with a battery and motor, or direct drive to a motor, providing five viable systems for further consideration. All system elements and the rope-pump itself were fully characterised through experimental testing. Computer-based simulations incorporating environmental conditions for Lilognwe, Malawi, were used to provide a 15 year lifecycle analysis. Results show that the use of PV powered system can deliver water reliably, at the lowest cost. For validation purposes, each rope-pump system was also analysed with the environmental conditions found in Bristol, UK providing comparison results, indicating the approach is systematic and rigorous enough to provide an effective decision making tool for the installation of rope-pumps anywhere, provided environmental data is available.

Keywords: *Rope-pump, renewable power, system modelling, system selection.*

1. Introduction

The rope-pump is a very simple type of water lifting device. The almost intuitive design is known by many other names including the paternoster (after the beaded prayer chain it resembles), liberation or rope-and-washer pump. It is a relatively recent development of the ancient chain-and-washer pump, which dates back two thousand years to feudal China [1]. In the 1980s the basic design was developed by numerous individuals [2, 3], taking advantage of low cost and versatile modern plastics to produce the modern rope-pump design, shown schematically in Fig.1. The rope-pump consists of a continuous loop of rope with plastic pistons spaced evenly along its length. When the rope is pulled up through the rising-main by a drive wheel located at ground level, the close fit of the pistons in the cylinder draws water up to a height of 30m potentially.

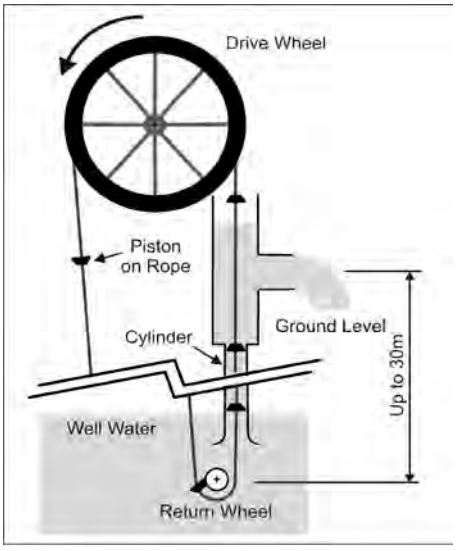

Fig.1. Schematic of a Rope-pump Powered Manually using a Drive Wheel.

The hand powered rope-pump has been highly successful across Africa and South America mainly due to attributes such as a high achievable head, low starting torque, low installation cost, ease of manufacture and minimal maintenance. These attributes identify the rope-pump as the most appropriate type of pump for automation, providing the remaining system components for automation still allow water to be delivered reliably at low cost. An affordable automated pump would allow a greater amount of water to be extracted than would be possible by hand alone, and this has many implications societally and economically for its users in developing countries. The extra water could be used to improve levels of sanitation and increase crop yields. This in turn would improve nutritional levels and provide a potential income from the sale of excess produce. It would also free up the time of users, which would otherwise be spent manually lifting limited amounts of water. This time could then be used for education and other income generating activities [4]. Various types of power supply for the rope-pump have previously been explored in order to replace manual operation, including: water wheel, pack animal, internal combustion engine and wind-turbine. This research aimed to simulate the performance of a range of automated systems with two renewable energy power sources (PV panel and wind turbine) in order that an economically viable rope-pump solution can be selected for any specific location and given set of environmental conditions.

2. Methodology

Economic, social and environmental factors associated with technical hardware prove to be crucial to the success or failure of the final rope-pump systems. Frequent maintenance and additional control systems required are likely to make the system impractical in locations where the necessary resources are unlikely to be available. The importance of a simple system, with a minimal demand on local expertise and supply chains and one that is appropriate to both the hydrological, geographical and social environment is crucial, a point stressed by industrial contacts and made clear from reviewing existing rope-pump systems.

A literature review, in combination with a dialogue with representatives of Solar-Aid (the main industrial contact on the project) identified the requirements of an automated rope-pump system, which were then summarised in a product design specification (PDS). Five system configurations capable of fulfilling this PDS were identified through a team-based exercise with all project stakeholders. These systems are shown schematically in Fig.2, and are a) direct connection of the motor to a PV panel; b) direct connection of the motor to a wind turbine; c) connection of the motor to a PV panel via a battery; d) connection of the motor to a wind turbine via a battery; and e) connection of both a PV panel and a wind turbine to the motor via a battery. The common component of all the system configurations devised is a suitably geared motor, but it would still be possible to decouple the motor from the rope-pump drive axle and provide manual operation through a hand-crank.

First, a theoretical force model for the rope-pump was developed based on a complete analysis of the frictional loads and energy flows present within the rope-pump. This could then define the electrical power and speed (gearing) requirements of the motor drive. Force and flow models were investigated empirically using a custom built motor driven rope-pump rig, designed to measure the rope tension, rope velocity and the discharge flow-rate, for two different pipe diameters and a range of heads up to 8m. The force model developed was found to be significantly more accurate than models proposed in previous literature, and the dependency of the flow-rate of the rope-pump on head and rising-main diameter was empirically confirmed to match an improved version of the model [**5**, 6]. The comprehensive treatment and analysis of frictional loads and energy flows within the rope-pump produced a key component of the system model performance model.

The remaining specific characteristic parameters of all system components were identified empirically from experimental testing; designed and built to accurately simulate the duty cycles of the components. The renewable energy power sources were chosen as a 150W PV panel (two RSM-75 from Shell Solar) and a 100W wind turbine with an axial flux generator, hand-built Hugh Piggott turbine type [7]. These system components were chosen due to availability and comparable (full) power rating to that of a human male, assuming a working duration of one hour. The wind turbine was fully characterised at different load conditions and wind speeds using a wind-tunnel providing new performance data for this turbine. Models of the motor, battery and PV panel were also identified and supported along with the turbine by empirical observations of their characteristics. The complete solar powered systems were tested under the local environmental conditions in Bristol, UK, but due to limiting wind speeds and radiation from the sun, the combined power sources had to be replicated using a power supply unit. A detailed description of the governing analytical equations and experimental characterisation for all system components is provided in [5] and [8].

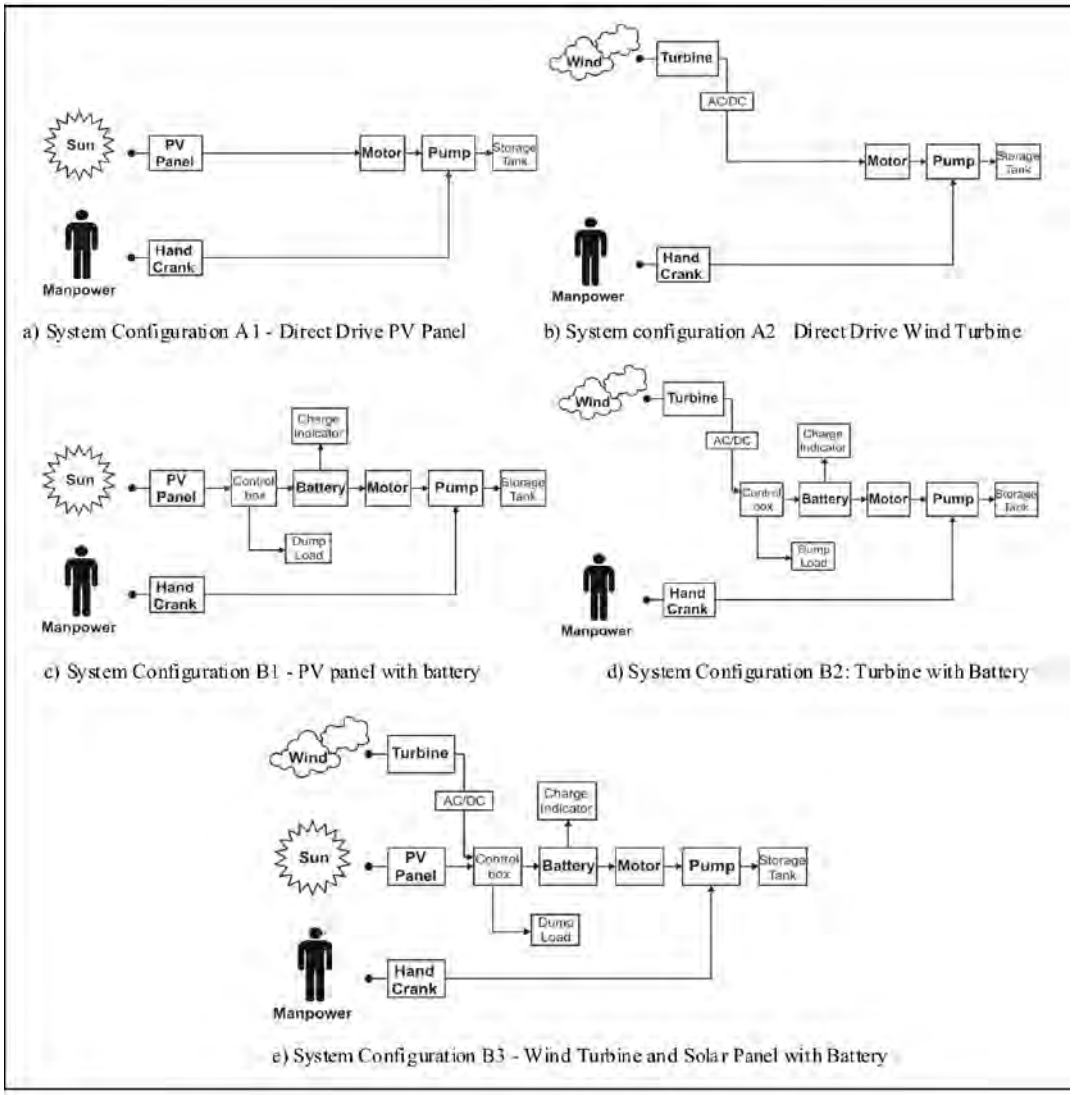

Fig.2. Five Automated Rope-pump System Configurations Considered for Simulation Studies.

From the comprehensive rope-pump system model, two computer programmes using MATLAB programming software were coded in order to investigate more efficiently a wide range of operational requirements for those systems with a battery and those without a battery,

as the computational stages are quite different for each. The computer programmes are provided in flowchart form (for one time-step) in Fig.3a) for those system configurations that use a battery, and Fig.3b) for those that do not i.e. directly driven by a motor, respectively. Together, these programmes are able to replicate the complete rope-pump system in direct drive or battery configurations, utilising a PV module and/or wind turbine as power inputs.

The PV panel model is based on the characteristic equations, and only requires inputs which are available on standard datasheets as this allows for easy comparison of alternative modules within the system. The wind turbine was modelled by directly uploading results from the turbine characterisation testing into the computer program. The program inputs are the independent local parameters (such as head and local weather data) and parameters which determine the size of the system (such as pipe diameter and number and characteristics of solar panels). This allows for the flow rate, and therefore the water volume lifted, to be estimated based on the capital cost available, as capital cost was identified as the a key differentiating requirement in the PDS.

A rigorous test regime showed the flow rates predicted by the computer model to be accurate to within 7% compared to the results from the experimental rope-pump. This is considered acceptable considering the unavoidable sources of error which would occur were the computer program to be used to size rope-pumps for use in the field. There are considered to be two major and unavoidable sources of error: firstly, the variation of local weather conditions from the average conditions used as program inputs will lead to the available power differing from the predicted values. For example, a decrease in the insolation available by 10% leads to a 4% decrease in the volume of water lifted for a direct drive PV powered system. Secondly, the empirical values derived for the pump and motor in the characterisation stage will not be identical for each rope-pump built. This is particularly true of the friction coefficient over the bottom guide, for which an increase from 1N to 10N leads to a 10% decrease in the volume water lifted for a head of 10m for a given internal rising-main diameter.

3. Results

The town of Lilongwe, Malawi and the city of Bristol, UK, are used as case examples for results analyses. Lilongwe is where the main industrial contact of the project, Solar-Aid, is based. Bristol is used to provide comparison data for presentation of the results and in order to demonstrate the robustness of the simulation software for a very different set of environmental conditions. The rope-pump is to be used to lift 1 to 10m^3 of water per day from a well 10m deep. This is a volume that is more than can be reasonably lifted by hand and a suitable amount for a typical small rural institution such as a school or hospital in Malawi. The environmental data used in the simulations were taken from a number of online sources [9-11].

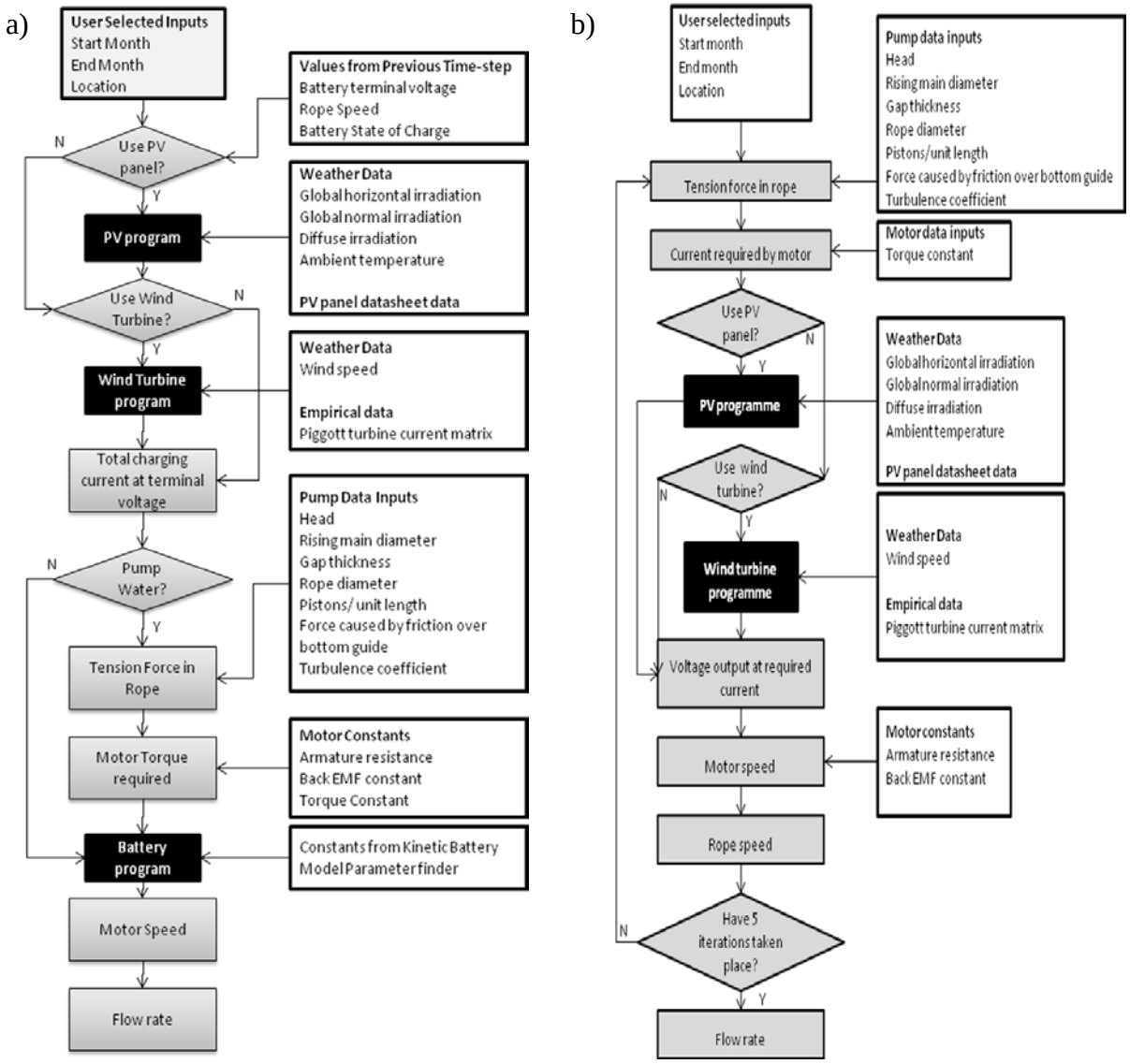

Fig.3. Simulation Flowcharts for Automated Rope-pump Configurations, a) battery systems, b) direct drive systems.

A 15 year life-cycle analysis was carried out for each of the five system configurations, including an additional variant of the direct driven rope-pump using a PV panel, called "A1–tilt", where the PV panel is manually oriented towards the direction of the sun periodically. The results of this life-cycle analysis for both Lilongwe and Bristol locations are shown in Fig.4. Where wind velocities are sufficient, the direct drive wind turbine rope-pump system has the potential to deliver water for the lowest cost (0.03US$/m^3 from 10m) in Lilongwe. However, the starting speed of the tested wind turbine was 3m/s, and makes this wind turbine component unsuitable for use in Malawi. The cost per m^3 of water lifted is capped at $0.14/m^3 for all rope-pump system configurations, and as Fig.4 shows, those systems using wind turbines in Lilongwe are the most costly. The use of a direct drive PV powered rope-pump system is then preferable as indicated by the low cost of A1. It is estimated that a direct drive PV system in Malawi weather conditions can deliver water at a cost of 0.05US$/m^3, again from 10m well. This cost can be reduced further with the A1-tilt system, although this system is not fully automated. In all cases the use of a battery was found to increase the cost per cubic meter of water lifted despite the increased volume of water delivered. For the PV powered rope-pump system, the cost was increased by 20%, for example.

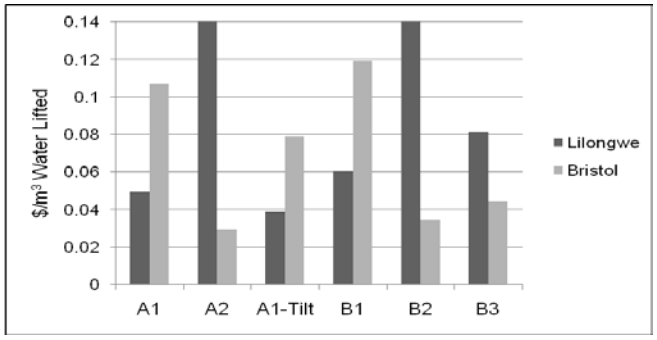

Fig.4. Cost of Water Lifted for Each Rope-pump Configuration in Lilongwe, Malawi and Bristol, UK.

Further results from the simulations are shown in Fig.5, where a daily volume of water in m^3 is provided for given inputted environmental data for a calendar year. These results are cost independent, and are purely performance based. Again, the solely wind turbine powered rope-pump systems A2 and B2 are determined as non-viable configurations for Lilognwe, as they do not appear on this chart at all. Systems B1 and B3 seem competitive in terms of water lifted, but B3 uses the wind turbine, and therefore it does not contribute to the system power due to a 3m/s starting wind speed, and should be disregarded. Similarly, B1 uses a battery and therefore is more costly overall for initial investment and long-term servicing, as previously estimated.

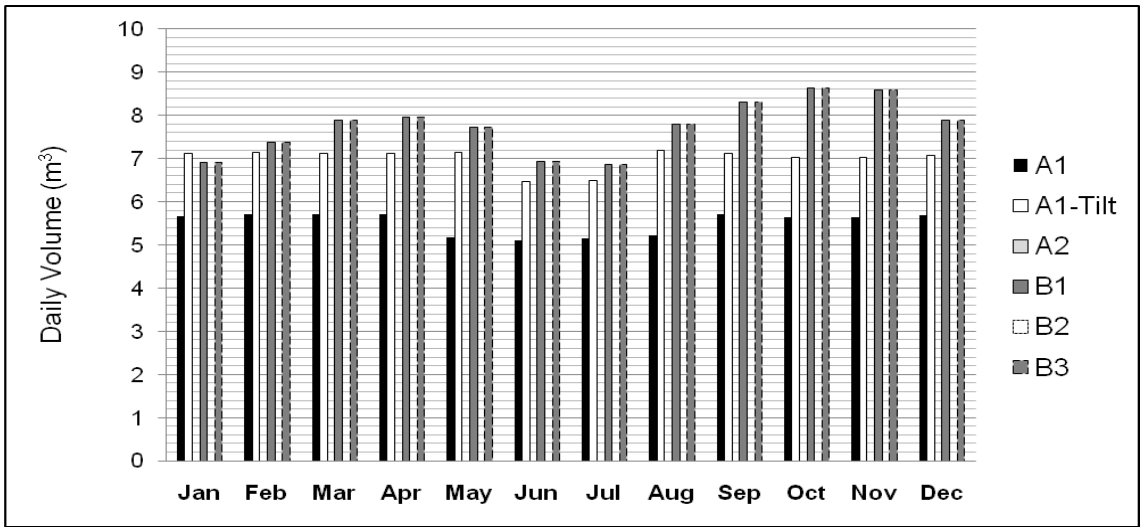

Fig.5. Daily Volume of Water from the Different Rope-pump Configurations for Lilongwe, Malawi Location (wind speeds in Lilongwe are lower than the cut in wind speeds for the tested turbine and so configurations A2 and B2 lift no water).

The results for Bristol are demonstrative of the range of location conditions that the simulation software can accommodate, with the only requirement of satisfactory data sets used for cost and environmental parameters. Overall, the results are very different to Lilongwe, as expected. All system configurations are technically viable at some part of the year, as indicated by Fig.6. A direct drive (A2) or battery powered (B2) wind turbine rope-pump configurations are the most cost effective as shown originally in Fig.4.

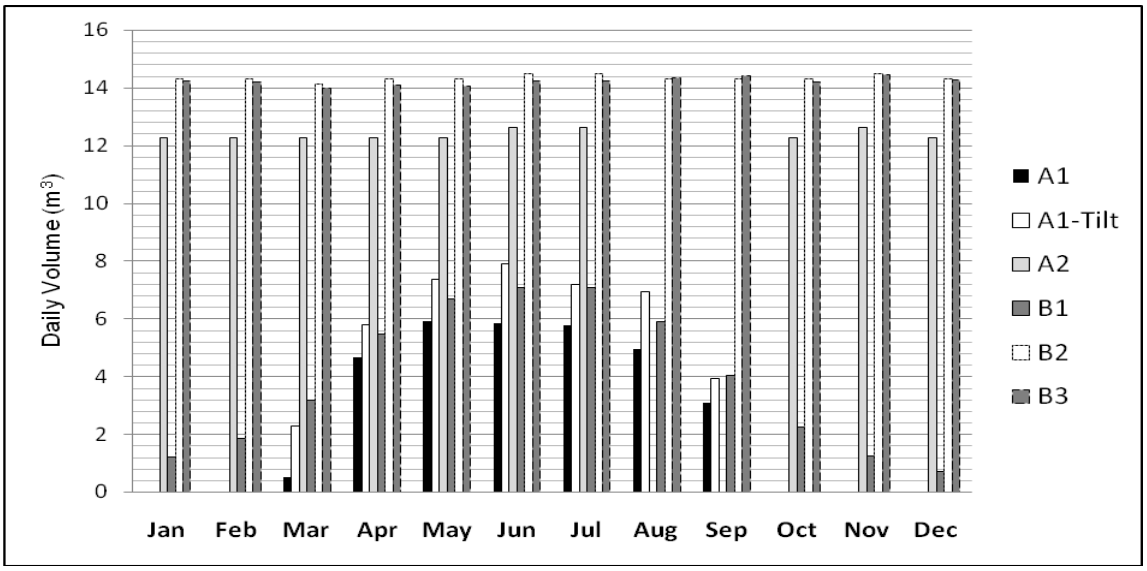

Fig.6. Daily Volume of Water from the Different Rope-pump Configurations for Bristol, UK Location.

4. Conclusions

Fully parameterised software, together with scalable hardware for physical testing of a variety of rope-pump systems has been produced in order to provide a decision making tool to select the most appropriate combination of system elements for technical and economic viability. The results shown confirm the simulation software has the flexibility to be applied to a variety of environments, duty cycles and rope-pump delivery requirements. An improved model for the rope-pump mechanical loads and flow-rates enables detailed specifications of sub-systems based around the rope-pump to be made, when previously a significant degree of trial and error was required. The method has been applied to different areas of the world to show the acceptability of other systems given their environmental data.

The use of a battery as the primary load on the PV module or wind turbine allowed for the efficient matching of the IV curves of the power source with the IV curves of the load, leading to an average of 40% more water pumped per annum for PV powered systems. However, the inherently short life-span of the battery leads to high capital and component replacement costs which lead to the cost per litre of water lifted being an average of 20% higher for systems utilising a battery than for the direct drive rope-pump systems. In locations where water source reliability is a concern, a reservoir should be used instead of storing energy in a battery, if installation costs permit. There has been considerable interest in the solar powered rope-pump for use in countries that have high-average sunshine levels, since its conception in 2007 [4]. The simulation has confirmed that a battery is not necessary for such locations. Based on other findings of the project, the possibility of integrating a wind turbine with a rope-pump may be given greater investigation for certain locations for installation, but requires a range of alternative turbine types to be evaluated. For example, the use of a small vertical axis wind turbine may offer a promising alternative to the one tested in this study.

There is potential for the computer program to be used by individuals and companies charged with the design and distribution of rope-pump systems. For this to be possible, the program would need to be loaded with weather data for a wide range of locations, and with power curves for a selection of available wind turbines. The process of selecting a PV module could also be improved if the program were linked to an available database of PV modules, such as that compiled by Sandia [12] removing the need to input a large amount of data from

datasheets. The program would be of most use in the early system design stages, to carry out feasibility studies for a number of system configurations. This will allow the user to determine the most suitable system for the location, which could then be designed in detail, with consideration given to the realities of component sourcing and maintenance. The modular nature of the program makes it possible to add additional 'modules'. Any component which can be fully characterised could be added. A suitable module would be a small grain mill: an item commonly used in developing countries which requires large amounts of man power to operate and has the potential to be powered by alternative sources. There is also potential for adding additional power source modules, for example, a diesel engine.

Acknowledgements
The authors would like to thank. Mark O'Riordan from Partners in Development, Bobby Lambert, Cardiff University and Solar-Aid, the project's industrial contact.

References

[1] P. Fraenkel and J. Thake, Water Lifting Devices: a handbook for users and choosers, Rugby: Intermediate Technology Publications Ltd, 3rd Ed., 2006.

[2] R.A. Lambert, How to Build a Rope-and-Washer Pump, Intermediate Technology Design Group, London, 1990.

[3] J.H. Alberts, The Rope-Pump: an example of technology transfer, Waterlines, 22(3), 2004, pp. 22-25.

[4] R.A. Lambert, Jumemaji: Solar Pumping for Sustainable Food Production Concept Paper, 2007 [Available from: bobby@bobbylambert.eul, 5th July 2007].

[5] A. Blanken, Measurements and Analysis on the Performance of the Rope-pump, University of Technology, The Netherlands, 2009 [http://www.msabi.org/docs/ropepump, viewed online 08/12/10].

[6] P. T. Smulders and R.P.P. Rijs, A Hydrodynamic Model of the Rope-pump, Veldhoven, The Netherlands, 2006 [http://www.arrakis.nl/reports/060923_Ropepump_Smulders-Rijs_lr.pdf, viewed online 08/12/10].

[7] H. Piggott, A Wind Turbine Recipe Book [http://www.scoraigwind.com, viewed online 13/12/10].

[8] A. Beattie *et al*, Rope-pump System Modelling using Alternative Power Combinations, UK, 2009 [http://www.msabi.org/docs/ropepump, viewed online 08/12/10].

[9] European Commission, Photovoltaic Geographical Information System (PVGIS) [http://re.jrc.ec.europa.eu/pvgis, viewed online 08/12/10].

[10] R. Hoare, World Climate [http://www.worldclimate.com, viewed online 08/12/10].

[11] The Weather Network, Statistics: Chitedze, Malawi [http://www.theweathernetwork.com/index.php?product=statistics&pagecontent=C0179, viewed online 08/12/10].

[12] Sandia National Laboratories, Photovoltaic System Research and Development [http://photovoltaics.sandia.gov, viewed online 08/12/10].

Machine learning approach for next day energy production forecasting in grid connected photovoltaic plants

L.Mora-López[1,*], I.Martínez-Marchena[1], M.Piliougine[2], M.Sidrach-deCardona[2]

[1] *Dpto. Lenguajes y Ciencias de la Comunicación. Universidad de Málaga. Málaga, Spain*
[2] *Dpto. Física Aplicada II. Universidad de Málaga, Málaga, Spain*
** Corresponding author. Tel: +34 952250362, Fax: +34 952131397, E-mail: llanos@uma.es*

Abstract: This paper presents a model for predicting the next-day energy production of a photovoltaic solar plant. The model is capable of forecasting the next-day production profile of such a system, merely by using the information obtained from the plant itself and the solar global radiation values for the previous operation days. This prediction is key in many photovoltaic systems in order to interact with conventional electrical grids. For example, Spanish legislation requires this type of information for large photovoltaic plants. In fact, the deviations from the predicted values are financially penalized. A three-stage procedure is used to build the model, which is capable of learning specific information about each facility and of using this information to fit the prediction. This model binds the use of regression techniques and the use of a special type of probabilistic finite automata developed from machine learning. The energy prediction yearly error is less that 20 percent which is a significant improvement over previous proposed models, whose errors are around 25 percent.

Keywords: *short term forecasting, photovoltaic energy production, machine learning*

1. Introduction

Process forecasting has become a key tool in many areas, such as competitive electricity or economic markets. In the short term, forecasting the expected values of certain variables can be an important tool for optimal systems management and to decide on the best operation strategies. Forecasting energy production by large plants has thus become a requirement in competitive electricity markets. In the short term, expected produced energy can help producers to achieve optimal management and can also help to implement efficient operation strategies based on the best way of interacting with conventional grid. For example, since 1998, the Spanish electricity market has moved from a centralized operational approach to a competitive on. It encourages the deployment of solar plants with a financial penalty for incorrect prediction of solar yields for the next day. In this global market, energy generated by these systems for the grid needs to be predicted as accurately as possible in order to ensure that solar energy systems are truly penetrated in the electricity market. Forecast regarding energy production is necessary to manage and schedule electricity grids. This prediction will facilitate the use of these systems as distributed generators in grid connected photovoltaic systems.

Estimating the energy generated by solar plants is difficult mainly due to its dependence on meteorological variables, such as solar radiation and temperature. In fact, photovoltaic production prediction is mainly based on global solar irradiation forecasts. The behavior of this variable can change quite dramatically on different days, even on consecutive days. This is because global solar radiation is not a deterministic variable due to the climatic conditions. Although the extraterrestrial solar irradiation -defined as the solar irradiation that reaches the extra atmospheric zones of the earth- is deterministic, once this irradiation penetrates in the atmosphere, different variable phenomena come into play and only a fraction of the extraterrestrial solar irradiation therefore reaches the surface of the earth. This fraction is known as solar global radiation. These phenomena include the presence of clouds in the atmosphere that can significantly reduce the solar irradiation reaching the earth. Accurately

forecasting the energy generated by these systems is difficult as solar radiation is the energy source of solar systems.

In general, a wide range of statistical and artificial intelligence techniques have been developed for process forecasting. Statistical time series methods are based on the assumption that the data have an internal structure that can be identify by using simple and partial autocorrelation, [1], [2], [3], [4]. Time series forecasting methods detect and explore such a structure. In particular, ARMA (autoregressive moving average), ARIMA (autoregressive integrated moving average) models have been widely used. Artificial intelligence techniques and, in general, machine learning models have been also used for process forecasting, [5], [6], [7], [8], [9]. Different approaches have likewise been specifically developed for forecasting global solar irradiation, [10], [11], [12], [13], [14].

We propose a model that is capable of learning the important facts in the prediction of photovoltaic plants energy production. A new approach based on the use of probabilistic finite automata and multivariate regression analysis is proposed here for short-term forecasting of the production of solar plants. The forecasting model is built in three stages and has been previously used for short-term forecasting of hourly global solar radiation, [15], [16]. The first and second stages of the procedure are used to identify and capture the significant information for predicting the production of a photovoltaic plant and to build the model using this information. In the first stage, the most significant independent variables are selected by using a multivariate regression analysis. In the second stage, probabilistic finite automata are built using the significant variables obtained in the first stage. The next values of the dependent variable are predicted using an algorithm for short term forecasting which is based on the information stored in the built model. In the third stage, the next-day solar energy production forecasting is calculated using the estimates values in the second step and the parameters of each solar photovoltaic plant. The methodology and the proposed model are described in the second section. In the third section, the results obtained when the model is used for next-day energy production forecasting in photovoltaic plants are presented. The conclusions of the paper are presented in the last section.

2. Methodology

This paper seeks to propose a model for forecasting next-day energy production in grid connected photovoltaic plants. The model is based on the model developed for short-term forecasting of hourly global solar radiation described in [15]. We propose the use of several independent variables to build the model; these variables are usually available in large photovoltaic solar plants: irradiation values and temperature. Moreover, specific parameters of the plant, such as power installed, orientation and tilt of the panel arrays, have been included in the final model. The model is built in three stages.

In the first stage, statistical techniques are used to determine the most significant information among the independent variables used. Using this information, the data are divided into different groups and for each group the new significant variables are determined. In the second stage, a special type of probabilistic finite automata is built for each group taking into account the significant variables of the group. In the third stage, the model of prediction is used for forecasting the energy produced by the photovoltaic solar plants for the next day.

The mathematical model proposed to store the information contained in solar irradiance is based on the use of a special type of probabilistic finite automata (PFA). The use of this mathematical model is envisaged to select both the most meaningful information included in a

stationary continuous time series and the information obtained from other sources. A detailed description of this model can be found in [15].
The power generated at the output of the inverter, P_{AC} can be estimated using the expression:

$$P_{AC} = \eta_{inv} * P_m^{STC} * \frac{G_\beta}{1000} * (1 + \gamma * (T_{\mathrm{mod}} - 25)) \quad (1)$$

where, η_{inv} is the efficiency of the inverter, $P_m{}^{STC}$ is the power generated by the photovoltaic generator in standard conditions of radiation and temperature (1000W/m^2, 25ºC), $G_{\beta t}$ is the global irradiance on the surface of the modules (W/m^2) – β is the inclination of the modules, γ is the temperature coefficient of P_m, and $T_{mod,t}$ is the module temperature. In the case of monocrystalline silicon, the value of the coefficient γ is 0.48%/ºC (these type of modules are used in all the facilities analyzed).

The irradiance on the surface of the modules is the most difficult parameter to estimate using Eq.(1). Moreover, this parameter presents a seasonal trend due to the changes in the relative sun-earth position. Using the values of clearness index is proposed to remove this seasonal trend. This parameter is estimated using the following expression:

$$k_t = \frac{G_t}{G_{0,t}} \quad (2)$$

where G_t is the global irradiance (Wh/m2) at time t and $G_{0,t}$ is the extraterrestrial solar irradiance at time t (Wh/m2); the expression for estimating $G_{0,t}$ can be found in [17].

2.1. First stage

In the first stage, the following linear regression model is estimated using ordinary least squares :

$$k_{t,d} = \beta_0 + \beta_1 k_{t,d-1} + \beta_2 k_{t,d-2} + \beta_3 k_{t,d-3} + \beta_4 S_{1,t,d} + \beta_5 S_{2,t,d} + \beta_6 ST_{3,t,d} + Error \quad (3)$$

where t means time, d means day and S_i , $i=1,2,3$, are three dummy variables to represent the season to which the observation $k_{t,d}$ belong (only three dummy variables are used to avoid multicollinearity problems). Among these independent variables, the most significant variable for predicting the next value of clearness index is used for splitting the observation into G groups. For each one of these groups, the Eq.(3) is again estimated to determine the significant variables of the group.

2.2. Second stage

For the observations of each group, a special type of probabilistic finite automata is built using the significant variables of the group. The continuous variables need to be discretized to use this model. A static discretization method has been used. The range of each continuous variable has been divided into q equals intervals. Several values of q have been proved for each group in order to select the best discretization, taking into account the performance of the probabilistic finite automata in the short-term forecasting of clearness index. The proportional mean prediction error (*PMPE*) has therefore been estimated, i.e.

$$PMPE = \sum_{t=1}^{N} \frac{| k_{t,d} - k_{t,d}^{*} |}{k_{t,d}} \quad (4)$$

where N are the number of observations in each group and $k_{t,d}^{*}$ is the predicted value of clearness index.

2.3. Third stage

In the third stage, the values of solar irradiance G_t are estimated from the values of clearness index predicted using the PFAs built in the second stage. With these values, the power generated at the output of the inverter is estimated using the Eq. (1). For evaluating the model, the mean prediction error for these values has been estimated, i.e.:

$$MPE = \frac{\sum_{t=1}^{N} | P_{AC,t} - P_{AC,t}^{*} |}{\sum_{t=1}^{N} P_{AC,t}} \quad (5)$$

3. Data

The data used have been recorded from four photovoltaic plants installed in different Spanish locations. The data used for these facilities are the following: power generated at the inverter output, irradiance on the surface of the modules and modules temperature. Moreover, the season to which each observation belongs has been included. Table 1 sets out a summary of the characteristics of each facility.

Table 1. Description of the data used.

Location	Latitude/Longitude	Peak power (kW)	Inclination of modules	Data
Location 1	43.30/-1.95	14.08 kW	20	01/10/2009-10/12/2010
Location 2	43.18/3.00	13.86 kW	20	01/10/2009-10/12/2010
Location 3	43.37/-1.85	20.16 kW	30	01/11/2009-10/12/2010
Location 4	43.37/-1.85	20.16 kW	30	01/11/2009-10/12/2010

4. Results

In the first stage, the linear regression model, Eq. (3), has been estimated using the ordinary least square (OLS) for the data of each location. In all cases, the most significant variable proves to be $k_{t,d-1}$, that is the clearness index for the same hour at the previous day (significance level=0.05).

Using this variable, the observations of each location have been split into 5 different groups depending on the value of this variable. The model, Eq. (3), has been estimated by OLS for each group.

Table 2 summarizes the significant variables for each group, taking into account the values of the t-statistic for a significance level of 0.05, for Location 3. As can be observed, these variables differ depending on the group. This result is similar for all locations.

Table 2. Significant variables for each group of observations (Eq.1, significance level=0.05) for Location 3

Interval	Significant variables
[0.0-0.2[	$K_{t,d-2}$, $K_{t,d3}$, $S_{3,t,d}$
[0.2-0.4[	$K_{t,d-2}$, $K_{t,d-1}$, $S_{3,t,d}$
[0.4-0.6[	$K_{t,d-2}$, $S_{3,t,d}$
[0.6-0.8[	$K_{t,d-2}$, $S_{1,t,d}$
[0.8-1.0]	$K_{t,d-1}$, $K_{t,d-2}$, $S_{1,t,d}$

A probabilistic finite automata (PFA) has been built for each location and group of observations using the significant variables and the procedure described in [15]. Using these PFAs, the values of clearness index have been estimated. The values of irradiance at the surface of the modules are also obtained using these estimates and the Eq.(2) . Finally, Eq.(1) is used to calculate the power generated at the inverter output for each instant and the daily profiles are also obtained. The mean prediction error has been estimated using Eq.(5) for the power generated at the output of the inverter for each location. These values are reported in Table 3.

Table 3. Mean prediction error of the proposed model.

Location 1	Location 2	Location 3	Location 4
0.18	0.14	0.17	0.16

5. Conclusions

We have developed a model to predict the energy that a photovoltaic solar plant will produce for the next day. This model only uses the information obtained in the own plant and the values of solar global radiation for the previous operation days. A three stage procedure was used to build the model. The model is estimated using the data from each facility and is capable of learning specific information about each facility and of using this information to fit the predictions.

This model binds the use of regression techniques and the use of a special type of probabilistic finite automata developed from machine learning. The mean prediction error of the energy predictions is less that 20 percent which is a significant improvement over previous proposed models, whose errors are about 25 percent.

Further research would lead to further information that is usually available at large grid-connected photovoltaic plants being included in the model

References

[1] G.E.P. Box, G,M. Jenkins, Time Series Analysis forecasting and control. USA. Prentice Hall, 1976.

[2] J.G. Gooijer, R.J. Hyndman, 25 Years of IIF Time Series Forecasting: A Selective Review," Tinbergen Institute Discussion Papers 05-068/4, Tinbergen Institute, 2005.

[3] P.J. Brockwell, A.D. Richard, Introduction to Time Series and Forecasting, Springer Texts in Statistics, 2002.

[4] J. Hwang, S.M. Chen, C.H. Lee, Handling forecasting problems using fuzzy time series. Fuzzy sets and Systems, 100, 1998.

[5] J.J. Guo, P.B. Luh, Selecting input factors for clusters of Gaussian radial basis function networks to improve market clearing price prediction, IEE Trans Power Syst, 18 (2), 2003, pp. 665-672.

[6] C.H.Wang, L.C. Hsu,. Constructing and applying an improved fuzzy time series model: Taking the tourism industry for example. Expert Systems with Applications 34, 2008.

[7] Q. Song, B.S. Chisson, Forecasting enrollments with fuzzy time series. Part I. Fuzzy Sets and Systems, 54, 1993.

[8] Q. Song, B.S. Chisson, Forecasting enrollments with fuzzy time series. Part II. Fuzzy Sets and Systems, 54, 1993.

[9] J. Hwang, S.M. Chen, C.H. Lee, Handling forecasting problems using fuzzy time series. Fuzzy sets and Systems, 100, 1998.

[10] R. Perez, K. Moore, P. Stackhouse, Forecasting solar radiation Preliminary evaluation of an approach based upon the national forecast database, Solar Energy, vol. 81, no. 6, 2007, pp. 809-812.

[11] L. Mora-Lopez, J. Mora, M. Sidrach-de-Cardona, R. Morales-Bueno, Modelling time series of climatic parameters with probabilistic finite automata. Environmental modelling and software, 20(6), 2005, pp. 753-760.

[12] B. Viorel (Ed). Modeling Solar Radiation at the Earths Surface. Recent Advances. Springer, 2008.

[13] R.A. Guarnieri, E.B. Pereira, S.C. Chou, 2006, Solar radiation forecast using articial neural networks in South Brazil, in Proc. 8 ICSHMO, Foz do Iguau, Brazil, Apr. 2428, 2006, 17771785, INPE.

[14] D. Heinemann, E. Lorenz, M. Girodo, Forecasting of solar radiation, Solar Energy Resource Management for Electricity Generation From Local Level to Global Scale, Hauppauge, NY: Nova, 2005.

[15] L. Mora-Lopez, J. Mora, M. Piliougine, M. Sidrach-de-Cardona. "An Intelligent Memory Model for Short-Term Prediction: An Application to Global Solar Radiation Data". LNAI 6098, 2010, pp. 596–605.

[16] L. Mora-López, M. Piliougine, J.E. Carretero, M. Sidrach-de-Cardona. Integration of Statistical and Machine Learning Models for Short-term Forecasting of the Atmospheric Clearness Index. International Congress on Environmental Modelling and Software Modelling for Environment's Sake, Fifth Biennial Meeting, Ottawa, Canada, Julio, 2010.

[17] M. Iqbal,An introduction to solar radiation. Academic Press Inc. New York – London, 1984.

PSpice Model for Optimization of battery Charging using Maximum power point Tracker

[*1]Md. Fahim Ansari,[2]Anis Afzal,[1]S.Chatterji,[2]Atif Iqbal,[3]N.K Nautiyal and [4]Padmanabh Thakur

1. NITTTR Chandigarh,
2.AMU Aligarh, ,
4 MNNIT Allahabad
3,GEU Dehradun,
** Corresponding author. Tel: +919761866637, E-mail: fahim402001@yahoo.co.in*

Abstract; the goal of this paper is to use the solar power to charge Lithium-ion (Li-ion) batteries, pulse width modulator (PWM) control method is implemented to design and build a solar battery charger prototype. Maximum power point tracking (MPPT) is used in the photovoltaic (PV) system to maximise the PV output power, irrespective of the temperature and irradiation conditions. MPPT system, consisting of a buck-type dc-dc converter, which is controlled by a microcontroller unit, is implemented. It is presented a model for the lithium-ion battery (Li-Ion) that is suitable for computer simulation. The used model can be easily modified to fit data from different batteries. The simulation results achieved by using *Pspice* programs and are in good agreement with the experimental results. These results allowed demonstrating the reliability and validity of the proposed MPPT technique. The battery charger prototype was tested and the results obtained allowed to conclude about the conditions of permanent control on the battery charger**.**

Keywords: *dc-dc converter, maximum power point tracking, microcontroller, photovoltaic systems, solar battery charger*

1. Introduction

Photovoltaic sources are used today in many applications such as battery charging [1], light sources [2], water pumping [3], satellite power systems [4], etc. Since PV modules still have relatively low conversion efficiency, the overall system cost can be reduced using high efficiency power trackers which are designed to extract the maximum possible power from the PV module (maximum power point tracking, MPPT) [5]. The main goal of this paper is to study the use of solar power to charge lithium-ion batteries. In the literature, many battery charging techniques are investigated and proposed [6]-[7]. These methods use a variety of battery characteristics like voltage and temperature to achieve a s afe and fast charging process. However, in this paper a simple maximum power point tracking technique, known as Voltage MPPT (VMPPT) [8], is simulated and constructed. The implementation and simulation of the proposed method uses a low-cost, low-power consumption microcontroller, which controls a buck type dc-dc converter and performs all control functions required by the MPPT process and battery charging.

Due to their high energy densities and long life times, Li-Ion batteries are increasingly used in systems such as portable electronics, electric vehicles [9], etc.

2. Description of system

The photovoltaic charger system consists of four subsystems, each with its own function. These four subsystems are connected in accordance with the block diagram shown in Figure 1. The first subsystem consists of solar panel of polycrystalline PV module from Solarex. This PV module has a rated power of 12 Watt and is formed by 18 photovoltaic cells connected in series. Second subsystem is charger unit which includes a dc-dc converter controlled by a PWM signal. Dc-dc converter is formed by two switches and an input and output filter [10].

Third subsystem (control unit), consists of a programmable interface circuit (PIC) microcontroller, model PIC18F4585, and an integrated circuit (IC), SG3524. PIC microcontroller is a high performance 8-bit reduced instruction set code (RISC) architecture, operates from 2V to 5.5V belonging to 40 pins family and IC is a 16 pin PWM switching regulator.

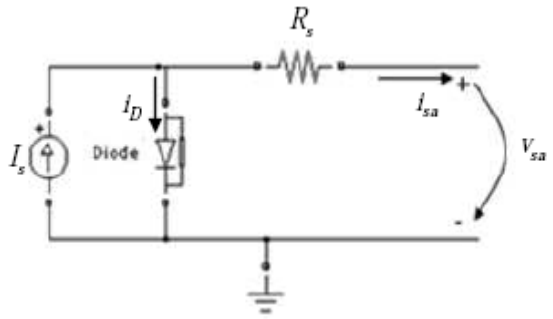

Fig.1.Equivalent circuit of solar cell

However, when it is connected to an external supply a current i_D called diode current will be present. A solar cell is usually represented by an electrical equivalent one-diode model [3] with a series resistance, as shown in Fig.1. The model contains a current source I_s one diode and a resistor R_s.The net current is the difference between the photocurrent I_s and the normal diode currenti_D. The diode current is given by equation (1).

$$i_D = I_0 \times \left\{ e^{\frac{V_{sa}+R_s}{m \times V_T}} - 1 \right\} \qquad (1)$$

Where:
I_0=diode current (strongly dependent on temperature);
V_{sa}=voltage imposed across the cell;
m =Ideal factor (ideal: m =1; real: m > 1);
V_T= Thermal potential =$\frac{K \times T}{q}$
R_s= Series cell resistance;

Where
K: Boltzmann constant, K =1.38X10^{-23}J / K;
T : cell temperature in K
q : electric charge of electron, q =1.6X10^{-19}C .
hence net current i_{sa} is given by

$$i_{sa} = I_s - I_0 \times \left\{ e^{\frac{V_{sa}+R_s}{m \times V_T}} - 1 \right\} \qquad (2)$$

2.1. Charger Circuit

Fig.2 gives a general description of the charging unit block. A dc-dc converter consists of a number of storage elements and switches that are connected in a topology such that the periodic switching controls the dynamic transfer of power from the input to the output, in order to produce the desired dc conversion. The two fundamental topologies of dc-dc converters are the buck and the boost converter as described [11]. The purpose of the dc-dc

converter is to transform a DC voltage from one level to another. This is done by varying the duty cycle, ∂. Dc-dc converters have two distinct operating modes; continuous conduction mode (CCM) and discontinuous conduction mode (DCM). The paper takes the advantage of dc-dc converter working in CCM.

The low pass filter (LPF) is a simple RC filter where the capacitor is in parallel with the load. The combination of resistance and capacitance gives the time constant of the filter:

$$\tau = RXC \tag{3}$$

The cut off frequency is given by

$$f_c = \frac{1}{2\pi RC} \tag{4}$$

2.2. Electrical Model for Li-ion Battery

The duration of the battery cycle is the total amount of discharge-charge cycle that a battery relieves before more power cannot be hold. The energy of the battery, expressed in Watt-hour, *Wh,* is the product of the capacity and the voltage of the battery, *V*. Fig.2 represents an intuitive and comprehensive electrical battery model.

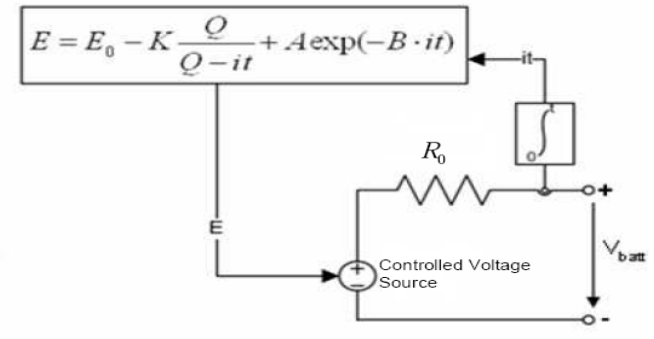

Fig.2 Equivalent circuit models of Li-ion battery

Where,
E = Internal voltage, V;
E = Constant voltage, V;
K = Polarization voltage, V;
Q = Battery capacity, Ah;
A = Exponential Voltage, V;
B = Exponential Capacity, Ah^{-1}
The terminal voltage V_{batt} is given by equation 5

$$V_{batt} = E - I_{batt} \times R_0 \tag{5}$$

3. Simulation results in Pspice

The use of Pspice is very useful in cases where there is the need to determine the values of voltage and current circulating in the circuit, in order to investigate the range of values of some components, or even just to make changes in topology. With the help of this simulation program it was possible to build a basic circuit of a step-down switching regulator with duty

cycle ratio control. The circuit is depicted in Fig.3 and allows the modulation of the dc-dc converter. Specification of the used components may be consulted in as shown below;

Voltage source
$V_0=V_1=V_2=10V_{dc}$

Resistances
$R_1=4k\Omega$ $R_4=5k\Omega$
$R_2=4k\Omega$ $R_5=5k\Omega$
$R_3=15k\Omega$ $R_{PV}=15\Omega$

DC-DC Converter components
$C_1=10\mu F$
$L_1=300\mu H$
$C_2=100\mu F$
Q_1 -MOSFET 2N6660
Diode - D1N5817

IC SG3524 components
$C_3=5nF$
C4=100nF

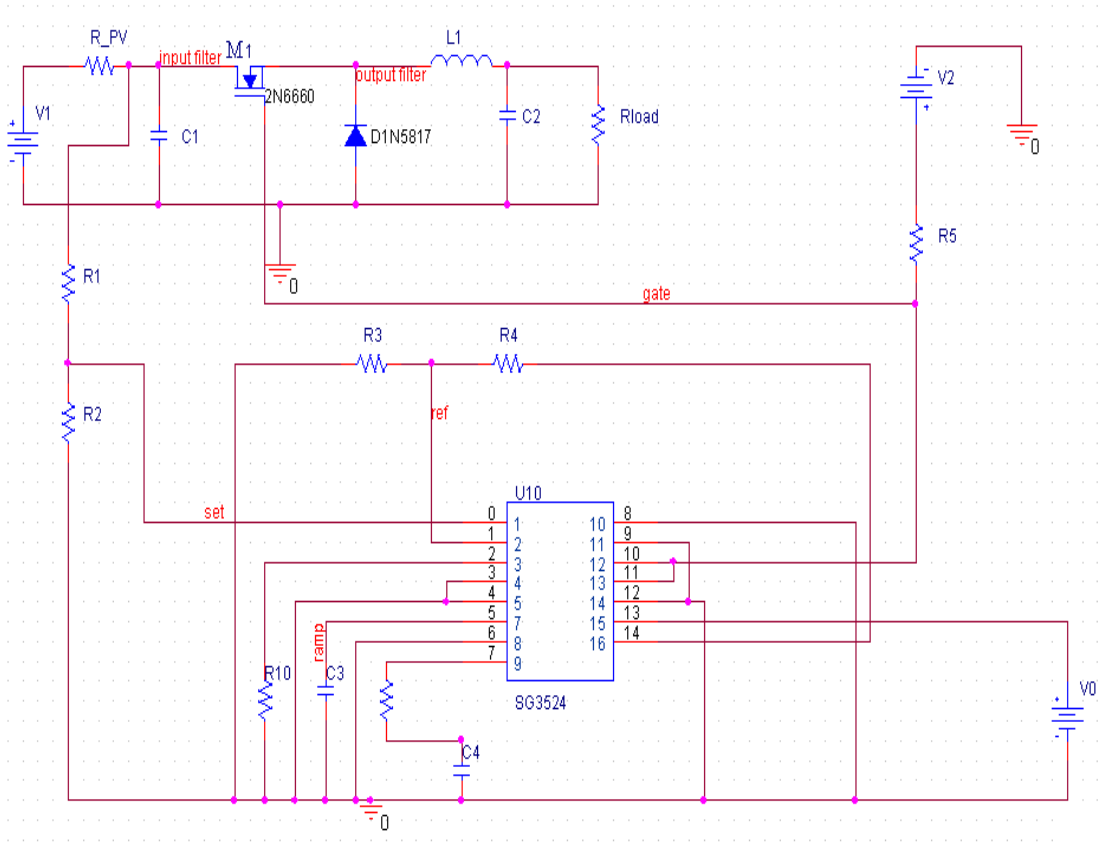

Fig.3–Step-down switching regulator circuit

Two schemes were simulated for both R_{load} = 20 Ω and R_{load} =40 Ω. It is assumed that the circuit is working on the MPPT point and that all the results obtained depend of it. The value of V_{set} ,output voltage of the solar panel is tending to this operation point which allows predicting that the circuit is being controlled: without knowing the value of the output voltage

and current the system evolves to the maximum power rate that the PV model allows VMPPT algorithm. There is a permanent control of the system duty cycle ratio control. Another important aspect worth to look at is the ripple value of the V_{set}voltage corresponds to the solar panel output voltage. In Fig.4 the maximum ripple obtained is nearly 3% of the voltage value $\nabla V_{C_1} = 0.1V = V$, which means that capacitor, C_1 is well dimensioned.

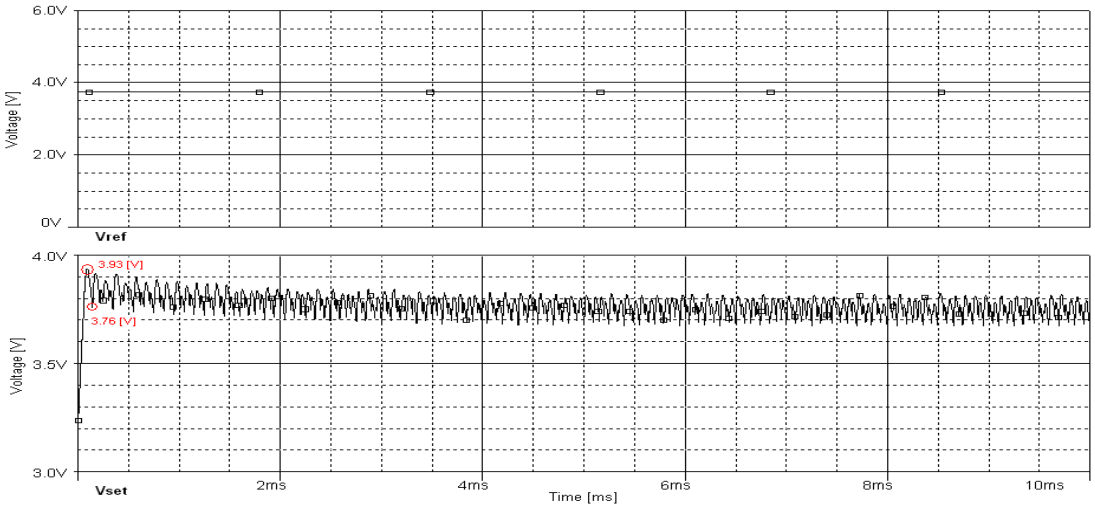

Fig.4variation of $\mathbf{V_{set}}$ *and Vref for* $\mathbf{R_{load}}$ *= 20* Ω

Fig.4 presents the result of the difference between V_{ref} and V_{set} The PWM signal gives us the final idea that the system is, in fact, being controlled. Variation of V_{set} , V_{ref} and V_{gate} are given in Fig.5

Fig.5 presents the voltage and current that is present in the load (R_{load} = 20 Ω),this resistive load reflects the ideal conditions for the charging process, taking into account the technical specifications of the chosen battery, presenting very good values for voltage $V_{R\,load}$ = 4.1V and current i_{load} = 205mA. The initial conditions ($V_{R\,load}$ =4.8V and i_{load}=240m A)

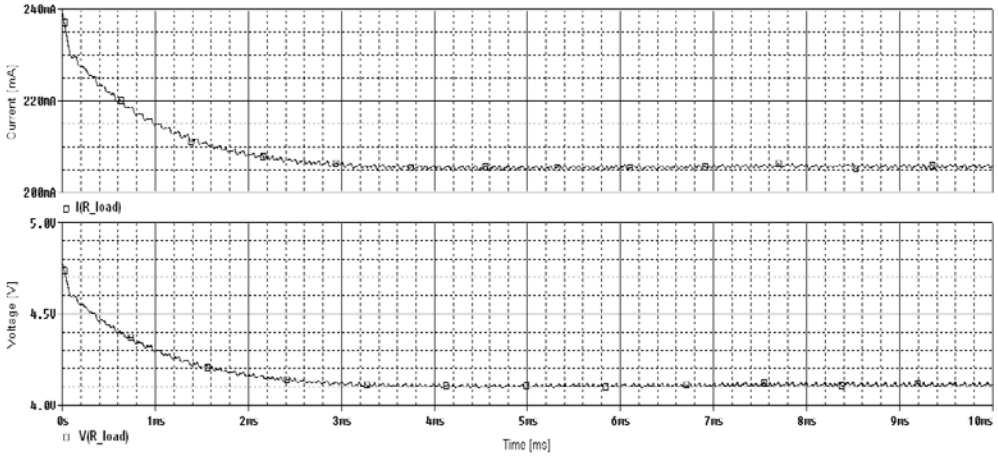

Fig.5 variation of I ($\mathbf{R_{load}}$*) and V (*$\mathbf{R_{load}}$*) at* $\mathbf{R_{load}}$ *= 20* Ω

Fig.6 presents current in inductor $L_1$and voltage across diode for R_{load} = 40 Ω.. Current in inductor is always $i_{L_1} > 0$ the converter is in CCM. When current in inductor decreases, the

diode is forward biased and hence converter is working correctly. This figure shows that current in the circuit is well dimensioned: current i_{L_1} does not go to complete zero which allows the circuit to work in CCM.

Fig.7 presents voltage across the resistance R_{load} = 40 Ω. Although the voltage is too high for the conditions stated in this paper and so the system is no longer controlling the ratio power between the input voltage sources which simulates the solar panel for the resistive load.

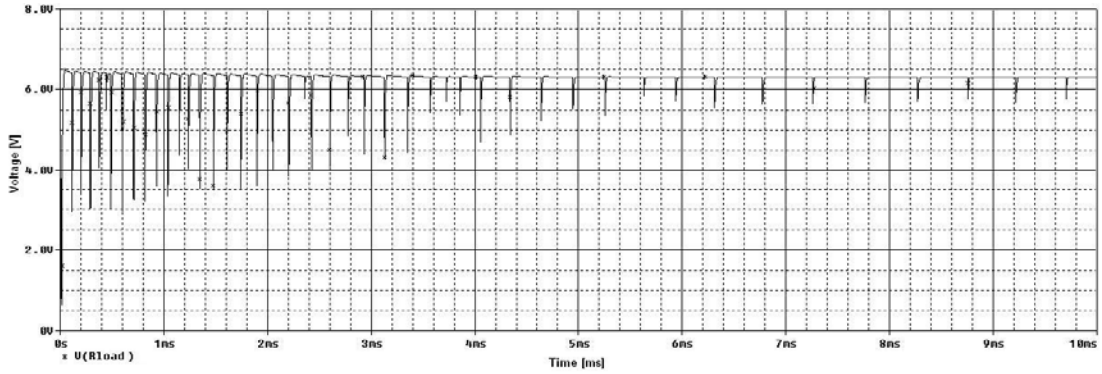

Fig.7 Voltage across load resistance R_{load} = 40 Ω

Fig.8 presents the situation where the system is being controlled for R_{load} = 20 Ω contrasting to Fig.9 where R_{load} = 40 Ω, the control is practically inexistent. If current i_L is lower than 150mA the system loses V_{gate} control and starts deficient control which shows that the current limit for control is achieved.

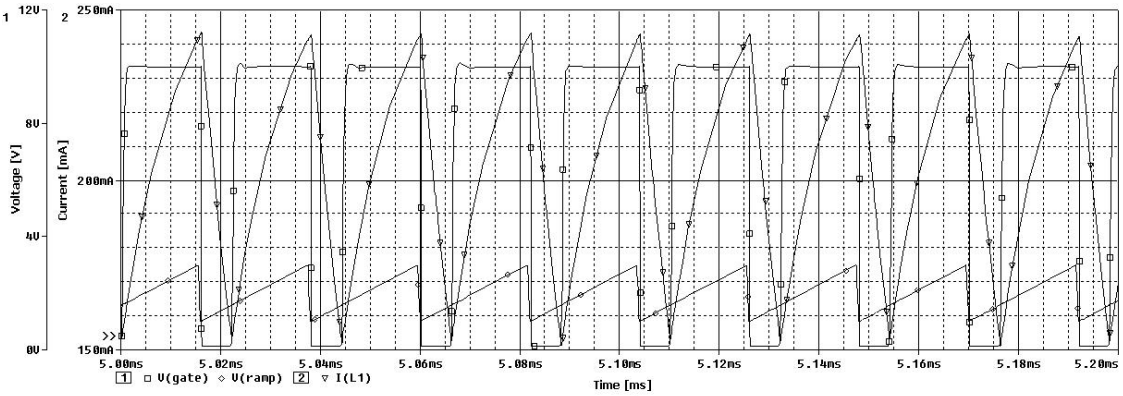

Fig.8 variations of V_{gate}, i_L and $V_{rampSG3524}$ R_{load} = 20 Ω

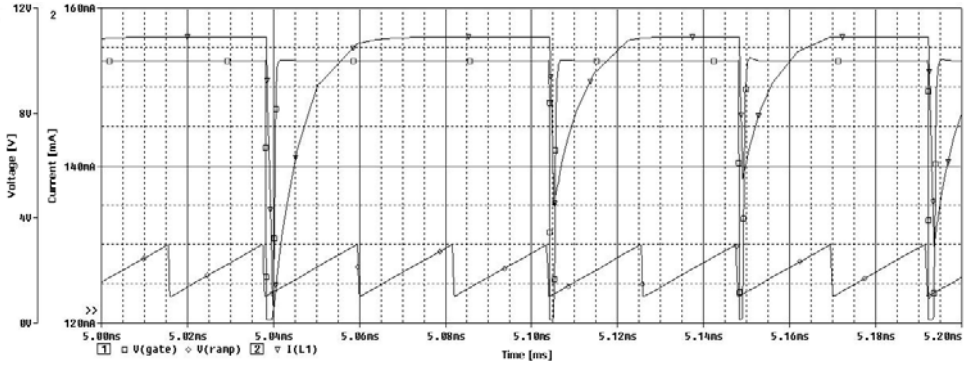

Fig.9 variations of V_{gate}, i_L and $V_{rampSG3524}$ R_{load} = 40 Ω

Fig.10 presents the maximum power transfer rate that operating in the maximum power point the solar panel provides, more or less $P_{max\,pv} \approx 1.2W$. Therefore, the representation of the solar panel by an ideal voltage source and resistance is reliable for this system.

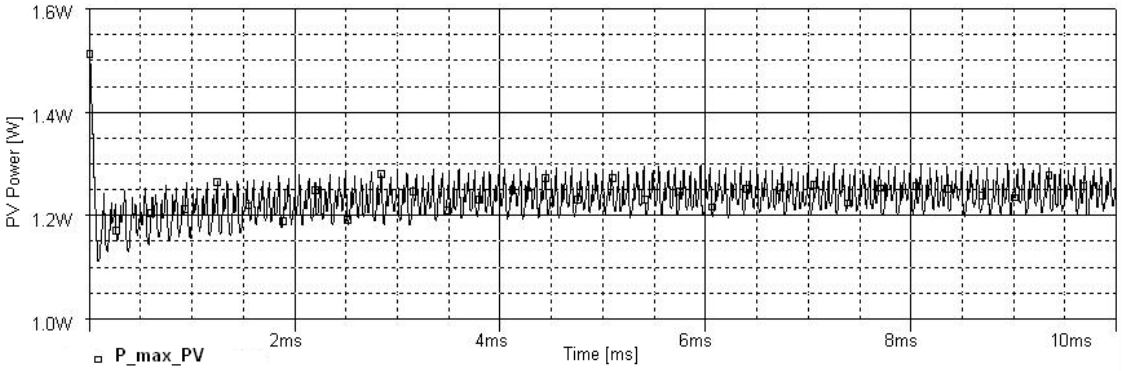

Fig.10 PV Output Power

Fig.11 and Fig.12 presents the power across the 20 Ω and 40 Ω load, respectively. In the individual graphs it is possible to look at the power loss: R_{load} = 20 Ω the system presents a power loss for 20 Ω load resistance ≈1.2-0.85=0.35W and power loss for 40 Ω load resistance ≈1.2-0.89=0.31W . With these results it is possible to conclude that the system is not ideal, even referring to a simulation program. Nevertheless, regardless of the load value, the system presents power conservation: the final power value achieved is very similar in both cases even if the system with R_{load} = 40 Ω loses control.

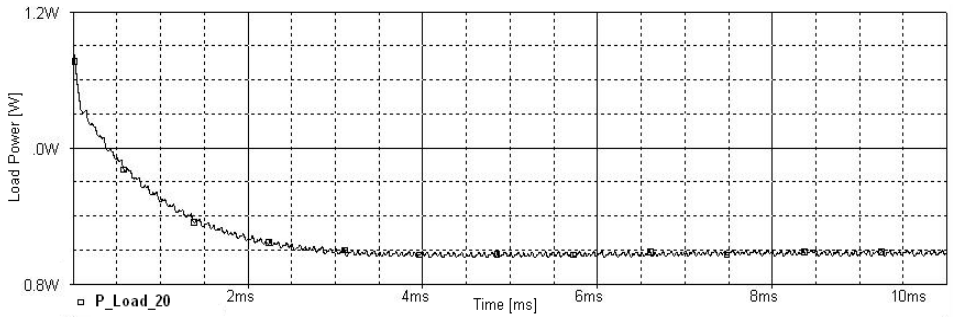

Fig.11 Load Power R_{load} = 20 Ω

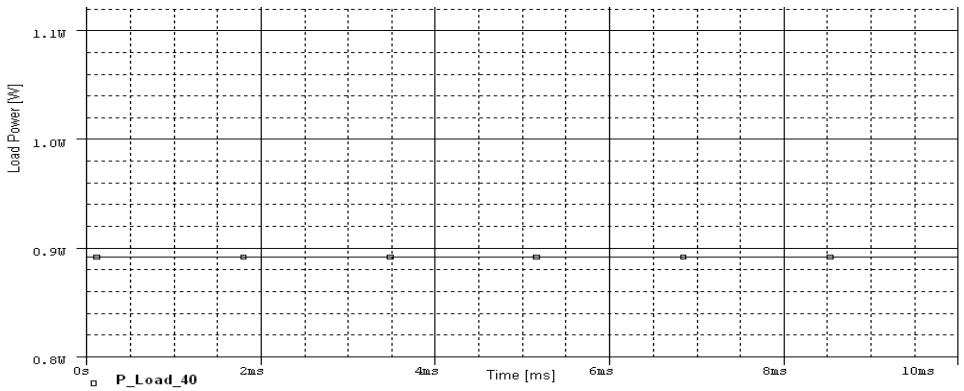

Fig.12 Load Power R_{load} = 40 Ω

4. Conclusions

The use of *Pspice* simulation program allows a better understanding of the system behavior when in the presence of variable loads. It can be generally stated that while the system is represented by a load of R_{load} = 20 Ω, it allows a controllable system. The duty cycle ratio control is a constant premise. For this reason the values obtained at the output of the system voltage and current are the ideal ones for an optimum battery charger in this case, optimum values for the type of battery chosen. Although the losses presented in the system, probably due to losses of the transistor switching and internal resistance, the system presents a very good behavior and a faithful representation of what will happen in reality. Since system is very sensitive to load variations. The system starts losing control for load values above 40 Ω presenting a load voltage higher than the one allowed to correctly charging the Li-Ion battery. The maximum voltage value in the load that allows the duty ratio control of this system is close to 5.2V.

References

[1] Mohamad A. S. Masoum, Seyed Mahdi Mousavi and Ewald F. Fuchs, "Microprocessor-Controlled New Class of Optimal Battery Chargers for Photovoltaic Applications", IEEE Transactions on Energy Conversion, Vol. 19, No.3, Sep. 2004.

[2] Md.Fahim Ansari,S.Chatterji and Atif Iqbal"AUTOMATIC PEAK POWER TRACKER FOR SOLAR PV MODULES USING d SPACE SOFTWARE". International Journal of Sustainable Energy,Taylor and Francis Vol. 29 No. 3 September2010 pp 151-163,

[3] Md.Fahim Ansari,S.Chatterji and Atif Iqbal "A FUZZY LOGIC CONTROL SCHEME FOR SOLAR PHOTO VOLTAIC SYSTEM FOR MAXIMUM POWER POINT TRACKER" International Journal of Sustainable Energy,Taylor and Francis 29: 4, 245 — 255,December 2010.

[4] K. Tanaka, E. Sakoguchi, Y. Fukuda, A. Takeoka, and H. Tokizaki, "Residential solar powered air conditioner", in Proc. Eur. Power Electronics Conf., Brighton, U.K., Apr. 1993, pp.127-132.

[5] E. Koutroulis and K. Kalitzakis, "Novel battery charging regulation system for photovoltaic applications", IEE Proc.-Electr. Power Appl, Vol. 151, No. 2, March 2004.

[6] Lijun Gao, Shengyi Liu, and Roger A. Dougal, "Dynamic Lithium-Ion Battery Model for System Simulation", IEEE Transactions on C omponents and Packaging Technologies, Vol. 25, No.3, Sep. 2002, pp1521-3331.

[7] Wei Zhang, Dale Skelton and Robert Martinez, Modelling and Analysis of an Off-line Battery Charger for single Cell Lithium Batteries", IEEE, Sep. 2004.

[8] Mohamad A. S. Masoum, Hooman Dehbonei and Ewald F. Fuchs, "Theoretical and Experimental Analyses of Photovoltaic Systems With Voltage and Current Based Maximum Power Point Tracking", IEEE Transactions on E nergy Conversion, Vol. 17, No.4, Dec. 2002.

[9] http://www.mathworks.com/toolbox/physmod/powersys/ref/battery.html, Apr. 2008.

[10] Min Chen and Gabriel A. Rincón-Mora, "Accurate Electrical Battery Model Capable of Predicting Runtime and I-V Performance", IEEE Transactions on E nergy Conversion, Vol. 21, No.2, June 2006.

[11] José Fernandes Alves da Silva, Sistemas de Energia em Telecomunicações: Texto de Apoio, Set 05-06, Instituto Superior Técnico, Área Cientifica de Energia, Portugal, May. 2006.

Photovoltaic for Rural Development: A study of policy impact and scope of market development in South Asian Region

Siddha Mahajan[1,*], Shirish Garud[2]

[1] *The Energy and Resources Institute, New Delhi, India*
[2] *Greenergy Renewables Pvt Limited, Mumbai, India*
** Corresponding author. Tel: +91 1124682100, +91 9873846092, Fax: +91 1124682144, E-mail: siddha.mahajan@teri.res.in*

Abstract: Growing energy demand, increase in carbon emissions due to increase in fossil fuels it becomes imperative for developing regions like South Asia to switch to non-conventional sources of energy. Being naturally blessed with the renewable energy resources it becomes easy for these countries to switch. The best resource to be harnessed in the region is the solar energy through Photovoltaic technology. The best part about this technology is its suitability for remote area rural electrification which is the need of hour in the region Access to electricity is essential to bring about equitable economic development in sustainable manner. But, there exist barriers which hold back the development of renewable energy resources. While some countries in this region like India, Sri Lanka and Bangladesh have been able to develop the markets for PV, other countries in the region are yet to develop policies and programs. Financial initiatives as a result of policy push have major role to play in developing the market. Un-electrified rural population being very high in this region, the countries like Nepal, Bhutan Pakistan and Maldives which seeks to develop the market can learn from the success stories of these countries.

Keywords: *Photovoltaic, South Asia, Policy, Rural development*

1. Introduction

Energy consumption is an indicator of socio-economic development of the country. With the increasing energy demands coupled with global warming and energy security issues, it becomes imperative for all the countries to switch from conventional carbon based fuels to low carbon sources of energy. This is especially important for the developing countries which are on development path. South Asia is one such region. It is on one hand, one of the major economic hubs of the world, and on the other, is home to a quarter of total world's population, majority of them in rural areas. Major portion of the population of this region still remains devoid of electricity due to infrastructural in-capabilities, high investments required for the development of infrastructure This holds back the development of this part of world. Abundance of sunshine throughout the year makes Photovoltaic (PV) technology a suitable and viable option to provide off-grid and decentralized electricity solutions is a long term cost effective solution that can help in equitable development. It also gives added advantages like rural employment, future energy security, and clean environment. Governments in India, Bangladesh and Sri Lanka have taken several steps ahead to create markets for this technology, through policy intervention in rural areas and there have been successful stories as well. While, Bhutan, Nepal and Maldives are still far behind in the development of market for the technology and can learn from successful stories of neighboring countries to develop a self sustaining market in their regions.

The purpose of this study is to bring out the advantages and impacts of policies on photovoltaic technology through various successful stories that can help in rural development. Also, to understand what are the various financing mechanisms developed for creating market. To achieve this purpose the objectives of this paper are:

- To conduct a cost-benefit analysis of the technology with the conventional sources
- To understand the existing PV deployment in the rural regions of South Asia

- To learn about the available financial incentives and schemes for its deployment.
- To understand the barriers in market development

2. South Asia

2.1. Current scenario

The South Asian region, which comprises of Bangladesh, Bhutan, India, Maldives, Nepal, Pakistan, and Sri Lanka[1] is home to more than 1.5 billion people, reaching almost close to a quarter of the world's population [1]. This geographical region is currently experiencing a rapid growth in energy demand, associated with economic growth and industrialization. Despite, such a growth, there is a huge gap between demand and supply of electricity. Table 1 and figure 1 together summarizes the current scenario. Nearly 613.9 million people in this region are un-electrified in this region (IEA/OECD 2009) consisting mainly of the rural region. This issue, further, is strongly linked to other major issues of poverty, education, and health and hygiene. The electricity production in this region is through coal, petroleum and crude oil imports [2]. Countries like Bangladesh and India do have substantial reserves of natural gas, coal and petroleum, despite that substantial amount is imported for sustaining the commercial and industrial sector for meeting the growing demands. Maldives, on the other hand, rely 100% on imported refined petroleum. Pakistan, Nepal and Bhutan, derive most of its energy needs through hydro and biomass. Pakistan is still heavily dependent on oil imports. All over in the region, hydro is mainly deployed for commercial power generation; biomass obtained from forests supplements the household energy needs of rural population. This is followed by small hydro and very miniscule amount of solar PV. Conventional fuels that are common among rural population are kerosene and diesel that are offered at highly subsidized rates. A study by UNDP shows that this region has medium to high Oil Price Vulnerability Index (OPVI)[2] point for all the countries. It has been found that the divergence of large amount of national investments towards the fuel imports side-lines the social development. Also, huge dependence on the foreign oil imports leads to insecurity of energy.

Table 1: Summary of South Asian countries energy scenario[3,4,5,6,7]

Country	Land area (sq. km)	Total Population (million)	Energy production (Mtoe)	Population without electricity (millions)	OPVI Index
Bangladesh	1, 47, 570	158	21.26	95.7	High
Bhutan	38,394	0.6	0.6804	NA	Medium
India	32,87, 263	1123	450.92	403.7	Medium
Maldives	8, 59, 000	0. 3	NA	NA	High
Nepal	1, 47, 181	28	8.53	16.5	High
Pakistan	8, 03, 950	162	63.64	68	High
Sri Lanka	65, 610	19	5.08	4.7	High

2.2. Solar energy deployment

South Asia being a tropical region is abundantly rich in solar energy, receiving an average solar radiation of 4-4.9 kWh/m^2 [8]. The most important contribution of this source is in the decentralised and off-grid power supply to the remote rural areas where grid connectivity is not possible. This will not only contribute to the rural development but also the equitable

[1] Afghanistan, though a part of South Asia has not been considered due to unreliability of data
[2] Oil price vulnerability index (OPVI). It is calculated with the help of three indices economic strength, economic of performance and economic growth with low share of oil

social and economic development of the rural parts, thus contributing to the overall development of the country as a whole.

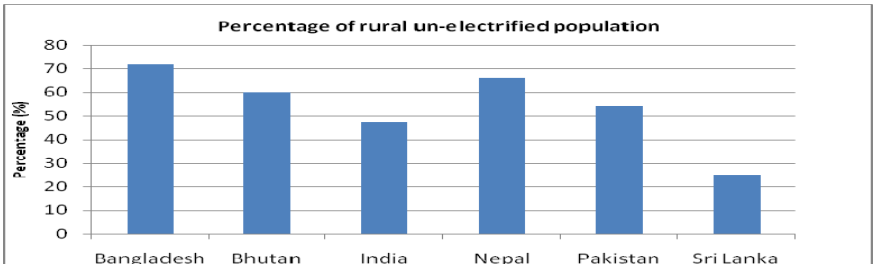

Fig. 1: Graph showing the total un-electrified population in South Asia. Data for Maldives is unavailable [9]

2.3. Photovoltaic technology

Photovoltaic (PV) is the technology through which the solar power can be harnessed. Photovoltaic is the array of cells, commonly known as solar cells, which convert solar energy into electricity. The commonly used end use applications of solar PV in rural areas are Solar Home Lighting Systems/Solar Home Systems, Solar Lanterns, Solar Street Lighting Systems, Solar PV Water Pumping system. These applications are put in use for various purposes like residential, rural communities, schools and hospitals electrification, for micro enterprises, water pumping, signalling remote telecommunication, captive power generation, back up power generation, urban applications, highway lightings and many more.

2.4. Choice of Solar PV as preferred technology

Harnessing of this resource is suggested above other resources because of the reliability, modularity and free and easy availability of the resource in the region, unlike wind, biomass and hydro energy which are highly site specific. The two most important benefits are:

1. It can be used for rural electrification in remote areas. This is the most potential reason for the South Asian countries to adopt this technology.
2. The fuel cost is zero and no fuel supply linkages are required as in biomass [Refer to Table 1].

This reduces the dependence on the fossil fuels and the large drain of money due to imports of fuels. Besides these, it is a silent process of energy generation and the installation of the technology does not require large space. In case of roof-tops it uses the unused spaces on the roof. It is easy to install and maintain; produced and consumed at the same place so no translocation charges. PV modules can be added to increase the capacity as needs grow.

3. Methodology

Literature study was done firstly to understand the basic energy scenario in each country through primary and secondary research. Stakeholder discussions and sector knowledge of the experts was also taken as secondary research that provided the dynamic of the sector. Open ended structured questionnaires were prepared and were mailed to the organizational heads in different countries. Questionnaires prepared for the countries were based on the current situation and the literature survey done during previous research. Two sets of questionnaires were prepared. One set was for India, Sri Lanka and Bangladesh and another set was for Pakistan, Bhutan, Maldives and Nepal. 13 respondents were mailed the questionnaire, out of which only three responded. These respondents belonged to Nepal, Bangladesh and Sri Lanka. Due to weak responses to the questionnaire the analysis for Bhutan, Pakistan and Maldives was based on the data collected during literature survey and stakeholder consultation.

The values taken for conducting cost benefit analysis has been mainly taken from the Indian market since the facts say that the market is most developed in India. The calculations are based on the study done by International Energy Studies in 2004 [10]. The results obtained would be used as a representative data for the region to understand the cost and benefits of the technology. The calculations have been carried out in USD with the conversion factor of 44.45, as per the currency conversion rate in April, 2010.

Thus, results produced are primarily based on the articles, reports, research papers, publications, stakeholder discussions and sector knowledge of experts. Various international conference presentations by national experts of different countries were also used in understanding, documenting, analyzing the PV market. The results have been produced in both quantitative and qualitative form.

4. Results and Discussions

4.1. Cost-benefit analysis of the technology with the conventional sources

The Cost Benefit Analysis (CBA) has been carried out between the off-grid solar PV rooftop and conventional power plants (thermal power plant, diesel and natural gas power plant) that would be providing the electricity to the un-electrified region through grid connection.

4.1.1. Total Cost of generation

Figure 2 compares the total cost of generation (TCoG) from four different fuel plants. TCoG for off-grid PV is found to be greatest among the four i.e. $ 0.4719/kWh followed by Diesel power generation and natural gas. It has come least for the coal generated power i.e. $ 0.0509/kWh. Higher TCoG of solar PV is mainly because of high capital cost of the technology.

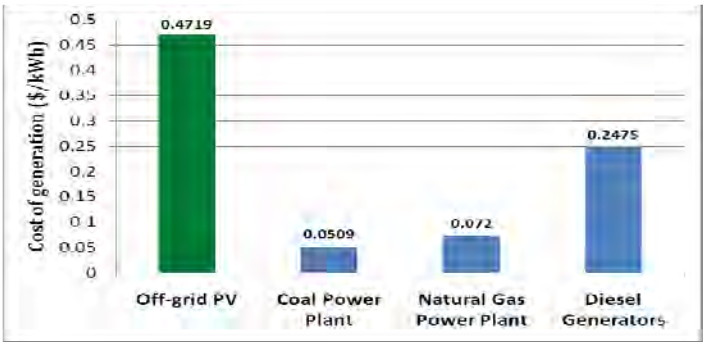

Fig. 2: Comparison of cost of electricity generation profit

4.1.2. Net Profits

Figure 3 and 4 compares the net profits on the cost of generation for electricity derived from the conventional and PV power plants before and after internalising the environmental cost, respectively. The costs have been calculated over the useful life of the plants. The useful life of Off-grid PV, coal power plant and natural gas power plant is 25 yrs [11]. It is found that that net profits over the remains positive in all the cases but it is higher by investing in off grid solar PV. Long-term profits further decrease in case of investments in conventional plants when environmental cost is internalized. Diesel power plant could not be assessed due to the lack of data but it can be understood with the combustion properties of diesel the NPV tends to come down if environmental cost in internalized.

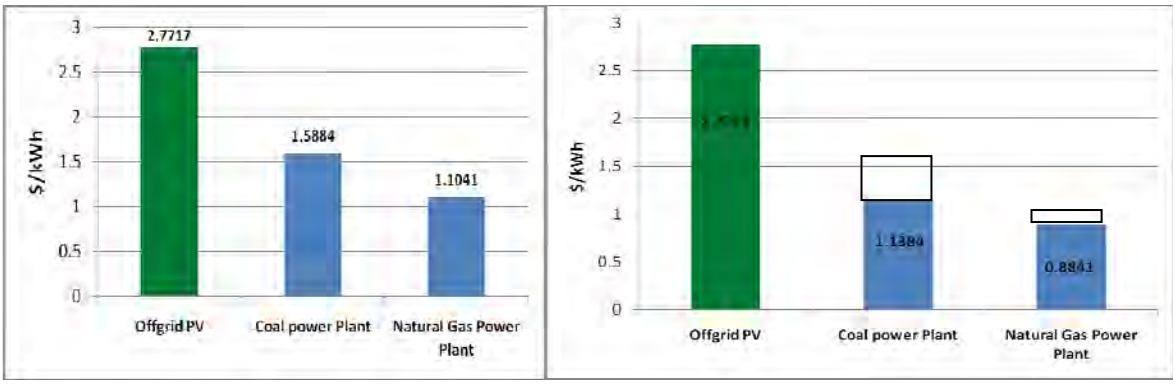

Fig. 3: Net profit before internalizing environment cost; Fig 4: Net Profit after internalising the environment cost

4.1.3. Net present value

Figure 5 shows that the net returns of today's investment in the PV project. Results show that investments in PV deployment would fetch greater returns than investments today in conventional plants.

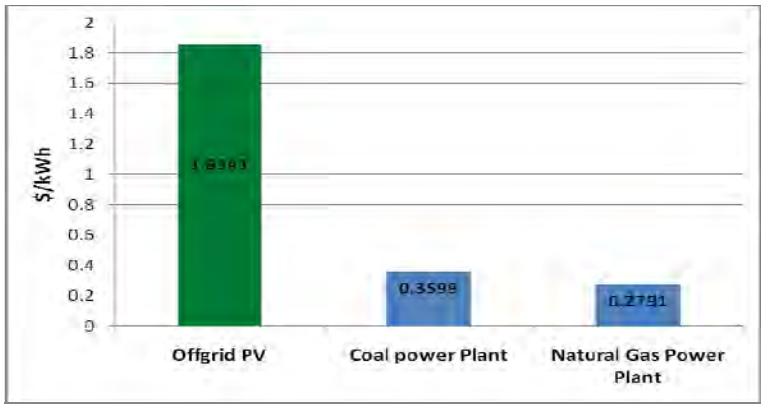

Fig. 5: NPV of various power generators

4.2. PV deployment

Table 3 and figure 6 are the summary of the PV installations done in South Asia. Out of all the PV off-grid installations, the most popular end use application is the Solar Home lighting Systems (SHSs). It has been installed in almost all the countries in South Asia. It is followed by the distribution of solar pumps. It is used in India, Bangladesh and Nepal. It is followed by solar lanterns distributed mainly in the rural areas which are un-electrified. Street lighting systems which has found more urban application is in use in India. In Bangladesh, it is still in the discussion phase. Over the years, with the developing market the number of installations has also increased. Thus it can be concluded from the above table and graph that PV market is most developed in India, followed by Bangladesh and Sri Lanka

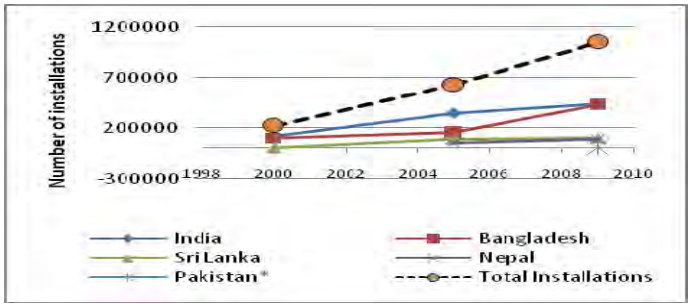

Fig 6: Total SHS installations in South Asia

Table 3: Various end use applications of PV

Country	Solar Home lighting Systems (SHS)	Solar Lanterns	Solar Street lighting systems	Solar Pumps
Bangladesh				
India				
Sri Lanka				
Pakistan				
Bhutan				
Nepal				
Maldives				

System installed In demonstration phase Not installed Data unavailable

4.3. Financial incentives available

Table 4 summarises various financial incentives offered in the South Asia region. The PV market set up in South Asia so far has been set up mainly in three countries: India, Sri Lanka and Bangladesh.Although, the market is small yet, it is growing up. The majority of the market share is that of off-grid installations. The two main financial mechanisms which have been effective in this market segments are :

Table 4: Off-grid financial schemes for PV

Country	Off-grid Schemes		
	Micro credit System	Capital Subsidy	Interest Subsidy
Bangladesh			
India			
Sri Lanka			
Nepal			
Bhutan			
Pakistan			
Maldives			

Practiced Being discussed Not practiced Data unavailable

Micro-credit System: This is mainly practiced in Bangladesh and has been successful in creating the rural market in the country. A community participation initiative taken on the basis of trust to make repayments of loans has been very successful in developing rural sector of the country (See figure 7). Initiative taken by the Grameen Bank in Bangladesh has helped the rural market to grow rapidly. It is interesting to note that today the villagers have 90% shareholding whereas; the government has 10% share holdings.

Capital Subsidy: This financial mechanism is practiced in India and Sri Lanka (See figure 8). While in case of India the subsidy given is supported by the Government, in Sri Lanka the subsidy given is supported mainly by the international support. The international support given to Sri Lanka for the promotion of Solar Home Lighting Systems had actually crossed the target set for installations and has been a major reason of success in the rural sector.

The above two financial models have been succesful in revolutionising SHSs in the respective countries and creating the market. Soft loans have also been extended to the consumers for achieving the targets of SHSs installations in Sri Lanka and India. Soft loan scheme is a interest subsidy scheme where interest charged on loan is lower than the prevailing market interest rate. It was introduced in India in the year 2002-2003 for financing the purchase of

solar photovoltaic systems by various categories of users. This is slowly replacing the upfront capital subsidy schemes which need huge budgetary support from the government.

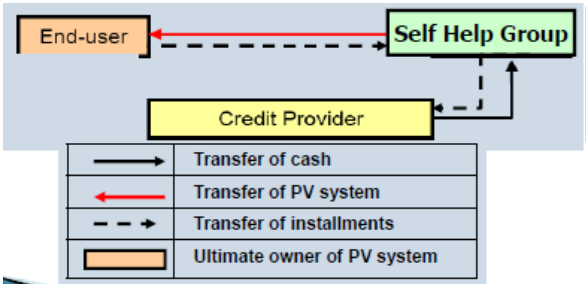

Fig 7: Micro-credit model

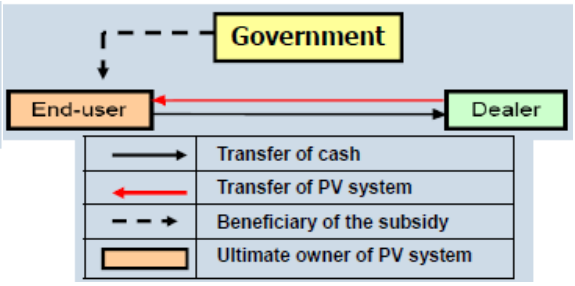

Fig 8: Capital Subsidy Model

4.4. Barriers

Table 5 summarises various barriers country wise. The two common barriers in the promotion of PV market in the South Asian countries are lack of R&D sector focussed on solar energy development and the funds availability. Also the people awareness and the availability of technologies are other barriers which hold back the growth of the market. Political inconsistency is one of the prime concerns of the funding given by the international funding agencies. But, with a successful example of Bangladesh one can learn that with more of people's willingness and interest in taking initiatives market could be created. Lack of information about the resource, needs, appropriate technologies are also major issues in developing the markets especially in Bhutan, Nepal, Maldives and Pakistan. Lack of suitable financing schemes has also held back the development of PV market in countries like Bhutan, Maldives and Pakistan.

Table 5: Barriers in various countries for PV

Barriers	Bangladesh	Bhutan	India	Maldives	Nepal	Pakistan	Sri Lanka
Financing schemes							
R&D							
Lack of Information							
Funds availability							
Institutional Framework							
Political instability							

Barrier Exist Barrier doesn't exist Information unavailable

In all these countries though the PV technology is used for the off- grid power generation yet, either the contribution compared to grid power is miniscule or nearly zero. SHSs have found easy way in the market because of affordable incentive schemes and favourable policy environment. In Bangladesh because of its properties like modularity, easy maintenance and with Self Help Group (SHG) practice in Bangladesh, the banks have been ready to provide loans for installation. The main policy push comes from the government, thus government plays a major role in penetration of the technology. The financial schemes to create and support the off-grid market like capital subsidy in India and Sri Lanka and microcredit system of Bangladesh made it easy for the rural consumers to meet their power demands and easy down payments have been supported by government. Central funding is still an issue as many countries are not able to afford the same. Besides, it is also seen the government does not allocate the funds for the development of solar energy technology and its harnessing.

5. Conclusion and Recommendation

The policies initiatives for flexible and easy flow of cash have a major role to play in the proliferation of PV technology into the market, especially when the market development is in the nascent stage and is dominated by the rural population. While in case of India and Sri Lanka, capital subsidy and soft loans succeeded to generate the market for Solar Home lighting installations, micro-credit system model succeeded in Bangladesh to develop market among rural sector. This has also helped in generating rural employment and averting poverty by promoting cottage industries. This, keeping into consideration the large un-electrified population, and increase in PV market through installations of SHS in India, Bangladesh and Sri Lanka, it is very much possible for other countries in South Asia to learn from the neighboring countries and work towards development of market. There are several disadvantages considered for the technology like it cannot be used during cloudy and rainy seasons and that its output is not comparable to the conventional sources but it is the government through policy should encourage capacity building and R & D to overcome barriers. Also, at the initial stage government should also provide lucrative offers to bank to promote adoption of PV at easy interest rates. This would not only help in building rural market but would also boost rural employment and avert other social issues.

References

[1] South Asia Environment Outlook 2009 http://www.roap.unep.org/publications/SAEO%202009.pdf [Accessed 12 November 2010]

[2] United Nations Development Programme, 2007. Overcoming vulnerability to rising oil prices options for Asia and the Pacific, Thailand.

[3] Energy and the Poverty in the Maldives, UNDP Report, Challenges and the way forward, 2007

[4] Development Effectiveness Brief Report of Bhutan, Asian development Bank

[5] Overview of Energy policies in Bhutan, Department of Energy, Ministry of Economic Affairs, RGoB March 2009

[6] International Energy Outlook, International Energy Agency, 2009

[7] http://tonto.eia.doe.gov/cfapps/ipdbproject/IEDIndex3.cfm?tid=2&pid=2&aid=2 [Accessed 22 February 2010]

[8] *http://www.oksolar.com/abctech/solar-radiation.htm*

[9] http://www.worldenergyoutlook.org/database_electricity/electricity_access_database.htm [Accessed 22 February 2010]

[10] Sayathe, J. & Phadke, A., 2004. Cost and carbon emissions of coal and combined cycle power plants in India: Implications for costs of climate mitigation projects in a nascent market, International Energy Studies, Berkeley, USA

[11] CERC (Terms and Conditions of Tariff) Regulations, 2009

[12]Summary report of the study " Post-Clearance Environment impacts and Cost benefit analysis for Power Generation in India" Conducted by National Environment Engineering Institute (2006) Available at: http://www.mospi.gov.in/research_studies_post_clearance.htm

Case Study: Modelling and sizing stand-alone PV systems for powering mobile phone stations in Libya

Salem Ghozzi[a*], Khamid Mahkamov[b]

[a]*Al madar Al jadid, Almadar Aljadeed Building, Gorgi Area, P.O. Box 83792, Tripoli Libya*
[b]*School of Comp., Eng. and Inf. Sciences, Northumbria University, Newcastle upon Tyne, NE1 8ST, UK*
** Corresponding author. Tel: +218 91-919-0500, E-mail: s.ghezzi@almadar.ly*

Abstract: A mobile telecommunication sector has experienced a rapid growth in Libya and Al-Madar Al-Jadid is one of largest companies providing services in this sector. Currently, PV systems are widely used for powering remote GSM communication stations in the country and number of Al-Madar Al-Jadid communication stations powered by such stand-alone PV systems was about 135 in 2009. A Simulink Matlab model was built to dynamically simulate the operation of the stand alone PV system powering one of Al Madar Al Jadid remote communication stations in desert conditions, taking into account variation of insolation and ambient temperature during a day. The results of mathematical modelling on the producible and produced power, charging and discharging battery power and the state of charge of the battery bank are in a good agreement with real experimental data recorded on the station with the use of a data-logger. Results obtained clearly indicated that the existing system, including PV panels and the electrical storage, is excessively large for the current electrical demand on the station and therefore could be reduced in the size by a factor of two.

Keywords: *Stand alone PV systems, Modeling stand alone PV systems, Powering mobile phone stations by stand alone PV systems.*

1. Introduction

The use of PV systems for powering remote communication stations is rapidly expanding in both developed and developing countries [1]. In Libya the photovoltaic power has been in use for the stations of communication networks since 1979. The use of the PV technology instead of diesel-generators reduces operational costs, since there is no need for fuel transportation, and is exhaust gas emissions (CO_2 and NO_x) free.

A typical PV system generally consist of an array of PV panels (a solar generator), an energy storage, which is very important for stand-alone systems, a power conversion system made of DC/DC converters and inverters, and an associated power flow control.

Dynamic modelling the operation and interaction of all system components, especially the PV generator and the electrical storage, is very important for the system assessment and its sizing. Mathematical models should be validated against the performance of the actual system in order to evaluate its accuracy and then can be used with a confidence to predict the overall performance of similar systems with different sizes. In this study, the PV generator and the electrical storage made of battery banks have been modelled in the Libyan environment using Simulink Matlab software and then the model results were compared to experimental data collected in one of Al-Madar Al-Jadid standalone communication stations.

2. Methodology

2.1. Modelling of the stand-alone PV system

The system model combines two sub-system models, the PV model and the battery storage system model, see *figure 1*. The model does not take into account the influence of air flow, due to its complexity, and calculates the DC output power of the PV array (P_{PV}) in watts as function of the solar irradiance, the PV cells temperature and the ambient temperature. The DC power output of the PV array is used as input data in the battery storage model. The

battery model simulates a lead-acid battery bank and calculates the electricity flow for situations when batteries are charged or discharged and also the surplus and deficient power values.

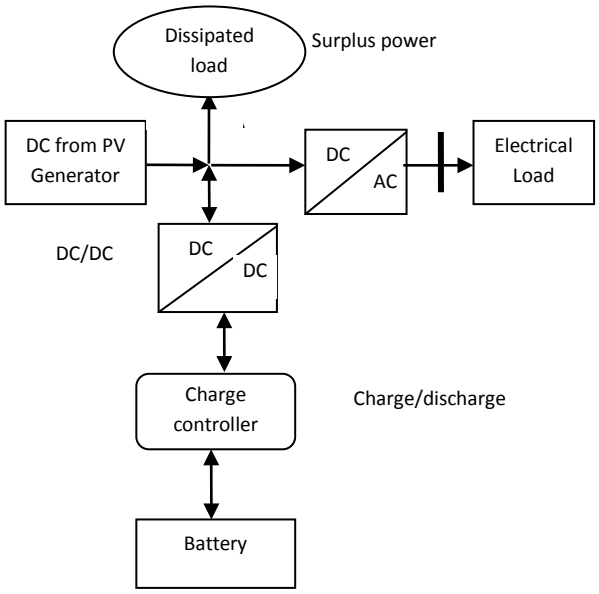

Fig. 1. The schematic of the electrical storage and electrical interface model

2.2. PV generator model

In order to achieve the best performance the PV modules must operate at the maximum power point (MPP). There are several methods to calculate DC power generated by the PV system and in this work this value was calculated as [2]:

$$P_{PV} = \eta_g \times N \times A_m \times G_T, \qquad (1)$$

where η_g is the instantaneous efficiency of the PV system, A_m is the area of a single PV module (m^2), G_T is the global irradiance incident on the titled plane (W/m^2) and N is the number of modules.

In the modelling it was assumed that connection and wiring losses and all other energy losses in the PV system are negligible.

The instantaneous efficiency of the PV generator is given as

$$\eta_g = \eta_r \times \eta_{TR}\left[1 - B_T\left(T_c - T_r\right)\right]. \qquad (2)$$

Here η_r is the PV generator reference efficiency, η_{TR} is the efficiency of the maximum power point tracker (MPPT), T_c is the solar cell temperature (°C), T_r is the solar cell reference temperature (°C) and B_T is the temperature coefficient, ranging from 0.004 to 0.006 per °C for a silicon cell.

The PV cell temperature is expressed as [3]:

$$T_c = T_a + G_T\left(\frac{\tau \times \alpha}{U_L}\right), \qquad (3)$$

where T_a is the ambient temperature (°C), U_L is the overall heat loss coefficient (W/m^2 °C), τ and α is the transmittance and the absorbance coefficients, respectively, of the PV cell.

In this investigation the simplified mathematical model of the PV generator has been adopted in Simulink Matlab in order to calculate the DC power output and this model is based on the following equation [4]:

$$P_{PV} = \eta_{PV} \times S \times A_{PV}\left(1 + \sigma_T\left(T_c - T_{c\_ref}\right)\right) \times \eta_{MPP\_PV}, \quad (4)$$

where P_{PV} is the DC power output of the PV generator, S is the solar irradiance incident on the surface of the solar cell, η_{PV} is the efficiency of the PV generator, A_{PV} is the area of the PV modules, σ_T is the temperature coefficient, T_c is the solar cell temperature, T_{c_ref} is the reference solar cell temperature and η_{MPP_PV} is the efficiency of the MPP tracker.

The input data for the Simulink Matlab model consists of the irradiance, the ambient temperature, the temperature of the cell, the area of the modules and the reference solar cell temperature. The Simulink Matlab model simulates the PV generator when it is working at the MPP.

The temperature of the PV cells is a function of the weather conditions and the PV cells characteristics. The PV cell temperature (T_c) is given as [4]:

$$T_c = T_a + \frac{S}{S_{ref}} \times \left(T_{c\_ref} - T_{a\_ref}\right) \times \left(1 - \frac{\eta_{PV}}{0.9}\right), \quad (5)$$

where S_{ref} is the reference solar irradiance and T_{a_ref} is the reference ambient temperature.

2.3. Electrical storage system model

The battery storage system, shown in *figure 1*, has been adopted from [6]. It is relatively simple model but is sufficient to achieve the purpose of these investigations, which is evaluation of the power flow between the PV generator and the load and batteries and between batteries and load when it is necessary to compensate the shortage in the power production. The model is based on a time resolution of 60 minute to simulate the generated power, the load demand, the electrical storage and the power losses in the inverters and the power electronic equipment. The model is a generic and can simulate different sizes of the electrical storage system by changing the nominal voltage of the system V_B and the storage capacity C_O.

The nominal DC voltage output V_B of the battery in the model is set to be 48 V to match the battery used in the Al Madar Al Jadid telecommunication station. The storage capacity C_O of battery bank of PV system used in the stations of Al Madar Al Jadid is 5964 Ah. The state of charge SOC can be defined from documentation provided by the manufacturer. It is recommended not to discharge the battery completely in order to increase the life span of the battery and to avoid the very high drop of the battery voltage. Manufacturers commonly recommend the SOC from 20% to 80% of the storage capacity C_O. However, in this model, SOC_{max} and SOC_{min} are taken as 100% and 20% of C_O, respectively, to guarantee an acceptable battery's lifetime (i.e. SOC_{max}=5964 Ah and SOC_{min}= 4771.2 Ah). It is recommended in the provided technical documentation that the maximum allowable discharging current should be equal to C/5 and that the maximum charging current should be

equal to C/10. Thus, in the battery bank the maximum allowable discharging current I_{Dmax} and the maximum allowable charging current I_{Cmax} are 1192.8 and 596.4 A, respectively.

Charging and discharging currents at any time (t) vary depending on the shortage or surplus in the available DC power from the PV generator, though, in order to ensure efficient performance of the battery, a charge controller limits these currents to the maximum and minimum amounts, I_{Dmax} and I_{Cmax}, respectively [5].

The surplus power P_+ at any time is the difference between the power of the PV generator (P_{PV}) and the electricity demand of the load P_{Load} at the same time [5]:

$$P_+ = P_{PV} - P_{Load}, \quad P_{PV} > P_D \tag{6}$$

where P_D is the electricity demand of the site at any time.

However, when the power produced by the PV generator P_{PV} is less than the demand, then a shortfall in power P_- can be calculated as follow:

$$P_- = P_{Load} - P_{PV}, \quad P_D > P_{PV} \tag{7}$$

The surplus power produced by the PV modules is used to charge the battery bank, unless it is already fully charged; the batteries charging current (I_{CO}) is limited by the charge controller to the maximum allowable charging current I_{Cmax} and SOC must be equal to or less than SOC_{max}. The charging current I_{CO} is calculated as [5]:

$$I_{co} = \frac{(P_+ \times \varepsilon_c \times \varepsilon_{B1})}{V_B}, \tag{8}$$

where ε_C is the charge controller efficiency (it is constant and equal to 0.98 in the model) [5]; ε_{B1} is the AC/DC converter efficiency, though it varies insignificantly with the load, it is assumed to be constant at 0.9; V_B is the system and the batteries voltage and equals to 48 V.

In the event when the power required by the demand exceeds the generated power the current from the battery I_{DO} contributes to compensate this shortfall power. I_{DO} is

$$I_{DO} = \frac{P_-}{(V_B \times \varepsilon_C \times \varepsilon_{B2})}, \tag{9}$$

Here ε_{B2} is the efficiency of the DC/AC converter or inverter [5].

The change in the battery capacity C_D with a period of time of Δt can be calculated as:

$$\Delta C = (I_C \times \Delta t) - C_D, \tag{10}$$

The battery state of charge SOC at any time *t* is calculated by the following equation:

$$SOC_t = SOC_{(t-1)} + \Delta C, \tag{11}$$

where $SOC_{(t-1)}$ is the battery's *SOC* at the time earlier than *t*, which is limited by the values of SOC_{min} and SOC_{max}.

The PV generator sources the load and charges the batteries during the day. In sunny periods, when the batteries are fully charged there will be more power produced than it is required. Therefore, the surplus power is dissipated in the Simulink model. The power demand supplied by the batteries at any time is calculated as [5]:

$$P_{batt} = I_D \times V_B \times \varepsilon_{B2} \times \varepsilon_C \qquad (12)$$

On the other hand, if there is surplus power P_+ and $SOC = SOC_{max}$ or $I_{CO} > I_{Cmax}$, the dissipated power P_{diss} will be determined as

$$P_{diss} = \left[\frac{I_{CO}}{\varepsilon_{B1} \times \varepsilon_C} - I_C\right] \times V_B \quad P_{diss} = \left[\frac{I_{CO}}{\varepsilon_{B1} \times \varepsilon_C} - I_C\right] \times V_B \text{ For } I_{CO} > I_C \quad (13)$$

The model calculates the SOC for every minute taking into account the charging and discharging currents determined in equations 8 and 9, the maximum and minimum limits of the charge, SOC_{max} and SOC_{min}, respectively. The power drawn from the battery C_D at any time estimated by multiplying I_D by Δt in hours. However, the efficiency of discharge at high rates is considerably lower than 100%, so the accurate discharge efficiency can be calculated as [6]:

$$C_D = \frac{I_D \times \Delta t}{\alpha}, \quad C_D = \frac{I_D \times \Delta t}{\alpha}, \quad 0 \leq \alpha \geq 1 \quad 0 \leq \alpha \leq 1 \qquad (14)$$

where α is the discharge efficiency determined as [5]:

$$\alpha = \frac{13.3 \times \ln\left(\frac{C_O}{I_D}\right) + 59.8}{100}, \quad 0 \leq \alpha \geq 1 \qquad (15)$$

It has been assumed in the model that the value of α cannot exceed the value which guarantees that the maximum charge removed from that battery at any time period Δt does not exceed the product ($I_D \cdot \Delta t$).

Although the same phenomenon is present during charging process, it does not significantly affect the efficiency of charging, especially with the charge current limited to C/10 (as highlighted earlier). So, such the effect has been neglected in the model. Consequently, the change in battery capacity C_D during any time period Δt is calculated as

$$\Delta C = (I_c - \Delta t) - C_D \qquad (16)$$

Thus, the battery SOC at any time *t* is calculated using the following equation:

$$SOC_t = SOC_{(t-1)} + \Delta C, \qquad (17)$$

Here $SOC_{(t-1)}$ is the battery's SOC at the time earlier than *t* and is limited by the values of SOCmin and SOCmax.

3. Experimental Part

Al Madar Al Jadid Company started using PV panels for power supply of stations in 2005, when 6 new stations were built in a rural areas and the General Company of Electricity refused to power these new sites since some of them were away from the national grid and the grid network in the vicinity of others were not powerful enough. The PV systems were supplied and installed by Total Company using Ericsson a sub-contractor. The PV systems and batteries with the voltage of 24Vdc were used to power the stations directly without DC/AC conversion. Recently, the network of Al Madar Al Jadid Company has expanded to cover rural regions, oil company sites and roads in the desert area. A project to built 350 stations including 135 sites powered by PV panels, was developed and accepted in 2009. The new stations will have AC air conditioning, so it is necessary to use DC-AC inverters.

The GSM station which was chosen to be used for evaluation in this study is located in the vicinity of the main road connecting country's north and south parts and is about 50 km away from the national grid. The actual data used in this study is acquired at the location of the station using a laptop base data acquisition system. The data has been collected over three times periods, namely in January, April and July.

4. Results and discussion

During numerical investigations the average hourly performance of the PV system was modeled for three periods, namely January, April and July, and then the theoretical results were compared with the corresponding experimental data. The climatic conditions were taken from NACA collected data and the highest discrepancy between theoretical and experimental results was observed in modeling of operation in January period. Even so, the theoretical model provides acceptable accuracy in simulation the performance of the PV system.

The load entered into the Simulink Matlab model is an actual load for the real PV generator operating in Libyan winter conditions.

Although the solar radiation on a horizontal surface in winter, particularly, in January and December is not high, the solar radiation on an inclined surface is fair and at noon reaches the level of about $700W/m^2$. The high value of the geometric factor for January and December months causes an increase in the solar radiation on inclined surfaces.

Figure 2 illustrates the DC power that can be produced by the PV generator. Overall, the both theoretical and experimental curves have the same trend and the output power, which is represented by the area under the curves, is almost equal. The main difference is that the curve of the experimental output power is shifted in time and the PV system starts to generate power at about 8:30 am and not at 7.30 as predicted by simulations. This is because of satellite data on solar irradiance used in this study which is hourly data for a fixed period from 7:30 to 16:30 for 12 months of the year.

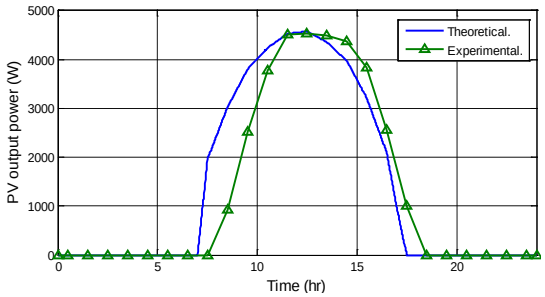

Fig. 2. Producible PV power

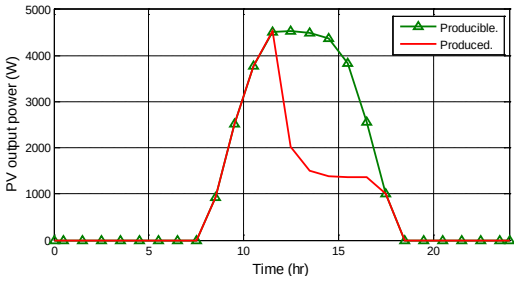

Fig. 3. Producible and produced PV power

Figure 3 shows the actual power produced by the PV generator and how much power is lost as a result of over sizing the PV system. The sum of the power consumed by the load and received by the electrical storage is about a half of the total producible power.

It can be seen in *figure 4* that the simulated battery charging curve is very similar to that of the experimental results. In both theory and experiment the batteries receive power as soon as it is started to be generated by the PV panels and it demonstrates that the power consumed by the load is very small compared to the power generated. On the other hand, the batteries are fully charged within few hours, because of the low power discharge, which is result in the huge capacity of the battery bank comparing with the load consumption. However, it can be observed from the experimental curve in *figure* 4 that the batteries charging is continued until the end of the day to compensate battery self-discharging process.

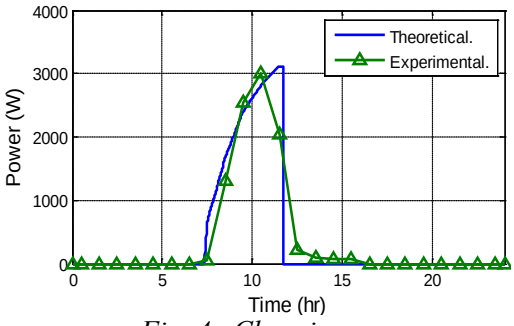

Fig. 4. Charging power

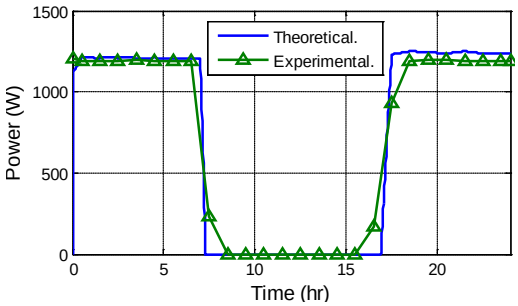

Fig. 5. Discharging power

Figure 5 presents the theoretical and experimental results on the battery discharging. As it can be seen from this figure, the curves are close, except at the beginning and the end of the day. Theoretically, the load is supplied either by the PV generator or the electrical storage; while in the real system, the shortage in the power from the PV generator is compensated by the power from the battery and this is reason for discrepancy between theoretical and experimental curves.

Figure 6 shows the SOC and processes of charging and discharging power in the summer period. It can be observed in this figure that, the batteries are fully charged within few hours, due to the small power drawn by the load during the night time. That emphasizes the excessive capacity of the battery bank compared with the load consumption.

As it is highlighted above, the power produced by the PV panels is disproportionately large when compared to the load consumption and the electrical storage. On the other hand, the capacity of the electrical storage is also very large with respect to the power consumed by the load. As a result, the deficit in the power is always zero. The dissipated power, which is represented by the red colour section in *figure 7*, is approximately two thirds of the total power that can be produced if the capacity of the battery bank is large enough, whereas the

produced power, which is represented by the blue colour section, is only about one third of the total power.

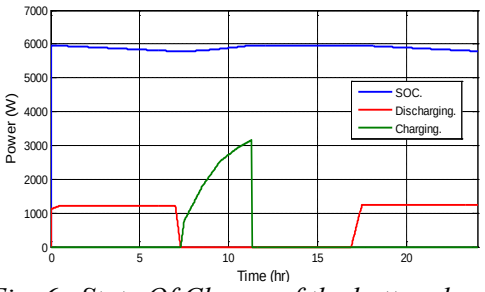

Fig. 6. State Of Charge of the battery bank

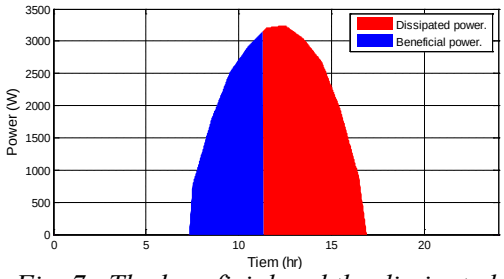

Fig. 7. The beneficial and the dissipated power

5. Conclusion

In this study the performance of standalone PV systems in telecommunication stations has been numerically evaluated. The simulation results illustrated that there is a considerable amount of the producible power is dissipated due to the over sized PV panels which can produce much more electricity than that could be stored in batteries bank. On other hand, the power drown from the battery bank at the normal rate is small and does not exceed 3% of the total stored power, which demonstrates the excessively large capacity of the electrical storage. Although zero solar radiation situations are very unlikely to have place such scenario taking place for 24 hours was simulated in order to calculate the power supplied by the battery and the SOC of the battery bank. The results from the simulation of such the scenario showed that only 10% of the total stored power is drawn from the battery in the winter, autumn and spring seasons, and in summer period this value is 11% of the total stored power. These results emphasize the large capacity of the battery bank. As a result of series calculations, it is found that the 60% of the existed PV modules area and 50% of the electrical storage capacity would be sufficient for powering the station. This would also result in significant reduction (by about 50%) of the capital cost of the PV system.

References

[1] Kaldellis, J.K. Optimum Hybrid Photovoltaic-based Solution for Remote Telecommunication Stations, Renewable Energy, Vol. 35, October 2010, PP 2307-2315.

[2] Markvart, T. Solar Electricity, 2nd edition, John Wiley & Sons,2000, pp. 6-132.

[3] Diaf, S. Diaf, D. Belhamel, M. Haddadi, M. and Louche, A. A methodology for Optimal Sizing of Autonomous Hybrid PV/Wind System, Renewable Energy, Vol. 35, November 2007, pp 5708-5718

[4] Ashraf, A. Ran, Li Bumby, J. Sizing and Best Management of Stand Alone Hybrid PV-Wind System Using Logistical Model, 2009, The University of Durham.

[5] Jenkins, D.P. Fletcher, J. and Kane, D. Model for Evaluating Impact of Battery Storage on Micro Generation Systems in Dwellings, Energy Conversion and Management, Vol. 49, August 2008, pp 2413-2424.

[6] Peacock, A.D. and Newborough, M. Effect of Heat-Saving Measures on t he CO2 Savings Attributable to Micro-Combined Heat and Power (μCHP) Systems in UK Dwellings, Energy, Vol. 33, April 2008, pp 601-612.

Designing a Photovoltaic Solar Energy System for a Commercial Building Case Study: Rosa Park Hotel in Khartoum-Sudan

Asim M. Widatalla[1,*], Heimo Zinko[2]

[1] *Linkoping University, Dept. of Thematic Studies, Water and Environmental Studies, Linkoping, Sweden.*
[2]*Linköping University, Department of Management and Engineering, Energy Systems, Linkoping, Sweden*
** Corresponding author. Tel: +46 707165268, E-mail: asiwi224@student.liu.se*

Abstract: Instability of electricity supply in Sudan is an increasing problem, especially in the capital and other larger cities. Commercial users such as hotels are looking for alternative solutions in order to be able to deliver adequate standards to their guests. In this study we investigate and optimize combined PV/Diesel system as a main electricity source for a hotel. There is significant potential for the use of the photovoltaic solar energy in countries like Sudan which receive abundant amounts of solar radiation around the year; the present work aims to design a rooftop photovoltaic solar system, or a hybrid system (Solar and Diesel) to produce 88100 kWh/yr of electricity for Rosa Park Hotel in Khartoum. The aim of this feasibility study was to find economic and useful combinations between Diesel and PV systems based on actual electricity consumption data of the hotel, taking into consideration both economic and environmental system aspects.
The study shows that, the PV systems can be used independently or together with the Diesel generator as a replacement energy resource. Due to the high initial cost of the installation of a PV stand-alone systems, the economic optimizations shows that a combination of a relatively small Diesel aggregates with a PV system can result in low system costs taking advantage of free and clean solar energy of PV and the system flexibility of a Diesel system.

Keywords: *HOMER, Hybrid system, Photovoltaic Solar Energy, Renewable Energy, Sudan.*

1. Introduction

Sudan Fig.2 is a country located in northeastern of Africa, with high solar radiation, according to Abdeen, (1997), the average sunlight hours in the capital– Khartoum - range between 8.7 hours per day in July and 10.5 hours per day in February [1], this gives a yearly average of sunlight hours 9.92 per day, and around 3600 hours/year. On the real side: the country faces a serious problem of instability of electricity supply especially in the capital and the main big cities. The hydro-power generators could not feed their rated electricity supply mainly in the rainy season - April to October - because of the accumulation of the mud in the dams. There are some other factors that make the problems of electricity supply and demand in urban areas bigger than similar problems in rural areas, such as the constant increase of population and building density.

Figure 1: Map of Sudan [2]

The aim of this study is to find out how the solar energy can be used to produce electricity for a hotel in Sudan, the task is to design a stand-alone PV system, and a Solar/Diesel system, and then to compare those regarding cost-effectiveness and environment.

1.1. Rosa park hotel

Rosa Park Hotel is a new four stars hotel located at the city center of Khartoum, there are 66 rooms spread across five floors, In addition to the health club service and fitness center.

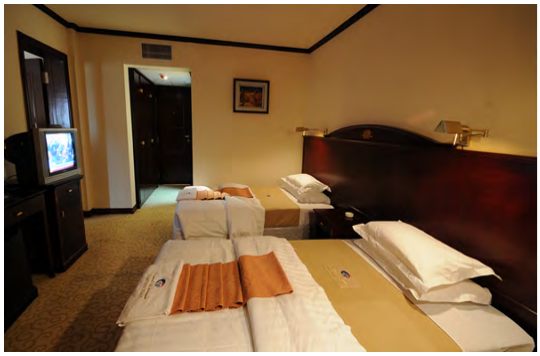

Figure 2: Photos from Rosa Park Hotel. [3]

1.2. Photovoltaic System

For this study, a commercial polycrystalline silicon solar cell was chosen at offered fixed price for the installation. Besides the solar cells, there are other important components in the PV-system, such as the inverter that is used to convert the direct current DC from the solar modules to alternating current AC, in our case synchronous with the grid. Furthermore, due to the variability of sunshine on both daily and seasonable basis, the mismatching between the production and the consumption of the electricity must be balanced by a battery system. [4].

1.3. Methodology

The methodology that we used for this study included the preparation of the inputs and calculations that are required for the simulation process. These inputs can be technical specifications of the PV panels, batteries, generators, etc., or the characteristics of the plant size, such as the weather data of the area where the system will be build on, the solar radiation density to which the plant site is exposed and the annual average temperature of the specific area. Also the economical inputs such as the capital costs and costs for replacement, operation and maintenance of the different equipment are of great importance for the financial evaluation.

A commercial software HOMER (Hybrid Optimization Model for Electric Renewables) was chosen for simulation purposes. HOMER is a computer model first developed by National Renewable Energy Laboratory, (USA-DOE). It is based on hour to hour simulation and this gives possibilities to control the battery status and to determine the sizing of the batteries [5]. The program determines the energy production for a given system over a defined period and calculates investment and operational costs. Because of the possibility of handling multiple inputs, HOMER can in short time calculate a multitude of optional system solutions and by that way an optimal system solution can be found.

2. Energy specifications

2.1. Electrical loads

The primary load distribution is essential for the designing process because the variation of the load through the day and night will affect the number of PV panels, and hence the capacity of storage battery and inverter:

- There are different loads for different seasons, the load will be 300 kWh/day for the tourists season (from October till February), and 200 kWh/day for the normal season (from March till September).
- The power consumption will vary according to the daily activities, for example; most of the work in the kitchen, rooms cleaning and the laundry used to be during the day.

The following tables show the loads for the two seasons per hour during day and night.

Table 1: The load of the tourist season

Time	Load kW	Time	Load kW	Time	Load kW	Time	Load kW
00:00 - 01:00	3.0	06:00 - 07:00	7.0	12:00 - 13:00	20.0	18:00 - 19:00	15.0
01:00 - 02:00	3.0	07:00 - 08:00	10.0	13:00 - 14:00	25.0	19:00 - 20:00	15.0
02:00 - 03:00	3.0	08:00 - 09:00	15.0	14:00 - 15:00	25.0	20:00 - 21:00	10.0
03:00 - 04:00	3.0	09:00 - 10:00	15.0	15:00 - 16:00	25.0	21:00 - 22:00	8.0
04:00 - 05:00	3.0	10:00 - 11:00	15.0	16:00 - 17:00	25.0	22:00 - 23:00	6.0
05:00 - 06:00	3.0	11:00 - 12:00	20.0	17:00 - 18:00	20.0	23:00 - 00:00	6.0

Table 2: The load of the normal season

Time	Load kW	Time	Load kW	Time	Load kW	Time	Load kW
00:00 - 01:00	2.0	06:00 - 07:00	3.0	12:00 - 13:00	13.0	18:00 - 19:00	10.0
01:00 - 02:00	2.0	07:00 - 08:00	6.0	13:00 - 14:00	18.0	19:00 - 20:00	10.0
02:00 - 03:00	2.0	08:00 - 09:00	10.0	14:00 - 15:00	18.0	20:00 - 21:00	8.0
03:00 - 04:00	2.0	09:00 - 10:00	10.0	15:00 - 16:00	18.0	21:00 - 22:00	4.0
04:00 - 05:00	2.0	10:00 - 11:00	10.0	16:00 - 17:00	18.0	22:00 - 23:00	3.0
05:00 - 06:00	2.0	11:00 - 12:00	13.0	17:00 - 18:00	13.0	23:00 - 00:00	3.0

2.2. Solar radiation

The average global solar radiation on the horizontal surface for each hour of the year will be needed for designing a PV system in a specific location. Here for this study, the solar plant was suggested to be located in Khartoum in Sudan at a location of 15° 31' N latitude and 32° 35' E longitude. The hourly solar radiation data was obtained from the NASA Surface Meteorology and Solar Energy web site [6]. The annual average of the daily solar radiation on a horizontal surface for this area is 6.31 (kWh/m^2/d).

3. Optimization

By feeding the software with the required basic input data, HOMER starts the work by running an hourly simulation of all possible configurations of different system types, and performs energy balance calculations for each hour in the year. The optimization process generates a list of configurations, sorted by net present cost, which can be used for the comparison of the different system design options [7]. An example is shown in Figure 3.
Three main types of system solutions have been investigated: PV stand-alone system, Hybrid system (PV + Diesel) and Diesel generator system (reference case). The size of PV system, Battery system and inverter system is depicted in Figure 3.

Sensitivity Results | Optimization Results

Double click on a system below for simulation results.

PV (kW)	engin (kW)	H3000	Conv. (kW)	Initial Capital	Operating Cost ($/yr)	Total NPC	COE ($/kWh)	Ren. Frac.	Diesel (L)	engin (hrs)	Batt. Lf. (yr)
20	10	12	20	$ 137,703	11,083	$ 279,380	0.251	0.42	18,481	5,629	8.3
	20	12	20	$ 47,430	18,559	$ 284,672	0.251	0.00	32,372	5,082	6.4
20	20		20	$ 134,374	20,225	$ 392,918	0.348	0.36	32,115	8,732	
	30			$ 29,181	29,745	$ 409,424	0.361	0.00	48,390	8,760	
61		48	40	$ 387,064	3,650	$ 433,729	0.399	1.00			13.8

Figure 3: Optimization results generated by Homer.
The headers in Figure 3 have the following meanings: engin - diesel engine, H3000 means 1 set of storage battery type of Hoppecke 24 OPzS (3000 Ah), Conv. is for converter, Ren. Frac. is for Renewable fraction of generated electricity, and Batt. Lf. is for battery lifetime, besides the symbols of PV panel, diesel engine, battery and converter are also included.

3.1. Economic parameters

The investment costs are described in Table 3. The costs include the hardware, the installation on the site and the connection to the grid. Beside the initial investment, we have to take into account replacement of equipment which is worn out. Hence replacement costs are added to the generation cost, when the lifetime of equipment has been reached. For batteries, the life time is different depending on the number of charging cycles and depth of the discharge. This is the reason for varying battery lifetimes in different systems. The time frame of the financial analysis of this project is 25 years. The interest rate was taken to 6 %.

The economical evaluation of the project can be calculated based on the inputs of financial aspects, which include the cost of the system components that the hotel's owner will pay, and on the other hand the benefits that the owner will earn from the projects.

- *Projected Benefits = Value of Generated Electricity + Value of Excess Energy + Value of CO_2 Reduced*
- *Electricity Costs = Capital Costs + Replacement Costs + Periodic Costs.*

The annuity calculations of all the benefits, the costs and also the Net Present Value were done based on assumed 25 years lifetime of the PV panels. The lifetime of the batteries is varying according to their use (see sect. 3.2.2) and the life time of the inverter is 15 years. Replacement costs are shown in Table 4.

3.1.1. Value of electricity

For the evaluation purpose of this system, we will use the electricity price that is achieved by the Diesel generator as a reference in order to calculate the projected benefit – because Diesel generators are widely used to produce the electricity in the areas of instable electricity supply. Therefore, According to the summary of the results in Table 7 the annual saving due to the electricity production is:

= the generated electricity through the year (kWh/yr) * Diesel generated electricity price ($)

= 88100 kWh/yr * 0.251 ($/kWh) = 22113.1 ($/yr).

Eventual excess energy (which is produced by the stand-alone system) is assumed to be sold to neighbors for the price of diesel-electricity.

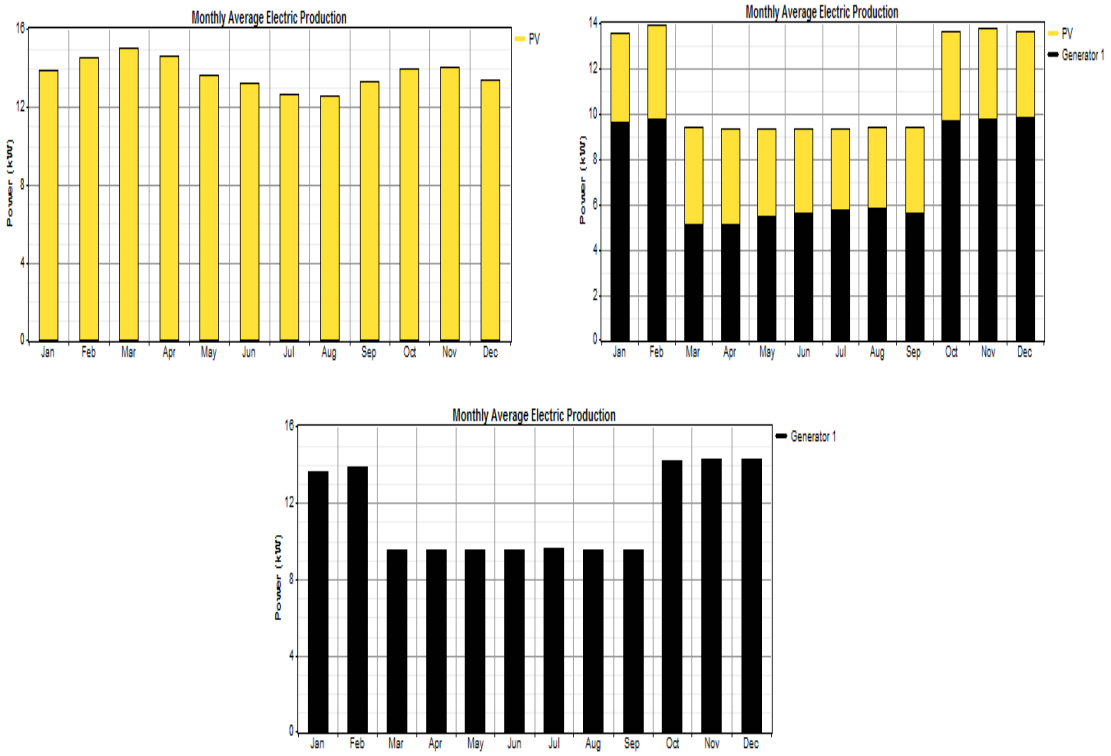

Figure 4: Monthly Average Electric Production for the three different System solutions.

3.1.2. Value of emitted CO_2

The reduced amount of CO_2 by the energy system has an economical value, due to the taxes that will paid for each kg of CO_2 that is emitted, even if there are at the moment no policies that control the emission of CO_2 in Sudan. The value for the CO_2 reduction is set to 15 $/ton.

3.1.3. Capital cost

Table 3 below shows the capital cost or the specific purchase price of the different components of the system (PV systems, Storage Batteries, Inverters and Diesel Generator):

Table 3: The Capital Cost

Unit	Size	Capital Cost	Ref.	Unit	Size	Capital Cost	Ref.
PV panels	1.0 kW	5000 $	[8]	Inverters	1 kW	746.4 $	[10]
Diesel Generator	1.0 kW	972.7 $	[9]	Batteries	1 set (3000 Ah)	1088.2 $	[11]

The PV panel's cost that mentioned above is the total cost of the system including panel, installation, connection to the house and so on, the panel's cost is about half of that.

3.1.4. Cost of Replacement, Maintenance and Fuel

The replacement cost is the cost of equipment that is purchased to replace a component when its lifetime is shorter than the project time set for this financial analysis. The solar cells have not to be replaced, but the inverters will be replaced after 15 years, battery's lifetime indicated in Figure 3. Battery's lifetime is greater when using PV standalone than the other systems because the number of batteries that used is four times greater, also the battery's annual throughput (the amount of energy that cycled through the battery bank /year) of this system is two times greater. Table 4 shows the replacement cost of the different components:

Table 4: The inputs of the specific Replacement Cost

Unit	Size	Replacement Cost	Unit	Size	Replacement Cost
PV panels	1.0 kW	0	Inverters	1.0 kW	$ 746.4
Diesel Gen.	1.0 kW	$ 680.9	Batteries	1set (3000 Ah)	$ 1088.2

The operating and maintenance (O&M) cost of the PV panel is expected to be $0.45 per m^2/year, [12], Table 5 shows the maintenance cost for the rest of the components:

Table 5: The Inputs of the Periodic Maintenance Cost

Unit	Size	O&M Cost $	Unit	Size	O&M Cost
PV panels	1.0 kW	$4.09/yr	Inverters	1.0 kW	0
Diesel Gen.	1.0 kW	$0.078/hr	Storage Batteries	1set (3000 Ah)	$20/yr

The total operating cost is the sum of the annual operation and maintenance cost, and the annualized replacement cost for remaining time of the equipment. The price of Diesel used in this study was selected based on the actual market price of 2006, for gasoline and Diesel in northern Kurdufan which was approximately (1.35 $/gallon), while the cost in villages is about (1.44 $/gallon) [13]. The total annual O&M costs are shown in Figure 3, showing the large difference between PV stand-alone at the Diesel system.

4. Results

A summary of the optimized results of the different categories are listed in Table 6. Based on the results, the selected economical evaluation methods will be discussed as shown below. It is interesting to note, that the Hybrid system shows the lowest Net Present Value of all the systems investigated. The systems are compared by means of three types of cost analysis, all three calculated using standard methods and standard definitions:

- *Net Present value NPV*
- *Payback Period (straight payback)*
- *Levelized Cost of Energy (COE)*

Table 6: Summary of the Simulation Results

System	Ann. Saving $	NPV $	Payback period	Levelizd COE ($)	Excess Electricity	CO_2 Emission kg CO_2/kWh
PV Stand-alone	29774.1	433729	13.1 yr	0.399	18.6 %	0
Hybrid System	24031.8	279380	8.3 yr	0.251	0	0.507
Diesel Gen.	22113.1	284672	5.0 yr	0.251	0	0.879

The annual saving is based calculated from the amount of the electrical energy produced per year and delivered to the hotel and in the case of the stand-alone system also to the neighbors. This is multiplied by the cost of electricity produced by the Diesel system (which is 0,251 $/kWh).

4.1. Net Present Value NPV

As shown in Table 7, the initial cost of the PV Stand-alone system is the highest among all the systems-almost 3 times compared with the hybrid system, and more than 8 times compared with the Diesel system. However, the PV system uses no fuel, and the other systems pay from $7000 and $12000 per year, respectively. Also, Diesel generators need to be replaced approximately 4 times during the project's lifetime. The storage battery holds for about 14 years in the stand-alone system; it needs to be changed 2 times at least for the other systems.

At the end of the project's economic running time, the total NPV of the PV stand-alone system is only about 1.5 times of both the hybrid and the diesel systems total NPV cost.

Table 7: The details of the NPV cost.

	Initial Capital $	O&M Cost $	Annual Fuel $	Total NPV $
PV Stand-alone system	387 064	1 204	0	433 729
Hybrid System	137 703	335	7 014	279 380
Diesel Generator	47 430	266	12 285	284 672

It can be seen that the NPV-analysis has a limited effect on the economical evaluation on the two systems (stand-alone and the hybrid), in spite of the big difference in the initial costs.

4.2. Payback period

The payback period can give an indication to the investor how fast he can get his money back. From the data of Table 6, one can notices that while the minimum time that is needed to recover the investment cost of the hybrid system and the Diesel generator system are 8.3 and 5 years respectively, the stand-alone PV system needs 13.1 years to recover its cost.

4.3. The Levelized Cost of Energy COE

The levelized cost of energy COE gives the average cost of producing one kWh of electricity, including all the different cost contributions. Table 7 shows that the PV stand-alone system has the highest COE per kWh ($ 0.399), while the COE of both Diesel and hybrid systems are the same ($0.251). This seems to be reasonable in respect to the NPV-levels of the systems.

4.4. Sensitivity analyses

In such analyses, the results are strongly influenced by the quality of the input. Therefore, sensitivity analyses can illustrate this influence. In our study, we have increased the oil price by 20 % , and reduced the PV panels cost by 20 %. In all cases, there was no change of the ranking of the three types of systems, but of course the gap becomes smaller. The Hybrid system turns out to be the system with lowest COE (0.25 $/kWh) in both cases, the PV stand-alone system remaining the system with the highest COE (0.359 $/kWh).

5. Discussion and/or Conclusions

Three categories of the power systems are suggested by this study to solve the instability of the power supply of Rosa Park Hotel in Khartoum, and to replace the grid/Diesel current options. From the simulation results, and the analysis of the annuity calculations, one can notice that both the stand-alone and hybrid PV/Diesel systems can be used and both of them sound profitable, with a straight payback period less than 9 years for the hybrid system, and less than 14 years -which is almost half of the project's lifetime- for the stand-alone system.

The study shows also that, the PV solar energy can be use separately or together with the Diesel generator as a replacement energy resource, to solve the power supply problems, and also to reduce the need of carbon-based energy. Due to the high initial cost of the installation of the stand-alone system, based on the economical evaluation of the systems, we think, the hybrid system is more viable option compared to the use of the Diesel generator separately.
However, the selection of such system should not be evaluated based only on the economic feasibility; also the expected environmental and social benefits need to be considered, since the three elements are important for the sustainable development assessment of any project.

From the economical analysis it is easy to notice that, the stand-alone PV is the most expensive way to generate electricity among the three systems, but in terms of carbon dioxide emissions, it is more environmentally sound because the system emits no CO_2 during the electricity production, while both the Diesel generator system and the hybrid system emit considerable amounts of the greenhouse gas, about 0.879kg of CO_2/kWh and 0.507kg of CO_2/kWh respectively. According to Simon, these emissions from fusel fuel-powered generators present a 'cost' that should be factored into energy system choices [14]. This might be difficult to be achieved in developing countries such as Sudan, but if the government would make the cost per kWh from the power generator more transparent and would remove the fuel subsidy, PV systems would be a competitive option also in this country [13].

References

[1]O. Abdeen, Compilation and Evaluation of Solar and Wind Energy in Sudan, Renewable Energy Vol. 12 (No.1), 1997, pp 47.

[2] Greenwich Mean Time website, (sited 29-10-2009, 21.58)

[3] Rosa Park Hotel website (sited 24/08/2010) http://www.rosaparkhotels.com/Photos.html

[4] (EUREC), PV in Building: The Art of Merging, the European Renewable Energy Research Centres Agency, 1997.

[5] Vanggaard, Morten Eghøj, Lund, Dan Toste, Design of a standalone PV system for Greenland, Dep. of Civil Engineering, Danmarks Tekn. Univ. (DTU), 2009, M.Sc: 7&8.

[6] The NASA Surface Meteorology and Solar Energy web site -.http://eosweb.larc.nasa.gov/cgibin/sse/homer.cgi?email=asim214@yahoo.com&step=1&lat=15+31&lon=32+35&submit=Submit&ms=1&ds=1&ys=1998&me=12&de=31&ye=1998&daily=swv_dwn

[7] National Renewable Energy Lab., Getting started Guide for HOMER Vers. 2.1,2005.

[8] Wholesale Solar Company website: sited 16/08/2010 http://www.wholesalesolar.com/products.folder/module-folder/bp/bp380U.html.

[9] Just Generators website: sited 16/08/2010 http://www.justgenerators.co.uk/pages/Stephill_SSDX11_3phase.htm.

[10] Wholesale Solar Company website: sited 16/08/2010. http://www.wholesalesolar.com/products.folder/inverter-folder/XP1100-12.html

[11] Wind & Sun company website: sited 16/08/2010. http://www.windandsun.co.uk/Prices/prices_batteries.htm

[12] Joan M. Ogden, Cost and performance sensitivity studies for solar photovoltaic / electrolytic hydrogen systems, Solar Cell, 30, 1991 pp 517.

[13] B. Croxford, M. Rizig, Is photovoltaic power a cost-effective energy solution for rural peoples in western Sudan? Solar 2006: renewable energy, key to climate recovery, American Solar Energy Society.

[14] International Energy Agency (IEA), Guidelines for economic evaluation of building integrated PV, Report IEA PVPS T7-05: 2002 p.12.

Analytical model and experimental validation of the heat transfer and the induced flow in a PV cooling duct in environmental conditions

R. Mazón[1,*], A.S. Káiser[1,*], B. Zamora[1], J.R. García[1], F. Vera[1]

[1] *Thermal and Fluid Engineering Department, Technical University of Cartagena, Doctor Fleming, s/n 30202, Cartagena, Murcia, Spain*
[*] *Tel: 34* 96832594 *rmh@alu.upct.es*
**Tel: 34 968325984, antonio.kaiser@upct.es*

Abstract: This paper describes a model to account for the heat transfer and the convective flow induced in the interior of a channel inclined 35° with respect to the horizontal, formed by a photovoltaic panel and an adiabatic plate. The model developed is validated experimentally by measurements made on an experimental prototype. The solar installation consists of two photovoltaic panels integrated with air ducts on the top of a building in southern Spain. The objective is to determine the temperature reached by the photovoltaic module in this configuration. This model considers the processes of heat transfer by radiation and convection on the outside for several atmospheric conditions (wind speed, ambient temperature and incident radiation) and for different geometrical and physical characteristics of the PV cooling duct (plate area, module performance, emission and absorption coefficients). Good agreement has been obtained between the experimental data and the results of this model.

Keywords: *PV cooling duct, solar experimental facilities, efficiency solar panels.*

1. Introduction

The performance of PV implemented on t he top of a building depends on t he panel temperature in addition to other factors such as insulation and shading. High panel temperatures resulting from overheating could occur due to low wind cooling effect compared with free standing installation. One cost effective method to regulate the temperature of rooftop integrated photovoltaic (PV) panels is to provide an open air channel underneath the panel.

To determine the equilibrium temperature of the modules, for different atmospheric conditions, it is necessary to solve simultaneously the heat transfer processes between the PV modules and the exterior and interior of the air duct, and the convective flow induced by buoyancy effects and by the suction of the external wind. Various studies have been carried out to assess the performance of roof-mounted solar (thermal or photovoltaic) panels. Some authors centered their research on the effect of the air gap between a solar panel and a roof [1], others suggested that a reasonable air gap for solar thermal collectors would be between 0.1 and 0.14 m [2] and also derived expressions for the mass flow rate, velocity and temperature rise in the air gap behind solar cells considering the effect of the geometry (aspect ratio of the channel) and location of these solar cells [3]. Other authors presented procedures of the heat transfer and the convective flow through a PV cooling duct to determine the equilibrium temperature of the module [4].

This work initially raises the set of equations that characterize the thermal and fluid dynamic process in the air gap behind the solar cells. Subsequently a selection of the characteristic values is made of the input variables in this model, based on t he existing literature and the available data on t he experimental prototype presented in this work. Once estimated the solution of the equations system is presented, with particular emphasis on how the temperature of the module changes as the incident radiation and the external wind change. To

solve this system of equations the ESS software has been used. The model is validated with experimental measurements obtained on the configuration under study.

2. Experimental facility

The solar installation consists of two photovoltaic panels arranged as shown in figure 1, first panel (panel A) is used as reference panel. Panel temperature at different points, voltage, and current are measured to understand the panel behavior under normal operating conditions and to compare with another one (panel B) which is modified to test different ducts with different cross sections. In this second panel, surface temperature at different points, voltage, and current are also measured jointly with the air temperature and air flow rate. In the solar panels, temperatures are measured with RTD, and duct air speed with hot film anemometers [5].

Fig. 1. Solar panels. Left panel (A), right panel (B).

The horizontal components of solar radiation are measured by two pyranometers. Other environmental conditions such as temperature, pressure, humidity and wind speed are measured with a meteorological station place on our laboratory roof just beside the experimental facility. All data is registered and recorded by means of a data logger.

3. Analytical model

3.1. The incoming heat flow to the channel

As mentioned, the procedure requires the simultaneous solution of two heat transfer equations. On one hand it has to solve the external equation, which represents the transfer of heat to the surroundings from the top face of the module and on the other hand the internal equation, which represents the transfer of heat into the duct. The module temperature links up both equations. In general, there may be a temperature difference between the two faces of the photovoltaic module, which is given by the expression [6]

$$T_o - T_m = \frac{E}{E_o}\Delta T \qquad (1)$$

where T_o is the cell temperature inside the module, T_m the lower face temperature, E is the irradiance measured, E_o is reference solar irradiance on the module (1000 W/m^2) and ΔT the temperature gap between cell and back surface measured with E_o = 1000W / m^2, whose value

depends on the module rear ventilation (in this case is usually 2-3 ° C). In the approach of our model we consider in the first instance that there is no temperature difference between the two sides of the module.

The external equation requires the following energy balance. At any point of the module, the heat flux that goes into the channel is given by the difference between the absorbed solar radiation minus the electrical output and losses to the surroundings. These losses are due on one hand, to the reflected and emitted radiation, and on the other hand to the external convection:

$$q = (\alpha_s - \eta) \cdot q_s - U_a (T_o - T_a) \quad (2)$$

being α_s the absorption coefficient, η the electrical efficiency, U_a the external loss coefficient and T_a the ambient temperature, and q_s the solar flux or irradiance. As guide values for electrical efficiency and the absorption coefficient we've considered α_s = 0,85 and η = 0,12 [7]. Other authors suggest a value of αs - η = 0. 8 and regarding the external loss coefficient (U_a), they also propose $U_a = h_{re} + h_{ce}$ [8] where

$$h_{re} = 4\varepsilon\sigma\left[\frac{T_o + T_a}{2}\right]^3 \quad (3)$$

$$h_{ce} = 1{,}3(T_o - T_a)^{1/3} + 4 \cdot V_{10} \quad (4)$$

with h_{re} as the radiation loss coefficient (where we assume that the surroundings are a cavity of adjacent air temperature and that the panel has an emittance of ε), h_{ce} is the external convection coefficient (it takes into account the existing exterior wind and it has been adjusted for the location of our facility studied considering the results of Palyvos [9]) and V_{10} is the external wind speed at the height of 10 meters. It is obvious that in general the heat flow q is not uniform over the surface of the module. However, as U_a, is usually taken as uniform, so the heat flow will be also in our model over the PV module.

The formulation of the equation of heat transfer inside the duct initially requires determining the buoyancy-induced flow and wind effects inside the channel when the photovoltaic module is subjected to a uniform solar radiation. In this process, the output variables are the wall temperatures, T_o (module temperature) and T_b (temperature of adiabatic wall) and its variation along the panels. The process requires an iterative calculation, given the existing degree of coupling.

3.2. The mass flow rate induced inside the channel

According to the investigations of Brinkworth [8], considering a constant heat flow in the module, determining the flow induced in the interior, is decoupled from the temperature of the channel walls, and can therefore be obtained separately. Therefore, we will raise the problem as decoupled and initially we will solve the induced mass flow (and hence the average speed) and then, based on this result, the heat transfer and temperature of the plates. To obtain the induced mass flow inside the channel, it is necessary to consider a balance of global forces on the air mass inside the same channel. The flow inside the duct is the result of driving forces (buoyancy-induced by natural convection and wind suction) and resistant forces (friction and

other hydraulic losses in the inputs and outputs). Below, this paper describes each of these forces.

3.3. Driving forces

The drop in pressure to conduct the air through the duct is the sum of buoyancy and wind effect [10]:

$$\Delta p_d = \Delta p_b + \Delta p_w \tag{5}$$

For flows that meet certain conditions, Boussinesq suggested that variations in fluid density can be neglected except in the gravitational term of the equation of conservation of momentum in the vertical direction, in which density appears multiplied by the gravity acceleration (g). This approach assumes that other fluid properties such as dynamic viscosity, conductivity and specific heat are constant. Supposing that the compressibility effects are small, so that density variations are due solely to the temperature changes, we can use the Boussinesq approximation, if the temperature variations in the fluid are small. Considering the Boussinesq's hypothesis the buoyancy term can be expressed as the difference between the base and the end point of the fluid column with a height of $Lsin\theta$:

$$\Delta p_b = \rho g \beta \left(T_{media} - T_i\right) L \ \sin\theta = \rho g \beta S \left(T_e - T_i\right) L \ \sin\theta \tag{6}$$

where $S(T_e - T_i)$ is the average increases of the temperature reached in the duct. The value of S depends on the temperature profile along the duct. For a linear increase in temperature, its value is about 0.5. This value is what we consider in this study as a starting point. On the other hand, the value of $(Te - Ti)$ can be expressed in terms of incoming heat as

$$qA = \dot{m} C_p \left(T_e - T_i\right) \tag{7}$$

If we solve eq. (7) for $(T_e - T_i)$, expressing the mass flow-rate, $\dot{m}$, in terms of the density,

$$\left(T_e - T_i\right) = \frac{qL}{\rho U H C_p} \tag{8}$$

and substituting in equation (6)

$$\Delta p_b = \frac{g \beta S q L^2 \sin\theta}{U H C_p} \tag{9}$$

where β is the coefficient of thermal expansion, L the channel length, U the average velocity of induced flow, C_p the specific heat of air and H the depth of the channel. The channel width is taken to be 1m.

As already mentioned, the external wind exerts a suction force on the channel so the mass flow increases. The pressure difference induced by wind can be represented by

$$\Delta p_w = C_{pi}\left(\frac{\rho V_{wi}^2}{2}\right) - C_{pe}\left(\frac{\rho V_{we}^2}{2}\right) \tag{10}$$

being C_{pi} and C_{pe} the wind pressure coefficients at the entrance and exit of the duct, and V_{wi} and V_{we} are the values of wind speed at the inlet and outlet of the duct. According to Brinkworth [8], assuming that the position of the duct is such that the wind causes an increase in mass flow, we can estimate the combined effect of wind on the channel as:

$$\Delta p_w = (+0.5)\frac{\rho V_{10}^2}{2} \tag{11}$$

with V_{10} the wind speed at the height of 10 meters above the channel (the coefficient of +0.5 is included in eq.11 to adjust experimentally the effect of the surroundings).

3.4. Resistant forces

The flow resistance expressed in terms of pressure differences (Δp_r) is given by the sum of the pressure drop due to friction (Δp_f) and other hydraulic losses (Δp_h). Friction losses can be expressed by the Darcy's equation

$$\Delta p_f = f(L/D)\frac{\rho U^2}{2} \tag{12}$$

where f is the friction factor in a duct of length L and the hydraulic diameter of the cross section is $D = 2H$, due to the width is 1m and H<<1. In general, the factor f is a function of the aspect ratio (L/D) and of the Reynold number ($Re_D = UD/\nu$). In the case of a channel the following expression is proposed:

$$f = f_o + \frac{f_1}{L/D} + \frac{f_2}{\mathrm{Re}^n} \tag{13}$$

With n ≈1, $f_0 \approx 0$, $f_1 \approx 1$ and $f_2 \approx 64$. Given these values, the expression $f\,(L/D)$ approaches to 1. On the other hand, the pressure drop due to hydraulic losses can be expressed in terms of coefficients K_h of the dynamic pressure in the form

$$\Delta p_h = \left(\sum k_h\right)\frac{\rho U^2}{2} \tag{14}$$

When there is a heat flow asymmetry on both walls in the channel. We may assume $\sum k_h \approx 1.5$ [10]. If we propose the balance of forces, the equation obtained is:

$$\frac{2gqSL^2 \sin\theta}{T_a \rho H C_p} = \left(f\frac{L}{D} + \sum k_h\right)U^3 - \left(\frac{2\Delta p_w}{\rho}\right)U \tag{15}$$

which is a cubic function of the average velocity induced in the channel.

$$A \cdot U^3 + B \cdot U^2 + C \cdot U + X = 0 \tag{16}$$

With $A = 1 + \sum k_h$, $B = 0$, $C = -V_{10}^2$ and $X = -2gqSL^2 \sin\theta / T_a H \rho C_p$.

3.5. The heat transfer inside the duct

The incoming heat flow q is transferred to the air through the convection at the two walls of the channel and may be expressed by $q = q_0 + q_b$. The first term, q_o, regards to the heat flow for convection of the PV module to channel air. This is given by

$$q_0 = (T_0 - T_m) \cdot h_0 \tag{17}$$

where h_o the convection coefficient of this panel, T_o temperature of the panel at a distance of the channel input in longitudinal direction and T_m the average temperature of the air-flow at this point. The second term, q_b, represent the heat flow for convection from the adiabatic module. This heat came from the radiation heat flow issued over this panel for the PV module. It can be represented with the next equation.

$$q_b = (T_b - T_m) \cdot h_b \tag{18}$$

This radiation heat flow can be well represented for an interchange direct equation that considers local temperature of the two facing surfaces, with a heat transferred coefficient linearized h_r, described by [8],

$$h_r = 4 \cdot \varepsilon_{eff} \cdot \sigma \left(\frac{T_0 + T_b}{2} \right)^3 \tag{19}$$

In this case, we assume that the plate facing the module is adiabatic and that the energy that it receives by the radiation is entirely transferred for convection to the flow. So, the average air temperature in the duct at a distance x from the input is given by

$$(T_m - T_b) = \frac{q\ x}{\rho_a C_p U\ H} \tag{20}$$

From the above equations, you can get the temperatures of the two walls thanks to the expressions (23) and (24). The convection coefficients h_o and h_b can be obtained from the following expressions

$$h_0 \cdot \left(1 - n\hat{\theta} \right) = h_c \tag{21}$$

$$h_b \cdot \left(1 - \hat{\theta}\ / n \right) = h_c \tag{22}$$

where h_c is the coefficient of convective heat transfer on the hot wall of a channel in where the other wall is adiabatic and we assume there is not heat flow by radiation. $\hat{\theta}$ is the influence coefficient which depends on the shape of the temperature profile of the plate that the duct is only heated on one side . The variable n is the ratio of heat flux between two walls

$$n = \frac{q_b}{q_0} = \frac{h_r (T_0 - T_b)}{h_0 (T_0 - T_m)} \tag{23}$$

To close the system, we need information about h_c (or of Nu_c) and $\hat{\theta}$. For turbulent flow in a channel with heat flow in a plate and the other being adiabatic, the following expression is referenced, where Re_D is the Reynolds number based on the hydraulic diameter:

$$h_c = 0{,}0186 \ \mathrm{Re}_D^{0{,}787} \ k / D \qquad (24)$$

With regards to the value of $\hat{\theta}$, we have estimated it, correlating the presented values for the case of Re_D = 10,000 according [11]

$$\hat{\theta} = 0{,}0452 \ln(L / D) + 0{,}0178 \qquad (25)$$

In spite of these values assumed by *hc* (or by Nu_c) and of $\hat{\theta}$, there is no criteria in bibliography to determine them. Therefore, a future task is to numerically determine its values for different conditions of heat flow between both walls and different angles of incidence.

4. Experimental validation of the model and results

The equation model proposed to resolve the heat transfer and the induced flow has been solved by means of the EES software used, for different real cases which have been measured experimentally in our solar facility. The following starting parameters have been considered: Cp = 1007 J/kg K, D_h = 0.27 m, ε = 0.88, ε_{eff} = 0.3, g = 9.8 m/s^2, η = 0.1353, H = 0.165 m, α_s = 0.85, K_h = 1.5, L = 1.956 m, σ= 5.670 x 10^{-8} W/m^{2}K^4, μ_a = 0.00001834 kg/ms, V_w = 1,86 m/s, Re_{Dh} = 17,351, ρ_a = 1.197 kg/m^3, S = 0.5 *y* θ_p = 35^o.

Figure 2 compares the experimental data of the temperatures of the module (T_o) and the adiabatic wall (T_b) as a function of the irradiance, with those obtained by the analytical model. Taking into account that the experimental data has been obtained varying the atmospheric temperature (between 298 and 303 K), the results of the analytical model have been presented for different atmospheric temperature conditions. Experimental correlations for module and adiabatic wall temperature have been also printed in the Fig. 2. On the other hand, it has been also studied experimental and analytically the effect of the air gap between the module and the adiabatic wall. It has been tested that its effect is not very important in the performance of the module, once a minimum value of the aspect ratio has been reached ($H/L \approx 0.1$).

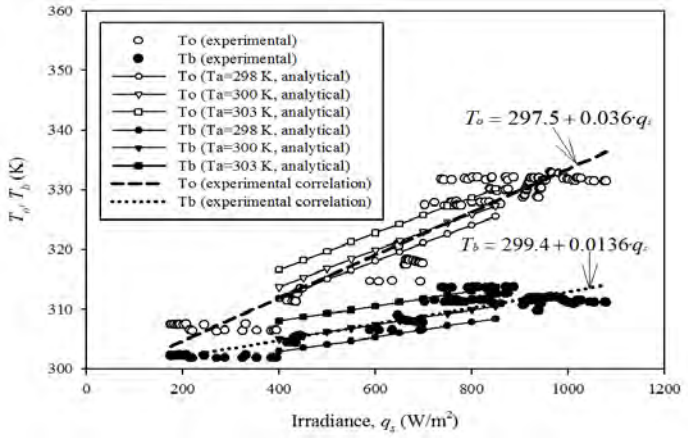

Fig.2. Experimental validation of the analytical model for different atmospheric temperatures and the experimental correlation of the photovoltaic plate temperatures.

5. Conclusions

A solar installation consisted of a photovoltaic panel and adiabatic plate in an inclined channel configuration has been experimentally tested. Experimental correlations have been proposed for the temperature of the module and the temperature of the adiabatic plate as a function of the irradiance, for an average wind velocity of 2 m/s and an average atmospheric temperature of roughly 300 K.

An analytical model of this configuration to study the heat transfer and the convective flow induced in it has been carried out and solved by EES software, considering some previous models of the bibliography and particular aspects of this experimental facility. The experimental measurements have been used to validate this analytical model. It has been tested that the effect of the air gap between the module and the adiabatic wall is not very important in the performance of the module, once a minimum value of the aspect ratio has been reached ($H/L \approx 0.1$).

Acknowledgements

The authors thank the local association Fundacion Seneca for its cooporation in this study, which has been supported by the company Apia XXI, so we'd like to show our gratitude to them.

References

[1] J. Khedari, J. Hirunlabh, T. Bunnag, Experimental study of a roof solar collector towards the natural ventilation of new habitations. Energy and Buildings 26, 1997, pp. 159–164.

[2] J. Hirunlabh, S. Wachirapuwadon, N. Pratinthong, J. Khedari, New configuration of a roof solar collector maximizing natural ventilation. Building Env. 36, 2001, pp. 383–391.

[3] M. Sandberg, B. Moshfegh, Buoyancy-induced air flow in photovoltaic facades. Effect of geometry of the air gap and location of solar cell modules. B. Env. 37, 2002, pp. 211–218

[4] B.J. Brinkworth, R.H. Marshall, Z Ibarah, A validated model of naturally ventilated PV cladding. Solar Energy 69 (1), 2000, pp. 67–81.

[5] R. Mazón, JR García, F Vera, A S. Kaiser, B Zamora, Development of an installation to reduce the temperature of photovoltaic modules and improve their efficiency, ICREPQ'10, 2010.

[6] D.L. King, W.E. Boyson, J.A. Kratochvil, Photovoltaic array performance model, Sandia National Laboratories, 87185-0752, 2004.

[7] F. Sarhaddi, S. Farahata, H. Ajama, A. Behzadmehra and M. Mahdavi Adelia, An improved thermal and electrical model for a solar photovoltaic thermal (PV/T) air collector, Applied Energy 87, 2010, pp. 2328-2339.

[8] B.J. Brinkworth, M. Sandberg, Design procedure for cooling ducts to minimize efficiency loss due to temperature rise in PV arrays, Solar Energy 80, 2006, pp. 89-103.

[9] J.A. Palyvos, A survey of wind convection coefficient correlations for building envelope energy systems´modeling, Applied Thermal Engineering 28, 2008, pp. 801-808.

[10] B.J. Brinkworth, Estimation of flow and heat transfer for the design of PV cooling ducts, Solar Energy 69, 2000, pp. 413-420.

[11] B.J. Brinkworth, Coupling of convective and radiative heat transfer in PV cooling ducts, ASME 124, 2002, pp. 250-255.

Design, fabrication and testing of micro-channel solar cell thermal (MCSCT) tiles in indoor condition

Sanjay Agrawal[1,*], S. C. Solanki[1], G. N. Tiwari[1]

[1]*Centre for Energy Studies, Indian Institute of Technology Delhi, New Delhi, India*
** Corresponding author. Tel: +91 9911428863, Fax: +91 1126591251, E-mail: sanju.aggrawal@gmail.com*

Abstract: In this paper design, fabrication and testing of micro-channel solar cell thermal (MCSCT) tiles has been discussed. Solar simulator for an indoor testing of micro-channel solar cell thermal tiles has also been developed. Fabricated MCSCT tile consists of single solar cell, micro- channel and fan for extraction of heat from bottom of solar cell. Single MCSCT tile has been termed as case-I. Similarly, two MCSCT tiles which are connected in series have been termed as case-II. The performance evaluation in terms of electrical efficiency, thermal gain, overall thermal energy and overall exergy of both cases has been carried out in indoor conditions on various intensities. It has been also found that the electrical efficiency is higher in case-I as compared to case-II. On the other hand the thermal out put of case-II is higher than case-I on same intensity and mass flow rate. It has been found that the average electrical and thermal efficiency of newly designed and fabricated MCSCT tile is 12.4% and 35.7% respectively. This economical solar simulator can be used by manufactures for testing of different type of photovoltaic tile as well as photovoltaic modules.

Keywords: *Full Photovoltaic thermal tile, Micro-channel, Solar simulator.*

Nomenclature

A_c *Area of MCSCT tile* ..... m^2
E *Electrical power* ..... W
$\dot{E}x$ *Exergy* ..... kW
$I(t)$ *Intensity*..... Wm^{-2}
$\dot{m}_f$ *Mass flow rate of* ..... $Kg\ s^{-1}$
C_f *Specific heat of air*..... $Jkg^{-1}\ K^{-1}$
$\dot{Q}_u$ *Rate of useful energy* .....kW
V *velocity of air inside micro-channel* ....$m{\cdot}s^{-1}$
V_{oc} *Open circuit voltage* .....*Volt*
V_L *Load voltage* .....*Volt*
I_{sc} *Short circuit current* .....*Amp*
I_L *Load current* .....*Amp*

T_{foN} *Outlet fluid i.e air temperature of* N^{th}*tile*..... ^0C
T_{fi} *Inlet fluid i.e air temperature* ..... ^0C
T_a *Ambient temperature* ..... ^0C

Subscript
n *number of MCSCT tile*
f *Fluid*
c *solar cell*
o *outlet*

Greek letter
η_e *Electrical efficiency*
η_{th} *Thermal efficiency*

1. Introduction

Photovoltaic technology (PV) is commonly known as one of the promising renewable energy technologies. It is well known fact that electrical efficiency falls as the temperature of the photovoltaic cells rises. The efficiency of the system falls about 0.0045 when cells temperature increased by 1°C [1]. The generation of both thermal and electrical energy simultaneously is known as hybrid photovoltaic thermal technology (PVT). Solar hybrid PVT system can generate more energy per unit area compared to the system of solar panel and thermal collector separately side by side [2]. Sopian et al. [3] and Prakash[4] have analyzed single pass solar collector with open channel absorber. The double pass solar collector with upper and lower channels has been fabricated by Garg et al. [5] and cox et al. [6]. Erdil et al. [7] fabricated a hybrid system consisting of a PV module and a solar thermal collector and tested it for energy collection in Cyprus. They found out that the ratio of gain to losses for

thermal energy is 50 times the electrical energy, which was measured between the periods of 12:00 and 16:00 hour.

An experiment to compare the efficiency of an integrated photovoltaic thermal solar (IPVTS) system with conventional solar water heater was carried out by Huang et al.[8]. Tonui and Tripanagnostopoulos [9] reported a cheap and simple method to cool the photovoltaic thermal (PVT) system. Sopian et al. [10] developed and tested a double pass PVT solar collector, which is suitable for solar drying purposes. Design, development and performance monitoring of a photovoltaic-thermal (PVT) air collector has been studied by Niccolo et al. [11] and they found that the simulation model, developed under this program predicts quite well the thermal and electrical performance of a PVT collector. The model, in general, can be utilized for any set of design and operational parameters for evaluating the performance of front cover direct flow PVT air collector, semitransparent with different solar cell density (i.e. the ratio between the area of the cells and the total laminate surface) or completely opaque (e.g. standard PV laminate like those employed in the experimental campaign presented). The relations between energy and exergy, energy and sustainable development, energy policy making, exergy and the environment and exergy in detail are reported by Dincer [12]. Energy and exergy analysis of hybrid micro-channel photovoltaic thermal module has been carried by Agrawal and Tiwari [13] and they concluded that micro-channel photovoltaic thermal module gives better results.

Till now, most researchers have carried out the electrical and thermal performance analysis on PVT system consisting of PV module and a duct. The objective of this study is to develop a micro PVT system known as MCSCT tile and solar simulator for testing of MCSCT tile. The performance evaluation of MCSCT tiles has been carried out on various intensity and constant mass flow rate. Comparative studies have been carried out between single MCSCT tile (case I) and two MCSCT tile connected in series (case II).

2. Experimental setup

Experimental test rig consisting of MCSCT tiles and solar simulator to test the performance of the MCSCT tiles on various operating parameter.

2.1. Micro-channel solar cell thermal tile

The MCSCT tile as shown in Fig. 1a consists of a single solar cell, rated at 2.2 Wp having 0.125m width and 0.125 m length and mounted on a rectangular wooden channel. The channel has a dimension 0.125m in length, 0.125m in width and 0.005m in depth. Small holes are provided at the cross edge of the channel to pass the hot air for utilization and also to connect other the MCSCT tile in series combination. The wooden micro-channel has been sealed with putty and adhesive tape to avoid air leakage. Similarly, another one MCSCT tile are fabricated and connected in series through PVC pipe. MCSCT tile are arranged in such a manner that outlet of first tile is inlet of second .The MCSCT tile have been placed on a mild steel platform with a mechanism for up and down movement for varying the light intensity. A DC fan of 6.0 V and 0.1A has been used for forced mode of operation to make flow the air through the channel of tile.

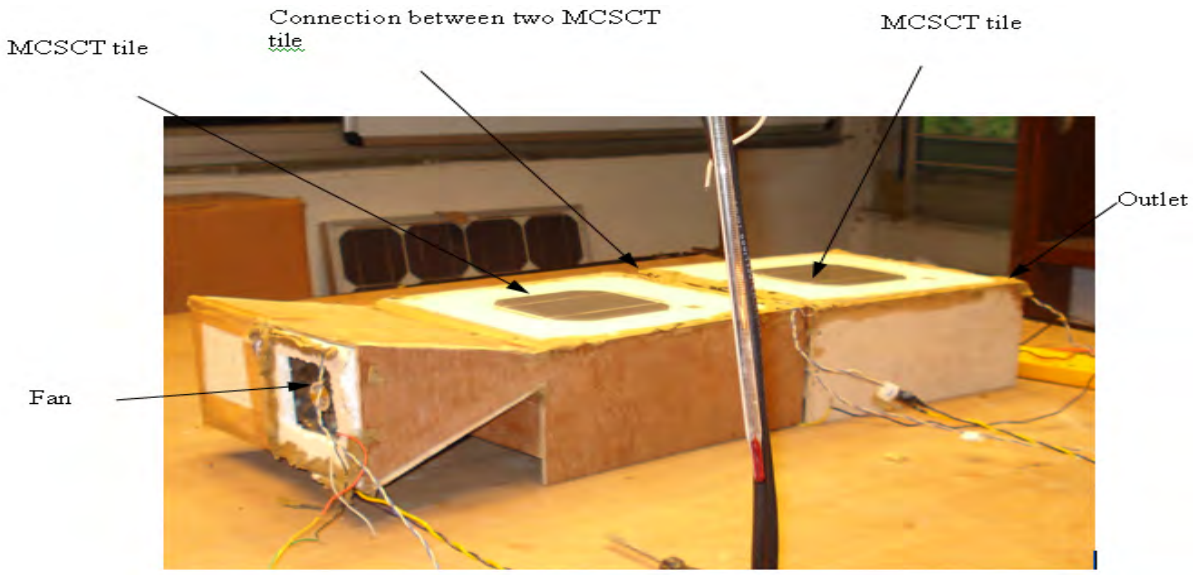

Fig.1a. Photograph of hybrid micro-channel solar cell thermal (MCSCT) tiles

2.2. Solar simulator

A solar simulator (Fig.1b) with a 3-phase lamp array is employed to imitate the necessary solar irradiation in the testing of micro-channel solar cell thermal tile. The solar simulator has 28 tungsten halogen lamps (Philips manufactured; Model: 392472) each having 500W, 9000 lumens and rated at 240V and 11A. The halogen lamps are arranged in 7 × 4 matrices for uniform distribution of irradiance on the MCSCT tile. An exhaust fan has also been provided in the laboratory wall to avoid the overheating of cell by withdrawing the thermal energy associated with it. The available area for testing is 1×2 m .The height of the simulator from the floor is 200 cm. The distance between platform and halogen lamp is 100 cm. Intensity of simulator can be varied between 300 W/m^2 to 1000 W/m^2 by decreasing the gap of halogen lamp and platform.

Fig.1b. Photograph of solar simulator with micro-channel hybrid MCSCT tiles

2.3. Instrumentation

The following instruments have been used during the experimentation:

(i)Thermocouples: A calibrated copper-constantan thermocouples and a digital temperature indicator are used to measure the temperature of several locations, namely, back surface, inlet and outlet air temperature of each collector and final outlet air temperature. Digital temperature indicator has least count of 0.1^{o}C.

(ii) Solarimeter: The intensity of solar radiation is measured by the solarimeter having a least count of 20W/m^2, manufactured by CEL, India Ltd, Sahibabad (UP), India. The solarimeter has been calibrated with the standard pyranometer.

(iii) Anemometer (Lutron-AM4201): It is a conventional instrument used to measure the velocity of flowing air. The least count of the instrument is 0.1 m/s.

(iv) Infrared thermometer: The infrared thermometer is used to measure the top surface temperature of PV module. The least count of the instrument is 0.1^{o}C.

(v) Clamp meter: It is used for measurement of a current and voltage. The least count of the instrument is 0.1A and 0.1V.

3. Methodology

The experiments have been conducted on various intensity namely 600,700 and 800 W/m^2 and maintaining the constant mass flow rate (0.000145 kg/s) to observe the effect of intensity on different performance parameters of single MCSCT tile (case-I) and two MCSCT tile connected in series (case-II). The following mathematical expressions have been used for analysis:

3.1. Electrical efficiency

The electrical efficiency of micro-channel solar cell thermal (MCSCT) tile can be obtained as, Tiwari [14],

$$\eta_{\mathrm{e}} = \frac{FF \times V_{oc} \times I_{sc} - I_L \times V_L}{N \times A_c \times I(t)} \tag{1}$$

where fill factor (FF) is a measure of sharpness of the *I-V* curve. It indicates how well a junction was made in the cell and how low is the series resistance. It can be lowered by the presence of series resistance and tends to be higher whenever the open circuit voltage is high

.

3.2. Instantaneous thermal efficiency

An instantaneous thermal efficiency of hybrid micro-channel solar cell thermal tile can be obtained as, Tiwari [14] and Duffie and Beckman [15] ,

$$\eta_{th} = \frac{\dot{Q}_{U,N}}{NA_c I(t)} \qquad \text{where } \dot{Q}_{U,N} = \dot{m}_f C_f \left(T_{foN} - T_{fi}\right) \tag{2}$$

3.3. Over all thermal energy

The energy analysis is based on the first law of thermodynamics, and the expression for overall thermal gain can be defined as,

$$\sum \dot{Q}_{u,overall} = \sum \dot{Q}_{u,thermal} + \frac{\sum \dot{Q}_{u,electrical}}{\eta_{cpower}} \quad (3)$$

where η_{cpower} is a conversion efficiency of thermal power plant which depends upon quality of coal (η_{cpower} =0.38 for good quality of coal).The range of η_{cpower} is varying between 0.20-0.40. This electrical energy has been converted to equivalent thermal by using electric power generation efficiency conversion factor as 0.20-0.40 for a conventional power plant, Huang et al. [8] and it depends on quality of coal. Usual value of this factor is taken as 0.38 for conversion

3.4. Overall exergy

The exergy analysis is based on the second law of thermodynamics, which includes accounting the total exergy inflow, exergy outflow and exergy destructed from the system.

$$\dot{E}x_{overall} = \dot{E}x_{thermal} + \dot{E}x_{electrical} \quad (4)$$

Where $\dot{E}x_{thermal} = \dot{Q}_{U,N}\left[1 - \frac{T_a + 273}{T_{fo} + 273}\right]$ and $\dot{E}x_{electrical} = \left[\frac{\eta \times A_c \times I(t)}{1000}\right]$

4. Results and discussions

In a series of experiments conducted, data have been recorded at different intensity for comparative evaluation for case-I and case-II. The experimental results of outlet air temperatures for both configurations (case-I and case –II) at various intensities 600 W/m^{2,} 700 W/m^2 and 800 W/m^2 have been shown in Fig. 2. It has been observed that outlet air temperature of case-II is higher as compared to case-I at same intensity and constant mass flow rate (0.000145 kg/s) and T_{fi} =38 ^{0}C. The Effect of intensity on outlet air temperatures of MCSCT tiles has also been shown in Fig. 2. One can be concluded that as intensity increases, the outlet air temperature increases for case-I. Similarly trends have also been observed for case-II. It has also been observed that as there is increase in duration of time, outlet air temperature is increased and approaches the steady state condition after approximately two hours. The maximum outlet air temperature of 90^0 C and 89^0 C on intensity of 800 W/m^2 have been observed for series combination and single MCSCT tiles respectively.

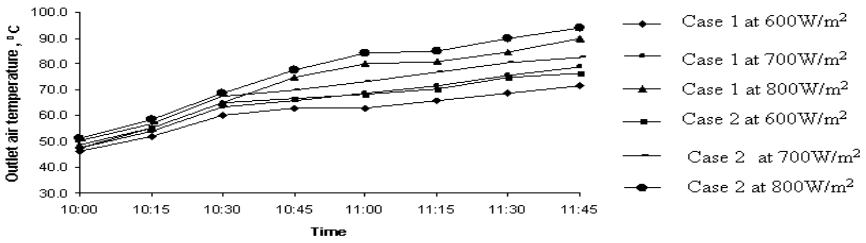

Fig. 2 . Variation of outlet air temperature at various intensity

Fig. 3 shows the time variation of solar cell temperature at different intensities 600 W/m^{2,} 700 W/m^2 and 800 W/m^2 for both cases. It can be seen that solar cell temperature of case-II is

significantly higher than case-I at lower intensity (600 W/m^2) but at higher intensity (700 and 800 W/m^2) the solar cell temperature of both cases are nearly same. It is obviously due to very small heat carrying capacity of air.

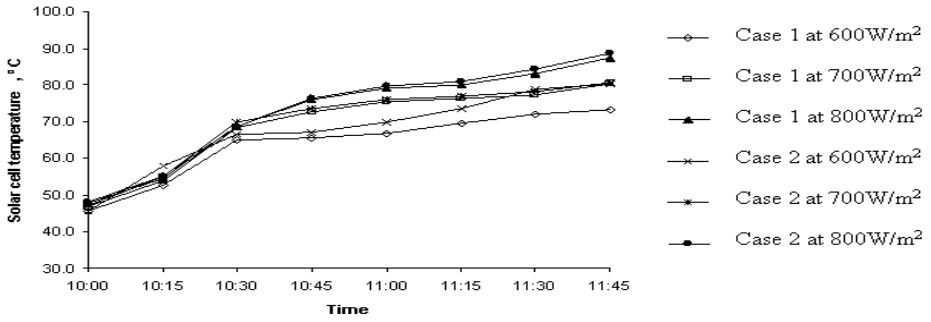

Fig. 3. Variation of solar cell temperature at various intensity

The electrical and thermal efficiency have been calculated with help of Eq. (1) and Eq. (2) for both cases at various intensities. Variations of electrical and thermal efficiency with respect to time have been shown in Fig. 4 and Fig. 5, respectively It has been found that as intensity increases, electrical efficiency decreases because of rise in cell temperature and this result is in accordance with result reported by earlier researchers, Zondag et al.[1]. The electrical efficiency for case-I is higher than case-II at lower intensity due to lower cell temperatures. Electrical efficiency in the range of 13.6 % to 11.7% and 13.6 % to 11.1% has been observed for case-I and case-II respectively. It has been found that as intensity increases, outlet temperature of MCSCT tile also increases and due to increase in outlet temperature , thermal efficiency is increased because inlet temperature T_{fi} =38 ^{0}C is maintained constant.

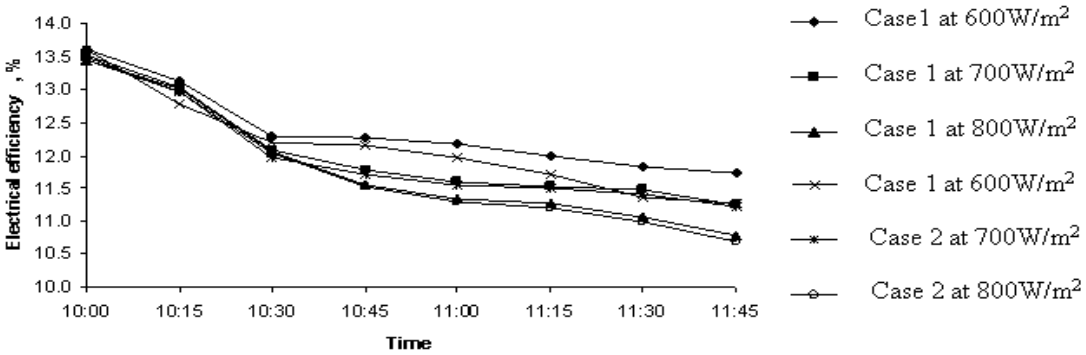

Fig. 4. Variation of electrical efficiency at various intensity

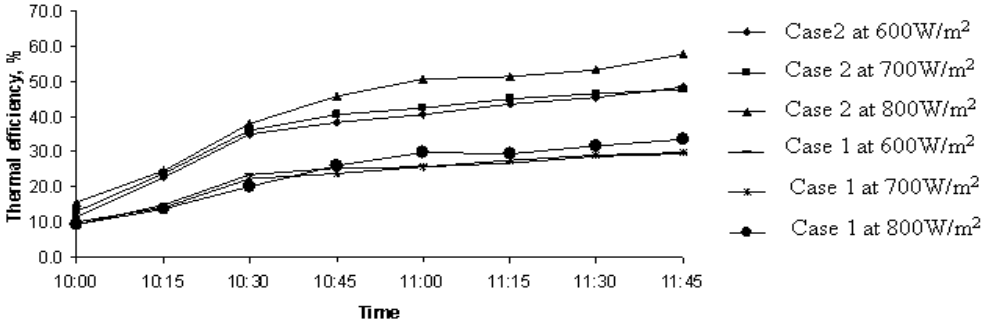

Fig.5. Variation of thermal efficiency at various intensity

Overall thermal energy and overall exergy have been calculated with help of Eq. (3) and Eq. (4) for both cases at various intensities Fig.6 shows that the variation of overall thermal energy at various intensities. It has been observed that increase in intensity will increase the overall thermal energy for MCSCT tiles for both cases and one can also conclude that overall thermal energy of series connected MCSCT tiles (case II) is significantly higher than single MCSCT tile (case I) .Similarly trends has also seen for overall exergy for both case as shown in Fig. 7.

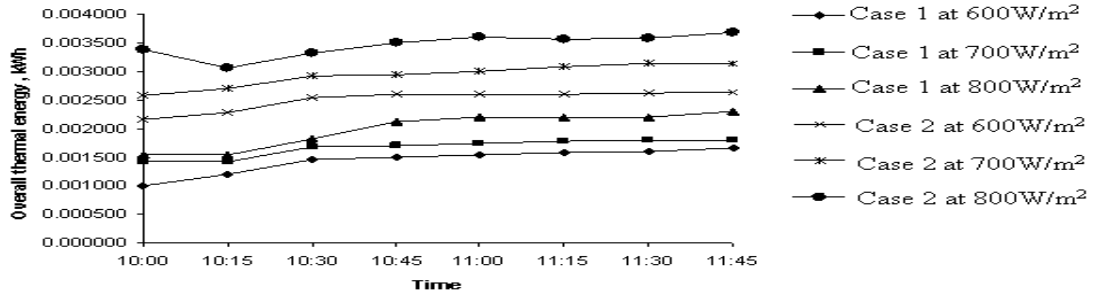

Fig. 6 .Variation of overall thermal energy at various intensity

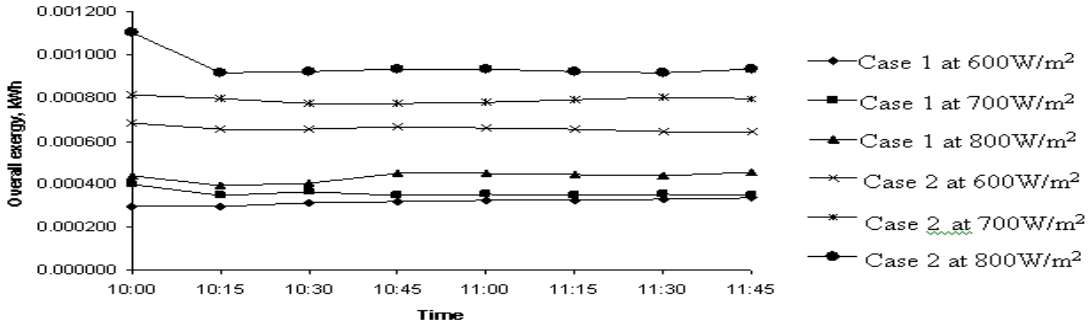

Fig. 7. Variation of overall exergy at various intensity

6. Conclusions

It has been concluded that the average electrical and thermal efficiency of newly designed and fabricated MCSCT tile is 12.4% and 35.7% respectively. This new present setup would have beneficial effect of permitting much less expensive installation for testing of PV tile. Hence the test procedure can be used by manufacturers for testing of different type of PV tiles and combination of PV tiles in order to optimize its products for better efficiency. The Limitations of MCSCT tile are ohmic losses in solar cell, temperature gradient along the thickness of solar cell.

References

[1] H. A. Zondag, D. W. de Vries, W. G. J. van Helden, R. J. C. van Zolingen, A. A. van Steenhoven, The thermal and electrical yield of a PV thermal collector, Solar Energy, 72 (2), 2002, pp.113–128.

[2] P.G. Charalambous, G.G. Maidment, S.A. Kalogirou, K. Yiakoumetti, Photovoltaic Thermal (PVT) collectors: A review, Applied Thermal Energy 27, 2007, pp. 275- 286.

[3] K. Sopian, K.S. Yigit, H. T. Liu, S. Kakac , T. N. Veziroglu, Performance analysis of photovoltaic thermal air heaters, Energy Conversion and Management 37,1996, pp. 1657-1670.

[4] J. Prakash, Transient analysis of photovoltaic thermal solar collectors for cogeneration of electricity and hot air/water, Energy Conversion and Management 35, 1994, pp. 967-972.

[5] H. P Garg, R. K Agarwal, A. K. Bhargava ,Study of a hybrid solar system-solar air heater combined with solar cells, Energy Conversion and Management 31, 1991, pp. 471-479.

[6] C. H. Cox III, P. Raghuraman, Design considerations for flat-plate photovoltaic/thermal collectors, Solar Energy 35, 1985, pp. 237-242.

[7] E. Erdil, M. Ilkan, F . Egelioglu , Renewable energy resources as an alternative to modify the load curve in Northern Cyprus, Energy 33, 2008, pp.1241 -2008.

[8] B. J. Huang, T. H. Lin, W. C. Hung, F S. Sun,Performance evaluation of solar photovoltaic/thermal systems, Solar Energy 70, 2001, pp 443–448.

[9] J. K. Tonui, Y. Tripanagnostopoulos , Air-cooled PVT solar collectors with low-cost performance improvements, Solar Energy 81, 2007,pp. 498–511.

[10] K. Sopian, H. T. Liu, S. Kakac, T. Veziroglu, Performance of a Double Pass Photovoltaic Thermal Solar Collector Suitable for Solar Drying Systems, Energy Conversion and Management 41, 2000, pp. 353 – 365.

[11] Niccolo, C. Giancarlo, V. Francesco, Design, development and performance monitoring of a photovoltaic-thermal (PVT) air collector, Renewable energy 33, 2007,pp. 914-927.

[12] Dincer, The role of exergy in energy policy making, Energy Policy 30, 2002, pp. 137-149.

[13] S. Agrawal, G. N. Tiwari, Energy and exergy analysis of hybrid micro-channel photovoltaic thermal module, Solar Energy, 85, 2011, pp 356-370.

[14] G. N. Tiwari, Solar Energy: Fundamentals, Design, Modeling and Applications. Narosa Publishing House New Delhi, 2004.

[15] J. A. Duffie, W. A. Beckman, Solar Engineering of Thermal Processes, John Wiley and Sons, New York, 1991

Using structured aluminum reflectors in flux scattering on module performance

Joseph Simfukwe *[1], Sylvester Hatwaambo[1], Kabumbwe Hansingo[1]

[1]*University of Zambia, Department of Physics, Box 32379, Lusaka, 10101, Zambia.*
** Corresponding Author: Tel: +260 211 293343, Email: josephsimfukwe@yahoo.com*

Abstract: The current energy production from fossil fuels and nuclear energy has environmental drawbacks. These drawbacks include the creation of nuclear waste, and the pollution associated with fossil fuels which lead to global warming and climate change. It is apparent that an alternative and sustainable source of energy must be found. A potential solution to this problem is solar electricity. Currently, solar panels are expensive and hence un-economical for most buyers**.** The use of solar concentrators creates a potential for less expensive electricity because concentrators raise the amount of incident radiation over a relatively small area of the absorber. The reduction in cost is achieved by reducing the module area and the use of low-cost reflectors. However, specular reflectors cause high concentrated heating and form hot spots on the solar module cells. These hot spots are a result of uneven concentration of radiation. The overall effect is the reduced fill-factor and overall efficiency of the system. In this paper, we report an alternative solution to the problem of non-even illumination by using locally available low-cost semi-diffuse reflector with four different groove orientations scribed on it so as to scatter the radiation flux onto the module. The groove orientations were plain sheet (NG), horizontal grooves (HG), vertical grooves (VG), and the crisscross groove (CG) orientations. Our results show that the locally purchased semi-diffuse aluminium structure can be used as a booster reflector compared with the commercial high specular reflector.

Keywords*: Semi-diffuse, specular, fill-factor, non-even illumination, low-concentration*

1. Introduction

The costs of solar panels compared to the amount of power they produce make their purchase un-economical for most end-users**.** The use of solar concentrators create a potential for producing less expensive electricity by replacing expensive solar cell area with inexpensive optical materials such as plastic refractors or metal reflectors. Currently, mirror-like reflectors (specular materials) are used for solar thermal applications while lenses are used in photovoltaic systems. The use of lenses in photovoltaic (PV) may not reduce the cost of electricity to affordable levels because they are expensive. Highly specular materials have high reflectance and are good in imaging optics for high concentration, whereas semi-diffuse reflectors are preferred in non-imaging optics for flux scattering. The module cost could be reduced if low-cost materials are used to concentrate solar energy flux across a small module area [1,2]. In this paper we address two of the problems faced with concentrating photovoltaic systems namely; non-even illumination and use of expensive lenses and specular materials as reflectors by designing, constructing and evaluating a low concentrator system, using locally available low-cost semi-diffuse aluminium structure reflector with four different groove orientations scribed on it to improve on the fill-factor (FF) of the module for low cost electricity. Fill-factor is an important parameter that tells the overall performance of the solar module. A solar module with a high fill-factor is able to produce high power for a longer period of time. Therefore, by improving the FF of the module we are increasing both the power output and the durability of the module [3].

2. Methodology

2.1. Design and construction of the compound parabolic concentrator (CPC)

We first designed the Compound Parabolic concentrator (CPC) using the standard polar co-ordinate system proposed by Winston [4,5]. The value of *a* which is the half width of the

exit aperture was determined after deciding on the size of the solar module string to be used after which the acceptance half angle θ of the CPC was decided while Φ varied from 5° to 107° in our case. The determined values of a and θ in this case were (a=5cm and θ=15°) which we then used in equations (1) and (2) to generate the X and Y co-ordinates. These co-ordinates were then plotted on the graph paper to design the CPC which was later constructed .Figure 1 shows the CPC designed (a) and the actual constructed Compound Parabolic Concentrator (b) used for the current-voltage (I-V) measurements.

$$x = \frac{2f\sin(\phi - \theta)}{1 - \cos\phi} - a \qquad (1)$$

$$y = \frac{2f\cos(\phi - \theta)}{1 - \cos\phi} \qquad (2)$$

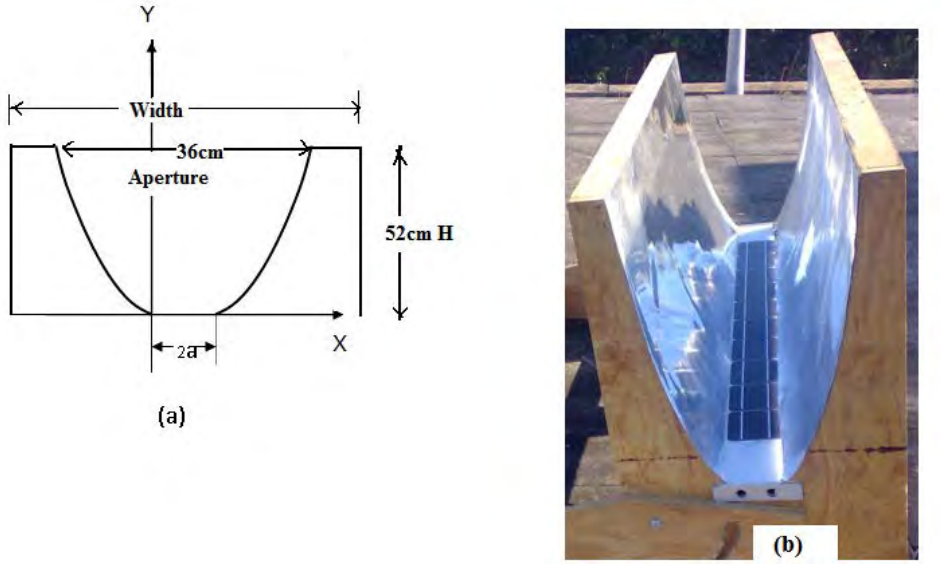

Fig 1. Shows the CPC design from polar co-ordinates into the X-Y co-ordinates system (a) and the actual compound parabolic concentrator constructed (b).

2.2. Spectral reflectance of structured aluminium

An ideal reflector material for solar electricity production should have a relatively high reflectance in visible and ultra violet regions of the solar spectrum and to maintain this relative high reflectance for the entire life of the solar system [6].

In this experiment we used one reflector material (semi-diffuse aluminium structures), but with four different orientations of the grooves namely; plain (NG) (no grooves), horizontal grooves (HG) vertical grooves (VG) and criss-cross groove (CG) orientations as shown in Figure 2. The groove sizes ranged between 2mm to 3mm. Our aim was to determine which of these four orientations was able to provide uniform illumination and a better fill-factor improvement using the named reflector .The optical properties of this reflector material were obtained from the Perkin Elmer spectrophotometer lambda 900. The total integrated

reflectance (TIR) was calculated from equation (3). The TIR gives the overall reflectance of the material the property that shows how much flux the material is able to scatter.

$$R_s = \frac{\sum_{305nm}^{2450nm} R(\lambda).G(\lambda).\Delta\lambda}{\sum_{305nm}^{2450nm} G(\lambda).\Delta\lambda} \qquad (3)$$

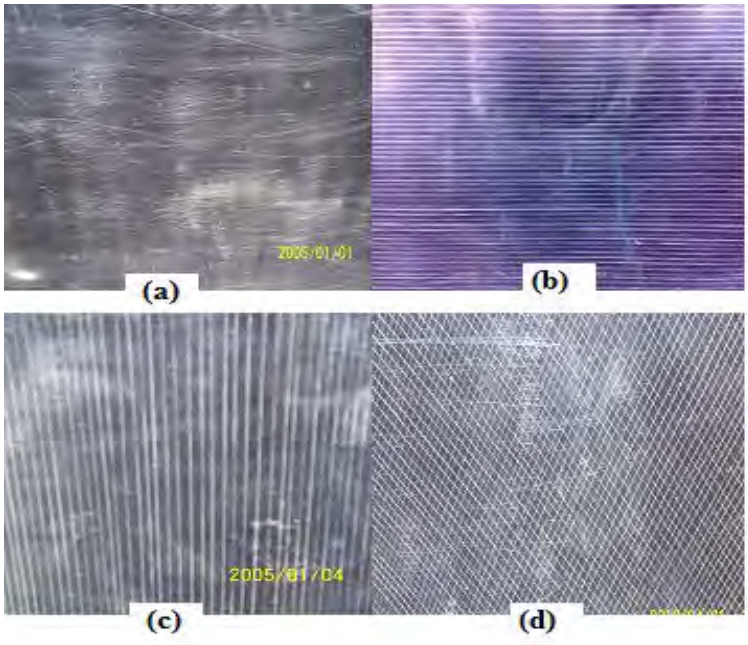

Fig 2. Showing the four different orientations of the grooves on the semi-diffuse structured aluminium:(a) plain sheet (NG) (b) horizontal grooves (HG) (c) vertical grooves (VG) and (d) criss-cross grooves (CG)

2.3. Current-voltage (I-V) curve measurement.

The current and voltage generated by the module under concentration was measured using the current-voltage tracker instrument obtained from Vattenfall, Sweden .The short-circuit current *Isc*, the open-circuit voltage V_{oc}, the power maximum P_m, the maximum current I_m, and the maximum voltage V_m were extracted from each I-V curve. The fill-factor (FF) was evaluated from equation (4).

$$FF = \frac{I_m.V_m}{I_{sc}.V_{oc}} = \frac{P_m}{I_{sc}.V_{oc}}. \qquad (4)$$

3. Results

3.1. Measurement of Total Integrated Reflectance(TIR)

Table 1 shows that the plain sheet (NG) was a better reflector with TIR of 89% followed by the criss-cross grooves (CG) orientations with 88%, the horizontal grooves (HG) orientation was the third best with 85% while the vertical orientations of the grooves on the aluminium structure was the least with 82%, as measured by the integrating sphere in the lab.

Orientation	Total Integrated Reflectance (TIR)
NG	89%
HG	85%
VG	82%
CG	88%

3.2. Fill-factor comparison at 0° (normal)

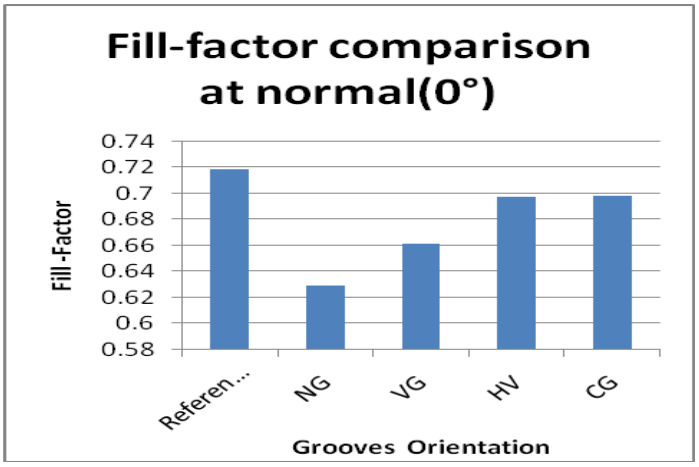

Fig.3 Fill-factor comparison at 0°

The results for the fill-factor comparison revealed that the criss-cross grooves (CG) gave the highest fill-factor followed by the horizontal grooves (HG) and then the vertical grooves (VG). The plain sheet had the least fill-factor. The results also shows that the drop in the fill-factor from the reference for the criss-cross grooves and the horizontal grooves orientations was about 3%, while that of the vertical grooves (VG) and the plain sheet was 8% and 12% respectively. The better results of fill-factor for the criss-cross grooves and the horizontal grooves can be attributed to the fact that, the orientation of the grooves in this manner provided evenly scattering of the solar flux on the module thereby reducing the hot spot formation and causing an even distribution of current within the solar cell . On the other hand, the reduced fill-factor for the plain sheet and the vertical grooves can be expalined in terms of the non-uniform irradiance leading to non even distribution of current within the solar cell. This causes hot-spot formation that leads to the overall degradation of the module.

3.3. Power comparison at 0° (normal)

Figure 4 shows the comparison of power at 0º with VG and NG giving the highest power output, but these are a result of high currents which cause hot spots and an overall reduction in the performance of the module. Hot-spot heating occurs when a large number of series connected cells cause a large reverse bias across the shaded cell, leading to large dissipation of power in the poor cell. Essentially the entire generating capacity of all the good cells is dissipated in the poor cell. The enormous power dissipation occurring in a small area results in local overheating, or "hot-spots", which in turn leads to destructive effects, such as cell or glass cracking, melting of solder or degradation of the solar cell[3].

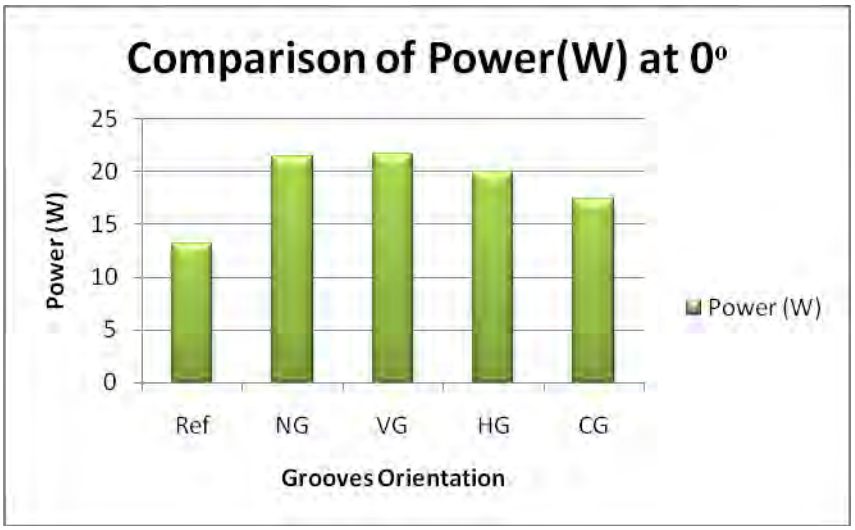

Fig. 4 bar charts showing comparison of the power for the four different grooves orientations and the reference (Ref) (without concentration).

4. Discussion and Conclusions

The performance of the CPC constructed using the locally available materials has been analysed and the results show that the locally purchased semi-diffuse aluminium structure can be used as a booster reflector in low cost photovoltaic system. The results also show that the criss-cross groove and the horizontal groove orientations were found to be the best orientations for the fill-factor improvement since they had only a 3% drop in fill-factor from the reference. The two orientations were able to scatter the solar flux evenly across the solar cell module. It is the even scattering that causes uniform distibution of currents within the solar cell thus reducing the hot spot formation. However, between the two orientations we would recommend the horizontal grooves(HG) because it is less costly when making the grooves but it gives a better fill-factor as much as that of the criss-cross grooves. The horizontal grooves also gave a higher power increase of 52% compared to 33% for the criss-cross grooves.

Acknowledgements

My deep and heartfelt appreciation to my supervisors:

Dr. Sylvester Hatwaambo and **Dr. Kabumbwe Hansingo** under whose guidance, patience, and genuine criticism, this work was successfully done. I am also indebted to the Solar Energy Materials (SEM) Project in the Department of Physics at the University of Zambia (UNZA) in conjunction with the International Science Programme (**ISP**) of the Uppsala

University in Sweden for granting me a scholarship. Many thanks to **Dr.H.V. Mweene,** The Head of Physics Department for taking care of our welfare.

References

[1] S. Hatwaambo et al, "Angular Characterization of low concentrating PV-CPC Using low cow-cost reflectors," Solar Energy Materials & Solar Cells Vol. 92,1347-1351.(Elsevier, 2008).

[2] S. Hatwaambo, H.Hakansson, A.Roos and B. Karlson ,Mitigating the non-uniform illumination in low concentrating CPCs using strctured reflectors," Solar Energy Materials & Solar Cells Vol. 93,202-2024 (Elsevier, 2009).

[3] http://pvcdrom.pveducation.org/MODULE/Hotspot.htm

[4] W. T. Welford and R. Winston, High Collection Non-imaging Optics,(Academic Press,1989).

[5] R .Winston, J. C. Miñano and P.Benitez , Non-imaging Optics,(Elsevier Academic Press,2005).

[6] Brogren, M., "Optical Efficiency of Low –Concentrating Solar Energy Systems with Parabolic Reflectors," (PhD. Thesis, Uppsala University, Sweden, 2004).

Semi-Virtual laboratory design for photovoltaic generator characterization performance

Hocine Belmili[1,*], Mourad Haddadi[2, **], Salah Med Aitcheikh[2], Ahmed Chikouche[1]

[1]*Group of research: Photovoltaic system, Unit of Development of Solar Equipments (UDSE) National road N°: 11 Bou-Ismaïl LP 365, Tipaza 42415, Algiers,*
[2]*Laboratory of communication devices and photovoltaic conversion (LCDPVC), Polytechnic National School, 10 Avenue Hacen Badi El Harrach Algiers,*
**belmilih@yahoo.fr , **mourad_haddadi@yahoo.fr*

Abstract: This paper present a study of the photovoltaic generator (PVG) performance. It basing on comparison between characterizations obtained in real time test and simulated ones using mathematical models. This study is evaluated by the design of a semi-virtual laboratory, which is composed on a hardware support based on the developed data acquisition system in real operating conditions and a software support based on mathematical models descriptions. T his laboratory permits to identify PVG parameters using correlation between measurements and simulated characteristics.

Keywords: *Simulation, photovoltaic generator, characterization, performance, hardware, software.*

1. Introduction

PVG or PV modules in general are formed by a co mbination of parallel and series connections of solar cells. The electrical characteristics of PV modules are rated at standard irradiance and temperature conditions. The standard conditions are AM1.5 spectrum, 1000 W/m2 at 25°C cell temperature, for terrestrial applications, whereas for the extraterrestrial standard conditions it is AM0 (1353 W/m2) at 25°C[1]. Therefore the user knows only the electrical parameters nominal values of the PV module, which may be different from the values during the operating conditions. The variation of the characteristics from one set of conditions to another is a problem faced by designers and users, who want to know the outputs of a PV installation in real conditions rather than those given by the manufacturer in standard conditions [2]. Several environmental factors act to influence the performance of photovoltaic devices such as the temperature, the solar angle of incidence, the total irradiance level, the irradiance spectrum and optical effects due to shading. Numerous performance analysis studies have been carried out to assess the magnitudes of these effects, yet there is still some debate about the relative importance of each factor. Due to strong correlations between each environmental driver, their separation for quantification has proved a major challenge that has not yet been met conclusively [3]. Figure 1 represents the block diagram of the semi-virtual laboratory design.

2. PVG model description

There are several description models for PVG. Some themes are analytical models; the other ones are empirical and semi-empirical model. In this context we present two PVG model descriptions. The first one is an analytical model basing on one-diode model and the second one is an empirical model which is developed by Sandia Laboratory.

2.1. One-diode PVG model

One-diode model of PVG is presented as an electrical circuit as showing the figure 2.

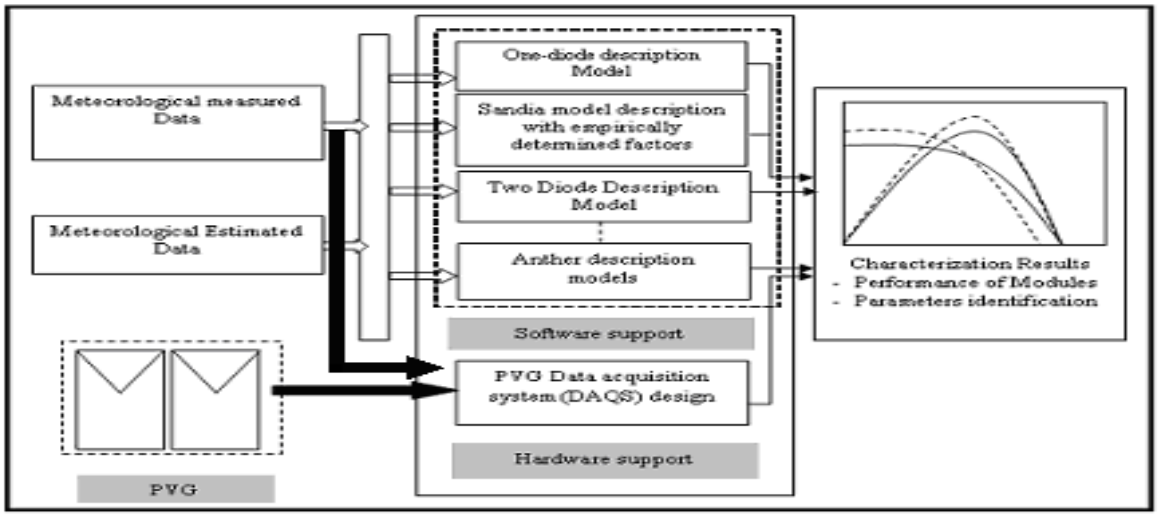

Fig.1: Semi-virtual laboratory design for PVG characterization performance.

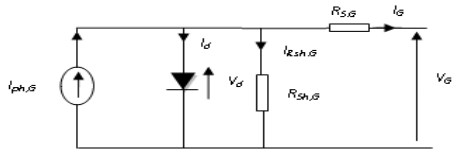

Fig. 2: one-diode equivalent circuit model.

At a fixed temperature and solar irradiation, the I-V curve of this circuit is given by equation:

$$I_G = I_{ph,G} - I_s\left[\exp\left(\frac{q\left(V_G + R_{S,G}\cdot I_G\right)}{n\ n_s kT}\right) - 1\right] - \frac{V_G + R_{S,G}\cdot I_G}{R_{Sh,G}} \qquad (1)$$

The parameters for this model, described elsewhere [4], can be found by either numerical or analytical methods. It has been shown that the circuit parameters I_{ph}, R_{sh}, R_s, I_s and the diode ideality factor 'n' at a particular temperature and irradiation can be computed from the V_{oc}, I_{sc}, V_m, I_m, R_{so} and R_{sho} values measured from the I-V characteristic. Several researchers have either investigated or developed numerical algorithms to determine the solar cells parameters by fitting measured I-V curves [5]. The difficulty to obtain the PV parameters, from the measured I-V curves, resides in the implementation of complex computer algorithms since the estimation of these parameters, somehow, are restricted to specific research laboratories as those studying fundamental physics device. However, analytical methods can be used as a design tool to derive the parameters from the basic data given by PV module manufacturers, or other readily available data. Under Simulink we present this model as following

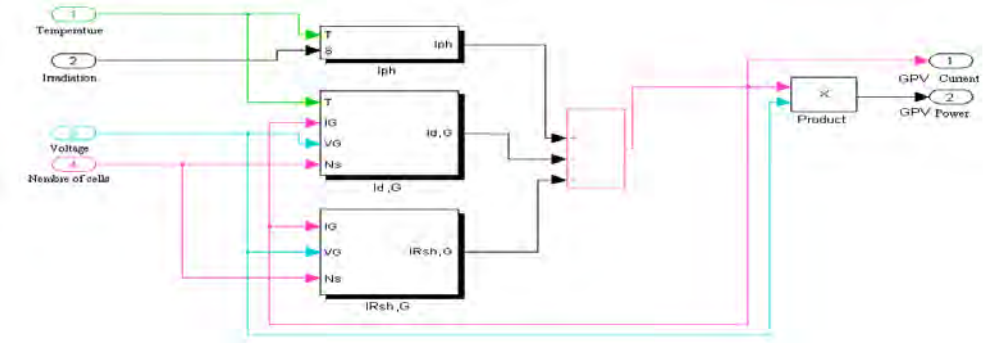

Fig.3: One-diode PVG model simulation under Simulink.

2.2. SNL model description

SNL (Sandia National Laboratory) performance model is an empirically based method. It achieves its versatility and accuracy from the fact that individual equations used in the model are derived from individual solar cell characteristics. The versatility and accuracy of the model has been demonstrated for different photovoltaic and concentrator modules, as well as for large arrays of modules. This model takes account of electrical, thermal, solar spectral and optical effects for photovoltaic modules [6]. The performance modeling approach has been well validated through extensive outdoor module testing, and through inter-comparison studies with other laboratories and testing organizations [7]. Recently, the performance model has also demonstrated its value during the experimental performance optimization of off-grid photovoltaic systems [8]. The following equations define the model used by the Solar Technologies Department at Sandia for the analysis and the modelling of the photovoltaic modules performances. The equations describe the electrical performances for individual photovoltaic cells, modules, and arrays. The solar resource and weather data required by the model can be obtained from tabulated databases [9] or from direct measurements.

$$\begin{cases} I_{sc}(E,T_c,AM_a,AOI)=(\dfrac{E}{E_0})\,f_1(AM_a).f_2(AOI)\{1+\alpha_{Isc}.(T_c-T_0)\} \\ Ee=I(E,T_c=T_0,AM_a,AOI)/I_{sc0} \\ V_{oc}(E_e,T_c)=V_{oc0}+C_3.\ln(E_e)+\beta_{V_{oc}}.(T_c-T \\ V_{mp}(E_e,T_c)=V_{mp0}+C_4.\ln(E_e)+C_5.\{\ln(E_e)\}^2+\beta_{V_{mp}}.(T_c-T_0) \\ I_m(E_{ea},T_c)=C_1+Ee\{C_2+\alpha_{I_{mp}}.(T_c-T_0)\} \\ P_{mp}=I_{mp}.V_{mp} \\ FF=P_{mp}/(I_{sc}.V_{oc}) \end{cases} \quad (2)$$

The following figure represents Simulink simulation of this model.

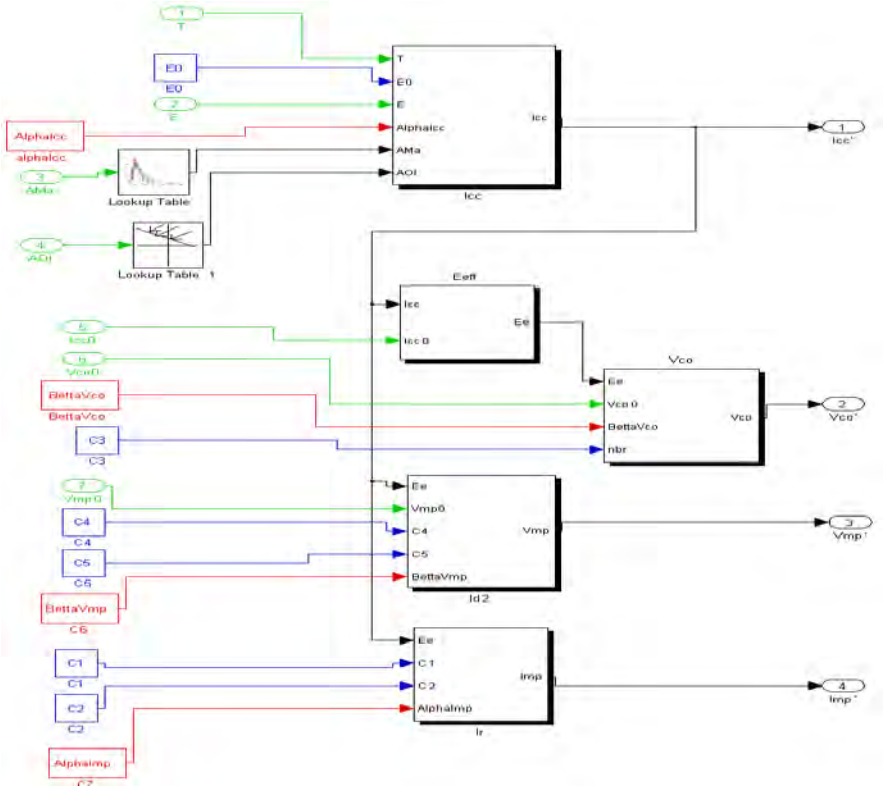

Fig.4: Sandia PVG model simulation under Simulink.

3. Hardware design and development of a real-time PVG characterizer

The Hardware part is based on a development of a data acquisition system for real time PVG characterization. T he data acquisition system (DAQS) is an important part of the experimental setup. A good experiment can be completely ruined if the data is not collected with the necessary precision and repetition. Figure 5, s hows the block diagram of the developed system. The DAQS is linked to a graphical user interface. The developed hardware parts basic element is the electronic load [10]. This electronic load can characterize an array of one or two solar modules connected in serial or in parallel, protected with a by-pass diode. Figure 5 show the block diagram of the developed hardware PVG testing unit.

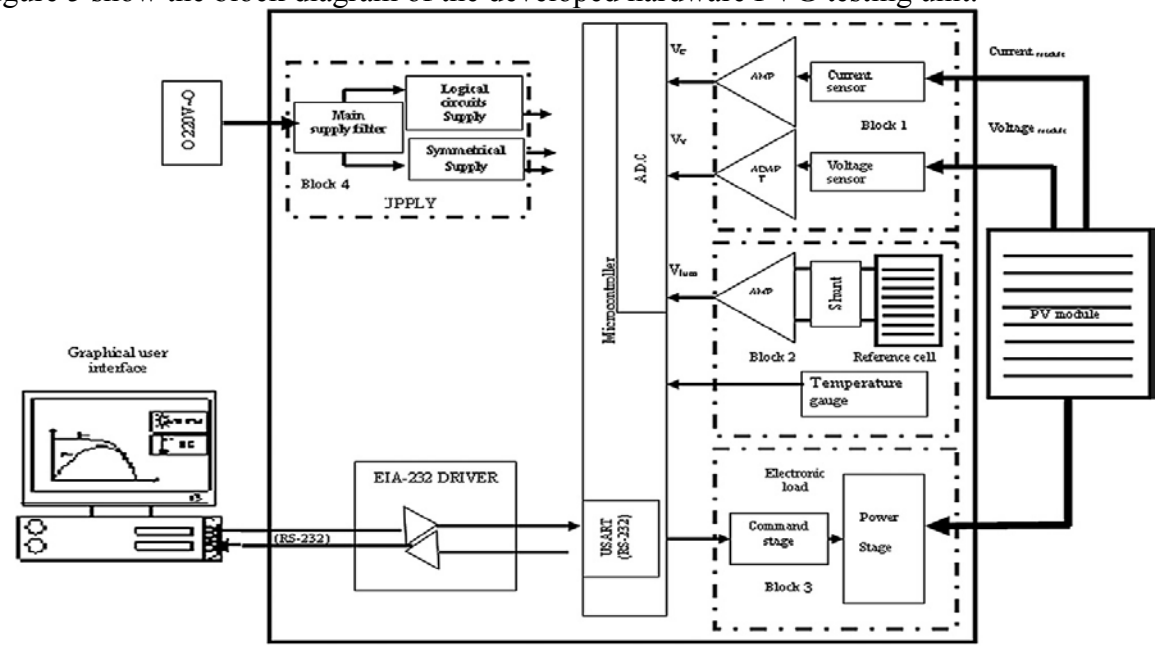

Fig.5: Block diagram of PVG testing unit.

4. Software design

The software has been developed using Object-Oriented Programming (O.O.P) under windows. This software based on t he development of a three principal programs (figure 6). The first one to estimate irradiation on PVG captor, the second to extract PVG parameters from manufactures data sheet and from other temperature and irradiation inputs and the third one we permits to identify PVG parameters using correlation between measured and estimate characteristics.

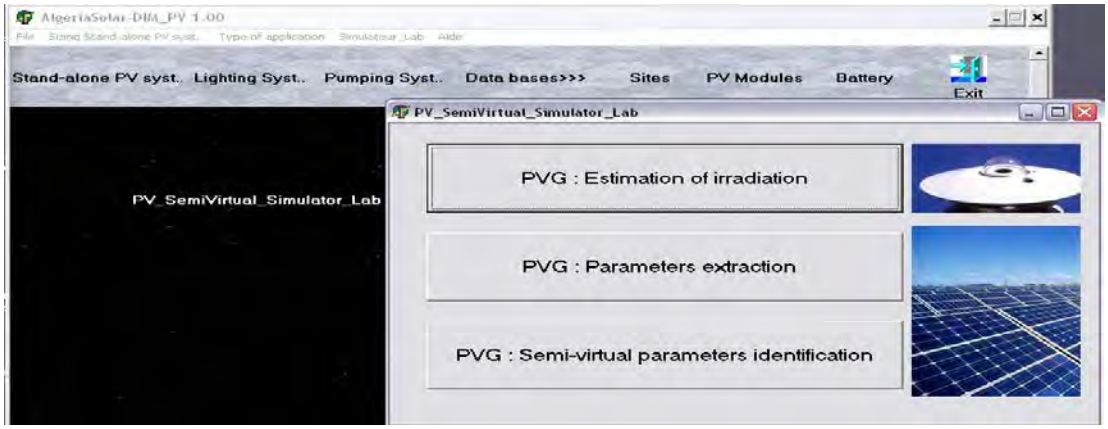

Fig. 6: software design.

4.1. Estimated irradiation program

In this context the developed software is based on a specific algorithm for irradiation simulation [11]. Figure 7 represent the input data window of the developed software for the daily and annual estimation irradiation for different locations. In the present window, sites are identified by the geographical location (latitude, longitude and altitude). With this program, we simulate global horizontal and inclined irradiation. The Albedo represents the diffusion coefficient. Its value belongs to [0.1, 0.9]. The user introduces the year day number and the angle of incidence (AOI) of the irradiation on the module. This software has a data base of different sites in the word. The user can introduce other sites, not configured in the data base, by introducing its geographical location. He, then, can estimate the global and inclined, daily and annual irradiation of the introduced site. The daily sunshine duration is also calculated when the user start execution of daily irradiation simulation.

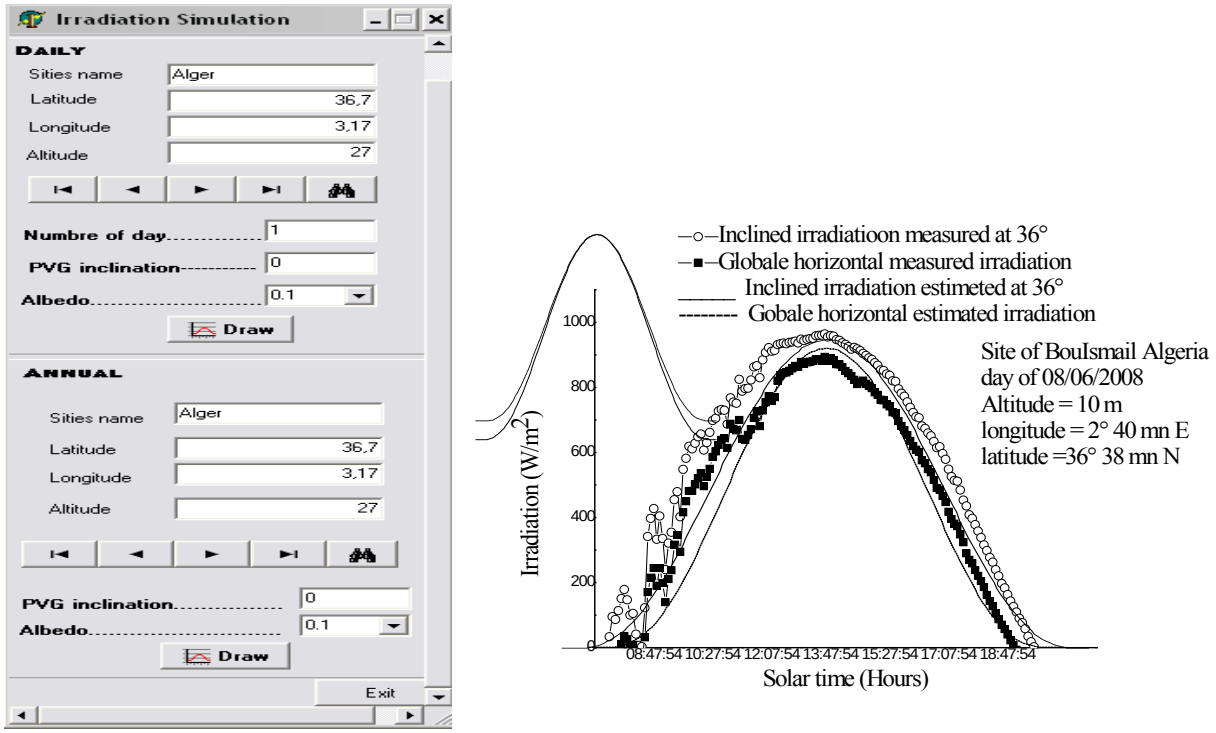

(a) *(b)*

Fig. 7: (a) Inputs data (latitude, longitude and altitude) window for daily and yearly irradiation simulation for sites characterization, (b) Measured and estimated irradiation comparison results.

4.2. Developed software for PVG Parameter extraction

Figure 8 shows the input/output data window for the PVG characterisation under STC conditions and under measured irradiation and temperature conditions. This software disposes of a user-friendly PV modules database for different manufacturers. Using one-diode description model for PV module, this program can identifying the five parameters models: ideal factor, serial resistance, shunt resistance, saturation current and photocurrent. The modules in the database are identified by the manufacturer reference and by their STC condition characteristics: Isc, Voc, Im, Vm and Pm. Besides, thru this software, we can add in the database other commercial modules and carry out their characterization, figure 8.

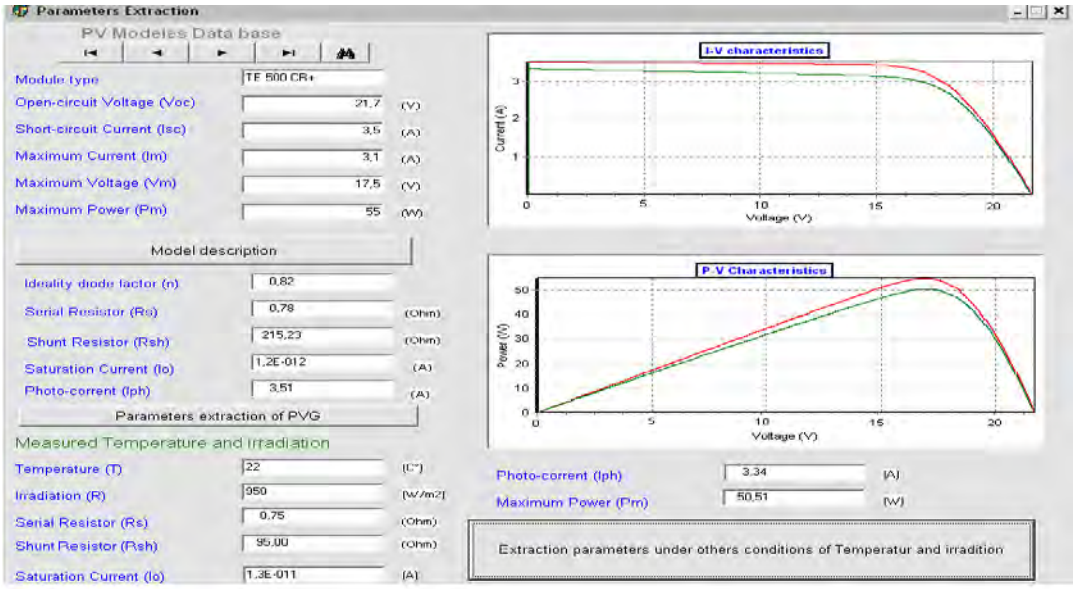

Fig.8: PVG parameter extraction from manufacture data in STC and from authors temperature and irradiation values.

4.3. PVG parameter identification platform using correlation with measured characteristics

After developing the data acquisition system for PVG characteristics measurements, we are very interested by the developing of software which permits the identification of PVG parameters in correlation with the measurements characteristics. The identification algorithm is based on the calculation of the correlation factor named "R^2" between measurements and simulated characteristics. This coefficient is given by the equation number (3).

$$R^2 = 1 - \frac{\sum \left(X_{\exp} - X_{sim} \right)^2}{\sum \left(X_{\exp} - \overline{X_{\exp}} \right)^2} \qquad (3)$$

The following figure shows this software. This software permits also the identification of the current and voltage coefficients of temperature.

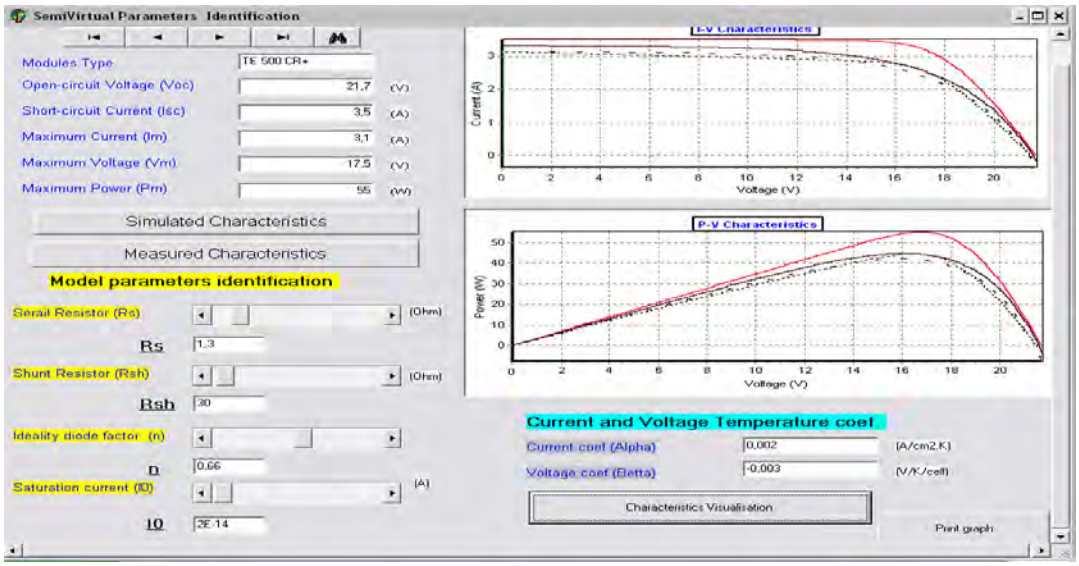

Fig.9: Software of PVG parameters identification using correlation between measurement and simulated characteristics.

5. Example for commercial PVG characterization

This example is study the PV commercial module "TE500CR+". It is multi-crystalline technology [12]. The following figure, shows the I-V and P-V characteristics for the SNL, one diode model and experimental measurement at T = 20°C, Ir=820W/m^2 and Ws= 3.5 m/s.

Table 2: Results of TE 500 CR+ module characterization

Manufactures results (STC conditions)		Isc(A)		Voc (V)		Pm (W)		Im (A)		Vm (V)	
		3,50		21.70		55		3,10		17,50	
Real Meteorological data measurement	Model used	Isc	E_{Isc} (%)	Voc	E_{Voc} (%)	Pm	E_{Pm} (%)	Im	E_{Im} (%)	Vm	E_{Vm} (%)
T = 20°C Ir=820W/m^2 *Ws= 3.5 m/s*	Measured results	3.406		19.463		46.64		2.88		14.78	
	RMSE	Measured results/ One diode model prediction								0,69	
		Measured results/ Sandia model approximation prediction								0.63	
FF	Manufactures results (STC conditions)									0.72	
	Measured results									0.64	
	One diode model prediction									0.70	
	Sandia approximation model prediction									0.67	

One-diode PVG model parameters identification										
TE 500CR+ module	Model parameters identification using correlation with measured values with R^2= 0,98					Model parameters extracted using manufactures data				
	I_{ph} (A)	I_0(A)	R_s(Ω)	R_{sh} (Ω)	n	I_{ph}(A	I_0(A)	R_s(Ω)	R_{sh}(Ω)	n
	3.10	2e-14	1,3	30	0.66	3.51	1.2e-12	0.78	215,23	0.82

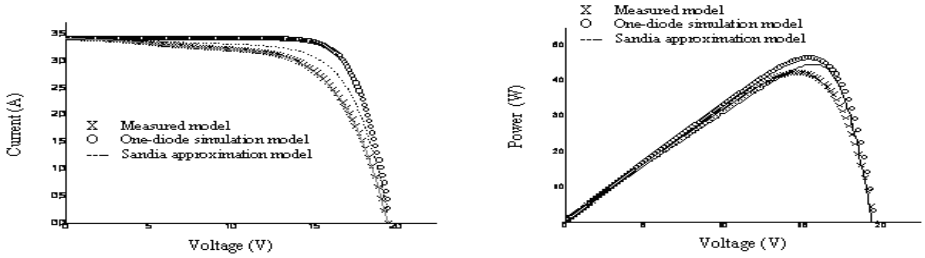

Fig.10: I-V and P-V TE500CR+ module characteristics comparison between Sandia approximations, One-diode estimated model and experimental results.

6. Conclusion

This work described the functioning of the designed semi-virtual laboratory for PVG performance characterization methodology. This laboratory based on the comparison between the predicted models results and experimental ones. I-V and P-V, characteristics are obtained and compared, in one hand. In the other hand the PVG parameters are obtained using predict models and experimental results for real and estimated meteorological data. The present example for measurement and modeling applied for the TE500CR+ modules can be used for characterized different PV commercial modules. The final objectives is to duplicated this results and choose modules gives good response when they are introducing in the PV installation and gives either a best installation dimensioning. In perspectives of this research is to introduce other PVG models in this semi-virtual laboratory and its compared with the studied ones

References

[1] Test Method for Photovoltaic Module Power Rating, FSEC Standard 202-05, Research institute of the university of central Florida, May 2005

[2] David L. King, William E. Boyson and al, "Application and Validation of a New PV Performance Characterization Method", 26th IEEE Photovoltaic Specialists Conference, September 29 October 3, 1997, Anaheim, California.

[3] W. Durisch ,J. Urban and G. Smestad, "Characterisation of solar cells and modules under actual operating conditions" California 93955-8001, California, U.S.A. WREC 1996

[4] Ali Nacer celik and Nasir Acikgoz, "Modeling and experimental verification of the operating current of mono-crystalline photovoltaic modules using four and five parameter models", Elsevier, Applied energy pp 84 (2007)1-15.

[5] D. S. H. Chan, J. R. Philips and J. C. H. Phang, "A comparative study of extraction methods for solar cell model parameters", Solid-State Electronics Vol. 29, No. 3. pp. 329-337, 1986.

[6] D. L. King et al, Photovoltaic system performance characterization methodologies, NREL/CD-520-33586, 543-546.

[7] A. Hunter Fanney, and al, «Comparison of Photovoltaic Module Performance Measurements". 152 / Vol. 128, MAY 2006 Copyright © 2006by ASME Transactions of the ASME

[8] D.L. King, J.A. Kratochvil, W.E. Boyson, and W.I. Bower, "Field experience with a new performance characterization procedure for photovoltaic arrays" , 2nd World Conference and Exhibition on Photovoltaic Solar Energy Conversion, 6-10 July 1998, Vienna, Austria.

[9] http://www.sandia.gov/pv/

[10] Hocine Belmili, Salah Med Aitcheikh, Mourad Haddadi, Cherif Larbas "Design and development of a data acquisition system for photovoltaic modules characterization" Elsevier Renewable energy 35(2010)1484-1492.

[11] Piedallu, C. and Gégout, J.C. "Multiscale computation of solar radiation for predictive vegetation Modeling". Annals of Forest Science, 64: 899-909. 2007.

[12] TE 500 CR+ Modules. www.total-energie.com.

Two Phase Change Material with Different Closed Shape Fins in Building Integrated Photovoltaic System Temperature Regulation

M. J. Huang[1,*]

[1] *University of Ulster, Newtownabbey, Co. Antrim, N. Ireland, UK*
** Corresponding author. Tel: +44 28 90366037, E-mail: m.huang@ulster.ac.uk*

Abstract: Photovoltaics (PVs) operate at around 40°C above ambient temperature in full sun. On a cold day in Europe the cell temperature will be at 30°C and compared to a summer temperature of up to 80°C. As each ten temperature increases the efficiency of the crystal silicon photovoltaic will reduce 10%. So considering the whole year, running at 25°C for Building Integrated Photovoltaic (BIPV) will be an ideal temperature target to achieve in order to keep PV cells at their peak efficiency in Europe. Passive heat removal technique was applied for thermal regulation of PV using Phase Change Material (PCM) integrated on the back of the PV. The temperature in PV can be effective regulated, but the low thermal conductivity of the PCMs is one of the main problems for this application. This paper details the results of a theoretical investigation and analysis of PV temperature control and solar thermal energy storage achieved using phase change materials with different types of fins, structure and PCMs. The predicted performance provides an insight into the effects of using various quantities of different PCM materials with different types of fins and thermal storage for selected ambient conditions of temperature and insolation. From this parametric study, optimum arrangements of the PV/PCM system with different type of fins are proposed, thereby improving the efficiency of the PV/PCM system.

Keywords: *phase change materials, Photovoltaic and Building Integrated Photovoltaics*

Nomenclature

C *Specific heat capacity* ..... $Jkg^{-1}K^{-1}$
E *Thermal energy* ..... Jkg^{-1}
H *Heat transfer coefficient* $Wm^{-2}K^{-1}$
H *Latent thermal energy*..... Jkg^{-1}
I_T *Insolation incident on photovoltaic cell* Wm^{-2}
K *Thermal conductivity* ..... $Wm^{-1}K^{-1}$
T *Time* .....
Δt *Time step*.....
T *Temperature* ..... ^oC
ΔT *Transition temperature of PCM* ℃
T_{PV} *PV Temperature* ..... ℃
T_{amb} *Ambient temperature* ..... ℃
T_m *PCM Melt temperature* ..... ℃
U_L *Overall heat loss coefficient,* $Wm^{-2}K^{-1}$
η_c *PV Electrical conversion efficiency*
τ *Transmittance of PV cover*
α *Absorptance of PV*

Subscripts
L *liquid phase*
S *solid phase*

1. Introduction

Building integrated photovoltaic systems (BIPVs) are widely recognised as the most cost effective form of PV power generation [1]. As well as producing electricity, BIPV panels can replace some of the conventional wall cladding and roofing materials, therefore reducing the net costs of the PV system. The elevation of the PV temperature reduces solar to electrical energy conversion efficiency by 0.4-0.5%K^{-1} for crystal silicon PV when it rises above the characteristic power conversion temperature of 25°C [2] [3]. Maintaining the silicon PV's temperature at a low temperature, preferably lower than or around 25°C will retain the maximum conversion efficiency of the PV for practical applications. Active and passive heat dissipations have been studied for decade [4] [5] [6].

PCM can absorb a large amount of energy during the phase change, and is therefore widely investigated for thermal storage. A review on thermal energy storage with phase change materials and application has been carried by Sharma, et al. [7] and Agyemin et. al. [8]. An

investigation of a system which uses PCMs to absorb energy as latent heat at a constant phase transient temperature and to regulate the rise in PV temperature (PV/PCM) has been carried out recently ([6], [9] and [10]). It was found that the PCM thermal conductivity and volume expansion during melting are the main barriers for this application. A series of arrangements with different types of fins inserted inside the PV/PCM system was also carried out experimentally [6]. Although the metal fins inserted inside the PCM can improve the heat transfer inside the PV/PCM system, the thermal regulation period declines as the volume of the PCM is substituted by the metal mass of the PV/PCM system. It was also found that during crystallisation the air cavity formed inside the PCM will increase the thermal resistance when used for temperature regulation during the day time. The further studies using different types of PCMs for the PV/PCM application, including a eutectic mixture of capric-lauric acid (CL), a commercial blend of salt hydrate and paraffin phase change material (SP22), a eutectic mixture of Capric Palmitic acid (CP) and a Calcium Chloride hexa hydrate ($CaCl_2$), have been carried out [11]. Eutectic Mixture of Capric-Palmitic Acid and CaCl2.6H2O with higher thermal conductivities than paraffin wax have a better thermal regulation performance on BIPV for indoor conditions and the outdoor climates of Ireland and Pakistan [11]. Further investigation on the corrosion of the container needs to be conducted.

In this paper an experimental validated numerical simulation model [9] has been modified to suit for two phase change materials for PV/PCM modeling. The thermal regulation of the PV/PCM system in triangular shaped cells and circular shaped cells (which optimise for reducing stress due to PCM expansion) have been studied. A range of different phase transient temperature PCMs under static state and realistic conditions have been discussed in this paper.

2. Methodology

The simulation model used in this work is a two dimensional temperature-based finite volume based conjugated heat transfer numerical model to moderate the temperature rise in BIPVs in a PV/PCM system. This model is based on the previously developed and experimentally validated model for a single PCM with straight fins in the PV/PCM system by the authors [9]. The non-linear transient model uses Boussinesq's approximation and allows convection and diffusion to be simulated. The developed model can be used to predict the transient temperature distribution and fluid flow field within a two-dimensional region in the PV/PCM system for different insolation, ambient temperatures, convective and radiative heat transfer boundary conditions ([9] and [10]). The modified PV/PCM model can be used for multiple PCMs with different transient temperatures and for triangular shaped PCM cells. The following assumptions are made:

(i) The heat conduction in the PV/PCM combined system is two-dimensional and the end sides at the top and bottom are adiabatic.
(ii) The thermal conductivity of the aluminum frame and PCMs in the solid and liquid phases are constant and do not vary with respect to temperature.
(iii) The PCM is homogeneous and isotropic.
(iv) The convection effect in the molten PCM is neglected for the thermal performance comparison, but has been considered for special case.
(v) The interfacial resistances are negligible.
(vi) The specific heat capacity "C_P" value of the PCM is considered as uniform during phase change process, though in actual practice, there is variation in C_P value within the small temperature range.

A brief summarization is as follows.
The energy equation for melt [9]:

$$\rho_L c_L \frac{\partial T}{\partial x} + \frac{\partial}{\partial x}(\rho_L c_L \vec{u} T - k_L \frac{\partial T}{\partial x}) + \frac{\partial}{\partial y}(\rho_L c_L \vec{\upsilon} T - k_L \frac{\partial T}{\partial y}) = 0 \quad (1)$$

The energy equation for solid:

$$\rho_S c_S \frac{\partial T}{\partial t} + \nabla \cdot (k_S \nabla T) = 0 \quad (2)$$

Where the same equations hold good for all the frame and cell wall material and PCMs by incorporating suitable k, ρ, C_p values. The instantaneous continuity of heat flux and temperature at the interfaces of frame and cell with PCMs are preserved.
In the exterior front boundary, where the PV/PCM system is exposed to solar radiation, the boundary condition is,

$$k\frac{\partial T}{\partial x}\bigg|_{x=0} = S + h_0(T_{amb} - T_{x=0})$$

In the exterior back layer of the PV/PCM system $x=L$, the boundary condition is

$$k\frac{\partial T}{\partial x}\bigg|_{x=L} = h_L(T_{x=L} - T_{amb})$$

Where h_0 and h_L are the heat transfer coefficients from the front and back surfaces of the PV/PCM system to the surroundings. S is the heat received by the PV/PCM system on the front surface from the incident solar energy.

Table 1. Thermophysical properties of RT21, RT27, RT31 [13]

	RT21	RT27	RT31	Aluminium
Melting temperature	21	27	29	N/A
Latent heat (kJ kg^{-1})	134	184	169	N/A
Density (kg m^{-3})				
Liquid	760	750	770	N/A
Solid	840	840	890	2675
Thermal conductivity ($Wm^{-1}K^{-1}$)	0.2	0.2	0.2	160
Viscosity ($mm^2 s^{-1}$)	25.71	26.32	28.57	N/A

The most significant thermal characteristics affecting the performance of the PV/PCM system are (a) the PCM heat capacity, (b) the phase transient temperature, (c) the location of the PCM and (d) the mass in the system fins arrangement. In this paper, the PV/PCM system has been designed with small metal cells to hold two types of PCMs considered to enhance heat transfer. The triangular and circular cell shapes are good for directing the bubbles produced during the melting process and thereby dissipates the stress due to the volume expansion which challenges many PCM applications. The schematic of the PV/PCM with metal cells is illustrated in Figure 1. The vertical position is used to mimic building integrated PV. The study here is just concentrated on the building wall integrated PV, the inclined PV systems beyond these limits. The 4 mm aluminium front/ back walls and the 1 mm aluminium alloy fins of the PV/PCM test system provided a high rate of heat transfer to the PCM. The interior dimensions of the containers were 0.132m high by 0.04m depth. The upper and lower ends of the PV/PCM system were assumed adiabatic. The incident energy I_T absorbed by the PV as heat is conducted through the high heat transfer cell wall to the PCM and dissipated from the rear of the PV/PCM system. The different thermal regulation characters of the PCMs can hold PV temperature at lower levels for longer periods. The PCMs that are commercially available

with different phase transient temperatures from 21 to 60°C are combined to regulate the PV temperature rising in the PV/PCM system. Different combinations of the PCMs used to augment the PV/PCM system are analysed for static conditions and realistic diurnal temperature and insolation boundary conditions in the England summer period and the heat transfer and temperature distribution are predicted. The thermal properties of the aluminium alloy and the four PCMs that can be combined into the types of PCMs from RUBITHERM [13] used as input data in the simulations are presented in Table 1.

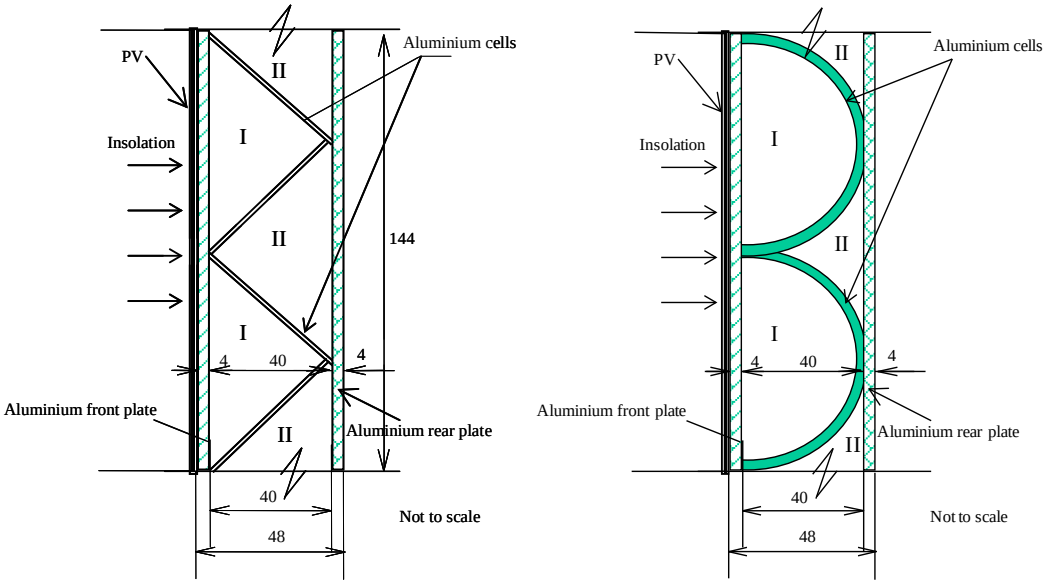

Figure 1. Schematic diagram of PV/PCM system with metal cells for different PCMs

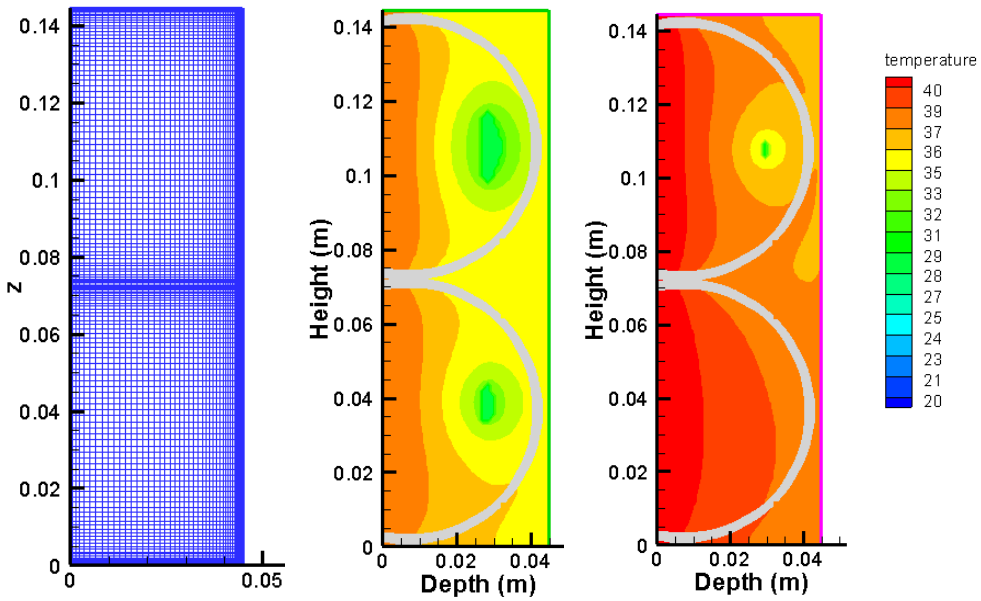

Figure 2. Grid and isotherms of circular cells with two phase change materials in PV/PCM system

The heat transfer coefficients from the front and back surfaces of the PV/PCM system are set at 10 $Wm^{-2}K^{-1}$ and 5 $Wm^{-2}K^{-1}$ (to simulate natural ventilation conditions) and the top and bottom boundaries of the system are assumed to be adiabatic. A fixed grid space of 1mm square for straight fins and variable grid for circular cell fins simulation with finite volumes and a variable time step with a minimum value of 0.0125 s are used for all the simulations. The total number of grid is 144x48 for simulation.

Simulating the behaviour of the PV/PCM system with the two different phase transient temperature PCMs is carried out under the static state and realistic conditions. In real thermal applications it is subject to the cyclic melting and solidification boundary conditions. To predict long-term temperature control, three days are simulated using weather data for the 21st June for the SE of England [14] on the vertical south-east oriented PV/PCM system when the insolation was greater than 120 Wm^{-2}. For the simulations, realistic ambient temperatures and insolation boundary conditions are regarded as invariant over 5 minute intervals. The simulation temperatures within the PV/PCM system are all initially set to the outdoor ambient temperature at 00:00 hr for the transient applied boundary condition.

3. Results and Discussions

In order to evaluate the PV/PCM performance, predictions of the temperature development with the two phase materials, a single PV plate is predicted as a reference for performance comparison. The predicted reference temperature is at 68.45°C with insolation 1000 W/m^2 and ambient temperature 20°C. The following four cases using different combinations of two PCMs with different melting temperatures and two shapes of fins (triangle and half circular fins) were simulated on setting static conditions of (a) insolation 1000 W/m^2 and ambient temperature 20°C and (b) realistic three days ambient conditions with repeating data on 1st June [14].

- RT27 with RT21 (triangle cells)
- RT27 with RT27 (triangle cells)
- RT31 with RT27 (triangle cells)
- RT31 with RT27 (half circular cells)
- RT60 with RT21 (triangle cells)

The variable grids of the simulation for the circular cell is listed in Figure 2 along with the isotherms of the circular cells in different time. The insolation absorbed on the front surface of the PV/PCM system and conducted through the PV increases the temperature of the metal cell wall. The metal wall of the cell provides good thermal transfer to the two PCMs. Similar situations can be seen on the triangle fins in Figure 3. As time elapses, it can be seen that the temperature on the front surface of the PV/PCM system has a lower temperature rise for the system with RT27-RT21 than that with the RT27-RT27 and RT31-RT27 filled system, and the thermal regulation period is shorter. It is easy to understand that the lower melting PCM can have better thermal regulation compared with the higher melting PCM. This can be observed from the predicted isotherms for the PV/PCM system cross-sections as shown in Figure 3. Metal fins in the PCM increase the heat transfer inside of the PCMs by increasing the surface area over which heat transfer to the PCM occurs and also act as a pressure release pathway for the melted PCM. After the first 30 minutes the temperature inside the system with RT27-RT21 is relatively lower than the RT27-RT27 and RT31-RT27 cases. After 60 minutes the front temperature on RT27-RT21 increases more rapidly to the insolation intensity than the RT27-RT27 and RT31-RT27 cases do, and the thermal regulation period is less. The position of the PCMs is an important factor in thermal regulation. When combined with low phase change transient PCM the temperature on the front surface of the PV/PCM system has a lower temperature rise.

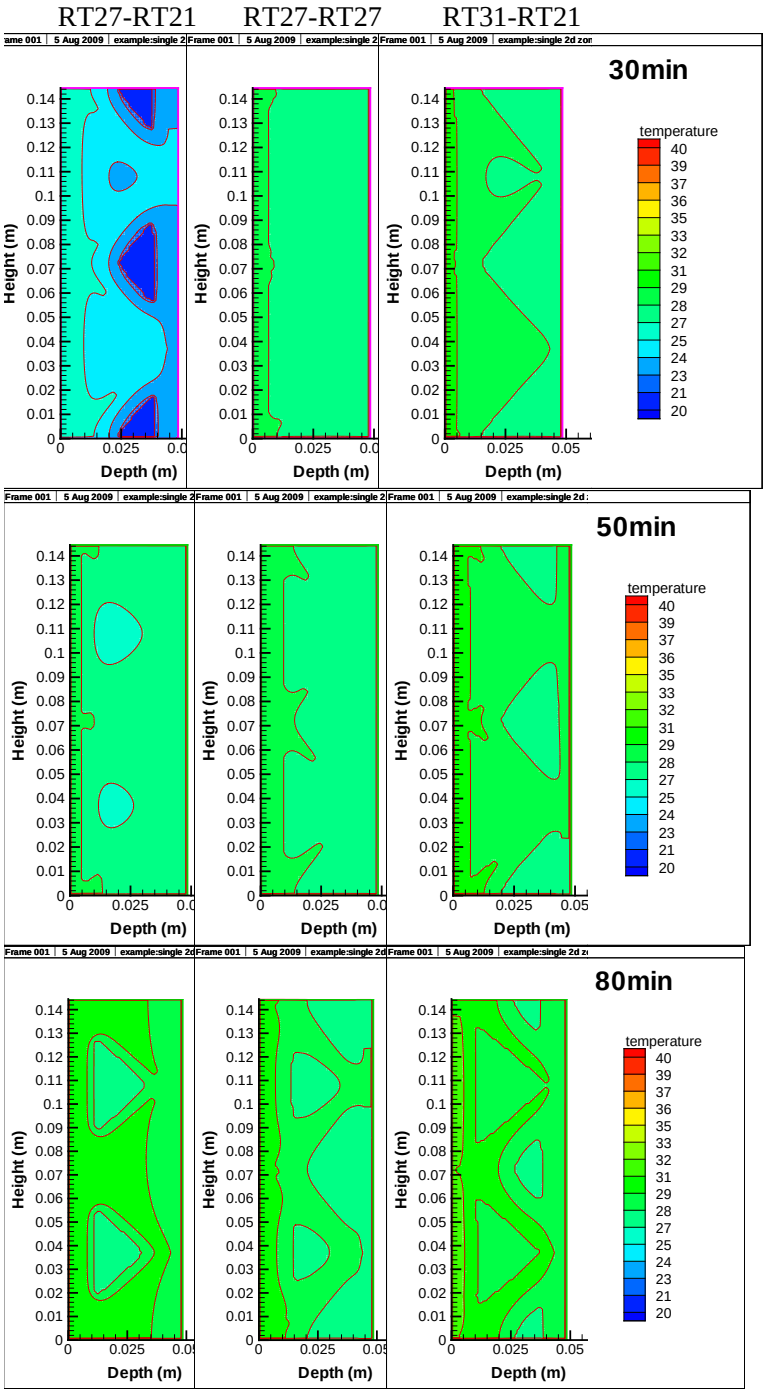

Figure 3. Predicted isotherms for the PV/PCM system with four cases of RT27-RT21, RT31-RT27 during the PCM phase change process

A three day simulation using the weather data on 21st of June has been undertaken to predict the heat accumulation in the PV/PCM system with a combination of two PCMs and is presented in Figure 4. The temperatures of the system respond more rapidly to the insolation than to the ambient temperatures. When no insolation is involved, it can be found that the temperature on the front surface of the system decreases with phase change properties. The temperature of the PV/PCM systems follows the incident insolation but lags with the properties of PCMs by more than 20 minutes. Absorbed solar energy is stored in the PCMs during high daytime temperatures and subsequently released to the ambient in the evening. The predicted temperatures for the second and third days for all the cases are the same, the

PCM has thus released all its latent heat to the ambient environment at night and returned to its solid phase at the start of each period of insolation. The RT31-RT27 system with triangle and circulate close fins can efficiently control the temperature on the PV under 30°C for the whole test period. For two different PCMs the lower phase transient PCM dominates the whole system performance. The phase transient performance is clear in the cooling stage.

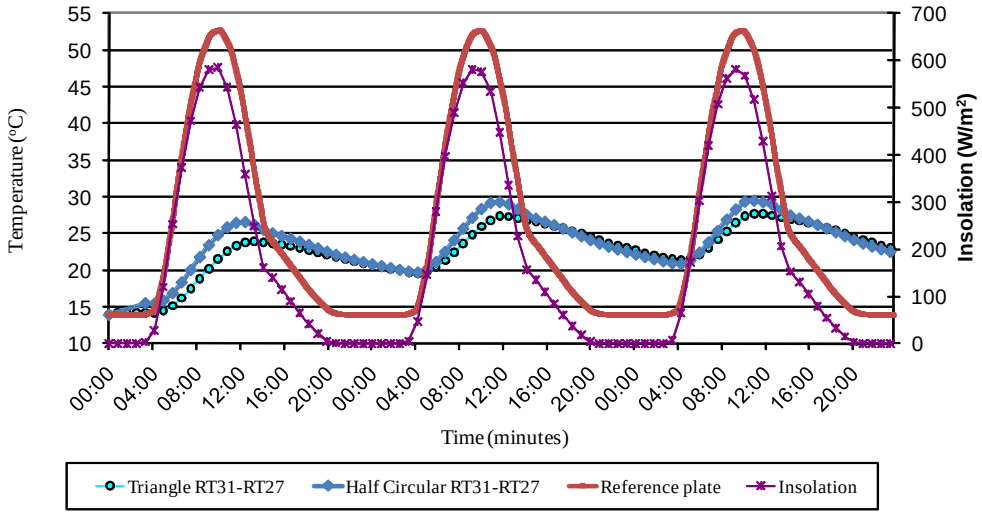

Figure 4 Average temperature evolution at the front surface of the PV/PCM system with the RT31 and RT27 combination for a three day simulation using the weather data on 21st of June SE England

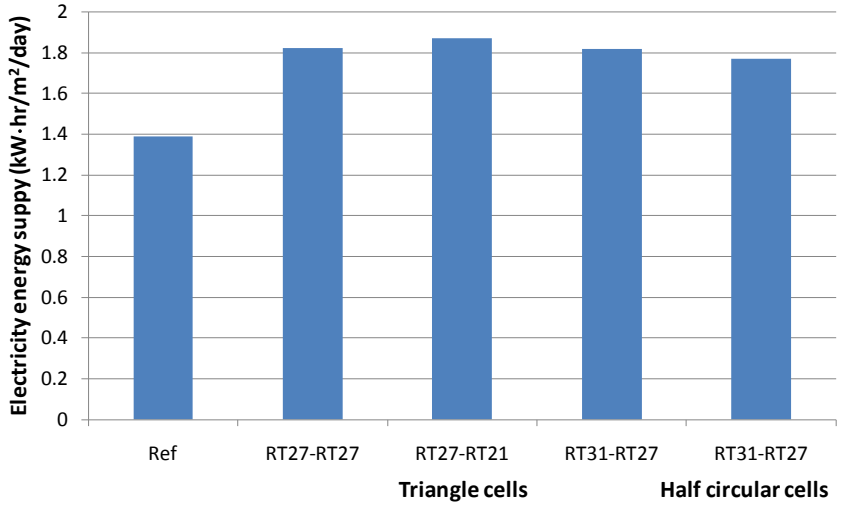

Figure 5 Electricity energy supply on the selected day in 23th June in SE England per square metre for different PCMs combine PV/PCM system along with reference PV module

The temperature regulation may be quantified in terms of the electricity supplied in a typical day in summer. Assuming that the useful electricity power can be produced only after the insolation is over 200 Wm^{-2}. Figure 5 shows the comparison of the electricity energy provided by the two PCMs combined PV/PCM systems with the reference PV module during one day's performance in 21st June in SE England. The PV/PCM systems with half circular cells and triangle cells have been compared as well. The effect of temperature regulation by PV/PCM combined system is clear. The difference between using the triangle and half circular cells is not significant with the selected PCMs combination.

4. Conclusions

The thermal performance of using two PCMs to regulate the temperature rising on PV/PCM system is studied. The PCMs with different transient temperatures can maintain the PV at operating temperature closer to its characteristic value of 25°C and thus lead to an improvement in solar-to-electrical conversion efficiency. The different thermal regulation characters of the PCMs can keep PV temperature at lower levels for longer periods. The PCMs evaluated at different combinations show that the thermal regulation performance of the PV/PCM depends on (a) the thermal mass of PCMs, (b) the positions of the PCMs inside the PV/PCM system and (c) the thermal characteristics of both the PCMs and the PV/PCM systems structure. Comparing different combinations, RT27-RT21 achieves the highest temperature reduction during the daily operation.

References

[1] NREL, (2008). National Renewable Energy Laboratory, A National Laboratory of the US Department of Energy Office of Energy Efficiency & Renewable Energy, http://www.nrel.gov/pv/building_integrated_pv.html.

[2] Ingersoll J. G., (1986). Simplified calculation of solar cell temperatures in terrestrial photovoltaic arrays. ASME J. Solar Energy Engineering 108, 95-101

[3] Krauter S., Hanitsch R. and Wenham S. R., (1994). Simulation of thermal and optical performance of PV modules, Renewable Energy, 5, 3, 1701-1703

[4] Tonui, J.K. and Tripanagnostopoulos, (2007). Air cooled PV/T solar collectors with low cost performance improvements. Solar Energy 81, 498-511.

[5] Fossa, M., Ménézo, C., Leonardi, E., (2008). Experimental natural convection on vertical surfaces for building integrated photovoltaic (BIPV) applications, Experimental Thermal and Fluid Science 32, 980-990.

[6] Huang M.J., Eames P.C. and Norton B., (2006). Experimental Performance of Phase Change Materials for Limiting Temperature Rise Building Integrated Photovoltaics, Journal of Solar Energy, 80, pp. 1121-1130.

[7] Sharma, A., Tyagi, V. V., Chen, C. R. and Buddhi, D. (2009). "Review on thermal energy storage with phase change materials and applications." Renewable and Sustainable Energy Reviews 13(2): 318-345.

[8] Agyenim, F., Hewitt, N., Eames, P. and Smyth, M. (2010). "A review of materials, heat transfer and phase change problem formulation for latent heat thermal energy storage systems (LHTESS)." Renewable and Sustainable Energy Reviews 14(2): 615-628.

[9] Huang M.J., Eames P.C. and Norton B., (2004). Thermal Regulation of Building-Integrated Photovoltaics Using Phase Change Materials, International Journal of Heat and Mass Transfer, 47, Pages 2715-2733

[10] Huang M.J., The Application of CFD to Predict the Thermal Performance of Phase Change Materials for the Control of Photovoltaic Cell Temperature in Buildings, PhD Thesis, University of Ulster, UK, 2002.

[11] Hasan, A. (2010), Phase Change Materials for Thermal Regulation of Building Integrated Photovoltaics, PhD thesis, Dublin Institute of Technology.

[12] Duffie J.A. and Beckman W.A., (1991). Solar Engineering of Thermal Processes, Wiley & Sons, Inc., USA.

[13] Anon, RUBITHERM data sheets for RT21, RT27, RT31 and RT60, RUBITHERM GmbH, Schumann company. (2011).

[14] CIBSE, (2006). CIBSE Guides A, Chartered Institute of Building Services Engineers, London, UK.

Performance-based analysis of a double-receiver photovoltaic system.

Alaeddine Mokri, Mahieddine Emziane

Solar Energy Materials and Devices Lab,
Masdar Institute of Science and Technology, Masdar City, PO Box 54224, Abu Dhabi, UAE
E-mail: amokri@masdar.ac.ae, memziane@masdar.ac.ae

Abstract: Concentrating photovoltaic (CPV) systems with three-junction solar cells are already in the market. In the CPV market, photovoltaic systems with four cells are needed to make CPV more cost competitive. This is because systems with four cells have more yield than the existing three cell systems. Technically, making a stack of four cells imposes constrains on the choice of the materials (i.e. energy bandgap and lattice constant) and it involves complex and costly fabrication techniques. This paper suggests a design of a CPV system with two separate double-junction solar cells (i.e. four PV cells). The system proposed enables the operation of the four cells independently. It also offers high flexibility in the choice of the materials for making the solar cells. The system described in this paper involves a double-junction cell made of AlGaAs/Si; and another double-junction cell made of: InGaAsP/InGaAs. This paper presents the modeling approach and the response of the system under the standard conditions.

Keywords: *photovoltaic, beam splitting, concentrating photovoltaic system.*

1. Introduction

Recently, efficiencies as high as 41.6 % have been measured on concentrating photovoltaic systems (CPV) with a t hree junction solar cell made of InGaP/InGaAs/Ge [1, 2]. Such converters are already in the PV market for terrestrial applications but with a share of less than 1%, while the other photovoltaic technologies (i.e. silicon and thin films) dominate the market [3, 4]. Though the performance of CPV systems with three cells is high, further improvements are still needed to bring down the cost of power from CPV systems and make it cost competitive with the other technologies, namely: silicon based technologies, thermal concentrating solar power and thin-films. One way to improve the response of CPV systems is to involve four-junction solar cells which are not in the market yet. As a matter of fact, the company Emcore is planning to use four-junction cells in their modules from the second quarter of 2011 to achieve 30% outdoors efficiency [5]. Theoretically, the limiting efficiency of a series connected solar cell with four sub-cells is 67.9% under the direct solar spectrum [6]. Making monolithic 4-junction solar cells is technically challenging imposes constrains on the choice of the material because the four cells need to have specific lattice constants and specific energy bandgaps for an optimum response. However, making 2-junction solar cells is relatively simple and can be made with less constrains.

In this work, we suggest a design to involve four cells to achieve a high efficiency with less constrains by using optical techniques. The idea is to design a multi-receiver system in which the cells are kept apart and the sunlight is split into different sub-beams. This type of multi-receiver systems tends to be complex shape-wise which makes wiring, mounting and cooling more complex. In the literature, many CPV systems with beam-splitting features are reported; however, three CPV systems only involve four solar cells [7-11]. United Innovations Inc. proposed a cavity receiver with four mono-junction cells coated with optical filters: InGaP, GaAs, InGaAsP and InGaAs (see configuration 1 in Table 1). The efficiency was calculated and estimated at 48.32 % under 100 suns [8]. Another receiver with four cells was demonstrated at the Fraunhofer ISE in Freiburg, Germany (see configuration 2 in Table 1) [9]. Two of the cells were made of InGaP and GaAs, and they were stacked together. The other mono-junction cells were made of Si and GaSb. An efficiency of 34% was measured [9, 11].

In configuration 3 in Table 1, a system built at the University of Delaware is shown. The system was tested under outdoors site-specific conditions and an efficiency approaching 40% was measured [10].

Table 1: Photovoltaic systems with four cells and beam-splitting features.

Configuration	Solar cells	Efficiency	Reference
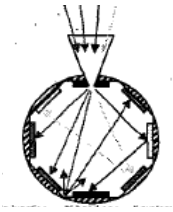 *Configuration 1*	InGaP, GaAs, InGaAsP, InGaAs	48.32 % under 100 suns (calculated)	*Ref. 8*
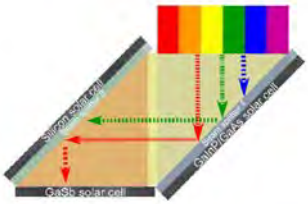 *Configuration 2*	GaInP/GaAs, Si, GaSb	34 % (measured)	Ref. 9
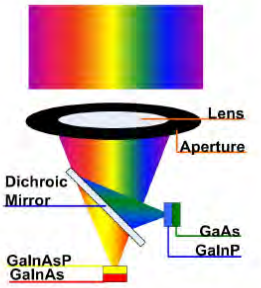 *Configuration 3*	InGaAsP/InGaAs, GaAs/InGaP	39.5 % under 30 suns and DNI = 360 W/m2 (not standard conditions)	Ref 10

We have looked at several systems with beam-splitting features, and based on the lessons learned from the designs proposed in the literature, we are proposing a design with four solar cells. Our system has concentration features. This is because concentration improves the response of solar cells and their yield. Also, concentrating systems use a small cells which reduces the amount of material required for making the solar cells; thus, reducing their cost. The proposed system has only two separate receivers in order to avoid multiple reflections, which is not the case in configurations 1 and 2 in Table 1. Having a system with four solar cells and two receivers imply that each receiver holds a double-junction tandem solar cell.

In this paper, the proposed system is presented. A modeling approach has been developed to estimate the response of the system under the standard conditions.

2. Description of the system

The proposed system is displayed in figure 1 and it is composed of a parabolic mirror, a plano-convex lens coated with a short-pass optical filter, and two tandem photovoltaic cells. The setup has two separate receivers: one receiver holds a double junction solar cell made of AlGaAs/Si and the other receiver holds an InGaAsP/InGaAs double-junction cell.

For the dimensions of the receiver, the diameter of the dish is 112 mm. The cells have circular shapes. The AlGaAs/Si cell has a radius of 7 mm; however, the cell at the opposite receiver has a radius of 10 mm.

The dish concentrates sunlight on the lens. The plano-convex lens is made of fused silica and it is coated with a short-pass multilayer optical filter. Ideally, the filter transmits photons with energies higher than the energy bandgap of Silicon and reflects photons with energies shorter than the energy bandgap of Silicon. We should remind that AlGaAs and Si have the following energy bandgaps of 1.817 eV and 1.124 eV. Therefore, photons with energies higher than 1.124 eV only can be absorbed and converted and those with energies lower than 1.124 eV are reflected to the InGaAsP/InGaAs solar cell. $In_{0.57}Ga_{0.43}AsP$ and InGaAs have energy bandgaps of 1.0 eV and 0.74 eV respectively. Therefore, photons with energies higher than 0.74eV and shorter than 1.124 eV can be absorbed and potentially converted.

For the sake of developing an accurate model, realistic optical properties for the reflective coating on the mirror and the short-pass coating on the lens for commercialized products were used in our model. The transmittance of the multilayer optical filter is presented in figure 2. The spectrum incident on each receiver is presented in figure 3.

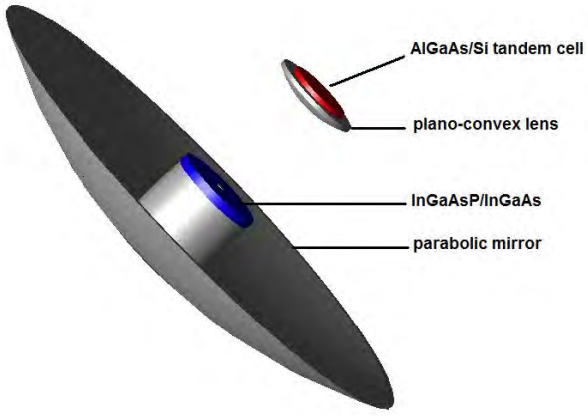

Fig. 1. Configuration of the proposed double-receiver system.

3. Modeling approach

To the best of our knowledge, there is no package dedicated to the modeling of CPV systems with multiple receivers. Therefore, we had to devise a multi-step procedure for modeling the different parts of the system: the light source, the opto-mechanical system, and the solar cells. For the details of the modeling procedure, reference [12] is recommended.

3.1. Modeling the light source:

For modeling the light source, the package SMARTS was used for generating a file for the standard solar spectrum AM1.5 D ASTM G173-03 [13, 14]. The output of the package consists of the wavelengths and the corresponding flux values in $W/m^2/nm$ in the other column. As we are modeling a concentrating photovoltaic system, only photons coming directly from the source (i.e. the sun) can be tracked. For this reason, spectrum of sunlight coming directly from the sun was generated (i.e. AM1.5D). To cover the maximum of the spectrum, we generated spectrum for wavelengths starting from 280 nm to 4000 nm. The spectrum is presented in figure 3.

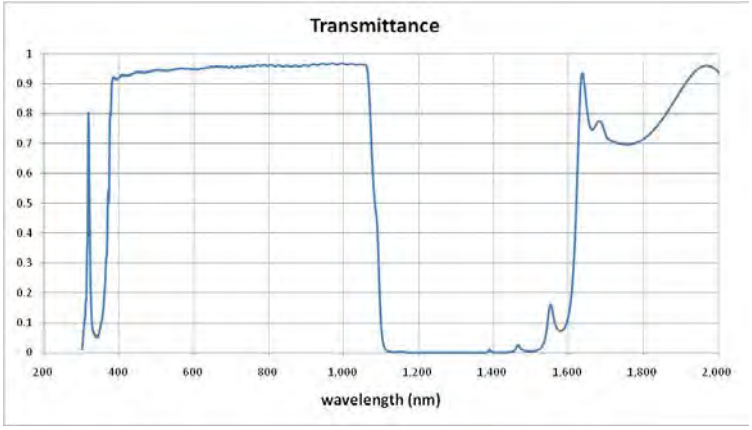

Fig. 2. Transmittance of the short-pass optical filter.

3.2. Modeling the opto-mechanical system:

The values obtained from SMARTS were used for modeling the light source in the ray tracing package TracePro Expert [15]. We used the ray tracing program to determine the flux received at the two receivers. The system presented in figure 1 was built in TracePro Expert and one million rays were launched from the source to find the power incident on each one of the two receivers. Though the acceptance angle should theoretically be 32', in our model, we considered it to be 0^o.

3.3. Modeling the solar cells:

After determining the flux incident on the receivers and the spectrum absorbed by the two solar cells, the cells were simulated in PC1D. PC1D is a package dedicated to modeling photovoltaic solar cells [16]. That is, two PC1D models were developed: one for the AlGaAs/Si solar cell and one for the InGaAsP/InGaAs solar cell, and both are double junction tandem cells. Numerical optimization of the cells is the subject of our previous studies [17, 18].

In PC1D, two spectrum files were generated to model the two solar cells. These files were obtained by modifying the spectrum files that correspond to AM1.5D. For each wavelength in the AM1.5D file, the value of the flux was multiplied by reflectance of the reflective coating and then multiplied either by transmittance (or reflectance) to obtain the flux incident on the AlGaAs/Si cell (or the InGaAsP/InGaAs cell).

After preparing the spectrum files in PC1D and after determining the flux incident on the two solar cells by using TracePro Expert, the PC1D model was run and the final results were obtained.

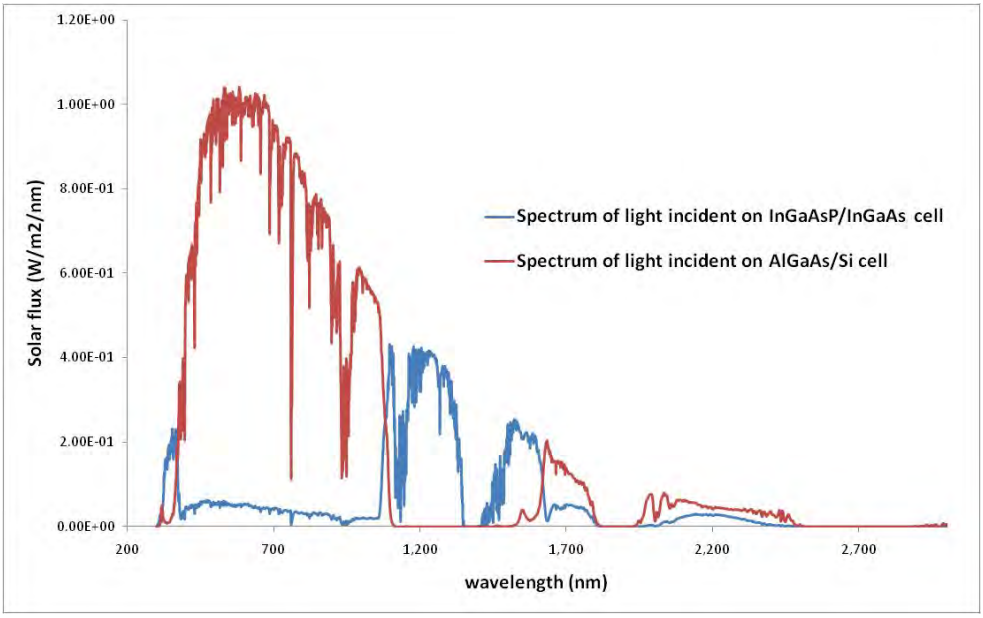

Fig. 3. Spectrum of light incident on the two receivers.

Table 2: Response of the cells in the system.

	AlGaAs	Si	InGaAsP	InGaAs
Energy bandgap (eV)	1.817	1.12	1.00	0.74
Isc (mA/cm2)	717	470	77.1	339.5
Voc (Volts)	1.352	0.752	0.624	0.425
Efficiency (%)	15.5	5.6	1.47	4.21

4. Response of the system:

After running the model, we found that under the standard conditions where the total flux incident on the dish is 850 W/m2 (i.e. a power of 8.374 W is received by the 112 mm wide receiver), 5.716 Watt of concentrated sunlight is received by the InGaAs/Si tandem cell and another 1.712 Watt of concentrated sunlight is received by the InGaAsP/InGaAs tandem cell. These values correspond to power densities of 37.13 kW /m^2 and 5.45 kW/m^2 on the AlGaAs/Si and InGaAsP/InGaAs cells, respectively. These numbers show that the optical efficiency of the system is 88.7 %. The response of the solar cells is summarized in Table 2.

The results in table 2 show that the overall efficiency of the system is 26.8 %. Under the standard conditions, this corresponds to a power density of 227.6 W/m^2. This also means that one dish generates 2.24 W under the standard conditions.

5. Conclusions

In this paper, a system with four solar cells was modeled under the standard conditions. The system involved four solar cells made of the following materials: AlGaAs (1.817 eV), Si (1.124 eV), InGaAsP (1.0 eV) and InGaAs (0.74 eV). The system has beam splitting features and an optical concentration of 63 suns. For modeling the system, we proposed a multi-step modeling procedure. The modeling results show that the efficiency of our proposed system is 26.8 % which corresponds to a power output of 2.24 W. Comparatively with systems with four solar cells reported in the literature, the efficiency of the system is low because of two reasons:

- The combination of the energy bandgaps is not optimum: changing the distribution of the energy bangaps can be done either by using other materials or by changing the composition of the materials used in this study. The optimum energy bandgaps can be determined by changing the cells.
- The optical concentration ratio: the concentration ratio of the system is 63 suns. Increasing this efficiency to very high values above 300 suns would enhance the efficiency of the system.

References

[1] M. A. Green, Keith Emery, Yoshihiro Hishikawa, Wilhelm Warta, "Solar cell efficiency tables (version 36)," Progress in Photovoltaics: Research and Applications, 2010, 18:346–352.

[2] R.R. King, A. Boca, W. Hong, X.-Q. Liu, D. Bhusari, D. Larrabee, K.M. Edmondson, D.C. Law, C.M. Fetzer, S. Mesropian, N.H. Karam," Band-Gap-Engineered Architectures for High-Efficiency Multijunction Concentrator Solar Cells," in Proceedings of the 24th European Photovoltaic Solar Energy Conference, 21-25 September 2009, Hamburg, Germany.

[3] International Energy Agency Report," Technology roadmap: solar photovoltaic energy", 2010.

[4] A. Extance, C. Marquez, "The Concentrated Photovoltaics Industry Report 2010," CPV Today, 2010.

[5] D. Buie, R. Hoffman, P. Blumenfeld, J. Foresi, J. Nagyvary, C. Dempsey, "A Review of Emcore's Third Generation Utility Scale CPV System," In the proceedings of the 6th International Conference on Concentrating Photovoltaic Systems, 07-09 April 2010, Freiburg.

[6] M. A. Green, "Third Generation Photovoltaics: advanced solar energy conversion", Springer, 2003, pp 59-68.

[7] A.G.Imenes, D.R.Mills, "Spectral beam splitting technology for increased conversion efficiency in solar concentrating systems: a review", Solar Energy Materials & Solar cells 84 (2004) 19-69.

[8] U. Ortabasi, A. Lewandowski, R. McConnell, D. J. Aiken, P. L. Sharps, B. G. Bovard "Dish photovoltaic cavity converter (PVCC) system for ultimate solar-to-electricity conversion efficiency general concept and first performance predictions," proceedings of the 29th Photovoltaic Specialists Conference 2002, pp 1616-1620.

[9] B. Groβ, G. Peharz, G. Siefer, M. Peters, J.C. Goldschmidt, M. Steiner, W. Guter, V. Klinger, B. George, F. Dimroth, "Highly efficient light splitting photovoltaic receiver," In the proceedings of the 24th European PV Solar Energy Conference and Exhibition, 21-25 September 2009, Hamburg, Germany.

[10] X. Wang, A. Barnett, "One lateral spectrum splitting concentrator photovoltaic architecture: measurements of current assemblies and analysis of pathways to 40% efficient modules", proceedings of the 35th IEEE Photovoltaic Specialists Conference, Honolulu, Hawaii, June 20-25, 2010.

[11] B. Mitchell, G. Peharz, G. Siefer, M. Peters, T. Gandy, J. C. Goldschmidt, J. Benick, S. W. Glunz, A. W. Bett, F. Dimroth, "Four-Junction Spectral Beam-Splitting Photovoltaic Receiver with High Optical Efficiency," Progress in Photovoltaics: Research and Applications, n/a. doi: 10.1002/pip.988.

[12] Mokri A., Emziane M., "An approach for modeling and optimizing multi-receiver photovoltaic systems with optical filters", Proceedings of the IEEE International Energy Conference, Manama, Bahrain, 18-21 December 2010.

[13] Gueymard, C., "Parameterized Transmittance Model for Direct Beam and Circumsolar Spectral Irradiance", Solar Energy, Vol. 71, No. 5, pp. 325-346, 2001.

[14] Gueymard, C., "SMARTS, A Simple Model of the Atmospheric Radiative Transfer of Sunshine: Algorithms and Performance Assessment". Professional Paper FSEC-PF-270-95. Florida Solar Energy Center, 1679 Clearlake Road, Cocoa, FL 32922, 1995.

[15] TracePro Expert - 6.0.4 Release, Lambda Research Corporation.

[16] PC1D, Version 5.9, © School of Photovoltaic and Renewable Energy Engineering at the University of New South Wales, Australia.

[17] M. Emziane, R. J. Nicholas, D. C. Rogers, J. Dosanjh, " Investigation of InGaAsP-based solar cells for double-junction photovoltaic devices," thin solid films 516 (2008) 6744-6747.

[18] M. Emziane, R. J. Nicholas, "Optimization of InGaAs(P) photovoltaic cells lattice matched to InP," Journal of Applied Physics, 101, 054503 (2007).

Improving the performance of solar panels by the use of phase-change materials

Pascal Biwole[1,*], Pierre Eclache[2], Frederic Kuznik[2]

[1] *University of Nice Sophia-Antipolis, Nice, France*
[2] *University of Lyon, Villeurbanne, France*
** Corresponding author. Tel: +33 492965029, Fax: +33 492965071, E-mail:phbiwole@unice.fr*

Abstract: High operating temperatures induce a loss of efficiency in solar photovoltaic and thermal panels. This paper investigates the use of phase-change materials (PCM) to maintain the temperature of the panels close to the ambient. The main focus of the study is the CFD modeling of heat and mass transfers in a system composed of an impure phase change material situated in the back of a solar panel (SP). A variation of the enthalpy method allows simulating the material thermo-physical change of properties. The buoyancy term in Navier-Stokes' momentum conservation equation is modified through an additional term which forces the velocity field to be non-existent when the PCM is solid. For validation purposes, isotherms and velocity fields are calculated and compared to those from an experimental set-up. Results show that adding a PCM on the back of a solar panel can maintain the panel's operating temperature under 40°C for around two hours under a constant solar radiation of 1000W/m².

Keywords: *Solar Panel, Operating Temperature, Phase Change Material*

Nomenclature

Cp	*specific heat* ..... $J\,kg^{-1}\,K^{-1}$	P	*pressure* ..... Pa
g	*gravitational constant* ..... $m\,s^{-2}$	T_m	*mean melt temperature* ..... K
H	*PCM container height* ..... m	u	*velocity* ..... $m \cdot s^{-1}$
k	*thermal conductivity* ..... $Wm^{-1}K^{-1}$	ΔT	*half range of melt temperatures* ..... K
L_F	*Latent heat of fusion* ..... $J\,kg^{-1}$	β	*coefficient of thermal expansion* ..... K^{-1}
L	*PCM container internal width* ..... m	ρ	*density* ..... $kg \cdot m^{-3}$
m	*mass* ..... kg	μ	*dynamic viscosity* ..... $kg \cdot m \cdot s^{-1}$

1. Introduction

The efficiency of solar panels depends on three factors: the intensity of the solar radiation flux, the quality of the semi conductor in use, and the operating temperature of the semi conductor cell. The variations of solar radiation cannot be controlled. Therefore the ongoing research focuses either on new material like copper, indium diselenium, cadmium tellurium and chalcopyrites, or on maintaining low operating temperatures. For PV panels, high operating temperatures create a drop in the conversion rate of about 0.5% per Celsius degree over the nominal cell operating temperature of 25°C [1], as defined by the industry standard STC (Standard Test Conditions). In summer, panel's temperature typically ranges from 40 to 70°C which makes a 7.5 to 22.5% drop in the conversion rate. In the same way, the efficiency of solar thermal panels decreases mainly because of radiation losses when their operating temperature is above the ambient.

To lower the operating temperature, one can either improve the free cooling on the back of the panel thanks to natural or forced convection, or try to absorb the excess heat by modifying the panel's architecture. The latter solution includes the use of PCMs situated on the back of solar panels. PCMs are materials that undergo reversible transition of phase depending on their temperature. They absorb or reject heat in the process. Only a few studies have been specifically devoted to passive cooling of solar panels by SP/PCM architectures. The hypothesis driving the research is simple: when the panels' temperature rises, the excess heat

must be absorbed until the PCM has completely melted. When the panel's temperature decreases, the solidification of the PCM should provide additional heat for the operating liquid in solar thermal panels, provide heat to the building or act as an insulation material. The SP/PCM solution is expected to be very useful for roof or facade integrated panels where space for ventilation is limited.

Huang et al. [2] studied the melting of PCMs in an aluminum container submitted to a solar radiation of 750 to 1000W/m². They used a finite volume model to resolve both the heat transfers diffusion and the Navier-Stokes equations. They later included cooling fins in the tank to improve the PCM bulk thermal conductivity [3] [4]. They found that the temperature rise in the system could be reduced by more than 30°C for 130 minutes. Cellura et al. [5] resolved the same architecture using a finite element PDE solver. However, they considered the PCM as pure, meaning that the PCM melting temperature is unique and does not change while the PCM is still melting. This property is not valid for most commercial PCMs which are generally mixtures of several different materials. By resolving only the heat transfers diffusion equation, they showed that a PCM with a melting temperature between 28°C and 32°C can improve the energy conversion efficiency by around 20% in summer time. Jay et al. [6] experimentally studied a layout where PCM were contained in a honeycomb grid to improve conduction in the container. They showed that after 6 hours and 30min of experiment under an artificial insulation of 800W/m² on real PV panels, the temperature of a PV/PCM system was still lower than that of a single panel, with a mean temperature difference of 24°C. They also found that the panel's temperature drop using a PCM with a melt temperature at 27°C was higher than using a PCM with a melt temperature at 45°C.

In this study, we consider the same geometry as [2]. The transient conduction and convection heat transfers as well as the Navier-Stokes equations are simultaneously resolved in the PCM domain using a finite element model on a fixed grid. The buoyancy term in Navier-Stokes' momentum conservation equation is modified through an additional term to force the velocity field to be zero when the PCM is solid. This scheme is validated using an experimental set-up. The model is then used for a parametric study of the SP/PCM architecture performances.

2. Methodology

2.1. Numerical case description

The geometry of the model is presented in Fig. 1. The thermo-physical properties of the simulated materials are presented in Table 1.

Table 1. Thermo-physical properties of RT25 and aluminum.

	Cp	k	ρ
Solid RT25	1800	0.19	785
Liquid RT25	2400	0.18	749
Aluminum	903	211	2675
Constant properties of RT25:			
L_F: 232000 J kg^{-1}			
T_m: 26.6°C, ΔT=1°C			
β: 1e-3K^{-1}			
μ: 1.7976e-3 $m^2.s^{-1}$			

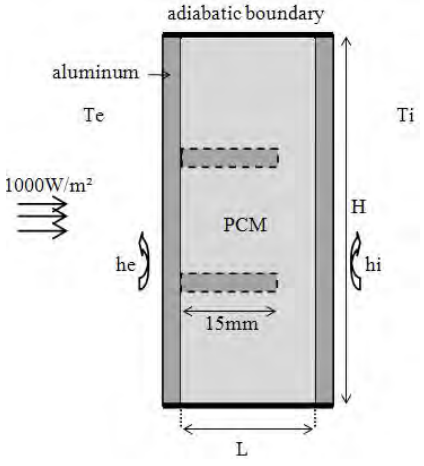

Fig. 1. Geometry of the numerical model.

2.2. Mathematical model

2.2.1. Modeling heat transfers

Over the front plate surface, we considered conduction, convection and radiation heat transfers as shown in Eq. (1). Long wave radiation with the sky was neglected in the model.

$$\rho C_p \frac{\partial T}{\partial t} = -k \frac{\partial T}{\partial x} + h_e (T_e - T) + \alpha E(t) \tag{1}$$

where α is the aluminum thermal absorptivity and E the solar radiation intensity. The heat transfers diffusion equation applies over the PCM, the air layer and the aluminum domains:

$$\rho C_p \frac{\partial T}{\partial t} + \nabla.(-k \nabla T) + \rho C_p \vec{u}.\nabla T = 0 \tag{2}$$

The velocity field ***u*** in Eq. (2) is given by Navier-Stokes equations for incompressible fluids. To model the changes in PCM RT25 thermo-physical properties occuring during the phase transition, we define function B_0 as the liquid fraction in the PCM domain. Let be T_m the mean melt temperature and ΔT the half range of melt temperatures:

$$B_0(T) = \begin{cases} 0 & , \quad T < (T_m - \Delta T) \\ (T - T_m + \Delta T)/(2\Delta T) & , \quad (T_m - \Delta T) \le T < (T_m + \Delta T) \\ 1 & , \quad T > (T_m + \Delta T) \end{cases} \tag{3}$$

Eqs. (3) show that B_0 is zero when the PCM is in solid and 1 when it is in liquid phase. B_0 linearly grows from zero to 1 between the two states. To ensure second order continuous differentiability of the liquid fraction over the temperature domain and to help numerical convergence, B_0 is approximated by a second order differentiable function B_1. $B_1(T)$ is the sixth-degree polynomial whose coefficients are calculated using the following conditions:

$$\begin{cases} B_1(T_m - \Delta T) = 0 \quad ; \quad B'_1(T_m - \Delta T) = 0 \quad ; \quad B''_1(T_m - \Delta T) = 0 \quad ; \quad B_1(T_m) = 0.5 \\ B_1(T_m + \Delta T) = 1 \quad ; \quad B'_1(T_m + \Delta T) = 0 \quad ; \quad B''_1(T_m + \Delta T) = 0 \end{cases} \tag{4}$$

where B_1' and B_1" are $B_1(T)$ first and second derivatives. B_1 is used to model the changes in the PCM thermo-physical properties as follows:

$$\rho(T) = \rho_{solid} + (\rho_{liquid} - \rho_{solid}) \cdot B_1(T) \tag{5}$$

$$k(T) = k_{solid} + (k_{liquid} - k_{solid}) \cdot B_1(T) \tag{6}$$

The modeling of the specific heat includes an additional term representing the latent heat of fusion absorbed during the melting process:

$$C_p(T) = C_{p\,solid} + (C_{p\,liquid} - C_{p\,solid}) \cdot B_1(T) + L_F \cdot D(T) \tag{7}$$

Where $$D(T) = e^{\frac{-T(T-T_m)^2}{\Delta T^2}} \Big/ \sqrt{\pi \cdot \Delta T^2} \tag{8}$$

Function D is a smoothed Delta Dirac function which is zero everywhere except in interval [T_m-ΔT, T_m+ΔT]. It is centered on T_m and its integral is 1. Its main role is to distribute the latent heat equally around the mean melting point.

2.2.2. Modeling mass transfers

We assumed that the PCM in the liquid phase is a Newtonian fluid. The mass, momentum and energy conservation equations were resolved simultaneously with the heat transfers diffusion equation. However, to model the phase transition, the momentum conservation equation was modified as follows:

$$\rho\frac{\partial\vec{u}}{\partial t}+\rho(\vec{u}.\nabla)\vec{u}-\mu.\nabla^2\vec{u}=-\nabla P+\vec{F}_b+\vec{F}_a \tag{9}$$

where $\mathbf{F_b}$ is buoyancy force given by the Boussinesq approximation:

$$\vec{F}_b=-\rho_{liquid}\left(1-\beta\left(T-T_m\right)\right)\vec{g} \tag{10}$$

And $\vec{F}_a=-A(T)\cdot\vec{u}$ (11)

with $A(T)=\frac{C(1-B_1(T))^2}{(B_1(T)^3+q)}$ (12)

The expression of A is inspired from the Carman-Kosensky relation in a porous medium where the value of C depends on the morphology of the medium. If we assume that the flow is laminar:

$$\nabla(P)=\frac{-C(1-B(T))^2}{B_1(T)^3}\cdot\vec{u} \tag{13}$$

In this study, C is given the constant value 10^5. This value is chosen arbitrarily high. Constant q is chosen very low in order to make Eq. (12) valid even when $B_1(T)$ is zero. The value of q was fixed at 10^{-3}. When the temperature of the MCP is higher than T_m+ΔT, the PCM is completely liquid. Therefore, B_1 is 1 and consequently, A and $\mathbf{F_a}$ are zero. In this case, the usual momentum conservation equation applies. During the transition state, $0 < B_1(T) < 1$. A(T) increases along with the melting process until the added force $\mathbf{F_a}$ becomes greater than the convection and diffusion terms in Eq. (9). The momentum conservation equation becomes similar to the Darcy law for fluid flow in porous medium:

$$\vec{u}=-\frac{K}{\mu}\nabla(P) \tag{14}$$

where the permeability K is a function of $B_1(T)$. When $B_1(T)$ diminishes, the velocity field also diminishes until it reaches zero when the PCM becomes completely solid. At that point, the MCP temperature is lower than T_m-ΔT. Therefore, B_1 is 0. Eq. (12) shows that the value of A(T) becomes very high. Consequently, all the terms in the momentum conservation equation are dominated by the added force. The only solution of the Navier-Stokes equations is **u=0** which corresponds to a solid medium.

2.2.3. Numerical method

A 2D finite element model was used. To satisfy the Brezzi-Babuska condition [7] three degrees of freedom were used on each element to approximate the pressure field and an additional degree of freedom was used by adding a node at the center of mass of each triangular element to approximate the velocity field. The maximum mesh size was 4.10e-4m. The final mesh had 135 240 elements and 465 857 degrees of freedom. No significant change of the results was observed when using a finer mesh. A Galerkin least-squares stabilization method was employed.

Fig. 2. Comparison of the simulated (left) and the experimental(right) liquid-solid moving boundary location

2.3. Elements of validation

2.3.1. Experimental set-up

The experimental set-up consisted of a 167mm x 167mm x30mm-large Plexiglass container without cooling fins and filled with a PCM. An air layer was left at the top of the tank to prevent it from breaking due to the PCM thermal expansion. A fixed temperature of Te = 20°C and Ti = 40°C was imposed on each side of the tank thanks to heating plates. The transient two-dimensional velocity field in the tank was measured thanks to a PIV apparatus including a Nd-Yag laser.

The experimental validation consisted of: firstly, a transient comparison of the moving liquid-solid boundary location (Fig. 2); secondly, a comparison of the simulated and measured velocity fields in the completely melted PCM (Fig. 3). Some discrepancies were noted between the simulated and the measured velocity fields. This may be due to the very low velocities in the tank which are of the order of 10e-4m/s. However, the transient locations of the simulated moving boundary closely matched the experimental one.

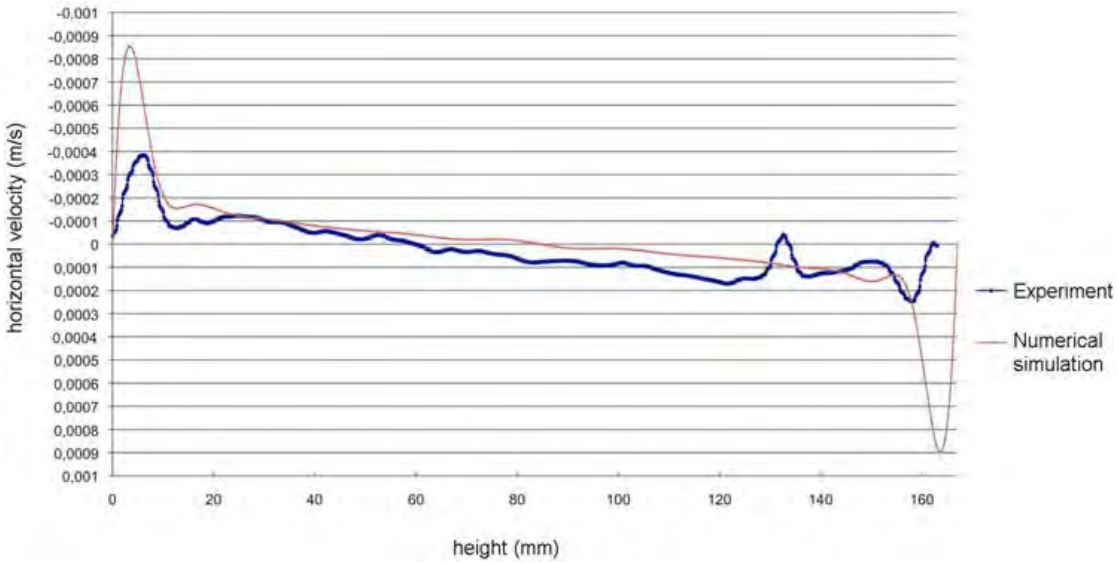

Fig. 3. Comparison of the PIV-measured and simulated velocity in the vertical mid cross-section of the PCM domain.

3. Results

All the simulations were conducted using he=10W/m².K, hi=5W/m².K and E = 1000W/m².

3.1.1. Temperature and velocity fields

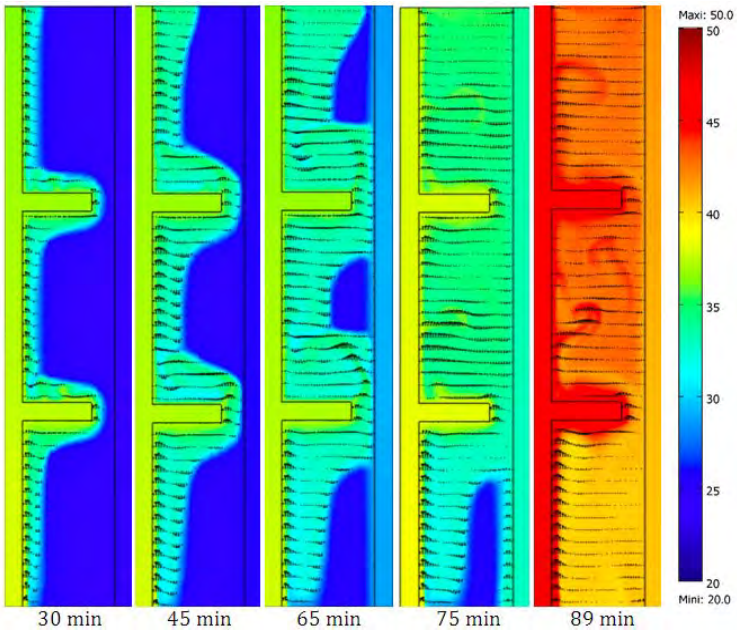

Fig. 4. Simulated transient isotherms and velocity fields in the SP/PCM system. H=132mm, L=20mm.

3.1.2. Parametric study

Table 2. List of simulated cases.

	(a)	(b)	(c)	(d)
L(m)	0	20	20	20
H(m)	132	132	40	132
Cooling fins	no	yes	no	no

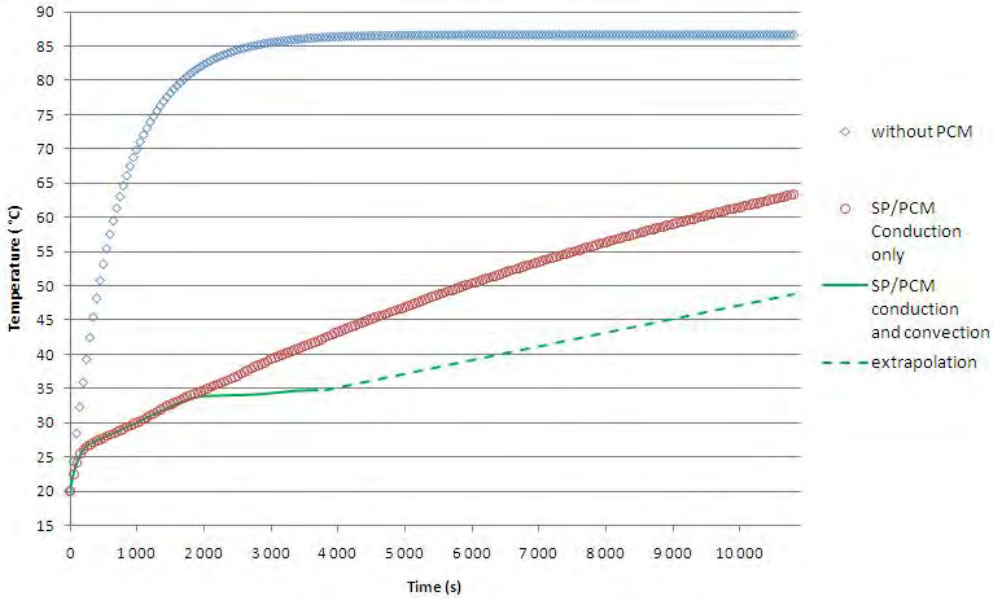

Fig. 5. Impact of convection heat transfers in the PCM on the panel's operating temperature. H=0.132m and L=0.049m.

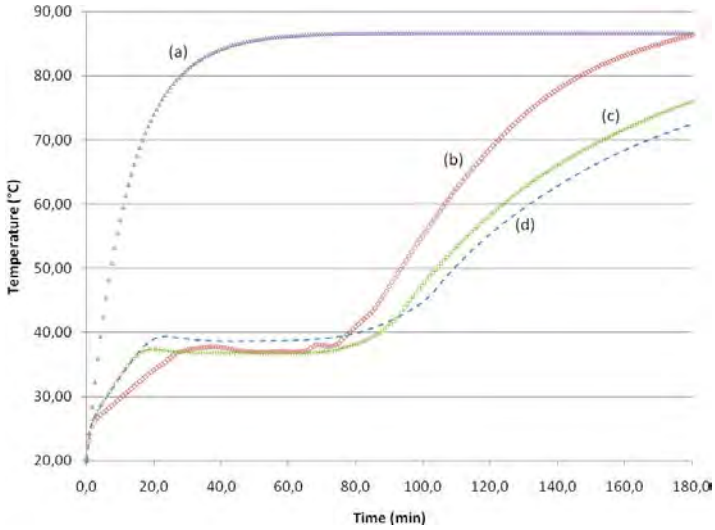

Fig. 6. Impact of the SP/PCM size on the panel's operating temperature.

4. Discussion and conclusion

The first limitation of this work rises from the representation of the solar panel by an aluminum plate. This simplification does not take into account the bulk specific capacity of real panels. The second limitation comes from the fact that the impact of sky temperature was not included in the numerical model, due to experimental validation difficulties. Despite those limitations, the following observations remain relevant:

The velocity field in Fig. 4 shows a circulation of the liquid PCM through the three parts of the container. Convection of the liquid PCM is observed upward close to the heated panel, and downward close to the liquid-solid boundary. The Rayleigh number in the liquid PCM was between 10^5 at melt start and 10^6 at melt end. This result is coherent with our initial assumption of a laminar flow and confirms the observation of [4]. Like [4], we also numerically observe a suspended solid PCM mass when the melting is nearly over.

Over the range of simulated sizes for the SP/PCM system, the temperature of the front plate always remains lower than 50°C after 89min under a constant radiation of 1000 W/m^2. The better performance is obtained with a 13.2 x 4.9cm large PCM container. In this case, the panel's temperature is 34.9°C after 1 hour. The same temperature is reached after 5min without PCM (Fig. 5). These observations are in good agreement with [3] and [5]. Three inflexions points can be observed on the transient operating temperature profile. The first one happens at the PCM melt temperature. After a steep increase, the panel temperature rises much more slowly from that point because of the start of the melting process.

Between the first and the second inflexion point, the PCM acts like an insulation material for the panel and heat transfers are dominated by conduction (Fig. 5). The second inflexion point indicates the start of the convection heat transfers which balances conduction heat transfers in the PCM. Fig. 5 shows that the simulated panel temperature may be overestimated by 20% after 3600s when conduction only is considered in the numerical model. On Figs. 5 and 6, the operating temperature remains more or less constant until the PCM has completely melted. The last inflexion point marks the end of the melting process. Heat transfers in the container are dominated by convection. Afterwards, the temperature rises more slowly than before the start of the melt because of the higher specific heat capacity of the liquid PCM.

The parametric study also shows that the operating temperature drops proportionally to the increase of the PCM width: after 3600s, T = 34.9°C when L = 0.049m whereas T=37°C when L = 0.02m. Comparing curves (c) and (d) shows that the same trend is observed when the panel height is increased but only when the PCM has completely melted. In brief, it is better to increase the PCM width than its height to lower the panel's temperature. Adding cooling fins in the PCM tank provides a faster attenuation of the operating temperature because the PCM bulk conductivity is increased. But this layout accelerates the phase transition too. When the PCM has completely melted, the operating temperature rises faster than for all other SP/PCM architectures (Fig. 6). This fact moderates the idea that adding cooling fins makes SP/PCM systems more efficient [4].

To conclude, adding PCM on the back of solar panels is an efficient way of improving panels' performance. Their operating temperature can be substantially decreased using that technology. Future work should include experimental validations of this first numerical model using real solar panels under real climate.

References

[1] K. Emery, J. Burdick, Y. Caiyem, D. Dunlavy, H. Field, B. Kroposki, T. Moriatry, Temperature dependence of photovoltaic cells, modules and systems, Proceedings of the 25th IEEE PV Specialists Conference, Washington DC, USA, May 13–19, 1996, pp. 1275–1278.

[2] M.J. Huang, P.C. Eames, B. Norton, Thermal regulation of building integrated photovoltaics using phase change materials, International Journal of Heat and Mass Transfers 47, 2004, pp. 275-2733.

[3] M.J. Huang, P.C. Eames, B. Norton, Phase change materials for limiting temperature rise in building integrated photovoltaics, Solar Energy 80 (9), 2006, pp. 1121-1130.

[4] M.J. Huang, P.C. Eames, B. Norton, Comparison of a small-scale 3D PCM thermal control model with a validated 2D PCM thermal control model, Solar Energy Materials and Solar Cells 90 (13), 2006, pp. 1961-1972.

[5] M. Cellura, G. Ciulla, V. Lo Brano, A. Marvuglia, A. Orioli, Photovoltaic panel coupled with a phase changing material heat storage system in hot climates. In: Proceedings of the 25th Conference on Passive and Low Energy Architecture, Dublin, Ireland, October 22-24, 2008.

[6] A. Jay, S. Clerc, B. Boillot, A. Bontemps, F. Jay, Utilisation de matériaux à changement de phase pour réduire la température de panneaux PV intégrés au bâti, Proceedings of the International Building Performance Simulation Association conference, Moret sur Loing, France, November 9-10, 2010.

[7] D. N. Arnold, F. Brezzi, M. Fortin, A stable element for the Stokes equations, Calcolo (21), 1984, pp. 337-344.

Assessing the impact of micro generation in radial low voltage distribution networks taking into consideration the uncertainty

Alvaro Gomes[1,2,*], Luís Pires[1]

[1]*Department of Electrical Engineering and Computers – University of Coimbra, Coimbra, Portugal*
[2] *INESC Coimbra, Coimbra, Portugal*
** Corresponding author. Tel: +351 934262925, Fax: +351 239796247, E-mail: agomes@deec.uc.pt*

Abstract: The increasing penetration of micro generation units in low voltage distribution networks and the need for evaluating the potential benefits and also the potential negative impacts of such penetration ask for detailed assessment tools and methodologies. The impacts of a single small-scale unit (<5,75kW) is, probably, negligible. However, the aggregate contribution of many small capacity units can be significant and an adequate assessment of the impacts is needed in order to prevent some undesirable effects and in order to accurately compute the benefits of such units. This paper presents a methodological approach that allows an adequate assessment of micro generation impacts on radial distribution networks based on Monte Carlo simulations to reproduce both demand and generation behavior, and using scenarios to deal with the uncertainty about micro generators placement. Besides, the use of both generation and demand diagrams of high resolution allows to adequately assess the voltage values variability in different buses.

Keywords: *Micro-generation, LV radial distribution networks, Losses and voltage profile assessment*

1. Introduction

In traditional power systems, without distributed generation or micro-generation units, power flows from substation to the end-user loads and power systems are designed for such behavior. The utilization of micro-generation units might, however, impact the flow of power and voltage levels and eventually cause reverse power flows. Thus, some problems may arise and should be taken into consideration when promoting this type of generation. For a given load and generation levels the impacts of micro generation on distribution networks depend, among others, on both the location and size of micro generation systems. Several methodologies dealing with different issues raised by the dissemination of micro-generation have been proposed in the literature [1]-[9]. However, load demand and the output of micro generation units vary widely over the time and typically micro generation systems location is not known in advance. The uncertainty associated with both generation systems location and load/generation levels makes hard an accurate assessment of the impacts of those generation systems on the radial distribution networks. Namely, the impacts on the voltage profile and power losses, but also eventual changes in power flows direction should be carefully accounted for. On the other hand, an adequate assessment of the impacts on voltage profiles asks for both an adequate time resolution in the representation of demand and generation and the usage of real load and generation diagrams not averaged ones. Averaged load diagrams and inadequate time resolution of load diagrams do not allow capturing the real impact on buses voltage profile. Even 15 minutes time resolution may provide only indicative values for changes in voltage profiles provoked by micro generation systems.

The main contribution of this work is the capability of making a daily basis analysis with a proper time resolution allowing for an adequate assessment of voltage impacts and the ability to deal with uncertainties that exist at both available generation and at the demand level.

The structure of the paper is as follows. In section 2 the methodological approaches to compute power flow and the demand and generation models are presented. Also, the different scenarios used to deal with the possible different locations of micro-generation units are

presented. Follows, in section 3, the case study while, in section 4, the results are shown. Finally, in section 5, some conclusions are drawn.

2. Methodology

In order to properly assess the impacts of micro-generations units on voltage profile and on the losses in a radial low voltage (LV) network, suitable demand and generation models and adequate power flow algorithms are necessary. Demand and generation models should be able to tackle the uncertainty that exist in both generation and in the demand, and the power flow algorithms need to take into consideration the intrinsic characteristics of distributions circuits which typically are unsymmetrical and unbalanced. Some proposals for dealing with some of these issues can be encountered in the literature [10][11]. However, a detailed analysis at the LV network level taking into consideration demand and generations variability is not available. The methodological approach followed in this work allows such detailed analysis, namely regarding the impacts on voltage levels and on power losses, while taking into consideration the uncertainties associated with both the demand and the generation. In order to deal with the uncertainty of both the demand and generation we use Monte Carlo simulations to generate all possible realistic load/generation diagrams. The Monte Carlo simulations carried out to obtain demand diagrams, different for each customer, were based on information collected from load profiles obtained during monitoring campaigns. Namely, for each time interval, a probability density function characterizing the behavior of the demand was identified and used in the Monte Carlo simulations. For every customer (bus) different load profiles, obtained from field surveys, are considered. In the study carried out, in order to account for different possible amounts (number) and locations (buses) of micro generation units several scenarios have been simulated. The developed software tool allows the use of any time resolution to represent load profiles and generation.

The variability of the demand is, most of times, associated with the utilization of energy services (heating, cooling, tv, computers, lighting, etc) according to the needs of the end-user. Consequently, energy consumption varies throughout the day and is different for different days (Figure 1). Adequate models for reproducing the demand taking into account such variability must produce realistic load curves and not averaged load curves and should have a proper time resolution that allowing capturing the impacts on the voltage levels. Therefore, average demand curves with a time resolution too high, for instance hourly demand models (Figure 2), are not adequate for such evaluation. In order to run Monte Carlo simulations, for every time interval adequate probability distributions have been identified based on data collected, thus allowing the generation of realistic load diagrams for different days of the week and different periods of the year. The uncertainty associated with the photovoltaic and wind generation is modeled also by using Monte Carlo simulations with normal distribution probability. Several scenarios regarding the number of micro-generation units and location have been analyzed. “A” is the scenario with no micro-generation units (MGU); in scenario B there are only 5 MGU, for evaluating the impacts of a low level MG penetration; in scenarios C – G there 10 MGU, located in different buses. In scenario C MGU distributed throughout the network; in scenario D (E) MGU are preferably located in buses far (near) from the distribution transformer (DT), allowing to evaluate the impacts as a function of the distance from DT; and in scenario F(G) MG units are mainly in the phase with higher (lower) demand, allowing to assess the impacts as a function of the demand level. These scenarios are summarized in Table 2. The implemented algorithm for computing power flows is the forward/backward sweep method based on successive sweeps until the convergence is achieved [12]-[15].

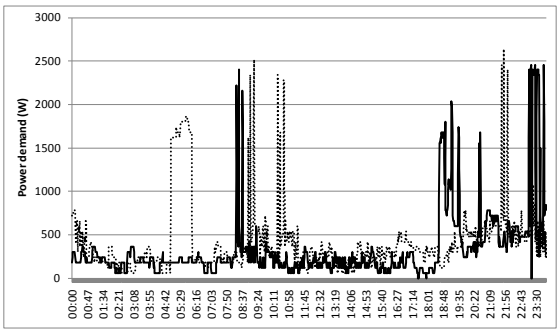

Figure 1- Energy consumption patterns in two consecutive days for the same residential consumer.

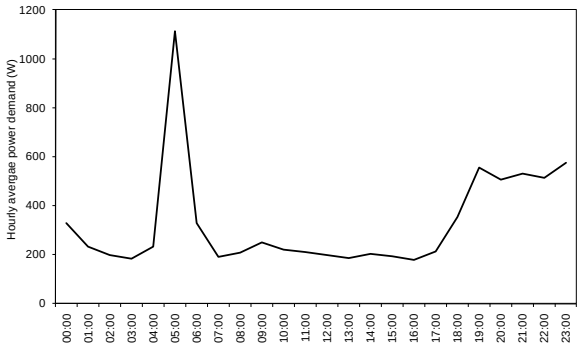

Figure 2- Hourly averaged load diagram for the residential consumer of Figure 1.

3. Case study

A real urban low voltage radial distribution network data has been used in this case study. The network has 38 buses, 28 feeding residential consumers and 8 distribution buses (points of connection). There are no losses at the distribution buses and the neutral is grounded in every bus. The distribution transformer is a 30kV / 400V-230V 160 kVA transformer. Figure 3 shows the layout of the network. Besides residential consumers we have also street light.

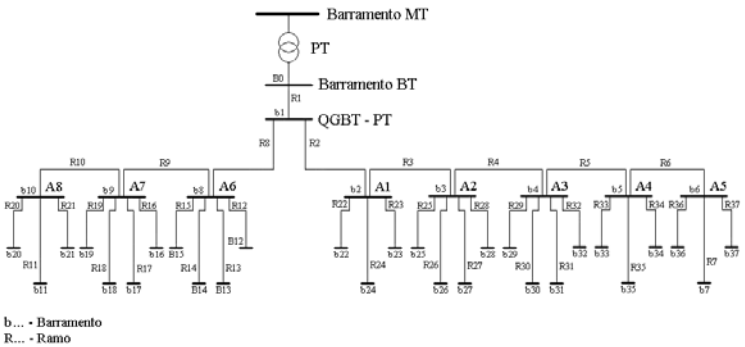

Figure 3- LV distribution network being analyzed.

Most residential customers are single-phase consumers. In Table 1 the contracted power and the phase for every consumer are shown. Phase "A,B,C" means a three-phase consumer. According to the Portuguese legislation (decree-law 363/2007) the aggregated power of all micro-generation units installed in a LV distribution network cannot exceed 25% of the distribution transformer capacity and in order to access special-regime (premium) of the PV feed-in-tariff scheme the individual capacity of the micro-generation units is limited to 3.68 kW, meaning that in this LV network can be installed at most 10 units. In this work all MG units have 3,68 kW capacity and are consumer owned.

Table 1- Placement of microgeneration units.

Bus	Phase	Contracted Power	Bus	Phase	Contracted Power
1	A	6,9 kVA	**24**	C	6,9 kVA
7	A	6,9 kVA	**25**	B	6,9 kVA
11	A	6,9 kVA	**26**	A,B,C	10,35 kVA
12	C	6,9 kVA	**27**	C	6,9 kVA
13	A	6,9 kVA	**28**	A	6,9 kVA
14	C	6,9 kVA	**29**	C	13,8 kVA
15	B	10,35 kVA	**30**	A	6,9 kVA
16	A,B,C	10,35 kVA	**31**	B	6,9 kVA
17	B	10,35 kVA	**32**	B	10,35 kVA
18	C	10,35 kVA	**33**	C	10,35 kVA
19	A	6,9 kVA	**34**	B	6,9 kVA
20	C	10,35 kVA	**35**	A	10,35 kVA
21	B	10,35 kVA	**36**	C	10,35 kVA
22	B	6,9 kVA	**37**	B	6,9 kVA
23	A	10,35 kVA			

In order to deal with the uncertainty of demand and of the generation, 300 simulations per interval of time have been done. Total computer time was 1200 seconds. Regarding the location of micro-generation units (MGU) 7 scenarios have been analyzed, as described in Table 2.

Table 2- Different scenarios for the placement of micro-generation units

Scenario	Characteristics
A	Reference scenario, with no micro-generation units.
B	5MGU, to assess the impact of low level MGU penetration.
C	10 MGU spread throughout the circuit.
D	10 MGU mainly connected in remote buses.
E	10 MGU mainly connected in buses near the distribution transformer.
F	10 MGU connected mainly in highly loaded phase (B).
G	10 MGU connected mainly in phase with lower demand (C).

4. Results

4.1. Power Flows

In the following table the average active and reactive power flows at the DT and the amount of energy drawn from the grid to feed the consumers are shown. The difference between each alternative scenario (B-G) and the reference scenario (A) is also presented. One can see the reduction of power drawn from the grid through power transformer as a result of micro generation units

In Figure 4 the power flows at DT for scenarios A-C are shown. Negative values mean that reverse power flows exist, as in scenario C (high photovoltaic penetration). Dealing with photovoltaic units means the main changes regarding the reference scenario occur during the day. As MGU are operating at unity power factor there are no differences regarding the reactive power flows.

Table 3- Power flow at the distribution transformer and energy drawn from the grid.

	Sce. A	Sce. B	Sce. C	Sce. D	Sce. E	Sce. F	Sce. G
Hourly averaged active power (kW)	17,96	13,89	9,81	9,81	9,80	9,82	9,81
Daily active energy (kWh)	430,99	333,28	235,48	235,55	235,20	235,74	235,38
Differences regarding scenario A(%)	0	-22,67	-45,36	-45,35	-45,43	-45,30	-45,39
Hourly averaged reactive power (kVAr)	12,99	13,01	13,02	13,03	13,01	13,04	13,20
Daily reactive energy (kVArh)	311,66	312,16	312,58	312,66	312,27	312,86	312,48
Differences regarding scenario A(%)	0	0,163	0,298	0,321	0,197	0,388	0,264

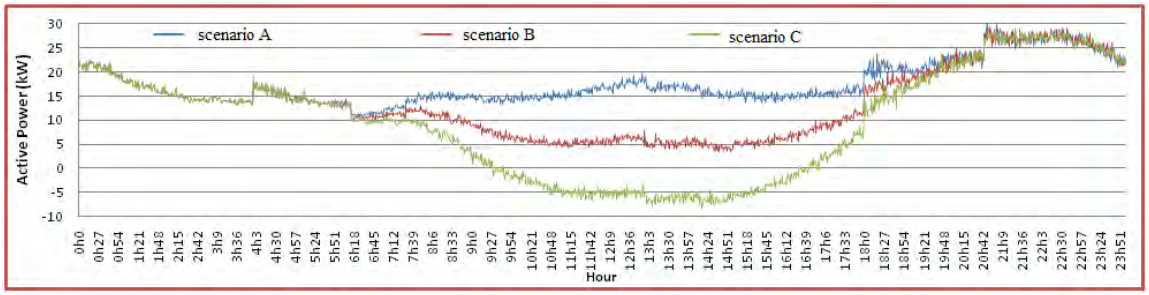

Figure 4- Active power flow at distribution transformer (scenarios A-C).

4.2. Power Losses

In Table 4 the active and reactive power losses are presented as well as the differences regarding the reference situation (scenario A). For low level MGU penetration (scenario B) there is a reduction in losses. However, when MGU penetration increases losses depend on the location of MGU. Typically there is a reduction in losses, not as big as in scenario B, but some situations, like in scenarios D and G, might present higher losses. In scenario G, MGU are connected mainly in the phase with lower demand (phase C) resulting in a strong current flow increase in this phase and thus an increase in losses. In scenario D, MGU are mainly connected at remote buses resulting in longer distances for power flows and thus higher resistance. An interesting situation that may occur when MGU penetration increases is that the power losses maximum value can occur during the higher outputs from MGU and not in the periods of higher demand.

Table 4- Losses for the different scenarios

	A	**B**	**C**	**D**	**E**	**F**	**G**
Active power losses (W)	87,78	79,77	83,65	88,92	85,05	84,60	93,70
Daily active losses (kWh)	2,107	1,914	2,008	2,134	2,041	2,030	2,249
Variation regarding A (%)	0	-9,13	-4,70	1,30	-3,11	-3,62	6,75
Reactive power losses (VAr)	23,81	21,05	21,73	22,90	22,03	22,29	24,93
Daily reactive losses (kVArh)	0,571	0,505	0,522	0,550	0,529	0,535	0,598
Variation regarding A (%)		-11,58	-8,72	-3,84	-7,48	-6,40	4,70

4.3. Voltage

Following figures show the voltage values in the 38 buses of the network at 12:00h, for the different scenarios. In general voltage profile improves when MGU are connected. Typically, higher voltage increase occurs in the buses and in the phases where MGU are connected. There is, however, a decrease in voltage values in phase B in buses 8, 9 and 10. These decrease might be due to the introduction of MGU in buses 11 (phase A) and 18 (phase C)

reducing the magnetic coupling between phases A and C and the phase B thus leading to a higher voltage drop in phase B. From Figure 6-scenario D) to Figure 6-scenario G) one can see that the voltage profile in the network is highly dependent on the location of MGU. When the MGU are located in remote buses (scenario D) the impact on voltage level is higher compared with the scenario in which MGU are connected near the DT (scenario E). When MGU are mainly located in a single phase (scenario F – phase B, high demand; scenario G – phase C, low demand) the voltage value in the phase increases strongly but is higher when MGU are located in the low loaded phase (scenario G).

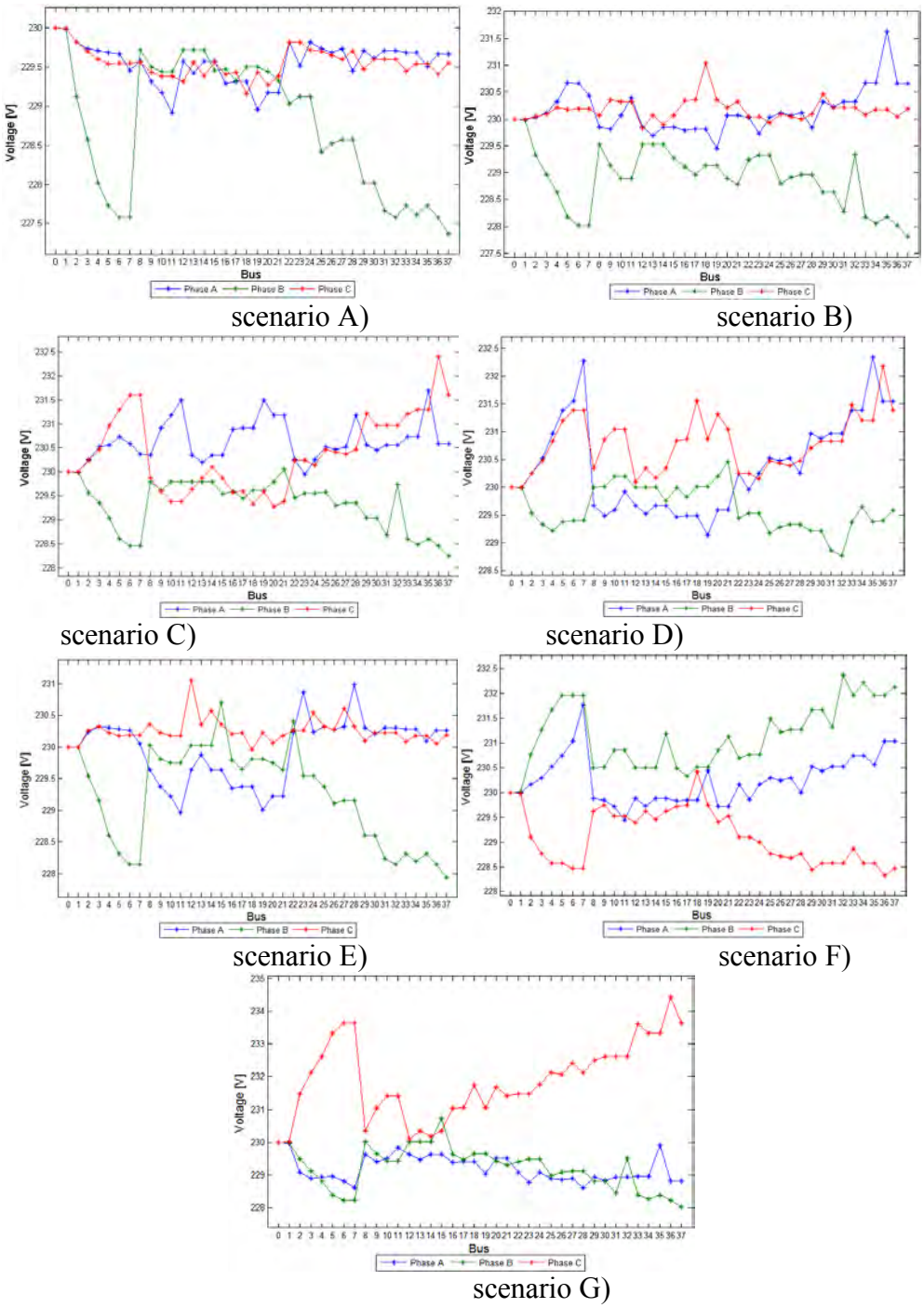

Figure 5- Voltage values at the different buses for all the scenarios

Figure 6 shows the variation in voltage profiles due to the variability of demand or/and micro-generation. For example, according to the collected data, voltage in bus 35 may vary between 229,6V and 234V. In some buses the voltage variation range is much higher (for example, in buses 7, 11, 35) than in other buses (for example, 8, 12, 14, 15). In figure 6 circles show the average voltage values in each bus.

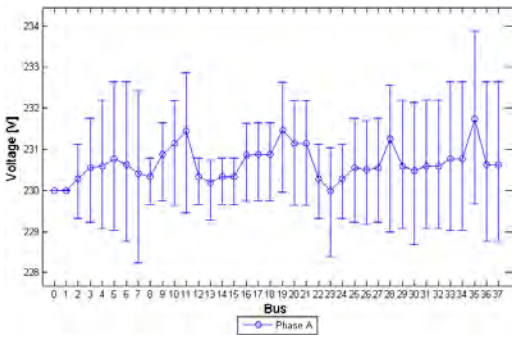

Figure 6- Variation of voltage profile at 12h in phase A due to demand uncertainty and micro-generation variability.

The single-phase nature of both most end-use loads and of micro-generation units at residential level together with the unsymmetrical nature of the LV distribution networks may result in unbalanced voltages. In Figure 7 the unbalance of voltage at bus 36 for the different scenarios is shown. G is the scenario presenting the highest voltage unbalance, resulting from micro-generation occurs mainly in the phase with the lower demand/higher voltage.

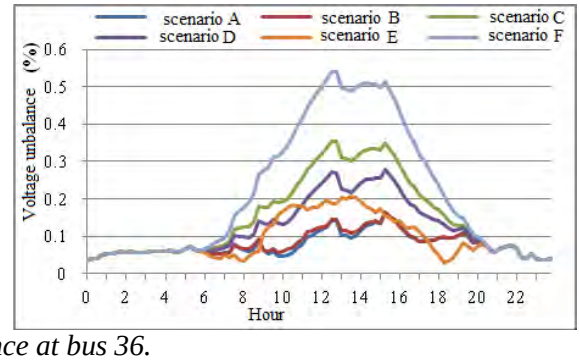

Figure 7- Voltage unbalance at bus 36.

5. Conclusions

The increasing penetration of micro-generation on LV distribution networks will impact the flow of power, with possible reverse flows, and voltage levels on the network. It is clear that besides the detailed assessment of those impacts, the accurate calculation of benefits pointed out to this type of generation, such as losses reduction, needed to be carried out. In this work Monte Carlo models have been used to reproduce the demand and available micro-generation in a LV distribution network, taking into account the uncertainty associated with both the demand and generation, in order to allow a detailed assessment of the impacts of MGU in the power flows, voltage levels and unbalance and in the power losses. By using load diagrams developed from interval metering in each consumer and Monte Carlo simulations it is possible to use realistic demand patterns with adequate time resolution.

References

[1] P. Costa, M. Matos, Avoided losses on LV networks as a result of microgeneration, Electric Power Systems Research, 79, 2009, pp. 629-634.

[2] E. Carpaneto, G. Chicco, J. Akilimali, Loss Partioning and Loss Allocation in Three-Phase Radial Distribution Systems With Distributed Generation, IEEE Transactions on Power Systems, Vol. 23, No. 3, August 2008, pp.1039-1049.

[3] P. Trichakis, P.C: Taylor, P.F. Lyons, R: Hair, Predicting the technical impacts of high levels of small-scale embedded generators on low-voltage networks, IET Renewable Power Generation, 2008, Vol. 2, No. 4, pp. 249-262.

[4] D. Zhu, R. Broadwater, K.-S. Tam, R. Seguin, H. Asgeirsson, Impact of DG placement on reliability and efficiency with time-varying loads, IEEE Transactions on P ower Systems, Vol. 21, No. 1, February 2006, pp.419-427.

[5] V. Quezada, J. Abbad, T. Román, Assessment of Energy Distribution Losses for Increasing Penetration of Distributed Generation, IEEE Transactions on Power Systems, Vol. 21, No. 2, May 2006, pp. 533-540.

[6] P. Barker, R. Mello, Determining the Impact of Distributed Generation on P ower Systems: Part 1 – Radial Distribution Systems, Power Engineering Society Summer Meeting, 2000, IEEE.

[7] J.-H. Teng, Modelling distributed generations in three-phase distribution load flow, IET Generation, Transmission & Distribution, 2008, Vol. 2, No. 3, pp. 330-340.

[8] M. Begović, A. Pregelj, A. Rohatgi, D. Novosel, Impact of Renewable Distributed Generation on Power Systems, Proceedings of the 34th Hawaii International Conference on System Sciences – 2001.

[9] P. Sritakaew1, A. Sangswang, K. Kirtikara, On the Reliability Improvement of Distribution Systems Using PV Grid-Connected Systems, ECTI Transactions on Electrical Eng., Electronics, and Communications Vol.5, No.1 February 2007.

[10] W. H. Kersting, The computation of neutral and dirt currents and power losses. s.l: IEEE Power Systems Conference and Exposition, 2004, pp. 213 - 218 (vol. I).

[11] W. H. Kersting, and Phillips, W.H, Distribution feeder line models, IEEE Transactions on Industry Applications, 1995, pp. 715 – 720.

[12] A. G. Bhutad, S. V. Kulkarni, S. A. Khaparde, Three-phase load flow methods for radial distribution networks. IEEE TENCON 2003, Conference on Convergent Technologies for Asia-Pacific Region. pp. 781-785, Vol. 2.

[13] G. W. Chang, S. Y. Chu, H. L. Wang, A Simplified Forward and Backward Sweep Approach for Distribution System Load Flow Analysis, IEEE PowerCon 2006, International Conference on Power System Technology. pp. 1–5.

[14] J. Nanda, et al., New findings on r adial distribution system load flow algorithm, IEEE Power Engineering Society Winter Meeting, 2000, pp. 1157 - 1161, Vol.2.

[15] R. M. Ciric, A. P. Feltrin, L. F. Ochoa, Power flow in four-wire distribution networks-general approach, 2003, IEEE Transactions on Power Systems. pp. 1283-1290.

Optimal Sizing of an Islanded Micro-grid for an area in north-west Iran Using Particle Swarm Optimization Based on Reliability Concept

H. Hassanzadehfard[1,*], S.M.Moghaddas-Tafreshi[1], S.M.Hakimi[1]

[1] *Faculty of Electrical Engineering, Khajeh Nasir Toosi University, Iran, Tehran*
** Corresponding author. Tel: +989124798639 Fax: +982188462066, E-mail: sm_hakimi@ieee.org*

Abstract: In islanded micro-grid design, a proper Distributed Energy Resource (DER) selection, sizing and effective coordination between resources are important and challenging optimization tasks. The types and sizes of renewable energy sources such as wind turbines, photovoltaic panels, fuel cell and the capacities of battery bank and the other distributed generators must be optimized in islanded micro-grid design. In this paper, the problem is formulated as a nonlinear integer minimization problem which minimizes the sum of the total capital, operational and maintenance and replacement cost of DERs, subject to constraints such as energy limits of each DER. This paper proposes Particle Swarm Optimization (PSO) for solving this minimization problem. The proposed methodology was used to design micro-grid for northwest of Iran. The simulation studies have shown that the proposed methodology provides excellent convergence and feasible optimum solution for sizing of islanded micro-grids using particle swarm optimization. In this paper some notions of reliability are considered for micro-grid, and the effect of reliability on total cost of micro-grid is evaluated.

Keywords: *Micro-grid, Optimal sizing, Particle swarm optimization, Reliability*

Nomenclature

P_{wind}	*power generated by wind turbines..... kW*	E_{bat}	*stored energy in battery banks ..... kWh*
P_{PV}	*power generated by PV generators ..... kW*	R	*lifetime of project ..... year*
P_{FC}	*power generated by fuel cells ..... kW*	L	*lifetime of each component..... year*
P_{Load}	*..... load power*	ir	*Interest rate ..... %*

1. Introduction

The increase in penetration of distributed generation depth and the presence of multiple distributed generators in electrical proximity to one another have brought about the concept of the micro-grid [1, 2]. Micro-grids comprise low voltage distribution systems with distributed energy sources, storage devices, and controllable loads, operated either islanded or connected to the main power grid in a controlled, coordinated way. Refs. [3, 4] introduce the benefits of micro-grid, such as, enhance local reliability, reduce feeder losses, support local voltages, provide increased efficiency through using waste heat combined heat and power, voltage sag correction or provide uninterruptible power supply functions. Proper selection of distributed energy resources and optimal sizing of them are important and challenging tasks in the designing of islanded micro-grids [5] because the coordination among distributed energy resources is very complicated. The problem can be formulated as a nonlinear integer optimization problem which can be solved by a suitable optimizing methodology. Our aim is to minimize the total costs of the system such that the demand is met. For standalone hybrid wind/PV power systems, a typical tangent method is used to fix the size of wind generator and optimize the size of PV panels and the capacity of batteries [5, 7]. Several research works have been done for selecting the parameters such as the size of wind generators, the size of PV panels and the capacity of batteries but the decision variables collectively taken without any optimizing methodologies [5- 12]. Recently, a genetic algorithm for the concerned problem has been proposed by Xu et al. [13] where genetic algorithm optimizes the size of wind generators, the size of PV panels and the capacity of batteries as decision variables. Although this method provides a better performance in comparison to the previous literature,

it is necessary to find a flexible generalized methodology for any kind of micro-grid designing with higher computational efficiency.
In this paper, the optimal sizing of a wind-PV-fuel cell-battery bank in micro-grid is considered. The optimization is carried out via Particle Swarm Optimization (PSO) algorithm. Generation of hydrogen by the reformer causes a higher reliability for the system.
First, we consider the micro-grid. And then the cost of the system presented by an objective function. Finally some simulation results are presented. This study is performed for Ganje site in northwest of Iran. It is located in a village with a population of 800.

2. Description of the micro-grid components

2.1. Wind turbine

The power of the wind turbine is described in terms of the wind speed by Ref [16]:

$$\begin{cases} 0 & V < V_{cut-in}, V > V_{cut-off} \\ P_{rated} \times ((V - V_{cut-in}) / (V_{rated} - V_{cut-in}))^3 & V_{cut-in} \le V < V_{rated} \\ P_{rated} & V_{rated} \le V \le V_{cut-off} \end{cases} \quad (1)$$

In which V_{cut-in}, $V_{cut-off}$, V, V_{rated} and P_{rated} are cut-in wind speed [m/s], cut-out wind speed [m/s], wind speed [m/s], nominal wind speed [m/s] and the rated power of wind turbine [kW] respectively. In this analysis, each wind turbine has a rated capacity of 1 kW. Cost of one unit is considered 2500$, while replacement and maintenance cost are taken as 1500$ and $75/year. Lifetime of a turbine is taken to be 20 years [14].

2.2. PV

The output power of the PV generator P_{PV}, can be calculated according to the following equation:

$$P_{PV} = \eta_g * N * A_m * G_t \quad (2)$$

Where η_g is the instantaneous PV generator efficiency, A_m is the area of a single module used in a system (m^2), G_t is the global irradiance incident on the titled plane (W/m^2) and N is the number of modules. In this analysis, each PV generator has a rated power of 1 kW. Cost of one unit considered is 6000$ while replacement and maintenance cost are taken as 5000$ and 0$/year respectively. Lifetime of a PV generator is taken to be 20 years [14].

2.3. Fuel cell

Proton exchange membrane (PEM) fuel cell is an environmentally clean power generator which combines hydrogen fuel with oxygen from air to produce electricity.
The capital cost, replacement cost and operational cost are taken as 3$k, 2.5$k and 175$/year for a 1-kw system, respectively. Fuel cell's lifetime is considered to be 5 years [14].

2.4. Battery storage

At any hour the state of battery is related to the previous state of charge and to the energy production and consumption situation of the system during the time from t-1 to t.
In all cases the storage battery capacity is subject to the following constraints:

$$E_{bat\min} \prec E_{bat}(t) \prec E_{bat\max} \quad (3)$$

Where $E_{bat\max}$ and $E_{bat\min}$ are the maximum and minimum allowable storage capacities. $E_{bat\min}$ is determined by the maximum allowable depth of battery discharge (DOD) as follows:

$$E_{bat\min} = (1 - DOD) * E_{bat\max} \quad (4)$$

In this analysis, each battery bank capacity is 552Ah. Cost of each battery is considered 264$ while replacement and maintenance costs are taken as 260$ and 2.64$/year. Lifetime of a battery is taken to be 3 years [14].

3. System modeling

The micro-grid consists of some wind turbines, PV arrays, fuel cells, reformers and battery banks (Fig. 1). Natural gas is used to produce fuel cells' required hydrogen.
It is desirable that the system meets the demand, the costs are minimized and the components have optimal sizes.

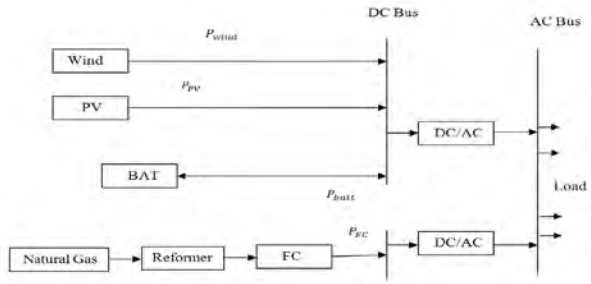

Fig.1. Schematic diagram of micro-grid

3.1. Strategy

We consider three situations for the system: A. generation power produced by renewable energy (wind + PV) meets demand, B. over generation and C. over demand.

3.1.1. Power generation produced by wind and PV meets demand

In this situation the power generated by the wind turbine plus the power produced by the PV array is equal to the demand ($P_{wind}(t) + P_{PV}(t) = (P_{Load}(t)/\eta_{conv})$), hence:

$$E_{bat}(t) = E_{bat}(t-1),\ P_{FC}(t) = 0 \quad (5)$$

It is notable that the time steps Δt are taken to be 1 hour in this study.

3.1.2. Over generation

The produced power of the wind turbine plus power produced by the PV array are more than the demand ($P_{wind}(t) + P_{PV}(t) \succ (P_{Load}(t)/\eta_{conv})$).
The excess power is utilized for charging the batteries:

$$E_{bat}(t) = E_{bat}(t-1) + (P_{wind}(t) + P_{PV}(t) - P_{Load}(t)/\eta_{conv}) * \Delta t * \eta_{cha},\ P_{FC}(t) = 0 \quad (6)$$

3.1.3. Over demand

The demand is more than the power generated by the wind turbines and power produced by the PV array ($P_{wind}(t) + P_{PV}(t) \prec (P_{Load}(t)/\eta_{conv})$).

In this situation we have two cases:
a. Available battery banks' energy and power generation of wind turbine plus PV array can meet demand ($P_{wind}(t) + P_{PV}(t) + (E_{bat}(t) - E_{bat\min}) * \eta_{dech} / \Delta t \succ (P_{Load}(t)/\eta_{conv})$).

$$E_{bat}(t) = E_{bat}(t-1) + (P_{wind}(t) + P_{PV}(t) - P_{Load}(t)/\eta_{conv}) * \Delta t / \eta_{dech}\ ,\ P_{FC}(t) = 0 \quad (7)$$

b. Available battery banks' energy and power generation of wind turbine plus PV array can not meet demand:

In this situation the battery banks are completely discharged and the energy in the battery banks is equal to $E_{bat\min}$. In this state, load requirements are supplied from the fuel cell:

$$E_{bat}(t) = E_{bat\min}\ ,\quad P_{FC}(t) = (P_{Load}(t)/\eta_{conv}) - P_{PV}(t) - P_{wind}(t) - (E_{bat}(t) - E_{bat\min}) * \eta_{dech} / \Delta t \quad (8)$$

3.2. System's cost

In this paper we consider the capital and replacement costs, the operation and maintenance costs of each component of micro-grid.
We choose Net Present Cost (NPC) for calculation of system's cost.

3.2.1. Net Present Cost

The Net Present Cost (NPC) of each component is defined as [15]:

$$NPC = N * (capital\_\cos t + replacement\_\cos t * K + operation\ \&\ maintenance\_\cos t * \frac{1}{CRF(ir,R)} \quad (9)$$

$$CRF(ir,R) = \frac{ir*(1+ir)^R}{(1+ir)^R - 1}\ ,\ K = \sum_{n=1}^{y} \frac{1}{(1+ir)^{L*n}} \quad (10)$$

L is the lifetime and N is the optimal number of each component.

3.2.2. The objective function

The objective function is the sum of all net present costs [16]:

$$NPC = NPC_{wind} + NPC_{PV} + NPC_{battery} + NPC_{FC} + NPC_{ref} + NPC_{conv} \quad (11)$$

The objective function must be minimized, such as minimization is done by PSO algorithm in this paper.

4. Simulation results

Lifetime of the project is 20 years. In this article, the optimum combination of the micro-grid considered shown in Fig.1 is calculated. The system data consists of the annual wind data and

solar radiation which belong to a region in northwest of Iran. The load curve which is actually an IEEE standard curve with 500 kW peak, the yearly wind speed and solar radiation are showed in fig.2. For the sake of simplicity, we have considered the weekly mean in input data in our simulation. The data is the wind velocity and the demand in every one hour in a day. So, an average of the input data in each hour is calculated during a week. The power of the wind turbine and PV array could be derived by Eq. (1.2) from the wind speed and solar radiation data. The optimal size of wind turbine, PV array, battery bank and Fuel cell are shown in table.1. Fig.3. shows the output power of wind turbine, PV array, fuel cell and Energy of battery storages. We see that at the time 940, fuel cell injects power to the micro-grid. Where the available battery storage energy is equal to minimum allowable storage capacity and output power of PV array is equal to zero. Also output power of wind turbine does not satisfy the micro-grid's demand, so fuel cell injects power to the micro-grid in order to compensate load requirements. Fig.4. Shows the system costs in terms of the iterations.

Table 1. Optimal size of each component.

Number Wind turbine	Number PV array	Number Battery bank	Number Fuel cell	Total cost $
351	1758	4217	187	17.838M

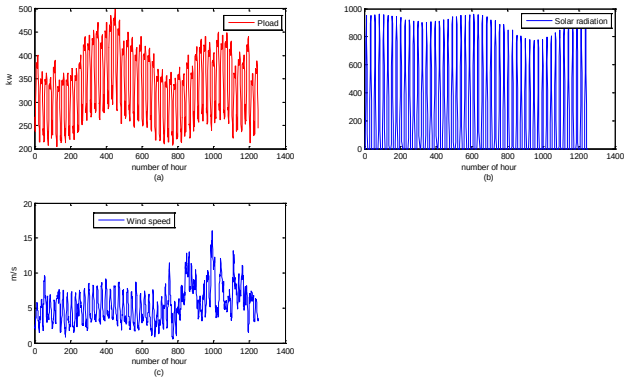

Fig. 2. (a). Load information. (b) Solar radiation information. (c) Wind speed information.

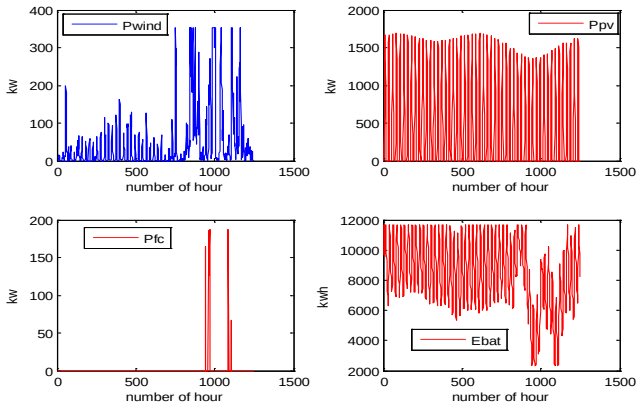

Fig. 3 (a) Output power of wind turbine. (b) Output power of PV array. (c) Output power of fuel cell. (d) Energy fluctuate of battery banks.

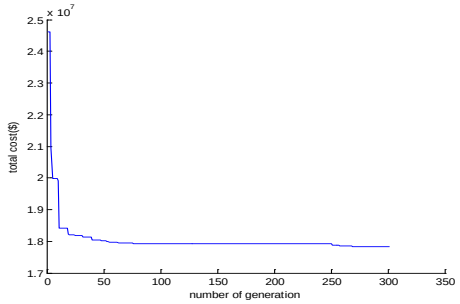

Fig. 4. The optimal cost of micro-grid in terms of the iterations

4.1. Effect of the capital cost of PV arrays on simulation results

In this section, the effect of capital cost of PV arrays, on the optimal size of each component and total cost of micro-grid is regarded. Table.2 shows that increasing the capital cost of the PV array causes the micro-grid costs to increase and the optimal size of PV array to reduce.

Table 2. Effect of capital cost of PV array.

Capital cost of PV unit	Wind turbine	PV array	Battery bank	Fuel cell	Total cost $
5000	337	1787	4154	193	16.149M
6000	351	1758	4217	187	17.838M
7000	383	1748	4263	172	19.558M
8000	523	1603	4732	106	20.646M

5. Reliability

Some notions of reliability are commonly used for systems with hourly demand and supply data. Loss of Load Expectation (LOLE), Loss of Energy Expectation (LOEE), Loss of Power Supply Probability (LPSP) and Equivalent Loss Factor (ELF) are some of them considered in this paper. ELF is described by:

$$ELF = \frac{1}{N}\sum_{t=1}^{N}\frac{Q(t)}{D(t)} \tag{12}$$

Where $D(t)$ is the total energy demand, $Q(t)$ is the loss-of-load and N is the number of hours. The ELF contains information about both the number of outages and their magnitude. In this paper we regard that ELF should be lower than 0.01 [17].

5.1. Simulation Result considering reliability parameters

In this micro-grid when the power of fuel cell to support the demand is greater than the optimal size, $Q(t)$ is described by:

$$Q(t) = P_{FC}(t) - N_{FC} * P_{Fuel-Cell} \tag{13}$$

Where N_{FC} is the optimum size and $P_{Fuel-Cell}$ is the rated power of fuel cell. The cost of electricity interruptions has been estimated. The value we use in our model is 5.6 $/kWh. Fig.5. depicts the flowchart of the algorithm simulating the micro-grid considering reliability. The optimal size of wind turbine, PV array, battery bank, fuel cell and the total cost of micro-grid are shown in table. 3.

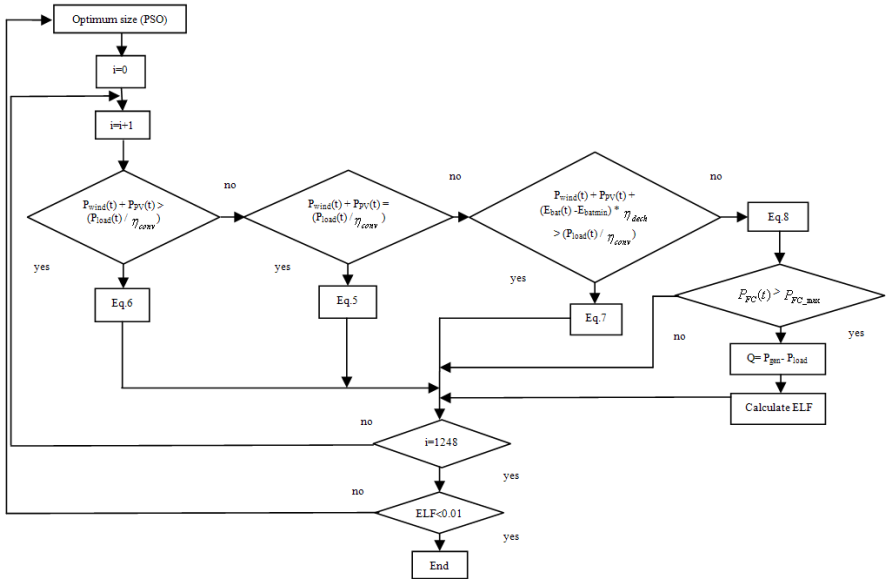

Fig.5. The flowchart of the algorithm simulating the micro-grid considering reliability.

Table.3. Optimal size of each component considering reliability parameters.

Wind turbine	PV array	Battery bank	Fuel cell	Total cost $
515	1660	3150	14	15.33M

Table.3 shows that considering reliability parameters such as ELF for micro-grid (some of loads in some hours are not satisfied) reduces the total cost of micro-grid. Figure 6 shows the loss of energy in each hour.

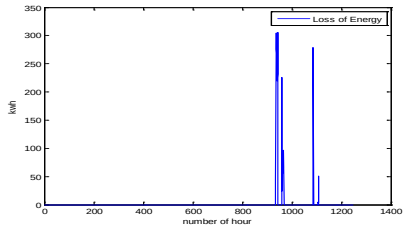

Fig. 6. Loss of energy in each hour.

We see that maximum loss of energy appears at the time between 900-1000.Where the available battery storage energy and output power of PV array to inject to the micro-grid is equal to zero. The value of some notions of reliability is shown in table. 4. Table 4 shows that ELF is in the acceptable confine.

Table 4. The amount of some notions of reliability

LOLE (hr/yr)	LPSP	LOEE (MWh/yr)	ELF	Penalty
24	$9.1098*10^{-3}$	3.8623	$9.999*10^{-3}$	0.21235M

6. Conclusion

In this paper the optimal sizing and operation strategy of micro-grid are considered. The system consists of wind turbines, PV arrays, fuel cells, battery banks, reformers and DC/AC converters. The micro-grid used in this study has high reliability because fuel cells are as a backup for wind turbines and PV arrays. The main problem of renewable energy source is that they are dependent on environmental conditions. So they could not cover the demand

perfectly. Entering storage component solves this problem significantly. In this study battery bank is used to cover the demand desirably. We assumed that in each hour micro-grid can interrupt loads subject to reliability constraint such as ELF. In this situation total cost of micro-grid reduces.

References

[1] R. Lasseter, A. Akhil, C. Marnay, J. Stephens, J. Dagle, R. Guttromson, A. Meliopoulos, R. yinger and J. Eto, “White paper on Integration of consortium Energy Resources. The CERTS MicroGrid Concept.”CERTS, CA, Rep.LBNL-50829, Apr.2002.

[2] MICROGRIDS: Large Scale integration of Micro-Generation to low Voltage Grids” EU contact ENK5-CT-2002-00610, Technical Annex, May 2002.

[3] Lasseter RH. MicroGrids. IEEE Power Eng Soc Transm Distrib Conf 2002(1):305–8.

[4] Marnay Chris, Venkataramanan Giri. Microgrids in the evolving electricity generation and delivery infrastructure. IEEE Power Eng Soc Gen Meet 2006:18–22.

[5] H. L. Willis and W. G. Scott, Distributed Power Generation: Planning and Evaluation, Marcel Dekker, New York, 2000.

[6] California Distributed Energy Resources Guide, Available at: http://www.energy.ca.gov/distgen/

[7] B. S. Borowy and Z. M. Salameh, "Methodology for Optimally Sizing the Combination of a Battery Bank and PV Array in a Wind/PV Hybrid System," IEEE Trans. On Energy Conversion, pp.367-375, 1996.

[8] M. A. Habib, S. A. M. Said, M. A. El-Hadidy and A. I. Zaharna," Optimization Procedure of Hybrid Photovoltaic Wind Energy System Energy," pp.919-929, 1999.

[9] J. K. Kaldellis, "Parametric Investigation Concerning Dimensions of a Stand-alone Wind-Power System," Applied Energy, pp.35-50, 2004.

[10] B. Ai, H. Yang, H. She and X. Liao, "Computer-aided Design of PV/wind Hybrid System," Renewable Energy, pp.1491-1512, 2003.

[11] M. A. Elhadidy and S. M. Shaahid, "Optimal Sizing of Battery Storage for Hybrid (wind+diesel) Power Systems," Renewable Energy, pp.77-86,1999.

[12] A. M. Al-Ashwal and I. S. Moghram, "Proportion Assessment of Combined PV-Wind Generating Systems," Renewable Energy. pp.43-51, 1997.

[13] D. Xu, L. Kang and B. Cao, "Optimal Sizing of Standalone Hybrid Wind/PV Power Systems Using Genetic Algorithms," Proc. of IEEE Canadian Conference on Electrical and Computer Engineering, Canada, pp. 1705-1708, 2005.

[14] M.J. Khan, M.T. Iqbal, "Pre-feasibility study of stand-alone hybridenergy systems for applications in Newfoundland", Renewable Energy 30 (2005) 835–854.

[15] <www.mahler-ags.com>

[16] Hakimi SM, Moghaddas-Tafreshi SM. "Unit sizing of a stand-alone hybrid power system using particle swarm optimization (PSO)". IEEE ICAL Aug 2007; 18–21:3107–12.

[17] Raquel S. Garcia, Daniel Weisser, "A wind–diesel system with hydrogen storage: Joint optimization of design and dispatch", Renewable Energy 31 (2006) 2296–2320.

Evaluation of the Solar Hybrid System for Rural Schools in Sabah, Malaysia

Abdul Muhaimin Mahmud

Public Works Department of Malaysia, Kuala Lumpur, Malaysia.
Tel: +603 92354399, E-mail: *muhaimin@jkr.gov.my*

Abstract: The impact of the implementation of solar hybrid system which was installed at Penontomon Primary School in Sabah, Malaysia has been analyzed in this paper. The project was initiated by the Malaysia's Ministry of Education with the target to electrify rural schools that do not have grid connected electricity in Sabah with alternative power supply; ie, the renewable energy. The paper looked into the users' experiences, technical and the economical aspects of the system and found that alternative resources from renewable energy offers better electricity in providing power supply to the rural schools than the old and conventional diesel generator system. The technology gives benefit and impact to the pupils and teachers by creating more comfortable lifestyle and conducive learning environment.

Keywords: *Solar hybrid, Rural schools, SCADA, Battery, Inverter*

1. Introduction

Malaysia, although moving rapidly towards being a developed nation, has a considerable number of under-developed rural areas. Most of these are tiny pockets of inhibited villages, sprawling over large areas of Sabah and Sarawak (the Borneo Island part of Malaysia). In general, basic infrastructures are inadequate and grid connected electricity supply is the major one. Out of more than 10,000 schools in Malaysia, 809 in Sabah and Sarawak still lacked 24-hour electricity supply and have to rely on decentralized diesel generator as the main source. The main reasons can be attributed to (1) the remote locations of these villages and (2) the community size is very small. These factors caused the investment cost for grid supply prohibitively expensive and un-economic. The cost of electricity using this method is very high – primarily due to the fuel transportation to the sites. Furthermore, consistent electricity cannot be guaranteed because of the climatic and geographical conditions that may hamper the fuel supply route. To ensure that these areas are not lagging behind in the country's modernization strategy, the Ministry of Education (MOE) has initiated a large electrification program for rural schools in Sabah. It is recognized that stable and reliable electricity supply is the key element for conducive learning environment and enables the use of computers, communication system, lighting and etc [2]. The government has allocated over RM1.15 billion (USD365 Million) to improve the basic infrastructure [1]. Fittingly, electricity supply is given top priority.

Despite the fact that the program has been going on for two years, there is no documented literature describing the design methodology, performance analysis, economics evaluation and the social impact of the installed systems. It is envisaged that the lessons learned from these experiences can provide valuable guidelines for future rural electrification programs using SHS. Hence this work is carried out. The study can be divided into two parts (1) to analyze the technical and the economical aspects of the system design and daily operation based on real data (2) to study and analyze the impact of the SHS on their lifestyle and the learning environment.

2. Methodology

This study used quantitative and qualitative methods in determining the impact of the Solar Hybrid System to the end users and to evaluate the system performance.

2.1 Impact On The Solar Hybrid System

Structured questionnaires were distributed to the 40 selected respondents, which consists of the teachers and pupils. The questionnaire was developed to ensure that the impact of the system can be analyzed base on;

a) Comparison of the users' experience before and after the system installed and how the system does affects their life and the learning environment.
b) Comparison of the users' knowledge of renewable energy especially the Solar Hybrid System before and after the installation.
c) Load management strategies which are being exercised by the users.
d) Users' opinions on how the system can benefit the entire community should the same system implemented for their village as well.

2.2 Implementation and Operation of the Solar hybrid System

The second part of the methodologies determines the Solar Hybrid System performance technically and economically. The design and actual load analysis compares the design load profile and the actual load profile (average) and the system operation analysis answers the sustainability and reliability issues of the system. The measurement data, recorded by the online monitoring system; ie, JKR Supervisory Control and Data Acquisition System (JSCADA) are used to analyze the system performance. The economic analysis includes both costs and benefits of the system. Parameters like investment cost, operating cost and cost of energy are used to measure the beneficial of the system as compared to the conventional diesel generator [4].

3. Solar Hybrid System

The solar hybrid system integrates two power sources. The system is designed to supply electricity for every building in the school like class rooms, computer lab, guard house and teachers' quarters. For the purpose of the analysis, Penontomon Primary School which is located in Keningau District in Sabah (N 4°52.73' E 116°15.9') has been identified to be the sample site for evaluation and analysis processes.

3.1 Description of Loads & Load Profile

The total installed rated load power for SK Penontomon is 15.23 kW [6]. The load usage has been distributed over 24 hours load profile which used to identify the maximum peak load during the day. The daily energy consumption for SK Penontomon was calculated from the load profile. During daytime, the energy demand is at 35,964 Wh which is 69.53% of the total daily energy demand. While at night it requires 30.47% of the daily energy demand (15,722 Wh). Daytime is considered from 06.00 hours to 18.00 hours which is the normal sun rise and sunset for the location.

3.2 System Configuration

As shown in Figure 1 below, the 20 kW_p PV array is used to supply power to the load and to charge the battery during day. Priority will be given to satisfy the day time load. A 3,500 Ah tubular vented deep cycle lead acid battery bank is used for storage and supply power to the loads mostly during night. The bidirectional inverter converts the DC-AC voltage and vice

versa. If there were insufficient power from the PV to charge the battery, the 27 kVA diesel generator will turn on automatically. Moreover, excesses electricity from the generator will be used to electrify the loads. The generator is configured to be automatically turned on for one hour every week to warm up and also once a month for several hours for battery equalization.

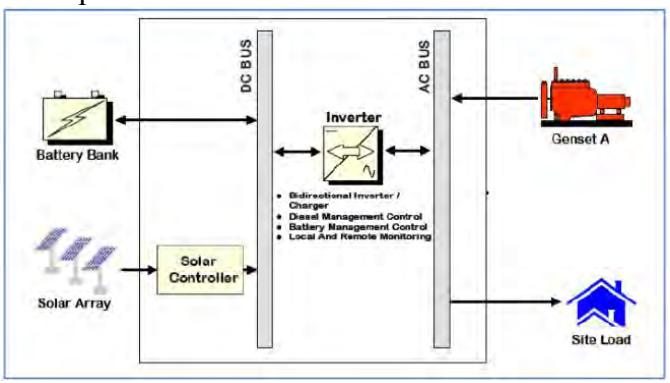

Figure 1 : The solar hybrid system configuration diagram [6].

4. Results and Analysis

4.1 User Experiences

4.1.1 Knowledge

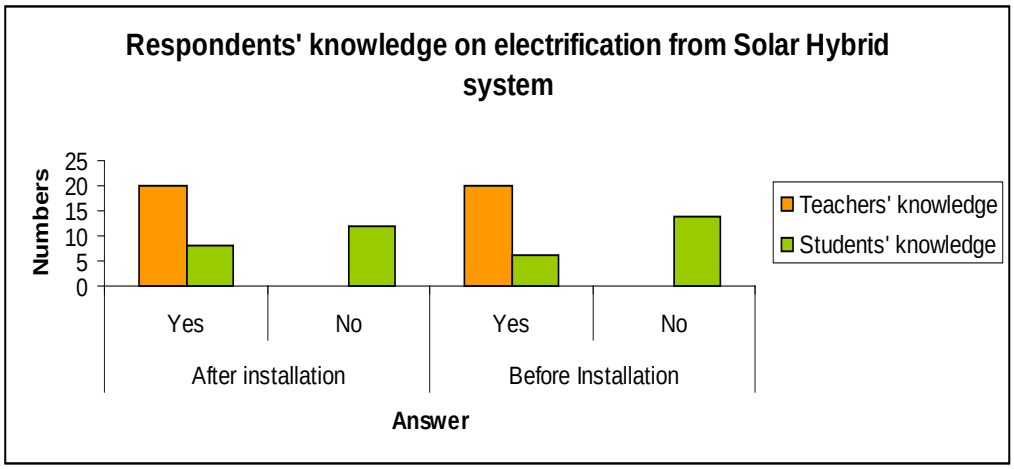

Figure 2 : Respondents' knowledge on electrification from solar hybrid technology system.

All of the teachers and only six pupils have some knowledge of the Solar Hybrid System before the installation of the system. The numbers of the pupils that gain information of the system after it is in operation increasing by 10%.

Books, magazines and newspapers are the popular sources of information of the system. 40% of the respondents have read about the technology. For the pupils, most of them knew about renewable energy by reading from the school library. Alternative information is from the internet as 20% of the respondents get the information from the World Wide Web (www.). The internet can be access from the school's computer lab or at other places/towns nearby.

35% of the respondents have seen the technology before at other places/villages. The technology was installed for village communities in several rural electrification programs like

Solar Home System (SHS) by Ministry of Rural and Region Development and Solar PV System for Rural ICT Centre by Ministry of Energy, Water and Communication.

The education system also provides some basic information on renewable energy system in standard six's Science subjects. 16% of the respondents learn/teach the subject and they are mostly the Science teachers and standard six pupils.

Four respondents replied that they get the information from other sources. Three of them by informal conversation and the other one have a standalone PV system installed at his house nearby.

4.1.2 User Training

At least a teacher from each school is required to attend training on solar hybrid technology. The teacher will be responsible to give the information on the technology to the other users. It is found out that only informal explanation was given to the users. As shown in figure 3 below, only 24 respondents were given informal information and eighteen respondents understand well about the technology, while another six respondents requested for more explanation and formal training.

The main barrier in implementing PV system in any rural electrification program is the operation period. PV system and its implementation are frequently looked upon in a very simplistic manner by a number of people which has resulted in a large number of failures [4]. Proper transfer of technology training program is required for the end users because the awareness and knowledge on the system technology are equally as important as the adequate financing and institutional framework.

4.1.3 Load Management Strategies

All of the respondents replied that they practiced load management when using the electricity. However, they do not have a schedule management or do not strategies their usage. All loads would only be turned on when required. For example, if during the class there was enough sunlight to light the room, lamps will not be used. All the loads in the school building would be turned off when there is no occupant in the room, except for the equipments that need 24 hours operation like refrigerator.

4.1.4 Users' Opinions

All of the respondents voted that technology gives benefit and impact to their lifestyle and the learning environment. Nowadays, the teaching and learning process is more comfortable as teachers can use interactive teaching methods using computers and projector at anytime during the school period. Besides, the teachers and pupils can get access to the internet from the already installed satellite communication system (Very Small Aperture Terminal – VSAT). There is no case of damage electronic equipments after the installation and for teachers who live in the teachers' quarters; they can access the latest news and entertainment from the television and radio, store food in the refrigerator, and stay awake for more time during the night. As for the pupils, they can have extra classes during the night especially for pupils who will sit for the national primary school examination.

The respondents believe that the nearby village should be connected by renewable energy technology especially the solar hybrid system. They believe that, electricity is an important element for developing a community and nation and therefore can bridge the development gap between the urban and rural areas in economy, education, lifestyle, communication and etc.

4.2 Design and Actual Load Analysis

Figures 3 and 4 below show the comparison of the load profile for both schools.

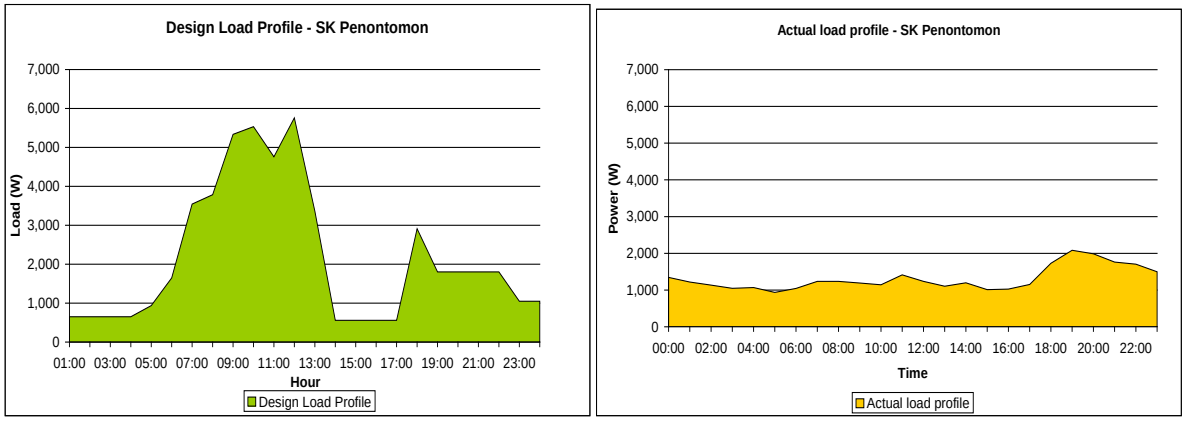

Figure 3 and 4 : The design load profile [6] (left) and t he actual load profile (right) for SK Penontomon. The actual load profile was calculated based on the load consumption in September 2009 recorded from the JSCADA system.

The actual base load (minimum load) for the school is double the value of the design base load. The maximum actual load is half the value of the design load. The maximum actual load for SK Penontomon occurred at night instead of day as assumed in the design profile.

The total daily energy consumption was less 30% than the design values. The actual energy consumption at SK Penontomon was higher at night. The reason is the teachers' quarters in SK Penontomon contribute 41% of the total load sharing.

4.2 System Operation Analysis.

Parameter that can determine the reliability of the PV system to supply electricity to the load is *Loss of Load (LL)*. Moreover, another two useful parameters are the *Generator Capacity, C_A* and the *Accumulator Capacity, C_S*. "C_A, is defined as the ratio of the daily energy output of the PV generator divided by the daily energy consumption of the load" [3]. "C_S is the maximum energy that can be extracted from the accumulator divided by the daily energy consumption of the load" [3]. Hence the equations will be;

$$C_A = \frac{E_{PV}}{L} \quad (1)$$

$$C_S = \frac{C_U}{L} \quad (2)$$

Where E_{PV} is the daily energy output of the PV generator, L is the daily energy consumption of the load and C_u is the maximum energy that can be extracted from the battery. For rural electrification purposes as mentioned in [3], the values of both C_A and C_S are commonly used as $C_A \approx 1.1$ and $3 \leq C_S \leq 5$. But C_A is also depending on the local solar climate condition.

Solar fraction, also known as renewable energy fraction, is the amount of energy provided by the solar technology system divided by the total energy required [5]. This shows the system dependency on the diesel generator as compared to the solar PV.

The *battery energy efficiency,* η_{Wh} is the ratio of the energy discharged from the battery to the energy charged to the battery within a certain period of time [3]. In this study, one month energy efficiency is calculated.

Table 1 : Summary of the system energy parameters for both systems.

Parameter	**Symbol**	**SK Penontomon**
Loss of load	LL	0 %
PV Generator capacity	C_A	1.57
Accumulator capacity	C_S	5.76
Solar Fraction	SF	92%
Battery Energy Efficiency	η_{Wh}	94%

The system satisfies the entire load required. Loss of load value of zero shows that the system which consists of PV, storage and generator is reliable and can produce sufficient and sustainable energy to satisfy the electricity demand by users.

The combination of the PV and the generator shows that the system is not very dependent on the usage of the generator and allows a significant lower quantity of diesel used during the measurement. The data also showed that the system can work without any major problems.

4.4 Economic Analysis

Generally, for either systems (diesel generator only or solar hybrid system), the Cost of Energy (COE) is depending on the size of the system. A bigger system capacity reduces the COE. But, it will also increase the investment cost.

The operating cost of both systems shows that the client will be burden by the higher cost for operating the diesel generator system compared to the solar hybrid system. For solar hybrid system, the service and maintenance routine should be done at least twice a year excluding the corrective maintenance. The generator has less services every year since the operation hours is minimum.

Table 2: Result from Homer simulation on the economic aspect [4].

Parameters	SK Penontomon	
	Diesel generator	**Solar Hybrid System**
Investment cost	€134,371.00	€568,131.00
Cost of Energy	€3.83/kWh	€5.86/kWh
Operating cost	€59,787.00/yr	€49,415.00/yr
Diesel Generator energy produced	29.36 MWh/yr	2.06 MWh/yr
Diesel consumption	12,514.00 L/yr	778.00 L/yr
Cost of Diesel[1]	€18,771.00/yr	€1,167.00/yr

Figure 5 below is the total cost of the project in twenty five years of its lifetime. It is based on the components cost including their replacement cost, civil works of building the power house, electrical works especially for mini grid installation, fuel cost and the operation and maintenance costs. Replacement of batteries is considered in every 6 years, diesel generator in 8 years and inverter and charge controller in 15 years [3]. It is clearly shows that the batteries are the most important component of the system as it contributes 45% of the lifetime project cost.

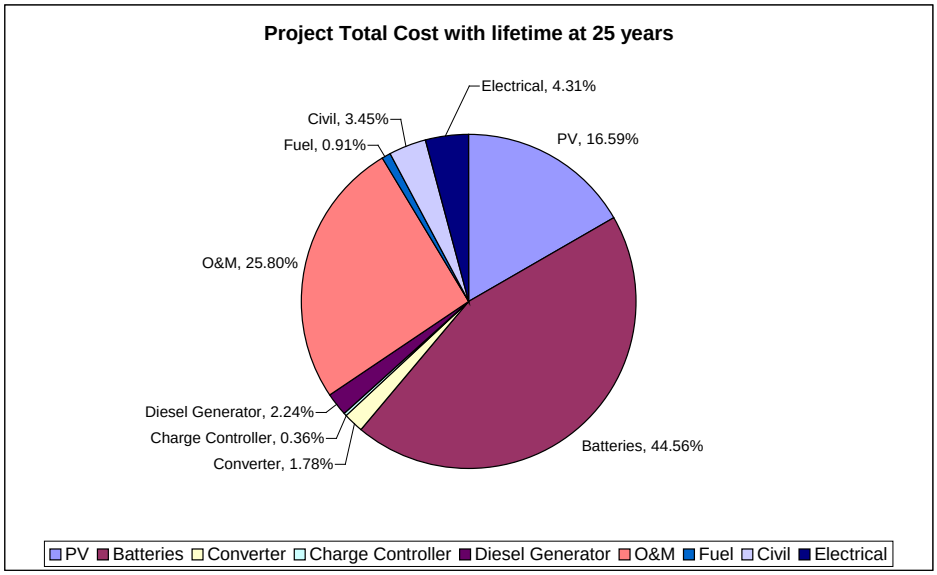

Figure 5 : Project total cost of the solar hybrid system. The project lifetime is at 25 years.

[1] Diesel price is assumed at €1.50 per litre of diesel at the sites. The diesel selling price in Malaysia is at € 0.34/litre due to subsidized by the government. The higher price as compared to the normal selling price is due to logistic cost to supply the diesel to the remote areas.

5. Conclusion

In general the solar hybrid system offers better electricity in providing power supply to the rural schools than the old and conventional diesel generator system. The technology gives benefit and impact to the pupils and teachers by creating more comfortable lifestyle and conducive learning environment.

The measurements and simulation of the system shows that the solar hybrid system can produce reliable power supply to meet the electricity need of rural schools. The system was designed and configured correctly but predicting the load pattern to be as accurate as the actual load consumption has always been the challenging part.

The combination of the PV-batteries-generator reduces the dependency of the fuel consumption and fully utilizes the clean energy from the sun. Even though a diesel generator system costs less than a solar hybrid system, but the fact that its operating costs in providing a proper service and maintenance makes the system less favorable compared to the solar hybrid system. The study shows that the heart of the system lies on the batteries as it contributes almost half of the total lifetime cost and almost half of the daily load consumption is served by the batteries. Improper conducts on t he system may directly affect the batteries performance which may lead to the failure of the system.

6. Acknowledgement

My deepest gratitude to my supervisor; Mr. Hans Gerhard Holtorf of University of Oldenburg, Germany, my family, officers/friends at Electrical Engineering Branch, Public Works Department of Malaysia, and Public Service Department of Malaysia for sponsoring my study. Also thanks to my entire PPRE and EUREC classmates.

References

[1] *National Green Energy Technology Policy*, (2009), Ministry of Energy, Green Technology and Water, Malaysia.

[2] United Nation Development Programme – Malaysia, *MDG7 – Achieve Universal Primary Education,* http://www.undp.org.my/

[3] Luque, L., Hegedus, S., (2003), *Handbook of Photovoltaic Science and Engineering*, Wiley.

[4] National Renewable Energy Laboratory, *HOMER – The Micropower Optimization Model*, http://www.nrel.gov/homer

[5] Wikipedia, *Solar Saving Fraction*, http://en.wikipedia.org/wiki/Solar_fraction

[6] Public Works Department of Malaysia, (2008), *Cadangan Merekabentuk, Membina, Membekal, Menyiapkan dan M enyelenggara Sistem Solar Hibrid Bagi Sekolah Luar Bandar Negeri Sabah P akej 1(Design, Build, Supply, Commission and Maintain of the Solar Hybrid System for Rural Schools in Sabah Package 1)*, Contract Document.

Analysis of dust losses in photovoltaic modules

J. Zorrilla-Casanova*[1], M. Piliougine[1], J. Carretero[1], P. Bernaola[1], P. Carpena[1], L. Mora-López[2], M. Sidrach-de-Cardona[1]

[1] *Dpto. de Física Aplicada II, Universidad de Málaga, 29071 Málaga, Spain*
[2] *Dpto. de Lenguajes y Ciencias de la Computación, Universidad of Málaga, 29071 Málaga, Spain*
** Tel: 34- 95-213-2772 , Fax: 34-95-213-1355, Email: ppz@ctima.uma.es*

Abstract: The accumulation of dust on the surface of a photovoltaic module decreases the radiation reaching the solar cell and produces losses in the generated power. Dust not only reduces the radiation on the solar cell, but also changes the dependence on the angle of incidence of such radiation. This work presents the results of a study carried out at the University of Malaga to quantify losses caused by the accumulation of dust on the surface of photovoltaic modules. Our results show that the mean of the daily energy loss along a year caused by dust deposited on the surface of the PV module is around 4.4%. In long periods without rain, daily energy losses can be higher than 20%. In addition, the irradiance losses are not constant throughout the day and are strongly dependent on the sunlight incident angle and the ratio between diffuse and direct radiations. When studied as a function of solar time, the irradiance losses are symmetric with respect noon, where they reach the minimum value. We also propose a simple theoretical model that, taking into account the percentage of dirty surface and the diffuse/direct radiation ratio, accounts for the qualitative behavior of the irradiance losses during the day.

Keywords: *optical losses, dust effects, energy losses*

1. Introduction

The accumulation of dust on the surface of the photovoltaic modules decreases the incoming irradiance to the cell and produces power losses (see [1] and references therein). Previous studies [2] show that in dry areas, these losses could reach 15%. In these cases the only solution is to clean the modules with water. In large-scale photovoltaic plants this task is often expensive, especially in those areas with water shortage.

Some approaches to analyze and quantify the effect of dust on photovoltaic modules have been proposed in the literature. The early studies about the relationship between dust and transmittance date back to a few decades ago, all of them in the context of solar thermal collectors. For example, in [3], the effect of dust on the irradiance received by various inclined surfaces of flat-plate collectors have been studied. The performances of one photovoltaic and two thermal panels during several months of outdoor exposure in Saudi Arabia have been measured in [4]. For the photovoltaic panel, the average degradation rate of the efficiency was 7% per month. The authors of [5] made an experimental study of the effect of accumulation of dust on the surface of photovoltaic cells. Several kinds of dust having different physical properties were used. Experiments were performed using a solar simulator. They concluded that the results depend on many factors like the principal dust material, the size of dust particles and dust deposition density. We can see in [6] a computerized microscope system that has been developed for studying the physics of dust particles, which adhere to the surface of solar collectors and photovoltaic modules. The device enables investigators to calculate the particle size distribution of dust and the fraction of surface area covered by dust. Some examples are given for the use of such a measuring system for the study of photovoltaic and solar-thermal collector surfaces. Wind tunnel experiments were described in [7] to study the effect of wind velocity and air dust concentration on the drop of photovoltaic cell performance caused by dust accumulation on such cells. I-V characteristics were determined for various intensities of cell pollution. The evolutions of the I_{sc}, V_{oc}, P_{max}, and FF were examined.

This work presents measurements of radiation losses produced by the accumulation of dust. The experiment has been carried out at the roof of the Photovoltaic Laboratory of the University of Málaga (latitude 36.7 °N, longitude 4.5 °W, altitude 50 m) in the south of Spain. The campus is located between a residential and an industrial area surrounded by open fields with shrubs, weeds and some olive trees. Several roads with heavy traffic flow are very close to the building. At the time of the measurements, some excavations have been conducted in the vicinity of the building, which has increased the amount of inorganic dust particles present in atmospheric air.

2. Methodology

The objective of this work is to quantify losses caused by the accumulation of dust on the surface of photovoltaic modules. With this aim, irradiance values measured by two mSi cells have been recorded every ten minutes during a year. These cells have been previously calibrated against a reference pyranometer Kipp and Zonen CMP21. One of the reference cells has been cleaned daily, while the other has not been cleaned throughout the experiment (one year). Other parameters, such as rainfall and wind speed have been also measured.

Each reference cell has a low value shunt resistor between its terminals, and then the voltage drop across the shunt must be proportional to the short-circuit current and so it is further proportional to solar irradiance on the cell. The determination of the calibration constant for each cell is based on a comparison with a reference pyranometer under natural sun along a clear-sky day (only values of irradiance greater than 200 Wm^{-2} have been taken into account). Both sensors (the reference cells and the pyranometer) are connected to an A/D module (cFP-AI-112) installed in Compact FieldPoint cFP-2120 data acquisition system that have been programmed to store a measure of all sensors at one-minute intervals. The manufacturer of the pyranometer provides a sensitivity constant that must be used to determine the actual irradiance value from the voltage its voltage output. Finally, a linear regression (setting offset to zero) between voltage values across each shunt and irradiance value have been performed to determine each constant.

Once the calibration procedure has been performed both cells remained installed and connected to the acquisition data system and measures of both of them have been recorded every three minutes along one year. The output value of each cell has been multiplied by the constant obtained by the calibration procedure in order to get the irradiance. Whereas one of them has been cleaned manually every day, the other cell has only been cleaned by rain. As well as registering irradiance values, the irradiation value along each day has been computed using trapezoidal integration too.

By comparing recorded irradiance values sensed by the two reference cells, dust influence on the received radiation can be quantified, and as consequence its effects on the solar energy received in the cell. Daily irradiation losses caused by dust are calculated comparing irradiation values sensed by the clean and the dirty cells. The two calibrated cells and the pyranometer are placed on a p lane whose tilt angle is 30º (see Fig. 1). The period of measurements comprises from 12/15/08 to 12/14/09. Along that period, summer was dry without any rain, and winter and spring had rainfall more frequent than usual for this period. An autumn with low rainfall completes the meteorological period. The availability of data for the studied period has been 96.4%.

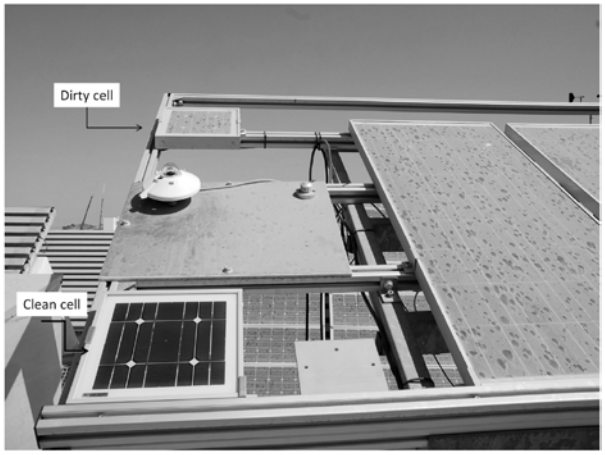

Fig. 1. The experimental setup used in the measurements.

3. Results

3.1. Irradiation daily losses

The evolution of the irradiation daily losses along the year of measurements is shown in Fig. 2. These losses (*HL*) represent the fraction of daily energy that a PV module will not receive as consequence of dust deposited on their surface, and are calculated as

$$HL(\%) = 100 \times \left(\frac{H_{CC} - H_{DC}}{H_{CC}} \right) \quad (1)$$

where H_{CC} is the daily irradiation measured by the clean reference solar cell (W h m^{-2}) and H_{DC} is the daily irradiation measured by the dirty cell (W h m^{-2}). As can be seen in Fig. 2, the losses produced by the presence of dust are strongly dependent on the rainfall. In rainfall periods, a good cleaning of the dirty cell is produced and it recovers its initial performance; even a light rain, below 1 mm, is enough to clean the cover glass, reducing daily losses *HL* below 5%. However, in long periods without rain, like summer, the accumulation of dust can cause daily losses exceeding 20%.

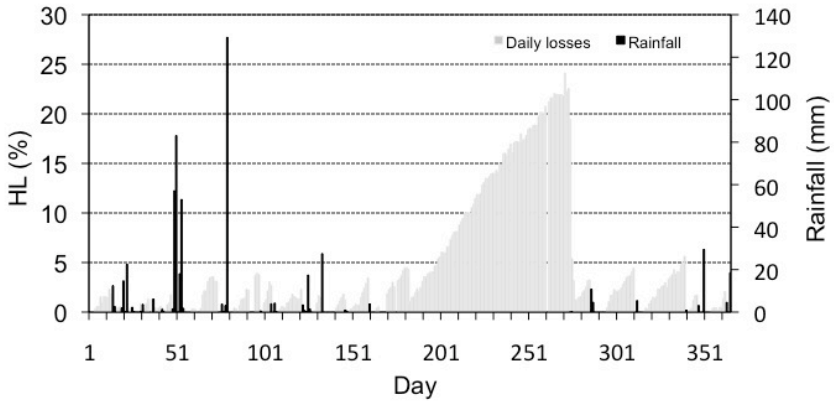

Fig. 2. HL values for all days of measurements along a whole year (left axis). We also plot daily values of rainfall (right axis).

The mean of the daily energy losses along a year caused by dust is 4.4%. Monthly averages of daily energy losses are lower than 2% except in summer months, when the lack of rain favors the accumulation of dust and causes the increase of losses above 15%. Note that the energy

production reaches its maximum in these summer months, and therefore the possible adverse effect of dust is very relevant.

3.2 Evolution of the dust losses along the day

As seen in the last section, accumulations of dust on the surface of a photovoltaic module reduce strongly the energy received. We have not observed any influence of the wind speed or direction on the losses, probably because the high relative humidity contributes to the adherence of the dust particles on the module surface. As shown in previous studies [7-10], these losses should not be constant during the day, but have to be dependent on the incidence angle of beam radiation. In order to study this dependency, irradiation values sensed by the clean and the dirty cells throughout the day are compared. In this case, relative irradiance losses are calculated as:

$$GL\ (\%) = 100 \times \left(\frac{G_{CC} - G_{DC}}{G_{CC}} \right) \qquad (2)$$

where G_{CC} is the irradiance value measured by the clean reference solar cell (W m^{-2}) and G_{DC} is the irradiance value measured by the dirty reference solar cell (W m^{-2}). It should be pointed out that losses caused by the dependence of the transmission coefficient of the glass cover on the angle of incidence does not affect in the calculation of *GL* since it is identical in both cells. However, the presence of dust modifies the angular dependence of the irradiance, which is different for the clean and the dirty cell, and precisely this effect is measured with *GL*.

These losses represent the fraction of irradiance that the cell will not receive, and in the case of PV modules, power losses. When cells are clean, losses are approximately constant during the day. As dirt is deposited on the dirty cell, the behavior of the losses is not constant throughout the day in clear sky days, becoming dependent on the angle of incidence. Daily evolution of dust losses on the 08/06/09 is shown in Fig. 3. This is a clear sky summer day, almost two months after the last rains; as consequence, dust level deposited on the dirty cell surface is high, causing daily losses of 14.8%.

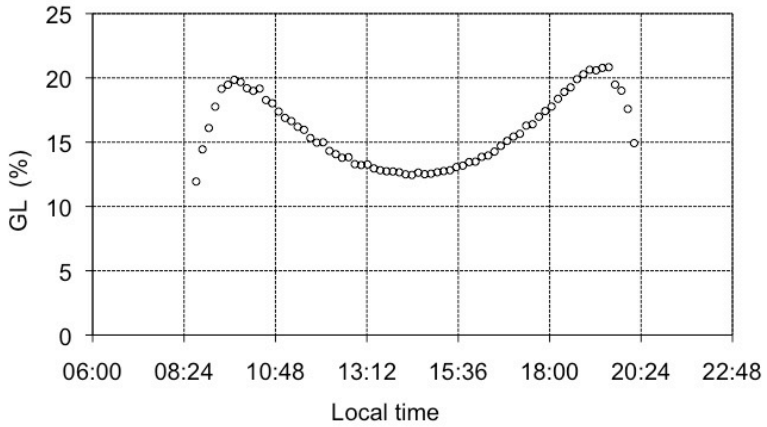

Fig. 3. Relative irradiance losses (GL) along a day.

The typical behavior of *GL* as a function of the incident angle (θ) is shown in Fig. 4. In this figure, we plot *GL* curves obtained in several days with different *HL* values (i.e. with different amounts of dust). As expected, losses are strongly dependent of the incident angle of radiation. Minimum transmittance losses occur at noon (12.4%) when the incident angle is

minimum. As incidence angle increases, losses increases slowly, but the growth rate increases as the angle. Nevertheless, from an angle of about 60º, losses remain almost constant for a window of about 10º and then, after a maximum of about 21%, they decrease. This occurs at first and last hours of the day, when incidence angle is between 60-80º and irradiance value is about 200 Wm^{-2}. (Note that morning maximum is slightly lower than afternoon maximum; the cause is that calibrated cells are no exactly in the same plane an there are a little bench between them). Dependence of dust losses with the angle is shown in Fig. 4.

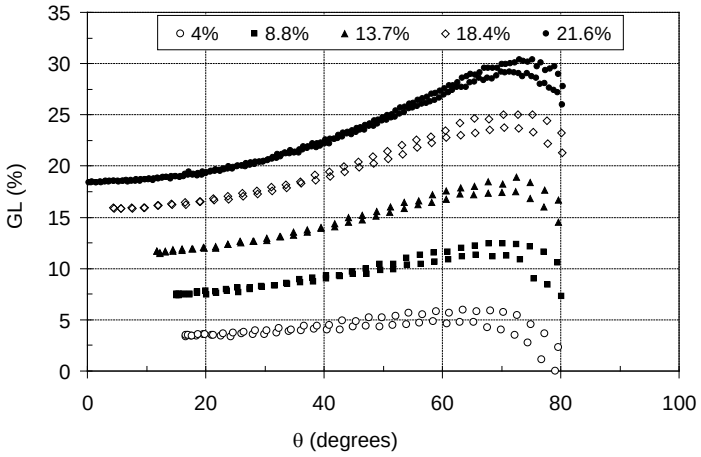

Fig. 4. Dependence of GL with the angle of incidence (θ) for several days with different HL values.

This behavior is related with the proportion of diffuse irradiance on global irradiance in the early morning and evening, when its value increases. In section 4, a theoretical model justifies this behavior. On cloudy days, when the global irradiance is mainly diffuse irradiance, losses remain almost constant throughout the day. Diffuse irradiance has not specific direction and hence losses are not dependent on the incidence angle.

Table I summarizes *HL*, θ and *GL* at solar noon and the maximum value of *GL* for each day shown in Fig. 4. Values of *HL* are between 4.0% for the first day and 21.6% for the last day. It can be noticed that all the shape of the curves is generic and it is not dependent on the *HL* value.

Table I. Measured parameters of Fig. 4

Date	*HL* (%)	θ at solar noon (degrees)	*GL* at solar noon (%)	*GL* maximum (%)
27/06/2009	4.0	17.0	3.5	5.9
13/07/2009	8.8	15.1	7.5	12.5
30/07/2009	13.7	11.7	11.7	18.9
23/08/2009	18.4	4.4	16.0	25.0
04/09/2009	21.6	0.2	18.4	30.4

4. Modeling the losses produced by the dirt

We have developed a simple model to justify the shape of the typical behaviour of the relative transmittance losses due to the presence of dust in the solar cell (see Fig. 3). The model is based on the following assumptions:

a) Dust grains are modelled as spheres homogeneously distributed on the surface of the panel.
b) Each sphere has a reflection coefficient R, which accounts for both specular and diffused reflection.
c) Total incoming radiation from the Sun (I_T) is composed of direct radiation (I_0) and diffuse radiation (I_D). We consider that this latter radiation comes homogeneously from any direction and it is kept constant along the day. Note that the total irradiance received by a clean solar cell is given by:

$$G_{CC} = I_0 \cos\theta + I_D \quad (3)$$

where θ is the angle of incidence of direct radiation on the panel. The albedo radiation has been neglected.
d) In the dirty solar cell, any sphere of dust shadows the panel thus reducing the light reaching it. However not all radiation reaching the spheres is lost because part of if is reflected (a factor R) and can be partially recovered by the panel. Both effects, the shadowing and the recovery of light, depend on the angle of incidence of the direct radiation and thus vary along the day. On the other hand, there is no such dependence in the diffuse radiation since we assume that I_D is constant along the day.

To quantify the irradiance losses *GL* due to the presence of dust in the solar cell we use Eq. (2). In order to understand the effect of the dust on the losses we have to analyse separately the direct and diffuse radiations.

4.1. Direct radiation

For the direct radiation the shadowing increases with the angle of incidence, reaching the maximum for $\theta = 90^o$. At the same time, the fraction of the light specularly reflected reaching the panel increases with θ up to a maximum value and finally decreases for very large θ. On the other hand, the fraction of light diffusely reflected reaching the panel is constant because the direction of the reflected rays is independent of the angle of incidence. The sum of all these contributions is not evident and therefore we simulate the phenomenon using a ray tracer [11]: For each angle of incidence θ we trace 10^6 rays reaching a square cell of unit area with a single sphere on its center. We impose periodic boundary conditions. The reflection coefficient of the spheres is set to $R = 65$ % (19.5 % specular and 45.5 % diffuse), and the radius of the sphere is set to $r = 0.315$ units, which is equivalent to a coverage of 31.17 % of the surface of the cell. In Fig. 5 we show *GL* as a function of the angle of incidence for this simulation (dashed line). The values of the parameters are physically acceptable and have been chosen in order to fit the experimental results (also shown in Fig. 5) for small angles of incidence. As can be observed, the model does not reproduce at all the behaviour of *GL* for large angles of incidence. In particular it gives a monotonously increasing *GL* while the experimental one reaches a maximum and decreases for very large angles of incidence.

4.2. Diffuse radiation

As we see, the contribution of direct radiation alone does not suffice to explain the experimental results. Therefore we incorporate the diffuse radiation to the model. Again we generate and trace 10^6 rays with directions uniformly distributed. The total amount of energy carried by these rays is equivalent to 23 % of the total radiation that would reach the cell under normal incidence. When these rays are included in the simulation (solid line in Fig. 5)

the result obtained for *GL* agrees fairly well with the experimental results and in particular, it reproduces the reduction of the losses observed at large angles of incidence.

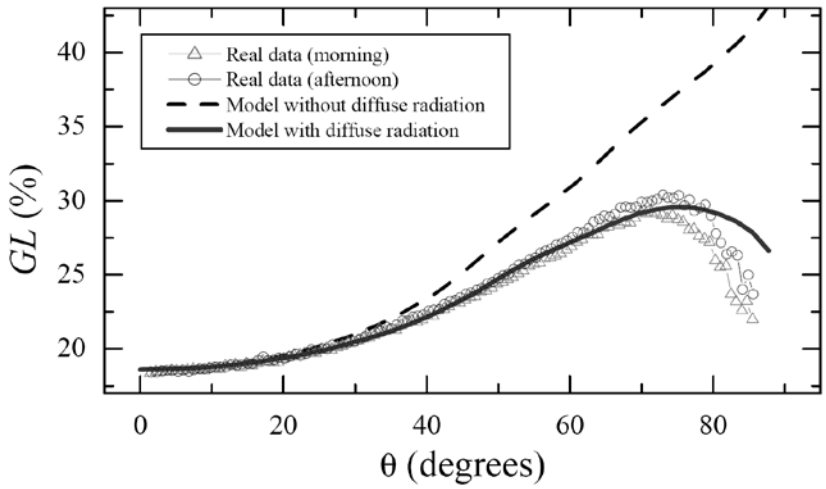

Fig.5. Relative irradiance losses of a dirty solar cell as a function of the angle of incidence of solar direct radiation. Hollow triangles (circles) correspond to real data measured in morning (afternoon) hours on the 4th of September, 2009 (Malaga, Spain). Dashed line corresponds to the results obtained with a simulation (see text for details) in which diffuse radiation is not considered whereas the solid one has been obtained by taking into account this radiation.

4. Conclusions

In this work we have studied in general the energy losses due to accumulated dust on the surface of photovoltaic modules. First, we present results about daily irradiation losses and we show that the mean value of this quantity along a whole year is about 4.4%. In rainfall periods, the rain water cleans the dirty cell and it recovers its normal performance: even a light rain, below 1 mm, is enough to clean the cover glass, reducing daily losses *HL* clearly below the average value of 4.4%. However, in long periods without rain, like summer, the accumulation of dust can cause daily losses exceeding 20%.

Second, we present results of the dust-caused irradiance losses *GL* and its dependence on the angle of incidence θ. The curve that describes the dependence of these losses on the angle of incidence has a very specific shape: *GL* has a minimum at solar noon, then increases with θ up to a maximum value found when $\theta \approx 75^{\circ}$, and then decreases for larger values of θ. This behavior can be explained by the influence of the diffuse radiation.

In addition, we have presented a simple model, simulated with the ray-tracing technique, to explain the behavior of losses in solar modules due to the presence of dust. With this model we have shown the relevance of diffuse radiation in order to understand the full behavior of losses as a function of the angle of incidence. Indeed, when only direct radiation is considered the model does not provide results comparable to experimental measures. On the other hand, when diffuse radiation is also taken into account, the model reproduces quite well the shape of the experimental data for reasonable values of the input parameters.

We conclude that the estimation of energy losses produced by the presence of dust have to be calculated in a different way for photovoltaic systems with fixed modules or with solar-tracking. In addition, the proportion of the diffuse component in the global radiation must be taken into account when estimating the energy losses produced by the dust on the system energy performance.

Finally, it is very important to quantify energy losses produced by dust in dry areas where such losses could reach large values and so producing a substantial decrease in the efficiency of photovoltaic systems. In these cases a regular cleaning of the modules would be necessary thus increasing maintenance costs.

Acknowledgements

We acknowledge the Spanish "Ministerio de Ciencia e Innovación" (grant No. ENE07-67248) and "Junta de Andalucía" (grant No. P07-RNM-02504) for financial support.

References

[1] M. Mani, R. Pillai. Impact of dust on solar photovoltaic (PV) performance: Research status, challenges and recommendations, Renewable and Sustainable Energy Reviews 14, 2010, pp. 3124-3131.

[2] M. Piliougine, J. Carretero, M. Sidrach-de-Cardona, D. Montiel, P. Sánchez-Friera. Comparative analysis of the dust losses in photovoltaic modules with different cover glasses. Proceedings of 23rd European Solar Energy Conference, 2008, pp. 2698-2700.

[3] H.P. Garg, Effect of dirt on transparent covers in flat-plate solar energy collectors, Solar Energy 15 (4), 1974, pp. 299-302.

[4] S.A.M. Said, Effects of dust accumulation on performances of thermal and photovoltaic flat-plate collectors, Applied Energy 37 (1), 1990, pp. 73-84.

[5] M.S. El-Shobokshy, F.M. Hussein, Effect of dust with different physical properties on the performance of photovoltaic cells, Solar Energy 51 (6), 1993, pp. 505-511.

[6] S. Biryukov, D. Faiman, A. Goldfeld, An optical system for the quantitative study of particulate contamination on solar collector surfaces, Solar Energy 66 (5), 1999, pp. 371-378.

[7] D. Goossens, E. Van Kerschaever, Aeolian dust deposition on photovoltaic solar cells: the effects of wind velocity and airborne dust concentration on cell performance, Solar Energy 66 (4), 1999, pp. 277-289.

[8] N. Martin, J.M. Ruiz, Calculation of the PV modules angular losses under field conditions by means of an analytical model, Solar Energy Materials & Solar Cells 70, 2001, pp. 25-38.

[9] M. García, L. Marroyo, E. Lorenzo, M. Pérez, Soiling and other optical losses in solar-tracking PV plants in Navarra, Progress in Photovoltaics: Research and Applications, DOI: 10.1002/pip.1004.

[10] N. Martin, J.M. Ruiz, Annual angular reflection losses in PV modules. Progress in Photovoltaics: Research and Applications 13, 2005, pp. 75-84.

[11] A.S. Glassner (Ed), An introduction to ray tracing, Academic Press, 1993.

An experimental study of combining a photovoltaic system with a heating system

R. Hosseini [1,*], N. Hosseini[2], H. Khorasanizadeh[2]

[1] *Amirkabir University of Technology (Tehran PolyTechnic), Tehran, Iran*
[2] *University of Kashan, Kashan, Iran*
** Corresponding author. Tel: +98 (21)64543433, E-mail:hoseinir@aut.ac.ir*

Abstract: Solar photovoltaic and thermal systems are potential solutions for current energy needs. One of the most important difficulties in using photovoltaic systems is the low energy conversion efficiency of PV cells and, furthermore, this efficiency decreases further during the operational period by increasing the cells temperature above a certain limit. In addition, reflection of the sun's irradiance from the panel typically reduces the electrical yield of PV modules by 8-15%. To increase the efficiency of PV systems one way is cooling them during operation period. In this experimental study combination of a PV system cooled by a thin film of water with an additional system to use the heat transferred to the water has been considered. Experimental measurements for both combined system and conventional panel indicate that the temperature of the photovoltaic panel for combined system is lower compared to the conventional panel. The results show that the power and the electrical efficiency of the combined system are higher than the traditional one. Also since the heat removed from the PV panel by water film is not wasted, the overall efficiency of the combined system is higher than the conventional system.

Keywords: *Cooling PV systems, Electrical efficiency, Combined system, Overall efficiency*

1. Introduction

Environmental problems due to extensive use of fossil fuels for electricity production and combustion engines have become increasingly serious on a world scale in recent years. To solve these problems, renewable energy sources have been considered as new sources of clean energy. Solar energy is one of the most important sources among the renewable energies. Generally, solar energy conversion systems can be classified into two categories: thermal systems which convert solar energy into heat and photovoltaic systems which convert solar energy to electricity.

Intensive efforts are being made to reduce the cost of photovoltaic cell production and improve efficiency and narrow the gap between photovoltaic and conventional power generation methods such as steam and gas turbine power generators. In order to decrease the cost of PV array production, improve the efficiency of the system and collecting more energy for unit surface area different efforts have been made.

The performance of the PV system is affected by several parameters including temperature. The part of absorbed solar radiation that is not converted into the electricity converts into thermal energy and causes a decrease in electrical efficiency. This undesirable effect which leads to an increase in the PV cell's working temperature and consequently causing a drop of conversion efficiency can be partially avoided by a proper method of heat extraction. PV/T solar systems consisting of photovoltaic modules and thermal collectors are applied to cool photovoltaic panel and use the heat generated by the panel and increase total energy output of the system. By proper circulation of a fluid with low inlet temperature, heat is extracted from the PV modules keeping the electrical efficiency at satisfactory values. The extracted thermal energy can be used in several ways, increasing total energy output of the system. Many researchers have investigated and proposed different methods for design and optimization of the PV/T systems to improve the

system efficiency by cooling PV module and collecting more energy. The main concepts of hybrid PV/T systems have been presented by several researchers since 1978 [1-5]. Tripanagnostopoulos [6] studied hybrid PV/T solar systems experimentally and used water and air to extract heat from the PV module rare surface. He used a hybrid system with air duct under the PV module for heat extraction with air circulation and another hybrid system with thermal unit of water circulation through a heat exchanger. In the system he tested, water was circulated in pipes with the flat surface of a copper sheet placed at the rear surface of the PV module and in thermal contact with it. Kalogirou and Tripanagnostopoulos [7] proved analytically the potential benefits of PV/T systems compared to typical PV modules and presented justification of energy and cost results regarding system application. Their method could be considered as an estimation of the cost effectiveness of new solar energy systems in practice.

One method for cooling photovoltaic module is to flow a film of water over the PV module to decrease its temperature. By using this method reflection would also be reduced and therefore the electrical efficiency will improve. Krauter [8] studied the effects of cooling photovoltaic array surface with film of water on the power generated by the array. Abdolzadeh and Ameri [9] improved the operation of a photovoltaic water pumping system by spraying water over the front of the photovoltaic cells. Kordzadeh [10] studied the effects of nominal power array of 90 and 135 W on 16 m head of water pumping system on panel efficiency as well as the panel efficiency for 135W nominal power output on different heads of pumping system. A thin continues film of water was running on the top of the PV panel without water being recirculated. The advantage of the later system (thin water running on top of the photovoltaic array) is obtaining better electrical efficiency because of decreasing the reflection loss, in addition to decreasing temperature of the array. The disadvantage of this system is that the heat gained by the water running on top of the photovoltaic array is wasted.

The aim of the present experimental research is to consider the combination of a PV system equipped with cooling system consisting of a thin film of water running on the top surface of the panel with an additional system to use the hot (or warm) water produced by the system.

2. Experimental procedure

The experimental setup is composed of two similar but separate PV solar photovoltaic panels each with area of 0.44 m^2. The maximum output voltage and current are respectively 23V, 2.61A and with maximum power output of 60W. One of the panels is used in a combined system with a film of water running over its top surface without front glass and an additional fabricated system to use the heat generated by the panel. The other panel is a conventional PV as a reference panel. To produce a film of water over the photovoltaic panel, a tube with a slit along it has been installed on the top end of the photovoltaic panel (see Fig. 1). Water pumped to the feeding tube, leaves the slit and flows over the panel as a thin film. Power of the pump for circulation of water is 0.25 hp. The water collected at the lower end of the panel passes through a finned tube used as a heat exchanger and consumer of heat gained by the water. Another role of this finned tube is to dissipate heat to the environment and produce a constant low water temperature. Therefore when the water is pumped back to the feeding tube it would be at a desired temperature level to flow on the panel surface. The flow rate is 1 lit/min. Pumping system and the heat exchanger which are used in the combined system are shown in Fig. 2.

Fig. 1. Front view of solar photovoltaic panel equipped with water film producer.

Fig. 2. Pumping system and the heat exchanger of experimental combined Photovoltaic/Thermal (PV/T) system.

Maximum power output was obtained by utilizing an optimized ohmic load (8.7 Ω). Current and voltage were measured by Omega type multimeter with accuracy of 1 miliamper and 1 milivolt respectively. Both panels were facing south with an angle of inclination of 29°. Irradiance was measured by a Kimo SL100 solar meter installed on the corner of one of the panels with the same angle of inclination. Ambient temperature was measured in the shade at specified intervals. Patch type thermocouples (k type) were installed on the back surface of the two panels. Temperature of the top surface of the reference panel was occasionally measured by a surface probe and was almost $1.5\,^{\circ}C$ above the temperature of the back surface of the same panel. Therefore, the temperature difference between top and back surfaces of both panels was considered to be about $1.5\,^{\circ}C$. Standard thermocouples (k type) were used for measuring the temperature of the water before running over the panel and at the lower end of the panel. Temperature of the water coming out of the heat exchanger was also measured by installing a standard thermocouple (k type) at the end of the finned tube. Measurements have been performed simultaneously over 14 days during September, 2010 in Tehran (latitude 35° 41' and longitude 51° 25') and recorded every 10 minutes.

3. Results

In this section results of measurements on the 18th of September, 2010 have been presented and analyzed. Variation of irradiance received by the surfaces of the panels during the test day is shown in Fig. 3.

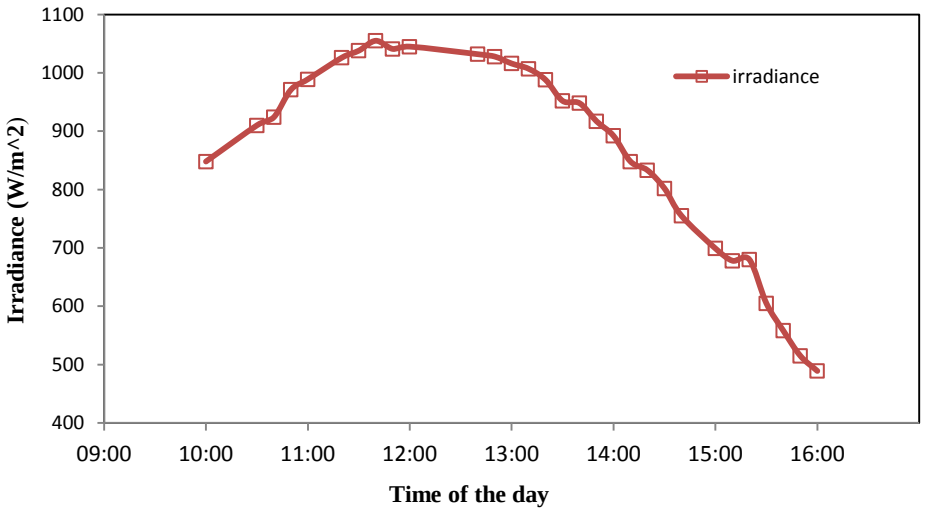

Fig. 3. Variation of irradiance during the test day.

Due to the water flow and additional cooling by water evaporation, the PV/T panel's operating temperature measured is much lower in comparison to the conventional reference panel. As could be seen in Fig. 4, maximum temperature difference of $18.7\,^{\circ}C$ is observed. This temperature reduction has caused a noticeable improvement for electrical efficiency as shown in Fig. 5, such that for some hours the relative difference is more than 33%.

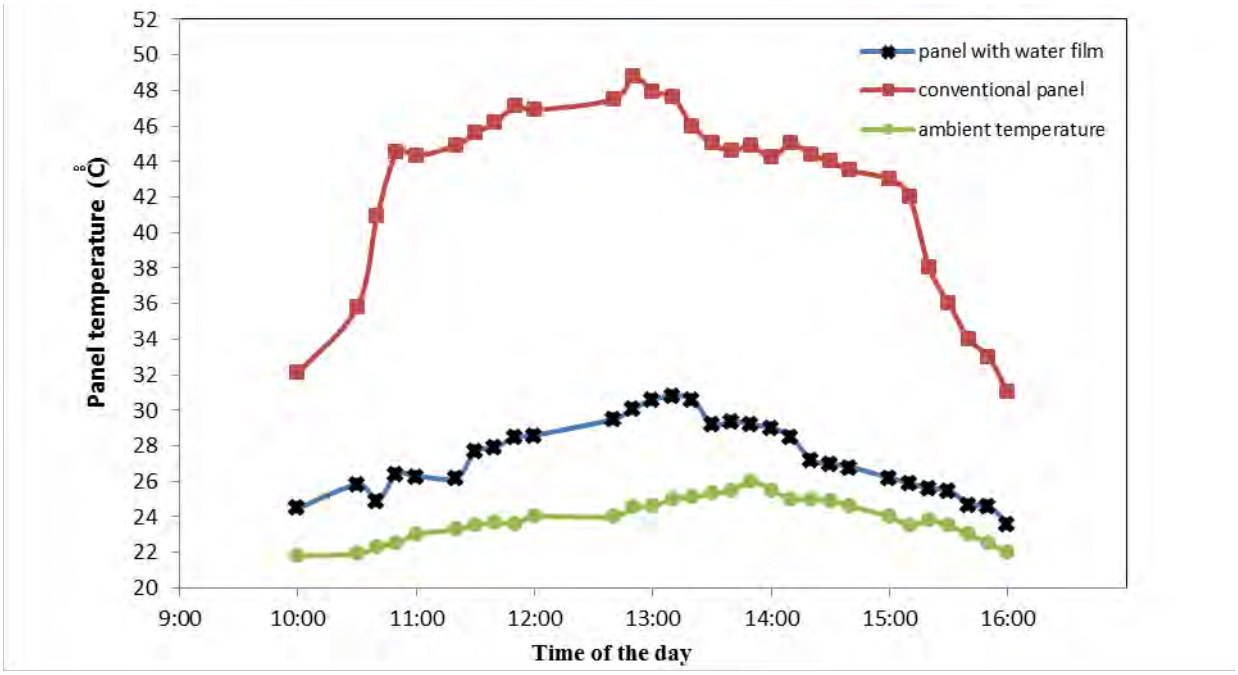

Fig. 4. Comparison of conventional photovoltaic panel temperature with the temperature of the panel in the combined system.

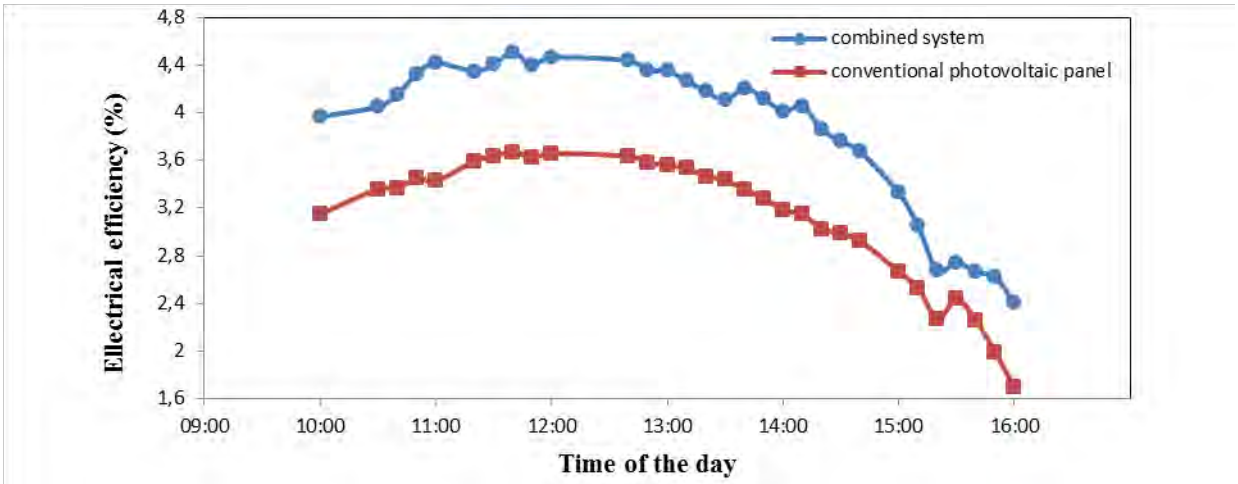

Fig. 5. Comparison of conventional photovoltaic panel electrical efficiency with the electrical efficiency of the combined system.

The experimental results showed that the continuous film of water on the surface of PV panel has two important effects on the operation of the system. First, it reduces the reflection of the solar irradiance. Second, it reduces the panel temperature by absorbing the heat generated by the panel. Temperature reduction is significant due to heat absorbed by the water. The heat removal from the PV panel by the water film increases the temperature of the water running over the panel surface and also causes evaporation. Calculations show that cooling is mainly by evaporation. In Fig. 6, temperature of the water before running down over the surface of the panel has been shown in comparison to temperature of the water collected at the lower end of the panel and temperature of the water coming out of the heat exchanger. As it is shown, the heat absorbed by

the water when running down the panel is removed when passing through the heat exchanger and the temperature reaches more or less to the water temperature at the top end of the panel.

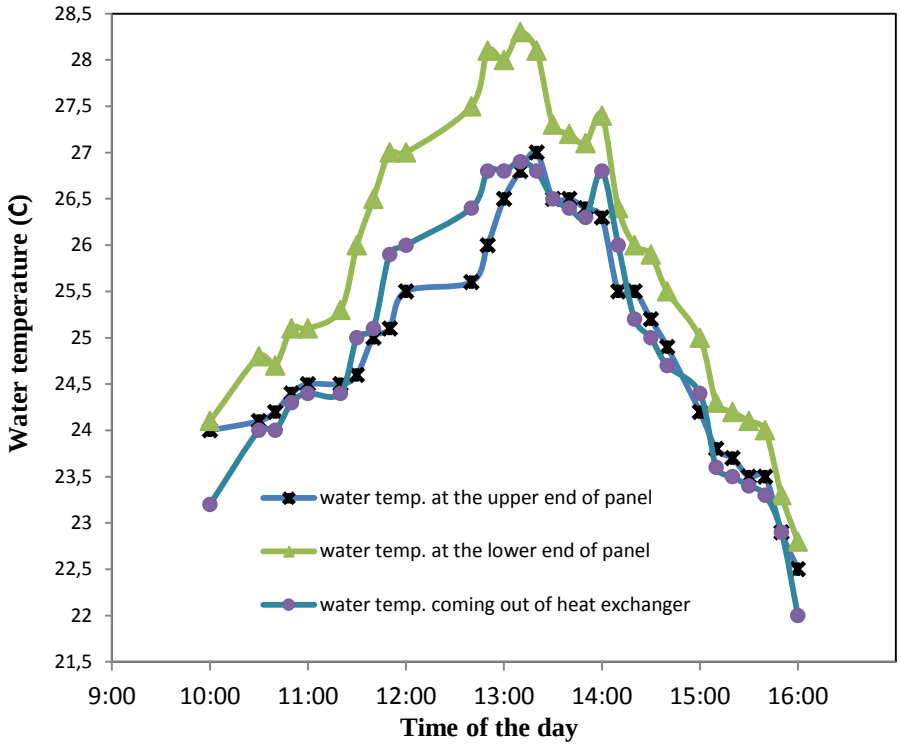

Fig. 6. Comparison of water temperature at the upper and lower ends of the panel and water coming out of the heat exchanger in the combined system.

Overall efficiency can be defined as the total energy output of the system compared to the radiant energy received by the system. For conventional system, total energy output of the system consists of electrical energy produced, but for the combined system it consists of both thermal and electrical energy produced. Thermal energy output is defined as the increase in the internal energy of the water running over the panel due to the increase in the temperature of the water ($\dot{m}\, c_p\, \Delta T$). Due to high specific heat of water the temperature increase is quite a bit. Also because of small surface area of the panel, the sensible heat added to water is a small amount. As could be seen in Fig. 7, there is a noticeable improvement in overall efficiency of the combined system in comparison to the conventional system.

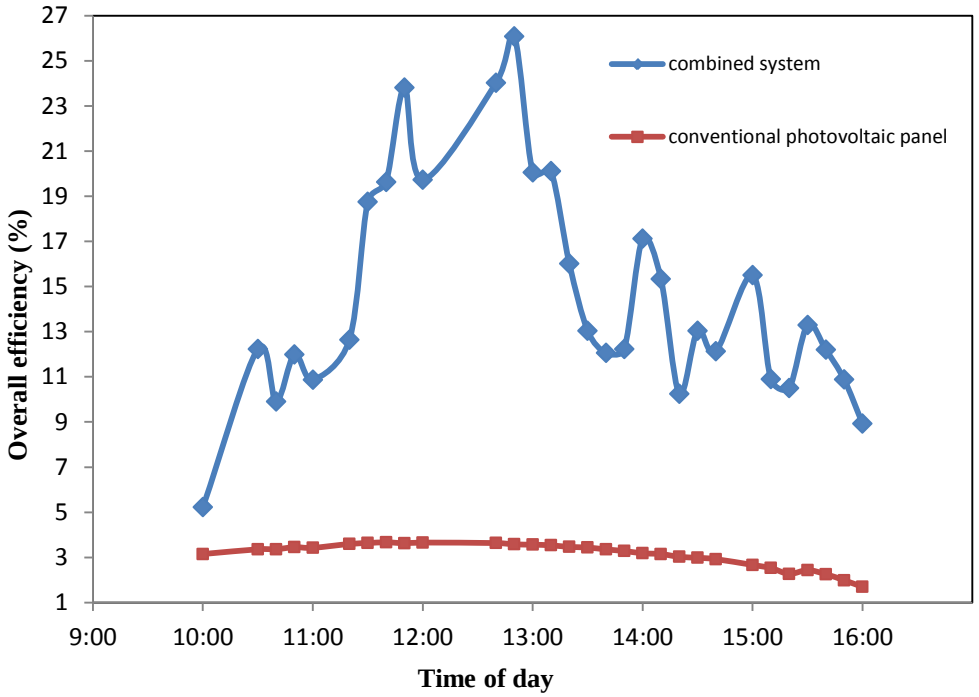

Fig. 7. Comparison of conventional photovoltaic panel overall efficiency with the overall efficiency of the combined system.

4. Conclusion

The photovoltaic panel efficiency is sensitive to the panel temperature and decreases when the temperature of the panel increases. One of the ways for improving the system operation is covering the panel surface with a thin running film of water which decreases both reflection loss and temperature of the panel. Results of present work showed that while the temperature of the panel could be controlled at a desired temperature level, the water collected at the lower end of the panel can be used as a utility for heating purposes. Therefore when the water is pumped back to the upper end of the panel it would be at a desired temperature level to flow on the panel surface. In the combined system tested in this work, aplying a film of water for cooling photovoltaic panel resulted in decreasing the temperature and reflection loss of the PV panel which increased electrical efficiency of the combined system. Also the heat removed by the water from the panel was used in a heat exchanger. Therefore, total energy output of the combined system (collected thermal and electrical energy for unite surface area) increased significantly compared to the electrical energy of the conventional photovoltaic panel. In this experimental study it has been shown that the overall efficiency of combined system at some hours is one order of magnitude more than the efficiency of conventional panel.

Acknowledgement

Special thanks to thermodynamic lab personals (technicians and instructors) in mechanical engineering department of Amirkabir University of Technology for their help and providing necessary facilities and measuring equipments. Also the financial support of Iranian Fuel Conservation Company is kindly acknowledged.

References

[1] E.C. Kern and M.C. Russel, Combined photovoltaic and thermal hybrid collector systems, Proceedings of the 13th IEEE Photovoltaic Specialists, 1978, pp. 1153–1157.

[2] S.D. Hendrie, Evaluation of combined photovoltaic/thermal collectors, Proceedings of international ISES Conference, 1979, pp. 1865–1869.

[3] L.W. Florschuetz, Extension of the Hottel-Whillier model to the analysis of combined photovoltaic/thermal flat plate collectors, Journal of Solar Energy 22, 1979, pp. 361–366.

[4] P. Raghuraman, Analytical predictions of liquid and air photovoltaic/thermal, flat-plate collector performance, Journal of Solar Energy Engineering 103, 1981, pp. 291–298.

[5] C. H. Cox and P. Raghuraman, Design considerations for flat-plate photovoltaic/thermal collectors, Journal of Solar Energy 35, 1985, pp. 227–241.

[6] Y. Tripanagnostopoulos, Hybrid Photovoltaic/Thermal Systems, Journal of Solar Energy 72, 2002, pp. 217–234.

[7] S.A. Kalogirou and Y. Tripanagnostopoulos, Industrial application of PV/T solar energy systems, Journal of Energy Conversion and Management 47, 2006, pp. 3368–3382.

[8] S. Krauter, Increased electrical yield via water flow over the front of photovoltaic panels, Journal of Solar Energy Materials & Solar Cells 82, 2004, pp. 131–137.

[9] M. Abdolzadeh and M. Ameri, Improving the effectiveness of a photovoltaic water pumping system by spraying water over the front of photovoltaic cells, Journal of Renewable Energy 34, 2009, pp. 91–96.

[10] A. Kordzadeh, The effects of nominal power of array and system head on the operation of photovoltaic water pumping set with array surface covered by a film of water, Journal of Renewable Energy 35, 2010, pp. 1098–1102.

Volume 12

Sustainable Cities and Regions

Promoting renewable energy through green procurement and impact assessment

Kedar Uttam[1,*], Berit Balfors[1], Ulla Mörtberg[1]

[1] *Royal Institute of Technology, Department of Land and Water Resources Engineering Stockholm, Sweden*
** Corresponding author. Tel: +46 87907328, E-mail:kedar@kth.se*

Abstract: With urbanization, the construction sector (CS) has been consuming great quantities of energy and contributing to almost 50 percent of the global GHG emissions. Thus, it is imperative for the CS to adopt a sustainable energy system (SES). Renewable energy (RE) is foreseen as a viable option to promote SES. However, adopting RE in CS involves challenges within the areas of both RE development and infrastructure planning (IP). These challenges call for research not only on technology, but also on policy aspects and systems thinking. Thus, the aim of this paper is to understand the scope for incorporating discussions on RE use within the policy instruments (PIs) used in the IP process. The method involved literature review from the perspective of the synthesis of PIs that have the capacities to accommodate discussions on sustainability during planning. The paper highlights a PI called green procurement (GP), which involves procuring services and products that meet environmental requirements. GP could go far to ensure that the energy procured is renewable. The paper indicates that the discussion on procuring RE could be routed through synthesis of GP and impact assessment, which is a PI for evaluating environmental impacts, with the capacity to assist IP.

Keywords: *Infrastructure, urbanization, sustainable energy, impact assessment.*

1. Introduction

The planning, construction and management of major infrastructure projects such as mass transit systems or international airport complexes essentially deals with large scale human-activity centred systems capable of continual growth and expansion [1], involves key players such as the construction sector (CS), and has accelerated urbanization. Consequentially, urbanization has been responsible for substantial consumption of energy, especially by the CS. Significant amount of energy is consumed during manufacturing and transportation of building materials, installation, construction activities [2] and operation. According to the Organization for Economic Co-operation and Development (OECD), the operation of buildings accounts for 25 to 40 percent of the total final energy use in OECD countries [3]. The CS annually generates 50 percent of the global greenhouse gases [4]. The use of non-renewable energy by the sector is one of the causes for its CO_2 emission [5]. However, the emission of CO_2 is noticeable during different phases of a building life cycle, such as, in the construction process, exploitation, renovations, and also during demolition stage [6]. Emissions are also associated with the *use of energy* in construction related activities that precedes site activities, primarily in the construction procurement supply chain [7]. As to what Dimoudi and Tompa [8] highlight, the energy required for construction and consequently, for the material production, is gaining importance. They argue that the selection of materials for the building construction is determinant for the energy required for the construction and for the environmental consequences. It is, therefore, imperative for the CS to adopt a sustainable energy system. Sustainable energy system can be regarded as a "cost-efficient environment-friendly energy system", which efficiently uses local resources and networks, and promotes the introduction of new techno-economic and political solutions [9]. The implementation of such a system by the CS calls for a decrease in the dependency on oil/ other fossil fuels, CO_2 emissions reduction, efforts to curtail social costs and a transition towards renewable energy (RE) such as wind energy or bioenergy.

However, the adoption of RE for construction activities involves challenges both within the ambit of RE development, and in the area of infrastructure planning. Thus, the effort needed to address these challenges and to shift towards a sustainable energy system requires research not only on technology, but also on policy aspects and systems thinking. The two important policy instruments, relevant to infrastructure planning, primarily from an environmental perspective, are *green procurement* (GP) and *environmental impact assessment* (EIA). Due to the links that GP and EIA have with infrastructure planning, this study focuses on them for the promotion of RE in the CS. Further, EIA adopts several analytical tools such as multi-criteria decision analysis (MCDA) in order to achieve its purposes. MCDA is highly suitable for analyzing the intersecting systems of energy and environment [10-13]. Although there is an increasing focus on integration and integrative approaches in EIA [14], the systems perspective needs to be strengthened during its application.

GP, within the context of this study, involves the procurement of construction projects that meet environmental requirements, which must be stipulated such that it facilitates the contractor to comply with them, and further enables verification by the client [5]. In the public sector, GP is termed as green public procurement, which according to the European Commission is a mechanism wherein public authorities intend to procure goods and services with a reduced environmental impact throughout their life cycle [15]. EIA is a process that evaluates the impacts likely to arise from a development project significantly affecting the environment [16], and involves the introduction of mitigation measures to avoid, reduce, remedy or compensate for any adverse impacts [17]. Sánchez and Hacking [18] highlight that ideally, EIA is applied during the planning stage of a new project so as to choose the economically and environmentally feasible technological alternative, and plan management measures to mitigate negative impacts and enhance positive effects. Several authors have investigated the link between EIA and planning (for instance, [19, 20]). The effective *implementation* of strategies and mitigation measures identified through EIA process (during planning), however, remains a challenge [21]. This is where the systems perspective in EIA needs to be strengthened. *In this study, we envisage that integrating GP and EIA could be one way to strengthen the systems perspective. This means that discussions on GP should commence at the stage of EIA. Such integration could be an option to strengthen the link between project planning and implementation.*

GP can go far to ensure that the energy used for construction is renewable and green [15]. It can also involve the procurement of low energy consuming materials for construction. Therefore, the central concern of this paper is to discuss on planning for GP at the stage of EIA. This discussion could be channeled through MCDA, which seeks to identify the plurality of perspectives [17]. MCDA includes "formal approaches" that intend to "take explicit account of multiple criteria" [22] during impact assessment. The decision making procedure under MCDA is based on the concept of making a choice between different actions or alternatives that the decision maker examines and assesses through a set of criteria [11]. These criteria could be defined by objectives or attributes [23], involve qualitative or quantitative data [24], include conflicting factors such as technological, economic, social, risk, and environmental, with different groups of decision makers participating in the process [10]. With these instruments and their synthesis as the focus, the aim of this study is to understand the 'scope' within the infrastructure planning process for incorporating discussions on the utilization of RE in the construction sector. The objective of the study is twofold. Firstly, to envisage the synthesis of GP and EIA. During this process, the paper uses the standpoint of "innovation system perspective" (ISP) [25], wherein networks, strategies and institutional mechanisms play an important role. While exploring the role of EIA and GP,

this study also attempts to understand the potential role of MCDA in presenting the deliberation on energy inclusive GP. The second objective is to explore the role that the construction sector could play in RE development. The paper also discusses areas for future research from the perspectives of both GP and EIA.

1.1. Methodology

The study is largely based on review of literature and content analysis. The review attempted to systematically examine previous research on innovation system perspective, EIA and planning, drivers and barriers for GP, MCDA adoption in energy planning, institutional mechanisms, and social innovation. This is in order to analyze the state of the art situation, and to investigate the scope for outlining the synthesis of the policy instruments under consideration. The study is explorative, in the sense that the literature has been reviewed from a systems perspective in order to establish how the policy instruments, concepts and institutional settings can allow and shape the synthesis. This also opened areas for future research for further understanding on the synthesis of the (policy) mechanisms. As described by Weber [26], the content analysis method was used to understand the focus in communication content. The European Commission's Communication on public procurement for better environment [15] was analyzed to understand the purview of GP. The method also involved semi-structured interviews, which included open-ended questions (cf. [27]), and were conducted with experts on energy issues. This was a pre-understanding process (cf. [28]) to investigate further on the second objective concerning the role that the construction sector could play. The analysis of the information obtained during the interview strengthened the key findings that emerged during the literature review. These key findings were useful in understanding the potential role of the construction sector.

2. Results

2.1. Synthesis of GP and EIA

In this study, the rationale behind the contemplation of synthesizing EIA and GP has its link with the ISP. Jacobsson and Johnson [25] highlight on ISP for investigating the change in energy system towards RE. The ISP emphasizes that the determinants of technology choice is present in an "innovation system". Such innovation systems facilitate as well as constrain the individual actors making a decision on the technology. In general, innovation systems consist of stakeholders, markets, networks and institutions, and many other components than the relative prices of various alternatives [29]. Innovation is not only about a new product; it could also be the introduction of an improved process, marketing method or organizational method in business practices [30]. As per OECD, dealing with innovation systems is about addressing systemic failures that block the functioning of innovation systems, and obstruct the information flow. These systemic disruptions emerge from institutional rigidities that are based on communication gaps, and lack of networking [29]. Such gaps and lack of integration are evident in the construction sector. The various stages of project development such as design and assessment, construction, operation and maintenance are not yet integrated. There may be considerable difference between project plans (and related EIA reports) and their implementation [30]. The "new environmentally friendly solutions" [31] set during the planning phase need to be effectively communicated at the project implementation stage. Thus, the link between EIA and the structure of the environmental tasks (during project implementation stage) need to be strengthened. For instance, in a Swedish tunnel project, requirements that were based on the environmental impacts identified in the EIA (report) were communicated to the construction contractors through the tender documents [32]. However, planning for GP during the EIA process is still not evident. *Such a planning can be related to*

the integration of project planning and EIA. For instance, in Sweden, during the first stage of the planning process, a decision is taken on whether the new investment in infrastructure is required or not. This stage is crucial because it clarifies the requirements for the EIA that will be carried out if the planning process proceeds [20]. *These requirements could provide the necessary space for emphasizing on the need for GP planning.* Also, since EIA has a legal mandate, by shouldering on EIA [14], there is an opportunity for GP planning to receive more attention than it receives as a stand-alone policy instrument. In the context of RE, as Gutermuth [33] highlights, legislation can have a direct beneficial effect on the diffusion of RE. Reciprocally, procurement policies have the potential to direct the search process of firms by recognizing the way forward for growth and through guiding the selection of technology [34], which indicates that GP planning within an instrument such as EIA might result in better environmental outcomes. According to the European Commission, green public procurement can be a powerful instrument to stimulate innovation that leads to enhanced environmental performance [15]. *This agenda of the Commission could add value to the integration of GP and EIA.*

This paper proposes a conceptual model (Fig.1) for RE procurement planning within the whole EIA process using a decision process flow chart designed by Haralambopoulos and Polatidis [10]. The first stage in this model should be collection and assessment of data.

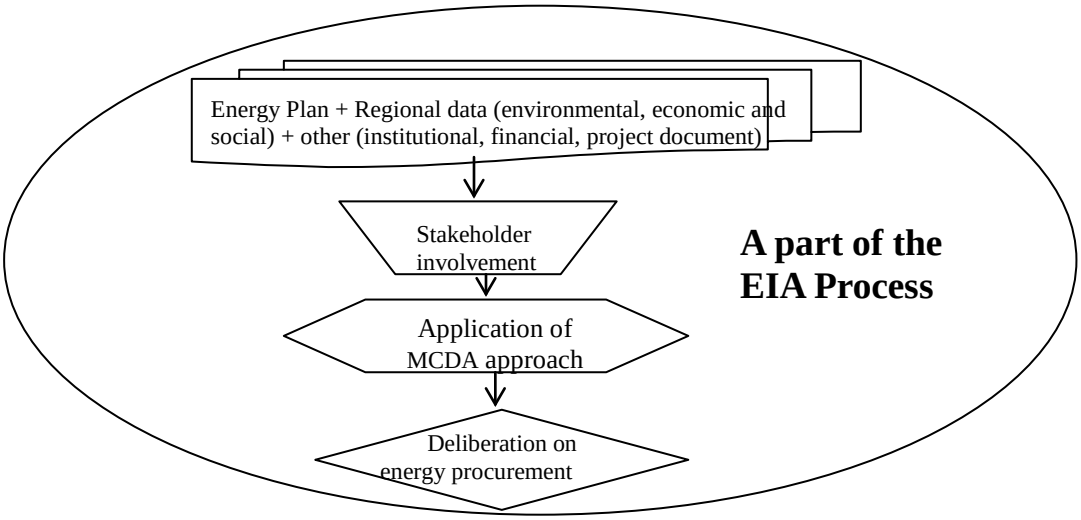

Fig.1. Conceptual model for renewable energy procurement planning within the EIA process.
Source: adapted from [10]

The data includes, inter alia, local energy plan. Tyskeng's [35] study on the Swedish local energy plans reveals that they discuss goals concerning oil reduction and reductions and/or restrictions on CO_2 emissions from a regional and local perspective, and also the use of different energy resources from both regional and local standpoint, energy efficiency, sustainable societies and biodiversity. Subsequent to the collection and assessment of data, the stakeholders need to be identified. The stakeholders consist of several people associated with planning, energy experts, public and statutory consultees, and "have the legitimate responsibility to participate and/or add a socio-political dimension to the decision-making process" [10]. During this stage of the model, it is also important to establish a "planning platform" for incorporating the socio-economic aspects of energy systems in conjunction with their technological attributes [12]. MCDA approach can facilitate the formation of this platform.

2.2. Multi-criteria decision analysis (MCDA) approach and group deliberation

Given the level of conflict that exists between criteria adopted for decision-making (DM), or the intensity of the debate between different stakeholders on the relevancy and the importance of different criteria, tools that seek to facilitate the deliberation and DM process are highly essential. MCDA approach is an umbrella term to describe such tools or methods that take into consideration multiple criteria and assist individuals or groups to explore decisions that matter [22]. It intends to "allow for a pluralist view of society, composed of diverse stakeholders with diverse goals and with differing values concerning environmental changes" [17] and can be an aid in making better decisions. An advantage of adopting MCDA is that it can simultaneously evaluate a number of alternatives, referring to an array of perspectives [11]. In the conceptual model (Fig.1), the MCDA approach has been proposed. However, the various methods that could be used under the MCDA approach needs to be further elaborated. These methods should be such that it can be easily accommodated within the mechanism of EIA integrated with GP. Also, it has to be noted that MCDA is not the only tool that could be used within EIA. There are several other tools such as geographical information systems and life cycle analysis that could be used within EIA (and in certain cases together with MCDA) [23,36]. Further, as Richardson points out, together with stakeholder participation in environmental assessment, there is a need to consider the ethics of practice [37]. *The stakeholder group deliberation on energy procurement, which is the last stage in the conceptual model, should evolve considering, inter alia, ethics and sustainability objectives.*

2.3. The role that the construction sector (CS) could play

The legitimacy of RE technology is a key issue, and might involve a political struggle between the new innovation system and the established one. Such a struggle calls for the participation of politically and financially strong actors, who can have a major influence on the innovation process. These actors can be called prime movers [29]. The CS could be 'prime movers' in promoting RE diffusion and development. Prime movers perform four crucial tasks to promote new technology: create awareness, plan and undertake investments, ensure legitimacy and diffuse the new technology. The new technology here refers to new renewables such as wind power and bioenergy that have not yet reached a wide spread market [25]. Carlsson and Jacobsson [38] indicate that if the consumer/user firms possess significant problem-identifying and problem-solving capabilities in the field of new technology and systems integration, then they can facilitate in strengthening the supplier industry. They noticed this type of user-supplier linkage in the system for factory automation in Sweden. The users in this Swedish factory automation example have been argued to be prime movers [25].
The CS as one of the large energy users would need to strengthen its link with the energy suppliers. Considering their financial and political capacities, the CS could contribute to the diffusion and development of RE. However, the influence of managerial concerns and stakeholder pressures play an important role in the contractors' green innovation [39]. Prime mover may also be cluster of actors if several actors share an interest in promoting a new technology [25]. *Thus, future research should identify other actors for this cluster and investigate the ideal conditions and framework for such a cluster to function effectively*.

3. Discussion

The synthesis of GP and EIA is novel and not a simple task. The conceptual model (e.g. Fig.1) that has been proposed and presented in this paper is a GP planning process that can be accommodated within the EIA process. However, the future questions and challenges are concerned with a strategic mechanism, that is where and how in the EIA should this synthesis with GP occur. EIA has three phases: predecision, post decision and transition [40]. The

phase that is of particular interest in the future study is the predecision phase, which involves designing, developing the EIA report, its review and decision-making. The predecision phase could provide the necessary space for RE planning, and this needs future investigation. The effort towards the synthesis of energy inclusive GP and EIA also requires sufficient scope in the local energy plans prepared by the municipality. So the objectives concerning RE in the local energy plans have an impact on the link between energy inclusive green procurement and EIA, which needs to be investigated further. If the CS through the synthesis of GP and EIA is able to push the development of sustainable energy systems, then it has not only demonstrated its role as a prime mover but also intervened with the issue of urbanization. Being a significant contributor to the process of urbanization, the efforts towards transitioning to a sustainable energy system is not optional, but an inevitability for the CS.

References

[1] Yeo K. Planning and learning in major infrastructure development: systems perspectives. International Journal of Project Management 13, 1995,pp. 287-293.

[2] Yan H, et al., Greenhouse gas emissions in building construction: A case study of One Peking in Hong Kong. Building and Environment 45, 2010,pp. 949-955.

[3] OECD. Environmentally Sustainable Buildings: Challenges and Policies. Paris, France: OECD Publications Service, 2003.

[4] Integrated Waste Management Board. Designing with Vision. California Environmental Protection Agency; 2000.

[5] Sterner E. 'Green procurement' of buildings: a study of Swedish clients' considerations. Construction Management and Economics 20, 2002, pp.21 - 30.

[6] González MJ, Navarro JG. Assessment of the decrease of CO_2 emissions in the construction field through the selection of materials. Building and Environment 41, 2006, pp.902-909.

[7] Acquaye AA, Duffy AP. Input-output analysis of Irish construction sector greenhouse gas emissions. Building and Environment 45, 2010,pp.784-791.

[8] Dimoudi A, Tompa C. Energy and environmental indicators related to construction of office buildings. Resources, Conservation and Recycling 53, 2008,pp.86-95.

[9] Alanne K, Saari A. Distributed energy generation and sustainable development. Renewable and Sustainable Energy Reviews 10, 2006, pp.539-558.

[10] Haralambopoulos DA, Polatidis H. Renewable energy projects: structuring a multi-criteria group decision-making framework. Renewable Energy 28, 2003,pp.961-973.

[11] Cavallaro F, Ciraolo L. A multicriteria approach to evaluate wind energy plants on an Italian island. Energy Policy 33, 2005,pp.235-244.

[12] Polatidis H, Haralambopoulos DA. Renewable energy systems: A societal and technological platform. Renewable Energy 32, 2007,pp.329-341.

[13] Løken E. Use of multicriteria decision analysis methods for energy planning problems. Renewable and Sustainable Energy Reviews 7, 2007,pp. 584-1595.

[14] Vanclay F. The Triple bottom line and impact assessment: How do TBL, EIA, SIA, SEA AND EMS relate to each other? J. Env. Asses. Pol. Mgmt 6. 2004, pp.265-288.

[15] Commission of the European Communities (CEC). COM (2008). Public Procurement for a better environment. 2008.

[16] Jay S et al., EIA: Retrospect and prospect. EIA Review 27, 2007,pp. 287-300.

[17] Glasson J, Therivel R, Chadwick A. Introduction to EIA. 3rd ed. NY: Routledge; 2007.

[18] Sánchez LE, Hacking T. An approach to linking EIA and EMS. Impact Assessment and Project Appraisal 20, 2002 pp.25-38.

[19] McDonald GT, Brown L. Going beyond EIA: Environmental input to planning and design. EIA Review. 15, 1995, pp.483-495.

[20] Isaksson K et al., From consultation to deliberation? Tracing deliberative norms in EIA frameworks in Swedish roads planning. EIA Review 29, 2009,pp.295-304.

[21] Slotterback CS. Evaluating the implementation of environmental review mitigation in local planning and development processes. EIA Review 28, 2008,pp.546-561.

[22] Belton V, Stewart TJ. MCDA. An Integrated Approach. Netherlands: Kluwer Publishers 2002

[23] Malczewski J. GIS-based multicriteria decision analysis: a survey of the literature. International Journal of Geographical Information Science 20, 2006,pp.703 - 726.

[24] Mendoza G, Martins H. Multi-criteria decision analysis in natural resource management: A critical review of methods and new modelling paradigms. Forest Ecology and Management 15, 2006,pp.1-22.

[25] Jacobsson S, Johnson A. The diffusion of renewable energy technology: an analytical framework and key issues for research. Energy Policy 28, 2000,pp.625-640.

[26] Weber R. Basic Content Analysis. Quantitative Applications in the Social Sciences. Newbury Park: Sage Publications; 1990.

[27] Frankfort-Nachmias C, Nachmias D. Research Methods in the Social Sciences. London: Arnold; 1996.

[28] Gummesson E. Qualitative methods in management research. California: Sage Publications; 2000.

[29] Bergek A. Shaping and Exploiting Technological Opportunities: The Case of Renewable Energy Technology in Sweden. Chalmers University of Technology, 2002.

[30] Bröchner J. Construction contractors as service innovators. Building Research & Information 38, 2010, pp.235 - 246.

[31] Swedish EPA. En mer miljöanpassad offentlig upphandling – förslag till handlingsplan. 2005.

[32] Varnäs A et al., Linking EIA,EMS and green procurement in construction projects: lessons from the City Tunnel Project in Malmo, Sweden. Impact Assessment and Project Appraisal 27, 2009,pp.69-76

[33] Gutermuth P. Regulatory and institutional measures by the state to enhance the deployment of renewable energies: German experiences. Solar Energy 69, 2000, pp.205-213.

[34] Johnson A, Jacobsson S. Inducement and blocking mechanisms in the development of a new industry: the case of renewable energy technology in Sweden.In:Technology and the market: demand, users and innovation. UK: Edward Elgar Publishing, Inc.; 2001. pp.

89-111.

[35] Tyskeng S. Environmental assessments of projects and local plans in the energy and waste sectors in Sweden - Practice and potential for improvement. 2006.

[36] Li X, Zhu Y, Zhang Z. An LCA-based environmental impact assessment model for construction processes. Building and Environment 45, 2010,pp.766-775.

[37] Richardson T. Environmental assessment and planning theory: four short stories about power, multiple rationality, and ethics. EIA Review 25,2005,pp.341-365.

[38] Carlsson B, Jacobsson S. Technological systems and economic policy: the diffusion of factory automation in Sweden. Research Policy 23, 1994,pp. 235-248.

[39] Lam PT, et al., Factors affecting the implementation of green specifications in construction. Journal of Environmental Management 91, 2010, pp 654-661.

[40] Morrison-Saunders A, Bailey J. Exploring the EIA/Environmental Management Relationship. Environmental Management 24, 1999, pp. 281-295.

Renewable Energy in Flanders. Current Situation, trends and potential for spatial planning

X.B. Lastra Bravo[1,*], T. Steenberghen[2], A. Tolón Becerra[1], B. Debecker[2]

[1] *University of Almería, Almería, Spain*
[2] *Katholieke Universiteit Leuven, Leuven, Belgium*
** Corresponding author. Tel: +34 950015902, Fax: +34 950015491, E-mail: xlastra@ual.es*

Abstract: In its energy policy, the European Union (EU) sets the target of a 13% share of renewable energy sources (RES) for Belgium. Several instruments have been implemented to reach this target. The objective of this study is analyze those instruments and it effectiveness and efficiency. To tackle this objective, we first analyze the current status of RES in Flanders. Second, we compare the situation in Flanders to the national situation in Belgium and to the other EU member states. Then, we analyze the potential of each type of RES. Finally, we discuss the opportunities and problems of RES related to spatial planning.
In Flanders, the main application of renewable energy is electricity production, of which the main source is biomass. An aspect of the Flemish energy policy worth mentioning is the green certificate system, which has stimulated the development of renewable energies. However, a greater effort to regulate this market and to decrease the cost of kWh produced has proven to be necessary.
The RES-electricity share of total consumption has increased by 3.2% between 1994 and 2008. But, compared to others EU countries, the share of RES to gross inland consumption in Flanders is small. Large-scale facilities are necessary to reach the EU targets. The development of large wind, biomass and solar projects is suggested as the preferred option for Flanders.

Keywords: *Renewable energy sources, EU Policy, Spatial planning, Flanders*

1. Introduction

The term 'renewable energy source' (RES), which is closely linked to sustainable development, is defined as any sustainable resource available in the long term in a simple long-lasting manner, found at a reasonable cost and applicable for any task without causing negative effects [1,2,3]. Several technologies are available for the production of clean, efficient and reliable energy from long-term renewable resources, such as wind, sun, water, biomass and biogas, tides and waves, hydrogen and geothermal energy [1,4].

Worldwide development of RES is currently limited by the high cost for development and implantation, uncertainty on local impact, insufficient funding for research and poor institutional and economic agreements, and limited availability of technological and economic know-how [5,6]. These problems can be solved by technical, economic, market, social and institutional means [2,6], but mainly through policies that incentivize and improve RES access to the power market [1,7].

The annual business volume of the renewable energy market in the European Union (EU) is 15 million €, equivalent to half of the world market, in which the EU is a leading exporter [8]. Furthermore, the EU is the second largest power market in the world (450 million consumers), but the contribution of RES continues to be relatively small, only 6% in 2000 [9,10]. In this context, at the proposal of the Commission, the European Council approved the so-called 20-20-20 goals [11,12]. The RES goals are 20% of EU energy consumption from RES and an increase in the share of biofuels to 10% of the transport fuel mix consumed in the EU by 2020. The EU target set for Belgium is an RES share of 13% [13]. The Belgian National Action Plan, published in November 2010, establishes the Flanders targets related to EU targets and the strategies to reach it in this sense.

The purpose of this study is to analyse the instruments implemented in Flanders to reach the EU RES target, and their effectiveness and efficiency. The analysis was done using available statistical data, and improved by interviews with a large number of people related to renewable energies in Flanders.

2. Renewable energies in Flanders

Solar water heaters, solar panels and wind turbines are becoming well established [14]. However, Flanders produces a lot more renewable energy from many lesser-known sources, such as biomass, biogas and even from waste. In the last years, the energy from wind and sun went through a larger development than the others types (Table 1). In Flanders, the main application of RES is electricity generation, and two-thirds of this comes from biomass [15].

Table1. Renewable energy inventory of Flanders (2005-2008).

Green electricity production (TJ) (net)	2005	2006	2007	2008
Hydropower	8.2	7.5	9.9	13.0
Wind energy	556.0	855.0	1,013.0	1,198.8
Solar (PV)	4.7	11.2	20.0	120.3
Waste incineration	574.3	749.5	922.0	961.6
Biomass	1,537.5	2,904.5	3,033.0	3,942.2
Biogas	800.7	624.2	907.5	954.4
Total green electricity	3,481.3	5,151.8	5,905.4	7,190.3
Gross electricity consumption (GEC)	210,327.8	216,441.1	217,430.6	215,960.9
Net green electricity / GEC (%)	1.7	2.4	2.7	3.3

Green heat production (TJ)	2005	2006	2007	2008
- by CHP plants		2,153	3,074	3,252
- by plants that produce only heat		6,446	6,704	6,960
Total green heat production		8,598	9,777	10,213
Total heat		503,266	466,569	486,359
Green heat / total heat (%)		1.7	2.1	2.1

Biofuels consumption (TJ)	2005	2006	2007	2008
Biofuels for transport	0	0	1,996	2,179
Total road transport consumption	176,477	176,462	179,030	180,630
Biofuels / energy consumption in road transport (%)	0.0	0.0	1.1	1.2

The Flemish Energy and Natural Resources Policy of 2004 and 2009 stipulated that by 2010, 25% of the electricity supplied in Flanders had to be generated by RES and cogeneration. Specifically, for renewable energy from wind, biomass and solar, the energy policy defines a 6% target of. The remaining 19% must be generated by Cooling Heating and Power Plants (CHP) [16]. The current government (2009-2014) decided to continue this policy until a new target for 2020 was drafted. Flanders finalized its Action Plan, and integrated it, and in consultation with the Federal Government, it was also integrated in the action plans of the other regions.

For the Flemish Government, biofuels are not a priority due to current problems with their production and their impact on agriculture, biodiversity, forests and land use changes. The

Flemish Government is looking for other alternatives and new advances in the production of second and third generation biofuels.

2.1. Location of Renewable Energy Facilities in Flanders

Wind turbines, especially large-scale, are usually located near urban or industrial centres, ports (Bruges, Gent and Antwerp) or larger-scale infrastructures such as highways and railways. Most wind turbines have been installed in the provinces of West Flanders, East Flanders and Antwerp. A map of potential areas for installation of future wind energy turbines in these provinces are shown in Figure 2 (in brown). Note that not all wind turbines (in yellow) are currently installed in these potential areas.

Large-scale biomass facilities (in green in Fig. 2) are mainly located near ports (Gent and Antwerp), because most resources required for biomass energy production are imported from other countries, mainly from France. In Limburg, plentiful agricultural resources available led to the installation of small and medium-scale facilities.

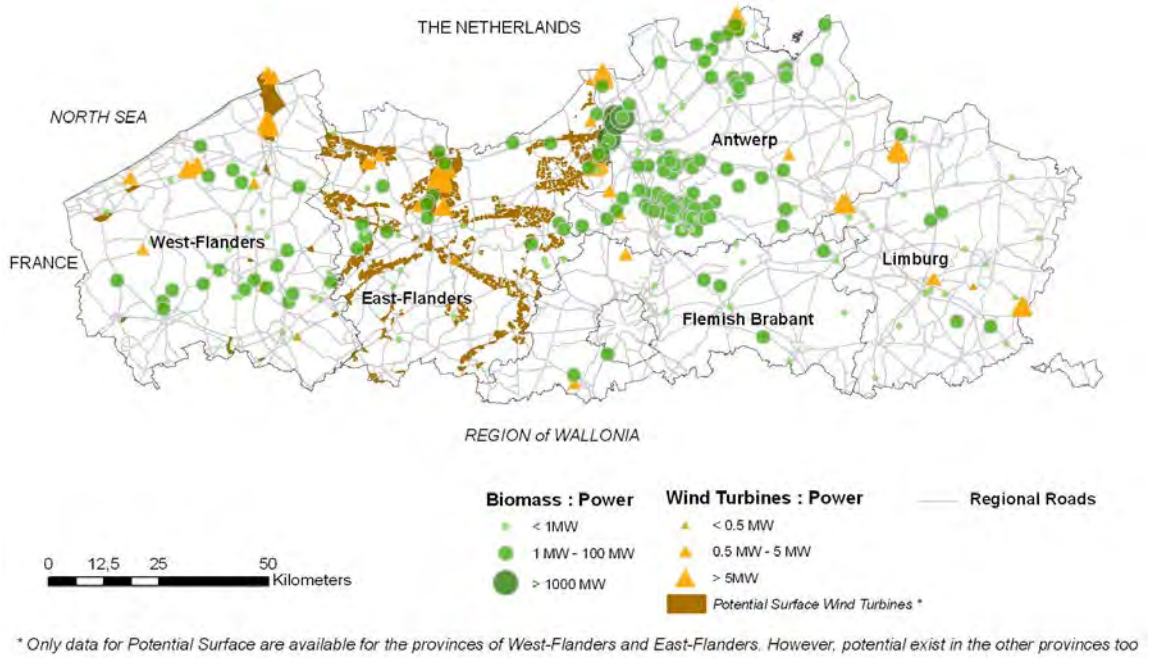

Fig. 2. Location of wind and biomass energy facilities in Flanders.

2.2. Green Electricity

The share of electricity from RES in total electricity consumption has increased to 3.3% in 1994-2008. Absolute values increased from 58 GWh to 1,997 GWh by 2008. According to the Flemish Energy Agency [14], 2,688 GWh of electricity were produced from green energy sources by 2009 (4.8% of total electricity consumption).

In 1994, the electricity from waste incinerators was the main source (Table 2), but in the last five years, the majority of green electricity comes from biomass [14]. Wind power was the second main source in 1994-2008. Although hydropower increased during this period, its share in the total electricity consumption has decreased.

Table 2. Evolution of the share of green electricity in total electricity consumption (1994-2008)

%	1994	1996	1998	2000	2002	2004	2006	2008
Biomass	-	-	-	-	21.8	31.1	56.4	54.8
Wind	15.6	11.6	8.8	9.1	17.1	15.2	16.6	16.7
Waste	78	69.2	77.9	77.4	42.5	21.6	14.5	13.4
Biogas	3.6	16.1	11.9	12.1	17.7	31.8	12.1	13.3
Solar	-	-	-	0.1	0.2	0.1	0.2	1.7
Hydro	2.8	3.1	1.4	1.3	0.8	0.3	0.1	0.2

In absolute terms, green electricity from biomass, wind, solar and hydro energy increased 1,331 times during 2002-2008. Biomass has been responsible for over 80% of green electricity since 2004, especially the selectively collected waste biomass (Fig. 3). In 2009, the electricity generated by biomass (2,160 GWh) represented 80.4% of the total amount of RES-electricity (2,688 GWh).

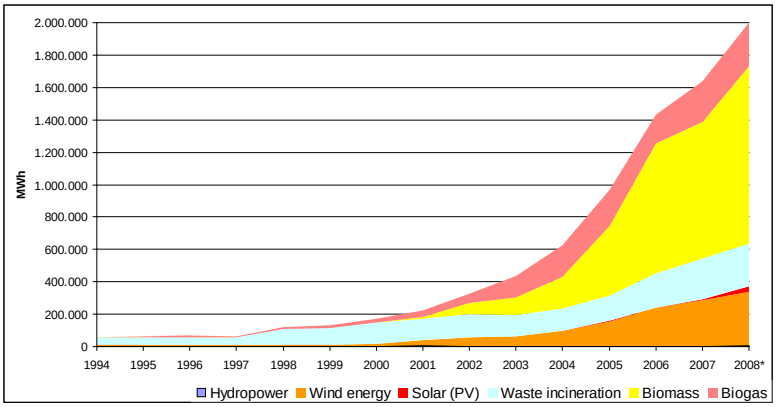

Fig. 3. Evolution of green electricity in Flanders from 1997 to 2008[16].

The largest increase was experienced by electricity from solar energy (6.7 times), but by 2008 it still only represented 1.7% of the total amount of green electricity. Wind energy, which provides almost 17% of the total green electricity production, increased by 750% in 2002-2008 (Fig. 3). In 2009, electricity from solar energy increased steeply to 138 GWh of the 2,688 GWh total green power produced (5%). Almost 3 million m² of solar panels for electricity production were installed. Moreover, 100,000 m² of solar collectors for heat production supplied sanitary water heating for 25,000 Flemish families.

2.3. Green Certificate System

The Flemish Region launched a Green Certificate System (GCS) on 1 January 2002. There are two kinds of green energy certificates, compulsory and optional EUR [14]. From 1 January 2002, all electricity suppliers are required to sell a minimum amount of energy from renewable sources. Strong growth of Flemish RES electricity generation from 0.8% of electricity sales in 2002 to 4.9% in 2007 brought the 2010 6% target within reach (Verbruggen, 2009) [17]. The number of Green power certificates issued in 2002-2007 has increased almost 18 times. The technology with the largest increase is PV, from five certificates in 2002 to 139,489 in 2009. This success is a consequence of high certificate prices in the first years of the system. The number of energy certificates decreased last year due to their lower prices (2,692,904 in 2009 and only 929,792 as of July 2010).

The GCS works better than traditional subsidies and is a relatively good option for developing renewable energies. The system achieved relatively good results right from the start,

especially in promoting the installation of wind turbines and PV solar panels. However, the overall performance of the Flemish support system (effectiveness, efficiency and equity) is assessed as poor, despite its good short-term targets, costs and profits [17]. Moreover, there are no clear transition trajectories to a sustainable power system, and RES electricity generation from old waste-processing facilities is of dubious quality (effectiveness). Moreover, dynamic efficiency is spurious because there is no link to a technological industrial policy (efficiency). Finally, the polluter-pays principle is not respected, but jeopardized in the waste management sector (equity).

3. Flanders and EU Benchmarking - Main Indicators

Denmark, Sweden, Finland, Germany, the Netherlands and Austria all made a great effort to reach their EU targets. Flanders had only a of 1.7% share of green electricity from RES in its total electricity consumption by 2005 (Fig. 4), and was still far from reaching the EU target (6.0%) for 2010. However, the whole country of Belgium had a 2.8% share by 2005, and if past performance could be continued in 2005-2010, the EU target would be reached by 2010 (5.3% in 2008).

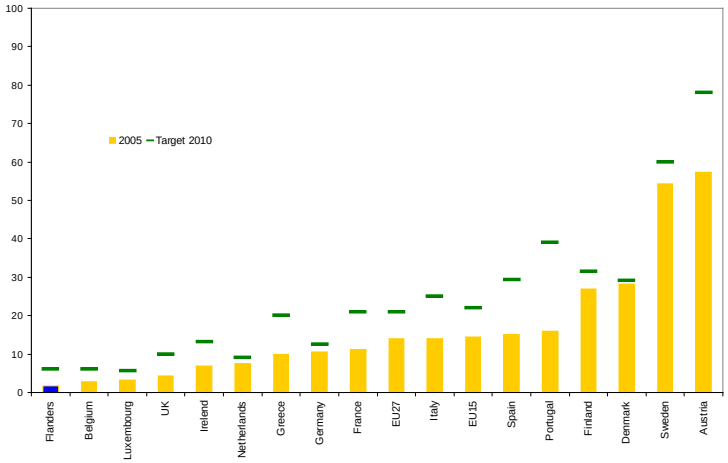

Fig. 4. 2010 EU electricity targets vs. 2005 green electricity production in Europe and Flanders (%).

The share of RES in Gross Inland Consumption in Flanders is small compared to the other EU countries. The relative share of RES-electricity in Flanders is half the relative share of all of Belgium. This means that the Walloon Region produces roughly 3 times more electricity from RES than Flanders. According to some experts interviewed in this study, this difference between the two regions is explained by the greater availability of biomass resources in the Walloon Region. Moreover, the relative Flemish share is only larger than the relative share of Estonia and Cyprus. In spite of this, the significant increase in its share from 0.21% in 2004 to 1.22% in 2007 highlights the effort made by the Flemish Government.

Of the different RES, biomass is the largest in both Flanders and all of Belgium. The share of biomass in Flemish RES production (82.3%) is the second largest in the EU after Hungary. The share of wind energy in Flanders is also relatively large (17,2%), and close to the EU27 share (19.8%). Electricity production from other sources (hydropower, solar and geotechnical) makes up less than 1% and is relatively insignificant.

4. Analysis of the Opportunities and Problems related to Spatial Planning

In the Flemish Region, the development of large-scale energy facilities is mainly limited by its high-density population and related factors, such as concentration of cities and infrastructures (roads, railroads, housing, factories, industrial areas, etc.). Other restricting

factors are landscapes values, relief (mainly in hydropower facilities), monuments, natural protected areas, air-restricted areas, and so on. Finally, the aesthetics of renewable energy facilities is an important factor related to public acceptance.

The "Projections on renewable energy and cogeneration to 2020" study [18] examined the potential of different technologies (electricity, heat and biofuels), and compared a business-as-usual scenario (BAU) with a Pro-active policy (PRO). The Flemish Government used the calculated potential in the PRO scenario in its Energy Plan (Table 3).

Table 3. Potential of renewable energies in Flanders.

Technology	2010 (GWh)	2020 (GWh)	Increase (%)
Wind onshore	521	1,905	265
Wind offshore	320	3,841	1,100
Solar energy (PV)	174	935	437
Solar thermal	224	1,193	433
Biomass plants for electricity production	97	217	124

In order to realise the potential of renewable energies in Flanders, the surface required for the installation of new facilities is calculated as follows. To reach the target of 1,000 MW, 300 new 2.5-MW wind turbines (+750 MW) are necessary. Since the current legislation prescribes a minimum buffer distance of 250 m from any dwelling (radius = 250m → area = 20 ha), a surface free of housing of 6,000 ha is required.

To reach the proposed 935 GWh by 2020, VITO[o] assumes that the efficiency of solar panels will improve from the current 110 kWh m^{-2} per year to 170 kWh m^{-2} per year. Therefore, an additional 800 ha are necessary to install the required panels. An increase in surface of 300 ha for installing solar water heaters is desired by 2020. However, the installation of PV and thermal panels does not require the acquisition of new land, which makes it a good option.

The main environmental problems related to biomass and CHP facilities are the emissions of greenhouse gases (GHG) and the effect of noise and smell, in addition to the visual impact. Therefore, rural areas are the most suitable for the installation of biomass and CHP facilities. For such an installation, the availability of resources and connection to the power grid are essential. Heat facilities have been observed to be the most used in the rural areas. A regulation related to the use of biomass sources (especially pellets) is needed.

Wind turbines have been installed near large structures, such as industrial areas and highways, and near high power grids. The choice of such locations helps reduce the visual impact and the problem of the noise of wind energy turbines. Most past installation projects were medium or small scale (3-4 turbines) because of existing limitations (mainly the available surface). Nowadays, small wind turbines are considered inefficient. The Windplan for Flanders was launched in 2001.It includes potential areas for the installation of wind turbines according to their wind potential way, the provinces of West Flanders, East Flanders and Antwerp made a more advanced multiple-criteria map of potential areas for the installation of wind energy turbines (residential and industrial areas, protected landscapes, agricultural areas, recreational areas). However, these areas are only designated as suitable, and the map is not legally binding.

The installation of solar panels (at small and medium-scale) has seen a boom in the last year, mainly due to its promotion by the GCS and benefits for private promoters. PV panels are the

most widespread. The installation of large-scale projects in Flanders (4-6 ha) is generally restricted by the limited availability of surface. The most suitable area for the installation of solar panels in Flanders is the North Sea coast (West Flanders Province). East of the Flemish region, the potential is reduced due to the proximity of higher lands and increased presence of clouds. Belgium is now the 6th most solar PV- intensive country in the world (defined by km^2 of solar panels).Price is the main limiting factor for installation of solar panels. Arestricting technical factor is the shadowing by nearby buildings. Around a 20% shadow on one solar panel suffices to stop the energy production of all the panels connected in the same loop.

5. Conclusions: Trends and Future challenges of RES in Flanders

The electricity generation is currently the main application of renewable energies, while heat production (from heat pumps, wind, geothermal, solar) has the highest potential for further application and development in Flanders. There are currently no concrete projects for developing geothermal energy. Should this be reconsidered, more effort by the regional government will be needed to develop this type of RES in the coming years.

The Flemish Government promotes RES through their green certificate pricing policy. First, wind facilities were promoted, followed by PV installations, and more recently biomass and CHP installations. With theses mechanisms, the Flemish Government strives to reach the EU 20/20/20 energy targets. However, a stronger effort to regulate the green energy market and to decrease the cost of kWh produced is necessary, because there are no clear transition trajectories to a sustainable power system. This situation requires broad agreement between the government, the power industry and the public. The RES market potential may be substantially increased by means of dedicated policies, implemented after consensus, such as, a better qualification system, different subsidies, levies and taxes to shift market prices, lowering the cost of RES, or helping abolish man-made barriers through technological innovation. But support for the development of RES through a modified or better GCS must continue in order to reach the EU targets and real sustainable development.

Benchmarking of relative Flanders and EU RES and RES-electricity consumption indicators shows that most of them are low. Despite this, increase in recent years has been significant and highlights the effort made by the Flemish Government.

Concerning spatial planning, the search for available suitable areas to install such facilities must be a priority for renewable energy policy makers. Ports, highways and industrial zones are priority areas for the installation of wind energy facilities. However, a more participatory approach for the development of renewable energy facilities is necessary, especially for the construction of wind turbines.

The large increase in PV solar energy production is accompanied by problems between producers and distribution companies, and further regulation is required in this field. In addition, a better distribution grid is needed, since the current grid is not well adapted to receive all the renewable energy produced.

In addition, the specific potential and conditions of each individual region should be considered when setting regional prices for green certificates, and installation of renewable facilities in areas with lower potential should be promoted (e.g., wind energy in Brabant-Flanders and Limburg). These measures would help decentralise energy production, bring production closer to consumers and avoid grid losses from long-distance energy transport.

Finally, better regulatory framework co-ordination between governmental departments and the energy is required for the EU, Belgian and Flemish targets to be met.

References

[1] A.M. Omer, Energy, environment and sustainable development, Renewable and Sustainable Energy Reviews 12, 2008, pp. 2265–2300

[2] I. Dincer, Environmental impacts of energy, Energy Policy 27, 1999, pp. 845-854.

[3] W.W.S. Charters, Developing markets for renewable energy technologies, Renewable Energy 22, 2001, pp. 217-222.

[4] F. Abulfotuh, Energy efficiency and renewable technologies: the way to sustainable energy future, Desalination 209, 2007, pp. 275–282.

[5] IPCC, Climate change 2001, UN International Panel on Climate Change, 2001.

[6] A. Verbruggen, M. Fischedick, W. Mooma, T. Weir, A. Nadaï, L.J. Nilsson, J. Nyboer, J. Sathaye, Renewable energy costs, potentials, barriers: Conceptual issues, Energy Policy 38(2), 2010, pp. 850-861.

[7] DEFRA, Energy Resources, Sustainable development and environment, 2002.

[8] EU, Green paper on an energy strategy for sustainable, competitive and secure energy, COM (2006) 0105.

[9] EU, Green paper on energy efficiency or doing more with less, COM(2005), 265 final.

[10] European Communities, Communication from the Commission to the European Council and the European parliament - An energy policy for Europe, COM(2007)1 final.

[11] Council of the European Union, Brussels European Council 8/9 march 2007, Presidency conclusions, (7224/1/07).

[12] D. Bouquet, T.B. Johansson, European renewable energy policy at crossroads-Focus on electricity support mechanisms, Energy Policy 36, 2008, pp. 4079- 4092.

[13] European Parliament and European Council, Directive 2009/28/EC of the European Parliament and of the Council on the promotion of the use of energy from renewable sources amending and subsequently repealing Directives 2001/77/EC and 2003/30/EC.

[14] Vlaams Energieagentschap, 2010, Available on: http://www.energiesparen.be/

[15] K. Briffaerts, E. Cornelis, T. Dauwe, N. Devriendt, R. Guisson, W. Nijs, S. Vanassche, Prognoses voor hernieuwbare energie en warmtekrachtkoppeling tot 2020. Studie uitgevoerd in opdracht van: Vlaams Energie Agentschap. 2009/TEM/R/. VITO.

[16] E. Cornelis, K. Aernouts, S. Van Geel, WKK-inventaris in Vlaanderen 2008. Studie uitgevoerd in opdracht van: 2009/TEM/R.

[17] A. Verbruggen, Performance evaluation of renewable energy support policies, applied on Flanders' tradable certificates system, Energy Policy 37(4), 2009, pp.1385-1394.

[18] Vlaamse instelling voor technologisch onderzoek, Prognoses voor hernieuwbare energie en warmtekrachtkoppeling tot 2020. Tussentijds Rapport. Studie uitgevoerd door Vito in opdracht van het Vlaams Energie Agentschap, 2009.

Sustainable Cities: Strategy and Indicators for Healthy Living Environments

Mohsen M. Aboulnaga[1,*], Sabah Abdullah[2]

[1] *Professor, University of Dubai, Dubai, UAE and Main Founder, Emirates Green Building Council*
[2] *University of the Basque Country, Environmental Economics Unit, Institute for Public Economics, 48015 Bilbao, Spain & University of Bath, Department of Economics, Bath, UK*
** Corresponding author. Tel: +971 506185217, PoBox 126166 Dubai, E-mail: mohsen_aboulnaga@yahoo.com*

Abstract: The impact of climate change on our cities has been clearly manifested. Cities do not only consume most natural resources but also produce air pollution and generate great amount of waste and waste water. This paper focuses on sustainable cities strategies and indicators for the case of Santa Monica city, US using a set of 29 sustainable indicators for some years 1990-2006. The study sheds light on the application of some sustainable development (SD) indicator and suggests more applicable and specific data to further examine other cities sustainable programmes. The six thematic dimensions: sustainable, economic, equitable, social, viable and livable, where 62% of the 29 indicators are presented. Indeed, the review of some of the 29 indicators for Santa Monica shows the various levels of SD before and after the Sustainable City Program (SCP).

Keywords: *Sustainable Cities, Strategies, Sustainable Development Indicators, Santa Monica.*

1. Introduction

Over the past century, cities and towns using various urban systems were developed and built in inefficient ways based on traditional ways of activities and life styles. Consequently, such models drove production and consumption of resources inefficiently. Indeed, the urban sprawl is an urgent and persistent problem when world's natural resources are scarce and pressured by human settlement. Moreover, such pressures particularly related to carbon emissions in urban areas/ cities involve power generation, transport, and waste. Nevertheless, creating buildings and designing cities is one of the most complex and sophisticated tasks.

Cities pressure natural resources and consume large amounts of energy and water as well as emitting air pollutants and generating waste. All these activities pose potential risks to our economic, health and environmental wellbeing and the prime global concern at the present time is the effect of human activities upon climate change particularly related to urban areas. Several studies published by the United Nations Habitat showed that in 2007-2008 a major shift occurred where more than half the world's population was classified as urban dwellers [1,2,3]. Globally, the number of people living in towns and cities at the end of 2008, was estimated at 3.3 billion and this is expected to increase to five billion by 2030 [4,1]. However, the main challenges to such increases are the pressure on natural resources as well as utilities such as on energy, water as well as waste management and mobility. For instance, the recent United Nations Environment Programme (UNEP) data on global energy demand suggested that nearly 45 percent will increase by 2030 [5].

It is vital to efficiently plan our cities to be sustainable by developing strategies and policies to promote sustainability. Significantly, capturing sustainable development indicators at local as well as global levels is relevant since the climate changes and pollutions are global problems. Moreover, emphasis should be stressed when it comes to cities' consumption patterns and their impact on other neighboring regions and ecosystems. Also, the accountability and responsibility for all stakeholders to assist in monitoring consumption patterns and addressing the requirements for a sustainable city is needed. Additionally, adaptive policies to reduce, recycle and re-use consumer goods are important strategies for

cities to achieve sustainability pathways [6]. As shown in Table 1, the list depicts some of the sustainable cities according to sustainable city network (SCN) 2007-2011 [7].

Table1. List of Sustainable Cities

Australia & Pacific	Americas	Europe
Adelaide	Ottawa	Berlin
Ballarat	Vancouver	Bristol
Maleny	Niagara	Cambridge
Melbourne	Florida	Geneva
Auckland	Greensburg	Malmö
Wellington	Moraga	Rotterdam
	Santa Monica	Stockholm
	Philadelphia	
	Tuscon	
	San Francisco	
	San Jose	
	Seattle	
	Silicon Valley	
	Bogota	
	Chiapas	
	Curitiba	

In the next sub-section namely sustainable indicators (1.1), we discuss briefly some components of such strategies which some cities have integrated in their mandate to become sustainable.

1.1. Sustainable Development Indicators (SDI)

According to Tanguay, et.al (2010), sustainable development indicators (SDI) are used intensively to illustrate sustainable development pathways particularly applying actual assessment and monitoring systems [8]. The authors also argued that the exploitation of the SDI remains problematic because of general definition of sustainable development as outlined in the Brundtland report (WCED, 1987). SDI varies from one place to another but the main components are listed in Table 2. SDI variation in the present time compared to say twenty years ago can be attributed to the priorities set in meeting the environment, social, economic, political and technological objectives of the local and regional needs. A case in point is in the EU where new and old member countries are requested to revise their National sustainable development strategies (SDS) in line with the renewed EU SDS which is likely to increase the degree of cohesion in defining and monitoring SDIs. As mentioned previously, SDI can differ at local levels but must also be analyzed from a global perspective.

Table.2. Indicators used to measure the sustainability of a city

- Sustainable Development Policy & Practice
- Biodiversity
- Climate Change
- Energy
- Environment
- Planning
- Transport
- Social Issues
- Pollution
- Urban Development
- Construction
- Waste Management
- Water

Moreover, sustainable cities may vary due to the countries or regional sustainable strategies. Take the case of US where according to the latest report by the Sustainable Cities Index (SCI) the sustainable cities namely the City of Portland, Oregon, were analyzed according to four major indicators: clean technology, green building development, overall quality of life, and sustainability planning and management [9]. In the case of UK cities, the assessment focused less on the equitable dimension. For Europe, cities can and should not only be highly resource-efficient but also safe, healthy, pleasant, fulfilling and inspiring places to live. Based on a strategy paper (2007–2013) by the European neighborhood and partnership, it concluded that at city level, the local strategies for sustainability require active participation and commitment of the local community who can provide effective actions [10]. Moreover, the challenge for Europe's cities to achieve sustainability objectives their governments must allow cities maximum freedom to apply suitable tools at local level [6]. Indeed, indicators are increasingly developing into a vital tool of communicating information to decision-makers and the public in a straightforward and robust manner.

The motivation of this paper is to review several indicators that measure sustainability of cities by examining one case study found at a local level in the United States. Our attempt is to illustrate the practical application of such indicators at the local levels. In fact, the need to measure sustainable development (SD) is based on robust indicators or evaluation criteria [8]. The comparison of theoretical and practical approaches is essential in illustrating the robustness of such criteria.

In this vein, Shen et al. (2011) point out that among the available urban sustainability indicators there are no single set of indicators equally suitable to all cities or communities. They further suggest the use of consistent indicators for monitoring and comparison purposes due to the fact that such indicators will allow cities to have a common grid to share and apply successful tools and measures [11]. Zhang, He, and Wen (2003) recommend that for urban sustainability indicators (USI), in other words, city sustainable indicators should offer no less than: a) explanatory tools to translate the concepts of sustainable development into practical terms; b) pilot tools to assist in making policy choices to promote sustainable development; and c) performance assessment tools to decide how effective efforts have been established [12]. This paper is outlined in 4 parts: introduction as presented above, section 2, methodology and sub-section focusing Santa Monica city as a case study. Section 3, presents the results and discussions of the application of sustainable development indicators for the case of Santa Monica, and section 4 concludes.

2. Methodology

Many models address sustainable cities in different taxonomies. However, strategy and policy, and appropriate assessment tools at national planning levels should be firmly developed and implemented to improve the key indicators in order to ensure cities are sustainable at the local levels. In Moussiopolous et al. (2010) study, they developed a dynamic tool for the management of environmental, social and economic indicators to evaluate sustainability in urban areas. In their study, the case study of Greater Thessaloniki Area, in Greece was selected with a set of indicators included 88 indicators in 13 discrete thematic areas. Additionally, guidelines were recommended for developing communication among local stakeholders [13].

Shen et al. (2011) critically examined and compared different sustainable urbanization practices when selecting urban sustainability indicators [11]. They further stated that measuring sustainability in urban areas requires strong local socio-economic development and

the key challenge for environmental managers and decision-makers is environmental decay. They further caution that indicators selected should be the ones that are essential and likely to produce the most accurate information about the status of practice. Tanguay et al, (2010) defined a number of SDI derived from 17 studies showing diverse conceptual frameworks and choices. In their study, a method, called SuBSelec, where 188 indicators extracted from the aforementioned 17 studies and reduced to 29 SDI. The SuBSelec strategy produced a new perspective to the debate related to the SDI selection. This is seen as a preliminary step aimed for planners and decision makers where a scientifically based and operational SDI Grid is established [8]. The authors acknowledge the subjective nature of this approach and believe that the classification allows the selection of recognized indicators which covers the various aspects of sustainable development broadly. Additionally, their conclusion is similar to Niemeijer and De Groot (2008) in that selection of indicators is invariably subject to arbitrary decisions at one phase of the process or another [14]. Such analyses demonstrate that current practices related to SDI cannot meet standard objectives and the need to obtain indicators which reflect local concerns.

In this study we follow the approach suggested by Tanguay et al. (2010) namely, Survey-based selection strategy (SuBSelec) which refers to 29 indicators divided into six dimensions: sustainable, liveable, equitable, social, economic and viable, for a given city [8]. The focus of next sub-section is to review and compare the Santa Monica Sustainable City Indicators (SCI) as found in SCP to the sustainable development indicators (SDI) given by these authors.

2.1. The case study: Santa Monica

In early 1990's the Santa Monica City Council took bold steps to address sustainability issues in the community adopting a Sustainable City Plan [15]. The Sustainable City Program (SCP) was initially proposed in 1992 by the City's Task Force on the Environment to ensure that Santa Monica could continue to meet its current needs–environmental, economic and social without compromising the ability of future generations to do the same. Such a programme comprised goals and strategies, for the City government and all sectors of the community. As shown in Table 3 (see Appendix) eight indicators' dimension with their respective categories were defined by the SCP. Indeed, the primary reason of selecting this city is because it boasts of comprehensive history to examine and discuss at local level. In reviewing the SCP, a span of several years ranging from 1990 to 2008 was selected, depending on the availability of data. In Table 4 (see Appendix), each indicator and the eight SD dimensions are depicted with the relevant notes for various years. It should be noticed that some indicators were not applied to all. For the comparison purposes the ratio between the years 2000 and 1990 were set to 1 for relative changes but not in absolute terms, this is because in some cases few years were not for 2000 and 1990 as explained above.

3. Results and discussion

This section exhibits the six dimensions: sustainable, economic, equitable, social, viable and livable, where 62% of the 29 indicators are presented. Indeed, the review of some of the 29 indicators for Santa Monica shows the various levels of SD before and after the SCP.

Fig.1 and Fig.2, illustrate the sustainable and economic dimensions respectively where in the year 1990 and 2000 greatly differs, where in 1990s the sustainable and economic situations were less than the year 2000. For the equitable dimension (Fig.3), it exhibits a better performance in 2000 compared to that of 1990 in terms of low crime rates and poverty levels. In Fig.4, the citizen participation increased nearly twice as those in 1990. Also, the rate of participation in municipal elections has slightly increased.

The viable dimension as shown in Fig.5 exhibits this dimension in terms of quantity of waste recycled. In this dimension, the ratio increased from ratio 0.2 (1999) to 1 (2000). This can be attributed to number of waste produced and/or the increase in technology in recycling such waste.

For the livable dimension as shown in Fig.6, both indicators the GHG emission and household waste in 2000 have increased compared to 1990. This maybe explained due to increase in populations or socio-economic activities during this time. Again, the indicators are subjective particularly when population and other economic variables are not considered in the picture.

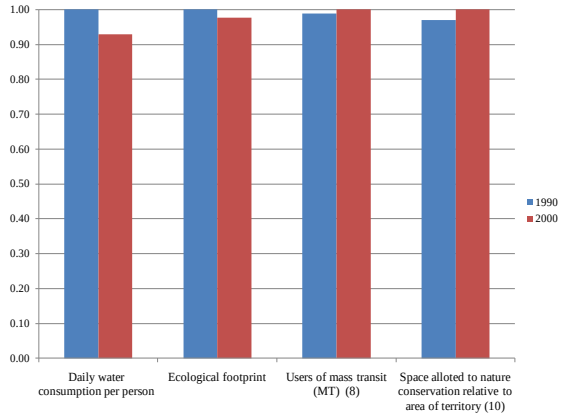

Fig.1 Sustainable Dimension

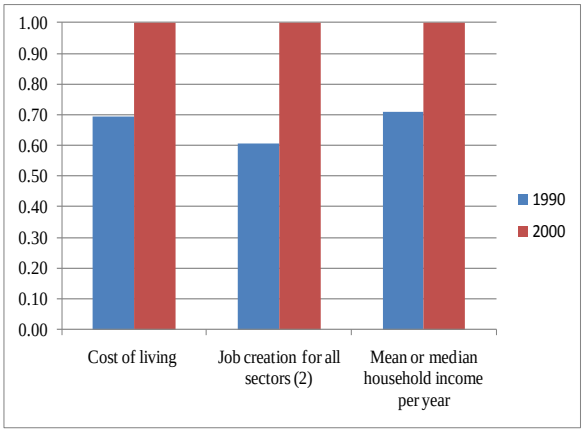

Fig.2 Economic Dimension

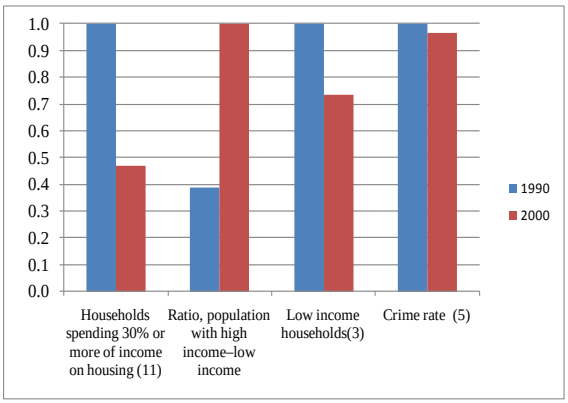

Fig.3 Equitable Dimension

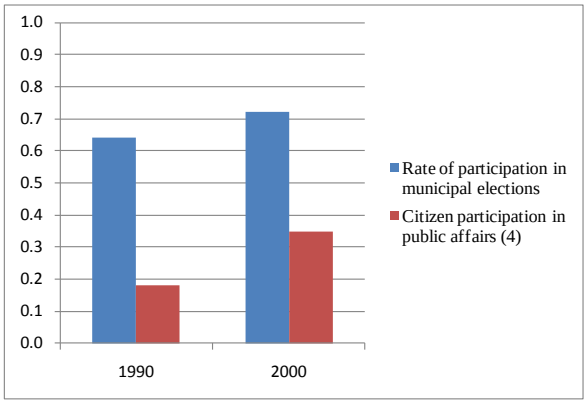

Fig.4 Social Dimension

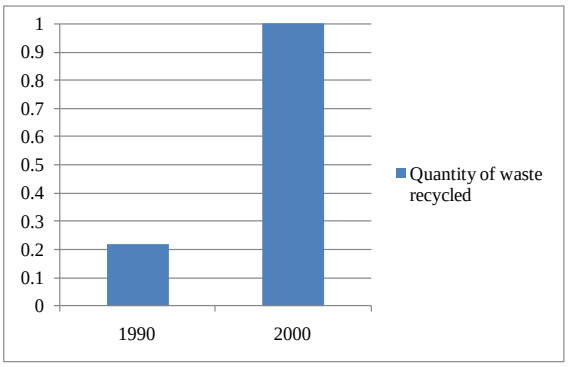

Fig.5 Viable Dimension

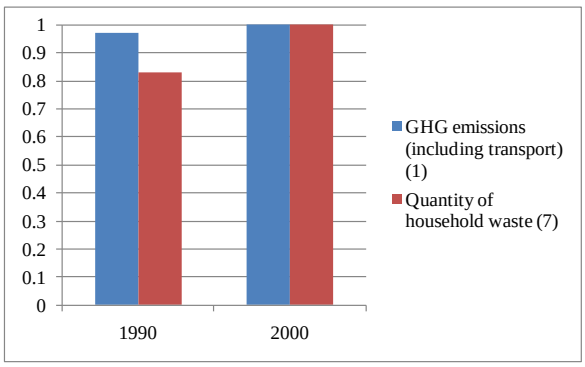

Fig.6 Livable Dimension

4. Conclusions

In this paper, we had used the case of Santa Monica city to review 29 indicators as suggested by Tanguay et al, (2010). The case of Santa Monica has demonstrated that the six thematic dimensions of sustainable development are not sufficient to measure the years between 1990-2000. This exercise suggests that continuous data collection needs to be exploited to assist the development and assessment of indicators to achieve their local sustainable objectives. Indeed, in most cases, these indicators are subjective they can be revised to vary from one city to another. Significantly, there is a need to identify the practical application of sustainable indicators at local levels. This can be a challenge at the present time in some cases, though these challenges can be overcome with the suitable indicators to address sustainability in the future.

Consequently, the development of an appropriate framework for a sustainable city requires a tailor-made model that considers the needs of the locals in the city at the same time meet the sustainable efforts of its participants. On one hand, there are advantages in establishing sustainable indicators but on the other hand, such a task is challenging as stated by Stiglitz et al. (2009) in a dossier [16]. This calls for urban sustainability to include all stakeholders within the local areas and devise appropriate tools and framework. Another challenge facing sustainable indicators is the access to local data available to public and various stakeholders' objectives in communities. In addition, the end-use activities in this case, consumption, which are strongly linked to CO_2 emissions and other pollutants, need specific local information. For instance, detailed data about industries such as manufacturing, oil and gas, roads and buildings in relation to sustainability at the local. Moussiopolous et al. (2010) highlighted one of the challenges in creating an efficient system of indicators is the selections of a manageable list of metrics to better describe sustainability. They further point out that developing indicators cannot be a purely technical or scientific process but should be an open communication and policy process [13]. In sum, it is recommended that future works include other cities in a comparison exercise using consistent sustainable indicators for the purpose of improving sustainable indicators for cities considering the socio-economic, political and environment conditions.

Appendix

Table.3. Description of sustainable dimensions found in Santa Monica progress report

Indicator dimension	Categories	Indicator dimension	Categories
Resource conservation	Ecological footprint	**Housing**	Affordable Housing
	Energy Use		Affordable Housing for Special Needs
	Green Construction		Distribution of Affordable Housing
	Green House Gases Emissions		Green Housing
	Renewable Energy		Livable Housing
	Solid Waste		
	Sustainable Procurement		
	Water Use		
Environmental and public health	Air Quality	**Transportation**	Alternative Fuel Vehicles - City Fleet
	City Purchase of Hazardous Materials		Average Vehicle Ridership
	Farmers' Market		Bike Lanes
	Food Choices		Bus Ridership
	Household Hazardous		Pedestrian - Bike Safety

	Waste		
	Local Produce at City Facilities		Sustainable Transportation Options
	Restaurant Food		Traffic Congestion
	Santa Monica Bay Health		Traffic Impact on Emergency Response
	Toxic Air Containment		Vehicle Ownership
	Urban Runoff		
	Vehicle Miles Traveled		
	Waste Water		
Economic development	Business Reinvestment	**Open space and land use**	Land Use and Development
	Cost of Living		Open Space
	Economic Diversity		Park Accessibility
	Income Disparity		Regionally Appropriate Vegetation
	Jobs - Housing Balance		Trees
	Local Employment of City Staff	**Community education/civic contribution**	Civic Participation
	Quality Job Creation		Sustainable Community Involvement
	Resource Efficiency of Local Business		Voter Participation
Human dignity	Ability to Meet Basic Needs		
	Basic Health Insurance		
	Crime Rate		
	Economic Opportunity		
	Education & Youth		
	Empowerment of Minorities		
	Homelessness		
	Incidents of Abuse		
	Incidents of Discrimination		
	Perception of Personal Safety		

Source: Santa Monica, Sustainable City Progress Report
http://www.smgov.net/Departments/OSE/progressReport/default.aspx.

Table.4. Application of Sustainable development indicators (SDI) for the case of Santa Monica

	Indicator	Description	SD Dimensions	2000	1990
1	SD policies or strategies	yes / no	Sustainable	1	0
2	Density of urban population		Sustainable	n.a	n.a
3	Daily water consumption per person	millions gallon per day	Sustainable	13.2	14.2
4	Ecological footprint	per acres	Sustainable	20.9	21.4
5	State of health reported by population (6)	percentage perception by	Sustainable	16%	n.a
6	Users of mass transit (MT) (8)	percentage of riders	Sustainable		9.10%
7	Space alloted to nature conservation relative to area	percentage of open space to	Sustainable	3.30%	3.20%
8	Cost of living	Cost living $ per household	Economic	79,890	55,300
9	Participation rate for all sectors		Economic	n/a	n/a
10	Job creation for all sectors (2)	number of jobs	Economic	2113	1283
11	Mean or median household income per year	Median household ($ / Yr.)	Economic	50,714	35,997
12	Households spending 30% or more of income on	% Percent of rent-controlled	Equitable	40%	85%
13	Population aged 18 and over with less than a high		Equitable	n.a	n.a
14	Unemployment rate		Equitable		
15	Ratio, population with high income–low income	ratio of high-low	Equitable	92.9	35.9

16	Population receiving social assistance		Equitable	n.a	n.a
17	Low-income households(3)	percentage of households	Equitable	25%	34%
18	Crime rate (5)	per capita crime rate	Equitable	4.35	4.51
19	Rate of participation in municipal elections	%	Social	72%	64%
20	Citizen participation in public affairs (4)	%	Social	35%	18%
21	Annual consumption of energy from renewable	%	Viable	18%	19%
22	Businesses with environmental certification		Viable	n.a	n.a
23	Quantity of waste recycled	tonnes per year	Viable	181,902	40,013
24	Concentration of PM10 particles		Liveable	n.a	n.a
25	GHG emissions (1)	per capita	Liveable	10.6	10.3
26	Population exposed to Lnigh>55 dB (A)		Liveable	n.a	n.a
27	Quality of waterways		Liveable	n.a	n.a
28	Quantity of household waste (7)	tonnes per year	Liveable	333,518	275,842
29	Participation in sports in parks & swimming pools (9)	% of households	Liveable	88%	n.a

Notes:(1) Including transport (2) here only for 2005 (19%) and 2006 (18%) data, here the job creation 2113 (2005), 1283 (2006 (3) less than 25,000K US (4) only for 2002, for the year 1990 without considering other attributes such farmer's market, pier's concert and festivals (5) only for 2006 (4.35%) and 2005 (4.51%) (6) only for 2002, for the other years undetermined (7) for 1995 (275,842) for waste and recycled for 1995 (40,013) (8) for 2007 (9.1) and 2008 (9.2) (9) for 2005 only, not participation but access (10) open space for parks, public gathering, green streets, gardens and other public places 2006 (3.3) and 2004 (3.2%) (11) for 1998 (85%) and 2008(40%).

References

[1] L. R. Brown, Plan B.4.0, Mobilizing to Save Civilization, Earth Policy Institute publication, W.W. Norton and Co: New York, 2009.

[2] M. Polase, Urban Population in 1900, Urbanization and Development, Development Express, no.4, 1997, U.N. Population Division, World Urbanization Prospectus: The 2007 Revision, UNPD: New York 2009.

[3] U.N. Population Division, World Urbanization Prospectus: The 2007 Revision Population Database, electronic database, 2007, available at: www.esa.un.org/unup.

[4] G. Metschies, Pain at the Pump, Foreign Policy, July/August 2007, World's Automotative Group, World Motor Vehicle Data: Southfield, Michigan, 2008

[5] A. R. Migiro, The U.N. Report on Water Crisis, U.N. Symposium on Water Security, News Services, 2009

[6] P. Anastasiadis and G. Metaxas, Environmental protection and the sustainable city, Proceedings of 1st World Conference on Technology and Engineering Education, Kraków, Poland, 14-17 September, 2010 WIETE, pp. 91

[7] Sustainable city network (SCN), available at: www.sustainablecitiesnet.com.

[8] G. A. Tanguay, J. Rajaonson, J.F. Lefebvre and P. Lanoie, Measuring the sustainability of cities: An analysis of the use of local indicators, Ecological Indicators 10, 2010, pp. 407–418.

[9] Climate action, available from: http://www.climateactionprogramme.org/news.

[10] European Neighbourhood and Partnership Instrument, Strategy Paper (2007-2013), Eastern Regional Programme, European Commission, available from: http://ec.europa.eu/world/enp/pdf/country/enpi-eastern-rsp-en.pdf.

[11] L. Shen, J. Jorge Ochoa, Mona N. Shah, and Xiaoling Zhang, The application of urban sustainability indicators e A comparison between various practices, Elsevier, Habitat International 35, 2011, pp. 17-29.

[12] K. Zhang, X, He, and Z, Wen, Study of indicators of urban environmentally sustainable development in China, International Journal of Sustainable Development 6 (2), 2003, pp. 170-182.

[13] N. Moussiopoulos, C. Achillas, C. Vlachokostas, D. Spyridi, and K. Nikolaou, Environmental, social and economic information management for the evaluation of sustainability in urban areas: A system of indicators for Thessaloniki, Greece, Cities, 27, 2010, pp. 377–384.

[14] D., Niemeijer, R.S. De Groot, A conceptual framework for selecting environmental indicators sets. Ecological Indicators 8, 2008, pp. 14–25.

[15] Santa Monica Sustainable City Program - Progress Report Office of Sustainability and Environment, Santa Monica, US, 2009 available from: http://www.smgov.net/Departments/OSE/progressReport/default.aspx.

[16] Stiglitz, JE, Sen, A & Fitoussi, JP. Report by the Commission on the Measurement of Economic Performance and Social Progress (Commission on the Measurement of Economic Performance and Social Progress, 2009.

Semantic Link with the Natural Environment: Sustainable and Healthy Artificial Environments for Hot-Humid and Warm-Humid Climates

Ahmet Kochan[1], Altay Colak[1,*], Tolga Uzun[1], Ayberk N. Berkman[2], Mustafa Yegin[1], Erkan Gunes[3]

[1]*Cukurova University, Faculty of Engineering and Architecture, Department of Architecture, Adana Turkey*
[2] *Cukurova University, Faculty of Economics and Administrative Sciences, Department of Economics*
[3]*Eser Architecture, Mersin, Turkey*
**Corresponding author Tel: +90 3223386084-2921, E-mail: acolak@cu.edu.tr*

Abstract: Architectural artificial environment; as a joint product of imagination and technical information and as a combination of ecological, social, political, aesthetical and moral values, is the balancing epistemological systematic for ecology, economics and society which comprises of the future generations and all other living creatures. In ecological architecture, it is essential to design artificial environment as an artificial ecological system. This study asserts regional principles for different climate zones and environmental conditions by determining environmentally-conscious general design principles of ecological and sustainable public housing design. The significance and authenticity devolved on ecological and sustainable public housings and settlements on local, regional and global scales are discussed. As a result, in the light of the foregoing information given on ecological and sustainable process model and climate-weighted ecological and sustainable social public housing design model, related suggestions are made.

Keywords: *Sustainability, Healthy Artificial Environment, Healthy and Sustainable Process Model.*

1. Introduction

In today's world, energy production and consumption are among the most important criteria for development. Since the biggest portion of daily activities occurs in the building, the number of buildings and the level of energy consumption are correlated. However, existing and newly-constructed buildings are the main reasons for some of the major problems of our present and future such as environmental pollution and exhaustion of natural resources. Especially in the 20th century, the effects of both industrial and technological power of mankind over nature have reached its highest levels, even to the extent that it might have destroyed the life on life as we know it.

Incidents such as global warming, thinning of ozone layer, glacier meltdown, diminishing of forest lands, air and water pollution, extinction of species, etc. indicate that today's life style is not only disappointing, but also far away from being an inspiration for the future. Especially, by considering imperative revision of the 20th century's life style, adoption and development of a life style with less energy usage in daily routine and guidance of the society toward that direction are necessary within the scope of interdisciplinary studies. In this context, architecture as an effective discipline for both nature and human life assumes fundamental duties. While human-centric design in architecture was subject to change, environmental consciousness and harmony with nature had become the main criteria for success.

Considering the usage percentages of global resources in buildings, housings clearly take place in life style of the 21th century's information society as prominent means for achieving ecological and sustainable objectives.

Table 1. The Usage Percentages of Global Resources in Buildings and The Percentage of Global Pollution Level caused by Buildings. (1)

Resource	2. % of Usage
Energy	50%
Water	42%
Materials	50%
Agricultural Areas	48%
Coral Reefs	50%

Pollution	Relation to Building
Air Quality (Urban)	24%
Global Warming Gases	50%
Drinking Water Pollution	40%
Superficial Solid Waste	20%
CFCs/HCFCs	50%

Historically, housing is an organized pattern of communication, interaction, space, time and significance. On the one hand, it reflects the characteristics, life styles, behavioral codes, ecological choices, images and time-space taxonometries of ethnic groups it belongs to, and on the other hand it reflects personality and concession of the individual via its users' essential images and propensity of self-expression (2). Housing, a by-product of settled living culture, has survived in different building forms as the result of different climate conditions, cultures in different regions. Artificial environment of traditional architecture had been an output of the balance of the challenge between nature and mankind. However, migration toward urban areas, due to labor demand of industrial system, attraction of urban life and various other factors have eventually disrupted that balance. Public housing became the solution for sheltering needs emerged due to industrialization, overpopulation and urbanization. However, as a result of new building materials, new construction techniques and over-consumption of resources especially with the misconception of cheap and seemingly inexhaustible fossil-based energy sources; hazardous wastes, environmental pollution and artificial environments that fail to meet the users' needs came into existence. Thus, today's housing acquisition policies have reached a turning point. The aim of increasing life quality of housing and environment is on the agenda, rather than the mere effort of providing a huge number of community members with housing facilities. Evidently, related studies and energy issues in accordance with mission they undertake are amongst the most important facts of the future.

2. Sustainable Society and Artificial Environments

Throughout the history, mankind had experienced mainly 3 revolutionary transitions: the first and the longest one; transition to settled life as an agricultural society, the second; the Industrial Revolution, and the third one; transition to an information society(3). Being an information society in the 21th century requires innovation and nurturing of new multi-disciplinary approaches and applicable models aiming for sustainable development for both present and future generations. Society / Economy / Ecology are 3 important components of Sustainable Society Structure (Fig. 1).

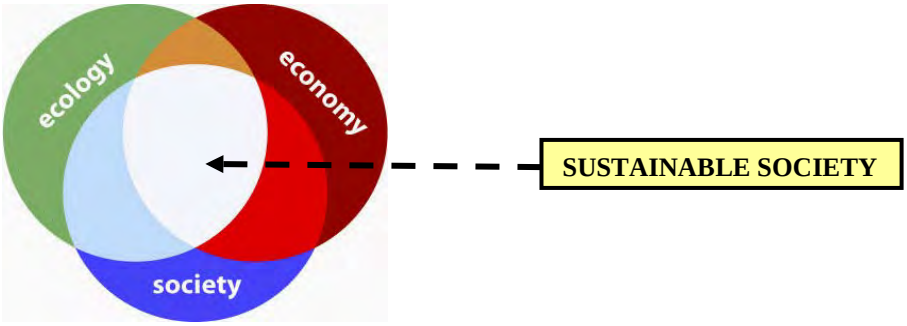

Fig. 1. Sustainable Society Structure (4)

Environmentally-conscious and sustainable artificial environments go through a long process to be formed, from the designing stage that begins with a preliminary sketch to the end of the physical life of building. Architectural artificial environments not only serve to meet sheltering needs of the society, but they also appear as mutual products of imagination, technical information and a combination of ecological, social, political, aesthetical and moral values. They are the balancing epistemological systematic for ecology, economics and society which comprises of the future generations and all other living creatures. They are formed with the moral necessity that requires the society to act as a whole for a common purpose (5).
Considering the role of environmentally-conscious architecture in solving global ecological and energy problems, 3 di mension of the mission undertaken by sustainable artificial environment designs are prominent; economical dimension, social dimension and ecological dimension. "Rationalistic and Salutary Sustainable Artificial Environments'' are present at the common denominator of ecology, society and economy, with an interactive and conscious balance, (Fig. 2).

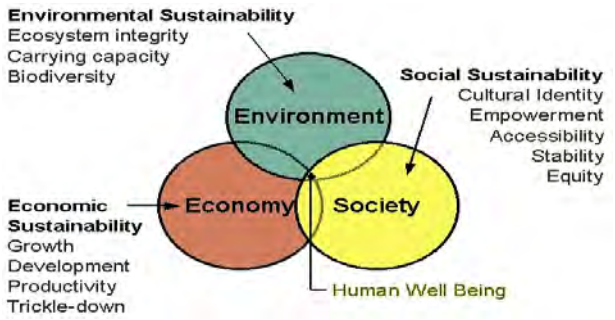

Fig. 2. Rationalistic and Salutary Sustainable Artificial Environment Model (6)

3. Methodology

3.1. Ecological Housing and Realization Potential for Sustainability

Designing, construction and usage of buildings take a long process and continuous consumption, accumulation of wastes are natural consequences. Therefore, the effects of architecture on ecological problems are present at the stages of designing, production, usage and until the end of physical life of architectural output. Nonetheless, in today's world it is almost mandatory to find new solutions in order to minimize adverse effects, or at least to keep them within reasonable boundaries. Architectural artificial environment should be viewed and designed as an artificial ecological system. Deterioration of ecological environment, as a concrete factor closely related to individual and societal welfare, has both quantitative and qualitative adverse effects on s ociety. In order to get rid of those adverse effects and to develop ecological consciousness, artificial environment design should abide by a series of criteria. These criteria are multi-dimensional social and physical components variable upon t ime and location conditions, covering the whole process from the designing stage of the building to demolition phase.
As of ecological and sustainable studies in general, the following are prerequisites for sustainable environment;

- Rational, productive and minimal resource consumption,
- Usage of recyclable materials and renewable resources,
- Conservation of energy stocks, usage of renewable energy sources which do not cause environmental pollution and,
- Recycling of wastes (7).

Pilot projects introduced as ecological and sustainable approaches are based on mainly 5 basic principles; (7)

i. Salutary Artificial Environment: Harmony with topography is restored, the former natural habitat is revived, and formation of an artificial ecosystem is aimed. Building materials with no toxic raw materials and hazardous gases and construction systems are used. Waste control and recycling are applied without polluting water and air.
ii. Sufficient and Efficient Energy Systems: Necessary precautions should be taken in order to keep energy usage at the lowest level for providing suitable vital conditions.
Heating, lighting and cooling systems are made of energy-efficient methods and products. Renewable energies are utilized as much as possible in active, passive or mixed systems.
iii. Environmentally-conscious Building Materials: In production, application, building materials and products with no hazardous waste that require less-energy are used. Usage of natural materials such as wood requires maximum diligence for energy efficiency. Especially, recyclable products and systems are used.
iv. Environmentally-conscious Form: Building forms and space organization are designed according to the structure of location and climate characteristics of the region. Ecological structure is respected. Interior comfort conditions are provided via rational and productive use of energy. Form is designed in such a way that a harmonic nexus between the user and nature is established.
v. Smart Design: Space usage, circulation, building form, mechanical systems and construction are designed to maintain productive, swift, harmonic and durable operation.

3.2. Ecological and Sustainable Housing Design

Sustainable, environmentally-conscious and energy-efficient public housing design can be defined under 2 headlines; unchanged 'General Principles', and 'Regional Principles' that are variable upon climate conditions of the region (8).

3.2.1. General Principles

General principles of sustainable public housing design also include some basic principles that are valid for all geographical areas. Despite different conditions; these are constant, sustainable and energy-efficient design decisions, which cover design, construction, usage and all other stages throughout the entire physical life of public housings. Following are 10 Basic General Principles;
i. Conception System and Design Principles; Environmental consciousness and energy conservation come into being on the table during the designing stage prior to physical existence of the building.
ii. Ecological Artificial Environment Design and Location Choice; Location choice, accurate interaction with environment, energy conservation and environmental consciousness are among the most crucial phases in sustainable public housing design. Design decisions are subject to have regional differences in accordance with climate conditions of the location.
iii. Construction and Resource Management; Resource and energy consumptions during construction phase have a huge share in total consumption. Thus, this phase has great importance for studies with the aim of sustainability in public housings.
iv. Building Envelope and Building Geometry; Building envelope and building geometry put forth the semantic nexus with natural habitat for consideration. Design decisions are subject to change according to regional differences.
v. Space Organization; Space organization in housing is one of the most important factors which affect the users' health and productivity. Living culture is determinant for interior function. Designing is subject to differ according to regional climate conditions of the location.
vi. Choice of Building Material and its Adequacy in terms of Building Physics; The concept of sustainable public housing combines all environmentally-conscious and energy

efficient methods throughout the entire stages of the building; from designing to the end of its physical life. Usage of sustainable and environmentally-conscious materials and products is one of the most important phases. Appropriate material choice in accordance with regional climate conditions is essential for success.

vii. Air-conditioning Systems; Air-conditioning of housings is one of the most important phases for providing the users' health and comfort, and for managing resource usage and energy consumption. Air-conditioning systems would differ according to regional climate conditions.

viii. Users' Comfort Needs; The concept of sustainable public housing aims to meet the users' comfort expectation at maximum level. Meeting the needs without destroying the environment is top priority.

ix. Waste Management; The adverse effects of wastes on natural environment necessitate sustainable and ecological design. Thus, waste management becomes a preferential objective of design. As a result, unmanageable wastes inflict damage to natural life along with human health.

x. Natural Life and Sustainable Society; Mankind cannot survive without nature. Therefore, the faster we destroy our natural environment, the sooner we approach to our own extinction.

3.2.2. Regional Principles

There are many different climate zones due to various geographic factors such as solar radiation reception, topographic structure and flora. Regional principle are sustainable and environmentally-conscious design decisions which contain regional differences on design, construction, usage and physical life of public housing resulting from variable climate conditions. Different climate conditions cause public housing and artificial environment location choices to be unique to the current region by the help of architectural differences in building envelope, building geometry, space organization, building material and air-conditioning systems. General principles; such as 'Location Choice and Ecologic Artificial Environment Design', 'Building Envelope and Building Geometry', 'Space Organization', 'Choice of Building Materials and their Adequacy in terms of Building Physics' and 'Air-conditioning Systems', contain some additional precautionary measures and principles in accordance with climate conditions of the location (Fig. 3).

4. Discussion

The rise of ecological and sustainable buildings, as an indication of technological improvement in Today's information society, does not only aim to meet people's sheltering needs. Ecological and sustainable design is not merely an arbitrary architectural interpretation from a group of environmentally-conscious architects. Being ecological and sustainable requires taking lessons from environmental catastrophes caused by the 19th century's Industrial Revolution and the 20th century's human-centric life style. A well-planned design is not the final phase for sustainability. It begins with design decisions on the table and continues until the end of physical life of the building. This process can be broken down into 8 phases;

i. Understanding the Location: Ecological and sustainable design begins with self-description of its concrete and abstract value via detailed analysis of the location.

ii. Understanding Natural Process–Respect to Nature: Ecology has a natural balance which provides and protects the continuity of life on earth. There is no place for waste in natural life; the by-product of a living organism serves as a food resource of another. Thus,

artificial environments formed by architecture should act as components of natural systems in order to maintain the continuity of life.

iii. Understanding the People: Architect should be familiar with the users who will be residing within the artificial environment that he/she designs. The users' habits, needs, sentiments, beliefs, cultures etc. should be analyzed and design should be modified in accordance with obtained information.

iv. Interdisciplinary Interaction / Team Work: Sustainable design is a conscious integration of architecture with electrical, mechanical and structural engineering and sociologists. Designer should interact with all other disciplinary fields, regard all related opinions and provide common solutions to problems.

v. Construction Planning: It begins with application of architecture's concrete effects on environment to designed output. Adverse effects of construction sites on the environment such as water, air and noise pollution are minimized and consumption of resources are controlled, so that the damaged portion of nature would be restored.

vi. Planning Tenancy Process: Resource consumption and wastes reach their highest levels during tenancy process of buildings. Systems with minimum adverse effects to environment are designed and used for meeting the needs, comfort conditions. Renewable energy sources are utilized at the highest possible level, while fossil fuel usage and wastes are controlled and minimized. Low-cost with high-efficiency is aimed.

vii. Conscious Society/Global Action: Success of ecological and sustainable studies depends directly on cooperation of societies and a global participation. Especially the countries which cause more global pollution should be more responsible for taking active roles in these studies.

viii. Foreseeing the Future: It is essential to preserve resources to be passed on to usage of future generations. For this purpose, rational and planned consumption of resources and recyclable material choice are foreseen. At the designing stage, physical lives of the buildings and demolition phases are predicted.

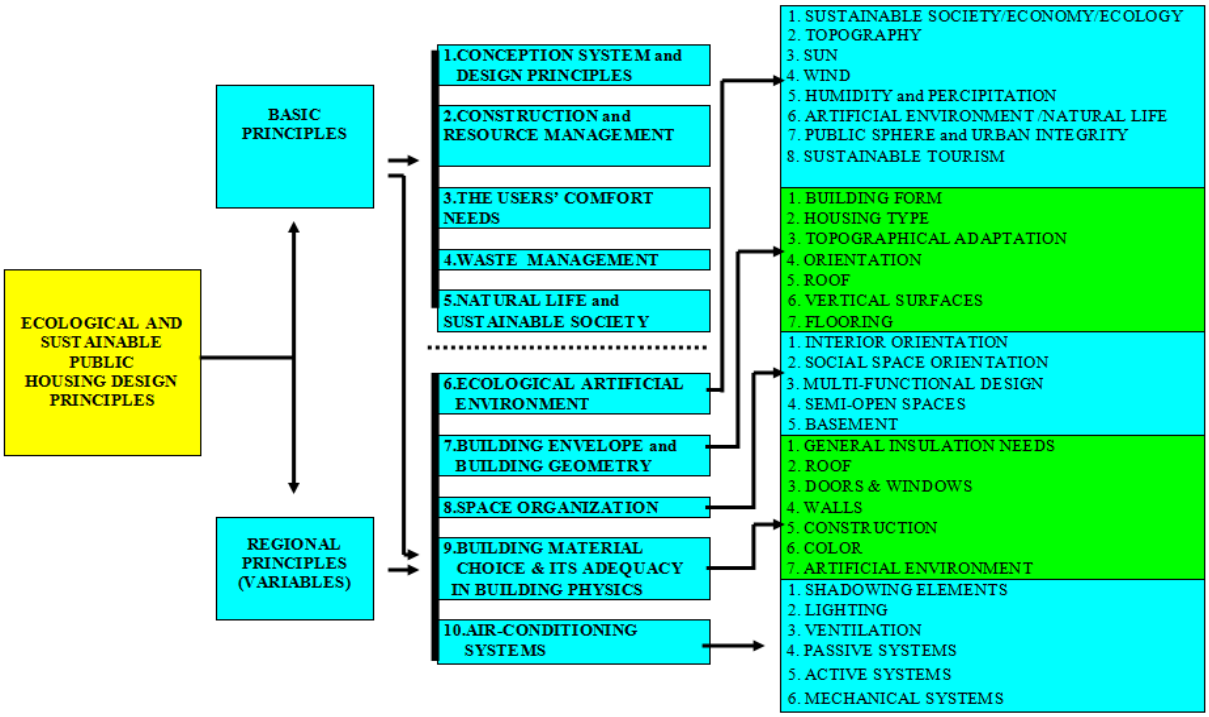

Fig. 3. Climate-Weighted Design Model in Ecological and Sustainable Public Housing (8)

5. Conclusions

Ecological and sustainable design is neither merely a style nor an architectural conception of a group of architects. Being ecological and sustainable is nominated as life style and understanding of the 21st century's information society accessorized with past experiences from environmental disasters caused by the 19th century's Industrial Revolution and the 20th century's economy-based and human-centric industrial society. After all, it is well-understood that human-kind would not exist without nature. That is to say, the faster we destroy our natural environment, the sooner we go extinct. Ecological and sustainable approaches aim to balance social, economic and environmental aspects of our present and future actions. The undertaken mission concerns a matter of existence or extinction, beyond any further achievement.

The users should be aware of characteristics and purposes of organizational, structural and factual design which brings existential integrity to architectural objects in architectural ecological artificial environment by the help of ecological and sustainable public housing design. For this purpose, every environmentally-conscious architectural innovation should be set up along with all its objective values with their abstract and concrete realities on sound basis. Local-regional-global significance and realities of ecological and sustainable public housing toward today's information society and future generations, namely, relative realities can be examined in 4 categories;

i. Existential Reality; is simply mankind's need for sheltering and protection against outer nature conditions. This reality involves the interdependence between the living organism and its habitat and sentimental and sensorial connections with domicile.
ii. Material Reality; is the provision of all necessities and objective needs as the basis for sensual perception and biological convenience in order to provide the most appropriate conditions for the users' health, productivity and comfort.
iii. Ideal Reality; is the formation of an artificial ecological environment along with architectural artificial environment by making appropriate design decisions and maintaining a balanced interaction between artificial environment and natural environment.
iv. Basic Reality; is the formation of environmentally-conscious and sustainable life style for the 21st century by establishing a rationalistic balance with respect to ecology-society-economy triangle within local, regional and global dimensions.

References

[1] B. EDWARDS, Green Architecture, Architectural Design 2001, Volume 71, Issue 4, pp. 30.

[2] Ş.Ö. GÜR, Doğu Karadeniz Örneğinde Konut Kültürü,Yapı Endüstri Merkezi Yayınları, Istanbul, Nisan 2000, pp. 11.

[3] Z. UTKUTUĞ, Mimarlık: Yaşamın İçinde Bir Serüven, Yeni Ufuklara, Bilim Ve Teknik, TÜBİTAK, Kasım 2002, pp. 22.

[4] www.clearcreekwater.org/watershed-management.html

[5] A. KOÇHAN, Sürdürülebilir Gelecek İçin Ekolojik Tasarım, Yapı 249, Ağustos 2002, pp. 45 – 53.

[6] http://www.arch.hku.hk/research/BEER/sustain.htm

[7] A. KOÇHAN, Doğal Çevreyle Kurulan Anlamsal Bağ: Sürdürülebilir Toplu Konut

Tasarımı, Yapı 256, Mart 2003, pp. 49 – 55.

[8] A. KOÇHAN, İklimsel Bölgelere Göre Ekolojik ve Sürdürülebilir Toplu Konut Tasarımında Düşünce Sistematiği, KTÜ Fen Bilimleri, Trabzon 2003.

Green Sustainable Island by Implementation of Environmental, Health, Safety and Energy Strategy in KISH Trading-Industrial Free Zones-IRAN

Amin Padash [1,*], M. Khodaparast [2], A. Zahirian [3], A. Kaabi Nejadian [4]

[1] *Iranian Academic Center for Education, Culture & Research – San'ati Sharif university branch, Environmental Engineering Centre, Tehran- Iran*
[2] *Contracts Department of National Iranian South Oil Fields Company, Ahwaz- Iran*
[3] *Islamic Azad University Khuzestan Science & Research Branch, Shiraz-Iran*
[4] *Consultant of Director General of Renewable Energy Organization of Iran*
** Corresponding author. Mob: +98912 3000 586, Fax: +98 21 88906044, E-mail: AminPadash@gmail.com*

Abstract: The sustainable development of green islands for implement Environmental, Health and Safety Management Systems for free trade zones required to confirm to ISO 14001, OHSAS 18001 and ISO 50001 standards. The Standard development of policy and strategy for business and tourism requires, in first instance, a vision. It needs to trace down what are the main threats, where do they come from, and what can be done about it. The green economy has been growing globally at great pace over the past five years. This is all the more impressive considering the severe global downturn of years 2006-2009. Ireland has, in recent times, gained a presence in this exciting sector, with enterprise opportunities in a wide variety of areas.

Sustainable development considers Social, Economic, Energy and Environmental needs. Trading-Industrial Free Zones (TIFZ) purposes and duty must be met in sustainable ways. However, TIFZ have a good track record of finding sustainable solutions whilst balancing these purposes and duty.

The method used in this article is comparative and matching method, by using ISO 50001 standards which is approved by ISO, and HSE-MS which is structured by Oil and Gas Production (OGP). Jointing of Energy management by HSE-MS is the main objective of this paper.

This case study has attempted the Implementation of EHSE Strategy in Kish Islands which is in Persian Gulf of Iran. EHSE modeling will overarch strategic document and central to the future of the Kish. It shows co-ordination and integration with other plans, strategies and actions in the Kish where they affect the TIFZ purposes and duty. It indicates how the TIFZ purposes and associated duty will be delivered through sustainable development. Matching requirements of the environment with energy safety and health is the ultimate goal of this research. In fact, the clean environment, with safe and healthy quality and with optimum energy consumption pattern, is the most ideal strategy for the management of a green region. Surely this concept of sustainable Green Island will be achievable in the near future. According to the result of this research, successfully management system in the way of sustainable development, is to attached and used efficiency all of the parameters such as Environment, Safety, Health and Energy in the same way and with the total carrying capacity. Such sensitive development at Green Island will ensure that resort guests and day visitors will continue to enjoy a quality nature based experience within a magnificent rainforest and reef environment.

Keywords: *Sustainable Islands–Environmental, Health, Safety and Energy Policy– KISH ISLAND*

1. Introduction

The man is the main pivot in the sustainable development. Possibility, planning, and implementation of any project or plan which include even technical or economical advantage, if there were any disadvantages or if the principles of health, safety and environmental rules were in danger, it is not advisable to be recommended. Thus, the national and international standards are generated [4. Sustainable development is a pattern of resource use that aims to meet human needs while preserving the environment so that these needs can be met not only in the present, but also for future generations. The term was used by the *Brundtland* Commission which coined what has become the most often-quoted definition of sustainable development as development that "meets the needs of the present without compromising the ability of future generations to meet their own needs."[11][10]

The field of sustainable development can be conceptually broken into three constituent parts: environmental sustainability, economic sustainability and sociopolitical sustainability. (fig.1) Requirements for health and safety and of environmental topics in the world are proof for anyone.In addition to, Energy has been playing an important role in the economic development all over the world. World population is expected to double by the middle of this century, and economic development will continue at a faster pace in the developing world than that in the developed world.[12]

Considering the matching of four mentioned subjects and their inevitable relations, in addition to their advantages of implementation, such as reducing the taxes and costs and being timesaver nowadays health, safety, environment and energy are studied and considered as a united group.If the system does not have an Environmental, Health, Safety & Energy Management System (EHSE-MS) in place now, it may be required to implement one soon.[7] Free trade zones are domestically criticized for encouraging businesses to set up operations under the influence of other governments, and for giving foreign corporations more economic liberty than is given indigenous employers who face large and sometimes insurmountable "regulatory" hurdles in developing nations. However, many countries are increasingly allowing local entrepreneurs to locate inside FTZs in order to access export-based incentives. Because the multinational corporation is able to choose between a wide range of underdeveloped or depressed nations in setting up overseas factories, and most of these countries do not have limited governments, bidding wars (or 'races to the bottom') sometimes erupt between competing governments. Free Trade Zones are also known as Special Economic Zones in some countries. [5]

TIFZ look like live Company size, resource availability or markets served will not necessarily dictate when and if implementation will happen. And even though organization may have many of the components in place already for an easy transition to ISO 14001 or OHSAS 18001 or ISO 50001 (fig.2), the road to an effective EHSE-MS can be fast, furious and paved with various pitfalls.There are many reasons why organizations implement Environmental Health Safety & Energy Management Systems that conform to ISO 14001 and/or OHSAS 18001 and ISO 50001 standards. Identifying occupational health and safety hazards and risks and the environmental impacts and also the procedure of usage the energy and also the energy efficiency of your company and employees is a given. However, more and more customers are demanding EHSE-MS as a requirement for doing business.

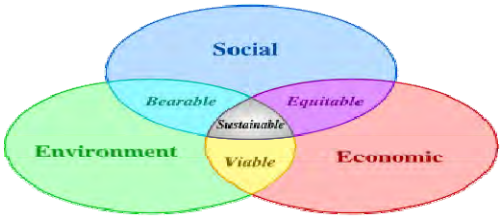

Fig.1- Scheme of sustainable development: at the confluence of three constituent parts.[4]

1.1. Location (Kish Island)

Kish is a resort island in the Persian Gulf. It is part of the Hormozgãn Province of Iran. Due to its free trade zone status it is touted as a consumer's paradise, with numerous malls, shopping centres, tourist attractions, and resort hotels. It has an estimated population of 20,000 residents and about 1 million people visit the island annually.[4]

The area of the island is 91.5 km². Kish Island is the purported to be the third most visited vacation destination city in the Middle East, after Sharm el-Sheikh and Dubai.

1.2. Geography and Environment

Kish is located in the Persian Gulf 19 km from mainland Iran and has an area of around 91 km² with an outer boundary of 40 km and a nearly elliptical shape. Along Kish's coast are coral reefs and many other small islands. The Island is positioned along the 1359 km long Iranian coastline north of the Persian Gulf, at the first quarter from the Hormuz entrance to the Persian Gulf. Its longitudinal and latitudinal positions are 26.32N and 53.58E degrees. The Island is 15.45 km long from west coast to the east coast (the distance between Mariam Complex and Hoor field). (See Pic.1)[8]

Picture1: Kish Island, Persian Gulf.

1.2.1. Kish, a Scenery coral Reef

The corals are considered as herbal and cylinder shaped animals which are mostly living as colony. Their Heads are located above cylinder in a way that a broad and wide screen exists in bottom part. These cells emit lime materials with the aim of fixing coral on a board. By emission of these materials, lime base will be created for coral. Aggregation and accumulation of corals and lime emissions from them, have played a very key role in various geological eras in appearance of Kish Island. Coral Islands and cylindrical forests enjoy the highest biodiversity in world ecosystems.[7][11]

1.2.2. Kish Large Recreational Jetty

Kish Large Recreational Jetty has been constructed by Iranian experts and engineers with the method of pipe driving and wooden deck with four- spacious satellite design. As long as 437 meters with 18 meters width and as large as 10,000 square meters, this jetty and quay has not any destructive effect on marine habitat in a way that tourists and sea voyagers can enjoy while standing on deck of this jetty and have a very pleasant time on visiting sceneries and breathtaking view of coral coasts of Kish Island.[9]

1.3. Human impact-Major Kish Island Projects

1.3.1. International oil bourse

The International Oil Bourse is a commodity exchange which opened on February 17, 2008.

1.3.2. Dariush Grand Hotel

Dariush, a $125 million five star hotel with over 200 guest rooms, is located near the eastern sandy beaches of the island. The hotel was built to be a reminder of Persepolis, a symbol of the glory and splendor of the ancient Iranian civilization. The hotel was designed and

developed by the European-Iranian entrepreneur and hotel tycoon, Hossein Sabet, who owns and manages several tourist attractions and hotels in the Canary Islands.[6]

1.3.3. Kish Hidden Pearl

In 1999, a project to build an underground complex was begun by 300 artists and excavation workers. After deep excavations rigid coral ceilings were discovered, and this was included in the final design. Once completed, the city will include restaurants, tourist resorts and underground therapeutic mud pools.

1.3.4. Kish Dolphin Park

The Dolphin Park is 10,000 square metres large and is surrounded by over 12,000 palm trees. The park includes a Dolphinarium, Butterfly Garden, Silkworm Compound, Exotic Bird Garden, Artificial Rain Forest, Volcanic Mountain, The World of Orchids and Cactus Garden.

1.3.5. Solar Powered Hotel

Hossein Sabet owner of the Sabet Hotels Group which includes the Dariush Grand Hotel and many other hotels on the island is set to build the first solar powered hotel in the Middle East on the island. Cyrus Hotel will be 7-star costing $520 million and will have 500 rooms, 23 floors in an area of 100,000 square meters. The hotel is set to be complete in October 2009.[7][6]

1.4. Extant Industries in Kish Island

These industries are located in five industrial townships as follows:

- ✓ Electricity and electronic industries
- ✓ Home appliances industries
- ✓ Metal and car manufacturing industries
- ✓ Oil industry technical and engineering services and logistics industries
- ✓ Garment and textile industries
- ✓ Food, pharmaceutical and hygienic industries
- ✓ Wooden and cellulose industries
- ✓ Mineral and non-metallic industries
- ✓ Chemical industries
- ✓ Heating and cooling industries
- ✓ Packing industries[12]

2. Methodology

The method used in this article is comparative and matching method, by using *ISO 50001*, *ISO 14001*, *OHSAS 18001* and *OGP for HSE-MS*. All of these models are an international model, but the main goal is to match the requirement of energy management in Health, Safety and Environmental Management. Important in this research is how to use and the 4 components of sustainable development goals. [2][3][6][14]. Therefore, in order to implement this right and fundamental components relying on international standards on the one hand and the principles of sustainable development other hand, this model has been proposed.

3. Results

According to the investigations and analyzing the requirements of ISO 50001, ISO 14001, OHSAS 18001 and matching to the main HSE Standards, this result has been proposed.

Following reviews carried out and matching of four main components environment, health, safety and energy, the proposed resulting model includes the following main axes: (Fig. 2)

1. Leadership and commitment
2. EHSE Policy and strategic objectives
3. Organization, resources and documentation
4. EHSE Risk Evaluation and management
5. Planning
6. Implementation and monitoring
7. EHSE Auditing and reviewing

Fig.2- A proposed Model contain Environmental, Health, Safety and Energy part for Island.

4. Discussion and Conclusion

By definition EHSE, sustainable development will run by Health, and Safety (social), Energy (economic) and environmental needs. Kish Island purposes and duty must will be met in sustainable ways. However, Kish has a good track record of finding sustainable solutions whilst balancing these purposes and duty in EHSE ways.

To provide and describe the characterization of EHSE Strategy, the full description of every stage has been provided step by step:

4.1. Leadership and commitment

It addresses Top-down commitment and company culture, essential to the success of the system: The Kish Island (KI) Management should create and sustain an organization culture that supports the EHSMS, based on:

- Belief in the Kish Island's desire to improve EHSE performance;
- Motivation to improve personal EHSE performance;
- Acceptance of individual responsibility and accountability for EHSE performance;
- Participation and involvement at all levels in EHSEMS development;
- Commitment to an effective HSEMS.[10]

4.2. EHSE Policy and strategic objectives

It addresses corporate intentions, principles of action and aspirations with respect to environment, health & safety. The Kish Island's management should define and document its EHSE policies and strategic objectives and ensure that they:

- are consistent with those of any parent company;
- are relevant to its activities, products and services, and their effects on EHS;

- are consistent with the Kish Island's other policies;
- have equal importance with the Kish Island's other policies and objectives;
- are implemented and maintained at all organizational levels; are publicly available;
- commit the company to meet or exceed all relevant regulatory and legislative requirements;[9]
- apply responsible standards of its own where laws and regulations do not exist; commit the Kish Island to reduce the impacts, risks and hazards to health, safety and the environment of its activities, products and services to levels which are as low as reasonably practicable;
- Provide for the setting of EHSE objectives that commit the Kish Island to continuous efforts to improve EHSE performance.

4.3. Organization, resources and documentation

It addresses Organization of people, resources and documentation for sound EHSE performance.
The Kish Island should define, document and communicate—with the aid of organizational diagrams where appropriate—the roles, responsibilities, authorities, accountabilities and interrelations necessary to implement the EHSE MS, including but not limited to:

- provision of resources and personnel for EHSE MS development and implementation;
- initiation of action to ensure compliance with EHSE policy;
- acquisition, interpretation and provision of information on EHSE matters;
- recording of corrective actions and opportunities to improve EHSE performance;
- recommendation, initiation or provision of mechanisms for improvement, and verification of their implementation;
- control of activities whilst corrective actions are being implemented;
- control of emergency situations.

4.4. EHSE Risk Evaluation and management

Risk is present in all human endeavors. This section addresses the identification of EHSE hazards and evaluation of EHSE risks, for all activities, products and services, and development of measures to reduce these risks.
The essential steps of hazard management:

1. Identify hazards and effects
2. Establish screening criteria
3. Document significant hazards and effects and applicable statutory requirements
4. Evaluate hazards and effects
5. Implement selected risk reduction measures
6. Set detailed objectives and performances criteria
7. Identify and evaluate risk reduction measures

4.5. Planning

This section addresses the firm planning of work activities, including the risk reduction measures (selected through the evaluation and risk management process). This includes planning for existing operations, managing changes and developing emergency response measures. The Kish Island should maintain, within its overall work programmer, plans for achieving EHSE objectives and performance criteria. These plans should include:

- a clear description of the objectives;

- designation of responsibility for setting and achieving objectives and performance criteria at each relevant function and level of the organization;
- the means by which they are to be achieved;
- resource requirements;
- time scales for implementation;
- motivating and encouraging personnel toward a suitable EHSE culture;
- mechanisms to provide feedback to personnel on EHSE performance;
- processes to recognize good personal and team EHSE performance
- mechanism for evaluation and follow-up.

4.6. Implementation and monitoring

This section addresses how activities are to be performed and monitored, and how corrective action is to be taken when necessary.
Activities and tasks should be conducted according to procedures and work instructions developed at the planning stage—or earlier, in accordance with EHSE policy:

- At senior management level, the development of strategic objectives
- and high-level planning activities should be conducted with due regard for the EHSE policy.
- At supervisory and management level, written directions regarding activities (which typically involve many tasks) will normally take the form of plans and procedures.
- At the work-site level, written directions regarding tasks will normally be
- in the form of work instructions, issued in accordance with defined safe systems of work (e.g. permits to work, simultaneous operations procedures, lock-off procedures, manuals of permitted operations).[10]

Management should ensure, and be responsible for, the conduct and verification of activities and tasks according to relevant procedures. This responsibility and commitment of management to the implementation of policies and plans includes, amongst other duties, ensuring that EHSE objectives are met and that performance criteria and control limits are not breached. Management should ensure the continuing adequacy of the EHSE performance of the Kish Island through monitoring activities. [10]

4.7. EHSE Auditing and reviewing

This section addresses the periodic assessment of system performance effectiveness and inherent suitability.[9]
The Kish Island should maintain procedures for audits to be carried out, as a normal part of business control, in order to determine:

- Whether or not EHSE management system elements and activities conform to planned arrangements, and are implemented effectively.
- The effective functioning of the EHSEMS in fulfilling the company's EHSE policy, objectives and performance criteria.
- Compliance with relevant legislative requirements.
- Identification of areas for improvement, leading to progressively better EHSE management.[10]

And at the end, as final conclusion, according to the proposed EHSE-MS model, it can improve environment, health, safety and energy performance resulting in pollution prevention, safer workplaces and fewer injuries in the islands. But even more than that, these

systems are being used by organizations to gain a competitive edge. And as corporate social responsibility initiatives gain momentum, EHSE-MS takes on an even more critical role within the organization.

The main purpose of this model is to plan the EHSE model for other island such as Kish, to show the established overarching strategic document and central to the future of the TIFZ. It shows co-ordination and integration with other plans, strategies and actions in the TIFZ where they affect the TIFZ purposes and duty. It indicates how the TIFZ purposes and associated duty will be delivered through sustainable development by improve EHSE performance resulting. In addition to, this is the first research that shows the intergradations of this for main subject in one model in the world.

References

[1] Adams, Jeff (1993, 16 April). "Twinning Breaks Pledge, Says Expert". Calgary Herald. p. B11.

[2] American National Standard Institute, ISO 50001 on Energy Management Systems Approved as Draft International Standard, ANSI Publication, 2010

[3] C. A. Brebbia, Environmental Health Risk V, WIT Press, 2009, pp.142-148

[4] Committee on Environmental Policy. 2006. Environmental Performance reviews, Organization for Economic Co-operation and Development, United Nations Economic Commission for Europe. Published OECD online bookshop, Page: 166.

[5] Economics: Principles in action. Upper Saddle River, New Jersey 07458: Pearson Prentice Hall. 2003. pp. 454. ISBN 0-13-063085-3.

[6] International Association of Oil and Gas Producers, HSE management guidelines, OGP Publication, 1999, pp.15-24

[7] "Iran Travel And Tourism Forecast", Economist Intelligence Unit, August 18, 2008.

[8] Kish Free Zone Organization http://www.kish.ir/

[9] Millen, Joyce and Timoth Holtz, "Dying for Growth, Part I, The Politics of Globalization, ed. Mark Kesselman, Hougton Mifflin, 2007

[10] Padash, Amin, "Principles of Health, Safety and Environment Management System" Kavosh Ghalam pub. 2007. pp. 174. ISBN 964-2517-03-5

[11] Pearson School http://www.pearsonschool.com/index.cf

[12] Sargent, John and Matthews, Linda. "China vs. Mexico in the Global EPZ Industry: Maquiladoras, FDI Quality and Plant Mortality" (PDF)

[13] Smith, Charles; Rees, Gareth (1998). Economic Development, 2nd edition. Basingstoke: Macmillan. ISBN 0333722280.

[14] Suzan Linn Jackson, ISO 14001 implementation guide: creating an integrated management system, John Wiley and Sons, 1997, pp.34-45

[15] United Nations. 1987."Report of the World Commission on Environment and Development." General Assembly Resolution 42/187, 11 December 1987. Retrieved: 2007-04-12

[16] World Summit 2005 Outcome Document, World Health Organization, 15 September 2005 http://www.who.int/hiv/universalaccess2010/worldsummit.pdf

An Analysis of two Sustainable projects in the light of the LEED-NC and LEED-ND rating systems

F. Roseta-Vaz-Monteiro[1,*], E. M. Karayianni-Vasconcelos[1]

[1] *CIAUD - Faculty of Architecture, Technical University of Lisbon, Lisbon, Portugal*
**Tel: +351 916746476, E-mail: froseta@fa.utl.pt (or) filipa.roseta@network.rca.ac.uk*

Abstract: The methodology used in this paper consists in studying how the 5 environmental categories of the LEED New Constructions and Major Renovation plus the 3 categories of the LEED Neighbourhood Development apply to the architectural and urban design strategies of two projects: Masdar City and "Forwarding Dallas". We chose two very different but at the same time similar projects which claim to be environmentally conscious. On one end, there is the self-intituled "world's first carbon-neutral city", Masdar, designed by Foster + Partners and one of the largest and most ambitious developments of its kind. On the opposite end, and in a significantly smaller scale, there is the "Re-Vision Dallas" competition winner project, "Forwarding Dallas", designed by a collaboration of two Portuguese architecture practices: DATA + MOOV. This competition promoted the idea of transforming a vacant inner-city block in Dallas into a carbon-neutral neighbourhood, creating, for that purpose, a prototype for an innovative, sustainable urban community.

This paper strives to highlight, through the comparative analysis of these two projects, how the desire to meet high standards of sustainability not only affects the practice of architecture and urban design, but might also generate a particular architectural language with identifiable physical characteristics.

Keywords: *Carbon-Neutral, Masdar City, Forwarding Dallas, LEED, Renewable Energy*

1. Introduction

This paper presents part of a research developed by a research unit, named "*+E-CO2*", or "*More Energy, Less Carbon"*, based in Lisbon, at *Faculdade de Arquitectura da Universidade Técnica de Lisboa*, which pursues the goal of understanding how the carbon neutral challenge is changing present day's urban design and architectural practices. Our purpose is to focus on the design process in order to assess two key questions: 1) How does the desire to meet high standards of sustainability affect the practice of architecture and urban design? 2) Will this global concern with a carbon-neutral future generate a particular architectural language with identifiable physical characteristics regardless of location?

2. Methodology

We have determined as research methodology for our *+E-CO2* research project the analysis of self-acclaimed carbon neutral and/or carbon reduction projects in order to detect how the carbon neutral challenge is affecting the practice of urban and architectural design. The projects which claim to be carbon neutral are the most relevant for our research because, in these projects, the practitioners are guided by the clear purpose of configuring architecture and urban space so as to meet the carbon neutral challenge.

Our analysis derives from the comparative process of design strategies in light of fixed criteria, enabling us to highlight specific design differences and/or resemblances in between the projects. For this paper, we have chosen as fixed criteria the 5 environmental categories of the LEED New Constructions and Major Renovation [1] plus the 3 categories of the LEED Neighborhood Development [2]. In light of these 8 categories, we analyze and compare two very ambitious projects in what regards the carbon neutral challenge.

The first project is the development of a block in Dallas designed by a collaboration of two Portuguese architectural practices (MOOV+DATA), which obtained the first prize in an international architectural competition promoted by the American non-profit organization named "Re-vision". The competition's brief challenged architects to design a project able to become LEED Platinum. Most information regarding the project has been provided by António Louro, one of the architects/partners managing the project [3]. The project's brief was to redesign an urban block in Dallas, including mostly housing, but also commercial spaces and urban equipments.

The second project is the Masdar City development designed by Foster+Partners which aims to become the first carbon neutral city to ever be built. The Masdar City development is located in Abu Dhabi, close to the international airport and was conceived to be carbon neutral, zero-waste, car-free city for 40,000 residents and 50,000 daily commuters. The city is designed for an area of six million square meters. Even if the city is currently under construction (the completion of the first building was announced in November 2010), its scale and ambitious program as a research and institutional hub dedicated to Renewable Energies make it a most relevant project to follow, as noted by Reiche [4]. Data cited in this paper has been gathered from other papers, from the information provided by the company responsible for the development, the Abu Dabhi Future Energy Company [5], by the architects responsible for the masterplan at Foster + Partners [6], and by articles included in architectural magazines [7]. Papers reviewed regarding Masdar City relate to specific technological innovations in the energy field [8], to policies supporting the development [4] or to specific buildings [9]. Prior to this paper, we have presented a paper on the possibility of using some of Masdar City's renewable energy strategies in a "bottom-up" type of development [10]. For the current paper, our approach is different as we aim to highlight the impact of the carbon neutral challenge on architectural and urban design.

We have determined as primary data the information coming from the practitioners or from the entities commissioning the projects. This data must be taken as a set of design guidelines which might not be possible to complete or might change with the project's development (as it has already happened in the Masdar City development with the experimental transport system, originally elevated and currently underground).

We chose to use the LEED categories as fixed criteria due to this rating system's holistic approach and to the system's ability of evaluating projects worldwide; however, unlike the LEED rating system, which aims to provide a quantifiable benchmark to compare each project's efficiency, we aim to assess the impact of the carbon neutral challenge on architectural design; hence, some categories might have no effect on architecture (such as the efficiency of appliances), while others will change the configuration of the city of the future. In Table 1, we present the relationship we created in between the LEED categories and the architectural and urban design strategies of the two case-studies selected. We created a rating system measuring the Impact on Architectural Design (IAD), presenting five classes ranging from IAD 0 to IAD4 where: IAD 0 classifies the strategy as having no or low direct impact on architectural design; IAD 1 classifies the strategy as affecting architectural surfaces using existing design strategies; IAD 2 classifies the strategy as affecting architectural surfaces using new technologies and/or innovative design strategies; IAD 3 classifies the strategy as affecting architectural form using existing design strategies; and IAD 4 classifies the strategy as affecting architectural form using new technologies and/or innovative design strategies.

Table 1. Relationship between LEED categories and architectural and urban design strategies

LEED Environ. Categories (NC=NewConstruction; ND= Neighborhood Development) *The categories which, on both case-studies, did not apply or had NINF were excluded for this paper*	Architectural and Urban Design Strategies *(NA=does not apply; NINF=not enough information; IAD Impact on architectural design 0-4))*	
	Forwarding Dallas	Masdar City
NC - Sustainable Sites		
Construction Activity Pollution Prevention	IAD 0	Impacts assessed + mitigation actions predicted [10] IAD 0
Site Selection	Block within built neighbourhood. IAD 3	6km, built mostly on former plantations land. IAD 3
Development Density and Community Connectivity	Optimizes pedestrian public space + connectivity public space for pedestrians+ bicycles inside the block. IAD 3	Optimizes pedestrian public space + connectivity public space for pedestrians+ bicycles inside the block. IAD 3
Alternative Transportation	No public transport system available. Promotes cyclable public spaces, car-pooling and bicycle parking. IAD 3	Car-free city. New transport system, 2 levels: LRT (aboveground), PRT (undergound). IAD 4
Site Development	Use of native vegetation in public spaces and rooftops. IAD 4	Compact footprint and limited, or walled, perimeter. IAD 3
Stormwater Design	includes vegetative roofs and pervious pavements IAD 4	NINF
Heat Island Effect	Roofs covered with vegetative surfaces. IAD 4	Roofs with shading structures covered by photovoltaic panels. IAD 4
LEED NC – Water Efficiency (WE)		
Water Use Reduction	Rainwater collected and used in agriculture + graywater used in toilets IAD 4	Rainwater collected +graywater used in toilets and cooling of public spaces. IAD 4
Water Efficient Landscaping	Native plant use + drop-by-drop irrigation system + on site measurements to assess irrigation needs. IAD 4	Native Plant use+ Intelligent irrigation systems. IAD 4
Innovative Wastewater Technologies	On-site waste water treatment by gravity-driven mechanical systems + sand and UV light filtration. IAD 4	NINF
Water Use Reduction	NINF	Initial use of desalinized water and recycling of most water in the system. IAD 3
NC -Energy and Atmosphere		
OptimizeEnergy Performance	High energy performing	NINF

	appliances + LED technology IAD 0	
On-site Renewable Energy	On the rooftop - Solar thermal energy + photovoltaic + wind energy. Roof design expands surface to maximize production. Solar cells on the façade. IAD 4	On the rooftop – almost 80% of the consumed energy will be solar. The entire city covered with panels. IAD 4
Enhanced Commissioning	Specialized consultants included. IAD 0	Specialized consultants included. IAD 0
Enhanced Refrigerant Management	Non-mechanical methods of ventilation (cross-ventilation in every apartment). IAD 3	Traditional methods of cooling (such as cooling chimneys) + mechanical cooling. IAD 3
Measurement/ Verification	IAD 0	IAD 0
Green Power	IAD 0	IAD 0
NC - Materials and Resources		
Storage and Collection of Recyclables	Includes area for Storage and Collection of Recyclables. IAD 0	50% waste will be recyclable, 17% will become fertilizers and 33% will not be recyclable. IAD 0
Construction Waste Management	100% pre-fabricated building systems to reduce on site impact and waste. IAD 2	NINF
Recycled Content	Recycled Wood. IAD 2	Materials with a 30% recycled content predicted. IAD 2
Regional Materials	Use of locally produced materials. IAD 1	NINF
NC-Indoor Envirn. Quality		
Minimum Indoor Air Quality Performance Required	Non-mechanical methods of ventilation (cross-ventilation in every apartment). IAD 3	Traditional methods of cooling (such as cooling chimneys) + mechanical cooling. IAD 3
Environmental Tobacco Smoke- Control Required	IAD 0	IAD 0
Outdoor Air Delivery Monitoring	IAD 0	IAD 0
Controllability of Systems—Lighting and Thermal Comfort	Operable Windows and Window Protections IAD 2	NINF
Thermal Comfort—Design/Verification	Northeast façades in high thermal mass straw walls. IAD 2	NINF
Daylight and Views	Block designed to maximize daylight and views. Windows consider southern orientation and permanent shading	NINF

	devices. IAD 3	
NC/ND -Innovation in Design		
Innovation in Design	Educational project IAD 0	Educational project IAD 0
LEED Accredited Professional	Goal to obtain LEED Platinum IAD 0	NINF
NC/ND-Smart Location and Linkage		
Smart Location	Block within existing neighborhood in Dallas. IAD 3	New development on previously planted land close to national transport infrastructure (airport). Max. walkable distance from the planned PRT stops is 150m. IAD 4
Imperiled Species and Ecological Communities	NA	Loss of existing habitats predicted. Mitigation actions predicted. IAD 3
Wetland and Water Body Conservation	NA	No significant effects predicted in the initial stages. IAD 0
Agricultural Land Conservation	NA	Located predominantly on abandoned plantations. IAD 3
Preferred Locations	Existing City. IAD 3	Located predominately on abandoned plantations – new infrastructures considered. IAD 3
Locations with Reduced Automobile Dependence	Included in city with high automobile dependence. IAD3	Car-free city. IAD 4
Bicycle Network and Storage	Predicted. IAD 3	Mostly walkable distances. IAD 3
Housing and Jobs Proximity	Mostly residential (dwellings and support areas = 303658 sq.f; commercial, equipments and greenhouses 101828 sq. f, parking 68867 sq. f). IAD 3	Mixed-use development (30% residential; 20% tax-free enterprises; 10% commercial services; 3% cultural equipments, 3%university , 34% with parking, services, recreational spaces, and other areas). IAD3
Site Design for Habitat or Wetland and Water Body Conservation	NA	Loss of existing habitats predicted. Mitigation actions: creation of new habitats with native species through the greenfingers + retention of desert habitat outside citywalls + healthy native plant specimens translocated to Masdar's nursery. IAD 3

Restoration + Long Term Conservation Management of Habitat or Wetlands and Water Bodies	NA	Mitigation actions predicted. IAD 3
ND-Neighborhood Pattern + Design		
Walkable Streets	Pedestrian space within the block. Ground level with commercial and other equipments with glass façades. IAD 3	Car-free city. Most of the transport system is underground to free public space for pedestrians. IAD 4
Compact Development	Increases footprint IAD 3	Compact footprint with rigid physical limit perimeter to prohibit urban sprawling. IAD 3
Connected and Open Community	Block designed (sectioned) to increase existing connectivity. IAD 3	Requirement to place every pedestrian at a distance of 150m from a PRT station in any given location increases connectivity. IAD 4
Mixed-Use Neighborhood Centers	NA	Mixed-use. Centers related to transit system. IAD 3
Mixed-Income Diverse Communities	Dwellings range from studio to 3 bedroom flats IAD 3	NINF
Reduced Parking Footprint	Reduced surface parking IAD 3	Parking outside city walls IAD 3
Street Network	Block designed (sectioned) to increase existing connectivity. IAD 3	Every pedestrian at a distance of 150m from a PRT station in any given location. IAD 4
Transit Facilities	Promotes cyclable public spaces, car pooling and bicycle parking. IAD 3	Car-free city. Underground Urban Transit to free public space. IAD 4
Transportation Demand Management	Promotes vehicle sharing. IAD 0	Use of Urban Transit System. IAD 4
Access to Civic and Public Spaces	Public space inside the block. IAD 3	Due to the underground characteristic of the transit system, most public space will be passive. IAD 4
Access to Recreation Facilities	Recreational facilities within the block. IAD 3	NINF
Visitability and Universal Design	Several types of dwelling units /concern with mobility. IAD 3	NINF
Community Outreach and Involvement	Calls for an holistic design approach. IAD 0	NINF
Local Food Production	Includes local food production on the rooftops. IAD 4	Includes local food production outside city perimeter IAD 3
Tree-Lined and Shaded Streets	Tree-lined streets. IAD 3	Main streets are tree-lined; other streets are shaded and

		narrow. IAD 3
ND-Green Infrastructure + Buildings		
Certified Green Building	Goal:LEED Platinum. IAD0	Goal= Carbon Neutral IAD 0
Water-Efficient Landscaping	(= LEED NC IAD 4)	(= LEED NC IAD4)
Minimized Site Disturbance in Design and Construction	NINF	Mitigation actions predicted. IAD 0
Heat Island Reduction	(= LEED NC. IAD 4)	(= LEED NC. IAD 4)
Solar Orientation	East-west axis 5xlonger than north-south axis. Block orientation greater than 15º from the geographic east-west. IAD 3	Narrow streets and compact design. IAD 3
On-Site Renewable Energy Sources	On the rooftop – Solar thermal energy + photovoltaic + wind energy. Roof design expands surface to maximize production. Solar cells on the southwestern façade. IAD 4	On the rooftop – almost 80% of the consumed energy will be solar. The entire city covered with panels. IAD 4
Solid Waste Management Infrastructure	Organic waste used as fertilizer (predicted). IAD 0	Organic waste used as fertilizer (predicted). IAD 0

3. Results

Two types of results can derive from Table 1. The first result is that all items classified as IAD 4 (with one exception) regard either the use of rooftops or the planned transport system (e.g. Table 1). The second result is a high frequency of strategies classified as IAD 3, followed by IAD 4 and IAD 0, with only a few items classified as IAD 1 or 2 (e.g. Fig.1).

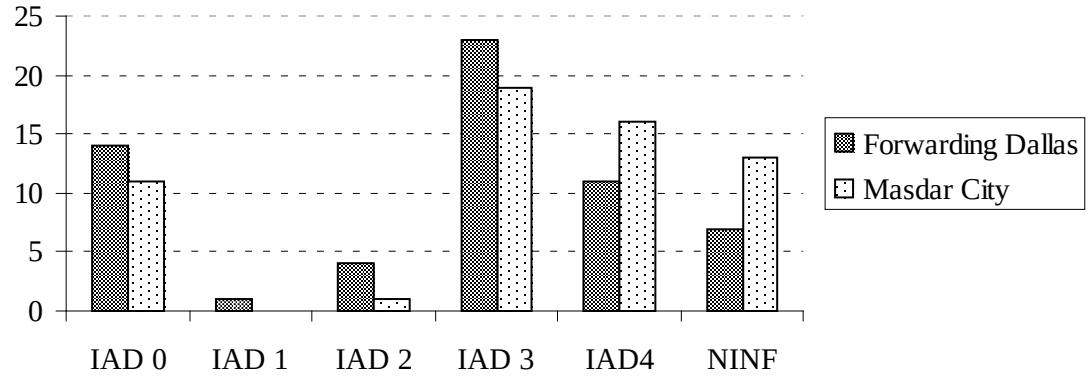

Fig. 1 Frequency of IAD (Impact on Architectural Design) according to classes (IAD 0 to IAD 4)

4. Discussion and Conclusions

Based on these results, we can argue three conclusions. The first conclusion is that two new technologies which might become a trademark of the city of the future are: the increased relevance of the rooftop as a "productive surface", with the potential to collect energy and rainwater, and to provide spaces for plantation; and the inclusion of intelligent urban transport systems, allowing public space to be car-free. This conclusion is based on the indication that

almost all strategies classified as IAD 4 are related either to rooftops or to the urban transport system. The second conclusion derives from the low frequency of IAD 1 and IAD 2, indicating that fewer design strategies are related to the surface of the architectural object (or to the architectural skin) as compared to the configuration of the architectural from. Most strategies used by the selected practitioners to comply with the LEED categories fall under IAD 0, IAD 3 or IAD 4; hence, there is either no impact on architectural design (IAD 0) or a profound impact on the configuration of architecture (IAD 3 and IAD 4). The third conclusion derives from the high frequency of strategies classified as IAD 3 (e.g. Fig.1), indicating that the selected practitioners are using existing or traditional design strategies to relate architecture effectively to climate and location.

What we believe to be particularly interesting about these results is that the first conclusion has the potential of becoming global in its application as practitioners all over the world (literally) turn their projects to the sun and build intelligent urban transport systems, while the third conclusion indicates a promotion of local characteristics; hence, the carbon neutral city of the future might present an architectural language which incorporates both global and local design characteristics, a language where tradition meets technology to achieve a most efficient architectural design.

References

[1] US Green Building Council, LEED 2009 for New Constructions and Major Renovations Rating System, 2009, pp. 1-88.

[2] Congress of New Urbanism, Natural Resources Defence Council and US Green Building Council, LEED 2009 for Neighborhood Development Rating System, 2009, pp. 1-122.

[3] MOOV+DATA, “Forwarding Dallas”, Technical drawings, Project Description and interviews conducted by the authors, 2010.

[4] Reiche, D., Renewable Energy Policies in the Gulf Countries: a case-study of the Carbon Neutral “Masdar City” in Abu Dabhi, Energy Policy, 2009, doi: 101016 / j.enpol.2009.09.28

[5] Masdar City, Abu Dhabi Future Energy Company, www.masdar.ae

[6] Foster+Partners, www.fosterandpartners.com.

[7] Habitat Futura, Masdar, La Ciudad del Futuro, n.24, 2010, pp. 37-46.

[8] Nader, S., Paths to a low-carbon economy – the Masdar Example, Energy Procedia 1 (2009) doi:10.1016/j.egypro.2009.02.99

[9] Boyer,JL et. al., Systems integration for cost effective Carbon Neutral Buildings: A Masdar headquarters case-study, Proceedings of the 4TH ASME International Conference on Energy and Sustainability, Vol.1, 2010.

[10] Roseta V.M., F. “From Critical to Carbon Neutral, Grassroots Sustainable Urban Planning” in C.A. Brebbia, et al (ed.) The Sustainable City VI - Urban Regeneration and Sustainability, Southampton: WIT Press, 2010, pp. 629/636.

[11] Hyder Consulting, “Environmental Impact Assessment Report”, Masdar Delivery Phase 1, April 2009, pp. i-xiv.

Energy demand and available technologies analysis for district heating cooling applications in a Science and Technology Park (PTA) in a Mediterranean country

R. Zubizarreta[1*],J.M. Cejudo[2], J.P. Jiménez[3]

[1] *Andalusia Institute of Technology, Málaga, Spain*
2 Grupo de Energética, Escuela Técnica Superior de Ingenieros Industriales, UMA. Málaga, Spain
[3] *Andalusia Institute of Technology, Málaga, Spain*
** Corresponding author. Tel: +34 952 02 87 10, Fax: +34 952 02 04 80, E-mail: rzubizarreta@iat.es*

Abstract: The purpose of this paper is to present the results of the feasibility study for a district heating-cooling network to cover the energy demand in a Science and Technology Park under Mediterranean climate conditions. To evaluate the energy demand a bottom-up strategy has been followed: a building inventory has been carried out to define several building types according to use, envelope and glazing. Energy + has been used to obtain heating and cooling demand profiles for each building type and orientation. According to municipal development plans for PTA and forecast in business growth, the energy demand evaluation in a 10-years timeframe has been carried out.

Most appropriate technologies has been analyzed and evaluated: Cogeneration (gas turbine and alternative internal combustion engines), biomass boiler and conventional technologies have been evaluated with TRNSYS to obtain consumption profiles, consumption rates, efficiency indicators and energy losses. Finally an economic analysis has been done to technologies in a 20 years period to evaluate technology that better economic results address.

The main objective of this work is the promotion of the efficient and effective energy supply in areas with high energy consumption. DCH technology is widely used in the North of Europe and this paper try to demonstrate that this technology could be apply in Mediterranean areas successfully.

Keywords: *District heating cooling: DHC; building energy analysis; energy demand; technical and feasibility study, district energy, thermal energy generation..*

Nomenclature (Optional)

A *effective area of supply* ..... m^2
EUI energy demand…… *kWh*
R *effective building type surface ratio*…… m^2*/building*
ATE artificial thermal efficiency
E_{el} *electric energy produced* ..... *kWh*
$E_{input\_by\_fuel}$ *energy introduced in engine by fuel*..... *kWh*
H *heat amount provided to users* ..... *kWh*
η *efficiency level, ratio between useful output and input amount in plant components*
P_{term} *thermal demand*..... *kWh*
E_{el_cons} *electrical energy consumed by the facility*..... *kWh*

1. Introduction

Currently, as a result of improved quality of life for both, developed and developing countries, global energy demand grows at very high rates. For this reason, the responsible use of energy resources is crucial for a sustainable model to ensure power supply without compromising the natural resource depletion.

Energy system, as known today, is responsible for large energy losses. These losses result from the different transfer processes taking place from production to consumption points, resulting in an overall process inefficient.

Within this framework, district heating and cooling, DHC in advance, is an alternative technology that improves power distribution processes as it is a local generation technology, and allow to incorporate different sources of energy supply (CHP, use of waste heat or solar thermal), thus constituting a technology that increases the efficiency of the complete cycle generation-consumption.

This paper presents the feasibility study of a DHC network to supply thermal energy to a group of companies located in Technology Park located in Málaga (Spain). It is remarkable the adaptation of this technology to Mediterranean climates in which winters are mild.

2. Methodology

2.1. Demand characterization

Energy demand evaluation is the starting and the most critical point to face a problem of this type, since it allows to determinate which are the heating and cooling needs in the consumption points to supply. The complexity in determining the demand for air conditioning in a group of buildings is not easy because the modelling a set of buildings is a complex tax. Several authors, such as Gustafsson [4], Heiple [5], Huang [6], Pedersen [7] or Segen [8] have developed various methods to solve this problem. In these papers, two types of strategies for estimating the demand could be found:

Top-down strategy: it is based on statistical methods for predicting the demand for a set of buildings based on aggregate data in large communities (cities or regions). Under this approach Pedersen [7] presents a method for calculating the demand for heat and electricity power planning adapted to large areas where heat demand is based on a regression analysis that uses the outdoor temperature as independent variable.

B**ottom-up strategy:** this case is the opposite that previous method, ie the starting point in this case is the estimated demand of different building types and total demand is calculated as the sum of the demands of each of the buildings that comprise. An inventory of buildings that are in the area of study is needed to use this method because each building is assigned to a "building type" that will carry the energy demand mean values. Mathematically:

$$Demand = \sum_{i=1}^{N} (A_i \cdot \sum_{j=1}^{M} EUI_j \cdot P_{ij})) \qquad (1)$$

Where A is the net surface in each building, EUI_j is annual energy demand for each building type (M different types) and P_{ij} is the matrix that set the relation between net building surface and building type.

Heiple [5], Huang [6] and Segen [8] have developed methods based on statistical data and numeric simulations with the aim of getting energy demand profiles for a set of buildings according to their location, envelope and use. In the same line, Chow [9] addresses the design of a distribution network by simulating energy demand for each building type using EnergyPlus [21] and analysing global system with TRNSYS software [22].

In this case, a bottom-up strategy has been chosen. Although it is unknown use and type of each actual building, it is known the surface of the extension (651,334 m^2), the % of the area for each use, the net area of each parcel and it is known that the type of construction is not very different from the buildings that are currently operating in the PTA (according to the municipal development plan).

A deep study has been developed for the buildings currently in the PTA to get the main characteristics that define each building type and that will allow to define the thermal behaviour of the new buildings, the characteristics that have been identified are:

- **Envelope characteristics.-** due to the large variety used in PTA, the minimum values according to actual laws have been taking.
- **Glass surface.-** Up to three categories based on the % of glass in the façade have been defined: low glazing (<10%), medium glazing (10-75%) and high glazing (>75%).
- **Orientation of buildings.-** defined by the final orientation of the building.
- **Use.-** considering the current business in PTA and the allocation for the several uses according to the partial plan, the following uses have been defined: hotel with shopping centres, babysitting, light industry and offices.

Several building types have been developed using Energy Plus based on these characteristics, this has allowed to obtain the hourly profiles for heating and cooling demand of each of them. In order to ensure the model convergences, the following conditions have been established:

- Load and temperature convergence tolerance value: 0,1.
- Heat balance algorithm: conduction transfer function [20].

The results obtained with the simulations have been validated and adjusted to reference values for the same purpose buildings that have been previously published by other authors [10], [11] and [12]. For instance table 1 show some reference values:

Table 1. Reference data consumption for buildings.

Use	Mean Consumption (kWh/m^2)	Cooling %	Heating %
Offices	131,57	42	4
Hotel	312,66	28	12

Once the different models of buildings have been adjusted in terms of thermal behaviour, the possible location of different types of building have been allocated according to the uses defined in the partial plan and the main characteristics of actual buildings in the PTA. This division has allowed evaluating the total demand of all buildings according to equation 1.

Another point considered in the analysis of the demand is the change in the occupation of parcels over time, this analysis will reveal the annual demand of thermal energy and thus affect the economic valuation of the proposed solutions. It has estimated by regression techniques based on the evolution experienced by PTA from its inception to the present. The result is shown in Figure 1:

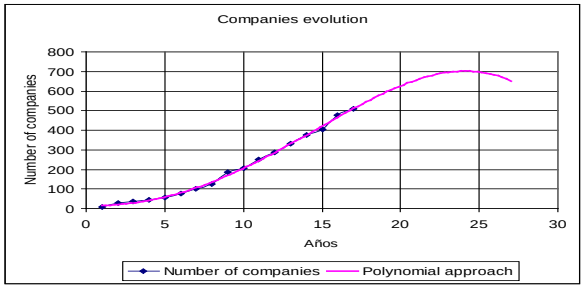

Fig 1. Number of companies installed in PTA

The regression curve of order 4 which adjusts the actual data with a regression coefficient of 0.9978 is:

$$y = -0{,}0031 \cdot x^4 + 0{,}0482 \cdot x^3 + 1{,}853 \cdot x^2 - 1{,}2072 \cdot x + 14{,}605 \quad [2]$$

The energy demand values for each type of building together with the annual distribution of occupation of parcels allow to establish energy demand scenarios with a horizon of 10 years and make a more realistic assessment and economic valuation of the investments required.

Distribution system design has been calculated using peak demand values. DHC network is composed by a set of infrastructures that allow getting energy from producer to end-users. The design has been done considering the peak demand in year 10 because the infrastructure will not change during the entire period of operation thereof. The following components have sized: pipes, accumulation tank and pumping equipment.

2.2. Generation technology alternatives

After presenting the methodology for calculating demand, next question to ask is how the needed energy will be generated to cover the estimated demand. TRNSYS software will be used to study the different generation technologies; this will help to evaluate the efficiency and consumption parameters. The convergence of the models developed in TRNSYS to study the different technologies has been ensured by mean of energy balances. These balances guarantee good results from the models.

Previously, different technologies have been analyzed based on the work of Cardona [13], Marimon [14], Ortiga [15] and Söderman [16]; this analysis has permitted to reject those technologies that do not properly fit for the future expansion of the PTA and to work in-depth analysis of those technologies that fit better. Technologies that have been discussed are:

Biomass boiler.- the system includes a 20 MW biomass boiler for hot water production that feeds heating network, and the cooling-generating system. As support systems a 9 MW gas boiler and 6 MW electric chillers is selected.

CHP.- cogeneration gas turbine and reciprocating internal combustion engine (ICE in advance) are the two types of systems that has been analysed, in both cases a 2 MW rated power equipment has been selected. Sizing has been performed considering the recommendations made by Cardona [13], Ortiga [15] and Söderman [16], using that system that maximizes the area under the aggregate demand curve. Besides Spanish legislative frame[18] should be ensured. The 2 MW rated power guarantees both the system efficiency and the legislative requirements. In both cases, use waste heat from the engine or exhaust gases to generate useful heat will be used to heat water that will allow, in one hand, meet the demand for heating and hot water, and in the other hand, feed the cooling-generating system. As support systems a 9 MW gas boiler and 6 MW electric chillers is selected.

Waste treatment.- this technology has not been considered because there is no waste treatment plant close to the park that could serve as energy source to feed the DHC network.

Solar thermal energy.- it has not been considered as an alternative in order to supply the energy required. Both, the high costs associate with this technology and the high free spaces required mean that technology economically unfeasible (Bruno [17]).

Cooling generation technology.- double effect LiBr-water absorption chillers technology has been selected to cover cooling demand; this choice has been based on the analysis of advantages and disadvantages conducted by Marimon [14]. In all cases, a double effect

absorption (BROAD 500) of 5.8 MW cooling capacity has been selected for cold water production. Additionally a water tank of 15,000 m^3 has been selected.

Finally, this paper has been focused on biomass boiler and CHP technology, these three technologies have been evaluated and compared with using conventional technologies, in which the cooling demand is satisfied by chillers and demand heating is covered by a gas boiler.

The following ratios are considered to quantify the results of the different technologies modelled in this paper:

For CHP technologies the following ratio will be used: ATE artificial thermal efficiency defined as:

$$ATE = \frac{E_{el}}{E_{input\_by\_fuel} - \frac{H}{\eta_{boiler}}} \quad (3)$$

Net primary energy consumption (NPEC).- it's defined to compare different technologies consumption rates. The mathematical expression for NPEC is:

$$NPEC = (E_{el\_cons} - E_{el}) \cdot C_1 + (E_{input\_by\_fuel}) \cdot C_i \quad (4)$$

where C_1 and C_i are the conversion coefficients for final energy (electric, gas and biomass) to primary energy in Spain; its values are 2,67, 1,06 y 1,25 respectively [19].

$COP_{instlallation}$ defined as:

$$COP_{installation} = \frac{P_{term}}{E_{el\_cons} - E_{el}} \quad (5)$$

These ratios will allow, in one hand, ensuring that minimum standards required by Spanish Royal Decree 661/2007 [18] are met and, in the other hand, knowing the overall performance of the system. This will facilitate the subsequent economic evaluation.

2.3. Economic analysis

The economic analysis has been performed considering the following topics:

- Depreciation cost for investments.
- Maintenance cost.
- Operating cost (energy, human resources, overall costs).
- Revenues from energy sales.

These topics have permitted to evaluate investments in terms of return on investment (ROI in advance), payback period and cumulative cash flow.

3. Results

Results obtained in the evaluation of demand, technology and economic assessment are as follows:

Energy demand and DHC Network design parameters.
Hourly profiles were obtained for heating and cooling demand in all buildings under study, considering the evolution of demand along the time as the occupation of the parcels is increasing. The monthly annual evolution for heating and cooling demand in the first 6 years is shown in Figure 2. It has been supposed that new buildings will be operative in the first six years. So, for years 7 to 10, the demand does not suffer modifications.

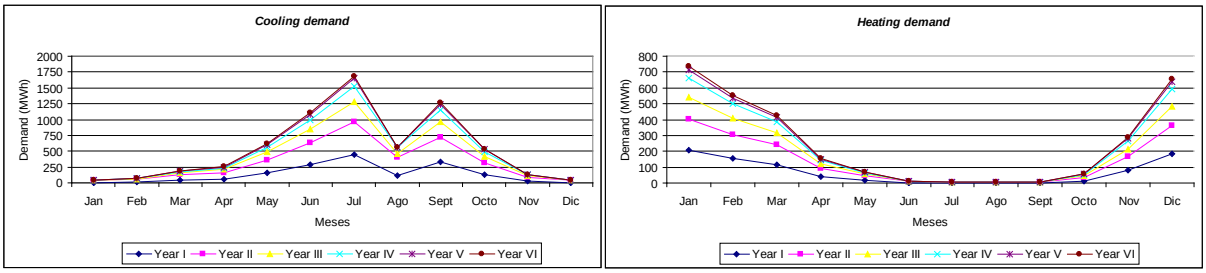

Fig 2. Cooling and heating demand evolution

As we can see, the cooling demand is highly reduced in August, since has been estimated the vacation period in this month.

In figure 3 the aggregate demand curve for heating and cooling in the year 10 is shown, this curve is very useful for sizing CHP equipment.

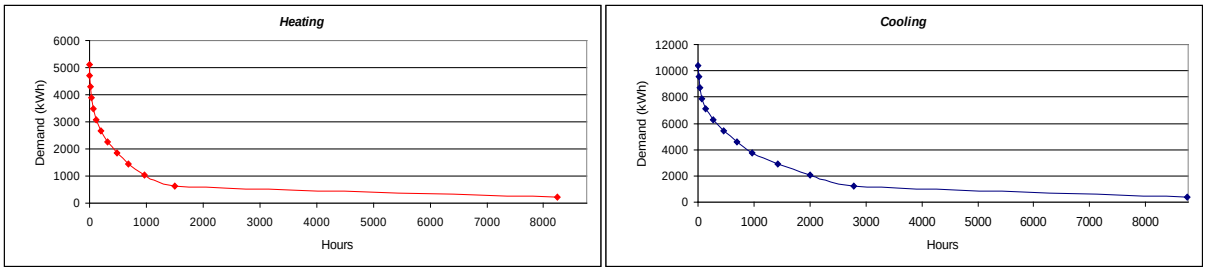

Fig 3. Aggregated demand curve for cooling and heating

As it is shown in the above figures, peak demand for year 10 has been set to 7.77 MW for heating and 12.22 MW for cooling. With those maximum power values and considering a temperature drop for heating of 30 ºC and 8 ºC for cooling, the maximum network flow is obtained: 61.8 kg/s for heating and 364.6 kg/s for cooling. These values along with the requirements of pressure loss in the network, and energy loss have led to size the diameter and thickness of insulation for the main pipe network and pumping system. Table 2 shows the design values of each of the components:

Table 2. Design DHC network parameters.

	Pipes DN (mm)	Isolate thickness (mm)	Power pumps (kW)	Tank volumen (m^3)
Cooling	600	7,1	315	15.000
Heating	350	5,6	75	-

Technologies evaluation

Table 3 show the results for technologies performance ratios calculated using TRNSYS.

Table 3. Design DHC network parameters.

	Net primary energy consumption (MWh)	COP installation	ATE
Conventional tech	27.030,55	0,353	-
Biomass boiler	29.117,90	0,328	-
Gas ICE	14.332,39	0,666	0,566
Gas Turbine	22.533,64	0,424	0,589

Economic analysis

Table 4 show the economic analysis for each of the technologies evaluated and figure 4 show cumulative cash flow for each technology:

Table 4. Economic analysis.

	ROI	Payback (years)
Conventional tech	< 0%	12,5
Biomass boiler	< 0%	16
Gas ICE	9,63 %	8
Gas Turbine	1,69 %	10

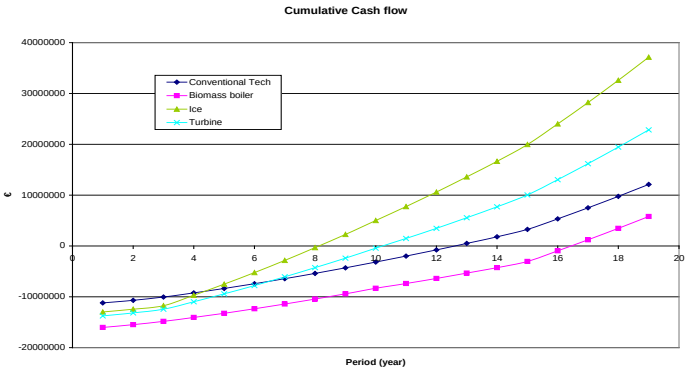

Figure 4. Cumulative cash flow analysis

4. Conclusions

As it could be seen in table 5, the technology that offer the minimum pay back period is the Gas ICE following by the Gas Turbine, this fact is consequence of the electricity production associate with those technologies that offer economical benefits. For Gas ICE, the benefits begin to be positive since year 8. It is obvious that infrastructure costs are very high in DHC. Economic figures are critical in the early years when buildings begin to establish in the technology park network and the energy demand is low.

The economic results showed support the implantation of a DHC network under the considerations done. The limitation for the feasibility resides in the future evolution of the new building openings. In this case the funding model of this type of technology must go through a public-private hybrid model in which the government support with soft credits to be repaid at the rate of new companies in the PTA are incorporating to DHC network, it will help owner company to obtain an acceptable incomes in the early years of operation.

References

[1] Directive 2009/28/EC of the European Parliament and of the Council of 23 April 2009 on the promotion of the use of energy from renewable sources.

[2] Directive 2002/91/EC of the European Parliament and of the Council of 16 December 2002 on the energy performance of buildings.

[3] Secretary of State for Energy, (2008). “The energy in Spain 2008”. Ministry of Industry, Tourism and Trade.

[4] S. Gustafsson. Optimal heating of large block of flats. Energy and buildings. 40 (2008) 1699-1708.

[5] S. Heiple. Using building energy simulation and geospatial modelling techniques to determine high resolution building sector energy consumption profiles. Energy and buildings. 40 (2008) 1426-1436.

[6] Y.J. Huang, H. Akbari, L. Rainer, R. Ritschard. Prototypppical Commercial Buildings for 20 Urban Market Areas. Lawrence Berkeley Laboratory, Berkeley 1991. LBL-29798.

[7] L.Pedersen, J. Stang, R. Ulseth. Load prediction method for heat and electricity demand in buildings for the purpose of planning for mixed energy distribution systems. Energy and Buildings, 40 (2008) pp. 1124-1134

[8] O. Segen, E.M. Franconi, J.G. Koomey. Technology data characterizing space conditioning in commercial buildings: Applications to end-use forecasting with COMMEND 4.0 LBL-37065 1995.

[9] T.T. Chow, K.F. Fong, A.L.S. Chan, R. Yau, W.H. Au, V. Cheng. Energy modelling of district cooling system for new urban development. Energy and Buildings, 36 (2004) pp. 1153-1162

[10] Ministry of Economy. Saving Strategy and Energy Efficiency in Spain, 2004-2012: Building Sector. November 2003.

[11] Bohdanowicz, Paulina, Martinac, Ivo. "Determinants and benchmarking of resource consumption in Hotels – Case study of Hilton International and Scandic in Europe". 2006.

[12] Pérez-Lombard, Luis, Adnot, Jérôme, Ortiz, José A.,Riviere, Philippe. "HVAC Systems energy comparison for an office building". 2004.

[13] E. Cardona, A. Piacentino "A methodology for sizing a trigeneration plant in mediteranean areas" April 2003.

[14] M.A. Marimón. Diseño y caracterización de configuraciones avanzadas de sistemas de trigeneración en edificios. DEA 2008.

[15] J.Ortiga, J.C. Bruno, A. Coronas. Review of optimization models for the design of polygeneration systems in district heating and cooling networks. 17th European Symposium on Computer Aided Process Engineering – ESCAPE17. 2007.

[16] J. Söderman, F. Pettersson. Structural and operational optimisation of distributed energy systems. Applied Thermal Engineering, 2006, 26:1400-1408.

[17] J.C. Bruno, J. López, J. Ortiga, A. Coronas. Techno-economic design study of a large scale solar cooling plant integrated in a district heating and cooling network. 61st ATI National Congress – International Session "Solar Heating and Cooling". Perugia, 2006.

[18] Royal Decree 661/2007 on the regulation of electricity in the special regime. BOE 126, p. 22846-86; 2007.

[19] Factores de conversión de consumo o producción a energía primaria (EP) y facot. IDAE. Instituto para la diversificación y ahorro de la energía. Ministerio de Industria, Turismo y Comercio; 2010.

[20] ASHRAE Handbook – Fundamentals. 2009.

[21] Energy Plus v5.0. Gard analytics. U.S. DOE Energy Efficiency and Renewable Energy (EERE)

[22] TRNSYS v16. TRaNsient SYstem Simulation Studio. Solar Energy Laboratory, Univ. of Wisconsin-Madison.

Sustainable Parameters for Latin American Cities

Oscar D. Corbella[1†], Gisele Silva Barbosa[2 *], Patricia R. C. Drach[3]

[1] *PROURB/ FAU, UFRJ, Rio de Janeiro, Brasil*
[2] *PROURB/ FAU, UFRJ, Faculdade Salesiana Maria Auxiliadora, Brasil*
[3] *PROURB/ FAU, UFRJ, Rio de Janeiro, Brasil*
** Corresponding author. Tel: +55 2127103135, Fax: +55 3232162313 E-mail:giselearquitetura@yahoo.com.br*

Abstract: Over the last few decades, Latin American cities have been undergoing a rapid process of population increasing. With scarce investments in infrastructure, they are unable to meet the demands. Some of the consequences of this excessive population growth include a failure of the transport system, inefficient public services, the formation of urban heat islands, among other consequences, all of them contributing to a steep fall in life quality and energy consumption increasing.
Given the precarious conditions observed in large Latin American cities, especially in metropolitan areas, and the disconnection between the urban built and natural environment surrounding them, there is a call for action, from intervention in the territory already consolidated, to the development of future cities through sustainable urban criteria.
This paper presents some parameters to guide contemporary urban design criteria in the planning of sustainable cities. It started from a theoretical approach guided by international authors with different views on such parameters. The methodology is based on a qualitative study considering urban design issues relating to sustainability, such as urban management, adequacy of climate and place, regionalism, physical limitations of the city, the mixed uses, productive city, integration between urban and rural, and no polluting mobility.

Keywords: *Sustainable Cities, Sustainable Parameters, Urban Design*

1. Introduction

The environmental problem today is a much discussed subject in academic circles. However, this theme is not introduced in the social consciousness as a result of scientific papers, but by the effect of environmental disasters aggravated by the unsustainability of current cities, mainly, in the metropolises of South America. Furthermore, the typical living standards are incompatible with the process of regeneration of the environment, the wide variety of population's consumption patterns of different countries and the increasing rate of social inequality in many of them contributes to the increased awareness of various social sectors on the need for new forms of intervention in the environment.

The possibility of actuation in existing cities and in the formation of new cities more sustainable guides this work, that have the purpose of thinking about urban design environmental parameters. Thus, it is proposed some categories that contribute to the systematization of the study: limiting urban environmental management, network of cities, regionalism, diversity of land use and productive cities. From the analysis of these categories it was searched to implement environmental parameters for urban actions in small and medium cities, and also in the formation of new cities.

The vast majority of developed countries, as much as those in development, are exploring the capacity of their natural resources to the limit. Depending on the level of industrialization of each country there are different problems. In developed countries, the migration of people from urban centres to the outer suburbs, which offer a natural more prosperous environment, has led to an increased use of automobiles, resulting in traffic jams and air pollution. Already

[1] † CNPq Researcher

in Latin American developing countries, environmental and social problems are intensified by the excessive growth of cities, the result of a centralist model of urbanization without accompanying infrastructure to support such increase.

The effects of global climate change brought environmental problems and put in focus the search for new solutions to the urban development process. The rational use of natural resources, consumer awareness, and social and environmental justice began to be treated as guidelines for urban planning, even if sometimes only theoretical.

Urban sprawl without limitation on the territory brings disastrous consequences for the environment, for example the reduction of the surrounding areas for agriculture and natural reserves, and also the intensified and confined use of natural resources without respecting the carrying capacity. Without urban limitation, the disastrous effects can be observed also for the population, such as failure of adequate services and infrastructure of several structural problems such as mobility, access to health and education.

Life in cities is the current preference of the vast majority of the population and cities are seen as centres of knowledge and culture. Thus, it is important to think about these urban agglomerations in a global and sustainable way, especially with regard to planning and urban design. It is believed that urban design can be a key ally to the possibility to plan more sustainable cities, besides the need for an urban management consistent with sustainable urban parameters.

2. The aim of the paper

The Latin American countries have experienced the swelling of their cities. This process guided by a centralist model of urbanization, coupled with a growing shortage of infrastructure and perspectives - as cities move far away from large centers, promotes the emergence of mega cities, full of big problems. The idea in this work is, starting from more sustainable principles, to seek parameters to point out the way to formation of new towns, and the acting in small and medium cities.

3. Methodology

From the theoretical framework relevant to the subject, from theories and information contained in different references on the general problems experienced by cities in the world today - due to lack of actions that are concerned with sustainable development - it was possible to define categories that deal with urban sustainability. From these categories it was developed a qualitative study looking for the determination of relationships among them and with the urban design, covering issues relevant to the development of a sustainable urban design for cities in Latin America.

4. Results and Discussion

It was possible to identify seven major categories that can delimitate the urban design and assist in their preparation. These categories are: urban management (consistent with sustainable development), limitation of the city, regionalism, mixed uses, productive city, integration between urban and rural, and mobility.

4.1. Urban Management

The first raised category was the **promotion of policies and actions** that might be able to generate a sustainability committed to social justice, focusing, therefore, on the rights and

basic needs of citizens. Through public policies and actions it is possible to reduce inequalities and ensure access to urban services. It is expected that a socio-political planning assures a decent income and a sustainable and balanced social and economic development and, in addition, combating speculation and privatization of natural resources. For this, the **society participation in the policy making** and in the oversight of government activities is of paramount importance. The democratic management oriented by sustainability paradigms requires responsible action of social actors.

The planning criteria that seek for sustainable development must be considered as one of the main objectives of the socio-economic balance of society, besides the improvement in quality of life, the management responsible for environmental preservation and rational use of the territory (The European Chart for land management - CEOT/CEMAT, 1983). Furthermore, it is necessary to **strengthen local autonomy** for the municipal power to manage the financial assets of the city, gearing to investments that ensure a **more just and secure city.**

For Rogers (1997), for the city to be sustainable the economic and sociology factors should be interwoven and integrated into urban planning. Moreover, the motivation of citizens and their participation in public decisions and policies must be guaranteed (the sense of belonging and democracy). In this regard, it is necessary to the actuation of technician expertise, and the diffusion of educational activities and the implementation of information tools to empower and enable the society activities with the State.

It is important to promote the citizen participation in shaping the territory seeking from the beginning, the major motivation of actors in policy making and urban areas, allowing greater community awareness about its urban space and educating the population on environmental problems.

4.2. Urban Limitation

It is important to call attention to that environmental impacts are interrelated and urban poor planning, or its lack, as well as an inadequate urban design can bring undesirable consequences in sequence; as, for example, public policies for urban periphery and the designs that emphasise the private automobile. Urban sprawl intensifies the need for automobile use, which increases the demand for infrastructure (roads) and fossil fuels. A lack of limitation may also contribute to urban deforestation, causing erosion and consequent siltation of rivers.

To ensure good governance and a population access to political decisions it is necessary to limit the size of the metropolis (CORBELLA, 1998). It is believed that the city should be limited by legislation to control land speculation. Moreover, the government should encourage investment in different areas, so that from a certain size of the first city the construction of another city should be encouraged. This capacity of the government allows it to act on local issues, focusing on the common good, linking capabilities, and regional and global needs. If, for example, other surrounding areas are encouraged and every city has around it a "green belt" of protected land speculation, used for both food production and for environmental conservation, urban areas will be delimitated[2].
These measures cannot be applied in large cities already moulded, but can be used in small and medium shape cities, preventing them from growing out of control [3]. The structure in

2 The green belt was firstly proposed in 1904 by Howard (HOWARD, 1996).
3 A deep analysis of the unsustainability of megacities was made by NEIRA ALVA (1998).

smaller cities connected together in a network is much more sustainable than large cities. The smaller number of inhabitants, and consequently, infrastructure, facilitates the public administration and increases society control over political power, reducing corruption.

However, it is no use limiting the city area to preserve the soil and facilitating the movement of pedestrian, and then densify it. It is necessary to refer both to limit the area built as well as the population. A small town, but still very dense, continues over-consuming and polluting with the same intensity.

One of the "so called sustainable" principles in recent years, mostly widespread by Rogers, is the formation of dense cities (ROGERS, 1997). However, densification may even represent an attempt to soften the urban and environmental problems caused by the macro scale, but at the same time, it causes new problems such as intense vertical cities, affecting ventilation and natural lighting, and the concentration of air pollution. Furthermore, in the case of the tropical Latin American cities, there is the issue of high temperatures, also improved by the lack of ventilation, allowing heat islands (BARBOSA, DRACH and CORBELLA, 2010).

It is known that large scattered cities generate big problems, but the densification of cities does not guarantee sustainability, although is still an attempt to avoid environmental problems in these cities. From the bioclimatic point of view, in the humid tropics, as stated above, the compact city promotes the formation of heat islands, with the consequent increase in electricity consumption for air conditioning and the production of pollution (BARBOSA, DRACH and CORBELLA, 2010).

Rogers (1997) considered that the "densification" of a city can bring ecological benefits, such as reducing air pollution by cars, that did not need to move large distances, the greater safety of urban centres, the reduction of the city expansion over the natural landscape and the integrated planning, that optimize the use of energy resources and reduce pollution. But if this city offers a quality of life for its city dwellers, it will soon undergo an exponential growth that will take out all the benefits achieved by its promoting big density.

Consequently the problem is not compactness, but the lack of physical limitation. The creation of limited new cities could help curb the population growth and to endorse the healthy migration from the unsustainable megacities. This design conception brings all the possible advantages of compact cities, without the problems caused by macro-scale, and it also promotes a better society participation in the policy decisions. A small city may be socially diverse, in which different social and economic activities can multiply and society could integrate more easily (MOORE, 1998).

It is appropriate that the city to be organised through reduced nodes (districts) to form a circular system that enables interaction between them. Still, resources and services all over the city and its surrounding territory should be redistributed, decentralizing services and urban equipment and creating a network of activities and information to assist in the reduction of dislocations with cars through polycentric neighbourhoods. This organization contributes to solve one of the serious problems of current planning - the linear cities that normally follow a highway. Linear growth can be avoided if other surrounding areas are encouraged. In addition to the internal network of the city neighbourhoods, a network of cities that fosters exchange of resources and services through a polycentric system should be considered.

4.3. Regionalism

The considerations about the natural and urban environment cannot be separated from social and political issues. Cities can be interpreted as parasites that absorb the region resources in order to survive, or can be designed to absorb the population growth and provide opportunities, instead of harming the region future. For this, we need to understand that the Earth is a system that took millions of years to accumulate resources such as fossil fuels and water and that these resources should be used rationally and sustainably.

For many years, especially in the last hundred years, these resources have been extracted and consumed without any criteria and, thus, producing pollution that causes serious environmental problems as acid rain and global warming. Remarkable is the "circular metabolism"[4] for cities, where consumption is reduced, improving performance and increasing the reuse. Cities today have a 'linear metabolism' in which there is an inflow of resources like energy and food, and the consumption of such materials within the city presents, in sequence, waste production and emission of toxic gases (Figures 1 and 2).

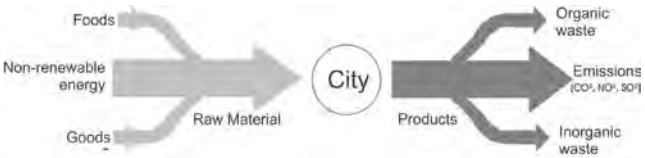

Fig. 1 – Linear Metabolism.
Source: Adopted from Rogers (1997)

Fig. 2 – Circular Metabolism.

The proposal for a "circular metabolism" is based on materials recycling, reducing energy consumption, the conservation of exhaustible energy and the use of renewable energy. These circular processes reduce waste and pollution, and improve the use of resources enabling the better use of consumer goods. To achieve a circular system, the best way is environmental sustainable urban planning. Also, we should promote the solution of environmental problems at every stage of the cycle from the beginning (incomes) to the end (exit of waste). By focusing on the "circular metabolism" through the conservation of energy and materials and by encouraging recycling, urban sustainability is promoting.

Environmental planning establishes a sustainable concept of integration between the built environment (buildings and cities) and the surrounding natural environment (climate, geomorphology, flora and fauna), in order to minimize the negative environmental consequences such as pollution of the environment and excessive production of solid and liquid wastes (HIGUERAS, 2006).

A detailed study of environmental and climatic characteristics of each place is the active part of this process of decision making and concrete proposal of planning. Regionalism is vitally important for a successful environmental planning. It is essential to profit the place weather characteristics to design and build the various components of urban and architectural elements as bioclimatic (CORBELLA and YANNAS, 2009). It must also be considered the issues on the territory that is analysed, about society, about the urban environment in question and also about the urban plans made earlier in the region.

[4] Concept addressed by Herbert Girardet (1993).

4.4. Incentives for mixed uses

The Zoning, heavily used by the modernists, tends to avoid the urban complexity by reducing the cities to simple divisions to obtain a greater ease in their management, from legally and politically point of view. But at the same time it prevents a healthier relationship between man and the environment and his fellows.

The work areas are normally located in urban centres that are deserted and dangerous at night, and housing and leisure are situated in more distant neighbourhoods connected by highways to the city centre. The environmental impact caused by this zoning is much greater than the impact of plans in which work, leisure and residential environments come into close, and often shared, places.

It is necessary to enhance the mixed use to mitigate energy consumption by reducing the distances between activities. This way of planning a city not only diminishes the excessive energy use and pollution, but also reduces the uncertainty in the urban centres for citizens to exercise control over their habitat.

4.5. Productive Cities - Work and Income

Another important category for a sustainable urban design is its conception as a productive city (MOORE, 1998). This condition gives characteristics of stability and sustainability to the city: the best way for a human being to settle down in a place is when he gets his livelihood from it.

It is essential that the population produces part of its food and its material needs, because it promotes pertinence as well as lowers transport spending and brokering, and it generates income and employment for the local society. It is important to balance food production and consumption, and also the need for all the cities to produce at least the basic and essential food for the local population. The incentive for production activities and services geared towards the promotion and preservation of the natural environment is an urban strategy that emphasizes both human welfare and nature. In rural areas it is important to enable people to work with agro-ecology and eco-tourism education.

It is essential the promotion of diverse manufactures of the productive cities, following the regional vocations in which different activities will inspire and promote a vital and dynamic community. The planners should understand, with the participation of citizens, the complex relationship between population, services, transportation policy and energy generation, as well as the impacts of these relationships on both the immediate surroundings and on the wider geographical domain.

As a result of the economic restructuration produced by globalization, a reduction of jobs has been produced and, this way, changed the urban landscape with the rise of the informal work. To enable productive cities that create jobs and income it is required: 1- policies for micro and small enterprises; 2- the encouragement of cooperatives in all branches of the system and the multiplication of business incubation; 3 - the training of different actors of society; and 4 - the encouraging the small farmer agriculture.

4.6. Integration of the natural environment, rural and urban

Nowadays there is a dichotomy between basic conditions in the city and the countryside, not only for the change in quality, velocity and temperature of the air, but the expectations of

humans, who prefer the city and move to it. The integration of the natural, rural and urban environment is then proposed as an improvement of the environment by introducing natural vegetation and creating regional corridors, and with the same importance in urban areas, promoting the balance between nature and city, preserving the natural cycles and putting green areas into the urban fabric. Thus, it also limited processes of uncontrolled urban sprawl, allowing a urban regeneration ecology.

The urban open spaces are very important because they serve as recreation areas and social use, in addition to provide more pleasant climates. These should be enlarged and properly designed to serve the people and to ease the negative urban environmental conditions. There is a necessity for properly planned urban spaces to allow the meeting and social exchange (VASCONCELLOS and CORBELLA, 2008). Hitherto such spaces, besides an architecture of quality, promote most beautiful cities. The quality of urban life can be encouraged through appropriate urban design, public safety and encouraging healthier environments, ensuring the physical and mental health of residents.

4.7. Mobility

In the traditional system of zoning, the automobile became the most important factor for urban planning. In the distribution of public spaces, all streets and avenues, and many times also parks, are designed to meet the needs of cars and not for pedestrians. The street, which was previously a local of exchange and social gatherings, today has been taken over by cars. To change this picture, besides the planning of mixed neighbourhoods it also must be encouraged public transportation or alternatives as cycling or walking to their own service, that are essential for a sustainable urban planning (CORBELLA, CORNER and BARBOSA, 2008).

The planning of smaller cities requires the end of the dominance of the automobile and the enhancement of pedestrian and public transport alternative. The city must grow through joint centres with mixt activities connected by public transportation with good quality, constituting an agglomeration of neighbourhoods with their own shopping areas and public parks.

5. Considerations and Recommendations

Over the past fifty years all the Latin American countries have experienced the problem of excessive growth of their cities. This swelling generated by similar processes and their problems were magnified by the growing scarcity of infrastructure and perspectives, a phenomenon that is incremented as cities move away from the big cities, and led, and continues to lead, to the formation of mega cities, full of great problems.

The assessment and determination of categories for the achievement of specific cases depend on the physical conditions of the region, the available place and the cultural and socioeconomic characteristics of future inhabitants, and with their participation it will be possible to define the solution of many issues related to sustainable cities. Most of the quantitative problems to be solved for the construction of sustainable cities have no general answers for the fact the solutions depend on the statement of the regional characteristics: the particularities of the region determine the numbers of local individuals who take in each category of analysis. Several factors are involved in these dynamics, and every minimal alteration of each of them may change the whole relationship of the structure.

The possibility of public power to intervene in the cities through policies and actions that promote the common good, paying attention to sustainability issues, makes it the greatest ally

in attempts to introduce strategies that are beginning to be delineated. The categories suggested here for the systematization of the study indicates a strong connection: limiting urban environmental management, network of cities, regionalism, mixed uses, productive cities, relationship between rural and urban mobility. Thus, by pointing out the strategies or environmental parameters for action in urban cities that are designed to be sustainable, the focus is related to finding ways for an effective public involvement.

References

[1] E. Higueras, Bioclimatic Urbanism (in Spanish), G. Gili, Barcelona, Spain, 2006, pp. 266-267.

[2] E. Neira Alva,(In)Sustainable Cities (Portuguese version), Ed. Dumara, Rio de Janeiro, Brazil, 1998, pp. 33-35.

[3] G. S. Barbosa, P. Drach and O. D. Corbella, Comparative Study of Sprawling and Compact Areas in Hot and Cold Regions: Way to Sustainable Development of Cities, Proc. of the World Renewable Energy Congress 2010 - WREC XI, Abu Dhabi, AUE, 2010, CD-room.

[4] H. Ebenerzer, City-Gardens for Tomorrow (Portuguese version), Hucitec, São Paulo, Brazil, 1996. (First edition in 1904).

[5] H. Girardet, Creating Sustainable Cities, Schumacher Briefings, UK, 1993. , pp. 56-57.

[6] O. D. Corbella and G. S. Barbosa, Towards Sustainability: Urban Environmental Principles, Proc. of the First Int. Conf. in Sustainable Cities, Morelia, Mexico, 2009, CD-room.

[7] O. D. Corbella, V. Corner and G. S. Barbosa, Urban Mobility fosters Sustainability, Proc. 25th PLEA Int. Conference, Dublin, Ireland, 2008, CD-room.

[8] O. D. Corbella, New Cities: Urbanism and Climate (in Spanish) Interior Ministry Publication, Buenos Aires, Argentina, 1998, pp. 80-88.

[9] O. D. Corbella and S. Yannas, Towards a Sustainable Architecture (in Portuguese with abstracts in English and Spanish), 305 pages, Ed. Revan, Rio de Janeiro, Brazil, 2009, pp. 145.

[10] R. Rogers,Cities for a Small Planet. Faber & Faber Limited, London, UK, 1997.

[11] V. Vasconcellos and O. D. Corbella, Open Space Planning: Relationships between Urban Morphology and Climate, in Urban Design and Ecology PUPH, G. Stewards and M. Ignatieva (Org.), St. Petersburg, 2008, CD-room.

[12] W. A. Moore, Eco-democracy: The Post-capitalism Model (in Spanish), Ed. Emed-Ceis, Buenos Aires, Argentina, 1998, pp. 45-47.

Urban microclimates and renewable energy use in cities

Erdal Turkbeyler[1], Runming Yao[1,*], Tony Day[2]

[1]*School of Construction Management and Engineering, the University of Reading, Whiteknights, PO Box 219, Reading, RG6 6AW, United Kingdom*
[2] *Centre for Efficient and Renewable Energy in Buildings (CEREB), Department of Urban Engineering, London South Bank University, London, SE1 0AA, United Kingdom*
** Corresponding author. Tel: +44 (0)1183786068, Fax: +44 (0)1189313856, E-mail: r.yao@reading.ac.uk*

Abstract: This paper presents an experimental measurement campaign of urban microclimate for a building complex located in London, the United Kingdom. The experiment was carried out between 19 July and 16 August, 2010 at the Elephant & Castle site. The wind and solar energy distributions within the London urban experimental site were assessed in detail for their potential use in areas of high-rise urban building complexes. The climatic variables were measured at every five minutes for the air temperature, the wind speed and direction, the air humidity and the global solar radiation for a period of four weeks. The surface temperatures were also measured on the asphalt road, pavement and building walls at every hour for the first week of the campaign period. The effect of the building complex on the urban microclimate has been analyzed in terms of the solar radiation, the air temperature and velocity. The information and observation obtained from this campaign will be useful to the analysis of renewable energy implementations in dense urban situations.

Keywords: *London, Urban Climates, Measurement*

1. Introduction

Effective urban planning and building design can have a beneficial effect on the urban climate and contribute towards reducing the intensity of urban heat island, improving living space, directly reducing the peak cooling load of a building and exploring potential implementation of renewable energy. Passive solar heating of houses in winters and passive cooling in summers provide low cost and sustainable solutions for these preferable outcomes. However, to achieve these solutions in high-rise and densely built urban environments are challenging due to the obstructions at close proximity and existing orientations of roads. Knowledge of microclimatic variables, particularly the urban wind and solar radiation can be used for developing better design options for renewable energy technologies within urban environment or determining their efficient operational conditions in cities.

In the literature, however, the microclimate within an urban complex is reported mainly in the context of air circulation and temperature distribution within urban street canyons, only. In these studies, the geometric characteristic of the urban layout is idealized as infinite parallel walls of street canyons. Santamouris et al. [1] studied the thermal characteristics in a deep (H/W=2.5) pedestrian canyon with a NW-SE axis, under hot weather conditions in Athens, during summer 1997. It has been observed a surface temperature difference of up to 19 °C, between opposite building walls. Air temperature difference near the two opposite facades varied up to 4.5 °C due to the impact of convection heat transfer from adjacent wall surfaces.

Similarly, Niachou and et al. [2] also reported an experimental study of a typical street canyon (H/W=1.7) oriented in ESE-WNW direction in Athens, again under hot weather conditions in 2002. The measured surface temperature difference across the street reached almost 30 °C and this caused the overheating of lower air levels. The microclimate in urban street canyons is also investigated by numerical studies [3, 4, 5,], with emphasis on pedestrian comfort, pollutant dispersion and natural ventilation. For an urban district, an experimental

investigation for the distribution of solar energy and wind energy for a general, random city layout was not available in the literature.
The present study investigates - unlike a simple layout of a street canyon, a general geometric characteristic of urban layout with high-rise and intensely spaced building complexes that are mixed with middle-rise buildings. The main objectives of this experimental investigation are: to quantify the temporal and spatial distribution of microclimatic variables for an urban site; to study the impact of the layout and orientation of buildings on these variables; and to assess the availability of the solar and wind energy within an urban building complex for their potential use, either actively or passively.

For this purpose, within a London urban district of the Elephant & Castle, the accessibility to the renewable energies- both the solar and wind energies, was studied experimentally by a field measurement campaign between 19 July and 16 August, 2010. The air temperature, the wind speed and direction, the air humidity and the global solar radiation were measured at four locations within a high rise building complex at the London site. The maximum distance between the measurement locations was 130m. Effects of the urban building complex on the thermal and airflow characteristics of the resulting microclimates were analyzed in detail. The surface temperatures of building walls and ground were also measured at these locations. The observed characteristics of urban microclimate at the London experimental site and the findings of the present study are presented in this paper.

2. Experimental method

2.1. Experimental site

London is located in the south of England, UK. , and has an elevation of 24m. It enjoys a temperate marine climate. The Elephant & Castle site has a global location of $51^{o}\,29'$ N and $0^{o}\,06'$ W. Figure 1 displays the London urban experimental site and the measurement points: 3, 4, 5 and 6. The experimental site was chosen for its high rise buildings and contrasting street layouts. The physical characteristics of the urban space are presented in Table 1. The London South Bank University Southwark campus occupies the central part of the experimental site. At the time of the experiments, a 32m high K2 building of the campus (Fig.1) had replaced previous low-rise buildings at the same location.

Four automatic weather stations (WS) were installed to the street-lighting columns that are located at the Ontario Street (3), Keyworth Street (4), the Thomas Doyle Street (5) and the Borough Road (6). The Keyworth Street (4) represents an urban street canyon linking Ontario Street (3) and Borough Road (6), and has a length of 230 meters. The weather station 3 that was installed at the dead end of Ontario Street faces the back of the surrounding buildings in every direction. The street level views of these four streets are displayed in Fig.2.

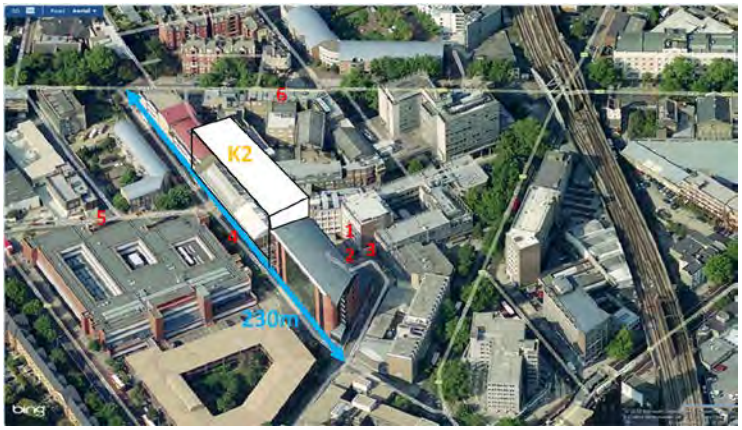

Fig. 1. London urban experimental site at Elephant & Castle (locations of weather stations: 3, 4, 5, 6)

Borough Road (WS-6)

Keyworth Street (WS-4)

End of Ontario Street (WS-3)

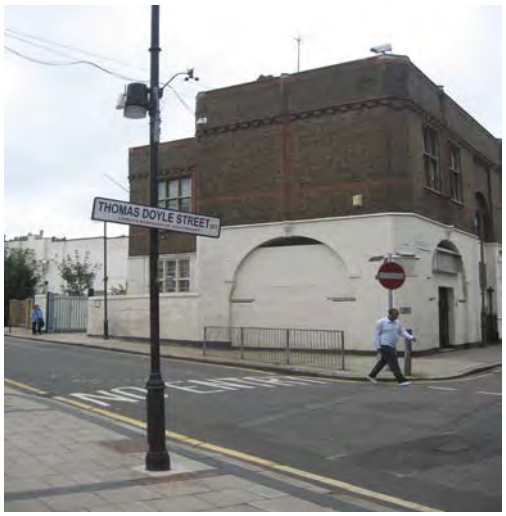

Thomas Doyle St. (WS-5)

Fig. 2 Street views of the London experimental site at Elephant & Castle Borough

Table 1. Characteristics of four streets at the London experimental site.

Street name	Street orientation	Weather Station No	Traffic conditions	Vegetation
Ontario St.	SSW to NNE	WS-3	Access only	None
Keyworth Street	SE to NW	WS-4	One way, low traffic	Trees at one side
Thomas Doyle St.	SW to NE	WS-5	One way, low traffic	None
Borough Road	WSW to ENE	WS-6	Two way, main road	Trees at both sides

Table 2. The geometry and material information of London experimental site

Street name	W(m): Street width	H/W: Ratios of building heights {H} to W	Building materials	Albedo
Ontario St.	14	0.57 – 2.00	Bricks, concrete	0.10 – 0.35
Keyworth Street	12	0.75 – 2.66	Bricks	0.20 – 0.35
Thomas Doyle St.	14	0.64 – 0.87	Bricks	0.20 – 0.35
Borough Road	22	0.45 – 0.68	Bricks	0.20 – 0.35

In table 2, for each street, the spacing between buildings (W) across the street including the pavements and the ratio of building heights (H) to spacing between the buildings (W) are listed alongside the type of building materials and their albedo values. The range of H/W ratios at each street represents all buildings along the street.

2.2. Parameters of measurements

At each measurement location (3, 4, 5 and 6), the air temperature, the wind speed and direction, the air humidity and the global solar radiation were recorded by an automatic weather station – Davis Wireless Vantage Pro2, Fig.3, which was attached at a height of 4m to a street-lighting column. The weather station 3 (WS-3) is located at the-dead-end of the Ontario Street, but, the other columns are positioned at the mid-distance of the streets. The accuracy of the integrated sensor suite (ISS) of the weather station for measuring each climatic variable is 0.56°C for air temperature, ± 5% for the wind speed, ± 7 deg for the wind direction, ± 3% for the air humidity and ± 5% for the solar radiation. At each street lighting-column location, the surface temperatures were also measured on the asphalt road, pavement and building walls at every hour. A K-type thermocouple digital thermometer – Model WK026, is used for the surface measurements.

Fig. 3 A view of the automatic weather station, positioned at 4m.

2.3. Duration of field measurements

The measurement campaign was carried out between 19 July and 16 August, 2010. The microclimatic variables were measured at every five minutes during the campaign period. During the first week of the campaign: 19 – 23 July, the surface temperatures were also measured every hour, over a period of five days.

3. Results

The experimental observations of the microclimatic variables at the London urban site are presented here for the air temperature, the air speed and the solar radiation. Figure 4 displays the evolutions of air temperatures at four locations over a 24 hours period from the midnight to midnight on 24 July 2010. During the day time, the air at the dead end of the Ontario Street (WS-3) is generally warmer than the air at the Borough Road (WS-6). The air temperatures at other locations remains between these bounding values of WS-3 and WS-6 However, the air temperatures at all locations get closer each other's value at the night time. The pattern in Fig.4 has observed also for the other days of the experimental campaign period. For example, Fig. 5 displays the air temperature evolutions at the locations of WS-3 and WS-6 for an interval of one week, between 2 and 8 August 2010. The factors affecting this pattern are discussed in section 4, below.

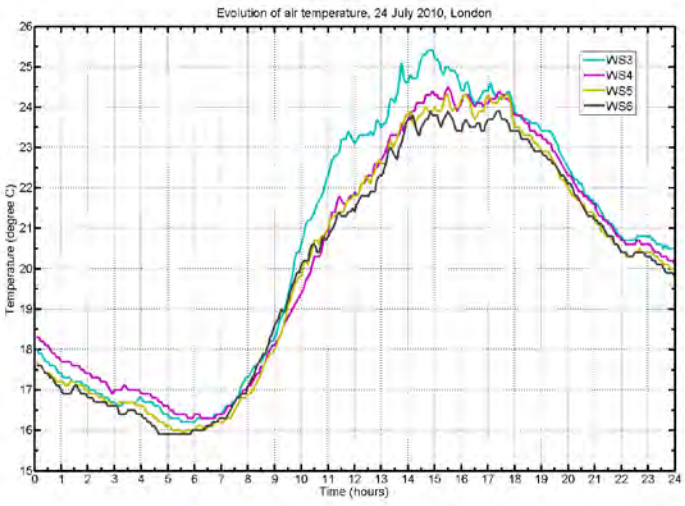

Fig. 4 Air temperature distributions at the London experimental site on 24 July 2010

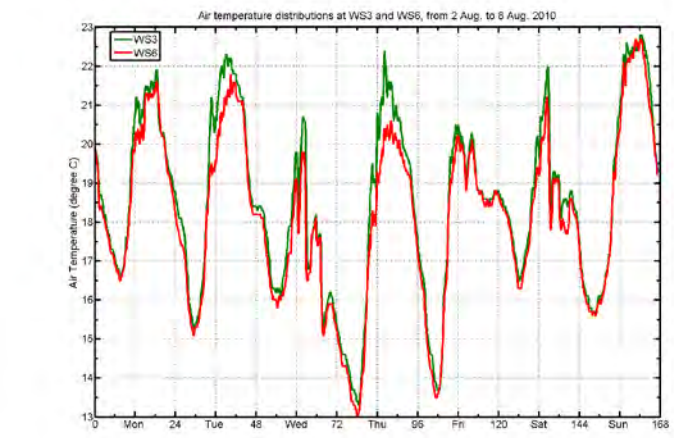

Fig. 5 Weekly air temperature evolutions at the dead-end of Ontario Street (WS3) and the Borough Road (WS6), 2 – 8 August, 2010

4. Discussion and conclusions

The layout of buildings and their orientations interact with the wind and the solar radiation and this interaction forms the different microclimates at each location. As is observed from these experimental results, Figs 4 and 5, the variation of air temperatures from location to location is an outcome of this interaction. Similarly, in an urban environment, the renewable energy use – solar or wind energy is also affected by spacing between buildings, building heights and their layout and orientations. For the measurement points of WS-3, WS-4, WS-5 and WS-6, the variation of the daily solar energy received by a horizontal surface over a period of one week and the variation of daily windiness over the same period are displayed in Figs. 6 and 7. Two new derived variables are calculated for this purpose; theyare wind run and the solar energy received at a given location over a time period.

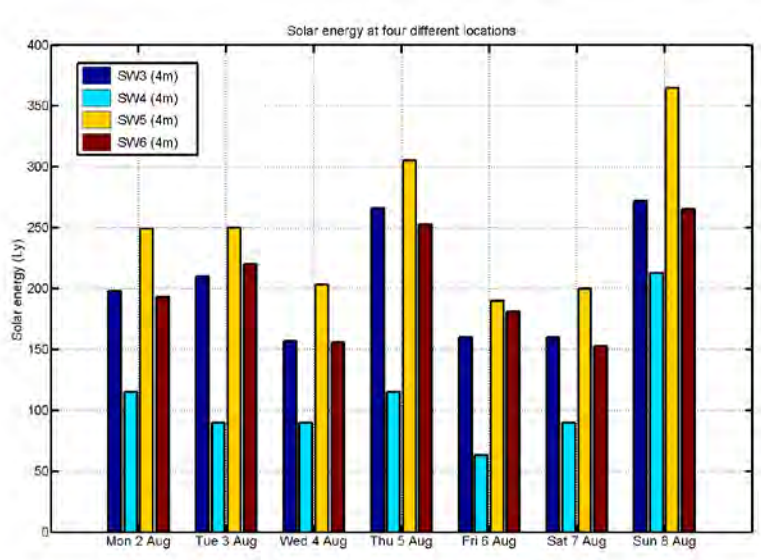

Fig.6 Daily solar energy variation at the London experimental site, from 2 to 8 August 2010

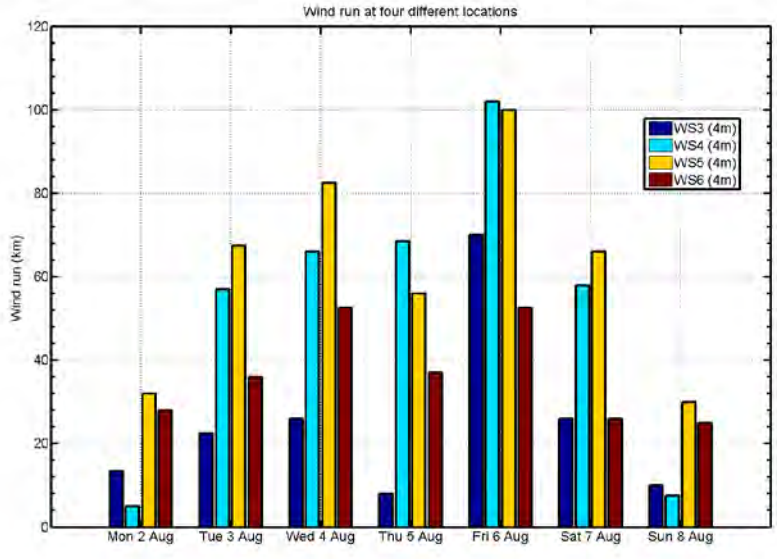

Fig. 7 Windiness of the London experimental site between 2 and 8 August 2010

Wind run presents the "amount" of wind passing the location of the weather station during a given period of time, expressed in "kilometers of wind". It is calculated by multiplying the average wind speed for each archive record by the archive interval of five minutes. By taking into account the variation of the solar radiation arriving at a location due to the position of the sun in sky, the passing clouds and shade movements, the resulting solar energy received over a time interval is also calculated. The average value of the solar radiation (watt per square meter) for each archive record is multiplied by the archive interval of five minutes to calculate the solar energy for the archive interval. The solar energy is measured in Langley (Ly): 1 Langley = 11.622 Watt-hours per square meter.

On Friday, 6 August, the dominant wind direction above the roof of K2 Building (32m) was in the SE direction, which coincides with the axis of the Keyworth Street (WS-4). As a result, WS-4 reaches the highest daily wind run value for this week, Fig.7. During the week, the dead-end of Ontario Street (WS-3) was the most sheltered one, and also having high values of the solar energy. As a consequence, the air at the dead end of Ontario Street (WS-3) warms up the most among all the locations, as was observed in Figs.4 and 5.

On the other hand, while the Thomas Doyle St. (WS-5) also receives a high value of solar energy due to the less obstruction against the sun light, this street also a windy one. As a result, the air at WS-5 does not warm up as much as like the air at Ontario Street (WS-3). The urban street canyon effect at the Keyworth Street (WS-4) can easily be observed from Fig.6 as the reduced solar energy at there.

In this paper, the results of the experimental measurement campaigns for studying urban microclimates for high-rise building complexes in London are presented. Implications on using the solar and wind energy in urban environments are analyzed. It has been demonstrated that the layout and orientation of buildings cause the variation of microclimate from one location to another. While, the tree-lined road was relatively cooler, the urban street canyon received the direct solar radiation only for a limited period, thus also remained relatively cooler. Whereas, the air in the non-green area has trapped the most heat and the air temperature has reached its highest value. It can be concluded that the buildings are operating against their own individual microclimatic variables rather than the meteorological weather data and that a buildings microclimate is affected by the existence of other buildings.

Acknowledgements

The authors would like to thank the finance support from the UK Engineering and Physical Sciences Research Council (EPSRC EP/F039867/1) and the support from the partners of the Chartered Institution of Building Services Engineering, Max Fordham, Short and Associates, MTT Consulting and Chongqing University.

References

[1] M. Santamouris, N. Papanikolaou, I. Koronakis, I. Livada, D.N. Assimakopoulos, Thermal and air flow characteristics in a deep pedestrian canyon and hot weather conditions. Atmospheric Environment, 33(1999) 4503-21

[2] K.Niachou, I. Livada, M Santamouris, Experimental study of temperature and airflow distribution inside an urban street canyon during hot summer weather conditions-Part I: Air and surface temperatures., Building and Environment, 43 (2008) 1383-1392.

[3] T. J. Williamson, E. Erell., Thermal performance simulation and the urban microclimate: measurements and prediction. , *Proc. of IBPSA Conference Building Simulation'2001,* pp.159-165.

[4] F. Sanchez de la Flor, S. Alvarez Dominguez., Modeling microclimate in urban environments and assessing its influence on the performance of surrounding buildings, Energy and Buildings, 36 (2004) 403-413.

[5] E. Bozonnet, R. Belarbi, F. Allard, Modeling solar effects on the heat and mass transfer in a street canyon, a simplified approach, Solar Energy 79 (2005) 10-24.

Development of a concept for ecological city planning for St. Petersburg, Russia

Åsa Nystedt[1,*], Mari Sepponen[1]

[1] *VTT Technical Research Centre of Finland, Espoo, Suomi*
** Corresponding author. Tel: +358 40570 3798, Fax: + 358 20722 7015, E-mail asa.nystedt@vtt.fi*

Abstract: The aim of EcoGrad, a research project conducted by VTT Technical Research Centre of Finland, was to develop a concept for the design of appropriate ecological neighborhoods for the city of St. Petersburg, Russia. A criteria list for ecological residential areas was developed together with local partners. Some differing aspects between Finnish and Russian criteria are pointed out in this paper. These are among others the attitude towards high-tech solutions, the norms regarding placement of services, and the lack of well functioning service concepts for operation and maintenance of facilities. Three pilot cases were also studied. A rough plan was made for the pilot areas including placement of buildings and services and transport solutions. Different scenarios for energy consumption and production systems were modeled and compared. Also emissions during the entire life cycle of the energy production processes were calculated with Global Emission Model for Integrated Systems (GEMIS). One of these pilot cases is described in this paper. During the project a questionnaire for residents in St. Petersburg was also made. It showed, among others, a poor willingness to pay for renewable energy and good indoor air. One of the major findings was a lack of policies and knowledge for certain renewable energy technologies and improved energy efficiency of buildings.

Keywords: *City planning, Russia, Energy-efficiency*

1. Introduction

In Russia the ecological planning is still in the early stage of development. Energy production based on renewable energy sources is also a quite unknown solution. However, there are already some regulations that support the guidelines of ecological urban planning. One of these is the regulation that orders maximum allowed distance from residences to the daily used services, such as day care centre, school, shops and health care centre.

The aim of EcoGrad, a research project conducted by VTT Technical Research Centre of Finland, was to develop a concept for the design of appropriate ecological neighborhoods for the city of St. Petersburg, Russia. Local features of the areas, such us Russian regulations, social and culture facts as well as local environment and weather conditions, formed the base data for the case studies. The project started in the beginning of 2010 and lasted until the end of the year 2010. The research report of the EcoGrad project will be published in English in the publication series VTT RESEARCH NOTES [1]. The objective of this paper is to present the development process used in the project and highlight some specific differences in ecological city concepts developed for Russia compared to Finland.

As partner on the Russian side was the Coordination Center for International Scientific-Technology and Education Programmes. The most important reason for having a Russian partner was to develop the contacts to the local government. Another reason was to get help with collecting necessary basic data. In addition a student from Saint-Petersburg State University of Architecture and Civil Engineering made a one month visit to VTT in order to help with data collection. A rough examination of the Russian building norms was made.

One of the guiding principles in the planning process was Globally Optimized, Locally Designed (GOLD) principle. Practically this means that the local conditions are taken into

consideration, when applying global optimized solutions into the EcoGrad concept. The aim was to find suitable solutions for Russia from those globally studied and applied technologies and concept solutions that are already approved to be sustainable, and suitable for ecocities.

The project included three pilot residential areas locating in St. Petersburg. A rough city plan was drawn and different energy systems were modeled and calculated. These plans included different building types in the area (residential, services and offices), floor areas of each building type, number of residents, the energy consumption level of buildings, green areas, suitable transportation solutions, and the structure of the area.

Based on the findings from the pilot studies and negotiations with the local authorities, a criteria list for an ecological city plan was made, presented, and iterated. It included aspects from the international LEED and BREEAM criteria and national Finnish criteria. The criteria list is divided into following sectors: energy, buildings, transportation, the structure of the area, land usage, landscape, waste and water solutions. There are three categories in the criteria list: general level criterion, details and specifications of the criterion and special notices from Russia. [1]

2. Methodology

2.1. Progress and collecting data

The approach was in the beginning to collect basic data and directly create plans according the EcoGrad concept for pilot areas. The general data needed was the energy efficiency level of houses being built today, ventilation systems normally used, energy prices and tariff systems, building norms, city planning process description, other relevant local regulations (such as distances to the daily services) etc. Case specific data needed was: existing transport solutions, maps of the areas, the stage of the city planning in the area, expected amount of inhabitants, etc. However, it turned out to be very difficult to get reliable base data, because it is hard to get energy consumption data on a single building level. Therefore the approach was changed. First a basic concept, based on Finnish base data, was developed. It was presented to the local authorities and adjustments were made based on the feedback received. The concept was made in more detail by adjusting it to three different pilot cases. The detailed concepts were again presented to locals and adjusted. The development process could be called an iteration process. As a result, the minimum emission saving potential in Russia could be evaluated. However, even larger emission savings may be achieved in St. Petersburg, since it is probable that the current Russian buildings consume more energy than buildings in Finland.

2.2. Questionnaire study for residents in Russia

Together with Finec, the St. Petersburg state university of Economics and Finance, a questionnaire for residents was made. The questions were made by VTT, and the questionnaire was performed by Finec. The questionnaire had 750 answers, 600 per email and 150 per telephone interview and face-to-face interviews. The survey was devoted to the living area conditions opinions, which included answers regarding the housing, buildings and living areas, transport etc.

The main finding was that almost all respondents (92 %) said that it is of no value for them to have their house heated with renewable energy. Less than half of the respondents (40 %) are willing to pay extra for good indoor quality, even though 80 % answered that they consider good indoor quality important. Security issues could also be highlighted, 72 % said that they do not feel safe in their neighborhood, which can be compared to a study made in Finland that

showed that 81 % of Finnish people living in urban areas felt really or quite safe [2]. The respondents want big apartments, over 100 m2, and they want to want to see parks, green areas and water when they look from their window. What also can be noted was that a rather big part, 44 % of the respondents do not own a car, mainly due to economical reasons.

2.3. Modeling of pilots

For each pilot case, a plan of the area was done, including the structure of the area, building types and location of services as well as transportation solutions. Different energy systems were modeled and compared. At first step, the base data was collected and a plan of the area was done. Number of inhabitants, buildings and necessary service spaces were settled.

At the second step, energy consumption of the entire area was calculated in different scenarios: base case scenario, low energy building and/or passive house level. The consumption level of base case scenario was assumed to correspond to the energy consumption level of Finnish building regulations in 2008, because reliable sources about Russian consumption levels were not available. Consumption level of low energy and passive houses were also based on Finnish definitions [3; 4]. The energy consumption of each type building was calculated using the WinEtana program which has been developed by VTT. WinEtana calculated the consumptions of different building types from the base data: the volume of the building, number of floors, the types, areas and U-values of ceilings, windows, roof and base floor, electrical equipments and their efficiency. These values for low energy and passive building levels are expert estimations by VTT.

Different options for renewable energy production were studied. Suitable production technologies were recognized, and then emissions produced during the entire lifecycle of the energy production process were calculated using the Global Emission Model for Integrated Systems (GEMIS), which is developed by The Öko-Institut e.V. The distribution losses were also included in the calculations. Results were compared with each other. According to IEA electricity transmission losses are 10 % and heat distribution losses 7 % [5].

Each pilot has its own characters and special aspects. First pilot was a residential area for 20 000 inhabitants. It was developed together with Pöyry Oy. The plan included different building types: one family houses, row houses and high rise buildings. The focus was on the factors affecting to the eco efficiency of the area (such as public transportation and walking and bicycling, green corridors, different building type areas, cultivation plots, placement of services and the entire area etc). This pilot has been presented shortly in this paper.

The second pilot was a residential area for 10 000 inhabitants, with residential high rise buildings. It was developed with a local building company. One starting point was to develop an ecological city plan without creating any extra investment costs. Focus was therefore put mostly on non-technical solutions, and the best suitable heat energy production was district heating with woodchip boiler. The third pilot was a smaller one, including only two blocks and less than 2000 resident and the focus was on the development of public-private partnership business models. It locates in the coast, on the Vasili island, in central St. Petersburg. Therefore, the water heat pump solution was considered interesting, since it could also be utilised for space cooling. The electricity could be produced with building integrated solar panels as well as with small building integrated wind turbines. However, most of the electricity demand should still be bought from the national grid. As another options solar collectors were also modeled.

3. Results

3.1. The EcoGrad concept

The EcoGrad concept was developed in the EcoGrad project. The target of the EcoGrad concept is an ecological urban planning process, which takes into account local Russian operational environment. A result of this process is to achieve an urban area, which is as eco efficient, functional and comfortable place to live, as possible. The fields included in the EcoGrad concept are: dense structure of the urban area, local environment and basis, energy efficient buildings, renewable energy production, sustainable transportation solutions, waste and water management and social facts. The aim is to utilize the concept also in the future projects in Russia.

One of the key issues of EcoGrad concept is an integrated planning process. This means that all urban planning fields are taken into consideration together already from the beginning of the planning process. In other words, the continuous co-operation of experts of different fields is really important. Then it is possible to find the solutions that are best for the entire system both environmentally and economically as well as functionally. [5]

In an energy system of the EcoGrad concept, the primary aim is to minimize the total energy consumption of the area. The main focus has to be concentrated on the energy usage of buildings as well as transportation, which are the most significant energy consumers. The energy consumption of buildings can be remarkably reduced with low energy and passive building technologies. On the other hand, the energy that is really needed in the area should be produced mainly from renewable energy sources. The optimization of the entire energy system, including heating, cooling, and electricity consumption and production, is important.

3.1.1. Factors affecting to the implementation of projects in Russia

The Russian building regulations can be found from the SNiP documents. The name is in Russia: СНиП - Строительные Нормы и Правила, which means Construction Rules and Regulations. SNiP is a set of regulations in the field of construction, enacted by executive state authorities, which contain obligatory requirements. SNiPs set general provisions, design requirements, rules of carrying out works and work acceptance, cost estimate guidelines. There are a large number of SNiPs, and each of them concentrates on one specific field. According to the Russian partners, the building regulations are under development process, which aim is to develop regulations toward European standards. In Russia, it is critical for all operations and projects to have knowledge about building codes and operation models.

Nowadays it is quite difficult to arrange the maintenances services of residential buildings in St. Petersburg. This is due to unclear ownership and management structures of facilities, as well as a poor level of the feature information of real estates and poor supply of services. It is unclear who should pay for the service and that often leads to the situation that the service is neglected. This needs to be considered when design includes technical aspects. This is one of the drivers that increase the interest for various Public Private Partnership business models.

Some solutions of EcoGrad concept are so multifaceted that it is necessary to have a private partner for maintaining and operating those. Without skilled private operator it cannot be assured that technical solutions operate efficient and ecologically enough, as planned. This is due to the fact that most of the solutions need special know-how and maintenance also after the construction phase. Depending on the used public private partnership model, private

partner can also be responsible for financing, investing, designing, building, and owning of services or necessary facilities. When designing and choosing suitable business model, it is important to consider ownership, responsibilities of the various parties and financial control.

3.2. The concept for the first pilot case

As an example the energy system, calculations of the first pilot are briefly introduced below. The plan of the first pilot area and the volumes are presented in the Figure 1. The planned number of inhabitants in the area is 20 000. The residential area is 30 m^2 per inhabitant, which means in total 600 000 m^2 floor area. There are five different building type areas: dense, low and dense, detached houses and villas. The inhabitation is most dense in the center of the area, which is really close to services and railway connection to the centre of St. Petersburg.

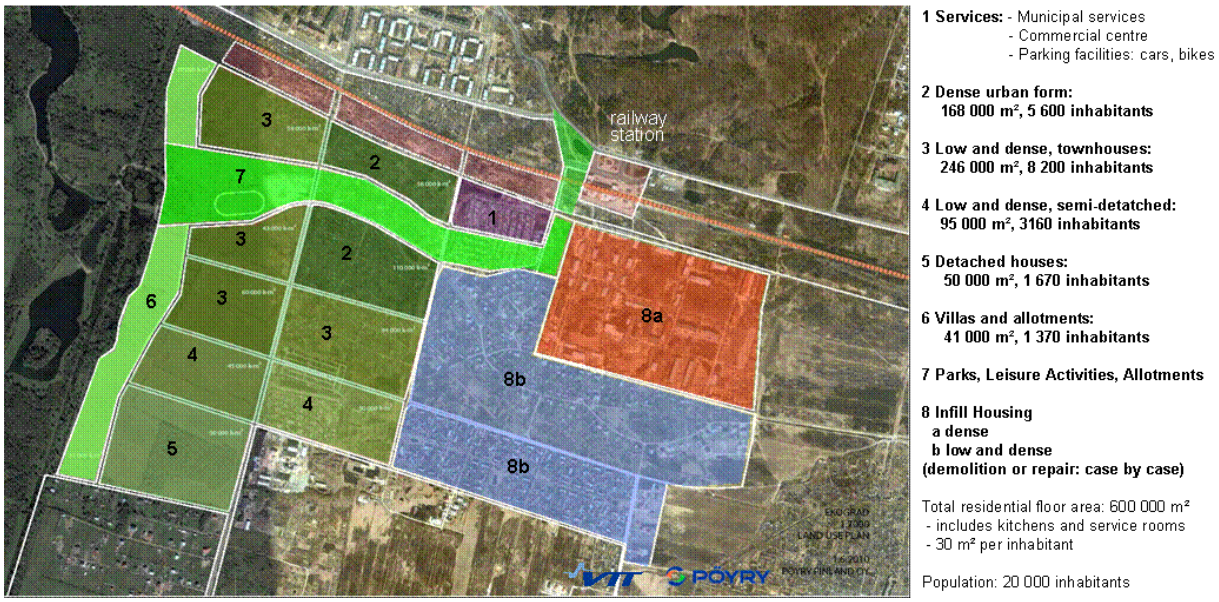

Fig. 1.Plan of the first pilot

The energy consumption has been calculated in three different scenarios: base case, low energy and passive building levels. The results can be seen from the Figure 2. M ost significant improvements are related to decreasing the heat consumption of buildings, and especially the heat consumption of space heating. It is more difficult to affect to the electricity or hot water consumption, because they depend more on the habits of the residents.

Next, different energy production options were studied. First option was quite ultimate with the target of using only renewable energy sources and achieving as low emission level as possible. That meant ground heat pumps, building integrated solar panels and wind power.

Heat collection pipes could be mounted on the golf court locating close to the pilot area. It was assumed that the COP of the heat pumps is 3, and the heat yield is 35 kWh/m2/a. One of the challenges was the fact that heat pumps consume electricity, which is also supposed to be produced within the area. If was further assumed that the entire area of roofs could be utilized with building integrated solar panels. It was calculated that the yield of solar panels would be 17 700 MWh/a. This means that there should also be a lot of wind energy: in a base case 28 804 MWh/a (the power capacity being 14,4 M W), low energy building level 20 200 MWh/a (with the power capacity of 10,1 MW) and passive building level 17 796 MWh/a (with the power capacity 8,9 MW). Power levels of wind power are calculated

with a capacity factor 23%. In this option the target was to produce as much energy as is consumed in the area, but it is assumed that the area is connected to the national electricity grid, which smoothes the differences between the production and consumption continuously.

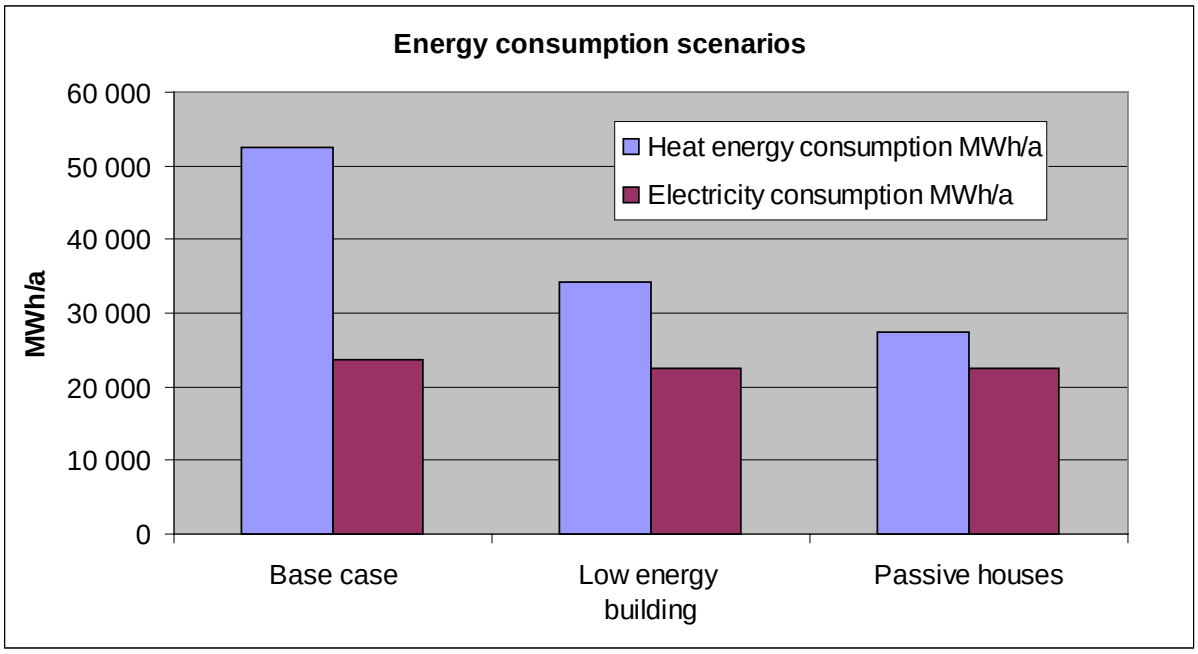

Fig. 2. Energy consumption of the pilot area in different scenarios

The second option was combined heat and power production (CHP) plant that is fuelled with woodchips. The third option was also a CHP plant, but it was fuelled with biogas produced from the wastes. It was assumed that the CHP plant is operated according to the heat demand in the area, as usual. In addition, it was assumed that the plant produces 80 % of yearly heat consumption, and the rest of the heat demand is covered with reserve plants, for example natural gas boiler. The used CHP processes were calculated with the information of real existing plants from the database of the GEMIS software. The plant using wood as a fuel produced 2 MWh of heat per 1 MWh of electricity, with the electrical efficiency of 27,5 % and operating time of 6000 h/a. The biogas CHP plant produced 1,5 MWh of heat per 1 MWh of electricity, and the efficiency and operating time were the same as the woodchip CHP plant.

The green house gas emissions of these different energy production options are presented in Fig. 3. The emission calculations include the emissions produced during the entire life cycle of their processes (including for example construction and transportation). These results were also compared to the base case, which represents the current situation in Russia. According to IEA, in Russia buildings are heated most commonly with district heating, in which the heat is produced from natural gas. The emissions of base case electricity are calculated with GEMIS from the base data of IEA [6].

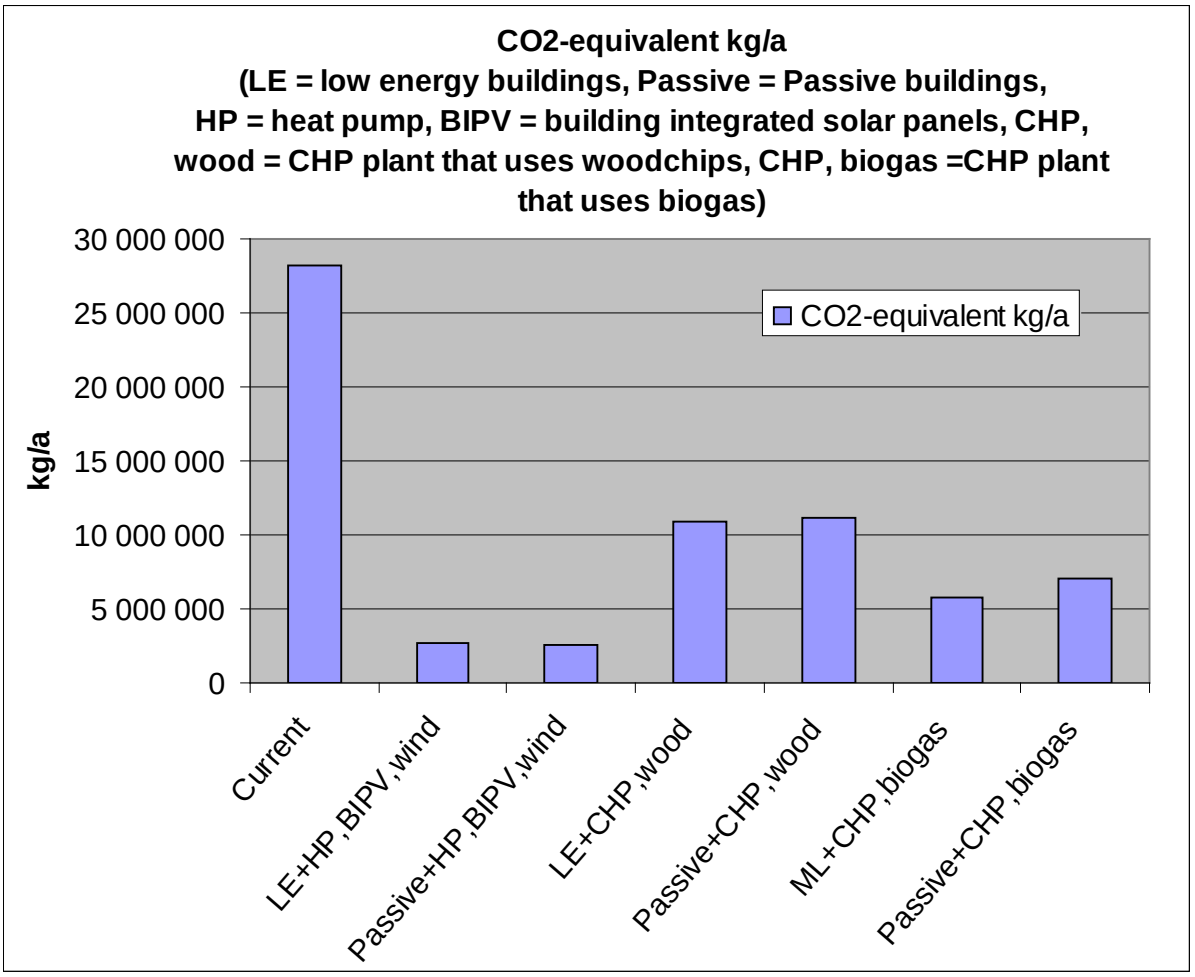

Fig. 3. Green house gas emission from different energy production options in the first pilot case. (LE = low energy buildings, Passive = Passive buildings, HP = heat pump, BIPV = building integrated solar panels, CHP, wood = CHP plant that uses woodchips, CHP, biogas =CHP plant that uses biogas)

4. Conclusions

After the whole project it can be concluded that ecological city planning principles can be applied in Russia. Ecological city plan was done for three pilot areas in St. Petersburg, and the energy consumption and production scenarios were modeled. One of the major findings was that it is important to aim buildings' energy consumption towards passive building level. Next, emissions during the entire life cycle of energy production process were calculated for each scenario with Global Emission Model for Integrated Systems (GEMIS). As a result a significant energy and emission saving potential was found. However, while modeling can be done, there are several issues that have to be considered in the planning process, and they need to be resolved before results of these modelings can be fully implemented. One of the most important further development steps is the actual implementation in these pilot areas.

It seems that there is a lack of knowledge and policies regarding renewable energy as well as technologies that improve the energy efficiency of buildings. The development of renewable energy systems is not yet common enough in Russia. Policies need to be clarified, for example the buffer zones for bio energy plants were not known by Russian partners. It was also unclear whether local legislation allows energy wells to be drilled for heat pumps. And as another example, an important part of the passive house concept is the mechanical ventilation

with efficient heat recovery. It needs to be emphasized that buildings cannot be built airtight and well insulated unless proper ventilation is insured. However, this is quite unknown solution according to the survey for residents, and the implementation may be difficult due to local policies. Generally speaking, the issues related to base data issues, ownership and operating conditions in existing buildings have to be resolved. Future efforts should be put on exporting knowledge and best practices about these issues. With better knowledge the local norms can be developed in a sustainable way and it will also support the development of the city planning process.

Taking the criteria developed in this project into the planning process is the next step in the development of new ecological areas. In contrast to similar studies conducted in Finland, the survey results suggested that while renewable energy is not a priority for Russians in new neighborhood developments, there is an interest in indoor quality and larger living spaces. Revealed challenges include the unwillingness to pay for improvements and low safety in neighborhoods, suggesting underlying economic and social issues that need to be addressed in addition to providing energy and environmental opportunities. Generally speaking, it seems that passive solutions that are not very technology dependent are valued higher in Russia. Technological solutions are not considered ecological. Smart metering systems for electricity consumption raised interest, but were still considered with skepticism.

During the project it was noticed that it is very important to have an active local partner in this type of development project. The local partners need to have their own funding for the project to ensure that the work is being prioritized. In addition, the results of the questionnaire made for residents in St. Petersburg imply that residents should be more involved in the planning process. This is another possible future implementation of the EcoGrad project.

References

[1] Nystedt Åsa, Sepponen Mari, Virtanen Mikko, Lahti Pekka, Nummelin Johanna, Teerimo Seppo. EcoGrad - Development of a concept for ecological city planning for St. Petersburg, Russia. VTT Reseach Notes.

[2] P. Suominen, Suomi - Euroopan turvallisin maa?. Reseach report. Poliisin ylijohdon julkaisusarja 7/2009, ISBN 978-952-491-434-5. Referred 12.12.2010. http://www.poliisi.fi/intermin/biblio.nsf/3D6379853B32E72DC225768C003279F0/$file/7-2009.pdf

[3] I. Strom, L. Joosten, Boonstra, J. Nieminen, M. Saari, E. Nykänen, Työraportti 1.2 Passiivisen talon ratkaisut. Work report of Promotion of European Passive Houses project. 2006. Referred 10.12.2010. Available: http://erg.ucd.ie/pep/pdf/Passive_House_Sol_Finnish.pdf

[4] J. Nieminen and K. Lylykangas, Passiivitalon määritelmä. Ohjeita passiivitalon arkkitehtisuunnitteluun. 2009. Referred 10.12.2010. Available: http://www.passiivi.info/download/passiivitalon_maaritelma.pdf

[5] Sepponen, Mari: Technologies and solutions for the energy system of an ecocity. Master's thesis 2010, Aalto University of Technology.

[6] IEA, Electricity/Heat in Russia Federation in 2008. R eferred 2.9.2010. Available: http://www.iea.org/stats/electricitydata.asp?COUNTRY_CODE=RU

Challenges for developing a system for biogas as vehicle fuel – lessons from Linkoping, Sweden

Björn Berglund[1,*], Carolina Ersson[1], Mats Eklund[1], Michael Martin[1]

[1] *Linköping University, Environmental Management and Technology, Linköping, Sweden*
** Corresponding author. Tel: +46 13285625, E-mail: bjorn.i.berglund@liu.se*

Abstract: Biofuels are being employed in nearly all the EU member states to fulfill the targets set up by the European Directive 2003/30/EC to have a 5.75% share of renewable energy in their transport sector by 2010. In Sweden ethanol is the leading biofuel, while biogas mainly depend on local initiatives with the city of Linköping as a case in point.

Our purpose with this article is to analyze the development of biogas in Linköping within a framework of technological transition theory. To this we add a set of concepts from large technical systems-literature to address and re-analyze two earlier studies on the biogas development in Linköping to achieve a deeper understanding of this success story. We argue that the establishment of a development trajectory for biogas depended on the ability of the involved actors to establish and nurture their social network, to create learning processes and stimulate the articulation of expectations and visions. It was also important that these three factors were allowed to influence each other for the system to gain a momentum of its own.

Furthermore, the biogas development in Linköping is found to be interesting in that the triggers for the development came from a variety of levels and angles. Initially, the rising fuel prices after the oil crises in the 1970's resulted in an increased interest in renewable fuels in general. Second, an anticipated national pipeline for natural gas planned through Linköping was considered a huge potential for methane exports. A part from these external energy incentives, the local trigger was the bad urban air quality caused by the public transport authority's bus fleet. The breakthrough came when it was discovered that by-product biogas from the wastewater treatment facility could be used as a fuel for transport.

When the plans for the national pipeline were rejected, a fruitful co-operation between the municipally owned production facility and the public transport authority was set up to meet the constructed demand from public transport. This cooperative pair-arrangement was the starting point for the biogas niche trajectory as other actors subsequently were enrolled to increase the size and agency of the network.

Nowadays, biogas and other renewable fuels play a significant role in the supply of transport fuels for Linköping. In 2009, a total of 9.5% of all transport fuels used in Linköping were from renewable sources, i.e. biogas (4.6%), ethanol and biodiesel. This puts the city well ahead of the European target of 5.75% renewable fuels by 2010.

Keywords: *Technological transitions, niche management, biogas, renewable energy, biofuels for transportation*

1. Introduction

Our purpose with this conference paper is to analyze the process of biogas development in Linköping using technological transition theory. We argue that the success story was an example of the interplay between three technological niche processes; social networking, learning processes and the articulation of expectations. Our focus is mainly local, but since national initiatives and plans also affected the process, some of these are included in the description. We suggest a local Swedish "style" of technological niche development as a topic for further research.

2. Methodology

To create a deeper understanding of the development of biogas in Linköping, we assemble a new theoretical perspective to re-analyze two earlier studies on this topic. The theoretical perspective stem from two bodies of literature; the main framework come from technological transitions-theory [1], [2], to which we add key concepts from large technical systems theory developed by Thomas Hughes [3], as well as findings from Swedish scholars within this field

[4], [5]. No new empirical material has been collected and the analysis veers more towards theory building than generalizable conclusions.

3. Theory

The basic conception of the paper is that technical systems are embedded in a societal context; they are socio-technical, which means that technical systems and societal actors both affect and are affected by each other [2]. This reflexivity is particularly evident in the case of emerging socio-technical systems, whose meaning and performance are still under negotiation in the process to reach a concluded design solution [6].

If successfully spread, an emerging socio-technical system may be taken up and evolve into a socio-technical regime, consisting of prevailing institutions and rule-sets (formal laws and regulations), which provide stability [7]. In a regime, relationships are since long established between for example suppliers, user and producer groups, research networks, public authorities and societal groups [2]. Different kinds of socio-technical systems often share the same characteristics within the same country. A typical feature of the Swedish way of constructing socio-technical regimes is the ”development pair”-configuration; a close, long-term relationship between an industrial company and a state customer regarding development projects on new technical systems. An example of this is the cooperation between the Swedish Powerboard (Vattenfall) and ASEA (later ABB) [5].

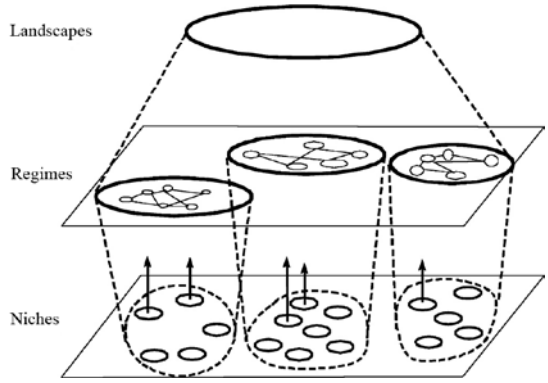

Fig 1. Multiple levels as a nested hierarchy[1]

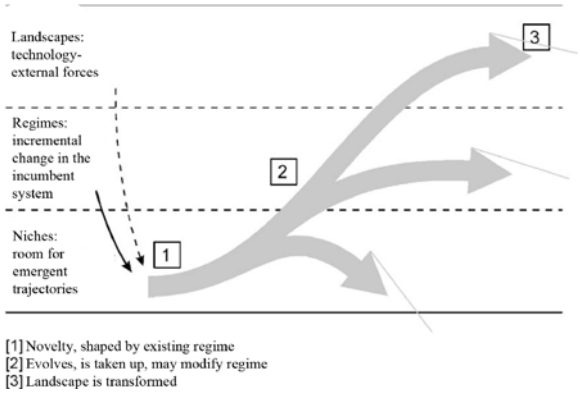

fig 2. Describing the niche trajectory[1]

Regimes are located at the meso-level in a heuristic model for socio-technical systems developed by Frank Geels, fig 1. Most changes in socio-technical regimes are of an incremental nature, so for major regime changes to occur, external pressure from outside of the regime level is needed [7]. An example of external pressure is when the oil crises during the 1970’s increased the transportation regime’s interest in renewable fuels.

The oil crises are examples of events in the socio-technical landscape. The landscape is located on a macro level in the model and is even more sturdy and hard to change than regimes. It contains technology-external factors such as financial fluctuations, diplomatic relations and international conflicts [2]. So while both the landscape and regime levels stabilize the incumbent practices of different socio-technical systems, they also create disincentives and barriers for disruptive technologies to develop [7].
The heuristic spaces for disruptive and/or emerging technical systems are the technological niches, found at the bottom of the socio-technical hierarchy. Here, change can still be radical, as uncertainties caused by socio-technical ”child diseases” must be overcome. It is important

to find an organizational form and agreements between the involved actors, for example through the formation of joint ventures. The technology must furthermore be trustworthy, the operational risks low, and subcontractors with the right components must exist on the market. [4]. Uncertainties at the niche level can be overcome by constructing a first and large enough secure market outlet to lower the economic risks involved in doing research on a yet immature technology. This is important as 'incubation room' where the nurturing can proceed without the pressures from mainstream market selection. The focus of this paper will be at the level of technological niches for which three crucial processes have been identified [2]:

1. The building of social networks with meaningful relational connections between involved actors. Such networks are the arena for users, decision-makers and other interest groups to give feedback about the technical system to firms, engineers and researchers, and vice versa.

2. The creation of learning processes is important, not only for technical aspects such as design and user preferences, but also from a societal point of view to understand for example regulation and infrastructure requirements.

3. Finally, the articulation of expectations and visions around a socio-technological system is important both to attract attention and resources from the social network, as well as to provide space for learning processes.

Achieving a successful interplay between the three processes is necessary to develop a development trajectory for a new radical socio-technical system [2]. If this is successful, the system can start to expand and require other systems and organizations to adapt. This is what Thomas Hughes calls 'momentum', a dynamic inertia that strives to enlarge the action space for and increase the number of activities in the socio-technical system. Momentum thrives on overcoming reverse salients, i.e. anomalies and/or uneven development that constrain the system from expanding. Reverse salients stimulate inventive activity and are thereby also important drivers for learning processes [3].

All socio-technical regimes have started out as niche trajectories. Regimes are the formalized results of social network activities, learning processes and achievements surrounding a technical system, which have gained enough momentum to overcome reverse salients and develop into a socio-technical regime in its own right, fig 2.

4. The biogas development in Linköping

4.1. Empirical data

The following description is in large parts collected from two reports. The first is a published paper by biogas researcher Magdalena Fallde [8], and the second is an unpublished report on the Linköping biogas development written by Undén [9], the former CEO of Svensk Biogas. We have taken into account that Undén have all the reasons to write a success story and have tried to stay away from bias in our description. The intention has been to re-frame these written accounts from a technological niche development perspective.

4.2. Context: biofuels in Sweden

Biofuels achieved attention on a national Swedish level after the oil crises of the 1970's. A large-scale methanol initiative characterized the first years of development without achieving much of a break-through. While methanol always remained a strictly top-bottom initiative, ethanol could to a larger extent be endorsed and played out locally [10]. The same was also

true for biogas; which still can be seen in the fact that most of Sweden's biogas facilities and the achieved competences most often remain within municipally owned companies [11].

4.3. Initial incentives

It was in many respects lucky circumstances that made biogas the option as the fuel for sustainable transportation in Linköping. Following the oil crisis (a critical event in the socio-technical landscape), the Swedish socio-technical regime discussions on environmental issues intensified on a national as well as local level. In Linköping, the discussion focused around the city center and especially the central bus stop square which was characterized by the smell of diesel exhaust and soot particles. Since the inner city was banned for other transportation vehicles than buses, the environmental problems could only be referred to them. This led to a joint will among the local politicians to improve the local transportation regime and the environment of the inner city in an economically feasible way. The local bus authority at the time, LITA, had problems convincing the citizens to continue using their buses, which had been regarded as the most sustainable transportation system in the city. The question became even more delicate for LITA since it coincided with both the expiration of the local authority monopoly for bus transportation and the widespread implementation of new catalytic exhaust technique in petrol driven private cars. On a deregulated market and with this technical alternative at hand, why would people choose their buses for transportation? LITA had only one choice, to change fuel in their buses [8]. All of these events in the local socio-technical transportation regime were influential in the biogas development process.

Parallel to these local triggers, there were plans to build a national natural gas pipeline through the county where Linköping is situated; a great possibility for both import and export of methane. This national project in the socio-technical energy regime, was part of Linköping's provider of regional services', Tekniska Verken AB (TVAB), search for alternative burning fuels. At the time TVAB had permission problems with their waste incineration plant, which the local authority threatened to close down. When the plans for the natural gas pipeline were rejected due to economical reasons, the idea of gas driven vehicles had stuck in the minds of the managers at LITA. Gas to them appeared as a new and unproven fuel but also attractive and with existing techniques for operation [8]. This interplay between national and local changes in different kinds of socio-technical regimes provided the ground for further initiatives for biogas on the local scale.

4.4. Early signs of a niche trajectory

When the bio-methane by-product in TVAB's wastewater treatment plant turned into a possibility, fuel for transportation was not at all their business idea. This was instead triggered by the fact that LITA was searching for new fuel for their buses. Replacing the missing natural gas with this existing source of bio-methane seemed obvious, even though bio-methane was mostly produced for reserve electricity purposes in Sweden at the time [8].

The two municipality-owned companies got the permission to perform a pilot study on refining the bio-methane from the wastewater treatment plant. The idea was to convert five diesel buses into bio-methane ones and put them in operation within regular traffic. This pilot study established the social network around the development project and added more concrete ways of practice. Part of the money invested in the project was a grant from the Swedish state; the rest came from the municipality of Linköping, the county, the regional bus authority, LITA and TVAB. Setting up this network of actors around a created offset market of bio-methane buses, proved successful as the first five rolled out in regular traffic in 1992. The work conducted in the pilot study was characterized by a steep learning curve. Several

technical issues concerning upgrading and distribution of bio-methane were solved and overcome during the scope of two years. The learning-by-doing process was considered fruitful to such an extent that the possibility of a full-scale operational project, from five to 20 buses, was discussed during the later part of the pilot study [9].

The wastewater treatment plant could not alone provide enough bio-methane for such an expansion, and had thus to be complemented by production from other substrates. Studies were carried out on different raw materials suitable for digestion at the same time as two other Swedish projects with bio-methane as fuel for transportation were about to start. This created a greater focus on the achievements done in Linköping and according to the CEO; a general wish of being pioneers was spread among both the personnel and politicians [9].

The calculations for the full-scale project of 20 buses showed that a switch to bio-methane would cost more than continued traffic with diesel buses. Nevertheless, the politicians made the decision to go ahead not only with 20 but the entire bus fleet of 65 buses, since economies of scale made the larger project less costly per driven kilometer. On the other hand, the capital risked in investments would also be bigger and with the implemented technology in the whole bus fleet of the inner city, a failure would be critical [9].

4.5. Technological momentum catching on

Around the same time, a new main supplier of raw material to the biogas digestion appeared in the form of the locally situated slaughterhouse Farmek. They had problems getting rid of their organic waste and biogas could be a way to secure their offset. Furthermore, the digested by-product from bio-methane production is a highly valuable fertilizer for farmland, so to secure the offset even further; LRF (the farmers association) was enrolled as an actor to take part in the social network surrounding the project as well. With this set-up, the bio-methane production system generated income at three times during the process: from receiving/treating the waste and the production of approved bio-fertilizer and bio-methane. Getting these actors to work together proved crucial, not the least since it at the same time confirmed the local authorities belief in the project. Successful enrollment of more actors proved that achievements and visions spread also outside of the established social network. This new setup of three stakeholders (TVAB, Farmek and LRF) started an associated company to TVAB with shared ownership, and a state grant was received to establish a first production facility for bio-methane in 1995. The plant was established during 1996 and provided a new space for further learning processes, so that the efforts made during the pilot study could be continued but on a larger scale [9].

In late December 1996, the first batch of substrate was loaded into the plant. During the first years of operation, experiences and breakthroughs were made about the operation of the whole system; from the controlling of digestion chambers, via the upgrading system and refilling stations to the everyday maintenance and operation of the bus fleet running in the inner city. Pioneering work became a part of the workforce's everyday and a strategy to allocate investments in personnel and to tie competence and not only technology to the project, was complemented with the sharing of experiences from other projects in Sweden [9].

Actors other than just the locally concerned thus shared the visions around the project, and the project gained a lot of attention both regionally and nationally. Between 1997 and 2008 the plant managed to manifold it's production of bio-methane due to conquests in process techniques and managed to keep the production steady by relocation during a period of difficulties in substrate deliverance. The plant also had to continuously increase the

production of bio-methane in order to meet the launching of converted bio-methane buses [9]. That the project had been able to manage and overcome these hardships, can be seen a sign of the niche trajectory building up a momentum. This was going to be put to the test when the project was seriously questioned for the first time since the start in 1990.

4.6. Reverse salients

The problem stemmed from the odor from the production site and proved very hard as well as important to solve, not the least since its solution was important in relation to the inhabitants of Linköping. A costly process was initiated by boxing in the incidence and an odor panel of local citizens was assembled to derive the cause of the problems and thereby undertake necessary measures at the plant. It took several years with an odor-reducing program until better levels for the surroundings were achieved [9].

At the same time as this process went along, the top management was changed and a new CEO was installed. The bio-methane production was not profitable enough so a new business idea was badly needed. A face-lift into yet another expansion phase was figured out to get more economically beneficial through size advantage. The expansion required large investments in both technology and personnel, and a crucial decision was taken to expand regionally and into the private market. The new CEO pushed the expansion plans through, although the political opinion was not throughout positive. This was due to that TVAB at the moment generated much better profit to the municipality than their other business areas [9].

Already during 2001 and 2002, two large investments were done in new upgrading units and the first public filling station. The entrance to the private market was announced through a public statement that bio-methane should be a fuel you can rely on in Linköping also for your private car. LRF and Farmek was not interested in this expansion and sold their ownership to TVAB, which became full owner of the new company that was now formed [9].

In 2003 TVAB planned to establish filling stations for private cars in every regional city to create a demand for bio-methane as quick as possible with as little investments as possible. The change of the name to Svensk biogas (Swedish biogas) coupled with logotype change packaged their new business idea, and the expansion first aimed at building a new production facility in the neighboring city of Norrköping. At the same time, they had also showed the possibility to transport compressed bio-methane to newly established bio-methane markets without local production, which was a new business practice by then. During the period of 2003-2006 Svensk biogas established 14 public fuelling stations regionally and grew the public market from 300 000 to 3 100 000 Nm^3 [9]. During these later stages of niche trajectory development, signs of a stabilizing momentum can be seen as more and more reverse salients are conquered and the socio-technical system achieves an expansive dynamic.

5. Results

The Linköping biogas case provides insights of how the intertwined process of social networking, learning processes and the articulation of expectations and visions can be configured for a technological niche development. Two initially important factors can be highlighted: the initial pilot study and the creation of an offset market in the form of the local bus fleet. This constructed an “incubation room” or niche, which could act as a protected arena for interactions and a starting point from which a trajectory could be developed.

Characterized by a steep learning curve, the pilot study years was successful enough in creating expectations and visions to overcome the crucial moment to further expand into a

second pilot study. At that point, the expectations created within the social network were strong enough to dare go into an even greater expansion than first planned for; 65 instead of 20 buses. Furthermore, the visions surrounding the project seemed hopeful enough to successfully enroll more actors to the network to provide a larger resource base of organic waste needed for the expansion.

The reconfigured social network and the larger second project provided yet another and extended arena for learning processes. New expectations and visions were in this process created around the project, which lead to the expansion into the private market. The dynamic expansion of the biogas project had begun to show signs of a technological momentum, as the enrolled actors had to adapt their processes to the biogas development. Furthermore, it conquered the first encounter with a reverse salient; the odor problems from the factory.

The biogas niche trajectory in Linköping was the combined result of the three processes. The relationship between the actors from different socio-technical regimes created a stabilized yet diverse local network. Although they had different incentives, they learned and developed the biogas technology and created a momentum through co-operation and a shared vision.

6. Discussion and Conclusions

An interesting feature in Linköping is the way that different socio-technical regimes affected the development of a biogas trajectory. Initially, pressure came from landscape change inflicted by the oil crises. Furthermore, the national gas pipeline project (the energy regime) had its implications as well as the earlier attempts and projects with other biofuels (the transportation regime) made in Sweden. These pressures, together with the local trigger event of bad air quality, opened up a window of opportunity for changes to occur locally. The biogas niche trajectory could develop as actors from different socio-technical regimes became enrolled and involved in the process: the wastewater treatment plant and agricultural sector found offsets for their by-products, while slaughterhouse waste became a resource provided by the food industry. Of course, the possibility of networking across regime borders stems from the fact that biogas (upgraded methane) is an energy source found as organic by-product in many different industrial processes. Still we believe it important, both for researchers and practitioners interested in socio-technical niche development, to look over the regime fences for possible exchanges as well as useful pressure mechanisms and offset markets.

The findings of this article furthermore suggest it reasonable for a slightly altered ”development pair”-concept to describe the development of biogas in Linköping. The co-operation between the municipally owned bus company customer on one side, and the municipally owned producer (TVAB) and the private actors they enroll to their network on the other, form the starting point for a niche trajectory. This cooperative pair-arrangement and their long-term collaboration form the basis of the development. It is important to stress that one observation alone is not enough to generalize any conclusions to be applicable also to other biogas cases in Sweden. Still, it is so that municipally owned companies run most biogas facilities and have the largest embodied competence on the subject in Sweden. We believe that it would be fruitful to conduct further research to seek out whether a local Swedish ”style” for technological niche development for biogas can be detected.

References

[1] Geels, F. W., Technological transitions as evolutionary reconfiguration processes: a multi-level perspective and a case-study, Research Policy 31, 2002, pp. 1257-1274.

[2] Geels, F. W. and R. P. J. M. Raven, Socio-cognitive evolution and co-evolution in competing technical trajectories: Biogas development in Denmark (1970-2002), International Journal of Sustainable Development and World Ecology 14, 2007, pp. 63-77.

[3] Hughes, T. P. Networks of power: electrification in Western society, 1880-1930. Johns Hopkins Univ.Pres, 1983.

[4] Kaijser, A. I fädrens spår: den svenska infrastrukturens historiska utveckling och framtida utmaningar, 1994.

[5] Fridlund, M. Den gemensamma utvecklingen: staten, storföretaget och samarbetet kring den svenska elkrafttekniken. B. Östlings bokförl. Symposion, 1999.

[6] MacKenzie, D. A. a. W., Judy. The social shaping of technology. 2. ed. Buckingham, Open University Press 1999.

[7] Ulmanen, J. H., Verbong, G.P.J., Raven, R.P.J.M., Biofuel developments in Sweden and the Netherlands: protection and socio-technical change in a long-term perspective, Renewable and Sustainable Energy Reviews 13(6-7), 2009, pp. 1406-1417.

[8] Fallde, M. Bakom drivmedelstanken: perspektiv på svenska biodrivmedelssatsningar, Univ., Institutionen för konstruktions-och produktionsteknik, Energisystem, 2007.

[9] Undén, P. BuSeNes Project, Biogas Businesses in Sweden and the Netherlands (BuSeNes) - Implications to Japanese gas supplier. Linköping, Linköping University, IEI, Division of Environmental Technology and Management, 2010, pp. 48-61.

[10] Jonasson, B. A. S. o. K. M. Variety Creation, Growth and Selection Dynamics in the Early Phases of a Technological Transition, The Development of Alternative Transport Fuels in Sweden 1974-2004. Göteborg, Chalmers university of Technology, Environmental systems analysis, 2005.

[11] Biogasföreningen, G. Biogas - Ett stort steg mot det hållbara samhället. Avfall Sverige, 2009.

Estimation of Renewable Energy Potential and Use- A Case Study of Hokkaido, Northern-Tohoku Area and Tokyo Metropolitan, Japan-

Tatsuya Wakeyama [1,*], Sachio Ehara [2]

[1] *Laboratory of Geothermics, Graduate School of Engineering, Kyushu University*
[2] *Laboratory of Geothermics, Faculty of Engineering, Kyushu University*
[*] *Corresponding author. Tel: +81 928023324, Fax: +81 928023324, E-mail: tatsuya-wakeyama@mine.kyushu-u.ac.jp*

Abstract: The present work is intended to evaluate renewable energy potential in Northern Japan area and Tokyo metropolis and to reveal possibility of supplying renewable energy from Northern Japan area to Tokyo metropolis. This evaluation method consists of three processes with GIS. The first process is simulation of the meteorological parameters such as river discharge and direct solar radiation. The second process is extraction of potential areas with restrictions such as meteorological conditions, geographical features and social environment. The third process is calculation of annual energy production. The application of the new method to Northern Japan area shows that the sum of renewable energy potential is 185,000 GWh/year, which contains 120,374 GWh/year of wind energy, 29,111 GWh/year of mini-micro hydropower, 986 GWh/year of solar power, 31,089 GWh/year of geothermal energy and 3,440 GWh/year of biomass energy. The geothermal and biomass energy potential were quoted from earlier study. The renewable energy potential in Northern Japan area is bigger than the 78,519 GWh/year of electricity demand in civilian sector in Tokyo. It is possible for the renewable energy potential in Northern Japan area to satisfy electricity demand not only in Northern Japan area but also in Tokyo metropolis.

Keywords: *Renewable Energy Potential Estimation, GIS, Wind Energy, Hydropower, Solar Energy*

Nomenclature

E_{pw} *Wind energy potential*..... $kWh \cdot year^{-1}$
V *Wind velocity*..... $m \cdot s^{-1}$
$f(V)$ *Weibull model*..... -
$P(V)$ *Power curve*..... kW
E_{ph} *Mini-micro hydropower potential* $kWh \cdot year^{-1}$
H *Height*..... m^{-1}
Q *River discharge*..... $kg \cdot s^{-1}$
μ_t *Waterwheel efficiency*..... -
μ_g *Generation efficiency* ..... -
E_{ps} *Solar energy potential* ..... kWh
N_h *Number of household*.....*family*
C_p *Capacity* ..... $kW \cdot family^{-1}$
S_e *System utilization*..... -

1. Introduction

The present work is intended to evaluate extensively renewable energy resources potential in Northern Japan area and Tokyo metropolis and to analyze locally renewable energy potential in Akita prefecture in order to reveal possibility of supplying renewable energy from Northern Japan area. In Japan, Tokyo metropolitan government and Northern Japan area, such as Aomori, Akita, Iwate, Yamagata and Hokkaido, have agreed on interregional cooperation for renewable energy use. The purpose of the agreement is to realize reducing CO_2 emission in Tokyo metropolis and revitalization of the rural economy and expansion of job opportunities by supplying renewable energy from the rural area to the huge city. There are differences of circumstance between rural areas that have a huge renewable energy potential and a big city that has huge energy demand behind.

In order to efficiently construct renewable energy facilities the systematic and accurate evaluation of renewable energy potential is important. Voivontas et al., for example, developed a decision support system by using GIS (Geographical Information System) for the evaluation of renewable energy sources potential and conducted financial analysis of

renewable energy investment in Crete, Greece [1]. The evaluation methods in earlier studies were designed locally for each specific area. In contrast, the authors intended to evaluate extensively renewable energy resources potential and to prove features in each area by comparison of evaluation results. Therefore the authors developed a new evaluation method by using GIS and publicly available digital spatial data in Japan [2].

2. Methodology

2.1. Study area

The study was carried out for Northern Japan area which includes Hokkaido and Tohoku area (Aomori, Akita, Iwate and Yamagata prefectures) and Tokyo metropolis in Japan. Fig. 1 shows that Hokkaido and Tohoku area lies in the northern part of Japan.

Fig. 1 Study area: Hokkaido, Tohoku area and Tokyo metropolis.

2.2. Software and data source

In the present work we used GRASS ver.5.3 and 6.2 as GIS software [3]. We also used GIS data from the database published by the Ministry of Land, Infrastructure, Transport and Tourism in Japan [4].We used 50 m grid elevation data, 1 km grid annual rainfall data, 100 m grid natural park data, 1 km grid number of family data, 100 m grid land use data and road vector data from the database.

2.3. Concept of estimation

In the renewable energy potential evaluation, we evaluate two kinds of potentials: “theoretical potential” and “practical potential.” A theoretical potential is an amount that all energy potential theoretically exist, for example, all solar energy and wind power. A practical potential is an amount that potential is evaluated with restrictions such as climate conditions, geographical features and social environment. In the present work we evaluate the practical potential with a common small number of restrictions to prove features in each area.

2.4. Procedure

This new evaluation method consists of three processes. The first process is simulation of the meteorological parameters such as river discharge and direct solar radiation. The second process is extraction of potential areas with restrictions such as meteorological conditions, geographical features and social environment. The third process is calculation of annual energy production. In this process we develop a s cenario for calculation of the power generation facility, annual energy production and number of introducing facilities.

2.4.1. Wind energy

First, wind property was quoted from the 500 m grid simulation result by NEDO [5]. Second, potential areas for wind energy were extracted under the consideration of the following restrictions;

- A minimum allowable wind speed of 5 m/s (in altitude of 30m) ;
- A maximum distance from roads of 200 m;
- A maximum slope from the level of 20 degrees;
- A maximum elevation of 1000 m.

The following areas were not considered for the installation of wind turbine;

- Construction areas for houses;
- Natural parks and national parks.

Third, in order to calculate electrical output of wind power generation, we developed a scenario that wind electrical output was calculated with power curve. The power curve is in proportion to the cubic of wind velocity and approaches 1000kW with 13m/s of wind velocity. Additionally, wind speed distributions were assumed as the Weibull model for calculation of annual energy production [5]. The number of introducing wind turbines was calculated on condition that wind turbines are set at 700 m interval in a potential area. The calculation for wind energy potential is described in Eq. (1). Wind energy potentials tend to be estimated bigger where extracted potential area is larger with this evaluation method.

$$E_{pw} = \sum \left(f(V) \times p(V) \right) \times 8760 \qquad (1)$$

where E_{pw} is the wind energy potential, V is the wind velocity, $f(V)$ is weibull model, $P(V)$ is power curve and 8760 is hours in a year.

2.4.2. Mini-micro hydropower

First, the river discharge was simulated from elevation and amount of an annual rainfall data with GRASS r.watershed module [3]. Second, potential areas for mini-micro hydropower were extracted under the consideration of the restriction that a minimum allowable river discharge is 0.01 m^3/s. Third, in order to calculate electrical output of mini-micro hydro electric generation, we developed a scenario that facilities is small scale hydropower: conduit type and afflux type power generation. This evaluation also assumed that hydro electric generators were set at 50m interval in each river in the target area and that the heights of facilities were calculated from maximum slope data and 50 m grid digital elevation model data. Additionally, we assumed that outflow rate of water from rainfall to river discharge is 30 % and that utilization ratio of river discharge is 20 % for calculation of annual energy production. The calculation for mini-micro hydropower potential is described in Eq. (2). Mini-micro hydropower potentials tend to be estimated bigger where output per unit is huge with this evaluation method.

$$E_{ph} = 9.8 \times H \times Q \times 0.20 \times \mu_t \times \mu_g \times 8760 \div 1000 \qquad (2)$$

where E_{ph} is the mini-micro hydropower potential, 9.8 is the gravity acceleration, H is height, Q is river discharge and 0.20 is utilization ratio of river discharge μ_t is waterwheel efficiency, μ_g is generation efficiency, 8760 is hours in a year and 1000 is unit conversion from W to kW.

2.4.3. Solar enegy

First, the direct solar radiation was simulated from elevation data with GRASS r.sun module [3]. Second, potential areas for solar energy were extracted under the restriction that a minimum allowable direct solar radiation is 0.1 kWh/m^2 a day. This restriction extracts almost all inhabitable areas as potential areas. Third, in order to calculate photovoltaic output, we developed a scenario that we introduce 1 kW photovoltaic cell to each household. Additionally, we assumed that PV system utilization is 12 % for calculation of annual energy production. The number of introducing photovoltaic cell was calculated with number of household in each 1 km grid. The calculation for solar energy potential is described in Eq. (3). Solar power potentials tend to be estimated bigger where population is huge with this evaluation method.

$$E_{ps} = N_h \times C_p \times S_e \times 8760 \quad (3)$$

where E_{ps} is the solar energy potential, N_h is Number of household, C_p is capacity, S_e is System utilization and 8760 is hours in a year.

3. Potential evaluation result

The results of renewable energy potential evaluation in Northern Japan area and Tokyo are summarized in Figs. 2 -4. These figures summarize each potential by each municipality and the municipalities in darker color have huge renewable energy potential.

3.1. Wind energy potential evaluation

Fig. 2 shows that each prefecture has several municipalities with huge wind power potential, which are over 1000 GWh/year, in Northern Japan area. These municipalities with huge wind potential mainly locate along the coastline and the mountains. In Tokyo metropolis, a few municipalities have wind energy potential, which are smaller than 30 G Wh/year. Municipalities with large wind energy potential locate along the coastline in Tokyo.

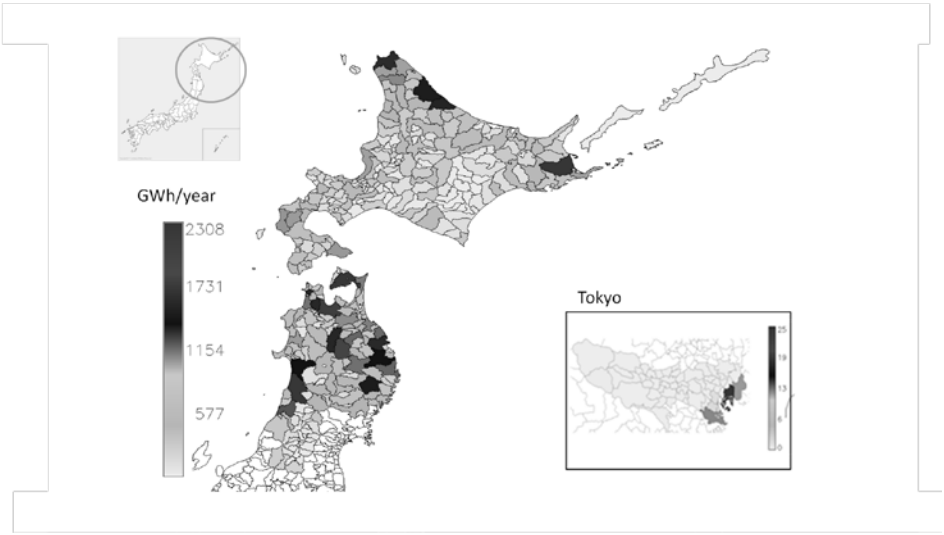

Fig. 2 Evaluation result of wind energy potential in Northern Japan area and Tokyo metropolis.

3.2. Mini-micro hydropower potential evaluation

Fig. 3 shows that a few municipalities with huge mini-micro hydropower potential locate in Hokkaido and Yamagata, which are over 800 GWh/year. Fig. 3 also indicates that many prefectures have large hydropower potentials, which are over 200 G Wh/year. These municipalities with large hydropower potential tend to be along the steep river with large river discharge and to have upper reach of a river. In Tokyo metropolis, municipalities with large mini-micro hydropower potential locate in western part of Tokyo. These municipalities have upper reach of a river and have mini-micro hydropower potential, which are around 100 GWh/year.

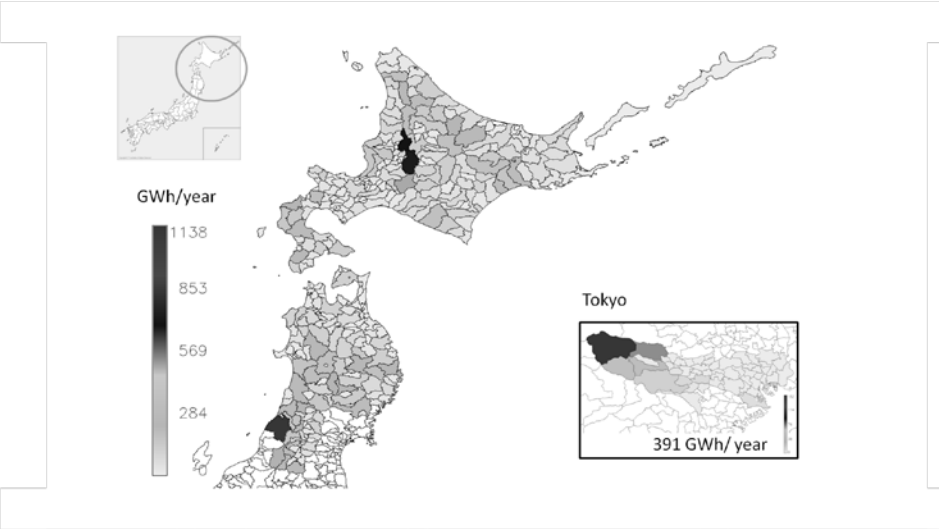

Fig. 3 Evaluation result of mini-micro hydropower potential in Northern Japan area and Tokyo metropolis.

3.3. Solar energy potential evaluation

Fig. 4 shows that a few municipalities with huge solar energy potential exist in Northern Japan areas, which are between 50 GWh/year and 120 GWh/year. These municipalities with large solar potential mainly locate along the coastline. In Tokyo metropolis, many municipalities have large solar energy potentials, which are over 50 GWh. Municipalities with large solar energy potentials locate in center area of Tokyo where populations are huge.

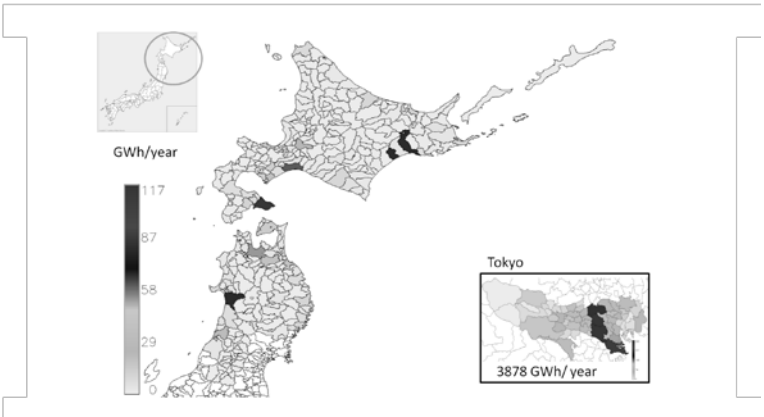

Fig. 4 Evaluation result of solar energy potential in Northern Japan area and Tokyo metropolis.

3.4. The sum of renewable energy potential

Table 1 shows the sums of wind, solar and hydropower potential with geothermal and biomass energy potential in Northern Japan area and Tokyo metropolis. The geothermal potential is quoted from Geothermal Potential Map in Japan [6]. The biomass potential is quoted from Biomass GIS Database [7]. The sum of renewable energy potential in Northern Japan area is 185,000 GWh/year, which contains 120,374 GWh/year of wind energy, 29,111 GWh/year of mini-micro hydropower, 986 G Wh/year of solar power, 31,089 GWh/year of geothermal energy and 3,440 GWh/year of biomass energy. The sum of renewable energy potential in Tokyo metropolis is 8,168 G Wh/year, which contains 52 G Wh/year of wind energy, 391 GWh/year of mini-micro hydropower, 3,878 GWh/year of solar energy, 675 GWh/year of geothermal energy and 3,173 GWh/year of biomass energy. On the other hand, Tokyo metropolis needs 78,519 G Wh/year of electricity demand in civilian sector [8]. The electricity demand of 78,519 GWh/year in Tokyo is almost equivalent to ten times of 8,168 GWh/year of the renewable energy potential. It is difficult to satisfy the electricity demand in Tokyo with renewable energy potential in Tokyo. However, the renewable energy potential of 185,000 GWh/year in Northern Japan area is enough to cover the electricity demand in civilian sector in Tokyo. It is important for Tokyo metropolis to make the most use of renewable energy potential in Northern Japan area in order to promote renewable energy use.

Table 1 Renewable energy potential evaluation result in Northern Japan area and Tokyo.

(GWh/year)	Hokkaido	Aomori	Iwate	Akita	Yamagata	Tokyo
Wind	56608	21589	23315	13752	5111	52
Mini-micro hydropower	13458	1778	5223	3398	5254	391
Solar	598	178	53	120	37	3878
Geothermal	20052	2330	3618	3005	2085	675
Biomass	1510	491	532	506	401	3173
Sum	92226	26366	32740	20780	12888	8168

3.5. Discussion on extensive renewable energy potential evaluation

The evaluation results show that extensive renewable energy practical potential evaluation with a common small number of restrictions proves features of each area and that renewable energy potential in Northern Japan area is important resource not only for Northern Japan area but also Tokyo metropolis. However, these evaluation results are not efficient to plan the specific project, because the evaluation method evaluates only one aspect of the renewable energy potential. Therefore, the authors conducted more detailed potential analysis for use in Akita prefecture in order to analyze features of the evaluated potential.

4. Wind energy potential analysis for use

4.1. Study area

The extensive renewable energy evaluation result showed that there is huge wind energy potential in Northern Japan area and that the wind energy potential in Akita prefecture is one of most important renewable energy potential in Table 1. Therefore, we analyzed locally wind energy potential with potential classification in Akita prefecture. The study area is Akita prefecture in Northern Japan area in Fig. 1.

4.2. Classification methodology of wind energy potential

We classified wind energy potential in order to analyze how to make use of wind energy potential. In this study, we classified wind energy potential with mean annual wind speed of over 6.0 m /s in altitude of 70m. The criteria for classification were decided based on feasibility of introducing wind energy facilities. In order to analyze feasibility of introducing wind energy facilities, the study area is divided into 10km square grids. We compared properties of grids that have installed wind energy facilities with the other grids. We focused attention on pr operties of average elevation and average slope. The areas with higher elevation or slope value are concerned about the possibility of increasing construction costs.
Fig. 5 shows comparison of properties in grids with wind energy facilities between in grids with no wind energy facilities. Fig. 5 (a) is a comparison of average elevation and Fig. 5 (b) is a comparison of average slope in each grid. Fig. 5 (a) indicates that the grids with installed wind energy facilities have average elevation of lower than 500m. The relationship is consistent with tendency of lower elevation to be encouraged in planning introducing wind energy facilities. Figure 5 (b) indicates that the grids with installed wind energy facilities have average slope of lower than 15 degrees. The relationship is also consistent with tendency of lower slope to be encouraged in planning introducing wind energy facilities. Therefore, the areas with following properties are seen as a strong possibility of introducing wind energy facilities.

- Average elevation is lower than 500 m in the grid.
- Average slope is lower than 15 degrees in the grid.

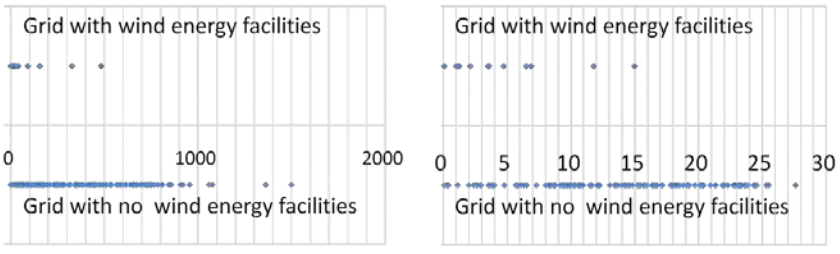

(a) Relationship between average elevation and installed wind energy facilities.

(b) Relationship between average slope and installed wind energy facilities.

Fig. 5 Comparison of properties in grids with wind energy facilities between in grids with no wind energy facilities.

4.3. Classification result of wind energy potential

Fig. 6 shows classification result of wind energy potential in Akita prefecture. Fig. 6 (a) shows the potential classified according to average elevation and average slope in Akita prefecture. Fig. 6 (a) shows the potential is 15,028 GWh/year with a minimum allowable mean annual wind speed of 6.0 m/s in altitude of 70m in Akita prefecture. The wind energy potential of 15,028 GWh/year includes potential of 11,090 GWh/year with average elevation of lower than 500m and average slope of lower than 15 degrees in each grid. On the other hand, the wind energy potential of 15,028 GWh/year also includes potential of 1,069 GWh/year with average elevation of higher than 500m and average slope of higher than 15 degrees in each grid. Fig. 6 (b) shows that the distribution of classification results in Akita prefecture. In Fig. 6 (b) darker gray shows hopeful grid. The hopeful grids colored with darker gray exist in several parts of Yamamoto area, Akita area, Yurihonjo area and Kazuno area, which are with lower elevation and slope. In fact, a portion of the wind energy potential is used there. In addition the grids with light gray exist around Kazuno area. The southern part

of Kazuno has potential with lower elevation and higher slope. On the other hand the northern part of Kazuno has potential with higher elevation and lower slope.

5. Conclusion

The sum of renewable energy potential in Northern Japan area is 185,000 GWh/year, which contains 120,374 GWh/year of wind energy, 29,111 GWh/year of mini-micro hydropower, 986 GWh/year of solar power, 31,089 GWh/year of geothermal energy and 3,440 GWh/year of biomass energy. Tokyo has 78,519 GWh/year of electricity demand, whereas only 8,168 GWh/year of total renewable energy potential. The renewable energy potential of 185,000 GWh/year in Northern Japan area is enough to cover the electricity demand in civilian sector in Tokyo. In Akita prefecture, wind energy potential of 11,090 GWh/year is with mean annual wind speed of over 6.0, with average elevation of lower than 500m and average slope of lower than 15 degrees in each grid. The hopeful wind energy potential exists in several parts of Yamamoto area, Akita area, Yurihonjo area and Kazuno area. It is possible for making use of the huge wind energy potential extensively there.

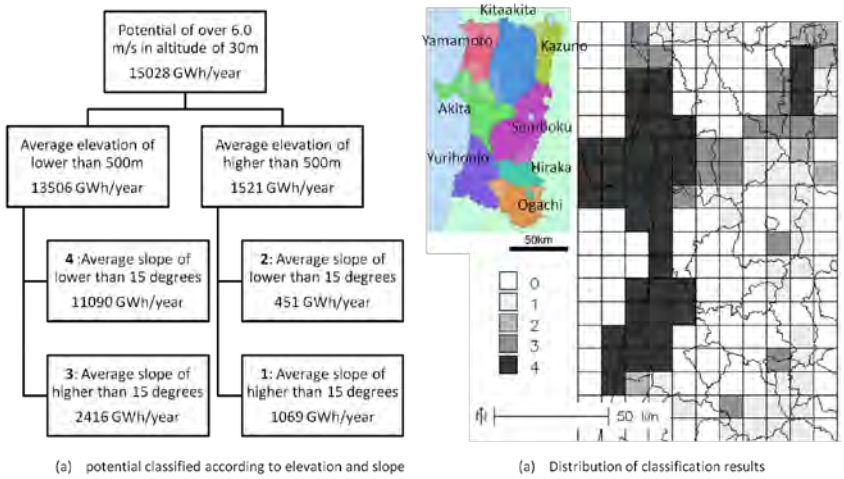

Fig. 6 Classification result of wind energy potential in Akita prefecture.

References

[1] D. Voivontas, D. Assimacopoulos, A. Mourelatos, J. Corominas, Evaluation of renewable energy potential using a GIS decision support system, Renewable Energy, 13, 1998, pp.333-344.

[2] T. Wakeyama, S. Ehara, Assessment of renewable energy by using GIS― A case study of Unzen city ―, Journal of the Japan. Institute of Energy, 88, 2009, pp.58-69.

[3] Grass development team, Welcome to GRASS GIS, 2010, http://grass.itc.it/

[4] Ministry of Land, Infrastructure, Transport and Tourism in Japan (MLIT), Digital national land information, 2010.

[5] New Energy and Industrial Technology Development Organization (NEDO), Local Area Wind Energy Prediction System, NEDO, 2006.

[6] Geological Survey of Japan, AIST, Geothermal Potential Map in Japan, AIST, 2009

[7] New Energy and Industrial Technology Development Organization (NEDO), Biomass GIS Database, NEDO, 2010

[8] H. Kurasaka, Sustinable Zone 2008, Research Center on Public Affairs, 2009

Evaluating the greenhouse gas impact from biomass gasification systems in industrial clusters – methodology and examples

Kristina M. Holmgren[1, 2,*], Thore Berntsson[1], Eva Andersson[3], Tomas Rydberg[2]

[1] *Chalmers University of Technology, Inst of Energy and Environment dep. of Heat and Power Technology, Gothenburg, Sweden*
[2] *IVL Swedish Environmental Research Institute Ltd, Gothenburg, Sweden*
[3]*CIT Industriell Energi, Gothenburg, Sweden*
** Corresponding author. Tel: +46 31772 85 37, E-mail: kristina.holmgren@chalmers.se*

Abstract Biomass gasification is identified as one of the key technologies for producing biofuels for the transport sector and can also produce many other types of products. Biomass gasification systems are large-scale industrial systems and it is important to evaluate such systems from economic, environmental and synergetic perspectives before implementation. The objective of this study is to define a methodology for evaluating the greenhouse gas (GHG) impact of different biomass gasification systems and to exemplify the methodology. The ultimate purpose of the methodology is to evaluate the GHG performance of different biomass gasification systems integrated in industrial clusters. A life cycle perspective is applied.
Most biomass gasification systems are multiproduct systems, simultaneously producing biofuels, heat at different temperatures and pressures and electricity. The value, in economic terms and in terms of GHG emissions, is well defined for some products (e.g. biofuels), whereas for other products (such as heat and electricity) it is more uncertain and in some cases dependent on time and location.

Keywords: *Greenhouse gas impact assessment, Biomass gasification, System analysis*

List of abbreviations

DH	*district heating*	*MTO*	*methanol to olefins*
FT	*Fischer-Tropsch*	*PE*	*polyethylene*
GHG	*greenhouse gas*	*PP*	*polypropylene*
GWP	*Global Warming Potential*	*SNG*	*Synthetic natural gas*

1 Introduction/background

Biomass gasification is seen as an important technology for the future production of biofuels. This paper is part of the project "***Advantages of regional industrial cluster formations for the integration of biomass gasification systems***" which aims to evaluate the economic performance and greenhouse gas (GHG) impact of different biomass gasification systems. The study is performed as a case study in south-west Sweden, focusing on the technical systems and opportunities for integration with existing industries and infrastructure. This paper discusses the methodology for evaluating the GHG performance of the different gasification systems from a life cycle perspective.

Life cycle assessments of bioenergy systems available in literature were analysed by [1] concluding that the use of different input data, functional units, allocation methods, reference systems etc. contributes to a wide range of results for similar systems and complicates the comparison between studies. Wetterlund et al. [2] show the effects of applying system expansion in the well-to-wheel CO_2 evaluation of biofuels. Our approach is similar to the one taken by [2], but we apply it to systems with a wider range of products and include non-CO_2 GHG emissions from all parts of the chain, and soil emissions from biomass production. We also describe how products with a longer lifetime can be handled in the evaluation.

2 Objective

This paper outlines and exemplifies a methodology for evaluating the GHG impact of biomass gasification systems integrated with other industries and infrastructure. The methodology is suitable for comparing alternative configurations and could also be applied to other bioenergy systems. The outlined methodology has a life cycle perspective, addressing the potential climate impact in terms of GWP (global warming potential)-summarised emissions. The methodology does not predict absolute environmental impacts.

3 The scope of the evaluation

Depending on scope, a GHG evaluation could answer different questions. The methodology of this paper includes two different aspects:

i) How much do the biomass-based systems reduce emissions compared to the conventional (often fossil-based) systems?

ii) In which applications does the biomass-utilisation result in the largest emission reductions?

We take a consequential approach and marginal data should therefore be used [3] for the assessment, since possible changes in the production could affect the directly or indirectly related marginal suppliers and competing products. Further, we include global emissions of carbon dioxide, methane and nitrous oxide, using GWP factors 1, 25, and 298 respectively based on [4]. *Fig. 1* shows the two systems to be compared in order to answer the first question above. Comparing several biomass-based systems to their reference (as in Fig. 1) can help answering the second question.

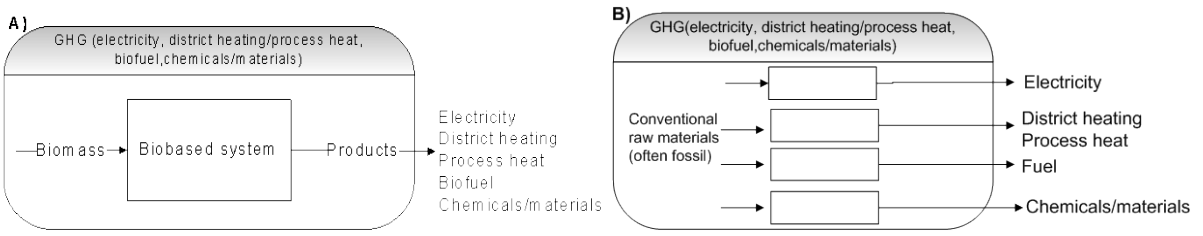

Fig. 1. Comparison between reference system (B) and biomass based system (A). The same amount of each product is produced in each system.

4 Methodological aspects

In this section we describe how important factors in the GHG evaluation process of the biomass gasification system should be treated, including; system boundaries, reference system and life cycle data from other studies. In the next section we exemplify our methodology.

4.1 System boundaries

Fig. 2 is a schematic view of the conceptual system and system boundaries of the biomass gasification system integrated with industry evaluated in this study. The geographical boundaries for the different parts of the system and the chosen time perspective should be taken into consideration [5]. The geographical boundaries could limit raw material supply, infrastructure for the transport and delivery of products and could also define the framework for the choices of reference systems. The time perspective can help to define the appropriate reference systems by giving a context for technology development. Even though focus is on the conversion system it is important to include both downstream and upstream systems.

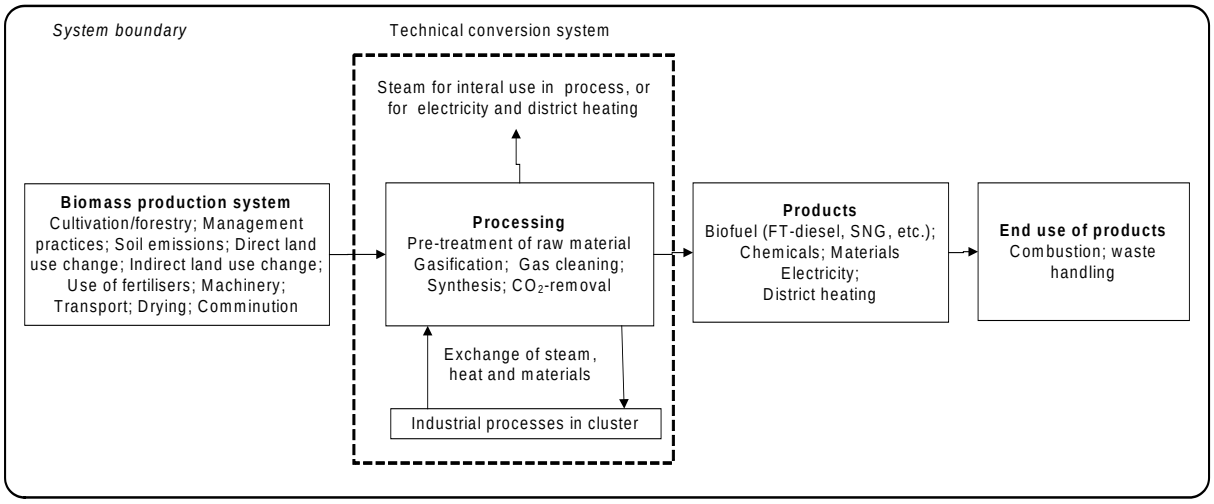

Fig. 2. Schematic view of conceptual system and system boundaries of the biomass gasification system evaluated in this study.

4.2 Functional unit

The functional unit is g $CO_{2eq.}MJ^{-1}$ biomass input. This unit was chosen since the evaluation focuses on the technical conversion system and the amount of input biomass is the same in all systems. For further discussion on the choice of functional unit, see [1,2].

4.3 Reference system

The reference system, *Fig. 1*B, is the conventional system to which the proposed biomass-based system, *Fig. 1*A, is compared. In the case of the biomass gasification system (and other multiproduct systems) the reference is not one single system but rather separate systems for each product. In most cases the reference is fossil fuel-based, but not necessarily. For future systems, such as in this study where different configurations of new installations are investigated, the definition of the reference system requires significant analysis.

4.3.1 Electricity

The reference for electricity should be the future marginal production technology determined by build margin [2]. Energy market scenarios with consistent assumptions for future prices and technologies could be used for determining the likely marginal production technology. Axelsson et al, [6], have developed a tool (ENPAC) for generating consistent energy market scenarios. The inputs to the tool are fossil fuel prices, levels of policy instruments (CO_2-charge, green electricity certificates) and available technologies and technology developments for electricity production. The output is scenarios that include future fuel prices, energy carrier prices and associated CO_2 emissions. The electricity price includes the cost for building new capacity and hence the marginal electricity production from the tool is the future build margin. This tool can be used in order to determine the appropriate marginal technologies for electricity production.

4.3.2 Heat

Prices from the ENPAC tool together with knowledge of local conditions for DH can be used to determine the appropriate reference for heat delivery. Infrastructure and possibilities for expansion are crucial for the performance (environmental and economic) of a bioenergy system with potentially large DH delivery [7]. Excess heat from a new biomass gasification unit running 8000 hours per year will constitute a base load to the DH system and the corresponding production technology for this load should be used as reference. The excess

heat from a gasification unit can even result in significant reductions in emissions when it replaces biomass-based DH, since the excess heat will save biomass that can be used elsewhere. Excess heat can also be delivered to an adjacent industry, whereby emission reductions then correspond to fuel or other resource savings.

4.3.3 Biomass

GHG emissions from the biomass production system could constitute a significant part of the overall emissions from the bioenergy system [8,9] and should take all sources into account, including soil carbon losses due to management and land use change. Biomass gasification generally requires significant pre-treatment of the biomass and all these treatments should be included irrespective of where they are performed. Since the amount of biomass available for energy purposes is, and will continue to be, limited it is important to include an alternative use of the biomass in the reference system [10,2]. In a European perspective the marginal biomass user is identified as coal power plants with co-combustion possibilities or possibly (if strong policy instruments are applied) biofuel producers [6]. Other marginal users, such as biomass combined heat and power plants could also be feasible under certain circumstances.

4.3.4 Biofuels

The reference for biofuels could be conventional fuels: diesel, petrol or a combination of the two. These are appropriate references even for future scenarios with a time frame of 10-20 years, since it is likely that these fuels will constitute a significant part of the use even in the coming decades. In *Table 2* the chosen reference for biofuels used in this study is presented.

4.3.5 Materials and chemicals

Biosyngas can also be used for the production of chemicals and materials. The reference for these products should be similar products produced by the conventional route. The end use could be complex since there might be several uses of the product although it will be similar to the conventional product. In our approach we take into consideration the incineration at the end of life and that some products act as carbon storages due to long lifetime by applying the method outlined in [11,12]. The latter point means that we apply a factor that reduces the GWP-value. The reduction of the GWP-value will be larger the longer the lifetime of the product. In the calculations we have used the simplified approach as suggested by [11].

4.4 Life cycle data from other studies

Our focus is on the technical conversion system (biomass gasification) and emission and energy consumption data for the other parts of the system and reference flows are taken from literature. However, these life cycle data need to be recalculated to ensure that assumptions are consistent for co-product allocation, marginal production of electricity etc.

5 Examples

In order to exemplify our methodology we show GHG emission reduction potential for three different types of biomass conversion systems; one biomass gasification unit producing FT-products [13], one biomass gasification unit producing bio-SNG (synthetic natural gas) [14] and one biomass gasification unit producing methanol [7] with a down-stream MTO-process (methanol to olefin) producing PE (polyethylene) and PP (polypropylene) [15]. The input and output to the installations are given in *Table 1* and the GHG emission reductions for different cases of assumptions for reference streams are shown in *Fig. 3*.The different cases are explained in *Table 2*. The plants have been scaled so as to have the same biomass input. In all cases, the input is wet (50 % wt.) forest residues that are dried using excess heat from the

conversion process. Emission factors for the different fuels and materials are taken from literature [16-23]. The assumed annual operation time is 8000 hours for all plants.

Table 1. Capacity data for example installations.

Conversion	**Input (MW)**		**Output (MW)**			
Plant	Biomass	Electricity	FT-products	SNG	PE/PP (kton yr^{-1})	Heat[a]
FT	371	9.8	167			50
SNG	371	-15.3		265		89
MeOH/PE& PP	371	37			32.1/15.7	134

[a] In the base case the maximum amount of deliverable DH is 300 GWh yr^{-1} for all biorefineries. In the case of heat delivery to industrial process the delivered amount is 711 GWh

6 Results

The results (*Fig. 3*) show that there is a significant difference between total impacts depending on assumptions made for the reference streams. Only one reference use of electricity is displayed but it constitutes a significant part of all chains. Also the GHG savings due to DH delivery constitute a significant part of the savings in most cases. Hence, it is important to make calculations for scenarios using different possible references for these flows

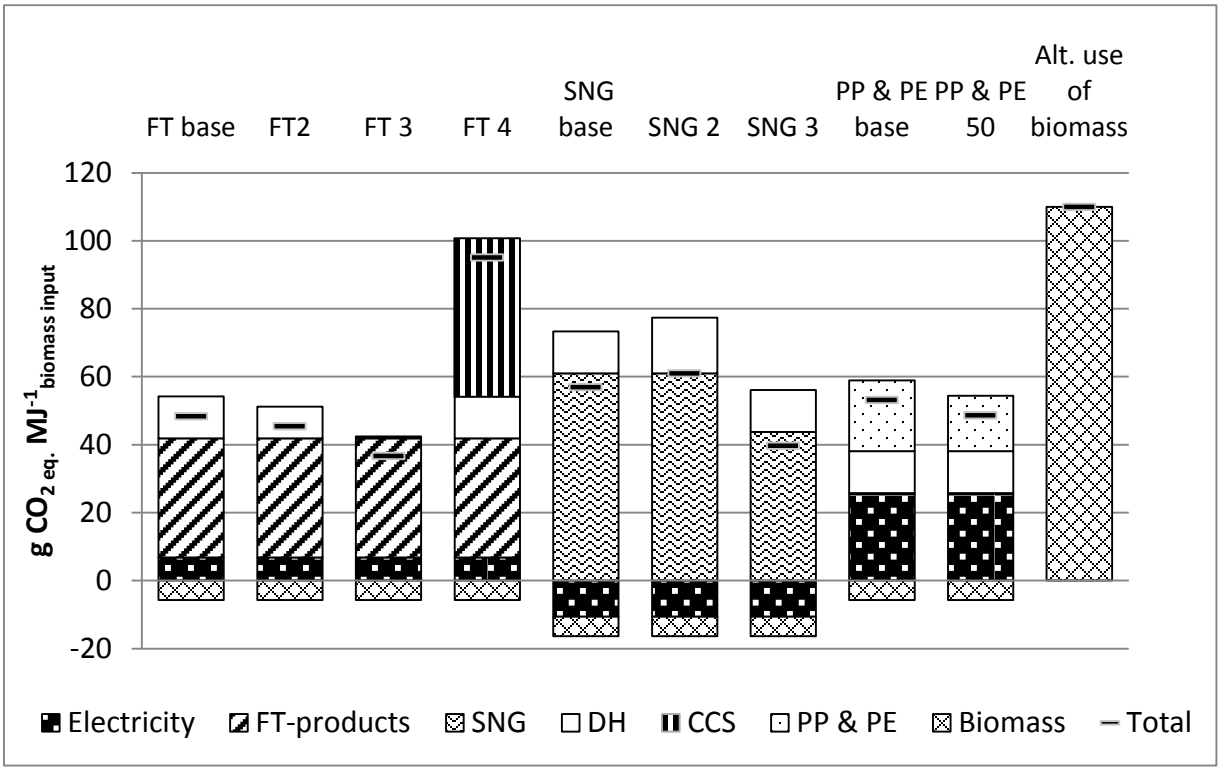

Fig. 3. GHG emissions savings for different reference systems for the different conversion systems. Positive values mean net savings of emissions compared to reference system. Alternative use of biomass is co-combustion in coal power plant.

In FT 3 we show the effect of not taking into consideration that biomass is a limited resource and thereby could save emissions by being used elsewhere. In FT 3 the emissions savings due to the DH delivery is reduced to the savings of not producing and utilising the biomass. The chosen reference systems of other products are of some importance e.g. case SNG 3, where the bio-SNG replaces natural gas in industry instead of petrol in cars. Case FT 4 shows that CCS at the biomass conversion plants is of significant importance. Our results also show that

the conversion to plastics results in significant savings compared to the fossil route. The significant electricity production in the methanol plant is an important part of the savings in these cases and in addition the electricity production possible from the end use of the materials (incineration) is also an important part of the total savings from the material part. The delay of emissions due to the lifetime of products had little impact, mainly since the delay will also occur in the reference system and the crediting for the electricity produced at incineration is delayed. Further, all of the gasification systems showed lower potential for GHG reduction than using the biomass for co-combustion in a coal power plant. This means that even though the biomass gasification systems result in net savings compared to the fossil systems, they are not optimal solutions for GHG mitigation when biomass is a limited resource.

Table 2. Assumptions for the different cases presented in Fig. 3.

Case	Assumptions
FT, SNG and PE & PP base	Reference electricity is produced in coal power plant. SNG replaces petrol in private cars. 85% of FT-products replace diesel in heavy duty vehicles and 15% replace petrol in private cars (based on [13]). Bio-based PE and PP replace fossil PE and PP based on naphtha, the end use is assumed to be short lived products (< 1 yr.). DH replaces biomass boiler; 300 GWh heat can be delivered from each of the plants. The delivery of DH leads to a reduction in biomass demand corresponding to the amount needed in the biomass boiler, which instead can be used in coal power plant.
FT 2, SNG 2	DH replacing natural gas boiler in industry. Greater amount of DH can be delivered due to higher number of operational hours in industry.
SNG 3	SNG replaces natural gas in industry
FT 3	Biomass resource is not considered limited. The reduction in biomass utilisation due to DH delivery does not lead to increased use in coal power plant.
FT 4	CCS is applied. 50% of coal in biomass could be stored away (based on [24])[a] .
PE & PP 50	The lifetime of the end products is assumed to be 50 years, and the carbon storage in products is taken into account according to method by [11,12]
Alt. use of biomass	Alternative use of biomass. Includes emissions from the life cycle of biomass and reductions from the saving of coal utilisation in co-combusted power plant.

[a] Assumption on electricity consumption for capture, separation and storage is based on [25].

7 Discussion

Few studies include a reference use of the biomass [2, 26] but our examples show that the biomass reference impacts results significantly. It is important to include either a reference use of the biomass or a reference land use [1]. Even though our results show that using biomass for co-combustion in coal power plants has higher potential of reducing GHG emissions, there are several reasons to further investigate the gasification systems. Transportation biofuels constitute an alternative to the limited fossil sources, and are thereby not only a solution to GHG mitigation. Further, conversion and efficiency data for our examples were taken from literature. However, the availability of data on optimized and integrated processes is limited and needs further investigation. For example, SNG processes with reduced or no electricity demand do exist at smaller scale and FT-processes have good possibilities for carbon capture. According to our results, such systems show GHG emission reductions comparable to the savings in a co-combustion plant. Knowledge of the methanol production plant with the downstream MTO process is very limited and needs to be investigated further. Our results show that reference electricity and DH production are important parameters for sensitivity analysis. A scenario approach using the tool from [6]

could be used for this. The LCAs of other reference products should also be adapted to the assumptions of the scenarios.

A LCA for a biorefinery concept, producing chemicals, based on switchgrass showed that the biomass production chain had a significant impact on the overall result [27]. However, in our case, using forest residues, both land use emissions and fertilisers are of little importance and hence the biomass production chain constitutes only a small part of total emissions. Since gasification units might use different biomass feedstock it is important to state which biomass has been used for a specific GHG evaluation.

8 Future work

Biomass gasification systems should be studied in more detail. Increased integration and optimal solutions could possibly increase emissions savings to levels comparable to those of using the biomass for coal co-combustion in power plants.

Acknowledgments

The research has been supported by Göteborg Energi, E.ON Gasification Development AB, Preem AB, Perstorp Oxo AB, Formas, the Swedish Environmental Protection Agency and the Swedish Energy Agency, which are gratefully acknowledged.

References

[1] Cherubini, F., Strømman, A.H. 2011. Life cycle assessment of bioenergy systems: State of the art and future challenges. Bioresource Technology, vol. 102, pp 437-451.

[2] Wetterlund, E., Pettersson, K. & Magnusson M. 2010. Implications of system expansion for the assessment of well to wheel CO_2 emissions from biomass-based transportation. International Journal of Energy Research, vol. 34 pp. 1136-1154.

[3] ISO 14044:2006 Environmental management – Life cycle assessment – Requirements and guidelines.

[4] IPCC (2007) Climate change 2007: The physical science basis. Contribution of working group 1 to the fourth assessment report of the International Panel on Climate Change. Cambridge University Press, Cambridge, UK

[5] ISO 14040:2006 Environmental management – Life cycle assessment – Principles and Framework.

[6] Axelsson, E., Harvey, S., Berntsson T. 2009. A tool for creating energy market scenarios for evaluation of investments in energy intensive industry. Energy, 34, pp. 2069-2074.

[7] Ericson K. & Börjesson, P. 2008. Potential utilization of biomass in production of electricity, heat and transportation fuels including energy combines –Regional analyses and examples. Lund University. Report no 64. (In Swedish; English summary).

[8] Zah, R., Böni, H., Gauch, M., Hischier, R., Lehmann, M., Wäger, P. 2007. Life Cycle Assessment of energy products. Environmental assessment of biofuels. Executive summary. EMPA – Technology and Society Lab. Switzerland.

[9] UNEP 2009. Towards sustainable production and use of resources: Assessing biofuels.

[10] Cherubini, F., Bird, N.D., Cowie, A., Jungmeier, G., Schlamadinger, B., Woess-Gallasch, S. 2009. Energy and greenhouse gas based LCA of biofuels and bioenergy systems: Key issues, ranges & recommendations. Resources, Conservation and Recycling, 53, 434-447.

[11] Clift, R. & Brandao, M 2008. Carbon storage and timing of emissions. Briefing Note dated 20th October 2008. Centre for Environmental Strategy, University of Surrey.

[12] PAS 2050:2008. Specification for the assessment of the life cycle greenhouse gas emissions of goods and services. BSI October 2008. ISBN 978 0 580 50978 0.

[13] Axelsson E., Overland, C., Nilsson, K. & Sandoff, A. 2008. Bioenergikombinat i fjärrvärmesystem. Svensk Fjärrvärme Rapport 2009:11. (In Swedish).

[14] Börjesson, M., & Ahlgren E.O. 2010. Biomass gasification in cost-optimized district heating systems – A regional modeling analysis. Energy Policy vol. 38 pp. 168-180.

[15] Nouri, S., Kaggerud, K. 2006. Waste-to-plastics: process alternatives. Chalmers University of Technology, Gothenburg, Sweden. CPM-report 2006:10.

[16] Edwards, R., Larivé, J-F. Mahieu, V. & Rouveirolles, P. 2007. Well-to-wheel analysis of future automotive fuels and powertrains in the European context. Well-to-wheels Report. Version 2c, March 2007. Available at http://ies.jrc.ec.europa.eu/WTW

[17] Uppenberg, S., Almemark, M., Brandel., M., Lindfors, L.-G.; Marcus, H.-O., Stripple, H., Wachtmeister, A. Zetterberg, L. 2001. Miljöfaktabok för bränslen. Bakgrundsinformation och Teknisk bilaga. IVL report B1334B-2, Stockholm, Sweden. (In Swedish).

[18] Gode, J., Martinsson F., Hagberg, L., Öman, A. & Höglund, J. Miljöfaktaboken 2010 Emission factors for fuels, electricity, heat and transport in Sweden. Värmeforsk; Sweden. (In prep.)

[19] Lindholm, E.-L., Berg, S., Hansson, P.A. 2010. Energy efficiency and the environmental impact of harvesting stumps and logging residues. Eur J For Res vol. 129, pp. 1223-1235.

[20] Liptow C., Tillman, A.-M., 2009. Comparative life cycle assessment of polyethylene based on sugar cane and crude oil. Chalmers University of technology, Dep. of Energy and Environment, div. of Environmental Systems Analysis. Report no 2009:14

[21] Kirkinen, J., Palosuo, T., Holmgren, K., & Savolainen, I. 2008. Greenhouse impact due to the use of combustible fuels: life cycle viewpoint and relative radiative forcing commitment. Environmental Management vol. 42, pp. 458-469.

[22] Lindholm, E.-L., 2010. Energy use and environmental impact of roundwood and forest fuel production in Sweden. Doctoral Thesis. Swedish University of Agricultural Sciences.

[23] Harding, K.G., Dennis, J.S., von Blottnitz, H. & Harrison, S.T.L. 2007. Environmental analysis of plastic production processes: Comparing petroleum-based polypropylene and polyethylene with biologically-based poly-β-hydroxybutric acid using life cycle analysis. Journal of Biotechnology vol. 130, pp. 57-66.

[24] Larson, E. D., Jin, H., & Celik, F.E. 2005. Gasification-based fuels and electricity from Biomass, with and without carbon capture and storage. Princeton Environmental Institute, Princeton University, Princeton, NJ, October 2005, 77 pp.

[25] Holmgren, K., Hagberg, L. 2009. Life cycle assessment of climate impact of Fischer-Tropsch diesel based on peat and biomass. IVL report B1833.

[26] Andersson, E., Harvey, S. 2007. Comparison of pulp-mill-integrated hydrogen production from gasified black liquor with stand-alone production from gasified biomass. Energy, 32 (4) pp. 399-405.

[27] Cherubini, F., Jungmeier, G. 2010. LCA of a biorefinery concept producing bioethanol, bioenergy and chemicals from switchgrass. Int J Life Cycle Assess, vol. 15, pp. 53-66.

Application of CHP Gas Engine Plant for a Detergent Factory: Energy and Environmental Aspects

Mohammad Ameri*, Seyed Mohammad Ali Afsharzadeh

Energy Engineering Department, Power and Water University of Technology, Tehran, Iran
** Corresponding author. Tel: +98 21 77312780, Fax: +98 21 77310425, E-mail: ameri_m@yahoo.com*

Abstract: In Middle East countries like Iran, energy intensity is higher than the other regions due to low energy prices. One of the good motives towards energy efficiency is energy prices and because of this fact Iranian government wants increase the energy prices. One of the best technologies in energy efficiency is combined production of heat and power (CHP). In this paper the feasibility study of utilizing a CHP unit in an Iranian detergent factory has been described. The thermal and electrical energy uses in the factory has been measured According to the energy consumptions. The CHP system has been selected based on reciprocating gas engines. The feasibility study for the CHP system has been performed with different energy prices and environmental effect like reduction in CO2 emission has been analyzed. The CHP system can save 6,500 tons of CO2 per annum. In the feasibility studies rate of return method has been utilized. According to the energy prices scenarios, the rate of return would vary between 13% and 33%.

Keywords: *CHP, Gas engine, Energy efficiency, Carbon dioxide emission, Feasibility study*

Nomenclature

AEL annual saving of electricity bill..... €
ANG annual fuel cost ..... €
i rate of return
AO&M annual operation/maintenance cost..... €
ARH recoverable heat from intercooler/oil... kW
CHP combined heat and power
CI capital investment..... €
ASNG annual saving of natural gas bill..... €
EUF energy utilization factor..... €
E30 30,000th hour maintenance cost.....€
E60 60,000th hour overhaul cost.....€
ELEC present worth of saving electricity production .....€
NGC natural gas consumption..... $m^3 \cdot h^{-1}$
MRH recoverable heat from water jacket..... kW
L percent of electrical full load

1. Introduction

After the first energy crisis in 1970s, OECD Countries decided to change their energy policies in order to reduce their dependence on imported energy from the Middle East. They utilized energy efficiency as an effective way to reach that goal. The best way to comprehend the presence of energy efficiency in a country or a region is to take a short look at its energy intensity curve. By utilizing energy efficiency in energy programming, the energy intensity will decrease every year (Fig.1).

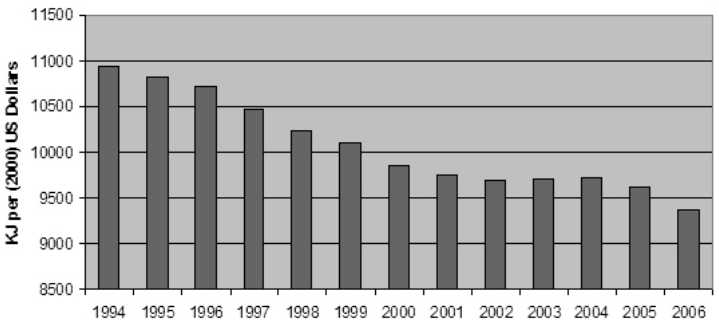

Fig. 1. World energy intensity [1].

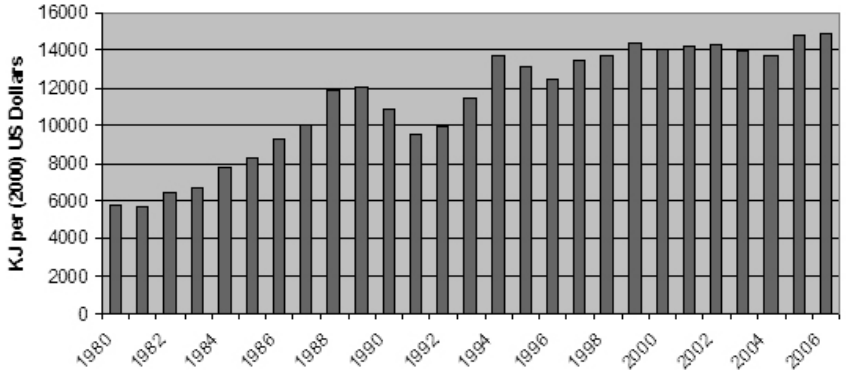

Fig. 2. Iran energy intensity [1].

On the other hand, Middle East Countries like Iran, which have rich energy resources, delayed utilizing the energy efficiency (Fig.2). In such countries, there is a huge obstacle on the path to reach an ideal energy efficiency, which is obviously the "low energy price". Low energy price always turns a profitable energy efficiency project to a lowly-lucrative one. In order to remove this obstruction, the Iranian government has planned policies to increase energy price in the near future. This project has sparked so many controversies amongst politicians because of its influential effect on the rate of inflation. However, because of the above-mentioned debates, it has not been enacted yet. Such an increase in energy prices is a nightmare for Iranian industries who are accustomed to low energy prices. The only way the industries may be able to come up with is by changing this threat to an opportunity through energy efficiency programs. One of the good practices in energy efficiency, which has been achieved since 1970s, is combined production of heat and power (CHP). In addition, distributed CHP systems in industries will result in reduction of electrical grid losses. The average thermal efficiency of thermal power plants in Iran is 36% and the loss in high and medium voltage electrical network is 4% [2]. Most of factories in Iran receive their electrical power by medium voltage network. Therefore, if the industries produce their own electrical demand by a CHP system, the grid losses, the fuel consumption and carbon dioxide emission will be lower. In this paper, application of a CHP system in a detergent factory in Iran is studied and discussed about the ratio between natural gas (as a fuel) and electricity prices and feasibility of the project. This factory is one of the largest detergent producers in the Middle East and produces over 132,500 tons of detergents per annum. The process of this factory requires electrical and thermal energy simultaneously. Therefore, CHP system is a perfect way to utilize energy efficiency in the factory, reducing energy bills and carbon dioxide emission.

2. Methodology

In the following section the energy demands of the factory, utilization of gas engines CHP system and economical analysis are described.

2.1. Energy demands of the factory

By installing a power logger in the main electrical feeder of the factory, electrical demand of the factory was measured. The electrical power demand of the factory is 3600 kilowatts and the annual consumption of electrical energy is 28,400,000 kilowatt-hours.

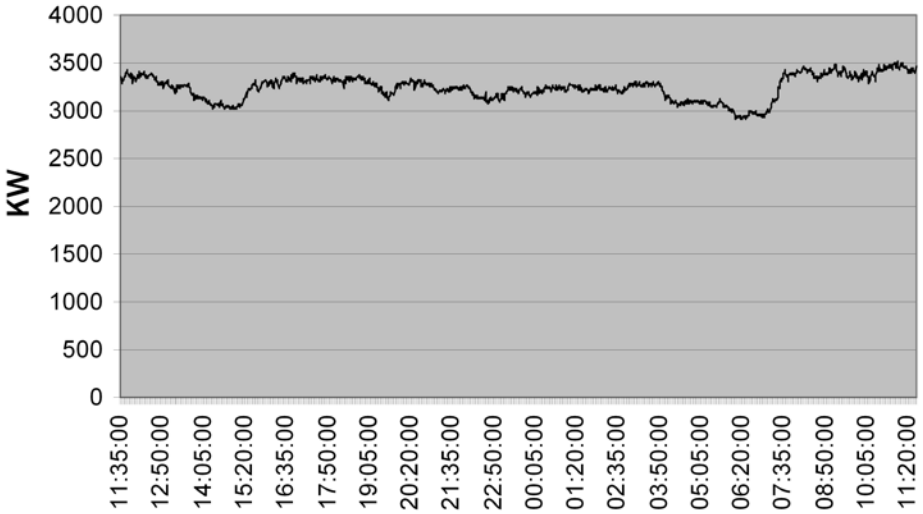

Fig. 3. Electrical demand of the detergent factory in a typical day.

The factory process consumes 244,931,438 kWh of thermal energy annually. Thermal energy source of the factory process is 45 tons per hour saturated steam at 1 MPa by 5 fire tube steam generator. The boiler's fuel is natural gas. The feed water enters the steam plant at $15^{\circ}C$ and it is heated by pegging steam in heat exchangers to $60^{\circ}C$. It enters the dearator to be heated to $95^{\circ}C$ in order to remove incondensable gases from feed water. For preheating the feed water in the steam plant, the factory needs 4.6 tons of steam per hour. All the produced steam is consumed within the process and there is no pipeline to return the condensate and recycle it as boiler feed water.

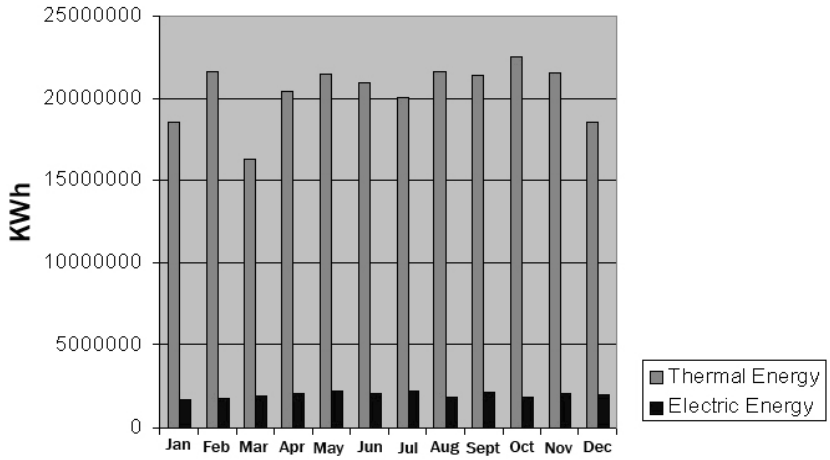

Fig. 4. Electrical and thermal energy usage in the detergent factory.

2.2. The choice of gas engine CHP system

In this case study, the authors selected a CHP system with 4 gas engine generating sets to cover the electrical demand. The nominal power of each gas engine is 952 kW therefore the overall nominal power of the plant is 3808 kW. The plant altitude is 1100 meters above the see level and in this site conditions the gas engines derate and actual power would be 4% and 3655 kW respectively [3]. For heat recovery of the system 2 plate heat exchangers are allocated for each gas engine. One of the plate heat exchangers recovers the waste heat from intercooler and engine oil and the other dedicates for waste heat of engine water jacket. The temperature of the intercooler/oil and water jacket are $60^{\circ}C$ and $95^{\circ}C$ respectively. The waste

heat of intercooler/oil is 844 kW (4 gas engines) and it can heat the feed water from $15^{\circ}C$ to $31^{\circ}C$ [3]. After preheating in intercooler/oil heat exchanger, the feed water enters the water jacket heat exchanger and gains 2520 kW thermal power and reaches to $80^{\circ}C$. Utilizing the waste heat of the gas engines will saves up to 3.8 tons per hour of steam in heat exchangers and dearator in steam plant. The electrical and thermal efficiency in full power at actual site conditions are 38% and 35%. Therefore the EUF of the plant is 73% at full power. However, the EUF, thermal and electrical efficiencies would vary with different electrical power output.

2.3. Energy analysis

According to Fig.3 the hourly electrical demand of the factory is fluctuating and the gas engines have to follow these fluctuations. With changing the electrical load of a gas engine, its waste heat will be different. Less electrical output of a gas engine means less amount of heat to be recovered. However, the variation in amount of recoverable heat is not linear with electrical output power. The electrical demand of the factory has been measured with the sampling time of 1 minute for 24 hours. To calculate the amount of recoverable heat from intercooler/oil and water jacket, the demand is divided between 4 gas engine generators. In Table 1 the thermal data sheet of the gas engine is mentioned. By interpolation between columns of Table 1, the correlations between the amount of recoverable heat from intercooler/oil and water jacket versus electrical output power have been developed. To reach this goal authors fitted a polynomial order 3 curves between the electrical output power versus the amount of recoverable heat from main and auxiliary water circuits.

$$MRH = 5 + 1216 \times L - 1112 \times L^2 + 520 \times L^3 \quad (1)$$

$$ARH = 76 - 81 \times L + 300 \times L^2 - 84 \times L^3 \quad (2)$$

$$NGC = 12 + 302.5 \times L - 125 \times L^2 + 62.5 \times L^3 \quad (3)$$

$$EUF = \frac{Electrical \quad Power + Heat \quad Power}{Inputed \quad Heat \quad by \quad Fuel} \quad (4)$$

Where L is the ratio between electrical load on each generator and maximum net actual power on the given site conditions for one gas engine generator. Using Eqs. (1) and (2), the amount of recoverable heat from intercooler/oil and water jacket is calculated every minute for 24 hours. In order to estimate the consumption of natural gas of the gas engines versus load, a correlation has been developed (Equation 3). Table 1 shows fuel consumption of the engines. In this table, fuel consumption is mentioned as heat power in kilo Watt. To transfer the heat power to flow rate of natural gas, the net heating value of natural gas is needed [4]. Energy utilization factor (EUF) for a CHP system is the amount of electrical power plus useful recovered heat from the system divided by the amount of heat input from the fuel (natural gas) to the system. Table 2 shows the amount of recovered heat from auxiliary and main circuits, natural gas consumption for 24 hours period of a typical day and a year. Table 2 reveals that the total recovered heat per year is 26,760,340 kWh, which is equivalent to 2,804,554 m^3 of natural gas per year. In addition, the total heat input to the CHP system per year is 76,428,645 kWh. Therefore, the EUF of the CHP system is 72.14%.

Table 1. The gas engine thermal datasheet [3].

Power rating		Full	Partial load		
load	%	100	80	60	40
Electrical power	KW	952	761	571	380
Fuel consumption	KW	2386	1952	1538	1105
Water jacket waste heat	KW	630	533	447	347
Intercooler/oil waste heat	KW	211	160	117	86
Heat in exhaust gases (120 C)	KW	388	328	268	194

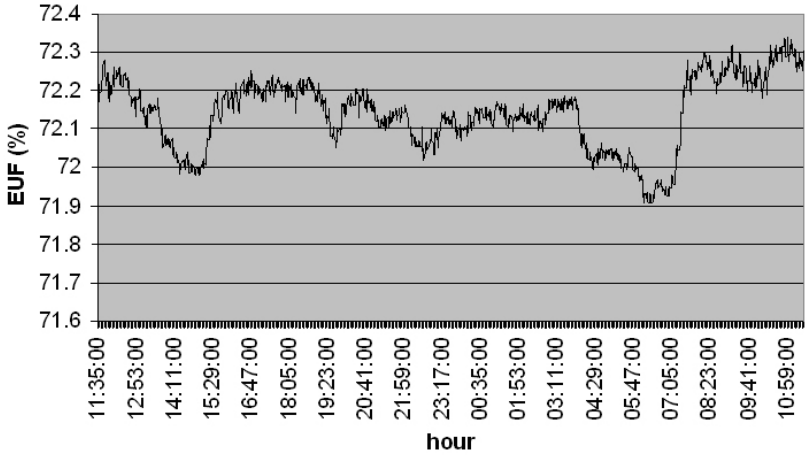

Fig. 5. Energy utilization factor of CHP System in a typical day.

Table 2. Energy parameters of CHP system.

	Unit	Per day	Per year
Natural gas consumption	m^3	21,945	8,009,925
Electrical energy production	kWh	77,754	28,380,210
Auxiliary circuit	kWh	17,743	6,476,195
Main circuit	kWh	55,573	20,284,145
Total heat recovery	kWh	73,316	26,760,340

2.4. Economical analysis

First step towards the economical analysis of a combined production of heat and power in the detergent factory is to determine the costs and benefits of the project. The costs of the project include the capital investment (which is 1.440.000 Euro), annual fuel cost, annual operation and maintenance (O&M) cost, and the 30,000th-hour maintenance and 60,000th-hour overhaul costs. The maintenance period of the selected gas engine is 60,000 hours, which includes 30,000th-hour maintenance and 60,000th-hour overhaul and the same periodic maintenance will be carried out quite regularly. The benefits of the project include saving the electricity bill and saving the natural gas bill as the result of recovering heat from the engines for preheating the boilers feed water instead of using pegging steam. The lifetime of the gas engine for continuous operation assumed to be 20 years. As it is discussed, the current energy price in Iran is low (natural gas: 0.011 Euro/m^3, Electricity: 0.014 Euro/kWh) and Iranian government is planning to increase it rapidly (natural gas: 0.0695 Euro/m^3, electricity: 0.0348 Euro/kWh) in the near future. Therefore, the benefits of the project need to be calculated with two different energy price references accordingly. Economical analysis carried out with rate

of return method. Rate of return method is based on time value of money. In this method, the net present worth of costs including capital investments, are placed to be equal to net present worth of benefits with a variable rate of interest (Equation 5). This variable rate of interest is called the rate of return.

$$AEL\times\left(\frac{(1+i)^{20}-1}{i\cdot(1+i)^{20}}\right)+ASNG\times\left(\frac{(1+i)^{20}-1}{i\cdot(1+i)^{20}}\right)=CI+ANG.\times\left(\frac{(1+i)^{20}-1}{i\cdot(1+i)^{20}}\right)$$
$$+AO\&M\times\left(\frac{(1+i)^{20}-1}{i\cdot(1+i)^{20}}\right)+E30\times\left[\frac{1}{(1+i)^{4}}+\frac{1}{(1+i)^{12}}\right]+E60\times\left[\frac{1}{(1+i)^{8}}+\frac{1}{(1+i)^{16}}\right] \quad (5)$$

3. Results

In this section reduction in carbon dioxide emission, costs and benefits of project, economical analysis based on rate of return method are discussed.

3.1. Environmental analysis

As mentioned before, the average efficiency of Iranian national thermal power plants are 36% and energy losses in high and medium voltage grid is 4%. Currently the factory receives 28,380,210 KWh of electrical energy per annum from medium voltage grid, which means that the national power plants have to generate 29,562,935 kWh annually to overcome the energy losses. For generation of 29,562,935 kWh of electrical energy, a typical Iranian thermal power plant consumes 8,606,316 m^3 of natural gas. On the other hand for producing the same amount of electrical energy in the factory, the specified CHP unit consumes 8,009,925 m^3 of natural gas with 26,760,340 kWh of useful recovered heat energy, which is equivalent to 2,804,554 m^3 of natural gas. Therefore, CHP unit saves 596,391 m^3 of natural gas as the result of reducing grid losses and improving the electrical energy efficiency and 2,804,554 m^3 of natural gas as the result of recovering the wasted heat from the engines, which are totally 3,400,945 m^3. Burning each cubic meter of natural gas produces 1.91407 Kg of carbon dioxide [4]. Therefore, an annual saving of 3,400,945 cubic meters of natural gas means saving 6,509 tons of carbon dioxide emission per annum.

3.2. Economical analysis

By solving the Equation 5, rate of return of the project is revealed. In table 3, the feasibility study result of the project for two different energy prices has been discussed.

Table.3. Annual costs and benefits of the CHP system

Item	Amount	Current price (€)	Price in near future (€)
Natural gas	8,009,925 m^3	88,999	556,244
O&M	-	77,250 [5]	
Maintenance at 30,000 hour	-	140,000 [5]	
Overhaul at 60,000 hour	-	160,000 [5]	
Saving the electricity bill	28,380,210 kWh	394,169	985,423
Saving the natural gas bill	2,804,554 m^3	31,161	194,760
Rate of return	-	12.6 %	33.3 %

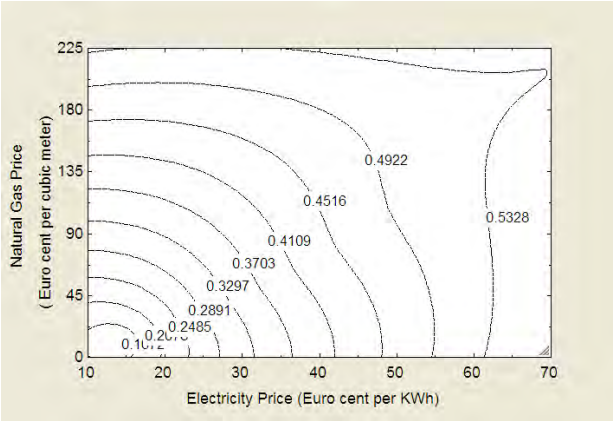

Fig.6. The sensitivity of energy prices versus rate of return.

Feasibility of the project is highly dependant to the energy prices. In the Fig.6, the effect of natural gas and electricity prices on the rate of return has been shown.

4. Conclusion

Application of a CHP system in the detergent factory was discussed from technical, economical and environmental point of views. Such a system can save 2,804,554 m^3 of natural gas and 6,509 tons of carbon dioxide annually without interrupting in the factory processes. The factory needs steam for its processes and the only way for direct steam generation with gas engines is utilizing heat from exhaust gases. The exhaust gases can produce only 2 ton of steam per hour but by utilizing low temperature heat from intercooler/oil and water jacket in order to preheat the feed water of boilers, 3.8 tons of steam per hour will be saved. This method of heat recovery is more efficient, simple and cheap. The feasibility of the project strongly depends on the fuel and electricity prices. Government should increase the energy prices in a conducted way to encourage the industries to utilize CHP system. Finally this study encouraged the owners of the detergent factory to install gas engines CHP plant and now the system is under operation.

References

[1] World Energy Intensity -- Total Primary Energy Consumption per Dollar of Gross Domestic Product 1980-2006, Energy Information Administration, International Energy Annual 2006.

[2] Iranian Energy balance, Iranian ministry of energy, 2008. See also http://iranenergy.org.ir/statistic%20info/energy%20balance/main840.htm

[3] POWER RATING SFGLD 560, document number: IC-G-B-IC-002, Guascor S.A.

[4] Analysis of Tehran natural gas, Reported by Iranian Research Institute of Petroleum Industry, June 21, 2008.

[5] Guascor S.A. Technical Communication, Spare part price list for SFGLD 560, TARIFA RECAMBIOS DO 2010 PVP.

Combined Optimal Placement of Solar, Wind and Fuel cell Based DGs Using AHP

A.K.Singh[1,*], S.K.Parida[1]

[1] *Department of Electrical Engineering*
Indian Institute of Technology, Patna, India
** Corresponding author. Tel: +91-612-2552040, Fax: +91-612- 2277383, E-mail: amit@iitp.ac.in*

Abstract: The integration of distributed generations (DGs) into grid has a great importance in improving system reliability. Many methods were proposed in the literature for finding best locations for DG placement considering various criteria. Sometime, it becomes difficult for combined placement of different kinds of renewable based DGs, such as solar, wind and fuel cell. The criterion of minimizing total system cost was used previously by many researchers for locating the optimal sites for DGs using OPF formulations. In this case, three different cost functions are formulated for different kinds of renewable energy sources (RESs). By taking combined cost function of all the RESs in the OPF to identify location for each different kind of sources becomes very cumbersome task. It would be difficult to find the exact locations for various kinds of RESs that is where to place which type of RESs. In order to solve this difficulty, three different objectives have been considered separately for determining the optimal locations for each kind of RESs using mixed integer nonlinear programming (MINLP) method. Having many alternatives with these three objectives, analytic hierarchy process (AHP) has been used to make a decision over getting the optimal locations for these different kinds of RESs. The proposed method for finding the optimal locations of solar, wind and fuel cell based DG placement has been demonstrated on 15 node distribution systems.

Keywords: *Analytic hierarchical process, Distributed generation, Mixed-integer non-linear programming, Optimal power flow, Renewable energy sources*

1. Introduction

The electric energy requirement has been rapidly increasing day by day throughout the global, Hydro and fossil fuel plants will continue to be the chief sources of electric supply for a few years. Electric supply authorities are likely to pay more attention to improve the generation technologies. Before the innovation of large generating units, small DGs were in use to supply electricity. But, due to economy of scale large generating systems were developed and the electricity is supplied at a cheaper price. However, there has been revival of interest in connecting DG to the distribution network. DG is often used to illustrate a small-scale electricity generator which can be owned and operated generally by customer to achieve sufficient volume of energy maintain the quality and reliability in electricity supply. It can be RESs, based on wind, photo-voltaic, biomass, fuel cell or hydroelectric power. RES may be either connected to the local electric power grid or isolated from the grid in stand-alone applications. RES plays an important role in providing clean energy along side reducing carbon foot prints, and hence a crucial constituent of future developments. The penetration of DGs in the network helps in achieving voltage control, reduction of power losses and improvement of system reliability.

Optimal location for the placement of DGs with minimization of losses using gradient and second order methods is presented in [1]. In [2], a linear programming approach to determine optimal allocation of embedded generation on distribution networks is proposed. Optimal location and sizing of distributed generation in a distribution networks using Genetic Algorithm (GA) is discussed in [3]. The allocation and sizing of DGs for social welfare maximization and profit maximization using Locational marginal price (LMP) is proposed in [4]. Optimal placement of distributed generation for profit maximization, reduction of losses

and improvement in voltage regulation at various load buses in the distribution network is shown in [5]. In [6], a GA based methodology for optimal DG allocation and sizing in distribution systems, in order to minimize network losses, and guarantee high level of reliability and voltage improvement was proposed. A method to allocate and determine the size of DG for minimization of the active losses of the feeders using tabu search algorithm is presented in [7]. In [8], Analytical Hierarchical Process (AHP) is used to decide the hierarchy of the planning process and members constituting the hierarchy are allowed to rate each other and relative grading of weights is discussed. AHP method is used to solve the DG planning with uncertainties and a different objective in a DG planning problem is discussed in [9]. The application of solid oxide fuel cell (SOFC) systems to generate electric power and thermal energy required for residential use is discussed in [12].

In this work, the planning of RESs has been carried out by using a hybrid method consisting of both optimization and analytic hierarchy process. Three different optimal power flow (OPF) problems have been formulated and solved using the mixed- integer non-linear programming (MINLP) method, which provides optimal bus locations for RES at various load serving nodes and ranking of each of the optimal bus location for the system. With numbers of alternative bus locations and rankings obtained from three OPF formulations, the overall priority indices have been obtained by using Expert Choice based on an analytic hierarchy process algorithm. The results of AHP clearly indicate the ranking of optimal location for various kinds of RESs. The effectiveness of the proposed approach has been tested on 15 node distribution systems [15].

2. Problem Formulation

For the planning of various kinds of RESs, three different OPF formulations have been used. The different objectives used in these formulations consider the minimization of cost of fuel cell, photo-voltaic system and wind turbine generation. With each of these objectives, the ranking of RES source locations has been obtained. Optimal placement of RES can provide both economical and operational advantages. The OPF formulations are given below.

2.1. Objective function

The three objective functions can be mathematically expressed as follows.

Case A: Minimizing fuel cell cost:

$$C_{fuel} = C_c + C_f + C_m \tag{1}$$

Case B: Minimizing solar system cost:

$$C_{solar} = C_{O\&M} * LF + (C_{CC} * FCR) / 8760 * CF \tag{2}$$

Case C*: Minimizing wind energy system cost:*

$$C_{wind} = (FCR * ICC) / AEP_{net} + AOE \tag{3}$$

where $C_c = C_{fc} * (i_r (1 + i_r)^n) / ((1 + i_r)^n - 1)$ (4)

$$C_f = (\gamma_{ng} * P_{dgi}) / \eta \tag{5}$$

$$AOE = LLC + (O\,\&\,M + LRC) / AEP_{net} \quad (6)$$

2.2. Equality Constraints

The network for the transmission of electric energy is modeled using the power balance equation at each node in the network. These include the usual load flow equations at each node and the power balance equation as given below.

$$P_{gi} - P_{di} = P_i \quad (7)$$

$$Q_{gi} - Q_{di} = Q_i \quad (8)$$

$$PLT = \sum_j P_{Lj} \quad (9)$$

$$QLT = \sum_j Q_{Lj} \quad (10)$$

2.3. Inequality Constraints

These constraints have considered the following.

Real and reactive power generation limits:

$$P_{gi}^{\min} \le P_{gi} \le P_{gi}^{\max} \quad (11)$$

$$Q_{gi}^{\min} \le Q_{gi} \le Q_{gi}^{\max} \quad (12)$$

Voltage and angle limits:

$$V_i^{\min} \le V_i \le V_i^{\max} \quad (13)$$

$$\delta_i^{\min} \le \delta_i \le \delta_i^{\max} \quad (14)$$

Distribution generation limits:

$$u.*P_{dg}^{\min} \le P_{dg} \le u.*P_{dg}^{\max} \quad (15)$$

where C_{fuel} is fuel cell cost function, C_{solar} is solar system cost function, C_{wind} is wind energycost function, C_c is annual investment cost, C_{fc} is total purchasing cost, γ_{ng} is the price of natural gas, η is the electrical efficiency, C_m is maintenance cost expressed as 4–10% of the purchasing cost, P_{dgi} represent DG generated power at bus i, $C_{O\&M}$ is the operating and maintenance cost, LF represent levelizing factor, C_{CC} shows the capital cost, FCR is fixed charge rate, CF is capacity factor, ICC represents initial capital cost, AEP_{net} is net annual energy production, AOE represents annual operating expenses, LLC and LRC are land lease cost and levelized replacement cost, i_r represents annual interest rate, n represents lifespan in years, P_i and Q_i represents active and reactive power injection at bus i, P_{Lj} and PLT represent individual real line loss and total real system loss, Q_{Lj} and QLT represent individual reactive

line loss and total reactive system loss, P_{gi}, Q_{gi}, P_{di} and Q_{di} are real and reactive power generation and demand respectively, P_g^{min}, P_g^{max}, Q_g^{min} and Q_g^{max} represent limits on real and reactive power generations, V_i and δ_i are the voltage magnitude and angle at the i th bus, V_i^{max}, V_i^{min}, δ_i^{max} and δ_i^{min} are the maximum and minimum limits on voltage magnitude and angle at bus i, u is the binary vector {0,1} that represent the absence and presence of DGs sources at a bus and P_{dg}^{max} and P_{dg}^{min} are limits of generated power from DG.

3. Analytic Hierarchy Process (AHP)

AHP is introduced by Saaty in [10]. AHP is a decision-making tool, which helps in finding goals or objectives among alternative courses of action. It is a systematic method for comparing a list of objectives and the alternative solutions satisfying respective objectives. First, pair wise comparisons are made between the objectives and, then, between alternative solutions with respect to each objective. For pair wise comparison, some weights are also assigned according to the importance, or preference of the objectives or the alternatives. A comparison of objectives/alternatives i and j utilizes a value b_{ij} , defined in Table 1.

Table 1. Relative importance, preference, or likelihood (b_{ij}).

1	Objective i and j are of equally importance
3	Objective i is weakly more important than j
5	Objective i is strongly more important than j
7	Objective i is very strongly more important than j
9	Objective i is extremely more important than j
2,4,6,8	Intermediate values

Further, if $b_{ij}=k$, then $b_{ji}=1/k$
Considering a decision-making problem to prioritize m alternatives with n objectives, the AHP algorithm has been shown in Table 2.

Table 2. Pairwise comparison matrix of objectives.

	*obj*1	*obj*2	…	*obj*n	Priority
ob_{j1}	b_{11}	b_{12}	…	b_{1n}	p_1
ob_{j2}	b_{21}	b_{22}	…	b_{2n}	p_2
.	.	.	.	.	.
.	.	.	.	.	.
ob_{jn}	b_{n1}	b_{n2}	…	b_{nn}	p_n

The relative weights of objectives can be computed as normalized geometric means of the rows (which are very close to the eigenvector corresponding to the largest eigenvalue of the matrix). The geometric means are computed as

$$h_i = \sqrt[n]{\prod_{j=1}^{n} b_{ij}} \tag{16}$$

The relative weight (priority) of the i th objective is obtained as

$$p_i = \frac{h_i}{\sum_{i=1}^{n} h_i} \tag{17}$$

Similarly, the pairwise comparison matrix can be defined for alternatives with respect to each objective. Therefore, with *m* alternatives for the *k*th objective, the priority of the *i*th alternative is obtained as

$$h_{ki} = \sqrt[m]{\prod_{j=1}^{m} b_{kij}} \tag{18}$$

$$p_{ki} = \frac{h_{ki}}{\sum_{i=1}^{m} h_{ki}} \tag{19}$$

The overall priority of the *m*th alternative is obtained as

$$p_m = \sum_{i=1}^{n} \sum_{k=1}^{n} p_i \, p_{km} \tag{20}$$

4. Case Study

The proposed hybrid method for RESs planning has been demonstrated and analyzed on 15 node distribution system [15]. The MINLP method has been used to obtain the optimal locations of DGs for each case separately. For ranking of optimal DG locations, all of the available DGs are taken simultaneously. In case A, which minimizes fuel cell generation cost with five numbers of DGs, the optimal locations are found at buses 13, 15, 12, 11, and 10. Reducing the maximum available source to four, buses 13, 15, 12, and 11 are found as the optimal locations. Hence, it can be concluded that bus 10 was ranked last, i.e., fifth. Again, by reducing the available sources to three, buses 13, 15, and 12 are found as the optimal locations, and, hence, bus 11 is ranked as fourth. Similarly, by reducing the available DGs, the ranking of optimal locations are obtained.

Table 3. Ranking of RESs locations based on different objective and overall locations.

Rank	Case A	Case B	Case C	Overall locations
1	13	12	15	15
2	15	11	14	13
3	12	10	13	14
4	11	9	12	12
5	10	13	11	11

Considering case B, which minimizes photo-voltaic generation cost, with five numbers of DGs, the optimal locations are found at buses 12, 11, 10, 9, and 13. While considering case C, which minimizes wind turbine generation cost, with five numbers of DGs, the optimal locations are found to be bus 15, 14, 13, 12, and 11. Table 3 shows the ranking of DG locations with different objectives (cases A, B, and C) are found and overall ranking for these three cases obtained by using the AHP. The scheme for obtaining the optimal locations of DGs is given in Figure 1. It can be observed from Table 3 that, with each objective, different rankings of optimal locations are obtained with a few common bus locations. Thereafter, as

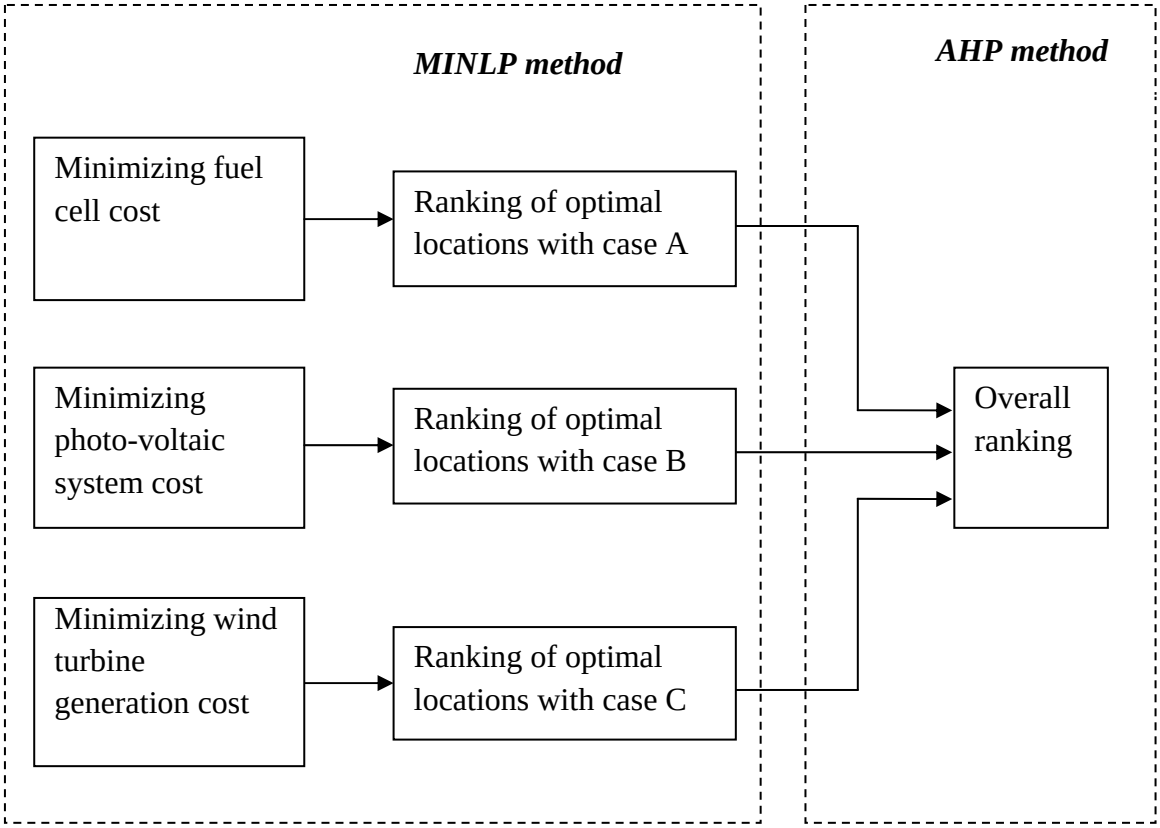

Fig. 1. Flow diagram of the hybrid method used for RESs planning.

given in the flow diagram in Figure 1, AHP algorithm is used to compute the overall ranking of optimal bus locations for RESs placement. The ratings considered for various types of RESs are 5 kW, 20 kW and 50 kW for fuel cell, photo-voltaic system and wind turbine generation system, respectively. Figure 2 shows the performance sensitivity graph with respect to criteria and goal. The objectives and alternatives are represented by the vertical and horizontal bars, respectively. The intersection of the alternative line graphs with the vertical criterion lines shows the priority of the alternative for the given objective, as read from the right axis labeled Alt%. The objective priority is represented by the height of its bar as read from the left axis labeled Obj%. The overall priority of each alternative is represented on the OVERALL line, as read from the right axis. It is observed from the graph that the suitable locations for wind, solar and fuel cell are 15, 13, 14, 12, 11, 10 and 9. The highest priority has been given to wind energy system whereas the solar system has got the lowest priority as shown in Figure 2. Finally we can conclude that wind energy system is the best for bus 15, fuel cell system is best suited for bus 13, wind energy system is best suited for bus 14 and solar energy system is best suited for bus 12, 11, 10 and bus 9, respectively.

Figure 3 shows the dynamic sensitivity of the different optimal bus locations, which indicates the priority in percentage for a particular bus. As per the Figure 3 the priority of bus 15, 14, 13, 12, 11, 10 and 9 is 28.4% (highest), 16%, 20.5%, 15.5%, 11.3%, 5.3% and 3% (lowest), respectively. Figure 4 shows the percentage of location for various types of RESs in the system. From this figure, it can be observed that 63.7% of the location is supplied by wind energy sources, 10.5% by solar energy and remaining 25.8% by fuel cell energy system.

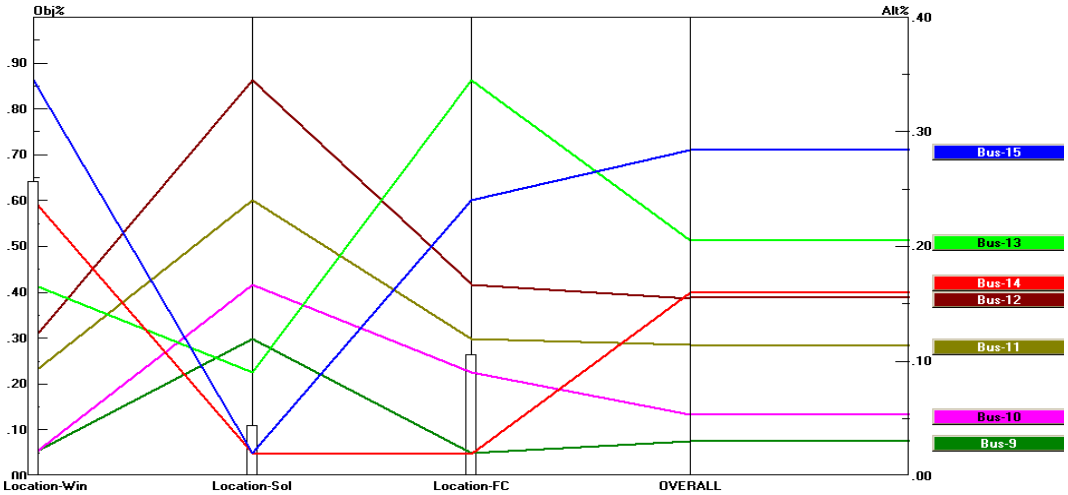

Fig. 2. Performance sensitivity graph with respect to criteria and goal.

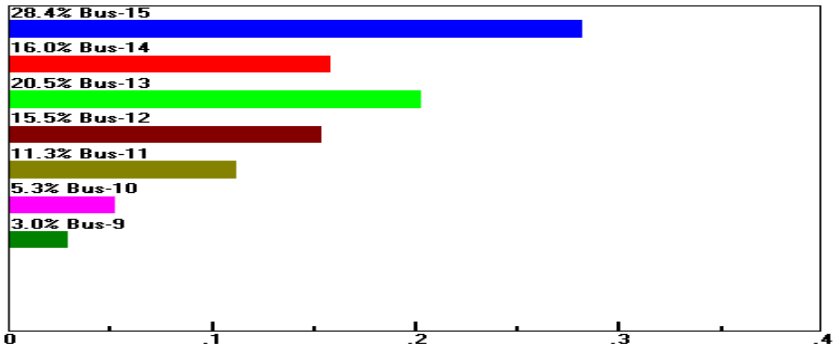

Fig. 3. Dynamic Sensitivity of the nodes.

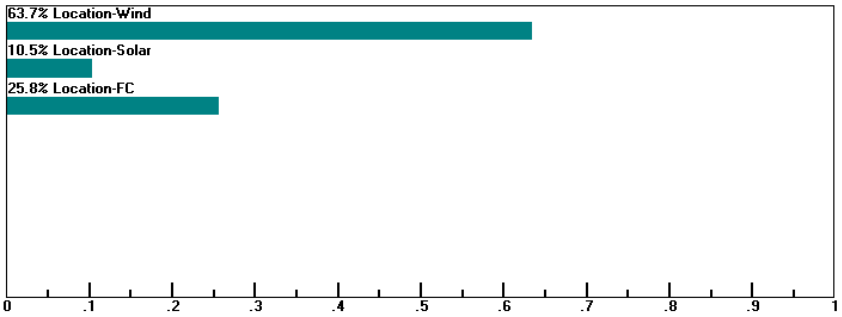

Fig.4. Distribution of RES locations based on different objective.

5. Conclusion

This paper proposes a hybrid method for DG planning taking various kinds of RESs simultaneously into account. This approach consists of two steps. In first step, the ranking of optimal locations are obtained by using MINLP method with an objective of minimizing the cost of respective RES. It has been observed that some of the optimal locations found to be same for different kinds of RESs, and which creates confusion over the placement of various types of RESs. Then, in second step AHP is used to distinguish the locations for various kinds of RESs by identifying the exact optimal location for a particular type of RES. These locations also indicate the placement and type of RESs. The results clearly indicate the overall ranking of bus locations and the type of energy sources to be placed there. In this planning work, wind, solar and fuel-cell energy has been used in the ratio of 63.7%, 10.5% and 25.8%,

respectively. If this sharing of various RESs changes then, the locations for different kinds of RESs also changes.

Acknowledgement

The authors acknowledge the financial support provided by Department of Science & Technology under SERC Fast Track Scheme Ref. # SR/FTP/ETA-074/2009 for carrying out the research work.

References

[1] N. S. Rau, and Y. H. Wan, Optimum location of resources in distributed planning, IEEE Transaction Power System, vol. 9, no. 4, Nov. 1994, pp. 2014-2020.

[2] A. Keane, and M. O'Malley, Optimal allocation of embedded generation on distribution networks, IEEE Transaction Power Systems, vol. 20, no. 3, Aug. 2005, pp. 1640-1646.

[3] I. Pisică, C. Bulac, and M. Eremia, Optimal distrbuted generation location and sizing using genetic algorithms, Proceeding of the 15th International Conference on Intelligent System Application to Power System (ISAP), 2009, Curitiba, Brazil.

[4] D. Gautam, and N. Mithulananthan, Optimal DG placement in deregulated electricity market, Electric Power System Research, vol. 80, no.7, July. 2010, pp. 828-837.

[5] R. K. Singh, and S. Goswami, Optimum allocation of distributed generation based on nodal pricing for profit, loss reduction, and voltage improvement including voltage rise issue, Electric Power System Research, vol. 36, no.6, July. 2010, pp. 637-644.

[6] C. L. T. Borges, and D. M. Falcăo, Optimal distributed generation allocation for reliability, losses and voltage improvement, Electric Power System Research, vol. 28, no.6, July. 2006, pp. 413-420.

[7] K. Nara, Y. Hayashi, K. Ikeda, and T. Ashizawa, Application of tabu search to optimal placement of distributed generators, IEEE PES Winter Meeting (2), 2001, pp. 918-923.

[8] A. P. Agalgaonkar, S. V. Kulkarni, and S. A. Khaparde, Multi-attribute decision making approach for strategic planning of DGs, Proceeding IEEE-PES GM, 2005, pp. 2213–2218.

[9] M. Sahraei-Ardakani, M. Peydayesh, A. Rahimi-Kian, Multi-Attribute optimal DG planning under uncertainty using AHP method, Proceedings of the IEEE-PES GM, July 2008, Pittsburg, PA, USA.

[10] T. L. Saaty, The Analytic Hierarchy Process, McGraw-Hill, 1980, New York.

[11] A User's Guide, GAMS Software, 1998.

[12] E. Bompard, R. Napoli, B. Wan and G. Orsello, Economics evaluation of a 5kW SOFC power system for residential use, Hydrogen Energy, vol. 33, 2008, pp. 3243-3247.

[13] G. M. Masters, Renewable and Efficient Electric Power Systems, John Wiley & Sons, 2004, New Jersey, U.S.A.

[14] L. Fingersh, M. Hand, A. Laxson, Wind Turbine Design Cost and Scaling Model, National Renewable Energy Laboratory Report, Dec 2006.

[15] D. Das, D. P. Kothari and A. Kalam, Simple and efficient method for load flow solution of radial distribution networks, International Journal of Electric Power and Energy Systems, vol. 17, no. 5, 1995, pp. 335-346.

Exploring the sustainability of industrial production and energy generation with a model system

Prakash R. Kotecha[1], Urmila M. Diwekar[1], Heriberto Cabezas[2,*]

[1] *Center for Uncertain Systems: Tools for Optimization and Management, Vishwamitra Research Institute, Clarendon Hills, Illinois, USA*
[2] *U.S. Environmental Protection Agency, Office of Research and Development, National Risk Management Research Laboratory, Sustainable Technology Division, Cincinnati, Ohio, USA*
** Corresponding author. Tel: +1 513-569-7350, Fax: +1 513-487-7787, E-mail: cabezas.heriberto@epa.gov*

Abstract: The importance and complexity of sustainability has been well recognized and a formal study of sustainability based on system theory approaches is imperative as many of the relationships between the various components of the system could be non-linear, intertwined, and non-intuitive. A mathematical model capable of yielding qualitative inferences can serve as an important tool for policy makers to: (1) explore various simulated important scenarios, and (2) evaluate different strategies and technologies. In this article, we consider a simplified ecological food web with an integrated macro-economic system, industrial production sector, an energy generation sector, and elements of a human society along with a rudimentary legal system. The energy sector is designed to supply energy to the other components of the system either by using a finite, non-renewable energy source or by a combination of a non-renewable source and biomass. Many of the components of the system depend directly or indirectly on the biomass used for energy production. Subsequently, this model is used to study the impact of using biomass for the production of energy on the sustainability of other components of the system under different scenarios such as population increases and per capita consumption increase.

Keywords: *Sustainability, Energy, Ecological Model, Scenario, Ecosystem*

1. Introduction

Sustainability or sustainable development has been generally defined (1) as "development that meets the needs of the present without compromising the ability of future generations to meet their own needs." From this definition, it can be noted that sustainable development can be achieved (and sustained) only by addressing various diverse issues making the study of sustainability an inherently complex and highly multi-disciplinary concept. The sustained effort of the scientific community has led to the realization that continued exploitation of the Earth's resources cannot be infinitely sustained and can severely endanger the existence of many of the biological species (2). This has led to a vast mobilization of efforts spanning all strata of human society including the scientific, political, and social. A growing body of research has been reported in literature (3-8). It has tried to comprehend the causes of various naturally occurring phenomena and attempted to predict some future consequences, along with suggesting remedial actions that need to be implemented over a period of time to avoid catastrophic events. It should be noted that sustainability is not a goal but a path or corridor through time, which has to be continuously followed and monitored. Sustainability is dependent on the interactions between the various dimensions of the system such as ecology, human society, economics, technology, and other aspects. Often, these interactions are nonlinear, intertwined, and non-intuitive in nature (7, 8). Additionally, the effects of many current actions manifest over a long period of time making the study of sustainability quite complex, requiring a systematic approach.

Stable mathematical models featuring the critical components of a real system can aid in the formal study of sustainability. Models capable of yielding qualitative inferences about sustainability under various simulated scenarios can assist policymakers when evaluating various strategies and technologies. A comprehensive review of some of these models can be

obtained from Whitmore et al. (5). The model proposed by Whitmore et al. (5, 6) integrated an economy under imperfect competition with a twelve-cell ecological model. Despite the unique features of the model, it had a limiting assumption as it presumed that an infinite amount of energy was available without any cost to the various components of the integrated system. This assumption warrants a cautious approach when extending the qualitative results of the model to any real world system, where it has been seen that factors related to energy not only have geo-political ramifications but also cause enormous stress on certain components of the system that could jeopardize sustainability.

An enhanced model, which considers various aspects, related to the production and utilization of energy from various types of energy sources in an integrated system has been presented in this article (8). This model can be used to simulate the production of energy based on a finite, non-renewable energy source or a combination of both a non-renewable energy source and biomass. The model is subsequently used to study the sustainability of different components of the integrated system due to the diversion of a part of biomass for the production of energy. Finally, we have used the model to study the sustainability of the integrated system under various plausible scenarios such as a population increases and an increase in the per capita material consumption levels of humans.

2. Integrated Ecological-Economic Model

The model consists of 14 compartments and represents a simplified ecological food web set in a macro-economic framework with farming, livestock raising, industrial production, energy generation, and a rudimentary legal system. The model shown in Fig. 1 consists of three primary producers (P1, P2 and P3), three herbivores (H1, H2 and H3), and two carnivores (C1 and C2) along with human households (HH). The Resource Pool (RP) represents a generic finite nutrient source while the Inaccessible Resource Pool (IRP) represents mass that is not biologically accessible to the rest of the system. The primary producers feed on RP and use energy from the Sun to make this mass available to the rest of the integrated system. A small amount of mass from IRP is recycled back into the system by P2 and P3, which symbolizes degradation by the actions of microorganisms. All nine biological compartments recycle mass back to RP through death. The Energy source (ES) represents a finite non-renewable energy source. The Energy Producer (EP) is an industry that uses labor to transform the energy source into a usable form of energy. This energy is supplied to HH and IS. EP is also capable of producing energy using P1, and this would represent the production of energy using biomass. The IS produces products valuable to HH using P1 and RP. The use of the IS products does not increase the mass of HH, but it instead passes through as this is used to increase the mass of IRP. Similarly, the use of mass by the EP to produce energy results in the increase of the mass of the IRP and a corresponding decrease in the mass of ES. The biological compartments of the system can be aggregated as shown in Fig. 1 into domesticated species that have economic value and wild species that have no economic value. A legal system assigns property rights to domesticated biological species, the product of the industrial sector, and the non-renewable energy source. Grazing rights are given to H1 to access P2, while the access of C1 to H1 is limited. Moreover, C1 is a protected species and cannot be hunted or consumed by other components of the integrated system. Similarly, the access of P1 by H2 is limited by using capital and labor, i.e. erecting barriers or “fences.”

The human workforce can choose to work in any of the four industries (P1, H1, IS or EP) and the wages are set by IS depending on the demand supply gap of the IS product along with the population, i.e. IS dominates the labor market. The demand for any product (P1, H1, and IS) by HH also depends on the price and demand for various other products. The demand for a

particular product (say P1) decreases with an increase in the price of that product (P1) and the demand increases (for P1) with an increase in the price of other products (like H1 and IS). The prices of the products depend on the wages paid for labor and the demand supply gap of that particular product. An increase in the wage levels or demand supply gap increases the price of the product. The price of energy depends on the labor and the amount of fuel that is available at the given point of time. An increase in labor cost increases the price of energy whereas a decrease in the amount of energy source would lead to an increase in the price of energy. The growth of the human population depends on the per capita human mass, the birth rate, and the mortality. The human birthrate in turn is assumed to be a negative function of the real wage as it represents the opportunity cost of opting to remain outside the labor force for the purpose of rearing children. The complete system is closed to mass so that it abstractly represents a planet. The food web is modeled by Locka-Volterra type expressions whereas the economy is represented by a price-setting model wherein firms and HH attempt to maximize their well-being. The aim of this model is to represent the critical elements of a real world system while keeping it simple enough for tractable mathematical analysis. Some of the salient features of the model include an organization based on trophic levels with fewer species and lower total mass for higher trophic levels, species specific preferences for food, cyclic variation in the growth of the primary producers, discharge fee on the industrial sectors and the ability to accommodate both non renewable mass and biomass to produce usable energy. Also, the model is flexible enough to allow for variation of the amount of energy produced from biomass. For this article, it was assumed that 30% of the total energy demand by the integrated system is being provided by the biomass. If sufficient amount of biomass is not available, the maximum available biomass is used for the production of energy and the remaining energy is produced from the non-renewable energy source. Moreover, it was assumed that there is no surplus or deficit in the energy levels as the EP produces as much energy as required by HH and IS. The dashed lines in Fig. 1 indicate mass flows that occur under anthropogenic influence. The dotted lines indicate the flow of energy from EP to HH and IS. The square dotted line between P2, P3, and IRP indicate slow transfers of mass as a result of microbial activity. For the sake of brevity, the complete mathematical model is not presented here and details including the base case results can be found in Kotecha *et. al.* (8)

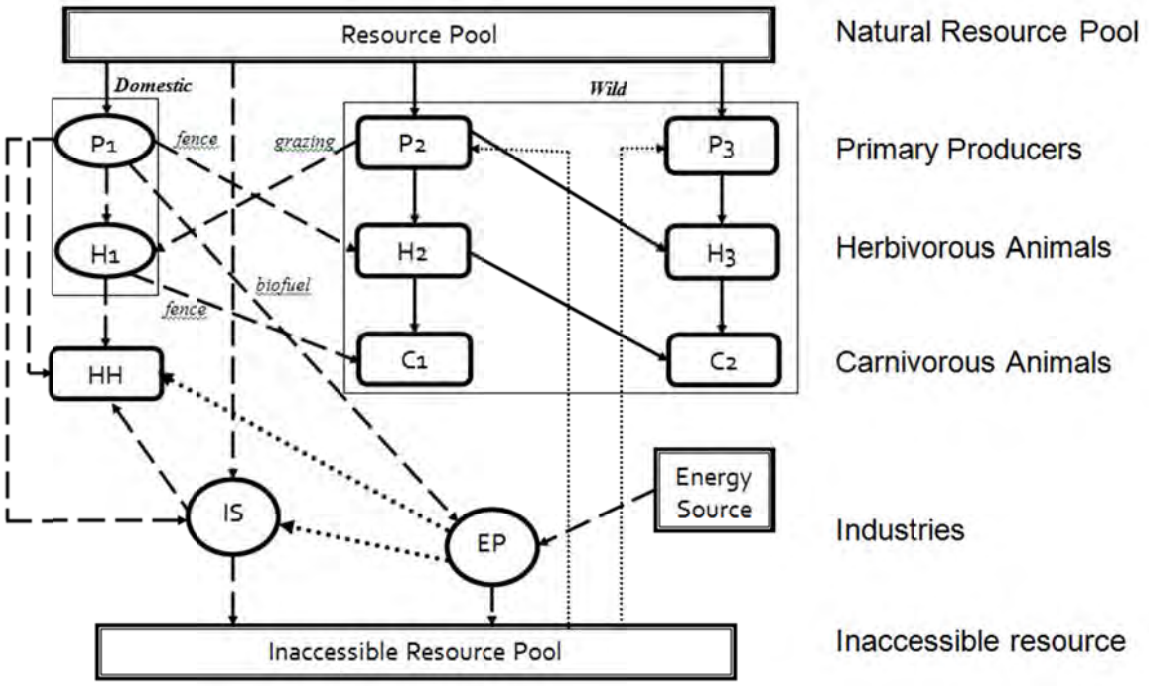

Fig. 1. Integrated Ecological Model

3. Scenario Analysis

Model based scenario analyses are an integral part of systems theory and help in understanding the dynamics of systems under various simulated scenarios without disturbing any actual system. Such analyses have been credited with helping make informed and rational decisions by their ability to offer insights into ramifications of current and possible future actions. However, the results of the scenario analysis should not be mistaken for actual forecasts, projections or predictions of the future as the future need not necessarily evolve based on the assumptions underlying the scenario analysis. At times, the actual future may involve a combination of different scenarios or even witness happenings not envisioned as possible scenarios. There have been a number of studies, which are based on scenario analysis and have been discussed in the literature (7, 8). We will consider here the two scenarios of an increase in human population and an increase in the per capita human consumption levels. For the sake of brevity, profiles of only the most important compartments have been provided.

3.1. Population Increase

Rapid population increase is one of the scenarios commonly envisaged by many environmentalists. The enormous growth of the human population has already placed severe stress on many finite resources of the Earth and may pose serious concerns on the sustainability of its ecosystem. It is widely believed that the human population will double from its current level and peak in the next 50-100 years (9, 10). This premise is largely based on the fact that mortality rates will be dropping due to better health care facilities whereas the birth rate will also get lowered due to better education of women and increased awareness of birth control techniques, particularly in the under developed countries. This period will be followed by a steady decline in the human population due to aging and a decrease in fertility rates (7, 8). As in previous published studies based on this model (7), the human mortality rate drop is modeled in a piecewise linear manner before settling at a final value while the coefficients in the birth rate function are nonlinearly varied. The issue of population is included here to provide a complete description of the system, but addressing it is well outside the purview of the U.S. EPA. This work should, therefore, not be construed as providing any guidance on population issues. The following discussion describes the dynamics of the various compartments of the integrated system.

From Fig. 2, it can be seen that the amount of P1 decreases faster initially when energy is produced using biomass. The price of P1 is initially higher for the scenario where bioenergy is used. Although, P1 is used for bioenergy, it does not decrease beyond a certain point because of market equilibrium. Due to an increased amount of resource pool mass, the amount of P3 increases with time whereas the amount of P2 declines due to an increase in the growth of H3. The increase in the growth of H3 is essentially due to an increased level of P3. From Fig. 2, it can be seen that there is a sudden decrease in the level of H1, and H1 never recovers. This sudden decrease occurs at the point where population growth is highest. At this stage, the resources for H1 to consume became limited due to consumption of P1 by humans as well as for its use for bioenergy. However, the level of H2 increases because the decrease in H1 leads to a decrease in the levels of C1, which in turn decreases the consumption of H2, and hence increases the compartmental mass of H2. From the figure, it can be seen that there is a drop in the level of C1 if a portion of the P1 is used for producing energy. This can be attributed to a drop in the amount of H1 that is being transferred to the C1 compartment due to a decreased level of H1, because of the production of energy using biomass. The amount of C1 drops due to the usage of P1 for producing energy even though C1 does not directly consume P1. Another important thing to notice is that though C1 is a protected species, its mass drops significantly because of the economics of P1. Similar observations also hold for C2. However,

it was observed that the species C1 or C2 do not become extinct due to the production of energy using biomass.

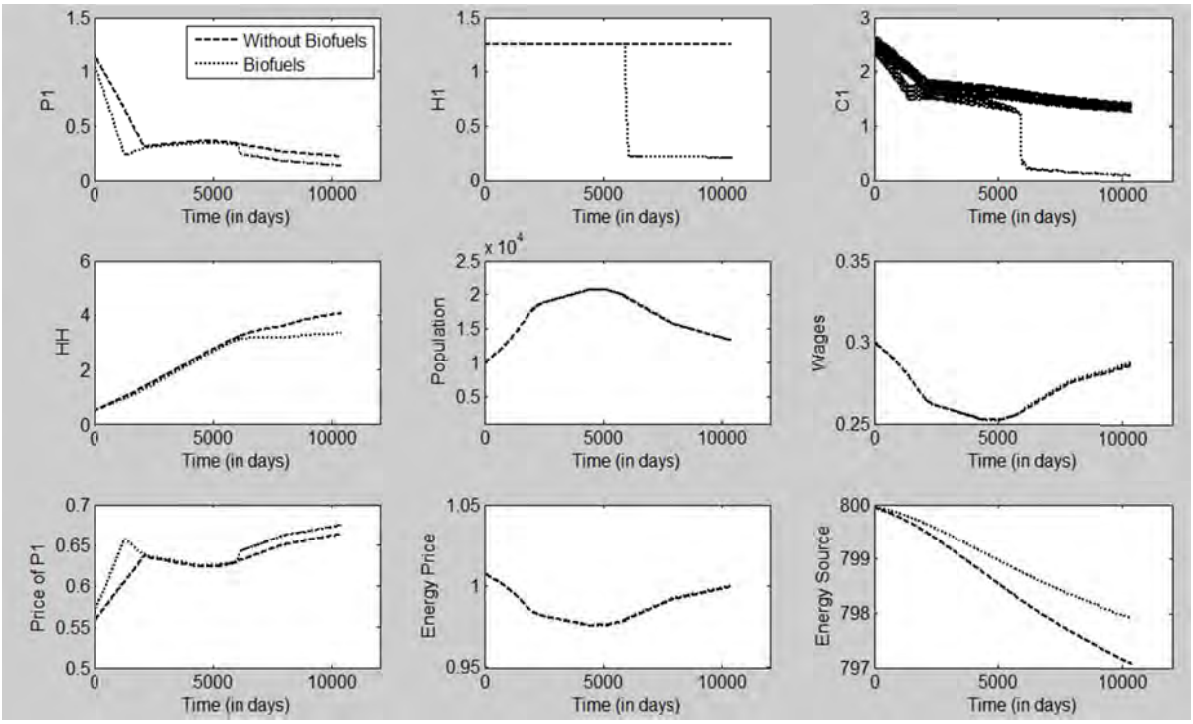

Fig. 2. Profiles of compartmental mass and price (population increase)

Figure 2 shows that the amount of human mass has slightly decreased due to the production of energy using biomass. The amount of human mass is directly dependent on the amount of P1 transferred to the HH compartment. Due to the production of energy using biomass, the amount of P1 decreases and hence the availability of P1 to feed HH decreases thereby causing the drop in human mass. Figure 2 also shows no change in the level of human population because of the production of energy using biomass. It can also be seen that the drop in the compartmental mass of human households is not translated into a reduction of the human population. This invariably indicates that the per capita mass of humans has decreased thereby corroborating both the decrease in human mass at similar levels of human population. Figure 2 shows that the production of energy using biomass does not lead to an increase in wages. Wages paid to human households is inversely proportional to the human population i.e., an increase in the human population decreases the wages of the human households. Thus, the wages are low when the population is high and increase with a decrease in the population.

Figure 2 shows that the decrease for ES is less if a portion of the energy is produced from biomass. This is because in the production of energy using biomass, P1 is used for producing energy and hence the non-renewable energy source is not used for that portion of energy thereby leading to a slower decrease in the amount of ES. The price of energy is similar in both cases. The price of energy initially decreases because the human population is increasing and leads to lower wages. Subsequently, the human population starts to decrease and wages start increasing as this gets reflected in the price of energy. This completes the discussion of the population scenario analysis, and we will now discuss the scenario of increase in the consumption levels of the humans.

3.2. Consumption Increase

Many of the resources that humans consume are non renewable and are finite in nature, and the resources which are renewable are often consumed at a rate much faster than the rate of

replacement. Such abnormal high consumption levels could severely affect the current composition of the ecosystem (11, 12). Moreover, with an increase in per capita income, the quality of life and disposable income have increased often leading to an increase in per capita consumption of both mass and energy. This continuous increase in consumption levels could not only exceed the capacity of the ecosystem to provide services, but endanger the longer-term sustainability of the system. For the model under study in this article, the increase in the consumption level of humans is modeled by linearly varying the constant coefficients involved in the estimation of per capita demand for resources. This strategy of modeling consumption increase is similar to the previous published work on a similar model by Shastri et al. (13). We will now present the discussion on the dynamics of various compartments present in the integrated system under increased levels of per capita consumption.

Figure 3 shows that increase in the consumption levels of humans leads to a decrease in the levels of P1, H1, and C1. The magnitude of decrease is more prominent when energy is produced using biomass. This is because a part of P1 is being used for the production of energy, and, thereby, is not available to the rest of the system. The increase in the price of P1 leads to a lower consumption of P1 by the H1 compartment. The level of P2 was also seen to decrease whereas the level of P3 increased due to increased levels of the resource pool. These changes in the primary producers have cascading effects on the other components of the integrated system. The herbivore H1 preys on P1 and a rapid decline in the levels of P1 leads to a rapid decline in the levels of H1. Similarly, the level of H2 falls rapidly when P1 is used for producing energy, since the levels of P1 and P2 are lower. However, the level of H3 remains the same in both the cases as it depends on the level of P3. The level of C1 and C2 in both cases decreases to significantly lower levels due to a decrease in the levels of H1 and H2. However, their decline is more rapid when P1 is used for the production of energy. For the case of population increase, the amount of C1 and H1 had also decreased but in the case of consumption increase, the mass of these two compartments not only decreases, but they become extinct. It should be noted that the extinction of C1 occurs despite the fact that it is a protected species. This is an example of the complex interaction between the various dimensions of sustainability, and how one or more dimensions can dominate the others. In this case, the economic dimension dominated the legal dimension, and this resulted in the extinction of the C1 species. It can be seen that the use of P1 to produce energy in an increasing consumption level scenario could accelerate the extinction of some species.

From Figure 3, it can be seen that the amount of human mass has increased substantially due to an increase in the consumption of P1 and H1. However, the use of P1 to produce energy leads to a lower increase in the mass of the human compartments. The figure shows that there is a drop in human population towards the end of the simulation horizon. The level of human population is slightly less when P1 is used as a source of energy for producing energy. This can be attributed to the fact that the non-availability of P1 leads to a decrease in the compartmental mass of the human households and subsequently manifests into a decreased population. The figure shows the prevailing wages as decided by the Industrial Sector (IS). The difference in the wage levels is a reflection of the difference in the population level for the two cases. Since the population is slightly lower when P1 is used for producing energy, the wage rates for this case are higher. The wage rates are constant for a considerable period of time and start to increase towards the end due to a decrease in the human population. This is consistent with the assumptions of the model wherein the wage rate remains constant with a constant population level and increases with a drop in the population.

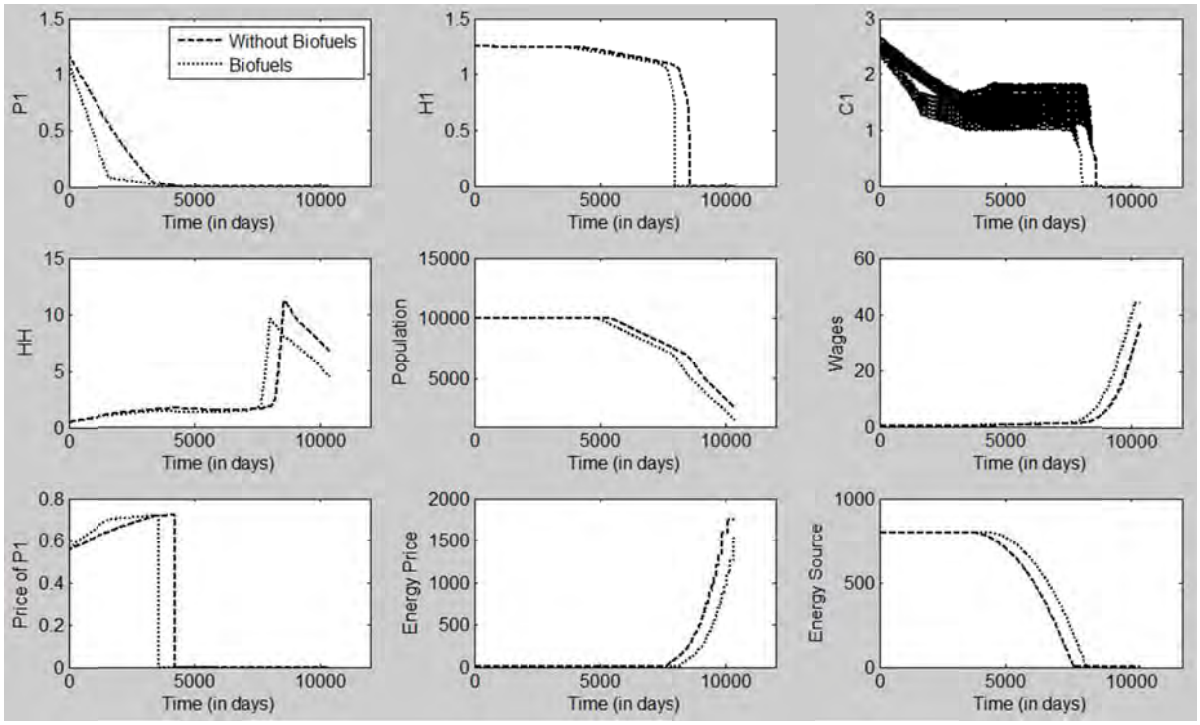

Fig. 3. Profiles of compartmental mass and price (consumption increase)

Figure 3 shows the price of P1 and energy along with the amount of non-renewable energy source available in the integrated system. As with the base case and the population increase scenario, the decrease for ES is less if a portion of the energy is produced from biomass. The use of P1 for producing a part of the energy decreases the utilization of the non-renewable energy source and hence the decline in it is moderated. However, in both the cases, the energy source faces decline, and the use of biomass for producing energy merely delays the exhaustion of the non-renewable energy source. The price of energy is a function of wages and the amount of energy source available in the system. Irrespective of the use of biomass to produce energy, the energy prices keep increasing. However, the use of biomass for producing a portion of the energy seems to lower the cost of the energy for this particular scenario of increasing consumption. This is because of the fact that the use of biomass helps in maintaining a higher level of the non-renewable energy source longer, and this, thereby, leads to a relatively lower cost of energy. It can be seen that the price of energy is significantly higher in the scenario of consumption increase than either the base case or population increase scenario. This is because the human population has decreased to very low levels thereby increasing the wage levels. Moreover, the scarcity of the energy source contributes to the increase in the price of energy.

4. Conclusions

An enhanced 14 compartmental model for an integrated system incorporating the generation and utilization of energy has been developed to aid in the formal study of sustainability and to derive qualitative inferences for various scenarios. Under the scenario of population increase, the use of biomass does not decrease the human population, but leads to a decreased per capita human mass, which may be inferred as an indicator for the quality of life. Moreover, the use of biomass for producing energy only delays the inevitable exhaustion of the non-renewable energy source and does not significantly impact the energy prices. For the scenario of per capita consumption increase, it was observed that the integrated system could not sustain high levels of human consumption. It was observed that the use of biomass for the production of energy delays the exhaustion of the non-renewable source, but can expedite

some of the catastrophic events such as the extinction of protected species and human well-being. The proposed model can be used to explore strategies, policies, and to evaluate the impact of alternate generic technologies on the long-term sustainability of the system. The inherent assumptions of the model have to be borne in mind, and a cautious and conservative approach should be practiced while extending these model inferences to reality.

Acknowledgments

Work was sponsored by U.S. EPA, Contract EP09C000220 under oversight of Norma Lewis.

References

[1] Brundtland, G. Our Common Future; World Commission on Environment and Development; Oxford University Press: Oxford, 1987; p 383.

[2] Raven, P. H. Science, sustainability and the human prospect. *Science* 2002, *297*, 954–958.

[3] McMichael, A.; Butler, C.; Folke, C. New visions for addressing sustainability. *Science* 2003, *302*, 1919–1920.

[4] Cabezas, H.; Pawlwoski, C.; Mayer, A.; Hoagland, N. Sustainability: Ecological, social, economic, technological, and systems perspectives. *Clean Technol. Environ. Pollut.* 2003, *5*, 1–14.

[5] Whitmore, H.; Pawlowski, C.; Cabezas, H. Integration of an economy under imperfect competition with a twelve-cell ecological model; Technical Report EPA/600/R-06/046, 2006.

[6] Cabezas, H.; Whitmore, H.; Pawlowski, C.; Mayer, A. On the sustainability of an integrated model system with industrial, ecological, and macroeconomic components. Resour. Conserv. Recycle 2007, 50, 122–129.

[7] Shastri, Y.; Diwekar, U; Cabezas, H; Williamson, J. Is Sustainability Achievable? Exploring the Limits of Sustainability with Model Systems. Environ. Sci. Technol. 2008, 42, 6710–6716.

[8] Kotecha, P,; Diwekar, U; Cabezas, H.; Model based approach to study the impact of biofuels on the sustainability of an integrated system. Submitted to Environ. Sci. Technol. 2010.

[9] Capistrano, D.; Samper, C. K.; Lee, M. J.; Raudsepp-Hearne, C. Ecosystems and Human Well-Being: Multi-Scale Assessments, Volume 4. In Millennium Ecosystem Assessment; Island Press: Washington DC, 2005.

[10] Cohen, J. E. Human population: The next half century. Science 2003, 302, 1172–1175

[11] Arrow, K.; Dasgupta, P.; Goulder, L.; Daily, G.; Ehrlich, P.; Heal, G.; Levin, S.; Maler, K.; Schneider, S.; Starrett, D.; Walker, B. Are we consuming too much. J. Econ. Perspect. 2004, 18, 147– 172.

[12] Imhoff, M. L. ; Bounoua, L.; Ricketts, T.; Loucks, C.; Harriss, R.; Lawrence, W. T. Global patterns in human consumption of net primary production. Nature. 2004, 429, 24, 870-873.

Natural Ionizing System of Electrical Protection against Atmospheric Discharges (Lightning)

L. Cabareda.[1]

[1] *Pararrayos Ionizantes, C.A., Maturín, Venezuela.*
**Luis Cabareda. Tel: +58 4148964010, Fax: +58 2916410616, E-mail: lcabaredaf@gmail.com*

Abstract: This is the New Highest Technology, 100% Venezuelan and Unique in the World, Technological Innovation, World Patent for Maximum Protection, Security and Zero Risk (0) to all Electrical and Power Generation Systems: Hydroelectric and Thermoelectric Power Plants; Wind, Nuclear and Solar Power Plants; others. It's the only technology around the world that has the potential to disperse and propagate to land mass the enormous energies associated to the Atmospheric Discharges (Lightning), which are in the order: 200,000 to 500,000 Amperes; 1,000 million Kilowatts and High-Level Transient Voltage of 100 million Volts. This New High Technology is the solution to the paradigm of Benjamin Franklin and it's the mechanism to end the "Blackouts" that produces so many damages and losses of billions of dollars to both: generators and users of electrical service, throughout the world.

Keywords: *Atmospheric Discharges, Lightning, Electrical Substations, Grounding Protection.*

1. Introduction

The Electrical Faults, Interruptions and "Blackouts" generated by Atmospheric Discharges (lightning) in Transmission Lines, Electrical Substations (High Voltage), Power Equipment and Electronic Equipment of High Sensitivity are the main problem in today's Electrical Engineering in the world.

The calculation and design of Protection Systems for Transmission Lines and Electrical Substations (Reticular Mesh of Grounding, Bars and others) that are currently used in Electrical Engineering are inefficient, because those calculations for Reticular Mesh of Grounding are made by taking into account only the electrophysical characteristics of Power Transformers and other items such as: transformers capacity, reactance, capacitance, inductance, secondary current, short circuit current symmetrical and asymmetrical, land resistivity, mesh geometry and others. In other words, Reticular Mesh of Grounding aren't designed or calculated to counteract the destructive effects of lightning.

The dispersion capacity of a Reticular Mesh of Grounding would be in the order of 10,000; 20,000 or 30,000 Amperes. In that sense, the energy values associated to lightning are in the order of: 500,000 Amperes, 1,000 millions of Kilowatts and High-Level Transient Voltage of 100 millions Volts that no Reticular Mesh of Grounding would be able to disperse.

The only existing device to disperse and propagate this huge energy is the Natural Ionizing System of Electrical Protection conformed by: Lightning Rod Ionizing Natural Ionca and Ionic Electrode Active Trimetallic Triac of Grounding, both High Technologies, 100% Venezuelan. (Cabareda, 2006. Science, Technology and Innovation Award, FUNDACITE, Science and Technology Ministry of the Bolivarian Republic of Venezuela). Finally, the only definitive and total solution to avoid Interruptions and Electrical Faults in Electrical Substations, Power Equipment and Electronic Equipment of High Sensitivity generated by Atmospheric Discharges (lightning) and to end "Blackouts" is by installing these devices on existing Towers and Transmission Lines, Electrical Substations and for those to construct.

2. The New Highest Technology, 100% Venezuelan,

2.1. Natural Ionizing Lightning Rod Ionca

It bases its operation on its electrophysical structure and the enormous differences of existing potential and the electrical field in the atmosphere in conditions of storm that allow to generate "crown effect" or "ionizing effect" that produce billions of high ion conductivity, because it has electrodes to atmospheric potential (atmospheric excitatory) and electrodes to grounding potential isolated to each other. This "ionizing effect" is increased by "hit effect" between air molecules and particles (ion) accelerated by the enormous existing electric fields during the storm. This natural ionization generates a "grounding direct discharge" which is the precursory current of lightning and that jointly with the stepped currents that derive from the interaction of the microparticles in the clouds, indicates the way and the trajectory for the Atmospheric Discharge (lightning), which will be lead through Lightning Rod Ionizing Natural Ionca and the Ionic Electrode Active Trimetallic Triac of Grounding to the land mass, scattering and spreading the enormous energies associated to this phenomenon, without causing damages. Electrophysical Characteristics: Height: 620mm. Diameter: 470mm. Weight: 6.4Kg. Material: Stainless Steel 304, Polytetrafluoroethylene (400°C). Vertical Penetration: 50 y 100m. Warranty: 20 years.

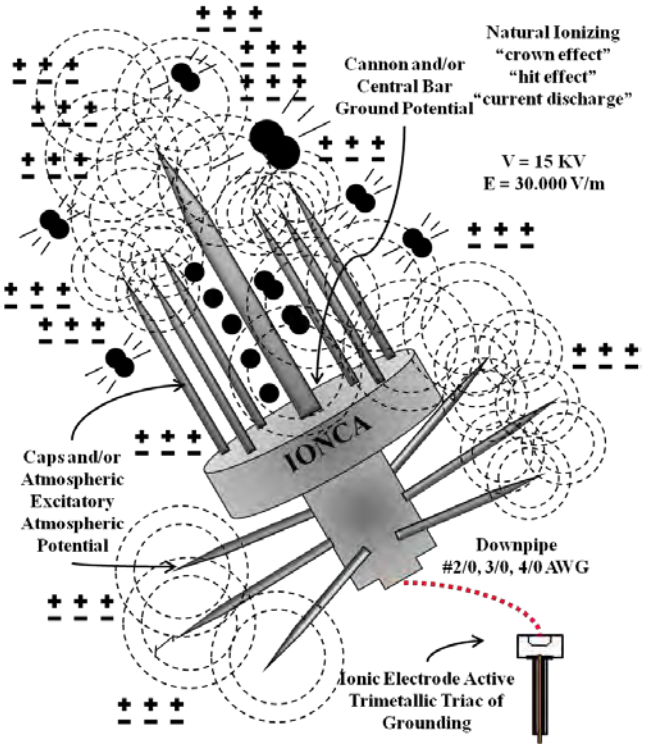

Fig. 1. Natural Ionizing Ligthning Rod Ionca. Electrophysical Basis.

One Natural Ionizing Lightning Rod Ionca can protect an area of 10,000m^2 (1 Hectare)

Fig. 2. Natural Ionizing Lightning Rod Ionca.

2.2. Active Trimetallic Ionic Electrode Triac of Grounding

It bases its operation and highest efficiency on its electrophysical characteristics that allow the total and complete adhesion to the land mass, whose land has been dealt chemically with high-electrical conductivity electrolytes that decrease the enormous resistivity and allows: water saturation and humidity retention, total adhesion to the land mass and high indices of alkalinity. The volume of the treated ground is from $18m^3$ to $27m^3$ approximately and is united to the land mass by the electrolytic and not mechanic adhesion, facilitating the way of dispersion and propagation of the enormous energies associated to the atmospheric discharges (lightning) and electrical faults, generally. Energy Dispersal Capacity to Land Mass: 500,000 Amperes, 1,000 million Kilowatts, Lowest Electrical Resistance R = 0.86 to 3 Ω (ohm). Land Characteristics: Lowest Land Resistivity, Porosity and Compaction, Maximum Humidity, Temperature, Station of the Year, Electrolytes, PH.

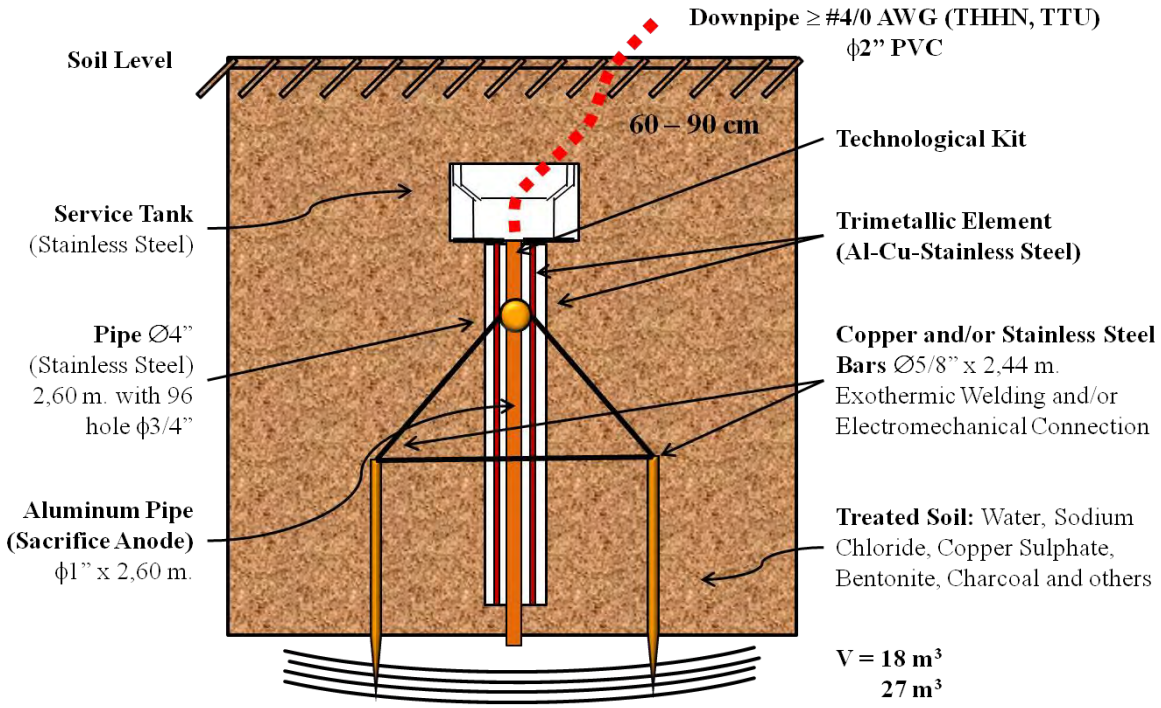

Fig. 3. Active Trimetallic Ionic Electrode Triac of Grounding. Cross Section.

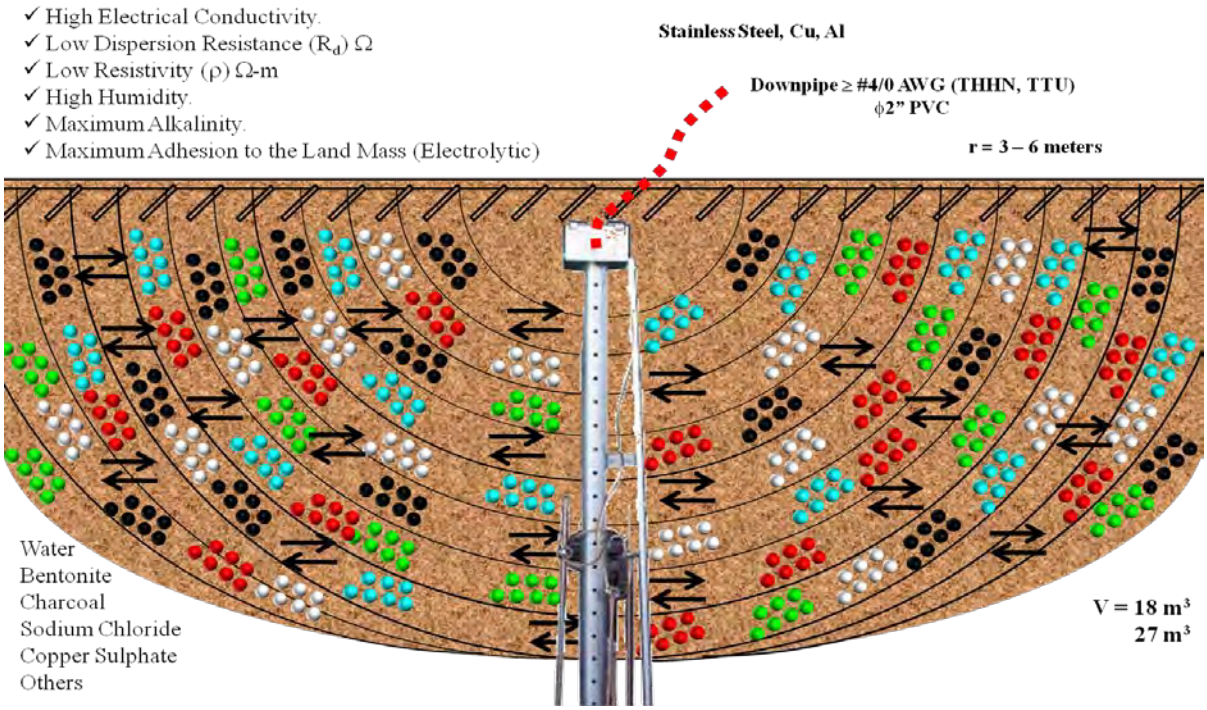

Fig. 4. Active Trimetallic Ionic Electrode Triac of Grounding. Electrophysical Basis.

HIGH CAPACITY OF DISPERSION OF THE ENERGY to the land mass:

-600,000 Amperes.

-1,000 million of Kilowatts.

-100 million of Volts.

-R = 0.86 a 3 Ω (ohmios)

Fig. 5. Active Trimetallic Ionic Electrode Triac of Grounding.

2.3. Energy of Lightning

Lightning, it's an interaction and transmission of elevated electrical charges between the atmosphere and the earth in conditions of storm or Atmospheric Disturbances. On Earth happens: 4,000 storms daily. 9,000,000 lightning daily. The Energy of Lightning is in this order: 200,000 to 500,000 Amperes; 1,000 million KW; 1 millions MW = 1.000.000 MW; 100 millions Volts.

The Energy generated for the biggest Hydroelectric's Dams around the world would only reach 10% of the Energy of a single Lightning: Hydro Québec (Canada) 36.810MW, Guri (Venezuela) 10.000MW, Macagua (Venezuela) 3.140MW, Caruachi (Venezuela) 2.160MW,

Tocoma (Venezuela) 2.160MW, Itaipu (Brazil-Paraguay) 14.000MW, Three Georges (China) 22.500MW, Hoover (USA) 2.080MW, Tehri (India) 2.400MW, Aswan (Egypt) 2.100MW, Inguri (Georgia) 1.300MW, Grand Dixence (Switzerland) 2.000MW, Nurek (Tajikistan) 4.000MW.

2.4. Consequences of Atmospheric Discharges (Lightning)

Damages to Constructions and Electricals Equipment, Electronic, Communications, Computation and Cybernetic, generally: Inductive and Conductive Effects that produce High Levels of Transitory Overvoltages (100 millions Volts). Damages to People: Cardiac and Respiratory arrest, Cerebral Injuries, Burns, Plow of the Eardrum, Pulmonary and Bony Injuries, Post-traumatic Stress. Losses of billions of dollars to both, generators and users of electrical service around the world.

2.5. Characteristics of Atmospheric Discharges (Lightning)

30 - 100 million Volts. 200,000 – 500,000 Amperes. 100 - 1.000 million Kilowatts. Electric Field: 30 Volt/m. Potential Gradient: 15KV. Air Impedance: 5KΩ. Atmospheric Pressure: 100 Atmosphere. Duration Time: 10 – 30 μseg. Energy: 3 x 10^9 J/m. Temperature: 15,000 to 30,000°C. Acustic Energy: 25% (thunder) Caloric Energy: 75% (electrical discharged)

2.6. The Lightning Rod

The Lightning Rod is a device conformed by one or several metallic bars with certain geometric disposition united to an grounding electrode by a downpipe conductor, that facilitates the way of the lightning from the cloud to the Earth, allowing the dispersion and propagation of the enormous energies associated, without causing damages to people and/or equipment.

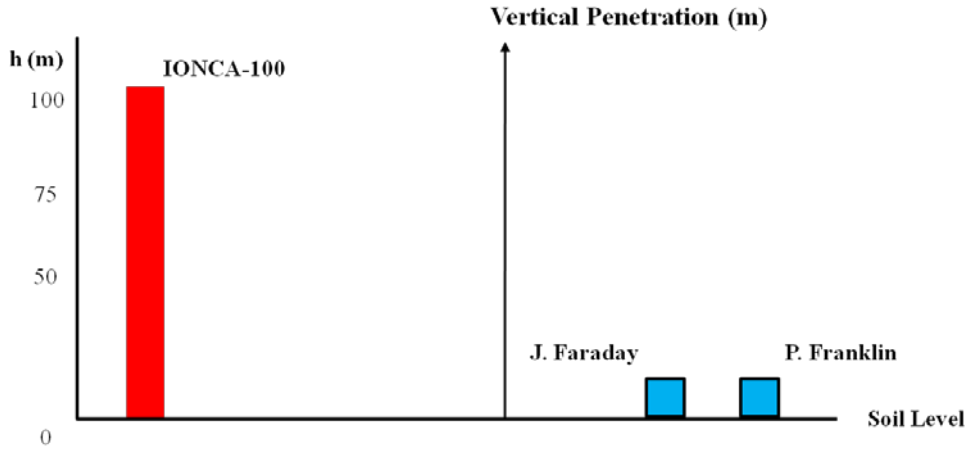

Maximum Security (∅=30°)	Protection Area (m^2)
IONCA-100	10.466 (1 Hectare)
Faraday Cage	300
Franklin Lightning Rod	100

Fig. 7. Traditional Lightning Rods and Natural Ionizing Lightning Rod Ionca comparison.

2.7. Grounding Systems

It's a set of metallic elements directly buried that allow and facilitate the dispersion and propagation of energy associated to a lightning and electrical faults, without causing damage. The adhesion to land mass of Traditional Systems of Grounding like Bars and Reticular Mesh of Grounding is mechanical. The adhesion to land mass of the Active Trimetallic Ionic Electrode Triac of Grounding is Electrolytic.

- It protects people and/or equipment (electrical, electronic, communication, computation).

- It protects against: Lightning, Transitory Overvoltages of Discharge and Low Level, Accidental Contact with Lines of High Tension (HT) and Low Tension (LW).
- It stabilizes the voltage of normal operation.
- It facilitates the switch operations.
- Equipotentiality: Touch Voltage and Step Voltage.
- It allows the dispersion and propagation to land of the associated energy (lightning) to electrical faults, leakage currents and Atmospheric Discharges.

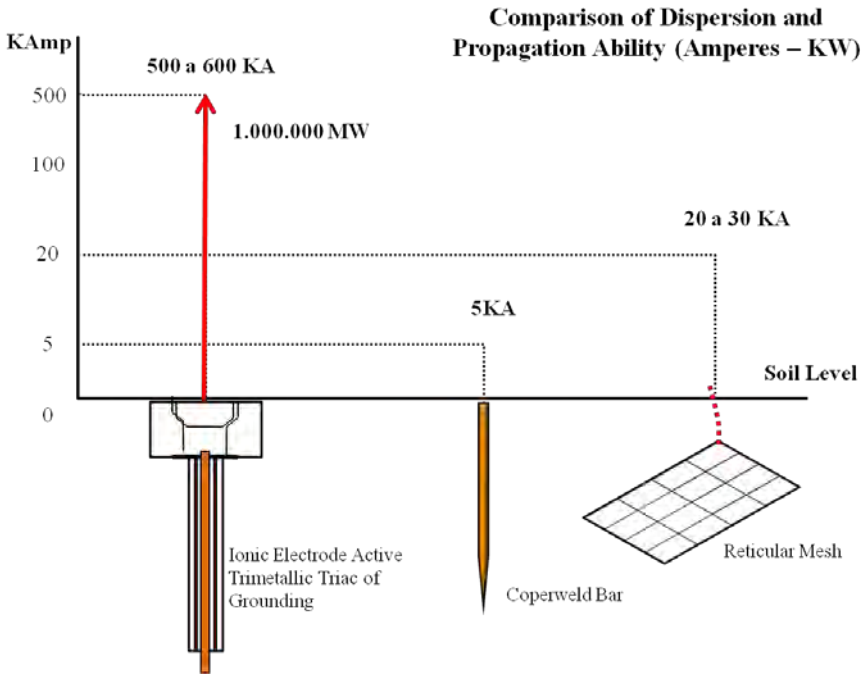

Fig. 8. Comparison of Traditionals Systems of Grounding with the Active Trimetallic Ionic Electrode Triac of Grounding.

2.8. Actual Electrical Substation

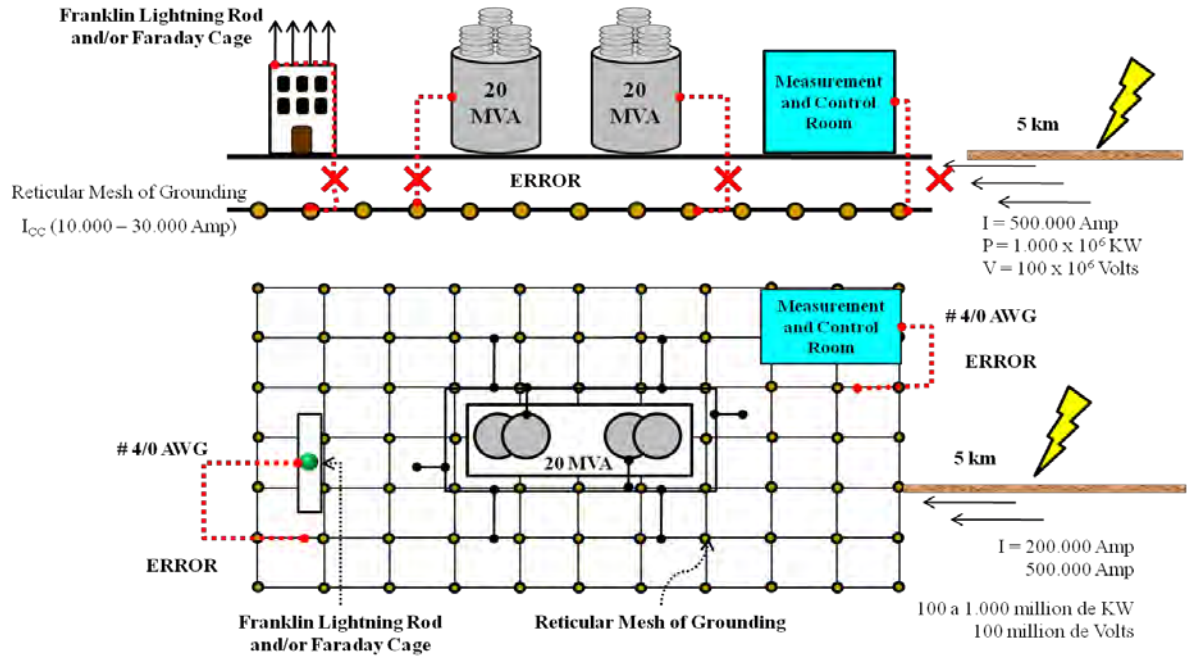

Fig.9. Actual and Traditional Systems of Grounding (ERROR)

2.9. Electrical Substation: The New Highest Technology

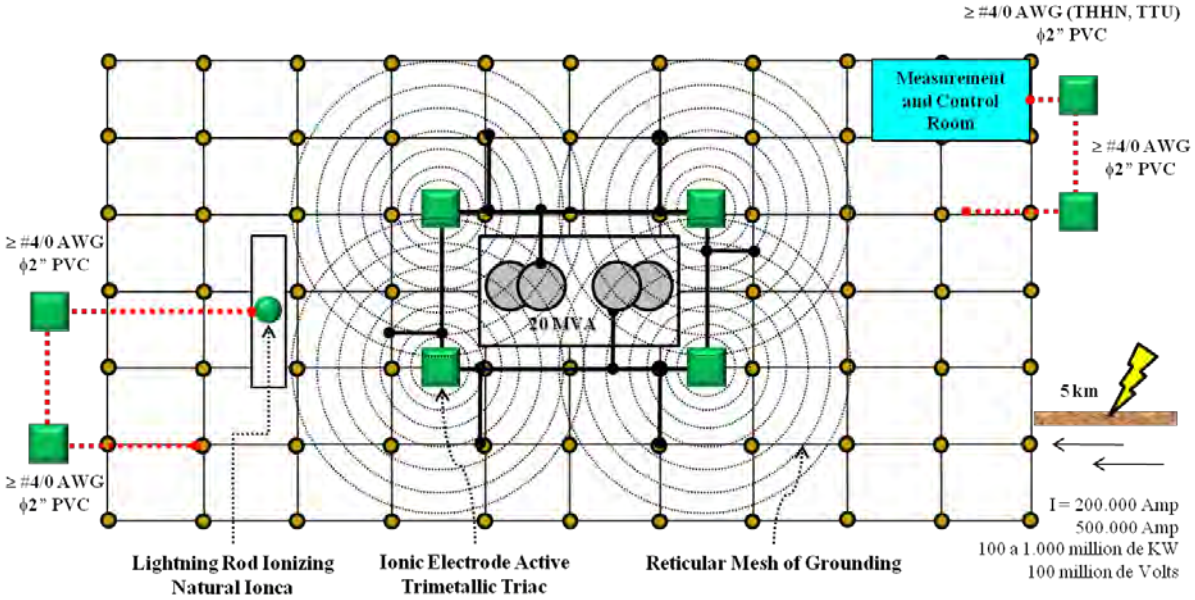

Fig. 10. Natural Ionizing System of Electrical Protection. New Concept, Design and Calculation of Engineering in Electrical Substations. (CORRECT)

3. Results/Conclusion

Power generation is vital and very important, but provide protection and security to the energy generated is perhaps even more important. We must avoid the energy losses with an efficient and effective protection. The 85% of major “Blackouts” and Electrical Faults in power generation, Power Equipment and Electronic Equipment of High Sensitivity in the world are produced by the destructive effects of Atmospheric Discharges (Lightning). This results in loss of lives and billions of dollars each year.

The New Highest Technology, 100% Venezuelan, Unique in the World, Natural Ionizing System of Electrical Protection conformed by the Lightning Rod Ionizing Natural Ionca and the Ionic Electrode Active Trimetallic Triac of Grounding of world-wide standard whose operation and electrophysical basis are based on phenomenon and events scientifically verified like: Atmospheric Discharges (lightning), “crown effect”, “hit effect”, “grounding direct discharge”, metallic and atmospheric ionization, electromagnetic and electric fields, ionizing potential and electronic affinity, electrical potential presented in the atmosphere in conditions of electrical storm, resistance and atmospheric pressure, tripole in the cloud, cosmic rays, physical state of the water (liquid, solid and gaseous), electrolytes, resistivity of the ground and resistance of dispersion, effects to improve the ground resistivity to give high degree of alkalinity), principle water humidity and retention (properties of the charcoal, copper sulphate, sodium chloride and the bentonite), substances, equipotential lines and equipotentiality of a system (properties of the steel, receives and aluminum like good electrical conductors), exothermic weld.

This New High Technology, 100% Venezuelan is the definitive and total solution against Electrical Faults and Interruptions generated by Atmospheric Discharges (lightning) and affect Electrical Substations, Power Equipment and Electronic Equipment of High Sensitivity, Oil Exploration, Drills, Tanks and Stations of Fuel Provision. At the same time, avoiding “the burning” of Electronics Cards in Electronics Equipment of High Sensitivity (Rx, CT, MRI). It’s the mechanism to end the "blackouts" that produces so many damages and losses of

billions of dollars around the world. It´s scientifically proved and globally accepted that the existing Electrical Systems of Protection at the moment like: Reticular Mesh of Grounding and Coperweld Bars don´t have capacity to disperse and propagate to land mass the enormous energies associated to the Atmospheric Discharges (lightning), which are in the order: 500,000 Amperes, 1,000 million Kilowatts and High-Level Transient Voltage of 100 million Volts, enormous energies that cannot be dispersed by Reticular Mesh of Grounding, which it has a maximum capacity between 20,000 and 30,000 Amperes. This is the principal cause of major Blackouts and Electrical Faults around the world.

Finally remarks

The Lightning Rod Ionizing Natural Ionca and the Ionic Electrode Active Trimetallic Triac of Grounding are Ecological, Natural, Don't Contaminate the Environment and fulfill all Electrical Codes and Norms International and National such as: IEEE, NFPA, ANSI, BSCP, WMO, NFC, NEC, CODELECTRA, COVENIN; and it has received the Certification and Recognition by: IEEE, The Institute of Electrical and Electronics Engineers, Latin America and The Caribbean Region. XXI World Energy Congress, WEC 2010, Canada, Author, Presenter, Venezuela Delegate. The New Highest Technology Paper: The International Energy Technology Data Exchange (www.etde.org); US Department of Energy Office of Scientific and Technical Information, OSTI, Library and Archives Canada and Scientific Libraries Worldwide. IEEE, XV International Congress of Electrical, Electronic and Systems Engineer, INTERCON 2008, Peru, Author, Presenter, Venezuela Delegate. Polytechnic Experimental National University "Antonio Jose de Sucre" (UNEXPO), Arbitrated University, Venezuela. Antenor Orrego Private University (UPAO), Peru. Science, Technology and Innovation Award granted by Foundation for the Development of Science and Technology (FUNDACITE), Ministry of Science, Technology and Intermediate Industries, 2006, Venezuela. General Department of Science and Technology Research, Ministry of Science, Technology and Intermediate Industries, Venezuela. National Center of Technological Innovation. CVG MINERVEN. National and Internationals Publics and Private Companies. Projects and Construction built: Church La Chiquinquira. CVG MINERVEN (Gold Mining). Promotora Minera Guayana (PMG), AGAPOV Group (Rusian) – Gold Mining. Corporación 80.000, C.A., AGAPOV Group (Rusian) – Gold Mining. CVG ALCASA (Aluminum). CVG VENALUM (Aluminum). Clinics: Medical Specialty Center, La Floresta, Chilemex, Maracay Medical Center. FIOR Venezuela (Iron Briquettes). CVG CARBONORCA (Anodes). Project: Toyota Venezuela (Toyomaya). Engineering Projects: Petróleos de Venezuela (PDVSA), PDVSA Boquerón, ENELBAR (Electrical Substations: Bárbula, Morón, Valle Seco, Chivacoa, Nirgüa, Yaritagüa), CADAFE (Electrical Substations: Tucupita, Temblador).

References

[1] M. De La Vega Ortega, Engineering Problems of Grounding, Limusa Noriega, 2006.

[2] P. Díaz, Practical Solutions for Grounding of Electrical Distribution System, McGraw Hill, 2001.

[3] IEEE Std, 80-1986, Guide for Safety in AC Substation Grounding.

[4] IEEE Std, 142-1991, Grounding of Industrial and Commercial Power Systems.

[5] IEEE, 0081P-1983, ANSI/IEEE Std, 81-1983, Guide for Measuring Earth Resistivity, Ground Impedance; and Earth Surface Potentials of Ground System.

Implementing bioenergy villages – a promising strategy for decarbonizing rural areas?

Till Jenssen[1*], Andreas König[2], Ludger Eltrop[1]

[1] *Institute of Energy Economics and the Rational Use of Energy (IER), Stuttgart, Germany*
[2] *German Academy of Science and Engineering (acatech), Munich, Germany*
* Corresponding author. Tel: +49 711 68587868, E-mail: till.jenssen@ier.uni-stuttgart.de

Abstract: An increasing number of rural municipalities want to meet their entire energy demand with biomass. This article gives a system analytic view on these "bioenergy villages" by balancing pros (GHG reduction potential) and cons (costs) using the example of a model municipality in Germany. The results indicate that a 100 % energy supply based on biomass potentials within the boundaries of a rural municipality is technically possible but less reasonable with respect to land-use competition and costs of energy supply. Whereas heat and power demand in bioenergy villages can be covered WITH RELATIVELY LITTLE LAND and to relatively low costs, the production of transport fuels based on energy crops (rape seed) leads to significant negative impacts. For a cost-efficient decarbonization of rural areas it can therefore be recommended to particularly expand the utilization of biomass for heat and power production.

Keywords: *rural supply concepts, sustainable energy, life cycle assessment*

1. Concept and status of bioenergy villages

Numerous bioenergy villages have been realized in rural areas of Central Europe over the last decade, for instance in Güssing (Austria), Jühnde (northern Germany) or Mauenheim (southern Germany). In Germany alone, planning and implementation of 55 additional bioenergy villages[1] is in progress or already completed [1]. These villages aim to maximize coverage of energy demand with biomass and to operate the bioenergy infrastructure independently. The German Agency for Renewable Resources (FNR) emphasizes that using fossil technologies for covering peak load demand can be compatible with the concept of bioenergy villages and specifies that – while balancing economic and environmental impacts – at least 50 % of heating demand and 100 % of electricity demand[2] should be met with biomass [2]. To fulfill the requirements of the concept, energy autarky (within the territory of a municipality) can be aimed but is not a mandatory goal [3]. It is rather emphasized that biomass provision should be „regional" or „decentral".

Table 1 highlights some pros and cons of bioenergy villages. Looking at the realized villages, it is interesting to see that they do not restrict themselves to biomass utilization and some even underline the implementation of additional renewable energy such as solar or geothermal energy. Moreover, it is noticeable that despite a relatively low energy demand density all bioenergy villages trust in district heating systems instead of using separate technologies for each building (such as split log boilers). This is because district heating systems offer the opportunity to gain economies of scale, to switch over to renewable energy fast and collectively as well as to keep the added value completely within the region (by using regional energy sources and operating the plant by local stakeholders). Besides, the rollout of district heating systems in rural areas often benefits from the lack of competing grid bound systems (e.g. pipelines distributing natural gas) [4].

[1] Moreover, more than 100 regions in Germany intend to cover 100 % of their future energy demand with renewable energy [11].
[2] the latter with regards to a yearly balance

And in fact, using renewable energy in rural areas seems to have advantages compared to urban areas. They have a good resource base, a case study of Baden-Württemberg for instance points out that in rural areas seven times more biomass (per capita) is available compared to large cities [5]. Moreover, market penetration is much higher, 60 % of Germany's installed bioenergy capacity is located in rural areas [6].

Table 1. Pros and Cons of bioenergy villages

pros	cons
Low fuel costs	High up front costs (Investments)
Stimulation of regional and rural economy	Transport of biomass (Traffic)
Reduction of energy related greenhouse gas emissions	Increase of „local" emissions (particulate emissions)
Shifting away from finite resources	
Reaching (to a large extent) independency from price development of fossil energy carriers	Increase of land use competition
Image building and strengthening of tourism	Acceptance of residents is an important pre-condition for economic feasibility

2. Research design

Against the background of the rapid development of bioenergy villages, this survey investigates the prospects of a range of bioenergy technologies such as fermentation biogas plants, district heating-plants and CHP[3]-plants (combustion and gasification), biodiesel plants and BTL[4] plants. The complete list of technologies is given in Table 2. The typology of bioenergy technologies is deduced from those technologies which are implemented in the cases of Güssing, Jühnde and Mauenheim. Alternative renewable energy sources such as solar and geothermal are not considered.
This article draws on a previous work [7]. It presents updated information, more detailled data on technologies and new evaluations and illustrations.

The analysis is carried out using the example of a rural "model municipality" representing an average German village and provides a system analysis focusing on costs and CO_2-reduction. The methodology is inspired by the pioneer of urban ecology Abel Wolman, who applied a similar approach in the 1960s to analyze the material flows of an US-American City [8]. The demand characteristics of the village result from a comprehensive evaluation of statistics and a literature review [5], [9], [10]. The analyzed model village has 1,050 hectares of agricultural land, 400 hectares of permanent grassland and 900 hectares of forest land. The number of inhabitants accounts for 3,000.

In a first step, a technology analysis is carried out to define the specific CO_2-emissions (g/kWh) and specific energy generation costs (EUR-cent/kWh) of biomass technologies as well as fossil reference technologies for the provision of heat, electricity and transport fuel. The analysis follows the principle of life cycle assessments (LCA) and – as illustrated in Fig. 1 – includes direct and indirect emissions (up- and downstream processes,

[3] CHP = Combined Heat and Power
[4] BTL = Biomass to Liquid

such as transport-diesel, fertilizer or deconstruction of facilities) as well as generating costs [11].

Table 2. Analyzed technologies for the provision of heat, electricity and transport fuel

Technology	Capacity	Fuel	End energy	Abbreviation
Fermentation biogas plant	150 kW_{el}/200 kW_{th}	Manure	heat/power	BG 150 M
	150 kW_{el}/200 kW_{th}	Corn	heat/power	BG 150 C
	600 kW_{el}/700 kW_{th}	Manure	heat/power	BG 600 M
	600 kW_{el}/700 kW_{th}	Corn	heat/power	BG 600 C
District heating plant	2.5 MW_{th}	Wood chips	heat	HP 2.5
	5 MW_{th}	Wood chips	heat	HP 5
	10 MW_{th}	Wood chips	heat	HP 10
	12.5 MW_{th}	Heating oil	heat	HP 12.5 HO
CHP plant (extraction condensing steam turbine)	max. 1.7 MW_{el} max. 3.5 MW_{th}	Wood chips	heat/power	CHP ST
CHP plant (gasification+gas engine)	2.0 MW_{el}/4.5 MW_{th}	Wood chips	heat/power	CHP gas
Biodiesel plant	3.6 MW/2.9 Mio. l/a	Rape seed	Biodiesel	RME
BTL plant	3.6 MW/2.8 Mio. l/a	Wood chips	BIODIESEL AND GASOLINE	BTL

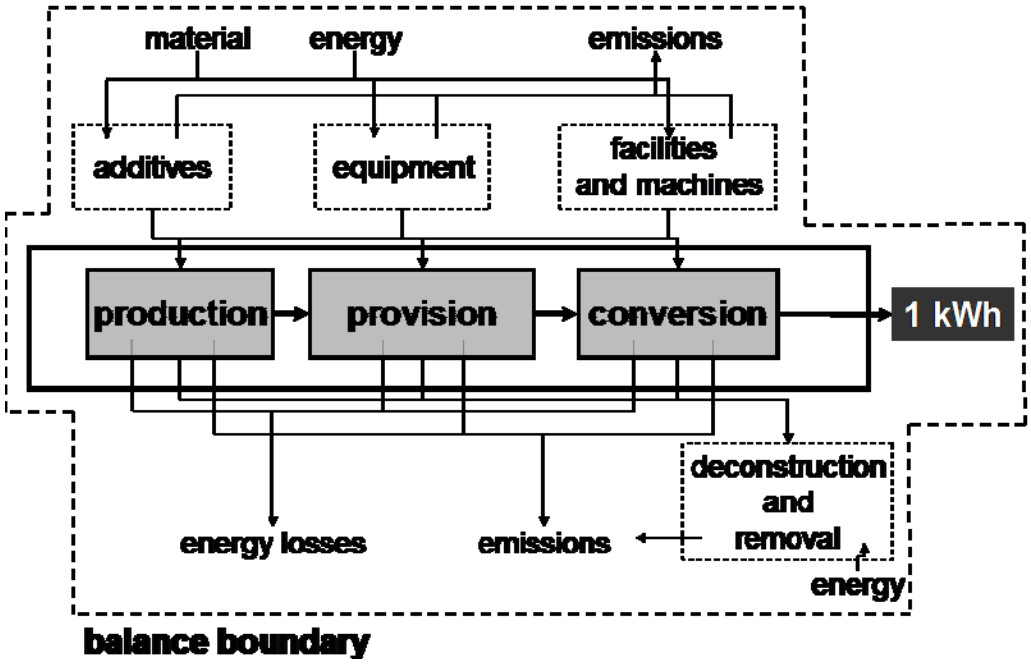

Fig. 1. Balance boundaries and elements of the life cycle assessment (LCA)

In a second step, six different combinations (BF1, BF2, BB1, BB2, BBB1 and BBB2) of the selected technologies are assessed. They are designed to cover the energy demand (heat, electricity, transport fuels) of the model village. The energy demand is considered as the cumulative energy demand during the period of one year. The actual coverage of the fluctuating energy demand during the period of a day or the four seasons is (with the

exception of heat supply) not considered. The six technology combinations are shown in table 3 and represent different cases for the substitution of fossil fuels:

- In BF1 and BF2 (Bio + Fossil) more than 100 % of electricity demand is provided by biomass technologies. At the same time, 30 % of heat demand is covered by fossil fuels[5] (peak load). Biofuels are not produced at all.
- In BB1 und BB2 (Bio + Bio) 100 % of heat demand and more than 100 % of electricity demand are covered by biomass-technologies. Biofuels are not regarded.
- In BBB1 and BBB2 (Bio + Bio + Bio fuel) 100 % of heat and fuel demand are covered by biomass technologies and surplus electricty is generated.

For every export and import of electricity (surplus production), an economic and environmental value is credited: The credits for emissions equate the electricity mix in Germany (576 g/kWh). The credits for costs are calculated in two ways: One credit (FIT) is based on the feed-in tariff of the German renewable energy law depending on the kind and capacity of the technology used (8.0 to 14.7 EUR-cent/kWh). The alternative credit (AVEL) is based on the average costs of the German electricity production (5.5 EUR-cent/kWh).

Finally, the results of the biomass utilization options are compared to a fossil reference supply system which is defined as follows: 60 % of heating demand are covered by individual boilers with fuel oil (371 g CO_2/kWh; 10.5 EUR-cent/kWh), 30 % by natural gas condensing boilers (226 g CO_2/kWh; 10.4 EUR-cent/kWh) and 10 % by boilers with split logs (12 g CO_2/kWh; 8.0 EUR-cent/kWh). Moreover, the electricity mix in Germany (576 g CO_2/kWh; 5.5 EUR-cent/kWh) as well as the shares of conventional diesel and gasoline in Germany's fuel mix (210 g CO_2/kWh; 3.7 EUR-cent/kWh) are taken into account for the reference supply system.

Table 3. Analyzed supply systems and technology combinations

Supply system	Abbr.	Combination of technologies	Coverage rate biomass [% of demand]		
			heat	elect.	fuel
Bio + Fossil	BF1	BG 150 M + 3x BG 600 C + HP 5 + HP 12.5 HO	70	133	0
	BF2	BG 150 M + 3x BG 600 C + CHP ST + HP 2.5 + HP 12.5 HO	70	272	0
Bio + Bio	BB1	BG 150 M + 3x BG 600 C + HP 2.5 + HP 5 + HP 10	100	133	0
	BB2	CHP ST + HP 2.5 + HP 5 + HP 10	100	116	0
Bio + Bio + Bio fuel	BBB1	BG 150 M + 3x BG 600 C + HP 2.5+ HP 5 + HP 10 + RME	100	133	100
	BBB2	HP 5 + HP 10+ CHP gas + BTL	100	131	100

3. Performance of technologies and technology combinations

Fig. 2 shows the results of the technology assessment. It contains the bioenergy technologies for heat, electricity and fuels without credits as well as the associated CO_2-emissions. There is quite a huge bandwidth of results, from 10 g/kWh (BG 600 M) to 116 g/kWh (RME) or (looking at costs with credits) 3.2 EUR-cent/kWh (BG 150 M) to 19.4 EUR-cent/kWh (BG 150 C).

[5] In these two cases the oil heating plant covers 63 % of the total capacity demand of 19.5 MW_{th}.

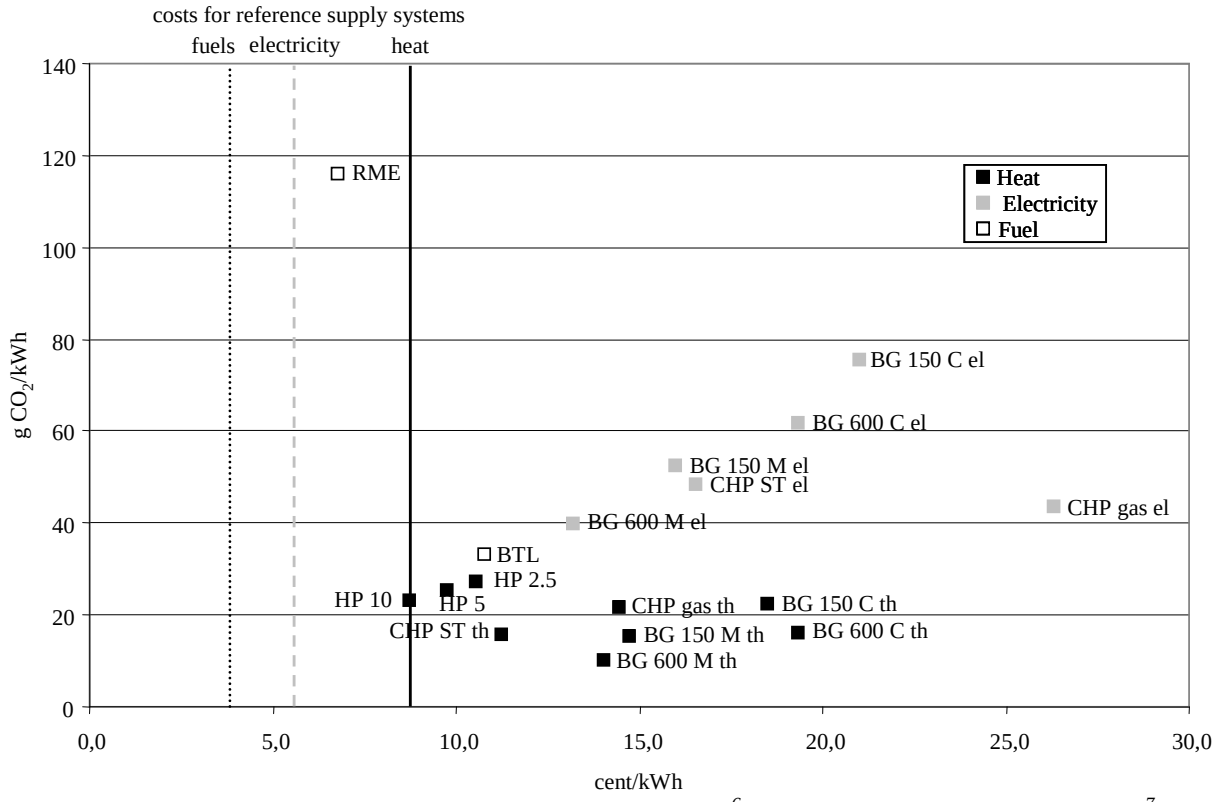

Fig. 2. Costs and CO_2 emissions of 11 bioenergy technologies[6] without credits (exergy allocation[7])

The results clearly indicate that:

- all bioenergy technologies come along with less CO_2 compared to the fossil reference technologies and (without feed-in tariffs) hardly achieve lower costs.
- heat provision is the most economic form of bioenergy and the provision of transport fuels comes along with the highest CO_2 emissions.
- using residues (manure) is much more favorable than energy crops. This is true for both, environmental and economic balances.

When looking at the six technology combinations in Fig. 3, the analysis furthermore proves that massive contributions to decarbonization of the rural energy supply can be achieved by implementing bioenergy villages. Even the least ambitious supply system (BF1) cuts emissions by 56 %, whereas the most ambitious approach (BBB2) reduces CO_2 emissions by even 97 %. Supply systems using biomass for peak load have considerably better results than systems with fossil peak load.

[6] The CO_2 emissions of the fossil reference technologies amount to 292 g/kWh (heating), 576 g/kWh (electricty) and 201 g/kWh (fuels).

[7] Exergy allocation attributes costs and emissions with respect to the share of energy that can be converted into any other from of energy ("available work"). Thus, the weight of useful heat depends on its temperature: the higher the temperature, the higher its weight. Due to thermodynamics, however, heat is always lower than 1. In turn, electricty always equals 1 per definition.

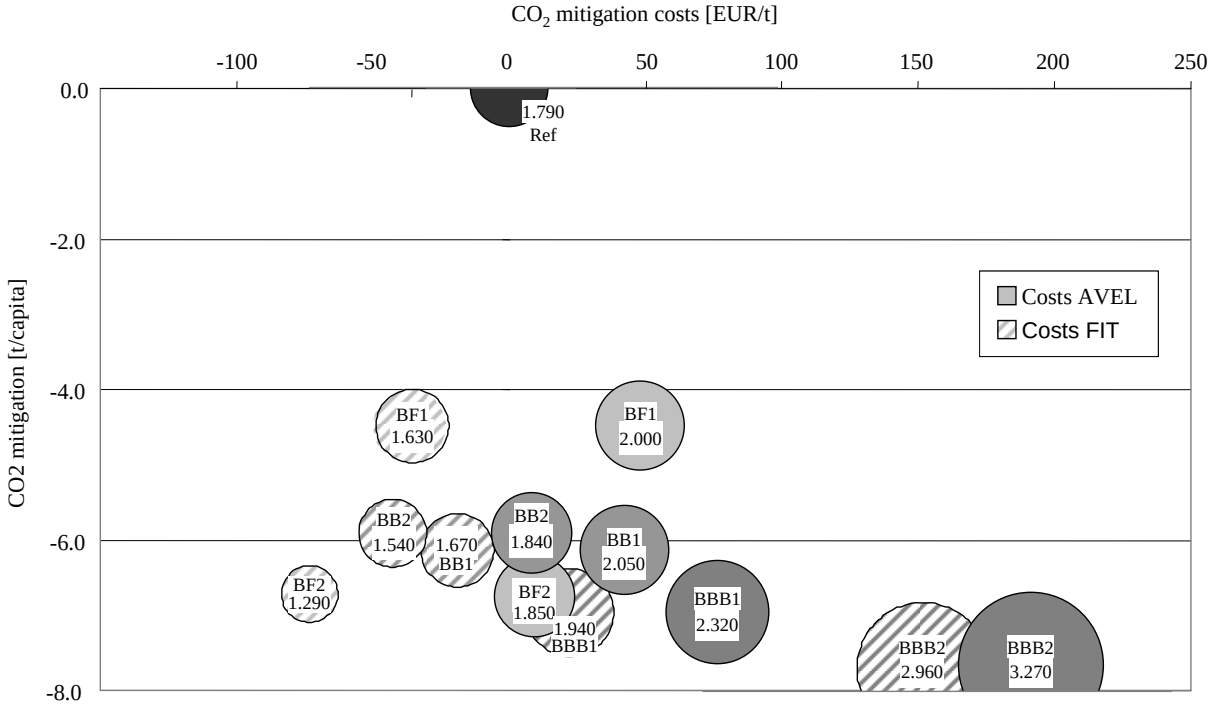

Fig. 3. CO_2 mitigation (compared to the reference supply system[8]), CO_2 mitigation costs and yearly costs per capita (bubble size, EUR/capita/a)

In contrast, under current prices for energy carriers, bioenergy villages hardly reach conventional supply systems without considering feed-in tariffs: the four cases BF1 (1,630 - 2,000 EUR/capita/a), BF2 (1,290 - 1,850 EUR/capita/a), BB1 (1,670 - 2,050 EUR/capita/a) and BB2 (1,540 - 1,840 EUR/capita/a) show higher costs (with regards to AVEL-costs) than the fossil reference system. In turn, costs based on credits for feed-in tariff certainly (FIT) are lower in BF1, BF2, BB1 and BB2 than the reference supply system.

In BB2 for instance costs are considerably lower compared to BB1 due to the utilization of less expensive woody biomass instead of energy crops. Comparing BB1 and BF1, only a small increase of costs (+2.5 %) can be seen. Therefore, it can be concluded that replacing a heating oil plant (peak load) with the wood chip heating plant can achieve moderate CO_2-mitigation costs. In turn, including transport fuels (BBB1 and BBB2) leads to a considerable increase of costs (up to 3,270 EUR/capita/a in BBB2).

Fig. 4 highlights that limits for the mass role out of bioenergy villages can appear with regards to resource base. In rural areas a 100 % supply with biomass – even though it is technically possible – can only be reached with unreasonably high competition to the food, fodder production, goods of the pulp and paper industry, and derived timber products. From this point of view, the combination with other renewable energy carriers ("renewable energy villages") should have good potentials to reducing the problems of spatial limits.

[8] 8.0 t/capita

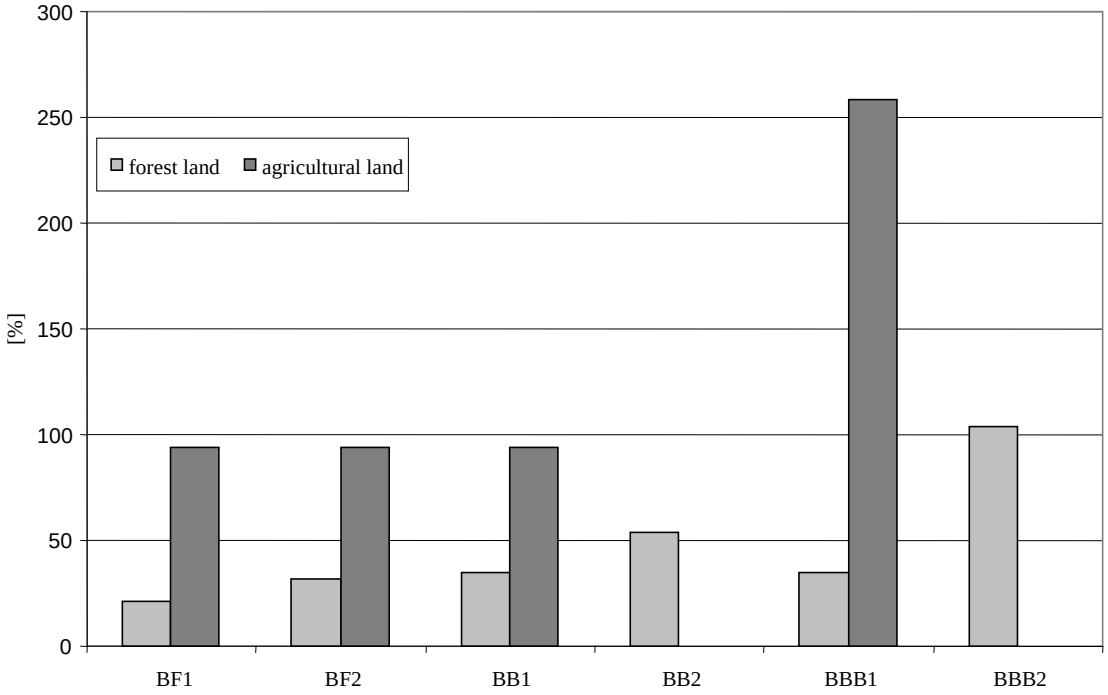

Fig. 4. Consumption of existing resource base (the share of all forest- and agricultural land is shown without considering non-energy use of forestry or agricultural products)[9]

4. Prospects for low carbon rural areas

The survey clearly proves that bioenergy villages offer good opportunities for achieving low carbon rural areas. In addition, most supply concepts – at least under current feed-in tariffs in Germany (FIT) – stood the economic test and (except the ambitious supply system BBB1 and BBB2) show negative CO_2 mitigation costs. Moreover, it demonstrates that a 100 % supply with heat, electricity and mobility is 'technically feasible' within the territory of an average German village. But such status can only be achieved if second generation biofuels are employed, which currently come along with significantly higher costs. Generally, energy autarky can only be reached with high competition to food- and fodder-production (conflict of aims). But it is possible to cover heating and electricity demand without causing significant land competitions.

Especially those municipalities which have large forest areas within their territory offer excellent prospects to become a bioenergy village. This is due to the circumstance that wood combustion technologies are the most developed and low-cost bioenergy technologies (see Fig. 2). In contrast, biogas technologies are competitive only due to the feed-in tariffs even when residues (manure) are used. The most expensive way of CO_2-mitigation is the production of biofuels. Therefore, the current strategy of most bioenergy villages (first providing heat and/or combined heat and power, then electricity and then fuels) is a wise approach.

Whereas a large resource base is given in rural areas, implementation of renewable concepts is facing serious drawbacks as low settlement densities lead to higher specific costs and losses

[9] Values < 100 % indicate that less biomass is used than can be provided within the boundaries of an average German rural municipality. In turn, values > 100 % imply that imports of biomass are mandatory to implement the respective bioenergy concept.

for heat distribution. Therefore, the implementation of individual technologies without heat distribution (e.g. pellet boilers) and the combination with other renewable energy carriers have good potentials to add to the concept of bioenergy villages.

References

[1] Bundesministerium für Ernährung, Landwirtschaft und Verbraucherschutz (BMELV), Wege zum Bioenergiedorf, http://www.wege-zum-bioenergiedorf.de/bioenergiedoerfer/karte.html, accessed November 9th, 2010.

[2] H. Ruppert, S. Eigner-Thiel, W. Girschner, M. Karpenstein-Machan, F. Roland, V. Ruwisch, B. Sauer, P. Schmuck, Leitfaden Wege zum Bioenergiedorf. Agency for Renewable Resources (FNR), Gülzow, 2008.

[3] K. Scheffer, Vom Bioenergiedorf zur autonomen Solarenerige-Region, Solarzeitalter 4, 2008: pp. 23-30.

[4] A. Paar, M. Duscha, H. Hertle, M. Pehnt, S. Ramesohl, M. Fischedick, W. Irrek, F. Merten, Vom Bioenergiedorf zur 2000 Watt Gesellschaft: Energiepolitische Zielkonzepte im Spannungsfeld zwischen erneuerbaren Energien und Energieeffizienz, Institut für Energie- und Umweltforschung (ifeu), Wuppertal-Institut für Klima, Umwelt, Energie, Heidelberg, Wuppertal, 2007.

[5] T. Jenssen, Einsatzmöglichkeiten der Bioenergie in Abhängigkeit von der Raum- und Siedlungsstruktur. Wärmetechnologien zwischen technischer Machbarkeit, ökonomischer Tragfähigkeit, ökologischer Wirksamkeit und sozialer Akzeptanz. Vieweg Teubner Research, Wiesbaden, 2010.

[6] A. Koch, L. Porsche, A. Wacker, Genügend Raum für den Ausbau erneuerbarer Energien? BBSR-Berichte KOMPAKT 13, 2010, pp. 1-16

[7] A. König, T. Jenssen, Bioenergy Villages – a blueprint for rural energy supply?, Journal of Environmental Management and Tourism, 1, pp. 4-7

[8] A. Wolman, The Metabolism of Cities, Scientific American 213, 1965, pp. 179-190

[9] Statistical offices of the Federation and the Länder (Statistical Offices), Statistik lokal. Daten für die Gemeinden, kreisfreien Städte und Kreise Deutschlands, Federal Statistical Office, Wiesbaden, 2006.

[10] M. Blesl, S. Kempe, M. Ohl, U. Fahl, A. König, T. Jenssen, L. Eltrop, Wärmeatlas Baden-Württemberg. Erstellung eines Leitfadens und Umsetzung für Modellregionen, BWPLUS, Stuttgart, 2008.

[11] A. König, Ganzheitliche Analyse und Bewertung der energetischen Biomassenutzung - Techno-ökonomische und ökologische Analyse konkurrierender energetischer Nutzungspfade für Biomasse im Energiesystem Deutschland bis zum Jahr 2030, Südwestdeutscher Verlag für Hochschulschriften, Saarbrücken, 2009.

[12] M. Bensmann, Auf dem Weg zu 100 Prozent, neue energie 06, 2009: pp. 30-40.

Sustainable regional development through the use of photovoltaic (PV) systems. The case of the Thessaly region

Roido Mitoula*, Konstadinos Abeliotis, Malvina Vamvakari, Athina Gratsani

[1] *Harokopio University, Athens, Greece*
** Corresponding author. Tel: +30 2109549213, Fax: +30 2109577050, E-mail:mitoula@hua.gr*

Abstract: The purpose of this study is the contribution of photovoltaic systems to the Sustainable Development of the region of Thessaly in Greece. The aim is to explore both the potential for further installation of PV systems in the region and to record the opinions, knowledge and attitudes of residents about them. To document the theoretical data was carried out fieldwork using questionnaires given to a sample of 200 residents of the region of Thessaly. The work attempts to clarify the term "Sustainable Development" and what are the factors that contribute to it. The advantages and disadvantages of PV systems and the European policy that is followed in Greece for them, are recorded. The work focuses on solar rooftops and special attention is given to the advantages and disadvantages of solar roofs. The search area is studied and the general characteristics are given. The research, the results of statistical analysis and the X^2 test for independence are described. In this way, we are given the possibility to approach the degree to which citizens are informed and sensitized on the issues of photovoltaics. In the last part of the study the results of statistical analysis are commented, the conclusions are recorded and proposals are formulated to improve the current situation and further spread and use of photovoltaic parks and solar roofs in the region of Thessaly.

Keywords: *Sustainable Regional Development, Photovoltaic Systems Renewable energy.*

1. Introduction

Nowadays, it has become acceptable that sustainable development is directly linked to energy development. The use and evolution of renewable energy can contribute to the sustainable development of a place, because this will mean environmental protection, and security for the financial resources for this place. (Mitoula, 2006)

Regarding photovoltaic systems, the photovoltaic parks made today at a regional level, produce electricity channeled through the Public Power Corporation (PPC) for the electrification of areas. (www.photovoltaicscom.gr) The same occurs with the installation of PV on the roofs of houses (so-called solar roofs). The advantages of such a practice are many, since firstly, the citizen produces his own electricity for the home and secondly, a profit because it is connected to the electricity network and the "excess" power is sold to it. In this way achieve faster depreciation of the cost of installation. (www.atlantisresearch.gr) (www.helapco.gr), (www.pv-home.gr)

The purpose of this study is the contribution of photovoltaic systems to the Sustainable Development of the region of Thessaly in Greece. The aim of this study is to explore both the potential for further installation of PV systems in the region and to record the opinions, knowledge and attitudes of residents about them. To document the theoretical data was carried out fieldwork using questionnaires given to a sample of 200 residents of the region of Thessaly. The work focus on solar rooftops.

In the last part of the study the results of statistical analysis are commented, the conclusions are recorded and proposals are formulated to improve the current situation and further spread and use of photovoltaic parks and solar roofs in the region of Thessaly.

2. Case Study: The region of Thessaly

The region of Thessaly is the central - eastern part of mainland Greece. It consists of the prefectures of Karditsa, Larissa, Magnesia and Trikala and occupies a total area of 14,036 km^2 (10.6% of the total area of the country). (www.thessalia.gov.gr) (Sivignon, 1992) (www.el.wikipedia.org)

In the region of Thessaly operates 19% of photovoltaic power plants in Greece. The greatest contribution of Thessaly in energy through photovoltaic systems for large power stations, from 150 to 2000 KWp, sector which occupies 31% of national production. 9% contribute to a small group to 20 K Wp and 14% in average power of 150 K Wp. Then data on the 4 prefectures of Thessaly are recorded.

In the prefecture of Magnesia, power stations are located, of which 14% of Thessaly contribution to the national average production of energy is produced. (www.anaptixiaki-anamth.gr)

The first photovoltaic park double-axis, power 94,5 Kw, (6 acres) was created in Stefanovikio of Magnesia in 2009 and its operation involves several elements of originality, since the construction is based on a tracking system of the sun (tracker double -axis), thanks to moving rather than stable panels follow the sun, ensuring maximum efficiency. (www.wordpress.com, www.qualitynet.gr). At the same time, authorized another photovoltaic power station same power (2MWp), adjacent to the operating station Industrial Area of Volos.

In the field of solar roofs, the Social Law Center South Pagason of Municipal Agency for Health and Social Affairs of the Municipality of Volos equipped with an integrated system for producing electricity from the sun. The PV panels are composed, produced more than 2.600 KWH per year, offsetting 2.3 tonnes of CO2 emissions in the same period. The PV system that was installed in front of this building is the first building unit of a municipal building in Greece and the PV modules are specially designed for buildings. (www.aleo-solar.gr) This system is innovative and the aim of Volos is the progressive intervention on existing buildings, contributing to environmental protection and energy security for the city. Having such a slogan "Volos-Green Town", the Municipal Authority has been gradually implementing an ambitious program to become the capital of Magnesia benchmark and a model "Green City".

The prefecture of Karditsa, has large areas of high sunshine, a favorable ground for development of this technology, which supports local development. As priority areas for siting installation of exploitation of solar energy are the areas that are barren or are not high productivity and preferably invisible from crowded places, and with opportunities of connectivity to the Network or System. (www.minenv.gr)

Example of installation of PV parks in the prefecture of Karditsa is in the municipality of Campos, where 5 PV parks were constructed, which produce 20 KW / h each. The funding was made by the Operational Programme "Competitiveness" of the Ministry of Development (45% subsidy from Ministry of Development and 55% own contribution). (www.oikosocial.gr) The project makes the municipality electrician producer. The benefits from the operation of this park are numerous and significant for the local community and the wider region. In 2008 established the "Energy Company of municipality of Campos". The local company that took over the project, pledged that 50% of profits will invested in environmental projects and the remaining or rest of 50% in activities of cultural, sporting and

environmental sector, namely development projects for the benefit of the municipality. (www.karditsanews.gr) Also, 2.5 acres used for the installation of PV is like to have created 200 acres of forest. This is because many would be needed to absorb 280 tones of CO2, the release of which prevent the PV. (www.oikosocial.gr)

Also in Artesiano of Karditsa two units of 100 KWp are built in neighboring areas of PV panels of high efficiency, with rated power 100 KWp each. (Www.aleo-solar.gr)

Under construction is PV station in the Industrial Area of Karditsa with power 1MW.

In addition has given a license installation of a power station by PV power systems 0,84 MW, in place of the industrial area of Karditsa, Palama Municipality of Karditsa (www.thessalia-espa.gr/Files/espa_episimi.pdf)

Regarding the prefecture of Larissa, in recent years contributes significantly to generating/producing electricity using not only PV parks and solar roofs.

In the municipality Kranona installed PV park, thanks to the special bases of support, following the sun in two directions (two-axles trackers). This provides 40% more power than conventional – stable installations. Already by 2/4/2009 have been saved 1.616,54 kg CO_2 emissions from the PV station rated power of 19.80 kW, which came into full production mode on 13/3/2008. The project was funded under the CSF by the "Competitiveness" of the Ministry of Development, at 55%. (www.greenproject.gr)

Also, in the municipality Polydamanta was authorized in 2009 by the Ministry of Development and the Region of Thessaly, the transmission of energy production license and, installation license of PV station, power 9,99 MW.

In February 2010, in place Kritiri of the municipality Farsala of Larissa, was issued permit installation of PV power station, power 1.998 MWp.

Finally, based on the same article, was issued another permit installation of PV power station, power 4.996 M Wp, in the municipality Narthakiou of Larissa. (www.photovoltaics.com.gr/solar-panel-pv-3.html)

As for the prefecture of Trikala, there is a rapid increase in installed PV systems.
Specifically, the Energy Regulatory Authority (RAE) approved the installation of PV systems with total power 95,04 KWp on the roof of the Technical Vocational High School of the city. This project covers not only the electricity needs of the school but the excess is sold to ΔΕΗ. The choice of school was for learning and energy purposes. (www.news.trikki.gr)

Also, in 2008 completed the installation of PV power system with power 99.30 KWp in Vasiliki of Trikala. Using the single-axis moving bases, frames are always oriented to the sun by increasing production by 32%. The whole system is supported by a metal circular track of 12 meters in diameter, and thus the suncarrier oriented to the sun every 10 minutes.

The first photovoltaic station in Trikala of "small class" (up to 20 kWp), built in 2008 in the municipality Paleokastro. (www.aleo-solar.gr)

In Pigi of Trikala a new photovoltaic park of 19,98 kW rated power is installed and the connection to the electricity network was held on August 12, 2009.

Also, in the prefecture of Trikala installed PV park on a flat roof of industrial building crafts an extent of 1500 square meters, rated power 19,80 kW. This is the first PV system in Greece installed in the roof using sun tracking system (tracker). Due to the limited installation space and to avoid shadows, preferred to use single-axis tracker, which delivers increased production compared to systems of stable bases (approximately 30-35%).

In 2009, completed another PV park rated power 19,98 kW in Faneromeni of Trikala. The project was funded under the third CSF by the program "Competitiveness" of the Ministry of Development, at 55%. (www.greenproject.gr)

The Municipality Ichalias of Trikala converted in solar center, where completed the installation of two more PV parks of 19,80 kW each, reaching a total of 4 parks in the area.

In 2010, another permit to construct plants producing electricity from PV systems was issued, with a power of 1,006 MW, in the municipality of Paliokastrou in Trikala.

3. Research

In the investigation of these issues, in region of Thessaly, a fieldwork was carried out during the period between February and April 2010. 280 completed questionnaires shared, while 200 of those were returned, of which 60 relate to people of Volos, 40 of Karditsa, 60 of Larissa, and 40 of Trikala (total population = 317105 residents). The number of questionnaires was proportional to the population of each district. Completion of the questionnaire was anonymous, while the sample was selected using the simple random sampling and attempted to cover all the scales of ages and educational levels. After the completion of questionnaires, were processed, followed by checking their validity, the coding of variables and their introduction in the statistical program Statgraphics. Using the statistical program Statgraphics found the percentages. The Excel has the ability to make charts of the percentages of the respective responses of the respondents. Of the 200 people, 46% are men and 54% are women. The majority of respondents are aged 20-29, the rest ranging from 30-59 years old and only 3% are aged 60 or over, which consists of pensioners. The education level of respondents varied, with 52% ranging from 15.000 € to 30.000 €, 12.5 % have an annual household income <15.000 €, 31% from 30.000 € to 45.000 €, and 4.5% of respondents with more than 45.000 €. One very important factor that could influence the views of respondents are professional jobs where just over half the respondents, 51.5% appears to be private and civil servants, 11.5% self-employed, the 20.5% students, 9% are employed in households, 4.5% were unemployed and 3% retired.

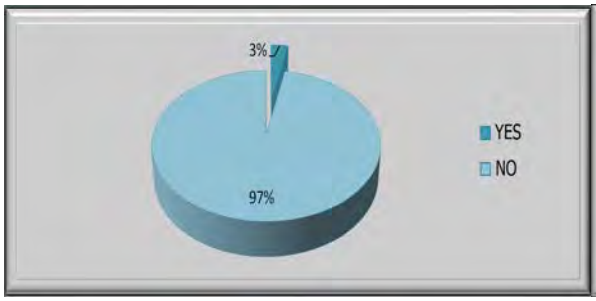

Fig. 1. Have you ever use PV?

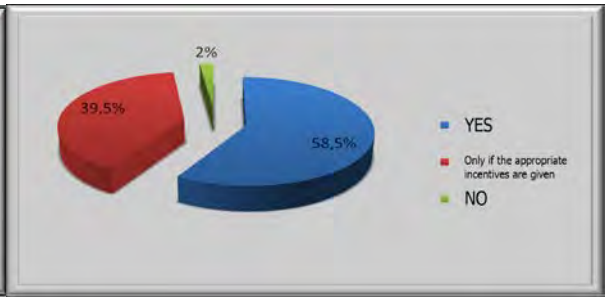

Fig. 2. Are you willing to help in reducing energy consumption by using solar energy through PV?

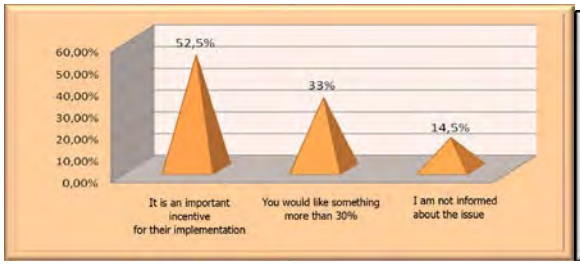

Fig. 3. What about the subsidy by the E.U. for the use of PV?

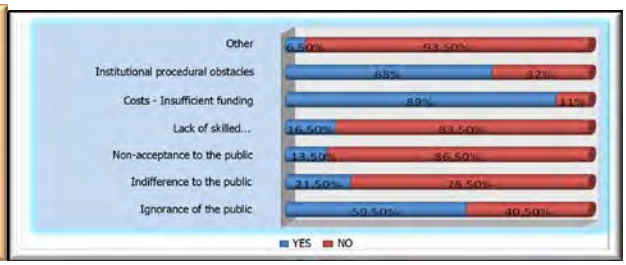

Fig. 4. Obstacles for the use of PV.

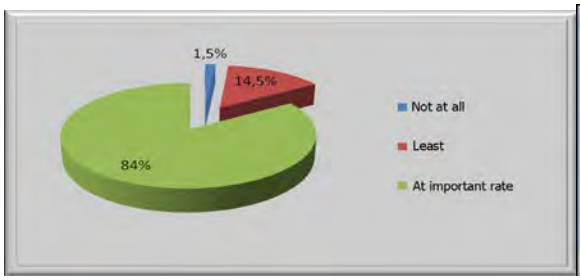

Fig. 5. How PV contribute the Sustainable Development?

Fig. 6. Would you install PV on your rooftops?

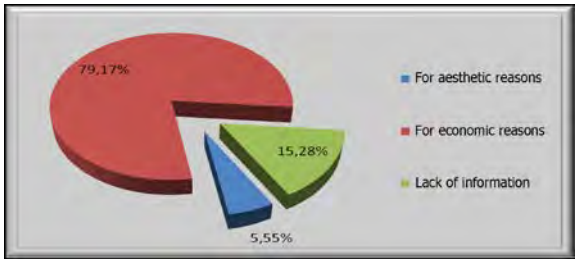

Fig. 7. The others who do not agree with the installation of PV on roofs.

To extract the best conclusion was necessary to examine whether the realization of an event influences another event. To test the degree of dependence between two qualitative variables the X^2 test is used. The X^2 test of independence is a method that allows us to determine whether two variables are dependent.

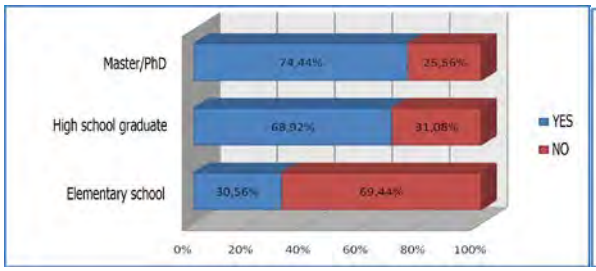

Fig. 8. Correlation of the variables "educational level" and "install PV on roofs"

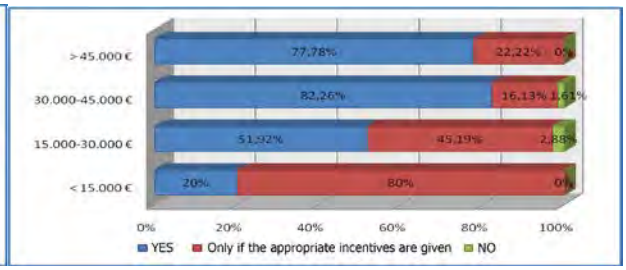

Fig. 9. "annual family income" and "help to reduce energy consumption by using PV

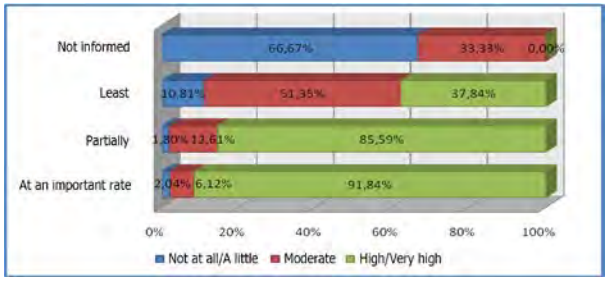

Fig. 10. "information" and "necessity of the installation of PV in the region of Thessaly"

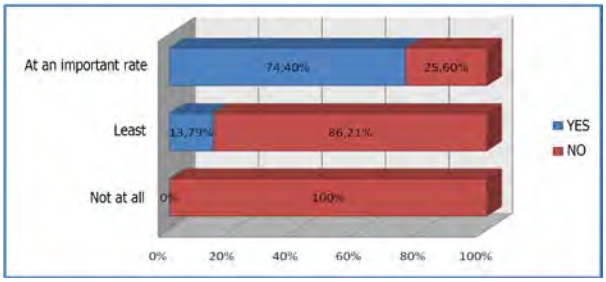

Fig. 11. The intensive use of PV contributed significantly to enhancing sustainable development in the region of Thessaly, the majority agree with the installation of PV on their roofs

4. Discussion

The above survey shows that residents are aware of issues of environmental protection. Furthermore, they are interested in the development of their country and are willing to accept the further use of photovoltaic systems.

97% of the sample have not used PV but are willing to shift to the use of solar energy through photovoltaic systems instead of conventional energy (polluting fuels). On the issue of EU subsidies for application of PV systems exist 2 views exist: in the one hand a subsidy is an important incentive, while on the other hand, a large proportion of the sample considers that the subsidy amount is small compared with the obstacles facing such an action. Also, in the opinion of the sample, there are major institutional problems (bureaucracy, etc.) problems of cost (design, purchase and installation). Therefore, the willingness, determination and environmental consciousness exists, but others are the factors that contribute to the further development of PV systems.

The survey showed that people propose funding from the government, further and better information about the account issues from media and press. Generally, regular information and awareness of public is demonstrated by research that leads to change human behavior, without neglecting the education/training from an early age.

Arguing that the PV systems contribute to sustainable development of the Region of Thessaly, the respondents indicate that the growth sectors that will most affected by the widespread application of PV as a renewable energy, is initially the economy. This is because new jobs, liquidity in the region and independence as a point of fueling are created. The impact on the environment will also be positive, due to reduced emissions, the friendly operation of PV on it, and the recyclability of construction materials. At the same time, the employment of many people working in research on environmentally friendly technology is enhanced.

The subject of the installation of PV on roofs (so-called solar roofs), is a very important part of research because from the results that carried out, is concluded that the largest percentage of respondents who would make installation, are based on the following reasons: they are environmentally friendly, provide reliability and long life, and of course the maintenance cost is very low. Note however that the reason why they would not install, is more economical.

Then, indicated that, the better the educational level of each respondent is, the greater and the eagerness to help in reducing energy consumption by using solar. This happens because the level of education means more knowledge, not just for one particular sector, but general as

long-term benefits, impacts, even in conjunction with other sectors. Moreover, in the case of solar roofs, it is concluded that the higher the educational level is, the higher the percentage of respondents are agreeing with the installation of PV on rooftops. It seems therefore, that this feature reduces the hesitation, financial or otherwise, for such an installation.

Another factor that contributes to the willingness of respondents to install PV is the annual family income, even if it undermines the protection of the environment. The higher the annual household income is, the percentage of people who are interested to help in the effort of reducing energy consumption by using PV increases. In addition the needs of one person to the other differ, also differ in their beliefs, willingness and interests that are directly affected by income. Moreover, employment, which is linked to income, is also a factor that influences the views of persons. The above observed from the fact that the majority of workers support the view that the subsidy that is given by the EU for the application of PV is an important incentive, unlike the pensioners, the unemployed and those employed as household who believe that although is a motive, they would like more subsidy. Implicitly/ Indirectly, then is confirmed that the higher the level of awareness of energy saving issues and renewable energy is, the positive attitude of respondents towards the necessity of installation of PV in the region of Thessaly increases, because of long-term benefits that they offer.

Therefore, for the installation of photovoltaic park in the region, openness and condescension increaese as increasing the willingness to the effort of reducing energy consumption by using solar energy through PV instead of polluting fossil fuels for electricity in the region. Finally, it turns out that sustainable development makes/gives a 'functionality', supports the invulnerable and endlessly point of this development over the years, reinforce local and regional development in conjunction with the RES, because the higher the percentage of respondents who believe that the intensive use of PV contributes to reinforcement of sustainable development is, the possibility of installation of PV on the roofs increases.

5. Conclusions

The region of Thessaly is largely dependent on f ossil fuel, but on the potential use of photovoltaic systems is satisfactory level. The above study also demonstrated the positive attitude of the residents of Thessaly toward this type of systems.

In conclusion, the use of photovoltaic systems is significantly close to the new perspectives of balanced development, which seeks to ensure environmental quality, economic development and improving social cohesion. Also emphasized that the region of Thessaly is the second in Greece in the frequency of using photovoltaics for electricity production, resulting in energy to contribute significantly to sustainable regional development.

References

[1] Mitoula R., "Sustainable Regional Development in the European Union and the Greek Reconstruction of Urban Environment, ed Stamoulis, Athens, 2006, p.27-30, 76

[2] www.photovoltaics.com.gr/solar-panel-pv-3.html

[3] www.atlantisresearch.gr/files/ap5820_ENHMEROTIKO_148.pdf

[4] www.helapco.gr/library/23_7_09/Solar_Roofs_Q&A_d.pdf

[5] www.pv-home.gr/

[6] www.thessalia.gov.gr/contents.asp?id=167

[7] Sivignon M. (1992), "Thessaly, a region of geographic analysis', Educational Institute of Agricultural Bank Translation: Julie Anastopoulou, Athens, p. 69-70

[8] www.el.wikipedia.org/wiki/Θεσσαλία

[9] www.anaptixiaki-namth.gr/index.php?option=com_content&task=view&id=5260&Itemid=65

[10] www.aleo-solar.gr/index.php?view=item&catid=207%3Agreece&id=128%3A2010-01-27-10-05-07&option=com_aleoreferenzen&Itemid=689

[11] www.minenv.gr/4/42/00/sxedio.kya.ape.pdf

[12] www.oikosocial.gr/index.php?option=com_content&view=article&id=221:2010-01-08-14-35-40&catid=43:2009-10-08-07-38-59&Itemid=81

[13] www.karditsanews.gr

[14] www.thessalia-espa.gr/Files/espa_episimi.pdf

[15] www.greenproject.gr/a8.html

[16] www.news.trikki.gr

Integrated Community Energy Modelling: developing map-based models to support energy and emissions planning in Canadian communities

Jessica Webster[1*], Brett Korteling[2], Brent Gilmour[3], Katelyn Margerm[3], John Beaton[4]

[1] *Natural Resources Canada, Ottawa, Canada*
[2]*Vive le Monde Mapping, Gabriola Island, Canada*
[3] *The Canadian Urban Institute, Toronto, Canada*
[4]*Strait-Highlands Regional Development Agency, Port Hawkesbury, Canada*
Corresponding author. Tel: +1 613 992 9532, Fax: +1 613 996 9909, E-mail: jessica.webster@nrcan.gc.ca

Abstract: Urban emissions represent approximately 40% of Canada's current GHG emissions and the need to implement Integrated Community Energy Solutions (ICES) is now broadly recognized. A more consistent approach for characterizing energy and emissions opportunities in communities and the provision of more accurate and comprehensive information to planning processes is required. Integrated Community Energy Models (ICEMs) employ Geographical Information Systems (GIS) to integrate spatial information on a community's land use, building stock, transportation and energy systems and socio-economic characteristics. Using future scenarios, ICEMs support the prioritization of opportunities for energy efficiency and renewable and district technology integration, better enabling planning, policy development and investment decisions.
This paper describes organizations forwarding ICES and ICEM development and selected enabling provincial legislation. Three case-studies are presented: the *Energy Density Mapping Strategy* for the cities of Guelph and Hamilton, Ontario, the *Spatial Community Energy Carbon and Cost Characterization (SCEC^3)* model for the City of Prince George, British Columbia and the *Energy Asset Mapping* project in the Strait-Highlands Region, Nova Scotia. For each, core model aspects, required data, highlighted results and their integration into community planning processes are discussed. The article concludes with next steps for implementation and future research and development of ICEMs in Canada.

Keywords: *Integrated Community Energy Modelling, Community Energy Planning, GIS*

1. Introduction

For several years Canadian communities have been developing Community Energy Plans (CEPs) and have demonstrated success in implementing actions within municipal operations. Preliminary studies suggest however, that targets established in plans for community-wide energy and emissions (E&E) reductions are not being consistently achieved. [1] To address this gap, there is a need for improved decision support for community-wide actions, aided by models flexible enough to assess the impacts of a variety of future scenarios.

Integrated Community Energy Models (ICEMs) support the spatial characterization and prioritization of energy efficiency and district and renewable energy opportunities in communities. The models developed in Canada to date have been used largely in the assessment of E&E reduction targets, policies and actions in CEPs, Official Community Plans (OCPs), Integrated Community Sustainability Plans (ICSPs) and for the accelerated deployment of renewable energy technologies.

It is hypothesized here that ICEMs used in the planning process help planning departments, utilities and the broader public to better comprehend energy end-use and renewable supply options within the built environment. Because energy-related decisions are made at various levels of geography [2] the spatial characterization of energy use and supply is seen as critical to the development of practical and effective reduction plans. The information required for comprehensive E&E reduction planning includes: land use zoning, the type and location of residential densities, employment centres and transportation networks; waste recycling systems and potential carbon sinks; and the capacity for renewable generation and district

energy systems. An integrated assessment of these landscape features enables targeted investment planning towards strategic energy infrastructure and E&E reduction initiatives.

This paper describes three Canadian ICEMs, each of which explores in different levels of detail some of these E&E information aspects: the Energy Asset Mapping (EAM) project undertaken for the Strait-Highlands Region, Nova Scotia, the Spatial Community Energy Carbon and Cost Characterization ($SCEC^3$) model developed for the City of Prince George, British Columbia and the Integrated Energy Mapping, Modelling and Financial Assessment (IEMMFA) strategy for the Cities of Guelph and Hamilton Ontario.

1.1 Community energy research and development objectives of leading organizations

Natural Resources Canada (NRCan) is a department of the federal government of Canada. The CanmetENERGY works with partners to develop more energy efficient and cleaner technologies. An objective of the Program of Energy Research and Development's Communities sub-program is to develop a standardized methodology for characterizing energy and GHGs at the community scale. In 2009, the House of Commons Standing Committee confirmed NRCan's mandate in this area, recommending that the department "…should continue to investigate the reliable measurement of energy in communities." CanmetENERGY is the proponent of the $SCEC^3$ model, and has supported various Canadian ICEMs, including IEMMFA and the Strait-Highlands EAM.

The Canadian Urban Institute (CUI) is Canada's applied urban policy institute dedicated to policy and planning solutions that enable urban regions to thrive and prosper. A Toronto-based not-for-profit organization, the CUI encourages the application and integration of E&E planning into the decision-making process at the municipal level. The Institute has led a program of research into long-term solutions for urban transportation, waste management and energy supply challenges. CUI is the main proponent of the IEMMFA strategy.

The Strait-Highlands Regional Development Agency (RDA) has facilitated economic development for communities and businesses since 1994. A strategic focus within its business plan is to foster a smart energy region. Key objectives include maintaining an energy and emissions inventory, conducting emissions forecasting, and partnering with municipal and community champions to set and achieve reduction targets. The Strait-Highlands RDA initiated the EAM when developing a local action plan, towards achieving Milestone 3 in the Federation of Canadian Municipality's Partners for Climate Protection program. [3]

1.2 Enabling legislation in the provinces of British Columbia, Ontario and Nova Scotia

Within Canada, provincial governments have the jurisdiction to develop legislation on energy and land use planning pertaining to municipalities.

British Columbia has passed a series of acts promoting energy efficiency and emissions reductions. Bill 27, the Local Government Statutes Amendment Act (2008) [4] links E&E to land use planning processes by requiring local governments to include GHG emissions targets, policies and actions in their Official Community Plans and Regional Growth Strategies. Bill 17, the Clean Energy Act (2010) [5], sets ambitious goals for energy reductions of 66% less increased demand and 93% of electricity to be derived from clean sources by 2020. To assist planning efforts, British Columbia has provided 27 regional districts and 163 local governments with their own Community Energy and Emissions Inventory (CEEI) reports, [6] and is fostering an emerging modelling community of practice.

The energy sector in Ontario is in the midst of a significant transformation, spurred on by an interest in an open market for energy production and distribution and the problems of an aging infrastructure and near brownouts. Introduced in 2008, the Green Energy and Economy Act (GEEA), makes it easier to bring renewable energy projects on-line and encourages a culture of conservation. Changes introduced with the bill include a Feed-In-Tariff (FIT), the establishment of conservation targets for utilities, and the requirement for public sector institutions to develop energy conservation plans. Municipalities and utilities have been assigned electrical demand reduction targets and are using energy mapping to assist with decision making on potential strategies to meet them.

The province of Nova Scotia through the enactment of Bill 146, the Environmental Goals and Sustainable Prosperity Act (EGSPA), [7] has set an ambitious target of 25% of electricity to be generated from renewable sources by 2015. A second target, although not yet backed by law, aspires to a 40% reduction in greenhouse gas emissions for 2020. Targets established under the EGSPA are accelerating renewable energy planning in Nova Scotia.

2. Core Model Aspects

2.1 Energy Asset Mapping (EAM)

The Strait-Highlands Region Energy Asset Mapping (EAM) identifies opportunities for the introduction of alternative and renewable energy sources to serve municipal, commercial and residential energy needs. The energy sources explored include: earth energy, wind energy, solar potential, waste heat from mines, geothermal, synergies between large industries, coal bed methane reserves and small-scale hydro potential. Existing information such as hydrology and wind energy profiles and newly created data including solar and waste resource assessments are represented geographically in map layers. These potential energy sources are evaluated based on annual energy output in kilowatt hours (KWh), estimated GHG reduction potential, and cost-effectiveness when compared with a future rise in conventional energy prices. Some sources, including earth energy, bio fuels and industrial synergies, are better represented non-spatially and were evaluated based on estimated values for the quality and quantity of energy available. There is an accompanying guide that provides other details on the technologies including installation costs and, in some cases, a simple payback analysis.

2.2 Spatial Community Energy Carbon and Cost Characterization Model (SCEC^3)

The SCEC^3 model enables the calculation and spatial characterization of present-day and future energy use, emissions and associated costs for residential, institutional, commercial and industrial buildings in the City of Prince George, British Columbia. It combines simulated energy information for selected housing and building archetypes with BC Assessment Authority (BCAA) building attribute information. The building archetype approach is consistent with that observed in projects internationally [8], [9].

Energy modelling for homes was completed in HOT2000, using ecoENERGY Retrofit Audit records collected in Prince George and held by NRCan. One objective of the research is to explore the use of existing federal government data and tools for community E&E characterization. Seven housing types were selected within the City of Prince George as representative of both the ecoENERGY Retrofit audit records and the housing stock as a whole. In addition to the community's baseline energy, GHGs and operating energy costs, 'low cost' and 'low energy' retrofit scenarios were developed. The model connects data tables containing energy, emissions and cost information to a GIS layer of the City's parcel boundaries via parcel ID (PID) numbers. A dynamic exploration of current and future energy use, emissions profiles and related cost scenarios is enabled through a series of custom queries

developed in an MS Access database and custom scripts developed in ESRI ArcMap GIS software. The SCEC[3] model facilitates the exploration of future energy, carbon and cost scenarios through the addition of new buildings in given locations and the retrofit of existing buildings in random locations. Retrofits can also be targeted to select neighbourhoods.

2.3 Integrated Energy Mapping, Modelling and Financial Assessment (IEMMFA)

The IEMMFA model, developed by the Canadian Urban Institute, works to provide communities with the ability to see a clear link between the energy consumption of land-use and transportation and renewable energy systems and utility strategies across an entire community. The approach begins by developing information on building by connecting simulated archetype or actual energy consumption information with building floor area and built form typologies derived from municipal building attribute information. An assessment for transportation follows, using information derived from local trip tables to enable an assessment of energy use for both private and public transit.

The model connects a range of data tables containing information on energy, emissions, cost, alternative technologies and renewable fuels, transportation efficiencies, job creation and other information linked to different GIS layers. The GIS layers are based on parcel boundary information for buildings and trip zones for transportation. The model allows for the ranking and evaluation of current and future scenarios based on different combinations of building efficiency improvements, transportation demand management approaches, emission profiles, as well as the assessment of different built form patterns and their associated energy use.

To assist community members to compare and strategically prioritize opportunities, backcasting and scenario building are central to the IEMMFA approach, as is financial cost sensitivity. Rate of return, and dollar per tonne ($/tonne) of GHGs reduced are key measures allowing identified energy strategies to be compared in their ability to achieve a community target for the multiple criteria including energy, energy cost, GHGs, or other objectives.

3. Results and Implementation

3.1 Energy Asset Mapping

With almost 80% of Nova Scotia's energy coming from imported coal, results from the Strait-Highlands EAM indicate enormous potential for both GHG emission reductions and economic opportunities in the region. Several areas on the coast are suitable for large scale wind energy projects with much of the rest of the region appropriate for smaller wind projects of less than 2 MW. Opportunities exist for commercial scale tidal electricity generation within the nearby Great Bras d'Or Channel with an estimated 2.8 MW of potential tidal power. Potential for PV electricity generation was conservatively assessed at 22,153 MWh per annum, corresponding to an 18% reduction in annual electricity consumption and 22,733 tonnes of equivalent CO_2 saved per year; mass deployment of PV technologies could lead to more than three times higher than in the conservative scenario. Potential SWH generation was an estimated 23,177 MWh annually, or approximately 43% to 58% of current annual domestic hot water use, with potential emissions reduction of 11,342 tonnes of equivalent $C0_2$ per year. The passive solar heating asset is estimated at 25,381 MWh annually constituting approximately 15% of the current annual space heating energy budget. A number of river systems were assessed to have a total output capacity of 28,122 MWh per year, with full implementation of hydro electricity resulting in a reduction of 24,409 tonnes of equivalent $C0_2$ per year.

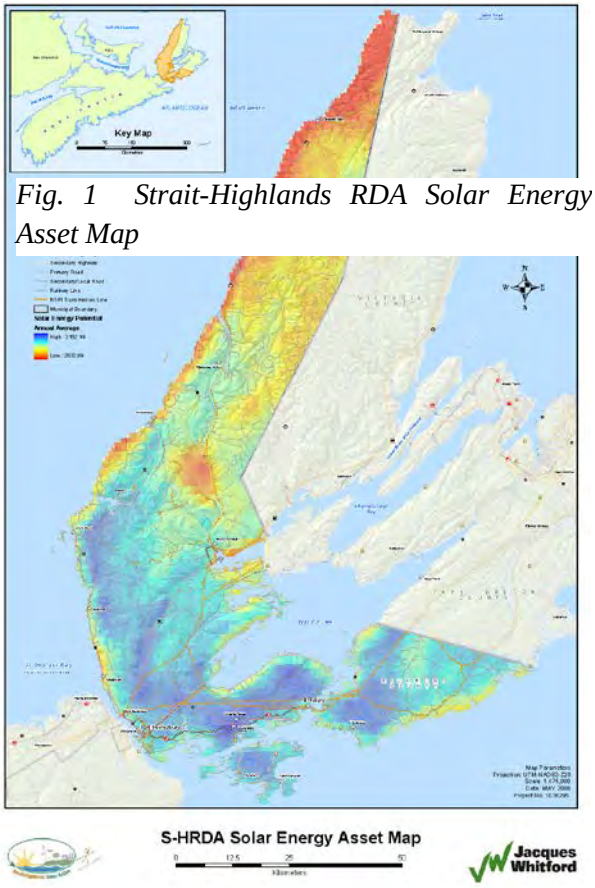

Fig. 1 Strait-Highlands RDA Solar Energy Asset Map

The Strait-Highlands EAM project concluded that capacity exists to supply the local clean energy required to meet a majority of future local energy needs from a number of different sources that could significantly diversify the energy mix in the region.

A consultation session was arranged with renewable energy development experts to discuss findings of the EAM project and determine barriers to development of renewable energy opportunities in the region. The report and map sets were used to develop directives for diversifying energy supply and increasing energy security under the ICSPs of the three partner municipalities. Custom maps were developed for targeted opportunities such as identification of municipally-owned properties ideal for wind energy development. Further to integration in planning, the EAM project has enabled renewable energy projects including solar thermal and PV applications and one demonstration project for a wind turbine in *Les Suetes*, a wind regime with speeds in excess of 150 km per hour. Planning is underway to develop a district energy system with a power plant and paper mill, using the nearby ocean for heating and cooling, a project initiated as a direct result of the EAM. Public consultation has led to a number of small and medium-scale renewable energy projects, including a building project that won the region's *Grass Roots Environmental Excellence Network Award*.

3.2 Spatial Community Energy Carbon and Cost Characterization Model

An example of the type of question that can be answered by the SCEC^3 model is: Will the residential sector in Prince George do its part to meet its community-wide target of 2% reduction from 2002 by 2012? When the 'low energy' scenario with multi-family growth for new construction was run, it was found that by 2018 the emissions from residential houses will be 112% of 2002 levels. It was only in 2028 that the residential housing stock would achieve 99% of 2002 levels. Even under the most aggressive scenario, it will be sometime after 2028 that the residential housing stock will meet a target that was to have been achieved by 2012. Based on these results, more widespread retrofits in residential houses, and the introduction of renewable energy technologies are required for the residential sector to do its part to achieve the community's target of 2% reduction from 2002 levels by 2012.

Fig. 2. Neighbourhood level output showing, for the residential sector, total annual energy use (GJ) per suite in the City of Prince George in 2038 under the low energy scenario.

Development of the model began in 2008 in conjunction with the Prince George *Smart Growth on the Ground* initiative to revitalize the city's downtown. [10] In the fall of 2009, Prince George City Council, city staff and community members embarked on myPG, a community-wide planning initiative comprising the development of an ICSP and update to the city's OCP. The SCEC[3] model initially developed data that was used for the baseline for the ICSP process, and provided a more accurate understanding of building energy consumption and associated GHG emissions specific to the Prince George context.

The City of Prince George was awarded the *2010 Community Energy and Climate Action Award* in the Community Planning and Development category; the community's use of innovative energy mapping mentioned in the context of the award. At the time of writing, in preparation for the city's community energy design charrette in the winter of 2011, 4 future land use scenarios developed by the community in the myPG process [11] are being run and information developed to forecast the impact of different types of policies and actions on E&E within the city's housing stock.

3.3 Integrated Energy Mapping, Modelling and Financial Assessment (IEMMFA)

A variety of insights have been gained during the initial use of the IEMMFA model in Guelph and Hamilton, Ontario. For Guelph, building and transportation energy efficiency improvements required for the city to meet its goal of a 50% reduction in energy use per capita were explored. An energy baseline of the existing built environment was established

and energy efficiency scenarios developed to identify the most cost effective approach in terms of $/tonne of greenhouse gas (GHG) emissions reduced. A 50% improvement in energy efficiency over the Ontario building code for all new buildings and a 25% improvement through retrofits of existing buildings would be required for Guelph to meet its goals. Results are being used to understand where larger scale energy systems can be most effectively integrated with long range planning. The city is also considering the use of the model to more discretely evaluate how different built forms and associated transportation trips can be maximized to meet the community's energy objectives. Resulting from the identification of the need to dramatically reduce transportation energy use within the existing built environment, policy and program options are being evaluated by the city Community Energy Manager for development through partnerships with the local utility and others.

For the City of Hamilton, the approach taken was to evaluate the most cost effective energy efficiency options that would allow the city to actively address peak oil concerns. The IEMMFA model was run to evaluate various combinations of building improvements and the use of alternative technologies and renewable fuels. A key component of the evaluation was to identify strategies providing a reasonable internal rate of return of 6% assuming different future energy price scenarios. For Hamilton, it was found that the application of GeoExchange across the city would be an optimal strategy for maximizing fossil fuel reduction while promoting resilience against rising energy costs. In terms of cost effectiveness, evaluated on an internal rate of return of 6%, it was found that a combination of alternative technology and renewable fuels, and building energy efficiency improvements for existing buildings and new construction could achieve a 36% reduction in energy consumption. Information is being used to support the Hamilton Community Energy Collaborative, a group comprised of city staff, councillors, local community groups, utilities and others, to develop a comprehensive community energy plan. The local electrical utility in Hamilton is using the baseline electricity map to identify areas that would benefit from conservation programs.

4. Summary

The ICEMs reviewed here are among the first developed in Canada, and although they are all developed with the help of digital map-based models, getting stakeholders thinking spatially about energy and emissions in communities can begin with a hands-on, paper-based exercise. This 'rough-sketch' collaborative approach is an effective means of soliciting local knowledge of and preferences for efficiency and renewable energy options in a community and can be used to kick-start the development of an ICEM in an E & E planning process.

The focus of the ICEMs featured here varied according to the goals of stakeholders, local geographical feature, land use patterns and available data. The Strait-Highlands EAM considered local energy assets towards achieving renewable supply targets and economic development. The SCEC^3 model leveraged existing data and simulation tools to assess the energy and emissions reduction potentials within existing and new buildings, demonstrating the use of existing federal datasets and tools to link modelling with policy implementation in communities. The IEMMFA model and strategy can be described as the most holistic of the three approaches, and connected building technology with transportation and land use change to explore the relative influence of changes to the built form, population densities and location, demand-side management and renewable energy generation. Its ability to conduct financial cost sensitivity analysis will be of interest to communities, policymakers and utilities seeking to assess the costs of various energy technology, land use and infrastructure options.

5. Conclusion

In the past few years, the development of Integrated Community Energy Models has emerged as an important piece of the strategic energy and emissions planning puzzle for Canadian communities. Lessons learned through the iterative development of these first map-based models have identified technical barriers and knowledge gaps around issues of data, modelling, visualization and communication of model outputs. Additional research is being initiated to mitigate these barriers and gaps. As required data becomes more accessible and ICEM best practices are developed, the capacity of communities and their collaborators to respond to new legislative requirements around energy and emissions will be enhanced. More importantly, the practice of developing ICEMs and the integration of their outputs into planning processes will assist communities in their quest for Integrated Community Energy Solutions. The use of ICEMs in community planning provides a promising decision support approach towards greater economic, environmental and social prosperity for all Canadians.

References

[1] Laura Tozer, Community Energy Plans in Canadian Cities, Master's Thesis. University Of Toronto, 2010, p.26

[2] M. Jaccard, Lee Failing and Trent Berry, From Equipment to Infrastructure: Community Energy Management and Greenhouse Gas Emission Reduction, Energy Policy, 25:13, 1997, pp. 1065 – 1074.

[3] Federation of Canadian Municipalities, Partners for Climate Protection Program, 2010. http://fmv.fcm.ca/Partners-for-Climate-Protection/ Accessed: 6/02/11

[4] Province of British Columbia, Bill 27: Local Government (Green Communities) Statutes Amendment Act, 2008. www.leg.bc.ca/38th4th/1st_read/gov27-1.htm Accessed: 6/02/11

[5] Province of British Columbia, Bill 17: Clean Energy Act, 2010. www.leg.bc.ca/39th2nd/1st_read/gov17-1.htm Accessed: 6/02/11

[6] Province of British Columbia, Community Energy and Emissions Inventories, 2010. www.toolkit.bc.ca/ceei Accessed: 6/02/11

[7] Province of Nova Scotia, Bill 146: Environmental Goals and Sustainable Prosperity Act, 2007. www.gov.ns.ca/nse/egspa/ Accessed: 6/02/11

[8] Prince, Thomas, Stefan Herbst. Demographic Indicators for Energy Demand. Presentation to ENERegion, University of Salzburg 26/06/08

[9] Heiple, Shem and David. J. Sailor. 2008. Using building energy simulation and geospatial modelling techniques to determine high resolution building sector energy profiles. Energy and Buildings 4. 1426 – 1436.

[10] Smart Growth BC, Prince George Smart Growth on the Ground, 2009, Available: www.sgog.bc.ca/content.asp?contentID=138. Accessed: 6/02/11

[11] HB Lanarc & the City of Prince George, Official Community Plan Growth Options, 2010, http://mypg.ca/progress/Documents/4%20Options%20Detailed%20Overview.pdf. Accessed: 6/02/11

Carbon Neutral Village: The Australian Model

Joanne Stewart, Martin Anda*, David Goodfield, Goen Ho, Kuruvilla Mathew

Murdoch University, Perth, Western Australia
** Corresponding author. Tel: +61 8 9360 6123, E-mail: m.anda@murdoch.edu.au.*

Abstract: This paper presents a model for carbon neutral land development as a mechanism to help drive innovation and emission reduction within the built environment sector. The carbon content model is comprised of the following:

- The greenhouse gas (GHG) embodied in the materials of the buildings and the infrastructure;
- The GHG emitted during the construction process with different approaches;
- The electrical power and natural gas used in the buildings for different building types;
- The transport fuels used in the construction and the on-going use by residents;
- The GHG produced in the full water cycle
- The GHG from the solid waste.

Understanding the interactions between the six elements of the model allows better decarbonisaton options to be developed. Two remote settlement cases are analysed. Firstly for a mine site camp, we introduce the "Smart Camp" digital control and monitoring concept . This includes sustainable village design, heating and cooling reduction, renewable energy, water use and reuse, and landscaping. Secondly, for the remote Aboriginal settlement, we address the need for sustainable livelihoods, including local food production and rangelands forestry and management.

Keywords: *Carbon neutral, Life cycle analysis, Accreditation*

1. Introduction

The built environment in Australia is currently responsible for around 20 percent of the nation's greenhouse gas emissions [1]). This is largely due to the energy consumed within buildings, as this energy predominantly comes from coal.

In Australia, carbon emission assessments for buildings are limited to operational energy. The Building Code of Australia (BCA) requires predictive calculations of operational energy use based on thermal performance modelling. The National Greenhouse and Energy Reporting (NGER) Act, 2007 requires actual emissions to be reported for facilities when the relevant energy or carbon emission thresholds are met. Analysing only operational emissions is similar to making an investment decision by solely examining the running costs of a building and ignoring the capital cost of development and construction.

If future construction is based on the need to reduce only the operational phase of the building, there is a real risk that further carbon emissions will be generated. from materials to increase operating efficiency. Hence, the proportion of emissions may be shifted from the operating phase to the 'before' and 'after-use' phases, without necessarily reducing overall emissions [2].

This paper is essentially a positioning paper that presents a model for carbon neutral land development as a mechanism to help drive innovation and emission reduction within this sector. The carbon content model is comprised of the following:

- The GHG embodied in the materials of the buildings and the infrastructure;
- The GHG emitted during the construction process with different approaches;
- The electrical power and natural gas used in the buildings for different building types;

- The transport fuels used in the construction and the on-going use by residents;
- The GHG produced in the full water cycle
- The GHG from the solid waste.

It is considered that these elements comprise the major sources of carbon emissions, but it is important to understand how each element interacts with the others in order to reduce overall emissions. This more inclusive and holistic approach to village design is likely to result in reduced carbon emissions over its life. Two cases are analysed with the model: the remote mine site camp and the remote Aboriginal settlement.

2. Methodology

A literature review was undertaken to determine the methodology best suited to analyse the proposed carbon model of settlements. This was conducted in conjunction with a review of available tools to assess the six elements in the model, with project partners Curtin University. Data collection methods to populate the model will include interviews with service providers, surveys with communities and mine site operators, plus an active research method with a remote Aboriginal community. The data collection methods are still being refined.

2.1. Carbon analysis method

In order to fully determine the carbon emissions associated with a building or community, it is necessary to ensure the embodied and operating emissions are both measured in an appropriate calculation method. It is imperative that the method allows for comparability across a range of buildings and settlement types.

Carbon emission calculations can be conducted by a lifecycle analysis (LCA) method as they are for a wide range of products and services. LCA is supported by the International Energy Agency as a valuable methodology for examining the carbon of settlement development and the special assessment needs, such as adaptability of buildings and recyclability of materials can be incorporated [3]. The AS/NZS ISO standard *14040:1998 Environmental Management-Life cycle assessment - principles and framework* outlines the requirements and process for undertaking a lifecycle impact assessment. The standard states that the assessment is conducted for impacts throughout a product's life, or "cradle to grave", including raw material acquisition, through production, use and disposal [4].

Carbon Profiling [2] is a modification of LCA that can also be applied to settlements. This method develops a metric that includes the energy associated with land development, such as embodied energy in existing buildings on site and highlights the importance of the lifespan of linked components within the building system. This method proposes that end-of-life aspects not be incorporated as they are generally not decided at the time of construction but could be incorporated if the site is redeveloped in the future.

On this basis it was decided that a life cycle approach was appropriate and that consideration should also be given to any existing carbon on site and the life spans of linked components. End of life aspects would not be calculated, however the recyclability of materials will be included in considerations. Also the adaptability and transportability of structures that have a longer life span than the settlement requires, such as short term mine sites, would need to be considered where appropriate.

2.2. Review of software

An extensive review of software was undertaken to evaluate their functionality to assess the six elements of the model [5]). The evaluation comprised a literature review to identify software designed to assess settlements, an evaluation of the software's ability to calculate carbon emissions related to each of the six elements and a pilot test of two to determine their appropriateness for mining and remote Indigenous settlements.

The review found that there are only a few software tools that provide the required functionality and none of them fully satisfied the six elements. However it was noted that recognition of life cycle analysis for settlement evaluation is growing and the USGBC has been investigating ways to incorporate an LCA module in its LEED evaluation tool (USGBC, 2006 [6]. The software chosen by the authors for the analysis of small-scale settlements was *eTool*, which satisfies four of the six element requirements: materials, construction process, operating energy and water systems. The software is currently being developed in Western Australia.

2.3. Model design

Based on the reviews above a model was developed to understand the interactions between the six key elements of settlements that generate carbon emissions. The model was then applied to the two remote settlement types: mine site camps and Indigenous communities.

The six elements of the carbon model are all interconnected and impact on each other. For example the choice of energy supply can impact on transport and waste energy. Remote settlements that are dependent on diesel generators for electricity require regular transport of diesel and services for maintenance of equipment and also have fuel drum waste to dispose of or recycle.

A schematic depiction of the key applications,is provided in ***Figure 1*** below.

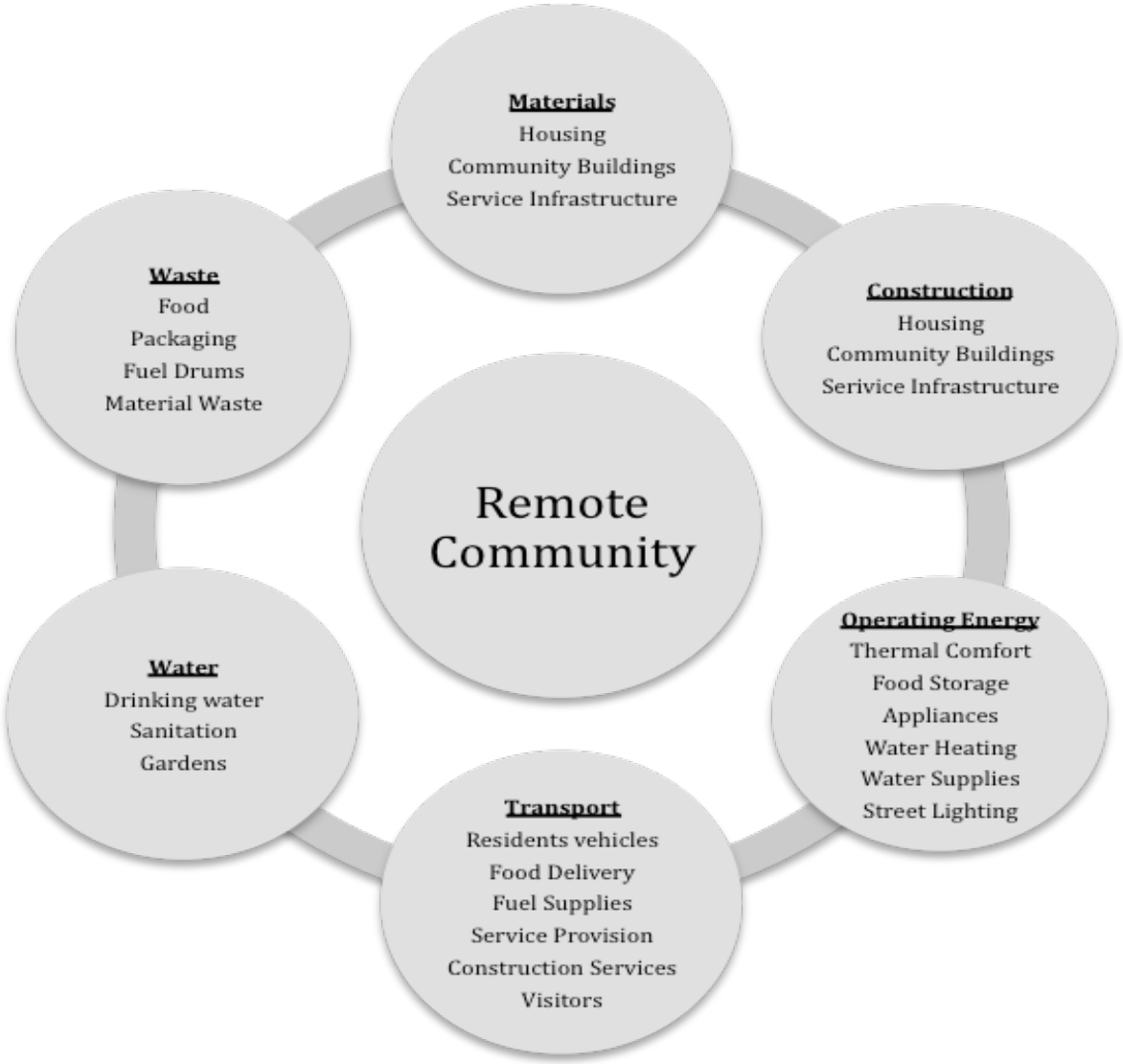

Figure 1 Carbon model with key applications of each element for both settlement types

2.4. Application to Mining Camps

Essentially a mine camp or village is a well defined organism and as such associated GHG emissions can be audited, monitored and controlled as a single entity. This research should, therefore, be able to provide a model for other types of remote community development where carbon reduction is an imperative.

The mining industry has a range of challenges to address in reducing its carbon emissions and providing a sustainable environment in its mine site camps and villages where they house their mining staff. Two known studies have been carried out where suggestions have been made for modifications to these camps and villages in order to reduce their carbon footprint [7, 8]. The majority of emissions in the referenced case studies come from diesel fired generation of electricity to operate camp services. No published audited figures exist. Mining operations are generally set up and budgeted for a specific life. This lifespan will determine the longevity of the accommodation to service it during three main phases, namely: establishment, operation and finally the decommissioning and rehabilitation phase. This research intends to apply the tools and metrics in order to optimise, from a sustainability and low-carbon standpoint, the form and function of mine site accommodation. This way the

mining companies are more likely to minimise their costs and maximise their return by creating the most appropriate type of accommodation to suit the prevailing circumstances.

Social behaviour clearly has its influence on carbon emissions research indicates that a change in behaviour will directly result in a reduction in these emissions. However, the task has been shown to be a none-too simple one [9]. This research intends to show that by changing the behaviour of the mine site employee, be they engineer or kitchen hand, that there will be considerable flow on effect in other areas of their lives, thus taking the carbon reduction strategy beyond that specific to the mine site accommodation itself [10].

Anecdotal evidence indicates the profligate use of energy in mine site accommodation is well known in the industry – for example air conditioners being left on in unoccupied buildings during a rostered-off period. Monitoring and control of operational energy is therefore a significant area where improvements could be made to make the camps and villages more energy efficient. In order to develop advanced monitoring and control solutions a collaboration between Furtwangen University, the Digital Ecosystems Business Intelligence Institute (DEBII) of Curtin University and this research has been formed. The interface between the digital world of control and monitoring systems is well established but this research will focus on the connection between them and the process of sustainable practice and education in a manner which to date is otherwise unexplored.

Stationary energy to service camp operations is generally generated using diesel as a fuel with high carbon polluting results. This research will also investigate the practical introduction of renewable energy systems to replace such fossil fuel consumption. These will include photovoltaic, solar thermal, geothermal, wind, and wave power (coastal only), and the appropriateness and sustainability of these technologies. From the mining company point of view a cost-benefit analysis will also need to be attached to the investigations.

2.5. Application to Indigenous Communities

In 2006 the Indigenous population of Australia was estimated to be 517,000, which is 2.5% of the Australian population. Of these it is estimated that 24%, approximately 124,000, live in remote or very remote areas as classified by the Australian Standard Geographical Classification (ASGC) [11]. The communities in these areas range in size from small outstations to town-sized populations with various amenities [12].

While there is little published data on the carbon profiles of these communities, it is expected they are highly carbon intensive, despite their relatively low-income status. This is due to their general reliance on diesel-powered electricity generators, fossil-fuelled vehicles that need to travel vast distances and provision of public housing that is often inappropriate for the climate. They are also often dependent on external service providers and supply systems, all of which increase the transport requirements for goods and service delivery.

Energy use by households in these communities can vary widely from 3 kWh to over 40 kWh per day. This is due to a wide variation in the number of occupants per household, which is often high, and the appliances being used, particularly for air-conditioning and water heating. A community with 100 to 150 people would use between 500 to 750 litres of diesel per day to generate electricity, which emits approximately 1.3 to 2 tonnes of CO_2e per day.

It is also reported that Indigenous communities in the north of Australia are likely to be highly impacted by the effects of climate change [13]. While decarbonising mainly aims to mitigate

the effects of climate change, some of the proposed strategies to be employed can provide the twin benefit of adaptation and therefore help negate some impacts.

There are certainly reasons to maintain remote communities as opposed to relocating the residents into urban areas. These include improved health outcomes, such as in the community of Utopia ([11], and opportunities for income generation through natural resource management and carbon offset services [14].

Given the carbon profile in communities is highly influenced by their dependency on external factors such as energy, housing, food and general service supplies and lack of internal resources it is worth investigating the effect of transitioning communities to a more self-sufficient 'sustainable livelihood' model to address carbon emissions and also provide a suite of other benefits.

The Sustainable Livelihoods Framework, provided in ***Figure 2*** below, has been used by international development agencies in attempts to address poverty in developing countries [15]. It also provides a framework within which to apply carbon management programs as livelihood strategies.

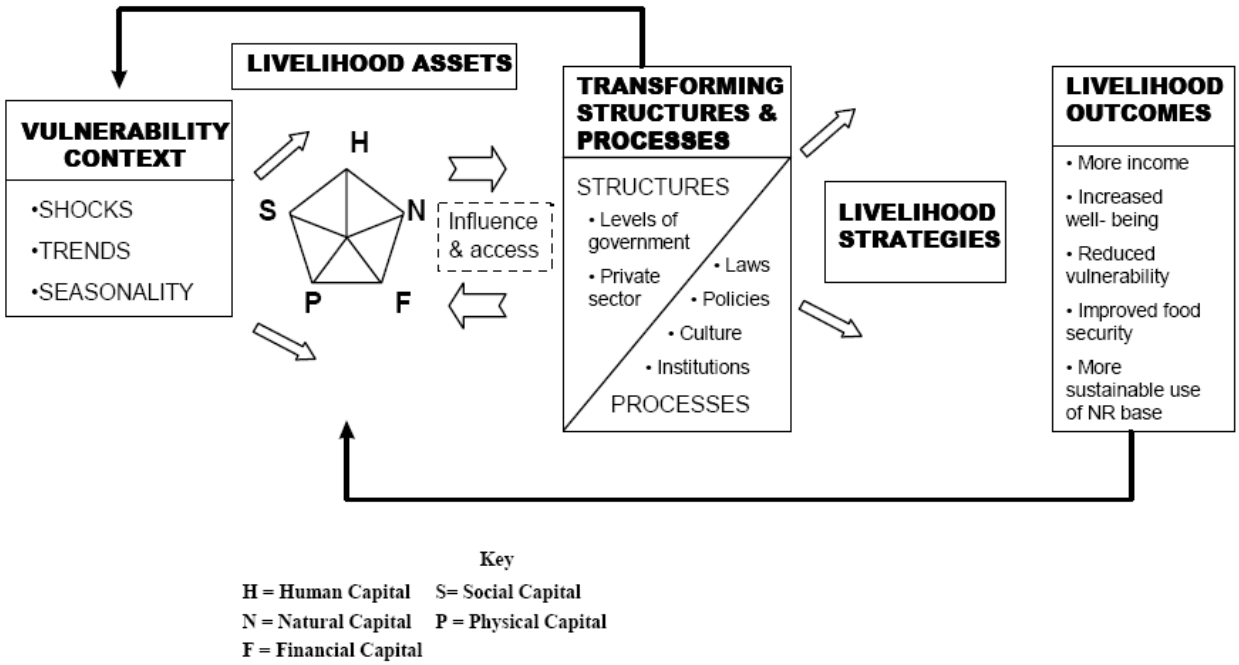

Figure 2 Sustainable Livelihoods Framework (source: Carney cited in [16])

By addressing the vulnerability factors and improving the five categories of assets (human, social, natural, physical and financial) a more sustainable community will develop. The connections to energy and carbon management are considerable. Firstly, using lifecycle analysis, the lifespan of a physical asset should be lengthened in order to maximise use of its embodied energy. The natural assets should be maintained to reduce energy use in relation to thermal comfort of buildings and food supplies and to generate carbon offsets, without upsetting the natural balance of other ecosystem services. Human and social assets are enhanced with skill development and network capability, which alleviate dependency on external goods and service provision, and therefore also transport needs.

3. Results

For both remote settlement types there are clearly links between the six elements in the model and their impacts on carbon emissions. While the general links and possible solutions have been identified, further investigation and analysis is required to understand the exact connections and extent of impact.

As the model has not yet been applied results will not be available until further investigation of the carbon profiles and interconnections between elements have been examined and quantified.

4. Discussion

The model requires verification in the form of energy and emission quantities for each element and the key integration points. This will be conducted using the life cycle analysis method discussed. Identification and quantification of the key contributors to carbon emissions can then be completed. Proposed strategies, including the Sustainable Livelihoods framework and the digital monitoring system, need further research with application in pilot studies at remote settlements, which is currently being arranged. The success of these strategies will also be evaluated using a comparative life cycle analysis. Successful implementation methods that are suited to varying regional circumstances will need to be identified. Finally an accreditation process that certifies and incentivises transition to low-carbon settlements will be investigated with research partners CUSP.

Acknowledgements:

Australian Research Council, Curtin University Sustainability Policy Institute (CUSP), Horizon Power and Parsons Brinckerhoff.

References

[1] Australian Sustainable Built Environment Council (ASBEC), *The Second Plank - Building a low carbon economy with energy efficient buildings*. 2008, Australian Sustainable Built Environment Council (ASBEC).

[2] Sturgis, S. and G. Roberts, *Redefining Zero: Carbon profiling as a solution to whole life carbon emission measurement in buildings*. 2010, RICS: London.

[3] International Energy Agency Annex 31 Project, *Life cycle assessment methods for buildings*. 2004: Ottawa.

[4] Standards Australia, *14040:1998 Environmental Management - Life cycle assessment - Principles and framework* 1998, Standards Australia: Homebush.

[5] Beattie, C., et al., *Carbon analysis of settlements and a review of appropriate tools.* In press, 2010.

[6] Trusty, W., *Integrating LCA into LEED: Working Group A (Goal and Scope) Interim Report #1*. 2006, US Green Building Council (USBGC).

[7] SKM, *Improving the Sustainability of Mining Camps, a report by Sinclair Knight Merz.* 2008.

[8] Anda, M. and D. Goodfield, *Sustainable Village Design: A Study of Options*. 2008.

[9] Druckman, A. and T. Jackson, *The Carbon Footprint of UK Households 1990 – 2004: A socio-economically dissagregated, quasi-multi regional input- output model.* Ecological Economics, 2009. **68**: p. 2066-77.

[10] Mulugetta, Y., T. Jackson, and D.v.d. Horst, *Editorial.* Energy Policy, 2010.

[11] SCRGSP (Steering Committee for the Review of Government Service Provision), *Overcoming Indigenous Disadvantage: Key Indicators 2009*, P. Commission, Editor. 2009, Productivity Commission: Canberra.

[12] Department of Indigenous Affairs (DIA), *Facts at a Glance: Indigenous Demographics*, D.o.I. Affairs, Editor. 2010, Government of Western Australia: Perth.

[13] Green, D., S. Jackson, and J. Morrison, *Risks from Climate Change to Indigenous Communities in the Tropical North of Australia*, D.o.C.C.a.E. Efficiency, Editor. 2009, Australian Government: Canberra.

[14] Alchin, M., E. Tierney, and C. Chilcott, *Carbon Capture Project Final Report: An evaluation of the opportunity and risks of carbon offset based enterprises in the Kimberley-Pilbara region of Western Australia*, D.o.A.a.F. WA, Editor. 2010, Department of Agriculture and Food WA: Perth.

[15] Fisher, S., *Applying the Sustainable Livelihoods approach in the*

[16] *Australian Indigenous context*, Centre for Appropriate Technology: Alice Springs.

[17] Measham, T., Y. Maru, and R. Murray-Prior, *Outback Livelihoods: Defining and linking social and economic issues affecting the health and viability of Outback regions: Sample Discussion Paper*. 2006, Tropical Savannas CRC and Desert Knowledge CRC: Darwin.

Improving energy and material flows: a contribution to sustainability in megacities

S. Mejía Dugand[1,*], O. Hjelm[1], L.W. Baas[1]

[1]*Division of Environmental Technology and Management - Department of Management and Engineering, Linköpings Universitet. Linköping, Sweden.*
[*]*Corresponding author. Tel: +46 13285639, E-mail: santiago.mejia.dugand@liu.se*

Abstract: As cities have become home for 50% of the world's population, urban systems have definitely caught public attention. The urban metabolism can be improved by transforming their linear behavior into a more circular one. This paper is based on a project initiated by the Division of Environmental Technology and Management at Linköping university, financed by Vinnova: *Megatech*. The aim is to study the megacities of Cairo and Mexico City in order to understand some of the problems they are facing. By improving their energy and material flows behavior, these megacities can benefit from the reduction of their dependence on fossil fuels and virgin materials; the protection of part of their social, economic and productive systems from external factors (e.g. political drawbacks, shortage/distribution problems, international prices); an increased effectiveness of their planning activities–as they would be based to a large extent on their own resources–and the reduction of their environmental burden. An *in situ* study will take place with the participation of local stakeholders. Information about environmental problems will be collected and potential solutions will be analyzed and suggested. A tentative model is presented, showing how the reinsertion of the outflows into the urban system could benefit these cities' overall environmental performance.

Keywords: *Flows analysis, Urban metabolism, Urban sustainability, Megacities.*

1. Introduction

Cities seem to be the future's structure for social and economic activities. Today, 50% of the world's population has moved into cities [1] and their uncontrolled growth has brought along problems and challenges. Some of these cities have reached once-unthinkable population levels and have been called 'megacities', after the Greek word 'mega' (μέγας – great).

These highly urbanized agglomerations concentrate people, materials, money, information and knowledge and continue to grow as more people are being attracted by the apparently endless possibilities of wealth and comfort that they offer. However, in a planet constrained by finite resources, unlimited growth is not possible [2]. Under today's circumstances, and especially given the technological and economical lock-in [3] that our societies are suffering from, most of these resources are facing short-term depletion. Nevertheless, from an industrial ecology perspective, urban agglomerations are not lacking resources–i.e. energy and materials; the problem is that important sources are being ignored or mismanaged.

Industrial ecology studies material and energy flows through different systems, with the intention of optimizing their cycles; considering them as an ecosystem, part of the biosphere surrounding it [4]. An analysis of these flows makes it possible to find options for their reinsertion into the social and economic system, while reducing the impact on t he environment and helping creating more sustainable urban settlements, where these three aspects are considered. The aim is then to propose a model describing how a better behavior of these flows–i.e. their circularization and reinsertion–reduces the environmental burden and contributes to building more sustainable societies. A description of common urban environmental challenges in two selected megacities is made, followed by a depiction of how industrial ecology can address some of them. Last, some potential results regarding energy use and CO_2 emissions reduction are shown and discussed.

2. Methodology

The *Megatech* project is an explorative research of sustainable business and clean technology markets in the megacities of Cairo and Mexico City. By using a bottom-up approach, the project's team studies these cities' dynamics from a holistic perspective, considering the social, economical and environmental spheres and analyzing their urban metabolism, aiming at detecting potential niches for Swedish CleanTech offerings.

The selection of the cities of Cairo and Mexico City was based on three criterions. The first one–as the definition of *megacity* suggests–was the population size; i.e. more than ten million inhabitants. The second criterion was the access to information, due to concerns of sufficiency and reliability. For this, strategic partners were looked at in each town in areas of interest to the project's objectives. Last, the socio-economic conditions were important for the selection, as important business opportunities can result from them. Specifically, emerging markets were of interest for the project's team, i.e. developing countries.

A case-study methodology was selected as appropriate for the analysis and understanding of the issues intended to be addressed by the project. By consulting official reports and publicly accessible information from, e.g. governmental and supra-governmental organizations, municipalities, environmental and economic councils/agencies, independent studies and local newspapers, an initial description of these settlements was developed, depicting problems and challenges from a sustainability/environmental perspective. With this information in hand, an initial identification of stakeholders gave the team an insight of the groups of interest and the indications for a first set of interviews, in order to confirm the previously acquired information, and especially in order to have the possibility of understanding these concerns from the perspective of those directly involved and affected by them. The latter would help the team build the desired bottom-up approach.

Once this information was collected and confirmed, an industrial ecology approach was used in order to analyze possible solutions for the circularization of waste flows. A tentative analysis was made by identifying sources, directions and disposal activities. Two types of results were obtained: the identification of specific problems in each town and the discussion of the benefits that could be obtained through a flow analysis and the application of the proper technologies and possible barriers and drivers for their implementation.

3. Current situation

Uncontrolled growth, both in the residential and in the industrial sector, is a big problem for megacities in developing countries. The available technical systems are not able to cope with this expansion and the increased demand of energy and waste treatment technologies are common challenges faced by their citizens and governments. More specifically, the problems detected in Cairo and Mexico City are as follows:

Cairo

Cairo has always been an important cultural, economic and commercial center of the Arab world. Such an important role has meant several challenges, embedded in the need of developing and giving its citizens a better quality of life, at the same time that it struggles to survive under the demands of a growth-addicted, competitive economic system.

The most representative environmental problems detected so far by the team are:

- *Water supply/quality.* The Egyptian culture flourished around the waters of the great Nile. However, a growing population and the political and economic demands of modern times have posed a lot of stress on this resource. Several countries share its waters and have their own development programs, which in one way or another affect Cairo–and Egypt in general, being located at the very end of its trajectory. Moreover, the high pressure on irrigation water for the production of wheat–the biggest source of protein in poor countries, thus very sensitive social-wise–is a big problem when the demand cannot be met by local resources and international prices skyrocket (see e.g. [5]). Also, wastewater treatment is not very effective, especially when more and more slum dwellers increase the burden due to their illegal and unplanned nature (see e.g. [6]).

- *Urban waste.* Solid waste is a huge problem in Cairo. The collection of waste in some areas has been outsourced to e.g. Spanish or Italian companies, who have had several problems [7, 8, 9]. Moreover, the traditional *Zabbaleen* people's activities–who make a living out of recycling or from recoverable items and by feeding their animals with the organic fraction–have been affected by the recent swine-flu paranoia, resulting in an overload of unpicked organic material on the streets [7, 10]. Despite of several efforts by the city's administration, 19 500 tons of waste produced everyday in Greater Cairo represent a huge challenge [11].

- *Traffic.* Uncontrolled traffic and air pollution are a big problem in Cairo. An average speed as low as 10 k m/h [12] reflects on higher fuel consumption and reduced productivity. In addition, industrial pollution and the natural characteristics of the region–i.e. sand blowing from the desert–add to the problems of the air's quality and public health.

- *Energy.* Fossil fuel dependency is not only a problem for the transportation and production sectors, as many families depend on them for cooking and heating purposes. It is mainly butane being distributed to households in pipes, highly subsidized by the government [13]. Shortages of this gas have caused discontent among the poorest sectors, unable to pay for higher prices [14].

- *Population.* As stated above, urban population has grown uncontrolled, especially during the last century. The last census (2006) counted around 13.5 million living in Greater Cairo [15]. Such an amount poses an enormous pressure on resources, food, housing and infrastructure in general.

<u>*Mexico City*</u>
The ancient city of *Tenochtitlán* was already an important place back in the 15th century. Today, this city lies hidden under the colossal Mexico City, which under an undoubtedly changed context, struggles to maintain its citizens' quality of life.

Today, Mexico City must face the following environmental challenges:

- *Water supply.* The level of overexploitation is estimated to be 35% [16], making the replenishment rate to be lower than needed [17] and requiring solutions that demand enormous amounts of energy, like pumping water from a 1 100-meters lower region, located 127 km away from the city [18]. In addition, the mentioned extraction has caused the underground layers to collapse, sinking infrastructure up to 40 cm in some

areas [16]. Finally, several sources of pollution, both natural and artificial, harm the liquid's quality [16], causing the citizens' distrust on the quality/quantity of the water they receive [20].

- *Air.* Road transport contributes to 50% of the emissions that cause air pollution. Industry and landfills 24% and 14% respectively, followed by combustion practices in residential areas with 10% [16]. In addition, the geographic characteristics of the Valley hinder the natural dilution of these emissions. Although Mexico City has a low average PM_{10} value–around 52 $\mu g/m^3$ [19]–compared to Cairo (roughly 150 $\mu g/m^3$ [21]) or Shanghai (around 110 $\mu g/m^3$ [21]), levels have reached figures as high as 164 $\mu g/m^3$ in some areas in recent years [19].

- *Mobility.* Around 4.5 million vehicles were registered in the city by 2010 [22], with a big share of privately owned cars. In the metropolitan area, there are 397 cars/1000 people, compared to, e.g. 38 in Shanghai [23]. Speed figures are as low as 3 km/h in some places during peak hours, with an average of 21 km/h [24]. Around 20 million work-hours/day are estimated to be lost in traffic or commuting [25], due to an average daily commute time of 2.5 hours–compared to e.g. 1.4 in London [23].

- *Solid waste.* An average of 12 500 tons/day are generated in the Federal District only [16]. The landfill used has already exceeded its capacity but has not been closed due to the lack of a good alternative. Although the administration has several campaigns–e.g. waste oil collection and organic waste-sorting/handling–activities like composting or recycling are still relatively small [26].

- *Energy.* As most of the cities around the globe, Mexico City suffers from fossil fuel dependency. Mexico was the 7th oil producer in the world in 2008 [27] and petrol is cheaper than mineral water [23].

- *Population.* The Metropolitan Area of Mexico City is one of the most populated urban areas in the world, with an estimated 19.9 million inhabitants in 2009 [28], 60% of them living in illegal and informal housing [23], which means gigantic challenges for public services like drinking water, sewage and electricity.

3.1. Bending the arrows: improving the city's metabolism and finding new energy sources.

Industrial ecology looks at the conversion of linear flows into circular flows, by studying both energy and materials in a system. Urban flows are of special interest here, given the important weight that cities have on the overall environmental crisis. Although the study has not reached a mature stage yet where specific figures are available, some insights (as describe above) can help building an initial model of what is happening and how a better flows' behavior can contribute to the goal of reaching more sustainable and independent societies.

Cities are very dependent on external resources for their everyday's functioning and are normally net consumers–energy and material-wise, meaning that they have a passive role in the whole material and energetic cycle (as shown in Fig. 1).

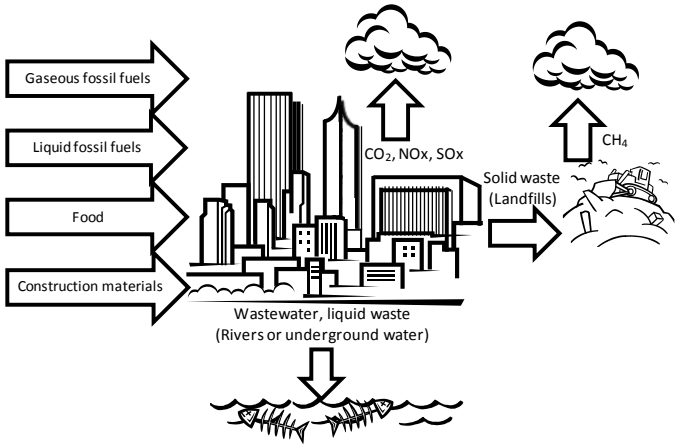

Fig. 1. All urban flows are linear and end up in natural sinks (i.e. water, air and soil).

However, environmental technology and sustainable practices have found innovative and effective solutions for most of these problems, "bending the arrows" and turning cities into more active actors, whilst reducing their environmental burden. Some examples of these solutions are:

- Urban gardening: vegetables production in green areas, roofs and urban greenhouses.
- Biogas from sewage sludge and organic waste: besides cleaning wastewater, reducing sludge volume and producing energy in the form of biogas are additional benefits. An organic fertilizer is a by-product, useful for both urban and rural agriculture.
- Waste incineration: with the proper technology, waste can be used for electrical and thermal energy production, reducing the need of landfilling and the volume of waste as much as 98%. Ashes can be used as a construction material.
- Methane capture in landfills: Landfills are a big source of methane, useful as a fuel.
- Biodiesel from used cooking oil: The collection and further processing of used oils helps reducing the pollution of water sources and the city's dependence on fossil fuels.

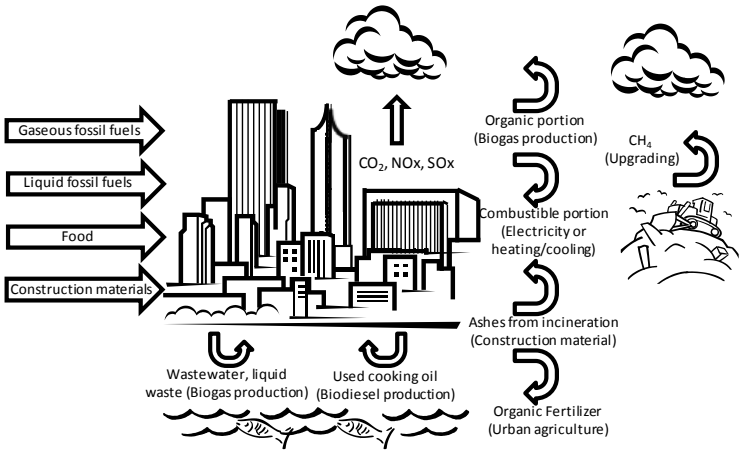

Fig. 2. By closing loops, cities improve their environmental performance.

As Fig. 2 intends to illustrate, flows entering the urban areas can be reduced, diminishing to some extent the city's necessity of external sources and protecting it against i.e. international prices, political drawbacks or unhealthy dependences. At the same time, the surrounding ecosystem is harmed to a lesser degree, manifested in the improvement of the air and water's quality and the remediation of soil.

4. Potential renewable sources and CO_2 emissions reductions

An indication of how a circularization of the urban flows could contribute partially to the solution of the energy and environmental crisis can be shown in the Mexico City's case, whilst data from Cairo is still to be collected.

A back-of-the-envelope estimation can be done regarding the potential production of biogas in the federal district, given the biological oxygen demand (BOD) content of its wastewater. Out of 118 m^3/s that were treated in 2008 in Mexico, 3.5 m^3/s (3%) are treated in the federal district [29]. Assuming that the BOD content is equally distributed all over the country (very likely to be higher given the industrial and economical activities and the population in the area), 270 300 tons BOD would be generated every year both by households and industry–out of 9 million nation-wide [29]. Each ton BOD can potentially generate 500 normal cubic meters (Nm^3) of methane by anaerobic digestion [30], meaning that around 135 MNm^3 could be produced annually only from wastewater, with an energy content of roughly 1.3 TWh/year. This is equal to the amount of energy needed by the Cutzamala system, which provides 18% of the potable water to the Valley of Mexico [29] and consumed 0.56% of the electricity produced in Mexico in 2008 [29], contributing roughly 630 000 tons CO_2 [31]. An important challenge arises considering that only 13% of Mexico City's wastewater is treated [32].

Other important sources of raw materials could back up these activities. For instance, 700 tons of organic waste are generated every day at *Central de Abastos* (wholesale market) [33], with a potential production of around 20 MNm^3 of methane/year, an energy content of 200 GWh [30] and an estimated reduction of 170 500 tons CO_2/year [33], not to mention the availability of a high-quality organic fertilizer. On the other hand, the government has plans to extract and take advantage of the methane emitted by the *Bordo Poniente* landfill, with a reduction on CO_2 emissions of roughly 1.4 million tons [33].

5. Discussion

There are technological solutions available for several of the problems that megacities suffer from, including the ones described above. However, the specific context plays a very important role if the actual feasibility of implementation was to be discussed. Social, economic and environmental factors are very variable depending on cultural, geographic and specific current conditions of the city being analyzed, reflected on barriers and drivers, enablers and challenges. For example, the importance of the informal economy both in Cairo and Mexico can become a challenge, especially when approaching the problem of waste management. Hundreds of people rely on the picking of sellable material from the collected waste both in official and parallel markets (e.g. *Zabbaleen* in Cairo and *Pepenadores* in Mexico City). Some powerful unions have been created, influencing greatly political decisions. Any attempt to modify the current situation would affect a lot of people if they are not taken into account in an integral plan that considers actions in order to keep–at least–the current income level of those doing the job and confront in an effective way the problem of illegal activities in the sector.

Another big barrier faced regarding waste management is sorting. In Mexico, for example, 43% [16] of the waste landfilled is organic and the situation in Cairo has gotten worse since pigs are not there anymore to take care of this fraction. Although there are some plans for the proper treatment of this type of waste, no significant activities are taking place currently. Regarding fuels, for example, the low prices of fossil fuels–due to subsidies–and the widely spread use of private transportation, creates a lot of economic disincentives for the production of biofuels from wastewater, used oil or organic waste. The high subsidies that governments

pose on these energy carriers and the important position that oil has on their respective country's economy put concerns on a very low level in the ladder of priorities.

Last, the socio-economic situation of developing countries represents a very big barrier for a lot of these technologies. Some of them require huge investments–unreachable for most of them–and long pay-back periods, thus long-term commitments: sometimes too long to be considered.

Nevertheless, governments are conscious of their role in creating a better environment for their citizens and the generations to come. They are aware of the huge opportunities that all these challenges represent and how much international interest they attract. Programs encouraging the use of solar power for heating purposes, landfill gas capture and use and energy efficiency measures in Mexico and the construction of concentrated solar thermal power plants and wind farms in Egypt are a proof of their commitment.

Acknowledgments

This project is financed by the Swedish governmental agency for innovation systems–VINNOVA–and is being performed at the division of environmental technology and management at Linköping's university.

References

[1] United Nations, World urbanization prospects – The 2007 revision, Economic and Social Affairs/Population division, 2006.

[2] T. Jackson, Prosperity without growth – Economics for a finite planet, London: Earthscan, 2009.

[3] P.A. David, Clio and the Economics of QWERTY. American Economic Review 75, 1985, pp. 332-337.

[4] S. Erkman, Industrial Ecology: an historical view, Journal of Cleaner Production, Vol. 5, No. 1-2, 1997, pp. 1-10.

[5] Al-Masry Al-Youm, Wheat shortage, thunderstorms in the south, aid to Gaza, 2010.

[6] IRIN, EGYPT: Health problems for residents of sewage-soaked shantytown, 2008.

[7] B. Sigvardsson, Sopkaos i Kairo när sopplockarna rationaliseras bort [Waste chaos in Cairo when waste-pickers are rationalized], Avfall och Miljö 3, 2010, pp. 35-37.

[8] Daily News Egypt, Cairo governorate amends waste management contracts, 2010.

[9] EFE, Empresas españolas atrapadas en la basura de El Cairo [Spanish companies trapped in Cairo's waste], 2004.

[10] The New York Times, Garbage piles up in Cairo after swine-flu pig slaughter, 2009.

[11] The Ministry of State for Environmental Affairs, Addressing the problem. Al-Ahram, 2009.

[12] R. Leila, Reaching an impasse. Al-Ahram, 2006.

[13] The Associated Press, Gas shortage raises Egyptians' anger at the government, 2010.

[14] Al-Masry Al-Youm. Today's papers: MBs arrested, butane shooting in Tanta, 2010.

[15] Central Agency for Public Mobilization and Statistics – CAPMAS, The final results for Population and Housing Census 2006, 2008.

[16] Gobierno del Distrito Federal. Transparencia Ciudadana [Citizen Transparency], www.transparenciamedioambiente.df.gob.mx, accessed 10 August 2010.

[17] The International Development Research Centre – IDRC, México, una ciudad sedienta [Mexico, a thirsty city], 2004, www.idrc.ca/en/ev-68034-201-1-DO_TOPIC.html, accessed 10 June 2010.

[18] Sistema de Aguas de la Ciudad de México - SACM. El camino del agua [Water's path], www.sacm.df.gob.mx/sacm/index.php, accessed 17 November 2010.

[19] Secretaría del Medio Ambiente, Registros históricos 2000-2010 [Historical records 2000-2010], www.sma.df.gob.mx/simat2/index.php?opcion=69, accessed 17 October 2010.

[20] El Universal, 77% no confía en agua capitalina [77% does not trust the capital's water], 2010, www.eluniversal.com.mx/ciudad/102971.html, accessed 15 October 2010.

[21] World Health Organization Europe, Air quality guidelines – Global update 2005, 2006.

[22] Secretaría del Medio Ambiente del Distrito Federal, Pierde DF sustentabilidad por autos [The Federal District loses sustainability because of cars], 2006, www.sma.df.gob.mx/imecaweb/boletin/bol0906/pdf/20.pdf, accessed 1September 2010.

[23] R. Burdett and D. Sudjic, ed., The endless city, London: Phaidon Press Ltd., 2007.

[24] The Clean Air Institute, Revisión crítica de información sobre proyecto de restricción sabatina [Critical informative revision of the sabbatine restriction project], 2007.

[25] La Jornada, Habitantes del valle de México pierden cinco años de su vida por congestiones viales: CTS [Inhabitants of the valley of Mexico lose five years of their lives due to traffic jams: CTS], 2010.

[26] Secretaría de Obras y Servicios, Recolección, transferencia, selección y disposición final [Collection, transfer, sorting and final disposal], www.obras.df.gob.mx/servicios_urbanos/residuos/rec_trans_sel_final.html, accessed 1 September 2010.

[27] U.S. Energy Information Agency, Country energy profiles, 2008, tonto.eia.doe.gov/country/index.cfm, accessed 16 November 2010.

[28] Consejo Estatal de Población, Zona Metropolitana del Valle de México [Metropolitan Zone of the Valley of Mexico], 2009.

[29] Comisión Nacional del Agua, Estadísticas del agua en México – Edición 2010 [Water statistics in Mexico – 2010 Edition], 2010.

[30] Svenskt Gastekniskt Center, Substrate handbook for biogas production, 2009, http://www.sgc.se/display.asp?ID=1242&Typ=Rapport&Menu=Rapporter, accessed November 15, 2010.

[31] Instituto Nacional de Ecología, Inventario nacional de gases de efecto invernadero 2006 [National inventory of greenhouse gases 2006], 2008, http://www.ine.gob.mx/descargas/cclimatico/inf_inegei_energia_2006.pdf, accessed January 3, 2011.

[32] Economist Intelligence Unit, Latin America Green City Index, 2010, http://www.siemens.com/entry/cc/features/greencityindex_international/all/en/pdf/report_latam_en.pdf, accessed November 10, 2010.

[33] Secretaría del Medio Ambiente del Distrito Federal, Mexico City Climate Action – Program 2008-2012/Summary, 2008.

Renewable energy mapping in Maharashtra, India using GIS

Sampada Kulkarni[1], Rangan Banerjee*

[1] *Indian Institute of Technology-Bombay, Powai, Mumbai-76, India*
** Corresponding author. Tel: +91 22 25767883, Fax: +91 22 25764890, E-mail: rangan@iitb.ac.in*

Abstract: Increasing negative effects of fossil fuel in addition to limited stock have forced many countries to switch to environmental friendly alternatives that are renewable and can sustain the increasing energy demand. In order to tap the potential of various renewable energy sources, there is a need to assess the availability of the resources spatially. Mapping potential sites for tapping renewable energy is the focus of this study. The study employs the Geographical Information System (GIS) to map various renewable energy sources. A case study of Indian state Maharashtra has been taken. Open source software, Quantum GIS (QGIS) is used to analyze the variability of renewable energy considering the spatial aspect. Maps of installed capacity have been prepared. Solar insolation data and wind speed data available for few sites in the state are mapped and then interpolated for the entire state. A macro survey is done to estimate the renewable energy potential available in the state. Spatial interpolation has been done for micro analysis to define the usefulness of such a system.

Keywords: *renewable energy, geographical information system, spatial mapping*

1. Introduction

Energy is one of the most important inputs for economic growth and human development. The sustainability of future energy systems is critical for sustainable development. Renewable energy is a key element for any sustainable solution. One of the first steps for the exploitation of any energy source is its estimation and mapping to identify the most suitable areas in terms of energy potential. To understand the current trend of the renewable energy, it is important to analyse the spatial variation of resources and their deployment.

A Geographical Information System (GIS) is a system that can handle and process location and attribute data of spatial features. Nguyen and Pearce [1] have used an open domain approach to compute insolation including temporal and spatial variation of albedo and solar photovoltaic yield. Ramachandra and Shruthi [2] have estimated the wind energy potential of Karnataka using GIS technology. Celik [3] has estimated monthly wind energy production using Weibull representative wind data for a total of 96 months from five different locations in the world (Cardiff, Canberra, Davos, Athens, Ankara). Sen [4] has used CSV (Cumulative Semi-Variogram) approach to predict the solar irradiation at any point from a given set of known data points. This paper provides a framework for analysing the status of renewable energy situation using GIS and illustrates this for Maharashtra state of India.

Maharashtra is situated in western part of India and covers the entire Deccan region. (Area 1,19,000 square miles, population 97 million as per 2001 census [5]) There are 35 districts in Maharashtra [5]. A district is an administrative division of an Indian state or territory. Maharashtra is the largest power generating state in India with an installed capacity of 22,435 MW [6]. The total renewable energy installed capacity in the State till March 2010 was 2,601 MW [7]. Open domain Quantum GIS (QGIS) is used to represent the spatial data.

2. Methodology

The general methodology for analysis of renewable energy framework using GIS approach is summarised in Fig. 1. Distribution of renewable resources; wind and solar, in terms of wind power density and hourly insolation values respectively is spatially interpolated for the state and maps are created for the same. Current installed sites of various renewable resources, viz.

wind power generation, bagasse co-generation and small hydro power plants are identified and represented on the map. Each site is linked to its corresponding database of location and installed capacity.

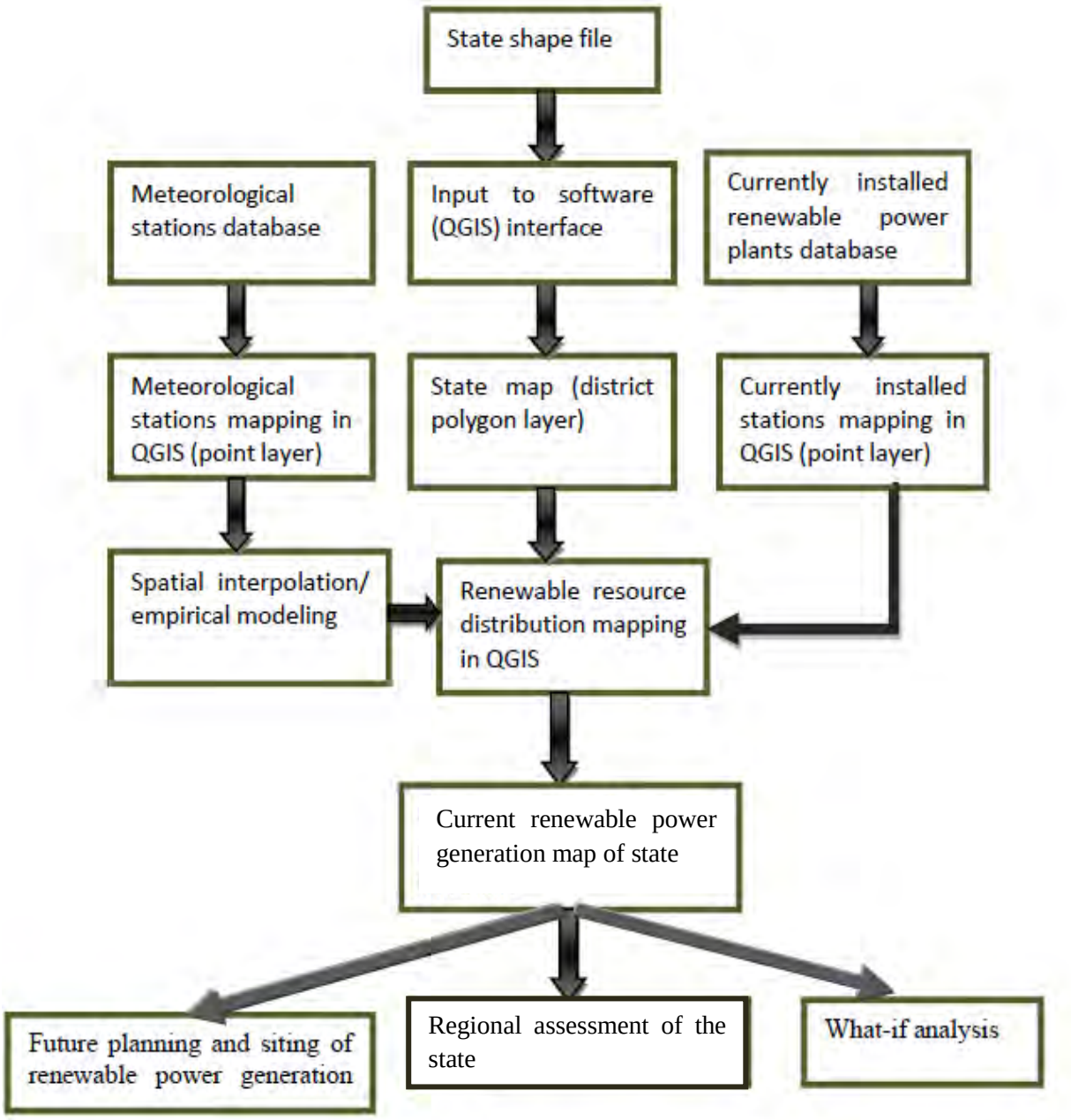

Fig. 1. General methodology to develop renewable energy framework

District shape file for Maharashtra state is taken as the first input to QGIS interface. This shape file may be created in C++ environment or may be directly downloaded. The shape file contains location attributes and area of these 35 districts. Database is obtained for currently installed renewable power generation sites, with their rated power output (MW) and location attributes. The meteorological stations for wind and solar are identified and the corresponding database of instantaneous values of parameters like wind speed, wind power density, Weibull parameters, etc. and global solar radiation are obtained. A summary of database for renewable power generation analysis in the state is organized in Table 1. Various input parameters used to create maps in reference to renewable resources and shape files are summarized in Table 2.

Table 1. Summary of database of renewable power generation in Maharashtra

Renewable energy source	Number of meteorological stations	Estimated potential (MW)	Installed capacity (GW) (2009-10+)	Number of installed power generation sites
Wind	7	4.58	2.01	31
Solar	3	-	-	-
Bagasse co-generation	-	1.25	0.35	39
Small hydro power	-	7.5	0.2	28

Table 2. Summary of input parameters used in QGIS interface

Input parameter	Information available
District shape file	35 districts; location attributes; area
Wind meteorological stations	7 stations, location attributes; hourly wind speed, hourly wind power density; Weibull parameters
Solar meteorological stations	3 stations; location attributes; hourly global, diffuse and direct solar irradiation for each month
Wind installed sites	31 sites; location attributes; installed capacity
Bagasse co generation installed sites	39 sites; location attributes; installed capacity; location of sugar factories
Small hydro power installed sites	28 sites; location attributes; installed capacity

Monthly average values of wind speed, wind power density and solar insolation for the unknown locations are predicted using interpolation techniques and empirical relations from the set of known values of meteorological stations. Predicted values are used to create raster maps in QGIS showing the distribution of wind power density and solar intensity over the state.

Currently installed renewable energy sites are mapped on the spatial layer of Maharashtra state to create point layer for each site in QGIS framework. Each point representing a renewable energy site is linked to its corresponding database of geographical coordinates and installed MW capacity. The Point layer of current installed renewable power generation sites is integrated with the resource distribution raster maps to get the current renewable scenario map for the state.

Usability of the system is defined in terms of future planning and siting of renewable power generation, micro modeling through regional assessment and district wise analysis of the state and what-if analysis to explore some major issues involved in integrating renewable energy framework with conventional electricity transmission network.

3. Renewable energy resource mapping

Distribution of wind power density and solar insolation is estimated for the state and represented as raster maps. Spatial interpolation technique, Kriging interpolation is used for predicting wind power density for unknown locations while Inverse Distance Weigthing (IDW) interpolation is used for predicting hourly solar insolation values for unknown locations.

3.1. Spatial interpolation for wind

Wind energy is the most explored renewable energy in Maharashtra. Out of an estimated potential of 4584 MW, almost 1990 MW has been achieved with an estimated capacity factor of 14% [7]. Seven meteorological stations are identified where actual measurement of various wind parameters (hourly wind velocity, Weibull parameters and average wind power density) are done. These stations are Lonavala, Malwan, Vijaydurga, Panchgani, Deogad, Vengurla and Chalkewadi. The database for the seven stations is obtained from the wind energy resource survey in India by Anna and Mani [8]. There are currently 31 wind power generation sites with their known installed capacities.

Map showing the distribution of wind power density over the state is created to aid in the selection of suitable region for wind turbine installation. Raster map showing the distribution of wind power density over the state is shown in Fig. 2. Current wind power generation sites are mapped to estimate the capacity target. The seven meteorological stations are also mapped and each station is linked to its corresponding data base of geographical coordinates and monthly instantaneous wind speed values. Quantum GIS (QGIS) is used to integrate the conventional database of the seven meteorological stations and 31 wind power generation sites with spatial features to get a complete pictorial representation of current wind power generation scenario.

Monthly average wind power density is predicted for all the districts in the state using the sampled values of seven meteorological stations. The seven stations are represented by ✚ and 31 installed sites are represented by ⚑ in Fig. 2. Raster map of wind power density distribution are created using these predicted values. Kriging interpolation is used for predicting wind power density values.

This is done by generating the experimental semi-variogram of the data set and choosing a mathematical model which best approximates the shape of the function from sample Cumulative Semi Variance (CSV) values [9]. Weights are obtained by converting CSV values into dimensionless values and subtracting from the maximum value, i.e. 1. This appears as a non-increasing function of dimensionless distance and is known as Standard Weighing Function (SWF)[9]

Dimensionless distance of each un-sampled location from each of the seven sampled locations is estimated using the distance tool in QGIS. The distance values are based upon the centroid values of latitude and longitude of locations. For each dimensionless distance; the value of weighing function is estimated from the plot of SWF [9]. Weighted average of the

corresponding value of wind power density, weights being the estimated values of weighing function, gives the predicted value of wind power density for unknown locations.

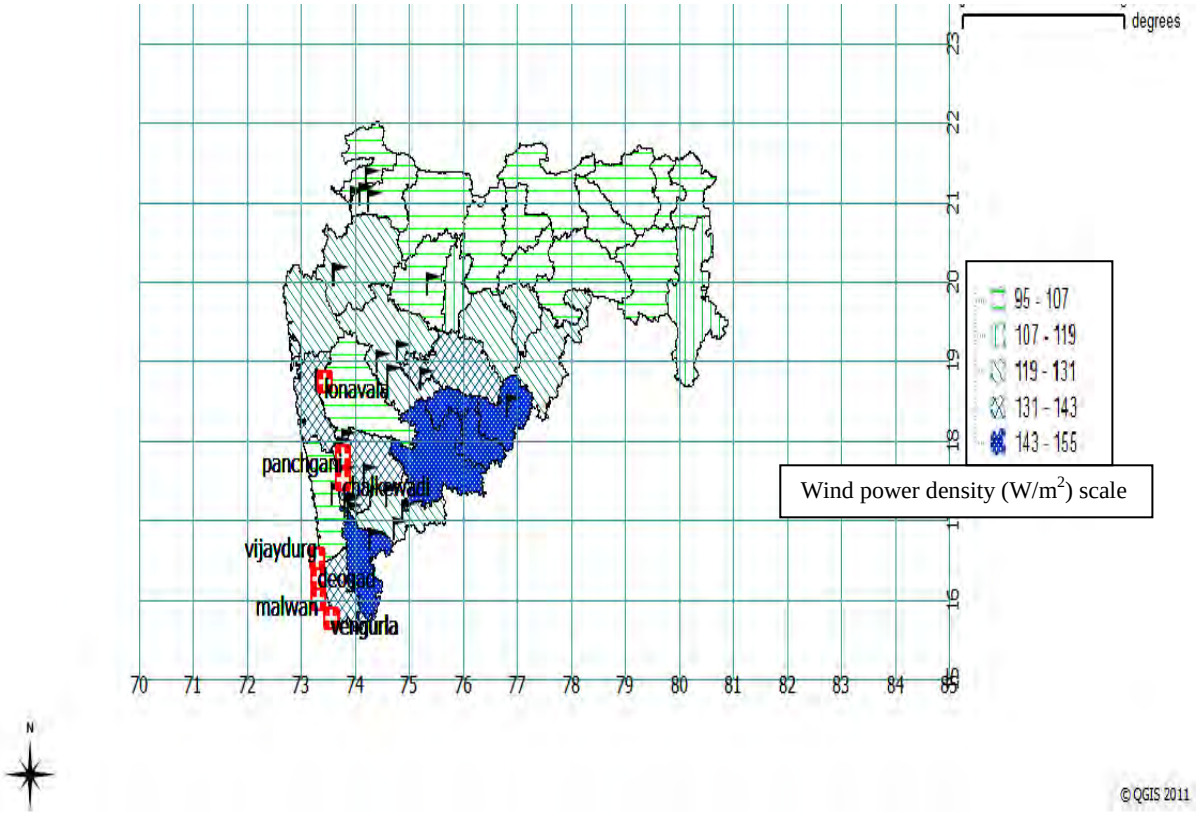

Fig. 2. Wind power density distribution over Maharashtra state

3.2. Spatial interpolation for solar resource mapping

For solar energy, three meteorological stations are identified, viz. Pune, Nagpur and Mumbai. Hourly values of global and diffuse solar radiation for the three stations are taken from solar energy resource survey in India by Anna and Mani [8]. Inverse Distance Weighting (IDW) interpolation [10] technique is used to predict hourly insolation values for un-sampled locations.

In IDW interpolation, weights are proportional to the inverse distance value between un-sampled location and sampled location. This proportionality varies with the power to which the distance is raised and is known as distance coefficient. Distance coefficient of two is taken here.

Raster map showing the distribution of solar energy resource is created using the IDW interpolation plugin in QGIS platform. Hourly global solar radiation estimated for the state are in the order of magnitude of 2000 kWh/m^{2}year which signifies a relatively low value. The variation of solar intensity over the state is also low. Variation of global solar insolation over a year for Mumbai station is shown in Fig. 3. The raster map showing the distribution of solar energy resource is not shown here although the three meteorological stations are represented by ◘ in Fig. 4.

Since the IDW interpolation technique is based on the distance value between the un-sampled location and the sampled location, the uncertainty in the predicted value increases with the increasing distance value. The three sampled locations for solar energy are at a considerable

distance from each other. Therefore using local correlations model for estimating the hourly insolation values would give better accuracy.

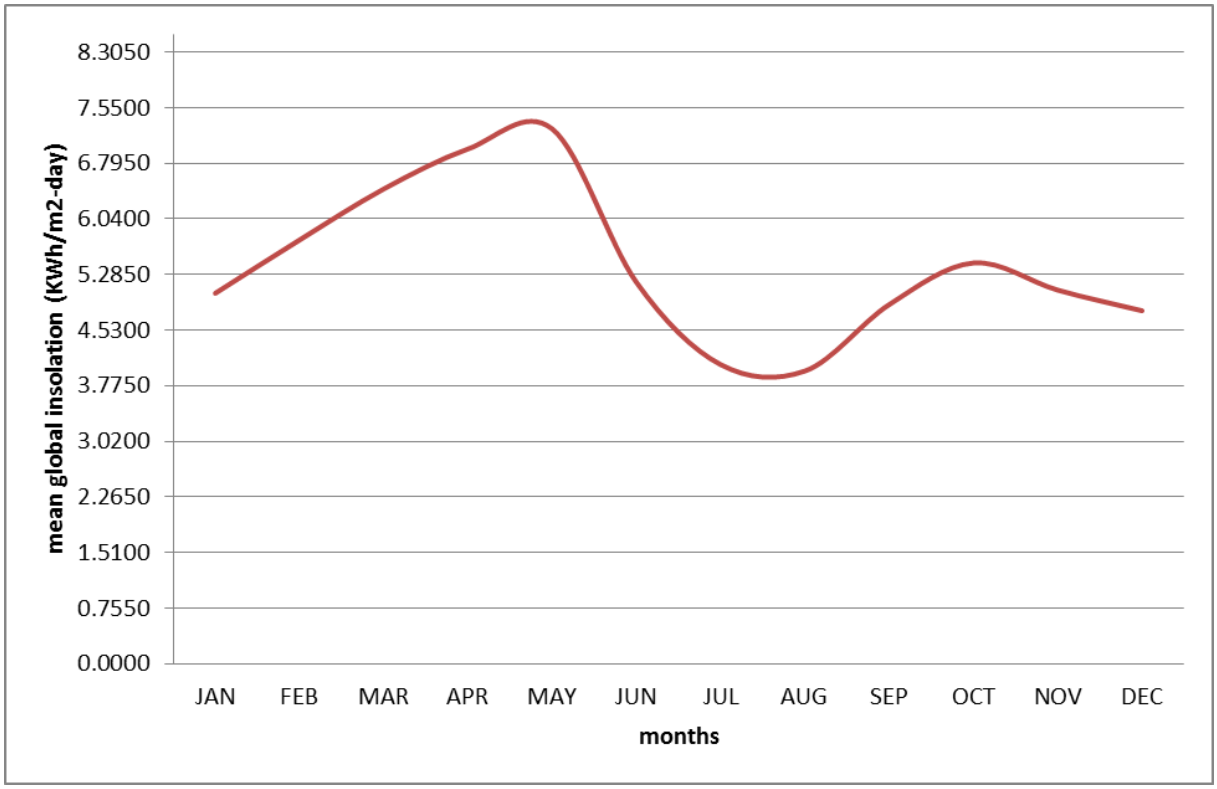

Fig. 3 Variation of global solar insolation for Mumbai

4. Renewable installed capacity mapping

In the field of green energy, the major renewable energy sources in Maharashtra are wind energy, small hydro power plants and bagasse co-generation plants with a small contribution of waste to energy power plants and biomass [6]. 31 sites of wind power generation, 39 sites of bagasse co-generation plants and 28 sites of small hydro power plants are identified and represented spatially [7]. A vector map showing the current installed sites of renewable power generation in Maharashtra is shown in Fig. 4.

Each station mapped is linked to its corresponding data base of geographical coordinates and monthly instantaneous parametric values. A complete database of hourly wind speed data of each month for seven wind meteorological stations (Lonavala, Malwan, Vijaydurga, Panchgani, Deogad, Vengurla and Chalkewadi) is linked with the corresponding location. Similarly database of hourly global solar radiation data of each month for three solar energy meteorological stations (Mumbai, Pune and Nagpur) is linked with the corresponding location. Maps are created representing the spatial data of current installed sites of wind power, bagasse co-generation and small hydro power plants (Fig. 4). Each site is linked with its corresponding database. Every district in the state is also linked to the database of district name, location attributes, i.e. longitude and latitude of the location and predicted values of monthly average wind power density, and monthly average solar insolation. One such database for Satara district in Maharashtra state is shown in Fig. 4.

Monthly average wind power density of seven wind sampled locations and monthly average solar insolation data of three solar sampled locations is used to predicts wind power density distribution and solar intensity distribution over the state respectively.

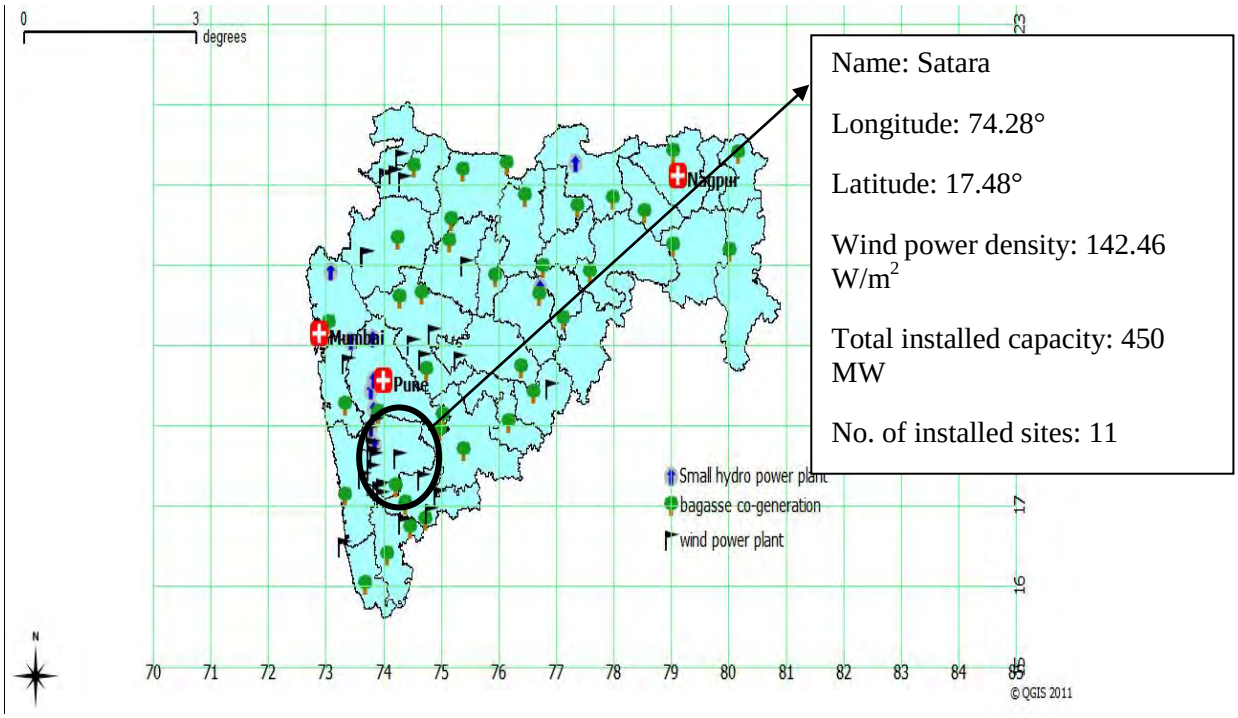

Fig. 4 Current status of major renewable power generation sources in Maharashtra and sample database for Satara district

The GIS approach used is helpful in estimating the renewable energy potential available in the state. Such a system could be useful in future planning and siting of wind power and solar power generation. It helps in analysing the potential areas where wind and solar energy resources can be used exhaustively. Regional assessment of state is also possible as can be seen from Fig. 4 that central region of the state is the major site of wind turbines installation and also the region of high wind capacity (Fig. 2). Satara district in the central region of the state is the site of maximum wind turbine installation with total installed capacity of approximately 450 MW. Eastern part of central region also has high wind potential and hence can be explored more. Similarly southern part of the state was found to be the region of high solar intensity. Bagasse co-generation power plants are distributed all over the state which is in accordance with the distribution of sugar factories in the state [11].

5. Conclusion

A framework is developed for mapping renewable energy resources using an open domain GIS (QGIS) and linking this with the databases for individual stations. Using this framework, it is possible to determine average wind and solar energy densities in selected regions. This is illustrated for Maharashtra state in India.

The QGIS platform is also used to represent the spatial distribution of installed capacities of different renewables. This permits determination of installed capacities for selected regions and renewable energy generation based on estimated capacity factors using the renewable energy resource data for the region.

The framework developed can be used to assist siting decisions. For any site selected, it is possible to determine through Kriging interpolation or empirical correlations the availability (and monthly variation) of wind and solar resource. This can enable determination of the annual capacity factor and the cost-effectiveness of new installed capacities.

Since the method is simple it will be useful, in general, for engineers, architects and solar system designers. The system is also helpful in what-if analysis: if certain percentage of electricity to be achieved through renewable only, is fixed, then what would it imply in terms of capacity of different renewable required to be installed, hybrid scenario of renewable power system, impact on conventional power system, operational and economic implications and capacity savings achieved with penetration of renewable power in the grid.

QGIS being open domain software, the framework can be extended to other states and countries as well and hence can be used extensively for renewable power generation siting and planning for any region.

Acknowledgement
The authors would like to thank Maharashtra Electricity Regulatory Commission [12] for sponsoring the M Tech fellowship and supporting the project and the Maharashtra Energy Development Agency [13] for providing access to renewable energy data.

References

[1] Nguyen H.T., Pearce J.M., Estimating potential photovoltaic yield with *r.sun* and the open source Geographical Resources Analysis Support System, Solar energy, 2010, pp 831-843

[2] Ramachandra T.V., Shruthi B.V., Wind energy potential mapping in Karnataka, India, using GIS, Energy conversion and management, 2005, pp 1561-1578

[3] Celik A.N., Energy output estimation for small-scale wind power generators using Weibull-representative wind data, Journal of wind engineering and industrial aerodynamics, 2003, pp 693-707

[4] Zekai Sen, Ahmet D. Sahin, Spatial interpolation and estimation of solar irradiation by cumulative semivariograms, Solar energy, 2001, pp 11-21

[5] http://en.wikipedia.org/wiki/Maharashtra

[6] Ministry of new and renewable energy, framework for programmatic CDM projects in renewable energy, May 2009

[7] Economic survey of Maharashtra 2009-10, directorate of economics and statistics, planning department, government of Maharashtra, Mumbai

[8] Anna and Mani, Wind energy resource survey in India, Department of non-conventional energy sources, New Delhi, India, edition 1995

[9] Zekai Sen, Ahmet D. Sahin, regional assessment of wind power in western Turkey by the Cumulative Semivariogram method, Renewable energy, 1997, pp 169-177

[10] S. Naoum, I K Tsanis, ranking spatial interpolation technique using a GIS based DSS, Global Nest, 2004, pp 1-20

[11] Renewable energy atlas cd, MEDA

[12] Maharashtra Electricity Regulatory Commission, http://www.mercindia.org.in/

[13] Maharashtra Energy Development Agency, http://www.mahaurja.com/

Project management and institutional complexity in domestic housing refurbishment with innovative energy solutions. A case study analysis.

Thomas Hoppe[1,*], Kris R.D. Lulofs[2]

[1] *CSTM, Institute for Innovation and Governance Studies,University of Twente, Enschede, the Netherlands*
[2] *CSTM, Institute for Innovation and Governance Studies,University of Twente, Enschede, the Netherlands*
** Corresponding author. Tel: +31 489 3242, Fax: +31 489 4850, E-mail: t.hoppe@utwente.nl*

Abstract: Applying innovative energy solutions (IES) in dense residential areas in the Netherlands is a challenge. This paper presents a typology that supports the analysis and understanding of policy implementation processes to encourage the adoption of innovative energy solutions in urban residential areas. The typology uses theoretical concepts from the social sciences, more specifically the disciplines of public administration and policy studies. The two main hypotheses in the paper are that: (a) a high degree of process management will lead to an increasing likelihood that such a policy will be successful implemented, whereas: (b) a high degree of institutionalized interest from other policy areas – especially urban renewal - will lead to failure to implement policy strategies aimed at the adoption of innovative energy solutions. The hypotheses are empirically tested by presenting four case studies in which fitting innovative energy solutions in domestic housing was on the residential site refurbishment project agenda. The paper adds further insights in the fields of environmental energy policy implementation, sustainable cities and energy transition.

Keywords: *Environmental energy policy implementation, Urban renewal, Sustainable cities, Housing, Case studies.*

1. Introduction

Larger energy efficiency can nowadays be achieved in existing dwellings, thanks to longer equipment lifecycles, slow replacement rates, and emerging technical innovations. Opportunities for large-scale energy conservation can thus now be found in neighbourhood revitalization projects [1]. These projects aim at improving the social and physical structure of post-War housing estates in which the houses and their environments are characterized by poor-quality, obsolete physical construction. An additional characteristic is that the poor-quality buildings are accompanied by a poor social structure, as indicated by high unemployment, above-average crime rates and a large proportion of ageing residents. To cope with those problems, neighbourhood revitalization projects are meant to improve both social and physical (construction) structures.

A national government (climate) policy that seeks to link into existing neighbourhood revitalization projects, offers advantages. Such sites contain a large number of dwellings owned by central actors (housing associations) and renovating them will be a major operation in any case, so there will be a low threshold for the house owners to adopt energy conservation measures. Local governments encourage the setting of ambitious goals as a stepping stone to realize high energy efficiency goals [1]. Improving energy efficiency proves to be a difficult task, though. Due to the absence of legal governmental instruments there is a need to rely on communicative and economic policy instruments to convince house owners and stakeholders. Moreover, only 'soft instruments' are used, such as information campaigns, covenants and subsidy schemes [2]. This means that governments are dependent on the willingness of their target groups. Although the description applied to the Dutch situation, it is similar to those encountered in other Western European countries [3].

Local governments are able to exercise influence and encourage the uptake of energy conservation appliances by making trade-offs with housing associations, with a strategic use

of urban renewal subsidies and legal permits. However, the local authorities remain firmly dependent on the willingness of housing associations and other property owners to cooperate. Lengthy and complex decision-making is unavoidable when a large-scale neighbourhood or building block renovation plan is being scheduled. In short, many institutional barriers exist that prevent the large-scale adoption of technical appliances to stimulate energy efficiency in existing housing [2].

The analytical focus in this paper is on the adoption of energy innovations in projects in which family dwellings are refurbished. The central question of the paper is how to understand and overcome the difficulties that adoption of energy innovations encounters in neighbourhood revitalization projects in urban residential areas. A typology based on theoretical insights derives from network governance and institutional complexity is introduced to support further comprehension. The typology is designed to improve analysis of complex contexts in which energy innovations - especially renewable energy systems - are adopted in highly institutionalized contexts, such as large-scale refurbishment projects in post-War urban residential areas.

2. Theoretical framework

Here we discuss the need to design a new typology to better understand the adoption of energy systems in a highly institutionalized context. The theoretical literature on environmental policy integration is presented as well as governance mechanisms to deal with complexity in similar contexts, drawn from the literature in the disciplines of public administration and policy studies of the management of complex networks, the aim being to achieve collective policy objectives in multi-stakeholder settings. The section ends with the introduction of a typology that covers two dimensions: (1) institutional complexity (as a lack of policy integration) and (2) project management of complex situations.

2.1. Institutional complexity

Environmental policies and energy efficiency goals are not prioritized in major urban settings. Moreover, social and economic aspects of the living environment and the climate for attracting business enterprises are often considered more important. Furthermore, environmental energy objectives may not be fully integrated or coordinated with other policy domains' objectives which also need to be fulfilled in such projects. This is no wonder since problems related to climate change – an environmental problem "at large" [4] – are not limited to a single sector or policy domain and hence are not coordinated optimally. This calls for environmental policy integration [5] - balancing the interests, concerns and priorities of the so-called three pillars: social, economic and environmental dimensions [6] - or arenas in which policy sectors are not competing for attention on the agenda, but which rather converge [7]. In many domains this is not yet the case [5, 8], such as revitalization of post-War neighbourhoods, a domain subject to urban renewal policy. These neighbourhoods are characterized by factors that hamper effective decision-making, such as distributed ownership rights, high 'social infrastructure', and hence complex regulations. For instance, regulation which requires tenants' approval to the project plans in large scale refurbishment projects. To deal with these complex issues many local revitalization projects receive earmarked financial support from government. In turn, local stakeholders are requested to ensure that the project meets urban renewal performance targets. Energy efficiency is no longer considered a significant target in urban renewal practice, at least not in the Netherlands.

2.2. Project management

Realizing the installation of innovative energy systems in local neighbourhood revitalization projects meets complexity in decision-making as multiple actors are involved who have interests and are mutual dependent. Actor-networks dominate negotiations and bargain about how to meet public goals. From a governmental perspective 'steering' towards the achievement of public goals, such as reductions in greenhouse gas emissions, then becomes a difficult task. In this regard, management of decision-making in a multi-actor setting becomes important. Due to the presence of multiple interconnected actors this can be perceived as 'governance of complex networks' [9]. Management of such public-private networks cannot be perceived as just a form of governmental 'steering' which has a broader meaning than strict, administrative control. Given the context, it may be better to define it more accurately as "directed influence" rather than steering [9]. The challenge, rather, is to realize policy in interaction with those other actors, which can engage social support, withstand the test of criticism, and connect other actors to policy efforts. Public agencies therefore fulfil the role of safeguarding that under-represented goals – such as environmental ones - and interests can participate in games. In a multi-actor, decision-making game this requires a balancing act if the actors involved are to achieve the goal(s) successfully and simultaneously [9]. It enables their perceptions to be aligned, visions to be converged, expectations to be discussed, mutual trust to be created, sharing of experiences (especially tacit knowledge), with reflection on how to achieve goals in a feasible manner, and keep environmental goals on the decision-making agenda. This requires a custom approach which fits the particular setting and its actors, for instance by gathering support from stakeholders to facilitate effective decision-making. In such settings, public actors may function as 'network managers': they may act as a 'facilitator' or 'process manager' by facilitating dialogues between actors and employ techniques such as workshops and brainstorming sessions to promote consensus building. By doing this they may attract skilled participants, and gather external resources (such as subsidies or loans), which enables professional leadership and favours learning conditions. Other game management strategies are: covenanting, influencing actor's perceptions, bargaining, introduction of ideas in furtherance of reflection, selective activating of actors (usually not present in the arena), furtherance of facilitation, brokerage, and mediation [9]. In the domain environmental energy 'change agents' [10] aim to have multiple actors adopt green energy technologies [11].

2.3. A typology

Based on the two dimensions introduced in the previous sections, a two-dimensional typology is adduced. The matrix has four quadrants, allowing predictions to be made concerning the outcome of the project's objectives on the adoption of energy innovations. A graphical presentation of the typology is presented in figure 1. The dimension "institutional complexity" is presented on the vertical axis, with the dimension "project management" on the horizontal one. In this study the unit of observation of the typology relates to neighbourhood refurbishment projects in urban residential areas. Besides application to the issue discussed here, the typology may also be applicable to other types of projects with multiple actors, interdependent actors that seek to achieve (collective) goal(s).

The two hypotheses relevant to the dimensions in the typology are that: (a) a high degree of process management will lead to an increasing likelihood of successful adoption of energy innovations by project stakeholders: whereas (b) a high degree of institutionalized complexity - from other policy domains, especially urban renewal - will lead to failure in the implementation of policy strategies aimed at the adoption of innovative energy systems.

The main hypothesis of this paper concerns a combination of these two hypotheses. On the basis of these propositions expectations can be formulated about the influence of the dimensions in terms of four possible outcomes. This is shown in figure 1. Whereas the optimum outcome can be expected in quadrant 4 (Q_4; low institutional complexity and a high degree of project management), the worst outcome can be expected in quadrant 1 (Q_1; high institutional complexity and low degree of project management). The outcomes in quadrants 2 and 3 will lie between the extreme outcomes in quadrants 1 and 4.

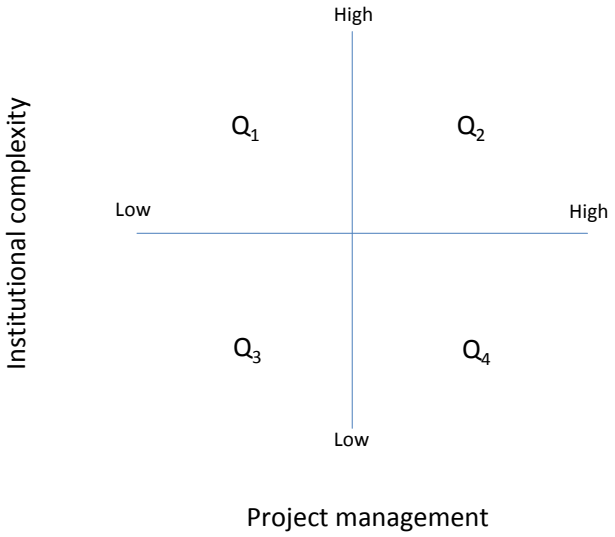

Fig. 1. Graphical representation of the typology.

3. Methodology

The empirical study comprised four case studies concerning residential district renovation projects that featured family housing. The cases were selected from an existing project set that provides information on urban renewal projects and ambitions for energy affairs [12]. The four case study projects all comprise domestic housing built in the late 1960's and early 1970's.

Different types of data were collected, both qualitative and quantitative. Among other things, 27 semi-structured interviews were conducted. Additional documentation on the cases was traced both before and after the interviews were conducted. The project documents retrieved included formal policy documents, advisory reports, annual reports, other informative papers, websites, feasibility study reports and geographical maps of project locations. Data were collected between October 2007 and April 2008.

In this study, a cross-case (comparative) research design was applied. The analysis was conducted in order to test the predictions based on the main hypothesis following the typology in the previous section. The dimensions 'project management' and 'institutional complexity were operationalized as 'ten-point-Lickert-scales. For the analysis the scores-per-case were assigned to the scales on the two dimensions. Next, the positions of the cases were plotted in a graphical display on the basis of the two-dimensional typology.

4. Results

In table 1 key data on the cases studies are presented. The table presents information on the initial objective (ambition) during the early stages of the project and actual outcome (in terms of innovative energy systems being applied). As it turns out, in three out of four cases no innovative energy systems were applied.

Table 1. Key data on four case studies.

Name of site	Name of town	IES (ambition)	IES (actually implemented)
Atol- en Zuiderzeewijk	Lelystad	None	None; only conventional measures
Bijvank en het Lang	Enschede	Solar thermal system	None; only conventional measures
Nieuwstad	Culemborg	Solar thermal systems or district heating from an industrial plant	None; only conventional measures
Groot Kroeven	Roosendaal	Collective biomass installations and heat pumps	Passive renovation

Figure 2 presents the result of the comparative analysis of the case studies. The positions of the cases in the figure relate to the scores on both dimensions 'institutional complexity' and 'process management', presented in a scatter plot. As can be seen, the cases in which a high degree of project management and a low degree of institutional complexity are present, innovative energy systems have been applied in existing apartment buildings. This is to say that the case in quadrant 4 (Groot Kroeven) has a positive outcome, as was predicted by the main hypothesis in section 2.3. The other cases, situated in quadrants 1 (Atol- en Zuiderzee-wijk), 2 (Bijvank en het Lang) and 3 (Nieuwstad) have negative outcomes.

4.1. Discussion

The results of the analysis allow lessons to be drawn. First, in all four cases innovative energy systems were not applied, and in the cases in which innovative energy systems were initially considered the initial objectives were not met. During the project trajectories plans were changed for different reasons. Only the refurbishment project in the Groot Kroeven case may be considered successful. Although the institutional complexity conditions favoured success – the local government did not own property near the site and no serious urban renewal performance targets focused on the project - the outcome was to a large extent due to clever project management. This resulted from a combination of professional leadership, an actor-network of motivated and skilled participants, a high level of trust between the stakeholders, the use of subsidies, and learning capacity. This last point was revealed as initial barriers were overcome. This came at a high price, though, as expertise and personnel capacity had to be hired from abroad, new construction measures had to be designed and tested – in fact

experimental houses were established and monitored -, and a difficult decision-making process had to be undertaken to convince tenants and thus to meet the legal '70 percent tenant-approval standard' for large-scale refurbishment projects. All these matters led to delay in the project schedule. Hence, additional costs were incurred. Nonetheless, the infrequently used concept of "passive renovation" was applied successfully in 134 houses. The initiative to adopt this innovative concept had its origin in the housing association (or actually the project manager in situ), not the local authority.

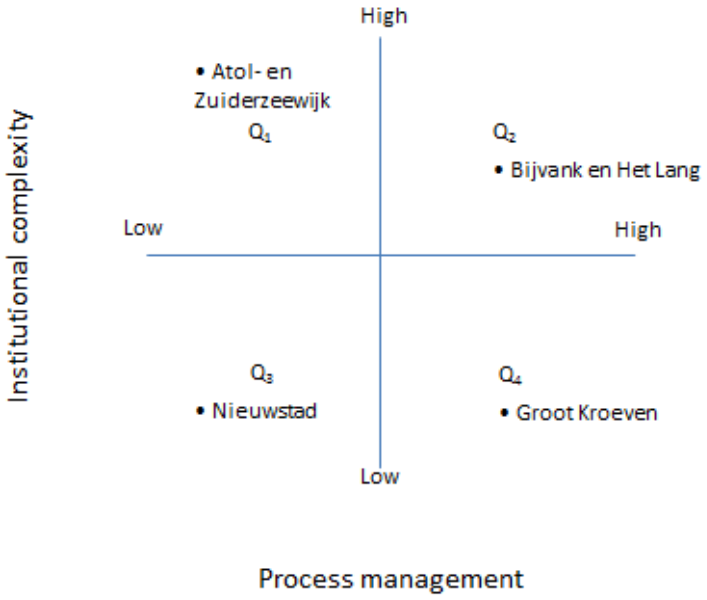

Fig. 2. Results of the case study analysis.

Second, if one's aim is to fit innovative energy solutions in renovation projects with a high degree of complexity, one is prone to encounter problems. When the housing property owner does not have the financial means to invest, on-site housing ownership rights are distributed among many different actors, and urban renewal objectives are given priority, the chances of successfully applying energy innovations are poor. The cases Atol- en Zuiderzeewijk and Bijvank en het Lang provide evidence that non-energy related urban renewal issues are assigned greater importance in the projects. When considered during the initial stages, the innovative energy appliance became an 'end of the bill' objective and was dropped from the agenda when cost estimations were done, and tenants feared monthly rent increases and delays to the project. The latter also applies to the Nieuwstad case.

Third, the cases revealed mistrust between the actors involved. Local authorities initiated a process to have energy innovations applied in local housing projects. They managed to have an energy audit report drafted by an external consultancy agency (paid for with a subsidy from national government). The advice in the audit report considered several options for on-site improvements to energy-efficiency. However, they were met with scepticism by the project stakeholders, especially the housing associations. To a large extent this related to the credibility of the energy audit reports. A difficulty, when the energy audit advice was taken into consideration, was that it remained on the decision-making agenda, especially when the actual costs of installing the systems were looked at. When the actual calculations were done it turned out that the audit report advices left out significant cost aspects, such as the installing costs and the replacement of energy-infrastructure (pipelines), as shown by Bijvank en het Lang and Nieuwstad cases.

In two cases (Bijvank en het Lang, and Nieuwstad) the housing associations complained about the unequal distribution of costs between stakeholders in the revitalization project in respect of the use of innovative energy solutions. Whereas the local authority aimed at having renewable energy systems, it did not participate in sharing in the costs. As a consequence, the housing associations were to bear the costs single-handedly, which was considered de-motivating. These two cases show that it is very important that local government and housing associations discuss a project plan seriously in the project's initial stages. In both cases the housing associations blamed the local governments for their high ambitions but their unwillingness to share in the additional costs, which bred mistrust. In that sense, it was no surprise that the ambitious energy objectives failed as the housing associations were confronted with the high costs of installing the systems, once they were seriously considered and calculated. Ergo, due to non-specific negotiations between the two parties in the initial stages of the projects, the financial feasibility of the objective was never discussed in detail.

Fourth, it may be stated that the cases show that energy innovations are preferably installed in projects that feature newly constructed houses rather than the renovation of existing houses (which means that one needs to cope with social and institutional 'infrastructure'). Theoretically speaking, new construction is favoured by the opportunity to make high investments for the long term, which needs to be done anyway, plus the absence of an existing energy infrastructure. This may also be the reason why the municipality of Lelystad – a national renewable energy frontrunner – did not formulate an ambition for the renovation of the existing neighbourhood Atol- en Zuidzeewijk, whereas there were many recently built residential sites nearby with innovative energy systems (wind power and district heating).

Finally, the cases also provide evidence that tenants fear innovative energy solutions. When requested in a vote, tenants did not accept an increase in their monthly rents as compensation for having a solar thermal system installed in their houses. The outcome of the vote was a reason for housing association to renounce the option of having the renewable energy system used in the project. The tenants' fear may have a background in their unfamiliarity to innovative systems, but may also be related to mistrust between the tenants and the housing association.

5. Conclusion

The installation of innovative energy solutions in urban areas is difficult, as local neighbourhood revitalization projects are highly complex. This paper has introduced a typology to support the analysis and understanding of local projects in which energy innovations are to be fitted. We used a comparative case study research design to test the predictions empirically against the typology. The research design comprised four case studies of local neighbourhood revitalization projects in the Netherlands, concerning refurbishment of domestic housing. The main hypothesis was confirmed as success as predicted only concerned a local project where a low degree of institutional complexity was combined with a high degree of project management.

This case, the Groot Kroeven project, shows that due to a combination of clever project management, professional leadership, learning capacity, an actor-network of motivated and skilled participants, the use of subsidies, and the absence of highly demanding urban renewal context and –project plans, barriers were overcome and positive project outcomes can be realized.

The external validity of the results is limited due to the few amounts of cases we were able to investigate. A case study design – with only four cases - was necessary, though, due to the need to analyse detailed data, which are difficult to collect and require many efforts. More research is necessary to apply our typology and to test its main hypothesis in research designs that feature more observations. This could very well be possible in other contexts, such as different types of buildings, neighbourhoods or geographical entities. One may consider applying the typology to challenges that impede the achievement of 'sustainable cities'.

References

[1] T. Hoppe, J. Bressers and K.Lulofs, Local Government Influence on Energy Conservation Ambitions in Existing Housing Sites – Plucking the Low-hanging Fruit?, Energy Policy, 2011, 39, pp. 916-925.

[2] T. Hoppe, and K. Lulofs, The Impact of Multi-level Governance on Energy Perfomance in the Current Dutch Housing Stock, Energy & Environment, 19(6), pp. 819 - 830.

[3] M. Elle, T. van Hoorn, T. Moss, A. Slob, W. Vermeulen, and J. van der Waals, J. Rethinking Local Housing Policies and Energy Planning: The Importance of Contextual Dynamics. Built Environment, 28(1), pp. 46-56.

[4] M. Hajer, The Politics of Environmental Discourse: Ecological Modernisation and the Policy Process. Clarendon Press, 1995.

[5] EES, "Environmental Policy Integration in Europe: State of Play and an Evaluation Framework", EEA Technical Report, European Environment Agency, 2005.

[6] J. Knudsen, Environmental Policy Integration and Energy, Ph.D. thesis, University of Twente, 2009.

[7] H. Lovell, H. Bulkeley and S. Owens. Converging Agendas? Energy and Climate Change Policies in the UK. Environment and Planning C: Government and Policy 27, 2009, pp. 90-109.

[8] A. Jordan and A. Lenschow, Environmental Policy Integration: an Innovation in Environmental Policy? In A.J. Jordan and A. Lenschow (Eds.). Innovation in Environmental Policy? Integrating the Environment for Sustainability. Cheltenham, UK: Edward Elgar, 2008, pp. 313-341.

[9] W. Kickert, E-H. Klijn and J. Koppenjan. Managing Complex Networks; Strategies for the Public Sector, Sage Publications, 1997.

[10] E. Rogers, Diffusion of Innovations, Third Edition, The Free Press, 2003.

[11] J. van der Waals, W. Vermeulen, and P. Glasbergen, Carbon dioxide reduction in housing: experiences in urban renewal projects in the Netherlands, Environment and Planning C: Government and Policy 21, 2003, pp. 411-427.

[12] T. Hoppe, CO_2 reductie in de bestaande woningbouw; een beleidswetenschappelijk onderzoek naar ambitie en prestatie, Ph.D. thesis, University of Twente, 2009.

Improvements in environmental performance of biogas production from municipal solid waste and sewage sludge

Ola Eriksson[1,2,*], Mattias Bisaillon[2], Mårten Haraldsson[2], Johan Sundberg[2]

[1] *University of Gävle, Gävle, Sweden*
[2] *Profu AB, Mölndal, Sweden*
** Corresponding author. Tel: +46 26 64 81 45, E-mail: ola.eriksson@hig.se*

Abstract: Management of municipal solid waste is an efficient method to increase resource efficiency as well as to replace fossil fuels with renewable energy sources. This is due to that (1) waste to a large extent is renewable in itself as it contains food waste, paper, wood etc. and (2) when energy and materials are recovered from waste treatment, fossil fuels can be substituted. In this paper some of the results from a comprehensive system study of future waste management in the Gothenburg and Borås regions are presented. Emphasis is put on biological treatment of easy degradable waste such as food waste, by-products from food industry and sewage sludge. The project has been performed in cooperation between Kretsloppskontoret (The municipal office for waste and water management), Göteborg Energi (The energy company in the city of Gothenburg), Renova (The waste management company in the Gothenburg region), Gryaab (A water management company in Gothenburg) and researchers from Profu (Environmental and Energy Consultancy).
Several treatment options for the organic waste have been investigated. Different collection and separation systems for food waste in households have been applied as well as technical improvements of the biogas process as to reduce environmental impact. The biogas replaces fossil fuels and the solid residue is pelletised and either used as fertiliser or as fuel. The method used is computer modelling with the ORWARE (Organic Waste Research) model for the waste management system. Deliverables from the model are environmental impact categories as developed within life cycle assessment and financial costs and revenues.
The results show that central sorting of a mixed fraction into recyclables, combustibles, biowaste and inert is a competitive option compared to source separation. The result is however based on several crucial assumptions. Separation and utilisation of nitrogen in the wet part of the digestion residue is made possible with a number of technologies which decreases environmental impact drastically, however to a substantial cost in some cases. There are several advantages with pelletisation of the solid digestion reside. Use of pellets is beneficial compared to direct spreading as fertiliser. Fuel pellets seem to be the most favourable option, which to a large extent depends on the circumstances in the energy system. Waste management integrated with local energy supply, wastewater treatment, agriculture and vehicle fuel supply is thus a cost efficient method to decrease greenhouse gases and promote the use of waste as a renewable fuel.

Keywords: *LCA, ORWARE, Biogas, Costs*

1. Introduction

In Sweden, biogas has been produced at municipal waste water treatment plants since the 1960's. The primary incentive was to reduce sludge volumes. However, the oil crises of the 1970's rang alarm bells, leading to research and development of biogas techniques, and construction of new plants in order to reduce environmental problems and dependency on oil. During the 1980's, several landfill plants started to collect and utilise biogas produced in their treatment areas, an activity that expanded quickly during the 1990's. Several new biogas plants have been constructed since the mid-1990's to digest food industry and slaughterhouse wastes, and kitchen wastes from households and restaurants. [1]

Statistics for 2009 from Swedish Energy Agency [2] shows that biogas to an increasing extent is produced in co-digestion plants and in farm facilities and then used as vehicle fuel. The major biogas production emanates from different types of waste such as sewage sludge, source separated food waste and waste from food industry. In all the production was 1363 GWh in 2009, approximately the same level as in 2008. In Sweden there are in total 230 biogas plants of which 136 are wastewater treatment plants, 57 are landfills, 21 are co-

digestion plants, 4 are placed on industries and 12 are farm facilities. The number of upgrading plants is 38 and biogas is injected to the natural gas grid at 7 places. The biogas production is predominantly present in the metropolitan areas. Compared to previous years a larger share of the produced biogas was utilised in 2009. Torching of biogas is decreasing and vehicle fuel production is increasing. The major use was for heat generation purposes (49 %) followed by vehicle fuel (36 %), electricity generation (5 %) and gas flame (torch) (10 %). Gasfuelled cars still constitute a minor share of the total vehicle fleet in Sweden, but the number of gas cars is increasing and more car producers offer more car models as gas cars. Vehicle gas is on average 60 % biogas in Sweden.

In order to illustrate the offset for biogas in Europe figures from 2005 [3] have been used. In 2005 recovered biogas was used for electricity (13 TWh), heat (8 TWh) and vehicle fuel (0.1 TWh). The majority of the heat- and power generation comes from Germany and Great Britain whereas almost all vehicle fuel was generated in Sweden. Figure 1 illustrates the distribution of energy from biogas production in each European country.

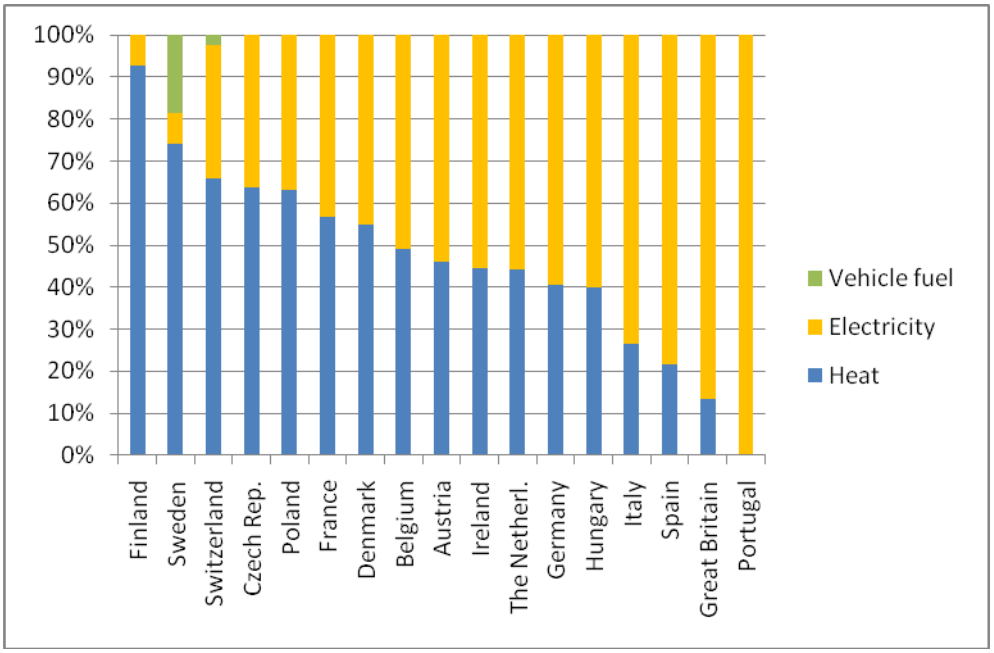

Fig. 1 Distribution for the generation of electricity, heat and vehicle fuel from landfill gas and biogas in each country in 2005. Sources: Switzerland [4], Sweden [5], others [6]

The biogas market is however not saturated. In a report from AvfallSverige (Swedish Waste Management) [7] the total biogas potential from domestic raw products, excl. raw products from forestry, amounts to 15.2 TWh/year, of which the total potential with limitations due to technical and economic reasons is assessed to 10.6 TWh/year. By-products from forestry represent a substantial potential for future bio methane production. Residues from forestry are estimated to 59 TWh/year. The total potential from food waste is 1346 GWh/year, of which 60 % is included above. Residues from industry and agriculture have a potential of 8-11 TWh/year depending on limitations. Digestion of sewage sludge is 7 % of the practically feasible potential.

In a waste management perspective, anaerobic digestion is a preferably immature technology in comparison to landfill disposal and waste incineration in terms of waste amounts treated, when the method entered the waste management market and also environmental and technical standards. That, in combination with high investment costs for biogas plants in comparison to

composting and also a historically low demand for vehicle gas (and thus willingness-to-pay), has pushed waste to enter the vehicle fuel market. The transport sector is however tightly bound to fossil fuels, to a higher extent than e.g. the residential sector, and the willingness-to-pay is high in this sector. In a future where the oil price will continue to increase, the incitements for bio-vehicle-fuels, including biogas, will grow. In fact the raw product - the substrate – may switch from waste (a cost for the waste owner) to a commodity (revenue to the supplier). The demands from society on environmental standards and resource efficiency in biogas systems will probably increase during this evolvement. That is why it is interesting to study what improvements can be achieved in such systems. For the interested reader other relevant studies on biogas in a systems perspective are reported in [8-10].

2. Methodology

The method used is life cycle assessment (LCA) [11] and financial cost calculation facilitated by computer modelling with the ORWARE (Organic Waste Research) model [12]. In this study only waste streams suitable for anaerobic digestion are included. ORWARE is a computer based tool for environmental and economic systems analysis of waste management. It was first developed for systems analysis of organic waste management, hence the acronym ORWARE (Organic Waste Research). The model is designed for strategic long-term planning of recycling and waste management and based upon s tatic conditions and on l inear programming (LP). The ORWARE model has been developed since the early 1990s in close cooperation between four different research institutions in Sweden (Royal Institute of Technology, Swedish Environmental Research Institute, Swedish Institute of Agricultural and Environmental Engineering and Swedish University for Agricultural Sciences). The waste management is followed from cradle (waste sources) via collection and transport to treatment plants and further to grave (utilisation of products from waste treatment). Treatment facilities included are incineration with energy recovery, composting, landfill, anaerobic digestion with biogas utilisation, spreading of organic fertiliser on arable land, sewage treatment, material recycling of plastic and paper packages, and some additional technologies. The model delivers substance flows, distributed to emissions to air and water, left in growing crops and in recycled material. Energy flows such as energy use and recovered energy is also provided. Single substances such as carbon dioxide or substances to water leading to eutrophication can be tracked, as well as the amount of plant-available nutrients and emissions of different heavy metals. Emissions are also characterised and weighted using Life Cycle Impact Assessment. At the same time, financial costs (investment and operational costs) and environmental costs and revenues including savings in the surrounding system can be calculated for the whole management chain.

In this particular study, treatment of biodegradable waste by anaerobic digestion producing biogas for vehicle purposes and solid and wet fertiliser is the system in focus. The goal of the project is to conduct a system analysis from economic and environmental perspectives to investigate (1) what is the best alternative for collection of substrate and (2) what is the best alternative for dealing with digestate and reject water. The plants used as the point of departure for the study are a planned biogas plant in Gothenburg and an existing biogas plant in Borås. The plant in Borås is planned to be included in an energy combine with ethanol production.

Upstream to the biogas plant two different collection and separation systems for food waste in households have been applied for the Gothenburg case:
A Kerb-side collection with source separation of food waste

B Co-mingled fraction of combustible and organic fraction which is thereafter mechanically separated

Case A refers to the most common method in Swedish municipalities to achieve source separation of food waste. Data on vehicles, costs etc. has been provided by members of the project group as to reflect existing plans on extended schemes for source separation and collection.

Case B comprises a technical solution present in Ludvika in Sweden [13]. A facility for central sorting of food waste, also called homogenisation plant, has been investigated and data adjusted to the Gothenburg waste management system. The plant is fed with residual waste from households (the remaining waste after sorting out newspapers and packages made of glass, plastic, metal and cardboard). After a sequence of sorting steps (drums) different materials are sorted out, leaving raw compost left to biological treatment. Concerning collection this alternative does not require vehicles with multiple trays.

Downstream to the biogas plant one method for refinement of the solid residue (bio fertiliser) and five methods for refinement of the wet residue have been applied for the Gothenburg case and to some extent also in Borås, see below:
C Drying and pelletisation of the solid digestion reside with application as fuel- or nutrient pellet
D Separation and utilisation of nitrogen in the wet part of the digestion residue

Case C contains different treatment options for the dewatered sludge from an anaerobic digester. There are several potential options for the digestate:
C1 Drying and pelletisation, then used as fuel in a waste incinerator constructed for RDF-fuel
C2 Incineration in a waste CHP without further drying
C3 Spread directly on arable land without further drying and pelletisation
C4 Drying and pelletisation and then spread on arable land as soil fertiliser
In the systems there are two types of sludge available for which the above methods have been applied: one from digestion of dewatered sewage sludge (C1-4) and one from co-digestion of food waste from households and business facilities (C3-4). The sludge dryer applied uses hot water from the district heating system as energy source, and data is taken from design plans.

Finally, in case D different methods for reducing ammonia in the wet part of the digestate are applied. In the reference scenario wet digestate (no dewatering) is spread on arable land. In all other scenarios the sludge is dewatered and the dry digestate is spread on arable land. Following technologies for treatment of the wet part have then been compared to this reference:
D1 The reject water is treated in a wastewater treatment plant (WWTP) (just Gothenburg)
D2 The reject water is first treated in a Sequencing Batch reactor (SBR) and then treated in a WWTP (just Borås)
D3 The reject water is first treated by deammonification in a Moving-Bed Biofilm Reactor (DeAmmon) and then treated in a WWTP (just Gothenburg)
D4 The reject water is first treated by air desorption and then treated in a WWTP
D5 The reject water is first treated by steam desorption and then treated in a WWTP
D6 The reject water is first treated in a membrane facility and then treated in a WWTP

More details on the different technologies are found in [13]. The environmental impact assessment uses CML 2001 baseline [15].

3. Results

Results for CO_2 emissions and costs are presented for the A-D cases. More detailed results (e.g. acidification and eutrophication) for A-C are found in [13] and for D in [14].

When central sorting of food waste (case B) is compared to conventional source separation (case A) there are only minor changes in environmental impact. This is due to that there are small changes in the actual waste treatment, which dominates over collection and transport in terms of environmental impact. The environmental impact is somewhat higher (+400 tonnes CO_2) when central mechanical sorting is applied due to decreased net electricity generation as the sorting facility uses some electricity. The lost electricity generation is compensated for by marginal electricity production (725 kg CO_2/MWh el) mainly consisting of coal condense power. This negative effect is to some extent (-200 tonnes CO_2) compensated for by increased heat and power generation from waste incineration due to a higher heat value of the supplied waste fuel. Hereby marginal electricity and other fuels for district heating are substituted. The higher heat value is explained by that in the sorting facility metals, landfill residue (grovel, sand and other incombustibles) and moisture are removed from the combustible fraction. The result for CO_2-emissions is a slight increase by 162 tonnes which is infinitesimal in relation to the 249 ktonnes of CO_2 from the whole waste- and district heating system. In an economic comparison the net costs are decreased by almost 20 MSEK/year (1 EUR ≈ 10 SEK). The sorting facility costs 16 MSEK/year, but 23 M SEK/year is avoided for the kerb-side collection system. Costs are also lower for waste incineration (11 MSEK/year) which together with some other minor savings adds up to -19 MSEK/year.

In the systems analysis of different treatment of the digested and dewatered sewage sludge and co-digestion sludge the options have been compared to C1 for sewage sludge and C3 for co-digestion sludge. The result is depicted in Table 1.

Table 1 CO_2-emissions and costs for different sludge treatments

GHG (kton CO_2 eq./year)	**Sewage sludge C4**	**Sewage sludge C2**	**Sewage sludge C3**	**Sewage sludge & co-digestion sludge C4**
Waste management system	0.0	-0.1	0.3	0.0
District heating system	2.3	-1.0	0.0	2.8
Background system	1.4	0.8	-1.5	2.5
Sum	3.6	-0.4	-1.2	5.3
Costs (MSEK/year)				
Waste management system	-18	-25	-18	-15
District heating system	7	-5	-1	9
Sum	-11	-30	-19	-6

Eventually the result for case D is presented in Table 2.

Table 2 Climate impact and net costs from system analysis of digestate treatment

Technology	**Climate impact (tonnes CO_2 eq./year)**		**Net costs (MSEK/year)**	
	Gothenburg	**Borås**	**Gothenburg**	**Borås**
D0: Un-dewatered biofertiliser for soil improvement	-940	-690	5.0	8.1
D1: Dewatering and WWTP	1340	-	24.8	-
D2: Dewatering and SBR	-	1270	-	6.1
D3: Dewatering and DeAmmon	750	-	5.2	-
D4: Dewatering and air desorption	620	580	7.0	7.5
D5: Dewatering and steam desorption	250	190	8.1	7.5
D6: Dewatering and membrane	590	610	6.6	7.7

The results of the system analysis of digestate treatment (Table 2) show that the best alternative for Gothenburg, both from an economical point of view (column 4) and when considering the climate impact (column 2), is to transport and spread the un-dewatered digestate directly onto arable land (D0). From the economic perspective, the best alternative for Borås (column 5) is to continue with the treatment method used today at the plant, that is, SBR (D2). From the perspective of climate impact (column 3), the best alternative is to spread the un-dewatered digestate directly onto arable land (D0). Now, these methods are aimed at reducing emissions of ammonia affecting eutrophication and acidification. On the basis of acidification and eutrophication potentials, the best alternative for Gothenburg is to treat the reject water with the DeAmmon process and for Borås the best alternative is to treat the reject water with some form of stripping method, or SBR.

4. Discussion and Conclusions

Organic waste (biowaste, food waste) is a renewable resource that should be used in order to avoid as much negative environmental impact as possible. A large benefit of anaerobic digestion of food waste is that the biogas substitutes other fossil vehicle fuels. Therefore, when analysing different methods for improvement of a biogas system, it could be expected that these improvements should reduce potential global warming. This is however not the case for the improvements studied, cf. Table 3

Table 3 Climate impact, costs and CO2-cost in the studied scenarios

	CO_2 eq. (tonnes)	Costs (MSEK)
B-A: Central sorting	+162	-19
C4-C1: Sewage sludge as nutrient pellets	+3600	-11
C2-C1: Sewage sludge incinerated in CHP	-400	-30
C3-C1: Sewage sludge spread direct	-1200	-19
C4-C1: Sewage sludge & co-digestion sludge	+5300	-6
D1-D0: Dewatering and WWTP	+2280	20
D2-D0: Dewatering and SBR	+1960	-2
D3-D0: Dewatering and DeAmmon	+1690	0.2
D4-D0: Dewatering and air stripper	1560 G 1270 B	2 G -0.6 B
D5-D0: Dewatering and steam stripper	1190 G 880 B	3.1 G -0.6 B
D6-D0: Dewatering and membrane	1530 G 1300 B	1.6 G -0.4 B

In most cases the emissions of CO_2 increases compared to the reference system. Costs are both increasing and decreasing in an interval of 50 M SEK. There are only two scenarios where the CO_2 emissions decreases, resulting in a *decreased* net cost! When assessing climate impact sludge should not be dried and pelletised, regardless of use as fuel pellet or nutrient pellet. This comes from that ammonia in the sludge is lost in the drying process and this loss has to be compensated for by conventional fertiliser that uses fossil resources. Other conclusions are drawn when looking at eutrophication and acidification.

An important conclusion from this comparison is that CO_2 cannot be used as the only indicator of which biogas system design is the most environmentally feasible. As the carbon in food waste is of biological origin, also other impact categories such as eutrophication and acidification have to be addressed to fully evaluate the environmental performance of these systems.

Another comment of concern is that it would be politically difficult to introduce mechanical pre-sorting (often called material recovery facility - MRF) on large scale in Sweden due to that source separation is a well established method. It can however be a cost efficient method in countries where source separation is not as well developed and implemented. It may also work as a co mplementary system, e.g. in remote areas where the marginal cost for introduction of kerb-side collection is high and for an additional sorting of waste from areas with poor sorting quality.

It should also be mentioned that upstream and downstream improvements of course can be combined. Future studies will focus on pre-treatment of waste (e.g. hydrolysis) as to increase the gas yield as well as new techniques for upgrading raw gas to vehicle gas. Other points for improvement that have been identified are dry conservation of waste, the performance of biofilters and also the use of sludge pellets in forestry.

References

[1] Swedish Biogas Association, Biogas – renewable energy from organic waste, 2004, broschure

[2] Energimyndigheten (Swedish Energy Agency), Produktion och användning av biogas år 2009 (Production and use of biogas in 2009), 2010, ES 2010:05, ISSN 1654-7543

[3] AvfallSverige (Swedish Waste Management), Energi från avfall ur ett internationellt perspektiv (Energy from waste in an international perspective), 2008, report 2008:13, ISSN 1103-4092

[4] BFE, Schweizerische Statistik der erneuerbaren Energien –Ausgabe 2005, 2006, Bundesamt für Energie

[5] Energimyndigheten (Swedish Energy Agency), Produktion och användning av biogas 2005 (Production and use of biogas in 2005), 2007, ER 2007:05; ISSN 1403-1892

[6] Eurobserver, Biogas barometer, 2007, SYSTÈMES SOLAIRES le journal des énergies renouvelables N° 179

[7] AvfallSverige (Swedish Waste Management), Den svenska biogaspotentialen från inhemska råvaror (The Swedish biogas potential from domestic raw material), 2008, report 2008:02, ISSN 1103-4092

[8] P. Börjesson, M. Berglund, Environmental systems analysis of biogas systems – Part I: Fuel-cycle emissions, Biomass and Bioenergy 30, 2006, pp. 469-485

[9] P. Börjesson, M. Berglund, Environmental systems analysis of biogas systems – Part II: The environmental impact of replacing various reference systems, Biomass and Bioenergy 31, 2007, pp. 326-344

[10] O. Eriksson, Environmental technology assessment of natural gas compared to biogas, Chapter 6 in the book "Natural Gas", 2010, SCIYO, ISBN 978-953-307-112-1

[11] ISO 14040 International Standard, Environmental management – Life cycle assessment - Principles and framework, International Organisation for Standardization, 2006, Geneva, Switzerland

[12] O. Eriksson, B. Frostell, A. Björklund, G. Assefa, J. -O. Sundqvist, J. Granath, M. Carlsson, A. Baky, L. Thyselius, ORWARE - A simulation tool for waste management, Resources, Conservation & Recycling 36/4, 2002, pp. 287-307.

[13] M. Bisaillon, J. Sundberg, M. Haraldsson, O. Eriksson, Systemstudie Avfall i Göteborg (A systems study of the waste management system in Gothenburg) (In Swedish with English summary), project report WR 21, WASTE REFINERY, SP Sveriges Tekniska Forskningsinstitut, 2010, ISSN 1654-4706

[14] P. Aarsrud, M. Bisaillon, H. Hellström, G. Henriksson, E. Jakobsson, T. Jarlsvik, U. Martinsson, C. Jensen, L-G. Johansson, M. Kanerot, D. Ling, Förädling av rötrest från storskaliga biogasanläggningar (Refinement of digestate from large scale biogas plants), (In Swedish), project report WR 20, WASTE REFINERY, SP Sveriges Tekniska Forskningsinstitut, 2010, ISSN 1654-4706

[15] Guinée J.B.(final editor), M. Gorrée, R. Heijungs, G. Huppes, R. Kleijn, L. van Oers, A. Wegener Sleeswijk, S. Suh, H. A. Udo de Haes, H. de Bruij, R. van Duin, M.A.J. Huijbregts, Life Cycle Assessment An operational guide to the ISO standards, Volume 1, 2 en 3, 2001, Centre of Environmental Science Leiden University, Leiden, the Netherlands

Environmental thermal impact assessment of regenerated urban form: A case study in Sheffield

Mohammad Fahmy[1,*], Abigail Hathway[2], Laurence Pattacini [3], Amr Elwan [1, 4]

[1] *Military Technical Collage, Department of Architecture, Cairo, Egypt*
[2] *University of Sheffield, Department of Civil Engineering, Sheffield, UK*
[3] *University of Sheffield, Department of Landscape, Sheffield, UK*
[4] *University of Sheffield, School of Architecture, Sheffield, UK*
** Corresponding author. Tel: + (202)2 40 29 382, Fax: + (202)2 26 21 908, E-mail: md.fahmy@live.com*

Abstract: Urban comfort is becoming increasingly important due to climate change, increasing population and urbanization. Greater use of mechanical cooling is not reasonable due to consuming more energy, discharging anthropogenic heat and CO_2 emissions which all can be minimized by passive strategies. As part of the EPSRC funded project Urban River Corridors and Sustainable Living Agendas, URSULA, two radically different urban regenerations for a site in Sheffield were passively designed and had to be microclimatically assessed upon their thermal impacts. Passive design strategy for the first is wind tunneling and solar shelter effects owed to compact form that provides river bank access by perpendicular streets. The second, park option, offers space for the river to flood into a green channel which provides evaporative cooling. Simulations using ENVI-met BETA4 applied four receptors to record different meteorology and the pedestrian comfort in terms of Predicted Mean Vote, PMV. The increased green coverage showed horizontal shifting of about 0.2 with 2h of urban time lag in PMV records from 14.00-16.00LST in some places. Results give advantage for the park option design but needs more emphasize on indoor performance.

Keywords: *Thermal impact assessment, urban thermal mass, urban time lag, urban regeneration*

1. Introduction

Temperature increases due to climate change are further exasperated within urban areas due to hard urban surfaces, reduced porosity, and deep canyons preventing radiation release and ventilation [1-4]. Careful design of urban form and the use of green infrastructure can mitigate this effect [5]; many studies showed the benefits of vegetation such as trees [6-9] and Parks [10-13]. However there are often many other, sometimes competing, drivers which affect the design of our urban forms. Urban forms are the fabric of a site along with its network and vegetation. From these standing points, a statistical study in Sheffield presented the distances to the nearest green node which is followed by the biometeorological green structure study, GreenSect, to confine UHI effects [14] by the application of park cooling island effect, PCI [15]. In this study, microclimate effects of two radically different urban form designs for one site in Sheffield took place as part of URSULA project. Site is located near the centre of Sheffield, in the temperate UK climate. Although the city is having high levels of vegetation it showed an UHI of 2C on a spring day [16]; with the potential for greater, and more frequent heat waves. Site is approximately 1.2 hectares (c.300mx400m) adjacent to the river Don. The riverside location offers recreational benefits, but also presents a high risk of flooding and the rationales for two urban form designs for this site have been developed in relation with these two issues. The first design alternative has been developed to facilitate and enhance access to the river, through the use of streets running perpendicular to the bank. On the river front the buildings have been stepped back from the river to create new urban squares looking onto the river, and also to reduce the risk of high wind speeds [17]. The streets are designed to a similar scale to the surrounding existing infrastructure and the open spaces have an urban character with hard landscape treatment and urban trees. In the second design the main objective is to make space for water as an adaptation method for present day climate change symptoms. As the risk of flooding was the initial driver, a channel for flood

water has been created through the middle of the site. In order to avoid obstruction when it floods, the channel is treated as a meadow planted with only grass and reeds. This long continuous open space is expected to provide cooling effect according to the principle that park land provides cooling up to approximately 300m from the park [7, 18- 20]. The two radically different proposals are designed also differently from passive strategies' point of view. Passive urban form design is believed to affect indoor energy consumption and thermal performance so that energy supplies can be minimized [3, 4, 7, 9]. As the main objective of passive design is to minimize indoor heat gain/loss so that energy is saved, first design case, C1 provide cooling/heating by compact form tunneling and thermal mass effects. The second design case, C2 provide evaporative cooling in summer by the more vegetated area. With respect to URSULA concerns about heat waves and floods in summer, the study was then to find which of both alternatives have the better thermal impact in comparison to their existing urban form.

2. Methodology

Methodology is composed of two steps; first, urban climate conditions of each case is simulated to have meteorological plots at same certain points in each case. Second, average outdoor meteorology for each case is calculated to ensure results from receptors as well as validating the averaging methodology and tool.

2.1. Method

Numerical simulations using ENVI-met were applied for its easy and few data entries as well as the understanding of urban climate it gives [21]. ENVI-met simulates the surface-plant-air interactions with a resolution of 0.5 to 10 m in space and 10 sec in time from microclimate to local climate scale using the fundamentals of thermodynamics and heat transfer as a CFD package [22, 23]. The model formatted on a number of on sub-models to model and analyze surface-plant-soil-air relations, its 3.1 version is validated for radiation and RH and still have limitations [9, 21]. The software is relevant to this study as it assesses the outdoor thermal performance in terms of different meteorological outputs along with pedestrian comfort levels using the modified Predicted Mean Vote, PMV following the work of Jendritzky [24-26]. ENVI-met gives results in terms of thematic maps extracted from results by the Leonardo tool or numerically in terms of meteorological records corresponding to each grid in the simulated urban form [22]. In order to ensure results of the receptors along with having a complete idea about whole outdoor spaces performance rather than only single receptor points, PolygonPlus has been used. PolygonPlus is a visual basic tool used after ENVI-met to generate reference averaged neighborhood meteorology rather than records at single non-representative points [13]. Moreover, comparisons of different urban designs upon their urban spaces meteorological averages can take place against receptors' outputs to validate PolygonPlus.

2.2. Parameterization

Table 1 shows the simulation input data for the 27th of July which is the extreme summer day for Sheffield, UK (Lat; 53.38, Long; -1.46), fig. 1 [28]. Two methods of recording outdoor meteorological data were used, snapshot receptors of ENVI-met and the averaging tool PolygonPlus. Four snapshot receptors were located at the boundaries and the middle of the site to record air temperature T_a, Relative Humidity RH, wind Velocity V, and PMV at 1.5m above ground level, fig. 1/b, c, d. The hypothesis assumes that pedestrian PMV of both cases will be different as the fabric, network and vegetation elements of the built environment are varying. Output were then compared with the whole site averaged records calculated by PolygonPlus tool developed by Fahmy [29] to represent a whole local scale urban spaces'

climate condition rather than single points, fig. 2. Due to no modeling measurements for trees foliage, urban trees, U1, U2 and U3, used in simulations were modeled after Fahmy [9] by the application of the value LAI=1, table 1.

Table 1: Inputs used in simulations based on [22, 30, 31].

Parameter	Value
Outdoor T_a	295.45 K
RH	60%
V	3.4 m/s at 10m height
Indoor T_a	293.15 K
Ground temperature	288.15 K from 0-0.5m and 286.35 K from 0.5-2m
Ground humidity	40% from 0-0.5m and 50% from 0.5-2m
U value Walls	1.0 for all buildings walls
U value Roofs	2.0 for all buildings roofs
Albedo Walls	0.475 for all buildings walls
Albedo Roofs	0.45 for all buildings roofs
Albedo Pavement	0.67
Albedo Asphalt	0.20
Human walking speed	1.1 m/s
Pedestrian Clo.	0.50
U1; Alunas cordota	10m total height – 1.8m height to canopy – 3 height of max diameter
U2; Alunas cordota	7m total height – 1.8m height to canopy – 3 height of max diameter
U3; London plane	20m total height – 2m height to canopy – 10 height of max diameter

Fig.1/a: Google maps capture for the site area and the existing fabric.

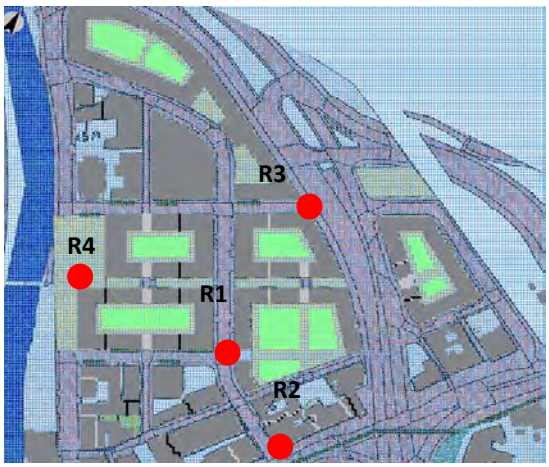

Fig.1/b: ENVI-met Graphical user interface; Modeling the urban form alternative 1 for the case area, R is abbreviation for the receptor placed at points 1-4.

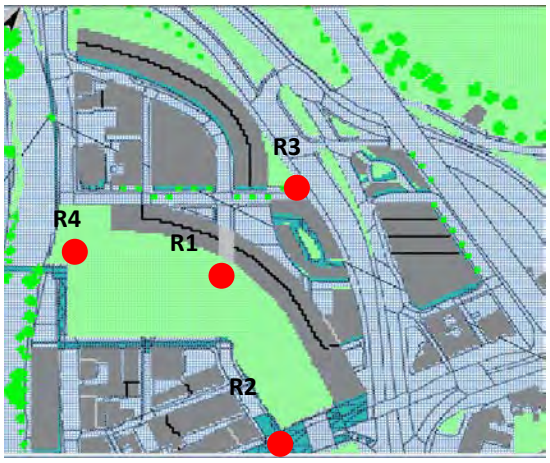

Fig.1/c: ENVI-met Graphical user interface; Modeling the urban form alternative 2 for the case area.

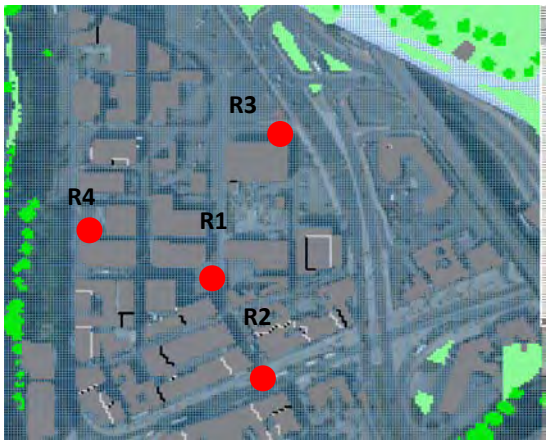

Fig.1/d: ENVI-met Graphical user interface; Modeling the urban form base case.

3. Simulation course

3.1. Results

Fig. 3 illustrates the comparison for T_a, RH, V and PMV extracted from the receptors plotted along with the averaged reference local climate condition calculated by PolygonPlus for 12h except the base case which simulation encountered a numerical flow error at the last simulated hour. However, it didn't affect the comparisons and the concluded remarks as there was 11 common hours from 8-18LST. Good agreement appeared between records from the individual receptors and the averaged values for T_a and RH, whereas considerable difference found between the receptors and the average value for V and PMV, demonstrating a microclimate manipulation on the local scale. All T_a and RH records show the same trend in all cases with reductions in C2 T_a due to the more vegetated area used in comparison to both C1 and BC. The opposite trend in RH occurred attributed also to the different vegetated area used. The sudden drop in PMV record of some cases like C1 at the receptor point R2 indicates the effect of shading. Wind speeds are much higher in C2 than both C1 and BC owed to open fabric used that removed the blockage effect might occur by the fabric in C1. And in combination with the reduced T_a in C2, and resulted more acceptable PMV records at receptors microclimate regardless the reduced PMV of the averaged local records of C2 than PMV at C2R3 as the averaged records is a reference for the whole neighborhood rather than for a single point. The effect of urban thermal mass firstly found by Fahmy [13] has been also found in this study despite the different climatic region. Regardless the close PMV trend of both alternatives' averaged values; increasing green coverage in the park option showed a minor urban thermal mass effect represented by a difference in PMV of 0.1-0.3 at peak time almost with no urban time lag. Receptor, R, no.1 and no.2 showed similar PMV horizontal shifting on the curve of about 0.2 with 2h of urban time lag from 14.00LST to 16.00LST. R3

showed vertical shifting indicating reductions due to the more vegetation in C2. R4 also showed vertical shifting but with increased PMV value at peak time due to the less trees in comparison to C1.

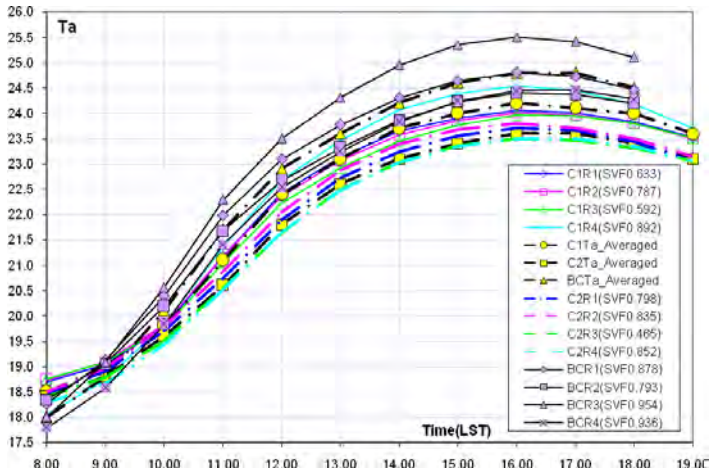

Fig.3/a: Comparison of averaged T_a and the receptors outputs for different cases.

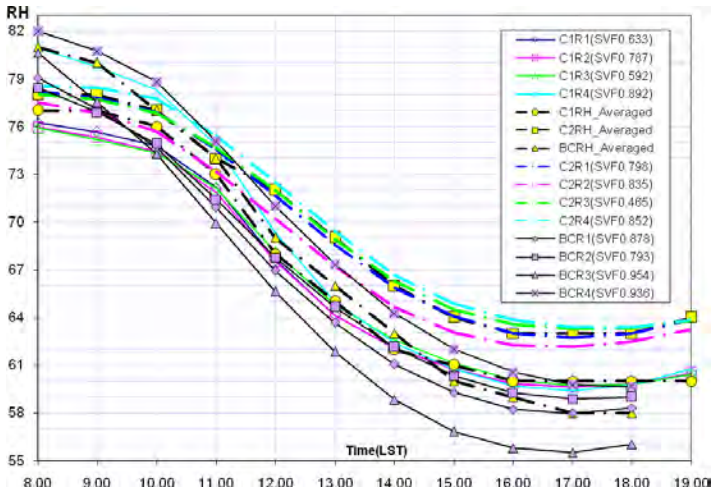

Fig.3/b: Comparison of averaged RH and the receptors outputs for different cases.

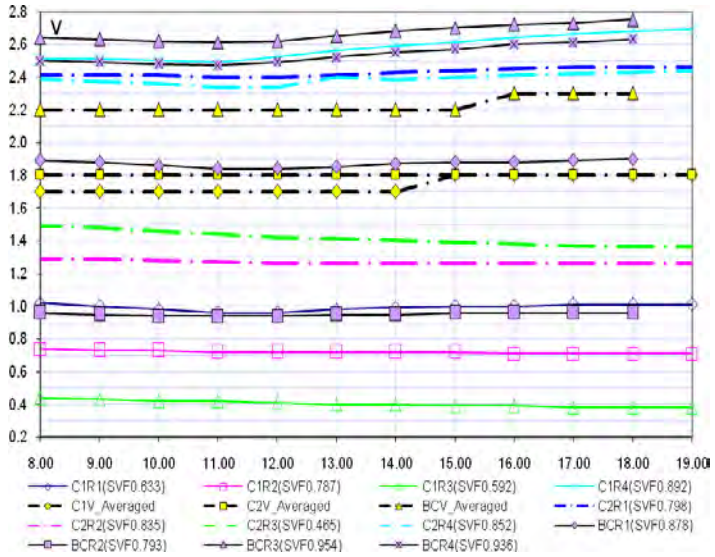

Fig.3/c: Comparison of averaged V and the receptors outputs for different cases.

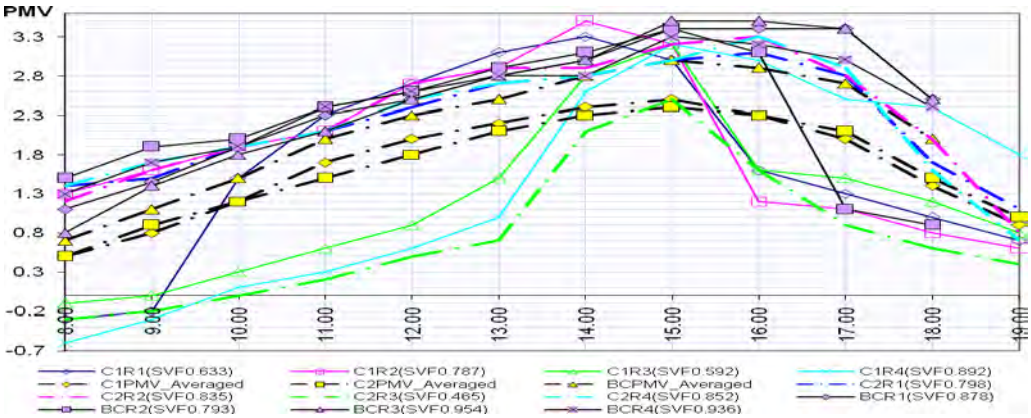

Fig.3/d: Comparison of averaged PMV and the receptors outputs for different cases.

3.2. Discussion and conclusion

This study aimed to assess the thermal performance of two radically different urban regeneration alternatives with their existing case in Sheffield in order to give on of the alternatives an advantage for execution. Methodology composed of two steps; first, urban climate conditions of each case is simulated to have meteorological plots at same certain points in each case. Second, average outdoor meteorology for each case is calculated to ensure results from receptors as well as validating the averaging tool, PolygonPlus. All averages' records occurred between the maxima and minima of receptors outputs of each case which validates PolygonPlus. The more vegetated alternative revealed reductions in the whole neighborhood pedestrian comfort records. This is owed to the open form that allowed more wind speed averages as well as more park cooling effect. On the other hand, an urban thermal mass effect has been noticed. It can be said that the whole C2 urban green structure turned the neighborhood form into *urban thermal mass* that shifted PMV curves from C1 as shown in fig.3 and agrees with Fahmy [13], p-138, regardless the different climate classification of Sheffield's case in this study. After all, outdoor climate assessment suggests that the second urban form design is probably more sustainable with reference to urban spaces simulated in the two alternatives in comparison to the existing site urban form, but further indoor analysis is required to study the impact of each urban form on the energy demand and the green house gases emissions; i.e. coupling whole neighborhood buildings' indoor thermal performances with their outdoors.

4. Acknowledgement

This paper is based on work undertaken within the URSULA project, funded by the UK Engineering and Physical Sciences Research Council (Grant number: EP/F007388/1) and the authors are very grateful for this support. The views presented in the paper are those of the authors and cannot be taken as indicative in any way of the position of the project sponsors or of colleagues and partners. Any remaining errors are similarly those of the authors alone.

References

[1] Grimmond, C.S.B. and T.R. Oke, Heat storage in urban areas: Local-scale observations and evaluation of a simple model. Journal of Applied Meteorology, 1999. **38**(7): p. 922-940.

[2] PRB, World Population Highlights; Key findings from PRB's 2007 world population data sheet Population Bulletin; a publication of the Population Reference Bureau, 2007. **62**(3).

[3] Rosenfeld, A.H., H. Akbari, S. Bretz, B.L. Fishman, D.M. Kurn, D. Sailor, and H. Taha, Mitigation of urban heat islands: materials, utility programs, updates. Energy and Buildings, 1995. **22**(3): p. 255-265.

[4] Stone, B. and M.O. Rodgers, Urban Form and Thermal Efficiency: How the Design of Cities Influences the Urban Heat Island Effect. Journal of the American Planning Association, 2001. **67**(2): p. 186 - 198.

[5] Gill, S.E., Handley, J.F., Ennos, A.R., Pauleit, S. , Adapting Cities for Climate Change: The Role of the Green Infrastructure. 2007. **33**(1): p. 115-133.

[6] Giridharan, R., S.S.Y. Lau, S. Ganesan, and B. Givoni, Lowering the outdoor temperature in high-rise high-density residential developments of coastal Hong Kong: The vegetation influence. Building and Environment, 2008. **43**(10): p. 1583-1595.

[7] Shashua-Bar, L. and M.E. Hoffman, Vegetation as a climatic component in the design of an urban street: An empirical model for predicting the cooling effect of urban green areas with trees. Energy and Buildings, 2000. **31**(3): p. 221-235.

[8] Yang, F., S.S.Y. Lau, and F. Qian, Summertime heat island intensities in three high-rise housing quarters in inner-city Shanghai China: Building layout, density and greenery. Building and Environment, 2010. **45**(1): p. 115-134.

[9] Fahmy, M., S. Sharples, and M. Yahiya, LAI based trees selection for mid latitude urban developments: A microclimatic study in Cairo, Egypt. Building and Environment, 2010. **45**(2): p. 345-357.

[10] Dimoudi, A. and M. Nikolopoulou, Vegetation in the Urban Environments: Microclimatic Analysis and Benefits. Energy and Buildings, 2003. **35**(1): p. 69-76.

[11] Jensen, M.B., B. Persson, S. Guldager, U. Reeh, and K. Nilsson, Green structure and sustainability -- developing a tool for local planning. Landscape and urban planning, 2000. **52**(2-3): p. 117-133.

[12] Lam, K.C., S. Leung, W.C. Hui, and P.K. Chan, Environmental Quality of Urban parks and open spaces in Hong Kong. Environmental Monitoring and Assessment 2005. **111**(1-3): p. 55-73.

[13] Fahmy, M., Interactive urban form design of local climate scale in hot semi-arid zone, in School of Architecture. 2010, University of Sheffield: Sheffield.

[14] Fahmy, M. and S. Sharples, Extensive review for urban climatology: Definitions, aspects and scales, in 7th International Conference on Civil and Architecture Engineering, ICCAE-7. 2008a: Military Technical Collage, Cairo May 27-29.

[15] Saaroni, H. and B. Ziv, The impact of a small lake on heat stress in a Mediterranean urban park: the case of Tel Aviv. International journal of Biometeorology, 2003. **47**(3): p. 156-165.

[16] Lee, S.E. and S. Sharples. Analysis of the Urban Heat Island of Sheffield - the Impact of a Changing Climate. in Proceedings of PLEA2008 - 25th Conference on Passive and Low Energy Architecture. 2008. Dublin: PLEA.

[17] Kofoed N U and G. M., Considerations of Wind in Urban Spaces. In: Designing Open Spaces in the Urban Environment: a bioclimatic approach. Ed. Nikolopoulou M. Available online at http://aplha.gr/ruros/. 2004 Greece.

[18] Yokohari, M., R.D. Brown, Y. Kato, and H. Moriyama, Effects of paddy fields on summertime air and surface temperatures in urban fringe areas of Tokyo, Japan. Landscape and Urban Planning, 1997. **38**(1-2): p. 1-11.

[19] Jauregui, E., Influence of a large urban park on temperature and convective precipitation in a tropical city. Energy and Buildings, 1990. **15**(3-4): p. 457-463.

[20] Oke, T.R., J.M. Crowther, K.G. McNaughton, J.L. Monteith, and B. Gardiner, The Micrometeorology of the Urban Forest [and Discussion]. Philosophical Transactions of the Royal Society of London. B, Biological Sciences, 1989. **324**(1223): p. 335-349.

[21] Ali-Toudert, F., Dependence of Out Door Thermal Comfort on the Street Design in Hot and Dry Climate. 2005, Institute of Meteorology: PhD. Thesis, Freiburg, Germany.

[22] Bruse, M., ENVI-met V3.1BETA4, a microscale urban climate model, [Online], Available: www.envi-met.com. Accessed 11/6/2010. 2010.

[23] Bruse, M., ENVI-met bulletin board [Online], Available: http://envi-met.de/phpbb/index.php. Accessed 17/3/2009. 2009.

[24] Jendritzky, G., W. Sönning, H.J. Swantes, d. Beiträge, and f. Akad, Ein objektives Bewertungsverfahren zur Beschreibung des thermischen Milieus in der Stadt- und Landschaftsplanung (Klima-Michel-Modell). Raumforschung und Landesplanung, 1979. **28**.

[25] Jendritzky, G. and W. Nübler, A model analysing the urban thermal environment in physiologically significant terms. Meteorology and Atmospheric Physics, 1981. **29**(4): p. 313-326.

[26] Jendritzky, G., A. Maarouf, D. Fiala, and H. Staiger, An Update on the Development of a Universal Thermal Climate Index. 15th Conf. Biomet. Aerobiol. and 16th ICB02, Kansas City 27 Oct - 1 Nov, 2002.

[27] Bruse, M., ENVI-met V3.1BETA4, a microscale urban climate model, [Online], Available: www.envi-met.com. Accessed 11/6/2010. 2010.

[28] AutoDesk. ECOTECT2010, [Online], Available at: http://www.autodesk.co.uk/adsk/servlet/mform?validate=no&siteID=452932&id=14205163. Accessed 19/4/2010.

[29] Fahmy, M., Interactive urban form design of local climate scale in hot semi-arid zone, in Architecture. 2010, University of Sheffeild: Sheffield. p. 254.

[30] Akbari, H., P. Berdahl, R. Levinson, S. Wiel, W. Miller, and A. Desjarlais, Cool Color Roofing Materials. 2006, University of California: California.

[31] Oke, T.R., Boundary layer climates. 1987, London: Methuen.

[32] Fahmy, M., A. Trabolsi, and S. Sharples, Dual stage simulations to study microclimate thermal effect on comfort levels in a multi family residential building., in 11th International Building Performance Simulation Association Conference 2009: University of Strathclyde in Glasgow, 27-30 July.

Mitigating Heat Gain Using Greenery of an Eco-House in Abu Dhabi

Khaled A. Al-Sallal[1,*], Laila Al-Rais[2]

[1, 2] *Dept. of Architectural Engineering, United Arab Emirates University, Al-Ain, United Arab Emirates*
** Corresponding author. Tel: +9713 7622318, Fax: +9713 7636925, E-mail: k.sallal@uaeu.ac.ae*

Abstract: Two fundamental design strategies should be taken into consideration when designing a residential building in desert climates, they are as follows: minimizing solar heat gain through shading and proper building envelope and maximizing passive cooling through natural ventilation. By introducing extensive vegetation yet carefully distributed, shading of building's facades or roofs will directly mitigate heat gain through building envelope. An eco-house was designed in Abu Dhabi with special attention to greenery. In this study, landscape elements were intensively analyzed with the aim of reducing heat gain and improving overall building energy performance. Landscape elements such as green roofs, grass ground cover and greenery next to external walls were simulated in order to achieve optimum energy performance. The use of outdoor landscape (grass ground cover and shade trees) has made a 9% improvement of performance over the reference case regarding the electrical energy use and greenhouse gas emissions. The energy use of the house dropped down by 16% for cooling and 18% for fan operation. With regards to the green roof scenario, a performance improvement of 19% over the base case has been achieved. The energy use of the house dropped down by 24% for cooling and 27% for fan operation.

Keywords: *Heat gain, Green roof, Grass ground cover, Energy performance*

1. Introduction

Cooling and air conditioning of buildings in Abu Dhabi accounts for 75% of electricity consumption in the summer months and are considered the major consumer of electricity [1]. This leads to very high levels of CO_2 and other greenhouse emissions. Landscape effect on heat gain mitigation on buildings has not been studied in the UAE. With the new policies in the UAE calling for green building such as Estidama guidelines and other codes, the consideration of landscape strategies to improve building environmental performance has become significant. Landscaping is considered as a challenging part due to its high water consumption and the scarcity of water resources especially in arid regions such as Abu Dhabi. In this study, the focus is on how landscape design contributes directly in enhancing the building energy performance; and thus lowering the overall energy consumption. Landscape elements such as green roofs, grass ground cover and greenery next to external walls were simulated to evaluate how it will integrate with other passive systems for an Eco-house design in order to achieve optimum energy performance. Where plants normally take a huge amount of water resources, the suitable plants type was carefully selected to consume least amount of water.

2. Background

Vegetation can reduce the heat reaching the building and penetrating its envelope by increasing the reflection of solar radiation and by providing shading. They can achieve evaporative cooling and taking the heat away through the process of transpiration. In this study, the effect of conventional landscape elements (i.e.; grass cover with shade trees) combined with green roof was investigated in terms of their thermal behavior.

2.1. Green roof

The term *"green roof"* generally represents vegetation and growing medium planted on the building rooftop. There are several environmental benefits associated with green roofs such as energy savings through building envelope thermal regulation, roof membrane protection and

thus prolonged building's life cycle, sound insulation as green roofs act as an acoustic barrier and finally other benefits at the urban level such as mitigating urban heat island effect and storm water retention. With introducing circular no. 171, green roofs and vertical landscaping by Dubai Municipality (DM) that became effective since July 2009 [2], both buildings consultants and contractors have to integrate green roofs into their new buildings design taking into consideration the selection of proper vegetation type, irrigation system, insulation materials and roof structural membrane system. Estidama also encourages applying the concept of green roofs and external landscaping in order to mitigate heat island effects [1]. NRC-IRC constructed a field roofing facility at its Ottawa campus to study the performance of garden roofs [3]. This energy demand was reduced from 6.5–7.0 to less than 1.0 kWh/day in the garden roof, a reduction of over 75%. The garden roof was more effective in controlling heat gain than in reducing heat loss because of the various thermal mechanisms involved, shading, insulation, evapotranspiration and thermal mass. It reduced heat gain by 95% and heat loss by 26%. The study also predicted that in warmer regions where cooling rather than heating is the main concern, the results could be more significant. The study also showed how garden roofs can lower the temperature and modify the temperature fluctuations experienced by the roofing membrane, which results in greater durability and an extended service life for the roof membrane. Another study [4] evaluated the life cycle environmental impacts of an eight story residential building, including the addition of a green roof (only 16% of the building's exposed surface area) located in downtown Madrid, Spain using computer simulation. Due to a lower absorption of solar radiation and lower thermal conductance, the addition of a green roof was estimated to reduce annual energy consumption by 1.2%. This was primarily due to summer cooling load reductions of over 6%. For the upper floors, the peak hour cooling load was reduced by as much as 25% relative to the common flat roof.

2.2. Shade Trees

Akbari et al. [5] quantified the effect of shade trees on the cooling costs of two similar houses in Sacramento, California and the results showed that the trees reduced seasonal cooling costs by between 26% and 47%. The same study modeled the effect of the trees on both houses using the DOE-2.1E3 simulation program and found that the model underestimated the energy savings of the trees by as much as twofold. Another study by Akbari and Taha [6], used simulation to study the effect of trees on energy use in four Canadian cities, concluded that increasing the vegetative cover of a neighborhood by 30% and increasing the albedo of houses by 20% would decrease heating costs by 10–20% and decrease cooling costs 30–100%. A simulation study by Simpson and McPherson [7] found that trees shading the west side of houses in California had the biggest effect on cooling costs and that adding shade trees to a house on the west side and east sides reduced annual cooling costs by 10–50%. Another study by McPherson and Simpson [8] used simulation modeling and aerial photography to estimate the energy savings of existing urban trees and new plantings in California indicated that existing trees could reduce peak energy load by 10% resulting in annual savings of $779 million. They estimated that planting an additional 50 million trees on the east and west sides of houses would further reduce peak load by an average of 4.5% over the next 15 years, which would result in total savings for consumers of $3.6 billion or $71 per tree. In a recent study Donovan and Butry [9] estimated the effect of shade trees on the summertime electricity use of 460 single-family homes in Sacramento, California. Results showed that trees on the west and south sides of a house reduced summertime electricity use by 185 kWh (5.2%), whereas trees on the north side of a house increased summertime electricity use by 55 kWh (1.5%). Results also showed that a London plane tree, planted on the west side of a house, can reduce carbon emissions from summertime electricity use by an average of 31% over 100 years.

2.3. Grass ground cover

Vegetation surfaces and pavement materials heavily influence outdoor thermal environments. Field measurements performed in Singapore revealed there were clear effects of hard versus vegetation surfaces on globe temperature and mean radiant temperature (MRT) [10]. The characteristics of heat and water transfer processes in porous block pavement, asphalt, grass and ceramic porous pavement was analyzed using numerical modeling. The model revealed that the surface temperature of permeable pavement is appreciably lower than that of impermeable pavement [11]. A filed experiment conducted in Eastern Saudi Arabia found a good correlation between pavement temperature and air temperature [12]. Other experiments in Singapore showed that granite slab, terracotta bricks and concrete interlocking blocks provide lower surface temperatures and heat output than conventional asphalt concrete pavements [13]. An empirical study was performed on five pavements in three areas of Taiwan to study the seasonal influence of pavement on outdoor thermal environments [14]. The study found that asphalt concrete and concrete have higher temperature than interlocking blocks or interlocking blocks with grass infilling, and grass always has the lowest air temperature. The surface temperature of artificial pavements was 10°C higher than that of vegetation surface at noon in the summer, but the difference among the various pavement types were not significant in winter.

3. Methodology

One of the most important and challenging architectural targets in this design exercise was the proper landscaping. Landscape design went hand in hand with other passive and active design components of the eco-house. Grass ground cover and greenery next to external walls (LS case) was simulated and considered as the first scenario. The effect of the green roof element was simulated in a separate scenario (GR case) and the results of both cases were compared against the reference house (REF case). All three cases were simulated using Enerwin-EC software [15]. The window to wall ratio (WWR) as 0.20, 0.15, 0.20, and 0.10 for North, East, South, and West facades, respectively, was used in all three cases.

Landscape design and location (whether horizontally or vertically) tend to maximize shading around the house especially near the windows, and minimize the load due to ground reflected solar radiation by using appropriate ground cover such as grass. The impact of the grass ground cover along with the shade trees on energy was evaluated in this eco-house. The exterior shade trees were set to provide only 50% shading on walls and windows. Where plants normally take a huge amount of water resources, the suitable plants type was carefully selected. Palm trees, ornamental trees and aqueous plants such as Yucca Filamentosa and Yucca Aloifolia were recommended [2]. These desert plants are suitable for intensive greening, yet consume least water. They are normally watered by drip irrigation and consume from 50-60 liters/day for palm and ornamental trees, and as little as 15-20 liters/m^2/day for the aqueous plants. According to Estidama credit (PW-2.1: Exterior Water Use Reduction: Landscaping) in areas with low rainfall or seasonal droughts, up to 60% of total seasonal water usage can be attributed to irrigation [16]. As mentioned earlier, the main system used of plants irrigation is drip irrigation (mainly for roof gardens) besides a bioswale for the house central courtyard. A bioswale is a densely vegetated open channel designed to attenuate and treat storm water runoff. It has gentle slopes to allow runoff to be filtered by vegetation planted on the bottom and sides of the swale (see Fig.1).

As for the green roof structure [17, 18], the whole roof area was 150 mm solid concrete slab, lined with a waterproof membrane insulated with Polyfoam Roofboard 200 mm thick

(2x100mm), covered with Polyfoam Slimline membrane. The Slimline membrane was overlaid with a root barrier/ moisture reservoir as specified ensuring there were no gaps and edges were overlapped. That was covered with a filtration layer, and growing matter as specified by Estidama [16] in order to match desert plants. That typical green roof section (see Fig. 2) has a U-value of 0.15 W/m^{2}K without considering the insulation value of the soil which varies with the water content.

Fig. 1. Landscape elements distribution in the Eco-House

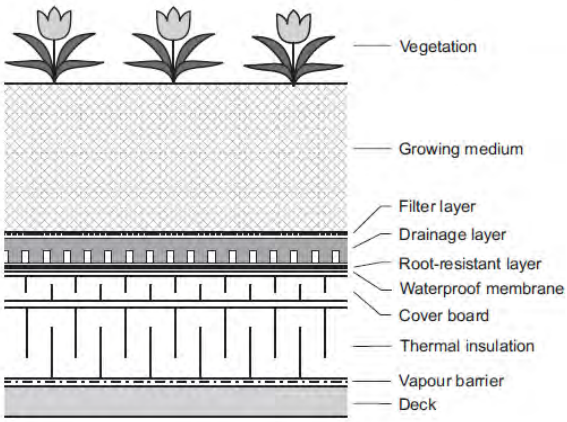

Fig. 2. Green roof structural elements, adapted from [17].

4. Results and Discussion

Typically at the UAE latitude (24° N), the heat gain through the roof component is usually the highest; then comes heat gain through the windows and walls; other building components have usually smaller effect compared to these main components. Thus, before improving the house performance by proper design of the greenery, it was necessary to optimize its form design so that distribution of load becomes a bit more uniform with smaller magnitude at each component, and thus easier to solve. That was done in a previous stage in which the courtyard form was tested and evaluated against a typical Emirati house [19]. The typical house yielded load distribution as follows: 25% for roof, 23.5% windows solar, walls 20%, and 30% for other components. The courtyard configuration (referred to as the reference house or REF case in this study) helped to distribute the cooling loads as follows: 24.3% for roof, 18.1% for windows solar, 27.4% for walls, and 30% for other components; this helped to decrease the windows solar and roof loads' contributions.

4.1. Landscaping results

The first decision was to minimize direct and reflected solar heat gain by maximizing shading on walls and windows and improve ground cover. This would help to reduce the walls and windows-solar loads. Landscaping has great potential to provide these benefits and in the meantime attain other Estidama credits such as LV-R1: Urban Systems Assessment, LV-R2: Outdoor Thermal Comfort, RE-1: Improved Energy Performance [16]. This resulted in great reduction of the windows-solar (63.7%), windows transmission (22.1%), walls loads (20.7%), and mass effect (16.9%); and 21.5% reduction in the total annual cooling load, compared to the base case. The energy use of the house (compared to the REF case) dropped down by 16% for cooling and 18% for fan operation. It also helped to reduce the greenhouse gas emissions and the electrical energy use by 9%.

4.2. Green Roof

The second decision scenario was to improve thermal resistance for the roof heat gain. This resulted in great reduction of the heat gain through roof (99.6%), compared to the reference case. The energy use of the house (compared to the reference case) dropped down by 24% for cooling and 27% for fan operation. It also helped to reduce the greenhouse gas emissions and the electrical energy use by 19%. See figures 3, 4, and 5.

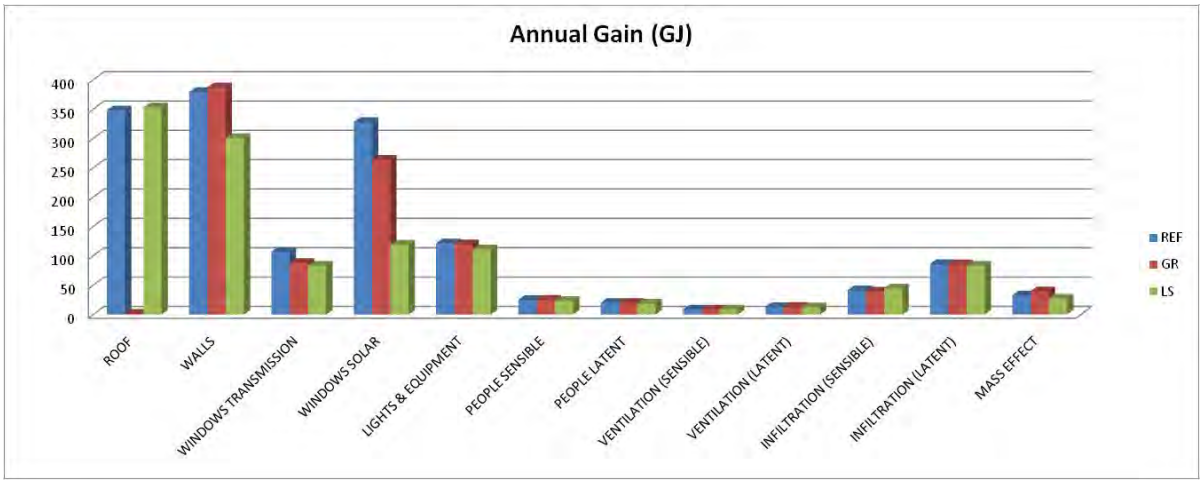

Fig. 3. Annual heat gain by component for the tested cases.

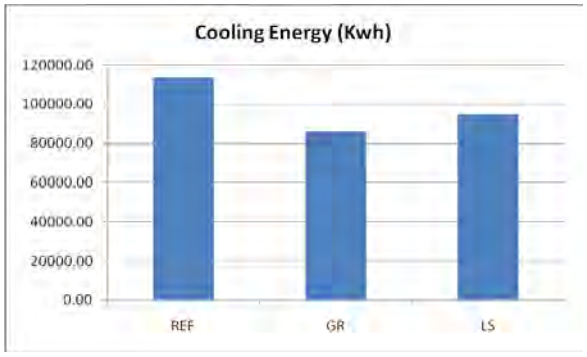

Fig. 4. Cooling energy of the tested cases.

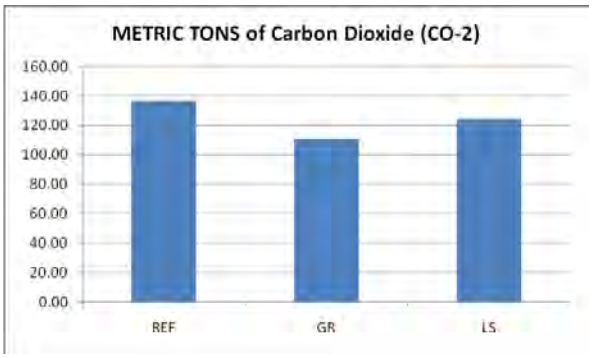

Fig. 5. CO_2 emissions of the tested cases..

5. Conclusion

In a hot climate such as Abu Dhabi for an envelope dominated building, most of the heat gain comes through the roof, the windows and the walls (approximately 70%). This indicated the critical need to minimize solar gain and improve the thermal conservation level of the building envelope. Using greenery to improve the building thermal performance can also result in other benefits such as improved air quality, visual comfort via daylight uniform distribution, noise reduction, prolonged building structure (as green roof), outdoor and indoor thermal comfort, and aesthetics. The use of outdoor landscape (grass ground cover and shade trees) has made a 9% improvement of performance over the base case regarding the electrical energy use and greenhouse gas emissions. The energy use of the house (compared to the reference case) dropped down by 16% for cooling and 18% for fan operation. With regards to the green roof scenario, a performance improvement of 19% over the base case has been achieved. The energy use of the house dropped down by 24% for cooling and 27% for fan operation. Such strategies and improvement of performance would eventually help to earn several points in Estidama Pearl Rating System for Villas such as: LV-R1: Urban systems assessment, LV-R2: Outdoor thermal comfort, LV-9: Indoor noise, IP-1: Innovative cultural

& regional practices, IP-2: Innovating Practice, IDP-R1: Integrated Development Strategy, IDP-1: Life Cycle Costing, NS-R1: Natural systems assessment & protection, NS-1: Landscape design & management plan, NS-2: Landscape enhancement, PW-2.1: Exterior water use reduction: Landscaping, PW-3: Stormwater management, and RE-1: Improved Energy Performance.

References

[1] Estidama Sustainable buildings and Communities and Buildings Program for the Emirate of Abu Dhabi- Design Guidelines for New Residential and Commercial Buildings, May 2008.

[2] Dubai Municipality, Green Roof Circular no. (171), 2009.

[3] K.Y. Liu, A. Baskaran, Using Garden Roof Systems to Achieve Sustainable Building Envelopes, Construction Technology Update No. 65, NRC-IRC - National Research Council of Canada, Institute for Research in Construction (2005).

[4] S. Saiz , C. Kennedy, B. Bass, K. Pressnail, Comparative life cycle assessment of standard and green roofs, Environmental Science & Technology 40 (2006) 4312-4316.

[5] H. Akbari, D. Kurn, S. Bretz, J. Hanford, Peak power and cooling energy savings of shade trees, Energy and Buildings 25 (1997) 139–148.

[6] H. Akbari, H. Taha, The impact of trees and white surfaces on residential heating and cooling energy use in four Canadian cities, Energy 17 (2) (1992) 141–149.

[7] J. Simpson, E. McPherson, Potential of tree shade for reducing residential energy use in California, Journal of Arboriculture 22 (1) (1996) 10–18.

[8] E. McPherson, J. Simpson, Potential energy savings in buildings by an urban tree planting program in California, Urban Forestry and Urban Greening 2 (2003) 73–86.

[9] G. Donovan, D. Butry, The value of shade: Estimating the effect of urban trees on summertime electricity use, Energy and Buildings 41 (2009) 662–668.

[10] N. Wong, Y . Chen, C. Ong, A. Sia, Investigation of thermal benefits of rooftop garden in the tropical environment. Building and Environment 2003;38(2):261–70.

[11] T. Asaeda, V. Ca, Characteristics of permeable pavement during hot summer weather and impact on the thermal environment. Building and Environment 2000;35(4):363–75.

[12] R. Ramadhan, H. Al-Abdul Wahhab, Temperature variation of flexible and rigid pavements in Eastern Saudi Arabia. Building and Environment 1997;32(4):367–73.

[13] S. Tan, T. Fwa, Influence of pavement materials on the thermal environment of outdoor spaces. Building and Environment 1992;27(3):289–95.

[14] L. Tzu-Ping, H. Yu-Feng, H. Yu-Sung, Seasonal effect of pavement on outdoor thermal environments in subtropical Taiwan. Building and Environment 42 (2007) 4124–4131.

[15] Enerwin-EC Software: Energy Simulation Software for Buildings with Life-Cycle Costs, professional version 5.9, Texas A&M University & Degelman Engineering Group, Inc.

[16] The Pearl Rating System for Estidama, Emirate of Abu Dhabi, Abu Dhabi Urban Planning Council, Version 1.0, April 2010.

[17] K. Liu, A. Baskaran, Using Garden Roof Systems to Achieve Sustainable Building Envelopes, Construction Technology Update No. 65, Institute for Research in Construction, National Research Council of Canada, September 2005.

[18] Knauf Insulation Ltd, Merseyside, United Kingdom, June 2010. www.knaufinsulation.co.uk

[19] K. Al-Salla, L. Al-Rais, M. Dalmouk, Designing a Sustainable House in the Desert of Abu Dhabi, Proceedings of the 11th World Renewable Energy Congress, 2010, pp. 404-409.

Solar energy in urban community in City of Salzburg, Austria

Helmut Strasser[1,*], Boris Mahler[2], Norbert Dorfinger[3]

[1] *SIR Salzburger Institut für Raumordnung und Wohnen, Salzburg, Austria*
[2] *Steinbeis Transferzentrum, Energie-, Gebäude- und Solartechnik, Stuttgart, Germany*
[3] *Salzburg AG, Salzburg, Austria*
** Corresponding author. Tel: +43 662 623455, Fax: +43 662 629915, E-mail: helmut.strasser@salzburg.gv.at*

Abstract: Lehen is the largest district of City of Salzburg, close to the city centre and with high quality of infrastructure of public transport. Since the last decades the district was confronted with essential changes. The use of the area of the former utility means a huge potential for further development of the district. High share of renewable energy should be the main focus of the project, considering existing heat supply with district heating. High standards of buildings and large-scale solar system are the main elements of the energy concept. The use of a heat pump ensures an efficient increase of solar gains and leads to low primary energy demand resp. CO_2-emissions. The new building area was also seen as a chance for modernization activities in existing building stock around. Energy efficient pumps and lightning as well as PV modules in the facades will ensure high share of renewable energy also for electricity demand. First results show the way for further projects – concerning effective steering of complex processes and technologies to achieve total CO_2-reductions in urban areas.

Keywords: *General development plan, Urban communities, Process of energy planning, Solar optimization*

1. Introduction

The district of Salzburg-Lehen is situated quite close to the city centre of Salzburg. The appearance of Lehen was for long years dominated by residential buildings from 1950 to 1970, high amount of school buildings, the main soccer stadium of Salzburg, the head-quarter of the utility and a main traffic road. Obviously caused by the living situation in mostly not renovated buildings and the traffic situation the district was endangered to get more and more social problems. Considering the very attractive location the potential for establishing a new and attractive district in Salzburg was seen. With the opening of a new train station Lehen is now connected to the new city train which means another improvement of living quality of the district. The movement of the utility and the football stadium to other sites mean new chances for further development. Meanwhile the main city library was established on the site of the former soccer stadium.

On the site of the former utility a new residential and commercial area was initiated. In a competition a master plan of the launched project "Stadtwerk Lehen" was developed. Residential buildings with apartments and commercial areas, a kindergarten, a student's hostel and a "Competence park" with four live science buildings, a hotel and the renovation of the former office building are foreseen. Besides that, there is an existing building stock around the areas of the utility with residential buildings from 1950 – 1960, most of them without any thermal renovation and equipped with individual heating system with oil or gas. So the new-built area was seen as a chance also for the surrounding retrofit areas. Energy efficiency of the buildings and the integration in the energy supply concept of the new buildings of "Stadtwerk Lehen" became a concrete perspective for city planners. This causes an over-all renovation as a requirement for the further project development.

Table 1. Key figures

Total area	155.000 m²
Owners	Social and commercial housing associations, city of Salzburg
Existing buildings	50.000 m²
Number of dwelling	623
Average age of existing buildings	60 – 70 years
Type of buildings	85% residential, 15% commercial
New buildings	105.000 m²
Number of dwellings	550
Type of buildings	80% residential, 20% commercial

Table 1 shows the key-figures of the area. Besides the goals of urban development and motivated by the discussion of a new communal development plan which fulfils criteria of sustainability the project of "Stadtwerk Lehen" was created as a pilot project for sustainable urban development. Main performance criteria concerning energy were defined as:

- Low energy standard for buildings
- Energy efficient pumps and lightning of public areas
- High rate of renewable energy for energy supply

In addition to that energy supply system and integration of renewable energy should also be optimized related to existing district heating system, since district heating is based on high shares of available industrial waste heat resources. Thus the main focus of project development was the optimization of the energy supply concept. As there are different approaches for new buildings and renovation, a couple of involved partners and clear targets defined by funding programs the definition of an optimized methodology for the realization process became an important issue. Project realization is scheduled for 2005 – 2013, Table 2 shows the concrete time-table.

Table 2. Time Table

Preparation phase	2005 – 2007
Planning phase	2007 – 2010
Construction phase	2009 – 2011 (for housing, commercial buildings will be finished later)
Completion	2013 (for housing, commercial buildings, renovation will be ongoing)

2. Methodology

Successful realization of the project has to be built on two main focuses. On the one hand the steering of the realization process with involvement of many institutions and stakeholders is essential for project success. On the other hand the optimization of technologies on energy efficiency and renewable energy is crucial for achieving performance criteria.

2.1. Realization process

Effective steering of the realization process needs first identification of the relevant players and their roles. Furthermore binding instruments for realization and effective monitoring of the process itself are essential.

Partners and their roles: Besides the City of Salzburg several social housing associations / project developers and the former utility that is/was owner of the area involved. This needs

clear identification of their roles in the project, because partly the partners have different roles in the project.

Quality agreement: A quality agreement was worked out and signed by all partners. This agreement includes a commitment to the performance criteria, minimum requirements of building standards and the obligatory fulfillment of the energy supply concept.

Steering group / Working groups: A monthly steering group of leaders of key actors was installed to monitor fulfillment of quality agreement. The steering group is chaired by the city of Salzburg. In addition to the steering group working groups were established.

Fig. 1 shows the different involvement of partners depending on their specific roles.

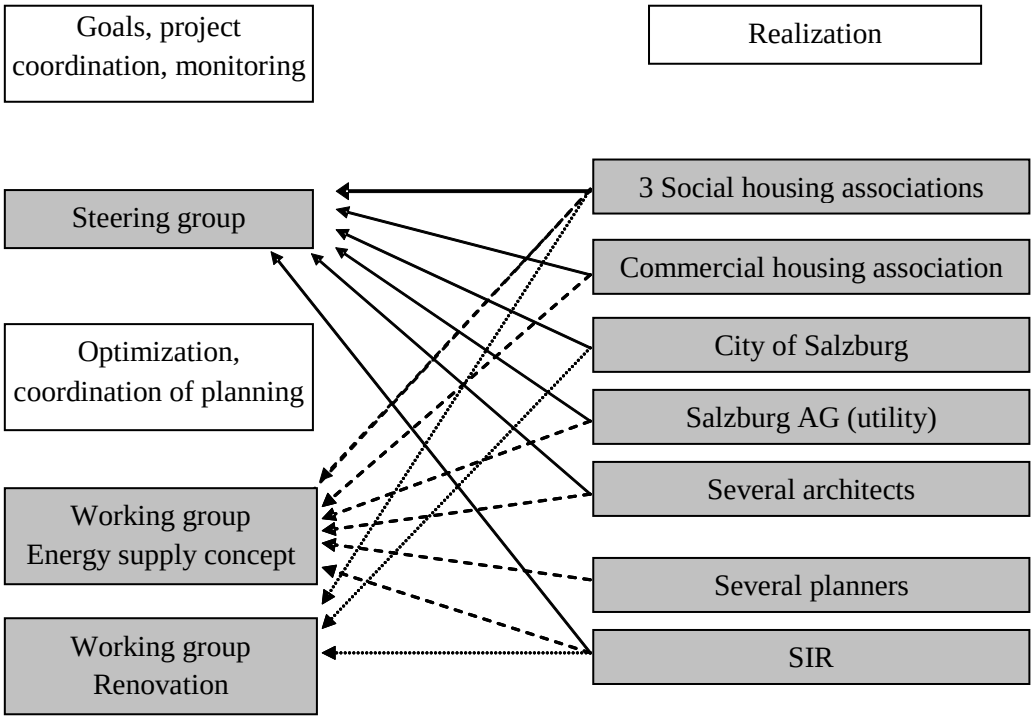

Fig. 1. Process organization

2.2. Building standards

Focus of Stadtwerk Lehen was put on high share of renewable energy, both for heat and electricity demand. Ambitious energy performance of the buildings was seen as the basis for achieving the targets. On the other hand there are existing rules of funding schemes which are limiting the investment costs for social housing. Thus low-energy standard was required as minimum instead of more ambitious passive house standard. Table 3 shows the targets for new buildings and renovation. Based on this target minimum U-values for new buildings and retrofit were defined.

Table 3. Minimum requirements of building standards

	Specific heat demand (kWh/m².a)
New buildings	< 20
Renovation	< 30

For new buildings required standards were contracted with involved housing associations and included in the calls-for-tender. For existing buildings project had to start with increasing motivation for renovation since there was no instant need for overall renovation within the tenants. Thus a detailed study on chances of modernization was done in one part of the existing area called "Strubergassensiedlung". This study was explicitly performed by an external expert, who has also no fear on possible conflicts and who has no expectation of further planning jobs. Goal of this study was to show the chances of renovation – concerning improvements in energy consumption but also related to issues of quality of life (quality of apartments, quality of public space …) and economic benefits. Based on detailed analyses of the buildings and concerned to energy standards several variants were analysed:

- Standard-renovation
- Factor 10- renovation
- Passive-house-standard-renovation resp. for addition of another storeys

Table 4 shows needed standards of main components of renovation.

Table 4. Thermal standards of main components of renovation

Building Component	Stock	Variant 1 Standard		Variant 2 Factor 10		Variant 3 Passive-house	
	U-value	Insulation	U-value	Insulation	U-value	Insulation	U-value
	W/(m^{2}K)	cm	W/(m^{2}K)	cm	W/(m^{2}K)	cm	W/(m^{2}K)
Outer wall	1,015	16	0,180	20	0,138	25	0,114
Basement ceiling	1,111	12	0,231	20	0,151	25	0,124
Ceiling above upper floor	0,812	20	0,143	25	0,119	30	0,101
Pitch of the roof	1,127	27	0,154	30	0,131	35	0,113
TH-wall to cellar	1,722	16	0,194	20	0,146	25	0,119
TH-wall to attic	1,722	16	0,194	20	0,146	25	0,119
Outside door	2,800		1,250		1,250		0,800
Interior door to unheated	2,800		1,250		1,250		0,800
Window			0,9		0,85		0,8
Outer wall to soil	1,596	16	0,192	20	0,158	25	0,129

Considering the different standard of each building of the "Strubergassensiedlung" and individual approaches concerned to actual standards a renovation plan for the whole area was elaborated. For buildings where criteria like quality of apartments are already high standard renovation is suggested. Other buildings where there will be total renovation necessary are suggested to be in passive house-standard.

2.3. Energy supply concept

The challenge to integrate renewable energy in existing supply system of the city was solved by following a strategy based on solar energy and district heating system. But there are additional improvements necessary to meet the goal of high share of renewable energy. Increase of solar fraction is achieved by installation of a heat pump in order to increase efficiency of solar collector fields. In addition to that also an own micro-net for heat supply of the whole area is foreseen. This micro-net in combination with planning directives for all of the housing projects allows low temperatures and thus higher solar gains. Fig. 2 shows the hydraulic scheme including the main components solar collector, storage tank, heat pump and micro-net.

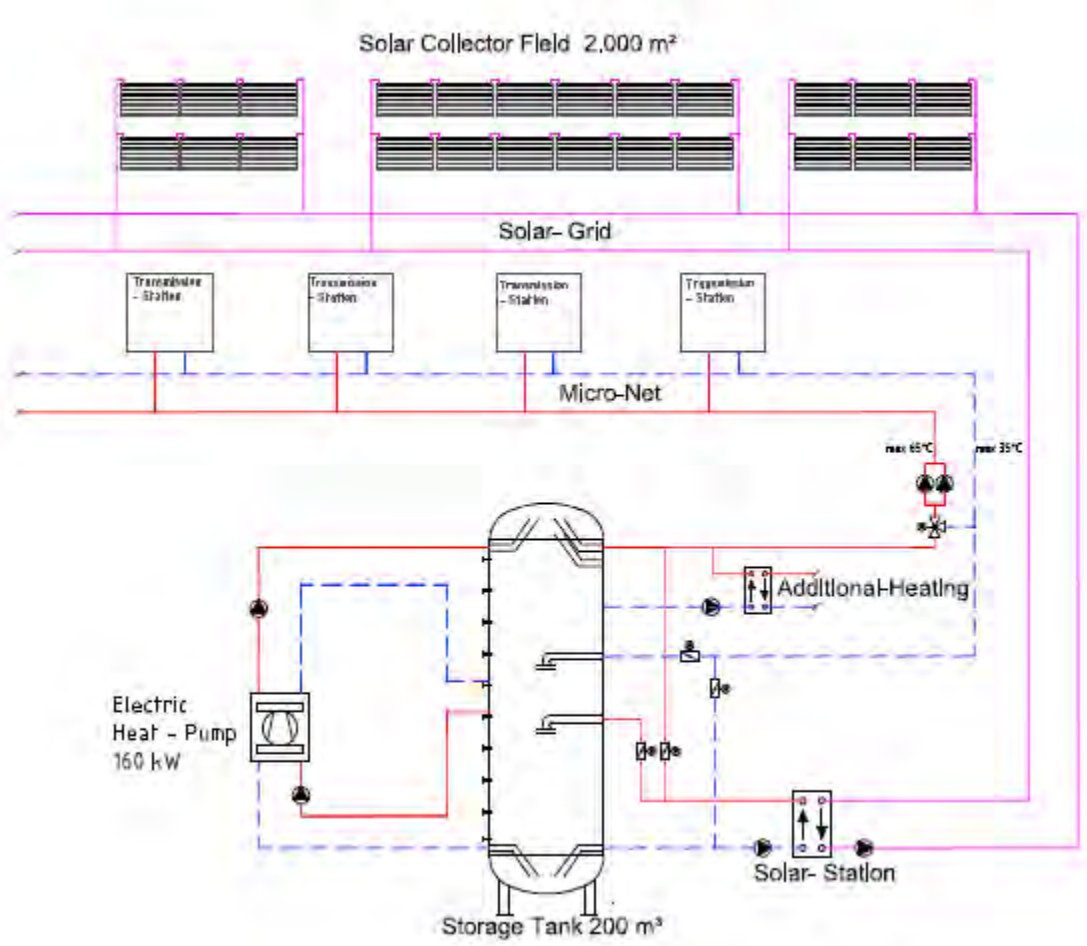

Fig. 2. Hydraulic scheme

Based on the heat-supply concept detailed simulation were done in order to optimize the whole system. Different scenarios were calculated:

- Assumptions of heat-demand because of different time-tables of planning (new residential buildings
- New commercial buildings, existing residential buildings
- Size of collector field
- Size of storage tank
- Size of heat-pump
- Return temperature of micro-net
- Type of heat pump (electricity, gas)

As an example Fig. 3 shows the influence of the return temperature of the micro-net on the collector yield. It is evident, that return temperature has generally a high influence on efficiency of the district heating system (high temperatures mean lower efficiency of solar system and lower capacity of storage tank). By using a heat pump the influence of return temperature on solar yield can be reduced. Simulation shows that there is a higher solar yield in case of 50°C return temperature and heat pump in comparison to solution with 30°C return temperature without heat pump.

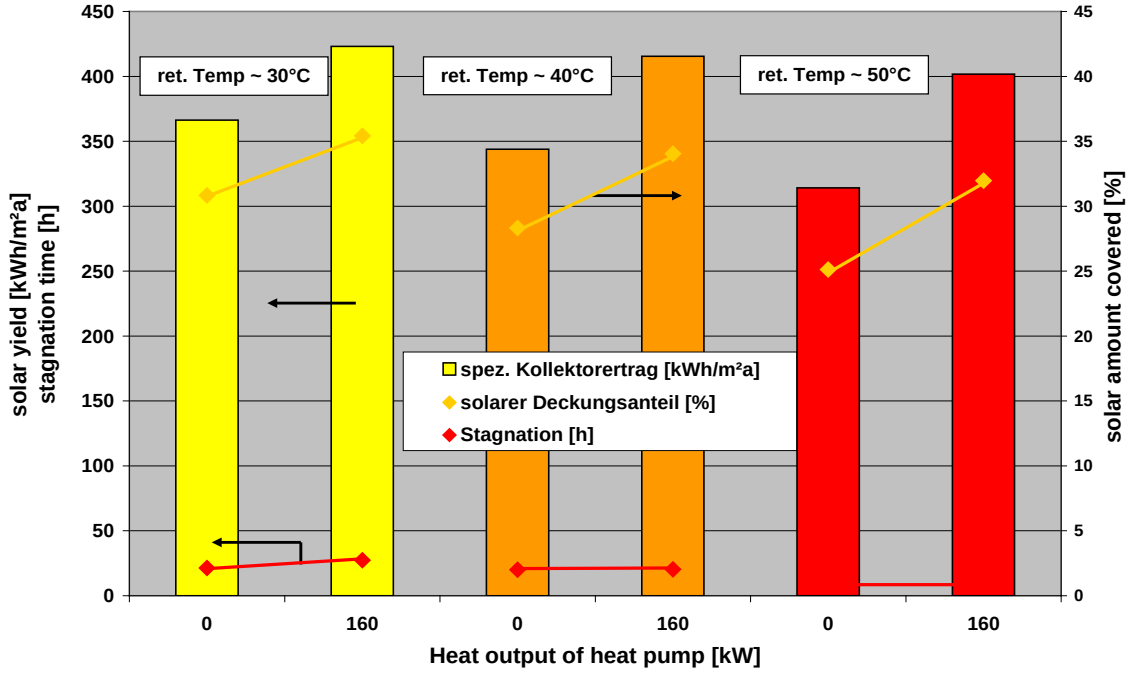

Fig. 3. Influence of return temperature

3. Results

Yet new buildings are under construction, required building standards will be achieved. Optimized energy supply concept is based on 2.000 m² solar collector fields and 2.000 m² of storage tank in combination with a heat pump and an own low-temperature-micro-net for heat distribution. The calculation of primary energy demand for several variation of energy concept (Fig. 4) showed, that system with solar collectors in combination with electric heat pump leads to the maximum reduction of non-renewable primary energy demand, compared to energy supply based on district heating and solar energy. But it is essential, that the result depends very much on the primary energy figures of the electricity.

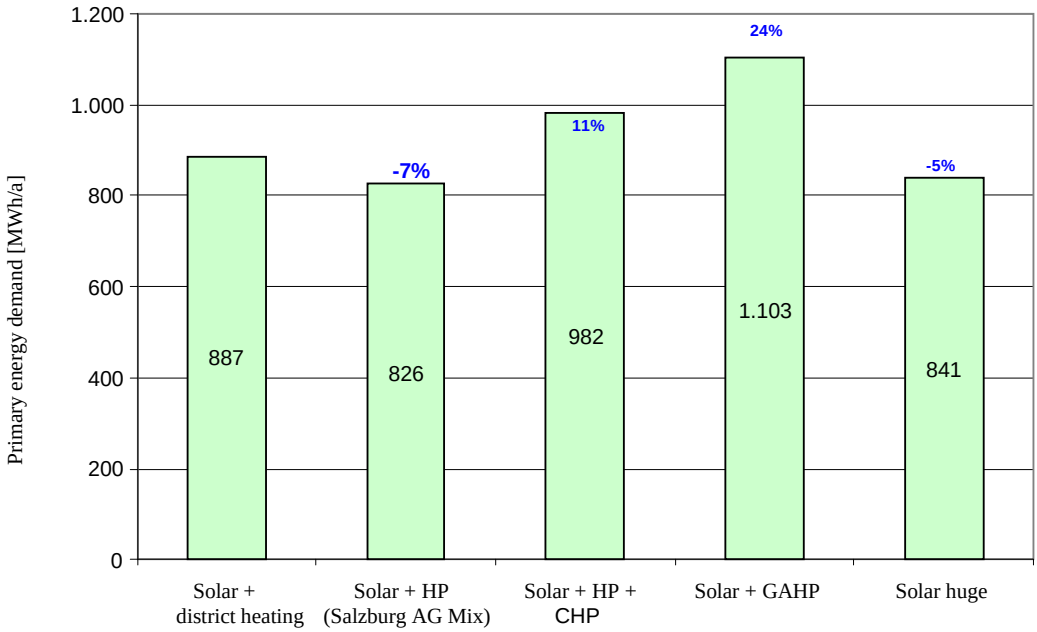

Fig. 4. Primary energy figures

At least, a reduced electricity demand for public areas will be achieved with efficient lightning systems and pumps. Demand will be covered with PV-modules on the several buildings.

4. Discussion and Conclusion

Driving forces
For project of "Stadtwerk Lehen" funding programs were the main driving forces at the beginning. Without this opportunity there would be no discussion on development of an ambitious project like it is now neither a development of an energy concept for new building areas and existing community. So for further projects driving forces have to be identified.

Clear roles
In addition to that funding-programs have led to a signed partnership of relevant institutions and persons. Furthermore roles of partners are defined; in particular there is the defined mission for developing an overall energy concept for the whole area and with defined interfaces to the several planners of the buildings.
Thus further projects which have do be developed need to have clarified before

- who will define the overall energy concept,
- purchased by whom,
- financed by whom,
- at which time of project development?

These questions can become an important issue for development departments of local administrations, although they may not understand as being responsible for energy planning.

Process design for successful renovation projects
Decision making for renovation of existing building stocks is a complex process if there are a couple of stakeholders with each with his own interest addressed. The implementation of a detailed showcase-study was very helpful to show the possibilities of total renovation and its

options for the overall refurbishment of the district. Thus renovation does not only include insulation of buildings. In fact modernization means more than renovation and offers more possibilities to address the expectations of the tenants. Furthermore it is important that specific interests of tenants are addressed with modernization activities, although they might not be energy-related. This helps to get tenants support for renovation process.

Ambition versus market situation
Renovation of multi-storey building is planned to achieve high energy standards. In opposite to social housing sector commercial buildings are highly depending on market situation. If there is less interest on commercial areas with high energy standards (and thus also higher rents) it is very difficult to implement ambitious projects.

Optimized energy concept for whole community
Energy concept for new buildings can be planned and optimized since relevant figures and stakeholders are known. Integration of building stock causes several further questions such like:

- Figures about actual heat demand
- Figures about expected heat demand after renovations / modernizations
- Schedule of renovation process

Thus optimization has to consider several uncertainties respectively planning has to be modular. Further it has to be discussed who has to take the risk for additional costs.

References

[1] SIR – Salzburger Institut für Raumordnung und Wohnen: "StadtUMBAU LEHEN", Salzburg, 2010

[2] Steinbeis Transferzentrum Energie-, Gebäude- und Solartechnik: "Energiekonzept Mikronetz - Simulation, Wirtschaftlichkeit, Emissionen", Stuttgart, 2009

[3] Dr. Burkhard Schulze Darup, Schulze Darup & Partner: "Rahmenplan für die Modernisierung der Strubergassensiedlung in Salzburg", Nürnberg, 2010

The project of "Stadtwerk Lehen" is funded by:

- European Union / Concerto
- BMVIT /Haus der Zukunft plus
- Land Salzburg / Wohnbauforschung

Towards a 2kW City – the case of Zürich

Urs Wilke[1,*], Maria Papadopoulou[1], Darren Robinson[1]

[1] *EPFL, Lausanne, Switzerland*
** Corresponding author. Tel: +41 693 4545, Fax: +41 693 2722, E-mail:urs.wilke@epfl.ch*

Abstract: In 2004 the Council of the Federal Polytechnics of Switzerland proposed that the country's per capita primary energy demand should be reduced by a factor of three from its current average of around 6kW to 2kW – the current global average – by 2150. During the past six years the semantics of this proposition have been much debated, but the concept has won overall favour, with several cities voicing their support. Indeed in November 2009 the inhabitants of the city of Zürich voted in favour of applying the 2kW city concept to their city, but targeting the year 2050. Thus, the city of Zürich is now committed to understanding which strategies should be employed and when, to achieve 2kW city status. But the city is not naïve, it fully appreciates that this target is ambitious and will only be realised through commitment and a multiplicity of transition strategies; some of which have already been implemented. But to understand, which are the most promising future strategies will require some form of predictive model. In this paper we describe one such model, which is currently under development, and the strategies that may be tested by it as well as outlining the already implemented strategies.

Keywords: *Urban sustainability, Environmental politics, Micro-simulation*

1. Introduction

In 2009, the total end energy use in Switzerland amounted to about 878 PJ [1] of which 55.1% are covered by petroleum products and 23.6% by electricity. Approximately 55.8% (*cf. Fig. 1*) of Switzerland's overall electricity conversion comes from hydropower, which forms the main part (96.5%) of electricity produced by renewables [2; 3]. Nuclear power plants account for 39.3% of domestic conversion and conventional thermal energy/other renewable energy plants for approximately 5% (*Fig. 1*). And while hydropower has been, historically, Switzerland's longest-serving and most important source of renewable energy, other renewables including solar, wood, biomass, wind, geothermal and ambient heat are starting to play an increasingly important role in Switzerland's energy supply [1; 2]. Private households, industry, services and the transportation sector account for almost 29, 19, 16 and 35% of Switzerland's energy use, respectively (*Fig. 1*).

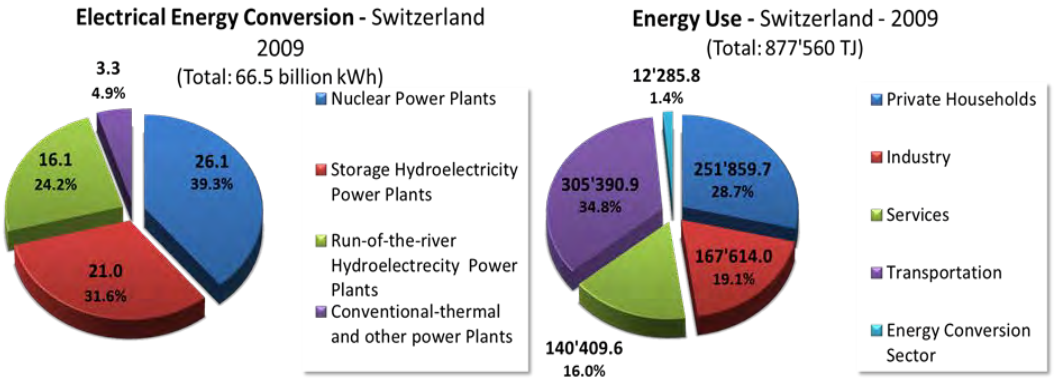

Fig. 1. Electricity conversion (left) and total energy use (right) by sector in Switzerland for 2009 [1; 2]

Ten years ago, the Swiss Federal Institute of Technology (ETH) in Zürich developed the vision of a "2000-Watt Society" which represents Switzerland's approach to tackling climate change and the upcoming conflict of resources. It is based on the idea that the Swiss citizens

limit their energy use to the global average value of 2000 watts by the year 2150. Should other developed countries follow suit, this would enable the per capita energy demands of developing countries to increase, to meet their inhabitants' aspirations for improved living standards, without further increasing the global average. Furthermore, renewable energies should be used to satisfy at least 75% of these 2000 Watts, so that on an annual basis only one tonne of carbon dioxide equivalent is emitted per capita and year. The use of nuclear energy should also be completely phased out [4]. The implications of this approach are summarised in Fig. 2.

By closely analysing the unexploited efficiency and substitution potentials in Switzerland, scientists of the Swiss Federal Institutes of Technology (ETH) and other institutions have shown that the vision of a 2000-watt society is indeed feasible. They concluded that a period of between 50 and 100 years would be needed for this to become a reality [4].

Following from this, the citizens of Zürich participated in a referendum in November 2009, with around three quarters voting in favour of committing to achieving the 2000 Watt society status, but by **2050** [4]. This follows from a long standing commitment in Zürich to reducing the city's energy use. Indeed in 2000 the city acquired the label "Energiestadt®", which has since become a Europe-wide initiative, the "European Energy Award®". Four years on, the city was recertified and obtained the label "Energiestadt® Gold" [5].

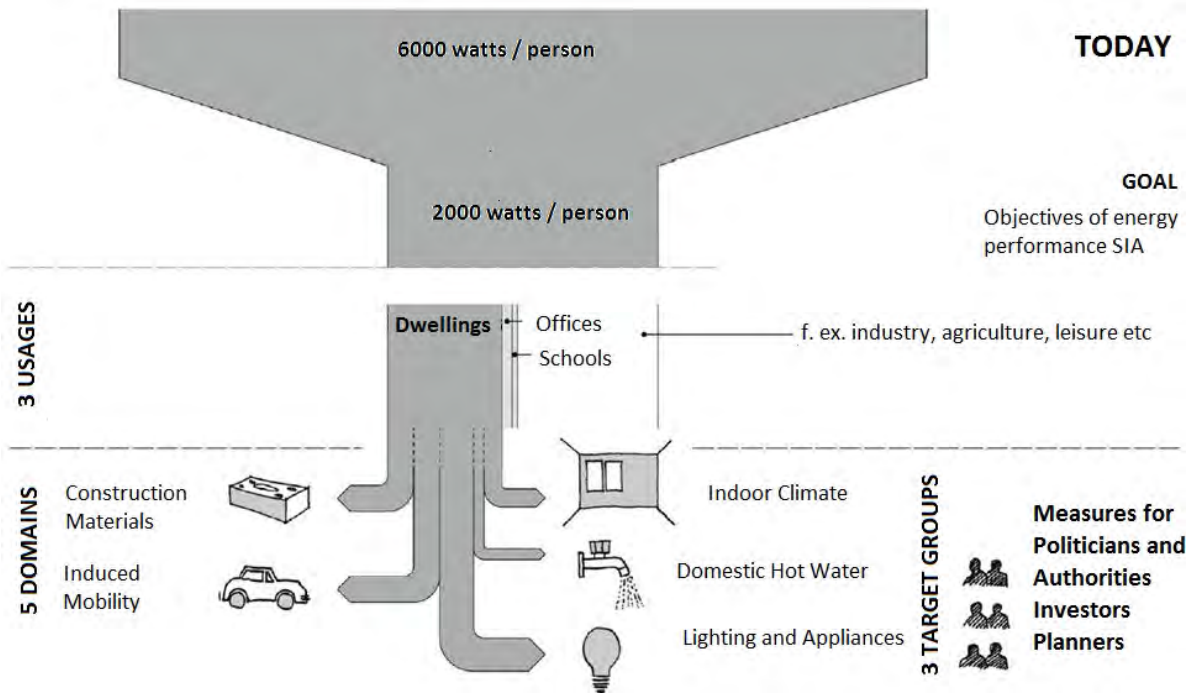

Fig. 2 The strategic plan to achieve a 2 kW-City-of-Zürich (original figure taken from [6])

2. 2 kW City of Zürich

2.1 Current energy breakdown: magnitude of improvements required

Private households and transportation are together responsible for around 60% of energy use in Zürich, with the remaining 40% being used by industry, commerce, services and retail sectors (economy and administration) (*Fig. 3*). Of these latter the non-industrial uses are dominant in Zürich. As such the city's efforts should be focussed upon transport, housing and other non-industrial building uses.

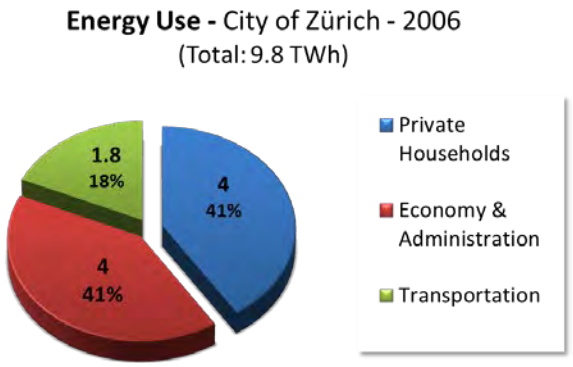

Fig. 3. Energy use by sector for the city of Zürich for the year 2006 [7]

The city has identified that, amongst the required improvements is reducing the energy use through better conservation and improving energy efficiency, while developing and exploiting innovative technical solutions. Thus, it is important to encourage the intelligent and efficient use of eco-friendly resources and materials, the utilization of waste heat and renewable energy, but also to promote social learning processes, new life styles and management concepts [8; 9].

Following from the above observations, the city is currently focusing on the following strategies to achieve its 2kW status:

- Building Sector: Implementation strategies regarding the use of better insulating construction methods and energy-efficient technologies. The target here is to demonstrate the feasibility by renovating and constructing "demonstration" buildings with low initial, running and maintenance costs, while ensuring a high quality of living [10].
- Mobility: Promotion of a more expansive and energy-efficient public transportation system whilst facilitating pedestrian and bike traffic. The city, in collaboration with the Canton of Zürich, has also proposed to launch a road pricing initiative to encourage the switch to more sustainable transport modes [10].

2.2 Initiatives under way since 2004

As part of its commitment to the European Energy Award the city has already established several initiatives which may be further reinforced during the coming years. And while Zürich promotes energy-efficient measures, companies and individuals can benefit from a vast variety of information and advice, including:

- Advising/educating/energy coaching: for eco-friendly lifestyle/behaviour in buildings and the induced mobility by various departments of the city to different actors (constructors, investors, operators and users) [11; 12; 13].
- Assessing existing buildings/construction projects: A methodology has been designed which makes use of the comprehensive international Life Cycle Inventory database "ecoinvent" [14]. This database contains indices relating to embodied energy and gaseous emissions (e.g. CO_2-equivalent) for a broad range of composite materials and their constituent parts [15].
- Environmental policy guidelines/regulations: Defining specific thresholds of energy use to assess the progress of energy savings in the building sector as well as its induced mobility [22]. The City Council also uses this document to formulate environmental policy

guidelines. For the construction sector, specific guidelines have been conducted regarding HVAC systems, electrical appliances and sanitary fittings [11].

- Financial Support:

  To promote and support the required transition strategies several incentive schemes have been established for energy-efficient investments. This includes subsidies provided to private citizens, firms as well as institutions, on a communal, cantonal and federal level:

  – Cantonal support program: Information and financial support (also for expertise of impartial consultants) of energy-efficient refurbishments [16].

  – Electricity Savings Fund of the City of Zurich: Subsidises investments for the efficient use of energy and the integration of renewables [17].

  – Subsidies from CO_2 tax on heating oil [18]: At the federal level, insulation improvement measures of the building envelope are subsidized for buildings which have been constructed before 2000. Furthermore, in the Canton of Zürich the use of renewable energy, modern building technology and the use of waste heat is supported [19].

  – Reduction of interest rates on credits for investments in energy-efficient measures: Environmental reductions up to 0.8% for new construction and renovation according to the MINERGIE® standard, investment in renewable energies, energetic refurbishments and other ecological projects [20].

  – Tax deductions: Investments in energy-saving renovation of old buildings can be partially deducted from tax [21].

3. A bottom-up model of urban energy flows

As noted above, the city of Zürich is very aware of the need for some rational basis to guide their decision making processes with respect to the choice and implementation of strategies for making the transition from the current per capita energy use of around 5kW to just 2kW within the next forty years. Ideally, this should be some form of model with which alternative hypotheses may be tested. Now, since the principle uses of energy within Zürich are to condition buildings, support the activities accommodated within buildings and to transport goods and people between buildings (see section 2.1), it follows that our decision making model should represent buildings and transport systems. Such a model may be spatially aggregated (or macroscopic), treating the city as an ensemble in which we model the stocks and flows of resources between compartments of this ensemble. Or we may have a spatially disaggregated model, in which we explicitly model individual buildings in their spatial context as well as individual transport journeys between these buildings. Or we may opt for some compromise between these two: for example grouping buildings into clusters and explicitly modelling an example from within each cluster and extrapolating to the remainder.

As part of a project funded by the Swiss National Science Foundation, we have elected to develop a spatially explicit or micro-simulation program, which combines the modelling capabilities of two complementary tools: CitySim for buildings and MATSim for transportation.

CitySim [22] is a detailed simulation program for predicting the energy demands of buildings as well as the supply of energy to them, whether using building-embedded or district scale energy conversion systems. It takes as input a 3D description of the scene to be simulated, in which each building is attributed according to the thermal and optical properties of its

construction, characteristics describing its occupants as well as the heating, ventilating and energy conversion systems. Either the buildings, or the district to which they belong, are then associated with characteristics describing their energy conversion systems. This scene description is parsed to an integrated dynamic model which simulates energy demands for heating, hot water, lighting, ventilating and cooling as well as for electrical appliances. These simulations account for the stochastic nature of occupants' presence and their interactions with the building envelope and its active systems as well as the effects of adjacent obstructions on surface radiation exchanges (accounting for occlusions to sun and sky as well as reflections from these occlusions). CitySim is thus a comprehensive and detailed program for simulating building-related energy flows at the urban scale.

In complement to CitySim, MATSim [23] simulates the sub-hourly transport of individual people within our urban scene. For this a geometric description of the scene is required, consisting primarily of the transport network nodes and the links between them as well as the locations of activities (work, home, education etc) located at or adjacent to these nodes / links. Using geo-coordinated census data a population of households may then be created. The members of this population are then associated with activity chains such as home-work-leisure-work-home and the locations and preferred timing of these activities. With this initialisation complete the scene may be simulated. Following from an initial shortest route finding algorithm, an optimisation algorithm is employed to optimise travellers travel plans: identifying departure times following each activity which maximise travellers utility, based on minimising travel time and maximising the time spent performing the required activities. With agents' daily travel plans chosen, their final journeys may be simulated and the associated fuel consumption calculated, using empirical performance data.

The means for coupling CitySim and MATSim is via the exchange of people. Upon launching a simulation a population of agents is generated, with each agent being associated with socio-economic characteristics, travel plans, building locations (e.g. residential and workplace) corresponding to these plans, environmental comfort preferences to be applied whilst within these buildings etc. MATSim is then launched to simulate agents' arrival and departure times at the geo-referenced buildings. These agent IDs and their arrival and departure times are then parsed to CitySim which simulates each buildings' energy demands as well as the supply of energy to them. Thus we have a comprehensive platform in which we are able to test a range of strategies, including:

- Inhabitants' investments in: building renovation measures, more efficient vehicles, public transport season tickets etc.
- Energy service company investments in distributed heating, cooling and power systems.
- Uptake of subsidies to encourage more widespread uptake of building-embedded renewable energy conversion systems.
- Changes in buildings' use to reduce transport energy demands and improve the match between energy demand and distributed energy supply system etc.

And of course the energy implications of the above measures.

Having now developed a first prototype of this coupled building-transport modelling platform we are currently in the process of testing this in conjunction with a district of the City. Our next step will then be to prepare and calibrate a whole city model and to test hypotheses for improving its energy performance; strategies that we will define in liaison with the City stakeholders.

4. Conclusions

Following from a longstanding commitment to reduce its use of energy and associated adverse environmental impacts, the citizens of the city of Zürich recently voted in favour of reducing its per capita primary energy use from its current level of more than 5kW to just 2kW within the next forty years. Other complementary commitments are to reduce per capita greenhouse emissions to below 1t CO_2 equivalent per Capita and to eliminate the use of electricity derived from nuclear sources. In pursuance of these objectives the city has already implemented a range of programs to contribute towards the required transformations, but so far these are relatively modest in their ambitions. The city understands that to achieve its ambitious objectives, will require serious commitment and a multiplicity of initiatives. To assist in this process the two Swiss Federal Institutes of Technology (Lausanne and Zürich) are collaborating in the development of a new urban energy modelling platform, integrating micro-simulation programs of buildings, distributed energy conversion and storage systems and transport systems.

A first prototype of this new modelling platform has been developed and is being applied to a sample district of the city. Following from this initial application a full scale city model will be prepared and a range of scenarios defined and tested, with the solicited contributions of key city stakeholders. It is also intended that a working model of the city will be handed over to the city, to support its continued updating and application to test future strategies.

References

[1] Schweizerische Gesamtenergiestatistik 2009. Swiss Federal Office of Energie SFOE. Bern : BBL, Vertrieb Publikationen. 805.006.09 d/f / 08.2010 / 2800.

[2] Schweizerische Elektrizitätsstatistik 2009. Swiss Federal Office of Energie SFOE. Bern : BBL, Vertrieb Publikationen. 805.005.09 d/f / 06.2010 / 2000.

[3] Swiss Federal Office of Energy. Renewable Energy. [Online] [Cited: 2010] http://www.bfe.admin.ch/themen/00490/index.html?lang=en#.

[4] The City of Zürich. 2000 Watt Society. [Online] www.stadt-zuerich.ch/2000-watt-society.

[5] Umwelt- und Gesundheitsamt (in English: Department for Environmental and Health Protection). Die Energiestadt® Zürich. [Online] [Cited: 14. 12. 2010.] www.stadt-zuerich.ch/energiestadt.

[6] Preisig, H. and Pfäffli, K. SIA Effizienzpfad Energie. Zürich : SIA, 2006. D 0216.

[7] Gesundheits- und Umweltdepartement (in English: Department for Environmental Protection). Energiebilanz. [Online] [Cited: 16. 12. 2010.] http://www.stadt-zuerich.ch/gud/de/index/umwelt/energie/energiekennzahlen/energiebilanz.html.

[8] Gesundheits- und Umweltdepartement, (in English: Department for Environmental Protection). Ziele & Grundsätze. [Online] [Cited: 17. 12. 2010.] http://www.stadt-zuerich.ch/gud/de/index.html.

[9] Novantlantis. 2000-Watt-Gesellschaft. [Online] http://www.novatlantis.ch/2000watt.html.

[10] novatlantis. Partnerregion Zürich. [Online] [Cited: 14. 12. 2010.] http://www.novatlantis.ch/partnerregionen/partnerregion-zuerich.html.

[11] Gesundheits- und Umweltdepartement (in English: Department for Environmental and Health Protection). Strategien & Umsetzungsmodelle. [Online] [Cited: 13. 12. 2010.]

http://www.stadt-zuerich.ch/gud/de/index/das_departement/strategie_und_politik/2000_watt_gesellschaft/was_macht_zuerich/strategie_umsetzung.html.

[12] Planungsbüro Jud. Energieeffizienz in der Mobilität, Schlüsselfaktoren bei Bauprojekten. Zürich : Tiefbauamt, 2008.

[13] Gesundheits- und Umweltdepartement (in English: Department for Environmental Protection). Sportlich zum Sport. [Online] [Cited: 14. 12. 2010.] http://www.stadt-zuerich.ch/gud/de/index/das_departement/strategie_und_politik/2000_watt_gesellschaft/sportlich_zum_sport.html.

[14] ecoinvent. database. Ecoinvent - Swiss Centre for Life Cycle Inventories. [Online] http://www.ecoinvent.org/database.

[15] City of Zürich, Federal Office of Energy, "EnergieSchweiz für Gemeinden" and Novatlantis. LSP 4 - "Nachhaltige Stadt Zürich - auf dem Weg zur 2000-Watt-Gesellschaft". Zürich : Stadt Zürich, 2009.

[16] Canton of Zürich. Jetzt – Energetisch Modernisieren. [Online] http://www.energetisch-modernisieren.ch/.

[17] electric power company Zürich. Stromsparfonds. [Online] [Cited: 14. 12. 2010.] http://www.stadt-zuerich.ch/ewz/de/index/energie/stromsparfonds.html.

[18] Gesundheits- und Umweltdepartement (in English: Department for Environmental Protection). Förderbeiträge. [Online] [Cited: 15. 12. 2010.] http://www.stadt-zuerich.ch/foerderbeitraege.

[19] Konferenz kantonaler Energiedirektoren EnDK (in English: Conference of Cantonal Energy Directors); Federal Office of Energy / for the Environment. Das Gebäudeprogramm. [Online] [Cited: 14 12 2010.] http://www.dasgebaeudeprogramm.ch/.

[20] Zürcher Kantonalbank. Umweltdarlehen. [Online] [Cited: 14. 12. 2010.] zkb.ch/umweltdarlehen.

[21] Amt für Abfall, Wasser, Energie und Luft (AWEL) (in English: Office for Waste, Water, Energy and Air), Abteilung Energie, Baudirektion,. Merkblatt des kantonalen Steueramtes über die steuerliche Behandlung von Investitionen, die dem Energiesparen und dem Umweltschutz dienen, bei Liegenschaften des Privatvermögens. Zürich : Amt für Abfall, Wasser, Energie und Luft (AWEL), Abteilung Energie, Baudirektion,, 2009.

[22] Robinson et al. Building modelling, In: Computer modelling for sustainable urban design. London : Earthscan press, 2011.

[23] Axhausen. Transport modelling, In: Computer modelling for sustainable urban design. London : Earthscan Press, 2011.

Application of mechanical heat treatment for the recovery of plastics as energy resource

Jyi-Yeong Tseng[1], Chia-Chi Chang[1], Zang-Sie Hung[1], Yen-Chi Wang[1], Dar-Ren Ji[1], Chun-Han Ko[2], Yi-Hung Chen[3], Je-Lueng Shie[4], Yuan-Shen Li[4], Chungfang Ho Chang[5], Sheng-Wei Chiang[1], Shi Guan Wang[6], Kuang Wei Liu[6], Ching-Yuan Chang[1,*]

[1] *Graduate Institute of Environmental Engineering, National Taiwan University, Taipei, Taiwan*
[2] *School of Forestry and Resource Conservation, National Taiwan University, Taipei, Taiwan*
[3] *Department of Chemical Engineering and Biotechnology, National Taipei University of Technology, Taipei, Taiwan*
[4] *Department of Environmental Engineering, National I-Lan University, I-Lani, Taiwan*
[5] *Department of International Trade, Chung Yuan Christian University, Chung-Li, Taiwan*
[6] *Environmental Analysis Laboratory, Environmental Protection Administration, Chung-Li, Taiwan*
** Corresponding author. Tel: +886 223638994, Fax: +886 223638994, E-mail: cychang3@ntu.edu.tw*

Abstract: The mechanical heat treatment (MHT) is one of the pre-treatment alternatives for conditioning the municipal solid waste (MSW) before its further separation, recovery and reuse. The MHT would result in the change of properties of constituents of MSW, making it suitable for separation. For example, the plastics may be softened and shrunken. Therefore, the MSW via the pre-MHT can be more easily separated into various fractions of resources such as metals, plastics, compost-like and primary refuse derived fuel (RDF) or bio-char for further re-utilization.

The objective of this study was to examine the efficiency and effective of energy recovery and volume downsize of plastics via MHT process. The commonly used plastic, high-density polyethylene (HDPE) was tested. The changes of weight, triple components, true density and calorific value of target plastic before and after the MHT with saturated steam at 100, 150 and 180 ^{o}C were examined. The effects of temperature on the performance of MHT were assessed. The results indicated that an increase of MHT temperature induces more significant shrinkage and higher volume density, enhancing its feasibility for the separation from non-plastic materials. The information obtained in this study is useful for the rational design and proper operation of MHT system for treating the used plastics in the MSW and separating it for the re-utilization as energy resource.

Keywords: *Energy resource, Mechanical heat treatment, MHT, Municipal solid waste, MSW.*

1. Introduction

The ultimate goal of the waste management aims at the complete collection of the garbage, proper treatment for the thorough energy recovery and material reuse targeting at a sustainable utilization of all resources. Traditional waste treatments processes include landfill, incineration and recycling. Incineration is a process which directly combust or incinerate the waste to generate heat and then recycle the energy through the production of steam or hot water with the help of heat recovering facilities. The incineration residues including sand, ceramic, glass, metal and little incomplete combustion of organic matter are sent to landfill. The process of incineration not only wastes a significant amount of reusable energy, but also produces secondary pollutants such as ash dregs or fly ash [1-3]. Further, if the plastics are directly recycled without any pretreatment, it will cause the lack of storage space and the consumption of transportation expense. Therefore, the new generation of energy recovery technique of the waste to replace incineration must take into consideration all kinds of factors such as the complex varieties and properties of the waste, the availability of waste as a resource, the technique for its transportation and storage, the constrain of economics and relevant regulations and the energy or environmental benefit for the whole systems. Thereafter, in addition to the enhancement of performance and the reduction of the cost, it has

become a trend converting the waste into energy of different forms. According to a report of Environmental Protection Administration of Taiwan (TEPA) in 2008 for the Municipal solid waste (MSW) composition, there are 44.54% of paper, 2.63% of fibrous cloth, 1.99% of wood, bamboo and fallen leaves, 30.56% of kitchen waste, 17.28% of plastics, 0.36% of leather and rubber, 0.33% of ferric metals, 0.33% of non-ferric metals, 1.11% of glass, 0.5% of ceramic sands and 0.48% of other combustible materials [4]. These data reveals that there is a high content of plastics in the MSW. With certain kinds of pretreatment techniques, the separation of MSW and the followed resources recovery and reutilization may become more complete and efficient. The so called cooking assorting or mechanical heat treatment (MHT) is one of the techniques that are worthwhile to be evaluated [5,6]. The MHT would result in the change of properties of constituents of MSW, making it suitable for separation. For example, the mass of non-plastics decreases while the volume density increases. The cellulose and hemi-cellulose of biomass in MSW are decomposed for easy torrefaction. The plastics may be softened and shrunken. Thus, the objective of this study was to examine the efficiency and effective of energy recovery and volume downsize of plastics via MHT process. In this research, we investigated over the changes of weight, triple components, true density and calorific value of high density polyethylene (HDPE) before and after the cooking process for the reference need in plastic recycling from MSW via cooking separation process.

2. Methodology

2.1. Devices

Cooking apparatus used for this experiment is illustrated in Fig. 1. This apparatus includes a steam generator that can produce saturated steam and a high temperature (398-593 K) and high pressure (5-205 kg cm^{-2}) autoclave equipped with stirring accessory. The autoclave is made by stainless steel 316 with inner volume of 1.5 L. The stirring axes are composed by outer and inner axes. The inner axis is enclosed in the outer axis and driven by the outer axis with magnetic force. The bearing is cooled by cooling water. The outer axis is connected to 0.25 hp motor. The upper cap has six holes with three for thermal couple, pressure gauge and release valve, while three for spare port. The steam generator is constructed by an autoclave and an oven. The heating wire of oven is made of nichrome. The oven temperature is controlled by a proportional-integral-differential (PID) controller with K-type thermal couple in the vessel.

2.2. Experimental conditions

HDPE, the most common plastic that can be found in MSW for the experiment, was selected. Then the cooking experiments was performed 60 minutes with 100, 150 (P_g = 5.15-5.4 kg cm^{-2}) and 180 ^oC (Pg = 8.05-10.25 kg cm^{-2}) saturated high temperature steams via cooking apparatus. The dry weight changes, triple components (including water, ash and combustible components), true density and calorific value for the HDPE before and after the cooking process were examined.

2.3. Analytical methods

The thermal stability of HDPE was analyzed by the thermal gravity analysis (TGA) (model TGA51, Shimadzu Co., Kyoto, Japan). The calorific value was measured by a calorimeter (model 6775, Parr Instrument Company, Moline, Illinois, USA). The triple components were analyzed by a high-temperature oven (model muffle furnace DF 40, Deng Yng Co., Taipei, Taiwan).

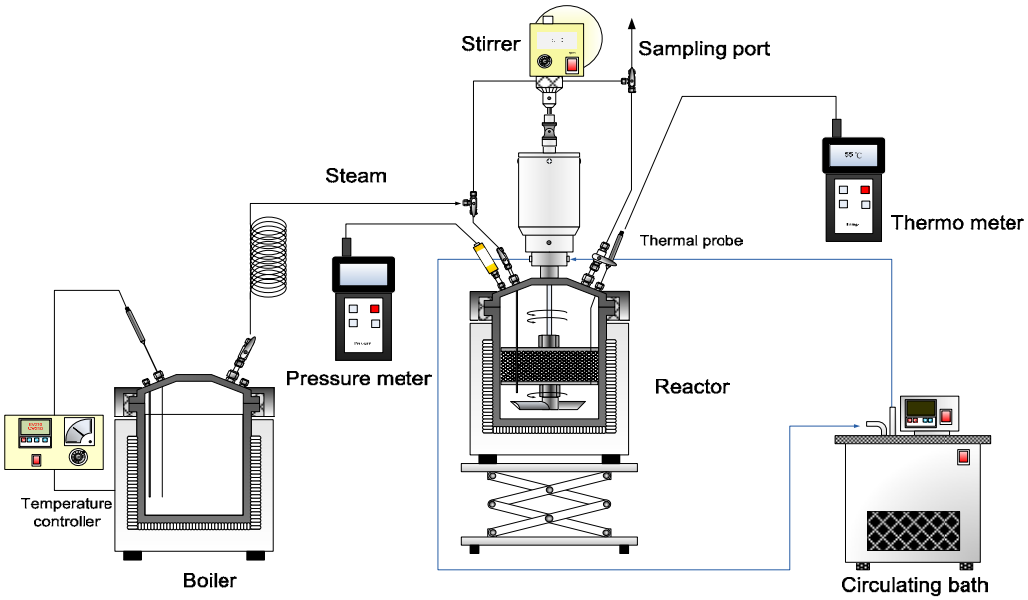

Fig. 1. Mechanical heat treatment (MHT) apparatus used for the recovery of plastics as energy resource.

3. Results

3.1. TGA of HDPE

TGA has proven to be a useful and efficient technique of the estimation of thermal stabilities of plastics. TGA is also widely used in studying pyrolytic processes. In this research, we investigated over the TGA to observe the degradation point and thermal behavior of HDPE. Fig. 2 is the TGA result generated on the HDPE at an applied heating rate of 10 ^{o}C min^{-1} before cooking process. As displayed in Fig. 2, weight loss curve is smooth, with one inflection point during reaction under nitrogen atmosphere. Figure 2 also shows that the decomposed point of HDPE is about 377 ^{o}C. Decomposition reactions for the heating rate of occurred at the temperature range from 630 K to 850 K.

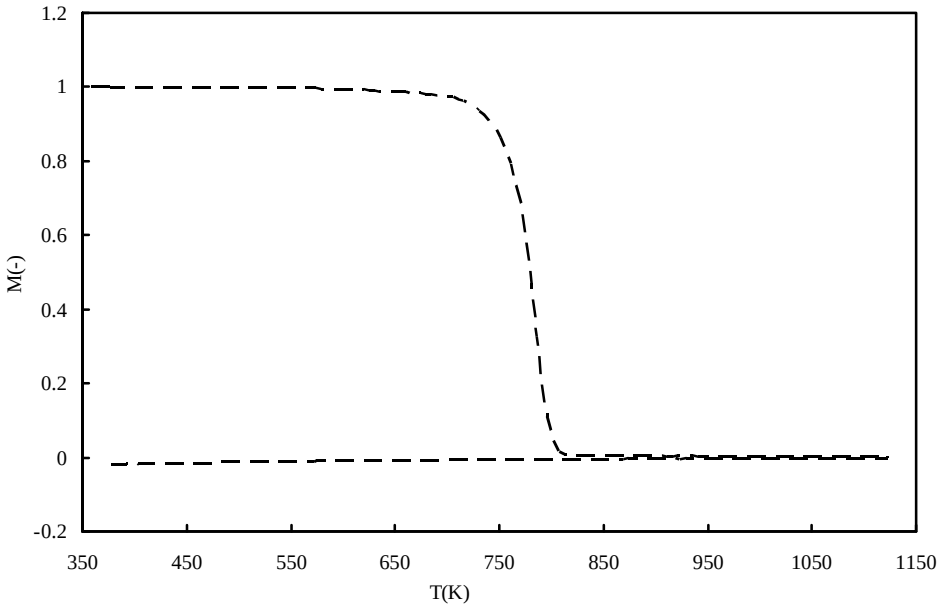

Fig. 2. The TGA curves for high density polyethylene (HDPE).

3.2. Dry weight changes after cooking

We can roughly speculate the thermal characteristics of the HDPE samples by the observation of weight changes in samples. As shown in Fig. 3, there is no significant dry weight change before and after cooking process in a steaming condition of 100, 150 and 180 ^{o}C. As HDPE has a melting point of 130-140 ^{o}C and a degradation point of 350-380 ^{o}C [7], the results indicate that the melting of HDPE at 150 and 180 ^{o}C has negligible effect on dry weight reduction.

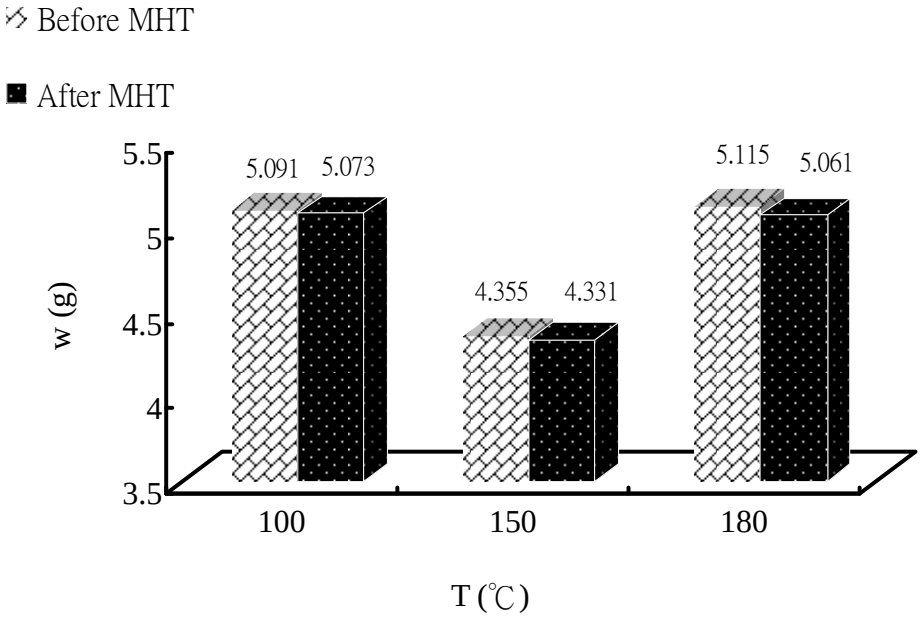

Fig. 3. Dry weight changes for HDPE before and after the MHT with saturated steam at 100, 150 and 180 ^{o}C. w: Dry weight.

3.3. Triple component analysis

With the analysis of triple components (including water, ash and combustible components), we can know if there's any change in the organic components of the samples. Moreover, a high quality of RDF would possess a higher value for the combustible component, and lower values for moisture and ash contents. Thus, the triple components analysis is also an important index to assess MSW if it is suitable to be utilized as RDF. The results of Fig. 4 show there is little change in the amount of combustible component existed in HDPE after cooking. The combustible component content is 99.62% before cooking and 99.02, 98.98, 98.21% after being cooked in saturated steam condition of 100, 150 and 180 ^{o}C, respectively. Therefore, we can conclude that the organic component does not reduce in those steaming conditions of 100, 150 and 180 ^{o}C. The results also indicate that the combustible component (> 98%) of HDPE is very high, which is larger than that of the unprocessed MSW (30-40%). Thus, if we recycle the plastics as energy resource or RDF via MHT process, the energy utilization of MHT will be more efficient and effective than that of direct incineration treatment of MSW.

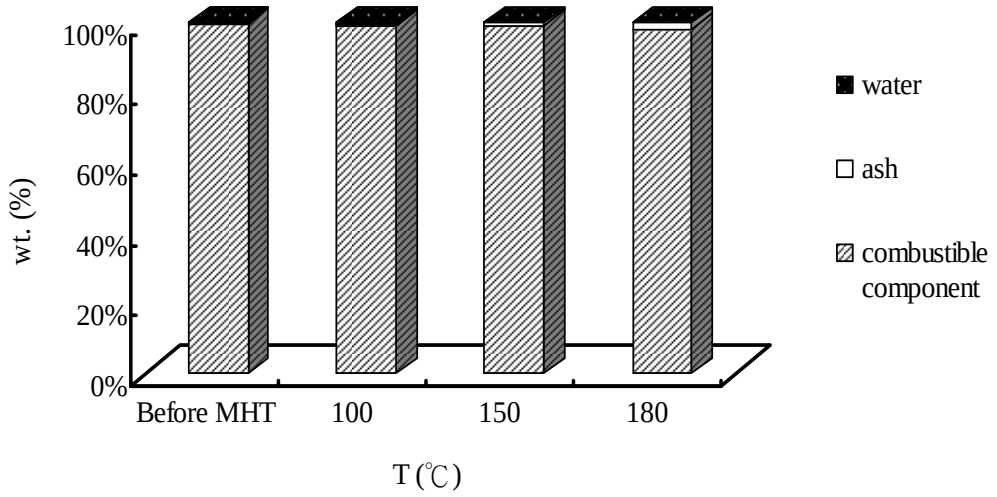

Fig. 4. Triple component analysis before and after the MHT with saturated steam at 100, 150 and 180 ^{o}C. *wt.: Weight percentage.*

3.4. True density changes

Figure 5 indicates that with an increase of temperature of steam introduced, the true density after cooking offers increases, reaching a value of 0.983 g cm^{-3} at 180 ^{o}C. This is due to that thermoplastic material fluidizes and swells after being heated. It then solidifies and shrinks from the melt status during cooling. Taking advantage of this characteristic, cooking process offers a very promising volume reduction effect for thermoplastics and can reduce the storage space and transportation expense drastically. Moreover, plastics soften and shrink into pellet shape with an increasing density and thus can be easily separated from other components existed in the MSW and enhancing recovery of plastics for utilization.

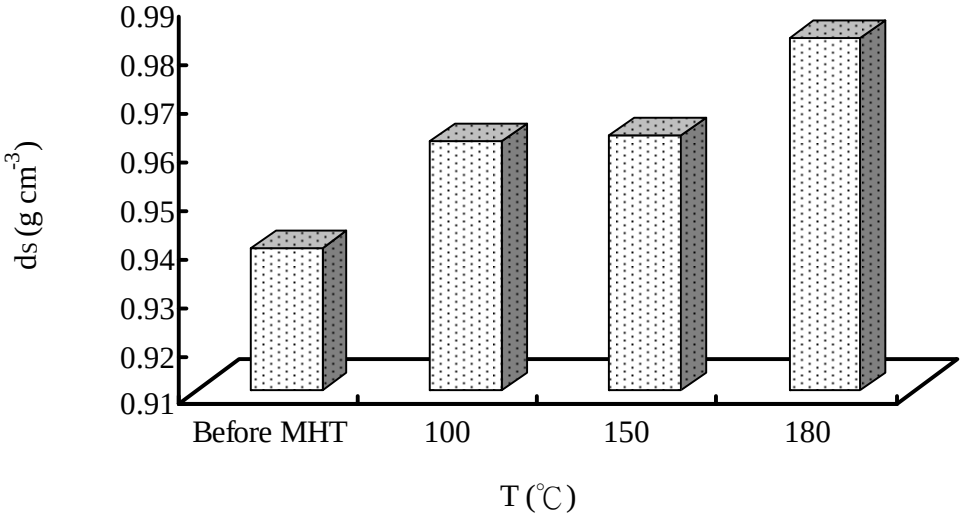

Fig. 5. True density changes before and after the MHT with saturated steam at 100, 150 and 180 ^{o}C. *d_S: True density.*

3.5. Calorific value changes

As shown in Fig. 6, the heating values (H_V) of HDPE before and after MHT are higher than that of coal of about 7000-8000 kcal kg^{-1} [8]. It has a value of 10654 kcal kg^{-1} before cooking and 10834, 10680 and 10669 kcal kg^{-1} after cooking in saturated steam condition of 100, 150 and 180 ^{o}C, respectively. We observed that H_V did not have a big change for the said cooking conditions. We can therefore conclude that the cooking process does not cause the degradation or other chemical changes of HDPE which may further influence its heating value. As contrasted with the H_v of 1889 kcal kg^{-1} of unprocessed MSW [4], it is clear that the separation of non-combustibles in the waste (glass and metals) can increase heating value and energy generation. From the point of view of maximization of energy recovery of MSW, MHT is a good pretreatment process for the separation of non-combustibles and energy recovery in MSW.

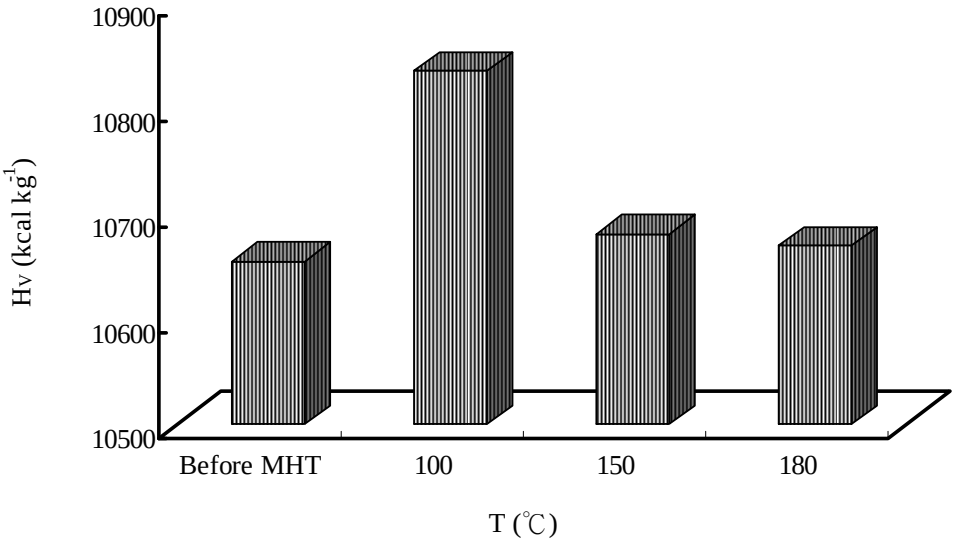

Fig. 6. Changes of heating value before and after the MHT with saturated steam at 100, 150 and 180 ^{o}C. H_V: Heating value.

4. Discussion and conclusion

In accordance with the theme of sustainable material management (SMM), the waste is viewed as the used material. The ultimate goal of SMM is targeted at total recycling and reuse without discharge of waste. To follow the appeal of SMM, this study applied the MHT for the recovery of waste plastics from waste stream, aiming at the feasibility of its recovery for the re-utilization as energy resource. As shown in Fig. 7, the recovered plastics can be directly utilized as RDF. The ferric materials and gravels can be separated via magnetic or gravity separations. The MSW containing cellulose (including organic fiber (fiber) and cotton (floc)) can partially hydrolyze after cooking to form bulk powder materials, which can help the decomposed cellulose granulation to produce renewable fuels. The treated MSW containing cellulose can be torrefied together with other agricultural and forestry materials to produce biocoal, or use as an agricultural soil improvement materials. Therefore, we can summarize that MHT has the following advantages including the disinfection, deodorization of the waste, ease of sorting and recycling and effective utilization of resources especially for energy use.

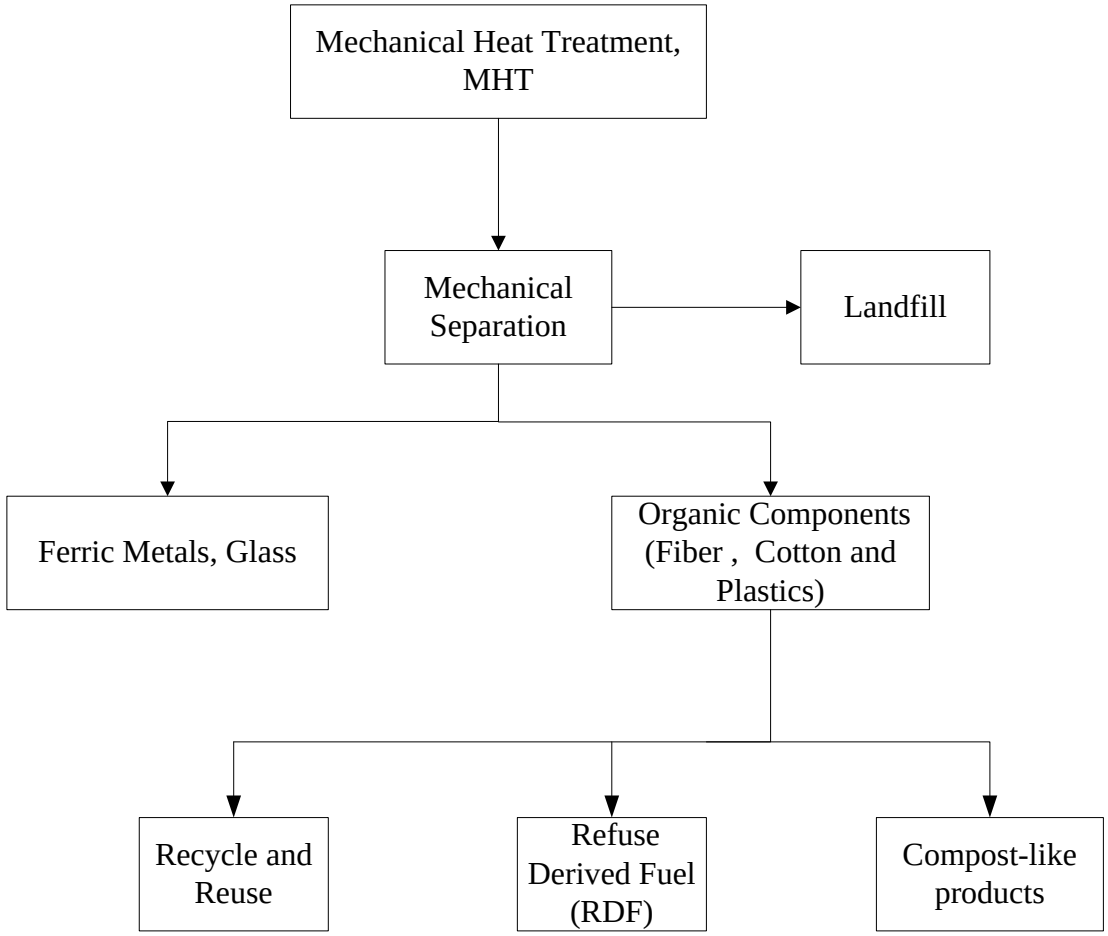

Fig. 7. The flow chart of Mechanical heat treatment (MHT) used for municipal solid waste (MSW).

Among these resources, the treated plastics can be easily separated, stored and transported, because the plastics are deformed and shrank into pellet shape with an increasing density after MHT. Further, the chemical characteristics, such as dry weight, combustible component and H_V, do not have significant changes for the said cooking conditions, which can be concluded that MHT is a good and interesting process to completely recycle the plastics as energy resource if compared to incineration treatment. The information obtained in this study is useful for the rational design and proper operation of MHT system for treating the used plastics in the MSW and separating it for the re-utilization as energy resource.

We can draw the following critical conclusions through the experimental results cited above.
(1) With the cooking technique, it can achieve a volume and size reduction of HDPE.
(2) The true density of HDPE reaches a high value of 0.983 g cm^{-3} with a 180 ^oC saturated steam condition.
(3) HDPE has a very high calorific value and exhibits no significant changes in dry weight, triple component composition and calorific value after MHT. It is very suitable to be used as RDF.
(4) As compared with the calorific value and combustible component of HDPE and unprocessed MSW, the energy utilization of MHT will be more efficient and effective than that of direct incineration treatment of MSW.

Acknowledgments

The authors are grateful for the financial supports provided by the National Science Council and the Environmental Protection Administration of Taiwan.

References

[1] R. Longcake, Waste Treatment Technologies, City of Bradford Metropolitan District Council, 2007, pp. 8.

[2] Y.S. Hung, Y.H. Chen, N.C. Shang, C.H. Chang, T.L. Lu, C.Y. Chang and J.L. Shie, Comparison of biodiesels produced from waste and virgin vegetable oils, Sustainable Environment Research 20, 2010, pp. 417-422.

[3] J.L. Shie, C.Y. Chang, C.C. Tzeng, P.Y. Hung, C.C. Chang, S.W. Chiang, J.Y. Tseng, W.K. Tu, M.H. Yuan, H.Y. Li and Y.J. Yu, Water-enhanced reforming of syngas to fuels and chemicals in a batch reactor, Journal of Environmental Engineering and Management 20, 2010, pp. 181-187.

[4] Taiwan Environmental Protection Administration (TEPA), Database of Taiwan's Environmental Statistics, http://210.69.101.110/WEBSTATIS/webindex.htm (accessed in Sep. 2009). (In Chinese)

[5] A. Papageorgiou, J.R. Barton, A. Karagiannidis, Assessment of the greenhouse effect impact of technologies used for energy recovery from municipal waste: a case for england, Journal of Environmental Management 90, 2009, pp. 2999-3012.

[6] A. Garg, R. Smith, D. Hill, N. Simms and S. Pollard, Wastes as co-fuels: the policy framework for solid recovered fuel (SRF) in Europe, with UK implications, Environmental Science & Technology 41, 2007, pp. 4868-4874.

[7] Q.B. Wang, H.J. Huang, B.H. Xie, W. Yang, M.B. Yang, Thermal degradation of HDPE in a batch pressure reactor: reaction time and mechanical stirring effect, Journal of Macromolecular Science, Part A 47, 2010, pp. 1123-1129.

[8] Wikipedia, Coal, http://en.wikipedia.org/wiki/Coal.

Integrated waste management as a mean to promote renewable energy

Ola Eriksson[1,2,*], Mattias Bisaillon[2], Mårten Haraldsson[2], Johan Sundberg[2]

[1] *University of Gävle, Gävle, Sweden*
[2] *Profu AB, Mölndal, Sweden*
** Corresponding author. Tel: +46 26 64 81 45, E-mail: ola.eriksson@hig.se*

Abstract: Management of municipal solid waste is an efficient method to both increase resource efficiency (material and energy recovery instead of landfill disposal) and to replace fossil fuels with renewable energy sources (waste is renewable in itself to a large extent as it contains paper, wood, food waste etc.). The paper presents the general outline and results from a comprehensive system study of future waste management. In the study a multifunctional waste management system integrated with local energy systems for district heating and electricity, wastewater treatment, agriculture and vehicle fuel production is investigated with respect to environmental impact and financial economy. Different waste technologies as well as management strategies have been tested. The treatment is facilitated through advanced sorting, efficient treatment facilities and upgrading of output products. Tools used are the ORWARE model for the waste management system and the MARTES model for the district heating system. The results for potential global warming are used as an indicator for renewable energy. In all future scenarios and for all management strategies net savings of CO_2 is accomplished. Compared to a future reference the financial costs will be higher or lower depending on management strategy.

Keywords: *LCA, Waste management, ORWARE, Martes, Costs*

1. Introduction

Management of municipal solid waste is an efficient method to both increase resource efficiency (material and energy recovery instead of landfill disposal) and to replace fossil fuels with renewable energy sources (waste is renewable in itself to a large extent as it contains paper, wood, food waste etc.).

In this paper the general outline and results from a comprehensive system study of future waste management in the Gothenburg region is presented. The purpose of the system study was to evaluate new waste treatment options for municipal and industrial waste from a system perspective. In the study a multifunctional waste management system integrated with local energy systems for district heating and electricity, wastewater treatment, agriculture and vehicle fuel production is investigated with respect to environmental impact and financial economy. Different waste technologies as well as management strategies have been tested. The treatment is facilitated through advanced sorting (source separation of recyclable materials and MRFs (Material Recovery Facility) for both bulky waste and source separated household waste), efficient treatment facilities (thermal and biological treatment) and upgrading of output products (biogas as vehicle fuel and pelletisation of digestion sludge for use as fuel or as fertiliser in fields or forestry). The future district heating system comprises waste CHP and waste heat (excess heat) as base load and bio-CHP, natural gas-CHP and heat pumps as intermediate load while oil is peak-load. Thermal and biological treatment of waste is included and several scenarios of future waste management have been developed comprising a number of parameters for the background system and different waste amount growth rates.

The project has been carried out as a part of the project Thermal and biological waste treatment in a systems perspective – WR21 [1]. The focus has been set to the waste and district heating system in Gothenburg. The project has been running for 2.5 years with an active group consisting of persons from Renova, Kretsloppskontoret, Göteborg Energi,

Gryaab and Profu. The work on development of models and of methods of handling strategic questions within the field has gone back and forth within the group.

2. Methodology

The method used is life cycle assessment (LCA) [2] and financial cost calculation facilitated by computer modelling with the ORWARE (Organic Waste Research) model [3] for the waste management system and the MARTES model [4] for the district heating system including CHPs (Combined Heat and Power). In this study waste streams suitable for thermal and/or biological treatment (including waste water treatment sludge) are included whereas fractions for material recycling are excluded.

ORWARE is a computer based tool for environmental and economic systems analysis of waste management. It was first developed for systems analysis of organic waste management, hence the acronym ORWARE (Organic Waste Research). The model is designed for strategic long-term planning of recycling and waste management and based upon static conditions and on linear programming (LP). The ORWARE model has been developed since the early 1990s in close cooperation between four different research institutions in Sweden (Royal Institute of Technology, Swedish Environmental Research Institute, Swedish Institute of Agricultural and Environmental Engineering and Swedish University for Agricultural Sciences). The waste management is followed from cradle (waste sources) via collection and transport to treatment plants and further to grave (utilisation of products from waste treatment). Treatment facilities included are incineration with energy recovery, composting, landfill, anaerobic digestion with biogas utilisation, spreading of organic fertiliser on arable land, sewage treatment, material recycling of plastic and paper packages, and some additional technologies. The model delivers substance flows, distributed to emissions to air and water, left in growing crops and in recycled material. Energy flows such as energy use and recovered energy is also provided. Single substances such as carbon dioxide or eutrophication substances to water can be tracked, as well as the amount of plant-available nutrients and emissions of different heavy metals. Emissions are also characterised and weighted using Life Cycle Impact Assessment. At the same time financial costs (investment and operational costs) and environmental costs and revenues including savings in the surrounding system can be calculated for the whole management chain.

MARTES is a model for district heating systems with production of heat, steam and electricity. The model simulates the use of different plants to satisfy the demand for district heating during a year. As a result the effects on costs and emissions are calculated, based on the energy conversion in the district heating system. The development of MARTES started on a mainframe computer at the Department of Energy Conversion in 1983. It has been commercially available on personal computer since 1990. Today it is the most widely used tool for strategic planning of district heating systems in Sweden, since it covers nearly 70 % of the produced heat [5]. The MARTES model captures operation of all facilities for district heating generation, given a exogenously given total need for heat. The heat demand is based on a load curve and described with a detailed time slice division into day and night periods. The model includes fuel and electricity prices and policy tools. The simulated plants are modelled with efficiencies (and with part load performance for CHP plants), minimum load for operation, availability, emissions of carbon dioxide, sulphur and nitrogen oxides. Annual fixed costs for equipment purchase and installation as well as variable and annual fixed costs for operation and maintenance are also included in the model. The output from the model is heat generation for all plants, power generation in CHPs, use of electricity in heat pumps and electrical boilers, fuel consumption and emissions to air.

As mentioned above the focus in the study has been the waste treatment and district heating system in Gothenburg. However, to generate a fully system analysis one also has to consider effects that occur in surrounding systems, such as the transport sector (biogas from waste substitutes petrol and diesel oil), the electricity production system (electric power from waste incineration with energy recovery replaces electricity generation from fossil fuels), the agricultural sector (nutrients from anaerobic digestion of waste and sludge are used instead of mineral fertiliser) etc. In this study; two different types of scenarios that reflects the situation of year 2030 has been set up: local scenarios and external scenarios [6]. In a local scenario we define the waste treatment processes that are assumed to be in operation in Gothenburg's waste treatment system in year 2030 (e.g. waste incineration, anaerobic treatment). Furthermore, an external scenario reflects the situation in the surrounding systems (e.g. price of electricity, fuels and CO_2-allowances). The local scenarios thereby describe developments that the actors in Gothenburg can influence, while the external scenarios describe developments that the actors have to adapt to. The main principles of the local scenarios that have been set up are as follows:

-Business-as-usual: This local scenario is characterized of a traditional development of the waste treatment system in Gothenburg, i.e. a significant share of waste incineration. The capacities in existing facilities are adapt to the amount of waste that are assumed to arise in year 2030. Today's central composting is still used for treatment of biological degradable waste from households. Sludge from the wastewater treatment plant is first treated in an anaerobic treatment facility, thereafter composted and finally sold as a soil product.

- Maximized return of nutrients: In this local scenario more of the arising waste is treated in biological treatment facilities, compared to "Business-as-usual". The capacity of the source separation system in Gothenburg is expanded and an anaerobic treatment facility is built that replaces the central composting. The capacity of the anaerobic treatment facility is set to 60 000 tonnes/year. The capacity of waste incineration is thereby decreased in comparison to the case in the local scenario "Business-as-usual". Sludge from the wastewater treatment plant is treated in an anaerobic treatment facility and thereafter used as fertilizer in the agricultural sector.

- Maximized electricity production: the source separation system is expanded and an anaerobic treatment facility is being built, similarly to the local scenario "Maximized return of nutrients". Furthermore a part of the combustible waste is going through a mechanical treatment process to create a refuse derived fuel. This fuel is used in a new waste incineration facility with a slightly higher electrical efficiency than the existing ones. Sludge from the wastewater treatment plant is treated in an anaerobic treatment facility. Thereafter the sludge is dehydrated and turned into pellets that are used as fuel in the new waste incineration facility.

Within the project a number of external scenarios capturing several parameters that describe the state in the economy, the energy system, the waste system (such as waste amounts etc.) etc. were discussed. Eventually three of these were selected for a more careful analysis.

- Reference: is a scenario that reflects a conservative development in the surrounding environment. The background system is changed but mainly the same impact and policy as of today prevails. The Reference scenario is not to be interpreted as the most likely scenario.

There is no valuation of which of the three external scenarios is the most likely one. All three projects constitute a "window of development" which is assessed as possible and realistic.

- Material lean growth: is a scenario that reflects a development where the society in general puts a lot effort in reducing environmental impact on a long term and evident environmental improvements are achieved compared to the system of today by policy measures and a change in values. The most important change in this study is that the trend of increasing waste amounts is broken and a decoupling effect (i.e. the waste amounts are no longer increasing at the same rate as economic growth) is present. This effect means that waste amounts follows the population trend in the region. This scenario also captures savings in energy use and more ambitious environmental targets which in turn affect the results of the system study. The magnitude of the economic growth is assumed to be on the same level as in the Reference scenario.

- Material intense growth: this scenario is characterized by an economic growth in society which exceeds the one in the other external scenarios, and a continuously increased consumption of material based products resulting in a higher growth rate for waste amounts than for the economy. This external scenario should not be looked upon as an opposite of material lean growth, also in this scenario there are assumptions on a development where the society is directed towards a decreased environmental impact.

A vast number of parameters have been studied and varied in the different external scenarios. A vital part that has been kept constant is however the tax system. Present levels of taxes on petrol, diesel, and natural gas to CHP etc. are used also in 2030. In reality these will probably change several times during the period to 2030. These changes are however very hard to predict, thus this conservative assumption.

3. Results

In table 1-2 aggregated results of the analysis for the three local scenarios is presented. Each local scenario has been evaluated from four different aspects: economy, climate, acidification and eutrophication of which the two latter is not presented here. The results are shown in scoreboards where the three scenarios have been given a gold, silver or bronze medal. The local scenario with the best result receives a gold medal while the worst result receives a bronze. The interval between these two results is then split into three. If the result for the local scenario not yet given a medal is placed in the upper third of the interval, the scenario receives a gold medal, a result in the middle interval return silver, while a result in the lover third gives a bronze medal. Each scoreboard is followed by a text that describes the results.

*Table 1. Scoreboard for the economic results from the systems study. The choices for development of the waste management system (the local scenarios) are compared to each other and scored by gold (**G**) silver (**S**) and bronze (**B**) bullets.*

Economy External scenario/ Internal scenario	Reference	Material lean growth	Material intensive growth
Business-as-usual	S	S	B
Maximized return of nutrients	G	G	G
Maximized electricity production	B	B	B

From the economic aspect, the local scenario "Maximized return of nutrients" present the best result irrespective of which external scenario that is being studied. Factors that contribute to

this result are revenues for biogas to the transport sector and avoided costs for expanding the waste incineration capacity. It's important to remember that we've been studying a situation around year 2030, which means that new investments in waste treatment capacity must come in place in order to meet a rise in waste amounts. This is another situation compared to today where existing treatment capacity is enough to meet the demand in the region.

The result is sensitive to some input data, where of one can mention the price of biogas, the investment costs for anaerobic treatment and waste incineration, the transport costs for wastewater sludge and sludge from anaerobic treatment to the agricultural sector and the costs for the source separation system.

*Table 2. Scoreboard for the results of emissions of climate gases from the systems study. The choices for development of the waste management system (the local scenarios) are compared to each other and scored by gold (**G**) silver (**S**) and bronze (**B**) bullets.*

Climate gases External scenario/ Internal scenario	Reference	Material lean growth	Material intensive growth
Business-as-usual	B	B	B
Maximized return of nutrients	S	G	G
Maximized electricity production	G	G	G

Table 2 shows that the local scenario "Maximized electricity production" receives the best results for emissions of climate gases. Also "Maximized return of nutrients" receives good results. The local scenario "Maximized return of nutrients" receives better results compared to "Business-as-usual" partly because this scenario includes production of biogas that keep out the use of fossil fuels in the transport sector. A second reason is that more electricity is generated within the system that keeps out electricity production outside the system with higher emissions of climate gases. The reason for the increased electricity production is that new waste treatment capacity partly consists of a facility for anaerobic digestion, which decreases the need for investments in waste incineration. With less waste incineration, more district heat will be produced from other combined heat and power plants within the district heating system. These units have a higher electrical efficiency compared to waste incineration, thus more electricity will be produced within the system. The local scenario "Maximized electricity production" receives even better results for emissions of climate gases. The reason for this is that in this scenario the electricity production from the system increases even further. This is partly because we in this scenario study the effects of investing in a waste incineration facility with higher electrical efficiency compared to existing. This is also because this scenario includes investments in a sludge dryer, heated by district heat. This causes an increase in the heat demand, thereby combined heat and power plants within the district heating system may run during a longer period of time.

The local scenarios "Maximized return of nutrients" and "Maximized electricity production" reduces the emissions of greenhouse gases by 4 -7 % (17 000 – 29 000 tonnes CO_2-eq./year) compared to "Business-as-usual". Another figure to relate to is the total emissions of CO_2 from Göteborg Energi, which in 2009 amounted to 545 000 tonnes CO_2 [7]. As seen before, the local scenario "Maximized return of nutrients" yield a decrease in the system cost, in other words the cost for reducing the emissions of greenhouse gases by choosing this path is negative. In contrast the system cost increases by the local scenario "Maximized electricity production", hence the cost for reducing greenhouse gases by the measures stapled in this

scenario can be calculated to between 80 and 550 SEK/tonne CO_2 (depending on which external scenario you choose to study).

4. Discussion and Conclusions

The following ten conclusions have been drawn from the project.

I. From an economic point of view, new waste treatment technologies have difficulties in the competition with the type of treatment options that already exists in Gothenburg today. The conclusion holds even when comparing new investments in new or existing technologies.

II. Having said so, we can consider that the only new technology found to be economically competitive to existing treatment options are anaerobic digestion of food waste. The conclusion holds for a situation when the treatment capacity has to increase in order to meet the demand in the region. This is not the situation of today, but it is most likely that the situation will arise in future because of increased demand for waste treatment or because the existing treatment facilities become too old.

III. Increasing the share of electricity generated from waste incineration is a clear advantage in order to realize a decrease of emissions of climate gases. This is partly because the fact that the electricity produced from the incinerator keep out other electricity production with higher emissions of climate gases. A second positive factor is that a higher share of electricity production results in a minor share of district heat production, which in turn results in increased production in other combined heat and power plants in the district heating system. Thereby even more electricity is being produced within the system, keeping out other electricity production with higher emissions of climate gases.

IV. Another good way to reduce climate gases is to produce biogas from waste and use it within the transport sector. The reason for this is partly that the biogas is used as a substitute for fossil fuels, but it is also because of the fact that the need for waste is decreased. As described above, this lead to increased use of other combined heat and power plants within the district heating system, resulting in more electricity produced from the system.

V. Results from the project show that today's composting of food waste and anaerobic digested sludge from wastewater treatment result in emissions of acidifying substances. A better option for treatment of food waste is anaerobic digestion followed by spreading of the digestate on agricultural land as fertilizer. The sludge should also be utilised as fertilizer, or alternatively used as fuel in waste incineration.

VI. In a comparison between source separation and central sorting of food waste, the latter turns out to be a better choice when regarding economic aspects. The main reason for this is that the capital costs related to central sorting are lower compared to the costs for a system with sources separation of the food waste. Regarding the environmental aspects, the two systems are almost equal. Uncertainties within the results primarily concern the performance of a central sorting system. Even though it's not evident, the assumption made is that the sorted fractions from the central sorting facility hold an equal quality with the one from a source separation system.

VII. When comparing waste incineration with gasification of waste the latter turns out to be in favour regarding emissions of climate gases. On the other hand, waste incineration is by far the best choice when regarding economy. The reason for the good result for gasification of

waste when comparing emissions of climate gases is first of all that the district heat output from the technique is much lower than the output from waste incineration. As described earlier, this results in increased electricity production within the district heating system, keeping out other electricity production with higher emissions of climate gases. Secondly, gasification of waste by itself has a higher output of electricity compared to waste incineration.

VIII. In the analysis we've blocked the possibility of importing waste to the system in study. This restriction has been evaluated in a sensitive analysis, which shows that import of waste for treatment in waste incineration within the system give positive effects on the emissions of climate gases. The main reason for this is that the import of waste results in a decrease of the amount of waste going to landfills outside the system. Since landfilling of organic waste result in high emissions of climate gases it is highly desired to decrease this activity.

IX. Composting of food waste and anaerobic digested sludge from wastewater treatment also result in emissions of substances that leads to eutrophication. However, spreading digested sludge and digestate from anaerobic digestion of food waste on agricultural land will also lead till eutrophication. From this perspective, it is better to use the digestate as fuel in waste incineration.

X. In a sensitive analysis regarding handling of anaerobic digested sludge the result shows that the best treatment method from an economic point of view is to spread the sludge on agricultural land. As discussed above (in conclusion IX), when considering eutrophication it is better to use the sludge as fuel in waste incineration. The different treatment options studied for sludge gives equal results when concerning acidification and emissions of climate gases.

In general we can conclude that the results are almost equal irrespective of which external scenario we choose to study. This means that the results hold even though changes occur in the surrounding systems. The external scenarios differ significantly and create varied prerequisites for the waste treatment system; nevertheless the results show that the same treatment methods should be chosen.

Having said so, we also have to be aware of the uncertainties that exist in the analysis. For example we've not studied how the economic results would react from a change in competitiveness for the waste treatment facilities. It is also important to notice that this, first of all, is a scientific project which points out interesting future waste treatment technologies. This means that the result should not be seen as a comprehensive material for an investment decision. Furthermore, the analysis is based on today's tax system, which of course is a simplified description of the situation of year 2030. It should also be noticed that it's difficult to find valuated data for new techniques. The data can both be overestimated, caused by to ambitious thoughts regarding the technique, and underestimated as further developments of the technique can result in decreased costs and increased performance.

Regarding the results for the aspect of climate change the assumptions for the development of the electricity production system plays a significant role. If the electricity production in northern Europe will transform into a system with less emissions of carbon dioxide the worth of electricity production in Gothenburg will decrease, and vice versa. Furthermore the results for acidification and eutrophication are difficult to interpret as these environmental problems are regional and not global. Therefore the question of where the emissions are made becomes

essential. This fact has not been taken into consideration in the main results, however an alternative analysis has been made that describes this factor in more detail.

We will emphasise that many but not all aspects have been analysed for the waste treatment and district heating system. For example we have not included toxic effects or the consumer perspective. Furthermore, we have not included effects from the fact that some natural resources used within the system may be limited on a global scale; this is for example the case for phosphor and biofuels.

Finally we conclude that the three external scenarios that have been created within the project reflect three very different outcomes of the situation in 2030. Most significant we see large differences in the amount of waste that arise and needs treatment. The increase of waste differ from + 24% up to + 80%, compared to the situation of today. This results in large differences in the costs and environmental effects for the waste treatment system. A conclusion from this is that minimization of the increase of waste is essential for a more sustainable development of the society. However, in this project the focus was set on different waste treatment options and regardless of the amount of waste the choice of waste treatment method is solid.

References

[1] M. Bisaillon, J. Sundberg, M. Haraldsson, O. Eriksson, Systemstudie Avfall i Göteborg (A systems study of the waste management system in Gothenburg) (In Swedish with English summary), project report WR 21, WASTE REFINERY, SP Sveriges Tekniska Forskningsinstitut, 2010, ISSN 1654-4706

[2] ISO 14040 International Standard, Environmental management – Life cycle assessment - Principles and framework, International Organisation for Standardization, 2006, Geneva, Switzerland

[3] O. Eriksson, B. Frostell, A. Björklund, G. Assefa, J. -O. Sundqvist, J. Granath, M. Carlsson, A. Baky, L. Thyselius, ORWARE - A simulation tool for waste management, Resources, Conservation & Recycling 36/4, 2002, pp. 287-307.

[4] A. Josefsson, J. Johnsson, C-O. Wene, Community-based regional energy/environmental planning, in: The International Workshop on Operations Research and Environmental Management 1993, Universitè de Genève and Fondazione Eni Enrico Mattei Milan, Geneva, Switzerland. Milan: Fondazione Eni Enrico Mattei, 1994. Nr. 78.94

[5] M. Olofsson Linking the Analysis of Waste Management Systems and Energy Systems, Thesis for the degree of Licentiate of Engineering, 2001, Department of Energy Conversion, Chalmers University of Technology, Göteborg, Sweden

[6] O.Eriksson, M. Olofsson, T. Ekvall, How model-based systems analysis can be improved for waste management planning,Waste Management and Research 2003:21, pp.488-500.

[7] Göteborg Energi, Annual report – part 1, 2010

Determination of the Operating Regimes of CHP Turbines with Stage-wise Heating of District Heating System Water

Zvonimir Guzović[1,*], Perica Jukić[2], Dražen Lončar[1]

[1] *University of Zagreb, Faculty of Mechanical Engineering and Naval Architecture , Zagreb, Croatia*
[2] *HEP-Proizvodnja d.o.o., Member of HEP Group, Thermal Power Plants, Zagreb, Croatia*
** Corresponding author. Tel: +385 16168532, Fax: +385 16156940, E-mail: zvonimir.guzovic@fsb.hr*

Abstract: Today, the district heating (DH) is often based on cogeneration power plants with steam turbines for combined heat and power production (CHP turbines and plants). As the heat is supplied as steam with the given parameters, so CHP steam turbines are realized with controlled steam extractions. In case of stage-wise heating of the district heating system water the entire heating is realized in a number of successively connected water heaters by steam extracted from the turbine. The aim of stage-wise heating is additional production of electricity, because the heating steam extracted for the first stage in the direction of system water flow has lower pressure than for the second stage. In this paper the results of determination of heat-supply operating regime with two-stage heating of the system water for CHP turbine of 120 M W power (T-100-110/130-3) installed in Cogeneration Power Plants Zagreb (TE-TO Zagreb), obtained by means of original developed computer program, will be presented both in analytic form (by equations) and by means of diagrams.

Keywords: *Cogeneration, CHP turbine and power plants, Operating regimes, District heating (DH), Stage-wise heating*

Nomenclature

c	*specific heat*……	$J \cdot kg^{-1} \cdot K^{-1}$	
$\dot{E}_1$	*specific production of electricity by heat-supply flow rate at one-stage heating*……	$MW_e \cdot MW_{to}^{-1}$	
h_{zvv1}	*enthalpy of condensate of the upper heating extraction*.....	$kJ \cdot kg^{-1}$	
h_{zvv1}	*enthalpy of condensate of the lower heating extraction*.....	$kJ \cdot kg^{-1}$	
q	*flow rate*.....	$kg \cdot s^{-1}$	
$\eta_{g.m}$	*electrical and mechanical efficiency*	-	
ϑ	*temperature*……	^0C	

Subscripts

m	*measured data obtained on the actual turbine during operation*
prog	*calculation results obtained by the program or equation*
v.z.	*ambient air*
w	*system water*

1. Introduction

District heating is a system for distributing heat generated in a centralized location for residential, public and industrial heating requirements such as space heating and water heating in a large area. The heat is obtained from a cogeneration power plant burning fossil fuels (but now increasingly from renewable energy sources such as biomass, as well as nuclear power). District Heating (DH) based on cogeneration power plants with simultaneous production of heat and electricity (also called Combined Heat and Power – CHP) provides high system efficiency, low emissions and higher degree of fuel flexibility than single-purpose energy systems (e.g. localized boilers).

The number of DH systems associated with CHP plants has been increasing in the last decade due to their energy savings (up to 30%), environmental improvements and reduction of life cycle costs [1]. New CHP plants have a power-to-heat ratio of about 1.0 compared with 0.4-0.5 for traditional condensing steam turbines. However, only 13% of electricity generated in EU today is based on CHP; however, it is regarded by the European Commission as a

possible way to improve energy efficiency and reduce the environmental impact. DH plays a minor role in the overall European energy system today, but it is significant in Denmark, Finland and Sweden [2].

Therefore, this paper pays special attention to DH based on CHP turbines (plants). The advantages of stage-wise heating of the district heating system water over one-stage will be presented. With the aim of studying further the possibilities of energy efficiency increase, first of all, by improvement of an operating regime in specific conditions of simultaneous production of power and heat, an original computational program for determination of the operating regime diagrams for different types of CHP turbines has been developed [3]. The program is based on operating regime diagrams (i.e. of energy characteristics), manufacturers' data, results of normative measurements and data obtained during exploitation. The results of calculation by means of the developed program will be presented for CHP turbine of 120 MW power installed in the Cogeneration Plant Zagreb (TE-TO Zagreb) for the heat-supply regime with two-stage heating of district heating system water.

2. Characteristics of CHP turbines and CHP plants

CHP steam turbines are characterized by a diversity of probable operating regimes which can be divided into two groups depending on the heating load: condensing regimes and heat-supply regimes. In a condensing regime, the steam flow rate to controlled extraction is equal to zero. This regime is identical to the operation of a condensing turbine. Heat-supply regimes are characterized by a certain heating load carried by the turbine. A heat-supply regime may be carried out by either heating or electric schedule depending on the nature of the heating load. In operation by heating schedule, the electric power is determined by the heating load and cannot be changed without changing accordingly the heat consumption. Under such conditions, a certain (minimal) quantity of steam is however passed through the low-pressure part of the turbine in order to absorb the heat of friction of the rotating elements. In operation by an electric schedule it is typical that turbine carries a certain heating load which limits the possibility of reducing the electric power blow to a certain minimum, but it is possible to increase the electric power up to the maximum by passing more steam to the condenser.

Thermodynamic characteristics, design, techno-economic indicators and other characteristics of CHP turbines and plants are described in more detail in [3-9].

The heating load is characterized by significant changes during the year and its value changes depending on the temperature of the ambient air. The maximum output of heat is at the minimal calculation temperature of ambient air which is determined on the basis of climatic conditions. During the summer period there will be only the heating load for the heating of hot water, which accounts for on the average two thirds of the mean value in winter [3-4].

The heating load and parameters of the district heating system water are connected by the equation

$$Q_{to}^{TE} = q_w c_w (\vartheta_{pol} - \vartheta_{pov}) \qquad (1)$$

where Q_{to}^{TE} is the heating load of the cogeneration power plant, ϑ_{pol} and ϑ_{pov} are the starting and the returned temperature of the system water.

The change in the starting and returned temperature of the system water in dependence on the ambient air temperature is called a t emperature diagram. Fig. 1 shows the temperature diagram constructed for the climate conditions in the city of Zagreb [3].

The steam of heat-supply turbine extractions is used for covering the heating load. Uniformity of load of turbine heat-supply extraction can be achieved if the extraction is used only for covering the base part of the diagram, and its peak is covered e.g. by peak hot-water boilers, Fig. 1 [3].

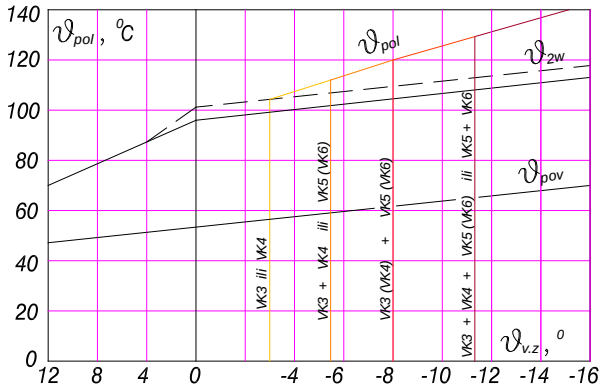

Fig. 1. Temperature diagram of the district heating system: VK3, 4, 5, 6 - peak hot-water boilers; -- -- -- -- - using the heat of steam leaving the condenser [3]

The ratio of heat load of the turbine heat-supply extractions and the total heating load of the cogeneration plant at minimal calculation temperature of ambient air is called the coefficient of heating α_{TE} [3-4]. With $\alpha_{TE} < 1$ part of the heating load is covered for example, by peak hot-water boilers, and in a thermal power plant with cogeneration also separate production of heat appears.

The temperature diagram of the district heating system and accepted coefficient of heating determine the starting temperature of the system water after regenerative heaters ϑ_{2w} which are fed with steam from the turbine heat-supply extractions. At the minimal temperature of the ambient air, the value is determined from the equation

$$\vartheta_{2w} = \vartheta_{pov} + (\vartheta_{pol} - \vartheta_{pov})\alpha_{TE} \tag{2}$$

For any given ambient air temperature is

$$\vartheta_{2w} = \vartheta_{pov} + \frac{Q_{to}^{TE}}{q_w c_w} \tag{3}$$

For the heat-supply period, when the peak boiler is switched off and the entire heat load is covered by turbine heat-supply extraction

$$\vartheta_{2w} = \vartheta_{pol} \tag{4}$$

In case of turbines with controlled extractions of steam, efficiency increase can be achieved by using heat of the steam leaving the condenser [3-6].

3. Stage-wise heating of district heating system water

In case of stage-wise heating of district heating system water (Fig. 2) the whole heating is realised in a number of successively connected water heaters by steam extracted from the turbine. The required pressure of the extracted steam is determined by the temperature of water at the exit from each heating stage. The steam, extracted for the first stage in the direction of the system water flow, has lower pressure than for the second stage, which ensures additional production of electricity in comparison with one-stage heating, when the whole steam is extracted at a pressure which is determined by the final heating temperature of the system water. Therefore, the aim of stage-wise heating is additional production of electricity by means of the heating steam [3-4].

Effectiveness of stage-wise heating of the system water is determined by a large number of factors, including the primary ones: the number of heating stages and the distribution of the heating load between stages; heating load values, flow rate and temperatures of system water and their change during the year; dimensions, design and temperature diagram of district heating system, climatic conditions and coefficient of heating, parameters of fresh steam, design of turbine and auxiliary plant, etc. [3-6].

Fig. 2 presents the stage-wise heating of the system water (two-stage) which corresponds to the type scheme of the modern CHP turbines with the following characteristics:

- System water heaters are supplied by steam from extractions of one turbine.
- There are no governing valves on the steam pipelines of extractions.
- The flow rate of the system water through all heating stages is equal.
- Condensate from single heaters of stage-wise heating by pumps is carried into the line of regenerative heating of feed water.

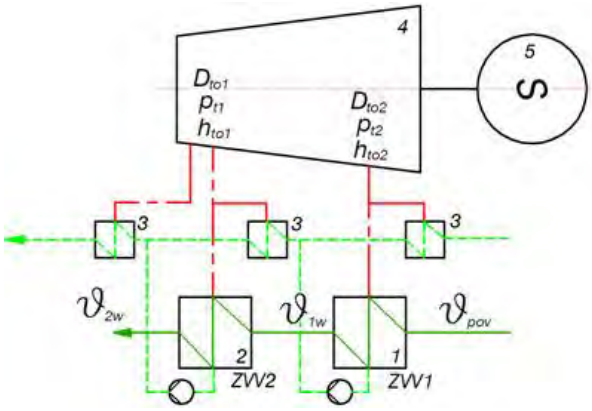

Fig. 2. Principal diagram of a CHP turbine with two heating steam extractions: 1- the lower heating extraction; 2- the upper heating extraction; 3- regenerative heaters; 4- turbine, 5- generator; D_{to1}, p_{t1}, h_{to1} - flow rate, pressure and enthalpy of the upper heating extraction; D_{to2}, p_{t2}, h_{to2} - flow rate, pressure and enthalpy of the lower heating extraction; $\vartheta_{pov}, \vartheta_{1w}, \vartheta_{2w}$ - temperatures of the returned system water, and after the lower and upper heating extractions

At transition from one-stage on two-stage heating of district heating system water, with unchanged heating load, the additional production of electricity ΔP is

$$\Delta P = D_{to2}\left[(h_{to1} - h_{to2})\eta_{g.m} + \dot{E}_1(h_{zvv2} - h_{zvv1})\right] \qquad (5)$$

and the additional specific production of electricity $\Delta\dot{E}_2$ by means of the heating steam

$$\Delta\dot{E}_2 = \frac{D_{to2}}{Q_{to}^{TE}}\left[(h_{to1} - h_{to2})\eta_{g.m} + \dot{E}_1(h_{zvv2} - h_{zvv1})\right] \qquad (6)$$

At a two-stage heating of district heating system water by scheme shown in Fig. 2 the optimum increase of water enthalpy is equal in both stages of heating [3-4].

4. Heat-supply operating regime of T-100-110/130-3 CHP turbine: two-stage heating of district heating system water

For T-100-110/130-3 CHP turbine on t he basis of theoretical principles, the design data obtained from the manufacturer of the UTMZ-Russia turbine, the data of normative and remaining measurements performed in the Cogeneration Plant Zagreb and on the basis of data obtained during exploitation, the uniform operating regime diagram has been designed in the graphical form in which all turbine working regimes are presented [3]. After that, the obtained operating regime diagram in graphical form is completely translated into the analytic form, i.e. described by analytic dependences in the form of energy characteristics. The energy characteristics are built into the algorithm of original computer program, by means of which it is possible to calculate all the operating regimes of T-100-110/130-3 CHP turbine [3]. These are the condensing operating regime and the heat-supply regimes with one-stage, two-stage and three-stage heating of district heating system water.

As in this paper the object of investigation is stage-wise heating of district heating system water, only the results for the heat-supply operating regimes with two-stage heating will be presented: both in analytic form (by equations) and by means of diagrams [3]. The heat-supply regime with two-stage heating is used when the need for heat is minimally 120 MW, and when the daily temperature is below 5^0C. The functional dependences are obtained on the basis of results from the region of CHP turbine heat-supply operating regimes with two-stage heating [3].

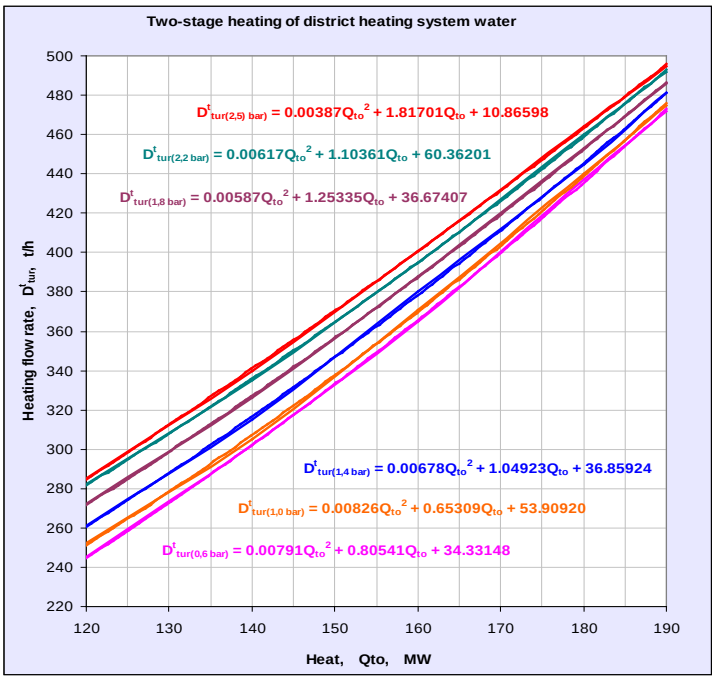

Fig. 3. Heat-supply operating regime of the T-100-110/130-3 CHP turbine - dependence of heat-supply flow rate on heat and on the pressure in the upper heating extraction at two-stage heating of system water [3]

The dependence of heat-supply flow rate $D^t_{tur_{dvo}}$ on heat Q^{dvo}_{to} and on the pressure in the upper heating extraction at two-stage heating (index *dvo* in the following equations) of system water is presented in Fig. 3, and can be described by the following equation

$$D^t_{tur_{dvo}} = a^{dvo}_D (Q^{dvo}_{to})^2 + b^{dvo}_D Q^{dvo}_{to} + c^{dvo}_D \quad (7)$$

The dependences of increasing parameters of the heat-supply flow rate $a^{dvo}_D, b^{dvo}_D, c^{dvo}_D$ on the pressure in the upper heating extraction p_{t1} at two-stage heating of the system water can be described by the following equations [3]

$$a^{dvo}_D = -0.004119\, p^5_{t1} + 0.025966\, p^4_{t1} - 0.05743\, p^3_{t1} + 0.051103\, p^2_{t1} - -0.015333\, p_{t1} + 0.008073 \quad (7.a)$$

$$b^{dvo}_D = 1.259133\, p^5_{t1} - 7.872131\, p^4_{t1} + +17.222733\, p^3_{t1} - 15.060567\, p^2_{t1} + 4.186251\, p_{t1} + 0.917671 \quad (7.b)$$

$$c^{dvo}_D = -92.54839\, p^5_{t1} + 572.1809\, p^4_{t1} - 1237.44892\, p^3_{t1} + 1072.77346\, p^2_{t1} - 273.77944\, p_{t1} + 12.73158 \quad (7.c)$$

The dependence of electricity produced by heat-supply flow $P^t_{e_{dvo}}$ on the heat Q^{dvo}_{to} and on the pressure in the upper heating extraction at two-stage heating of the system water is presented in Fig. 4, and can be described by the following equation

$$P^t_{e_{dvo}} = a^{dvo}_P (Q^{dvo}_{to})^2 + b^{dvo}_P Q^{dvo}_{to} + c^{dvo}_P \quad (8)$$

The dependences of increasing parameters of the electricity produced by heat-supply flow rate $a^{dvo}_P, b^{dvo}_P, c^{dvo}_P$ on the pressure in the upper heating extraction p_{t1} at two-stage heating of the system water can be described by the following equations for the pressure range 0.6-1.4 bar [3]

$$a^{dvo}_P = 0.000428\, p^2_{t1} - 0.001145\, p_{t1} + 0.001499 \quad (8.a)$$

$$b^{dvo}_P = 0.100437\, p^2_{t1} + 0.212762\, p_{t1} + 0.386902 \quad (8.b)$$

$$c^{dvo}_P = 4.4641\, p^2_{t1} - 8.9851\, p_{t1} - 7.5197 \quad (8.c)$$

and for the pressure range 1.4-2.5 bar by the following equations [3]

$$a^{dvo}_P = 0.01746\, p^5_{t1} - 0.172862\, p^4_{t1} + 0.673167\, p^3_{t1} - 1.287444\, p^2_{t1} + 1.208139\, p_{t1} - 0.444287 \quad (8.d)$$

$$b^{dvo}_P = -6.03471\, p^5_{t1} + 59.848\, p^4_{t1} - 233.57253\, p^3_{t1} + 448.01589\, p^2_{t1} - 422.14618\, p_{t1} + 156.85117 \quad (8.e)$$

$$c^{dvo}_P = 402.1153\, p^5_{t1} - 4006.05631\, p^4_{t1} + 15686.88113\, p^3_{t1} - 30157.54742\, p^2_{t1} + 28457.0162\, p_{t1} - 10560.43274 \quad (8.f)$$

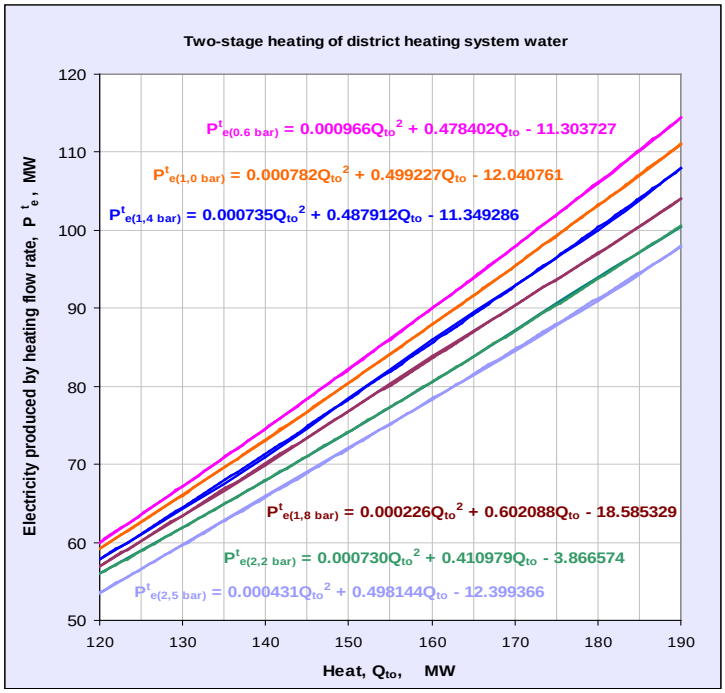

Fig. 4. Heat-supply operating regime of the T-100-110/130-3 CHP turbine - dependence of electricity produced by heat-supply flow on heat and on the pressure in the upper heating extraction at two-stage heating of system water [3]

5. The equations reliability

Equations given in the paper are checked by comparing the results of the calculation obtained by the program using the measured data obtained on the actual turbine during operation for the same ambient air temperatures. The results of comparisons for the regime with two-stage heating of the returned system water are given in Table 1.

Table 1. Comparison of the calculation results obtained by the program with the measured data obtained on the actual turbine during operation for the same ambient air temperatures for the regime with two-stage heating of the district heating system water [3]

Ambient air temperature,	Program			Measured data obtained during operation			Electricity deviation
$\vartheta_{v.z.}$	$(P_e)_{prog}$	$(D^t_{tur\,dvo})_{prog}$	$(D^t_{kon_{dvo}})_{prog}$	$(D_{tur})_m$	$(p_{t1})_m$	$(P_e)_m$	ΔP_e
4^0C	84 MW	278 t/h	62 t/h	340 t/h	1.0 bar	82 MW	+2.4%
2^0C	92 MW	317 t/h	83 t/h	400 t/h	1.4 bar	91 MW	+1.1%
0^0C	94 MW	352 t/h	68 t/h	420 t/h	1.6 bar	93 MW	+1.1%
-2^0C	96 MW	387 t/h	53 t/h	440 t/h	1.8 bar	95 MW	+1.0%
-4^0C	98 MW	423 t/h	37 t/h	460 t/h	2.0 bar	97 MW	+1.0%
-6^0C	101 MW	458 t/h	32 t/h	490 t/h	2.2 bar	99 MW	+2.0%
-8^0C	100 MW	461 t/h	29 t/h	490 t/h	2.4 bar	98 MW	+2.0%
-10^0C	99 MW	472 t/h	18 t/h	490 t/h	2.4 bar	97 MW	+2.0%
-12^0C	99 MW	472 t/h	18 t/h	490 t/h	2.4 bar	97 MW	+2.0%
-14^0C	99 MW	472 t/h	18 t/h	490 t/h	2.4 bar	97 MW	+2.0%

Since in case of heat-supply operation regime on the turbine it is not possible to measure only the electricity obtained on the basis of heat-supply steam extractions but rather the total electricity, in this case the electricity obtained on the basis of the total steam flow through a turbine is compared with total electricity that is given by the program. As can be seen from

Table 1, the results obtained by using the program provide a good match with the measurement data obtained on the actual turbine: the deviation is in the range of +1.0% to +2.4%. It can also be seen that the sum of computed steam flow of heat extraction and computed steam flow to the condenser fully agree with the measured steam flow at the entry into the turbine. Therefore, it can be concluded that the results of the calculations provided by the program are reliable, including therefore also the equations based on these results.

Single equations are valid only for a specific turbine, but by taking into consideration single specific characteristics similar equations can be obtained for different CHP turbines.

6. Conclusion

The paper presents some results of the original computational program by means of which it is possible to calculate all the operating regimes of T-100-110/130-3 CHP turbine. The energy characteristics, which are obtained by translating the previously designed uniform operating regime diagram from graphical to analytic form, are built in the algorithm of the program. The computational program is successfully used in the Cogeneration Plant Zagreb (TE-TO Zagreb) for the prediction of the relevant parameters of single operating regimes with the aim of work optimization of the CHP turbine. Simultaneously it makes possible to investigate the different operating regimes with the aim of improving their economy (e.g. the introduction of stage-wise heating of system water of district heating). The algorithm is also applicable for other types of CHP turbines, and by taking into consideration single specific characteristics, a program for calculating the operating regimes of the concrete turbine is obtained (condensing turbines with one or two controlled steam extractions; turbines with back-pressure, including the turbines with back-pressure and controlled steam extraction). The comparison of the results of the calculations provided by the program with the measured data obtained on the actual turbine during operation indicates that the equations presented in the paper are reliable, i.e. their accuracy is acceptable for the engineering application.

References

[1] S. Ghafghaziet et al., A multicriteria approach to evaluate district heating system options, Applied Energy 87, 2010, pp. 1134-1140.

[2] A. Joelsson and L. Gustavsson, District heating and energy efficiency in detached houses of different size and construction, Applied Energy 86, 2009, pp. 126-134.

[3] P. Jukić, Improvement of operating regimes of CHP turbine, M.Sc. Thesis, Faculty of Mechanical Engineering and Naval Architecture, University of Zagreb, 2005, Zagreb, [in Croatian].

[4] E.I. Benenson and L.S. Ioffe, CHP steam turbines, Energiya, 1986, Moscow [in Russian].

[5] A. Kostyuk and V. Frolov, Steam and gas turbines, Mir Publishers, 1988, Moscow.

[6] A.D. Truhniy, Stationary steam turbines. Energoatomizdat, 1990, Moscow [in Russian].

[7] H. Bloch and M. Singh, Steam turbines: design, application and re-rating, McGraw-Hill Professional, 2008, New York.

[8] J.H. Horlock, Combined power plants: including combined cycle gas turbine (Ccgt) plants, Krieger Publishing Company, 2001, New York.

[9] I.S. Ertesvag, Exergetic comparison of efficiency indicators for combined heat and power (CHP), Energy 32, 2007, pp. 2038-2050.

Potential for low-temperature energy usage at power plant's cold end in order to increase energy efficiency

Vladimir I. Mijakovski[1,*], Nikola Mijakovski[2]

[1] *University "St. Kliment Ohridski", Faculty of Technical Sciences, Bitola, Macedonia*
[2] *xSoft engineering, Skopje, Macedonia*
** Corresponding author. Tel: +389 47 207748, Fax: +389 47 203370, E-mail: vladimir.mijakovski@uklo.edu.mk*

Abstract: Thermal power plant (TPP) 'Bitola' is the largest electricity producer in the Republic of Macedonia with installed capacity of 3x225 MW. It is a lignite fired power plant, in operation since 1982. Most of the installed equipment is of Russian (former Soviet) origin. Power plant's cold end consists of a condenser, pump station and cooling tower. The power plant was built without considerations regarding energy efficiency and usage of waste heat energy.
A possibility to increase energy efficiency through low-temperature heat usage from the power plant's cold end is shown in this work. The system includes connection of heat pump to the power plant's cold end for heating of greenhouse (orangery) complex located close to power plant's cooling towers. An analysis presenting economic feasibility of the concept for two different refrigerants used in the heat pump is also presented.
Comparison between separate production of heat energy in a boiler - house and combined – merged system consisting of three heat pumps working in parallel proves the applicability of the heat pumps concept in terms of increased energy efficiency and pay-back period of investment.

Keywords: *Power plant, Heat pump, Energy efficiency*

1. Introduction

Orangery or greenhouse is a building with microclimate quite different from the external, meaning its internal temperature is substantially different from the external air temperature. Part of the solar energy is absorbed by plants and soil, part is transformed to heat energy, hence heating up the internal air. That is the reason, depending on local climate conditions, heat radiation covers 30 to 60 % of the total heat energy needs of the orangery.

Greenhouse complexes built so far in Macedonia are supplied with heat mainly by boilers using heavy oil as a fuel. At the moment, price of oil on the world market has negative impact on the price of end product. Price of the fuel, for some products, contributes to as much as 70% in the total price of the product, [1]. That does not mean that the rate of growth of orangeries should decrease. It is necessary to substitute the oil with fuel available in the country, especially in the Bitola region.

2. Low temperature heat energy from the cooling towers

One of the possible ways to raise the efficiency of orangery production is by using part of the low temperature waste heat from cooling towers of lignite fired power plant "Bitola".
A complex (combined) system is proposed, comprised of low temperature system (heat pumps) and system with boilers.

One, two or more (up to 10) parallel systems can be located next to the cooling tower of TPP "Bitola". Each system should consist of 21 module, each with 1,5 ha of greenhouses with dimensions: length 21x35 = 735 m and width of 428,6 m. Total area covered by one system is 21x15 000 = 315 000 m^2 or 31,5 ha.

Techno economic analysis presented in the article refers to one orangery complex comprised of 21 module with an area of 1,5 ha in each module. Creation of other parallel systems results in equal economic results.

According to [2], the required installed heat energy for heating of the complex, (for 1,5 ha, required heat energy is 3 457 kW), for total area of 31,5 ha are:

$$Q_{OC} = A_{OC} \cdot q_{OC} = 31{,}5 \cdot 2\,305 = 72\,600 \text{ kW} \quad (1)$$

Two systems, with three heat pumps in each system, should be installed in combination with boiler house for back-up heating of the medium (running on hot water 75/35 °C).
Cooling tower of one of the blocks of thermal power plant "Bitola" works with following design parameters of cooling water:

- volume flow of water through cooling tower q_w = 30 000 m^3/h;
- temperature of hot water entering cooling tower t_{w1} = 33 °C;
- temperature of cold water exiting cooling tower t_{w2} = 25 °C.

Low temperature system of heat pumps is supplied with water from the cooling tower's basin, e.g. Fig. 1. Basin has a volume of 10 100 m^3, [3]. Water with temperature of 33 °C enters in parallel in every evaporator of the heat pumps where it is cooled down to a temperature of 25 °C and through a common pipeline brought back into cooling tower's basin.

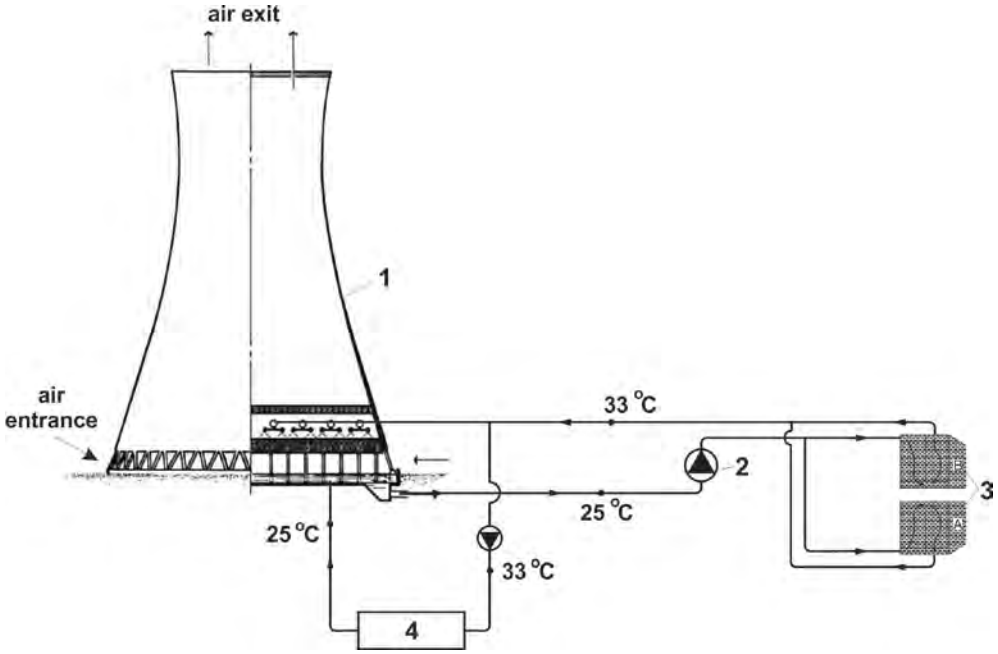

Fig. 1. Heat pumps connected to Thermal Power Plant's cold-end; 1 – cooling tower; 2 – circulation pump station; 3 – condenser; 4 – heat pumps

Mass flow of water from the cooling tower to the heat pumps is 3x359 = 1 077 kg/s, or 12,9% of designed flow of water in the system cooling tower – condenser.

In evaporator of every heat pump, the quantity of heat transferred from the water to the refrigerant is:

$$Q_1 = \dot{m}_{w1} \cdot c_p \cdot \left(t_{w1} - t_{w2}\right) = 359 \cdot 4{,}186 \cdot (33\text{-}25) = 12\,022{,}192 \text{ kW}$$

Total transferred heat for one system (made of 3 heat pumps):

$$Q_{total} = 3 \cdot Q_1 = 3 \cdot 12\,022{,}192 = 36\,066{,}576 \text{ kW} \quad (2)$$

Evaporators of all three heat pumps are connected in parallel (in respect to circulating water from cooling towers), while corresponding condenser units are connected in series (in respect to orangery's' heating medium 75/35 °C), e.g. Fig. 2.

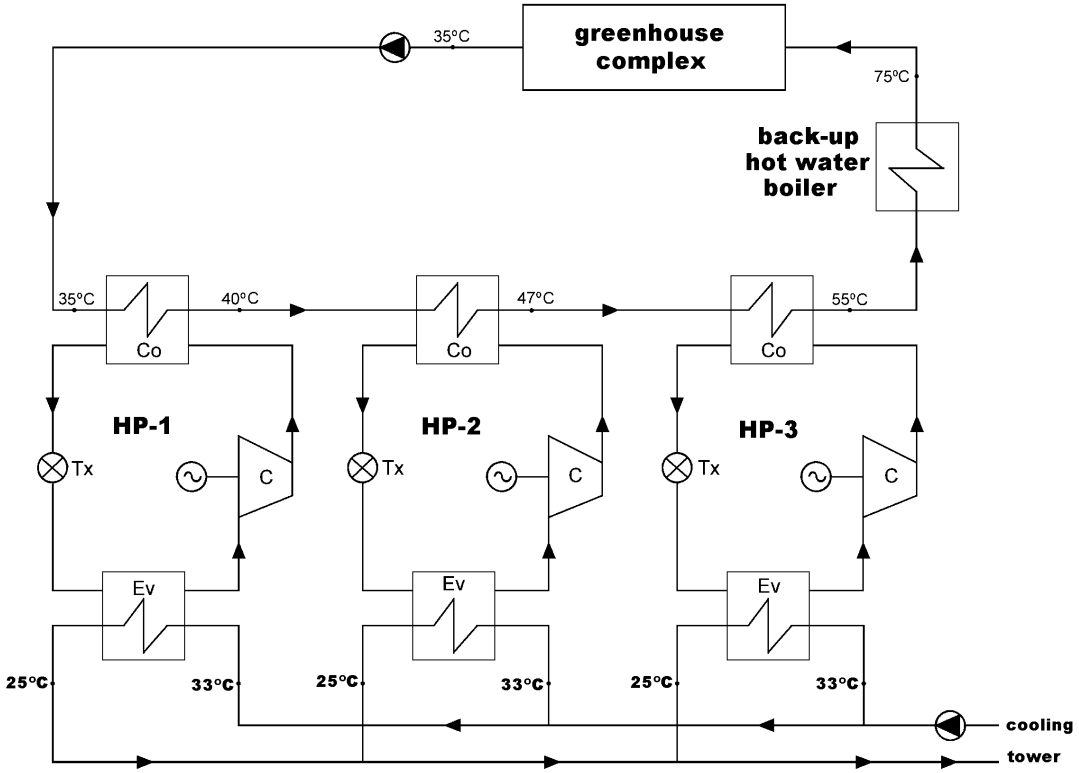

Fig. 2. Combined heating system: heat pumps and back-up boiler house

Although calculations for two refrigerants (HFC-134a and R410A) and two different condensation temperatures (3 K and 5 K) were performed, due to limited space for the article only an example of calculation for one medium and one condensation temperature will be presented completely. Results from other calculations, a review of the operating characteristics of heat pumps for different working fluids, [4], [5] and [6], and condensation temperature of $\Delta t_c = 3$ K, is given on Table 1.

Parameters from techno-economic analysis are shown hereafter, [7].

Total annual consumption of fuel for separate production of heat energy (boilers running on lignite with efficiency 90%) is:

$$Q_{tot,yr} = 132{,}5 \text{ GWh/year} \;;\; B_{yr} = 69\,920{,}844 \text{ tons of lignite/year} \quad (3)$$

where $Q_{tot,yr}$ is the total demand for heat energy per year and B_{yr} is the total annual consumption of fuel if separated system is used.

Table 1. Review of operating characteristics of heat pumps for different cooling fluids

Refrigerant	HP No.	Δt_c , K	l_i , kJ/kg	q_c , kJ/kg	m_f , kg/s	N_e , kW	COP_{avg}
HFC-134a	1	5	21,91	168,27	53,93	1 312,84	6,220
HFC-134a	2	5	29,82	164,68	77,15	2 501,76	4,565
HFC-134a	3	5	31,39	154,05	94,25	3 287,23	3,975
HFC-134a	1	3	22,36	171,82	52,82	1 341,63	6,088
HFC-134a	2	3	27,44	166,10	76,49	2 332,10	4,903
HFC-134a	3	3	35,49	161,45	89,93	3 546,24	3,685
R410A	1	5	24,01	178,63	50,80	1 355,23	6,026
R410A	2	5	32,46	184,08	69,02	2 489,31	4,593
R410A	3	5	47,06	168,08	86,38	4 516,70	3,900
R410A	1	3	27,41	185,93	48,81	1 486,53	5,494
R410A	2	3	28,64	173,06	73,41	2 336,10	4,895
R410A	3	3	36,56	162,78	89,20	3 623,50	3,606

Combined system (comparison for heat pumps with HFC-134a and R-410A and Δt_c = 5 K):

HFC-134a ; Δt_c = 5 K R-410A ; Δt_c = 5 K

$Q_{BH,yr}$ =33,13 GWh/year

$Q_{TOT,HP}$ = 99,37 GWh/year

$B_{TOT,yr}$ = 17 482,85 t /year

COP_{avg} = 4,92 COP_{avg} = 4,84

E_{COMP} = 20,197 GWh/year E_{COMP} = 20,531 GWh/year

$B_{COMP,yr}$ = 12 150,17 t/year $B_{COMP,yr}$=12 351,10 t/year

B = 29 633,02 t/year B = 29 833,95 t/year

ΔB = 40 287,82 t/year ΔB = 40 086,89 t/year

where $Q_{BH,yr}$ is the total annual production of heat energy of the boiler house, $Q_{TOT,yr}$ is the total annual production of heat from heat pumps, $B_{TOT,yr}$ is the total annual consumption of fuel of the boilers, COP_{avg} is the average value of the coefficient of performance for a heat pump system, E_{COMP} is the total annual energy consumed by heat pump's compressors, $B_{COMP,yr}$ is the total annual consumption of lignite for heat pump's compressors, B is the total consumption of fuel of a combined system and ΔB is the annual savings of fuel if a combined system instead of separated system is used.

3. Economic efficiency

Values for specific investment costs, maintenance costs and average price of coal for year 2006, [8] and [9]:

- Lignite price 0,0556 EUR/kg
- Heat pump investment 142 907,5 EUR/1 MW
- Hot water boiler house investment 43 125 EUR/1 MW

3.1. Investment costs

A. For separate production of heat in a boiler-house:

$$72{,}6 \cdot 43\,125 = 3{,}130875 \cdot 10^6 \text{ EUR}$$

B. Combined system

- heat pumps: $36{,}3 \cdot 142\,907{,}5 = 5{,}187542 \cdot 10^6$ EUR

- hot water boiler house: $36{,}3 \cdot 43\ 125 = 1{,}565437 \cdot 10^6$ EUR

3.2. Exploatation costs

3.2.1. Cooling fluid HFC-134a and Δt_c = 5 ℃

- Fuel
  - A. $69\ 920\ 844 \cdot 0{,}0556 = 3{,}8876 \cdot 10^6$ EUR/year
  - B. $(17\ 482\ 850 + 12\ 150\ 174) \cdot 0{,}0556 = 1{,}647596 \cdot 10^6$ EUR/year
- Maintenance costs
  - A. $0{,}06 \cdot 3{,}8876 \cdot 10^6 = 0{,}233256 \cdot 10^6$ EUR/year
  - B. $0{,}06 \cdot 1{,}6476 \cdot 10^6 = 0{,}100476 \cdot 10^6$ EUR/year

3.3. Total annual costs

3.3.1. Cooling fluid HFC-134a and Δt_c = 5 ℃

A. Total annual costs for purely boiler system are equal regardless of the cooling medium used,

$$\Sigma T_A = \left(\frac{3{,}130875 \cdot 10^6}{8} + 3{,}8876 + 0{,}233276\right) \cdot 10^6 = 4{,}512216 \cdot 10^6 \text{ EUR/year}$$

B. Investment costs $\frac{(5{,}187542 + 1{,}674596) \cdot 10^6}{8} = 0,\ 8577673 \cdot 10^6$ EUR/year

- Fuel $(17\ 482\ 850 + 12\ 150\ 174) \cdot 0{,}0556 = 1{,}674596 \cdot 10^6$ EUR/year
- Maintenance costs $0{,}06 \cdot 1{,}674596 \cdot 10^6 = 0{,}100476 \cdot 10^6$ EUR/year

Total annual costs for the combined system are:

$$\Sigma T_{B,com} = (0{,}8577673 + 1{,}674596 + 0{,}100476) \cdot 10^6 = 2{,}632839 \cdot 10^6 \text{ EUR/year}$$

Energy unit (specific) price:

$$C_A = \frac{4{,}512216 \cdot 10^6}{132{,}5 \cdot 10^3} = 34{,}055 \text{ EUR/MWh}$$

$$C_B = \frac{2{,}632839 \cdot 10^6}{132{,}5 \cdot 10^3} = 19{,}87 \text{ EUR/MWh}$$

The rest or ‘the savings' are:

$$\Sigma T_A - \Sigma T_{B,com} = (4{,}512216 - 2{,}632839) \cdot 10^6 = 1{,}879377 \cdot 10^6 \text{ EUR/year}$$

Investment payback period:

$$\tau = \frac{(5{,}187542 + 1{,}565437) \cdot 10^6}{1{,}879377 \cdot 10^6} = \frac{6{,}752979 \cdot 10^6}{1{,}879377 \cdot 10^6} = 3{,}59 \text{ years}$$

4. Conclusion

For the defined optimal orangerie's complex comprised of 21 modules, each having 1,5 ha or 31,5 ha in total, and needed heat energy of 72,6 MW for heating up the complex, two systems are proposed:
A. Separate system, comprised of boilerhouse for production of hot water which meets the total requirements for heating of the complex (72,6 MW, system 75/35 °C), and
B. Combined (merged) system, comprised of low-temperature system with heat pumps (capacity of the pumps 36,3 MW) that will cover around 75% of the total annual heat energy requirements, and boilerhouse with capacity of 36,3 MW that will cover the remaining 25% of the annual heat energy needs. Calculations are done for two cooling fluids, HFC-134a and R410A and at two condensation temperatures (Δt_c = 3 K and Δt_c = 5 K).

Fuel used in the boilerhouse is lignite from the "Suvodol" basin (fuel used by the TPP) with lower calorific value of H_d = 7 580 kJ/kg.

Techno economic analysis is performed under equal energetic efficiencies of both systems. Total annual costs for both systems are compared and results are shown on Table 2:

Table 2. Comparison table for total annual costs for both systems

System type	Energy unit price (EUR/MWh)	Total annual costs (EUR/year) (in millions)	Savings (EUR/year) (in millions)	Investment return period (in years)
System A	34,055	4 512 216	/	/
System B HFC-134a;Δt_c=5K	19,87	2 632 839	1 879 377	3,59
System B HFC-134a;Δt_c=3K	19,90	2 636 624	1 875 592	3,60
System B R410A ; Δt_c=5K	20,33	2 693 458	1 818 758	3,70
System B R410A ; Δt_c=3K	20,88	2 766 522	1 745 694	3,84

From the analysis presented in the article, one can conclude that the combined (merged) system, that is the system that uses HFC-134a as a cooling fluid and Δt_c = 5 K is the most applicable in the turns of savings and investment payback period.

Despite all the benefits of such a system, only basic structure for one greenhouse module was built near one of the cooling towers of above mentioned power plant. Unfortunately, neither pipelines nor other elements of the proposed system were ever built or installed.

References

[1] Mijakovski V., Thermo technical effects from application of thermal basis elements in the Republic of Macedonia, MSc. Thesis, Faculty of Mechanical Engineering, Skopje, 2001 (in Macedonian).

[2] Šarevski V., Optimization of low temperature energy systems for orangery's' heating, PhD. thesis, Faculty of Mechanical Engineering - Skopje, Macedonia, 1993 (in Macedonian).

[3] Pecakov S., Petreski T., Hristov T., Local instructions for exploitation of circulational pump stations and technical water systems at TPP – Bitola, Public enterprise "Macedonian power plants", Skopje, Macedonia, 1999 (in Macedonian).

[4] Ciconkov R., Refrigeration-Solved Examples, Faculty of Mechanical Engineering-Skopje, 2000.

[5] Thermodynamic properties of DuPont Suva 410A (R-410A) refrigerant, DuPont Fluorochemicals, USA, 2004.

[6] Thermodynamic properties of HFC-134a, DuPont Fluorochemicals, USA, 2004.

[7] Mijakovski V., Possibility for utilization of waste heat energy from the cold end of a power plant, Proceedings from the 11th meeting of Society of Thermal Engineers of Macedonia, 2008, pp.62-71 (in Macedonian).

[8] Vattenfall Annual Report 2006, Vattenfall AB, Stockholm, Sweden.

[9] Energy security and climate policy, assesing interactions, International Energy Agency, 2007.

An Evaluation of Internal Combustion Engines as the Prime Movers in CHP Systems

Mehdi Aghaei Meybodi and Masud Behnia*

School of Aerospace, Mechanical and Mechatronic Engineering, The University of Sydney, NSW 2006, Australia
** Corresponding author. Tel: +61 2 9036 9518, E-mail: m.behnia@usyd.edu.au*

Abstract: Optimum selection of prime movers in combined heat and power (CHP) systems is of crucial importance due to the fact that inappropriate choices reduce the benefits of CHP systems considerably. In the selection procedure the performance characteristics of prime movers as well as economic parameters should be considered. The aim of this paper is to present a thermo-economic approach to selecting the optimum nominal power and planning the operational strategy of internal combustion engines in a medium scale combined heat and power system is presented using the Net Annual Cost (NAC) criterion. Three modes of operation have been considered, namely one-way connection (OWC) mode, two-way connection (TWC) mode, and heat demand following (HDF) mode. The proposed method has been used for a case study. It has been observed that the optimum nominal powers in the case of using gas engines are 3.3 MW, 3.2 MW, and 1.2 MW and in the case of using diesel engines are 3.4 MW, 3.4 MW, and 1.4 MW for TWC, OWC, and HDF modes respectively. The proposed method may be also used for other types of prime movers as well as various sizes of combined heat and power systems.

Keywords: *Combined Heat and Power System, Internal Combustion Engines.*

Nomenclature

ACT	*annual carbon tax* ..... *$/year*	*LT*	*lifetime* ..... *year*
C	*cost* ..... *$/kWh*	*MC*	*maintenance cost per hour* ..... *$/hr*
CC	*capital cost* ..... *$*	*N*	*number of time intervals*
COF	*cost of fuel per hour* ..... *$/hr*	*NAC*	*Net Annual Cost* ..... *$/year*
$\dot{H}$	*heat rate* ..... *kW*	*P*	*electric power* ..... *kW*
HRB	*heat recovery boiler*	*SV*	*salvage value* ..... *$*
i	*interest rate* ..... *%*	τ_m	*time interval of demand profile* ..... *h*
k	*number of equipment*		

Subscripts

b *buying electricity*
el *electricity*
f *fuel*
h *heat*
r *required*
s *selling electricity*

1. Introduction

Combined heat and power (CHP) systems are considered to be one of the most important ways to consume the fossil fuels efficiently. These systems emit less pollution compared to the separate production of the same amount of electricity and heat. This paper presents a thermo-economic method for optimum sizing of internal combustion engines to serve as the prime movers of medium scale (500 kW-5,000 kW) combined heat and power systems. Three modes of operation: one-way connection (OWC) mode, two-way connection (TWC) mode, and heat demand following (HDF) mode are examined. In all three modes, buying electricity from the grid is possible while selling electricity to the grid is allowable in TWC and HDF modes. The objective of HDF mode is to minimize the waste of energy; therefore the engines

work in a condition at which the excess generated heat is minimal. A backup boiler can be installed to supply heat in all three modes.

2. Methodology

The applied method is one of the standard engineering economy approaches which is called annual cash flow (ACF) analysis. In ACF method, all costs and benefits are converted to equivalent uniform annual cost (EUAC) and equivalent uniform annual benefit (EUAB). To compare the various options, the difference of EUAC and EUAB (EUAC-EUAB) is calculated and the one which results in the minimum value is the most economical choice [1]. Based on the annual cash flow method, the proposed objective function (Net Annual Cost (NAC) $/year) is defined as:

$$\text{NAC}=\left[\sum_{j=1}^{k}(CC_j - SV_j(\frac{1}{(1+i)^{LT}}))\right](\frac{i(1+i)^{LT}}{(1+i)^{LT}-1})+\text{ACT}+\sum_{m=1}^{N}[\sum_{j=1}^{k}(MC_j + COF_j) + P_b \times C_{el,b} - P_{CHP,r} \times C_{el} - \dot{H}_{CHP,r} \times C_h - P_{CHP,s} \times C_{el,s}]_m \times \tau_m \quad (1)$$

2.1. Selection and planning of operational strategy

To determine the optimum nominal power and the operational strategy of internal combustion engines as prime movers of CHP systems based on the specific electricity and heat demand profile, the following procedure is adopted:

- For nominal powers from 500 kW to 5,000 kW and for each time interval of demand profile (τ_m) with changing of partial load from 20% to 100%.
- Calculating NAC for a given partial load (this is represented by NAC_m).
- Comparing the calculated NAC_m values and choosing and saving the minimum value ($\text{NAC}_{m,\,min}$) and its associated partial load.
- Calculating NAC by adding up the $\text{NAC}_{m,\,min}$ values for all time intervals.
- Choosing the nominal power which results in the minimum NAC as the prime mover's nominal power of the CHP system.
- For the selected nominal power and for each time interval the partial load at which the $\text{NAC}_{m,\,min}$ is obtained is the operational strategy of CHP system.

3. Results

To illustrate the Net Annual Cost method, we have chosen a case study. It is noted that adoption of the specific operational mode directly depends on the method of connection to the grid which determines the possibility of selling electricity. Fig. 1 shows the electricity and heat demand profile for the case study based on operational data of a local educational institute [2].

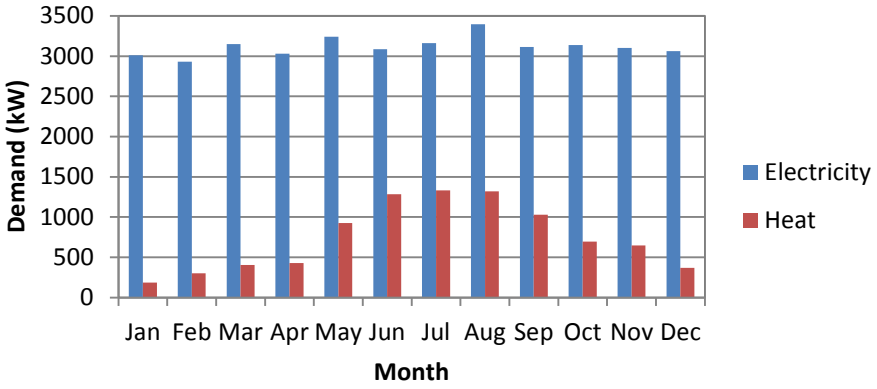

Fig 1. Demand profile for the case study

Table 1 lists the costs of natural gas, diesel fuel, and electricity as well as the value of generated electricity and heat [3-5]. A nominal Carbon tax of $30 per emitted tonne of CO_2 equivalent is assumed [6].

Table 1. Price list

Items	Price ($/kWh)
Buying electricity ($C_{el,b}$)	0.18
Natural gas	0.045
Diesel fuel	0.117
Selling electricity ($C_{el,s}$)	0.15
Generated electricity (C_{el})	0.18
Generated heat (gas engine) (C_h)	0.05
Generated heat (diesel engine) (C_h)	0.138

Figs. 2-4 illustrate the variation of Net Annual Cost versus nominal power of gas engine in three modes of operation. In TWC mode a 3.3 MW gas engine, in OWC mode a 3.2 MW gas engine, and in HDF mode a 1.2 MW gas engine have resulted in the minimum NAC values.

Fig. 2 Variation of Net Annual Cost versus gas engine nominal power in TWC mode

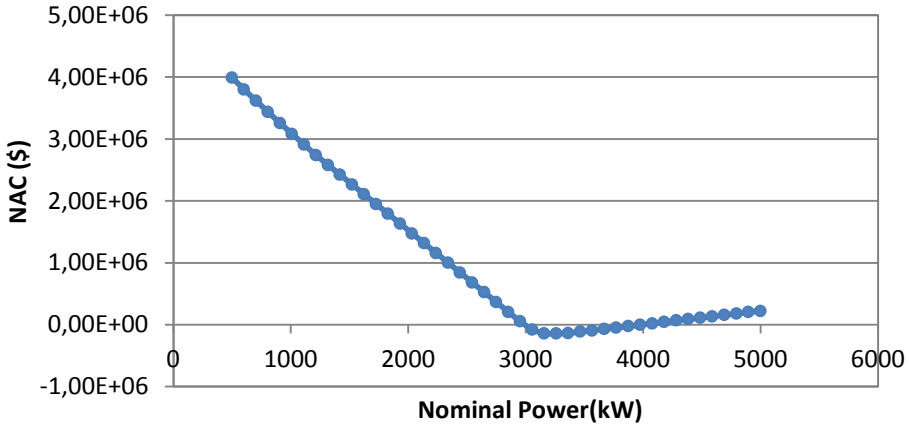

Fig. 3 Variation of Net Annual Cost versus gas engine nominal power in OWC mode

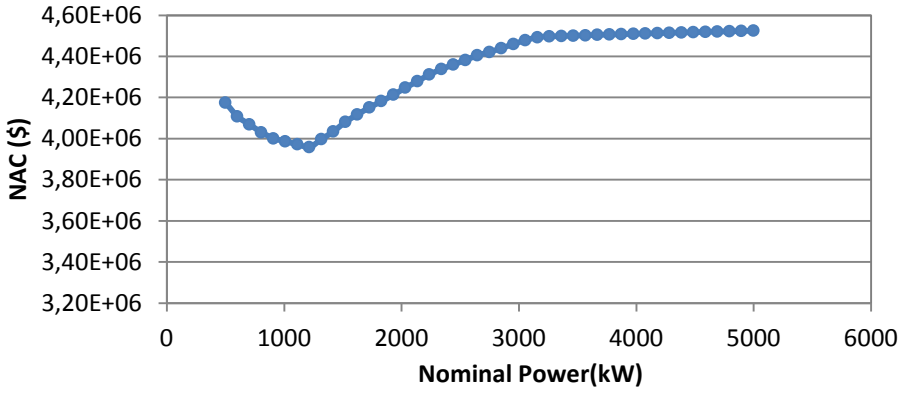

Fig. 4 Variation of Net Annual Cost versus gas engine nominal power in HDF mode

The variation of NAC with nominal power of diesel engine for three modes of operation is shown in Figs. 5-7. The optimum nominal powers in TWC, OWC, and HDF modes are 3.4 MW, 3.4 MW, and 1.4 MW, respectively.

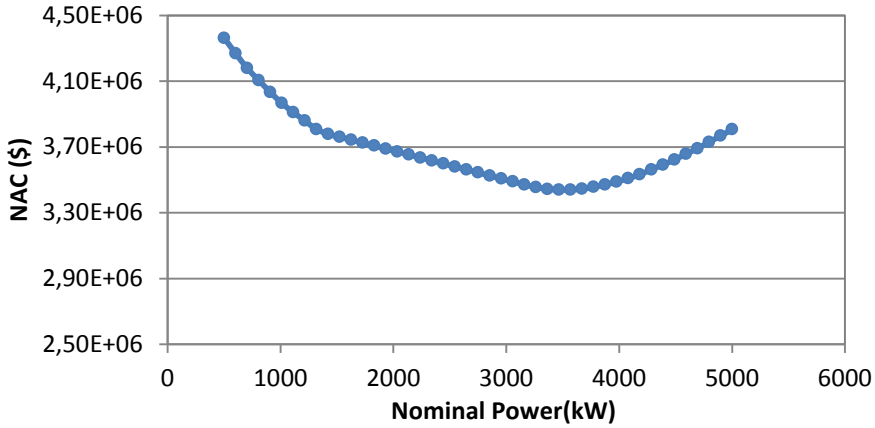

Fig. 5 Variation of Net Annual Cost versus diesel engine nominal power in TWC mode

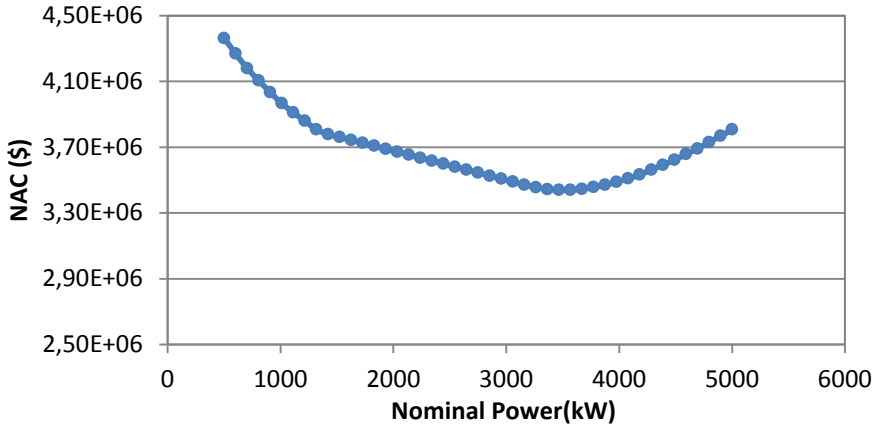

Fig. 6 Variation of Net Annual Cost versus diesel engine nominal power in OWC mode

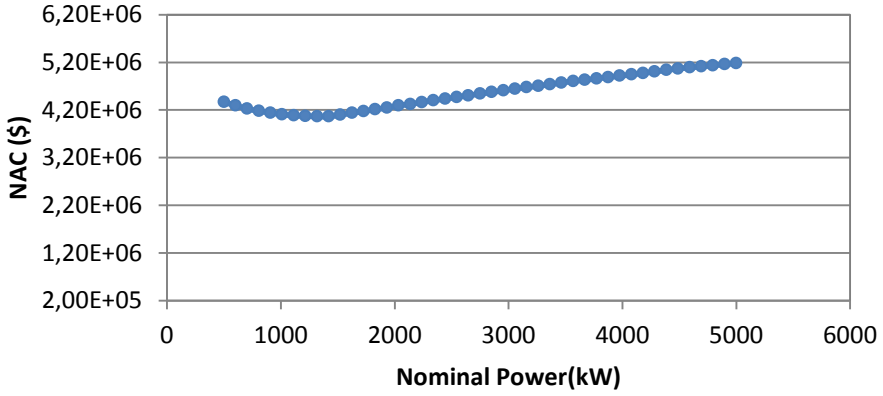

Fig. 7 Variation of Net Annual Cost versus diesel engine nominal power in HDF mode

The operational strategy of selected gas engines and diesel engines in the three modes of operation is shown in Figs. 8-13.

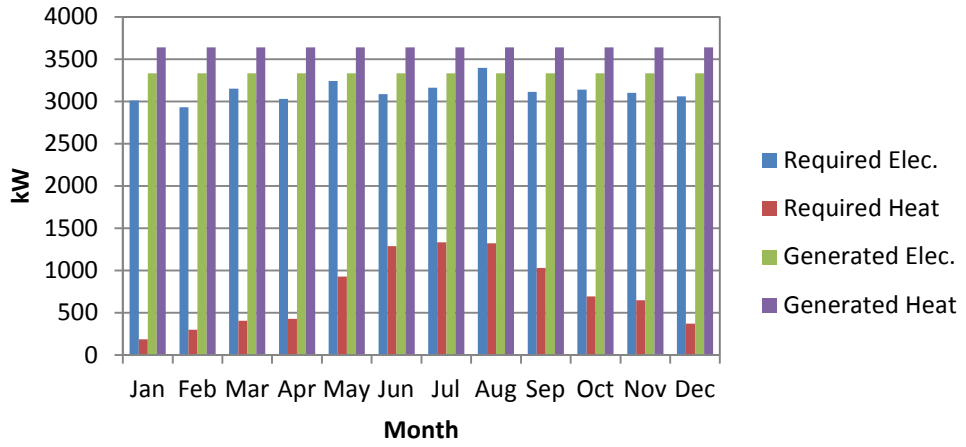

Fig. 8 The operational strategy of selected gas engine in TWC mode of operation

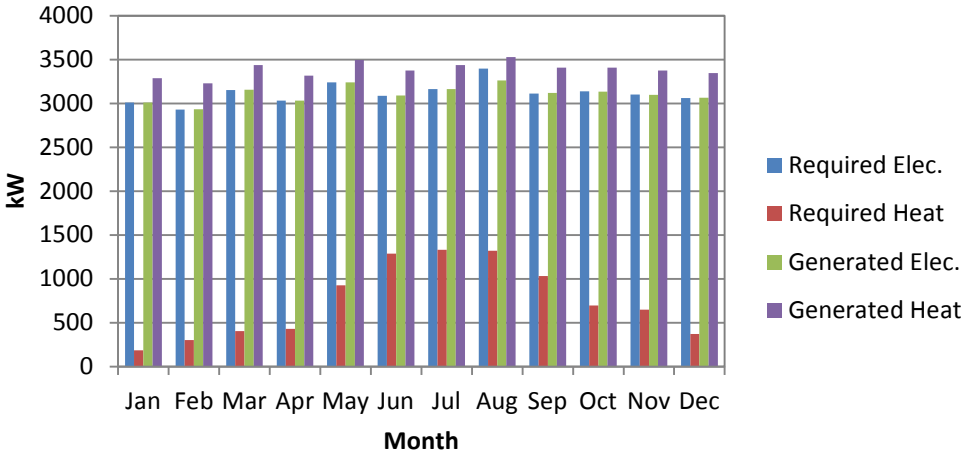

Fig. 9 The operational strategy of selected gas engine in OWC mode of operation

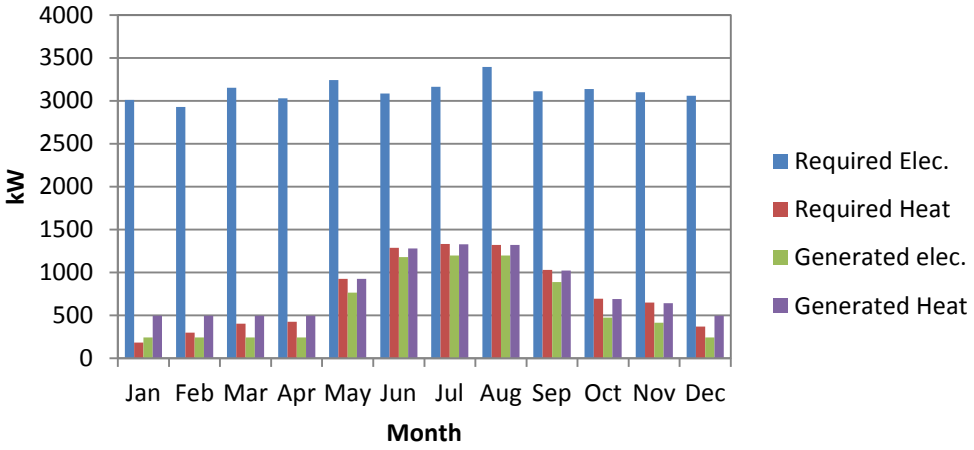

Fig. 10 The operational strategy of selected gas engine in HDF mode of operation

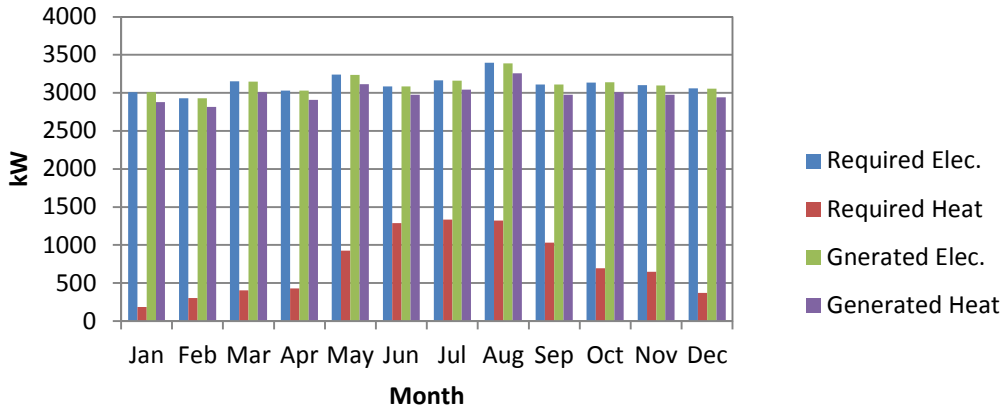

Fig. 11 The operational strategy of selected diesel engine in TWC mode of operation

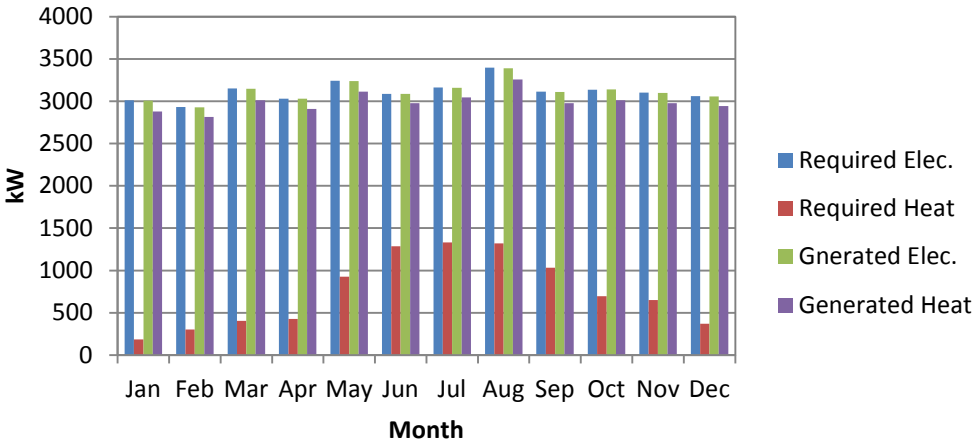

Fig. 12 The operational strategy of selected diesel engine in OWC mode of operation

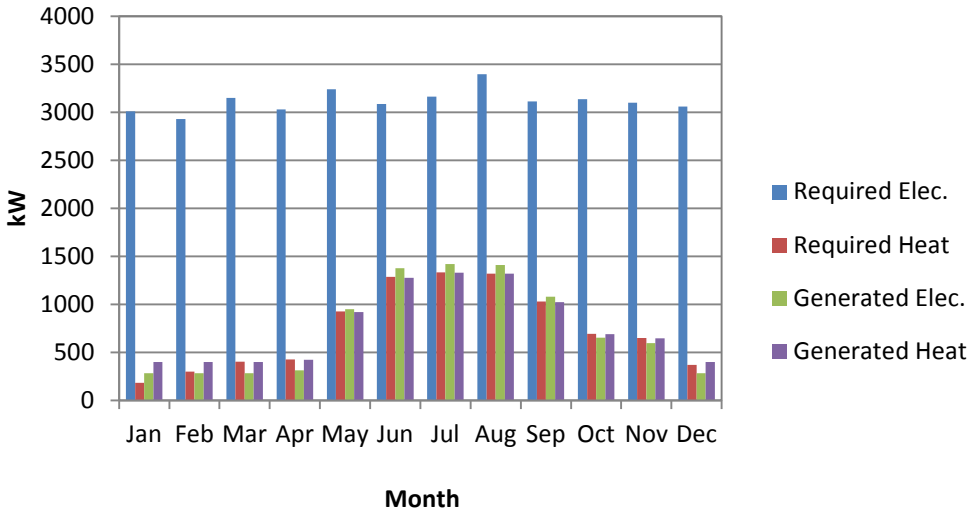

Fig. 13 The operational strategy of selected diesel engine in HDF mode of operation

4. Discussion

The figures for the operational strategy of selected gas engines show that in TWC mode, in which selling the excess electricity is allowed, the prime mover works at full load condition during the year. In OWC mode, the prime mover follows the electricity demand profile and produces as much electricity as required. In HDF mode, a large amount of electricity should be bought due to the fact that to produce as much less heat as possible the prime mover works in low load conditions.

It is noted that because of high price of diesel fuel, in TWC mode of operation the diesel engine follows the electricity demand profile and there is no excess electricity to be sold. Therefore, the values of NAC and consequently the operational strategy results are the same for TWC and OWC modes. Similar to gas engine, the prime mover works in low load condition in HDF mode.

5. Concluding remarks

In this paper, a thermo-economic method for the optimum sizing and planning the operational strategy of internal combustion engines in a medium scale combined heat and power system is presented introducing the Net Annual Cost (NAC) criterion. The methodology has been adopted for an operational case study and the proposed method can be used for all types of prime movers as well as various sizes of the system.

References

[1] D. G. Newnan, T. G. Eschenbach, J. P. Lavelle, Engineering Economic Analysis, Oxford University Press, 9th Edition, 2004.

[2] www.uow.edu.au/about/environment/energy/ planning

[3] www.integral.com.au

[4] www.originenergy.com.au

[5] www.aip.com.au

[6] J. Humphreys, Exploring a Carbon Tax for Australia, The Centre for Independent Studies, 2007, Available from: http://www.cis.org.au.

Air gasification of palm empty fruit bunch in a fluidized bed gasifier using various bed materials

Pooya Lahijani[1], Ghasem D. Najafpour[2,*], Zainal Alimuddin Zainal[1], Maedeh Mohammadi[2]

[1] *School of Mechanical Engineering, Engineering Campus, Universiti Sains Malaysia, 14300 Nibong Tebal, Penang, Malaysia*
[2] *Faculty of Chemical Engineering, Noushirvani University of technology, 47147 Babol, Iran*
[*] *Corresponding author: Fax: +98 111 321 0975, E-mail address: Najafpour@nit.ac.ir*

Abstract: Use of lignocellulosic biomass as an alternative, renewable and sustainable source of energy has fulfilled part of the growing demand for energy in developed countries. Amongst various technologies applied to convert biomass wastes to biofuel and bioenergy, biomass gasification has attracted considerable attention. In this work, gasification of palm empty fruit bunch as a potential lignocellulosic waste was investigated in a pilot scale air-blown fluidized bed. Silica sand and dolomite were used as bed material. The bed temperature was varied in the range of 650 to 1050 ^{o}C. The quality of the producer gas (H_2, CO, CO_2 and CH_4) and gasification performance was assessed in terms of heating value, carbon conversion efficiency, dry gas yield and cold gas efficiency. It was concluded that high temperatures improved the quality of producer gas; maximum heating value of 5.3 and 5.5 MJ/Nm^3 were achieved using silica sand and dolomite. Maximum dry gas yield of 1.84 and 1.79 (Nm^{3}gas/kg biomass), carbon conversion of 91 and 85% and cold gas efficiency of 69 and 65% were obtained for silica sand and dolomite, respectively. Although the quality of the produced gas was considerably improved at high temperatures, however formation of the bed agglomerates was the major concern at temperatures above 800 and 850 ^{o}C for silica sand and sawdust.

Keywords: *Biomass gasification, Fluidized bed, Gas producer, Palm empty fruit bunch*

1. Introduction

In recent years, rapid development of modern industry has greatly increased the demand for energy. Today, fossil fuels are the most common energy sources in the world. Most countries which use such conventional fuels are facing major air pollution problems as it has been estimated that the world's oil reserves will get depleted by 2050 [1]. Besides, significant amount of pollutants including CO_2, NO_x and SO_x are emitted from fossil fuels into the atmosphere. Meanwhile, the cost of fossil fuel is globally increasing [1, 2]. Considering theses issues, boosts the importance of finding and exploring alternative, renewable and sustainable energy resources.

Lignocellulosic biomass is one of the potential renewable energy resources which is receiving great worldwide attentions. Malaysia as the largest producer of palm oil generates a large amount of lignocellulosic residues including palm empty fruit bunch (EFB), palm shell and mesocarp [3]. These lignocellulosic biomass feedstocks can be efficiently utilized in various thermo-chemical conversion processes to yield energy and fuels. Among various biomass conversion technologies, special attention has been paid to biomass gasification due to its high conversion efficiency [4-6].

A survey of literature reveals successful application of lignocellulosic biomass in various types of gasifiers including fixed beds [7], entrained flow [8] and fluidized beds [9-13]. However, amongst different categories of gasifiers, fluidized beds have offered advantages such as efficient mixing of gas and solid, improved reaction rate and conversion, and low tar content of the producer gas. Various gasifying agents including air, steam, oxygen-steam, air-steam, O_2-enriched air and oxygen-air-steam have been utilized in fluidized beds [6, 8, 14, 15]. Although a very high quality producer gas is not attainable through air gasification, however is boosts the feasibility of the biomass gasification for industrial application.

Although various biomass feedstocks have been gasified in fluidized beds, little data has been published on g asification of EFB in catalytic fluidized beds. Current research aims to investigate the gasification of EFB in a pilot-scale air blown bubbling fluidized bed. Calcined dolomite and silica sand were used as bed material and their effect on the quality of the producer gas was investigated.

2. Methodology

2.1. Biomass feedstock and its characterization

The biomass used in the current study was palm empty fruit bunch which was obtained from a local palm oil mill factory. The raw feed containing high amount of moisture was air dried for 2 days. The dried feed was then crashed and ground to the fibers with the mean length of 2-6 mm.

Ultimate and proximate analysis was conducted on a sample of EFB to determine the elemental composition of the biomass. The heating value of EFB was measured by a bomb calorimeter. The obtained results and data analysis are presented in Table 1.

Table 1. Ultimate and proximate analysis of EFB

Ultimate analysis (wt %)	
Carbon	43.52
Hydrogen	5.72
Oxygen	48.90
Nitrogen	1.20
Sulfur	0.66
Proximate analysis (wt %)	
Moisture	7.80
Volatiles	79.34
Ash	4.50
Fixed carbon	8.36
HHV, MJ/kg (dry basis)	15.22

2.2. System description and operation

An air blown bubbling fluidized bed gasifier with the height of 1050 mm and internal diameter of 150 mm was operated for EFB gasification. Air was introduced into the gasifier

using a 0.75kW blower. Silica sand and calcined dolomite with mean size of 600 µm were used as bed material. The biomass was continuously fed into the reactor through a screw feeder conveyer equipped with an inverter. The temperature of different operating zones of the gasifier was monitored by several type K thermocouples. The operated experimental setup is represented in Fig. 1.

At start up, the system was heated up to the desired temperature of 500 ^{o}C. There was a heating chamber supplied by LPG below the distributer plate to provide the necessary heat. As the temperature of reactor reached to 500 ^{o}C, air was introduced and the biomass feeding was started. To avoid the pyrolysis of biomass inside the screw feeder, there was a cooling jacket surrounding the conveyor and cooling water always passed during the process.

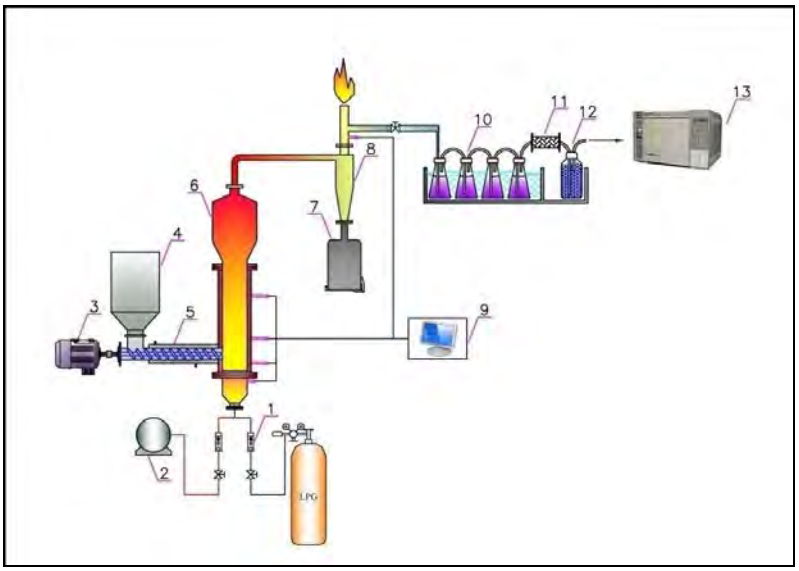

Fig. 1. Schematic representation of the pilot-scale BFB gasifier:
1. Mass flow controller; 2. Blower; 3. Variable frequency driver; 4. Feeding hopper; 5. Water cooled screw feeding system; 6. Fluidized bed reactor; 7. Particle holder; 8. Cyclone; 9. Temperature monitoring unit; 10. Condensers; 11. Fiber filter; 12. Silica gel; 13. Gas chromatograph

2.3. Gas sampling and analysis

The gasifier was operated at atmospheric pressure. The gasifier was equipped with a cyclone and the dirty outlet gas containing ash, char, tar and dust particles entered the cyclone separator. The cyclone removed ash and chars from the hot gas and derived them into the bin connected to the cyclone. Producer gas was exited from the cyclone to the incinerating device while a part of it was sent to the gas sampling unit. The gas samples were collected in several gas sampling Tedlar bags for further analysis using Gas Chromatograph (GC). The GC (Agilent Technology, 4890) was equipped with a thermal conductivity detector (TCD). A packed Carboxene 1000 (Supelco, USA) column (15 ft × 1/8 in, 80/100 mesh) was used to measure the mole fraction of permanent gases. External standard method obtained from 6 tanks of simulation gas was used to calculate the composition of the producer gas. Temperature programmed GC analysis was carried out with initial oven temperature set at 35 °C, then it was gradually increased to 210 °C at a rate of 20 °C/min. The injector and detector temperatures were 150 and 220 °C, respectively. Helium was applied as carrier gas at a rate of 35 ml/min.

3. Results and Discussions

3.1. Producer gas composition

In order to investigate the effect of temperature and bed material on the composition of producer gas, the bed temperature was varied in the range of 650 to1050 ^{o}C. The results are depicted in Fig. 2 (a) to (d). As observed in Fig. 2 (a) increasing the bed temperature from 650 to 1050 ^{o}C improved the H_2 content of the producer gas from 7.3 to 12.4% and 11.1 to 16.8% for silica sand and dolomite, respectively. Such increase in the H_2 level of the producer gas was due to the improvement of the endothermic reactions (1-3) involved in the gasification process:

$CH_4 + H_2O \leftrightarrow CO + 3H_2$ ΔH= +206 kJ/mol (1)

$CH_4 + 2H_2O \leftrightarrow CO_2 + 4H_2$ ΔH= +165 kJ/mol (2)

$CH_4 + CO_2 \leftrightarrow 2CO + 2H_2$ ΔH= +247 kJ/mol (3)

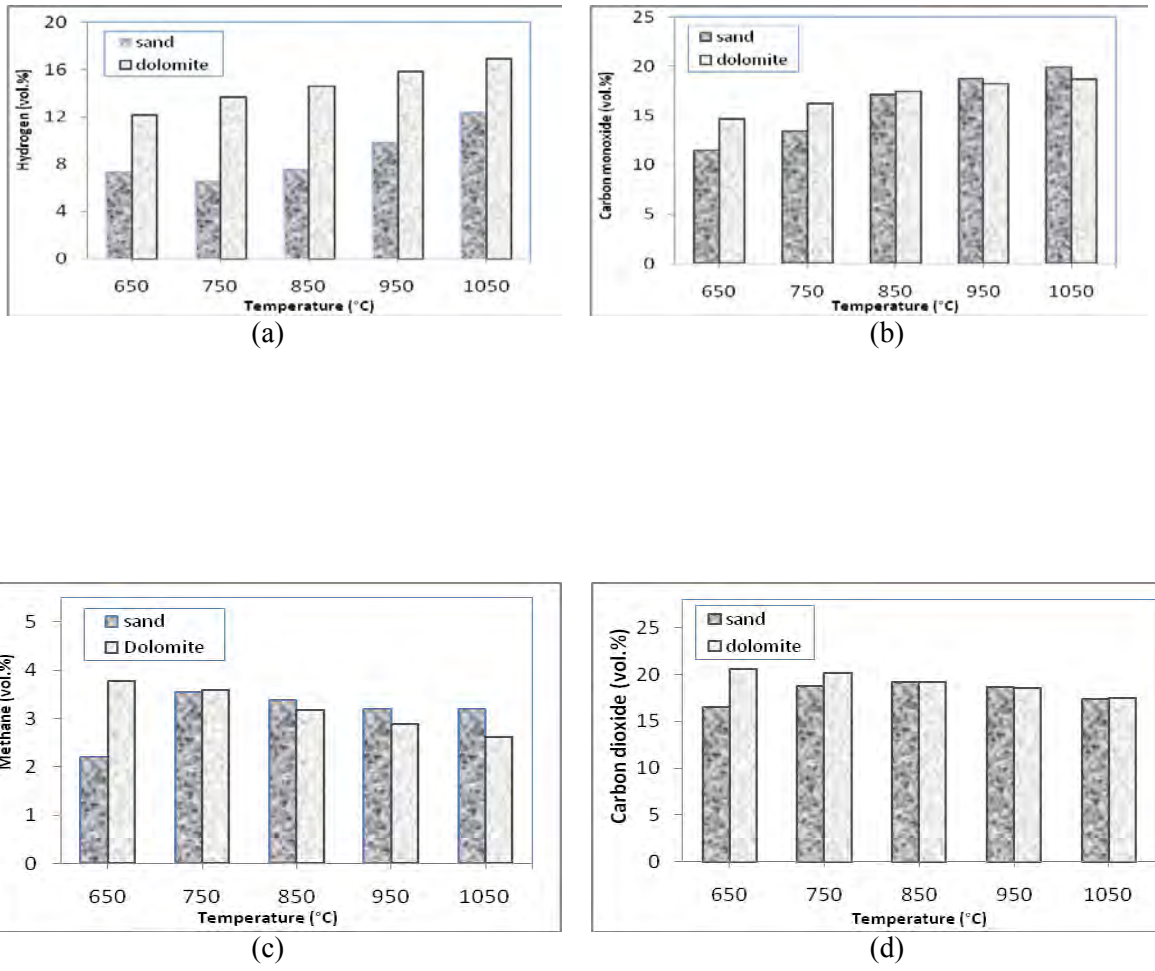

Fig 2. Effect of bed temperature and bed material on producer gas composition

Beside the contribution of the endothermic reforming reactions in increasing the H_2 concentration, the remarkable higher H_2 concentration obtained using dolomite in comparison to sand was confidently related to the improved tar cracking reactions (4-6):

$$C_nH_m\ (tar) + nH_2O \leftrightarrow (n + m/2)\ H_2 + nCO \qquad \Delta H > 0 \qquad (4)$$

$$C_nH_m\ (tar) + nCO_2 \leftrightarrow (m/2)\ H_2 + 2nCO \qquad \Delta H > 0 \qquad (5)$$

$$C_nH_m\ (tar) \leftrightarrow (m/2)\ H_2 + nC \qquad \Delta H > 0 \qquad (6)$$

The variation of CO level of the producer gas with respect to the bed temperature is presented in Fig. 2 (b). The obtained result revealed the positive effect of the bed temperature on CO content. As the bed temperature was raised from 650 to 1050 ^oC, the CO level increased from 11.5 to 19.8% and 16.2 to 18.7 for silica sand and dolomite, respectively. It was inferred that improved char gasification reactions (7 and 8) as well as methane reforming reactions (1-3) were the main cause of such increase at high temperatures [12]:

$$C + H_2O \leftrightarrow CO + H_2 \qquad \Delta H = +131\ kJ/mol \qquad (7)$$

$$C + CO_2 \leftrightarrow 2CO \qquad \Delta H = +172\ kJ/mol \qquad (8)$$

Fig. 2 (C) shows the CH_4 level of the producer gas at various applied bed temperatures. The maximum CH_4 level of 3.8 and 3.6% was obtained at 750 ^oC for silica sand and 650 ^oC for dolomite, respectively. The results showed that the CH_4 content of the producer gas follows a reducing trend for both silica sand and dolomite at high gasification temperatures. High temperature favors endothermic methane reforming reactions, thus reducing the CH_4 content of the producer gas.

The variation of CO_2 level of the producer gas with respect to the bed temperature is presented in Fig. 2 (d).The high concentration of CO_2 was observed at low temperatures and then a drastic decrease at temperatures above 850 ^oC was experienced for both sand and dolomite. At low temperatures, CO_2 is produced through water-gas shift reaction (9) but high temperature promoted its evolution via methane reforming (2). However, the generated CO_2 was consumed through methane dry reforming (3), tar cracking (5) and Boudouard reaction (8) to yield more H_2 and CO and lead to a decrease in CO_2 level at temperatures above 850 ^oC. The lowest CO_2 content of 17.4 was achieved at 1050 ^oC for both sand and dolomite.

$$CO + H_2O \leftrightarrow CO_2 + H_2 \qquad \Delta H = -41.98\ kJ/mol \qquad (9)$$

3.2. Gasification performance

Fig. 3 (a) illustrates the effect of bed temperature on high heating value (HHV) of the producer gas for sand and dolomite. As explained earlier, high temperatures enhanced the evolution of combustible gases especially H_2 and CO which in turn resulted in an increase in HHV of the producer gas. The HHV of the producer gas increased from 3.3 to 5.3 MJ/Nm^3 and 4.9 to 5.5 MJ/Nm^3 for silica sand and dolomite, as the bed temperature was increased from 650 to 1050 ^oC.

Variations of dry gas yield with respect to bed temperature are shown in Fig. 3 (b) for silica sand and dolomite. Increase of the bed temperature improved the dry gas yield from 1.3 to 1.8 Nm^3/kg and 1.5 to 1.8 Nm^3/kg for dolomite, respectively. Increase in dry gas yield may be

originated from the promotion of initial pyrolysis rate at high temperatures which increased the gas production as well as steam cracking and reforming of tars at high temperatures. In addition, endothermic reactions of char gasification at elevated temperature (7 and 8) improved the dry gas yield [11].

The result of carbon conversion calculation is presented in Fig. 3(c) for sand and dolomite. As expected, high temperatures enhanced carbon conversion efficiency due to the improvement of water-gas and Boudouard reactions (7 and 8) through which more carbon is converted to gaseous products. However, increase of the bed temperature beyond to 850 ^{o}C did not enhance carbon conversion due to the reduction of CO_2 content despite CO production.

Improvement of cold gas efficiency with increasing the bed temperature for EFB and sawdust is depicted in Fig. 4 (d). The highest cold gas efficiency of 69 and 65% was achieved at 1050 ^{o}C for sand and dolomite due to the high dry gas yield and heating value.

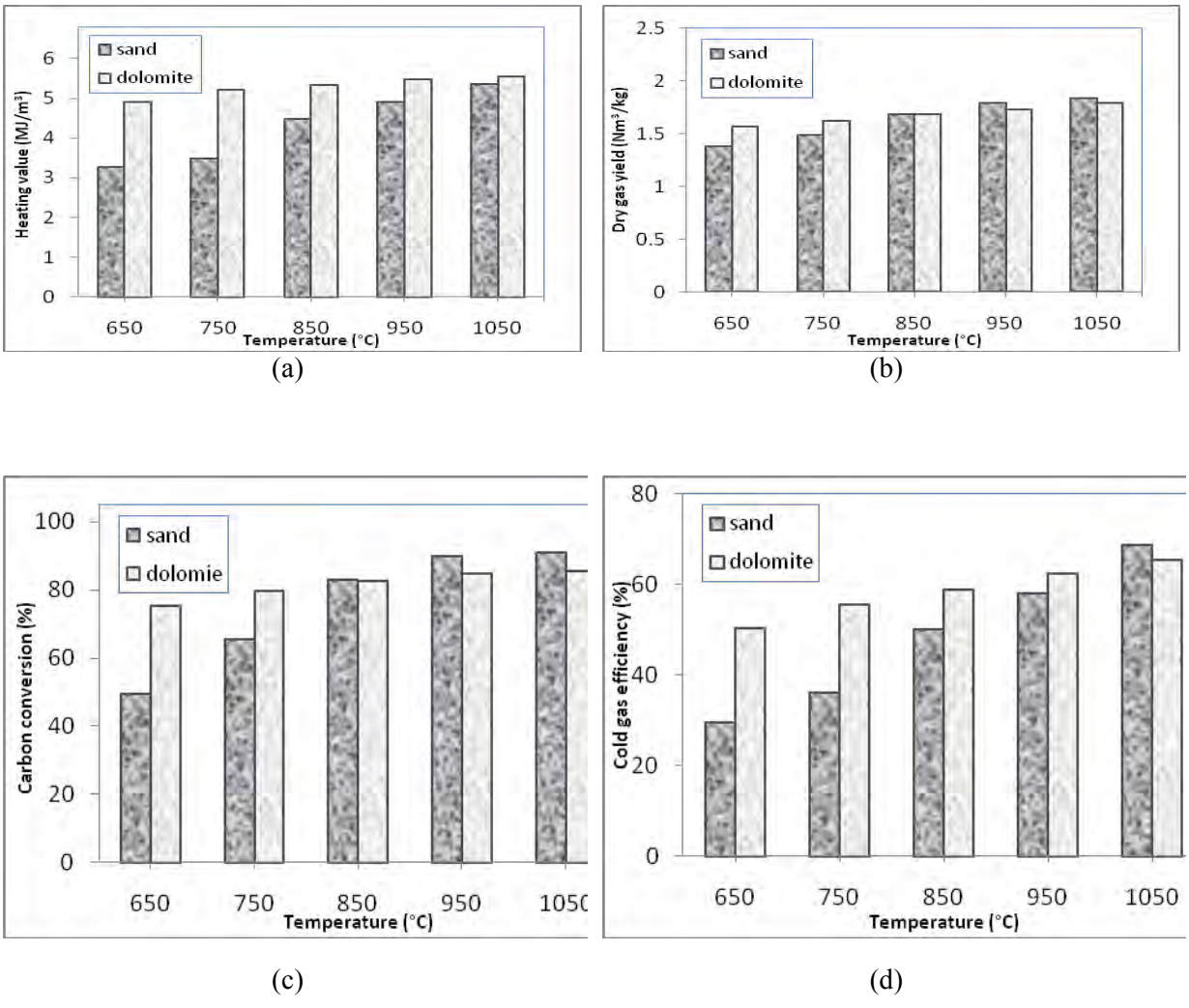

Fig 3. Effect of bed temperature and bed material on gasification performance

Agglomeration of the bed material was observed as the major concern in EFB fluidized bed gasification, especially at high temperatures. Such undesired phenomenon originated from the high K_2O content of EFB (44%) which deteriorates the sintering and agglomeration tendency of the bed materials to form low melting eutectics [16]. Increase of the bed temperature

beyond to 800 and 850 ^{o}C for silica sand and dolomite, resulted in the growth of bed particle. However, agglomeration with dolomite was not severe and the size of agglomerates was not considerable in comparison to silica sand agglomerates.

4. Conclusions

Gasification of EFB as an abundant lignocellulosic waste was studied in an air blown pilot-scale bubbling fluidized bed gasifier. The effect of bed temperature and catalytic bed material on the quality of the producer gas was assessed. The achieved results proved the potential of this biomass to generate energy as the HHV of 5.5 MJ/Nm^3 was obtained with dolomite. However, the agglomeration evolved at high temperatures was the main concern in EFB gasification. Thus, the EFB gasification experiments should be performed at temperatures below 850 ^{o}C to ensure the avoidance of any agglomeration.

References

[1] R. Saxena, D. Adhikari, H. Goyal, Biomass-based energy fuel through biochemical routes: a review, Renewable and Sustainable Energy Reviews 13, 2009, pp. 167-178.

[2] J. Escobar, E. Lora, O. Venturini, E. Yáñez, E. Castillo,O. Almazan, Biofuels: Environment, technology and food security, Renewable and Sustainable Energy Reviews 13, 2009, pp. 1275-1287.

[3] S. de Souza, S. Pacca, M. de vila, J. Borges, Greenhouse gas emissions and energy balance of palm oil biofuel, Renewable Energy 35, 2010, pp. 2552-2561.

[4] M. Paisley, Biomass gasification system and method. 2001, Google Patents.

[5] I. Narvaez, A. Orio, M. Aznar, J. Corella, Biomass gasification with air in an atmospheric bubbling fluidized bed. Effect of six operational variables on the quality of the produced raw gas, Industrial and Engineering Chemistry Research 35, 1996, pp. 2110-2120.

[6] Z.A.B.Z. Alauddin, P. Lahijani, M. Mohammadi, A.R. Mohamed, Gasification of lignocellulosic biomass in fluidized beds for renewable energy development: A review, Renewable and Sustainable Energy Reviews 14, 2010, pp 2852-2862.

[7] R. Warnecke, Gasification of biomass: comparison of fixed bed and fluidized bed gasifier, Biomass and bioenergy 18, 2000, pp. 489-497.

[8] J. Zhou, Q. Chen, H. Zhao, X. Cao, Q. Mei, Z. Luo, K. Cen, Biomass-oxygen gasification in a high-temperature entrained-flow gasifier, Biotechnology advances 27, 2009, pp. 606-611.

[9] R. Moghadam, A. Alias, Air Gasification of Agricultural Waste in a Fluidized Bed Gasifier: Hydrogen Production Performance, Energies 2, 2009, pp. 258-268.

[10] K. Mansaray, A. Ghaly, A. Al-Taweel, F. Hamdullahpur,V. Ugursal, Air gasification of rice husk in a dual distributor type fluidized bed gasifier, Biomass and bioenergy 17, 1999, pp. 315-332.

[11] F. Pinto, C. Franco, R. Andre, C. Tavares, M. Dias, I. Gulyurtlu, I. Cabrita, Effect of experimental conditions on c o-gasification of coal, biomass and plastics wastes with air/steam mixtures in a fluidized bed system, Fuel 82, 2003, pp. 1967-1976.

[12] P. Lv, Z. Xiong, J. Chang, C. Wu, Y. Chen, J. Zhu, An experimental study on biomass air-steam gasification in a fluidized bed, Bioresource Technology 95, 2004, pp. 95-101.

[13] G. Xu, T. Murakami, T. Suda, Y. Matsuzaw, H. Tani, Two-stage dual fluidized bed gasification: Its conception and application to biomass, Fuel Processing Technology 90, 2009, pp. 137-144.

[14] M. Campoy, A. Gḿez-Barea, F. Vidal, P. Ollero, Air-steam gasification of biomass in a fluidised bed: Process optimisation by enriched air, Fuel Processing Technology 90, 2009, pp. 677-685.

[15] G. Schuster, G. Lffler, K. Weigl, H. Hofbauer, Biomass steam gasification-an extensive parametric modeling study, Bioresource Technology 77, 2001, pp. 71-79.

[16] P. Lahijani, Z.A. Zainal, Gasification of Palm Empty Fruit Bunch in a Bubbling Fluidized Bed: A Performance and Agglomeration Study, Bioresource Technology 102, 2011, pp. 2067-2076.

Future-Proofed Design for Sustainable Urban Settlements: Integrating Futures Thinking into the Energy Performance of Housing Developments

Maria-Christina P. Georgiadou[1,*], Theophilus Hacking[2]

[1] *Centre for Sustainable Development, Engineering Department, University of Cambridge, CB2 1PZ, Cambridge, United Kingdom*
[2] *Development Director, University of Cambridge Programme for Sustainability Leadership, Cambridge, United Kingdom*
** Corresponding author. Tel: +44 (0)1223 333321, Fax: +44 (0)1223 765625, E-mail: mcg36@cam.ac.uk*

Abstract: This paper investigates sustainable building and low energy housing at a neighbourhood or city district scale. In particular, it examines how futures thinking on the energy performance can be integrated into the selection of building components, materials and low or zero carbon technologies. A multiple case study is undertaken in European housing developments that represent sustainable communities of 'best practice'. A literature review on the need for long-term thinking in the built environment research is followed by the definition of 'future-proofed design' and its application to the energy performance of housing developments. The extent to which building strategies in selected urban settlements have been 'future-proofed' is assessed. The analysis of the case studies includes a set of identified trends and drivers affecting the energy performance of buildings by 2050. The building strategies that explicitly accommodate these future aspects in these projects are also examined. Results suggest that the vast majority of building decisions focus predominantly on cost-effective solutions, such as energy efficiency measures. The use of renewable energy technologies, low embodied energy components, and new methods of construction relate to a demonstration project or any specific regulatory requirements. It is shown that 'best practices' accommodate predictable trends and drivers rather than exploring a wider spectrum of plausible futures. This reveals the tendency to neglect long-term thinking due to the complexity of dealing with uncertainty and the short-term mindset of the building industry. It is concluded that building strategies need to be more flexible to adapt to climate change, accommodate future changes and follow the increasingly stringent building regulations. A new generation of decision-support tools that combine futures techniques with mainstream sustainability assessment methods should also be developed.

Keywords: *Sustainability, Housing developments, Energy performance, Future-proofing, Building strategies.*

1. Introduction

The building sector has the greatest potential to deliver long-term, significant and cost-effective Greenhouse Gas (GHG) emissions compared to other major emitting sectors, such as transport and industry [1]. It is estimated that 64% of the world's economic production, consumption and environmental pollution is associated with the urban built environment in developed countries, where people spend around 80-90% of their time indoors [2-3]. At present, the building sector accounts for around 40% of total energy consumption worldwide, which translates to about 30% of global carbon dioxide emissions [4].

Sustainable development is 'development that meets the needs of the present without compromising the ability of future generations to meet their own needs' [5]. Sustainable building has emerged as an integrated approach to urban design with the evaluation of social, economic and environmental aspects surrounding the use of natural resources, energy consumption, environmental performance, functional quality, and the consideration of future values [6]. The latter entails the concept of 'future-proofing', which refers to an explicit and systematic appraisal of future possible options. In practice, however, little research has been conducted into the issue of how to design and construct buildings considering long-term implications of the energy performance and carbon footprint, due to the dominant short-term mindset that prevails in much of the property and construction sectors [7].

This paper introduces the concept of 'future-proofed design' and presents its application to the energy performance of European housing developments of 'best practice'. It seeks to assess the extent to which exemplary projects integrate futures thinking into the selection of materials, building components and low or zero carbon technologies. The objective is to uncover building strategies that can 'future-proof' the energy performance of residential buildings against long-term impacts of climate change, technological innovation, demographics, energy behaviours and market forces. The term 'energy performance' refers to energy efficiency, on-site renewable energy generation, and the embodied energy[1] of materials and building components. There is a growing trend towards 'sustainable communities', which refer to eco-developments of various scales, such as eco-neighbourhoods, eco-towns or eco-cities. In this paper, the term relates to urban settlements at the neighbourhood or city district scales that demonstrate pioneer thinking, political leadership, a whole systems approach, innovative financial solutions, low carbon innovation, multi-stakeholder collaboration, and community engagement [8]. Unlike individual buildings, community-led processes offer greater opportunities for a step change in sustainability through the integration of community energy networks and better economies-of-scale for novel Renewable Energy Technologies (RET) [9].

2. Methodology: Case study approach

The research adopts a 'real-life' perspective to understand the opportunities, practical constraints, and trade-offs in the selection of materials, building components and RET. The literature review focuses on the justification and conceptualisation of 'future-proofing'. A multiple case study method is employed in turn and 'best practice' European housing developments from 200 to 11,000 residences are selected. Table 1 provides a list of the case studies, along with a short project description. These projects are expected to provide the best platform for planning and design techniques from which to develop any improvements with regard to 'future-proofing'. Case studies entail both desk-based research and fieldwork. An ongoing survey via a structured questionnaire in parallel to expert interviews and focus groups via a semi-structured questionnaire are carried out since October 2010. The target audience includes planners, developers and local authorities involved in these projects.

3. The concept of future-proofed design in urban settlements

3.1. The need for futures thinking

An underlying reason to 'future-proof' buildings is that design choices cannot be easily revised and that the cost of inaction significantly outweighs the cost of timely action [14-15]. Futures thinking should be systematically integrated into the early planning and design stages, thus avoiding social, economic, and environmental costs associated with modifying settlements once they have been built. 'Although upfront design and construction costs may represent only a fraction of the lifecycle costs, when just 1% of a project's upfront costs are spent, up to 70% of its lifecycle costs may already be committed […] that first 1% is critical because, as the design adage has it, all the really important mistakes are made on the first day' [16].

[1] Embodied energy is the energy used to extract, process, manufacture and transport building materials and components.

Table 1: Selected 'Best-Practice' Housing Developments in Europe.

Project	Description
Hammarby Sjöstad, Stockholm, Sweden [8]	The 2010 European Green Capital. A mixed-use development of 11,000 apartments with energy, waste, and water following a unique eco-cycle. The City's long-term goal is to be fossil fuel-free by 2050.
Malmö, Sweden [10]	Bo01 and Västra Hamnen are two 'green' neighbourhoods (around 600 homes). By 2020, the City aims to be climate neutral and by 2030 the whole municipality will run on 100% renewable energy.
Freiburg, Germany [8]	Vauban (5,000 homes) and Rieselfield (4,200) homes are two district demonstrating pioneer thinking in solar energy.
Hanham Hall, Bristol, UK [9]	The first development of around 185 homes to meet zero carbon standards (Code for Sustainable Homes Level 6) in the UK.
Northstowe, Cambridgeshire, UK [11]	A new carbon neutral town of approximately 9,500 new homes, a town centre, offices and schools at a pre-design stage.
First wave of the Eco-town Programme UK [9,12]	Four new mixed-use developments of around 5,500 zero carbon homes and 40% of affordable housing at a pre-design stage: - Whitehill Bordon, East Hampshire - China Clay Country, St.Austell, Cornwall - Rackheath, Norfolk - Northwest Bicester, Oxfordshire
One Planet Communities UK [13]	- BedZED, London Borough of Sutton: around 100 zero carbon homes and 50% affordable housing. - One Brighton: a new mixed-use development of around 175 zero carbon apartments, office units and community facilities.

Another key motivation for future-proofing is the slow turnover of the stock. Buildings have generally an economic life of 50 to 60 years and a design life of 40 to 100 years [17-18]. Long lifecycles are due to high upfront costs of retrofitting, practical difficulties associated with deconstruction or demolition, and social attachments due to historical or cultural reasons, even if this was not explicitly the intention [19]. However, change is inevitable and caused by operational and maintenance processes, which determine refurbishment, deconstruction or demolition. It is estimated that 70% of the existing stock will be standing in 2050, thus each new building constructed in an energy-wasting manner or retrofitted to a suboptimal level will lock us into a high carbon-footprint future.

3.2. Definition of future-proofed design

Future-proofing is defined as 'designing something that can be resilient to future developments including both mitigation of negative impacts and taking advantage of future opportunities' [20]. This concept is promoted implicitly within the increasingly stringent environmental legislation, building standards and regulations at European and national levels, such as the recast of the European Performance Building Directive and the UK Climate Change Bill [21-22]. When applied to the context of energy and buildings, future-proofing refers to building strategies made at early stages which can be connected to long-term energy solutions, such as ability to accommodate new technologies or space for energy storage, thus achieving optimum energy performance throughout the lifecycle [23].

A future-proofed design strategy entails 'stress-testing' against a range of possible futures to ensure that building decision remain robust of the lifecycle and simultaneously ensuring effective management of future energy requirements. There are two key characteristics that underline this concept:
- The level of uncertainty surrounding the trends and drivers that could influence the energy performance of buildings, which can vary between predictable trends and unknown aspects that cannot be anticipated based on present forecasts.
- The level of availability in product and process innovation; i.e. technical solutions and decision processes to accommodate future aspects of the energy performance.

Future-proofed building strategies should manage both uncertainty and the need for innovation. This will aid the selection of materials, building components and low or zero carbon technologies that will be cost-effective and flexible in accommodating future changes or requirements. The benefits of sustainable building can only be realised over the long-term and, therefore, failure to incorporate futures thinking may result in poor levels of energy performance for decades.

4. Results

A review of policy documents and consultation reports for the identified case studies, along with data gathered via the ongoing survey and interviews, have revealed the extent to which 'best practice' urban settlements accommodate futures thinking in energy-related decisions.

4.1. Trends and drivers affecting the energy performance of urban settlements

Figure 1 reveals that the investigated housing developments acknowledge predominantly four trends and drivers from a broad spectrum of issues affecting buildings by 2050. These include: i) demographic changes due to increase in urban populations and social changes in housing unit and tenure types, ii) the increasingly stringent environmental legislation, building standards and regulations, iii) innovative economic incentives and funding mechanisms for energy efficiency, RET, and community energy networks, and iv) the launch of new technical solutions.

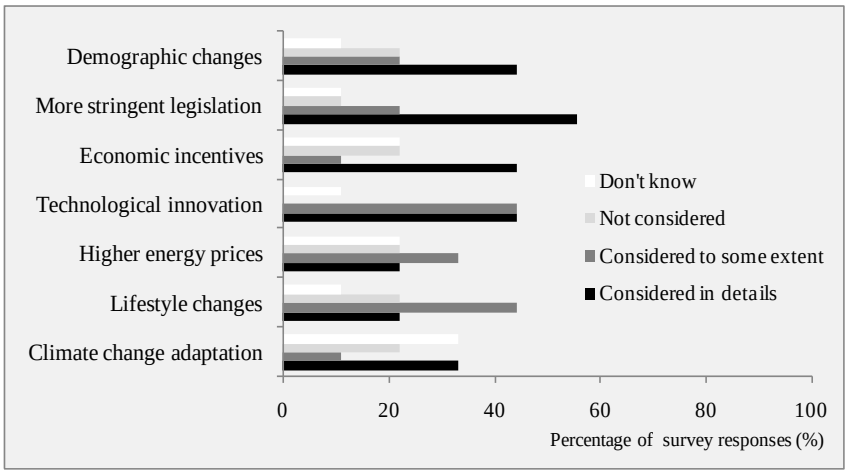

Fig.1. Trends and drivers affecting the energy performance of urban settlements by 2050.

Higher energy prices and lifestyle changes are considered to some extent. The latter refers to the energy-intensive behaviours associated with higher energy consumption, such as the

purchase of more appliances, higher preferred lighting levels or room temperatures, and the occupancy of larger living spaces per person. Nonetheless, it is shown that 'best practices' do not fully consider adaptation to a changing climate change, as this trend is not considered or even overlooked in about two thirds of the survey data. Many future impacts of the energy performance of housing developments are already 'locked-in', as result of past GHG emissions. Figure 1 shows that adaptation to a changing climate is not yet a priority at the design stage, as building strategies have mainly focused on mitigation; i.e. reducing GHG emissions via energy efficiency measures and the use of RET.

4.2. Future-proofed building strategies

This section includes a list of building strategies adopted in the selected case studies as shown in Table 2, along with observed limitations and directions for future research. These future-proofed building strategies aim to accommodate the trends and drivers affecting the energy performance of buildings by 2050 (see Figure 1). In addition, Table 2 provides an understanding of the decision-making process behind them. Survey data reveals that the majority of the building strategies are selected due to the commonly used and cost-effective environmental design techniques; i.e. strategies to mitigate GHG emissions with energy efficiency measures.

Table 2: Future-proofed building strategies used in the case studies.

Building strategies	Main reason for selection
Energy efficiency of the building fabric: • Passive systems: location and orientation, natural daylighting, external shading, natural ventilation • Active systems: optimum insulation, thermal mass, and advanced glazing • Low energy lighting • Low energy appliances • Control systems: building management systems and smart metering	Standard practice, cost-effective
Low and zero carbon technologies: • Individual buildings: solar thermal panels, photovoltaic (PV) panels, micro-wind, heat pumps • Local energy networks - Gas-fired and biomass-fuelled Combined Heat and Power (CHP) plants - District heating and/or cooling systems - Large wind turbines outside built-up areas	Demonstration project
Low embodied energy materials and building components	Demonstration project, regulatory requirement
New methods of construction (e.g. prefabricated solutions, green roofs and walls, cool roofs, phase change materials, smart facades)	Demonstration project, regulatory requirement, marketing or 'green' image

Apart from the abovementioned environmental design features, the analysis of the case studies shows that 'best practices' integrate economic aspects of sustainability to enhance long-term affordability in the building layouts, functions, materials, building components and

energy systems. This is achieved by process innovation in business models for the commercialisation of new technologies or the establishment of energy partnerships and community trusts. An example can be the establishment of an Energy Service Company (ESCO), which engages in a long-term arrangement with a developer to cover both the financing and management of the energy-related costs over the development's upfront and running costs. Furthermore, 'best practices' demonstrate social aspects of sustainability, by ensuring buildings for all types of occupants with a variety in housing unit and tenure types and by enhancing health and well-being. Social acceptability of low or zero carbon technologies is also achieved via community engagement and public participation.

Nevertheless, Table 2 reveals a lack of adaptation strategies that could bring flexibility into the building design and enhance the ability to undergo the impacts of future changes. The case studies do not fully demonstrate a diversified mix of energy sources and the ability to accommodate future changes or mandatory requirements regarding new technologies, such as PV-ready roofs or space for energy storage. Adaptable building strategies that address socioeconomic issues, such as internal space flexibility to support new behavioural patterns (e.g. home-based working) should also be incorporated in the building design. Another issue that is not considered in detail is a specific strategy for the decommissioning stages at the early lifecycle stages. Demolition should be avoided and designers should opt for materials and building components that can be disassembled for re-use and recycling. Improvements in energy efficiency have led in reduced energy consumption at the operational stage, and therefore the relative significance of embodied energy has increased, as it forms a higher proportion of the total amount of energy used during the lifecycle [24]. The findings, however, reveal that embodied energy is not integrated systematically, as this choice is related to a demonstration project and the establishment of any mandatory or prescriptive requirements for such calculations.

5. Concluding discussion

Future-proofed building strategies aim to ensure the delivery of resilient and flexible buildings that foster low carbon development and have potential for cost savings, lower running costs, and added-value in the future. To date, the case study research demonstrates that a starting point to future-proof a housing development is to be one step ahead of the building regulations with high energy efficiency measures and installation of cost-effective RET. It also highlights the importance of stakeholder engagement and the need for a step change from short-term mindsets to long-term strategic thinking and full lifecycle considerations, since it is the early decisions that determine whether a project will be sustainable and future-oriented or not. Nonetheless, when 'best practices' think about future-proofing, they focus predominantly on mainstream and cost-effective building strategies, such as energy efficiency, low energy lighting, and control systems. More innovative features, such as novel RET, local energy networks, embodied energy considerations, and new methods of construction, are still not mainstream solutions and are mainly considered due to a demonstration character, regulatory requirements, marketing or 'green' image purposes of a project, when testing novel energy solutions.

At present, it is challenging to deal with uncertainty and long-term decision-making on the building design. Interviewees agree that there is still no single, truly holistic sustainability assessment method that can integrate futures thinking into the evaluation of the energy performance, thus bringing flexibility to the building design. The case studies reveal that futures techniques have only been applied to a limited fashion in urban settlements. Futures

techniques can help identify both anticipated and uncertain outcomes, bring together different perspectives, challenge current thinking, and aid robust decision-making. They are a family of tools that have not been developed with sustainability in mind but their orientation is of direct relevance to future-proofing. For instance, Scenario Planning is one commonly used technique, which has become increasingly dominant in business strategy and long-term planning of products, processes and industrial sectors [25].

The case studies have revealed the lack of a comprehensive technique to integrate futures thinking into *ex ante* sustainability assessment methods. At present, mainstream techniques and tools, such as Environmental Impact Assessment (EIA) or building rating tools (e.g. BREEAM, Code for Sustainable Homes, LEED, etc.), give emphasis to particular environmental themes rather than social and economic and focus predominantly on predictable energy trends and drivers. Therefore, they tend to overlook reasonably foreseeable or unknown dimensions of the energy outlook. A new generation of decision-support tools should be developed, which will adopt a hybrid approach combining mainstream sustainability assessment methods (e.g. EIA) with futures techniques (e.g. Scenario Planning) for the appraisal of the energy performance of housing developments.

Acknowledgments

The first author would like to thank the Engineering and Physical Sciences Research Council (EPSRC) and the Alexander S. Onassis, Public Benefit Foundation in Greece, for making possible this PhD research. This paper is a work in progress based rather than a completed piece. It is based on preliminary results, as this research is in the data collection stage. Material of interviews, surveys and correspondence is available upon request.

References

[1] Intergovernmental Panel on Climate Change, IPCC Fourth Assessment Report, 2007.

[2] D. Devuyst, L. Hens, and W. De Lannoy, How Green is the City? Sustainability Assessment and the Management of Urban Environments, Columbia University Press, 2006.

[3] J. Burnett, City Buildings – Eco-Labels and Shades of Green!, Journal of Landscape and Urban Planning 83(1), 2007, pp. 29 – 38.

[4] United Nations, Sustainable Development Innovation Brief: Buildings and Construction as Tools for Promoting more Sustainable Patterns of Consumption and Production, Department of Economic and Social Affairs, Division for Sustainable Development, 2010.

[5] United Nations, Our Common Future, World Commission on Environment and Development (WCED), 1987, p. 43.

[6] SESAC, 'Sustainable Buildings, Low Energy Housing', Sustainable Energy Systems in Advanced Cities, CONCERO Initiative, European-funded project, available from: http://www.concerto-sesac.eu/spip.php?rubrique81, 2010 [cited 22 January 2011].

[7] J. Ravetz, Integrated Assessment for Sustainability Appraisal in Cities and Regions, Journal of Environmental Impact Assessment Review 20(1), 2000, pp. 31 – 64.

[8] Homes and Communities Agency, Eco-Town Report: Learning from Europe on Eco-Towns, London, 2008.

[9] Town and Country Planning Association (TCPA), Creating Low Carbon Homes for People in Eco-Towns: Eco-Towns Housing Worksheet, London, 2009.

[10] City of Malmö, Sustainable City Development, available from http://www.malmo.se/English/Sustainable-City-Development.html, 2010 [cited 22 Januart 2011].

[11] South Cambridgeshire District Council, Local Development Framework: Northstowe Area Action Plan, Development Plan Document, 2007.

[12] Department of Communities and Local Government, Planning Policy Statement: Eco-Towns A supplement to Planning Policy Statement 1, London, 2009.

[13] One Planet Communities: Earth Greenest Neighbourhoods, One Brighton, UK, available from: http://www.oneplanetcommunities.org/communities/one-brighton/, 2010 [cited 17 August 2010].

[14] P. Stasinopoulos, M. Smith, K. Hargroves, C. Desha, Whole System Design: An Integrated Approach to Sustainable Engineering, Earthscan, 2009.

[15] E. Wilson and J. Piper, Spatial Planning and Climate Change, the Natural and Built Environment Series, Oxford Brookes University, Routledge, 2010.

[16] P. Hawken, A. Lovins, L. H. Lovins, Natural Capitalism: Creating the Next Industrial Revolution, Earthscan, 1999.

[17] T. Malmqvist, M. Glaumann, S. Scarpellini, I. Zalbaza, A. Aranda, E. Llera, S. Diaz, Life Cycle Assessment in Buildings: the ENSLIC Simplified Method and Guidelines, Journal of Energy, 2010.

[18] R. Shaw, M. Colley, R. Connell, Climate Change Adaptation by Design: A Guide for Sustainable Communities, Town and Country Planning Association (TCPA), 2007.

[19] T. Hacking, Improved Energy Performance in the Built Environment: Unpicked 'Low-Hanging Fruit'?, Proceedings of the Conference on Building Physics and the Sustainable City, University of Cambridge, Cambridge, 2009.

[20] J. Jewell, H. Clarkson, J. Goodman, I. Watt, The Future Climate for Development: Scenarios for Low Income Countries in a Climate-Changing World, Forum for the Future, London, 2010.

[21] European Commission, 'Directive 2010/31/EU of the European Parliament and of the Council on the Energy Performance of Buildings (recast)', 2010.

[22] Department of the Environment, Food and Rural Affairs, Draft Climate Change Bill, The Stationery Office, Cm 7040, London, 2007.

[23] Department of Communities and Local Government, Code for Sustainable Homes: Technical Guide Version 2, London, 2009.

[24] B. Boardman, Examining the Carbon Agenda via the 40% House Scenario, Journal of Building Research and Information 35(4), 2007, pp. 363 –378.

[25] Foresight, Horizon Scanning Centre Toolkit Exploring the Future: Tools for Strategic Thinking, available from: http://www.foresight.gov.uk/microsites/hsctoolkit/, 2008 [cited 17 January 2010].

Space-time of solar radiation as guiding principle for energy and materials choices

Embodied Land instead of primary energy as universal performance indicator

Ronald Rovers[1,*], Wendy Broers[2], Katleen de Flander[3] ,Vera Rovers[4]

[1] *RiBuilT, Research Institute Built environment of Tomorrow, RiBuilt/Zuyd university, Heerlen The Netherlands*
[2,3,4] *RiBuilT/Zuyd University, Heerlen The Netherlands*
** Corresponding author. Tel: +31 645064180, , E-mail:r.rovers@hszuyd.nl*

Abstract: Renewable energy is based on using a direct route from solar radiation to consumption, as an efficiency improvement from a long term route via fossils. However, both routes put a claim on space/land and the time of use of that land/space to intercept and convert it to useful forms. However, the same solar radiation is needed, to produce materials in a similar change from fossil materials to renewable materials, and materials are needed as well to produce the conversion devices for renewable energy. Similar processes take place in the realizing sustainable buildings, especially 0-energy buildings: : there is space time involved to generate the renewable energy, but also to generate for instance the renewable material based insulation materials, or the wooden construction.
These insights lead to the notion that looking to production of renewable energy only is sub- optimization of systems, and could in fact be counterproductive. This has defined our research to explore new ways of evaluation of activities, and in our case buildings. We have developed a indicator called Embodied Land, to evaluate the time and space occupied by generating both renewable energy and renewable materials. This has been tested in two cases, and runs out to be a interesting approach, showing clearly how the optimization of land and space use over a certain time period relates to choices in materials and energy together, and makes it possible to optimise from both resources together, using an minimum of land occupation.

Keywords: *Exergy , Exergetic space, Embodied land, Primary energy, Maxergy, Space time evaulation, Building assessment,*

1. Introduction and research questions

In reducing the impact of Buildings and built environments, what we want in the end is to measure whether we are really moving towards a more balanced use of materials and energy at a fundamental level and to see whether this can provide a approach and strategy that will transform the activities in a way to be maintained for many generations to come. It is however not the absolute use or burden we are interested in but whether the use within a certain space (system) and time (frame) can be continuous , with regeneration of quality instead of net depletion of systems potentials over the time of use. Studying the different possibilities of such a approach creates an inconvenient feeling with current calculation methods, performance indicators and assessment Tools . These exist in many forms however seldom measure real improvement of the global impact or resource situation. Nearly all tools use relative or subjective weighting, historic benchmarks and more, including even LCA (Life Cycle Assessment) tools . Other studies have provided similar conclusions: “Many research studies show the vulnerability of tools when accumulating indicators are used to reach a sole value”. [1] [2] Lowe has attempted to see if we could define absolute environmental limits for the built environment. Lowe concluded that there are also many uncertainties and problems when applying. [3] Another issue is that, for practical use, most tools and assessment methods are not very convenient, and provide too much detail according to the influences of the specific stakeholders’ position as has also been experienced in practice and concluded in research: “the non-transparency of tools for use in practice”. [1,2]
We will have to see if we can find new ways of calculating and accompanying tools and approaches that overcome these disadvantages..

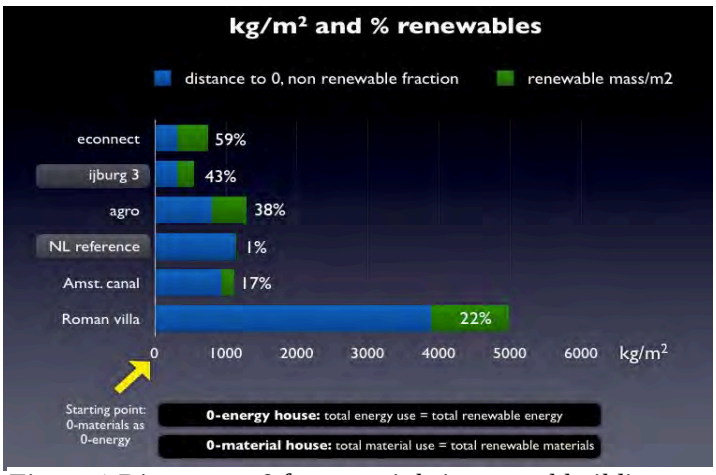

Figure 1 Distance to 0 for materials in several buildings

A first step to improve from looking at energy alone has been made in research on how to define a closing cycles approach, firstly focussing at materials. [4,5,6] . Materials are under threats of scarcity as well, and are a m ain cause of CO2 emissions in production. Materials should therefore , similar to energy, after centuries of growing depletion, start to fit in to a closed cycle approach. The logic step is to define a material neutral building as one that is been made of renewable materials. There are still resources involved, but only ones that ca be regenerated over the time of their use. It's a similar approach as for E nergy, when applying solar radiation . The difference is that the renewable energy is i nstantaneously regenerated, for renewable materials the time span is much longer. (but so is their application)

At that point a few questions were phrased:

A) If a 0-energy building is created, (fossil-) energy for operations and CO2 emissions are no issue anymore (besides in production of devices)[7] However, the embodied (fossil) energy of construction materials have become the major cause of the resource depletion and CO2 emissions related to erect and construct a building…! This poses questions like: Should we add more insulation (with still energy and CO2 impacts) or remain a higher heating load (requiring more –renewable-energy), what is best? [8] In other w ords: looking only into operational energy has become obsolete and is sub-optimisation, . But and how to combine both energy and materials in a evaluation? [1]

B) renewable materials are only renewable if they are renewed, and how would that work out in defining a 0-materials building, one that regenerates the resources on site?

C) both energy approach and materials approach , be fore de scribed, is still a quantitative approach. How would this change if we look at specific qualities needed? (heat, structural materials etc).

This paper further explores answers to these questions, introduces a approach and a exploration of two cases to test the approach.

2. MAXergy

One of the main question to address, in order to get answers, is to explore how energy and materials can be combined in a closed cycle approach , what would be a common denominator, one that automatically requires that different qualities are integrative addressed[2].

This forces us to look more in-depth at an overarching approach, that of exergy, which explores the quality potentials in a system. Energy can not be depleted, however its exergy ,

[1] The production of materials requires enormous amounts of energy, (cement production alone is responsible for 7 pct of all worldwide CO2 emissions, and growing [9] the total burden on fossil fuels is due to materials use! [10]

[2] This link between materials and energy has been explored in research on exergy, among others in The SREX programme in The Netherlands {http://www.exergieplanning.nl/} [11]

the qualities of energy (to provide work) that can get lost . The approach is mainly to see how decrease of the quality can be reduced. The usual approach is that a system is trying to be optimised from the inside: re-use of waste heat for instance (get more out of the same energy flow). More important however, the analyses is usually based on a "fossil" notion of exergy: that of oil and gas of high exergetic quality , available in a system. These however have only a high exergy/quality, since they are 'available'. It is seldom asked how they *became* available… These notions require a redefinition of quality in a system and how to maintain it. The following observations and arguing help redefine this.

2.1. Ecosystems, quality and humans

Natural ecosystems generate the highest quality. However one can argue if the word quality is the right word to use. Nature in fact has no quality, nature just is. Physically its about thermodynamic stored potential, however only quality in terms of human use if made available *to do "work*". Its humans that value qualities since they make use of it. To explore the *human valued* quality, in different forms, we will explore in how far humans can make a potential available , and to have maximum use of it, maximum in the sense of lowest exergy loss (or better: to balance exergy *consumption* with exergy *growth* in time and space in a human managed system.)

2.2. Systems

the system addressed is usually limited ie a part of the earth. If quality is a main evaluating criterion for mankind's inhabiting of the earth, then its no use looking at a limited system: the largest system that is bordering human influence is the earth. There is no neighbouring system that can provide resources[3]. There is only one connection outside that system: that of solar radiation, the driver of our whole system, and the only source capable of preventing equilibrium(total decrease of quality). (besides a little gravity)

2.3. Redefining the oil route: solar radiation

Following this argument, the origin of Oil in fact is solar radiation (from outside the largest human addressed system) , converted to biomass, ending up as sediments and under heat and pressure changed in Oil (or gas or coal) This reveals that oil is in fact not the ultimate source for (100%) exergy calculations but just a specific state into a process of using/decreasing quality in the system as a whole. . If we calculate this, (total known oil stocks, 65 million years process, over total earth surface) , we can find that oil is renewably generated at a speed of approximately 14000 liter per day globally!. One step further we can derive the relation of oil gas and coal with space and time: the speed of generation and the earth surface use over time (for the biomass involved) . In fact electricity via the fossil fuel route (average of oil gas and coal) comes out at ~0,0017 kWh per ha per year. As comparison : electricity from solar panels provides ~1.000.000 kWh per ha per year . Its two different routes from solar radiation to electricity, with different impacts in land use and time. This creates a direct link to the use of a source and the space- time involved. And directly from that, the space time occupied by the use of it. Or in other words: if we do not use more oil as regenerated it's a lasting process, a sustainable operation. Based on the input of land and time to convert solar radiation. Via a different route Tran and Vale come to the same question of involving land in measuring sustainability and renewable energy production.. [12]

[3] Many of our system analyses are based on looking at a limited system, with imported resources un quantified, however having a burden on a neighbouring system loosing quality. This is only acceptable is the neighbouring system is also a well managed system. In the end its at the scale of the earth it all comes together, and no neighbouring system is available anymore.

2.4. And what about mass?

Energy and mass are two of the same, as Einstein already concluded and both share thermodynamic laws. In modern ecosystem approach its even mainly mass recognised as the main potential and process for capturing quality (as was biomass for oil…) [13, 14] Connect this to the fact that a shift to a *renewable* materials approach is based on solar energy as well, for materials to be (re-)generated on land, in a certain time period, and we have our first direct relation to evaluate energy and materials in one assessment. : the land use over time to produce the (human valued) quality. For food and water similar approaches apply.

Ultimately it is the solar radiation that decides on the quality in a system that directly translates into forming of mass and energy out of solar radiation, and both have direct effect on the land-use to make these conversions take place. In a change for a renewable sources based society-(closed cycles) there is in fact 1 principle basic to both, which is the ability to convert solar radiation into useful forms of exergy: quality in the form of mass and/or energy. (and food and water, however is not the scope of this paper)

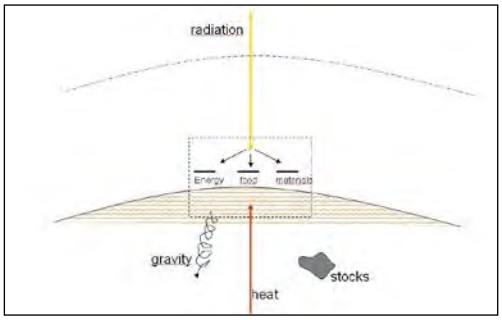

Figure 2 solar radiation access as the main structuring value

Important aspect of this approach is the relation with space needed to produce these resources and the time aspect in which they will regrow.

The questions we posed before can now be answered .
Ad A1 how can energy and materials be evaluated in a common system, is to explore the time space use that is involved in maintaining a closed cycle management, based on renewable resources. the question on energy and materials sub optimisation can be answered by using a common nominator for their impact: m2 solar radiation access over time to (re-)generate the demand (and the different qualities).:(or restore quality)

Ad B What is a 0-materials building, can be answered as one that re-generates the resources *on site*: it has to include space over a certain time to be able to regrow the resources used to construct the building, and the time relates to do so before their end of use.: In other words: the land to be appointed for their regrow should be included in the building site (similar to roof surface for PV for example)

Ad C The issue of qualities in stead of quantities has become obsolete in this approach: Its not an issue, it's the production potential to fulfil a function, with least time space occupation that is decisive for our possibilities , staying within closed cycle limits. Its all a matter of m2 solar access, which helps makes choices, also in qualities.

3. The Exergetic Space approach

Mass and energy , in a closed cycle operated society, have become one and the same, and can be only optimised in a combined way, in relation to their claim on solar radiation access via land/space over time. This can be phrased as The Exergetic Space , required for some function: The space-time needed to produces certain qualities over the time of use of a function fulfilled.

And the only real value to address this quality, or better the prevention of decrease in potential quality, is the m2, and our capability to create quality (convert solar radiation into human valued resources) in (at least) the same pace as it is consumed.

Or to turn it around: any system, no matter what size defined, has a maximum capacity to generate quality. If activities inside the system uses more quality then generated, it depletes resources and will face collapse in the end. Or in other words: one can determine the maximum activities in a system, to be maintained for ever by incoming potential and converted to useful forms.
Optimising for space-time, on the basis of converting energy/mass into useful carriers for human used value, leads to a complete different approach as so far. It requires reserving areas of space for generating a meaningful volume of the the most wanted quality.
And preserving the highest quality in a system, is not established by starting from cascading inside sources, but by starting from the system entering solar radiation and capture and convert in the highest valued mix of needed qualities

3.1. New indicator: Embodied land

Going back to our fist exploration into kg's of material involved in construction - the distance to 0 where all materials required were provided on a renewable basis - we can now quantify the impacts of the need to regrow these resources, without depleting a system: it's the land over a certain time involved : or the Embodied Land (EL).

4. Pilot cases

The approach developed can be used in two different ways. One is to evaluate the performance of different buildings ("the exergetic space need" or Embodied Land, for providing the building m2's) .

The other way is to explore in how far an existing and consuming urban environment can be re-developed into a 0-impact area, using the time space need as structuring element. This has been explored in a parallel case in which we develop the Urban Harvest + approach, and tested in a pilot Kerkrade West, a district in the south of The Netherlands. Its described in detail in other papers { 15}

4.1. The methodology

The methodology is structured as in the illustration (fig 3): first to explore the space need involved with generating the renewable materials. A database has to be developed to record yields for different resources. The results will be part of another publication, the illustration shows some basic findings (these are climate related of course). Next step is to include the embodied energy of the materials, and translate this into Embodied land.

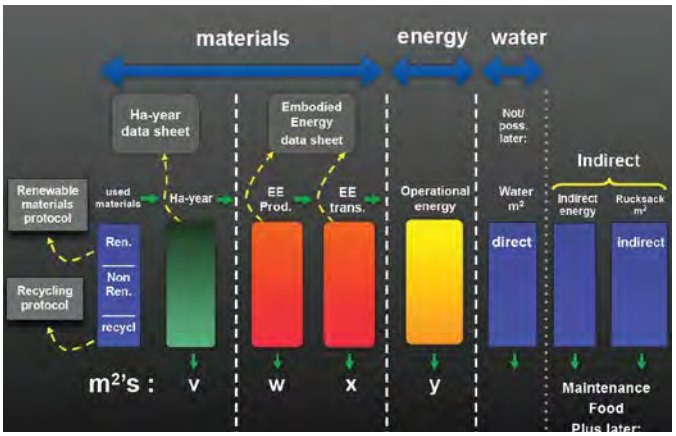

Figure 3 the methodology

For Embodied Energy figures, this research bases itself on the Inventory of Carbon & Energy (ICE) from the University of Bath version 1.6a .
As an example we both re-calculated the land use for fossil energy as well as with renewable energy. The third step is to add the operational energy to the calculation, giving a total land

need over a certain period of time to compensate for the exergy load/ quality loss in the system. In a further research also water will be added as well as secondary resource use and maybe food.

4.2. The cases and results

One case was a 5 level prefab Timber frame and straw bale house, designed for Amsterdam's new canal house district Ijburg.. Its based on 43 % of renewable materials
The materials use and energy related data were brought together and the embodied land was calculated for the above mentioned fractions.

Materials embodied land
In the case of Ijburg , the production of (43% renewable) materials require 916 m 2-year to produce , per m2 of living area. This can be produced in 1 year on 916 m2, or , if we take the lifecycle of a house as 50 years, on 18.3 m2 for the continuous period of 50 years. The space time occupation of embodied land significantly drops when lifetime of the house increases.

Energy embodied land
This has been recalculated for both fossil based energy and renewable based energy. To produce the energy for materials production by fossils, a land use of 43 million m2 per m2 of living area is involved (on a 50 year regeneration basis…!) . A huge amount, of course. To do so with modern biomass energy generation 2,16 m2 is needed, and via PV panels 0,06 m2.(both in 50 years) (only direct energy, not including yet indirect energy, for storage for instance) But it shows already the immense difference in effectivity whether fossils or renewables are used. For operational energy similar calculations are made: for Ijburg-3 0,08 m2 per m2 living area is needed. (solar generated, or 57 million m2 when fossils are used)

	Ijburg 3 50 years lifetime 1 m2 living area 550 kg/m² 43% renewables			Dutch Ref House 50 years lifetime 1 m2 living area 1145 kg/m² 1% renewables		
EL	18,33 m² - year			0,24 m² - year		
	PV	biomass	fossil	PV	biomass	fossil
EE	0,06	2,16	43.527.315	0,07	2,24	45.209.601
OE	0,08	2,83	57.013.505	0,49	16,51	332.914.466

Figuur 4: Embodied land for reference house and house from Straw and wood: for materials generation(EL) and for three energy sources providing Operational energy (OE) and embodied energy (EE)

From this point on its already clear that in the case of a ch ange to renewable materials , with still using fossil fuels as energy source, the last one is by far the most devastating to our land use : A 100 m illion m2 for EE and OE per m2 living area, compared to 18.33 m2 for materials (t he 43%, maybe twice as much for a 100 pct renewable materials house). However, if we include the fact that we have to change for 100% renewable energy, the picture is completely turned upside down: 0,14 m2 for EE and OE compared to 18,33 m2 for the materials fraction (on a 50 year calculation, but the relation remains the same) This already shows that decisions regarding materials have far more impact then those related to energy, in a renewable resources based world. As we will see later more in detail. In a second case study we started at the other side: that of an existing district which consumes more energy and mass as is produced in the area, or in other words, has huge embodied land occupied outside its own "jurisdiction", providing its own water and materials as well. This will require strong reduction of demand, and maximise production. This has been done following a 5 step model (the Urban Harvest plus approach [Rovers 2010] .For example: The energy plan assumes all houses are renovated towards passive house standards, requiring

large amounts of insulation materials and a new structural façade. However from materials point of view these are not available, and require a large extra amount of land. A calculation shows that there is need for 135 ha of extra land to supply all materials for the whole district over a period of 20 years. On the other side it only requires 17 ha of Solar collector "land" to supply the heat for un-insulated houses. The choice is clear: no insulation and extra heating is the most effective choice. The finding were surprising even for the researchers, and even when expecting that materials might be more important then energy in a closed cycle and renewable source based society. It should be noted that only direct energy and mass has been calculated: materials for collectors, or process energy for materials have not been included yet. A follow up study should detail this issue, and probably find an optimum between insulation and heating. Both examples show that it is possible to combine energy and mass in one objective approach and relate directly to the sole sources for both qualities in the earthen system: m2 access to solar radiation, or "Embodied Land" . The model developed proved useful, and shows no un beatable barriers. Nevertheless some issues still have to be specified: The land relation for non renewable materials, as far as they are still used, the valuing of recycled materials (16), the detailing of choices, using indirect energy and materials, and other issues.

5. Conclusions and Consequences:

First of all the attempt to combine both energy and materials in one objective calculation has been proven possible though details still have to be settled. It turns out that direct solar access and the space time involved is the real value to relate decisions of environmental effectively and operation within a closed cycle process. Even food can be included in this evaluation (though not explored here) since it is in the same way depending on solar access. A second conclusion is that materials are as expected more influential in the environmental performance as (renewable) energy , though even far more as expected by the researchers.
Further findings and conclusions are:

- Quality is not a direct issue anymore: Since the evaluation starts from the potential available(in a given district) or the potential needed and the land to be included, in case of a new development qualities are to a certain extent given facts, and not directly structuring.
- Embodied Land seems a very good and understandable indicator to judge the impact of any activity .
- Optimising space and time in capturing the needed qualities, is what has to be valued , in order to establish a highest level of materialised welfare . How high is depending on our pattern of consumption of qualities, and the amount of individuals striving for that level of welfare, ie acquiring the useful functionalities.
- Optimising for space time, on the basis of converting energy/mass into useful carriers for human use, leads to a complete different approach as so far. It requires reserving areas of space for generating a meaningful volume of the most wanted quality.
- Preserving the highest quality in a system, is not established by starting from cascading inside sources, but by starting from the system entering energy and capture and convert in the highest valued mix of needed qualities

There is a few consequences to this approach. First of all: The notion " primary Energy " has become a historic artefact and thrown in the rubbish bin, since a historic relic from a fossil fuel driven society. When real values and impacts are calculated, the reference has become the sun, and the time space involved to generate quality from its radiation, and the capability

to convert that in useful forms for humanity[4]. It also shows that trying to optimise the energy cycle, looking at (renewable) energy alone, , is sub optimising. The role of materials is far more important . So far the exploration has only involved a 2 D approach, in m2 land available for a specific amount in time. However in fact we face a 3D problem: How to deal with shading, how to deal with excavations, quarries in this approach? Think of a troglodyte house: The underground houses found in dry climates, like Tunisia, and including some underground villas by the Romans. They in fact produce materials, in stead of consuming by way of excavating soil to create living space. Or to include height in the form of hydropower potential . A more general approach for this has to be explored, in relation to the study of the use of non renewable materials .

References

[1] Kellenberger 2005, et all, comparison of European LCA –based buildings assessment and design tools, SB07 New Zealand Paper number: 029
[2] Humbert 2007 et all, Leadership in Energy and Environmental Design (LEED). A Critical Evaluation by LCA and Recommendations for Improvement, the Int J LCA Special Issue Vol. 12, No. 1, 1 − 78.
[3] Lowe 2006, Defining absolute environmental limits for the built environment., BRI (2006) 34 (4)
[4] Rovers, R., (2007) Urban Harvest , and the hidden building resources, Paper CIB2007-474 -CIB world congress 2007, www.cibworld.nl
[5] Rovers,R et all, 2008, 0-energy or Carbon neutral? Discussion paper on systems and definitions, www.sustainablebuilding.info
[6] Rovers,R. 2009, Material-neutral building: Closed Cycle Accounting for building Construction, paper SASBE conference, Delft, The Netherlands 2009
[7] Schmidt, M. (2009). "Global Climate Change: The Wrong Parameter."
[8] Gommans, L. J. J. H. M. (2009). "The use of material, space and energy from an exergetic perspective." Proceedings Sasbe 2009 Conference on Smart and Sustainable Built Environments.
[9] Taylor M. et all Energy Efficiency and CO2 Emissions from the
Global Cement Industry, International Energy Agency, Energy Efficiency and CO2 Emission Reduction Potentials and Policies. in the Cement Industry, IEA, Paris, 4-5 September 2006
[10] Sartori I. , et all , 2006, Energy use in the life cycle of conventional and low-energy buildings: A review article. Department of Architectural Design, History and Technology, Norwegian University of Science and Technology (NTNU), 7491 Trondheim, Norway Received 11 April 2006; received in revised form 27 June 2006; accepted 10 July 2006
[11] SREX , 2007-1011, long term research in to planning and exergy, Dutch university consortium , http://www.exergieplanning.nl
[12] Tran, Han Thuc, et all, 2010, Measuring sustainability, carbon or land? ,SB0 Helsinki conference, September 2010.
[13] Jorgensen Sven Erik, 2006-2007, An integrated ecosystem Theory, Eur. Acad. Sci (2006-2007) Liege, EAS Publishing house 19-33
[14] Jorgensen Sven Erik 2007, Evolution and exergy, Environmental chemistry
[15] Rovers 2010, Urban Harvest Plus apporahc for 0-impact built environments, case Kerkrade West, proceedings SB10 Western Europe conference, Maastricht 2010, http://www.ribuilt.eu/Kennis/EuregionalConferenceSustainableBuilding.aspx
[16] Rovers 2011 valuing recycling and non renewable materials , to be published.

[4] Nature has no qualities. It is however thermodynamic stored potential, however only quality in terms of human use if made available to do “work”) . To explore the human related quality, it is explored in how far humans can make a potential available , and to have maximum use of it, maximum in the sense of lowest exergy loss (or better: to balance exergy consumption with exergy growth in time and space in the addressed system. (from the SREX research)

Energy Efficient Building in Third Climatic Region of Turkey

M.H. Çubuk[1,*], Ö.Emanet[1], Ö.Agra[1]

[1] *Yıldız Technical University, Mechanical Eng.Dep., İstanbul, Turkey*
** Corresponding author. Tel: +90 212 383 2817, Fax: +90 212 261 6659 E-mail: hcubuk@yildiz.edu.tr*

Abstract: Residential and commercial buildings consume a considerable amount of the energy produced in Turkey. 82% of that consumed energy is heating related. A reduction to 25% to 50% of energy consumption is possible with only proper insulation of these buildings. Fossil fuels such as coal and petroleum produce CO_2. Tests have shown that CO_2 levels have reached 360 ppm in Turkey. In this context, buildings that are efficiently designed and configured will provide energy savings. Energy efficiency in buildings in Turkey, has gained prominence recently with the adoption of the Directive on Energy Performance of Buildings in 2008. The object of this study is to convert a building, located in the 3rd climatic region in Turkey, to an energy efficient one. Analysis of the building has revealed that it does not accommodate the TS 825 s tandards. New thermal insulation design has cut energy consumption estimates to 37,09 kWh/m^3, which is within the limits of regulation codes.

Keywords: *Energy Efficient Building, TS 825, Energy Performance of Building.*

1. Introduction

Fossil fuel reserves that provide a significant amount of world's energy requirement are rapidly coming to an end. Using energy resources efficiently is significant. It has been emphasized in several studies that only by using energy efficiently provide savings on energy consumption at the rate of 30% annually.

In Turkey, 82% of energy is used for heating. It is possible to provide 25% to 50% fuel savings only by building insulation. It is seen that the released CO_2 level as a result of fosil fuel burning is 360 ppm nowadays. Carbondioxyde is relatively 55% more efficient than other greenhouse gas on c ausing global warming. Therefore it is required that the living environments must be designed and configured to provide energy savings and efficient energy usage. In this study, by taking into consideration the requirements mentioned above, it has been intended to turn a building which is in Ankara, Gölbaşı in the third region, on the lakeside of Lake Mogan, away from the tall buildings, frontal to highway, having its own garden, independently oriented; consisted of a ground floor, one normal floor and a penthouse to an "Energy Efficient Building".

2. Heat insulation project

2.1. Heat insulation project for the current building

Considering the indoor temperature as 19°C in accordance with TS 825 Heat Insulation Regulations, conformity to standard has been reviewed by designing heat insulation project for the current non-insulated building. In the analysis for the current building, while the limited energy requirement is 33,77 kWh/m^3, calculated energy requirement for the building was 86,40 kW h/m^3. As it stands the building is not confirmed to TS Standard no 825 on Rules of Heat Insulation in Buildings in Turkey.

2.2. Variations on the architectural project and insulation application

To provide the building's conformity to TS 825 and reduce the energy consumption, various variations on external structure and roof has been proposed. Changes has been occured on the walls, windows and roof of the building as a result of the reconsiderations mentioned below

and the analysis has been repeated in accordance with TS 825. Reconsiderations for the building were:

Window space has been increased on the south frontage of the building. 62% of window space increase on south frontage and 45% on total has been provided.

Roof gardening has been applied on the South and North frontages of the roof.

As a result of roof gardening application, the South frontage space of the building and the penthouse window space have been increased.

As a result of roof gardening application, "open air roof space" has been emerged.

Shadowing has been done on the North side of the building by planning evergreen plantation.

As a result of the studies made to provide conformity to TS 825 for the building, rockwool of 6 cm thickness for outdoor air contacted areas and 8 cm thickness for unheated inside walls have been used. 12 cm thick glaswool on the roof areas of the ceiling and 10 cm foamboard on open air roof because of the roof gardening application have been used in accordance with the fire code. Thickness of insulating material on flor has been calculated, considering the energy balance of the building, as 10 cm of foamboard. 10 cm floating floor boards have been used on floors next to unheated areas.

Instead of double-glass used in current situation, Low-E plated heat insulation bridged aluminum windows which has an Up value of 2,4 W/m^2K have been used. 3 cm thick cement mortar has been used on the external wall in current situation. In the new insulated condition of the building; 7 mm thick anorganic based palstering made of lightweight aggregates has been applied on insulation instead of cement mortar because of the nonconformity to structure physics.

2.3. Heat insulation project for the new condition

As the heat insulation done in accordance with TS 825 Heat Insulation Regulations energy requirement for the building has been reduced from 86,35 kWh/m^3 for current condition to 37,09 kWh/m^3. Therefore energy requirement for the building has been reduced from 37,12 kWh/m^3 as presented in the standard and confirmed to TS 825 standard. Annual energy requirement of non-insulated building has been reduced from 71544 kWh to 28572 kWh, provided energy savings of 60% and reduced CO_2 release with the insulation.

The comparison of heat loss values for construction element before and after insulation can be seen in Figure 1.

3. Alternate energy sources

Troubles, affecting whole world such as global warming, climate change and greenhouse effect caused by the usage of increasing amount of fossil fuel and so energy usage, prompts communities to develop new and clean alternate energy sources. Accordingly, new solution offers for active and passive systems to reduce the energy consumption in the current building are as follows.

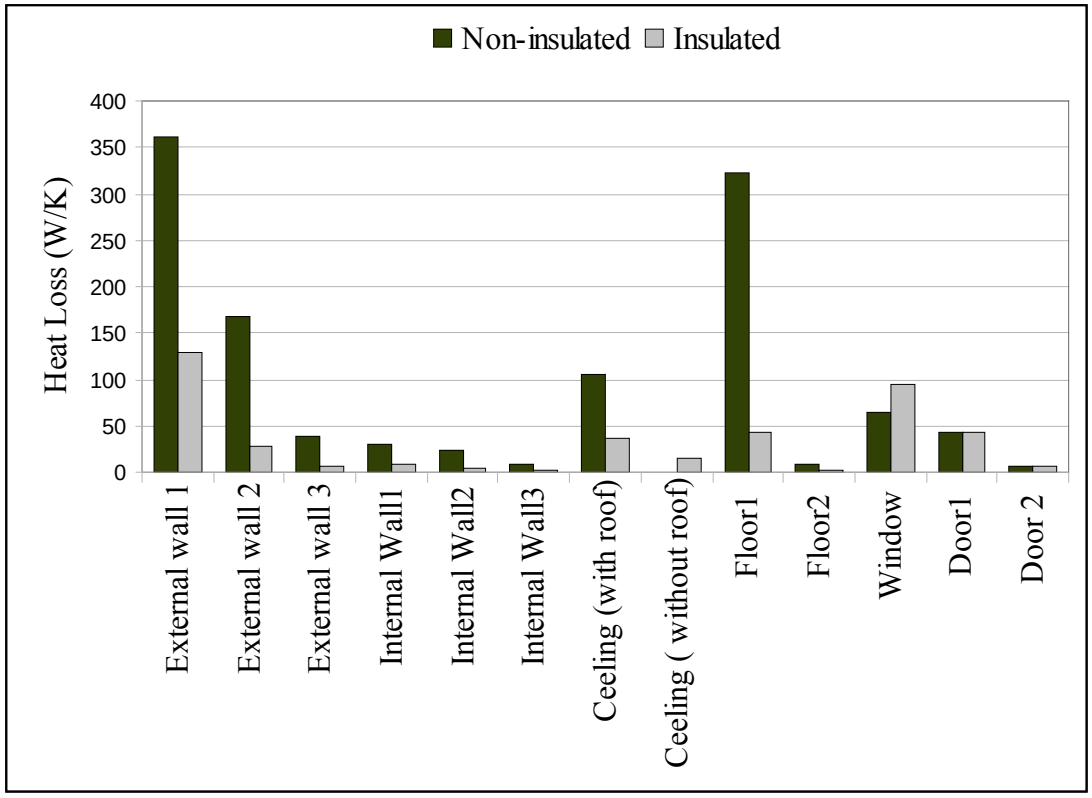

Fig.1. Heat loss for insulated and non-insulated conditions

3.1. Ground source heat pump application

To do heat insulation in accordance with TS 825 standard and to provide the annual building heating and cooling requirements which are reduced to minimum in virtue of passive methods applied, vertical type ground source heat pump application has been approved.

Energy requirement for the building has been calculated in accordance with TS 825 as mentioned above and distributions by months have been determined. As this distribution is reviewed it is seen that in January at the value of 20.497.178 kJ (7,9 kW) maximum energy requirement is occurred. Heat pump with 14,6 kW heating and 2,4 kW (EER=5,1) cooling capacity has been selected according to heating load. By calculating the cooling load of the building, solar collector has not been applied because in the system designed to be used both in heating and cooling seasons the heat pump will provide the required energy for both heating and cooling water usage. Analysis results for this design are presented in Table 1. Payback period for the planned system has been calculated as 11 years and 11 months.

When geological structure in Lake Mogan surrounding in Ankara-Gölbaşı region has been investigated, it has been understood that after a significant boring depth underground water is reachable [1]. Accordingly, specific thermal contraction capacity of stratas with underground water has been determined as 70-90 W/m [2]. It has been seen that 102 m borehole is required as a result of calculations below based on the peak load a heat contraction capacity. Investment cost (device, pipe, boring and labor cost included) for this system is determined as 8472 TL. Fuel requirement is removed the heat pump will completely provide the energy needed for heating the house and generating hot water.

3.1.1. Economic analysis of active systems

Investment calculations, fuel savings and other additional cost (electricity consumption) belong to above mentioned active systems have been calculated and economically reviewed. Interest rate for the economic analysis has been considered 10% and "payback period" of the system has been calculated also considering the time value of Money.

The results obtained are presented below on Table 1. By considering interest rate as i = 10% and also considering the time value of Money, it has been seen that the system will return to profitability in 11 years and 11 months.

Table 1. Energy audit of the new investment and monetary values

	Heating	Domestic Hot Water	Cooling		Investment	Saving	Additional Cost
	(m^3 N.Gas)	(m^3 N.Gas)	(kW)	(TL)	(TL)	(TL)	(TL)
Current situation	7647	340	12,3	1004			
Insulation	-4592				13722	2572	
Heat pump (heating)	-3395				10500	1901	-1356
Heat Pump (cooling)			-12,4	-393			+611
PV					1090		
TOTAL	0		0	+611	25312		-745
						Net Utility (NU) =	3728

Payback period (PP) is calculated according the equation below:

$$PP = \frac{\ln\left(\frac{NetUtility}{NetUtility - i * Investment}\right)}{\ln(1+i)} \qquad (1)$$

$$PP = \frac{\ln\left(\frac{3728}{3728 - 0.10 * 25312}\right)}{\ln(1+0.10)} = 11 \text{ years } 11 \text{ months}$$

3.2. Heat storage in greenhouse, water wall and bedrock

Thermal storage is significant in direct solar energy recovery systems. Thermal masses allow storage and later usage of solar energy.

3.2.1. Greenhouse application

As one of passive heating systems greenhouse application has been applied on the building (Fig.1, Fig.2). Greenhouse is a structure which is on the South frontage, adjacent to the building. It has one-way inclined roof and its all areas are consisted of glass. Roof pitch is designed as 50° in accordance with incidence angle of sun beams for Ankara in winter. Therefore heat gain occurs in the areas next to the greenhouse. Glass used on greenhouse is a Standard insulation glass with a U value of 2,6 W/m^2K. By using this glass sun radiation has been utilized more effectively. At the same time heat loss from the glass has been tried to minimize. In virtue of the vents that positioned on the upside and underside of the

greenhouse, it has been targeted to reduce the negative contribution to cooling load of the greenhouse by providing an air stream in hot summer days. Also with the help of shadowing components (jalousie) that will be placed on glass surface of the greenhouse and deciduous trees, it has been provided to reduce sun radiation that affect the greenhouse surface. As a result of thermal analysis of the design the total heat gain provided from the greenhouse has been calculated as 17,444 kW.

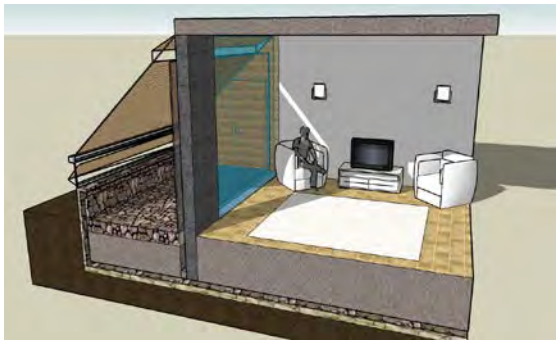

Fig. 1. Greenhouse, summer application (jalousie closed, went open)

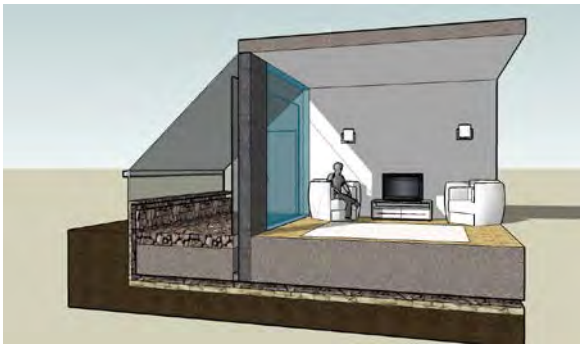

Fig. 2. Greenhouse, winter application (jalousie open, went closed)

3.2.2. Water wall application

Both to store thermal energy and to reduce light transmittance the wall that separates the greenhouse from the site has been transformed to a thermal mass by using two plane plexiglas board. In this application, by using water, which is a supply that has one of the highest thermal capacity (4160.103 kJ/m^{3}K), more heat has been stored and also it has been provided to increase the amount of sun beams entering the site because of the transparent surface [3]. With this thermal mass that is placed on south frontage sun radiation affecting the surface will be stored to able to be used in hours that we can not utilize the sun enough or none.

3.2.3. Heat storage application on bedrock

Bedrock has been formed as a thermal mass on the greenhouse or house floor to support passive heating of the house. It has been anticipated that by means of this thermal mass storing of excess heat accumulates in the greenhouse during the insulation and utilizing this energy when insulation is not enough [4,5,6].

It is provided to transform heat to rocks by sending the hot air which is drafted from between the water columns with a glass panel placed on front side of water columns, by means of the fan that is placed on the intersection point of the greenhouse floor and water columns. In virtue of two sensors, one is placed inside the greenhouse and the other on rock surface, fan only will work when the temperature in greenhouse is higher than rock heat. By this means, it is provided to prevent this cool air to reduce the heat of the bedrock. It has been targeted to rise apparent ambient temperature in virtue of the heat stored on rocks which cause a temperature rise on floor heat.

3.3. Other passive system applications

Window spaces on the south frontage of the building have been increased to utilize incident rays in winter. Window space increase has been provided at the rate of 62% on south frontage and a total of 45%.

To prevent living spaces from extreme heating in summer because of new windows which have been placed to utilize the sun beams more effectively in winter, window shades in specific sizes have been placed on top of the windows. These components let the light in which comes with oblique angle in winter but reflect the light out which comes with right angle in summer.

Two lines forestation has been done on north to protect the building from north winds. No forestation has been done on South frontage of the building.

Natural air conditioning – vents have been place on North frontage to provide natural air conditioning in the building. These vents have been placed on stairs column, penthouse bedroom and living room walls. Pressure difference required for these vents to work will be occurred when the Windows on South frontage are open and by that air circulation will be provided.

Light shelf systems – Light shelf is a component which is designed to prevent the sun light entering and direct it to the ceiling and placed horizontal or almost horizontal on inner surface or exterior surface of the window. These components will be added to top sides of the windows afterwards.

Two-leaf glass frontage application – Glass frontage cladding has been applied on first floor bedroom and first floor living room to utilize the sun beams on south frontage and two vents are used on the walls. These vents have been placed on top corners and bottom corners of the wall as enter and exit.

Power generation with Photovoltaic panels (PV) – It has been seen that payback period for the system will be too long as a result of feasibility study on whether all energy requirement of the building that becomes independent on heating and providing hot water can be provided with renewable energy or not. In that case, it has been designed to provide electricity requirement for fire exit way illumination and smoke sensors with PV panels instead of entire energy requirement of the house. For this purpose a package unit that consists of 180 W solar battery, 1 charge regulator and control unit, 1 solar accumulator and 4 light bulbs (11 W, 12 V) has been selected to be placed on roof. Investment cost for this unit is 1090 TL and it is presented in economical analysis tables mentioned above.

Heat insulated garden roof terrace – Besides looking beautiful, roof gardening, which is very common in western Europe, also provides substantial economical and ecological benefits if it is applied with a safe water insulation and well planning [7,8,9]. Considering the draught in Ankara, water has become significant and roof gardening application has been decided.
Water saving and recycling – To reduce the utility water usage in the house it has been suggested to use type-A water saving sinks and double stage reservoir in bathrooms and to store the rain water handled in gutter and roof gardening to use in both toilet flush tank and watering the garden.

Chimney flue – No change has been made in the chimney which is on the North side of the current house. It has been thought that using the chimney in winter will provide heat gain on the colder north side of the house and also to utilize flue gas heat. Discharge shaft has been designed as a heat transformer to do that. In that design, by placing a second layer on flue gas brick it is targeted to heat the flowing air in between and return it to the environment. Therefore reduced heat requirement for the environment has been provided.

Phototubes (Cold light in hot day) – Sun light has the top quality light among lighting devices. Day light for first floor North bathroom, garage, mechanical room and the penthouse which has been made by roof gardening application has been provided by this system. Therefore there will be electricity saving at the rate of 30%-70%.

4. Conclusion

It is a fact that a significant part of energy consumption is occurred at our living environments, houses and working places. Therefore designing and configuring the living environments to provide energy saving and efficient energy use is a necessity.

In this study in virtue of heat insulation, active and passive methods applied to the building both energy saving and economical benefits has been provided. Energy generated, transmissioned and commercialized in our country has been used without squandering. When the applied methods are considered as a whole, 7987 m^3 natural gas and 10320 kg CO_2 release saving has been provided. In the second system that also the cooling load of the building is considered as well as the heating requirement 7987 m^3 natural gas saving and reduced electricity consumption has been provided. In that case CO_2 release saving has been 11847 kg.

Current building has been transformed into an "Energy Efficient Building" by applying heat insulation as well as other several active and passive systems and its ecological footprint has been reduced.

References

[1] Topkaya, B., Türkiye Göl ve Rezervuarları İçin Veri Tabanı Hazırlanması, TÜBİTAK İNTAG Proje No: 825, 2008, Akdeniz Üniversitesi, Antalya, Turkey

[2] IYEM Seminar Notes, VIESSMANN Isı Pompaları

[3] Günerhan, H., Duyulur Isı Depolama ve Bazalt Taşı, Mühendis ve Makine Dergisi, 2004, pp.540

[4] Çakmanus, İ., Bilgin, A., Güneş Enerjisi İle Binaların Pasif Isıtılması, TTMD Journal, 2005, Issue 36

[5] Wilson, A., Thermal Storage Wall Design Manual, New Mexico Solar Energy Association, 1979, New Mexico.

[6] Guobing Z., Yinping Z., Kunping ., Wei X., Thermal analysis of a direct-gain room with shape-stabilized PCM plates, Renewable Energy, 33(6), 2008, pp.1228-1236.

[7] ZinCo GMBH, The Greenroof Directory, 2008, www.greenroofs.com

[8] Gel, M.K., Bahçe teraslarda su yalıtımı, Türkiye Mühendislik Haberleri, 2003, Issue 427, pp.123-126.

[9] Korgavuş, H., Teras ve çatı bahçelerinde su yalıtımı, 2003, Istanbul, Turkey

Urban materials for comfortable open spaces

Valentina Dessì

Politecnico of Milan Dept. BEST, Milan, Italy
Tel: +39223995128, Fax: +39223995150, E-mail: valentina.dessi@polimi.it

Abstract: All the elements present in open areas contribute to define the microclimate and they have to be designed to mitigate the microclimate. In particular urban materials have to be selected on the basis of the urban space use and its thermal behavior.
This paper shows the influence of urban pavements and building facades materials on the open spaces environmental performance and on thermal comfort conditions. In order to evaluate the contribution of the materials thermal simulations in dynamic regime were carried out of simplified configurations (corner of squares and streets. The paper shows how the urban space thermal performances change when only one or two walls are considered and if differences occur when the analyzed area is near or far from the wall, as well as when building height changes. This first part of analysis considers the open space as reference case and evaluates how the thermal performances change according to the changing context (from open space to the corner of the square). The second part points out the differences among the materials due to the physical properties, like albedo, thermal capacity and density. The last analysis concerns the evaluation of these configurations in terms of thermal comfort.

Keywords: *Microclimate mitigation, urban materials, thermal comfort, open spaces.*

1. Introduction

Pavement and building facades represent the recognizable support of urban space, i.e. the scenario of collective memory and social life built by movements, trading, meetings and communication. These spaces should represent more than the possibility to cross or reach destinations: they should satisfy the users need dealing with the perception of the space [1] [2]. Pavements and facades have another role. Urban space materials, as well as urban morphology, define the urban heat island. Nowadays the insufficient attention to physical properties of materials and the free development of the built environment induce to increase this phenomenon. It affects the unpleasant microclimate in contemporary cities, especially during the summer. It is important to know natural materials properties in order to classify them on the basis of energy performances.

To understand the energy behaviour of materials in urban space an analysis was done comparing energy performance of some urban configurations by changing pavements and facades materials. Thermal simulations in dynamic regime were carried out with the software Solene [3] in order to define the role of materials and observe their behaviour in particular urban contexts. Simulations were done for a latitude of 45° (Milan, Italy) in a sunny day (clear sky). The microclimate is determined also by the materials' thermal properties and can be evaluated in order to foresee suitable environmental performance and acceptable thermal comfort conditions of urban space, in case of new project or urban renewal.

2. Methodology

Thermal simulations in dynamic regime have the advantage of highlighting each element contribute one by one. For this reason it is possible to evaluate the pavement colour impact on energy performance of the urban space as well as the heat capacity. In other words it allows to understand if it is better to pave a square with red granite or wood, with clear or dark stone.

Cases simulated with Solene and reported in the paper describe the thermal behaviour of specific locations in a urban space (centre of a square, the corner or areas differently oriented) by varying paving and facades materials.

Nevertheless before analysing thermal performance of materials in specific urban configurations, the most common paving materials should be analyzed to better understand differences [4]. To reach this goal we use a urban space not surrounded by buildings. This situation will be next considered as reference case.

Table. 1. Pavements materials used for the simulations. (A is albedo)

	N°	Material	cm	Conductivity (W/m°C)	Specific heat (J/kg°C)	Density (Kg/m^3)
ASPHALT A= 0.2 	1	Wear layer - asphalt	2.5	0.7	920	2100
	2	Tout venant – (gravel)	7	1.2	840	1700
STONE A= 0.5 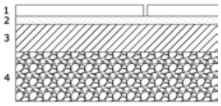	1	Red granite slab A= 0.5*	≥3	4.1	840	3000
	2	Mortar	3-4	0,58	840	1200
	3	Hot flush	15	0.94	880	1800
	4	Road-metal	20/40	0.6	840	1700
* alternative coating	1	Marble A= 0.8	≥3	3	840	2700
	1	Lime A= 0.7	≥3	1.5	840	1900
PORPHYRY A= 0.3 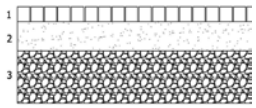	1	Cubes of porphyry	5	2.9	880	2200
	2	Sand and concrete layer	10	0,35	840	1800
	3	Road-metal	20/40	0.6	840	1700
BRICK A= 0.4 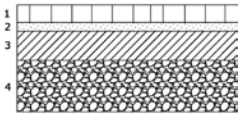	1	Sestini di laterizio	6	1.7	840	2400
	2	Mortar	2,5	0,58	840	1200
	3	Hot flush	15	0.94	880	1800
	4	Road-metal	20/40	0.6	840	1700
COLORED CLS A= 0.5 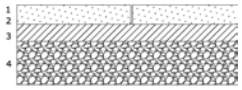	1	Slurry	8	1.2	880	1800
	3	Hot flush	7	0.94	880	1800
	4	Road-metal	20-40	0.6	840	1700
WOOD (LARIX) A= 0.6 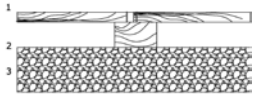	1	Larix stave*	4/5	0.12	2700	550
	2	Joist transverse				
	4	Road-metal				
* alternative coating		Cedrum stave	4/5	0.19	2390	700

It's important to keep in mind that with solar radiation, the characteristic with highest impact on thermal behavior is the solar reflection coefficient, the albedo (A), which depends on color and texture [5] . Material surface temperatures on horizontal plan are more close to the solar radiation trend then the air temperature.

A first assessment was done on several stone materials – granite, porphyry, lime stone and marble. Specific heat in stone materials is quite similar, while conductivity and density can be quite different. A second study was done on other urban materials (asphalt, concrete, wood).
The analysis will be completed after evaluating the previous simulations into a urban context. Each urban space, i.e. a square, a road or a courtyard is a distinct system that should be analyzed every time. In this work just parts of urban spaces were considered, like a position close to a wall (dihedral) or the niche (trihedral) representing the corner in a square. Simulation results were compared with the reference case (pavement in open space, i.e. without facing buildings).

In order to include geometrical and material aspects in the same analysis the mean radiant temperature MRT was considered, i.e. the all surfaces temperature multiplied by the view factors of buildings and pavement.

The urban space is usually considered "closed", i.e. the sum of view factors is equal to 1. In this analysis only pavement and facades were considered, (dihedral and trihedral configuration) (fig.1).

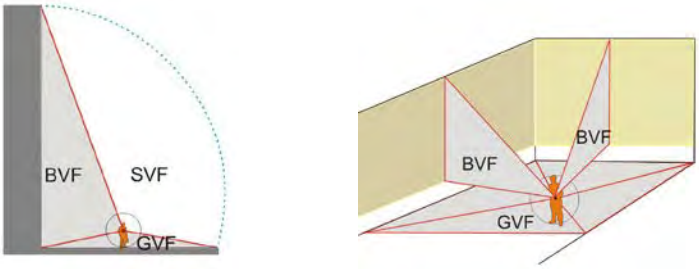

Fig.1: Dihedral and trihedral sections with angles representation for view factors calculations. BVF= building view factor; GVF= ground view factor; SVF= sky view factor (1- BVF-GVF).

Table. 2. Physical characteristics of façade materials used for the simulation

	N°	Material	cm	Conductivity (W/m°C)	Specific heat (J/kg°C)	Density (Kg/m^3)
"LIGHT"	1	wooden floor	2	0.15	2500	560
	2	polystyrene	20	0.04	1000	25
	3	wooden floor	2	0.15	2500	560
MASSIVE	1	plaster	1.5	0.9	840	1800
	2	bricks	20	0.8	840	2000
	3	plaster	1.5	0.9	840	1800
GLASS WALL	1	Double glass	2.2	1	837	3500

The two configurations in the four orientations were analysed and observations were made to understand what happens when the point is near or far from the wall and what happens if the wall is 4 or 20 metres high. It is possible to investigate the role of vertical surfaces, it means to understand what happens when the wall is a glass' one, brickwork (heavy) or highly insulated (light) one, associate to a paving with albedo A = 0.5.

3. Results

3.1. Materials' energy behaviour in open space

The comparison among stone materials shows that the porphyry is the stone with the worst environmental performance because of the high conductivity and relative low density. If we consider only density and conductivity e not the albedo parameter, marble and granite would be quite similar and with best environmental performance (fig.2). During the day surface temperatures would arise over the air temperature (>10°C) while in the night it would go under air temperature, to about 4-5 °C.

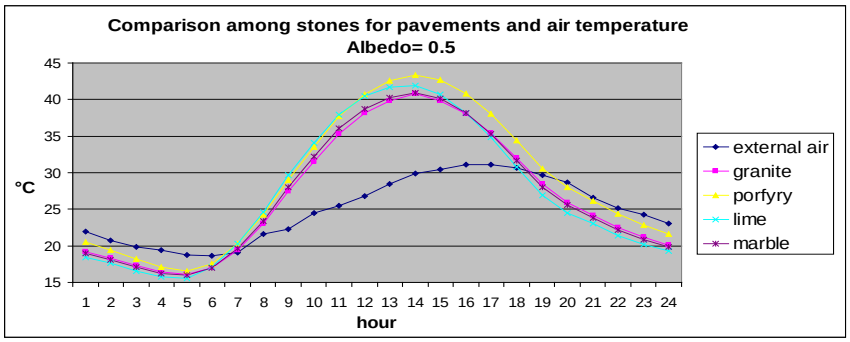

Fig.2: air temperature and stone pavements surface temperature. All stone materials are considered with the same albedo

Lime stone with relative low density and low conductivity has the surface temperature higher than the marble's and granite's ones and during the night it is the coolest material.
Regarding the other materials, wood has the worst performance, few differences if it is citron or larch. The asphalt is similar to the concrete and it isn't the worst material as usual (fig.3).

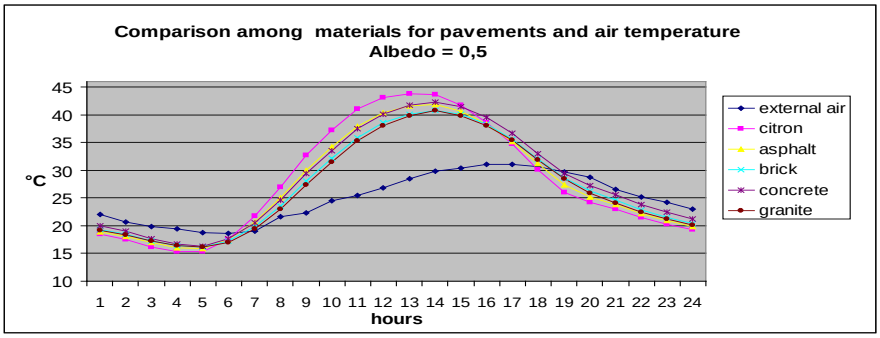

Fig.3: air temperature and surface temperature. All materials are considered with the same albedo

Considering realistic albedo values the red granite temperature is between porphyry and lime stone's ones (fig.4), quite higher than the marbles one (>10°C). According to [7], it is evident that higher is the albedo, lower is the surface temperature, in spite of the other physical characteristics of the materials. The white marble for instance has the albedo value close to 0.8 and his surface temperature is lower than the air temperature. On the other hand asphalt is absolutely the worst, due to the low albedo. With a simple observation we can confirm that asphalt should be avoided in pedestrian areas.

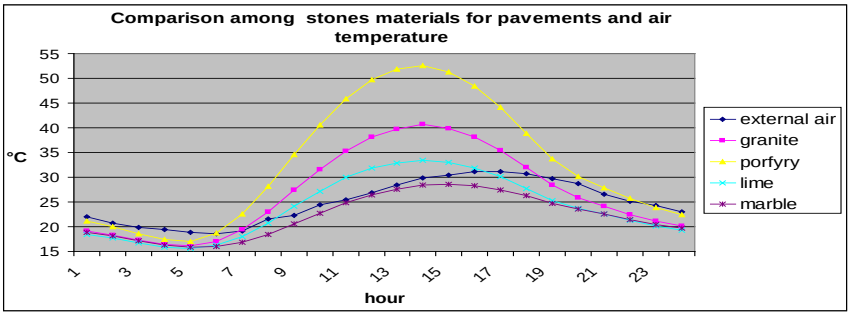

Fig.4: air temperature and stone pavements surface temperature

Wood hasn't good performance as well and if we want to use it, it would be better to paint it otherwise to use it with water as for cool pavements.

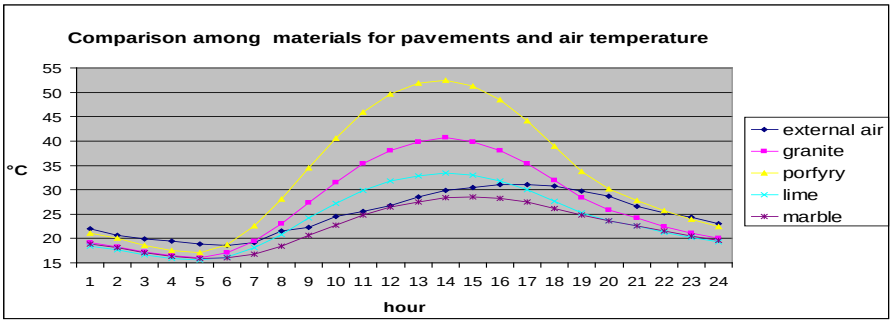

Fig.5: air temperature and pavements surface temperature

In general we can see that during the day the difference between materials and air temperatures could be also about 23°C (the higher difference at 2 p.m., in fig.5), but in the night the air temperature is always higher than the pavements materials' one. Figure 5 also shows that even in this case there are significant differences during the day when a big amount of solar radiation is present. In these hours the albedo influence is evident. During the night differences are due to density and conductivity (specific heat is similar for them).

3.2. Materials' energy behaviour in simplified urban configurations

The graphs display air and mean radiant temperature in a dihedral and trihedral shape.

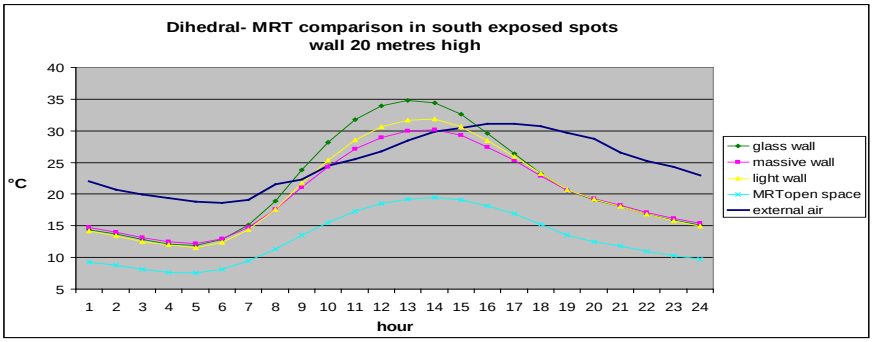

Fig.6: air temperature and mean radiant temperature (MRT) in an open space and dihedrals shape with massive light and glass wall. The point is south exposed 10 metres far from the wall 20 m high

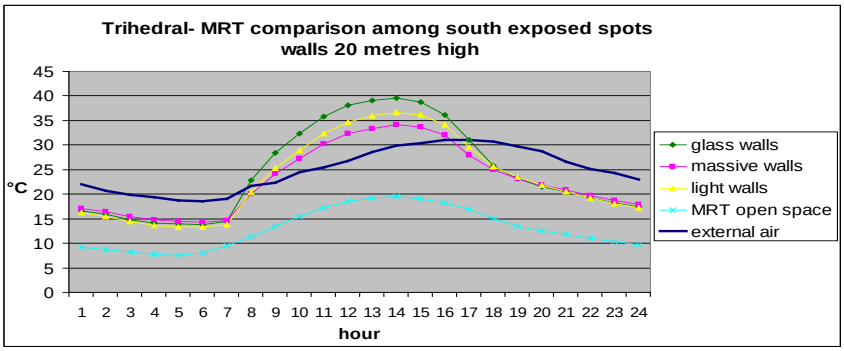

Fig.7: air temperature and mean radiant temperature (MRT) in an open space and trihedrals shape with massive light and glass wall. The point is south exposed 10 metres far from the wall 20 m high

Both in the dihedral and the trihedral with a glass wall the MRT is higher than in massive and light walls During the day, especially between 8 a.m. and 5 p.m. the MRT with glass wall is maximum 3 °C higher than in the light wall and till 5 °C than in the massive wall(fig.6, fig.7).. The farther we move from the wall the lower the surface difference will be; this is due to different wall materials. 10 metres far from the wall the differences are insignificant.

When the wall height decreases also the surface temperature decreases and consequently the MRT too. Differences of temperature between a wall 4 metres high and another one 20 metres high are about 4-5°C for every orientation (fig.8, fig.9). By comparing MRT of dihedral and trihedral with MRT in open field – with only pavement- the contribution is clearly evident. For instance at 2 p.m. a south oriented dihedral with the glass wall 20 metres high has the MRT 20°C higher than MRT in open field as the MRT in the configuration with glass wall 4 metres high is 7°C higher than one in open field.

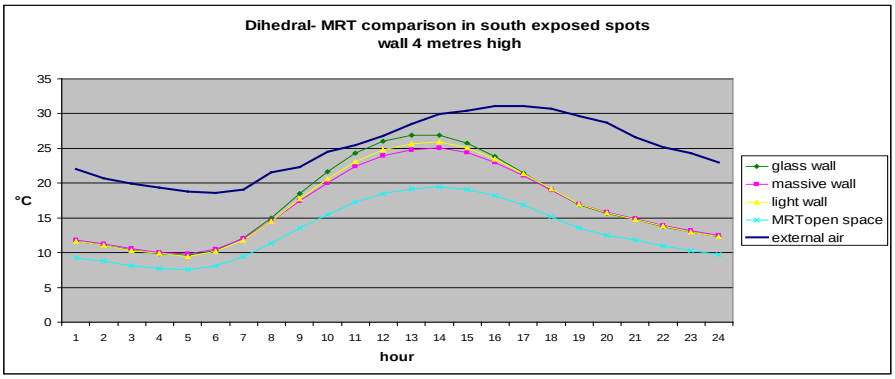

Fig.8: air temperature and mean radiant temperature (MRT) in an open space and dihedrals shape with massive light and glass wall. The point is south exposed 10 metres far from the wall 4 m high

It is possible to observe same differences in the other orientations even though temperature trends are different.

The MRT in the dihedral with the north oriented wall is always under the air temperature because it isn't never reached by solar radiation. The one with west oriented wall is the worst because of the large amount of solar radiation that reach the wall.

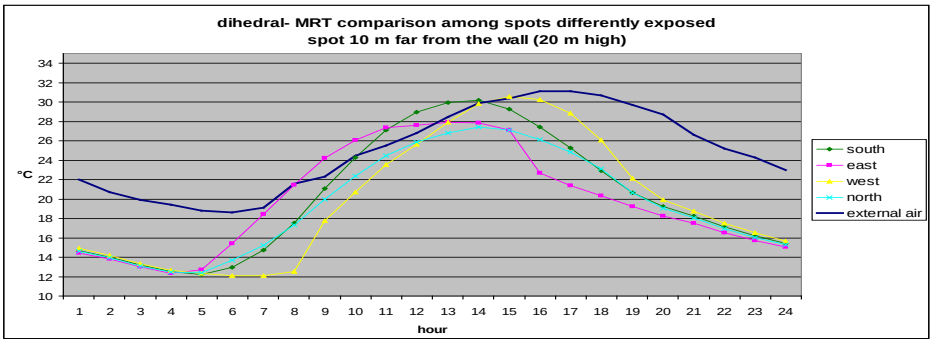

Fig.9: air temperature and mean radiant temperature (MRT) in an open space and dihedrals shape with massive wall. The points are south east and west exposed 10 metres far from the wall 20 m high

3.3. Thermal comfort

Finally a thermal comfort analysis was carried out to define configurations environmental performance in terms of people well-being. Surface temperature and MRT parameters are only a part of urban space configurations used to evaluate environmental performance. In order to evaluate thermal comfort we need to "close" this configuration by considering the sky view factor and the sky temperature. Thermal comfort was considered in terms of PET. With this evaluation it is possible to see any changing in people behaviour when they walk on a street like a "belvedere", for instance, or when getting close to a square corner. Graph reported below considers the dihedral and trihedral with facing walls 20 metres high and the analysed position 10 metres far from the wall.

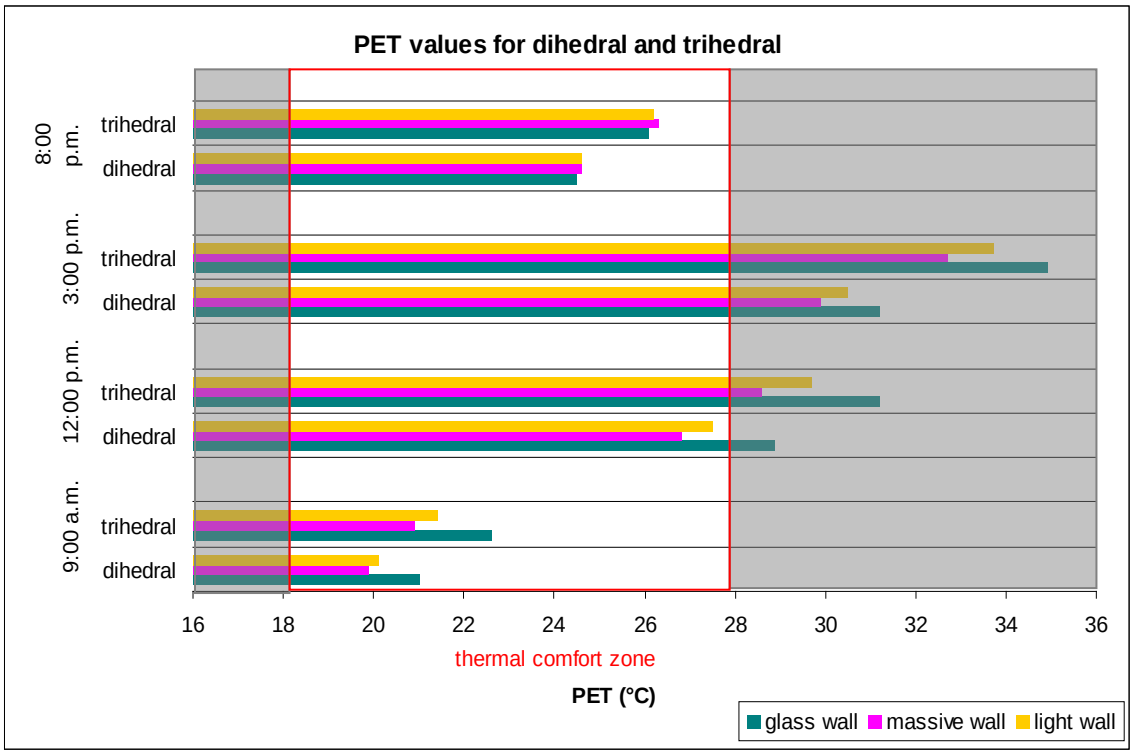

Fig.10: PET of the south exposed dihedral and trihedral with glass, massive and light wall.

For the trihedral we have the same trends of the dihedral but at mid-day and early in the afternoon PET is about 4°C higher then in dihedral. It is strongly recommended not to use glass wall and to be careful with the light wall too. Massive structures should be preferred.
According with the previous analysis west oriented configurations have the worst comfort conditions due to the incident radiation on the facades in the hottest hours of the day.

4. Discussion and conclusion

Lot of investigation have been done considering performance of materials in terms of surface temperature. The target of these researches are mainly focused on the heat island effect [6] [7]. According to this it would be easy to have simple conclusions on the choice of the best performing urban material. Nevertheless we need to clarify possible misunderstandings.

As we have seen, during a sunny day the surface temperature increases as the albedo decreases; in other words dark colours correspond to higher temperature and vice versa.

Clear and smooth materials like the marble have surface temperature are similar to the air temperature thus they behave as they are in shadow. One of the most popular strategies to reduce the heat island effects consists of using clear materials because they don't heat and reflect solar radiation. Nevertheless some problems are faced by using clear materials and when considering the idea to white as much as possible the urban surface. Problems can be the dazzling and the visual discomfort in addition to problems related to the urban traffic.

The other issue is related to the thermal comfort. The solar radiation reflected from a clear surface, like the marble, can be easily redirect to a space user. In the heat balance we have the surface temperature (as MRT) with the whole radiation including the reflected one. It's true that the marble absorbs 20% of radiation and its surface temperature is always quite low, but we cannot ignore that the 80% go back to the environment and can hit other urban surface on the space users. Material choice has to be done by keeping in mind all the elements trying to combine the "bad" material in terms of thermal comfort, with cooling strategies, like shading devices or water cooling system. A Thermally positive material surfaces temperature should be close to the air temperature during the day, with surfaces temperature similar to the surfaces temperature of materials always shaded.

References

[1] Scudo G., Dessì V., Rogora A., "Evaluation of radiant conditions in urban space" In: Designing open spaces in the urban environment: a bioclimatic approach. Ed. CRES, Athens, 2004

[2] Dessì V., Progettare il comfort urbano. Soluzioni per un'integrazione tra società e territorio, Napoli, Sistemi editoriali Se, Esselibri. Napoli, Esselibri, 2007

[3] Antoine M.-J, Groleau D., "Assessing solar energy and environmental variables in urban outdoor spaces: a simulation tool", in: Rebuild the European cities of Tomorrow: Shaping our European cities for the 21st Century. Proc. of the 2nd European Conference, ETA, Florence, 1998

[4] Doulos L., Santamouris M., Livada I., "Passive cooling of outdoor urban space. The role of materials", in: *Solar Energy* n° 77, Elsevier, 2004

[5] Santamouris M., "Appropriate materials for the urban environment" in: *Energy and climate in the urban built environment*. Asimakopoulos D.N. et alii, Mat Santamouris ed., 2001

[6] Akbari H., et al., 1992 Cooling our community. A guidebook on tree planting and light coloured surfacing, EPA, Lawrence Berkeley Laboratory, 1992

[7] Akbari H., Menon S., Rosenfeld A., "Global cooling: effect of urban albedo on global temperature". In: 2nd Palenc Conference, Santamouris Wouters ed., Athens, 2007

The Franklin district of Mulhouse: first French experience of low energy building renovation in a historic area of the city centre

Benoit Boutaud[1,*], Andreas Koch[1], Pascal Girault[1]

[1] *European Institute for Energy Research, Karlsruhe, Germany*
** Corresponding author. Tel: +49 (0) 721 61 05 17 06, Fax: +49 (0) 721 61 13 32, E-mail: boutaud@eifer.org*

Summary: The project for the Franklin district of Mulhouse is the first French experiment in the renovation of old buildings in the context of a deteriorating urban area with a historic character to preserve incorporating firm energy objectives. Its first phase has just been completed with the publication of a feedback report [1] regarding its energy concept, large parts of this paper are based on these findings. The latter is in line with the Annex 51 programme of the International Energy Agency, *Energy Efficient Communities: Case Studies and Strategic Guidance for Urban Decision Makers*. The aim of this paper is to clarify the main elements enabling this project and to present the first results after two years of monitoring.

Keywords: *Urban Renovation, planning instruments, financing schemes, historical area*

In the European context a large part of the activities in urban development planning focus on the rehabilitation of existing areas. Today's approaches for rehabilitation schemes have to address the urgent environmental questions by increasing the energy efficiency of our cities but at the same time have to find answers to social difficulties and in many cases respect historic characteristics of the city. These were the main objectives for the City of Mulhouse in 2004 when it began to renovate a large part of its city centre and simultaneously intensify its sustainable development policy, especially focusing on climate change. Much of the city centre at that time was experiencing social difficulties and the inhabitants saw their everyday surroundings deteriorate. For this reason, the city chose to combine urban renovation and low energy use concepts by launching out one of the first projects in France regarding renewable energy in a historic city area formed by the legacy of the city's working-class past. The Franklin scheme is in line with the definition and the set-up of sustainable development policies at the national and European level. The aims at the outset were high and the conditions for getting there were difficult. This paper will discuss the first results and show that the project succeeded to nut just conduct a renovation programme but to fit and interlock with a policy and city planning logic on the agglomeration scale. Energy efficiency is thus closely linked with social and economic considerations. First results from the time span between 2004 to 2010 are discussed here based on a follow up report published in May 2010 [1], first of all by presenting the contextual specifics on which the operation depends; by focusing on the elements necessary for setting it up and finally, by presenting the necessary determining factors in the success of low energy building renovation measures that this experiment produced.

1. Context and energy targets

1.1. Operational Context

The district of Mulhouse (112 000 inhabitants) and its metropolitan area m2A (Mulhouse Alsace agglomeration - 255 000 inhabitants) occupies a unique geographic position in close proximity to Switzerland (Basel) and Germany (Freiburg). In the early 20th century it was one of the biggest European industrial centres. After de-industrialisation and the sweeping economic changes which followed this age, the town experienced harder times which it has been trying to overcome for many years. In order to achieve this, it can count on a young population and recognised technological know how mainly in the automobile industry.

Having something of an image problem, and looking to make the area more attractive, the Mulhouse agglomeration was one of the first actively to embark on sustainable city planning. Its climate plan, drawn up in accordance with the National Climate Plan, is one of the first in France (2007). This first step also includes the hope to revitalise the agglomeration's centre and to slow migration of commercial activity and the middle classes towards the periphery. To this end, work was undertaken in 2001 as part of a vast programme to renovate the city centre which included public spaces, economic activity and housing. It is within this framework that the local authority decided to renovate a number of particularly run-down buildings in line with low energy use targets. Thus first and foremost it is an approach linked to city policy, within which an environmental and energy aspect is formulated.

1.2. Energy Objectives

The Franklin district was built by the leaders of the Mulhouse textile industry between 1880 and 1910 to house their workers. It was very run-down and heading towards abject poverty, which resulted in a sizeable lack of renovation of buildings, some of these becoming outdated without a corresponding fall in housing costs falling behind in terms of comfort and basic facilities as well as security problems. In 2004, the city therefore launched a consultation process as part of the city centre's renovation. The local authority wanted to preserve the strong working-class identity of the area while implementing a thorough renovation which could have a practical impact on the urban environment and on the inhabitants' quality of life. Eventually the low energy building standard (BBC[1]) was set as target. Back then, and still today, renovating buildings according to the BBC standard is regarded ambitious in the French context, with energy use twice as low as the requirement of new buildings at that time. This level was set by the ALME (Agence locale de la maîtrise de l'énergie – Local Energy Agency) one of the very first French agencies created within the framework of the 1999 European SAVE programme. The ALME was given a mandate by the city of Mulhouse to develop energy optimisation and the use of renewable energies on the buildings to be renovated in Franklin. It also coordinated and led the operation, being responsible for accompanying the contracting authorities and project managers in applying their energy limits.

The neighbourhood consists of 300 buildings of which 106 were identified as not being in an adequate condition. Almost a third of the 106 buildings were potentially involved in the renovation work. Most of the dwellings in question are identical terraced town houses (i.e. adjoining on two sides) which contain 2 to 4 levels. To reduce the primary energy demand from an average of 450 kWh/(m²a) in primary energy to the set target, a modest intervention was not enough. From the outset, ALME, which engaged the services of a specialist energy research department (ENERTECH), decided to develop "standard technical solution" (solution technique universelle - STU) [2] in order to gain simplicity and efficiency in the implementation and also to reduce the costs. An initial comparison based on the dynamic simulation of individual buildings allowed assessing different combinations of existing efficiency technologies in order to define the targets which would be adapted to the Alsace region. To reach the BBC level, several main themes were defined. Insulation was reinforced for the walls and windows (triple glazing), taking summer comfort into account. External insulation was preferred where possible but the historic character of the façades or the encroachment onto the pavements often rendered this solution impossible.

[1] The French BBC standard limits primary energy use to 50 $kWh_{primary}/(m^2a)$. This value includes heating and cooling needs as well as energy for domestic hot water, ventilation and lighting.

The existing distribution system (i.e. radiators) were maintained but supplied by new wall mounted condensing gas boilers. The air exchange was ensured via mechanical ventilation with heat recovery, centralised for each building. From the point of view of electricity consumption, savings were identified in specific uses of electricity (appliances on standby, buying class A appliances or better). Domestic hot water (ECS) was taken care of by solar water heaters, from 5 to 7 m² per building, representing about 40% of the needs. At the same time, devices reducing water consumption were installed (e. g. pressure reducers).

Integrating all these solutions into a renovation project was sometimes complicated. The installation of some particular devices such as the double flux ventilators required ducts inside the dwellings. Alongside these technical problems, complexity also arose around the set-up of the project which had to obtain the maximum amount of financial backing and attain the energy targets.

2. A combination of mechanisms for the renovation scheme

2.1. The process

The city of Mulhouse delegated the project's implementation and management to SERM, a local mixed enterprise for developments in the Mulhouse region. The firm was mandated by the city of Mulhouse to carry out the operation in strict collaboration with ALME.
SERM was in charge of the renovation operation in 2004 for the old historic parts of town. Within this perimeter, some buildings from the Franklin district were particularly run-down, which meant their owners could have been forced to carry out renovations on their property. If they weren't capable to do so, the work would be declared in the public interest for these buildings, which allowed SERM to acquire the buildings. The buildings were then resold at the market rate to private landlords with an obligation to carry out the work according to the low energy standards contained in the conditions of the contract. The resulting incremental costs for investors were compensated by the community authority through subsidies and tax benefits. To support them in the application of the contractual conditions, the investor and his project manager received free assistance from ALME throughout the realisation of the project in order to respond to their enquiries and to ensure conformity for the intended work. The aim was to integrate the energy constraints and to form teams contributing to the installation of the technology. ALME also carried out checks during construction time and was available for the entire operational phase. This monitoring led to an optimisation along the way, following difficulties which arose during the implementation of technology which at that date was not in widespread use. Once the buildings were finished and the inhabitants had taken possession of them, ALME supported the tenants by informing them about the aims of this low energy renovation and by explaining how to operate the devices.

So that these aims and this support would be feasible and financially realistic, the local parties involved sought to take advantage of the financial opportunities the project was able to claim.

2.2. The implementation

In this paper the main focus is put on the implementation process. Therefore technical aspects will be treated in a lesser detail while primarily planning and financial instruments applied in the project will be described. Urban renewal operations as the one described depend on a sizeable number of financial aids to be called upon for the actors within the given area who do not have the necessary funds at their disposal (local authorities as well as private property owners). The necessity as traditional mechanisms to renovate buildings are ineffective (e.g. the property market or economic activity). As a result, the success of a project such as the one

in Franklin relies on the ability of the project manager to obtain financial backing and its effective usage. The city of Mulhouse – and indirectly the private investors in the district – managed to do this. In addition to their own funds, they received significant subsidies which the diagram below summarises, indicating the level of origin and whether or not they were transferred directly to the public project manager.

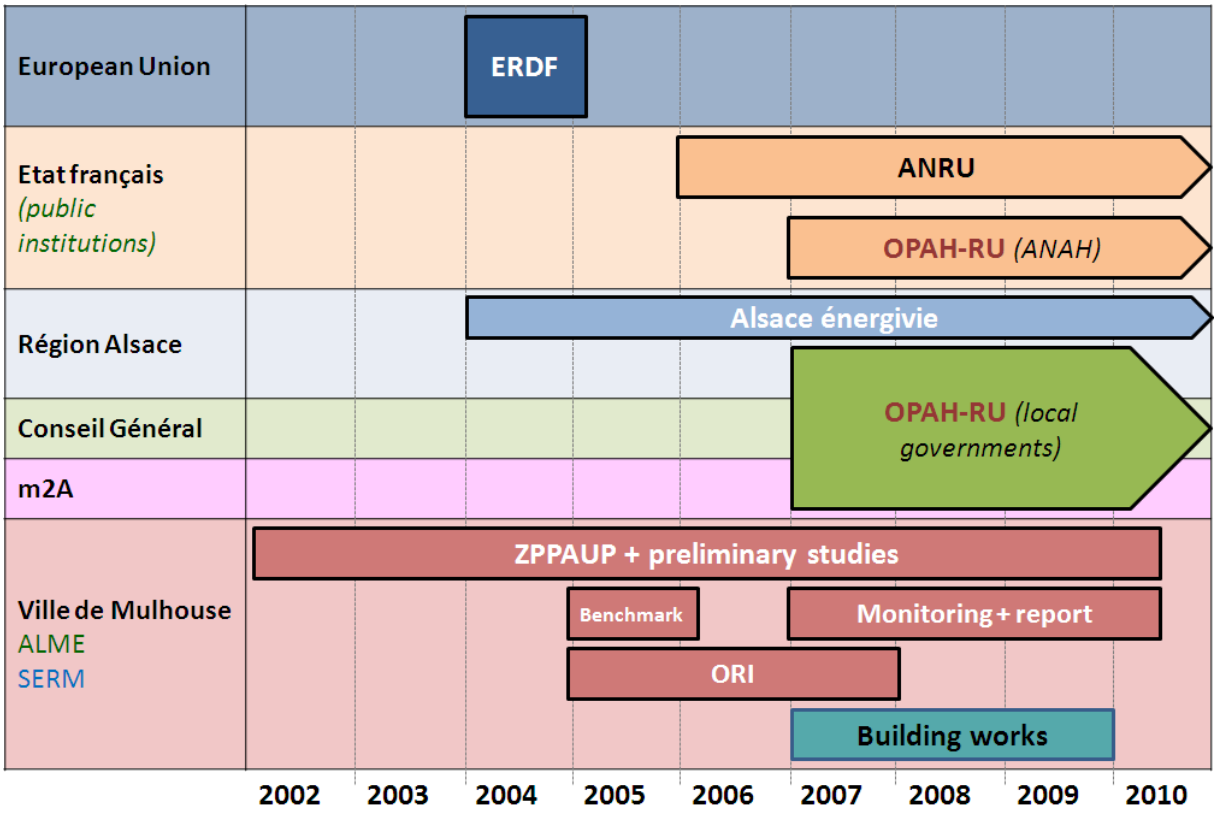

Figure 1 : Summary diagram of programmes and financial schemes in place within the Franklin district project

The European Union contributed via the European Regional Development Fund (FEDER) by financing for two years the preliminary research and the benchmarking. It was also a partner in the programme *"Alsace énergivie"* [4] led by the Region of Alsace in partnership with the ADEME which funded all the organisational engineering and the project's technical support assistance between 2004 and 2010. This programme has been designed since 1998 to promote energy saving and renewable energy by supporting private entities as well as local governments in their projects (awarded the 2008 European Commission Regiostars prize). Alongside this involvement, the state plays a specific role both by contributing direct funds to the local authority, but also by subsidising private entities. The City of Mulhouse came to choose the Franklin district project because it presented an ideal configuration, allowing urban renovation funds set up by the French state to be drawn on as part of the implementation of a city policy. This area is affected by four main mechanisms which are strongly interrelated.

An agreement was signed with the National Agency for Urban Renovation (ANRU) concerning the old city-centre districts such as Franklin (€270m of which 18m were allocated to the programme in 2006). ANRU is a public institute charged with funding and setting up the urban renovation programme across the country in urban zones which have experienced

difficulties (lack of social/functional mix, lack of opening up to the rest of the city, etc.). In the Franklin district and the old districts surrounding it, it was expected that the housing on offer would be renewed, and that a series of public places would be rearranged: the Franklin public square, several schools, extracurricular centres, etc. The ANRU funds went directly to the public body charged with carrying out the work.

Furthermore, a scheme designed to improve the housing sector (OPAH) has been launched, dedicated to zones containing a high number of buildings potentially hazardous to health, run down (both internally and externally), empty or subject to social dysfunction. The OPAH-RUs (Urban Renewal, specific to urban zones), solely dedicated to the rehabilitation of urban zones, are organised as a partnership between districts, local authorities and the state. Here, it's the Alscace regional authority, the agglomeration of Mulhouse m2A and the City of Mulhouse who contributed to the funding. The ANAH subsidies rose to about €350/m² transferred to the new owners of the property for a renovation cost of €1450 /m² (exclusive of tax).

The fourth mechanism is the setting-up of an scheme for property restoration (ORI) for old districts, which can be applied when the building is especially dilapidated and after a public investigation has been carried out. It is applicable within a reduced perimeter and differs from the OPAH-RU operation because of its coercive character. In fact, the owners, once they have been notified of the requirement for work, run the risk of expropriation in the event of non-compliance. This was one of the levers used in order to impose a thorough renovation in the Franklin district.

Finally, tied in with this ORI, the municipality demarcated an architectural and urban heritage protection zone (ZPPAUP) which made it possible for owners to exempt a part of the cost of the renovation work subject to them by renting the building out.

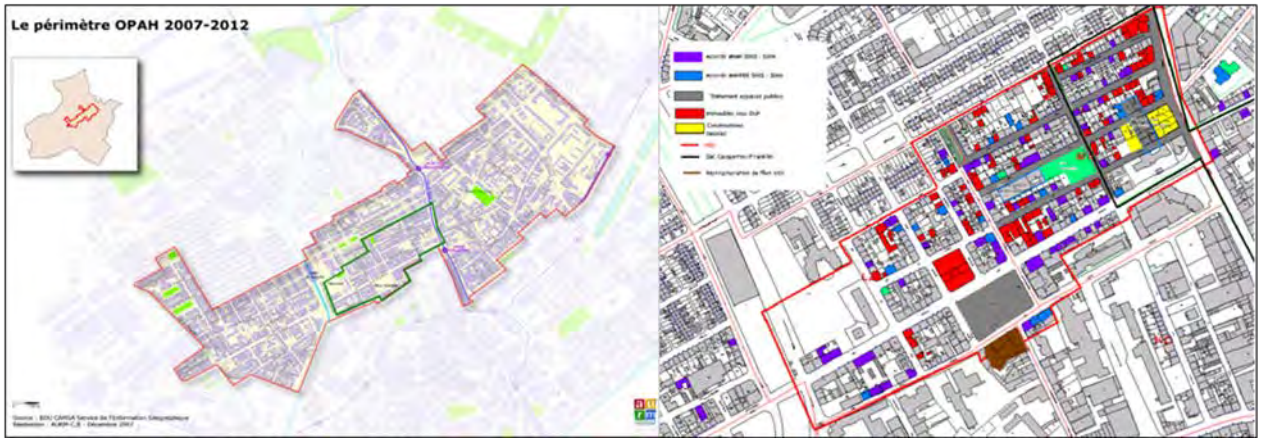

Figure 2 : The boundary of the OPAH and, that of the ORI (Source: ALME, AURM)

Within the framework of the aforementioned financial sources, SERM offered to help the owners for free. Firstly by providing for a dossier allowing all available subsidies to be claimed. Secondly by transferring the part directly subsidised to companies in form of upfront capital fund so that the owner wouldn't have to pay in advance. It therefore created a one-stop-shop for private entities. This action made the process of distributing subsidies easier, and so increases the attractiveness for private investors.

3. Energy efficiency at the linking technology and behaviour

3.1. The occupant, key element in low energy schemes

From the outset of the project, the Franklin district was intended above all to be a city planning experiment for renovating a city centre, as well as a turning-point taken by the agglomeration in terms of sustainable development. To follow its progress and develop it was therefore the motor for the management of the project. A very unusual approach which could even give rise to disappointment faced with the uncertainty of the results. However, aside from a few pitfalls, the positive outcome of the renovation scheme could clearly be demonstrated.

In financial terms, the additional costs associated with the requirement for low energy renovation ("universal technical solution ", STU) was estimated in 2006, at the start of the project's implementation, at €315/m² (exclusive of tax) relative to usable surface (figure 3). Other costs linked to energy rise to €524/m² (excl. tax) for a total cost for the implemented measures of €1551/m² (excl. tax). The individual measures are described in figure 3 and included the insulation of the roof and the walls, mechanical ventilation and exchange of the boiler.

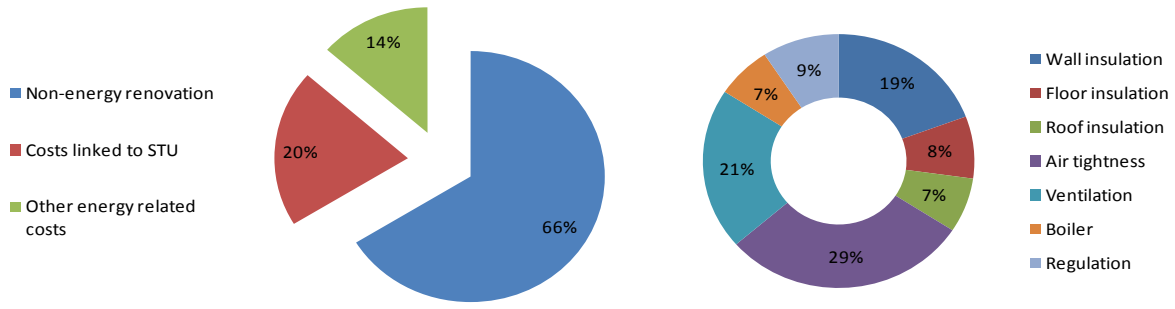

Figure 3: Cost breakdown of the renovation and ventilation of STU average costs in € and € /m² (excluding tax) of liveable surface area [3].

The investment costs, however, have had a tendency to go down since the start of the implementation in 2006 (-20% between 2009 and 2010). In addition, it became desirable to give up on some technical features which remained expensive such as triple glazing, and to develop air tightness in compensation which was found to provide for a higher energy efficiency potential [3] for the same investment. Concerning energy mechanisms, the 12 first buildings were the object of a thermal assessment and 2 years' monitoring. In addition, ALME's presence and its observations identified problems on site which couldn't be measured by instruments.

Yet Franklin is above all a city planning operation which, with or without ambitious energy targets, was a necessity for the neighbourhood. Its primary objective was the renovation of a run-down area improving the quality of life of its residents. The first return of experience on this subject is encouraging. The quality of using the dwellings has been improved: reduction of noise problems thanks to the insulation, greater thermal comfort, etc. This is accompanied by a significant lowering of costs for tenants who today pay rents similar to those in force prior to renovation but with charges considerably reduced (heating costs divided by 8). This advantage is vital because it sizably diminishes the vulnerability to energy price. More generally, the whole set of energy efficiency measures offers an added resale value for investors and increases the maintenance of the buildings over time.

From a specifically energy related perspective, one of the primary factors for success or, alternately, for failure, lies in the residents' acceptance of the systems put in place. An observation which has been highlighted in other analyses already carried out on new construction like in Grenoble's De Bonne district. The first results confirm that technology alone does not reach the full potential of the energy efficiency measures. First of all, the trial of communal areas for washing and drying made up part of the recommendations. However, this solution showed itself to be a failure as the designated spaces were not used very much. Also, some of the residents didn't follow the advice given to them during their moving in and kept the same habits as in a traditional dwelling (e.g. opening windows in winter, high heating temperature). The summer comfort was generally good but the results could have been even better with improved habits (e.g. night time ventilation). As often observed the users regulated the heating system to a higher indoor temperature as was initially assumed - heating to 20°C compared with the recommended 19°C. The final report cites the neutralisation of the thermostatic radiator valves regulated to a maximum of 19°C or the obstruction of the ventilator openings [3]. Besides traditional behavioural problems, one of the factors identified in this misuse lies in the problem of communication with the tenants. Sometimes this was linked to a poor command of the French language (suspicion regarding the measuring devices in the apartments, unworkable advice). In a more general sense sometimes the ALME had difficulties to stay informed of the arrival of new tenants which is due to the magnitude of owners and landlords in the area. However, the options for tackling this area of problems remain few, and their results hypothetical.

3.2. Energy efficiency: know-how and quality of implementation

Another behavioural factor depends on the implementation of the chosen energy efficiency measures. In Franklin, no revolutionary technology was used. On the other hand, in 2004 they were quite unusual compared to those traditionally used in French refurbishment market.
Some of the engineering offices in their approach did not distinguish between low energy buildings and traditional buildings. That notably led to an over sizing of the heating installations and therefore a poor efficiency. Moreover, the monitoring drew attention to the need, from the start up and the receiving of the dwellings, to take particular care of the auxiliary energy as well as ventilation or domestic hot water production.

Moreover some of the building professionals had not been informed about the installation quality required to achieve the low energy objectives. Problem also known in traditional construction yet its consequences become more visible when it comes to achieving this level of performance. Explanatory information had indeed been put together but it didn't work very well, notably because of the fluctuation of involved companies. This lack of care led in some examples to a poor air tightness of the building envelope. After the first applications this point has been added to the contractual conditions. Due to this, energy consumption for heating varied from one building to another partly caused by differences of air tightness. The average energy use is about 70 $kWh_{primary}/m^2$ of usable surface area per year in primary energy. Electricity consumption on the other hand was well managed, excluding that which was consumed by general maintenance services. A malfunction linked to incorrect application of the engineering office's instructions (e.g. continual running of pumps, ventilators) is strongly suspected and will be subject to further investigation. Finally, the thermal solar panels made it possible to attain the domestic hot water objectives.

Monitoring of the construction work will eventually allow the problems to be limited without however managing to avoid them completely. The aim therefore was achieved, which represents a success. Another positive note, the companies involved got used to the specific requirements of low energy buildings and are today more operational than when the project

started. Creating a skills centre on low energy building ("pôleBBC") is one of the means by which this is managed today. This centre is in close contact with the previously mentioned Alsace centre for energy [4]. Thus an important aspect of the Franklin district remains its capacity building aspect as a place for the application of energy efficient building techniques. It makes it possible to crystallize experiences, to create a space for discussion and to draw on other similar experiences from professionals. The benefits are threefold: acquire a recognised low-energy skill, bring this economic sector to life and create jobs.

4. Conclusion

The renovation of buildings in the Franklin district contributed a lot to the diffusion of low-energy buildings in Mulhouse and met many of the targets which were originally set. Numerous links have been set up in France and in Europe between Mulhouse and other cities facing similar problems via conferences and visits. The reproducibility of such an operation, which brings together the financial support mechanisms, is however scarcely conceivable in its present state. Some of the funds received were within the framework of promoting renewable energy or energy efficiency. But above all, these were only possible in derelict urban areas. As a result, what made it a success might to a degree be responsible for its non-reproducibility. These measures were chosen partly according to the prerogatives given to the public project manager to impose certain kinds of renovation, and partly according to the subsidies they could obtain with a view to making the project viable and attractive for private investors.

Franklin has become a part of the city's sustainable development policy which now can draw upon a set of good practices and lessons learned. In addition it bears testimony to the synergies between questions of energy efficiency, traditional urban renewal and, to a certain extent, the policy pursued on the scale of an entire agglomeration. Beyond the contribution to improving the urban quality of the city centre and social cohesion, core elements of the project, this experiment focussed above all on energy efficiency in an existing urban area, which remains today the real challenge to which we must respond.

Acknowledgements

The authors would like to thank the *Agence de l'environnement et de la maîtrise de l'énergie* (ADEME) [4] and Anne Grenier in particular, the local Energy Agency of the Mulhouse Region (A*gence locale de la maîtrise de l'énergie de la région mulhousienne* - ALME), the department for urban renewal of the City of Mulhouse (service du Renouvellement urbain de la Ville de Mulhouse)[5] and the *Société d'équipement de la région mulhousienne* (SERM) and the City of Mulhouse.

References

[1] Alsace énergivie, *Rénovation d'immeubles d'habitation au niveau BBC. Retour d'expérience sur les opérations menées dans le Quartier Franklin à Mulhouse de 2004 à 2010*, Mai 2004.

[2] ENERTECH, *Evaluation technico-économique de réhabilitation « basse consommation » d'immeubles d'habitation*, rapport final, mars 2010.

[3] Sidler, O., *Rénovation à basse consommation d'énergie des logements en France*, ENERTECH, 2007

[4] Alsace énergivie, *Etude sur la basse énergie appliquée aux anciens bâtiments*, 2005.

[5] http://www.ademe.fr

[6] http://www.mulhouse-alsace.fr

Energy Efficient Communities – A Collaboration Project of the International Energy Agency IEA

Reinhard Jank [1]

[1] *Volkswohnung GmbH, Karlsruhe, Germany*
Tel: +49 (0) 721 3506 238, E-mail: reinhard.jank@volkswohnung.com

Summary: The background and purpose of a project to evaluate international experiences on planning and implementation of "Energy Efficient Communities" is explained. First results are presented, showing approaches and successes/failures on different levels of "communities", and conclusions to be drawn.

Keywords: *Urban energy planning, energy system models, IEA ECBCS R&D projects*

1. Introduction

Since in general over 40 % of the end energy use in OECD countries is caused by the built environment, an increase of the energy performance in this sector, together with the increased use of renewables for electricity generation, will be the key to a successful energy and climate change policy in the industrialized world. 80 % of our built environment is located in towns and cities. For this reason, it is decisive that cities, small or large, will be able to achieve such ambitious energy goals, and this will entail enormous changes in urban fabric and urban energy use patterns in the future. During recent years, new energy standards like the German "Passivhaus" or the Swiss "Minergie", or even "Net Zero Buildings", have been introduced successfully, which have facilitated a reduction of end energy consumption by a factor of 2 or more compared to conventional new buildings. Is this the solution of the problem? Looking at the existing buildings in our cities and considering the fact, that some 80 % of them will still be there in 2050, and their current primary energy consumption for heating, cooling, hot water and electric appliances is in most cases beyond 300 kWh_{PE}/m^2, a reduction by 80 % would require a primary energy use level of about 60 kWh_{PE}/m^2. While this is technically feasible with today's technologies, there are economic limits due to a non-linear increase of costs. To reduce the economic burden, cost-efficient alternatives must be found to simply decreasing U-values below economic limits.

Due to economies of scale, a number of technologies, like cogeneration or combined heat and power, waste heat recovery, biomass, geothermal energy, solar heating (and cooling), and others, are more efficient – in technical and economic terms – when used in large installations instead of small ones. Taking advantage of these technologies where locally available will enable the primary energy consumption (or GHG emissions) achieved by an optimized system to fall possibly to the best available standards (in terms of kWh/m^2 or kg CO_2/m^2) for new buildings, but with lower cost and with the advantage of a feasibility at community scales. A successful urban climate change policy will only be available if such options can be found and realized; otherwise, it will just be too expensive. Therefore, communities will have an essential role to play in the future to make this happen.

As the number of cities with successful climate change policy is still very low, it is obvious that there are powerful barriers that prevent cities from recognizing and implementing their potentials. A strategy to bypass these barriers is needed, in the form of integrated energy planning for neighbourhoods or energy master plans for whole cities – and the corresponding implementation strategies. Contrary to individual pilot or demonstration buildings, the aim of community-wide energy concepts must be to find an optimized solution *in economic terms* rather than introducing cutting-edge technical innovations, otherwise implementation would

not be achievable. This makes a big difference between community projects and projects that are involved just with one single building. This has been recognized in several countries, where national programs for urban energy planning projects have been initiated. To benefit from experiences made by those national Case Studies, an international project (an "Annex") was commenced within the framework of IEA's "Energy Conservation in Buildings and Communities" Implementing Agreement. The title of this ECBCS-Annex 51 is "*Guidelines and Case Studies for Energy Efficient Communities"*. The work has begun in 2009 and will be finished until autumn 2012. 11 countries participate in this Annex.

2. Objectives and Project Structure

In Local or Urban Energy Planning, there are no standard solutions. An optimized design and implementation strategy must be found in every new case. The subject of Annex 51 is to identify methods how to find such solutions and to provide successful examples: Its aim is to provide stakeholders in communities with the necessary information to be able to achieve their local climate policy goals more successfully than in the past. This objective has defined the work plan of Annex 51:

- explore the state-of-the-art of local energy planning with respect to methods, tools and strategies: *Subtask A*
- exchange experiences from projects ("Case Studies") carried out within the ongoing national "city" programs: *Subtask B* for neighborhoods and *Subtask C* for whole cities
- summarize the outcome of this work in the form of a guidebook that serves as a source of methodological knowledge and practical examples for local decision makers and planners, and supply a simplified planning tool for decision makers to be used in the early planning phase: *Subtask D*

3. Annex 51 – Subtasks

3.1 Subtask A: Review on Existing Planning Tools and Implementation Strategies

Subtask A will be finished until summer 2011. The Subtask leader is France, represented by P. Girault and A. Koch from EiFER – European Institute for Energy Research (a research subsidiary of EdF in Karlsruhe). In this Subtask, selected successful Local or Urban Energy Planning projects ("LEP" or "UEP") from the participating countries, and planning methods and tools used in practice are evaluated, but more importantly, implementation strategies and instruments are discussed and conclusions will be drawn.

3.1.1 LEP – Neighbourhood Scale Projects

The LEP projects showed a large variety in terms of size, uses, targets, building constructions and energy systems involved, such as inner city revitalisation projects, as Western Harbour in Malmö or Regent Park, Toronto, or a commercial downtown district in Yokohama, until greenfield residential developments like Burgholzhof in Stuttgart. The number of residents or users is between 1.000 and 10.000 in most cases. While most of the cases have been finished, others are still in some stage of implementation.

The technical descriptions of the LEP projects presented in Subtask A have a big value in itself, because they show the large variety of solutions and approaches that can be used to achieve the energy or GHG goals strived for in the different projects. Due to the fact that in most cases there was no direct access to detailed data in Subtask A (planning data, measured data after completion, cost and price structures etc.), a quantitative evaluation is impossible for the Subtask A cases. In particular, it was not possible in most of the projects to compare

the initial targets in terms of energy efficiency or GHG reduction with the reality after project completion. This should be different in Subtasks B and C, because the respective reviewers in most cases are directly involved with the Case Studies considered there. Conclusions to be drawn from Subtask A in terms of planning and implementation processes of LEP projects, show that five major influences seem to be common as success factors:

- a decision maker being directly involved in the specific project and acting as a driver in terms of technical innovations, energy / sustainability targets, feed-back to stakeholders etc.
- bilateral/personal information transfer from comparable other community projects that have been successfully implemented
- a "contract" at the initial phase of the project that is signed by all involved actors in mutual agreement and where the main targets of the LEP project are laid down
- the perspective of grants or allowances for the project according to some public funding program (whereas the absolute amount of money received seems to be less important)
- an "integrated approach", aiming at a holistic view of the long-term perspective of the neighbourhood or district under consideration in terms of the three components of "sustainability": social, economic and ecologic development.

In every specific LEP project, there might be other important issues that need proper solutions, but if all these five favourable points as mentioned above are valid in a project, the perspectives for successful implementation seem in general to be good.

3.1.2 UEP - City Scale Projects

A detailed discussion of the conditions and approaches of city Case Studies in terms of energy or GHG policy is being done in Subtask C. In Subtask A, only 2 cities have been presented as cases, Lyon in France, and Freiburg in Germany. While Lyon has began only recently with the establishment of a "climate plan", in the City of Freiburg a continuous municipal energy policy has taken place since almost 30 years. Four phases can be identified: an initial period of political dispute (1980ies), a phase of first quantification of urban energy saving and renewable potentials and targets (1990 – 1996), a learning phase of practical implementation (until 2003) and a phase of re-adjustment to ensure successful achievement of the energy targets (until 2007). These last two phases may repeat periodically during implementation. The following chart presents wishful and real GHG developments in Freiburg over 20 years of time, showing that successful GHG policies for whole cities need a very long time and continuous adjustments to make sure that there is a move towards the targets set.

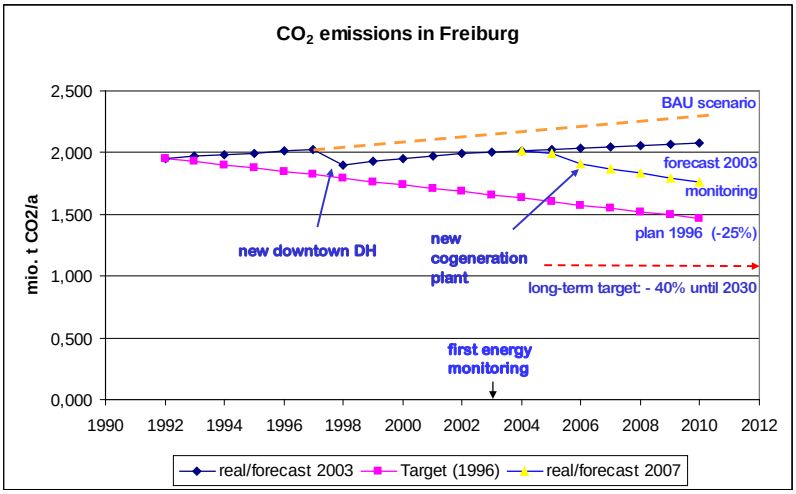

Fig. 1: Projected and real development of CO_2-emissions in Freiburg1992 - 2010

Fig. 1 illustrates the results of these phases in terms of urban GHG emissions in Freiburg, beginning with the first quantification phase in 1995. Based on this, a target of minus 25 % CO_2-emissions until 2010 (compared to 1992) was decided in 1996 by the City Council, while focusing its policy to *solar energy* and on ambitious standards for *new buildings*.

When a first evaluation of this policy, made in 2003, proved that the target until 2010 would be clearly missed, a new phase of analysis of more detailed and realistic energy scenarios was initiated. A first conclusion taken was that it would be necessary to track periodically the effects of measures made in the framework of the municipal energy policy. For that purpose, a tailor-made municipal energy and GHG balancing scheme was developed. However, developing a successful implementation policy based on local energy conservation and renewables potentials was a difficult step, which needed extensive discussions. To enable a detailed discussion of different policies, a spread sheet model with four "scenarios" was developed, which was used to quantify different assumptions or combinations of measures over a given timeline. As a result, in 2008 an almost unanimous decision was taken by the City Council to define a new GHG target of "minus 40 % until 2030" compared to 1992. This decision was combined with the presentation of a "climate change roadmap". The municipal administration was appointed to be responsible to report periodically on their implementation.

Most important points on the "climate change roadmap" were the support of a retrofit program of the building stock making use of federal building modernisation pro grams, enforcement of neighbourhood scale district-heating schemes using cogeneration, biomass or biogas, substitution of all remaining coal uses, support of electricity saving programs for private households, and a diversity of measures in the mobility sector. Eventually, an ambitious modernization program of the municipal buildings was decided to serve as a model also for other investors in the commercial sector.

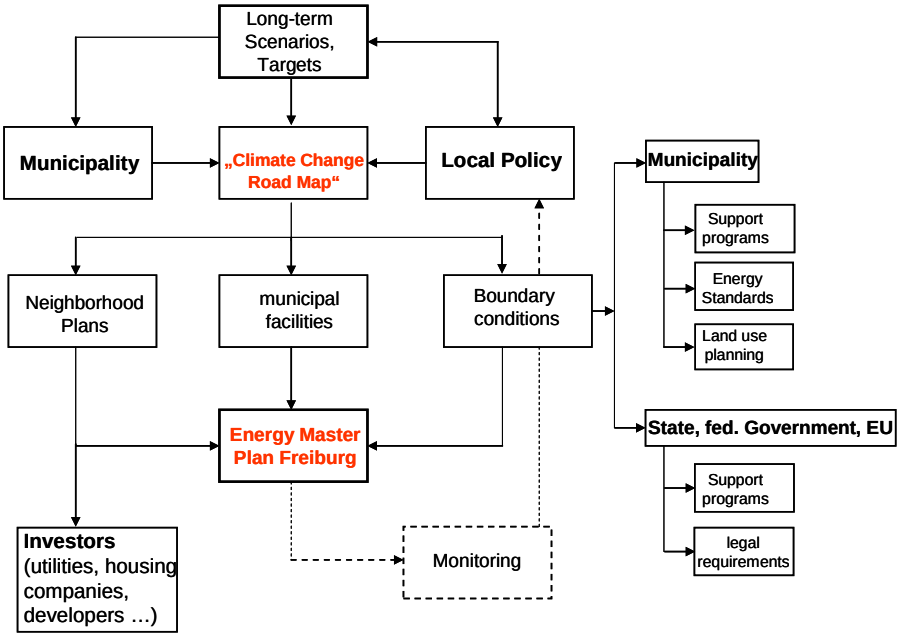

Fig. 2: Climate change policy in Freiburg 2008 - Organisational Structure

Fig. 2 shows a sketch of the decision making structure that can be outlined. The experiences in Freiburg have shown that the pre-requisites of a successful municipal energy and GHG policy will consist of a

- detailed information base on local potentials and options
- realistic target-setting based on achievable results
- detailed delegation of responsibilities and obligations
- continuous monitoring and communication
- installation of a project management (authority, energy agency, …) responsible for work organisation, reporting and feed-back to involved stakeholders.

As can be learned from the experiences in Freiburg, the definition and implementation of a community energy policy is a task, which requires a certain continuity in know-how and management capacities over many years of time. If successful, it will contribute to local economic development and quality of life as well.

3.1.3 Methods and Tools

On the scale of neighbourhoods or cities, different questions are to be answered by the planner compared to the scale of one individual building. While a number of *building planning tools* are available, which have proved their practicability to achieve useful results - examples are the "Passivhaus Planning Package" (PHPP) in Germany, or eQuest in the US, HOT3000 in Canada, Enorm in Sweden etc. – for neighbourhoods or districts, the situation is different. It was one purpose during Subtask A Case Study evaluation to explore, which planning methods and tools are currently in use (or in demand). On the scale of neighbourhoods or districts, the question of energy (and GHG) balances for demand and supply, annual and diurnal variations, economic optimization of both supply and demand measures are relevant for the planner. To be able to include a consideration of energy distribution, an interface with GIS would be useful, such as an energy map. However, on this scale, commercial energy models are not really available so far. Planners often use several different self-made calculation tools, with the disadvantage of intransparent calculation methods and lack of interfaces to existing data bases. As a result, every LEP project is a singular project. However, the situation with energy modelling of neighbourhoods (or cities) is better than currently apparent in planning practice, since several energy system models are "there" and used by academic experts in projects which have often the character of research projects. Two "models" are currently in widespread use, at least in Germany, Austria and Switzerland, one of them "GEMIS", which is used most often as a reference database for primary energy and GHG factors for a wide range of energy systems, but is also capable to be used to "model" energy systems, including default cost values [2] and the other "model" is ECORegion, a tool primarily intended to make up energy and GHG balances of cities [3]. Two additional balancing tools, BilanCarbon of ADEME (France) and "Energy Balance" in Denmark have been used in Subtask A Case Studies, as well as pure simulation tools of energy supply systems, such as GOMBIS or EISAB, that are applied in Subtask B Case Studies (Germany, Japan) and will be evaluated there. Comprehensive energy system models, such as TIMES, POLIS or PERSEUS, are powerful, but complex optimization models that need skilled users and are in general not used by conventional planners (one application of POLIS is presented in [8]). It would be an important task of the future to develop such tools in a way that they can be used also beyond academic circles of model developers. One different approach has been developed by [4], where a physical model (buildings, spaces between the buildings, orography; climate) is blended with GIS and scanning data to simulate the annual energetic development of a whole neighbourhood including thermal energy demand, solar gains and energy system components and (statistical) user behaviour.

A simplified energy benchmarking approach for neighbourhoods was discussed in Case Studies in Germany [5]. Here, the idea was to extend the existing methods of building energy per-

formance rating, where the specific thermal energy demand of a building, $q_H + q_W$ (q_H = space heating demand, q_W = DHW demand, both in $kWh_{th}/(m^2 \cdot a)$), is covered by an energy system with an end energy use ratio e_{EE} (kWh_{EE}/kWh_{th}). The term $p = (q_H + q_W) \cdot e_{EE}$ ($kWh_{EE}/(m^2 \cdot a)$ is used for the energy performance rating of the building.

Looking at a neighbourhood, typical uses (residential building types, others) have to be identified and the term $p = (q_H + q_W) \cdot e_{EE}$ as mentioned before has to be weighted according to the use areas to calculate an average value of p for the neighbourhood. At this scale, also the quality of the end energy delivered to the neighbourhood has to be considered. This can be thermal energy from a central heating plant, using a biomass boiler in the base load, or a cogeneration plant, a geothermal heat pump, waste heat utilization etc. In every of these cases, the "quality" of the end energy supply process, characterized by f_{EE} (kWh_{PE}/kWh_{EE}), can be described by an appropriate formula. For a central heating station for instance, operated with wood chips in base load and with a gas peak boiler, one may be interested in the "quality" of the end energy supply provided via a neighbourhood heating scheme in terms of fossil energy consumed (kWh_{foss}/kWh_{th}). In this case, f_{EE} is given by $f_{EE} = (1 - f_{ren})$, where f_{ren} is the fraction of renewable energy used in the central station (for instance, $f_{ren} = 0{,}80$). The resulting energy performance factor p ($kWh_{PE}/(m^2 \cdot a)$) of the neighbourhood is then given by

$$p = (q_H + q_W) \cdot e_{EE} \cdot f_{EE} = (q_H + q_W) \cdot e_{EE} \cdot (1 - f_{ren})$$

In the case of a cogeneration plant instead of the wood-chip boiler, f_{EE} (kWh_{PE}/kWh_{th}) would be calculated from

$$f_{EE} = \frac{1+s}{\eta_B} - \frac{s}{\eta_{el}}$$

with

s … ratio of electric to thermal output of the cogeneration plant (kWh_{el}/kWh_{th})
η_B … overall efficiency of the cogeneration system (kWh_{EE}/kWh_{PE})
η_{el} … average electric efficiency of the regional power plant mix.[1]

In other cases, such as a heat pump for instance, different formulae for f_{EE} would have to be used.

One task of Annex 51 is to evaluate the current situation of planning tools and their practical use (or development needs). The basic requirements for such a tool to be applied for LEP projects would be

- description of energy demands (hourly, monthly, annually) and supply systems and their future developments at neighbourhood scale
- balances in terms of costs and GHG on neighbourhood level
- scenario building (business as usual as reference and scenarios using different technical options) for neighbourhoods and cities
- costs and economic assessment (e.g. using LCA) as basis for economic optimization
- continuous monitoring of implementation.

[1] In real applications, the fact that only the base load will be made from cogeneration, and the existence of losses in heat distribution and electric transmission would have to be considered, which makes the formula more complicated.

It remains to be shown if existing tools can be used by conventional planning consultants, perhaps after adequate re-designing of the user interface, or if there is a need for a completely new planning tool still to be developed.

2.2 Subtask B: Case Studies on Energy Planning for Neighbourhoods

This is a continuation of the work carried out in Subtask A, with the difference that in Subtask B the focus is on recent or ongoing Case Studies with explicitly innovative character, be it technically, methodically or with respect to the implementation approach. 14 Case Studies in 11 countries are evaluated, which cover existing neighbourhoods as well as new ones, and residential as well as mixed use neighbourhoods. Another difference to Subtask A is that the Case Study reviewers here are in most cases directly involved and therefore have access to detailed information as to cost structures and prices, business models or implementation strategies. This will allow for a much more detailed evaluation compared to Subtask A. This work is ongoing, led by the University of Linköping (Prof. B. Moshfegh, Prof. H. Zinko). Three of the Subtask B Case Studies are being presented at the WRE Conference [6-8].

2.3 Subtask C: Energy and Climate Change Strategies for Cities and their Implementation

With respect to international long-term energy and climate change targets, successful urban climate change policy is a key to success: without massive GHG mitigation in all cities, climate change targets can not be achieved. Compared to neighbourhoods, climate change strategies on city scale are much more complex and need much more time. Ongoing initiatives, such as the International Climate Alliance, ICLEI or the C 40 Initiative have been formed in the past, and more recently the EU-based "Covenant of Mayors", to support members of their organisations in the development of urban climate change strategies. However, really successful cities are still the exception rather than the rule.

As in Subtask B, methods and implementing strategies shall be evaluated using successful cities as Case Studies, but still more important is a description of the transition processes that cities have to undergo in terms of organisation and local implementation of their climate change master plan.

The Subtask C Leader is Prof. Kimman from Hogeschool Zuyd in Herleen (NL). Cities that are being evaluated in Subtask C are Tilburg and Apeldoorn (NL), Ludwigsburg (D), Stockholm, Zurich, St. Johann (A) and the City of Prince George (CAN). Results of this Subtask will be available in 2012.

2.4 Subtask D: Guidebook and Energy Model for Decision Makers

The main deliverables of Annex 51 for the general public will be provided by this Subtask, containing the essential results and conclusions drawn from the other Subtasks. The intention of the "Guidebook to Successful Urban Energy Planning" is to provide the necessary background of methods and usable planning tools to urban planners and decision makers, to select and explain the most interesting Case Studies of Subtasks B and C, which can serve as good examples for other cities, and to provide to the user a "Pathway on How to make an Urban Climate Change Action Plan and Implement it Successfully".

3. Conclusions

First results and experiences of the work made in Annex 51 have shown that for both Local and Urban Energy Planning, there is a lack in generally acknowledged and practically used

methods and planning tools as part of the necessary knowledge base of planners and decision makers in municipalities. In addition, there is a need for learning processes from municipalities or cities that have proven to be successful in establishing a local energy and climate change master plan and transition into a successful implementation phase. Through the work being made in Annex 51, both needs shall be satisfied, with the aim to provide to this target groups a practical guidebook that is really beneficial in their every days work.

4. Acknowledgements

The author would like to thank all Annex 51 participants (being too large in number to be explicitly mentioned here) for continuous discussions during the course of our common project. In particular, I want to mention my Subtask Leaders, A. Koch and P. Girault from EiFER in Karlsruhe, Prof. B. Moshfegh and H. Zinko from the University of Linköping, Prof. J. Kimman with his assistant, W. Broers, Hogeschool Zuyd in Herleen, and H. Erhorn-Kluttig, Fraunhofer Inst. für Gebäudephysik, Stuttgart. In addition to these, I want to mention Prof. D. Robinson, ETH Lausanne, and Prof. U. Eicker, FH Stuttgart, for valuable discussions on the sometimes cumbersome issue of "energy models". My own contributions would not have been possible without the financial support of the Secretary of Economics and Technology, Germany, which has supported R&D in energy since decades in general and IEA co-operative projects in particular.

References

[1] IEA ECBCS Annex 49,´, D. Schmidt et al.: *Low Exergy Systems for High Performance Buildings and Communities*; www.ecbcs.org

[2] U. Fritsche et al.: GEMIS – Globales Emissions-Modell Integrierter Energie-Systeme, Version 4.6 – www.oeko.de/service/gemis/de/indes.htm

[3] EcoSpeed AG, Zurich: ECO*Region – Energie- und Treibhausgas-Bilanzierung für Städte*; www.ecospeed.ch

[4] D. Robinson et al.: *CitySim: Comprehensive Micro-Simulation of Resource Flows for Sustainable Urban Planning*, Int. IBPSA Conference on Building Simulation, Glasgow 2009

[5] H. Erhorn-Kluttig et al.: *Energetische Quartiersplanung*, Fraunhofer IRB Verlag, Stuttgart 2011

[6] B. Boutaud et al.: *The Franklin District of Mulhouse: First French Experience of low energy Building Renovation in a historic area of the City Centre*, WREC 2011, Linköping

[7] R. Kuzuki et al.: *Study on Non-Energy Benefits of Area-Wide Energy Utilization and Evaluation of the Marginal Abatement Cost*, WREC 2011, Linköping

[8] A. Zhivov et al.: *Towards a Net-Zero Building Cluster Energy Systems Analysis for the US army Installations*, WREC 2011, Linköping

[9] IEA ECBCS Annex 49, H. Erhorn-Kluttig et al.: *Retrofitting in Educational Buildings: Energy Concept Adviser for Technical Retrofit Measures*, www.ecbcs.org

Experimental investigation of the use of lignite ash for roof solar cooling

Eftychios Vardoulakis, Dimitris Karamanis*

Department of Environmental & Natural Resources Management, University of Ioannina, Agrinio, Greece
** Corresponding author. Tel: +30 26410 74210, Fax: +30 26410 39576, E-mail: dkaraman@cc.uoi.gr*

Abstract: The moisture sorption properties of fly or bottom ash and their application prospect as evaporative coolers of roof surfaces were studied. Initially, samples were characterized through techniques like elemental analysis, x-ray diffraction, thermogravimetry, reflectance measurements and water vapor adsorption isotherms. Moreover, the water adsorption properties and the associated temperature variations were determined in a specific wind tunnel with controllable environmental conditions. The adsorption isotherms were of type III indicating hydrophobic materials with low water vapor adsorption. However, all samples were capable of lowering their surface temperatures due to water evaporation and the release of the latent heat. The maximum differences in temperature increase under simulated solar irradiation between fly ash and concrete were 3.8, 4.1 and 6.4 °C for the surface, middle and bottom, respectively of 3 cm material thickness. The toxicity assessment of materials implication in buildings roofs was performed by radioactivity and metal leaching experiments with rain water. According to the results, mixing of fly ash with either an inert material like soil or a green roof material or multifunctional nanocomposites is proposed in order to minimize its environmental impact.

Keywords: *Evaporative cooling, Solar cooling, Water vapor sorption, Fly ash, Lignite*

1. Introduction

The increased temperature in the summer time of the so called "urban heat island" effect is a major energy and environmental problem of urban areas. The effect leads to the increase of electricity generation for cooling purposes and the subsequent higher pollutants emission, the chemical weathering of building materials and the increase of the discomfort and even the mortality rates. Among the mitigation measures, building integrated evaporative cooling is an alternative and sustainable way to cool the surfaces of a building or the pavement of outdoor spaces by taking advantage of the sorption properties of porous materials. Stored water or night sorbed moisture inside the pores are evaporated during the hot day and the porous surface temperature is reduced due to the release of the latent heat [1-2]. Lower surface temperatures contribute to the reduction of air temperature since the intensity of heat transfer through the cold surface is lower while the heat flow inside the building is reduced. The method of roof evaporative cooling is considered to be the most effective method for roof and indoor temperature reduction [3]. Indirect benefits associated with the installation of roof integrated porous materials for evaporative cooling include water retention in heavy rainfall, increase of the thermal insulation pollutants uptake, reduction of roof materials' degradation and carbon sequestration.

The materials' rate of water vapor sorption and the sorption capacity are the primary factors in the selection of the porous materials. However, the outdoors stability, the affordable price, the local availability and the environmental non-toxicity are secondary parameters that should also be taken into consideration in the selection of the suitable material for evaporative cooling applications and for commercial use.

Moreover, around 37 and 4.8 million of tonnes of fly and bottom ashes (FA and BA) are produced every year in Europe while more than 20% of these are produced in Greece (10 million tonnes FA per year) [4]. Fly ash is beneficially used mainly in the building industry and road construction applications such as cement or asphalt additive, autoclaved aerated concrete block, concrete admixture or aggregate and highway ice control. The average ash

utilization rate in Europe is 47% [4]. Other applications are zeolites synthesis and hazardous waste removal, blasting grit, flowable fill material, masonry block, structural fill, grouting etc. In spite of these applications, the largest proportion of the produced fly ash is directly discharged into landfills, increasing in this way the concern of environmental pollution. Therefore, the development of alternative applications and further means to facilitate the recycling of fly ash are urgently needed. To the best of our knowledge, the potential application of fly or bottom ash as a stand-alone material or roof additives for solar cooling has not been studied yet.

In this work, the moisture sorption properties of fly and bottom ashes from the major thermoelectric power plant in Greece were determined. Prior to moisture sorption experiments, materials were characterized by x-ray diffraction, thermogravimetry, reflectance measurements and water vapor sorption isotherms. Moreover, the water sorption properties and the associated temperature reductions were determined in a specific wind tunnel with controllable environmental conditions. Finally, an initial evaluation of the environmental impact of the fly ash application was performed by radioactivity and metal leaching experiments.

2. Methodology

2.1. Ash samples

Fresh lignite by-products of fly and bottom ashes, coded ADFA and ADBA, were obtained from the lignite power plant of Agios Dimitrios (1595 MW). Fly ashes were collected in a dry state from the electrostatic precipitators of the power stations while bottom ashes were air-dried at room temperature. All samples were ground by hand and sieved to a fragment size less than 200 μm.

2.2. Characterization

The major chemical constituents and trace elements of raw ashes were determined with the spectrometric methods of X-ray fluorescence (XRF) and proton-induced gamma-ray emission (PIGE) [5]. PIGE measurements were carried out at the 5.5 MV terminal voltage of the Tandem accelerator of the National Center for Scientific Research "Demokritos". Characteristic γ-rays emitted from the deexcitation of the residual nuclei following (p,p'γ) reactions, were used for the determination of light elements as Al, Si, Mg and Na. XRF measurements were performed by a vertical Si(Li) detector and a ring shaped radioisotope source (^{109}Cd or ^{241}Am) for providing the exciting radiation [5]. Cation exchange capacity was determined by cesium sorption isotherms, traced with ^{137}Cs [6].

X-ray diffraction patterns of the prepared materials were collected on a Bruker AXS D8 Advance Bragg–Brentano geometry with Cu sealed tube radiation source plus a secondary beam graphite monochromator. A step of 0.02 ° and a time of 6 s step^{-1} were selected. The thermogravimetry (TG) measurements were performed on a STA 449C (Netzch-Gerätebau, GmbH, Germany) thermal analyzer. The heating range was from ambient temperature up to 450 °C, with a heating rate of 5 °C min^{-1} under synthetic air flow rate of 40 cm^3 min^{-1}. The spectral reflectance of fly ash in comparison to that of a typical soil was measured using UV/VIS/NIR spectrophotometer (Varian Carry 5000 fitted with a 150 mm diameter, integrating sphere (Labsphere DRA 2500) that collects both specular and diffuse radiation) over the solar spectrum (200-2500 nm).

2.3. Water vapor sorption experiments

In the moisture sorption isotherms, samples were placed in desiccators with saturated salt solutions for controlling relative humidity (32.8, 57.6, 78.6 a nd 93.6 %) while temperature was air-conditionally controlled at 25 °C . Prior to measurements, samples were dried to constant mass in an air-circulated oven at 105 °C. In order to determine the sorption isotherms and kinetics, the samples were periodically weighed and the moisture content was calculated as the difference of mass measurements in different time periods and the initial dry state. The water sorption properties and the associated surface temperature reduction were conducted in a home-made wind tunnel of controllable conditions of air relative humidity, temperature and wind flow [7]. Wind flow (m^3 h^{-1}), relative humidity (%) and temperature (°C) of air inside the tunnel, weight of sample and temperatures of T-type thermocouples at the surface, middle and bottom layers of the sample cell were recorded by a CR1000 datalogger (Campbell Scientific). The solar radiation was simulated with a metal halide lamp of 400 W (Radium HRI-BT 400W/D).

2.4. Toxicity assessment experiments

The average fly ash yield of lignite burning is 10-15 percent by weight. Therefore, the concentration of most elements (radioactive and toxic) in solid combustion wastes will be much higher than in lignite. In this frame, the concentration of radioactive isotopes and toxic metals in the ADFA sample was determined by means of γ- and XRF spectrometry, respectively [8]. Furthermore, leaching experiments with rain water were conducted by mixing 5 g of fly ash with 200 ml of rainwater under stirring for 24 h. After vacuum filtering, leached metals was measured with XRF after preconcentration with ammonium pyrrolidine dithiocarbamate [8].

3. Results and Discussion

3.1. Ash characterization

Chemical analysis showed that SiO_2 is the dominant oxide, with appreciable Al_2O_3 in both ashes (Table 1). More than 90% of the composition of the studied samples consisted of Si, Al, Fe, Ca, Mg, Na, and K. Due to the high CaO content, the ashes were classified as Class C.

Table 1. Concentration of major elements in the fly ash (ADFA) and bottom ash (ADBA) samples.

Oxide	ADFA (%)	ADBA (%)	Oxide (%)	ADFA (%)	ADBA (%)
SiO_2	42.71	51.97	MgO	5.66	4.11
Al_2O_3	16.49	19.14	K_2O	2.24	1.44
Fe_2O_3	4.29	6.42	Na_2O	0.88	0.72
CaO	31.31	14.89	TiO_2	0.27	0.45

After lignite firing, the concentration of major compound of amorphous aluminosilicate glass is high in the produced ashes (up to 90%) and there are no intense crystalline phases in the XRD patterns, especially in the region of 20-30° (Fig. 1A). The minor crystalline structures are quartz (Q-SiO_2), anhydrite (An-$CaSO_4$), lime (CaO), calcite (C-$CaCO_3$) (mainly in the bottom ash samples), hematite (H-Fe_2O_3), maghemite (M-$FeO.Fe_2O_3$) and complexes like gehlenite (G-$Ca_2Al_2SiO_7$) (Fig. 1A). The cation exchange capacity of the samples was found 0.02-0.03 meq g^{-1}, much lower than the corresponding of smectites and zeolites. The results of thermal analysis are shown in Fig. 1B. Because of the sampling of fly ash materials directly from the electrostatic filter, the moisture content of fly ash was very small and the change in

its mass was limited up to 400 °C (1 wt%). The bottom ash showed higher reduction in weight, with values up to 6%.

The spectrophotometric reflectance data shown in Fig. 2 revealed that the tested sample exhibited a low reflectance in the entire spectrum. Moreover, the solar reflectance of the sample was calculated by weighted-averaging, using the ASTM G173-03 reference solar spectrum as the weighting function. The values of solar reflectance for each sample are shown in Table 2. In the same table, the calculated solar reflectance values for the ultra violet (UV), visible (VIS) and near infrared (NIR) part of the spectrum are also included. The reflectance of the fly ash sample was found to be higher than the reflectance of a typical soil sample. The highest difference was observed in the visible part of the spectrum since the ADFA was closer to the grey-white color than the dark-brown of the soil. Both the samples presented high absorptance in the UV and their highest reflectance in the near infrared part of the spectrum.

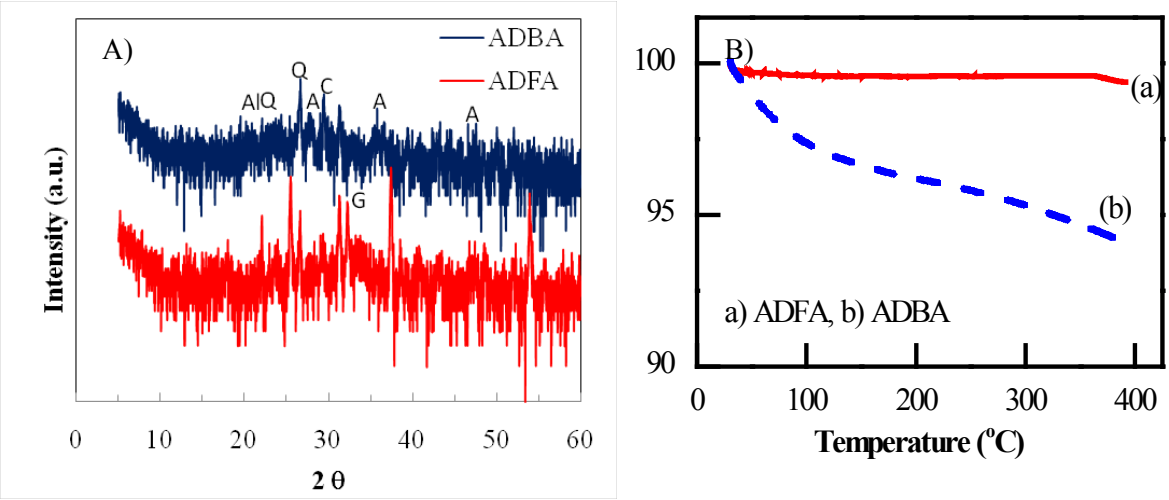

Fig. 1. A) X-ray diffraction patterns and B) TGA/DTA curves of the ash samples.

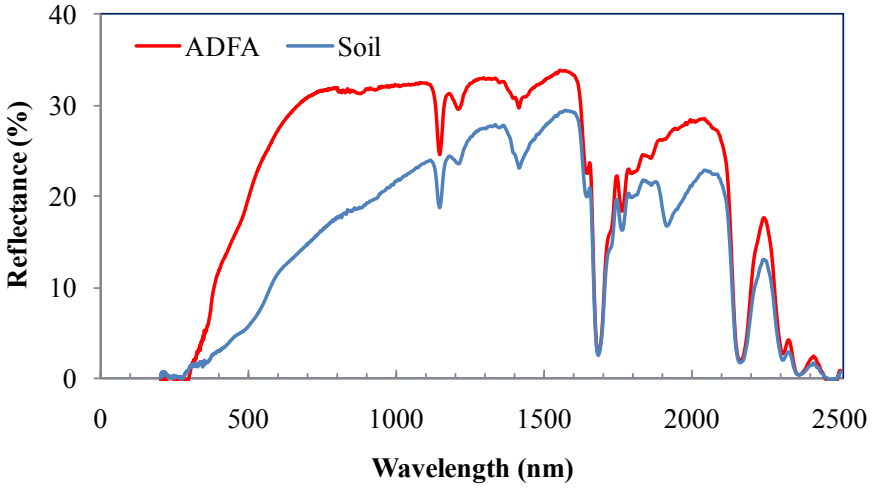

Fig. 2. Spectral reflectance of the ADFA and soil samples.

3.2. Water vapor adsorption

The kinetics of the two ash samples (ADFA and ADBA) and soil are shown in Fig. 3A. Upon comparison, the pseudo-second-order rate equation yielded the best results for water vapor

adsorption on the samples. The fast rate of a few hours was responsible for more than 90% of water vapor sorption while the slow rate accounted for the rest of the adsorption.

Table 2. Solar reflectance values (SR, 280-2500 nm) and solar reflectance values in the UV (280-400 nm), VIS (400-700 nm) and NIR (700-2500 nm) part of the spectrum of the ADFA sample and a typical soil.

Sample	SR (%)	SR_{UV} (%)	SR_{VIS} (%)	SR_{NIR} (%)
ADFA	25	8	24	30
Soil	12	2	9	19

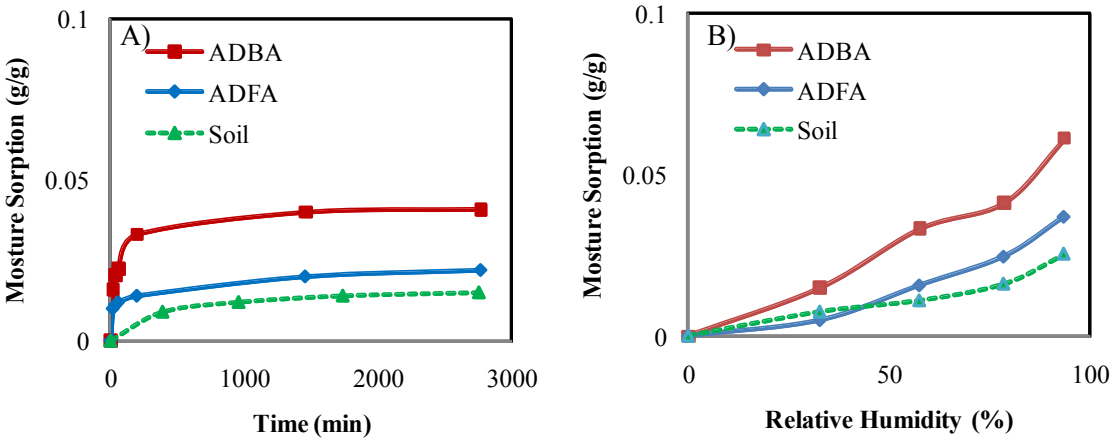

Fig. 3. Water vapor sorption A) kinetics at 60% RH and B) isotherms of the ash materials and soil at 25 °C.

According to the results of the kinetics experiments, water vapor adsorption in the pores of the ash samples was very low. This was further confirmed in the static measurements of sorption isotherms shown in Fig 3B. At low relative humidity, a small fraction of water was adsorbed on the samples (less than 7%). Bottom ash possessed a higher adsorption capacity than fly ash and soil which can be attributed to adsorption sites at the unburned carbon. However, water vapor adsorption at relative humidity more than 50% (normal outdoors) was higher in both ash samples than the soil. The isotherms of the ash samples were of type III indicating the hydrophobicity of the materials with chemisorption rather than physical sorption and monolayer sorption even at high relative pressure. This result is in agreement with the hydrophobic indices, recently published for Greek fly ashes [9]. It should be mentioned that the water-holding capacities in fly ashes are much higher than those of typical soils while water sorption on fly ash is strongly affected by its organic carbon as well as by the inorganic minerals of the fly ash, which have hydrophilic properties [10].

3.3. Evaporation cooling

The materials were further tested in the wind tunnel under simulated solar irradiation. The radiation was provided by a metal halide lamp over the top of the wind tunnel. The incoming radiation at the test cell position was measured 50 W/m^2 with a portable digital solar meter. Every material test lasted for 48 hours. Initially, 3 ml of water were sprayed on the surface of the material and left overnight. In the morning the lamp was turned on for a period of 12 hours and the cycle was repeated for one more day. All samples were capable of lowering their surface temperatures due to water evaporation and the release of the latent heat. Fig. 4 A)-C) shows the measured temperature increase for the three positions in the cyclic

experiments with simulated solar radiation of two continuous cycles, starting from the first lamp on as the zero time. A volume cell of 3 cm thickness was used in all the samples while the relative humidity was raised from 60% to 80% at night with lamp off. The maximum difference of temperature increase under simulated solar irradiation was observed between the

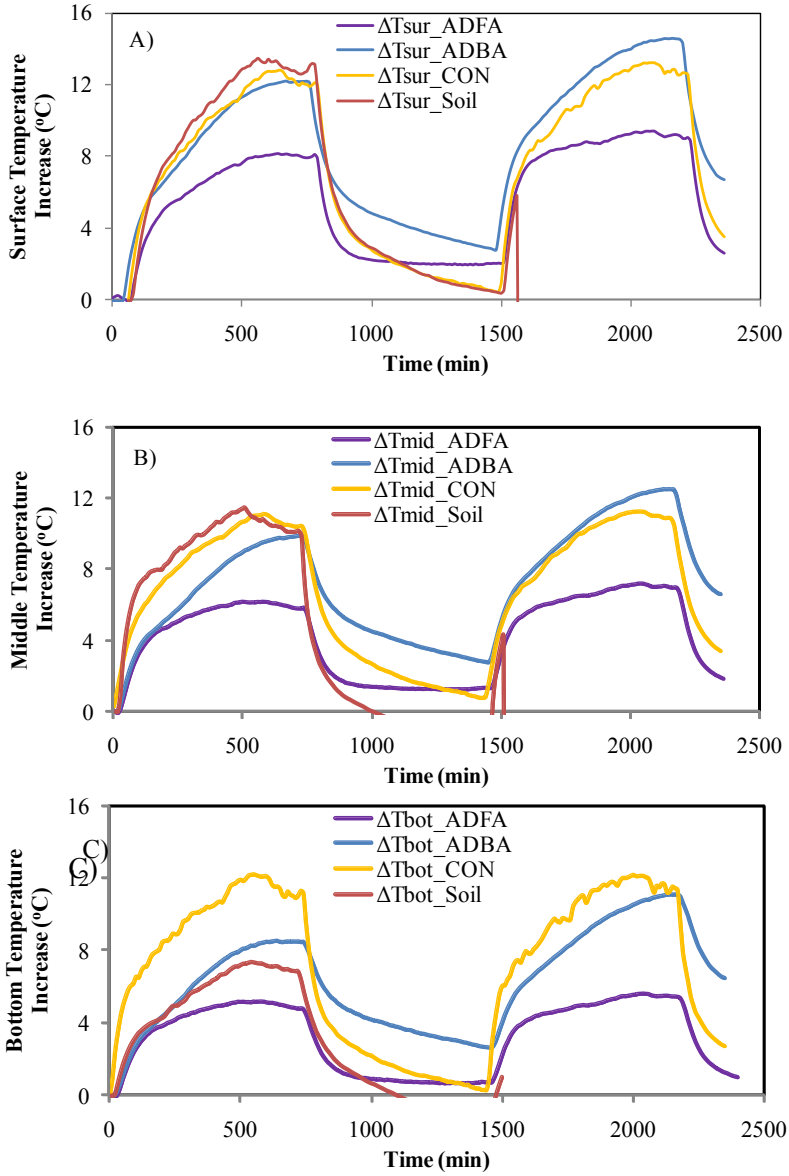

Fig. 4. Increase of the temperature at the A) surface, B) middle and C) bottom position of materials ADFA, ADBA, Concrete and Soil) cell due to simulated solar irradiation. (The cycle starts with the addition of 3 ml of water in order to monitor the retention property of its material in the first cycle. 1st cycle: 0-720 min-lamp on-RH 60%,720-1440 min-lamp off-RH 80%; 2nd cycle: 1440-2160 min-lamp on, 2160-2400 min-lamp off).

fly ash sample and the concrete with values of 3.8, 4.1 and 6.4 °C for the surface, middle and bottom position, respectively. These results indicate the material's suitability for the proposed application of evaporative cooling and further research regarding also the performance of the fly ash samples under the more realistic conditions of open fields will be performed.

3.4. Toxicity assessment

The toxicity of materials implication in buildings roofs was assessed by radioactivity and metal leaching experiments with rain water. For the proposed application, the risk from the use of fly ash is associated with three main reasons: a) outdoor exposure from the radioactive isotopes in the ash, b) internal exposure from the radioactive isotopes and toxic elements after inhalation of particulates and c) leaching of radioactive isotopes and toxic elements and contamination of water bodies. Regarding the direct exposure, the risk was estimated by the calculation of the radium equivalent activity (REA), the annual equivalent dose (AED) and the index of radiation protection (IRP) [8, 11]. Prior to the calculation, the concentration of minor elements, toxics and radioisotopes was determined by the methods described in Ref [8]. According to the results shown in Table 3, the AED and IRP can be higher than the existing limits and therefore the fly ash sample should be mixed with an inert material in order to minimize the risk. The second way of inhalation can be eliminated by material aggregation with a binder, reducing in this way any possible wind resuspension. Regarding the third reason, leaching experiments in a w orst case scenario of heavy rainfall, indicated the availability of some of the metals even at the high pH of the Class C fly ash [12]. Therefore and in order to minimize the environmental impact of the use of ashes for solar cooling purposes, mixing of the fly ash with either an inert material like soil or a green roof material or multifunctional nanocomposites with high water vapor adsorption [13] is proposed.

Table 3. Concentration of minor elements and radioisotopes in the ash samples and radiotoxicity indices.

Element (mg/kg)	**ADFA**	**ADBA**	**Element (mg/kg)**	**ADFA**	**ADBA**
V	41.4	BDL	Rb	26.8	68.0
Cr	169. 9	138.5	Sr	292. 6	255.1
Mn	299.2	396.2	Y	7.9	16.7
Ni	299.0	1824.2	Zr	129.2	171.8
Cu	13.9	42.1	Nb	11.2	20.4
Zn	38.9	31.5	Mo	3.2	2.4
Isotopes (Bq/kg)			**Isotopes (Bq/kg)**		
^{226}Ra	645±20	390±12	^{235}U	30±3	16±2
^{232}Th	43±2	38±2	^{40}K	222±12	224±13
REA (Limit 370 Bg/kg)	722	460	AED (Limit 1 mSv/y)	0.41	0.26
IRP (Limit <1 or 6 and 1 mSv/y)	2.44	1.56			

4. Conclusions

The extended use of air-conditioning and electricity to compensate the increased temperatures during the summer time has raised the need for the development and application of passive and efficient ways to cool down urban surfaces. In this work, fly and bottom ashes were tested as alternative applicators of the evaporative cooling principle. Cycle experiments with controllable laboratory conditions and under simulated solar irradiation, showed maximum differences between fly ash and concrete of 3.8, 4.1 and 6.4 °C for the surface, middle and bottom temperature increase, respectively. The substantial temperature reductions with the

use of the fly ash material indicate their significant potential for cooling applications. Since, the environmental assessment revealed non negligible impact due to the high concentration of radioisotopes, further research on the treatment of fly ash for the removal of toxic elements and the increase of water vapor adsorption are in progress.

Acknowledgment

This work was supported by the John S. Latsis Public Benefit Foundation.

References

[1] Q. Meng and W. Hu, Roof cooling effect with humid porous medium, Energy and Buildings 37, 2005, pp. 1-9.

[2] S. Wanphen and K. Nagano, Experimental study of the performance of porous materials to moderate the roof surface temperature by its evaporative cooling effect, Building and Environment 44, 2009, pp. 338–351.

[3] J. Alvarado, W. Terrell, M. Johnson, Passive cooling systems for cement-based roofs, Building and Environment 44 , 2009, pp. 1869-1875.

[4] Ecoba, Production and utilisation of CCPs in 2008 in Europe (EU 15), http://www.ecoba.com/ecobaccpprod.html, Accessed 8/10/2010.

[5] D. Karamanis, X. Aslanoglou, P.A. Assimakopoulos, N.H. Gangas, PIGE and XRF analysis of an ano-composite pillared layered clay material for nuclear waste applications, Nuclear Instruments Methods B 181, 2001, pp. 616–621.

[6] D. Karamanis and P.A. Assimakopoulos, Efficiency of aluminum pillared montmorillonite on the removal of cesium and copper from aqueous solutions, Water Research 41, 2007, pp. 1897-1906.

[7] E. Vardoulakis, D. Karamanis, G. Mihalakakou, M.N. Assimakopoulos, Moisture sorption properties of modified porous clays for roof evaporative cooling applications, Proceedings of 3rd International Conference PALENC, 2010, pp. 1-11.

[8] D. Karamanis, K. Ioannides, K. Stamoulis, Environmental assessment of natural radionuclides and heavy metals in waters discharged from a lignite-fired power plant, Fuel 88, 2009, pp. 2046-2052.

[9] O.K. Karakasi, A. Moutsatsou, Surface modification of high calcium fly ash for its application in oil spill clean up, Fuel 89, 2010, pp. 3966-3970.

[10] P. Hartmann, H. Fleige, R. Horn, Physical properties of forest soils along a fly-ash deposition gradient in Northeast Germany, Geoderma 150, 2009, 188-195.

[11] G. Skordas, P. Grammelis, E. Kakaras, D. Karangelos, M. Anagnostakis, E. Hinis, Quality characteristics of Greek fly ashes and potential uses, Fuel Processing Technology 88, 2007, 77-85.

[12] D. Karamanis, E. Vardoulakis, G. Antonopoulou, Ash as a Material of Passive Cooling of Buildings and Open-Air Areas, Final report of Project Funded by John S. Latsis Public Benefit Foundation, 2010 (In Greek).

[13] D. Karamanis, N. Okte, E. Vardoulakis, T. Vaimakis, Water vapor adsorption and photocatalytic pollutant degradation with TiO_2-sepiolite nanocomposites, Applied Clay Science (in press).

Building refurbishment to passive house standards of the quarter Brogården in Alingsås, Sweden

Heimo Zinko[1*]

[1] *Linköping University, Linköping, Sweden*
** Corresponding author. Tel: +46 155 58344, Fax +46 155 282545, e-mail: zinko@algonet.se*

Abstract: In Sweden, the transition of the society from agricultural to industrial occupation caused millions of people to move from the country-side into cities and in the 1960-ies and 1970-ies a broad building construction program was performed in order to build 1 million new dwellings in Sweden. However, these buildings are now after 40 years under urgent need of refurbishment and therefore offer a great opportunity for being supplied with modern and efficient construction details and heating systems. An example of such a project is the refurbishment of residential buildings in the quarter Brogården of Alingsås, were 16 buildings with 300 dwellings are to be converted from 1970-standards to modern passive house standards. The housing company Alingsåshem has in partnership with the construction company Skanska and under the consultancy of efem architects and the local Passive House Centrum started a refurbishment project for Brogården. The project involves the extensive renovation of the buildings with passive house techniques, and includes the installation of new façades and roofs, thicker insulation and new ventilation systems. The refurbished buildings do not use conventional heating systems and require very little energy for space heating. Hot water is primarily produced by solar energy, peak load energy is supplied by district heating,

Keywords: *Building refurbishment, Passive house, Energy efficiency, Urban development*

1. Introduction

In order to fulfil EU's action Plan for Energy Efficiency from 2006 it is important to apply energy saving measures not only to new buildings but also to existing buildings. In Sweden, like in many other countries, this is a very important issue with a high potential as reduced energy use for heating purposes is concerned. The transition of the society from agricultural to industrial occupation caused millions of people to move from the country-side into cities and in the 1960-ies and 1970-ies a heavy building construction program was therefore performed in order to create 1 million new dwellings in Sweden. However, these buildings are now after 40 years under urgent need of refurbishment and therefore offer a great opportunity for getting renovated and supplied with modern and efficient construction details and heating systems [1]. In Sweden, this could mean that EUs plans for energy efficiency for both 2020 and 2050 could well be met.

1.1. Objective

This paper presents the refurbishment project in Alingsås, Sweden, performed by the municipality-owned housing company Alingsåshem, which is in train to renovate 16 buildings with 300 apartments to passive house standard. The project is affecting about 650 people. It started 2008 with the renovation of the first building with 18 apartments indented to serve as a demonstration and for motivating the tenants to undergo the total construction work and to accept all the inconveniencies during the refurbishment. Up to the end of 2010, 4 of the 16 buildings have been renovated and again taken into use.

In this paper, the important features of the refurbishment task and its planning is shortly described as well as first experiences from living in the new apartments.

2. General project information

The ***housing company Alingsåshem*** is owned by the municipality Alingsås which applies a policy of *"serving the tenants with the different needs which occur in the housing sector and to contribute to a sustainable habitation*". The owner has a. o. specified that Alingsåshem should

- offer the inhabitants of the city an attractive and secure residence
- offer a varying and interesting selection of dwellings
- offer good availability and integration for everyone
- be responsible for that planning and construction of dwellings meets the demands.

Figure 1: The apartment houses of the Brogården area.

The principal working form of Alingsåshem is *Partnership*, which means that the cooperating companies are selected for a period of five years in order to give the partners enough time for together developing and applying new ideas and methods. The renovation work in Alingsås is facilitated by the fact that a renowned *Passive House Company* with a leading passive house Architect *Hans Eek* is located in Alingsås. Hans Eek and Ing-Marie Odegren, the general manager of Alingsåshem have a similar view on housing refurbishment: *"Our general view means to include economy, health, sustainability and quality in the total optimisation"*.

In the case of Brogården (Figure 1), the partnership consists of the following companies:

Construction work

- Building owner: Alingåshem AB
- Main entrepreneur: Skanska Sverige AB

- ***Design team***
- Architect: efem arkitekter (Hans Eek)
- Structural engineer: WSP Byggprojektering AB
- Electricity consultant: COWI AB
- HVAC consultant: Andersson och Hultmark AB
- Measurements: SP Technical Research Institute of Sweden
- Advice and evaluation: Lund University, Energy and Building Design

Skanska Sverige AB is one of the larger Swedish construction companies and contributes to the project by further developing the initially selected methods for refurbishment and energy saving.

3. Specific information about the settlement/neighbourhood structure

3.1. The buildings

The dwellings of Brogården consist of a suitable mixture of 2-, 3- and 4-room apartments, plus kitchen, hall and sanitary rooms. The neighbourhood is a relatively open green area of

100 000 m^2, of which 6000 m^2 are occupied by buildings (Figure 1). The total living area is 18500 m^2, resulting in an average dwelling size of about 60 m^2. This occupancy is typical for the living situation in minor cities in Sweden and is contributing to the relatively high living quality in Swedish provincial towns. The average age of the buildings in year 2010 is 37 year. The buildings in the quarter of Brogården are for pure residential applications, i.e. service and commercial locals are not foreseen there.

3.2. Reason for refurbishment

Due to the age of the buildings, the need for a refurbishment program was getting more and more accentuated. The tenants complained about draughts and low indoor temperatures. Earlier renovation of similar buildings showed that these complaints did not disappear after the renovation process; the buildings needed to be made more air-tight. Also the sanitary equipment was worn out and the general feeling was that the apartments were draughty and noisy. And last not least, the façade was in an urgent need of repair, façade bricks were just braking out of the façade (Figure 2).

Furthermore, the annual energy and maintenance were increasing with time. The house-owner's capital cost for the houses in the Brogården area were at the same order as the annual energy costs. *Therefore it was the basic idea that the apartments should be renovated aiming at the energy levels of passive houses and that by saving energy costs the rent received could instead be used for amortizing the investments for the renovation.*

Figure 2: Details of the façades of the old building

4. Sustainable building construction

4.1. The philosophy of sustainable construction

The base for the refurbishment project Brogården is the consciousness of achieving a *sustainable environment*, which a. o. means also a reduced energy use on a sustainable level. The driving force for Alingsåshem was a generalised view about the role of a public company in the society, i. e. not only to achieve maximum profit for the company but to strive for the maximum profit of *company and the society*. Thus for the first time, such a generalised planning philosophy could be realised in Alingsås, after having fallen prey to short time profits on many other places.

In practice, the idea of sustainability was threefold:
Economy: In total, the project must be economic, otherwise the company will not survive and the tenants will be the looser.
Ecology: Environmental sustainability is one of the main issues which nowadays come into vogue at some places, but in the long term it is a necessity in all construction work.
Social welfare: The Stockholders (Municipality of Alingsås) have put the directive on Alingsåshem to work for the best of the tenants, with a long-term perspective on sustainability and not only looking on short run margins.

4.2. The realization

The old buildings have been examined regarding possible moisture problems and air leakage. Even though the brick façade is worn out, there was no trace of moisture in the wooden wall construction. The new wall construction is based on a steel frame which allows an increased insulation area. For the outer protection, a new ceramic façade material is chosen, which gives the buildings the same architectural expression as the old brick façade, but which is able to withstand the influences of the climate for a long time. The floor of the balconies in the old construction consisted of the same concrete slab as the rest of the floor. This caused a large thermal bridge that now is eliminated by moving out the façade and balconies and hanging the balconies on the outside of the building. The result of this reconstruction is seen in Figure 3. This new solutions gives also a new, friendly look to the houses.

Figure 3: Renovated building in Alingsås with new façade material and new balcony construction.

A big effort has been put on insulation and air tightness of the buildings. Figure 4 illustrates the construction and the ventilation system with incoming/exaust air heat exchangers. The air leakage rate is below 0.3 l/s,m^2 at ±50 Pa. In winter time, the air is preheated by district heating (which is existent from before).

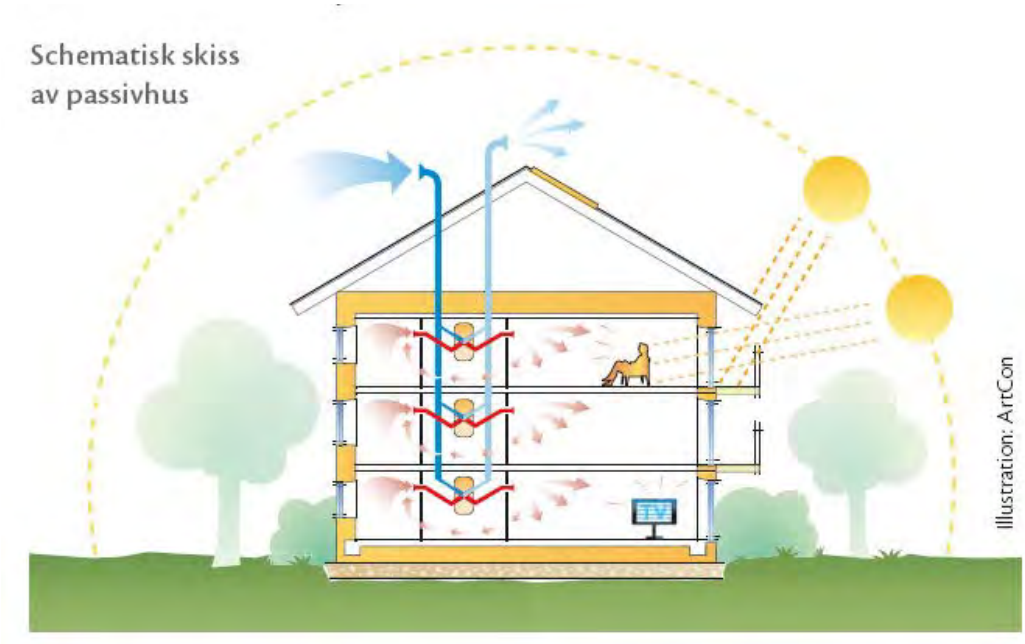

Figure 4: Principle of ventilation air heating system. Fresh air is transported via heat exchangers of each apartment to living room and sleeping rooms. Used air is taken from bath and kitchen. Attic insulation is 40 cm, wall insulation 44 cm and ground floor insulation 20 cm. Solar collectors provide domestic hot water. Balconies help to regulate solar radiation. Windows are of highest insulation standard.

In all, the following measures were undertaken in connection with refurbishment:

- Thermal insulation on the ground floor and the outer walls
- Acoustic insulation on inner walls
- New façade material
- New (3-glass) windows
- Increased air-tightness, building envelope
- New ventilation with exhaust air heat exchanger
- Energy-efficient household appliances
- Solar collectors for domestic hot water (providing 50% of DHW on annual basis)
- Moved balconies
- Entrance vestibules
- Increased access to indoor stores
- IT - access
- Individual heat metering - DHW and household electricity
- Handicap adapted entrance staircases, elevators and doors.

4.3. Social aspects

Beside energy efficiency, the project 'Brogården' aims to create a sustainable area of housing that promotes social integration. The projects main principles are *accessibility, social structure and environment*. The project started with a survey of the area to illustrate Brogården's qualities and its 'soul'. Through this survey, inadequacies in these aspects could be identified and the needs of Brogården's tenants documented. Customer focus groups with residents and various partnerships were created, f. i. with the elderly care services, municipal social management, child care services and schools, association activities and the social welfare administration. The customer focus groups were arranged through meetings with an idea workshop for the residents. It turned out that for the tenants it is was very important that families and single peoples could meet each other and - if possible - could also keep the physical neighbourhood. Another important factor for the living quality was the improved accessibility for handicapped people. That means that elderly people can stay longer time in their familiar environment.

5. Savings on energy and environment

Alingsås is situated about 100 km north-east of Gothenburg, i.e. in the southern Swedish climate zone. The annual mean temperature is about 6.5ºC, the mean monthly minimum temperature is – 3.1ºC in February and the mean monthly maximum temperature is 15.6ºC in July. The normal Sunshine time is 1715 hours/year and the annual global irradiation on a horizontal surface is about 960 kWh/m^2.

The Brogården quarter was in the last years heated by district heat from the district heating company Alingsås Energy. This company runs since 1996 a biogas heating plant which drastically reduced the CO_2 emission compared to the oil plant used before. In 2009 the specific CO_2 emission from district heat production in Alingsås was 0.032 kg CO_2/kWh_{th} heat (including a primary energy factor of 1.7 [2]) and we assume the same value for the expected savings. For the impact of the use of electricity in Sweden, different ways are used for assessing the primary energy for energy calculations, essentially depending on two different ways to think about the energy use: Marginal use of energy or average use. When considering individual projects, it is recommended to use the *marginal electricity* use which is

based on coal condensing power imported from Denmark and Germany. Hence the primary energy factor for the saved kWh electricity is relatively high. According to the State Energy Administration [3] the primary energy factor = 3.0 (3 kWh_{th}/kW_{el}) and the related CO_2 emission is 1 kg CO_2/kWh_{el}. So far, the evaluation of the new construction is only based on simulations, but measurements are going on. The supply of solar heat to the tap water system is based on expectations. Measurements and simulation results are summarised in Table 1:

Table 1: Energy demand, before and after renovation, if the proposed measures will be applied.

Energy Demand (kWh/m^2,yr)	**Before** (Measured average) (kWh/m^2,yr)	**After** (Calculated) (kWh/m^2,yr)
Space Heating	115	30
DHW	30	25
Household electricity	39	27
Electricity, common areas	20	13
Sum	**204**	**95**

It can be seen from Table 1 that the expected energy use will be considerably decreased. The highest reduction belongs to the passive house conversion which reduces the need for bought energy by 74 %. The posts for household electricity and the electricity for operating the common areas are of course very uncertain estimates because they depend strongly on the lifestyle of the tenants. The operating energy of the fan-driven air heating system is included in the heat balance. The total electricity consumption is expected to be reduced by 32 %.

Table 2: Use of primary energy and CO_2 emissions of the Brogården project

Specific energy use	**Before**		**After** (kWh/m^2)		**Saving**	
	Bought	Primary	Bought	Primary	Bought	Primary
Heat	115	195,5	30	51	85	144,5
Electricity	89	267	65	195	24	72
Sum	**204**	**462,5**	**95**	**246**	**109**	**216,5**

Spec. CO_2 emission	(kg/m^2)		
Heat	3,7	1	2,7
Electricity	89	65	24
Sum	**93**	**66**	**27**

As can be seen from Table 2, the total use of primary energy will be almost reduced to the half (53 %) whereas the resulting CO_2 emission is reduced by 29 %. That means that the Brogården project in total will reduce CO_2 emissions by 500 tons a year.

6. Cost information

The management of Alingsåshem divides the renovation cost into three parts. One part is *energy saving*, the second *is investment in higher standard in the apartments* (f. i. larger bathroom, new surface materials, etc.) and the third is the *maintenance cost*, the cost for renovations anyway needed. Since the need of renovation was so extensive, the cost for making the building energy efficient at the same time is not dominating.

Because we are dealing with an on-going project and continuous developments within it, the management is reluctant of telling exact costs for the moment. A cost indication gives the

following estimates: Planned total costs are 300 – 400 Million SEK, which is a cost of SEK15000 - 20000/m^2 living area. The costs of new apartments in Sweden are about the double of that. The reason for the high renovation costs is of course the fact that both outer walls and roof are substantially reconstructed.

These costs can be allocated to the following positions:
- 30 % renovation
- 50 % increase of standard and comfort
- 30 % energy saving measures.

The saving of used energy corresponds to about 109 kWh/m^2 or totally about 2 GWh/yr, worth for the tenants ca. 3 Million SEK/year. Hence the amortisation time for the energy part is around 30 years. Another part concerns comfort, for which the tenants have to pay an increased hire with 1000 SEK/month. The remaining position 'maintenance' goes on the expense of Alingsåshem which replaces direct service costs by depreciation of investment (at least in the next years). Alingsåshem expects that these costs will be depreciated in 20 years. In the recently decided next refurbishment stage for 3 buildings of Brogården, the costs were calculated to 55 million SEK for 65 flats, i.e. 850.000 SEK/flat.

7. How the tenants react

The organization plan has foreseen that the buildings should be renovated in a certain time sequence and the first building served as both demonstration and exercises object for the entrepreneurs. A demonstration apartment was also created in the first completed building, which allowed Brogården residents to visit and understand how their apartments were to be redeveloped. At most are three buildings under reconstruction at the same time. The duration of the refurbishment work is about 8 months. The tenants were supposed to move around in the areas empty flats. An important feature is therefore the continuous feedback from Alingsåshem to the tenants and vice versa. The tenants were informed about the special features and the economical consequences of the refurbishment work.

For this purpose, Alingsåshem publishes an in information folder on bimonthly basis and holds regularly information meetings with the tenants. The main entrepreneur Skanska participates with detailed explanations about the new techniques used in the refurbishment process. The tenants can express their degree of satisfaction with the different measures and their own situation.

Some people mentioned that it took a while until they understood the severity of the interference in their life, both economical and regarding the living. But in the long term, they think, it will be to their advantage. After the first buildings have been accomplished, there were claims about low winter and high summer temperatures as well as odours and noise from neighbour apartments [4]. Lessons from that were taken into the construction of the consequent buildings.

The biggest change for the individual tenant belongs to the economy, the hire is higher and the energy use (which earlier was included in the hire) has now to be paid separately. That means that a bath in the tub costs about 1 €, which is a new experience to Swedish tenants. On the other hand the energy costs are lower than before and compensate partly for the increased hire bill. The total increase of the bill for hire and energy is around 1000 SEK per month.

8. Summarising conclusions

- An important feature of the passive house refurbishment project is the political and social vision of the public (municipality) stockholders in the housing company, namely to apply an integrated view regarding an optimal solution for the living including economy, health, sustainability and live quality. An additional achievement is the internal selling of the project to the people who finally had to pay for it.
- A further ingredience is the engagement of an interested construction company in a winn/winn partnership with the building owner. The goals with the partnership is to develop working methods and building processes according to a learning curve which could be applied in a continuous way to the 300 apartments of the whole quarter. This partnership helped to start the project by minimizing risks and gives both partners economic and technical incentives according to the lessons learned during the project.
- An additional important feature in the project is the mutual communication with the tenants by keeping them informed by means of newsletters and meetings and by listening to their arguments and comments. This participation of the tenants increased their comprehension of the passive house ideas, the implications for the future living in these houses and finally the acceptance of the increased hire connected with the refurbishment.
- The benefit to the society is a demonstration that it is possible to reduce the energy use of existing buildings and especially of these mass produced buildings of the Million Programme that would have been worn out in the next 20 years. Hence it is demonstrated that they can be refurbished by satisfying strong new construction and environmental standards.
- The annual energy use was shown to be reduced by more than 100 kWh/m^2 flat area, summing up to about 6 – 7 MWh/per flat, which corresponds roughly to a reduction of 1,5 tons CO_2 per flat and year. This is a relatively low value for achievable saving due to the fact that the heating energy is based entirely on renewable energy (biogas). The energy saving is mainly by achieved additional insulation, application of highest window standards, solar water heating and a low flow air-heating system. District heat is only used for peak power.
- The critical issue of the project is its relatively high costs, i.e. about half the cost for a completely new construction. However, the Standard of the buildings is that of new construction and it can be argued that if the tenants had to leave their homes and move in to newly constructed buildings, their hire would become higher. However, in order that this argument holds, the longevity of the refurbished buildings has to be demonstrated.
- Summarising, we can state that the expected heating energy is with 55 kWh/m^2 annual heating energy relatively close to the passive house standard 45 kWh/m^2 for southern Sweden. If this value will be reached in practice, it would stand for a real breakthrough as far as refurbishment projects for the Million Programme buildings are concerned.

References

[1] Janson, Ulla: *Passive houses in Sweden*, Licentiate Thesis, Lund University (2008). Report EBD-T--08/9.

[2] Swedish Energy Adminstration STEM: Koldioxid värdering av Energianvändning (*Carbon dioxid evaluation for energy use).* Eskilstuna 2008.

[3] Climate presentation of Alingsås Energi, 2009.

[4] Brogårdsbladet, nr. 25, oct 2010. www.alingsashem.se/index.php?page=brogardsbladet.

Energy performance indicators for neighbourhoods applied on CONCERTO projects

Olivier Pol

Austrian Institute of Technology, Vienna, Austria
Tel: +43 505506592, Fax: +43 505506592, E-mail: olivier.pol@ait.ac.at

Abstract: Current practice of energy efficient neighbourhoods shows that building energy performance ratings are commonly used to characterise the energy performance of the neighbourhood itself. The main inconvenient of this practice is that this indicator usually does not consider the energy efficiency of the neighbourhood energy infrastructure and does not allow for comparisons between neighbourhoods with different characteristics (urban form etc.). In the context of the new neighbourhood developments in CONCERTO, a set of more suitable indicators was developed. The paper presents the calculation methodology for these indicators and their application to chosen CONCERTO neighbourhoods. Given the relative small number of neighbourhoods considered, it is not yet possible to propose benchmarks for energy efficient communities in different European countries. The next step in this direction would be to apply this assessment framework to a statistically relevant number of neighbourhoods in Europe.

Keywords: *Energy performance indicators, neighbourhoods, CONCERTO*

Nomenclature

RES Renewable Energy Sources .....
TEC Thermal energy carrier .....
B Number of buildings in a neighbourhood..-
A_b Gross floor area of building b ..... m²
EPR Energy performance rating ..... kWh/m².a
F Number of facilities in a neighbourhood...-
E_f Energy use of facility f ..... kWh/a
FE Specific final energy demand ...kWh_{FE}/m².a
PE Specific primary energy demandkWh_{PE}/m².a
DE_{el} Electrical energy delivered .....kWh_{FE}/a
DE_{tec} Thermal energy delivered.....kWh_{FE}/a
GE Generated electricity from RES..... kWh/a

1. Introduction

Whereas the use of energy performance indicators is rather diffused for buildings and overall indicators as total CO_2 emissions are frequently used at city level, few dedicated indicators are currently used at neighbourhood scale. Usually a description of the energy performance standards of the buildings located in the neighbourhoods is used to characterise the neighbourhoods' energy performance [1]. This approach reaches its limits when it comes to comparing neighbourhoods having different urban forms and consisting of different building types with different building energy performance standards. As urban development is usually interpreted in terms of neighbourhood developments, using simplified aggregated indicators expressed at neighbourhood scale would help urban planners to assess the energy performance of different master plan configurations and in particular to assess the impact of urban form on the neighbourhood's energy performance [2].

Following the needs to propose benchmarks of energy efficient neighbourhoods based on the experience of the European CONCERTO initiative [3], indicators had to be developed and calculated for all neighbourhood projects assessed. In the CONCERTO initiative, one of the requirements was to select geographical areas "within which all of the dynamic interactions and relevant energy flows between centralised and decentralised energy supplies and demands [could] be identified for measurement and assessment purposes" [4]. This could lead to a satisfactory amount of data for calculating energy performance indicators at neighbourhood scale.

After a presentation of the proposed indicators and their relevance, the indicators are calculated for all new neighbourhood development projects of the CONCERTO initiative. Based on these results and a statistically relevant amount of data available, benchmarks for energy efficient neighbourhoods can be proposed in future.

2. Methodology: proposed set of indicators

2.1. Requirements for indicators

2.1.1. Considering energy performance of buildings

At first place an energy performance indicator for a neighbourhood should refer to the energy performance level of the buildings located in the neighbourhood. There are two possibilities to implement this requirement.

On the one hand, the distribution of the energy performance ratings (EPR) of the entire building stock of the neighbourhood can be graphically represented, using a typical distribution curve as shown by Fig. 1. The EPR can refer to energy needs or energy use, expressed for heating, cooling (space heating and domestic hot water) and electricity, and can be obtained from monitoring data or energy performance calculation. A set of diagrams based on Fig. 1. provides therefore a detailed picture of the energy performance of a building stock in a neighbourhood. The effect of the urban environment on the building energy performance can be considered if this factor is taken into account in the building energy performance calculation.

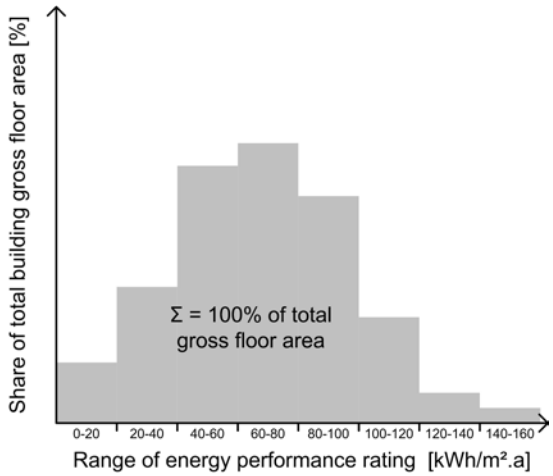

Fig. 1. Example of the distribution of energy performance ratings of the entire building stock in a neighbourhood

On the other hand, the weighted average of the EPR of each building in the neighbourhood can be calculated. This has the advantage to summarise the energy performance of many buildings and facilities (public lighting etc.) in one indicator, thus easing comparisons between projects. The EPR for a neighbourhood based on the energy use of buildings and facilities would be expressed by applying Eq. (1). Like for Fig. 1, the EPR can be calculated for heating, electricity, and possibly cooling energy use.

$$EPR = \frac{\sum_{b=1}^{B} A_b \times EPR_b + \sum_{f=1}^{F} E_f}{\sum_{b=1}^{B} A_b} \quad (1)$$

Another advantage of using an overall indicator consists in being able to integrate the energy use of facilities, i.e. applications which are not assigned to buildings but are to be included in the energy performance assessment of a neighbourhood (e.g. public lighting). Expressing them as ratio to the total gross floor area of buildings in the neighbourhoods is a way to relate the public facilities to the buildings (and people) they serve.

2.1.2. Considering the efficiency of energy supply in the neighbourhood, in particular the use of onsite RES

A second requirement for a neighbourhood energy performance indicator would be that is has to consider the efficiency of the energy supply infrastructure. In a low-density neighbourhood supplied by a district energy system, the relative thermal distribution losses are higher than in a high density neighbourhood where network piping length is reduced due to high settlement compactness. This influences also the electricity demand of pumps and therefore has to be considered in the indicator.

In addition to this, the contribution of onsite renewable energy technologies has to be considered as well because it influences the theoretical neighbourhoods' dependency from energy flows from outside the system boundaries.

The most suitable approach for including these requirements is to use an efficiency indicator of the overall energy transformation chain, considering extraction, conversion, storage and distribution to the final end-user. The primary energy factor for an energy system, defined in the sense of [5] seems to be the most appropriate factor. It can be determined also for district energy systems [6] and therefore can be used at the scale of a neighbourhood.

2.1.3. Considering the geographical extension of the neighbourhood and the settlement density

Last but not least, it is important to quantify the energy intensity in relation to the settlement density and to point out the links between land and energy use. For a given area, one of the main requirements for urban master plans consists in specifying the targeted plot ratio, defined as the "ratio of total gross floor area of a development to its site area" [7]. Comparing the EPR of different master plans proposed for a given plot ratio is a way to quantify the land-use efficiency in energy terms.

2.2. Proposed indicators

Based on these considerations, it is clear that a combined set of indicators needs to be used to express the energy performance of a neighbourhood:

- using only building EPR based on final energy use would not take into account the renewable energy sources available onsite and the efficiency of the energy supply infrastructure

- using only EPR based on primary energy use would not make building energy efficiency visible, since a low primary energy use due to high contribution of renewable energy sources would possibly hide a low building energy efficiency

It is therefore proposed to graphically represent couples of indicators in order to consider all relevant parameters and obtain an appropriate assessment of the energy performance of a neighbourhood considering the dimensions previously mentioned.

2.2.1. Combined representation of specific average final and primary energy use

Following the general principles already presented in [8], the combined representation of specific average final and primary energy use requires the calculation of specific final and primary energy use ratings at neighbourhood scale.

Applying Eq. (1) in a way to consider all energy flows delivered to the buildings (electrical and thermal energy flows) leads to Eq. (2). In this case the EPR of the neighbourhood is expressed as specific final energy demand.

$$FE = \frac{\sum_{b=1}^{B}\left(DE_{b,el} + DE_{b,tec}\right) + \sum_{f=1}^{F} E_f}{\sum_{b=1}^{B} A_b} \quad (2)$$

The primary energy demand of a neighbourhood is then calculated by weighting the delivered energy flows by the primary energy factors of the related energy carrier, as shown by Eq. (3). All thermal energy carriers are to be considered here: renewable energy carriers, district heating, heat from small-scale combined heat and power plants and non-renewable energy carriers. The electricity yield from onsite renewable energy technologies in monovalent processes is substracted from the total after multiplication by the primary energy factor for electricity.

$$PE = \frac{\sum_{b=1}^{B}\left(DE_{b,el} \times PEF_{el} + \sum_{tec=1}^{TEC_b} DE_{b,tec} \times PEF_{tec}\right) + \left(\sum_{f=1}^{F} E_f - GE\right) \times PEF_{el}}{\sum_{b=1}^{B} GFA_b} \quad (3)$$

In case of small-scale combined heat and power plants located in the neighbourhood, the primary energy benefits from electricity generation are assigned to the heat based on Eq. (4).

$$PEF_{Heat,CHP} = \frac{Q \times PEF_{gas} - W \times PEF_{el}}{H} \quad (4)$$

where Q is the calorific value of natural gas multiplied by the amount of gas yearly used in the CHP, W the yearly amount of electricity generated by the CHP and H the yearly amount of heat generated by the CHP and used in the building.

The set of indicators consists in representing the energy performance of the neighbourhood placing *FE* (Eq. (2)) on the x-axis and *PE* (Eq. (3)) on the y-axis.

2.2.2. Combined representation of specific average final energy use and plot ratio

The combined representation of specific average final energy use and plot ratio does not require a particular additional effort in data collection, but a special care in calculating the plot ratio and in particular the site area. The same conventions should be used in all projects assessed, mainly regarding the non-built spaces (roads, parks…).

When this is done, the set of indicators consists in representing the energy performance of the neighbourhood placing the plot ratio on the x-axis and *FE* (Eq. (2)) on the y-axis.

2.2.3. Normalised indicators

Assuming that a statistically relevant number of communities would be available for benchmarking, final and primary energy performance ratings could be normalised referring to the benchmark, mainly depending on building type and climate conditions. In this context, a neighbourhood energy performance index can be calculated based on Eq. (5).

$$EPI = \frac{\sum_{b=1}^{B} \frac{Q_b}{Q_b'} \cdot A_b}{\sum_{b=1}^{B} A_b} \qquad (5)$$

where *EPI* is the energy performance index of the neighbourhood, Q_b the specific final or primary energy demand of the building b, Q_b' the benchmark for energy performance rating, depending on building type and climate conditions and A_b the gross floor area of building b.

3. Results

The methodology presented here was applied to the CONCERTO communities which included new neighbourhood developments or neighbourhood renovation as demonstration projects. In the following, the results are presented for the new neighbourhood development projects and are only related to buildings. Other facilities (e.g. public lighting) located in the neighbourhoods are not included since they were not considered in CONCERTO.

3.1. Specific average final and primary energy use

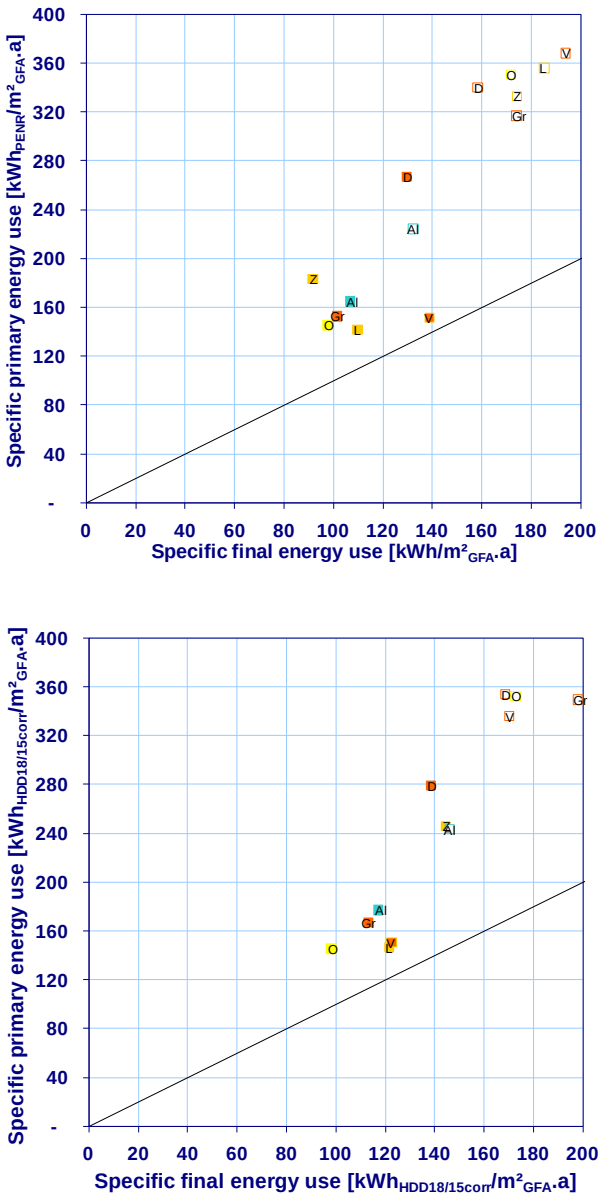

Legend

Reference situation: without CONCERTO

Situation with CONCERTO

Each square represents the performance of a neighbourhood, calculated as a **weighted average** of all buildings of the neighbourhood.

Conventions used for calculations:

- Energy use for **heating, cooling and all electrical appliances** is considered.
- If electricity use for appliances is not available, **average figures** are taken from projects providing data.
- All energy performance ratings are expressed as ratio to the **Gross Floor Area** (gross floor area of heated spaces).
- Only the **non-renewable part** of primary energy is considered.
- Common **EU-wide primary energy factors (PEF)** are used for **gas (1,36) and electricity (3,14)**.
- PEF are **calculated** for each district heating network, if **energy balance is known**.
- **A default value (0,8)** is used as PEF for district heating networks **if energy balance is not known**.

List of neighbourhoods considered:

- **Al: Almere**
  - Neighbourhood „Noorderplassen West“
  - Neighbourhood „Columbuskwvartier“
- **D: Delft**
  - Neighbourhood „Harnaschpolder“
- **Gr: Grenoble**
  - Neighbourhood „De Bonne“
- **L: Lyon**
  - Neighbourhood „Confluence Lots A, B, C“
- **O: Ostfildern**
  - Neighbourhood „Scharnhauser Park“
- **V: Växjö**
  - Neighbourhood „Biskopshagen“
- **Z: Zaragoza**
  - Neighbourhood „Valdespartera“

Fig. 2. Specific final and primary energy use of new neighbourhood developments in CONCERTO (top: without heating degree days correction / bottom: with heating degree days correction).

Specific final and primary energy use figures for the new neighbourhood developments in CONCERTO are presented in Fig. 2. The bottom graph considers a correction of all heating energy use figures by normalizing them to the average heating degree days in Europe.

The best neighbourhood energy performance levels are reached when both the primary energy use and the final energy use reach low values, i.e. the points are located on the bottom-left part of the graph. The neighbourhoods of Scharnhauser Park (Ostfildern (D)) and Confluence (Lyon (F)) reach high levels of performance in this comparison, mainly because they combine energy efficient building standards (ambitious compared to 2005 levels) with a high share of heat generated from biomass (district heating in Scharnhauser Park and individual boilers in Confluence). The De Bonne neighbourhood in Grenoble (F) reaches comparable energy performance standards and the use of small-scale gas CHP plants allows for a high primary energy performance.

3.2. Combined representation of specific average final energy use and plot ratio

As shown by Table 1, there is a high variety of urban settlement typologies in the chosen CONCERTO neighbourhood projects, ranging from low-rise terraced house (Almere, neighbourhoods Columbuskwartier and Noorderplassen West) to rather dense urban forms with multi-storey building blocks (Lyon, neighbourhood Confluence (Lots A, B, C)).

Table 1. Settlement typologies in the chosen CONCERTO neighbourhoods

			
Almere	Zaragoza	Grenoble	Lyon

Following the plot ratio definition of [7] and considering the entire land area of the developments (i.e. including all internal roads, parks etc.), Fig. 3 shows the various plot ratios obtained for the neighbourhood developments of Table 1 and the average specific final energy use of these neighbourhoods (without considering any heating degree days correction).

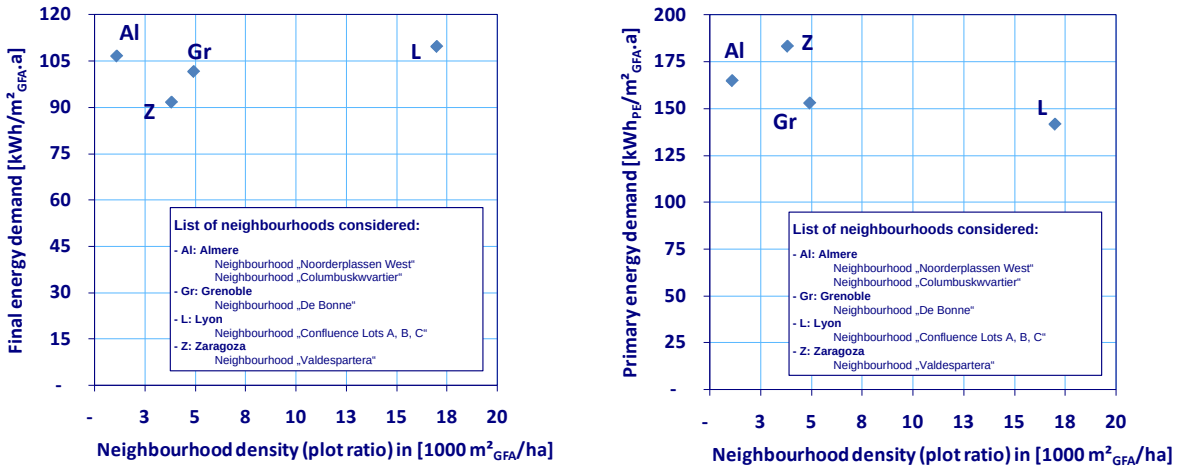

Fig. 3. Specific final energy demand and plot ratio.

Fig. 3 clearly shows that in the Confluence (Lots A, B, C) neighbourhood in Lyon, a high plot ratio is associated to ambitious energy performance standards, whereas the other neighbourhoods are not so densely built, even having similar performance levels. Considering final energy and on the basis of these examples, one could say that this level of energy performance can be reached independently of the plot ratio chosen. However, it would be interesting at this point to compare the energy performance of other neighbourhoods having the same plot ratio as Confluence, in order to compare the effect of different master plans proposed at a given plot ratio.

4. Conclusion and outlook

An attempt to establish benchmarks for energy efficient neighbourhoods was presented in this paper, mainly based on the definition of new sets of indicators and their application to some of the CONCERTO communities.

The proposed sets of indicators allow for considering the most relevant dimensions when it comes to energy use in the built environment of neighbourhoods, which are the final and primary energy use calculated on the basis of unified conventions for balancing energy flows, and the plot density as indicator of land-use intensity.

In the case of CONCERTO, the neighbourhoods combining ambitious energy performance standards in buildings with a high share of biomass in heat generation or combined heat and power reach the highest levels of neighbourhood energy performance. The high range of plot ratios in the neighbourhoods assessed show the different ways of dealing with land-use in CONCERTO.

Nevertheless, given the relatively low number of neighbourhoods assessed, the statistical relevance of the assessment results is rather limited. It will be necessary in future to apply this methodology to a high number of neighbourhoods, considering in particular a range of settlement typologies, different climate zones and sets of technologies.

In future, the energy demand for the overall public infrastructure (public lighting, street cleaning, gardening etc.) should be included in the indicators, as mentioned in Eq. (1).

Aknowledgement

The author thanks all participants in the CONCERTO initiative for sharing their experience, knowledge and data about their projects, and particularly for this paper the project teams in Almere, Delft, Grenoble, Lyon, Ostfildern, Växjö and Zaragoza. He thanks also Darren Robinson for his ideas and improvements.

References

[1] A. Koch et al., Description of the state-of-the-art of energy efficient projects on the scale of neighbourhoods, Subtask A report of IEA ECBCS Annex 51: Energy Efficient Communities - Case Studies and Strategic Guidance for Urban Decision makers, 2011

[2] K. Steemers, Energy and the city: density, buildings and transport, Energy and Buildings 35, 2003, pp. 3-14

[3] O. Pol, D. Österreicher, Evaluation methodology to assess the theoretical energy impact and the actual energy performance for the 27 communities of the European CONCERTO initiative, proceedings of the eceee summer study 2007

[4] FP6 work programme, European Commission, 2003

[5] EN 15603:2008, Energy performance of buildings – Overall energy use and definition of energy ratings, European Committee for Standardization, January 2008

[6] EN 15316-4-5:2007, Heating systems in buildings – Method for calculation of system energy requirements and system efficiencies, Part 4-5: Space heating generation systems, the performance and quality of district heating and large volume systems, European Committee for Standardization, July 2007

[7] V. Cheng, Understanding density and high density, in Designing high-density cities for social & environmental sustainability, Edited by Edward Ng, ISBN 978-1-84407-460-0, 2010, pp. 3-19

[8] O. Pol, S. Shoshtari, A simplified method to assess the quality of integration between activities targeted to increase energy efficiency and use of renewable energy sources in urban areas: example of the CONCERTO initiative, CISBAT 2009, Lausanne

Towards a Net Zero Building Cluster Energy Systems Analysis for US Army Installations

Dr. Alexander Zhivov[1], Dr. Richard J. Liesen[1], Dr. Stephan Richter[2], Dr. Reinhard Jank[3], Mr. David M. Underwood[1], Mr. Dieter Neth[4], Mr. Alfred Woody[5], Dr. Curt Björk[6], Mr. Scot Duncan[7]

[1] *U.S. Army Engineer Research & Development Center; Champaign, IL, USA*
[2]*GEF Ingenieur AG, Leimen, Germany*
[3]*Volkswohnung GmbH, Karlsruhe, Germany*
[4]*Senergy GmbH, Mossingen, Germany*
[5]*Ventilation/Energy Applications, PLLC, Norton Shores, Michigan*
[6]*Curt Björk Consulting, Naxos Island, Greece*
[7]*Retrofit Originality Incorporated, Lake Forest, California*
**Corresponding author. E-mail: Alexander.M.Zhivov@usace.Army.mil*

Abstract: U.S. federal agencies are required by law to eliminate fossil fuel use in new and renovated facilities by 2030, and to reduce overall facility energy usage by 30% by 2015 (EISA 2007). Army policy is to achieve 5 net zero energy installations by 2021, 25 net zero energy installations by 2031 and for all installations to achieve net zero energy status by 2058.

The Army operates what are essentially small campuses, or clusters of buildings on its installations. The US Department of Energy (DOE) is focused on the national grid scale or on individual buildings, while the commercial focus is on retrofits to individual buildings. There is a lack of tools and there are only few case studies worldwide that address dynamics of energy systems at the community scale. The Army's future building energy requirements is a mixture of ultra-low and high energy intensity facilities. Achieving net zero energy economically in these clusters of buildings will require a seamless blend of energy conservation in individual buildings and building systems automation, utility management, and control, power delivery systems with the capability to offer integration of onsite power generation (including renewable energy sources) and energy storage.

When buildings are handled individually each building is optimized for energy efficiency to the economic energy efficiency optimum and then renewables are added until the building is "net zero." This process works for buildings with a low energy intensity process for its mission, such as barracks and administrative buildings. When the mission of the building requires high energy intensity such as in a dining facility, data center, etc., this optimization process either will not end up with a net zero energy building, or large amounts of renewables will be added resulting in the overall technical solution that is not cost effective. However when buildings are clustered together, after each building is designed to its economic energy efficient option, the building cluster is also energy optimized taking advantages of the diversification between energy intensities, scheduling, and waste energy streams use. The optimized cluster will minimize the amount of renewables needed to make the building cluster net zero. This paper describes this process and demonstrates it using as an example a cluster of buildings at Fort Irwin, California.

Keywords: *Energy efficiency, Energy generation and distribution, Building cluster, Renewable energy source, Integrated optimization process.*

1. Army Energy Policy Overview

Buildings contribute to a large fraction of energy usage worldwide. In the United States alone, buildings consume about 40% of total energy, including 71% of electricity and 54% of natural gas. Army alone spends more than $1 billion for building related energy expenses. The Army Energy Security Implementation Strategy sets the general direction for the Army including elimination of energy waste in existing facilities, increase in energy efficiency in new construction and renovations, and reduced dependence on fossil fuels. The 2005 Energy Policy Act requires that federal facilities be built to achieve at least a 30% energy savings over the 2004 International Energy Code or ASHRAE Standard 90.1-2004 as appropriate, and that energy efficient designs must be life-cycle cost effective. According to the Energy Independence and Security Act (EISA 2007), new buildings and buildings undergoing major renovations shall be designed so that consumption of energy generated offsite or on-site using fossil fuels is reduced, as compared with such energy consumption by a similar building in fiscal year 2003 (as measured by Commercial

Buildings Energy Consumption Survey (CBECS) or Residential Energy Consumption Survey (RECS) data from the Energy Information Agency), by 55% in 2010, 80% by 2020, and 100% by 2030.

In an increasingly energy constrained world, the Army and its logistic support envisions a future where its energy needs are designed and fulfilled by a suite of ultra low energy solution options that can be tailored for adaptation at any Army installation depending on climatic zone, mission needs, mix of building types, availability of different sources of renewable energy, etc. Presently there is no overarching power "delivery/energy storage/demand" architecture and methodology to accomplish this. Commanders also need the capability to meet their energy use reduction goals with the requirements for energy security, affordability, environmental footprint, occupant well-being and productivity, and building sustainability (as appropriate) depending on the threat conditions, mission needs, utility market prices, etc.

2. Integrated Optimization Process

The Army is rapidly changing its views on energy usage to reconsider energy conservation and efficiency [1]. Army installations are essentially small campuses, comprised of clusters of buildings. Energy efficiency requirements dictate a serious tracking of all waste energy flows, their use, and their storage within the "Installation Boundaries," with consideration of realistic thermodynamic constraints for all rejected energy. To accomplish these ends is neither straightforward nor inexpensive. The concept of improved standards and increased energy efficiency in buildings can help individual buildings achieve more efficiency. However, it is difficult to adapt existing buildings to achieve Net Zero Energy (NZE) goals on their own. Net Zero Energy cannot be met with efficiency increases alone; there must be efficiency gains on the conversion, supply, and distribution side as well. Achieving NZE cost effectively will be possible if an optimum mix of demand reduction, energy distribution, energy supply, and renewable sources are put in place at a community (installation) or building cluster scale.

The knowledge base needed to build, renovate, and maintain Army installations with the highest levels of energy efficiency do not penetrate far enough into the market. There are a multitude of available technologies [2] related to the building envelope, ventilation, advanced "low exergy" heating and cooling systems, central energy plants with co- and tri-generation, hybrid and high efficient lighting systems designs and technologies, integrated solar thermal and electrical systems, etc. Due to economies of scale, a number of technologies, like cogeneration or combined heat and power, waste heat recovery, biomass, geothermal energy, solar heating (and cooling), and others, are more efficient —in technical and economic terms— when used in large systems rather than in small or individual building systems. Taking advantage of these technologies will enable an optimized system to reduce the primary energy consumption achieved (including demand and supply) to the best available standards, and also to lower costs.

Community energy planning and central system optimization do not require development of a new approach. Energy planning methods in the past were used to design the components of the energy supply systems, e.g., a district heating network connected to local combined heating and power plant was often planned by the local utility using an "optimization strategy." Existing energy planning methods used energy balancing methods and available planning models that include environmental models. This approach was then, and is still today, unfamiliar to energy planners. An important feature that is necessary in community-wide energy planning is the integrated consideration of supply and demand, which leads to optimized solutions. Therefore, it is the objective to apply the principles of such a holistic approach to community energy planning and to provide the necessary methods and instruments to master planners, decision makers, and stakeholders.

Thermal Energy Systems consist of three major elements: generation of energy, distribution of energy, and the demand of energy. The goal is to find the optimum for the entire energy system, where each element requires consideration. This process can be outlined in a several step analysis:

2.1. Site Setup and Analysis

Determine building locations, geography, utility locations, etc.:

1. Gather Building Energy Data for Benchmarking – gather utility bills, available energy demand data, etc., for all new and existing buildings.
2. Characterize All Buildings in Inventory – determine the building type and use characteristics and determine appropriate building model to simulate for demands.
3. Pre-Planning and Data Gathering – Gather all building and site data from stakeholders and partners. Gather all of the data with no pre-conceived answers.

2.2. Building Simulation

Simulate base and efficient cases for each building type selected in the site inventory:

1. Determine Baseline Model – simulate each building classification type identified in the building characterization step from the inventory.
2. Energy Efficiency Measures (EEM) – determine the appropriate building energy efficiency measures for each simulated building type.
3. Simulate the Energy Efficiency Cases – simulate the energy efficiency scenarios and produce the optimization curve for each building type.
4. Generate the EEM Project List – during the optimization process generate the project list to bring the building to net zero ready status.
5. Produce Building Energy Use Profiles with Peaks – Develop hourly, monthly, and annual use profiles for all demand energy

2.3. Distribution and Supply Optimization

Take data from the building efficient cases to setup the load and network design to determine the optimal distribution and supply network:

1. Integrate All Building Energy Demands – use the efficient case for the building cluster to be analyzed.
2. Develop Load Duration Curves – integrate all energy demands for the building cluster to be optimized and produce curves.
3. Use Hydraulic Simulation – develop the hydraulic parameters for integrated heating and/or cooling systems.
4. Determine Supply Equipment Inventory – Determine all of the existing and planned boilers, chillers, solar thermal, generators, renewables, etc. locations, sizes, age, etc.
5. Use Electric Distribution Simulation - do a grid analysis and determine the optimized distribution of the electrical system and electric renewable energy supplies.
6. Use Supply & Distribution Optimization Simulation – use a model like “POLIS” to determine the optimal distribution and supply systems for both the thermal and electrical and the integrated loads to calculate primary energy demands with the included distribution losses.
7. Determine Centralized and De-Centralized Options – optimization needs to consider both sets of scenarios

2.4. Financial and Emission Analysis

Integrate energy and fuel usage using the efficient buildings and optimized distribution systems and supply scenarios calculate the fuel costs and associated emissions. Using energy, fuel, distribution and supply costs, the initial costs, investment costs, and annual income, yearly and cumulative cash flows are calculated for the project life for each scenario.

2.5. Overall Scenario Results and Project Recommendations

Estimate the sensitivity of important financial indicators in relation to technical and financial input assumptions and develop final results for each of the scenarios investigated. Display overall scenario results showing risk and reward for the project and make scenario/project

recommendations with the development of the project business plan. The primary goal is to calculate the amount of energy delivered, in various forms, by the energy systems. The challenges of the model are to assess the system's energy needs in terms of heating, cooling and power generation; and then to estimate how those needs can be met by the various energy systems that are ultimately chosen. The model is devoted to calculating the system's load and energy use and to evaluating how they can be optimally met.

2.6. Building Level Optimization

The Army's present and future building stock is comprised of a variety of building types. Energy requirements in some of them (i.e., barracks, office buildings, child development centers, maintenance facilities and hangars) are dominated by climate (heating, cooling and humidity control) with a smaller effect from plug-in loads. Other buildings (e.g., command and control facilities, hospitals, training facilities with simulators, dining facilities, laboratories) have high energy loads dominated by internal processes and high ventilation requirements.

While some energy use reduction methods in most of these facilities are similar and well understood (building envelope improvement, better lighting systems designs and technologies, etc.), in buildings with high internal loads, energy use reduction can result only with intervention into specific processes use of energy efficient appliances and use of significant waste streams [2], which is currently rarely addressed. More work is needed to address energy uses and wastes at such energy intensive facilities like data centers, laboratories, training simulators, hospitals, etc.

The energy demand determines the amount of energy that needs to be provided by the distribution and supply generation side. Building level energy simulation and optimization can be accomplished using models such as EnergyPlus, ESPr, TRANSYS, or another accurate hourly energy analysis program. When a community or a cluster of buildings is evaluated there are more opportunities available for energy savings and more challenges for analysis and optimization. In addressing buildings as a community, you not only need to deeply evaluate each building, but you also need to take the individual analysis and apply it to a community, or cluster, with possibilities for integrated supply services.

The building optimization process starts with identifying typical buildings and energy systems on Army installations and existing energy wastes and inefficiencies related to these buildings and systems [2], developing load profiles for typical base case buildings and identifying an analysis of suites of technologies for ultra-low energy installation to include waste recovery and energy conserving (ultra-low energy), energy generation and storage technologies that could be applied to buildings and the energy systems that support those buildings to minimize traditional electrical and fossil energy use.

There is a debate over whether to conserve energy first or just generate energy with renewable alternatives. Figure below shows the theoretical path for optimization and the process for each individual building and building cluster optimization process.

Point 1 is the base case building that is either required to be built by the local code body requirements or is an existing building. If renewables are added at this point, the total annual cost of the net zero energy building will be as shown in point 8, using a constant cost for a unit of photovoltaic system ($/m^2 of a PV panels or $/kWh electricity produced). Another alternative from point 1 will be to add energy efficiency technologies at the building level, which will require investing in these technologies (additional first cost) and eventually point 2 is reached with the lowest total annual cost. One would not add renewables at this point since many more energy efficiency technologies can be added that are more cost effective than adding renewable generation. Point 3 is reached when the same total annual cost as existing building or base case building built to code, but this building is now much more energy efficient and in many cases much more comfortable to inhabit. By continuing to add energy efficiency improvements to the building, the building will eventually reach point 4, where adding more energy efficiency

measures will result in diminishing returns, or cost more than adding renewable generation. For an individual building analysis, this building would be at the Net Zero Ready point. For different types of buildings and climate locations, fossil fuel based energy reduction will vary [3] for each case.

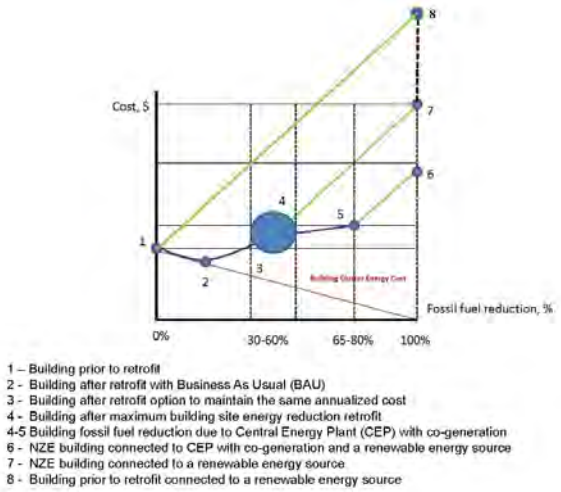

Fig. 1. Building fossil fuel reduction optimization process

In buildings with low internal energy loads, reduction of fossil fuel can be significant (50 to 75%), but only 20 to 30% in buildings with high internal loads. This is true even for buildings built or retrofitted to "passive house" requirements and using advanced "low exergy" systems to satisfy remaining heating and cooling needs. The remaining energy requirements will be dominated by electrical power needs for lighting, appliances and internal processes and by domestic hot water needs, i.e., for showers and other domestic needs. Adding renewables from point 4 will result in the total annual cost, shown by point 7. Depending on the building internal load, building fossil fuel based energy reduction can reach 30 to 60%.

Alternatively, the building characterized by point 4 can be connected to co-generation plant serving either this individual building or cluster of buildings. This will require a smaller investment compared to the cost of decentralized boilers and chillers for single buildings, and the cost of larger renewable generation equipment [9], but result in a significant fossil fuel reduction due to use of waste heat accompanying electricity generation. This heat can be used either to satisfy heating, cooling, and domestic hot water needs of the building cluster, or be exported to another building cluster. Connecting to a Combined Heat and Power (CHP) plant, fossil fuel usage by the building cluster (point 5) can be further reduced by another 20-25%. When CHP uses biomass or biogas as a fuel, the connected building(s) become "Net Zero" fossil fuel. Typically at point 5, buildings do not require additional thermal energy from renewable energy source, but may require additional electrical power. After point 5, adding solar or wind generated electrical power becomes a cost-effective supply option, and this point, by definition, states that the building cluster is "Net Zero Ready." As one can see from the graph, path 1-2-3-4-5-6 is the lowest cost path for building improvement leading toward net-zero fossil fuel based energy strategy.

When this process has been completed for each building, the results from all of the individual buildings are integrated and put into annual load duration curves. The load duration curve shows the cumulative duration for different loads in the system over a full year. Due to diversity of energy use in buildings comprising the cluster (community), the peak of the resulting load curve is much smaller than the sum of peaks of individual buildings and thus the needed generation and a back-up capacity is much smaller.

2.7. Building Cluster or Installation Analysis

To develop the community energy concept, energy models can be used that optimize distribution of energy from central generation/production to the energy usage by the buildings and systems. The building simulation gives results for demand curves for domestic hot water consumption, electricity consumption, heating, and cooling for those buildings at existing climatic conditions and these are passed to the next step. These models will minimize energy waste and losses and optimize first and operating costs (First Cost + Operating Cost = Total Cost). Based on this concept, a Master Planning process can be developed that will provide an orderly approach to changing the typical Army installation to an ultra low energy consuming community.

2.8. Distribution and Supply Optimization

Simulation of supply systems can be done using an energy system optimization model like POLIS [4]. Between energy generation and energy demand points (at each building level), a distribution system is used to transport the energy via a hot or chilled water system. While "energy balancing" means just calculating the correct energy flows (and perhaps also carbon emissions) in a system, to estimate energy costs and to benchmark with other similar systems, simulation and optimization is necessary for system planning. For principal comparisons of available alternatives, a simpler simulation approach will be favorable, one that provides a possibility to make an energy balance for the whole system and to compare the effects of different demand or supply side measures in terms of energy efficiency, capital and energy costs, and GHG (Green House Gas) emissions with the simulated demand curves from the building simulation optimization step.

For this purpose, energy system models might be applied that have been developed for the optimization of large systems. However, to be used as a regular planning tool, skilled planners are needed that are familiar with them. POLIS models an energy system as a closed system including the entire chain from demand, the distribution system, to supply systems. Every element like buildings, boilers, generators, grids, etc. are described as "knots"; energy- and cost-related parameters are linked together to an interconnected system in which different usages are interlinked. Power supply, heating, and air-conditioning is modeled in a common system. This offers the opportunity to compare efficient technologies like co-generation (power + heat) and tri-generation (power + heat + cooling). The result of this type of model offer the best suited solution to reduce the energy usage of a building cluster, and leads the way to net zero installations with least cost. More than that, the approach of optimizing building clusters will offer new and/or additional options that reduce the fossil energy footprint of community systems cost efficiently.

In POLIS, an energy system can be modeled by using prototypes of generation equipment, distribution systems, and load profiles. Cost, emissions, and technical parameters are used to describe existing or future elements of the system. Simulation is performed using hourly load profiles for the thermal and electrical energy demand throughout a year (8760 hours), which is generated from the summation of the building cluster energy simulations. POLIS allows calculation of the best suited combination of paths to meet the load with the objective to minimize total system costs, or minimize total GHG-emissions. Since the distribution systems play a significant role in an overall thermal energy system, a hydraulic flow model should be used to analyze critical capacities and flows in the system. Through an iterative process, these two models will determine whether an optimization of the energy system (POLIS results) will lead to a feasible optimized supply and generation system.

3. Fort Irwin, CA Building Cluster Case Study Results

The integrated energy optimization process described to this point includes analysis of building energy efficiency improvements and optimization of energy generation and distribution. The tools required to optimize an individual building were applied to the analysis of eight types of Army buildings. The goal was to meet or exceed EPACT 2005 requirements for new construction [5,6,7] as well as for the "Integration of Energy/Sustainable Practices into Standard Army

MILCON Designs" study [3] of five common types of Army buildings with aggressive goals to achieve 60 to 80% energy use reduction against CBECS 2003. Continuing the discussion started in [8], this section of the paper illustrates the proposed approach using the example of the building cluster to be renovated at Fort Irwin.

Fort Irwin is located in the High Mojave Desert midway between Las Vegas, NV and Los Angeles, CA. The energy required to serve the needs of more than 1600 buildings located on the installation is not generated on site; it must be conveyed over long distances. Electric power is transmitted from distant generators through the power grid; LPG for heating and domestic hot water (DHW) is trucked to Fort Irwin in bulk.

The Engineer Research and Development Center, Construction Engineering Research Laboratory (ERDC-CERL), with support from a group of industry experts, conducted an energy study [9] at Fort Irwin with a focus on a representative group (cluster) of buildings that included five barracks buildings, a dining facility, and a central energy plan to which all these buildings were connected. The integrated optimization process used in this analysis includes optimization of each building in the cluster to meet its economic energy efficient optimum. The building cluster is then energy optimized taking advantage of the diversification between energy intensities, scheduling, and waste energy streams use between the buildings.

3.1. Modeling of Buildings and Systems

The modeling of the buildings, the systems within the buildings, and the systems supporting the buildings was done by using the eQuest – an hourly annual building energy analysis tool that provides professional-level results with an affordable level of effort.

The estimated energy use of the five barracks and dining facility as operating during the site visit was 3.1 million kWh/yr and 9193 million Btu (2,694,202 kW-hr) of LPG gas. The data generated by computer analysis indicate that a typical upgrade of a barracks building only saves 8% of the electricity use compared to the barracks "as we found them" and 7% of the heating energy. In other words, a typical barracks upgrade is not very energy efficient.

The results of further analysis (Table 1) show that upgrades to Net Zero energy ready buildings allow the reduction of the energy consumed to heat, cool, and ventilate the cluster facilities by 44 to 49% of electrical use and 30 to 59% of heating use with paybacks of 2 to 10 yrs depending on the alternative chosen. Since the proposed energy efficiency work includes the implementation of DOAS and high efficiency dehumidification systems that would dramatically reduce the potential for biological growth, in climates where mold is an issue, the avoided costs of mold mitigation can decrease the payback to 1.2 yrs.

A renewable energy use analysis to achieve "Net- Zero" energy status building cluster must provide the remaining energy amount using renewable energy sources. For the location of Fort Irwin, the most attractive renewable energy sources are solar and waste products. For development of the renewable energy concepts the following exiting conditions were used. The Barracks and the Dining Facility are connected to the Central Heating Plant (Bldg 263) by a district heating grid. Three LPG boilers, 2060 MBtu/hr (603 kW) each, are generating heat for domestic hot water DHW needs and space heating (SPH). No water storage tanks are installed in the Central Heating Plant. DHW storage tanks with a capacity of approximately 1500 gal (5678 L) are installed in each building. The LPG and electricity prices are the actual values given during the energy assessment. Renewable energy opportunities for the building cluster, including installing solar thermal, biomass (wood chip), and PV electrical generation systems can save 4832 million Btu/yr (1,416,119 kW-hr/yr) and generate 41,630 KWh/yr. Renewable thermal energy generation is cost effective and has a simple payback period of less than 10 years. Using photovoltaic panels to generate renewable electrical energy is not a cost effective solution since it has a significant payback period of 47 years.

4. Conclusions

The integrated optimization process is being developed under the Army research and development project "**Modeling Net Zero Installations-Energy (NZI-E)**" [11] and the International Energy Agency (IEA) Energy Conservation in Buildings and Community Systems (ECBCS) Annex 51. The process includes optimization of each building clustered together to meet its economic energy efficient option; then the building cluster is also energy optimized taking advantages of the diversification between energy intensities, scheduling, and waste energy streams use. The optimized cluster connected to CHP plant will minimize the amount of renewables needed to make the building cluster Net Zero fossil fuel energy.

The recommended, integrated energy solution demonstrates that vastly improved energy efficiency and greenhouse gas reductions are feasible in the context of a normal scale development using proven approaches from the United States and elsewhere.

"Business as usual" leads to individual boilers and chillers for each building, which leads to significant total overcapacity, and over time, to a wide range of boiler inefficiencies and chiller COP's with limited overall system control to meet the diverse demands of an installation. Alternatively, district heating and cooling systems link buildings in common networks that eliminate inefficient boiler and chiller over-capacity, and allow the integrated system to meet the integrated peak loads instead of individual peak loads. The addition of efficient technologies now, allows future technologies to be added to one location instead of to each building at the location.

References

[1] Army vision for Net Zero. Net Zero is a force multiplier, Washington, DC: Office of the Assistant Secretary of the Army (Installations, Energy & Environment), 15 December 2010, www.asaie.Army.mil

[2] Energy and Process Assessment Protocol, *International Energy Agency (IEA) Energy Conservation in Buildings and Community Systems (ECBCS) Annex 46*, http://www.annex46.org/

[3] USACE Report on EISA Study, *Army MILCON Energy Enhancement and Sustainability Study of Five Buildings*, (A collaboration by USACE, ERDC-CERL, NREL, PNNL).

[4] Richter, S., and T. Hamacher. "URBS: A Model for Investigations on Future Urban Energy Systems." *PowerGen Europe, Conference Proceedings*. International Conference and Fair. CCD Düsseldorf, Germany, May 2003.

[5] Zhivov, A., D. Herron, and M. Deru. "Achieving Energy Efficiency and Improving Indoor Air Quality in Army Maintenance Facilities." *ASHRAE Transactions*. LO-09-094, 2009, Vol 115, Pt 2.

[6] Herron, D., A. Zhivov, and M. Deru. "Energy Design Guides for Army Barracks," *ASHRAE Transactions*, 2009, LO-09-093, Vol 115, Pt 2.

[7] Deru, M., D. Herron, A. Zhivov, D. Fisher, and V. Smith, "Energy Design Guidelines for Army Dining Facilities," *ASHRAE Transactions*, LO-09-095, 2009, Vol 115 , Pt 2.

[8] Zhivov, A, R. Liesen, S. Richter, R. Jank and F. Holcomb, "Towards a Net Zero Building Cluster Energy Systems Analysis for a Brigade Combat Team Complex." *Proceedings of ASME 2010 4th International Conference on Energy Sustainability*, ES2010-90487, 17-22 May 2010. Phoenix, AZ, USA.

[9] David M. Underwood, Alexander Zhivov, Scot Duncan, Alfred Woody, Curt Björk, Stephan Richter, Dieter Neth, Dan Pinault, and Reinhard Jank. *Working Towards Net Zero Energy at Fort Irwin, CA*. ERDC/CERL TR-10-24. Champaign, IL: ERDC-CERL, 2010, http://www.cecer.Army.mil/techreports/ERDC-CERL_TR-10-24/ERDC-CERL_TR-10-24.pdf

A Study of Urban Form and the Integration of Energy Supply Technologies

Vicky Cheng[1,*], Sandip Deshmukh[2], Anthony Hargreaves[1], Koen Steemers[1], Matthew Leach[2]

[1] *Department of Architecture, University of Cambridge, Cambridge CB2 1PX, UK*
[2] *Centre for Environmental Strategy, University of Surrey, Guildford GU2 7XH, UK*
** Corresponding author. Tel: +44 1223762549, Fax: +44 1223332960, E-mail: bkc25@cam.ac.uk*

Abstract: Buildings account for a substantial share of the energy consumption and CO_2 emissions in the UK. Reduction of energy consumption and the use of low carbon technologies in buildings constitute a vital part in achieving the government's CO_2 reduction goals. Based on six existing urban form examples in the UK, this paper explores the potential for integrating different low carbon technologies for buildings taking into account factors relate to built forms. The study suggests that dwelling density has a significant influence on energy demand; however, it is not the only factor that influences the potential for low carbon energy supply. The combination of dwelling density and site coverage are the crucial built form factors that determine the potential of CO_2 reductions from low carbon technologies. The initial findings suggest that medium to low density housing may in some cases enable a greater saving in CO_2 emissions than higher density development because of the greater amount of space for collection of renewable energy. However, the effects of density on the energy use by other sectors such as transport, water and waste management, also needs to be considered and this integrated approach is part of our ongoing research on the ReVISIONS project.

Keywords: *Urban Form, Integrated Energy Supply, Renewable Energy, Low Carbon Technologies*

1. Introduction

Buildings in the residential, commercial and public sectors account for an estimated 48% of the total final energy consumption and 42% of all carbon emissions in the UK. The UK government has made a commitment in the Climate Change Act 2008 that the carbon account for the year 2050 is to be at least 80% lower than the 1990 baseline [1]. Reduction of energy consumption and the use of low carbon technologies in buildings constitute a vital part in achieving the government's carbon emission reduction goals. The Code for Sustainable Homes [2] requires that new homes are zero carbon by 2016. However, the rate of new house building in the UK is less than 1% per year compared to the existing housing stock and so around two thirds of the housing stock of 2050 already exists. Therefore, a substantial reduction in the carbon emissions from the existing housing stock is vital for achieving carbon reduction targets.

Energy use in buildings can be attributed to three main factors: building design, systems performance and occupant behaviour. Building design parameters such as plan, section, orientation and façade design account for a 2.5x variation in energy consumption. Services system parameters such as the efficiencies of lighting, boiler and other equipments contribute a 2x variation and occupant behaviour for a 2x variation. These factors cumulatively lead to a total variation of tenfold in energy consumption of buildings with similar functions [3]. Clearly, the design of built form and service systems has significant energy implications; they not only influence the energy demand but also determine the potential for renewable energy supply and the use of low carbon technologies. The government has committed to delivering 15% of energy from renewables by 2020 in accordance with the European Union Renewables Directive [4]. In order to achieve this goal, a significant increase of small-scale to community-scale renewable electricity and heat generation is expected [5]. The UK government launched a consultation in 2009 on its Heat and Energy Saving Strategy [6] which proposed that by 2030 all homes would have received a 'whole house' package including all cost effective energy saving measures plus renewable heat and electricity measures as appropriate. The policies are still tentative at this stage because there are a range of uncertainties about how

these measures will be implemented. There are some exploratory ongoing schemes such as the Carbon Emissions Reduction Target 2009-2012 (CERT) and the Community Energy Saving Programme 2009-2012 (CESP) which place obligations on energy supply companies to reduce carbon emissions and improve energy efficiency. The aim is to achieve a 30% reduction in carbon emissions from households by 2020 compared to 2006. However, there are a number of uncertainties about how large scale retrofitting of existing dwellings can be achieved and guidance is required on what measures are appropriate and cost effective for different urban forms and densities.

Many of the energy-efficient and renewable energy technologies available today (such as solar thermal, photovoltaic, micro-wind turbine, heat pumps, CHP, etc.) have already been in development for several decades; we have profound understanding of the science and engineering of these technologies. However, our knowledge concerning the integration and optimization of these technologies in buildings with respect to built form and spatial layout is limited. In the current planning practice, the decision about the built form for a particular target density is often driven by a combination of economic, social and cultural factors. The final form however would ultimately govern the potential of renewable energy sources that could be exploited on-site. In order to deliver a sustainable low carbon development, the design of built form, its energy implications and the potential for renewable and low carbon technologies needed to be considered together with other non-environmental factors in an integrated manner.

This study explores the potential for integrating different low carbon microgeneration technologies for buildings taking into account factors relate to built forms and spatial layouts. This paper represents our first step in understanding the interaction between energy demand and the supply technologies. This work forms part of the ReVISIONS project[1], a wider study investigating the inter-relationship between spatial planning and infrastructure policies for transport, water, waste and energy at the regional and local scales.

2. Existing urban form examples

Six existing urban form examples in Cambridge and London in the UK are selected for this study (Figure 1). The examples are largely domestic areas built up from Census output areas. Census output areas are statistical geography developed by the Office for National Statistics (ONS) as part of the 2001 Census in the UK; they are generated in consideration of population size, mutual proximity and social homogeneity. Land use information in each of the example area is sourced from General Land Use Database (GLUD) and the number of dwellings and dwelling type data are sourced from Neighbourhood Statistics Database.

The six urban form examples exhibit a diversity of densities and morphologies:

1. Comprises mainly rows of two-storey terrace houses at a gross residential density[2] of 55 dph. Each dwelling has its own private garden but communal open space is scarce in close vicinity. This setting is commonly found in many urban residential areas in England.
2. Comprises mainly detached and semi-detached houses at a density of 18 dph; this setting is typical of suburban areas where dwelling density is low and the dwelling plot size is large.

[1] ReVISIONS Regional visions of integrated sustainable infrastructure optimized for neighbourhoods project website: http://www.regionalvisions.ac.uk

[2] The residential density measure used throughout this paper is expressed in dwelling per hectare (dph) and is the gross density within selected Census output areas of predominantly residential use. It is calculated as the ratio of total number of dwellings to entire selected site area; the measure of site area takes into account all land use types (e.g. domestic, non-domestic, road, green space, etc.)

3. Is characterized by a courtyard-form layout which comprises mainly four-storey terrace houses and flats at a density of 33 dph. This spatial arrangement results in large areas of communal open space whilst private garden area is limited.
4. Represents a mixed urban form at a density of 27 dph. It has semi-detached houses with large private garden in the west, courtyard-form apartment blocks with communal open space in the east and rows of terraced houses in the middle.
5. Comprises a ten-storey courtyard-form apartment block which houses over 1200 flats; it has a very high density of 523 dph. Although primarily domestic, the development contains spaces for other uses: however this paper focuses on the built form of dwellings and does not consider non-domestic spaces.
6. Consists of three distinctive built forms: a fifteen-storey high-rise tower (~181 dph), a cluster of terraced houses (~93 dph) and a group of multi-storey slab-block flats (~97 dph). The entire study area has a gross residential density of 100 dph. The high density and diverse spatial arrangements may give rise to the potential of communal infrastructures for low carbon energy generation.

Fig. 1. The six urban form examples selected for this study (shown on the same scale).
© Crown Copyright/ database right 20(10). An Ordnance Survey/EDINA supplied service.

3. Domestic energy demand

The domestic energy demand of each urban form example is estimated using the Domestic Energy and Carbon Model (DECM) developed as part of the ReVISIONS project [7]. DECM consists of two major components: a housing stock database and a building energy model. The housing stock database is primarily developed based on the English House Condition Survey 2007. The survey contains 16194 sample dwellings covering a range of typical domestic building types in England. The building energy model is based on SAP-2005 with modifications to improve the energy estimation. DECM incorporates regional climate data and performs monthly calculations for electricity, water heating and space heating demands. Comparison of the model prediction with national statistics published by the UK Department

of Energy and Climate Change (DECC) confirms the capability of DECM in providing good estimations at both national and Local Authority (LA) levels. At national level, the model estimation of CO_2 emissions and gas and electricity consumptions are respectively 4.5%, 3.4% and 1.0% higher than the DECC figures. At the LA level, the correlations between the model estimations and the DECC records are statistically significant and substantial (all $r_s>0.9$ and $p<.01$).

Using DECM, average dwelling energy demand and CO_2 emissions for the four main dwelling types are produced (Table 1)[3]. The heat and electricity demands for each urban form example are estimated by multiplying these figures by the corresponding number of dwellings in each example. This method assumes the energy demand of dwellings in the urban form examples do not significantly deviate from the national averages. This is a rough estimation because the occupancies per dwelling will vary locally depending on the supply and demand for housing in different areas. Table 2 summarizes the key building parameters and estimated energy demand of each example area. It shows that energy demand per dwelling decreases with increased gross residential density ($r_s=-0.829$, $p<.05$). It is mainly due to the changes in dwelling mix; more flats and fewer houses at high density and vice versa in low density. This observation is consistent with a wider analysis conducted by the main author based on national housing stock and domestic energy consumption statistics.

Table 1. Annual average dwelling energy demand and CO_2 emissions for four main dwelling types

	Detached	**Semi-detached**	**Terraced House**	**Flat**
Floor area (m^2)	137.7	94.4	85.4	62.2
Occupants (number)	2.6	2.5	2.5	1.8
Energy demand (kWh)				
Space heating	14064	10490	9553	5547
Water heating	2469	2010	1901	1590
Electricity	3949	3105	2932	2320
CO_2 emissions[4] (tonnes)	7.4	5.7	5.3	4.0

Table 2. Key building parameters and estimated annual energy demand of each urban form example

Urban Form	**1**	**2**	**3**	**4**	**5**	**6**
Site area (ha)	8.0	8.3	8.1	9.3	2.4	4.8
Gross density (dph)	55	18	33	27	523	100
Site coverage[5]	0.3	0.1	0.2	0.2	0.5	0.3
Dwelling mix (number)						
Detached	20	40	8	34	0	3
Semi-detached	42	64	25	70	0	0
Terraced	322	18	159	39	0	51
Flat	55	29	73	110	1236	426
Total	439	151	265	253	1236	480
Energy demand (kWh)						
Water heating	833294	307712	488298	473674	1965438	781755
Space heating	4103152	1566740	2298678	2195206	6855780	2892334
Electricity	1281106	476748	744790	721207	2868070	1149888
Energy per dwelling	14163	15571	13327	13400	9457	10050
CO_2 emissions[6]	2311t	870t	1334t	1293t	4925t	1990t

[3] Energy demand refers to the energy required to meet the various end-uses; it is different from energy consumption as the latter also takes into account system efficiency.
[4] Emission factors: gas (0.184 $kgCO_2/kWh$), electricity (0.47 $kgCO_2/kWh$), oil (0.265 $kgCO_2/kWh$) and solid fuel (0.333 $kgCO_2/kWh$).
[5] Site coverage is calculated as the ratio of total domestic building footprint area to entire site area.
[6] Existing CO_2 emissions (tonne/year) are estimated based on average dwelling emissions as shown in Table 1.

4. Urban form and low carbon energy generation technologies

The low carbon energy technologies considered in this paper include solar thermal panel, photovoltaic (PV) panel, ground source heat pump (GSHP) and combined heat and power (CHP) device. Table 3 provides a general view and the spatial requirements of these technologies [8]. Micro wind turbine is not considered in this study owing to the limited wind potential in urban areas.

Table 3. Low carbon technologies and their requirements

Technology	Requirements		Typical cost of one unit	Typical size in kW
Photovoltaics	Roof or space facing SE/SW	Can export electricity if connected to grid, more cost effective if high on-site demand	£5k to £25k upwards	1 to 4 upwards
Solar thermal	Roof or space facing SE/SW	Hot water demand on-site	£2k to £5k	2 to 3
Ground Source Heat Pump	Land area for ground collector or a water source	Building with a space heating (and possibly cooling) demand and low temperature heating system (e.g. under-floor)	£5k to £25k upwards	3.5 kW to 15 kW upwards
Micro-CHP and CHP	Domestic or communal space	Proportional heat and electricity demand, scope for heat network	£500 to 800 /kWe and £660/kWe	kW to MW

The government has plan to significantly increase the uptake of low carbon and renewable energy technologies; the lead scenario set out in the RES suggests that over 30% of our electricity (including 2% from small scale generation) and 12% of heat demand supplied by renewable sources [5]. Using the urban form examples, we examine the prospect of achieving these targets, the potential savings in CO_2 emissions and cost effectiveness of the installations. Table 4 shows the proposed energy supply technology mix for each urban form example[7]. The technologies are selected on the basis of economics (mainly costs), technological suitability (scale and scope), environmental (associated emissions), resource potential (availability), and social (acceptance and policy) factors. The proposed options are considered in conjunction with the national electricity grid so that surplus or shortage of electricity can be exported to or imported from the grid.

[7] The following assumptions are used in the calculation: solar thermal panel of typical 100 litre capacity requires 2.03m^2 of roof space; PV panel of 210We capacity requires 1.64m^2 roof/facade space; and GSHP of 23.1 kW_{th} capacity. The heat and power ratios for micro-CHP and large-scale CHP are 3.0 and 1.8 respectively; they are assumed to be powered by gas and the overall efficiencies are 85% and 75% respectively. Excessive heat demand is assumed to be met by conventional gas boiler with efficiency 76%.

Table 4. Low carbon energy supply options for each urban form example

Urban Form	**1**	**2**	**3**	**4**	**5**	**6**
Water Heating Demand (kWh)	Solar thermal: 437 panels of 100 (lit) capacity	Solar thermal: 148 panels of 100 (lit) capacity	Micro-CHP: 488298	Micro-CHP: 340400; GSHP: 133274	CHP: 1965438	CHP: 781755
Space Heating Demand (kWh)	GSHP: 4158000; electricity required: 864000	GSHP: 1663200; electricity required: 345600	Micro-CHP: 1746072	GSHP: 2195206; electricity required: 483840	CHP: 3197088	CHP: 1288043; GSHP: 1663200; electricity required: 345600
Electricity Demand (kWh)	PV: 1026205	PV: 720804	Micro-CHP: 744790	PV: 691619; Micro-CHP: 113467	CHP: 2868070	CHP: 1149888
Renewable/ low carbon supply	6017498 kWh	2691716 kWh	2979160 kWh	3473966 kWh	8030596 kWh	4823977 kWh
Other supply (kWh)	Grid elect.: 1118901	Grid elect.: 101543	Gas: 4232007	Grid elect.: 399961 Gas: 533961	Gas: 20399786	Grid elect.: 345600 Gas: 6431969
Renewable/ low carbon	84%	96%	41%	79%	28%	42%
CO_2 savings (tonnes/year)	1757	777	409	943	325	381
Capital & operations costs	£9.1M	£5.1M	£0.8M	£5.0M	£2.7M	£3.7M
Effective costs (£/tCO_2 saved)	£259	£328	£98	£265	£416	£486

5. Discussion and Conclusion

The fraction of total energy demand which can be supplied by renewable and low carbon technologies varies remarkably from 28% to 96% across the six urban form examples; the variation is dependent of built form as exhibited in different dwelling types. Houses in general provide more opportunities for the application of low carbon technologies (especially renewable technologies) as they have suitable roof and garden areas where natural energy can be harvested. Urban Form 1 and 2 with high proportion of houses in the dwelling mix facilitate the use of solar thermal, PV and GSHP and result in the highest proportions of renewable and low carbon supplies. The spatial layout of apartment buildings significantly limits the exploitation of renewable energy; the strategy of low carbon supply lies on efficient cogeneration of heat and electricity. The high concentration of energy demand and the generally high proportion of heat to electricity demand in apartment buildings are conducive to the use of cogeneration systems. As illustrated in Urban Form 5, assuming a 20-year lifetime for the CHP system, an estimated 258 tonnes of CO_2 can be saved on average annually by switching the conventional centralized energy supplies to a cogeneration system; the saving is equivalent to around 6% of the total emissions produced by the existing centralized system to 2030.

The capital and operational costs of the proposed technology mix for each urban form example vary widely from less than £1 million to £9 million. The high costs shown in Urban Form 1, 2 and 4 are mainly due to the use of PV panels. The use of PV technology, although seemingly expensive, results in remarkable reduction in CO_2 emissions. Table 5 presents an alternative energy supply option for Urban Form 1, 2 and 4 where the use of PV is excluded; the demand for water heating is provided by solar thermal systems and space heating provided by GSHP. The entire electricity demand is assumed to be met by the national grid.

In order to gain a fuller picture of the cost effectiveness of the proposed technology mix, the effective costs which represent the costs per tonne of CO_2 saved are examined. The effective costs are calculated based on an average 20-year lifetime of the technologies applied in conjunction with the UK government projection of the carbon dioxide emission factors for different fuels for 2030 [9]. The government expects to see a substantial reduction of coal-fired power plants and a considerable increase of renewable sources in the national electricity generation in 2030. As a result, the emission factor of grid electricity is projected to fall from the current 0.47kgCO_2/kWh to 0.19kgCO_2/kWh in 2030; whilst for fuels other than electricity, the emission factors are assumed to remain constant to 2030.

Table 5. Carbon savings and effective costs for energy supply options without PV.

	1	2	4
Renewable/ low carbon supply	4991294 (70%)	1970912 (71%)	2802154 (70%)
CO_2 savings (tonnes/year)	1401	527	767
Capital & operations costs	£4.1M	£1.5M	£2.2M
Effective costs (£/tCO_2 saved)	£145	£144	£143

As shown in Table 4, the effective costs vary between £98 and £486 for every tonne of CO_2 saved across the urban form examples. The application of micro-CHP to supply all of the electricity and heating for Urban Form 3 results in the option with the lowest cost per tonne of CO_2 saved but uses gas which not renewable and this technology will become less cost effective as gas supplies become scarcer and more expensive. The proposed technology mix for Urban Forms 5 and 6 is the least cost effective because communal CHP at this scale of application works out more expensive than the micro-CHP used for Urban Form 3. On the other hand, the technologies for Urban Forms 1, 2 and 4 are relatively expensive but achieve a much greater reduction in CO_2 emissions and are therefore more cost effective per tonne of CO_2 saved than Urban Forms 5 and 6. The complete elimination of direct fossil fuel use in the proposed technology mix for Urban Form 1, 2 and 4 derive the most benefits from the government's decarbonisation strategy for grid electricity but the cost per tonne saved is far greater than the 2030 value of £70 per tonne of carbon mitigation by DECC [10]. Table 5 shows that if PV is omitted from the technology mix for Urban Forms 1, 2 and 4 then the cost per tonne of CO_2 saved is substantially reduced but is still around twice the DECC value. These renewable energy technologies may become better value for money if their costs can be reduced and if grid electricity can be decarbonised to a greater extent than assumed in this paper. The above comparisons suggest that the most cost effective building-scale technologies are those that supply heat. Further research is now being carried out by our ReVISIONS project on how these low carbon technologies could function as part of wider systems and how technologies such as CHP may become more cost effective when considered at a wider communal scale. This research will continue to focus on how urban spatial form affects the feasibility of these technologies.

Dwelling density has a significant influence on energy demand per household; however, it is not the only factor that influences the potential for low carbon energy supply. For instance, Urban Form 1 is more than three times as dense as Urban Form 2 but both show high potential for the application of these renewable and low carbon technologies. The combination of both dwelling density and site coverage are the crucial built form factors that determine the potential reductions in carbon emissions from these technologies. The small number of urban form examples recruited in this study limited the feasibility of a quantitative analysis of the effects of morphological parameters such as site coverage and plot ratio on the potential of low carbon supply. The examples shown in this paper suggest that medium to low density housing may in some cases enable a greater saving in carbon emissions than higher density development because of the greater amount of space for collection of renewable energy. However, the effects of density on the energy use by other sectors such as transport, water and waste management, also needs to be considered and this integrated approach is part of our ongoing research on the ReVISIONS project.

Acknowledgements

Research for this paper was supported by funding from the UK's Engineering and Physical Science Research Council (EPSRC) for the project entitled 'ReVISIONS: Regional Visions of Integrated Sustainable Infrastructure Optimised for NeighbourhoodS'.

References

[1] H.M. Government, Climate Change Act 2008, 2008.

[2] Department for Communities and Local Government (CLG), The code for sustainable homes: setting the standard in sustainability for new homes, 2008.

[3] Baker, N. and K. Steemers, Energy and environment in architecture: a technical design guide, E. & F. N., 2000.

[4] European Union Renewables Directive, Official Journal of the European Union L140/16: on the promotion of the use of energy from renewable sources, 2009.

[5] H.M. Government, UK Renewable Energy Strategy, 2009.

[6] Department of Energy and Climate Change (DECC), Heat and energy saving strategy consultation: executive summary, 2009.

[7] Cheng, V. and K. Steemers, Modelling domestic energy consumption at district scale: A tool to support national and local energy policies, Environmental Modelling and Software (submitted for review) 2010.

[8] Enviros Consulting Limited, Utilising renewable energy resources within south Cambridgeshire, 2008.

[9] Market Transformation Programme (MTP), BNXS01: Carbon dioxide emission factors for UK energy use: version 4.2, 2010.

[10] Department of Energy and Climate Change (DECC), Carbon valuation in UK policy appraisal: a revised approach (June 2010 update), 2010.

IEA-ECBCS Annex 51: energy efficient communities. Experience from Denmark

A. Dalla Rosa[1,*], S. Svendsen[2]

[1] *Technical University of Denmark, Kgs. Lyngby, Denmark*
[2] *Technical University of Denmark, Kgs. Lyngby, Denmark*
** Corresponding author. Tel: +45 45251939, Fax: +45 45881755, E-mail: dalla@byg.dtu.dk*

Abstract: The paper describes the Danish contribution to the IEA-ECBCS Annex 51: "energy efficient communities". We present three case studies, two from Annex subtask A (state-of-the-art review) and one from subtask B (ongoing projects). The first case study is "Samsoe: a renewable energy island". In a ten-year period, the community achieved a net 100% share of renewable energy in its total energy use, relying on available technical solutions, but finding new ways of organizing, financing and owning. The second project is "Concerto class I: Stenloese Syd". The buildings in the settlement are low-energy buildings class I (Building Regulation 2008). The project envisaged the implementation of selected key energy-supply technologies and building components and carried out an evaluation of user preferences to give suggestions to designers and constructors of low-energy houses. The third case study is: "low-energy neighborhood in Lystrup, Denmark". The project integrates sustainable solutions both for the building sector and the energy supply side, which in the case consists on a low-temperature district heating network. The analysis of the successful/unsuccessful factors in the projects contributes to develop the instruments that are needed to prepare local energy and climate change strategies and supports the planning and implementation of energy-efficient communities.

Keywords: *energy efficiency, urban planning, renewable energy, district heating*

1. Introduction

The main objective of the IEA-ECBCS Annex 51: "energy efficient communities" is the design of integrated long-term energy conservation and greenhouse gas (GHG) mitigation strategies within a community, with optimal exploitation of renewable energy (RE) [1]. A holistic approach is used, comprehending generation, supply, transport and use of energy. Annex 51 explores effective paths that implement technical innovations in communities with an increased rate, enabling communities to set up sustainable energy structures and identify the specific actions necessary to reach ambitious goals. We consider both short-term and long-term plans, and their economic feasibility. Furthermore, we prepared recommendations, best-practice examples and background material for designers and decision makers.

2. Methodology

The title of subtask A is "existing organizational models, implementation instruments and planning tools for local administrations and developers – a state-of-the-art review". Each participating country describes the national legislative and economic framework for urban energy and climate change policies and prepared a review of data acquisition methods and tools for monitoring municipal energy and GHG balances. Next, we consider local energy system modeling and simulation tools and their combination with conventional planning tools for the design of energy supply systems and demand calculation. Finally, we discuss successful examples of community energy planning projects within the participating countries. The focus is on methods and planning principle, implementation strategies and the final comparison and evaluation of approaches in different countries.
In subtask B, "case studies on energy planning and implementation strategies for neighborhoods, quarters or municipal areas", we describe methods to characterize the actual state of a project in terms of energy and GHG performance. We investigate scenarios and planning alternatives arisen during the case study timeframe, and we report cost structures and

cost/benefit analyses. The process organization, the role of the decision makers and the implementation strategy are put into focus. Finally, we report R&D issues, methods and tools used by the decision makers and the results achieved, with regard to GHG targets and economic feasibility.

3. Results and Discussion

3.1. Samsø: a renewable energy island

In 1997 Samsø island (114 km^2, 4124 inhabitant in 2010) won a competition, announced by the Danish Ministry of Energy. It dealt with the choice of a local community with the most feasible plan for the transition to energy self-sufficiency with exploitation of RE.

3.1.1. Objectives and milestones

The objective was to study what share of RE a well-defined area could achieve using available technology, and without extraordinary state subsidies. The master plan described the available resources and how the transition could be made, with descriptions of both technical and organizational figures. Reduced energy consumption in all sectors, i.e., heating, electricity and transportation was an essential requirement. The degree of local participation was another top priority for the project: the business community, local authorities and local organizations had to support the proposed master plan to give it credibility. It was expected to envisage new ways of organizing, financing and owning the sub-projects proposed.

Table 1: Comparison between energy and economical figures in Samsø, period 1997-2005.

Energy and economical figures	**Master Plan (1997)**	**Achieved (2005)**
Share of renewable energy [%]	100	99.7
Degree of energy self-sufficiency [%]	100	35
Share of district heating [%]	65	43
Heat use [TJ/year]	140 (+ 0%*)	155 (+10%*)
Electricity use (no for heat) [TJ/year]	70.0 (-12%*)	77.3 (-3%*)
Onshore wind turbines [TJ/year]	86	100
Offshore wind turbines [TJ/year]	260	285
CO_2 emissions [tons/year]	-14000	-15000
Private investment [€·10^6]	78.7	53.3
Public subsidies [€·10^6]	9.3	4.0
Private investment [€/inhabitant]	20000	13500
Public subsidies [€/inhabitant]	2300	1000

*Reference year: 1997

3.1.2. Energy conservation

Campaigns were made concerning energy savings, among those the "pensioner project". The Danish Energy Authority granted funds (50% of the investment, max. 3250 EUR) to pensioners for energy saving renovations in their private houses. Informative letters were sent to the 444 pensioner families of Samsø and a free visit by an energy adviser was offered. 43% of the families made use of it. Local business increased its turnover by 1.1 million EUR. Nevertheless, the total energy use (electricity, heat and transport) increased by 4% in the period 1997-2005, from 305.4 TJ to 318.6 TJ, mainly due to an increased heat demand (+10%, partly because of a cold winter in 2005) and energy use for transportation (+ 7%).

3.1.3. Energy supply

The municipal council guaranteed the mortgage loans that financed the district heating (DH) plants, whose fuel (straw and wood chips) is produced by local farmers. Buildings built in

areas with existing or planned DH were compelled to connect to the system, while the houses that complied at least with the low-energy class 2 standard (Building Regulation 98, [2]) were exempt. Outside DH areas, the actual planning process began when 70% of consumers using regular oil furnaces or boilers had signed up for the conversion to DH. The energy utilities introduced a new financial model, who was an exception to normal practice. The consumer paid a connection fee of around 10 EUR, if registered before the establishment of the network, while the fee increased up to 5000 EUR afterwards. This method guaranteed a high degree of connection and aimed at encouraging end-users' energy savings, due to higher energy supply costs. The production increased from 39.6 TJ in 1997 to 82.4 TJ in 2005 [3]; at the same time, the expansion of the existing networks caused the distribution heat losses to increase from 19.9% to 24.2% of the delivered energy. The main figures about the DH systems are shown in Table 2. A cooperatively owned regional utility, NRGi, own and operates two DH systems; another system is owned by a local commercial operator, while the consumers themselves own and finance the last system.

Table 2: District heating in Samsø (2005).

Location	Nordby/Mårup	Tranebjerg	Ballen/Brundby	Onsbjerg
Ownership	NRGi*	NRGi*	Consumer-owned	Private
Consumers	178	400	240	76
Investment costs [€*10^6]	2.7	3.5	2.2	1.1
Subsidy [€*10^6]	1.2	-	0.3	0.4
Peak power [MW]	1.6	3.0	1.6	0.8
Energy [MWh/year]	n.a.	9500	3300	1500
Solar collector area [m^2]	2500	-	-	-
Solar storage tank [m^3]	800	-	-	-
Year of establishment	2002	1993	2005	2002
Resources	Biomass/ solar	Biomass	Biomass	Biomass
Fuel consumption [tons/year]	1250	n.a.	1200	600
Fixed fee [€/(consumer·year)]	344	362	345	350
Price [€/MW]	92	104	90	90
Connection fee* [€]	3350	3350	6000	6000
Connection fee* [€/m$_{pipe}$]	150	150	-	-

* Only for customers who connect after the establishment of the DH network

Individual solutions were applied in areas not reached by DH networks: 860 solar thermal systems, 35 heat pumps and 120 biomass-based units were installed [4]. To cover the electricity demand, 11 onshore wind turbines were installed, with a total peak capacity of 9 MW_{el}. An offshore wind turbines park was dimensioned with a capacity of 23 MW_{el}, corresponding to the difference between the actual energy use in the transport sector and the energy savings to be realized in the master plan. Five of the 10 off-shore wind turbines are owned by the municipality of Samsø. The proceeds from the windmills are reinvested in future energy projects as Danish law does not allow local municipalities to earn money by generating energy. Three of the off-shore turbines are privately owned by local farmers. Nine offshore wind turbines are owned privately by small groups of farmers and two are owned by local cooperatives with up to 1500 shareholders [5]. Spreading the ownership improved citizenship acceptance for the construction of the wind turbines. Electricity production prices are regulated by law and include a ten-year fixed price agreement which is the same for all the wind turbines on the island. The agreement stipulates a guaranteed price of about 0.08 EUR for the first 12000 full-load running hours and afterward about 0.06 EUR, until the ten year period expires.

3.1.4. Analysis

The strengths, weaknesses, opportunities, and threats (SWOT) analysis is shown in Table 3.

Table 3: SWOT analysis for the Samsø case study.

	Helpful	**Harmful**
Internal origin	*Strength* - Political support - Internal energy market - Local coordination - Local ownership - Organizational structure - Local resources - Challenging jobs	*Weakness* - Minor energy savings - No cogeneration - Municipality administration - Uncertainty of energy prices - Training and education - Protests against placement of wind generators and DH plants
External origin	*Opportunity* - External investments - EU incentives - Lower tax for electricity from RE - Creation of new employment opportunities - El. contracts avoid price fluctuations - Positive effect on tourism	*Threat* - Removal of subsidies by new government - Immaturity of electric car technology - Lack of suppliers and companies for maintenance

3.2. Concerto class I: Stenløse Syd

The project Class1 began in 2007, after the municipality of Egedal decided to strengthen the energy requirements for a new settlement to be erected in the municipality [6]. The project is part of the "EU Concerto initiative project" [7]. During the years 2007-2011 a total of 442 dwellings were or are designed and constructed with a heating demand corresponding to the Danish "low-energy class I". This means that the energy consumption will be 50% below the energy frame set by the Danish Building Regulation (DBR 08). The energy frame is calculated with the following formula, where A is the heated floor area:

$$\text{Energy frame} = 70 + 2200/A \text{ in kWh/m}^2\text{/year} \quad (1)$$

Figure 1: Site area (left) and status of the settlement in 2010 (right).

During the first year of the project, the municipality itself has constructed a kindergarten in compliance with the above restrictions and a social housing association has completed an ultra low-energy house project (heating demand of 15 kWh/(m2.year)) – comprising 65

dwellings. Besides, the constructions of the elderly centre and 13 single family houses have commenced. The Class 1 project focuses on selected key technologies and building components: slab and foundation insulation, window frames, mechanical ventilation with heat-recovery combined with heat-pumps, biomass-CHP, heat distribution for local DH and user-friendly building energy management systems.

3.2.1. Evaluation of user preferences and legislative analysis

One part of the demonstration activities deals with the evaluation of the user preferences to improve target future buyers/builders of low-energy houses. The methodology was determined and the initial interviews were carried out. The final report is available in [6]. Proactive attempts have been identified and documented to understand legislative and planning means in the process of promoting sustainable community projects [8].

3.2.2. Key-product development

Industrial partners have made progress in developing new and/or improved products suitable to low-energy buildings: a low energy window, whose production costs were reduced by 30% by process changes and machinery investment and a ventilation unit with heat recovery and integrated heat pump for low-energy houses. Moreover the low-rise, dense building sites will be supplied by a local low-temperature DH network. During the summer period the bio-mass CHP plant will be closed down and the solar heating systems will deliver the heat for domestic hot water (DHW).

Table 4: SWOT analysis for the Stenløse Syd case study.

	Helpful	**Harmful**
Internal origin	*Strength* - Integration of different sectors - Comparison of strategies in the different participating countries	*Weakness* - No obligatory monitoring concept implemented in all the sub-projects
External origin	*Opportunities* - Mix of energy savings and renewable energy policies, R&D and dissemination activities - Intelligent management and monitoring of water and energy consumption	*Threats* - Coordination of many partners

3.3. Low-energy neighborhood in Lystrup

The project deals with the realization and evaluation of a sustainable housing area in Lystrup, Aarhus. The residential area B was completed in "Lærkehaven" in May 2008 and represented the first step towards the vision of a sustainable housing development, with a total of 122 low-energy buildings. The residential area C was completed in early 2010. The last stage (residential area A) will be finalized in 2011. The main characteristics of each area are [9]:
A: 32 two-storey family houses according to the German Passive House Standard.
B: 33 two storey houses (Danish low-energy class I) and 17 single-storey houses (Danish low-energy class 2), LED lighting, phase change materials (PCM), common solar cell facility.
C: 40 residences (Danish low-energy class I, expected energy demand of 30 kWh/m^2, total heated floor area: 4115 m^2), connected to a low-energy DH network.
In the paper, we focus on the area C. The project integrates sustainable solutions in the end-user side (building sector) and in the energy supply side (DH network). The former deals with finding cost-effective solutions for the construction of low-energy buildings and at the same time promoting high architectural quality and comfort; the latter refers to the demonstration of

the technical and economical feasibility of DH applied to areas with low heat demand densities and to the testing of two heating unit designs with focus on return temperature.

3.3.1. The low-energy and low-exergy district heating system

The project is among the first in the world, where a low-temperature DH network is applied. The DH network (total trench length: ~800 m) was designed according to low-temperature operation in the supply pipe (55°C) and in the return pipe (25°C). The application of the low-exergy concept to the DH technology aims at three main targets. The first one is to guarantee comfort, with regards to delivery of DHW and to space heating requirements, by exploiting low-grade energy sources and RE. The second objective is to match the exergy demand of such applications with the necessary exergy available in the supply system, by making the temperature levels of the supply and the demand closer to each other. Finally, it aims at reducing the heat loss in the distribution network, so that the total profitability is ensured from the socio-economic point of view. The main design concepts are:

-Low-size media pipes. This is achieved by allowing a high pressure gradient in the branch pipes connected to the unit with instantaneous DHW preparation or by installing units with storage of DH water. The latter one consists on a heat exchanger coupled to a water storage tank on the primary side, which ensures low continuous water flow from the DH network and therefore media pipes of lower size in the distribution lines.

- Low-operational temperatures: down to 50-55°C in the supply line and 20-25°C in the return line.

- Twin pipes are used. Furthermore flexible plastic pipes replace steel pipes, wherever it is possible. This leads both to lower investment costs for the civil works connected to the laying of the pipeline and to lower total heat loss.

- Installation of a circulation pump. The pump ensures an increase of the available differential pressure in the network and it compensates for the choice of small-diameter media pipes.

Figure 2: Sketch of the DH network with the location of the meters (adapted from [10]).

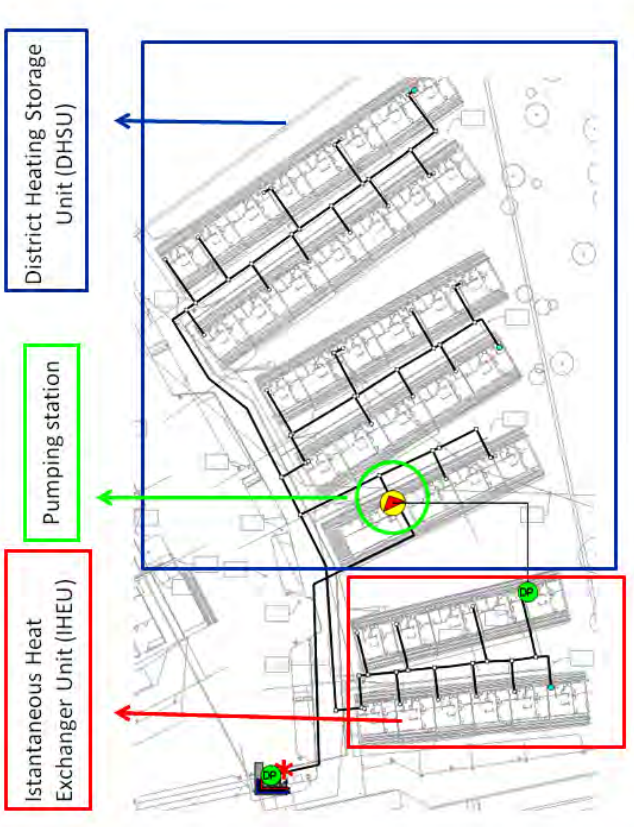

Two types of DH substations are installed: 30 Instantaneous Heat Exchanger Unit (IHEU) and 11 District Heating Storage Unit (DHSU). This former utilizes a heat exchanger between the primary side (DH loop) and the secondary side (DHW loop) for instantaneous production of DHW, while there is a direct system for space heating. The unit is equipped with an external by-pass, meaning that the by-pass water does not flow through the heat exchanger. The latter includes a storage tank and a heat exchanger. Heat is stored with DH fluid as medium. The DHW is produced by a heat exchanger, supplied from the tank. A flow switch detects a water flow and starts the pump. There is no need for by-pass flow in this type of unit. The DHSU are all placed on the same street line so that it is possible to measure both the performance of

the unit itself and the implications at street level. The total investment cost for the whole network, including the substations, lies between 350000 € and 400000 €.

3.3.2. Analysis

We highlight here the main findings, with regards to the planning process.
- The project took profit of the extensive collaboration among different partners: the housing association, industrial partners, architectural and engineering consultants, research institutions and governmental agencies.
- The international architectural competition and the import of prefabricated building envelopes from abroad succeeded to ensure high standards and reasonable economy.
- To some extent, the Danish building construction tradition has been a barrier for planning the community as a whole, more than as a collection of individual building units. In fact, the tendency in the sector, related to low-energy buildings, is to provide solutions based upon individual energy supply systems, mainly heat pumps, and the building types are often not developed with a friendly interface to DH systems. On one hand, this means that standard and reliable offers for low-energy buildings already exist; on the other hand, it could hinder the chance of implementing a sustainable and holistic vision that gathers both the end-user' side and the energy supply side.
- A conflict between different goals arouse during the planning and implementation process. A target pertained to the high expectations about reaching the "climate goal", which for Denmark is defined by the political will of developing an energy system based on 100% RE by 2050 and it is translated to action at national, regional and local level. Another objective was connected to the need of finding solutions that can lead the process in a cost-effective way. The conflict was critical at least in two phases: during the definition of the budget for the construction of the low-energy buildings in the residential area A, and during the planning of the energy supply system for the residential area C. In the first case, the maximum allowed budget was constrained by the requirements of the social housing in Denmark, whose requirements limit the economical burden for the tenants. The implementation phase was then delayed and the construction started only when it was decided to exceed the maximum budget. In the preliminary plan for the energy supply system for the residential area B, the planners chose a traditional DH network based on a pair of single pipes, directly connected to the main network in Lystrup (T_{supply}= 80°C and T_{return}=40°C). The cost-effectiveness of such network was questioned, so that individual solutions, such as heat pumps were considered as alternative. The final decision was taken when an external R&D project took over the planning responsibility, bringing along also more capital to be invested. The final outcome was successful, since it was demonstrated not only that the low-temperature DH concept is applicable to low-energy buildings, but also that the total long-term economy (30 years) improved in comparison to the original design solutions.
- The recognition of the existence of a market in Denmark in relation to sustainable, energy-efficient and environmental-friendly houses was an additional motivation for starting the project, from the housing association point of view. In fact, the completed dwellings were fully occupied by tenants faster than in other newly established areas, despite the housing sector suffered a crisis in that period.

4. Conclusions

We conclude by summing up the main findings, which will be extensively discussed in the final report of IEA-ECBCS Annex 51. The case study of Samsø demonstrates how a community can base its whole energy system on RE, without extraordinary external subsidies. The process towards such communities benefits from local participation and local ownership. Taking the results from the experience in Samsø and simply transferring it to a national level,

the transition towards a fully RE-based nation would cost about 90 billion EUR, giving savings for 8 billion EUR/year and a pay-back time of about 11 years (considering 2005 figures). Although these data are encouraging, the Danish average energy use per inhabitant is 25% higher than in Samsø, while the potential biomass per inhabitant is one third. Moreover, the potential of wind energy is lower in the rest of the country. Therefore, substantial energy conservation efforts are needed to achieve the goal of 100% share of RE in the country as a whole. Such issue is central in the project in Stenløse Syd, where proactive attempts have been identified and documented to understand legislative and planning means in the process of promoting sustainable low-energy community projects [8]. With regard to energy planning, the "neighborhood approach" is more profitable and can achieve better results than the "local approach", as demonstrated by the project in Lystrup. The best social-economy is obtained only if the energy plan is done for the community as a whole, instead of considering local plans for the single housing units. Moreover, the combination of energy saving policies in the building sector and an energy efficient supply system based on RE, such as a low-temperature DH network, is seen as a promising concept for achieving ambitious climate goals.

References

[1] www.annex51.org (2010).

[2] www.ebst.dk (2010)

[3] PlanEnergy and Samsø Energy Academy, Samsø – a renewable energy island, 10 years of development and evaluation, 2007.

[4] J.P. Nielsen, J. Jantzen, Summary of work 2005-2008, Samso Energy Agency, 2009.

[5] www.energiakademiet.dk (2010).

[6] www.class1.dk (2010).

[7] www.concertoplus.eu (2010).

[8] L. Castellazzi, M. Citterio, and others, National guidelines for residential buildings presented as grid of applicability in participating countries, Concerto Class 1 project, Work Package 4, Deliverable 22, 2009.

[9] www.bf-ringgaarden.dk (2010).

[10] Ledningsdimensionering og konceptuelt layout ("Pipe dimensioning and conceptual design"), COWI A/S, 2009.

Towards optimization of urban planning and architectural parameters for energy use minimization in Mediterranean cities

Neophytou, M.,[1,*], Fokaides, P.[1], Panagiotou, I.[1], Ioannou, I.[1], Petrou, M.[1], Sandberg, M.[2], Wigo, H.[2], Linden, E.[2], Batchvarova, E.[3], Videnov, P.[3], Dimitroff, B.[3], Ivanov, A. [3]

[1] *University of Cyprus, Department of Civil and Environmental Engineering, Cyprus*
[2] *KTH Research School, University of Gävle, Sweden*
[3] *Bulgarian Academy of Science, National Institute of Meteorology and*
** Corresponding author. Tel: +35722 892266, Fax: +35722 892295, E-mail: neophytou@ucy.ac.cy*

Abstract: This paper reports observations and first experimental results from a field measurement campaign at the neighbourhood/urban scale, which was conducted in July 2010 in Nicosia (Cyprus) under the European Research Project TOPEUM funded by ERA-NET (Urban-Net Call). The ultimate goal of this work is to investigate the influence of urban design and architectural parameters in the resulting urban climate and the resulting energy usage. The field measurement campaign was carried out in the capital city of Cyprus, Nicosia, reflecting a typical Mediterranean city both in relation to buildings architecture and fabrics, street geometry and neighbourhood morphology. The field measurements include meteorological measurements as well as on-ground and aerial thermography, covering a range of spatial scales, from local-street canyon to meso-scale. The measurements record the meteorology, the thermal response of the buildings in the field site area and the resulting local microclimate particularly in the street.

Keywords: *Urban Heat Island, Intensive Observation Period, Field Measurements, CFD Modelling, Wind Tunnel Measurements*

1. Introduction

Urbanization has been increasing at an alarming rate: while in the 1800's, only 3% of the world's population lived in urban areas, by the 1950's the urban population increased to 30% and in 2000 it reached 47%. With this ever increasing growth, numerous issues have been raised, such as air quality issues, sustainable use of energy, maintenance of waste materials and socio-economic status of urban inhabitants [1]. All these issues depend on the sustainable urban planning, the type of materials used in buildings [2] as well as the organisation of economical and social life. The complexity of the task to aim at ideal sustainable city goes through accounting for contradictory effects by any kind of measures. Therefore, basic and applied research is needed in order to investigate the city as human-made environment. The task is to achieve sustainability in the use of energy, food, waste, air and water quality. Recent studies on the influence of climate change on Northern–European cities suggest that within 50 years they may experience a climate close to that of South-European cities today. This has enormous resource implications when the design and layout of the urban fabric and the individual buildings are not well suited to mitigate extreme conditions [3,4] There is therefore a strong need for strategic designs to be developed which would mitigate such environmental changes. For example, whilst the general cause of overheating of cities is known, it is not well understood how much influence different urbanization characteristics and building materials have on the intensity of the city overheating [5,6].

In this study the energy exchange processes between buildings and air in a typical South-European city as well as the ventilation properties in relation to urban-planning and architectural parameters, for the purpose of energy use minimisation are examined. The complexity of this problem requires complementary methods to be employed. In a boundary layer wind tunnel the basic flow under neutral conditions of different generic city configurations will be studied. The wind tunnel data will serve also as calibration data for

CFD simulations which will in turn be utilised to evaluate heating effects and material properties. The computational fluid modelling will predict the effect of city layout and building materials on temperatures. Based on predicted temperatures the energy use for air conditioning will then be assessed. Heat absorption phenomena occurring at building surfaces have a major impact on the urban climate: field measurements of surfaces heat flux and material thermal properties will be carried out for urban sites in Cyprus. For these reasons an intensive observation period of 1 month was carried out in which a series of measurements were taken both for the air, solar radiation and humidity as well as the building surfaces.

2. Methodology

2.1. Multidisciplinary approach

The methodology for the implementation of this study consists of the following steps:

1.Selection of the site under investigation: The identification of the site to be investigated was performed under prescribed criteria based on the building materials, the geometry and the location of the buildings.

2.The field measurements involved meteorological measurements at three different scales (from meso-scale to micro-scale), while the thermal response of buildings was simultaneously recorded through thermography (both aerial and on-ground) as well as in-situ measurements of temperature and moisture. In this paper the results from this field measurement campaign are presented, the analysis and interpretation, as well as results from supporting studies in the wind tunnel and computational simulations to assist in the understanding and derivation of guidelines for "climatically-informed" urban design.

3.Laboratory experiments: The selected city blocks will be scaled down and applied in a wind tunnel, where ventilation and heat efficiency effects will be investigated. The determination of the velocity field will be achieved by employing Laser Doppler Anemometry (LDA) and Particle Image Velocimetry (PIV).

4.CFD modelling will contribute to the study, by examining the air flow as well as the thermal performance of building materials taking into account the structure of the modelled urban areas. It will raise the opportunity to understand the contribution of heat conduction and heat radiation in the generation of thermal discomfort in urban canyons for the case of Cyprus.

2.2. Site Selection

In terms of the site selection, the parameters of building height, building density and paved and unpaved area coverage were examined. This analysis provided fundamental data for all the subsequent tasks and actions. The objective was to create a complete database of the investigated area in order to assess the status of urban environment in Cyprus. Hence, major groups of building blocks (approximately 350 building blocks) were analyzed and scaled down for the applied channel, in order to support the parameterization studies for the investigated scenarios. Within this task, the geometries under investigation were also be modelled for the purposes of the CFD study. The building energy behaviour and performance are heavily influenced by the density of the building space that is why the facades chosen have different SVF. For example facades that are placed in front of an open parking area ($H/W<1$) can be compared with some others that are placed in a canyon. Some other important factors were the orientation of the chosen facades and the properties of the surrounding surfaces in the same canyon.

Among the investigated neighbourhoods, the old city centre of Nicosia appeared as being the most representative for the Mediterranean-like architecture, therefore it was decided that the

field campaign should be carried out in this area (see Fig. 1). The old town centre, which is the historical centre of the city, is delimited by Venetian type walls. It is generally characterized by narrow canyons with Mediterranean-style planning but also includes some buildings of contemporary architecture and also some large squares. From the West to East, four major sub-neighbourhoods (SN) could be identified according to homogeneity and packing building density SN1 to SN4. SN1 includes some larger open spaces/parking lots so that it has an overall lower packing density and it is less homogeneous. SN2 is homogeneous over relatively large distances in neighbourhoods units. SN3 has some broader avenues and squares so that it has a lower packing density. SN4 has a very large packing density being also relatively uniform.

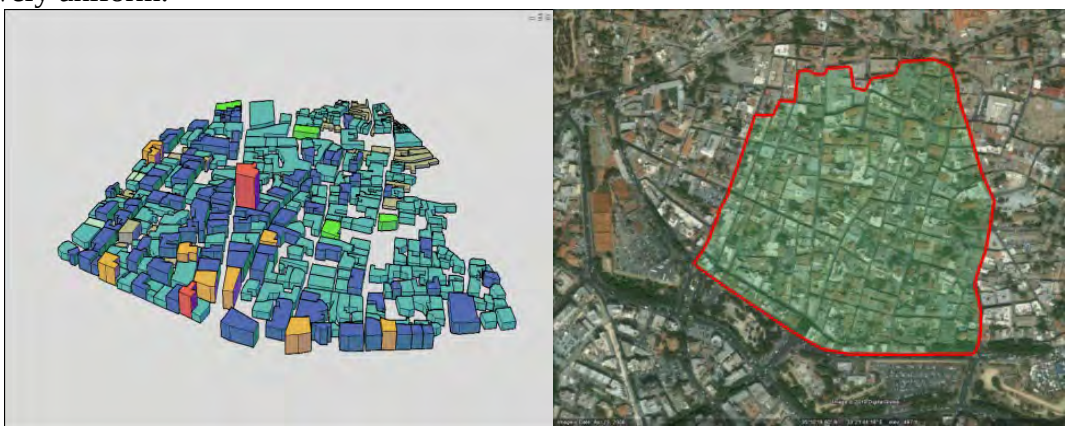

Fig.1. Investigated Site

2.3. Intensive observation period

During the intensive observation period, measurements in neighbourhood, micro- and meso-, scale were performed. Regarding the meso-scale, an upper air sounding system was employed. The sounding system provided the profile of the air pressure, temperature and humidity as well as of the wind speed and direction from ground level up to 2 km altitude. Sets of the measured data were sent down to a receiving station (ground station) as the radiosonde was carried aloft by a balloon. The characteristics of the micro-scale were determined by means of aerial thermography and a weather station consisting of a hypersonic anemometer and instrumentation for temperature and humidity measurements. InfraRed thermal and visual images were captured via a high-resolution (640x480) FLIR P640 IR-camera from a helicopter at approximately 500 m above the ground. The aerial thermography measurements were performed along a flight path of a total length of 7 (km) traversing from the eastern rural area, over the urban area of the town centre and up to the western rural area. The measurement schedule was based on the time lag of the building materials with respect to the sunrise calendar of the location and the solar exposure of the materials. For the meteorological data, stations with temperature and humidity sensors were installed close to the sonic anemometers. Surface temperature and moisture measurements, as well as measurements of the ambient temperature, humidity and wind speed and direction were performed. Surface temperatures were determined by means of building IR thermography, as well as with the use of thermocouples and a FLUKE 62 Mini IR thermometer with an accuracy of +/- 0.1 °C. For the measurement of the buildings moisture an EXTECH moisture meter (model MO250) with an accuracy of +/-0.1% was employed. IR thermal images of surface temperature were captured with a FLIR T335 camera at specific locations within the city. The thermal images of the building façades were acquired over the space of an hour, every two hours during the time period from 10th to 12th of July 2010 at 3 different locations. At each location, 4 thermocouples were used (one at ground level and 3 at heights of 40, 120 and 200cm from ground respectively).

3. Results

3.1. Meso-scale measurements

In Fig.2a, the measurement of the temperature in the meso-scale above the city centre is provided. According to these results, the surface is very hot and therefore super adiabatic gradient is observed in the first 300m above ground. This is, in fact, the surface layer in terms of temperature. Above 300m, and up to 2000m a well-mixed (convective) layer is formed. In order to clarify the observed temperatures, the schematics of the boundary layer over an urban area is also provided (Fig.2b). The upper zone represents the urban internal boundary layers where advection processes are important. The regime below shows the inertial layers that are in equilibrium with the underlying surface and where Monin-Obukhov scaling applies. The lower region is the roughness layer that is highly inhomogeneous both in its vertical and horizontal structure. Finally the region between the inertial layer and the roughness layer represents adjustment between neighbourhoods with large accelerations and shear in the flow near the top of the canopy [7]. The same clear top of the convective boundary layer was also observed also in the relative humidity profiles and thus the entrainment zone was very shallow. The air mass above the convective layer was dryer and the wind direction was found to change substantially.

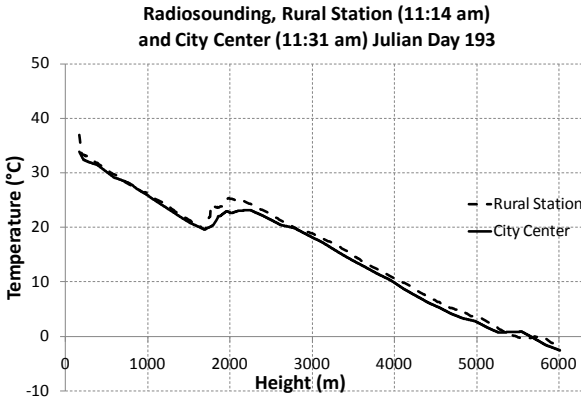

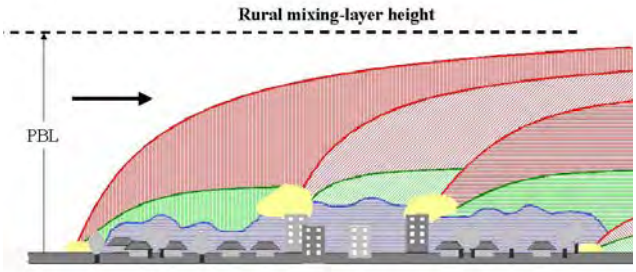

Fig.2a. Radio-sounding temperature measurement above city centre
Fig.2b. Boundary layer over an urban area

3.2. Micro-scale measurements

In Fig.3 the ultrasonic anemometer measurements of the wind speed and direction, over the intensive observation period at Ledras Street on the rooftop level are provided. The analysis of the sonic data shows clear difference in the regime of wind during the day and the night. The sonic on the roof shows weak easterly wind every night (24 – 6) and much stronger westerly wind during the day (9-18). Therefore, two different regimes can be simulated, easterly wind of 2 m/s and westerly of 5 m/s. The transition periods are rather short around 9 in the morning and 21 in the evening. From the time series of wind direction we can note that during the intensive observation period (Julian Day 190-193) the flow is slightly disturbed, and is predominantly easterly, also during the day. The friction velocity measured by the sonic at the roof is much higher than the value ($u^*=0.08u$) suggested by similarity theory. The mean value for the 2 weeks of measurements is $u^*=0.14u$. This is a value typical for urban areas. The wind direction within the street canyon is strongly modified by the buildings, but the two regimes (day and night) are distinguished as well. The wind speed is between 0.5 and 7 m/s.

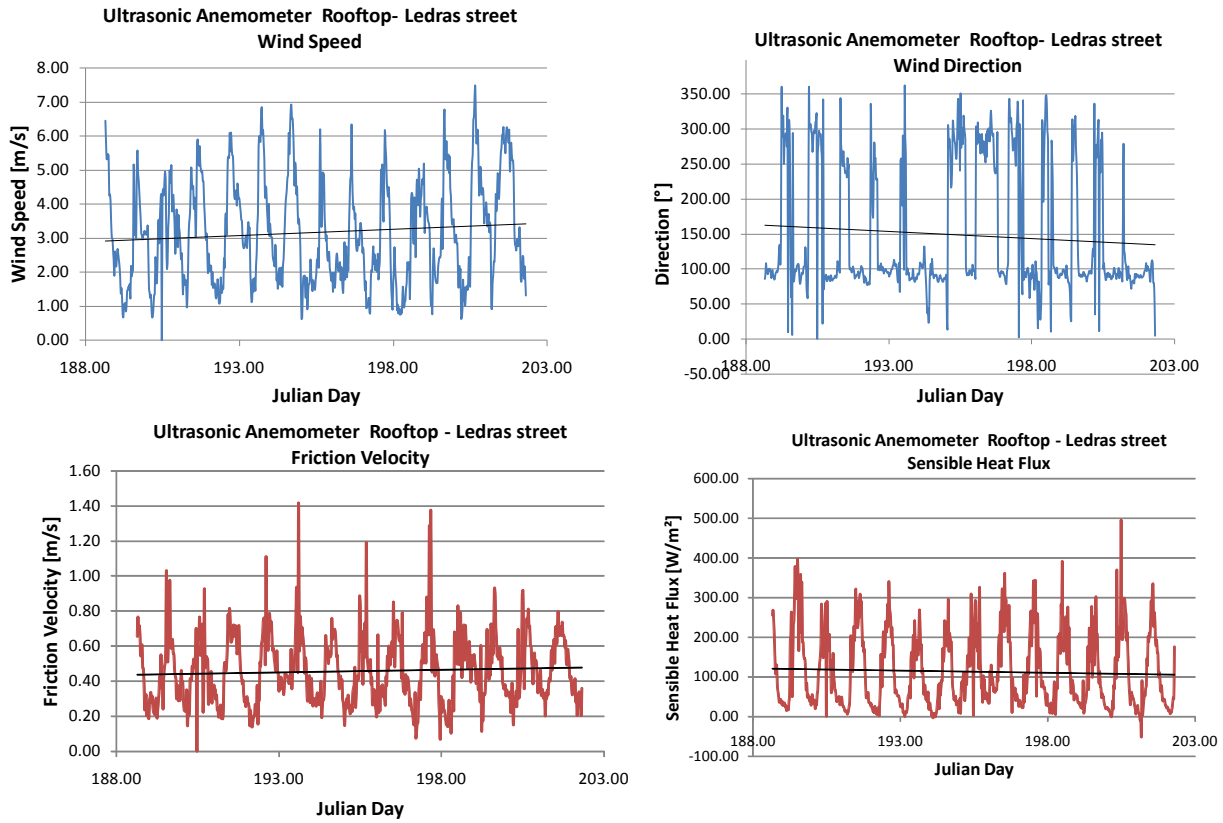

Fig.3. Ultrasonic Anemometer Measurements, Ledras Street, Rooftop Level

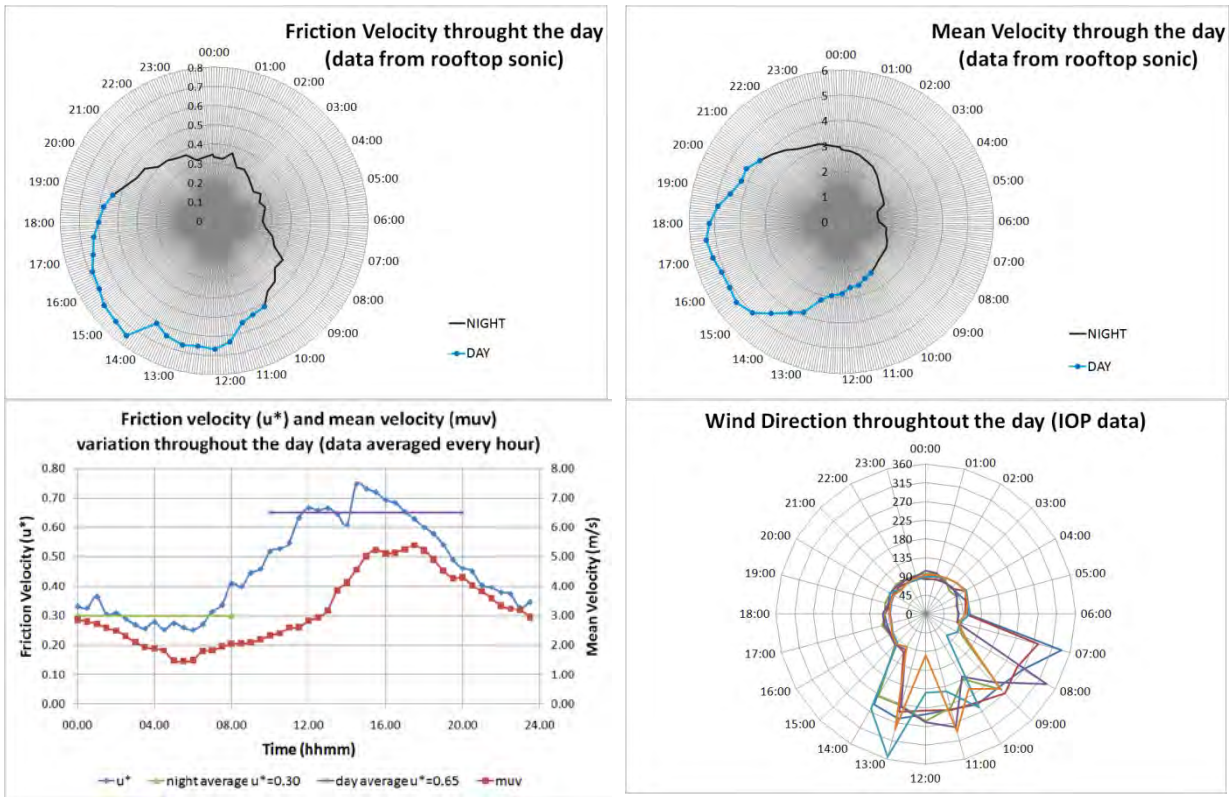

Fig.3. Ultrasonic Anemometer Measurements, Ledras Street, Rooftop Level

Aerial Thermography was also performed in order to determine the intensity of the heat radiation emmited by the built environment in the investigated field. For this purpose, a statistical analysis of the temperature intensity was performed by means of the SPSS software. The temperature distribution was compared for several city environment providing some useful conclusions regarding the importance of thermal radiation resulting from the applied building materials.

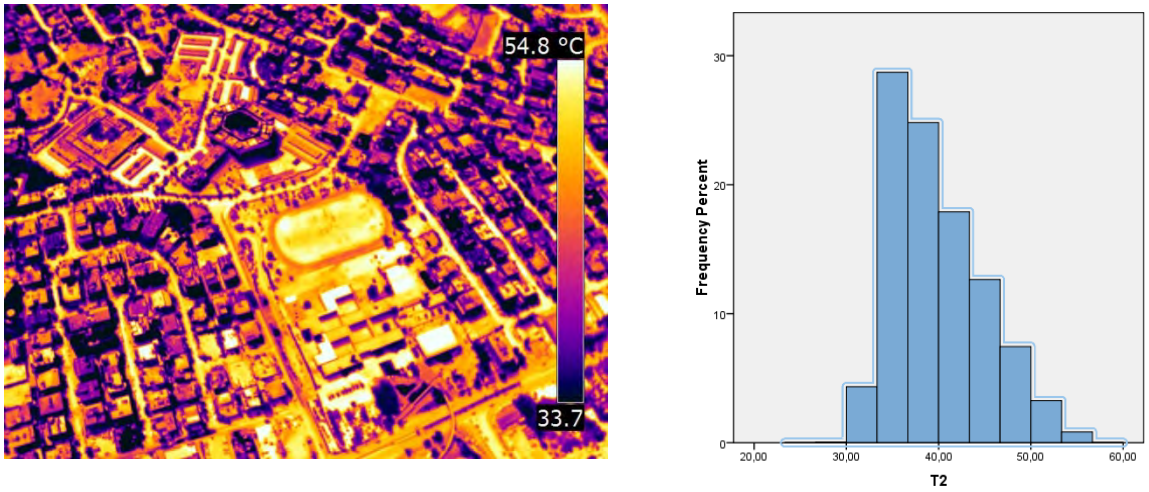

Fig.4. Aerial thermography and statistical analysis of temperature distribution

3.3. Neighbourhood scale

The Urban Heat Island Intensity (UHII) was also identified by means of data comparison from the weather station in the investigated site and from a rural weather station 5km outsite the city. According to these measurement UHII was found equal to 4 °C, especially during the midday (see Fig. 5).

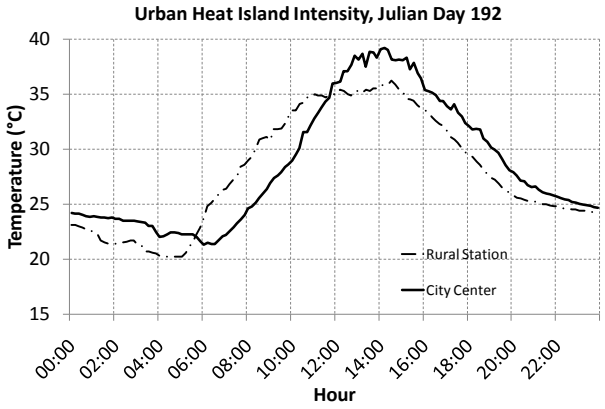

Fig.5. Urban Heat Island Intensity.

The impact of the building materials on the intensity of the urban heat island intensity was approached by means of measurements of surface temperature of building materials at the field site. Fig.6 and 7 presents the temperature profile during the IOP. In the first case the ambient temperature was measured at the rooftop of the building, whereas in the latter case it was measured next to the building element, and was, as expected affected by the environment radiation. The measurement in Fig.6 was performed on a wall constructed with forced cement, and the measurement in Fig.7 on a stone wall. The thermal emissivity of both materials is

almost equal (around 0.85), whereas in the latter case, the heat capacity of stone wall is increased, compared to the heat capacity of forced cement. Therefore, although the temperature peaks were observed more or less to be equal, the duration of the peaks was greater in the case of stone wall. Another important outcome of this measurement was that the contribution of thermal radiation as well as of the anthropogenic emissions in the street canyons led to an important temperature increase, which was observed throughout the day.

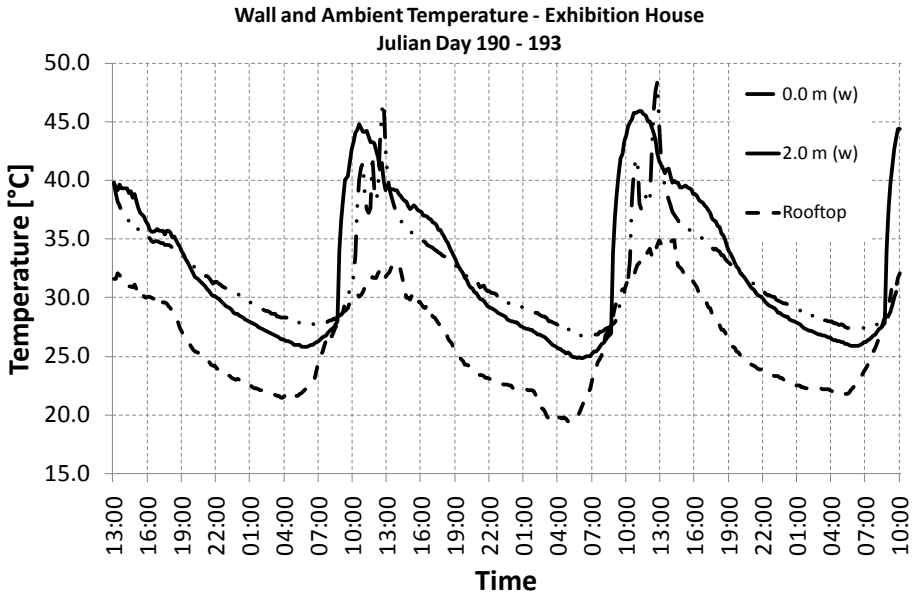

Fig.6. Wall temperature Measurement

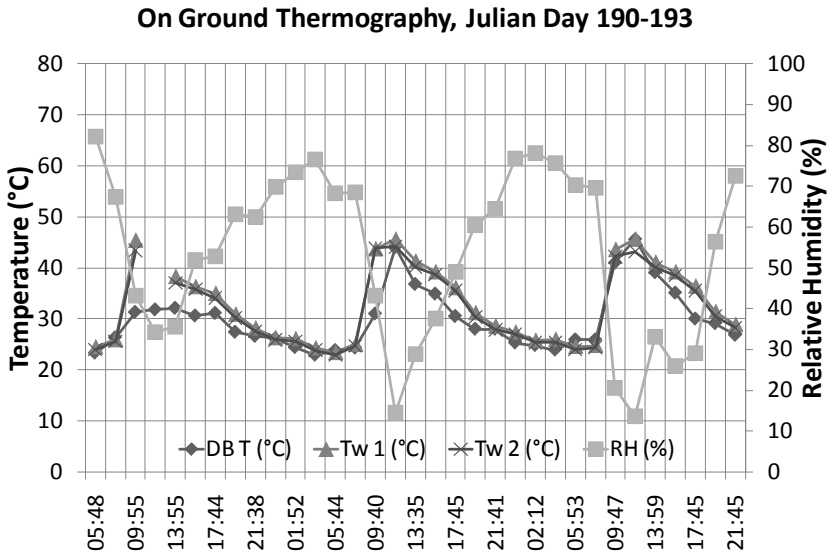

Fig.7. Wall temperature Measurement – on ground Thermography

4. Conclusions and future work

A series of simultaneous measurements of urban meteorology and the associated thermal response of buildings has been conducted in Nicosia, reflecting a typical Mediterranean setting for climate and urban architecture. Some preliminary observations show a consistent temperature difference in the ambient air between the urban and rural areas of about 2K with

an approximate temperature difference for the thermal response of the buildings in their corresponding peaks and lows of 5 to 8 K (wall surface temperature). Simultaneous diurnal measurements of the moisture of the buildings show also a direct correlation with the corresponding wall surface temperatures. Further post-processing and analysis are in progress and in addition complementary methods will be employed; therefore, the field measurement campaign will be followed by detailed experimental and numerical studies. The investigated city blocks will be scaled down and applied in a wind tunnel, where ventilation and heat efficiency effects will be investigated using Laser Doppler Anemometry (LDA) and Particle Image Velocimetry (PIV). In order to calibrate the CFD modelling the pressure on the ground around the buildings will be measured in 400 points. Thus, the experimental results, as well as the results of the field measurement will be used in order to optimize the adopted models used to performed numerical simulations by means of Reynolds-Average Navier-Stokes (RANS) modelling. The experimental feedback will enable also the performance of further investigations concerning radiation effects from building surfaces assuming unsteady state conditions.

Acknowledgements
The authors wish to acknowledge a number of organisations and persons for their contribution and assistance during the field measurement campaign, without which this work would not have been possible: Cyprus Police for providing the helicopter for 4 flights and assistance during the flights, Nicosia District Mayor, Cyprus Meteorological Service, United Nations, Prof. Joe Fernando (from Notre-Dame University, USA) for sharing experience and advice in Urban Heat Island Experiments, as well as a large number of volunteers who helped at various stages in various ways for this work to be realised. The project is funded through ERA-NET (Urban-Net Call) and the Cyprus Research Promotion Foundation under the contract ΔΙΕΘΝΗ/URBAN-NET/0308/02.

References
[1] Akbari, et al. (1996): Policies to reduce heat island: magnitudes of benefits and incentives to achieve them, in proceedings ACEEE Summer Study on Energy Efficiency in Buildings, vol. 9,. Pp. 177.

[2] Santamouris (2001): „Energy and Climate in the Urban Building Environment. James and James Science Publishers, London".

[3] Jian Hang et al.: Studies of wind environment in simple compact square, round or long cities by CFD simulation and wind tunnel measurements, Project No. HKU 7145 /07E

[4] De Ridder Koen, et al., 2006: The impact of urban sprawl on air quality and population exposure: a case study in the German Ruhr area; EURASAP Newsletter 60, April 2006, ISSN-1026-2172, 13-29.

[5] T.R. Oke et al. (1991): „Simulation of surface urban heat islands under ‚ideal' conditions at night. – Part 2: Diagnosis and causation, Boundary Layer Meteorology, Vol. 56. pp.339-358

[6] Synnefa et al. (2005): A study of the thermal performance of reflective coatings for the urban environment, Solar Energy, Vol. 80, pp. 968-981.

[7] Batchvarova and Gryning (2006). Progress in Urban Dispersion Studies. Journal of Theoretical and Applied Climatology, Vol. 84, Nos. 1-3, pp 57-67.

[8] Kakoniti, A.: „The effect of radiation heat transfer in the urban heat island phenomenon using computational fluid dynamics simulation", Master Thesis, University of Cyprus, Deparrment of Civil and Environmental Engineering

Case study on the effects of smart energy community construction at Kanazawa seaside district in Yokohama

Satoshi Yoshida[1,*], Satoru Sadohara[1], Yuichi Ikuta[2], Ryota Kuzuki[3], Toru Ichikawa[3]

[1] *Yokohama National University, Yokohama, Japan*
[2] *Japan Environment Systems, Tokyo, Japan*
[3] *Tokyo Gas Corporations, Tokyo, Japan*
** Corresponding author. Tel: +81 453394247, Fax: +81 453381016, E-mail: syoshida@ynu.ac.jp*

Abstract: This research worked on the measure against CO_2 reduction according to the characteristics of the area for the Kanazawa seaside area in Yokohama city. This area consists of a collective housing complexes and a minor scale industrial complex, and also locates a waste incineration plant, a wastewater treatment plant, and a sludge treatment facility. Having been chosen as a measure with the large amount of CO_2 discharge reduction, it is the system which feeds into an incinerator the methane gas by carrying out mixed digestion of the kitchen garbage together with sewer sludge, and supply heat from a waste incineration factory through the transmission line. However, since this system has large initial cost for construction of transmission line, marginal abatement cost (MAC) for CO_2 emission reduction is very as large as 166.16 [USD/CO_2]. Then, when the pay-back year of the transmission line was changed from 20 years to 31.5 years which is equivalent to 70% of legal durable years, MAC was reduced to 104.40 [USD/CO_2]. Moreover, when Non Energy Benefit (NEB) by system introduction, such as job creation and an environmental improvement of the area, was taken into consideration, MAC was greatly reduced to -124.22 [USD/CO_2].

Keywords: *Exhaust heat from waste incineration plant, Solar energy, Digestion of sewage sludge mixed with kitchen garbage, CO_2 reduction cost*

1. Introduction

1.1. Background and objectives of research

As the countermeasures against the issues of global climate change, it is essential to reduce CO_2 emissions from building sectors. To promote the reduction of CO_2 emissions from building sectors, various countermeasures should be executed, not only for building sectors but also for the community. The Kyoto Protocol Target Achievement Plan was materialized in Japan in April, 2005 [1]. Until then, main measures for the energy conservation such as heat-insulation and introduction of efficient equipments were implemented on individual buildings only. In this plan, measures for advance energy saving and low carbonation in the community were also specified in addition to the measures for individual buildings. For advance energy saving and low carbonation in the community, the mutual cooperation of various stakeholders of the community is indispensable. It is important to make the process which shares the target of energy saving and low carbonation, distributes profits impartially, and shares a risk equally within the community. Therefore, the objective of this study is to propose the measures for energy saving and low carbonation and examine the technique of presenting the effects (benefits) and risk (cost) clearly for Kanazawa seaside district in Yokohama city.

In this study, the countermeasures for the CO_2 emission reduction in the community are focused. There are lots of options for the reduction of CO_2 emissions at the community scale, such as PV's, solar thermal use, biomass, exhaust heat from waste incineration plant, and so on. But these options may not be suitably introduced anywhere. Thus, it is very important to recognize characteristics of the community to introduce the suitable countermeasure options. The case study area is Kanazawa seaside district in Yokohama City, Japan.

The main purpose of this research is to determine the countermeasures for CO_2 emission reduction which is appropriate for this community, and to analyze the cost effectiveness of these countermeasures.

1.2. Study area

The case study area is Kanazawa seaside district in Yokohama city. This district is reclaimed land with an area of 121.9ha [2] where collective housings were sold in lots from around 1970. A railway runs through the center of this district to the south north. Residential area is located at the west side of the railway. At present, 7,500 households with the population of about 20,000 persons are living in this district [2]. It had been about 30 years after a sale in lots and now many housing complexes are aged and expected to be reconstructed and repaired. On the other hand, the east side of the railway is industrial complex area for middle to minor scale factories. There are some urban facilities in this area, such as a waste incineration plant, a sewage treatment plant, and a sludge treatment plant.

Kanazawa waste incineration plant incinerates about 300,000[t/year], and generates 130 [GWh/year] electric power by using exhaust heat of waste incineration [3]. Kanazawa wastewater treatment plant has treatment capacity of 265,900 [m^3/day] [4] , and generates treated water (recycled waste water). Nanbu sludge treatment plant has treatment capacity of 14,700 [m^3/day], and generates methane gas through digestion tank [5]. In addition, there are some office building, hotels, and the campus with the hospital of Yokohama City University.

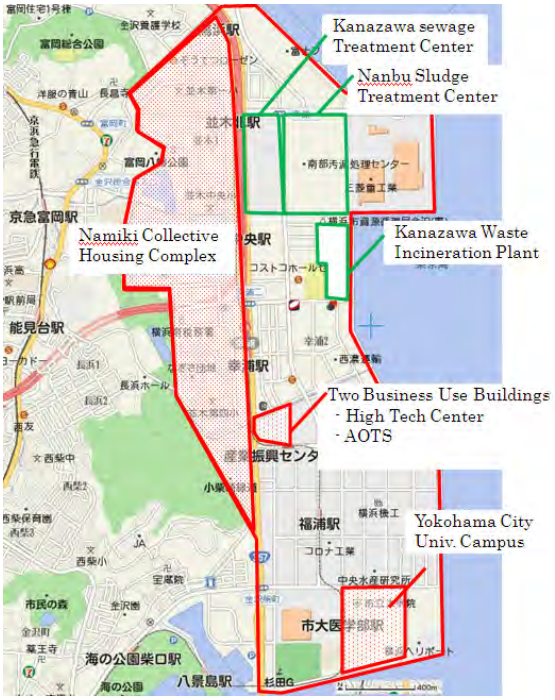

Figure 1 Kanazawa Seaside Area

In the road map for environment model city realization, Yokohama city government regards this area as an important area, and the Yokohama Green Valley project is in operation. The amount of CO_2 emission from energy consumption in this area is assumed about 72,000 [t-CO_2/year]. About 60% of this emission is due to energy use in residential and business sectors.

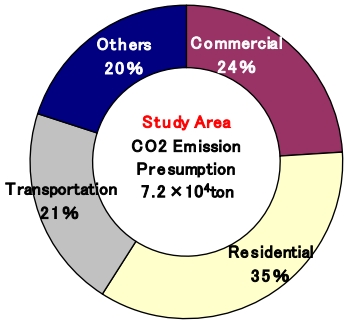

Figure 2 Estimated CO_2 emission of Kanazawa seaside area

2. Countermeasures for smart energy community

2.1. Outline

Figure 3 shows the smart energy network in the proposed area. Four stages were assumed as present condition (2010), the first stage (2015), the second stage (2020), and final stage (2025). Various countermeasures for each building promoted by Japanese government were executed, and also the other measures for community scale were tried to be executed. While planning the smart energy network in this area as a whole, the effective use of urban facilities such as sewage treatment plant, waste incineration plant etc. were considered to have significant role.

Table1 Present energy demand of subject buildings in this area

		Total Floor Area ㎡	Demand (Present)			
			Electricity GWh/year	Heating TJ/Year	Cooling TJ/Year	Hot Water TJ/Year
Namiki Collective Housing Complex	House	721,400	32.75	51.26	54.28	144.74
High-Tech Center	Office&Hotel	50,000	8.06	13.29	14.59	16.40
AOTS	Office&Hotel	12,000	1.73	4.78	3.36	10.78
Yokohama City University	Hospital&University	107,000	10.48	40.79	20.62	78.37

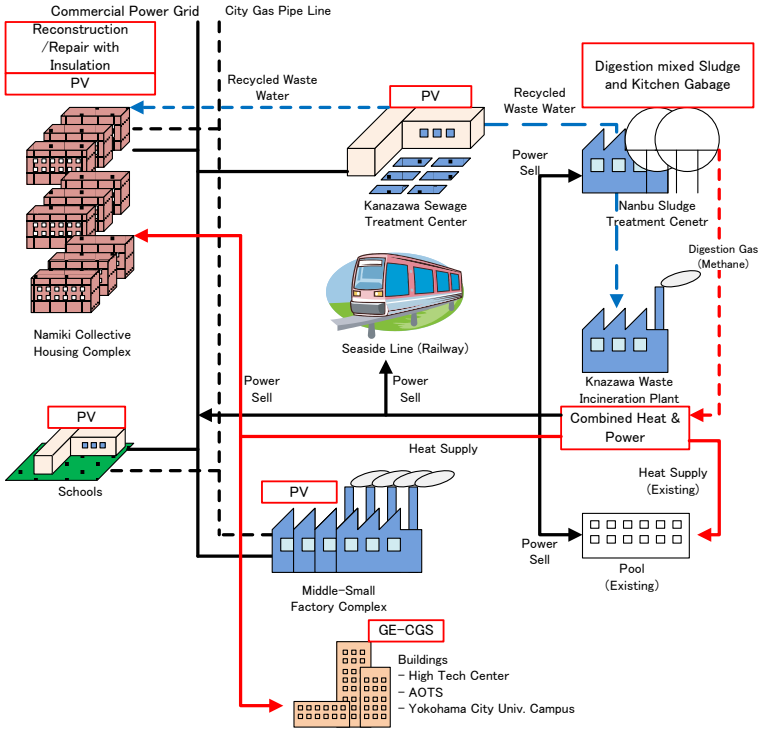

Figure3 Proposed smart energy network at Kanazawa seaside area

2.2. Remote ownership of Photo Voltaic Panel

In the Electricity Enterprises Law of Japan, the photovoltaic generation panels set up in places other than home are not permitted to be owned [6]. Therefore, families living in high-rise housing complexes don't have their own roof and so cannot own the PV panels.

However, the development of smart meter and smart grid technology may solve this problem in near future. In this case study, the remote ownership of PV panels is proposed. People living in high-rise housing complexes can set up PV panels on the roof of factories, sewage treatment plant, and schools.

2.3. Exhaust heat from waste incineration plant

Today, exhaust heat from waste incineration is used for power generation. As incinerated waste includes wet kitchen garbage, the energy loss for the latent heat is caused. It was proposed that wet kitchen garbage to be collected separately and sent to sludge treatment plant for the methane generation by mixed digestion with sewage sludge. Generated methane is supplied to waste incineration plant as input to the boiler. Although the waste incineration plant supplies only electricity in the present condition, it was considered to supply heat also in this case study. If wet kitchen garbage is not incinerated, by rough estimation, calorific value of wet kitchen garbage and the energy loss for the latent heat decrease. When the kitchen garbage is not incinerated with other garbage, the quantity of heat generated by the

incineration will decrease by a calorie of kitchen garbage. When the kitchen garbage is also included, an additional quantity of heat is required to evaporate its moisture content. Hence, if the additional quantity of heat is avoided then there will be no change of heat in total. Ministry of Land, Infrastructure, and Transportation in Japan had examined to increase the speed and the quantity of methane generation by digestion of sewage sludge mixed with slurry of kitchen garbage. This project was named LOTUS project [7]. Result of this LOTUS project was that it was possible to digest the kitchen garbage slurry which was equivalent to 13% of the sewage sludge, in addition two times of methane was generated compared to the case without the kitchen garbage slurry. Methane gas generation potential was calculated in the condition that the amount of mixed digested kitchen garbage was set half of the amount of kitchen garbage incinerated in the current condition because the cost for collecting the kitchen garbage separately was very large. Cost for the collection of kitchen garbage separately, removal of impurities contained in the garbage, and making of the garbage slurry were calculated.

2.4. Cogeneration installation for business use

Three large business use buildings were installed with GE-CGS in this study. Those buildings were hotels, offices, and university campus. Campus of Yokohama City University has also hospital building, and 700kW of GE-CGS was installed as part of ESCO project in 2009. High-Tech Center has hotel, office, and research laboratory, and 360kWof GE-CGS was installed in this study. AOTS is training facility with lodging for foreigners, and 90kW GE-CGS was installed in this study. This GE-CGS's were operated from 8:00am to 9:00pm.
The initial cost of CGS was considered as 2,000 USD per kW, and the annual maintenance cost as 2.0 USD per 100 kWh.

2.5. Thermal transmission network

Heat supply transmission line was newly constructed in this district that connected sludge treatment plant, waste incineration plant, Namiki-collective housing complex area, and three larger business use buildings. Construction cost of the transmission line was considered, but the distribution pipes from the transmission line were not considered in the cost calculation.
This transmission line supply steam from waste incineration plant and sludge treatment plant as a heat load for Namiki- collective housing complex area, and three larger business use buildings. The quantity of heat that can be supplied from a garbage incineration plant and the amount of methane generated increased after the mixed digestion of sewage sludge and kitchen garbage were large enough. Therefore, it could provide all of the hot-water demand of the collective housing complexes, and the required heat demand of three business-use buildings.

3. The result of CO_2 Reduction effect

Table 2 shows calculated reduction potential of CO_2 emission by each countermeasure that had been considered in this case study. The amount of CO_2 emission reduction by implementation of the countermeasures in each building was divided proportionally from statistical approach, such as population of the region, based on "Local government environmental report 2007 [8]". CO_2 reduction potential through steam supply by transmission line was the largest of all measures. Of course, increment in the methane generation by the digestion of the mixture of raw sludge and kitchen garbage was also included in this measure.

Table2 CO_2 emission reduction potential

		Measures	CO_2 Emission Reduction Potential [t-CO2/year]
①	[Residential]	Changes in Lifestyle	454
②	[Commercial]	Changes in Workstyle	131
③	[Residential]	Lighting Efficiency Improvements, etc	565
④	[Residential]	Heating and Cooling Efficiency Improvements	753
⑤	[Commercial]	Lighting Efficiency Improvements, etc	311
⑥	[Commercial]	Air Conditioning Equipment Efficiency Improvement	233
⑦	[Residential]	Introduce of HEMS	444
⑧	[Commercial]	Power and Other Efficiency Improvements	109
⑨	[Commercial]	Use of Solar Thermal Energy	870
⑩	[Commercial]	Commercial Cogeneration	848
⑪	[Commercial]	Introduce of BEMS	19,344
⑫	[Joint Commercial and Residential]	Incineration Plant Waste Heat and Sludge Treatment Plant Digestion Gas	1,010
⑬	[Residential]	Household appliances efficiency improvements	2,447
⑭	[Commercial]	Photovoltaic power generation	105
⑮	[Residential]	Photovoltaic power generation	1,815
⑯	[Residential]	Higher insulation in newly constructed housing	412
⑰	[Residential]	Improved existing insulation	108
Total			**29,959**

4. Cost-benefit Analysis

4.1. Additional cost curve for reduction of CO_2 emission

Based on the method of the marginal abatement cost (MAC) curve advocated by McKinsey [9], the amount of CO_2 discharge reduction in this area and the relation of that measure cost are analyzed. Subsequent analysis has adopted the analytical idea of MAC and the method in consideration of NEB which Kuzuki and others proposed [10].

4.1.1. Case of short pay-back time

Figure4 shows the case which calculated MAC based on short pay back year.
This short pay-back year refers to the value used by the Central Environment Council [11], the Ministry of Environment, in order to calculate the MAC of CO_2 emission reduction. It was about 3 to 5 years. In this case, as the initial cost including the MAC of photovoltaic, heat insulation repair of building and thermal transmission line was large enough; the MAC will also be higher. The average MAC of all measures was 237.11 [USD/t-CO_2] for a year, and installation is difficult as long as there is no financial support of the subsidy etc.

4.1.2. Case of long pay-back time

On the other hand, since a building and a thermal transmission line were used over a long period of time, it could be thought that 3-5 years of the pay-back year was too short.
Then, 70% of legal durable years were re-set as the pay back years of each measure. Pay back years become longer and were from 20 years to maximum of 31.5 years.

Figure5 shows the calculated MAC based on these long pay back years. In the case of these long pay back years, the MAC per year decreased sharply, and the average MAC of all measures was 124.57 [USD/t-CO_2] per year. Especially MAC of thermal transmission line reduced greatly to 104.40 [USD/t-CO_2] from 166.16 [USD/t-CO_2], because pay back years changed from 20 years to 31.5 years.

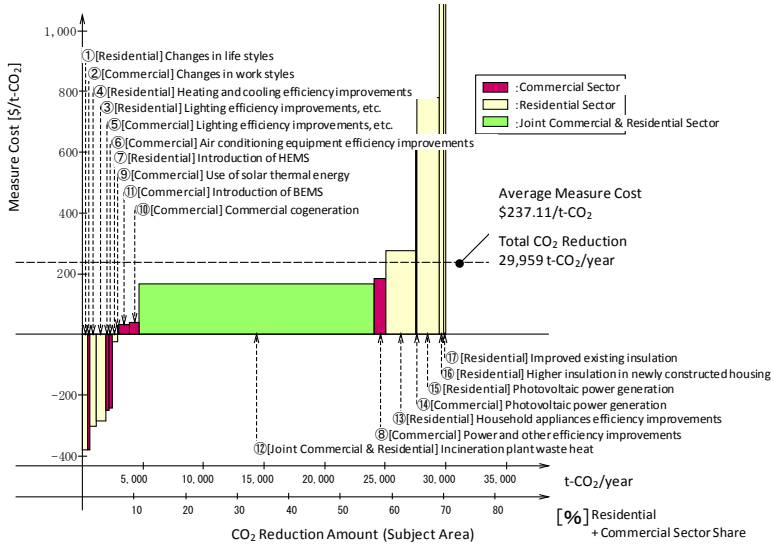

Figure4 Calculated MAC based on short disinvestment years

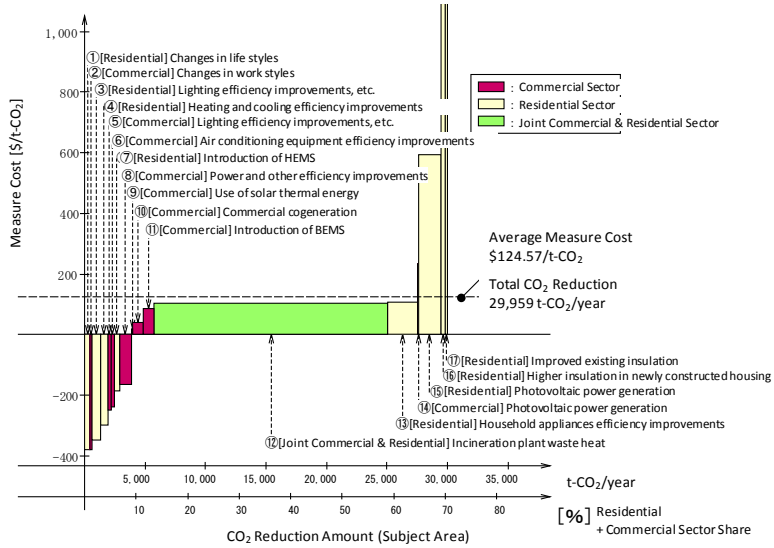

Figure5 Calculated MAC based on long disinvestment years

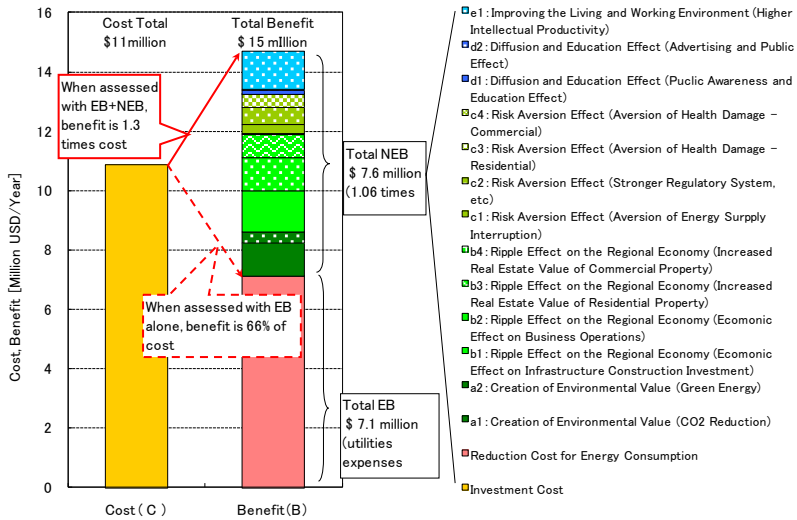

Figure6 B/C including NEB

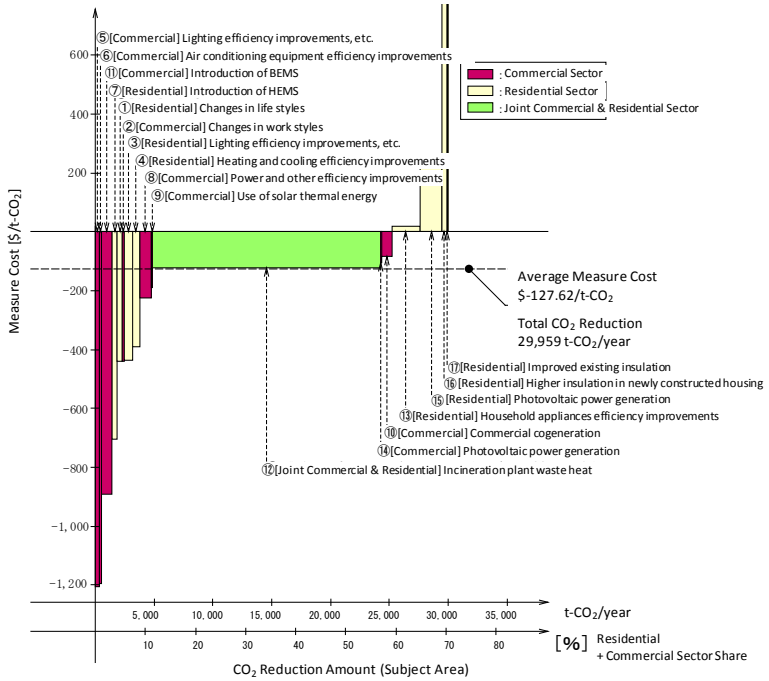

Figure7 Calculated MAC based on long disinvestment years in consideration of NEB

4.2. Non-Energy Benefits

These measures against CO_2 emission reduction resulted the benefits of not only the decrement in energy cost but also the job creation, the environmental improvement of this area, etc. Then, NEB (Non-Energy Benefit) by the implementation of CO_2 emission reduction measures in this area was computed based on the calculation method of the NEB which R. Kuzuki and others has advocated [4].

Figure6 shows the relation between annual cost and NEB. The B/C including only direct benefits such as cut in fuel, lighting, and water cost by a measure was 0.66. Then the B/C including indirect benefits such as for example job creation etc., increased to 1.35.
Moreover, the calculation result was divided proportionally for each measure, and the MAC curve was created.

Figure7 shows the MAC curve in consideration of NEB. As a result of dividing indirect benefits proportionally for each measure against low carbon and re-creating a marginal abatement cost curve, CO_2 reduction cost of each measure decreased greatly, and average measure cost reduced to -127.62 [USD/t-CO_2].

5. Conclusions

From the results of this case study it became clear that the measures against low carbon of the community according to the characteristic of areas raised CO_2 emission reduction potential. The effective countermeasures were thermal transmission line using methane gas produced by the digestion of mixture of sewer sludge and kitchen garbage sludge, and use surplus steam from waste incineration plant. It was also found that taking NEB into consideration improved B/C greatly and increased feasibility.

References

[1] Cabinet Secretariat Japan, Global Warming Prevention Headquarters, "Kyoto Protocol Target Achievement Plan," April 2005

[2] Statistic Division of Ministry of Internal Affairs and Communications, National Census of Japan, 2005

[3] Waste and Recycle Division of Yokohama City, The amount of garbage incineration and power production according to incineration factory, 2008 http://www.city.yokohama.jp/me/pcpb/data/dat30.html#syoukyakuryo(In Japanese)

[4] Yokohama City, Kanazawa Wastewater Treatment Plant (Pamphlet) http://www.city.yokohama.lg.jp/kankyo/gesui/centerinfo/06wtc/shiryo/pamphlet.pdf(In Japanese)

[5] Yokohama City, Nanbu Sludge Treatment Center (Bio-Land Kanazawa) http://www.city.yokohama.lg.jp/kankyo/gesui/centerinfo/13src/ (In Japanese)

[6] Ministry of economy, trade and industry of Japan, Electricity Business Act, the last revision 2006 http://law.e-gov.go.jp/htmldata/S39/S39HO170.html(In Japanese)

[7] Ministry of Land, Infrastructure, and Transportation, "Lotus Project", http://www.mlit.go.jp/kisha/kisha04/04/040917_.html(In Japanese)

[8] Coalition of Japanese Local Governments for Environment Initiative and the Institute for Environmental Planning Inc., "2008 Local Government White Paper on the Environment," Coalition of Local Governments for Environment Initiative Secretariat, May 2008

[9] McKinsey & Company: "Pathways to a Low-Carbon Economy: Version 2 of the Global Greenhouse Gas Abatement Cost Curve," January 2009

[10] R. Kuzuki, et al, Study on the Non-Energy Benefit (NEB) of Area-Wide Energy Utilization and Evaluation of the Marginal Abatement Cost , World Renewable Energy Congress 2011 – Sweden, Urban Energy (UE), 8-11 May 2011, Linköping, Sweden

[11] Central Environment Council, Global Environment Committee, Targets Reduction Scenario Subcommittee, Mid-term Report, June 2001

Study on Low Carbon Energy Supply to the District Heating & Cooling Plants and Buildings with a Waste Heat Pipeline in Yokohama City

Toru Ichikawa[1,*], Ryota Kuzuki[1], Satoshi Yoshida[2], Satoru Sadohara[2]

[1] *Tokyo Gas Co., Tokyo, Japan*
[2] *Yokohama National University, Yokohama, Japan*
** Tel: +81 354007761, Fax: +81 354007766, E-mail: toithi@tokyo-gas.co.jp*

Abstract: District heating and cooling (DHC) in Japan's major cities are required to further lower their carbon emission. This study proposes to supply zero-carbon steam from a nearby waste incineration plant to the DHCs in the center of Yokohama, Japan's second largest metropolis by constructing a pipeline between them. To maximize environmental effects of the project, efficient cogenerations will also be integrated extending low carbon heat supply to large buildings along the pipeline. Construction cost of five alternative pipeline routes, revenue from steam sales and the environmental value of reduced CO_2 emission were estimated. Then the loan repayment period was calculated to figure out how to finance and manage the project. Because statistical data are used to calculate heat load, actual primary energy consumption and reduction of CO_2 emission may differ. Also, without a detailed field survey, assumed construction cost may not correspond to the actual amount to be financed. From the study it became clear that steam pipeline with cogeneration will reduce 3.6 PJ of primary energy use and 300,000 tons of CO_2 emission annually. The project will become feasible with loan repayment period of 8 and 10 years with and without subsidy by minimizing the construction cost.

Keywords: *district heating and cooling, low carbon, waste heat, CO_2 emission, steam pipeline*

1. Introduction

District heating and cooling (DHC) has been introduced to Japan's major cities from 1970s achieving efficient and reliable supply of energy compared to the installation of small appliances to the individual building. However, additional effort is being required to further lower the carbon emission nowadays. This study proposes to supply zero-carbon steam from a nearby waste incineration plant to the center of Yokohama, Japan's second largest metropolis, by constructing a pipeline between them. Environmental and economic benefits of the project have been examined in order to evaluate its feasibility.

1.1 Site review

Yokohama city center is one of most densely built up metropolis in Japan with good access to public transportation. Because density of energy consumption in the area is high, a few district heating and cooling plants are already in operation and most of the blocks have been assigned for urban renewal promotion area. Therefore it is easy to recognize that the area has a good potential of providing necessary heat more efficiently by networking the supply pipeline. If these networks are connected to the untapped low carbon heat sources, the entire city can reduce its energy use and CO_2 emission dramatically. This is why the study proposes to transport zero-emission heat source from a nearby waste incineration plant to two DHC plants and buildings in Yokohama city center. Following are the outline of the DHC plants.

1.1.1 Yokohama West DHC

It Started operation in 1998 with 6.5 hector of supplying land area and 350,152m^2 total floor area. Customers include department stores, hotels and a train station. Chilled water and middle pressure steam (0.8 – 1.0 MPa) are supplied by absorption chillers, boilers and two 1MW gas turbine cogenerations.

1.1.2 Minato Mirai 21 DHC

It Started operation in 1989 with total supplying floor area of 2,311,000 m^2 as of 2008. Major customers include 23 office and commercial buildings, hotels, public facilities and 6 apartments. Chilled water and middle pressure steam are produced by steam and electric turbo chillers, absorption chillers as well as boilers and delivered through utility tunnels.

2. Steam network pipeline

Besides above DHCs, the network will be extended to the separate buildings by to the following stages.
Stage 0: Waste incineration plant and DHCs are connected by a steam pipeline
Stage 1: Buildings over 10,000m^2 of floor area are connected to the pipeline
Stage 2: Buildings over 5,000m^2 of floor area are connected to the pipeline
Extension of pipeline will be planned by the distribution of the buildings (Fig.1). Because DHCs and most of the buildings use middle pressure steam as major heat sources for space heating, hot water supply and air conditioning (cooling), the network will deliver steam (up to 2.0 MPa) to them.

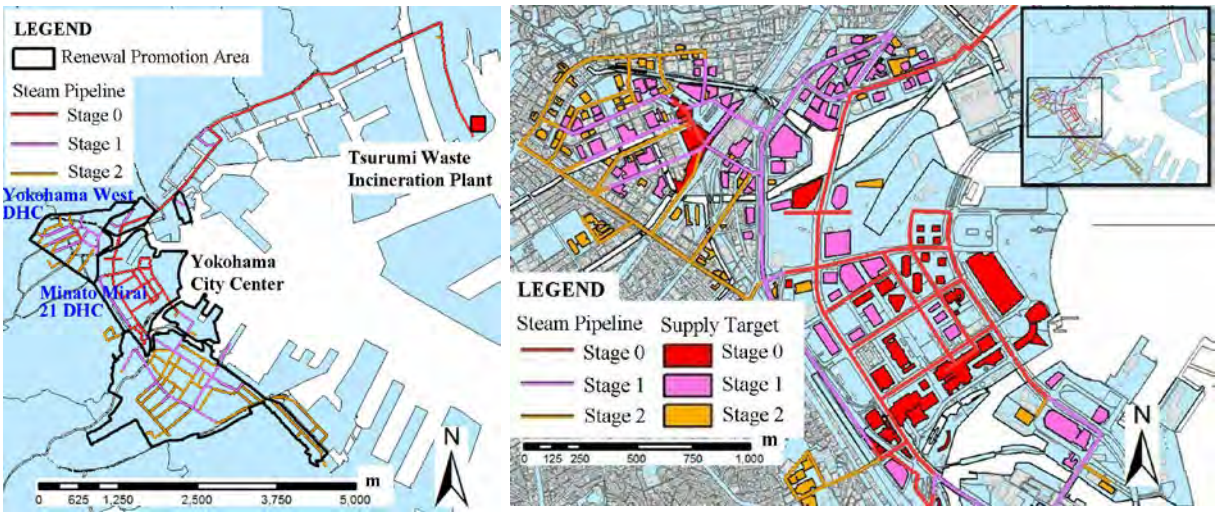

Fig. 1. Site map, steam pipeline and target buildings in Yokohama city center

2.1 Assumed heat supplying floor area by stage

Assumed floor area for supplying heat is 2,430,000m^2 at stage 0, 8,530,000m^2 at stage 1 and 10,620,000m^2 at stage 2. As for floor type shares, business, commercial and residential use rank top three with 36%, 33% and 19% of the total floor area respectively.

2.2 Assumed energy consumption

By multiplying assumed floor area and statistical unit energy consumption [1], energy consumption by purpose were calculated by hour, day, month and year. Because business and commercial floors with huge exhaust heat from appliances and human bodies prevail, annual cooling demand exceeds heating by about 50%.

3. Use of low carbon heat from waste incineration and cogeneration

3.1 Available heat from waste incineration

Three waste incineration plants are in operation in the vicinity of Yokohama city center. They are Kanazawa, Tsurumi and Asahi plants with 290, 270 and 120 thousand tons of annual handling amounts. These plants are equipped with total capacity of 66,000 kW of generators

which produce 293GWh of electricity annually. These generators, however, have low efficiency ranging from 13 – 18% because of the temperature restriction to avoid corrosion of the equipment. Therefore the study proposes among other options to halt generation and to supply entire amount of available heat to the city center by steam pipeline. This alternative will enable the plants to send 5,243 TJ of heat to the city center. (Table 1)

Table 1. Garbage Incinaration Plants nearby Yokohama City center

Plant Name	Handling Amount (t/year)	Generation Capacity (kW)	Generation Efficiency (%)	Generated Electricity (MWh/year)	Garbage Calorific Value (kcal/kg)	Incinerated Heat Value (TJ/Year)	Available Steam (TJ/Year)
Kanazawa	289,187	35,000	18	144,660	2,468	2998	2098
Tsurumi	266,640	22,000	16	107,181	2,838	3178	2225
Asahi	125,631	9,000	13	41,199	2,492	1315	920

Considering heat demand gap among seasons and daily hours, it is necessary to set appropriate supply capacity according to the base demand in order to avoid excess heat supply. Therefore the study cases accept steam only from the Tsurumi incineration plant with shorter pipeline to be built than with other plants. Assumed amount of heat to be supplied from Tsurumi is 2,225TJ/year.

3.2 Covered rate and used steam rate

Efficiency of steam driven appliances such as absorption chillers are determined to calculate demand of steam to be supplied by the network. Then the ratio of network steam to the demand is defined as “covered rate”. Also, the ratio of the used steam to its supply is defined as “used steam rate”. Both rates are calculated annually and monthly (Tables 2 and 3).

Table 2. Covered rate and steam share (Annual)

	Heat Demand (TJ/year)	Available Steam (TJ/year)	Usable Steam (TJ/year)	Covered Rate (%)	Used Steam Rate (%)
Stage 0	1,702	2,225	1,690	99%	76%
Stage 1	5,872	2,225	2,225	38%	100%

Table 3. Covered rate and steam share (Monthly)

	April		August		January	
	Covered Rate (%)	Used Steam Rate (%)	Covered Rate (%)	Used Steam Rate (%)	Covered Rate (%)	Used Steam Rate (%)
Stage 0	100%	53%	94%	100%	100%	96%
Stage 1	60%	100%	26%	100%	31%	100%

Annual covered rate of Tsurumi plant is about 100% at stage 0, while it drops to 38% at stage 1. Looking by season, at stage 1, covered rate decreases to 26% in August while it increases to

60% in April, a off-peak month. With heat storage during night hours, used steam rates reach 100% at stage 1. Hourly heat demand and supply from three waste incineration plants are shown in Fig.2. During daytime hours network steam is not sufficient to meet the heat demand.

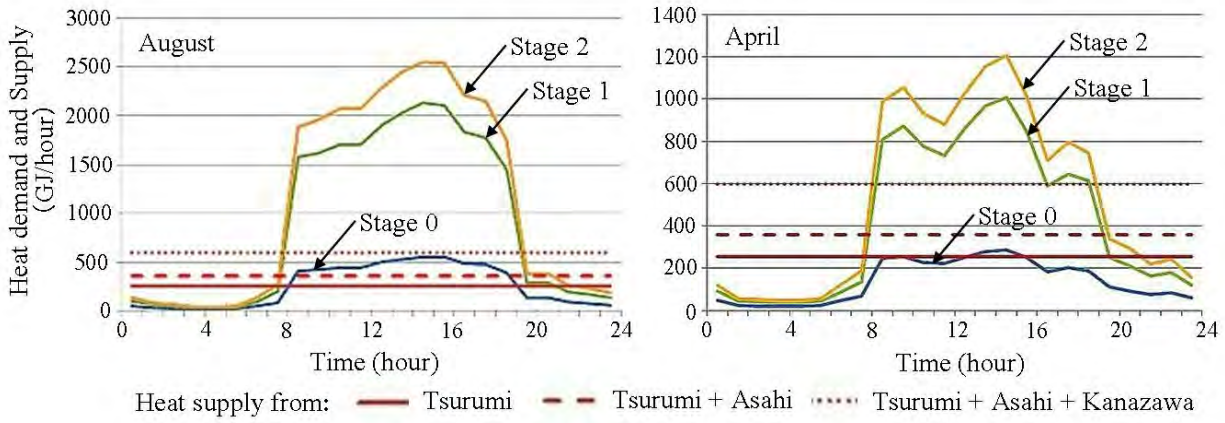

Fig. 2. Heat demand and supply from three waste incineration plants

3.3 Integrating cogeneration

Since daytime heat demand exceeds amount of steam supplied from Tsurumi throughout a year, it is appropriate to install and integrate cogenerations in the DHC plants and buildings along the network. To maximize the CO_2 reduction, gas engines with high generating efficiency and steam recovery capability from exhaust heat should be introduced instead of gas turbines. Capacities of gas engines were set so that they can meet most of the remaining steam demand at each stage. Covered rates will significantly increase by integrating cogeneration into the network.

4. Environmental effects expected by the network

Primary energy conservation and CO2 emission reduction by the network are calculated with following assumption.

4.1 Assumed condition for calculation

a) Priority of network steam use are: Cooling > Hot water supply > heating
b) Cogenerations operate to meet the electricity demand of the plants and buildings where they are installed. Priority of recovered steam use is same as a).
c) Chilled and hot water produced from excess steam during night hours are stored and used during daytime hours. Some steam accumulators, widely used in the factories, will be used too.
d) Marginal CO_2 emission factor is used for generated electricity by cogeneration. Flat emission factor is used for consumed electricity in the DHC plants and buildings as well as generated electricity at waste incineration plants.
e) Following alterative use of heat produced from waste incineration are compared
Case 0: discharged with no heat use
Case 1: exclusively used for electricity generation
Case 2: exclusively used for steam supply through network
Case 3: exclusively used for steam supply through network with cogeneration in buildings

4.2 Results

4.2.1 Energy conservation

At stage 0, primary energy conservation rate will be doubled from 18% to 35% by switching from electricity generation to steam supply. Also, if cogeneration is integrated in case 3, 3,616 TJ/year or 15% primary energy reduction will be attained at stage 2 compared to case 1 (Table 4).

4.2.2 Reduction in CO_2 emission

At stage 0, reduction in CO_2 emission will increase by 33% from 73,955 tons/year to 98,412 tons/year by switching from generation to network steam supply. By integrating cogeneration into the system, reduction will be increased by 36% or 252,595 tons/year at stage 1 and by 35% or 298,906 tons/year at stage 2 compared to case 1 (Table 4).

Table 4. Environmenal effects of the pipeline

		Stage 0				Stage 1				Stage 2			
		Case 0	Case 1	Case 2	Case 3	Case 0	Case 1	Case 2	Case 3	Case 0	Case 1	Case 2	Case 3
Primary Energy Consumption	(TJ/year)	5,776	4,723	3,765		20,869	19,815	18,630	16,621	25,144	24,091	22,927	20,474
Primary Energy Reduction	(TJ/year)		1,054	2,012			1,054	2,239	4,248		1,054	2,217	4,670
Primary Energy Reduction Rate	(%)		18	35			5	11	20		4	9	19
CO_2 Emission	(t-CO_2/year)	216,340	142,385	118,197		776,137	702,182	672,991	449,587	937,389	863,434	835,597	564,528
CO_2 Emission Reduction	(t-CO_2/year)		73,955	98,412			73,955	103,146	326,551		73,955	101,792	372,861
CO_2 Emission Reduction Rate	(%)		34	45			10	13	42		8	11	40

5. Business scheme and feasibility

5.1 Pipeline route alternative

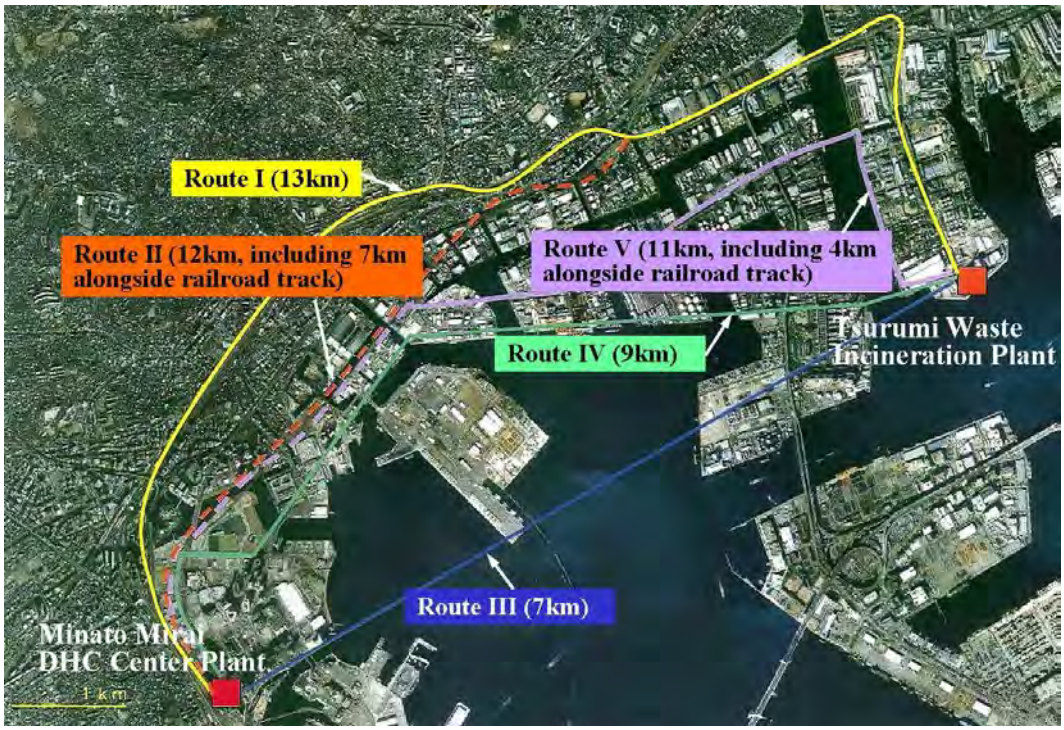

Fig. 3. Steam pipeline route study

Following alternative routes were proposed (Fig 3) and reviewed for case studies.

a) Route I: Laying pipes shallow underground along existing road (length: 13km)
b) Route II: Laying pipes shallow underground along existing road and railroad track (length: 12km)
c) Route III: Laying pipes deep undersea by excavating a tunnel (length 7km)
d) Route IV: Laying pipes under or over the private land on the waterfront (length 9km)
e) Route V: Laying pipes either under or over the green belt along the railroad track (length11km)

5.2 Assumptions for calculation

Costs and Prices in Japanese Yen are also converted to US dollars/cents using the rate of 1$US=82 yen as of February 4, 2011 and shown in parentheses.

a) Available amount of steam from Tsurumi Plant: 2,225 TJ/year
b) Acceptable amount of steam at DHCs and buildings: 1,690 TJ/year (Stage 0), 2,225 TJ/year (Stage 1)
c) Steam pricing: purchase price is set at 0.6 yen (0.73 cent) /MJ [2], 0.3 yen (0.37 cent)/MJ less than the base price assuming burning gas, wholesale price is set at 1.45 yen (1.77 cent)/MJ and 1.6 yen (1.95 cent)/MJ [3] assuming entire or a half of the surplus from the base price is to be refunded to the steam buyers respectively.
d) CO_2 emission reduction 24,188 tons/year for stage 0, and 252,595 tons/year for stage 1
e) Steam pipe size: 400 - 500mm in diameter for supply and 100- 150 mm for return
f) Construction cost [4]
   Route I : 1,500,000 yen ($18,293)/m for underground shallow plumbing along conventional road
   Route II : 800,000 yen ($9,756)/m for overground plumbing beside railroad track, 1,500,000 yen ($18,293)/m for u shallow underground plumbing along the conventional road
   Route III: 2,000,000 yen ($24,390)/m for undersea shielded tunnel construction and plumbing
   Route IV: 1,200,000 yen ($14,634)/m average for plumbing under and over the private land
   Route V: 800,000 yen ($9,756)/m for plumbing under or over the green belt along the railroad track
g) Subsidy: none (Case A), 1/3 of construction cost (Case B) parallel to the ongoing subsidy by the Ministry of Land Transportation and Tourism
h) Carbon credit: 2000 yen ($24)/t-$CO_2$ or 3000 yen ($37)/t-$CO_2$ credit added to the revenue
i) Managing expenditure
   - personnel cost: 6 million yen ($73,171)/year each for 4 operators, 8 million yen ($97,561) /year for a concu-
     rrent manager
   - road occupancy fee: 2,000 yen ($24)/m year
   - pipeline management cost: 1% of the construction cost each year
   - overhead expenses: 10% of personnel cost
   - depreciation period: 30 years with remaining book value of 10%

5.3 Business scheme

Following alternative are assumed.

a) PFI (Private Finance Initiative): Yokohama municipal government sells steam to a PFI enterprise. It will construct the pipeline, transport and sell the steam to its customers.
b) Private enterprise: Private companies will construct the pipeline by an open bid. They will also buy steam from Yokohama municipal government and sell to its customers.

c) A joint venture company: Yokohama municipal government and private enterprises cooperate to establish a so-called "third-party company" to construct the pipeline and operate the business.

5.4 Specifications of the business

a) Construction cost:
Route I (shallow underground): 19,500 million yen ($238 million)
Route II (overground and shallow underground): 13,100 million yen ($160 million)
Route III (deep undersea): 14,000 million yen ($171 million)
Route IV (underground and overground) 10,800 million yen ($132 million)
Route V (shallow underground and overground) 8,800 million yen ($107 million)
b) Terms of construction: Three years for connecting Tsurumi plant and two DHCs after start of construction at stage 0, another 2 to 3 years for connecting to the buildings at stage 1
c) Funding: 70% of the loan to be raised by senior bonds with an interest rate of 3 or 4%, 30% by subordinated bonds with an interest rate of 5 or 6%.
d) Insurance premium: 0.25% of the construction cost to be budgeted
e) Property tax: 1.4% of the opening book value can be exempted for the BTO (Build-Transfer-Operate) case of the PFI scheme

5.5 Results

Based on the basic case with relatively strict conditions, business feasibility under various conditions are compared. Loan repayment period will be extended to 24 years from 17 years without subsidy suggesting its availability will give a significant impact to the feasibility of the project.

5.5.1 Basic and Alternative cases

a) Routes: Loan repayment period will significantly shorten with reduction in construction cost. 17 years for the basic case (Route I) will be shortened by half to 9 years for Route IV and 8 years for Route V.
b) Steam price: Loan repayment period will shorten by three years to 14 yeas if a half of 0.3 yen (0.37 cent)/MJ surplus obtained by the steam purchase from Tsurumi plant is reserved for the enterprise rather than giving all out to the end users
c) Carbon credit: Loan repayment period will shorten by one year if the carbon credit price will be increased from 2,000 yen ($24)/t-$CO_2$ to 3,000 yen ($37)/t-$CO_2$.
d) Subsidy: Loan repayment period will be extended to 24 years without subsidy. However, even in that case, retained earnings which is a sum of the profit after tax and depreciation will be kept in black suggesting it is possible to run the business if long-term loan can be raised at a low interest rate.
e) Property tax: BTO case of the PFI scheme, in which the pipeline and facilities will be transferred to the Yokohama municipal government after completion, property tax will be exempted shortening the loan repayment period by three years.
f) Interest rate: Loan repayment period will be extended by one year if the interest rate of both senior and subordinated bonds increase to 4 and 6%.
g) Schedule: Even if the start of operation for stage 1 is extended from 2 to 3 years after the completion of stage 0, loan repayment period will not change significantly.
h) Surplus: No significant effect will be expected by investing surplus with 3% annual gain.
All above alternative are listed in Table 5.

Table 5. Loan repayment period for basic and alternative cases

Condition Loan Payback Period	Deteriorating Cases	**Basic Case**	Improving Cases			
Route/Construction Cost（million Yen）		I/ 19,500	II/ 13,100	III/ 14,000	IV/ 10,800	V/ 8,800
		17years	11years	12years	9years	8years
Steam sales price（Yen/MJ）		1.45	1.6			
		17years	14years			
Carbon credit（Yen/t-CO2）	None	2,000	3,000			
	19years	17years	16years			
Subsidy ratio to the construction cost	None	1/3				
	24years	17years				
Property tax on the opening book value		1.4%	None			
		17years	14years			
Interest rates of senior and subordinated bonds	4%,6%	3%,5%				
	18years	17years				
Stage 1 operation start (after stage 0 completion)	3years	2years				
	17years	17years				
Interest rate of surplus investment (%)		None	3%			
		17years	16years			

Currency rate: 1$US=82yen as of February 4, 2011

5.5.2 Combination of alternative cases

If most of the favorable alternative are applied together, loan repayment period will be shortened to 8 years. In that case, even without subsidy, the project will retain its profitability with loan payback period of 10 years.

6. Conclusions

A steam pipeline network is planned to transport zero-emission heat from Tsurumi waste incineration plant to the Yokohama city center. The study made it clear that by integrating cogeneration into the network, 3.6PJ or 15% of primary energy reduction as well as reduction of 300,000 tons of CO_2 emission will be achieved annually for the district heating plants and buildings over 5,000m^2 of floor area. The network will be able to provide inexpensive carbon-free heat with loan payback period of only 8 to 10 years by lowering the construction cost with an appropriate pipeline route selection. However, following limitations must be stated on the accuracy of above conclusions: (a) Because statistical data such as energy consumption by unit floor area are used instead of measured data to calculate heat load, actual primary energy reduction and reduction in CO_2 emission may decrease; (b) Without a field survey, assumed construction cost may not correspond to the actual amount to be financed, which may affect the feasibility of the project. These limitations should be cleared in a more detailed study to be followed.

References

[1] Japan District Heating & Cooling Assication, District Heating Technology Guide (Rrevised Edition) , 2002
[2] Tokyo's 23 Wards Cleaning Association, Working Report of the Waste Incineration Plants in FY 2009, 2010
[3] The Japan Heat Service Utilities Association, Heat Supply Business Handbook, 2009
[4] Japan District Heating & Cooling Assication, Feasibility Studies of Exhaust Heat Utilization from Waste Incineration plants in Central Tokyo District, 2010
[5] Japan Environmental Systems Co., Basic Research on the Improvement of Urban Thermal Environment by the Reduction of Anthropogenic Heat Disposal, 2009
[6] Japan District Heating & Cooling Association, Research on the Application of Untapped High-temperature Energy Sources in Japan's Metropolis, 2010

Study on the Non-Energy Benefit (NEB) of Area-Wide Energy Utilization and Evaluation of the Marginal Abatement Cost

Ryota Kuzuki[1,*], Shuzo Murakami[2], Toshiharu Ikaga[3], Satoru Sadohara[4], Satoshi Yoshida[4], Toru Ichikawa[1], Yoshio Kato[5], Tsutsumi Tanaka[5], Yuichi Ikuta[6], Ken Aozasa[7]

[1] *Tokyo Gas Co., Ltd., Tokyo, Japan,* [2] *Building Research Institute, Tsukuba, Japan*
[3] *Keio University, Yokohama, Japan,* [4] *Yokohama National University, Yokohama, Japan*
[5] *Nihon Sekkei Co., Ltd., Tokyo, Japan,* [6] *Japan Environmental Systems Co., Ltd., Tokyo, Japan*
[7] *Institute of Building Environment and Energy Conservation, Tokyo, Japan*
** Corresponding author. Tel: +81 354007752 Fax: +81 54007766, E-mail: kuzuki@tokyo-gas.co.jp*

Abstract: To achieve the Kyoto Protocol target of carbon reduction in Japan, additional measures beyond individual building-scale are strongly required. Area-wide energy utilization is expected to play an important role, not only in improving energy efficiency, but also in enhancing utilization of renewable energy and unused thermal energy toward a low-carbon society. But so far there have been few initiatives that have been realized. One of the major hurdles is the lack of methods to convince stakeholders to collaborate towards implementation. This study focuses on non-energy benefits (NEBs), which are indirect benefits such as stimulating regional economies and environmental protection, as distinguished from the direct energy-benefit (EB) of utility costs reduction.

Through the development of methods to classify and quantify various NEBs and to assign monetary values in the marginal abatement cost (MAC), area-wide energy utilization has been deemed to be more competitive among various carbon reduction measures. Customized marginal abatement cost curve evaluation has proven effective for encouraging stakeholders to implement.

Keywords: *Area-wide energy utilization, Non-energy benefit, Marginal abatement cost, Cost benefit ratio, Payback time*

1. Introduction

1.1. Area-wide energy utilization of scale measures for carbon reduction

In the commercial and residential sectors, further reductions of carbon emissions are being sought toward the realization of a low-carbon society. To respond to this issue, area-wide carbon-emission reduction measures must be promoted for blocks of buildings, communities, districts and for cities, which go beyond individual buildings. The Kyoto Protocol Target Achievement Plan[1)] in Japan begins with area-wide energy utilization as its first measure, in terms of further energy saving beyond individual buildings and for promoting a large increase in the utilization of neighboring unused energy sources and renewable energy sources.

1.2. Necessity of evaluating measures from a middle-to-long-term perspective, considering local characteristics

In 2008, the Mid-term Targets Examination-Committee of the Cabinet Secretariat's Council on the Global Warming Issue (hereafter, the "Mid-term Targets Committee") discussed measures for the nation to reduce carbon emissions over the middle term through marginal abatement cost (MAC). [2)]
The image is shown in Fig.1.

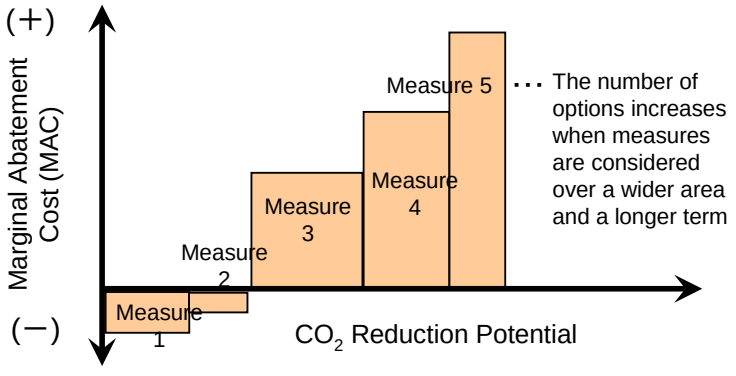

Figure 1 Marginal abatement cost curve (image)

MAC is defined as the cost required per additional unit reduction of CO_2 (e.g., per ton CO_2) from the present conditions, under a given area (e.g worldwide, nationwide, district-wide, etc.). McKinsey & Company[3] and some other organizations have evaluated the MAC of a variety of carbon reduction measures and have published reports presenting MAC curves, which is a useful method to determine the selection of cost-effective measures. However, for discussions on area-wide energy utilization, the current evaluation method has some problems, as listed below;

1) Measures whose costs vary greatly due to distinct regional characteristics (such as differences in energy infrastructure and in access to locally generated, locally consumed energy) are too detailed to discuss on a nationwide scale.
2) Measures which require large initial investments, but which are effective for a long time (such as insulation of buildings and infrastructure development) are evaluated as comparatively expensive options if the payback time is set at a relatively short uniform period.
3) MAC has been defined as the net cost of measures, deducting direct energy benefits (EB) of energy-utilities cost reduction from the total costs. However, even if there are also diverse indirect benefits, such as stimulation of regional economies and environmental protection resulting from the measures, which some researches collectively refer to as "non-energy benefits" (NEBs)[4),5)], they have not been considered in the MAC evaluation.

1.3. Research objectives

The objective of this research is to establish methods of accurately determining area-wide energy utilization in comparison with other carbon reduction measures, and methods of evaluating cost-benefit ratios (B/C) and MAC, focusing on non-energy benefits (NEBs) in order to encourage stakeholders to implement.

2. Methodology

2.1. Estimation of CO_2 reduction potential considering the regional characteristics

Specifying the particular region where the measures for a low-carbon society will be advanced clarifies the specific figures concerning any unused energy sources (incineration-plant waste heat, etc.) that can be accessed in the concerned district, such as solar heat collectors and photovoltaic power generation equipment in accordance with heat and electricity-demand density and patterns according to time band, and on-site cogeneration. Those figures are then used to calculate the CO_2 reduction potential of the concerned district. The initial and running costs of each measure are set referring to prior knowledge[2),6)] published by the Japanese government. The values for measures with different costs by region, by necessity, are set on a case-by-case basis. Subsidies and other grants are not included.

2.2. Setting the payback time considering the duration of the measure's effects

The MAC of each measure is calculated as the annual cost ([yen/year] / [t-CO_2/year]) under the following procedure; considering the initial costs (including renewal costs) for implementing each carbon-emission reduction measure, the running costs, and the reduction in utilities expenses gained from energy conservation. The expressions of the procedure are as follows, and Fig.2 presents an image of the MAC structure.

The payback time should be set appropriately for each measure from the viewpoint of the middle-term and long-term improvement of social capital and with consideration for the

technology use conditions. Referring to the option that the National Institute for Environmental Studies proposed to the Mid-term Targets Committee (a setting of 50-70% of the functional lifetime of each measure)[2], McKinsey & Company report[3], in this study the payback time is set at a number of years equivalent to 70% of the lifetime of each measure.

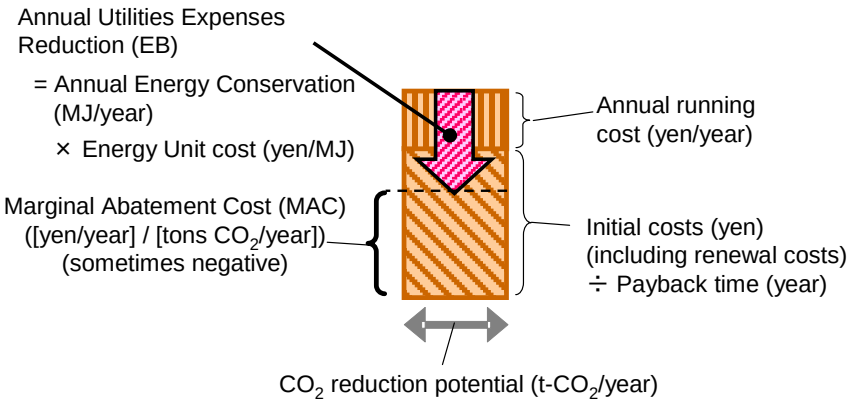

Fig. 2. Structure of marginal abatement cost (MAC) of a carbon reduction measure

Table 1 presents a summary of the classification of CO_2 reduction measures and their MAC.

Table 1. Carbon reduction measures and MAC setting by measures

Carbon reduction measures in this study (Set based on the 2008 Local Government White Paper (Japan) on the Environment)		MAC and payback time under prior Knowledge [2),6)]			Proposed MAC with payback time set at 70% of functional lifetime of each measure			
		MAC (yen/ t-CO_2)	Payback time (years)		MAC (yen/ t-CO_2)	Payback time (years)	References of lifetime	
Commercial Sector								
(1)	Air conditioning equipment efficiency improvements	-24,000	3		-24,000	10.5	15	*
(2)	Lighting efficiency improvements, etc.	-25,000	3		-25,000	14.0	20	*
(3)	Power and other efficiency improvements	19,000	3		-16,491	17.5	25	*
(4)	High-efficiency water heaters	32,000	3		0	10.5	15	*
(5)	Improved insulation in newly constructed buildings	69,000	9		16,143	21.0	30	***
(6)	Improved insulation in existing buildings	69,000	9		35,964	14.0	20	***
(7)	Building and energy management systems (BEMS)	3,000	8		8,714	7.0	10	*
(8)	Use of solar thermal energy	2,000	10		2,000	11.9	17	***
(9)	Photovoltaic power generation	62,000	9		23,378	11.9	17	**
(10)	Changes in work styles	-38,000	-		-38,182	-	-	****
(11)	Commercial cogeneration	-8,500	10		-8,500	10.5	15	****
Residential Sector								
(12)	Heating-and-cooling efficiency improvements	-30,000	3		-30,000	4.2	6	**
(13)	Lighting efficiency improvements, etc.	-28,000	3		-34,789	14.0	20	*
(14)	Household appliances' efficiency improvements	28,000	3		10,629	4.2	6	**
(15)	High-efficiency water heaters	143,000	3		11,343	7.0	10	*
(16)	Improved insulation in newly constructed housing	430,000	9		239,870	15.4	22	**
(17)	Improve existing insulation	430,000	9		266,607	14.0	20	***
(18)	Home energy management systems (HEMS)	-2,000	3		-18,457	7.0	10	*
(19)	Solar water heaters	17,000	8		-22,328	11.9	17	**
(20)	Photovoltaic power generation	78,000	10		59,319	11.9	17	**
(21)	Changes in life styles	-38,000	-		-38,000	-	-	****
(22)	Residential cogeneration	30,000	10		30,000	7.0	10	*
Community-Wide Energy Utilization								
(23)	Wind power generation	12,000	-		12,000	11.9	17	**
(24)	Woody biomass	4,000	20		4,000	14.0	20	****
(25)	Waste products power generation	2,000	-		2,000	14.0	20	****
(26)	Heat-and-electric power exchange among buildings*****	-	-		17,488	14.0	20	****
(27)	Incineration plant waste heat*****	16,616-28,329	20		9,890 - 14,925	31.5	45	****
(28)	Regional cogeneration*****	2,586	15		-2,082	21.0	30	****

2.3. Definition and Monetizing NEBs

As described above, there are various NEBs among the carbon reduction measures received by the stakeholders. In terms of the way of estimating monetary value, the classification and quantification of the NEBs are proposed. Five major categories are defined (a - e), and they are additionally classified into fourteen categories. Table 2 shows the details.

Table 2. Monetization of EB and NEBs by category

Benefit	Monetization Outline	Referenceis
<Energy Benefit (EB)>		
Reduction in utilities expenses	Reduction in utilities expenses (yen/year) = energy reduction volume (yen/year) X energy unit cost (yen/MJ)	**Energy unit cost** set based on supply agreements and supplementary supply agreements from city gas and electric power utilities
<Non-Energy Benefit (NEB)>		
a. Benefit from creation of environmental value		
a1. CO2 reduction value	CO_2 reduction value (yen/year) = CO_2 reduction amount (t-CO_2/year) X CO_2 price (yen/ t-CO_2)	**CO_2 price** set (e.g., 4,000yen/t-CO2) "Point Carbon "Carbon 2009" (March 2009)"
a2. Green energy creation value	Green energy creation value (yen/year) = green energy use volume (MJ/year) X green energy unit price (yen/MJ)	**Green energy unit price** set (e.g., 15yen/kWh) "Examination Committee on VER Japanese Certification Standards Used in Carbon Offsets" (for photovoltaic power generation)
b. Benefit from the ripple effect on the regional economy		
b1. Economic ripple effect from infrastructure construction investment	Economic ripple effect from infrastructure construction investment (yen/year) = initial infrastructure construction investment (yen) X gross value added ratio ÷ ripple effect period (years)	**Gross value added ratio** set (e.g., 0.5) with reference to public investment gross value added estimates from various industry-related analyses by local governments **Ripple effect period** set at 70% of the lifetime of business facilities lifetime (e.g., 10.5 years ~ 31.5 years)
b2. Economic ripple effect on business operations	Economic ripple effect on business operations (yen/year) = business operating expenses (yen/year) X (ripple effect multiplier – 1)	**Ripple effect multiplier** set (e.g. 1.3) with reference to public works ripple effect multiplier, estimates from various industry-related analyses by local governments
b3. Increased real estate value effect (residential property)	Area real estate value increase effect (¥/year) = standard land price (yen/m^2) X subject land area (m^2) X (real-estate-value increase rate (%)/100) ÷ increase effect period (years)	**Standard land price** uses the figures from Ministry of Internal Affairs and Communications, Statistics Bureau, "2009 Statistics on Cities, Wards, Towns and Villages" **Real estate value increase rate** set (e.g., 0.5%) with reference to the rent increase rate (0-5% for model case rent) in the "CASBEE Real Estate Use Manual (provisional version) (July 2009)" **Increase effect period** set at 70% of the lifetime of business facilities lifetime (e.g., 10.5 years ~ 31.5 years)
b4. Increased real estate value effect (commercial property)		
c. Benefit from risk aversion		
c1. Contribution to the business and living continuity plan (BLCP); energy supply interruption aversion effect	Energy supply interruption aversion effect (yen/year) = energy supply interruption unit damage (yen/kW-hour) X decentralized power source capacity (kW) X supply interruption period (hours/interruption) X damage occurrence probability (times/year)	**Supply interruption damage** (yen/kW-hour), **Supply interruption period** (hours/interruption) **Damage occurrence probability** (times/year) set considering prior research[5]
c2. Risk aversion effect from stronger regulatory system, higher standards, etc.	Risk aversion effect from stronger regulatory system (yen/year) = utilities expenses (yen/year) X risk aversion expense ratio ÷ 100	**Risk aversion expense ratio** set with reference to "Sumitomo Trust & Banking Co. Ltd. "Outline of Business Awareness Survey Regarding Environmental Buildings" (July 2009)
c3. Health damage risk aversion effect (residential sector)	Health damage risk aversion effect (yen/year) = insurance benefits (yen/person) X subject population (persons) X occurrence ratio	**Insurance benefits** set using the figures from Japan Institute of Life Insurance "Nationwide Life Insurance Fact Survey" (e.g., 20.33 million yen/person for death benefits) **Occurrence ratio** set (e.g., 0.01%) Tokyo Medical Examiner's Office)
c4. Health damage risk aversion effect (commercial sector)	Health damage risk aversion effect (yen/year) = work absence ratio (days/person-year) X salary income (yen/year-person) ÷ work days (days/year) X affected persons (persons) X occurrence probability	**Salary income** uses figures from National Tax Agency "Fiscal 2005 Salary Income Survey" (e.g., nationwide average of ¥4.37 million/person [including bonuses, etc.])
d. Benefit from the diffusion and education effect		
d1. Leading model project public awareness and education effect	Public awareness and education effect (yen/year) = subject population (persons) X cost required for public awareness and education (¥/person-year) X effective period coefficient	**Subject population** is the population residing in the subject district **Cost required for public awareness and education** set (e.g. 3,000yen/person) referring to the costs for attending seminars implemented by non-profit organizations **Effective period coefficient** set (e.g., 3 years, 10 years) as the ratio of the periods in which projects are still leading projects
d2. Leading model project advertising and publicity effect	Advertising and publicity effect (yen/year) = costs required for the measure (yen/year) X advertising and publicity effect coefficient X effective period coefficient	**Advertising and publicity effect coefficient** set (e.g., 2%) referring to the cases (e.g., an effect equivalent to 2% of total environment-related costs) for company case studies "FY2005 Environmental Accounting Guidelines Reference Materials" **Effective Period Coefficient** set the same as in d1
e. Benefit from improving the living and working environment		
e1. Higher worker intellectual productivity effect	Higher worker intellectual productivity effect (yen/year) = affected persons (persons) X personnel expenses (yen/person-year) X productivity improvement coefficient X effective period coefficient	Productivity Improvement Coefficient set (e.g., average of 0.5%) referring to the case study analysis (16 environmental buildings in the U.K. with an intellectual productivity change ranging from -10% to +11%) in Diana Urge-Vorsatz, et al., "Mitigating CO_2 Emissions from Energy Use in the World's Buildings," Building Research & Information (2007) 35(4), pp. 379-398
e2. Resident health promotion effect	Residents' health promotion effect (yen/year) = subject persons (persons) X amount intended to spend (yen/person-year) X effective period coefficient	**Subject persons** are the number of residents in the subject district **Amount intended to spend** is set based on a questionnaire survey of the residents

3. Case study

A case study of implementation on a specific district was conducted using the evaluation policy presented above.

3.1 Overview of the case-study district

Fig.3 presents an outline of the case-study-subject district. The district (hereafter, "District A") is an existing mixed-use urban area centered around a large train station and offices, stores, housing, hotels, universities and other facilities, and an incineration plant located nearby. The case study assumes the following infrastructure arrangement of the District A energy system, as district-scale measures, together with other carbon reduction measures at the individual building level, considering the presence of the incineration plant, which is an unused energy source nearby, as well as area-wide energy utilization that is already being implemented in part of the District.

1) Area-wide utilization of unused high-temperature energy sources (incineration plant heat)
2) Development of area cogeneration as a foundation of an area-wide energy system, together with area-wide development within the district
3) Formation of a smart energy network for the effective use of heat and electricity in response to demand fluctuations, with linkage to the existing district heating and cooling infrastructure

District A Overview

District with a high concentration of large-capacity, primarily commercial buildings

- District area: 398ha
- Building floor space: 8.8 million m^2
- Population: 40,700 persons
- Households: 22,000

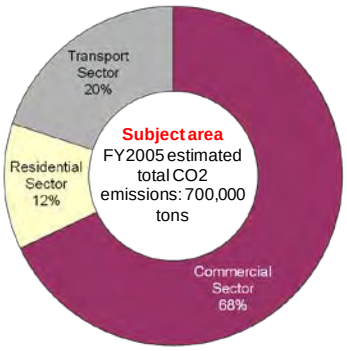

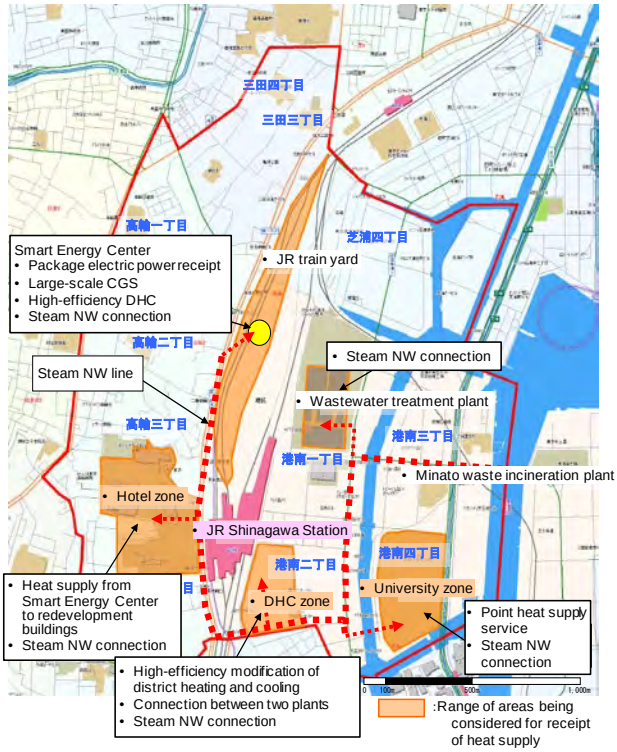

Fig.3. Case study district characteristics and annual CO_2 emissions breakdown

3.2 Carbon reduction measures and CO_2 reduction potential

Carbon reduction measures and the CO_2 reduction potential considering that the characteristics of District A are estimated based referring the 2008 (Japanese) Local Government White Paper on the Environment[7]. The total CO_2 reduction potential of all the assumed carbon reduction measures is approximately 160,000 t-CO_2/year.

3.3 Results - Cost-benefit ratio (B/C) considering NEBs

Fig.4 presents the cost-benefit ratio (B/C) trial calculation results for District A, considering NEBs. The total cost when all the measures are implemented is about 4.8 billion yen/y, the EB is approximately 3.7 billion yen/y, and the total monetized NEB is about 4.3 billion yen/y. The B/C is just 0.77 when only the EB is included, but rises to 1.7 when the NEBs are also considered.

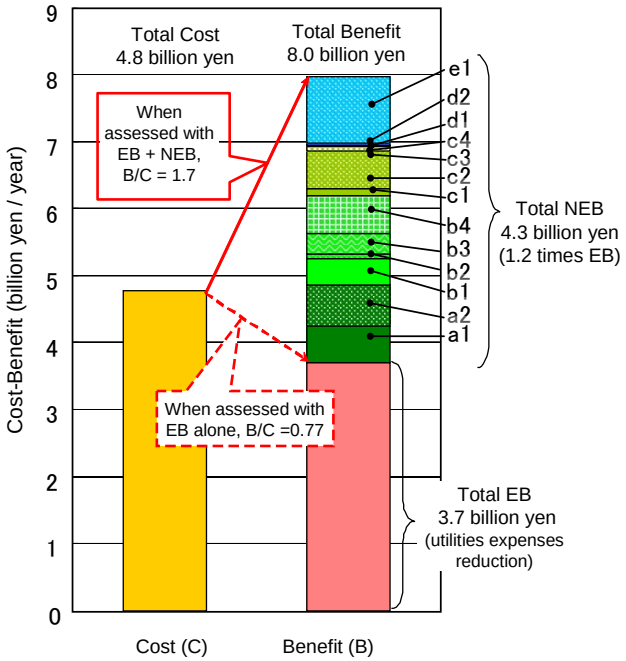

Fig.4. Total cost-benefit ratio (B/C)

3.4 Results – Marginal abatement cost curve considering NEBs

Fig.5, Fig.6 and Fig.7 present the results of estimated MAC curves. Fig.5 shows the MAC calculated with uniform payback time of 3 years, or of about 10 years. Fig.6 shows the results calculated by use of payback time set at 70% of the functional lifetime of the measures. Fig.7 is the result by considering the NEBs allocated to MAC of each measure in addition to Fig. 6.

As shown by the cross-hatched sections of each figure, in District A, arranging community-wide energy utilization by making use of the regional characteristics (including the effective use of incineration plant waste heat and the existing district heating and cooling network) has a high economic priority.

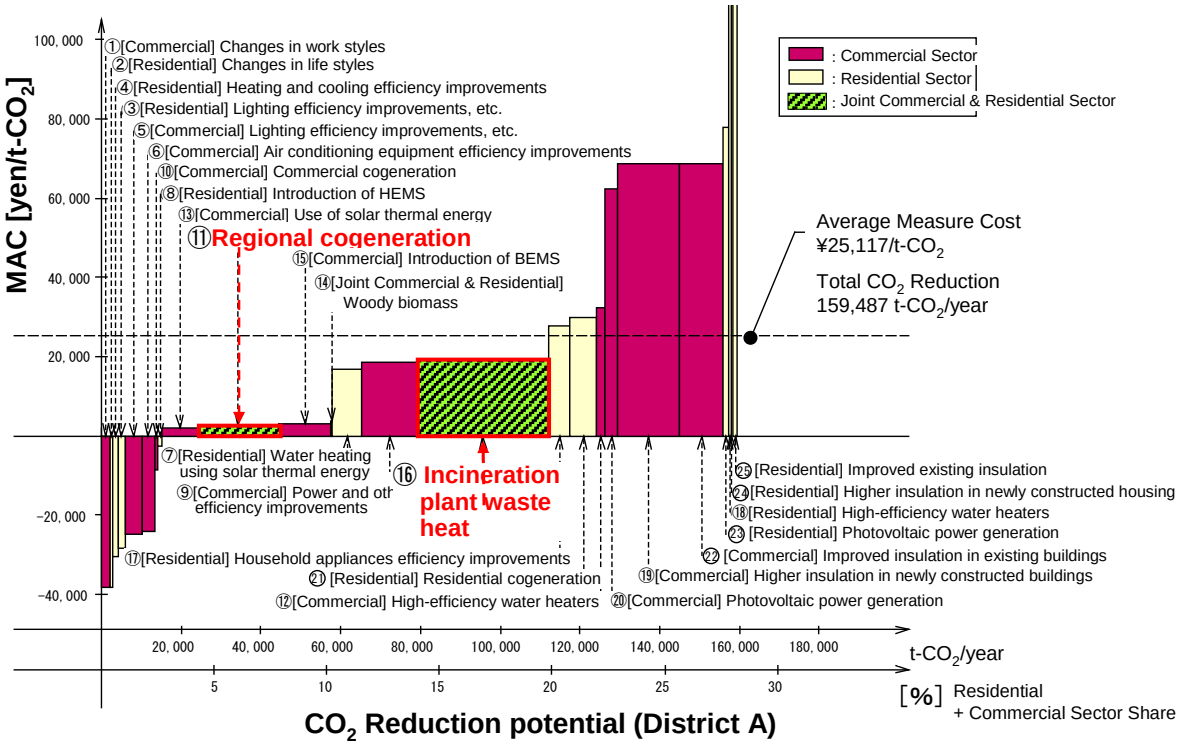

Fig.5. District A's marginal abatement cost curve (Uniform payback time of 3 years, or of about 10 years)

Comparison between Fig 5 and Fig6, it is clearly shown how setting the payback time appropriately for each measure greatly decreases the average cost of the measures (25,117 -> 6,739yen/t-CO_2).

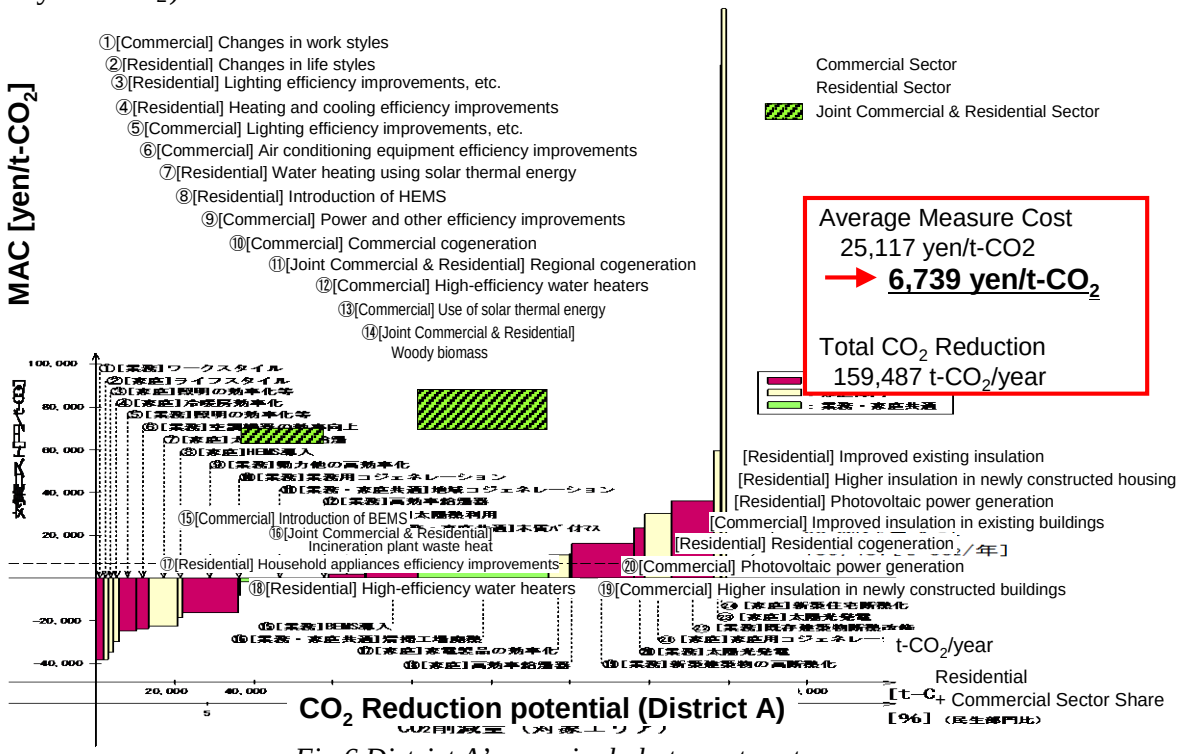

Fig.6 District A's marginal abatement cost curve (payback time set at 70% of the measure lifetime)

In addition, by reflecting the NEB to Fig.6, as Fig.7 shows, the MAC becomes negative for most measures (i.e., the benefits exceed the expenses over the payback time), and the average measure cost is estimated at around (+6,739 -> -20,006 yen/t-CO_2).

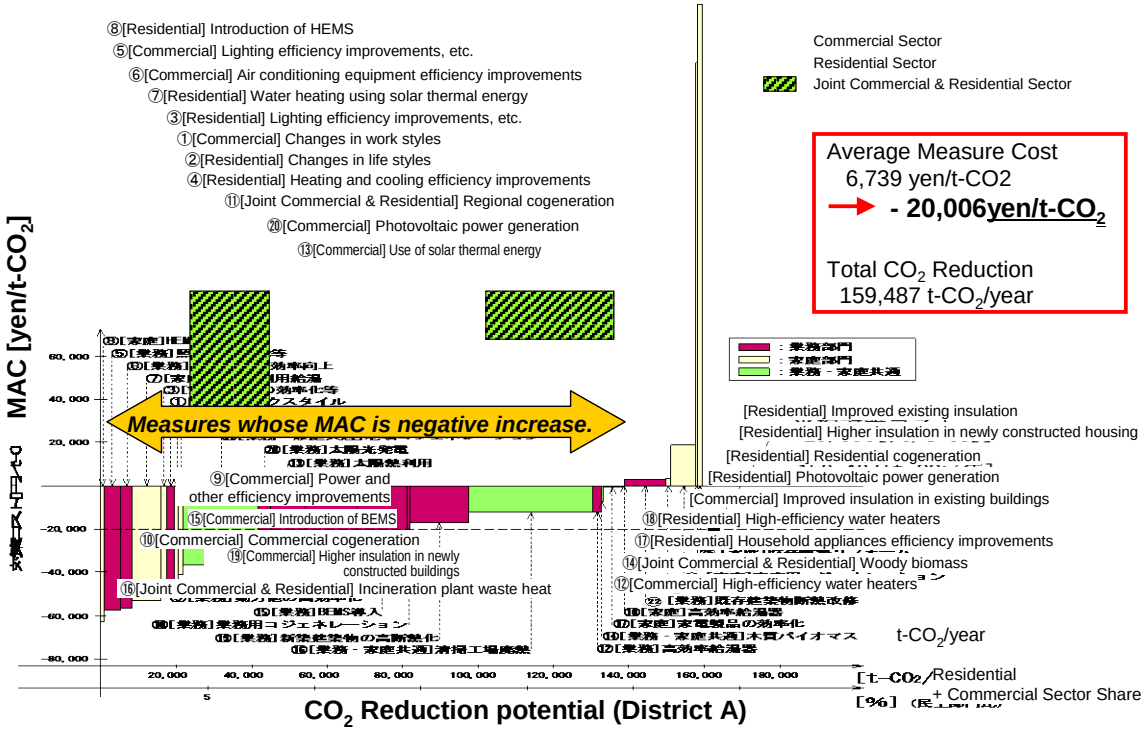

Fig.7 District A's marginal abatement cost curve (reflecting payback time set at 70% of the functional lifetime and NEB of each measure)

4. Conclusion

To promote area-wide energy management, this study proposes the approach of using a marginal abatement cost (MAC) from a middle-term and long-term perspective and conducting cost-benefit ratio (B/C) calculations considering the non-energy benefits (NEBs) generated from various carbon reduction measures. The findings are as below:

1) It was clarified that the CO_2 reduction potential of area-wide energy utilization and the utilization of unused energy sources are much competitive measures in the marginal abatement cost curve for a specific district. This was verified through a case study on utilization of incineration-plant waste heat.
2) It is proposed that evaluation of the MAC for each measure should should be used to set the payback time appropriately from the viewpoint of the middle-term and long-term improvement of social capital, with consideration for the conditions under which the technology is used. 70% of the functional lifetime of the measures is proposed as the payback time. Through a case study, it was clarified that this improves the MAC assessment for measures with high initial investments, such as improving building insulation and area-wide utilization.
3) This study presents an approach to monetizing the non-energy benefits (NEBs) that result from area-wide energy utilization, which can explain a higher B/C. This study also proposes an approach to revising MAC through allocation of the NEBs to each measure, and demonstrates through a case study how this results in the assessment of more of the measures within the subject areas as economically promising.

Acknowledgements

This paper is part of the results of activities conducted by the Carbon-Minus High-Quality Town Research Committee, established with the Japan Sustainable Building Consortium as the secretariat. The authors would like to express their gratitude to all the concerned parties for their contributions.

References

[1] Cabinet Secretariat Japan, Global Warming Prevention Headquarters, “Kyoto Protocol Target Achievement Plan,” April 2005

[2] Cabinet Secretariat Japan, Council on the Global Warming Issue: submitted papers at “Mid-term Targets Examination Committee” (Nov. 2008 - April 2009).

[3] McKinsey & Company: “Pathways to a Low-Carbon Economy: Version 2 of the Global Greenhouse Gas Abatement Cost Curve,” January 2009

[4] Bement Dawn and Lisa A. Skumatz: “New Non-Energy Benefits (NEBs) Results in the Commercial/Industrial sectors,” ECEEE 2007 Summer Study Proceedings, pp.1551-1559, June 2007

[5] R. Kuzuki, S. Murakami, et. al.: Improving Sustainability of Building Blocks by Extended Use of Decentralized Combined Heat and Power Systems, Proceedings of the 2008 World Sustainable Building Conference Vol.2, pp.3347-3354, 2008.12

[6] Central Environment Council, Global Environment Committee, Targets Reduction Scenario Subcommittee, Mid-term Report, June 2001

[7] Coalition of Japanese Local Governments for Environment Initiative and the Institute for Environmental Planning Inc., “2008 Local Government White Paper on the Environment,” Coalition of Local Governments for Environment Initiative Secretariat, May 2008

Regional climate and energy strategies: actors, responsibilities, and roles

J. Palm

Department of Thematic Studies – Technology and Social Change,
Linköping University, Linköping, Sweden.
Tel: +46 13285615, Fax: +46 13284461, E-mail: jenny.palm@liu.se

Abstract: Since 2008, the Swedish regional authorities, i.e., the County Administrative Boards (CABs), have been exhorted to produce regional climate and energy strategies indicating how sustainable energy systems might develop in the future. I analyze the CAB role and mandate to coordinate and promote the development of regional climate and energy strategies. How do other regional and local actors perceive the CAB role, mandate, and legitimacy in relation to work on regional climate and energy strategies? Case studies were conducted in two counties where CAB representatives, municipal politicians, municipal climate and energy consultants, and Regional Energy Agency and Regional Cooperation Council representatives were interviewed in-depth.

The results of the interviews indicate that it was difficult for interviewed actors to explain how the tasks and responsibilities differed between the CAB, Regional Energy Agency, and Regional Cooperation Council; the representatives of these three bodies also experienced this difficulty. The CAB's leading role in the energy strategy work was accepted by the other stakeholders, but only because the other regional actors currently lacked the resources to take on such work. In the future, the Regional Cooperation Councils will be the main legitimate CAB competitors, willing to take over the strategic energy work.

Keywords: *regional planning; strategy; accountability; legitimacy, network; planning theory, governance*

1. Introduction

In Sweden, the regional administrative level has generally been weak while the municipalities have been in a strong position. However, since 2008 the Swedish regional authorities, i.e., the County Administrative Boards (CAB), have been exhorted to produce regional climate and energy strategies indicating how sustainable energy systems might develop in the future. In this paper, I will discuss these strategic plans in relation to questions concerning their legitimacy and accountability.

The central government wants to strengthen the role of CABs in developing sustainable energy systems, and accordingly chose to assign them coordination responsibility [1]. The CAB role and tasks were debated by the Committee on Public Sector Responsibilities (Ansvarskommittén). From 2003 to 2008, this Committee was commissioned to analyze the current system of public administration and to determine whether changes were required in the division of responsibilities and in structural arrangements in order to meet the challenges public sector services will face in the future [2]. To remedy these structural deficiencies, the Committee proposed a new regional system of public administration with clearer roles and a clearer division of responsibilities, and regionalization that is the same for the state and the local government sector. As regards regional development, development tasks characterized by self-governance were distinguished from tasks that were more purely a matter of carrying out government agency mandates. Consequently, it was proposed that County Councils be replaced by directly elected regional authorities with overall responsibility for regional development and health and medical care.

The Committee on Public Sector Responsibilities wanted this regional development mandate to be assigned to the newly established regional authorities. At the same time, the CAB tasks and mandate would be concentrated, focusing on central government coordination,

supervision, permits and other legal applications, follow-up, evaluation, and cross-sectoral knowledge creation. The Committee's proposals were, however, not realized. As we will see, their investigation has had consequences for how local and regional actors reason about their responsibility and legitimacy in relation to developing regional energy and climate strategies.

In this context, I will analyze the CAB role and mandate to coordinate and promote the development of regional climate and energy strategies. How do other regional and local actors perceive the CAB role, mandate, and legitimacy in relation to work on regional climate and energy strategies? Over the past decade, several public actors in the regional arena have wanted to take responsibility for regional energy issues. These include the Regional Cooperation Council, organized by the municipalities in a county, which wants to assume overall responsibility for regional development. In addition, more regions have acquired a Regional Energy Agency with a regional focus on energy issues. Then we have local officials and politicians who want to keep their power of self-government on these issues. This paper will examine four actors: municipal politicians, municipal climate and energy consultants, Regional Energy Agencies, and Regional Cooperation Councils. I am interested in how these actors perceive the division of issues and responsibilities between actors at the regional administrative level in the energy system.

1.1. Methodology and material

Two case studies were conducted in two counties, Dalarna and Östergötland, where I interviewed regional and local actors concerned with the CABs' ongoing work on regional climate and energy strategy.

I interviewed one CAB representative in Östergötland and two in Dalarna. The CABs are state-controlled regional authorities that, among other tasks, are commissioned by the central government to develop regional climate and energy strategies.

In Dalarna, I also interviewed one representative of the Regional Energy Agency (REA). REAs are financed by the Swedish Energy Agency, EU, CABs, and Regional Cooperation Councils. They are commissioned to promote energy efficiency and the use of renewable energy sources.

The Regional Cooperation Councils (RCCs), mentioned above, handle regional cooperation between the municipalities in a county and the County Council (landstinget). RCCs are a politically controlled municipal interest organization commissioned to support the municipalities and facilitate cooperation and coordination between them. I interviewed one RCC representative from Östergötland and one from Dalarna.

I also interviewed nine municipal climate and energy consultants from Östergötland and five from Dalarna. They provide municipal energy guidance, disseminating objective knowledge of environmentally friendly energy sources, energy distribution, and energy use. We also interviewed six municipal politicians from Östergötland and five from Dalarna. Altogether, 31 interviews were conducted.

Interviews were used to gain an understanding of actor perceptions of the process and outcomes of developing regional energy strategies. I am interested in the background stories of and in-depth information on participants' experiences of this process. In the analysis, I compare the actors' descriptions of the process and search for patterns. While quantitative data concern differences in degree of aspects of a studied entity, qualitative data concern

similarities or dissimilarities between studied entities. Interview analysis is descriptive, and aims to go beyond merely describing the responses to the interview questions. The analysis entails the researcher, through reflection, abstracting from the descriptions and seeking patterns and dysfunctions in light of earlier studies or theories [3]. Taking the particular conclusions relating to Östergötland and Dalarna and generalizing them to other regions is not of interest; what is of general interest is analysing the actors' roles, responsibilities, legitimacy, and inclusion in and exclusion from the process. In other words, analytical generalization is of interest here, not statistical generalization [3].

2. Regional strategic planning: legitimacy and responsibility

Swedish CABs have been commissioned to develop regional climate and energy *strategies*. The meaning of *strategic planning* is an empirical question, and depends on what efforts particular actors put into it. Healey [4] emphasizes that strategic work aims to change the direction of an activity (in this case, a technical system), open up new possibilities and potentials, and move away from previous positions. These strategies are social products embedded in the governance cultures of particular regions [4,5]. A regional strategy functions by articulating an orientation shared by many stakeholders in a regional development process. Because strategies are social products formed in networks within governance structures, questions concerning legitimacy and accountability are vital for working strategies that influence the direction of regional energy systems.

According to CAB budget documents, regional sustainable energy systems are to be developed by creating arenas and processes where regional actors can meet and develop common strategies and goals. Such processes are often collectively labelled governance. Theories of governance often draw attention to how and why actors that are not part of the political sphere participate in forming politics in the broad sense, and to how new arenas and coordination forms are created and used [6,7].

Democratic legitimacy concerns how the governed are interested in and understand political legitimacy. A policy is seen as legitimate by concerned actors if there is principal consent, i.e., if concerned parties think the policy is legitimate and if they agree on norms and values. Legitimacy can also be conferred by active consent, referring to acts indicating approval, such as actor participation in projects, reference groups, etc., initiated by the actors seeking legitimacy [8].

In a government context, accountability is generally regarded as a chain extending from the electorate to the elected politicians and from the politicians to the public administration. The new localism and complexity of governance structures make accountability intertwined and multiple [9], imbuing it with new meanings. The role of government then changes: it becomes just one player among many [10]. Governance structures have developed in response to the state's increased need to mobilize actors, and their resources, outside their formal contexts to formulate and implement public policy [11].

Mitchell and Shortell [12] argue that accountability is "defined as a process by which a party justifies its actions and policies and is a key aspect of governance". The increasing complexity of governance through partnership permits a broader understanding of accountability, including bureaucratic/hierarchical, legal, professional, political, and moral/ethical dimensions [13].

In developing sustainable energy systems, CABs have been commissioned to establish strategic planning initiatives at the regional level. In practice, this means that they are responsible for promoting the issue; they should not do everything on their own, but work in cooperation with other actors. I will next discuss how this is done in practice.

3. Dalarna and Östergötland counties work on regional climate and energy strategies

Dalarna is often portrayed as a pioneer in regional energy work. Even before the government's 2008 budget document, it had worked to coordinate regional actors to deal with various energy issues. A regional energy programme had been developed from 2004 to 2005, "Energy Intelligent Dalarna – programme for regional energy coordination",[1] in which representatives of municipalities, industries, and organizations in the region participated. Dalarna's first climate and energy strategy was completed in October 2008. The strategy is supposed to integrate visions and goals from Energy Intelligent Dalarna and provide a common overview of the entire region [14].

Östergötland's climate and energy strategy was developed in 2008, also in consultation with external stakeholders. In Östergötland, a special advisory group was formed, including the CAB, RCC, and the County Council, which met several times [15].

3.1. Actor perceptions of roles, tasks, and responsibilities

The representatives of the CABs of both Östergötland and Dalarna said that they were happy that the CABs had been responsible for working on the climate and energy strategies, saying that the work was in line with the CABs' long-standing commitment to environmental issues. The Östergötland representative offered one reason why the CABs had been assigned this task:

> The CABs are the outstretched arm of the state in the regions, so that it is not so surprising, really. And the CABs have a coordination function in other contexts, too, and also in this cross-sectoral work.

Another option would be to allow the RCCs to coordinate regional energy planning. One representative of the Dalarna CAB, however, said that it could be difficult for the government to give an assignment to an RCC, which is funded by and works on behalf of the county's municipalities. If the state wanted to commission the RCCs to develop regional planning, it would also need to fund the assignment; that was not necessary when the assignment went to the CABs.

It can generally be concluded that the vast majority of interviewees were aware that their CAB had worked on a climate and energy strategy. However, the actors had difficulties specifying what the CAB had worked on more exactly or the objectives associated with the strategy. The answers were more general, the CAB's work being described thus: "they should take a holistic approach", "review the region's energy balance", and "work on sustainable development". The Dalarna CAB's work was slightly better known by the regional actors than was the Östergötland CAB's work. The regional actors in Dalarna could more easily cite concrete examples of the content and aims of the Dalarna energy strategy. The participants best remembered matters on which they had worked specifically with the CAB, for example,

[1] EnergiIntelligent Dalarna – program för regional energisamverkan

when the CAB had developed a template text for municipal energy plan, or held a seminar on a specific issue.

A common opinion among the municipal politicians was that the climate and energy strategy would convey the state's views on energy issues. Several also emphasized that the CAB was a *state* rather than a regional actor, and that it acted mainly as a supervisory authority.

3.2. Division of tasks between regional actors

The Östergötland CAB representative said that issues concerning both responsibility and implementation in relation to the strategy's goals and vision were not easy to sort out:

> This is not easy – if one looks at the control, control over the actions, since there are many who must do things.

The CAB representatives from both Östergötland and Dalarna stressed the importance of cooperation and that a diversity of actors, for example, the business community and the university, needed to be coordinated. The Dalarna CAB established a legitimation process in which actors could participate by creating a steering committee that included the county governor, RCC president, and key sector representatives. This committee was a way to create legitimacy and commitment by involving regional actors.

The division of responsibilities between the various regional actors, such as the CABs, RCCs, and REAs, was not very clear to any of the interviewees. One of the municipal climate and energy consultants commented on the difference between the CAB and the REA's GDE-Net:

> No, I don't know. They're the same … I cannot see any distinct difference. (Climate and energy consultant Dalarna, 5)

In addition, a more integrated strategy was asked for at the regional level:

> There are so many players now who work in the same direction. First, there's now the County Administrative Boards in general. Then we have the Environmental Protection Agency, with climate coaching, and then comes the Energy Agency with their 'sustainable municipality' programme. Actually, I think there are too many players. There should probably be just one regional player. (Climate and energy consultant Dalarna, 1)

3.3. The difference between the CAB and the RCC

The two regional players that were the biggest competitors in formulating and developing regional climate and energy strategies were the CAB and the RCC. According to the representative of Dalarna's RCC, the difference between the RCC and the CAB was that the CAB was a "clearly defined authority"; the RCC, on the other hand, "takes responsibility for regional development" in general, which is similar to the arguments of the Committee of Public Sector Responsibilities.

The representative of Östergötland's RCC Östsam said that the difference between the CAB and the RCC was unclear, but that they dealt with this periodically by recurring negotiations:

> It is never clear who is doing what, but the point is that you need to talk to each other and inform each other of what you are doing at the moment. And sometimes we can engage them in our activities and vice versa. But it isn't anything cast in stone, where you can say that this is the CAB's task and that is Östsam's. It may evolve over time, but now it's more that people talk to one another.

The municipal politicians discussed the problem of having two regional players, both driving the energy issue:

> Yes, I'm one of those who may feel that, as it is today, it has become a little bit like parallel actors, with both Östsam and the County Administrative Board. And it has become a kind of dual control, which I find a bit unnecessary. (Municipal politician Östergötland, 1)

The politicians would like to see the roles streamlined, and said that the CAB's role should be to monitor issues, and that a different kind of regional player should be responsible for regional development.

The RCC representatives from both Dalarna and Östergötland wanted to run the climate and energy strategy in the future, as this was seen as an important development issue for the Council. Even the elected municipal politicians advocated an increased role for the RCCs. In Östergötland, all the politicians wanted the CABs to be mainly regulatory in function in the future, and wanted Östsam to be solely responsible for regional development. The same was true in Dalarna, but here the politicians wanted to see a clearer distinction between supervision and development in the long run.

Dalarna's RCC representative felt that energy was an important development issue for which they should be responsible; that, however, would require that the Council receive additional resources. In the current situation, the RCC lacked sufficient resources, and until the financial situation was resolved, the representative thought it was positive that the CAB was responsible for developing a regional energy strategy.

Östsam would like to see a trend towards greater responsibility being transferred to the RCC, and would like to see this transfer start immediately.

4. Conclusions

By means of a government directive in the 2008 budget document, the state indicated that regional energy strategic planning was important. The CAB's mission was made clear, and the CABs in Dalarna and Östergötland have taken initiatives to develop common goals, visions, and strategies in the regions.

In the current situation, the CAB has no real "competitor" in either Dalarna or Östergötland. In the future, it is primarily the RCCs that might compete with the CABs and would like to assume responsibility for energy strategy work. Both the RCCs and leading local politicians identified the RCC as the party that should handle this strategic work. This is because local politicians and RCCs would like to see development handled in line with the recommendations of the Committee on Public Sector Responsibilities, according to which

CAB activities are limited to control issues and the RCCs would be responsible for regional development. This division of responsibilities can only be realized in the future due to the current lack of resources for RCCs. This lack also means that local politicians will continue to accept the CABs' current work and role until viable alternatives are available.

The roles of these actors, including the REA, are unclear. It was difficult for the interviewed actors to clarify their tasks and responsibilities. The representatives of the RCCs and CABs said that they divided tasks and responsibilities through ongoing dialogue with each other. When a question entered the agenda, they simply contacted each other to see how the issue could best be handled and by whom. This pragmatic system, however, is not very transparent to the actors excluded from the informal dialogue. With such an informal system, it is unclear how decisions are made and for what reasons, or who is accountable for a given decision. In addition, issues can fall through the cracks when no one is explicitly responsible for them.

Other issues raised are what will happen when the climate and energy strategies are to be acted on and the goals implemented. What legitimacy does a CAB strategy have in a county? Will it be just another document, among others, that the municipalities must take into account, and that will disappear among all the other documents? Assuming that a strategy reaches out to stakeholders, the problem of putting the goals and measures into practice remains. Another obstacle is that a CAB strategy may lack legitimacy and only be accepted because of lack of alternatives. The municipalities would like to see other agencies develop and implement regional goals and visions; it is too early to say what significance this might have for implementation, but it is an obvious hindrance and threat to united action in a region.

Local politicians are involved in the RCCs, which gives the Councils legitimacy and direct access to the municipal decision-making processes. In a situation of competition regarding future policies, CAB strategies will probably not attract support, because CABs are perceived as representatives of the central government rather than the regions. The RCCs, on the other hand, are working to create regional identities from below and represent local interests and not the state, which will benefit them in any future competition.

Acknowledgements
The research for this paper forms part of the research programme, Energy Choices in Households: A Platform for Change. This research was funded by the Swedish Energy Agency.

References

[1] Governmental Bill 2008/09:1, Budgetpropositionen.

[2] SOU 2007:13 (Swedish Government Official Reports), Regional utveckling och regional samhällsorganisation.

[3] R.K. Yin, Case Study Research: Design and Methods, Studentlitteratur, 1994.

[4] P. Healey, In search of the "strategic" in spatial strategy making, Planning Theory & Practice 10, 2009, pp. 439–457.

[5] L. Albrechts, Strategic (spatial) planning reexamined, Environment and Planning B: Planning and Design 31, 2004, pp. 743–758.

[6] J. Pierre, Debating Governance: Authority, steering and democracy, OUP, 2000.

[7] P.A. Sabatier & H. Jenkins-Smith, Policy Change and Learning: An Advocacy Coalition Approach, Westview Press, 1993.

[8] J. Johannsson, Regionförsök och demokrati: Demokratisk legitimitet och regionalt utvecklingsarbete i Skåne och Västra Götaland, Forskning i Halmstad no. 10, Högskolan i Halmstad, 2005.

[9] G. Stoker, 2004, New localism, progressive politics and democracy, The Political Quarterly 75, pp. 117–129.

[10] J. Pierre & G. Peters, Governance, Politics and the State, Macmillan, 2000.

[11] M. Considine, Making Public Policy, Polity Press, 2005.

[12] S. Mitchell & S. Shortell, The governance and management of effective community health partnerships: A typology for research, policy and practice, The Milbank Quarterly 78, 2000, pp. 241–289.

[13] L. Dicke & S. Ott, Public agency accountability in human services contracting, Public Productivity & Management Review 22, 1999, pp. 502–516.

[14] Länsstyrelsen Dalarna, Klimat- och energistrategi för Dalarna, version 1, October 2008.

[15] Länsstyrelsen Östergötland (2008), Ett vinnande klimat: Klimat- och energistrategi för Östergötland.

Wave Power Resource in Iran for Electrical Power Generation

Jawad Faiz[1,*], M. Ebrahimi-salari[2]

[1] *Center of Excellence on Applied Electromagnetic Systems, School of Electrical and Computer Engineering University of Tehran*
[2] *Young Researchers Club, Islamic Azad University, Najafabad Branch, Isfahan, Iran*
** Corresponding author. Tel: +98 21 61114223, Fax: +28 21 88633029, E-mail: jfaiz@ut.ac.ir*

Abstract: This paper presents the physics of ocean waves and its governing mathematical equations. The potentials of the Seas in Iran for wave's energy conversion into electrical energy using linear permanent magnet generators are discussed. The characteristics of the Seas and the useable regions for wave energy conversion are recognized. Finally economics of this energy conversion is analyzed.

Keywords: *Wave Energy, Electrical Power Generation, Iran*

1. Introduction

Direct-driven linear permanent magnet generator (LPMG) is a wave energy converter which has a simple structure, easy fixing, low volume, high efficiency and capability of converting the calm waves into electrical energy [1-4]. Falnes [5] introduced several theories for direct wave energy conversion systems and studied different forms of buoys for such energy extraction. LPMG consists of a movable and a fixed part. The magnetic field of the generators is provided by permanent magnet fixed on the moving piston. As shown in Fig. 1, the generator is fixed at the bottom of the sea and its piston is connected to a buoy on the sea level by a rope. The waves move the shaft, induce voltage in the armature windings and it is rectified and transmitted to the coasts by underwater cables.

Different techniques for converting wave's energy into electrical energy are categorized into three parts based on the distance from the shore as 1) shoreline, 2) near shore and 3) offshore. The shoreline systems have advantages such as easy fixing and low maintenance and they do not need very deep water or underwater cables; however, their generated power are too low because of low energy of the waves approaching the shore. Therefore, it is sometimes non-economical to install such system for wave energy conversion. The offshore systems enable to convert more wave's energy due to the stronger waves in the deeper water. LPMGs are considered as offshore devices which must be installed deeper than 15 m in order to gain an optimal efficiency. The existing wave energy depends directly on the wave height and its time period. One of the most important stages in the design, simulation and analysis of LPMG is the wave characteristic and modeling for the region in which the generator is fixed.

This paper considers the physics of the ocean waves and their stored energy. Characteristics of the seas in Iran are investigated. The attempt is made to recognize the regions in which the use of LPMG is suitable based on the sea depth, distance from shore and waves height. Also these characteristics can be included in the process of the design of LPMG. Finally, economics of the wave energy conversion is studied and compared with other forms of renewable energies.

2. Ocean Waves Energy

The total waves energy in the world coasts is estimated to be 10^6 MW and if only 2% of this energy is extracted it can supply the total world energy demand [1]. Generally ocean waves are categorized into wind-sea and swell waves. The wind-sea is used for the waves that generated

by the local winds, and waves move in the direction of these winds. The waves with long period generated in the stormy regions are called swell waves. The swell waves with very low energy losses spread from coast to coast. The typical wave length of swell waves, particularly in deep water, is 100-500 m, while the wind-seas are few meters up to 500 m depending on the wind velocity. In the installing LPMG in the deep water those waves are taken into account that has the depth larger than a half wave length **[5]**. In the deep water, the bottom of sea has no noticeable influence on the waves and their effects are ignored. Normally at a specific time, many waves' pulses are generated over offshore in different directions and periods. Wind-sea and swell may present simultaneously. A real ocean wave consists of the waves with different frequencies and directions. The mean stored energy in the unit area of the sea surface is as follows [1-13]:

$$E = \rho g H_{m0}^2 /16 = \rho g \int_0^\infty S(f)\, df \tag{1}$$

where ρ=1030 kg/m^3 is the sea water density, H_{m0} is the water height in the natural case and g=9.81 m/s^2.This stored energy is equally divided into the kinetic and potential energies. In (1), $S(f)$ is the wave spectrum in m^2/Hz. Integration of $S(f)$ shows the effects of frequencies of different waves upon the waves energy. In practice, (1) is substituted by sum of the limited number of waves frequencies. For sinusoidal waves having amplitude of 0.5H (H is the height of the wave, vertical distance between the lowest and highest points of the wave) H_{m0} is substituted by $H\sqrt{2}$ in (1) to calculate E. The approximate natural wave of $S(f)$ is defined using Fourier analysis by measuring the wave at a given time. To obtain the long-term statistics, measurement and analysis are taken every three year. For growth wind seas, the empirical Prison-Moskowitz spectrum agrees well with the practical spectra and calculated as follows:

$$S(f) = (A/f^5)\exp(-B/f^4) \tag{2}$$

where $A=BH_{m0}^2/4=0.0005m^2Hz^4$, $B=(5/4)f_P^4=0.74g^4/(2\pi U)^4$. $f_P=1/T_P$ is the peak frequency and U is the mean velocity of the wind at height of 15 m above the sea level. For a low reaction between the wind and sea level, the use of JONSWAP spectrum is more common; the band width of this spectrum is narrower than that of the Prison-Moskowitz spectrum. The torque of j-order wave moment is $m_j = \int_0^\infty f^j S(f) df$. Therefore, the significant wave may be defined versus 0-order torque spectrum as $H_{m0}=4\sqrt{m_0}$. To simplify the investigation it is assumed that the wave is propagated in x direction. For a sinusoidal wave with frequency f, the energy of the wave is transferred with velocity c_g (group velocity). The wave power level, defined as transferred energy over every unit width of the propagating front wave, is equal to $J=c_gE=c_g\rho gH^2/8$. For real sea waves, the level of wave power versus wave spectrum is:

$$J = \rho g \int_0^\infty c_g(f)\, S(f)\, df = \rho g^2 m_{-1}/4\pi = \rho g^2 T_J\, H_{m0}^2/16 \tag{3}$$

Eqn. (1) is true in deep water, where $c_g=gT/4\pi=g/4\pi f$ and energy period as $T_J=T_{-1,0}=m_{-1}/m_0$. The level of the wave power can be estimated by integrating the power density flow: $J=\int I(z)dz$ in z direction (direction of water flow). The peak wave power density is as follows:

$$I(0) = 2\pi \rho g m_1 = (\frac{\pi}{8})\rho g H_{m0}^2 / T_{0,1} \tag{4}$$

under water level z=0, the wave power density has its maximum value and it is more decreased by moving lower sea level. For perfectly growth wind-seas, we have the following based on Prison-Moskowitz spectrum:

$$I(0) = 0.0325\rho g^{3/2} H_{m0}^{3/2} = 5I_{wind} \tag{5}$$

where I_{wind} is the peak wind energy. For a sinusoidal wave in deep water, H_{m0} is substituted by $H\sqrt{2}$, T_J and $T_{1,0}$ by T in (4) and (5). The power density varies proportional with z. $I(z)=I(0)\ exp(2kz)$ where $k=2\pi/\lambda$ is the wave number, and $\lambda=gT^2/2\pi=(1.56m/s^2)T^2$ is the wave length. 96% of J is calculated from integrating between $z=-\lambda/4$ and 0. Decreasing water depth means approaching the wave near shore. In this case wave length reduces uniformly. However, c_g rises 20% compared with the deep waters. Value of $c_{g\ is}$ decreased by reduction of h and it nearly diminishes when approaches the shore (zero wave energy). In the shoreline, the wave energy is used to overcome the friction between the waves and shore bottom and depth-induced braking force.

In latitude of 40-50 degrees, the average annual wave's power levels in off-shore water are between 30 and 100 kW/m. The low power level waters are mostly in the north and south. In most equatorial waters, the average wave power level is lower than 20 kW/m. The offshore wave power levels are between kW/m up to MW/m (in the case of variable storm). Finally, a general equation for estimation of the stored energy in the real sea waves, propagated in different directions, is as follows:

$$E = \rho g H_{m0}^2 / 16 = \rho g \int_0^{\infty} \int_{\beta_1}^{\beta_2} S(f,\beta)\, df\, d\beta \tag{6}$$

where $S(f, \beta)$ is the oriented energy spectrum, and β is the propagation angle in respect to x-axis. The transferred power density from the waves to a floating cylinder with diameter equal to 1 m and normal (vertical) path in θ direction is as follows:

$$J_\theta = (\rho g^2 / 4\pi) \int_0^{\infty} \int_{\beta 1}^{\beta 2} f^{-1} S(f,\beta) \cos(\beta - \theta) df\, d\beta \tag{7}$$

For sinusoidal waves in deep waters, the transferred power density from the waves to 1 m diameter floating cylinder and its wave length are as follows;

$$J = \rho g^2 T H^2 / (32\pi) \quad W/m \tag{8}$$

$$J_\theta = (\rho g^2 / 4\pi) \int_0^{\infty} \int_{\beta 1}^{\beta 2} f^{-1} S(f,\beta) \cos(\beta - \theta) df d\beta \quad W/m \tag{9}$$

3. Characteristics of Sea Waves in Iran

3.1. Persian Gulf

Persian Gulf is situated between the north attitude of 25 and 32 degrees and between east attitude 49 and 56 degrees. The Persian Gulf area is about 850 km^2 which has been connected to the Oman Sea by the Hormoz Channel. The depth of the Persian Gulf increases from north-west to south-east and reaches to 100 m and lower depth in the Hormoz Channel. The water depth in Khozestan and Saudi-Arabia shores is very low and at most 10 m along tens km of the shores; while in the east of Khozestan, particularly in Kangan Port up to Gheshm Island,

the average depth is larger. The average depth of the Persian Gulf is basically about 40 to 50 m and is lower toward to the shores. There are sometimes high depth in the shores (around 40 m) which are small and a limited number of cavities and they cannot be considered as the real depth of the shore. The common depth in the shores is 18 to 29 m. So the Persian Gulf shores are generally flat and at the same time the deeper shores are in the north of the Persian Gulf [14, 15].

Fig. 2 exhibits the Persian Gulf map [16]. It shows that the depth of water over tens km of the shore is not larger than 10 m, this is the reason that most parts are not suitable for installing LPMGs. Because, the regions deeper than 15 m are very far from the shore and this increases the energy transmitting cost to shore. Also due to the limitation of deep areas in Persian Gulf, most of these areas are used as path for passing the large ships. However, in Asaloyeh, Gavbandi and particularly Hormoz Channel the deep regions are closer to the shore and suitable for installing the generators.

Fig. 3 shows the waves height in the Persian Gulf during 100-year period [17]. The stored energy in the waves has a direct relationship with the wave height. As indicated in Fig. 3, the waves height in areas close to the shores of Iran are higher than other points. According to Fig. 3, the west regions of the Persian Gulf up to the Gheshm Island and particularly Hormoz Channel with wave height of 4.5-5 m, up to 5 km of the shore are suitable regions for installing LPMGs. Considering sinusoidal waves with period of 4 s, the peak energy of the waves in these regions is estimated by (4), which is between 79.74 and 98.44 kW/m.

3.2. Oman Sea

Oman Sea is part of the Indian Ocean and is only open Sea of Iran. Persian Gulf in connected to Oman Sea via Hormoz Channel. The tropic of cancer passes the north of Oman Sea. It is one of the warmest seas on the south-west of Asia. The minimum water temperature in August is 33 and minimum in January 20 degrees. The area of the Oman Sea is 903 square km. This Sea is deeper than Persian Gulf particularly in the shores of Iran. Its depth around Chabahar Port is around 3380 m. There are many notches in the Oman Sea forming small Gulfs locally such as Chabahar Gulf and Govatr Gulf. However, most of these small Gulfs have low depth and they are not useable for large ships because their shores are sandy For this purpose, it is necessary to establish docks [14, 16]. Fig. 4 exhibits the map of Oman Sea [17]; which includes the depth of the Sea in different regions. Fig. 5 shows the peak height of the wave in the Oman Sea over 100-year

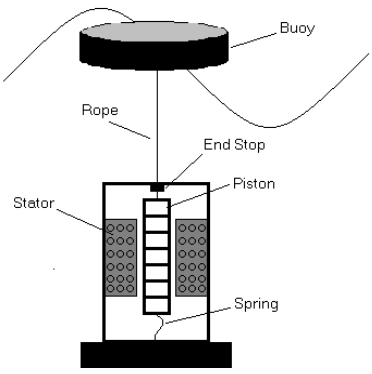

Fig.1. Direct wave energy conversion system

Fig. 2. Map of Persian Gulf

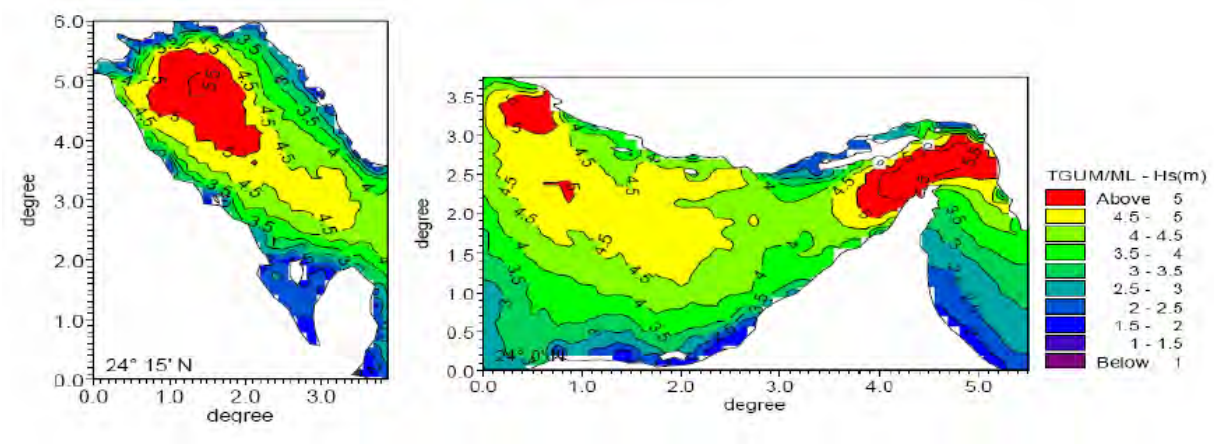

Fig. 3. Peak waves energy in Persian Gulf in 100-year period [17].

period [17]. In this Sea the deep areas (deeper than 15 m) are closer to the shores. However, the peak height of the waves is lower than that of the Persian Gulf and is between 3 and 4 m.

Considering sinusoidal waves with period of 4 s , the peak energy of the waves in these regions based on (9) is estimated between 35.44 and 63 kW/m. The advantages of deeper Sea close the shores are that the cost of transmitting the generated electrical power to the shores is lower. Finally most of the shores particularly Chabahar shores are suitable to install LPMGs.

3.3. Caspian Sea

Caspian Sea in the north of Iran has 424000 km^2 area and is the largest lake of the earth and that is why it is called the Sea. This is the largest remaining portion of the ancient Sea of Tetis which extended from the North Pole to Indian Ocean in the 1st to 3rd geology ancient time. The depth of the Caspian Sea in the north region is very low and about its 4/5 area has lower than 10 m depth. The peak depth of this Sea in the north is 15 m and in the south is 1000 m. The average depth of this Sea is 325 m. Basically, Caspian Sea is not a calm Sea. It is in the path of the air flow in many days of the year and is wavy. The waves created by the north which extended from the North Pole to Indian Ocean in the 1st to 3rd geology ancient time.

Fig. 4. Map of Oman Sea [16].

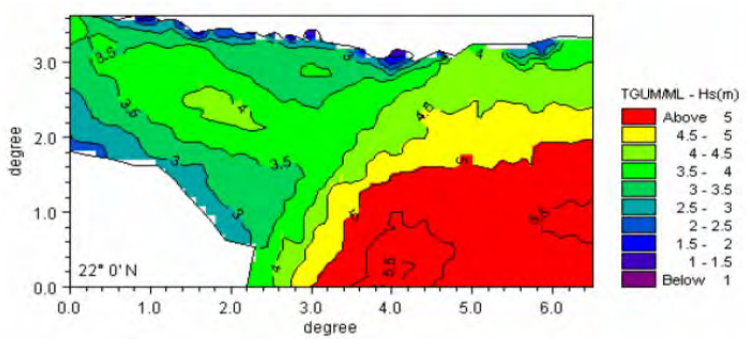

Fig. 5. Peak height of the wave in the Oman Sea over 100 years period [17]

The depth of the Caspian Sea in the north region is very low and about its 4/5 area has lower than 10 m depth. The peak depth of this Sea in the north is 15 m and in the south is 1000 m.The average depth of this Sea is 325 m. Basically, Caspian Sea is not a calm Sea. It is in the path of the air flow in many days of the year and is wavy. The waves created by the north winds often have 25 m/s velocity, 11 to 12 m height and 200 m wave length. The major part of these waves is formed by these waves. The frequency of the waves is larger in the west and middle parts and therefore these parts are more non-calm compared with other parts [18, 19]. This wavy Sea has large potential for waves energy conversion. Fig. 6 and Fig. 7 show the Caspian Sea map and the peak height of the waves in 100-year period respectively [16, 17]. Referring to Fig. 7, the height of the waves particularly close to the shores in Iran is very large which indicates the large potential of this Sea for converting the waves energy into electrical energy. In Caspian Sea the regions with high wave height and depth larger than 15 m are close to the shore and their distances to the shore are less than 5 km. This feature reduces the cost of electrical energy transmission. Considering sinusoidal waves with period of 5 s, the peak energy of the waves in these regions is estimated between 123 and 315 W/m by (9).

4. IV. Economics of Wave Energy Conversion

To estimate the economics of the available renewable energy conversion the following merit index has been defined:

$$\alpha = \frac{P_{ave}}{P_r} = \frac{W}{8760 P_r} \tag{10}$$

where α is the merit index, P_r is the rated power, P_{ave} is the mean developed power in kW, W

Fig. 6. Caspian Sea map

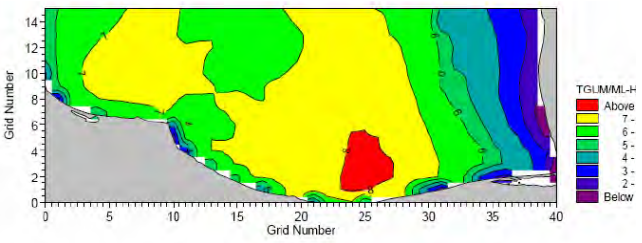

Fig. 7. Peak height of the wave in the south of

Caspian Sea over 100 years period

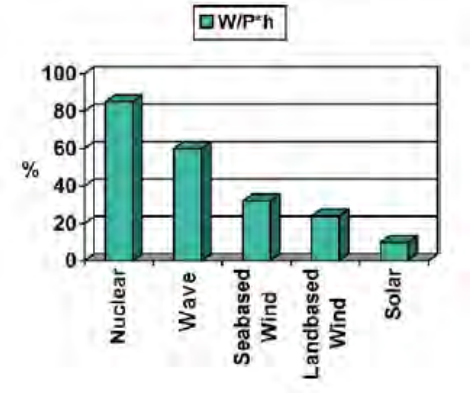

Fig. 8. Merit index for different types of renewable energies [20].

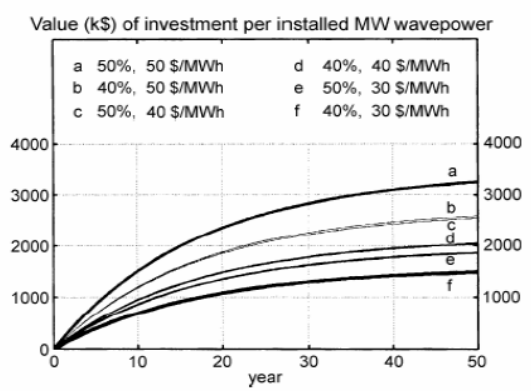

Fig. 9. Value of investment per installed MW wave power for different values of the utility factor and electricity price [20]

is the generated energy over one year in *kWh* and 8760 is total hours of the year [20]. Fig. 8 shows the merit index for different renewable energy systems. It shows that the waves energy has 60% merit index and places in the second rank after the nuclear energy. The wave energy is superior to the wind energy from generation time period and generation level points of view. The wave's energy is damped very calmer than that of the wind energy. Also the peak power density of wave under the sea level is 5 times of $I_{wind}=(\rho_{air}/2)U^3$ at 19.5 m above the Sea level. For wave energy density of 3.2 kW/m^2 and the mean wind velocity of U=10 m/s, the wind power density at 19.5 m above the Sea level is 0.6 kW/m^2 [14]. Fig. 9 shows that the investment for converting the waves energy into electrical energy is 40-50 $/MWh [20] where 3 $/MWh is for the maintenance. Of course direct conversion systems have not been included in this table. If direct conversion system is used a lower investment is required.

5. Conclusion

Physics of Seas waves and their governing equations were studied and then conditions of these Seas for wave's energy conversion into electrical energy were investigated. Persian Gulf is not suitable to install LPMGs due to its very low depth and its deep regions are far from the shore. The Oman Sea is deep and the deep areas are close to the shores and it is capable to generate electrical energy from the wave's energy using LPMGs. The Caspian Sea is wavy due to the path of the air flows in many days of the year and the height of the waves approaches 12 m and its wave length is very long. Also the depth of water in the south and west sides in Iran is high, therefore Caspian Sea has more potential to convert the waves energy into electrical energy using LPMGs. In order to include the characteristics of the Seas in Iran in simulation and design of LPMGs, it is necessary to have data about the wind velocity, average height of annual waves, and average wave length and time period of the waves. The mentioned data are required to use equations in section 2 of the paper and estimate the power level of these waves and design the generator suitable for this power level.

References

[1] K. Rhinefrank, et. al., Novel ocean energy permanent magnet linear generator buoy, Journal of Renewable Energy, vol. 31, 2006, pp. 1279-1298.

[2] Y. Masuda, An experience of wave power generator through tests and improvement, IUTAM Symposium on Hydrodynamics of w ave energy devices- Lisbon, Portugal, Springer Verlag, Berlin,1985, pp.1-6.

[3] N.N. Panicker, Power resource potential of ocean surface waves, Workshop of the wave and salinity gradient, Newark, Delaware, USA, 1976, pp. J1-J48.

[4] H. Polinder , M. Scuotto, Wave energy converters and their impact on power system, International Conf. on Future power systems, vol. 18, Nov. 2005, pp.9-11.

[5] J. Falnes, A review of wave-energy extraction, Journal of Marin Structures, vol. 20, no. 4, Oct. 2007, pp. 185-201.

[6] L. J. Duckers, Wave energy; crests and troughs, Renewable Energy, vol. 5, no. 2 , 1994, pp. 1444 – 1452.

[7] J. Falnes and J. Lovstedt, Ocean wave energy" Energy Policy, vol. 19, no. 8, 1991, pp. 768 – 775.

[8] H. Bernhoff, E. Sjöstedt, and M. Leijon, Wave energy resources in sheltered sea areas: A case study of the Baltic Sea, Renewable Energy, vol. 31, no. 13, 2006, pp. 2164–2170.

[9] D. Ross, Power from the Waves, Oxford University Press, 1995.

[10] I. Glendenning, Ocean wave power, Applied Energy, vol. 3, no. 3, July 1977, pp. 197–222.

[11] T.T. Janssen, J.A. Battjes, A note on w ave energy dissipation over steep beaches, Coastal Engineering, vol. 54, no. 9, Sep. 2007, pp. 711–716.

[12] D. Mollison, Wave climate and the wave power resource, - IUTAM Symposium on Hydrodynamics of wave energy devices- Lisbon, Portugal, Heidelberg: Springer-Verlag, 1986, pp. 133–56.

[13] J. Falnes, Radiation impedance matrix and optimum power absorption for interacting oscillators in surface Waves, Appl. Ocean Res., vol. 2, no. 2, 1980, pp. 75–80.

[14] M.B. Zomorodian, Geomorphology of Iran, Ferdowsi University of Mashad, Press, 3rd Ed., 2007.

[15] A. Faraji, A complete Geography of Iran, Iran Printing and Publishing Publisher, 1st Ed., 1988.

[16] Microsoft Encarta Reference Library Premium 2005, available in www.Encarta.com.

[17] Iran Ports and Ship Organization, Modeling of Waves in Iran, WWW.pso.ir.

[18] L. Mafkham Payan, Caspian Sea, Hedayat Publishers, 1998.

[19] A. Barimani, Mazandaran Sea, University of Tehran Press, 1977.

[20] M. Leijon, H. Bernhoff, M. Berg, and O. Agren, Economical considerations of renewable electric energy production—especially wave energy, Journal of Renewable Energy, vol. 28, no.8, July 2003, pp. 1201–1209.

Effects of environmental taxation on district heat production structures

Leif Gustavsson[1,2], Nguyen Le Truong[2], Ambrose Dodoo[2,*], Roger Sathre[2]

[1] *Linnaeus University, 35195 Växjö, Sweden*
[2] *Mid Sweden University, 83125 Östersund, Sweden*
** Corresponding author. Tel: +46 63165383, Fax: +46 63165500, E-mail: ambrose.dodoo@miun.se*

Abstract: In this study, we explore how different environmental taxation regimes influence the design of cost-optimal district heat production systems and the primary energy use for district heat production. Our calculations are based on the heat load duration curve of a district heat production system in Östersund, Sweden. Using the system's measured daily district heat load curve from 1st May 2008 to 30th April 2009, we model four cost-optimal district heat production systems based on four environmental taxation scenarios. The design of the district heat production under the different taxation scenarios is based on expected utilization time and on the production units which give the lowest heat production cost. We find that primary energy use varies strongly when different technologies and fuels are used under the different environmental taxation scenarios. However environmental taxation has a minimal effect on district heat production cost for optimally designed district heat production systems. Fossil fuels become less competitive as the environmental taxation increases. However, light fuel oil boiler for the peak load production remains viable due to low utilization time and investment cost.

Keywords: *District heat production, CHP, Boilers, Fossil fuel, Biofuel, Environmental tax, Primary energy, Cost*

1. Introduction

Energy security and the impact of energy systems on the global climate are important energy policy concerns in the European Union, including in Sweden. Several strategies can be used to address these concerns, including promotion of more efficient energy production technologies, and conversion to renewable and low carbon fuels. District heating based on combined heat and power (CHP) production is primary energy efficient [1], and can use biomass-based fuels.

In Sweden, district heating with CHP is increasingly common, and is the main source of heat for multi-story residential and non-residential buildings [2]. In 2008, district heating accounted for 50% (about 50TWh) of the total space and tap water heating [3]. The energy input for the Swedish district heat production is dominated by biomass, which accounted for 48% of total input in 2008 [4]. The Swedish government energy policy aims at further increasing the share of biomass. Policy instruments to realize this include environmental taxes on fuels, tradable green electricity certificates (GEC) and obligated quota mechanism of GEC for customers [2].

The utilization time of district-heat production units varies and is very small for the units that cover peak-load demand. Therefore, the investment costs of these units are much more important than the operation costs. Low investment fossil fuel-based technologies are often used even though they are associated with higher external cost. Environmental taxation can be an important policy instrument to restructure district heating systems into more sustainable form. Such policy instrument may influence the choice of technologies and fuels for district heat production units.

In this study we explore how different environmental taxation regimes influence district heat production structures. We investigate the choice of production units and fuels for cost-optimal district heat production for the different environmental taxation scenarios, and calculate the primary energy use and the cost of district heat production.

2. Method and assumptions

Our analysis is based on the measured daily district heat load curve of a district heat production system in Östersund, Sweden from 1st May 2008 to 30th April 2009. Figure 1 shows the measured heat load of the production system during this period, arranged in descending order. During this 12 month period, the output of the production system was 210 GWh electricity and 612 GWh heat. Based on the district heat load curve, we model four cost-optimal district heat production systems based on four environmental taxation scenarios. Figure 2 presents a schematic diagram of the study.

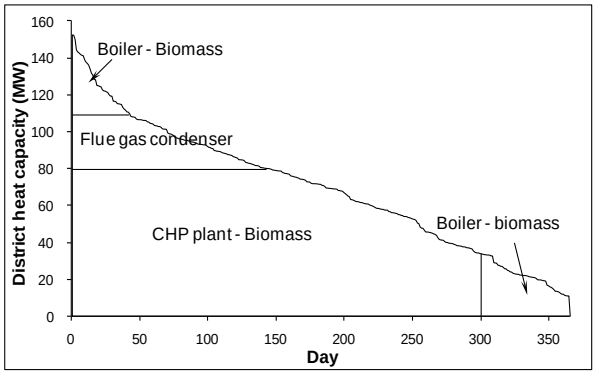

Fig. 1. Reference heat load duration curve

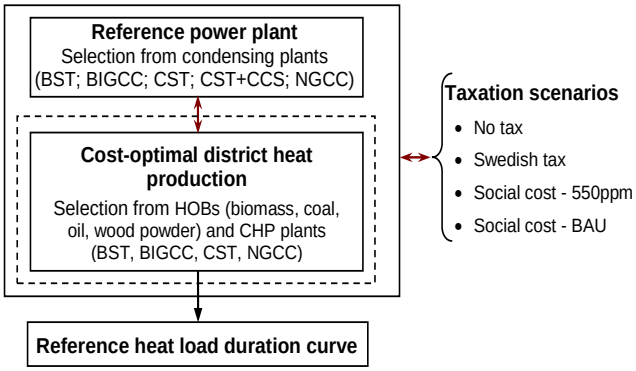

Fig. 2. Schematic diagram of the analysis

We use four environmental taxations scenarios to explore their effect on the structure of district heat production. The taxations scenarios are: (i) the *No tax* scenario with the year 2008 Swedish price of fuels with zero taxes; (ii) the *Swedish tax* scenario with the year 2008 Swedish prices and taxes on fuels, comprising of a carbon tax of €386/t CO_2 for emissions related to non-electricity production, an energy tax that varies for different fossil fuels used for non-electricity production, and an average green electricity certificate (GEC) benefit of €12.5/MWh_e of produced green electricity [5]; (iii) the *Social cost-550 ppm* scenario with the year 2008 fossil fuel prices excluding taxes, plus a carbon damage cost of €20.55/t CO_2 ($30/t CO_2) corresponding to the 550 ppm emission scenario by Stern [6]; (iv) the *Social cost-BAU* scenario with the year 2008 fossil fuel prices excluding taxes, plus a carbon damage cost of €58.23/t CO_2 ($85/t CO_2) corresponding to the business as usual (BAU) emission scenario by Stern (2006). The costs of the fuels under the various scenarios are shown in Table 1.

Table 1. Fuel costs under the various scenarios (€$_{2008}$/MWh)

	Scenarios			
Fuel type	No tax	Swedish tax	Social cost-550 ppm	Social cost - BAU
Fuel oil	29.7	62.9	36.1	47.7
Coal	8.0	46.3 (17.4)[a]	15.5	29.3
Forest fuel	16.3	16.3	16.5	16.8
Natural gas	33.7	37.6 (37.9) [a]	37.9	45.6
Wood powder[b]	26.1	26.1	26.4	26.9

[a] CHP plant.
[b] Estimated based on forest fuel cost.

We select the district heat production units for each taxation scenario based on the utilization time and lowest district heat cost. We consider the fuels and technologies shown in Table 2. The technologies consist of CHP plants and heat only boilers (HOB). The CHP plants are

based on biomass steam turbine (BST); biomass integrated gasification combined-cycle (BIGCC); coal steam turbine (CST); and natural gas combined-cycle (NGCC) technologies.

Table 2. Investment cost, fixed and variable costs and conversion efficiency of different technologies. The data is based on lower heating values (LHV).

Technology	Capacity	Investment cost	Fixed O&M cost	Variable O&M cost	Efficiency (%)	
					Heat	Elect.
Heat-only boiler (HOB):	*(MW_{heat})*	*(€/kW_{heat})*	*(€/kW_{heat})*	*(€/MWh_{fuel})*		
Biomass[a]		646	12.92	1.95	110	-
Wood powder[b]		430	8.6	1.95	95	-
Oil[a]		300	4.5	0.65	90	-
Coal[c]		690	17.3	2.59	90	-
CHP plants:	*(MW_{heat})*	*(€/kW_{heat})*	*(€/kW_{heat})*	*(€/MWh_{fuel})*		
BST[c]	80	1150	17.3	2.6	80	30
BIGCC[a]	80	1700	42.5	3.1	47	43
NGCC[a]	80	950	23.8	1.0	43	46
CST[c]	80	1350	33.8	3.1	59	30
Condensing power plant:	*(MW_{elec})*	*(€/kW_{elec})*	*(€/kW_{elec})*	*(€/MWh_{fuel})*		
CST[c]	400	1200	24.9	3.12	-	47
CST with CCS[c]	400	1900	74.8	5.2	-	37
NGCC[c]	400	620	18.7	1.04	-	58
BST[d]	400	1200	20	2.39	-	45
BIGCC[a]	100	1680	42	3.12	-	47

[a] Encompasses forest fuels; estimated from [7] with adjustment for the difference in investment cost between [8] and [7]
[b] Swedish Wood Fuel Association and Swedish Energy Agency [9], with 170% adjustment
[c] Hansson et al. [8]
[d] Estimated from CEC [7]

The calculation of the heat production cost is based on the following equation from Gustavsson [10]:

$$C_{heat} = \frac{C_{vom}}{\eta_{heat}} + \frac{C_{fuel}}{\eta_{heat}} - V_{elec} \times \alpha + \frac{CRF \times C_{cap} + C_{fom}}{t} \qquad (1)$$

where C_{heat} is the heat production cost (€/MW_{heat}), C_{vom} is the variable operation and maintenance (O&M) costs of the plant (€/MWh_{fuel}), η_{heat} is the efficiency of heat production of the plant, C_{fuel} is the fuel cost of the plant (€/MWh_{fuel}), V_{elec} is the value of produced electricity (€/MWh_{elec}), α is the electricity-to-heat ratio of the plant, CRF is the capital recovery factor of the plant, C_{cap} is the capital cost of the plant (€/MW_{heat}), C_{fom} is the annual fixed O&M costs of the plant (€/MW_{heat}), and t is the utilization time of the plant.

For district heating systems with CHP production, the production cost of heat may be determined by subtracting the value of the cogenerated electricity from the total production cost of the CHP plant [11]. We calculate the value of cogenerated electricity using the subtraction method, where we consider the cogenerated electricity as by-product and assume

its value to be equivalent to the cost of electricity produced with a reference condensing power plant [12]. We calculate the cost of the cogenerated electricity as the lowest production cost from the condensing power plants (Table 2) for each taxation scenario. We assume the same technologies as for cogeneration but also add carbon capture and storage (CCS) for the CST technology. Data for condensing power production from CST with CCS is from Hansson et al. [8]

We calculate the primary energy use and the heat and electricity generated by the cost-optimal district heat production systems based on the operation schedules, production units and fuels. We consider fuel cycle energy inputs in our calculations.

For all the production units, we assume a discount rate of 6%, an economic plant life of 25 years and a maximum operating period of 7200 hours per year. We use exchange rates of EUR/SEK = 9.62 and USD/SEK= 6.59, based on the average rates for 2008.

3. Results and discussion

The calculated cost of electricity from the condensing power plants under the various taxation scenarios is shown in Table 3. The numbers in bold show the lowest production cost for each taxation scenario, and hence become the reference condensing power plant for each scenario. CST emerges as the reference condensing power plant for electricity production in all scenarios except for the *Social cost-BAU* scenario. For the *Social cost-BAU* scenario, BST emerges as the reference condensing power plant. However, the cost difference between BST and CST is small for the *Swedish tax* and *Social cost-550 ppm* scenarios.

Table 3. The cost of electricity production for the various taxation scenarios (€/MWh).

Technology	*No tax*	*Swedish tax*	*Social cost-550 ppm*	*Social cost-BAU*
CST	**40.2**	**44.6**	**56.1**	85.4
CST, CCS	66.7	66.7	68.9	72.9
NGCC	69.2	76.5	76.4	89.7
BST	57.4	44.9	57.8	**58.6**
BIG/CC	65.4	52.9	65.8	66.5

Figure 3(a-d) shows the cost of district heat production units as a function of the utilization time under the different taxation scenarios. The units with the lowest heat production cost are applied to the heat load profile to minimize the overall heat production cost (Figure 4a-d). For the *No tax* scenario a CHP-CST for base load, coal boiler for medium load and light-fuel oil boiler for peak load give the cost-optimal system (Figure 3a). Five different units give the cost-optimal system for the *Swedish tax* scenario (Figure 3b), including CHP-BST and CHP-BIGCC for base load, wood powder boiler and biomass boiler for the medium load, and light fuel oil boiler for the peak load. However, the CHP-BIGCC may not be technically feasible as the technology is still at the demonstration stage and is not yet commercialized [13]. Therefore we select the CHP-BST plant for the base load production but show the results if CHP-BIGCC is used in a sensitivity analysis. During periods when the base load unit is shut down (after 300 days) heat demand has to be met by the medium load unit, increasing the utilization time for that unit. If this utilization time is also considered, the wood powder boiler becomes less competitive than the biomass boiler for the medium load production. Therefore a combination of CHP-BST plant for base load, biomass boiler for medium load and light fuel oil boiler for peak load gives the minimum heat production cost for the *Swedish tax* scenario

(Figure 4b). Similar analyses for the *Social cost-BAU and Social cost-550 ppm* scenarios give the selections the production units shown in Figure 4c and d.

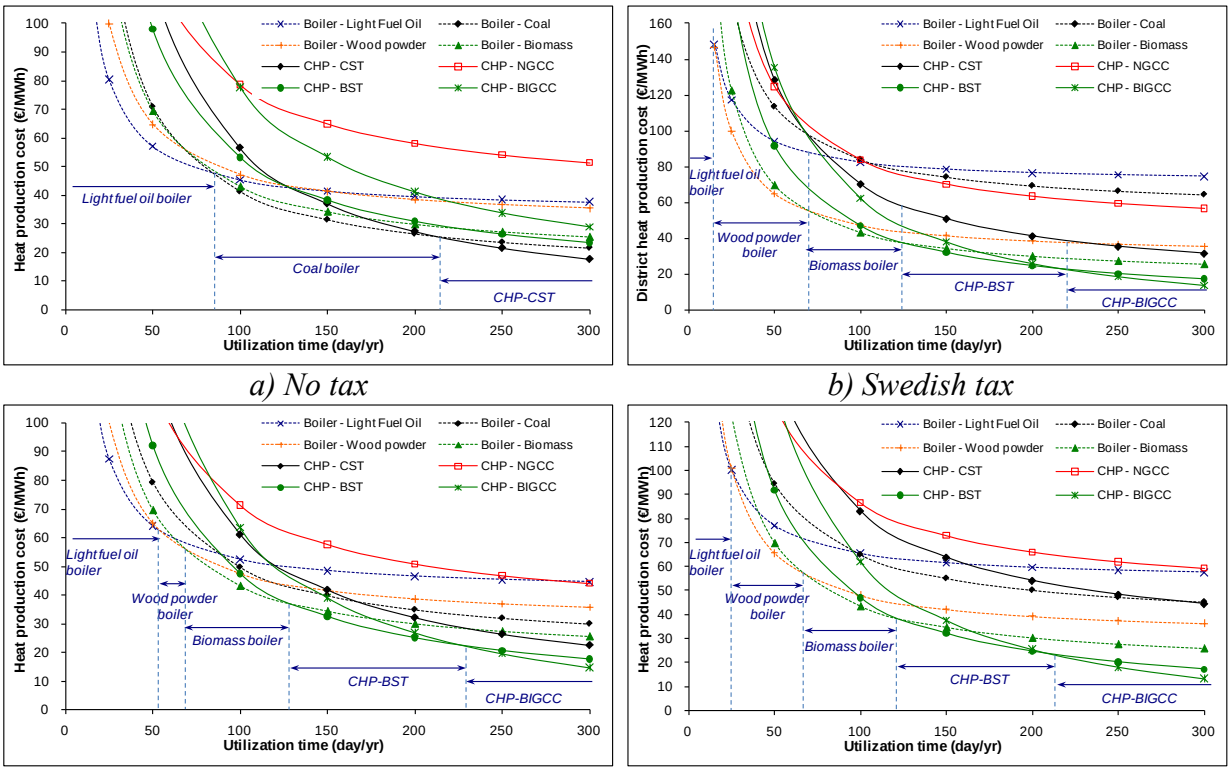

a) No tax *b) Swedish tax*

c) Social cost – 550ppm *d) Social cost – BAU*

Fig. 3. Performance of district heat production units under different taxation scenarios

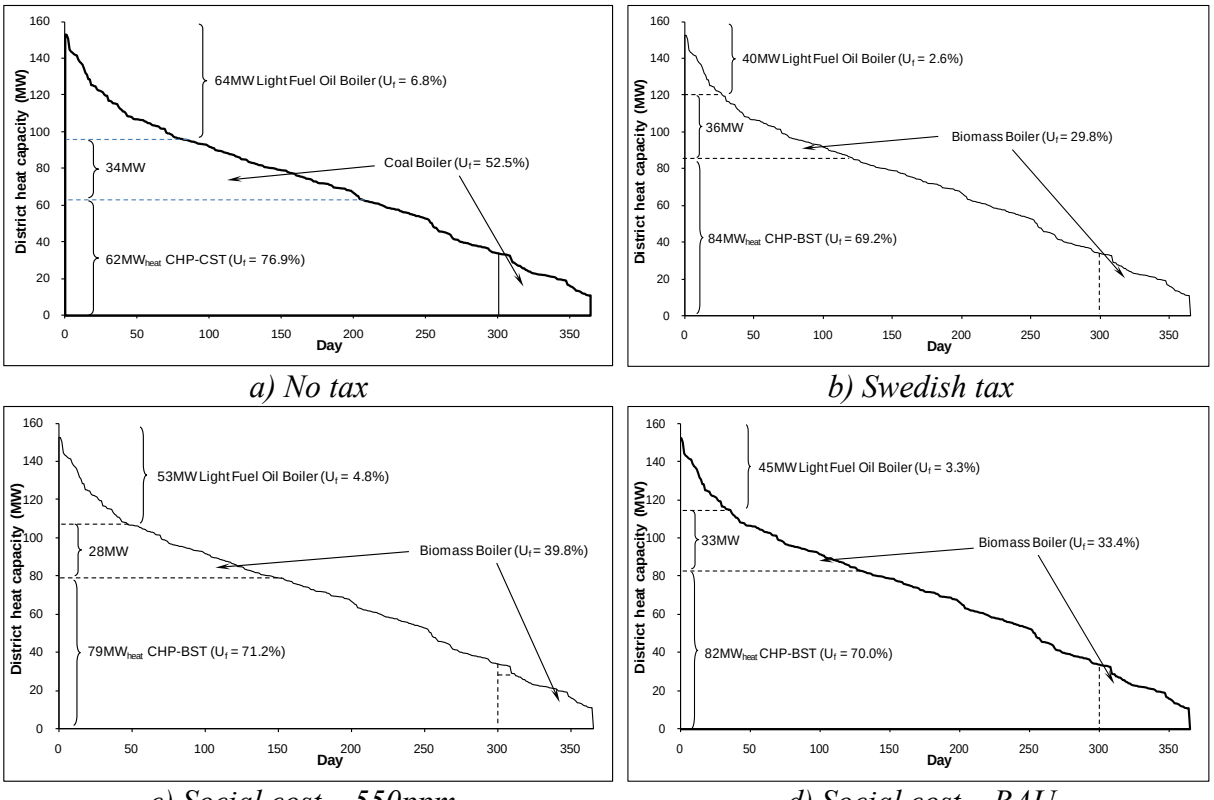

a) No tax *b) Swedish tax*

c) Social cost – 550ppm *d) Social cost – BAU*

Fig. 4. The cost-optimal production units satisfy heat load demand under different taxation scenarios

Table 4 shows the production units and the capacities of the cost-optimal district heat production systems as well as the annual heat and electricity production and the annual primary energy use. District heat production is based on only fossil fuels under *No tax* scenario whereas in the other scenarios district heat production is based mainly on biomass, accounting for 96.4% in *Social cost-550ppm* scenario and 98.5% in *Swedish tax* scenario. Hence fossil fuels become less competitive as the environmental taxation increases. However, light fuel oil boiler for the peak load production remains viable due to low utilization time and investment cost.

Table 4. The cost-optimal district heating systems under different taxation scenarios.

Production unit of district heat	*Capacity (MW_{heat})*	*Heat generation (GWh)*	*Elect. generation (GWh)*	*Primary energy use (GWh)*
No Tax:				
CHP-CST	62	418.0	212.0	793.0
Boiler-coal	34	156.0		159.0
Boiler-oil	64	38.0		47.0
Swedish tax:				
CHP-BST	84	509.0	191.0	658.0
Boiler-biomass	36	94.0		88.0
Boiler-oil	40	9.0		11.0
Social cost - 550ppm:				
CHP- BST	79	492	185.0	637.0
Boiler-biomass	28	98		92.0
Boiler-oil	53	22		27.0
Social cost - BAU:				
CHP- BST	82	503	188.0	650.0
Boiler-biomass	33	96		91.0
Boiler-oil	45	13		16.0

Table 5 shows the district heat production cost and primary energy use for heat production under the different scenarios. The district heat productions with CHP-BST have similar district heat production cost, ranging from €25.6 to €25.8 per MWh regardless of taxation scenarios. This is slightly higher than that of the cost-optimal system under *No tax* scenario, which is €25.0 per MWh. The primary energy use is about 50% higher in the *No tax* scenario compared to the other scenarios. This is mainly because CHP is less cost-effective without any taxation, resulting in a higher use of the less efficient boilers.

Table 5. District heat production cost and primary energy use of cost-optimal systems.

Scenario	*District heat production cost (€/MWh)*	*Primary energy for heat production (GWh)*
No tax	25.0	440.6
Swedish tax	25.8	325.8
Social cost – 550ppm	25.6	335.9
Social cost – BAU	25.6	311.6

4. Sensitivity analysis

To demonstrate the potential of CHP-BIGCC technology if it is commercialized, the CHP-BIGCC plant is used for the base load production for the *Swedish tax, Social cost-550 ppm* and *Social cost-BAU* scenarios as it gives the lowest district heat production cost. The optimal capacities for the production units with CHP-BIGCC are given in Table 6. The capacities of the production units and the heat generated decrease when CHP-BIGCC is used instead of CHP-BST. This is because the CHP–BIGCC system is more efficient than the CHP–BST but also more capital intensive. However, the cogenerated electricity is about twice as much for CHP- BIGCC than for the CHP-BST.

Table 6. The cost-optimal district heating systems under different taxation scenarios if CHP-BIGCC is used.

Production unit of district heat	*Capacity (MW_{heat})*	*Heat generation (GWh)*	*Elect. generation (GWh)*	*Primary energy use (GWh)*
Swedish tax:				
CHP-BIGCC	74	473	433.0	1042.0
Boiler-biomass	46	130		122.0
Boiler-oil	40	9.0		11.0
Social cost - 550ppm:				
CHP-BIGCC	72	465.0	425.0	1024.0
Boiler-biomass	33	124.0		117.0
Boiler-oil	55	23.0		29.0
Social cost - BAU:				
CHP-BIGCC	75	477.0	437.0	1051.0
Boiler-biomass	36	118.0		111.0
Boiler-oil	49	17.0		20.0

Table 7 shows the district heat production cost and primary energy use if CHP-BIGCC is used. The district heat production cost is 5-8% lower than when CHP-BST is used. The primary energy for district heat production is also significantly reduced compared to when CHP-BST is used. This is due to the benefits from the increased cogenerated electricity.

Table 7. District heat production cost and primary energy use of cost-optimal systems if CHP-BIGCC is used.

Scenario	*District heat production cost (€/MWh)*	*Primary energy for heat production (GWh)*
Swedish tax	24.0	254.7
Social cost – 550ppm	24.3	288.6
Social cost – BAU	23.6	247.1

5. Conclusions

In this study, we explore how different environmental taxation regimes influence the design of optimal cost district heat production system. We find that primary energy use varies strongly when different technologies are used under the different taxation scenarios. CHP is less cost-effective without any taxation, resulting in a higher use of the less efficient boilers. Fossil fuels become less competitive as the environmental taxation increases. However, light

fuel oil boilers for the peak load production remains viable due to low utilization time and investment cost. Varying the environmental taxation has a minimal effect on the heat production cost when the biomass-based district heat production is designed for the given taxation.

CST emerges as the reference condensing power plant under all taxation scenarios except for the *Social cost–BAU* scenario, in which BST is the reference condensing power plant. CHP-BIGCC is an emerging technology for efficient use of biomass for district heat production as this technology increases the power-to-heat ratio of CHP-based district heat production. Policy instruments that provide incentives for and eliminate barriers against this technology may be needed to implement the technology. Hence, environmental taxation can be an important policy instrument to increase the competitiveness of biomass-based CHP.

References

[1] A. Joelsson, and L. Gustavsson, District heating and energy efficiency in detached houses of differing size and construction, Applied Energy, 2 86(2), 2009, pp. 126-134.

[2] Swedish Energy Agency (SEA), Energy in Sweden 2009, SEA, Sweden, 2010, pp. 167.

[3] Swedish District Heating Association, Verksamhetsberättelse 2008/2009, Svensk Fjärrvärme, 2009, pp. 52. Web accessed at www.svenskfjarrvarme.se in August, 2010.

[4] Svensk Fjärrvärme, Statistik 2008 - tabeller och diagram, Svensk Fjärrvärme AB, 2010. Web accessed at www.svenskfjarrvarme.se in August, 2010.

[5] Swedish Energy Agency, Energy in Sweden 2008, SEA, Sweden, 2008.

[6] N. Stern, Stern review on the economics of climate change, 2006. Web access at www.hm-treasury.gov.uk in February, 2010.

[7] CEC (Chalmers EnergiCentrum), Biokombi Rya biomass gasification project, final report. (Biobränsleförgasning satt i system, slutrapport), report 2007:3, Chalmers University of Technology, Göteborg, Sweden, 2007.

[8] H. Hansson, S.E., Larsson, O. Nystroem, F. Olsson, B. Ridell, Electricity from new plants. Elforsk AB, Stockholm (SE), 2007.

[9] Swedish Wood Fuel Association and Swedish Energy Agency, Heating with wood powder, 2001. Web accessed at www.energimarknadsinspektionen.se on June 08, 2009.

[10] L. Gustavsson, District heating system and energy conservation – Part I. Energy, 9(1), 1994, pp. 81-91.

[11] J. Sjödin, and D. Henning, Calculating the marginal costs of a district heating utility. Applied Energy, 78(1), 2004, pp. 1-18.

[12] L. Gustavsson, and Å. Karlsson, CO_2 mitigation: On methods and parameters for comparison of fossilfuel and biofuel systems. Mitigation and Adaptation Strategies for Global Change, 11, 2006, pp. 935-959.

[13] I. Obernberger, and G. Thek, Combustion and gasification of solid biomass for heat and power production in Europe - State-of-the-art and relevant future developments, Proceeding of the 8th European Conference on Industrial Furnaces and Boilers, Vilamoura, Portugal, 2008.

Energy Neutral Districts ?
Key to Transition towards Energy Neutral Built Environment !

Eric M.M. Willems[1,*], Bronia Jablonska[2], Gerrit Jan Ruig[2], Tom Krikke[3]

[1] *Cauberg-Huygen Consulting Engineers BV s-Hertogenbosch, The Netherlands*
[2] *ECN Petten, The Netherlands*
[3] *Technical University Eindhoven, The Netherlands*
* *Corresponding author. Tel: +31 737517900, Fax: +31 73 7517901, E-mail:e.willems@chri.nl*

Abstract: The Dutch project 'Transition in Energy and Process for a Sustainable District Development' focuses on the transition to sustainable, energy neutral districts in 2050, particularly in energy concepts and decision processes. The research results in six innovative energy concepts for 2050.
Firstly, fourteen variations of six general energy concepts have been developed and calculations conducted on the energy neutrality by means of an Excel model designed for this purpose.
Three concepts are based on the idea of an energy hub (smart district heating, cooling and electricity networks, in which generation, storage, conversion and exchange of energy are all incorporated). Calculations show the energy neutrality ranges from 130 % to 164% excluding transport of persons within the district.
In this approach, different districts have different sustainable energy potentials that have their peak supply at different times. The smart approach therefore is not an autarkic district, but an exchange of surplus sustainable energy with neighbouring districts and import of the same amount of energy in case of a shortage.

Keywords: *Energy neutrality, District, Energy concept, Energy hub, All-electric*

1. Introduction

One third of the current Dutch (and European) energy demand is caused by the built environment. The target of the Dutch government, in accordance with the European targets, is to reach 20% renewable energy supply in 2020 [PEGO, 2009]. The document [New Energy for the Netherlands, 2009] contains a plea of the leading political parties in favour of a completely renewable energy supply in 2050.

A characteristic of the built environment is that it changes very slowly. Each year, 1% of the floor area of existing building stock is added to the total building stock. With a minimal lifespan of buildings of one hundred years we need to take action today to reach this vision before 2050 or even this century if we wish to break our addiction to fossil fuels. We need to develop innovative and integral energy concepts for renovation and new housing and apply them to entire districts.

Energy neutral houses are already demonstrated mainly as villa's or special designs [1]. In ordinary cities, existing buildings and newly built districts it is impossible to reach energy neutral houses on a large scale with these common technologies. For offices it is even more difficult to gain energy neutrality [2]. Only within district energy neutrality can be achieved. It can be concluded that there is a need for using sustainable sources on an district scale.

2. Future Energy Housekeeping

The starting point for establishing the energy demand of the energy neutral concepts is based on the Building Future Potential Study 2050 [2] and [4]. According to this study, the main features of a energy neutral district are as summarized below (Fig. 1):

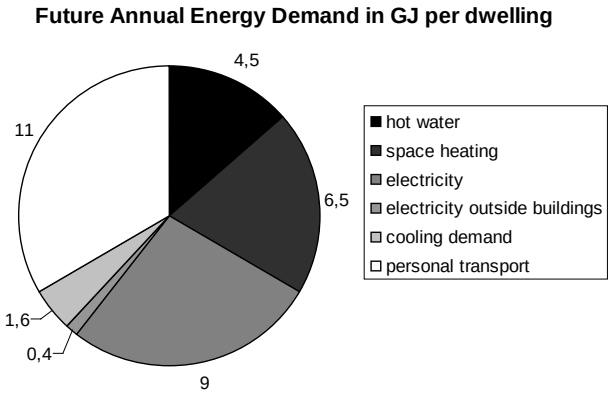

Fig. 1: Annual energy demand of a house in GJ, assessed for 2050 [ECN, 2009]

The energy demand of a district separated into the following components: (1) Buildings, (2) Transport for persons within the district and (3) the surroundings of the district. Due to a far-reaching reduction of demand in future, the total average energy demand of a dwelling will be approximately 33 GJ annually, separated into:

- Domestic Hot water (4.5 GJ or 185 m^3 natural gas)
- Space heating (6.5 GJ or 300 m^3 natural gas)
- Space Cooling (1.6 GJ or 300 kWh_e)
- Electricity for lighting and household appliances (9 GJ or 2,450 kWh)
- Electricity demand for street lighting etc (0.3 GJ)
- Transport of persons (11 GJ).

Energy losses due to distribution of heat:

- high temperature (90-70 C): 5 GJ per meter with high performance insulation
- low temperature (50-30 C): 2.5 GJ per meter

The energy demand for transportation of persons within a district is established as 34 GJ primary energy use of 11 GJ electricity [5].

3. Understanding energy neutral districts

An (energy neutral) district, as defined in this research, follows the boundaries of the built area and consists of a mix of residential and commercial buildings. This implies that energy sources from outside the district, such as wind turbines (for example offshore) and biomass (forests, agricultural sources) are not taken into account. It is assumed that the energy for industry and transport other than personal transport is generated outside the district boundaries. One exception is waste heat from large-scale incineration and combustion plants, which process mainly waste from the district such as domestic and company refuse.

We consider a district as energy neutral if, on a yearly base, no net energy import is necessary from outside the district. An energy neutral district is not an autarkic district that does not exchange any energy with its surrounding districts. Surplus of energy can be exported and, in case of energy shortage, the same amount of energy can be imported from the surrounding districts. It is better to import or export electricity than to store it. This definition is according to PEGO [6].

3.1. Technologies used in energy neutral concepts

Technologies needed to be deployed in energy neutral concepts can be classified as existing, future (on the market within app. 10 years) and still to be developed technologies (market ready after 2020). Existing renewable technologies comprise of high and low temperature

district heating networks, geothermal sources, heat and cold buffering in storage tanks, Aquifer Thermal Energy Storage (ATES), flat plate and vacuum tube solar collectors, heat pumps, heat-driven cooling, PV (photovoltaic modules), urban wind energy and biomass CHP. The future technologies are, among others, organic rankine cycle (ORC), heat pump booster, electricity hub, heat and power matcher, thermal chemical heat storage (TCS) and hydrogen as carrier and storage of sustainable energy. Still to be developed technologies are, among others, bi-directional district heating networks, heat/cold hub and energy hub.

In addition to this it is assumed that the primary energy use per produced kWh electricity delivered to the power grid will decrease. Nowadays the energy-efficiency has an average of about 39%. This efficiency will increase in 2050 towards 50%.

3.2. Energy hubs

An energy hub is defined as a central point in a district where all energy distribution systems come together and energy can be converted to other energy carriers. In addition vehicles can be refuelled with (bio)gas or liquid bio-fuel there, for example. (Bio)-gas can be used for combined heat and power systems in order to generate heat and electricity. Electricity can be used to charge electric vehicles and to generate heat or cold with heat pumps. Energy hubs will probably be equipped with seasonal storage of heat and cold. Energy management, based on the PowerMatcher™ (Figure 2a) and HeatMatcher (Figure 2b, under development) technology will be used to coordinate the generation, supply and demand of all energy flows and conversions. The energy hub makes sure that the entire renewable energy generation potential of all connected systems will be exploited to its maximum.

Fig. 2a: Supply and demand matching with the PowerMatcher™ [ECN, 2009]

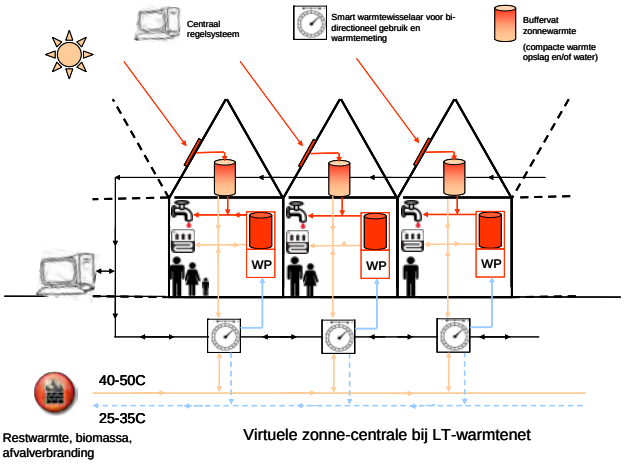

Fig. 2b. Part of a smart heat grid with solar collectors (under development; Willems, 2010)

4. Quantification energy neutrality and sustainable energy surplus

The results are expressed in terms of "degree of energy neutrality" (or energy self-sufficiency). The degree of energy neutrality is defined as the renewable energy generated in a district, divided by the energy demand of that district. If the degree of energy neutrality is higher than 100%, this means that the district can export energy surplus in terms of heat, cold or electricity. Values under 100% mean that the district needs to import renewable (or fossil) energy in order to meet its annually energy demand. Shortage and surplus are expressed in primary energy. It can be shown that the energy neutrality is not strictly depending on the energy demand but of the combination of demand en supply of sustainable energy.

5. Six concepts for energy neutral districts

Six types of energy concepts on a district scale have been developed by means of well considered combinations of the above mentioned technologies. The names of the concepts are derived from its main sustainable energy source: Geo hubs, Bio hubs, Solar hubs, All-electric Natural gas concepts and Hydrogen concepts. Within these six general concepts, fourteen variations have been elaborated. The energy performance, as expressed as the degree of energy neutrality, has been calculated for each concept variation for the years 2020, 2035 and for 2050. These steps give as an example insight in what steps de maximum energy performance can be increased in time.

5.1. Description and performance

The first step in all energy concepts consists of limiting the energy demand by means of refurbishing or renovating according to the passive house standard for existing buildings (Renovated houses have a higher heat demand: 28 kWh/m^2 of floor area annually.). Newly built buildings reach the passive house standard by an excellent building envelope (insulation and air tightness), low temperature space heating and heat recovery from ventilation air. The heat demand for newly built passive dwellings is 15 kWh/m^2 of floor area annually. Both types of dwellings also have heat recovery from waste water. The average roof area suitable for solar energy generation systems such as solar collectors, PV and PVT (combined thermal solar collector and PV) is assumed to increase in time up to 28.1 m^2 per dwelling. This increase mainly is caused by making use of southern orientation of the roofs or other construction possibilities that provides the use of solar energy. On the supply side the main sustainable district sources are thermal energy: geo, bio and solar; electrical energy through PV-panels and urban wind turbines.
In view of the aspiration of an imaginary municipality, concept 4 (all-electric) combined with concept 3 (low temperature storage with ORC or heat pumps) is given as an example of the applications of the developed concepts (Figure 3).

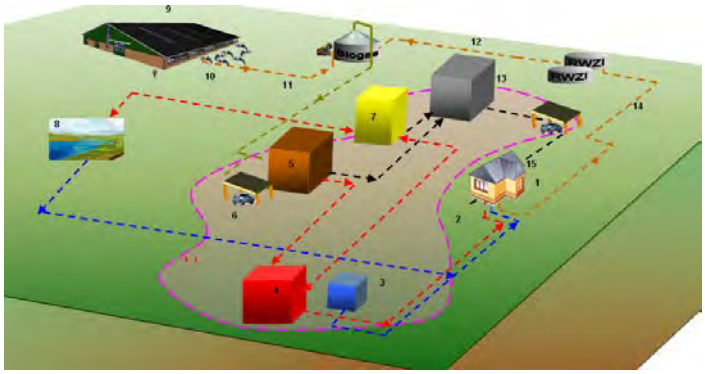

Fig. 3: Energy flows in an imaginary district

1 – Dwellings
2 – Solar heat
3 – ABS chiller
4 – Heat hub
5 – CHP
6 – Fuel tank
7 – ORC
8 – Canal/surface water
9 – Stables
10 – Fertilizer
11 – Biogas
12 – Sludge
13 – Electricity Hub
14 – Sewage
15 – PV-panels

The energy performance of the energy concepts has been calculated in an Excel model.

The performance of the main energy concepts and their related variations are presented in Table 1 below.

Table 1: Degree of energy neutrality of the concepts in 2020, 2035 and 2050 [ECN]

				Degree of energy neutrality [%]					
				2020		2035		2050	
	ENERGY CONCEPTS	Individual or collective	Cooling			Transport			
				excl	incl	excl	incl	excl	incl
1	**Waste Heat and/or Geothermy (Geo-Hubs)**								
	High temperature waste heat utilization or geothermy	District heating	Compression cooling by PV or sorption cooling by solar	96	61	120	73	**164**	**96**
2	**Waste Heat and/or Biomass (Bio-Hubs)**								
	Moderate temperature waste heat utilization	District heating	Compression cooling by PV or sorption cooling by solar	93	60	119	72	**163**	**95**
3	**All-Solar concepts (Solar-Hubs)**								
	High temperature storage of solar heat	District heating	Compression cooling by PV or sorption cooling by solar	53	34	73	45	**130**	**76**
	Low temperature storage with ORC or heat pumps			47	30	72	43	**131**	**76**
4	**All-Electric concepts**								
	Individual electric heat pumps, PV and solar collectors	Individual	Free cooling by ground heat exchanger	71	45	102	61	**150**	**87**
	Individual electric heat pumps and PV			73	47	106	64	**157**	**92**
5	**Conventional concepts with PV**								
	Individual gas boilers with PV	Individual	Compression cooling by PV	36	23	64	38	**112**	**65**
	Individual gas boilers, solar collectors and PV		Compr. or sorpt. cooling by solar	38	24	65	40	**114**	**67**
6	**Hydrogen concepts**	Individual	Free cooling by ground heat exch.	15	7	57	30	**115**	**54**

In 2050, all concepts can provides in a energy surplus, unless personal transport in the district is included.

5.2. Interaction between district energy concepts and scale

The actual size of a district is determined by the energy losses of the heat transport grid. Too long transportation pipes (heat) give high losses (about the same quantity) compared to the energy demand. Several energy concepts together perform energy neutral districts on a larger scale than apart due to energy exchange by energy hubs where a meso scale develops. On a macro scale we can imagine geothermal energy and large scale wind turbines. The areas between the built environment (e.g. agricultural land, oceans) can provide in wind, bio mass and hydro power for other purposes than the built environment (industry transport etc). Examples are given in table 2.

Table 2. Techniques per scale of energy concepts

Micro level (1-40 houses)	Meso level (40-4.000 houses)	Macro level (> 4.000 houses)
Solar energy	Bio mass	Bio mass
ATES / ground source heat pump	ATES	Mine water energy
PV-panels	Geothermal energy	Geothermal energy
Urban wind turbines		Large scale wind turbines

In figure 4 visualisation of the interaction between energy neutral concepts is given. Smallest circle is representing the scale of an energy concept on micro level. In this vision energy concepts based on natural gas only have a function if only a part of the built environment is energy neutral. Through energy hubs the surplus of sustainable energy can be used in other districts. In case of only energy neutral districts except one there is a surplus on renewables and still using natural gas, an unwanted situation.

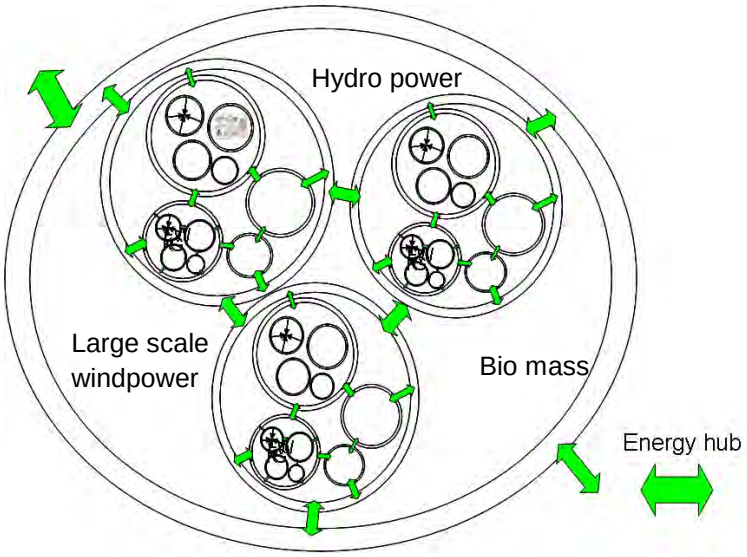

Fig. 4.Visuliasation of the scale and interaction between energy neutral district concepts (Willems 2010 [7]).

5.3. Robustness and sensitivity

Sensitivity analysis are grouped in three classes: screening methods like OAT-method (One-Parameter-At-a-Time), local sensitivity methods and global sensitivity methods [8]. In the sensitivity analysis of the Excel tool, a screening method is used, because is a relatively simple method that can identify and qualitatively rank the parameters that has the most influence of the tool's outcome. To evaluate the robustness of the calculations on the energy concepts energy performance a short sensitivity analysis is performed. These values are specified in Table 3 as averages per dwelling.

Table 3. Input parameters used in the sensitivity analysis, including the stratified samples per parameter

Parameter	Unit	Discrete values				
ATES efficiency	[-]	*20%*	*40%*	*60%*	*80%*	*100%*
Space Heating	[GJ_t]	4.5	6.5	8.5	10.5	12.5
Domestic electricity usage	[GJ_e]	*70%* 8.8	*85%* 10.7	*100%* 12.6	*115%* 14.5	*130%* 16.4
Percentage renewables national generation	[GJ_{pe}/GJ_e]	*20%* 1.6	*30%* 1.4	*40%* 1.2	*50%* 1.0	*60%* 0.8

The sensitivity index is defined as a percentage of the output difference of the extreme values according to:

$$SI = \frac{\text{Emax} - \text{Emin}}{\text{Emax}} x100\% \qquad (1)$$

where the maximum and minimum degree of energy neutrality are represented by respectively E_{max} and E_{min}. The results of the screening analysis are illustrated in Table 4.

Table 4. Sensitivity Index of the varied parameters per concept first impression analyses

Parameter	Concept													
	1	2	3	4	5	6	7	8	9	10	11	12	13	14
ATES efficiency					56%	57%	30%	30%						
Space heating	16%	16%	16%	16%	25%	16%	25%	24%	19%	20%	39%	37%	37%	19%
Domestic electricity usage	25%	25%	25%	25%	25%	25%	25%	25%	25%	25%	25%	25%	25%	40%
Percentage renewables national generation	13%	13%	13%	13%	4%	3%	3%	4%	9%	11%	29%	21%	21%	1%

Energy concepts with heat hubs have a surplus in sustainable heat. They are less sensitive to energy demand of heat. Energy concept that have a surplus on electricity are very sensitive to de efficiency of the power grid as well as very sensitive to de heat demand. The figures in table 4 show that de heat-hub concepts are more robust than the all-electric and natural gas concepts.

6. Conclusions

The aim of a built environment without any need of fossil fuels is still ambitious but becoming a realistic goal. Building techniques and energy storage will become market ready in 10-20 years an will provide the missing links in the energy concepts.

Based on the conducted research the following conclusions can be drawn:

- Energy neutrality of the built environment can only be reached by an extensive reduction in energy demand. Sun oriented new buildings and new and renovation building development according to the passive house standards and development of high-performance heat recovery from warm waste water are essential.
- In 2050, energy neutrality is feasible with several energy concepts. The geo and bio hubs and the all-electric concepts lead to the highest degree of energy neutrality, followed by solar hubs. Conventional and hydrogen concepts realise the energy neutrality only barely. The fact that all elaborated concepts lead to energy neutrality in 2050 or earlier means that the transition based on the current energy infrastructure is possible. This way, the investments already made can remain profitable.
- Based on the assumptions made here, energy neutrality of the built environment including personal transport is not feasible within a district. Because the production of renewables in maximized only energy neutrality with personal transport can be reached by reducing transport or increasing efficiency of transport vehicles.
- Energy concepts with sustainable heat form local sources (ground, biomass, solar) are more robust due to changes in energy demand and efficiency of the power grid. It can be derives that diversification of sustainable energy sources is preferred above all-electric.

7. Follow-up steps

The research will be continued on various aspects of the above-mentioned energy concepts. The energy hub concepts seem very promising. It would be interesting to elaborate various types of energy hubs to a level of preliminary design for certain cases in communities and districts as presented by ECN [9].

An energy hub will be dynamically simulated in order to prove the added value of the exchange, conversion and storage of the energy flows within a district.
Next to the energy and CO_2 reduction, a further research can be done on clever utilisation of temperature levels of energy flows within an energy hub.

For future investigation it appears that the availability of sustainable sources becomes more important than the specific efficiency rates in energy conversion. In case of complete energy neutral districts only availability of the appropriate cost effective energy carrier for a specific energy demand is of importance, not the way it is generated or converted.

Acknowledgements
The authors would like to thank the Ministry of Economic Affairs of The Netherlands for their financial support of this research within the Energy Research Subsidy regulation (EOS-LT) – long term.

References

[1] Energy neutral houses in Groningen and Amersfoort, The Netherlands, www.nulwoning.nl (2010).

[2] E.M.M. Willems, Energieneutrale kantoren? Kijk eens om je heen! (Energy neutral offices? Look around you! TVVL-magazine The Netherlands (2010).

[3] F.G.H. Koene, Knoll B., Renovation concepts for saving 75% on total domestic energy consumption, Eurosun Conference, Lisbon, Portugal (2008).

[4] H. Visser, Koene, F.G.H., Paauw, J., Opstelten, I.J., Ruijg, G.J., Smidt, R.P. de, Sustainable energy concepts for residential buildings, Packages of current and future techniques for an energy neutral built environment in 2050, ECN-E--09-021. ("Building Future Potential study 2050"), ECN Petten, The Netherlands (2009).

[5] A. Dohmen, Mullenders F., *Auto's rijden gemiddeld 42 kilometer per dag*, (Cars do drive an avarage of 42 km a day) Centraal Bureau voor de Statistiek, Voorburg/Heerlen; CBS Webmagazine, www.cbs.nl (2006).

[6] PEGO Stevige ambities, klare taal (Strong ambitions, clear language). Platform Energy Neutral built Environment (2009).

[7] E.M.M. Willems, Presentation Annex 51 3rd meeting Tokyo, www.annex51.org (2010).

[8] P. Heiselberg, Annex 44 Expert Guide Part 1. Responsive Building Concepts, Aalborg University Denmark (2009).

[9] B. Jablonska Ruijg, G.J., Opstelten, I., Willems, E.M.M., Epema, E, Transition to Sustainable Energy Neutral Districts before 2050: Innovative Concepts and Pilots for the Built Environment 7th Biennial International Workshop, Barcelona (2010).

A Forecast of Effective Energy Efficient Policies for the Building Sector in Shanghai through 2050

Rui Xing[1,*], Toshiharu Ikaga[1], Manfred Strubegger[2]

[1]*Keio University, Yokohama, Japan*
[2]*International Institute for Applied Systems Analysis (IIASA), Vienna, Austria*
**Corresponding author. Tel.: +81 45 566 1808, Fax: +81 45 566 1770, E-mail: xingrui@a6.keio.jp*

Abstract: Currently in China, the energy consumption of buildings is increasing rapidly. In this study, we used a macro-model to forecast the energy consumption of buildings in Shanghai through 2050. Total energy consumption from 2000 to 2050 and the potential energy savings were projected for both the residential and commercial sectors. For urban residential buildings, we developed a forecast model for 2050 to estimate the potential energy savings of residential measures. Compared to the business-as-usual (BaU) scenario, implementation of residential measures achieved a 24% reduction in energy consumption. The reduction rate rose to 65% by combining the implementation of residential and electrical measures. For commercial buildings, we first used official statistical data to determine the energy intensities of air conditioning, lighting, computing, and other thermal uses for the base year 2000. Then, estimates of the labor force, GDP, and floor area were predicted through 2050 according to past growth patterns and the literature. Likewise, estimates for energy intensities through 2050 were projected. Energy-saving scenarios also were integrated into the commercial model. Compared to BaU scenario, implementation of commercial measures achieved an 80% reduction in energy consumption. The reduction rate increased to 99% by combining commercial and electrical measures.

Keywords: *Shanghai, Energy consumption, Buildings, Forecasting*

1. Introduction

At the UN Climate Conference in Copenhagen in 2009, the European Union formulated the goals that temperature increase by no more than 2 °C, that global emissions peak no later than 2020, and that by 2050 global emissions be reduced to a level that is at least 50% below the figure for 1990. These goals require action by both industrialized nations and developing countries (Gaines and Jager, 2009). In the Copenhagen Accord, the Chinese government announced mitigation action to reduce CO_2 emissions per unit of GDP by 2020 to 40-45% of the 2005 level. This target was reaffirmed at the 2010 UN Climate Conference in Cancun. However, the most efficient way to achieve this reduction goal remains an unsolved problem.

In recent years, the economy of China has developed rapidly, which encourages demand for higher living standards and energy consumption. In this paper, we focus specifically on urban buildings in Shanghai, which is one of the biggest cities in China and has the highest GDP among all Chinese cities. First, we investigated the environmental performance of both residential and commercial buildings in Shanghai. Then, to quantify their sustainability, we developed macro-models to forecast CO_2 emissions for both residential and commercial buildings. The forecasts include global warming countermeasures and are intended to support decision making for determining reasonable CO_2 emission reductions.

2. Methodology

2.1. Residential Projections

2.1.1. Summary of the macro-model

The macro-model used for the residential sector has been modified from the "Estimation Macro-model for Residential Energy Consumption" (Ikaga, 2004). The flow chart in Fig. 1

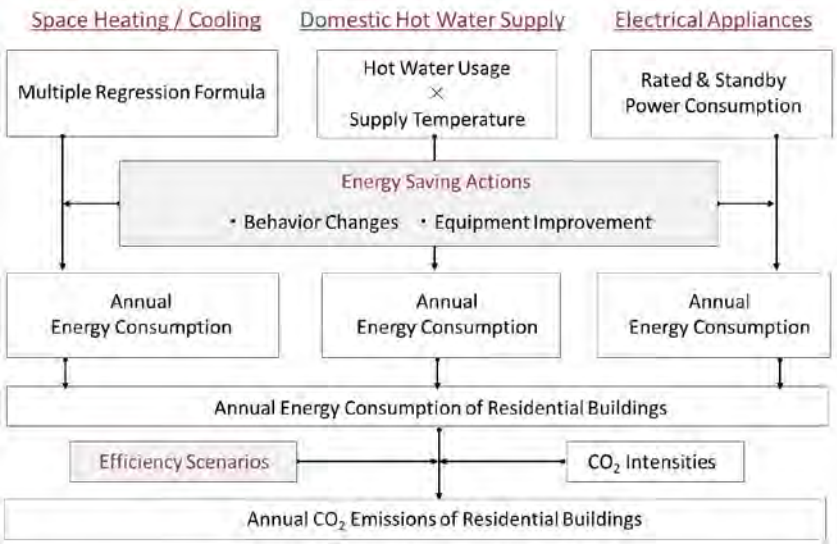

Fig. 1. Flow chart of the residential sector macro-model.

provides an overview of the model. It is a simulation model that estimates changes in energy consumption on the basis of family type, application, and energy source for each year. Estimation methods are described below.

Space heating/cooling: Annual load per household was calculated using a multiple regression equation for heating and cooling load. The annual total load of each city was computed multiplying the number of households of each household type by the energy use for the respective household type and taking the summation.

Domestic hot water supply: The total load of each city was calculated using the frequency of hot water use, the number of households and the average temperature of tap water for each month. Furthermore, energy consumption was calculated using the ratio of owned equipment and the average coefficient of performance (COP) by fuel type.

Other electrical appliances: Energy consumption was calculated as the product of the cumulative energy consumption per household per day and family type, the number of households, and the number of days in each month.

Total CO_2 emissions: By totaling the results of the three functions calculated above and multiplying by the CO_2 intensity of electricity for each energy source, we calculated the annual total CO_2 emissions.

2.1.2. Model parameters

The present model is based on a macro-model that was used to calculate the national residential CO_2 emissions in Japan. For the case of Shanghai, we switched the entire calculation database. The parameters that were set include the number and size of households, average gross floor area, and several pieces of household data. The parameters come either from official statistics or are based on the Chinese government development plan.

There were several parameters for which we could not find a source. To set these parameters we referred to data for the Japanese city of Fukuoka in place of Shanghai, as the two cities have similar latitudes and climates.

2.1.3. Scenarios

In this study, two scenarios are examined: one for residential measures and another for electrical measures. In the residential scenario, we recommend behavioral changes and equipment improvements as global warming countermeasures, having taken into account the social conditions and citizens' lifestyles in China. All the measures are listed in Table 1.

Table 1. Residential measures.

Scenario	Measure	Implementation rate (by 2050)
Behavioral changes	1. Regulation of room air temperature (Heating: STD -2 °C; Cooling: STD +1 °C) 2. Regulation of space heating and cooling operation time (STD×0.75) 3. Reduction of hot water supply temperature (STD +1 °C) 4. Reduction of hot water use 5. Using cold water during summer 6. Unplugging electrical equipment when not in use 7. Only washing clothes when there is a large load 8. Washing clothes using shorter cycles 9. Closing the lid of warm-water cleaning toilet seats 10. Adjusting the temperature setting of warm-water cleaning toilet seats	Implemented by 50% of all households
Equipment improvement	1. Old air conditioners replaced by energy-efficient models	Increase of COP: Heating from 3.0 to 8.0; Cooling from 4.0 to 8.0
	2. Enhancement of thermal insulation level	All houses meet new standard
	3. Water heaters replaced by heat pumps	Increase of COP: 3.0 → 6.0
	4. Use of water-saving shower heads	Implemented by 50% of all households
	5. Kerosene water heaters replaced by heat pump models	Electrification rate increases 2.5% every 5 years
	6. Replacement of incandescent bulbs with compact fluorescent lamps	Implemented by 50% of all households
	7. Accelerating the adoption of eco-appliances	Reduction of power consumption: 70% reduction of refrigerators, 75% reduction of TVs (compared to 2005)

As for electrical measures, the electric utilities made contributions to global warming mitigation. The CO_2 intensity of electricity in Shanghai was 1.027 kg-CO_2/kWh in 1990, which we use as the baseline figure (100%). The NDRC scenario was based on data from the National Development and Reform Commission (NDRC) of China. According to NDRC,

the emissions rate will decrease to 80% of the baseline amount by 2030. The METI scenario was proposed by the Ministry of Economy, Trade and Industry (METI) of Japan. In the METI scenario, the reduction rate of the CO_2 intensity of electricity will be even larger, to 40% of the baseline amount by 2050.

2.2. Commercial Projections

2.2.1. Summary of the macro-model

Figure 2 shows the estimated flow chart of the macro-model applied to the commercial sector. Total energy consumption was divided into two parts: air conditioning and other electrical appliances. Air conditioning includes cooling and heating; other electrical appliances include lighting, computers, and other heating devices. The macro-model is a simulation model that estimates changes in energy consumption according to building type (retail space and hotels, office buildings, warehouses, education facilities, hospitals, and personal services facilities and others) and application (air conditioning, lighting, computing, and others) over a 5-year period.

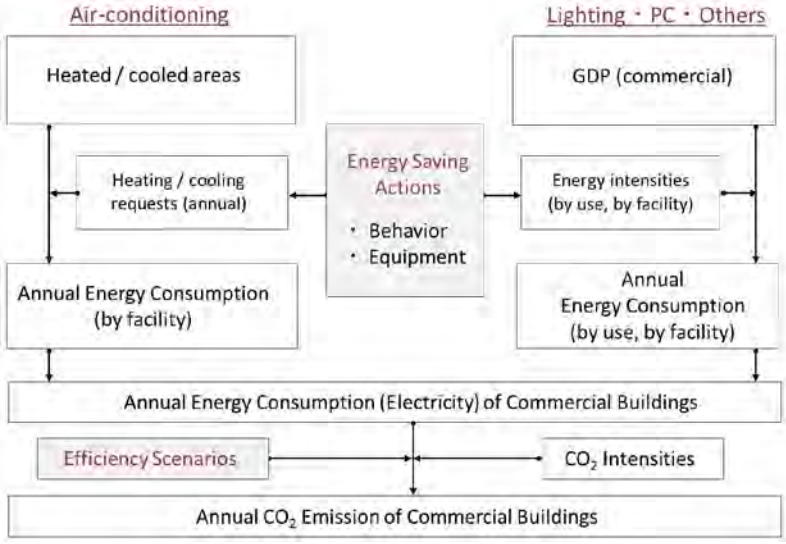

Fig. 2. Flow chart of the commercial sector model.

The commercial model is also a bottom-up engineering model that estimates energy consumption similarly to the residential model. Hence, we analyzed the connection between GDP and penetration rates of electrical appliances in the past 10 years to project penetration rates though 2050.

2.2.2. Model parameters

Because this is prediction research, every parameter was set through 2050. The data for 2000 and 2005 were primarily from the *Shanghai Yearbook*. Parameters for future years were based on relevant literature and the author's assumptions.

For the GDP projection, we referred to research results from the Department of Foreign Affairs and Trade (Wu, 1997) that suggested Chinese GDP will continue growing sharply and overtake the GDP of the United States by 2020. We then looked at the historical growth patterns of another Asian country, namely, Japan. Japan has also been through a period of high growth and development, starting with the "Golden Sixties" and ending with the "Lost Decade." After this period, growth became stable and the trend line became flat. China is now

going through a period of high growth. On the basis of the two perspectives above, we assumed that this unusually high growth in China will last until 2030, at which time it will start slowing down. The GDP of Shanghai's service sector was projected through 2050 using this same trend line, as shown in Fig. 3 (left). Using a similar approach, we also projected the labor force and gross floor space for the next 40 years. For the labor force projection, we referred to the population projection by the Shanghai Municipal Population and Family Planning Commission (SMPC) and calculated labor force as a share of the overall population. For gross floor area, we analyzed the growth pattern over the past 10 years (Xing, 2010) and projected future gross floor area through 2050, as shown in Figure 3 (right).

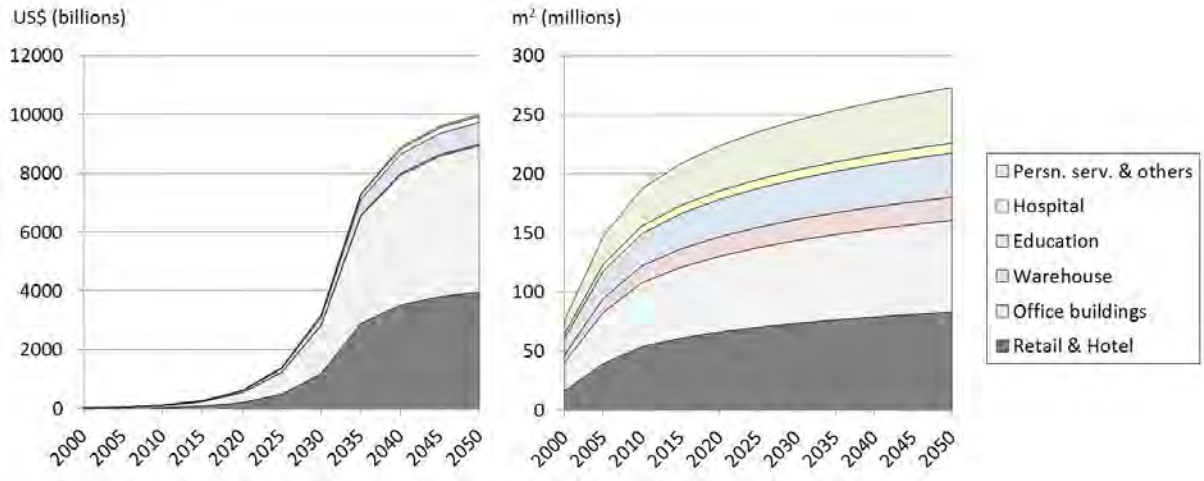

Fig. 3. Projected GDP (left) and floor space (right) through 2050.

Table 2. Commercial measures.

Electrical application	BaU	Energy saving scenarios	
		Behavioral changes	Equipment improvement
Air conditioning	Heating 18 °C, cooling 26 °C COP: 3.54	Heating 17 °C, cooling 27 °C Operational time × 0.75	COP: 3.54 → 8.0
Lighting	Lighting is used all day	Turn off the lights when away	Adoption of LED lighting
Computer	PC enters sleep mode after work	Shut down PC after work	Adoption of ECO-PC
Other heating devices	Waste of standby power	Unplugging electrical equipment when not in use	None

COP: Coefficient of Performance

2.2.3. Scenarios

Two projection scenarios for the commercial sector were also examined: one for commercial measures and another for electrical measures. As for the residential sector, we recommend behavioral changes and equipment improvements as global warming countermeasures for the commercial sector. Table 3 shows the operating power settings for electrical applications by building type under different energy use scenarios. In the Global Energy Assessment (GEA) electrical scenario, the CO_2 intensity of electricity will decrease to 10% of the baseline amount by 2050.

Table 3. Operational power settings by application and building type

	Air condition (COP)		Lighting (W/m^2)	
	BaU (DAIKIN, ZEAS 2000)	Energy saving (METI)	BaU (GB50189)	Energy saving (Hitachi Lighting)
Retail and hotel			16,00	1,60
Office building			15,00	1,50
Warehouse			5,00	0,50
Education	3,54	6,00	15,00	1,50
Hospital			15,00	1,50
Personal services & others			12,00	1,20

	Computer (W/hour)				Other heating devices (W/hour)	
	BaU (NEC standard)		Energy saving (NEC eco model)		BaU	
	In use	Sleep	In use	Sleep	(GB50189) In use	(LBNL) Standby
Retail and hotel					15,00	
Office building					20,00	
Warehouse					5,00	
Education	300	30	240	24	20,00	0,98
Hospital					20,00	
Personal services & others					12,00	

METI: Ministry of Economy, Trade and Industry, Japan; GB50189: Design Standard for Energy Efficiency of Public Buildings, China Construction Division, July 2005; LBNL: Lawrence Berkeley National Laboratory

3. Results

We first compared the estimation results with government statistics to verify the reliability of the macro-model (Fig. 4). In the years 1990, 2000, and 2005, total annual energy consumption estimated by the macro-model was very close to the government's statistics, suggesting that this model is reliable.

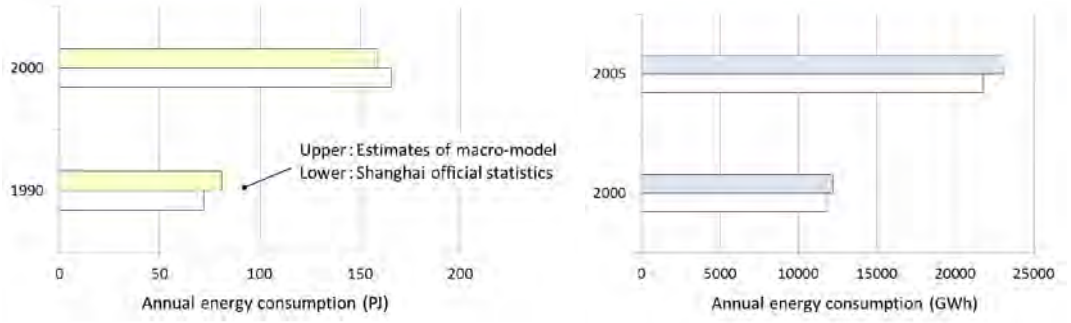

Fig. 4. Macro-model estimates and official statistics for the residential sector (left) and the commercial sector (right).

3.1. CO_2 Emission Reduction of Residential Buildings

The BaU scenario showed a 2.7 fold increase in CO_2 emissions above the 1990 level by 2050. Under the scenario where residential measures are adopted, behavioral changes caused a 6% reduction in CO_2 emissions by 2050 c ompared with BaU. Equipment improvements contributed an additional 18% reduction, which increased the total benefit of residential measures to 24% below the BaU scenario for 2050. When we combined residential measures with the NDRC scenario, the total emissions reductions reached 40%. Residential measures combined with the METI scenario reduced emissions by 65%. Figure 5 (top) shows the projected CO_2 emission reductions for the residential sector by electrical application.

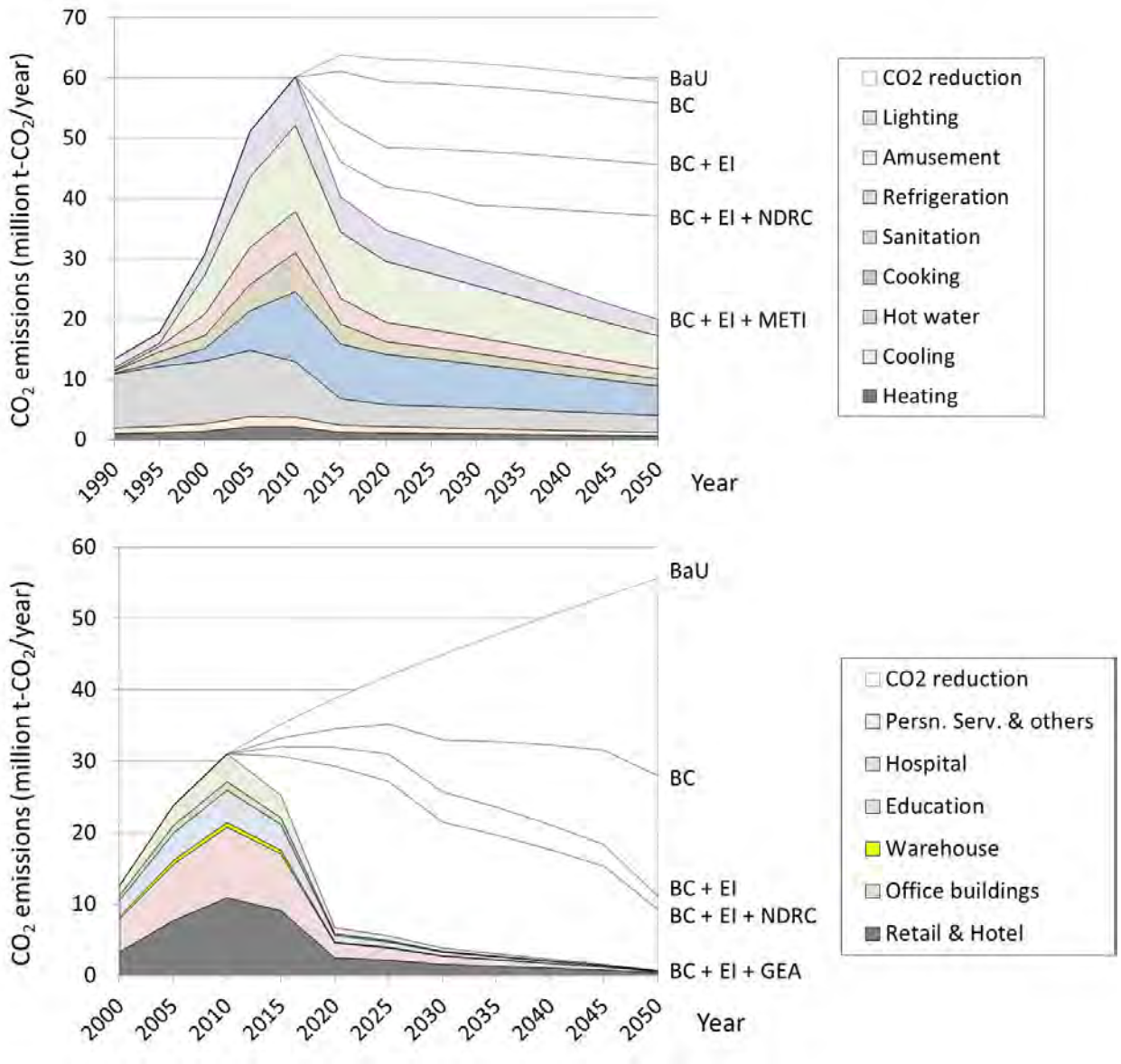

Fig. 5. Projected CO2 emissions for residential buildings (top) and commercial buildings (bottom). BC: Behavioral Changes; EI: Equipment Improvement; NDRC: National Development and Reform Commission of China; METI: Ministry of Economy, Trade and Industry of Japan; GEA: Global Energy Assessment, High case, CPA, WiP 0.5.1

3.2. CO_2 Emission Reduction of Commercial Buildings

Similar to the residential sector, the BaU scenario saw a 3.43 fold increase in CO_2 emissions by 2050 for the commercial sector above the 2000 level. The CO_2 emission estimates for commercial buildings were projected by building type and electrical application. Figure 5 (bottom) shows the results for commercial buildings by building type.

Under the scenario where commercial measures are implemented, behavioral changes caused a 50% reduction of CO_2 emissions compared with the BaU scenario by 2050. Equipment improvements contributed an additional 30% reduction, which increased the total benefit of residential measures to 80%. When we combined commercial measures with the NDRC scenario, total emissions reductions reached 83%. Commercial measures with the GEA scenario reduced emissions by 99%, which means near-zero contributions of CO_2 emissions from commercial buildings.

4. Discussion and Conclusions

In this study, we developed a model to predict the CO_2 emission reduction potentials by 2050 for diverse climates and policy scenarios. For energy savings in commercial buildings, we found that behavioral changes appear to be more efficient than equipment improvement. This finding will likely be appreciated in a developing country like China, since there is a limited budget for large-scale replacement of equipment.

In general, the projections in this research are theoretical. There is no evidence showing that all the suggested energy saving actions could be fully implemented as described in the scenarios projected. However, we hope the results of this research will help decision makers when they look for solutions to achieve CO_2 emission reduction goals in the future.

For the model parameters, we generally relied on the literature and official statistics. In future research, we will schedule local surveys and field measurements in Shanghai. These efforts are expected to improve the accuracy and reliability of the projection model.

Acknowledgment

This work was supported in part by a Grant-in-Aid for the Global Center of Excellence Program for the "Center for Education and Research of Symbiotic, Safe and Secure System Design" from the Ministry of Education, Culture, Sport, and Technology, Japan.

References

[1] J. Gaines & Stefan Jager, A Manifesto for Sustainable Cities, Prestel Publishing, 1st Edition, 2009, pp. 66.

[2] T. Ikaga et al., Development of Macro Simulation Method on Household Energy Consumption and CO_2 Emissions by Each Administrative Division: Journal of Technology and Design, Architectural Institute of Japan, 2005, Vol. 22, pp. 264-268.

[3] Hurry X. Wu, Measuring China's GDP, Department of Foreign Affairs and Trade of Australia, Briefing Paper Series No. 8, 1997, pp. 24.

[4] Rui Xing, Effective Energy Efficient Policies for Commercial Building in Shanghai, Young Science Summer Program (IIASA), 2010

The Institutional dimension of rural electrification in the Brazilian Amazon.

Maria Gómez[1,*], Semida Silveira[1]

[1] *Energy and Climate Studies School of Industrial Engineering and Management, KTH, Brinellvägen 68, 100 44 Stockholm, Sweden*
** Corresponding author. Tel: +46 87907431, E-mail: maria.gomez@energy.kth.se*

Abstract: The Brazilian government aims at providing complete electricity coverage for all citizens as a means to achieve development and reduce poverty. More than 2 million people living in the Amazon have benefited from the rural electrification program Luz Para Todos (LPT – Light for all), mainly through a grid-extension approach. Yet, there is general agreement on the need for an off-grid scheme in order to supply isolated areas. How can the actual institutional framework support the process of supplying electricity to these communities so that the trend of improving electricity access and quality of life continues? We aim at exploring the existing institutional dimension connected to LPT and identifying potential forms of organization for decentralized solutions in the Amazon region. Our analysis is based on current energy policy in Brazil, existing institutional framework, achievements of LPT and potentialities of the isolated areas in terms of resources. Our conclusions draw attention to potential approaches for the next step within LPT context. We argue that the off-grid approach must be based on the uniqueness of the isolated areas in the Amazon. We emphasize the relevance of renewable energy sources in the process of supplying electricity and securing inclusion of isolated areas in universal access.

Keywords: *Rural electrification, off-grid solutions, renewable energy*

In Brazil, significant governmental efforts have been put in place to enhance electricity access in rural areas since the 1990s. The last of these initiatives is called Luz para Todos (LPT – Light for all). It was launched in 2003 and has so far benefited about 11 million people, two of which live in the Amazon region. In general, grid-based systems have been used for the purpose of providing electricity to new users in Brazil, and the interconnected national grid supplies the majority of the population. Hydropower has been the most important energy source for electrification in the country. Despite its continental dimensions, Brazil has been successful in its program for electricity provision and has achieved about 88% of electricity access in rural areas. This makes Brazil the leader of universal electricity access in Latin America [1]. Traditionally, the availability of huge hydro resources and the search for economies of scale for power generation has promoted the development of a centralized electricity system. The fact that the government has allocated exclusive service territories for concessionaires has further promoted this centralized system [2]. Also the results obtained through the recent development of LPT are in line with the centralized approach, and mainly associated with grid extension for electricity provision. These results have not benefited yet an important group of people living in the Amazon region.

The Amazon region is assimilated hereby to the North region, as per defined in the macro-region division of Brazil. This has been usual practice in studies on the Brazilian Amazon. The Amazon region is the home of nearly 14 million people. and covers about 4 million km^2. This implies a population density of less than 4 inhabitants/km^2. The region is also characterized by a very sensitive eco-system. Extending the grid in this area is neither realistic because of the local topography and natural conditions, nor cost-effective because high investments would be required to benefit a few citizens with low income and consumption rates. Within this context, the target remaining in the Amazon is to provide electricity access to one million people who are still not connected [3]. Current challenges in terms of energy access are related to the exhaustion of the grid-extension model and mainly associated with

the provision of services in isolated areas where grid extension is not economically viable. Though a very small percentage of the Brazilian population, the dispersed inhabitants of the Amazon serve the important role of guaranteeing the sustainability of this rich and very sensitive eco-system. Poverty exposure can jeopardize their task. Thus reaching this population in their local environment is important. But here, a different scheme is required, based on decentralized systems and the exploration of renewable energy resources. The decentralized approach is characterized by the generation of power in a location closer to the final users, focusing essentially on meeting local energy needs. But, how to organize the electricity delivery institutionally, and guarantee its technical, economic and environmental sustainability?. There is a well-structured institutional framework which has proved effective for the purpose of improving energy access in Brazil. This institutional framework has successfully provided electricity access to 11 million people throughout the country in a short period of time [3]. However, these results have been achieved through grid extension. The government has recognized the need for developing an off-grid approach in order to provide electricity to the dispersed rural communities living in the Amazon region. Nevertheless, there is a gap between the institutional arrangements in place, which are focused on a model of centralized electricity provision, and the institutional capacity required to develop an off-grid, decentralized model of electrification. This gap needs to be overcome if universalization is to be achieved in the Amazon region [4].

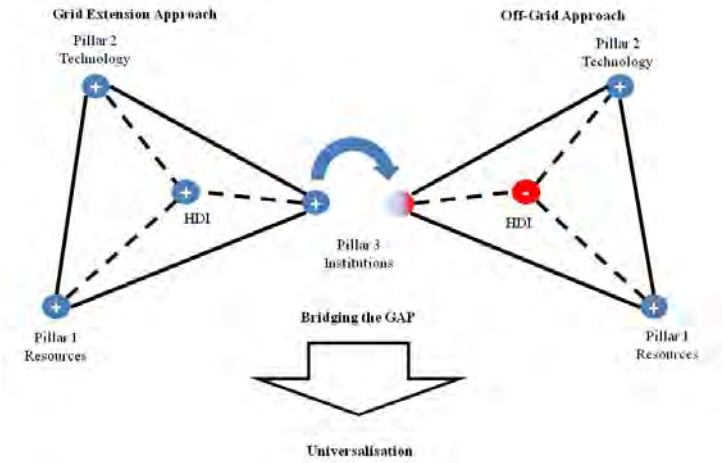

Fig. 1. Bridging the institutional gap for universalization in the Amazon region.

This paper explores the institutional characteristics of LPT and identifies improvements needed for the purpose of implementing decentralized solutions in the Amazon region. Our study has evolved around the analysis of three pillars of the electrification models applied based on grid-extension and off-grid approaches: (i) the resource availability; (ii) the technology applied and (iii) the institutional framework created to support the efforts (See Figure 1). How can the actual institutional framework support the process of supplying electricity to isolated communities so that the trend in improving electricity access and quality of life continues? The three pillars are crucial for the purpose of achieving human development. (see Figure 1). They are analyzed for both grid extension and off-grid approaches in the Amazon region. The isolated systems in the Amazon consider those electricity systems that are not connected to the national interconnected system. Though not interconnected, the majority of these systems have followed a centralized model that replicates, at a smaller scale, the national scheme. Electricity is provided through different approaches: (i) sub-grids that provide the main capital cities and nearby villages, also called Capital Isolated Systems and being developed through a grid-extension approach; (ii) mini-grids that provide electricity to small and remote villages and (iii) stand alone systems. The

extension of the sub-grids corresponds, for the purpose of this paper, to a grid-extension approach. On the other hand, the off-grid approach is related to minigrids and stand alone systems.

1. Pillar 1. The Amazon region: the potential of available resources

In face of the unfeasibility of extending the national interconnected grid, smaller but also centralized power plants were installed in order to provide electricity to the main cities in the Amazon. The grid extension approach has relied mainly on fossil resources and today about 60% of the installed power generation in the Amazon is based on diesel power plants. At a lower scale (less than 1 MW capacity per unit), suitable for off-grid applications, about 80% of the generated power is produced using diesel. The remaining 20% is produced using hydro resources [14]. Thus, while offering an opportunity to provide energy access without significantly impact the environment in the Amazon region, renewable sources have not been explored enough. In terms of hydro resources, the Amazon basin shows the largest potential for electricity generation in the whole country, corresponding to about 106 GW, that is, 42 % of the national potential [5]. But a nominal potential of about 1,7 GW has been quantified as appropriated for using small, off-grid hydro power plants [4]. According to the National Electricity Agency –ANEEL, 15 small hydropower plants are already installed. This implies a total installed capacity of just 12 MW in the region and illustrates the magnitude of the unexplored potential [14]. A number of opportunities connected to biomass resources have also been identified and actually implemented. For example, floating residual wood being carried by the rivers is already being collected in order to avoid danger for navigation. It might be used for power generation [15]. The possibility of using vegetable oils either in natura or processed as biodiesel has also been studied and applied at the level of pilot projects [6]. Though seven biomass-based power plants with an installed capacity of about 72 MW are in place in the region, just two of them have an installed capacity of less than 1 MW [7] A wide variety of native species are yet to be explored. Regarding solar radiation, the potential for every location is not well known yet due to the extension of the area and the difficulties in terms of accessibility. However, there is evidence of an average radiation of 5.5 kWh/m^2. This potential has low inter-seasonal variability, which makes it suitable for the purpose of implementing hybrid systems [10]. Finally, wind resource is found mainly in the coastal area and in Roraima, close to the border between Brazil and Venezuela. The average annual wind speed there is higher than 5m/s, suitable for the installation of small scale wind turbines with capacity at the order of 100kW [4].

To summarize, the grid extension and the off-grid approaches in the Amazon have relied on fossil fuels. Given the sensitiveness of the eco-system in the Amazon, widely available renewable energy sources offer an opportunity for fulfilling universalization goals that is still to be explored.

2. Pillar 2: technologies to provide electricity in the Amazon

The traditional grid-extension is not self-sustainable and does not promote sustainable development [10]. Some estimation exist that reveal the need for an additional installed capacity of between 456 MW and 1 GW for the purpose of attending isolated systems [11, 12]. Unlike the majority of the national inhabitants, most of the Amazon population is today supplied through the Isolated Systems. They are characterized by (i) the predominance of diesel-driven power plants; (ii) consumers that are highly dispersed; (iii) the inexistence of economies of scale and; (iv) significant difficulties of logistics for fuel supply in the region

Thermal and hydropower plants have been the main technologies used for both, the grid extension and the off-grid approach in the Amazon. The most significant difference between them is the scale. Since the grid-connected power plants supply the main cities and nearby villages, they usually have a capacity higher than 1 MW. On the other hand, the off-grid options, that is, mini-grids and stand alone systems, are related to power plants with a smaller capacity. The number of installed diesel-based power plants with a capacity inferior to 1 MW is more than ten times that of small scale hydro power plants (Figure 2). Regarding stand alone systems, diesel-based systems with capacities ranging from 10 to 66 kW are the most common. In most of the cases, communities are responsible for the installation and operation of these power plants. Some estimation exists that reveal the presence of about 3000 small-scale diesel driven power generators just in the Amazonas state. Unfortunately, these power plants are not registered in the official records [11, 12].

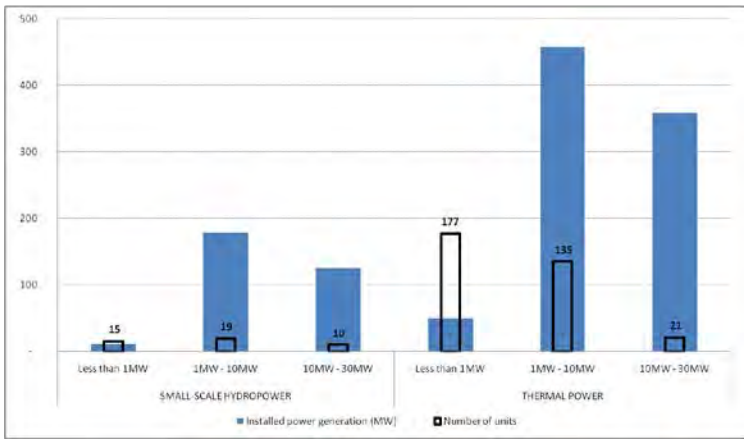

Fig. 2. Installed capacity and number of thermal and hydropower units in the Amazon (Less than 30 MW of installed capacity per unit). Source: [11]

Renewable technologies have in many cases proved cheaper and more appropriate than national grid extension when used in rural electrification [4, 13, 15, 21]. However, except for small hydro power plants, they are not used in the Amazon. The official records register just one photovoltaic system of 20 kW [14]. Biodiesel-based power generation has already shown its feasibility in stationary engines and gains importance in face of the vast biomass resources [6]. Photovoltaic technologies are suitable for lower demands than small hydro or biomass technologies. They have proved effective to provide services such as lighting and clean drinking water. On the other hand, wind energy technologies offer a good cost-competitive opportunity, in some cases with prices below those of PV, particularly effective for hybrid systems (PV-diesel) [10]. In any case, the simplicity, reliability, robustness, environmental aspects and low costs of operation and maintenance are key factors for the selection of the proper technology or mix of technologies (in the case of hybrid systems) to be implemented in a specific location.

3. Pillar 3: The existing institutional framework

LPT has obtained remarkable results in terms of poverty alleviation and human development, measured through the Human Development Index (HDI). These results have been achieved through a significant mobilization of political will and a precise definition of policies to promote full coverage [3] Resource availability, proven and mature technologies for electricity provision and a proper institutional framework have forged the success of LPT under a grid extension model. Isolated areas too have plenty of renewable energy sources that can be explored for electricity generation such as solar power and biomass. But the challenges

here are different to harness the resources and provide the technology at the local level. Can the achievements of the grid extension approach serve as the foundation for developing a decentralized approach?. If so, how can the institutional gap be covered so that the goal of universalization can be reached?.

LPT is a national program reflecting a national goal. It has created an institutional structure in which the roles of diverse players are specified at regional and local levels. Along this institutional line of action, responsibilities are attributed to organizations at the various levels, and activities are defined from planning to monitoring. At national level, a National Commission of Universalization (NCU) is in charge of defining the policies that lead to full coverage in the country and use electricity access as a driver for development. The multi-sectorial support of the policies, as per exemplified by the participation of as many as 13 ministries, together with the operationalization of the policies guaranteed by the regulator (The National Energy Agency -ANEEL), and the financial support of Brazil's major development bank are noteworthy. The National Management Committee (NMC) acts transversally, coordinating, supervising and monitoring the actions of the programme throughout the country. The coordination role is in the hands of the Ministry of Mines and Energy (MME). Eletrobras, a federal company controlled by the Brazilian government, is responsible for the Operational Secretariat and administers the financial resources provided by the corresponding sectorial funds At the regional level, the Territorial Committee accompanied by the State Management Committee (SMC) identifies and prioritizes electricity demand. The SMC receives and analyzes the demand requirements that are provided by the communities. At the local level, the concessionaires, together with the civil society act in the implementation of the program through specific projects. They work in close cooperation for the purpose of identifying actual energy needs. [8] .The monitoring activities have received particular attention and institutions at three levels have been designated to develop them. Eletrobras and ANEEL are in charge of watching over the statement of commitment signed between the Federal Government, states and implementing agents

Table 1 shows the main competences of the existing institutions involved in the development of LPT. Whilst this matrix does not show the entire spectrum of competences in every institution, it does give a good illustration of the main capabilities that serve the LPT at three different levels, national, regional and local, with the purpose of accomplishing 100% electricity coverage in the country. It also shows the preponderant role of the concessionaires at the local level, as they are the only ones directly involved in the implementation activities. This is the result of the regulation considering exclusive service territories for concessionaires. It also emphasizes a strong connection between existing technologies and implementing agents. In other words, concessionaires' expertise has grown based on the implementation of hydro and diesel-based power plants. In the search for universal access and based on the existing interconnected electricity system, Brazil has built a well structured rural electricity policy that is anchored at national, regional and local levels. However, the traditional and strongly grid-oriented approach has reached physical and economic limits in the Brazilian Amazon. It cannot be further developed. In terms of institutions, this approach has enhanced a concession model that is in its nature exclusive and creates difficulties for new stakeholders to come into the system. There is a need for a new approach focused on the demand-side and a decentralized approach, requiring different technologies and a different institutional framework. How will that be delivered?

In the process of providing universal access, the government has recognized the need for these new players and has taken action, creating some possibilities for them to be active. The

government has started the process to close the existing gap and the law has allowed the participation of new players within the existing concessions, where the concessionaires are not able to fulfill universalization targets. These possibilities are restricted where exclusivity contracts have been signed and further action from the government is limited by this fact. Yet, it is also possible for the concessionaires to establish commercial agreements with technology providers [2].

Table 1. Main competence of the institutions connected to LPT.

		Competences							
Level of action	Institutions	Policy	Regulation	Coordination	Integration	Prioritization	Operational Secretariat	Implement.	Monitoring
National	National Commission of Universalization NCU)	x							
	National Agency of Electricity (ANEEL)		x						
	Ministry of Mines and Energy			x					
	National Management Committee				x				x
	Eletrobras						X		x
Regional	Regional Coordinators			x		x			x
	State Management Committee								x
Local	Implementing Agents (concessionaires)							x	

Prepared by authors based on [8, 9]

4. Bridging the gap. Discussion and conclusions

The need for an off-grid approach has been generally recognized. Yet, the institutional framework for promoting the electricity access has not been modified or complemented for the purpose of appreciating the peculiarities of the isolated communities in the Amazon [9]. The Amazon is rich in renewable energy sources and various technologies can be applied for the purpose of providing electricity to isolated communities. These technologies have been identified by the government as critical for the purpose of reaching universalization [1, 18, 19].but the concessionaires do not have knowledge related to their installation and operation. This means that knowledge on a wide range of technologies could be better adjusted to the off-grid needs. The question is then if this implies the need for new agents for implementation, operation, maintenance and monitoring of the new off-grid systems. In this context, technology providers, community organizations and academic institutions, knowledgeable on specific renewable technologies, could add to the capacity that has been built by concessionaires in terms of management and operation of small scale thermal and hydropower plants. However, their action is limited by the existence of long-term contracts that give exclusivity to concessionaires.

Nevertheless, the concessionaires do have valuable information on the location and energy consumption trends in some of the isolated areas where they have been active and have worked in cooperation with local communities. This communication channels have been opened thanks to LPT. Local organizations, closer to the isolated communities, could then be responsible for some of the activities that today are in the hands of the concessionaires and that imply costly operation, maintenance and after-installation activities, due to the fact that concessionaires are located far away from the final users.

Thus, in order to reach universalization, the involvement of the concessionaires needs to be complemented with actions from other agents that can provide their expertise. An opportunity for existing institutions and new agents emerges for the purpose of providing electricity to the isolated areas. Actions from these new agents integrated with those from existing stakeholders could enhance the development of the required off-grid approach. Clear responsibilities for both private and public stakeholders are required to generate, distribute and supply electricity to rural inhabitants under a decentralized approach. Now, the need for a clear set of rules for new comers arises. It also does for concessionaires in connection to their new role. They could work at local level in cooperation with organizations with knowledge on the required new approaches and technologies. Technology providers, international entities and universities are examples of this type of organizations. The fact that communities are isolated and usually located far from the concessionaires raises the need for the participation of community organizations that are closer to the communities and can communicate with them easily. Such is the case of NGOs or cooperatives that have not been very active due to the existing centralized approach. Further, due to the size of the off-grid systems, management and operational skills requirements are less strict than those required to operate and manage centralized facilities. This could encourage the participation of local communities using local skills to operate the off-grid systems.

The design and implementation of the required institutional framework is complex due to the intervention of diverse public and private actors such as electricity companies, final users, funding, controlling and regulating institutions, national and local governments among others. Each of these agents has particular goals and creates the need for a clear set of rules to act. In this sense, actions from the government are crucial. There is no unique solution rather a combination of solutions that can be adopted. There are strengths that can support the process of universalization if properly complemented with the action of existing agents and new comers to be considered within the framework of LPT. Yet, clear rules are needed in order to build an enabling framework that brings together potential institutions and stakeholders when it comes to off-grid electrification of isolated villages. The governmental commitment exists and the recognition of the role that electricity access can play in addressing and achieving development goals is already in place. Now, the time has come for leading the establishment of a clear set of rules that facilitate action from the required agents and can support the development of a new and urgently needed approach.

Acknowledgements

This paper was written as part of a research program on Global Energy and Climate Studies funded by the Swedish Energy Agency.

References

[1] IEA, 2009. International Energy Agency. The Electricity Access Database. Available at http://www.worldenergyoutlook.org/database_electricity/electricity_access_database.htm on April 16, 2010

[2] Zerriffi, H., 2008. From açaí to access: distributed electrification in rural Brazil. International Journal of Energy Sector Management 2(1), 90-117.

[3] Gómez, M.F., Silveira, S., 2010. Rural electrification of the Brazilian Amazon – Achievements and lessons. Energy Policy 38 Volume 38 (10), 6251-6260.

[4] Di Lascio M., Barreto E., 2009. Energia e desenvolvimento sutentável para a Amazônia rural Brasileira. Kaco gráfica e Editora Ltda. Brasilia.

[5] ANEEL, 2009. NationalEnergyAgency.Atlas de Energia elétrica doBrasil.3 ed.Brasilian Electricity Regulatory Agency.

[6] González, W.A et al., 2008. Biodiesel e Óleo Vegetal in Natura. Soluções Energéticas para a Amazônia. Ministry of Mines and Energy. Brasilia.

[7] ANEEL, 2010; Power generation database available at http://www.aneel.gov.br/aplicacoes/capacidadebrasil/CombustivelPorClasse.asp?Classe= Biomassa on December 12, 2010.

[8] MME, 2009a. Ministry of Mines and Energy Manual de operacionalização. Programa Luz Para Todos. Review 6

[9] MME, 2009b. Ministry of Mines and Energy. Manual de Projetos especiais do Programa Luz Para Todos.

[10] Duarte, A.R., Bezerra, U.H., Tostes, M.E., Duarte A.M., Filho, G.N., 2010. A proposal of electrical power supply to Brazilian Amazon remote communities. Biomass and bioenergy 34, 1314-1320.

[11] IICA, 2008. Agroenergia e Desenvolvimento de Comunidades Rurais Isoladas Instituto Interamericano de Cooperação para a Agricultura. Available at http://webiica.iica.ac.cr/bibliotecas/RepIICA/B0849p/B0849p.pdf on September 26, 2010.

[12] Pimentel F.M., 2008. Obstáculos e oportunidades para uma política de generação de enrgía con fontes alternativas: o programa do universalização e os sitemas isolados. Master thesis. Universidade Salvador (UNIFACS).

[13] Schmid, A.L., Hoffman, C.A., 2004. Replacing diesel by solar in the Amazon: short-term economic feasibility of PV-diesel hybrid systems. Energy Policy 32, 881–898.

[14] ANEEL, 2010; Power generation database available at http://www.aneel.gov.br/area.cfm?idArea=15&idPerfil=2 on August 30, 2010.

[15] Bacellar, A.A., Rocha, B.R.P., 2010. Wood-fuel biomass from the Madeira River: A sustainable option for electricity production in the Amazon region. Energy Policy 38, 5004–5012.

[16] Andrade, C.S., Rosa, L.P. Da Silva, N.F., 2011. Generation of electric energy in isolated rural communities in the Amazon Region a proposal for the autonomy and sustainability of the local populations. Renewable and Sustainable Energy Reviews 15. 493–503.

[17] MME, 2008. Ministry of Mines and Energy. Biodiesel e Óleo Vegetal in Natura. Soluções Energéticas para a Amazônia

[18] Goldemberg J., Coelho S., Lucon O., 2004. How adequate policies can push renewables. Energy Policy 32 (9), 1141–1146.

[19] Pereira M., Freitas M., Da Silva N., 2010. Rural electrification and energy poverty: Empirical evidences from Brazil. Energy Policy. 14(4), 1229-1240

[20] De Castro, J. C., 2005. Atendimento Energético a Pequenas Comunidades Isoladas: Barreiras e Possibilidades. T&C Amazônia, Ano III, Número 6, January 2005.

[21] Mainali, B., Silveira, S., 2010. Financing off-grid rural electrification: Country case Nepal.Energy. Available on line 12 August 2010.

The Mágina Project. The renewables potential for electricity production in the province of Jaén, southern Spain

J. Terrados[1,*], J.A. Ruiz-Arias[2], L. Hontoria[3], G. Almonacid[2,3], P.J. Pérez, D. Pozo-Vázquez[4], F.J. Gallego[1], P. Gómez[5], E. Castro[6], A. Martín-Mesa[7], M.J. del Jesús[8]

[1] *Dept. Graphic Engineering, Design and Projects, University of Jaén, Jaén, Spain*
[2] *Commissioner for the Centre of Advanced Studies in Energy and Environment*
[3]*Dept. Electronic and Automatic Engineering*
[4]*Dept. Physics*
[5]*Dept Electric Engineering*
[6]*Dept. Chemical, Environment and Material Engineering*
[7]*Dept. Economy*
[8]*Dept. Computer Science*
** Corresponding author. Tel: +34 953212825, Fax: +34 953212334, E-mail: jcepeda@ujaen.es*

Abstract: Nowadays, the global energy generation system relies mostly on fossil fuels. However, their foreseen depletion for the forthcoming decades puts at risk the current schema and suggests a gradual transition to a more self sustainable system. Consequently, the European Union (EU) committed in March 2007 to set a binding target for 20% of the EU's total energy supply to come from renewables by 2020. In this work, we tackle the study of the renewables' potential for electricity production in the province of Jaén (southern Spain), which has a pronounced unbalance between its inner electricity production and consumption. The potential of biomass from olive trees, solar photovoltaic (PV) and wind power has been analyzed using Geographical Information System tools. As a preliminary result, it has been proposed the installation of 5 biomass facilities, with an estimated production of 735 GWh per year, 10 PV facilities, with an estimated production of 534 GWh per year, and 50 windmills, with an estimated production of 172 GWh per year. Overall, these three resources together would be able to increase the rate of produced to consumed electricity in the province from a 30% to a 77%.

Keywords: *renewable energies, electricity, distribution grid, regional development*

1. Introduction

The foreseen depletion of fossil resources is forcing us to seek for new energy springs. However, the climate change issue claims for non-pollutant solutions that help in mitigating the global warming. Even more, due to the world's economic development, it is expected that the worldwide demand for electricity will increase by 80% between 2006 and 2030 [1]. This global scenario makes unavoidable the transition to more and more renewable energy shares.

Therefore, promotion of renewable energies will play a major role as it is also indicated by the European Union (EU) objectives by 2020. They set a binding target for 20% of the EU's total energy supply to come from renewables by 2020 (6.5% in 2007). Furthermore, they set a firm target of cutting 20% of the EU's greenhouse gases emissions by 2020 relative to 1990. Additionally, Europe has a marked dependence on outer energy imports (50%) provided its lack of own fossil resources. In Spain, particularly, the dependence is even higher, reaching the 85%. Hence, the national government has promoted in the last years the renewables through various ambitious national plans [2] which, additionally, pretend to accomplish with the EU's commitments through, among other, a 30% target contribution of renewables for electricity production.

The province of Jaén is situated in the southern part of the Iberian Peninsula (Fig. 1). It occupies an extension of roughly 13 500 km^2 with a population totaling 669 000 inhabitants. Its economy is principally based on the olive oil industry. Actually, the olive oil production in Jaén is the 20% of the worldwide production and the 50% of the Spanish one. Its territory is

divided in two different topographic regions: the south-eastern and the northern façades, which are traversed by mountainous systems, and the region in between, a well-flat area which houses the higher part of the Guadalquivir river basin. The highest peak is the Mágina Peak, in the southern façade, with 2 167 meters above sea level.

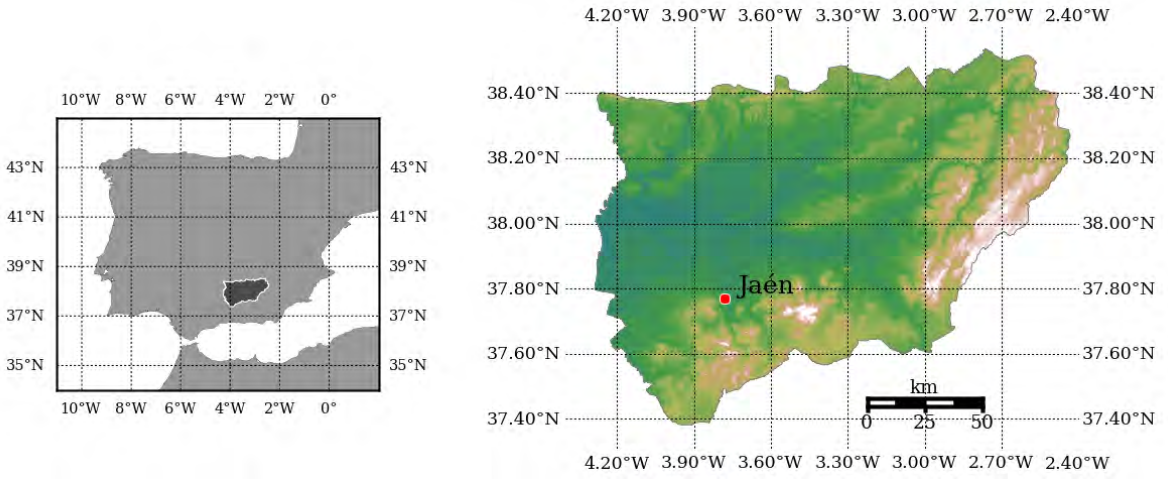

Figure 1. Geographical location and topography of the province of Jaén.

As the rest of Europe and Spain, Jaén has a high dependence on fossil fuels. As far as electric energy concerns, the region has a negative balance in production/consumption. Particularly, in 2008 the actual inner production of electricity was only about 940 GWh, against a consumption of about 3 080 GWh in this same period [3]. This situation strongly contrasts with the rest of Spain, where the electricity production/consumption is well-balanced. Particularly, in 2008, total production and consumption were about 296 000 and 275 000 GWh, respectively [3].

In order to correct this unbalance in the province, fossil fuels should not be a choice. Instead, local renewable resources are a real alternative with huge potential still to be developed. However, in spite of the high potential, currently, about 84% of the electricity is produced in thermal plants, most of them, combined heat and power plants. Out of this 84%, only a small rate comes from biomass residuals. The rest of the electricity share is produced by hydro-power stations (9%), solar photovoltaic (PV) (4%) and wind power (3%) [3].

Biomass is an important energy spring in the province, mainly, from agricultural residuals as prune wastes and olive stones, for instance. Currently, it represents around a 20% of the primary energy consumption, mainly for heating [4]. However, just the biomass from the olive prune is estimated to be about 3 tons per hectare and year [5]. Hence, the more than 600 000 ha of olive crops in the province are a resource that deserves to be exploited. Additionally, the province also has a considerable potential from solar and wind resources. Particularly, Jaén is one of the sunniest regions in Spain, with more than 1 700 sunshine hours a year. The electric production from wind farms is also a feasible approach as it has been already demonstrated by some plants that operate in the region.

In this work, we intend to tackle an estimation of the real potential for electricity production in the province of Jaén from local renewable resources: biomass, solar PV and wind power. It pretends to be a solid background to develop an optimum plan for a massive intervention in the electric grid that correct the current unbalance between electricity production and consumption based purely on renewable energies. We here propose a preliminary distribution

of the production plants based on multiple criteria as the resources distribution, availability of feed-in points in the grid or even distribution of the plants along the region. However, this initial distribution is still subject to modifications based on on-going tasks, as a deeper investigation of the current state of the local electric grid or environment and economic issues.

2. Methodology

Firstly, the different resources availability has been independently evaluated using a suitable approach in each case. Afterwards, they have been jointly analyzed by using geographical information systems (GIS) tools. With these tools, digital models with the spatial distribution of the resources have been created considering restrictive criteria as topographic features or soil type and use. These maps allow estimating the real potential for electricity production from renewable resources and a subsequent analysis based on environment, social and economic criteria; currently, an on-going task.

2.1. Biomass potential from olive tree residuals

This part of the study has involved two different stages: (i) the evaluation of the total amount of biomass residuals available from olive trees and, (ii) the evaluation of the electric performance that could be achieved.

The first stage required an intensive use of GIS tools. Firstly, soil use maps of the province were used to isolate the olive crops in the region. Among them, only those areas with a terrain slope less than 20% were considered as useful for exploitation. The rationale behind is that terrains with higher slopes make difficult the use of agricultural machinery, thus considerably increasing the management and transport costs of the residuals. Once the total (useful) area of olive crops available for exploitation was determined (S_{crops}), the total amount of residuals (*BR*, biomass residuals in kg per year) was evaluated based on the biomass residuals production index (*BRI*) for olive trees. It indicates the biomass residuals availability per ha and per year. Therefore:

$$BR = S_{crops} \times BRI. \quad (1)$$

The value of the *BRI* parameter for olive trees was extracted from previous research works conducted by the Andalusian Energy Agency and the Agricultural Department of the Regional Government of Andalusia [6, 7]. Following the recommendations of these studies, two different *BRI* values were used for irrigated and dry lands. This terrain classification was conducted based also on the soil use maps of the region.

In order to assess the potential electricity that can be generated from these biomass residuals, we were based in the operation data accumulated in some biomass plants that are already operating in the province and the rest of Spain.

2.2. Photovoltaic potential

The solar PV potential assessment also implied a two steps procedure: (i) the evaluation of the solar resource potential and, (ii) the electricity potential generation based on the resource availability.

In order to evaluate the solar resource, the clear-sky solar radiation model of the European Solar Radiation Atlas (ESRA) was used in its version implemented in the GRASS GIS

platform [8]. The ESRA model has been profusely used in practical applications as the determination of solar radiation maps from satellite imagery [9] or the generation of databases from ground measurements as the PVGIS web platform. This model parameterizes the effect of the atmosphere based on the Linke turbidity coefficient (T_L), which represents the number of Rayleigh atmospheres radiatively equivalent to the actual atmosphere. The Linke turbidity is a climatic and dimensionless parameter which has been traditionally calculated on a monthly basis from satellite and ground measurements. It is freely available in wide databases as the SODA dataset.

The second step involved the assessment of the potential electricity produced from this solar resource. The evaluation was based on a traditional fixed PV system with panels inclined 30º degrees over the horizontal and permanently oriented to the south. This reference configuration is close to the optimal for the latitudes of the region, thus enabling us to estimate the real PV potential. The recovered energy, E_{PV}, was estimated considering the practical rule that installation of 1 MW_p requires approximately a parcel of 2 ha. Therefore:

$$E_{PV} = \frac{G}{G_p}\frac{1MW_p}{2\,ha}P_R, \qquad (2)$$

where G is the total irradiance that strikes the PV panel, G_p=1000 Wm^{-2} and P_R is the performance ratio, which accounts for the different system losses. Based on our own experience, we took P_R = 75%.

The use of this methodology presents various advantages. On the one hand, as the model is integrated within a GIS, it is able to account for the topographic shading effect of surrounding terrain elevations. On the other hand, it allows us to calculate the solar radiation components with a high temporal resolution (in this case, every 12 minutes) which is essential to evaluate the total solar radiation on the tilted plane of the PV panels. Nevertheless, note that the clear-sky model is not accounting for the extinction caused by clouds. Thus, an evaluation of the model has been carried out based on long-term measurements of global solar radiation in the study region.

2.3. Wind potential

As in the former cases, the assessment has involved two steps: (i) the evaluation of the wind potential in the region and, (ii) the evaluation of the potential electricity that can be obtained from this resource.

Wind is a highly fluctuating resource both in space and time. This makes very difficult its estimation over a wide region exclusively from ground measurements since it would be required too many experimental stations which, additionally, should also record the wind at different altitudes above surface (typically, from 20 to 80 meters). Overall, this approach is often prohibitive from the economic point of view. Therefore, nowadays, the use of numerical weather prediction models is a common practice. They are able to generate comprehensive long-term data bases of the state of the atmosphere at high spatio-temporal resolutions. To do it, they make a spatial and temporal disaggregation based on physical laws (known as dynamical downscaling) over the previously assimilated datasets from worldwide measurements of the atmosphere.

In this study, we have used the Weather Research and Forecast (WRF) model [10], one of the most profusely used models for regional weather studies. A simulation over the southern half of the Iberian Peninsula was conducted for the whole 2007, thus avoiding boundary effects over the province of Jaén. The output was saved every 9 km and every hour. In the vertical, which is very important for wind assessment, the atmosphere was described based on 27 unevenly-distributed layers. A higher layers-density was set near the surface in order to achieve a better description of the turbulent transport processes that occur in these regions, which give rise to a high variability of the wind profile near the ground. Since most of the current windmills install their turbines at, roughly, 80 meters above surface, the output for wind speed from WRF was interpolated every hour at this vertical level. Afterwards, a refinement of the maps was carried out by spatial interpolation up to a grid spacing of 3 arc minutes (approximately, 5.4 km).

Finally, the wind potential for electricity generation was based on the power curves of two standard commercially available windmills developed by Gamesa (http://www.gamesa.es). If the power curve, *P(v)*, of the wind turbine is known, the potential energy generated, E_W, can be easily calculated from the local wind speed distribution, $\Phi(v)$, as:

$$E_W = \int_{v_s}^{v_c} \Phi(v)\mathrm{P}(v)\,dv, \qquad (3)$$

where v_s is the velocity at which the turbine starts to work and v_c is the cut-off velocity, above which it is locked for safety. Usually, the performance and suitability of a windmill in a given placement is measured based on the number of equivalent hours, H_e, which represents the number of hours that the wind turbine must be working at maximum power, P_n, in order to produce the actual energy which is produced along a natural year. It is calculated as E_W/P_n.

3. Results

Results will be presented separately for each resource: biomass, solar PV and wind power.

3.1. Biomass energy

The total area of olive crops in the province amounts to 680 000 ha and, up to 482 000 ha of them correspond to useful terrains for exploitation (terrain slope below 20%). The *BRI* values, given as a function of the terrain slope and for irrigated and non-irrigated lands, are shown in Table 1.

Table 1. Biomass residuals production index for olive crops in tons per ha per year.

Terrain Slope	Dry crops	Irrigated crops
less than 10%	1.6	1.7
greater than 10%	1.4	1.6
greater than 20%	excluded	

According to these values, the total potential volume of biomass residuals from olive crops was found to be about 720 000 tons per year. After revising the historical production records of some biomass power plants which are already operating in Spain, it was concluded that facilities with a power of 16 and 25 MW consume around 120 000 and 170 000 tons per year, respectively. Therefore, multiple number and size of facilities, as well as different distribution layouts, could be selected. In this case, using GIS techniques, three different schemes were evaluated considering multiple criteria as: volume of biomass residuals available in the

proximities of the plant, ease access to the facilities with heavy machinery, ease access to feed-in points in the grid or distance to cities. Particularly, the different layouts tested were: (i) 4 plants of 25 MW, (ii) 6 plants of 16 MW and (iii) 2 plants of 16 MW and 3 plants of 25 MW. The latter probed to be the best one according to the criteria established. Table 2 shows the operating details for each plant and Fig. 2 shows their geographical distribution and influence area.

Table 2. Installed power, biomass consumption and electricity production of the biomass power plants proposed in this study.

Facility (nearest city)	Installed Power (MW)	Biomass consumption (tons/year)	Production (GWh/year)
Linares	25	167 411	187.5
Vva. del Arzobispo	16	115 349	120.0
Peal del Becerro	16	115 349	120.0
Arjonilla	16	115 349	120.0
Martos	25	167 411	187.5
Total	98	680 867	735.0

3.2. Solar PV energy

The solar radiation potential was estimated using the ESRA's clear-sky model, which does not account for the very important role of the clouds. In order to evaluate the validity of this approach, the clear-sky estimates were compared against a 5 years-length record of global solar radiation data registered at the experimental station of the University of Jaén. During spring and summer months, when the solar resource is higher, the difference between the measurements and the model keeps always below 1 $kWhm^{-2}$. During the 5 years record, the experimental station registered an average daily value of 5.95 $kWhm^{-2}$, while the corresponding simulated value was 5.50 $kWhm^{-2}$. Interestingly, the simulated value is below the observed one. This seems to indicate that SODA database reported an excessively high value in the province over the whole year. Anyway, the annual error is below 8%.

Figure 2. Proposed distribution of the biomass, PV and wind power plants.

The difference between the maximum and the minimum yearly sum of irradiance over the whole region is a 5%. This is attributable to the topographic spatial variability caused by the mountains. In the flat area over the Guadalquivir river basin, the solar resource is relatively homogeneous around 2 075 $kWhm^{-2}$, which is equivalent to a PV generation of 78 $kWhm^{-2}$. Extended over the whole province, the PV potential is more than 300 times higher than the annual consumption of electricity in the region.

Based on these results, we propose the installation of 350 MWp spread over 10 PV facilities. Overall, these power plants would produce 534 GWh per year, occupying around 70 km^2, the 0.5% of the province's extension. Again, GIS tools have been used to delimitate those areas useful for housing the power plants. Now, based on soil use and type, the next areas were excluded: urban, industrial, leisure and commercial areas, dumping sites and wet, irrigated and protected lands. Finally, the PV plants were distributed as shown in Fig. 2 based on the next criteria: (i) the plants must be close to suitable feed-in points, (ii) they must be evenly distributed over the electric grid and, (iii) complementary to the windmills sites proposed in the next section.

3.3. Wind energy

In average, according to the simulation with the WRF model, the areas with the highest wind speed at 80 meters above surface are the southern and eastern mountainous systems. This result shows the existence of a certain complementarity with the PV solar energy, which is more suitable in flat lands without topographic shading. The yearly average wind speed over the mountains ranges from 6.5 to 7.5 ms^{-1}. In the flat areas around the river basin, the resource drops up to 4 ms^{-1}.

The amount of electricity that can be generated from this resource depends on the wind turbine which be used. We selected two commercially available standard windmills, the G80 and the G87, developed by Gamesa, with the turbine placed at 80 meters above surface. Both windmills give a maximum (nominal) power of 2 MW. By using Eq. (3) we calculated the energy produced by each turbine over the whole province and, then, the number of equivalent hours. Overall, the G87 model fitted better the local wind resources. Particularly, all mountains in the province have more than 1500 equivalent hours and, the eastern façade, more than 2000 hours.

Deployment of wind farms must accomplish a severe environmental normative. Actually, it is usual that several projects be rejected by the competent authority. Therefore, in this study, we based our proposal for the wind farms distribution on a previous work carried out by the provincial department of energy of Jaén [11] which describes a series of sites that already account with legal support for its suitability to house small wind farms. Overall, the installation of 50 windmills over 13 small wind farms is proposed (Fig. 2). All of them are placed along the south – south-eastern façades of the province, outside protected natural parks. The average number of equivalent hours is 1 702 and the estimated amount of electricity generated with these wind turbines is about 172 GWh.

4. Discussion and conclusions

Compared to Andalusia and the rest of Spain, the province of Jaén has a marked unbalance between its inner electricity production and consumption. Nevertheless, it has a promising potential to increase its production quota based solely on local renewable resources which, additionally, contribute to reduce pollutant emissions to the environment. On the one side, its

industry is mainly based on the olive oil, being the major worldwide producer. This industry generates a huge amount of wastes that can be used as fuel in biomass power plants. On the other side, the province also counts with large solar and wind resources.

In this work, we have analyzed the potential for producing electricity from these three renewable sources. We have study a preliminary distribution of the production plants based on geographical and territory criteria. Hence, it is worth to note that this proposal does not aim to be the optimal energy mix in the region since we are not considering social and economic constraints, for instance. Overall, with this proposal, around 1 450 GWh could be produced every year. Consequently, the rate of produced to consumed electricity would increase from a 30% to a 77%. At the same time, the use of renewables instead of fossil-fuel-based technologies, would avoid the emission of almost one million tons of CO_2 to the atmosphere.

Currently, the project has other on-going tasks aiming a deeper knowledge of the current state of the electric distribution grid to identify the improvements required to support this intervention, as well as the environmental, social and economic implications of the plan. First results seem to recommend a smooth implantation of the facilities along a decade and should end with a first proposal of optimal energy mix.

References

[1] International Energy Agency, World Energy Outlook 2006

[2] Ministerio de Industria, Comercio y Turismo, Plan de Energías Renovables de España 2005-2010, Instituto para la Diversificación y el Ahorro de la Energía

[3] Junta de Andalucía, Anuario Estadístico de Andalucía 2010. Instituto de Estadística de Andalucía. Consejería de Economía, Innovación y Ciencia

[4] Terrados, J., Metodología para la planificación y el desarrollo de las energías renovables en el ámbito regional. Caso de aplicación: la provincia de Jaén, 2005. Tesis Doctoral dirigida por el Dr. Gabino Almonacid Puche.

[5] Sánchez, S., Moya, A.J., Moya, M., Romero, I., Torrero, R., Bravo, V., San Miguel, M.P., Aprovechamiento del residuo de poda del olivar, Ing. Quim., 34(391), 2002, pp. 194-202

[6] Junta de Andalucía, Potencial energético de la biomasa residual agrícola y ganadera en Andalucía, 2008, Consejería de Agricultura y Pesca

[7] Junta de Andalucía, Potencial y Aprovechamiento energético de la biomasa del olivar en Andalucía, 2007, Agencia Andaluza de la Energía

[8] Šúri, M., and Hofierka, J., A new GIS-based solar radiation model and its application to photovoltaic assessments, Transactions in GIS, 2, 2004, pp. 175–190

[9] Rigollier, C., Bauer, O., Wald, L., On the clear sky model of the ESRA—European Solar Radiation Atlas—with respect to the Heliosat method, Solar Energy, 68(1), 2000, pp. 33-48

[10] Skamarock, W., et al., A description of the Advanced Research WRF Version 3, 2008, Technical Report, National Center for Atmospheric Research, Boulder, CO, USA

[11] Diputación Provincial de Jaén, Proyecto de Promoción de Parques Eólicos Singulares en la Provincia de Jaén, 2007, Agencia de Gestión Energética de Jaén

Different regional scenarios of renewable energies analyzed with the use of Analytic Network Process

Elena Comino[1,*], Vincenzo Riggio[1] , Maurizio Rosso[2]

[1] *Dipartimenti di Ingegneria del Territorio dell'Ambiente e delle Geotecnologie – Politecnico di Torino, C.so Duca degli Abruzzi, 24, 10129 Torino, ITALY*
[2] *Dipartimento di idraulica, trasporti e infrastrutture civili – Politecnico di Torino, C.so Duca degli Abruzzi, 24, 10129 Torino, ITALY*
** Corresponding author. Tel: +39 011 5647647, Fax: +39 015646997, E-mail: elena.comino@polito.it*

Abstract: In March 2007 Europe Union fixed strong environmental objectives for all its members, and for the 2020 it will be required a reduction of 20% of energy consumption, a 20% quota of energy consumption obtained by renewables and a 20% reduction of greenhouse gases. The Piedmont Region administration lunched a roadmap either for the industrial side that for the civil one, but our Region has several territory scenario strongly linked with the geomorphology and many technical solutions can't be used as a standard. With this work our aim is to make a comparison of the most used renewables technology in our territory like biomass, hydroelectric and photovoltaic with a multi-criteria analysis. The paper shows the application of Analytic Network Process (ANP), a multi-criteria technique, according to complex network, in order to select the most sustainable solution for the different scenario. The models enable all the elements of the decision process to be considered, namely technological factors, environmental aspects, economic costs and social impacts, and to compare them to find the best alternative. All the data used in the model are taken from public sources and the required elaboration were self-made.

Keywords: *Multi-criteria analysis, Renewable energy, Analytic Network Process.*

1. Introduction

In the last years the Piedmont Region started to considered the energies from renewable sources as a priority in the new government energy policies. As a result a deep study was conducted based on economics and technological models, to realize a strategic energy document useful for the sectorial demand and supply, forecasts of the trends of input-output items, and a list of actions, collecting several measures voted to fulfill the main aims of the energy plan [1]. This plan is addressed to reach the main goal of a 20 – 20 – 20 scenery (energy saving, production from renewable sources, reduction of greenhouse emissions), according to the many constraints and factors. To fully comply these needs could be useful the adoption of a multicriteria approaches in the selection of the most appropriate actions among all the available alternatives. The selection of the alternative options derives from the goal set identified by the decision – maker, with regard to the technical, economic and environmental spheres. Different multicriteria methods have been developed during the last 30 years for providing support to decision makers facing conflicting, or not so clear, decision situations. Recent literature surveys have shown that Multi-Criteria Decision Analysis has been used in energy planning [2,3], with some cases dealing with the comparative assessment of energy scenarios [4,5]. This paper presents a decision support approach, called Analytic Network Process [6], for energy planning application. The investigation takes place on a case study of different renewable energy technologies provision for local government in Italy, taking as its base the area of Piedmont, a region placed in the north-western part of the country.

2. Methodology

2.1. The ANP

The ANP model consists of control hierarchies, clusters and elements, as well as interrelations between elements [6,7]. The ANP allows interactions and counter-interactions between clusters to be studied and supplies a network structure that is able to connect clusters and elements in any manner in order to obtain priority scales from the distribution of the influence between the elements and clusters. The ANP requires a network structure to represent the problem, as well as a pairwise comparison to establish the relationships within the structure. The analytical tools provided by the ANP are very useful to support the decision making process; nevertheless, it is always important to supply a great deal of information or many experts to the model in order to arrive at a better solution. The literature in the ANP field is quite recent and some publications can be found in strategic policy planning [8], market and logistics [9], economics and finance [10] and in civil engineering [11], while research activity on territorial and environmental assessment is still poor [12,13,14,15]. From the methodological point of view, the model can be divided into several main stages as follow: Step I: Development of the structure of the decision-making process; Step II: Pairwise comparison; Step III: Supermatrix formation; Step IV: Final priorities.

2.2. Case study

2.2.1. Application of the Analitic Network Process to energy planning in Piedmont

This work presents an application of the ANP for the selection of the most suitable technologies in a RET (renewable energy technologies) diffusion plan for the Piedmont Region [1]. A group of technologies of energy conversion has been chosen in order to asses environment, energy and economic effects, which are associated with their actual and future (2020) diffusion in Piedmont. This set has been further restricted to macro technologies oriented to renewable resource use. Table 1 shows the selected alternatives/actions.

2.2.2. Definition of evaluation cluster

Aside the cluster filled with the alternatives a diffusion process of an innovative technology needs the following requirements: a) consistence with the local energy demand predictions, required to confirm or reject the expectations of lasting development for the considered improvement; b) affinity with the local economic and technical condition, which derives on the local capacity of managing the innovation both at financial and technical levels; c) compatibility with the political, legislative and administrative situation; d) compatibility with the actual environmental and ecological constraints. Agreeing with the above considerations, 13 criteria are identified and collected under 3 macro criteria as shown in Table 2.

2.3. Description of the criteria for the analysis

Regional scale objective of primary energy saving (A): It is an estimation of the amount of primary energy that a given action allows to save. This saving can be estimated by means of reduction of final energy consumptions, under the same operating conditions. This criteria is defined as the awaited annual saved energy in the potential scenario [1], which derives from fossil fuels, as ktep/year.

Technical reliability, maturity (B): It is fundamental based on the state of the art of the applied technology. The judgment is expressed by means of a score included within the range [1,5]. A level order is applied, with increasing preference from 1 to 5, as follows: 1. Laboratory level; 2. Pilot plants, where the demonstrative goals is correlated to the experimental one, referring to the operating and technical conditions; 3. Improvements are still possible; 4. Theoretical limits of efficiency are near to be reached; 5. A very efficient technology.

Table 1. List of the selected actions to be diffused

Number	Energy source	Technologies/actions	Macro technologies
1	Hydraulic energy	Hydro plants in derivation schemes Hydro plants in existing water distribution network	Hydro plants
2	Biomass energy	Electric power from solids biomass Electric power from liquids biomass Electric power from biogas Biofuels CHP plants fed by biogas CHP fed by solids biomass CHP fed by liquids biomass	Biomass
3	Solar energy	PV roofs: grid connected system generating electric energy	PV
4	Solar energy	Solar water heating for large demands at low levels of temperature Domestic solar water heaters	Solar water heaters
5	Geothermal energy at low enthalpy	GSHP, SGV, GWHP, plants that use lakes and drainage basin water to fed the circuit	Geothermal
6	Wind energy	Wind turbines (grid connected)	Wind turbines

Number of installation and maintenance requirements with local technical know-how (C): It is a qualitative comparison between the complexity degree of the considered technology, and the capacity of local actors of assure an appropriate support. The following qualitative scale is used: 1. Inadequate technical background for installation and maintenance; 2. Moderate technical background for installation and maintenance; 3. Good technical background for installation and maintenance.

Efficiency and predictability of performances (D): It is very important to know if exist a pattern of not continuous operational conditions. This situation is often strongly linked to the specific technology and does not indicate a factor of unreliability. Obviously when malfunctioning conveys toward condition of unpredictability, it could be a sign of weakness. The following scale of judgment is used for the evaluation: 1. Erratic and not constant operation; 2. Probable but not constant operation; 3. Probable and constant operation.

Impact on the local employment (E): The estimation of potential labor, due to employment of RET, was not possible using literature data, mostly due to a lack of information at Italian regional and national levels. This value was obtained for every technology [1,5] as the difference between the awaited installed power at the minimal energy scenario and the potential one [1]. Where 1 is the lowest grade and 5 the highest.

Regional economic incentives (F): Is the criteria that takes in consideration how much the generated electricity is paid with the economic incentives. It is a reference index expressed in €/MWh.

Affinity with political, legislative and administrative situation (G): The national normative promotes several innovative strategies of energy saving and conversion. The different strength of these national incentives represents a judgmental element among different alternative

interventions. The examined criterion assesses the qualitative relevance of the above actors, and the policy of public information. The overall value judgment is expressed in the following way: 1. Lacking; 2. Middle; 3. High.

Market opportunity (H): This criterion evaluates the market availability and the status in the penetration process of a given technology, materials and services associated with the considered action. The adopted scale is the following: 1. Market availability of the technology for more than 10 years; 2. Market availability of the technology for less than 10 years; 3. Start of market availability; 4. Pilot plants; 5. Not present on the market at least in an experimental stage.

Scheduled lines of research (I): In the Regional energy plan every technology has several research fronts [1],this information is used to create a qualitative index [1-3] where 1 represent the lowest grade of active research channels and 3 the highest.

Sustainability reported to greenhouse pollutant emissions (L): The criteria is taken in consideration to measure the equivalent emission of CO_2, which will be avoided by the examined action in the potential scenario at 2020. Therefore it is a reference index expressed in kt of reduced CO_2.

Sustainability reported to greenhouse pollutant emissions (M): Pollutants taken in consideration are divided in the following categories: a) air emissions mainly due to combustion process; b) liquid wastes, which are associated mainly with secondary products; c) solid wastes, which are generated during the life cycle of actions. Category and volume of emissions, and costs associated with wastes treatment are considered. To obtain a synthetic index, the score is expressed through the following qualitative ranks: 1. Very high emissions, each category is relevant; 2. High emissions, at least two category are relevant; 3. Middle emissions, at least one category is relevant; low emissions, all the emissions category are insignificant or do not exist.

Estate requirement (N): This is probably one of the most critical factors for the intervention site, especially when the human activities are relevant factors of environmental pressure. Some technologies requires strong demand of and this could determinate an economic losses, which are proportional to the specific value of site and the possible attendant alternative needs. For the large scale of proposed actions it is difficult to perform specific evaluation and a mean index is assessed as m^2/kW of installed power. Local scale evaluations could describe better drawbacks or possible benefits, but this is not the scope of the present work.

Sustainability reported to other environmental impacts (O): In this criteria are evaluated all the relevant impacts like landscape, acoustic emissions, electro-magnetic interference, bad smells and microclimatic change. The synthetic judgment is expressed through the following rank: 1. Very high intensity; 2. High intensity impacts; 3. Middle intensity impacts; 4. Low intensity impacts; 5. Not existing impacts. All the scores, obtained from the application of the criteria to each action, are grouped in the table below (Table 3).

2.4. The network model

This model consists of elements grouped into cluster. The elements of a cluster can be related to elements of another cluster or to elements of the same cluster (feedback). The alternatives form an additional cluster.

Table 2. Groups of criteria

Technological criteria	Economic and social criteria	Environmental and energy criteria
Regional scale objective of primary energy saving	Impact on the local employment	Sustainability reported to greenhouse pollutant emissions
Technical reliability, Maturity	Regional economic incentives	Sustainability reported to other pollutant emissions
Number of installation and maintenance requirements with local technical know-how	Affinity with political, legislative and administrative situation	Estate requirement
Efficiency and predictability of performances	Market opportunity	Sustainability reported to other environmental impacts
	Scheduled lines of research	

Table 3. Synthesis of evaluation of alternatives, according to the fixed criteria.

Alternatives	A	B (1-5)	C (1-5)	D (1-3)	E (1-4)	F (€/MWh)	G (1-3)	H (1-5)	I (1-3)	L (kt)	M (1-4)	N (m2/KW)	O (1-5)
Hydro plants	272	5	5	2	2	220	3	1	1	844.7	4	-3.8	2
Biomass	-70.2	4	4	1	2	180-280	1	4	2	2089.8	2	-80.5	3
PV	26.6	2	2	1	1	251-402	2	4	2	82.7	4	0.0	4
Solar water heaters	67.2	4	4	1	1		1	2	3	196	4	0.0	4
Geothermal	30.5	3	3	2	4	200	1	5	1	53.6	4	0.0	5
Wind turbines	30.3	4	2	1	3	300	1	5	1	94.1	4	-10.0	3

2.4.1. Determination of the network.

In ANP, numerical data can be represented graphically and thus show the influence pattern of the network. This step is essential for the further development of the process because if all the complexity of the real-world case study is to be transferred to the model, it is fundamental to accurately identify the influences of some elements upon others based. The risk is that if one influence is not identified, the model will not take it into account and some valuable information will be lost. The decision model was built with the help of the Super Decisions v 2.0.8 software (www.superdecisions.com). Fig. 1 shows the relationships among the clusters.

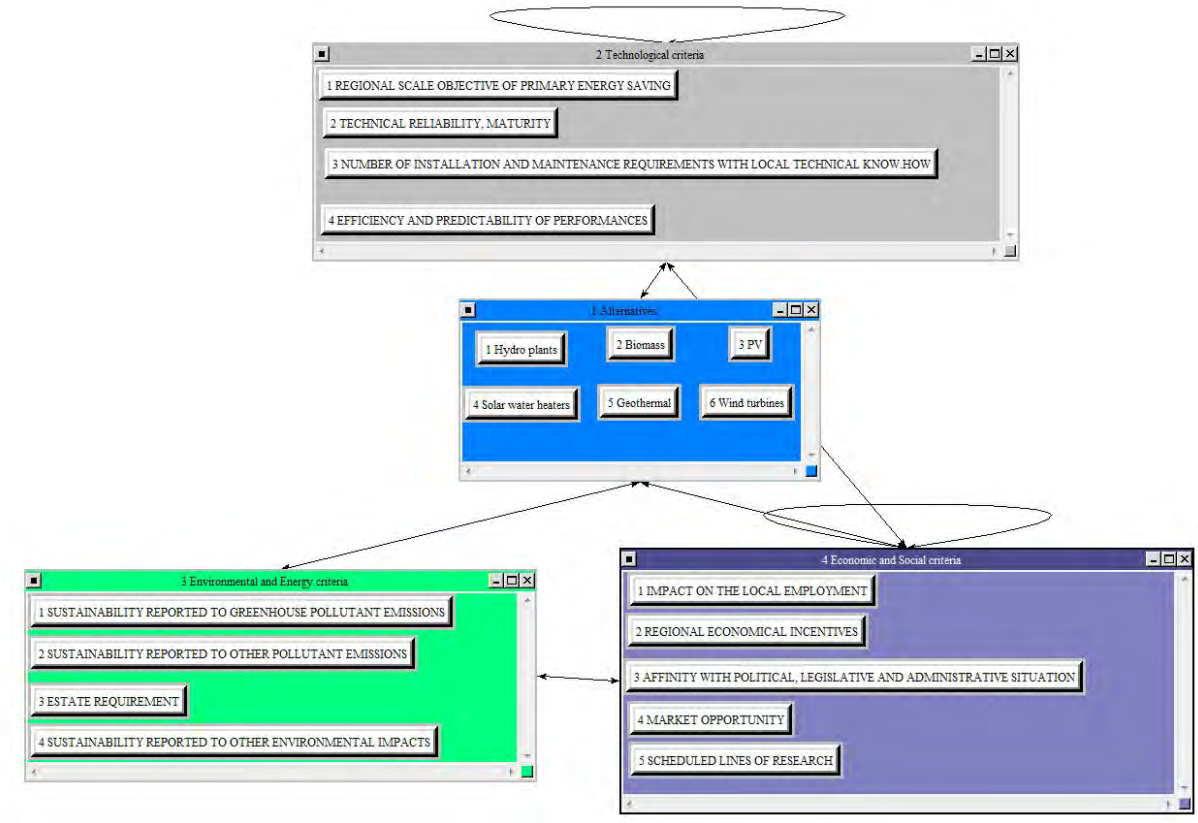

Fig. 1. ANP model scheme with inner and out dependencies.

2.4.2. Determination of element and cluster priorities

This stage includes all the steps of the ANP model. The first step consists of assigning priorities to related elements in order to build the unweighted supermatrix. For this end, each node is analyzed in terms of which other node have influence upon it; then the corresponding pairwise comparison matrices of each cluster are generated in order to obtain the corresponding eigenvectors. As in the case study different node from different clusters have influences on one cluster the unweighted matrix is nonstochastic by columns. All clusters that exert any kind of influence upon each group have to be prioritized using the corresponding cluster pairwise comparison matrices [16]. The value corresponding to the priority associated with a certain cluster weights the priorities of the elements of the cluster on which it acts (in the unweighted supermatrix), and thus the weighted supermatrix can be generated.

2.4.3. Calculation of the limit matrix and resulting prioritization.

By raising the weighted supermatrix to successive powers the limit matrix is obtained. The results of the model are shown in Fig.2.

Name	Graphic	Ideals	Normals	Raw
1 Hydro plants		1.000000	0.206519	0.06292
2 Biomass		0.946465	0.195463	0.05955
3 PV		0.680408	0.140517	0.04281
4 Solar water heaters		0.795539	0.164294	0.05005
5 Geothermal		0.709340	0.146492	0.04463
6 Wind turbines		0.710419	0.146715	0.04469

Fig. 2. Final results where the Raw *column gives the priorities from the limiting supermatrix, the* Normals *column shows the results normalized for each component and the* Ideals *column shows the results obtained by dividing the values in either the normalized or limiting columns by the largest value in the column.*

2.4.4. Phase of evaluation of results

Fig. 2 shows the results obtained with model of the study. The "best" alternative is the one with the "highest" score. The alternative selected by the model as the best options is the hydro plants technology, which is the action with the best behavior throughout the execution process, from project formulation to final score. The result shows the great complexity of the problem. In ANP the priorities are effected by the influences among clusters.

3. Discussion

It is clear that the results obtained from the model must be read in the correct way. Even if the model selected an action amongst the others it does not meaning that technology is always the preferred solution. Indeed the meteorology monitoring of the past few years has shown that precipitation in the Region are not so plentiful to allow a full energy production from the installed hydro plant. Nothing let us believe that this situation will change in the nearest future. So the second and the third actions could be very interesting in a planning situation, both biomass and solar water heaters are good potential technology. Biomass contains a big potential that could be express both in electricity and thermal power. At the same time solar water heating, even if a well know technology, could be implemented in more efficiency ways as the research in the optimization of thermal transformation proceeds.

4. Conclusions

An ANP model is applied in order to asses groups of actions focused on the implementation of several RET innovative technologies voted to use energy renewable resources. The introduction of a multicriteria approach makes a decisional process more flexible and transparent. In this case study 13 evaluation criteria grouped in 3 cluster have been defined, in order to increase the flexible approach to the decision-making. From the obtained results is clear as the RET represent in all forms a strong response to the limits imposed for the 2020 scenario.

References

[1] V.A., Relazione programmatica sull'energia 2009, Regione Piemonte, 2009.

[2] Hobbs B.F., Meier P., Energy decisions and the environment: a guide to the use of multicriteria methods. Dordrecht: Kluwer Academic Publishers, 2000.

[3] Diakoulaki D., Antunes C.H., Martins A., MCDA and energy planning, in: Figueria J., Greco S., Ehrgott M., editors, Multi-criteria decision analysis: state of the art surveys. New York: Springer, 2005, pp. 859-98.

[4] Jones M., Hope C., Hughes R., A multi-attributive value model for the study of UK energy policy, J. Oper Res Soc, 1990, 41:919-29.

[5] Pan J., Rahman S., Multiattribute utility analysis with imprecise information: an enhanced decision support technique for the evaluation of electric generation expansion strategies. Electr Power Syst Res, 1998, 46:101-9.

[6] Saaty T.L.,Vargas L.G., Decision making with the Analytic Network Process – Economic, Political, Social and Technological application with Benefits, Opportunities, Costs and Risk., Springer Science + Business Media LLC, 2006, pp. 1-20.

[7] Saaty T.L., Theory and Applications of the Analytic Network Process. RWS Publications, Pittsburgh, 2005.

[8] Ulutas, B.H., Determination of the appropriate energy policy for Turkey. Energy, 2005, 30 (7), pp. 1146-1161.

[9] Agarwal A., Shankar R., Tiwari M.K., Modelling the metrics of lean, agile and leagile supply chain: an ANP-based approach. European Journal of Operational Research, 2006, 173 (1), pp. 211-25.

[10] Niemura M.P., Saaty T.L., An analytic network process model for financial –crisis forecasting. International Jpurnal of Forecasting, 20 (4), 2004, pp. 573-87.

[11] Neaupane K.M., Piantanakulchai M., Analytic network process model for landslide hazard zonation. Engineering Geology, 2006, 85 (3-4), pp. 281-94.

[12] Promentilla M.A.B., Furuichi T., Ishii K., Tanikawa N., Evaluation of remedial countermeasures using the analytic network process. Waste Management, 2006, 26 (12), pp. 1410-1421.

[13] Bottero M., Lami I.M., Lombardi P., 2008, Analytic Network Process. La valutazione di scenari di trasformazione urbana e territoriale, Alinea: Firenze, 2008.

[14] Bottero M, Mondini G., An appraisal of analytic network process and its role in sustainability assessment in Northern Italy, International Journal of Management of Environmental Quality, 2008, 19 (6), pp. 642- 660.

[15] Wolfslehner B., Vacik H., Evaluating sustainable forest management strategies with the Analytic Network Process in a Pressure-State-Response framework. Journal of Environmental Management, 2008, 88 (2), pp. 1-10.

[16] Saaty T.L., Decision making with independence and feedback: the analytic network process. Pittsburgh: RWS Publications, 2001.

The Händelö area in Norrköping, Sweden
Does it fit for Industrial Symbiosis development?

Saeid Hatefipour[1, *], Leenard Baas[1], Mats Eklund[1]

[1] *Division of Environmental Technology & Management - Department of Management & Engineering, Linköping University, Linköping, Sweden*
[*] *Corresponding author. Tel: +46 (0) 13 28 56 27, E-mail: saeid.hatefipour@liu.se*

Abstract: Today, sustainable cities/regions are playing an important role in sustainable development projects. The overall aim of the current paper is to demonstrate an Industrial Symbiosis development in the Händelö area of Norrköping city in the Östergötland county of Sweden. It is part of a research program called "Sustainable Norrköping" focusing on developing links between the industrial and the urban part of the city. As analysis of the current situation is important for understanding the future development, the paper tries to map the current industrial symbiosis links and symbiotic network to identify potentials exist. To achieve this, paper gives a general view of how this area has been developed, constructed, and grown. The next stage is devoted to an inventory of different actors, stakeholders, and companies, their processes and relationships in the form of energy, materials and by-products exchanges, flows and streams into and out of the Händelö area considering the Händelö/Norrköping as system boundaries. In addition, by describing different tools, elements and approaches of industrial symbiosis and considering and applying two main key tools as industrial inventories and input/output matching the paper also tries to show that whether the already industrial activities formed inside the Händelö fits for an industrial symbiosis development.

Keywords: *Sustainable Regions, Norrköping, Händelö Area, Industrial Symbiosis (IS)*

1. Introduction

Eco-industrial and sustainable regional/industrial developments are terms that now a days researchers, regional planners and business developers are encountered with. During the recent years, a substantial amount of research works has been conducted through emerging field of industrial ecology and one of its major applicable parts, industrial symbiosis. Almost both fields' aims are addressing sustainable development through systems at different levels and approaches. Hence, industrial symbiosis has been suggested as an efficient and applicable tool for sustainable regional/industrial development. Going back to historical view of industrial ecology, Erkman [1] proposed an analogy between industrial systems and natural ecosystems in which industrial systems and its processes are explained as mimicking the nature. The main elements of an industrial system are introduced as energy, materials, and information that flow inside the system. Chertow defined that industrial ecology preforms at three levels; "facility or firm", "inter-firm", and "regional/global" level. Moreover, as industrial symbiosis involves exchange cases amongst several firms, hence industrial symbiosis operates at "inter-firm" level. In a system perspective, by definitions, Chertow has defined key elements to IS as, "the keys to IS are collaboration and the synergistic possibilities offered by geographic proximity" and "Industrial symbiosis engages traditionally separate industries in a collective approach to competitive advantage involving physical exchange of materials, energy, water, and/or by-products" [2]. Ristola & Mirata enhanced the sustainability of localized industrial systems using industrial symbiosis. Moreover, regional scale of industrial symbiosis is currently applied worldwide as a tool with the aim of developing more sustainable regions [3]. In a Swedish case study of the Landskrona industrial symbiosis project, the industrial symbiosis networks and its contribution to regional environmental innovation has been investigated by Mirata & Emtairah [4].

The present study is somehow intertwined with two current research projects at the division of environmental technology and management at Linköping University. From one side, it is part of a research program called "Sustainable Norrköping" which tries to study links between the industrial and urban part of the city. On the other side, it can be part of the Industrial Ecology Research Program (IERP), a research program developed in the framework of a 10-year funding agreement between TEKNISKA VERKEN (the energy corporation in Linköping) and Linköping University. IERP mainly focuses on regional Industrial Symbiosis development in Östergötland county of Sweden. It will show how and whether industrial symbiosis has the potential and capability to be an applicable tool towards regional sustainable development. Furthermore, it will practice how industrial symbiosis can contribute to a sustainable Östergötland development network. However, the Händelö area project is a real case as a sub-local development that can be expanded to a local (Norrköping city) and regional (Östergötland county) development. Hence, the current paper tries to find how industrial symbiosis fits in industrial activities of Händelö area at city of Norrköping. In the next phase, we analyze material exchange types at a spatial/organizational scale of Industrial Symbiosis by the application of a geographic information system (GIS) tool. Moreover, concepts like contribution to a CO_2-neutral eco-industrial park, moving toward maximize sharing of renewable energy resources will be also investigated in the next development stages of our research.

2. Methodology

The paper is being formulated based on the following approaches. First of all, a literature review with the subject of industrial ecology/industrial symbiosis projects and regional sustainable development has been performed, aiming at recognizing the main characteristics, challenges, and opportunities that other industrial symbiosis projects and regional development cases were encountered with. In the next stage, an inventory of the actors or an industrial inventory as one of the useful industrial symbiosis tools is introduced [2]. In this regard, an inventory of participating actors along with their processes is provided and analyzed. These types of information are mainly collected from interviews with key actors, field visits, and by setting up a technical meeting with responsible organizations involved in a regional project. Using a case study is another methodology used in this paper. As there are several actors in the city of Norrköping and the city consists of different parts and areas that have some technical, business and social relation with each other, the focus in this paper is mainly devoted to Händelö area and the energy cluster at Händelö as the nominated area for industrial symbiosis.

3. Results

3.1. Lessons learned from industrial symbiosis concepts and applications

Being deeper in most of recent and current industrial symbiosis or eco-industrial park projects worldwide, it is evident that there are some key items, concepts, approaches, tools and elements which have been used, discussed, and applied during those projects. Amongst several industrial symbiosis projects world wide, the Kalundborg in Denmark was pioneer in experiencing an industrial symbiosis model to create an eco-industrial park [2]. In this regard, it is shown that the Kalundborg's achievements not only energy, water, and waste exchanges, which have lead to better environmental and economic performances, but also social-human dimensions, equipment and information sharing were involved as well. On the basis of literature and projects experiencing in the field of industrial symbiosis [2,5], approaches, measures, key items, elements, applicable tools and definitions of different aspects of industrial symbiosis and industrial symbiosis projects have been found. With this knowledge in the first round of research can be identified whether an industrial area and the participants

in the symbiosis can be matched with industrial symbiosis or not. Those elements and key items are summarized below.

3.1.1. Industrial Symbiosis tools

Regarding industrial symbiosis tools, Chertow [5] has defined several useful tools in industrial symbiosis analysis like industrial inventories, input/output matching, stakeholder processes, and material budgeting. It is suggested that, as soon as an industrial area is considered of interest for industrial symbiosis, the first step through an industrial symbiosis analysis can start with an inventory of local actors and relevant organizations. In the same literature, input/output matching has been introduced as "key to symbioses" for links of companies. Three methods: written surveys, interviews and utilizing simulation softwares, are mentioned for data gathering and analysis. Another industrial symbiosis tool is defined as materials budgeting, in which the aim is to map the energy and material flows through an industrial system. As the tool can help to map the route of flows and stocks, it could be fundamental to an industrial symbiosis analysis. Moreover, it is defined that, "The material budgeting can be a basic building block of an industrial symbiosis analysis" [5].

3.1.2. Elements of Industrial Symbiosis

Items such as embedded energy and materials, life cycle perspective, cascading, loop closing, and tracking material flows have been introduced by Chertow as elements of industrial symbiosis [5]. Embedded energy and materials is an industrial symbiosis element which shows that the sum of materials and energy consumed to generate a new product is equal to the amount of embedded in that product. Hence, "reusing by-products" in industrial symbiosis links, maintains the embedded materials and energy for a longer time within the industrial systems. Environmental impacts which appear at every stage of product life cycles, considered as life cycle perspective. According to industrial symbiosis, life cycle perspective is used to evaluating symbiotic opportunities. When energy or water recourses are consumed many times in several different relevancies, cascading is appeared. Cascading has been defined as a prevalent policy for industrial symbiosis; hence the environmental advantages of cascading are several. A special type of cascading is loop closing, where it is considered more ring-shaped. The environmental and economic advantages of loop closing are alike to those in cascading. Tracking of energy, water and material flows has been defined as another key to industrial symbiosis analysis. It is shown that applying material tracking at different levels has contributed to definite industrial ecology tools: substance flow analysis (SFA) and material flow analysis (MFA).

3.1.3. Material exchange types versus Spatial/organizational scale of industrial symbiosis

As different exchanges has different proximity and the distance amongst partners and organizations in industrial symbiosis plays an important role, hence another aspect of industrial symbiosis is devoted to the spatial scale of industrial symbiosis. The geographic proximity amongst firms refers directly to the spatial scale. In this regard Chertow proposed a methodology based on taxonomy of 5 different material exchange types to consider both components, spatial scale and materials exchange [2,5].

Type 1: through waste exchanges
Type 2: within a facility, firm, or organization
Type 3: among firms co-located in a defined Eco-Industrial Park
Type 4: among local firms that are not co-located
Type 5: among firms organized virtually across a broader region

In addition, Chertow argued a "3-2 heuristic" definition in which at least three different actors exchanging at least two distinct material/resources; differentiating industrial symbiosis from linear one-way exchanges [6]. More than that, it is discussed that types 3-5 "can readily be identified as industrial symbiosis" [2].

3.1.4. Exchange types and synergistic possibilities

The most common type of exchanges are considered as resource exchanges in which energy, raw material, waste handling, and by-products are cycling amongst different actors and firms based on a predefined collaboration. Considering several literature and researches [2,5], the concepts such as synergies and synergistic possibilities are argued. "Synergistic possibilities offered by geographic proximity" has been defined as key to industrial symbiosis. Synergistic possibilities may refer to both material exchanges and by-product exchanges. Chertow showed that by-product exchanges can be transported in a longer distances while the material exchanges (steam, hot water…), cannot be economically applied in longer distances and crossing the boundaries of symbiotic network [2]. In this regard, in the case of collaboration between different firms, industries and organizations, the synergistic possibilities may refer to business and economic synergies as well. A classification of different exchanges in the form of synergies amongst firms and industries has been defined by the Center of Excellence in Cleaner Production (CECP) [7]. They categorized the exchanges as supply, by-product, and utility synergies.

3.1.5. Industrial symbiosis project development

Chertow [2] discussed several examples of industrial symbiosis projects along with eco-industrial park projects in which different definitions regarding to project development, types of industrial symbiosis networks, and planning stages are being defined. In this regard, the symbioses can be developed based on a planned and structured process in contrast with continually spontaneously evolved projects in which several firms and partners in the symbiosis have developed and evolved simultaneously over time. Furthermore, the participants in industrial symbiosis can be defined as conscious or unconscious network regarding to the environmental characteristics of their exchanges. According to planning stages and development progress of industrial symbiosis projects, a sampling of twelve industrial symbiosis projects reviewed by Chertow [2], shows that most of the industrial symbiosis projects can be categorized in the phases: late planning, implementation phase, operational stages, and project completed. In addition, in the case of a planned project, different approaches are applicable. A project could be considered and performed as "Stream-Based" or "Business-Based". Similarly, an eco-Industrial park as a planned project would begin based on "New or Existing Operations". As an example it is implied that the case of the industrial district in Kalundborg Denmark, was a continually spontaneously developed project in which different partnerships in the symbiosis have evolved during the years. More than that, it is concluded that the spontaneous projects in contrast with planned and structured eco-industrial parks, "are proving to be more robust and resilient to market dynamics", [5].

3.2. History and background of the Händelö area

Händelö is a 600-hectare island in the Baltic Sea, just outside the city of Norrköping in the county of Östergötland in Sweden. The Händelö Island is surrounded by Motala River and Bråviken Bay. Historically, Händelö farm has registered on 1322, 60 years before Norrköping became a city. Vast areas of the former farm have been built by industries during the recent years. Now, over the years, the farm itself may be developed into a center of environmental technology, which owned green companies and clean technologies to generate sustainable economy. Due to the nature of Händelö, the area is also called as coexistence between

conservation of nature and industrial sites both locates on an island with high business and economy potentials as well as high nature value, which makes the Händelö area being as a meeting point for nature and technology in a sustainable way. For around three decades, it is planned for large and new establishment of industries and infrastructure. Norrköping municipality owns Händelö area. Nowadays, the Händelö Island has vast and distinct facilities inside. Because of that it attracted the interests of business planners/developers, local authorities, and academia researchers. Facilities like the center of logistics companies, the renewable energy cluster and Natura 2000 conservation areas. More than that, the strategic position of the area such as access to the railway and vicinity to the harbor is another order of merits of the Händelö area.

3.3. An overview of an industrial ecosystem in Norrköping, Sweden

The current paper is a case study to examine industrial symbiosis in a sustainable development application at Händelö area in Norrköping. Nevertheless, for deeper understanding and further realization of relations between different parties inside and outside the border of Händelö, a brief description about the current situation of industrial ecosystem at Norrköping is given. Figure 1 shows a schematic relation and collaboration between different actors and organizations in Norrköping. The involved exchanges include mainly energy, materials/waste, and by-products. Municipal wastes from Norrköping city feed into E.ON, the combined heat and power plant that produces heat, electricity, and process steam. Heat is delivered to the district heating network, electricity to the grid, and steam to the nearby ethanol production plant (Agroetanol). Wheat from the agriculture sector feeds to the Agroetanol Company, which produces pure ethanol. The produced ethanol is used as vehicle fuel. Stillage, a by-product from the ethanol plant, is delivered to a biogas production plant, Svensk Biogas to produce vehicle biogas and bio-fertilizer for the agriculture sector.

Econova is an enterprise in the environmental technology sector and its main activities focus on products and services in the field of biomass, landfills, waste & by-products, and gardening. In this regard, Econova basically runs on two distinct business areas called Econova Energy and Econova Garden. The first one's activities are utilizing and processing waste and by-products from municipalities and the forest industry. The second one‘s activities are based on producing and selling environmentally friendly garden products. Hence, the company's main strategies are based on "eco-cycle" thinking and effective use of resources in an environmentally and economically efficient way. The business strategies of Econova facilitate that more and more customers organize their activities in local cycles. Furthermore, those strategies contribute to more efficient environment, better social relationships along with increasing resources economy. The main business partners of Econova are the agriculture sector, who receives bio-fertilizer, the forest sector which exchange biomass and bio ashes, the waste water treatment plant for sludge exchange, the municipalities for organic and household waste, and the CHP plant for exchanges of ashes and biomass [8].

Returpack and Cleanaway are neighbor companies with an unique strategy in closed eco-cycle system for depositing, handling, collecting, recycling of pet bottles and aluminum cans at Händelö in Norrköping. Returpack is the company in charge of the Swedish pet bottles and aluminum cans deposit system since 2003. They selected Norrköping for its vast facilities in logistics. Around 20,000 tonnes per year of pet bottles are delivered to Returpack. The daily processing is about 3.6 million Aluminum cans and pet (9). The transportation costs for sending this amount of pet bottles and Aluminum cans for recycling to other regions were too high so it was decided to follow the "Next door" strategy to build the Cleanaway Company close to Returpack to avoid logistic/transportation costs. Cleanaway, business partner of

Returpack is a company in charge of cleaning and recycling of pet bottles, and is constructed in 2006. Cleanaway delivered about 8 tonnes per day of pet bottles and around 27,000 of pet bottles per annual of which 20,000 tonnes brought in from Returpack and rest comes from Norway and Finland [9]. Around 75% of cleaned pet materials are used for producing new pet bottles, and the rest is used for producing other plastic products. The process waste is sent to the E.ON CHP plant at Händelö as combustible materials. The key successive items through collaboration between Cleanaway and Returpack is the "wall to wall" strategy which contribute to a set-up based on an agreement "among firms collocated in a defined eco-industrial perk".

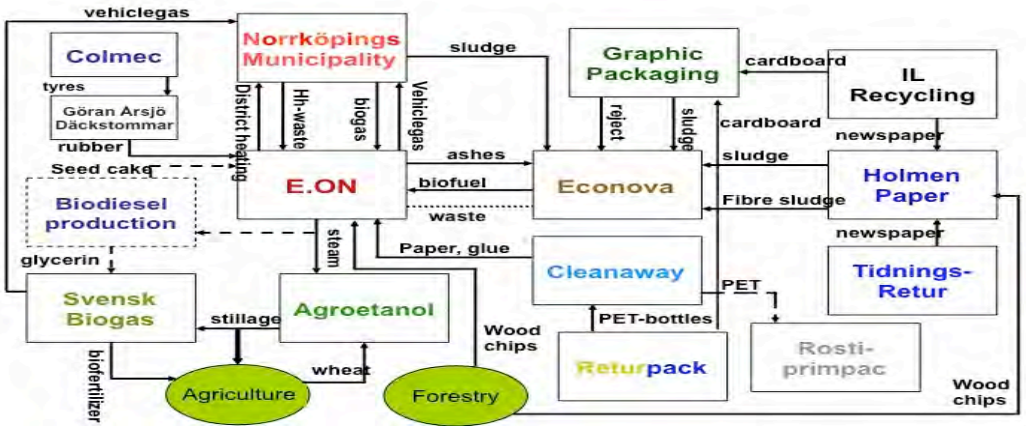

Fig. 1. Industrial eco-system at city of Norrköping (10)

3.4. Industrial symbiosis tools applicable at Händelö

As stated, an industrial inventory (inventory of the actors) is introduced as one of the useful industrial symbiosis tools. As soon as an industrial area is nominated as a possibility for industrial symbiosis, the first step through an industrial symbiosis analysis could be starting with an inventory of local actors and relevant organizations. Another industrial symbiosis tool is defined as materials budgeting, in which the aim is to map the energy and material flows through the nominated area. As the tool can help to map the route of flows and stocks, it could be fundamental to an industrial symbiosis analysis [5].

The energy services company, bio fuel (biogas, bioethanol) production companies, the agriculture sector, forestry, logistic companies, pet bottles, aluminum cans, and rubber tires recycling companies are major green partners through their links and the applications of clean technologies. Händelö became the center of industrial symbiosis and environmental technology to stimulate a sustainable economy in the area. As there are several actors and industrial companies in different sectors at Händelö that share some technical, business and social relationships with each other, the focus in this paper is mainly on the Händelö area and the energy cluster as the nominated area for industrial symbiosis. In this regard, an inventory of participating companies in the area and their processes containing energy, material, waste, and by-products exchanges along with mapping the energy and material flows through the area is provided and analyzed.

3.4.1. Industrial inventory at Händelö energy cluster

As discussed earlier, the energy cluster at Händelö area is part of the eco-industrial complex in Norrköping city. The primary partners at Händelö energy cluster are E.ON CHP plant, Lantmännen Agroetanol (ethanol production company), and Svensk Biogas (bio-gas production company) [9].

The E.ON combined heat and power plant as the engine, is a part of energy cluster at Händelö. E.ON produces heat and electricity that is delivered to the municipality of Norrköping. In addition E.ON produces process steam for the nearby ethanol production plant (Lantmännen Agroetanol). The municipality of Norrköping provides household waste to E.ON to use in their waste incineration plant. The main fuels to E.ON are wood/return chips, wood waste, rubber tires, and sorted household waste. The fuels contain 53% of biomass, 43%waste, 4%coal, and small amounts of oil during peak loads. The waste consumption of the incineration plant is about 20 tones per hour at full power. The overall heat capacity of the plant is around 1.1TWh including steam. The power production of the unit reaches to 300GWh. Of the total energy produced, 57% is processed into heat and is delivered to the district-heating network, 29% is processed into steam, which is delivered to the ethanol production plant, and 14% is processed into electricity that is delivered to the grid. Lantmännen Agroetanol is Sweden's only large-scale producer of grain-based fuel ethanol and has a large production plant at Händelö. Due to high demand for ethanol as a fuel in Sweden, it has expanded its production plant in Norrköping. The plant is also one of the Sweden's largest producers of protein-rich crops and feedstuff for animal feeding. At the Norrköping plant, wheat is the main raw material. The first batch of ethanol was delivered from the plant in 2001. In November 2008 the second production line started. This yields to an expansion in capacity to produce 210 million liters of bio-ethanol and 195 thousands tones of protein feed (DDGS) annually. The production is based on 550,000 tones of cereals. Lantmännen Agroetanol has several industrial, commercial, and social links with other companies in and outside the Norrköping region. E.ON, Svensk Biogas, oil companies, farmers, and animal feed factories are the main Lantmännen Agroetanol counterparts.

Svensk Biogas (Swedish Biogas) at Händelö has started in 2007. Biogas is produced from organic waste and residues. Sewage sludge, stillage, grains, crops, and plants from the agriculture sector are the most frequently used raw materials for biogas production plant at Händelö. Stillage is provided from the nearby ethanol production company and sewage sludge is a by-product of the wastewater treatment plant. Amongst different by-products of the biogas plant, the most important ones are bio-fertilizer and bio-manure which both return to the agriculture sector again. The produced biogas is refined and is fed into city gas filling stations for both private and public transportation. The biogas plant at Händelö produces around 2.6 million Nm^3/year biogas.

4. Discussion and Conclusions

Having a look upon the business partners, actors and their processes at Händelö, it is evident that the most common type of material exchanges through the symbiotic network is a combination of both types tree and four, in which the exchanges are mainly, occurs "among firms co-located" in a symbiotic network. Stillage the by-product of the ethanol company is feed to both biogas plants at Händelö in its geographic proximity as well as to a more distant plant in Linköping, "over the fence". As the primary partners are linked together within a few-mile vicinity and have advantages of exchanging energy and materials, it can be classified as a type four exchange. As spatial/organizational scale of industrial symbiosis plays an important role in issues like material exchange types and geographic proximity amongst actors, the "Geographic Information System (GIS) tool" can be added as a new component to industrial symbiosis analysis. Considering two definitions of eco-industrial parks by USA/EPA and President's Council on Sustainable Developments (PCSD) [2], the Händelö area can be classified and evaluated as an eco-industrial park. Based on further steps in the research and its analysis, new definitions like CO_2-neutral eco-industrial parks through maximize sharing of renewables energy resources can be found.

Performing an industrial inventory as a starting point through an industrial symbiosis analysis shows how local actors depend on each other through the entire network. In this regard, Händelö is a clear sample of "cooperation between different industries by which the presence of each increases the viability of the others, and by which the demands of society for resource savings and environmental protection are considered" [2]. Having a look from an industrial symbiosis perspective at Händelö, it is easily seen that collaboration and synergistic possibilities within a geographic proximity are entirely embedded through the area. More than that, reusing by-products is a dominant process through the whole network where embedded energy and materials links as an industrial symbiosis tool is already performed. In addition the synergistic possibilities and exchanges are mainly devoted to by-product synergies and utility synergies. It is evident that the participants in the Händelö energy cluster have generated a conscious network with regard to the environmental characteristics of their exchanges. More than that it seems that the Händelö symbiotic network and the symbiosis is a type of continually spontaneously evolving projects in which several new firms and partners in the symbiosis have developed and evolved simultaneously over time. Rather than that, the Händelö energy cluster seems to be a sample of an "integrated bio-system" in which the involved processes mainly come from industry and agriculture [2]. Finally, an overview of industrial activities in both local (Norrköping city) and sub-local (Händelö area) level and specifically the energy cluster at Händelö shows social-human dimension of industrial symbiosis such as trust and communications are the most key factors in cooperation between the participants at the Händelö symbiotic network. In addition, amongst several current samples of industrial symbiosis projects and eco-industrial parks worldwide, the keyword industrial symbiosis, can be coined to green economies and clean technologies that have already formed at Händelö.

References

[1] Erkman S., Industrial ecology: an historical view, J. of Cleaner Prod. Vol.5, pp. 1-10

[2] Chertow, M., Industrial Symbiosis: Literature and Taxonomy. Annual review of energy and environment, 25, 313-337

[3] Ristola P., Mirata, M., Industrial symbiosis for more sustainable, localized industrial systems, Progress in Industrial Ecology- An International Journal, Vol. 4, Nos. ¾, pp.184-204

[4] Mirata M., Emtairah T., Industrial symbiosis networks and the contribution to environmental innovation: the case of the Landskrona industrial symbiosis program, Journal of Cleaner Production 13 (10-11), 993 - 1002

[5] Chertow, M., Lifset, R.,Industrial symbiosis,www.eoearth.org/article/industrial_symbiosis

[6] Chertow, M. "'Uncovering' Industrial Symbiosis." J. of Industrial Ecology, 11(1): 11-30

[7] Center of Excellence in Cleaner Production (CECP), Regional resources synergies for sustainable development in heavy industrial areas: An overview of opportunities and experiences, Perth, Australia, Curtin University of Technology, 2007

[8] Econova AB (2010). Econova AB Homepage. 2010, www.econova.se

[9] Cleantech Östergötland (2009), the energy complex at Händelö. Cleantech magazine-environmental technology in the twin cities of Sweden, 1, pp.16-17

[10] Nicklasson, D., Industrial ecology for development and marketing of trade and industry in Norrköping, Master thesis, LIU-IEI-TEK-A--07/00259—SE

Dynamics of Energy Consumption Patterns in Turkey: Its Drivers and Consequences

Gülden Bölük[*1], A.Ali Koç[2]

[1] *Akdeniz Univesity, Department of Economics, Antalya, Turkey*
[2] *Akdeniz Univesity, Department of Economics, Antalya, Turkey*
** Tel: 90 242 3106407, Fax: +90 242 227 44 541, E-mail:guldenboluk@akdeniz.edu.tr*

Abstract: Turkey has a characteristics with very young population, high annual population growth rate, rapid urbanization and relatively high economic growth rate. Turkey's population has reached about 73 million in 2010 The country has faced with growing demand for energy during last two decades and primary energy demand is projected to reach 220 mtoe in 2020 which means 150 percent increase from current level. But primary energy supply met about 28 percent of energy demand in 2009. Increasing import dependency highlights the energy security problem for the country and also poses important burden on economy such as foreign current deficit. Total energy import increased nearly six folds for last 15 years with 12 percent annual average growth rate. The share of energy in total import has exceeded 20 percent in recent years. Increasing GHG emissions is another issue which has substantially increased during last two decade, particularly emitted from energy production. Therefore, energy dependency and GHG emission issues entails investment in renewable energy sources such as wind, biomass, hydro and solar to both reducing energy dependency and emission. In addition, ensuring greater energy efficiency will contribute energy security since current level of efficiency is rather low.

Keywords: *Turkey's energy consumption dynamics, drivers of energy demand, impacts of energy policies.*

1. Introduction

Turkey has been rapidly growing country for decades. The gross national product of country has grown at an average annual rate of 5 percent since 1983 . Turkey's energy demand has also risen rapidly as a result of economic growth and development. Turkey has an economy challenging by a growing demand for energy while its self sufficiency rate in primary energy sources are very low. Total primary energy production met about 28 percent of the total primary energy demand in 2009.

Turkey is heavily dependent on expensive energy imports which impose significant burden on the economy. As a result of increasing energy consumption, air pollution has been causing severe environmental issues in the country. Furthermore, to meet criteria of Kyoto Protocol, consumption pattern needs to be modified. As a candidate country, Turkey will have to adopt the bio-energy and bio-fuel directives of the EU in case of membership. In this regard, promoting renewable energy resources seem to be one of the effective energy policies in Turkey which also entails substantial investments.

The aim of this article is to analyze the dynamics of the energy consumption patterns in Turkey and evaluate the impacts of energy demand patterns change both on energy sector and whole economy. Furthermore, this paper aims to contribute the national energy sources management and policy decision by analyzing the energy demand patterns change and its macroeconomic consequences. The paper is organized as follows. In the second section, macroeconomic drivers of energy demand in the economic development process and national energy policy are presented. In the third section energy sector and energy consumption structure are analyzed. In the fourth section implications for energy consumption patterns change is evaluated. Final section concludes important results.

2. Energy Policies in Turkey and Macroeconomic Drivers for Energy Demand

Turkey is situated at the meeting point of the three continents (Asia, Europe and Africa) and is adjacent to regions which pose over 70 % of the world's proven oil and natural gas reserves. Moreover Turkey sits on major international waterways. Therefore Turkey is an important transit state for world energy resources [1]. Turkey's size 779,452 km^2 and Turkey's population was about 73 million in 2010. Moreover fast migration from rural regions to industrial and/or tourism regions has continued and fast growing urbanization is leading more energy consumption. Turkey is rapidly growing economy, and over the past decade it's Gross Domestic Product (GDP) has increased an exceptional rate compared to other OECD countries. Turkey is 17th largest economy expanded on average by 4.7 % a year [2].

Since 1980 (in liberal period), public investments including electricity investments has been gradually cut down to reduce the public share in the economy. Moreover, the Turkish government initiated some legal regulations to attract the private investors to the economy [3]. By the end of the 1990s, it was understood that quasi-privatization policies were not going on to be feasible given the rapidly deteriorating fiscal situation. Thus, Turkey adopted a radically different framework for the design of the energy markets. In 2003, Electricity Market Law (EML, No:4628) came into force [4]. The EML was designed to establish a competitive electricity market, to promote private participation and improve the efficiency in electricity supply [3]. In parallel with the electricity market reform, some other reforms were also initiated in other segments of market. In 2001, Natural Gas Market Law (NGML, No: 4646) also came into force to achieve similar goals in natural gas industry. The new regime established the Energy Market Regulatory Authority (EMRA). Also, Petroleum Market Law (PML, No:5015) and Liquefied Petroleum Gas Market Law (LPGM, No:5307) was enacted in 2003 and 2005 respectively. EMRA has responsibility for regulation of these markets as well [4].

Table 1: Population, Economy and Energy in Turkey, 1973-2020.

Year	Population (1000)*	Population Increase, (% o)	GDP per capita, ($**)	GDP, at current prices, (billon USD)	Total Energy Consumption, (Mtoe)
1973	38,073	20.7	2,369.00	90.2	20.04
1990	55,120	17.0	3,859.52	202.38	40.55
1995	59,756	15.4	6,693.43	223.74	63.21
2000	64,259	13.8	8,149.60	265.18	82.2
2005	67,903	13,0	11,005.80	482.78	92.5
2010	72,698	11.0	15,392.16	729.05	97.31
2020	80,257	8.8	19,748.55	1,344.29	220.0

* Mid-year population data; ** IMF, International USD PPP equivalent
Source: [5, 6, 7, 2, 8].

Turkey's GDP is expected to grow at a rate 5 % in 2012 and 5.5 % in 2013 [9]. Turkey is also expected to fastest medium-long term growth in energy demand among the IEA counties. The total energy consumption is expected to reach 220 Mtoe by the year 2020. But, Turkey's energy consumption per capita is still relatively low compared to developed countries [2]. As mentioned before, Turkey is a candidate country to EU. Therefore all candidate countries need to harmonize with the European Union energy policies. Moreover all candidate countries should have adequate legislation and well functioning institutions. In this regard, Turkey adopted a strategy which consists of a privatization and integration into European and global economy. EU energy policies essentially include the improvement of competiveness, security

of energy supply and protection of environment [10]. In this context, some efforts for sustainable energy, energy efficiency and environmental issues have been observed in Turkey [11]. As a matter of fact, the Renewable Energy Law (REL, No:6094) was enacted by the Turkish Grand National Assembly in December 28, 2010.

3. Dynamics of Energy Patters

Energy consumption of Turkey has grown substantially since the beginning of the 1970s. The quantity of consumption almost quintuplicated between 1973 and 2010 from 20.4 to 97.31 millions tons of oil equivalent (Mtoe). Turkey's energy consumption is rapidly growing, but it's domestic primary energy sources (especially oil and natural gas) are relatively low. According to the Ministry of Foreign Affairs [7], primary energy demand is projected to reach 220 million toe in 2020, revealing 150 percent increase as compared to the current figure.

Table 2: Production, Supply and Consumption of Energy Sources in Turkey, thousand TEP,2008.

Energy	Domestic Production	Primary Energy Supply	Total Final Energy Consumption
Hard Coal	1204	14179	7010
Lignite	15205	15003	4138
Oil	2268	31784	28732
Natural Gas	931	33807	13957
Hydroelectric	2861	2861	0
Wood	3679	3679	3669
Biofuels	66	66	66
TOTAL	29257	106338	79559

Source: [13].

According to the MENR statistics (2008), petroleum products, natural gas and coal consist of the bulk of the primary energy consumption in Turkey. Although the consumption of oil has been increasing for the several decades, because of the natural gas, this rate was started to decrease. Roughly 90 percent of Turkey's oil supply is being imported. But oil is still the dominant energy source in Turkey. In the past four decades oil's shares were 42.3 %, 45.5 %, 41.1 % and 36.1 % for 1970, 1990, 2000 and 2008 respectively. Turkey oil consumption was 28,732 thousand TEP in 2008 [13]. Turkey's oil production in 2008 met only 7.9 of total in consumption [5]. The oil deficit between production and final consumption was met by imported oil from Saudi Arabia, Libya, Iran, Iraq, Russia, Syria and Algeria.

Turkey is a transforming country, so energy usage has shifted towards to manufacture sector and cycle and energy sector. While the manufacture sector share in total energy consumption was 24.5 % in 1970, this share nearly doubled in 2006. Moreover share of the cycle and energy sector increased more than two folds from 1970 to 2006. The shares of cycle and energy sector were 12 % and 28.6 % for 1970 and 2006 respectively. Shares in total energy demand for households, transportation, agriculture and out of energy were 30.7%, 19.3 %, 4.6 % and 5.4 % respectively. In the power sector it is expected that oil-fired power plants will continue to be replaced by other forms of power plant technologies [2].

Natural gas consumption has risen substantially in recent years in Turkey. The shares for natural gas in energy consumption for 1970, 1980, 1990 and 2008 were 0%, 5.9%, 17.5% and 31.6 % respectively. Natural gas has been particularly important in the power sector which has risen to tenfold from 1990 to 2008. Gas usage is expected to continue to increase rapidly in all sectors for medium and long term (61 bcm in 2020). Turkish natural gas is anticipated to

increase rapidly over the next years with the most important consumers expected to be natural gas fired electric power plants and industrial users. Total natural gas production only met 6.7 % of gas consumption and the rest of the natural gas consumption (93.3 %) was imported. Natural gas has been imported mainly from Russia, Algeria, Iran and Nigeria. Turkey produces only a small amount of natural gas and therefore natural gas imports have increased rapidly [14]. Coal has been a major fuel source in energy consumption in Turkey after the oil and natural gas since 1970s. The share of coal (hard coal plus lignite) in consumption was 15.4 % in 1970 and declined to 14.4 % in 2008. Around 87 percent of domestic lignite is used for generating electricity in 2008. Power generation, industry (including coke ovens and blast furnaces) household usage accounted 46, 44 and 9 percent respectively in hard coal plus lignite consumption in 2007 [2].

There has been also rapid increase in electricity consumption. It has grown 9-10% per year except for recent economic crises. Electricity demand reached 194,079.1 Gwh[1] in 2009 and increased tenfold over the last 25 years [15]. Although significant increase realized in electricity consumption per capita in 2009 (2699 kwh/year), it is still under the EU average (6500 kwh/year) and developed countries average (8900 kwh/year) and just above the world average (2500 kwh/year) [16]. Electricity consumption increase is expected to continue over the next 15 years [17]. Besides natural gas, another fast growing source for electricity is coal. From 2000-2009, gas fired generation grew by 48 Twh, accounting for 72 % of total power generating. Coal fired grew by 17 Twh, accounting for 25 % of demand [2]. Demand projections up to 2018 indicate that annual average increase in demand will be 7 % and 6.3 % in high and low demand scenarios respectively [18].

4. Implications of Energy Consumption Pattern

As mentioned before, demand for energy has been rapidly increasing [19]. But Turkey's self sufficiency rate in primary energy source is very low. Total primary energy production met about 28 percent of total primary energy demand in 2009 and Turkey has no significant oil and natural gas reserves. So the first inevitable result of energy consumption in Turkey is energy security issue. Turkey is highly dependent on imported primary energy sources. Energy import by the sectoral break down is presented in Table (3).

Table 3: Energy Import by ISIC Rev 3 of Turkey, million $, 1996-2010

Energy/Year	1996	2000	2006	2007	2008	2009	2010
Hard Coal, cooking coal and briquette	623,5	676,3	2054,5	2666,5	3411,7	3113,4	2518,5
Petrol and petroleum based products	3998,3	5642,7	16608,3	19339,4	27034,4	15171,8	16921,2
Natural gas and manufactured gas	1280,4	3078,6	10177,7	11856,5	17819,3	11602,7	11185,2
Total energy import	5913,9	9529,3	28858,7	33882,8	48280,9	29905,1	30640,0
Energy import share in total import.	13,5	17,5	20,7	19,9	23,9	21,2	20,7

Source: [5].

[1] Gross demand is obtained by Gross Generation + import-export (15).

The highest dependency rate with 93.3 percent is in natural gas. Dependency rate for oil and hard coal are 92 % and 91 % respectively. It is projected that the production will decrease and meet the 23 % of total energy demand in 2020 which was 28 percent in 2009. This energy import dependency poses important burden on economy. The oil and natural gas import is expected to substantially increase over the next decade. The natural gas share in total import is expected to be 33 % in 2020 [2, 20]. Turkey's total energy import has increased nearly six folds for last 15 years and reached to 48281 million US Dollar in 2008 and 30640 million US Dollar in 2010. Energy import bill has nearly grown with annual average 12 percent except 2009. Economic crises in 2008 let to decrease in energy import in 2009 but this slowdown reversed again in 2010. The energy import share in total energy import also increased during last 15 years and constitutes about 20 % of the country total import. Because of the high import dependency rate, the government has developed an energy policy aimed at diversifying energy sources and suppliers and attracting private capital in Turkey [21]. Hence domestic energy sources of Turkey become strategically important. Although Turkey has no large oil and natural gas reserves, it has promising significant energy sources like coal (mainly in lignite), hydro and geothermal [10]. Turkey has also the great remaining potential for hydro. It is stated that Turkey's hydro electric potential can meet 33-46 % of electricity demand in 2020. Based on the electricity supply and demand projections, it has been targeted that the share of the nuclear power plants in electricity production will be 5% by the 2020. For this purpose, Construction and Operation of Nuclear Power Plants and Law on Sale of Energy (No:5710) came into force in 2007. An intergovernmental agreement was signed between Turkey and Russia for the construction a nuclear power plant in Mersin-Akkuyu [12]. In the context of the energy diversification issue in Turkey, alternative energy sources such as biofuels became an important focus in recent years. Furthermore, as a candidate country, Turkey will have to adopt the bio-energy and bio-fuels directives of EU in case of membership. Turkey has potential for ethanol based biofuels [22]. European Commission introduced a legislative framework to promote the achievement of 20% target for renewable energy in 2020 [23]. According to the [12], the renewable energy share in electricity energy is planned to be 30 % in 2023 in Turkey.

Table 4: GHG by Sectors in Turkey, 1990-2008, million tones CO_2 equivalent

Sectors	1990	1995	2000	2005	2008
Energy	132.13	160.79	212.55	241.75	277.71
Industrial Process	15.44	24.21	24.37	28.75	29.83
Agricultural activities	29.78	28.68	27.37	25.84	25.04
Waste	9.68	23.83	32.72	33.52	33.92
Increase to 1990 (%)	-	26.99	58.80	76.37	95.96

Source: [5].

In Turkey, the highest growth of CO_2 emission between 1990 and 2008 was observed in energy industries with 114% in 2008. It is followed by manufacturing industries with 79%. Approximately 91% of total CO_2 emission has been emitted from energy sector and the rest portion, which is %9, was originated from industrial processes in 2008. However, 59% of CH_4 emission is originated from waste disposal and 31% from agricultural activities while 72% of N_2O emission is from agricultural activities. In terms of fuel combustion, 36% of total CO_2 emissions is originated from energy industries while 19% from manufacturing industries, 16% from transport and 21% from other sectors in 2008. Energy related CO_2 emissions have more than doubled since 1990 and it will most likely to continue to increase fast over the medium and long term because of the increasing energy demand [5].

Turkey is a Party to United Nations Framework Convention on Climate Change (UNFCCC) and a Party to Kyoto Protocol in 2009. However, as developing economy with low emission per capita, Turkey has preferred not to determine quantitative overall target to limit emissions. Although Turkey has no legal compulsory commitment, she has been working on further developing it's post 2012 approach and determining it's commitment. For example it has set a unilateral quantitative target for $C0_2$ emissions from energy sector (- 7 % from scenario level in 2020) as determined in it's 2009 National Climate Change Strategy report [2]. Both biofuels targets and greenhouse emission commitments will bring important implications in agriculture, industry and household sector. There has been increasing effort in energy production from biomass, but, unfortunately official statistics are not available to evaluate its contribution to energy supply and GHG emission reduction.

5. Conclusion

Turkey has no large oil and natural gas reserves and it's domestic energy supply is low relative to total demand. Hence Turkey is dependent on imported energy sources that constitutes big burden on the economy. Turkey has potential for further growth in energy demand as a result of social and economic development. Growing energy consumption combined with the insufficient primary energy sources negatively effects not only the foreign trade balance and greenhouse emissions but also energy security. Moreover growing demand makes additional investments inevitable in energy sector. These issues constitute dilemma for energy policy in Turkey.

If the precautions cannot be taken in time, Turkey will be at the risk of energy deprivation and volatility of energy prices. Electricity energy demand also has been growing so it has pressure on other primary energy resources and also investment needs. Investments in electricity generation capacity have to be enhanced. Improvement in electricity market in terms of competition would have positive impact on increasing the domestic and foreign private funds in the sector. Much more exploiting hydro and other renewable resource such as wind, biomass, solar for electricity generation would contribute both in generating capacity and also energy security. Increasing the renewable energy usage and supporting the R&D studies in renewable energy technologies would improve the energy independency and economic development. Geothermal energy is a promising energy source for the future. Turkey has to develop the usage of solar and wind energies because the potential for these energies is good. Ensuring the sufficient energy supply for economic development should be the government's main target. According to the recent research [24], Turkey has potential about 25% for the efficient energy usage. In this context, government should stimulate the efficient energy using in the country and prepare additional regulations for the Renewable Energy Strategies. Environmental concern has risen because of the high value GHG especially emitted from energy sector. Although there is a development in energy efficiency in Turkey, the efficiency of energy is not as important as in Europe. Although Turkey has no official target for CO_2 emissions, eventually she will have to prepare its plan. In this context, emission targets will bring important commitments on households and industries.

References

[1] Shaffer B., Turkey's Energy Policies in a Tight Global Energy Market, 2010, http://belfercenter.ksg.harvard.edu/files/insight_turkey_shaffer_energy.pdf, acces date 9/10/2010.

[2] IEA, Energy Policies of IEA Countries: Turkey 2009 Review, OECD/IEA 2010, France, 2010.

[3] Ozkivrak O., Electricity restructuring in Turkey, Energy Policy, 33(10), 2005, pp.1339-1350.

[4] Erdogdu E., Regulatory reform in Turkish energy industry: An analysis, Energy Policy, Vol.35, 2007, pp.984-993.

[5] TURKSTAT, Statistics, 2010, www.turkstat.gov.tr, acces date 1/11/2010.

[6] IMF, Country Information:Turkey, 2010, www.imf.org.tr, Access date 4/11/2010.

[7] MFA, Ministry of Foreign Affairs,The Republic of Turkey, Turkey's Energy Strategy, 2006, http://www.econturk.org/Turkisheconomy/energy_turkey.pdf, Access date 4/12/2010.

[8] Toklu E., Guney M.S., Isık M., Comakli O. and Kaygusuz K., Energy Production, consumption, policies and recent developments in Turkey, Renewable and Sustainable Energy Reviews, Vol.14, 2010, pp.1172-1186.

[9] SPO, State Planning Organization, Medium Term Program (2011-2013), Main Macroeconomic and Fiscal Targets, Turkey, 2010, www.dpt.gov.tr, acces date 24/1/2011.

[10] Balat M., Security of energy supply in Turkey:Challenges and solutions, Vol. 51, 2010, pp.1998-2011.

[11] Soyhan H.S., Sustainable energy production and consumption in Turkey:A Review, Renewable and Sustainable Energy Reviews, Vol.13, 2009, pp.1350-1360.

[12] MENR, Nuclear Energy, 2010a, http://www.enerji.gov.tr,, Access date 5/12/2010.

[13] MENR, Sectoral Energy Consumption 1970-2006, 2010b, http://www.enerji.gov.tr/EKLENTI_VIEW/index.php/raporlar/raporVeriGir/4043/2 , access date 2/12/2010.

[14] Demirbaş A., Turkey's Energy Overview beginning in the twenty-first century", Energy Conversion and Management, Vol.43, 2002, pp.1877-1887.

[15] TEIAS, Electricity Generation & Transmission Statistics of Turkey 2009, 2010, http://www.teias.gov.tr/istatistik2009/index.htm, access date 24/11/2010.

[16] Turkyilmaz O., "Türkiye'nin Enerji Profili", Türkiye'nin Enerji Gerçekleri ve Çıkış Yolları Sempozyumu, (The Energy Profile of Turkey, Syposium on Energy Realities of Turkey and Way Outs), 3 December 2010. MMO Antalya/Turkey, 2010.

[17] Kilic C.F. and Kaya D., Energy production, consumption, policies, and recent developments in Turkey, Renewable and Sustainable Energy Reviews, Vol.11, 2007, pp.1312-1320.

[18] Deloitte, Turkish Electricity Market: Developments and Expectations 2010 – 2011, 2010, https://www.deloitte.com/assets/Dcom-Turkey/Local%20Assets/Documents/turkey-tr_ er_ElektrikEPiyasasi2010_090710.pdf, Access date 10/5/2010.

[19] Ulutas B.H., "Determination of the appropriate energy policy for Turkey", Energy, Vol.30, 2005, pp.1146-1161.

[20] DTM, Türkiye'de Enerji Üretimi ve Tüketimi, (Undersecretariat of Prime Ministry for Foreign Trade, The Energy Production and Consumption in Turkey), 2010, http://www.dtm.gov.tr/dtmadmin/upload/EAD/KonjokturIzlemeDb/teut.doc, access date 15/12/2010.

[21] Demirbaş A., Energy Balance, Energy Sources, Energy Policy, Future Developments and Energy Investments in Turkey, Energy Conversion and Management, Vol.42, 2001, pp.1239-1258.

[22] Boluk G. And Koç A., Biofuels in World and Turkey: Production, policies, cost and impacts, ,Iktisat, Isletme ve Finans, 23(269), 2008, pp.25-50.

[23] EC, Communication from the Commission to the European Parliment, The council, The European Economic and Social Committee and the Committee and the Regions, Energy 2020 A strategy for competitive, sustainable and secure energy, 2010, www.europa.eu.int, Access date 10/10/2010.

[24] Keskin T., "Türkiye'nin Enerji Verimliliği İmkanları", Türkiye'nin Enerji Gerçekleri ve Çıkış Yolları Sempozyumu, (The Energy Efficiency Possibilities of Turkey, Symposium on Energy Realities of T urkey and Way Outs), 3 D ecember 2010. MMO Antalya/Turkey, 2010.

Optimization of a renewable energy supply system on a remote area: Berlenga Island case study

L. Amaral[1], N. Martins[2] and J. Gouveia[3]*

[1]Department of Economics, Management and Industrial Engineering; Research Unit on Governance, Competitiveness and Public Politics (GOOVCOP) University of Aveiro; Campus Universitário de Santiago, 3810-193 Aveiro, Portugal*
[2]Department of Mechanical Engineering; Centre for Mechanical Technology and Automation (TEMA); University of Aveiro; Campus Universitário de Santiago, 3810-193 Aveiro, Portugal
[3]Department of Economics, Management and Industrial Engineering; Research Unit on Governance, Competitiveness and Public Politics (GOOVCOP); University of Aveiro; Campus Universitário de Santiago, 3810-193 Aveiro, Portugal
**Correponding Author. Tel: +351 234 370 830, Fax: +351 234 370 953, E-mail: lpgamaral@ua.pt*

Abstract: HOMER software was used to technical and economically assess two renewable energy supply (RES) system configurations – PV-only (80 kW) and PV (34 kW)/WT (36 kW), both with a three day storage capacity and requiring 11kW of electric power – proposed by a partnership project responsible for the implementation of sustainable measures on a Portuguese small island. HOMER calculation showed insufficient storage capacity for both RES system proposed, so extra storage capacity should be added. Economically, life cycle cost (NPC) of the cheaper configuration (PV/WT) resulting from HOMER calculation was significantly lower (20%) than the one advanced by the project. On a second stage, HOMER was used to compute an optimal RES system configuration to attend water desalination and street lighting electric additional loads. The optimal configuration – PV (25 kW)/WT (18kW) – costs 18% less than the equivalent PV/WT system proposed by the project when the same additional load is considered. Sensitivity analysis on the electric load showed the cost difference between project's and HOMER's proposals fading as the load increased. Variation on wind speed average demonstrated the significance of data accuracy: using NASA's average wind speed data the NPC increased on 15% compared to using wind speed values revealed on a monitoring campaign on the island.

Keywords: *Remote off-grid energy systems, Optimization software, Sensitivity analysis*

1. Introduction

Decentralized energy generation systems have become a recent trend on the development of energy systems. Concerns related to energy security and climate change have been fostering the implementation of projects that allow the production of power and heat closer to the point of use [1], as the current and dominant approach of centralized energy production, based on fossil fuels, lead to inequities, external debts and significant environmental degradation [2]. Sustainability of energy systems is based on the energy hierarchy principles: top priority is energy conservation, next the adoption of renewable resources for energy production, and last the use of fossil resources [3].

Planning energy systems represents a major issue on the development process of our society. Available computational energy models can support energy planners to decide the best configuration for an energy supply system, as they allow simulating different solutions and working conditions, and checking their technical and economical feasibility in an early stage of the decision process. Optimization models, namely linear programming mathematical models, are usually used to solve cost minimization problems subject to specific technological, political and demand satisfaction constraints given by energy models [4]. This is the case of HOMER®, a software developed by the US National Renewable Energy Laboratory to address the need for a hybrid system design tool accurate enough to predict energy system performance. It has been used on several situations all over the world: a feasibility study for the implementation of a zero home energy in a Canada's city [5]; study of

wind penetration into an existing diesel plant of an Saudi Arabia village [6]; analysis of the technical and financial viability of grid-only, renewable energy supply (RES)-only and grid/RES hybrid power supply configurations for a large-scale grid-connected Australian hotel [7].

2. Methodology

2.1. HOMER Software

HOMER is primarily an optimisation software package which simulates different RES system configurations and scales them on the basis of net present cost (NPC), which is the total cost of installing and operating the system over its lifetime. Depending on the input data and constrains imposed by the user, HOMER firstly assesses the technical feasibility of the RES system (i.e. whether the system can adequately serve the electrical and thermal loads and any other constraints imposed by the user), and then estimates the system's NPC [7]. Besides the electric load to attend, the user has to specify the "search space", i.e., the sizes and/or quantities of the different components of the RES system (wind generators (WT), photovoltaic array (PV), batteries, inverters, electrolyser, generator…) that will be used to calculate the optimal system design. It also performs sensitivity analysis to evaluate the impact of a change in one or more of the input parameters.

HOMER was used on this paper with three purposes: first, to assess the technical and economical performance of two predetermined RES system configurations; second, to optimise a RES system based on wind and solar resources on the Berlenga Island; and third, to assess the impact of the variation on electric load and the average wind speed has on the optimal RES system configuration.

2.2. Case Study: Berlenga Island

The Berlengas Archipelago is located 6 miles away from the Carvoeiro cape on Western Portugal, and has approximately 100 ha. Its island is called Berlenga Island. There is no resident population on this small group of islands, which contributed for the preservation of singular species of flora and fauna. Despite the absence of resident population, there is some human activity on Berlenga Island all year long: lighthouse workers are present on the island 24H/7day during all year. They work on rotation teams and spend several days in a row all year long; some Peniche's municipality workers spend some periods of time on the island form March to November; from May to October nearly 30 fisherman and restaurant workers stay full time on the island. Besides these "permanent" residents, there is a legal limitation of 350 islands visitors [8].

Before 2007, when a partnership program called "Berlenga – Sustainability Lab" (from now on called Berlenga Project) started, electricity generation was based on diesel generators (130 kW), producing 30 MWh/year and consuming nearly 15000 L/year (roughly 40 ton CO_2 emissions/year) [9]. This system had several drawbacks: high O&M diesel costs due to the aggressive environment on the island; limited energy supply schedule; island development compromised due to electrical limitations (water treatment systems) [9-10]. As so, Berlenga Project intended to develop a zero CO_2 emission electric system to supply the Berlenga Island. Two possible configurations were proposed: Configuration A – PV/WT system; Configuration B – PV-only system. Accordingly to Berlenga Project, Configuration A is less expensive than Configuration B (600 k€ and 750 k€, respectively), however it has an higher environmental impact (mainly because of WT's visual impact and sound pollution) [10].

2.2.1. Berlenga Project Electric Load

In an early stage of Berlenga Project, island's electric monthly load profile was monitored – Fig. 1. Island's electric load profile shows irregular electricity consumption due to the "tourist invasion" during summer months. This domestic electric load profile refers to electricity use on households only. From December to February the only residents on the island are the lighthouse workers. The lighthouse already had a PV array installed and that justifies the absence of electric load on those months. To perform a HOMER simulation, a monthly load profile is not accurate enough. It is required an hourly electric load profile. For that purpose it was used a typical household hourly load profile – Fig. 2 – in order to calculate an hourly load for an average day of each month of the year. The maximum electric power considered was 11 kW and the electric load is subject to 5% standard deviation on daily averages and 10% deviation between the difference of hourly data and the average daily profile.

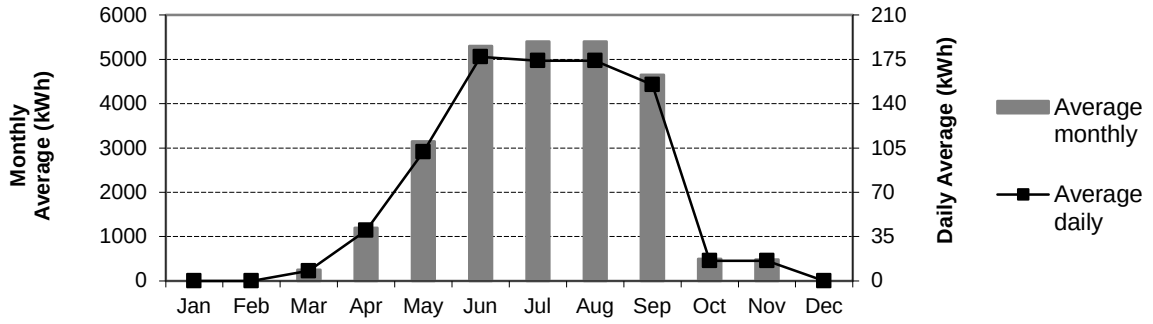

Figure 1. Monthly and daily average domestic electric load profile – adapted from [9].

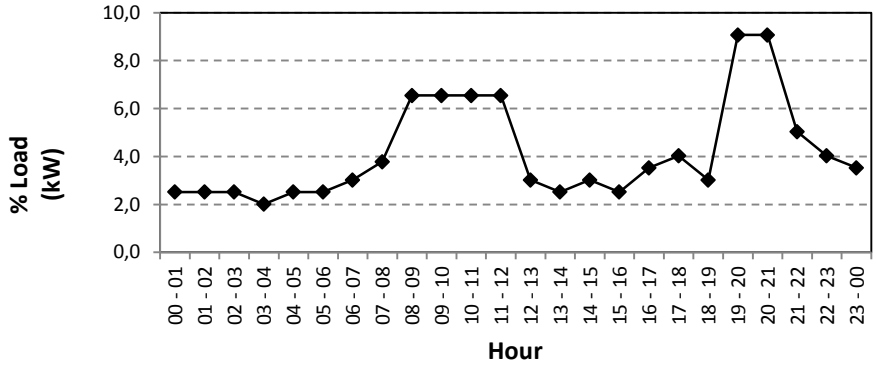

Figure 2. Hourly load percentage distribution during a typical day – adapted from [11].

2.2.2. Additional Electric Loads

Installation of street lighting on the island was assessed on this study. The street lighting system should include 10 street lamps with 125W each working on average 10h/day (3650 hours/year). During winter (Oct-Mar) street lightning works 12 hours/day (from 19:00 to 07:00) and on summer period (Apr-Sep) only 8 hour/day (from 22:00 to 06:00).

The island doesn't have fresh water reserve aquifers. Fresh water is supplied to the island through an 8 m^3 container, by the ship that takes the visitors to the island [12]. According to the last report on this matter [12], fresh water consumption on the island during high season (July and August) was 3 m^3/day and 2 m^3/day on 2007 and 2008 respectively. The fresh water load and electric load required to produce it using a reverse osmosis equipment, are shown on Fig. 3. This electric load was considered as a *deferrable load*, i.e. electrical load that must be

met within some period of time, but the exact timing is not important.

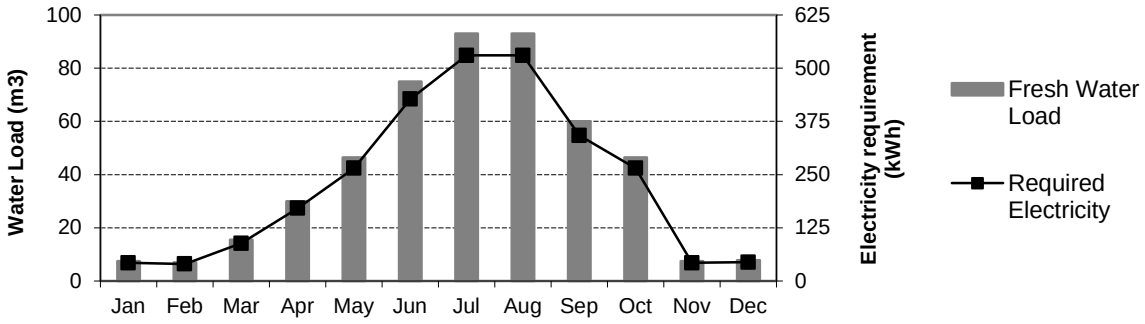

Figure 3. Fresh water consumption and required electricity to produce it.

2.3. Renewable Resources – Wind and Sun

Two sources of information were available on wind average speed. Through NASA's website on data information on surface meteorology and solar energy [13] it's possible to get a monthly profile according to the geographic coordinates of a certain location. To the location of Berlenga Island the database indicate a baseline annual average of 5,16 m/s. In addition to this information, wind potential on the island was evaluated through a monitoring campaign from December 2006 to September 2007 [14]. The campaign's reported an average wind speed of 6,74 m/s, significantly higher than NASA's baseline annual average. As so, it was used 6,74 m/s as a scaled annual average value on the simulation. The scaled data retains the shape and statistical characteristics of the baseline data, but may differ in magnitude.

Solar data information provided by HOMER database was used, according to the geographic coordinates of the island – 4,092 kWh/m2/day and 0,518 Clearness Index.

2.4. Equipments

To perform HOMER simulations, RES system equipments shown on Table 1 were considered.

Table 1. Capital and operation and maintenance costs of a RES system's equipment.

Equipment	Capital Cost	O&M Cost
6 kW Wind Turbine	29445 €/unit [15]	600 €/year [16]
15 kW Wind Turbine	76700 €/unit[15]	850 €/year [16]
Photovoltaic Array	5500 €/kW [17]	10 €/kW [18]
Battery 6CS – 7,6 kWh	850 €/unit [19]	10 €/year [19]
Battery 4KS – 6,94 kWh	770 €/unit [19]	10 €/year [19]
Inverter/Converter	550 €/kW [19]	-

3. HOMER simulation results

Solar and wind data, electric loads and equipments required to build a RES system were described on the previous sections. The project lifetime is 25 years.

3.1. Berlenga Project Configurations

The Berlenga Project originally proposed two alternative configurations for the required RES system: Configuration A – PV (34 kW)/Wind Turbine (36 kW); Configuration B – PV (80 kW). In order to meet Berlenga Project constrains, both configurations should attend the

required domestic electric load and include batteries with capacity to bear three days of average consumption, i.e., 230 kWh [9-10]. After running the simulation with this storage capacity, the only feasible configuration resulted on a PV (80 kW)/WT (36 kW) system, mainly due to high electric demand on summer days. As so, it was necessary to extend the storage capacity to enable the simulation of both Configurations A and B – Table 2.

3.2. Additional electric load scenario

Configuration A and B were simulated to attend the domestic electric load monitored on the scope of the project as shown on Fig. 1. It was simulated a RES system configuration to attend additional street lighting and water desalination electric loads – Current Load Scenario – resulting on Configurations C and D, as shown on Table 2. Adding these two additional loads resulted in higher Initial Capital Cost (IC) and NPC, basically due to the requirement of extra storage capacity and respective O&M costs, however the cost of energy (COE) dropped. HOMER defines COE as the average cost per kWh of useful electrical energy produced by the system. The lower COE shows more efficient use of the electricity produced, as the same amount of electricity is produced and more energy is effectively used.

Table 2. RES systems configurations proposed by Berlenga Project.

RES Config	PV (kW)	WT 6kW (unit)	6CS (unit)	4KS (unit)	Conv (kW)	IC (k€)	O&M ($/yr)	NPC (k€)	COE ($/kWh)
3 day storage	80	6		30	21	642	8789	764	1,415
A	34	6	35		19	390	5744	506	0,937
B	80			65	21	495	4168	579	1,073
C	34	6		40	19	398	6101	520	0,757
D	80			80	21	508	4874	606	0,882

3.3. Optimal configuration by HOMER

As an alternative solution to the originally proposed configurations, above referred as A and B, HOMER was used to shape an optimal RES system based on PV panels, wind turbines and a battery bank to store electricity in order to attend the same domestic electric load shown on Fig 1. It was included a 15 kW wind turbine on this simulation in addition to the 6kW wind turbine. The optimization results are shown on Table 3. Three different configurations result to be possible for the implementation of a RES system on the Berlenga Island: Configuration 1 – PV (25kW) + WT (3x6kW); Configuration 2 – PV (65 kW); Configuration 3 – WT (9x6kW). Configuration 1 represents the HOMER optimal configuration – lowest NPC. The RES system based on PV-only (Configuration 2) is significantly more expensive than mixing PV and WT. A third option (Configuration 3) is available using wind turbines only. This one has a lower IC than configuration 2, but the higher O&M costs results on a higher NPC.

Table 3. HOMER optimal configuration when attending the domestic, water desalination and street lighting loads.

RES Config	PV (kW)	WT 6kW (unit)	WT 15kW (unit)	4KS (unit)	Conv (kW)	IC (k€)	O&M ($/yr)	NPC (k€)	COE ($/kWh)
1	25	3		85	22	298	6374	426	0,620
2	65			95	21	438	5430	548	0,796
3		9		100	19	350	10387	559	0,813

Comparing Berlenga Project's original configurations C (PV/WT) and D (PV-only) with configurations 1 (PV/WT) and 2 (PV-only) resulting from HOMER optimization, it is clear that the last ones present better financial indicators, especially the PV/WT configuration.

3.4. Sensitivity Analysis by HOMER

3.4.1. Electric Load

The effect of higher electricity requirement on HOMER optimal configuration was assessed through a sensitivity analysis, by creating two additional electric load scenarios: 10% Increase Scenario – 10 % increase on domestic and water desalination electric load; 20% Increase Scenario – 20 % increase on domestic and water desalination electric load. Street lighting remained unchanged on both scenarios. A PV/WT system resulted to be the optimal configuration for both scenarios. The NPC increases linearly with the electric load – Fig. 3. Comparing configuration C (34 kW PV/36 kW WT) with HOMER optimal configuration for each electric load scenario, it can be stated that the greater the electric load the closer is the economic performance of both configurations even though the optimal configuration proposed by HOMER is always cheaper – Fig. 4.

With 10% load increase scenario the three possible configurations for the RES system showed on Table 3 are feasible. As the electric load increase 20%, PV-only solution becomes unfeasible.

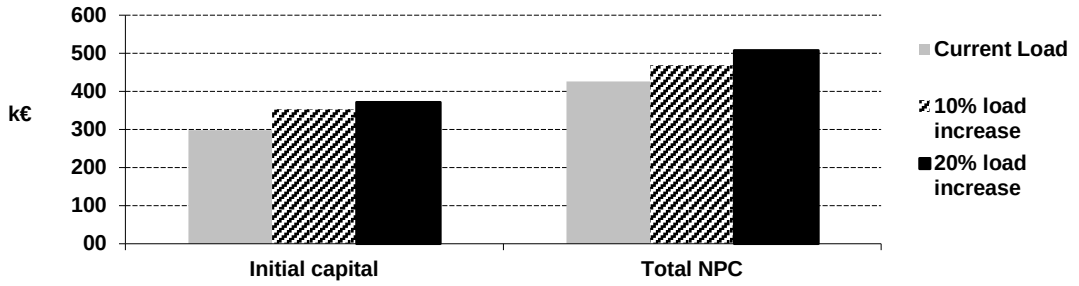

Figure 4. Effect of increasing electric load on RES system costs.

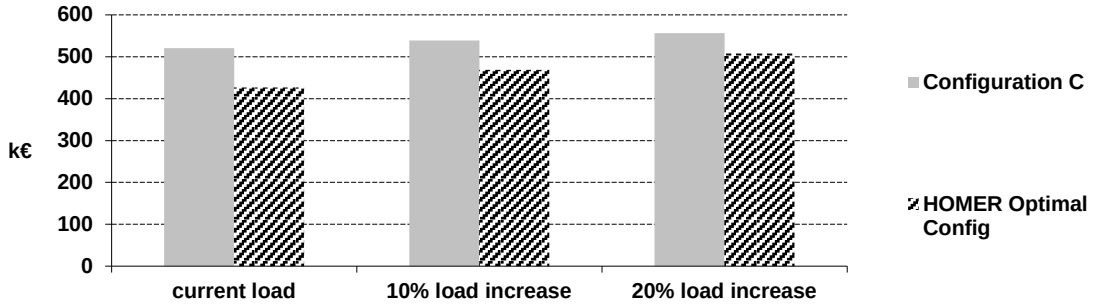

Figure 5. NPC comparison between Configuration C and Configuration 1.

3.4.2. Wind speed

As occurred with the electric load sensitivity analysis, a PV/WT system resulted to be the HOMER optimal configuration when assessing wind speed influence. The economic impact of the average wind speed on the optimal RES system can be assessed on Fig. 5. Using NASA's database value for annual average wind speed, NPC increased around 11% on all three electric load scenarios.

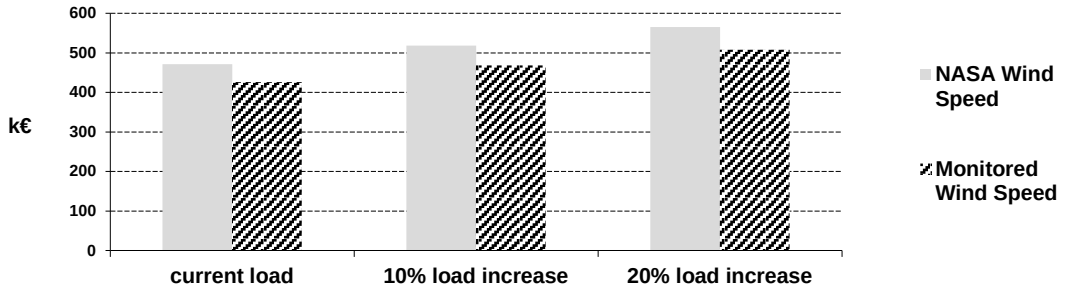

Figure 6. Effect of the average wind speed on system's NPC for each of the electric load increase.

For the current load scenario, the feasibility of the three possible configuration systems is not affected despite the WT-only system results to be almost 80% more expensive than the PV/WT optimal configuration. As the load increase 10% the WT configuration becomes no longer feasible and with 20% electric load increase PV/WT is the only feasible configuration.

4. Conclusions

One of the assumptions made by Berlenga Project's authors was to use a three day storage capacity (230 kWh). HOMER's system simulation showed that this storage capacity not enough for the proposed RES system configurations (A and B) mainly because of the high demand on summer months.

Information on system's cost issued by the Berlenga Project is not completely obvious. A cost of 600 k€ for configuration A (PV/WT) and 750 k€ for configuration B (PV-only system) was assumed, but it is not clear if those are IC or NPC [9]. Assuming those values as NPC and that the aim is to attend the domestic electric load monitored under the Berlenga Project, the costs resulting from HOMER simulation for both system configurations are lower than those proposed by the Berlenga Project: 506 k€ for configuration A and 579 k€ for configuration B. When attending additional street lighting and the water desalination loads (configurations C and D) the costs rose, due to higher storage capacity needed, but they still were far from the costs advanced by the Berlenga Project. This cost gap can be explained, at some extent, by the fact that the costs advanced by the Berlenga Project were from 2007, three years ago. When performing the "free" optimization to attend domestic, water desalination and street lighting loads (Current Load Scenario), the optimal configuration (configuration 1) includes 25 kW photovoltaic panels and three 6 kW wind turbines. Both PV/WT and PV-only optimized configurations resulted to be cheaper than the ones proposed by the Berlenga Project.

Two sensitivity analyses were performed to assess the impact of electric load deviation and average wind speed on the RES system cost and configuration attending domestic, street lighting and water desalination loads. As the electric load rises, the closer is the economic performance of both Berlenga Project (configuration C) and HOMER optimal configurations, even though the latter is always cheaper. This means that the configuration proposed by the Berlenga Project was oversized for the present electric load requirement. This may be an assumed choice, having in mind the future load growth, when new electric loads were included in the grid, the only equipments to add on the RES system should be batteries to store electricity. Despite using NASA's data to profile the average monthly wind speed, a scaled value for the wind speed based on the monitoring campaign made on the Berlenga Island was used to compute the simulation, for a better representation of local conditions. Higher average wind speed means more available wind resource and less costs to generate the same amount of electricity. The higher wind speed value results on a 10% lower NPC for the optimal PV/WT configuration. This is true both for current load and for load increase

scenarios. This analysis stresses the importance of use valid reliable data, namely renewable resources availability data, when performing a technical and/or economical assessment of a RES system.

References

[1] Wolfe, P., The implications of an increasingly decentralised energy system. Energy Policy, 2008. 36(12): p. 4509-4513.

[2] Hiremath, R.B., S. Shikha, and N.H. Ravindranath, Decentralized energy planning; modeling and application - a review. Renewable & Sustainable Energy Reviews, 2007. 11(5): p. 729-752.

[3] Association, R.E., et al., Sustainable Energy Manifesto. 2006.

[4] Antunes, C.H., A.G. Martins, and I.S. Brito, A multiple objective mixed integer linear programming model for power generation expansion planning. Energy, 2004. 29(4): p. 613-627.

[5] Iqbal, M.T., A feasibility study of a zero energy home in Newfoundland. Renewable Energy, 2004. 29(2): p. 277-289.

[6] Rehman, S., et al., Feasibility study of hybrid retrofits to an isolated off-grid diesel power plant. Renewable and Sustainable Energy Reviews, 2007. 11(4): p. 635-653.

[7] Dalton, G.J., D.A. Lockington, and T.E. Baldock, Feasibility analysis of stand-alone renewable energy supply options for a large hotel. Renewable Energy, 2008. 33(7): p. 1475-1490.

[8] Portaria nº 270/90 de 10 de Abril, M.d.A.e.R. Naturais, Editor. 1990.

[9] Maciel, J., Berlenga Sustainability Laboratory - A free-Carbon Energetic Solution. 2007.

[10] Estanislau, S. Berlenga – Sustainability Lab/Plans. in 2007 C3P & NASA Technical Workshop Partnership for Energy and Environmental Stewardship. 2007. Peniche.

[11] Fritz, W. and D. Kallis, Domestic Load profile measurtements and analysis across a disparate consumer base, in 18th International conference on the "Domestic Use of Energy". 2010.

[12] Correia, C.S., Projecto “Berlenga – Laboratório de Sustentabilidade” Soluções de Abastecimento de Água e Saneamento, in Departamento de Ciências e Engenharia do Ambiente. 2008,: Lisboa.

[13] NASA. Surface meteorology and Solar Energy. A renewable energy resource web site (release 6.0) sponsored by NASA's Earth Science Enterprise Program Available from: http://eosweb.larc.nasa.gov/sse/.

[14] Simões, T., P. Costa, and A. Estanqueiro. Wind resource assessment in Berlengas Island. in European Wind Conference. 2007. Berlin, Germany.

[15] Proven Energy website. 2008; Available from: http://www.provenenergy.co.uk/our_products.php.

[16] Canada Wind Energy Association Website. 2008; Available from: http://www.smallwindenergy.ca/en/Overview/Costs/CostComparison.html.

[17] Suneffect website. 2009; Available from: http://www.suneffects.net/index_m.html.

[18] Partnership, P.R. Public Renewables Partnership website. Available from: http://www.repartners.org/solar/pvcost.htm.

[19] SolarBuzz. SolarBuzz website. 2010; Available from: http://www.solarbuzz.com.

Pathway to a fully sustainable global energy system by 2050

Yvonne Y Deng[1,*], Sebastian Klaus[1], Stijn Cornelissen[2], Kees van der Leun[1], Kornelis Blok[1]
[1] *Ecofys, London, United Kingdom,*
[2] *Ecofys, Nuremberg, Germany,*
[3] *Ecofys, Utrecht Netherlands*
[4] *ZinInZin, Utrecht, Netherlands*
** Corresponding author. Tel: +44 20 7423 0984, Fax: +44 20 7423 0971, E-mail: y.deng@ecofys.com*

Abstract: We present a possible pathway to a global, sustainable energy system by 2050. This new energy scenario follows a comprehensive examination to all aspects of energy use across the entire world and the possible means of supplying this energy from the sustainable sources we have available to us. It does so, from the perspective of actual, physical activities that require energy: our industrial processes, our cars, our buildings.

For each of these activities, the scenario asks the questions:

- What is the minimum amount of energy required to deliver these functions?
- How can we supply this energy in a sustainable way?

The key aspects of this new Energy Scenario are:

- It is an ambitious, but feasible pathway for all sectors; we *can* build an energy system by 2050 which sources 95% of its energy from sustainable sources.
- This energy system will use only a small fraction of each of the sustainable energy sources, making this a robust scenario.
- We can progress towards a world that still sustains comfortable lifestyles, despite consumption patterns, demonstrating a more efficient use of energy and other resources, particularly in developed countries.
- Energy efficiency is the key requisite to meeting our future energy needs from sustainable sources. Total energy demand in 2050 is lower than in 2000, despite the growth of population and energy services.
- Electricity is the energy carrier most readily available from sustainable energy sources and therefore, electrification is key.
- All bioenergy required, (primarily for residual fuel and heat demands) can be sourced sustainably, provided the appropriate management practices and policies are in place.
- The scenario's energy system will have large cost advantages over a business-as-usual system because the initial investments will be more than offset by savings made on energy costs, in later years.

The scenario is based on a comprehensive energy model, developed by Ecofys, to establish a scenario for future energy demand and supply worldwide. Unlike many world models, it is based on physical activity indicators and takes a comprehensive look at all aspects of energy demand and supply across all sectors.

The work pays particular attention to the implementation speed of sustainable energy technologies and assesses energy at the detailed carrier and sub-sector level.
It also contains a comprehensive assessment of biomass as a sustainable energy source, with a multitude of different source options and conversion technologies, subject to stringent sustainability criteria.

Keywords: *Sustainability, Renewable energy, Energy efficiency, Scenario, Global*

1. Introduction

The last 200 years have witnessed a substantial increase in energy use by societies worldwide. In recent decades, it has become clear that the way this energy is supplied is unsustainable and now both, short- and long-term energy security, are at the top of the political and societal agenda.

Evidence suggests that we should be able to meet our energy demand from renewable sources, given their abundance: Worldwide energy use, in units of final energy (after conversion from

primary fuels), was ~310 EJ in 2007 (~500 EJ in primary energy terms) [1] whereas technical potentials range from 100s to 1000s of EJ/a (see Fig. 3).

In an attempt to reconcile these figures, the energy scenario provides a comprehensive view of the energy system. It incorporates and examines all energy uses; all quantities, locations, carrier forms (e.g. electricity or fuel) and all purposes (heat in buildings or heat in industry)

This level of detail is (partially) captured in the various energy scenario models that are currently used to predict the most likely energy future for the world and the possible alternative scenarios. However, because cost-optimisation is often the driving algorithm, not many of the models have been used to push the share of renewable sources in the energy system to the highest technically possible levels. One of the few studies which has prioritised renewable sources, is the Energy [R]evolution published by Greenpeace. [2] Even this scenario however, falls short of reaching a fully sustainable energy system by mid-century.

The fundamental question that guided this study was:

"Is a fully sustainable global energy system possible by 2050?"

We find that an (almost) fully sustainable energy supply is technically and economically feasible, given ambitious, yet realistic growth rates of sustainable energy sources. The path to achieving this system deviates significantly from 'business as usual' and the difficult choices that must be made on the way are discussed in this article.

This article is a summary of three full-length publications. The reader is referred to the full publications.[3]–[5]

2. Methodology

Energy demand is the product of:

- the volume of the activity requiring the energy (e.g. travel or industrial production), and
- the energy intensity per unit of activity (e.g. energy used per volume of travel).

This energy scenario forecasts future global demand and supply by inherently following the paradigm of Trias Energetica:

1. Reducing energy demand to the minimum required to provide energy services
2. Providing energy by renewable, where possible, local, sources first
3. Providing remaining energy from 'traditional' energy sources as sustainably as possible.

The Trias Energetica approach was translated into this calculation logic:

1. Future energy demand scenario
    a. Future demand side activity was based on existing studies or projected from population and GDP growth.
    b. Future demand side energy intensity was forecasted assuming fastest possible roll-out of most efficient technologies.
    c. The resulting energy demand was aggregated by carrier (electricity, fuel, heat).
2. Future supply scenario
    a. The potential for supply of energy was estimated by energy carrier

b. Demand and supply were balanced in each time period according to the following prioritisation:
    i. Renewables from sources other than biomass (electricity and local heat)
    ii. Biomass up to the sustainable potential
    iii. Traditional sources, such as fossil and nuclear which were used as 'last resort'.

Energy flows have been characterised by carrier type and differentiated into electricity, heat and fuels, consistent with the energy carriers reported in the IEA energy balances, to which this work is calibrated, with 2005 as the base year. [6]
Unless stated otherwise, all energy in this publication is final energy.

2.1. Sector definitions

There are many different ways of analysing energy demand. We have chosen to distinguish between energy demand in industry, buildings and transport. (These sectors are congruent with the sectors for which the International Energy Agency (IEA) reports energy statistics, which form the basis of this work.) These three sectors, which cover ~85% of total energy use, were studied in detail. The remaining sectors, (including agriculture, fishing, mining etc.) are included in this study, but were not examined separately. Non-energy use of energy carriers was excluded from this analysis.

In the Industry sector, we distinguish between 'A' sectors, for which actual activity measures are available (Iron & steel, non-ferrous metals, non-metallic minerals, paper & pulp) and 'B' sectors, for which activity has to be based on proxy indicators, such as value added (Chemical & petrochemical, food & tobacco, all others).

3. Results – Part 1: Demand

For each of the sectors, we established an activity and energy intensity forecast, to arrive at a final demand projection for the period to 2050.

3.1. Activity

Activity forecasts were made as follows:

- Industry: Population and GDP forecasts were coupled with assumptions on the evolution of per capita production of industrial products.
- Buildings: Population and GDP forecasts were coupled with assumptions on the evolution of per capita residential and commercial building areas.
- Transport: Modal shifts, (from road and air to rail transport) are incorporated into an existing BAU transport scenario [7].

The overall evolution of activity is given in Fig. 1.

3.2. Intensity

The most significant means of reducing energy demand is the efficient use of energy, i.e. the reduction of energy intensity to a minimum.
We describe our approach to each sector's energy intensity below.

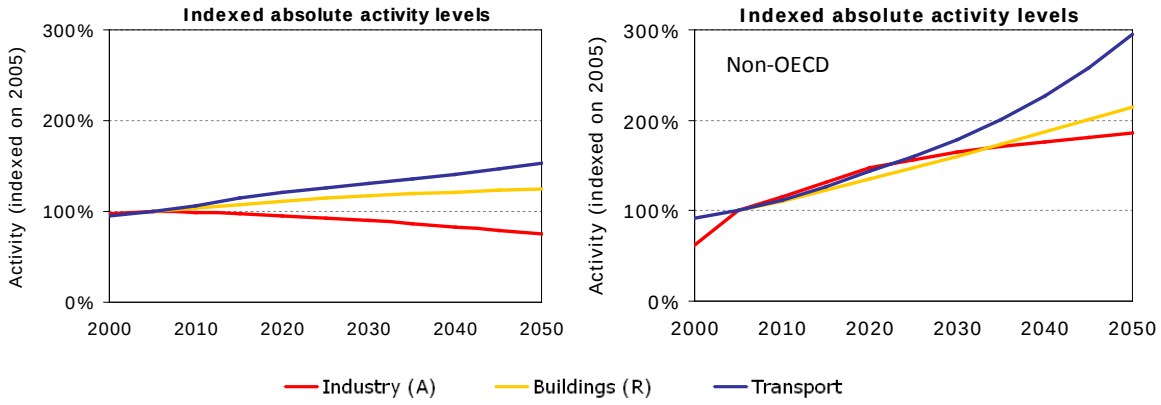

Fig. 1 Activity levels indexed on 2005 in absolute terms. Shown industrial production volumes in the 'A' sectors (Industry), residential floor space (Buildings), and passenger kilometers (Transport).

3.2.1. Industry

Future energy intensity is projected based on key marker processes. We adopt a decrease in energy intensity, measured in energy per tonne produced for 'A' sectors [8]–[11], and in energy per economic value for 'B' sectors.

'A' sectors

The energy intensity evolution was examined in detail for the four 'A' sectors, yielding, on average, a ~50% reduction in energy used, per tonne of material produced in 2050 against the 2000 figures. Although the individual technologies vary by sector, all sectors follow these common assumptions:

- Increased use of recovered input materials or alternative routes
  - i.e. recycling of steel, paper and aluminium and alternative input materials into the clinker process in cement production
- Ambitious refurbishment of existing plants to meet performance benchmarks
- Stringent requirements for using best available technology (BAT) in all new plants.
- Continuing improvements of BAT over time

'B' sectors

For the 'B' sectors, an annual efficiency improvement of 2% was adopted, which may be obtained through improved process optimisation, more efficient energy supply, improved efficiency in motor driven systems and lighting and sector-specific measures.

3.2.2. Buildings

The following steps are followed to project the future evolution of energy intensity, i.e. the possible future heat and electricity demand per square metre of living or commercial floor space.

Existing buildings stock

1. All existing buildings will have to be retrofitted by 2050 to ambitious energy efficiency standards. This requires retrofit rates of up to 2.5% of floor area per year, which is high (compared to current practice), yet feasible.
2. For any given retrofit it is assumed that, on average, 60% of the heating requirements are abated by insulating walls, roofs and ground floors, replacing old windows with

highly energy efficient windows and by installing ventilation systems with heat recovery mechanisms.
3. A quarter of the remaining heating and hot water need is met by local solar thermal systems and the rest, by heat pumps.
4. Cooling is provided by local, renewable solutions, where possible.
5. Increased electricity needs per floor area due to increased cooling demand, increased use of appliances (per area) and heat pump powering have been partially offset by increasing efficiency.

New building stock

1. Increasingly, new buildings will be built to a 'near zero energy use' standard, reaching a penetration of 100% of new buildings by 2030.
2. The residual heat demand is met by passive solar (radiation through windows) and internal gains (people, appliances), renewable energy systems in the form of solar thermal installations and heat pumps.
3. This building type only requires electric energy.
4. The near zero-energy concept is applied to warm/hot climates, often returning to traditional building approaches.
5. There is a residual cooling demand in warm/hot climates. Increased electricity needs from increased cooling and appliances, as well as the use of heat pumps, have been estimated and included in this scenario.

3.2.3. Transport

The following steps ensure that the scenario employs the most efficient transport modes that have the greatest possible share of renewable energy in the energy supply:

1. Moving to efficient technologies and modes of employment, e.g. trucks with reduced drag, improved air traffic management or reduced fuel needs in hybrid buses.
2. Electrifying the mode as far as possible, e.g. electric cars in urban environments and electric rail systems.
3. Finally, providing the fuel from sustainable biomass, where possible (see next section).

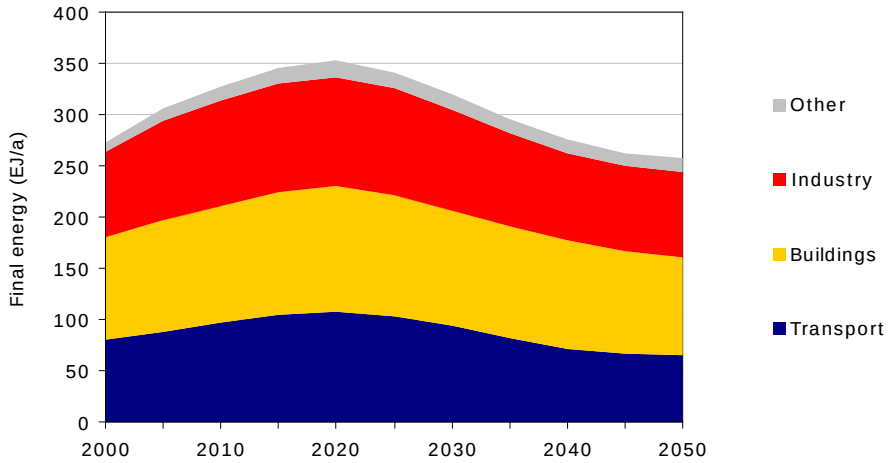

Fig. 2 Global energy demand across all sectors, from 2000 to 2050.

Noteworthy assumptions are:

- A complete shift to plug-in hybrids and/or electric vehicles as the primary technology choice for light-duty vehicles.

- Long-distance trucks undergoing significant efficiency improvements due to improved material choice, engine technology and aerodynamics, rather than a complete electrification of freight road transport (due to the prohibitive size and weight of batteries required with current technology). Delivery vans covering 'the last mile' are electrified, leading to an electric share estimate of 30% for trucks.
- A (small) share of shipping fuel gradually being replaced by hydrogen, won from renewable electricity. This has been deemed a feasible option because of the centralised refuelling of ships.

3.3. Summary

The activity and intensity assumption detailed above lead to the following overall evolution of energy demand (Fig. 2)

4. Results – Part 2: Supply

4.1. Renewable sources excluding bioenergy

Once total demand has been established, demand must be matched with energy supply.

This scenario is based on the deployment potential shown in Fig. 3. This is the potential which can be captured at any time, considering technical barriers and ambitious, yet feasible market growth developments. The deployment potential does not necessarily represent the most cost-effective development, i.e. it does not account for market barriers or competition with other sources.

The realisable potential (R.P.) is the fully achievable potential of the resource with a long-term development horizon.

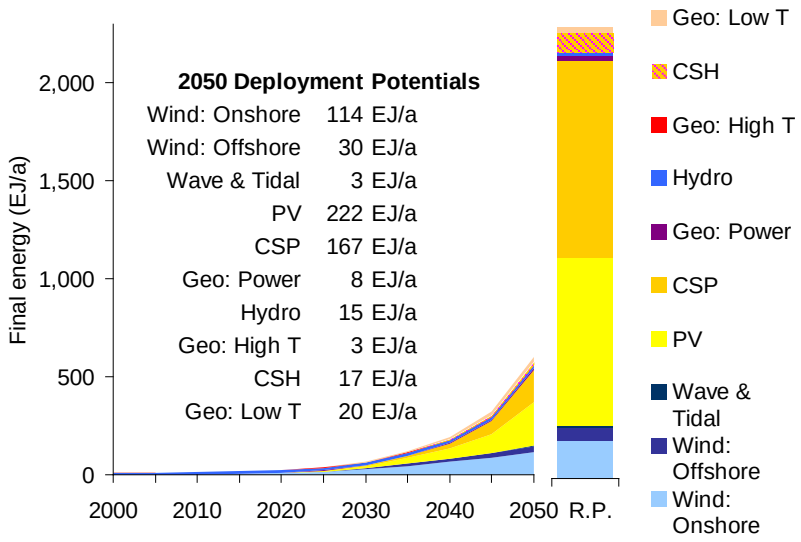

Fig. 3 Global renewable energy potentials (excl. bioenergy), from 2000 to 2050. [5], [12]–[29]

4.2. Bioenergy

The scenario incorporates a significant share of sustainable bioenergy supply to meet the remaining demand once other renewable energy options have been employed. The scenario only includes bioenergy supply that is sustainable and leads to high greenhouse gas emission

savings in comparison to fossil references. The complete approach the scenario takes to bioenergy is discussed in a separate publication. [4]

4.3. Results of balancing demand and supply

Following the strict prioritisation of options described in the Methodology section, the overall evolution of energy supply is determined, as shown in Fig. 4.

Stabilising energy demand, driven by strong energy efficiency, coincides with fast renewable energy supply growth in later years, resulting in an energy system that is 95% sustainably sourced.

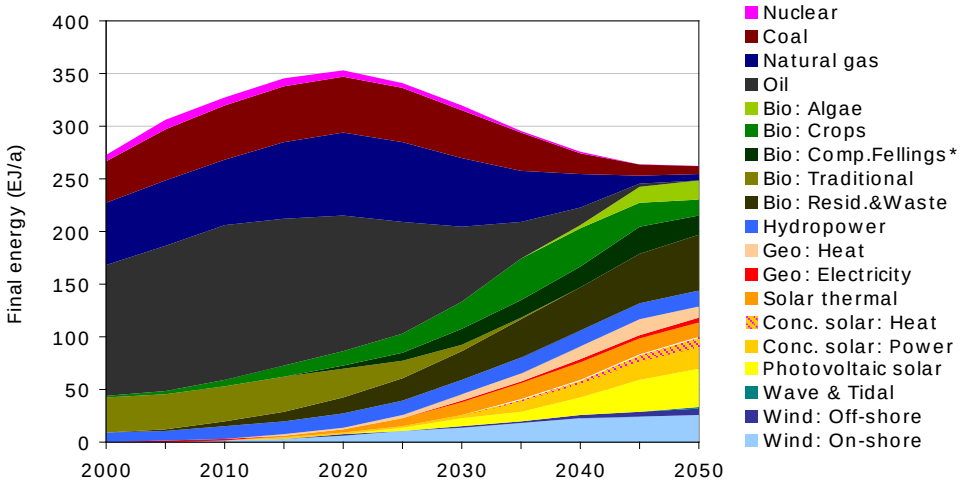

*Fig. 4 Global energy supply in the Scenario, split by source. (*Complementary fellings include the sustainable share of traditional biomass use.)*

5. Discussion

The energy scenario we have presented combines the most ambitious efficiency drive with a high-growth of renewable source options to reach a fully sustainable global energy system by 2050. Both sides of the equation are important: the transition to a renewable energy system cannot be achieved on the supply side alone.

This energy scenario examines the feasibility of a fully renewable energy future by taking a bottom-up, physical approach to the energy system. It does not necessarily present the most cost-efficient way of achieving this goal. It is however, insightful to estimate the associated investment and savings of this energy system in comparison to a BAU energy system.

This cost study is presented in a separate publication. [5] The key findings are, that upfront investments are estimated at less than 2% of global GDP and the energy system proposed in this scenario would be significantly cheaper to operate than BAU by 2050.

References

[1] International Energy Agency (IEA), World Energy Balances, OECD and nonOECD databases, 2009 Edition

[2] Krewitt et al., Energy [R]evolution 2008—a sustainable world energy perspective, Energy Policy (2009), doi:10.1016/j.enpol.2009.08.42

[3] Deng et al.,Transition to a fully sustainable, global energy system, 2011, [in preparation]

[4] Cornelissen et al., The role of bioenergy in a fully sustainable, global energy system, 2011, [in preparation]

[5] Klaus et al., Costs and benefits of a fully sustainable, global energy system, 2011, [in preparation]

[6] IEA, World Energy Balances, OECD and nonOECD databases, 2008 Edition

[7] IEA/SMP, Model Documentation and Reference Case Projection for WBCSD's Sustainable Mobility Project (SMP), 2004

[8] N. Martin et al., Emerging Energy-Efficient Industrial Technologies, Lawrence Berkeley National Laboratory , 2000, DC (LBNL-46990).

[9] Kim et al., Energy Policy 30, 2002, p. 827

[10] Worrell et al., World Best Practice Energy Intensity Values for Selected Industrial Sectors, Lawrence Berkeley National Laboratory, LBNL-62806, 2008

[11] IEA, Tracking Industrial Energy Efficiency and CO2 Emissions, 2007

[12] Ecofys, 2008, [internal assessment]

[13] Global Wind Energy Council - GWEC, Global Wind Report 2007, 2007

[14] Hoogwijk et al., Global potential of renewable energy sources: a literature assessment, Ecofys Netherlands, 2008

[15] Leutz et al., Technical offshore wind energy potentials around the globe, European Wind Energy Conference and Exhibition, Copenhagen, Denmark, 2001

[16] Global Status Report, REN21 (Renewable Energy Network for the 21st Century), 2010

[17] China Wind Power Report, ISBN: 978-82-90980-29-9, WWF China, Chinese Renewable Energy Industries Association, 2008

[18] Climate Solutions, WWF, 2006

[19] European Ocean Energy Roadmap, European Ocean Energy Association, 2010

[20] IEA, Implementing Agreement on Ocean Energy Systems, 2009 Annual Report, 2010

[21] EPIA, Solar Generation V, 2008

[22] EPIA, Global Market Outlook for Photovoltaics until 2013, 2009

[23] Hofman et al., The potential of solar electricity to reduce CO2 emissions, Report no. PH4/14 for the Executive Committee of the IEA Greenhouse Gas R&D Programme, 2002

[24] Li et al., 2007 China Solar PV Report, China Environmental Science Press

[25] DLR, Concentrating Solar Power for the Mediterrenean Region, MED-CSP, 2005

[26] Lund et al, Geothermics 34, 2005, p. 691–727

[27] Bertani, Geothermics 34, 2005, p. 651

[28] Bertani, EGC 2007, Unterhaching, Germany

[29] "The Investor's Guide to Geothermal Energy", 2008

Volume 13

Sustainable Transport

The Use of Sustainable Travel Planning Strategies within Remote Cities

Mohamed H Ismail[1]

[1] *Technologies for Sustainable Built Environments Centre, University of Reading, United Kingdom and Hereford Futures Limited, Hereford, United Kingdom*
** Corresponding author. Tel: +447912044831 E-mail: Mohamed@herefordfutures.co.uk*

Abstract: The paper considers sustainable travel strategies for remote cities that form a regional centre for a wider area. The strategies aim to minimise private vehicle traffic within the city centre arising from both city residents and commuters in from outside regions, but without adversely impacting on the total inflow of people to the city for business, leisure or educational purposes so as not to affect the city's economic viability.

The primary case study within the paper is Hereford, United Kingdom – an ancient Norman city within rural Herefordshire. Significant research has previously been conducted as to the transport problems within the city and such research is summarised and built on in the current paper by proposing potential solutions to the problems.

The paper concludes that sustainable travel strategies in such cities are best aligned in zones, with key strategies for the inner zones being walking and cycling and key strategies for the outer zones being "park and walk" schemes to the inner walking/cycling zones.

Keywords*: Sustainable Travel, Soft Measures, Remote Cities*

1. Introduction

Cities located within a rural area are often the primary source of employment, higher education, retail and other facilities for a wide local area, which may result in a net inflow of daily visitors due to:

- residents of the city remaining within the city for work, shopping and other needs; and
- residents of the rural area outside the city coming into the city on a daily basis for work, shopping and other needs

Should the primary means of transport be private vehicle, this may result in significant congestion within the city (which has consequent detrimental economic and social impacts) as well as other adverse environmental, social and economic impacts such as increased carbon emissions; air pollution; poor public health; and reduced incentive to invest in the area.

Therefore, careful travel planning is essential to minimise private vehicle usage without dissuading people from coming to the city, as it is important (particularly in the current economic climate) to maintain and increase the economic prosperity of the region. The focus in this paper is on sustainable travel solutions for commuters to work, as these form a significant proportion of peak time journeys.

2. Case study: Hereford, UK

2.1. Background

The main case study within the paper is the ancient cathedral city of Hereford, United Kingdom, located within the predominantly rural county of Herefordshire. Hereford has a population of

55,700 whilst the other principal towns within Herefordshire (Leominster, Ross-on-Wye, Ledbury, Bromyard and Kington) have much smaller populations, ranging from 3,200 to 11,100[1]. The nearest large city to Hereford is Worcester, which is 21 miles away, whilst the major cities of Cardiff, Birmingham and Bristol are 58, 61 and 65 miles away respectively. These geographical circumstances have led to Hereford becoming the county's centre for employment, administration, health, education facilities and shopping, resulting in significant pressure on its urban highways and its historic city centre, in which it retains an 11th Century cathedral and other historic buildings.

2.2. Geographical Factors

An additional geographical complication for Hereford city is that the River Wye divides the city between the North and the South. There is only one principal road bridge, at which the A49 crosses the river. This crossing point suffers from significant congestion which causes significant delays during peak commuter travel time[2]. There are also two further pedestrian bridges, one of which carries an important cycle route (the Great Western Way).

However, an important positive factor is Hereford's pleasant and compact city centre, with a pedestrian-only main shopping street (High Town) and numerous historic buildings, which make it a very "walkable" environment.

2.3. New Development

Hereford is currently undergoing a significant redevelopment at the Edgar Street Grid, a 40ha site to the north of the city centre, which will entail new residential, retail, office and leisure facilities. Therefore, it is important that any travel planning options take into account the impact of the new development, in terms of additional residents to the area and additional employment opportunities within the city centre. In total, Hereford plans to increase the number of households by 8,500 by 2026 (including those at the Edgar Street Grid)[2].

2.4. Journeys to Work

76% of Hereford residents work within Hereford and 65% of residents' journeys to work are less than 5km. Therefore, there appears to be significant scope for encouraging more sustainable means of travel to work, given the short distance of typical work journeys. 57% of residents take their private vehicle to work (with an additional 7% being car passengers); 18% walk to work and 8% cycle. Only 6% use public transport to travel to work, all of which consists of bus use.

The figures below[2] show that the choice of transport mode to work is strongly affected by the area of the city in which the resident lives. The majority of car journeys to work arise from the outskirts of the city whilst the majority of journeys on foot arise from within the city centre. This may indicate that a key employment zone is within the city centre:

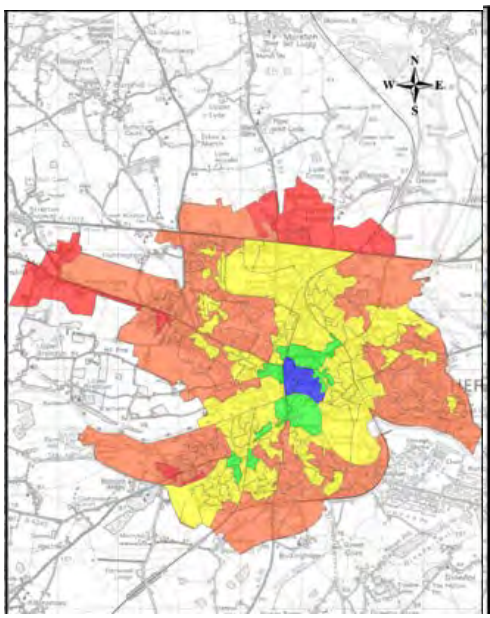

Fig 1: Car journeys to work

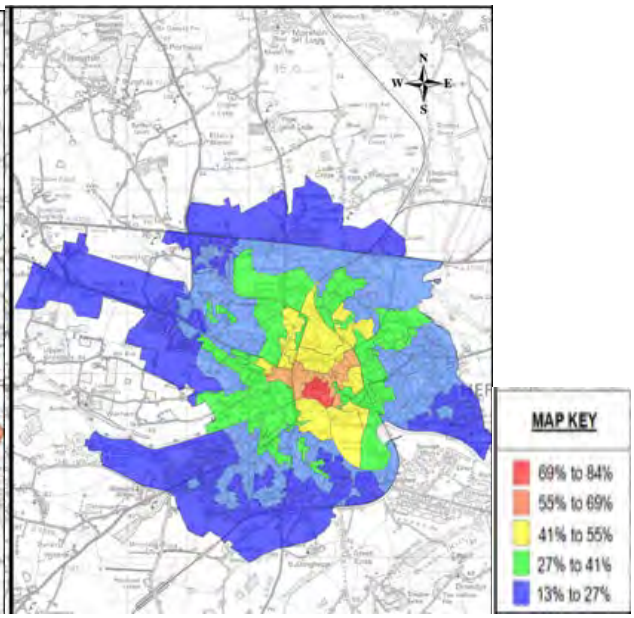

Fig 2: Journeys to work on foot

2.5. Hereford Travel Objectives

From the above background, it can be seen that the key objectives for Hereford are to:

- maintain and encourage the relatively high levels of walking and cycling to work within the city centre
- reduce private vehicle use from the city outskirts into the city centre
- protect the city's historic core against increased vehicle use
- reduce the significant congestion on the A49 crossing point over the Wye river

However, due to the current economic climate, and the reduced public sector funding now available for transport issues, low-cost approaches will be favoured to strategies which involve significant capital expenditure or long-term operation and maintenance costs.

3. Methodology

The focus of the research is on "soft measures". Such measures do not involve investment in new transport infrastructure or technologies but instead focus on changing people's behaviour so that they make better use of currently available resources. Following a review of available soft measures, a city-wide sustainable travel plan is devised to suit Hereford and other similar cities, which is set out in the Discussion.

4. Results

A summary of available soft measures[4], which can potentially be used to encourage a behavioural change in choice of transport mode, are set out below and discussed in section 5.

Table 1: Available Soft Measures

Strategy	**Details**	**Potential Financial Implications on the Local Authority**
Pedestrian-only zones	Converting the city centre to pedestrian-only zones would prevent private vehicle use in the inner zones of the city.	Cost of converting roads into pedestrian-only zones Additional car parking on the outskirts of the pedestrian-only zone
Reduced car parking	Reducing availability of city centre car parking could encourage private vehicle drivers to use different modes of transport due to the inconvenience of locating a parking space.	Reduced car parking income Additional car parking on the outskirts of the city centre
Car parking duration	Limiting city centre parking to a maximum duration (up to 3 hours) could minimise use by commuters without deterring other day visitors such as shoppers.	Reduced car parking income Additional car parking on the outskirts of the city centre
Car parking charges	Increasing city centre car parking charges could minimise use by commuters but could also deter other day visitors.	Reduced car parking income Additional car parking on the outskirts of the city centre Reduced income from day visitors, and potentially reduced business investment
Park and Ride	Car parking on the outskirts of the city centre and public transport connections into the city centre.	Additional car parking facilities and re-routing of public transport vehicles (primarily bus)
Reduced public transport costs	Local authority subsidies of public transport charges to offer reduced rates or season ticket discounts.	Cost of subsidising public transport
Public transport promotion and marketing	Greater awareness of available public transport options could increase public transport use.	Promotion/marketing cost
Walking / cycling promotion and marketing	Campaigns such as “Walk/Cycle to Work Week” can positively encourage people to switch to walking or cycling.	Promotion/marketing cost
Bicycle parking facilities	Availability of good quality and secure bicycle parking can encourage cycle use.	Cost of bicycle stands (approximately £35 to £100 per stand)
Car share schemes	Providing car share websites or other databases allows people living in the same area and travelling to the same area to share their car use.	Cost of maintaining website / databases

5. Discussion

5.1. Reduction of Private Car Use

It is self-evident that converting the city centre into a pedestrian-only zone will prevent private vehicle use within the area. However, such a measure may be unduly restrictive and unworkable for residents and outside visitors. An alternative therefore may be to enforce driving restrictions within the city centre for specific time periods, rather than a full conversion of the city centre into a pedestrian-only zone.

Parking restrictions within sustainable travel plans have been reported as effective in reducing commuter car use by an average of 24% or more, whilst the reduction in commuter car use was only 10% or more without parking restrictions[4]. From Table 1, the three strategies relating to parking restrictions (reducing car park availability, reducing parking duration, and increasing parking charges) may all be effective in reducing private vehicle use. However, only reduction of parking duration specifically targets commuter driving, whilst the other two methods impact on day visitors as well as commuters.

5.2. Sustainable Travel Alternatives

A potential sustainable alternative to private vehicle use is public transport use. It has been reported that offering public transport discounts can be highly effective in encouraging reduced car use[4]. Hereford has a railway station within its city centre but no other stations in the outskirts of the city, thus preventing commute to work by rail for Hereford residents. Therefore, the primary existing public transport option for Hereford is bus.

As mentioned above, only 6% of residents commute to work by bus, which seems a relatively low proportion. This may, potentially, be explained by the inability (due to space restrictions) to provide bus priority measures (such as exclusive bus lanes) within the historic city centre core. Therefore, bus users may be subject to the same congestion as faced by private vehicle users, but with the added inconvenience of public transport use (such as waiting at bus stops for the bus to arrive).

Given the compact nature and pleasant environment of Hereford city centre, it is therefore considered that sustainable travel options which favour walking and cycling within the city centre, rather than increasing bus use over current levels, are the optimum choices.

5.3. Hereford City Proposal

Figures 1 and 2 above show that private car use and walking are more popular respectively in different parts of the city. It is therefore useful to consider the city centre as "Zone 1" and the outer regions as "Zone 2" with different travel planning strategies for each zone.

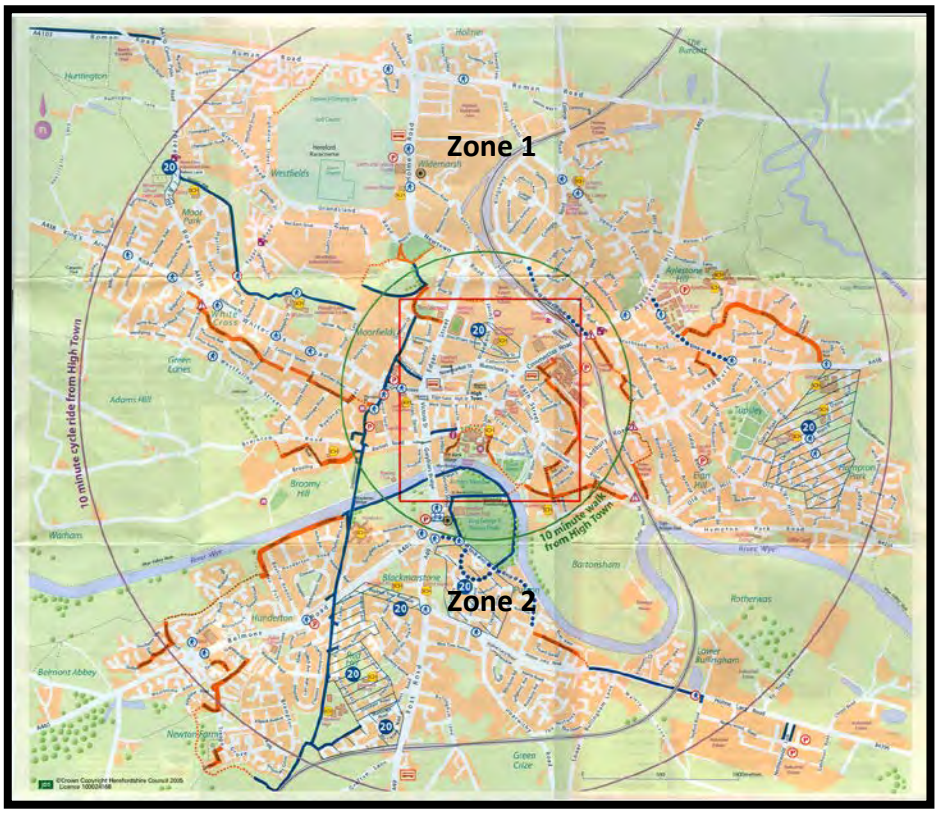

Figure 3: Map of Hereford with travel planning zones[5]

Zone 1 (circled in green - from the Wye Bridge to Hereford railway station) is 0.9 miles in length. The Herefordshire City Council mini-map[5] states the area within the red square in Zone 1 is within 10 minutes walk from High Town (the main city centre shopping street). From the above discussion, it is considered that the key approach for Zone 1 is to implement some form of parking or driving restriction within Zone 1 and couple this with measures to encourage increased walking and cycling within the Zone.

Whilst parking restrictions may encourage reduced private car use, driving restrictions would guarantee reduced private car use, and may therefore be the more effective option. However, it is not desirable to adversely impact on day visitor numbers to the city. Instead, the key target is commuters into the city for work to tackle peak time congestion. Therefore, a potential solution is to enforce driving prohibitions in the city centre only during peak commuter travel time. A proposed time frame could be, for example, 7.30am to 9.30am and 4.30pm to 6.30pm. The driving restrictions would only be within the red square in Zone 1, so as not to exceed a reasonable walking distance for most people. Naturally, there would be exceptions for disabled drivers, emergency vehicles and buses.

Enforcement of the driving restrictions could involve the placement of CCTV cameras at key road junctions within the city which would record vehicle use. Residents of Zone 1 who need to commute outside of Zone 1 during peak hours may apply for a special permit to be displayed on their vehicle to avoid receiving any penalty should they be recorded on the CCTV cameras. As it is only relatively low proportion of Hereford residents who commute outside of Hereford for work (and not all of them live within the city centre) it is considered that their vehicle use would not detract from the overall advantages of creating the peak time driving restriction zone within the city centre.

Outside of peak time hours, shoppers, tourists and other day visitors would be permitted to use their private vehicles. Whilst this may be disadvantageous from an environmental viewpoint, the potential adverse impact from an economic viewpoint of deterring such visitors may counter-balance this.

This system would therefore reduce road traffic congestion (a significant concern within Hereford); create a more pleasant walking atmosphere; and reduce carbon emissions. In order to encourage residents to accept and appreciate the change (rather than feeling that it has been imposed upon them) promotion and marketing campaigns ought to be used in the lead-up to the change, to promote the positive outcomes of the peak-time pedestrianisation.

Due to the driving restrictions to be implemented within Zone 1, drivers into the city centre from Zone 2 (as well as from outside Hereford) will need parking facilities on the outskirts of Zone 1. It is proposed that such facilities be located just before the A49 road bridge crossing the river Wye, which is currently the main congestion hotspot in the city area. This, it is anticipated, will lead to drivers from Zone 2 who wish to reach the city centre driving up to the parking facility and then walking or cycling into the city (using the pedestrian footbridges) rather than attempt to drive across the river on the A49 road bridge.

Therefore, the only drivers who will continue to use the A49 river crossing will be those who do not intend to drive into the city centre, but will instead continue past the city centre heading either to the north or south of the city.

Reducing vehicle numbers on the river crossing in this way would, it is anticipated, result in reduced congestion, so as to allow drivers who wish to bypass the city centre and reach the north or south of the city to move more easily. This would therefore alleviate the economic and social adverse impacts caused by congestion, as well as to reduce carbon emissions by the reduced private vehicle users.

Additional strategies suitable for Zone 2 include strategies to encourage cycling within the city centre. For example, efficient, smart-card operated bicycle hire facilities could be made available at the river crossing car park, to enable drivers to hire a bicycle daily to continue their commute to work once parked. At the city centre, secure bicycle parking would also need to be provided at key locations to assist such additional cyclists.

Further, the setting up and promotion of car share schemes could be valuable in encouraging reduced private vehicle use from Zone 2 (and beyond) to the river crossing facility.

6. Conclusions

Whilst it is a straightforward matter to set out a list of potential travel planning "soft measures" which may encourage sustainable transport use, a more complex issue is selecting which measures are suitable for particular circumstances. In the case of rural cities, such as Hereford, the importance of the city as a centre for a much wider local area cannot be underestimated, and so any selection of measures must take into account and balance the economic impacts, as well as the environmental and social considerations. As such, it is considered that the package of measures proposed above can be applied effectively to rural cities in the same or similar circumstances as Hereford, and can achieve the appropriate balance between environmental, economic and social aims.

The focus in this paper has been on reducing congestion and carbon emissions from private vehicle traffic caused by commuters to Hereford city centre for work. The proposals do not resolve other travel issues which may affect Hereford, primarily the concern that the A49 currently takes "through traffic" directly into the city centre. Current proposals include the development of a new bypass road to allow outside traffic passing through Hereford to bypass the city centre. However, these issues are beyond the scope of this paper.

The views expressed in this paper are mine alone, as an independent researcher, and do not represent the views of Hereford Futures Ltd or Herefordshire County Council.

References

[1] Herefordshire Council, The Population of Herefordshire, November 2009

[2] Delivering a Sustainable Transport System Stage 2 Study for the West Midlands Region, Growth Point Connectivity Stage 1, April 2010

[3] Census Data, 2001

[4] Cairns, S., Sloman, L., Newson, C., Anable, J., Kirkbride, A., Goodwin, P. (2004), Smarter Choices – Changing the Way We Travel, Department for Transport

[5]Herefordshire Council, Mini-Map, http://www.herefordshire.gov.uk/docs/Hfd_Mini_map_07.pdf

Not planning a sustainable transport system – Swedish case studies

Göran Finnveden[1,*], Jonas Åkerman[1]

[1] *KTH Royal Institute of Technology , Sweden*
** Corresponding author. Tel: +46 8 79073 18, E-mail:goran.finnveden@abe.kth.se*

Abstract: The overall objective of the Swedish transport policy is to ensure the economically efficient and sustainable provision of transport services for people and business throughout the country. More specifically the transport sector shall contribute to the achievement of environmental quality objectives where the development of the transport system plays an important role in the achievement of the objectives. The aim of this study is to analyse if current transport planning supports this policy. This is done by analyzing two recent cases: the national infrastructure plan 2010-2021 and the planning of Bypass Stockholm, a major road investment. Our results show that the plans are in conflict with several of the environmental quality objectives. Another interesting aspect of the planning processes is that the long-term climate goals are not included in the planning processes, neither as a clear goal nor as factor which will influence the future transport system. In this way the long-term sustainability aspects are not present in the planning. We conclude that the two cases do not contribute to a sustainable transport system. Thus, several changes must be made in the processes, including putting up clear targets for emissions.

Keywords: *Transport, Planning, Energy Use*

1. Introduction

One of the pillars of the Swedish environmental policy is Environmental Policy Integration, suggesting that environmental factors must be integrated into all operational areas [1]. An expression for this is the sector responsibility for environmental issues that among other things entails that a number of agencies have responsibility to follow the environmental development within their sectors.

The overall objective of the Swedish transport policy is to ensure the economically efficient and sustainable provision of transport services for people and business throughout the country. More specifically the transport sector shall contribute to the achievement of the environmental quality objective *Reduced climate impact* and to other environmental quality objectives where the development of the transport system plays an important role in the achievement of the objectives. The objective *Reduced climate impact* requires significant reductions of greenhouse gases. In Sweden, the government's target is that emissions should decrease by 40%, of which 2/3 in Sweden, by 2020 compared to 1990, and that the net emissions should be zero by 2050 [2]. These goals will require powerful economic instruments [2]. To be in line with the 2-degree target for climate change, the transport sector needs to reduce the emissions by 40 % to 2020, 80 % to 2030 and 95 % to 2050, compared to 1990 according to the Swedish Road Administration [3].

The aim of this study is to analyse if current transport planning supports the Swedish transport policy and also to what extent environmental factors are integrated into the decision making processes.

2. Methodology

Two case studies were chosen for the analysis: The national infrastructure plan 2010-2021 and the planning of Bypass Stockholm, a major road investment which is also a part of the infrastructure plan. These plans are reviewed and analysed in relation to the transport policy goals and the integration of environmental aspects in the plans. As a criterion for a sustainable

transport system we use in this paper the transport policy goal that the transport system shall contribute to a Reduced climate impact and other relevant environmental quality objectives. There are other criterion related to social and economic aspects of a sustainable transport system that could be added, but in this paper we focus on the ecological dimension.

3. Results

3.1. *Bypass Stockholm*

3.1.1. *Choice of alternatives*

The Swedish Road Administration has proposed in a statement to the Government that permission be granted for Bypass Stockholm [6]. It is interesting to study what alternatives were considered, and why Bypass Stockholm was recommended. In the Road Analysis [7], it is stated that the purpose of the road analysis is... to find the road corridor that best... ties together the north and south parts of the Stockholm County, creates a bypass for long distant traffic, improves the availability on the access roads, improves the possibilities for a common work and housing market for the region, allow a multi-nuclear region, and give possibilities for development in a region with growth. None of these goals touches on climate, environment, or sustainable development.

In the Road Analysis, three main alternatives are analysed:

- Bypass Stockholm without congestion charges
- Diagonal Ulvsunda without congestion charges. This is also a road alternative but located closer to Stockholm's inner-city than Bypass Stockholm.
- The Combination Alternative that includes congestion charges, public transport investments, and less road construction.

The Combination Alternative was developed by the Road Administration although it may not be the most competent organisation to develop that alternative since it is not responsible for public transport systems including railroads. The system for congestion charges included in the Combination Alternative is not the system that is used today. The structuring of the Combination Alternative has also met criticism [22] for having chosen expensive and inefficient investments in new tracks.

In the Road Analysis, the Combination Alternative is later rejected. The motivation is that it is not considered to meet the project goals. Here several key observations are possible. Already in the goal formulation it is set down that a road must be found. Other solutions for the foreseen transport problems are not of interest. In the Supplementary Report [6], it is stated also that “the Combination Alternative does not offer sufficient road capacity.”

The main purpose of the Road Analysis was thus, according to the above, to find a road corridor. At the same time, there are the transport policy goals to adhere to. These entail that the transport system must both be effective from a socio-economic perspective and be long-term sustainable. In the Road Analysis, there is no direct evaluation made with regard to the transport policy goals, but several aspects of these are taken up. For example, environment and climate is evaluated for the alternatives and it is concluded that the Combination Alternative is better than the Bypass Stockholm. Also related to other goals such as safety, travel times and gender aspects, the Combination alternative is preferable [8].

A number of conclusions can be drawn from this discussion:

- In the Road Analysis, the goal was to find a road corridor, not to find the best solution for Stockholm's traffic and transport problems. Thus, there is still a need to analyse alternative solutions for Stockholm's traffic problem.
- The Combination Alternative is rejected with reference to its not meeting the project goals. The choice of project goals is therefore central.
- None of the project goals in the Road Analysis is focused on environment, climate or sustainable development. If it had been so, then Bypass Stockholm could have been rejected with reference to its not meeting the project goals.
- Had the transport goals been guiding for the choice of alternatives, then Bypass Stockholm would hardly have been recommended [8].

3.1.2. *Traffic volumes*

New roads do not only lead to traffic moving from one road to another. New roads also generate new traffic [9-12]. There are several mechanisms for why new roads generate new traffic, and one can distinguish between effects in the short and long term. In the short term, new roads can lead to car-use being more attractive relative to other transport forms, and to travel itself becoming more attractive relative to alternative activities. In the long term, new roads can lead to new localisations. It can for example be attractive to develop new areas if there are better road connections, which then leads to increased traffic volumes.

The Swedish Road Administration's prognosis [6] includes short term effect on passenger vehicles. The traffic prognoses show that Bypass Stockholm leads to increased traffic volumes and decreased share of public transport. Increased traffic because of new localisation patterns is not included, however. For freight traffic, no consideration is made that new roads generate new traffic.

Thus, conclusions from this section are that:

- Bypass Stockholm leads to increased traffic volumes
- the Road Administration has likely underestimated these increases. This in turn imply that:
- congestion is underestimated
- travel times are underestimated
- accessibility is overestimated
- environment impact, including CO_2 emissions, is underestimated
- effects of development of new areas on, for example, natural environments and emissions, are not considered fully

3.1.3. *Emissions of greenhouse gases*

According to the Swedish Road Administration [6], Bypass Stockholm will increase the emissions of greenhouse gases. In our estimation this increase is underestimated. An important reason is that Bypass Stockholm likely leads to higher traffic volumes than what the Road Administration has supposed (see above). Some additional reasons are discussed below.

A failure of earlier analyses of Bypass Stockholm [7] is that these did not include emissions from the construction of the road itself [13]. This was also one of the points that the Government Offices wanted to have supplementary information on [6].

The Road Administration has in the Supplementary Report [6] analysed energy consumption and emissions from construction of the road, but unfortunately in an incomplete way. The

analysis that the Road Administration commissioned [14] includes energy consumption and greenhouse gas emissions for the road's construction, but not for the production of the materials. The construction of tunnels requires concrete and steel that are not included. An initial analysis indicates that the energy consumption for the production of these materials can be at least as large as the energy consumption that is already included in the analysis [8]. The effect on the calculations of emissions of CO_2 can thereby be significant.

In connection with analyses of environmental impacts, it is sometimes discussed how one should assess energy use and its consequences. An example relates to emissions from electricity production. The different emissions from for example hydropower, nuclear power, wind power, and coal power vary tremendously of course. Thus a discussion often arises about what electricity production should be used in the analyses, e.g. [14-16]. There are two types of data that can be chosen: average data and marginal data. Average data relate to the average electricity production during a certain time period in a certain area, for example average production in Sweden in 2008. Marginal data relate to that specific electricity production that is changed, if electricity consumption increases or decreases. Identifying the marginal electricity source may be difficult [16] and may depend on the chosen time perspective and on what decisions future politicians make. It has therefore been suggested that sensitivity analysis should be made using both low-carbon and high-carbon electricity [23].

The choice of average data or marginal data depends to a large extent on the type of analysis and question one poses, e.g. [16-19]. If the analysis is to perform an environmental accounting of a system, then the average data for the system being studied is the most suitable. If instead the analysis is for assessing impacts of changes and measures that affect energy consumption, then marginal data are the most suitable choice.

What then is relevant in this context? Environmental impact assessment focuses on analysing the consequences of a decision. If a decision entails that energy consumption changes, data for the production that changes, not the average production, should be used. That is, marginal data should be used in environmental impact assessments. CBAs also focus on analysing effects of changes. The mathematical basis for analyses is differential equations. That is, even in this case, marginal data should be used rather than average data.

However, in the analysis that Stripple makes [14], average data are used as the primary alternative. This is questionable according to the above. Instead, marginal data should be used. That is also done by Stripple in a sensitivity analysis. There he uses coal condensation power as an example of marginal electricity production. The result then becomes radically different and the emissions of carbon dioxide from construction, maintenance and operation of the road become significantly higher. With average data the emissions are 0.248 million tons CO_2 compared with 5.83 million tons when the figures for marginal electricity production are used [14].

In the Swedish Road Administration's Supplementary Report [6], a prognosis is used for future vehicles and their emissions of CO_2 [20]. In the prognosis, it is assumed that the share for renewable fuels will be circa 20% in 2020. Furthermore, it is assumed that the share of plug-in hybrids among new car sales will be 45% in 2020, and that the total share of plug-in hybrids will be about 10% that year. These assumptions are very optimistic,. The prognosis that the share of vehicles driven with renewable energy will be 20% in 2020 can be compared with the Swedish Government's target of 10% renewable fuels in transport by 2020. Furthermore, the prognosis for plug-in hybrids (circa 10% in 2020) can be compared with the

Swedish Energy Agency's prognosis of 85 000 vehicles (all-electric and plug-in hybrids together), which corresponds to circa 1.5%.

In the calculations of CO_2 emissions, two simplifications are then made that cause underestimations. One is that all vehicles that can use alternative fuels are driven exclusively with these [20]. The other simplification is that only emissions during the operation of the vehicle are considered. Excluded, therefore, are the emissions during:

- production of renewable fuel (which can be significant)
- production of electricity (which can be significant)
- production of the vehicle itself (which is larger for electric cars and plug-in hybrids than for conventional vehicles)

This leads to clear underestimations of the CO_2-emissions.

To summarise, by the Swedish Road Administration's own assessment [6], Bypass Stockholm leads to increased emissions of the greenhouse gas CO_2. This increase is underestimated, for the following reasons:

- the increase of traffic volume is likely underestimated.
- the production of materials for the roads has not been included.
- marginal data for the emissions should have been used.
- the introduction of vehicles fuelled with electricity and renewables has been overestimated.
- it has been assumed that vehicles that can use alternative fuels will be driven exclusively with these.
- emissions from the production of fuels and electricity for the operation of vehicles, have been excluded.
- emissions from the manufacturing of vehicles have been excluded.

3.1.4. *Cost-benefit analyses*

In an earlier report [13], we have discussed the use of CBAs both from a general perspective and in previous analyses of Bypass Stockholm. The reflection built on earlier CBAs [21]. In the Swedish Road Administration's Supplementary Report [6], a new CBA is made. The conclusion is reached that the CBA of Bypass Stockholm yields a positive result. There are, however, a number of deficiencies and uncertainties in the calculation. One is the underestimation of the CO_2-emissions as discussed above. Another is the zero value given to encroachment onto natural and cultural environments, some with national importance. Another important aspect is how the future developments are included. In the analysis, future powerful economic instruments that are required to reach the Reduced climate change objective are not included. It is likely that if such policy changes were included, the benefits of a new road would decrease. This is because powerful economic instruments would probably reduce traffic volumes and thus reduce benefits from time savings. In an earlier CBA [21] it was also showed that an increased oil prices would significantly reduce the benefits of a new road.

3.2 National infrastructure plan

The national infrastructure plan includes suggestions for new investments and maintenance for the Swedish transport system corresponding to approximately 50 billion euro. It was developed by the Swedish transport agencies and submitted to the government [4]. An environmental assessment of the plan was also submitted [5].

There are two overarching aspects of the Swedish transport policy, it should be economically efficient and it should support a sustainable provision of transport services. However, these two goals do not seem to have the same importance in the planning. In the plan, it is stated that the economic efficiency, measured by cost-benefit analyses, has been guiding the work [4]. The corresponding comment is not made regarding sustainable transport service. One reason for this may be the existence of established methods for evaluating the economic efficiency. For sustainability, corresponding tools are according to the plan lacking, and it is therefore difficult to evaluate [4].

The environmental assessment [5] concludes that the national infrastructure plan will

- lead to increased impacts on the biological diversity (which is relevant for the environmental quality objective A Rich Diversity of Plant and Animal Life),
- only in a limited way contribute to the achievement of the environmental quality objective Clean Air,
- not lead to a decreased number of people being affected by noise above reference values decided by the parliament and thus not contribute to a sustainable development with regards to human health and a good environment.

In relation to emissions of greenhouse gases, it is claimed that the plan will lead to small emission reductions [4, 5]. It is thus clear that the planned projects do not contribute to the significantly decreased emissions that are required. Furthermore, the agencies have underestimated the energy use and greenhouse gas emissions in several ways. They have

- not at all, or only to a limited extent, included energy use and emissions from building of infrastructure.
- assumed large fractions of vehicles which can use renewable fuels or electricity.
- assumed that all vehicles that can use renewable fuels do that all the time.
- assumed zero emissions from production of renewable fuels.
- assumed low emissions from electricity when electricity use is increasing and high emissions when electricity use is decreasing.
- only partially included the increased transport volume caused by new infrastructure.

It is therefore likely that the plan instead will lead to increased emissions of greenhouse gases.

The plan was accompanied by an environmental assessment[5] in line with European directives [24]. It is however unclear to what extent the assessment has influenced the plan since it is noted in the assessment that the suggestions in the plan is in conflict with the environmental quality objectives and thus in conflict with the transport policy.

The environmental assessment also has some limitations in relation to the requirements formulated in the directive [24]. One such requirement is that the plan should be compared with a zero-alternative that is the likely development without the plan. The zero-development (as well as the plan) includes the so called EET-strategy, a strategy until 2020 for efficient energy and transport systems developed by several Swedish agencies. In the infrastructure plan it is however concluded that it is not likely that this strategy will be implemented. Thus the zero-alternative includes a non-likely development. Furthermore, no policy measures are assumed after 2020. Although it is clear that in order to reach the Reduced climate change goal, significant policy measures are required, no such measures are assumed in the plan. Thus the transport agencies either do not believe in the goals the Parliament has decided on, or the zero-alternative does not represent the likely development. This has implications for the comparisons between the plan and the zero alternative, and also for the cost-benefit analysis

performed. Another requirement is that the environmental assessment should include also other reasonable alternatives. The proposed document did however only include an alternative with minor modifications.

4 Conclusions

The National Road Authority suggested the Bypass Stockholm in spite of this alternative being worse than other alternatives from a climate and environmental perspective and according to their own evaluation leading to increased emissions of greenhouse gases. Also the suggested infrastructure plans do not fulfill important environmental quality objectives. Since these two cases do not contribute to the fulfillment of relevant environmental quality objectives, we conclude that the two cases do not contribute to a sustainable transport system and are thus not in line with the transport policy objectives.

Another interesting aspect of the planning processes is that the long-term climate goals, or other sustainability issues, are not included in the planning processes, neither as a clear goal nor as factor which will influence the future transport system. In this way the long-term sustainability aspects are not present in the planning. Thus, several changes must be made in the processes. Examples of such changes are:

- When goals for projects and plans are formulated, environmental and sustainability aspects should be included.
- If environmental and sustainability project or policy goals are not met, new alternatives should be developed and analysed.
- Project goals should not define the solutions (as for example the goal to find a road corridor in the Bypass Stockholm case), but be open to different possibilities.
- Environmental assessments should be performed using state-of-the art methods and data.
- Long-term environmental and sustainability goals should be included in the planning as a factor that might influence the future transport system.
- Methods for assessing the sustainability of transport systems should be developed.

References

[1] Nilsson, M. and Eckerberg, K. (Eds.), Environmental Policy Integration in Practice. Shaping Institutions for Learning, Earthscan, 2007.

[2] Sweden Government Offices, En sammanhållen klimat- och energipolitik – klimat. Regeringens proposition 2008/09: 162. Regeringskansliet, 2009.

[3] Swedish Road Administration, Vägverkets handlingsplan för begränsad klimatpåverkan. Publikation 2009:82. Vägverket, 2009

[4] Swedish Road Administration, Nationell plan för transportsystemet 2010-2021. Vägverket, 2009

[5] Swedish Road Administration, Miljökonsekvensbeskrivning för Nationell plan för transportsystemet 2010-2021. Vägverket, 2009.

[6] Swedish Road Administration, Komplettering i tillåtlighetsärendet Förbifart Stockholm. Med bilagor. Vägverket, 2009.

[7] Swedish Road Administration, Nord-sydliga förbindelser i Stockholmsområdet. Vägutredning. Vägverket, 2005.

[8] Finnveden, G. och Åkerman, J., Förbifart Stockholm, klimatet och miljön – en fallstudie inom vägplaneringen. TRITA-INFRA-FMS 2009:2. KTH, 2009.

[9] The Standing Advisory Committee on Trunk Road Assessment, Trunk Roads and the Generation of Traffic. The Department of Transport. London, HMSO, 1994.

[10] Goodwin, P.B., Empirical evidence on induced traffic. A review and synthesis. Transportation, 23, 1996, 35-54.

[11] European Conference of Ministers of Transport, Infrastructure-induced mobility. OECD, 1998.

[12] Noland, R.B. and Lem, L.L., A review of the evidence for induced travel and changes in transportation and environmental policy in the US and the UK. Transportation Research Part D, 7, 2002, 1-26.

[13] Finnveden, G. and Sterner, T., Reflektioner på samhällsekonomiska analyser i allmänhet och på kalkylen för nord-sydliga förbindelser i Stockholm i synnerhet. TRITAINFRA-FMS- 2007:1. KTH, 2007.

[14] Stripple, H., Kompletterande underlag för tillåtlighetsprövning – en översiktlig miljöstudie av väginfrastrukturen i projekt Förbifart Stockholm. IVL Svenska Miljöinstitutet. 2009.

[15] Sköldberg, H. och Unger, T., Effekter av förändrad elanväning/elproduktion. Rapport 08 30. Elforsk, 2008

[16] Swedish Energy Agency, Koldioxidvärdering av energianvändning. Vad kan du göra för klimatet? Energimyndigheten, 2008.

[17] Ekvall, T., Weidema, B.P., System Boundaries and Input Data in Consequential Life Cycle Inventory Analysis. Int. J. LCA. 9, 2004, 161-171.

[18] Finnveden, G. and Moberg Å., Environmental systems analysis tools – an overview. *J Cleaner Production.* 13, 2005, 1165-1173.

[19] Tillman, A.-M., Significance of decision-making for life-cycle assessment. Environmental Impact Assessment Review, 20, 2000, 113-123.

[20] WSP, Bilparksprognos i Åtgärdsplaneringen. EET-scenario och referensscenario. Rapport 200825. WSP Analys och Strategi, 2008..

[21] Transek, Samhällsekonomiska kalkyler för Nord-sydliga förbindelse i Stockholm. Rapport 2006:18. Transek, 2006.

[22] Swedish Society for Nature Conservation, Synpunkter från Naturskyddsföreningen i Stockholm län på kompletterande underlag inför en eventuell tillåtlighetsprövning enl 17 kapitel Miljöbalken av ”Effektivare Nord-sydliga förbindelser i Stockholmsområdet”. Naturskyddsföreningen i Stockholms län, 2009.

[23] Finnveden, G, A World with CO_2-caps. Electricity production in consequential assessments. Int J LCA, 13, 2008, 365-367.

[24] European Parliament and Council of the European Union, Directive 2001/42 on the assessment of the effects of certain plans and programmes on the Environment, Brussels.

Sustainable bus transports through less detailed contracts

Helene Lidestam[1,*]

[1] *Department of Management and Engineering, Linköping, Sweden*
** Corresponding author. Tel: +46 13282433, Fax: +46 13281101, E-mail:helene.lidestam@liu.se*

Abstract: The purpose of this paper is to investigate both environmental effects and cost effects of using less specified contracts regarding bus sizes in public bus transports. The process of choosing the best bid in the public procurement of bus transports is easier if the demands of the qualifications are well specified and detailed. On the other hand, detailed contracts can force the entrepreneurs to use less environmentally friendly and uneconomical alternatives. The process of choosing the best bid in the public procurement process will be more complicated when the contracts are less detailed compared to current situations. Indeed, using less detailed contracts leads to decreased emissions and probably costs for all parts involved. A mathematical model with binary variables is developed in order to evaluate the environmental and the economic effects of using less detailed contracts in the public procurement of bus transports and in turn more suitable bus sizes. Computational results with data from a Swedish bus service provider are presented. The results of the model indicate that the emissions decrease considerably by using less detailed contracts. The results of a sub case indicate that the costs could be reduced as well, depending on how efficient the additional buses can be planned.

Keywords: *Environmental sustainability, Bus transports, Public procurement, Mathematical modeling*

1. Introduction

Many nations have converted their public transport systems from monopoly transit systems to competitive tendering. One of the first regions to use fully-tendering regime was London in 1985 [1]. An overview of international successful and less successful ways to use competitive tendering as a possibility to decrease the subsidies within the business of public bus transports has been presented [1]. The competitive tendering system has worked satisfactory in most of the European countries. Two exceptions are Italy and France where the transfer to the competitive tendering system has not affected the transports costs at all [2]. However, the costs have a tendency to be low at the first time competitive tendering is used and then instead increase for the second and third time the system is used [1]. This form of tendering often leads to changes of the structure of the actors involved in the process. Going from a market including many small actors, the actors are now few and large [1]. The system for public procurement in Sweden started through a national resolution in 1985, which led to a law coming into effect in 1989 [3]. The process for the regulations for procurement of public bus transport in Sweden is based on EU public-procurement guidelines. The most common form of contracts used in Sweden is gross contracts, where the bus entrepreneur only gets paid for the costs and is not involved in the ticket revenues. The most common way to choose the winning bid is to use so called first-price auction, which is to choose the bid with the lowest price as a winner. By using this combination the final contracts will often be very detailed. An earlier study showed that the CO_2-emissions can be reduced considerably by using less specified contracts with respect to bus sizes in the public bus transports [4]. The part of traffic being involved in the public procurement processes has increased drastically since and is now (2010) around 90%. The process of choosing the best part in the public procurement of bus transports is easier if the demands of the qualifications are well specified and detailed. On the other hand, detailed contracts will lead to limitations and could force the entrepreneurs to use uneconomical, but most of all, less environmentally friendly alternatives. The resulting contracts are indeed very detailed and there is not much inbuilt flexibility regarding for example the bus sizes. Using large buses with many bus seats for transporting few persons is

expensive, both in economic terms and most important in emission terms The trade organizations within the public bus transports area in Sweden have a common goal to double the public transports to 2020 and this ambition is in line with the aim in EU declaring that the emissions should decrease considerably. The purpose of this research was to study the cost effects of using more environmental-friendly bus traffic. The economic and environmental consequences are two of three essential aspects in sustainability. The third aspect concerns the social area. As increased emissions can lead to diseases, also this aspect is affected negatively when using non environment-friendly solutions. The outline of the paper is as follows. The methodology is presented in Section 2 and in Section 3 the mathematical model for the problem is formulated. Data from a real-life case is studied and presented in Section 4. The computational results are presented in Section 4 and finally, in Section 6, some concluding remarks are viewed.

2. Methodology

A mathematical optimization model with binary variables is developed to evaluate the environmental and cost effects of more optimized bus sizes. The mathematical model is carefully described in Section 3. We have used the program, AMPL, for modeling the problem and the commercial program CPLEX, version 10.2.0, is used to solve the model. These programs are suitable when the mathematical models include binary or integer variables. Data needed for the study is collected for one region in Sweden and is provided by a large Swedish bus entrepreneur, called Nobina Bus AB. All distances from one stopping place to the next stopping place on all chosen bus tours have been used as well as different kind of buses and their capacity in terms of number of seats. Finally, the levels of CO_2-emissions (kilogram per kilometers) and costs (Swedish crowns per kilometers) for each kinds of bus type are considered. Two opposite scenarios have been tested in order to evaluate the environmental effects of more details in contracts. The scenarios are shortly described below:

Scenario A – This is the basic scenario and it shows the current situation in the chosen region. The contract for bus traffic in the area defines which type of buses those have to be used on which bus tours.

Scenario B– The possibility to use additional buses along the lines is tested. Sometimes a large bus can drive empty from the starting place to the second last stopping place and then it can get a lot of passengers for the last part of the line. No restrictions regarding the choice of bus type. The results in this scenario show the level of CO_2-emissions when as small buses as possible, with respect to CO_2 emissions, are used. The possibility to use other bus types is also tested.

The economic effects of using more flexible and less detailed contracts in the public procurement process are evaluated in the specific case described in Section 4. This case is a sub case of the general case. In order to get a more lifelike situation, some restrictions are added into the relevant scenarios. They are further described in Subsection 4. The results from the sub case are compared to the current daily planning by the involved bus entrepreneur. The results of the model will give a solution that uses as small bus sizes as possible with respect to the costs.

3. Mathematical model

In this section we present the mathematical model for the problem of evaluation of public procurement of bus transports. The model is used in order to find as small buses as possible to use of each part of the bus tours. The model consists of an objective function, binary

variables, parameters and constraints. We first describe the parameters and the variables. Thereafter the objective function is presented and finally, the constraints are described. The original model is earlier presented [4].

Parameters

$h_i = CO_2$ emissions measured in kilogram per kilometer from bus type i.

a_{jk} = the distance from stopping place k to the next stopping place at line j.

e_{jk} = the number of people getting on the bus at stopping place k at line j.

r_{jk} = the number of people getting off the bus at stopping place k at line j.

P_i = the capacity for bus type i measured in number of seating places.

Variables

$$\boldsymbol{B_{ijk}} = \begin{cases} 1, & \text{if bus type } \boldsymbol{i} \text{ is used from stopping place } \boldsymbol{k} \text{ to the next stopping place on line } \boldsymbol{j} \\ 0, & \text{else.} \end{cases}$$

i = 1..m, j =1..n, k = 1..h

Objective function

$$\text{Min} \sum_{\boldsymbol{i}} \sum_{\boldsymbol{j}} \sum_{\boldsymbol{k}} \boldsymbol{a_{jk} h_i B_{ijk}}$$

Constraints

$$\sum_i P_i B_{ijk} \geq e_{j1} \quad \forall j, \forall k : k = 1 \quad (1)$$

$$\sum_i P_i B_{ijk} - \sum_{k=1}^{k-1} e_{jk} + \sum_{k=1}^{k} r_{jk} \geq e_{jk} \quad \forall j, \ \forall k : k \geq 2 \quad (2)$$

$$B_{ijk} \geq B_{ijk-1} \quad \forall k \geq 2, \forall i, \forall j \quad (3)$$

$$B_{ijk} \in \{0,1\} \quad (4)$$

The objective function minimizes the CO_2-emissions. The distance between all stopping places at the lines is multiplied with the CO_2-emissions from the different bus types, respectively. The constraints (1) make sure that the capacity of the used buses is enough that is that all of the people that get on the bus at the starting point have a seat place on the bus. The constraints (2) ensure that all the people getting on the buses at the forthcoming stopping places gets a seat place on the used buses. The fact that one bus has to following the whole line after it has started is described in the constraints (3). The constraints (4) express that all variables are binary, that is they could either be 1 or 0. Constraints (3) also allow buses to start on a later stopping place along the line, but it has to continue to drive to the end of the line. If there is no possibility to add buses along the line the constraints (3) can instead be described as constraints (5) given below:

$$B_{ijk} = B_{ijk-1} \quad \forall k \geq 2, \ \forall i, \ \forall j \quad (5)$$

To evaluate the specific case and to reach the lowest level of included costs, the objective function in the model is modified in the following way:

$$\text{Min} \sum_{i} \sum_{j} \sum_{k} a_{jk} c_i B_{ijk} ,$$

where c_i = costs measured in Swedish crowns per kilometer regarding bus type *i*. The costs refer to variable driving costs. The fixed capital costs, mainly for depreciations, are added afterwards in order to compare different scenarios. The constraints used for the specific case are the same as above (1-4). The model does not consider any limitations of the number of buses that can be used for different lines. The distance between one stopping place at a line and a starting place at another line and the distance to the bus garage is not regarded in the problem. The different times for the lines are counted only as different lines so the time aspect and any possible limitations of the use of different bus types has not been considered as well in the problem.

4. Case study

Nobina AB, earlier called Concordia Nordic Bus AB, is the largest bus transport company in the Nordic countries and one of the ten largest in Europe. Nobina AB works for different public authorities in Sweden. The name of the public authority for the region considered in this study is Västtrafik. The general case included 103 different lines. The lines are divided into several sub lines depending on the number of stopping places along the line. For each line there are different variants of the line. The variants differ regarding the included stopping places and their order. Each variant of a line is used several times in a 24 hour. In total it is 2 044 tours including 2 037 stopping places during a day in the selected area and the number of counted people getting on (and off) the buses is 34 312. Seven types of buses are used by Västtrafik and taken into account in the scenarios. The capacity of the different type of buses is from 23 seats to 56 seats and the levels of CO_2-emissions range from 0,83 kg/km to 0,99 kg/km. For each bus type, the related seat capacity and CO_2-emissions are given. The CO_2-emissions are defined by kilogram per kilometer. The presented model will minimize the level of CO_2-emissions.

The calculations of the emissions are based on road driving with few stops. The most important factor to consider in this paper is the difference in emissions due to the size of the bus type, which in this case is measured in number of seats in each bus type. Therefore the other depending factors, for example type of engine and driving properties are equal in of all the bus types. The considered engine in all of the bus type is a euro3 engine. The newer engine euro5 has fewer emissions but the difference is mostly related to the NOx-emissions and SOx. The figures on CO_2-emissions are considered proportionate to fuel-consumption. The fact that a full bus has more CO_2-emissions compared to an empty bus has not been considered in the optimization, however, it can be calculated and evaluated after the optimization has been made if needed. In scenario B, two additional bus types are possible to use; one large bus taking 65 passengers with 1,15 kg/km of CO_2-emissions and one small bus taking only eight passengers with 0,3 kg/km of CO_2-emissions.

An area of bus traffic is chosen from the general case in order to investigate the economic effects on a given real planning situation. One hundred tours (around 5 %) of 2 044 in total

are included in the specific case. The total length of these tours is 5 750 kilometers to compare to the total length of the general case which is 44 790 kilometers. The bus traffic for the specific case is chosen in cooperation with the planning manager at the involved company Nobina AB. One reason for choosing this area and these tours was that the traffic is expected to be heavy and the buses are supposed to be more full compared to an average tour in the area of the general case. The 100 used tours are divided into 14 bus trips. The bus trips describe the day of each bus. The current situation at the chosen region is that 14 large buses (Express buses) are used on the 100 tours. The bus goes from the garage in the morning and back to the garage at the evening. The bus trips can include from five to nine different tours. A typical example of a bus trip is illustrated in Figure 4.1. This bus trip (on the x-axis) includes seven different bus tours (the piles) represented in time order, that is the first tour represents the early morning and the last tour represents the late afternoon or evening for the bus trip. The y-axis shows the number of passengers on each tour. Each bus tour includes a number of lines between the stopping places and the number of passengers in Figure 4.1 refers to the highest number of passengers on the each tour. That means that the situation can be that the bus drives empty most of the distances and drives with many passengers, for example 50, only on one of the included lines. Then the number of passengers, in Figure 4.1 below, will be 50 on that tour. Most of the bus trips look like the one below in that sense that number of passengers on the tours included varies a lot. As mentioned before only type of large buses are used today in this area. The average number of the highest level of passengers is 24 on the 100 included tours.

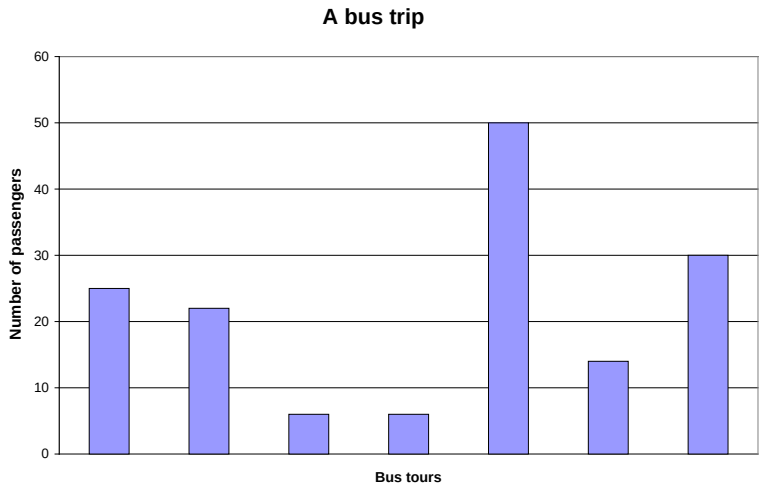

Figure 4.1 Example of a bus trip

Alternatives to use only large Express-buses can be to use as small buses as possible on the fourteen tours. That is further on called using adaptive bus sizes and that will of course also lead to the use of fourteen buses. Another alternative that will be investigated on the specific case is to use another bus type, here called Middle-bus, as a standard bus and then use smaller buses, here called Mini-buses, as additional buses that can be used whenever needed between one or several stopping places. The capacity of the Middle-bus, in terms of seats, is 32 and the capacity of the Mini-bus is 15. The CO_2-emissions from the Middle-bus and the Mini-bus are 0,45 and 0,35 kilogram per kilometers, respectively, compared to the level of 0,96 kilogram per kilometers from the Express-bus. Regarding the alternative of using adaptive bus sizes, the bus type Ordinary is also taken into account. The level of CO_2-emissions from that bus type is 0,93 kilogram per kilometers and the number of seats is 46. The considered variable costs are referred to costs for operating the bus and costs regarding the bus driver. The

included fixed costs are capital costs, mainly with respect to the depreciations and based on the purchase cost. The levels of the different costs are collected and evaluated by the planning manager for Nobina AB in the area of the specific case.

5. Results

The resulted levels of CO_2-emissions from the scenarios in the general and the specific case are presented in Table 5.1. The level of CO_2-emissions is calculated based on the level of emissions per 24 hours workday. The bus traffic on workdays is on average four times more intense compared to the bus traffic on Saturdays and Sundays. We have estimated the number of workdays in a year to 245 and the official holidays, including Saturdays and bridges days, to 120. The differences compared to Scenario A are given in percent.

Table 5.1 Comparison of the two cases.

Case	Scenario	CO_2 kg/year	Difference
General	A	11 765 150	0 %
General	B	7 653 800	- 34 %
Specific	A	1 554 300	0 %
Specific	B	1 183 050	- 24 %

The results from the two scenarios, indicate a clear relation between CO_2-emissions and contract-flexibility. By letting the number of passengers decide which bus size to use instead of following the contract regulations, the CO_2-emissions can be decreased by 34 %. The possibility to add buses along the tours create a need for more small buses. A disadvantage by using smaller buses is the fact that more buses have to be used. The buses will in total be used on shorter distances but indeed more buses on a line results of course in more bus drivers. It is a trade-off between the fixed costs of having several bus drivers and the ambition to drive as small buses as possible in order to reduce the CO_2-emissions. The fact that the difference between Scenario A and Scenario B in the general case is larger compared to the difference between the same scenarios in the specific case indicates that the chosen area for the specific case is not fully representative for the general case. The results above also tell that there are other areas in the general case that would gain more, with respect to lower CO_2-emissions, by using more flexible and less regulated contracts. The solution times regarding the general case are less than 20 minutes and the solution times for the specific case are all very small, below one minute.

The current situation, only use Express-buses, is compared to other alternatives regarding the specific case. The first alternative to investigate was to adaptive bus sizes. To find and use the smallest bus for each trip resulted in seven Express-buses, six Ordinary-buses and one Middle-bus and these changes would lead to 5 % lower CO_2-emissions on the same number of active kilometers compare to the current situation. The second alternative investigated was to use another type of base bus, Middle-bus on all trips and then when necessary use additional, Mini-buses, on parts of the tours. By using fourteen Middle-buses and seventeen Mini-buses the CO_2-emissions can be reduced by as much as 47 %.

The results, however, only present the CO_2-emissions from the active driving in the tours. The driving from the bus garage to the first tour in the morning and the driving from the last tour in the evening back to the bus garage are not taken into account. Also the fact that the buses used on one or several sub distances between stopping places on one tour also are used for other sub distances on other tours lead to additional CO_2-emissions. These extra CO_2-

emissions are not been taken into consideration in the above table. The circumstances of using additional buses on the trips lead to a larger number of active kilometers, 6 677 compared to 5 750. The plan of where different buses will be used has been showed to the planning manager. He has, from his point of view, estimated the practical need for buses in the current area to be 10 additional Mini-buses. Therefore the calculations regarding costs are made for using 10 additional buses. The results measured in emissions and costs for using different kind of combinations of bus types on the fourteen bus trips are presented in Table 5.2.

Table 5.2 The results regarding CO_2-emissions and costs from the specific case.

Used buses	Active kilometers	CO_2 kg/year	Difference	Total costs (SEK/year)	Difference
14 Express	5 750	1 518 000	0 %	30 449 000	0 %
7 Express 6 Ordinary 1 Middle	5 750	1 438 000	- 5 %	28 009 000	- 8 %
14 Middle 10 Mini	6 677	800 786	- 47%	24 997 660	- 18 %

The calculations made by the planning manager showed that adding 10 more buses in the current situation will increase the costs by 10 %. There is apparently a gap from decreasing the costs by 18 % to increasing the costs by 10 % due to how the additional buses can be scheduled. However, the value of lowering the emissions and in turn improving the environment is hard to measure and compare to the increasing related costs.

6. Conclusions

The results of the mathematical model indicate that all parts involved in the public procurement process, the public authority, the entrepreneur and the customers, will gain from more flexible and less detailed contracts. The results from the general case expose notable lower levels of CO_2-emissions when the contracts are more flexible and without detailed restrictions. The levels of CO_2-emissions decrease by 34 % from the current situation to the most flexible scenario (Scenario B). The results from the specific case indicate that the costs could be reduced as well, depending on how efficient the additional smaller buses can be planned. The results indicate that the emissions can be reduced up to 47 % by using smaller buses in traffic and the costs can in worst case increase by 10 %. Anyway, there are possibilities to decrease the costs as well if the operations planning changes. That could be done for example by expanding the planning area for the buses in order to increase the possibility to make use of returns to scale and coordination advantages. Other kinds of entrepreneurs, such as taxicabs, could also be used in addition to the ordinary buses. That will lead to more flexibility. Another base for getting lower cost could be to plan the bus trips in a different way. The occupancy level on the buses in general could probably be higher if the tours for a bus trip have more equal occupancy levels. The number of on and off-going people in the studied bus trips in the specific case varies a lot along the trip. The possibility to use parking places for the buses along the tours in addition to the bus garage could also decrease the bus driving. Directions for future research could therefore include the above suggestions in order to show the possibility to reduce both the CO_2-emissions as well as the costs considerably. In order to get a more complete view, other aspects, for example the traveler behavior connected to the level of occupied buses should be further investigated. The results from the optimization model show that detailed rules in the public procurement process lead to increased CO_2-emissions and probably higher overall costs, and therefore it would be

highly motivated by the politicians to evaluate the Swedish system. The research will therefore contribute to the operation management planning in order to achieve the overall aim to reduce CO_2-emissions. The actors in the public bus transport business should as well be interested in getting insight in how fewer restrictions in the contracts will affect them.

References

[1] D.A. Hensher and I.P. Wallis, Competition tendering as a contracting mechanism for subsidising transport – The bus experience, Journal of Transport Econimics and Policy 39, 2005, pp. 295-321.

[2] A. Boitan and C. Cambini, To bid or not to bid, this is the question: the Italien experience in competitive tendering for local bus services, European Transport 33, 2006, pp. 41- 53.

[3] P. Elvingson, Bättre kollektivtrafik, ISBN 91 558 6951 3, Svenska Naturskyddsföreningen, 2005. (in Swedish)

[4] H. Lidestam and M. Abrahamsson, Mathematical modeling for evaluation of public procurement for bus transports in terms of emissions, Management of Environmental Quality 5(3), 2010, pp. 645-658.

Analysis of alternative policy instruments to promote electric vehicles in Austria

Viktoria Gass[1,*], Johannes Schmidt[1], Erwin Schmid[1]

[1] *Department of Economics and Social Sciences, University of Natural Resources and Life Sciences, Feistmantelstrasse 4, A-1180 Vienna, Austria*
[*] *Corresponding author, Tel: +43 147654 3594, Fax: +43 1476543692, E-mail: v.gass@students.boku.ac.at*

Abstract: The large amount of CO_2 emissions and of fossil fuel consumption by the transportation sector makes the sector central for attaining the EU energy and climate policy targets. Consequently, new propulsion systems are developed in the automotive industry, which currently have cost disadvantages compared to conventional internal combustion engines (ICE). The article provides a review on support measures for electric vehicles which have been currently implemented within the European Union. In a case study analysis for Austria, we analyze different policy instruments including a CO_2 tax aiming to support the introduction of electric vehicles in Austria. We have calculated and compared total costs of ownership (TCO), which includes all costs associated with the ownership of an automobile including costs of purchasing, operating and maintaining, charges and taxes as well as costs of recycling and disposal. A survey on main specifications of electric vehicles has been conducted among the main automobile manufacturers and importers in Austria. Based on this survey, TCO have been calculated dynamically from 2011 to 2020 for a business as usual (BAU) scenario considering currently implemented taxes and subsidies for ICE and electric vehicle systems. Three alternative policy support measures have been assessed to promote EV to ICE until 2015. We conclude that an up-front price support seems to be favorable over taxation systems. The paper focuses only of the effectiveness of the three policy support measures but does not analyze their efficiency.

Keywords: *Electric vehicles, Total cost of ownership (TCO), Fiscal policy instruments, Break-even*

1. Introduction

Currently, 98% of the transportation sector in the EU depends on fossil fuels. The sector is responsible for approx. 21% of the greenhouse gas (GHG) emissions, with more than half of the emissions produced by passenger cars [1]. The EU Directive (2009/33/EC) on the promotion of clean and energy efficient road transport vehicles has been released to foster a broad market penetration of environmentally-friendly vehicles in order to decarbonize the transportation sector and to reduce oil dependency.

Several new propulsion systems as plug-in hybrids, range extenders as well as electric vehicles have emerged and entered the market or are ready to enter the market in the near future [2]. However, in order to achieve a shift in the transportation sector the cost disadvantages of the newly emerged propulsion systems have to be overcome. Economic viability and a successful introduction of alternative propulsion systems will mainly depend on economic aspects such as relative costs. The gap between the total cost of ownership (TCO) of alternative transportation systems and ICE should be temporarily closed by appropriate policy interventions to promote environmentally-friendly vehicles.

Current research regarding the economic viability of electric vehicles (EV) focused mainly on lifecycle cost analysis [3,4,5]. Thiel et al. [3] compared the well-to-wheel CO_2 emissions, costs and CO_2 abatement costs of passenger light duty vehicles including gasoline vehicles, diesel vehicles, diesel hybrid vehicles, plug-in hybrid and battery electric vehicles [3]. A static comparison has been conducted for the years 2010, 2020 and 2030 under a new energy policy scenario for Europe. They conclude that electric vehicles can clearly contribute to a decarbonization of the transportation system if renewable electricity is used. According to [3],

current cost disadvantages of electric vehicles can be overcome by adequate policy support instruments to attain payback periods of less than five years.

Ogden et al. [4] conducted an analysis of the societal lifecycle cost of transportation including the purchase price, fuel costs, externality costs of securing oil supply and damage costs for emissions of air pollutants and greenhouse gases which are calculated over the full fuel cycle. Thomas [5] developed a dynamic computer simulation model that compares the societal benefits of replacing conventional gasoline cars with vehicles that are partially electrified, including hybrid electric vehicles. He concludes that electric vehicles in combination with hybrids, plug-in hybrids and biofuels will be necessary to achieve an 80% reduction in greenhouse gas emissions below 1990 levels by simultaneously cutting dependence on imported oil and eliminating nearly all controllable urban air pollution from the light duty vehicle fleet. However, to increase market shares, market barriers have to be overcome. Therefore, the consumer perspective and thus effective and efficient policy instruments should be the focus of further research. Taxation systems regarding vehicles vary strongly between countries.

The aim of the article is to analyze different policy instruments by comparing total cost of ownership (TCO) of EV and ICE in Austria. TCO are calculated dynamically from 2011 to 2020 for a business as usual (BAU) scenario considering currently implemented taxes and subsidies for ICE and EV in Austria. In contrast to lifecycle cost analysis of alternative propulsion systems, our analysis focuses mainly on the total cost of ownership and places the consumer perspective in the center of the analysis. The consumer perspective is placed in the center of our analysis as only early adopters are willing to accept the current cost differential between ICE and EV. As such instruments necessary to close the gap are considered to be necessary in order to achieve a mass market introduction.

The article is structured as follows. Section 2 provides an overview of the support schemes currently launched in the EU-15. Section 3 presents the methodology and data. An analysis on different policy support instruments to equalize the TCO of EV and ICE in Austria is shown in Section 4 and section 5 presents major conclusions from our analysis.

2. Implemented support schemes for EV in the EU-15

Many EU member states have introduced national targets for the EV driving stock, the expansion of charging infrastructure, or production targets of electric vehicles [6]. Most EU member states overcome the cost disadvantage of alternative vehicles by introducing policy instruments such as an up-front price support in order to increase the affordability of electric vehicles by reducing the marginal capital cost, which is considered as one of the key barriers for consumers [7]. Within the EU-15, passenger cars have mainly been the target of a tax reform that takes into account the CO_2 emissions of vehicles. Policy instruments that are currently implemented in order to stimulate the up-take of alternative propulsion systems consist of [7]:

- *Registration or purchase taxes*
  Registration or purchase taxes are an up-front cost and can have a strong impact on CO_2 emissions and the market, if costs are differentiated with regard to the specific CO_2 emissions of the vehicles. In France, a bonus/malus system has been introduced whereby vehicles above certain CO_2 emission thresholds have to pay a malus and vehicles under the threshold receive a bonus. Such a system may increase the political acceptability as well as of consumers, because it can be designed in a revenue neutral manner [7].

- *Circulation or motor taxes*
  Circulation or motor taxes have according to [7] a limited effect on the purchase decision as they are annual or monthly charges. Although they are considered to be politically acceptable, their impact to promote EV is rather low as the cost range of such measures is limited.
- *Fuel taxes*
  Fuel charges have limited short-term effects, because they do not change the purchasing decision of consumers in the longer term [8]. Furthermore, they are considered to be politically prohibitive.

Policy instruments to stimulate the up-take of alternative propulsion systems are subsidies, taxation of benefits in kind and treatment of depreciation (relevant for company cars) and in use and parking charges [8]. Table 1 provides an overview of the currently implemented support measures [7-10].

Table 1: Policy instruments to supporting EV in the EU-15

Country	**Economic instruments for the support of EV**
Austria	Exemption from fuel consumption tax Exemption from monthly vehicle tax
Belgium	Purchasers of electric cars receive a personal income tax reduction of 30% of the purchase price (with a maximum of EUR 9,000)
Finland	Exemption of fuel tax
Italy	A tax incentive of EUR800 and a two year exemption from annual circulation tax is granted for the purchase of a new passenger.
Denmark	Exemption from registration tax and annual circulation tax. Further EV qualify for free parking
Germany	EV exempt from the annual road tax for a period of five years from the date of the first registration
Spain	Various regional governments grant tax incentives for the purchase of alternative fuel vehicles including EV – approx. EUR 6,000
France	Bonus-Malus System; New Cars with CO2 emissions below 125 g/km receive a premium. EV receive currently EUR 5,000
Greece	EV exempt from registration tax. If engine capacity below 1929 cc, exemption from road tax. Further EV are even allowed to drive in Athens when parts of the city are restricted to ICE to reduce traffic congestion.
Ireland	EV exempt from registration tax – approx. EUR 2,500.
The Netherlands	approx. EUR 6,400 reduction from the registration tax
Portugal	Exemption from registration tax
Sweden	Exemption from annual road tax for a period of 5 years upon first registration
United Kingdom	Exemption from annual road tax
Ireland	Exemption from registration tax
Luxemburg	Annual circulation taxes based on CO_2 emissions

3. Data and Methodology

Total cost of ownership (TCO) includes all costs arising with the ownership of an automobile including costs of purchasing, operating and maintaining, charges and taxes as well as costs of recycling and disposal over a specified timeframe under consideration of opportunity costs. TCO is defined as following:

$$TCO = -I + \sum_{t=1}^{N} c\,(1+r)^{-t} + R\,(1+r)^{-N} \quad , \qquad (1)$$

where *I* represents the purchase price, *c* maintenance and operating costs, *r* the discount factor and *R* the resale price. Maintenance and operating costs include infrastructure charges, insurance, fuel consumption tax (NoVA) and the monthly engine related vehicle tax (motorbezogene Versicherungssteuer).

TCO have been calculated for limited vehicle options based on a survey conducted with the main automobile manufacturers and importers in Austria. The survey includes data on technical specifications and costs. The EVs included in the analysis are either already available for sale or will be in the near future. The survey has been conducted with the automotive offices of Nissan, Peugot, Renault, Mitsubishi and Think City in Austria. The ICE have been chosen of similar size and technical specifications, which are the most often sold cars in the vehicle class [11]. Technology and performance assumptions for ICE have been derived from the respective automobile manufacturers [12,13]. Table 2 provides an overview of the main specifications as well as the main resulting performance and cost figures of EV and ICE for which the TCO have been calculated dynamically over the period 2011 until 2020.

Table 2: Technical, performance and cost assumptions of analyzed vehicles

	VW Golf Rabbit	**VW Golf Rabbit**	**Nissan Leaf**	**Peugeot iOn**	**Mitsubishi i-Miev**
Technology					
ICE engine displacement (l)	1.6	1.2	-	-	-
Turbocharger (yes/no)	yes	yes	-	-	-
PT power (kW)	77	77	-	-	-
Electric motor power (kW)	-	-	80	47	49
Battery capacity (kWh)	-	-	24	16	16
Energy source	Diesel	Gasoline	Electricity	Electricity	Electricity
Performance					
Weight (kg)	1,314	1,314	1,545	1,120	1080
Acceleration 0-100 km/h (in s)	11.3	10.6	-	-	-
Top speed (km/h)	190	190	140	130	130
Fuel consumption (l/100km)	4.1	5.2	-	-	-
Electricity consumption (kWh/100km)	-	0	15	15	15
Tailpipe CO_2 emissions (g/km)	107	121	-	-	-
Costs					
Vehicle incl. VAT and NoVA (EUR)	20,350	22,120	39,600	36,000	35,900
NoVA (fuel consumption tax in % of purchase price)	4%	4%	0%	0%	0%
Battery cost (EUR/kWh)	-	-	600	600	600
Battery cost (EUR)	-	-	14,400	9,600	9,600
Loss in value p.a.	17%	16%	32%	32%	32%
Maintenance cost (EUR/100km)	4.6	4.1	2.5	2.5	2.5

The TCO have been calculated over a period of five years assuming that 15,000 km are traveled annually. According to the survey, automobile manufacturers expect that the battery of EV needs to be replaced after approx. 75,000 km. We assume that vehicles are sold after

five years, because no estimates on battery replacement costs are currently available. Both assumptions refer to results of [13] and have been confirmed by the survey. The percentage loss in value p.a. as well as maintenance costs are guesstimates of manufacturers received in the survey. Average figures are applied to all EV, because the guesstimates from the respective manufacturers differ slightly and empirical values are not available yet. We also assume that the purchase price of ICE will not change over time, because further efficiency gains in ICE are costly [2]. Furthermore, learning effects from increased production volumes decrease the purchase price. The learning effects have been depicted from an analysis conducted by [15] and are consistent with [3,14,16]. Currently, battery costs amount to approx. 600 EUR/kWh and shall decrease to approx. 300 EUR/kWh by 2015 if the projected production volumes are reached. Projected productions volumes are reflected in the assumed learning rate and have not been separately been calculated. As such price reductions resulting from an increase in production volume are already reflected in the calculation of the TCO.

The current gasoline price in Austria amounts to 1.3 EUR/l and for diesel to 1.1 EUR/l including taxes and charges. The gasoline and diesel prices are assumed to be consistent with the projected oil prices in the Annual Energy Outlook. The electricity price for Austrian households amounts currently to 0.15 EUR/kWh including taxes and charges. The average increase in the electricity price (EEX Phelix baseload) from 2000 until now has been approx. 2.8% p.a. Similar price developments are assumed to 2020.

4. Results

The three policy scenarios consist of an up-front price support, a CO_2-tax as well as a fuel consumption tax for ICE, respectively. The level of incentive to make EV competitive from 2011 onwards is shown for each policy instrument.

In a BAU-scenario, the EV becomes cost-competitive with ICE in the year 2015. TCO of ICE are increasing over time mainly due to rising fuel costs. The decrease in TCO of EV is mainly attributed to the projected decreases in battery costs. The TCO time line for EV and ICE is shown in Fig. 1.

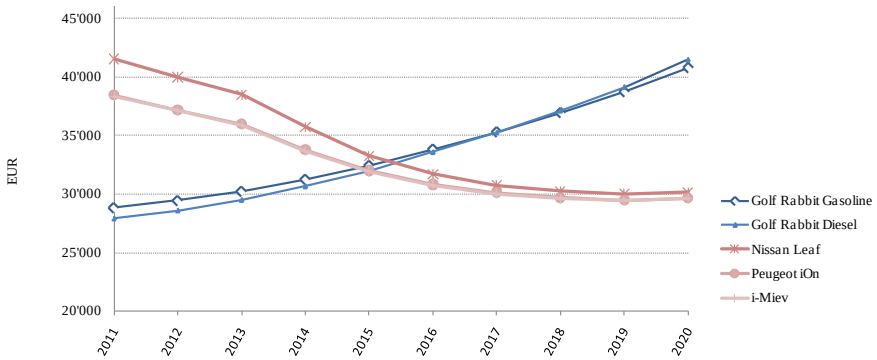

Fig. 1: TCO – BAU-scenario

The BAU scenario implies that TCO of ICE and EV will converge in 2015. However, it only may convergence if the projected volumes are produced to realize the necessary economies of scales. Consequently, subsidies may be necessary to realize the projected production volumes. As shown in Section 2, many countries have currently implemented or are considering to implement an up-front price support (e.g. usually in the form of an exemption of the registration tax) for alternative propulsion systems. An up-front price support is considered as an effective policy instrument, because consumers put much larger emphasis on the purchase

price of a vehicle than on the resulting maintenance and operating costs [8]. However, by introducing an up-front price support for EV, the question arises of how much price support is necessary to incentivize sufficient uptake of EV.

In our analysis, we have calculated alternative levels of upfront price support to offset the gap between ICE and EV TCO (table 3). It is assumed that covering the entire price differential would require large amounts of subsidies despite remaining technical limitations such as limited range that may lead to higher costs [8]. However, a regressive price support system would minimize windfall profits. Nevertheless, the interviewed representatives of automotive manufacturers clearly stated that final purchase prices are set under consideration of governmental support and that EV will be available for sale only in countries with governmental support measures at a level that is considered sufficient from the perspective of car manufacturers. The level of price support should be adjusted annually to account for learning effects. High political and public acceptability is attributed to an up-front price, however some moral hazard problem will remain [7].

Table 3: Levels of up-front price support until 2015 in Euro

	2011	2012	2013	2014	2015
up-front price support	10'000	8'000	5'500	3'000	0

In a second scenario, we have analyzed the level of a CO_2 tax for the transportation sector in order to promote EV. A CO_2-tax is generally considered to be an effective policy instrument from an environmental point of view, because it contributes to lowering CO_2 emissions. Furthermore, it is a cost-effective policy instrument as it generates revenues for the government that can be used to subsidize cleaner technologies [18]. Besides reducing greenhouse gas emissions, a CO_2-tax has the capacity to reduce other external costs of ICE such as changing driving habits, reducing traffic congestions and other emissions e.g. fine dust [18].

A CO_2 tax can be levied by directly taxing gasoline and diesel corresponding to the carbon content of the respective fuel. This implies that a CO_2 tax would result in an increase in the respective fuel price. The level of CO_2 price necessary to sufficiently promote EV is shown in Table 4 and Table 5 shows the resulting gasoline and diesel prices.

In our analysis, the implementation of a CO_2 tax becomes effective, if the CO_2 price is approx. 2’000 EUR/t. Currently, the CO_2 price on the EU Emission Allowances spot market trades at 15 EUR/t. Increasing the CO_2 tax to up to 2’000 EUR/t is seen as politically infeasible. Therefore, the introduction of a CO_2 tax as sole policy instrument to reduce the price differential and to achieve a certain market penetration of EV is not considered viable.

Table 4: Required levels of CO_2 tax until 2015 in EUR/t

	2011	2012	2013	2014	2015
CO_2 tax	2'500	2'300	2'250	1'000	0

Table 5: Resulting gasoline and diesel prices until 2015

	2011	2012	2013	2014	2015
Golf Rabbit Gasoline					
CO_2 emission g/km	121	121	121	121	121
Fuel consumption l/ km	0.052	0.052	0.052	0.052	0.052
CO_2 emission g/l	2'327	2'327	2'327	2'327	2'327
CO_2 tax ct/g	0.250	0.230	0.225	0.100	0.050
ct/l	581.7	535.2	523.6	232.7	116.3
Golf Rabbit Diesel					
CO_2 emission g/km	107	107	107	107	107
Fuel consumption l/ km	0.041	0.041	0.041	0.041	0.041
CO_2 emission g/l	2'610	2'610	2'610	2'610	2'610
CO_2 tax ct/g	0.250	0.230	0.225	0.100	0.050
ct/l	652.4	600.2	587.2	261.0	130.5

The necessary levels of the fuel consumption tax (NoVA) have been analyzed as third policy option. Currently the NoVA amounts to 4% of the purchase price for the cases under consideration. As shown in Table 6, the NoVA would need to be increased by up to 45% in order to sufficiently support EVs from 2011 onwards. Similarly to the CO_2-tax, an increase in the NoVA as sole policy instrument is considered to be politically infeasible and it may cause adverse effects on the total automotive market.

Table 6: Required level of NoVA in %

	2011	2012	2013	2014	2015
NoVA	45	40	35	30	0

5. Concluding Remarks

Several TCO have been calculated for EV and ICE. The BAU-scenario shows that EV shall be competitive with ICE in the year 2015 if no additional policy actions are taken. However, significant learning effects are assumed to decrease costs of electric cars. Such learning effects can be mainly triggered if policy makers sufficiently support research and development of new environmentally friendly vehicle technologies. The analysis shows that both CO2 and NoVA taxes, which increase the costs of ICE, have to be prohibitive to make electric cars competitive. Introducing such levels of taxes seems not politically feasible besides other adverse effects on the vehicle market. Therefore, up-front price support systems (e.g. direct financial support, exemption from registration tax, bonus/malus system, etc.) seem to be favorable over the taxation systems. These results are confirmed by literature. Even though cost disadvantages can be overcome by policy support instruments, technical limitations of EV such as limited range and relatively long charging times remain. In addition to closing the TCO gap between EV and ICE and to overcoming technical limitations, policy makers shall focus on providing infrastructures for a large-scale take-up of EV.

References

[1] EU Insight, Driving toward a more sustainable future, Issue No. 29, 2009.

[2] S. Schmid, P. Mock, H. Friedrich, Welche Antriebstechnologien prägen die Mobilität in 25 Jahren, Zeitschrift für Energie Markt Wettbewerb, 4, 2010, pp.6-11.

[3] C. Thiel, A. Perujo, A. Mercier, Cost and CO_2 aspects of future vehicle options in Europe under new energy policy scenarios, Energy Policy, 2010, pp. 7142-7151.

[4] J. Ogden, R. Williams, E. Larson, Societal lifecycle costs of cars with alternative fuels/engines, Energy Policy, 2004, pp. 7-27.

[5] C.E. Thomas, Fuel cell and battery electric vehicles compared, International Journal of Hydrogen Energy, 2009, pp. 6005-6020.

[6] F. Kley, M. Wietschel, D. Dallinger, Evaluation of European electric vehicle support schemes, Working Paper Sustainability and Innovation No. S 7/2010, Frauenhofer ISI, 2010.

[7] AEA Energy & Environment, Hybrid Electric and Battery Electric Vehicles: Measures to Stimulate Uptake, Version 2, 2008.

[8] AEA, Market Outlook to 2022 for Battery Electric and Plug-in Hybrid Electric Cars, Issue 1, 2009.

[9] European Automobile Manufacturers' Association (ACEA), Overview of Tax Incentives for Electric Vehicles in the EU, 2010.

[10] Joint Research Center, Well-To-Wheels analysis of future automotive fuels and powertrains in the European context, Version 3, 2008.

[11] OEAMTC, Zukünftige Elektrofahrzeuge, 2010.

[12] VW, Der Golf – Preise, Austattungen, Technische Daten, November 2010.

[13] K. Handa, H. Yoshida, Development of Next Generation Vehicle „i-MiEV", Mitsubishi Motors Technical Review, No.19, 2007.

[14] The Boston Consulting Group, The Comeback of the Electric Car? How Real, How Soon, and What Must Happen Next, 2009.

[15] PricewaterhouseCoopers, Elektromobilität in Österreich, internal paper, 2010.

[16] McKinsey, Roads toward low-carbon energy future: Reducing CO2 emissions from passanger vehicles in the global road transportation system, 2009.

[17] Element Energy, Strategies for the uptake of electric vehicles and associated infrastructure implications, 2009.

[18] H. Hammer, S. Jagers, What is a fair CO_2 tax increase? On fair emission reductions in the transport sector, Ecological Economics, 2007, pp. 377-387.

Comparative Analysis of Performance and Combustion of Koroch Seed Oil and Jatropha Methyl Ester blends in a Diesel Engine

Tapan K. Gogoi[1,*], Shovana Talukdar[1], Debendra C. Baruah[2]

[1] *Tezpur University ,Tezpur, Assam, India*
[2] *Tezpur University ,Tezpur, Assam, India*
** Corresponding author. Tel: +913672267004, Fax: + 913672267005, E-mail: tapan_g@tezu.ernet.in*

Abstract: The present study analyzes the performance and combustion characteristics of 10%, 20%, 30% and 40% blending of Koroch Seed Oil Methyl Ester (KSOME) and Jatropha Methyl Ester (JME) with diesel as fuels in a diesel engine. The brake specific fuel consumption (BSFC) was more for the methyl ester blends and particularly for the JME blends. The brake thermal efficiency (BTE) was slightly lower for the biodiesel blends and for the JME blends it was less compared to that of the KSOME blends. The indicated power was more in case of the blends; however it reduced significantly for the 40% blend of KSOME. Both the KSOME and JME blends exhibited similar combustion trend with that of diesel, however, the blends showed an earlier start of combustion with shorter ignition delay. The ignition delay was less and the combustion duration was more for the JME blends as compared to the KSOME blends. The overall observation was that the KSOME blending up to 30% showed an acceptable performance and combustion trend whereas the JME blends showed favorable combustion trend but due its comparatively higher fuel consumption characteristics, finally the engine BTE was less with the JME fuel blends.

Keywords: *Biodiesel, diesel engine, Koroch seed oil, Jatropha*

1. Introduction

Biodiesel obtained from non edible plant species such as Jatropha *curcas (Ratanjot), Pongamia pinnata (karanj)*, *Calophyllum inophyllum (Nagchampa)*, *Madhuca indica* (*Mahua*), *Hevea brasiliensis* (*Rubber seed)* are gaining importance as possible renewable alternate fuels in India. Biodiesel is non toxic, biodegradable, and environmentally friendly as it contains minimum sulfur and aromatics. However, its higher viscosity leads to poor atomization of the fuel spray and incomplete combustion, coking of the injector tips, oil ring sticking and thickening and gelling of the engine lubricant oil. Its lower calorific value and lower volatility are regarded as its disadvantages. Therefore, the 5-20% (by volume) blending with standard diesel has been considered as suitable at present for using in existing diesel engines without any modifications. Many researchers have evaluated the performance of conventional diesel engines fuelled by bio-diesel and its blends. Raheman and Ghadge [1] while evaluating the performance of a single cylinder, four stroke Ricardo E6 engine with various biodiesel blends and pure biodiesel from Mahua seed oil found higher BSFC and lower BTE in case of the blends. Ramadhas et al. [2] used Rubber seed oil and its blend in a single cylinder diesel engine and observed that the blends containing 20–40% of rubber seed oil in the blend yielded an engine performance closely matching that of diesel oil. Raheman and Phadatare [3] used karanja methyl ester and its blends in a single cylinder, four-stroke, direct injection (DI) diesel engine and observed slightly higher torque in case of 20% blending (B20) and 40% blending (B40) while lower torque was observed with 60% blending (B60) to pure biodiesel (B100) when compared to diesel. BSFC was lower for B20 and B40 and found to be higher for blends ranging from B60–B100. The BTEs were also higher for B20 and B40. Sahoo and Das [4] made a combustion analysis using neat biodiesel from Jatropha, Karanja and Polanga; and their blends (B20 and B40) at various loads. Saravana et al. [5] observed lower delay period, lower maximum rate of pressure rise and heat release with 20% blending of crude rice bran oil methyl ester (CRBME) in a stationary small duty DI diesel engine. The BSFC of CRBME blend was found to be only marginally different from

that of the diesel. Qi et al. [6] evaluated combustion and performance of a single cylinder four stroke diesel engine (rated power 11.03 kW, rated speed 2000 rpm) with biodiesel produced from crude soybean oil. However, the performance and combustion trend vary depending upon the type of biodiesel used, engine configurations, test conditions, and the method of analysis. Also, the appropriate blend that would give optimum engine performance and best combustion characteristics may vary from biodiesel feedstock to feedstock, its production processes and the type of engine in which it is used. For the present investigation, biodiesel was prepared from Koroch seed and Jatropha curcus oil using a two step acid base catalyzed trans-esterification process in a laboratory scale. The properties of the various blends prepared by mixing biodiesel in various volumetric proportions with diesel obtained from Numaligarh refinery limited (NRL) are summarized in Table 1. The properties were determined at the Quality and Control Laboratory of NRL. Koroch is a tree found in abundance in the forests of north east India and oil obtained from Koroch seed has its own unique characteristics as a potential source of biodiesel. The author of this paper has not come across any study on diesel engine performance and combustion involving KSOME and its diesel blends. Although related literatures are available for JME, still blends of JME have been chosen as fuels for a comparative analysis.

Table 1. Properties of NRL diesel and various biodiesel blends

Fuel	NRL diesel	KB10	JB10	KB20	JB20	KB30	JB30	KB40	JB40
Density at 15°C (gm/cc)	0.8460	0.8500	0.8474	0.8548	0.8512	0.8594	0.8552	0.8661	0.8574
Kinematic Viscosity at 40°C (cSt.)	2.34	2.64	2.58	2.84	2.62	3.07	2.74	3.28	2.85
HHV (kJ/kg)	45553.0	45489.9	45682.4	45418.1	45471.9	45348.9	45379.0	45247.4	45161.2
Cetane index	46.60	46.34	47.48	46.50	48.01	46.34	48.54	45.39	48.61
Flash point (°C)	46	47	47	49	52	53	54	55	53
Pour point (°C)	3	-3	3	0	-3	3	-6	6	-6
Sulpher content (ppm)	489	440	452	390	370	302	308	274	292

2. Methodology

Tests were performed in a single-cylinder; four-stroke, naturally aspirated, DI diesel engine and its specifications are given in Table 2. The test engine is provided with necessary instruments for combustion pressure, fuel pressure and crank-angle measurements. The in-cylinder and the fuel pressure are sensed by two piezo sensors. Signals from these pressure transducers are fed to a charge amplifier. A high precision CA encoder is used to give signals for top dead centre (TDC) and the CA. The signals from the charge amplifier and the CA encoder are supplied to a data acquisition system which is interfaced to a computer through engine indicator for obtaining pressure CA diagram. There are provisions in set up also for interfacing airflow, fuel flow and load measurement. The engine is coupled with an eddy current dynamometer for controlling the engine torque through computer. A Lab view based engine performance analysis software package evaluates the on line engine performance. The tests were conducted at steady state and 100% load at average engine speed of 1,535 rpm where the average engine torque was 21.85 Nm. This yielded an average brake power (BP) of 3.5 kW in each fuel test. Three test runs were performed under identical conditions to check for the repeatability of all the results. The repeatability of the results was found to be within an acceptable limit. The test results were then averaged and the average test results have been reported.

Table 2. Engine Specifications

Make and Model	Kirloskar –TV1
Rated power and speed	3.5 kW and 1500 rpm
Type of Engine	1 cylinder, DI type, 4Stroke
Compression ratio (CR)	12-18:1
IV Opening	4.5° before TDC
IV Closing	35.5° after BDC
EV Opening	35.5° before BDC
EV Closing	4.5° after TDC
Bore & Stroke	87.5mm and 110mm
Nozzle opening pressure	220 bar
Cooling Medium	Water cooled

3. Results and Discussion

3.1. Performance Characteristics

3.1.1. Brake thermal efficiency

Fig. 1 shows the BTE of the test engine for the tested fuels. It was observed that the BTE with the methyl ester fuel blends were comparatively less. The BTE decreased with increasing proportion of methyl ester in the blends. Further, the BTE for the JME blends were less compared to that for the KSOME blends. The BTE values with NRL diesel, KB10, JB10, KB20, JB20, KB30, JB30, KB40 and JB40 are 25.63%, 24.86%, 23.89%, 24.34%, 23.24%, 24.13%, 22.41%, 22.35% and 22.18% respectively. K and J here refer to KSOME and JME respectively. Compared to KSOME blends, slightly lower BTEs for the JME blends was mainly due to their increased fuel consumption rates for maintaining a constant BP output. Since the density and viscosity values of the JME blends were lower and the HHVs were higher compared to their corresponding KSOME blends, fuel consumption for the JME blends should have been lower than those of KSOME blends. Similarly the BTEs of the JME blends should also be more due to better combustion resulting from lower viscosities of JME blends compared to their KSOME counterparts. But the opposite trend in fuel consumption and BTE could not be understood. An energy balance study determining the various energy losses could be an appropriate future work for confirming this opposing trend.

3.1.2. Brake specific fuel consumption

The BSFC for the blends of JME and KSOME are compared with NRL diesel and is shown in Fig. 2. It was seen that the BSFC for the biodiesel blends was more. BSFC was marginally higher in case of the JME blends. This is due to higher fuel consumption rate in case of the JME blends. The fuel consumption rate for NRL diesel, KB10, JB10, KB20, JB20, KB30, JB30, KB40 and JB40 are 1.15 kg/h, 1.187 kg/h, 1.23 kg/h, 1.214 kg/h, 1.27 kg/h, 1.228 kg/h, 1.32 kg/h, 1.328 kg/h and 1.34 kg/h respectively.

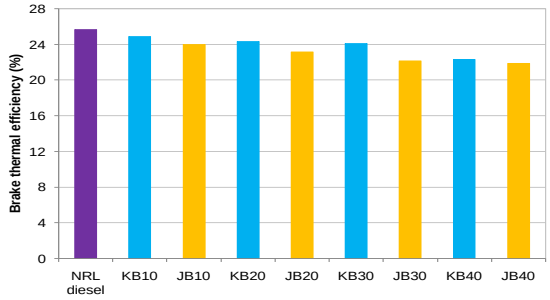

Fig. 1. BTE for the tested fuels

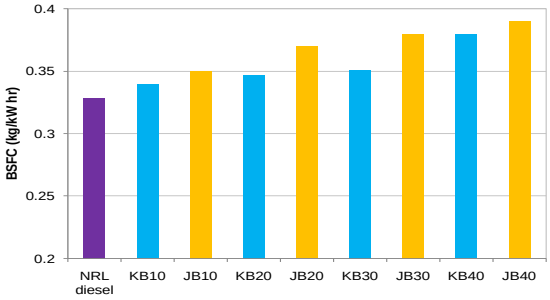

Fig. 2: BSFC for the tested fuels

3.1.3. Indicated power

From Fig. 3 it is observed that the engine IP operated with the blends is slightly more except for the blend KB40. The engine IP produced with NRL diesel, KB10, JB10, KB20, JB20, KB30, JB30, KB40 and JB40 are 5.6 kW, 5.76 kW, 5.7kW, 5.80 kW, 5.83kW, 5.92 kW, 6.02kW, 5.42 kW and 6.09kW respectively. It was observed that the loop work i.e. the work done during the gas exchange process and the compression work were less while the combustion and expansion work were more in case of the blends. Hence the net work done during the cycle was more and this resulted in higher IP. Slightly higher IP with the methyl ester blends may also be due to combustion of relatively more amount of fuel in case of the blends. Although the calorific values of blended fuels were lower than that of NRL diesel, the fuel energy was more for the blends and particularly for the JME blends due to relatively higher fuel consumption rate. Lower IP with KB40 was due to increase in the compression and loop works and decrease in the expansion work. The viscosity of KB40 was higher and may be due to poor combustion of this fuel blend it resulted in cylinder pressure variation leading to lower IP. Again, the IP with the JME blends was comparatively more than that with the KSOME fuel blends. It was due to higher energy input in respect of these blends and also due to higher net works done during the cycle as can be seen from the Table 3 shown below.

Table 3. Various works done during the cycle

Fuel	NRL diesel	KB10	JB10	KB20	JB20	KB30	JB30	KB40	JB40
Combustion and Expansion work (kJ)	724.13	728.18	721.84	719.64	734.99	743.05	748.1	692.86	749.90
Comprssion work (kJ)	309.80	300.51	285.98	286.15	288.43	294.92	288.63	311.35	280.55
Loop work (kJ)	24.16	20.12	10.42	18.32	8.48	14.64	13.84	42.97	8.55
Net work (kJ)	390.17	407.55	425.44	415.17	438.08	433.49	445.63	338.54	460.80

4. Combustion characteristics

4.1. Pressure crank angle diagram, peak pressure and rate of pressure rise

The pressure CA variation at full load is shown in Fig. 4 for the tested fuels. It was observed that pressure rise takes place early in case of the biodiesel blends. As compared to the KSOME blends, the pressure rise was earlier in case of the JME blends. Early pressure rise for the JME and KSOME blends may be due to their lower ignition delay which can be found out and will be discussed separately in section 3.2.4. Early pressure rise with JME blends in comparison to that with the KSOME blends implies relatively lesser ignition delay for the JME blends. It was also seen that more the amount of biodiesel in the blend, early is the pressure rise that occurs. Fig. 5 shows the peak cylinder pressure for the tested fuels. The peak pressure depends on the amount of fuel taking part during premixed combustion which in turn depends upon the delay period and the spray envelope of the injected fuel. Larger the ignition delay more will be the fuel accumulation, which finally results in a higher peak pressure. It was seen that the peak pressure for NRL diesel as well as the KSOME blends was almost the same at full load, the peak pressure values for KB10, KB20, KB30 and KB40 being 57.35, 57.62, 57.31 and 57.16 bar respectively, as against a peak pressure value of 57.43 bar for NRL diesel. However, the peak pressure for the JME blends were slightly less and these being 57.02, 56.98, 56.04 and 55.93 bar for JB10, JB20, JB30 and JB40 respectively. This is again due to combustion of relatively less amount of fuel during premixed phase of combustion as a result of lesser ignition delay period associated with the JME blends. The CAs at which these peak pressures occurred were 370, 370, 370, 370, 370, 369, 370, 369 and 369 degree CA for NRL diesel, KB10, JB10, KB20, JB20, KB30, JB30,

KB40 and JB40 respectively. Even though the pressure rise was occurring earlier in case of the JME and KSOME blends, but the peak values occurred almost at the same CA for these blends at full load. This may be due to lower rate of pressure rise in case of the biodiesel blends which is shown in Fig. 6. Rate of pressure rise was slightly more in case of the biodiesel blends towards the end of compression and it was more in case of the JME blends as compared to the KSOME blends. The pressure rise rate first decreased during the delay period for all the fuels and then it increased before the start of combustion (SOC) with a sharp rate of rise after SOC. However the peak of the rate of pressure rise was less and it also advanced in case of the biodiesel blends. Compared to the KSOME blends, the peak of the rate of pressure rise was less in case of the JME blends with early occurrence of the same.

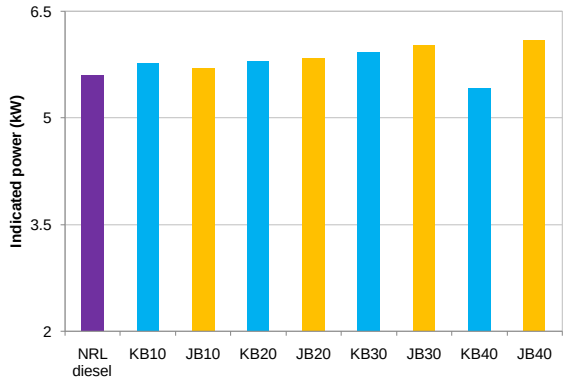

Fig. 3. Indicated power for the tested fuels

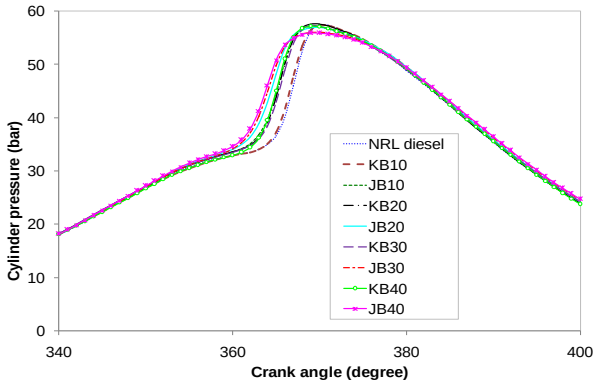

Fig. 4. Pressure crank angle variation for the fuels

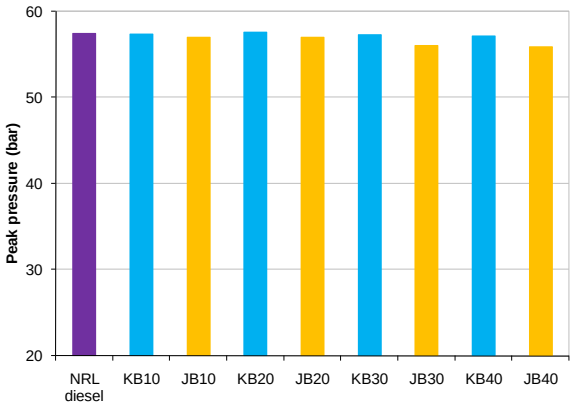

Fig. 5. Peak pressure for the tested fuels

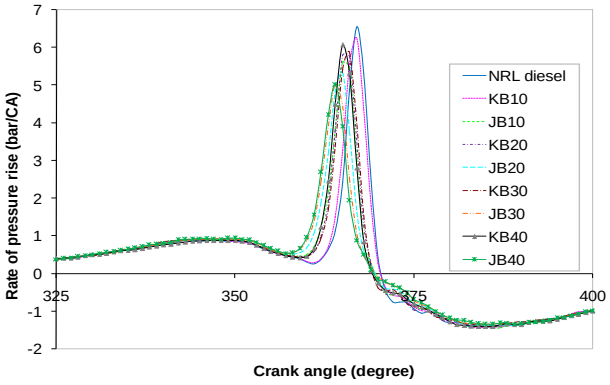

Fig. 6. Rate of pressure rise for the tested fuels

4.2. Net heat release rate

The heat release rate was calculated by first law analysis of the pressure CA data. The apparent net heat release rate which is the difference between the apparent gross heat release rate and the heat transfer rate to the walls is given by Equation (1) as given below.

$$\frac{dQ_n}{d\theta} = \frac{\gamma}{\gamma - 1} p \frac{dV}{d\theta} + \frac{1}{\gamma - 1} V \frac{dp}{d\theta} \qquad (1)$$

An approximate range for γ (specific heat ratio) for diesel engine heat release analysis is 1.3 to 1.35. However the values of γ which will give more accurate heat release information are not well defined [7]. In the present analysis value of γ for all the fuels were taken as 1.35. Lower heat release rate was observed in case of methyl ester blends at full load as can be seen from Fig. 7. In the equation (1), it is the second term in the right hand side which mainly influences it over a w ide range of TDC and therefore the rate of heat release is directly

proportional to the rate of pressure rise. Since the pressure rise was earlier in case of the biodiesel blends and also due to the early occurrence of the peak of the rate of pressure rise which was also lower for the blends it is seen in Fig. 7 that the net heat release rate also followed the same trend. As obviously the rate of net heat release raised early in case of the JME blends as compared to that of the KSOME blends. Similarly the peak of net heat release rate was also less for the JME blends. It was also seen that the net heat release rate was higher particularly for the JME blends during the reaction controlled diffusion and late combustion phases.

4.3. Cumulative heat release

Cumulative heat release is shown in fig. 8 for the tested fuels. It was observed that cumulative heat release was more for most of the biodiesel blends towards the later part of the combustion process which means that greater amount of heat was released in case of the blends for producing a given output. This was due to greater heat release as a result of diffusion combustion in case of the blends. As the amount of fuel taking part in combustion was more in the case of the KSOME and JME blends therefore it resulted in higher amount of heat release with the biodiesel blends. This is also the reason of higher IP associated with these blends. Although the calorific value of the KSOME and JME blends was less compared to that of NRL diesel but the lower calorific value of these fuel blends were compensated by their higher fuel flow rate and hence cumulative heat release increased in case of the blends. In case of the JME blends both the fuel consumption rates and the calorific values were more compared to their KSOME counterpart. Therefore the cumulative heat release was also more for the JME blends. Slightly lower cumulative heat release in case of JB10 was due to lower heat release during later part of its diffusion combustion. Exceptionally the cumulative heat release for the blend KB40 was significantly lower towards the later part of combustion. Although the fuel consumption rate was higher but may be due to incomplete burning of this particular fuel blend together with its lower calorific value it resulted in low cylinder pressure and low rate of pressure rise during the later part of combustion. This ultimately affected the cumulative heat release. The reason for incomplete burning can be its higher viscosity due to which it led to poor atomization and ultimately resulted in lower heat release. The same can also be the reason of lower engine IP produced with this particular fuel blend.

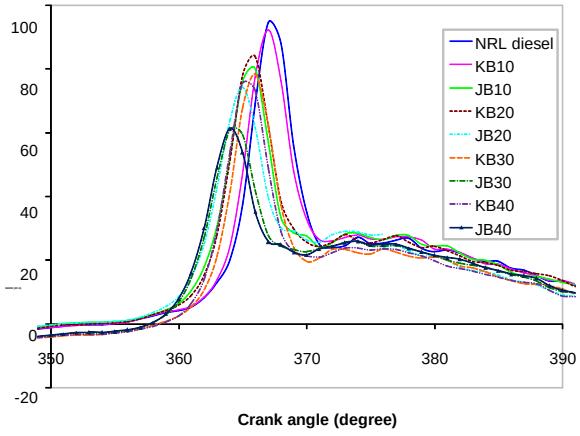

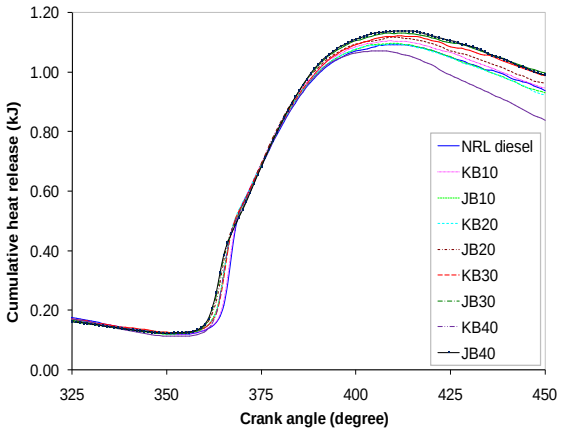

Fig.7. Net heat release rate for the tested fuels *Fig.8. Cumulative heat release for the tested fuels*

4.4. Igniton delay

Ignition delay is the time period between start of injection (SOI) and SOC. The point of SOI was determined from measurement of the fuel injection pressure profile. SOI is usually taken

as the time when the injector needle lifts off its seat. As no needle lift sensor was fitted to the injector, therefore the CA at which the fuel pressure in the fuel line reached its maximum value followed by a sudden drop in pressure, was considered as the SOI. Criterion based on $\max\left(d^2p/d\theta^2\right)$ is widely used to predict SOC [7] and was also used in the present study to determine SOC. Fig. 9 shows the ignition delay for NRL diesel and various biodiesel blends at full load. It was found that the ignition delay period for the KSOME and JME blends was less. Further, the delay period was found to be less for the JME blends compared to the KSOME blends and the prediction made in pressure CA and heat release analyses was found to be correct. Cetane index of the KSOME and JME blends were higher and therefore the ignition delays were less for the biodiesel blends. Cetane index of the JME blends were comparatively higher and hence delay periods were lower for the JME blends compared to KSOME blends. Moreover, biodiesel typically contains unsaturated fatty acids and these get oxidized when exposed to oxygen environment. May be due to presence of higher oxygen content, biodiesel blends get ignited earlier than that of diesel. Another reason could be the rapid preflame chemical reaction of the biodiesel mixed fuel with high temperature air during injection and also the thermal cracking due to which the high molecular weight ester (biodiesel) breaks down to lighter compounds and ignites earlier resulting in shorter ignition delay.

4.5. Combustion duration

Determination of combustion duration of a diesel engine is a difficult task because the total combustion process consists of phases such as rapid premixed combustion, mixing controlled combustion and the late combustion of fuel present in the fuel rich combustion products. It can be defined as the time interval from the start of heat release to the end of heat release [4]. Banapurmath et al. [8] evaluated the combustion duration considering the CA interval between the SOC and 90% cumulative heat release. They observed higher combustion duration with Honge, Jatropha and Sesame oil methyl esters which they attributed to the longer diffusion combustion phase of the esters. Rao et al. [9] however observed lower combustion duration with JME blends and it was stated to be due to early start and faster rate of combustion. In the present study the CA at which the cumulative heat release is the maximum has been considered as the end of combustion. Fig. 10 shows the combustion duration for NRL diesel and the various methyl ester blends at full engine load. It was seen that, the combustion durations of KB30 and NRL diesel were the same (47° CA duration) and it was slightly less for the other KSOME blends. Even though the amount of injected fuel was more for the KSOME blends but slightly lesser combustion duration may be due to fact that biodiesel is oxygenated in nature which helps in early completion of combustion of the blends as it was the case for KB10. But with the increase in the amount of biodiesel in the blend, combustion duration increased for KB20 and KB30 which may be due to increase in the amount of fuel injected. But again the combustion duration decreased in case of KB40, which may be due to higher viscosity of this particular blend. However for the JME blends, the combustion durations were slightly more compared to the KSOME blends and these were 46, 47, 50 and 50° CA for JB10, JB20, JB30 and JB40 respectively. Slightly higher duration of combustion particularly with respect to JB30 and JB40 could be due to earlier start of combustion and relatively longer diffusion combustion for these blends.

5. Summary and Conclusion

Compared to NRL diesel operation, the KSOME and JME blends resulted in slightly poor performance in terms of BTE and BSFC. However the IP produced with the methyl ester

blends was more except for the blend KB40. Although the fuel consumption with KB40 was higher, but may be due to higher viscosity it resulted in poor fuel atomization leading to incomplete combustion, lower heat release and hence lower IP. All the blends revealed almost similar pressure CA characteristics, however early pressure rise and lower ignition delay was observed in case of the blends. Compared to the KSOME blends, the ignition delay period and the pressure rise were early in case of the JME blends. The JME blends also showed better combustion trend with improved rate of pressure rise and heat release due its lower viscosity, increased fuel consumption and slightly higher calorific value. However, BTE values were slightly lower for the JME blends.

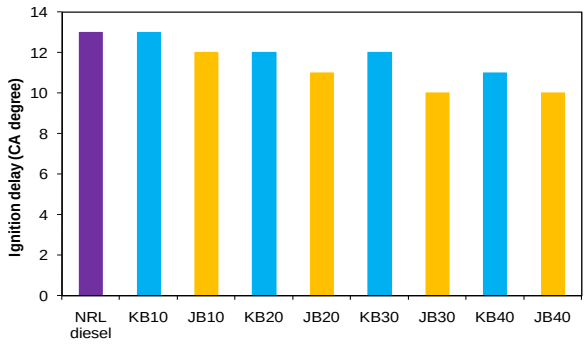

Fig.9. Ignition delay of the various fuels

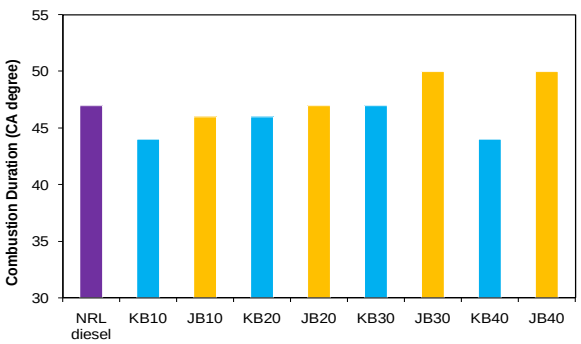

Fig. 10. Combustion duration of the fuels

References

[1] H. Raheman, S.V. Ghadge, Performance of compression ignition engine with mahua (Madhuca indica) biodiesel. Fuel 86 (2007) pp. 2568–2573

[2] A.S. Ramadhas, C. Muraleedharan, S. Jayaraj, Characterization and effect of using rubber seed oil as fuel in the compression ignition engines, Renewable Energy 30 (2005) pp. 795–803

[3] H. Raheman, A.G. Phadatare, Diesel engine emissions and performance from blends of karanja methyl ester and diesel, Biomass and Bioenergy 27 (2004) pp. 393 – 397

[4] P.K. Sahoo, L.M. Das, Combustion analysis of Jatropha, Karanja and Polanga based biodiesel as fuel in a diesel engine, Fuel 88 (2009) pp. 994–999

[5] S. Saravanan, G. Nagarajan, G. L. N. Rao, S. Sampath, Combustion characteristics of a stationary diesel engine fuelled with a blend of crude rice bran oil methyl ester and diesel, Energy 35 (2010) pp. 94–100

[6] D.H. Qi, L.M. Geng, H. Chen, Y.ZH. Bian, J. Liu, X.CH. Ren, Combustion and performance evaluation of a diesel engine fueled with biodiesel produced from soybean crude oil

[7] J.B. Heywood, Internal combustion engine fundamentals. New York: McGraw-Hill;1988.

[8] N.R. Banapurmath, P.G. Tewari, R.S. Hosmath, Performance and emission characteristics of a DI compression ignition engine operated on H onge, Jatropha and Sesame oil methyl esters. Renewable Energy 2008; 33:1982-8

[9] G.L.N. Rao, B.D. Prasad, S. Sampath, K. Rajagopal, Combustion Analysis of Diesel Engine Fueled with Jatropha Oil Methyl Ester - Diesel Blends. Int J of Green energy 2007; 4:645–58

Performance Study of a Diesel Engine by using producer gas from Selected Agricultural Residues on Dual-Fuel Mode of Diesel-cum-Producer gas

D.K.Das[1], S.P.Dash[2], M.K.Ghosal[1*]

[1] *Department of Farm Machinery and Power, College of Agricultural Engineering and Technology, Orissa University of Agriculture and Technology, Bhubaneswar-751003, Orissa, India*
[2] *Orissa Lift Irrigation Corporation, Government of Orissa, Orissa, India.*
** Corresponding author. Tel: +91 9556271208, E-mail: mkghosal1@rediffmail.com*

Abstract: Of all the alternative sources of energy for rural areas, producer gas from biomass appears to have the greatest potential. As an agricultural country, India has large supply of biomass resources. It is estimated that about 40 to 60 percent of agricultural residues are either lost or put to inefficient use. This calls for better utilization of these resources by thermo-chemically converting into producer gas in the current context of limitedness of petroleum based fuels for use in internal combustion engines. Diesel engines are widely used in Indian agricultural farms for a variety of stationary and mobile operations. The usual approach of producer gas utilization in diesel engines consists of operating existing compression ignition engines on producer gas cum diesel dual-fuel mode. There is also a lack of information on the use of different types and conditions of biomass to generate producer gas as a supplement fuel for diesel engines. Therefore, an effort was made to develop a gas producer system utilizing the locally available biomass materials to power a diesel engine that can be used on small horse power tractors and stationary machines. Experiments were conducted to study the performance of a diesel engine (four stroke, single cylinder, 5.25 kW) with respect to its thermal efficiency, specific fuel consumption and diesel substitution by use of diesel alone and producer gas-cum-diesel (dual fuel mode) through a downdraft gasifier. Performance of the engine was studied by keeping biomass moisture contents as 8%, 12%, 16%, and 21%, engine speed as 1600 rpm and with variable engine loads. The gas producer system developed for a 5.25 kW diesel engine was found to perform satisfactorily by using three types of biomass such as wood chips, pigeon pea stalks and corn cobs. The average value of thermal efficiency on dual fuel mode was found slightly lower than that of diesel mode. The specific diesel consumption was found to be 60 to 64 % less in dual fuel mode than that in diesel mode for same amount of energy output. The average diesel substitution of 64% was observed with pigeon pea stalks followed by corn cobs (63%) and wood chips (62%). Based on the performance studied, the producer gas may be used as a substitute or as a supplementary fuel for diesel conservation, particularly for stationary engines in agricultural operations in the farm.

Keywords: *Biomass gasification, Producer gas, Downdraft gasifier, Diesel engine.*

1. Introduction

The escalating oil prices and scarcity of fuel oils coupled with exploding population have resulted in serious energy crisis. There is thus a pressing need to develop technology for utilizing the renewable energy sources that can make significant contribution to the economy and the well being of the rural people.

Of all the alternative sources of energy for rural areas, producer gas from biomass appears to have the greatest potential. As an agricultural country, India has large supply of biomass resources. It is estimated that about 40 to 60 percent of agricultural residues are either lost or put to inefficient use. This calls for better utilization of these resources by thermo-chemically converting into producer gas in the current context of limitedness of petroleum based fuels for use in internal combustion engines. Producer gas is generated from solid carbonaceous fuels such as wood, charcoal, coal, agricultural and forest residues and also animal wastes by gasification process (Hindsgaul C et.al., 2000, Dogru M. et.al., 2000, Bhattacharya S.C. et.al., 2001, G. Sridhar et.al., 2001, Das and Pandey, 1993 and Pathak and Jain, 2004). Gasification is an irreversible thermo-chemical process by which feed stock is thermally decomposed and the end products are principally in gaseous form, the main combustible components being carbon monoxide and hydrogen. The main advantages of gases as a fuel over liquid or solid

fuels are that (i) gases burns with higher efficiency than the solid or liquid fuels, (ii) they have a higher rate of heat release (iii) the rate of energy output is easily controlled and adjustable, and (iv) gaseous fuels with good energy utilization can be used for power sources. A good quality producer gas has an energy content of about 5200 kJ/Nm^3. A gas producer requires 2.5 to 3 kg of wood to generate about the same energy as 1 liter of diesel (Tiwari and Ghosal, 2007).

Diesel engines are widely used in Indian agricultural farms for a variety of stationary and mobile operations. The usual approach of producer gas utilization in diesel engines consists of operating existing compression ignition engines on producer gas cum diesel dual-fuel mode. The thermal efficiency of gasifiers in which producer gas is produced has been found to be 70-80 per cent and that of the gasifier-engine system to be 16-20 percent (Tiwari and Ghosal, 2007). The problem is more acute and serious in nature when producer gas is used to run motor vehicles particularly for agricultural operations. Past studies indicate that a very little effort has been made in this direction. There is also a lack of information on the use of different types and conditions of biomass to generate producer gas as a supplement fuel for diesel engines. Therefore an effort was made to develop a gas producer system utilizing the locally available raw materials to power a 5.25 kW (7 hp), single cylinder diesel engine that can be used on small horse power tractors, known as power tillers. The major objectives in this study were as follows:

(i) To fabricate the different components of a gas producer system to operate a 5.25 kW (7 hp) diesel engine.
(ii) To evaluate the performance of the above engine with respect to thermal efficiency, specific diesel consumption and diesel substitution by using different types of biomass.

2. Fabrication of gas producer system

A gas producer system consisting of a gasifier, a cooler cum cleaner unit, a filtration unit and a mixing device was designed and fabricated to operate a 5.25 kW diesel engine on dual fuel mode (Fig.1). A downdraft type gasifier operating under suction induced flow was designed for a maximum engine gas requirement of 10.70 Nm^3/h taking a maximum hearth load of 0.9 Nm^3/cm^2-h. The upper part of the gasifier was the fuel container and the lower part was the hearth with ash pit. The hearth section of the gasifier was V-shaped.

The primary air intake was through a pipe extended from top to the hearth with a provision to adjust the air inlet height. The ignition tube was passed through the hearth which was closed during gasification and opened only while starting to introduce fire. Ash pit was covered with a metal filter known as grate through which ash and soot particles were collected. A hand blower was attached to the gasifier for initial charging. The cooler-cum-cleaner unit consisted of a radiator to radiate heat from hot water, a venturi to provide sufficient space for cooling the gas and a water tank. The other attachments to the cooling system were a fan driven by a 0.375 kW motor to lift water from the tank to the radiator. A two stage filtering unit was developed to filter the dust and soot particles. The first stage consisted of gravel, charcoal, coconut coir and cotton layers each of 15 cm thickness where as the second stage consisted of only two layers of cotton each of 15 cm thickness. Both the filtering units were packed in different boxes.

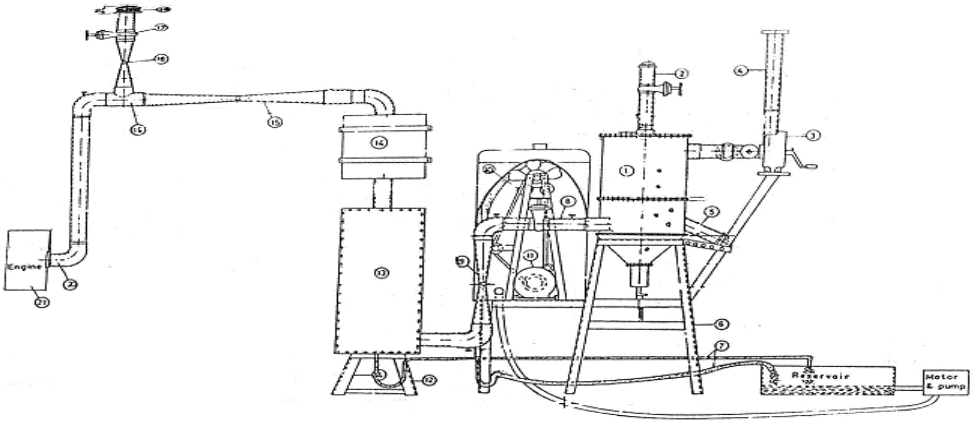

1. Gasifier
2. Air inlet pipe
3. Blower
4. Blower outlet
5. Ignition pipe
6. Gasifier stand
7. water pipe with U bends
8. Gas outlet
9. Gas cooling venturi
10. Radiator and fan
11. Fan motor
12. Filter stand
13. Primary filter
14. Secondary filter
15. Gas flow venturi
16. Air flow venturi
17. Air control gate valve
18. Air filter
19. Air gas mixing device
20. Intake manifold
21. Diesel engine

Fig. 1 A gas producer system.

3. Methodology

A single-cylinder 4-stroke 5.25 kW diesel engine of a commercial power tiller was used for the experiment. The intake manifold of the engine was modified using a T-section to introduce the mixture of air and gas into the engine during suction stroke. The quantities of gas and air flowing to the engine were measured separately with the help of two venturi sections provided in the T-section. The U-tube manometers were connected to the venturi section with polythene tube to measure the pressure drop across them. The original fuel supply of the engine from its fuel tank was cut-off for the operation on dual fuel mode and the diesel fuel was supplied from an auxiliary tank provided with a fuel measuring set-up. In order to measure the load applied to the engine, a prony brake dynamometer was used. A strain gauge transducer was used to measure the temperatures of oxidation and reduction zones in the gasifier and the exit gas from the gasifier and the filtration unit.

3.1. Performance evaluation of engine

The diesel engine (specifications given in Table-1) was tested on diesel as well as on dual fuel mode at the engine speed 1600 r/min and six loads (7.5N, 12.5N, 20N, 30N, 40N and 50N). The composition of the gas was also studied (CO=22.8%; CO_2= 7.2%; O_2=0.5% and other gases= 69.50%). For dual fuel operation, the types of biomass used were wood chips, pigeon pea stalks and corn cobs. Three materials were used at four different moisture contents (8, 12, 16 and 21 percent on wet basis). Each test was conducted for a period of 5 minutes with two replications. During each test on diesel, the engine load, engine speed and fuel consumption were measured. The observed data were utilized to calculate the engine thermal efficiency, specific diesel consumption and percent diesel substitution. The performance of a diesel engine operated on dual-fuel mode was generally evaluated in terms of specific diesel consumption, engine thermal efficiency and per cent diesel substitution. These parameters were determined as follows,

a) Specific diesel consumption (SCD) : SDC is given by

$$\text{SDC} = \frac{3600 v_d \rho_d}{1000 t\ p} = 3.6 \frac{v_d \rho_d}{t\ p} \quad (1)$$

where SDC = specific diesel consumption, g $kW^{-1}h^{-1}$; v_d = volume of diesel consumed, cm^3, ρ_d = specific weight of diesel, kg/l; t = time required to consume v_d in second; and p = engine power, kw.

b) Thermal efficiency: The thermal efficiency is expressed as the ratio of output power to the power supplied by the fuel.

i) Thermal efficiency of engine on diesel alone: Thermal efficiency of engine on diesel alone is given by

$$\eta_t = \frac{\text{Brake power}}{\text{Power input from fuel}} \quad (2)$$

The power input from fuel in eqn. (2) is given by

$$p_f = \frac{cv_d \times \rho_d \times f_c}{3600} \quad (3)$$

Where p_f = Power input from fuel, kW; cv_d = calorific value of diesel = 39 MJ/kg ρ_d = densityof diesel = 640 kg/m^3; and f_c = fuel consumed, cm^3/h. Substituting the values of cv_d and ρ_d, the eqn (3) yields

$$\text{P}_\text{f} = \frac{39 \times 840 \times \text{f}_\text{c}}{3600} = 9.1\ f_c \quad (4)$$

Using eqn (4.), eqn (2) gives

$$\eta_t = \frac{\textit{Brake}\ \text{power}}{9.1 f_c} \quad (5)$$

ii)Thermal efficiency of engine on dual fuel mode

The formula used for calculating the thermal efficiency of engine on dual fuel mode is given by

$$\eta_t = \frac{\text{Brake power}}{\text{Power input from pilot diesel} + \text{power input from gas}} \quad (6)$$

Power input from producer gas is given by

$$p_g = \frac{CV_g \times g_c}{3.6} \quad (7)$$

where p_g = power from producer gas, kW; cv_g = calorific value of producer gas, KJ/Nm^3; and g_c = gas consumption, Nm^3/h. Substituting eqns. (5) and (7) in eqn. (6),

$$\eta_t = \frac{\textit{Brake}\ \text{power}}{9.1 f_c + \frac{CV_g \times g_c}{3.6}} \quad (8)$$

iii) Diesel substitution: The per cent diesel substitution is given by

$$ds = \frac{D_d - D_{dg}}{D_d} \times 100 \qquad (9)$$

Where ds = diesel substitution, per cent; D_d = diesel consumption by the engine on diesel alone, cm^3/h; and D_{dg} = diesel consumption by the engine on dual fuel mode, cm^3/h.

Table-1 Specifications of gas producer engine system under test

I. Engine		
(a)	Type	4-stroke cycle diesel engine
(b)	Number of cylinder	1
(c)	Cylinder capacity (cc)	450
(d)	Bore (mm)	80
(e)	Stroke (mm)	90
(f)	Crank shaft speed (rated), r/min	2200
(g)	Rated capacity (kW)	5.25
(h)	Grade of oil	SAE 30
(i)	Fuel	High speed diesel
(j)	Cooling system	Water-cooled
II. Gasifier		
(a)	Type	Moving bed, co-current Down draft
(b)	Material of construction	Mild steel
(c)	Hearth opening (mm)	60
(d)	Grate mesh size (mm)	10
(e)	Total weight (kg)	37

4. Results and discussion

The relationship between engine load and thermal efficiency at the four levels of moisture content (8%, 12%, 16% and 21%) for the different types of biomass (wood chips, pigeon pea stalks, corn cobs) is shown in Figs. 2 , 3 and 4 at engine speed of 1600 r/min. The trend shows that the thermal efficiency increased with a decreasing rate with increase in engine load for all the biomass fuels at all the biomass moisture levels tested. This may be due to better combustion of relatively rich gas-air mixture at higher loads. It is also observed that with increase in biomass moisture from 8 to 21 per cent, the thermal efficiency also increased marginally from 28 to 31 per cent with wood chips, 30 to 32 per cent with pigeon pea stalks and 29 to 32 per cent with corn cobs. The slight increase in thermal efficiency from 8 to 21 per cent moisture range might have been caused due to better combustion of premixed mixture of gas and air on dual-fuel mode resulting in reduced requirement of total energy input at different loads.

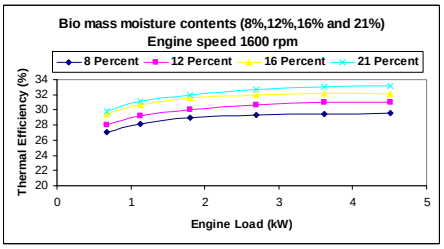

Fig. 2 Variation of thermal efficiency with engine load on dual fuel mode at different moisture contents of wood chips

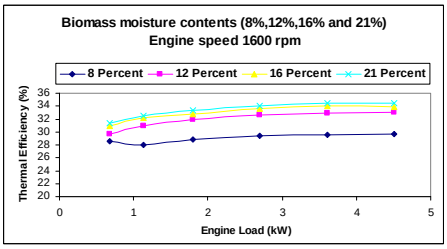

Fig. 3 Variation of thermal efficiency with engine load on dual fuel mode at different moisture contents of pigeon pea stalks

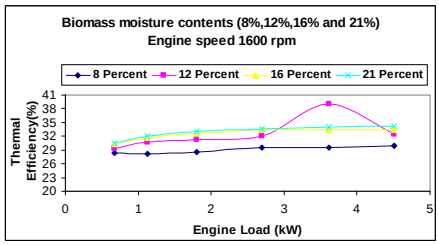

Fig. 4. Variation of thermal efficiency with engine load on dual fuel mode at different moisture contents of corn cobs

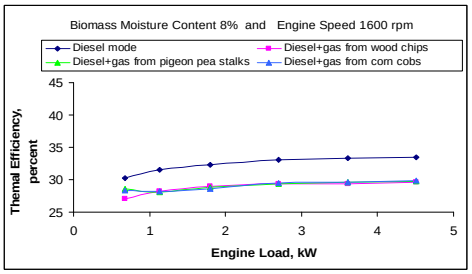

Fig. 5 Effect of engine load on thermal efficiency with different types of fuel

The effect of different types of fuel on engine thermal efficiency at 1600 r/min is shown in Fig. 5. The trend showed that there was a slight drop in thermal efficiency of engine on dual-fuel mode, compared to that on diesel alone. Based on mean values, it may be reported that the thermal efficiency of diesel engine when tested, dropped from 32.3 per cent on diesel fuel mode to 30.5 per cent on dual-fuel mode using wood chips. However, the efficiency of engine on dual-fuel mode using pigeon pea stalks and corn cobs was found almost at par with that on diesel mode. This showed that the combustion of air-gas mixture while using pigeon pea stalks and corn cobs was better compared to wood chips, even though the energy content of wood chips was relatively high. The variation of specific diesel consumption and diesel substitution with engine load on dual-fuel mode of a diesel engine at different biomass moisture levels has been shown in Figs. 6 through 11. The trend of the curves showed that the specific diesel consumption, in general, decreased with increase in engine load at different moisture levels for all the three types of biomass used. However, a definite trend of variation of diesel substitution with engine load has not been established. It has shown increasing trend with load in most of the cases, whereas in a few cases a decreasing pattern has also been observed. This kind of trend is not uncommon in the existing literatures. It is usually reported that if the energy content of the gas remains relatively stable, a higher load means a higher consumption of diesel fuel and thus a lower percentage of diesel fuel displacement. But if the quality of the gas in terms of its energy content is not stable, an increase in load can also increase the percentage of diesel fuel substitution. The decrease in specific diesel consumption with load is primarily due to increase in diesel fuel consumption at a decreasing rate. From the mean values of specific diesel consumption and diesel substitution in the test engine at different operational parameters (taking all loads into consideration), it was observed that the specific diesel consumption of engine on dual-fuel mode using wood chips decreased from 87.9 g/kWh at 8 per cent moisture level to 75.9 g/kWh at 12 per cent moisture level beyond which it again increased and rose to 161.8 g/kWh at a biomass moisture level of 21 per cent. The diesel substitution on the other hand, varied from 50.5 to 68.8 per cent in the same moisture range showing maximum value of 72.3 per cent at a moisture level of 12 per cent. Similar trends of variation of specific diesel consumption and diesel substitution were also noticed in case of the other two biomass fuels. For the sake of comparison, the minimum values of specific diesel consumption using pigeon pea stalks and corn cobs were observed to be 82 and 87 g/kWh respectively, whereas the maximum values of diesel substitution for these fuels was found to be about 71.3 per cent at a moisture level of 12 per cent. This showed that the minimum values of specific diesel consumption were derived at a particular biomass moisture level (12 per cent) where diesel substitution was maximum. This was perhaps due to better quality of gas obtained at this moisture level as reflected by its higher CO content resulting in better combustion of air gas mixture. The variation of specific diesel consumption with engine load for the test engine on diesel mode as well as on dual-fuel mode using different types of biomass is shown in Fig. 12 for a particular set of operating

parameters. The data indicated a slight decrease in specific diesel consumption with engine load both on diesel as well as on dual fuel operations. As expected, the specific diesel consumption on diesel mode is much higher than that on dual-fuel mode for all the engine loads tested. Comparing the performance of engine on the basis of the mean values of specific diesel consumption, it was observed that the engine consumed 60 to 64 per cent less diesel on dual-fuel mode than that on diesel mode for the same amount of energy output. The effect of engine load on per cent diesel substitution for different types of biomass is shown in Fig. 13. The trend showed increasing pattern of diesel substitution with engine load as explained earlier. Based on the mean values of diesel substitution, it can be pointed out that the average diesel substitution of 64 per cent was found with pigeon pea stalks followed by corn cobs (63 per cent) and wood chips (62 per cent) throughout the range of biomass moisture. From the results discussed above, it can be stated that the gasifier system developed for 5.25 kW diesel engine has indicated satisfactory performance by showing, on an average 60 to 65 percent saving in diesel consumption while utilizing three types of locally available biomass fuels.

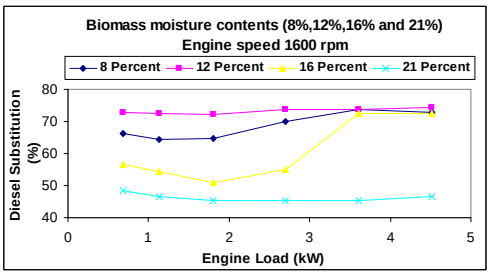

Fig. 6. Variation of specific diesel consumption with engine load on dual fuel mode at different moisture contents of wood chips

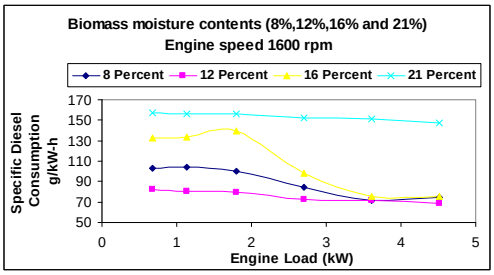

Fig. 7. Variation of diesel substitution with engine load on dual fuel mode at different moisture contents of wood chips

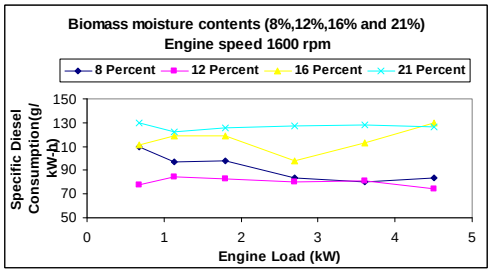

Fig. 8. Variation of specific diesel consumption with engine load on dual fuel mode at different moisture contents of pigeon pea stalks

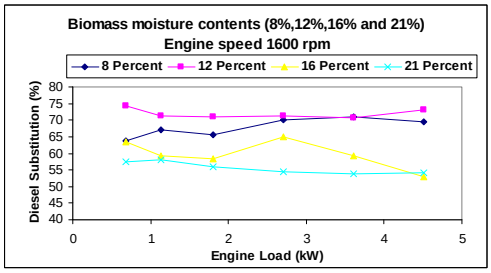

Fig. 9. Variation of diesel substitution with engine load on dual fuel mode at different moisture contents of pigeon pea stalks

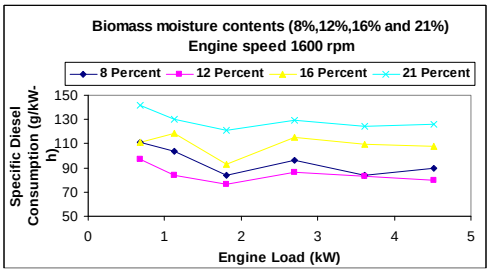

Fig. 10. Variation of specific diesel consumption with engine load on dual fuel mode at different moisture contents of corn cobs

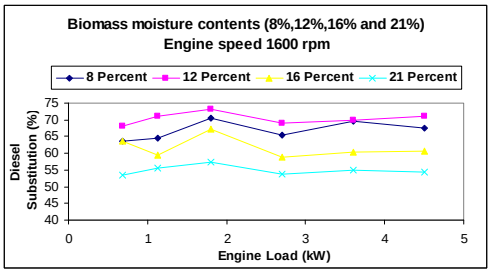

Fig. 11. Variation of diesel substitution with engine load on dual fuel mode at different moisture contents of corn cobs

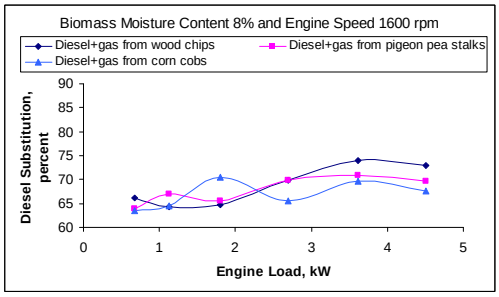

Fig. 12. Effect of engine load on specific diesel consumption with different types of fuel

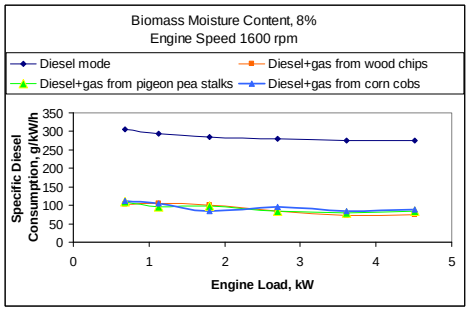

Fig. 13 Effect of engine load on diesel substitution with different types of fuel

5. Conclusions

Based on the studies conducted, the following conclusions may be drawn.

(i) The gas producer system designed and developed for a 5.25 kW diesel engine was found to perform satisfactorily by using different types of biomass such as wood chips, pigeon pea stalks and corn cobs.

(ii) The average value of thermal efficiency of engine was found to drop slightly from 32.3 percent on diesel mode to 28.7 percent on dual fuel mode using wood chips as biomass fuel. However the efficiency found on dual fuel mode with pigeon pea stalks and corn cobs was comparable to that on diesel mode.

(iii) The mean values of specific diesel consumption of engine on dual-fuel mode for all the three biomass fuels were less compared to diesel mode and their diesel substitution was more.

(iv) The average diesel substitution in a 5.25 kW diesel engine was found in the range of 62 to 64 percent using three types of biomass fuels.

The above findings presented in this paper would provide useful information to all those engaged in design, manufacture and use of gasifier system for satisfactory and mobile operation of stationary engine used in agricultural purposes.

References

[1] C. Hindsgaul, J. Schramm, L.Gratz, U. Henriksan, and J.D. Bentzen, Physical and chemical characterization of particles in producer gas from wood chips, Bio Resource Technology 73, 2000, pp. 147-155.

[2] M. Dogru, C.R. Howarth, G. Akay, B. Keskinler and A.A. Malik, Gasification of hazelnut shells in a downdraft gasifier, Energy, 27, 2000, pp. 415-427.

[3] S.C.Bhattacharya, Hla. San Shwe, and Hoang-Luang. Pham, A study on a multi-stage hybrid gasifier-engine system. Biomass and Bioenergy 21, 2001, pp. 445-460.

[4] G.Sridhar, P.J.Paul, and H.S.Mukunda, Biomass derived producer gas as a reciprocating engine fuel—an experimental analysis. Biomass and Bioenergy 21, 2001, pp. 61–72.

[5] D. K. Das, and K P. Pandey, Some studies on biomass based gas producer system for a diesel engine. Unpublished Ph.D. thesis, 1993, Agril.Engineering Department, IIT, Kharagpur.

[6] B. S.Pathak, and A. K.Jain, Engine quality producer gas from leucaena leucocephala and selected agricultural residues. J. of Agril. Engineering 21(3), 2004, pp. 43-50.

[7] G.N.Tiwari and M.K.Ghosal, Fundamentals of Renewable Energy Sources: Basic Principles and Applications. Narosa Publishing House, New Delhi, 2007.

Comparative Study on Performance of Straight Vegetable Oil and its FAME with respect to Common Diesel Fuel in Compression Ignition Engine

Soumya Sri Sabyasachi Singh[1], Dwijendra Kumar Ray[1], Sunasira Misra[2], Soumya Parida[2], Debendra Kumar Sahu[2,*]

[1]*Department of Mechanical Engineering*
[2]*Department of Chemistry, C.V. Raman College of Engineering, Bidyanagar, Mahura, Janla, Bhubaneswar-752054, India*
** Corresponding author. Tel:+91-674 2460043, 93, Fax: +91- 674 2460093, Email: drdksahu62@rediffmail.com*

Abstract: A comparative study has been carried out on the performance of compression ignition engine (CI) using common diesel fuel (CDF) blended with both refined soybean (Glycin max) and sunflower (Helianthus annus) oil as straight vegetable oil (SVO) as well as their corresponding fatty acid methyl esters (FAME) with respect to CDF. Low cost methyl esters of vegetable oil were prepared using own patented technique where ultrasonic energy has been found to be beneficial. SVOs and corresponding FAMEs were blended with CDF separately at different proportion to act as fuel for research CI engine. Both engine performance and fuel combustion characteristics were evaluated from the present study at different loads with varying compression ratios. Graphical relationships of load (kg) in engine against various engine performance parameters such as: brake thermal efficiency (%), brake specific fuel consumption ((kg/kWh), brake mean effective pressure (bar), cumulative heat release (kJ) and emission characteristics have been plotted for each set of fuels with respect to CDF. The relationship developed identifies the advantages of using blended FAME prepared with the patented processes over their corresponding SVO and CDF in the CI engine.

Keywords: *CI engine, Straight vegetable oil, FAME, Blended fuel, CDF*

1. Introduction

The Energy and Environment will determine the fate of mankind in this century. The alarming rise of energy demand in the growing civilization is mainly met by fast depleting fossil fuel. The transport sector is the highest consumer of fossil fuel as common diesel fuel (CDF) requiring more than 29 per cent of its total consumption. Due to its high sulphur, aromatics and nitrogen content the CDF is considered to be the single largest polluter of the environment. As the agro based vegetable oil is carbon neutral of renewable energy source and free of sulphur as well as aromatics, it behaves environmental friendly biofuel. However, the straight vegetable oil (SVO) fails to act as ideal fuel primarily because of its high viscosity and poor atomization in fuel spray for its low volatility. It often leads to deposit and chocking of injector, combustion chamber and valves [1]. These hurdles are reduced to minimum by subjecting the vegetable oil mainly to the process of dispersion or Transesterification. Dispersion of SVO with common diesel fuel, also called blending is to provide a simple as well as cheap fuel for the CI engine.

1.1. Transesterification of vegetable oil and animal fats

Chemically, vegetable oil and animal fat are triglycerides in which one glycerol molecule is esterified with three molecules of different long chain fatty acids [2] each with 15-20 carbon numbers raising its average molecular mass over 800amu. This reason might be responsible to inherit high kinematic viscosity and lowers vapour pressure. The process adopted to transfer one heavier ester to three lighter esters (esters of three different fatty acids with lower aliphatic alcohols) is called Transesterification reaction. Combination of these different

FAME molecules with viscosity and carbon equivalent to CDF is able to replace fossil fuel as ideal fuel for CI engine, popularly called Biodiesel [3].

1.2. Fuel for the performance of Unmodified Compression Ignition Engine:

CDF is a mixture of hydrocarbon molecules with varying carbon chain of C_6-C_{18}. The presence of smaller hydrocarbon chains with their high vapour pressure contributes to lower flash point of CDF to below 60^0C which is ideal to start ignition under common compression. While FAME of particular fatty acid (biodiesel), a compound of fixed carbon number 15-18 acquires very low volatility is contributing high flash point (>130^0C) thus fails to get atomized in unmodified CI engine for early ignition. The hurdle is minimized by blending the biodiesel with CDF. A system known as the "B" factor is generally used to state the amount of biodiesel in CDF fuel mixture such as: 100% biodiesel is referred to as B100, while 20% biodiesel when mixed with 80% CDF is labeled B20 and so on. Obviously, the higher the percentage of biodiesel, the more eco-friendly is the fuel. Blended fuel up to B20 has successfully used in unmodified engines [4-7].

The aim of the article is to evaluate the acceptability of biodiesel prepared at reduced parameters by employing ultrasonication at various steps of the composite process such as the purification of crude vegetable oil, transesterification, separation of FAME from the reaction mixture and purification of crude FAME to make ASTM standard. An unmodified CI engine setup with variable compression ratio is adopted to study the engine performance and combustion of fuel for different fuel and evaluate brake power (kW), brake thermal efficiency (%), brake specific fuel consumption (kJ/kW-hr), brake mean effective pressure (bar), of engine against various engine loads (especially lower loads). A comparative statement would be prepared for each set of four combinations of SVO-CDF, their corresponding FAME-CDF in different ration against CDF to find out the most acceptable fuel for the CI engine.

2. Methodology

2.1. Materials

Refined Soybean oil of Nature fresh (India) and refined sunflower oil of Fortune brand (India) are collected from retail outlets and analysed to evaluate the free fatty acid (FFA), phospholipids and moisture content following ASTM 6751 method. Refined varieties of soybean oil and sunflower oil were found to contain such impurities within permissible limit to prepare biodiesel. Fatty acid methyl esters (FAME) of refined soybean oil and sunflower oils were prepared following in house patented process [8]. CDF collected found to have the acceptable range of fuel specification for CI engine [9]. Low energetic (1kW) Ultrasonic Processor Sonapros PR-1000 model (M/s Oscar Pvt. Ltd., Mumbai, India) was used for transesterification at various steps of the composite process.

2.2. Preparation of fuels for the comparative studies

Four sets each of both soybean oil and sunflower oil were prepared by blending 5% and 10% of the two SVOs and their corresponding FAMEs with rest quantity of common diesel fuel (CDF). Samples of soybean and sunflower oil blends (as shown in ***Table 1***) were taken to evaluate the fuel properties in CI engine and make a comparative study with 100% CDF. Physical properties of this fuel were measured following ASTM 6751 method. Results within a range for both the fuels were reported in ***Table 2***.

Table 1. Set of fuels for the comparative study in CI engine

Vegetable oil	CDF %	Percentage of SVO in blended common diesel fuel		Percentage of FAME in blended common diesel fuel	
		05% SVO	10% SVO	05% FAME	10% FAME
Soybean oil	100	SVO SB B05	SVO SB B10	FAME SB B05	FAME SB B10
Sunflower oil	100	SVO SF B05	SVO SF B10	FAME SF B05	FAME SF B10

Table 2. Physical properties for Common Diesel Fuel (CDF), SVOs (soybean and sunflower oil) and corresponding methyl esters (Biodiesel)

Sl. No.	Properties of Fuel	CDF	Vegetable oil	Biodiesel
01	Kinematic Viscosity(cSt) at 40^0 C	2.5-5.5	35-65	5-8
02	Gross caloric value (kJ/kg)	42000	39,000-48,000	30000-39477
03	Density at 20^0 C, kg/m^3	0.835	0.825-0.894	0.865-0.877
04	Flash Point (^{0} C)	38	>200	130-175
05	Cetane Number	45	40-50	40-58

A Research engine, make Kirloskar type, 1 cylinder, 4 strokes diesel, water cooled with variable compression ratio (VCR) of M/s Apex Innovation Pvt. Ltd., Sangril, Maharashtra, India was procured to study the CI engine performance. The engine is of constant speed (1500 rpm) type having maximum load 12kg with a capacity of 661.1cm^3. The engine performance with various sets of fuels (shown in Table 1) was studied at lower loads of 2, 4, 6 and 8 kg under different compression ratios (16, 17 &18). The data acquisition system was used to create pressure-crank angle plot for both diesel and cylinder pressure. Also the pressure-volume plot was obtained to study the power generated by the engine at various compression ratios. Brake Specific Fuel Consumption and Brake Thermal Efficiency were obtained from load and fuel consumed etc. The engine Brake Power was measured by Eddy current dynamometer. Air inlet flow was measured using pressure transmitter and water flow by rotameter. Exhaust emission analysis was done with a multi gas analyser, M/s Netel (India) Ltd. under varying operating conditions.

3. Results and Discussion

3.1. Brake Specific Fuel Consumption (BSFC) of Soybean and Sunflower oil

Results on BSFC (i.e. the ratio of fuel mass flow of an engine to its output power) for all four sets of both soybean and sunflower fuel blends and CDF with engine loads of 2 to 8 kg against each compression ratio (16-18) are drawn but only CR 18 is shown in ***Fig. 1*** and ***Fig. 2*** respectively. It is observed that the BSFC(kg/kWh) is highest for B05 of both FAMEs when the engine load is only 2kg and CR 16, which further decreases linearly at higher CRs (17 and 18). BSFC for all fuels decrease uniformly when engine load increases to 8 kg because combustion improves due to increases in pressure and temperature.

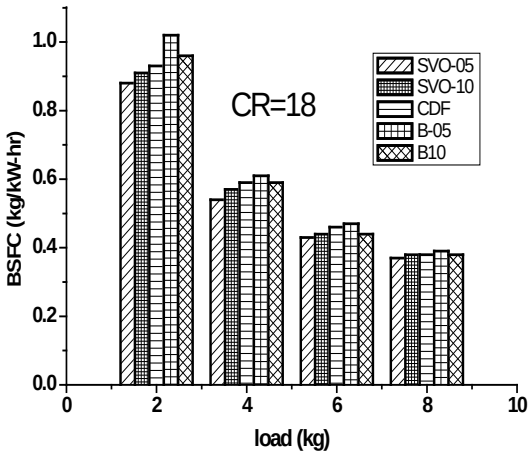

Fig.1. BSFC (kg/kWh) vs variable engine loads (kg) plot at CR-18 for four fuel blends of soybean oil and CDF

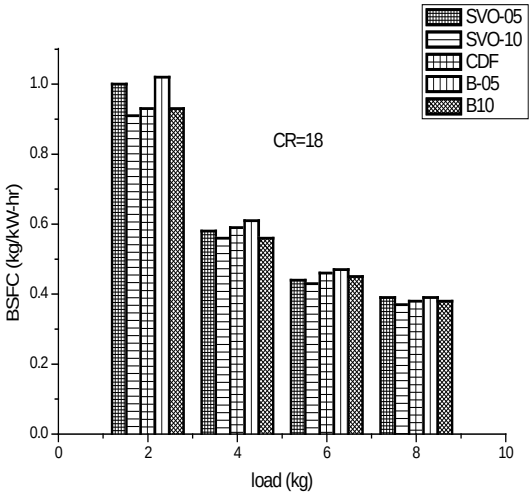

Fig. 2. BSFC (kg/kWh) vs variable engine loads (kg) plot at CR-18 for four fuel blends of sunflower oil and CDF

On comparing the results of ***Fig. 1*** (soybean oil) with ***Fig. 2*** (sunflower oil) it is observed that BSFC values for both fuel sets are almost identical at engine load 8 kg. Values for B10 of both fuel blends are less than that of B05 but almost equal to CDF. With low gross calorific values of biodiesel, it is expected to have high BSFC for the B10 blended fuel. The presence of easily combustible linoleic and oleic acids with unconjugated and unsaturated fatty acids in respective FAME probably balanced such negative effect.

3.2. Brake mean effective pressure for soybean oil and sunflower oil

Brake mean effective power (BMEP) is the measure of the useful power output of the engine and may be represented by the equation (1).

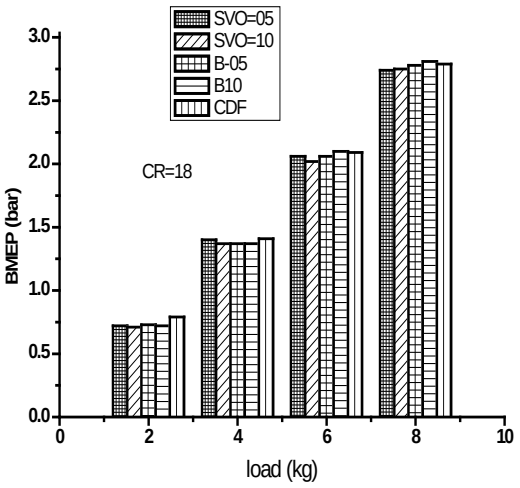

Fig. 3. BMEP (bar) vs variable engine load s(kg) plot at CR-18 for four fuel blends of soybean oil and CDF

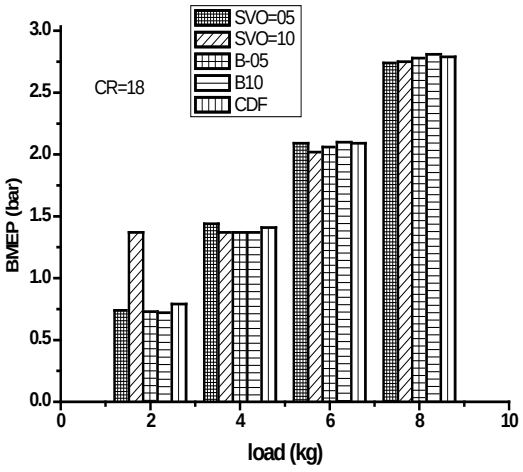

Fig. 4. BMEP (bar) vs variable engine loads (kg) at CR-18 plot at CR-18 for four fuel blends of sunflower oil and CDF

$$BMEP = 2\pi T n_C / V_d \quad (1)$$

where T = torque(Nm), n_c = number of revolution per cycle and for 4 stroke engine it is 2, and V_d = displacement in volume.

Experimental results of brake mean effective pressure for each fuel of soybean set are drawn against engine load of 2-8 kg for each CR values of 16-18. The power outputs for all fuels are increasing with rise of engine load but shows same trend for all compression ratios. The BMEP comparison plots with respect to CDF at CR 18 for soybean and sunflower fuel blends are shown in ***Fig. 3*** & ***4*** respectively. BMEP is found to be much high for B10 of both soybean-FAME and sunflower-FAME at compression ratio 18 with 8 kg engine load.

3.3. Brake thermal efficiency

The variation of brake thermal efficiency with engine load of 2-8 kg at compression ratio 18 for both soybean and sunflower fuel sets are presented in ***Fig. 5*** and ***6*** respectively. It increases with increase in load under all compression ratios for both the fuel systems along with that of CDF. This may be due to the reduction in heat loss and increase in power with increase in load. The brake thermal efficiency for B05 and B10 for both fuel systems are less than that of CDF. This lower brake thermal efficiency obtained could be attributed to lower GCV values of biofuels. Hence it may be concluded that the performance of the unmodified CI engine with biodiesel prepared [10] with less operating parameter is comparable with conventional common diesel fuel.

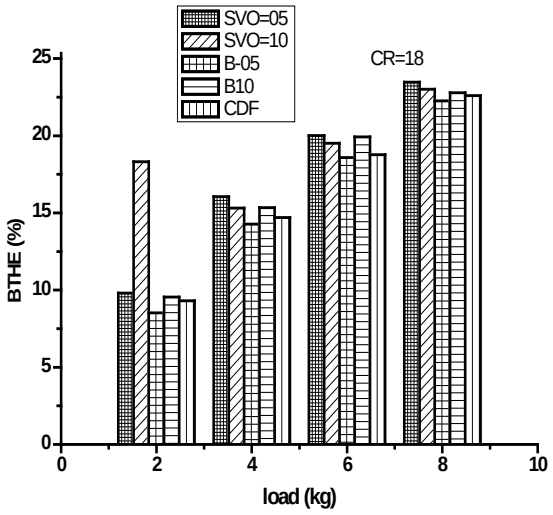

Fig. 5. BTHE (%) vs va riable engine loads (kg) plot at CR-18 for four fuel blends of soybean oil and CDF

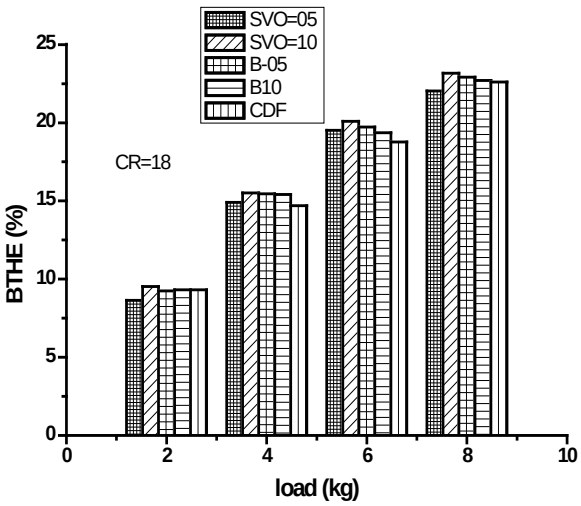

Fig. 6. BTHE (%) vs va riable engine loads (kg) plot at CR-18 for four fuel blends of sunflower oil and CDF

3.4. Brake power

The power output for all fuels increase with rise of engine load but shows same trend for all compression ratio at higher loads. ***Fig. 7*** shows FAMEs give slightly better power with respect to SVOs.

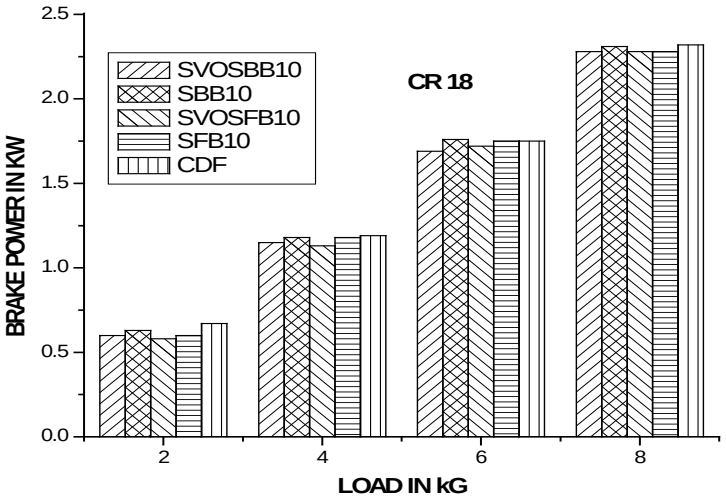

Fig.7. Brake power (kW) vs various engine loads (kg) plot at CR-18 for SVO and FAME (Biodiesel 10) fuel blends of soybean and sunflower oil with respect to CDF

3.5. Cumulative Heat Release

From ***Fig. 8*** it is clear that heat release of CDF is more than soybean SB B10 and slightly lower than sunflower SF B10 since biodiesels have less calorific value whereas out of these two biodiesels sunflower derivative is easily combustible than that of soybean.

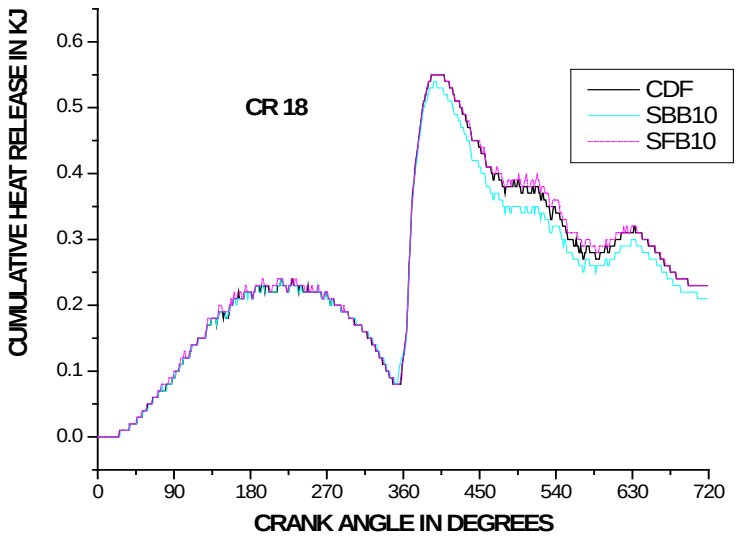

Fig.8. Cumulative heat Release (kJ) vs Crank angle (degrees) at 8kg engine load with CR-18 for CDF, soybean B10 and Sunflower B10

3.6. Exhaust emission characteristics

Exhaust emission profile for Common Diesel Fuel (CDF), and methyl esters (Biodiesel) of soybean and sunflower (B10) at CR 18 were studied and the results are given in Table 3. Combustion efficiency of these fuels under study increases with rise in engine load. It is seen that the combustion efficiency of B10 of both soybean and sunflower FAME are much better than that of CDF. SB B10 FAME is found to be more efficient fuel than SF B10. However, NO_x emission increases at higher loads due to rise in temperature in the compressor.

Table 3. Exhaust emission characteristics for Common Diesel Fuel (CDF), and methyl esters (Biodiesel) of soybean and sunflower (B10) at CR 18

Engine Load (kg)	CDF			Soybean (SB B10)			Sunflower (SF B10)		
	% CO_2	% O_2	NO_X (ppm)	% CO_2	% O_2	NO_X (ppm)	% CO_2	% O_2	NO_X (ppm)
2	1.7	18.2	72	2.9	16.1	144	2.4	17.2	106
4	2.0	17.5	116	3.5	15.6	235	2.8	16.6	162
6	2.6	16.8	161	3.9	15.0	290	3.1	16.1	226
8	2.9	16.2	208	4.6	14.0	321	3.4	15.7	269

4. Conclusion

The fatty acid methyl esters prepared from soybean and sunflower oil with own patented composite process employing ultrasonication has been successfully tested in unmodified compression ignition engine. Amongst various engine performance data evaluated, the BSFC parameters although suggest biofuel to be inefficient than CDF, however, considering the exhaust emission factor biofuel is acceptable. SVOs possess better performance, but taking the viscocity into account FAMEs look better fuel from the present study. From BMEP studies biofuels show better performance than CDF. With reference to the studies on BTHE, brake power and emission characteristics B10 soybean-FAME fuel is most acceptable fuel amongst the all studied nine fuels including CDF for the CI engine with lower load up to 8 kg at compression ratio 18. Hence it may be recommended as renewable fuel and prominent replacement for CDF in unmodified compression ignition engine.

References

[1] Meher L.C.,Vidyasagar D, Naik S.N., Technical aspects of biodiesel production by transesterification-a review. Renewable and Sustainable Energy Reviews10 2006, pp. 248-268

[2] Dmytryshyn S.L., Dalai A.K., Chaudhuri S.T., Mishra H.K, Reansey M., Synthesis and characterization of vegetable oil derived esters: evaluation for their diesel additive properties, Bioresource Technology 92, 2004, pp.55-6

[3] Ma F., Hanna M.A., Biodiesel production: A review, Bioresource Technol 70, 1999, pp.1-15

[4] Celikte, I., Koca, A., Arslan, M.A., Comparison of performance and emission of diesel fuel, rapeseed and soybean oil methyl esters injected at different pressure, Renewable Energy 35, 2010, pp. 814-820

[5] Sahoo, P.K., Das, L.M., Babu, M.K.G., Naik, S.N., Biodiesel development from high acid value polang seed oil performance evaluation in CI engine, Fuel 86, 2007, pp. 448-54

[6] Godiganur, S., Murthy Ch. S., Reddy, R.P., Performance of emission characteristics of a Kirloskar HA394 diesel engine operated on fish oil methyl ester, Renewable Energy 35, 2010, pp. 355-359

[7] Raheman H. and Ghadge S.V. Performance of Diesel engine with biodiesel at varying compression ratio and ignition timing, Fuel 87, 2008, pp. 2659-66

[8] Sahu D.K. and Parida S., A Process Technology for the Production of Low Cost Biodiesel, Indian Patent Application no- 165/KOL/2009 of dated 29.01.2009

[9] Diesel fuel ISI specification 1460, 1974

[10]Sahu, D.K. and Parida, S., Application of process of sonoication for single phase stability of straight vegetable oil-diesel blended fuel, presented in WREC2009-Asia, pp. 56

An Experimental Investigation on Performance and Emissions of a Multi Cylinder Diesel Engine Fueled with Hydrogen-Diesel Blends

Duraid F. Maki[1,*], P. Prabhakaran[2]

[1]*Mechanical Engineering Department, Faculty of Technology and Engineering, The M. S.University of Baroda Vadodara 390 002 – Gujarat - India*
** Corresponding author. Tel: +91 9974620190, E-mail:duraid_m@yahoo.com*

Abstract: Diesel engines are major contributors of air pollution by its exhaust gasses such as particular matter, carbon oxides, oxides of nitrogen, and sulfur compounds. Also, the diesel as a fossil fuel is threatened to decay with depletion of its sources. Hydrogen as a renewal energy and promising fuel might use to solve that troubles and crisis. A multi cylinder, natural aspiration, four stroke, compression ignition, and water cooled engine is tested under hydrogen diesel different blends and at different operating conditions. A hydrogen induction set up is built in the lab with all of the acquitting sensors and measuring instruments. The safety rules are considered. A continuous hydrogen induction in the inlet manifold is selected technique for this investigation. Experimental tests are done to investigate engine thermal performance and exhaust emission constituents under those blends circumstances. The optimum operating conditions and optimum parameters for those blends are found. The investigation led to find that, the optimum rate of hydrogen induction is 7.5 lpm. This optimum rate reduced the diesel fuel consumption by 20 % and increased the brake thermal efficiency by about 8-9%. The NO_X emission is reduced.

Keywords: *Hydrogen, Compression ignition engine, Performance, Exhaust emission, Dual Fuel.*

1. Introduction

Since 1878 to this day, diesel engine played the role of one primary source of power in human life. Many life sectors are depended on diesel engine such as agriculture and transportation. Diesel engine possesses a high reliability and durability with reasonable fuel consumption. Unfortunately, diesel engine is the main contributor to world's pollution. It has smoke and NO_X as major exhaust emissions. Numerous research efforts are concentrated on finding solutions to this problem. In 1970, the energy crisis ignited the competitions and research to find new energy sources or renewable energies. For both challenges, save our environment and save the energy sources, hydrogen is found as a promising solution. Hydrogen is nearly ideally suited as energy carrier because of its physical and chemical properties. It can be produced from water and conversely, on combustion forms water again in a closed cycle with very low formation of NO_X. It seems that the improvement in the engine performance under steady conditions is mainly attributed to the contribution of the hydrogen properties to the combustion process. The use of hydrogen with diesel engine might supplement wholly or partially without substantial hardware modification in arrangement of diesel engine [1]. The replacement of diesel by hydrogen totally needs high compression ratio above 29 along with a drop in the engine power and efficiency. Duel fuel mode or hydrogen diesel blends are more preferable [2]. The idea of using hot diesel drops as an igniter to air- hydrogen blend is applied. Many techniques have been studied and tested to inject or induct the hydrogen in air manifold or air intake passage. Carburetions, timing intake injection and induction, continuous injection or induction are the techniques mostly used [3].

Each technique has advantage and disadvantage. However, indirect injection or induction techniques pose no requirement of high compression ratio to run the engine under hydrogen-diesel blend. Verhelst at el. [4] used air port injection method to investigate the hydrogen effect on SI engine which might apply in diesel engine as well. Masood et al [5, 6] investigated direct injection and in port induction with modeling to those blends. Saravanan et

al. [7-10] investigated different techniques in the hydrogen injection and induction with recycling to exhaust gas and tested the timing and duration of hydrogen injection.

In this paper, a continuous induction of hydrogen in the air inlet manifold of a multi cylinder, compression ignition engine is adopted to investigate engine performance and exhaust gas emission constituents experimentally under different hydrogen induction rates and loads.

2. Experimental set-up

The experimental set up used for the present investigation consists of a four cylinder, four stroke, water cooled, indirect injection, naturally aspirated, and compression ignition engine developing a rated maximum power of 37 hp or 26.7 kW and running at varied speed equipped with a hydrogen induction system and an eddy current dynamometer with variable loading arrangement. The eddy current dynamometer gives the value of load in terms of Amp. only. The engine is coupled directly to the dynamometer and is mounted on a test bed with suitable connections for lubricating and cooling systems. The specification of the engine used for the study is given in Table 1.

Fig. 1 illustrates the schematic of the set up. Hydrogen induction system consists of high pressure hydrogen gas cylinder at 14.6 bar pressure, regulating valves, fine valve and digital mass flow meter to measure hydrogen flow rate. Nitrogen gas cylinder, flame arrestor, flame trap, non-return valve are used as a protection devices. PT 100 thermometer type is used to measure the exhaust temperature. Diesel weight flow rate is measured using strain gauge. Air surge tank with vertical water manometer is used to measure air pressure difference and to calculate the airflow rate in inlet manifold pipe. While a non contact tachometer is used to measure the engine speed. All the instruments are calibrated against traceable standards.

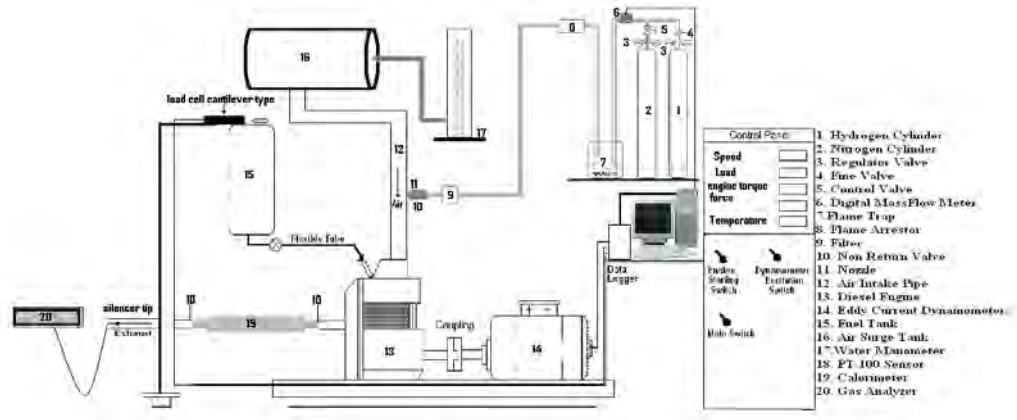

Fig. 1. The experimental setup

Table 1. Engine specification

Make and model	Stride Engine 1.5 E2 DSL
General details	Four cylinder, four stroke, compression ignition, vertical, water cooled, indirect injection
Bore	73 mm
Stroke	88.9 mm
Compression ratio	23:1
Max. power	27.6 kW @ 4000 rpm
Max. torque	83.4 Nm @2250 rpm
Capacity	1489 cm^3

3. Experimental procedure

The following step by step procedure is followed during the experimental investigation:
Start and run the diesel engine at 1500 rpm (most of previous investigations tested the diesel engine at this rate speed) for about 15 minutes to warm the engine and attain steady state condition before the data is acquired.

1. Set the fuel supply system in only diesel mode and record the data of fuel consumption rate, air difference pressure, engine speed, exhaust gas temperature, and exhaust gas constituents under no-load condition.
2. Repeat the observations under different load conditions at the eddy current dynamometer with loadings at 0.5, 1, 1.5, and 2 Amp. of load.
3. Run the engine on diesel mode. Then, set the induction of hydrogen in the an inlet manifold at a specified rate of 1 lpm and run the engine under dual fuel mode to attain steady state condition.
4. Record the data of fuel consumption rate, air pressure difference, engine speed, exhaust gas temperature, and exhaust gas constituents under 0.5 Amp. load condition.
5. Repeat the procedure in steps 4 and 5 under different load conditions at the dynamometer with loadings at 1, 1.5 and 2 Amp.
6. Repeat the experiment for different hydrogen induction rates of 2, 3,…, up to 18 lpm.
7. Close the hydrogen cylinder valve and open the nitrogen cylinder valve and purge the hydrogen gas from the induction system to avoid any burning of residual hydrogen gas.
8. Stop the induction of nitrogen and bring the engine to no load condition before switching off the engine.

4. Results and discussion

From an initial experimental study, it is found that the maximum rate of hydrogen induction at a given loading is to be restricted up to 18 lpm and the maximum loading possible on the engine is 2 Amp. due to engine load capacity restriction. This is the constraint within which the present experimental investigation is carried out.

Fig. 2 illustrates the relation between brake thermal efficiency and hydrogen induction rate at 1500 rpm speed and various loads. The brake thermal efficiency calculated by [1]:

$$brake\ thermal\ efficiency\ (\%) = \frac{Brake\ Power}{(m_f \times CV_D + m_{H2} \times CV_{H2})} \quad (1)$$

It is seen that, the brake thermal efficiency significantly increases with hydrogen induction rate. The rate of increase in brake thermal efficiency with continuous hydrogen induction is found to be higher at higher loads of 1, 1.5, and 2 Amp. load, while, there is no significant change in the efficiency with load of 0.5 Amp. The reason may be attributed to the higher caloric value of hydrogen which is approximately twice that of diesel. For a given load and speed condition, the influence of extra energy addition due to hydrogen induction on brake thermal efficiency is apparent from Eq. (1). The extra energy induction decreases the need of diesel fuel required. At full load, there is 20% increasing in brake thermal efficiency when the hydrogen induction rate changed between 0 lpm and 18 lpm.

Fig. 3 gives the variation in diesel fuel consumption with hydrogen induction rate for various loading (0, 0.5, 1, 1.5, and 2 Amp.) of diesel engine running at 1500 rpm. The engine running at constant speed needs less amount of diesel at a specified brake load due to extra energy available from hydrogen. It can also be noticed that the rate of reduction in diesel fuel consumption is higher at higher loading. At high load condition, the rate of reduction in diesel

fuel consumption is found to be about 40% between hydrogen induction rate from 0 to 18 lpm. This is observed to be true for higher loading of 1, 1.5, and 2 Amp. However, at no loading or light loadings of 0 and 0.5 Amp respectively, the reduction in diesel fuel consumption for hydrogen induction rate from 0 to 18 lpm is found to be about 25-30 %.

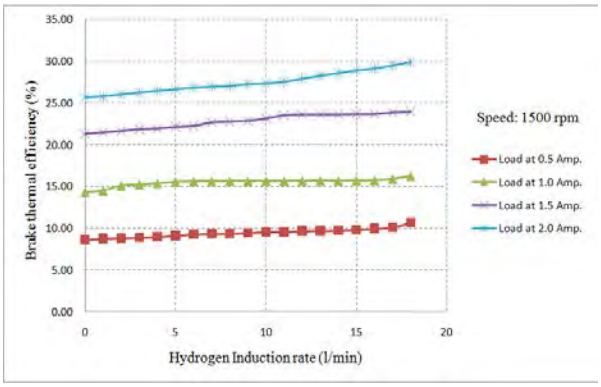

Fig. 2 Variation of brake thermal efficiency with hydrogen induction rate for various loading of diesel engine

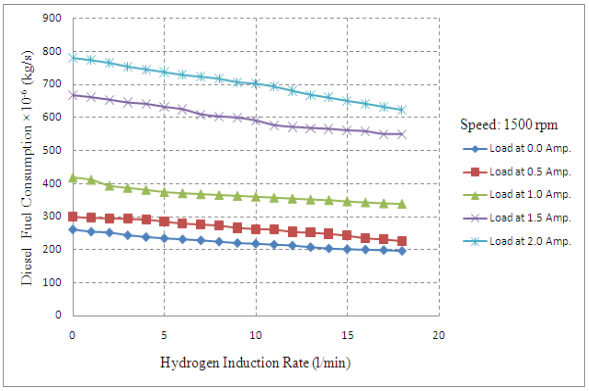

Fig.3 Variation of diesel fuel consumption with hydrogen induction rate for various loading of diesel engine

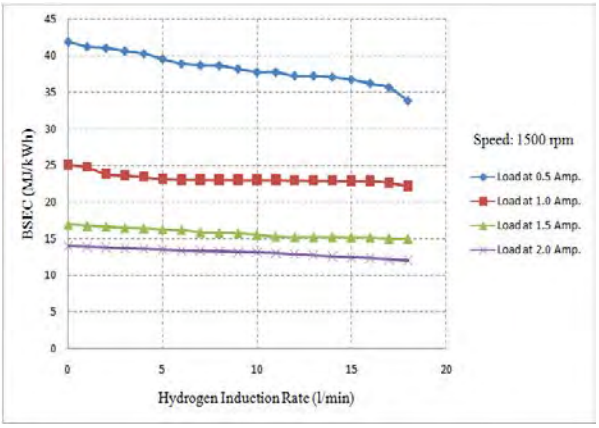

Fig. 4 Variation of brake thermal efficiencywith hydrogen induction rate for variousloading of diesel engine

The variation of the brake specific energy consumption (BSEC) with hydrogen induction rate at different loading conditions is shown in Fig. 4. It is seen that the hydrogen induction in the atmospheric air intake manifold of the engine enhances the consumption of energy to produce more usable power. Basically, the BSEC decreases with increase in load with the engine running at a given constant speed. The same trend is observed with various hydrogen induction rate also. With the induction of hydrogen, the decrease in BSEC is more significant when the load applied is beyond 1.0 Amp. At constant induction rate, the decrease in BSEC is of the order of about 3 times when the load is increased from 0.5 Amp. to 2.0 Amp.

Fig. 5 illustrates the effect of hydrogen induction rate on the exhaust temperature of diesel engine at different loading conditions with speed held at 1500 rpm. The increase in exhaust temperature is an indicator of combustion process behavior. The increment in exhaust temperature is directly indicating to the increment in the energy released increment in the combustion chamber. It can be noticed a margin increase in exhaust temperature due to the high caloric value of hydrogen.

The effect of hydrogen induction rate on volumetric efficiency is represented in Fig. 6. It is observed that irrespective of the loading condition, volumetric efficiency decreases by about 10% when the hydrogen induction rate increased from 0 to 18 lpm. The reason for such a trend may be attributed to the following. A naturally aspirated diesel engine working at a constant speed is found to operate with constant air suction rate. The rate of suction air decreases with increase of load resulting in a decrease of volumetric efficiency. In the range

of loading under consideration, the decrease is found to be a maximum of about 5%. However, at a constant speed and load, the volume intake of air decreases when hydrogen induction rate is increased which results in decrease of volumetric efficiency. The reduction in suction air rate leads to incomplete combustion affecting obviously the emission characteristics.

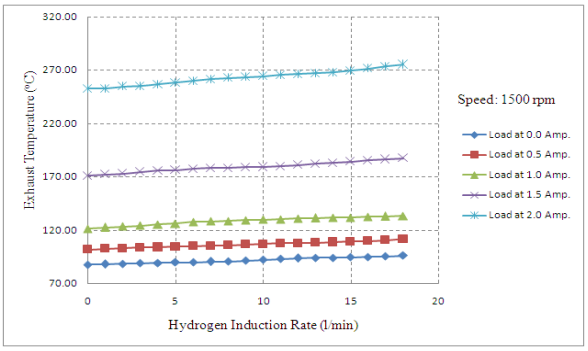

Fig. 5 Variation of exhaust temperature with hydrogen induction rate for various loading of diesel engine

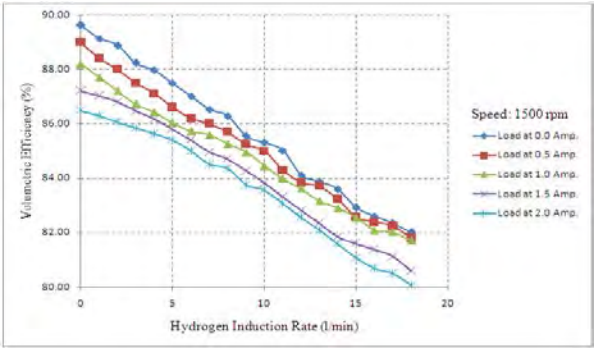

Fig. 6 Variation of volumetric efficiency with hydrogen induction rate for various loading of diesel engine

Fig. 7 shows the variation of equivalence ratio with continuous hydrogen induction rate for various loading of diesel engine running at constant speed. The trend is in consistent with that observed in Fig. 3. For diesel hydrogen duel fuel system, the equivalence ratio is calculated using Eq. (2) [12]. The equivalence ratio increases with loading increase. The equivalence ratio decreased as hydrogen induction rate increased for a given load.

$$\emptyset = \frac{\frac{[G]}{[Air]-\frac{[H_2]}{\left(\frac{[H_2]}{[Air]}\right)_{st}}}}{\left(\frac{[G]}{[Air]}\right)_{st}} \qquad (2)$$

Where, ϕ is equivalence ratio, [G], [Air], and [H_2] are respectively diesel, air, and hydrogen molar concentrations. Subscript 'st' stands for stoichiometric. The thermal performance evaluation of the effect of continuous hydrogen induction in inlet manifold to naturally aspirated multi cylinder water cooled diesel engine running at a constant speed of 1500 rpm indicates improvement in brake thermal efficiency. The notable feature of the effect of the hydrogen induction is the significant reduction in diesel consumption rate required. However, an optimum hydrogen induction rate could not be ascertained for maximizing thermal efficiency and minimizing diesel consumption rate as hydrogen induction rate beyond 18 lpm poses serious flash back problems.

In view of the above observations, experimental investigations are further carried out to quantitatively estimate the emission characteristics and evaluate whether there should be an optimum hydrogen induction rate, which does not seriously affect pollutant emission rates. Figs. 8-12 represent the effect of continuous hydrogen induction rate on the emission of the various exhaust constituent gases such as CO, CO_2, HC, NO_X, and O_2 when the engine is run at different load.

It is seen from Fig. 8 that, the hydrogen induction rate has significant effect on CO emission. The reason for such a trend is due to the proportionate decrease in the content of inlet manifold air. In the case of fuel rich mixture, the CO emission increases while for that of lean

fuel mixture, it remains fairly constant. As diesel engines are operated with lean fuel mixture, CO emission is generally low [13]. However, with hydrogen induction rate increased from no induction to 18 lpm, the CO percentage emissions increases from about 0.15% to 0.95% with the loading of 2 Amp. Similarly, it is found that there is significant effect of hydrogen induction rate on CO emission for the engine running at 0, 0.5, 1 and 1.5 Amp. loads.

Since diesel consumption rate increases with increase in loading. There is an increase in CO_2 emission by about three times (i.e from about 2.5% to 7.5%) with no hydrogen induction. Further, similar trends are observed with hydrogen induction rate, Fig. 9. Further, it is seen that there is no significant effect on CO_2 emission when hydrogen induction rate increased from 0 to 18 lpm for engine running at constant speed and load.

Fig. 10 illustrates the effect of hydrogen induction rate on unburned hydrocarbon (HC) emission. It is observed that there is a considerable increase in HC emission when hydrogen induction rate is increased beyond 7.5 lpm. At 18 lpm hydrogen induction rate the HC decreased by about 8 times when the load varied between 0 and 2 Amp.

Hydrocarbons, or more appropiately organic emissions, are the consequence of incomplete combustion of the hydrocarbon fuel. The level of HC in the exhaust gases is generally specified in terms of total hydrocarbon concentration expressed in parts per million carbon atome or volume percentage (as in present work). While total hydrocarbon emission is a useful measure of combustion inefficiency, it is not necessarily a significant index of pollutant emissions. Engine exhaust gases contain a wide variety of hydrocarbon compounds. Hydrocarbon compounds are divided into different categories and scales. The simplest scale, which divides the HC into classes as methane and non methane hydrocarbons, probably best approximates the end result for all HC emissions. All hydrocarbons except methane react, given enough time. In diesel the HC constituents vary from methane to the heaviest hydrocarbons. The multi gas analyzer used into present work measured the HC on basis of the methane. Unburned hydrocarbons or partially oxidized hydrocarbons emission levels from diesel vary widely with operating conditions, and different HC formation mechanisms are likely to be most important at different operating modes. Engine idling or low speed and light load operations produce significantly high hydrocarbon emissions than full load or high speed operation [11]. These notes can be observed in the Fig. 10. The increment in hydrogen induction rate causes reduction in the intake air which results in a displacement of some volume of the intake air. With increase in load , therefore, the percent content of CO in exhaust gases slightly decreases for a given hydrogen induction rate. This slight reduction in per cent content of CO in exhaust gases may be either due to the formation of lean mixture when only diesel is used as base fuel or/and due to the conversion of CO to CO2.

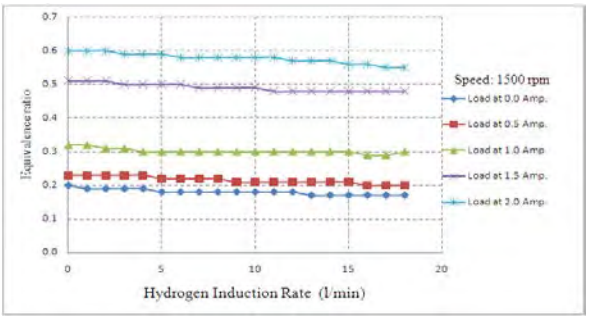

Fig. 7 Effect of hydrogen induction rate on equivalence ratio

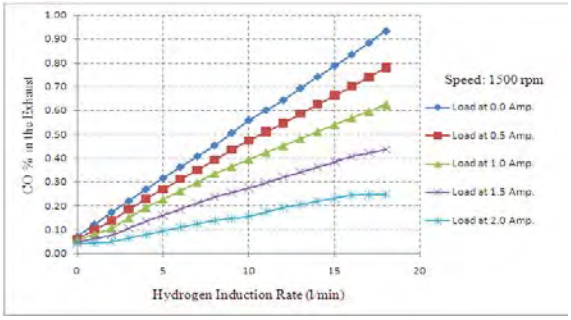

Fig. 8 Effect of hydrogen induction rate on on CO emission at difference loading

The effect of hydrogen induction rate on NO_X emission is given in Fig. 11. It is seen that there is 20% decrease in NO_X emission at smaller loading of 0, 0.5, and 1 Amp. from the condition of no induction to 7.5 lpm hydrogen induction rate. However, at higher loading, the decrease in NO_X emission is only about 6-7% between the same ranges of hydrogen induction rate. The constituent gases of NO_X emission are mainly NO and NO_2. Although the amount of the NO_2 is increased with higher hydrogen induction rate, the decrease in the amount of constituent gas NO plays a dominant role in the decrement in NO_X formation. The reduction in the amount of intake air has contributed to the reduction in NO_X emission in spite of the increase in the exhaust temperature. Fig. 12 illustrates the effect of hydrogen induction rate on O_2 emission. It is observed that there is only a marginal decrease in O_2 emission with increase in hydrogen induction rate. However, as the load on the engine is increased from 0 to 2 Amp., there is a 30 – 35 % decrease in O_2 emission.

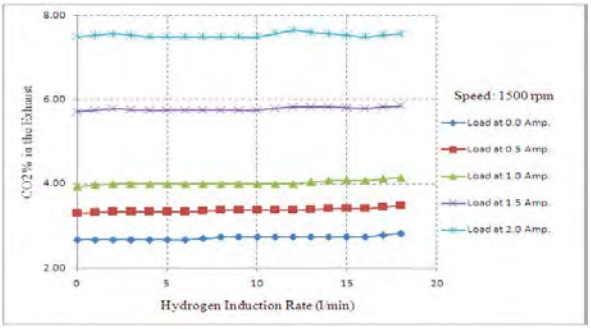

Fig. 9 Effect of hydrogen induction rate on CO_2 emision at difference loading

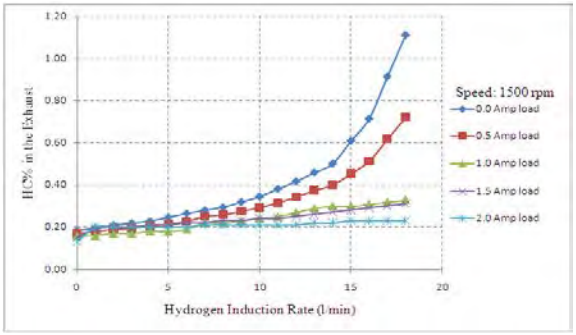

Fig. 10 Effect of hydrogen induction rate on HC emission at difference loading

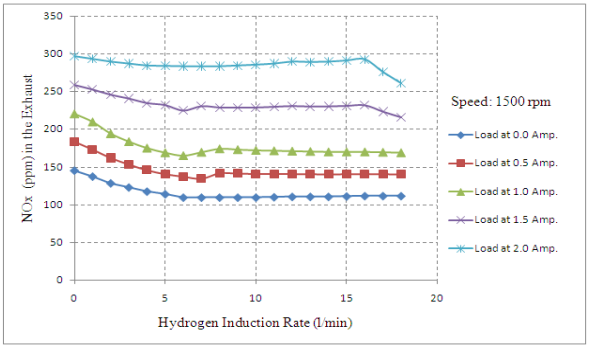

Fig. 11 Effect of hydrogen induction rate on NO_X at difference loading

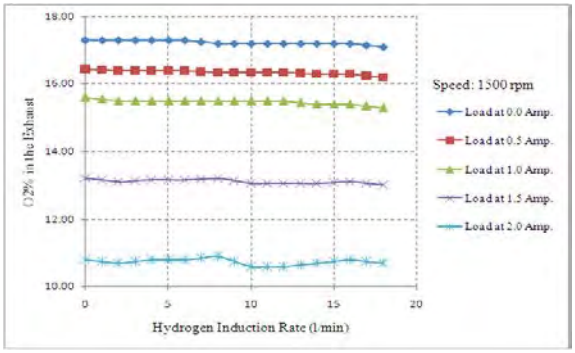

Fig. 12 Effect of hydrogen induction rate on O_2 emission at difference loading

5. Conclusion

Based on the experimental studies conducted on the thermal performance and pollutant emissions using a indirect injection multi cylinder naturally aspirated diesel engine with and without continuous hydrogen induction in the inlet manifold, the following conclusions are drawn:

1. A continuous hydrogen induction into the inlet manifold is a unique way of addressing simultaneously issues related to thermal performance and pollutant emission from diesel engine operated with diesel as a fuel. The system may be treated as hydrogen diesel dual fuel system as energy from hydrogen is also utilized.
2. There is a monotonous effect of continuous hydrogen induction rate on thermal performance parameters such as brake thermal efficiency, diesel fuel consumption rate and volumetric efficiency. And hence thermal performance tests alone cannot predict optimum hydrogen induction rate needed.

3. Based on both thermal performance and pollutants emission studies, it is seen that hydrogen induction rate about 7.5 lpm gives an optimum performance keeping the emissions level at a reasonable low levels. At 7.5 lpm, the levels of CO, CO_2 and HC are not increase significantly while the NO_X is reduced. The 7.5 lpm hydrogen induction rate approximately reduced the diesel fuel consumption by 20% and increased the brake thermal efficiency by about 8~9%.

References

[1] H. S. Yi, K. Min. and E.S. Kim, The Optimised Mixture Formation For Hydrogen Fuelled Engines, Int. J. of Hydrogen Energy, Vol. 25, Issue 7, 2000, pp. 685-690.

[2] Probir Kumar Bose and Dines Maji, An Experimental Investigation on Engine Performance and Emissions of a Single Cylinder Diesel Engine Using Hydrogen as Inducted Fuel and Diesel as injected Fuel with Exhaust Gas Recirculation Int. J. of Hydrogen Energy, Vol. 34, Issue 11, 2009, pp. 4847-4854.

[3] L. M. Das, Hydrogen Engine: Research and Development (R&D) Programmes in Indian Institute of Technology (IIT), Delhi, Int. J. of Hydrogen Energy, Vol. 27, Issue 9, 2002, pp. 953-965.

[4] S. Verhelst and R. Sierens, Hydrogen Engine Specific Properties, Int. J. of Hydrogen Energy, Vol. 25, Issue 9, 2001, pp. 987-990.

[5] M. Masood, S. N. Mehdi and P Ram Reddy, Experimental Investigation on a Hydrogen – Diesel Duel Fuel Engine at Different Compression Ratios, Transactions of ASME, Journal of Engineering for Gas Turbines and Power, Vol. 129, 2007, pp. 572578.

[6] M. Masood, M.M. Ishrat, A.S. Reddy, Computational Combustion and Emission Analysis of Hydrogen–Diesel Blends with Experimental Verification, Int. J. of Hydrogen Energy, Vol. 32, Issue 13, 2007, pp. 2539-2547.

[7] N. Saravanan and G. Nagarajan, An Experimental Investigation on Performance and Emissions Study with Port Injection Using Diesel as an Ignition Source for Different EGR Flow Rates, Int. J. of Hydrogen Energy, Vol. 33, Issue 16, 2008, pp. 4456-4462.

[8] N. Saravanan and G. Nagarajan, Performance and Emission Study in Manifold Hydrogen Injection with Diesel as an Ignition Source for Different Start of Injection, Renewable Energy, Vol. 34, Issue 1, 2009, pp. 328-334.

[9] N. Saravanan, G. Nagarajan, G. Sanjay, C. Dhanasekaran and K. M. Kalaiselvan, Combustion Analysis on a DI Diesel Engine with Hydrogen in Dual Fuel Mode, Fuel, Vol. 34, Issue 1, 2009, pp.328-334.

[10] N. Saravanan and G. Nagarajan, Experimental Investigation in Optimizing the Hydrogen Fuel on a Hydrogen Diesel Dual-Fuel Engine, Energy & Fuels, Vol. 23, 2009, pp. 2646–2657.

[11] Heywood, J.B., Internal Combustion Engine Fundamentals. 1988, New York: McGrew-Hill Book Company.

[12] Y. Hacohen and E. Sher, On the modeling of a SI 4-stroke cycle engine fueled with hydrogen enriched gasoline, Int. J. Hydrogen Energy, Vol. 12, No4., 1987, pp214-220.

[13] N. Saravanan, G. Nagarajan, K. M. Kalaiselvan and C.Dhanasekaran, An Experimental Investigation on Hydrogen as a Dual Fuel for Diesel Engine System with Exhaust Gas Recirculation Technique, Renewable Energy, Vol. 33, Issue 3, 2008, pp. 422-427.

Combustion Characteristics of an Indirect Injection (IDI) Diesel Engine Fueled with Ethanol/Diesel and Methanol/Diesel Blends at Different Injection Timings

Ali Turkcan [1], Mustafa Canakci [1, 2, *]

[1] *Department of Automotive Engineering Technology, Kocaeli University, 41380 Izmit, Turkey*
[2] *Alternative Fuels R&D Center, Kocaeli University, 41275 Izmit, Turkey*
**Corresponding author; Tel: +90 262 303 22 85, Fax: +90 262 303 22 03, E-mail:* mustafacanakci@hotmail.com

Abstract: In this study, the influence of methanol/diesel and ethanol/diesel fuel blends on the combustion characteristic of an IDI diesel engine was investigated at different injection timings by using five different fuel blends (diesel, M5, M10, E5 and E10). The tests were conducted at three different start of injection {25°, 20° (original injection timing) and 15° CA before top dead center (BTDC)} under the same operating condition. The experimental results show that maximum cylinder gas pressure (P_{max}) and maximum heat release rate $(dQ/d\theta)_{max}$ increased with advanced fuel delivery timing for all test fuels. Although the values of P_{max} and $(dQ/d\theta)_{max}$ of E10 and M10 type fuels were observed at original injection and retarded injection (15° CA BTDC) timings, those of the diesel fuel were obtained at advanced injection (25° CA BTDC) timing. From the combustion characteristics of the test fuels, it was observed that ignition delay (ID), total combustion duration (TCD) and maximum pressure rise rate $(dP/d\theta)_{max}$ increased with advanced fuel delivery timing. The ID increased at original and advanced injection timings for ethanol/diesel and methanol/diesel fuel blends when compared to the diesel fuel. It was also found that increasing methanol or ethanol amount in the fuel blends caused to increase in ID and to decrease in TCD at all injection timings. At original injection timing, the $(dP/d\theta)_{max}$ increased with increasing methanol or ethanol amount in the fuel blends. To see the cycle to cycle variation, the fifty cycles of each fuel were also investigated at the different injection timings. It was found that, at the advanced injection timing, cyclic variability of the test fuels was higher when compared to the original and retarded injection timings. The maximum cyclic variability was observed with the M10 at the advanced injection timing.

Keywords: *Ethanol, Methanol, IDI diesel engine, Injection timing, Combustion characteristics*

1. Introduction

Compression ignition (CI) or diesel engines are widely used for transportation, automotive, agricultural applications and industrial sectors because of their high fuel economy and thermal efficiency. The existing CI engines operate with conventional diesel fuel derived from crude oil. It is well known that the world petroleum resources are limited and the production of crude oil is becoming more difficult and expensive. At the same time, with the increasing concern about environmental protection and more stringent government regulation, the researches on the decreasing of exhaust emissions and improving fuel economy have become a major research issue in the engine combustion and development. A lot of research related to the emissions reduction has been performed by using different injection parameters such as injection time and injection pressure, exhaust gas recirculation and oxygenated alternative fuels. In the recent years, methanol and ethanol are attractive oxygenated alternative fuels for diesel engines. The oxygenated alternative fuels such as methanol and ethanol have provided more oxygen during combustion. Therefore, the oxygenated alternative fuels and blends with gasoline and diesel fuel are more clean combustion processes than that of diesel and gasoline fuels [1-7]. The studies related to the alternative fuels should be enhanced for diesel engines especially for indirect injection (IDI) diesel engines. Because, they have a simple fuel injection system and lower injection pressure level. They do not depend upon the fuel quality and have lower ignition delay (ID) and faster combustion than direct injection (DI) diesel engines.

For a diesel engine, the fuel injection timing is a major parameter that affects the combustion and exhaust emissions. If the start of fuel injection timing is earlier, the initial air temperature and pressure will be lower, so that the ID will increase. The increase in the ID period causes to increase in the premixed burning phase, the cylinder gas temperature and the NO_x emissions. However, this trend decreases PM emissions. If the start of fuel injection timing is later (when piston is closer to TDC), the temperature and pressure will be slightly higher, therefore the ID will decrease. For this reason, injection timing variation has a strong effect on the combustion characteristics and exhaust emissions, because of changing maximum pressure and temperature in the cylinder.

Canakci et al. [2] experimentally investigated the combustion and exhaust emissions of a single cylinder diesel engine at three (25, 20 original injection timing and 15° CA BTDC) different injection timings when methanol/diesel fuel blends were used from 0 to 15%, with an increment of 5%. The results indicated that the P_{max} decreased and the ID increased with the increase of methanol mass fraction at all injection timings. The increment in the ID caused to the deteriorating combustion thereby reduced the P_{max}. Also advanced injection timing boosted the P_{max} and the rate of heat release because of the increase in ID. Huang et al. [8, 9] used the diesel/methanol blend and combustion characteristics and heat release analysis in a CI engine. According to the experimental results, the increase in methanol mass fraction in the diesel/methanol blends resulted in an increase in the heat release rate at the premixed burning phase and shortened the combustion duration of the diffusive burning phase. The ID increased with increasing of the methanol mass fraction. This trend was more obvious at low engine load and high engine speed. TCD and P_{max} increased by advancing fuel delivery timing. The P_{max}, the $(dP/d\theta)_{max}$ and the $(dQ/d\theta)_{max}$ of the diesel/methanol blends obtained a higher value than that of diesel fuel. Yao et al. [10] researched the effect of diesel/methanol compound combustion (DMCC) fuel injection method on combustion characteristics. In this fuel injection method, the methanol was injected into the air intake of each cylinder. The diesel fuel was injected into the cylinder to ignite a methanol/air mixture. This system was tested on naturally aspired diesel engine. The test results showed that the ID increased and the cylinder gas temperature reduced with the DMCC fuel injection method due to the high latent heat of methanol.

Xing-cai et al. [11] conducted research on the heat release and emissions of a high speed diesel engine fuelled with ethanol/diesel blend. They found that the ID increased and TCD shortened for ethanol/diesel fuels when compared to diesel fuel. It was observed that the maximum heat release rate of ethanol/diesel blends were lower than that of diesel fuel. In the other studies, Rakopoulos C.D. et al. [12] investigated the effect of ethanol/diesel blends with 5%, 10% and 15% (by vol.) ethanol on the combustion and emissions characteristics of a high speed direct injection diesel engine. According to the experimental results, the ID for the E15 blend was higher than pure diesel fuel; also there was no significant difference among the P_{max} for each load conditions.

The combustion characteristics of IDI diesel engines are different from the DI diesel engines, because of greater heat-transfer losses in the swirl chamber. This handicap causes the brake-specific fuel consumption (bsfc) of the IDI engine to increase and the total engine efficiency to decrease compared to that of a DI diesel engine. Because of these disadvantages of the IDI diesel engines, most engine research has focused on the DI diesel engines. However, IDI diesel engines have a simple fuel injection system and lower injection pressure level because of higher air velocity and rapidly occurring air-fuel mixture formation in both combustion chambers of the IDI diesel engines. In addition, they do not depend upon the fuel quality and produce lower exhaust emissions than DI diesel engines [13].

From the literature review, it was concluded that the combustion characteristics of an IDI diesel engine have not been clearly investigated when using methanol/diesel and ethanol/diesel fuel blends at different injection timings. For this reason, this study experimentally investigated the effects of methanol/diesel and ethanol/diesel fuel blends on the combustion characteristics of an IDI diesel engine and compared them with those of diesel fuel.

2. Materials and method

In this study, a naturally aspirated, water-cooled, four cylinders IDI diesel engine was used as a test engine. The test engine specifications are compression ratio: 21.47, the maximum brake torque (95 Nm) was obtained at 2000 rpm and the maximum power 38 kW at 4200 rpm, start of injection timing: 20^{o} CA BTDC and injector opening pressure: 130 bar. A hydraulic dynamometer was directly coupled to the engine output shaft. Fig. 1 shows the schematic diagram of the experimental setup. The following parameters were recorded during the each test: engine speed, load, fuel consumption, air flow rate, and ambient, cooling water inlet-outlet, and oil and exhaust temperatures. Conventional diesel fuel, methanol and ethanol were used, and their properties are shown in Table 1. To obtain cylinder gas pressure and fuel line pressure data, piezoelectric-type sensors were used. The cylinder gas pressure sensor was installed on the first cylinder of the engine head. The cylinder gas pressure was obtained by using a Kistler water-cooled piezoelectric sensor type 6061B. An AVL quartz pressure sensor 8QP500c was mounted on the fuel line of the first cylinder to measure the fuel line pressure. The outputs of the pressure sensors were amplified by a Kistler charge amplifier 5015A type. The output of the charge amplifier and a signal from the magnetic pick-up were converted to digital signals and recorded by an Advantech PCI 1716A data acquisition card, which has a 16-bit converter and 250 kS/s sample rate. The pressure and crank angle data were stored in a computer. A computer program was written to collect the pressure data, with a resolution of 0.25° of crankshaft angle. To analyze the cylinder gas pressure, a combustion analysis program was written. To eliminate cycle-cycle variation, the cylinder gas pressure data of 50 cycles were averaged using a computer program. Then, the pressure data was used to calculate the heat-release rate. Experiments were performed after the test engine reached to the steady-state conditions. The steady-state conditions were determined with the engine oil temperature (~70 °C). The test engine was run at least 5 min after the test engine was loaded, and then data was collected for each test. The test procedure was repeated 3 times to verify the each engine test condition, and the results were averaged.

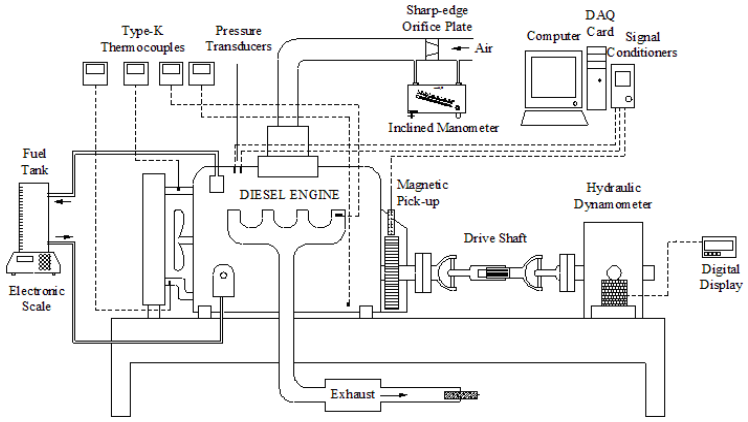

Fig. 1: Schematic diagram of the experimental set-up

Table 1. Properties of the test fuels

	Methanol	Ethanol	Diesel
Formula	CH_3OH	C_2H_5OH	$C_{10.8}H_{18.7}$
Molecular weight (kg/kmol)	32	46	170
Boiling temperature (^oC)	64.7	78	180 – 330
Density (g/cm^3, at 20 ^oC)	0.79	0.78	0.83
Auto-ignition temperature (^oC)	470	423	235
Lower heating value (MJ/kg)	20.27	26.8	43
Cetane number	4	5-8	50
Viscosity (mm^2/s, at 25^{o}C)	0.59	1.2	2.6
Heat of vaporization (MJ/kg)	1.11	0.856	0.280

3. Heat release analysis

The heat release analysis was based on the changes of the cylinder gas pressure and cylinder volume during the cycle. Therefore, some assumptions were made to calculate the heat release rate. It was assumed that no passage throttling losses exist between both chambers. Large temperature gradients, pressure waves, leakage through the piston rings, fuel vaporization and charge mixtures were ignored. Hence the intake and exhaust valves assumed to be closed. After using these assumptions, the heat release rate is calculated by using the following formula:

$$\frac{dQ}{d\theta} = \left[\frac{k}{k-1}\right] P \frac{dV}{d\theta} + \left[\frac{1}{k-1}\right] V \frac{dP}{d\theta}$$

Where: $(dQ/d\theta)$ is the combination of heat-release rate, P is cylinder gas pressure, V is cylinder volume, θ is the crank angle, k is the ratio of specific heats.

The parameters of combustion characteristics are ID, start of combustion, TCD which are obtained from heat release curve. The heat release curve in a diesel engine examines ID and TCD. The ID is defined as the time between the start of injection and the start of combustion. The start of injection time is determined by the fuel line pressure reached the injector nozzle opening pressure. The start of combustion is defined as the point where the heat release rate turns from negative to zero. The TCD is defined as the time from the start of combustion to the end of the heat release.

4. Results and discussion

In this study, the engine test was conducted at three different start of injection {25^o (advanced), 20^o (original) and 15^o (retarded) CA BTDC} under 1400 rpm and 40 Nm. The maximum fuel/air ratio was observed at 1400 rpm for diesel fuel, therefore the test condition was chosen as 1400 rpm. The relationship between the combustion characteristics and injection timings were focused by using conventional diesel fuel (D), E5, E10, M5 and M10. These fuel blends content of methanol or ethanol in different mass ratios (e.g., E5 contains 5% ethanol and 95% diesel fuel by mass). In this study, the combustion characteristics defined as the cylinder gas pressure and heat release rate were analyzed as shown in Fig. 2. The ID, TCD, $(dQ/d\theta)_{max}$, $(dP/d\theta)_{max}$, and the variation of the fifty consecutive P_{max} were also investigated as shown in Figures 3 and 4.

Fig. 2 illustrates the cylinder gas pressure and heat release rate of test fuels at three different injection timings under the same engine operating conditions. As shown in Fig. 2, it can be clearly seen that the cylinder gas pressure and heat release rate increased by advancing fuel

injection timings for all test fuels. This behavior was such that, as injection started earlier, the cylinder gas pressure and the heat release rate become higher due to more fuel injected during the ID period. In addition, the location of P_{max} and the start of combustion points occurred early with advanced fuel injection timing. Therefore the premixed combustion phases occurred earlier and also this phase finished before TDC at 25° and 20° CA injection timing. Diffusion or controlled combustion phase of the M10 and E10 formed lower burning than that of other test fuels at original injection timing. The lower viscosity and density of M10 and E10 led to high atomization and vaporization, so the lower burning was observed in the diffusion combustion phase. At the same time, the fraction of the heat release in the premixed or uncontrolled burning phase of the E10 and M10 blends decreased and the peak of premixed combustion phase of these blends increased at original injection timing. These results can be explained by increasing ethanol and methanol mass fraction in the blends.

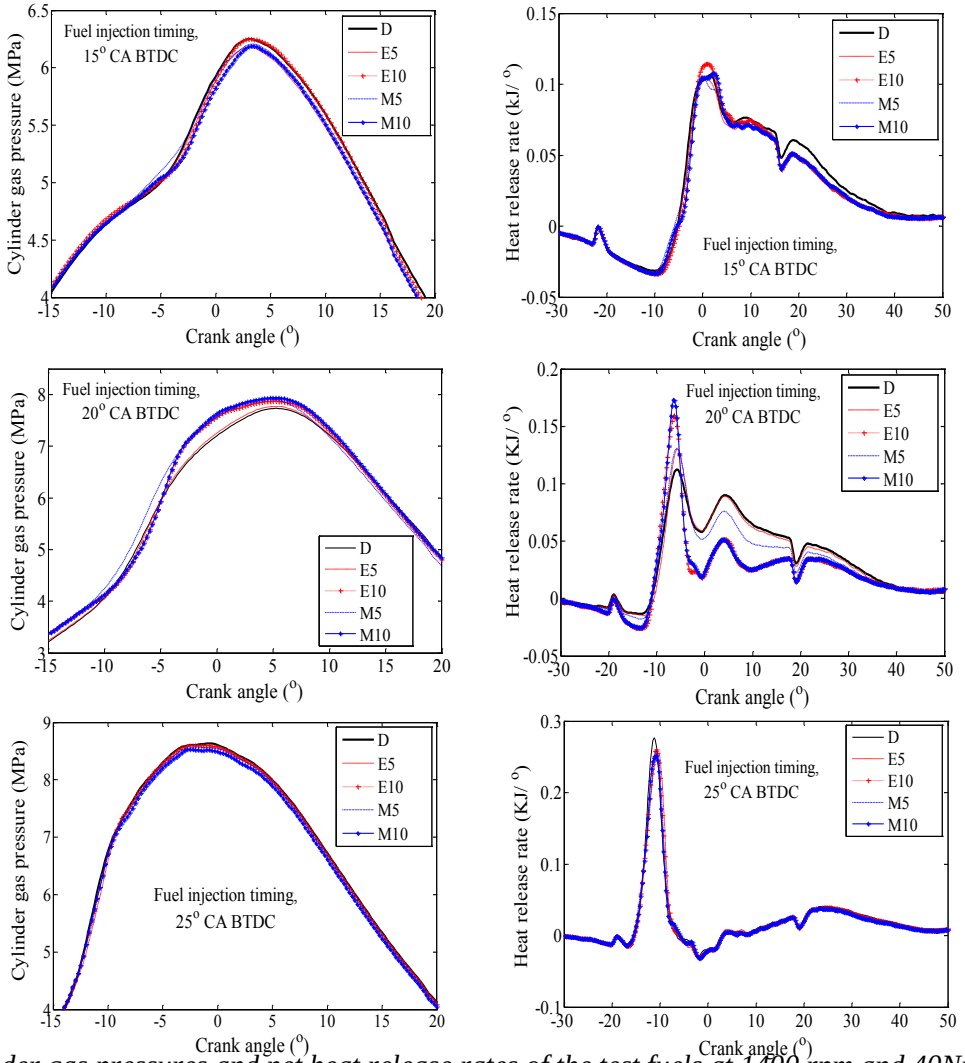

Fig.2 Cylinder gas pressures and net heat release rates of the test fuels at 1400 rpm and 40Nm

Fig. 3 shows the variation of ID, TCD, $(dQ/d\theta)_{max}$ and $(dP/d\theta)_{max}$ under three different injection timings. It was observed that the ID decreased with retarded injection timing for all test fuels. This behavior can be explained by the pressure, temperature and vaporization in the cylinder increased with retarded injection timings. It was found that, at advanced and original injection timings, the IDs of the blends are longer than that of conventional diesel fuel. This effect was interpreted by two different reasons. The first reason is that cetane numbers of the

blends which are lower than that of conventional diesel due to the cetane number decreased with the increase in methanol and ethanol mass fraction in the fuel blends. The second reason is that the methanol and ethanol have higher heat of vaporization than that of conventional diesel fuel. It was observed that the IDs of the E5 and M5 were shorter than that of E10 and M10 due to lower cetane number of the E10 and M10 blends. The TCD decreased with retarded fuel injection timing for all test fuels. The reason for the decrease in TCD is the increase in the premixed or uncontrolled combustion phase due to long ID and decrease in the diffusion or controlled combustion phase. It was revealed that, at all injection timings, TCD with blends was longer than that of conventional diesel fuel. This result can be explained by the increasing amount of the oxygen in the blends. It is known that the increase in amount of the oxygen enhances the combustion and causes to the diffusion combustion phase which becomes shorter.

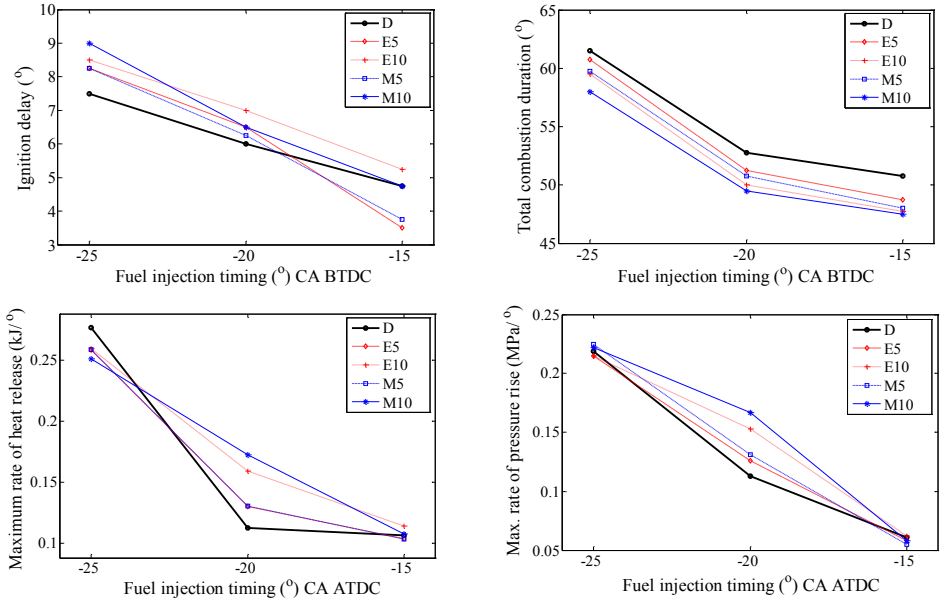

Fig.3 Effect of injection timing on the ID, TCD, $(dQ/d\theta)_{max}$ and $(dP/d\theta)_{max}$ at 1400 rpm, 40 Nm for each test fuel

As shown Fig. 2, the net heat-release profile has a slight negative dip during the ID period, which is mainly heat loss from the cylinder during the fuel vaporizing phase. It is more obvious at retarded injection timings. Because of the temperature in the cylinder increasing with retarded injection timing, the injected fuel during the ID period causes an increase in the evaporation heat. Therefore, the $(dQ/d\theta)_{max}$ decreased with retarded injection timings for all test fuels. The $(dP/d\theta)_{max}$ increased with the advancing injection timing as shown in the Fig. 3. This can be attributed to the increase in the injected fuel into the engine cylinder during the ID period, and so that produced higher the $(dP/d\theta)_{max}$ and the cylinder gas pressure. Also, there is no significant difference among the $(dQ/d\theta)_{max}$ and the $(dP/d\theta)_{max}$ of the test fuels at advanced and retarded injection timing, while at original injection timing, the $(dQ/d\theta)_{max}$ and the $(dP/d\theta)_{max}$ of the blends were higher than that of conventional diesel fuel. The main reason for this situation is that in order to obtain the same bmep from the blends, more fuel was injected into engine cylinders due to the blends have lower heating value than that of conventional diesel fuel. At the same time, it w as observed that the $(dQ/d\theta)_{max}$ and the$(dP/d\theta)_{max}$ increased with the increase in the mass fraction methanol and ethanol in the blends at original injection timing. This was caused by E10 and M10 fuel blends which have

more oxygen rate than E5, M5 and conventional diesel fuel. Thereby, the combustion became better and the $(dQ/d\theta)_{max}$ and the $(dP/d\theta)_{max}$ increased.

Fig. 4 shows the average of the P_{max} achieved from 50 consecutive cycles for all test fuels and all injection timings. It was observed that the cyclic variability decreased with the retarding fuel injection timings. Specially, at 25° CA injection timing, the cyclic variability of the M10 test fuel was higher than those of other injection timings. As shown in Fig.4, similar cyclic variability and the smooth operation of the engine can be achieved by using E5, E10, M5 and M10 blends when compared the conventional diesel fuel.

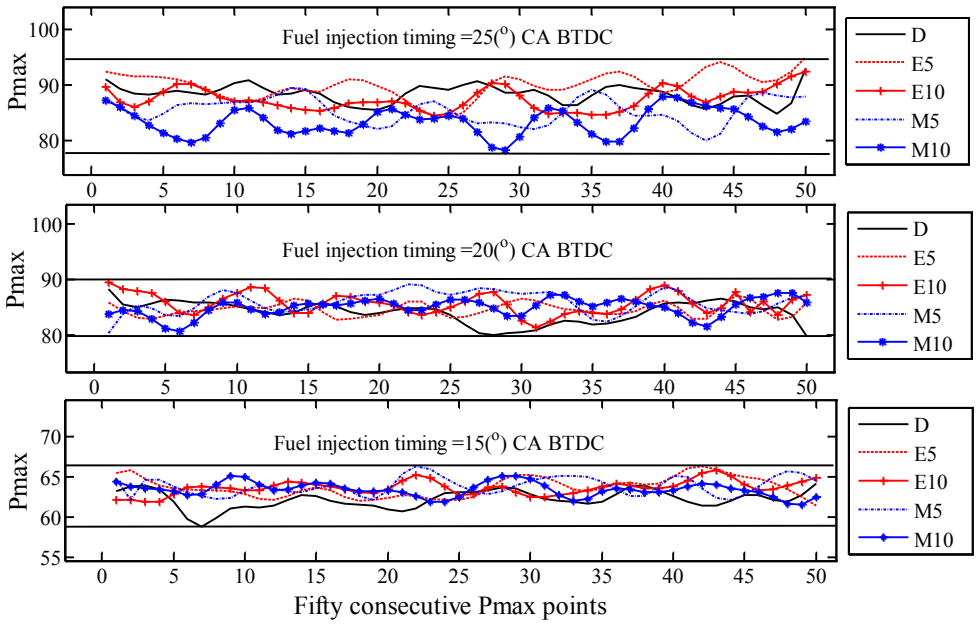

Fig.4 Effects of blends and fuel injection timing on the variation of maximum cylinder gas pressure

5. Conclusion

The paper presented the results of experimental research on the effects of injection timing on the combustion characteristics of an IDI diesel engine using the ethanol and methanol blends with diesel fuel. The following conclusions can be drawn from the current paper:

(1) The P_{max} and premixed combustion rate increased with advanced fuel injection timings for all test fuels.
(2) The location of P_{max} and the start of combustion points occurred early with advanced fuel injection timing.
(3) The ID and TCD decreased with retarded injection timing for all test fuels.
(4) It was determined that the IDs of the blends were longer than that of conventional diesel fuel at originally and advanced injection timings.
(5) An increase in the mass fraction of the methanol and ethanol in the fuel blends generally caused to increase in ID, but it decreased TCD.
(6) The retarding of injection timing decreased the $(dQ/d\theta)_{max}$ and the $(dP/d\theta)_{max}$ for all test fuels.
(7) It was found that the characteristics of $(dQ/d\theta)_{max}$ and $(dP/d\theta)_{max}$ of the blends are higher than that of conventional diesel fuel. These characteristics increased with the increase of methanol and ethanol mass fraction in the fuel blends at original injection timing.
(8) It was observed that the cyclic variability decreased with the retarding fuel injection timings. Also, the maximum cyclic variability was observed with the M10 at the advanced injection timing. The fuel blends used in the current study may replace with

conventional diesel fuel in terms of the combustion characteristics, cycle to cycle variation and smoothness of the engine operation.

References

[1] M. Canakci, C. Sayin, A.N. Ozsezen, and A. Turkcan, Effect of Injection Pressure on the Combustion, Performance, and Emission Characteristics of a Diesel Engine Fueled with Methanol-blended Diesel Fuel, Energy and Fuels 23, 2009, pp.2908-2920.

[2] M. Canakci, C. Sayin, and M. Gumus, Exhaust Emissions and Combustion Characteristics of a Direct Injection (DI) diesel Engine Fuelled with Methanol-Diesel Fuel Blends at Different Injection Timings, Energy and Fuels 22, 2008, pp.3709-3723.

[3] C.Y. Choi, R.D. Reitz, An experimental study on the effects of oxygenated fuel blends and multiple injection strategies on DI diesel engine emissions, Fuel 78, 1999, pp.1303-1317.

[4] L.J. Wang, R.Z. Song, H.B. Zou, S.H. Liu, L.B. Zhou, Study on combustion characteristics of methanol-diesel fuel compression ignition engine, Proc Inst Mech Eng D-J Auto 33, 2008, pp.1314-1323.

[5] Ö. Can, İ. Çelikten, N. Usta, Effects of ethanol addition on performance and emissions of a turbocharged indirect injection Diesel engine running at different injection pressures, Energy conversion and Management 45, 2004, pp.2429-2440.

[6] M. Eyidogan, A.H. Ozsezen, M. Canakci, A. Turkcan, Impact of alcohol-gasoline fuel blends on the performance and combustion characteristics of an SI engine, Fuel 89, 2010, pp.2713-2720.

[7] M.A. Ceviz, F. Yüksel, Effects of ethanol-unleaded gasoline blends on cyclic variability and emissions in an SI engine, Applied Thermal Engineering 25, 2005, pp.917-925.

[8] Z.H. Huang, H.B. Lu, D.M. Jiang, K. Zeng, B. Liu, J.Q. Zhang and X.B. Wang, Combustion characteristics and heat release analysis of a compression ignition engine operating on a diesel/ methanol blend, Proc Inst Mech Eng D-J Auto 218, 2004, pp.1011-1024.

[9] Z.H. Huang, H.B. Lu, D.M. Jiang, K. Zeng, B. Liu, J.Q. Zhang and X.B. Wang, Combustion behaviors of a compression-ignition engine fuelled with diesel/methanol blends under various fuel delivery advance angles, Bioresource Technology 95, 2004, pp.331-341.

[10] C. Yao, C.S. Cheung, Y. Wang, T.L. Chan, S.C. Lee, Effect of Diesel/methanol compound combustion on diesel engine combustion and emissions, Energy Conversion and Management 49, 2008, pp.1696-1704.

[11] L. Xing-cai, Y. Jian-guang, Z. Wu-gao, H. Zhen, Effect of cetane number improver on the heat release rate and emissions of high speed diesel engine fuelled with ethanol-diesel blend fuel, Fuel 83, 2004, pp.2013-2020.

[12] C.D. Rakopoulos, K.A. Antopoulos, D.C. Rakopoulos, Experimental heat release analysis and emissions of a HSDI diesel engine fueled with ethanol-diesel fuel blends, Energy 32, 2007, pp.1791-1808.

[13] A.A. Abdel-Rahman, On the emissions from internal combustion engines: a review, Int. J. Energy Res. 22, 1998, pp.483–513.

Land use, greenhouse gas emissions and fossil fuel substitution of biofuels compared to bioelectricity production for electric cars in Austria

Johannes Schmidt[1, *], Viktoria Gass[1], Erwin Schmid[1]

[1] *Institute for Sustainable Economic Development, University of Natural Resources and Life Sciences, Vienna, Austria*

** Corresponding author. Tel: +43 650 2151579, Fax: +43 1 47654-3692, E-mail: johannes.schmidt@boku.ac.at*

Abstract: Bioenergy is one way of achieving the indicative target of 10% renewable energy outlined in the EU Directive 2009/28/EC. This paper assesses the consequences for land use, greenhouse gas (GHG) emissions and fossil fuel substitution of increasing the use of bioenergy for road transportation. Different technologies, including first and second generation fuels and electric cars fuelled by bio-electricity are assessed in relation to existing bioenergy uses for heat and power production. The paper applies a spatially explicit energy system model that is coupled with a biomass production model to allow estimating impacts of increased biomass utilization for energy production on agriculture and forestry. Uncertainty is explicitly considered with the help of Monte-Carlo simulations of input parameters. Results indicate that second generation fuels perform better with respect to land use than first generation ethanol and that costs are lower. Biodiesel is also a cheap option, although the total potential is limited at a low level due to constraints in feedstock production. Electric vehicle mobility minimizes land use, however, costs are still high and prohibitive. First generation ethanol production is effective in reducing domestic GHG emissions because it does not induce feedstock competition with existing bioenergy uses (i.e. heat and power production). However, land use change is significant.

Keywords: *biofuels, electric cars, e-mobility, 2020 goals, spatially explicit optimization*

1. Introduction

Directive 2009/28/EC requires all member states of the EU to guarantee a share of 10% of renewable fuels in transportation by 2020. The target may be reached by various measures, including an increase in the share of biofuels and an increase in the share of renewably produced electricity in the transportation sector. However, since the large scale introduction of biofuels in the US and Europe an extensive discussion has evolved because the large land requirements were identified as cause for direct and indirect greenhouse gas (GHG) emissions [1], [2] and as the driver for increasing competition between food and fuels [3], [4]. In Austria, bioenergy has played traditionally an important role. It provided around 8% of the primary energy demand in 2006, mainly for heating purposes [5]. Other uses of bioenergy developed in recent years, include biofuel and power production. Austria has complied with the 5.75% indicative EU biofuel target since late 2008 and used around 4.00 TWh of biodiesel and 0.60 TWh of ethanol in 2008 [6]. A further increase of the supply of biofuels will be difficult to achieve, particularly if only domestic biomass supply is considered. However, new technologies are emerging that aim to increase biofuel productivity and diversify feedstock supply. Second generation biofuels that may use ligno-cellulosic feedstock for fuel production are regarded as a sustainable alternative to first generation biofuels which are mainly produced from food and feed crops [2], [7]. A technological alternative is electric cars. Technical and economical barriers currently prevent the large scale introduction of electric cars, however, future potentials are considered significant [8], [9]. Electric cars will only contribute to renewable energy targets if the electricity for cars is produced in a renewable manner. Biomass is one possible source for this purpose. An existing study estimates [10] that the utilization of biomass resources for electricity generation and subsequent utilization in electric cars is a far more effective way of using limited land resources for transportation than the conversion of food and feed crops to first generation ethanol. However, the assessment relied merely on technical details without considering economics and alternative uses of biomass in

the energy sector – e.g. for heating. This paper contributes to research by applying a spatially explicit agricultural-bioenergy-system model to evaluate several technological options for the transportation sector, including first and second generation fuels and electric cars, with respect to land use, GHG emissions and fossil fuel substitution. The techno-economic characteristics of future biofuel production as well as of electric cars are not well known yet. Also, high uncertainty is attached to future price energy scenarios. We therefore apply a Monte-Carlo simulation of input parameters to explicitly include uncertainty in the modeling process.

2. Methodology

2.1. Model and Model Boundaries

A spatially explicit, techno-economic mixed integer program is developed and applied to assess the costs, land use and GHG emissions of different bioenergy conversion routes. The model minimizes the costs of supplying Austria with transportation fuels, heat and electricity from either bioenergy or fossil fuels. It is static and simulates one year of operation. The current model version considers domestic biomass supply and energy demand only and does not allow imports and exports of biomass or bioenergy commodities. The model determines which bioenergy plants of a specific size and specific location shall be built and which demand regions are supplied with bioenergy and/or with fossil fuels. Each plant produces various energy commodities, e.g. the heat produced in a combined heat and power (CHP) may be delivered to district heating networks (Figure 1). By-products of biofuel plants are sold as animal feed. Biomass supply curves endogenously determine the price of feedstock from forestry and agriculture, while prices of fossil fuels and energy demand are defined exogenously. Taxes currently applied to both fossil and bioenergy fuels are not included in the model.

2.2. Technologies

We assess several bioenergy technologies which are able to replace fossil fuels in the transportation sector along with technologies that convert biomass to heat and power. First generation biofuels are classified into ethanol produced from fermentation of starchy and sugar crops (e.g. wheat and corn) and biodiesel which is produced from vegetable oil derived

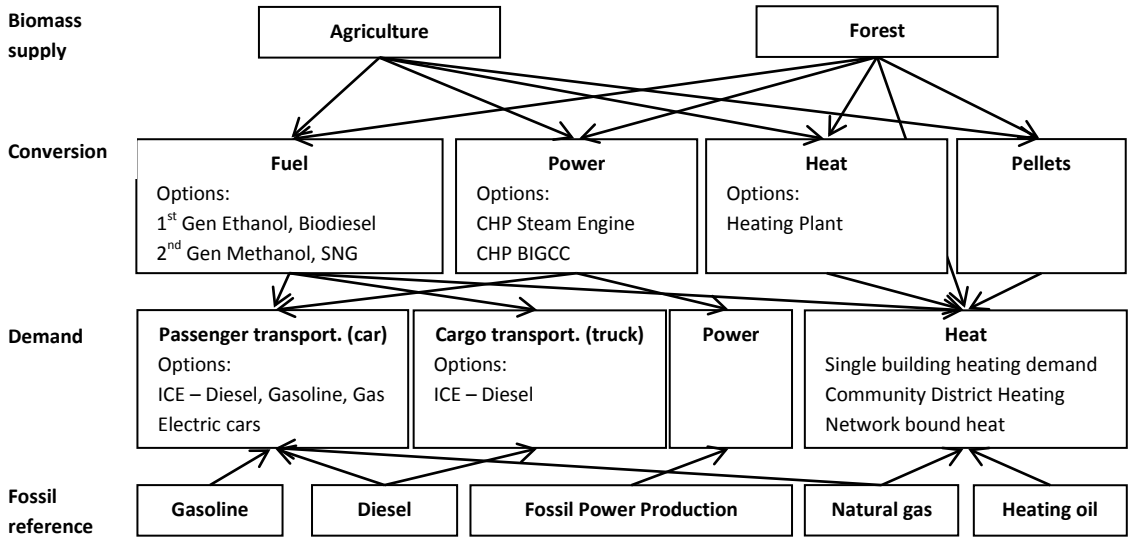

Figure 1: Diagram of the mixed integer programming model.

from oil crops (e.g. sunflower and rapeseed). Both technologies are commercially available and are currently used for the production of biofuels in Austria**.** Ethanol is blended with gasoline. A blend of 5% ethanol and 95% gasoline is considered safe to be used in all cars,

while all cars sold currently on the market are also able to handle a blend of 10% of ethanol. Similar limitations apply to biodiesel [11]. Second Generation biofuels are able to use cellulosic feedstock and even waste for the production of biofuels. There are two major technological options [7]. The biomass can be gasified and subsequently upgraded to liquid transportation fuels such as methanol or synthetic natural gas (SNG) which can also be used as transportation fuel. The second option is the hydrolysis of cellulose to sugars that are fermented to ethanol afterwards. We assess gasification only as it is estimated to be economically more viable than hydrolysis with fermentation [12], [7]. Second generation production technologies are currently under research and first pre-commercial installations are being built. US legislation requires 572 TWh of yearly cellulosic biofuel production until 2022 [13], therefore a rapid increase in the construction of second generation facilities can be expected. Current cars cannot run solely on methanol and the amount of methanol that may be blended to gasoline is, similar to ethanol, limited. SNG requires significant modifications to the car, including the installation of a gas tank. Electric cars are currently globally under research, however, costs and ranges of batteries are major economic and technical obstacles to full implementation of the technology. Ranges of above 150 km are currently only achieved at very high costs [9]. Also, electric cars need the large scale deployment of charging stations. Metering of power and billing still has to be developed. The model considers investment costs for electric cars. Costs associated with additional infrastructure necessary for electric cars are not included. With respect to power production, the model allows two technologies: steam engines and biomass integrated gasification combined cycle (BIGCC) plants. While steam engines are well established in Austria and the installed capacity exceeded 300 MW in 2007 [5], BIGCC is a technology that is still under research. It allows higher electrical conversion efficiencies than steam engines but capital costs are also significantly higher. We assume that power can be either used to fuel electric cars or that it is simply sold on the electricity market at a fixed price. Heating technologies modelled include fuel wood furnaces, pellet furnaces and heating plants for district heating networks.

2.2.1. Total Cost of Ownership – Cars

We use the concept of total cost of ownership (*tco*) to assign different costs to different cars in the model. Costs for fuels are endogenously determined by the model and are therefore not included in the calculations of *tco.* The *tco* per km is described by equations (1)-(3):

$$tco = \frac{C\frac{i(1+i)^t}{(1+i)^t-1}+B}{km} + om \qquad (1)$$

$$t = \min\left(\frac{maxKm}{km}, 10\right) \qquad (2)$$

$$B = \frac{i(1+i)^{tb}}{(1+i)^{t}b-1}\sum_{tb\in y}\frac{bc}{(1+i)^{t'}} \qquad (3)$$

The *tco* is determined by the annuity of capital costs *C* of the car, assuming an interest rate *i* and a lifetime *t*. For electric cars, the battery cost *B* is additionally considered as explained below. Total necessary yearly investment costs are divided by the kilometres *km* driven annualy. Additionally, operation & management costs per km of *om* are assumed. These costs are assumed to be lower for electric cars because maintenance of the electric motor is less complex than for an internal combustion engine (ICE) [9]. The lifetime of the car is limited to ten years, however, if the car is driven a lot (i.e. more than *maxKm*), the lifetime is further reduced as indicated by equation (2). The lifetime of a battery is significantly less than that of the carriage. A change of the battery within the lifetime is therefore probable and is modelled

by equation (3): the annuity of battery costs is derived by adding up the discounted battery costs over the whole life time, assuming that one battery costs *bc*. The battery is changed in year *y* when the driven kilometres since the last change exceed the lifetime of the battery. The *tco* depends significantly on the kilometres driven each year. A higher amount of kilometres implies lower specific capital costs per km. We therefore estimate ten classes of annual car utilization based on data provided by ÖAMTC. ÖAMTC, the biggest Austrian Automobile Association, checks approximately 10% of all cars for their technical liability each year. The total driven kilometers and the year of the first registration of the car are collected in the examination of the cars. An approximate estimate of the yearly driven kilometers can be derived from this data. We classified the cars by the annual driven kilometers into ten classes (0 km - 10,000 km, 10,001 km - 20,000 km, …, 90,000 km – 100,000 km). For each class, the mean of the yearly driven kilometers by car and the mean of the sum of driven kilometers by all cars in the class are determined. The sum of driven kilometers is linearly extrapolated from the ÖAMTC data with data of total Austrian car ownership from Statistik-Austria to allow an estimate for whole Austria as ÖAMTC data only covers around 10% of all registered cars.

2.3. Demand

We estimate current transportation demand from the ÖAMTC data and assume that the demand for transportation remains constant until 2020. We assume a total of 60 billion annual kilometres for personal transportation and total of 24 billion tonne kilometres for cargo transportation by truck. Although transportation fuel consumption has historically seen significant increases in the last years, the increase was significantly caused by "tank tourism" due to lower fuel taxes in Austria. We exclude demand from "tank tourism" from our analysis and also assume that public transportation will take a higher share of the overall transportation supply, thus allowing that road transportation remains constant. While the model allocates biomass resources to various conversion routes depending on energy prices and production costs, the demand for biomass heating is assumed to not fall under 17 TWh in the simulations. This is a possible decline of 5 TWh from current consumption levels. Setting a lower bound for biomass consumption for heating is reasonable because adjustment of individual heating devices to new economic conditions generally takes a lot of time.

2.4. Uncertainty

Most of the parameters in the study are of high uncertainty. Uncertainties on the performance and costs of various technologies as well as uncertainty about future energy prices are high. We explicitly address this issue by performing Monte-Carlo simulations of the MIP model and conducting an extensive sensitivity analysis. We first define plausible ranges for the uncertain parameters from a literature research and assume that the parameters are distributed uniformly within that range. For energy and CO_2 prices, correlation between the prices of oil, gas, gasoline and CO_2 are determined from historical spot prices**.** The input data for the Monte-Carlo simulation is generated by performing a Latin Hypercube Sampling procedure and combining it with the Iman-Conover method to guarantee correlation of correlated parameters in the procedure [14]. Latin Hypercube Sampling is used to guarantee that the whole parameter range is covered in the Monte-Carlo simulations. Results are given in form of probability distributions and a stepwise regression analysis is performed to examine the sensitivity of results to input parameters. The assumption on the distribution of the most important parameters is reported in Table 1. Further parameters modelled stochastically are biomass costs, conversion efficiencies and investment costs of bioenergy plants.

Table 1: Main model parameters and uncertainty ranges

	Lower Bound	Upper Bound
Price of oil (€ MWh^{-1})	40	60
Price of gas (€ MWh^{-1})	30	50
Price of gasoline (€ MWh^{-1})	42	62
Price of electricity (€ MWh^{-1})	54	74
Price of carbon (€ MWh^{-1} tCO_2^{-1})	21	55
Battery costs (€)	4,000	6,500
Replacement distance battery (km)	70,000	90,000
Investment costs electric cars (w/o battery) (€)	14,000	16,500
Investment costs gasoline cars (€)	16,500	16,500
Investment costs diesel cars (€)	17,000	17,000
Investment costs gas cars (€)	17,500	17,500
O&M costs electric car (€ km^{-1})	0.02	0.025
Conversion efficiency car – Gasoline (km MWh_{fuel}^{-1})	2,000	2,200
Conversion efficiency car – Diesel (km MWh_{fuel}^{-1})	2,250	2,450
Conversion efficiency electric car (km MWh_{elec}^{-1})	5,600	7,000

2.5. Scenarios

We model one baseline scenario, that assumes no policy intervention at all, and 7 policy scenarios. Three of the scenarios assume that 5% (*S5*), 10% (*S10*) and 15% (*S15*) of the transportation sector are supplied by bioenergy, allowing all technologies to be selected by the model. The other four scenarios examine the impact of a 10% target of renewable transportation fuels, if only single technologies (i.e. ethanol (*eth*), methanol (*met*), sng (*sng*), electric mobility (*emo*)) are allowed. Biodiesel is not modelled in these scenarios because domestic feedstock production is too low to supply 10% of the transportation sector with biofuels.

3. Results

3.1. Technologies and fuel utilization

The first three scenarios allow free choice of technologies. Biodiesel and methanol supply the biofuels in these scenarios. Biodiesel is however limited at around 0.5 TWh due to restrictions in feedstock supply of oil-crops. Second generation methanol is the supplement to biodiesel to complete the full target. E-Mobility plays a role in the first three scenarios - however, variation is very high and the contribution is significantly lower than that of methanol. Ethanol and SNG are not selected in the first three scenarios. These results indicate that methanol production can be considered superior to ethanol in terms of costs – although the variation of results is generally high, the dominance of methanol over ethanol is stable. Competing bioenergy technologies (i.e. heating and power production) are mainly reduced in *S15, met* and *SNG*. This is due to the high demands for woody biomass for biofuel production which increases prices for the feedstock and therefore makes production of power and heat partly unprofitable. The ethanol scenario has less influence on the woody biomass market as ethanol feedstock competes with food and feed crops. Biodiesel is mainly used in the freight sector where it substitutes diesel. Ethanol and methanol are used for personal transportation in driving classes with low annual distances because fixed capital costs contribute more to the total costs of transportation in those classes than the distance dependent fuel costs. Higher classes with higher annual driving distances are more likely to be supplied by electric cars where the influence of the high capital costs of the car and the battery decrease and the fuel costs become more important.

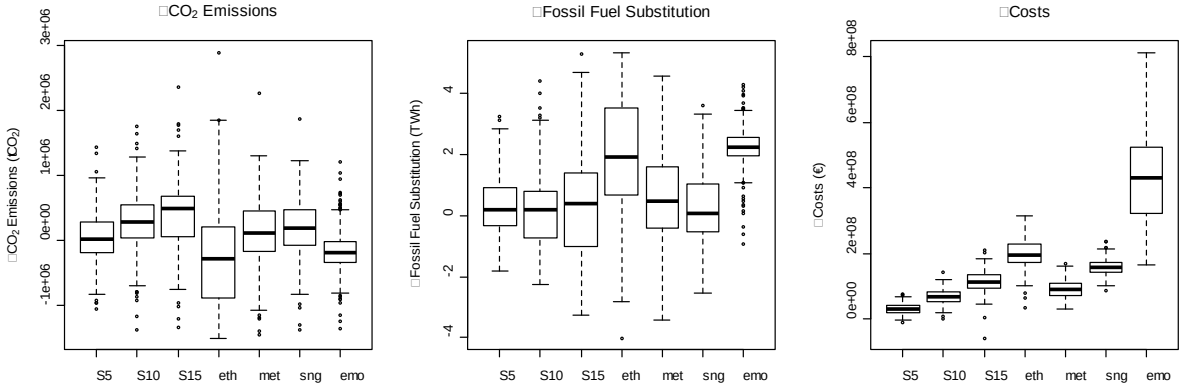

Fig. 2: Differences in CO_2-Emissions, Fossil Fuel Substitution and Costs between the baseline and the biofuel scenarios.

3.2. CO_2 Emissions, Fossil Fuel Substitution and Costs

Figure 2 shows CO_2 emissions, fossil fuel substitution and costs calculated as the difference from the baseline scenario. A significant reduction in CO_2 emissions and an increase in fossil fuel substitution are achieved by the *eth* and the *emo* scenario. These two scenarios also have highest costs. The variance of costs is highest in *emo* due to the large uncertainties in the development of the costs of electric vehicles. However, the model only considers domestic GHG emissions while effects of indirect land use change on GHG emissions are not modeled.

3.3. Land use

While the *eth* policy substitutes a lot of fossil fuels, the land use effects are also substantial in comparison to the other policy scenarios (See Figure 3). Up to 200,000 ha of agricultural land are converted to energy crop production while all other scenarios stay well below 50,000 ha. This implies that food and feed production is reduced significantly in the *eth* scenario while all other policies have rather low impacts on the production of other agricultural products. There are two reasons for this: first, productivity is higher for second generation fuels and for electric mobility due to higher total conversion efficiencies (see Figure 3). Second, these technologies rely on lignocellulose resources that may come from additional forest harvesting or that may otherwise be used for power and heat production (see Figure 3, bottom-right). There are also important differences between the *S10*, *met*, *sng* and *emo* scenarios. Combining biodiesel and methanol for the biofuel goals as in *S10* reduces land use change in comparison to the methanol only scenario. Biodiesel therefore plays a small, but important role in the technological portfolio. Figure 3 shows that *SNG* is more efficient in converting biomass than methanol. Electric mobility has by far the lowest impact on land use change and on additional forest wood utilization.

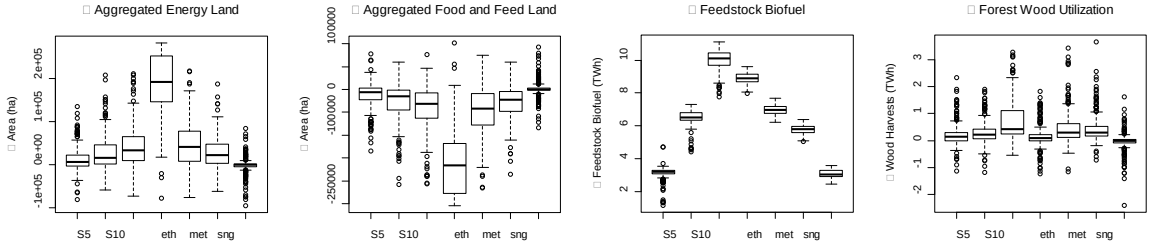

Fig. 3: Differences in Land Use, Feedstock Utilization and Forest Wood utilization between the baseline and policy scenarios.

3.4. Sensitivity Analysis

Table 2 show the results of the sensitivity analysis performed on the results of the *S15* scenario. We checked for the influence of parameters on the deployment of electric mobility to show which factors mainly influence the competition between second generation fuels and electric mobility by performing a regression of the input parameters on the output variables (a stepwise regression procedure is used). The regression coefficients are normalized. The most important input parameters regard the cost for the electric car (i.e. battery costs, investment costs, O&M). The carbon price and the kilometers until replacement of battery also prove to significantly influence the results while the gasoline price does not show significant influence on results.

4. Discussion

Results of our study are in line with other studies that estimate lower land use for bio-electric-cars than for biofuel production [10]. They are also in line with studies that come to the conclusion that battery replacement costs are currently the biggest economic barrier to the large scale introduction of electric mobility in the transportation sector [8], [9]. However, there are additional barriers to electro-mobility that were not modelled within this study: the change from cars that are refuelled at gas stations in very short time to cars that need hours of recharging and that have a comparably low driving range probably plays a more important role than sole considerations of the *tco*. The model results indicate that drivers who use their car a lot are more likely to choose electric cars than those with low car utilization because of lower fuel costs. However, technical reasons may impede the utilization of electric cars for those drivers: the low range and the high recharging times may render electric cars impractical for them. With respect to economics, renewable electricity production from wind or small water power plants may produce electricity at much more competitive costs than biomass powered thermal plants. Therefore, electric cars may be more competitive than stated in this study due to lower fuel costs from renewables. The GHG emission effects of biofuel policies have to be considered in conjunction with the land use change that is caused by the expansion of biofuel production. The GHG emissions stated in this paper do not include indirect or leakage effects of the policies. However, it can be clearly stated that fuelling electric cars with electricity produced from biomass induces by far the least change of land use and can therefore be considered to also minimize leakage effects.

*Table 2: Results of sensitivity analysis. Confidence levels: *** 0.999, ** 0.99 and * 0.95*

	Coefficient	
Amount of electric mobility (R^2 0.49)		
Battery Costs	-0.54	***
Investment costs electric car	-0.28	***
O&M costs electric car	-0.12	*
Gasoline price	0.08	
Kilometers until replacement of battery	0.15	**
Carbon price	0.17	**

5. Conclusions

Second generation biofuels have less impact on land use than first generation ethanol due to two reasons: yields of biofuel per hectare are higher for agricultural land and the feedstock may additionally come from forests. Biodiesel has high yields per hectare, but the total domestic potential is limited at a low level. The lowest land use is implied by the utilization of

electric cars, which, at current technological standards, are still very costly in comparison to cars fuelled by liquid fuels. With respect to policies for promoting second generation biofuel production, one has to consider that investments in second generation biofuel production will have a long-term effect on the utilization of biomass resources. The results of the study indicate, however, that the gains in efficiency in relation to first generation fuels are relatively low while significant efficiency increases can only be expected when developing a transportation system based on electricity. A large scale introduction of second generation biofuels has to be considered very carefully therefore and in the light of a possible total restructuring of the transportation sector within the next 20 to 30 years.

References

[1] T. Searchinger et al., "Use of U.S. croplands for Biofuels Increases Greenhouse Gases Through Emissions from Land Use Change," *Science*, vol. 319, no. 5867, pp. 1238-1240, 2008.

[2] P. Havlík et al., "Global land-use implications of first and second generation biofuel targets," *Energy Policy*, p. doi:10.1016/j.enpol.2010.03.030, 2010.

[3] B. A. Bryan, D. King, and E. Wang, "Biofuels agriculture: landscape-scale trade-offs between fuel, economics, carbon, energy, food, and fiber," *GCB Bioenergy*, vol. 2, no. 6, pp. 330-345, 2010.

[4] P. Dauvergne and K. J. Neville, "Forests, food, and fuel in the tropics: the uneven social and ecological consequences of the emerging political economy of biofuels," *Journal of Peasant Studies*, vol. 37, no. 4, p. 631, 2010.

[5] L. Kranzl and R. Haas, *Strategies for the optimal development of biomass potentials in Austria until the year 2050 aiming at a maximal reduction of green house gas emissions (Strategien zur optimalen Erschließung der Biomassepotenziale in Österreich bis zum Jahr 2050 mit dem Ziel einer maximalen Reduktion an Treibhausgasemissionen).* Energy Economics Group, University of Technology Vienna, 2008.

[6] R. Winter, *Biokraftstoffe im Verkehrssektor in Österreich 2008 (Biofuels in the transportation sector in Austria 2008)*. Umweltbundesamt, 2010.

[7] J. Lange, "Lignocellulose conversion: an introduction to chemistry, process and economics," *Biofuels, Bioproducts and Biorefining*, vol. 1, no. 1, pp. 39-48, 2007.

[8] C. Sandy Thomas, "Transportation options in a carbon-constrained world: Hybrids, plug-in hybrids, biofuels, fuel cell electric vehicles, and battery electric vehicles," *International Journal of Hydrogen Energy*, vol. 34, no. 23, pp. 9279-9296, 2009.

[9] C. Thiel, A. Perujo, and A. Mercier, "Cost and CO2 aspects of future vehicle options in Europe under new energy policy scenarios," *Energy Policy*, vol. 38, no. 11, 2010.

[10] J. E. Campbell, D. B. Lobell, and C. B. Field, "Greater Transportation Energy and GHG Offsets from Bioelectricity Than Ethanol," *Science*, p. 1168885, 2009.

[11] O. van Vliet, M. van den Broek, W. Turkenburg, and A. Faaij, "Combining hybrid cars and synthetic fuels with electricity generation and carbon capture and storage," *Energy Policy*, vol. 31, no. 1, 2011.

[12] S. Bram, J. De Ruyck, and D. Lavric, "Using biomass: A system perturbation analysis," *Applied Energy*, vol. 86, no. 2, pp. 194-201, 2009.

[13] Environmental Protection Agency, *Regulation of Fuels and Fuel Additives: Changes to Renewable Fuel Standard Program; Final Rule*. 2010.

[14] A. Saltelli and MAT, *Sensitivity Analysis*. Chichester [u.a.]: Wiley, 2000.

Technological challenges for alternative fuels technologies in the EU. A well-to-Tank assessment and scenarios until 2030 considering technology learning

Felipe Toro[1*], Martin Wietschel[2]

[1] *IREES GmbH, Schoenfeldstraße 8, 76131 Karlsruhe, Germany*
[2] *Fraunhofer Institute for Systems and Innovation Research, Karlsruhe, Germany*
**Felipe Toro. Tel: +49-721-915263621, Fax:+49-721-915263611, email: f.toro@irees.de*

Abstract: The initial step of this analysis corresponds to the evaluation of the current state of the art (SoA) for various alternative fuels (AFs) and alternative sustainable automotive technologies (ASATs) across Europe, taking into account their detailed energetic, environmental and economic variables. The method to assess economic and environmental performance of AFs and ASATs corresponds to a well-to-tank (WTT) and tank-to-wheel (TTW) assessment complemented by scenarios until 2030, with projections of reference and high prices of major input variables of analysis. This analysis determines short and long term economic performance taking into account technology learning. 2nd generation biofuels offer potentials for meeting future fuel-energy demand, and are currently supported by main governments and programs. Initial results of this study also indicate that second generation biofuels offer promising solutions in terms of environmental performance but production costs, conversion efficiencies and by-products are major challenges that can influence the overall economic performance considerably. In addition, price volatilities for first generation biofuels feedstock play a major role on the competitiveness and economic performance of these fuels.

Keywords: *Sustainable transport, Low carbon fuels, Alternative fuels, Mobility technologies, Economic assessment*

1. Introduction

Biofuels and alternative fuels (AFs) have emerged strongly since last one decade as sustainable alternatives for the reduction of fossil fuel energy demand and emissions in the transport sector. Various AF production options include 1st generation biofuels (biodiesel and bioethanol) obtained from well established fermentation, oil extraction and trans-esterification processes, as well as emerging 2nd generation biofuels via BTL, gasification, CTL and other processes. Currently, several technological challenges and bottlenecks exist in different AF production options at different levels across the whole supply chain. Biomass supply constraints, inefficient and capital intensive production processes, fuel transportation and supply, onboard usage related problems and many others are such challenges that affect the success and proliferation of these AFs. The expected economic and environmental performance of these alternatives require not only a clear understanding of the current state of the art, but also a comparison between various alternatives along the complete supply chain as "well-to-tank" and "tank-to-wheel" analysis. Within this study, scenarios for the future development of the most important input variables in different AF production pathways have been defined with feedstock costs and production-scale effect variations that influence the overall economic performance.

2. Methods and modelling structure

The current state of the art and developments of AFs and ASATs have been studied by various authors in different projects and studies. In this study, the characterization of technologies along the whole technology cycle included an extensive literature review including research papers, studies, industrial information, etc. from 2003 until 2010, as well as expert's interviews and assessments in order to screen the state of development of alternative fuel technologies along the technology cycle curve (S-Curve) [1,4]. State of the art updates and projections until 2030 were collected for 26 different AFs pathways through

techno-economic databases including information on biomass feedstock requirements, production process input characterizations (inputs, quantities, efficiencies, costs, emissions) and other techno-economic and techno-environmental parameters. The main formulas and assessments used in this study include the annual cost of capital (ACC):

$$\mathbf{ACC} = \frac{IR}{1-\left(\frac{1}{(1+IR)^{Te}}\right)} * Ti * 1 - \left(\frac{1}{(1+IR)^{Te}}\right) * \left(\left(\frac{Tt-Te}{Tt}\right)\right)$$

Ti corresponds to total investments, *Te* to economic lifetime and *Tt* to technical lifetime while IR is the interest rate. For this particular research it was established as 8% for all AF technologies; however it could be higher for 2nd generation and other unavailable technologies due to risks related. Total costs have been estimated as the sum of capital costs and O&M costs which were either found in existing examples or estimated based on the technical configuration of plants and assuming operating conditions (e.g. annual operation hours) by taking into account maintenance due to associated risks of new technologies [1,2,4].

2.1. Technology Learning

Technology learning is projected in the future development of specific investment costs based on the cumulative number of plants in relationship to an assumed progression ratio [4,5,6,7,8]. The currently existing plants especially for 2nd generation AF technologies are either very new or with short commercial history thus making it difficult to have reliable data and technology experience. Therefore, this parameter has been built as an adjustable progress ratio (***Pr*)** as experienced in case of other industries like aviation, machinery, wind mills etc. and it reflects a maximum of 10 to 30% progress ratio differentiated in small and large scale plants. The following equation indicates the specific investment costs ***(SIC)*** taking into consideration total investments ***(Ti)*** and installed capacities ***(Ic).*** The indicator ***TPI*** corresponds to a technological progress indicator based on the assumed cumulative number of plants as function of time within 5 years periods.

$$\mathbf{SIC} = \frac{\mathbf{Ti}}{\mathbf{Ic}} * \mathbf{TPI} * \left(\frac{\mathbf{Log\ Pr}}{\mathbf{Log\ 2}}\right)$$

2.2. Well to Tank (WTT) and Tank to Wheel (TTW) assessment

The WTT assessment in this study relates to the amount of energy expended and the associated GHG emitted in various steps involved in production and delivery of the fuel. The economic assessment of the pathways considers the scale of production and revenue generated through by-products and other associated production costs. Depending on inputs, WTT economic performance [c€/kWh] and CO_2 emissions have been calculated with the steps involved in producing one kWh of alternative fuel and the corresponding inputs (like electricity, heat, fuel and biomass feedstock) as well as the corresponding emissions factors for each particular input variable. This detailed WTT analysis of the pathway(s) describes various processes involved in cultivation of the feedstock until the distribution of finished fuel at the filling station. The TTW assessment accounts for the energy expended and the associated GHG emitted by the fuel and vehicle technology combinations. In this assessment, the internal combustion engine vehicles were considered to propel with pure biofuel (such as ETBE, FT-diesel) or blended with conventional fossil fuel (E85, B5) [3,4,11]. Complete WTW CO2 emissions were assessed by combining the emission generated during the fuel production pathways WTT [gCO2eq/km] and TTW [gCO2eq/km] emissions generated by combustion of fuel at the level of vehicle. The data that WTW assessment includes are the WTT emitted GHG and expended energy (i.e. excluding the energy content of the fuel itself)

per unit energy content of the fuel [MJf/100 km] and the TTW energy consumed by the vehicle per unit of distance covered.

3. Assumptions

3.1. WTT – Technology Pathways

Biofuel technology pathways were pre-selected by carrying out a pathway analysis based on the evaluation of costs and emissions performance at various stages of production until delivering biofuel at the filling stations. Year 2010 was selected for comparison between conventional and advanced biofuels, as AFs were to have a commercial start up onwards. In the respect of WTT assessment, 26 biofuel pathways were analyzed in this research and they are described in detail below.

Biodiesel pathways stated include rapeseed and sunflower grain cultivation and transportation to the extraction of oil in small scale (SS) or large scale (LS) extraction plants, production of biodiesel in small scale (SS) or large scale (LS) plants, distribution by trucks and storage at filling station (FS). The consideration of by-products for the assessment result in *8 pathways* for the case of biodiesel as indicated below.

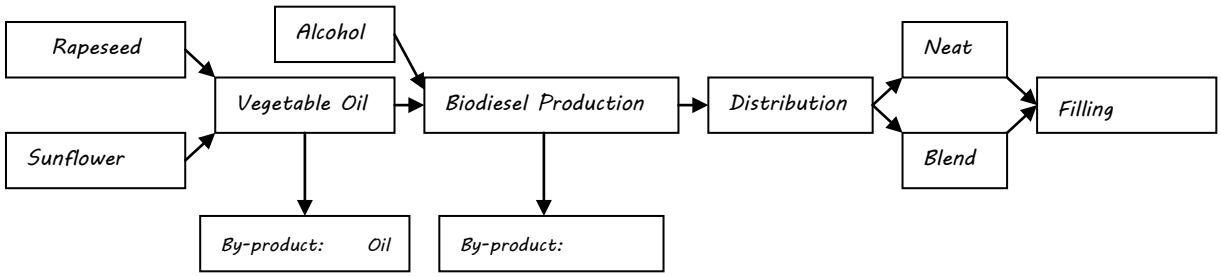

Figure 1: Biodiesel WTT pathways
Source: [1,2]

For bioethanol, *12 WTT pathways* were analysed for both conventional (1st generation) and advanced options (2nd generation) considering biomass production and transport, bioethanol production and distribution until the filling station (FS). Bioethanol production is modelled in small scale (SS) and large scale (LS) plants and the revenues generated from by-products were considered for the assessment (separate pathways for by-products revenues). For lignocellulosic ethanol, by-products have been considered along all the pathways but the differences lie among the feedstock used.

The six BTL Pathways (Figure 3*)* take into account the scale of production plants (small scale, medium scale and large scale) as well as the use of by-products (electricity, heat) however, the differences lie on the biomass pre-treatment techniques using either pyrolysis oil or woodchips pre-gasification in small, medium and large scale F-T Diesel production plants. Power generation data is currently based on demonstration or CHP standard configurations on efficiency and costs. The use of power generation by BTL has the highest contribution to reduce emissions and increase competitiveness.

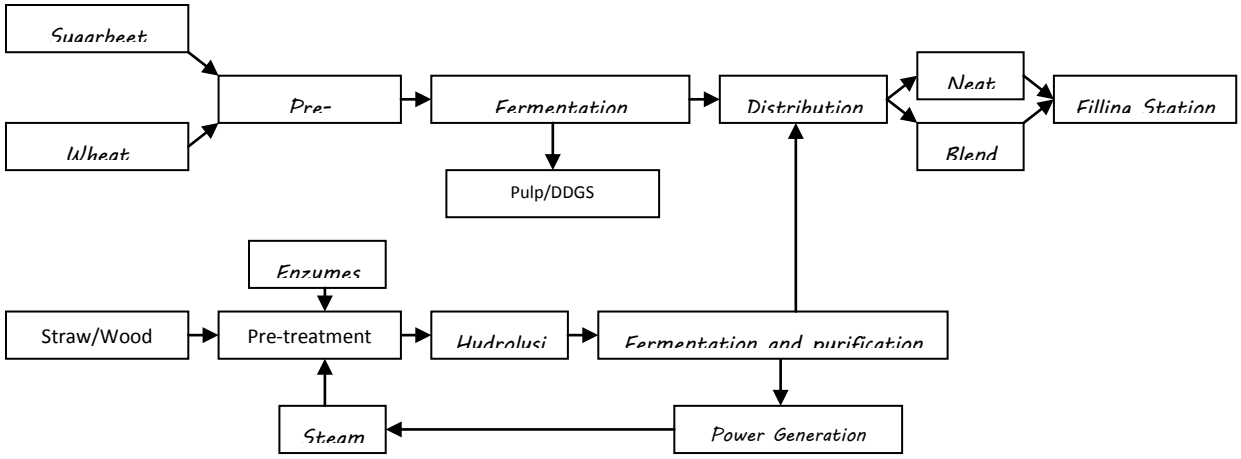

Figure 2: Bioethanol WTT pathways
Source: [1,2]

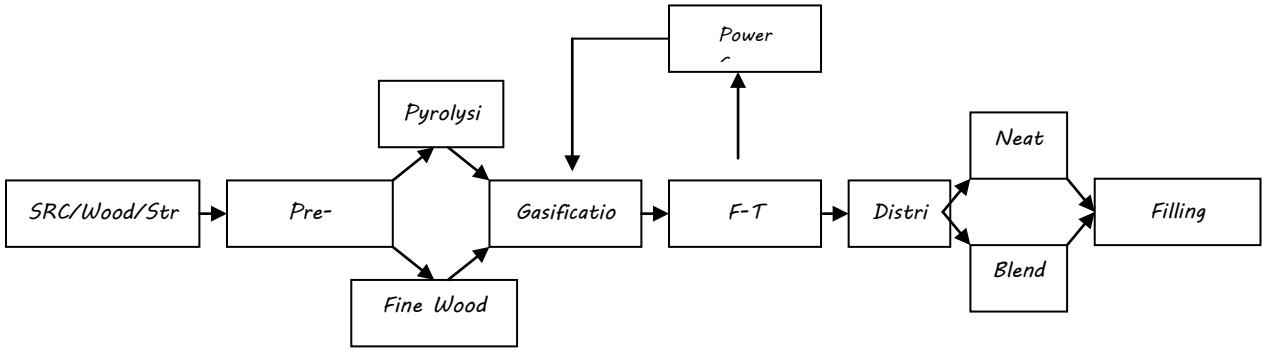

Figure 3: Biomass-to-Liquids Pathways
Source: [1,2]

3.2. Scenarios definition

One *reference and* one *high price* scenarios are defined in this research including the projection of the most important drivers for the production development of alternative fuels AF (e.g. feedstock prices, input prices, co-products). This is a new approach combining not only a mere techno-economic characterization of several technologies but simulating future economic performance under changing the most important parameters dynamically in 5 years steps until 2030. The scenario I (reference) projects until 2030 the most important input materials for alternative fuels production such as biomass feedstock prices, electricity, heat and fuels. The projection reflects conditions before the economic crisis for scenario I considered as a *reference* projection. Scenario II reflects a high prices environment for the same parameters.

With respect to the technology learning the progress ratio, shown as indexed changes in percentage below, reflects enhanced learning as cumulative capacities and production are achieved (scenario II). However, the technology learning projections partially simulate a normal and enhanced learning conditions for AF technologies not directly correlated with the price development of scenario I and II. The values for the major inputs projections for both scenarios and progress ratios are shown in Figure 4 in [c/kWh] and Figure 2 in [%].The projections have been cross checked with experts' assessments and the review of several studies on feedstock prices since 2004 until 2010 [1,2,4,9,10,11]; however, Figure 4 projections assumptions have been made based in correlation with the development of the

projected diesel prices for both reference and high price environments. Two progress ratios changes for technology learning are assumed for modelling technology learning possibilities as shown in Figure 5.

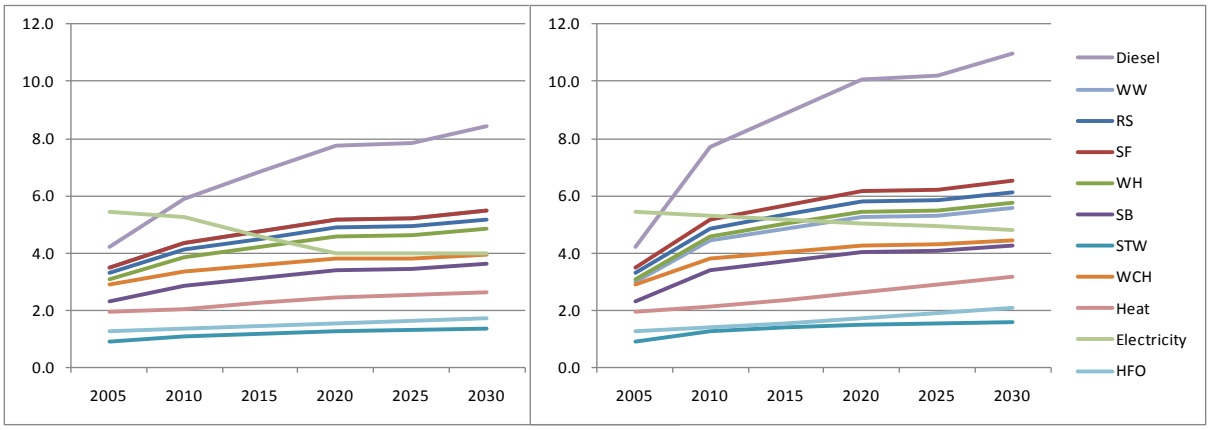

Figure 4: Assumed price changes for AF technologies inputs for scenario I (left) and II (right) until 2030 – [c/kWh]

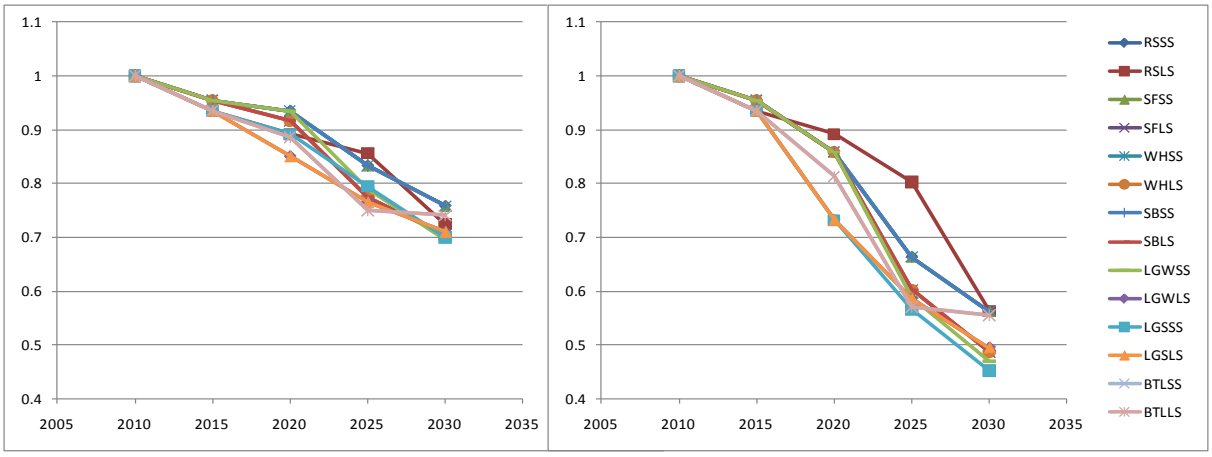

Figure 5: Changes in progress ratios (PR) for AF technologies (large and small scales) for scenario I (left) and II (right) until 2030- [% - index year 2010]

The scenario assumptions should be carefully interpreted as they have strong interaction with other variables (e.g. yields, climate conditions, dietary changes, etc) not directly modelled in the present construct. These scenarios have been defined for all pre-selected pathways, in particular with their inputs such as feedstock for 1st and 2nd generation biofuels, heat, electricity or heavy fuel oil (HFO) among others. In addition, a further assumption is done for technology learning with lower or higher progress ratios in 5 years steps differentiated for small and large scale units.

4. Results and discussion

Results of WTT assessment are illustrated for biodiesel and bioethanol pathways in Figure 6 and Figure 7. BTL results are also available but omitted in graph form due to space limitation. Both figures illustrate the economic performance changes of AFs pathways for both the *reference and high price* scenarios as well as due to the considerations in enhanced technology learning progress ratios for the years 2010 until 2030 in 5 years steps. The number below the graphs corresponds to the number assigned to the pathway for each particular

alternative fuel analysed. Pathway 1[1] (2010) and 27 (2030) for example are identical in configuration but 27 reflects 2030 results. Production economic performance increases 17% in scenario *reference* while almost 20% in scenario II compared to 2010 values. A 2.5% annual increase of rapeseed prices until 2030 (high prices) increases in 16% the costs for oil extraction and biodiesel production when compared to the *reference scenario*. The learning effects are observed in the right side graphs where pathway number 27 reduces its cost performance in further 2% by learning with high progress (experience) ratios of 75% for large scale plants and 80% for small scale plants.

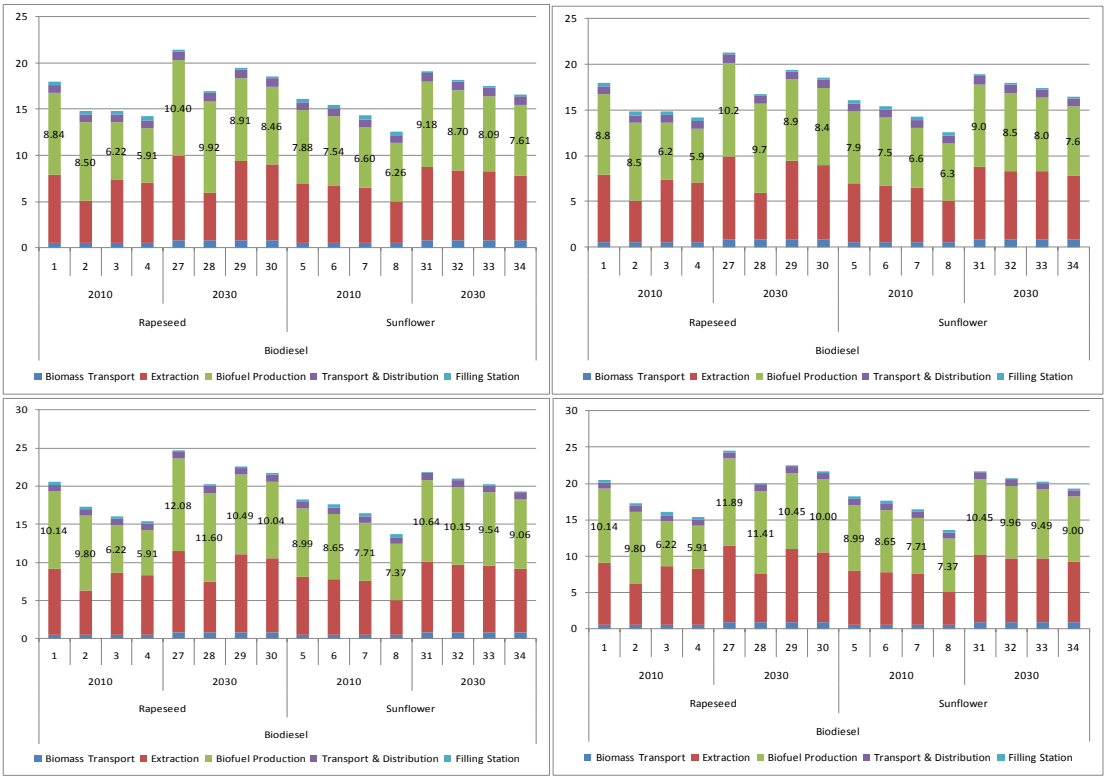

Figure 6: Results of the integrated WTT analysis (economic performance) for Biodiesel pathways for scenario I and II (up) and technology learning (right side graphs)- [c/kWh]

For biodiesel, as observed in the figures, pathways corresponding to large scale facility production, taking into account by-products credits, perform better with respect to economics (and emissions). The major part of the costs for all pathways corresponds to the extraction and production, especially the biomass feedstock prices varying from 50 to 85% of total producing costs. Oil extraction and subsequent biodiesel production are highly sensible to the variation on agricultural production costs.

Bioethanol pathways are grouped for starch (cereals) and sugar-beet crops and lignocellulosic biomass options (straw-2nd generation). The results indicate that the largest part of the costs for all options correspond to bioethanol production, of which the biggest share corresponds to the biomass costs and delivery at the bioethanol production facilities. Non-agricultural biomass feedstock (e.g. Straw) is less vulnerable to feedstock prices changes than the agricultural feedstock for 1st generation bioethanol, exhibiting higher vulnerability to volatile sugar and cereals markets. The benefits from increased learning rates remain marginal for

[1] Biodiesel from Rapeseed in *large scale* facility without by-products credits. Pathway 2 considers by-products also large scale. Pathway 3 and 4 are small scales with the same by-products considerations.

most of the producing options despite of a strong increase in experience (lower ratios) and therefore lower costs.

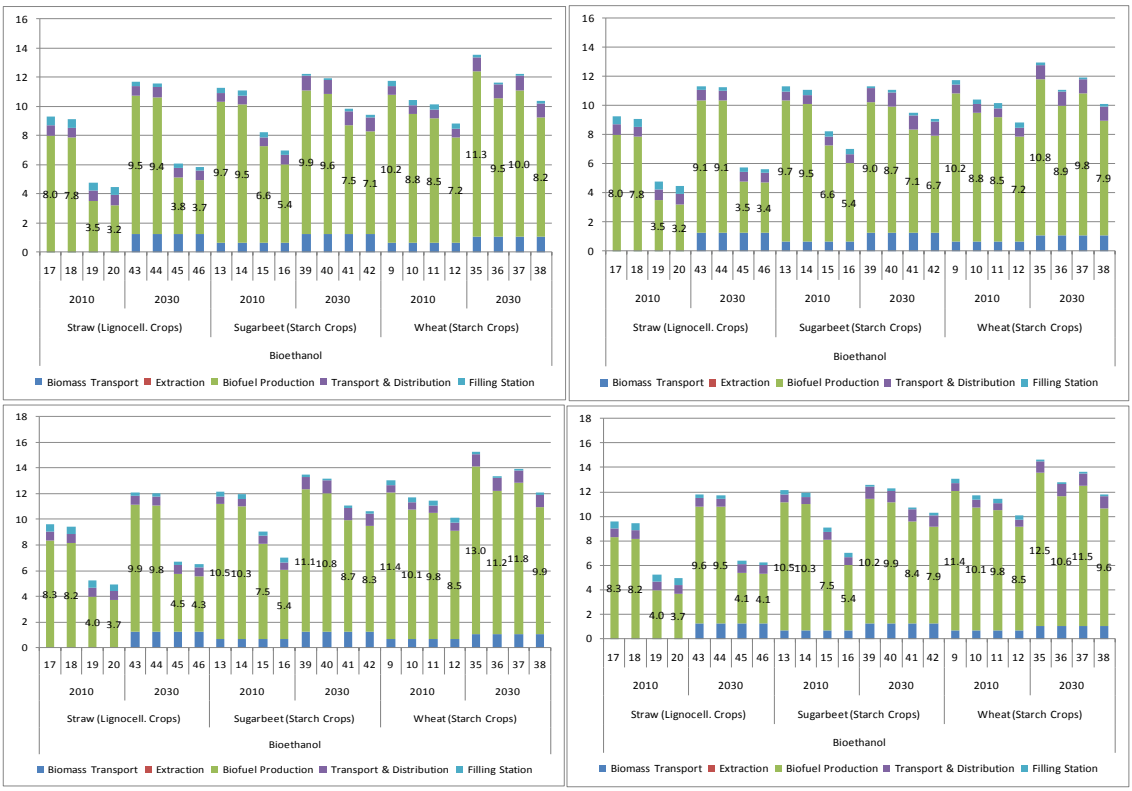

Figure 7: Results of the integrated WTT analysis (costs) for Bioethanol pathways for scenario I and II and technology learning (right side graphs)

The best cost performance corresponds to large scale plants considering by-products credits for animal feed substitution for both cereal and sugar crops. Large scale lignocellulosic bioethanol performs also better in 2010 while in 2030 it also demands logistically an organized supply of straw, however outperform compared to 1st generation options in *reference and high price* scenarios. However, such a facility does not exist currently in the market and this is just an indicative value of the cost ranges of these technologies. Furthermore, short rotation crops (wood) as feedstock for the production of bioethanol with similar plant characteristics have been used in the analysis. This technology is still in development phase and it could mean that higher capital expenditures, especially for large capacities are needed. This technology will enter the market only around 2010 and onwards, and efficiency improvements as well as capacity enlargements are expected to reduce costs in the future. Within the results, the highest emission reduction potentials are obtained for BTL facilities as the energy spent in the process is recovered using the co-generated gas to produce electricity and heat that can be reused internally in the process (self-sufficiency). Followed by the BTL facilities, the second highest reduction potentials are obtained from lignocellulosic ethanol. For biodiesel and bioethanol further emissions improvements are achieved when considering by-products credits as they substitute other materials.

5. Conclusions

The strong dependency of 1st generation alternative fuels on agricultural feedstock is observed in the results for their reference and high price scenarios developments. These technologies have still the potential to achieve costs reductions through learning, increase production, economies of scale; however, the results presented here only show a marginal benefit to increase economic performance. The high volatility of agricultural markets combined with

strong climatic changes and increase in food demand poses higher pressures to producers to develop strategies that keep supply prices down. However, the results of this analysis indicate that large scales plants might have the possibility to perform better than smaller producers, partially also reflected on the possibility to have stocks (not modeled here), however, there are high direct increases in the economic performances of these options in these kind of fuels in high price scenarios prospects. Bioethanol pathways (2^{nd} generation (4-9.5 c/kWh) and starch/cereals 8-11 c/kWh) are close to get competitive with diesel projected prices in 2030 for both large and small scale configurations with by-products credits. Biodiesel inputs are strongly correlated with diesel prices increases and therefore results indicate that these pathways remain uncompetitive. BTL results for high price scenario considering stronger technology learning (ca. 7.8 - 12 c/kWh) are closer to be competitive to diesel projected prices in 2030 for large scale configurations with centralized biomass treatment concepts.

Furthermore, advanced AFs (2^{nd} generation biofuels) that are in R&D and Demonstration phase (non commercial technologies) pose higher risks for investors despite of the fact that they could have faster technology learning when entering the markets especially for certain portions of second generation routes such as lignocellulosic, BTL and Hydrogen. These options are high capital intensive with still unresolved technological challenges on biomass supply possibilities; meet end-use properties like energy content, chemical stability, refueling infrastructure, storage and ex-ante feedstock price projections. The better economic performance observed in these results are partially true in case lower biomass waste streams are used or high value by-products (co-generation) add to the income flows. However, these results should be considered cautiously as the input data for the simulation is based on data that is to be proved in real operating conditions that at the moment can only be obtained by demonstration or pilot projects. In emissions terms, pathways performing better relate to the ones where by-products credits are taken into account especially co-generation plants which definitely will reflect emissions reductions, requiring on the other hand more investments for additional facilities.

References

[1] Toro F, Hasenauer U, Wietschel M, Schade W (2008): Technology trajectories for transport and its energy supply.
[2] Toro, F. Techno-Economic Assessment of Biofuels in Europe, Working Paper Fraunhofer ISI, 2004, 2005.
[3] CONCAWE, EUCAR, JRC EU Commission, Well to Tank Reports, 2006, 2007, 2008.
[4] Toro, F. A., Reitze, F., Ajanovic, A., Hass, R., et al. (2010). State of the art for alternative fuels and alternative automotive technologies. Karlsruhe, Germany.
[5] Argote, Linda; Beckman, Sara L.; Epple, Dennis, 1990. 'The Persistence and Transfer of Learning in Industrial Settings'. Management Science 36(2): 140-154
[6] Dutton, John M.; Thomas, Annie, 1984. 'Treating Progress Functions as a Managerial Opportunity'. Academy of Management Review 9(2): 235-247
[7] Resch, G., Faber, T., Haas, R., and Huber, C. (2004): Experience Curves vs Dynamic Cost-Resource Curves. In: Energy & Environment, 15, pp. 309-321.
[8] Resch, G., Held, A., Toro, F., Haas, R., et. al., (2008): Potentials and prospects for renewable energies at global scale. In: Energy Policy, 36 (11), pp. 4048-4056.
[9] Toro, F.; Held, A., Ragwitz, M.; (2009): Assessment of the Potentials for Renewable Energy Sources. In: Ball, M.; Wietschel, M. (eds.): The Hydrogen Economy. Cambridge University Press, Cambridge, pp. 135-168.
[10] E4tech (2008): Biofuels Review: Greenhouse gas saving calculations; for the Renewable Fuels Agency, June 2008.
[11] OECD/FAO (2009). OECD-FAO Agricultural Outlook 2009-2018

Impact of Plug-in Hybrid Electric Vehicles on Tehran's Electricity Distribution Grid

S. M. Hakimi[1,*], S. M. Moghaddas-Tafrshi[2]

[1] *K. N. Toosi University, Terhran, Iran*
[2] *K. N. Toosi University, Terhran, Iran*
Energy Management and Distribution Lab
** Corresponding author. Tel: +989124798639, Fax: +982188462066, E-mail: sm_hakimi@ieee.org*

Abstract: Hybrid electric vehicles (HEVs) are commercialized and plug-in hybrid electric vehicles (PHEVs) are becoming more popular. PHEVs are charged by plugging into electric outlets or on-board electricity generation. These vehicles can drive at full power in electric-only mode over a limited range. As such, PHEVs offer valuable fuel flexibility. The charging of PHEVs has an impact on the distribution grid because these vehicles consume a large amount of electrical energy and this demand of electrical power can lead to extra large and undesirable peaks in the electrical consumption. The improvements in power quality that are possible by using coordinated charging are emphasized in. It also indicates that not coordinating the charging of PHEVs decreases the efficiency of the distribution grid operation. Several automakers are preparing for the next generation of passenger transportation, Plug-in Hybrid Electric Vehicles (PHEVs). Using data from the Tehran Regional Electric Company (T.R.E.C), this study sought to understand how different charging scenarios for PHEVs could impact electricity demand in Tehran.

Keywords: *Plug-in hybrid electric vehicles; Charging scenario; Distribution grid*

1. Introduction

Plug-in hybrid electric vehicles (PHEVs) are a new and upcoming technology in the transportation and power sector. As they are defined by the IEEE, these vehicles have a battery storage system of 4 kWh or more, a means of recharging the battery from an external source, and the ability to drive at least 10 miles in all electric mode [1]. These vehicles are able to run on fossil fuels, electricity, or a combination of both leading to a wide variety of advantages including reduced dependence on foreign oil, increased fuel economy, increased power efficiency, lowered greenhouse gas (GHG) emissions and vehicle-to-grid (V2G) technology [2–4]. These claims are backed by data suggesting that fueling a PHEV would cost the equivalent of 70 cents per gallon of gasoline when electricity costs 10 cents per kWh [4] and that an all electric driving range of 40 miles could lower oil consumption by two-thirds [4]. Currently, there is little storage available in the power grid so demand and generation must be perfectly matched and continuously managed to avoid frequency instabilities. PHEVs have an energy storage capacity which is rather small for each individual vehicle, but the number of vehicles will be large, yielding a significant energy storage capacity. At any given time, at least 90% of the vehicles are theoretically available for V2G [5,6]. These vehicles must be connected to the grid when idle. There must be enough vehicles plugged in during the day to provide grid services therefore it could be beneficial to give incentives to vehicle owners to stay plugged in. Most of the weekdays, vehicles follow a schedule which does not vary much from week to week [5]. The electrical storage of PHEVs could provide grid services via V2G concept and add a surplus value to the vehicle owner [7]. The reason for choosing Tehran for this study is the air pollution. Cut oil subsides in Iran is another reason for choosing Tehran for this study. At such low prices, domestic demand for energy in Iran has grown very rapidly. With the price reform, you will dampen domestic demand, which means more efficient energy use domestically, more energy available for profitable exports, and higher revenues for the country. From a domestic perspective, if prices are higher, the energy sector in Iran will become more profitable and hence be able to invest,

extract, and produce more. Furthermore, if the Iranian people are able to restrain their consumption, this will have a positive side effect on the global oil market. This will also push the domestic automobile industry to modernize itself. The country produces about 1.5 million cars per year, targeting the domestic market of 74 million people. Since gasoline is almost free, carmakers have little incentive to make their product energy efficient. But when gasoline price rises to the international level, Iranian car manufacturers will have to change the way they operate and increase the energy efficiency of their vehicles. Once this happens, Iranian-made cars will be more competitive on the export market.

2. Transition from conventional vehicles to Plug-in Hybrid Electric Vehicles (PHEV)

For the first time it was German inventor, Nikolaus Otto, who made it possible to use combustions engines in cars for the first time by the invention of the first four-stroke internal combustion engine in 1862. These types of engines are continuously being used in so-called conventional vehicles. The low-efficiency of ICE (Internal Combustion Engines) and high emission production are the most negative points about these types of vehicles. In the figure 1, the recent development in car industry is been shown.

Figure1. Schematic on development in car industry

As it can be seen from the figure (1), the first important breakthrough in car industry after the implementation of ICE in vehicles is the transfer from conventional vehicles to hybrid electric vehicles. These types of vehicles are first commenced in 1997 in Japan by the introduction of Toyota Prius. The main specification of this type of vehicle is the operation of the ICE on its efficient interval by means of a regenerative braking system. The latest generation of the vehicle is introduced in the market recently. They are mostly called PHEVs (Plug-in Hybrid Electric Vehicles) with additional capability to be charged from the grid.

3. Plug-in Hybrid Electric Vehicles (PHEV)

A PHEV is basically has the same structure as a Hybrid Electric Vehicles (HEV) but the grid charging capability is additional feature which consequently result in the necessity of higher battery capacity.

Grid connection capability in PHEVs will make it possible to coordinate energy resources for domestic consumption and also will lead to lower emission production from private cars in the business and residential areas.

The large percentage of the total emissions production is from the low-duty cars which are private and company cars. Reducing emission production is a big challenge for both developed and developing countries. On the other hand, the other major challenge in today's world in the high consumption of fossil fuels with increasing price and diminishing number of resources. Low-duty cars are one of the major sources of fossil fuel consumption. Therefore,

high fuel consumption and emission production are the major incentives to make changes in the low-duty car sector. Moreover, the new ways of electricity generation can be considered as an incentive for introduction of PHEVs.
Global green house gas emissions from the different sectors are show graphically in Figure 2. These gases are included Carbon Dioxide (72% in total), Methane (72% in total) and Nitrous oxide (26% in total) [8].

Table 1. Charging Times for Different PHEV-20s Vehicle Classes under Various Circuit Voltage and Amperage Levels

Vehicle Type	Pack Size (kWh)	Rated Pack Size (kWh)	Charging Circuit	Charging Size (kW)	Charger Rate (kWh/hr)	Time to Charge Empty Pack (hours)
Compact Car	5.1	4.1	120 V 15 Amp 120 V 20Amp 240 V 40 Amp	1.4 1.9 7.7	1 1.3 5.7	4 3 0.7
Mid-Sized Sedan	5.9	4.1	120 V 15 Amp 120 V 20Amp 240 V 40 Amp	1.4 1.9 7.7	1 1.3 5.7	4.7 3.5 0.9
Mid-Sized SUV	7.9	6.3	120 V 15 Amp 120 V 20Amp 240 V 40 Amp	1.4 1.9 7.7	1 1.3 5.7	6.3 4.7 1.1
Full-sized SUV	9.3	7.4	120 V 15 Amp 120 V 20Amp 240 V 40 Amp	1.4 1.9 7.7	1 1.3 5.7	7.4 5.6 1.3

As shown in the figure 2, 14 percent of the emissions are produced by transportation sector which is close to the industrial sector. This means that by removing the emissions from the transportation sector, the total emissions can be reduced approximately as much as industrial sector. The introduction of PHEVs can be even more interesting when the emissions from power station are low and the electricity is generated from clean resources.

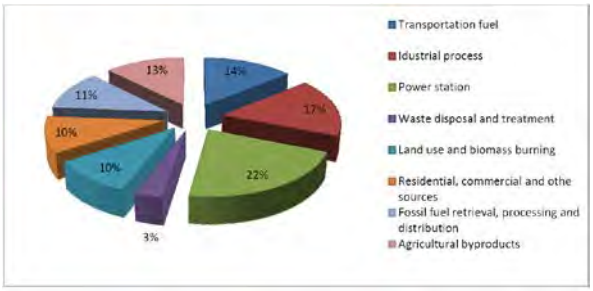

Figure2. Global Green house gasses emissions [8].

Conversion of the cars from the ones with fossil fuel consumption to the ones with electricity consumption is not just interesting from the car sector but also it is interesting from the grid point of view. The high intermittency of the electricity from renewable resources can be synchronized with the intermittency of consumption of electric cars. However, new generation is needed in order to charge the electric cars. The technical parameters of different plug-in vehicles are summarized in Table 1.

4. Plug-in Hybrid Vehicle Charging Scenarios

Electric Power Research Institute (EPRI) has performed studies regarding the energy requirements for potential PHEV vehicle designs. This information, which is summarized in Table 1, provided a basis for the charging scenarios. Figure 3 shows the power demanded for different PHEV-20 vehicle classes using a standard household electrical circuit of 120 volts and 15 amperes.

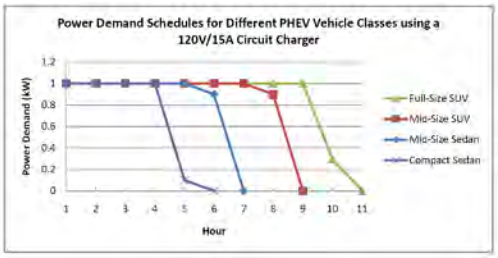

Figure 3. Power Demand Schedules for Different PHEV Vehicle Classes using a 120V/15A Circuit Charger.

The power demand schedules in Figure 3 show a consistent draw of power for the first few hours and then a partial power demand during the last hour of charging. For example, the Compact Sedan PHEV-20 requires 4.1 kWh of energy to fully recharge the battery from a 20% SOC. 1.0 kW of power is needed over the first 4 hours, and 0.1 kW during the 5th hour. This compact sedan therefore would require 4.1 hours to recharge at a rate of 1.0 kW per hour. Since most household outlets already contain 120 volt/15 amp outlets, it was assumed that most PHEVs that reach the market will charge through these circuits. Mid-sized sedan plug-in hybrids with all-electric ranges of 20 miles were used as the standard in the baseline scenarios. Variations to the electric range were used later in this paper. Using the information on charging rates and battery capacity, PHEV power demand curves were generated based around three types of charging scenarios.

The three scenarios representing how vehicle owners might charge their vehicles in the course of a day are summarized below:

Simultaneous Charging: All PHEV owners charge their vehicles at a specified time. This scenario is an adequate upper limit since recharging all the vehicles at one time maximizes the power demanded by plug-in hybrids

.

Continuous Charging: A random percent of PHEVs are connected to the grid throughout the day, requiring a continuous demand of power. A random value between 1% and 50% were established for each hour, representing the percent of PHEVs that are connected to the grid.

Normal Distribution Charging: PHEV charging follows a normal distribution around a specific hour of the day (or mean hour). This represents a scenario between the two limits.

For the simultaneous and normal distribution charging scenarios, an evening charge time of 6 pm is used for the baseline. In the simultaneous charging scenario all PHEVs plug in at 6 pm. For the normal distribution recharge, most of the PHEVs begin charging between the hours of 4 pm and 8 pm (mean hour of 6 pm and standard deviation of 2 hours). Combining the charging scenarios above with the time of day charge and charging circuit size provided the baseline scenarios for this study. Each of these is scenarios are summarized in Table 2.

Table 2. Description of Baseline Scenarios

Scenario	
Scenario 1	All mid-sized sedan PHEV-20s begin charging at 6 pm using 120V/15A charging circuits.
Scenario 2	A random percent between 1% and 50% of mid-sized sedan PHEV-20s charge throughout the day, using 120V/15A charging circuits.
Scenario 3	Mid-sized sedan PHEV-20s charge as a normal distribution about mean hour 6 pm, with a standard deviation of 2 hours, using 120V/15A charging circuits.

Different penetrations of plug-in hybrids were used with each of the charge scenarios above. The PHEVs penetrations represented 5%, 10%, 15%, and 20% of the number of registered vehicles in Tehran.

5. Baseline Charging Scenarios

Using knowledge from previous EPRI studies on lithium-ion battery technology and power demand (table 1), baseline scenarios were created and applied to electricity load demand from the Tehran Regional Electric Company (T.R.E.C). The results from the different baseline scenarios are presented with peak load day. As a reference, the average load in August 2010 is also shown. Figure 4 provides a visual representation of how different penetrations of PHEV-20s recharging at typical household electrical outlets might affect electricity load in Tehran.

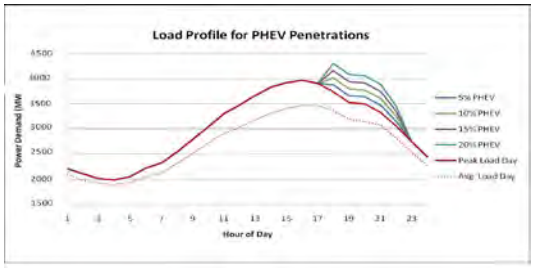

Figure 4. Load profile for PHEV-20 with varying penetrations charging under Scenario 1.

As shown by the peak load day and average August load curves, electricity load is the lowest (below 2500MW) between midnight and 8 am. Electricity generation begins to ramp up starting at 4 am up until 4 pm where it peaks. Electricity load decreases at a faster rate than its initial ramp-up and between the hours of 7 pm and 9 pm, load levels are sustained for a brief period. Peak hours roughly occur between 2 pm and 6 pm. The scenario above represents vehicle owners that all recharge at the same time in the evening (6pm) resulting in a sudden spike in demand.

Figure 5 represents a continuous charging scenario, where up to 50% of PHEV owners could begin to recharge their vehicles at any one particular time. While its probable that PHEV owners will follow a more structured recharge pattern, this scenario helps demonstrate how free access to recharging can spread the demand throughout the day, with slight fluctuations.

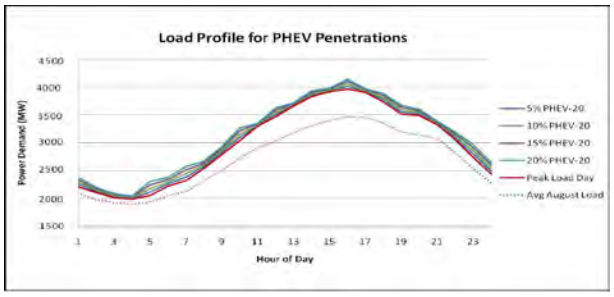

Figure 5. Load profile for PHEV-20 with varying penetrations charging under Scenario 2.

The amount of PHEV-20s that are allowed to charge at any given time is constrained to 50% in the above figure. Open access to the power grid for PHEV owners in this scenario distributes the additional power demand throughout the day, creating a completely new load profile curve.

A more realistic scenario is represented in Figure 6, where recharging occurs as a normal distribution around a specific time period. In this case, it is assumed that most PHEV-20 owners will begin recharging once home from work, around 6 pm.

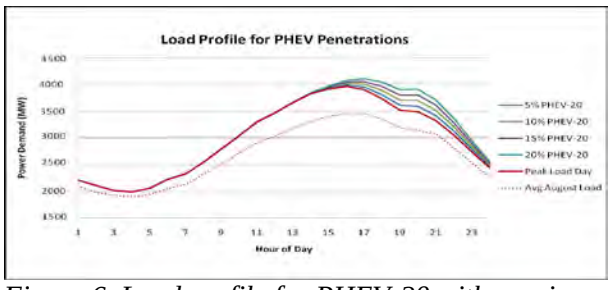

Figure 6. Load profile for PHEV-20 with varying penetrations charging under Scenario 3.

Under Scenario 3, the initial wave of PHEV owners begin charging at 3 pm, and at 6 pm, almost 20% of the owners begin charging. Since the PHEV-20s that connected to the grid between 3 and 5 pm still have not finished fully charging, this lengthens the amount of load necessary to meet demand. The maximum additional electricity demand in this scenario occurs around 8 pm and the last set of PHEV-owners charge at 10 pm, requiring additional power into the late nighttime hours.

The additional power demand at any given hour for the simultaneous scenario represents the load that is sustained for the duration of the charge, in this case, over four hours. Whereas the

simultaneous demand occurs over a short period, the continuous charging maintains a consistent load on the grid throughout the day with much smaller power required. The range for the normal distribution scenarios display the lowest power demand when the fewest PHEV-20s are charging, and the largest demand which occurs at 8 pm, when most vehicles are connected to the grid.

6. Time of Day Charging Variations

The first variation from the baseline scenario is altering the time of day that charging of plug-in hybrid vehicles begin. Shifting the charging to the morning creates the potential for additional load during peak hours. Figure 7 below shows the load profile for the peak day, applying a morning (mean hour of 9 am) charge to the load curve.

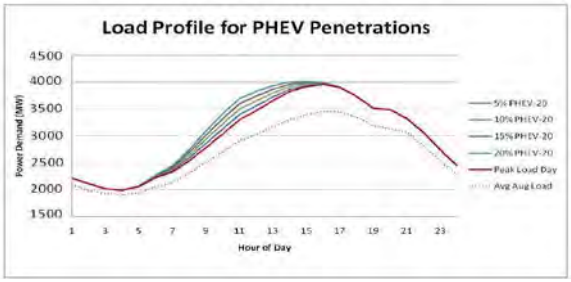

Figure 7. Load profile for PHEV-20 with aarying penetrations charging under a morning (9 am) normal distribution scenario.

As the morning charging scenario demonstrates additional that could occur when PHEV owners plug-in their vehicles after the morning commute leg, the following scenario shows how a nighttime charging scenario might impact Tehran's grid, as shown in Figure 8.

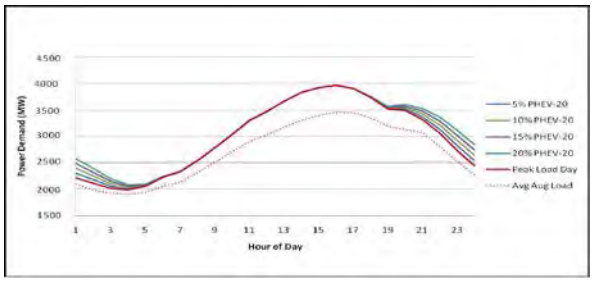

Figure 8. Load Profile for PHEV-20 with Varying Market Penetrations Charging under a Nighttime (10 pm) Normal Distribution Scenario.

Charging the PHEV-20s around a mean hour of 10 pm creates additional demand during the hours when load is diminishing, and reaches into hours when load is the lowest (3 and 4 am). Although the additional demand by PHEVs will ultimately require more electricity generation, charging during the nighttime hours, as shown above, helps to flatten the load curve. Utilizing electricity generation resources into hours when load is low and some electricity is unused, improves efficiency. Although more electricity supply is necessary to meet the demand from PHEVs in all cases, charging at night reduces the need for generating resources to be turned off and back on again.

7. Discussion

Under the simultaneous charging sharp increases can incur and although this is unlikely, it is important to understand this as a potential worst case scenario. The second recharge scenario, where less than 50% of PHEV owners are actively charging their vehicles, the overall load

profile experiences a shift to meet the elevated demand. Although vehicle owners may have the capability to recharge their vehicles multiple times per day, due to the smaller battery power capacity of PHEV-20, vehicle owners may not frequently recharge. For longer electric range PHEVs, such as a PHEV-60, or larger vehicle designs, such as Sport Utility Vehicles (SUVs) which require more energy, the battery may require multiple recharges throughout the day, if the goal is to fully utilize electric drive capability. The final recharge scenario, where recharging follows a normal distribution around 6pm, demonstrates a more realistic behavior pattern. While no sharp increases in demand are expected, it is anticipated that a gradual ramp up in load demand occur during the late afternoon hours and that these resources would be utilized into the evening hours.

8. Conclusion

The results of the study have provided insight into the how Tehran's electricity grid may be impacted from the introduction of plug-in hybrid vehicles. Hours of the day when recharging is expected to occur in large numbers, such as when commuters arrive home from work, can have significant impacts on demand. In the absence of dramatic infrastructure changes with respect to charging stations for PHEVs, most owners will recharge using standard 120V/15A electrical outlets. The charging of PHEV-20 under a 120V/15A circuit would not inconvenience most vehicle owners. The time of day for recharging plug-in hybrid vehicles is an important factor to be considered when planning for this new technology. Late evening hour recharges create additional demand when electricity generation begins to ramp down, only requiring existing generating units to be utilized for a longer duration. If the addition of recharge stations in parking lots where incorporated into the scenario, it would be possible for a portion of vehicle owners to recharge when generation is beginning to ramp up, as shown in the morning charging scenarios.

References

[1] IEEE USA. Plug-in electric hybrid vehicles. Position statement adopted by IEEEUSA board of directors; 2007.

[2] Duvall M. Comparing the benefits and impacts of hybrid electric vehicle options for compact sedan and sport utility vehicles. Technical Report of EPRI 2002.

[3] Li X, Lopes LAC, Williamson SS. On the suitability of plug-in hybrid electric vehicle (phev) charging infrastructures based on wind and solar energy. IEEE Power & Energy Society General Meeting 2009; 1–8.

[4] Dickerman L, Harrison J. A new car, a new grid. IEEE Power and Energy Magazine 2010; 8(2):55–61.

[5] S.D. Jenkins, J. Rossmaier, M. Ferdowsi, Utilization and effect of plug-in hybrid electric vehicles in the united states power grid, in: IEEE Vehicle and Propulsion Conference (VPPC), 2008.

[6] S.G. Wirasingha, N. Schofield, A. Emadi, Plug-in hybrid electric vehicle developments in the US: trends, barriers, and economic feasibility, in: IEEE Vehicle Power and Propulsion Conference (VPPC), 2008.

[7] P. Denholm, S. Letendre, Grid services from plug-in hybrid electric vehicles: a key to economic viability? National Renewable Energy Laboratory, Tech. Rep.

[8] Rosmarino, Tanyalynnette. A Self-Funding Enterprise Solution to Reduce Power Consumption and Carbon Emissions.

Analysis of the CO_2 and energy demand reduction potentials of passenger vehicles based on the simulation of technical improvements until 2030

Felipe Toro[1*], Felix Reitze[1], Sulabh Jain[2], Eberhard Jochem[1,3]

[1] *Institute for Resource Efficiency and Energy Strategies IREES, Karlsruhe, Germany*
[2] *TU Bergakademie Freiberg, Freiberg, Germany*
[3] *Centre for Energy Policy, ETH Zurich, Switzerland*
**Felipe Toro. Tel: +49-721-915263621, Fax:+49-721-915263611, email: f.toro@irees.de*

Abstract: In Europe, passenger cars use over 65% of total transport fuel energy and produce around 12% of total EU carbon emissions. Under such circumstances advanced technologies and modifications in multiple powertrain technologies in passenger cars hold an important key to reduce emissions and energy demand into future. This study compiles a set of efficiency improvement technologies and makes use of a 'Bottom-up simulation' to assess the effects of introduction these technologies on total energy demand and CO_2 emission from passenger cars up to 2030 in the EU-27. The integration of improvement technologies in vehicle will serve the purpose of increasing fuel efficiency, enhancing performance and provide further technical and environmental benefits, but it will also result in incremental costs over the vehicle baseline prices. This research also assesses changes in specific driving costs, cost of CO_2 avoidance and the payback period of incremental costs on the vehicle's economic performance. The technical improvement potentials' options considered in this study show that a 5% to 22% increase in fuel economy of car is possible. And based on assumed diffusion of technologies across total gasoline and diesel vehicles, this study infers a potential of 19% to 34% savings in energy demand and CO_2 emission by 2030.

Keywords: *Low carbon vehicles, Vehicles innovation, Energy efficiency, Bottom-up modelling, Technology market diffusion*

1. Introduction

Across Europe cars have given the public greatest mobility that is adjustable to different usages, driving locations and preferences, and this trend will continue to grow into future. Over the last few years, increasing environmental concerns, rising oil prices and continuous urge for technological developments have stimulated industries and nations across the world to move towards better efficiency and sustainable practices in the transport sector. To tackle the problems associated with constantly increasing transport fossil fuel demand and greenhouse gas (GHG) emission, it has become very important to consider the alternative fuels and alternative cars for meeting environmental benefits.

In the last few years, the European car manufacturers have invested significant amount of money in the technology R&D, and have introduced more than 50 advanced technologies into the cars for the purpose of efficiency gain and emission reduction. In addition to the varied upcoming vehicle technologies like battery electric vehicles and hydrogen fuel cell vehicles, nowadays a large number of vehicle and powertrain improvement technologies are aimed at increasing the fuel economy and efficiency of the existing conventional vehicles through technical improvements. The core analysis of this paper is based on such 'technical improvement potentials'. This paper is an extension of an ongoing research under the project ALTERMOTIVE, contracted under Intelligent Energy Europe.

Currently, a huge diversity of fuels and advanced powertrain technologies are available in Europe. Table 1 states various alternative automotive mobility technologies (AAMTs) mapped under different developmental stages along the technology curve (Research, Demonstration and/or Commercial state). In Table 1 it can be seen that in addition to the conventional diesel and gasoline cars, few other AAMTs like Natural Gas Vehicles and Flexi

Fuel Cars already exist in the European market on commercial level. These technologies also show continuous process of developments for achieving higher vehicle efficiency and better customer satisfaction. The technologies included under Demonstration phase are not at commercial scale yet, but depending on the speed of progress and overcoming market and cost barriers these may come to commercial phase in next few years. The technologies exhibiting the R&D phase will continue to progress to overcome technical challenges and incompatibilities, and will come to commercial phase no sooner than 2020-2025.

Table 1: Alternative Automotive Mobility Technologies - State of the Art in Europe (2010)

	Commercial	Demonstration	R&D
Technologies	**NG (LNG/CNG)** **Flex-Fuel Vehicle** *(conventional fuel + BD/BE)* **Bi-fuels** *(NG + Gasoline/Diesel)* **Gasoline-Electric Hybrid** **Electric Vehicles:** *Micro-Mild Hybrid* *BEV (only light vehicles, no convertor, DC Motor, Range<100 km*	**Solo/High blend BE** **Diesel-Electric Hybrid** **Electric Vehicles:** *Enhanced HEV-PHEV* *BEV (with convertor, AC Motor, Range > 100 km)* *Full Hybrid* **FC hybrids** *(conventional fuel + hydrogen)*	**Solo/High blend BD** **Biogas** **Electric vehicles:** *FCV- PHEV (Plug-In functionality for FCV/HEV)* *BEV (with convertor, AC Motor)* **FCV**

Source: (Toro, et al., 2010)

Abbreviations = NG: Natural Gas, LNG: Liquid NG, CNG: Compressed NG, BD: Biodiesel, BE: Bioethanol, EV: Electric Vehicle, HEV: Hybrid EV, BEV: Battery EV, PHEV: Plug-in Hybrid EV, DC: Direct Current, AC: Alternative Current, FC: Fuel Cell, FCV: FC Vehicle

2. Methodology

The method implemented for this study starts with the review of various technical improvement potentials in the European passenger cars along with their potentials in enhancing the vehicle efficiency. In next step, this study selects two sets of innovative improvement technologies called as 'Technology Option 1 & 2' and assesses the impacts of their integration on vehicle's energy demand, CO_2 emission, and economic performance. The main assessments applied in this study with the bottom-up simulation and economic estimations are:

1. Assessing the improvements in the vehicular energy consumption and consecutive CO_2 emission as a result of integration of Technology Options – Techno-Environmental assessment.
2. Assessing the changes in economic performance of the car as a result of incremental costs and technical improvements – Economic assessment.
3. Assessing the potentials of technologies in overall energy demand and emission reduction at assumed diffusion rates across EU-27 car fleet – Techno-Environmental assessment.

2.1. Techno-Environmental assessment:

The techno-environmental assessment carried through the bottom-up simulation is done to assess the energy demand and CO_2 emission by the total European passenger cars (including all types' such as gasoline, diesel, hybrid, bioethanol etc.) for a fixed annual driving distance. For setting up an energy demand baseline, energy demand projections and car fleet size

forecasts in EU-27 until 2030 were derived from Fiorello, et al., (2009). Then the bottom-up simulation tool was built up by using different vehicular data and other input values (like fuel economy, average annual traveling etc.) to assess the overall energy demand and CO_2 emission up to 2030. The general formula for the assessment is:

$$ED_t = \sum\left(F_{i,t} \times D_{i,t} \times FE_{i,t}\right) \quad [\text{PJ}] \quad \text{Eq. 1}$$

Where, ED_t is the total energy demand (including different fuels *Fu*) in the year *t*, *i* is the model year, *F* is the number of vehicles of a model year *i* running in year *t* on fuel *Fu*. *D* is the annual distance travelled by a car of model year *i* in year *t* using fuel *Fu. FE* is the average fuel economy (MJ/100km) of the car for a model year *i*, using fuel *Fu* running in year *t.*

Changes in fuel economy: It was considered that when the technical improvements occur into the car by implementation of *'Technology Options'*, the fuel economy increases by a certain %. The equation used to assess changes in the fuel economy is:

$$FE_e = FE_b \times (1 - \%E_{TO}) \quad [\text{MJ/100km}] \quad \text{Eq. 2}$$

Where, FE_e is the enhanced fuel economy, FE_b is the baseline fuel economy of the vehicle and $\%E_{TO}$ is the percent (%) by which the *'Technology Option'* enhances the vehicle efficiency.

2.2. Economic assessment:

The fuel efficiency of the vehicle can be enhanced by implementation of advanced innovative technologies, but the introduction of new technologies in vehicle will cause extra upfront investments and additional costs to the manufacturers and these costs will add extra price over the vehicle price (McKinsey, 2009). Thus, it is technically feasible to reduce the fuel consumption of new vehicles, but additional costs will be incurred. In this study, following assessments were done.

Incremental Cost of technology options: The concept of Retail Price Equivalent Multiplier (RPE factor) that represents the average additional price consumers would need to pay for an advanced technology was used to assess the incremental costs of technologies.

$$IC_{TO} = C_M \times RPE\ factor \quad \text{Eq. 3}$$

Where IC_{TO} is the incremental cost of Technology Option, C_M is the manufacturer cost of technologies (derived from AEA, 2009) and *RPE factor* is the retail price equivalent multiplier (derived from Vyas, et al., 2000; NRC, 2010).

Specific Driving Costs: the cost of driving per kilometer of vehicle. This cost in the analysis was interpreted as an aggregate construct of vehicle investment costs linked to 8% annual O&M costs, fixed annual driving distance and the vehicle lifetime of 10 years.

$$\boldsymbol{SC_d = \frac{I_a + O\&M}{D_{annual}}} \quad [€/\text{km}] \quad \text{Eq. 4}$$

Where, SC_d is the specific driving cost, I_a is the annual investment cost, *O&M* is the operation and maintenance cost and D_{annual} is the annual distance travelled by the car.

Average payback Period: It is the time period in which the incremental costs can be compensated by the monetary savings that occur as a result of decreased fuel demand by technical improvement.

$$PB_{avg} = \frac{C_i}{YS_{€/a}} \quad \text{[Years]} \quad \text{Eq. 5}$$

Where, PB_{avg} is the average payback period, C_i is the incremental cost and $YS_{€/a}$ is the annual monetary saving (€/a) per year through reduced fuel expenditure.

Cost of CO_2 avoidance or CO_2 abatement costs: It is assumed that for a technically improved vehicle the driver has to bear extra investment costs over the vehicle price. So, how much does it cost (in €) to the driver for saving each tonne of CO_2 is called the cost of CO_2 avoidance. It is calculated by the following formula.

$$CO_2\ abatement\ cost = \frac{C_i}{Tonne\ CO_{2\ saved}} \quad \text{[€/tonnne]} \quad \text{Eq. 6}$$

Where, C_i is the incremental cost and Tonne CO_{2saved} is the CO_2 saved within vehicle life time.

2.3. Sources, Data and Assumptions:

2.3.1. iTREN Reference Scenario (Deliverable-4, 2009): Fiorello, et al., (2009)

This report was chosen for fleet characteristics and energy demand projections as it delivers the quantified data in Europe until 2030 and more importantly the assessment carried in the study does not consider any technical improvements of the cars after 2008. Table 2 states the data and values extracted from Fiorello, et al., (2009).

Table 2 : Baseline values and assumptions (EU-27 passenger car fleet)

	Unit	2005	2010	2020	2030
Total no.of cars-EU-27	1,000 vehicles	211,062	228,120	265,628	294,220
Total Energy Demand	PJ	8,435	9,251	9,630	10,301
CO_2 emissions*	Million tonnes/year	624	684	712	761
Emissions	MillionTonnes/year	793	760	833	840
Gasoline Price	€/litre	1.07	1.40	1.27	1.34
Diesel Price	€/litre	0.92	1.25	1.16	1.24

*Source: (Fiorello, et al., 2009), *Calculated by Authors*

2.3.2. Concawe (WTW, Version-2b, 2006 and TTW, Version-3, 2008)

Average characteristics and data for the European passenger cars like vehicle price, engine power, fuel economy, fuel specific emission factor of the fuel etc. were derived from the Concawe reports mentioned above. Table 3 states the data derived for gasoline and diesel cars.

Table 3: Data and values derived from Concawe reports

	Unit	Gasoline	Diesel
Vehicle Price	€	19,000	20,000
Capacity Fuel/Engine Power	kW	77	74
Av. Travelling distance*	Km/yr	18,000	20,000
GHG emission	gm CO_2 eq.per km	165	140
Specific driving costs*	€/100 km	24.18	22.90

Source: (Concawe, 2008)*; *Authors' assumption/calculations*

2.4. Efficiency Improvement Technologies

There are many efficiency improvement technologies that can be introduced in today's vehicles without changing the vehicle's basic type, general size, or performance. Virtually all of the technologies are capable of increasing vehicle efficiency and reducing fuel demand, but they all are not equally ready for the commercial production. The technologies grouped as Technology option 1 and 2 in Table 4 were chosen based on their readiness as they are applicable into the conventional diesel and gasoline passenger cars within 2010-2012 timeframe.

Table 4: Technology Options considered for the study

	Technology Option 1	*Technology Option 2*
Technology Combination	1. Reduced engine friction losses 2. Improved aerodynamics 3. Low rolling resistance tyres	1. Improved aerodynamics 2. Vehicle Weight reduction 3. Optimized transmission 4. Mild downsizing with Turbo Charging 5. Start-stop-system 6. Use of advanced devices (tyre pressure monitoring system, gear shift indicator etc.)
Expected efficiency increase	Around 5%	Around 22%
Source - eff. Increase	(EPA, 2008)	(McKinsey, 2009)
Tech. cost assumption*	10% over car baseline price	30% over car baseline price
Status in Europe	Integrated into new cars by most manufacturers	High consideration for application

**Source: (TNO, 2006), (AEA, 2009)*

2.5. Technology Diffusion Assumption

The term technology diffusion in this study refers to the widespread integration of Technology Options into the new European gasoline and diesel cars up to 2030. For the simulation, the diffusion was considered only within gasoline and diesel cars because both the Technology Options are compatible into these cars without rendering any change to the size or performance of the car. Moreover, gasoline and diesel cars represent the biggest share in the total EU-27 car fleet and this trend of majority will continue to increase at least until 2030.

To build the stock of new cars in EU-27 until 2030, a review of historical vehicle registration data and socio-economic developments was done. Then the review was complemented with the expected GDP growth to establish the expected trend of new car registrations in EU-27.

The two scenarios considered for this study are:

Scenario 1: Technical Potential - Assessment of the maximum energy demand and CO_2 emission reduction potential offered by the technologies under the assumption that Technology Option 2 diffuses extensively across the fleet.

Scenario 2: Autonomous Potential - Assessment of the reduction potential form the technologies under the assumption that the Technology Option 2 diffuses to a limited extent within the new fleet, however followed by autonomous technological progress the Technology Option 1 diffuses widely across the fleet.

Table 5: Technology Diffusion Assumption

		2010	2015	2020	2025	2030
Scenario 1 (Tech.Pot)	Diffusion of Tech. Op 2 into new cars	10%	30%	50%	75%	100%
	Diffusion of Tech. Op 2 into old cars	10%	20%	25%	30%	25%
Scenario 2 (Auto.Pot)	Diffusion of Tech. Op 2 into new cars	10%	15%	20%	30%	35%
	Diffusion of Tech. Op 2 into old cars	10%	15%	18%	20%	20%

3. Results

The results presented in Table 6 are derived by considering the integration of Technology Options into the vehicle. The assessment methods for the techno-environmental and economic assessment take into account all the salient aspects like baseline vehicle price, additional investment costs Technology Options, engine size and fuel capacity, yearly driving distance, diesel and gasoline fuel price projections until 2030 from (Fiorello, et al., 2009).

Table 6: Results of techno-environmental and economic assessments at the vehicular level

Assessed value	Unit	Baseline value (G)	Gasoline Car		Baseline value (D)	Diesel Car	
			Tech. Op.1	Tech. Op.2		Tech. Op.1	Tech. Op.2
Average cost of *'Technology Option'*	€	-	350	2,800	-	350	2,450
Sp. Driving Costs	€/100 km	24.18	24.62	27.74	22.90	23.30	25.71
Fuel economy	MJ/100km	220	209	171.6	190	180.5	148.2
Specific CO_2 emission	gCO_2/km	165	156.8	128.7	140	133	109.2
Fuel expenses*	€/100km	9.49	9.02	7.40	6.63	6.29	5.17
Fuel economy	km/litre	14.7	15.5	18.9	18.9	19.9	24.2
Fuel economy	l/100km	6.78	6.44	5.29	5.30	5.04	4.13
Yearly energy demand	MJ/yr	39,600	37,620	30,888	38,000	36,100	29,640
Yearly CO_2 emissions	Tonnes CO_2/yr	2.94	2.80	2.30	2.79	2.65	2.18
Cost of CO_2 avoidance	€/Tonne	-	238	432	-	250	398
Average payback period*	Years	-	4.1	7.4	-	5.3	8.4

*Source: Assessed by authors, * considering 2010 fuel price from (Fiorello, et al., 2009)*

The energy demand and emission potential results presented in Table 7 show as what could be achieved when technologies are implemented into the assumed percentage of the EU-27 new gasoline and diesel cars. The scenarios developed within this study show that 19% to 34% reduction in total energy demand and subsequent CO_2 emission can be achieved by 2030.

Table 7: Results of total energy demand and emission saving potential

Results	2010	2015	2020	2025	2030
Baseline – Energy Demand (PJ)	9,253	9,439	9,630	9,959	10,300
Technical Potential (S1)	9,121	8,197	7,935	7,550	6,797
Autonomous Potential (S2)	9,186	8,600	8,514	8,344	8,328
Scenario 1/Baseline	-1.43%	-13.16%	-17.59%	-24.19%	-34.01%
Scenario 2/Baseline	-0.72%	-8.89%	-11.59%	-16.21%	-19.14%
Baseline - CO_2 emission (Mil.tonne)	684	698	712	736	761
Technical Potential (S1)	674	606	587	558	502
Autonomous Potential (S2)	679	636	629	617	615
Scenario 1/Baseline	-1.41%	-13.11%	-17.59%	-24.15%	-34.03%
Scenario 2/Baseline	-0.70%	-8.84%	-11.57%	-16.16%	-19.14%

Source: Own calculations

It is important to note that diffusion assumptions explained here are based on authors' views supported by technology readiness and expected technical developments. In reality there may be several interactions and measures (like EU policies, market behavior, cost of technologies, consumers' preference etc.) that will affect the relative effectiveness of technologies and their deployment within industry (Skinner, Essen, Smokers, & Hill, 2010). To summarize the results, Figure 1 shows the overall potentials in energy demand and CO_2 emission savings assessed within this study. The figure is converted in % savings for the ease of understanding and combining the energy demand and emission changes until 2030.

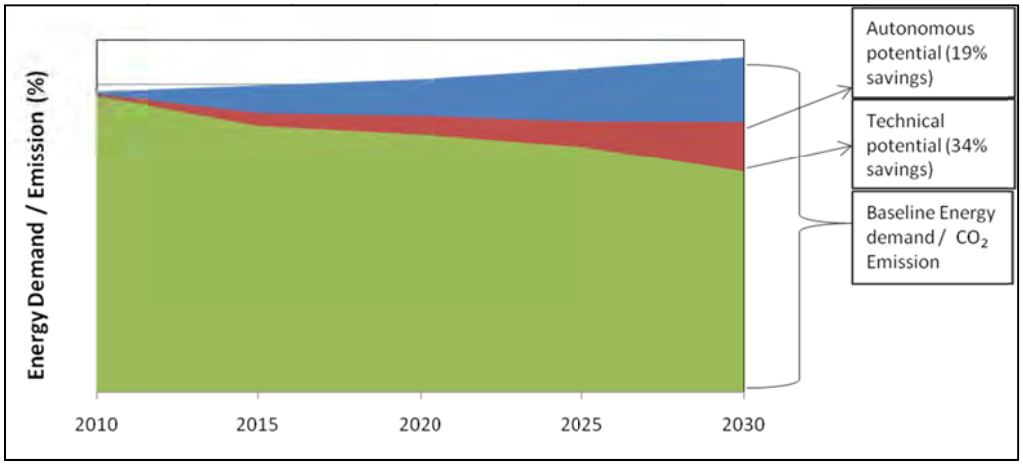

Figure 1: Total energy and CO_2 emission saving potentials
Source: Own calculations and elaboration

4. Discussion and Conclusions

The results and analysis detailed in this paper show the potentials of energy demand and CO_2 emission reduction; however, there are certain limitations in the analysis. The technologies considered in the study are based on the theoretical values and potentials for vehicle efficiency increase, but the results may vary significantly during vehicle segment applications (e.g. small, medium or large cars) and under different on-road driving conditions. Secondly, the technologies included in this study are not the only options that European car manufacturers are considering. There are many other technologies and measures that have varied degree of technology readiness and implementation within cars for the purpose of efficiency increase.

An important aspect regarding the aforementioned results is the compliance of the emission values with the EU regulations on average gCO_2/km emission. The European Commission has established the emission limiting targets by averaging emissions (g/km) of all car models weighted by the sales volumes of the manufacturers. Therefore, when the baseline emission values are compared to the EC targets then this does not imply that all the cars drive at the same mileage and emit same amount of CO_2. All car models across the Europe possess varying mileage range, therefore different vehicle models, car segments and the fuel used in them contribute differently to the average on-road CO_2 emission.

Technical improvement technologies can result in substantial improvements in new car fuel economy and subsequent GHG emission. While virtually all of the technologies are capable of enhancing vehicle efficiency, they are not equally ready for production and integration into the vehicle. Technologies included in Technology Option 1 have been widely introduced into the market until now. And, the technologies included in Technology Option 2 posses high

degree of technology readiness and high consideration by the manufacturers for integration within the current production lines.

Results stated in this study (in Table 6) have shown the increasing pattern of fuel economy in gasoline and diesel cars. Technology Options 1 & 2 have the potential to enhance vehicle efficiency by 5% and 22% respectively, which can save between 0.14 and 0.64 tonneCO_2/year per car for a fixed driving cycle. Results of economic assessment show the decreasing pattern of fuel expenditure in terms of €/100km or €/Year. The assessment shows that both the Technology Options may increase vehicle cost by 10% and 30%, but as a result of increased fuel economy and reduced fuel expenditure, the additional investment can be reimbursed within the certain time period considered as the 'Payback period'. The Technology Options are projected to result in a net cost benefit to the owner over a 10 year vehicle lifetime because the cumulative fuel expenditure savings offset the higher incremental costs. The results of technology diffusion based on bottom-up simulation show that there is a potential of between 19% and 34% reduction in the energy demand and CO_2 emission in the EU-27 up to 2030.

References

[1] Toro, F. A., Jain, S., Reitze, F., Ajanovic, A., Hass, R., Furlan, S., et al. (2010). State of the art for alternative fuels and alternative automotive technologies. Karlsruhe, Germany: Project ALTERMOTIVE: Deriving effective least cost policy strategies for alternative automotive concepts and alternative fuels.

[2] Fiorello, D., De Stasio, C., Koehler, J., Kraft, M., Newton, S., Purwanto, J., et al. (2009). *The iTREN-2030 reference scenario until 2030: Deliverable 4 of iTREN-2030.* Milan, Italy: Project co-funded by European Commission 6th RTD Programme.

[3] McKinsey. (2009). Der Trend zu energie - effizienten Pkw, Implikationen für die deutsche Automobilindustrie. McKinsey&Company.

[4] Concawe. (2008). *Weel to Wheel Analysis of Future Automotive Fuels and Powertrains in the European Context.*

[5] EPA. (2008). *EPA Staff Technical Report: Cost and Effectiveness Estimates of Technologies Used to Reduce Light-duty Vehicle Carbon Dioxide Emissions.* United States Environmental Protection Agency. US-EPA.

[6] AEA. (2009). *Assessment with respect to long term CO2 emission targets for passenger cars and vans.* AEA - Deliverable D2: Final Report.

[7] TNO. (2006). *Review and analysis of the reduction potential and costs of technological and other measures to reduce CO2-emissions from passenger cars.* Delft: TNO Science and Industry.

[8] Skinner, I., Essen, H. v., Smokers, R., & Hill, N. (2010). *Towards the decarbonisation of the EU's transport sector by 2050.* London, UK: AEA.

[9] TNO. (2006). *Review and analysis of the reduction potential and costs of technological and other measures to reduce CO2-emissions from passenger cars.* Delft: TNO Science and Industry.

[10] Skinner, I., Essen, H. v., Smokers, R., & Hill, N. (2010). *Towards the decarbonisation of the EU's transport sector by 2050.* London, UK: AEA.

Experimental performance of an R134a automobile heat pump system coupled to the passenger compartment

M. Direk[1], M. Hosoz[1,*], K.S. Yigit[2], M. Canakci[1], A. Turkcan[1], E. Alptekin[1], A. Sanli[1], A.F. Ozguc[3]

[1] *Department of Mechanical Education, Kocaeli University, 41380 Kocaeli, Turkey*
[2] *Department of Mechanical Engineering, Kocaeli University, 41040 Kocaeli, Turkey*
[3] *Department of Mechanical Engineering, Istanbul Technical University, Istanbul, 34437, Turkey*
** Corresponding author. Tel: +90 2623032279, Fax: +90 2623032203, E-mail: mhosoz@kocaeli.edu.tr*

Abstract: This study presents experimental performance of an R134a automotive heat pump (AHP) system driven by a diesel engine and capable of utilizing the heat absorbed from the ambient air, engine coolant and exhaust gas. The experimental setup was developed from the components of the air conditioning system of a compact-size car, and tested by changing the engine speed, engine load and air temperatures entering the condenser and evaporator. The steady-state and transient performance characteristics of the AHP system for each heat source were evaluated by applying energy analysis to the system based on experimental data. Then, the performance parameters of the AHP system for three different heat sources were compared with each other and with those of the baseline heating system. The results show that the AHP system using engine coolant provides higher heating capacities and air temperatures at the register outlet in the first five minutes of the tests. However, the baseline heating system usually performs better than the AHP system when the steady-state is achieved. The AHP system caused an increase in the engine brake specific fuel consumption within the range of 4–54% depending on the engine load.

Keywords: *Automotive heat pump, R134a, Refrigeration, Air conditioning, Automobile*

1. Introduction

Passenger vehicles equipped with a water-cooled internal combustion engine usually utilize the engine waste heat in order to perform comfort heating of the passenger compartment under cold weather conditions. However, this coolant-based heating system cannot provide an appropriate thermal comfort in the passenger compartment until the coolant temperature rises to a certain value. This problem is more critical for the vehicles employing high-efficiency diesel engines due to the lack of sufficient waste heat within an acceptable duration of operation after the engine is started up. With the intention of obtaining thermal comfort rapidly, some vehicles utilize heaters using fuel or electricity. However, these systems have disadvantages such as high initial and operating cost, low efficiency and leading to air pollution as well as global warming. On the other hand, the problem of insufficient heating can be solved by adding some low cost components to the present air conditioning system of the vehicle to operate it as a heat pump. The automotive heat pump (AHP) system can heat the passenger compartment individually, or it can support the present heating system of the vehicle. In the literature, there are several investigations on the performance of AHP systems. Among these studies, Domitrovic et al. [1] simulated the steady-state cooling and heating operations of an automotive air conditioning (AAC) and heat pump system using R12 and R134a, and determined the change of the cooling and heating capacities, coefficient of performance (*COP*) and power consumption with ambient temperature at a fixed compressor speed. Hosoz and Direk [2] evaluated the performance of an air-to-air R134a AHP system, and compared its performance with the performance of the air conditioning system. Rongstam and Mingrino [3] evaluated the performance of an R134a AHP system using engine coolant as a heat source, and compared it with the performance of a coolant-based heating system at an ambient temperature of –10ºC. Scherer et al. [4] reported an on-vehicle performance comparison of R152a and R134a AHP systems using engine coolant as a heat source.

Antonijevic and Heckt [5] developed and evaluated the performance an R134a AHP system, which was employed as a supplementary heating system. They carried out the tests at very low ambient temperatures and compared the performance of the AHP system with that of other supplemental heating systems.

In this study, an experimental AHP system capable of providing a conditioned air stream by utilizing the heat absorbed from the ambient air, engine coolant or exhaust gas was developed. In the experimental system, after passing through the indoor unit, the conditioned air stream was sent to the vehicle passenger compartment through a flexible air duct. In the experiments, the engine speed, engine load and air temperatures entering the condenser (indoor unit) and evaporator (outdoor unit) were controlled and concisely adjusted. The investigated performance parameters were the air temperature at the compartment front register outlet, mean air temperature in the passenger compartment, heating capacity, coefficient of performance and the increase in the brake specific fuel consumption (*BSFC*) of the engine caused by the operation of the AHP system.

2. Methodology

The experimental AHP system was usually made from the original components of an AAC system of a compact size car. As schematically shown in Fig. 1, it employs a seven-cylinder fixed-capacity swash-plate compressor, a parallel-flow micro-channel outdoor coil, a laminated type indoor coil, two thermostatic expansion valves, a reversing valve to operate the system in reverse direction in heat pump operations, a brazed plate heat exchanger between the engine coolant and the refrigerant to serve as an evaporator and another plate heat exchanger to extract heat from the exhaust gas.

All lines in the refrigeration circuit of the system were made from copper tubing, and insulated by elastomeric material. The indoor and outdoor coils were inserted into separate air ducts of 1.0 m length. In order to provide the required air streams in the air ducts, a centrifugal fan and an axial fan were placed at the entrances of the indoor and outdoor air ducts, respectively. These ducts also contain electric heaters located upstream of the indoor and outdoor coils. The indoor and outdoor coil electric heaters can be controlled between 0–2 kW and 0–6 kW, respectively, to provide the required air temperatures at the inlets of the related coils. The refrigeration circuit was charged with 1600g of R134a. In order to gather data for the performance evaluation of the experimental AHP system, some mechanical measurements were conducted on it. The employed instruments and their locations are depicted in Fig. 1, and the characteristics of the instrumentation are reported in Table 1.

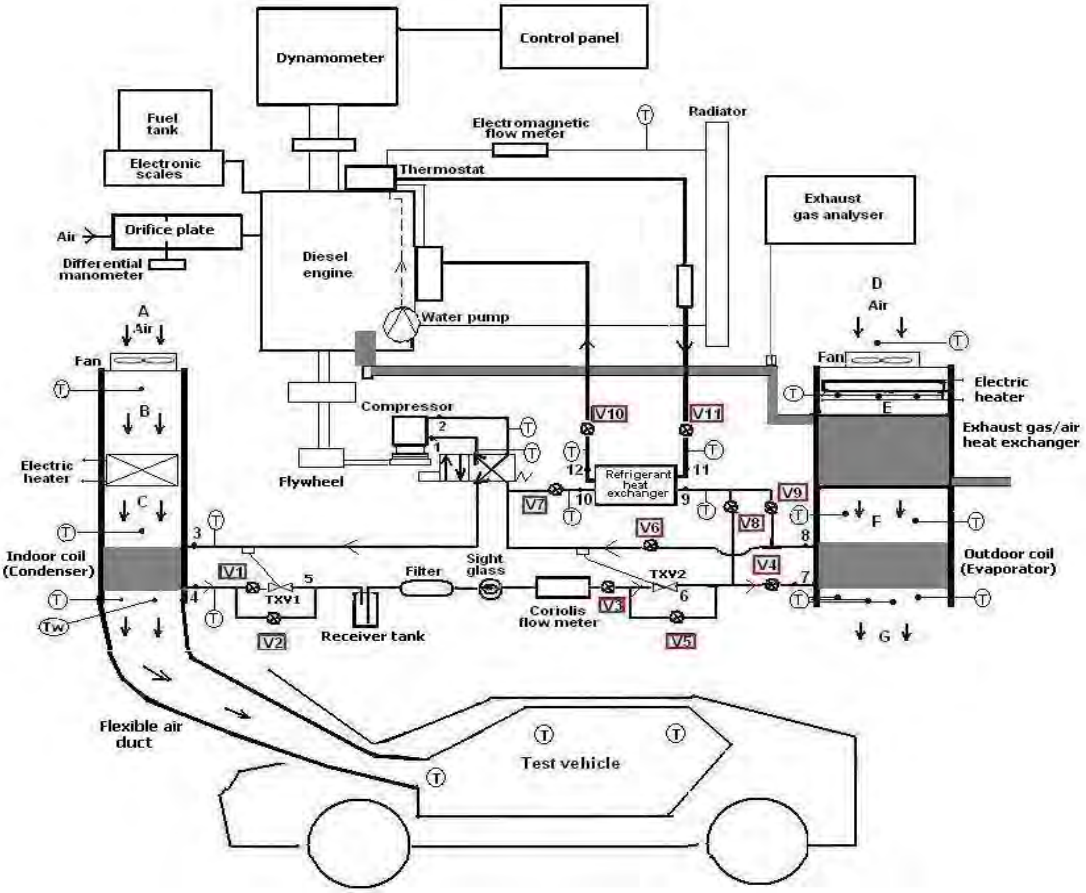

Fig. 1. Schematic illustration of the experimental AHP system and test vehicle (The arrows show the flow paths in the heat pump operations using ambient air and exhaust gas as a heat source).

Table 1. Characteristics of the instrumentation.

Measured variable	Instrument	Range	Uncertainty
Temperature	Type K thermocouple	–50–500 ºC	± % 0.3
Pressure	Pressure transmitter	0–25 bar	± % 0.2
Air speed	Anemometer	0.1–15 m s^{-1}	± % 3
Refrigerant mass flow rate	Coriolis flow meter	0–350 kg h^{-1}	± % 0.1
Compressor speed	Digital tachometer	10–100000 rpm	± % 2
Torque	Hydraulic dynamometer	5–750 Nm	± % 2

The refrigerant mass flow rate was measured by a Coriolis mass flow meter. The temperatures of the refrigerant and air at the inlet and outlet of each component were measured by K-type thermocouples. The refrigerant pressures at the inlet and outlet of the compressor were measured by both Bourdon gauges and pressure transmitters.

The AHP system was driven by a Fiat Doblo JTD diesel engine with a cylinder volume of 1900 cc and a maximum power of 77 kW at 4000 rpm. The engine torque and speed were measured by means of a hydraulic dynamometer with a maximum measuring power of 100 kW, a maximum torque of 750 Nm and a maximum speed of 6000 rpm. The fuel consumption was measured using an electronic scale and a chronometer. Most of the measurement data were acquired through a data acquisition system and recorded on a computer.

The conditioned air stream discharged from the condenser duct was supplied to the passenger compartment of the test automobile Renault Safrane. The connection between the evaporator

duct and the compartment was performed using an insulated flexible air duct. In order to measure the compartment temperatures, a thermocouple was located at the outlet of the front register, another one was suspended in the air close to the front left seat at the driver neck level, and the last one was suspended in the air close to the rear right seat at the passenger neck level.

Fig. 1 also illustrates the refrigerant flow paths in the experimental heat pump system for the cases of using ambient air or exhaust gas as a heat source. In order to perform the heat pump operation, the reversing valve is energized. Then, the reversing valve directs the high temperature superheated vapour refrigerant discharged from the compressor to the indoor coil. Afterwards, the refrigerant condensed in the indoor coil enters the outdoor unit (evaporator) through the thermostatic expansion valve (TXV2). The refrigerant evaporates by absorbing heat from the ambient air stream, which can be preheated by the exhaust gas/air heat exchanger in the heat pump operations using the exhaust gas as a heat source. Finally, the evaporated refrigerant is drawn by the compressor through the reversing valve.

In order to operate the experimental system as a heat pump using engine coolant as a heat source, the refrigerant is directed to the refrigerant/coolant heat exchanger after passing through the TXV2. In this case, the refrigerant absorbs heat from the engine coolant and has a high superheat at the exchanger outlet. In order to test the baseline heating system, the heater core is located downstream of the indoor coil and connected to the proper terminals of the engine thermostat. Further information on the experimental AHP system and its instrumentation can be found in references [6, 7].

The performance parameters of the experimental AHP system can be evaluated by applying the first law of thermodynamics to the system. Using this law for the indoor coil (condenser), the heating capacity of the experimental AHP system can be evaluated from

$$\dot{Q}_{cond} = \dot{m}_r (h_{cond,in} - h_{cond,out}) \quad (1)$$

where $\dot{m}_r$ is the refrigerant mass flow rate and h is the enthalpy of the refrigerant.

Assuming that the compressor is adiabatic, the compressor power absorbed by the refrigerant can be obtained from

$$\dot{W}_{comp} = \dot{m}_r (h_{comp,out} - h_{comp,in}) \quad (2)$$

The energetic performance of the AHP system is found by evaluating its *COP*, defined as the ratio between the heating capacity and compressor power, i.e.

$$COP = \frac{\dot{Q}_{cond}}{\dot{W}_{comp}} \quad (3)$$

The power output from the engine, which is called the engine brake power, can be determined from the product of the engine torque and engine speed, i.e.

$$\dot{W}_{brake} = T \frac{\pi n}{30} \quad (4)$$

The brake specific fuel consumption of the engine can be evaluated from

$$BSFC = 3600 \frac{\dot{m}_F}{\dot{W}_{brake}} \quad (5)$$

where $\dot{m}_F$ is the fuel consumption rate of the engine.

3. Results

In order to perform the tests, the diesel engine was operated at five different speeds, namely 850, 1200, 1550, 1900 and 2250 rpm. Because the diameters of the crankshaft and compressor pulleys are the same, the engine speed is equal to the compressor speed. The tests at 850 rpm were performed at the dynamometer loads of both 5 Nm (idling operation) and 60 Nm, while tests at other speeds were performed only at the dynamometer load of 60 Nm. In all tests, the air flow rate at the front register outlet was adjusted to its maximum (0.403 m^3s^{-1}). In the tests using ambient air and exhaust gas as a heat source, the air flow rate passing through the outdoor coil was also adjusted to its maximum (0.52 m^3s^{-1}). Before performing the tests, the air temperatures at the inlets of the indoor coil ($T_{ind\ coil,\ ain}$) and outdoor coil ($T_{outd\ coil,\ ain}$) both were fixed to 5 °C. Meanwhile, the relative humidity of the air stream entering the outdoor coil was between 50 and 70%. After these adjustments, the diesel engine was started up and the engine speed along with dynamometer load was rapidly adjusted to the required values. Using data acquired in the test operations, the steady-state performance of the AHP system was evaluated from the Eqs. (1–5), while the air temperature at the outlet of the front register and the mean air temperature in the compartment were considered as the parameters showing the transient behaviour of the system.

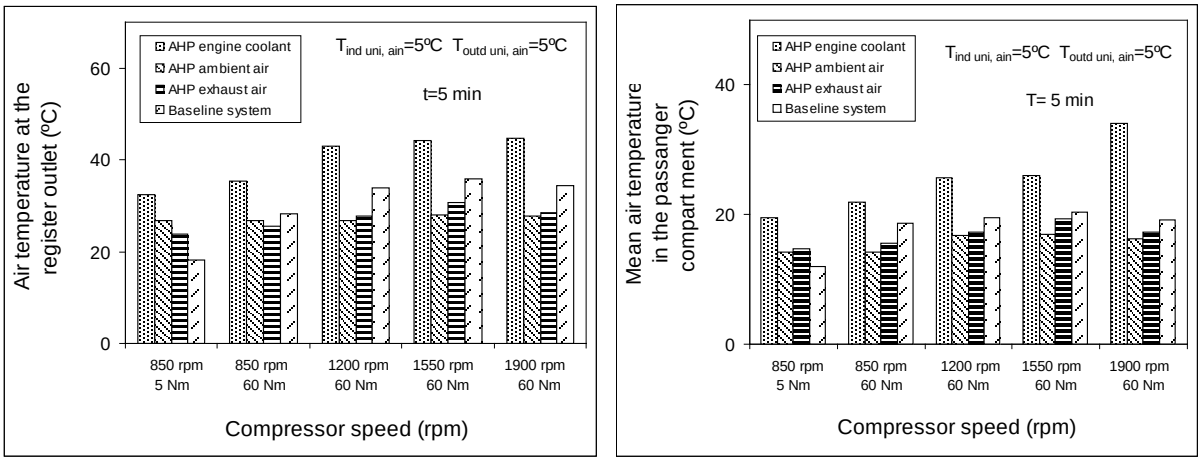

Fig. 2. The change of the air temperature at the compartment front register outlet (a); the change of the mean air temperature in the compartment (b) (both temperatures were recorded at the end of five-minute operation period).

Fig. 2 (a) shows the comparison of the fifth minute air temperatures measured at the front register outlet of the vehicle for the AHP systems and baseline heating system for different compressor speeds and dynamometer loads. It can be seen that the AHP system using engine coolant has higher air temperatures at the front register outlet compared with the AHP systems using ambient air and exhaust gas as well as with the baseline heating system. As the engine coolant temperatures increases, the evaporating temperature also increases, thus yielding higher condensing temperatures and conditioned air temperatures. It is seen that in

the heat pump operations, the air temperature at the front register outlet rises immediately after the compressor is started up. At 850 rpm speed and 5 N m load conditions, the AHP system using engine coolant provides a fifth minute air temperature at the front register outlet of 32°C, while the AHP system using ambient air and exhaust gas yields 26 and 23°C, respectively, and the baseline heating system provides only 18 °C, which is unacceptably low.

The air temperature at the front register outlet rises for all AHP systems when the engine speed and load are increased. In the AHP systems using engine coolant and exhaust gas, this increase is due to the elevated coolant and exhaust gas temperatures, respectively. As the engine speed increases, the refrigerant mass flow rate also increases, thus providing higher heat rejection in the condenser and higher air temperatures at the front register outlet for all AHP systems. Although the AHP system using engine coolant yields higher fifth minute conditioned air temperatures than the baseline heating system, the AHP systems using ambient air and exhaust gas cannot usually provide so high temperatures. Fig. 2 (b) demonstrates the changes of the fifth minute mean air temperatures in the passenger compartment as a function of compressor speed. When the engine speed and load are increased, the mean air temperature in the passenger compartment rises for all AHP systems and the baseline system. For the operations with the engine coolant, this increase is due to the elevated coolant temperature.

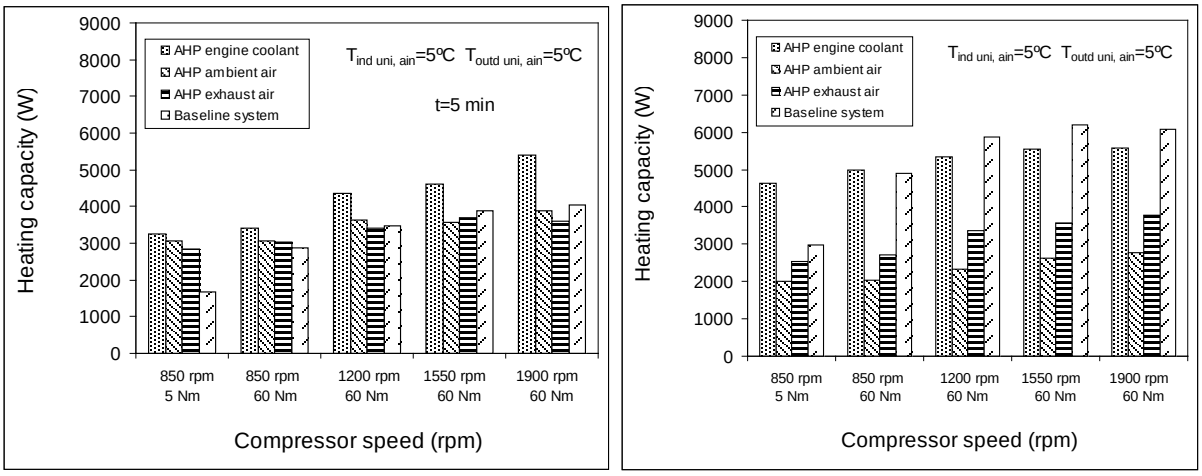

Fig. 3. The change of the heating capacity at the end of five-minute operation period (a); the steady-state heating capacity (b).

Fig. 3 (a) indicates the variations in the fifth minute heating capacity as a function of compressor speed. The heating capacity at the end of the five-minute operation period increases with the compressor speed at a constant engine load. At 60 Nm load conditions, the coolant based AHP system has the highest fifth minute heating capacity at all engine speeds, which is usually followed by other heat pump systems and baseline heating system. Fig. 3 (b) demonstrates that the steady-state heating capacities are usually higher than the fifth-minute ones. In the AHP system with the engine coolant, the refrigerant absorbs a greater amount of heat from the coolant heat exchanger, thereby providing considerably higher heating capacities compared with the AHP system with ambient air or exhaust gas. In the tests performed at 850 rpm and 5 Nm, the coolant based AHP system has the highest steady-state heating capacity, which is followed by the baseline heating system, AHP system using exhaust gas and AHP using ambient air in descending order. However, as the compressor speed is increased, the heating capacity of the baseline heating system gets higher.

Fig. 4(a) indicates the variations in the coefficient of performance of the experimental AHP system as a function of compressor speed based on steady-state data. It is seen that the *COP* for heating decreases by increasing the compressor speed since the compressor power increases faster than the heating capacity does with increasing compressor speed. The AHP system using engine coolant provides the highest *COP* compared with the AHP systems using ambient air and exhaust gas. Fig. 4 (b) shows the impact of the operation of AHP systems on the brake specific fuel consumption at different compressor speeds and engine loads. The *BSFC* increase caused by the AHP operations is very low when the engine speed and load are at high values because most of the power provided by the engine is applied to the dynamometer at these conditions. On the other hand, most of the power provided by the engine is used by the compressor of the AHP system when the engine is operated at low speeds and loads. Therefore, the increase in the *BSFC* due to the operation of the AHP system ranges between 4% and 54% depending on the engine speed and load.

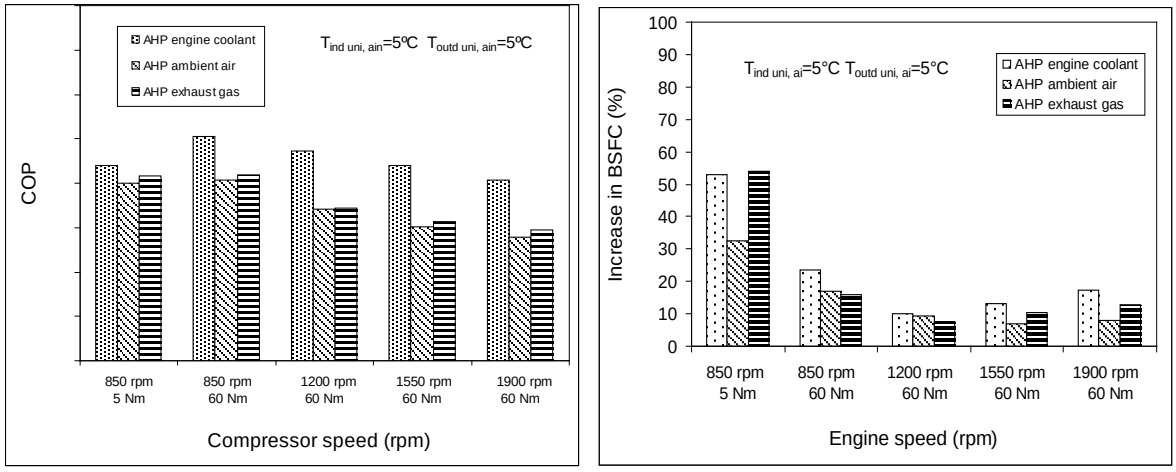

(a) *(b)*

Fig. 4. The change of the COP (a); the increase in the brake specific fuel consumption caused by the operation of the AHP system (b).

4. Discussion and conclusions

Both transient and steady-state performance parameters of an experimental automotive heat pump system charged with R134a and using ambient air, exhaust gas and engine coolant as a heat source have been evaluated. The AHP system was coupled to the passenger compartment of a test vehicle by means of a flexible air duct in order to supply the conditioned air stream to the compartment. The performance of the AHP system for each source was revealed by performing tests at various compressor speeds and engine loads. The performance parameters of the AHP system for each heat source were compared with those of the system using other heat sources and with those of the baseline heating system. Based on experimental data, the heating capacity, coefficient of performance, air temperature at the front register outlet, mean air temperature in the compartment of the test vehicle and the increase in the *BSFC* caused by the operation of the AHP system were presented as a function compressor speed. The following conclusions can be drawn from this investigation:

- When the engine is operated at idling conditions (n=850 rpm and T=5 Nm), the AHP system using engine coolant provides the highest steady-state conditioned air temperatures and heating capacities compared with the AHP system using ambient air and exhaust gas and with the baseline heating system.

- On increasing the engine torque and speed, the baseline heating system provides higher heating capacities after the steady-state has been achieved.
- The AHP system using any heat source yields higher conditioned air temperatures and heating capacities than the baseline heating system at the end of five-minute operation period when the engine is operated at the idling conditions.
- Only, the AHP system using engine coolant as a heat source provided a better fifth-minute heating capacity than the baseline heating system at speeds over 850 rpm when the engine load is 60 Nm.
- The AHP system using the engine coolant yields the highest *COP*s, while the AHP system with ambient air results in the lowest ones.
- The AHP system causes an increase in the *BSFC* of the engine within the range of 4–54% depending on the engine speed and load.

Compared with the baseline heating system, when the engine speed and load are at low values, the use of all considered AHP systems at transient phase are advantageous in terms of heating capacity and conditioned air temperature. Because the AHP system using the engine coolant provides higher heating capacities than other alternatives, this system can heat the passenger compartment individually, or it can support the present heating system of the vehicle in expense of increased *BSFC*.

Acknowledgement

The authors would like to thank The Scientific and Technological Research Council of Turkey (TUBITAK) for supporting this study through a Research Project (Grant No. 108M132).

References

[1] E.R. Domitrovic, V.C. Mei, F.C. Chen, Simulation of an automotive heat pump. ASHRAE Transactions, 103, 1997, pp. 291−296.

[2] M. Hosoz, M. Direk, Performance evaluation of an integrated automotive air conditioning and heat pump system. Energy Conversion and Management, 47, 2006, pp. 545−559.

[3] J. Rongstam, F.A. Mingrino, A coolant-based automotive heat pump system, Vehicle Thermal Management Systems Conference (VTMS6) Proceedings, 2003, SAE Paper Code: C599/067/2003.

[4] L.P. Scherer, M. Ghodbane, J.A. Baker, P.S. Kadle, On-vehicle performance comparison of an R-152a and R-134a heat pump system, SAE Technical Papers, 2003, Paper code: 2003-01-0733.

[5] D. Antonijevic, R. Heckt, Heat pump supplemental heating system for motor vehicles, International Journal of Automobile Engineering: Part D, 218, 2004, pp. 1111–1115.

[6] M. Hosoz, M. Direk, K.S. Yigit, M. Canakci, E. Alptekin, A. Turkcan, Design and instrumentation of an automotive heat pump system using ambient air, engine coolant and exhaust gas as a heat source, 16th International Conference on Thermal Engineering and Thermogrammetry (THERMO), 2009, Budapest, Hungary.

[7] M. Hosoz, M. Direk, K.S. Yigit, M. Canakci, A. Turkcan, E. Alptekin, A. Sanli, A.F. Ozguc, Experimental performance of an automotive heat pump system for various heat sources, Congress on Automotive and Transport Engineering (CONAT 2010), 2010, Brasov, Romania, Paper code: CONAT 20104046.

Prospects for eliminating fossil fuels from the electricity and vehicle transport sectors in New Zealand

Jonathan D Leaver[1,*], Luke HT Leaver[2]

[1] *Unitec NZ, Auckland, New Zealand*
[2] *Asia Pacific Energy Research Centre, Tokyo, Japan*
** Corresponding author. Tel: +64 98494180, Fax: +64 98154372, E-mail: jleaver@unitec.ac.nz*

Abstract: New Zealand is a small isolated country in the South Pacific with a population of 4.3 million people that has a strong commitment to reducing greenhouse gas emissions stemming both from its drive for global branding of principal export commodities and a desire to invest in new green technologies. New Zealand's renewable electricity generation reserve using biomass and wind alone is as much as 11 times the 2009 annual electricity demand. In this study the practical limits of fossil fuel reductions in the electricity and road transport sectors of the New Zealand economy are investigated using the multi-region partial equilibrium economic model UniSyD to examine a low carbon scenario in which oil reaches a maximum of US$200/bbl in 2030 in conjunction with a carbon tax of US$200 per tonne of carbon dioxide equivalent. In this scenario biofuel and electric drive vehicles are found to constitute 8% and 36% of the light vehicle fleet in 2050 respectively, with the balance of 56% still being fossil fuel vehicles. Government regulation is likely needed to reduce the proportion of fossil fuel vehicles to below 30% of the total fleet.

Keywords: *Alternative fuel vehicle, battery electric, hydrogen fuel cell, emissions*

1. Introduction

New Zealand is a small isolated country in the South Pacific with a population of 4.3 million people that has a strong commitment to reducing greenhouse gas emissions stemming both from its drive for global branding of principal export commodities and a desire to invest in new green technologies. As part of the commitment to reduce greenhouse gases New Zealand is one of the 187 countries to sign the Kyoto Protocol [1], one of 126 countries that agreed to the Copenhagen Accord [2], and in 2010, joined 28 other countries that have an emissions trading scheme [3].

In 2009 New Zealand produced 72.5% of its electricity from renewable energy [4] with the government aiming to increase this to 90% by 2025 [5]. Based on data from [6] and [7] New Zealand's potential renewable electricity generation reserve using biomass and wind alone is as much as 11 times the 2009 annual electricity demand with this being reduced to a factor of four if a wholesale electricity price limit of 8.4 USc/kWh is imposed. This provides opportunity to consider excluding fossil fuels from the electricity generation and transport sectors except where necessary to provide stability to the national electricity grid.

Studies on the economic impacts of alternative vehicle technologies on the New Zealand economy ([8], [9], [10]) have shown that a hydrogen fuelled fleet offers significant savings over a long range (320 km) battery electric vehicle (BEV) fleet. To achieve up to 80% reductions in greenhouse gas emissions from the transport sector a transition to all-electric vehicles will be necessary. This transition will include the adoption of a range of vehicle technologies [11].

Replacing fossil fuels in the electricity generation mix in New Zealand was shown to be possible for the period 2005-2007 [12]. The key factor in optimizing supply was the effective use of hydro in conjunction with wind. Wind energy spillage, peak load shifting and back-up fossil based peaking plant, were also important elements.

In this study the practical limits of fossil fuel reductions in the electricity and road transport sectors of the New Zealand economy to 2050 are investigated using the multi-region partial equilibrium economic model UniSyD4.4. The term "practical limit" in the context of this study means the utilization of all the available renewable energy resources of New Zealand that are economically viable within the scenario parameters. These resources include hydro, geothermal, wind, biomass (lignocellulose, rape seed) and solar.

2. Methodology

To explore the practical limits of fossil fuel reductions in the electricity and road transport sectors two scenarios were constructed. Each scenario excluded plug-in hybrid vehicles (PHEV) on the basis that these are an intermediate technology between conventional internal combustion engine vehicles (ICEV) and full electric drive vehicles. The scenarios are:

(i) Fossil Future (FF) in which no electric vehicles except hybrids (HEV) compete with the ICEV fleet before 2050. The carbon tax is US\$15/t-CO_{2eq} and the oil price rises at 2% per annum in real terms to a maximum of US\$120/bbl by 2030.
(ii) Renewables Future (RF) in which BEVs with a 320 km range and HFCVs compete for market share in the vehicle fleet along with HEVs. The carbon tax is US\$200/t-CO_{2eq} and the oil price rises at 4.7% per annum in real terms to a maximum of US\$200/bbl by 2030. No coal fired fossil fueled electricity generation is permitted.

The scenarios were simulated using the multi-regional partial equilibrium model UniSyD4.4 [8]. This is a system dynamics based model with a high degree of technological specificity in the electricity generation and transport sectors of the New Zealand economy. Each energy sector considers existing technologies and those that are contending to come on-stream to 2050 such as co-generation of hydrogen and electricity from coal or natural gas with sequestration as an option [8]. The model contains about 1150 variables and equilibrates supply and demand in fortnightly time steps in four primary markets in 13 geographic regions of New Zealand. These four markets comprise electricity generation, hydrogen generation, lignocellulose from purpose grown forests and the vehicle fleet. The model incorporates dynamic interactions based on the elasticity of prices with demand. The primary energy resource base for the model consists of hydro, geothermal, wind, biomass (lignocellulose, rape seed), natural gas, coal and solar.

The electricity market regions generate, import and export electricity based on the price of regional production and grid transmission costs. Options for electricity generation or energy saving on a domestic scale include micro-cogeneration of electricity and heat using either hydrogen or natural gas along with rooftop photovoltaics and solar thermal water heating. Temporal fluctuations in wind are neglected.

In the hydrogen market there are four centralised plant types of biomass gasification, coal gasification, large steam methane reforming and coal co-generation of hydrogen and electricity with sequestration of emissions using a solid oxide fuel cell topping cycle. There are five sizes for each plant to match supply with change in demand. Plants in the electricity and hydrogen markets are built by extrapolating demand growth from the previous three years up to four years in the future.

In the lignocellulose market, supply from forests is directly related to the forest residuals and purpose grown forest supply curve based on data from [6]. The biomass cost is determined on a marginal pricing system set in competition between the use of biomass for hydrogen,

bioethanol production and electricity generation. The decision to build a new biomass based plant is determined by the same mechanism as the hydrogen market.

The vehicle market model uses a standard logit choice, also known as a conditional logit model [13] to determine the market share of any particular vehicle technology. The market share is a function of elasticities of fuel cost, purchase price as shown in Fig. 1, maximum range and consumer driving distance.

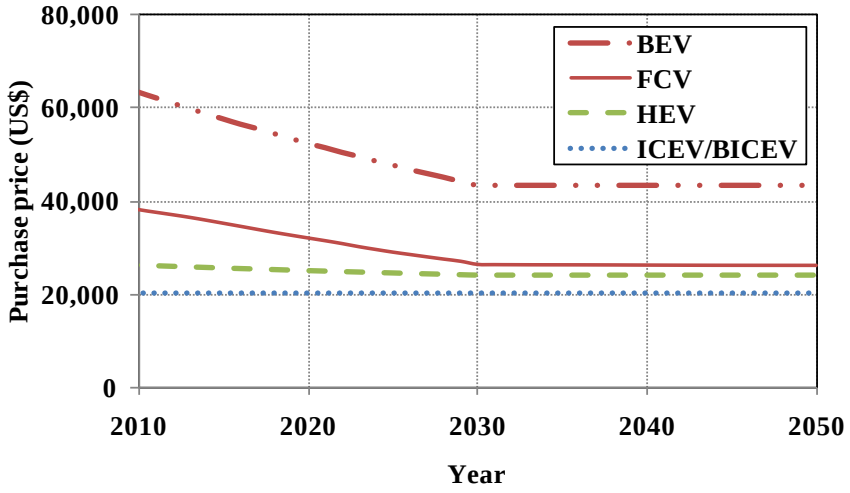

Fig. 1: Purchase price of alternative vehicles.

The standard logit choice model used in this study gives the market share of item i (S_i), as a function of the price (p_i), the price elasticity (β_i), and the intrinsic preference parameter (γ_i). The market share, S, is given by [13]:

$$S_i = \frac{e^{(\beta_i p_i - \gamma_i)}}{\sum_j e^{(\beta_j p_j - \gamma_j)}} \quad (1)$$

A significant feature of Fig.1 is that the long term purchase price of BEVs with a 320 km range is likely to be 80% higher than the mean of the other options. In the vehicle market ICEVs, HEVs, FCVs, and BEVs compete for market share. As imported vehicles represented 48.6% of the light fleet in 2009 [14] the imported and New Zealand new light vehicle fleets are modeled separately.

3. Results

The model results for the Fossil Future and Renewables Future scenarios are shown in Figs. 2 and 3 respectively. Under the FF scenario Fig. 2a shows electricity generation from wind increases rapidly after 2025 with the mandated phasing out of fossil fuels. Wind penetration in 2050 is 35% of total generation by 2050 with hydro 38%, geothermal 18% and 9% other renewable generation such as biogasification. In Fig. 2b the electricity price averages about 7.0 USc/kWh after 2030 with the price spike in 2022 reflecting a short term electricity shortage due to the phasing out of coal production that is independent of carbon tax policy. In Fig. 2c, bioethanol production from forest resources provides fuel for 12% of the vehicle fleet by 2050 (Fig. 2e and 2f) with the balance of 88% being fossil fueled. In Fig. 2d GHG emissions decrease by 7% between 2010 and 2050 with a 34% reduction during the period 2020 to 2030 with the reduction in fossil fueled electricity generation. Improving fuel

economy in the vehicle fleet limits increases in GHG emissions for the period 2030 to 2050 to 17%.

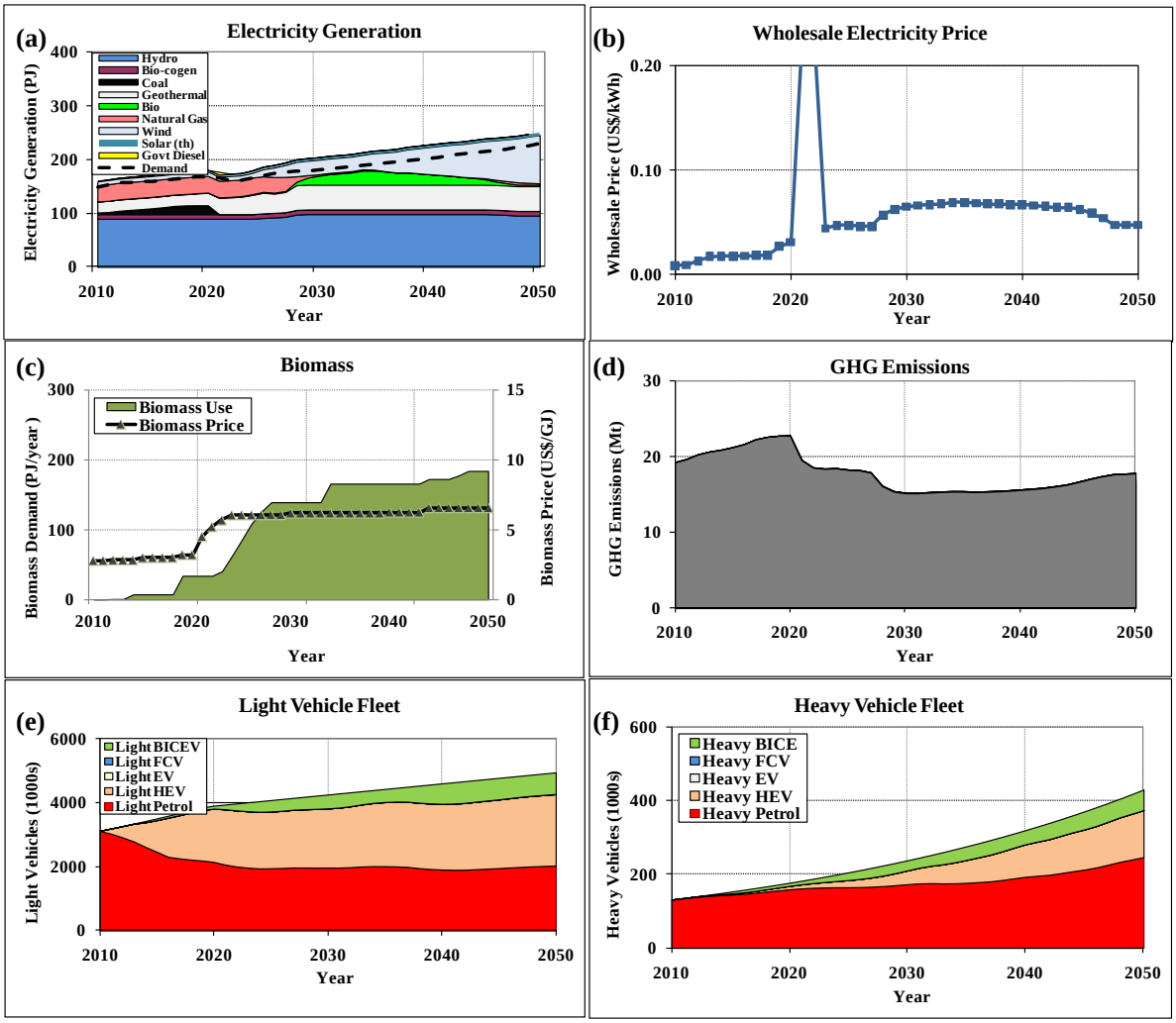

Fig. 2: For the Fossil Futures scenario: (a) Electricity generation profiles. (b) Hydrogen production profiles. (c) Wholesale electricity price. (d) Wholesale hydrogen price. (e) Biomass demand and price. (f) GHG emissions. (g) Light vehicle fleet. (f) Heavy vehicle fleet (g) Fuel economy. (h) Fuel cost per k of travel.

Under the RF scenario in Fig. 3a the high carbon tax eliminates coal fired generation and natural gas generation ceases by 2018. By 2050 the generation profile consists of 41% wind, 36% hydro, 14% geothermal and 9% other renewable generation such as biogasification. Total renewable generation is 97%. In Fig. 3b the electricity price rises to a high of 13 USc/kWh in 2013 with the sudden rise in carbon tax from US$15/t-C to US$200/t-C. Prices average about 7.2 USc/kWh after 2030. In Fig. 3c hydrogen production commences with forecourt electrolysis in 2015 with large scale hydrogen production from biogasification commencing in 2020. Fig. 3d shows that the hydrogen production price is close to US$5.00/kg after 2020. In Fig. 3e biomass use rises sharply from 2016 to 2020 as a primary fuel for hydrogen production by biogasification. In Fig. 3d, GHG emissions decrease by 58% between 2010 and 2050. In Fig. 3g light BICEVs, HFCVs, and EVs constitute 8%, 28% and 8% respectively of the light vehicle fleet in 2050, with the balance of 56% being ICEVs and HEVs. In Fig. 3h, heavy BICEVs and HFCVs constitute 14% and 44% respectively of the heavy vehicle fleet in 2050, with the balance of 42% being ICEVs and HEVs.

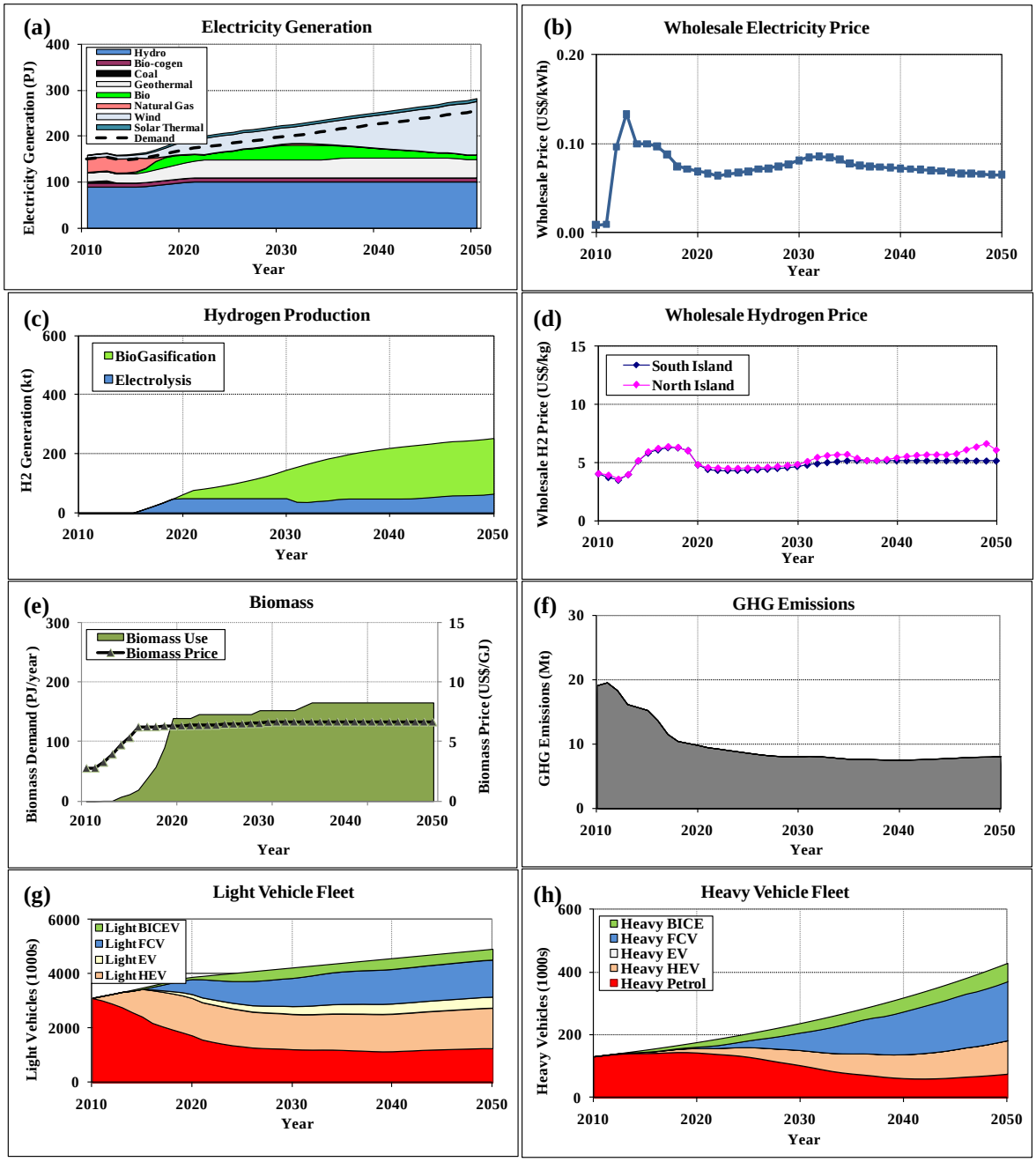

Fig. 3: For the Renewables Future scenario: (a) Electricity generation profiles. (b) Wholesale electricity price. (c) Hydrogen production profiles. (d) Wholesale hydrogen price. (e) Biomass demand and price. (f) GHG emissions. (g) Light vehicle fleet. (f) Heavy vehicle fleet (g) Fuel economy. (h) Fuel cost per k of travel.

4. Discussion

Two primary consequences emerge from a comparison of the Fossil Future and Renewables Future scenarios. Firstly in 2050 in both scenarios all generation excluding backup peak load generation is renewable. The only effect of the high carbon tax in the RF scenario is to reduce geothermal generation by about 4% and replace this with wind. All GHG emissions are from the vehicle fleets. GHG emissions in the RF scenario are 54% less than in the FF

scenario by 2050 which equates to a 54% reduction by weight in fossil vehicle fuel. Secondly the proportion of light ICEVs under the RF scenario of 56% is 32% less than that under the FF scenario of 88%. The fact that the combined penetration of ICEV and HEV in the RF scenario remains high at 56% is a result of the improving fuel economy of ICEVs and HEVs that enhances the competitiveness of these technologies and delays their replacement by all electric BEV and HFCV technologies. Reducing the penetration of ICEV and HEV to less than 30% of the total fleet may require government regulation to encourage adoption of electric vehicles. The primary focus of any regulation should be to reduce the purchase price of electric vehicles with subsidies while recovering the subsidy as a fuel tax. The motive behind this is that purchasers value an incremental reduction in purchase price at twice that of a reduction in running costs [15].

The average electricity price under RF remains stable at about 7.2 USc/kWh despite the increased electricity demand for hydrogen production by electrolysis and subsequent recharging of electric vehicles. This increase in electricity price is buffered by the large wind resource available at less than 8.4 USc/kWh referred to earlier in this study.

Wind penetration in the RF scenario is 41% by 2050 which poses significant issues for the stability of New Zealand's electricity grid. In Denmark the Danish Transmission System Operator is planning for up to 50% wind penetration in the transmission system [16]. However New Zealand cannot import electricity from neighboring countries.

Mason et al. [12] examined wind penetration in the New Zealand electricity system of up to 35% during 2005-2007 when demand totaled 54% of expected demand in 2050. The study concluded that penetration rates of 19% could be achieved by utilizing the existing hydro system to balance periods of low wind generation with almost no reduction in electrical energy from hydro generation.

Wind penetration of 18% has been estimated [17] to incur integration costs of 0.6 USc/kWh as shown in Table 1.

Table 1. Wind integration cost (adapted from [17]).

Year	2010	2020	2030
Installed wind power capacity (MW)	634	2066	3412
Wind energy (PJ)	8.3	24.1	39.1
Wind energy as % of total generation	5	12.5	18
Additional wind integration cost (USc/kWh)	0.14	0.14	0.61

Recent wind integration studies [17, 18] suggest enough standby generation must be available to meet a 'no wind' scenario. Analysis of a 19-year daily synthetic wind speed dataset [19] showed that no wind generation is likely to occur for two days every three years under a geographically diverse wind portfolio. In order to cater for the 'no wind' scenario requirement at 41% wind penetration in 2050, New Zealand will require active demand side management, smart flexible gas contracts and peaking based hydro management coupled with fast start standby thermal generation. This could include remote shut-down of selected hot water heating installations, and short term diversion of electricity and gas supplies from selected large industrial electricity users such as aluminum [20] and methanol [21] production plants. Diversion from large industrial plants has the potential to provide additional backup electricity generation of up to 50% and 66% respectively of predicted wind generation in 2050 under the RF and FF scenarios. Further measures may involve a mixture of pumped hydro storage using off peak electricity, or changing the operating limits of hydro lakes for very short periods.

To ensure grid stability a number of load balancing generation and load shifting options will be needed. Load balancing options would principally include hydro with support from fossil fuelled peaking plants. Load shifting options could include remote shut-down of selected hot water heating installations, pumped hydro storage using off peak electricity, and smart metering that allows real time electricity billing to encourage fast consumer response to electricity price.

This study used an upper bound carbon tax of US$200/t-C to examine renewable energy penetration limits. Marginally lower penetration rates of renewable energy may be possible with a carbon tax of US$100/t-C although a detailed study of this option is outside the scope of this paper.

5. Conclusions

New Zealand's has the potential to achieve over 90% electricity generation from renewables by 2050 but maintaining or exceeding this target to 2050 will require complex integration of peak load backup generation to balance the variability of wind generation. This target is largely independent of the carbon tax due to the large and economically viable wind resource. In the vehicle fleet, in the absence of plug-in hybrid vehicles and without government regulation, 44% of the light vehicle fleet is expected to be electric drive by 2050. The penetration rates of electric vehicles will be enhanced with purchase price subsidies capitalised from fuel taxes.

References

[1] United Nations Framework Convention on Climate Change, Status of Ratification of the Kyoto Protocol, http://unfccc.int/essential_background/kyoto_protocol/status_of_ratification/items/5524.php. Accessed 1 October 2010.

[2] United Nations Framework Convention on Climate Change, Report of the Conference of the Parties on its fifteenth session, held in Copenhagen from 7 to 19 December 2009. Report 3F0C CMCa/rCchP /22001009 /11, 30 March 2010. p. 36.

[3] New Zealand Ministry for the Environment. The New Zealand Emissions Trading Scheme. http://www.climatechange.govt.nz/emissions-trading-scheme/. Accessed 1 October 2010.

[4] New Zealand Ministry of Economic Development, New Zealand Energy Data File: 2009 Calendar Year Edition, ISSN 1177-6676, 2010, p. 174.

[5] New Zealand Ministry of Economic Development, Draft New Zealand Energy Strategy: Developing our energy potential, ISBN 978-0-478-35862-9, 2010, p. 34.

[6] Scion, Bioenergy Options for New Zealand: Situation Analysis, ISBN 0-478-11019-7, 2007, p. 83.

[7] Connell Wagner, Transmission to Enable Renewables: Economic wind resource study, Report 31362/001, 2008, p. 27.

[8] J.D. Leaver, K.T. Gillingham, L. Leaver, Assessment of primary impacts of a hydrogen economy in New Zealand using UniSyD. International Journal of Hydrogen Energy 34 (7), 2009, pp. 2855-2865.

[9] J.D. Leaver, K.T. Gillingham, Economic impact of the integration of alternative vehicle technologies into the New Zealand vehicle fleet. Journal of Cleaner Production, 18, 2010, pp. 908-916.

[10] R. Whitney, T. Clemens, A. Gardiner, J. Leaver, Transitioning to a Hydrogen Economy in New Zealand: An EnergyScape Project, Proc. XXI World Energy Congress, Montreal, 2010, p. 20.

[11] C. Thomas, Transportation options in a carbon-constrained world: Hybrids, plug-in hybrids, biofuels, fuel cell electric vehicles, and battery electric vehicles, International Journal of Hydrogen Energy 34, 2009, pp. 9279-9296.

[12] I.G. Mason, A 100% renewable electricity generation system for New Zealand utilizing hydro, wind, geothermal and biomass resources, Energy Policy, 38, 2010, pp. 3973-3984.

[13] D.L. McFadden, Conditional Logit Analysis of Qualitative Choice Behavior. In P. Zarembka (ed.), Frontiers in Economics, 1973, New York: Academic Press, pp. 105-142.

[14] Ministry of Transport, The New Zealand Vehicle Fleet: Annual Fleet Statistics 2009, ISBN978-0-478-07228-0, 2010, p. 68.

[15] K.E. Train, EM Algorithms for nonparametric estimation of mixing distributions, Journal of Choice Modelling, 1(1), pp. 40-69.

[16] K. Sperling, F. Hvelplund, B. Vad Mathiesen. Evaluation of wind power planning in Denmark: Towards an integrated perspective, Energy (in press), 2010, p.12.

[17] G Strbac, D Pudjianto, A Shakoor, MJ Castro. New Zealand Wind Integration Study. Meridian Energy, April 2008. Accessed 8 November 2010. http://www.meridianenergy.co.nz/NR/rdonlyres/345B3A36-1434-4CAF-95AC-. 10.

[18] B Smith, Wind integration – the long view, Report. The New Zealand Electricity Authority, April 2009.

[19] New Zealand Electricity Commission. Analysis of wind integration – synthetic wind data. April, 2009, http://www.ea.govt.nz/industry/modelling/analysis-of-wind-integration/. Accessed 17 November 2010.

[20] A. Bennett, Meridian boss hails deal with smelter, http://www.nzherald.co.nz/energy/news/article.cfm?c_id=37&objectid=10467340. Accessed 8 November 2010.

[21] Contrafed Publishing Co. Ltd, A train in want of gas, Energy NZ, No.11 2009.

Advanced Research Strategy for Designing the Car of the Future

Konstantinos Gkagkas[1,*], Jonas Ambeck-Madsen[1], Ichiro Sakata[1]

[1] *Toyota Motor Europe NV/SA, Brussels, Belgium*
** Corresponding author. Tel: +32 27123435, Fax: +32 27123325, E-mail:Konstantinos.Gkagkas@toyota-europe.com*

Abstract: This paper describes a novel concept regarding the method for research and development of future vehicles. It is shown that the traditional rate of progress cannot keep up with the increasingly pressing issues of global warming and social sustainability. A new, holistic approach which takes into account the form, operation and social aspects of the future society is suggested. This approach tries to remove the boundaries between different sections of science and also accelerate the rate and speed of adoption of new technologies into the final, mass-produced vehicle. Such an approach can pave the way for the creation of a vehicle that reaches our goal of zero accidents and zero emissions.

Keywords: *Sustainable Transport, Social Sustainability, Future Mobility and Technology*

1. Introduction

The issue of global warming and its relation to human-induced emissions is well known. In 2009, both the European Union and G8 leaders agreed that CO_2 emissions must be cut by 80% by 2050 in order to stabilise the concentration of greenhouse gas (GHG) emissions in the atmosphere at a level of 450 ppm of CO_2 equivalent and keep global warming below the level of 2ºC. Transport accounts for about one-fifth of global energy use and one-quarter of energy-related CO_2 emissions [1]. To achieve the necessary deep cuts in greenhouse gas emission by 2050, transport must play a significant role and achieve 95% decarbonisation. Car ownership worldwide is projected to triple to over two billion by 2050 and, without strong global action, a respective growth of energy use and CO_2 emissions will occur [1]. Fig. 1 shows estimation for EU total greenhouse gas emissions. It can be seen that, following the baseline scenario which already includes large efficiency improvements, especially in industry, the emissions are expected to remain constant. The amount of additional effort that must be put in each sector in order to achieve the necessary emission cuts is clearly visible [2].

Fig. 1. EU total GHG emissions forecast for 2050 and comparison to target.

Similarly, annual global road-traffic fatalities sum to more than 1 million and injuries to more than 50 millions [3]. Awareness, technological advances and stricter legislation have lead to

the reduction of injuries and fatalities in developed countries as can be seen in Fig. 2; however the increasing level of car adoption, especially in developing countries, means that the global number of fatalities and injuries is likely to increase [3]. The cost of road accidents, in both social and financial terms is not negligible. For example, the cost of fatalities in EU-27 during 2006 corresponded to approximately 2% of the total GDP [4].

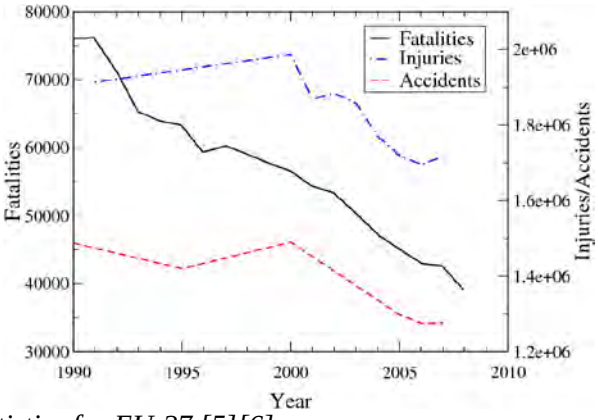

Fig. 2. Road accident statistics for EU-27 [5][6].

Current automotive technology improves at incremental steps, as conventional, long-existing concepts are optimised towards their theoretical limits. Compared to previous decades, current cars provide higher levels of safety and have a similar or lower environmental footprint at the same time. Stricter legislation and industrial competition have supported this trend by leading to the introduction of new or improved technologies in the course of the years. However, growing concerns of the climate change mean that this rate of progress is not viable, as shown in Fig. 1.

The introduction of the mass-produced automobile represented a revolution in affordable, highly flexible mobility and convenience. This flexibility makes its use appropriate especially in cases where large investments in mass transportation are not viable. Its usage has led to significant changes in society and has contributed to economic growth, supporting the growth of small and medium-size businesses over the years. Currently, transport is one of the backbones of European economy, accounting for about 7% of GDP and more than 5% of total employment in the EU. How can we continue to enjoy the benefits of car mobility in a sustainable way, without the associated risks of traffic accidents and accelerated climate change? In the following sections we try to share selected elements of our vision for research carried out in Toyota Motor Europe for creating the future image of automotive transportation, as well as the necessary technologies to make this sustainable. More specifically, in Section 2 we describe our research methodology. In Section 3 we outline our perceived image of the future car and present key technologies that will render it possible. Finally, in Section 4 we summarise our findings.

2. Research strategy

The automobile has evolved over several decades into a practical and reliable product by following a solid approach of thinking and engineering. This traditional approach is starting to become a limitation to the rate of further technology improvement, unable to keep up with the requirement for drastic changes shown in Section 1. The automotive industry is faced with a lot of challenges to deliver innovative products to its customers, and some will likely require a big innovation jump. Currently developed and emerging technologies need to be implemented in new vehicles rapidly, at a rate and on a scale that is unprecedented in the last 40 years of

transport evolution. New technologies that deal with weight reduction, performance optimisation and efficient usage of energy resources need to be developed for reversing the trends of the past decades and achieving our targets in GHG emission cuts, without a negative impact on existing levels of quality and comfort. This will require answers to paradoxical questions such as how can we produce a vehicle which is extremely lightweight and completely safe at the same time? How can we manufacture a vehicle which provides complete freedom and pleasure to the driver and passengers, without any environmental impact? Such questions are indeed paradoxical when following the traditional way of thinking. A fresh, "out of the box" approach is therefore needed to provide answers and solutions which are realistic and feasible in a short timeframe compatible with our extremely challenging targets.

2.1. Limitations of current methodology

Before describing a new research strategy, we first reflect on the more than 100 year long automotive history in order to understand the logic and the potential of the current direction for improving the environmental performance of cars. Fig. 3(a) shows the history of average fuel consumption in Europe and the US for the period 1975-2002. In comparison, fuel consumption of the first mass-produced vehicle, Ford Model T, in 1908, was around 11-18 lt per 100 km [7]. It can be seen that after period of a relatively strong improvement in average fuel economy during the 70s, homologated consumption has roughly stabilised in the US and drops only slowly in EU. This can be explained by Fig. 3(b), which shows the relative evolution of vehicle mass, power and engine size in EU for the same period. It is clear that during the same period, vehicles have become heavier, more powerful and relatively faster. Increases in engine size and vehicle mass can partly be attributed to dieselisation (as diesel vehicles have a lower power/mass ratio), but even so it is evident that the trend for bigger, faster and theoretically safer cars has off-set the gains in efficiency.

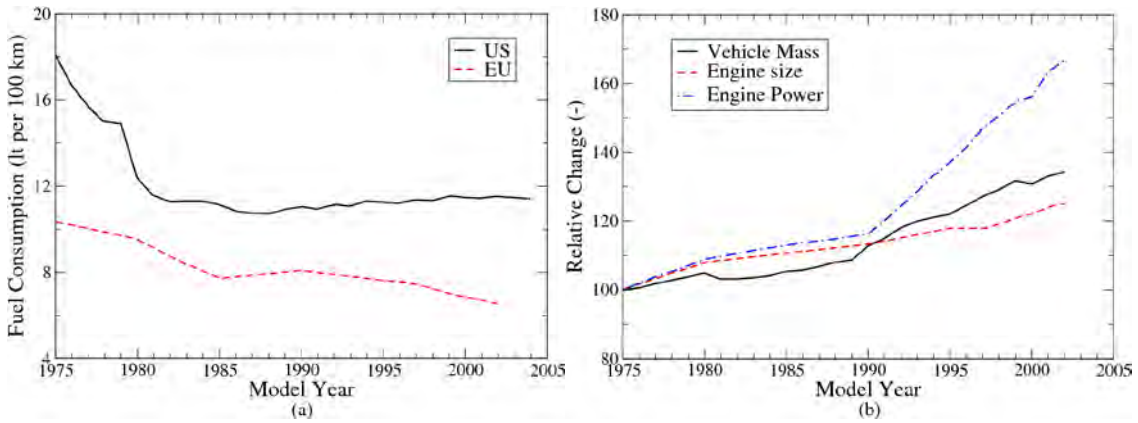

Fig. 3. Evolution of (a) US and EU motor vehicle economy from 1975 to 2003 and (b) average weight, power and engine size of new cars sold in EU from 1975 to 2002[8]

As a second example, Table 1 shows the evolution of a typical vehicle over the last decades. As specifications can vary a lot over different countries and model generations, some typical values are shown, corresponding to a compact sedan vehicle, with comparable acceleration performance. The trend of increasing weight and dimensions is obvious, with a current vehicle being more than 0.5 meters longer, and almost double the weight, compared to 40 years ago. It is also interesting to note that the average fuel consumption has had small fluctuations over the years, with significant reductions being achieved in the last decade, bringing us back to the levels of 1960's. These numbers also verify the findings of the average vehicle evolution trends, with the levels of safety and comfort improving considerably over

the last decades at the expense of potential improvements in performance and fuel consumption.

Table 1. Evolution of Toyota Corolla Sedan typical specifications. Figures obtained from internal TME material.

Year	Length (mm)	Weight (kg)	Engine size (lt)	Power (kW)	Acceleration (s)	Cd (-)	CdA (m^2)	Fuel consumption (lt/100km)
1966	3848	700	1.2	50	13.7		0.6	6.4
1970	3945	801	1.4	63	11.6		0.61	6.82
1974	3995	930	1.6	61	12.6	0.43	0.776	7.92
1979	4048	821	1.5	55	11.5	0.43	0.798	7.51
1983	4135	920	1.6	62	11.6	0.37	0.696	7.22
1987	4191	955	1.6	70	11	0.33	0.62	7.22
1991	4270	1000	1.6	81	10.4		0.631	
1997	4295	1035	1.6	81	10.7	0.33	0.644	7.81
2000	4365	1125	1.6	81	10.3			
2006	4540	1310	1.6	97	10	0.3	0.73	6.4

The design and production of a car is a very challenging exercise, with many contradictory demands. Such demands, limited by existing practices and infrastructure investments, lead invariably to compromises in the final product, and do not allow the full potential of technology to be exploited. The shortcomings of this approach can also be noticed in the current development of new generation, alternative drive-train vehicles, which are essentially developed on the platform of traditional ICE cars with a direct replacement of engine and the addition of energy storage or conversion devices in space which could opportunistically be used for the comfort of the passengers or as optimised shape for drag reduction. Similarly, the current strategy of tackling the possible dangers that inherently quiet electric vehicles may pose to pedestrians by adding artificial noise is another example of lack of "new thinking" in what could be a chance for a significant reduction in urban noise pollution.

2.2. New approach

It becomes clear from subsection 2.1 that in order to induce the required paradigm shift, a new way of thinking and performing research is necessary. Since several years, we try to seek inspiration in all kinds of science around us. Such inclusive thinking incorporates cutting edge research in engineering. We can find interesting concepts in the work of several research groups. A recent example is the development of a battery which can also be used as a structural material [9], therefore removing significant duplication of the weight. Research from NASA has led to a self-sustainable marine vehicle [10], while Lotus Engineering has recently shown that a significant weight reduction can be achieved using relatively standard technologies and with a minimum impact in cost [11]. However, our truly multidisciplinary research approach extends beyond the conventional limits of engineering to concepts not directly related to vehicles, such as biology and social sciences, and can provide new seeds of technology which are not limited by topic and therefore also not in scope. In nature we observe many truly amazing technology-like functions, and we have long been looking here for inspiration to solve some of our fundamental engineering challenges related to both vehicle safety and sustainable energy efficiency. Another pillar of our approach is that we take into account the future society structure and operation and thus our real target becomes to increase the efficiency of the whole system, rather than a single component, as done traditionally. In such a holistic approach, we consider the automobile not as an individual unit,

but as a living part of a bigger organism. This way, many of the existing obstacles can be overcome and a higher rate of development can be achieved.

In addition, we consider practical aspects such as the cost of new technology, investments in infrastructure, local energy resources availability, as well as human aspirations and market diversity. Sustainable mobility, apart from dealing with environmental and energy issues, must also satisfy the individual customer needs, meaning that it must maintain or improve upon the current acceptable levels of performance, safety, comfort and practicality. It must also respond and adapt to changes in lifestyle, such as urbanisation and network connectivity, converting such changes into opportunities for further improvements. Finally, it must maintain and extend the personal freedom of the driver and the passengers, keeping the aforementioned benefits of private transportation, in a socially and environmentally responsible manner.

Such a quest for a potentially sustainable automotive transportation technology, as described in Section 1, is slowly starting to gain traction globally. A recent example is the LA Auto Show Design Challenge which has been providing a platform for presenting new ideas over the past seven years. A different theme, relevant to different aspects of future car usage, is employed each year, and some interesting ideas can already be seen [12].

3. Image of the sustainable vehicle

Following the approach described in Section 2, we estimate that the amount of energy needed for car transportation by 2050 is possible to be one order of magnitude lower than current levels and the emitted greenhouse gases close, if not equal, to zero. By removing inefficiencies in all the subsystems and introducing new technology concepts, we are aiming at creating a vehicle which can propel itself without any fossil fuel derived energy support while maintaining the current levels of vehicle performance and occupants comfort.

3.1. Evolving society

The large-scale availability of affordable liquid fuels has essentially sparked a modern industrial revolution over the 20th century and shaped the transportation sector. Today transport is at a transition point, as it is starting to become a victim of its own success. The genesis of our image for the future car should therefore be viewed in the context of its existence inside the future society. A society which we believe will be characterised by the lack in cheap resources, growing levels of population and urbanisation. This future society will be more extrovert and will strive to remove inefficiencies following a global optimisation approach. In such an environment, information will constantly be transferred and exchanged, allowing each subsystem to automatically adapt its operation in order to support a smooth global operation. New information technologies, providing immense wealth of information, are already starting to move in this direction [13].

Apart from the information exchange, which is necessary for a smooth coexistence of the different structures in a society, another important concept which needs to be materialised is that of energy exchange. By this, we mean the constant adaptation of energy resources used, in order to achieve the most efficient energy production, as well as the constant energy re-usage process, during which energy is converted into different forms without loss. The successful combination of energy and information exchange processes will ensure the achievement of such a smart and self-regulating entity.

3.2. Shaping the future car

In such exchanging society, different means of transportation have their own role to play. We believe that the desire for the pleasure, freedom and practicality of personal mobility will not be eclipsed, and therefore the personal car will continue to have an important role. By actively taking advantage of opportunities presented in the future society, automotive transportation can adapt and be optimised in order to achieve successful merging and co-existence in the daily life of its citizens.

A self-sustainable vehicle has, first of all, to remove the past inefficiencies. Fig. 4 shows the energy losses in two usual driving scenarios, according to [14]. It can be seen that the energy which finally results in the actual mobility of a conventional car corresponds to less than 20% of the available energy from the fuel. A lot of new technologies aim at reducing or removing such energy losses, although, arguably, the most significant of these losses is inherent to the historical operation of the thermal engine and is the hardest to tackle. Another source of inefficiency is the mass of the vehicle itself and the associated inertial effects. As shown in Section 2, the improvements in engine technology have been offset by the weight increase over the last decades, with the fuel economy not being able to improve as drastically as it could. It is highly paradoxical that a vehicle of more than 1000kgs is needed for the transportation of an 80kg person. It is clear that different technology is required in the design of future vehicles.

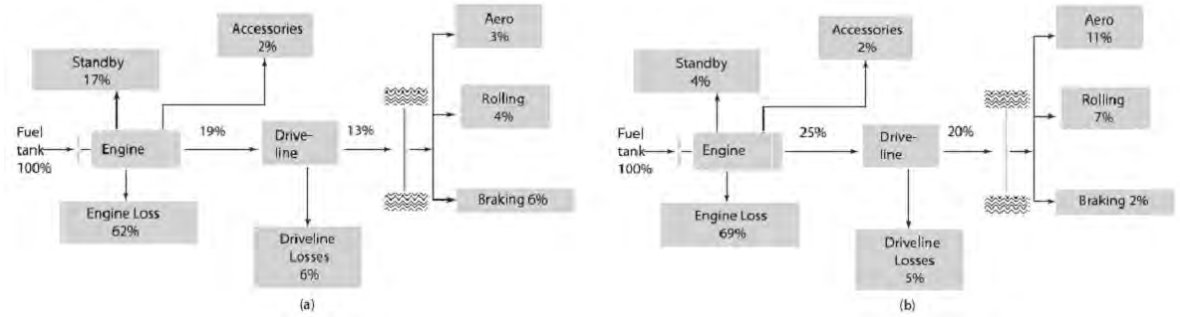

Fig. 4. Energy dissipation in (a) urban and (b) highway driving [14]

Completely in line with our image of the future society, the future vehicle takes advantage of all the available information and energy forms in order to maximise its potential and optimise its operation. Like the combined intelligence of a school of fish that travel together in a way that offers them safety and ensures the minimum drag during their movement in the water, our future vehicle can communicate with its surroundings and adapt its operation in a way that removes the danger of accidents, while respecting the individuality and the preferences of the driver. Moreover, this communication and adaptation allows the usage and re-usage of the available energy in the best possible way without losses, but with continuous transformation from one form to another.

A significant gain can be achieved by reducing the mass of the vehicle considerably. We envisage a five-fold reduction in this sector. A combination of ideas will be necessary for this target to be achieved. First of all, the novel intelligent safety systems will ensure that it is possible to avoid any dangerous situation at all times, and therefore reduce the reliance on increasingly stronger individual vehicle structures, which can be parallelised more to the sturdiness of an elephant, rather than the elegance and nimbleness of a bird. Then, a new generation of materials, inspired by nature and based on simple, cheap building blocks which gain their strength by their internal microstructure will allow the creation of vehicles which

are more in line with their natural surroundings. The human organism consists of materials which do not necessarily have significant individual strength or potential. However, due to their relative organisation and control under powerful sensory and cognitive skills, they can be protected by catastrophic damage and are capable of achieving comparatively amazing results. Finally, the integration of multiple functions in fewer structures or components can remove unnecessary weight.

Such optimizations can significantly reduce the amount of energy which is necessary for mobility. This has initially a positive impact on the rate of existing resource depletion. More importantly, though, it can enable an era of desired self-sustainability, where the naturally occurring energy streams can be harvested and exchanged efficiently, thus minimising the link to fossil fuel consumption.

Fig. 5. Example of image enhancement by novel night vision algorithm: (a) Original frame. (b) Tone mapped version. (c) After noise reduction. (d) After noise reduction with sharpening.[15]

Fragments of such ambitious thinking can already be seen in cutting edge research. An example of research is a novel night vision system, inspired by the eyes of nocturnal insects [15]. The algorithm developed in this project was born from understanding how an insect can hunt for food which is beautifully coloured flowers at night, navigating with its normal eyes. A sample result is shown in Fig. 5. Whereas traditional technologies might saturate in terms of performance, results obtained from such a holistic research framework can have the potential to leap-frog beyond current frontiers.

3.3. Contribution of the engineer

We are faced with the tough challenge of adapting this totally new knowledge back into existing systems and applications of our industry, to fully measure and evaluate its true potential, but it is a challenge which we are working hard to overcome. To do so, first we try to play a binding role by bringing different kinds of science together and removing the borders between them. Secondly, we try to identify the potential and feasibility of each technology, and quickly pursue its development and application into the final product through interaction with development, production engineers, marketing etc. For successful guidance in such an approach, we set a clear future target, like the one we are presenting in the current paper. We believe, based on our experience from ongoing projects, that this concept will allow a revolutionary design and integration of subsystems, paving the way to radically new implementations.

4. Summary

We have a dream of zero accidents and zero emissions for our future car. The pressing sustainability issues mean that our dream is relevant more than ever. In this paper, we propose the development of technologies which support the process of exchanging energy and information as a way to reach this target. By such challenging of traditional thinking we aim

to spark innovation for game-changing technologies, leading to a truly sustainable mobility solution, from both an environmental and social point of view.

References

[1] International Energy Agency, Transport Energy and CO2: Moving towards Sustainability, OECD Publishing, 2009, pp. 29 – 41.

[2] EIA (US Department of Energy, Energy Information Administration), International Energy Outlook 2010, DOE/EIA-0484(2010), 2010, p. 6.

[3] World Health Organization, World Report on road traffic injury prevention, Geneva, 2004, pp. 33-38.

[4] Commission of the European Communities, Impact Assessment of the Communication "Keep Europe Moving". Sustainable mobility for our continent. Mid-term review of the European Commission's 2001 Transport White Paper, Brussels, 2006, p. 74.

[5] Commission of the European Communities, A Sustainable Future for Transport: Towards an integrated, technology-led and user friendly system, Brussels, 2009.

[6] C. Nicodème, K. Diamandouros, J. Luiz Diez, I. Fusco, M. L. Lorente Miñarro, European Statistics 2010, European Union Road Federation, 2010, pp. 50-55.

[7] Media.ford.com, Model T Facts, Retrieved 2010-12-15, Available at: <http://media.ford.com/article_display.cfm?article_id=858>.

[8] T. Zachariadis, On the Baseline Evolution of Automobile Fuel Economy in Europe, Energy Policy 34, 2006, pp. 1773-1785.

[9] Imperial College London, Cars of the future could be powered by their bodywork thanks to new battery technology, 2010, Available at: <http://www3.imperial.ac.uk/newsandeventspggrp/imperialcollege/newssummary/news_5-2-2010-10-26-39>.

[10] NASA/Jet Propulsion Laboratory, NASA demonstrates novel ocean-powered underwater vehicle, ScienceDaily, 8 April 2010. Available at: <http://www.sciencedaily.com-/releases/2010/04/100405142152.htm>.

[11] Lotus Engineering, Lotus Engineering Study Concludes Vehicle Mass Improvement of 38% by 2020 vs a Conventional Current Vehicle Can Be Achieved at Only 3% Cost, Green Car Congress, 27 April 2010, Available at: <http://www.greencarcongress.com/2010/04/lotus-20100427.html>

[12] LA Auto Show, Design Challenge 1000lb car, 2010, Available at: <http://www.laautoshow.com/DC10/>

[13] C. Heipke, Crowdsourcing geospatial data, ISPRS Journal of Photogrammetry and Remote Sensing 65, 2010, pp. 550-557.

[14] The National Academies, Tires and Passenger Vehicle Fuel Economy, Transportation Research Board Washington D.C., 2006, p. 40.

[15] H. Malm, M. Oskarsson, P. Clarberg, J. Hasselgren, C. Lejdfors, E. Warrant, Adaptive enhancement and noise reduction in very low light-level video, IEEE 11th International Conference on Computer Vision, 2007

Electric Vehicle with Charging Facility in Motion using Wind Energy

S.M. Ferdous[2,*], Walid Bin Khaled[1], Benozir Ahmed[2], Sayedus Salehin[1], Enaiyat Ghani Ovy[1]

[1] *Department of Mechanical & Chemical Engineering*
Islamic University of Technology, Board Bazar, Gazipur-1704, BANGLADESH
[2] *Department of Electrical & Electronic Engineering*
Islamic University of Technology, Board Bazar, Gazipur-1704, BANGLADESH
** Corresponding author. Tel: +8801912669030, E-mail: tanzir68@gmail.com*

Abstract: The main disadvantage of Electric Vehicle is the lack of capability of storing sufficient energy to run the vehicle for a long time. The energy storage capacity of battery used in electric vehicle is very low compare to conventional fuels used in modern automobiles. The operation, performance and efficiency of motor driven electric vehicles are much better than engine driven vehicles, at the same time electric vehicles are very much environment friendly. Still electric vehicles are falling behind in the automobile industries due to the problem of storage of energy. This paper is based on the concept of charging the batteries of an electric vehicle when it is in motion or propelling. This may be done by using the energy of wind which is caused by the relative motion between the vehicle and the wind surrounding it. Wind turbines can be mounted on the body structure of the vehicle to generate electricity in such a way that it must not create any additional drag force (rather than the existing drag force due to frontal area and skin friction) upon the vehicle. An elaborate aerodynamic analysis of the structure of the vehicle along with the flow pattern and wind turbine is presented in the paper. Some techniques and methods are proposed to minimize the drag imposed by the introduction of the turbines as much as possible. Optimum values of different design parameters and rated velocity of the vehicle are of prime concern. With this concept it may be possible to increase the mileage of an electric vehicle up to 20%-25% and it will also save the charging time of the battery to a great extent. Flow pattern over the vehicle is simulated using software called ANSYS CFX.

Keywords: *Electric Vehicle, Wind Energy, ANSYS-CFX, Wind Turbine, Drag Reduction*

1. Introduction

When a vehicle moves it experience wind resistance which are classified in two different forms- frictional drag and form drag. Frictional drag arises due to viscosity of air and form drag arises due to variation of air pressure in the front and rear side of the vehicle [1]. As the vehicle moves forward, it lefts the air stream behind. A turbulence or disturbance is created on the wind when a vehicle moves through it. If stationary wind turbines are placed near the road then energy can be extracted from the wind stream generated due to the movement of the vehicle. Such a study had been carried out in University of Arizona by a group of students. If it is possible to capture those wind streams within the vehicle itself then it can be used to recover some of energy that has been used to overcome the form drag (aerodynamic drag) of the vehicle. If this wind energy is used to extract some power in such a way that it does not create any component of force or thrust opposite to the direction of the propulsion of the vehicle, then this gained energy can be used to produce electricity to charge up the battery of the electric vehicle itself. At the same time drag can be expected to be reduced by passing this air to the rear side (Low pressure side) of the vehicle. Air stream sliding over the body of the vehicle cannot enter into the rear side due to vortex shedding [1]. If air streams are allowed to flow in this region by any means then the form drag will be reduced by some amount and at the same time it may be possible to generate electricity using the kinetic energy of wind. Several studies had been carried out in this field but none of them are proved to be scientific. During the Second World War, wind turbines are used in submarines to charge up the batteries when they remained static and float in the water. At present it is also common to use turbines in ships, caravans and vehicles when they are parked. But to extract power from a

moving vehicle is quite difficult as the turbine will act as a load for the vehicle. Most of the design showed that the turbines are placed over the vehicle roof without considering the fact that it will impose an additional load for the vehicle and on the other hand no measures had been taken to reduce it. A design by Rory Handel and Maxx Bricklin showed that it has four tactically placed air intakes which will channel the air flow over the car's body towards the turbine. No such detailed design was available.

In this paper the topic is dealt by considering all the scientific facts and laws of energy conversion. A new approach is proposed and simulation of the design is carried out to analyze the behavior of the model. Some theoretical formulas have been used for the purpose of calculations.

2. Basic Theory

It is assumed that the vehicle is moving in a calm and steady wind stream with zero wind velocity. If the vehicle is moving at a constant speed of 15 m/s (54 km/h), then we can think a wind stream with15 m/s is flowing around the vehicle. Normally this wind will cause a drag force which is opposite to the direction of the propulsion of the vehicle. At constant speed (zero acceleration) the energy requirements to move the vehicle forward are –To overcome the frictional force (rolling resistance of road) and to overcome wind resistance [1]. At this Condition, if the air stream flowing around the vehicle (which was not interacting with the vehicle previously) is allowed to enter inside and let it flow down to the rear side; then it may be possible to use these air streams to generate power. The vehicle has already interacted with this wind and it deflects the stream of wind at the two sides of it by stagnation at the front. This is the energy that had been lost from the vehicle to overcome the aerodynamic resistant. Now if these stream generated by the interaction of the wind and vehicle is captured within the vehicle in such a way that it would not impose an additional drag at the direction of propulsion of the vehicle, some of the energy can be recovered and fed back to the battery by means of conventional energy conversion processes. Placing a wind turbine can serve the purpose. At the same time it will help to increase the pressure at the back side (according to Bernoulii's equation pressure will be increased if velocity is decreased and velocity will be reduced at the back side of the turbine after energy extraction) which will reduce the drag force that existed before with the conventional design of the vehicle. So, vortex shedding will be reduced at the rear side. For this it is necessary to modify the design of a vehicle which gives provision of air flow through the vehicle. On the other hand positioning of the turbines will also be important because they must be placed in such a way that they do not impose or create any additional drag on the vehicle. Symmetrical positioning of the turbine can do the trick as the thrust acting on the turbines will cancel each other.

3. Design and Modeling

We can consider a vehicle which is redesigned to allow airflow and wind turbine can be set up to extract energy. Wind turbines are set in parallel with the flow of air. This set up will not create any additional thrust at the direction of propulsion. Two basic equations will be needed to explain the air flow and power extraction.
The air flow through the vehicle is given by, [2]

$$Q = C_v A v \qquad (1)$$

Where, Q = flow rate in cubic meter per second.
C_v = opening effectiveness

[Value for C_v is 0.5 - 0.6 for perpendicular flow and 0.25 – 0.35 for skewed flow] [2]
A = Area in square meter
v = air velocity in m/s
This equation (1) will determine the amount of air flow through the vehicle inlet area.
Output power from a wind turbine is given by [4],

$$P_T = 0.5\, C_P\, \rho\, Q\, v^2 \qquad (2)$$

Where,

P_T = Power output from the turbine in watt.
C_p = Power co-efficient
(Assuming, C_p = 0.4 for the design) [4]
ρ = air density; 1.225 kg/m^3.
Q = air flow in m^3/s.
v = air velocity in m/s.

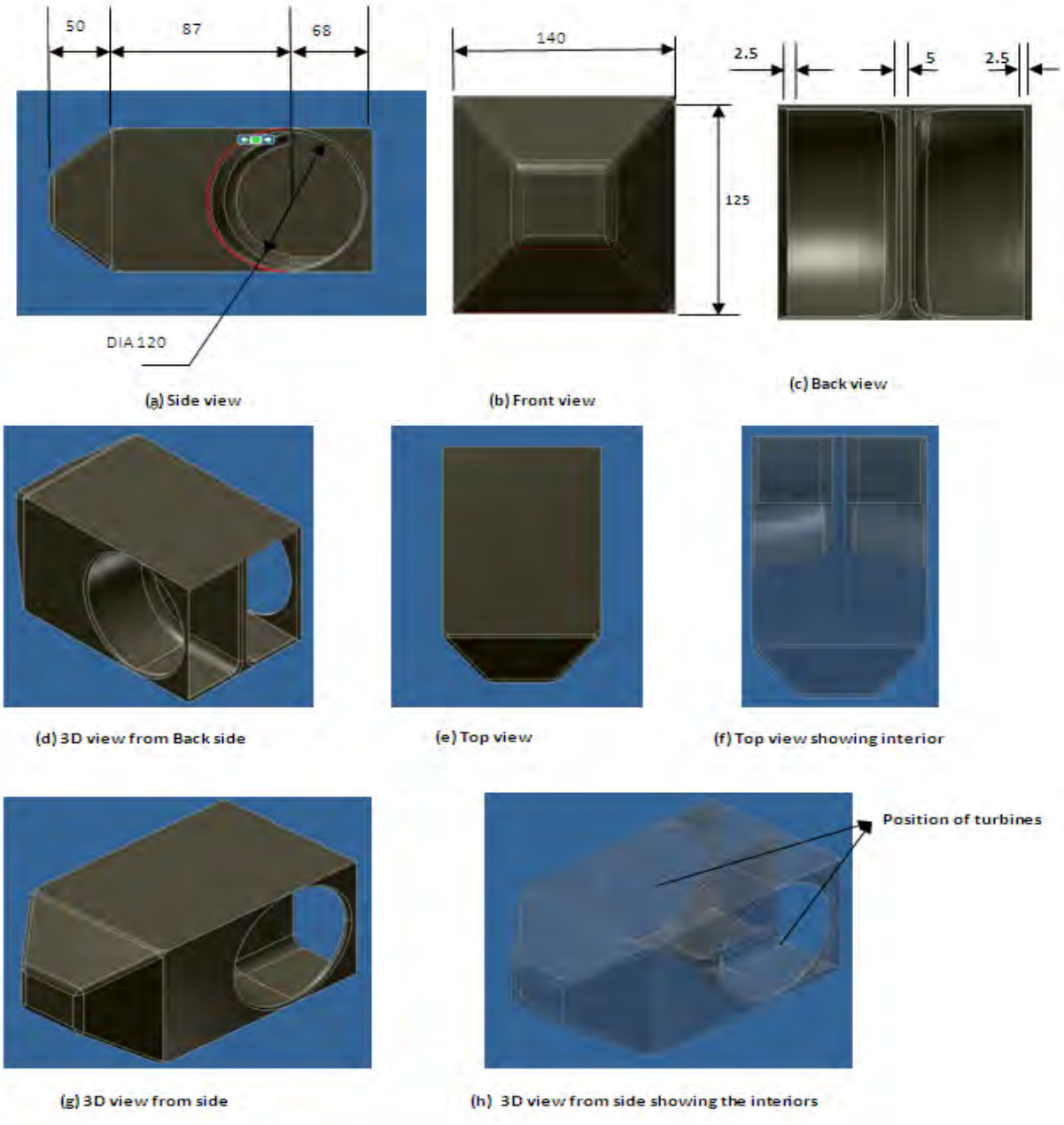

Fig. 1. 3D and isometric views of the model. The diameter of the turbine is 120 cm which is placed at the rear side of the vehicle. The length of the vehicle is 255 cm. All dimensions in the diagram are in centimeters.

In conventional vehicle air cannot go to rear side of the vehicle due to presence of boundary layers and vortex shedding. If a high-pressure and a low-pressure region can be connected via a neutral zone, then air can flow in between these pressure regions. Our design will allow the air to flow in this manner. The detail designs with dimensions are shown in the fig.1.

The vehicle is run by a 1.5 KW DC motor which has five 12V, 120 A-h D.C battery to supply power to the motor. The vehicle has to move at a velocity of 54 km/h i.e.15 m/s. The design of the vehicle is shown here with all dimensions. In this design the wind turbines are set in such a way so that the axial thrusts on the turbines are 180° apart to each other which results in the cancellation of two thrusts. In this way this symmetrical positioning of the turbines will create no additional drag component over the vehicle. Placing the turbines on the top will increase the frontal area as well as the drag acting on the vehicle. So that approach is not scientific. Rather some solar panels can be placed on the top to aid the recharging of the vehicle, both in motion and parked position. In addition if the vehicle is parked in a place where the wind velocity is above cut in speed then it is possible to charge the vehicle and thus it could aid the total charging system and hence charging time can be reduced.

4. Wind turbine

The wind turbine chosen for power generation has the features stated bellow [5] –

- Two blades (for low solidity).
- Horizontal axis.
- Lift type.
- High lift to drag ratio with efficiency ranging from 0.4 to 0.45. They need a relatively high tip speed ratio ($\lambda = \omega R / v_w$). For our design we have chosen $\lambda = 6$. For this value of λ it can be assumed that the value of C_p will be 0.4 to 0.45.

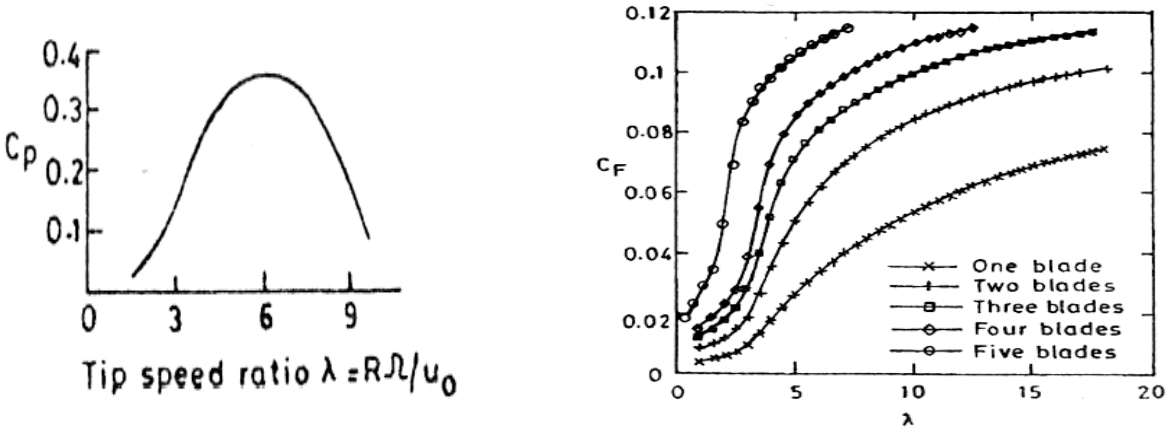

Fig. 2: Power Coefficient and Axial Thrust Coefficient for HAWT [6].

From $C_p - \lambda$ and $C_F - \lambda$ curve we can see $C_p = 0.4$ and $C_F = 0.055$ [6]

Where,

C_F = axial thrust co-efficient.

So, $C_p/C_F \approx 7$

This implies that as at perfect dynamic matching generated power will be greater than the power spend due to thrust. In other words the generated power by a turbine will be greater

than the thrust acting on the blade as an aerofoil section has high lift to drag ratio. On the other hand, turbines are placed in parallel to the flow rather than perpendicular to the flow.

5. Generator

We want to use an A.C. generator with 3-Φ windings with increased no. of poles. The poles will be permanent magnets and the no. of poles will be 8.

$\lambda = 6 = \omega R / v_w$; $\omega = 6\ v_w/R = \frac{6 \times 15}{0.6} = 150$ rad/s; R.P.M, $N = \frac{60 \times \omega}{2\pi} = 1433.12$;

This eliminates the need of a gear box in the system.
We shall use a three phase A.C. to D.C. converter to charge the batteries. Cúk converter is used to give a constant 60V at the output. The current of the converter will vary with the variation of the speed of the vehicle or the r.p.m of the turbine keeping the terminal voltage fixed.

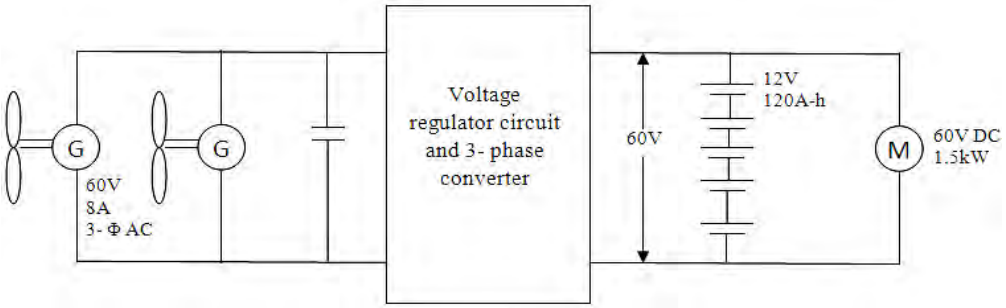

Fig. 2. Charging and control circuit of the battery. 3Φ windings are used to reduce the ripples. A motor control circuit can be used to control the motor and it will also introduce the provision of Regenerative Braking. Simple Power diodes can be used for designing the converter circuit. The cut-in velocity (minimum wind velocity to generate power) of the turbines is 5m/s.

6. Calculation

Using equation (1) we can calculate the amount of air flow,
$Q = C_v\ A\ v \quad = 0.25 \times 0.8 \times 1.131 \times 15 \times 2 = 6.8\ m^3/s$

Here, $A = \pi r^2 = 3.1416 \times 0.6^2 = 1.131\ m^2$

$v = 54$ kmph $= 15$m/s

Here multiplier of C_v is 0.8 as ratio of the inlet and outlet area is 1.38. C_v is chosen as 0.25 as it is a skewed flow [3].

So, Power, $P_w \quad = \frac{1}{2} \rho\ Q\ v^2 = \frac{1}{2} \times 1.2 \times 6.8 \times 15 \quad = 918$ W

Assuming, $C_p \quad = 0.4$ Then we have,

$P_T \quad = 918 \times 0.4 = 367.2\ W \approx 360\ W$

So, each turbine will produce a power of 180 W. This much power will be fed back to the battery when it is moving at a constant velocity of 15m/s.

So increase in mileages = (1500-1140)/1500 x 100% = 24%. This is due to the feeding back of some of the energy captured by the turbine which is spend to overcome the aerodynamic drag. That means the turbines are capturing some fractions of the energy which has already been spend by the vehicle to overcome the aerodynamic drag.

7. Simulation Result

The Flow pattern over the model is simulated using ANSYS CFX. Two models had been chosen for simulation. One is the conventional design and another one is modified design which includes turbines on the vehicle. Using the simulation result the pressure difference and force acting in the direction of flow (i.e. the thrust acting against the direction of propulsion) is calculated. The simulation results are shown and analyzed in the following figures.

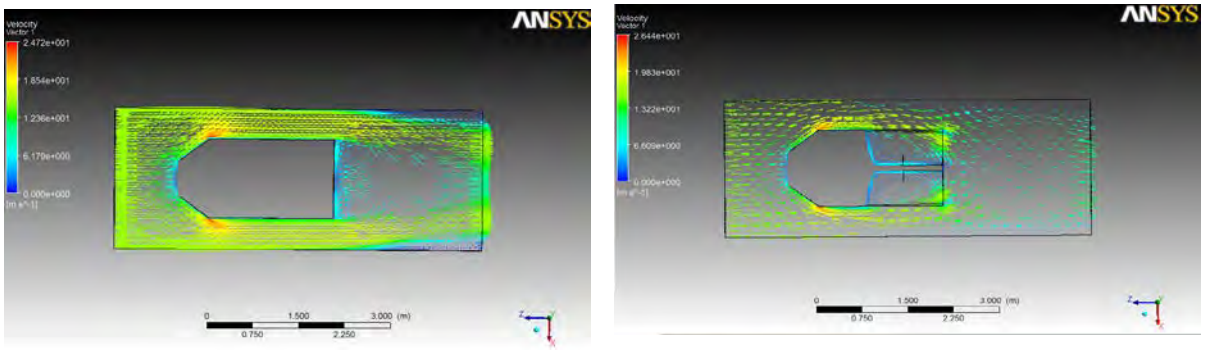

(a) Conventional vehicle model without ducts for turbine **(b) Modified vehicle model with ducts for turbine**

Fig. 3. Flow pattern around the vehicle using the velocity vectors. Wind is entering inside the vehicle and going out. Energy will be extracted from this flow.

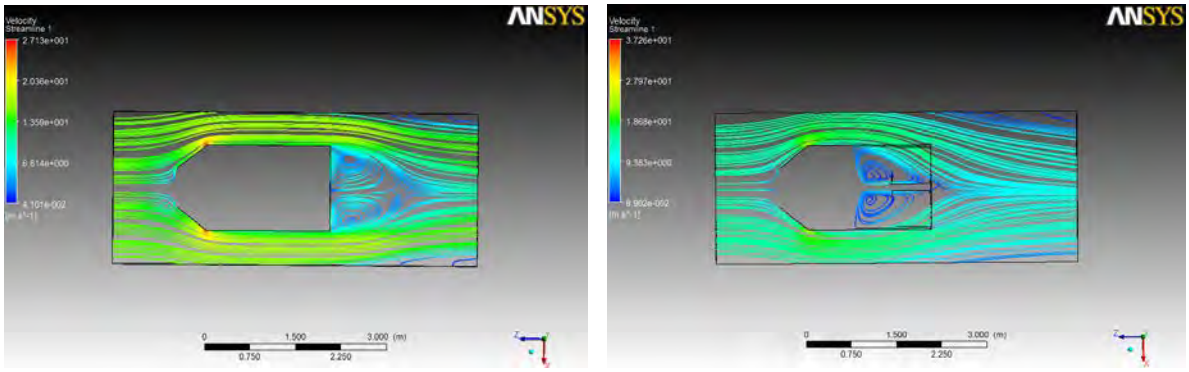

(a) Conventional vehicle model without ducts for turbine **(b) Modified vehicle model with ducts for turbine**

Fig. 4. Streamline of flow over the two different models of the vehicle. It may be noted that the vortexes on the modified design is reduced. On the other hand an additional propulsive thrust can be obtained as the streamlines are leaving the vehicle.

Analyzing figure 3 and 4, it can be seen that the wake region and vortexes are reduced for the modified design which implies that the force (form drag) that existed before is reduced. So it can be concluded that the prediction of flow through the duct and hence reduction of drag should be possible with this modified design. On the other hand, turbines can be placed in these ducts for extraction of some of the kinetic energy contained in the flow. The inlet and outlet pressure along with forces of these two models found from simulation are tabulated in Table 1.

Table 1. Simulation results for pressure and forces

Comparison Parameters	Conventional Design		Modified Design with ducts for turbine	
	Inlet	Outlet	Inlet	Outlet
Pressure(Pa)	2.29185	-1.24196	2.28742	0.240414
Force(Drag)(N)	45.9144	6.5354	15.5202	11.605

Table.1 shows the plane force and pressure over the two designs have been tabulated. The variation of force and pressure are identical for the both designs, but there are variations in the magnitudes of the parameters. The outlet pressure is increased for the modified design which indicates a reduction in form drag.

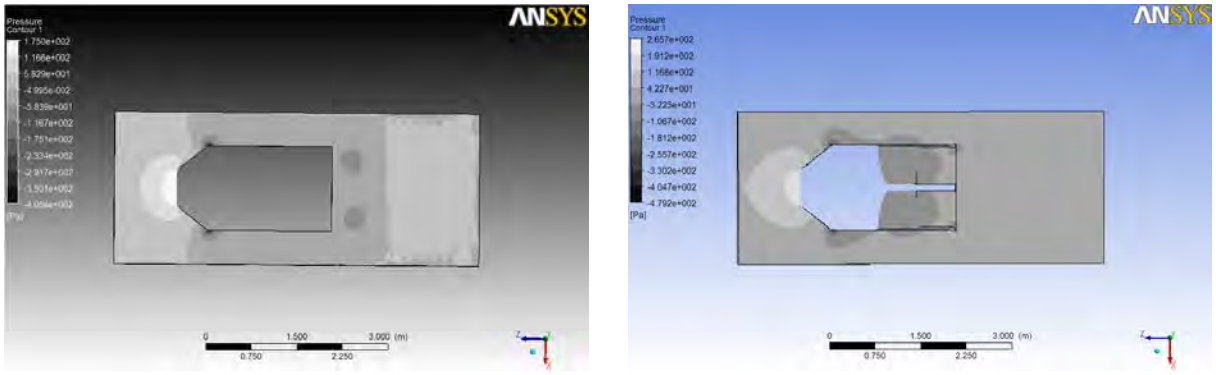

.

(a) Conventional vehicle model without ducts for turbine **(b) Modified vehicle model with ducts for turbine**

Fig. 5. Pressure contour around the two models.These figures indicate that the variation of pressure and generation of force due to this pressure variation would be identical but opposite in direction. This symmetry in the design should cancel out the additional thrust crated on the vehicle.

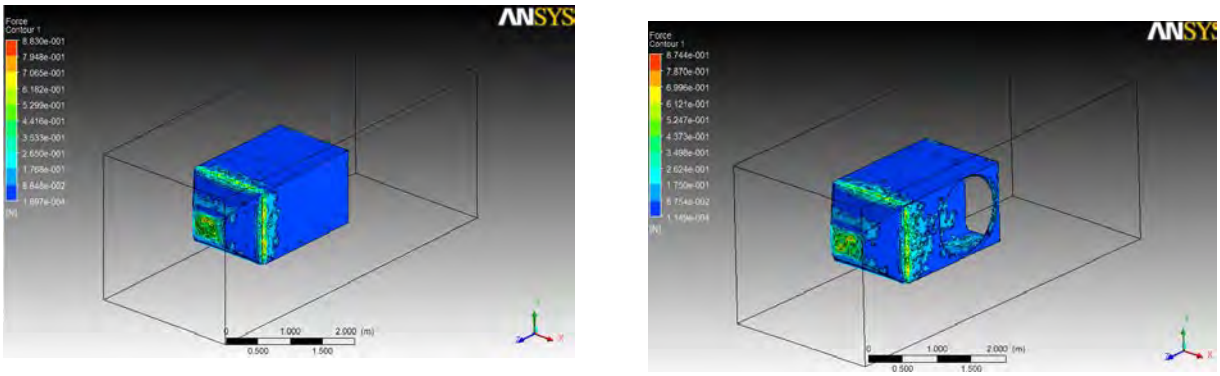

(a) Conventional vehicle model without ducts for turbine

(b) Modified vehicle model with ducts for turbine

Fig. 6. Force contour showing force exerted by the air on the two vehicles which are almost same.

Further analyzing the diagrams we can see (from Fig.3) that the thrust will not be on the axis of the turbine. That means an additional drag force will arise due to placement of the turbines. We predicted that the thrust will be 180 degree apart and hence cancel out each other. But

from velocity vectors we found that the thrusts are not fully at opposite rather they are in a skewed direction. The horizontal components will cancel each other but the vertical components will impose a resultant force. Hence a resultant thrust will be generated against the direction of propulsion on the turbine.

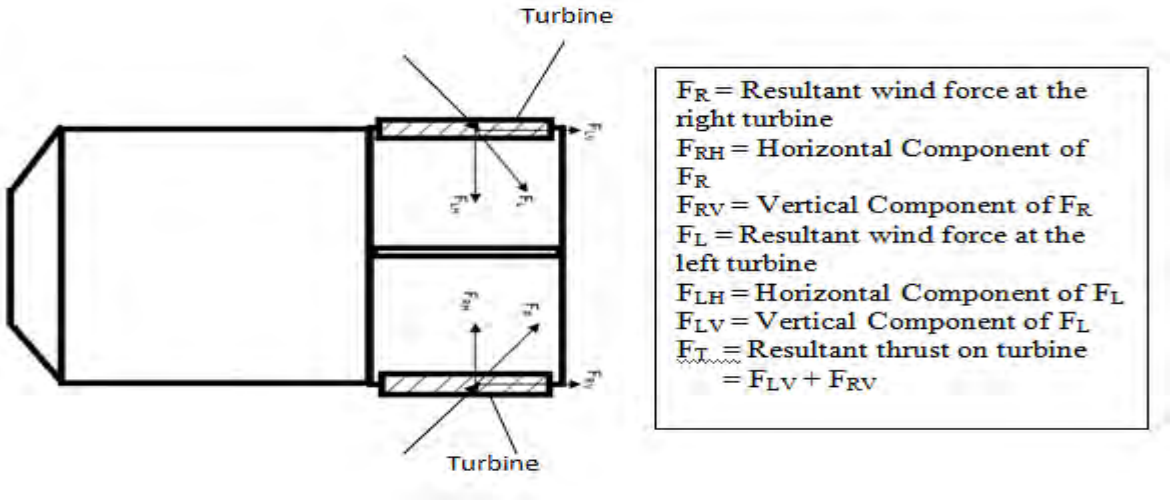

Fig. 8 : Resultant thrust generated on the turbines due to air flow through the ducts.

8. Conclusion

The prime concern with this model is that whether this design will create any additional resistive force components opposite to the direction of the propulsion. It has been found by the simulation that a drag will be induced due to addition of turbine. Overall simulation result along with graphs from Fig.3 will suggest that the overall effect will be same which means the modified design will experience almost same amount of drag compare to the conventional one. But the addition of turbines may give the provision of capturing some energy which will offer some benefits for the vehicle as discussed earlier. A physical structure of the design should be used to carry out wind tunnel tests which are yet to be done. At first the system may resembles with perpetual motion. But a careful observation may indicate that the system is trying to recover some of the energy spend to overcome the aerodynamic drag. The concept of placing symmetrical turbines is presented for the very first time by us. We believe it requires more research and elaborate analysis which we expect to continue in future.

References

[1] Thomas D. Gillespie, “Fundamentals of Vehicle Dynamics”, Society of Automotive Inc.

[2] Terry S. Boutet,” Controlling Air Movements- A Manual for Builders and Architects”, McGraw- Hill Book Company.

[3] Victor Olgyay, “Design with climate”, Princeton University Press, 1963, p.104

[4] Godfrey Boyle, “Renewable Energy- Power for a sustainable future”, Oxford University Press.

[5] Dr. Amalesh Chandra Mandal, Dr. Md. Quamrul Islam, “Aerodynamics and Design of Wind Turbines”, Published by BUET.

[6] G.N.Tewari, A.K. Bansal, “Renewable Energy Resources”, Narosa Publishing House.

[7] Martin O.L. Hansen, “Aerodynamics of Wind Turbines”, Earthscan, London.

[8] Bent Sorensen, “Renewable Energy” Academic Press, USA.

[9] Mukund R. Patel, “Wind and Solar Power Systems” CRC Press, USA.

[10] John D. Anderson, “Fundamentals of Aerodynamics”, McGraw Hill Book Company.

Whole-system Optimisation for Carbon Footprints Reduction of Corn Bioethanol

Andrea Zamboni[1], Nilay Shah[2], Fabrizio Bezzo[1,*]

[1] *CAPE-Lab, Dipartimento di Principi e Impianti di Ingegneria Chimica, Università di Padova,via Marzolo 9, 35131, Padova, Italy*
[2] *CPSE – Centre for Process Systems Engineering, Imperial College London, South Kensington Campus, SW7 2AZ London, UK*
** Corresponding author. Tel: +39 0498275468, Fax: +46 0498276461, E-mail: fabrizio.bezzo@unipd.it*

Abstract: Whether biofuels production from starchy biomass can actually be environmentally is still an open question. A modelling approach for strategic systems design combining lifecycle analysis (LCA) and supply chain optimisation (SCO) analysis can significantly contribute to clarify the question. Here we discuss the possibility of managing and optimising the biomass cultivation stage and its integration through the entire production network in order to tune the environmental performance of bioethanol production. The design task is addressed through a quantitative modelling tool, which aims at steering crop management towards the best fertiliser usage and distillers dried grains with solubles (DDGS) end-use in order to ensure optimal whole system performance in terms of both profit and greenhouse gas (GHG) emissions.

Results shows how a crop management strategy devised from a whole systems perspective can significantly contribute to reduce biofuels carbon footprints. In particular, it is observed that through whole systems optimisation, the GHG emissions of so-called first-generation biofuels can approach those associated with second generation ones.

Keywords: *Bioethanol, Whole system optimisation, Supply chain, GHG emissions*

1. Introduction

Over the past years biofuels for transport have been acknowledged as one of the key issues within the world energy agenda. Among the alternatives, bioethanol through first generation productions was first hailed as the most appropriate solution aiming at a partial substitution of oil-based fuels. Although the initial verve, founded on the potential economic benefits as well as on the energy supply security ensured by a broad range of suitable feedstock (i.e sugar cane and starchy biomass), the first generation pathway has recently known oppositions by both the public opinion and part of the academic community. The core of the question revolves around ever increasing doubts on whether bioethanol could effectively ensure the expected potential in terms of global warming mitigation, particularly when the energy vector derives from the conversion of starchy biomass [1,2].

This did contribute to heat up an already existing debate on the actual carbon footprints of these productions. Most of the studies addressing the question [1-6] state that ethanol derived from starchy biomass can actually contribute to a partial oil displacement [3,4,6], although the effective environmental impact tightly relates to the technological and geographical context in which the system performs, and to specific details in the operation of the overall supply chain. For example, GHG emissions from corn-based ethanol production can be estimated between 3% and 86% [5] lower than the emissions from gasoline production, depending on how the ethanol is produced. This large variability is mainly related to biomass production conditions: climate, properties of soil, cropping management and cultivation practice in general [3] can generally contribute to about 45% of the overall GHG emissions [7]. The raw nerve is represented by mineral fertilisers (mainly nitrogen-based ones) as their extensive application in biomass cultivation stage is the primary source of GHG such as nitrous oxide (N_2O) [8]. On the other hand, nitrogen dosage would also entail *direct effects* on biomass production

parameters and, as a consequence, *indirect effects* on the subsequent stages of the network itself. Technically, increasing the nitrogen input per unit of cultivated land causes: *i*. a direct increase in the corn yield, and, indirectly, in the ethanol yield; *ii*. a direct increase in the yield of grain protein to the detriment of starch content of corn grains, and, indirectly, improving the by-products (i.e. DDGS) yield to the detriment of the ethanol yield; *iii*. a direct increase in costs related to fertilisers, but indirectly to reducing operating overheads as an indirect consequence of the potential increase in both ethanol and DDGS yield; *iv*. an indirect increase of the total global warming impact due to greater GHG emissions coming from both fertiliser production and N_2O release from soil.

Another important aspect of the lifecycle emissions relates to the end-use of valuable sub-products (e.g. heat and power or DDGS), and the assumptions about the products that they displace (e.g. coal-derived energy and soya meal) [7]. This is influenced by nitrogen application, too: the potential increase in by-products yield coming from the over-dosage of mineral fertiliser can cause an indirect increase in emission credits coming from products displacement.

All these issues evidence a conflicting situation which cannot be cleared up by means of a mere heuristic evaluation of the pros and cons of fertiliser application. Thus, it raises the obvious need for a fully integrated analysis embodying all those issues (i.e. global warming mitigation together with economic and financial feasibility) that may help defining a more comprehensive and quantitative view of the interactions along the entire biofuels production system so as to assist both crop and fuel producers and, most importantly, policy makers in their strategic decisions. To the best of our knowledge, no analysis has so far been presenting the adoption of modelling tools to *optimise* the overall bioethanol supply chain by taking into account the entire set of production stages in the supply chain including biomass cultivation.

Some of our prior works have addressed the development of optimisation tools linking LCA and SCO models (i.e. Multi-objective Mixed-Integer Linear Programming - MoMILP), and specifically devised for the optimisation of both the environmental and economic performance of biofuels production [7]. Here we discuss the possibility of managing and optimising the biomass cultivation stage, too, and its integration within a quantitative MoMILP model which aims at tuning the environmental performance of bioethanol production so as to identify strategies for deep, system-wide reductions of GHG emissions.

Eventually, the emerging biomass-based ethanol production in Italy is assessed as a real world case study to demonstrate the actual approach capabilities in steering the crop management toward the best overall nitrogen fertiliser usage and DDGS end-use technical choice ensuring best whole-system performance in terms of both profit and GHG emissions.

2. Methods and modelling assumptions

The modelling framework here described is conceived as an optimisation problem in which the production chain is required to comply with both profit maximisation and impact minimisation criteria. Key components of the optimisation problem include biomass production response to nitrogen dosage (yields, costs, etc); biofuel production facilities capital and operating costs as a function of biomass characteristics; transport logistics costs and emissions; environmental burdens of biomass and biofuel production as a function of nitrogen dosage as well as of the DDGS end-use options; and energy market features (energy purchase prices and green credits).

The objective is to determine the optimal system configuration in terms of financial profitability (NPV) and GHG emissions. Therefore, key variables to be optimised include nitrogen dosage over the biomass crop field, DDGS end-use solution, system financial performance over a 10 years horizon and system impact on global warming.

The problem is referred to a fixed land surface (30,000 ha) fully cultivated to supply the biomass needs of a unique production plant of flexible capacity, anyway ranging within a consistent interval, namely 80–120 kt/y.

2.1. Mathematical formulation

The mathematical formulation of the proposed framework is based on the modelling approaches adopted in the design of multi-echelon SCs [9,10], by also introducing multi-period features to address the financial analysis (which is performed over a 10-years time horizon).

2.1.1. Objective functions

The first objective considered is the NPV (Obj_{NPV} [€]) of the business to be established. This imposes the maximisation of profit-related indexes, and hence the Obj_{NPV} value is required to be written in its negative form:

$$Obj_{NPV} = -NPV = FCC - DNI \quad (1.a)$$

where *FCC* [€] are the facility capital costs and *DNI* [€] represents the discounted net incomes.

The second objective is to minimise the total daily GHG impact (Obj_{TDI} [kg CO_2-eq/d]) resulting from the SC operation. Thus, the definition of Obj_{TDI} needs to consider each life cycle stage contribution, as expressed by the following equation:

$$Obj_{TDI} = \sum_s I_s \quad (1.b)$$

where I_s [kg CO_2-eq/d] are the stage-related environmental impacts resulting from the operation of the single stage *s*.

2.1.2. Economics

The *FCC* term accounts for the capital investment required to establish a new fuel conversion facility. However, this model allows for the choice between two different technological options according to the two mentioned options proposed for DDGS use: k =1, which involves the standard conversion technology in which DDGS is processed as a simple by-product to be sold to the animal fodder market; or k = 2 which envisages the construction of a CHP station fuelled by DDGS to produce heat and electricity.

According to this, *FCC* can be calculated by alternatively assigning the capital investment value (CI_k [€]) corresponding to the technological features adopted, as expressed by:

$$FCC = \sum_{n,k} CI_k \cdot W_{n,k} \quad (2)$$

where $W_{n,k}$ is the binary decision variable controlling whether to establish a production facility of type k when a nitrogen dosage n is applied: a value of 1 allows for the construction of the plant type k, otherwise 0 is assigned.

The discounted net incomes *DNI* is defined as the sum over the 10 year operating period of the annual profit before taxes (*PBT* [€/y]) plus the annual depreciation charge related to the capital investment (*D* [€/y]) minus the taxation charge for each year *t* (*TAX* [€/y]), as expressed by the following equation:

$$DNI = \sum_t (PBT - TAX + D) \cdot \varepsilon_t \quad (3)$$

All the terms on the right hand side of Eq. (3) have been discounted through the application of a discount factor (ε_t) defined as [11].

The profit before taxes *PBT* represents the gross annual profit and has been defined as the difference between the total annual revenues *TAR* [€/y] and the total operating costs *OC* [€/y] for year *t* minus the depreciation charge *D*. Accordingly:

$$PBT = TAR - OC - D \quad (4)$$

TAR represents the annual incomes which depend on both ethanol and DDGS sales:

$$TAR = MPe \cdot \sum_{n,k} Pe_{n,k} + \sum_{n,k} Pd_{n,k} \cdot MPd_{n,k} \cdot \omega_k \quad (5)$$

where *MPe* is the bioethanol market price (set equal to 709 €/t according to [12]); $Pe_{n,k}$ [t/y] and $Pd_{n,k}$ represent, respectively, the ethanol and DDGS production rate related to plant technology *k* when a nitrogen dosage *n* is applied to crop biomass; $MPd_{n,k}$ is the DDGS market value and depends on the DDGS end-use solution *k*. When DDGS is used as soy-meal substitute in the animal fodder market ($k = 1$), $MPd_{n,1}$ is the market price that also depends on the nitrogen dosage *n*. On the other hand, if power generation is chosen as the end-use option ($k = 2$), $MPd_{n,2}$ identifies the average market price per unit of electric energy sold to the grid. This does not depend on the nitrogen dosage *n* in any case. This modelling solution also requires the application of a conversion factor, $\omega_{n,k}$, to quantify the amount of by-product produced per unit of DDGS. Thus, when power generation is chosen as end-use solution ($k = 2$), $\omega_{n,2}$ [$kWh_e/t_{10\%m}$] identifies the amount of energy that can be sold to the grid per unit of DDGS produced. On the other hand, when DDGS is used as a soy-meal substitute in the animal feed market ($k = 1$), the amount of by-product to be sold should be equal to the overall DDGS production. In order to comply with Eq. (5), $\omega_{n,1}$ [t/t] has been set equal to 1.

OC is given by the sum of the annual operating costs over the entire supply chain. This has to account for the contribution of all the supply stages (*s*), i.e. biomass production (BP), ethanol and DDGS production (EP) and transports (for biomass, BT, and ethanol, ET), minus the by-products allocation credits (BC). Accordingly:

$$OC = \sum_{n,k} \begin{bmatrix} (Pb_{n,k} \cdot UPCb_n)_{BP} + (Pe_{n,k} \cdot UPCe_n)_{EP} + (UTCb \cdot Pb_{n,k})_{BT} \\ + (UTCe \cdot Pe_{n,k})_{ET} - (Pe_{n,k} \cdot UCRd_{n,k})_B \end{bmatrix} \quad (6)$$

where $Pb_{n,k}$ represents the biomass production rate supplying a conversion plant of type *k* when a nitrogen dosage *n* is applied to crop fields, $UPCb_n$ [$€/t_{DM}$] and $UPCe_n$ [€/t] are respectively the unit production costs for biomass and ethanol, *UTCb* [$€/t_{DM}$] and *UTCe* [€/t] define the unit transport costs for biomass and ethanol respectively, and $UCRd_{n,k}$ is the cost reduction per unit of DDGS used as a valuable alternative *k* and produced when a nitrogen dosage *n* is applied.

The last factor defining *PBT* in Eq. (4) is the depreciation charge *D* evaluated by simply dividing the total capital investment (*FCC*) by 10 (thus assuming a constant depreciation strategy).

2.1.3. Environmental impact

The definition of stage-related environmental impacts I_s [kg CO_2-eq/d] resulting from the operation of the single stage *s* is calculated as follows:

$$I_s = \sum_{n,k} f_{s,n,k} \cdot F_{n,k} \quad \forall\, s \tag{7}$$

where $f_{s,n,k}$ is the a g lobal emission factor representing the carbon dioxide emissions equivalent at stage *s* for technology *k* and nitrogen dosage *n* per unit of reference flow; whereas $F_{n,k}$ uniquely defines the reference flows for each individual life cycle stage and expresses them explicitly as a function of the design variable controlling the optimisation problem. In this problem $Pb_{n,k}$ represents the reference flow for biomass production and biomass transport, $Pe_{n,k}$ for ethanol production and ethanol transport, whereas $Pd_{n,k}$ refers to the emissions credits.

2.1.4. Logical constraints and mass balances

All the variables defined in the above are linked to the specific SC features through the definition of a set of constraints that must be satisfied in each of the SC stages.
A set of relations is formulated to constrain the goods production rate together with the binary variables. In particular, $Pb_{n,k}$ is the dominant production variable and is defined as follows:

$$Pb_{n,k} = LA \cdot GY_n \cdot W_{n,k} \quad \forall\, n,k \tag{8}$$

where *LA* [ha] is the land availability (30,000 ha, as declared in the previous section) and GY_n [t_{DM}/ha] the grain yield per hectare when a nitrogen dosage *n* is applied.

Once the biomass production is quantified, the ethanol and DDGS production rates can be derived by simply applying a specific conversion factor. Accordingly:

$$Pe_{n,k} = Pb_{n,k} \cdot \gamma_n \text{ and } Pd_{n,k} = Pb_{n,k} \cdot \delta_n \quad \forall\, n,k \tag{9}$$

where γ_n [$t_{biofuel}/t_{biomass}$] and δ_n [$t_{10\%m}/t_{biomass}$] are respectively the alcohol and DDGS yields when biomass is cropped by applying a nitrogen dosage *n*.

2.2. Response curves

The definition of the variables response to nitrogen dosage is based on the comprehensive work by Smith et al. [13], which, however, refers to wheat. Since no complete sets of data could be retrieved on corn, it was decided to tune up the wheat data set to corn cultivations on the few data available. Correlations for wheat reported in [13] have been used to define both the graphical and the mathematical dependence of corn grain yield (*GY*), grain protein content (*PY*), DDGS yield (*DDGSY*) and alcohol yield (*EY*) on nitrogen dosage (*ND*). The entire set of model parameters and their inherent dependence on ni trogen application have to be estimated on the basis of these response curves. Because we wish to maintain model linearity, we use a piecewise linear dependence of key variables on ni trogen dosage. The nitrogen dosage variable is discretised into a number (=12) of intervals *n* (25 kg_N/ha of extension). Note that in general climatic and land characteristics may have an impact on the actual crop

response to nitrogen dosage and this should be taken into account when applying the methodology.

The technological related parameters, i.e. GY_n, δ_n, γ_n and μ_n, have been directly obtained by the corresponding response functions. In particular, μ_n is the soy-meal replacement factor representing the amount of soy-meal that can be replaced by DDGS. Thus, in this work we do not assume an allocation by energy on DDGS, but a substitution as fodder at iso-nitrogenous and iso-energetic conditions. According to [14], this has involved the application of a substitution ratio of about 0.68 $kg_{soy\text{-}meal}/kg_{DDGS}$ (defined assuming a DDGS protein content of about 76% compared to soy-meal). Then, the DDGS protein content (and, hence, the substitution ratio response to nitrogen) has been scaled according to the nitrogen dosage applied.

On the other hand, both economic and environmental parameters has been defined adapting the approaches of [7,15] by varying the nitrogen-dependent inputs according to the trend in the response curves.

3. Results and discussion

The modelling framework as presented was used to determine the optimal system configuration according to the two conflicting objectives discussed in the above. Design variables (the nitrogen dosage over the biomass crop field and the DDGS end-use option) were optimised by means of the CPLEX solver in the GAMS® modelling tool [16]. The model considers two technological options for DDGS end-use: *i)* soy-meal substitute to be sold in the animal fodder market, or *ii)* fuel fed to a combined heat and power (CHP) station.
A first instance has been assessed by assuming standard market conditions for the electricity selling price ($MPd_{n,2}$ = 91.34 €/MWh_e). The sub-optimal set of solutions (◆) coming from the trade-off between the environmental (total impact, TI, expressed in kt CO_2-eq) and the financial (Net Present Value, NPV, expressed in M€) criteria is reported in Fig. 1.

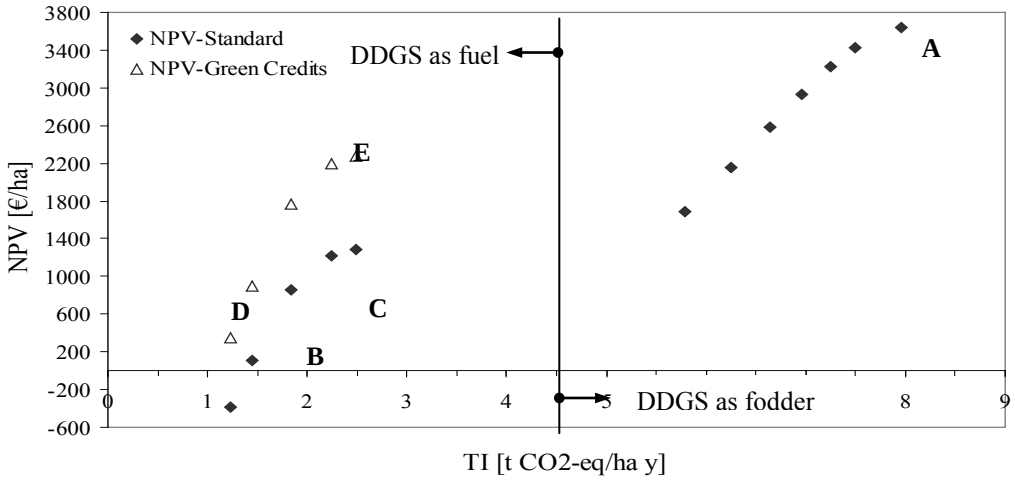

Fig. 1. Pareto set of solutions: NPV vs. Total Impact (TI)

Point A on the diagram represents the best optimum in terms of economic performance that can be obtained by applying a nitrogen dosage of 237.5 kg_N/ha and using DDGS as animal fodder substitute. However, this is not a feasible solution if we consider the EU targets (which impose a minimum of 50% of emission savings with respect to conventional fuels by 2017): point A, indeed, corresponds to a GHG emissions reduction of about 21% that totally amount to 238.9 kt CO_2-eq (about 67.6 kg CO_2-eq/GJ_{EtOH}). The mentioned target is never met if we

keep using the DDGS as animal feed substitute. Thus, it is worth to investigate on the other alternative, namely the use of DDGS to fuel a CHP station. In this case, we assist to a sensible GHG emissions reduction by still remaining within the economic feasibility region. It is possible to obtain payback times lower than 6 years from point B up to point C. The environmental optima (that also assures feasible economic conditions) involves a nitrogen dosage of 87.5 kg_N/ha (point B) so allowing for a GHG emissions reduction of about 80% (17.1 kg CO_2-eq/GJ_{EtOH}) with respect to gasoline and realising an NPV of about 25.7 M€ (the payback time is still reasonable and amounting to about 6 years). On the other hand, the financial optima (still assuring feasible environmental performance) involves a greater nitrogen dosage (162.5 kg_N/ha, point C) so resulting in higher GHG emissions, although still more than acceptable (21.2 kg CO_2-eq/GJ_{EtOH}, corresponding to 75% of emissions savings with respect to gasoline), and realises an NPV of about 38.5 M€ (the payback time is now 5.5 years).

The situation might be even more profitable if the bioethanol business would be supported by governmental subsidies, as it is actually envisaged according to the latest Italian regulation on renewable energy: accordingly the electric energy produced from renewable energy sources can be sold at a price of 180 €/MWh_e. The positive effect of these subsidies is evident from the set of sub-optimal solutions (△) reported in Fig. 1. Considering the solution involving DDGS as animal feed substitute, the situation does not change because green credits do not affect the financial features of this option. On the other hand, the financial performance is actually enhanced if DDGS is used to fuel a CHP station: the points between D and E represent feasible options in terms of both economic and environmental criteria. For instance, by applying a nitrogen dosage of 37.5 kg_N/ha (point D) the environmental optima entails a GHG emissions reduction amounting to about 82% (15.8 kg CO2-eq/GJ_{EtOH}) with an economic profit of about 27 M€ over a 10 years horizon (the payback time is about 6 years, still). However, if the profit maximisation is preferred, it is possible to apply up to 162.5 kg_N/ha (point E) so as to keep within the environmental feasibility region (the GHG emissions reduction would be 75% with respect to gasoline) and realising excellent financial performance: as shown in Figure 7.6, the NPV now amounts to 68.4 M€ so allowing for the lowest payback time (4 years).

4. Conclusions

It is clear that the analysis of biofuels production is a complex task, particularly when environmental issues are taken into account. Broader information, analysis tools, interactions between different types of expertise are necessary to obtain a full comprehension of such a multifaceted problem. If the final goal is fuel instead of food, the overall chain might have to be operated in a different way and the boundary between "first-generation" and "second-generation" biofuels may start blurring. This is why decision makers should be provided with tools capable of evaluating how the system may react to different options and how its design may change if optimised towards specific goals. On the one side, it is important to identify the existing optimal points; on the other hand, we need to assess how flexible the system is in terms of profitability, GHG emissions and environmental and social impacts.

In this contribution we showed how whole-system optimisation tools can be exploited to address these issues. We considered the nitrogen balance optimisation and the technology selection in a first generation bioethanol supply chain according to economic and environmental goals. Results demonstrate that the only way to meet the EU standards (50% of GHG emission savings by 2017) on corn bioethanol in Italy is to adopt a technological solution envisaging the construction of a CHP station to be fuelled with DDGS. This requires

moderate nitrogen dosage as a mineral fertiliser (about 160 kg_N/ha) so as to reach GHG emission savings of about 75% with respect to gasoline production. It is also worth mentioning that a more thoughtful use of mineral fertiliser would also reduce other environmental impacts associated with fixed nitrogen application to agricultural soils (i.e. eutrophication and acidification of the ecosystem). However, this would require support through the deployment of governmental subsidies so as to ensure all the competitiveness and economic efficiency requirements imposed by the global market.

Over the years, the discussion has broadened by incorporating the analysis of the entire supply chain and more recently even the indirect effects of land use change. In fact, future work will need to deal the analysis and modelling of the effects that the land conversion from crop-for-food to crop-for-fuel would generate.

References

[1] J. Fargione et al., Land clearing and the biofuel carbon debt, Science 319, 2008, pp. 1235–1238.

[2] T. Searchinger et al., Use of U.S. croplands for biofuels increases greenhouse gases through emissions from land-use change, Science 319, 2008, pp. 1238–1240.

[3] S. Kim and B. Dale, Life cycle assessment of fuel ethanol derived from corn grain via dry milling, Bioresource Technology 99, 2008, pp. 5250–5260.

[4] E.C. Petrou and C.P. Pappis, Biofuels: A survey on pros and cons, Energy & Fuels 23, 2009, pp.1055–1066.

[5] S.C. Davis et al., Life-cycle analysis and the ecology of biofuels, Trends in Plant Science 14, 2009, pp. 140–146.

[6] E. Gnansounou et al., Life cycle assessment of biofuels: Energy and greenhouse gas balances, Bioresource Technology 100, 2009, pp. 4919–4930.

[7] A. Zamboni et al., Spatially explicit static model for the strategic design of future bioethanol production systems. 2. Multiobjective environmental optimization, Energy & Fuels 23, 2009, pp. 5134–5143.

[8] G.P. Robertson et al., Sustainable biofuels redux, Science 322, 2008, pp. 49–50.

[9] N.V. Sahinidis et al., Optimization model for long range planning in the chemical industry, Computers & Chemical Engineering 13, 1989, pp. 1049–1063.

[10] P. Tsiakis et al., Design of multi-echelon supply chain networks under demand uncertainty, Industrial & Engineering Chemistry Research 40, 2001, pp. 3585−3604.

[11] S.M Peters et al., Plant design and economics for chemical engineers, McGraw-Hill, 2003.

[12] Agra Informa website: www.agra-net.com.

[13] T.C Smith et al., Wheat as a Feedstock for Alcohol Production, HGCA, 2006.

[14] U. Meyer et al., Effects of by-products from biofuel production on the performance of growing fattening bulls, Animal Feed Science and Technology 161, 2010, pp. 132–139.

[15] G. Franceschin et al., Ethanol from corn: A technical and economical assessment based on different scenarios, Chemical Engineering Research & Design 86, 2008, pp. 488–498.

[16] R.E. Rosenthal, GAMS - A Users' Guide (Version 22.5). GAMS Development Corporation, 2006.

Effects of Biodiesel Fuel Use on Vehicle Emissions

Larry G. Anderson[1,*]

[1] *University of Colorado Denver, Denver, Colorado, USA*
** Corresponding author. Tel: +1 3035562963, Fax: +1 3035564776, E-mail: larry.anderson@ucdenver.edu*

Abstract: Many countries are using and considering the increased use of biodiesel blended fuels to slow their growth of fossil fuel use for transportation purposes. Before the use of biodiesel fuels increase, it is critical that we understand the effect of using biodiesel blends on vehicle emissions, so that we better understand what air quality impacts to expect. Many previous reviews of biodiesel effects on emissions have combined all of the emissions data available to construct a single value for the effects on pollutant emissions. This includes combining emissions data from both light-duty and heavy-duty diesel vehicles and engines, combining vehicle data from chassis dynamometer and on-road emissions testing. In this review, we will analyze the effects on vehicle emissions of switching from petroleum diesel fuel to biodiesel blended fuels for light-duty and heavy-duty vehicles, separately. We will not include engine emissions data in this analysis. For the heavy-duty vehicles, we will also separate results for on-road emissions testing from chassis dynamometer testing. The emissions of regulated pollutants will be evaluated, including hydrocarbons (HC), nitrogen oxides (NOx), carbon monoxide (CO) and particulate matter (PM), as well as carbon dioxide (CO_2) emissions and fuel economy. In these analyses, we have found some statistically significant differences in the effects of biodiesel use on the emissions between heavy-duty vehicles based on dynamometer and on-road emissions testing, and light-duty vehicle dynamometer data. For vehicle emissions from heavy-duty vehicle tested using a dynamometer and on-road emissions techniques, the emissions of CO, CO_2 and PM were found not to be significantly different for B20, but the HC, NOx and fuel economy results were significantly different. The results of the heavy-duty and light-duty dynamometer emissions were found to not differ significantly for any pollutant, other than PM emissions when B20 blended fuels were used. When the results of the emissions studies were not significantly different, the results were combined to determine the effect of biodiesel use on vehicle emissions.

Keywords: *Renewable fuels, Biodiesel, Vehicle emissions, Regulated air pollutants, Hazardous air pollutants*

1. Introduction

Many countries are evaluating a variety of alternative fuels for use in motor vehicles in an attempt to reduce greenhouse gas emissions and to improve the energy security of the country. Biodiesel and other biofuels are substitute fuels capable of replacing fossil fuels on a large scale in the transportation sector. Although biodiesel currently accounts for a small portion of the total diesel fuel used, increasing its use requires that we understand the impact that biodiesel could have on vehicle emissions, and ultimately on air quality.

Vehicle emissions are affected by the fuel that is used. There have been several reviews of the effects of biodiesel fuel use on emissions, but many of these have used engine emissions tests in addition to or instead of vehicle emissions tests [1-4]. Emission measurement methods include engine and chassis dynamometer tests, tunnel studies, and more recently, remote sensing and portable (or on-board) emissions monitoring systems. Engine dynamometer systems are quite useful for research purposes, but because these systems test only the engine, they are missing many factors that may affect the real-world emissions of vehicles. Chassis dynamometer studies test the entire vehicle and can use realistic driving cycles which are expected to produce more representative emissions results. Chassis dynamometer testing is more complicated and expensive than engine testing, so less of that data is available. Remote sensing and on-board emissions measurements have also been used to assess the effects of using different fuels on vehicle emissions. Remote sensing uses spectroscopic measurements of a vehicle that passes through the light beam to measure the concentrations of emitted pollutants. These measurements provide only a snapshot of the emissions at a particular

location and thus cannot characterize an entire operating cycle for a vehicle. On-board emissions measurement systems offer the advantage of being able to capture real-world emissions during an entire operating cycle for the vehicle. In this review, we will focus on the analysis of vehicle emissions data that is more representative of real-world operating conditions, from chassis dynamometer and on-board emissions measurement systems.

2. Analysis Approach

In this paper, we will assess the impact of biodiesel fuel use by looking at the relative value of a property, such as pollutant emissions from a biodiesel blended fuel divided by that from conventional diesel fuel use for a particular vehicle. This reduces some of the variability in analyzing vehicle emissions data, since vehicles that emit larger or smaller quantities of a pollutant when using diesel fuel are expected to also emit larger or smaller quantities of that pollutant when using a biodiesel blended fuel. If the use of biodiesel fuels does not affect the property being studied the relative value will be 1. For example, a value of 1.12 indicates that the property has increased by 12% with biodiesel fuel use and a value of 0.89 would indicate a decrease by 11% with biodiesel fuel use. In this analysis, at least twenty measurements were required to assess statistical significance. This minimum number of measurements was used in an attempt to assure the representativeness of the data. These relative emissions and fuel economy data were tested for normality using the Lilliefors test. These data were found not to be significantly different from a normal distribution. This allows the use of conventional statistical techniques in these analyses.

3. Heavy-Duty Diesel Vehicle Emissions

Quite a bit of data exists for biodiesel blended fuels in heavy-duty (HD) diesel vehicles where the emissions were measured using chassis dynamometers and on-road using portable emissions monitoring systems (PEMS). These two different sources of emissions data will be analyzed separately.

3.1. Heavy-Duty Diesel Chassis Dynamometer Studies

The data used to assess the effect of biodiesel fuels use on HD vehicles from dynamometer studies comes from 19 different studies and includes 124 different tests. Much of the data on the emissions effects of biodiesel blended fuels from chassis dynamometer studies of HD diesel vehicles was for 20% blends of biodiesel with petroleum diesel (B20) and neat biodiesel (B100) fuels. Since a total of twenty valid measurements are required in order to assess the significance of the effect of biodiesel blended fuels on a measurement, only hydrocarbons (HC), nitrogen oxides (NOx) and carbon monoxide (CO) had sufficient data for the assessment of both B20 and B100 biodiesel, while sufficient data was also available for B20 blends to assess the significance of the effects on carbon dioxide (CO_2), particulate matter (PM) and fuel economy. For these HD vehicles, the use of biodiesel led to a decrease for hydrocarbon emissions of 5.7 ± 4.4% (95% confidence interval) for B20 and 23.0 ± 9.2% for B100, a decrease for CO emissions of 4.1 ± 6.4% (not significant) for B20 and 24.0 ± 7.2% for B100, and an increase in NOx emissions of 3.5 ± 2.3% for B20 and 9.0 ± 2.8% for B100. The use of B20 blended fuels also led to a decrease for CO_2 emissions of 0.4 ± 1.0% (not significant), for PM emissions of 13.3 ± 5.1%, and for fuel economy of 2.6 ± 1.2%. There was an insufficient quantity of emissions test data for other biodiesel blends to characterize the variability in the emissions data, and to allow one to reliably assess the significance of the effects on the emissions of HD vehicles tested using chassis dynamometers.

3.2. Heavy-Duty Diesel On-Road Vehicle Emissions Studies

The data used to assess the effect of biodiesel fuels use on HD vehicles from on-road studies comes from 14 different studies and includes 94 different tests. Almost all of the data for these on-road vehicle emissions tests of HD diesel vehicles are for B20 blends. For these HD vehicles, the use of B20 blends led to a decrease for hydrocarbon emissions of 21.7 ± 4.4% (95% confidence interval), a decrease for CO emissions of 6.6 ± 5.4%, and a decrease in NOx emissions of 3.3 ± 3.4% (not significant). The use of B20 blended fuels also led to an increase for CO_2 emissions of 3.0 ± 3.6% (not significant), a decrease for PM emissions of 15.2 ± 6.0%, and an increase for fuel economy of 6.3 ± 8.1% (not significant). One of the major complications of the on-road PEMS testing for evaluating different fuels is the much poorer matching of the operating conditions of the vehicles with these different fuels. This generally leads to increased variability in the results.

3.3. Differences between Chassis Dynamometer and On-Road Heavy-Duty Vehicle Emissions Data

The chassis dynamometer and on-road vehicle emissions data for HD vehicles were tested to determine if the results were significantly different for these two testing procedures. It was found that there was no significant difference in the results of the emissions test methods for the CO, CO_2 and PM data using B20 blends. However, the results were significantly different for the HC, NOx and fuel economy data between the two data sets. For the HC data, B20 blends led to a significant decrease in HC emissions in both cases, but only about 5.7% for the dynamometer studies and 21.7% for the on-road studies. The decrease from the on-road studies with B20 were similar to the effects of B100 seen with the dynamometer data. For the NOx data, B20 blends led to a significant increase in NOx emissions of about 3.5% for the dynamometer studies, while there was a 3.3% decrease (not significant) in NOx emissions in the on-road studies. The data continues to support an increase in NOx emissions with biodiesel blends in HD diesel vehicles. In the case of the fuel economy data, B20 blends led to significantly lower fuel economy of about 2.6% from the dynamometer studies, but led to a 5.7% increase (not significant) in fuel economy for the on-road studies. The data continues to support a decrease in fuel economy with B20 biodiesel blends in HD vehicles.

Since there was no significant difference in the results of the dynamometer and on-road emissions studies using B20 blends for the HD vehicle emissions of CO, CO_2 and PM, these data sets were combined and the significance of the effects on this larger pooled data set were assessed. For the CO emissions data with B20, a 4.1% decrease (not significant) was found from the dynamometer studies and a significant 6.6% decrease was found from the on-road studies. With the combined data set, a significant decrease of 5.3 ± 4.1% was found for CO using B20 blends. For the CO_2 emissions data with B20, a 0.4% decrease (not significant) was found from the dynamometer studies and a 3.0% increase (not significant) was found from the on-road studies. With the combined data set, a 1.6 ± 2.2% increase (not significant) was found for CO_2 using B20 blends. These data support the conclusion that the use of B20 biodiesel fuels has no significant effects on the emissions of CO_2. For the PM emissions data with B20, a significant 13.8% decrease was found from the dynamometer studies and a significant 15.2% decrease was found from the on-road studies. With the combined data set, a significant decrease of 14.5 ± 3.9% was found for PM using B20 blends.

4. Light-Duty Diesel Vehicle Emissions using Chassis Dynamometers

The data used to assess the effect of biodiesel fuels use on light-duty (LD) vehicles from dynamometer studies comes from 47 different studies and includes 259 different tests. LD

diesel vehicle emissions have been measured almost exclusively by use of chassis dynamometers. PEMS have not been used extensively in the study of LD diesel vehicle emissions. The available data consists of a number of studies conducted in North America, Europe, Asia and Australia. The studies conducted in North America tend to be dominated by studies of larger vehicles, including pickup trucks, while those elsewhere in the world include a larger fraction of cars, passenger and delivery vans. This data set also includes biodiesel fuels that are made from different biooil feedstock (soy, rapeseed, canola, palm, coconut, used cooking oils, animal fats, etc.). The emissions test data for light-duty vehicles contains many more tests with varying biodiesel percentages, not largely B20 and B100.

Fig. 1 shows the relative emissions of HC, NO_x, CO, CO_2, PM and fuel economy effects of using various biodiesel blended fuels based on chassis dynamometer testing of LD vehicles from a number of different studies. From this figure it is clear that there is a relatively large quantity of data available with different biodiesel percentages, and that there is considerable variability in the individual measurements of the relative emissions effects of biodiesel blended fuels. Similar figures are seen when one looks at the HD diesel emissions data. For the regulated pollutant emissions, there are more that 20 sets of test results available for the B5, B10, B20, B30, B50 and B100 biodiesel blends. This allows the evaluation of statistical significance of the effects of these blends on vehicle emissions.

For the LD diesel vehicle emissions we observed the following effects of the biodiesel blended fuels. For the HC emissions the effects of the biodiesel blends is an increase of 1.6 ± 4.5% (95% confidence interval) for B5, an increase of 4.2 ± 5.2% for B10, a decrease of 4.1 ± 5.5% for B20, a decrease of 0.3 ± 5.4% for B30, a decrease of 0.9 ± 10.3% for B50, and a decrease of 5.8 ± 14.8% for B100. None of the observed effects on hydrocarbon emissions are statistically significant. For NOx emissions the effects of the biodiesel blends was an increase of 1.1 ± 2.7% for B5, of 5.1 ± 2.3% for B10, of 5.8 ± 2.2% for B20, of 7.2 ± 2.7% for B30, of 7.3 ± 3.5% for B50, and of 6.5 ± 3.5% for B100. The biodiesel blend effect on NOx emissions is consistently a statistically significant increase for all of these blend levels, except B5. The effect of the biodiesel blends on CO emissions show a decrease of 0.7 ± 2.9% for B5, an increase of 2.7 ± 5.9% for B10, a decrease of 5.5 ± 3.5% for B20, an increase of 4.8 ± 6.0% for B30, an increase of 4.7 ± 10.8% for B50, and an increase of 12.9 ± 14.3% for B100. For the CO emissions, none of the biodiesel blends above had a statistically significant effect, except the decrease observed for the B20 blend. For the CO_2 emissions the effects of the biodiesel blends was a decrease of 2.0 ± 2.3% for B5, a decrease of 1.1 ± 0.9% for B10, a decrease of 0.4 ± 1.2% for B20, an increase of 1.1 ±1.4% for B30, an increase of 1.2 ± 1.3% for B50, and an increase of 0.8 ± 1.4% for B100. This data shows a small statistically significant decrease in CO_2 emissions only for the B10 blend. None of the other results are statistically significant. The effect of the biodiesel blends on PM emissions show a decrease of 1.0 ± 5.0% for B5, a decrease of 14.8 ± 3.5% for B10, a decrease of 5.8 ± 4.9% for B20, a decrease of 16.0 ± 3.6% for B30, a decrease of 9.1 ± 8.6% for B50, and a decrease of 7.0 ± 14.8% for B100. The decrease observed for the B10, B20, B30 and B50 blends are statistically significant, and they are relatively large effects in the range of 6-16% decrease, but none of the other biodiesel blend levels resulted in a statistically significant effect. For the fuel economy results, only the B5, B10, B20, B30 and B50 blends had a sufficient quantity of data (more than 20 values) to assess the significance of the effects. The fuel economy was found to decrease (or fuel consumption increased) by 0.4 ± 1.2% for B5, by 0.3 ± 1.0% for B10, by 1.0 ± 1.8% for B20, by 1.3 ± 2.0% for B30, and by 1.9 ± 2.5% for B50. None of the fuel economy effects are statistically significant.

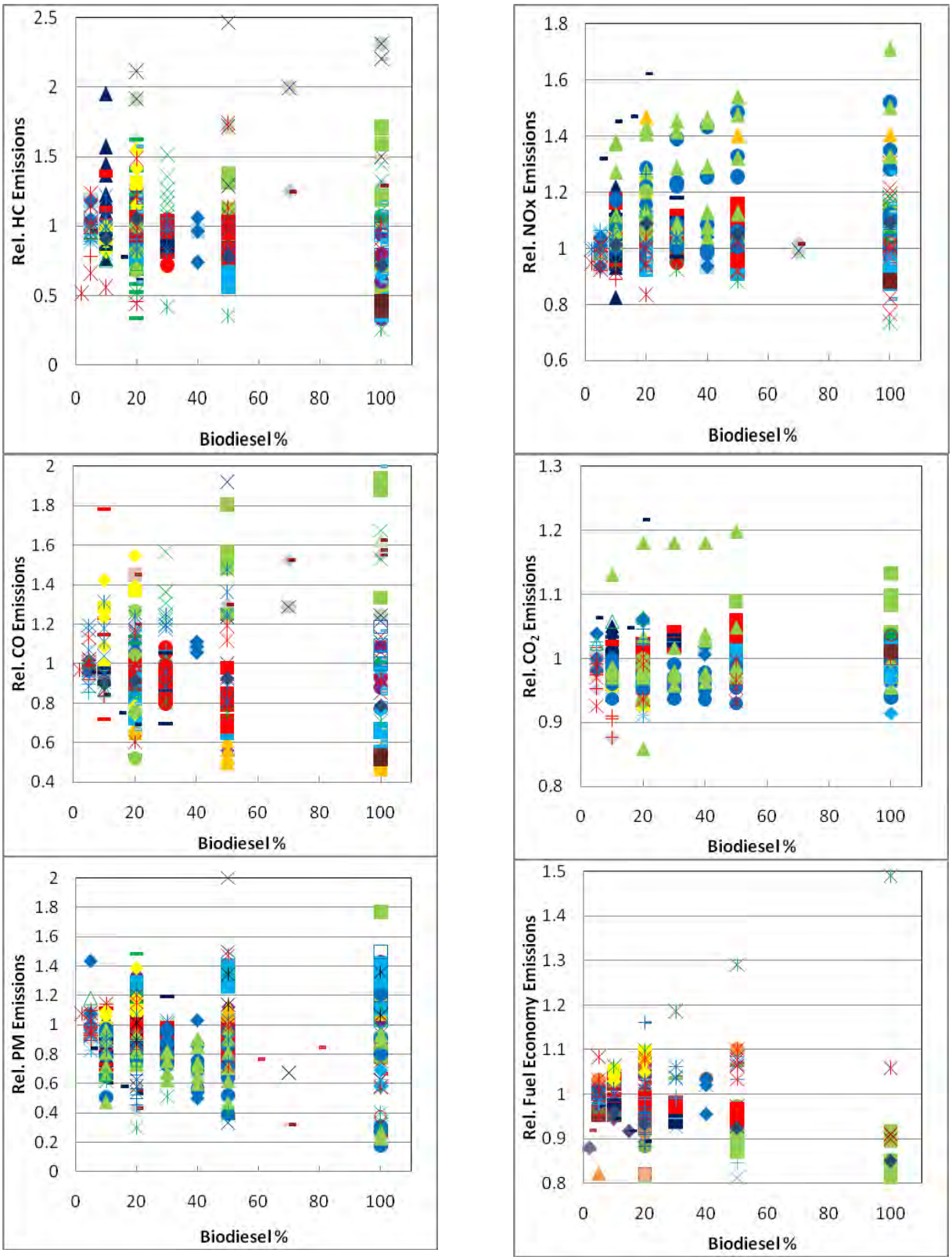

Fig. 1. Chassis dynamometer test results of relative emissions of hydrocarbons, nitrogen oxides, carbon monoxide, carbon dioxide, particulate matter, and vehicle fuel economy for biodiesel fuel relative to diesel fuel in light-duty diesel vehicles.

Sufficient data exists to allow one to begin to explore the effects of biodiesel fuel use on the emissions of formaldehyde, acetaldehyde and total polycyclic aromatic hydrocarbons (PAH) for LD vehicles. The effects of the biodiesel blends on formaldehyde emissions were increases of 28.9 ± 17.1% for B10, 27.5 ± 21.8% for B20 and 34.9 ± 8.7% for B30, while the effects on acetaldehyde emissions were increases of 40.7 ± 76.1% for B10, 69.9 ± 126% for B20 and 23.1 ± 7.2% for B30. All of the increases found for formaldehyde emissions were statistically significant, but only the acetaldehyde emissions increase for B30 was statistically significant. The results for the effects of the biodiesel blends on the emissions of total PAH were confusing, with the total PAH emissions reduced by 8.3 ± 6.4% for B10 and 8.9 ± 9.8% for B20, while for the B30 and B100 blends, the total PAH emissions increased by 21.2 ± 18.4% and 33.4 ± 53.7% respectively. Only the results for B10 and B30 were statistically significant.

5. Comparison of Heavy-Duty and Light-Duty Diesel Vehicle Emissions

The only comparisons that can be made between HD and LD diesel vehicle emissions are for B20 blends, where sufficient data exists for the HD diesel dynamometer and on-road and LD dynamometer tests, and for HC, NOx and CO emissions where sufficient data exists for HD and LD dynamometer tests with B100 fuels. For the HC emissions, we have found that the emissions from HD vehicles in the on-road emissions studies are significantly lower that the HD dynamometer test results. The HD on-road emissions results are also significantly lower than the LD dynamometer results, and the HD and LD dynamometer results are not significantly different from each other. The HD and LD dynamometer results have been combined for the B20 blend, resulting in an overall HC emissions decrease of 4.9 ± 3.5% from the combined dynamometer data. Again for NOx emissions, the HD on-road emissions results were significantly lower than the HD dynamometer results and were significantly lower than the LD dynamometer results. There was no significant difference between the HD and LD dynamometer results for NOx. The HD and LD dynamometer results have been combined for the B20 blend, resulting in an overall NOx emissions increase of 4.7 ± 1.6%. For the CO emissions, the HD on-road emissions results were not significantly different that the HD dynamometer results, and the combined HD emissions results were not significantly different than the LD dynamometer results. The HD dynamometer and on-road emissions results, and the LD dynamometer emissions results were combined for the B20 blend, resulting in an overall CO emissions decrease of 5.4 ± 2.9%. For the CO_2 emissions, the HD on-road emissions results were not significantly different that the HD dynamometer results, and the combined HD emissions results were not significantly different than the LD dynamometer results. The HD dynamometer and on-road emissions results and the LD dynamometer emissions results were combined for the B20 blend, resulting in an overall CO_2 emissions increase of 0.9 ± 1.5%. For the PM emissions, the HD on-road emissions results were not significantly different that the HD dynamometer results, but the combined HD emissions results were significantly lower than the LD dynamometer results. The HD dynamometer and on-road emissions results were combined for the B20 blend, resulting in an overall PM emissions decrease of 14.5 ± 3.9%. The fuel economy from HD vehicles in the on-road studies are significantly higher than the HD dynamometer test results. The HD on-road fuel economy results are not significantly different from the LD dynamometer results, and the HD and LD dynamometer results are not significantly different from each other. The HD and LD dynamometer results have been combined for the B20 blend, resulting in an overall fuel economy decrease of 1.8 ± 1.1%.

For the HC emissions from B100 blends, we have found that the emissions from HD and LD dynamometer data are not significantly different. The HD and LD dynamometer results have been combined for the B100 blend, resulting in an overall HC emissions decrease of 13.4 ±

9.2%. For the NOx emissions from B100 blends, the emissions from HD and LD dynamometer data are not significantly different. The HD and LD dynamometer results have been combined for the B100 blend, resulting in an overall NOx emissions increase of 7.5 ± 2.4%. For the CO emissions from the B100 blend, the heavy duty dynamometer results are significantly lower than the LD dynamometer results.

6. Conclusions

Most reviews of the effects of biodiesel blended fuels use on vehicle emissions combine all of the available data engine and vehicle, LD and HD to assess the effects. As has been found in this work this is not always a valid approach. In this work, we have only used vehicle emissions data, no engine data, and we have found some significant differences in subsets of this vehicle data.

In this work, it was found that there some of the emissions for HD diesel vehicles tested using dynamometers and on-road were significantly different. For B20 blends, the HC emissions for both test procedures led to significant decreases emissions in these emissions of 5.7% for the dynamometer studies and 21.7% for the on-road studies. In the cases of NOx emissions studies, a statistically significant increase in NOx emissions was found for B20 blends from the dynamometer data, while the on-road studies resulted in a 3.3% decrease that was not significant. For fuel economy, the dynamometer data for B20 showed a significant decrease in fuel economy of 2.6%, while the on-road data gave a 5.7% increase that was not significant. For each of these three measures for the two different sources of HD vehicle emissions data, the dynamometer data was significantly different from the on-road data. It is not be valid to combine data from the dynamometer and on-road studies of B20 blended fuels for HC and NOx emissions and fuel economy to determine the effects of using these fuels in HD vehicles. But since the B20 data for CO, CO_2 and PM emissions derived from these two different test procedures are not significantly different, it is valid to combine these data sets to assess the overall effects of B20 on these emissions from HD vehicles.

In comparing the results of studies on LD and HD vehicles for B20 blends, we have found no significant differences in HC and NOx emissions and fuel economy between the LD and HD dynamometer studies, and we have found no significant differences in emissions of CO and CO_2 between the LD dynamometer and the combined HD dynamometer and on-road test data. But the PM emissions for B20 fuels are significantly different between the LD dynamometer and the combined HD dynamometer and on-road test data. Table 1 summarizes the statistically significant results for B20 blended fuels, where the HD and LD data are combined when there is no significant difference between the subsets of the data.

Being able to partition data to allow one to explore subsets of vehicle emissions data requires large quantities of data. Many other factors need to be explored, but there is a shortage of adequate data to be representative of these other factors. There is inadequate data available to allow one to assess the effects of biodiesel fuel use on emissions of hazardous air pollutants, such as benzene, 1,3-butadiene, etc. As seen in this work, there is sufficient data to begin exploring the effects on LD vehicle emissions of formaldehyde, acetaldehyde, and polycyclic aromatic hydrocarbons. We need much more data to begin assessing the effects of biodiesel fuel use on ultrafine particulate emissions, especially, particle number and particle size distributions in emissions. Different biodiesel feedstocks are more commonly used in different areas of the world, such as soy oil in North America, rapeseed oil in Europe and palm oil in southern parts of Asia. Additional vehicle emissions data is necessary to explore the effects of different biodiesel feedstocks on vehicle emissions.

Table 1. Summary of statistically significant results for B20 and B100 biodiesel blends for combined LD and HD dynamometer (dyno) and HD on-road emissions data.

Emission	Biodiesel Blend	Tests	Biodiesel Effect	95% Confidence Interval	Number of Measurements
HC	B20	HD & LD Dyno	-4.9%	±3.5%	204
HC	B20	HD On-road	-21.7%	±4.4%	89
HC	B100	HD & LD Dyno	-13.4%	±9.2%	122
NO_x	B20	HD & LD Dyno	+4.7%	±1.6%	227
NO_x	B100	HD & LD Dyno	+7.5%	±2.4%	143
CO	B20	HD, LD Dyno & HD On-road	-5.4%	±2.9%	286
PM	B20	HD Dyno & HD On-road	-14.5%	±13.9%	137
PM	B20	LD Dyno	-5.8%	±4.9%	109
Fuel Economy	B20	HD & LD Dyno	-1.8%	±1.1%	94

References

The literature that was reviewed in this analysis included 19 published studies using dynamometers for HD vehicles, 14 studies using on-road data for HD vehicles, and 47 studies using dynamometers for LD vehicles. Due to space limitations these references are not included in the reference list, but are available upon request.

[1] R. L. McCormick, The impact of biodiesel on pollutant emissions and public health, Inhalation Toxicology 19, 2007, pp. 1033 – 1039.

[2] M. Lapuerta, O. Armas, J. Rodriguez-Fernandez, Effects of biodiesel fuels on diesel engine emissions, Progress in Energy and Combustion Science 34, 2008, pp. 198- 224.

[3] J. Yanowitz, R. L. McCormick, Effect of biodiesel blends on North American heavy-duty diesel engine emissions, European Journal of Lipid Science and Technology 111, 2009, pp. 763-772.

[4] S. K. Hoekman, A. Gertler, A. Broch, C. Robbins, Investigation of biodistillates as potential blendstocks for transportation fuels, Coordinating Research Council, CRC Project No. AVFL-17, 2009.

First experiences of ethanol hybrid buses operating in public transport

Martina Wikström[1,*], Anders Folkesson[2], Per Alvfors[1]

[1] *Chemical Engineering and Technology, Division of Energy Processes, Royal Institute of Technology, Stockholm, Sweden*
[2] *Sustainable Solutions, Buses and Coaches, Scania CV AB, Södertälje, Sweden*
** Corresponding author. Tel: +46 8 790 65 51, Fax: +46 8 732 08 58, E-mail: marbjor@kth.se*

Abstract: With the ambitions to further increase its share of more sustainable vehicles, Stockholm Public Transport Authority (SL) carried out a project to evaluate the performance of ethanol hybrid buses together with bus manufacturer Scania and bus operator Nobina. Ethanol hybrid buses were operating in regular suburban public transport traffic in Stockholm between May 2009 and June 2010. The purpose of this paper is to evaluate the potential of the ethanol hybrid buses in general and their energy efficiency in particular. The evaluation is based on experimental data, mainly from standardised duty cycle tests, but also general experiences during the trail, for example error reports. The buses have a series hybrid powertrain with super capacitors as energy storage. At favourable conditions the fuel reduction is approximately 20 %. The potential additional fuel savings of the start/stop software has been tested and adds at least another 10 % fuel reduction. Not all of the hybrid system's components are yet robust enough, thus they need further development to fully commercial. Hybrid city buses have great potential but are currently not technically mature and proven, nor have the overall costs over the lifetime of the vehicle reached a commercial level as yet.

Keywords: *Ethanol hybrid bus, Series hybrid, Duty cycle, Urban public transportation, Energy analysis*

1. Introduction

Six ethanol hybrid buses and one reference bus were operated during a one-year field test to evaluate the robustness and energy saving potential of their hybrid powertrain. Partners in the project were the Stockholm Public Transport Authority (SL), the bus manufacturer Scania and the bus operator Nobina and it was carried out with funding from the Swedish Energy Agency. This is a unique project because it is one of the first times renewable-fuelled hybrid buses have been tested and operated in real traffic. The buses were operating in Stockholm's south suburban areas but were also taken out of traffic to perform standardised duty cycle tests on a test circuit, tests intended to better reflect inner-city driving. The objective of the field test from Scania's perspective was to test the hybrid powertrain in real traffic early in the development process in order to find weaknesses in the hybrid system. From SL's and Nobina's point of view the project aimed to evaluate the status and the potential of hybrid buses and was a way to enhance the development of even more environmentally friendly vehicles in their fleets. Already today (2010), SL has the world largest fleet of renewable-fuelled buses with more than 400 ethanol buses and 100 biogas buses in operation out of a fleet of around 2000 buses. The target is that 50 % of all buses should run on renewable fuels at the end of 2011 and 100 % by 2025 [1]. In this paper the general operational findings are presented with focus on evaluation of robustness of the powertrain (one-year field test) and the energy efficiency potential (duty cycle tests).

2. Methodology

The objectives are to evaluate the robustness and the energy efficiency potential of ethanol hybrid buses. In order to evaluate the robustness of the hybrid powertrain, the drivers and technicians filed error reports during the one-year field test. To attain reproducible experimental data in order to evaluate the energy efficiency potential, duty cycle tests were carried out. More details about the experimental set-up, see section *5. Experiments and results.*

3. Towards sustainable urban transportation

There are many reasons for promoting more sustainable urban transportation:

- To reduce emissions harmful to public health such as NOx, particulates and noise.
- To reduce emissions of greenhouse gases, most important fossil CO_2.
- To secure energy supply for the transport sector in the long term.

Additionally, by increasing the share of public transportation the problems with traffic congestion decrease. Traffic congestion becomes worse as the population in urban areas increases and cities become more densely populated while simultaneously more transports of people and goods must be carried out in the same or even less space than before.

The CO_2 emissions are, apart from increasing the share of public transport, tackled cost-efficient by shifting from fossil to renewable fuels. This has positive impact also on the energy security issue, especially if bio fuels may be produced locally. Bio fuels may sometimes be used as low-blends in fossil fuels, and sometimes as high-blends or pure fuels. There are political targets and also legislation for introduction of bio fuels in various regions, e.g. the EU is to have 10 % renewable fuels by 2020 [2]. A local example is the Swedish Government's vision that the Swedish transport sector should be independent of fossil fuels by 2030 [3]. Most widely spread renewable fuels are ethanol and biodiesel but other fuels, such as biogas are also getting increased attention in some markets [4].

At the same time as more bio fuels are introduced in the transport sector, vehicles must be as energy or fuel efficient as possible, irrespective of the fuels used, i.e. fossil and/or renewable. Striving for fuel efficiency is an ongoing process and has been the single most important force of competition in the commercial vehicle industry for decades – fuel efficiency improvements are introduced when commercially feasible. Commercially feasible refers to the lifecycle cost of an improvement in comparison with its expected benefits. This is for fuel efficiency improvements the development and production costs, expected lifetime, replacement cost if the lifetime of a new component is short as well as additional repair and maintenance costs measured against fuel cost saving or CO_2 saving. Hybridisation is one proposed method for vehicle fuel savings. A hybrid powertrain also gives the potential to improve the vehicle by other means and to make it more attractive for the passengers, e.g. noise impact can be minimised during start and acceleration since the internal combustion engine is assisted by one or more electric motors. If the vehicle has a series hybrid powertrain, i.e. a completely electric propulsion system, the powertrain usually offers a completely step less, and thereby very comfortable, drive without any jerks at all due to gear shifts. In this powertrain, there are also possibilities to improve the vehicle design and layout because there are basically no restrictions imposed by a mechanical transmission, prop shafts, cardan angles etc [5]. Even though hybrid buses seem to have a good potential there is no production of hybrid buses in common commercial terms, only small series production as tests and demo fleets, or politically driven and heavily subsidised fleets. In North America there are a few thousands hybrid buses running in Seattle, New York City, San Francisco and Toronto among other cities, all heavily subsidised by the government or local municipalities. The extra cost for hybridisation is usually very high, in the range of 100,000 € or even more extra per vehicle [6] and the technology is not yet proven, especially the energy storage systems (e.g. battery). Even so, hybrid buses, if designed and implemented in a clever and cost-efficient way, may play an important role in a future sustainable transport system due to their potential for energy saving, especially if combined with renewable fuels.

4. The bus

The ethanol hybrid bus is a Scania OmniLink, a three axis, 13.7 meter long low-entry city/suburban bus with a rear boggie. The internal combustion engine (ICE) is a diesel engine slightly adapted (e.g. higher compression ratio) to combust ethanol according to the diesel combustion process. The renewable fuel (ED95) used for the engine consists of 95 % ethanol and 5 % additives (ignition improver, lubricating additive etc). This is the third generation of ethanol engines from Scania since start of production in the late 1980s. So far around 700 ethanol buses have been delivered, mainly to Stockholm but also to number of cities worldwide.

The hybrid buses are equipped with a series hybrid powertrain, i.e. with fully electric propulsion. A 150 kW electric motor propels the mid axle of the bus. A high power and high torque generator is mounted on the internal combustion engine. The electric motor, generator and power electronics are delivered by Voith. The energy storage system in the hybrid powertrain consists of super capacitors, not batteries. Four 125 V modules from Maxwell connected in series offer total usable storage capacity of 400 Wh.

Fig 1. The Scania OmniLink ethanol hybrid bus and a schematic illustration of the series hybrid powertrain [Photo: Stefan Wallin, SL]

A reference bus with an identical ethanol engine but equipped with a conventional six-speed hydraulic automatic gearbox with retarder from ZF was also operated during the field test. The reference bus has the same identical exterior dimensions (excluding the roof hood containing the energy storage) and interior design as the hybrid bus. The only difference is that the hybrid buses have one seat missing in front of the rear door of the bus due to a conduit for cabling and coolant pipes to the power electronics and the energy storage system mounted on the roof. The hybrid bus is approximately 1.5 tonnes heavier than the reference bus.

Type: Scania OmniLink Low-entry city bus	Description
General	
Dimensions *(L × W × H)*	13.7 m × 2.55 m × 3.54 m
Kerb weight	16 tonnes
Max weight	26 tonnes
Passenger capacity	115 (40 + 75) (minus one seat in hybrids)
Internal Combustion Engine	Diesel ethanol engine
Fuel	ED95
Maximum Power output	198 kW (270 hp)
Maximum Torque	1 250 Nm
Emission level	Euro V / EEV
Hybrid components	
Type	Series hybrid
Electric motor	Voith TFM
Maximum Power	150 kW
Maximum Torque	2 750 Nm
Generator	Voith TFM
Maximum Power	220 kW
Maximum Torque	1 250 Nm
Energy Storage Unit	Maxwell Super Capacitors
Number of modules	4
Total capacity (useable)	400 Wh
Maximum voltage per unit	125 V
Maximum voltage in total	500 V

Fig 2. Technical description of the ethanol hybrid bus

5. Experiments and results

The one-year field test generated considerable experience as regards the robustness of the hybrid powertrain. In order to evaluate the energy efficiency potential, duty cycle tests were carried out to obtain experimental data representing various traffic situations. The nature of the suburban route did not produce data relevant for an energy flow analysis for city traffic.

5.1. Evaluation of powertrain robustness from one-year field test

Based on error reports filed by the drivers and technicians during the field test, the main malfunctions were divided into three categories: 1) ICE, internal combustion engine 2) the bus in general and 3) hybrid powertrain-related errors. To further evaluate the hybrid powertrain, this section is divided into four subgroups (a – d) to evaluate the robustness of its main areas. Compilation of results from error report is shown in Figure 3.

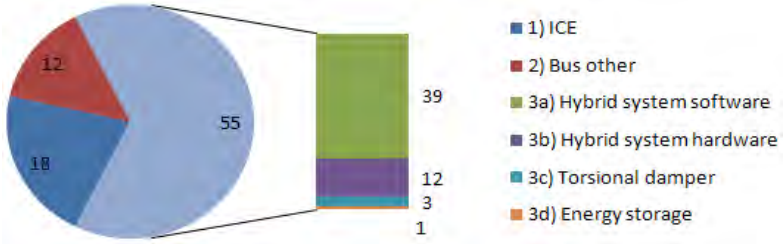

Fig 3. Error reports filed during the one-year field-test.

The robustness of the hybrid powertrain is the focus for this paper, but just to mention something about the other two categories, also the internal combustion engine underwent development during the field test period, e.g. the fuel injections system was improved. Upgrading the engine eliminated many of the errors reported during the first part of the test period. The hybrid software is still under development; during the field test it was too sensitive to interference from e.g. abnormal parameter values sent from other hybrid components as well as the 24 V system voltage level. Through maintenance charging of the 24 V start battery; the number of software reports was reduced. Malfunctions due to hardware are caused predominantly by three components: the direction sensor on the electric motor, the electric motor itself and the torsional damper between ICE and generator. Due to the hybrid management road safety system, incorrect indication of torque to the direction sensor will immediately shut down the system. Some sensors were malfunctioning and therefore replaced and other reported errors were just false alarms. The construction of the electric motor in the tested version was not durable enough for this 3-axle hybrid bus application and had a life of about 15 000 – 20 000 km in several buses causing many filed error reports. This problem arose rather late in the project and was not yet resolved when the field test ended, but is defined and considered possible to tackle with further development. The torsional damper (3c) was initially too weak and when replaced by a stronger one the problem was solved. The only problem reported concerning the energy storage was a fan failure and therefore not caused by the super capacitors. The super capacitors may, as far as this one-year field test is concerned, be regarded as suitable energy storage for the application as regards robustness.

5.2. Evaluation of energy efficiency potential by standardised duty cycle test

In order to evaluate the potential of the hybrid powertrain, standardised duty cycle tests, according to SORT – Standardised on-road tests cycles (developed by the International Association of Public Transport, UITP), were carried out. The key parameters in a traffic situation are the average speed and the number of stops per kilometre, see Table 1. Variations due to topography are neglected to make the test repeatable, hence duty cycles are assumed to be completely flat.

Table 1. Characteristics of the three SORT duty cycles, from UITP 2004 [7]

	SORT 1	SORT 2	SORT 3
Average speed [km/h]	12.6	18.6	26.3
Stops per kilometre	5.8	3.3	2.1
Time idling [%]	39.7	33.4	20.1
Cycle type	Urban	Mixed	Suburban

Figure 4 shows the three performed duty cycles' continuous velocity profile coupled with the energy content in the super capacitors expressed as the state-of-charge (SOC) where 100 % is fully charged and the lowest level is restricted to 25 % (half nominal voltage) to decrease the risk of chemical side reactions and thereby increase capacitor service life. Experiments show that the super capacitors obtain a high round-trip efficiency, generally above 90 %. Super capacitors have high power density [8] and are therefore a suitable energy storage units for heavy vehicles equipped with regenerative braking. The kinetic energy accumulated during deceleration, is converted in the electric motor into electric power charging the super capacitors. If not stored in the super capacitors, it will be used to propel the ICE via the generator or, last of all, dumped in the resistor as heat to the cooling system, see Figure 1. SORT 1 tests show dynamic energy storage management without long time periods of completely charged or empty super capacitors. As seen in Figure 4 already during the SORT 2 test the energy storage will be restricted in terms of size (400 Wh), i.e. the energy storage system is fully charged. During SORT 3 tests, the charge oscillates between its extreme values. The capacity of the energy storage system is therefore a limiting factor for a bus in driving situations similar to SORT 2 and 3 but feasible for SORT 1, urban operation.

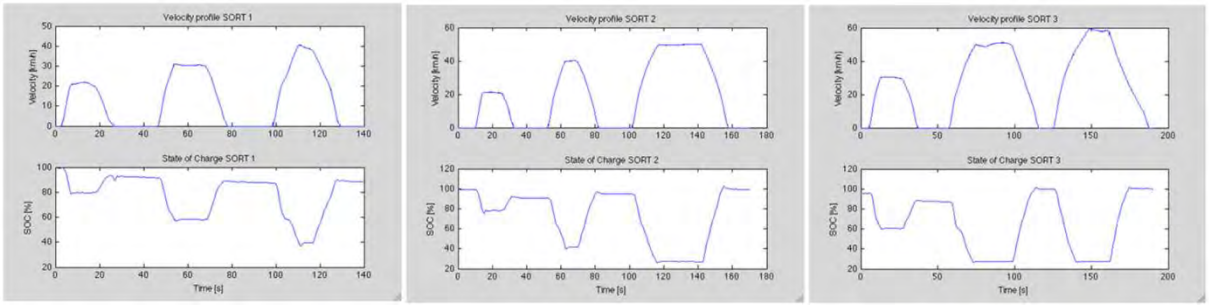

Fig 4. Velocity profile (top) and corresponding SOC profile (bottom) for SORT 1-3 test cycle

Performed SORT cycle tests with the reference bus enable quantification of the absolute fuel consumption reduction generated by the hybridisation, see Table 2.

Table 2. Fuel consumption SORT duty cycles.

	Reference Fuel consumption [litre/ 100 km]	Ethanol hybrid bus Fuel consumption [litre/ 100 km]
SORT 1	89.5	72.5
SORT 2	79.0	63.0
SORT 3	71.0	63.0

A significant fuel consumption reduction is attained for the cycles SORT 1 and SORT 2, 19 %, and 20 %, from 89.5 to 72.5 l/100 km and 79 to 63 l/100 km, respectively. The fuel consumption reduction for SORT 3 corresponds to 11 %, from 71 to 63 litre/100 km. In order to increase the level of detail, the energy spent per driving mode was explored, see Figure 5.

The four driving modes were defined as:

Idling – vehicle speed (υ) is zero, $\upsilon(i)=0$
Deceleration – when not idling and acceleration is negative $\upsilon(i) > \upsilon(i+1)$
Acceleration – when not idling and acceleration is positive $\upsilon(i) < \upsilon(i+1)$
Cruising – when not idling and acceleration is zero. $\upsilon(i) = \upsilon(i+1) \neq 0$

Fig 5. The energy and time spent per driving mode for duty cycle tests with hybrid bus according to the three SORT-cycles

Even though a large time is spent idling (about 1/3 of the time), the fuel consumption during this driving mode is moderate (between 5 and 15 %). The most fuel-consuming driving mode is acceleration where approximately 60 % (varies between 57.7 and 62.8 %) of the total fuel consumption is utilised during about 30-35 % of the time.

5.2.1. Start/stop

To further decrease the fuel consumption it is possible to install a software start/stop feature, which automatically turns of the ICE when idling. Analogous to the time spent as in Figure 5 the fuel consumption when the start/stop software operated was measured. The fuel consumption during idling drops drastically, now only consuming between 2.97 % (SORT 1) and less than 1 % (SORT 2 and 3). Decreasing the fuel demand during idling (which for the SORT cycles, corresponds to approximately 30 % of the time and in real traffic sometimes up to 60 % or more) has a significant impact on the overall fuel consumption, seen in Table 3:

Table 3. Fuel consumption during SORT duty cycles with the buses

	Reference [litre/ 100 km]	Ethanol hybrid bus [litre/ 100 km]	Ethanol hybrid bus with start/stop [litre/ 100 km]
SORT 1	89.5	-19 %	-33 %
SORT 2	79.0	-20 %	- 21 %
SORT 3	71.0	-11 %	- 13 %

5.2.2. Energy flow analysis using Sankey diagram

The energy flows through the electrified powertrain, see Figure 1, for the urban SORT cycle are illustrated in Figure 6 by a Sankey diagram. The Sankey diagram presents an average overview of the energy flows, and is not representative for a specific time during the cycle but is illustrative for the complete cycle. The energy flows in and out of key hybrid components are on-board measured data. The total power input is calculated from the instantaneous amount of fuel injected, in gram per stroke, using the lower heating value and density of ED95, 26.8 MJ/kg and 820 g/l, respectively. Losses for the ICE correspond to energy losses such as heat, mechanical and transmission losses. The energy consumption for running the auxiliary systems is also accounted for as an energy loss over the ICE. The efficiency in the generator is defined as the ratio between electrical power output and mechanical input. The generator and its inverter has experimentally proven to have an average efficiency of around 92 %.The energy storage efficiency, when SOC-balanced just as the round-trip efficiency, is calculated as the ratio between the total energy storage output and total energy storage input.

The energy storage efficiency is consistently about 90 % for all the three cycle tests. When decelerating, the electric motor operates as a generator and recovers brake energy. The share recovered brake energy almost exceeds 20 % of total power input. The efficiency of the electric motor is defined as the ratio between the average power input from the powertrain and the mechanical power output. The experimental average efficiency of the electric motor is approximate 92%. The share of power dumped upon the resistor during the SORT 1 cycle is small which indicates adequate energy storage size. The share, which is not regenerated, constitutes the term of losses due to aerodynamic drag, rolling resistance, transmission losses and wheel brakes.

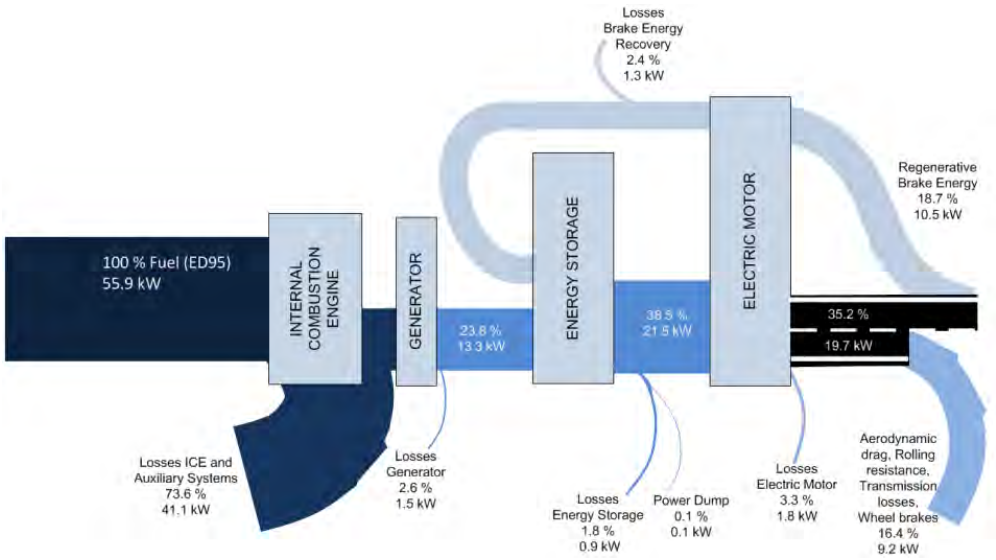

Fig 6. Sankey diagram of average, experimental power (energy) flows for the SORT 1 cycle

5.3. Field test – Urban Stockholm

The SORT 1 cycle tests indicated that the series hybrid system has high potential for significant fuel consumption savings. This lead up to a one-day field test in central Stockholm, during rush hour, to evaluate the potential of transferring the SORT results onto public transportation. Both the ethanol hybrid bus and the reference bus operated two routes: 2 and 66. To perform only a one-day test results in statistically uncertain values but still generates data that hopefully may indicate potential for urban regular transport. Due to organisational and legal reasons, since the bus operator participating in the project was not responsible for the inner-city bus routes, the city field test could not be prolonged.

Table 4. Characteristics of routes 2 and 66 in Stockholm

	Route 2	Route 66
Average velocity [km/h]	12.2	12.4
Stops per kilometre	6.15	5.0
Time idling [%]	25.4	22.36

The fuel consumption reductions are not of the same order as for the SORT tests. For route 66 the hybrid powertrain gives an insignificant (less than 1%) fuel consumption reduction. The fuel consumption may be reduced by 9.3 % for route 2. An explanation to the poor result might be related to the test method used, that the buses were operated nose-to-tail, a method that normally works well in a controlled environment such as a test track. However, in dense real traffic when, apart from consider the other bus, other vehicles and pedestrians as well as traffic regulations, the bus is subjected to weak accelerations and decelerations, which results in poor brake-recovery for the hybrid bus.

5.3.1. London Hybrid Bus Trials

The results from both the duty cycle tests and the field test are similar to the results of an extensive diesel hybrid bus trail in London, hosted by Transport for London (TfL), which also had difficulties in obtaining the significant fuel consumption reduction achieved during duty cycle test for regular public transport [6]. Based on the Millbrook proving ground's London Transport Bus (MLTB) test cycle the average fuel consumption reduction was 31 %, an average attained from series, parallel and mixed hybrid buses, both single and double-decked. During the hybrid bus trail in London, 56 hybrid buses operated 10 routes. The results were scattered between almost reaching the TfL 30 % reduction target and an actual increase in fuel consumption. For all vehicle manufactures, the results indicated a much smaller (or non-existing) fuel consumption reduction than expected. This indicates that fuel consumption reductions due to the hybridisation, when operating on public urban routes oscillate depending on the prevailing traffic situation since there are parameters in real-life traffic which can not be transferred to a test situation. A general conclusion from operation of hybrid buses in London is that the overall costs over the lifetime of a hybrid vehicle are not on a commercial level yet, i.e. the fuel savings do not equal the extra cost of the vehicles.

6. Experiences and conclusions

The series hybrid powertrain have experimentally shown potential for reducing the fuel consumption in urban traffic by up to 20 % and additionally 10 % when utilising the start/stop software. In conformity with similar experiments with hybrid buses, it is not evident that the fuel reduction potential may be realised on real life routes since the fuel reduction potential is dependent on the route characteristics. A recommendation for the next project is that the real inner-city fuel saving potential should be validated in real operation on inner-city bus routes. Some components of the hybrid system still need some development as regards robustness. The super capacitors did work consistently during the whole field test and may so far be considered to be suitable as energy storage for this hybrid vehicle application.

References

[1] Stockholm Public Transport (SL) web page, www.sl.se, accessed 2010-12-18

[2] Directive 2009/28/EC of the European Parliament and of the Council of 23 April 2009 on the promotion of the use of energy from renewable sources and amending and subsequently repealing Directives 2001/77/EC and 2003/30/EC, Brussels

[3] The Swedish National Action Plan for the promotion of the use of renewable energy in accordance with Directive 2009/28/EC and the Commission Decision of 30.06.2009

[4] REN21, Renewables 2010, Global Status Report. Available at <www.ren21.net>, accessed 2010-12-14

[5] L. Overgaard, Scania hybrid concept – with robust technology into the future, Proceedings of 57th UITP World Congress, 2007

[6] Mike Weston, London Hybrid Bus Trials, Proceedings of Low Carbon Vehicle Partnership (LowCVP) Conference 2010, available at < www.lowcvp.org.uk >

[7] UITP, International Association of Public Transport, SORT – Standardised on-road test cycles, 2004. Available for purchase at < www.uitp.com >

[8] V. Paladini, T. Donateo, A. de Risi, D. Laforgia, Super-capacitors fuel-cell hybrid electric vehicle optimization and control strategy development, Energy Conversion and Management, Volume 48(11), 2007, Pages 3001-3008

Local production of bioethanol to meet the growing demands of a regional transport system

Lilia Daianova[1]*, Eva Thorin[1], Jinyue Yan[1, 2], Erik Dotzauer[1]

[1]*School of Sustainable Development of Society and Technology, Mälardalen University, Västerås, Sweden*
[2]*Royal Institute of Technology, Stockholm, Sweden*
** Corresponding author: Tel: +46 (0)21 10 15 38, Fax: +46 (0)21 10 14 80*
E-mail: lilia.daianova@mdh.se

Abstract: Energy security and the mitigation of greenhouse gas emissions (GHG) are the driving forces behind the development of renewable fuel sources worldwide. In Sweden, a relatively rapid development in bioethanol usage in transportation has been driven by the implementation of national taxation regulations on carbon neutral transport fuels. The demand for bioethanol to fuel transportation is growing and cannot be met through current domestic production alone. Lignocellulosic ethanol derived from agricultural crop residues may be a feasible alternative source of ethanol to secure a consistent regional fuel supply in Swedish climatic conditions. This paper analyzes how the regional energy system can contribute to reducing CO_2 emissions by realizing local small scale bioethanol production and substituting petrol fuel with high blend ethanol mixtures for private road transport. The results show that about 13 000 m^3 of bioethanol can be produced from the straw available in the studied region and that this amount can meet the current regional ethanol fuel demand. Replacing the current demand for petrol fuel for passenger cars with ethanol fuel can potentially reduce CO_2 emissions from transportation by 48%.

Keywords: *Agricultural crop residues, Straw, Bioethanol, Transport fuel, Greenhouse gas emissions (GHG)*

1. Introduction

According to the EU Directive, the target share of renewable energy sources as a percentage of gross final energy consumption in Sweden in 2020 is 49% [1]. Over the period 1990-2006 the proportion of renewable energy in final energy use has increased from 33.9% to 43.3%. Renewable electricity generation and renewable energy from the industrial sector contribute most to the proportion of renewable energy in final energy use in Sweden today with 18% and 14% respectively. Renewable energy use in the transport sector accounts for less than 1% of the final energy use [2].

Road traffic dominates in domestic Swedish transportation and contributes 93% of the total energy use in the transport sector (2009) [3]. Road transportation, which consists of private transport (mainly passenger cars), public transport and trucks, uses mostly fossil fuels, petrol and diesel. Use of renewable fuels such as ethanol, FAME (fatty acid methyl ester), biogas, and renewable electricity increased to 5.4% of the total energy use in transport by the end of 2009. Ethanol fuel made up 50% of liquid biofuels used in 2009 [3]. In 2007-2008 the corresponding share of ethanol fuel was almost 60% [4]. Along with a reduction in petrol fuel use in the last few years, ethanol use has also increased because almost all petrol is now a low blend E5 ethanol mixture. At the same time use of FAME and biogas increased by 8% and 1% respectively.

In Swedish transportation, the main current use of ethanol is as a 5% additive to petrol fuel (E5) or as high blend ethanol mixtures (E85, ED95). According to data presented by [3], from 2003-2009 the share of E5 in petrol fuel in Sweden increased from 45% to 95%. Total ethanol use in the Swedish transport sector increased from about 150 000 m^3 in 2003 to 391 000 m^3 in 2009 [5]. The use of low blend ethanol fuel (E5) grew from 125 000 m^3 to 229 000 m^3, whereas the use of high blend ethanol fuels (E85, ED95) grew from 25 000 m^3 to 162 000 m^3 during the period 2003-2009 [5].

However, domestic commercial ethanol fuel production in 2009 was 221 150 m^3. Currently, bioethanol is produced by Lantmännen Agroetanol in Norrköping by fermentation of wheat grains with a capacity of 210 000 m^3, which almost meets the demand for low blend ethanol. SEKAB in Örnsköldsvik produces 16 000 m^3 ethanol from sugary liquor from sulphite pulp from Domsjö Factories, and the SEKAB pilot plant [6] produces 150 m^3 ethanol from wood residues.

Ethanol demand in Sweden is much higher than domestic ethanol production. In the Swedish climate, cultivation of lignocellulosic biomass for bioethanol production is a possible alternative but there are still hurdles to overcome for the conversion of lignocelluloses to biomass. Consequently, realizing local small scale ethanol production can help regions to become more fossil fuel independent. This can also contribute to decreasing local environmental impact caused by transportation when replacing petrol fuel with renewable fuel. GHG emissions from road traffic totalled 29.1 million tonnes CO_2 eq in 2006, 63.6 % of the total Swedish transport sector emissions [7]. It is therefore of great importance to increase the use of biofuels in road transport, to make transport less dependent on fossil fuels and reduce GHG emissions.

GHG benefits of ethanol are discussed by Börjesson, where GHG emissions are estimated for the current Swedish grain-based ethanol production system [8]. Studies on technical performance of ethanol production integration with existing combined heat and power (CHP) plants have been published in recent years [9-11]. Models analysing road traffic energy demand and GHG emissions from transportation are developed for transport systems in China, Greece and Denmark [12, 13].

This paper focuses on analysing the potential for CO_2 emissions savings by substituting petrol use in the region with ethanol fuel, and does not consider the details of ethanol production. Based on an analysis of straw supply, current and potential ethanol and petrol fuel demand, we evaluate the possibilities for a self-sufficient road transport fuel system.

The present paper addresses the following questions. What is the regional demand for bioethanol, in 2009 and in 2020? Is there sufficient cereal straw available for local ethanol fuel production in the studied region in 2009 and 2020? What proportion of CO_2 emissions can be avoided in the region by substituting petrol use with ethanol fuel?

2. Methodology

In this study, input data is predominantly obtained from Swedish Official Statistics (SOS), which is also presented by state authorities (e.g. Swedish Energy Agency, Swedish Board of Agriculture) responsible for dissemination of statistical data in their respective areas. Input data collection is performed according to the structure shown in Figure 1.

The study region comprises the Sala-Heby municipalities, with around 35 000 inhabitants and a total area of 2 443 km^2 [5]. They are typical small municipalities with a predominantly service oriented economy. There are also small scale and decreasing farming and production industries and some tourist activities. A large part of the working population commutes to larger cities outside of the study region. Sala and Heby are neighbouring municipalities that belong to different counties (Västmanland and Uppsala) and are situated about 100 km northwest of Stockholm.

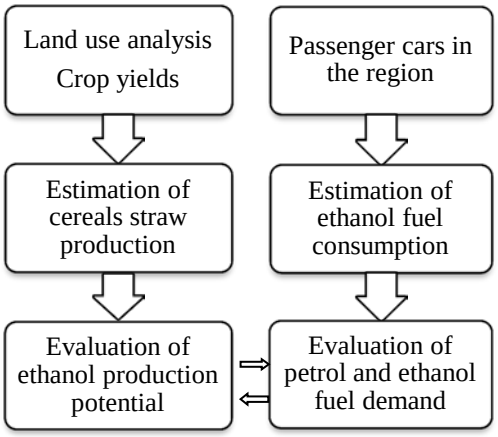

Fig. 1. A schematic flowchart for the local ethanol production study.

This paper focuses on analysing the potential for CO_2 emissions savings in the region by substituting petrol with ethanol fuel in transportation, ignoring the technological aspects of local small scale bioethanol production. The input year of the analysis is 2009. As cereal straw is considered as a feedstock for ethanol production in this study, all estimates are made for straw-based ethanol replacing regional petrol fuel demand. The study only considers fuel use by passenger cars as this is the dominant form of transport in regional road traffic.

In the Sala-Heby region, a total of 25 buses that run on diesel and biogas are used in public transportation. In Sala, the local public transportation company, Västmanlands Lokaltrafik, plans to substitute at least 10 of its 12 buses for biogas fuelled buses by 2014 [14]. In Heby, all 13 buses run on diesel and will be substituted with biogas buses during 2011-2012 according to the company's plan [15]. Buses are therefore excluded from the current analysis as none of the buses currently run on ethanol fuel and there are no plans for them to do so in future. Data on bus transportation in municipalities is obtained from local collective transportation companies as official statistical databases only present data on a regional level.

2.1. Data and assumptions

2.1.1. Straw supply and ethanol production potential

Input data is obtained from official statistics databases presented by the Swedish Board of Agriculture [16]. In this study, straw from wheat, barley and oats are considered as a feedstock for ethanol production as these types of cereals are the most commonly cultivated in the region. These cereals made up nearly 97% of the total cultivation area for cereals in the region in 2009 [16].

The ethanol production potential in the region (B) is calculated for each cereal type (wheat, oats and barley) using Eq. (1):

$$B = \sum_{i=1}^{4} S_i Y_i R_i A Y_{EtOH} \qquad (1)$$

where B is straw-based ethanol production potential (MWh), S_i is the cereals cultivation area (ha), Y_i is the cereals yield in the respective county (kg/ha), R_i is the crop to residue ratio for each cereal type, A is the straw availability, Y_{EtOH} is the ethanol production yield from straw (litre/kg), and i is the type of cereal crop.

Input data for estimation of straw supply and ethanol production potential is presented in Table 1 and in the text below.

Table 1. Input data for straw supply in the Sala-Heby region, 2009.

Parameter	**Unit**	**Type of biomass**				**Reference**
		winter wheat	spring wheat	barley	oats	
$\mathbf{R_i}$	1	1.3	1.3	1.2	1.3	[17]
$\mathbf{C_i}$	tonnes/year	14 733	12 464	41 137	30 549	Based on data from [5,15]

* Cereals production, $C_i = S_i * Y_i$

Cereals production (C_i) is calculated based on cultivation areas and average yields for cereal crop production. Cereal yields (Y_i) for Sala and Heby municipalities correspond to average yields in the counties that the municipalities belong to. As a proportion of straw has to be ploughed back into the soil to maintain the soil fertility and avoid erosion, only about 57% by weight (A in Eq. 1) of the total amount of straw produced can be used for fuel production [17]. The energy content of pure ethanol is 6.24 kWh/litre [18].

The future straw supply in the region is analyzed for the following scenarios:

- Scenario 2020-P1 – all the parameter values remain the same except areas for cereals cultivation. The total straw production is assumed to increase by 20% through use of fallow land for ethanol straw cultivation. Fallow land currently accounts for 29% of arable land for cereals production in the Sala-Heby region.
- Scenario 2020-P2 – all the parameter values remain the same except the yield for ethanol conversion from straw, which is assumed to increase to 0.35 (litre/kg) (Y_{EtOH}) due to improvements in the process technology.
- Scenario 2020-P3 – combines scenarios 2020-P1 and 2020-P2.

2.1.2. Transport fuel demand

There is a lack of statistics on motor fuel usage at the municipal level. We calculate the average distance covered per car and average fuel consumption per kilometre driven, and therefore the use of motor fuel based on the number of passenger cars registered in the municipalities of Sala and Heby. Input data was obtained from Swedish Official Statistics [5, 19]. The Swedish Energy Agency is the state authority responsible for disseminating statistics in the field of energy use in transportation, and Transport Analysis (Trafa) produces statistics on vehicles types and distances covered. The development of passenger car use in Sala-Heby region is shown in Figure 2 (based on data from [19]).

Ethanol fuel demand in the Sala-Heby region (D) is estimated for E5 and E85 ethanol mixtures using Eq. (2):

$$D = \sum_{i=1}^{2} N_i S_i Q_i C_i E \qquad (2)$$

where D is estimated ethanol fuel demand (MWh), N_i is the number of vehicles in use during a year, S_i is the distance covered per vehicle in the respective county in a year (km), Q_i is the fuel consumption per type of fuel and kilometre driven in each county (litre/km), C_i is the ration of pure ethanol to petrol in each type of fuel blend used, and E is the energy content of the fuel (kWh/litre). For E5 fuelled passenger cars i=1, and for E85 fuelled passenger cars i=2.

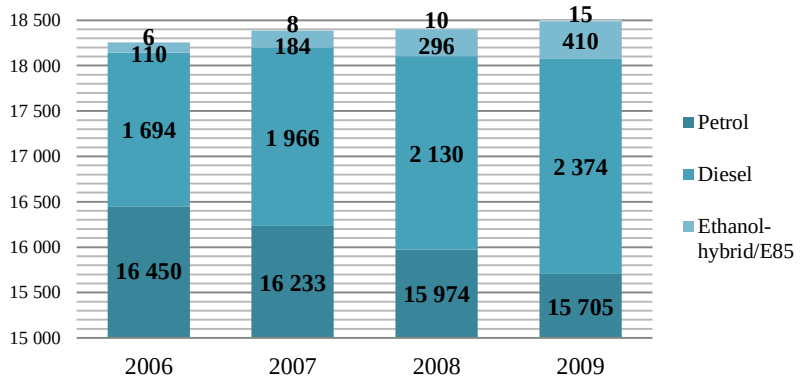

Fig. 2. Passenger cars in use by fuel type in 2006 -2009 in Sala-Heby. Based on data from [19].

It is assumed that all petrol fuel in the region is E5 fuel, as the share of low blend petrol in Sweden is 95% according to [3] and more detailed data on the regional share of E5 fuel and petrol fuel is not available.

To evaluate current and future regional demand on transport the following scenarios were analyzed:

- Scenario 2020-D1 – all the parameters remain the same except the numbers of passenger cars fuelled by petrol and ethanol fuels. The number of E85 fuelled cars increases and the number of E5 fuelled cars decreases, following the same trend as during the period 2006-2009 for each vehicle type. In this way, the total number of E5 and E85 fuelled vehicles is projected to be 17 814, a reasonable increase of 10.5% the 2009 figure.
- Scenario 2020-D2 – all the parameters remain the same except the amount of ethanol blended with petrol fuel, which is assumed to increase from 5% to 10% of the petrol fuel mixture, meaning that passenger cars are fuelled E10 with instead of E5. As in scenario 2020_1, the total number of cars is 17 814, following the trend in car numbers for the period 2006-2009. Petrol fuel consumption per driven kilometre is assumed to decrease following the trend from 2006-2009 (-1.2%), and is 0.074 l/km in 2020.
- Scenario 2020-D3 – this is the most extreme scenario, where it is assumed that all passenger cars are to be fuelled by E85 ethanol fuel.

2.1.3. CO_2 emissions from transportation

Estimates of CO_2 eq. emissions from passenger cars are based on the results presented by Johansson and Fahlberg [18]. Emissions rates in [18] and those presented in Table 2 are lifecycle based and include emissions from fuel combustion, production and distribution. The CO_2 eq. emissions factors on which further calculations are based are presented for E5, E85 and E10 (see Table 2).

Table 2. Total CO_2 eq. emissions factors by type of transport fuel [18].

CO_2 eq. emissions by type of fuel, (g/kWh)	
E5	277.48
E10	269.34
E85	110.54

3. Results and discussion

Regional straw production is estimated using Eq 1 and the input data presented in section 2.1.1. This calculation estimates 98 924 tonnes of straw in 2009. Thus, current straw-based ethanol production potential in Sala-Heby is 13 015 m^3 or 81 210 MWh as presented in Table 3 for 2009 and future Scenarios.

Table 3. Estimate of straw based ethanol production in Sala-Heby region.

Parameter	Unit	2009	2020-P1	2020-P2	2020-P3
$B_{ethanol}$	MWh/year	81 210	97 452	98 012	117 615

Regional ethanol fuel demand is estimated using Eq. 2 and the assumptions from the scenarios presented in section 2.1.2., and is presented in Table 4.

Table 4. Estimate of ethanol fuel demand in Sala-Heby region. Parameters for year 2009 are input parameters obtained from statistical databases and reports. Values in bold are changed from 2009.

Parameter	Unit	2009	2020-D1	2020-D2	2020-D3	Reference
N_1	1	15 705	**13 251***	13 251	**0**	[19]
N_2	1	410	**4 563****	4 563	**17 814**	[19]
S_1	km	14 267	14 267	14 267	14 267	[19]
S_2	km	14 267	14 267	14 267	14 267	[19]
Q_1	l/km	0.084	0.084	**0.074**	not relevant	
Q_2	l/km	0.126	0.126	0.126	0.126	[18]
C_1	1	0.05	0.05	**0.1**	not relevant	
C_2	1	0.85	0.85	0.85	0.85	
E_1	kWh/litre	8.598	8.598	8.474	8.598	[18]
E_2	kWh/litre	6.612	6.612	6.612	6.612	[18]
$D_{ethanol}$	MWh/year	12 234	52 927	57 955	179 977	-

*Average annual decrease in petrol fuelled passenger cars is 1.5%. Based on this rate the number of E5 fuelled passenger cars is estimated at 13 251.
**Average annual increase in E85 fuelled cars during 2006-2009 is 39%, whereas assumed average increase after 2014 is 20%. It is assumed to be unlikely that the early increase of 39% is maintained until 2020.

Distance covered per car and year for the whole Sala-Heby region is calculated from weighted averages of distances covered per car and year in each municipality. Distances covered by car in each municipality are obtained from [19] and are assumed to remain the same over the study period. Fuel consumption per driven km is assumed to decrease following the same trend as 2006-2009. E85 fuel consumption (Q_2) is assumed to remain the same. In scenario 2020-D2 E10 fuel is assumed to be used (C_1=0.1). For Scenario 2020-D2, the energy content of the fuel (E_1) corresponds to the energy content of the E10 ethanol mixture based on the assumption made for this scenario.

Summarized results for straw based ethanol supply and ethanol demand are presented in Figure 3. These figures indicate that the regional transport system can become self-sufficient in ethanol fuel by implementing local small ethanol production from locally produced cereal straw. The system could become fossil fuel free by 2020 using this approach.

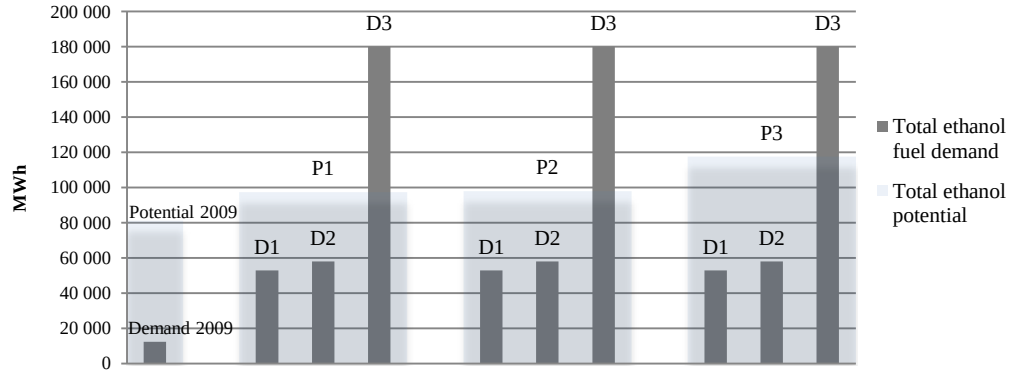

Fig.3. Ethanol supply potential and ethanol fuel demand in the Sala-Heby region (MWh).

The CO_2 eq. emissions from passenger cars were estimated (see Table 5), based on the same scenarios and approach as for the estimate of the ethanol fuel demand (see section 2.1.2.). Current CO_2 eq. emissions from transport are 45 446 tonnes. Assuming that the number of passenger cars in the region continues to increase according to the trend of the last 5 years, and assuming that all cars will run on E85 in 2020, the total CO_2 eq. emissions can be reduced to 23 591 tonnes CO_2 eq., a reduction of 21 855 tonnes CO_2 eq. or 48% from 2009.

Table 5. Estimate of CO_2 eq. emissions from passenger cars in Sala-Heby region.

Parameter	2009	2020-D1	2020-D2	2020-D3
Total CO_2 emission from passenger cars fuelled by petrol and ethanol fuel, tonnes	45 446	43 930	38 938	23 591

Börjesson [8] studied the reduction of GHG emissions obtained from using ethanol instead of petrol, including GHG emissions from producing ethanol. Using wheat grain based ethanol produced in Sweden results in an 80% GHG emission reduction compared to petrol fuel, while ethanol from Brazilian sugarcane gives 85% emission reduction [8]. Börjesson concluded that the results are very much dependent on the structure of the individual system. Assuming some different scenarios for the type of cultivation land, use of by-products from ethanol production, the reduction of using ethanol from current production in Sweden can be as low as 55% [8]. This paper focuses on GHG emission savings from road private traffic if replacing current petrol use with locally produced straw based ethanol assuming different scenarios for future car fleet development and ethanol supply. The CO2 eq. emission factors presented in [18], on which the calculations in this paper are based, correspond to 76% total CO2 eq. emission savings for pure ethanol compared with pure petrol fuel.

4. Conclusions

This study shows that the available cereal straw in the studied region is sufficient to meet local ethanol demand for 2009. However, it is not sufficient for a scenario where all passenger cars are fuelled with E85. If passenger car numbers increase according to the current trend until 2020, 3% CO_2 eq. emissions reductions can be achieved by using locally produced ethanol from cereal straw. CO_2 eq. emissions can be reduced by 14% by replacing all petrol fuel with fuel containing 10% ethanol (E10 fuel), and by 48% if all passenger cars in the studied region use E85 fuel.

This paper analyzes how the regional energy system can contribute to reducing CO_2 eq. emissions by realizing local small scale bioethanol production and substituting petrol with ethanol fuels in road transportation.

References

[1] Directive 2009/28/EC of the European Parliament and the Council of 23 April 2009 on the promotion of the use of renewable sources and amending and subsequently repealing Directives 2001/77/EC and 2003/30/EC

[2] Energy Indicators 2008. Theme Renewable Energy, Swedish Energy Agency, Report ET2008:21, Västerås, 2008, 97 pp.

[3] Energy Use in Transport Sector - 2009, Swedish Energy Agency, Report ES2010:04, Eskilstuna, 2010, 28 pp.

[4] Energy Use in Transport Sector - 2008, Swedish Energy Agency, Report ES2009:04, Eskilstuna, 2009, 24 pp.

[5] Statistics Sweden (SCB), 2010 - http://www.ssd.scb.se/databaser/makro/start.asp

[6] Swedish Energy Agency, Report ER 2009 27 (in Swedish), "Kvotpliktsystem för biodrivmedel - Energimyndighetens förslag till utformning", Eskilstuna, 2009

[7] European Environment Agency (EEA), October 2008

[8] Börjesson P., Good or bad bioethanol from a greenhouse gas perspective – What determines this?, Applied Energy, Vol. 86, Issue 5, pp. 589-594, 2009

[9] Starfelt, F., Thorin, E., Dotzauer, E., Yan, J. Performance evaluation of adding ethanol production into an existing combined heat and power plant, Bioresource Technology, 101 (2010) pp. 613–618

[10] A. Wingren, M. Galbe and G. Zacchi, Energy considerations for a SSF-based softwood ethanol plant, Bioresource Technology, 99 (2007), pp. 2121–2131

[11] Seabra, J., Tao, L., Chuma, H.L., Macedo, I. C. A techno-economic evaluation of the effects of centralized cellulosic ethanol and co-products refinery options with sugarcane mill clustering, Biomass and Bioenergy, 34 (2010), pp. 1065-1078

[12] Ou, X., Zhang, X., Chang, S. Scenario analysis on alternative fuel/vehicle for China's future road transport: Life-cycle energy demand and GHG emissions, Energy Policy, 38 (2010), pp. 3943-3956

[13] Papagiannaki, K., Diakoulaki, D., Decomposition analysis of CO_2 emissions from passenger cars: The cases of Greece and Denmark, Energy Policy, 37 (2009), pp. 3259-3267

[14] Upplands lokaltrafik, personal communication, 2010

[15] Västmanlands lokaltrafik, personal communication, 2010

[16] Swedish Board of Agriculture, 2010 - http://statistik.sjv.se/

[17] Johansson, J., and Lundqvist, U. Estimating Swedish biomass energy supply. Biomass and bioenergy, 1999; 17(2): 85-93

[18] Johansson, S., Fahlberg, K., 2009, Methods for strategies and assessment of climate change mitigation initiatives at local and regional levels, Emission Factors – Statistical Datasheet, http://www.ima.kth.se/klimatswe/html/rapporter.htm

[19] Transport Analysis, Trafa, 2010 - http://www.trafa.se/Publikationer/

Volume 14

Solar Thermal Applications

Environmental Regulation, Solar Energy Technology Components and International Trade

- An Empirical Analysis of Structure and Drivers

Felix Groba[1,*]

[1] *German Institute of Economic Research, Berlin, Germany*
** Corresponding author. Tel: +49 30 89789681, Fax: +49 30 89789113, E-mail: F.Groba@diw.de*

Abstract: Dynamics of the global renewable energy market are mostly described in terms of investment and added capacity. The role and characteristics of cross border trade flows with renewable energy system components, however, remains blurred. While national environmental regulation and innovative capacity is important for the promotion of renewable energies the effect of regulation and innovative efforts on export dynamics remains ambiguous as empirical studies on the pollution haven and the Porter hypothesis reach diverging conclusions and rarely focus on the renewable energy sector. This paper closes the gap by: First, focusing on solar energy technology components, structure and development of international trade since 1996 is analyzed. Second, determinants of OECD exports are identified in an econometric panel study estimating a gravity trade model. The results unveil a highly dynamic global market for solar energy technology components since 2002, with Europe as dominant market and increasingly strong exports from China. Additionally, the analysis supports the Porter hypothesis as countries with a strong framework supporting renewable energies have gained a comparative advantage in exporting solar technology goods. Analyzing the importer side shows that tariff reduction and FDI inflows have increased imports.

Keywords: *Renewable Energies, International Trade, Trade Barriers, Regulation*

1. Introduction

Diffusion and transfer of climate friendly energy technologies remain decisive topics in international climate negotiations as they play an important role in the nexus of economic development and a sustainable energy system transformation. Therefore, the development of the global renewable energy market is monitored in numerous studies. These studies commonly either refer to added capacity or investments into renewable energy projects to describe growth, structure and market development [1]. Although international trade has been identified as a decisive channel for technological change the role of the manufacturing sector, producing necessary components, and the international trade system in this production process is mostly neglected. While the interaction between trade flows and environmental regulation and the issue of clean technology transfer have become prominent literature strands, little effort has been put into accessing drivers and dynamics of global trade with specific renewable energy components. Additionally, current negotiation obstacles in WTO talks on environmental goods liberalization unveil that the relationship between trade, technology transfer and clean energy technologies are relevant.

The objective of this paper is to analyze the structure and identify drivers of clean energy technology trade with a specific focus on solar energy technology components. This step is necessary before trade effects such as technology diffusion and sustainable development can be studied in later research. After outlining the methodology, this paper describes structure and development of the international market for solar energy technology components. Subsequently, potential drivers of these specific technology exports from OECD countries to the world are characterized in a panel study estimating a standard gravity model. Three hypotheses are empirically tested: First, as components for solar energy systems are research intensive, the innovative capacity in exporting countries affects the export performance with respective goods. Second, following the Porter hypothesis, countries with a strong policy

framework of supporting renewable energies have gained a comparative world market advantage as such a framework is likely to support a national renewable energy industry that is a striving for export markets. Third, barriers to trade and an unreliable policy environment in receiving countries are obstacles to clean technology trade as additional costs to exporters are imposed.

2. Data description and methodology

Numerous empirical studies adopted the gravity model to explain the relationship between international trade flows and environmental regulation with respect to various goods and sectors. Introduced by Tinbergen [2] the model became the workhorse of trade relation analysis. The popularity can be explained by its successful empirical performance and by strong theoretical foundations outlined in the literature [3]. The general formulation of the gravity model (1) describes trade flows (F) from exporting country i to destination country j at time t as a function of economic masses (M), distances (D) and an error term (η). It furthermore takes a gravitational constant (G) into account depending on the units of measurement for F_{ijt}, $M_{it,jt.}$

$$(1) \qquad F_{ijt} = G\frac{M_{it}^{\beta_1} M_{jt}^{\beta_2}}{D_{ij}^{\beta_3}\eta_{ijt}}$$

As the aim of the study is to determine the drivers of international trade with solar energy technologies, the dependent panel variable is the bilateral export flow (EXP_{ijt}) from i to j at time t. The i-exporting countries are Australia, Austria, Belgium, Canada, Czech Republic, Denmark, Finland, France, Germany, Greece, Ireland, Italy, Japan, Korea, Netherlands, Norway, Portugal, Spain, Sweden, Switzerland, the United Kingdom and the United States. An analysis of developing country exports such as Chinese exports is excluded due to a lack of data on control variables. Nevertheless, the sample represents approximately 80 % of global exports in 2008. The sample of j-importing countries includes 129 states, including OECD countries. The time period analyzed with the balanced panel goes from 2000 to 2007. Empirical computation requires the gravity model to be transformed into logs, establishing a linear relationship between variables. This also allows interpreting the percentage change in the dependent variable due to a change in explanatory variables. Based on the explanatory variables, as explained in the subsequent sections, the exact gravity model applied has the following from:

$$\begin{aligned}(2) \qquad \ln SolarEXP_{ijt} = {} & \beta_0 + \beta_1 \ln(GDP_{it}GDP_{jt}) + \beta_2 \ln(POP_{it}) + \beta_3 \ln(POP_{jt}) + \beta_4 \ln(Dist_{ij}) \\ & + \beta_5 Border_{ij} + \beta_6 Language_{ij} + \beta_7 Contig_{ij} + \beta_8 Import\_Tariff_{jit} \\ & + \beta_9 \ln(FDI_{jt}) + \beta_{10} RoL_{jt} + \beta_{11} \ln(Envirregulation_{jt}) \\ & + \beta_{12} \ln(EnergyIntensity_{it}) + \beta_{13} \ln(Envirregulation_{jt}) + \beta_{14} \ln(RDBSolar_{it-1}) \\ & + \beta_{15} \ln(PatentStock_{it}) + \alpha_i + \varepsilon_{ijt}\end{aligned}$$

2.1.1. Development of solar energy technology component exports

Solar energy technology components are defined as investment goods and associated products needed in solar energy systems. This includes solar thermal and photovoltaic components. Reliable cross country data on trade flows with renewable energies are hardly available. National industry polls, commonly asking for sales as well as imports and exports, are likely to be biased as the number of companies active in the renewable energy market is unclear and poll return might be interest driven. Therefore, the representativeness of these polls is limited and can only be used as a rough indicator for national branch development. Furthermore,

industry polls do not guarantee data comparability. Therefore, international trade data based on the Harmonized Commodity Description and Coding Systems (HS 1996) using the UNCTAD COMTRADE database serves as the source of the dependent variable.

The classification with respect to environmental goods and energy technologies has been well defined by the OECD [4]. Nevertheless, the aspired solar energy technology differentiation requires addressing data validity. A product group based on 6-digit HS 1996 codes, under which solar system components are traded, has been generated (Table 1). The problem is that data might be inflated as the products environmental end use cannot be monitored, i.e. goods that are used for renewable energy systems and goods that might be used otherwise are traded under a common HS code and the renewable energy goods share under one HS code might vary between countries. However, the method used constructs the best available proxy for cross time cross country analysis as data is available on an international common methodology. Furthermore, contrary to industry polls, imports of inputs are likely to be captured allowing a more comprehensive picture of the market. Finally, product similarity can be assumed making the actual end use irrelevant.

Table 1. Nomenclature of solar energy technologies, HS 1996.

HS Code	Explanation
Solar Thermal	
841911	Instantaneous gas water heaters.
841919	Other instantaneous or storage water heaters, non-electric.
840219(ex)	Steam or other vapor generating boilers [Other vapor generating boilers, including hybrid boilers].
841950(ex)	Heat exchange units [Heat-exchange units for solar thermal or geothermal applications].
900290	Concentrator systems to intensify solar power in solar energy systems, other optical elements of any material mounted
Solar Photovoltaic	
850440(ex)	Static converters [Inverters (for converting DC power to AC power)] - change solar energy into electricity.
850720(ex)	Other lead-acid accumulators [solar batteries], i.e batteries for energy storage in off-grid photovoltaic systems.
854140(ex)	Photosensitive semiconductor devices, including photovoltaic cells whether or not assembled in modules or made up into panels; light emitting diodes.

The data show that exports have grown considerably from 1996 to 2008, whereas the largest growth occurred since 2002. Figure 1 supports the finding that the production of clean technology goods is highly skewed towards high income countries [5]. However, East Asian Pacific countries (LDCEAP), mainly China, have gained considerable market share. Interestingly, the data also show that the share of solar energy technology components in trade with industrial goods has been increasing since 1996. Although still low between 0,5 and 1,5% this indicates a quite dynamic market as the solar component trade growth rate has been larger than industrial goods trade growth rates. Another insight is that although the OECD countries are major exporters, the group runs an increasing net trade deficit hinting to the dominance of only some countries. An analysis of the trade direction between regions underlines that main import markets are in high income OECD countries with most of the trade occurring between OECD countries. Another important trade direction is from developing countries to developed counties. Trade between developing country regions remains marginal. Overall, it becomes obvious that the international market for solar energy

technology components is dominated by Europe and China as the main exporting players. Europe furthermore is the dominating importer with most of the global trade occurring within Europe itself.

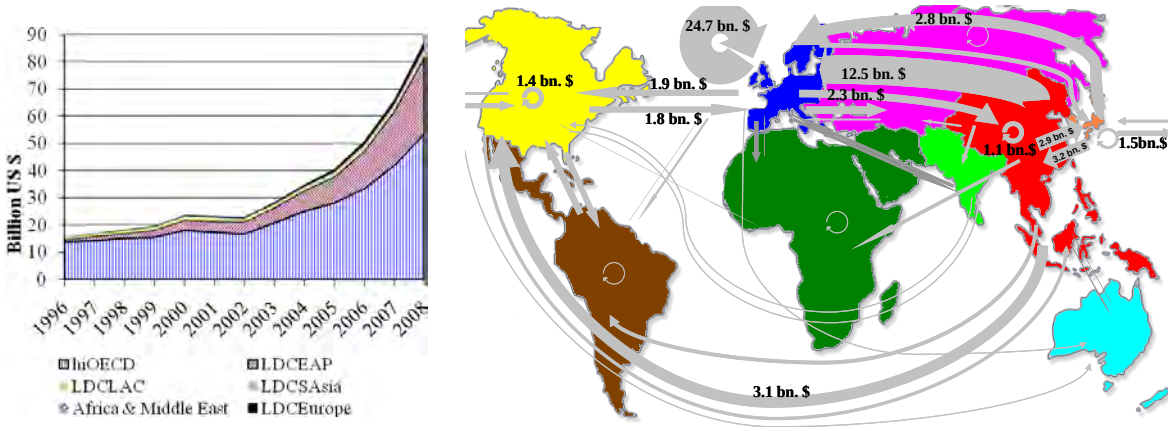

Figure 1. Development of Solar energy technology component exports by country group 1996-2008 and market structure 2008 (Source: UNCOMTRADE)

The analysis of country specific export flows and market shares underlines the dynamics and outlines the dominance of only some counties as well as the increasing importance of developing countries. Although, with a high increase in market volume the development of market export shares over time indicates a crowding out of some OECD exporters mainly due to strong export growth of China.

2.1.2. General parameter of trade analysis

The gravity model predicts that the bilateral trade volume is positively related to a countries' income ($GDP_{it}GDP_{jt}$) [6]. A counter force in this respect is population size as countries with a larger population (POP_{it} , POP_{jt}) are expected to trade less. The reason is that available resources and the domestic market size are expected to be positively correlated with the population size. The anticipated sign is thus negative as the market is able to rather produce goods itself. Theoretically, with increasing distance ($DIST_{ij}$), trade and transportation cost increase, reducing trade volume and causing the expected sign to be negative. Further determinants of bilateral trade flows that are empirically justified are included. Sharing an official language ($LANG$) and having a common border (ADJ_{ij}) is expected to increase bilateral trade flows as goods can be transported at lower costs. Data for these variables have been retrieved from the World Bank World Development Indicators (2009) and from the CEPII's Gravity Dataset (2010).

2.1.3. The role of environmental regulation

The empirical literature on the interaction between trade and environmental regulation remains ambiguous regarding the support of either the polluter haven or the Porter hypothesis [7]. According to the Porter hypothesis, shocks produced by new, stricter regulation creates external pressure on the firms which are subsequently fostered to created new products and processes that positively affect the dynamic behaviour of that economy and hence its international competitiveness. Thus, countries with a stringent environmental regulation may become net exporters of clean technology. The lead market literature, which supports the Porter hypothesis, indicates that an early introduction of adequate technology support policies can create an industry with a competitive world market advantage. A contrary theoretical effect of introducing environmental regulation is that specific clean technology demand is

generated causing additional imports as, in an open economy, foreign producers may provide technology either better or cheaper.

This studies' focus is on the effects of regulation on specific trade flows rather than on overall trade flows. Numerous policy instruments that increase the demand and supply of renewable energy technologies have been identified. The IEA report on 'Renewable energy market and policy trends' provides an overview of policies and time of introduction. Due to the heterogeneous character of these policies across countries the database does not facilitate an evaluation of regulatory stringency or renewable energy supportiveness in a panel context. Therefore, different measures of environmental stringency or renewable energy supportiveness, respectively, are used. In their study on export dynamics of energy technologies, Constantini and Crespil (2008) point out that an indirect measure of environmental stringency, such as CO_2 emissions per unit of GDP is adequate to investigate the Porter hypothesis as well as the political importance of energy saving strategies [7]. The variables $EnergInt_{it}$ and $EnvirREG_{it}$ give the relative environmental strictness in exporting countries. The underlying assumption is that countries implementing stricter environmental regulation exhibit a positive effect on export dynamics of solar energy technology components. The measures are based on the following environmental indicators:

- Level of Energy intensity 1996 – 2008 in tons of oil equivalent per thousand units of purchasing power parity GDP extracted from the IEA Energy Balance database;
- Level of Carbon intensity 1996 – 2008 in kg per thousand units of purchasing power parity GDP extracted from the Carbon Dioxide Information Analysis Center database.

Subsequently, following the literature, sample countries have been ranked on these relative and dynamic measures (1990 =100) assigning the lowest rank to the worst performer. In the given panel structure this ranking method better allows for a comparison of relative environmental strictness than a comparison of levels of energy use and emissions.

The introduction of further variables controlling for environmental regulation and thus a renewable energy friendly policy environment is neglected. Although statistics suggest that the Kyoto Protocol induced more innovation there seems to be no significant effect of the Protocol on technology transfer and thus trade.[5] In addition, other proxies of environmental regulation such as environmental private and public expenditures, environmental tax revenues and public environmental protection expenditures are likely to be captured by applied controls. The same is true for expected returns on energy investment, which is generally best reflected by electricity price trends. But, as total primary energy supply and therefore the energy market size of a country, is included in the estimation, incentives to invest in renewable energies are respected to some extent.

2.1.4. The role of the innovation system in exporting countries

In general, innovation is assumed to be a product of knowledge generating inputs [8]. As this study focuses on highly innovative technology goods, two variables controlling for the role of the innovation system in exporting countries are included.

First, a variable measuring a countries public technology specific research and development spending ($RDBsolar_{it}$) is introduced. In theory, research and development increases exports as new technology might be developed which, in an open economy, is available to the world market as well. The variable enters the analysis lagged by one period assuming that the process of technology development takes some time until a new product is ready for market entry. Data is obtained from the IEA (2010) Energy Technology Research, Development and

Demonstration database. The data show that combined OECD public spending on s olar energy has been constant since 1990 and is decreasing since 2006. Yet, there is substantial country level variation leaving the actual effect on export performance unclear.

Second, productivity of new knowledge is assumed to depend on the existing stock of ideas [8]. The patent stock of a country is the best proxy for knowledge stock in this respect. Therefore, patent counts for renewable energy have been extracted from the OECD (2010) Science, Technology and R&D Statistics database. Aiming at comparability and an unbiased estimation, only patent applications by inventor country issued under the international patent cooperation treaty have been included (Figure 2).

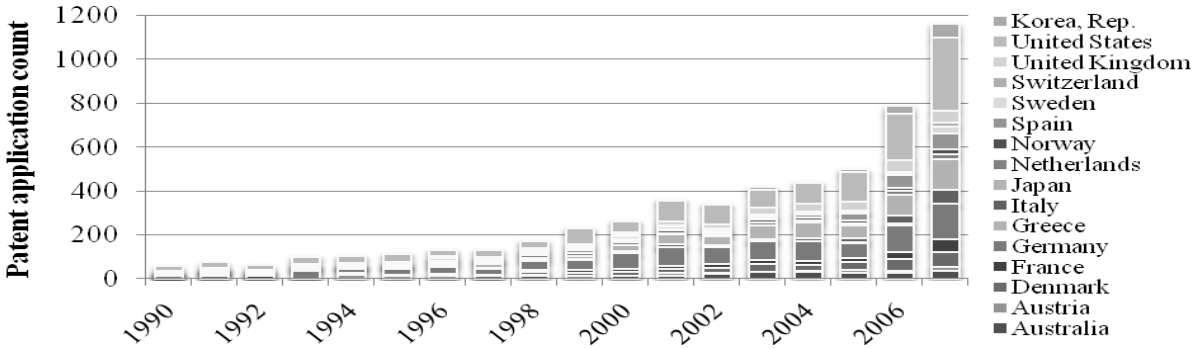

Figure 2: Renewable Energy Patent applications by country of origin 1990 – 2007

Based on the patent counts the countries' patent stock has been calculated with depreciation rate α of 15% as is commonly done in the literature[8]:

(3) $$PatStock_{it} = (1-\alpha)PatStock_{it-1} + Patents_{it}$$

Naturally, the stock of knowledge with respect to renewable energies differs substantially between countries. Therefore, the assumption to be tested empirically is that countries with a higher renewable energy knowledge stock export more to the world market.

2.1.5. The role of barriers to trade and regulation in importing countries

A general assumption is that tariff and non-tariff barriers inhibit trade while a positive general policy environment as well as environmental friendly regulation in importing states supports cross border flows of the specific high technology goods which are the focus of this study. Hence, import tariffs ($Import\_Tariff_{jt}$) applied to the compounded product group of solar goods are introduced as an explanatory variable. Data on the effectively ad valorem tariff applied by the importing country *j* to solar technology component exports from *i* in percent of the import value is obtained from the UNCTAD TRAINS database. The indicator serves as control for the potential impact of a liberalization of environmental goods as discussed in the WTO Doha negotiations and denounces the reduction of additional trade cost over time. The expected coefficient sign is negative as bilateral trade flows are high with lower tariffs as exporters face reduced trade costs. The development of tariffs over time seems to support the theoretical underpinning. While solar energy technology component exports of OECD countries increased significantly, the mean tariff applied by the samples importing counties decreased substantially from 10% in 1996 to 5% in 2008.

Environmental regulation and renewable supportiveness in receiving countries potentially plays a role as demand for clean technologies can be satisfied through the world market.

Hence, the environmental stringency variable $EnergREG_{jt}$ is introduced as control for such regulation using the same method as for exporting countries described above. The study also includes the World Bank's rule of law indicator (ROL_j) as a proxy for the quality of institutions and the capacity to respect legal rules which might be relevant for exporters.

As currently the solar energy market development is often described in terms of investments, controlling for such investments to explain technology component export flows is necessary. Adequate solar technology specific investment data on a cross time cross country level is not yet available. Therefore, the best proxy in this respect is net foreign direct investment inflow in importing countries (FDI_{jt}). Trade flows are tightly linked to foreign direct investments flows [9]. Following the literature on trade flows and foreign direct investments the coefficient should be positive as a higher attractiveness of a county for FDI also exhibits a higher attractiveness for exports.

3. Results

The gravity model as stated in equation (2) has been estimated using random and fixed effects in order to control for country heterogeneity with robust standard errors clustered on country level. However, the significance of the Hausman test clearly indicates that exporting country individual effect (α) and the repressors are correlated. Thus, only the consistent fixed effect estimation coefficients on the repressors are reported in Table 2. Adequate tests for the robustness of the results have been conducted.

Table 2. Gravity model and the role of environmental regulation, innovation and trade parameters

	(1)	(2)	(3)	(4)	(5)	(6)	(7)	(8)
ln GDP_{ijt}	1,57***	1,58***	1,18***	1,59***	1,55***	1,55***	1,65***	1,53***
ln POP_{it}	-6,81*	-7,19*	-6,49*	-6,89*	-8,31*	-6,81	-5,02	-11,63**
ln POP_{jt}	-0,42***	-0,44***	-0,06	-0,45***	-0,43***	-0,43***	-0,46***	-0,41***
ln $DIST_{ij}$	-1,01***	-0,98***	-0,99***	-1,00***	-1,01***	-1,00***	-0,99***	-0,93***
ADJ_{ij}	0,01	0,06	-0,05	-0,01	0,15	0,16	-0,22	0,038
$LANG_{ij}$	1,15***	1,19***	1,01***	1,13***	1,11***	1,10***	1,19***	1,06***
$Import\ Tariff_{ijt}$	-0,01***							
ln FDI_{jt}		0,17***						
RoL_{jt}			0,02***					
ln $EnvirREG_{jt}$				0,11*				
ln $EnergInt_{it}$					0,24*			
ln $EnvirREG_{it}$						0,15*		
ln $RDBsolar_{it-1}$							0,03*	
ln $PatStock_{it}$								0,03
Time dummies	yes	yes	yes	yes	yes	yes	yes	yes
N	22382	21630	22550	22550	21793	19475	21263	36092
R^2	0,68	0,69	0,70	0,68	0,67	0,67	0,70	0,64

note: significance level *** p<0.01, ** p<0.05, * p<0.1

The results show that standard control coefficients of trade flow analysis such as income, population and distance have the expected impact. Thus, this set of controls is taken as basis for the analysis of the remaining control variables. These specific control variables also

behave as expected. A one unit increase in tariffs decreases imports by 0.01 units. Thus, Higher tariffs significantly decrease import flows while the relationship between investment inflows and the institutional quality in receiving countries is positive. The impact of environmental regulation in importing countries on trade flows is weak but positive. The role of the innovation system in exporting countries remains ambiguous. On the one hand public spending in solar energy technology has a positive significant impact on export flows. On the other hand the renewable energy patent stock has no significant impact. The results of the study support the Porter Hypothesis as countries with a more stringent environmental regulation and a better energy intensive score export more solar energy technology components to the world market and thus seem to have gained a competitive advantage.

4. Discussion and Conclusion

This study applies an empirical gravity model to identify the main drivers of trade with solar energy technology components. Finding evidence for the Porter hypothesis and the importance of the innovations system the results are in line with findings of related work on environmental regulation and trade as well as with the OECD`s strategy on environmental regulation, innovation and green growth. Yet, besides the issues related to a potential dual use of products under one HS-code the effects might be biased by the use of rather broad control variable specifications such as general renewable energy patents instead of solar specific patents to construct the knowledge stock. Nevertheless, the results are interesting from a global climate negotiation perspective as it is shown that the regulatory context in receiving countries is decisive for clean technology imports and thus potential technology transfer.

Consequently, the remaining research agenda should focus on technology transfer in trade with these clean energy technologies as well as the study of potential trade effects. Within this context the construction of regulation measures capturing renewable energy supportiveness of a country more directly should be developed.

References

[1] REN 21, 2009. Renewables Global Status Report: 2009 Update, 2009, Paris.

[2] Tinbergen, J., 1962. Shaping the World Economy, Twentieth Century Fund, New York.

[3] Jug, J.; Mirza, D., 2005. Environmental regulations in gravity equations: evidence from Europe, World Economics 28(11), pp.1591-1615.

[4] OECD, 1999. The environmental goods and services industry manual for data collection and analysis, Paris.

[5] Dechezleprêtre, A.; Hascic, I., 2008. Invention and Transfer of Climate Change Technology on a Global Scale: A Study Drawing on Panel Data, Paris, 2008.

[6] Harris, M.; et al., 2002. Modeling the Impact of Environmental Regulation on Bilateral Trade Flows: OECD, 1990 -1996, in: The World Economy, vol.25 (3), 2002, pp.387-407.

[7] Constantini, V.; Crespi, F., 2008. Environmental regulation and the export dynamics of energy technologies, in: Ecological Economics 66(2008), pp. 447-460.

[8] Braun, F.; et.al., 2010. Innovative Activity in wind and solar technology: empirical evidence on knowledge spillovers using patent data, DIW Discussion Paper XI992/2010, Berlin.

[9] Makki, S., 2007. Impact of Foreign Direct Investment and Trade on Economic Growth, Washington.

Environmental Impacts of Solar Thermal Systems with Life Cycle Assessment

Alexis de Laborderie[1*], Clément Puech[1], Nadine Adra[1], Isabelle Blanc[2], Didier Beloin-Saint-Pierre[2], Pierryves Padey[2], Jérôme Payet[3], Marion Sie[3], Philippe Jacquin[4]

[1] *Transénergie, Ecully, France*
[2] *MINES ParisTech, Sophia Antipolis, France*
[3] *Cycleco, Ambérieu, France*
[4] *PHK Consultants, Ecully, France*
** Corresponding author. Tel: +33 472860407, Fax: +33 472860400, E-mail: a.delaborderie@transenergie.eu*

Abstract: Solar thermal systems are an ecological way of providing domestic hot water. They are experiencing a rapid growth since the beginning of the last decade. This study characterizes the environmental performances of such installations with a life-cycle approach. The methodology is based on the application of the international standards of Life Cycle Assessment. Two types of systems are presented. Firstly a temperate-climate system, with solar thermal collectors and a backup energy as heat sources. Secondly, a tropical system, with thermosiphonic solar thermal system and no backup energy. For temperate-climate systems, two alternatives are presented: the first one with gas backup energy, and the second one with electric backup energy. These two scenarios are compared to two conventional scenarios providing the same service, but without solar thermal systems. Life cycle inventories are based on manufacturer data combined with additional calculations and assumptions. The fabrication of the components for temperate-climate systems has a minor influence on overall impacts. The environmental impacts are mostly explained by the additional energy consumed and therefore depend on the type of energy backup that is used. The study shows that the energy pay-back time of solar systems is lower than 2 years considering gas or electric energy when compared to 100% gas or electric systems.

Keywords: *Environmental impact, LCA, Solar thermal systems*

1. Introduction

Solar thermal systems have encountered a high interest over the last ten years in many locations worldwide [1,2]. Indeed, it is a robust, efficient and simple technology to implement for individual households: solar thermal relies on well known process and materials. Its capacity in reducing energy load for domestic hot water (DHW) is significant in locations with high irradiation level.

Some studies have been carried out on thermosiphon solar water heaters in different countries [3-6] but none was focused on solar thermal systems with auxiliary energy source. This study is focused on this second type of installation since they often are preferred for Northern-European countries (collector and storage with integrated backup).

The main purpose of the work is to characterize the environmental impacts of solar domestic hot water systems, or solar water heaters (SWH), integrating auxiliary heating (electric or gas heaters). Furthermore, this study also aims at identifying the most discriminating parameters to support implementation solutions. These systems' performances are analyzed as case-studies both for temperate climates (typically in France) and for tropical climates (typically in the Caribbean).

Life Cycle Assessment (LCA) methodology is used for this environmental evaluation. Among several LCA impact indicators, this study focuses on primary energy consumption, global warming potential, effect on ecosystem quality and human health issues. Greenhouse gas emissions (expressed in CO_2 equivalent) and non-renewable energy consumption are considered here as key LCA outputs.

Environmental performances of the different SWH with gas-backup, electrical-backup or no backup (for tropical zone's systems) are compared with standard hot water systems without any solar contribution.

2. Methodology

This Life Cycle Assessment (LCA) study was performed in compliance with the ISO standards 14040 and 14044 [7,8].

2.1. Scope of the study

This study has been carried out on individual solar thermal systems applied in the case of temperate and tropical climates. For temperate locations, four systems have been studied, namely two traditional systems without solar systems considering only electricity or gas heater, and two systems with solar system and integrated backup energy (electricity backup see Fig. 1 or gas backup). Due to the irregular solar irradiation all over the year, this kind of solar thermal system requires a backup system to reach the target temperature.
For tropical climates, one thermosiphonic solar system (without backup energy) has been analyzed (Fig. 2).

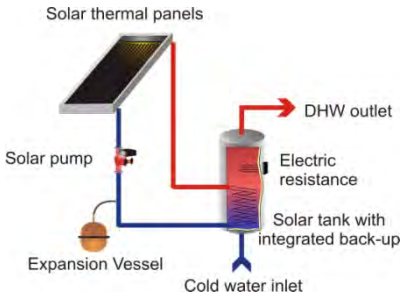

Fig. 1. Sketch-plan of temperate-type solar water heaters (electric backup)

To study both temperate and tropical systems, two climatologically average located places have been determined, namely Lyon (continental France) for temperate climate and Le Lamentin (Martinique, overseas France) for tropical climate.

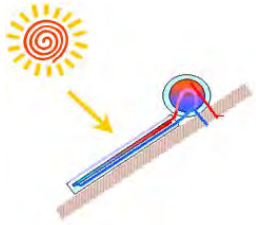

Fig. 2. Sketch-plan of tropical-type solar water heaters

The solar systems configuration and backup energy uses are different according to the climatic conditions. Therefore, two different Functional Units have been defined:

The temperate climate Functional Unit: Production of DHW for a four-person household, (assessed to be 140 litres of 60°C) in temperate climate and 20 years of life expectancy.

The tropical climate Functional Unit: Production of DHW for a four-person household, (assessed to be 200 litres of 50°C) in tropical climate and 20 years of life expectancy.

Given that tropical-type SWH does not include backup energy, the target temperature (50°C) is an indicator required to calculate solar energy but it does not represent the real outlet water temperature.

Corresponding irradiation levels and electricity mixes have been considered.

2.2. Inventory

2.2.1. Inventory building strategy and sources

Many hypotheses are necessary to evaluate the life cycle environmental impacts of DHW production. These hypothesis have been defined with the expertise of the consulting and

engineering partner[1] as well as technical data collected from public industrial actors. Thus, the different systems' component has been determined and sized. On the second hand, inventories for the electricity mix have been determined for the temperate-climate system.

For this study, the ecoinvent 2.0 LCI database [9] was used. Ecoinvent 2.0 contains international industrial life cycle inventory data on a various range of activities (energy supply, resource extraction, transport services,…). However, most of the SWH components are not defined exactly in the existing database. Thus, it has been necessary to modify or create new processes. When components' inventories were available in the database they were assessed in order to determine the validity of this inventory regarding the components' origin and main characteristics (materials used, manufacturing process and weight). When necessary, some inventories were modified by applying a weight or size ratio. Some inventories have also been completed by specific technical data collected within this project. When no inventory was available for a component, a new inventory has been built by the project team to estimate the required data.

As for the construction of the inventory, the composition of each component comes from different sources, which are described in Table 1.

Table 1. Data collection for infrastructures in scenarios

Component	Sources
Solar panel	Ecoinvent modified (to match with the surface defined for the scenarios)
Water Pump	Ecoinvent modified (estimates, from the mass of material)
Expansion Vessel	Ecoinvent (slightly oversized compared to usual design, but minor impact)
Hot water tank	Ecoinvent modified (from a 2000 l tank)
Solar regulation	Rough estimate (from the mass of the material, mostly electronics)
Mounting support	Datasheets from manufacturers, completed by estimates when necessary
Plumbing	Experience and estimates from the consulting and engineering partner
Electrical backup	Ecoinvent (slightly oversized, but minor impact)
Gas backup	Ecoinvent modified (to exclude the impacts related to domestic heating)

2.2.2. System boundaries

The system boundaries are described in Fig. 3. They include the solar panels manufacturing (panels, mounting systems), water tanks, internal heat exchanger, pipes, hydraulic components (pumps, valves, expansion vessel), regulation, cabling and solar fluid. In addition, they also include the use phase (backup energy consumption for temperate-climate SWH) and the recycling of components.

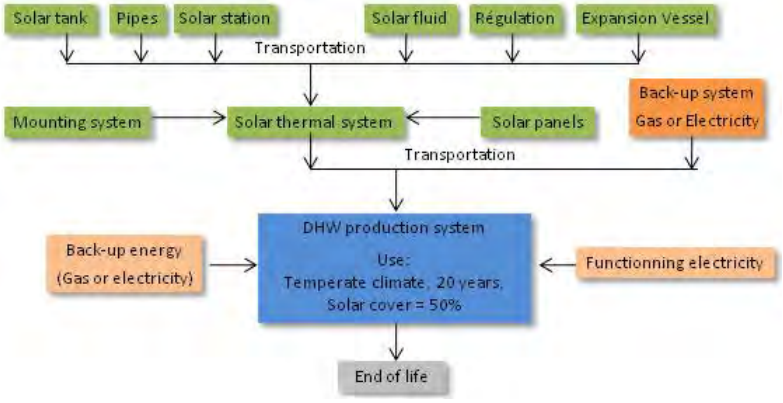

Fig. 3. Scheme of system boundaries

[1] Transénergie, http://www.transenergie.eu

2.2.3. Scenarios

Table 2 describes the four scenarios (scenarios 1-4) built for this study used for temperate climate systems. Scenario 5, standing as a reference for other scenarios results, comes from the ecoinvent 2.0 database.

Table 2. Scenarios for temperate climates

Temperate climate Scenarios					
	Scenario 1	Scenario 2	Scenario 3	Scenario 4	Scenario 5
System	Solar Thermal + Gas	Solar Thermal + Electricity	Gas heater	Electric heater	Solar Thermal + Gas
Solar Panels	Flat plate collectors[2]				Flat plate collectors[3]
Water tank	300 litres vertical tank	300 litres vertical tank			400 litres vertical tank
Backup system	Individual gas heater and heat exchanger[4]	Electric resistance[5]	Individual gas heater	Electric heater tank	Individual gas heater and heat exchanger[5]
Other components	Mounting system, pipes, regulation and solar station		Pipes		Mounting system, pipes, regulation and solar station
Overall lifetime energy consumption	205 000 MJ				~330 000 MJ
Solar coverage	50%		None		58,4%
Life expectancy	20 years				25 years

Table 3 describes the scenario built for this study for tropical SWH which is based on a thermosiphonic solar system. Flat plate collectors inventory is an average of the three main products that exists on the Caribbean market.

Table 3. Scenarios for tropical climate systems

Tropical climate Scenarios	
System	Thermosiphon
Solar Panels	Flat plate collectors[5]
Solar tank	200 l horizontal tank
Other components	Mounting system, pipes
Overall lifetime energy consumption	147 000 MJ
Life expectancy	20 years

2.3. Payback time indicator

Energy Payback Time (EBPT) has been calculated with the following definition:

$$EPBT = \frac{E_p^{fabrication} + E_p^{backup}}{avoidedE_p^{production}} \quad (1)$$

[2] Collector Area = 4,4 m² with solar panel coefficients : B=0,75 ; K=4,5 W/(m².K)
[3] Collector Area = 4 m² with unknown solar panel coefficients
[4] Integrated in the upper part of the tank
[5] Collector Area = 2 m² with solar panel coefficients : B=0,75 ; K=4,5 W/(m².K)

$E_p^{fabrication}$: Non-renewable primary energy used for the fabrication of the installation.

E_p^{backup} : Non-renewable primary energy used for the backup system.

$avoidedE_p^{production}$: Non-renewable primary energy avoided (thanks to the backup energy used, in case of electric backup, specific electricity mix of the country avoided where the SWH is installed.

In the case of electric backup or the comparison with the full electric system, this method of calculating EPBT gives results only valid for the country where the solar panels are installed.

3. Results and analysis

Results have been calculated according to the impact 2002+ (v2.04) [10] method available in SimaPro 7.1 PhD and the database ecoinvent 2.0.

3.1. Temperate climate-type systems

3.1.1. Overall environmental impacts

Scenarios are compared among all impact categories in figure 4. Figures 5 and 6 present the results for the most significant impact categories with the details of their origin.

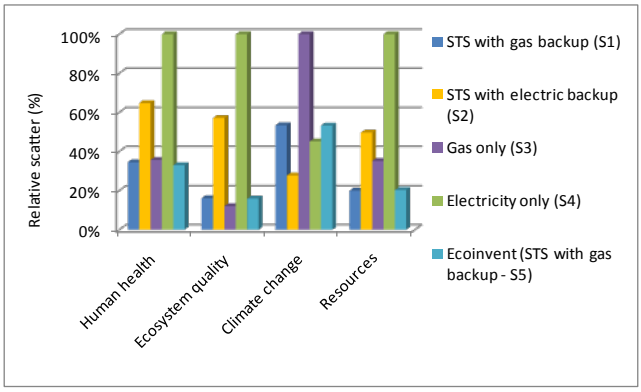

Fig. 4. Comparison of the temperate-climate-type scenarios on the complete lifetime

It strikes that the necessary water auxiliary heating has a strong influence on the overall impact indicators. In the case of a SWH with electric backup (scenario 2), CO_2 equivalent emissions are significantly cut down compared to a SWH with gas backup (scenario 1).
However, considering the other three impact categories, SWH with gas backup appears as the best impact reduction potential option compared to "traditional systems" (scenarios 3 and 4: respectively gas only or electricity only) as well as SWH with electric backup.

It is important here to point out that the electricity mix chosen here influences thoroughly the environmental performances of the ST installation, as well as the comparison with the electricity only scenario. Indeed, according to ecoinvent 2.0, the French electricity mix has particularly low carbon content: 103g/kWh. Thus, the energy backup's choice is critical according to the environmental impact reduction targeted.

3.1.2. Distribution of environmental impacts

The graphs below presents the climate change and non-renewable primary energy impacts. They show the distribution of the impacts of each scenario for the different main life cycle components.

In each of the five scenarios, transports (of materials to the manufacturing plant, as well as of the products to the installation location) play a minor role in non-renewable primary energy consumption. The electricity consumed for the operation of the SWH accounts for a smaller amount of non-renewable primary energy too. Backup energy consumptions stand by far

(>80-90%) for the most important part of for the climate change and non-renewable primary energy consumption impacts. Components of the solar thermal systems (solar thermal panels, pumps, solar tank and regulation system) finally make up for a lesser part of overall impacts, and once produced, consume very little electricity in the operating phase while providing 50% of DHW energetic demand.

In the case of electric backup, CO_2 equivalent emissions are low because the electricity mix chosen is mainly based on nuclear energy (France) and has particularly low CO_2 emissions. On the other hand, the French electricity mix has an important primary energy use (13.6 MJ of primary energy per kWh, according to ecoinvent 2.0), which is why, in this precise configuration (scenario 2), electric backup stands for 91% of non-renewable primary energy (see Fig. 5).

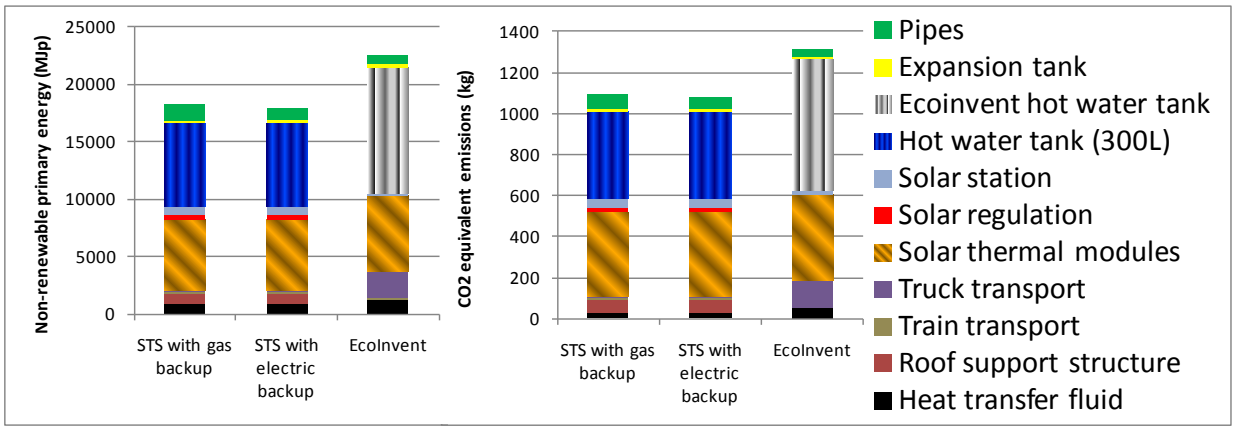

Fig. 5. Distribution of environmental impacts on climate change and non-renewable primary resources for the first four scenarios for temperate-climate-type SWH

Figure 6 shows the impacts of the fabrication of the solar thermal systems' components for the three scenarios with SWH. The results for those three scenarios show the same trend: solar thermal panels and the hot water tank are the major contributor to the environmental impacts of the two analyzed impact categories. Going further into details, it shows that the use of a large amount of steel stands for the most important part of the impacts of the hot water tank. As for solar thermal panels, it is aluminum (mainly for the frame) that causes most of the

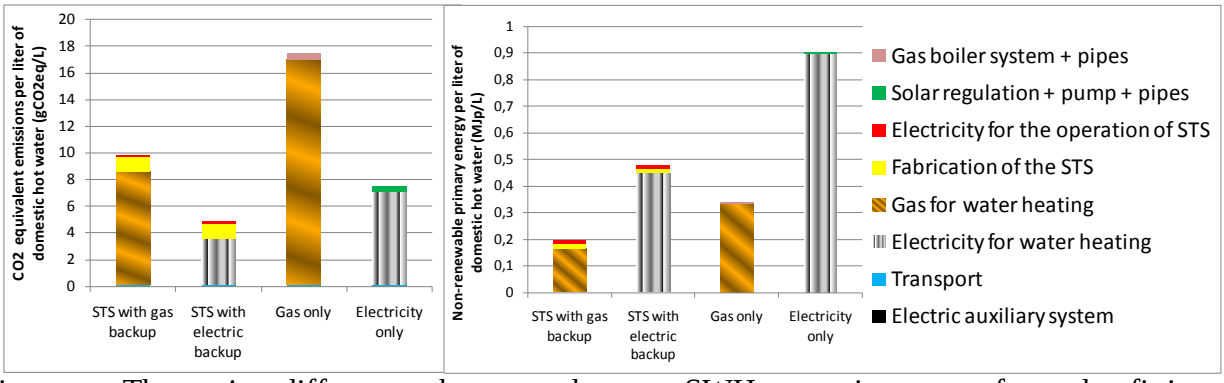

impacts. The major differences between the two SWH scenarios come from the fitting between the hot water tank and the boiler for the gas backup (fitting that is not necessary in the case of electric backup, which is integrated in the hot water tank).

Fig. 6. Detailed environmental impact potential of temperate-climate solar thermal system on climate change and non-renewable primary resources

3.1.3. Comparison with ecoinvent 2.0

Scenario 5 (the ecoinvent scenario) shows significant different results compared to the first two scenarios. This is due to the water tank used which is 1/3 larger in scenario 5 (400 l instead of 300 l). Besides, the transports hypotheses are much less favorable in scenario 5 compared to the first two. On the other hand, the supposed solar coverage ratio (SCR) is noticeably higher in the ecoinvent scenario while the solar thermal panels surface is lower: respectively 58.5% instead of 50% for the SCR, and 4 m² instead of 4.4 m². A further examination indicates that the main differences of results between the two sets of scenarios comes from hypotheses and choice of study parameters (lifetime, SCR, annual energy demand), and therefore shows the coherence between scenarios 1 (gas backup) and 2 (electrical backup) and the ecoinvent scenario (scenario 5).

3.1.4. Energy payback time

Energy payback time (cf. its definition in paragraph 1.3) has been studied in order to compare the energy required for the fabrication of SWH, to the energy avoided thanks to these systems while providing the same service (cf. functional unit). For the sake of clarity, only SWH with gas backup (scenario 1) has been compared to "traditional systems" (scenarios 3 and 4). Energy payback time is 1.5 years when comparing SWH with gas backup to gas only (scenario 1 to scenario 3), and less than 1 year when comparing SWH with gas backup to electricity only (scenario 4).

3.2. Tropical-type scenario

3.2.1. Environmental impacts and distribution

As detailed in Table 2, the solar thermal systems studied here as the tropical-type scenario shows specific differences with the systems used in temperate-climate conditions. Considering that the impact of gas or electricity consumption makes up the major part of overall impacts in the previous scenarios, the impacts of this scenario are significantly different from the previous in terms of distribution.

Fig. 7 shows the distribution of the impacts for each category. The water tank strikes as the major contributor to the impacts of the SWH, between 31% and 60% of each impact.
The other significant contributions are made by the solar thermal panels (about 20% of the impacts), the pipes (mostly because of the copper used), 23% and 31% respectively for human health and quality of ecosystems. The support structure accounts for 7% to 11% according to the impact category.

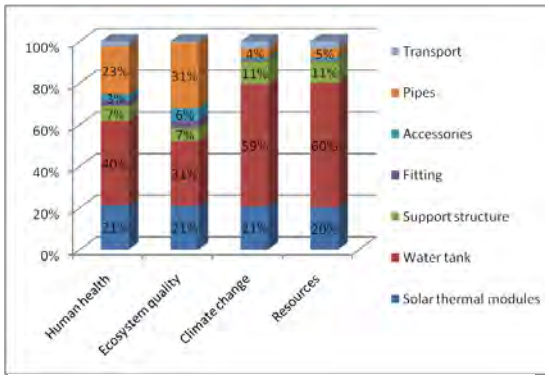

Fig. 7. Distribution of environmental impacts of the tropical-type SWH for each category of impact

3.2.2. Energy Payback Time

Payback time of tropical SWH (with no auxiliary energy) ranges between 5 and 6 months.

4. Conclusions, recommendations and perspectives

This study clearly shows that solar thermal systems are a very interesting solution to reduce the environmental impacts of domestic hot water production.
The impact assessment results for temperate climate systems highlight the backup energy as the major factor on environmental impacts. However, this study does not end with a clear-cut

environmental hierarchy among the different SWH systems: electricity or gas as a backup energy. This is mainly due to characteristics of the French electricity mix that has a low CO_2 content but an important primary energy ratio.
For all SWH, regardless of backup energy, solar panels, water tank and pipes emerge as the key environmental components.

Therefore, considering those results, technical improvement related to the main impacting components can be realized to lower the environmental impacts of the solar thermal part of SWH.

This project has been followed by a LCA on larger solar thermal installations to determine their related environmental impacts and compare with domestic solar systems[6].

Acknowledgments

ADEME (French Environment and Energy Management Agency) is co-financing this project which brings together different French specialists from the solar thermal industry and LCA fields.

References

[1] Eurobserv'er, Solar thermal Barometer, SYSTÈMES SOLAIRES - le journal des énergies renouvelables N° 191, June 2009

[2] Solar Thermal Markets in Europe Trends and Market Statistics 2009, ESTIF, 2010

[3] Soteris Kalogirou, Thermal performance, economic and environmental life cycle analysis of thermosiphon solar water heaters, Solar Energy 83, 2009, pp. 39–48

[4] Fulvio Ardente, Life cycle assessment of a solar thermal collector: sensitivity analysis, energy and environmental balances, Renewable Energy 30, 2005, pp. 109–130

[5] Crawford, R. H., Net energy analysis of solar and conventional domestic hot water systems in Melbourne, Australia, Solar Energy 76, 2004, pp. 159-163

[6] Soteris Kalogirou, Environmental benefits of domestic solar energy systems, Energy Conversion and Management 45, 2004, pp. 3075-3092

[7] International Standard Organization. ISO 14040. Environmental management – Life Cycle Assessment – principles and framework. 2006

[8] International Standard Organization. ISO 14044. Environmental management – Life Cycle Assessment – requirements and guidelines. 2006.

[9] Swiss Center for Life Cycle Inventories. The life cycle inventory data version 2.0. http://www.ecoinvent.ch. 2008.

[10] O. Jolliet, M. Margni, R. Charles, S. Humbert, J. Payet, G. Rebitzer, R. Rosenbaum. Impact 2002+: A new life cycle impact assessment methodology, International Journal of Life Cycle Assessment. 2003. Volume: 8, Issue: 6, Pages: 324-330

[6] More information are available on http://www.esthace.eu

Solar energy measurement on the South African east coast

E. Zawilska[1,*], M.J. Brooks[2]

[1] *Department of Mechanical Engineering, Mangosuthu University of Technology, Durban, South Africa*
[2] *Sustainable Energy Research Group, School of Mechanical Engineering, University of KwaZulu-Natal, Durban, South Africa*
** Corresponding author: Email: ewa@mut.ac.za, Tel: +27 319077233, Mobile: +27 825864123*

Abstract: This study presents the record and analysis of solar radiometry and selected meteorological parameters for Durban, South Africa over a full one-year period from January to December 2007. The results comprise of the key components essential in an assessment of the solar energy resource including global horizontal irradiance, global irradiance on a north-pointing tilted plane at 30° latitude angle, direct normal irradiance and diffuse horizontal irradiance. In addition, the ambient air temperature, humidity and rainfall records are presented and discussed. Selected solar radiometry variables obtained from the STARlab study were compared with data available from various sources including the HelioClim dataset, the NASA SSE database and the literature. The ongoing aim of this study is to build a reliable record of the solar resource for planning, engineering design and effective operation of solar energy systems and applications.

Keywords: *Solar energy potential, Radiometry data, Meteorological data, Renewable energy*

1. Introduction

The development and deployment of sustainable energy technologies across the globe continues at a growing pace, and of the various options available, solar energy remains among the most promising. As a developing nation, South Africa possesses an abundant solar resource, yet the country has traditionally been a carbon-intensive economy. For example, coal provided 70% of its primary energy in 2004, and 90% of the country's electricity [1]. In 2003, a government White Paper on Renewable Energy (WPRE) addressed future energy needs by committing the nation to achieving 4% of its anticipated power requirements from renewable sources by 2013 [2]. This target includes the deployment of end-use technologies such as solar powered water heaters, which South African power utility Eskom estimates could contribute 23% of the target. Eskom has since rolled out a large-scale solar water heating program, offering an incentive to consumers to replace existing electric geysers with the solar alternative [3]. In all these cases, however, an accurate and reliable understanding of the solar resource at the chosen geographic location is essential. Obtaining high-quality irradiation measurements poses a challenge due to the high cost of setting up and maintaining ground-based solar monitoring stations. As a consequence, only a limited number of solar resource assessment studies have been carried out in South Africa in recent years, which either possess inadequate resolution for use in coastal areas, or which have focused on sparsely populated desert regions in the Northern Cape province where concentrating solar power potential is greatest [3-5]. Densely populated urban areas on the east coast have largely been overlooked, yet this is where demand-side reduction programs could contribute greatly to lessening the country's reliance on grid electricity.

Durban is the largest city on the east coast of South Africa and in the province of KwaZulu-Natal (KZN). Despite high population density, growth and energy consumption few comprehensive studies have been done to characterize Durban's solar resource [6,7]. Lefevre et al. [8] compared

satellite-derived data with ground-based irradiance data using 35 ground stations in Africa but only Pretoria and Cape Town are included.

This study is part of a broader radiometric research program at Mangosuthu University of Technology, Durban, South Africa. Data were measured at a ground station located 3 km inland of the Indian Ocean coastline and is considered to be representative of the South Africa east coast region. This paper presents the record and analysis of the solar resource along with meteorological parameters for the period of January to December, 2007. In addition, the ambient air temperature, humidity, wind and rainfall records are presented and discussed. Selected solar radiometry variables obtained from the study are compared with the Meteosat-derived HelioClim dataset, NASA's SSE resource, as well as the literature. The ongoing aim of this study is to build a reliable record of the solar resource for planning, engineering design and effective operation of solar energy systems and applications. The database is also intended to support research in radiometric modeling. We anticipate expanding the database to geographic areas beyond Durban to cover more of the South African eastern coastal region. These efforts are intended to support the deployment of renewable energy resources and reduce the burden on the South African electrical grid.

2. Methodology

The data were recorded at the Solar Thermal Applications Research Laboratory (STARlab) which is an outdoor solar energy research centre in Durban, South Africa (29°58'N; 30°55'E). The station is at 105.5 m above sea level. STARlab is equipped with instrumentation for solar and meteorological monitoring, including thermopile radiometers and a weather station. The serial numbers, mounting and parameters of the radiometry instrumentation are listed in Table 1. The STARlab control room houses solar radiometry and meteorology data logging instrumentation. This includes two Agilent Technologies 34970A data acquisition units (one as back-up) with 34901A 20-channel multiplex modules connected to a desktop computer. Monitoring equipment is connected via an uninterruptible power supply unit. Data logging is controlled by custom-developed LabVIEW application that records point values at 30 sec intervals, with each set of values written to a spreadsheet file that is date- and time-stamped with day, month, year as well as local clock time and a corresponding solar time. In this study the PSA Algorithm was used for locating the solar vector [9] and generating key information such as declination, azimuth, zenith and hour angles. The radiometry data are recorded in terms of solar time, with solar noon occurring when the zenith angle is at a minimum. To obtain irradiation values, the irradiances are integrated over time. Weather variables such as temperature, wind speed and direction, rainfall, humidity and atmospheric pressure are recorded at 30 minute intervals for each 24-hour daily period. STARlab instrumentation is subject to a daily maintenance routine. For the period of this study less than 4% of data were missing due to unavoidable equipment malfunctions. A simple linear interpolation technique, similar to that reported in [6,10] was employed to replace missing information. A flowchart of the solar data monitoring system used in this study is given in Fig. 1.

The results of this study comprise key components essential to an assessment of the solar energy resource including global horizontal irradiance (G_t) global irradiance on a north-pointing tilted plane at 30° latitude angle (G_{tS}), direct normal irradiance (G_{DN}) and diffuse horizontal irradiance (G_d).

Table 1. Specification of STARlab radiometric instrumentation

Instrument	**Serial number**	**Mounting**	**Parameter**
Eppley PSP	# 34332F3	Horizontal plane, unshaded	Total global irradiance (G_t) in the wavelength range 285 nm to 2800 nm
Eppley PSP	#33583F3	Inclined at 30° slope to the horizontal, aligned true north, unshaded	Total global irradiance in the wavelength range at a 30° tilt angle (G_{tS})
Eppley NIP	#31955E6	Mounted on a ST-1 motorised solar tracker	Direct normal irradiance in the visible wavelength range (G_{DN})
Eppley TUVR	#34623	Horizontal plane	Ultra violet irradiance in the range 295 nm to 385 nm

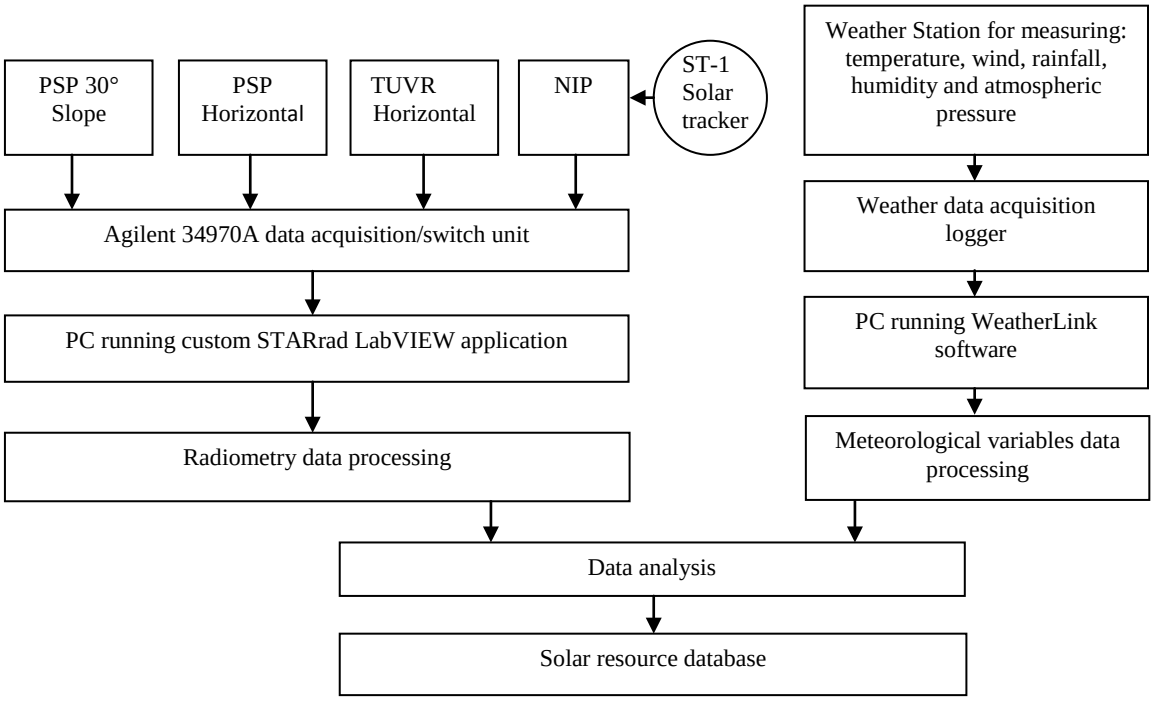

Fig. 1. Flow chart of the method applied in generating the STARlab solar resource database

In addition, the air ambient temperature, humidity, wind and rainfall records are discussed. Selected solar radiometry variables obtained from the STARlab ground-based records are compared with corresponding data available from HelioClim [11], NASA SSE [12] and sources in the literature. Data derived from Meteosat satellites have been used for comparison in a number of studies [8,13] and are currently in use by South African practitioners.

3. Results and Discussion

3.1. Radiometric analysis

Records of global horizontal irradiance G_t (W/m^2), global irradiance on a north-pointing tilted plane at 30º G_{tS} (W/m^2) and direct normal irradiance G_{DN} (W/m^2) were acquired from STARlab radiometers between January and December of 2007. The diffuse solar irradiance G_d (W/m^2) is calculated using the closure equation [14].

$$G_d = G_t - G_{DN} \cos\theta_z \quad (1)$$

where θ_z is the solar zenith angle. Daily cumulative irradiance values for G_t, G_{DN}, G_{tS}, and G_d are obtained by numerical summation of point values, to give H_t, H_{DN}, H_{tS}, and H_d, each representing a measure of energy per square meter (J/m^2). Daily values are averaged for each calendar month in the study to yield monthly average daily irradiation per square meter. Monthly average daily irradiation is often quoted as an indicator of energy availability for renewable energy activities. As a southern hemisphere country, South Africa's daily global horizontal irradiation trends higher between November and March. The winter period between April and October is characterized by clearer skies, but lower solar radiation intensity. The selected Durban results obtained from STARlab are compared with HelioClim-3 database values and NASA SSE datasets using the mean bias error (MBE) and root mean square (RMSE) approach to quantify difference .The MBE and RMSE are defined as follows:

$$MBE = [\sum(H_{sat} - H_{meas})]/n \quad (2)$$

$$RMSE = \{[\sum(H_{sat} - H_{meas})^2]/n\}^{1/2} \quad (3)$$

where H_{sat} is the predicted monthly average daily irradiation value for Durban from either HelioClim dataset or the SSE, H_{meas} is the measured monthly value from STARlab and n is the number of calendar months. The MBE and RMSE percentage values are calculated using the measured annual averages for each irradiation component for Durban. It should be noted that MBE and RMSE represent differences between the measured and modeled values, and not fundamental measurement uncertainty of the instrumentation.

The results show a typical trend for the southern hemisphere. For the eastern coastal region around Durban, two broad seasons can be identified: summer from November through March and winter from April through October. The monthly average of the daily global irradiation on the horizontal surface for summer and winter periods recorded at STARlab for 2007 were 5.62 kWh/m^2 and 3.6 kWh/m^2 respectively with the annual average value of 4.45 kWh/m^2. The highest value of 6.39 kWh/m^2 was recorded in January while the lowest value of 2.81 kWh/m^2 was measured in June. Similarly, the monthly average daily direct normal irradiation for summer and winter periods were measured as 5.25 kWh/m^2 and 4.94 kWh/m^2 respectively, with the maximum value of 5.90 kWh/m^2 recorded in February. The values of irradiation measured on the 30° incline are higher than those on the horizontal from March through October. Between November and February, the values on the horizontal exceed those on the incline. For example, the monthly average daily of the global irradiation on the 30° incline for May, June and July was 5.48, 4.30 and 4.89 kWh/m^2, with an annual average of 5.04 kWh/m^2. The corresponding values on the horizontal were 3.64, 2.81 and 3.17 kWh/m^2 respectively. The annual averages of daily

global irradiation components recorded at STARlab are found to be in reasonably close agreement with values obtained from HelioClim-3 and the NASA SSE datasets. The MBE and RMSE statistics are given in Table 2 and Table 3.

Table 2. Mean bias error and root mean square error for recorded data versus HelioClim data (Durban, 2007)

Solar radiation component	**MBE kWh/m^2**	**MBE %**	**RMSE kWh/m^2**	**RMSE %**
H_t	0.6	13.4	0.7	15.1
H_{DN}	-0.4	-9.1	0.6	15.6
H_d	0.2	9.0	0.3	17.1

Table 3. Mean bias error and root mean square error for recorded data versus NASA SSE data (Durban, 2007)

Solar radiation component	**MBE kWh/m^2**	**MBE %**	**RMSE kWh/m^2**	**RMSE %**
H_t	0.3	5.6	0.6	12.5
H_{tS}	0.1	2.4	0.5	10.1

Solar energy availability is often characterized by the diffuse fraction which provides a useful statistical distribution of the global irradiation at a location [6,14]. The diffuse fraction is particularly helpful in evaluating performance of systems such as flat-plate collectors. The monthly average diffuse fraction K_d is the ratio of monthly average daily diffuse irradiation on a horizontal surface (H_d) to the monthly average daily global total irradiation on a horizontal surface (H_t), as given in equation (4) [14], where H_d and H_t are measured in (kJ/m^2).

$$K_d = \frac{H_d}{H_t} \qquad (4)$$

The ratio of monthly average daily diffuse to global irradiation is presented in Fig. 2. This shows the expected seasonal trend for the Durban coastal region, with the diffuse fraction decreasing over the dry winter season, then increasing towards the humid summer season.

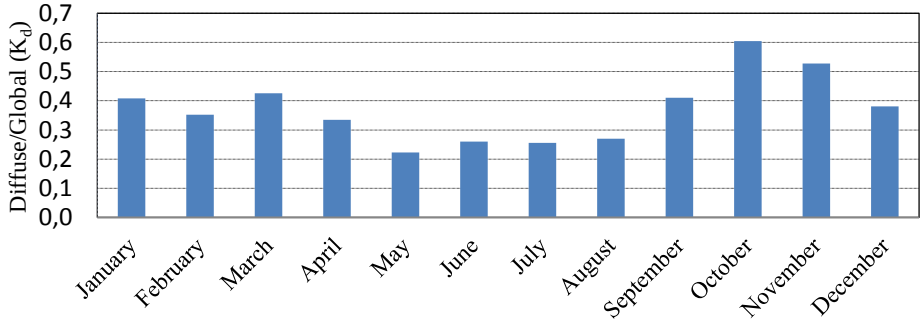

Fig. 2. Monthly average daily diffuse fraction values at STARlab

The measured annual average diffuse fraction for Durban in 2007 was 0.38. The annual cumulative values of solar energy measured in the year under consideration were 5881.85 MJ/m^2 for total global irradiance on a horizontal surface and 6592.09 MJ/m^2 for total global irradiance on a northward pointing 30° incline. The latter represents a 13% increase in energy availability, confirming the value of tilting flat-plate collectors in Durban at an angle equal to the latitude. For this assessment of solar resource potential it is useful to do a comparison with other areas around the world. Table 4 includes measured cumulative total global irradiation in the horizontal plane for 10 global cities, against which the Durban results are compared. It should be noted that not all values in Table 4 for other locations were obtained in 2007. The comparison is nevertheless indicative of Durban's relative solar potential. Arizona's desert is often considered as a benchmark when evaluating a location's solar resource and offers some of the highest solar potential in the world. Although this location has a significantly higher resource compared with Durban, the South African city exhibits similar solar energy potential to Sanary in France, Singapore and Miami (USA). Results suggest that Durban's solar potential is considerably higher than those of Seattle and Coeur d'Alene (USA), as well as Melbourne, Australia.

Table 4. Comparison of Durban measured annual total global irradiation in the horizontal plane with selected other locations

Location	Latitude	Reference	Year	Annual totals [MJ/m^2]	Relative solar resource
Durban, South Africa	29º58'S	STARlab data	2007	5881.9	100%
Coeur d'Alene, Idaho	47º72'N	[15]	1982-86	4485.6	76%
Eugene, Oregon	44º05'N	[15]	1975-97	4791.6	81%
Hermiston, Oregon	45º82'N	[15]	1979-97	5396.4	92%
Ely, Nevada	39º15'N	[16]	1961-90	6462.0	110%
Phoenix, Arizona	33º32'N	[16]	1961-90	7545.6	128%
Seattle, Washington	47º68'N	[16]	1961-90	4392.0	75%
Miami, Florida	25º34'N	[17]	2007	6242.0	104%
Sanary, France	43º08'N	[17]	2007	5996.1	104%
Singapore	01º22'N	[17]	2007	6030.0	103%
Melbourne, Australia	37º49'S	[17]	2007	5385.0	93%

3.2. Meteorological parameters

The meteorological parameters recorded and analyzed in this study were temperature, humidity, wind speed and direction as well as rainfall. Data were collected at 30 minute intervals over each 24 hour daily period. Fig. 3 shows the maximum, minimum and average daily ambient air temperature while Fig. 4 shows maximum, minimum and average daily humidity throughout the year under study. Durban has a subtropical climate with hot and humid summer and mild winter. Maximum monthly average daily temperatures of 24.0 ºC, 24.9 ºC and 23.4 ºC were recorded in January, February and March respectively. The lowest monthly average daily temperatures were recorded in June and July at 18.5 ºC and 18.2 ºC respectively. Humidity remains high for most of the year due to the influence of the warm Mozambique current flowing along KwaZulu-Natal's coast. The annual average monthly daily humidity recorded is 74.9%. Total rainfall recorded for

the year was 972 mm with a maximum value of 231.2 mm recorded in November and minimum of 1.4 mm measured in May.

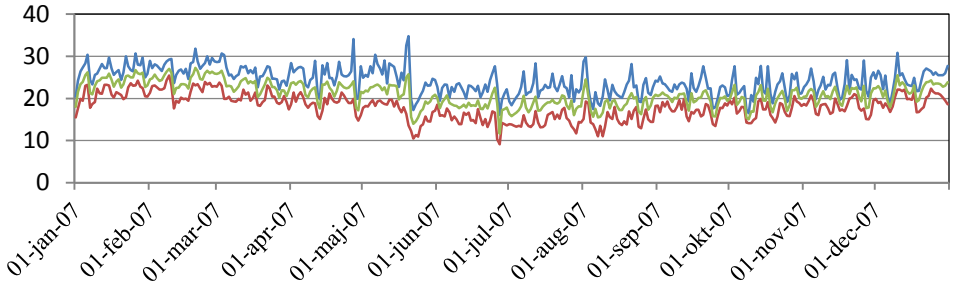

Fig. 3. Durban's daily average, minimum and maximum temperatures throughout the year

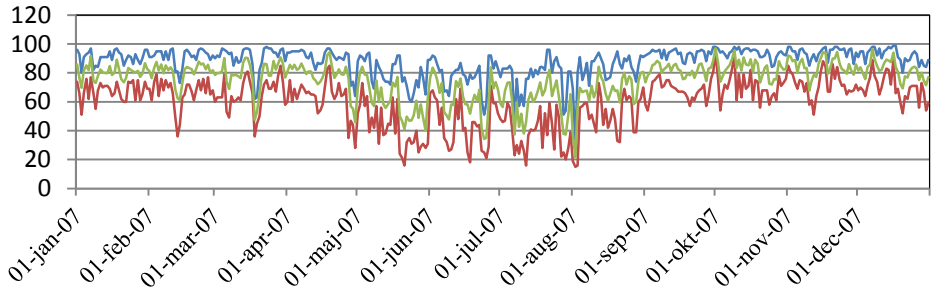

Fig .4. Durban's daily average, minimum and maximum relative humidity throughout the year

4. Conclusions

With a population density exceeding the national average, the east coast of South Africa around the city of Durban offers good potential for reducing demand on the electricity grid by switching to sustainable technologies like domestic solar water heaters and energy-efficient architecture. For urban planners, engineers and equipment suppliers there is a growing need for reliable solar radiation data on which to base technical and economic projections. In this study we show that two satellite-based software tools, HelioClim and NASA SSE offer reasonable estimates of the solar resource and each might be considered a good 'first stop' for estimating available energy. For 2007, mean bias differences in the satellite-based data versus measured values for annual average daily global irradiation were 13.4% for HelioClim and 5.6% for SSE. Random mean square differences were 15.1% and 12.5% respectively, suggesting that the SSE database is slightly more accurate. The HelioClim database tended to underestimate direct normal irradiation by 9.1% with random mean square difference of 15.6%. SSE is also able to predict annual irradiation on a tilted surface. The bias and random errors for the NASA database versus measured readings from a sloping pyranometer at 30° latitude tilt were 2.4% and 10.1% respectively. The measured annual average of daily global horizontal irradiance for 2007 was 4.45 kW/m^2 while the annual cumulative value was 5881.85 MJ/m^2. Overall, the solar resource for Durban is comparable to that of Singapore and Miami, marginally better than Melbourne's and about 28% weaker than that of Phoenix, Arizona. We anticipate expanding measurement activities to cover more of South Africa's eastern seaboard, via the recently established

GRADRAD network. These efforts are intended to aid radiometric research and reduce South Africa's dependence on fossil fuels for power generation.

Acknowledgements

The authors thank Dr. A. Mienie of Mangosuthu University of Technology and the University of Stellenbosch's Centre for Renewable and Sustainable Energy Studies for their assistance.

References:

[1] http://www.dme.gov.za/energy [accessed 5 October 2010]

[2] Whitepaper on Renewable Energy, Department of Minerals and Energy of South Africa, November 2003, http://unfccc.int/files [accessed 5 October 2010]

[3] http://www.eskom.co.za [accessed 5 October 2010]

[4] Munzhedi, R., Sebitosi, A.B., Redrawing the solar map of South Africa for photovoltaic applications, Renewable Energy 34: 165-169, 2009

[5] Fluri, T.P., The potential of concentrating solar power in South Africa, Energy Policy 37: 5075-5080, 2009

[6] Lysko, M., Measurement and Models of Solar Irradiance. Norwegian University of Science and Technology, PhD Thesis, 2006

[7] http://www.weathersa.co.za, South African Weather Service

[8] Lefevre, M., Wald, L., Diabate, L., Using reduced data sets ISCCP-B2 from the Meteosat satellites to assess surface solar irradiance, Solar Energy 81: 240-253, 2007

[9] Blanco-Muriel, M., Alarcon-Padilla, D.C., Lopez-Moratalla, T., Lara-Coira, M., Computing the solar vector, Solar Energy 70: 432-441, 2001

[10] Muzathik, A.M., Wan Nik, W.N.M., Samo, K., Ibrahim, M.Z., Reference Solar Radiation Year and Some Climatology Aspects of East Coast of West Malaysia, American J. of Engineering and Applied Sciences, 3 (2): 293-299, 2010

[11] http://www.sodais.com/ [accessed 1 November 2010]

[12] http://eosweb.larc.nasa.gov/sse [accessed 2 September 2010]

[13] Cros, S., Albuisson, M., Lefevre, M., Rigollier, C., Wald, L., HelioClim: a long-term database on solar radiation for Europe and Africa, Proceedings of Eurosun 2004, published by PSE GmbH, Freiburg, Germany, pp. (3) 916-920, 2004

[14] Iqbal, M., An Introduction to Solar Radiation, Academic, Toronto, 1983

[15] http://solardat.uoregon.edu/ [accessed 1 November 2010]

[16] http://rredc.nrel.gov/solar/old_data/nsrdb/ [accessed 1 November 2010]

[17] http://www.atlaswsg.com [accessed 1 November 2010]

Investigation of Solar Collector systems use in Latvia

P. Shipkovs[1,*], K. Lebedeva[1], G. Kashkarova[1], L. Migla[2], M. Pankars[2]

[1] *Institute of Physical Energetic, Energy Resources Laboratory, Riga, Latvia*
[2] *Riga Technical University, Riga, Latvia*
* *Corresponding author: Tel:* +371 67553537, Fax: +371 67553537, *shipkovs@edi.lv*

Abstract: Solar energy is the biggest energy resource on the earth. Latvia environment is very potential for solar usage, but there are many reasons why consumers have skepticism and a perception that the environment in this region is not suitable for solar energy usage.
To have broken this stereotype, this study is conducted. The aim of this program is to explore the suitability of Latvian environment with the use of solar collector. For the attainment of objective monotype house will be modeled, the house will be equipped with the combined solar heat system, which will be placed in different regions. There are various amounts of sunny days in different regions, as well as diverse average temperature, wherewith the amount of heat differs. For the modeling of building, modeling program model of solar collectors will be used, which is provided for several solar heat systems, inter alias for the calculation of combined solar heat supply system and for the solving of several relevant tasks. Program is simulation program for the thermal solar energy systems. It suits both for determination of hot water use and heating system use.
There are countries which are located in sunny regions and which history of solar energy usage is very longstanding, wherewith also technological achievements are high. Yet our contemporary rapid technology development enables to use ever more solar energy in the regions which are not so rich with the solar radiance, for example in Latvia. Interest about the usage of solar energy in Latvia increase – partly it is explicable to unpredictable and essential price rise of fossil firing resources and partly to the desire to invest in technologies which could reduce this rise in price in the future.

Keywords: *Modeling, Simulation, Solar Energy, Renewable Sources, Combined systems*

1. Introduction

During last few years significance of environmental problems increase. Wherewith, activation of environmental problems increases humans' interest about different environmentally friendly technologies. One of the biggest air polluters are fallouts resulted from burning of fossil firing. That is why urgent becomes utilizations of renewable resources for the energy obtaining, which are less nocuous to environment. Latvia's total final energy consumption is secured from local energy resources and the flow of primary resources from Russia, the CIS countries, the Baltic countries, EU and other countries. Currently, three types of energy resource making up approximately equal proportions dominate in the delivery of Latvia's primary resources – oil products, natural gas and wood-fuel. Like many other European Union countries, Latvia is dependent on imports of primary resources. The share of RES has traditionally been significant in Latvia's energy supply and in 2008 it comprised 29.9% of the total final energy consumption. Interest about the usage of solar energy in Latvia increase – partly it is explicable to unpredictable and essential price rise of fossil firing resources and partly to the desire to invest in technologies which could reduce this rise in price in the future. That is the reason why is it necessary to investigate solar energy potential in Latvian conditions.

Global radiance consists of direct and diffused radiance. Direct radiance is connected with the direction of sunbeams. Diffused radiance develops when molecule and particles in atmosphere disperse sunbeams in all directions. The duration and intensity of solar radiance depends on season, climatic conditions and geographical location. Global radiance of the earth on the horizontal area in the regions of solar zone may reach 2200 kWh/m^2. Maximal volume of solar radiance in North Europe is 1100 kWh/m^2. We can conclude that even in such

small country as Latvia are several different solar sliding duration zones. In the zone along the Baltic Sea is the longest solar sliding duration – more than 1900 hours, in its turn in Vidzeme heights it is the least – less than 1700 hours. Volume of Solar radiance is the main factor of solar energy usage in Latvia. [2]

2. Methodology

In order to define, how great volume of heat from building total use of the heat is possible to secure using solar heat energy, the model of the building will be created using modeling program. With the help of this program it is possible to carry out research, the modeling, the calculation of heat supply solar systems. Simulation of all type heating supply solar system is based on independent meteorological data. Time step of simulation is possible starting with one second even until one hour, it depends on situation, in its turn, there are a lot of versions of model simulation time periods – starting from one day until several years. The calculation basis in program has been integrated from subprogram Meteonorm. Using preferences of simulation program have been cleared up most effective location for solar collector in Latvian conditions. Comparatively, effective solar radiation may catch solar collector that is placed 55° anent to horizon or slope and 0° anent to the South or orientation and which has clean horizon, nothing puts a slur and otherwise do not affect the activity of collector, that is why received amount of solar heat takes as average from all models that are placed in corresponding place and location. However first of all foreseeable tables has been made. Data about the volume of receivable heat from 1 m^2 solar collector that depends from location, to be more precise in what angle as to the ground it has been put and in what orientation as to the South solar collector will catch the greatest volume of heat, has been put in the table.

Table 1. Percipient heat volume from 1 m^2 of solar collector in Riga dependence of location, kWh/m^2.

Orient. \slope	0°	15°	30°	45°	55°	60°	75°	90°
0°	259	325	382	417	**426**	425	401	348
15°	259	320	376	412	422	423	406	359
30°	259	325	380	412	417	414	385	324
45°	259	310	362	396	407	408	395	357
60°	259	322	370	396	397	393	358	294
75°	259	297	341	370	380	381	370	335
90°	259	314	355	373	369	363	325	262

Such location is the most effective and in the table 1 there are the same data, then we can conclude that program is comparatively precise for the calculation in the Latvia conditions. The least received heat volume is when the solar collector is located 0° anent to the Earth horizon. This location is the most inappropriate for the detection of solar radiance. To 0° anent to horizon at any orientation, the volume of received heat is constant, because ray angle falling form the Sun anent to the area is constant at any orientation of solar collector. In the Table 1 it is clearly seen how volume of received heat change and its changes are twice as much bigger. Therefore the precise setting up of solar collector has significant meaning. Although this calculation was done only for one type collectors, though the calculation corresponds to previously defined, we can conclude that in wholesale it is similar to all collectors.

The collector efficiency mainly depends on the difference between the mean collector temperature and the ambient temperature *Tm - Ta*. If this difference is high then the heat radiation and the convection losses are high. At small temperature differences the efficiency can reach 90%. If the mean collector temperature drops below ambient temperature because of a cold heat transfer medium then the efficiency can exceed even 100%. In this case the heat transfer medium is not only heated by the sun, it's also heated by the ambient air. [1] The efficiency is described by the efficiency curve. The temperature difference (*Tm - Ta*) divided by the irradiation normal to the collector (*Gk*) is the variable (*x*).

$$X = \frac{Tm - Ta}{Gk} \qquad (1.)$$

Following a typical efficiency curve of a regular glazed flat collector:

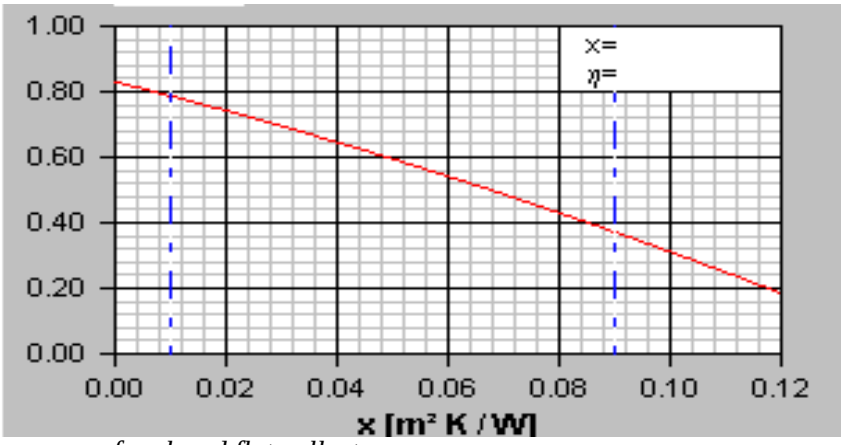

Fig. 1. Efficiency curve of a glazed flat collector.

The higher the mean collector temperature lowers the efficiency. The irradiation is 800 W·m^{-2}. This curve is described by a 2nd order Polynom with sufficient accuracy. This Polynom is clearly defined by three parameters, c_0, c_1, c_2 (or a_0, a_1, a_2; values measured under wind speed of 2-4 m·s^{-1}):

$$\eta = c_0 - c_1 x - c_2 G_k x^2 \qquad (2.)$$

where η – efficiency of collector; c_0, c_1, c_2 – coefficient of polynomial set in model; G_k – tightness of solar radiation, that falls athwart to the surface of collector,

The efficiency value amounts to c_0, if the mean collector temperature and the ambient temperature are equal. This value should be high. c_1 and c_2 describe a combination of different loss factors. These values are low if a collector is well insulated. It is worth to mention that such polynomial is used in modeling program for the calculation of efficiency. [1]

3. Results

Since program isn't potted to the conditions of Latvia, there isn't meteorological data, which are necessary for activity simulating of the combined heat supply of solar system in the Latvian conditions in its data basis. Since this program contains meteorological data from all world, in order to get this necessary information, accurate coordinates from different towns of Latvia, which are located in different zones of sun shining: Riga, Liepaja, Daugavpils has been entered. For the more visible efficiency determination of heat supply solar system, also

coordinates of typical sunny south city Bremen (Germany) and cool northern city Boden (Sweden). Wherewith, computer models will be created for different climatic zones and conditions in the European Union countries.

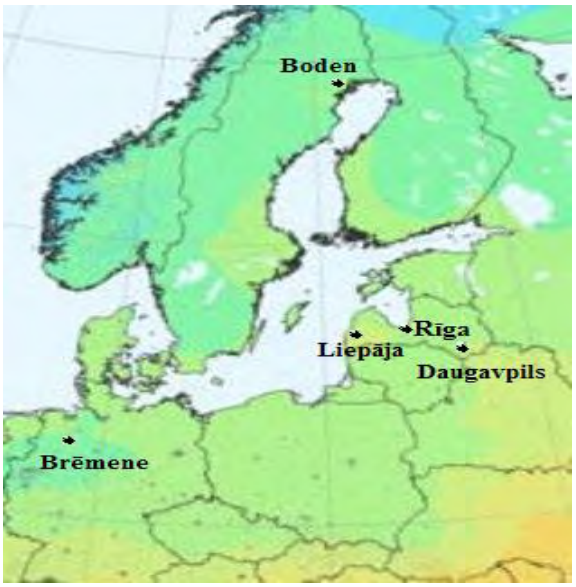

Fig. 2. Locations of cities that are used for modeling

Those data of communities that are used for the modeling of combined solar heat supply system are shown in table 2.

Table 2. Meteorological data for Meteonorm

Place of location	Latitude	Degrees of longitude	Elevation above sea level, m
Riga, Latvia	56,88°	24,13°	14
Liepaja, Latvia	56,49°	21,02°	1
Daugavpils, Latvia	55,87°	26,52°	105
Boden, Sweden	72,80°	12,58°	121
Bremen, Germany	65,78°	21,67°	31

Initially model one family building with the floor space 150 m^2, 4 persons will live in that building. Heat loss through demarcation constructions of building (external walls, roof, windows etc.) makes essential part form total use of heat energy. Power efficiency of demarcation constructions is able to evaluate when thermal coefficient of given construction is U ($W/m^2 \cdot K$). Because in Latvia there is relatively cool climatic conditions, than building must be well isolated with heavy constructions. Walls are made from bricks and from outside they have 0.2 m heavy insulation. Air exchange 0.6 l/h, and radiant 400W. Require heating capacity 6.1 kW at -8°C. Looking closely at balance sheet of used and acquired heat of each place we can conclude that in all chosen places development of heat use during year is similar, only volume of heat differs.

Table 3. Heat energy consumption for space heating depending from location, kWh/m^2 per year.

Place of location	Common use of heat energy for room heating (kWh per year)	Use of heat energy for room heating on 1 m^2 (kWh/m^2 per year)
Riga, Latvia	12 650	85
Liepaja, Latvia	12 500	80
Daugavpils, Latvia	13 615	92
Bremen, Germany	9 652	65
Boden, Sweden	27 342	182

In warmer climatic zone use of thermal energy reduces. Because Bremen is located closer to equator and its average temperature is superlative for all viewed cities, for that reason required volume of thermal energy is the least. Yet looking closely at Boden, which is located close to the North, it is contrary. Distinction among Riga, Liepaja and Daugavpils brings about location of those towns' towards the sea. Temperature at the sea in winter is warmer wherewith volume of thermal energy for room heating is different, yet towns are located relatively close to each other, wherewith volume of thermal energy is not very different. As in the building lives 4 persons and it is known that on one person provides 2 m^2 solar collectors, than for the building model use 8 m^2 flat area collectors. Previously we found out that solar collector works most effective when its slope angle is 55°C anent to horizon and 0°C anent to the South. We estimate position along vertical of solar collector modules. Wherewith, we can define thermal conductivity and thermal capacity of pipes, as well as the stream speed in pipes. Pump and system described values are calculated automatic after input of necessary data. In this case inputted values are the following: flow of pump, flow speed of their process 120 l·h^{-1} and back process 0, 06 m ·s^{-1}. Also one more important parameter of efficiency determination of combined solar heat supply system is heat carrier data of used solar collector. Usually water is used like heat carrier, due to its availability, low price and suitable physical qualities. In combined heat supply solar systems, water can be used only in the inner supply of heat and water. For the very reason in Latvia conditions pipes are excluded as heat carrier in exterior contour. Therefore glycol solutions must be chosen as the heat carrier in pretence model. Necessary volume of heat for the preparation of hot water in all climatic conditions is nearly identical 4069 kWh in a year. In some places suspended volume of solar heat is different.

Table 5. Perceptive solar heat volume, kWh/in a year.

Place of location	Common use of heat energy for room heating (kWh per year)	Use of heat energy for room heating on 1 m^2 (kWh·m^{-2} per year)
Riga, Latvia	3 200	400
Liepaja, Latvia	3 345	418
Daugavpils, Latvia	3165	395
Bremen, Germany	2930	366
Boden, Sweden	2890	360

It is not possible to unequivocal assert that solar collectors works more effective closer to the South and to the North they do not work effective. The most effective works solar collector that is located in Riga and not the solar collector in Bremen that is closer to the South. It is explained by the less requirement of system for heating, because during the year in all models the volume of warm water for the preparation of hot water and containers heat loss is equal. In a period when heating is necessary but available volume of solar heat

energy is sufficient not only for the preparation of hot water but also for the room heating, combined solar system has been used valuable. In the Northern models such periods are longer, wherewith the volume of used solar energy is greater. Riga's model in comparison with Bremen model volume of used solar energy is greater, because the air temperature in Bremen at the beginning and at the end of the year is a bit lower, but available solar heat is greater, wherewith the volume of used solar thermal energy increase. In all versions the volume of produced heat in auxiliary boiler is greater than necessary for the building. It is explained by the extra load of auxiliary boiler for the production of hot water. Because several simulations with different combinations has been carried out with different capacity auxiliary boilers and electricity, then average result has been accepted as the volume of produced heat of auxiliary boiler.

Table 6. Heat volume from auxiliary boiler, kWh/year.

Place of location	Heat volume from auxiliary boiler (kWh in a year)
Riga	15 400
Liepaja	14 800
Daugavpils	16 080
Boden	11980
Bremen	27120

In existing versions of auxiliary boilers more to the North, the volume of produced heat increase on the count of necessary volume of the heat for the production of hot water. At the beginning of colder season auxiliary boiler has been started later, because sufficient volume of the heat is stocked up in the container, which ensures room heating and preparation of hot water for the short period. In that way heat has been stocked up for the later use, which is one of the formation preconditions of the combined heat supply solar system. It is not important to evaluate the productivity of solar collector but the relations of produced capacity in the power balance of the building. As models of Riga, Daugavpils and Liepajas is relatively similar and let the chart is more obvious only Riga, Bremen and Boden will be compared.

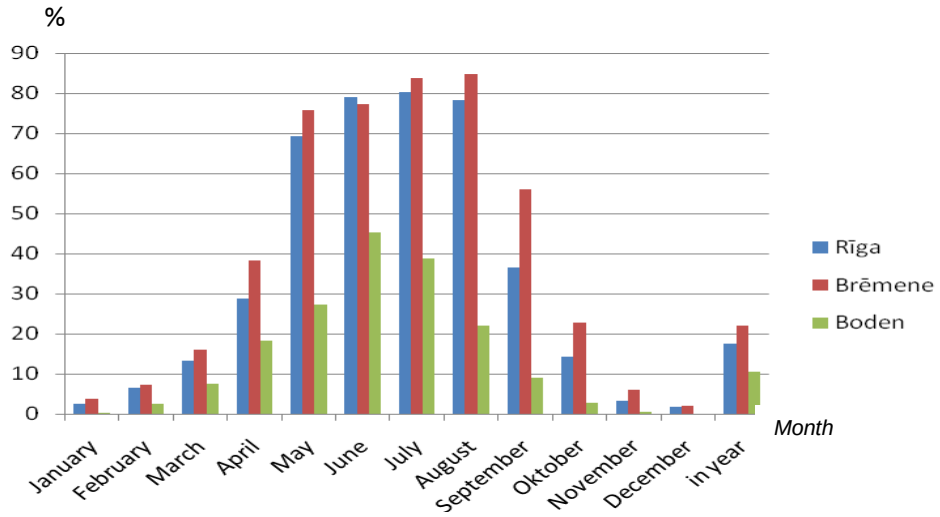

Fig.3. Percentage of produced heat from solar collector, %

Solar collectors may cover the necessary volume of heat during the summer month. Capacity of heat is not necessary for the room heating during the summer month, capacity of heat is necessary only for the preparation of hot water. It is important that solar collectors of Riga's

model produce practically the same volume of heat energy from building heat balance as it is in Bremen. To be more precise solar collectors in Riga's model produce more heat energy than Bremen model but heat loss of building is greater in Riga. The decrease of heat volume necessary for room heating reflects not only in the volume of used heat but also partly in not received volume of solar heat. In its turn, the volume of solar heat that is used in the preparation of hot water is growing, because the volume of solar heat is available. For that reason the bigger part of the solar heat energy is observed in used volume of heat. Important conclusion in that during the winter month volume of received heat is minimal and very similar to all viewed models. Consequently during those months combined solar heat supply system has reduction of usefulness. Probable it is worth to consider on solar collector unlock during the cooler season, in such a way raising its usefulness. Though already in early spring solar collectors may provide 30% from the use of building heat for the room heating and hot water. The volume of suspended solar heat do not show real possible volume of solar heat energy that may be used, because conveying of solar heat energy to the storing container happens during almost all light period of day, only disconnecting circulation pumps of model in short periods.

The Developed models were viewed on the other side. Heat exchanger effect on System efficiency was determinate. The system affects the handling characteristics, such as heat exchangers. They fulfill the important function as a heat-transfer. The resulting solar collector heat storage tank is given by the mixing of heat already is there or whether the fluid is more effective when the heat from the solar collector storage tank into the system through a heat exchanger. The heat storage tank heat loss is smallest when the system has been equipped with heat exchanger for Domestic hot water. Previously was found how to place the solar collectors to receive the maximum amount of solar radiation.

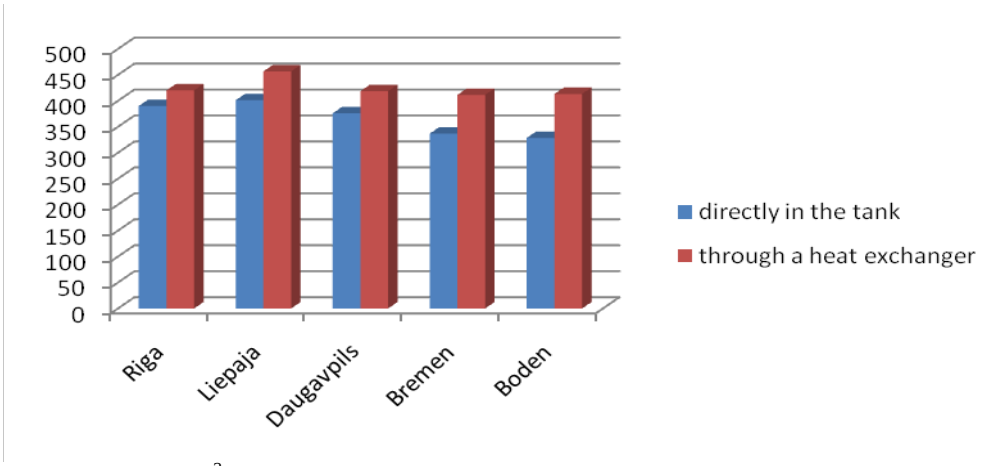

Fig. 4. Heat quantity W/m^2 depending of heat transforms type in system

The heat transfer from the solar collector system to the heat storage tank through a heat exchanger is about 14% efficiently than in cases where heat transfer occurs mixing of solar collector fluid transforms the heat in the tank. This is explained by the fact that the liquid flowing through the heat exchanger is less than the local losses. As well as more efficient heat exchange takes place.

4. Conclusions

The activity of the system depends on the weather conditions of particular place, which have an impact of the geographical fix, available volume of solar heat. It depends also on the individualities of particular place: the hills, the sea, the wind direction etc. In addition, the

great importance has the users of combined solar heat supply system, their way of life. Wherewith, comparing of simulation models located in different places is conventional.

The greatest volume of perceived solar heat in Riga is in the situation when solar collector is placed 55° against horizon and 0° orientation against the South

The combined solar heating system provides for constant domestic hot water and seasonally variable space heating demand ensuring in annual terms. As well as changing hot water and constant heating demand ensuring in daily. Combined solar heating system operation depends on various technical specifications and performance characteristics of system components, such as the installed area of solar collectors, size of thermal storage tank, heat conductivity, as well as other parameters of system. During the winter months such a system is not useful, but it pays off in the summer months, producing enough heat for domestic hot water and pre warming for space heating. Effect on system's efficiency gives availability and location of heat exchanger. The heat transfer from the solar collector system to the heat storage tank through a heat exchanger is about 14% efficiently than in cases where heat transfer occurs mixing of solar collector fluid transforms the heat in the tank.

Difference between accumulated solar collector's heat of the Latvian, Sweden (Boden) and Germany (Bremen) models are not significant. But Consumed heat for space heating and domestic hot water is drastically different. Hence contribution varies of solar thermal system in consumer balance sheets. As the building model of Boden has the highest heat consumption, than solar collector contribution in balance sheet are relative the smallest.

References

[1] Polysun 3.3. Documentation 2003. Solar Energy Laboratory SPF;

[2] P. Shipkovs, Atjaunojamo energoresursu izmantošana Latvijas apstākļos, RTU, Rīga, P. 2007, pp. 67;

New Method for Predicting the Performance of Solar Pond in any Sunny Part of the World

Adel O. Sharif*, Hazim Al-Hussaini, Ibrahim A. Alenezi

Centre for Osmosis Research & Applications, Chemical & Process Engineering Department, Faculty of Engineering & Physical Sciences, Surrey University, UK.
** Corresponding author: Tel: +44(0)1483 686584; F: +44(0)1483 686584; email: a.sharif@surrey.ac.uk*

Abstract: The solar pond is considered one of the most reliable and economic solar systems. The collecting and storing of the solar energy is in one system, so the heat in summer can be utilised in winter in the same system. To predict the potential of solar pond at any part of the world a mathematical model is established to calculate the parameters affecting the performance of the solar pond through a computer programme.. The solar radiation input to the pond is calculated using the daily monthly average method. One dimensional steady state and transient assumptions in the gradient zone are used to predict the effect of any parameter on the solar pond performance. The results show excellent agreement with the experimental data under the steady state assumption. Many parameters affecting the performance of the solar pond such as shading effect, depths of the upper, gradient and storage zones, ground temperature and covered insulation for different climates and different latitudes have been studied. The results show that the solar pond has high potential even for colder climates such as that of the UK, where the heat could be used for a number of applications including domestic and industrial.

Keywords: *Solar Pond, Solar Energy, Modelling*

Nomenclature

N *the number of the day in the year*
φ *latitude of the location……degree*
θ *the Incident angle ……..... degree*
I_{sc} *Solar constant …….. W.m^{-2}*
I_o *the average daily extraterrestrial solar irradiance …….. W.m^{-2}*
δ *the declination angle ……. degree*
ω_s *hour angle …….. degree*
I_{od} *is daily total direct normal extraterrestrial radiation…… W.m^{-2}*
IBF *the fraction of the extraterrestrial radiation*
Fc *the monthly correction factor*
$\bar{H}_T$ *the monthly daily- average total irradiation on a horizontal surface ……. W.m^{-2}*
H_{oT} *the total extraterrestrial radiation on a horizontal surface …….. W.m^{-2}*
ρ *water density….. kg·m^{-3}*
C_p *specific heat ……..J.kg^{-1}.^{o}C^{-1}*
A *Area …… m^2*
x *the depth …..m*
T *temperature.. ……. ^{o}C*
Q_{sru} *absorbed heat of solar radiation in the upper zone…….. W.m^{-2}*
Q_{uw} *heat loss from the sides in the upper zone…….. W.m^{-2}*
Q_{ub} *heat gained from the bottom in the upper zone…….. W.m^{-2}*
Q_{uc} *he at loss by convection in the upper zone…….. W.m^{-2}*
Q_{ur} *he at loss by radiation in the upper zone…….. W.m^{-2}*
Q_{ue} *heat loss by evaporation in the upper zone…….. W.m^{-2}*
Q_{srs} *absorbed heat of solar radiation in the storage zone…….. W.m^{-2}*
Q_{sw} *heat loss from the sides in the storage zone…….. W.m^{-2}*
Q_{sb} *heat loss from the bottom in the storage zone…….. W.m^{-2}*
Q_{st} *heat loss from the top in the storage zone…….. W.m^{-2}*
Q_{se} *heat loss by heat extraction in the storage zone…….. W.m^{-2}*

1. Introduction

Natural water temperature gradients was observed and reported first time by Kalecsinsky in the Medve Lake in Transylvania in 1902 [1,2]. This observation suggested the possibility of constructing and using the ponds as solar energy collectors and storage areas. Tabor (1964), Weinberger (1964), and Tabor and Matz (1965) reported a series of theoretical and experimental studies of these salt gradient ponds [3].

The solar pond is one of the simplest methods that can directly collect and convert solar energy to thermal power. Moreover, it is a solar power collector and a thermal storage unit at the same time. All Ponds convert solar radiation to heat although most of them lose that heat as a result of convection and evaporation. In nature when the sun's rays fall on the lake or the pond, the temperature of water increases gradually towards the bottom of the pond. Therefore, the water in the bottom becomes warmer then it rises to the surface and loses its heat to the atmosphere, a phenomenon called convection. However, the solar pond technology inhibits this phenomenon by dissolving salt into the bottom layer of this pond, making the fluid too heavy to rise to the surface, even when being hot. This idea can increase the temperature of the bottom layer up to more than 100 oC [4]. Once a high temperature is obtained, the bottom layer can be used as a heat source to provide continuous heat through a heat exchanger at any time. The solar pond principle is to prevent vertical convection and/or evaporation according to the type of the solar ponds [5].

A typical salinity-gradient solar pond consists of three main zones as shown in Fig. 1:

- The Upper Convecting Zone (UCZ) which has the least cost, salinity, temperature, and is close to ambient temperature. The thickness of this zone is typically 0.3 m and it should be kept as thin as possible. The cost of constructing the UCZ is usually reasonable.

- The Non-Convecting Zone (NCZ) which is located between the upper and the lower zones of the pond. Since the temperature and salinity increase with depth, this layer is not homogeneous. If the salinity gradient is large enough, the NCZ inhabits a convection phenomenon even when the lower zone is hotter.

- The Lower Convecting Zone (LCZ), which is a homogenous layer and has a relatively high salinity and high temperature. Heat is stored in this zone and can be exchanged in or out of the pond. As the LCZ's depth increases, the heat capacity increases and the temperature variation decreases.

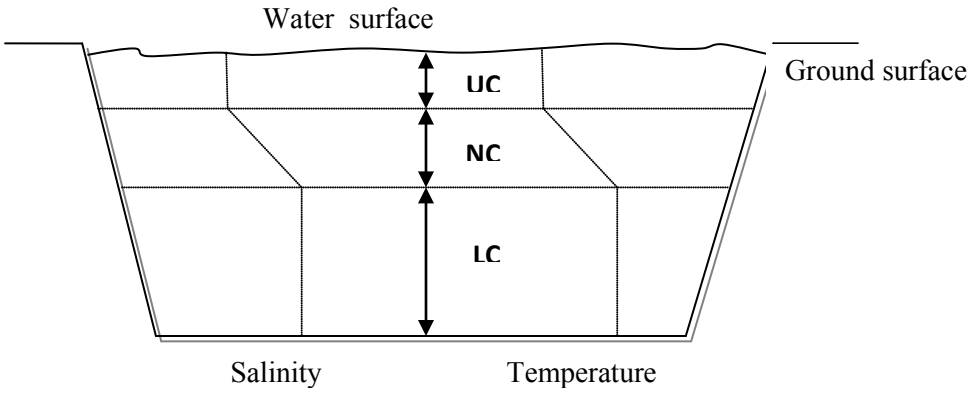

Fig. 1. Salinity and temperature profiles through the salinity gradient solar pond zones.

Non-convective solar ponds can provide heat for domestic, agricultural, industrial, power generation and desalination purposes. More details about solar pond c onstruction and limitation can be obtain from [1], [2] and [4].

2. Methodology

Solar irradiation data have been widely measured and recorded for almost every region in each country in the world for many years. Nevertheless, the predictions and calculations of the irradiation are sometimes required to obtain a good approximation of the irradiation.

According to a solar pond l ocation, the sun path in the sky is changed seasonally thus the sun's altitude and azimuth angle and the daily sunshine period are varied and cause a great effect on the amount of the incident solar radiation and then on the performance of the solar collector.

It is found that monthly averaged data are the most effective for representing the climate changes and calculations, since hourly and daily calculations and measurements are changed from year to another and are quite short to represent a general impression about the climate. In addition to this, seasonal and yearly readings cannot accurately represent the climate computations. Thus, averaged monthly measurements or computations have been adapted in this study.

Matlab computer software has been used to build a multi-scripts programme to solve ordinary differential equations by finite difference method for steady state models. This programme takes into account the changes of boundary conditions and surround factors with time.

This solar radiation computation program requires only a latitude value to predict sunrise, sunset and sunshine period to compute the solar radiation equations. A new predicted empirical equation has been added to this script to give a good agreement and it has been tested for three different locations in the middle east which are Kuwait, Riyadh and Jerusalem. The incident solar radiation values, based on m onthly average daily amounts can be obtained from the available references or the 22 years average values which are recorded in NASA website [6].

Since the earth-sun distance varies each season, the apparent extraterrestrial solar irradiation changes during the year. Therefore, the solar irradiation intensity depends on t he number of the day in the year. The average daily extraterrestrial solar irradiance is given by

$$I_o = I_{sc}\left[1 + 0.0033\cos\left(\frac{360N}{370}\right)\right] \qquad (1)$$

Solar constant (Isc) value has been measured by many researchers since the beginning of the 20th century. Abbot [7] and his team in Smithsonian Institute after many research proposed the value of 1353 W/m^2 to be the value of the solar constant. Many further investigations were made on ground-base and high altitude measurements and eventually 1353 W/m^2 has been accepted to be the standard for the solar constant. NASA, after many measurements on the space, has recommended this value as well [8]. It has very recently been published in NASA's

website that the generally accepted value of the solar constant is 1368 W/m^2 as a satellite measured yearly average, which is close to the standard value.

The total daily extraterrestrial radiation on a horizontal surface can be computed by

$$H_{oT} = \frac{I_{od}}{\pi}\left[\cos\theta\cos\delta\ \sin\omega_s + \frac{2\pi\omega_s}{360}\ \sin\varphi\sin\delta\right] \qquad (2)$$

Where I_{od} is daily total direct normal extraterrestrial radiation and can be obtained by yielding the value of extraterrestrial radiation solar irradiation throughout the day as the following

$$I_{od} = 24I_o \qquad (3)$$

To use these equations for computation of the monthly daily-average total extraterrestrial radiation on a horizontal surface $\bar{H}_{oT}$, the month representative-day is needed and given by lunde[9] in addition to other useful equations in solar radiation calculations. The new empirical equation which works with available solar radiation equations to estimate the solar radiation based on a single input parameter is

$$IBF = \frac{1.5\varphi - 14.25}{\varphi}\ Fc \qquad (4)$$

Where Fc is a predicted monthly correction factor validated accurately for the Middle East with NASA published date and the above equation can be utilized in the following formula;

$$\bar{H}_T = IBF(\bar{H}_{oT}) \qquad (5)$$

Eq(5) is a well known formula in the solar radiation equations which are expansively explained in [9] based on the cloudiness (or clearness) index, however, the index here is substituted by the predicted factor ,IBF, which is obtained by linking the field solar radiation data with longitudes in a special computer programme.

The steady state model for a solar pond has been widely adopted by the most famous researchers in the SGSP field such as Weinberger [10], Rabl and Nielsen [11], Kooi [12], Ali [13], Wang and Akbarzadeh [14] and many of other researchers. A downward one-dimensional flux model is often used for simplification purposes. The convective zones (upper and storage layers) are assumed to be well thermally mixed i.e. lumped systems. The upper layer steady state equation is:

$$\rho_u\, C_{pu}\, A\, x_u \frac{dT_u}{dt} = Q_{sru} + Q_{ub} - Q_{uc} - Q_{ur} - Q_{ue} \qquad (6)$$

The gradient layer is considered as a conduction slab and all absorbed solar radiation is consumed in building and maintaining the temperature profile in this layer. The storage zone steady state correlation will be

$$\rho_s\, C_{ps}\, A\, x_s \frac{dT_s}{dt} = Q_{srs} - Q_{st} - Q_{sb} - Q_{sw} - Q_{se} \qquad (7)$$

More details about each parameter in Eq(6) and Eq(7) are given by Lunde[9], Rable and Nielson[11] and Ali[13].Model validation is possibly the most essential step in the model building stages. In this study, the model validation is applied to Ali's study in Kuwait [13].

3. Results

The single input program is used to calculate the solar radiation in Kuwait, Riyadh and Jerusalem. The output of this script is compared with NASA average 22 year measurements data and the results are really good and shown in Fig. 2 for Kuwait, Fig. 3 for Riyadh and Fig. 4 for Jerusalem solar radiations.

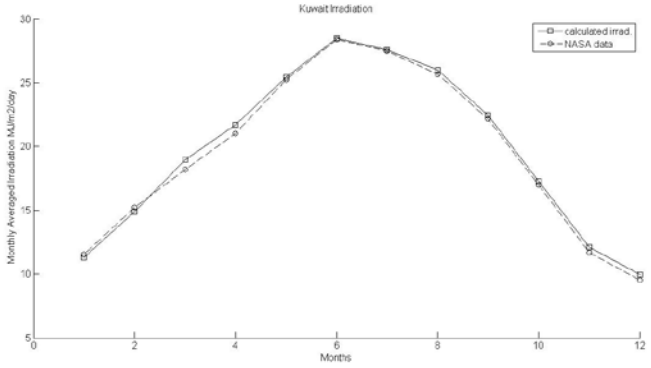

Fig. 2. NASA data and calculated solar irradiation for Kuwait.

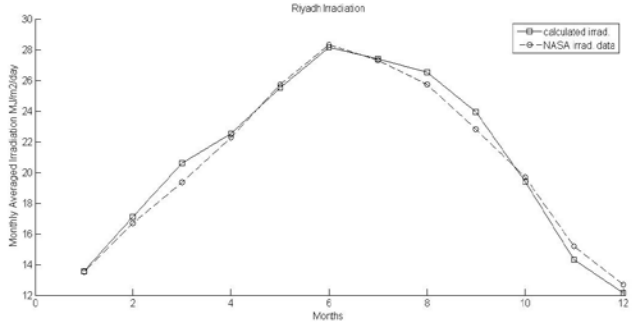

Fig. 3. NASA data and calculated solar irradiation for Saudi Arabia, Riyadh.

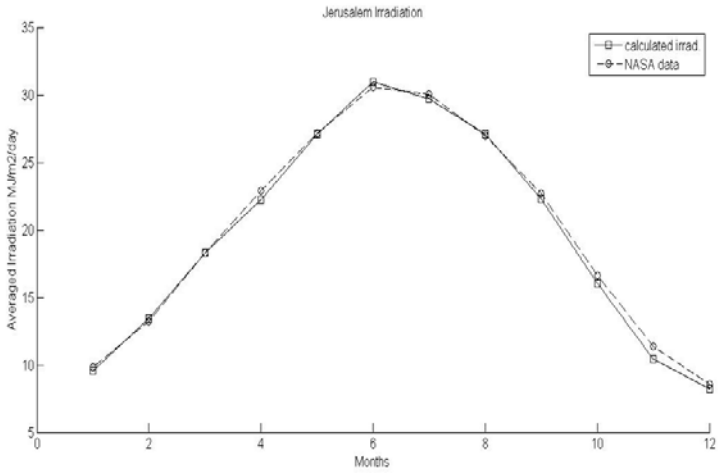

Fig. 4. NASA data and calculated solar irradiation for Jerusalem.

The obtained solar radiation data is used for one-dimensional time-dependent steady state program to predict the solar pond temperature behaviour in the storage zone during a year and an excellent agreement is obtained comparing with real temperature measurements by Ali [13] and this output and measured data are illustrated in Fig. 5.

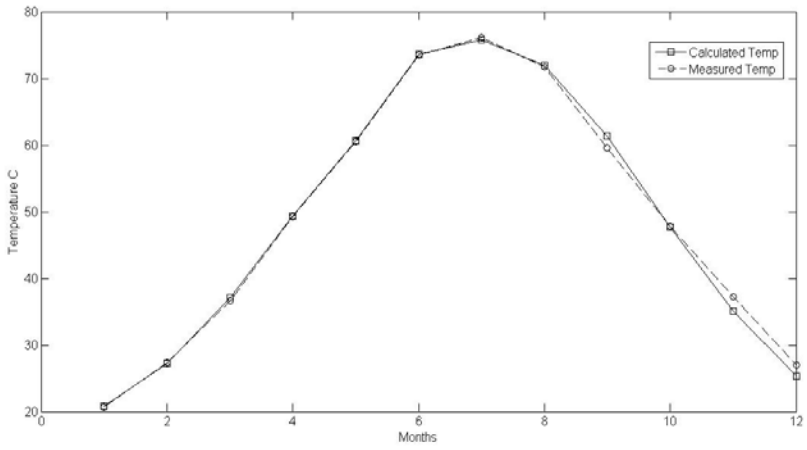

Fig. 5. Measured and calculated storage zone temperature in Kuwait solar pond.

The program can predict the performance of a solar pond in a cold climate location and for this purpose the University of Surrey in the UK has been chosen. The result is plotted in Fig. 6 and the storage zone temperature behaviour can be improved by changing the depth of the solar pond layers to reach 80 ^{o}C .

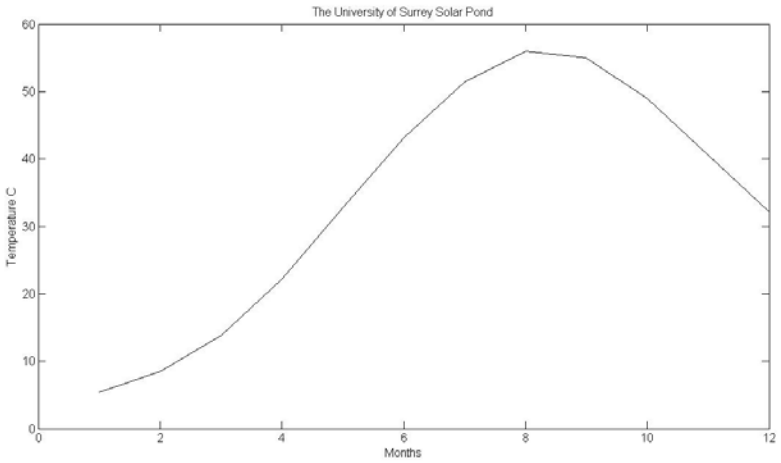

Fig. 6. Surrey storage zone(1m) temperature at 1m depth of gradient zone.

4. Conclusions

The proposed method provides an accurate prediction of the solar radiation based on a single input data which is the location latitude. The predicted results are validated by comparison with NASA 22 years averaged data in three various locations in the Middle East, where very close agreement has been obtained. The one-dimensional time-dependant steady state model has shown excellent agreement with Kuwait solar pond m easurement data. The transient model was investigated as well. However, it was found that the steady state model provided more realistic results. The solar pond performance in cold climate locations such as the UK has been studied and the pond temperature can reach 80 ^{o}C levels using some designs.

References

[1] W. C. Dickinson and P. N. Cheremisinoff, ‘’Solar Energy Technology Handbook’’ Marcel Dekker, New York, (1980) 374.

[2] J. F. Kreider and F. Kreith "Solar Energy Handbook" McGraw-Hill, New York (1981) 10-2

[3] J. A. Duffie, and W. A. Beckman ‘’Solar Engineering of Thermal Processes’’ 3rd Ed. , John Wiley & Sons (2006) 652.

[4] H. M. Lu, A. H. P. Swift, H. D. Hein and J. C. Walton, ‘’Advancements in salinity gradient solar-pond technology based on sixteen years of operational experience’’ J. Sol. EnergyTrans. ASME 126 (2004) 759-767.

[5] J. F. Kreider and F. Kreith ‘’Solar heating and Cooling Active and Passive Design’’ (1982) 284.

[6] NASA’s Website http://www.eoearth.org/article/Solar_radiation

[7] C.G. Abbot ‘’The Solar Constant’’ Solar Energy 9(2) (1965) 166-167.

[8] H. P. Garg ‘’Treatise on Solar Energy’’ V1, John Wiley & Sons (1982).

[9] P. J. Lunde ‘’Solar Thermal Engineering’’ John W New York (1980).

[10] H. Weinberger, ‘’The physics of solar ponds’’, Solar Energy 8 (1964) 45.

[11] A. Rabl and C. E. Nielsen, "Solar Ponds for Space Heating" Solar Energy 17 (1975) 1-12.

[12] C. F.Kooi, ‘’The steady state salt gradient solar pond’’ Solar Energy 23 (1979) 37-45.

[13] H. M. Ali ‘’ Mathematical modeling of salt gradient solar pond performance’’ Energy Research 10 (1986) 377-384.

[14] Y. F. Wang and A. A. Akbarzadeh, ‘’A parametric study on solar ponds’’ Solar Energy 30 (1983) 555-562.

Choice of solar share of a hybrid power plant of a central receiver system and a biogas plant in dependency of the geographical latitude

Spiros Alexopoulos[1,*], Bernhard Hoffschmidt[1], Christoph Rau[1], Johannes Sattler[1]

[1] *Solar-Institut Jülich, University of Applied Sciences Aachen, Jülich,Germany*
** Tel: +49 241600953551, Fax: +49 241600953570, E-mail: alexopoulos@sij.fh-aachen.de*

Abstract: The potential of renewable energies varies significantly from North to South Europe. Southern Europe has a high solar potential and is ideal for the implementation of solar concentrated power plants. To this group of solar thermal power systems belong the solar tower, parabolic trough, solar dish and linear Fresnel systems. North European countries, especially the Scandinavian countries, have a high biomass and hydropower potential. This paper focuses on calculation of the power production for hybrid systems of solar tower with gas turbine in Southern Europe and biogas-only operation in Northern Europe.
The solar tower system consists of a heliostat field, which concentrates direct solar irradiation on an open volumetric central receiver. The receiver heats up ambient air to temperatures of around 700°C. The hot air's heat energy is transferred to a steam Rankine cycle in a heat recovery steam generator (HRSG). The steam drives a steam turbine, which in turn drives a generator for producing electricity. In order to increase the operational hours of a solar tower power plant, a heat storage system and/ or hybridization may be considered.
The advantage of solar-fossil hybrid power plants, compared to solar-only systems, lies in low additional investment costs due to an adaptable solar share and reduced technical and economical risks. On sunny days the hybrid system operates in a solar-only mode with the central receiver and on cloudy days and at night with the gas turbine only. As an alternative to methane gas, environmentally neutral biogas can be used for operating the gas turbine. Hence, the hybrid system is operated to 100% from renewable energy sources.
An advanced software tool library has been developed for modelling such solar hybrid power plants. This library includes the components of the solar-heated hot gas cycle and the steam cycle. Moreover, a choice of different gas turbine and duct burner components is given. When developing a simulation model for the calculation of a small hybrid power plant, components from the library are inserted into the model. The software tool features the possibility of either calculating the energy output of individual operating points or of time intervals in the range of days up to an entire year.
With this simulation tool, hybrid solar tower systems are calculated for various locations with high solar potential within Europe. In addition, locations in North Scandinavian countries with high biomass potential are investigated and power plants with biogas as fuel without solar input are calculated.

Keywords: *solar tower, central receiver, hybridization, biogas, renewable energy*

1. Introduction

The potential of renewable energies varies significantly from North to South Europe. Southern Europe has a high solar potential and is ideal for the implementation of solar concentrated power plants. North European countries, especially the Scandinavian countries, have a high biomass and hydropower potential.

Since 1980s, power production with solar thermal power plants and the increasing use of biogas has been a promising option for reducing the consumption of fossil fuels.

The development of solar thermal technologies has gone into many directions, which can be exemplified with the various heat transfer media that are deployed in existing systems. Many solar thermal power plants contribute to the electricity generation in various European countries. To this group of solar thermal power plants belong the solar tower, parabolic trough, solar dish and linear Fresnel systems. Parabolic trough and solar tower systems are the most developed technologies as well as the most economical solar thermal plants at this moment of time.

A solar tower consists mainly of a heliostat field, a central receiver and a conventional steam Rankine cycle. Various central receiver technologies have been developed throughout the world. The software tool described in this paper models a solar tower with a open volumetric receiver. This type receiver has been deployed in the Solar Tower Jülich (STJ), Germany, since its completion in 2008. The subsequent explanations are valid for this type receiver only. At the STJ, the heliostat field, a field of sun-tracking mirrors, reflects and concentrates the direct solar irradiation onto the open volumetric receiver. This receiver consists of porous ceramic absorber modules. Incident sun rays enter the porous receiver, are absorbed inside and heat it up. To remove the heat, ambient air is continuously sucked through the porous receiver and is heated up to almost 700°C. The hot air is passed through a heat recovery steam generator (HRSG) in which it passes its heat to a water-steam cycle. The steam is expanded in a steam turbine and the rotation of the turbine's shaft drives a generator to produce electricity. Utilization of air as heat transfer fluid (HTF) secures a high plant efficiency due to the reason that air can be heated to very high temperatures, which in turn enables higher steam temperatures in the Rankine cycle and thus a better Carnot efficiency. Moreover, it allows a fast start-up to operating conditions; it is non-toxic and is available at no costs in unlimited amounts.

In order to increase the operational hours of a solar tower power plant, a heat storage system and/ or hybridization e.g. with biofuels must be considered.

As an alternative to methane gas, environmentally neutral biogas can be used as fuel for operating a gas turbine. Hence, the hybrid system is operated to 100% from renewable energy sources. The gas turbine not only delivers electricity but also heat in the waste gas, which can be reused.

2. Methodology

This paper focuses on the calculation of different important characteristic quantities, which include the annular power production, the solar share and the annual fuel consumption. The combination of two renewable technologies, namely biogas and solar concentrated energy, is investigated. Therefore the operation of a hybrid system consisting of a solar tower power plant and biogas-fuelled gas turbine is investigated.

2.1. Considered technologies

2.1.1. Solar tower plant

Germany's first solar tower power plant, which has a rated power output of 1.5 MW_e, was constructed and completed in 2008 in the town of Jülich [1]. It commenced solar operation in spring of 2009. The plant was built by the general contractor Kraftanlagen München and is operated by the local utility Stadtwerke Jülich. The Solar-Institut Jülich (SIJ) and the German Aerospace Center (DLR) conduct the accompanying research. The project is funded by the economic ministries of the German states of Northrhine-Westphalia and Bavaria, as well as by the German Federal Ministry for the Environment, Nature Conservation and Nuclear Safety.

The objective of the power tower project in Jülich is to demonstrate the entire system in commercial-like operation over a longer period of time, to develop control and plant management strategies and to further improve performance and reliability of the key components. Jülich was chosen as the favoured location because it is situated close to the involved research institutions and due to its fluctuating direct solar irradiation conditions. The latter reason has the advantage that it allows and requires the investigation into the system

operation strategy under transient conditions, especially with regard to optimizing the charging and discharging process of the thermal storage [2].

2.1.2. Biogas

Biogas is produced by the biological breakdown of organic matter in the absence of oxygen. It can be produced by anaerobic digestion or the fermentation of biodegradable materials such as biomass, manure or sewage, municipal waste, green waste and energy crops. Biogas is composed of 45-85% methane and 15-45% carbon dioxide, depending on the conditions during production. Moreover, biogas comprises small amounts of hydrogen sulphide, ammonia and nitrogen. Its field of application includes combustion engines, burners as well as gas turbines for electricity generation and co-generation of heat and power. Biogas can be further enhanced from low-quality to natural gas quality before it is fed in the public gas grid. This article considers biogas-fuelled gas turbines only.

2.1.3. Biogas potential

In all Scandinavian countries, biomass has a high potential. In the TRANS-CSP study [3] the theoretical potential of biomass is estimated for Norway at 26 TWh/a, for Sweden at 80 TWh/a and for Finland at 54 TWh/a.

Taking Sweden as an example, the country has approximately 233 biogas facilities with a total biogas production of 1.3 TWh/a [4]. Biogas can be produced at large-scale centralized plants, where different feed stocks materials are digested, and at small farm-based plants, which use and digest mainly agricultural feed stocks.

The theoretical potential of biogas production in Sweden lies at around 14-17 TWh/a, which is more than 10 times that of the present annual production [5]. From the feed stocks materials 70% is manure and farm waste, 13% is industrial waste, 9% is household waste and the remainder is garden waste and sewage sludge.

For Italy, the best biogas performance is recorded in the northern part of the country especially in the regions of Lombardy, Emilia Romagna, Trentino A.A, Veneto and Piedmont. With a share of 23.8%, the region of Lombardy is the biggest producer of biogas in Italy and dominates the biogas market. Moreover, Lombardy has the biggest biogas potential, which is estimated at 4,643 GW. As for the production of biogas from manure, 3,800,000 pigs and 1,600,000 heads of cattle were counted for the region of Lombardy in the ISTAT census in 2001. Together this amounts to 44% of the total domestic animal breed in Italy [6].

2.1.4. Hybrid system

To improve the availability and the capacity factor of a solar tower power plant, a hybridization of the plant is considered. In regions with very high irradiation, solar thermal power plants with heat storage facilities can reach a maximum of 3,000 to 4,000 nominal load hours per year. Hybridization, for example with the combustion of biogas, enables the operator to produce electricity day and night for up to 8,600 hours per year. It is expected that such hybrid power plants will have a high potential for the market introduction in the next decade.

The upgrade of a solar tower power with air receiver technology to a hybrid system by combining it with a gas turbine is shown in Fig. 1.

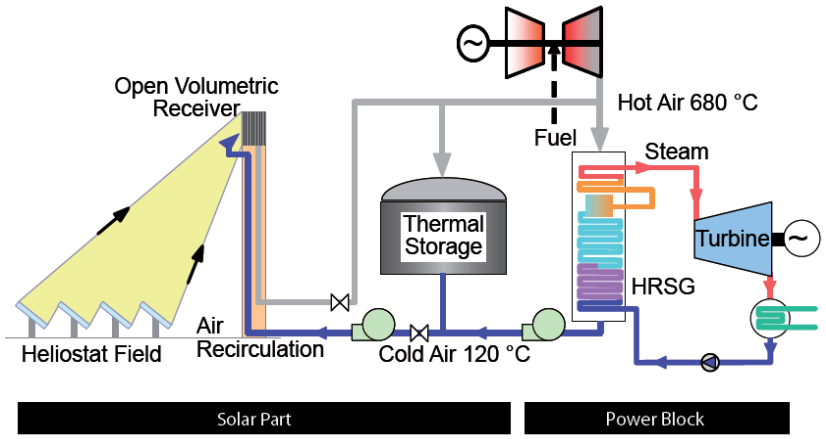

Fig. 1: Schematic diagram of a solar tower demonstration plant hybridised with a gas turbine

The operating strategy for the hybrid plant involves an alternating operation of the gas turbine and the air receiver. On sunny days the air receiver is operated in a solar-only mode. On days with very low direct solar irradiation (very cloudy conditions) the thermal energy provided by the heliostat field is not sufficient for operating the plant. On those days the gas turbine must be operated. The hot exhaust gas from the gas turbine is directed through the heat recovery steam generator (HRSG) for steam generation [7]. Throughout the nights, solely the gas turbine is operated.

2.2. Simulation

2.2.1. Implementation of the model

The implementation of the solar tower power plant model has been realised in the MATLAB/Simulink environment. MATLAB is a high-performance language for technical computing. It integrates computation, visualization, and programming in an easy-to-use environment, where problems and solutions are expressed in familiar mathematical notation. Simulink is a toolbox in MATLAB that provides an environment for modelling, simulating, and analyzing dynamic systems. It supports linear and nonlinear systems, modelled in continuous time or a sampled time. The implementation of systems can also occur at a multi-rate, i.e. have different parts that are sampled or updated at different rates [8].

2.2.2. Model library

The simulation models are based on thermodynamic theory using assumptions for simplification in order to maintain a fast simulation time while retaining good accuracy. Several components like the steam turbine, generator, burner, solar receiver, heliostat field, etc. are included in the model library. They include mostly energy and mass balance equations as well as additional algebraic equations. Most components models are optimized for steady-state operation. However, components with high thermal inertia, such as a part of the HRSG, are implemented as dynamic models.

The model library (Fig. 2) was developed with consideration of the following characteristics [9]:

- compatibility of the components related to the connection of one to the other
- possibility of choosing different geographical locations for performing the calculations
- applicability for different power plant sizes
- adjustability to different transport media: e.g. air, gas, exhaust gas

- ease of modification
- usability for short time intervals (minutes)

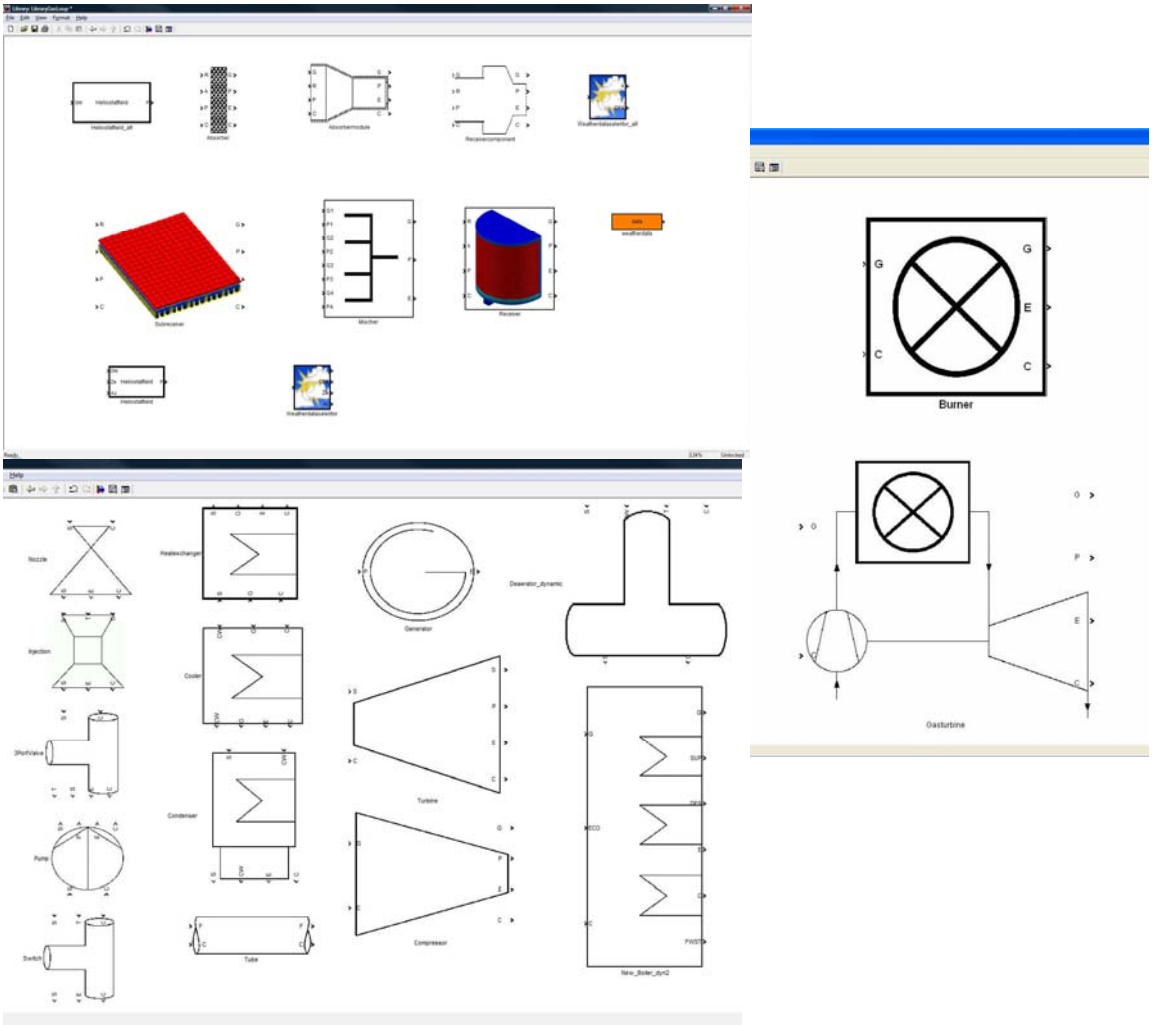

Fig. 2: Model libraries for the steam cycle, the solar and hybridization components

Gas and steam properties can be integrated in each model. The various state variables for water and steam are computed with polynomials taken from the industry standard IAPWS-IF97. For calculating the state variables for different gas mixtures, algorithms stated in the VDI (Verein Deutscher Ingenieure - engl.: Association of German Engineers) guideline 4670 [10] and provided by NASA Technical Memorandum 4513 [11] are integrated.

With the developed software, the annual performance and the electrical power output of small solar hybrid tower plants, combined cycle with gas turbine and solar-only operated solar tower with or without storage can be calculated.

2.2.3. Validation of library components

The components of the model library were validated mainly with calculation results of other simulation software [12]. They were also verified with results from different design points. The three thermodynamic cycles, namely the steam, air and water cooling cycle, were tested separately before they were combined to a complete power plant system.

3. Results

A comparison of energy production and fuel consumption was made for a combined-cycle plant in Sweden and a hybrid solar tower power plant located both in Jülich and North Italy. The combined-cycle plant in Sweden was taken as reference. It operates with a gas turbine, which utilizes biogas as fuel. The selected gas turbine is a Centrax 501-KB3 [13], which generates a nominal power of 2.68 MW_e. The hot exhaust gases are directed through a boiler for steam generation. In the steam cycle, the steam is expanded in a steam turbine. The generator, which is driven by the steam turbine, produces an additional 1.34 MW_e.

For all states and power plants, the biogas is composed of 56% methane, 40% carbon dioxide and other constituents. The configurations and main simulation parameters are shown in Table 1.

Table 1. Main simulation parameters

Place	Scandinavia	Jülich	Northern Italy
Nominal Power GT [MW_e]	2.68	2.68	2.68
Nominal Power ST [MW_e]	1.34	1.50	1.50
Heliostats [-]	0	2,150	2,150
Mirror area [m²]	-	8	8
Maximum air/flue gas temperature [°C]	571	680	680

Original weather data has been used for the locations Jülich and Milano (Italy). For Jülich, data from the year 2007 in a time resolution of 15 min was integrated. For Milano, data of the year 2006 in a one hour resolution has been used. The quasi-steady-state simulations are computed in time steps of maximum 60 seconds. The steam turbine and generator of the steam cycle for both locations have a generation capacity of about 1.5 MW_e. For the hybrid mode, the same gas turbine as simulated for the combined-cycle plant in Sweden (2.68 MW_e) was integrated.

The calculation for the location in Scandinavia (Sweden) was performed for a nominal plant operation with 8,760 hours of gas turbine operation. For the hybrid solar tower power plants, the calculation was realized with alternating operating mode. Hence, in the solar-only mode, nominal parameters could not always be reached. The results presented in Table 2 have an estimated error of about ±10%.

Table 2. Simulation results for the three sites.

Place	Energy Production [GWh]	Fuel Consumption [t]
Scandinavia	35.21	20,385
Jülich	25.17	14,004
Northern Italy	21.30	11,761

The results show that a Conventional Combined Power Plant in Scandinavia generates the estimated energy of 35.21 GWh at a fuel consumption of 20,385 t. The hybrid solar tower power plants instead produce less electrical energy, because only the steam turbine generates energy in daytime. Thus again means, that also less fuel is consumed. The difference between the two locations Jülich and Italy reflects this coherence. Locations with high insolation are associated with the less fuel consumption and less electricity production. This effect occurs if an alternate hybrid operation is considered.

In Fig. 3, which shows a good day regarding solar radiation (DNI), a typical operation of the hybrid plant in alternate mode is illustrated. The specific electrical (index EL) power of the steam turbine resp. gas turbine are shown. Furthermore, the thermal (index TH) power of the receiver (index Rec) and the heat input at the HRSG (index HRSG).

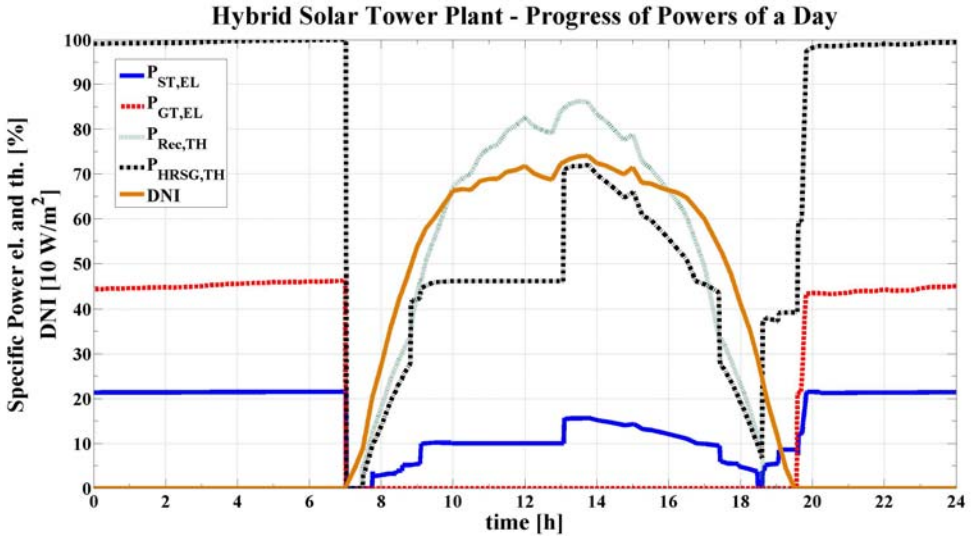

Fig. 3: Hybrid solar power tower plant operation for the 27th March 2007

At night the gas turbine provides continuous electricity and heat to the HRSG, so that a combined-cycle operation is conducted. When solar irradiation increases the gas turbine is shut down. Because of the clear switch to solar operation the electricity generation by the steam turbine may diminish. When solar radiation increases the electricity production increases, too. At a certain stage, by the receiver produced heat is send to the storage. The heat input to the HRSG is kept constant. When the storage is charged to a certain level, the charging is terminated and the full heat input is provided by the receiver (cf. fig 3. Jump at 13 h). When the sunset starts the storage is discharged slowly and the heat for the HRSG is supplied by the storage. In the evening the shift from storage operation to gas turbine operation is executed. This demonstrated operation strategy needs still optimization to ensure a maximum yield of power production and a continuous operation. Therefore weather dependent operation strategies and controlling has to be developed.

4. Discussion and Conclusions

Numerical procedures should be applied for the calculation of the annual energy yield of solar tower power plants. With the simulation tool, hybrid solar towers at different locations with high solar potential in Europe are calculated. Moreover, locations with high biogas potential in North Scandinavian countries are considered and power plants with biogas as fuel without solar input are investigated. The results of the simulation analysis show that the created model library is a solid basis for the simulation of hybrid concepts for solar tower systems.

In next steps a detailed investigation and analysis of the simulation results is planed. The simulation models and especially the operation strategies will be optimized in order to get even more accurate results.

In further steps an additional site in South Europe, for example in South Italy on the island of Sicily, will be investigated. For that reason weather data will be selected and a solar-only operation of a solar tower power plant will be regarded.

Acknowledgments

The authors gratefully acknowledge the financial support of the German Federal Ministry for the Environment, Nature Conservation and Nuclear Safety (BMU), the ministries of economic affairs of the German states of North Rhine-Westphalia (NRW) and Bavaria in the solar tower demonstration project. The research into hybridization is supported by the German Federal Ministry of Education and Research (BMBF).

References

[1] K. Hennecke, P. Schwarzbözl, S. Alexopoulos, J. Göttsche, B. Hoffschmidt, M. Beuter, G. Koll, T. Hartz: SOLAR POWER TOWER JÜLICH The first test and demonstration plant for open volumetric receiver technology in Germany, Proceedings of the 14th Biennial CSP SolarPACES Symposium, Las Vegas, Nevada, 4-7 March 2008, London.

[2] Alexopoulos, S., Goettsche, J., Hoffschmidt, B., Rau, C., Sattler, J., Schmitz, M., Warerkar, Sh., Hennecke, K., Schwarzboezl, P., Beuter, M., Koll, G., Hartz Th. (2009): SOLAR TOWER POWER PLANT JUELICH First experience with an open volumetric receiver plant and presentation of future enhancements, Proceedings Renewable Energy World Europe Conference, Cologne, Germany.

[3] Trans-Mediterranean Interconnection for Concentrating Solar Power, DLR, 2006

[4] Swedish energy agency. Production and use of biogas, 2005.

[5] Lantz, M., Svensson, M., Björnsson, L., Börjesson, P.: The prospects for an expansion of biogas systems in Sweden: Incentives, barriers and potential, Energy policy, 35:1830-1843, 2007

[6] Ceriani, A.: "Le energie alternative e rinnovabili in Lombardia nell'ambito delle attività produttive", Instituto Regionale di Ricerca Della Lombardia, Milan, January, 2010

[7] S. Alexopoulos, B. Hoffschmidt, C. Rau, P. Schwarzbözl: Simulation results for a hybridization concept of a small solar tower power plant, SolarPACES Symposium, Berlin, 15-18 September 2009

[8] MATLAB/Simulink Manual, http://www.mathworks.com, 2010

[9] S. Alexopoulos, B. Hoffschmidt, C. Rau, M. Schmitz, P. Schwarzbözl, S. Pomp: Simulation results for a hybridised operation of a gas turbine or a burner for a small solar tower power plant, SolarPACES Symposium, Perpignan, France, 21-24 September 2010

[10] McBride, B. J., Gordon, S., Reno, M. A.: Coefficients for calculating thermodynamic and transport properties of individual species, Nasa Technical Memorandum 4513, 1993

[11] VDI: Thermodynamische Stoffwerte von feuchter Luft und Verbrennungsgasen - VDI 4670, 2003

[12] S. Alexopoulos, B. Hoffschmidt, J. Göttsche, C. Rau, P. Schwarzbözl: First simulation results for the hybridization of small solar power tower plants, 1st International Conference on Solar Heating, Cooling and Buildings, Lisboa, Portugal, 7-10 October 2008

[13] ASUE - Arbeitsgemeinschaft für sparsamen und umweltfreundlichen Energieverbrauch E.V.: Gasturbinen-Kenndaten-Referenzen, 2006

Building-integrated Solar Collector (BISC)

Bin-Juine Huang [1,*], Yu-Hsing Lin[1], Wei-Zhe Ton[1], Tung-Fu Hou[1], Yi-Hung Chuang[1]

[1] *New Energy Center, Department of Mechanical Engineering National Taiwan University, Taipei, Taiwan*
** Corresponding author. Tel: +886 2 2363-6576, Fax: +886 2 2363-6576, E-mail: bjhuang@seed.net.tw*

Abstract: The present study intends to develop building-integrated solar collector (BISC). The storage tank inside is designed in multi-function. BISC combines the solar collector and the water storage tank together with one face acting as the solar absorber. A double-glazing design is adopted to reduce the heat loss. A PC-based automatic operating system is designed and built to monitor the long-term performance of the BISC system with 8 collector units. Hot water discharge is controlled from 18:00 until 22:00 to simulate the hot water load of a family. The discharge rate is at 60 L/hr. A 30 L backup electric water heater was connected to the BISC system. The long-term test results in winter season show that about 50 % energy saving was achieved in clear days. The monitored results have also shown that the daily-total solar irradiation on a 75° tilted surface (the BISC installed angle) is higher than the horizontal surface, about 40-50 % higher at Ht > 10 MJ/m^2day. This assures that BISC will produce more hot water in winter. This proves that the use of BISC as parapet or sun-shading canopy of a building (installation angle > 75°) is technically feasible. The characteristic efficiency of the installed BISC with different colors is 0.34-0.39.

Keywords: *Solar thermal, Building-integrated collector, Solar collector.*

Nomenclature

η	*the daily-total thermal efficiency of BISC*	η_{dc}	*the heat removal efficiency*
η^*	*the characteristic daily thermal efficiency of BISC*	τ_f	*spent time when heat removal*
α_o	*solar collecting efficiency (when T_i=T_a)*	m_e	*the heat removal flow rate*
U_s	*the heat loss coefficient*	C_p	*specific heat of water*
T_i	*initial temperature when collect heat*	T_e	*water outlet temperature*
T_a	*average ambient temperature*	T_{wi}	*water inlet temperature*
H_T	*the daily-total solar irradiation*	M_t	*total mass of water storage*
		T_{intial}	*initial temperature of water storage tank*

1. Introduction

The solar building involves advanced solar collector technology for heating and hot water supply. Our research intends to develop a building-integrated solar collector (BISC) as parapet or sun-shading canopy of a building, Figure 1.1. BISC has a dual function of solar utilization and building constructing material, which can greatly reduce the cost.

As part of the building constructing material, the design of BISC needs to consider the thermal performance, the mechanical strength, installation method on building, and outlook. We focus on the research of the thermal performance including heat utilization efficiency of hot water and the heat insulation of the front side.

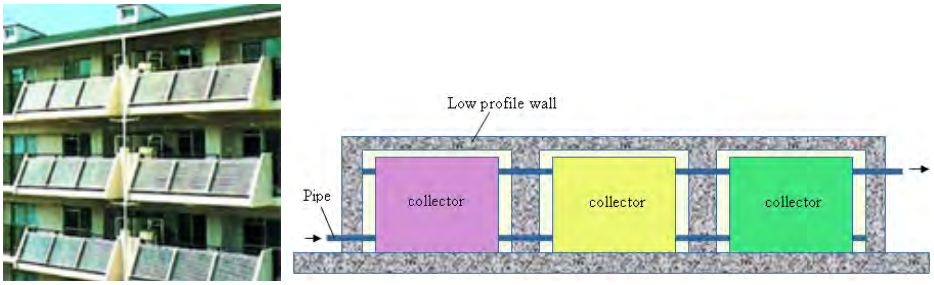

Fig. 1.1 BISC for parapet or sun canopy of a building

We have developed the first generation product of BISC. The special design features of BISC include:

1) Color glass cover: BISC uses the color glass cover in order to be compatible with building. It will match the architecture appearance by choosing the glass color.
2) Modular design: The solar water heater is designed as a module and easy to install. It only needs to fix on the wall or the ground and connect the water supply lines.
3) Multi-function water storage tank: The BISC combines the solar collector and the water storage tank together. It combines the solar collector and the water storage tank together. One surface of the water storage tank is the solar absorber which absorbs solar energy and directly conducts to the water inside the storage tank.
4) Double air-layer insulation: The BISC has a double-layer insulation, with two air gaps in front of the collector. This can reduce the heat loss.

2. Methodology

Design of BISC

The design specification of the BISC unit is as follows:

- outside dimension: 100cm x 70cm x 20cm
- solar absorber dimension: 90cm x 60cm
- storage tank: 90cm x 60cm x 7.5cm
- water storage: 40 liter
- glazing: 2 layers, 4mm color glass + 6mm PC
- glass color: clear, ocean blue, French green
- front double air layer insulation: 3cm/3cm
- heat exchanger: PC 6mm, 60cm x 90cm, 3 rows, 3.2m^2

There were 8 units of BISC were installed in the building for demonstration and field test. Figure 2.1 is the 3D drawings of BISC. Figure 2.2 is the real BISC. Figure 2.3 is the building installation of BISC.

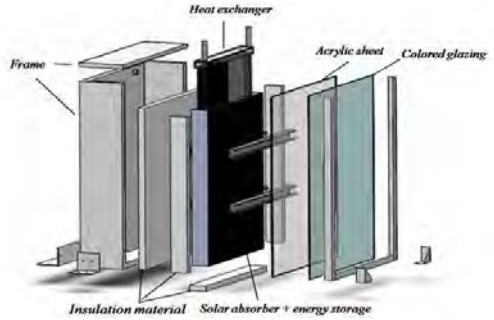

Fig. 2.1 3D drawings of BISC.

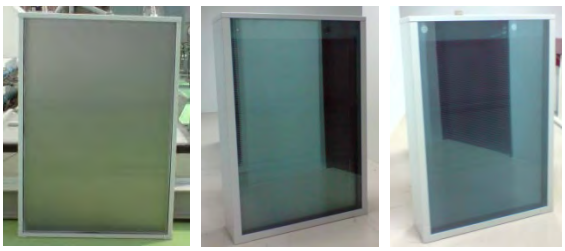

Fig.2.2 Color glass: clear, green, blue.

Equations (1) and (2) are used to determine the daily-total thermal efficiency of BISC (equation 1) and heat removal efficiency (equation 2):

$$\eta=\alpha_o - U_s \frac{T_i - T_a}{H_T} \quad (1)$$

$$\eta_{dc}=\frac{\int_0^{\tau_f} m_e C_p [T_e(t) - T_{Wi}]dt}{M_t C_p (T_{inital} - T_{Wi})} \quad (2)$$

The heat removal efficiency η_{dc} is defined as the ratio of the withdraw of total amount of useful heat compared to the total heat stored at sunset. Testing equipment for the measurement of daily-total thermal efficiency of BISC was designed and built in the research.

The equipment setups are shown in Figure 2.4. This testing equipment is automatic from early in the morning to sunset.

Design of a BISC system for a family

Figure 2.5 is the BISC system design to supply hot water for a family.

Fig. 2.3 BISC installation

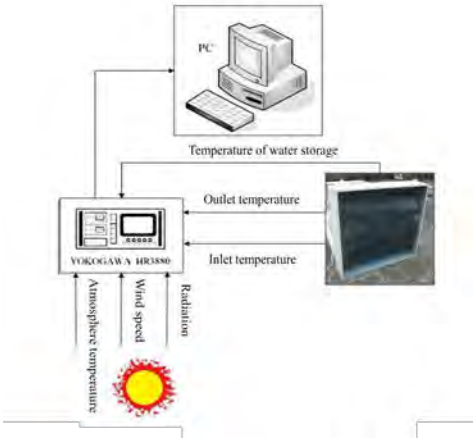

Fig. 2.4 BISC test equipments

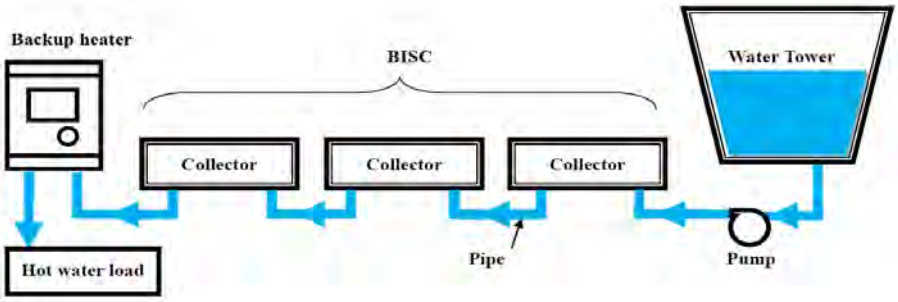

Fig. 2.5 BISC system.

Design of BISC system automatic monitoring system

A PC-based automatic operating and control system is designed and built to monitor the long-term performance of the BISC system built in the research. The operating system (Figure 2.6) monitors the instantaneous performance of the BISC system all day. Hot water discharge is controlled from 18:00 to simulate the hot water load of a family. The discharge rate is 30 L at every 15 minutes with 15 minutes stop after each discharge until 22:00. That is, the discharge rate is at 60 L/hr. A 30 L backup electric water heater was connected to the BISC system. The temperature setting of the backup heater is 55 ^{o}C.

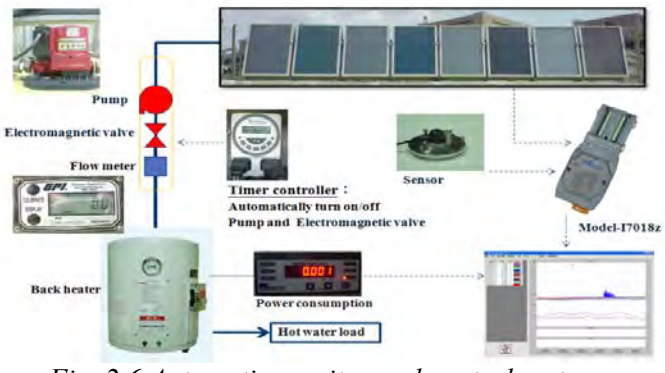

Fig. 2.6 Automatic monitor and control system

Figure 2.7 shows the water outlet temperature from BISC system. Figure 2.8 shows the electric consumption of the backup water heater. Figure 2.9 shows the daily performance pattern.

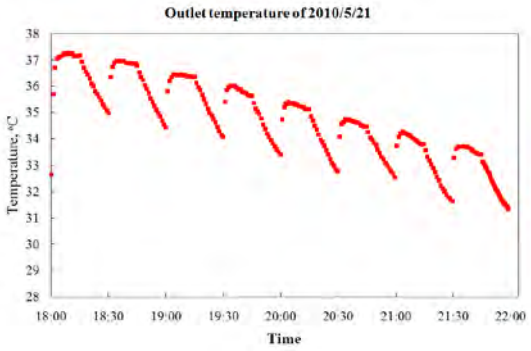

Fig. 2.7 BISC system outlet temperature

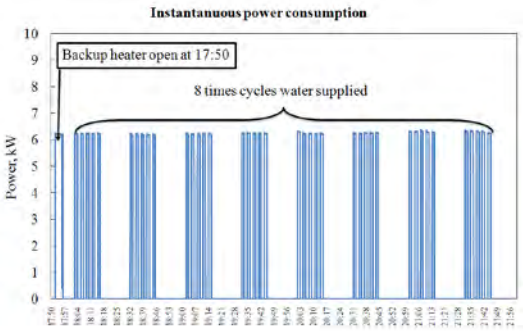

Fig. 2.8 Backup heater power consumption

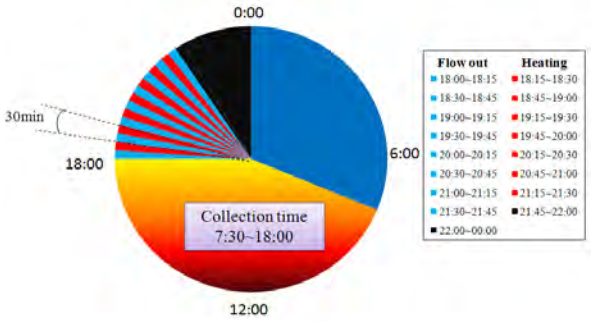

Fig. 2.9 Daily operation of BISC system.

3. Results

3.1. Measurement of daily thermal performance of BISC installed in building

Daily-total thermal efficiency test at 75° tilt

The data collected from the BISC system installed in building can be used to analyze the thermal performance of BICS at the installed tilt angle (75°), using the testing standard CNS B7277 developed by Huang [1-5]. The daily-total thermal efficiency tests were performed for BISC installed at 75° tilted angle with different color glazing, all facing south.

The daily-total efficiency is calculated using the measurement of daily-total energy stored in the storage tank and the total solar irradiation. Figure 3.1-1~Figure 3.1-5 and Table 3.1-1 present the daily-total thermal efficiency of BISC. The test results show that the characteristic efficiency of BISC with different colors which are installed in building with 75° tilt angle is 0.34-0.39 which is lower than the conventional solar water heater (0.50) with clear glass and tilted at lower angle (25°).

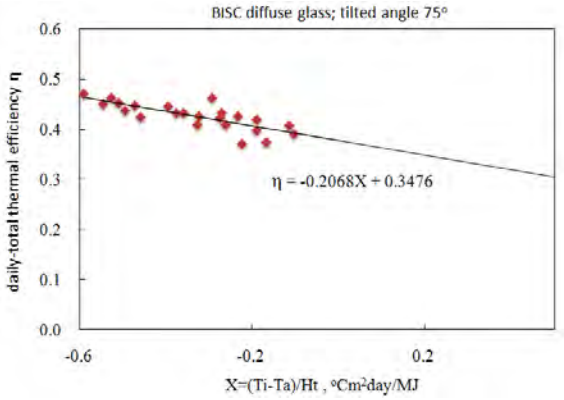

Fig. 3.1-1 Daily-total efficiency of BISC (diffuse glass).

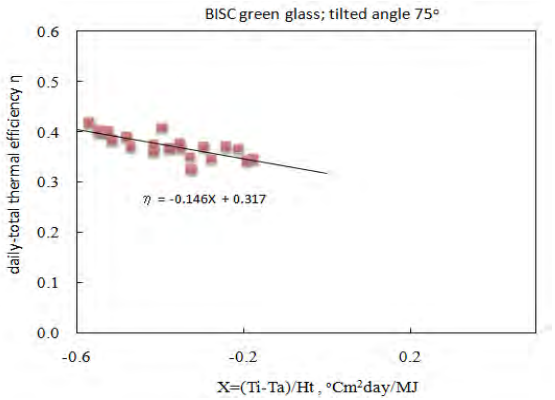

Fig. 3.1-2 Daily-total efficiency of BISC (green glass).

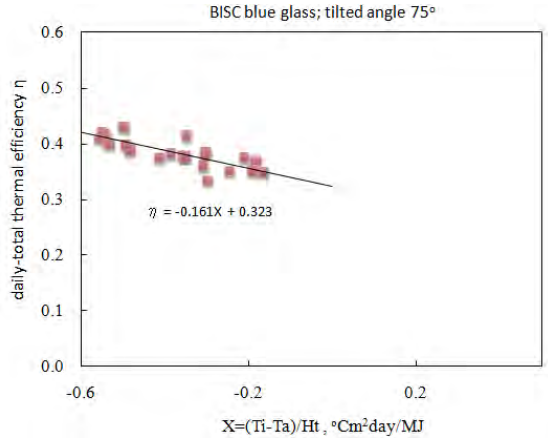

Fig. 3.1-3 Daily-total efficiency of BISC (blue glass).

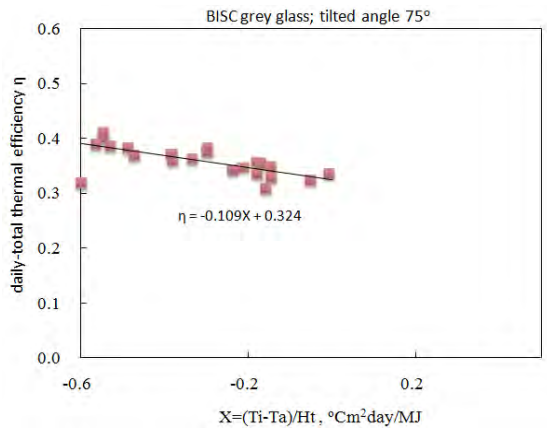

Fig. 3.1-4 Daily-total efficiency of BISC (grey glass).

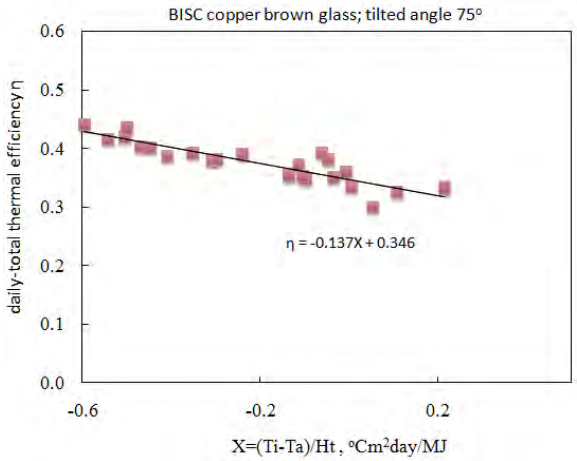

Fig. 3.1-5 Daily-total efficiency of BISC (brown glass).

Table 3.1-1 Test results of daily-total efficiency of BISC.

BISC facing South	U_s	α_o	η^*
Diffuse glass, tilted 75°	0.207	0.348	0.39
Green glass, tilted 75°	0.147	0.318	0.35
Blue glass, tilted 75°	0.161	0.323	0.35
Grey glass, tilted 75°	0.109	0.325	0.34
Copper-brown glass, tilted 75°	0.137	0.346	0.36

3.2. Long-term thermal performance test of BISC

The BISC system installed in building is tested by simulating the daily operation for a family. To estimate the energy saving of the backup electric heater, a baseline test was carried out to measure the daily energy consumption of the electric heater without using BISC. At daily solar irradiation 0.62 MJ/m^2 which is assumed as no s olar radiation (rainy, the daily electricity consumption is 11.1 k Wh. At daily solar irradiation 21.7 MJ/m^2 (the best weather), the daily electricity consumption is 4.0 kWh.

The first long-term performance monitoring is in winter season. Figure 3.2-1 shows the long-term monitoring results of BISC. It is shown that BISC can save 40 % to 50 % of electricity per day in winter. Figure 3.2-2 shows the variation of daily energy consumption and collected water temperature with solar irradiation in winter season. In spring season, the test results are shown in Figure 3.2-3 and Figure 3.2-4.

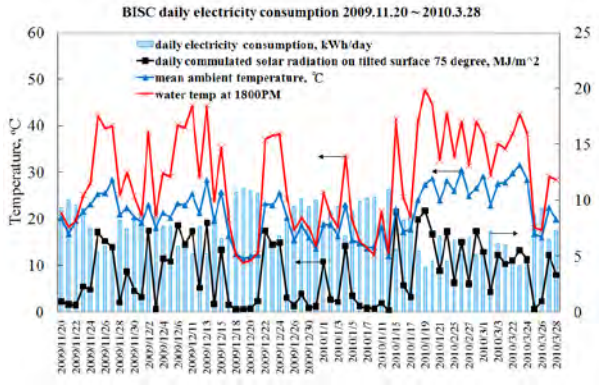

Fig. 3.2-1 Long-term monitoring results of BISC at Taipei 2009.11.20~2010.3.28.

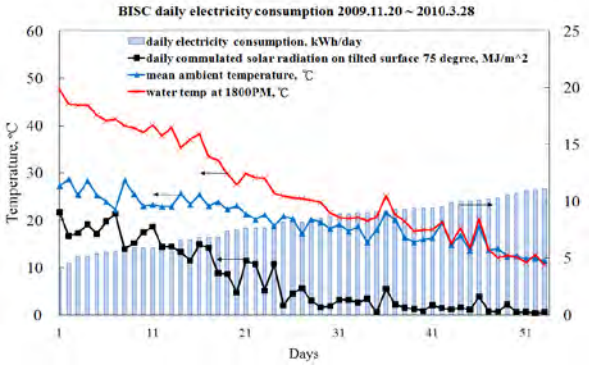

Fig. 3.2-2 Variation of daily energy consumption and collected water temperature with solar irradiation at Taipei 200911.20~2010.3.28

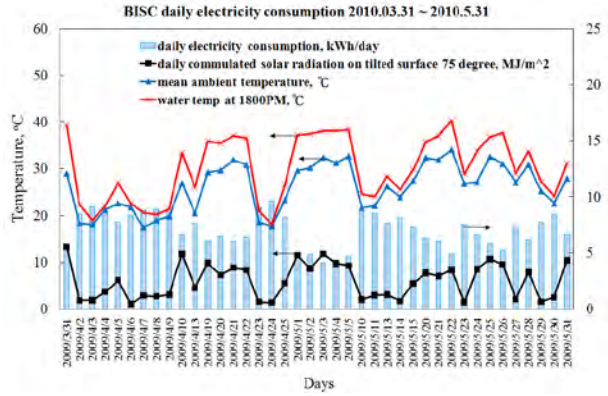

Fig. 3.2-3 Long-term monitoring results of BISC at Taipei 2010.3.31~2010.5.31

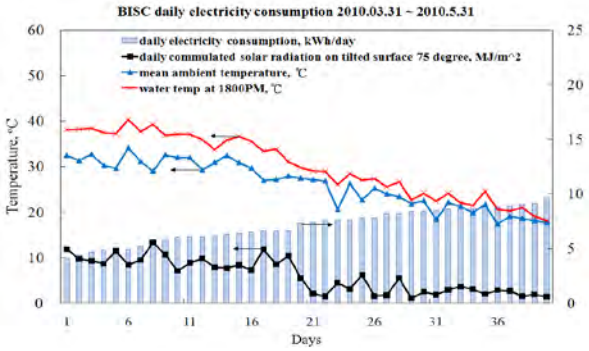

Fig. 3.2-4 Variation of daily energy consumption and collected water temperature with solar irradiation at Taipei 2010.3.31~2010.5.31

Figure 3.2-5 and Figure 3.2-6 shows the variation of daily-total solar irradiation on 75° and horizontal surfaces. The monitored results have also shown that the daily-total solar irradiation on a 75° tilted surface (the BISC installed angle in building) is higher than the horizontal surface, about 40-50 % higher at Ht>10 MJ/m^2day. This verifies that the use of BISC for parapet or sun-shading canopy of a building (installation angle > 75°) is feasible. In summer, it is expected that the solar irradiation on 75° surface will be less than the horizontal one and the heat collection efficiency will be lower. However, the hot water load in summer decreases about 50 % in summer. Therefore, the use of BISC as parapet or sun-shading canopy of a building is feasible.

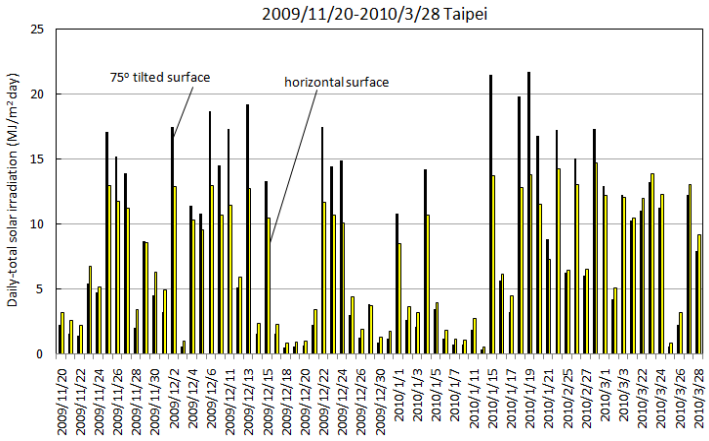

Fig. 3.2-5 Variation of daily-total solar irradiation 75° and horizontal surfaces.

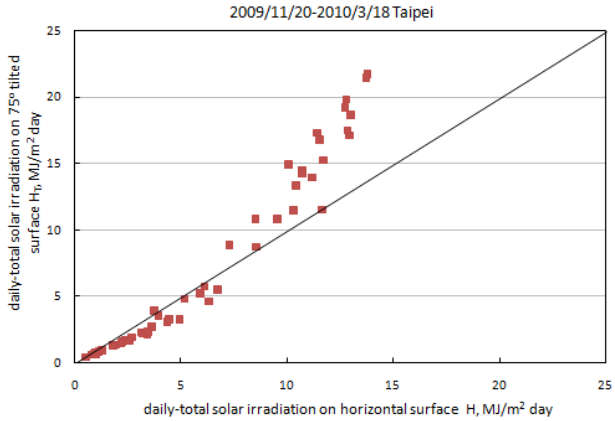

Fig. 3.2-6 Variation of daily-total solar irradiation on 75° and horizontal surfaces.

3.3. Heat removal efficiency test

The heat removal efficiency test is carried out to determine how much energy can be extracted from the tank rated at the total water extraction identical with the storage volume. With the Figure 3.4-1 By the equation (2), we can see the numerator is the real instantaneous removal heat (similar a trapezoid area), and the denominator is the total storage heat (rectangle area), then the heat removal efficiency calculate about 0.72.

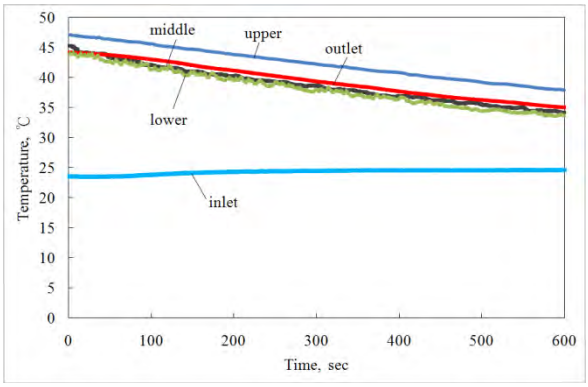

Fig. 3.4-1 Heat removal efficiency test.

4. Discussion and Conclusions

Our research intends to develop building-integrated solar collector (BISC). The BISC is designed to be part of construction material of a building. The storage tank inside is designed

in multi-function. BISC combines the solar collector and the water storage tank together with one face acting as the solar absorber which absorbs solar energy and directly conducts to the water inside the storage tank. A double-glazing design is adopted to reduce the heat loss. The outer transparent cover (glass) is made of color glass for architecture requirement. 8 units were installed on the roof of the lab at the Innovation and Incubation Center of NTU for field demonstration and test.

A PC-based automatic operating and control system is designed and built to monitor the long-term performance of the BISC system installed in the research. The system monitors the instantaneous performance of the BISC system all days. Hot water discharge is controlled from 18:00 to simulate the hot water load of a family. The discharge rate is 30 L at every 15 minutes with 15 minutes stop after each discharge until 22:00. That is, the discharge rate is at 60 L/hr. A 30 L backup electric water heater was connected to the BISC system. The temperature setting of the backup heater is at 55 ℃ which is fixed. The long-term test results in winter season show that about 50 % energy saving was achieved in clear days. The monitored results have also shown that the daily-total solar irradiation on a 75° tilted surface (the BISC installed angle in building) is higher than the horizontal surface, about 40-50 % higher at Ht>10 MJ/m^2day. This assures that BISC will produce more hot water in winter. This proves that the use of BISC as parapet or sun-shading canopy of a building (installation angle > 75°) is technically feasible. The test results show that the characteristic efficiency of BISC with different colors which are installed in building with 75° tilt angle is 0.34-0.39, lower than the conventional solar water heater (0.50).

The monitoring of long-term performance will be continued to find out the defects and efficiency of the system. Since BISC is part of the building, it needs a BISC with high quality in art design, high thermal performance, good manufacturing technique, and long service life (reliability). The reliability issue will be the focus of forthcoming research.

Acknowledgment

This publication is based on work supported by Award No. KUK-C1-014-12, made by King Abdullah University of Science and Technology (KAUST), Saudi Arabia

References

[1] B. J. Huang and S. C. Du, ”A performance test method of solar thermosyphon system”, ASME Journal of Solar Energy Engineering, Vol.113, pp.172-179.(1991)

[2] Test Standard CNS B7277, Method of Test for Solar Water Heater System, 1988. Taiwan.

[3] B. J. Huang, ”Performance rating method of thermosyphon solar water heaters”. Solar Energy, Vol.50, No5, pp.435-440.(1993).

[4] J. M. Chang, “A Proposed Modified Efficiency for Thermosyphon Solar Heating Systems”, Solar Energy, Vol. 76, No. 6, pp.693-701. (2004)

[5] J. M. Chang,”A Criterion Study of Solar Irradiation Patterns for the Peroformance Testing of Thermosyphon Solar Water Heaters,” Solar Energy, Vol. 73, No. 4, pp.287-292.(2002)

[6] B. J. Huang,”Development of Long-Term Performance Correlation for Solar Thermosyphon Water Heater”. ASME Journal of Solar Energy Engineering, Vol.111, pp.124-131. (May 1989)

Passive solar design in schools for the protection of the environment Greece: a case study

Agisilaos Economou[1,*]

[1] *National Technical University of Athens, Athens, Greece*
** Corresponding author. Tel: +03 9345386, Fax: +039345386, E-mail: aghs@mail.ntua.gr*

Abstract: The survey focuses on the passive solar schools units that have been built to date in Greece. It investigates on the one hand the bioclimatic principles applied to several school units with regard both to the building shell and the layout of the schoolyard area, and on the other hand the energy saving schemes that have been introduced to reduce energy consumption. This investigation is followed by a comparison with conventional schools in order to assess the economic and environmental benefits that the implementation of passive solar design bring to Greek schools.
The present survey relies on statistical data collected from passive solar design and conventional school buildings taking into account, among others, energy consumption, school building plots and implemented bioclimatic principles. Furthermore, in order to collect information about various issues and the cost of these new school units, the survey relies on personal interviews with staff members of the School Building Organization which is responsible for the construction of these schools.
The survey has shown that passive solar design used in the building of schools in conjunction with the installation of electronic control equipment to reduce consumption and the use of renewable energy, achieves a larger degree of environmental protection.

Keywords: *Passive solar design in schools, Save energy.*

1. Introduction

In Greece, school buildings, according to past interventions for energy saving and protection are divided into neoclassical buildings of the interwar period until 1950, school buildings built prior to the application of the General Building Rules (GBR)(1950-1980), school buildings constructed under the new implementation of the (GBR) (1979) [1] until 1998 when new measures were taken and terms were set to improve energy efficiency of buildings [2]. After Directive 2002/91/EC [3] of the European Union for the energy performance of buildings new measures were taken to reduce energy consumption in buildings, more specifically law 3661 [4], the Regulation of Energy Efficiency of Buildings [5] and law 3855 [6] in accordance with the directives of the European Union for energy saving.

Initially, the proposals for interventions in school buildings (from 1950 to 1980) refer to the closure of open corridors, to the insulation of the roof, replacement of window and door frames, the addition of RES, ventilation cooling and shading. Thermal bridges reduction was added to school buildings from 1980 to 1998 [7]. The bioclimatic design in school buildings was implemented on a pilot basis. Generally, the measures applied were thermal insulation, green roofs, and minimization of northern openings exposure during the winter,. On the other hand, during the summer, the measures applied were the minimization of western openings, shading and cross ventilation. Other passive systems such as solar atriums, skylights, cooling chimneys and soil pipes, were implemented [8].

Take into account that most schools have been built before the year 2000, it is shown that heat losses are much larger than those of school buildings constructed after 2000, which have implemented more stringent requirements for insulation and appropriate choice of materials.

Especially from 2007 and onwards, all schools in Greece are built in accordance with the principles of bioclimatic design related to both the architectural design and the choice of

location of the school. Also the extension of bioclimatic design in courtyards contributes more to the improvement of environmental conditions in schools and the better use of space and climate conditions.

In addition, the pilot application for the introduction of technology on energy saving systems in schools such as BMS systems, opens new horizons in energy saving.

Generally, the new design of schools, taking into account the bioclimatic principles both in the building shell and in the exterior space as well as energy-saving technologies in conjunction with the strictest standards for heat insulation, will contribute to good weather conditions with the minimum of energy consumption. The degree to which this new way of designing schools unit contributes to energy saving, will be analyzed below.

We note that the new standards for energy conservation should not be in conflict with bioclimatic design principles, but to complement them.

2. Methodology

First a reference to the policies implemented so far for the construction of schools in Greece is made. Next, the survey compares the fuel consumption between conventional schools and new schools with passive systems. Taking into account the thermal and climatic conditions in the region, the implementation or not of bioclimatic principles, an effort to estimate to which degree the use of passive solar systems can contribute to saving energy and protect the environment is made.

Thus, statistical data on the area and fuel consumption in selected schools are used in the survey. Also, the survey was supplemented with new data on the current policy for the construction of schools units. This information have been obtained through personal interviews of the directors of the School Building Organization, which is responsible for the construction of schools in Greece. The creation of maps is achieved by using data from Geographic Information Systems (GIS).

3. Results

The survey focused on schools units which are built according to the principles of bioclimatic design, as well as on conventional schools. Specifically, the research focused on the energy consumption for heating, taking into account the thermal, climatic conditions in the area and the buildings were designed.

From a survey made to the staff of the School Building Organization which are responsible for the construction of schools in Greece it is found that:

- Nowadays, the lack of suitable land in areas with increased urbanization, creates problems in the design of schools according to the principles of bioclimatic design.
- The old schools units need both maintenance and upgrading of heat insulation and sun protection.
- All schools built since 2007, and onwards follow the bioclimatic design principles, taking into account the location and orientation of the building. Techniques for sun protection, natural lighting, shading, natural ventilation (ventilation, traction phenomenon, solar chimney and cooling tower) and thermal insulation are applied. Green materials, wooden structures as well as green roofs and high planting are used (Fig. 1).
- Introduction of new insulating materials and automation programs for saving energy.

- Expansion of the use of natural gas in schools units in order to save energy and reduce emission of pollutants.
- Exploitation of strong sunlight via the use of photovoltaic systems. Due to good weather conditions and sunshine, in Greece, the design of school buildings different from those of northern European Union countries with different climatic conditions.
- Introduction of geothermal energy for heating and cooling in special school units, which are constructed for children with special needs, requiring greater energy consumption.
- Introduction of the new regulation on the energy performance of buildings in school buildings in order to obtain an energy building certification.

3.1. Schools units in Greece

New passive solar building constructed from 2007 onwards in Greece are presented in the following map (Fig. 1).

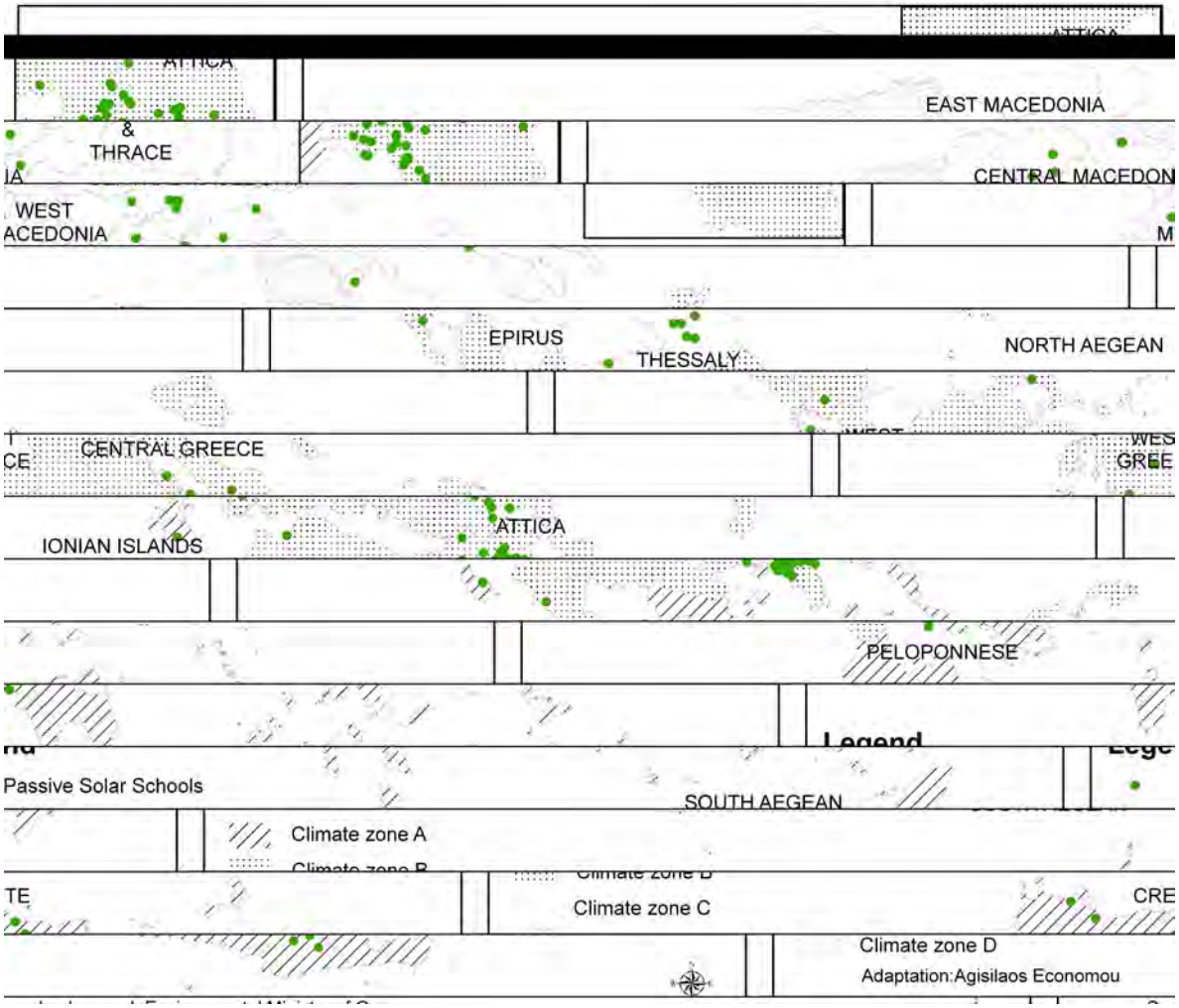

Fig. 1. Passive solar schools in Greece from 2007 up-today.

3.2. Schools units in Athens

As conventional schools, schools in Athens which are listed in the table below have been selected (Fig. 2), (Table 1). On the other hand, from the new modern schools the 6th Nursery school in Paleo Faliro, which is the first school designed with passive systems was selected. It features specific provisions for sun protection, shading, ventilation with carbon dioxide sensors to upgrade and clean the air, greenhouse and two green roofs.Also, it has lighting

control systems which take into account the sunshine outside and for heating, natural gas is used. Also a photovoltaic systems has been installed on the school for electricity production.

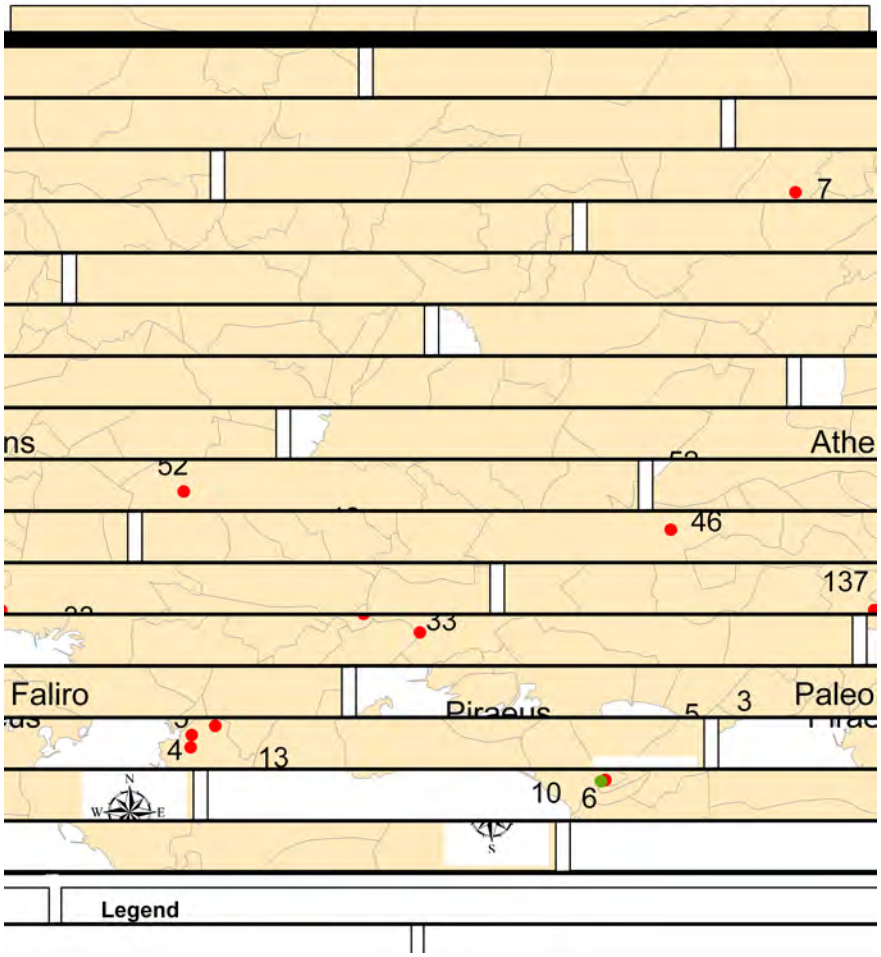

Fig. 2.Schools units in Athens

The survey found that in conventional school units there are different levels of consumption, depending on heat insulation and on the time period during which the boiler is operating for heating purposes.

In contrast in the 6st nursery school of Paleo Faliro (passive solar) a significant decrease in fuel consumption, compared to other schools in the same period was found.

Similar reductions were made to other schools in the past. For example, in the school unit of A. Kapon in Andros in 1989, which has an area of 513.5 m^2 with Tromble walls and 10 cm polystyrene insulation, the consumption was 12.36 Kwh/m^2. While in the school unit of I. Kalligeris in Rethymno in 1987, which has an area of 893.7m^2, through the use of greenhouses and shading, the consumption was at 6.73 Kwh/m^2.[8]. In other school units systems for solar gain, solar terraces, double glazing and others have been implemented.

Table 1. Use of natural gas for heating in school units in Athens during the period time 9/2009-8/2010 [9,10]

Schools units	**Year of construction**	**Total floor area (m^2)**	**Total volume of building**	**Consumption of natural gas (Kwh)**	**(Kwh/ m^2)**
46 High School of Athens	1917	2698.00	9421.00	70990.85	26.31
52 High School of Athens	1970	2714.45	9734.35	50091.29	18.45
7 Secondary of Metamorfosi	1980	1244.00	4552.00	62691.07	50.39
33 High School of Athens	1984	2451.07	12429.12	42235.80	17.23
5 High School of Paleo Faliro	1986	3835.80	7448.85	42012.18	10.95
13 Secondary of Paleo Faliro	1992	1896.24	7600.00	48663.39	25.66
3 Nursery of Paleo Faliro	1993	210.50	800.00	5444.56	25.86
137 Secondary of Athens	1993	1626.00	5962.00	36700.86	22.57
10 Secondary of Paleo Faliro	1995	1700.00	6652.00	38724.61	22.77
4 High School of Paleo Faliro	2000	3835.80	7448.85	21728.73	5.66
6 Nursery of Paleo Faliro	2005	600.20	2640.90	3063.00	5.10

Also, the use of natural gas in the schools units has further reduced the emissions of CO_2 in contrast to oil (Table 2)

Emission of CO_2, natural gas 0.20 kg/kWh, diesel fuel oil 0.26 kg/kWh) [11]

4. Discussion

Fuel consumption for heating of school grounds, varies depending on:

The climatic conditions of each region: Based on heating degree days and altitude, we have four climatic zones. From the hottest to the coolest (Fig. 1).

Heating time: The duration of the heating season ranged from 60 days to the region of Crete and reaches 210 days in the areas of Macedonia and Thrace [5].

Heat insulation: The heat insulation of buildings and the way of construction such as the orientation of the building, insulation of walls, floors and roofs, thermal insulation materials used and the use of openings.

Also, many schools and big complexes are attached to the operation of one boiler, which means that the above operation of a school or a department requires the operation of the boiler for more time as a result of which school units are heated unnecessarily.

Nowadays, in conventional schools interventions are made in order to increase the insulation during the winter and to ensure sun protection, ventilation and cooling during the summer months.

Table 2. Consumption in school units and emission of CO_2

Schools units	Consumption of natural gas[10] (Kwh)	Emission of CO_2 (ton) (if we used natural gas) (ton)	Emission of CO_2 (if we used oil) (ton)
46 High School of Athens	70990.85	14.19	18.45
5 High School of Paleo Faliro	50091.29	10.01	13.02
7 Secondary of Metamorfosi	62691.07	12.53	16.30
33 High School of Athens	42235.8	8.44	10.98
5 High School of Paleo Faliro	42012.18	8.40	10.92
13 Secondary of Paleo Faliro	48663.39	9.73	12.65
3 Nursery of Paleo Faliro	5444.56	1.08	1.41
137 Secondary of Athens	36700.86	7.34	9.54
10 Secondary of Paleo Faliro	38724.61	7.74	10.06
4 High School of Paleo Faliro	21728.73	4.34	5.64
6 Nursery of Paleo Faliro	3063	0.61	0.79

The above data shows (Table 1) that new schools planned in accordance with the principles of bioclimatic design and new energy saving measures, require less energy to operate than conventional schools.

In addition, the use of natural gas has reduced energy consumption due to the higher calorific value of gas compared to oil. Even the use of renewable energy sources in new school units it will contribute more to the protection of the environment.

5. Conclusions

New school units require less energy than conventional schools. An important role in energy consumption is played by the location of the school unit, thermal insulation as well as the use of passive solar systems. As it turned out, the implementation of new laws on heat insulation has increased significantly the reduction of energy consumption.

The survey showed that the existing conventional schools who consume large amounts of energy, are in need of improvement.

Also, the use of renewable energy sources such as photovoltaic systems, saves important natural resources, while the introduction of geothermal energy to schools, will reduce energy consumption even further.

Conclusively, not only do passive solar schools contribute to energy consumption reduction, but they also contribute to the conservation of natural resources and the reduction greenhouse gases emissions to the atmosphere. Nowadays, new techniques applied in schools and new energy-saving systems create a new field of research in the forthcoming years.

References

[1] Official Journal of the Hellenic Republic, 362/D/07.04.1979, pp.3960-4035 http://www.et.gr/search_publication

[2] Official Journal of the Hellenic Republic, 880/B/19.08.1998, pp.10071-10077 http://www.et.gr/search_publication

[3] Commission of the European Communities, Directive 2002/91/EC of the European Parliament and of the Council of 16 December on the energy performance of buildings, OJ, L1/65, Brussels, 2003, pp. 1-7.

[4] Official Journal of the Hellenic Republic, 89/19.05.2008, pp.1371-1377 http://www.et.gr/search_publication

[5] Official Journal of the Hellenic Republic, 407/B/09.04.2010, pp.5333-5346 http://www.et.gr/search_publication

[6] Official Journal of the Hellenic Republic. 95/A/23.06.2010, pp.1955-1964 http://www.et.gr/search_publication

[7] Ministry of Environment Energy & Climate Change/ Directorate of Urban Affairs and Housing – Center for Renewable Energy Sources (CRES), Action Plan for energy saving in residential sector "Energy 2001", 1995.

[8] E. Lazari, Center for Renewable Energy Sources (CRES), Bioclimatic Design in Greece: Energy efficiency and guidelines for implementation, Pikermi, 2002, pp.1-40.

[9] SBO (School Building Organization S.A.), Statistics Data Units 2007-2010, Athens, 2010.

[10] EPA, Provider of natural gas, Statistical Data on natural gas consumption in Attica buildings during the year 2009, Athens, 2009.

[11] Papanikas D., Natural Gas Technology, Media Guru, M.&Fr. Papanika Editions,Vol I, 2nd edition, Athens, Greece 2007, pp.156-157.

Modeling of the Seawater Greenhouse Systems

G.R. Salehi [1,*], M. Ahmadpour [2], H. Khoshnazar[3]

[1]*Islamic Azad University Nowshahr Branch,Nowshahr,Iran*
[2]*Islamic Azad University Takestan Branch,Takestan,Iran*
[3] *Shiraz university,Shiraz,Iran*
** Corresponding author. Tel: +989122031671, E-mail: rezasalehi20@gmail.com*

Abstract: The Seawater Greenhouse system uses sunlight, seawater and air to provide freshwater and cooled and humid air, so that in addition to provide the water required for greenhouse, supply more sustainable environmental condition from cultivation of crops in arid coastal regions. In this system ambient air is passed through the two evaporative cooling pads, which plant growth area is placed between those pads, by fans that placed end of the building, and then returned taking humidity on the tube-and-fin condenser. In order to decrease the entrance heating load to the plants, use pipe arrays to provide shade. This paper tries to describe simulation the Seawater Greenhouse considering condition of the Bandar Abbas City in IRAN. it shows that by increasing entrance air relative humidity, the water production and floor temperature increases and the differential temperature decreases. Also with increasing seawater flow rate, the water production increases and differential temperature and floor temperature decreases. With increasing entrance air flow rate, the water production water production and floor temperature decreases and differential temperature increases. Different cycle is developed and investigate in this paper and shows that in cycle that is water exist from first evaporator is passed under the greenhouse floor, is the effective cycle and produces more water than other cycle.

Keywords: *Seawater greenhouse, cycle design, condenser*

Nomenclature

D	*Pipe diameter*	*m*
E	*Pipe thickness*	*m*
F	*Seeing surface*	
g	*Acceleration due to gravity*	$m \cdot s^{-2}$
h	*enthalpy*	$kjkg^{-1}$
h	*heat transfer coefficient*	$wm^{-2}k^{-1}$
I	*solar radiation intensity*	wm^{-2}
k	*Thermal conductivity*	$wm^{-1}k^{-1}$
M	*mass*	*kg*
M^0	*flow rate*	$lits^{-1}$
Nu	*Nusselt number*	
p	*pressure*	*pa*
pr	*Prandtl number*	
Q	*Heat transfer*	*kj*
Re	*Reynolds number*	
T	*Temperature*	*k*
U	*Specific energy*	$kjkg^{-1}$
V	*velocity*	$m \cdot s^{-1}$
V	*viscosity*	$m \cdot s^{-1}$
V	*transmittance*	$m \cdot s^{-1}$
ω	*stefan-boltzmann constant*	$wm^{-2}k^{-4}$

1	*Entering air to first evaporator*	
2	*Entering Water to first evaporator*	
3	*Water out from first evaporator*	
4	*Air out from first evaporator*	
5	*Entering Water to pipes array*	
7	*Entering air to growing space*	
8	*Air out from roof space*	
9	*Air out from growing space*	
10	*Entering water to second evaporator*	
11	*Entering air to second evaporator*	
12	*Water out from second evaporator*	
13	*Air out from second evaporator*	
14	*Entering water to condenser*	
15	*Water out from condenser*	
16	*water production*	
17	*Air out from condenser*	
α	*absorptance*	
ε	*Emittance*	
φ	*Relative humidity*	
ω	*Water content*	

1. Introduction

The earliest solar distillation plant on record was designed and built in 1872 by Charles Wilson in Chile [1]. It was further developed at the University of Arizona in 1961 in cooperation with the Georgia Institute of Technology and the University of Sonora, Mexico at Puerto Peñasco,New Mexico. A well detailed study about sun fresh water making plans and

policies was investigated [2, 3, 5, 6]. But, the seawater Greenhouse history returned to 1991. The first experimental project started in Tenerife in 1994. This prototype Seawater Greenhouse was planned in England and constructed in Tenerife[7].

The increasing water requesting growth and water providing resources shortage are two certain and predictable problems in 21 century. Now, the great areas in the world suffer from drought. The deserts are developing and in comparison, raining has a fixed movement. While water requesting have been two times in present 20 years, request forwarding from refreshing resources amount is following at the same way. About 70% total water uses are in farming and then water crisis can be review in so close relationship with food materials producing and economy development and creating. Custom and traditional farming which just need few hundred liters water just produces one kg output and it is because of this farming style inefficiency in water management. The farming and its increasing water requesting will be an important pressure point in which seawater Greenhouse will help using and incorporating natural processes in order to provide low-cost resolution for presenting permanent and similar model in arid coastal regions to decrease this pressure. Seawater Greenhouse provides an ambient in which plants sweating is as low as possible. So, Greenhouse produces its needed sufficient water during sun distillation operation.

2. Seawater greenhouse process description

The greenhouse seawater system uses the sun, the sea and the atmosphere to produce fresh water and cooled air to the growth of crops in the greenhouse. The idea of its operation depends on creating the natural water cycle in controlled environment. First seawater pumped into a cold seawater tank after filtration. The seawater pumped to the condenser before reaching the first cooling pad evaporator at the front side of the greenhouse. The seawater greenhouse consist of two evaporator that planting area is located between them. The seawater passes through first evaporator from top to bottom, while air passes perpendicular direction to the flow of water. This evaporator faces the prevailing wind. Also fan assist and control air movement. The humidified and cooled air passes through planting area and combined with hot dry air from the cavity under the roof. The mixture passes through a second evaporator and creating hot saturated air which then flows through the condenser. The seawater is pumped to a pipe array which is installed in the cavity below the plastic cover and warmed up by solar energy and passes through second evaporator from top to bottom. It noted that only small fraction of solar radiation involved in photosynthesis since the roof traps infrared heat while allowing light through to promote photosynthesis. The saturated humid air from second evaporator passes through the condenser which is cooled by seawater flow. The temperature difference creates fresh water to condense out of air stream. The resulting condensate collected for using in irrigation of crops.

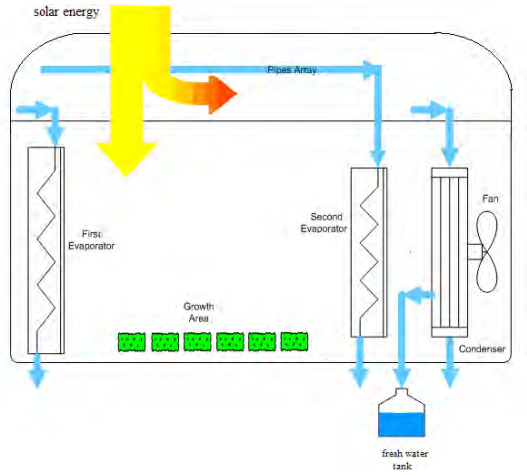

Fig1. Seawater greenhouse process schematic diagram

3. Modelling and Optimisation

Seawater greenhouse is consist of two evaporator, which is planting area located between them, condenser, and pipe array, which is feed the second evaporative pad through water which heated by the sun, is located in cavity under the greenhouse plastic cover. In analyzing the green house all of these parts must be modeling.

The first evaporator:

Energy and mass balance for evaporator cooling pad in the front of greenhouse gives:

$$\dot{m}_1 h_1 + \dot{m}_2 h_2 = \dot{m}_3 h_3 + \dot{m}_4 h_4 \quad (1)$$

$$\dot{m}_1 + \dot{m}_2 = \dot{m}_3 + \dot{m}_4 \quad (2)$$

The entrance air mass obtained with equation 3:

$$\dot{m}_{Air} = \frac{\dot{m}_1}{1+\omega_1} \quad (3)$$

The evaporative water amount will take from:

$$\dot{m}_4 - \dot{m}_1 = \dot{m}_{Air}(\omega_4 - \omega_1) \quad (4)$$

$$h_1 = f(T_1, P_{Ambient}, \omega_1) \quad (5)$$

$$\omega_1 = f(T_1, P_{Ambient}, \varphi_1) \quad (6)$$

$$h_2 = f(T_2, P_{Ambient}) \quad (7)$$

$$h_3 = f(T_3, P_{Ambient}) \quad (8)$$

$$T_4 = f(h_4, P_{Ambient}, \varphi_4) \quad (9)$$

$$\omega_4 = f(T_4, P_{Ambient}, \varphi_4) \quad (10)$$

The growth area:

Air after passing through the evaporator enters the growth space. Before air entering in plants growth space, part of it directs to the space in up. This part has an important role in freshwater production and simulate as follow:

The roof:

$$\alpha_{Body} I - h_{Out}(T_{Roof} - T_1) - h_{Up}(T_{Roof} - T_{Up}) - F_{Roof.Pipe}.\sigma.\varepsilon_{Body}(T_{Roof}^4 - T_{Pipe}^4) - F_{Roof.Sky}.\sigma.\varepsilon_{Body}(T_{Roof}^4 - T_{Sky}^4) = 0 \quad (11)$$

The left:

$$\alpha_{Body} I - h_{Out}(T_{Left} - T_1) - h_{Down}(T_{Left} - T_{Down}) - F_{Left.Pipe}.\sigma.\varepsilon_{Body}(T_{Left}^4 - T_{Pipe}^4) - F_{Left.Sky}.\sigma.\varepsilon_{Body}(T_{Left}^4 - T_{Sky}^4) - F_{Left.Floor}.\sigma.\varepsilon_{Body}(T_{Left}^4 - T_{Floor}^4) = 0 \quad (12)$$

The right:

$$\alpha_{Body} I - h_{Out}(T_{Right} - T_1) - h_{Down}(T_{Right} - T_{Down}) - F_{Right.Pipe}.\sigma.\varepsilon_{Body}(T_{Right}^4 - T_{Pipe}^4) - F_{Right.Sky}.\sigma.\varepsilon_{Body}(T_{Right}^4 - T_{Sky}^4) - F_{Right.Floor}.\sigma.\varepsilon_{Body}(T_{Right}^4 - T_{Floor}^4) = 0 \quad (13)$$

Pipes carrying seawater:

$$\alpha_{Pipe}.\rho_{Body}.I - h_{Pipe}(2T_{Pipe} - T_{Up} - T_{Down}) - F_{Pipe,Left}.\sigma.\varepsilon_{Pipe}(T_{Pipe}^4 - T_{Left}^4) - F_{Pipe,Right}.\sigma.\varepsilon_{Pipe}(T_{Pipe}^4 - T_{Right}^4) - F_{Pipe,Floor}.\sigma.\varepsilon_{Pipe}(T_{Pipe}^4 - T_{Floor}^4) - F_{Pipe,Roof}.\sigma.\varepsilon_{Pipe}(T_{Pipe}^4 - T_{Roof}^4) - \frac{2T_{Water} - T_{Up} - T_{Down}}{\frac{1}{h_{Water}} + \frac{e}{k}} \quad (14)$$

The Floor:

$$\alpha_{Floor}.(\rho_{Body}.\rho_{Pipe} + 2\rho_{Body})I - h_{Down}(T_{Floor} - T_{Down}) - F_{Floor,Left}.\sigma.\varepsilon_{Floor}(T_{Floor}^4 - T_{Left}^4) - F_{Floor.Right}.\sigma.\varepsilon_{Floor}(T_{Floor}^4 - T_{Right}^4) - F_{Floor,Pipe}.\sigma.\varepsilon_{Floor}(T_{Floor}^4 - T_{Pipe}^4) \quad (15)$$

The Greenhouse out air h:

$$h_{Out} = \frac{Nu_{Out}.k_{Out}}{L} \quad (16)$$

$$Nu_{Out} = (0.037\,\mathrm{Re}_{L,Out}^{4/5} - 871)\,\mathrm{Pr}_{Out}^{1/3} \quad (17)$$

$$\mathrm{Pr}_{Out} = f(T_1) \quad (18)$$

$$\mathrm{Re}_{L,Out} = \frac{V_{Out}.L}{\mu_{Out}} \quad (19)$$

$$\mu_{Out} = f(T_1, P_{Ambient}, \omega_1) \quad (20)$$

$$V_{Out} = \rho_1.\dot{m}_1 \quad (21)$$

$$\rho_1 = f(T_1, P_{Ambient}, \omega_1) \quad (22)$$

$$k_{Out} = f(T_1, P_{Ambient}, \omega_1) \quad (23)$$

The passing water h from the pipes:

$$h_{Water} = \frac{Nu_{Water} k_{Water}}{D_{Pipe}} \quad (24)$$

$$Nu_{Water} = 3.66 + \frac{0.0668\frac{D_{Pipe}}{L}\mathrm{Pr}_{Water}\,\mathrm{Re}_D}{1 + 0.04(D_{Pipe}\,\mathrm{Pr}_{Water}\frac{\mathrm{Re}_D}{L})^{2/3}} \quad (25)$$

$$\mathrm{Pr}_{Water} = f(T_{Water}, P_{Ambient}) \quad (26)$$

$$\mathrm{Re}_D = \frac{4\dot{m}_{10}}{\pi D_{Pipe}\mu_{Water}} \quad (27)$$

$$\mu_{Water} = f(T_{Water}, P_{Ambient}) \quad (28)$$

$$k_{Water} = f(T_{Water}, P_{Ambient}) \quad (29)$$

In this stage, by taking two control volumes around the Greenhouse up and down space that separating by the pipes carrying seawater, we have the following equations.

$$\dot{m}_6 h_6 + h_{Up}(T_{Roof} - T_{Up}) + h_{Pipe}(T_{Pipe} - T_{Up}) - \dot{m}_8 h_8 = 0 \quad (30)$$

$$\dot{m}_7 h_7 + h_{Down}(T_{Floor} + T_{Left} + T_{Right} - 3T_{Down}) + h_{Pipe}(T_{Pipe} - T_{Down}) - \dot{m}_9 h_9 = 0 \quad (31)$$

$$T_8 = f(h_8, P_{Ambient}, \omega_8) \quad (32)$$

$$T_9 = f(h_9, P_{Ambient}, \omega_9) \quad (33)$$

$$T_{Up} = \frac{1}{2}(T_6 + T_8) \quad (34)$$

$$T_{Down} = \frac{1}{2}(T_7 + T_9) \quad (35)$$

$$T_{Water} = \frac{1}{2}(T_5 + T_{10}) \quad (36)$$

The entering air divided into two branches that flowing down branch has the duty of humidification and cooling of the ambient and the up branch has the duty of by removing the heat gained from sun by pipe arrays and applying it increasing humidity capacity of air in exit. These two branches were mixed by near the second evaporator and caused increasing air temperature and moisture capacity. These combinations write as follow:

$$\varphi_{11} = f(T_{11}, P_{Ambient}, \omega_{11}) \quad (37)$$

$$h_{11} = f(T_{11}, P_{Ambient}, \omega_{11}) \quad (38)$$

The second evaporator:
This evaporator analyzes such as the first one

Condenser:
According figure 3, the governing equations are as following:

$$\dot{m}_{13}h_{13} + \dot{m}_{14}h_{14} = \dot{m}_{15}h_{15} + \dot{m}_{16}h_{16} + \dot{m}_{17}h_{17} \quad (39)$$

$$\dot{m}_{13} - \dot{m}_{17} = \dot{m}_{Air}(\omega_{13} - \omega_{17}) \quad (40)$$

$$\dot{m}_{13} = \dot{m}_{16} + \dot{m}_{17} \quad (41)$$

$$h_{14} = f(T_{14}, P_{Ambient}) \quad (42)$$

$$T_{15} = f(h_{15}, P_{Ambient}) \quad (43)$$

$$h_{16} = f(T_{16}, P_{Ambient}) \quad (44)$$

$$\omega_{17} = f(T_{17}, P_{Ambient}, \varphi_{17}) \quad (45)$$

$$h_{17} = f(T_{17}, P_{Ambient}, \omega_{17}) \quad (46)$$

Finally, all of these equations stimulate and solved by EES program.

4. Result and conclusion

Bandar Abbas have chosen as stimulation reference, and was simulated based on the following the following conditions[8]:

$P_{Ambient} = 100KPa$, $V_{Out} = 10m/s$, $I = 250W/m^2$, $L = 42m$, $\varphi = 0.64$, $\dot{m}_1 = 20kg/s$, $\dot{m}_2 = 3Lit/s$

Figure 2 shows the difference temperature between the inlet and outlet of the first evaporator as function of the mass flow rate and relative humidity of entrance air. With increasing mass flow rate, Re and h was increased and it caused more evaporation and the temperature of air was decreased.

Figure 3 shows the difference temperature between the inlet and outlet of the first evaporator as function of the mass flow rate of sea water and the relative humidity of entrance air. As shown in the figure, the more increasing mass flow is lead to the more decreasing temperature drop. Furthermore, the more increasing humid, the more decreasing temperature difference. Figure 4 shows water producing according to entrance air mass flow and various air humid. As you see in this figure, entrance air increasing has affected water producing tendency increasingly and has had an important step toward its decrease.

Figure 5 shows water producing mass flow based on seawater mass flow and various airs humidity. As have shown seawater mass flow increasing causes differential temperature dropping, then more warm air goes to the roof and its entrance will be warmer and caused the exit water will be warmer, this increases water inclination to evaporation and humid absorbing more. These events in addition to warmer air gets condense better in condenser will increase producing water in it and also we see clearly increasing in seawater mass flow will increase the producing water.

Figure 6 shows the temperature of Greenhouse floor as a function of seawater mass flow and various airs humid. It is cleared that the increasing water producing mass flow has increased soil temperature. It happens more in much humid

Figure 7 shows Greenhouse floor temperature based on entering air mass flow and various air humid. As have considered, increasing entrance air mass flow will decrease the outlet temperature of the first evaporator, and it results in more heat transfer to greenhouse floor and

decrease its temperature. In addition, entrance air mass flow increase affects Re and Nu and increasing h and absorbs multiple heat, so we can say the higher humid will be as the same as more soil temperature. As we see in this figure, entrance mass flow increasing has decrease heat, and more humid, will increase Greenhouse floor in a certain air mass flow.

.The difference cycles was simulated here to find the optimum cycles in this Greenhouse. The stimulations were done according the Bandar Abbas conditions. The first cycle which has shown by C1 in the figures, is the simplest one and the other plan is based on changes changes in this plan. C2 is a plan for decreasing the greenhouse floor temperature. The air which exits the condenser will be passed the under of the growth space in order to decrease Greenhouse floor temperature. C3 is a similar plan with the same goal by another approach. In this cycle, the water which exit the first evaporator is passed the under of Greenhouse floor space, like previous plan, for decreasing the temperature. C4, C5 and C6 have considered in order to low cost and each of them includes these changes: condenser feeding from the first evaporator exit water, pipes array feeding through condenser exit and finally pipes array feeding by the second evaporator exit. Now, we study these graphs in detail: Considering present cycles we can see with increasing humidity the water producing was increased. Another important result will obtain from this graph is C3>C2>C6>C5>C4>C1

Figure 8 shows water producing in different cycles according to various air humid, and describe cycle 3 is the best in water production and providing pleasure heat for greenhouse floor (in this way and through thermal transmitting increasing to the air produces water) and also says condenser feeding through exit water from operator just low cost and hasn't so profits in water producing. Figure 9 shows water producing in different cycles based on various entrance air mass flow rate. This graph interpretation is like graph 8 and the alone point which isn't mentioned is in all cycles increasing entrance air mass flow water producing is decreased. Figure 10 shows the location of different places in basic cycle.

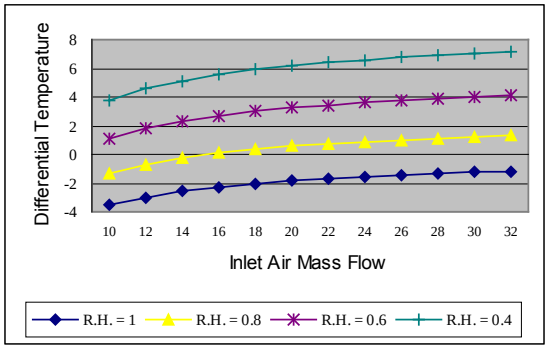

Fig 2- effect of heat inlet mass flow in Diff. T.

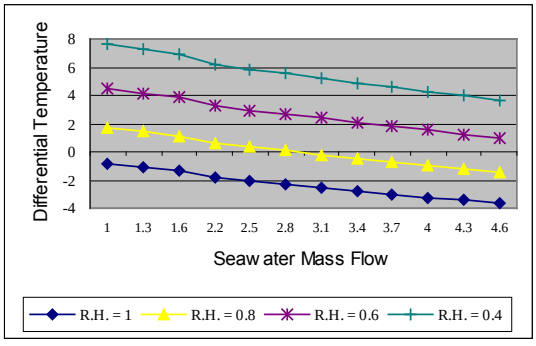

Fig 3- effect of sea water mass flow in Diff. T

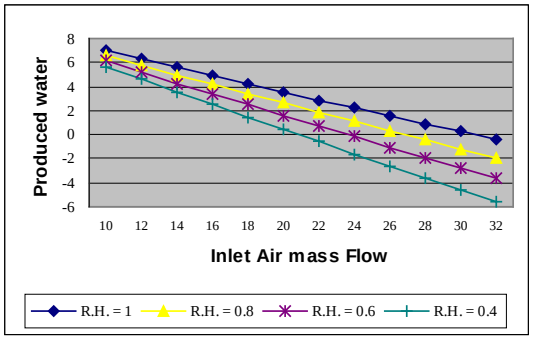

Fig 4- effect of inlet mass flow in produced water

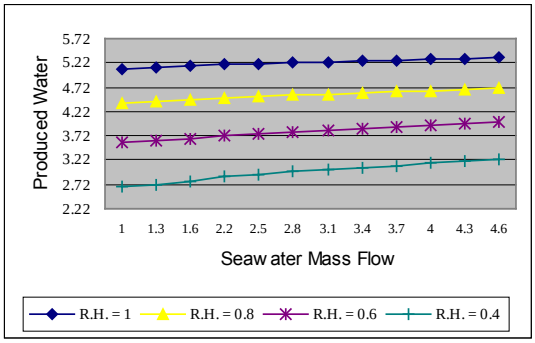

Fig 5- effect of sea water mass flow in produced water

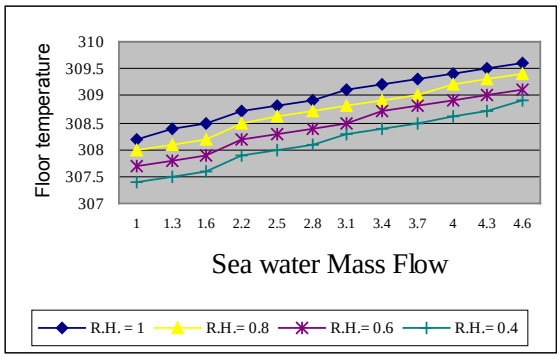

Fig 6-effect of sea water mass flow on floor temp.

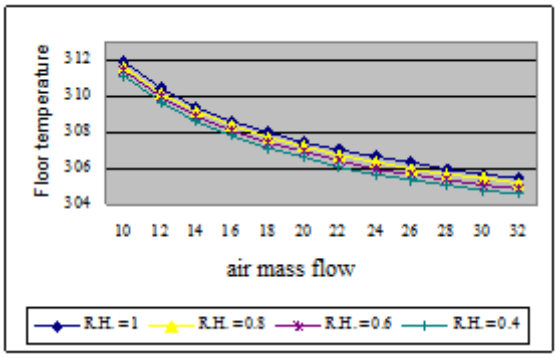

Fig 7-effect of air mass flow on Floor Temperature

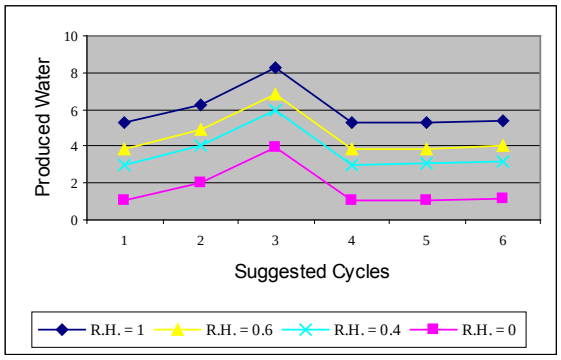

Fig 8- effect of suggested cycles in produced water

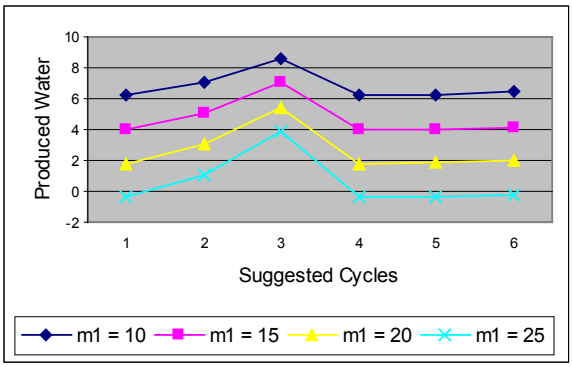

Fig 9- effect of suggested cycles in produced water in mass

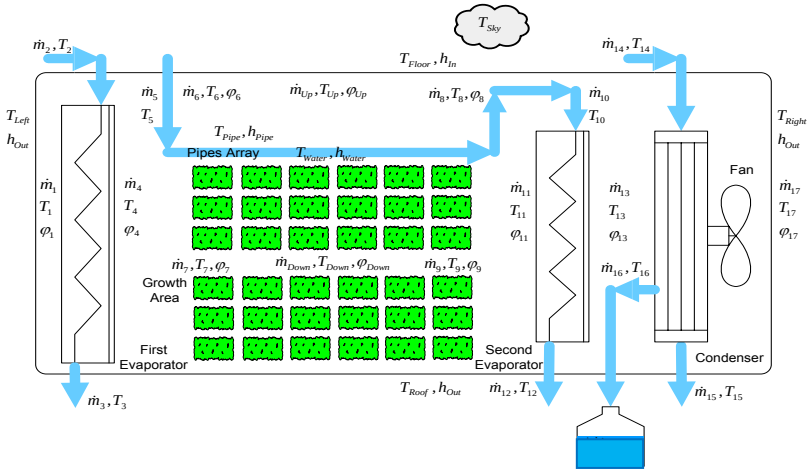

Fig 10. Location of basic cycle

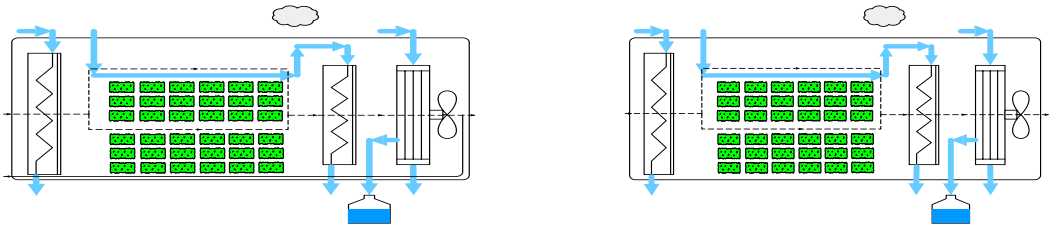

C1 *C2*

Fig 11. Location of different places in basic cycle

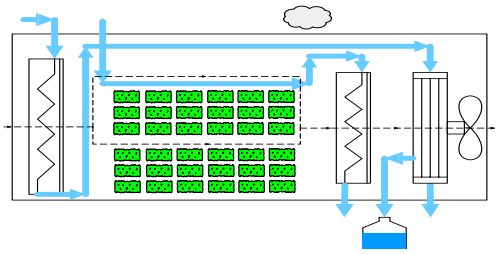

C3

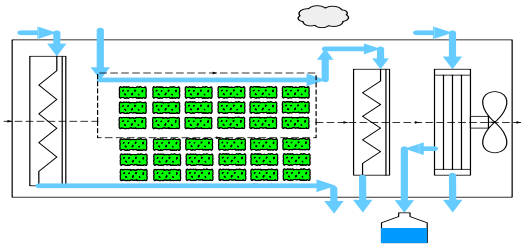

C4

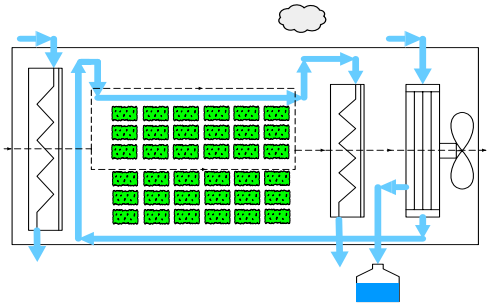

C5

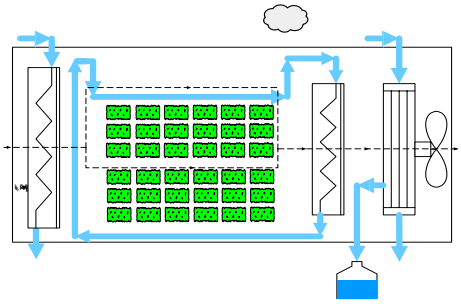

C6

Fig 11. continue

5. Conclusion

The seawater greenhouse was investigated in the Bandar Abass wether conditions.it shows that by increasing entrance air relative humidity, the water production and floor temperature increases and the differential temperature decreases. Also with increasing seawater flow rate, the water production increases and differential temperature and floor temperature decreases. With increasing entrance air flow rate, the water production water production and floor temperature decreases and differential temperature increases. Also different cycle is developed and investigates in this paper and shows that in cycle C3 which is water exist from first evaporator is passed under the greenhouse floor, is the effective cycle and produces more water than other cycle.

References

[1] Talbert, S. G., Lof, C-M Wong and E. N. Sieder, 1970. Manual on solar

[2] Yadav. Y. P. and L. K. Jha, 1989. A double-basin solar still coupled to a collector and operating in the thermo siphon mode. Energy, 14(10): 653–659.

[3] Hamed, O. A., E. I. Eisa and W. E. Abdullah, 1993.Overview of solar desalination. Desalination, 93: 563–579.

[4] Farid, M. M. 1999.Recent developments in solar desalination. In: Water Management, Purification and Conservation in Arid Climates. Vol. II.Water Purification. M. F. A.

[5] Goosen and W. H. Shayya. Technomic Publishing Co., Lancaster, PA, pp. 277–296.

[6] Goosen, M. F. A., S. S. Sablani, W. H. Shayya, C. Paton, and H. Al-Hinai, 2000.Thermodynamic and Economic considerations in solar desalination. Desalination, 129: 63–89.

[7] Paton, A. C. and P. A. Davis, 1996. International Engineering Conference (IEC) “Mutah 2004”, Mutah University, JORDAN, April 26-28. Pages 523-540.

[8] Data Processing Center, Annual Weather Report of the Year 2000

An exergy based unified test protocol for solar cookers of different geometries

Naveen Kumar[1*], G. Vishwanath[1], Anurag Gupta[1]

[1] *IIITD&M Kancheepuram, IIT Madras Campus, Chennai-600036, Tamil Nadu, India.*
***** *Corresponding author. Tel: +914422578555, Fax: +914422578555, E-mail: nkumar@iiitdm.ac.in*

Abstract: It is good for the consumer to have solar cookers of various varieties in terms of geometrical designs, performance and price but it is a challenge to develop a uniform test standard for evaluating the thermal performance of the cookers irrespective of their geometrical construction. Due to the lack of uniform test protocol, consumer cannot compare the quantitative performance of the cookers of different configuration and become confused. For this end, we plotted graphs between exergy output and temperature difference, for solar cookers of different designs and it resembled a parabolic curve for each design. The peak exergy (vertex of the parabola), can be accepted as a measure of devices' fuel ratings. The ratio of the peak exergy gained to the exergy lost at that instant of time can be considered as the quality factor of the solar cooker. Besides, the exergy lost is found to vary linearly with temperature difference irrespective of the topology of the device and the slope of the straight line obtained through curve fitting represents the heat loss coefficient of the cooker. The proposed parameters can lead to development of unified test protocol for solar cookers of diversified designs.

Keywords: *Solar Cookers, Test Protocol, Exergy Analysis*

Nomenclature

A	*gross area of glazing surface* m^2	G	*instantaneous solar insolation* W/m^2
c	*specific heat capacity of water* $J/kg\ K$	m	*mass of water* kg
E_o	*output energy* J	T_{am}	*instantaneous ambient temperature* K
E_{Xi}	*input exergy* kJ	T_f	*final water temperature* K
E_{Xo}	*output exergy* kJ	T_i	*initial water temperature* K
F_1	*first figure of merit* $m^2\ K/W$	T_s	*surface temperature of sun* K
F_2	*second figure of merit*	Δt	*time interval* s

1. Introduction

Solar cookers are a very useful and popular thermal device which is available throughout the world. It is one of the few renewable energy thermal gazettes which are portable, user friendly, easily operable, meant to fulfil the very basic need and economically competitive. Its affordable price makes it very attractive commercially, especially among the rural populace in the developing countries. In order to meet the demands of broad spectrum of the society and penetrate the market, different novel varieties of solar cookers have become available in accordance with peoples' need and purchasing capacity. Solar box type cookers (SBC) are available for domestic as well as community based applications. Similarly, SK-14, SK-10 and Scheffler paraboloid type concentrating cooker are also present in the market for fast cooking for domestic/community and industrial applications. In addition parabolic trough type concentrating cookers are being reported in recent studies for both domestic as well community type applications. Depending on the topology of the cooker construction, different test procedures and thermal indicators have been established, which act as benchmark thermal performance evaluators for various geometrical varieties of the cooker. On one hand it is good for the customer to have solar cookers of diversified designs in terms of geometry, performance and price but on the other hand it is a challenge to develop a uniform test standard for evaluating the thermal performance of the cookers irrespective of their geometrical construction. In the absence of such unified test/standard protocol, it is very confusing for the customer to compare the performance of these devices. In addition, to

promote renewable energy technologies (RETs), many governments throughout the world, are adopting environment friendly policies. This includes the provision of providing direct/indirect subsidies and other benefits to the user on the usage of the RETs. Many a times, manufacturers are not able to receive the subsidy benefits because the parameters set for eligibility criterion matches one design of solar cooker and not the others. Through the present manuscript, we propose an exergy based unified test protocol for solar cookers of different geometries. In this protocol, the test methodology for conducting full load test for solar cookers remains the same but the analyzing procedure has been altered so as to fulfill the above necessities. In order to develop a realistic and unified test protocol, we utilize the reported data from different well known published manuscripts and analyze it comprehensively to cater to the above mentioned needs.

2. Methodology

In order to test the performance of the solar box type cooker, two figures of merit (FOM) viz. F_1 and F_2 are generally calculated, as given by Mullick [1]. The first FOM, F_1 is defined as the ratio of optical efficiency to the heat loss factor by bottom absorbing plate and is a measure of the differential temperature gained by the absorbing plate at a particular level of solar insolation. The second FOM, F_2 is more or less independent of climatic conditions and gives an indication of heat transfer from absorbing plate to the water in the containers placed on the plate. Bureau of Indian standards have also accepted these parameters as performance indicators for SBC [2]. However, as per international test protocol for solar box cookers, the performance should be estimated in terms of its standardized cooking power as given by Funk [3], which is calculated through extrapolation of the curve/data. The value of the cooking power determined through this procedure comes out to be high and does not represent the actual cooking potential of the cooker. Internationally, the procedure for measuring the efficacy of cooking of solar cookers based on parabolic trough and Scheffler concentrating type topology is not very well known, nevertheless Scheffler concentrators are generally employed for very large scale cooking/industrial operations. As per Ministry of New and Renewable Energy (India), thermal performance of SK-14/SK-10 type cookers should be determined by its heat loss factor, optical efficiency and cooking power [4]. In all above mentioned thermal performance evaluation processes, energy based approach is employed. But, the benchmark parameters derived from the energy based method does not provide complete information and are inadequate performance indicators because their values can be misleadingly high or low depending on the temperature difference between source and sink, even though input energy condition may remain same. Exergy is a measure of the potential of the system to extract heat from the surroundings, as the system moves closer to the equilibrium with its environment [5]. After the system and the surroundings reach equilibrium, the exergy becomes zero. In the present manuscript, we would take the case of each of the different solar cookers of the above mentioned geometries and apply the exergy based approach so as to reach a holistic/uniform approach for deciding the common thermal indicators irrespective of the cooker design topology. The exergy of solar radiation, as the exergy input E_{Xi} to the solar cooker, can be calculated using the available solar energy flux ($GA\Delta t$) and is expressible through Eq. (1) which has the widest acceptability [5, 6].

$$E_{Xi} = G\left[1+\frac{1}{3}\left(\frac{T_{am}}{T_s}\right)^4 - \frac{4T_{am}}{3T_s}\right]A\Delta t \qquad (1)$$

where T_{am} is instantaneous ambient temperature, T_s is surface temperature of sun, G is instantaneous solar insolation, A is aperture area of cooker, and Δt is time interval. The sun's black body temperature of 5762 K results in a solar spectrum concentrated primarily in the 0.3−3.0 μm wavelength band [5, 7, 8]. Although the surface temperature of the sun (T_s) varies due to the spectral distribution of sunlight on the earth's surface, the value of 5800 K has been considered for the T_s. The energy gained by water in the vessel, kept inside the cooker, due to rise in temperature can be considered as the output energy (E_o) of the system and is mathematically given as

$$E_o = mc(T_f - T_i) \tag{2}$$

In the expression above, the output energy depends only on the difference in initial and final values of temperatures $(T_f - T_i)$ but in actual practice, ambient temperature as well as the initial and final temperature values also play the role in deciding the efficiency of the system, and this kind of qualitative effect can not be accommodated in the energy based approach. The exergy gained by water in the vessel kept inside the cooker due to rise in temperature can be considered as the output exergy (E_{X0}) [5, 6, 7, 9] of the system and is expressible through

$$E_{Xo} = E_o - mcT_{am} \ln\frac{T_f}{T_i} \tag{3}$$

The beauty of the exergy analysis/approach is self evident in the expression above as it considers the effect of ambient temperature as well as the absolute values of initial and final temperature in addition to $(T_f - T_i)$. The second term on the right hand side of this expression signifies the exergy losses elucidating the true potential of the system in converting the input energy. Thus, exergy analysis is a more complete synthesis tool because it accounts for the temperatures associated with energy transfers to and from the cooker, as well as the quantities of energy transferred, and consequently provides a measure of how nearly the cooker approaches ideal efficiency. Here, we propose to plot a graph between output exergy power and temperature difference and fit the data points with second order polynomial; temperature difference is the difference in the instantaneous water temperature and ambient temperature. From the fitted curve, it is easier to obtain the peak value of exergy, which is very near to the actual value of the peak exergy. The temperature difference gap corresponding to the half exergy points of the curve can be determined. The exergy lost during the test period can also be plotted against temperature difference so as to estimate the overall heat loss coefficient of the cooker. In order to determine the above mentioned parameters, we are taking the data from various manuscripts for each of the different solar cookers geometries.

3. Results and Discussion

Four different geometries of solar cookers are considered for depicting their thermal performance on the basis of exergy based parameters. These geometries are domestic box type cooker, domestic SK-14 type cooker, Scheffler community type cooker, parabolic trough type cooker. The proposed four exergy based parameters, which can be considered as the benchmark indicators of the performance of the cookers are as follows, (i) Peak Exergy, (ii) Quality factor, (iii) Exergy temperature difference gap product, (iv) Heat loss coefficient. Peak exergy is the highest/maximum exergy output power obtained through curve fitting by plotting the graph between exergy output power and temperature difference. This can be realistically considered as a measure of its fuel ratings. The ratio of the peak exergy gained to the exergy lost at that instant of time can be considered as the quality factor of the solar cooker. A higher quality factor is always desirable. The product of the temperature

difference gap corresponding to the half power points and the peak exergy power can also considered to be another benchmark indicator in this kind of analysis. Higher temperature difference gap means the lesser heat losses from the cooker. This kind of scheme is generally considered in electronics for expressing the performance of a BJT amplifier, as gain bandwidth product and also a quality factor in case of a notch/band pass filter. The heat loss coefficient of the device can be calculated by dividing the value of the slope of the line, obtained through linear curve fitting of exergy lost variations with temperature difference, by the value of glazing/focal area. In this approach, we are not dependent much on extrapolation and all the parameters were realistically calculated from the graphs/data. Calculations of the above mentioned topologies of the solar cooker are described in the subsequent sub-sections.

3.1. Domestic solar box type cooker

The variation in the exergy output as a function of temperature difference for domestic SBC of aperture area 0.25 m^2 is presented in Fig. 1, which depicts the case when the amount of water inside the cooking vessels/pots is 2.5 Kg. The maximum exergy power obtained through curve fitting is 6.46 W and the temperature difference gap corresponding to the half power points is 46.2 K. The peak exergy and temperature difference gap product for this case is found to be 298.5 WK. The experimental data, for performing calculation and obtaining the thermal parameters, is taken from Kumar [11].

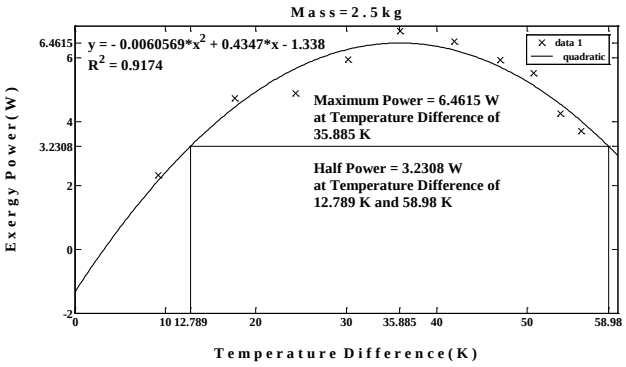

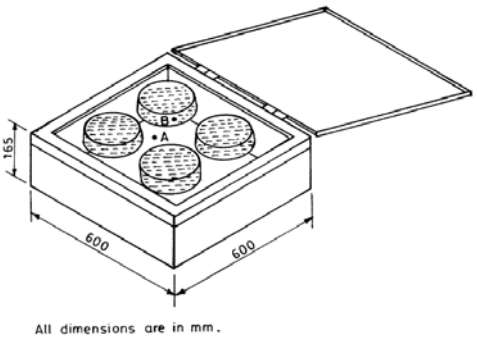

Fig. 1. Variation of Exergy output power with Temperature Difference for Domestic SBC with its schematics.

The curve between the exergy lost v/s temperature difference is plotted in Fig. 2. Heat loss coefficient is obtained by dividing the slope of the curve (which depicts the exergy lost per change in temperature, i.e., W/K), by the gross aperture area. The heat loss coefficient and quality factor, for 2.5 kg mass of water, are found to be 5.24 W/K m^2 and 0.123, respectively. The specific heat loss coefficient for this cooker is found to be 2.096 W/K m^2 kg.

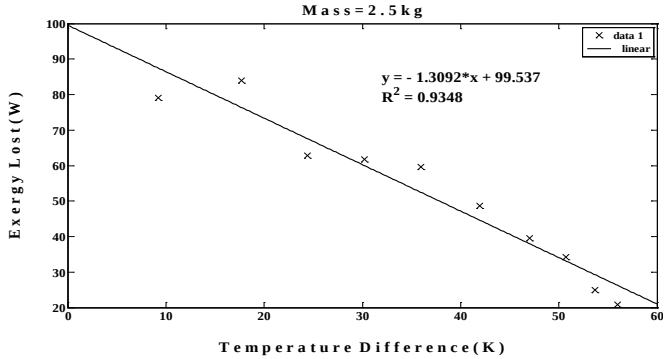

Fig. 2. Variation of Exergy power lost with Temperature Difference for Domestic SBC.

3.2. SK-14 type cooker

The variation in the exergy output as a function of temperature difference for domestic SK - 14 type of gross aperture area 1.47 m^2 and a focal area of 0.134m^2 is presented in Fig. 3, which depicts the case when the amount of water inside the cooking vessels/pots is 5 Kg. The reflective area of the cooker is 1.47 m^2 with its focal length equal to 0.28 m. The maximum exergy power obtained through curve fitting is 18.21 W and the temperature difference gap corresponding to the half power points is 40.374 K. The peak exergy and temperature difference gap product for the two cases is found to be 735.3 WK. The experimental data, for performing calculation and obtaining the thermal parameters, is taken from Kaushik [7]. The curve between the exergy lost v/s temperature difference is plotted in Fig. 4. The heat loss coefficient and quality factor, for 5 kg mass of water, are found to be 40.35 W/K m^2 and 0.106, respectively. The specific heat loss coefficient for this cooker is found to be 8.07 W/K m^2 kg.

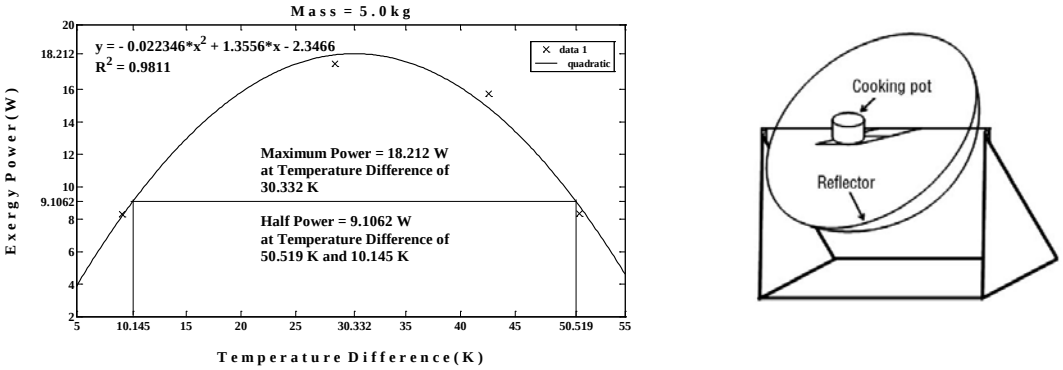

Fig. 3. Variation of Exergy output power with Temperature Difference for SK-14 type cooker with its schematics.

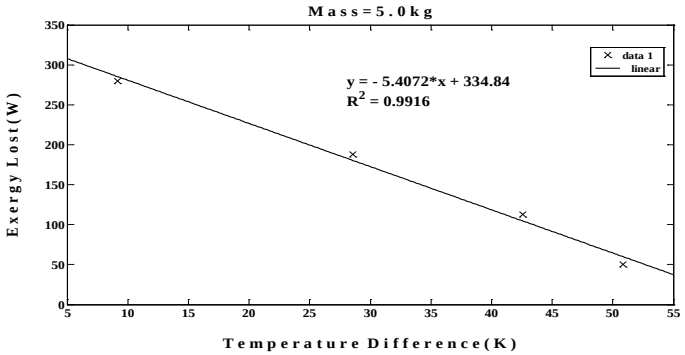

Fig. 4. Variation of Exergy power lost with Temperature Difference for SK-14 type cooker.

3.3. Scheffler Community type cooker

The variation in the exergy output as a function of temperature difference for Scheffler community type of gross aperture area 8.21 m^2 and a secondary focal area of 0.36 m^2 is presented in Fig. 5, which depicts the case when the amount of water inside the cooking vessels/pots is 20 Kg. The primary reflector area of the concentrator is 7.3 $m^2$with aperture diameters of 3.8 m lengthwise and 2.75 m widthwise and has depth of 0.3 m. The reflective area of secondary reflector is 0.36 m^2. The maximum exergy power obtained through curve fitting is 55.75 W and the temperature difference gap corresponding to the half power points is 39.62 K. The peak exergy and temperature difference gap product for the two cases is found to be 2208.815 WK. The experimental data, for performing calculation and obtaining the thermal parameters, is taken from Kaushik [7]. The curve between the exergy lost v/s temperature difference is plotted in Fig. 6. The heat loss coefficient and quality factor, for 20 kg mass of water, are found to be 54.125 W/K m^2 and 0.099, respectively. The specific heat loss coefficient for this cooker is found to be 2.706 W/K m^2 kg.

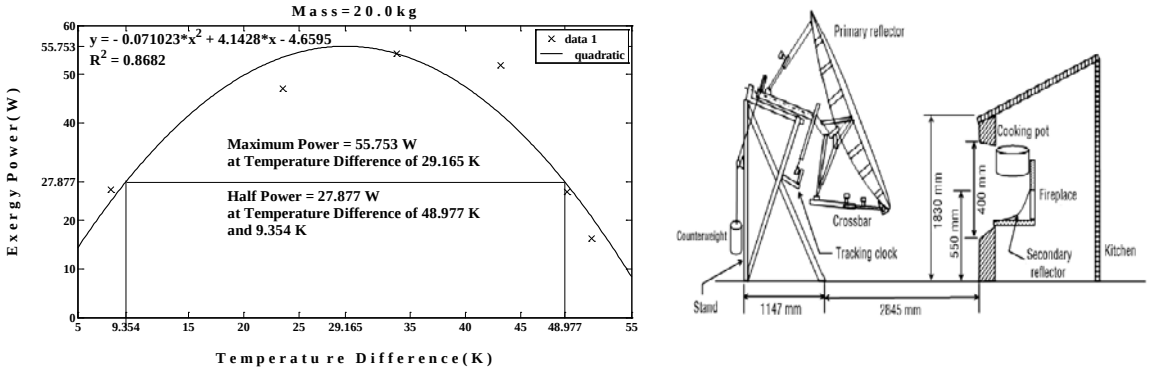

Fig. 5. Variation of Exergy output power with Temperature Difference for Scheffler type cooker with its schematics.

.

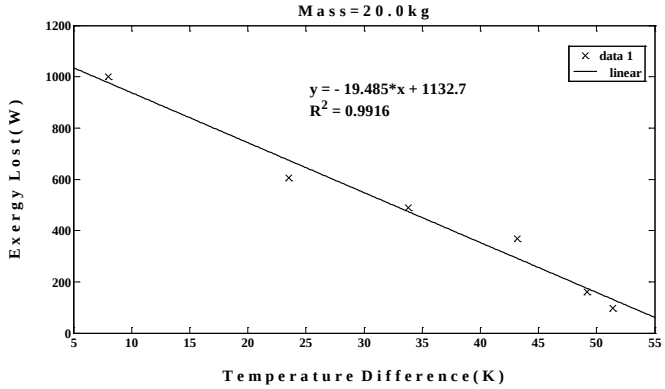

Fig. 6. Variation of Exergy power lost with Temperature Difference for Scheffler type cooker.

3.4. Parabolic trough type concentrating cookers

The variation in the exergy output as a function of temperature difference for parabolic trough type concentrating cooker of aperture area 0.9 m^2 and focal area of 0.088m^2 is presented in Fig. 7, which depicts the case when the amount of water inside the cooking vessels/pots is 6.3 Kg. The maximum exergy power obtained through curve fitting is 6.92 W and the temperature difference gap corresponding to the half power points is 23.15K. The peak exergy and temperature difference gap product for the two cases is found to be 160.198 WK. The experimental data, for performing calculation and obtaining the thermal parameters, is taken from Ozturk [8]. The curve between the exergy lost v/s temperature difference is plotted in Fig. 8. The heat loss coefficient and quality factor, for 6.3 kg mass of water, are found to be 47.73 W/K m^2 and 0.087, respectively. The specific heat loss coefficient for this cooker is found to be 7.58 W/K m^2 kg.

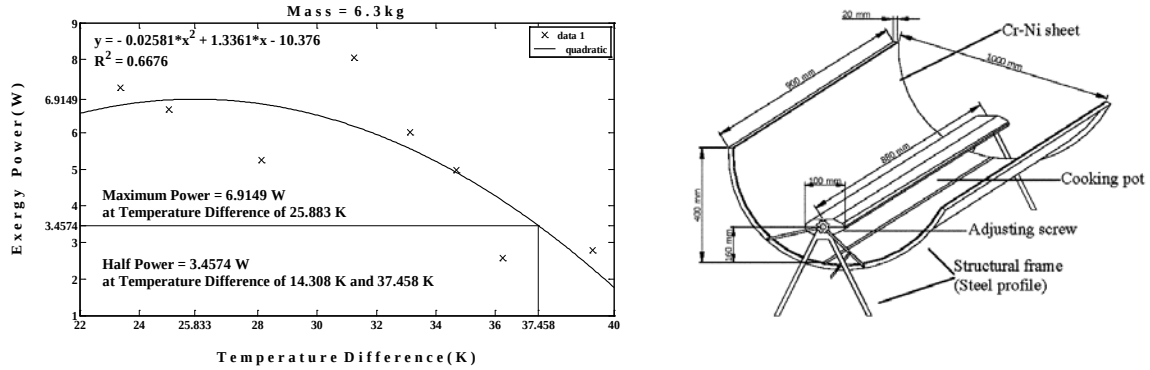

Fig. 7. Variation of Exergy output power with Temperature Difference for parabolic trough cooker with its schematics.

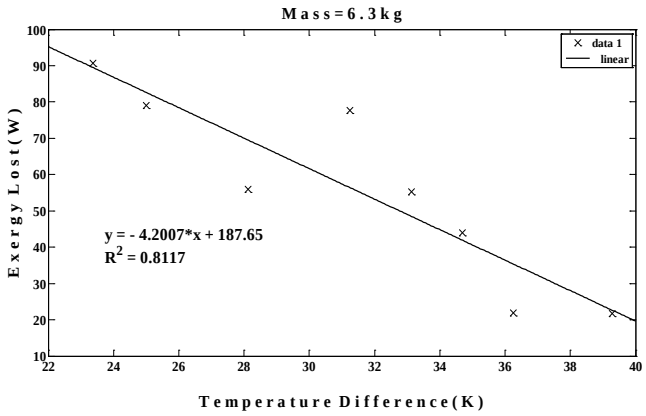

Fig. 8. Variation of Exergy power lost with Temperature Difference for parabolic trough cooker.

The cooker which attains higher exergy at higher temperature difference is the better one. It has been also noticed that the variation in the exergy lost with temperature difference is more linear when temperature of water varies in the range of 60°C to 95°C (see Fig. 2, 4, 6, 8). This range of temperature is also generally used in calculation/determination of F_2 *(second figure of merit)*, which is an important and well known performance indicator for SBC [1, 12]. The amount of heat energy at higher temperature is more valuable than the same amount of heat energy at lower temperature and in energy analysis it is not possible to take into account such qualitative difference. The exergy analysis is a more complete synthesis tool because it

account for the temperatures associated with energy transfers to and from the cooker, as well as the quantities of energy transferred, and consequently provides a measure of how nearly the cooker approaches ideal efficiency.

4. Conclusion

An exergy based analysis is applied to solar cookers of different designs. Variations in exergy output and exergy lost with respect to temperature difference are studied and four thermal performance indicators, viz. peak exergy, quality factor, exergy temperature difference gap product and heat loss coefficient, are proposed. The approach presented through this manuscript is comprehensive, realistic and flexible for it can easily accommodate the effect of variations in solar insolation (peak to valley) which can be greater than 300 W/m^2. The exergy output power, if required, can be converted into standardized exergy power on par with standardized cooking power. To establish a test standard for different types of solar cookers, one may require more comprehensive testing and data analysis. However, the proposed parameters may stimulate the discussion and strengthen the case for exergy based test standards.

References

[1] Mullick, S.C., Kandpal, T. C., Subodh Kumar, 1996. Testing of box-type solar cookers: second figure of merit F_2 and its variation with load and number of pots. Solar Energy 57(5), 409-413.

[2] BIS 2000. IS 13429 (part 3): 2000. Indian Standards Solar – Box Type- Specification Part 3 Test Method (First Revision) New Delhi: Bureau of Indian Standards.

[3] Funk, P. A., 2000. Evaluating the international standard procedure for testing solar cookers and reporting performance, Solar Energy. 68(1), 1-7.

[4] S.C. Mullick, T. C. Kandpal and Subodh Kumar, 'Thermal test procedure for a paraboloid concentrator solar cooker', Solar Energy, 46(3), 139- 144, 199.

[5] Petela, R., 2003. Exergy of undiluted thermal radiation. Solar Energy, 74, 469-488.

[6] Petela, R., 2010. Engineering Thermodynamics of Thermal Radiation for Solar Power Utilization, McGraw-Hill, New York.

[7] Kaushik, S.C., Gupta, M. K., 2008. Energy and exergy efficiency comparison of community-size and domestic-size paraboloidal solar cooker performance, Energy for Sustainable Development. 3, 60-64.

[8] Ozturk, H.H., 2004. Experimental determination of energy and exergy efficiency of solar parabolic-cooker. Solar Energy, 77, 67-71.

[9] Ozturk, H.H., 2007. Comparison of energy and exergy efficiency for solar box and parabolic cookers. J. Energy Engg., 133(1), 53-62.

[10] http://www.mnre.gov.in/pdf/test-proc-dish-cooker.pdf

[11] Subodh Kumar, 2004.Thermal performance study of box type solar cooker from heating characteristic curves. Energy Conversion and Management, 45, 127-139..

[12] Mullick, S.C., Kandpal, T. C., Saxena, A. K., 1987. Thermal test procedure for box-type solar cookers. Solar Energy 39(4), 353-360.

Evaluation of an integrated photovoltaic thermal solar (IPVTS) water heating system for various configurations at constant collection temperature

Rajeev Kumar Mishra[1,*], G.N.Tiwari[1]

[1] *Centre for Energy Studies, Indian Institute of Technology Delhi, New Delhi, India*
** Corresponding author. Tel: +91 9717720464, Fax: +91 1126591251, E-mail: bhu.rajeev@gmail.com*

Abstract: Photovoltaic thermal (PVT) technology refers to the integration of a PV and a conventional solar thermal collector in a single piece of equipment. In this paper, an integrated photovoltaic thermal solar (IPVTS) water heating system for various configurations has been evaluated for constant collection temperature. Analysis is based on basic energy balance for hybrid flat plate collector in terms of design parameters for a solar water heater installed at Solar Energy Park, IIT Delhi, India and climatic parameters provided by India Meteorological Department Pune, India. It is observed that the daily thermal energy gain of IPVTS system decreases with increasing the constant collection temperature. It is also observed that for collectors partially covered by PV modules, daily thermal energy increases with decrease of collector area covered by PV module. The exergy analysis of IPVTS system has also been carried out.

Keywords: *Hybrid PV thermal, Thermal energy, Exergy.*

Nomenclature

A *Area*…….. ……..m^2
C *Specific heat*…… *J/kg K*
F' *Flat plate collector efficiency factor*……..*dimensionless*
F_R *Flow rate factor*……..*dimensionless*
h *Heat transfer coefficient*……..W/m^2
PF_1 *Penalty factor first*……..*dimensionless*
PF_2 *Penalty factor second*……..*dimensionless*
I (t) *Incident solar intensity*……W/m^2
K *Thermal conductivity*……..*W/m K*
$\dot{m}_f$ *Rate of flow of water mass in collector*……..*kg/sec*
Q_u *Rate of useful energy transfer*……..*kW*
T *Temperature*……..^oC
$U_{t\,c,a}$ *Total heat transfer coefficient from solar cell to ambient through glass cover*……..W/m^2 *K*
$U_{L,m}$ *An overall heat transfer coefficient from blacken surface to ambient*……..W/m^2 *K*
V *Air velocity*……..*m/s*

Subscripts
A *ambient*.....
c *solar cell* .....
f *fluid*……
fi *inlet fluid*……
fo *outlet fluid* ……
g *glass*……
m *module* ……
N *number of collectors*……..

Greek letters
α *absorptivity*..-……
$(\alpha\tau)_{eff}$ *product of effective*.....
β *packing factor*……..
η_i *an instantaneous* .....
τ *transmittivity* .....

1. Introduction

Photovoltaic thermal (PVT) technology refers to the integration of a photovoltaic (PV) module and a conventional solar thermal collector in a single piece of equipment. The reason behind the hybrid concept is that more than 80% of the solar radiation falling on PV cells is either reflected or converted to thermal energy. This leads to an increase in the PV cell's

working temperature as much as 40-50^{o} C above the ambient temperature. Because of this temperature increase there can be two undesirable consequences: (i) 0.3% to 0.6 % of efficiency loss per degree C rise in PV cell temperature and (ii) a permanent damage in the structure of PV module if the thermal stress remains for a long period of time. In applications of PVT system, the production of electricity is the main priority, and therefore, it is necessary to operate the PV modules at low temperature in order to keep the PV cell electrical efficiency at a sufficient level. The temperature of the PV module in the hybrid PVT system can be reduced by cooling the base of PV module by allowing water/air to flow below it (Prakash [1], Tripanagnostopoulos et al. [2], Zondag et al. [3], Jones and Underwood [4], Chow [5], and Infield et al. [6]). Thermal energy available from PV module can be used for many applications namely water and air heating for domestic, agricultural sectors and buildings for thermal heating/cooling.

In this paper, the performance of the N collectors connected in series is evaluated by considering the three different cases, namely: Case A: All the collectors are fully covered by glass and connected in series. Case B: All collectors are partially covered by PV modules and connected in series and Case C: All the collectors are fully covered by PV module (glass to glass) and connected in series.

2. Methodology

For the present study conventional tube-in-plate-type collector of area of 2m^2 is considered. The design parameters of photovoltaic thermal (PVT) collectors are shown in Table 1. The glazing surface of the collector is either glass or PV module depending upon the requirement of the user. To increase the absorption of solar radiation the absorber plate of collector is blackened by black paint.

Energy balance equations:

In order to write the energy balance equation of PVT solar water collectors connected in series, the following assumptions have been made:

- One dimensional heat conduction is good approximation for the present study.
- The specific heat of water remains constant. It does not change with rise in temperature of water.
- The system is in quasi-steady state.
- The ohmic losses in the solar cell and PV module are negligible.

Energy balance for solar cells of PV module (glass-glass),

$$\alpha_c \tau_g \beta_c I(t) W dx = \left[U_{tc,a} \left(T_c - T_a \right) + h_{c,p} \left(T_c - T_p \right) \right] W dx + \eta_c \beta_c I(t) \cdot W dx \tag{1}$$

From Eq.(1) the expression fro cell temperature is

$$T_c = \frac{(\alpha\tau)_{1,eff} I(t) + U_{tc,a} T_a + h_{c,p} T_p}{U_{tc,a} + h_{c,p}} \tag{2}$$

Energy balance for blackened absorber plate below the PV module,

$$\alpha_p (1-\beta_c) \tau_g^2 I(t) W dx + h_{c,p} \left(T_c - T_p \right) W dx = h_{p,f} \left(T_p - T_f \right) W dx \tag{3}$$

From Eq. (3), the expression for plate temperature is

$$T_p = \frac{(\alpha\tau)_{2,eff} I(t) + PF_1 (\alpha\tau)_{1,eff} I(t) + U_{L1} T_a + h_{p,f} T_f}{U_{L1} + h_{p,f}} \tag{4}$$

Energy balance for water flowing through an absorber pipe below the PV module,

$$\dot{m}_f C_f \frac{dT_f}{dx} dx = F' h_{p,f} \left(T_p - T_f\right) W dx \tag{5}$$

In the present study three different configurations of PVT solar water collectors have been considered

Case A: All collectors are fully covered by glass and connected is series:

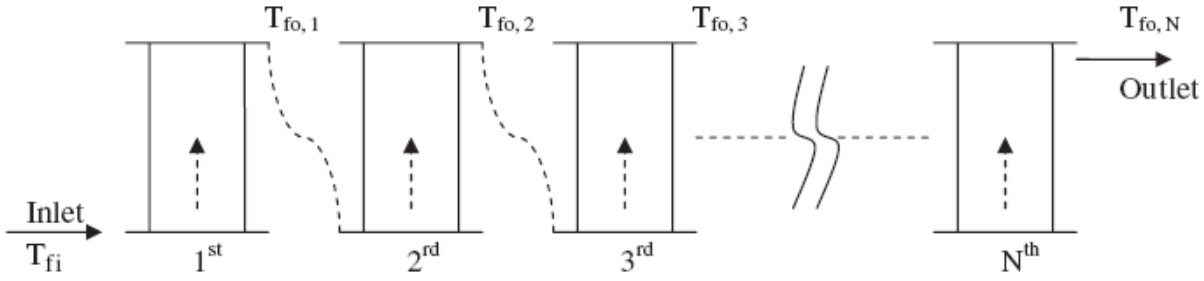

Fig. 1. Collectors fully covered by glass and connection in series.

Following Duffie and Beckman [7] and Tiwari [8] the mass flow rate for N collectors connected in series can be obtained as:

$$\dot{m}_f = \frac{F' N A_c U_{L,c}}{C_f \left[\log\left\{ T_{fi} - \left(\frac{(\alpha\tau)_{c,eff} I(t)}{U_{L,c}} + T_a \right) \right\} - \log\left\{ T_{foN} - \left(\frac{(\alpha\tau)_{c,eff} I(t)}{U_{L,c}} + T_a \right) \right\} \right]} \tag{6}$$

Case B: The collectors are partially covered by PV modules and connected in series

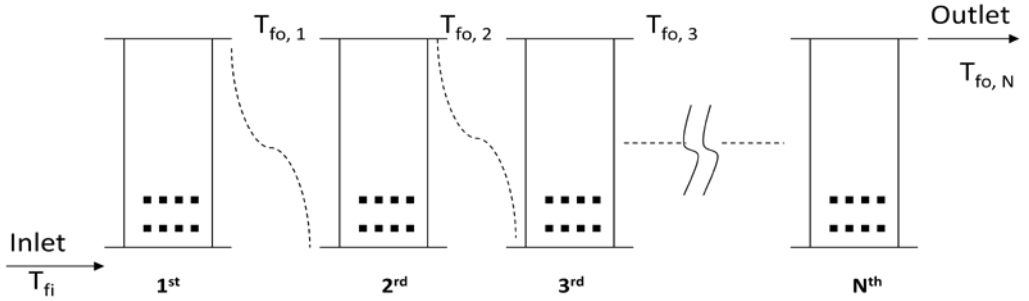

Fig. 2. Collectors partially covered by PV module and connected in series.

Following Dubey and Tiwari [9] the outlet water from N such collectors connected in series can be given as:

$$T_{foN} = \frac{\left(A F_R (\alpha\tau)\right)_1}{\dot{m}_f C_f} \left(\frac{1 - K_K{}^N}{1 - K_K} \right) I(t) + \frac{\left(A F_R U_L\right)_1}{\dot{m}_f C_f} \left(\frac{1 - K_K{}^N}{1 - K_K} \right) T_a + T_{fi} K_K{}^N \tag{7}$$

where,

$$K_K = \left[1 - \frac{\left(A F_R U_L\right)_1}{\dot{m}_f C_f}\right]$$

$$\left(A F_R(\alpha\tau)\right)_1 = \left[A_m F_{R\,m} P F_2(\alpha\tau)_{m,eff}\left(1 - \frac{A_c F_{Rc} U_{L,c}}{\dot{m}_f C_f}\right) + A_c F_{R\,c}(\alpha\tau)_{c,eff}\right]$$

and

$$\left(A F_R U_L\right)_1 = \left[A_m F_{Rm} U_{L,m}\left(1 - \frac{A_c F_{Rc} U_{L,c}}{\dot{m}_f C_f}\right) + A_c F_{Rc} U_{L,c}\right]$$

Case C: All the collectors are fully covered by glass to glass type PV module and connected in series

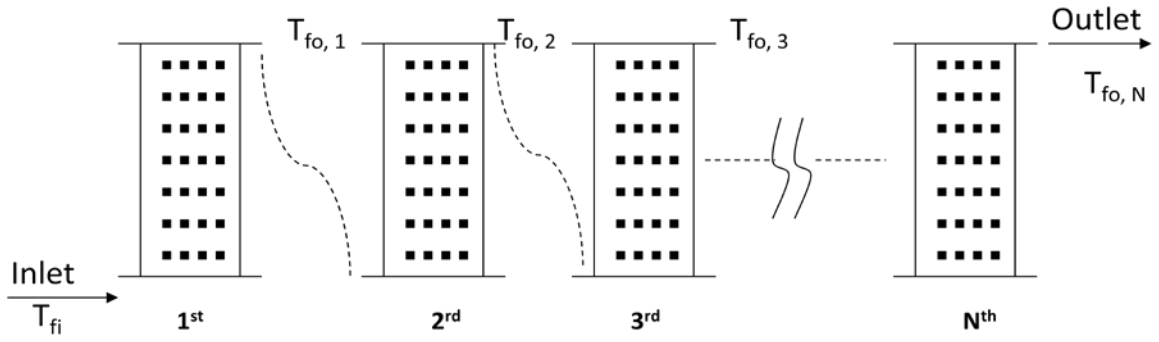

Fig.3. Collectors fully covered by PV modules and connected in series.

Following Dubey and Tiwari [9] Mass flow rate for N collectors partially covered with PV modules connected in series can be obtained as,

$$\dot{m}_f = \frac{N F' A_m U_{L,m}}{C_f\left[\log\left\{T_{fi} - \left(\frac{PF_2(\alpha\tau)_{m,eff} I(t)}{U_{L,m}} + T_a\right)\right\} - \log\left\{T_{foN} - \left(\frac{PF_2(\alpha\tau)_{m,eff} I(t)}{U_{L,m}} + T_a\right)\right\}\right]} \quad (8)$$

The rate of useful thermal energy obtained from N identical collectors connected in series can be given as

$$\dot{Q}_u = \dot{m}_f C_f\left(T_{foN} - T_a\right) \quad (9)$$

Electrical Efficiency of solar cell depends on solar cell temperature and can be given by Evans [10] and Schott [11]

$$\eta_c = \eta_o\left[1 - \beta_o\left(\overline{T_c} - T_o\right)\right] \quad (11)$$

Table 1. Design parameters of photovoltaic thermal (PV/T) collector

Parameters	Values	Parameters	Values
A_C	$2.0m^2$	U_{LC}	3.0 $W/m^{2o}C$
A_m	$0.605m^2$	U_{Lm}	3.44 W/ $m^{2o}C$
C_f	4190 J/kgK	$U_{t\,c,a}$	9.5 $W/m^{2o}C$
F'	0.968	V	1.0 m/s
F_{Rc1}	0.95	W	0.125 m
F_{Rc2}	0.94	α_c	0.90
F_{Rm}	0.96	τ_c	0.95
$h_{c,p}$	5.7 W/m^2	β_c	0.89
$h_{p,f}$	100 W/m^2	η_o	0.12
PF_1	0.357	α_p	0.80
PF_2	0.965	τ_g	095
K	204 W/m^oC		
$\dot{m}$	0.06 kg.sec		

3. Result and Discussions

The variation of solar intensity and ambient temperature for a typical day in the summer month (January) is shown in Figure 4.The values of design parameters of flat plate collector are given in Table 1. Here, the results of the three cases, case A (fully covered by glass) and case B (partially covered by PV modules) and case C (fully covered by PV modules) are discussed in detail. Equations 6, 7 a nd 8 have been computed using MATLAB software for evaluating the mass flow rate at different outlet water temperatures for a typical day during the month of January for a given design and climatic parameters (Table 1). Figures 5a and 5b represent the hourly variation of mass flow rate for case A and case B respectively at various constant outlet temperatures. The result shows that for constant collection temperatures 30-60^{o}C the mass flow rate of water in tubes decreases from 0.1 - 0.01 kg/s in case A, 0.08-0.01 kg/s in case B. Figure 5c gives the hourly variation of mass flow rate for case C. Figure shows that in this case one cannot get the outlet water temperature more than 40^{o}C in January month and the mass flow rate decreases from 0.04 to 0.01 kg/s for case C.

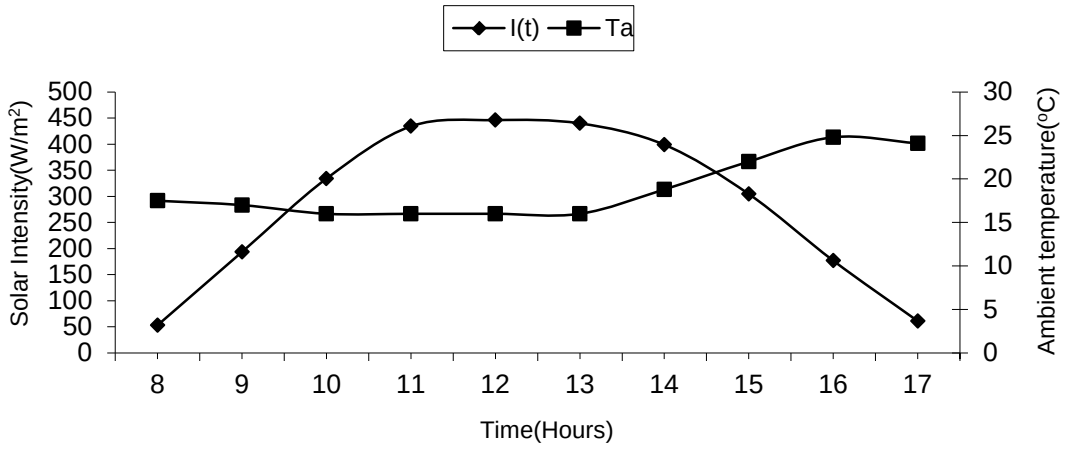

Fig. 4. Hourly variation of solar intensity and ambient temperature of a typical day in the month of January.

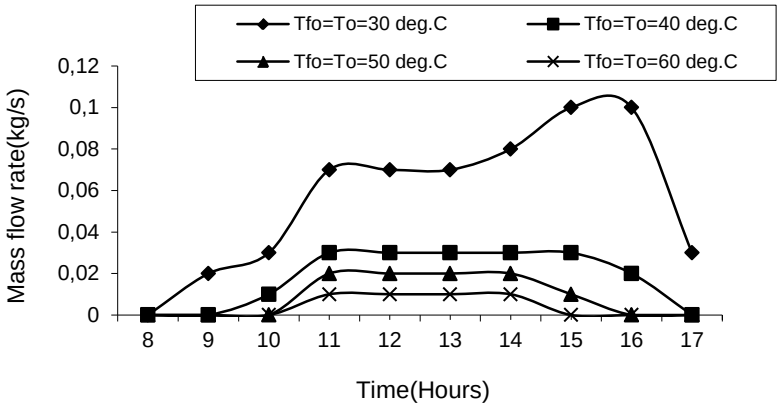

Fig. 5a. Hourly variation of mass flow rate at different outlet temperature for case A.

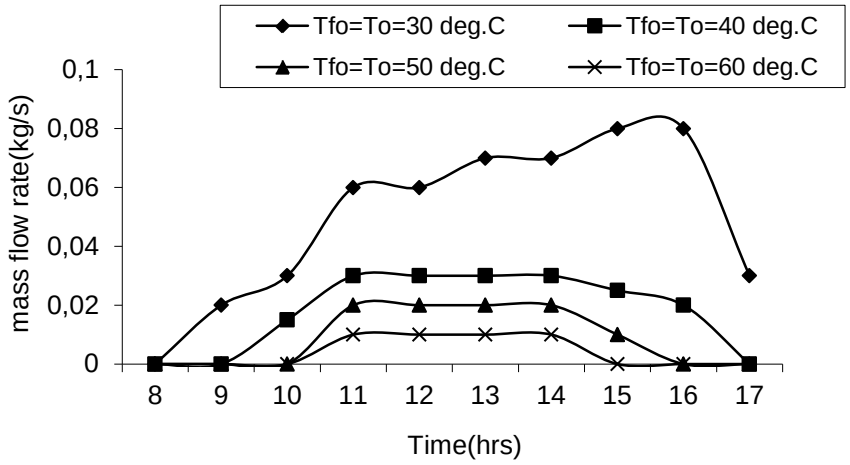

Fig. 5b. Hourly variation of mass flow rate at different outlet temperature for case B.

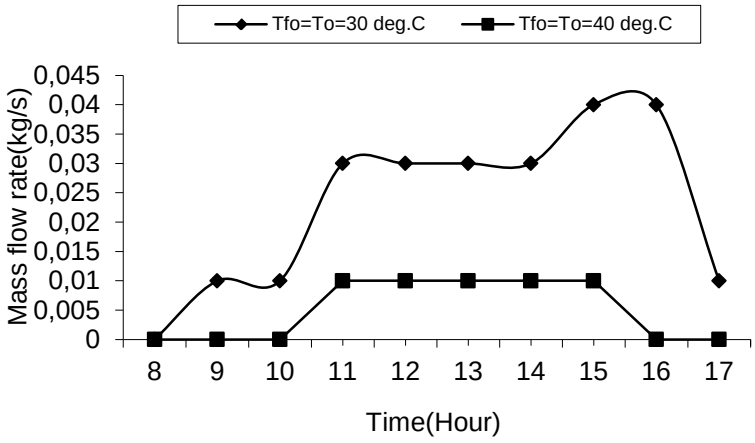

Fig. 5c. Hourly variation of mass flow rate at different outlet temperature for case C.

Fig. 6a and 6b represent the hourly variation of thermal energy gain and electrical energy gain respectively for various configurations of PVT collectors. The figures show that as the

collector area covered by PV modules increases the thermal energy gain decreases whereas the electrical energy gain increases as the collector area covered by PV modules increases.

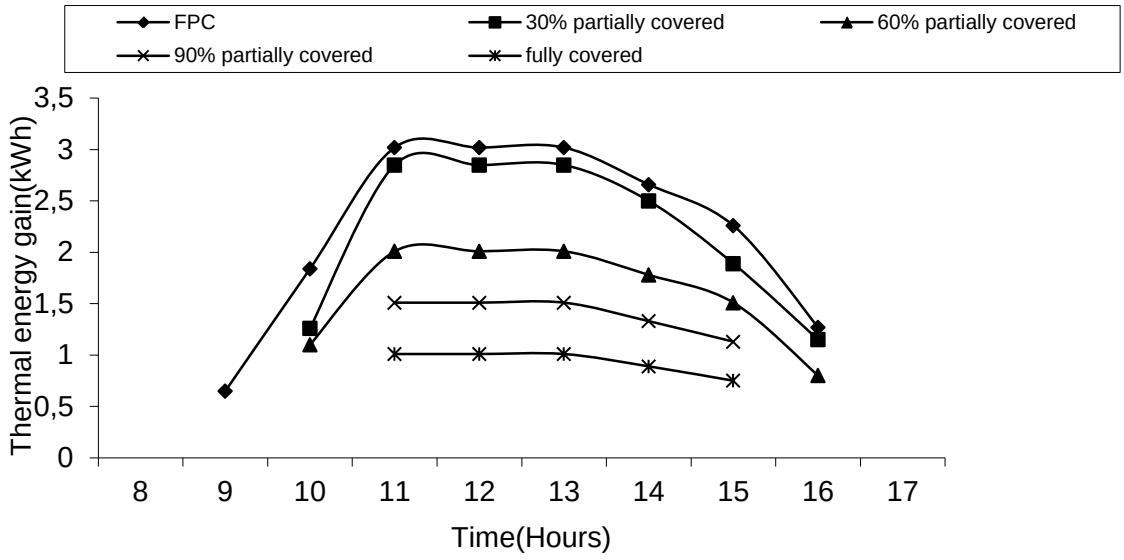

Fig. 6a. Hourly variation of thermal energy gain for different configuration.

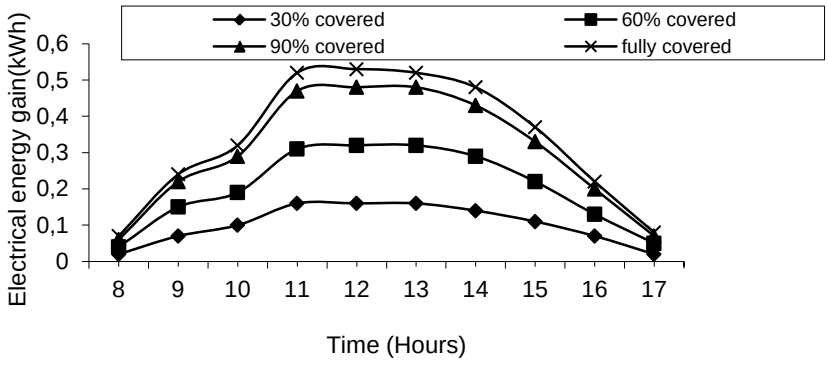

Fig. 6b. Hourly variation of electrical energy gain for different configurations.

4. Conclusion

The maximum thermal energy gain is obtained when collectors fully covered by glass cover; however maximum electrical energy gain is obtained when collectors are fully covered by PV modules.

References

[1] Prakash, J., Transient analysis of a photovoltaic-thermal solar collector for co- generation of electricity and hot air/water. Energy Conversion and Management. 35, 1994 pp. 967 - 972.

[2] Tripanagnostopoulos, Y., Hybrid photovoltaic/thermal solar system, Solar Energy 72(3), 2002, pp. 217-234.

[3] Zondag, H.A., de Vries, D.W. de, van Helden, W.G.J. ,van Zolengen, R.J.C., Steenhoven, A.A., The thermal and electrical yield of a P V-thermal collector. Solar Energy 72 (2), 2002, pp. 113-128.

[4] Jones, A.D., Underwood, C.P., A thermal model for photovoltaic systems. Solar Energy 70 (4), 2001, pp. 349-359.

[5] Chow, T.T., Performance analysis of photovoltaic-thermal collector by explicit dynamic model. Solar Energy 75, 2003, pp.143-152.

[6] Infield, D., Mei, L., Eicker, U., Thermal performance estimation of ventilated PV facades, Solar Energy, 76(1-3), 2004, pp. 93-98.

[7] Duffie, J.A., Beckman, W.A., 1991. Solar Engineering of Thermal Processes. John Wiley and Sons, New York.

[8] Tiwari, G.N., Solar Energy: Fundamentals, Design, Modeling and Applications. Narosa Publishing House, New Delhi, 2004.

[9] Dubey, S. and Tiwari, G.N., Analysis of different configurations of flat plate collectors connected in series, International Journal of Energy Research, 32, 2008, pp. 1362-1372.

[10] Evans, D.L., Simplified method for predicting PV array output. Solar Energy 27, 1981, pp. 555-560.

[11] Schott, T., Operational temperatures of PV modules. In: Proceedings of 6th PV Solar Energy Conference, 1985, pp. 392-396.

Design of a Latent Heat Energy Storage System Coupled with a Domestic Hot Water Solar Thermal System

Robynne Murray[1, 3], Louis Desgrosseilliers[1, 2, 3], Jeremy Stewart[1], Nick Osbourne[1], Gina Marin[1], Alex Safatli[2], Dominic Groulx[1, 3*], Mary Anne White[2, 3]

[1] *Department of Mechanical Engineering, Dalhousie University, Halifax, Canada*
[2] *Department of Chemistry, Dalhousie University, Halifax, Canada*
[3] *Institute for Research in Materials, Dalhousie University, Halifax, Canada*
** Corresponding author. Tel: +1 902 494-8835, Fax: +1 902 423-6711, E-mail: dominic.groulx@dal.ca*

Abstract: Solar domestic hot water (SDHW) can be used to reduce energy bills and greenhouse gas emissions associated with heating domestic water. However, one of the most significant barriers to further deployment of solar thermal applications is the space and weight required for storage of the energy collected. Phase change materials (PCMs) are advantageous for daily energy storage with SDHW due to their high storage density and isothermal operation during phase transitions, and would overcome these obstacles.

The aim of this paper is to outline the initial steps in the development of a SDHW energy storage system using PCMs, with emphasis on the numerical and experimental studies used to access the phase change and thermal behaviour of the selected PCM. Lauric acid was selected as the PCM based on the melting temperature range which was targeted by studying solar data from an existing solar hot water system in Halifax, Nova Scotia, Canada. Due to the low thermal conductivity of PCMs, additional work is required to develop and validate a design to enhance heat transfer to the storage material using fins. The selected design will be built and installed in an existing large scale solar thermal system on an apartment building in Halifax. The system will be instrumented in order to acquire continuous data (temperatures, flow rates, pressures, etc.) to fully characterize the system.

Keywords: *Latent heat storage, Solar domestic hot water, Phase change materials, Heat transfer enhancement*

1. Introduction

Solar thermal energy for domestic hot water heating is one of the most cost effective and efficient areas of alternative energy exploitation [1]. The use of phase change materials (PCMs) in latent heat energy storage systems (LHESS) can reduce the volume and weight of storage due to their high storage density, and overcome major obstacles in the further deployment of solar thermal energy [1]. LHESS have high energy densities compared with sensible heat storage systems [2], and have been shown to store up to 14 times more heat per unit volume than sensible heat storage materials [3]. Fig. 1 shows a simple schematic of a SDHW system with PCM energy storage.

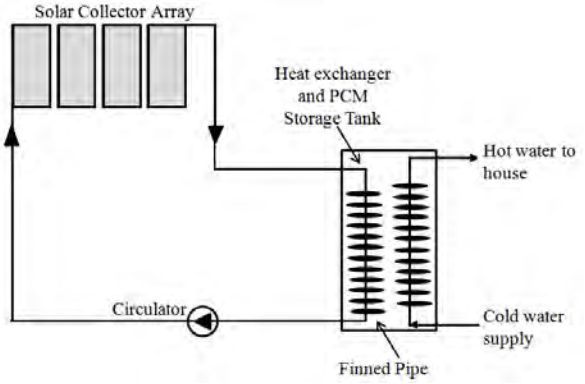

Fig. 1. Schematic of a LHESS for SDHW.

Energy storage using PCMs in combination with solar collectors has been studied mathematically [4] and experimentally [5] and shown to be advantageous. However, missing from previous works is a working prototype of a SDHW system for a large scale application [6].

This paper presents a phase change heat transfer study performed using a PCM, lauric acid, in a small-scale experimental LHESS using fins to enhance the overall heat transfer process. A numerical model was also created and its results are compared and validated with experimental results. Results of this study are to be used in the design of a SDHW system, with the numerical model to be used further in design optimization, mainly for fin configurations, of the LHESS. The resulting LHESS design will be built and installed in an existing large scale solar thermal system on an apartment building in Halifax by Scotian Windfield Inc.

2. Phase Change Material Selection

The PCM is selected based on its phase change temperature range and the operating temperatures of the SDHW system. A melting temperature range of 42 to 48°C and solidification temperature range of 35 to 40°C were targeted by studying the solar data from an existing SDHW system in Halifax, Canada. Several PCMs were considered based on their appropriate melting temperatures, low toxicities, and cost. The most promising materials were tested using a differential scanning calorimeter (DSC) to study their melting and solidification temperature ranges. Salt hydrates (e.g. Glauber's salt and sodium acetate) tested in the DSC showed significant supercooling, which is a common and undesirable phenomenon for these materials [7].

The DSC curve for lauric acid (dodecanoic acid; $CH_3(CH_2)_{10}COOH$; crude [< 80% pure], Fisher Scientific), presented in Fig. 2, shows a melting temperature range of 43.3 to 45.7 °C and solidification temperature range of 38.8 to 35 °C. The DSC curve for this lower purity sample compared well with literature curves for pure lauric acid [8]. Other fatty acids that were tested had either incompatible phase transition regions or toxicities and cost that were undesirable.

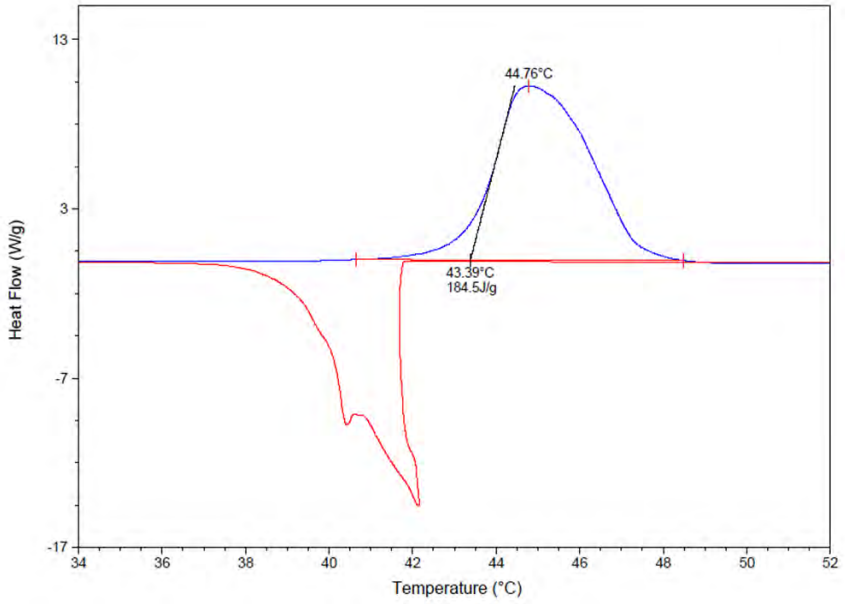

Fig. 2. DSC Curve for Lauric Acid (80% purity) measured at 10 K/min.

Lauric acid was selected based on its melting temperature range, high heat of fusion, minimal supercooling and safety. The material properties are displayed in Table 1.

Table 1. Thermal and Physical Properties of Lauric Acid [8,9].

Molecular Weight	200.31 (kg/kmol)
Density of Powder at 20°C / Liquid at 45°C [§]	869 / 873 (kg/m^3)
Fusion Temperature	42 (˚C)
Latent Heat of Fusion	182 (kJ/kg)
Heat Capacities Solid/Liquid [†]	2.4/2.0 (kJ/kg·K)
Thermal Conductivities Solid/Liquid [†]	0.150[*]/0.148 (W/m·K)
Viscosity [†]	0.008 (Pa·s)

[*] Value obtained from present experiments.
[†] Nominal properties calculated near the melting point.
[§] Density used in the numerical model presented = 880 kg/m^3.

To insure stable properties after many melting/solidification cycles, lauric acid was thermally cycled from 37 to 63 °C. After 800 cycles, there were no obvious signs of degradation. Lauric acid is also safe to use in conjunction with a SDHW system because it is a food grade substance and only a mild irritant [9].

3. Experimental Setup

The experimental setup used to study the melting and solidification behavior of lauric acid in a cylindrical container with horizontal copper fins is shown schematically in Fig. 3a. A Solidworks 3D rendering of the container is shown in Fig. 3b. Eight type T probe thermocouples are connected to a National Instruments 16-channel thermocouple module (NI9213) CompactDAQ data acquisition system. Temperatures are recorded using LabView. Thermocouples are located inside the lauric acid (T2 to T7) as well as on the inlet and outlet (T1 and T8), as seen in Fig. 3a. A pulse counter flowmeter from Omega is connected to a counter/pulse generation module (NI9435) on the DAQ system and read by LabView. The container is made of ¼-inch acrylic plastic and is un-insulated to allow visual study of the system.

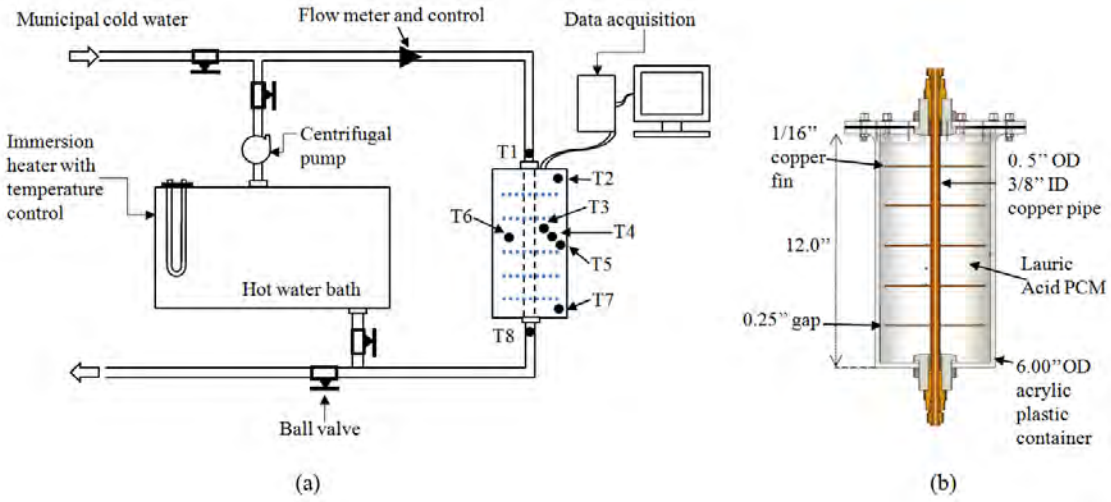

Fig. 3. (a) Schematic of the experimental setup and (b) PCM container.

The conditions under which the experiments were performed are summarized in Table 2.

Table 2. Experimental parameters.

Hot Water Inlet Velocity	1.5 (m/s)
Cold Water Inlet Velocity	3.5 (m/s)
Hot Inlet Temperature	55 ± 1 (^{o}C)
Cold Inlet Temperature	12 (^{o}C)

At the beginning of the experiment, lauric acid was solid in the container at room temperature. Hot water from the constant temperature water bath was pumped through the finned copper pipe, eventually melting the lauric acid. T he charging portion of the experiment was completed when the system reached steady state. At this point, cold water from the municipal water supply was pumped through the system to solidify the lauric acid and recover the stored thermal energy. The experiment concluded when the lauric acid was at room temperature. The results obtained with this setup were compared to results of numerical simulations.

4. Numerical Study

COMSOL Multiphysics (version 4.0a) was used to build a 2D axisymmetric numerical model of the experiment using the *Heat Transfer in Solids* physics to model the copper and lauric acid, and the *Laminar Flow* and *Heat Transfer in Liquids* physics to model the flowing water. The thermophysical properties of water and copper used in the model are those given by COMSOL. For lauric acid, the thermophysical properties used are those presented in Table 1. In this first numerical study, natural convection in the lauric acid was neglected to reduce computing time. An extremely fine mesh was used, with a maximum element size of 2.58×10^{-9} m^2. The following boundary and initial conditions were used:

i. Initial temperature of 295 K;
ii. All outside walls have radiation heat losses to the surroundings and natural convection losses are accounted for on the side wall;
iii. No-slip condition on the inner pipe wall;
iv. Inlet temperature and water velocity as in Table 2;
v. No viscous stress and convective flux at the pipe outlet.

Groulx and Ogoh's method of numerically modeling the melting process was used [10]. The simulated time for melting was 11.5 hou rs, and 10 hour s for cooling. Simulations took approximately 8 hours to run.

In the experimental setup, two thermocouples (T4 and T6) were placed symmetrically between horizontal fins at the same height but spaced 180^{o} apart in order to confirm symmetry in the experiment. In the numerical model, a reference point was added to extract information at this location, as shown in Fig 5.

5. Results and Discussion

5.1. Charging Process (Melting)

Figure 4 presents the temperatures measured experimentally by thermocouples T1 to T8 during the charging process. Refer to Fig. 3 for thermocouple positions.

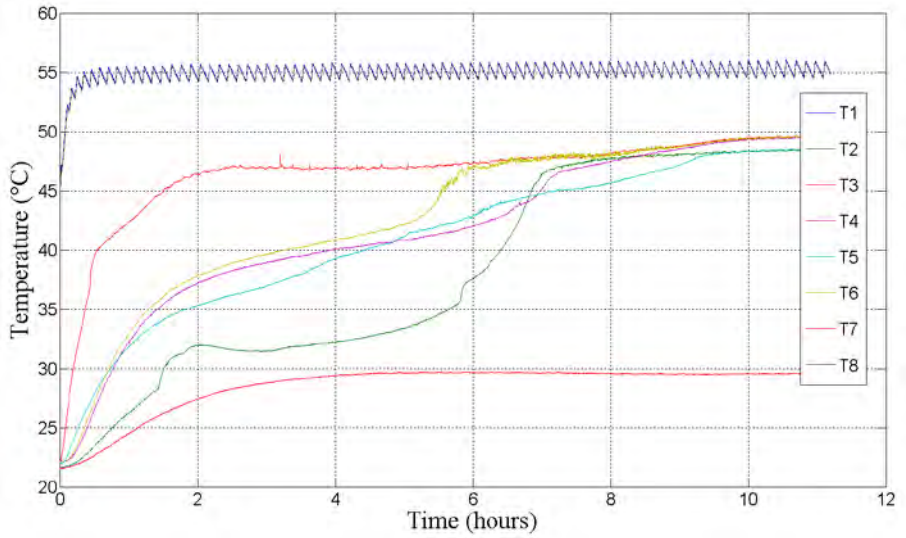

Fig. 4. Experimental temperatures during charging.

The inlet temperature (T1) fluctuates during the charging process due to the emersion heater on/off fluctuations, the outlet temperature (T8) logically follows the same trend. The temperature increases more rapidly close to the pipe and fins (T3), where it takes a longer time for the lauric acid to heat up and melt in regions farther from the pipe, T4 and T6, followed by T5. The region in the upper corner of the container experiences a fast increase in temperature (T2) after 6 hours, mainly due to the onset of natural convection in this region. The lauric acid does not reach the melting temperature in the bottom corner (T7).

Figure 5 shows the numerically obtained temperatures in the system during charging. The black contour line represents the melting interface.

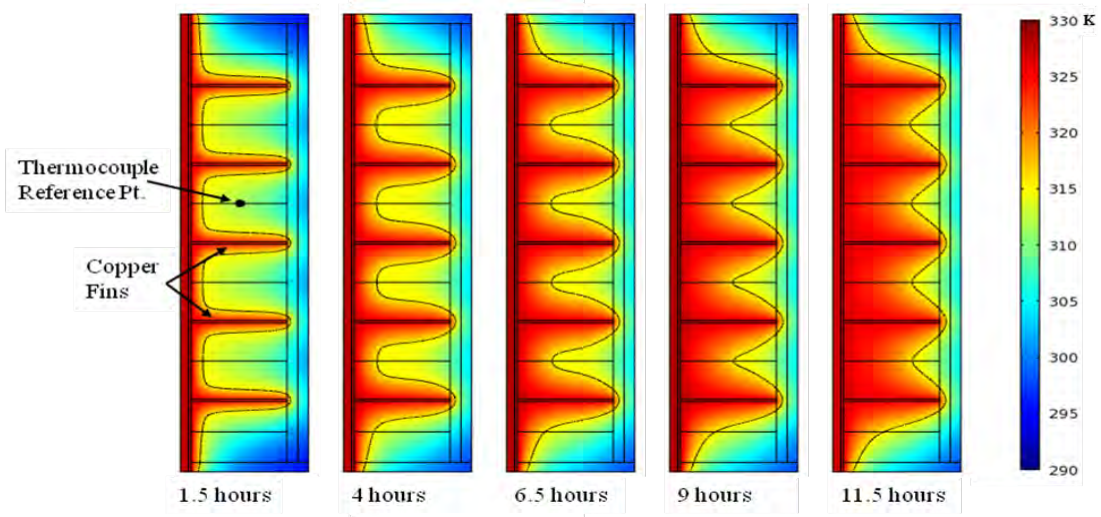

Fig. 5. Numerical temperature plots during charging after 1.5, 4, 6.5, 9 and 11.5 hours.

In Fig. 5, it can be observed that after 1.5 hours the melting process started near the pipe and fin surfaces first, with fairly small temperature increases everywhere else. The heat transfer has been enhanced by adding fins, which is clearly evident by looking at the overall temperature increases far from the pipe. After 11.5 hours of charging, solid lauric acid was still present around the inside wall of the container and in the corners. Experimentally, after 11.5 hours, solid lauric acid was only found in the bottom corners. This difference is thought

to be due to the effect of natural convection in the system, which increases the overall rate of heat transfer.

The experimentally measured (green and blue lines) and numerically calculated (red line) temperatures during the charging process are presented in Fig. 6.

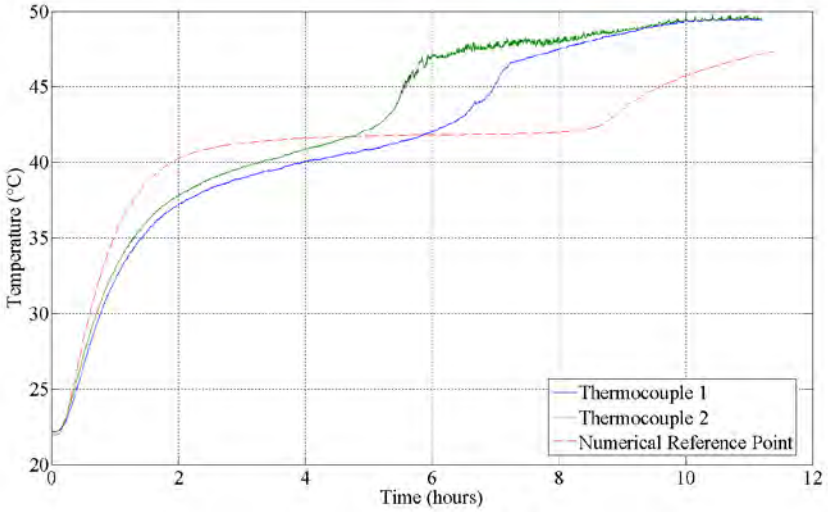

Fig. 6. Numerical validation of melting process in PCM container.

Thermocouples T4 and T6 showed slightly offset temperatures due to asymmetry in the fin assembly which caused one side of the container to heat up faster than the other. Melting occurred between 3 and 8.5 hours in the numerical model. The melting point was reached experimentally after 5 and 6 hours, with fairly constant temperature increases leading to this point; this is consistent with the formation of a mushy region around the thermocouple probes. Complete melting of the lauric acid numerically took longer, possibly due to the lack of natural convection in the model. Experimental results showed a sudden temperature increase in the liquid lauric acid just after melting; this rate of temperature increase in the liquid lauric acid was predicted well by the model.

The numerical model predicted higher effective heat transfer rates initially, leading to a faster temperature increase in the first 2 hours of charging; this is thought to be due to the ideal contact conduction between pipe, fins and lauric acid in the model. In the experimental setup, contact resistances between pipe and fins, as well as between copper surfaces and the solid lauric acid, may have resulted in decreased heat conduction rates at startup.

5.2. Discharging Process (Solidification)

Because of the higher flow rate of cold water used during the discharging process, solidification happened over a shorter period of time than melting: 3.5 hours compared to 11. Figure 7 shows the temperatures in the system during discharging, obtained numerically. The white contour line represents the solidification interface. Solidification of the lauric acid in the numerical model took 4 hours, as seen in Fig. 7.

Figure 8 shows the experimental (blue and green lines) and numerical (red line) cool down temperatures during discharging.

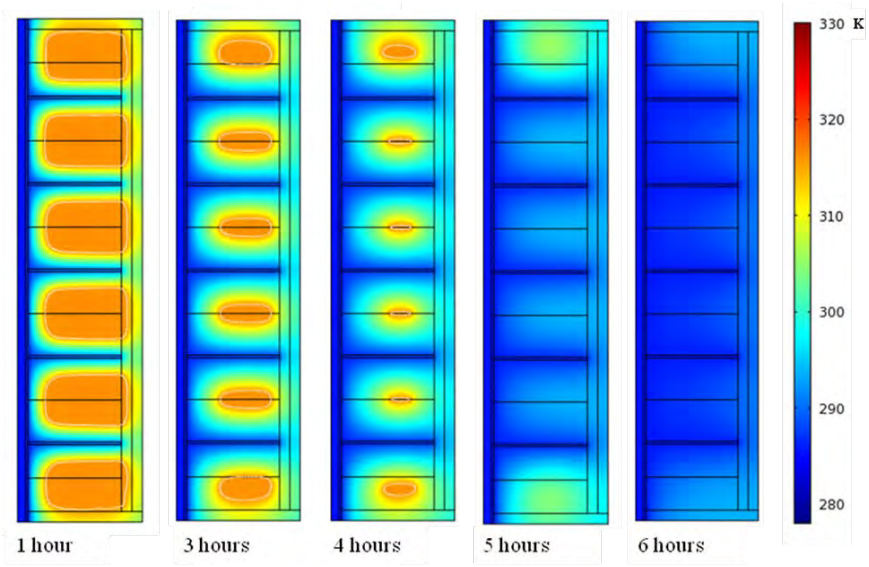

Fig. 7. Numerical temperature plots during discharging after 1, 3, 4, 5 and 6 hours.

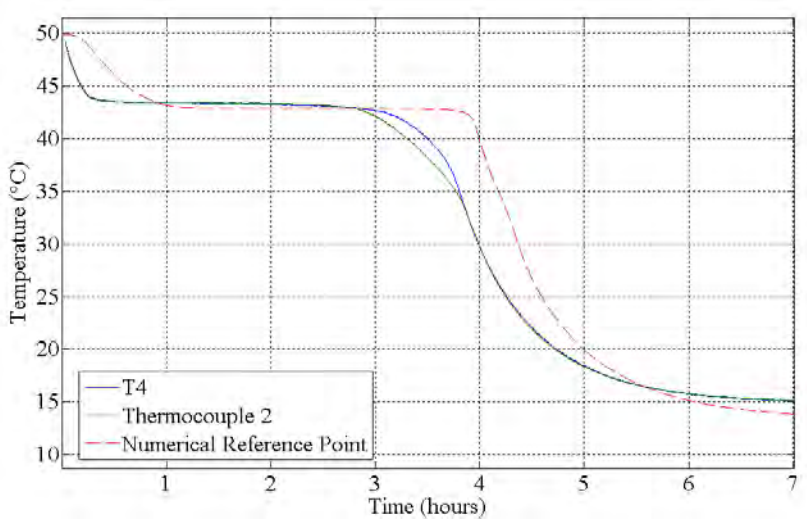

Fig. 8. Numerical validation of solidification process in PCM container.

Of importance to note, the lauric acid solidified at a temperature of 43°C, different from the predicted DSC measurements, which normally have a certain degree of supercooling. Nucleation happened in the first 15 minutes of cooling during the experiment, due to the presence of the thermocouple probes; this cannot be predicted numerically. However, the model does predict a solidification plateau similar to the one observed experimentally, and only slightly over predicts the time required for solidification at that point in the system.

Throughout the experiment, an insignificant amount of volume change from the solid to liquid phase was observed. Lauric acid did react weakly with copper, taking a bluish color in the liquid state; however this mild reaction does not lead to corrosion in any significant form [11].

6. Conclusion

The melting and solidification behavior of lauric acid inside a cylindrical container with a horizontal finned pipe was examined experimentally and numerically. Results for the charging experiment, when compared to the numerical simulations, clearly showed that a mushy region appeared in the system. The presence of natural convection in the liquid melt played a significant role in speeding up the heat transfer and melting process. During

discharging, the numerical results predicted fairly well the cooling and solidifying behavior observed in the experimental measurements; demonstrating that the effect of natural convection during solidification is for the most part negligible.

Acknowledgments

We thank Scotian Windfields for their support and expertise, as well as for funding for this project; Eco-Nova Scotia and the Natural Sciences and Engineering Research Council of Canada for their financial support; and the Dalhousie's Mechanical Engineering Department for research space and a flowmeter. The DSC is part of the Facilities for Materials Characterization managed by the Institute for Research in Materials at Dalhousie University.

References

[1] F. Agyenim, N. Hewitt, P. Eames and M. Smyth, A review of materials, heat transfer and phase change problem formulation for LHTESS, Renewable and Sustainable Energy Reviews 14, 2010, pp.615–628

[2] A.I. Fernandez, M. Martı´nez, M. Segarra, I. Martorell and L.F. Cabeza, Selection of materials with potential in sensible thermal energy storage, Solar Energy Materials & Solar Cells 94, 2010, pp. 1723-1729

[3] A. Sharma, V.V. Tyagi, C.R. Chen and D. Buddhi, Review on thermal energy storage with phase change materials and applications, Renewable and Sustainable Energy Reviews 13, 2009, pp. 318–345

[4] H. El Qarnia, Numerical analysis of a coupled solar collector latent heat storage unit using various phase change materials for heating the water, Energy Conversion and Management 50, 2009, pp. 247–254

[5] A. Sarı, and K. Kaygusuz, Thermal and heat transfer characteristics in a latent heat storage system using lauric acid, Energy Conversion and Management 43, 2002, pp. 2493–2507

[6] A. Shukla, D. Buddhi and R.L. Sawhney, Solar water heaters with phase change material thermal energy storage medium: A review, Renewable and Sustainable Energy Reviews 13, 2009, pp. 2119–2125

[7] Sandnes, B., and Rekstad, J., Supercooling Salt Hydrates: stored enthalpy as a function of temperature, Solar Energy 80, 2006, pp. 616-625

[8] Chemical Properties Handbook, edited by C. L. Yaws, McGraw-Hill, 1999

[9] A11672 – Dodecanoic Acid, Material Safety Data Sheet, Alfa Aesar, 2009, www.alfa.com/en

[10] D. Groulx and W. Ogoh, Thermal behavior of phase change material during charging inside a finned cylindrical latent heat energy storage system: Effects of the arrangement and number of fins, Proceedings of the International Heat Transfer Conference, Washington, DC, USA, 2010

[11] A. Sari and K. Kaygusuz, Some fatty acids used for latent heat storage: thermal stability and corrosion of metals with respect to thermal cycling, Renewable Energy 28, 2003, pp.939-948

Retrofitting Domestic Hot Water Tanks for Solar Thermal Collectors A theoretical analysis

Luís Ricardo Bernardo[1,*], Henrik Davidsson[1], Björn Karlsson[2]

[1] *Energy and Building Design, Lund Technical University, Lund, Sweden*
[2] *Mälardalen University, Västerås, Sweden*
** Corresponding author. Tel: +46 462227606, Fax: +46 462224719, E-mail: Ricardo.Bernardo@ebd.lth.se*

Abstract: One of the most expensive components of a solar thermal system is the storage tank. Retrofitting conventional domestic hot water heaters when installing a new solar hot water system can decrease the total investment cost. In this study, retrofitting of existing water heaters using forced circulation flow was investigated. A comparison with a standard solar thermal system is also presented. Four simulation models of different system configurations were created and tested for the climate in Lund, Sweden. The results from the simulations indicate that the best configuration consists on connecting the collectors to the existing heater throughout an external heat exchanger and adding a small heater storage in series. For this retrofitted system, preliminary results show that an annual solar fraction of 53% is achieved. In addition, a conventional solar thermal system using a standard solar tank achieves a comparable performance for the same storage volume and collector area. Hence, it is worth to further investigate and test in practice this retrofitting. Furthermore, using the same system configuration, solar collectors can also be combined with new standard domestic hot water tanks at new installations, accessing a world-wide developed and spread industry.

Keywords: *Solar thermal, Storage tank, Water heater, Retrofit, Domestic hot water*

Nomenclature

$T_{auxilia}$ *Preset temperature of the auxiliary heater.....(°C)*
T_{out} *Collector outlet temperature.....(°C)*
T_{solar} *Solar hot water temperature in the upper part of the retrofitted tank ….....(°C)*
t *Time during stagnation periods……(h)*

1. Introduction

Only in Sweden there exist more than half a million electrically heated single family houses that use conventional water heaters for domestic hot water production [1]. Since the solar tank is one of the most expensive components in a solar thermal system, retrofitting existing domestic water heaters when installing a new system can decrease its total investment cost. Previous research approached similar retrofitting using natural convection systems [2]. Thermosyphon systems became popular in several parts of the world such as Eastern Asia and Australia mainly due to its simplicity and reliability [3]. The thermosyphon driving force depends on the pressure difference and frictional losses between the heat exchanger side-arm and the tank. Hence, the generated flow will be complex function of the state of charge of the tank, the temperature profile along the heat exchanger and pipes, the height difference between the top of the heat exchanger and the top of the tank and the pressure drop in the heat exchanger, piping and connections [4].

Such dependence on the heat exchanger pressure drop and tank characteristics limits how the retrofit is carried out and which storage tanks can be used. Moreover, Liu and Davidson (1995) [5] showed that, when properly designed, forced circulation systems can generally achieve higher performances compared to natural convection driven systems.

In this research forced circulation was used to connect solar collectors to conventional domestic water heaters. This was carried out by means of two pumps, one in the tank loop and the other in the solar collector loop. Four different system configurations were simulated in TRNSYS [6]. Since forced circulation is used, almost any kind of storage tank can be retrofitted when installing a new solar thermal system. For a better understanding of the research contribution to the field and to increase the paper readability, the main objectives of the study are stated bellow:

- To compare the performance of different alternatives on r etrofitting conventional domestic water heaters when installing a solar thermal system;
- To compare the performance of the retrofitted system with the performance of a standard solar thermal system.

2. Methodology

Four different simulation models of the retrofitted system were created in TRNSYS software [6] in order to estimate the configuration achieving the highest performance. A comparison with a conventional flat plate system was also performed. The retrofitted system models range from simple connections to more advanced configurations. However, the complexity was never raised up to a level that would be technically difficult to build such a system in practice. Also, it was avoided to design configurations that would predictably cause such a rise on the investment cost that would be hardly paid back by the increase in energy savings. Some of the systems' details are not revealed due to patent pending. Each system model is made up of a solar collector array, storage tank/s, auxiliary heater, heat exchanger between the collector and the tank loops, circulation pump/s, and radiation processor.

The main boundary of this investigation was to use the most common type of existing heater in single family houses in Sweden. This information is very important for the system design but also very hard to attain. To the best of our knowledge, there is no official data concerning the most common tank size in such houses. According to the Swedish domestic water heater manufacturers, installers and researchers in the field, the most common Swedish single family house tank size is 200-300 litres, depending on the family size. In any case, the tank volume tends to be proportional to the family size. Thus, the trend is that higher loads also correspond to higher available storage volumes and the system design strategy does not change. On the other hand, the average domestic hot water load in single family houses is documented. Preliminary results showed that retrofitting a 300 litre tank for such a domestic hot water load would achieve a higher annual solar fraction than using a 200 l itre tank. Hence, to work on the safe side, it was decided to retrofit a 200 litre tank. If such a system achieves satisfactory performances the same should happen if a 300 litre tank is retrofitted instead.

An auxiliary heater power of 3 kW was used in all models since this is also the most common. The auxiliary heater keeps the top volume of the storage at 60˚C. This is a recommendation of the Swedish building regulations to avoid legionella problems [7]. The same document legislate that it is mandatory that the hot water temperature available at the tap is not less than 50°C. As a design guideline it is recommended that the domestic hot water system can be able to deliver two times 140 litres of 40°C water in one hour [7]. If the temperature setting is increased, all the different simulated systems reach approximately this peak on consumption. In practice, the thermostat is set to 60°C which ensures that ordinary loads are fulfilled. In case of extraordinary large draw-offs, the user has the possibility to steer the set point temperature. This is also normally the case for stand-alone conventional heaters.

The domestic hot water load profile consists on seven different draw-offs during the day. It is a simplification of the hourly profile described by [8] but scaled down to the latest data on the Swedish average hot water consumption of 42 litres/person/day [9]. Simulation results show that using a detailed hour profile would have a minimum impact on the results and would only increase the simulation total time. The measured average cold water temperature in the taps was 8.5°C. The consumption variation during the year was also introduced [10]. The daily and yearly domestic hot water profiles used in the models are shown in Figure 1. The average number of inhabitants in Swedish single-family houses is three [11]. Hence, the domestic hot water annual consumption in these houses was estimated to be 2050 kWh/year.

Since long stagnation periods affect the system's long-term reliability and can cause serious permanent damages on its components [12], the criteria used to design the collector array was based on the maximum solar fraction possible to be achieve under a certain overproduction limit. This deterioration factor was set to 5000 °C.h/year and integrates the number of hours which the collector was under stagnation and how much the collector outlet temperature raised over 100 °C during that period. This was calculated in the following way:

$$\Sigma\ (T_{out}-100)\ t \quad (°C.h) \text{ (during stagnation periods)} \qquad (1)$$

Stagnation period was defined by the time period during which both the top of the storage tank and the outlet collector temperature was above 100°C. During this period the pump on the collector loop is stopped. As shown in equation 1, it was assumed that stagnation time and collector outlet temperatures above 100°C have a linear influence on this parameter. 5000°C.h/year was considered to represent a reasonable practical maximum overproduction. This corresponds to, for example, 100 hours at stagnation where the collector outlet temperature was 150°C. Hence, by means of simulation, the maximum collector area that ensures maximum solar fraction under the overproduction limit was determined for each system configuration at a 50° collector tilt from horizontal. This design criteria is further discussed in the "Results and Discussion" chapter.

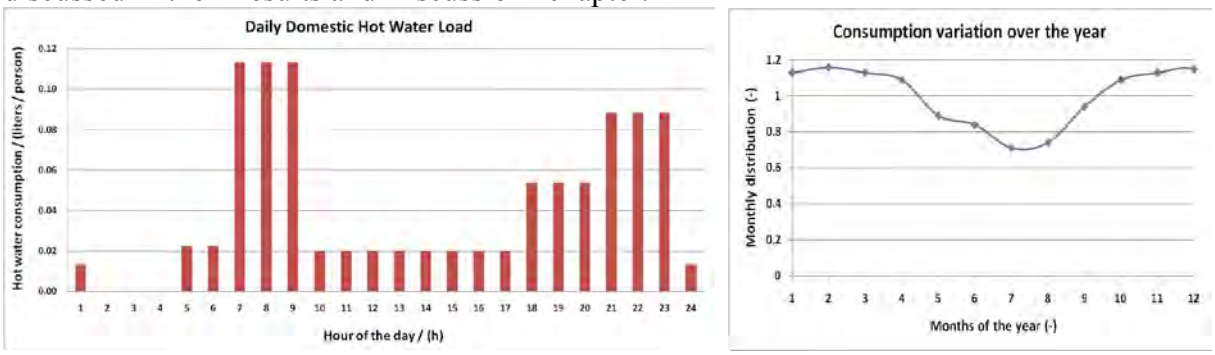

Fig. 1. Daily and yearly domestic hot water profile.

2.1. Standard system

A model of a standard solar thermal system was created and is described by the sketch in Figure 2. The figure illustrates a solar tank with and internal heat exchanger and auxiliary heater. The storage volume is 255 litres in order to match the volume of the retrofitted system that has the best performance (retrofitted system 4, Figure 6). There are three temperature sensors that control the pump, two placed on the tank's surface and the other at the collector outlet.

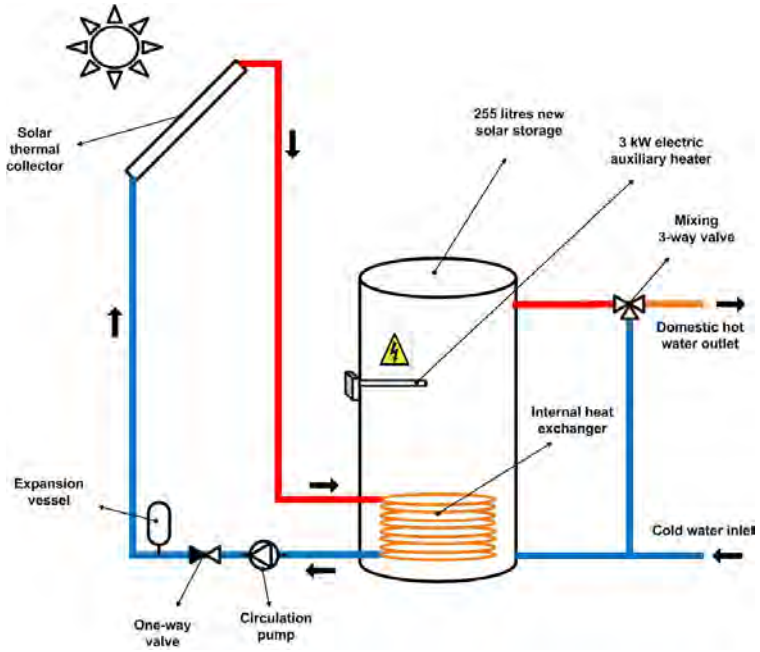

Fig. 2. Sketch of the standard solar thermal system.

2.2. Retrofitted system 1

Figure 3 describes one of the most simple and direct ways of assembling solar collectors to existing tank heaters. The connection is carried out by means of an external side-arm heat exchanger between the collector and the tank loops. Also, two temperature sensors are placed on the tank's surface in order to control both the collector and the tank pumps. As exemplified in Figure 2, solar storages are specially designed for solar thermal applications with, at least, two connections for the domestic hot water and two others for the solar collector loop. On the other hand, conventional tank heaters have only the two connections for domestic hot water (see Figure 3). In order to overcome this technical challenge, the working period of the pump placed on the tank loop must be controlled with the domestic hot water draw-offs so they do not coincide. When no hot water is required, the pump is able to charge the tank. When draw-offs take place, the pump is turned off and the incoming cold water is pressed in the bottom of the tank replacing the outgoing domestic hot water at the top.

2.3. Retrofitted system 2

In this system, a new 3 kW auxiliary water heater is added to the side-arm heat exchanger (Figure 4). Alternatively, if possible, the old auxiliary heater at the bottom of the existing tank can be used. The aim is to achieve stratification in the tank. The heater and the pump on the tank loop are turned on when the temperature in the sensor placed on the top of tank falls below the set point temperature minus the dead band. Consequently, the cold water in the tank bottom flows through the heat exchanger and is heated up in the side-arm heater before entering the top of the tank. The heater is turned off when the temperature on the upper sensor is higher than the set point temperature plus the dead band.

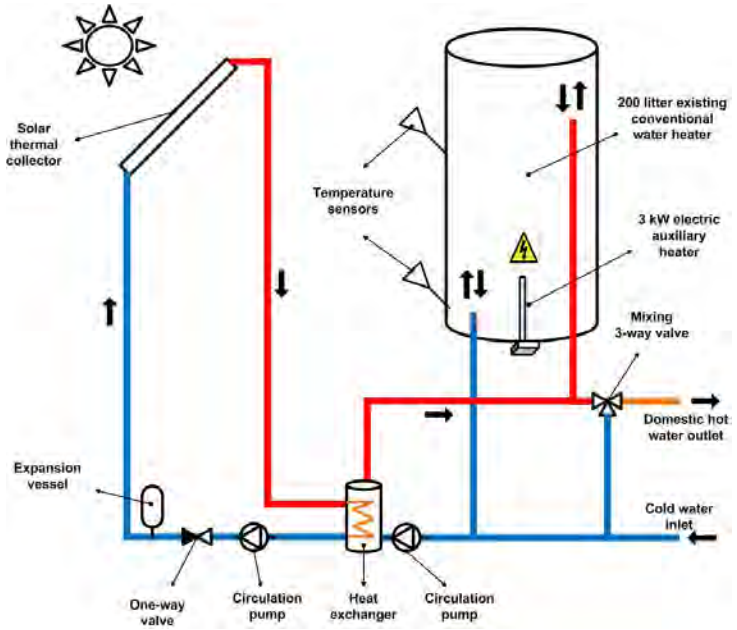

Fig. 3. Retrofitted system 1 - simple retrofitting of existing hot water heaters.

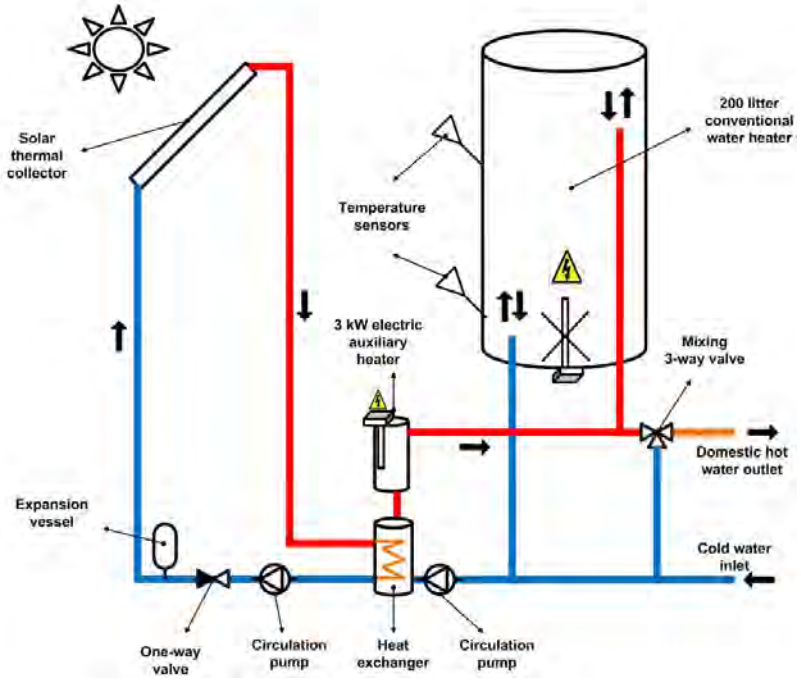

Fig. 4. Retrofitted system 2 - retrofitted system with auxiliary heater on the side-arm.

2.4. Retrofitted system 3

In retrofitted system 3, a small 55 litre auxiliary heater storage was added to the system (Figure 5). This means that the retrofitted storage is exclusively used for solar hot water. The volume of 55 litres was chosen based on design guideline for the domestic hot water load. The 4-way valve was modelled in TRNSYS using type 221 [13]. The valve has three inlets, two from hot sources and one from a cold source. It is programmed in order to use as much water volume as possible from the colder hot source which, in this case, corresponds to the solar storage. Hence, as long as there is available solar hot water in the retrofitted storage at the same temperature or above the domestic hot water load temperature, the water inside the auxiliary heater tank will not be used.

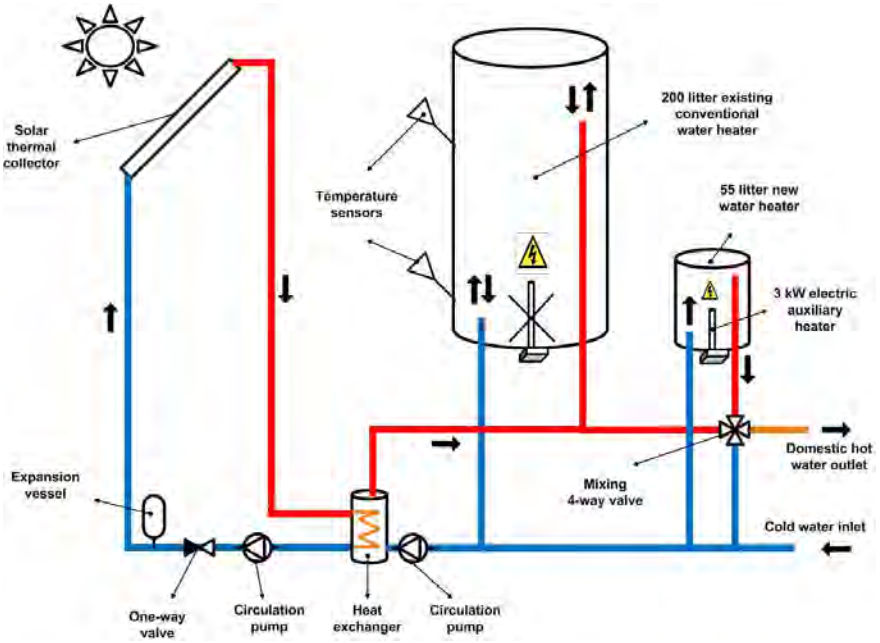

Fig. 5. Retrofitted system 3 - retrofitted system with an additional tank heater connected in parallel.

2.5. Retrofitted system 4

The last retrofitted system consists of connecting the small heater storage to the existing heater in series instead (Figure 6). Thus, when hot water is drawn off by the user, the water at the top of the solar storage is pushed to the bottom of the small heater.

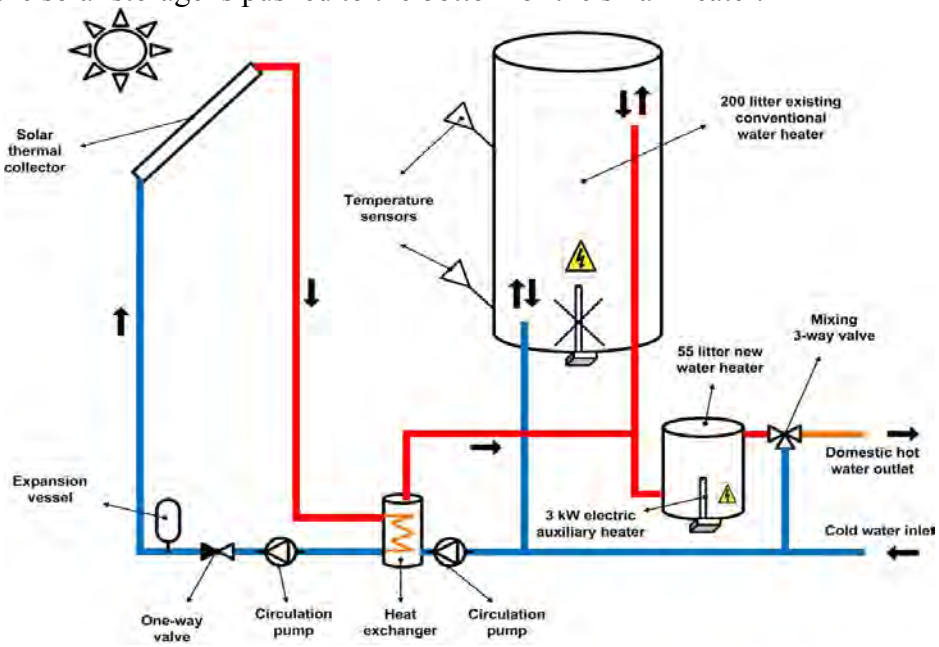

Fig. 6. Retrofitted system 4 - retrofitted system with an additional tank heater connected in series.

3. Results and Discussion

The assumed design criterion limiting the collector area takes into account not only the number of stagnation hours but also the collector outlet temperature. This deterioration factor was set to 5000 °C.h/year. Obviously, this design criterion can be questioned, especially when it comes to the particular chosen number of 5000 °C .h/year. Also, it is uncertain if temperature and time during stagnation periods should have equal weight on t his factor.

Hence, further research is needed to understand how to quantify this factor and what should be its weight on the system design. However, the intention is to take into account a deterioration factor when designing a new solar thermal system. The assumed design guideline should be seen as a first iteration step in that direction. The important analysis at this stage is result comparison between these two different collector systems rather than conclude about the absolute value of the solar fraction results. As both systems were designed in the same way, inaccuracies that occur in one system will occur in the same way in the other one. This makes it significantly more reliable to take conclusions about the systems performances. In a future analysis the system should be design to minimize the costs per produced energy unit.
The simulation results of the annual solar fraction for every system are presented in Table 1.

Table 1. Annual solar fraction of the various retrofitted systems and the standard solar system.

System name	Annual solar fraction (%)
Standard system	52%
Retrofitted system 1	6%
Retrofitted system 2	15%
Retrofitted system 3	42%
Retrofitted system 4	53%

Retrofitted system 1 shows a very low annual solar fraction of 6%. This can be explained by the auxiliary heater placing at the bottom of tank which makes it impossible to establish any tank stratification. In addition, the cold water pushed in the bottom of the tank is directly heated to the set point temperature of 60°C demanding constantly auxiliary energy every time a draw-off takes place. Also, the inlet collector temperature is 60°C practically all year long which decreases the working hours and its efficiency.

In retrofitted system 2 the auxiliary heater is moved to the tank side-arm aiming to increase stratification. The results show that the annual solar fraction increases only to 15%. This is mainly explained by the small stratification increase. In this configuration, the upper volume of the tank is always at least at 60°C while the bottom is fairly cold most of the time. This is because hot water is extracted during the whole day and replaced by cold water at the bottom. Hence, the collector pump works many hours when the collector outlet temperature is higher than the tank bottom but lower than 60°C. Due to the inlets geometry of the retrofitted tank, water heated by the collector is placed at the very top of the tank. Consequently, the tank top temperature will decrease and destroy stratification making the auxiliary heater run during most of the year.

Simulation results of retrofitted system 3 show that the solar fraction increases to 42%. Since it is difficult to achieve stratification with the connections of the retrofitted tank it is more advantageous to place the heater in another tank. This prevents the heater to be turned on almost continuously when the collector is working at temperatures under 60°C. Hence, the retrofitted tank will work at lower temperatures increasing the collector working hours and efficiency. In addition, a new well insulated hot temperature tank provides the extra energy when solar energy is not available. Having the larger tank working at lower temperatures and the smaller tank at higher temperatures, decrease significantly the heat losses. One can say that the system "stratification" is achieved by two tanks with low stratification but working at different average temperatures.
The estimated annual solar fraction for retrofitted system 4 is 53%. The reason why the solar fraction of the series connected system is higher than the parallel connection is not obvious.

The main reason is that, during the summer period when solar hot water is available over 60˚C, the total solar storage volume of the series connected system is increased to 255 litres, since both tanks are connected in series and no auxiliary energy is needed.

4. Conclusions

Four different system configurations on how to retrofit existing domestic hot water heaters were theoretically analysed. The simulation results show that the best configuration for the retrofitting consists on using the existing tank for solar hot water storage and connect it in series with a small auxiliary heater tank. The system annual performance was compared with that of a conventional solar thermal system. Preliminary results show that its annual solar fraction is 53% compared to 52% of a standard solar thermal system with the same storage volume. This means that both system performances are comparable. Hence, it is worth to further investigate and develop this retrofitting in practice. In the future, the model validation and an economical assessment will be performed. If it proves to be cost-effective, this solution can be very interesting since it can be applied not only in retrofitting existing tank heaters but also in combination with new heaters accessing a world-wide industry.

References

[1] Swedish Energy Agency, Energy statistics for one- and two- dwelling buildings in 2008, 2009.

[2] Cruickshank, C. and Harrison, S., Analysis of a Modular Thermal Storage for Solar Heating Systems, Proceedings of Canadian Solar Buildings Conference, 2004.

[3] Lin, Q., Analysis, Modelling and Optimum Design of Solar Domestic Hot Water Systems, Ph.D. thesis, 1998, ISBN 87-7877-023-8.

[4] Fraser, K. F., Hollands, K. G. T. And Brunger, A. P., An Empirical Model for Natural Convection Heat Exchangers in SDHW Systems, Solar Energy 55(2), 1995, pp. 75-84.

[5] Liu, W. and Davidson, J., Comparison of Natural Convention Heat Exchangers for Solar Water Heating Systems, Proceedings of American Solar Energy Society Conference, 1995.

[6] Klein, S. et al., TRNSYS, a Transient System Simulation Program, University of Wisconsin, Madison, 1999.

[7] Swedish Building Regulation, Regelsamling för byggande, BBR 2008, ISBN 978-91-86045-03-6.

[8] Widén, J., Lundh, M., Vassileva, I., Dahlquist, E., Ellegård, K. and Wäckelgård, E., Constructing load profiles for household electricity and hot water from time-use data—Modelling approach and validation, Energy and Buildings 41(7), 2009, pp. 753-768.

[9] Stengård, L., Mätning av kall- och varmevattenanvändning i 44 hushåll, 2009.

[10] Swedish Energy Agency, FEBY – Krav Specifikation för Minienergihus, 2009.

[11] Statistics Sweden, Boende och boendeutgifter 2006, BO 23 SM 0801, 2006.

[12] Hausner, R. and Fink, C., Stagnation behaviour of solar thermal systems, IEA SHC, task 26, 2002.

[13] Nordlander S. and Bales C., TRNSYS type 221, distributed by the Solar Energy Research Centre, Sweden, 2007.

Travelling Energy Collectors

Ernst Kussul*, Tatiana Baidyk, José Saniger, Felipe Lara, Neil Bruce

CCADET, UNAM, Mexico city, Mexico
** Corresponding author. Tel: +52 55 56228602 ext.1204, Fax: +52 55 55500654, E-mail: ekussul@servidor.unam.mx*

Abstract: Almost all modern solar and wind energy plants can be used only as auxiliary energy sources because of their intermittent character. On the other hand, geothermal systems can produce energy continuously. However, geothermal power plants need expensive wells, and the well will not always give high temperature underground water. It is possible to improve the performance of the plant by combining the different features of these mentioned systems. It is possible to obtain hot water not from drills but by using solar and wind energy installations placed on mobile platforms (travelling energy collectors) that will transport hot water to the power plant, where it will be stored in special tanks. A similar procedure is possible for cold water. To transform thermal energy, stored in the hot water and cold water tanks to electric energy it is possible to use conventional equipment of geothermal power plants. In this paper we give estimations of some parameters of the proposed power generation system based on travelling energy collectors. The estimations show that the power plant based on travelling energy collectors can be considered as a base load source of electric energy.

Keywords: *Solar energy, Wind energy, Travelling energy collector*

1. Introduction

Solar energy and wind energy can be considered as complementary. Solar energy can be captured only during daytime. Wind energy at a height of more than 80 meters is more intensive at night time. In summer it is possible to obtain more solar energy than in winter, and in winter there is more wind energy. So, it is useful to make power plants based on both solar and wind energies.

If we want to create a base load power plant that uses solar and wind energy we also need to store energy for at least some days. The best type of energy storage for such a period is Thermal Energy Storage (TES). Many types of thermal energy storages have been proposed. In this article we will suppose that the TES is based on hot and cold water. Water is the cheapest material and it has high heat capacity.

The proposed solar-wind power plant will work as follows: solar concentrators will prepare hot water for TES, and wind powered refrigerators will produce cold water for TES. Sometimes wind powered heaters can be added to produce an additional amount of hot water. Hot water and cold water from the TES will be used to produce the electric energy with the same equipment that is used for geothermal power plants. The hot water from the TES can also be used for space heating and the cold water can be used for air conditioning purposes.
In principle, the solar concentrators can be placed in a compact area, but the wind power installations must be distributed in a relatively large region because of the turbulences that each installation produces. Moreover, wind speed is higher over the sea surface, and the power plant is to be located on the shore. For these reasons we propose Travelling Energy Collectors (TEC) that will collect solar and wind energy on the sea surface and transport this energy in the form of hot and cold water to the power plant. The distance of transportation (or service radius) will depend on economical considerations and can vary from some kilometers to many tenths of kilometers.

2. Methodology

2.1. Power plant based on travelling energy collectors

The scheme of the power plant based on travelling energy collectors (TEC power plant) is shown in Fig.1.

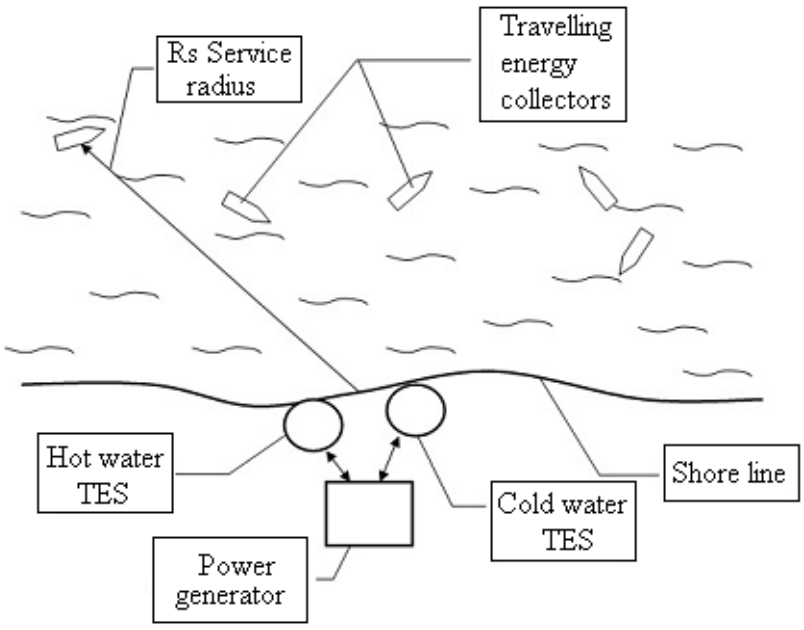

Fig. 1.Power plant based on travelling energy collectors.

It contains a power generator, hot water TES, cold water TES, and a multitude of thermal energy collectors (TECs). The TECs collect the solar and wind energy from the circular segment that has radius R_s, transform these energies to the hot water and cold water, and transport them to the hot water TES and cold water TES. The water from the hot water TES is supplied to the vapor generator that produces energy in the heat engine with the Organic Rankine Cycle (ORC). This type of engine is used for geothermal power plants. The water from the cold water TES is used for heat engine cooling. The Carnot efficiency of the power generator will be:

$$\eta_c = (T_h - T_c)/T_h \qquad (1)$$

where T_h is the temperature of hot water and T_c is the temperature of cold water. The total efficiency of the power generator will be:

$$\eta = \eta_c \cdot \eta_r \qquad (2)$$

where η_r is the relation of power generator efficiency to its Carnot efficiency. For ORC heat engines η_r usually has the values in the range of 0.5 – 0.67 [1]. In this article we will use a value η_r = 0.55.

If the temperature of the hot water is 90° C and the temperature of the cold water is 5° C, the efficiencies of the power generator will be:

$$\eta_c = 0.234, \quad \eta = 0.129 \qquad (3)$$

If we put the hot water TES at a depth of 50 m below the sea surface to obtain overpressure of 5 bar, it will be possible to increase the hot water temperature up to 140° C. The temperature of the cold water can be decreased down to – 20° C, if we use an ice-water mixture of salted water. In this case the power generator efficiencies will be:

$$\eta_c = 0.387, \quad \eta = 0.21 \qquad (4)$$

The efficiency 0.21 is at the level of the highest efficiencies of silicon photovoltaic panels, but in our case the power generator can supply the energy continuously.

2.2. Travelling energy collectors

A travelling energy collector (TEC) will be made as an unmanned sail catamaran. The scheme of the TEC is presented in Fig.2.

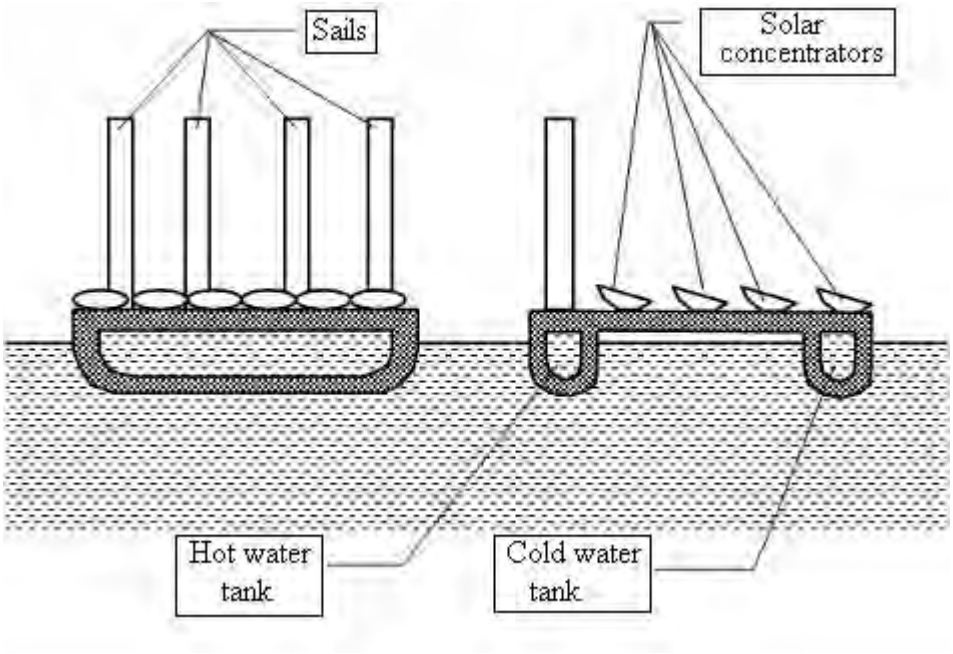

Fig.2. The scheme of the TEC.

The TEC contains sails, solar concentrators, small wind turbines, hot water tank and cold water tank. There are different types of maritime wind collectors. Some of them contain large wind turbines on the ship, others use the sails to move the ship, and submerged water turbine produce the electric energy [2].We propose to use small wind turbines, because large wind turbines have large weight, and the scheme containing the submerged water turbine has low efficiency. Small wind turbines can be placed into the sails (Fig.3).

In this case the film roll and the rope roll will be placed in the leading edge of the sail. When the TEC is working in the mode of wind energy collection, the sail film is wound to the film roll and small wind turbines are open for the wind. If the sail is to be used to move the catamaran, the ropes will be wound to the rope roll. These ropes run around the rear roll and pull the film from the film roll to close the wind turbine space and to form the sail air foil. The TEC will work in solar energy mode in the presence of direct solar radiation; otherwise it will work in wind energy mode, in transport mode, or in discharge mode.

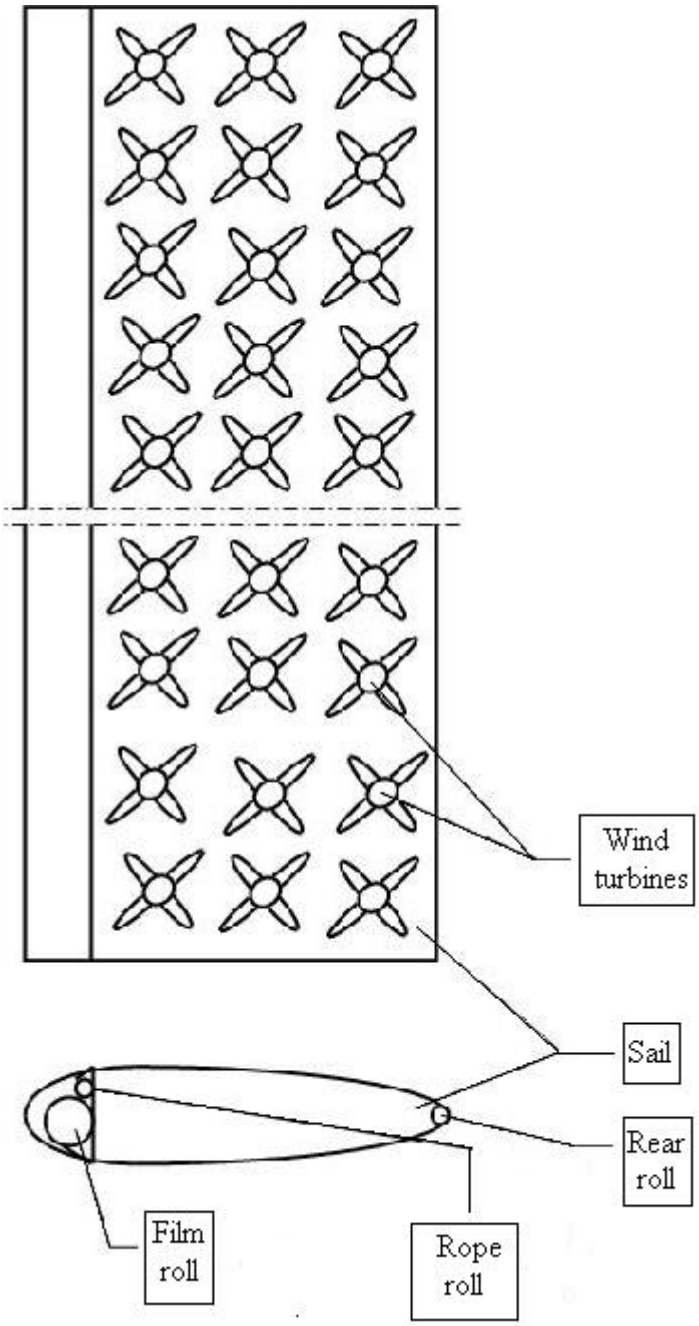

Fig.3. Small wind turbines.

In the solar energy mode the solar collectors will heat the water in the hot water tank. In the wind energy mode the energy from the wind turbines will feed the chiller to cool the ice-water mixture in the cold water tank and increase the amount of ice in the mixture. The approximate proportion of hot water energy to the cold water energy is:

$$E_h / E_c = T_h / T_c , \qquad (5)$$

where E_h is the energy of the hot water stored in the hot water tank, E_c is the energy of the ice-water mixture stored in the cold water tank, T_h is mean temperature of the hot water tank, and T_c is the temperature of the cold water tank.

The hot-water energy can be calculated using the equation:

$$E_h = M_h \cdot C_w \cdot (T_{h1} - T_{h2}), \quad (6)$$

where E_h is the hot water energy, M_h is the hot water mass, C_w is specific heat capacity of the water, T_{h1} is the temperature of the hot water after the heating in the solar concentrators, T_{h2} is the temperature of the hot water before heating in the solar concentrators.
To calculate the cold water energy we will use the following equation:

$$E_c = M_i \cdot q_i, \quad (7)$$

where E_c is the cold water energy, M_i is the mass of the ice in the ice-water mixture, and q_i is the latent heat of ice melting.

3. Solar Concentrators

Low-cost light-weight solar concentrators are needed for travelling energy collectors to heat the water in the hot water tank. At present we are developing these concentrators [3]. Each concentrator will contain a multitude of flat triangular mirrors that approximate a parabolic surface. A prototype of the support frame for the mirrors is shown in Fig.4.

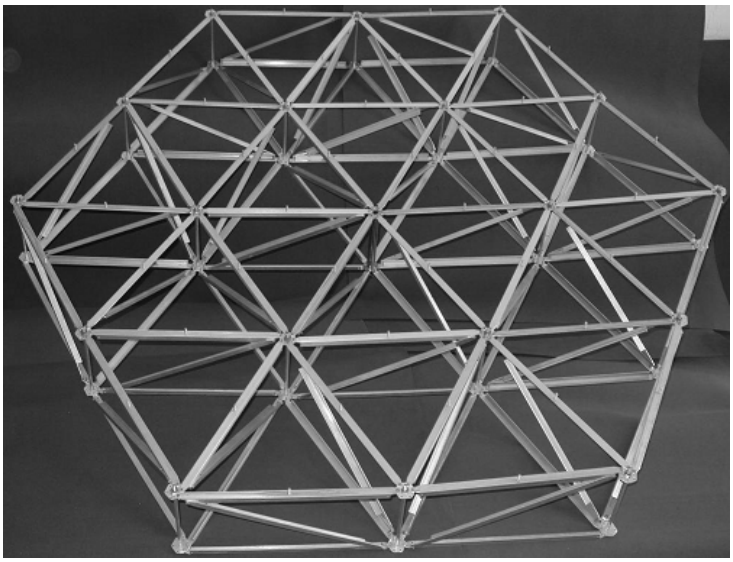

Fig.4. Support frame for the mirrors of solar concentrator.

The cost of mass production of these concentrators can be as low as 50 dollars for square meter of mirror surface [4].

3.1. Solar energy mode

The travelling energy collector will work in the solar energy mode in the presence of direct solar radiation. Let the TEC have a deck area of 1000 m^2. In this case the total area of solar concentrators can be approximately 500 m^2. Let us suppose that 1 m^2 of solar concentrator produces 700 Wt of heating power (concentrator efficiency is 0.7), and direct solar radiation is present during 4 hours per day. In this case the hot water will obtain the energy of

$$E_h = 504 \cdot 10^7 \text{ J/day.} \quad (8)$$

Let the initial temperature of hot water be T_{h2} = 403° K, the final temperature of hot water will be T_{h1} = 423° K. In this paper we will consider a TEC that discharges the hot and cold water each day. Using equation (6) it is possible to calculate the mass of hot water needed to store the heat energy in the hot water tank. In our case we will have:

$$M_h = 60000 \text{ kg} = 60 \text{ ton,} \quad (9)$$

3.2. Wind mode

In the nights and during cloudy days the TEC will work in the wind mode. For this purpose the TEC is to be oriented perpendicular to the wind speed, the sails are to be opened, and small wind turbines will produce the electrical energy for the ice machine. The ice machine will increase the amount of ice in the cold water tank. Using equations (5) and (8) we obtain:

$$E_c = E_h \cdot (T_c / T_h) = 504 \cdot 10^7 \cdot (253/413) = 308 \cdot 10^7 \text{ J/day} \quad (10)$$

Here we suppose that T_c equals – 20° C and T_h equals 140° C.
The power of wind turbines can be evaluated using the equation:

$$P_t = \eta_t \cdot S_t \cdot (\rho \cdot u^3)/2 \quad (11)$$

where η_t is turbine efficiency, S_t is the total area of the small wind turbines, ρ is the air density, and u is the wind speed. In this paper we will assume that η_t = 0.3, S_t = 500 m^2, ρ = 1.25 kg/m^3 and u = 8 m/s. In this case we will have:

$$P_t = 48000 \text{ Wt,} \quad (12)$$

We will suppose that the transport and the discharge modes will take 3 hours per day. The solar mode takes 4 hours per day, so the wind mode will take 17 hours per day. Not all this time will be used for power generation, because the TEC has a drift that must be periodically compensated. For drift compensation the sails are to be closed as for transport mode and the TEC is to be moved against the wind. We will assume that drift compensation will take 30% of the total time in the wind mode. The power generation in the wind mode will take t_g = 11.9 hours per day. The energy generated by the wind turbines will be:

$$E_t = P_t \cdot t_g \cdot 3600 = 206 \cdot 10^7 \text{ J/day,} \quad (13)$$

If coefficient of performance of the ice machine is 1.5, the total cooling energy produced in the form of ice will be E_c = 308 * 10^7 J/day. This is sufficient to obtain the balance of heating and cooling energies in the power plant. To store this amount of energy it is necessary to produce the following mass of ice:

$$M_i = E_c / q_i, \quad (14)$$

where E_c is the cooling energy, q_i is the latent heat of water freezing. Water has the value of q_i = 332 kJ/kg. For our example M_i will be:

$$M_i = 9300 \text{ kg}. \quad (15)$$

We will assume that the mass of the ice-water mixture is:

$$M_{iw} = 40000 \text{ kg} = 40 \text{ ton}, \quad (16)$$

In this case the total weight of hot water and cold water in the tanks will be 100 ton.
Different geographic areas have different relations between the amount of solar and wind energy, thus for each area different parameters of the power plant should be selected. The main parameter is the cold-water tank temperature. Increasing this temperature, it is possible to decrease the amount of wind energy to obtain good balance for example in tropical areas, where the wind energy can be relatively poor.

3.3. Transport and discharge modes

In transport mode the sails move the TEC from the power plant and after collection of energy return it to the power plant. The maximum distance of movement is:

$$R_s = t_{tr} \cdot u_{tr} / 2, \quad (17)$$

where R_s is the service radius of the power plant, t_{tr} is the time of the transportation mode, u_{tr} is the transportation speed. In our example t_{tr} = 2 hours. If the transportation speed is 10 km/h, the service radius will be:

$$R_s = 10 \text{ km}. \quad (18)$$

In the discharge mode the TEC discharges the hot water to the large hot-water tank of the power plant. The temperature of the discharged water is T_{h1}. After this the TEC loads its hot water tank from the large hot-water tank of the power plant with water that has the temperature T_{h2}. In parallel the ice-water mixture that contains M_{i1} kilograms of ice is discharged to the large cold-water tank of the power plant and a new ice-water mixture that contains M_{i2} kilograms of the ice is loaded to the small cold-water tank of the TEC.

3.4. TEC number

One TEC produces the energy of 504 * 10^7 J / day. This corresponds to a mean power P_{TEC} = 58330 Wt. If we want to create a power plant of power P_{pp}, we need the following number N_{TEC}:

$$N_{TEC} = P_{pp} / (P_{TEC} \cdot \eta), \quad (19)$$

where P_{pp} is the output power of the power plant, P_{TEC} is the power of one TEC, η is the efficiency of the power plant. If P_{pp} = 10 MWt, η = 0,21, we need:

$N_{TEC} = 816.$ (20)

This calculation shows that each TEC cannot be driven by an operator. It must be made as an autonomous robot, and its cost is to be as low as possible.

4. Discussion

A power plant for continuous electrical energy supply is proposed. In this power plant the conventional equipment from geothermal power plants is used for electricity generation. Instead of drilling deep wells to obtain hot water we propose the use of moving platforms (TECs) that contain solar concentrators for hot water production and small wind turbines for cold water production. Moving platforms transport the hot and cold water to the power plant located on the sea shore. Approximate calculations show the feasibility of this system.

5. Conclusion

Travelling energy collectors will permit solar and wind energy collection from sea areas near the shore, transform it to heat energy and store in hot water and cold water thermal energy storages. These storages will permit continuous energy production using the equipment of geothermal power plants. The travelling energy collector will be implemented as a catamaran with sails that include a multitude of small wind turbines. The solar concentrators will be placed on the deck of the catamaran. The catamaran will contain a hot water tank and a cold water tank to transport the heat energy to the power plant. It is necessary to make a large number of travelling energy collectors for one power plant. For this reason the catamaran must have an autonomous control system that will allow operation without human interaction.

Acknowledgment

This work was supported partially by projects CONACYT50231, PAPIIT IN110510-3, PAPIIT IN119610 and the project ICyTDF 330/2009.

References

[1] K. Rafferty, Geothermal power generation. A primer on low temperature, small-scale applications, http://geoheat.oit.edu/pdf/powergen.pdf.

[2] Y.Terao, K. Watanabe, M. Wakita, A feasibility study of an ocean power plant using a mega yacht system, Proceedings of the Second International Conference on Marine Research and Transportation, 2007, pp. 55-62.

[3] Kussul E., Baidyk T., Lara F., Saniger J., Bruce N., Estrada C., Micro facet solar concentrador, *International Journal of Sustainable Energy*, 2008, Vol.27, Issue 2, pp.61-71.

[4] Kussul E., Baidyk T., Makeyev O., Lara-Rosano F., Saniger J.M., Bruce N., Flat facet parabolic solar concentrator, The 2nd WSEAS/IASME International Conference on Renewable Energy Sources (RES-08)-2008, October 26-28, 2008, Corfu, Greece, pp.46-51.

Configuration of daylighting system via fibers and experiments of concentrated sunlight transmission

Song JF[1,*], Yang YP[1], Hou HJ[1], Zhang MX[1]

[1] *The New and Renewable Energy of Beijing Key Laboratory, North China Electric Power University, Beijing, 102206, China*
** Corresponding author. Tel: +86-10-61772816, Fax: +86-10-61772816, E-mail: songjifeng@ncepu.edu.cn*

Abstract: A daylight concentrating and transmission system via plastic fibers based on dual axis sun tracker to lighting indoor has been built and investigated. The sunlight tracking and concentrating platform adopting horizontal coordinate system combined with photosensitive sensor can realize high position resolution. A sunlight concentrating and transmission experiment has been carried out using 6m long PMMA plastic fibers based on that platform. It is found that color temperature of light transmitted by fibers is 600K lower than that of nature light. The spectrum of light transmitted by fibers is similar to that of nature light. This similarity also exists in chromaticity coordinate, color rendering index, dominant wavelength between light transmitted by fibers and nature light. A quantitative determination of flux loss has been carried out and the results show that there is an attenuation about 2db existing on the interface of fiber.

Keywords: *Sun tracking, Fibers, Concentrated, Transmission*

Nomenclature (Optional)

NA	*numerical aperture*	ψ	*longtitude*
α	*altitude angle*	T	*colour temperature* (K)
γ	*azimuth angle*	λ	*intrinsic attenuation constant* (db/m)
φ	*latitude*	z	*length of fibres* (m)
δ	*declination*	γ	*loss coefficient on fibers' facet* (db)
P_{out}	*output light flux* (lumen)	η	*total loss coefficient* (db)
P_{in}	*input light flux* (lumen)	I	*illumination* (lux)
τ	*time adjustment* (s)	D	*diameter of fibers* (m)

1. Introduction

The daylighting system is an optic-mechanical-electric technology that collects day light outside to transmit into basement and room lacking nature light by fibers in high concentrated level [1-2]. The infrared portion of solar radiation has been separated and eliminated by lens and fibers so that the output flux is a cool light. There are two major benefits from daylighting. The first benefit is the reduction in purchased electricity needed to light the building, and the second benefit is a reduced cooling load due to the high efficiency of light. Another potential benefit of daylighting is the advantageous factors for healthy of natural lighting but this effect is difficult to quantify. The excellent color rendering properties of daylight and its close match to the photopic response of the human eye make it an ergonomic light source that is generally preferred for pleasant working conditions[3-4]. There are two types of daylighting systems including light guide pipe and fibers. The latter is the research hotspot at present due to its smaller and few penetrations on the roof which means saving on the building's heating, cooling, and maintenance bills. T he purpose of this particular study is to evaluate the feasibility and performance of the technology. The day light concentrating and transmission system via fibers consists of a two-axis sun tracker and concentrating collector that gather direct normal solar radiation into the fibers. The key to realize stable flux output is high precision sun tracking which need a trade-off with fabrication cost[6]. And, at the present time, the optical parameters of sunlight transmission system via fibers have not get adequacy quantitative determination. Those problems provide the investigation motivation of this

research work. According to the structure forms, there are two ways of focalization including optical fiber bundle and single fiber. For the former, concentrator with large diameter is used to produce large focal spot, and so it can use optical fiber bundle to receive the concentrated radiation[7-9]. For the latter, the concentrator is lens with small diameter which produces small focal spot only suiting for single fiber. It is critical to obtain high accuracy position tracking in respect that small focus error will cause a large amplitude reduction of out flux due to single fiber's small diameter. Although much research has been devoted into sunlight concentrating and transmission system via fibers, there are still lots of problems and unknown characterizes awaiting solutions, such as quantitative study of the spectrum of output light. In order to try to answer above questions, a dual-axis sun tracking system has been investigated by the combined use of horizontal coordinate system and photosensitive sensor designed specially, based on that corresponding research has been done.

2. Dual axis sun tracking and concentrating system

2.1. Configuration of hardware

The system mainly is composed of support, reducing gears, motor, lens and control module. It must be emphasized that small deviation of focusing spot will lead to significant instability attributed to no light preserved module existing in the daylighting system. To satisfy above strict demand, orbit calculation method and optical sensing method are integrated into control flow. The prototype of the dual axis tracking and concentrating system is shown in Fig 1.

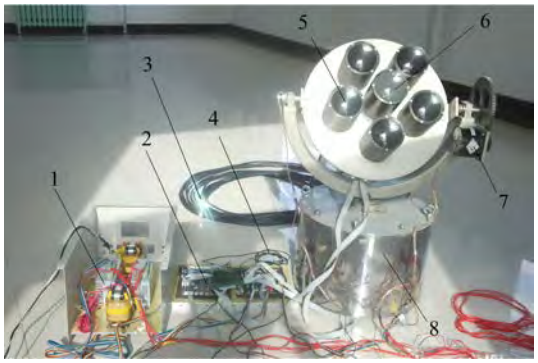

Fig. 1. Double-axis sun tracking system

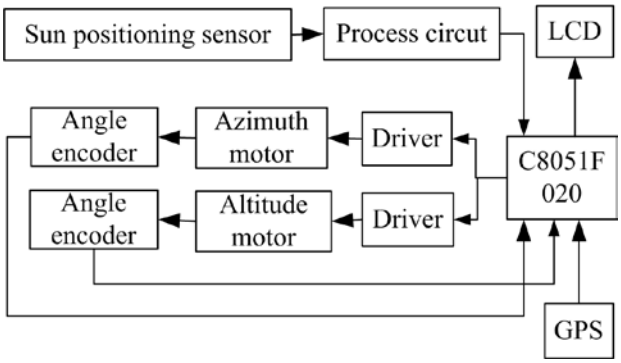

Fig. 2. Control system frame

In fig.1, the components numbered are step motor drivers, control board, plastic fibers, GPS module, lens, sun positioning sensor, altitude motor, substructure for installing azimuth motor successively. In practical, it is too difficult to realize accuracy positioning about 0.1° only depending on orbit calculation due to the varied limits, such as installation error and gravity deformation, et al, although it is possible in theory. The misalignment between geodetic coordinate and device coordinate led by installation error and gravity deformation will result in an inevitable calculation error in sun position[10]. So an optical sun positioning sensor is designed specially to eliminate the error accumulation and initial error, which uses photosensitive elements array to sensing the location of the focusing spot generated by lens. By comprehensive utilization of two methods, it is able to realize stability and high precision profit from orbit calculation method and sun optical positioning sensor respectively. The control system is designed to work automatically. Step motors are used to drive the tracking action and angle encoders are applied to feedback the real angle information of the mechanical components. Global positioning system module is adopted to provide exact time and latitude and longitude which are the parameters to calculate the sun position. With the help of GPS module, the tracking system can figure out the sunrise and sunset time to realize full automatic tracking without manual operation, meaning remarkable reduction of

maintenance. For convenience, a LCD display screen is installed to show real-time working state. Plano convex lenses made of K9 optical glass are adopted to concentrate sunlight which has a transmission coefficient that is no less than 0.9 at visible spectrum range. It is no cooling problem for lenses and fibers because there is nonexistence of hot spots due to their high transparency. Performance parameters of the hardware have been described in tab 1. To facilitate the precision drive, sinusoid subdivision drivers are used to improve step motors to achieve 12800 pulses per cycle, about 0.028°/pulse. In addition, gear pairs are applied to further improve the fine adjustment; however nonlinearity caused by gear clearance emergences isochronously. To ensure stable tracking, it is needed to introduce intelligent algorithm to compensate the nonlinearity. For instance, database is recorded in the program memory to distinguish different situations of nonlinearity. The concentrator is convex lens made of super white glass which transmittance is 0.92. According to the sun's

Table.1 Parameters of double-axis sun tracking and concentrating platform

Name	Unit	Amount	illustration
Torque of azimuth motor	N.m	3.6	Step motor
Torque of altitude motor	N.m	1.2	Step motor
Reduction ratio of azimuth		1:3	Straight gear
Reduction ratio of altitude		1:5	Straight gear
Tracking type			Orbit and optical sensor
Tracking accuracy	°	±0.15	
Range of altitude	°	0～90	
Range of azimuth	°	0～360	
Diameter of lens	m	Φ0.1	K9 material
Focal length	mm	180	Adjustable
Concentration ration		900-10000	Adjustable
Transmittance of lens		0.92	Visible band

2.2. Control method

As for the optical sun positioning sensor, it is used to detect detailed deviation and feedback the signal to microcontroller to realize exact tracking. The most important advantage of the optical sun positioning sensor is the ability to eliminate the error accumulation caused by errors from motor or reducing gears. The optical sun positioning sensor is good at dealing with error accumulation but bad at anti-climate impacts while the orbit calculation method is opposite. So it is wise to adopt combined utilization of both methods to obtain good tracking accuracy and anti-interference ability meanwhile. The flow chart of sun tracking process is shown in Fig 3. Because of complexity in practice, the flow chart has more fine regulation actions than that listed out in Fig 3.

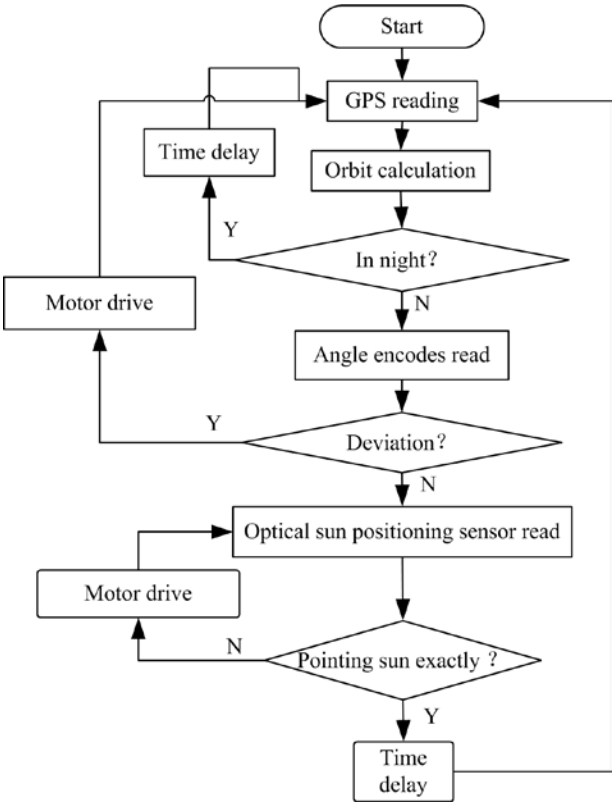

Fig.3. Control flow chart of sun tracking process

3. Plastic fibers

The diameter of fibers used for concentrated sunlight transmission is flexible and two orders of magnitude higher than that of fibers used for distant communication, whose range is 1-6mm generically. The materials of fibers include polymethyl methacrylate(PMMA), polystyrene and special quartz. Light attenuation is severe, about 0.25db/m, only suiting for close distance transmission not longer than 30m. Some parameters of the fibers tested in the work are described in Tab 2. The fiber tested in this research is made of PMMA, and has absorption peaks in 620nm and 705nm which is shown in Fig 4. The advantages of PMMA fibers are flexible and big numerical aperture which is very in favor for light focusing. Unfortunately, the upper limit for work temperature is only $70^{o}C$ which restricts the upper limit of concentration ratio, about 2500 without water cooling. But this upper limit could be extended to 10000 for quartz fiber which is used in solar furnace.

Table.2 Parameters of PMMA fibers

Name	Unit	Amount	illustration
Diameter	mm	2.5	
Length	m	6	
Numerical aperture		0.5	Ranger of angle of incidence is ±30°
Average attenuation	db/m	0.25	380nm～760nm

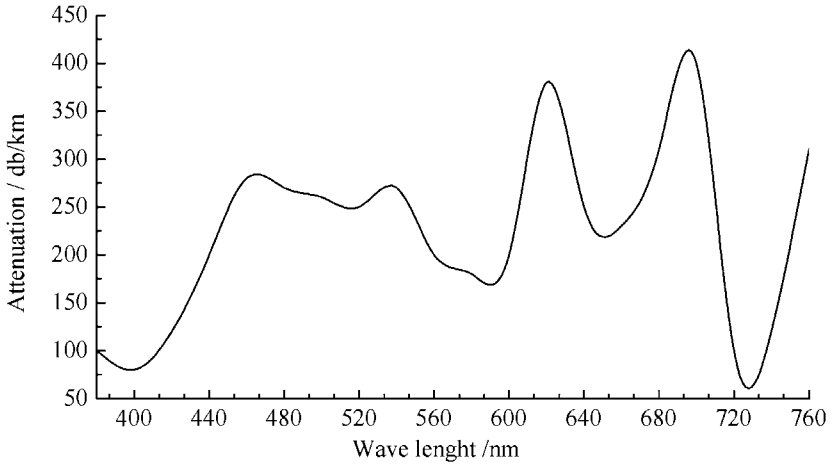

Fig.4. Curve of intrinsic attenuation of PMMA fibers

4. Results

The experimental system consists of the dual axis tracking and concentrating system, fibers, illuminometer and HAAS-2000 spectral radiometer, as in Fig 5. A sunlight concentrating and transmission experiment lasted for 9 hours has been carried out using 6m long PMMA fibers .

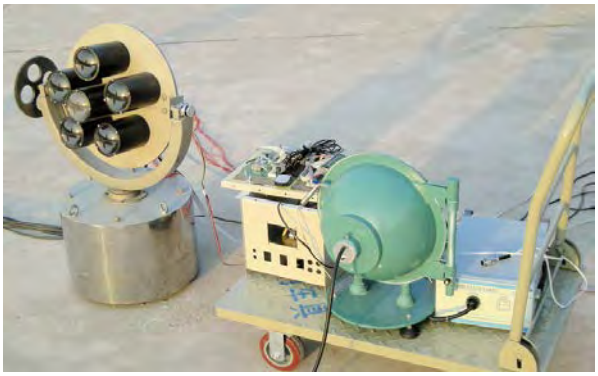

Fig.5 Optic testing system of concentrated sunlight transmission system

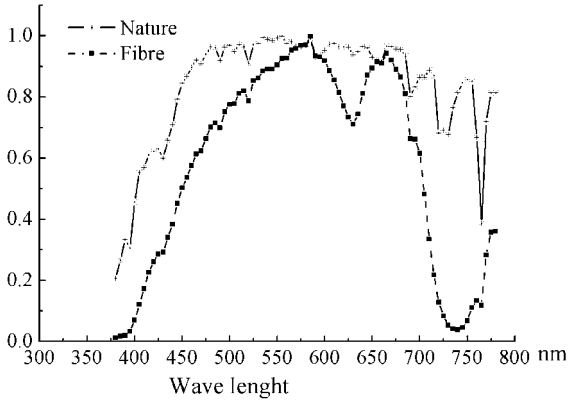

Fig.6 Spectrum comparison of nature light and light transmitted by fibers in visible band

The spectrum of light transmitted by fibers is similar to that of nature light, as shown in Fig 6. Although the deviation between two curves is evidence in 705nm led by absorption peaks of fibers, it influences the visual perception slightly because it is away from green band which is most sensitive for eyes. This similarity also exists in chromaticity coordinate, color rendering

index, dominant wavelength between light transmitted by fibers and nature light, as described in Tab 3.

Table.3 Parameters comparison between nature light and light transmitted by fibers

Parameters	Light out fibers	Daylight	Difference
Color temperature	4444K	5037K	-11.8%
Dominant wave length	571.6nm	569.4nm	+0.4%
Peak wavelength	585nm	538nm	+8.7%
Width of half wave	255.8nm	360.6nm	-29%
Color coordinate X	0.3688	0.3446	+7%
Color coordinate Y	0.3972	0.357	+11.2%
Color rendering index	88.9	99.3	-10.5%
Red light ratio	17.9	18.8	-4.8%

As identified in Tab 3, the flux transmitted through fibers is approximate to nature light, so it can satisfy the need of drawing office, indoor plant cultivation and shady bedroom.
As for the transmission loss, it is consists of three parts which are intrinsic loss, loss on end faces of fibers and loss led by bend. Among them, the intrinsic loss is a constant while loss on face is a large variation, determined by roughness mainly. In fact, the loss on face takes an essential ratio of total loss. So it makes sense to make certain that how much loss on face is. A experiment for determining the value of loss on face is designed, which separates the intrinsic loss from total loss by a series calculations.
For fibers without bend, we have

$$P_{out}(z) = P_{in}(0)e^{-\lambda z}e^{-\gamma}$$

Here $z = 6m$. As for the total η, it can be described as followed

$$\eta = 10\lg\frac{P_{out}(z)}{P_{in}(0)} = -10(\lambda z + \gamma)\lg e$$

Traditionally it is a custom to use decibel in attenuation analysis, so we have

$$\begin{cases}\overline{\lambda} = (10\lg e)\cdot\lambda \\ \overline{\gamma} = (10\lg e)\cdot\gamma\end{cases}$$

It is easy to get following conclusion after a further derivation

$$\begin{cases}\eta = -\overline{\lambda}z - \overline{\gamma} \\ \overline{\gamma} = -\eta - \overline{\lambda}z\end{cases}$$

$\overline{\lambda}$ is a constant known as $0.25\,db/m$ and $P_{out}(z)$ can be measured by integrating sphere and spectroradiometer while $P_{in}(0)$ can be worked out by the following formula

$$P_{in}(0) = I \cdot \pi D^2 / 4$$

Measured data of luminance outdoor and output flux of fibers is shown in Fig 7. Two curves are anastomotic through one day.

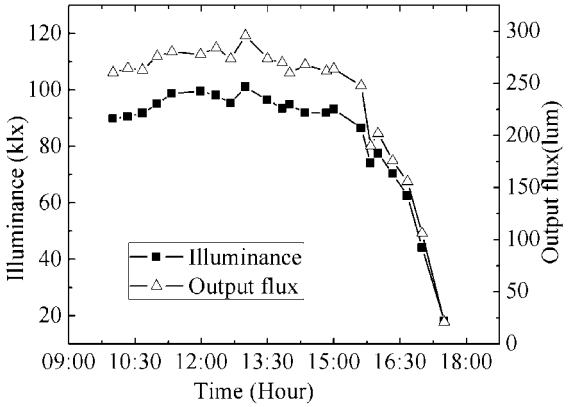

Fig.7 Corresponding relation of illumination outside and output flux of fibers

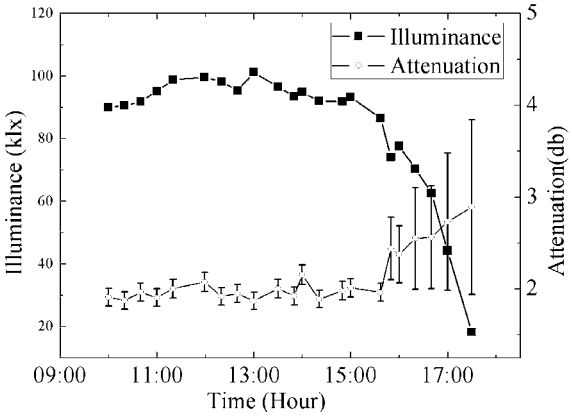

Fig.8 Corresponding relation of illumination outside and attenuation on interface

From measured data recorded in Fig7, the loss on face can be calculated out as shown in Fig 8. The loss on face can be regarded as a constant about 2db approximately which is accord with the optical principle. As to the increasing after 16:00pm, it can be explained that scattering radiation takes more and more proportion in total sunlight and this scattering radiation cannot be focusing onto the fibers, so above formulas in this situation produce large result.

5. Conclusions

Combination of orbit calculation method and sun optical positioning sensor posses accuracy and stability simultaneously in sun tracking which is the key to ensure the output flux of fibers stable. Different from solar thermal and photovoltaic application, there are no measures to storage nature light and so it is fatal when tracking error exceeds the allowable range. It must be pointed out that low speed drive is very beneficial to obtain high precision positioning in sun tracking which affords more time for the microcontroller to analyze the tracking status and implement compensation motions. This strategy makes full use of the feature of sun slow-moving. It is also relatively economic to adopt low power motors owe to the features of this strategy.

The spectrum of light transmitted by fibers is similar to that of nature light which make it favorable for places needing daylighting. Color temperature of the output light transmitted by fibres is about 600K lower than that of nature light which is caused by the selective absorption of plastic fibers. Fortunately, this selective absorption does not cause severe influence to the optical quality of sunlight transmission. The color rendering index still keeps a high value about 88.9 which is far better than those of incandescent lamp, fluorescent lamp and white LED. What's more, the loss on face of fibers cannot be neglected which is about 2db that is meaning 40% loss. The loss on face is relative to the roughness and incident angle. It requires precise measurement and mathematical modeling to establish the quantitative description of concentrated sunlight transmission.

Acknowledge

Financial support from National Natural Science Foundation of China (No.61004084) and Fundamental Research Funds for the Central Universities (09QG18) and State Key Development Program of (for) Basic Research of China (No. 2009CB219801) are appreciated.

References

[1] C. Kandilli, K. Ulgen, Review and modelling the systems of transmission concentrated solar energy via optical fibres[J], Renewable and Sustainable Energy Reviews, Volume 13, Issue 1, January 2009, Pages 67-84.

[2] Cemil Sungur, Multi-axes sun-tracking system with PLC control for photovoltaic panels in Turkey[J], Renewable Energy, Volume 34, Issue 4, April 2009, Pages 1119-1125.

[3] Schlegel, G.O., et al., Analysis of a full spectrum hybrid lighting system[J]. Solar Energy, 2004. 76(4): p.359-368.

[4] Tzempelikos, A., A.K. Athienitis, and P. Karava, Simulation of facade and envelope design options for a new institutional building[J]. Solar Energy, 2007. 81(9): p. 1088-1103.

[5] Teolan Tomson. Discrete two-positional tracking of solar collec-tors Original Research Article, Renewable Energy, Volume 33, Issue 3, March 2008, Pages 400-405.

[6] Tekelioglu, M. and B.D. Wood, Solar light transmission of po-lymer optical fibers. Solar Energy, 2009. 83(11): p. 2039-2049.

[7] Tsangrassoulis, L. Doulos, M. Santamouris, et al, On the energy efficiency of a prototype hybrid daylighting system[J], Solar Energy, Volume 79, Issue 1, July 2005, Pages 56-64.

[8] G. O. Schlegel, F. W. Burkholder, S. A. Klein, et al., Analysis of a full spectrum hybrid lighting system[J], Solar Energy, Volume 76, Issue 4, April 2004, Pages 359-368.

[9] Earl, D.D., Maxey, C.L., Muhs, J.D., 2003. Performance of new hybrid solar lighting luminaire design[J]. In: International Solar Energy Conference, Kohala Coast, Hawaii Island, March 15–18.

[10] H.Arbab, B.Jazi,M.Rezagholizadeh, A computer tracking system of solar dish with two-axis degree freedoms based on picture processing of bar shadow[J], Renewable Energy, Vol34(2009) 1114-1118.

Type12 and Type56: a load structure comparison in TRNSYS

Helena Persson[1,*], Bengt Perers[2], Bo Carlsson[1]

[1] *School of Pure and Applied Natural Sciences, Linnaeus University, SE 39182 Kalmar, Sweden*
[2] *Department of Civil Engineering DTU, DK-2800 Kgs. Lyngby, Denmark*
** Corresponding author. Tel: +46 731424645, E-mail: helena.persson@lnu.se*

Abstract: An investigation of the accuracy, advantages and disadvantages of using the simpler degree day house load-model Type 12 as a replacement for the more complex multi-zone Type 56 has been made. Results show that Type 12 provides sufficient accuracy for all systems including a storage tank capable of holding at least one day load. A discussion whether Type 12 is an accurate model for other situations is made.

Keywords: *TRNSYS, Renewable energy, Solar Combi, Programming, Type, 56*

1. Introduction

The modeling of solar combisystems in the academic community is often done in a commercially available fortran based simulation environment named TRNSYS [1]. These systems often contain some form of heating system (heat pumps, solar collectors) and some form of load that uses the energy created (building, hot water load). The load is often connected to some form of weather data, deciding the ambient conditions. The interaction between the heat sources and loads form a TRNSYS deck, a series of component models connected to each other to provide information about a system. Here we seek to investigate the impact of the house load model that is chosen. The load structures that will be investigated are the two most common types of buildings used in TRNSYS: the very simple single-zone degree day model with internal gains described by Type 12, and the much more complex multi-zone model Type 56.

Previous work includes Olof Hallström [2], who in his thesis compared Type 12 to a much more complex model developed at Lund University. He found that even though Type 12 was surprisingly accurate for most conditions, especially during low indoor house temperatures, the drawbacks of the type made the choice between Type 12 and Type 56 hard to determine. He identified these drawbacks as the constant heat loss coefficient and the difficulty to include stored solar radiation. It can be noted however, that Type 56 also has a constant heat loss coefficient. Previous simplifications of TRNSYS models have among many others been performed by T. P. McDowell [3], completing a ground source model and by P. T. TSILINGIRIS [4] and his solar heating designs. In both cases a drastically decreased calculation time at low accuracy cost was reached.

Simplifying a deck has the advantage of a decreased calculation time, which can be a major problem in decks taking many hours or even days to complete, especially if a large amount of runs are desired for statistical or optimization purposes. A simpler deck is also highly advantageous for applications directed at the industry, installers and education, such as Climate Well [5] or Winsun Villa [6]. Winsun Villa contains a slightly modified version of Type 12. The conclusions of this publication will be used for the Flexi-Fuel project [7], which has strong connections to the industry and its installers and customers. The objective of the following paper is to determine the accuracy, calculation time and complexity of Type 56 and Type 12 under different conditions.

2. Methodology

2.1. TRNSYS

TRNSYS is a system simulation computational tool developed by Wisconsin University that allows for dynamic simulation of systems using variable time steps. It allows for systems, particularly heating systems, to be created by connecting several components, known as types. These types are mathematical subroutines, i.e. programs, which describe for example a pipe, a house or a heat pump. Apart from the possibility of self-made types, TRNSYS contains a large number of readymade types, and a large number of types are also developed by different institutes and available commercially or for free.

2.1.1. Available load-describing Types

There are several commercially available load models available, but we limit ourselves to observing those Types that are included in the basic TRNSYS package. These are: Type 12, the simplest model, Type 88, a version of Type 12 that also includes some internal gains, (It may be noted that these internal gains are being modeled directly in Type 12 under "misc heat gain", for the investigations performed in this paper.) Type 56 which is a very complex and thorough multi-zone building model, and finally Type 19 a single zone building that is less complex then Type 56, but still requires the input of a large number of parameters. We choose to observe Type 12 and 56 since they are the source of the other models and represent the extremes in simplicity/speed and complexity/accuracy.

2.1.2. TYPE 56

Type 56 describes a building with multiple thermal zones, i.e. rooms. The model uses data from wall and window materials and thicknesses. Each room has a homogenous temperature, and radiation heat between the rooms is based on the room area. Heat addition from solar direct and diffuse radiation is calculated for each room depending on window and heat transfer properties.

2.1.3. TYPE 12

Type 12 is a simple degree-day, single-zone, single capacitance building model with internal gains. The model uses an effective heat capacity for the entire building together with the difference between indoor and outdoor climate to create a heating need. The load is corrected for internal gains. The use of a single heat capacity does not provide any information on solar radiation, which can have significant impact during summer. In this work the solar radiation is added to the internal gain, time step by time step. Duffie and Beckman reasons that since heat capacity effects are difficult to model with a single node when the outdoor temperature is fluctuating around the indoor temperature, Type 12 becomes less reliable for cooling loads. [8]. This has not been investigated here.

2.2. The House

As a reference building the IEA Task 32 building which is based on the IEA Task 26 reference building was used. [9] The reason for this choice is simply that it is a well defined and known building suitable for comparison purposes. Two levels of insulation are chosen to simulate an energy need of 60 or 100 kWh/m²a. The building consists of a two storey house with the specifications described in Table 1, 2 and 3.

Table 1. Building Properties.

		SFH60 [m]	SFH100 [m]	[kg/m³]	[W/mK]	[kJ/kgK]	SFH60 [W/m²K]	SFH100 [W/m²K]
external wall	plaster inside	0.015	--	1200	0.600	1.00		
	Viertl brick	0.210	--	1380	0.700	1.00	0.154	0.491
	EPS	0.120	0.060	17	0.040	0.70		
	plaster outside	0.003	--	1800	0.700	1.00		
	Σ	0.468	0.288					
ground floor	Wood	0.015	--	600	0.150	2.50		
	plaster floor	0.060	--	2000	1.400	1.00	0.157	0.561
	XPS	0.120	0.060	38	0.037	1.45		
	Concrete	0.150	--	2000	1.330	1.08		
	Σ	0.445	0.285					
roof ceiling	Gypsumboard	0.025	--	900	0.211	1.00		
	Plywood	0.015	--	300	0.081	2.50	0.119	0.380
	Rockwool	0.200	0.060	60	0.036	1.03		
	Plywood	0.015	--	300	0.081	2.50		
	Σ	0.335	0.115					
internal wall	Clinker	0.200	--	650	0.230	0.92	0.962	0.962

Table 2. Window Area.

	window area [m²]	window quotient [%]	total area [m²]
South	12.0	24.0	50.0
East	4.0	9.9	40.5
West	4.0	9.9	40.5
North	3.0	6.0	50.0
Summary	23.0	12.7	181.0

Table 3. Window Properties

building	UWINDOW [W/m²K]	g-Value [-]	UFRAME [W/m²K]	construction [mm]	WindowID
SFH60	1.4	0.622	2.3	4/16/3	2004
SFH100	2.83	0.755	2.3	4/16/4	1202

A more detailed description on the house's architectural design, internal load and ventilation can be found in [9].

2.2.1. Estimating UA-values

Type 12 uses a single overall UA heat transfer value for the entire house. This value can be estimated by summarizing the U-values from all walls and windows in the building. An effective UA value for the ventilation can be added as this has the same temperature difference as the transmission losses.

$$UA = U_{WALL1} * A_{WALL1} + U_{WALL2} * A_{WALL2} + U_{WALL3} * A_{WALL3} + U_{WALL4} * A_{WALL4} + U_{WINDOWS} * A_{Windows} + \\ + U_{Roof} * A_{Roof} + U_{Floor} * A_{Floor} + V_{house} * n * \frac{1}{3600} * (1 - \eta_{hx}) * \rho_{air} * c_{p\_air} \quad (1)$$

2.2.2. Estimating solar radiation gain

In Type 12, Solar gains through windows can be estimated by adding the window area for each direction and multiply it with a transmission value (In this publication 0.6 has been used for all cases) as described in (2)

$$S = trm(WA_N + WA_E + WA_W + WA_S) \quad (2)$$

Where
trm = transmission constant
WA = Window area in the specified direction

This solar radiation gain value is then inserted into Type 12 through internal gains.

2.2.3 Effective thermal capacitance of the house
An effective thermal capacitance of the type 12 house can be estimated by adding up the thermal capacity for the individual parts of the house. Duffie and Beckman [8] give approximate values of 0.153 MJ/m2/K for a medium house and 0.415 MJ/m2/K for a heavy house and up to 0.810 for a very heavy building. This corresponds in this case (with 140 m2 total floor area) to 21 MJ/K , 58 MJ/K and 113 MJ/K.

3. Measurements

Type 12 is deemed to be the less accurate model, and so when Type 56 and Type 12 are compared, any deviation from each other is considered to be due to an inaccuracy of Type 12.

3.1. The Timescale

Fig 1 shows the output of Type 12 and Type 56, as well as the difference between them. At first glance, the heating load required by Type 12 appears to be very inaccurate for both the well and the less insulated building as we see in the upper part of Fig.1. The whole line depicting the difference between the two types is in the order of 50% for most of the year.

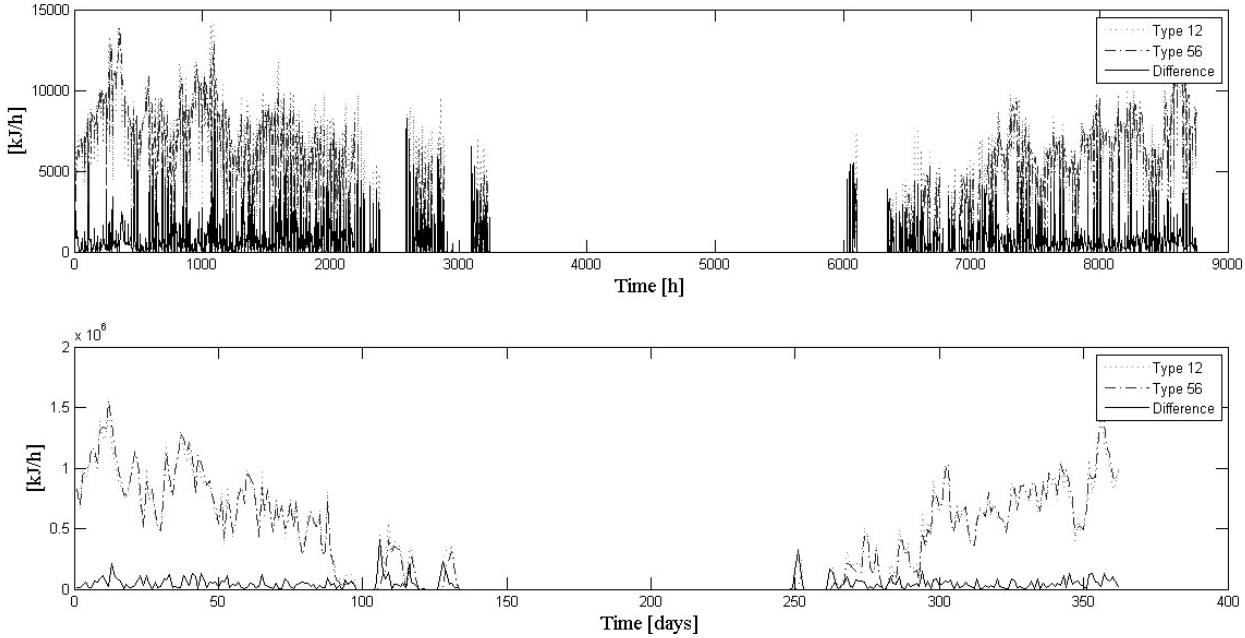

Fig.1 The output from Type12 and 56 with 12min time step (upper diagram) and 12h time step (lower diagram)

Possible heat pumps or solar collectors connected to a system are highly dependent on the temperature of the incoming flow. To gain sufficient accuracy for such heat sources a time step of a few minutes is required. The flow to such sources is often connected to some form of storage, such as a tank, between the load and the heat source. If for example a storage tank has the capacity of storing the energy required for heating a house for one day, a heat demand for one day is sufficient. When we integrate the output of both Type 56 and Type 12 over one day, we see a definite increase in agreement between the models as shown in the lower part of Fig.1.

3.2. The Accuracy of Type 12

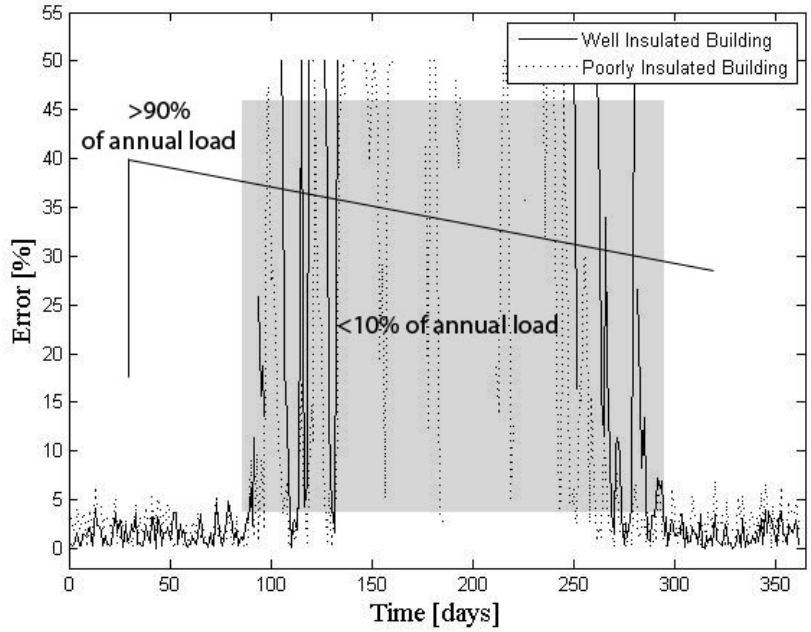

Fig. 2. The Difference in output for Type 12 and 56 for a poorly and a well insulated building

Fig.2 shows the error in percentage over one year. For the colder periods of the year the percentual error keeps below 7% for both levels of insulation. 7% is most likely a smaller error then those arising from building uncertainties such as cracs in the building shell or moisture in the isolation. Even though the error grows large in summertime, less than ten percent of the annual energy requirement occurs during this period. This means that for over 90% of the annual load, Type 12 performs acceptably. The yearly error becomes approximately 8%.

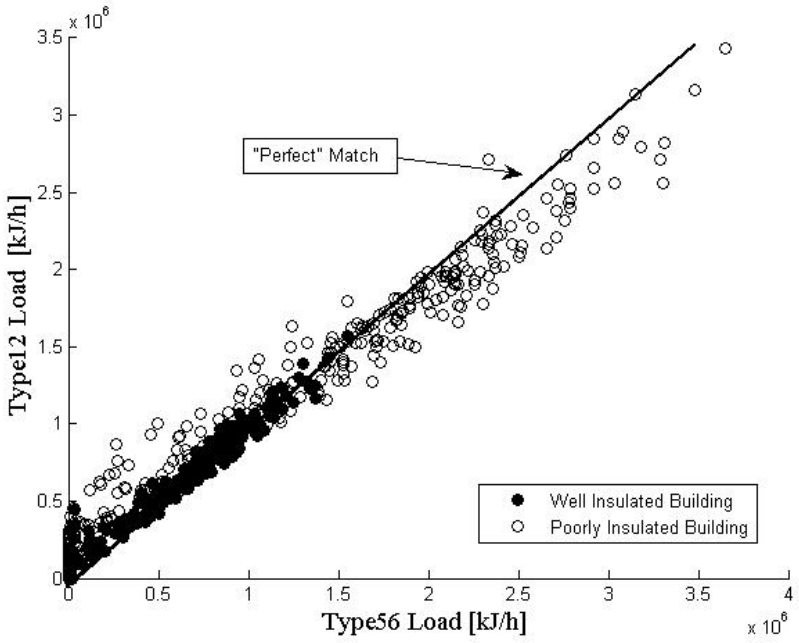

Fig. 2. Type 12 vs. Type 56 for a poorly and a well isolated building

Fig. 3 shows the output from the models plotted against each other. The error in output seems to be evenly distributed at the base of the line. The filled circles showing the well insulated building are closer to the line indicating that the overall UA value was a good guess for this case. At higher values we see a drift downwards, indicating that Type 12 underestimates the energy requirement for cold days, and overestimates it for warm days. This may be due to the fact that Type 12 does not store solar heat in the interior of the building.

3.3. The Phasing of Type 56

The difference in how the models react to outdoor temperatures is described in Fig. 4 and Fig. 5. Fig. 4 shows a zoomed in view of 3 days with the light gray line as outdoor temperature, the highly oscillating line as Type 12 and the less oscillating as Type 56. In this simulation, all windows, internal load and ventilation has been removed to get the crudest model possible. As seen in the image, Type 56 has a slight delay compared to the outdoor temperature, as might be expected by a more complex building model.

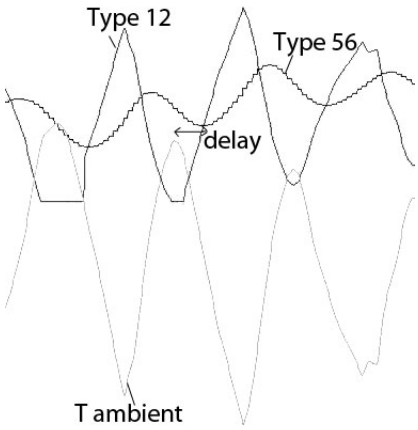

Fig. 4. The Delay of Type 56 when no windows are present

Fig. 5 shows two days but this time windows have been added to both models. Radiation coming through windows provides an instantaneous addition of heat, resulting in a model that responds much faster to outdoor weather. It could be argued that adding radiation through windows and ventilation provides a Type 56 that behaves more like Type 12.

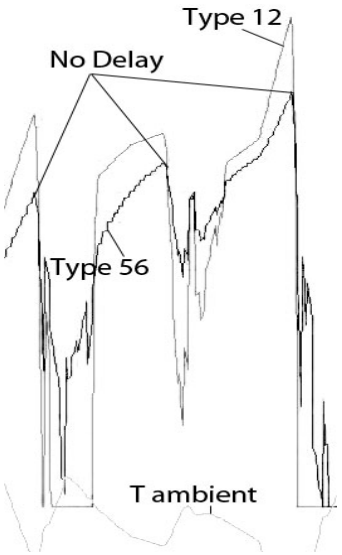

Fig. 5. No Delay of Type 56 when windows are present

3.4. Calculation Speed

Type 12 takes approximately half the simulation time for one year compared to Type 56 (23s against 42s). The time step was then rather long, 12minutes. In a full deck the tank may call the load several times before it converges, 10 times or more is not unusual. Also if a very short time step is used, this difference in calculation speed can have a significant impact on the usability of the deck.

4. Discussion

Considering the results presented above, Type 12 seems to be a good approximation under the right circumstances. It can be recommended for systems including a tank or other form of storage, or for systems that do not require high temporal resolution. The usage of Type 12 can not be recommended in applications consisting of heat sources without any storage. Type 12

only requires one UA parameter, which can be estimated as described above. In practical applications, the complete drawings of a building may not be easily accessible, or as in the case of the Flexi-Fuel project [7], it may prove very disadvantageous for a salesman to ask the client for every constructive layer in the wall before being able to demonstrate his/her products. In a real building the heat load will also be influenced by the wind dependent infiltration rate and quality of insulation work, as well as user behavior concerning choice of room temperature and for example open windows in some rooms periods of the day or night. The simulation model in the flexifuel project is aiming at fast but realistic system simulations and then type 12 may be the best choice.

References

[1] Klein et al., 2000, http://sel.me.wisc.edu/trnsys/

[2] O. Hallstrom, Solar Cooling Dimensioning, Modelling of Solar Cooling Installations Using a Thermal Chemical Accumulator from Climate Well AB, Thesis, 2008

[3] T. P. McDowell, J. W. Thornton, and M. J. Duffy, Comparison of a Ground-Coupling Reference standard model to simplified approaches, Eleventh International IBPSA Conference Glasgow, Scotland July 27-30, 2009

[4] P. T. Tsilingiris, Solar Water Design – A new simplified dynamic approach, Solar Energy Vol. 57, No. 1, pp. 19-28, 1996

[5] ClimateWell AB. www.climatewell.com 20070121.

[6] Winsun Villa, www.ebd.lth.se

[7] H. Persson, B. Carlsson, B. Perers, P Olsson and Å. Hjort, Test Plant and Development of Tools for Design of Combi-Heating Systems for large building, Eurosun2010

[8] Duffie, J. Beckman, W., Solar Engineering of Thermal Processes, John Wiley & Sons, Inc. 2006.

[9] R. Heimrath, M. Haller, A Report of IEA SHC - Task 32, 2007

Reducing energy consumption in Natural Gas Pressure Drop Stations by Employing Solar Heat

Mohammad Rezaei[1], Mahmood Farzaneh-Gord[2,*], Ahmad Arabkoohsar[2], Mahdi Deymi Dasht-bayaz[2]

[1] *Mazandaran Gas Company, Sari, Iran,*
[2]*The Faculty of Mechanical Engineering, Shahrood University of Technology, Shahrood, Iran*
** Corresponding author. Tel-Fax: +98 2733395440, E-mail:mahmood.farzaneh@yahoo.co.uk*

Abstract: In Iran (and probably in most countries) natural gas is transported through transmission pipeline at high pressures (5-7 Mpa) from production locations to consuming points. At consumption points, or when crossing into a lower pressure pipeline, the pressure of the gas must be reduced. This pressure reduction takes place in CGSs. At CGSs, the pressure is reduced from (5-7 Mpa) to (1.5-2.0 Mpa) (typically 1.7 Mpa) in high-pressure intrastate pipelines. Currently, gas pressure reduction is accomplished by using throttle-valves in all of Iran's CGSs, where the constant-enthalpy expansion takes place and a considerable amount of energy is wasted. The gas must be heated before it enters throttle valves to ensure that it remains above the hydrate-formation zone and dew point, so that no liquid or solid phase condenses at the station exit. The heaters are consuming a considerable amount of natural gas flowing though the CGS as fuel to provide the required heat for preheating the natural gas stream. As the low temperature heat is required for preheating the natural gas in a CGS, this makes a CGS as perfect place to utilize solar energy and to meet low temperature heat demand. As the low temperature heat is required for preheating the natural gas in a CGS, A solar collector array is proposed to be utilized in the CGS in order to displace heating duty of the heater and to reduce amount of fuel consumption. The proposition includes a modified design of an in-use CGS to take advantage of freely available solar heat.
The proposed system has been applied to study the thermal behaviour of a CGS within Iran. The results show that the cost effectiveness of the proposed method with an array of 450 collector modules is resulted in fuel saving with variation between 0 to 20 USD/hr. The annual fuel saving is about 10678 USD and as the capital cost is about 76500 USD, the payback ratio is calculated to be around 9 years. The number of collector modules has been determined based on cost analysis.

Keywords: *Natural gas pressure drop station, Line Heater, Solar energy, Solar thermal storage*

Nomenclature

CGS City Gate Stations,.....
T_{NG-1} *Natural gas temperature before heater* ^0C
T_{NG-2} *Natural gas temperature after heater..* ^0C
T_{NG-2} *Natural gas temperature after valve .* ^0C
$\dot{m}_{NG}$ *mass flow rate*.....$kg.s^{-1}$
$\dot{m}_{NG}$ *mass flow rate of fuel heater*..... $kg.s^{-1}$
$\dot{Q}_{solar}$ *Heat transfer rate produced by solar KW*
$\dot{Q}_{heater}$ *Heat transfer rate produced by heater KW*
h_{NG-1} *Enthalpy of Natural gas before heater W/kg*
h_{NG-2} *Enthalpy of Natural gas after heater W/kg*
T_W *Temperature of water in the tank*.....^0C
static pressure Pa
LHV Lowering heating value of fuel..... $kj.kg^{-1}$
η_h *Heater efficiency*
$\dot{m}_f$ *mass flow rate consumed heater* $kg.s^{-1}$

1. Introduction

Solar thermal technologies utilise the heat from the sun to offset the heating demand for many applications. The main component of any solar thermal technology is the solar collector. The device absorbs heat form solar radiation and transfers this heat to a circulating fluid (usually water). The heat absorbed by collectors then utilized in many applications. Kalogirou1 presented a survey of the various types of solar thermal collectors and applications. These includes Solar water heating systems, Solar space heating and cooling, Solar refrigeration,

Industrial process heat, Solar desalination systems, Solar thermal power systems, Solar furnaces and Solar chemistry applications[1].

The utilization of solar energy for providing process heat in industrial applications is not common especially for low temperature cases and a few researches have been carried out in this subject. Norton [2] presented the most common applications of industrial process heat. The history of solar industrials and agricultural applications are presented and practical examples are explained. A system for solar process heat for decentralised applications in developing countries is presented by Spate et al. [3] The system is suitable for community kitchen, bakeries and post-harvest treatment.

In Iran (and probably in most countries) natural gas is transported through transmission pipeline at high pressures (5-7)MPa from production locations to consuming points. At consumption points, or when crossing into a lower pressure pipeline, the pressure of the gas must be reduced. This pressure reduction takes place in CGSs. At CGSs, the pressure is reduced from (5-7)MPa to 1.5-2.0 MPa (typically1.7 MPa) in high-pressure intrastate pipelines. Currently, gas pressure reduction is accomplished by using throttle-valves in all of Iran‘s CGSs, where the constant-enthalpy expansion takes place and a considerable amount of energy is wasted (Farzaneh-Gord et al. [4]). The gas must be heated before it enters throttle valves to ensure that it remains above the hydrate-formation zone and dew point, so that no liquid or solid phase condenses at the station exit. Indirect Water Bath Gas Heaters (known as line heater) are employed in the CGS to preheat the natural gas. The heaters are consuming a considerable amount of natural gas flowing though the CGS as fuel to provide the required heat for preheating the natural gas stream. As the low temperature heat is required for preheating the natural gas in a CGS, this makes a CGS as a perfect place to utilize solar energy and to meet low temperature heat demand.

In this study, the objective is to reduce amount of the heater fuel consumption in the CGS by utilizing solar energy. A solar collector array is proposed to be utilized in order to displace heating duty of the line heater. The proposition includes a modified design of an in-use CGS to take advantage of freely available solar heat. The modification has been done in line to minimize the CGS design alteration and availability of the CGS to continue its tasks with or without additional solar system.

2. Methodology

When a natural gas pipeline approaches a city, the high-pressure gas has to be reduced to a distribution level. A city gate station (CGS) is a. Inlet Gas has a high temperature (T_{NG-1}) which is typically related to the ambient temperature (T_{am}). The gas must be heated before it passes through throttle valves to ensure that it remains above the hydrate-formation zone and dew point, so that no liquid or solid phase condenses at the output temperature (T_{NG-3}). The standard preheated gas temperature (T_{NG-2}) is in range of 30-55^{o}C but its value highly depended on inlet pressure and temperature. The heaters are comprised of four basic components, the heater shell, the fire tube, the gas coil and the water expansion section.

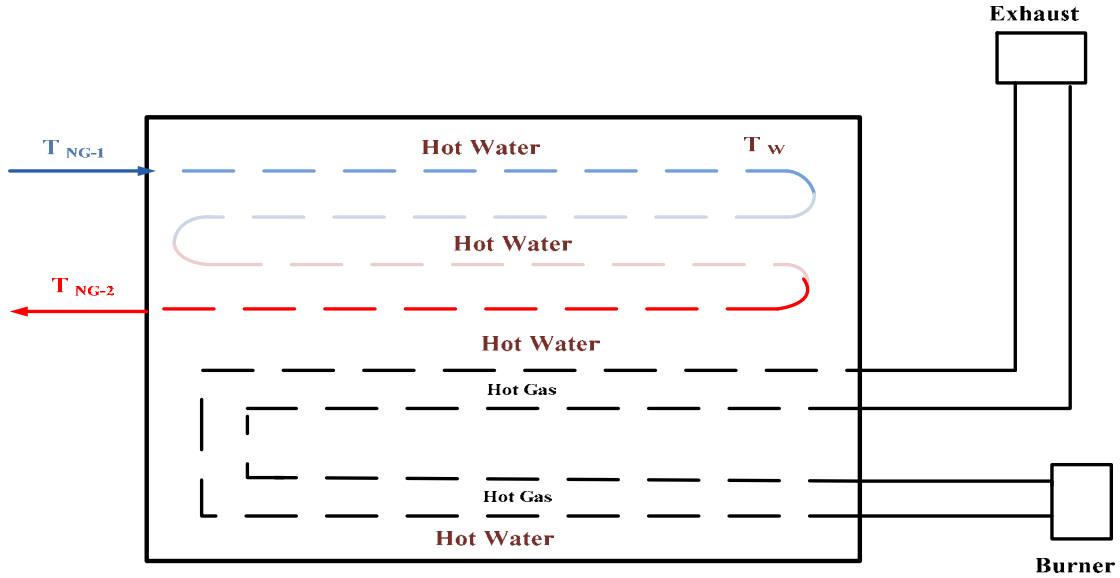

Fig. 1. A schematic diagram of an Indirect Water Bath Gas Heater (Line heater) employed in a CGS for preheating the gas

The heating duty of the heater and the water bath temperature could be estimated by knowing the station inlet and outlet gas temperature and pressure as discussed as follow.

Based on the standard outlet station gas pressure (250 psig or 17 barg) and the natural gas compositions, the hydrate gas temperature (T_{hyd}) could be calculated from thermodynamics models. The outlet station gas stream temperature (T_{NG-3}) is then selected 5 °C above the hydrate temperature [5]. By knowing the outlet station gas stream temperature, the gas temperature at the heater exit could be calculated as below:

$$T_{NG-2} = \overbrace{T_{hyd}}^{T_{NG-3}} + 5 + \Delta T_{tv} \qquad (1)$$

In which, $\Delta T_{tv} (=T_{NG-2} - T_{NG-3})$, is temperature drop due to pressure drop though the throttling valves. The amount of temperature drop is affected by the station inlet pressure and the natural gas compositions. Once, the gas temperature (and pressure) at the heater exit is known, the heater heating duty could be calculated as below:

$$\dot{Q}_{gh} = \dot{m}_{NG}(h_{NG-2} - h_{NG-1}) \qquad (2)$$

As the gas travels a long distance before reaching to the station trough a buried pipeline at depth of 1.2 m, the gas temperature assumed to be equal to the surrounding soil temperature (Edalata and Mansoori,[6]). The soil temperature varies with environment temperature and locations. Najafi-mod et al.11 proposed an empirical correlation for a simple and rational relationship between ambient temperature and soil temperature at different depths. The soil temperature for depth higher than 1 m for Iran could be simplified as follow (Najafi-mod et al.[7]) :

$$T_{NG-1}(^{o}C) = T_{soil} = 0.0084 T_{am}{}^{2} + 0.3182 T_{am} + 11.403 \qquad (3)$$

The heating duty of the heater is provided by burning natural gas as fuel. Considering a value for thermal efficiency, η_h ,of the heater, the fuel mass flow rate, $\dot{m}_f$,could be calculated as below:

$$\dot{m}_f = \dot{Q}_{gh} / (\eta_h LHV) \qquad (4)$$

In which, LHV , is lowering heating value of the fuel (here Natural gas). It should be pointed out that the heater heat lost to ambient is considered through the heater thermal efficiency. The current thermal efficiency of conventional heaters are low and in range of 0.35 to 0.55. In this research, thermal efficiency of the heater is assumed to be 0.45.

As the water bath temperature wouldn't need to be higher than 70°C and the line heater are most needed during winter, in this study an array of flat plate solar collector are proposed to be installed parallel to the heater as shown in Fig.2. The solar flat plat collectors received the water, heated it up and finally returned it to the heater. As it could be realized, a current CGS could be easily modified to take advantages of solar thermal energy as proposed in the Fig.3. The heater is able to continue its normal take with or without solar collectors.

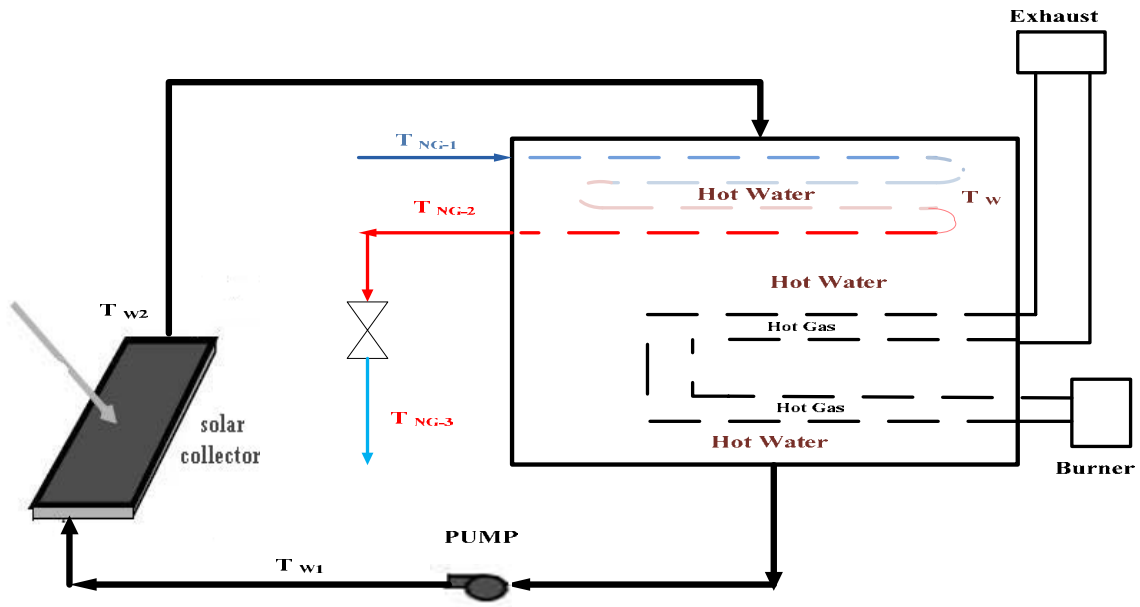

Fig. 2. A schematic diagram of the proposed system to utilize solar energy in the pressure drop stations

The governing equation for a perfectly mixed storage tank could be written as:

$$m_w C_{pw} \frac{dT_w}{dt} = \dot{Q}_{solar} + \underbrace{\dot{m}_f LHV \eta_h}_{\dot{Q}_{heater}} - \dot{Q}_{gh} \qquad (5)$$

In which, m_w C_{pw} , is the system thermal capacity, T_w , is bath temperature and $\dot{Q}_{solar}$ is rate of useful solar energy which is absorbed by the solar collector array and transferred into circulated water. $\dot{Q}_{gh}$ is heating duty of the heater or solar load in the system.

$\dot{Q}_{heater}$ is the rate of thermal energy provided by burning fuel. It should be noted that heat lost from the heater is considered in this term by introducing heater thermal efficiency. There are possibility of two scenarios at this point as a)a heater with automatic controllable $\dot{Q}_{heater}$ b) a heater with fixed $\dot{Q}_{heater}$. It should be pointed out that although all line heaters (within Iran) could be controlled and the rate of $\dot{Q}_{heater}$ could be varied, but these heaters are not equipped with automatic control unit. Here it is assumed that the heaters are equipped with automatic control unit and scenario a (a heater with automatic controllable $\dot{Q}_{heater}$) has been applied. In this scenario, the gas temperature at heater exit is fixed.

Fixed gas outlet temperature could be achieved by controlling rate of $\dot{Q}_{heater}$. $\dot{Q}_{heater}$ could be estimated by making some simple assumptions and applying a "Euler" integration technique. For this, it will be assumed that the values of $\dot{Q}_{gh}$ and $\dot{Q}_{solar}$ are only a function of storage tank temperature at the start of the hour and that (m_w C_{pw}) of the storage is fixed. Therefore, assuming one hour time period (i.e. 3600 seconds), $\dot{Q}_{heater}$ could be estimated by integrating both sides of equation(5). The final equation will be as below:

$$\dot{Q}_{heater} = m_w.C_{pw}(T_{w(i+1)} - T_{w(i)})/3600 + (\dot{Q}_{gh} - \dot{Q}_{solar})_{(i)} \qquad (6)$$

The above equation could be employed to find altered value of the heater fuel mass flow rate as below:

$$\dot{m}_f = (m_w.C_{pw}(T_{w(i+1)} - T_{w(i)})/3600 + (\dot{Q}_{gh} - \dot{Q}_{solar})_{(i)})/LHV\eta_h \qquad (7)$$

Equation (6) or (7) could be rearranged to estimate the hourly variation in water bath temperature as below:

$$T_{w(i+1)} = T_{w(i)} + \frac{(\dot{Q}_{solar} + \dot{Q}_{heater} - \dot{Q}_{gh})_{(i)} \times 3600}{m_w \cdot C_{pw}} \qquad (8)$$

3. Results

The heating duty should be supplied by heater either completely by fuel energy or by combination of solar and fuel energy. As discussed previously, the heater burns natural gas as fuel to preheat the gas. The rate of burning fuel would be useful for studying feasibility of the proposed solar system. Fig 3 shows the averagely daily rate of fuel (natural gas) burned in the heater for months of 2009.

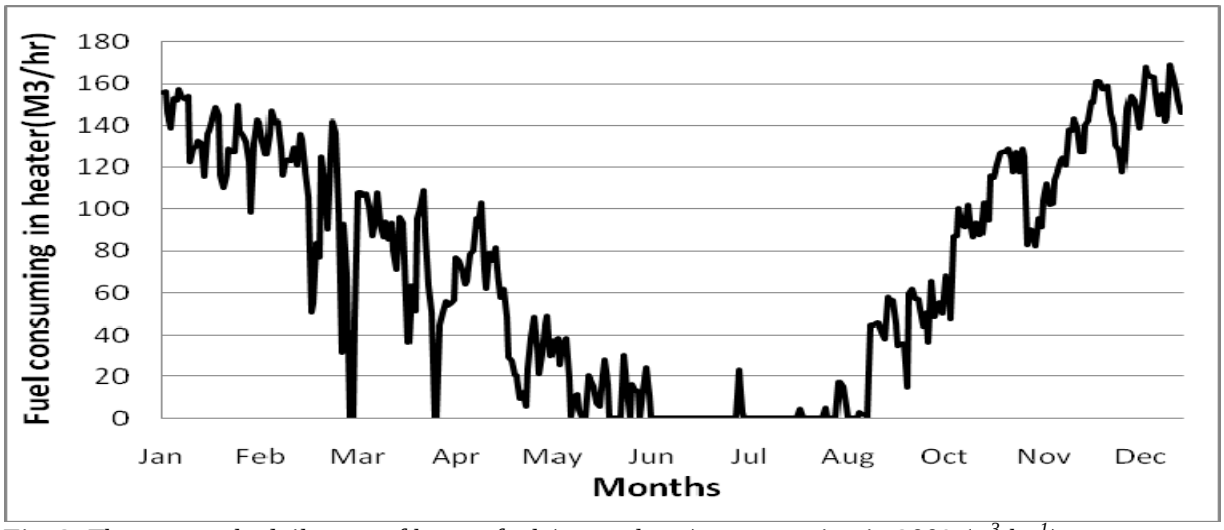

Fig. 3. The averagely daily rate of heater fuel (natural gas) consumption in 2009 ($m^3.hr^{-1}$)

As discussed previously, some part of required preheat energy in the heater is proposed to be replaced by energy gained in solar collector array. The average monthly of absorbed solar energy that gained in Akand Station area shown in Fig 4. It could be realized that the maximum absorbed solar energy is reached in Jun and The lowest value is in October.

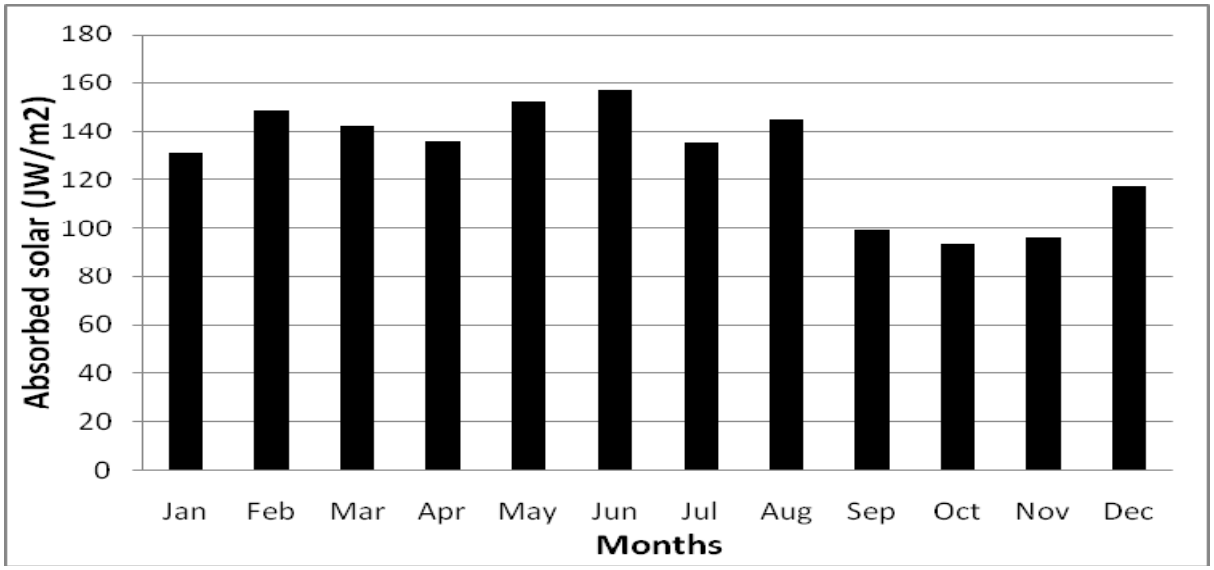

Fig. 4. Average monthly of absorbed solar energy in 2009

The capital cost of the proposed solar system or the array of collector modules could be actually calculated by multiplying the number of collector modules and cost of one module. The cost of one flat plate collector module is about 230 USD in Iran. As number of collector modules in the array increases, the capital cost increases but the heater fuel cost decreases. The variation of annual fuel cost of the heater and solar energy system capital cost against number of collectors modules are displayed in Fig.5. Considering the figure, one could select 450 as an optimum value for the number of collector modules.

It should be noted that the fuel cost calculation is based on current natural gas price which is 0.28 USD for each cubic meter.

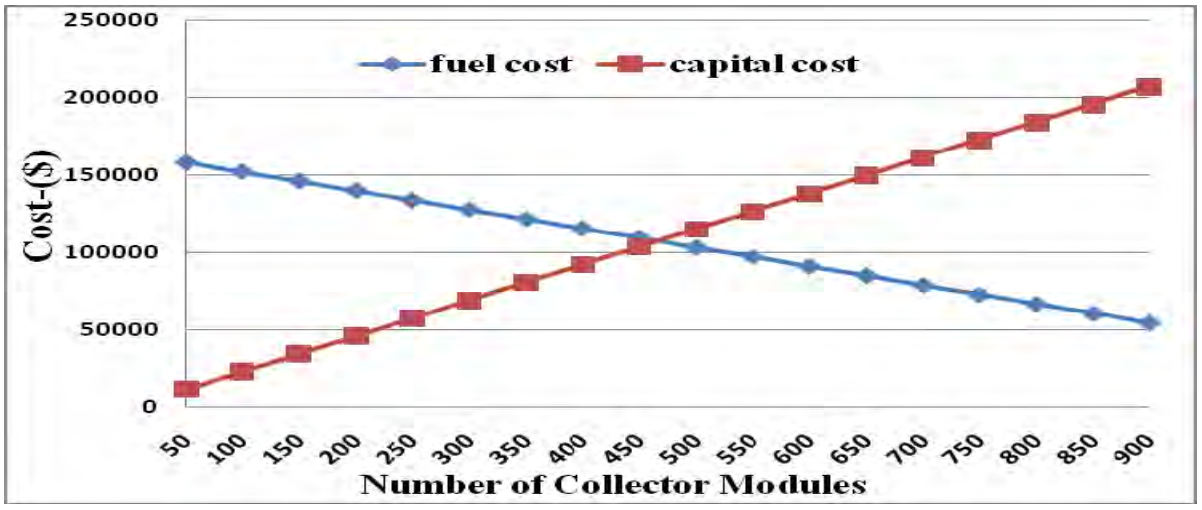

Fig. 5. Variation of solar system capital cost and fuel cost for against number of collector modules

To evaluate the desirability and to investigate the cost effectiveness of the proposed method with an array of 450 collector modules, Fig.6 shows the daily average heater fuel consumption required for preheating gas in 2009 in case of utilizing solar system or without solar system. The distinction between fuel consumptions, shows saving in fuel ($m^3.hr^{-1}$). Annually fuel cost saving can calculate by multiply this amount in 0.28 USD.

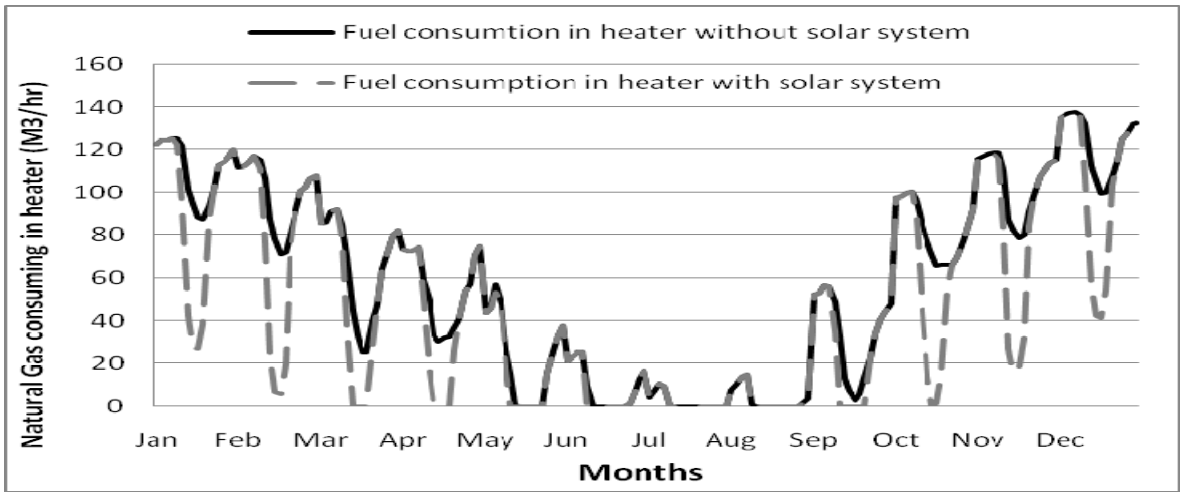

Fig. 6. The heater fuel (natural gas) consumption required for preheating gas in 2009

The annual fuel saving is about 10678 USD and as the capital cost is about 76500 USD, the payback ratio could be calculated as below:

$$Payback\ Ratio = (Capital\ \cos t)/(Benefit) = 9.2\ years \qquad (9)$$

4. Discussion

The natural gas pressure must be reduced to distribution pressure when reaches its end users. The gas must be heated before it enters throttle valves to ensure that it remains above the hydrate-formation zone and dew point, so that no liquid or solid phase condenses at the station exit when pressure and temperature reduced. Currently in all Iran's CGSs, the gas is preheated through a bath type heat exchangers (known as line heater) which burns a portion of the gas for providing heating duty to warm up the natural gas. As the low temperature heat is required for preheating the natural gas in a CGS, A solar collector array is proposed to be

utilized in the CGS in order to displace heating duty of the heater and to reduce amount of fuel consumption. The proposition includes a modified design of an in-use CGS to take advantage of freely available solar heat. The proposed system has been applied to study the thermal behaviour of a CGS within Iran (Akand City Gate Station). The results show that the cost effectiveness of the proposed method with an array of 450 collector modules is resulted in fuel saving with variation between 0 to 20 USD.hr^{-1}. The annual fuel saving is about 10678 USD and as the capital cost is about 76500 USD, the payback ratio is calculated to be around 9 years. The number of collector modules has been determined based on cost analysis.

References

[1] Soteris A. Kalogirou, Solar thermal collectors and applications, Progress in Energy and Combustion Science 30, 2004,231–295

[2] Norton B. Solar process heat: distillation, drying, agricultural and industrial uses. Proceedings of ISES Solar World Congress, Jerusalem, Israel on CD-ROM, Jerusalem, Israel; 1999.

[3] Spate F, Hafner B, Schwarzer K. A system for solar process heat for decentralised applications in developing countries. Proceedings of ISES Solar World Congress on CD-ROM, Jerusalem, Israel; 1999.

[4] Farzaneh-Gord, M., Hashemi, S., Sadi, M., Energy destruction in Iran's Natural Gas Pipe Line Network, Energy Exploration and Exploitation, Volume 25, Issue 6, 2009.

[5] Arnold, Ken; Stewart, Maurice, Surface Production Operations (2nd Edition) Volume 2 - Design of Gas-Handling Systems and Facilities, 1999 Elsevier.

[6] Mohsen Edalata; G. Ali Mansoori, Buried Gas Transmission Pipelines: Temperature Profile Prediction through the Corresponding States Principle, Energy Sources, Part A: Recovery, Utilization, and Environmental Effects, Volume 10, Issue 4 1988 , pages 247 - 252

[7] MH, Najafi-mod, Amin Alizadeh, Azadeh Mohamadian, Javad Mousavi, Investigation of relationship between air and soil temperature at different depths and estimation of the freezing depth (Case study: Khorasan Razavi), *Journal of water and soil of Ferdowsi University of Mashhad*, Vol. 22, No. 2, 2008

Performance of hybrid photovoltaic thermal (HPVT) biogas plant

Prabhakant[1*], Rajeev Kumar Mishra[1], G.N.Tiwari[1]

[1]*Centre for Energy Studies, Indian Institute of Technology Delhi, New Delhi, India*
** Corresponding author. Tel: +91 9810651484, Fax: +91 1126591251, E-mail: prabha.kant@nic.in*

Abstract: In this paper, the energy balance equations for the different components of hybrid photovoltaic thermal (HPVT) biogas plant have been written for quasi - steady state conditions to develop a thermal model. An analytical expression for slurry temperature has been obtained as a function of design and climatic parameters namely mass of the slurry, mass flow rate of fluid in collector, number of collectors, solar intensity, ambient temperature etc. Numerical computations have been carried out for climatic conditions of Srinagar, India. Based on mathematical computations it has been observed that the optimum slurry temperature (~ 37^{o}C) is achieved for a given set of design parameters of biogas plant and hybrid collectors (M_S =2000, $\dot{m}_f$ = 0.05kg/s, L = 25m). It has been observed that number of hybrid PVT collector has significant effect on slurry temperature.

Keywords: *Hybrid PV thermal collector, Thermal modeling, Biogas plants.*

Nomenclature

$I(t)$ Solar intensity at any time t. .....Wm^{-2}
T temperature..... ^{o}C
M mass……Kg
L length of the heat exchanger……m
N number of collectors…….dimensionless
$\dot{m}_f$ mass flow rate of water……Kgs^{-1}
r_1 Inner radius of the tube in heat exchanger…… m
h heat transfer coefficient ..... ……$Wm^{-2}{}^{o}C^{-1}$
α absorbitivity of the black absorber plate....
α' absorbitivity of the gas holder plate.....
β temperature coefficient of efficiency .....
τ transmittivity of the glass plate.....
h_1 heat transfer coefficient from gas holde plate to gas……$Wm^{-2}{}^{o}C^{-1}$
h_2 heat transfer coefficient from gas holder plate to ambient……$Wm^{-2}{}^{o}C^{-1}$
h_3 heat transfer coefficient from gas to slurry ……$Wm^{-2}{}^{o}C^{-1}$
h_c heat transfer coefficient from gas holder to slurry …….. $Wm^{-2}{}^{o}C^{-1}$
h_4 heat transfer coefficient from slurry to ground …… $Wm^{-2}{}^{o}C^{-1}$
$hrps$ radiative heat transfer coefficient… ……$Wm^{-2}{}^{o}C^{-1}$
T_{so} slurry temp at time t = 0 …… …… ^{o}C
A_h horizontal area of the gas holder exposed to solar radiation……m^2
Av veritcal area of the gas holder which is exposed to Solar radiation…… m^2
Ah' vertical area of sulrry……m^2
$A_{v'}$ submerged area of gas holder.…… …. m^2
h_s heat transfer coefficient from tube to slurry …… ……$Wm^{-2}{}^{o}C^{-1}$
U_{lc} over all heat transfer coeff… .....$Wm^{-2}{}^{o}C^{-1}$

Subscript

v vertical
h horizontal
o outlet
i inlet
s slurry
a ambient
c solar cell
p plate
f_i inlet fluid (water)
f_o outlet fluid (water)
m module
g glass

1. Introduction

Biogas is the gas emitted from cow dung in its anaerobic decomposition. Biogas provides fuel for cooking, thus saves the forests and also women from fetching and carrying heavy loads of fuel wood. Biogas is also used for lighting and space heating purpose in rural villages. Thus improves the quality of life. Finally, anaerobic digestion also yields bio-slurry and bio-dregs rich in nutrients, minerals and biologically active compounds. This forms the excellent organic fertilizer for crops and fodder for pig and fish. Production of biogas is maximum when slurry temperature is between 32 to 37 ^{o}C.

In order to increase the slurry temperature in harsh cold climatic condition, the researchers have proposed the following techniques:

(i) Erection of canopy green house over the biogas plant [1-6].
(ii) Integration of solar water heater/ solar still with dome [7-10].
(iii) Hot water charging the slurry before fedding into digester [11].
(iv) Integration of flat plate collector to digester through heat exchanger inside slurry, generally referred as active heating [12-15].

In their study, either floating or fixed dome type biogas plant has been considered. On the basis of their finding, it has been concluded that active heating of slurry in digester is more effective in comparison with other heating methods [12-15]. The temperature of slurry can be increased upto optimum level (~ 37^{o}C) by optimizing the area of flat plate collector for a given capacity of the slurry. It is further important to mention that only forced mode of operation for thermal heating is viable. Neto et al. [16] have suggested biogas/photovoltaic hybrid power system for decentralized energy supply of rural areas. Also, Dubey and Tiwari [17] have presented a hybrid photovoltaic flat plate collector (hybrid PV water collector) for forced mode to produce electrical as well as thermal energy. If such hybrid PV water is integrated to slurry through heat exchanger as shown in Figure 1a, then one can achieve the following:

(i) Increase in slurry temperature for higher yield in harsh cold climatic condition.
(ii) Hot water for domestic use.
(iii) Electricity production for lighting.

In this case the proposed system can be proved to be more economical than single application in rural area in decentralised manner.

2. Design of hybrid photovoltaic thermal (HPVT)-biogas Plant:

There are two types of biogas plat namely floating gasholder type and fixed dome type. In this paper floating gas holder type biogas plant has been considered.

2.1. Hybrid floating type biogas plant:

Hybrid photolytic thermal (HPVT)-biogas plant has been shown in the Fig. 1. It consists of (i) a floating type biogas plant; (ii) partially PV covered solar collectors connected in series and (iii) a coil type heat exchanger. Heat exchanger is connected with partially PV covered solar collectors connected in series and is immersed in the slurry as shown in the Fig. 1a. The hot fluid (water) at outlet of hybrid collectors is allowed to flow through heat exchanger and then transferring the heat from heat exchanger to slurry and hence the slurry gets heated.

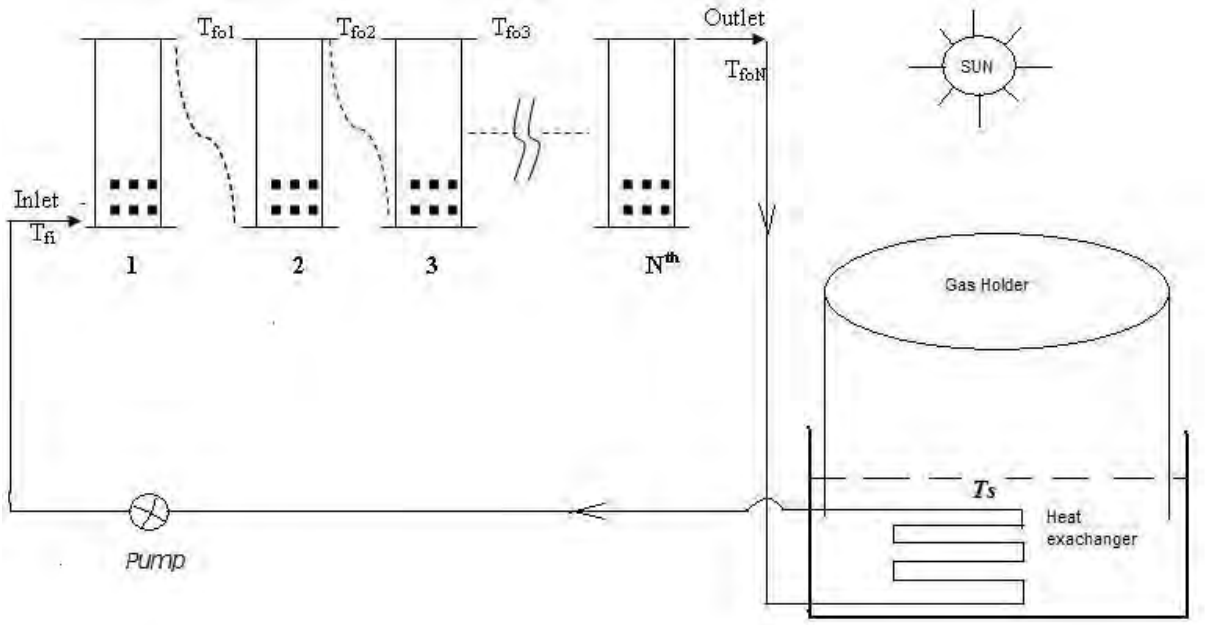

Fig.1 A conventional biogas plant integrated with hybrid PVT solar water collector.

3. Problem Identification

In this paper an attempt has been made to optimize the number of partially covered collectors, size of the heat exchanger and mass flow rate of the water in the heat exchanger for a given size of the biogas plant under a given climatic condition.

4. Thermal Modelling

4.1. Assumptions

In order to write the energy balance equation of hybrid photovoltaic thermal biogas plant, the following assumptions have been made:

- The biogas plant is of floating dome type
- Each component of the system is in quasi – steady state condition
- There is no stratification along the depth of the slurry and the gas column
- Thermal capacity digester and dome of the biogas plant has been neglected

4.2. Energy Balance Equations

The energy balance equations during sunshine hours have been formulated as follows.

For gas holder:

$$\alpha'\left[A_h I(t) + I(t)_v \frac{A_v}{2}\right] = h_1 A_t (T_p - T_g) + h_{rps} A_h (T_p - T_a) + A'_v h_c (T_p - T_s) + h_2(t) A_t (T_p - T_a) \quad (1)$$

For biogas: $$h_1 A_t (T_p - T_g) = h_3 A_h (T_g - T_s) \quad (2)$$

For slurry:

$$M_s C_s \frac{dT_s}{dt} = h_3 A_h (T_g - T_s) + A_h h_{rps} (T_p - T_s) + A'_v h_c (T_p - T_s) - h_4 A_h (T_s - T_\infty) - h_{sa} A'_h (T_s - T_a) - A'_h \dot{Q}_{es} + \dot{Q}_u \quad (3)$$

where,

$$\dot{Q}_{es} = h_{ew} (T_s - T_a) \quad (4)$$

and,

$$h_{ew} = \frac{0.016 h_{sa} \left\{ P(\overline{T}_s) - \gamma P(\overline{T}_a) \right\}}{(\overline{T}_s - \overline{T}_a)}.$$

Now, the rate of heat transfer from flowing fluid in the heat exchanger to the slurry can be written as

$$\dot{Q}_u = U 2\pi r_1 L \left(\overline{T}_w - T_s \right) = \dot{m}_f c_f \left(1 - \exp\left(-\frac{2\pi r_1 U}{\dot{m}_f c_f} L \right) \right) (T_{foN} - T_s) \quad (5)$$

Following Dubey and Tiwari [4], for N identical collectors partially covered by PV modules connected in series, the outlet fluid temperature at the end of N[th] collector can be given as,

$$T_{foN} = \frac{(AF_R(\alpha\tau))_1}{\dot{m}_f C_f} \left(\frac{1 - K_K{}^N}{1 - K_K} \right) I(t) + \frac{(AF_R U_L)_1}{\dot{m}_f C_f} \left(\frac{1 - K_K{}^N}{1 - K_K} \right) T_a + T_f i \, K_K{}^N \quad (6)$$

With the help of Eqs (4) & (5) , Eq (3) can be solved for the slurry temperature

4.3. Electrical output:

The electrical output generated by proposed hybrid photovoltaic thermal biogas can be evaluated by the following expression

$$E_{daily} = \sum_{i=1}^{n} \eta_m \times I_i \times A_m \times N \quad (7)$$

where,

$\eta_m = \eta_{mo} \left[1 - \beta \left(\overline{T}_f - T_a \right) \right]$, $\overline{T}_f = \frac{T_{fON} + T_{fi}}{2}$, η_{mo} =0.12 and β =0.0045 .

4.4. Thermal output:

The rate of thermal energy available from the proposed hybrid photovoltaic thermal biogas plant can be obtained as:

$$\dot{q}_u = \dot{m}_f \dot{c}_f \left(T_{fON} - T_{fi} \right)$$

The daily thermal energy is given by

$$Q_u = \sum_{i=1}^{n} \dot{q}_{ui}; \quad \text{n is sunshine hour.} \tag{8}$$

The daily exergy is given by

$$Ex_{daily} = Q_u \left[1 - \frac{\bar{T}_a + 273}{\bar{T}_{fON} + 273} \right] \tag{9}$$

For a set of design and climatic parameters, outlet temperature of n^{th} collector and Slurry temperature has been calculated using MATLAB software.

5. Results and discussions

Hourly variation of solar intensity on the horizontal and vertical walls of the dome has been calculated by using Liu and Jordan formula with the help MATLAB software. Fig. 2 shows the variation of solar intensity and ambient air temperature with time. Fig 3 gives the variation of outlet temperature from N^{th} collector and slurry temperature during 24 hours period of day and night. Figure shows that there is increase in slurry temperature (T_s) with time of the day as more thermal energy is available from hybrid PVT collectors. It attains maximum temperature (T_{smax}) of about 30^{o}C at 4 pm due to heat capacity of the slurry. This temperature can be further increased by decreasing the mass of the slurry. Further, it is to be noted that the outlet fluid temperature is achieved upto about 80-90^{o}C at noon time as expected. Fig.4 shows the variation of peak slurry temperature (T_{smax}) with mass flow rate. The peak slurry temperature (T_{smax}) increases rapidly with increase of mass flow rate of the fluid due to fast transfer of heat into the slurry. It is observed that there is not much variation in peak slurry temperature (T_{smax}) after mass flow rate 0.05kg/s and hence one can conclude that the optimum mass flow rate is 0.05 kg/s for design parameters given in Table 1 and climatic parameters shown in Fig. 2. Fig.5 shows the variation of peak slurry temperature (T_{smax}) with the mass of the slurry (M_s). This figure shows that peak slurry temperature (T_{smax}) decreases with increase of the mass of the slurry (M_s). It is observed that for the given design and climatic parameters , the optimum mass of the slurry is 2000kg. The variation of peak slurry temperature (T_{smax}) with number of PV/T collectors N is shown in Fig.6. This figure shows that peak slurry temperature (T_{smax}) also increases with increase of number of collectors due to increase of thermal energy provided by PVT collectors to the slurry. It is observed that there is not much variation in peak slurry temperature (T_{smax}) after 50 numbers of collectors and hence the optimum number of collectors for a design and climatic parameters under consideration is about 50.

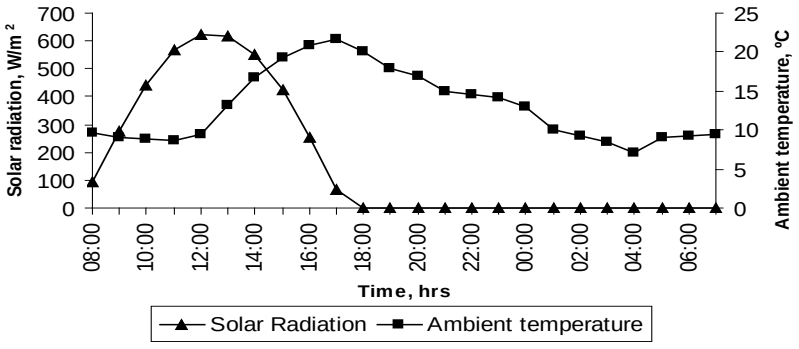

Fig.2. Variation of solar intensity and ambient temperature with time.

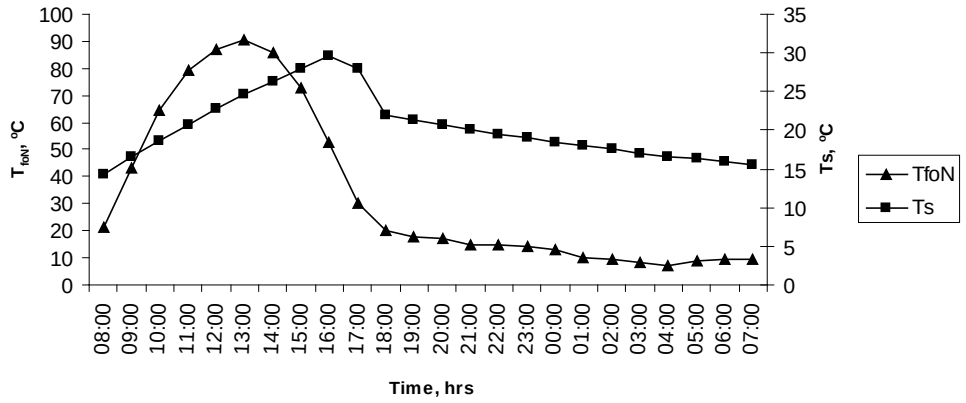

Fig.3. Variation of outlet water temperature (T_{foN}) and slurry temperature (T_s) with time (M_S=2500, $\dot{m}_f$ = 0.02kg/s, L = 25m, N=40)

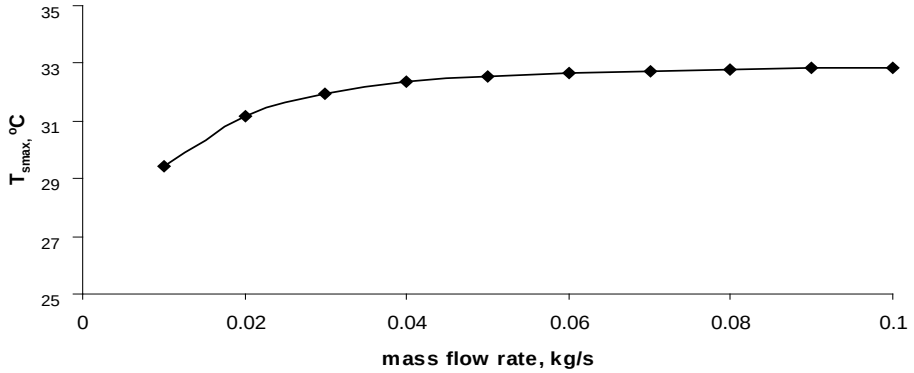

Fig.4. Variation of maximum slurry temperature with mass flow rate of the slurry.

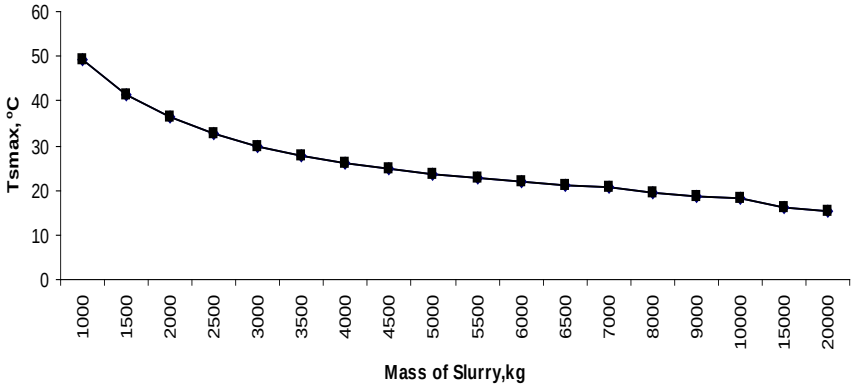

Fig.5: Variation of maximum slurry temperature with mass of slurry for N=40 and mass flow rate=0.02 kg/s.

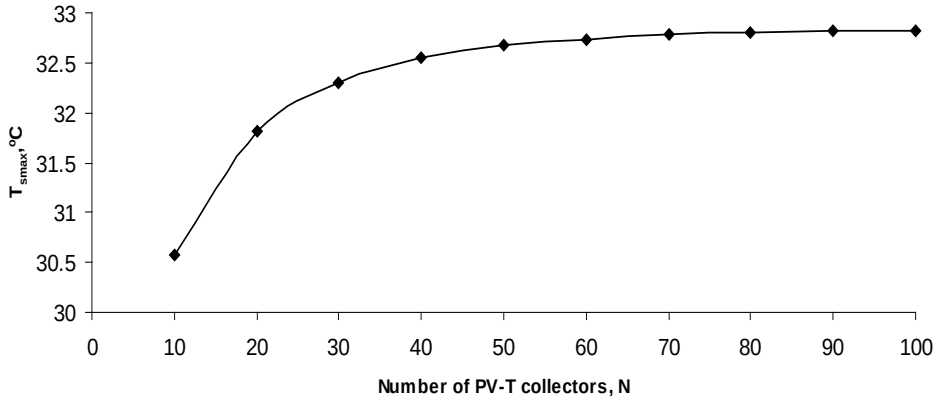

Fig.6. Variation of maximum slurry temperature with number of PV-T water collectors.

6. Conclusions

On the basis of present studies, one can conclude that:

(i) The design parameter of PVT integrated biogas plant can be optimised for a given capacity by using the present thermal model.

(ii) The present system is most suitable and self sustainable for cold climatic condition where ambient air temperature is much less than the optimum operating temperature (~37^{o}C) of the biogas plant.

References

[1] M.S. Sodha, S. Ram, N. K. Bansal and P. K. Bansal. Effect of PVC greenhouse in increasing the biogas production in temperate cold climatic conditions. Energy Conversion and Management 1987; 27 (1): 83–90.

[2] K. Vinoth Kumar , R. Kasturi Bai Solar greenhouse assisted biogas plant in hilly region – A field study, Solar Energy. 2008; 82: 911–917.

[3] N.K. Bansal, S.C. Bhand, S. Ram and K. K. Singh. A study of a greenhouse concept on conventional biogas systems for enhancing biogas yield in winter months. International Journal Energy Resources. 1985; 9: 119–128.

[4] M. Dayal, K.K.Singh, P.K. Bansal and S. Ram Solar assisted biogas digesters I: thermal analysis. International Journal Energy Resources 1985; 9: 455–462.

[5] K. Vinoth Kumar , R. Kasturi Bai Solar greenhouse assisted biogas plant in hilly region – A field study, Solar Energy. 2008; 82: 911–917.

[6] J.A.Usmani, G.N.Tiwari and Avinash Chandra. Performance Characteristic of a greenhouse integrated biogas system. Energy Conservation and Management 1996;

37(9):1423-1433.

[7] A. Kumar, N. Reddy, C.R. Prassad, P. Rajabapaiah, S.R.C. Satyanarayan.. Studies in biogas technology Part II – A novel biogas plant incorporating a solar water heater and solar water hater and solar still. Proceedings of Indian Academy of Sciences C2 (Part-3). 1979; 387–393.

[8] A.K.N. Reddy, C.R. Prasad, P. Rajabapaiah, S.R. Sathyanarayan. Studies in biogas technology, Part IV. A novel biogas plant incorporating solar water heater and solar still. Proceedings of Indian Academic Science. 1979;C2: 387–393.

[9] D. Singh, K.K. Singh, N.K. Bansal. Heat loss reduction from the gas holder/fixed gas dome of a community-size biogas plant. International Journal Energy Resources. 1985; 9: 417–430.

[10] G.N.Tiwari, A. Chandra. Solar assisted biogas systems: a new approach. Energy Conversion and Management 1986; 26 (2): 147–150.

[11] D.J. Hills, J.R. Stephens. Solar energy heating of dairy-manure anaerobic digesters. Agricultural Wastes. 1980; 2 (2):103–118.

[12] G. N. Tiwari, S. K. Singh and Kailash Thakur. Design criteria for an active biogas plant. Energy 1992; 17(10):955-958.

[13] G.N. Tiwari. Enhancement in daily production of biogas systems. Energy Conversion and Management. 1986; 26 (3/4), 379–382.

[14] G. N. Tiwari, S. B. Sharma and S. P. Gupta. Transient performance of a horizontal floating gas holder type biogas plant. Energy Conversion and Management. 1988; 28(3): 235-239.

[15] A. Axaopoulos and P. Panagakis, Energy and Economics analysis of biogas heated livestock building, Biomass and Bioenergy, 2003,24,239-248.

[16] M.R.Borges Neto, P.C.M. Carvalho, J.O.B. Carioca, F.J.F. Canafi's stula, Biogas/ Phtotvotaic hybrid power system for decentralized energy supply of rural areas, Energy Policy 2010; 38: 4497-4506.

[17] Prabhakant and G. N. Tiwari. Analysis of Return on Capital for Bio Gas Plants with and without Embodied Energy. Journal of Energy Storage and Conversion, Jan-June. 2009; 1: 61-78.

Air bottoming cycle for hybrid solar-gas power plants

Fouad Khaldi*

Department of Physics, University of Batna, Batna, Algeria
** Corresponding author. Tel: +213 33819895, Fax: +213 33819895, E-mail: f.khaldi@univ-batna.dz*

Abstract: Several solar-gas hybrid power plants based on the parabolic trough system are under construction in the MENA region and in Spain. The thermodynamic cycle of these plants is divided into topping cycle and bottoming cycle according to their temperature range. Since the solar collectors supply heat at a medium temperature level, up to 400°C, the existing technology uses a steam bottoming cycle (steam turbine). The present study aimed at investigating the thermodynamic feasibility of using air bottoming cycle (gas turbine) instead of the steam bottoming cycle. A thermodynamic scheme of solar air bottoming cycle was proposed. The case study considered an existing small size capacity gas turbine (<50 MW) as a topping cycle. The thermodynamic performance of the proposed solar air bottoming cycle was compared to two reference cases, without solar energy, a steam bottoming cycle and a conventional air bottoming cycle.

Keywords: *Solar-gas hybrid power plant, Air bottoming cycle, Thermodynamic analysis.*

Nomenclature

Acronyms

ABC	*Air Bottoming Cycle*	*GR*	*Gas Recuperator*
AC	*Air Compressor*	*GT*	*Gas Turbine*
ATC	*Air Topping Cycle*	*GTC*	*Gas Topping Cycle*
MENA	*Middle East and North Africa*	*HRSG*	*Heat Recovery Steam Generator*
C-ABC	*Conventional Air Bottoming Cycle*	*IC*	*Intercooler*
		PM	*Pump*
CC	*Combined Cycle*	*S-ABC*	*Solar Air Bottoming Cycle*
CD	*Condenser*	*SBC*	*Steam Bottoming Cycle*
CS	*Combustion System*	*SGHPP*	*Solar-Gas Hybrid Power Plant*
DE	*Deaerator*	*SH*	*Superheater*
DR	*Drum*	*SHX*	*Solar Heat Exchanger*
EC	*Economizer*	*ST*	*Steam Turbine*
EV	*Evaporator*		

1. Introduction

Algeria, located in the Middle East and North Africa (MENA) region, is counted among the best insolated areas. Over the country land, estimated at 2.4 millions Km^2, the Sahara represents 86%. It is exposed yearly to a direct sun irradiation higher than 2000 kWh/m^2 gain from 3500 hours of sunshine. These solar potential and land resources are optimal for the implementation of concentrating solar power plants (CSPPs) [1]. In 2009 the power generating capacity in Algeria was over 9 GW, 98% of this capacity is provided by gas-fired plants, guaranteed in 46% by gas turbine power plants [2]. In according to the Algerian energy policy fixing the share of renewable energy to 5% by 2010, augmented afterwards to 8% by 2020 [2], and since Algeria's natural gas resources are among the largest in the world, solar-gas hybrid power plant (SGHPP) is more suitable than solar-only power plant. The former technology allows for guaranteed power delivery to the grid without the thermal storage needed for compensating the solar energy intermittency day/night [3].

Currently, a 150 MW plant is expected to start run very soon in Algeria with about 25 MW from solar field. Similar power stations are under construction in other MENA region countries [4], Egypt [5], Morocco, whereas in Iran [6, 7] and Jordan [8] SGHPPs are under

consideration. The technology is based on the integrating of parabolic trough systems into combined cycles (CC) with gas topping cycle (GTC) and steam bottoming cycle (SBC). The parabolic trough systems represent the most mature solar thermal power technology, from both commercial and technical viewpoints, for mid-to-large scale grid connected power plants [9, 10]. The parabolic trough collectors can supply to the SBC a hot heat transfer fluid at medium temperature level of about 400 °C [11].

In recent years, intensive research works have been directed toward developing advanced bottoming thermodynamic cycles [12, 13]. The examined thermodynamic schemes were based on the combination of air cooling, intercooling, gas to gas recuperation and reheating [14-20]. For large-scale power generation, greater than 50 MW, it is proven that SBC is the most effective thermodynamic scheme than any other bottoming cycle [21-23]. However, for small-scale power gas turbines, generating less than 50 MW, suffering from limited efficiency, ABC can be competitive, thanks to size and economic constraints rendering unfavorable the use of SBC.
The present paper presents a conceptual analysis of SGHPP based on ABC. Air, instead of steam, is used in the bottoming cycle to recover both partially the energy supplied by the solar field and the energy from the gas turbine topping cycle exhaust. This plant will be dispensing with all the equipments related to steam power plant (high-pressure steam generator, steam turbine, condenser, pumps, water treatment plant, cooling towers, etc.). Hence, it is expected that the SGHPP based on ABC to be compact and less complex. In comparison to the steam turbine plant the gas turbine plant has some advantages: low capital investment cost and operating and maintenance cost, compact size, short delivery, high flexibility and reliability, fast starting and loading. In addition, gas turbines, free of water requirement, are more suitable to be implemented in high solar irradiation regions, limited in water resources.

A solar-air bottoming cycle (S-ABC) is proposed, analyzed and compared to two reference bottoming cycles (without solar energy), conventional air bottoming cycle (C-ABC) and steam bottoming cycle (SBC). The comparison is based on three main parameters, net output power, energy efficiency and exergy efficiency. For all scenarios, the same topping cycle was considered, an existing small size power turbine gas.

The thermodynamic simulations were performed by the flow-sheet program, “Cycle-Tempo”. This software is a freeware advanced tool for the analysis and optimization of energy systems, developed at the Delft University of Technology [24].

2. Thermodynamic simulations and evaluations

2.1. Thermodynamic bottoming cycles

In the evaluation, for the three considered bottoming cycles the same gas turbine topping cycle was used. The GE M&I LM5000-PC(1) gas turbine model was chosen [24], it is a simple open cycle composed of a compressor (AC), a gas turbine (GT), a generator (G); all linked by a shaft, and a combustion system (CS). The cycle generates 34.450 MW, at ISO conditions (1.013 bars, 15°C, RH 60%, and CH4 as fuel), with exhaust temperature and mass flow, respectively, 432.22 °C and 124.738 Kg/s. The energy and exergy efficiencies are respectively, 36.57% and 34.86%.

2.1.1. Solar-air bottoming cycle

The schematic flow diagram of the cycle is shown in Fig. 1. To limiting the number of heat exchangers incorporated in the cycle, just one intercooler (IC) was applied between two

compressors, (AC1) and (AC2). The intercooler cooled the air exiting the first compressor (AC1) down to 40°C. After exiting the second compressor (AC2) the air was heated to 370°C in the solar heat exchanger (SHX). Afterwards, after expanding in the first gas turbine (GT1) the air penetrated into the recuperator (GR) for recovering some energy from the topping cycle flue gas before expanding in the second turbine (GT2). The effectiveness of the solar heat exchanger was set at 90%, whereas the air recuperator had the effectiveness of 85%. It assumed that the hot heat transfer fluid, coming from the solar collector, entered into the solar heat exchanger with about 395°C and then leaved with about 295°C. For the two compressors, the optimum pressure ration was 3.16 and 2.41, respectively. Both compressors and the turbine had an isentropic efficiency of 90%. The relevant air mass flow was estimated at 143 kg/s.

Heat delivered to the air in the solar heat exchanger is:

$$\dot{Q}_a = \dot{m}_a \Delta h, \qquad (1)$$

where $\dot{m}_a$ is the mass flow rate of air, and Δh is the specific enthalpy gain of the air across the SHX. The solar irradiation input to the solar collector is calculated as:

$$\dot{Q}_s = \frac{\dot{Q}_a}{\eta_{sf}}, \qquad (2)$$

where η_{sf} denotes the efficiency of the global conversion of solar irradiation to heat. This includes both the optical efficiency of the solar collector and the thermal efficiency characterizing the heat transportation from the solar collector to the SHX. The value of η_{sf} is chosen to be 0.75, appropriate for the LS3 collector technology [25, 26].

The exergy input through the solar irradiation is determined by the formula [27, 28]:

$$\dot{E}x_s = \left[1 - \frac{4T_0}{3T_s}\left(1 - 0.28\ln(f)\right)\right]\dot{Q}_s, \qquad (3)$$

the symbols T_0 and T_s are, respectively, the ambient temperature and the temperature of the Sun (5777 K), and f is the dilution factor (1.3×10^{-5}).
The energy and exergy efficiencies of the cycle are defined, respectively, as follows:

$$\eta_e = \frac{P_{el}}{LHV\dot{m}_f + \dot{Q}_s}, \text{ and} \qquad (4)$$

$$\eta_{ex} = \frac{P_{el}}{E\dot{x}_f + E\dot{x}_s}, \qquad (5)$$

where P_{el} is the total net power delivered by the cycle, and LHV, $\dot{E}x_f$ and $\dot{m}_s$ are, respectively, the lower heating value, the exergy rate and the mass flow rate of fuel.

2.1.2. Conventional air bottoming cycle

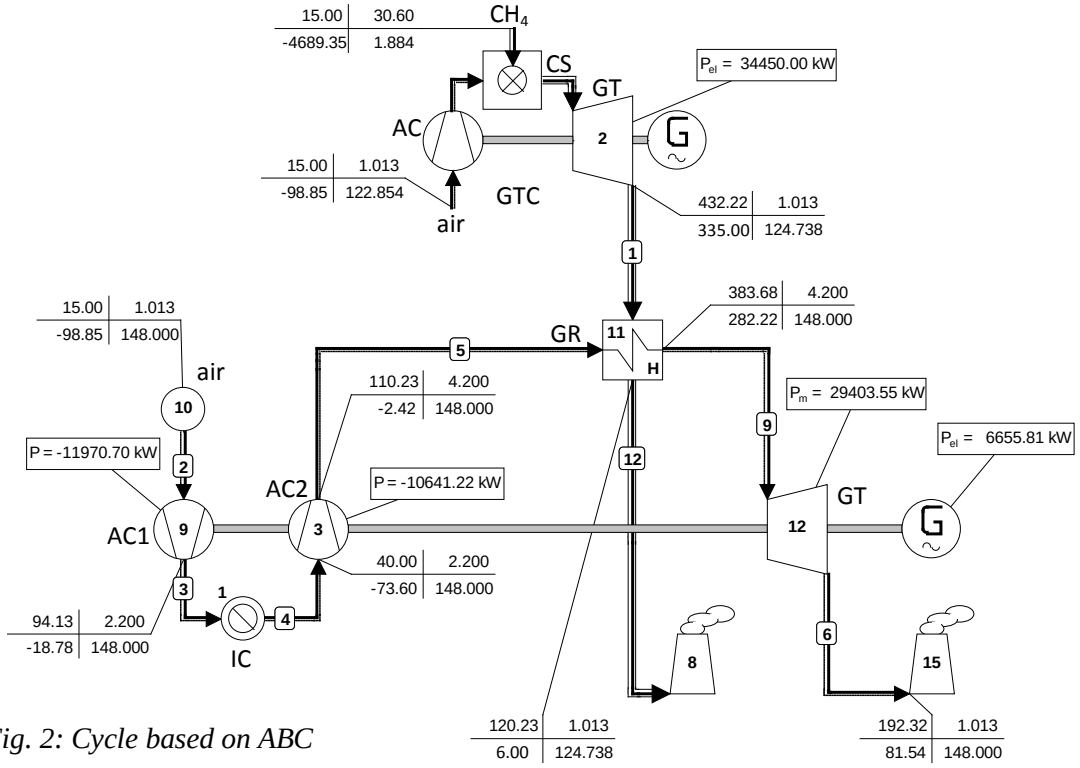

Fig. 2: Cycle based on ABC

As shown in Fig. 2, the air bottoming cycle without solar energy was examined. The C-ABC had the same characteristics as the S-ABC, except that the optimum pressure ration was 2.17 and 1.91, respectively. Also the air mass flow was fixed at148 kg/s.

2.1.3. Steam bottoming cycle

Since the gas turbine topping cycle is of small size (<50 MW), a single-pressure HRSG was chosen. The HRSG was composed of an economizer (EC), an evaporator (EV), a superheater (SH) and a drum (DR). It had the pinch temperature of 20 °C and the approach temperature of 14°C. The superheater had the effectiveness of 87%. The superheated steam entered into the turbine (ST) at 404°C and 19 bars. The isentropic efficiency of the turbine was 85%. The pressure in the condenser (CD) was fixed at 0.074 bars, corresponding to saturation temperature of 40°C. Also, the deaerator (DE) pressure was set at 1.2 bars. More details about the cycle are presented in Fig. 3.

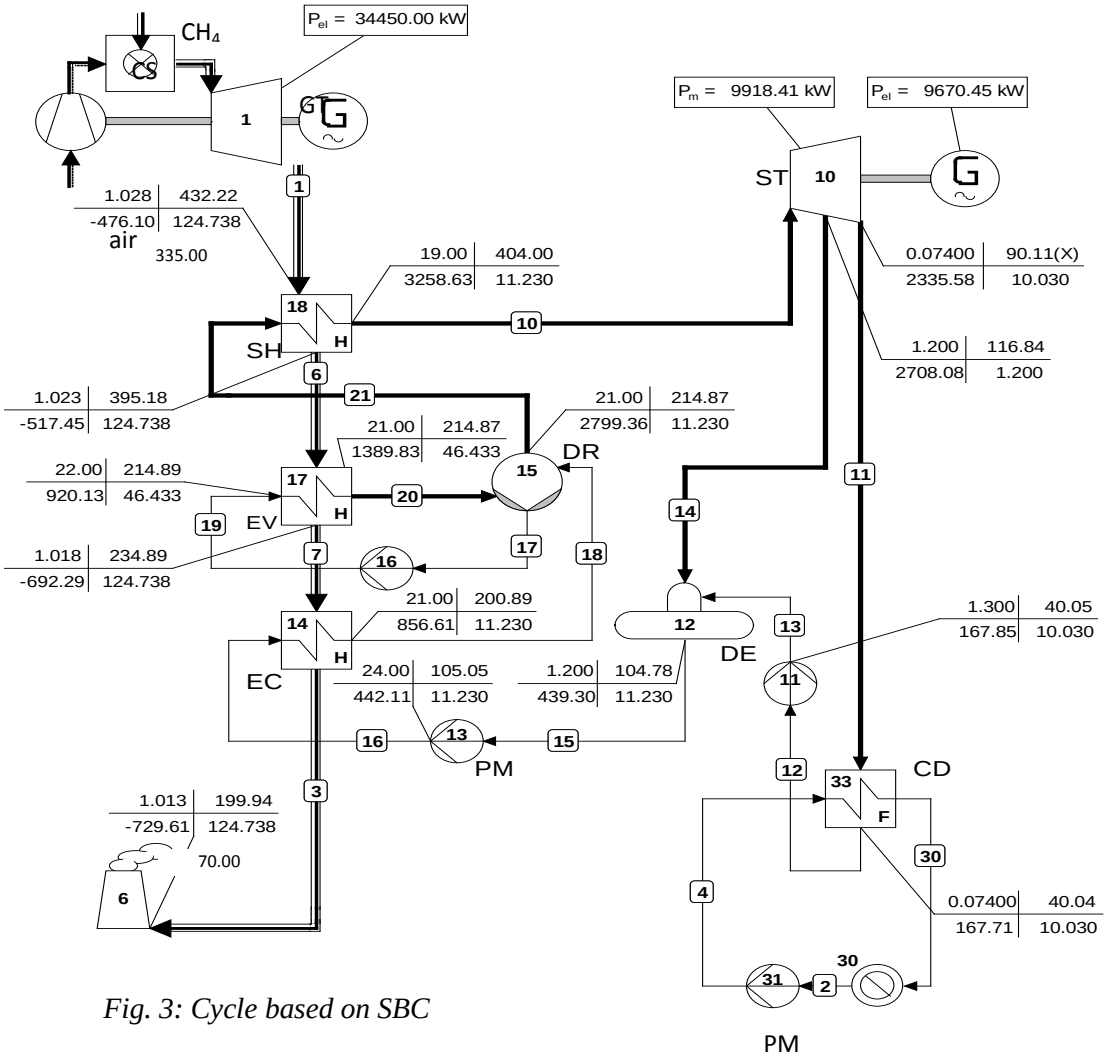

Fig. 3: Cycle based on SBC

3. Results and discussion

Main thermodynamic data related to the cycle performance, for the three examined bottoming cycles, are presented in Table 1. The S-ABC and SBC have nearly the same net output power; contributing to generate 44686 kW for the former and 44120 kW for the last, overtaking by far the C-ABC which delivers 41106 kW. However, the S-ABS is the less efficient cycle, with reference to the topping cycle, it augmented the cycle power by 28.07%, but it decreased the cycle efficiency from 36.56% to 31.87%. In contrary, the SBC is the more efficient cycle; with an energy efficiency of 46.78%, increasing then the topping cycle energy by 10.21 points. With energy efficiency of 41.60% the cycle based on the C-ABS improved the power generation by 19.32%. In term of exergy efficiency, relatively to the simple gas topping cycle the SBC and the C-ABC increase the cycle exergy efficiency from 34.36% (topping cycle), respectively, to 44.66% and 41.60%, the S-ABC decreased it slightly to 33.82%. Note that the cycle exergy efficiency associated to the S-ABC is greater than the energy efficiency.

The comparison between all the examined thermodynamic schemes depend on the relatively high number of thermodynamic parameters and combinations which can modify the performance of the cycle, i.e. turbines and compressors isentropic efficiency, heat exchangers effectiveness, pinch and approach temperature, condenser pressure, etc. The performance of the S-ABC can be improved by more cooling the air down in the intercooler, to less than 40°C, but this level of temperature is typical for cooling by dry air, adequate in regions poor in water resources. Further, at least one intercooler can be added, also an air to air recuperator

can be incorporated to recover some energy of the exhaust air bottoming cycle (143 kg/s at 231 °C). Eventually, the complexity degree of the cycle presents a constraint for any possible modification.

Even, if the S-ABC and the SBC have a comparable performance, potentially the S-ABC can offers 143 k/s of relatively hot air, 230°C, which can be adequate for heat processes requiring pure air.

Table 1. Performances of the three bottoming cycles, S-ABC, C-ABC and SBC.

	S-ABC	C-ABC	SBC
Net output power (kW)	44686	41106	44120
Energy efficiency (%)	31.87	43.63	46.78
Exergy efficiency (%)	33.82	41.60	44.66

4. Conclusion

A case study of solar-gas hybrid power plant has been analysed thermodynamically. The topping cycle of the plant was chosen to be of small size capacity gas turbine (35 MW). An air-bottoming cycle has been proposed instead the well recognized steam topping cycle. Its thermodynamic scheme was based on the combination of intercooling, reheating and gas to gas recuperation. The performance evaluation of the examined cycle was based on the comparison to two reference cases (without solar energy), steam bottoming cycle and conventional air bottoming cycle, in terms of net output power and energy and exergy efficiencies. It was found that the solar-air bottoming cycle and the steam bottoming cycle (without solar energy) had comparable net out powers; whereas the conventional air bottoming cycle (without solar energy) had the smaller capacity generation. However, the steam bottoming cycle is the most efficient cycle, followed by the conventional air-bottoming cycle and afterward by far the solar-air bottoming cycle. The difference in efficiency between the solar-air bottoming cycle and the steam bottoming cycle is due to the definition of energy and exergy efficiency related to the solar cycle. Since the solar heat is provided from the solar irradiation which is free and never depleted, it is may be more practical to don't consider the solar heat energy/exergy as an additional input energy/exergy in the calculation of the energy/exergy efficiency concerning the S-ABC. In that case, the S-ABC becomes the more efficient cycle, with cycle energy and exergy efficiency, respectively, 47.43% and 45.50%.

References

[1] V. Quaschning, Technical and economical system comparison of photovoltaic and concentrating solar thermal power systems depending on annual global irradiation, Solar Energy 44, 2004, pp. 171-178.

[2] Commission de Regulation de l'Electricité et du Gaz (Electricity and gas authority of Algeria), www.creg.org.dz, Annual Report 2010 (in French).

[3] Concentrated Solar Thermal Power-Now, European Commission, European Communities, 2005.

[4] A. Poullikkas, Analysis of power generation from parabolic trough solar thermal plants for the Mediterranean Region- A case study for the Island of Cyprus, Renewable and Sustainable Energy Reviews 13, 2009, pp. 2474-2484.

[5] M. A. H. El-Sayed, Solar supported steam production for power generation in Egypt, Energy Policy 33, 2005, pp. 1251-1259.

[6] R. Hosseini, M. Soltani, G. Valizadeh, Technical and economic assessment of the integrated solar combined cycle power plants in Iran, Renewable Energy 30, 2005, pp. 1551-1555.

[7] A. Baghernejad, M. Yaghoubi, Exergy analysis of an integrated solar combined cycle system, Renewable Energy 35, 2010, pp. 2157-2164.

[8] M. S. Al-Soud, E. S. Hrayshat, A 50 MW concentrating solar power plant for Jordan, Journal of Cleaner Production 14, 2009, pp. 625-635.

[9] Concentrating Solar Power-From research to implementation, European Commission, European Communities, 2007.

[10] Energy Technology Perspectives-Scenarios&Strategies to 2050, www.iea.org, 2008.

[11] A. Fernández-García, E. Zarza, L. Valenzuela, M. Pérez, Parabolic-trough solar collectors and their applications, Renewable and Sustainable Energy Reviews 14, 2010, pp. 1695–1721.

[12] Y. S. H. Najjar, M. S. Zaamout, Performance analysis of gas turbine air-bottoming combined system, Energy Convers. Mgmt. 37(4), 1996, pp. 399-403.

[13] M. Korobitsyn, Industrial application of the air bottoming cycle, Energy Conversion and Management 43, 2002, pp. 1311-1322.

[14] Y. S. H. Najjar, Comparison of performance for cogeneration systems using single-for twin-shaft gas turbine engines, Applied Thermal Engineering 17(2), 1997, pp. 113-124.

[15] Y. S. H. Najjar, Gas turbine cogeneration systems: a review of some novel cycles, Applied Thermal Engineering 20, 2000, pp. 179-197.

[16] P. A. Pilavachi, Power generation with gas turbine systems and combined heat and power, Applied Thermal Engineering 20 (15-16), 2000, pp. 1421-1429.

[17] Y. S. H. Najjar, Efficient use of energy by utilizing gas turbine combined systems, Applied Thermal Engineering 21, 2001, pp. 407-438.

[18] L. Chen, Y. Li, F. Sun, C. Wu, Power optimization of open-cycle regenerator gas-turbine power-plants, Applied Energy 78, 2004, pp. 199-218.

[19] A. Poullikkas, An overview of current and future sustainable gas turbine technologies, Renewable and Sustainable Energy Reviews 9, 2005, pp. 409-443.

[20] C. Ruixian, J. Lixia, Analysis of the recuperation gas turbine cycle with a recuperator located between turbines, Applied Thermal Engineering 26, 2006, pp. 89-96.

[21] A. L. Polyzakis, C. Koroneos, G. Xydis, Optimum gas turbine cycle for combined power plant, Energy Conversion and Management 49, 2008, pp. 551-563.

[22] A. Franco, C. Casarosa, On some perspectives for increasing the efficiency of combined cycle power plants, Applied Thermal Engineering 22, 2002, pp. 1501-1518.

[23] C. Carcasci, B. Facchini, Comparison between two gas turbine solutions to increase combined power plant efficiency, Energy Conversion & Management 41, 2000, pp. 757-773.

[24] Cycle-Tempo Release 5.0, 2007, Delft University of Technology, The Netherlands.

[25] G. Elsaket, Simulating the integrated solar combined cycle for cower plants application in Libya, MSc Thesis, 2007, Cranfield University, UK.

[26] M. J. Montes, A. Abánades, J. M. Martínez-Val, M. Valdés, Solar multiple optimization for a solar-only thermal power plant, using oil as heat transfer in the parabolic trough collectors, Solar Energy 83, 2009, pp. 2165-2176.

[27] E. Hu, Y. Yang, A. Nishimura, F. Yilmaz, A. Kouzani, Solar thermal aided power generation, Applied Energy 87 (9), 2009, pp. 2881-2885.

[28] M. V. J. J. Suresh, K. S. Reddy, A. K. Kolar, 4-E (Energy, Exergy, Environment, and Economic) analysis of solar thermal aided coal-fired power plants, Energy for Sustainable Development, 14 (4) 2010, pp. 267-279.

Economic Implications of Thermal Energy Storage for Concentrated Solar Thermal Power

Sharon J. Wagner[1*], Edward S. Rubin[1]

[1] *Carnegie Mellon University, Pittsburgh, PA, United States of America*
** Corresponding author. Tel: +1 412 592 6986, E-mail: sjwagner@andrew.cmu.edu*

Abstract: A 110-MW parabolic trough power plant operating in California was modeled to observe the effect of molten salt thermal energy storage capacity on plant performance, cost, and profitability. A plant with no storage (PT-NG) was modeled to match the hourly and annual electricity output of a comparable plant with storage (PT-TES). The solar field area for the PT-TES plant was selected to minimize the unsubsidized levelized cost of electricity (LCOE). For each storage capacity modeled here (1-12 hours), PT-NG resulted in a larger solar field area and higher O&M costs than the respective PT-TES option. PT-TES generally had higher capital costs than PT-NG, and the PT-NG levelized cost of electricity (LCOE) varied from 6% higher compared with smaller TES capacities to 6% less compared with larger TES capacities. The profitability of PT-NG compared to PT-TES followed a similar trend to the LCOE with larger margins of difference in select scenarios. These results were achieved with 3-22% of the net electric output from natural gas in the PT-NG plant. The 30% investment tax credit (ITC), currently in place for solar energy in the United States, lowered the capital costs and LCOE for each configuration. Electricity pricing through a power purchase agreement (PPA) of $200/MWh was more profitable than hourly real-time electricity pricing, which resulted in a net annual loss for all configurations. Both the PPA and ITC were required to achieve a positive annual profit, and the maximum annual profit achieved was $US 11 million per year with 0 hours of storage.

Keywords: *concentrated solar power, thermal storage*

Nomenclature

Q	thermal energy	MJ	
M	mass	kg	
T	temperature	^oC	
K	piping thermal losses	J/m^2	
T_o	ambient temperature	^oC	
L	length of pipe in solar field	m	
l_{gap}	length of gap between solar collector assemblies (SCA)	m	
w_{sca}	SCA width	m	
l_{br}	length of space between SCA rows	m	
A_{SCA}	SCA aperture area	m^2	
l_{sca}	SCA length	m	
n_{sca}	number of SCAs per row		
θ	incidence angle	^{o}	
η_{opt}	SCA optical efficiency		
IAM	incidence angle modifier		
F_s	mirror soiling factor		
d_o	outer diameter of solar field pipe	m	
m	mass flow rate	kg/s	
Δh	enthalpy change	J/s	
t	hour of TES storage capacity	hrs	
h_i	enthalpy at inlet	J/s	
h_e	enthalpy at exit	J/s	
η	efficiency or effectiveness		
h_{es}	enthalpy of isentropic state at exit	J/s	
w	work per unit mass	J/kg•s	
W	power	J/s	
Cp	specific heat	J/kg	
r	density	kg/m^3	
CF	plant capacity factor	%	
$W_{tdesign}$	design turbine output	MJ	
D_{htr}	natural gas-fired heater heat duty	MJ/hr	
k	loan interest rate	%	
j	loan lifetime	years	
C	cost	$US2009	
i	discount rate	%	
n	plant lifetime	years	
F_{debt}	debt portion of capital cost	%	
F_{equity}	equity portion of capital cost	%	
NPV	net present value	$	
LAC	levelized annual capital cost	$/yr	
C_{OM}	annual operation and maintenance cost	$/yr	
p	price of electricity	$/MWh	

1. Introduction

Solar energy is an attractive renewable energy source because the sun's energy is plentiful and carbon-free. Cost and intermittency issues have prevented widespread deployment of

solar power plants, but these issues may be partially mitigated with the addition of thermal energy storage (TES). Molten salt TES can be used in lieu of a natural gas boiler to provide backup energy for a parabolic trough concentrated solar thermal power (PT) plant during cloudy periods and nighttime. TES can enable a PT plant to provide reliable peak or baseload electricity without sacrificing carbon neutrality by relying on a natural gas backup system. However, the additional equipment associated with a TES system can add substantially to the already high capital cost of PT. An investor will only accept the additional cost of these components if the potential exists for an economic benefit that exceeds the extra cost. This study examines the economic implications of TES through an engineering-economic model. The model calculates the levelized cost of electricity and expected annual profit of a PT plant with varying TES capacities and compares these results to a similar PT plant with natural gas backup.

2. Methodology

An engineering-economic model was developed to simulate the hourly and annual performance and cost of a PT plant. A visual representation of the engineering portion of this model is presented in Figure 1. Typical meteorological year (TMY3) direct normal radiation (DNR) and ambient temperature data for Daggett, California [1] were used as inputs to a series of component-based mass and energy balances to simulate the thermodynamic operation of the system. Two separate and distinct engineering models were created: 1) PT-TES, which models a PT plant that uses a TES system, and 2) PT-NG, which models a plant that uses a natural gas-fired heat transfer fluid (HTF) heater in place of a TES system.

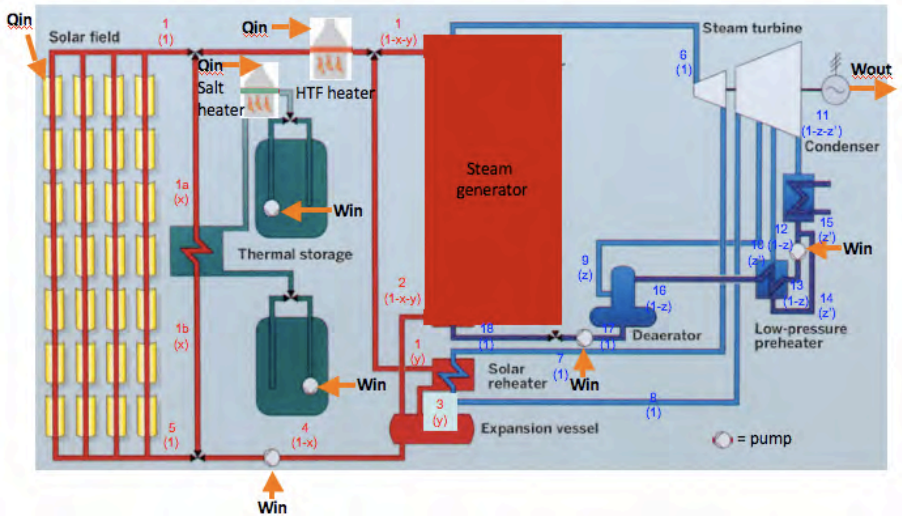

Fig. 1. Parabolic Trough Plant Schematic (adapted from [2]).
Hourly DNR enters the solar field and is concentrated on the heat transfer fluid (HTF) in the receiver tubes (red). The HTF is pumped to the power cycle where energy is transferred to steam (blue) via the steam generator and reheater. The heat from the steam drives the turbines to generate power (Wout) and the cooled HTF returns to the solar field. When the TES system is charging, some HTF flows to the heat exchanger to transfer energy to molten salt. Hot salt is stored in one tank and cold salt in the other. When the ambient temperature threatens to freeze the salt, the salt heater is activated to maintain the temperature above freezing. The HTF heater is used to maintain the HTF temperature above freezing when altering the HTF mass flow rate fails to prevent freezing. The HTF heater is used as an alternative to the TES system in the PT-NG plant. The heat energy input to the two heaters from natural gas combustion is represented as Qin. Five pumps are used in the system, and the work required to operate them is shown as Win. Red numbers refer to HTF states, blue numbers refer to steam states, and numbers in parentheses represent mass flow fractions.

The PT-TES model incorporates seven distinct operation modes, which are presented in Table 1. The hourly simulation selects operation modes based on whether all criteria are satisfied, following the hierarchy shown in Table 1. For example, if Day_TESC fails, the simulation will attempt to run Day_SOLAR. If Day_SOLAR fails, the simulation will attempt Day_TESD, and so on. The PT-NG model only uses Day_SOLAR, Night_SD, and Night_FP, and incorporates an additional mode similar to Day_TESD that uses the HTF heater in place of the TES system. The PT-NG model uses as inputs the T_1, W_{net}, and W_{sold} results from the PT-TES model (see equations 30 and 31), and the solar field area for PT-NG is selected to minimize the difference between W_{sold} from each model, in order to simulate two different power plants that generate comparable amounts of hourly and annual electricity.

Table 1. Plant operation modes.

Mode ID	Description	Criteria
Day_TESC	Only the solar field delivers thermal energy to the power cycle; excess solar energy "charges" the TES system	$Q_{SF} > \min$ $M_{salt} < \max$
Day_SOLAR	Only the solar field delivers thermal energy to the power cycle; the TES system is idle	$0 < Q_{SF} \leq \min$ $M_{salt} \leq \min$
Day_TESD	The solar field and the TES system deliver thermal energy to the power cycle	$0 < Q_{SF} < \min$ $M_{salt} > \min$
Night_TESD	Only the TES system delivers thermal energy to the power cycle; HTF circulates through the solar field at a minimum mass flow rate to stay warm	$Q_{SF} \leq 0$ $M_{salt} > \min$
Night_SD	The power cycle is idle; HTF circulates through the solar field at a minimum mass flow rate to stay warm	$Q_{SF} \leq 0$ $M_{salt} \leq \min$
Night_TESFP	The power cycle is idle; HTF circulates through the solar field at a minimum mass flow rate, and the TES system protects the HTF from freezing	$Q_{SF} \leq 0$ $M_{salt} > \min$ $T_{HTF} \leq \min$
Night_FP	The power cycle is idle; HTF circulates through the solar field at a minimum mass flow rate, and the natural gas-fired heater protects the HTF from freezing	$Q_{SF} \leq 0$ $M_{salt} \leq \min$ $T_{HTF} \leq \min$

The hourly simulation uses an iterative process that selects an operation mode based on the net energy captured by the solar field (Q_{SF}), the total mass of salt in the "hot" TES tank (M_{salt}), and the temperature of the HTF. The minimum Q_{SF} for the 110-megawatt (MW) system modeled here is 245 megawatt-hours (MWh). The hourly Q_{SF} value depends on hourly ambient conditions and HTF temperature, as shown in equations 1 through 3. The solar field area (A) is specified at the beginning of each simulation and varied to achieve the lowest levelized cost of electricity (LCOE). Equation 2 is a simplified version of the calculation used to determine the length of pipe in the solar field, which is a required input to equation 3.

$$K = a + b \bullet (T_{HTF} - T_o) + c \bullet (T_{HTF} - T_o)^2 \quad (1)$$

where a, b, and c are empirical thermal loss coefficients [3]

$$L = l_{gap} + 2 \bullet w_{sca} + 2 \bullet l_{br} + (A \div A_{SCA}) \bullet ((l_{sca} \bullet w_{sca} - A_{SCA}) \div w_{sca} + l_{sca} + l_{br} \div (A_{SCA} \bullet n_{sca}) + (2 \bullet w_{sca} + 2 \bullet l_{br}) \div n_{sca} - (2 \bullet A_{SCA} \bullet (w_{sca} + l_{br}))/A) \quad (2)$$

$$Q_{SF} = A \bullet DNR \bullet \cos(\theta) \bullet \eta_{opt} \bullet IAM \bullet F_s - K \bullet \pi \bullet d_o \bullet L \bullet (T_{HTF} - T_o) \quad (3)$$

where l_{gap}=1m, w_{sca}=5.77m, l_{br}=15m, A_{SCA}=817.5m^2, l_{sca}=149m, n_{sca}=4, d_o=0.07m, and η_{opt}=82% [3]

Equation 4 shows how the model calculates the total amount of M_{salt} using the design values presented in [4]. The HTF factor (F_{HTF}) was selected as 1.5 after several iterations of the model indicated that the hourly m_{HTF} rarely exceeded 1.5 times the design value. The number of hours of TES capacity refers to the number of hours the turbine could operate at full rated capacity using only the thermal energy from the storage system. The extra salt factor (F_{salt}) represents the amount of salt that must remain in the TES tanks at all times. In this study, the nominal value for F_{salt} was 1.14 [4].

$$M_{salt} = -((3600 \bullet (m_{HTF} - m_{HTFo}) \bullet F_{HTF} \bullet (\Delta h_{HTF})) \bullet t \bullet F_{salt}) / (\Delta h_{salt}) \quad (4)$$

where m_{HTF} = 1,206 kg/s, m_{HTFo} = 121 kg/s, F_{HTF} = 1.5, F_{salt} = 1.14

The model calculates the design states and mass flow rates of all fluids in the system shown in Figure 1 through a series of component mass and energy balance equations based on the First Law of Thermodynamics, assuming steady-state conditions and zero kinetic or potential energy flows (equations 5-29). The key design inputs to these equations include: T_1 = 393°C, T_3 = 225 °C, T_5 = 293 °C, T_6 = 373 °C, pressure $(p)_4$ = 110 kPa, p_5 = 620 kPa, p_6 = 10,001 kPa, p_7 = 1,900 kPa, p_8 = 1,700 kPa, p_9 = 700 kPa, p_{11} = 8 kPa, p_{12} = 200 kPa, p_{18} = 10,200 kPa, $\eta_{turbine}$ = 85%, η_{pump} = 80%, $\eta_{preheater}$ = 80%, TES heat exchanger effectiveness of heating and cooling = 88%. The hourly simulation also uses equations 5-29 to set the hourly states, beginning with a starting T_5 value of 100 °C.

Heat exchangers (steam generator/ reheater, condenser, LP preheater, TES heat exchanger, salt & HTF heaters):

$$h_i = (\eta \bullet h_{es} - h_e) \div (\eta - 1) \quad (5)$$

$$h_e = h_i + \eta \bullet (h_{es} - h_i) \quad (6)$$

$$h_e = h_i + (m_{steam} \bullet (h_{i\_steam} - h_{e\_steam})) \div m_{HTFadj} \quad (7)$$

$$Q = m \bullet (\Delta h) \bullet 3600 \quad (8)$$

where, η = heat exchanger effectiveness, adj = mass flow rate adjusted with fractions shown in Fig. 1

Turbines:

$$w = \eta \bullet (h_i - h_{es}) \quad (9)$$

$$h_e = h_i - w \quad (10)$$

$$W = w \bullet m_{steam} \quad (11)$$

Rankine cycle pumps:

$$w = (h_i - h_{es}) \div \eta \quad (12)$$

$$h_e = h_i - w \quad (13)$$

$$W = w \bullet m_{steam} \quad (14)$$

Expansion vessel:

$$h_4 = (1-y) \bullet h_2 + y \bullet h_3 \quad (15)$$

Solar field pump:

$$W = m_{HTF} * (r_4^{-1} * (p_4 - p_5) \div \eta) \quad (16)$$

$$h_5 = h_4 - w \quad (17)$$

Mass flow rates and fractions:

$$z = (h_{17} - h_{16}) \div (h_9 - h_{16}) \quad (18)$$

$$z' = (z \bullet (h_{16} - h_{14}) + h_{14} - h_{16}) \div (h_{14} - h_{12}) \quad (19)$$

$m_{steam} = W_e \div (h_6 + h_8 - h_7 - z \bullet h_9 - z' \bullet h_{12} - (1 - z - z') \bullet h_{11})$ (20)
$m_{HTF} = (Q_{SF} \bullet 1000000) \div (h1 - h8)$ (21)
$y = (m_{steam} \bullet (h_7 - h_8)) \div (m_{HTF} \bullet (h_1 - h_3))$ (22)
$x = (h_1 - h_{1a} \bullet m_{HTF}) \div (h_{1b} - h_1)$ (23)
$m_{salt} = -(x \bullet m_{HTF} \bullet (\Delta h_{HTF}) \div (\Delta h_{salt}))$ (24)

Therminol VP-1 (HTF) and nitrate salt properties [5]:
$Cp_{HTF} = 7.888e\text{-}4 \bullet T^2 + 2.496 \bullet T + 1.509e3$ (25)
$Cp_{salt} = 1.72e\text{-}1 \bullet T + 1.443e3$ (26)
$h_{HTF} = 1.377 \bullet T^2 + 1.498e3 \bullet T - 1.834e4$ (27)
$h_{salt} = 8.6e\text{-}2 \bullet T^2 + 1.443e3 \bullet T$ (28)
$r_{HTF} = -7.762e\text{-}4 \bullet T^2 - 6.367e\text{-}1 \bullet T + 1.0740e3$ (29)

The net electricity generated by the system is calculated using equation 30, and then separated into electricity sold and bought (equations 31 and 32) for the cost model. The power losses due to auxiliary equipment such as electronic motors, drives, computers, etc (W_{aux}) are calculated using the series of equations described in [6]. Equation 33 calculates the capacity factor based on electricity sold, while equation 34 calculates capacity factor based on net electricity generated (after subtracting electricity used by pumps during nighttime hours).

$W_{net} = W_{turbines} - W_{pumps} - W_{aux}$ (30)
$W_{sold} = W_{net}$ when $W_{net} > 0$ (31)
$W_{bought} = abs(W_{net})$ when $W_{net} < 0$ (32)
$CF = W_{sold} \div (W_{tdesign} \bullet 8760)$ (33)
$CF_{net} = W_{net} \div (W_{tdesign} \bullet 8760)$ (34)
where W_{aux} refers to power losses through auxiliary loads

The economic model calculates the total capital cost of the plant and the annual operation and maintenance (O&M) costs using a slightly adapted version of the National Renewable Energy Laboratory's (NREL) Solar Advisor Model (SAM) cost model [7], which was developed for a plant with a solar field area of 854,000 m^2. In order to apply this model to a variety of solar field sizes, a scaling factor (the ratio of the solar field area to the reference solar field area) is used for area-dependent O&M cost items. Calculations were added for the capital cost of the HTF and salt heaters as well (equations 35 and 36).

$D_{htr} = (\max (Q_{htr}) \bullet 0.00094781712) \div 1000000$ (35)
$C_{htr} = 13402 \bullet D_{htr} + 367158$ (36)

The levelized cost of electricity (LCOE) is calculated using equations 37-40. An alternative, subsidized levelized annual capital cost (LAC) is also calculated with the current United States federal investment tax credit (ITC) for solar energy investments. This ITC is applied as a cash grant, i.e., a deduction, of 30% of the total plant capital cost.

$C_{loan} = (k \div (1-(1+k)^{-j})) \bullet C_{cap} \bullet F_{debt}$ (37)
$NPV_{loan} = \Sigma (C_{loan} \div ((1+i)^{year}))$ (38)
$LAC = (i \div (1-(1+i)^{-n})) \bullet (NPV_{loan} + C_{cap} \bullet F_{equity})$ (39)
$LCOE = (LAC + C_{OM}) \div W_{sold}$ (40)

The expected annual profit (P) is calculated using equation 41 and hourly historic electricity pricing data from the California Independent System Operator (CAISO) from 2008 [8]. This calculation assumes that the power plant receives the real-time price of electricity from the

CAISO. An alternative P is calculated under the assumption that the plant owner enters into a power purchase agreement (PPA), and this calculation is shown as equation 42.

$$P = \Sigma (W_{sold} \bullet (p - LCOE)) \quad (41)$$

$$P_{PPA} = \Sigma (W_{sold} \bullet (p_{PPA} - LCOE)) \quad (42)$$

3. Results

The solar field area for PT-TES was selected to minimize the LCOE, while the solar field area for PT-NG was selected to minimize the difference between W_{sold} in the two models. Figure 2 shows that the solar field area increased with increasing storage capacities in order to capture enough energy for the TES system. The solar field area for the PT-NG plant increased even more because it was required to meet the hourly solar-generated electricity output of the PT-TES plant without being able to store excess solar energy during high DNR hours. The capacity factor for each plant was almost identical since PT-NG was designed to match PT-TES. The net capacity factor for each system was smaller because it subtracts nighttime pump energy from the annual electricity generation. Overall, capacity factor increased with storage capacity as the plants operated for more annual hours. The PT-NG plant generated 3-22% of its annual electricity with the NG heater.

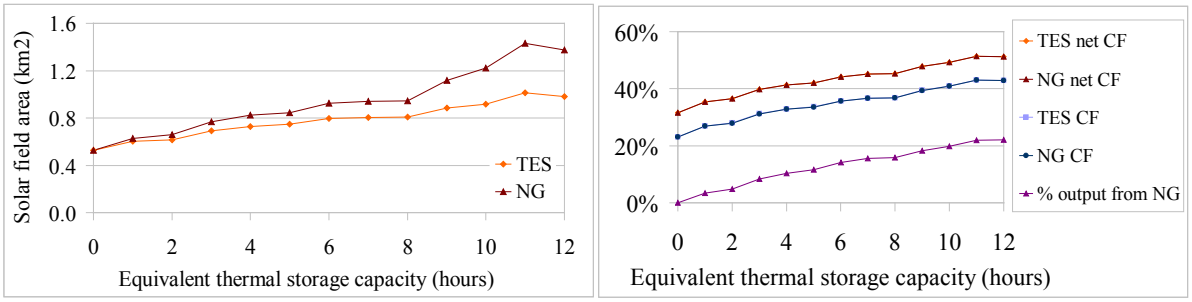

Fig. 2. Solar Field Area (left) and Plant Capacity Factor (right).
The first graph shows the solar field area selected for PT-TES to minimize LCOE and the area selected for PT-NG to match PT-TES electricity output. The second graph shows the corresponding plant capacity factors and the percent of output from natural gas in the PT-NG plant.

Figure 3 shows that the capital costs increased for both plants with increasing equivalent storage capacity, as a larger solar field was required. PT-TES with 1 hr TES had slightly lower capital costs than PT-NG as the latter required a slightly larger solar field. PT-TES with 3-12 hrs TES had higher capital costs than PT-NG as the cost of the TES system outweighed the larger solar field area required by PT-NG. O&M costs increased with storage capacity, as a larger solar field required more workers and maintenance. The O&M costs were higher for PT-NG because of the additional annual fuel purchase.

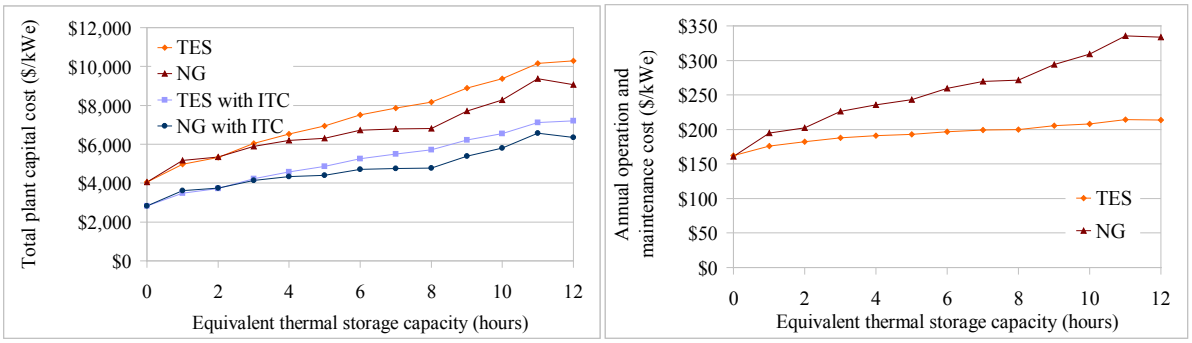

Fig. 3. Total Plant Capital Cost (left) and Annual Operation and Maintenance Cost (right).

The first graph shows the total plant capital cost for each plant with and without the 30% investment tax credit (cash grant). The second graph shows the annual O&M costs for each plant. Assumptions: natural gas = $US 5.92/MMBtu, auxiliary electricity = $US 135.15/MWh.

In Figure 4, the LCOE generally increased with storage capacity, and the LCOE of PT-NG varied +/- 6% from the LCOE of PT -TES. With smaller storage capacities, higher PT-NG O&M costs outweigh higher PT-TES capital costs to result in lower PT-TES LCOE. With higher storage capacities, higher PT-TES capital costs outweigh higher PT-NG O&M costs to result in higher PT-TES LCOE. This second effect was lessened with the ITC as the high PT-TES capital cost decreased, but the high PT-NG O&M cost remained unchanged. Based on these costs, a carbon price of $US 153-$383/tonne CO_2eq would be required for PT to be competitive with coal, depending on plant specifications.

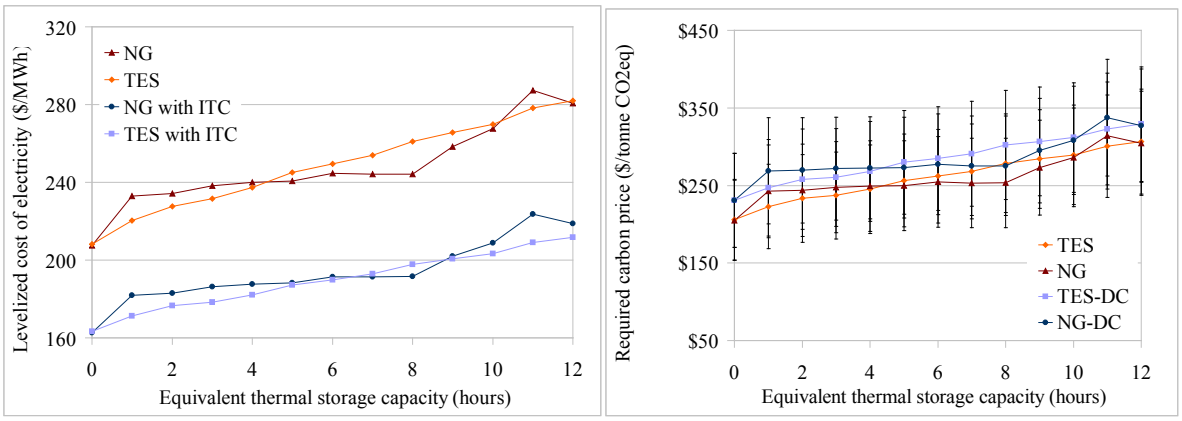

Fig. 4. Levelized Cost of Electricity (left) and Required Carbon Price (right).
The first graph shows the LCOE of each plant with and without the ITC. Assumptions: k=7%, j=20 years, F_{debt}=60%, F_{equity}=40%, i=12%, n=30 years. The second graph shows the carbon price that would be required for these plants to be competitive with coal electricity generation in the United States. Assumptions: coal LCOE=$US 64-74/MWh [9], coal greenhouse gas (GHG) emissions = 0.84-0.88 tonnes/MWh [10], and PT GHG emissions = 0.01-0.185 tonnes/MWh [11]. The bars represent the range of results associated with GHG emission and coal cost bounds.

Figure 5 shows that expected annual profit decreased with increasing storage capacity, and the only scenario that achieved positive annual profit was PPA/ITC with 0-8 hrs TES equivalent, highlighting the importance of guaranteed pricing and financial incentives. Hourly CAISO pricing with no ITC resulted in the largest annual loss, and similar trends were observed across storage capacities as those seen in the LCOE results: PT-TES was more profitable than PT-NG at storage capacities of 1-4 & 11 hr with no ITC, and 1-6 & 9-12 hr with the ITC. At the extremes, the profit of PT-NG with PPA/ITC was 4 times greater than 8 hr PT-TES and three times less than 11 hr PT-TES.

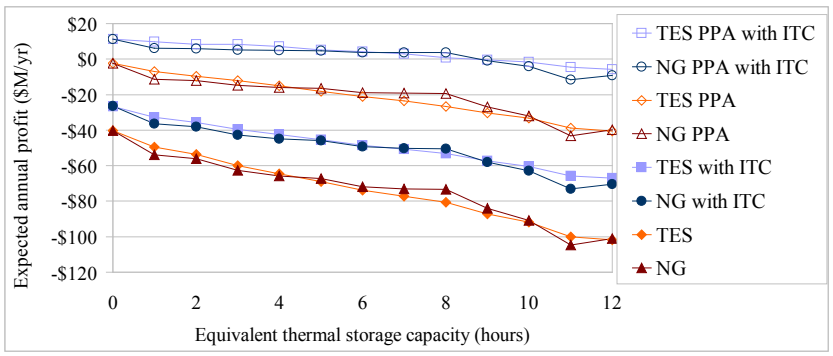

Fig. 5. Expected Annual Profit.
This graph shows the expected annual profit for each plant, using the unsubsidized LCOE, the subsidized LCOE (with ITC), hourly electricity pricing, and power purchase agreement pricing (PPA of $US 200/MWh).

4. Discussion and Conclusions

The results of this analysis are subject to the specific assumptions and calculations outlined above. The uncertainty inherent in these assumptions and the sensitivity of results to changes in nominal values has not yet been explored, but is the subject of future analysis. Nonetheless, the limited scope presented here offers some insights for solar energy policy. Encouraging PT power plants to serve as baseload generators could result in cost increases and profit decreases, whether the additional generation is met by NG or TES. However, a small amount of TES (1-4 hours) is likely to be slightly more profitable and less costly than attempting to achieve similar annual generation with NG backup. If the policy goal is to encourage the deployment of PT power plants as baseload generators, incentives such as the U.S. federal 30% investment tax credit (ITC) or a generous power purchase agreement (PPA) are necessary to reduce the LCOE and result in a positive expected annual profit. The ITC favors TES compared to NG because it reduces the high TES capital cost but does not affect the high NG O&M costs. A price of $US 153 per tonne CO_2eq or higher could make PT competitive with coal electricity generation.

References

[1] Wilcox, S. and W. Marion. 2008. User's Manual for TMY3 Data Sets, NREL/TP-581-43156. April 2008. Golden, Colorado: National Renewable Energy Laboratory.

[2] Price, H., ed. Assessment of Parabolic Trough and Power Tower Solar Technology Cost and Performance Forecasts. Rep.No. SL 5641. Sargent & Lundy LLC Consulting Group. Chicago, IL: NREL, 2003.

[3] Kreith, Frank, and D. Yogi Goswami, eds. Handbook of Energy Efficiency and Renewable Energy. New York: C R C LLC, 2007

[4] Estimated value from: Kelly, B. and Kearney, D. Thermal Storage Commercial Plant Design Study for a 2-tank Indirect Molten Salt System. Final Report, May 13, 2002 - December 31, 2004. Golden, CO.: National Renewable Energy Laboratory (2006).

[5] National Renewable Energy Laboratory, Solar Advisor Model User Manual, 2009

[6] National Renewable Energy Laboratory, Solar Advisor Model Reference Manual for CSP Trough Systems, 2009

[7] Turchi, C. Parabolic Trough Reference Plant for Cost Modeling with the Solar Advisor Model (SAM), National Renewable Energy Laboratory Technical Report No. NREL/TP-550-47605, July 2010.

[8] California ISO, version 5.7.7, http://oasis.caiso.com, accessed October 15, 2010.

[9] Integrated Environmental Control Model 6.2.4 (with advanced features selected), http://www.netl.doe.gov/technologies/coalpower/ewr/pubs/cmu-iecm.html.

[10] Jaramillo, P., W.M. Griffin, and H.S. Matthews. 2007. Comparative life cycle air emissions of coal, domestic natural gas, and SNG for electricity generation. Environmental Science & Technology. 41(17):6290-6296.

[11] Lechón, Y., C. de la Rúa, and R. Sáez. 2008. Life cycle environmental impacts of electricity production by solarthermal power plants in Spain. Journal of Solar Energy Engineering. 130. 021012-1-7.

Social and technical aspects in solar system design

Dorota Wójcicka-Migasiuk [1,*], Andrzej Chochowski [2]

[1] *Lublin University of Technology, Faculty of Fundamental Engineering, Lublin, Poland*
[2] *Warsaw University of Life Sciences, Warsaw, Poland*
** Tel: +48 81 5384453, Fax: +48 81 5384706, E-mail: d.wojcicka-migasiuk@pollub.pl*

Abstract: The paper defines and describes factors that should be considered when hybrid energy supply systems that incorporate solar systems in particular are planned. In the first point, the author establishes the hierarchy of criteria to apply at subsequent phases of the decision processes carried out when renewable energy systems are to be used. To do this, the authors take the advantage of shortly described case studies: a solar hot water system in an elderly house and an integrated system of steam boilers together with heat recovery from a cooling system in connection with solar heating in a food production plant, etc. Then, the paper indicates the necessity of energy simulations prior to taking up the decisions of localization and to final verification of the project. The example of the simulation method called equivalent thermal network is mentioned in the comparison to the advantages and disadvantages of the other software described. Some forms of promotion are presented, which can be applied to positively stimulate the sustainable development of the use of renewable sources in the European central eastern region on the background of a short comparison.

Keywords: *local availability, hybrid systems, sustainable development*

1. Introduction

Hybrid systems in relation to energy supply are the systems that incorporate different media such as electric current, flowing fluids or solid massive elements to carry out different forms of energy from various sources either renewable or conventional. They are also called integrated systems and can combine a traditional boiler gas fired, a heat pump transferring ground heat or the heat from solar thermal collectors, a usually small photovoltaic system supplying electrical energy for circulation pumps and somehow integrated a passive system such as e.g. solar walls. The particular composition is determined by operational conditions, energy source localization, availability and its form, and by other factors that influence the rational use of energy. The decisions can be taken up after thorough consideration of:

-local climatic conditions,
-social aspects that influence the cycle of energy demand,
-object character,
-technological aspects resulting from selected devices designed for the system,
-economical factors that determine investment capabilities in the frame of the analyzed enterprise and
-the cost of operation of the whole hybrid system.

The paper presents the description of the influence of selected factors on design and decision processes related to appropriate energy supply system and on the realization of objects that use solar energy. There is a vast diversity of social aspects and problems of matching between the demand and solar energy availability in a perspective characteristic for mid-severe climate, characteristic for central - eastern Poland. The procedure of careful analysis describes the most important contracting factors such as:

-high solar gain and low ambient temperature,
-high social acceptation and cost exaggerating investment capabilities in the region,
-standard regulations characteristic for the country and the region and availability of simulation tools, and with special attention
-the applicability of available simulation tools.

2. Methodology

The selection and decisive criteria can be divided in some hierarchy. It is obvious for engineers that the good will of having a system to supply renewable energy cannot be decisive for selection of components for the particular object. It is questionable, however, if the negative will (quite common in some societies) can be decisive for the resignation and if the decision should not be taken by local authority on the basis of justified technical reasons and natural conditions, having in mind the rational use of energy and environment protection. It is a distant goal to reach the situation when such justification is obligatory to potential investors. On this distant way to reach this goal either social mentality must undergo its process of evolution towards higher responsibility for the environment or legislation and standards must be established to rule new attempt to the selection of energy sources. The widely understood education drawing the attention to all mentioned determinants could be very helpful on this way to assume proper hierarchy in the processes of investment, design, realization, maintenance of systems and exploitation of resources to reach the final result established as sustainable development.

Usually, attempting the design process for a particular object, its localization and character is already established, but sometimes, we have a chance to adjust the localization for better exposition to solar radiation or for advantageous distribution of ground collectors and slightly adjust the waveform of load to the cycle of energy availability through some change of habits or technology. The principal idea of hybrid systems is not the most extensive use of all renewable energy sources (res) in one system but the most reasonable integration of those that are convenient for the localization and the object character. Country regions are comparatively flexible in fitting the localization to the needs of effective heating systems and this meets another fact that the systems that are used there are usually outdated and contain low effective boilers fuelled with coal or are expensive such as boilers fuelled with liquid gas or gasoil because of the cost of these fuels. In the first phase of design the availability and economics of resources is considered. The paper is focused on solar energy thermal conversion integrated within hybrid systems because widely understood conversion of solar energy has its special conditions and restrictions worth analyses.

The systems that use direct and dispersed beam require south oriented exposition with possible adjustment to horizontal plane, and thus should be placed on the ground or tilted roofs. They need the coincidence of load waveform and the cycle of availability as much as possible to avoid damage resulting from overheating of elements or heat loss because of extended accumulation. These systems are used:

- for hot water systems: in food industry, for sanitary and living purposes in permanently occupied buildings (SDHW) and to contribute low temperature heating systems, especially
- floor heating systems,
- to heat process water: in fish breeding ponds, to water glasshouse plants and to heat the ground,
- in drying processes of many purposes to contribute technological halls (air collectors and passive solar systems), especially biomass drying for solid biofuels,

Systems that cooperate with heat pumps in heating systems either in central heating or hot water systems require additional supply from electric grid and providing cooling power from the bottom source of so called bottom energetic potential i.e. from the ground, for example. They can have the form of:

- ground water wells, which require proper soil absorption to receive water from absorption wells, proper localization in a distance to each other and good quality of soil to protect durability of drilled objects,

- horizontal and vertical heat exchangers that require big undeveloped land area. One should remember that undeveloped does not mean unused. The terrain with ground collectors underneath can serve as a parking place, sports yard, nice flower bed or grass and only big root trees must be avoided.

Boilers can be fuelled with biofuels but each case must be considered if the particular localization is economically justified in the aspect of transport cost. It is difficult to describe biofuels as one source of energy because they are diversified as much as biomaterials and processes used for their generation. Shortly describing, the generation can also be understood as origin and is the classifying factor for biofuels. The first generation biofuels are produced directly from eatable plants in fermentation and trans-estrification processes and have similar limitations as food raw material. The second generation biofuels are produced from biomass or non eatable seeds having in mind that waste material is its origin. The third generation biofuels use the same material as the second one but after additional treatment, processing and modifications. The fourth generation biofuels are rather a perspective target employing such advanced technologies as in photo bioreactors and the use of intermediary organisms, e.g. algae, during production processes. In Poland, the second generation biofuels will soon have the dominant role over the first one which is positive and desired tendency.

Heat recovery systems from production processes of many types, e.g. from ventilation, from cooling, quite frequent in food industry and rarely from air conditioning as it is not very popular in Poland, or heat recovery from litter in animal farmhouses.

Photovoltaic systems, usually recognized as expensive, become reasonable when traditional connection to grid is more expensive than standards, especially when increased power demand in a farm or a household requires additional investment from regional distribution company which in turn is transferred to a user. They are treated as additional support to supply devices of low demand in complex hybrid systems (e.g. PV panels for circulation pumps in solar domestic hot water – SDHW - systems). Environmental protection aspects can be sometimes decisive if the localization is situated in nature parks. The most famous localization of this type in our country is the mountain shelter in the Valley of Five Polish Tarns. Moreover, it is also practical to install PV panels in periodically occupied small objects such as forest shelters, guest rooms and shepherd's huts but there is a need to provide an energy store system and protection in the period of no use by e.g. spare duty lighting. The potential of photovoltaics is recognized as capable to reach 12% share in total production of energy in Europe by 2020 year. Unfortunately, in Poland, there are no favorable circumstances to promote PV systems [1].

Solar walls in our climate should be completed with TIM (Transparent Insulation Material) modules besides typical massive elements and air gaps because this additional insulation protects the building envelope during fall-winter seasons against thermal losses at low ambient temperatures. It is necessary that the whole insulation of these buildings is of best quality ranging u value between 0.1 and 0.3 at maximum and that the terrain around is properly adapted. Several case studies can be mentioned on the basis of the author's research [5, 7] and the other reference [1]. Particular conclusions can be derived in relation to the application of such passive structures as Trombe-Mitchell's walls in eastern mid-European regions [7]. This typical construction cannot be successfully used for the whole year because:

- insulation even by two glass panels is insufficient for winter and
- solar radiation in summer often exceeds the needs.

In the intermediary season of fall (spring/autumn), solar walls prove their usefulness and thus make possible to reduce heating period and energy demand in total thanks to the solar gain in several weeks within the range of the whole heating period. There is also a very useful solution to the problem of insulation, i.e. transparent panels. Thanks to the capillary structure they let radiation in and prevent from thermal losses because of air trapped within capillary and its material – organic glass - of insulation properties. Moreover, the shading can be realized by means of insulated folded blinds and with the help of leaf trees.

Because of low intensity of heat flux coming from renewable sources such as ground or solar radiation, the renewable systems have comparatively long pipelines and this is one of the reasons of thermal loss from active elements. That is also why designs should strictly reduce collective pipeline length placing collectors as close as possible to the receivers. Moreover, in comparison to traditional heating, the effectiveness of renewable systems depends more on the cycle of load. In particular, the systems that work at loads lower than calculated in the design, have much lower energy effectiveness which influences directly the cost-effectiveness. The research carried out by Chochowski A. and Czekalski D. [1] prove that energy parameters outstand the predicted ones on the basis of static characteristics. Unequal load of the system in subsequent days leads to the reduction of conversion efficiency even of 50%.

3. Results

At first, the exemplary case study of an elderly house for women in a village can be shortly described. The design of this system avoids long pipelines because the boiler room is on the ground floor directly under the roof where collectors are to be installed with proper exposition on south oriented tilted roof. The design process of this hybrid system was carried out when the total modernization of the whole object was considered, including the change of fuel from liquid gas stored in tanks on the backyard to natural gas from local network. The designed solar system was to contribute to the main supply. The designed system consists of the battery of twelve flat plate thermal collectors and nine collectors have been planned on the south tilted roof and the other three on the west roof surface with additional construction for south-west exposition. Optional expansion of the battery into another eight collectors could be possible after removal of gas tanks. The condition of source availability is fulfilled this way. Another criterion for consideration was matching the load waveform to the cycle of heat production. In this aspect there is an ideal phase coincidence either in annual cycle or daily use of hot water and heat production from the solar system. This is possible because of special care that must be carried for the residents, i.e. – because the residents are of advanced age and through this debilitated and less resistant to temperature changes, their bathing in winter must be limited to the necessitate minimum. In summer, when there is a lot of sun radiation there are no such threats as low temperature, cold draughts etc., the balneological care can be more frequently applied. There is also some good coincidence in daily treatment because the baths are taken in the afternoon hours when the house service staff have managed with cleaning and cooking and the water storage tank is full of water heated from collectors at the maximum for the day. In the evening hours, the water storage starts slowly cooling off and the staff except for the person on duty, goes home. Moreover, the residents in elderly houses do not go for holidays as housing estate inhabitants or do not go home in the afternoon as people working in offices. It is only a pity that at so many favourable circumstances, this design has been abandoned.

Czekalski D. [1] points out also some other solutions of good coincidence: a seminary with boarding house, a monastery or a convent with retreat centers, a school with a swimming

pool, etc. Academic centers are especially vulnerable to the pressure of educative aspects of renewable energy applications and they should extremely thoroughly consider the matter of coincidence. The good solution could be a guest room house combined with a sports center containing a swimming pool available for usage during holidays. It seems not justified to supply lecture buildings from solar energy because the largest amount of energy is to be used potentially when the real use drops to zero. Then it is necessary to employ this energy somehow to avoid the destruction of the whole system. Overheated collectors are damaged and hot water stored for too long than a few days is the environment for bacteria growth. This problem has to be solved also for single family houses. In this aspect municipal applications in blocks of flats are advantageous because the part of inhabitants stays at home for the whole year and it is not a problem if this is not the same group when hot water is prepared centrally. The remaining usage is usually sufficient to ensure continuous medium flow through collectors.

Another attempt to the problem of coincidence is the consideration of the integration of an individual system with municipal grids and networks, however at the present state of formal regulations and technical practice, it is an extremely difficult enterprise in our country, available rather to bigger energy producers than just families or single farms. So far, the connection of geothermal source with the heat distribution network and the integration of boilers fuelled by biofuels with gas boilers supplied from gas distribution network or with the heat distribution network has had the best practical experience. In the case of the integration with gas boilers, the network does not receive the energy from the renewable system, only gives the possibility to reduce the amount of supplied fuel. The connection together with the receipt of energy is especially desired in the case of photovoltaic systems and the grid. The two aspect can be covered there: one of autonomous operation of a renewable system and the regular profile of power supply.

The next example of good coincidence could be the idea of integration between the production processes and solar thermal collectors studied for the case of meat production plant. Because of the meat processing, hot water of 80 ^{o}C is used to wash production rooms (intensive use at about 3 p.m.) and water of 60 ^{o}C for hygienic purposes and another processing continuously during two shifts. Hot water is supplied from cooling system recovery and steam boilers that provide also central heating in the object. The hybrid system concept suggests the integration between cooling system heat recovery and solar collectors where load cycle fits the solar daily availability waveform and conventional support from steam gas boilers.

4. Discussion

Some evaluation if the selected modules of a composed hybrid system is possible in advance by means of simulations. The most advanced simulation techniques are useful for designers, who in the case of not standard objects can verify their effectiveness. It is worth mentioning that RES systems are mostly unique because of the local applications, sometimes differing even between neighbor farms or buildings.

The most representative is the following software that is available in European location but with some limitations:
ESOP [4] developed by Viessman – very well prepared software, intended for use by designers but suitable also for local authority representatives. It provides calculation for some typical SDHW systems with the possibility to calculate carbon dioxide emissions and comparisons among different fuels, available in Polish version.

TRNSYS [2] developed by University of Winconsin – advanced software to calculate transient states in the variety of systems, with the reference to geographic and climatic conditions, very useful also for advanced use such as scientific analysis and for designers, however comparatively expensive and Polish version is not available. It is worth mentioning that the university provides some possibilities for free download from internet and even these limited versions are very educative and thus very useful for didactics. The software is grouped in packages for different media and RES and enables cost calculation on the basis of design system and selected devices from USA market.

WUFI [3] developed by Fraunhoffer Institute – software suitable for passive systems such as multi-layer wall structures, available in Polish version also for free download for the purpose of didactics but with limitations, provides some information to know particular producers of the used materials and thus can be useful to calculate the cost of the system.

Moreover, the authors can also mention simulation algorithms based on equivalent thermal network developed in cooperation by Lublin Technical University and the University of Life Science in Warsaw [5, 6]. These algorithms at the current state are suitable for advanced users, perform calculations also for transient states and have not been commercialized yet. The use of these algorithms is undoubtedly more time consuming but the user can decide on all simplifications introduced to the system model and to the calculations. The method enables modeling of energy flow by means of different media and thus is suitable for integrated systems, provides results of calculated energy flux, flows and temperature reached in the system units in time for different days of a year in the form of graphs and matrices. The other algorithms have been developed for solar walls by means of FEM analysis.

What is even more important the ease of simulation analysis can add the value to the planned refurbishments and all purpose modernizations in many municipal sectors in the phase prior to the design instead of time consuming and expensive existing building inventorying in situ. This should be particularly taken into account when numerous objects are to be rebuild in the regions where older technology have been applied so far.

References

[1] D. Chwieduk, R. Domański, et al., Renewable Energy. Innovative Technology and New Ideas., Chwieduk D., Domański R., Jaworski M. (editors) Warsaw 2008, p. 476.

[2] http://sel.me.wisc.edu/trnsys Oct.'10.

[3] http://www.wufi.de Oct.'10.

[4] Viessmann, ESOP v.2.0 CD, 23.03.2003

[5] Wójcicka-Migasiuk D., Modelling hybrid systems in rural regions, (in Polish) Inżynieria Rolnicza 1(89)/24, KTR PAN PTIR, Kraków 2007, p. 120.

[6] Wójcicka-Migasiuk D., Nodal potential simulation for the analysis and design of SDHW systems. (in Polish) Acta Agrophysica No. 39/2001, Inst. Agrofizyki PAN, Lublin 2001, p. 106.

[7] Wójcicka-Migasiuk D., Heat transfer through solar walls, (in Polish) LTN, Lublin 2008, p. 112.

On the Significance of Concentrated Solar Power R&D in Sweden

Torsten Strand[1*], James Spelling[1], Björn Laumert[1], Torsten Fransson[1]

[1]*Department of Energy Technology, KTH Royal Institute of Technology, Stockholm, Sweden*
**Corresponding Author. Tel : +46 70 268 4024, E-mail : torsten.strand@punkt.se*

Abstract: Concentrated Solar Power (CSP) is an emerging renewable energy technology that has the potential to provide a major part of European energy needs at competitive cost levels. Swedish industry is strongly involved in CSP-based energy production either in the form of growing providers on the European energy market or as developers and producers of key components for CSP power plants. The growing industrial interest is reflected and accompanied by state of the art research in this field at the Department of Energy Technology at KTH. In the present paper the main challenges and opportunities for CSP R&D are presented and linked to the industrial environment and interests in Sweden. Related to these challenges, an overview of the latest research activities and results at the Department of Energy Technology is given with examples concerning CSP plant operation and optimisation, techno-economic cycle studies and high temperature solar receiver development.

Keywords: *solar thermal power, Sweden, research and development*

Nomenclature

A	*area* ..... $[m^2]$	I_o	*incident solar flux* ..... $[W/m^2]$
C	*cost* ..... [€]	LEC	*Levelised Electricity Cost* ..... $[€/kWh_e]$
DNI	*Direct Normal Irradiation*	n	*payback time* ..... *[years]*
E	*electrical energy* ..... $[kWh_e]$	α	*annualisation factor* ..... [-]
i	*interest rate* ..... [-]	ε	*efficiency* ..... [-]

1. Introduction

At first glance, concentrated solar power (CSP) may not seem of great interest to Sweden, which receives only weak solar irradiation with few sunny days in winter when power is needed most. However, seen from the wider perspective of a sustainable energy system, with input from many different energy sources (such as hydro, wind and biomass) across Europe, North Africa and parts of Middle East, CSP could form a dominating part of the solution to future energy shortages and the problem of rising CO_2 emissions [1].

Sweden is today increasingly integrated in the European energy grid and major Swedish providers (e.g. Vattenfall, Fortum, E·ON) are growing on the continental energy market. Furthermore, many Swedish companies (e.g. Siemens Industrial Turbomachinery, ABB) are actively involved in the production of components for CSP plants such as steam turbines, mirrors for the collector fields and many more. As such, Sweden's interest in CSP is due not only to its wider environmental credentials, but also its direct economic importance to the country. There is thus good reason for Swedish energy institutions, authorities, industry and universities to actively take part in development to further strengthen the established position in this field.

2. Concentrated Solar Power Technology

In its most basic form, a CSP plant consists of solar collector field with mirrors that concentrate the solar radiation to one or more receivers where this radiation is converted to high temperature heat [2]. This high temperature heat source can be used to drive conventional power generation

equipment (such as steam cycles, Stirling engines, micro gas-turbines, etc.) to produce electricity. Significant amounts of waste heat are also available which are currently wasted but could be used to drive other processes.

The levelised cost of electricity (LEC) of CSP-based power plants has been shown to be amongst the most competitive of all renewable energy technologies [3], with a significant cost advantage over PV when deployed on a large scale. However, CSP technology has not yet matured to the point of grid-parity with conventional power generation systems, although this is predicted to occur within the next 15 years [4]. Rapid reductions in the LEC of CSP-based systems are expected, as shown in Table 1, whereas the cost of fossil-fuel based power is expected to rise with increased fuel prices and the introduction of CO_2 cap-and-trade schemes.

Table 1. Current and Predicted LEC of Selected Power Generation Technologies [4], [5]

LEC [€cts/kWh$_e$]	Parabolic Trough	Solar Power Tower	Dish Stirling	Solar PV	Coal
Current (2010)	17.2	24.1	28.1	28.4	8.4
Future (2025)	12.8	9.7	14.0	14.8	10.8

Direct solar irradiation is an abundant renewable energy source [1] but is available only at low flux densities: large areas must be used to collect enough energy. Even so, the area necessary to satisfy all of Europe's electricity needs using currently available CSP technology would be only a small fraction of the North African deserts [1]. The most suitable areas for CSP deployment are within the tropics, where irradiation is good, almost all days are cloudless and the land is of desert type with low population [3]. Suitable areas for CSP are shown in Fig. 1.

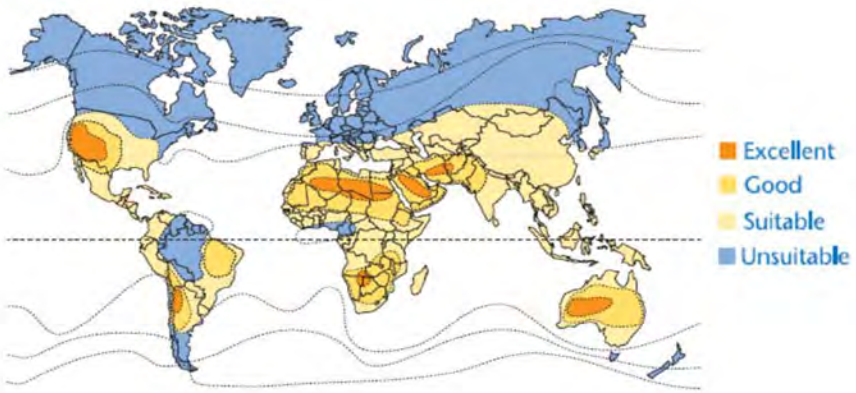

Fig. 1. Distribution of Sites Suitable for Solar Thermal Power Production
Source: German Aerospace Centre (DLR)

In Europe the requirements for economic electricity production with CSP are fulfilled for a number of countries around the Mediterranean Sea but the real "European Sun-belt" is in North Africa. A group of leading European industries have established the DESERTEC foundation [1] for promoting the deployment of CSP-technology in the North-African deserts, with the stated aim of providing 15% of the European electricity requirements [1], as well as meeting local demand. The total investment in CSP plants and transmission lines is expected to be in the region of €400 billion, to be realised by 2050.

2.1 Conventional CSP Technology

The dominating CSP technology: linear parabolic trough mirrors with collectors producing steam for conventional steam turbine plants, as shown to the left of Fig. 2, has been commercial for about 30 years [4]. The power range for these systems has been 30-80 MW_e with solar-electric efficiency around 15-20% [2]. A high number of 50 MW_e plants of that type are presently being put into operation in Spain [5]. Plants in the power range of 400 MW_e are built in the USA and planned for North Africa. Currently almost all steam turbines for solar thermal power plants are delivered from Sweden by Siemens Industrial Turbomachinery.

The technology is well proven and the present development trends are:

- Higher turbine inlet temperatures by developing heat transfer media with the ability to withstand higher temperatures
- Extension of operating time by hybrid operation, energy storage and shorter start-up times
- Efficiency improvements on mirrors and receiver pipes by optimised glass qualities and surface coatings

The cost break down of such a plant shows that the solar field is the most costly part, around 50% and that the thermal conversion unit is only around 24% [4].

2.2 Solar Towers: the Emerging Technology

Solar towers surrounded by heliostats, as shown to the right of Fig. 2, have higher solar concentration factors than parabolic troughs and can thus reach higher temperatures [2]. The size of the heliostat field around a tower has an optimum determined mainly by the height of the tower and the losses from the most distant mirrors. Today the optimal thermal power from a tower seems to be around 100 MW_{th} with a 160 m tower and some 830 heliostats with a 121 m^2 mirror area per unit [5]. Larger systems can be expected considering possible advancement in mirror and receiver efficiencies and control system precision.

Fig. 2. Conventional (left) and Emerging (right) CSP Technology
Source: Solar Millennium/Abengoa Solar

Presently the receivers are placed on top of the tower, which means the heat has to be transported by some means to the power block on the ground down the height of the tower. For small size units (up to around 6 MW_e) the power generation unit could be placed at the top of the tower, close to the receivers. The tower arrangement can be used with steam turbines, providing higher

live steam temperatures than the parabolic trough solar fields. More interesting is that gas-turbines can also be considered for the conversion of heat to electricity. Gas-turbines are cheaper, simpler to install, potentially more efficient and do not need water.

3. Challenges and Opportunities in CSP R&D

CSP remains an emerging technology, with an active R&D community working to improve the viability and effectiveness of the concept. On-going research activities at the Department of Energy Technology (EGI) of the Royal Institute of Technology, Stockholm have highlighted what the authors believe to be some key challenges in the development and deployment of CSP technology at the current time.

3.1 Increasing Economic Competitiveness

Solar thermal power technology cannot yet be considered to be directly competitive with conventional power generation technology (such as those based on the combustion of coal or natural gas) but later most probably with new nuclear power. In the current energy market, deployment of CSP technology is supported by government incentives such as feed-in tariffs and loan guarantees. Increasing the competitiveness of CSP technology is a key challenge in solar R&D and will go hand-in-hand with increased CSP deployment [2]. As such, any reduction in the cost of this technology represents a major opportunity for the industry.

Since the incident solar radiation is free, the cost of the electricity from a CSP plant is dependently solely on the depreciation of the initial investment cost C_{inv} and the annual plant maintenance cost $C_{O\&M}$. The standard definition of levelised electricity cost (LEC) used in solar thermal calculations [4] is based on the net electrical output E_{net} and an annualisation factor α, assuming a rate of interest i, a payback time n in years and an annual insurance rate k_{ins}. The net electrical output is a function of the total collector area A_{col}, the incident solar flux I_o and three efficiency factors ε_{col}, ε_{rec}, and ε_{cyc} for the collector field, solar receiver and power generation cycle respectively.

$$LEC = \frac{\alpha \cdot C_{inv} + C_{O\&M}}{E_{net}} \text{ with } \alpha = \frac{i \cdot (1+i)^n}{(1+i)^n - 1} + k_{ins} \text{ and } E_{net} = A_{col} \int_{year} \varepsilon_{col} \varepsilon_{rec} \varepsilon_{cyc} I_o dt \qquad (1)$$

Any reduction in the LEC will increase the economic competitiveness of the technology and equation (1) brings to light key ways in which reductions can be made:

- The first focus can be placed on reducing the cost of the power plant components (both in term of initial investment C_{inv}, as well as the maintenance $C_{O\&M}$). As the solar field components represent over 50% of the total investment cost, priority should be placed on reducing the cost of these components. Fortunately, these components are still in the early stages of their learning curve and costs are dropping rapidly.
- A second focus can be placed on increasing the net electrical output E_{net} for a given power plant. This can involve optimizing plant design, reducing parasitic consumption as well as improving operational strategy, all of which serve to increase the integrated annual value of ε_{cyc}.

- The final focus can be placed on new power plant concepts. This can involve moving to more efficient thermodynamic cycles (generally requiring higher temperatures), new receiver designs and improved collector field layouts with the aim of increasing the three efficiencies ε_{col}, ε_{rec}, and ε_{cyc} and thus E_{net}. This can result in lower values of LEC for the plant, as long as the increase in E_{net} compensates for any increase in the cost.

3.2 Reducing Water Consumption

The deployment of CSP technology is most effective in areas with high direct normal irradiation (DNI). This fact, coupled with the large land requirements for CSP plants would seem to make desert locations very attractive for deployment [1]. However, the high DNI of desert regions comes with a significant draw-back, in that these regions suffer from a severe scarcity of water resources [6] which will place a limit on the number sites found suitable for deployment of this technology.

The current generation of solar thermal power plants, based on conventional steam-cycles, require water for a number of purposes:

- For the cooling of the condenser, with especially large volumes for evaporative cooling
- To replace that lost from the cycle during steam drum blowdown
- To maintain a high efficiency of the solar field: the mirrors need to be kept clean to ensure a high reflectivity

In order to facilitate the increased deployment of solar thermal power in water-scarce areas it will become necessary to reduce the water footprint of CSP plants, shown for a number of contemporary plants in Table 2. A number of options for achieving this have been highlighted:

- Replacing evaporative or once-through cooling systems in steam-cycle power plants with dry or indirect cooling systems, including options for cold-water storage
- Moving towards higher-temperature solar receivers, allowing the use of gas-turbine cycles, eliminating the use of water as a working fluid as well as the need for cooling
- Moving towards high-efficiency power generation cycles, reducing the size of the collector field per unit electrical output, reducing the water use due to mirror washing

Table 2. Water Consumption of contemporary Rankine CSP Plants [8]

Power Plant Type	Water Consumption [m^3/MWh_e]		
	Evaporative	Hybrid Dry/Wet	Air Cooling
Parabolic Trough	3.0	0.4 – 1.7	0.3
Solar Power Tower	1.9 – 2.8	0.4 – 1.0	0.4

3.3 Increasing Availability/Dispatchability of CSP Plants

The output from a solar thermal power plant is strongly dependent on the available solar flux, which varies due to both the predictable daily evolution of the Sun's position as well as the more unpredictable variations in local weather conditions. This raises two key issues for CSP plants:

- In order to maintain an acceptable lifetime for the power plant components (turbine, steam generators, etc.) the duration of transient operation should be minimized. To improve the dispatchability of CSP plants, it is also of interest to accelerate the start-up of the turbines in order to bring power rapidly onto the grid once solar energy is available
- In order to increase the flexibility and economic viability of a solar power plant in a liberalised electricity market, it is advantageous for the plant to be able to produce power during times of peak demand, which are not necessarily in phase with times when the solar flux is available.

Both these issues require a decoupling of the energy supplied to the power generation cycle from the incident solar radiation. Over a short time period, thermal energy storage can ensure a constant power output to the cycle during solar transients resulting from cloud cover or other meteorological phenomena [2]. Larger storage volumes can also allow dephasing of the electrical output, permitting increased operational flexibility.

At the current time, certain conventional CSP units are built as hybrid plants, using natural gas fired boilers or gas-turbine waste heat recovery boilers for additional steam production when solar radiation is insufficient or absent. With a gas-turbine in the cycle, power production becomes very flexible with the possibility not only to meet peak power demand and to operate at night, but also to reduce the size of the mirror field.

4. Opportunities for CSP R&D in Sweden

Swedish industry is heavily involved in the supply of steam turbines for solar thermal power applications (through Siemens Industrial Turbomachinery) and it can be seen that many of the key opportunities for solar R&D lie in the field of turbomachinery. As all commercial CSP plants are based on the use of steam-cycle technology, improvements in steam-turbine operational strategy present attractive opportunities for R&D. Swedish companies such as ABB are involved in supplying tracking systems and others such as Cleanergy supply Stirling engines for solar dish systems.

The challenges presented in §3 highlight the potential advantages in moving towards gas-turbine-based CSP plants. Use of gas-turbines reduces water consumption and opens the possibility for the use of more flexible hybrid plants as well as higher efficiency combined-cycle systems. Swedish industrial companies are ideally placed to provide gas-turbines in the power ranges suitable for solar thermal applications.

5. Research focuses at the Department of Energy Technology

On-going research activities at EGI are focused on responding to the key challenges identified in §3 as well as supporting Swedish industrial partners in addressing the opportunities created. The following sections present key current projects.

5.1 Solar Steam Turbine Operation

Due to the variable nature of the solar supply and the daily operating cycle of solar power plants, the number of turbine starts per year for solar steam turbines is an order of magnitude higher than for base-load turbines. As a result, the speed with which the turbines can be started assumes a

greater importance in CSP plants and modifications allowing turbines to start faster are examined as part of on-going research.

The speed at which the turbines can reach full load is based on the lowest metal temperature measured before start-up begins. As such, if the steam turbine can be kept hot during idle periods, the duration of the next start-up can be reduced without impacting negatively on the lifetime. A number of modifications that can be made to the turbines to maintain their temperature during idle periods have been evaluated. Heat blankets were shown to be the most effective measure for keeping the turbine casing warm, whereas increasing the gland steam temperature was most effective in maintaining the temperature of the rotor [7]. By applying a combination of these measures the dispatchability of the turbine can be improved significantly: electrical output can be increased by above 9% for both long and short cool-downs, as is shown in Fig. 3.

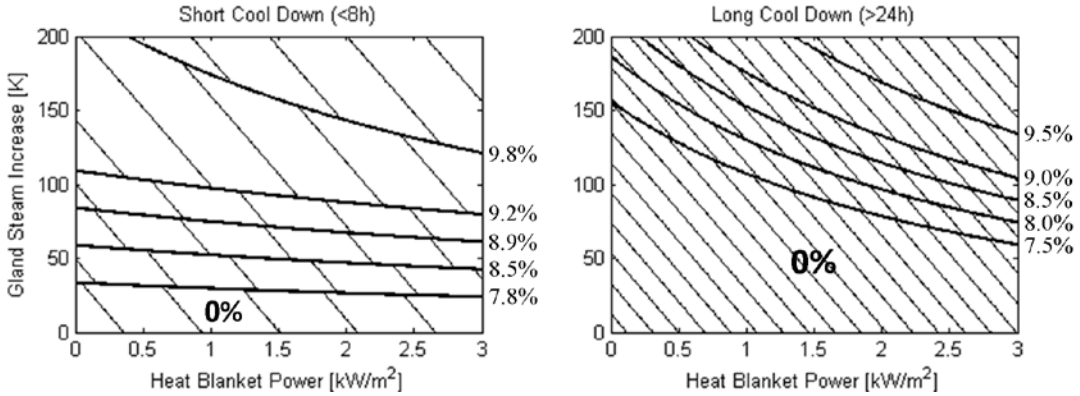

Fig. 3. Impact of applying a combination of heat blankets and gland steam temperature increase on the daily output of the plant on the day following the cool-down period [7]

5.2 Solar Power Plant Thermo-Economics

All operational commercial solar thermal power plants are based on the use of Rankine cycles, which are limited in the efficiencies they can achieve by the relatively low temperatures at the receiver. However, developments in the field of high temperature receivers [8] have opened up the possibility to use more advanced thermodynamic cycles, especially the use of gas-turbines. In order to evaluate the potential of new power plant concepts, thermo-economic models are used to predict investment and levelised electricity costs, as well as other important factors such as annual electricity production, water consumption, exergy efficiency, land use and many more [9]. Coupled with a multi-objective optimisation routine, Pareto-optimal power plant designs can be established and the trade-off between economic and environmental objectives analysed. Polygeneration concepts, mainly using waste heat for production of e.g. clean water, cooling or biogas for local consumption can also be positive factors both for acceptance and economy.

5.3 Solar Receiver Design and Testing for Gas-Turbine Integration

In order to support on-going solar gas-turbine research at EGI, small-scale but high temperature receivers are being design and tested for use with micro gas-turbines. Availability in Sweden of sunlight strong enough for testing is very limited and therefore a small indoor solar lab has been built, shown schematically in Fig 4. An artificial Sun consisting of strong Xenon lamps produces 11 kW of radiation which is directed to a parabolic dish of 1.8 m diameter and used to test small receivers of different innovative designs. Presently two receivers are being investigated:

- A medium temperature receiver in which materials with high thermal conductivity and coatings for good solar absorption are essential for high efficiency
- A generic high temperature volumetric receiver in which different types of heat exchange materials can be tested both for overall heat transfer data and detailed information on solar penetration depth, temperature gradients, pressure drops, etc.

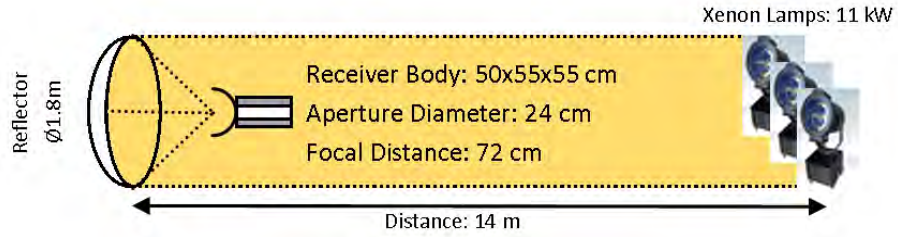

Fig. 4. Basic Layout of EGI's Receiver Test Facility

6. Conclusion

Amongst the plethora of renewable energy technologies on offer, CSP emerges as a promising option for sustainable power generation in the Sun-belt regions of the world. A diverse R&D community supports the refinement of the technology and commercial CSP plants are beginning to appear worldwide. Swedish industry is well-placed in the market, providing almost the entirety of the steam turbines for conventional CSP plants, as well as a number of ancillary components. Within Sweden, the nurturing of active R&D is essential to maintain this dominant position. EGI is actively pursuing key issues on different CSP systems such as techno-economic optimization, polygeneration arrangements, receiver components and their integration with the conversion unit.

References

[1] G. Knies, U. Möller, and M. Straub, "*Clean Power from Deserts: The DESERTEC Concept for Energy, Water and Climate Security"*, Hamburg, 2007

[2] C. Philibert, "*The Present and Future Use of Solar Thermal Energy as a Primary Source of Energy"*, International Energy Agency, Paris, 2005

[3] K. Ummel and D. Wheeler, *Desert Power: the Economics of Solar Thermal Electricity for Europe, North Africa, and the Middle East*, Center for Global Development, 2008.

[4] R. Pitz-Paal, J. Dersch, and B. Milow, *"ECOSTAR: European Concentrated Solar Thermal Road-Mapping"*, Deutsches Zentrum für Luft- und Raumfahrt, 2004

[5] C. Richter (Editor), *"Solar Power and Chemical Energy Systems: Annual Report"*, Deutsches Zentrum für Luft- und Raumfahrt, Köln, 2008

[6] US Department of Energy, *"Reducing Water Consumption of CSP Electricity Generation"*, Report to Congress, 2001

[7] J. Spelling, M. Jöcker and A. Martin, *"Thermal Modeling of a Solar Steam Turbine with a focus on Start-Up Time Reduction"*, ASME TurboExpo, Vancouver, 2011

[8] B. Hoffschmidt, F. Tellez, J. Fernandez., *"Performance Evaluation of the 200kWth HiTRec-11 Open Volumetric Receiver"*, Solar Energy Engineering, vol. 125 (2003), pp. 87-97

[9] J. Spelling, D. Favrat, A. Martin et al., *"Thermo-Economic Optimisation of Solar Tower Thermal Power Plants"*, International ECOS Conference, Lausanne, 2010.

Experimental heat transfer research in enhanced flat-plate solar collectors

R. Herrero Martín[1], A. García Pinar [1], J. Pérez García*[1]

[1] *Technical University of Cartagena, Cartagena, Spain*
** Corresponding author. Tel: +34-968-32.59.85, Fax: +34-968-32.59.99, E-mail: pepe.perez@upct.es*

Abstract: Enhancement techniques can be applied to flat-plate liquid solar collectors towards more compact and efficient designs. Tube-side enhancement passive techniques can consist of adding additional devices which are incorporated into a smooth round tube (twisted tapes, wire coils), modifying the surface of a smooth tube (corrugated and dimpled tubes) or making special tube geometries (internally finned tubes). For the typical operating flow rates in flat-plate solar collectors, the most suitable technique is inserted devices. Based on previous studies from the authors, wire coils were selected for enhancing heat transfer. This type of inserted device provides better results in laminar, transitional and low turbulence fluid flow regimes.
To test the enhanced solar collector and compare with a standard one, an experimental side-by-side solar collector test bed was designed and constructed. The testing set up was fully designed following the requirements of EN12975-2 and allow us to accomplish performance tests under the same operating conditions (mass flow rate, inlet fluid temperature and weather conditions). In this work the preliminary results obtained are presented and the standardized efficiency curve is shown for both tested solar collectors. A relevant improvement of the efficiency has been reported and quantified through the useful power ratio between enhanced and standard solar collectors.

Keywords: *heat transfer enhancement, wire-coil inserts, liquid flat plate solar collector*

Nomenclature

A_A	Absorber area ..... m^2	ρ	Fluid density..... kg/m^3
α_{A1}	Thermal losses coefficient..... W/m^2K	t_a	Ambient temperature..... $ºC$
c_p	Specific heat of working fluid ..... J/kgK	t_{in}	Inlet temperature ..... $ºC$
Q_{useful}	Useful power..... W	t_{out}	mOutlet temperature ..... $ºC$
Q	Flow rate ..... m^3/s	t_m	Mean temperature $t_m = t_{in} + \Delta t/2$ ..... $ºC$
G	Global irradiance..... W/m^2	T^*_m	Nondimensional temp. $T^*_m = (t_m - t_a)/G$
η	Thermal efficiency	τ	Transparent cover transmittance
η_A	Thermal efficiency based on absorber area	α	Absorptance of absorber plate
η_O	Optical efficiency coefficient	F_R	Heat removal factor
η_{OA}	Optical efficiency coefficient		

1. Introduction

In industrial applications, a set of enhancement techniques are widely used to improve the performance of heat exchangers. Enhanced surfaces can be used to increase heat exchange, reduce the size of equipments or save pumping power. Thermal liquid solar collectors are potential candidates for enhanced heat transfer, but not many studies have focused on this aspect. The vast majority of works carried out applying enhancement techniques to improve solar collector performance deal with air collectors, mainly inserting artificial roughness within the exchange surfaces [1, 2, 3].

Regarding liquid solar collectors just a few studies have focused on enhancement techniques. Kumar and Prasad [4] presented a remarkable work inserting twisted tapes in a serpentine solar collector. They investigated the effect of the twisted-tape geometry, different mass flow rates and intensity of solar radiation on thermal performance. The authors observed that heat losses were reduced (due to the lower value of the plate temperature) and consequently an increase on the thermal efficiency was observed.

Recently, Jaisankar et al [5] performed an experimental investigation of heat transfer, friction factor and thermal performance on a tube-on-sheet solar panel with twisted-tape insert devices. They also investigated the effect of the twisted-tape geometry for different Reynolds and intensity of solar radiation. The concluded that when twist ratio is increased, the swirl generation is decreased and both heat transfer and friction factor are minimized. Jaisankar et al also carried out several experimental investigations of heat transfer, friction factor and thermal performance of thermosyphon solar water heater systems fitted with twisted- tape insert devices. [6, 7, 8] The authors found that the heat transfer enhancement in the twisted tape collector was higher than in the standard collector.

Also Hobbi and Siddiqui [9] conducted an indoor experimental study to investigate the impact of several insert devices on the thermal performance of a flat-plate solar collector. They studied different passive heat enhancement devices: twisted strips, coil-spring wires and conical ridges. They observed no appreciable difference in the heat transfer to the collector fluid and concluded that the applied passive methods based on the enhancement of shear-produced turbulence were ineffective in augmenting heat transfer to the collector fluid.

In spite of the fact that many of the previous works within liquid collectors employed twisted tapes as inserted devices, basically due to the existence of well known design correlations [10, 11, 12], the use of other passive tube-side techniques such as wire coils still unexplored. Regarding the aforementioned fact, Webb and Kim [13] also pointed out that the existence of design correlations does not mean, however, that the twisted tape insert is the best insert device. As Garcia mentions [14, 15], wire coils are especially suitable for enhancing heat transfer in laminar, transition and low turbulent flow regimes. In a previous work from the authors, a numerical simulation methodology to study the heat transfer enhancement in a tube-on-sheet solar panel with wire-coil inserts, using TRNSYS as the simulating tool was developed. A parametric study was also performed to relate the fluid and flow characteristics with the heat transfer enhancement by wire-coil inserts. It was shown that the enhanced collector increased useful power in the whole range of mass flow rate when using water as the working fluid [16].

The purpose of the present work is then to characterize a flat-plate solar panel with wire-coil insert devices in terms of heat transfer, friction losses and thermal performance and compare this enhanced collector with a standard collector under the same operating and weather conditions. To test the enhanced solar collector and compare with a standard one, an experimental side-by-side solar collector test bed was designed and constructed. The testing set up was fully designed following the requirements of EN 12975-2 [17]. A relevant improvement of the standardized efficiency curve has been reported. Furthermore, the ratio of useful power and pressure drop between the enhanced and the standard solar collector for different flow rates and operating conditions were computed.

2. Experimental set-up

The experimental setup was designed to carry out simultaneously the thermo-hydraulic characterization of two solar collectors (an enhanced collector with wire-coil inserts and a standard collector) under the same operating (mass flow rate, inlet fluid temperature) and weather conditions. It is located in Cartagena, southeastern Spain (Latitude N'3736, Longitude W'00059). Furthermore, this facility was built in agreement with the requirements of standard EN 12975-2 [17]. A schematic layout of the test bed constructed is shown in Figure 1.

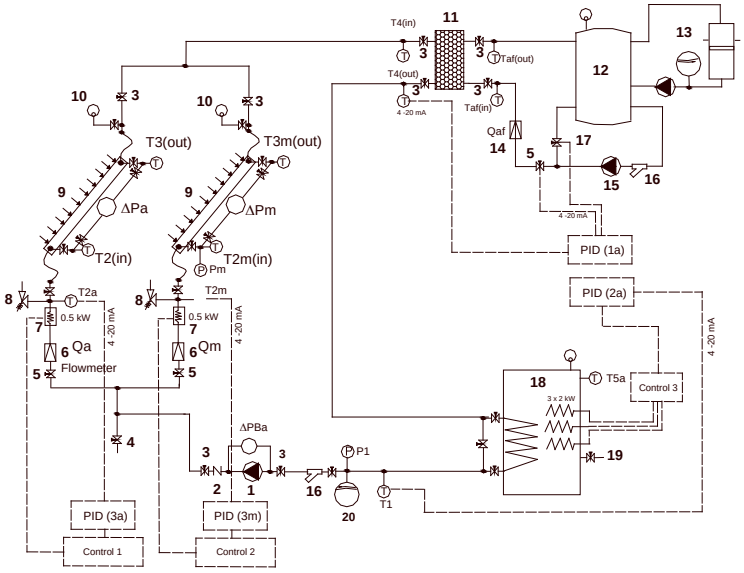

1	In-line pump (Hot water)
2	Check-valve
3	Ball valve
4	Drain Valve
5	Control solenoid Valve (0-10 VDC)
6	Electromagnetic flowmeter (SIEMENS MAG 1100)
7	Heating Resistance (0.5 kW)
8	Relief valve
9	Flat-Plate solar collector
10	Air vent valve
11	Heat Exchanger
12	Cold water storage tank
13	Water-chiller
14	Turbine flowmeter
15	In-line pump (Cold water)
16	Filter
17	By-pass solenoid valve (0-10 VDC)
18	Hot water storage tank (Heating reistance 3x1 kW)
19	Filling valve
20	Expansion tank

Fig. 1. Experimental set-up

The main components of the experimental setup are the two sheet-and-tube flat-plate solar water heaters with 9 parallel tubes (risers) on the back of the absorber plate, as it is detailed in Fig. 2. T he risers are connected at the top and bottom by headers to homogenize flow distribution and static pressure at inlet and outlet sections. Both collectors have a single glass cover; their technical specifications are summarized in Table 1.

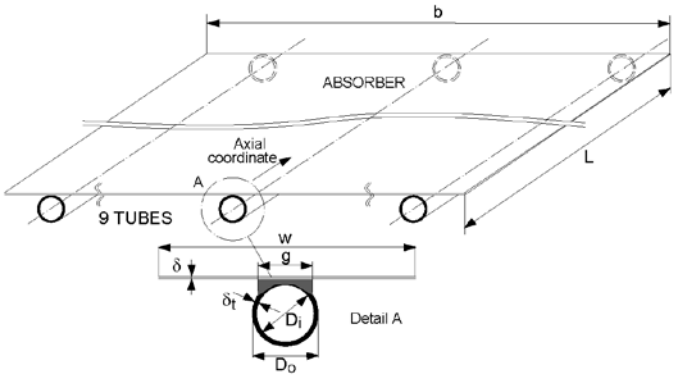

Fig. 2. Sheet-and-tube tested solar collector configuration

Table 1. Main characteristics of the flat-plate solar collectors

Material properties		**Geometrical data**			
k_{abs}	209.3 W/mK (Aluminum)	D_i	0.007 m	N_G	1
k_{tube}	372.1 W/mK (Copper)	w	0.1227 m	N_{tubes}	9
ε_g	0.88 (Glass)	g	0.0035 m	A_C	2.022 m^2
τ_g	0.93 (Glass)	δ_{abs}	0.0005 m	A_{edge}	0.2348 m^2
k_{ins}	0.05 W/mK	δ_{tube}	0.0005 m	L_t	1.83 m
ε_{abs}	0.05 (Miro-Therm)	δ_{ins}	0.025 m	β	45º
		α_{abs}	0.95 (Miro-Therm)		

One of the solar collectors was modified inserting wire–coils within their risers. A wire coil of dimensionless pitch p/D=1 and wire-diameter e/D=0.0717 was chosen (Fig. 3). This geometry showed good overall thermohydraulic behaviour for the operating conditions in solar collectors according to Garcia [15] work.

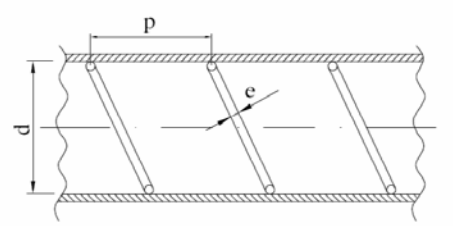

Fig. 3. Sketch of the helical-wire-coil fitted in the raisers of the modified solar collector.

2.1 Instrumentation

The instrumentation was selected and mounted according to the standard EN 12975–2 requirements. Thermorresistance Pt100 class 1/10 DIN A were used to measure the inlet and outlet fluid flow temperatures. To measure the flow rate and the pressure drop through the collectors, electromagnetic flowmeters (Siemens MAG1100 DN 3) and differential pressure transmitters (SMAR) with different configurable ranges were used. Regarding the weather conditions: 3 PSP class I thermoelectric pyranometers were employed to measure the solar irradiance (global irradiance in the aperture plane, global irradiance on the horizontal plane and the other one has a shading band to measure diffuse horizontal solar irradiance). Velocity and wind direction were measured with an ultrasonic anemometer (Windsonic from Gill Instruments Ltd). Ambient temperature, humidity and pressure were also measured. In Table 2 the main characteristics of the selected instrumentation are summarized.

2.2 Uncertainty propagation

We follow the criteria of ISO GUM (Guide to the expression of Uncertainty in Measurement) [18] to derive the equation for thermal efficiency proposed in EN 12975-2 and uncertainty propagation assessment. When the tests are accomplished in steady state, the thermal efficiency can be expressed as Eq. (1).

$$\eta_A = \frac{\dot{Q}_{\text{useful}}}{GA_A} = \frac{Q\rho_{(t)}c_{p(t)}\left(t_{out} - t_{in}\right)}{GA_A} \tag{1}$$

The standard uncertainty of each magnitude is shown in Table 2. The uncertainty of each magnitude is a combination of the uncertainties of Type A evaluation, associated to the standard deviation of the mean of the repeated observations, and of Type B, evaluated from scientific statement based on the calibration available information. According to the uncertainty propagation study carried out, it can be concluded that the initial uncertainties are slightly amplified and the expanded uncertainty at a 95% confidence level are ±0.1% for non-dimensional temperature T^*_m and ±0.9% for thermal efficiency η.

3. Thermal performance calculations according to standard EN 12975-2

The useful power is calculated according to Eq. (2).

$$\dot{Q}_{useful} = Q\rho_{(t)}c_{p(t)}\left(t_{out} - t_{in}\right) \tag{2}$$

where, the fluid density and the specific heat are evaluated at the mean fluid temperature $t_m = t_{in} + \Delta t/2$, and the thermal efficiency can also be expressed according to Eq. (3) as a function of global irradiance intercepted, absorber area and useful power.

$$\eta = \frac{\dot{Q}_{useful}}{GA_A} \tag{3}$$

Table 2 . Instrumentation description and uncertainty.

Magnitude	Sensors	Instrumentation	Uncertainty
Solar Irradiation	3	1st Class Kipp&Zonnen CMP6 Pyranometer Shadow band (Diffuse Irradiation)	±0.,1%
Ambient Temperature	1	Pt100 3w	±0.1ºC
Ambient Pressure	1	Piezorresistive barometer	± 0,4 mbar a 20ºC
Humidity	1	Capacitive sensor	±2%
Wind velocity and direction	1	WindSonic Gill Instrument (Vel. interval 0-60 m/s) (Vel. Direction 0-359º)	± 2% Velocity ± 3% Direction
Inlet and Outlet Fluid Temperature	4	Pt100 4w Class 1/10 DIN A	± 0,03 ºC
Flow Rate	2	Electromagnetic Flowmeter Siemens MAG 1100 Transmitter MAG 6000	± 0,25 %
Differential Pressure	2	Differential pressure transmitter SMAR D0 type (-4 to +4 inch H_20) Standard collector D1 type (0-20 inch H_20) Enhanced collector	± 0,1 % of Span
Absolute pressure	1	Piezorresistive transducer	± 0,5 %

The thermal efficiency η can be correlated with the reduced temperature, $T^*_m=(t_m-t_a)/G$ using linear $\eta = \eta_0 - a_1 T_m^*$ or quadratic regressions $\eta = \eta_0 - a_1 T_m^* - a_2 G T_m^{*2}$, based on absorber or aperture area. The experimental data obtained show a good linear correlation (R^2=0.9874 for the standard solar collector, and R^2=0.9282 for the enhanced solar collector). These linear correlations are simpler and more useful in engineering applications. Additionally, their coefficients are independent of global irradiance.

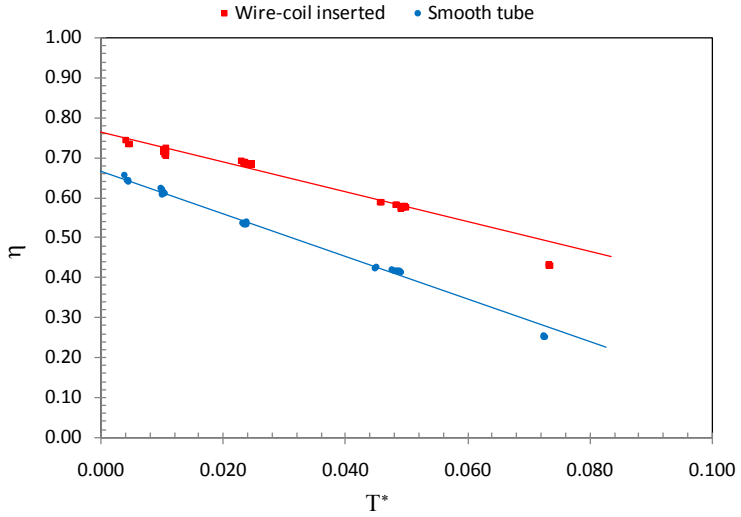

Fig. 4. Thermal efficiency curves for standard and enhanced flat-plate solar collectors (0.04 kg/s)

In Fig. 4 the standardized thermal efficiency curves for both standard and enhanced flat-plate solar collectors are shown. It can be observed that a significant improvement in the thermal efficiency of the solar collector with wire-coil inserts is achieved. Note that in the enhanced solar collector the optical efficiency coefficient η_{OA} is about 15% higher and the thermal losses coefficient α_{A1} is lower than in the standard one (Table 4). This effect can be due to the enhancement of heat transfer between the absorber plate and the working fluid which reduces its temperature and as a consequence, the thermal losses decrease. The uncertainty of the regression coefficients have also been assessed according to the methodology proposed by Coleman and Steele [19].

Table 4. Linear correlation coefficients and their uncertainties (95% I.C)

	Standard collector		**Enhanced collector**	
	Coefficient	Uncertainty	Coefficient	Uncertainty
η_{0A}	0.6670	0.44 %	0.7654	3.97 %
a_{1A}	-5.3410	1.71 %	-3.7640	0.52 %

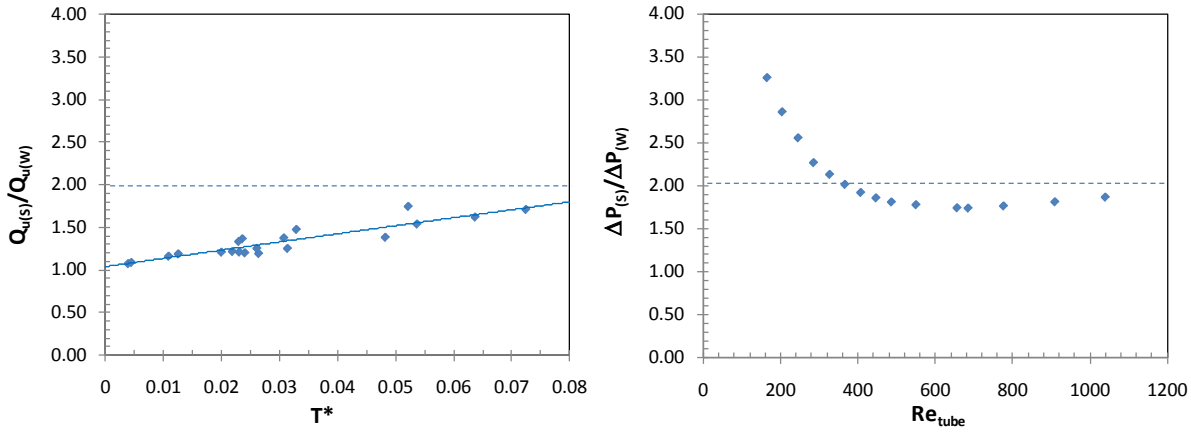

a) *b)*

Fig. 5. Ratios between standard and enhanced solar collectors a) Useful power versus non-dimensional temperature, and b) Loss pressure versus Reynolds number inside raisers

In Fig. 5 a) the useful power ratio between the enhanced and the standard solar collector is showed for different flow rates (0.016÷0.04 kg/s) and operating conditions ($520 \le \mathrm{Re}_{\mathrm{tube}} \le 2340$). It can be observed that there is a linear dependence between the useful power ratio and the non-dimensional temperature. For increasing values of T^* the ratio of useful power is higher. This is due to the fact that the wire-coil insert lowers the absorber temperature reducing the thermal losses. This confirms the results from the previous numerical simulations carried out by the authors. [16] In Fig. 5 b) the pressure loss ratio between both collectors is represented. For Reynolds numbers higher than 500, inside the raisers, the pressure loss ratio remains constant at about 1.8. This increase in pumping power is compensated with an improvement in thermal efficiency, which would be especially suitable for large installations in which several solar collectors are connected in parallel. In this type of configuration an accumulative increase in thermal power is obtained, while the pressure loss remains the same in all the solar collectors, and thus, this configuration would enable optimum operation and would be the best-practice approach.

Nevertheless, in order to establish the optimum operating range within enhanced solar collectors with wire-coil inserts, a heat exchangers performance evaluation criterion has to be employed. A modified criterion (R3m) was proposed by the authors [16]. This criterion stands for the increasing useful power obtained in the enhanced and the standard collector at equivalent operating regimes to satisfy the constraint of equal pumping power. To compute this parameter further efficiency and friction factor tests are being carried out.

4. Conclusions

An experimental side-by-side solar collector test bed was designed and constructed to characterize the thermo-hydraulic behaviour of a standard and an enhanced solar collector under the same testing conditions (operating parameters and radiant conditions). The facility

was built in agreement with the requirements of standard EN 12975 to carry out thermal performance and pressure drop tests.

The thermal efficiency curves of two solar collectors, a standard and an enhanced collector were obtained. The enhanced collector was modified inserting spiral wire coils of dimensionless pitch p/D=1 and wire-diameter e/D=0.0717 within each riser. The thermal efficiency increments depend on the operating flow rates. For a flow rate of 144 l/h (0.04 kg/s) the efficiency optical factor was found to increase by 15%. The collector with wire-coil inserts enhances heat transfer and as a consequence the absorber temperature is reduced. This means a reduction in the thermal losses as well as a decrease of the loss coefficient by 30%. However, an increase in terms of friction losses is observed and thus pumping power rises.
In order to account for the overall enhancement (thermo-hydraulic performance) that wire-coil inserts promote in the solar collector, the ratio of useful power and pressure loss between both solar collectors were computed. For increasing values of T* the ratio of useful power is higher and reaches values up to 1.8. For Reynolds numbers higher than 500, inside the raisers, the pressure loss ratio remains constant at about 1.8. The increase in pumping power is compensated with an improvement in thermal efficiency, which would be especially suitable for collectors connected in parallel. This configuration would enable optimum operation and would be the best-practice approach.

As a final conclusion, according to the present work, wire-coil devices can be successfully inserted within the flow tubes in solar water heaters for enhancing heat transfer rate.

Acknowledgements

This research is supported by the Spanish Regional Agency "ARGEM" (Agencia de Gestión de la Energía de la Región de Murcia) and by the "Fundación Séneca" in the frame of the research project "Design and development of an enhanced flat plate solar collector. Thermal efficiency evaluation and thermohydraulic characterization" Reference number: 08731/PI/08.

References

[1] A. Kumar, J.L. Bhagoria, R.M. Sarviya, Heat transfer and friction correlations for artificially roughened solar air heater duct with discrete W-shaped ribs. Energy Conversion and Management, 50 (8), 2009, pp. 2106-2117.

[2] S. B. Bopche, M. S. Tandale. Experimental investigations on heat transfer and frictional characteristics of a turbulator roughened solar air heater duct. International Journal of Heat and Mass Transfer, 52 (11-12), 2009, pp. 2834-2848.

[3] K.R. Aharwal, B. K. Gandhi, J.S. Saini. Heat transfer and friction characteristics of solar air heater ducts having integral inclined discrete ribs on absorber plate. International Journal of Heat and Mass Transfer, 52, (25-26), 2009, pp. 5970-5977.

[4] A. Kumar, B. N. Prasad. Investigation of twisted tape inserted solar water heaters—heat transfer, friction factor and thermal performance results. Renewable Energy, 19 (3), 2000, pp. 379-398.

[5] S. Jaisankar, T.K. Radhakrishnan, K.N. Sheeba. Experimental studies on heat transfer and friction factor characteristics of forced circulation solar water heater system fitted with helical twisted tapes. Solar Energy, 83 (11), 2009 , pp. 1943-1952.

[6] S. Jaisankar, T.K. Radhakrishnan, K.N. Sheeba. Studies on he at transfer and friction factor characteristics of thermosyphon solar water heating system with helical twisted tapes. Energy 34, 2009, pp. 1054–1064.

[7] S. Jaisankar, TK. Radhkrishnan, KN. Sheeba. Experimental studies on heat transfer and friction factor characteristics of thermosyphon solar water heater system fitted with spacer at the trailing edge of twisted tapes. Applied Thermal Engineering, 29(5–6), 2009, pp. 1224–31.

[8] S. Jaisankar, T.K. Radhakrishnan, K.N. Sheeba, S. Suresh. Experimental investigation of heat transfer and friction factor characteristics of thermosyphon solar water heater system fitted with spacer at the trailing edge of Left–Right twisted tapes. Energy Conversion and Management, 50 (10), 2009, pp. 2638-2649.

[9] A. Hobbi, K. Siddiqui. Experimental study on the effect of heat transfer enhancement devices in flat-plate solar collectors. Int. J. of Heat and Mass Transfer 52, 2009, pp. 4650–4658.

[10] P.S. Bandyopadhyay, U.N. Gaitonde, S.P. Sukhatme. Influence of free convection on heat transfer during laminar flow in tubes with twisted tapes. Exp. Therm. Fluid Sci. 45, 1991, pp. 577–586.

[11] R.M. Manglik, A.E. Bergles. Heat transfer and pressure drop correlations for twisted-tape inserts in isothermal tubes: Part II –transition and turbulent, J. Heat Transfer, 115, 1993, pp.890–896.

[12] R.M. Manglik, S. Maramraju, A.E. Bergles. The scaling and correlation of low Reynolds number swirl flows and friction factors in circular tubes with twisted tape inserts, J. Enhanced Heat Transfer, 8, 2001, pp. 383–395.

[13] R. L. Webb , N-H. Kim. Principles of Enhanced Heat Transfer, 2nd ed., Taylor & Francis, New York, 2005.

[14] A. García, P.G. Vicente, A. Viedma. Experimental study of heat transfer enhancement with wire coil inserts in laminar-transition-turbulent regimes at different Prandtl numbers. International Journal of Heat and Mass Transfer, 48 (21-22), 2005, pp. 4640-4651.

[15] A. García, J. P. Solano, P. G. Vicente, A. Viedma. Enhancement of laminar and transitional flow heat transfer in tubes by means of wire coil inserts. International Journal of Heat and Mass Transfer, 50, (15-16), 2007, pp. 3176-3189.

[16] R. Herrero Martín, J. Pérez-García, A. García, F. J. García-Soto, E. López-Galiana Simulation of an Enhanced Flat-Plate Solar Liquid Collector with wire-coil insert devices. Manuscript accepted for publication in Solar Energy.

[17] EN 12975-2:2006 "Thermal Solar Systems and Components –Solar Collectors – Part 2 test methods".

[18] ISO/IEC Guide 98, G uide to the Expression of Uncertainty in Measurement (GUM), International Organization for Stand. (ISO), Geneva, Switzerland, 1995, pp. 9–78.

[19] Coleman, H.W, Steele, W. Experimentation and Uncertainty Analysis for Engineers, John Wiley & Sons. 1999, 2nd Ed., New York. ISBN 0-471-12146-0, pp 202-235

Closed Environment Design of Solar Collector Trough using Lenses and Reflectors

Kazy Fayeen Shariar[1,*], Enaiyat Ghani Ovy[2], Tabassum Aziz Hossainy[2]

[1] *Department of Electrical & Electronic Engineering*
Islamic University of Technology, Board Bazar, Gazipur-1704, BANGLADESH
[2] *Department of Mechanical & Chemical Engineering*
Islamic University of Technology, Board Bazar, Gazipur-1704, BANGLADESH
** Corresponding author. Tel: +8801713083079, Fax: 880-2-9291260, E-mail: eshankonerbaiu@yahoo.com*

Abstract: Concentrated sunlight has been used to perform useful tasks from ancient time. There are number of varieties of collector trough being used to perform these tasks. Each Varity comes with advantages as well as disadvantages. The aim of this research project is to improve the design of collector trough in terms of efficiency, lessen the heat declination, and eliminate the sun tracker mechanism. Most of the existing solar concentrators use open type trough which cause the rapid heat declination. The design attempted in this paper is to lessen this rapid declination and improve the efficiency by introducing Closed Environment Collector Trough (CECT). The CECT consists of spherical collector trough having a reflective bottom surface, five evenly distributed lenses, 30^o apart from each other, on the upper half of the sphere to eliminate the sun tracker and hexagonal glasses to make the environment closed and impose greenhouse effect on the system. The CECT acts like a heat trap and keeps the heat inside the chamber for a longer period of time which basically lessens the heat declination. The reflective surface and lenses concentrate the sun light directly on the fluid pipe. In this paper novel design has been proposed to improve the overall performance of solar collector troughs.

Keywords: *Solar Thermal Collector, Concentrated Solar Power, Closed Environment Collector Trough.*

Nomenclature

A_a = *absorber area…….. (m^2)*
A_f = *collector geometric factor*
A_r = *receiver area…….. (m^2)*
D_s = *direct irradiation…….. (W/m2)*
f_w = *wind or exposure factor*
f_c = *construction type or quality factor*
n_o = *collector optical efficiency*
Q_u = *rate of useful energy delivered by collector (W)*
T_a = *ambient temperature…….. (K)*
T_r = *receiver temperature…….. (K)*
t_i = *inside design temperature…….. (K)*
t_o = *outside design temperature…….. (K)*
U_L = *heat loss coefficient*
α = *absorptivity*
$\bar{d}$ = *average bond thickness …….. (m)*
ρ = *mirror reflectance*
τ = *absorber transmittance*

1. Introduction

Researches have been carried out to utilize the concentrated solar power in various fields. To utilize the solar energy different patterns of the collectors have been designed previously considering advantages as well as disadvantages [4]. From the previous literature survey it was found that parabolic concentrating collectors were developed to use the solar energy in an efficient way. Non tracking concentrator was also designed to avoid the handling of a tracking device [1, 3]. To increase the performance innovative design was also proposed and modeled with reflectors without increasing the system cost. In that research work aluminum-polymer-laminated steel reflector for use in solar concentrators was evaluated with respect to its optical properties, durability, and reflector performance in solar thermal and photovoltaic systems [2]. In this paper a novel and innovative design of a solar collector which is basically Closed Environment Collector Trough (CECT) has been proposed. This novel CECT system lessens

the rapid heat declination and improves the system overall efficiency. This paper mainly focuses the detail designing of the collector with accurate explanation.

2. Methodology

2.1. Description of the system

This paper proposes a new design of compound solar collector trough. The collector effectively combines Lenses, Reflectors and Closed Environment. The general structure of the trough is sphere shaped with two halves consisting a pipe at the center (Fig: 1). Different parts of the trough are labeled on the figure. A detailed description of different parts of the collector trough is given below.

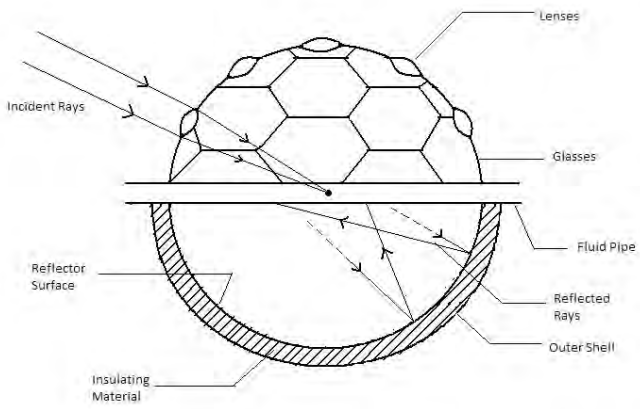

Figure 1: Closed Environment Collector Trough

The whole sphere shaped is main constructional shell of the system. It consists of two parts: Upper Shell and Lower Shell.

Lower Shell: Lower shell of the system is made of glazing metal (i.e. Aluminum). The outer surface is blackened and the inner surface is a reflector. There is another half sphere outside of this surface which is made of non-heat conductor material (i.e. asbestos). The inner diameter of the sphere is 40 c.m and outer diameter is 50 c.m. The space between the two surfaces is filled with cotton or rubber type materials (Fig: 2)

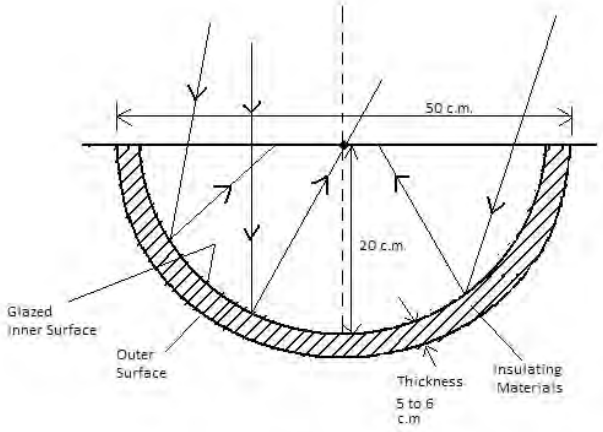

Figure 2: Lower shell

Upper Shell: The upper shell of the system is made of metal three dimensional lattice of hexagonal shape (Fig: 3). These shapes will accommodate small pieces of mirrors, which will allow the visible light to enter into the chamber but will trap the longer wavelengths of the infrared re-radiation from the heated objects are unable to pass through the glasses. The trapping of the long wavelength radiation leads to more heating and a higher resultant temperature.

There will be five lenses, evenly distributed on the upper surface of the mirror section. The lenses will be 30^o apart from each other (Fig.4). The center lens will be at 90^o angle. These lenses will concentrate the sunlight in to center line (for the lenses the center line will be the focus plane) of the sphere.

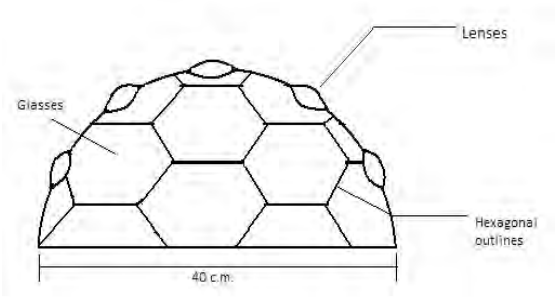

Figure 3: Upper Shell

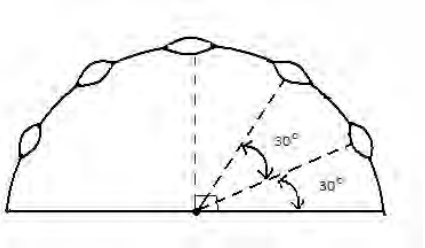

Figure 4: Arrangement of Lenses

Fluid Pipe: At the center of the sphere there will be a fluid carrying pipe. The fluid pipe will be consisted of two concentric pipes (Fig.5). The material of the outer pipe will be of transparent material (i.e. glass).The inner pipe will be metallic (i.e. Aluminum). The space between these two pipes will be evacuated. The inner pipe will carry the Heat Transfer fluid.

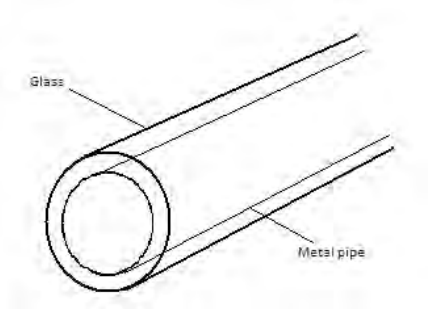

Figure 5: Fluid pipe

2.2. Calculation of Sun's Position in Bangladesh

To eliminate solar tracking mechanism effectively we have to calculate the sun's position throughout the year. Sun's position depends on local solar, elevation and azimuth angles. The equation to find the elevation and azimuth angles are given below:

$$\text{Elevation} = \sin^{-1}\left[\sin\gamma\sin\phi + \cos\gamma\cos\phi\cos HRA\right] \qquad (1)$$

$$\text{Azimuth} = \cos^{-1}\left[\frac{\sin\gamma\cos\phi - \cos\gamma\sin\phi\cos HRA}{\cos\alpha}\right] \quad (2)$$

Where HRA is the Hour Angle

Sun's position throughout a year is given in Fig.6

As from the figure we can see that sun follows a specific path throughout the year, the solar tracking mechanism can be effectively eliminated by preparing a solar chart at a specific interval. The solar trough can be setup as shown in the Fig.7 and can be manually tracked daily basis [5].

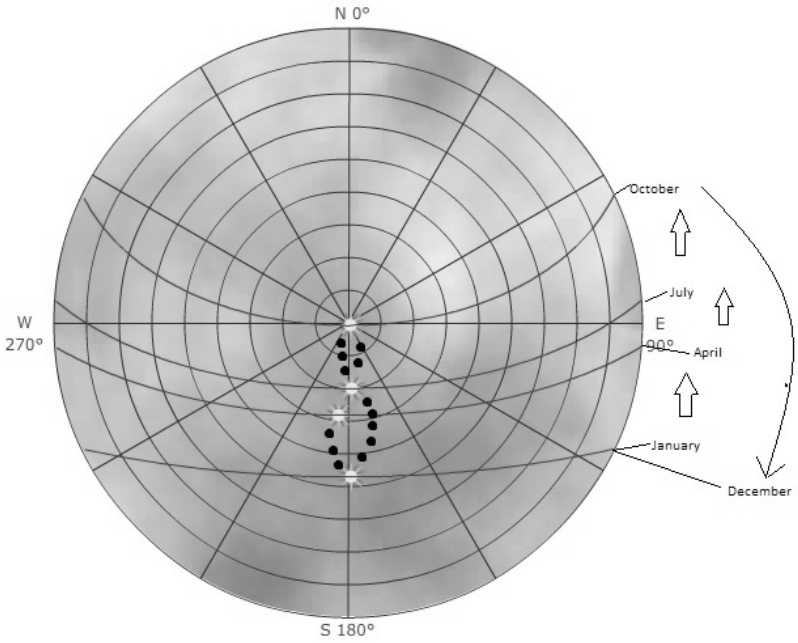

Figure 6: Sun's Position at 3 months interval. Dots represent the solar path

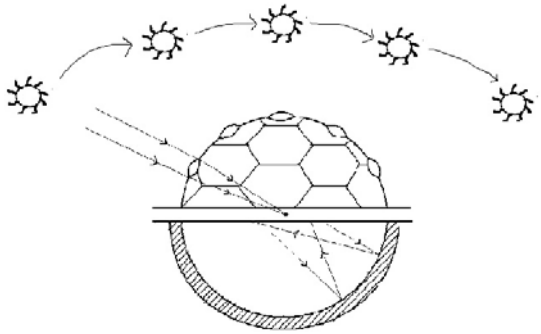

Figure 7: Collector position with respect to sun

2.3. Calculation of Solar Insolation in Bangladesh

Bangladesh is situated at 24° 00' North latitude and 90° 00' East longitude. At this position the amount of hours of sunlight each day throughout a year is shown in the following graph (Fig.8). The highest and the lowest intensity of direct radiation in W/m² are also shown in the

Fig.9. This data shows that using solar collector for high temperature is feasible in Bangladesh.

3. Calculation of useful energy delivered by the Collector

The generation of heat inside the chamber will occur in three different methods:

Lens concentrator: The lenses placed on the surface of the upper half of the heat chamber will concentrate the sunlight directly in to the focus plane of the lenses which in this case is the center of the heat chamber where the fluid pipe will be placed Fig 10. This will directly heat up the heat transfer fluid.

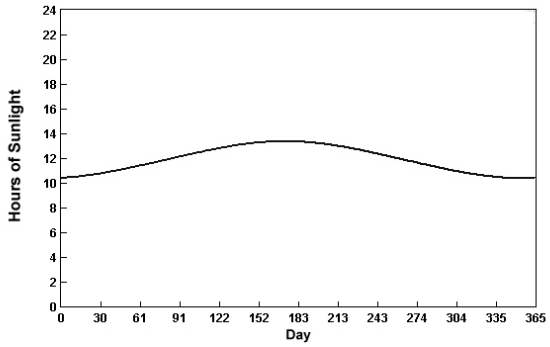

Figure 8: The amount of hours of sunlight in Bangladesh

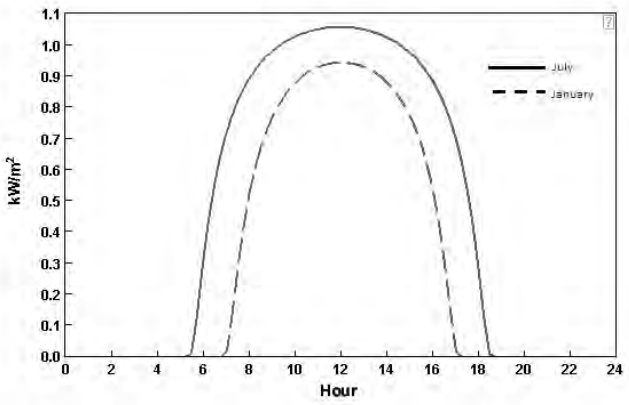

Figure 9: The highest and the lowest intensity of direct radiation in W/m²

The heat (in joules) generated by the lenses could be found by the following equation:

$$Q = ms\ (T_i - T_f) \qquad (3)$$

Where Q is generated heat in joules, m is mass of fluid in KG, T_i is initial temperature of fluid in Kelvin and T_f final temperature of fluid.

Reflector concentrator: This method will heat both the fluid pipe and the inner environment of the heat chamber. The concave bottom surface will act like a reflector mirror and most of the sunlight will be again concentrated on the pipe. This will result a thorough pipe heating (Fig. 11).

The Green House: The hexagonal glasses of the upper half of the heat chamber will allow entering the visible light, but will trap the longer wavelengths of the infrared re-radiation from the heated objects. The trapping of the long wavelength radiation leads to more heating and a higher resultant temperature. This will keep the temperature of the chamber high.

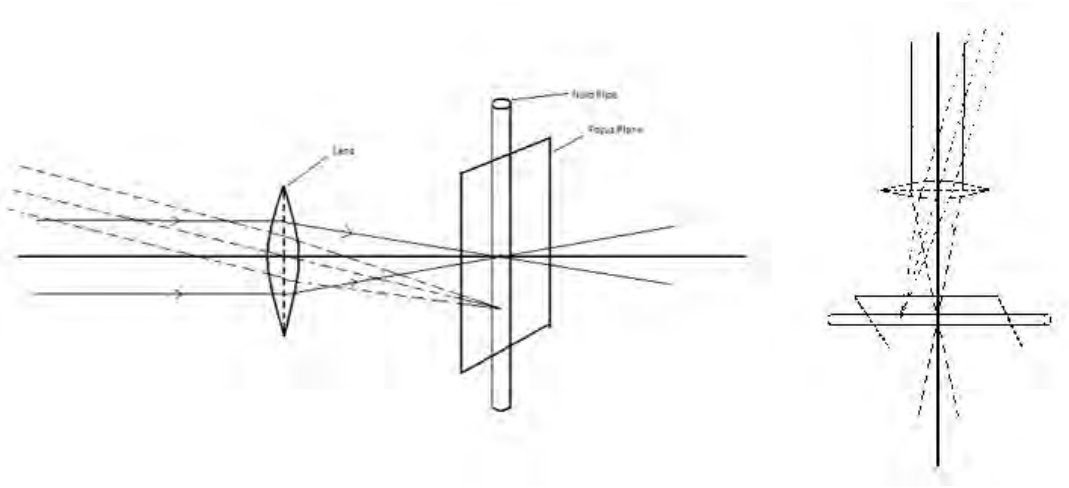

Figure 10: Lens and fluid pipe position

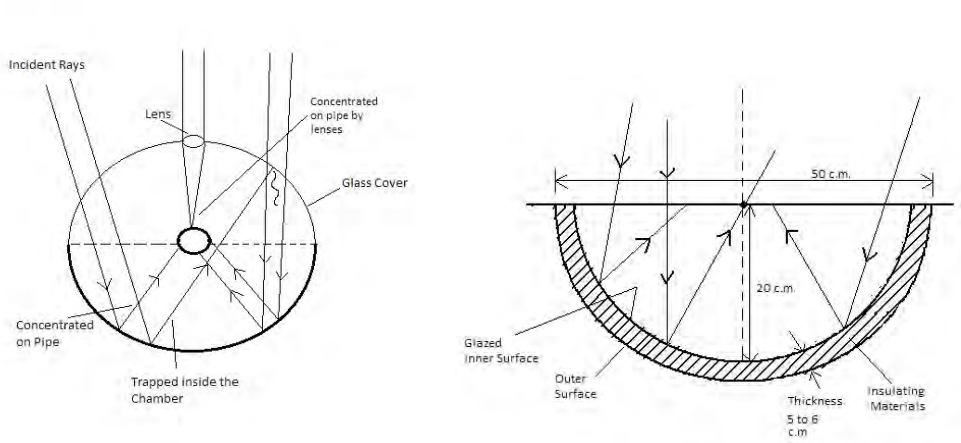

Figure 11: Front view and Section view of the collector

3.1. Overall energy calculation

The rate of useful energy delivered by the collector is governed by the following equation:

$$Q_u = D_s n_o A_a - A_r U_L (T_r - T_a) \quad (4)$$

As the system is a combination of Parabolic Collector Trough (PCT) the optical efficiency can be found from the PCT optical efficiency from the following equation:

$$n_o = \rho \tau \varepsilon \partial [(1 - A_f \tan(\varphi)) \cos(\varphi)] \quad (5)$$

As the system use a green house the heat loss coefficient is determined by the following equation:

$$U_L = \left[\frac{A1}{R1} + \frac{A2}{R2}\right] (t_i - t_o)\, f_w f_c \qquad (6)$$

4. Results

A preliminary screening of the CECT is conducted in order to identify the best match of the load. The result is shown on a plot of efficiency as a function of the heat loss parameter in the following graph.

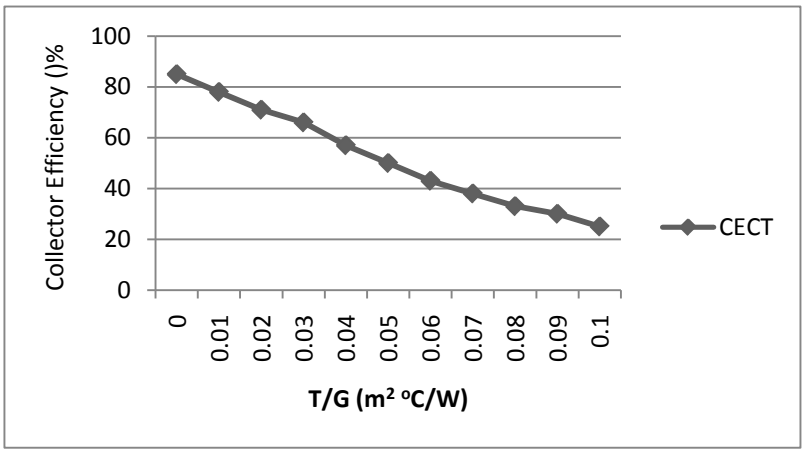

Figure 12: Collector efficiency

5. Discussion

Although Closed Environment Collector Trough is relatively a new concept, the system was expected to be more efficient than that of preliminary screening data. The future work should be based on the improvement of current design and optical as well as thermal optimization.

References

[1] H. E. Imadojemu, Concentrating parabolic collectors: A patent survey Energy Conversion and Management, Volume 36, Issue 4, April 1995, Pages 225-237
[2] Maria Brogren, Anna Helgesson, Björn Karlsson, Johan Nilsson, Arne Roos, Optical properties, durability, and system aspects of a new aluminium-polymer-laminated steel reflector for solar concentrators, Solar Energy Materials and Solar Cells, Volume 82, Issue 3, 15 May 2004, Pages 387-412
[3] A. Thomas, Solar steam generating systems using parabolic trough concentrators Energy Conversion and Management, Volume 37, Issue 2, February 1996, Pages 215-245
[4] Soteris A. Kalogirou, Solar thermal collectors and applications Progress in Energy and Combustion Science, Volume 30, Issue 3, 2004, Pages 231-295
[5] http://pvcdrom.pveducation.org/SUNLIGHT/SUNCALC.HTM

Optimum integration of a large size collector to a solar thermal power plant

M. Yaghoubi[1,*], S. Zarrini[1], S. Mirhadi[2]

[1] *Engineering School, Shiraz University, Shiraz, Iran*
[2] *Renewable Energy Organization of Iran, Tehran, Iran*
** Corresponding author. Tel: +98 7116133028, Fax: +98 7112301672, E-mail: yaghoubi@shirazu.ac.ir*

Abstract: In this paper the problem of increasing the capacity of an already constructed solar thermal power plant has been studied through the concept of lost available work. The required increased capacity has been proposed to be achieved by means of a new large size collector and an auxiliary boiler. Two different schemes along with an extra scheme for night operation of the power plant have been considered in the present work. For each scheme, three different operating conditions have been assumed, resulting in a total of nine operating options. For these options, results of analysis based on the second law of thermodynamics have been presented. These results might then be used to choose the optimum solar hybrid power plant configuration.

Keywords: *Renewable energy, Solar thermal power plant, Parabolic trough, Exergy, Entropy generation*

Nomenclature

$\dot{W}$	*work interaction* ..... *kW*	$\dot{S}_{gen}$	*entropy generation rate* ..... $kW.K^{-1}$
$\dot{Q}$	*heat interaction* ..... *kW*	P	*pressure* ..... *bara*
$\dot{m}$	*mass flow rate* ..... *kg/s*	s	*specific entropy* ..... $kJ{\cdot}kg^{-1}.K^{-1}$
T	*absolute temperature* ..... *K*	h	*specific enthalpy* ..... $kJ{\cdot}kg^{-1}$
T_0	*dead state temperature* ..... *K*	v	*specific volume* ..... $m^3.kg^{-1}$
C_p	*constant pressure specific heat* .. $kJ.kg^{-1}.K^{-1}$		

1. Introduction

1.1. Problem description

Renewable energies play the key role in sustainable development and are the most promising remedy to the problem of air pollution worldwide. Among various sources of renewable energy, the usage of solar thermal energy in generating electricity can be regarded as the most reliable and developed one in the path of commercialization [1].

In Shiraz, Iran, the first solar thermal power plant (STPP) has been designed and constructed for 250 kW power generation [2]. For the first phase of development, this plant has been constructed and tested only to produce high pressure and high temperature steam (21 bar, and $250\,^{o}C$). This steam is then fed into the steam turbine of a conventional Rankine cycle. Based on the new feasibility study, it has been decided to increase the nominal capacity of this plant to 500 kW by adding a new large size (100 meters long) parabolic trough collector and employing an auxiliary boiler to provide the deficiency of steam as well as running the system during night periods (or day periods in which the solar radiation is insufficient).

Various schemes are possible to integrate the new collector to the field of available collectors. In this paper, two different cases (A, B) along with a night case are considered to be suitable for the new system. Assuming three different operating conditions (by setting the turbine outlet pressure) for each case, a total of nine configurations have been analyzed. The three outlet pressures considered are 10, 25 and 100 kPa.

In the present article, these options are studied based on the first and second laws of thermodynamics. Each configuration has some advantages and disadvantages regarding

overall thermal performance, installation and operating costs. To assess the overall performance of various configurations in a comparative manner, exergy method has been applied to the corresponding cycles (as a representative of the second law analysis). Exergy and exergoeconomic methods have received considerable attention during the past decade in the analysis and optimization of power plant cycles to achieve higher efficiencies and to reduce the operating cost of the corresponding power plants [3,5].

For each case of the aforementioned cycles, results of exergy analysis are presented and exergetic losses due to various components (e.g. turbine, boiler, condenser etc) have been calculated. Finally the system with the best exergy efficiency to combine the new collector and increase the power rate of the plant is suggested for construction and operation.

1.2. Current Configuration

Shiraz solar thermal power plant consists of two separate cycles namely the oil cycle and the steam cycle. The oil cycle absorbs the solar radiation through collector field and transmits the harvested thermal energy to the steam cycle which is a classic Rankine cycle. The energy transfer between the two cycles takes place at three heat exchangers in series (E-201, E-202 and E-203). The collector field is composed of 8 parallel loops, each consisting of 6 collectors in series. The current configuration is able to produce 0.671 kg/s of steam at 21 bar and $250\,^{o}C$. This steam will be termed "field generated steam" as opposed to "boiler generated steam" which is the steam that is expected to be generated by the auxiliary boiler. A schematic of the plant is shown in Fig 1.

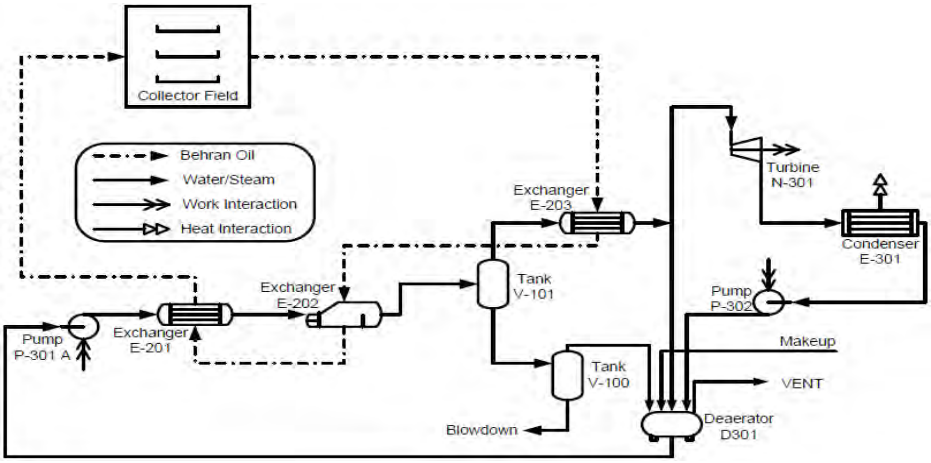

Fig. 1. Schematic of the current solar power plant.

1.3. Integration of the new collector

The new collector has been designed to bring Therminol VP-1 from 294^{O}C to 313^{O}C, supplying 200 kW of energy to the system. This energy can be introduced into the current configuration in a variety of ways. Two different approaches have been considered in the present work namely case A and case B. In case A the boiler provides steam at 21 bar 250^{O}C. This steam is then mixed with the field generated steam and the mixture is then becomes more superheated (to 294^{O}C) using available extra energy from the new collector in an extra heat exchanger (E-204). However, in case B, the boiler produces steam at 21 bar 294^{O}C and in exchanger E-204, only the field generated steam becomes more superheated. The remaining energy from the new collector is then used to make the outlet oil from the field warmer, thus, increasing the amount of field generated steam. Therefore another extra exchanger is needed

in case B to bring the VP-1 oil from the new collector and the Behran oil from the existing farm into thermal contact. Simplified depictions of cases A & B are shown in Fig 2 and Fig 3.

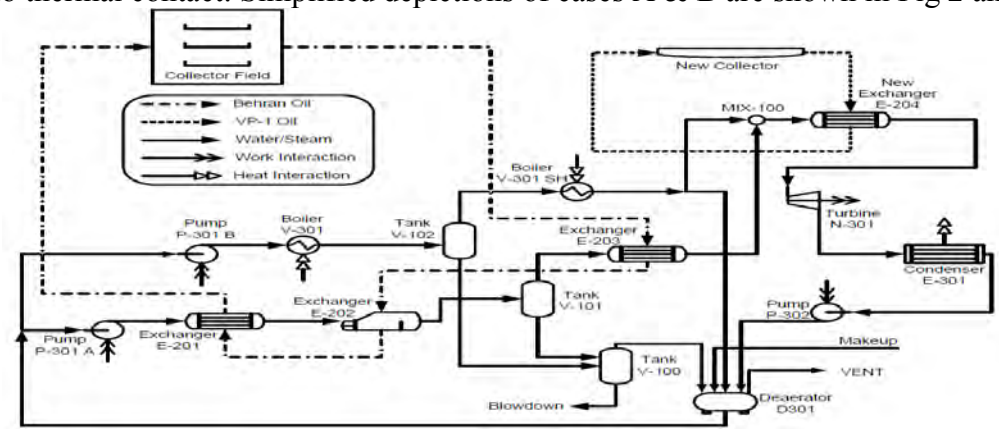

Fig. 2. Schematic of the proposed case A.

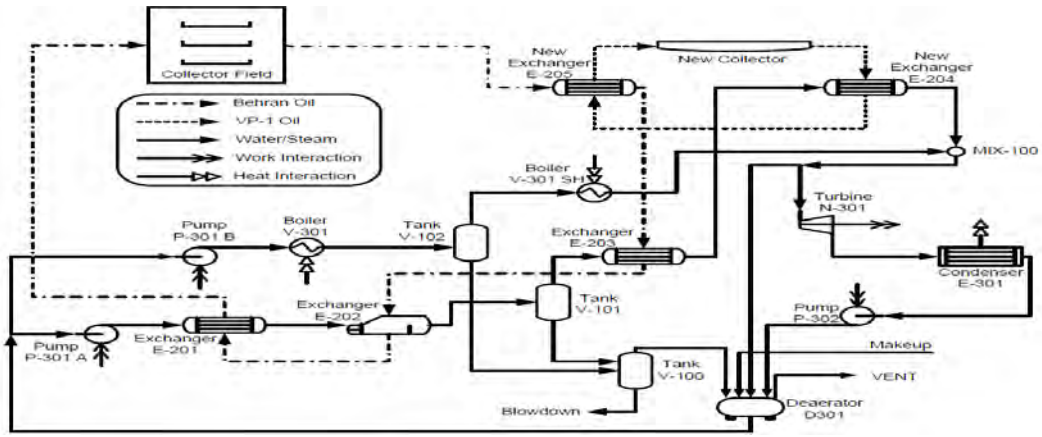

Fig. 3. Schematic of the proposed case B.

2. Methodology

As shortly explained in the preceding section, the problem at hand is a sort of semi-fixed system in which very few parameters are allowed to be altered. This is a direct consequence of the fact that we are dealing with a designed and constructed system and our attempt is to integrate a device into such a system which was not considered before. Thus we're not dealing with an ordinary optimization process in which particular parameters are allowed to vary in order to find the optimum set of parameters. Rather we are investigating the optimum case among a predefined set of choices. In other words, instead of optimizing the cycle, various predefined cases are compared based on the second law and the best can be *chosen*. The assessment of available options is done based on the destructed exergy associated with various components in each option. The destructed exergy (lost available work) is closely related to the rate of entropy generation through the following equation [4]:

$$\dot{W}_{lost} = T_0 \dot{S}_{gen} \qquad (1)$$

where T_0 is the lowest temperature available for the system to reach theoretically (dead state). In this work the dead state has been assumed to be at $25\,^{o}C$ and atmospheric pressure. Thus by calculating the rate of entropy generation for each component, the contribution to lost available work due to that component can be determined. The rate of entropy generation for

each component is readily derived from the general statement of the second law for open systems [4]:

$$\dot{S}_{gen} = \frac{dS_{cv}}{dt} - \sum_{i=0}^{n} \frac{\dot{Q}_i}{T_i} + \sum_{out} \dot{m}s - \sum_{in} \dot{m}s \qquad (2)$$

where $\dot{Q}_i$ is the i[th] heat interaction of the corresponding component with the surrounding (positive when heat transfer takes place from surrounding to the control volume) and T_i is the temperature of that portion of the control surface through which the i[th] heat interaction occurs. In calculating last two terms on t he right hand side of Equation (2) one may frequently encounter the case of calculating Δs terms for steam and oil. For steam the corresponding terms are read from standard thermodynamic tables while for oil (both the collector field oil and the new collector oil) the Δs terms are determined using their specific heats as a function of temperature. Starting from the well-known first law relation [4] and treating oil as an incompressible liquid the Δs term associated with oil can be written as:

$$Tds = dh - vdP \xrightarrow{dP=0} ds = dh/T \xrightarrow{dh=C_p dT} ds = C_p \, dT/T \qquad (3)$$

$$\Delta s = \int_{T_{in}}^{T_{out}} \frac{C_p}{T} dT \qquad (4)$$

It should be noted that in the use of equation (4), the temperatures should be considered in an absolute temperature scale (Kelvin in this work). Having the complete set of states for the current configuration and assuming that the states of steam cycle remain unchanged (which seems reasonable) the new intermediate temperatures have been determined by applying energy balance using an available solver code.

3. Results

After satisfying energy balance for the whole system in every configuration, the state at each node becomes fixed. Knowing the fixed states, the values of entropy generation and subsequently the values of lost available work can be readily determined. In the following four tables the values of $\dot{W}_{lost}$ for the main components in each configuration have been presented.

Example calculation 1:

The lost available work for exchanger E201 in case B for a turbine outlet pressure of 10kPa:

$\dot{m}_h = 14\,kg/s, \dot{m}_c = 0.7525\,kg/s, T_{h,i} = 231.6^o C, T_{h,o} = 221.1^o C, T_{c,i} = 98.53^o C, T_{c,o} = 217.9^o C$

$P_c = 22.3bara \Rightarrow s_{c,i} = 1.28866\,kJ/kg.K, s_{c,o} = 2.49896\,kJ/kg.K \Rightarrow \Delta s_c = 1.2103\,kJ/kg.K$

For hot fluid (Behran Oil): $C_p = 0.8132 + 3.706 \times 10^{-3}(T + 273) \Rightarrow \Delta s_h = -0.05601\,kJ/kg.K$

$\dot{Q}_{c.v.} = 0 \Rightarrow \dot{S}_{gen} = \dot{m}_h \Delta s_h + \dot{m}_c \Delta s_c = 0.1266\,kW/K$

$T_0 = 25^o C = 298K \Rightarrow W_{lost} = 37.72kW$

Table 1. Values of lost available work for cases A & B with turbine outlet pressure of 10 kPa.

case A			case B		
Component Type	Component Name	$\dot{W}_{lost}$ (kW)	$\dot{W}_{lost}$ (kW)	Component Name	Component Type
Exchanger	E201	35.30	37.72	E201	Exchanger
	E202	45.02	48.44	E202	
	E203	3.14	3.67	E203	
	E 204	5.90	3.39	E 204	
	-	-	2.82	E205	
Boiler	V301	143.81	237.47	V301	Boiler
	V301 SH	0.69	15.53	V301 SH	
Deaerator	D301	63.32	64.14	D301	Deaerator
Condenser	E301	146.75	150.01	E301	Condenser
Turbine	N301	321.59	318.58	N301	Turbine
Pump	P301A	0.42	0.46	P301A	Pump
	P301B	0.25	0.22	P301B	
	P302	0.96	0.89	P302	
Tank	V-100	3.30	4.43	V-100	Tank
	V-101	0.00	0.01	V-101	
	V-102	0.08	0.16	V-102	
Mixer	MIX-100	0.43	0.71	MIX-100	Mixer

Table 2. Values of lost available work for cases A & B with turbine outlet pressure of 25 kPa.

case A			case B		
Component Type	Component Name	$\dot{W}_{lost}$ (kW)	$\dot{W}_{lost}$ (kW)	Component Name	Component Type
Exchanger	E201	34.69	39.85	E201	Exchanger
	E202	44.94	48.14	E202	
	E203	2.35	1.49	E203	
	E 204	7.12	3.93	E 204	
	-	-	4.45	E205	
Boiler	V301	348.17	320.46	V301	Boiler
	V301 SH	0.92	21.22	V301 SH	
Deaerator	D301	43.01	43.74	D301	Deaerator
Condenser	E301	311.02	310.46	E301	Condenser
Turbine	N301	300.20	300.27	N301	Turbine
Pump	P301A	0.41	0.43	P301A	Pump
	P301B	0.33	0.29	P301B	
	P302	0.12	0.10	P302	
Tank	V-100	3.53	3.59	V-100	Tank
	V-101	0.12	0.21	V-101	
	V-102	0.00	0.16	V-102	
Mixer	MIX-100	0.53	0.00	MIX-100	Mixer

Example calculation 2:

The lost available work for condenser E301 in case A for a turbine outlet pressure of 25kPa:

$\dot{m}_h = 1.1375 kg/s, P_{h,i} = 0.25 bara, T_{h,i} = 65.0^o C, P_{h,o} = 0.2 bara, T_{h,o} = 60.09^o C, x_{h,o} = 0.967$

$$\Rightarrow s_{h,i} = 7.59958\,kJ/kg.K, h_{h,i} = 2540\,kJ/kg, s_{h,o} = 0.83217\,kJ/kg.K, h_{h,o} = 250\,kJ/kg$$

$$\Rightarrow \Delta s_h = -6.76741\,kJ/kg.K$$

$$\dot{Q}_{c.v.} = \dot{m}\Delta h_h = -2605kW \Rightarrow \dot{S}_{gen} = -\frac{-2605}{298} + 1.1375(-6.76741) = 1.04368\,kW/K$$

$$T_0 = 25^oC = 298K \Rightarrow W_{lost} = 311.02kW$$

In the above calculation, the dryness fraction at the turbine outlet has been determined by considering an isentropic efficiency of 60% for the turbine which is a reasonable value for a turbine of this capacity.

Table 3. Values of lost available work for cases A & B with turbine outlet pressure of 100 kPa.

case A			case B		
Component Type	Component Name	$\dot{W}_{lost}$ (kW)	$\dot{W}_{lost}$ (kW)	Component Name	Component Type
Exchanger	E201	35.34	37.72	E201	Exchanger
	E202	44.32	48.44	E202	
	E203	1.75	3.67	E203	
	E 204	8.33	3.39	E 204	
	-	-	2.82	E205	
Boiler	V301	555.16	517.80	V301	Boiler
	V301 SH	13.49	33.84	V301 SH	
Deaerator	D301	4.23	3.84	D301	Deaerator
Condenser	E301	689.24	684.55	E301	Condenser
Turbine	N301	273.29	273.37	N301	Turbine
Pump	P301A	0.41	0.46	P301A	Pump
	P301B	0.53	0.49	P301B	
	P302	0.00	0.00	P302	
Tank	V-100	4.43	4.62	V-100	Tank
	V-101	0.16	0.01	V-101	
	V-102	0.00	0.00	V-102	
Mixer	MIX-100	0.17	1.47	MIX-100	Mixer

Table 4. Values of lost available work for Night case with turbine outlet pressures of 10,25 and 100 kPa.

Component Type	Component Name	$\dot{W}_{lost}(kW)$		
		10 kPa	25 kPa	100 kPa
Boiler	V301	707.79	780.60	985.28
	V301 SH	46.90	51.68	65.26
Deaerator	D301	73.33	43.76	3.96
Condenser	E301	151.74	310.46	689.24
Turbine	N301	318.96	300.27	273.29
Pump	P301B	0.65	0.71	0.90
	P302	0.09	0.10	0.00
Tank	V-100	3.27	3.59	4.54
	V-102	0.17	0.00	0.00

It is worth mentioning that, generally in solar thermal power plants the major fraction of total exergy loss takes places in the collector field (mainly due to the ultra high temperature of the

sun)[5]. However, in the present work, the operating conditions of the collector field are the same in all configurations. Thus the exergy loss due to the collector field is not reported for comparison. It should also be noted that the night cycle is essentially either cases A or B in which no collector is at service and boilers are the only suppliers of thermal energy to the system. A quick study of tables 1-4 reveals the fact that, generally by decreasing the turbine outlet pressure, the value of lost work decreases in the corresponding devices. Moreover reducing the turbine outlet pressure increases the amount of power which can be extracted from the turbine. But, as expected, these advantages have their own counterparts; the need for creating vacuum condition for condenser, the need to change the condenser type from air-cooled to water-cooled, etc. Another implication is that in each configuration the dominant sources of lost work are boilers, condensers and turbines and that the contribution made by pumps, mixers and tanks are negligible.

From another point of view, comparing the values of lost available work for same devices, one may conclude that, in the same operating conditions, case A is thermodynamically superior to case B.

4. Conclusions

- The concept of lost available work has been utilized to select the best choice of integration of a hybrid solar power plant.
- Regarding various cases, it is found that case A is thermodynamically the preferred case for integration.
- Case A has the advantage of requiring one less extra heat exchanger to be integrated into the current configuration.
- For optimum integration, one must also take into account the economic aspect of each case. In other words, a thorough thermo-economic analysis might be proper to further assess these two proposed cases.
- Moreover one should also consider water consumption rate for each case. Water is rarely available especially for regions where solar energy is considerable and such limitation might sacrifice higher efficiencies or lower available lost work for the final decision.

References

[1] R. Shinnar, F. Citro, Solar thermal energy: The forgotten energy source, Journal of Technology in Society 29, 2007, pp.261-270

[2] K. Azizian, M. Yaghoubi, R. Heasmi, S. Mirhadi, Shiraz pilot solar thermal power plant design, construction, installation and commissioning procedure, Proceedings of 7th International Conference on Heat transfer, Fluid mechanics and Thermodynamics, 2010

[3] A. Baghernejad, M. Yaghoubi, Multi-objective exergoeconomic optimization of an integrated solar combined cycle system using evolutionary algorithms, International Journal of Energy Research, 2010

[4] A. Bejan, Advanced Engineering Thermodynamics, Wiley, 2nd Edition, 1997

[5] M.K. Gupta, S.C. Kaushik, Exergy analysis and investigation for various feed water heaters of direct steam generation solar thermal power plant, Journal of Renewable Energy 35, 2010, pp.1228-1235

Theoretical Modelling of a Dynamic Solar Thermal Desalination Unit with a Fluid Piston Engine

B. Belgasim and K Mahkamov*

*School of Computing, Engineering and Information Sciences, Northumbria University, Newcastle upon Tyne, NE1 8ST, UK**
**Corresponding author. Tel:+44 191 2274739, Fax: +44 191 2437630, Email: khamid.mahkamov@northumbria.ac.uk*

Abstract: Results of theoretical simulations of the steady-state operation of the dynamic solar thermal desalination unit with a fluid piston are presented in this paper. A laboratory prototype of a dynamic thermal water distillation unit was developed and it was built around an engine with fluid pistons. In the calculation scheme, the internal circuit of the desalination unit was split into several control volumes, namely the evaporator, the condenser and the cylinder. The lumped parameter mathematical model was derived based on the differential energy and mass conservation equations written for each of the control volumes and describing heat and mass transfer processes taking place during water evaporation and condensation under the cyclic variation of the pressure and temperature inside the system when the engine operates. The solution of the set of governing equations produces information on the variation of temperatures and pressure inside the system over the thermodynamic cycle and on the water desalination capacity of the unit.

Keywords: Solar water desalination, mathematical modelling

1. Introduction

The shortage in clean drinkable water supply has become one of the most important problems due to the continued growth in the world's population. Kalogirou [1] states that the fresh water represents only about 3% of all water on the earth. Approximately 0.25% of fresh water can be directly used from lakes and rivers and the rest is in the ice form or deep ground water which is difficult to reach. As a result, novel drinkable water production technologies are being continuously developed to resolve this important problem.

Desalination techniques are among feasible solutions to produce fresh water from saline water but such technologies require significant amount of energy. Using fossil fuels for water desalination results in high plant running costs and causes a considerable negative environmental impact. As a consequence, numerous studies are being performed on utilisation of an alternative energy source, namely renewable energy, for running desalination plants. The aim of the above research studies is to make the process of water desalination with the use of renewable energy safer for the environment and sustainable.

The literature review performed in this subject demonstrates that the majority of research carried out has been focused on the static solar stills in which the saturation pressure and temperature remain constant during the desalination process. Shatat and Mahkamov presented theoretical and experimental study of a static solar thermal distillation unit in [2]. The effect of the design parameters on the performance of the unit was investigated and an optimization of unit's design parameters have been conducted. Mahkamov and Belgasim described in [3] the concept of the dynamic solar distillation system in which an evacuated tube solar collector was coupled with a fluid piston thermal engine. The laboratory prototype of the proposed system was built and tested to demonstrate its functionality and preliminary experimental results were very encouraging. Furthermore, a comparative study between static and dynamic solar distillation systems was performed in the same study which demonstrates considerably higher fresh water production capacity of the dynamic system.

2. Model Description

The dynamic solar thermal desalination unit integrated with fluid piston engine is described in *fig.1*. This unit operates under a cyclic change in the pressure and temperature during the operation of the unit due to the expansion and the compression of the volume of the fluid piston engine. Such working conditions considerably intensify the desalination processes and fresh water production.

The plant's operation can be described as follows. Saline water is heated up and evaporated in the solar collector (1) causing pressure rise in the system. The initial increase of the pressure initiates oscillations of water columns (3) and (4) of the fluid piston engine and the whole system operates as a dynamic thermal oscillation system, in which the water evaporation is intensified by volume and pressure variations in the internal circuit. In its turn, this sustains oscillations of water columns. In this particular design, the distilled water is formed in the condenser (2) surrounded by the water jacket with the saline water and the condensate is collected in the distilled water vessel (6). The heated saline water from the water jacket of the condenser is pumped to the water storage tank.

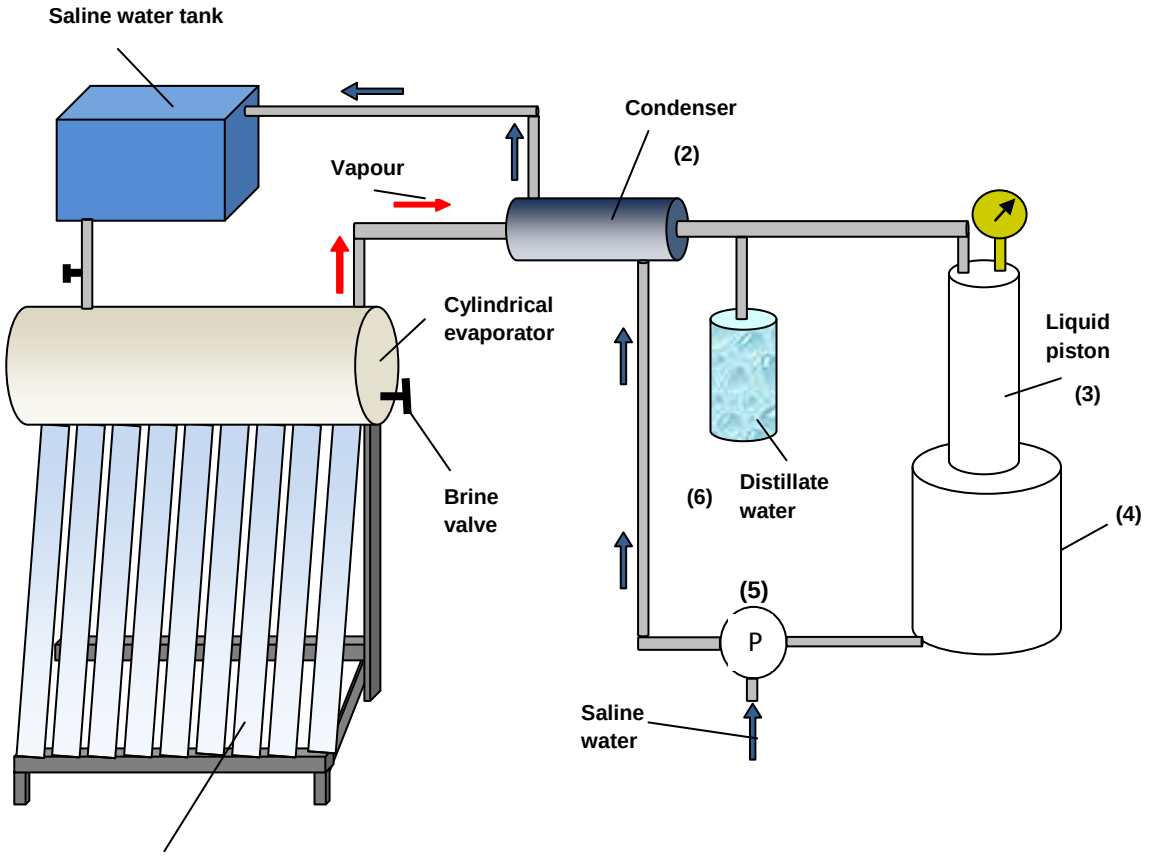

Fig. 1 **(1) Evacuated tube solar collector**

The above system was tested under a number of constant heat flux conditions created with application of a sun simulator: an array of 110 halogen floodlights placed above evacuated tubes. The heat flux magnitude is set using a three-phase transformer which controls the voltage of the electrical current supplied to the floodlights. Preliminary results obtained clearly show that such dynamic system has a considerable advantage in fresh water production capacity over conventional static systems. Currently the unit is being equipped with sensors to record oscillations of the liquid piston, temperature and pressure variations in components of the installation.

3. Theoretical Modelling

In order to perform the theoretical analysis, the unit was divided into three separate control volumes, namely the evaporator, the condenser and the fluid piston cylinder. The lumped mathematical model was derived based on energy and mass conservation differential equations written for each control volume taking into accounts the cyclic variation of the pressure and temperature inside the system during its operation.

3.1. Evaporator

The mathematical model of the system consists of the mass and energy balance equations written for each component. The mass conservation equation could be written as

$$\frac{d}{dt}(\rho V) = (\rho \dot{v})_{sw} - (\rho \dot{v})_{v} - (\rho \dot{v})_{b} \quad (1)$$

where t is time, V is volume, ρ is density and $\dot{v}$ is volume flow rat.

The initial condition for the above equation is the amount $(\rho V)_0$ of the seawater at the beginning of the operation. Two assumptions are made: the amount of saline water inside the evaporator is constant; all the vapour produced in the evaporator will be then condensed in the condenser.

The salt concentration conservation equation is

$$\frac{d}{dt}(\rho V c) = (\rho \dot{v} c)_{sw} - (\rho \dot{v} c)_{b} \quad (2)$$

where c is salt concentration.

The initial amount of salt is $(\rho V c)_0$

Finally, the energy conservation equation can be derived by applying the energy balance principle for the same control volume.

$$\frac{d}{dt}(\rho V c_p T) = Q_{in} + (\rho \dot{v} c_p T)_{sw} - (\rho \dot{v} h_{fg})_{v} - (\rho \dot{v} c_p T)_{b} - Q_{loss} \quad (3)$$

where Q is the heat flow, T is temperature h is enthalpy and c_p is heat capacity at constant pressure.

The energy $(\rho V c_p T)_0$ is at the starting time. In this equation the heat capacity of the system material has been neglected so no heat storage is considered in the evaporator substance.

3.2. Condenser

It was assumed in the simulation process that all the produced vapour is converted into fresh water. The condenser design represents the counter flow tube-in-tube heat exchanger in which the condensation process takes place on the internal surface of the inner tube while the cooling water passes through the outer tube. In order to enhance the productivity and the thermal efficiency of the system, the seawater fed to the evaporator is first used as cooling water in the condenser's water jacket to gain the latent heat of condensation.

The mathematical description of the condensation process depends on a number of factors including the condenser shape, the flow pattern and the condensation rate. The inner heat transfer coefficient in the case when the condensation rate is low and the vapour has a low velocity in a short condenser, can be calculated as [4]

$$h_i = 0.555\left[\frac{g\rho_l(\rho_l-\rho_v)k_l^3 h_{fg}^{'}}{\mu_l(T_{sat}-T_s)D}\right]^{1/4}$$

where the modified condensation heat is $h_{fg}^{'} = h_{fg} + \frac{3}{8}c_{p,l}(T_{sat}-T_s)$

The outer heat transfer coefficient is mainly effected by Nusselt Nu number which is a function of the flow pattern and depends on the Reynolds number Re. If $Re < 2300$ the flow is laminar and if $Re > 2300$ then the flow is turbulent. The outer heat transfer coefficient can be calculated as $h_o = \frac{k_l}{D_h}Nu_i$ [5]. Therefore, the overall heat transfer coefficient is $U = \frac{h_o h_i}{h_o + h_i}$

The condenser is considered as a control volume and using the mean temperature difference technique, the governing energy equation for the condenser can be written as:

$$Q = UA_s\frac{\Delta T_2 - \Delta T_1}{\ln(\Delta T_2/\Delta T_1)} = \dot{m}c_{p,sw}\left(T_{c,in} - T_{c,out}\right) \quad (4)$$

where U is the overall heat transfer coefficient, A surface area, $\dot{m}$ is mass flow rate, $\Delta T_1 = T_{sat} - T_{c,out}$ and $\Delta T_2 = T_{sat} - T_{c,in}$

In the above equation, the produced fresh water is assumed to be condensed at the saturation temperature.

3.3. Fluid piston engine

The fluid piston engine consists of two concentric cylinders attached to the collector at the top of the inner cylinder. The two cylinders are filled with water to work as a piston in both cylinders. After the solar collector starts to heat up the saline water, its temperature gradually increases leading to the rise in the pressure in the system. The pressure continue to rise until the inner cylinder piston, which is at the top position in the beginning of heating process, is pushed down. This results in expanding the volume of the system. The expansion process continues until the air pressure at the top of the outer cylinder balances the system pressure and then the system returns to the original position under the effect of the water weight and air pressure leading the cycle to be repeated again.

The expansion and compression processes are repeated continually allowing the unit to work under variable volume and pressure conditions. The change in the volume is important to estimate the change in pressure and in this study, the volume has been assumed to vary harmonically:

$$V_{tot} = V_{dead} + \pi A\frac{D^2}{8}\left[1 - cos(\omega t)\right] \quad (5)$$

where V_{dead} is the dead volume of the system, A is the amplitude of the fluid piston oscillations; D is the diameter of the piston and f is the frequency of oscillations.

The relationship between the change in volume and in the pressure is calculated as

$$\Delta P = P_{sat}\left[\left(\frac{V_{tot(1)}}{V_{tot(2)}}\right)^{k} - 1\right] \quad (6)$$

where ΔP is the pressure change due to the variation in the total volume of the system.

It was assumed that the expansion and the compression processes are isentropic processes.

4. Results and Discussion

The governing equations of the theoretical model are the set of ordinary differential equations with the time being the independent variable. The input parameters of the system include the initial conditions, the properties of water, the value of constant solar radiation and dimensions of the unit. In order to simulate the operation of the system, a MATLAB program has been written which uses Euler technique to solve the differential equations with a time step $\Delta t = 0.01\ sec$.

The theoretical simulations have been carried as set of a number cases with constant heat flux values, which are typical for different hours of the mid-summer day in the Middle East region.

The theoretical results on pressure and temperature variations inside the system for the heat flux corresponding to 12 noon are illustrated in *fig. 2* and *fig. 3*, respectively. During the expansion in the cylinder, the pressure drops to approximately 0.7 *bar* (minimum pressure) and rises to 1.15 *bar* (maximum pressure) during the compression stroke. These values are also close to experimental values of the minimum amd maximum pressures in the cycle, measured using a manometer. The temperature during the cycle varies between 92 and 105 degrees C.

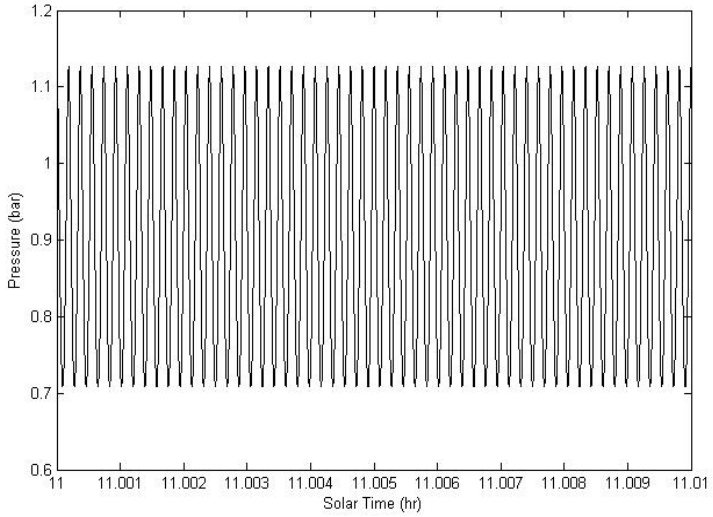

Fig. 2 The saturation pressure oscillation.

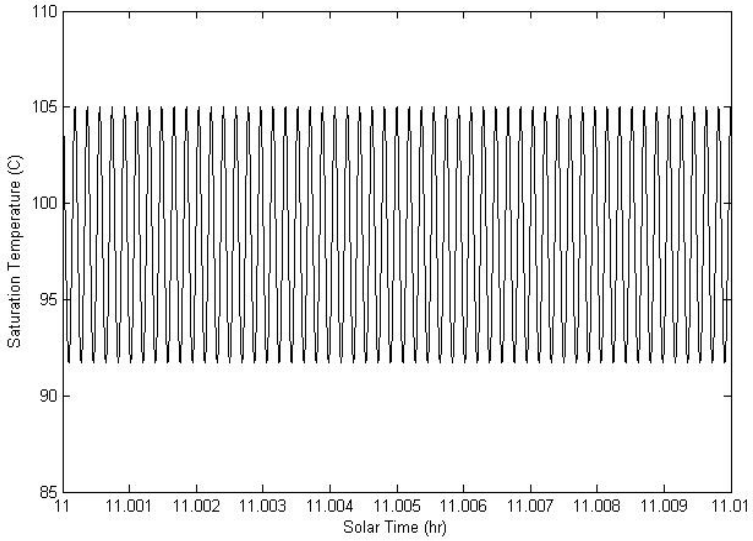

Fig. 3 The saturation temperature oscillation.

Theoretical results on the fresh water production capacity obtained by using the above mathematical model for a number of constant heat fluxes typical for different periods of the mid-summer day were used to produce the variation of the fresh water production capacity over the day, as shown in *fig 4*.

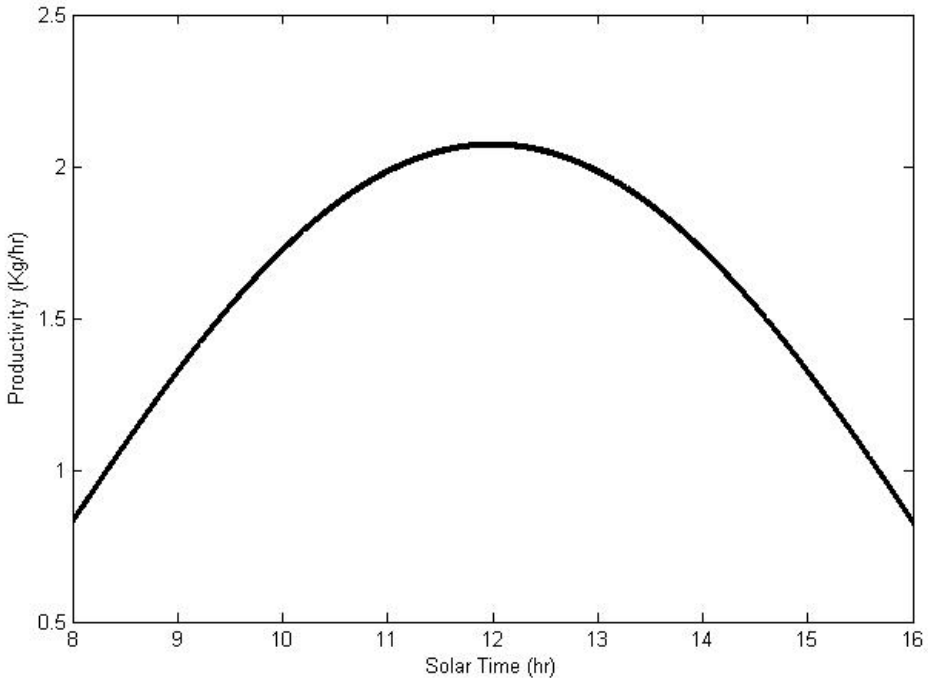

Fig.4 The productivity variation during the mid-simmer day

The theoretical value for the daily fresh water production capacity is obtained by integration water production capacity curve in *fig. 4* and it is about 9 litres, which is greater than 6 litres for the conventional static solar stills. During preliminary experiments at the same heat flux value the fresh water production capacity was about 8.2 litres.

5. Conclusions

The paper presents results of theoretical modelling of the steady-state operation of the proposed dynamic water desalination system with a number of constant heat flux values upon the evacuated tubes of the solar collector. The heat flux values used are typical for a different periods of the mid-summer in the Middle East region. The fresh water production, obtained from this study, was found to be about 9 litres/day which is greater than the most of conventional static solar distillation designs. The theoretical data obtained on the fresh water production capacity is in a good agreement with data obtained on the test rig which was run simulating variation of insolation over the summer day.

Currently the unit is being equipped with sensors to record oscillations of the liquid piston, temperature and pressure variations in components of the installation. Such experimental information can be used for calibration of the mathematical model.

It is planned to conduct modelling of unsteady operation with at variable heat flux conditions in the future. The unsteady model also will describe processes taking place in the evaporator and condenser in more details making it possible to take into account the effect of the insolation variation on the levels of the saturated pressure and temperature.

The further development of the mathematical model will also include an optimization procedure for design parameters of the unit.

References

[1] S. Kalogirou, Seawater desalination using renewable energy sources, Progress in Energy and Combustion Science 31, 2005, pp. 242-281.

[2] M. Shata and K. Mahkamov, Determination of rational design parameters of a multi-stage solar water desalination still using transient mathematical modelling, Renewable Energy 35, 2010, pp. 52-61

[3] K. Mahkamov and B. Belgasim, Experimental study of the performance of a dynamic water desalination system with a fluid piston engine, In: The 14th international Stirling engine conference, November 16-18, 2009, Groningen, The Netherlands.

[4] S. Maroo and D. Goswami, Theoretical analysis of a single-stage and two-stage solar driven flash desalination system based on passive vacuum generation, Desalination 249, 2009, pp. 635-646.

[5] F. Incropera and D. De Witt, Fundamentals of heat and mass transfer, New York: John Wiley&Sons, 3rd edition.

Theoretical study of the aspect ratio of a solar still with double slopes

A.Madhlopa[1,*], J.A. Clarke[1]

[1] *Energy Systems Research Unit, University of Strathclyde, James Weir Building, 75 Montrose Street, Glasgow G1 1XJ, United Kingdom.*
** Corresponding author. Tel: +44 1415483204, Fax: +44 141548, E-mail:a.madhlopa@strath.ac.uk*

Abstract: Clean water is essential for good health which influences the social and economic development of any nation. However, there is limited access to safe water on a global scale. This challenge can be overcome through a multi-faceted approach, including the development of appropriate technologies for water treatment and decision-making tools. Solar distillation is one of the commonest non-conventional methods for improving the quality of water. In this vein, the most widely-exploited solar distillation system is a conventional solar still, which has a thin layer of saline water in a shallow basin with a transparent cover over the water and one or two slopes. The productivity of a solar distillation system is influenced by design, climatic and operational factors, with solar radiation being the most influential meteorological parameter. It is therefore necessary to optimize solar radiation that effectively reaches the base of the solar still. Previous attempts have sought to improve the design characteristics of conventional solar stills through the consideration of system geometry and optical properties of construction materials. One of the important geometric parameters is the ratio (R) of length to width (aspect ratio) of the still base. For a single-slope solar still (SSS), R has been examined in preceding studies. Nevertheless, there is a paucity of information on the aspect ratio of a double-slope solar still. In this study, a state-of-the-art software (ESP-r) was used to simulate the variation of effective insolation with R for a double-slope solar still (DSS) in the east-west and north-south orientations and a SSS facing south. Meteorological data captured at the University of Strathclyde (55^o 52′ N, 4^o 15′ W) and Guantanamo Bay (19^o 54′ N, 14^o 51′ E) was employed in this analysis. Simulation results show that the optical performance of a DSS was lower (in both orientations) than that of a SSS at both sites. The DSS collected more solar energy in the east-west than north-south orientation, for a given value of R. In addition, effective insolation increased with R to an optimum level for both the DSS and SSS. Approximate optimum values of R were 3.0 and 2.0 for the University of Strathclyde and Guantanamo Bay respectively. However, the optimum value of R was not sensitive to the orientation of the DSS at the two sites. Further, the DSS and SSS exhibited the same optimal value of R at a specific site. It appears that R significantly affects solar collection in a DSS.

Keywords: *Aspect ratio, Effective insolation.*

Nomenclature

A	*area of still base*	m^2
B	*width of still base*	*m*
G	*irradiance*	Wm^{-2}
H	*mean annual daily effective insolation*	Jm^{-2}
I	*hourly effective insolation*	Jm^{-2}
L	*length of still base*	*m*
Q	*solar gain*	*(%)*
R	*aspect ratio*	*dimensionless*
x	*distance along x-axis*	*(m)*
y	*distance along y-axis*	*(m)*
z	*distance along z-axis*	*(m)*
α	*absorptance*	*dimensionless*
β	*tilt angle*	*degree*
ϕ	*latitude*	*degree*
θ	*zenith angle*	*degree*
ρ	*reflectance*	*dimensionless*
τ	*solar direct transmittance*	*dimensionless*

Subscripts

1	*transparent cover 1*
2	*transparent cover 2*
b	*basin liner*
g	*ground*
w	*wall*

1. Introduction

Clean water is essential for good health which influences the social and economic development of any nation. However, a large proportion of the available water on the earth's surface is saline [1]. This problem is exacerbated by environmental pollution predominantly

caused by anthropogenic activities. Consequently, there is limited access to clean water, especially in developing countries [2]. Solar distillation is one method of producing fresh water from salty water.

A conventional solar still is the most-widely exploited solar distillation system. It has a thin layer of water in a horizontal basin, transparent cover over the water with one or two slopes (Fig.1). The single-slope solar still (SSS) has a back wall which acts as an internal reflector while the double-slope solar still (DSS) has no back wall. Transparent covers in a DSS may be symmetrical ($\beta_1=\beta_2$) or symmetrical ($\beta_1\neq\beta_2$), with a gable along each breadth. In both the SSS and DSS, saline water in the basin is heated by solar radiation passing through the transparent cover and absorbed by the water and bottom part of the still basin. Vapour flows upwards from the hot water and condenses when it comes into contact with the cooler inner surface of the transparent cover. The condensate (clean water) is collected in a channel fitted along the lower edge of the transparent cover. For a given set of system design parameters, the distillate output from the system is influenced by climatic and operational factors, and a SSS intercepts a higher proportion of solar radiation than a DSS at locations with both high and low latitudes [3]. Moreover, solar radiation is the most influential environmental parameter [4], and the DSS is economically more viable than the SSS [5]. So, it is necessary to optimize the design of the DSS in order to maximize its capability of solar collection.

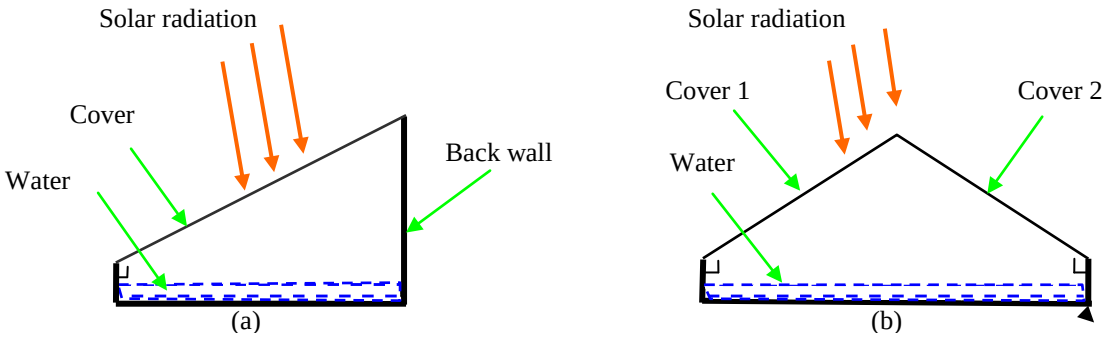

Fig.1: Cross-section of a basic solar still with a) single slope and b) double slopes.

Attempts have been made to establish materials with suitable optical properties of various components of a basin-type solar still. The cover absorbs and reflects part of the incoming solar radiation, with the remaining fraction being transmitted onto the still walls, the surface of saline water and basin liner. So, transmittance is the most important optical property of the cover layer, which may be plastic or glass. Different cover materials for solar stills have been investigated in previous work [6, 7]. It was found that solar stills with glass covers perform better than those with plastic covers. In addition, the internal surfaces of the walls of the still absorb and reflect part of the received solar radiation onto the surface of water. The reflectance of the walls of a solar still influences the effective insolation on saline water in the basin [8]. The basin liner also absorbs part of the solar radiation intercepted by the transparent cover. Consequently, the absorptance of the basin liner is an essential optical property. The various still components are assembled into a structure with specific geometry which affects the optical performance of the distillation system.

A solar still may be mounted on a tracker or fixed plane. A tracking solar still follows the sun on daily (one-axis) or daily and seasonal (two-axis) basis to maintain a low angle of incidence and thereby increase the transmission of solar radiation through the transparent cover. However, tracking solar systems are costly and unsuitable for large-scale production of

distilled water. In contrast, there is no cost associated with tracking in stationary solar stills. So, this variety of solar stills is more feasible for practical applications. The transparent cover of a fixed solar still is inclined at an angle (β) to the horizontal plane. It is reported that the optimum value of β is 10^{o} which just enables the distillate to flow downwards on the inner surface of the cover without dropping back into the basin [3, 9]. Nevertheless, β also affects the transmission of solar radiation through the cover [10]. So, $\beta > 10^{o}$ is sometimes used depending on the latitude (ϕ) of the site [4]. Generally, $\beta=\phi-10^{o}$ for summer season ($\phi>10^{o}$), $\beta=\phi$ for annual performance and $\beta=\phi+10^{o}$ for winter season [11]. In addition, a stationary DSS is oriented with the covers facing the east and west directions to optimize solar collection [12, 13]. On the other hand, a stationary SSS is commonly mounted facing the Equator for optimum performance. Capture of solar energy is also affected by the ratio of the length to width of the still base (R). Optimization of R is reported for a SSS [14] but there is a paucity of information on the aspect ratio of a DSS. The objective of this study was therefore to overcome this limitation

$$R=L/B \quad (1)$$

2. Methodology

2.1. System description and computational tool

Solar collection in a DSS with symmetrical slopes and a SSS has been studied theoretically. The major components of the systems were a) a horizontal basin, b) transparent covers and c) opaque walls and base (Fig.1).The basin liner was constructed from a steel material (0.001 m thick) while the covers were constructed from clear float glass (0.004 m thick) to allow solar radiation reach the internal surfaces of the still. Each cover was inclined at 55.9^{o} to the horizontal at the University of Strathclyde (55^{o} 52′ N, 4^{o} 15′ W) and 19.9^{o} to the horizontal at Guantanamo Bay (19^{o} 54′ N, 14^{o} 51′ E) to optimize solar collection on annual basis. The same slope was used for the DSS and SSS at a given site. Each wall was triple-layered with expanded polystyrene (0.05m thick) sandwiched between two plywood layers (0.005 m thick, each layer). Similarly, the base of each still was also triple-layered with plywood external (0.005 m thick), expanded polystyrene middle (0.05 m thick) and steel internal layers. The surface area of the base remained constant for different values of the aspect ratio. In addition, the height of the lower vertical sides was fixed at 0.05 m above the still base while the height of the higher vertical sides varied with R. Other design parameters are presented in Table 1.

Table 1. Design parameters of a double-slope solar still.

Parameter	Unit	Value
A	m^2	1.00
α_b	dimensionless	0.90
ρ_g	dimensionless	0.2
ρ_w	dimensionless	0.2
τ_1, τ_2	dimensionless	0.837

A state-of-the-art software (ESP-r, version11.9) was used to compute hourly irradiance on the basin liners of the DSS and SSS. This software has a robust algorithm for computation of insolation and shading effects [15]. Beam and diffuse components of solar radiation are treated separately, and optical view factors and multiple reflections are taken into consideration. A geometric construction of each solar distillation system was made in ESP-r with the origin at x=0, y=0 and z=1 m to simulate the system in a mounted mode (the x-, y- and z-axes are mutually perpendicular, z-axis is vertical and x-y plane is horizontal). The still

base was in the x-y plane, with the diagonals of the base intersecting at the origin. The orientation of the DSS was varied by rotating the system about the vertical axis through the origin (x=0 and y=0). For each system configuration, view factors were calculated by using the ray tracing technique, and the computed optical view factors were used in the computation of effective irradiance on the base of the solar still in any given hour. The DSS was simulated with the covers oriented in the east-west and north-south directions while the SSS faced south at both sites. Effective hourly insolation (I_i) was computed from irradiance on each still base. The total annual effective insolation (E) was determined by summing up the hourly insolation for a given value of the aspect ratio (R). Then, the mean annual daily insolation (H) was computed from E. In addition, the area of the still base remained constant as R was varied from 0.5 to 4.0. At successive increments in R, the percentage solar gain (Q) was calculated. Equations for these calculations were as follows:

$I_i=3600G_i$ for i=1, 2, 3, …, m (2)
where m=number of hours in a year.

$E=\sum_{i=1}^{i=m} I_i$ (3)

$H=E/j$ (4)
where j=number of days in a year.

$Q_k=100(H_k-H_{k-1})/H_i$, for k=1, 2, 3, … (5)

Mean hourly normal-incident beam and diffuse irradiance data, captured at the University of Strathclyde and Guantanamo Bay, was used in this study. This data covered the periods from 1 January to 31 December 2001 at the University of Strathclyde and 1 January to 31 December 1971 Guantanamo Bay. It should be noted that the University of Strathclyde and Guantanamo Bay are at high and low latitudes respectively.

2.2. Some assumptions

The following assumptions were made:

a) the distribution of incoming diffuse radiation was anisotropic. So, an anisotropic model was employed in calculating the amount of diffuse radiation received by a given surface. It should be mentioned that anisotropic models are more accurate in estimation of diffuse radiation than isotropic models [16],
b) the ground reflected diffusely because it is rough and so the reflected radiation is scattered,
c) the basin liner was black on the interior surface to optimize solar absorption on the still base, and
d) the solar still was not obstructed by other structures within the vicinity to reduce the effect of shading from these structures.

3. Results and discussion

The variation of mean annual daily effective insolation (H) on the base of the DSS and SSS simulated at the University of Strathclyde is shown in Fig.2. It is observed that the DSS collects less solar radiation than the SSS for a given value of the aspect ratio (R). This observation is attributed to the presence of a back wall in the SSS. The back wall reflects part of the incoming solar radiation onto the still base [8]. Garg and Mann [3] also found that the

DSS was optically less efficient than the SSS. In addition, the DSS captures more solar radiation in the east-west orientation than the north-south orientation, probably due to the effect of shading from the gables. For the east-west orientation, the gables are on the north and south of the still. So, one of these gables would cast a shadow on the still base when the sun is due north or south of the solar still, except when the sun traverses the sky over the local latitude. The sun traverses the sky to the south of the University of Strathclyde throughout the year. In this case, the southern gable would cast a shadow on the still base. However, solar radiation would be able to directly reach the still base even at low solar altitudes in the morning or afternoon. For the north-west orientation, the gables are on the east and west of the still. Thus, one of the gables would cast a shadow on the still base in the morning or afternoon times, except at local solar noon. The effect of shading is significant at low solar altitudes in the morning or afternoon, which accounts for the observed effect of orientation on the optical efficiency of the DSS [12, 13].

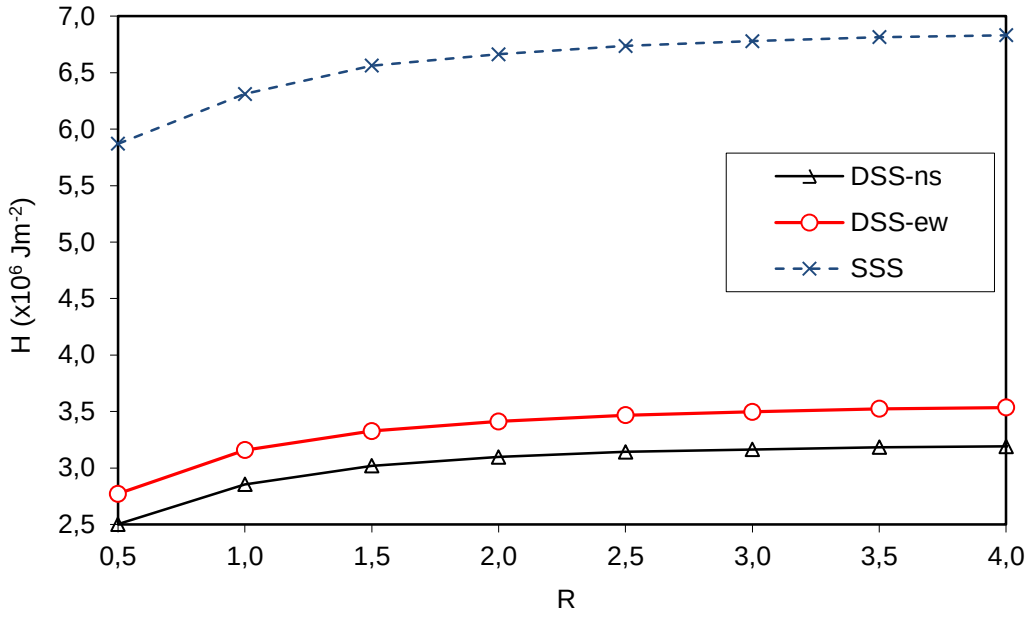

Fig. 2. Variation of mean annual daily effective insolation (H) with aspect ratio (R) for the DSS oriented east-west (DSS-ew) and north-south (DSS-ns), and the SSS facing south at the University of Strathclyde.

Fig.2 also shows that H increases with the aspect ratio (R) of the still base to an optimum level for both the DSS and SSS. This observation is ascribed to a reduction in self-shading arising from the wall along the breadth of the stills. It should be mentioned that R increases as the width (B) of the still decreases, leading to a decrease in the height and area of the slanted wall of the still (for a constant slope) and its shading effect on the internal part of the still base in both the DSS and SSS. Under the prevailing meteorological conditions, the optimum value of R (when Q<1.0 %) was approximately 3.0 for the DSS (in both the east-west and north-south orientations) and SSS. For the SSS, El-Swify et al. [14] reported an approximate optimum value of R=2.0 for climate data from Cairo (30° 3′ N, 31° 10′ E), which is lower than the present optimum value probably due to variations in site parameters. The latitude and longitude of a site affect solar angles and the distribution of solar radiation in a still.
Fig.3 shows the variation of H on the base of the DSS and SSS for the climate data from Guantanamo Bay. It is again observed that the DSS collects less solar energy than the SSS for a given value of R. In addition, the DSS captures more solar radiation in the east-west

orientation than the north-south orientation, in agreement with results for the climate data from the University of Strathclyde. For the east-west orientation, one of the gables would cast a shadow on the still base when the sun is due north or south of the solar still, except when the sun traverses the sky over the local latitude. It should nevertheless be noted that the sun traverses the sky over head, to the south and north of Guantanamo Bay during certain times of the year. In this case, a gable would cast a shadow on the still base when the sun is not crossing the sky over head but beam radiation would be able to directly reach the still base even at low solar altitudes in the morning or afternoon. For the north-west orientation, one of the gables would cast a shadow on the still base in the morning or afternoon times, except at local solar noon. Solar radiation would be unable to directly reach the still base at low solar altitudes during certain times in the morning or afternoon, which accounts for the observed effect of orientation on the optical efficiency of the DSS.

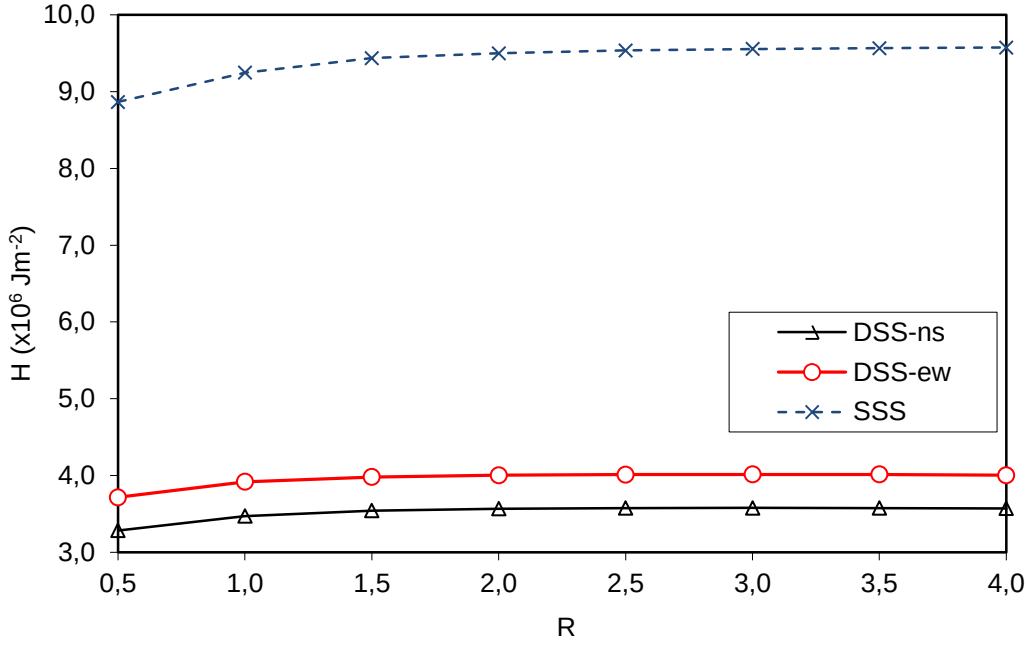

Fig.3. Variation of mean annual daily effective insolation (H) with aspect ratio (R) for the DSS oriented east-west (DSS-ew) and north-south (DSS-ns), and the SSS facing south at Guantanamo Bay.

It is also observed from Fig.3 that H increases with R to an optimum level for both the DSS and SSS. This observation is again attributed to a reduction in self-shading arising from the walls along the width of the stills. Under the prevailing meteorological conditions, the optimum value of R (when Q<1.0 %) was approximately 2.0 for the DSS (in both the east-west and north-south orientations) and SSS, which is in close conformity with findings of El-Swify et al. [14]. This observation is probably because of the influence of site parameters. The the latitude of Guantanamo (19^{o} 54′ N) is closer to that of Cairo (30^{o} 3′ N). It should be mentioned that the zenith angle (θ) is low around solar noon during most of the days at low latitude, with θ=0 at solar noon during some days of the year. Low values of θ would tend to reduce the effect of shading and optimal values of R. In contrast, θ is relatively high around solar noon during most of the days at high latitude, with θ>0 at solar noon throughout the year. High values of θ would tend to increase the effect of shading and optimal values of R. These findings show that site parameters influence the optimum value of R.

4. Concluding remarks

The effect of aspect ratio (R) on solar collection in a double-slope solar still (DSS) has been simulated by using ESP-r software. Optical performances of the DSS and single-slope solar still (SSS) were compared under the same meteorological conditions. The DSS was studied with its transparent covers facing the east-west and north-south directions while the SSS faced south. Meteorological data captured at the University of Strathclyde (high latitude) and Guantanamo Bay (low latitude) was employed in this analysis. Simulation results show that the optical performance of a DSS (in both orientations) was lower than that of a SSS at these sites. The DSS collected more solar energy in the east-west than north-south orientation, for a given value of R. In addition, effective insolation increased with R but the increase was insignificant for values of R>3.0 for both the DSS and SSS at a high latitude. Similarly, effective insolation increased with R but the increase was insignificant for values of R>2.0 for both the DSS and SSS at a low latitude. It is therefore concluded that a) R significantly affects the collection of solar energy by a DSS, b) the approximate optimum value of R is sensitive to site parameters, c) the orientation of the DSS does not affect the optimum value of R, and d) the optimum value of R is approximately the same for the DSS and SSS at a given site.

Acknowledgements

Authors are grateful to Newton International Fellowships Scheme for the financial support.

References

[1] G.N. Tiwari, H.N. Singh, R. Tripathi, Present status of solar distillation, Solar Energy 75, 2003, pp.367-373.

[2] WHO, World Health Statistics 2008, World Health Organization, 2008.

[3] H.P. Garg, H.S. Mann, Effect of climatic, operational and design parameters on the year round performance of single-sloped and double-sloped solar still, under Indian arid zone conditions. Solar Energy 18, 1976, pp.159-164.

[4] A.S. Nafey, M. Abdelkader, A. Abdelmotalip, A.A. Mabrouk, Parameters affecting solar still productivity. Energy Conversion and Management 41, 2000, pp.1797-1809.

[5] K. Mukherjee, G.N. Tiwari, Economic analysis of various designs of. conventional solar stills. Energy Conversion and Management 26, 1986, pp.155-157.

[6] B.W. Tleimat, E.D. Howe. Comparison of plastic and glass condensing covers for solar stills. Solar Energy 12, 1969, pp.293-304.

[7] H.M. Qiblawey, M. Banat, Solar thermal desalination technologies. Desalination 220, 2008, pp.633-644.

[8] R. Tripathi, G.N. Tiwari, Performance evaluation of solar still by using the concept of solar fraction. Desalination 169, pp.2004, 69-80.

[9] P.I. Cooper, W.R.W. Read, Design philosophy and operating experience for Australian stills. Solar Energy 16, 1974, pp.1-8.

[10] P.I. Cooper, The absorption of radiation in solar stills, Solar Energy 12, 1969, pp.333-346.

[11] M.A. Samee, U.K. Mirza, T. Majeed, N. Ahmad. Design and performance of a simple solar still. Renewable and Sustainable Energy Reviews 11, 2007, pp.543-549.

[12] A.K. Singh, G.N. Tiwari, P.B. Sharma, E. Khan, Optimization of orientation for higher yield solar still for a given location, Energy Conversion and Management 36, 1995, pp.175-187.

[13] V.K. Dwivedi , G.N. Tiwari, Experimental validation of thermal model of a double slope active solar still under natural circulation mode, Desalination 250, 2010, pp.49-55

[14] M.E. El-Swify, M.Z. Metias, Performance of double exposure still, Renewable Energy 26, 2002, pp.531-547.

[15] J.A. Clarke, Energy simulation in building design, Butterworth-Heinemann, 2nd edition, 2001, pp.212-255.

[16] R. Perez, P. Ineichen, R. Seals, J. Michalsky, R. Stewart, Modelling daylight availability and irradiance components from direct and global irradiance, Solar Energy 44, 1990, pp.271-289.

Concentrating solar power plants for electricity and desalinated water production

Soteris A. Kalogirou[1,*]

[1] *Department of Mechanical Engineering and Materials Science and Engineering, Cyprus University of Technology, P. O. Box 50329, 3603 Limassol, Cyprus*
** Corresponding author. Tel: +357 2500 2621, Fax: +357 2500 2637, E-mail:Soteris.kalogirou@cut.ac.cy*

Abstract: Electricity and water are two commodities which are usually both required in arid countries having a high solar insolation. A number of technologies exists for both systems, which are briefly reviewed in this paper. Among the most matured and suitable concentrated solar power (CSP) plants for electricity generation are the solar tower (ST) and the parabolic trough collector (PTC) systems, whereas for desalination these are the multiple effects distillation (MED) type evaporator and the reverse osmosis (RO). The paper shows also the possibilities that exist and the ways that these technologies can be combined in order to produce simultaneously electricity and water. The equipment required to be used for these systems (steam cycle components, MED or RO) is usually very expensive therefore, the system is required to operate continuously without complete shut down during the night. Such a system would be very suitable for arid countries, which due to the water shortage problem they face, locate power plants in coastal areas in order to use the seawater for the cooling needs of the steam cycle system (condenser). Therefore, in this case it would be comparatively easy to combine the power system with desalination as the resource for such a system, i.e., seawater would be readily available.

Keywords: *Parabolic trough collectors, power tower, multiple effect boiling, reverse osmosis, desalination*

1. Introduction

Cyprus does not have at the moment any sources of energy and depends exclusively on imported oil for its energy needs. The only inexhaustible natural source of energy that Cyprus posses abundantly, is solar energy. It is well known that other forms of renewable energy, like the wind energy, wave energy and biomass have limited potential in Cyprus. Cyprus Government decided to erect a solar thermoelectric power generation station with a capacity of about 50 MW. The characteristics that need to be considered when selecting the right type of thermoelectric system are the cost of electricity produced and the land area that would be required to install the solar plant. The latter is very important as Cyprus has no desert land near the sea but on the contrary seaside areas are very expensive as they are used for touristic development. It should be noted that all existing power stations are located near the sea so the solar power station should also be located near to one of those stations to ease access to the grid and for the use of the seawater for the condenser.

2. Concentrating solar power

Concentrating solar power plants, use mirrors to generate high temperature heat that drives steam turbines traditionally powered from conventional fossil fuels. Some of these systems incorporate also heat storage which allows them to operate during cloudy weather and night-time. The main systems that are operational today in various countries are the parabolic trough collector (PTC) system and the central receiver or power tower system. More details about these systems can be found in [1].

2.1. Parabolic trough collector system

From the technologies available the most industrially matured is the parabolic trough system. This is mainly due to the nine large systems installed and operating in California, USA since 1985, which have a total installed capacity equal to 354 MWe. Mainly due to the plants

operating in California for more than 20 years, parabolic trough is the most proven technology and today they produce electricity at about US$ 0.10/kWh. The success and durability of these plants has demonstrated the robustness and reliability of the parabolic trough technology. Compared to other technologies, this system has a high solar-to-electrical efficiency and low area per MWh requirement.

Parabolic trough collectors are the most mature solar technology to generate heat at temperatures up to 400°C for solar thermal electricity generation or process heat applications. Parabolic trough technology proved to be tough, dependable and proven. Today the second-generation parabolic troughs have more precise mirror curvature and alignment, which enables them to have higher efficiency than the first plants erected in California. Other improvements include the use of a small mirror on the backside of the receiver to capture and reflect any scattered sun rays back onto the receiver, the direct steam generation into the receiver tube to simplify the energy conversion and reduce heat losses, and the use of more advanced materials for the reflectors and selective coatings of the receiver.

2.2. Power tower systems

Power towers or central receiver systems use thousands of individual sun-tracking mirrors called "heliostats" to reflect solar energy onto a receiver located on top of a tall tower. The receiver collects the sun's heat in a heat-transfer fluid (molten salt) that flows through the receiver. This is then passed optionally to storage and finally to a power-conversion system which converts the thermal energy into electricity and supply it to the grid. In many solar power studies it has been observed that the collector represents the largest cost in the system, therefore, an efficient engine is justified to obtain maximum useful conversion of the collected energy. The power tower plants are quite large, generally 10 MWe or more, while the optimum sizes lie between 50-400 MW. It is estimated that power towers could generate electricity at around US$ 0.04/kWh by 2020 [2].

The heliostats should reflect solar radiation to the receiver at the desired flux density at minimum cost. A variety of receiver shapes has been considered, including cylindrical receivers and cavity receivers. The optimum shape of the receiver is a function of radiation intercepted and absorbed, thermal losses, cost and design of the heliostat field. For a large heliostat field a cylindrical receiver is best suited to be used with Rankine cycle engines. Another possibility is to use Brayton cycle turbines which require higher temperatures (of about 1000°C) for their operation and in this case cavity receivers with larger tower height to heliostat field area ratios are more suitable. For gas turbine operation, the air to be heated must pass through a pressurized receiver with a solar window. Combined cycle power plants using this method could require 30% less collector area than the equivalent steam cycles. Rankine cycle engines driven from steam generated in the receiver operate at 500 to 550°C.

2.3. Heat storage and hybridization

An interesting feature of parabolic troughs and power tower systems is that it is possible to store heat, which enables them to continue producing electricity during the night or cloudy days. For this purpose, concrete, molten salts, ceramics or phase-change media can be used. The parabolic trough and the power tower systems produce superheated steam which is used to drive the turbines of a conventional Rankine type power station or an Integrated Solar Combined Cycle System, i.e., they replace the conventional steam boiler with the solar collection system. It has been proved in a previous publication that a system with four hours of storage is the optimum for Cyprus [3]. Both systems can also be operated with fossil fuel (usually natural gas) so as to continue the production of electricity at low irradiation hours and

during the night. This is due to the fact that the equipment involved is expensive and it is not viable to leave the systems to cool down and stay idle for a long time.

All existing power stations in Cyprus are located near the sea. Such a solar power system should also be located near the sea close to an existing power station to ease access to the grid and for the use of the seawater for the condenser. The erection of such a system inland is not possible due to the lack of water required for the condensation of the steam. This is because Cyprus suffers from a water shortage problem, so it has no adequate water supply inland and the proximity of the solar to an existing station means it will also be close to existing power lines and maintenance personnel form the station. Moreover, the location of the solar plant near the sea will enable it to be combined with solar desalination, for the production of fresh water which is also a required commodity for the island.

3. Desalination processes

Desalination can be achieved by using a number of techniques. Industrial desalination technologies use either phase change or thermal processes, or involve semipermeable membranes or single-phase processes to separate the salts from the seawater. All processes require a chemical pre-treatment of raw seawater to avoid scaling, foaming, corrosion, biological growth, and fouling and also require a chemical post-treatment. Here only two desalination methods are considered the multiple effect boiling system, falling in the first category, and the reverse osmosis system, falling in the second. These are the most suitable for the application considered as will be presented in the following sections.

3.1. The MED process

The multiple effect distillation (MED) process is composed of a number of elements, which are called effects. The steam from one effect is used as heating fluid in another effect, which while condensing, causes evaporation of a part of the salty solution. The produced steam goes through the following effect, where, while condensing, makes some of the other solution evaporate and so on. For this procedure to be possible, the heated effect must be kept at a pressure lower than that of the effect from which the heating steam originates. The solutions condensed by all effects are used to preheat the feed [4]. In this process, vapour is produced by flashing and by boiling, but the majority of the distillate is produced by boiling. The MED process usually operates as a once through system without a large mass of brine recirculating around the plant. This design reduces both pumping requirements and scaling tendencies [5].

Early plants were of the submerged tube design and used only two to three effects. In modern systems, the problem of low evaporation rate has been resolved by making use of the thin film designs with the feed liquid distributed on the heating surface in the form of a thin film instead of a deep pool of water. Such plants may have vertical or horizontal tubes.

Another type of MED evaporator is the Multiple Effect Stack (MES) type. This is the most appropriate type for solar energy application. It has a number of advantages, the most important of which are its stable operation between virtually zero and 100% output even when sudden changes are made and its ability to follow a varying steam supply without upset [4]. In Fig. 1, a four-effect MES evaporator is shown. Seawater is sprayed into the top of the evaporator and descends as a thin film over the horizontally arranged tube bundle in each effect. In the top (hottest) effect, steam from a steam boiler or from a solar collector system condenses inside the tubes. Because of the low pressure created in the plant by the vent-ejector system, the thin seawater film boils simultaneously on the outside of the tubes, thus creating new vapour at a lower temperature than the condensing steam.

The seawater falling to the floor of the first effect is cooled by flashing through nozzles into the second effect, which is at a lower pressure. The vapour made in the first effect is ducted into the inside of the tubes in the second effect, where it condenses to form part of the product. Furthermore, the condensing warm vapour causes the external cooler seawater film to boil at the reduced pressure. The evaporation-condensation process is repeated from effect to effect in the plant, creating an almost equal amount of product inside the tubes of each effect. The vapour made in the last effect is condensed on the outside of a tube bundle cooled by raw seawater. Most of the warmer seawater is then returned to the sea, but a small part is used as feedwater to the plant. After being treated with acid to destroy scale-forming compounds, the feedwater passes up the stack through a series of pre-heaters that use a little of the vapour from each effect to raise its temperature gradually, before it is sprayed into the top of the plant. The water produced from each effect is flashed in a cascade down the plant so that it can be withdrawn in a cool condition at the bottom of the stack. The concentrated brine is also withdrawn at the bottom of the stack.

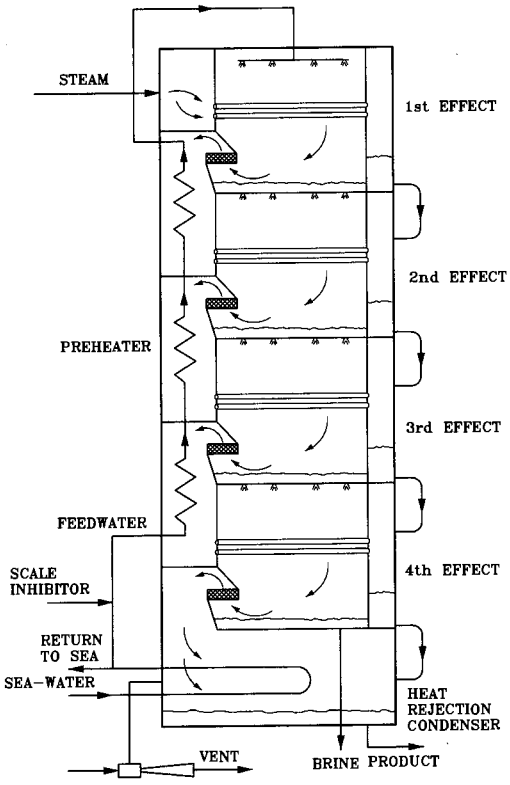

Fig. 1. Schematic of the MES evaporator.

The MES process is completely stable in operation and automatically adjusts to changing steam conditions even if they are suddenly applied, so it is suitable for load-following applications. It is a once-through process that minimises the risk of scale formation without incurring a large chemical scale dosing cost. The typical product purity is less than 5 ppm total dissolved solids (TDS) and does not deteriorate as the plant ages. Therefore, the MED process with the MES type evaporator appears to be the most suitable for use with solar energy.

3.2. The reverse osmosis process

The reverse osmosis (RO) system depends on the properties of semi-permeable membranes which, when used to separate water from a salt solution, allow fresh water to pass into the brine compartment under the influence of osmotic pressure. If a pressure in excess of this value is

applied to the salty solution, fresh water will pass from the brine into the water compartment. Theoretically, the only energy requirement is to pump the feed water at a pressure above the osmotic pressure. In practice, higher pressures must be used, typically 50-80 atm, in order to have a sufficient amount of water pass through a unit area of membrane [4]. With reference to Fig. 2, the feed is pressurised by a high-pressure pump and made to flow across the membrane surface. Part of this feed passes through the membrane where the majority of the dissolved solids are removed. The remainder, together with the remaining salts, is rejected at high pressure. In larger plants, it is economically viable to recover the rejected brine energy with a suitable brine turbine. Such systems are called energy recovery reverse osmosis (ER-RO) systems.

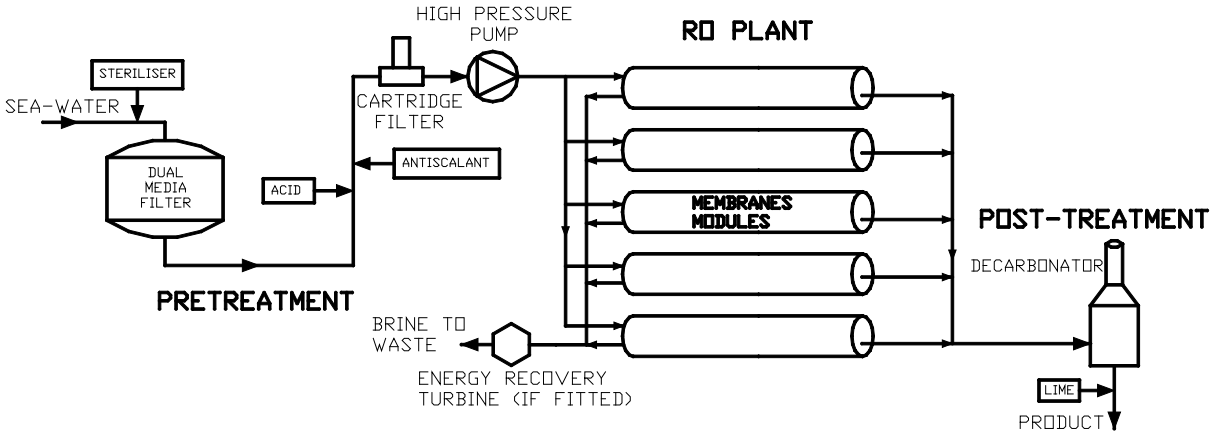

Fig. 2. Principle of operation of a reverse osmosis (RO) system.

Solar energy can be used with RO systems as a prime mover source driving the pumps or with the direct production of electricity through the use of photovoltaic panels. As the unit cost of the electricity produced from photovoltaic cells is high, photovoltaic-powered RO plants are not considered here. The membranes are in effect very fine filters, and are very sensitive to both biological and non-biological fouling. To avoid fouling, careful pre-treatment of the feed is necessary before it is allowed to come in contact with the membrane surface.

3.3. Characteristics of both processes

The identification and evaluation of the renewable energy resources (RES) in an area, is the primary step to be performed when designing a RES-driven desalination system. Such systems should be characterized by robustness, simplicity of operation, low maintenance, compact size, easy transportation to site, and simple pre-treatment and intake system [6].

The energy required for the two desalination processes considered, as obtained from a survey of manufacturers' data, is shown in Table 1 [4]. It can be seen from Table 1 that the process with the smallest energy requirement is RO-ER followed by RO and the MED.

Table 1. Energy consumption of desalination systems.

Process	Heat input (kJ/kg of product)	Mechanical power input (kWh/m^3 of product)	Prime energy consumption (kJ/kg of product)[1]
MED	123	2.2	149.4
RO	-	5-13 (10)	120
ER-RO	-	4-6 (5)	60

Notes: 1. Assumed conversion efficiency of electricity generation of 30%
2. Figure used for the prime energy consumption estimation shown in last column

A comparison of the desalination equipment cost and the seawater treatment requirement, as obtained from a survey of manufacturers' data, is shown in Table 2. The MED is the cheapest of all the indirect collection systems and also requires the simplest seawater treatment. RO although requiring a smaller amount of energy is expensive and requires a complex seawater treatment.

Table 2. Comparison of desalination plants.

ITEM	MED	RO
Scale of application	Small-medium	Small-large
Seawater treatment	Scale Inhibitor	Sterilizer, Coagulant Acid, Deoxidiser
Equipment price (Euro/m^3)	900-1700	900-2500 Membrane replacement every 5-6 yrs
Note: Low figures in equipment price refer to bigger size in range indicated and vice versa.		

4. Options considered

In this section, various options are considered to combine CSP with desalination. The first option considered is a thermal desalination system shown schematically in Fig. 3. In this option a solar field is used which provides thermal energy to a MED evaporator to produce fresh water. This solar heat can be given directly to the MED unit or in days with good irradiation the excess energy can be stored for use in periods of low sunshine and during the night. The system can also be hybridized using conventional fuel to run the desalination sub-system during the night. A very small quantity of electrical energy (compared to thermal) is required by the MED unit to drive the pumps. As the present RES system is thermal only, this quantity of electricity can be produced either from a PV system or obtained from the grid.

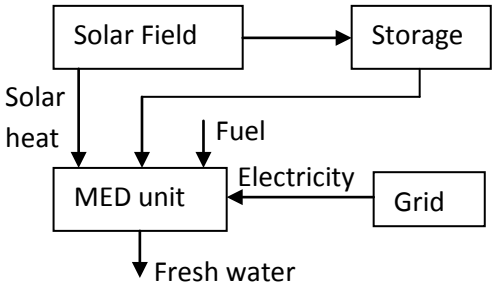

Fig. 3. Combination of a solar thermal system with MED for desalinated water production only.

The second option, shown in Fig. 4, concerns a solar thermoelectric system producing electricity with a CSP system. In this case some of the electricity produced can be used to drive a RO desalination system and the rest is supplied to the grid. This system has the advantage that the operators can decide according to the demand to produced either both, fresh water and electricity, or one of the two only. Any form of hybridization can go directly to the power plant as is normal to all such systems, when the storage is depleted a few hours after sunset, according to the size of the storage used.

The third option, shown in Fig. 5, is a combination of a normal solar thermoelectric power system with a MED unit to produce both electricity and fresh water. The MED requires thermal energy to operate in the form of high temperature hot water (>100°C) or low temperature steam. Therefore, this energy can be supplied either directly from the CSP system or from the waste heat of the power plant system, in the form of condensation heat. For this purpose the MED evaporator can be an integral part of the steam condenser of the Rankine

power plant cycle. In this option the hybridization is done directly on the power plant as is normal to all CSP power systems. The small quantity of electricity required by the MED is taken from the power plant.

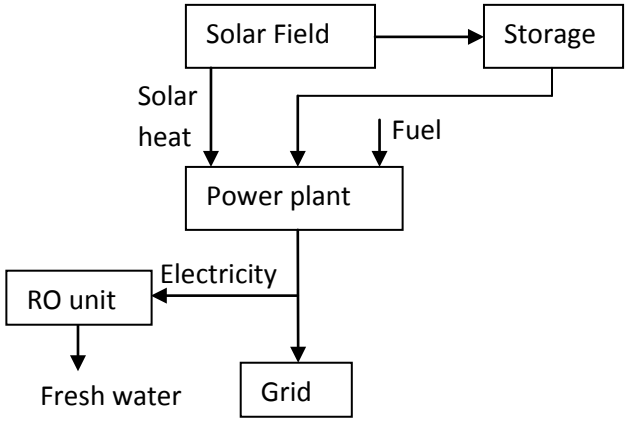

Fig. 4. Combination of a solar thermoelectric power system with RO to produce both electricity and fresh water.

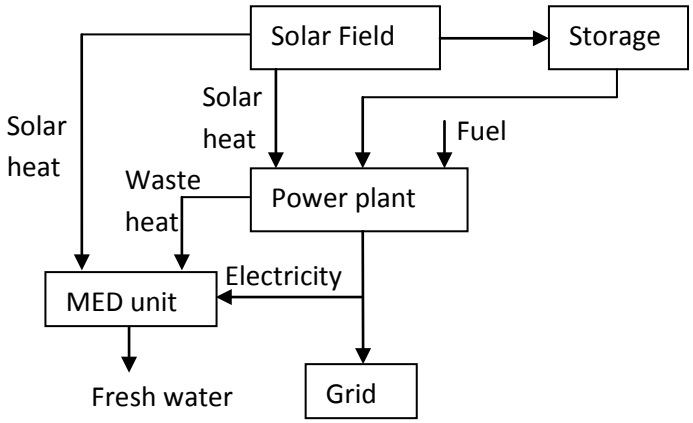

Fig. 5. Combination of a solar thermoelectric power system with MED, operated from solar and waste heat, to produce both electricity and fresh water.

The fourth option, shown in Fig. 6, is a combination of a solar thermoelectric power system with MED and RO systems for fresh water production. The RO unit operates as in the second option with the electricity produced by the CSP system, whereas the MED subsystem, which requires thermal energy to operate, can use either some of the thermal energy produced by the CSP system or the waste heat from the power plant, therefore the MED is part of the condensation system of the power plant. Again here the hybridization is done directly on the power plant as is normal to all CSP power systems. This option gives a larger number of operation options concerning the production of electricity and water according to the demand of each commodity however, it is a more expensive system as both MED and RO need to be purchased and installed.

All CSP systems shown in the above figures can use either a parabolic trough collector or a power tower system. As can be seen from the configurations presented above, there are a number of options to be considered when either only desalinated water or both electricity and fresh water are required. The choice of which system to apply for a particular case should depend on the particular requirements of each commodity and the characteristics of the load and water demand. Due to the high cost of the required equipment however, all systems needs

to be hybridized so as to operate the plants round the clock to reduce the idle time, the energy required to bring the systems to their operating limit and the problems associated with the frequent starts and stops of the equipment and thermal cycling. Before considering any hybridization though, the optimum size of storage needs to be used to minimize the adverse effects of the burning of fossil fuels on the environment. For this purpose a less polluting fuel needs to be employed, like the natural gas.

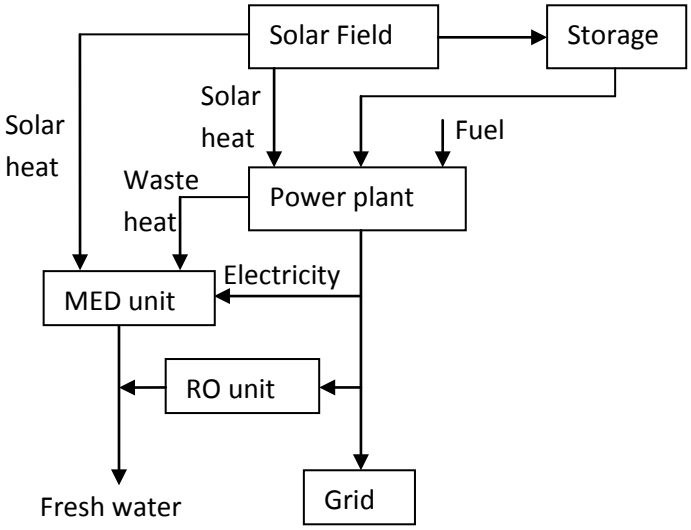

Fig. 6 Combination of a solar thermoelectric power system with RO and MED to produce both electricity and fresh water.

5. Conclusions

The parabolic trough and the power tower systems produce superheated steam which can be used to drive the turbines of the common Rankine cycle. Both systems can be supplied with conventional fuel (usually natural gas) so as to operate during hours of low irradiation and during night-time. For the reasons explained above such a solar plant need to be located near the sea. In such a case the solar plant can be combined with solar desalination to produce fresh water from seawater which is also a precious commodity for Cyprus. As shown in this paper a number of options exist for the combination of a CSP system with a desalination one to produce both electricity and water.

References

[1] S.A. Kalogirou, *Solar Energy Engineering: Processes and Systems*, Academic Press, New York, 2009, pp. 521-552.

[2] S. Taggart, Hot stuff: CSP and the power tower, *Renewable Energy Focus,* May/June issue, 2008, pp. 51-54.

[3] S.A. Kalogirou, Solar Thermoelectric Power Generation in Cyprus, Selection of the Best System, *Proceedings of the World Renewable Energy Congress XI on CD ROM,* Abu Dhabi, UAE, 2010.

[4] S.A. Kalogirou, Seawater Desalination Using Renewable Energy Sources, *Progress in Energy and Combustion Science,* 2005, Vol. 31, No. 3, pp. 242-281.

[5] S.A. Kalogirou, Survey of solar desalination systems and system selection, *Energy-The International Journal,* 1997, Vol. 22, No. 1, pp. 69-81.

[6] E. Tzen, R. Morris, Renewable Energy sources for desalination, *Solar Energy,*2003 Vol. 75, No. 5, pp. 375-379.

Analysis of solar lithium bromide-water absorption cooling system with heat pipe solar collector

Amir Falahatkar[1,*], M. Khalaji Assadi[1]

[1]*Department of Energy Engineering, Science & Research Branch, Islamic Azad University, Tehran, Iran*
**Corresponding Author. Tel: +98 912 2506923, Email: eng.falahatkar@srbiau.ac.ir*

Abstract: Solar energy applications in Iran for supplying domestic hot water, space heating and cooling have been considered severely in last decade. The purpose of this research is to analysis of solar single effect lithium bromide-water absorption cooling system in a typical office building in Tehran. The solar energy is absorbed by heat pipes and stored in an insulated storage tank. This system has been designed to supply the cooling load of mentioned typical office building where the cooling load is 35.17KW (10 tons of refrigerant) which events in July. Results demonstrate that depending on the Tehran climate and the specification of the building by means of optimized design of solar heat pipe collectors, up to 2400 m^3/year Natural Gas energy saving can be reached by use of solar absorption cooling system. Achieving this purpose requires utilizing 16 collectors which everyone compromises 30 tubes with total absorber area of 45 m^2 which is the optimum collector area for this plant in Tehran. According to this replacement the investment payback rate would be 13 years which would be much shorter than the payback time of a solar cooling system combined with conventional all air systems.

Keywords: *Absorption cooling, Heat pipe collector, Solar energy*

Nomenclature

$\dot{m}$	mass flow rate	$kg.s^{-1}$	
Q	thermal capacity	w	
c_p	specific heat	$j.kg^{-1}.c^{-1}$	
ΔT	temperature difference	$°c$	
q_u	useful energy	$j.m^{-2}$	
η	thermal efficiency	%	
$\overline{H}.$	monthly average daily total solar radiation on a horizontal surface	$j.m^{-2}$	
ϕ		degree	
β	slope	degree	
ρ_g	diffuse reflectance of the ground	degree	
δ	deviation angle	degree	
C	capital cost	$	
E	energy saving	$.year^{-1}$	
PB	payback time	year	
i	energy inflation	%	
ω_s	sunset hour angle	degree	

1. Introduction

The energy demand for refrigeration and air-conditioning appliances has been increased continuously in last decades. World energy demand-and CO_2 emissions- is expected to rise by some 60% by 2030 respect to the beginning of this century [1]. The cooling load in summer is associated with high solar energy, which offers a suitable opportunity to utilize solar energy for cooling. Conventional vapor compression chillers require high quality energy, electricity which is produced from initial energy resources. Furthermore, vapor compression cooling systems use chlorofluorocarbons (CFCs) and hydrochlorofluorocarbons (HCFCs) as working fluids. These materials will lead to global warming and ozone depletion. Thermal-driven air-conditioning systems are using heat as motive energy to provide cold energy. These systems can be categorized on absorption systems, adsorption systems, duplex rankine, desiccant cooling and ejector refrigeration systems. The heat could be obtained from waste heat sources, combined heat and power technologies (CHP), and solar energy. Lithium Bromide (LiBr)-water absorption cooling systems are conventional in thermal-driven air-conditioning systems and have too many benefits in comparison with other cooling

systems; because their performance is good and cost is low. The single effect LiBr-water absorption systems operate at a generator temperature range 70 to $95\,°c$ and the coefficient of performance (COP) of these systems are between 0.6 to 0.8, which are higher than NH3-H_2O absorption cooling systems [2].

Sparber et al [3] reported that till 2007 there were 81 installed large scale solar cooling systems, eventually including systems which are currently not in operation. 73 installations are located in Europe, 7 in Asia, China in particular, and 1 in America (Mexico). 60% of these installations are dedicated to office buildings, 10% to factories, 15% to laboratories and education centers, 6% to hotels and the left percentage to buildings with different final use (hospitals, canteen, sport center, etc). They also cited that 56 installations are belong to absorption systems and the overall cooling capacity of the thermally driven chillers amounts to 9 MW 31% of it is installed in Spain, 18% in Germany and 12 % in Greece.

Bong et al [4] designed and installed solar absorption chiller in Singapore. The system included 7KW absorption chiller, heat pipe collectors with a total area of 32 m^2, a hot water storage tank, an auxiliary heater and a 17.5 KW cooling tower. They cited that the overall average cooling capacity provided was 4KW, solar fraction of 39% and COP of 0.58.

Balghouthi et al [5] accomplished a simulation using TRNSYS program in order to select and size different components of solar absorption chiller. They reported that solar absorption cooling systems were suitable for Tunisian's condition.

Alizadeh et al [6] simulated and optimized a solar LiBr-water absorption cooling system that has been design for Malaysia using evacuated tube solar collectors. The modeling of the solar absorption chiller was accomplished with TRNSYS program.

Yeung et al [7] designed and installed a solar driven absorption chiller at the University of Hong Kong. This system included 4.7KW absorption chiller, flat plate collectors with a total area of 38.2m^2 , a cooling tower, a 2.75m^3 hot water storage tank and the other equipments. They reported that the collector efficiency was estimated at 37.5%, the annual system efficiency at 7.8% and an average solar fraction at 55%, respectively.

The objective of this work is to evaluate and investigate the energy conservation capacity of a sample office building in Tehran, using solar LiBr-water absorption chiller and heat pipe solar collector. Furthermore, the payback time for initial investments of the system has been calculated.

2. Methodology

A cooling system possessing solar-operated absorption chiller provides the cooling demands for the typical office building in Tehran-Iran. Tehran is located at $35.68\,°N$ and $51.32\,°E$. Figure 1 demonstrates both the variability of ambient temperature and relative humidity and in figure 2 the monthly solar radiation on horizontal surface is demonstrated. The office has a single storey and its floor area is 280m^2. The daily occupancy schedule is from 8:00 to 17:00, totally 9hours and the daily cooling system schedule is considered during June 1 to September 22. The daily average of global solar radiation of Tehran is about $23\,{Mj}/{m^2}$ for the summer months [8]. The major components of the plant are heat pipe solar collectors, a 35.17KW (10 RT) single effect LiBr-water absorption chiller, a hot water storage tank, a cooling tower, a control system and some other auxiliary equipments.

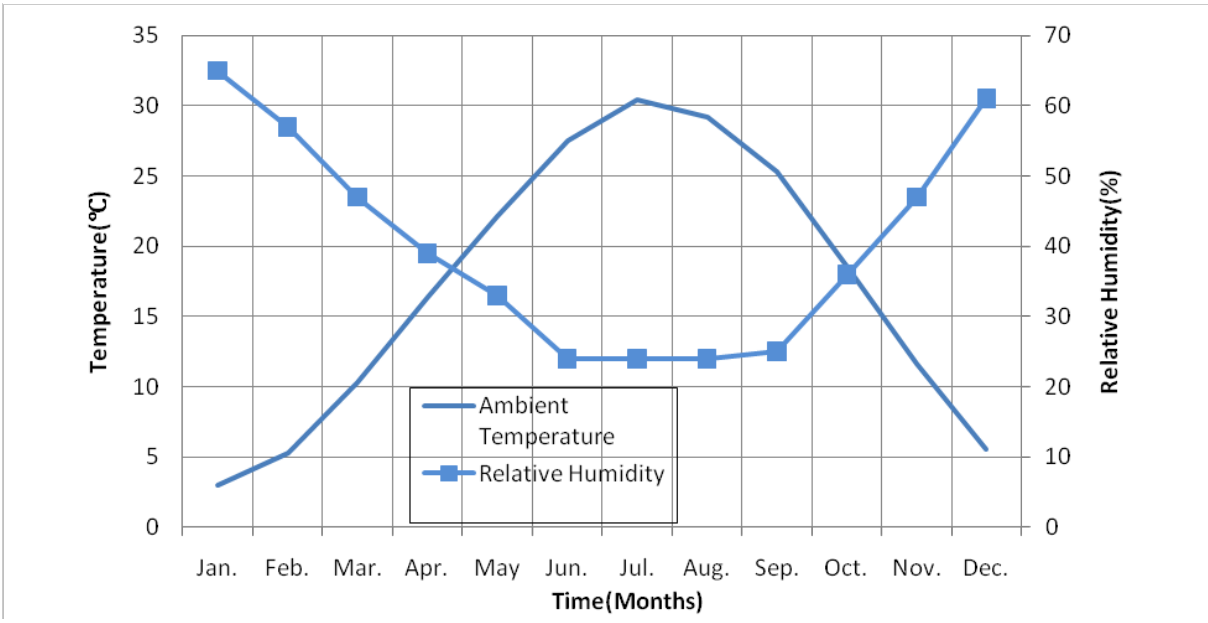

Fig. 1. Variability of ambient monthly temperature and monthly relative humidity for Tehran.

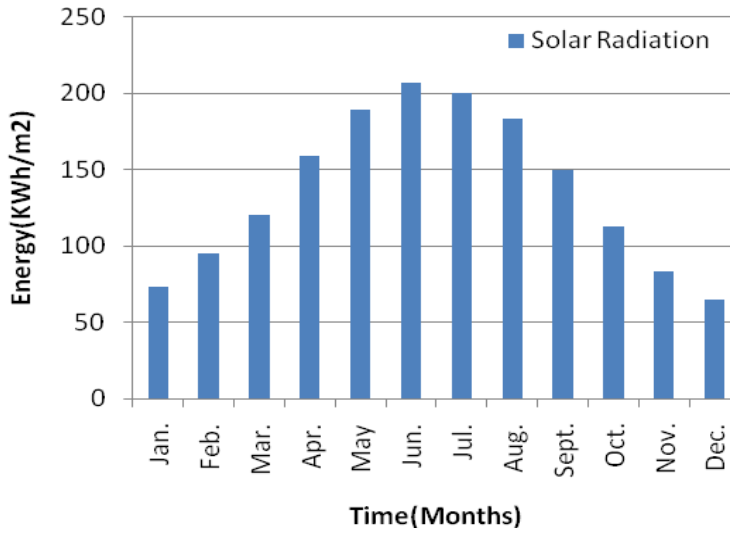

Fig. 2. Monthly solar radiation on horizontal surface in Tehran.

2.1. Solar Energy

The plant primary energy source is the solar energy, which is absorbed by heat pipe solar collector and stored in an insulated storage tank. Heat pipes are widely used for heat recovery and energy saving in various ranges of applications because of their simple structure, special flexibility, high efficiency, good compactness and excellent reversibility [9]. The heat pipe vacuum tube collects heat from the sun at high efficiency. It is important that heat pipe solar collectors must be installed with a tilt of at least $25°$. They operate like a thermal diode where the flow of heat is in one direction only [10]. This type of collector commonly filled with alcohol or water in a vacuum and operates in two versions, one with a dry and one with a wet connection [11]. The most important difference between evacuated tube solar collectors and heat pipe solar collectors is that the heat carrier fluid inside of the copper heat pipe is not connected to the solar loop. The heat pipe collectors are mounted on a roof and tilted by $25°$ with the roof to utilize more radiation in summer and it is produced by APRICUS.

2.2. Absorption chiller

A water fired chiller (WFC) with a related capacity of 35.17KW cooling (10RT) produced by YAZAKI when it is operating at a hot water driving temperature of $88°c$, coolant water temperature of $31°c$ and output chilled water at $7°c$. The coefficient of performance (COP) of this chiller is 0.7 as reported by the manufacture.

2.3. Presentation of parameters

The thermal capacity of the equipments is determined by Eq. (1):

$$Q = \overset{\circ}{m}.c_p.\Delta T\,, \tag{1}$$

Where $\overset{\circ}{m}$ is the mass flow rate, c_p is the specific heat at constant pressure and ΔT is the temperature difference.
The energy during a fixed period is determined by Eq. (2):

$$E = \int_{ti}^{to} Q dt\,, \tag{2}$$

Where t_i is initial time and t_o is final time. Afterwards, the efficiency of solar collectors is obtained by Eq. (3) [2]:

$$\eta = \frac{q_u}{\overline{R}.\overline{H}}\,, \tag{3}$$

Where q_u is the useful energy output of a collector per square meter, $\overline{H}$ is monthly average daily total solar radiation on a horizontal surface. It should be noted that the efficiency of solar heat pipe collector is about 63% as reported by the manufacture. $\overline{R}$ is the proportion of monthly average total radiation on tilted surface on the monthly average total radiation on horizontal surface which is determined by Eq. (4) [2]:

$$\overline{R} = \left(1 - \frac{\overline{H_d}}{\overline{H}}\right)\overline{R_b} + \frac{\overline{H_d}}{\overline{H}}\left(\frac{1+\cos\beta}{2}\right) + \rho_g\left(\frac{1-\cos\beta}{2}\right), \tag{4}$$

Where $\overline{H_b}$ is monthly average daily beam solar radiation on a horizontal surface, $\overline{H_d}$ is monthly average daily diffuse solar radiation on a horizontal surface, ρ_g is the diffuse reflectance of the ground and β is the slope of the collector, $\overline{R_b}$ is the ratio of the average daily beam radiation on the tilted surface on that on a horizontal surface which is determined by Eq. (5) [2]:

$$\overline{R_b} = \frac{\cos(\phi-\beta)\cos\delta\sin\omega_s' + \left(\frac{\pi}{180}\right)\omega_s'\sin(\phi-\beta)\sin\delta}{\cos\phi\cos\delta\sin\omega_s + \left(\frac{\pi}{180}\right)\omega_s\sin\phi\sin\delta} \quad (5)$$

Where ω_s' is the sunset hour angle for the tilted surface for the mean day of the month and ω_s is the sunset hour angle, which are obtained by Eq. (6) and Eq. (7) [2]:

$$\omega_s' = Min\begin{bmatrix}\cos^{-1}(-\tan\phi\tan\delta)\\ \cos^{-1}(-\tan(\phi-\beta)\tan\delta)\end{bmatrix} \quad (6)$$

Where φ is the latitude and δ is the solar deviation angle.

$$\omega_s = \cos^{-1}(-\tan\varphi\tan\delta) \quad (7)$$

3. Results

3.1. Determining the optimum solar collector area

With calculating $\overline{R}$ through equations 4 to 7, the useful energy output of a collector is determined. Figure 4 demonstrates the monthly energy derived from one square meter of collector in Tehran. The surface area for the heat pipe collector is determined by the proportion of the required energy for cooling the environment on the useful energy output of the collector.

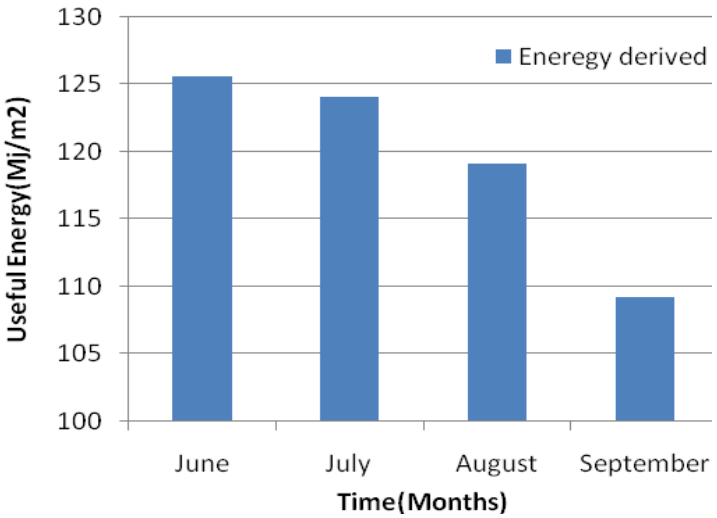

Fig. 3. Monthly energy derived from one square meter of collector in Tehran from June to September

Optimized solar collector area depends on some important factors such as: Solar radiation, intensity, cost increasing and amount of consumption [12]. To estimate the optimal surface of heat pipe solar collector, we should determine the solar cooling fraction (SCF). The solar cooling fraction is described as the ratio of solar heat yield to the total energy required to drive solar absorption chiller.

Finally, the optimum surface of heat pipe collectors for typical office building in Tehran is determined in each situation as presented as figure.4.

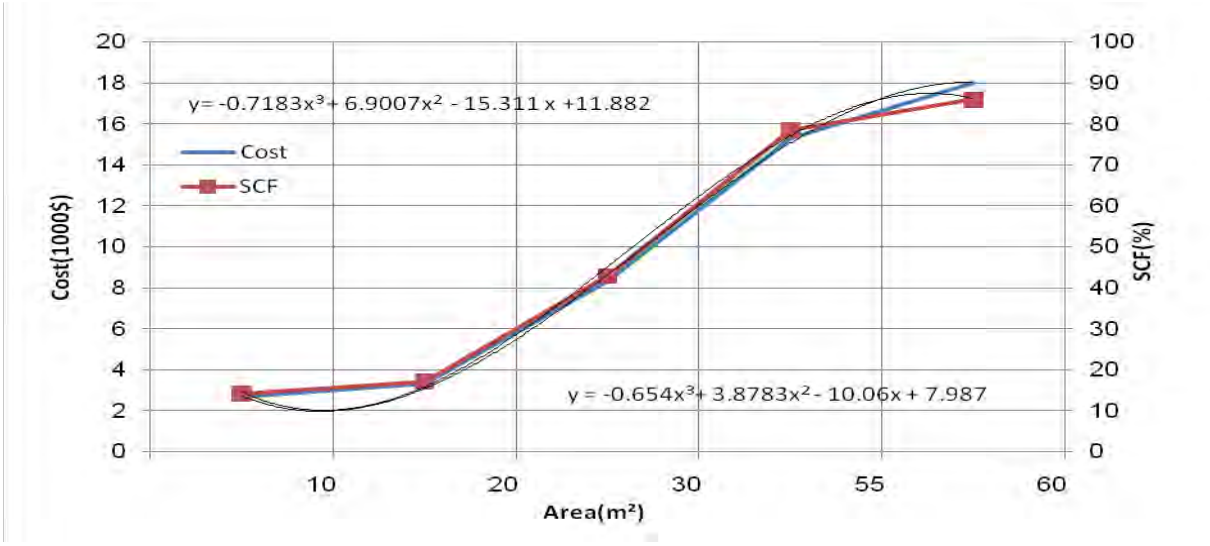

Fig. 4. Estimation of optimum solar heat pipe collectors for typical office building in Tehran

3.2. Economic analysis

Solar systems are commonly known by high investment and low operating cost. In order to estimate the payback time, total annual energy saving must be determined.
The payback time is determined by Eq. (8) [13]:

$$PB = \frac{\log\left[\frac{C}{E}.\frac{i}{100}+1\right]}{\log\left[1+\frac{i}{100}\right]} \qquad (8)$$

Where C is the capital cost of installed solar cooling equipment, E is the energy saving, i is the energy inflation and PB is the payback time.

The cost of equipments are summurized in table 1 and the cost of energy is shown in table 2.

Table 1. Cost of equipments

Equipment	Cost
LiBr-H_2O Absorption chiller	500 \$/KW
Heat pipe solar collector	278 \$/m^2absorber area
Auxiliary heater	50 \$/KW
Storage tank	790 \$/m^3
Cooling tower	65 \$/KW

Table 2. Cost of Energy

Energy	Cost
Electricity	0.330 \$/KWh
Oil	1.580 \$/t
Natural Gas	0.40 \$/m^3(2010)

Furthermore, during the economic analysis some basic assumptions are needed, such as maintenance costs, installation costs, the energy inflation and natural gas heating value. The maintenance costs are 1% of investments cost [13], installation costs are 12% of the equipment costs [14], the energy inflation is about 2% [5] and natural gas heating value is about 38376 Kj/m^3.

Consequently, the total energy and money saving are shown in table 3.

Table 3. total energy and money saving

Annual energy saving (MWh)	Annual money saving ($)	Annual natural gas saving (m^3)
25.5	960	2400

Thus, with calculating PB through equation 8, the payback time is estimated approximately 13 years which would be reasonable for solar cooling systems.

4. Conclusions

In this investigation the technical and economical analysis for single effect LiBr-water solar absorption system was done. The analysis was accomplished for a typical office building in Tehran. The plant provided air conditioning for a floor space of 280m^2. Furthermore, the plant included an auxiliary fossil system and its capacity was about 13KW. The most important advantage of this system is that it offers the highest environmental benefits. The other advantage is that we utilize the highest total energy saving.

It was shown that the solar cooling fraction for mentioned office building was 64.3% and the optimum solar heat pipe collector area was 45m^2. It means that this plant utilizes 16 collectors which everyone compromises 30 tubes. Finally, the payback time of this plant was estimated about 13 years.

.

References

[1] P. Bermejo, F. Javier Pino, F. Rosa, Solar absorption cooling plant in Seville, Solar Energy 84, 2010, pp. 1503-1512.

[2] JA. Duffie, WA. Beckman, Solar engineering of thermal processes, Wiley, Third edition, 2006, pp. 579-587

[3] W. Sparber, A. Napolitano, P. Melograno, Overview on worldwide installed solar cooling systems, Proceedings of 2nd international conference on Solar air conditioning, 2007, Spain

[4] T.Y. Bong, K.C. NG, A.O. Tay, Performance study of a solar powered air conditioning system, Solar Energy 39, 1987, pp. 173-182.

[5] M. Balghouthi, M. Hachemi Chahbani, A. Guizani, Solar powered air conditioning as a solution to reduce environmental pollution in Tunisia, Desalination 185, 2005, 105-10.

[6] F. Assilzadeh, SA. Kalogirou, Y. Ali, K. Sopian, Simulation and optimization of a Libr solar absorption cooling system with evacuated tube collectors, Renewable Energy 30, 2005, pp. 1143-1159.

[7] M.R. Yeung, P.K. Yuen, A. Dunn, L.S. Cornish, Performance of a solar powered air conditioning system in Hong Kong, Solar Energy 48, 1992, pp. 309-319.

[8] B. Safaie, M. Khalaji Aassadi, H. Taghizadeh, A. Jilavi, G. Taleghani, M. Danesh, The evaluation of solar radiation potential in Iran, Proceeding of 19th international conference on Power System, 2004, Iran.

[9] R. Parand, B. Rashidian, A. Ataei, KH. Shakibi, Modeling the transient response of the thermosyphon heat pipes, Journal of Applied Sciences 9(8), 2009, pp. 1531-1537.

[10] J. Facao, A.C. Oliveira, Analysis of a plate heat pipe solar collector, International Journal of low carbon technologies.

[11] The German solar energy society, Planning and installing solar thermal systems, Earthscan, Second edition, 2010, pp. 30-33

[12] A. Ataei, M. Khalaji Assadi, R. Parand, N. Sharee, M. Raoufinia, A.H Kani, Solar combi-systems a new solution for space heating in buildings, Journal of Applied Sciences 9(8), 2009, pp.1458-1465.

[13] G. Zidianakis, Th. Tsoutsos, N. Zografakis, Simulation of a solar absorption cooling system, proceeding of 28th conference on building low energy cooling and advanced ventilation technologies in the 21st century, 2007, 1187-1194

[14] M. Peters, K. Timmerhaus, R. West, Plant design and economic for chemical engineers, McGraw-Hill, Forth edition, 1991.

Design analysis for expansion of Shiraz solar power plant to 500 kW power generation capacity

K. Azizian[1,*], M. Yaghoubi[1], R. Hesami[1], P. Kanan[2]

[1] *Mechanical Engineering School, Shiraz University, Shiraz, Iran*
[2] *SUNA, Iran Renewable Energy Organization, Tehran, Iran*
** Corresponding author. Tel: +989173029791 Fax: +987112301672, E-mail: kian_azizian@yahoo.com*

Abstract: Various projects have been developed to use solar energy and some of them are in the course of developing all around the world. In Iran a 250 kW pilot solar power plant is constructed using parabolic trough collectors from 2001 to 2006. Results of thermal tests of the plant leads to the generation of steam with 250 ^{o}C temperature and 2 MPa pressure. Based on several years of experiments (from 2006-2010) it is decided to expand the solar thermal power rate to produce 500 kW electricity by combining the present system with a larger size collector and an auxiliary boiler. This article, explains the thermal design of the new collector and then various design options for combination of the new collector to the present plant have been studied and the most practical method of producing 500 kW is selected applying first law of thermodynamics utilizing a hybrid system.

Keywords: *Solar power plant, Shiraz solar Thermal Power Plant (STPP), solar parabolic collector, plant expansion*

1. Introduction

One of the most important problems for industrial countries in the upcoming decades is the replacement of fossil fuel energy sources with renewable energy technologies. Environmental pollutions, increasing price rate of fossil fuels and their limited sources has led to the development of new design and concepts for their replacement with cheap and available environmental friendly energy sources. Among them solar energy is one of the most important and available source of renewable energy all around the world and especially in Iran. The use of solar energy is daily growing in different fields such as generation of electricity [1]. In Iran several projects are defined to use this source of energy along with other countries of the world [2]. Among them, Shiraz solar Thermal Power Plant (STPP) is the first parabolic trough solar power plant constructed and tested successfully at Fars province at south of Iran. After the basic design and simulations [3-4], construction, installation and start-up of this power plant has been done to produce superheated vapor. For this plant different studies and simulations are made to find the overall performance of the plant [5-11]. Table 1 shows general specifications of the 250 kW STPP(Refer to [12] for more information on existing system operation).

After the successful` testing of this parabolic solar power plant (from2006-2010), it is decided to promote the system with advanced technologies and use an advanced parabolic trough collector for steam generation. This is made by beginning the constructing and installing a new parabolic trough collector with larger dimension and combining it with the existing system while increasing the power rate to 500 kW. The existing 250 kW Shiraz solar power plant, having been successfully tested for steam generation, uses old design, small parabolic trough collectors. Achieving the technology of parabolic trough collectors in the 250 kW power plant the following decisions were made:

1- Design and construction of a new collector, in the same dimensions as used in the new solar power plants of the world (such as Andasol plants).
2-Electicity generation

Table 1. Specification of 250kW Shiraz solar thermal power plant

Capacity	250 kW	Electricity generation System	Turbine+ Generator
Collectors Type	Parabolic Trough	Collector's Field Inlet Oil Temperature	231°C
No. of Collectors	48	Collectors Field Outlet Oil Temperature	265°C
Collector's Dimension	25×3.4 m^2	Oil Mass Flow Rate	13.7 Kg/s
Collectors' Driven System	Hydraulic	Steam Mass Flow Rate	0.673 Kg/s
Collector's Structure	Truss with Torsion Bar	Generated Steam Temperature	250°C
Heat Transfer Fluid	Thermal Oil	Generated Steam Pressure	2 MPa

These steps would lead to an increase in power plant capacity from 250 kW to 500 kW and at the same time design and construction of a new collector in length of 94 m and aperture width of 5.27 m. The main problem in the way of developing the power plant (except for the cost increase due to low capacity of turbo-generator system and high price of electricity generated) id the method of combining the new collector with the existing system. Due to the high operating temperature of the new collector compared to the existing system, optimal usage of the absorbed heat is the most important issue in the process of combining the two system of heating the old cycle primary fluid (oil) or its secondary fluid (superheated steam) or a combination of the two above. In addition to the above mentioned issue, the next step would be the selection of the appropriate turbo-generator considering the efficiency and price at the same time. Some explanations in this regard will follow. The most important equipment in the existing plant include the parabolic trough collectors field, heat storage and expansion tanks, three heat exchangers, deairetor and etc. To achieve the 500 kW power generation the equipment that shall be added to the system would be the new 100m collector, turbo-generator, storage and expansion tanks, fossil fuel boiler and condenser. In the following sections further explanation and results of thermodynamic analysis of the new design system are presented.

2. Design of new parabolic trough collector

After preliminary assessments [12] it was decided to construct and install a new collector and increase the capacity of the plant from 250kW to 500 kW. Based on these available technologies the design of the new collector of Shiraz solar power plant is made by following steps:

1-Thermal and thermodynamic design of collector
2-Design of structure and hydraulic system
3-Design of control and tracking system

2.1. Thermal design of Shiraz thermal solar power plant (STPP) with new collector

For thermal design and simulation of the new collector a program has been developed with Matlab software [13]. This program takes some primary data into account such as collector rim angle, optical properties of the mirror like its thickness and reflectance coefficient, errors in construction and installation of the collector, temperature of inlet and outlet of oil from the collector, temperature rise in the collector, date and day of design and its relevant data such as cloud factor, wind speed and ambient temperature, geographical location of the design point

and length of the collector. Some other information for the receiver tube such as absorbtivity coefficient of the tube, transmisivity coefficient of the glass tube, thickness of the glass cover tube and its diameter would be considered as input data to this program. The input data screen of software is shown in Fig.1.

Fig. 1. Data input of developed collector design software

The output of this simulation program include the total optical error, concentrating ratio, direct radiation (based on Daneshyar model[5]) effective length , oil mass flow rate, optical and thermal efficiency, heat loss and heat absorbed in each m^2 of the receiver tube surface. The allowable total error for the design of collector is calculated based on [14].

Collector design is based on Rabl et al. [15] procedure. The details of calculation procedure are explained in [13]. The thermal design of the collector is made for September 23rd at in the noon time for Shiraz (with latitude of 29.53°). Solar radiation is modeled from [5] relations, wind speed is assumed to be 7 m/s and ambient temperature is considered 30^{o}C. Regarding the limitation of construction of collector structures hydraulic system and etc it is decided to construct a new collector parallel to the existing field of collectors, therefore the length of new collector is considered to be 100 m equal to the available space in the field. Results of calculation and specifications of the new collector of Shiraz solar power plant is presented in Table 2.

3. Combining the new collector with present system

The next step after designing the collector is to combine the collector to the present system showing in Fig 2. Regarding the differences between the oil used in the present collectors field (Behran thermal oil) and the new collector (VP1) and also the higher oil temperature of fluid in the new collector, combining the new collector to the present system need some considerations such as the transferring the absorbed heat in new collector to the secondary

fluid (the oil in the present cycle or produced steam), selection of turbine type, new control philosophy, etc. Therefore it was decided to study the two important issues of the new cycle:

1- The way of using the absorbed heat (either transmitting the absorbed heat to the steam in order to superheat it or to heat the oil or a combination of these two).
2- Selecting the exhaust pressure of steam turbine.

Table 2. Specifications of the new collector of Shiraz solar power plant

Input Parameters			
Rim Angle(Degree):82	Length (m): 94	Absorber Tube Dia. (m): 0.07	Absorber Emmitance: 0.15
Absorber Absorbance: 0.94	Mirror Reflectance:0.90	Glass Transmittance: 0.9	σ- contour (mrad): 2.5
σ- specular (mrad): 2.5	σ- tracking (mrad): 3	σ- displacement (mrad): 3	T-ambient (K): 303
T-inlet (K): 567	T-rise (K): 19	Design Day: 23rd Sep.	Latitude Angle: 29.53
Output Parameters			
Avg. direct radiation (W/m2): 647.3	Avg. diffuse Radiation (W/m2): 84	Noon. Direct radiation (W/m2): 817.4	Noon diffuse Radiation (W/m2): 145.4
Concentrating ratio: 23.97	Mass flow rate (kg/s): 4.53	σ- total (mrad): 4.1	Mirror aperture width (m): 5.27

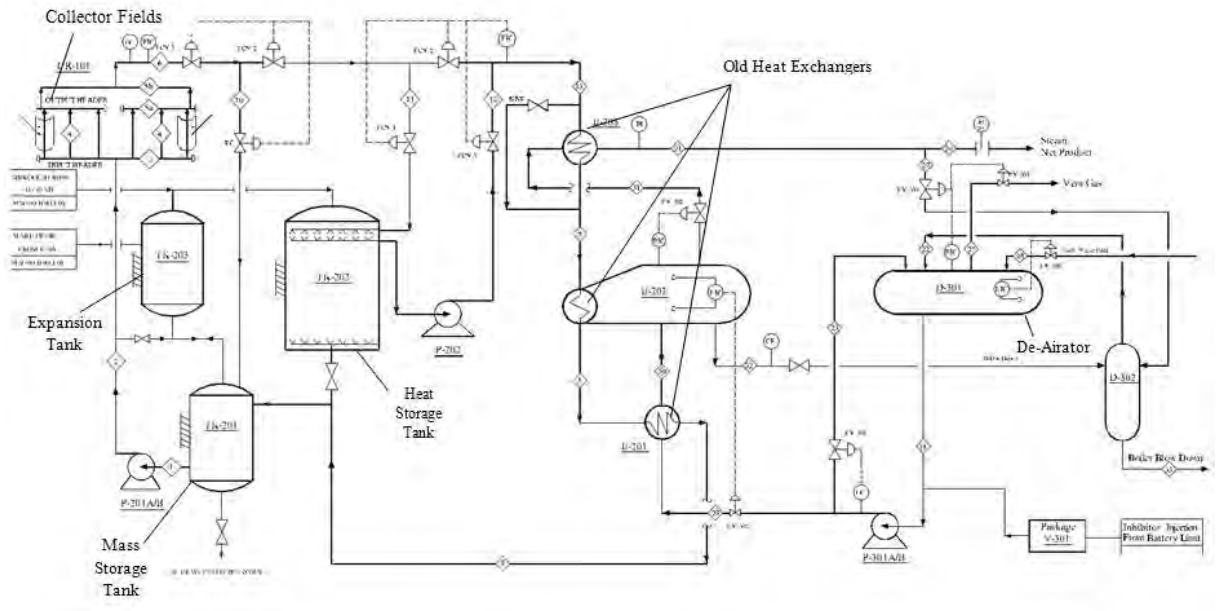

Fig. 2. The present PFD (Process & Flow Diagram) of STPP

Regarding the above objects, thermal design of the integration is made for two cases A and B. In case A, it is assumed that all the heat absorbed by the new collector would be transferred by an exchanger to heat generated steam in the present cycle and generated steam in the boiler, that leads to temperature rise of operating fluid in the new cycle. The heat absorbed will consequently lead to increasing steam temperature which leads to producing more electricity. In case B, the assumption is that a part of the heat absorbed in the new collector would be used to increase the temperature of superheated steam from the existing system and the rest of absorbed heat is used for heating up the outlet oil of existing collector field in order to increase the steam mass flow rate and consequently increasing the electricity generation. In this case 120 kW of the absorbed heat in the new collector is transferred to raise oil temperature and the rest (about 80 kW) will be used for superheating the generated superheated steam in the present cycle.

For each of the above cases 3 turbine outlet steam pressures of 100 kPa , 25kPa (using back pressure type turbine) and 10 kPa (using condensing type turbine) has been considered and the thermodynamic analysis for each case is carried out separately.

Considering the goal to produce 500 kW electricity power from the combination of the present plant and the new system, it is decided to add an auxiliary boiler to the system in order to compensate the superheat steam for generating 500 kW electricity and to provide possibility of using the power plant at night time. Fig. 3 shows results of thermodynamic analysis and condition for various cases studied. The estimated capacity for each equipment in each condition are provided in this table.

CASES		Farm Generated Steam			Boiler						Turbine				Condenser
		Temp (°C)	Press (kPa)	Flow rate (kg/h)	Working Capacity (kg/h)	Installed Capacity (kg/h)	Boiler load (%)	Press. (kPa)	Temp. (°C)	Considered Shaft Power (kW)	Inlet Press. (kPa)	Inlet Temp. (°C)	Exhaust Pressure (kPa)	estimated steam consumption (kg/h)	Duty (kW)
CASE A	100 kPa	250	2130	2399	3112	6000	52	2130	237	532	2100	294	100	5490	3429
	25 kPa	250	2130	2437	1951	5000	39	2130	215	532	2100	294	25	4095	2605
	10 kPa	250	2130	2486	1466	4500	33	2130	215	532	2100	294	10	3566	2286
CASE B	100 kPa	294	2130	2573	2912	6000	49	2130	294	532	2100	294	100	5467	3409
	25 kPa	294	2130	2573	1792	5000	36	2130	294	532	2100	294	25	4096	2605
	10k Pa	294	2130	2573	1336	4500	30	2130	294	532	2100	294	10	3558	2279

Fig.3. Results of calculators for the 6 primary plans cases

4. Selection of the appropriate plan

After considering the primary plans and the economical evaluation, one of the plans should be selected as the design plan. Each plan has some advantages and disadvantages. A list of the most important ones are summarized in Table 3.

The next step to choose a proper plan based on cost and other parameters. The most expensive equipments are condenser, turbine and boiler. Price quotations are gathered from local and international manufacturer for these three equipments. The relative cost with respect to case A of 100 kPa turbine outlet pressure is presented in Table 4.

Table 3. Results Advantage and disadvantages of case A and B

Case	Advantages	Disadvantages
A	Higher thermodynamic efficiency for exhaust pressure of 10 kpa Lower expenses due to use of a single heat exchanger Shutting down of present collectors there will be a possibility of using the heat absorbed by the new collector Boiler working at a lower temperature Lower boiler loss for lower exhaust pressures.	Dependency of electricity generation on the solar part Impossibility of complete heat absorption of the new collector in the system Impossibility of separating contribution of solar part & fossil fuel part power generation Un-available of the new collector, steam for turbine would not be at design condition Lower performance of one exchanger compared to two exchangers Impossibility of the new collector operation without boiler for produce power
B	Possibility of performance tests of new collector without boiler Equal importance of solar part and fossil fuel part Independency of solar and fossil fuel parts Possibility of electricity generation in case of an availablity of solar part Possibility of electricity generation with lower capacity in case that new collector is out of service Better performance of two exchangers compared to one exhanger Lower capacity of boiler in the exhaust pressure of 25 Kpa	Two heat exchangers needed Complicated control system With shutting down of present collectors field the new collector can be used to heat the oil in collectors field

Table 4. The relative cost of the new cycle for various cases

Case	Boiler	Turbine	Condenser	Total
A (Pout=100 kPa)	1	1	1	1
A (Pout=25 kPa)	0.8704	2.5129	2.0218	1.8140
A (Pout=10 kPa)	0.8055	2.5086	0.5523	1.4142
B (Pout=100 kPa)	1	1	1	1
B (Pout=25 kPa)	0.8704	2.5129	2.0218	1.8140
B (Pout=10 kPa)	0.8055	2.5086	0.5523	1.4142

One of the most important issue to be addressed before selection of a proper case is the type of condenser needed for the 3 exhaust pressures of the steam turbine. According to the estimations and calculations for turbine with 100 kPa and 25 kPa exhaust pressure the condenser needed could be air cooled type condenser, whereas for 10 kPa exhaust pressure, the condenser should be water cooled type. In case of using water cooled type condenser water a significant amounts of will be vaporized in the cooling tower.

According to Table 5, for the 3 items (turbine condenser and boiler) for each case A and B the final cost. A direct function of turbine price and consequently the boiler and condenser. Therefore it is observed that for both cases A and B for the different exhaust steam pressure the final cost is equal but regarding Fig. 3 the load of boiler in case of 10 kPa exhaust pressure is less than the case of 25 kPa exhaust pressure. In the same manner less than 100 kPa steam exhaust pressure, which would lead to lower fuel consumption and less fuel cost in the long term. But it must be mentioned that the weakness of 10 kPa exhaust pressure in comparison to the two other exhaust pressures is the requirement of water to cool the exhaust steam from turbine. Calculations show that the consumption of water in the power plant with capacity of 500 kW would be approximately 6.8 m^3/hr. Due to the great limitations of water in the present plant location and for most part of Iran the case B with an exhaust steam pressure of 25 kPa has been selected as the final plan. This is due to relatively higher efficiency, lower water consumption and lower risk with air cooled condenser in spite of higher final cost. Fig. 4 shows the PFD (Process Flow Diagram) of the selected plan.

5. Conclusion

For Expansion of STPP the case B with exhaust turbine of 25 kPa is selected based on following advantages:

1-The selected power plant configuration has lower water consumption, which is critical for the arid region of Iran. This will be more economical to install large plant in the semi-arid region of Iran with no available water sources.
2-In the selected configuration, lower fossil fuel needed for generating 500 kW electricity energy (because of lower boiler load).
3-Solar and fossil part of the plant can operate and be assessed separately.
4-Performance of new designed collector can be measured during normal operation of the plant or individually.

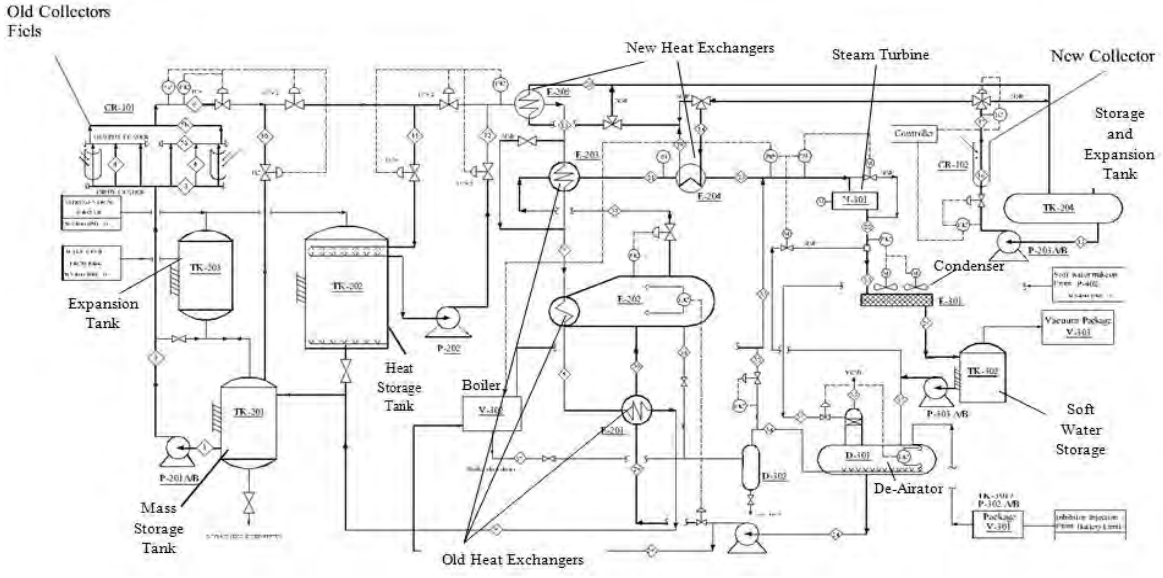

Fig. 3. PFD of the integrated 500 kW Shiraz parabolic trough solar power plant

Reference

[1] C. Ramos, R. Ramirez, J. Laguns, Potential assessment of concentrating solar technologies for electricity generation in Mexico, Proceeding of SolarPACES 2009, Berlin, Germany, September 2009.

[2] N. Supersberger, Energy scenario analysis of the Iranian energy system: role of renewable energy, Proceeding of SolarPACES 2009, Berlin, Germany, September 2009.

[3] M. Yaghoubi, R. Mehryar, Design and Performance simulation of a 250 kW solar Thermal power plant for Shiraz, Iranian Journal of Energy, Vol. 3, 1999.

[4] A. Kenary, M. Yaghoubi, F. Doroodgar, Experimental and numerical studies of a solar parabolic trough collector of 250 kW pilot solar power plant in Iran. Sharjeh Solar Energy Conference, Sharjeh, UAE, February 2001.

[5] M. Yaghoubi, K. Azizian, A. Kenary, Simulation of Shiraz solar power plant for optimal assessment, Renewable Energy, Vol.28, 2003.

[6] M. Yaghoubi, K. Azizian M. Salim, Shiraz solar power plant simulation with variable heat exchanger performance, Proceeding of ESDA04, 7th Biennial Conference on Engineering Systems Design and Analysis, Manchester, United Kingdom, July 2004.

[7] N. Naeeni, M. Yaghoubi, Analysis of wind flow around a parabolic collector (1) fluid flow, Renewable Energy, Vol.32, 2007.

[8] N. Naeeni, M. Yaghoubi, Analysis of wind flow around a parabolic collector (2) heat transfer, Renewable Energy, Vol.32, 2007.

[9] M. Yaghoubi, A. Mokhtari, R. Hesami Thermo-economic analysis of Shiraz solar thermal power plant, Proceedings of the Third International Conference on Thermal Engineering: Theory and Applications Amman, Jordan, May 2007.

[10] K. Azizian, M. Yaghoubi, J. Ghadiri, Optimal performance of Shiraz solar thermal power plant by exergy analysis, Proceedings of the Fourth International Conference on Thermal Engineering: Theory and Applications, Abu Dhabi, UAE, January 2009.

[11] I. Niknia, M. Yaghoubi, Transient analysis of integrated Shiraz hybrid solar thermal power plant, Proceeding of World Renewable Energy Congress, Abu Dhabi, UAE, September 2010.

[12] K. Azizian, M. Yaghoubi, R. Hesami, S. Mirhadi, Shiraz pilot solar thermal power plant design, construction, installation and commissioning procedure, Proceeding of HEFAT2010, 7th International Conference on Heat Transfer, Fluid Mechanics and Thermodynamics, Antalya, Turkey, July 2010.

[13] M. Yaghoubi, M. Vazin, A. Kenary, Optimal assessment of parabolic trough collectors design, Proceeding of 17th International electricity engineering conference of Iran PSC 2002, Tehran, Iran, May 2002.

[14] A. Vadeei, M. Yaghoubi, R. Hesami, P. Kanan, Optical assessment of Shiraz solar power plant collectors, Proceeding of 15th International mechanical engineering annual conference of Iran ISME 2007, Tehran, Iran, May 2007.

[15] A. Rabl, P. Bendt, H. W. Gual, Optimization of parabolic trough solar collectors, Solar Energy, Vol. 29, No.5, 1982.

Thermal regimes in solar-thermal linear collectors

Javier Muñoz*, José M. Martínez-Val, Rubén Abbas

Grupo de Investigaciones Termoenergéticas ETSII- Madrid Polytechnic University
** Corresponding author. Tel: +34 913363128, Fax: +34 913363079, E-mail: jamunoz@etsii.upm.es*

Abstract: In this paper the physics of linear receivers is analyzed. This analysis is oriented to evaluate the dependence of the thermal performance of the receiver on the characteristics of the concentrated solar radiation. It will be seen that two thermal regimes can be distinguished in that dependence, what will point out the need of studying at depth the features of systems with moderate concentration factors.
A fundamental question can be formulated as follows: what is the concentration factor required for obtaining the best solar energy exploitation within a design window established by some technical constraints?
In this performance analysis it has been found that moderate concentration factors (about 20 to achieve 400ºC) can be close to optimal in a cost benefit analysis, taking into account temperature constraints. Beyond these values, thermal and exergetic efficiency curves advice to limit the concentration factors to values that could be achievable by linear Fresnel reflecting collectors, avoiding mobile parts such as ball-joints or flexible joints that could be important leak-points, as well as metal-glass welds, which are another cause of failure in trough collectors

Keywords: *Renewable energy, Concentrated solar energy, Linear receiver, Fresnel*

Nomenclature

α	selective coating absorptivity	-	
C_f	concentration factor	-	
DNI	direct normal radiation	W/m^2	
ε	selective coating emissivity	-	
η	efficiency	-	
η_{ex}	exergetic efficiency	-	
η_{th}	thermal efficiency	-	
$\eta_{th\rightarrow e}$	thermo-electrical conversion efficiency	-	
h	heat transfer coefficient	$W/m^2 \cdot K$	
Q_{conv}	convection thermal losses	W/m^2	
Q_{rad}	radiation thermal losses	W/m^2	
Q_{sun}	available thermal power	W/m^2	
Q_{use}	transferred power to the fluid	W/m^2	
T_a	bulk temperature of the air	K	
T_c	absorbing surface temperature	K	
T_{env}	environment temperature	K	
T_f	heat carrier temperature	K	
T_{grnd}	ground temperature	K	
T_{sky}	high atmosphere temperature	K	

1. Introduction and background

One of the most critical decisions in the design of a solar thermal power unit is the choice of the radiation concentration geometry [1] [2], which is in turn connected with the thermal flux needed in the receiver for fulfilling the objectives of the plant. In this context, technical coherence is a major word. In particular, if a high value is chosen for the concentrated radiation thermal flux, the global heat transfer coefficient of the transfer from the receiver surface to the heat carrier fluid must have a similarly high value [1] [2]. Otherwise, the temperature difference between the receiver and the fluid would be very large, which would enhance thermal losses from the receiver. Besides that, large temperatures differences between different parts of the receiver will convey important differential dilation effects, which can be a major cause of concern in the durability of a solar power collector.

There are two main approaches for concentrating solar radiation [1] [2]:

- Parabolic troughs [3] and linear Fresnel concentrators [4], with one axis tracking.
- Revolution parabolic disks and central tower receivers [1], with a two axes tracking system.

The latter is out of the scope of this article, aimed at analysing the thermal features of linear technologies. The receivers involve a long pipe (or a set of parallel pipes, in a general approach) with a selective coating [5] covering its absorbing surface, i.e., the surface where the concentrated solar radiation impinge. This coating is chosen for having a high absorptivity to solar photons and a low emissivity for photons of the planckian spectrum at similar temperatures to the working ones in the receiver.

Inside the tube, the heat carrier fluid circulates from one end to the other. In most of the cases, collectors are placed in a parallel lay-out, with a high pressure header for distributing the fluid from the central block of the plant (the BOP) and a low pressure header that collects the streams of all the parallel solar receivers and sends the total hot stream into the BOP.

A third line of solar power plant configuration can be cited, the Solar Boiler [6], which is based on a central tower, but without a single central receiver in the top of the tower. The receiver is a bundle of tubes going up along the wall of the tower. This set of tubes can be considered as a linear receiver, although radiation would be concentrated by reflection from a field of heliostats very similar to the central receiver case.

The selective coating is the radiation absorbing element, and it is the component reaching the highest temperature. The useful heat is carried by the fluid and its actual exergy value will depend on the temperature achieved when it leaves from the collector. In some applications, boiling inside the receiver tube is considered, and the steam title will also be a relevant parameter. In general, the increase in specific enthalpy and the mass flow are the variables characterizing the heating of the fluid. In this context, two energy balances must be taken into account: the overall heating of the fluid, which is equal to the total energy transferred from the absorbing surface to the heat carrier fluid, and the detailed heat transfer balance, which depends on the temperature map attained in the collector due to the transmission processes among the components of the collector, with two main results:

- Heat transfer to the carrier fluid, which is the basis of the overall energy balance
- Losses to the environment, mainly through convection to air and radiation to the surroundings

Heat transfer to the carrier fluid depends on its velocity. The convection coefficient between the tube and the fluid can be increased by increasing its speed, but this fact has other effects, as an increase in pressure drop and pumping power [7] [8]. For liquids, this effect can be of second order as compared to the thermal problem. For gases, the mechanical problem can be as important as the thermal one, and the pumping power needed to keep the gas flow at the level required by the thermal requirement, can be as large as the power collected from the sun, what makes the plant useless.

Another important point in the design of the system is the actual limitations in the temperature of the different components. This is the case of the selective coating, which sets up a ceiling to the maximum temperature allowed in the collector. Coatings resisting 500 ºC without degradation are commercially available, but this is not usually the binding limitation, because in current trough-collector power plants, the most popular heat carrier fluid is synthetic oil, such as Therminol VP1 and the maximum working temperature is below 400 ºC.

Those limitations in temperature convey similar limitations in the maximum thermal flux impinging on the receiver, and therefore in the concentration factor. Nevertheless, those

limitations in the temperature of some materials have to be assessed in the full analysis of the system. If it is effective in transferring the heat to the carrier fluid, and the flow is large enough for guaranteeing a controlled heating, all temperatures will be within the corresponding limits. However, this guarantee relies on the proper circulation of fluid, and it embodies the afore-mentioned problem of the required pumping power.

This coupling of thermal and hydraulics constraints can be characterized in the case of linear collectors, to identify optimum solutions in some design windows, particularly aimed at reducing the cost of solar power plants. This optimization process will embody an exergy analysis of a system featured by the working temperature reached by the heat carrier fluid.

2. Methodology: A linear collector model

There are detailed physical and numerical models to calculate trough collectors and reflection Fresnel devices [6] [9] [10]. They are particularly useful to feature a power plant in nominal conditions, which include the set of variables to define the calculation of the collector for the reference conditions chosen as nominal ones, and they can also be used for integrating the performance along the year.

The model used for this study works in similar form to that used in Muñoz et al [6], but does not take into account neither the way used for concentrating the solar radiation, nor the natural aperture of the sun beams, which is an important factor when the concentration geometry involves large distances.

This model can be described as a lumped-parameters representation of the collector. It includes an expression for featuring the useful heat, which is associated with a temperature in the carrier fluid at the collector outlet. The model can be used for investigating the relative importance of some parameters, or equations coefficients, and for identifying relevant trends in the evolution of the system when the boundary conditions change, including the change in the concentration of solar radiation.

The simplicity of the model does not allow using it for designing purposes, or for optimizing a system, but the model is easily followed, unlike many computational codes, which are managed as black boxes. The model is based on the equations listed below, and it can be used to feature general trends in the behaviour of the linear receivers. It is obvious that some hypotheses can not be kept in detailed computations, which are needed for calculating a given design in specified conditions.

The model is an integrated energy balance where the impinging radiation on the receiver goes to useful heat or to thermal losses (convection through the air and radiation to the background). Both thermal phenomena involve several heat transfer mechanisms, but they can be lumped into a single step, expressed in terms of the difference between relevant temperatures, and they include a coefficient, to which an effective value must be assigned. Those values can be estimated from previous detailed calculations of similar systems or from the bibliography. Moreover, sensitivity calculations can easily be carried out by varying those values and other parameters characterizing the boundary conditions.

Four temperatures are sufficient to define the model:

- The temperature T_c of the absorbing surface (selective coating) where the concentrated radiation impinges. It represents an average value of the coating temperature

- The temperature of the heat carrier fluid as an average value as it is heated along the receiver, T_f
- The bulk temperature of the air, T_a
- The temperature of the background radiation or environment, T_{env}. It can represent either the temperature of the earth's surface, T_{grnd} , or the temperature of the high atmosphere [1][11], T_{sky}, each one being affected by their corresponding view factor from the receiver (detailed analysis of this matter demonstrates that for the considered values this dependence has no r elevant effect on the results)

Additional parameters of the model are the following ones. (Values assumed for the first set of calculations are given within brackets.):

- DNI = direct normal irradiation (1 kW/m^2)
- C_f = concentration factor (variable)
- ε = selective coating emissivity (0.1)
- α = selective coating absorptivity (0.9)
- U = global coefficient for convection losses (8 W/m$^2\cdot$K)
- h = g lobal coefficient for heat transfer from the absorbing surface to the heat carrier fluid (2 kW/m$^2\cdot$K)

In general, for all calculations the boundary conditions temperatures are:

- T_{air} = 25 ºC (=298 K)
- T_{grnd} = 25ºC (=298 K)
- $T_{sky} = 0.0552\cdot T_{air}^{1.5}$ [K] [11]

The model is defined by the following equations:

$$Q_{sun} = Q_{conv} + Q_{rad} + Q_{use} \quad (1)$$

$$Q_{sun} = C_f \cdot \alpha \cdot DNI \quad (2)$$

$$Q_{conv} = U \cdot (T_c - T_{air}) \quad (3)$$

$$Q_{rad} = \varepsilon \cdot \sigma \cdot (T_c^4 - T_{env}^4) \quad (4)$$

$$Q_{use} = h \cdot (T_c - T_{use}) \quad (5)$$

The absorbed energy and losses that are produced by convection and radiation, adding the cooling effect of the heat transfer fluid (thermal oil) determines the temperature level and the energy efficiency in the receiver itself that can be given, in function of the enthalpy increase in the heat transfer fluid (Q_{use}) by:

$$\eta_{th} = \frac{Q_{use}}{Q_{sun}} \quad (6)$$

Thermal efficiency is not sufficient to characterize a s ystem designed to yield useful work against the environment: we also use the exergetic efficiency (η_{ex}) that take into account the

required blower power (W_b) with $\eta_{th\rightarrow e}$ is the conversion efficiency from thermal to electrical energy, evaluated as 33% [6]:

$$\eta_{ex} = \frac{Q_{use} - W_b / \eta_{th\rightarrow e}}{Q_{sun}} \cdot \left(1 - \frac{T_a}{T_{use}}\right) \quad (7)$$

3. Results

This physical model has been applied to some simplified cases with the coefficients already given (first series of calculations) and the results are depicted in Fig. 1 and Fig. 2. It is worth commenting on the shape of the efficiency curve (thermal and exergetic), with two branches that are associated to two thermal regimes: a first branch with rapid increase in efficiency, followed by an almost horizontal second branch, where the heat transfer process from the collector's absorbing surface to the heat carrier fluid is saturated, and the efficiency value reaches a maximum value. A threshold can be marked as the beginning of the second regime. This threshold can be featured by the value of the slope of the curve, or by the relative value to the asymptotic level of the efficiency. In the case 400ºC of fluid temperature the threshold of the second regime can be marked around a concentration factor of 20. If the fluid temperature is 300 ºC, the threshold in the concentration factor is about 15. With a fluid temperature of 1000 ºC the threshold is at 70.

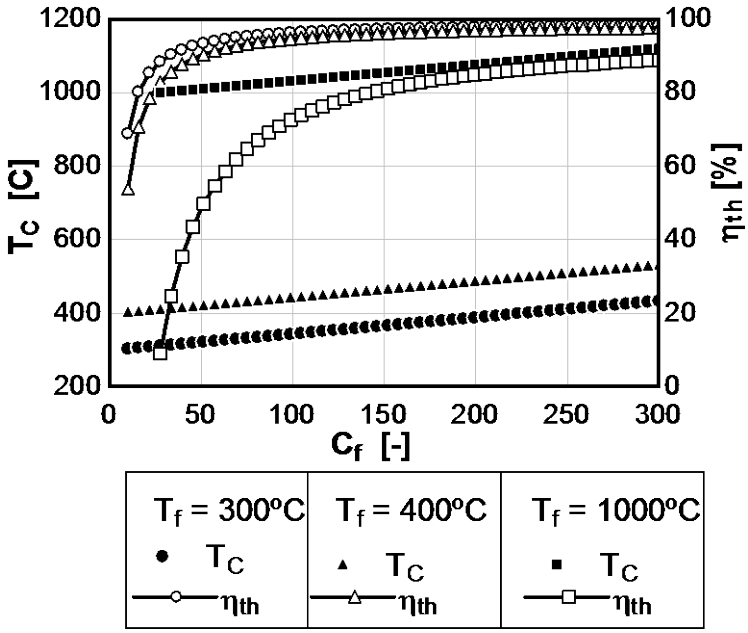

Fig. 1. Collector thermal efficiency and absorbing surface temperature Vs. concentration factor, for three values of T_f: 300 ºC, 400 ºC and 1000 ºC. The global coefficient for heat transfer from the absorbing surface to the fluid, "h", has a value of 400 W/m^2·K

It should be noted as well that the collector's absorbing surface temperature increases linearly with the concentration factor. This effect is influenced by some obvious limitations, because all materials, from the selective coating to the heat carrier fluid, have maximum operational temperatures (which can also depend on the mechanical stresses, in the case of structural materials).

As an initial advice from this analysis, it can be stated that linear collectors should be designed to operate in the saturated regime, limiting the concentration factor in order to limit

the temperatures. Moreover, the design point can be placed slightly above the threshold for that regime, if this option conveys a significant cost reduction because a lower concentration factor can be achieved with simpler and more robust collectors. Of course, this advice must be properly checked in a cost/benefit analysis, after reviewing in detail the thermo-physical features of collecting solar radiation in linear receivers.

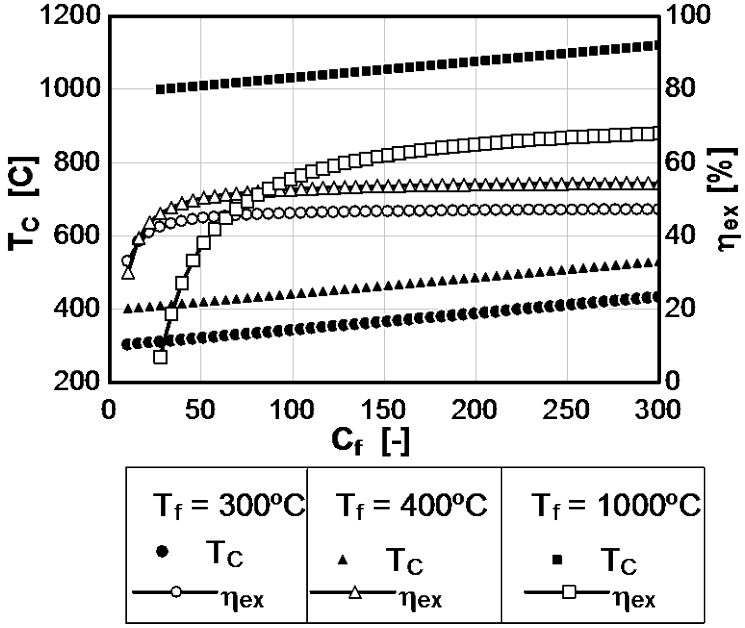

Fig. 2. Collector thermal efficiency and absorbing surface temperature Vs. concentration factor, for three values of T_f: 300 °C, 400 °C and 1000 ° C. The global coefficient for heat transfer from the absorbing surface to the fluid, "h", has a value of 400 W/m^2·K

This finding opens a new way for Concentrated Solar Power, because a Fresnel of large size can be used for heating synthetic oil up to 390 ºC, for activating a Rankine cycle similar to those of current power plants with parabolic trough collectors as Fig. 3 shows, with five Fresnel systems, each one of one total length, and all with the same impinging power: 2.5MW$_{th}$. The intensity goes from 5 to 25 kW/m^2, corresponding to lengths varying from 500 m from the former to 100 m for the latter.

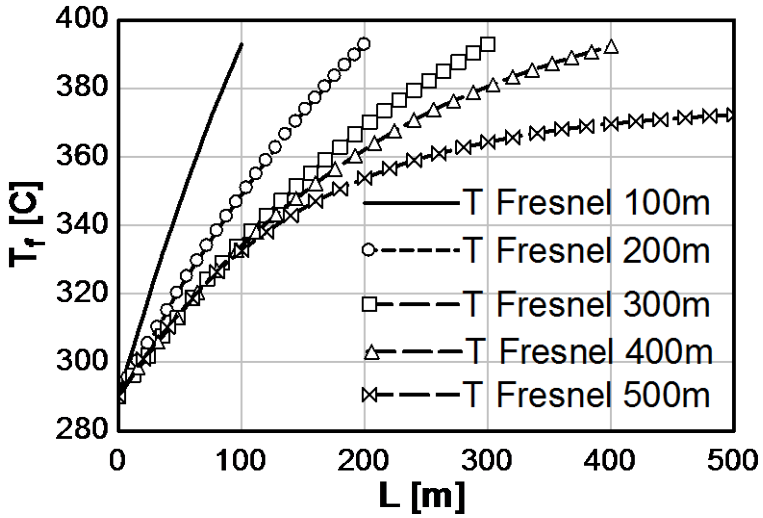

Fig. 3. Evolution of the fluid temperature along the collector length for a set of linear collectors receiving the same total power, with different radiation intensities and lengths.

It is seen that the case of 5 kW/m^2 does not reach the objective T (392 ºC, corresponding to Therminol VP1 as heat transfer fluid), which implies that this case is below the threshold. Energy and exergy efficiencies are shown in Fig. 4, and it is seen how fast they decrease as the radiation intensity goes down. It must be said that this effect is produced, to a large extent, by the objective of achieving a final T of 392 ºC.

It is obvious that requiring higher temperatures in the fluid makes the receiver less efficient, because the temperature gap from the irradiated surface to the bulk of the fluid is shorter than the gap of less demanding collectors, and thermal losses to the surrounding materials increase, as it remains the same. So, if the fluid temperature required for a particular plant is much higher than 400ºC, a Fresnel is not likely to be suitable, because its efficiency will be modest.

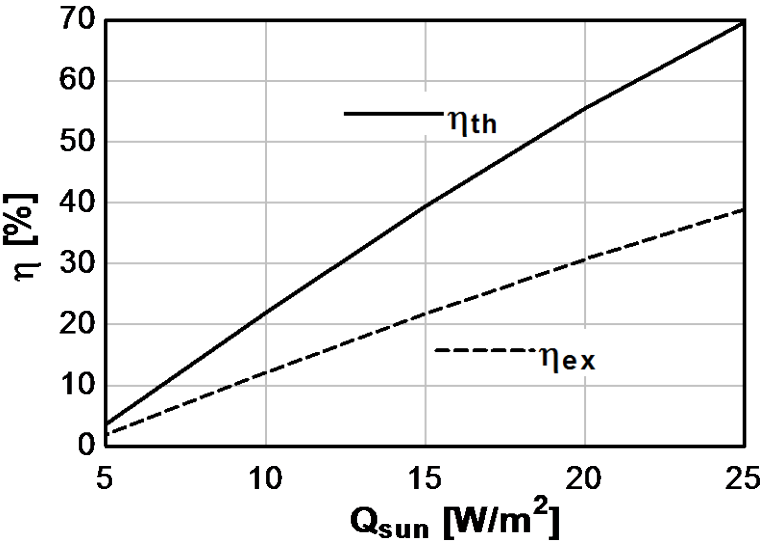

Fig. 4. Energy and exergy efficiencies of the collectors of the set introduced in the previous figure.

4. Conclusions

The analysis of thermal performance of linear collectors in the field of concentrated solar power shows the existence of two regimes: a lower regime, corresponding to small values of intensity impinging on the receiver and an upper regime, where the relevant thermal variable (notably, the efficiency) is almost saturated, opposite to the lower regime, where it increases very rapidly as radiation intensity does. The change from the lower to the upper regime is usually very well identified by a value, or a short range of values. It exists therefore a threshold for reaching the saturated regime. All these features depend on the temperature required in the heat-carrier fluid.

In this performance analysis it has been found that moderate concentration factors can be close to optimal values, due to temperature constraints. Thermal and exergetic efficiency curves show that beyond these values, i.e. increasing the concentration factor, the threshold is exceeded, and therefore efficiency increases slowly.

In the specific case of 400ºC as objective temperature – usual in current solar thermal plants with through collectors that uses thermal oil – the concentration factor takes the value 20 approximately.

This observation must be properly exploited by identifying the simplest and most robust concentration scheme able to attain the upper regime of a given application, for feeding the

boiler of a Rankine cycle with given working temperatures. This is the case of linear Fresnel reflecting collectors, which avoid mobile parts such as ball-joints and flexible joints that could be important leak-points, as well as metal-glass welds, which are another cause of failure in trough collectors

References

[1] J.A. Duffie & W.A. Beckman, Solar Engineering of Thermal Processes, John Wiley and Sons, New york, 2nd ed., 1991, pp. 330-378

[2] D. Mills, Advances in solar thermal electricity technology, Solar Energy, vol. 76, no. 1-3, 2004, pp. 19-31

[3] A. Fernández-García, E. Zarza, L. Valenzuela & M. Pérez, Parabolic-trough solar collectors and their applications, Renewable and Sustainable Energy Reviews, vol. 14, no. 7, 2010, pp. 1695-1721

[4] D.R. Mills & G.L. Morrison, Compact Linear Fresnel Reflector solar thermal powerplants, Solar Energy, vol. 68, no. 3, 2000, pp. 263-283

[5] M. Farooq & I.A. Raja, Optimisation of metal sputtered and electroplated substrates for solar selective coatings, Renewable Energy, vol. 33, no. 6, 2008, pp. 1275-1285

[6] J. Muñoz, A. Abánades & J.M. Martínez-Val, A conceptual design of solar boiler, Solar Energy, vol. 83, no. 9, 2009, pp. 1713-1722

[7] F.P. Incropera, Fundamentals of heat and mass transfer, John Wiley & Sons, Danvers, USA, 6th ed, 2007, pp 485-517

[8] R.L. Mott, Applied fluid mechanics, 6th ed., Pearson Prentice Hall, Upper Saddle River, 2006, pp 226-245

[9] R. Forristal, Heat Transfer Analysis and Modelling of a Parabolic Trough Solar Receiver Implemented in Engineering Equation Solver, NREL Technical Report, Golden, Colorado, USA, 2003

[10] M.J. Montes, A. Abánades & J.M. Martínez-Val, Performance of a direct steam generation solar thermal power plant for electricity production as a function of the solar multiple, Solar Energy, vol. 83, no. 5, 2009, pp. 679-689

[11] W.C. Swinbank, Long-wave radiation from clear skies, Quarterly Journal of the Royal Meteorological Society, vol. 89, no. 381, 1963, pp. 339-348

[12] J.M. Martínez-Val, Thermal solar energy collector, Es 2 231 576, P CT/ES2009/000557, WO2010/076350 08 July 2010 (08.07.2010)

Surface temperature distribution and energy gain from semi-spherical solar collector

Ilze Pelece*, Imants Ziemelis, Uldis Iljins

Latvia University of Agriculture, Jelgava, Latvia
**Corresponding author: E-mail: ilze.pelece@llu.lv*

Abstract: Usual constructions of solar energy receivers are not efficient enough in Latvia and others northern countries, and new constructions are required, that would be able to collect energy from all sides as well as to use the diffused radiation more efficiently.
The aim of the paper is to elaborate method for calculation of energy received by solar collector, usable for developing of new constructions of solar collectors, and to develop a new construction of solar collector using this method.
Such new construction can be a semi-spherical solar collector. Such collector has been made, and measurements of water heating have been carried out.
Method of calculations of received energy has been elaborated. Theoretical calculations of the energy gain from semi-spherical solar collector have been performed and verified by comparison of calculated daily energy sums with measured ones, and good coincidence has been obtained.
Method of calculations allows calculating not only integral received energy, but also distribution of the received energy along the surface. The measured distribution of surface temperature of the semi-spherical solar collector corresponds to the calculated one. There are no spot on the semi-spherical surface which would never get warm.
Such semi-spherical solar collector could be appropriate for use of solar energy in Latvia and other countries with similar geographical and climatic conditions.

Keywords: *Solar collector, Semi-spherical, Distribution of surface temperature, Energy gain*

Nomenclature

E_W	daily energy gain from solar collector ..... J	I	intensity of the solar radiation ..... $W\,m^{-2}$
E	daily energy sum at cloudy conditions..... J	I_D	intensity of the diffused radiation..... $W\,m^{-2}$
E_C	daily energy sum at clear sky conditions.. J	z	zenith angle of the sun..... rad
c	specific heat of water.....$J\,kg^{-1}\,K^{-1}$	δ	altitude of the sun ..... rad
K	productivity of the water pump..... $kg\,h^{-1}$	Φ	azimuth of the sun..... rad
t_1	temperature of inlet water ..... °C	S	solar constant ..... $W\,m^{-2}$
t_2	temperature of outlet water ..... °C	P	lucidity of the atmosphere ..... r.u.
Δt	time between two measurements.....s	m	air mass ..... r.u.
β	angle of incidence of solar rays .....rad	M	nebulosity .....grades

1. Introduction

Align with decrease of reserves of fossil fuel, as well as impact of use of fossil fuel on climate, in the world more attention has been paid to renewable sources of energy, including solar energy.

Also in Latvia the solar energy has been used, mostly in solar collectors for hot water production [1,2]. However in Latvia because of its geographical and climatic conditions there are some features in comparison with traditional solar energy using countries [3, 4]. Latvia is located at 57° northern latitude and 24° eastern longitude near the Baltic Sea. In Latvia at summer the length of day excides twelve and maximally reaches seventeen hours, accordingly is also long path of sun, but rather small altitude of sun (maximally 56 degrees above horizon) and therefore also small intensity of solar radiation. There is also frequently considerable nebulosity.

At winter the altitude of sun is very small (10^o) and the length of day 7 h, therefore use of solar energy at winter in Latvia is not possible.

Because of mentioned above features traditional flat plate collector without tracking to sun is not appropriate enough for use in Latvia, but new collector constructions are required, that would be able to collect the energy from all sides as well as to use the diffused radiation more efficiently. To these requirements a collector with a semi-spherical absorber considered in this article could correspond [5]. Energy gain from such collector is similar to that from flat plate collector tracking to sun, but tracking device is complicated, expensive and hard to exploit, while semi-spherical collector is rather simple, with good appearance, durable against wind.

For a better elaboration and evaluation of new constructions of solar collectors, also new, more precise, complete and convenient methods for calculation and forecasting of the received energy are required, capable to calculate received solar energy of surface of any shape and orientation, taking into account also the nebulosity. Such method is proposed in this article. Calculations consist from three steps. At first, solar coordinates at every moment must be calculated. These calculations are based on astronomical considerations [6]. Second step is calculations of the energy received by some surface, depending on its shape and orientation. Third step is evaluation of impact of clouds. There is a new improved model of taking into account impact of the nebulosity used in these calculations.

The method has been verified by comparison of results of calculations with experimentally measured values. A collector with the semi-spherical absorber has been used in these measurements.
Method of calculations allows calculating not only integral received energy, but also distribution of the received energy along the surface. The measured distribution of surface temperature of the semi-spherical solar collector corresponds to the calculated one. There are no spot on the semi-spherical surface which would never get warm.

2. Methodology

Calculations and measurements of the solar radiation as well as the received energy of the solar collector have been performed in this article.

2.1. Measurements

Measurements of the global solar radiation have been performed using an ISO 1. class pyranometer from “Kipp&Zonen”. Measurements have been performed automatically, taking intensity of radiation after every 5 minutes and accumulating data in a logger. Thereafter from these data the daily energy density has been calculated. Measurements have been carried out from April 2008 till November 2010.

Data on the nebulosity from "Latvian Environment, Geology and Meteorology Centre" have been obtained. The nebulosity is evaluated visually in grades from 0 (clear sky) to 10 (entirely overcast) accordingly the World Meteorology Organization methodology after every 3 hours.
Measurements of the received energy of the solar collector have been performed using a new construction – solar collector with a semi-spherical absorber, shown in Fig. 1.

The collector is made from a copper sheet shaped as semi-sphere and coloured black. Inside the dome is a copper tube shaped close to dome. Diameter of the tube is 10 mm, length 21 m. In this tube flows heat remover – water, transporting heat to the reservoir. The collector is covered with transparent polyethylene terephthalate (PET) dome. Radius of the collector is

1.12 m, what corresponds to 1 m^2 base area. In order to determine the received energy of collector temperatures of incoming and outgoing water have been measured after every 5 min. Water flow ensured a pump, which productivity was 30 l/h. Measurements with the semi-spherical solar collector have been carried out at 2009 from 1 August to 31 October and at 2010 from 1 Jun to 30 August.

Energy gain from solar collector has been calculated from Eq. (1)

$$E = \sum c \cdot K(t_2 - t_1) \cdot \Delta t \cdot 10^{-6} \quad (1)$$

where E is daily energy gain from solar collector (J), C is specific heat of water (4190 J kg^{-1} K^{-1}), K is productivity of the water pump (kg/h), t_1 and t_2 are inlet and outlet water temperatures respectively (°C) and Δt is time between two measurements. All positive E values must be summed.

Fig. 1. Semi-spherical solar collector.

The distribution of the surface temperature of semi-spherical solar collector also has been investigated. For this investigation there are 30 thermocouples mounted onto surface of the semi-spherical solar collector at even distances from each other. Measurements of temperatures have been carried out using termologgers Pico TC08. Surface temperature investigations have been carried out with and without water flow in tubes.

2.2. Theoretical calculations

For the theoretical calculation of the received energy of some surface [7] at first solar coordinates (declination and azimuth) must be calculated at every moment (we used interval 15 min). From solar coordinates and the orientation of the surface (normal of the surface) the angle of incidence of solar rays β can be calculated. Then the intensity of the radiation received of a surface element can be calculated from Eq. (2).

$$I = SP^m \cos\beta + I_D \quad (2)$$

where S is solar constant (equal to 1367 W m^{-2}), P is lucidity of the atmosphere, r.u., m is air mass, r.u., and I_D is intensity of the diffused radiation, assumed to be constant and equal to 75 W m^{-2}.

The air mass *m* accordingly to literature [8] can be calculated from empirical expression Eq. (3).

$$m = \frac{1.002432\cos^2 z + 0.148386\cos z + 0.0096467}{\cos^3 z + 0.149864\cos^2 z + 0.0102963\cos z + 0.000303978} \quad (3)$$

where z is zenith angle of the sun.
In order to determine the daily energy sum received by some surface the intensity calculated from Eq. (1) have to be integrated (summed up) in time from sunrise to sunset as well as over all irradiated surface.

Calculation of the clear sky energy according to Eq. (2) and (3) has been explained in our previous works [3,4,7] and therefore is not considered here.
Impact of clouds has been taken into account using a new empirical model Eq. (4) with experimentally evaluated numerical coefficients A, B and C.

$$E = E_C\left(A - B\exp(CM)\right) \quad (4)$$

where E is daily energy sum at cloudy conditions (J), E_C is the same at clear sky conditions, and M is nebulosity (grades).

Comparison of calculated and measured values has been done using graphical method. The model can be evaluated from the scatter plot of calculated daily energy sums via measured ones. About correspondence of calculated values to measured ones indicate slope (must be close to one) and intercept (must be near to zero) of best-fit line, as well as coefficient of determination R^2 (must be close to one).

3. Results

3.1. Impact of clouds

Impact of clouds has been taken into account via Eq. (4). Coefficients A, B and C has been evaluated from comparison of calculated daily energy sums with those measured with pyranometer, then the model for calculating of daily energy sum at cloudy conditions is Eq. (5)

$$E = E_C\left(1.01 - 0.0425\exp(0.295M)\right) \quad (5)$$

Such model gives good coincidence of calculated daily energy sums with measured ones, shown in Fig. 2.

The slope of the best-fit line in this case is 1.005, i ntercept 1.13, and coefficient of determination R^2= 0.88.

3.2. Surface temperature distribution of semi-spherical solar collector

Energy received by semi-spherical solar collector surface element, which is determined with spherical coordinates θ and φ, can be calculated from Eq. (2), where β is angle of incidence of solar rays and can be expressed as scalar product of two vectors: surface normal $\vec{n}$ and solar rays direction $\vec{l}$, Eq. (6).

$$\cos\beta = \vec{n}\cdot\vec{l}_1 = \sin\theta\cos\varphi\cos\delta\cos\Phi + \sin\theta\sin\varphi\cos\delta\sin a + \cos\theta\sin\delta = \\ = \sin\theta\cos\delta\left(\cos\varphi\cos\Phi + \sin\varphi\sin\Phi\right) + \cos\theta\sin\delta \quad (6)$$

where δ is the altitude of the sun and Φ is the azimuth of the sun.

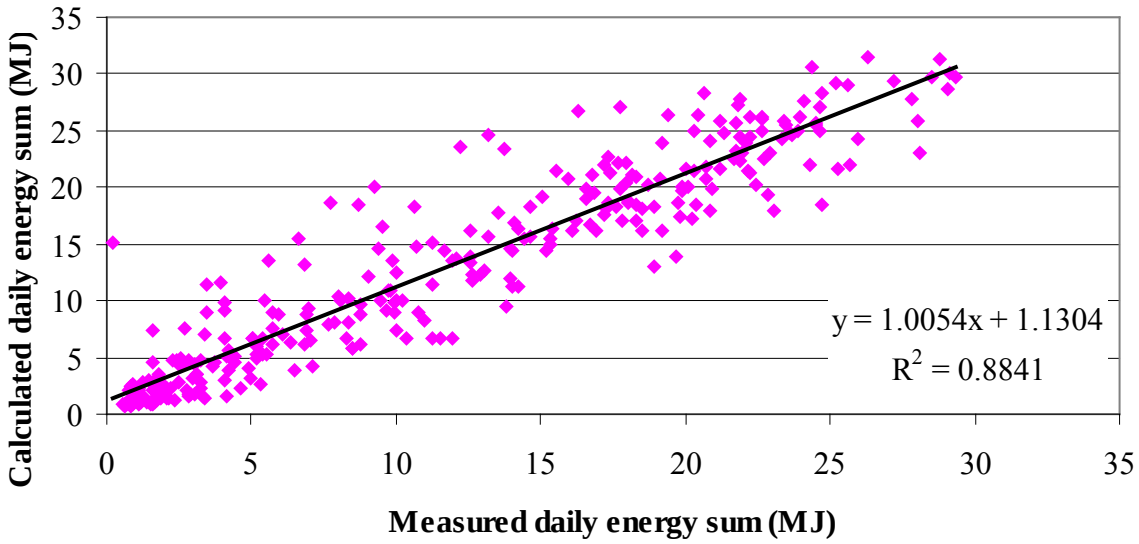

Fig. 2. Comparison of daily energy sums of solar energy, calculated from Eq. (5) with those measured with pyranometer from 1 January 2009 to 31 October 2009.

Results of these calculations in Fig. 3 b ha s been shown in comparison with measured distribution of surface temperature of semi-spherical solar collector Fig. 3 a.

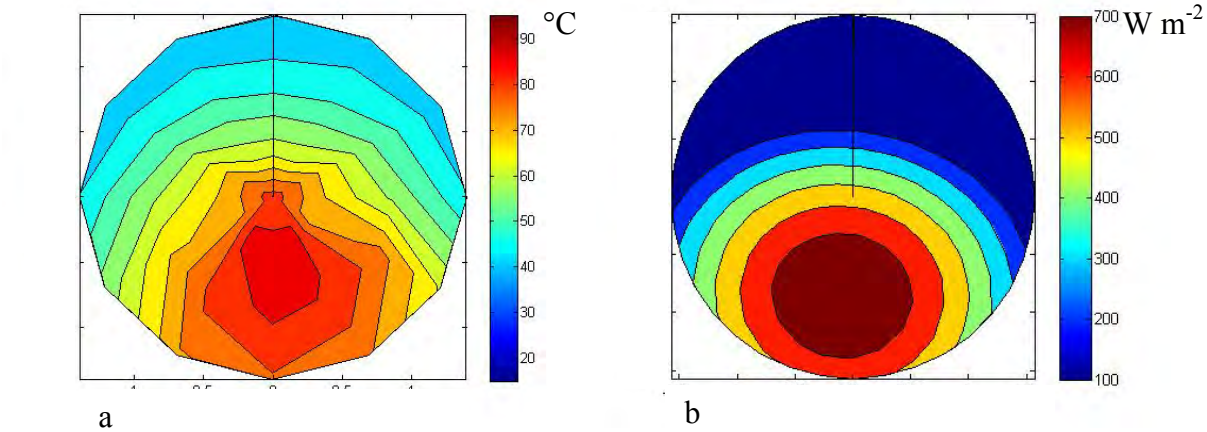

Fig. 3. Distribution of: (a) measured surface temperature and (b) calculated received energy of semi-spherical solar collector at 11 April 2010 at 13:00

Picture shows good correspondence between calculated and measured distributions. Measured distribution is more even because of heat conduction and convection in collector.

Fig. 4 shows daily mean distribution of measured surface temperature (a) and calculated received energy (b). Also good correspondence has been obtained.

Fig. 5 shows daily course of mean temperature at eastern and western sides (arithmetical mean from measurements of 6 thermocouples mounted at corresponding side) of semi-spherical solar collector, but Fig. 6 of northern and southern sides. Of course, eastern side receives more energy at morning, but western side at evening. It is not explained yet why maximal temperature at eastern side is higher than that at western side. Temperature of southern side is certainly higher than that of northern side, with the exception early at morning at late at evening in the middle of summer, when sun rises at northeast and sets at northwest.

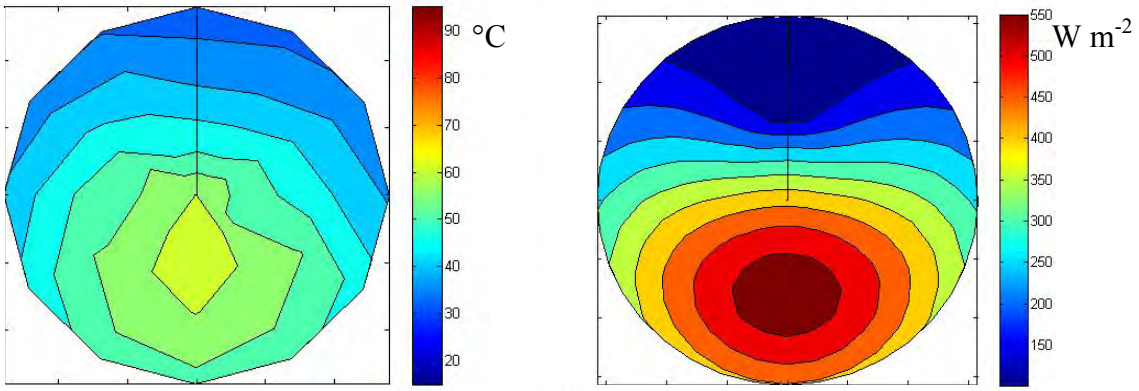

Fig. 4. Distribution of daily mean values of: (a) measured surface temperature and (b) calculated received energy of semi-spherical solar collector at 11 April 2010

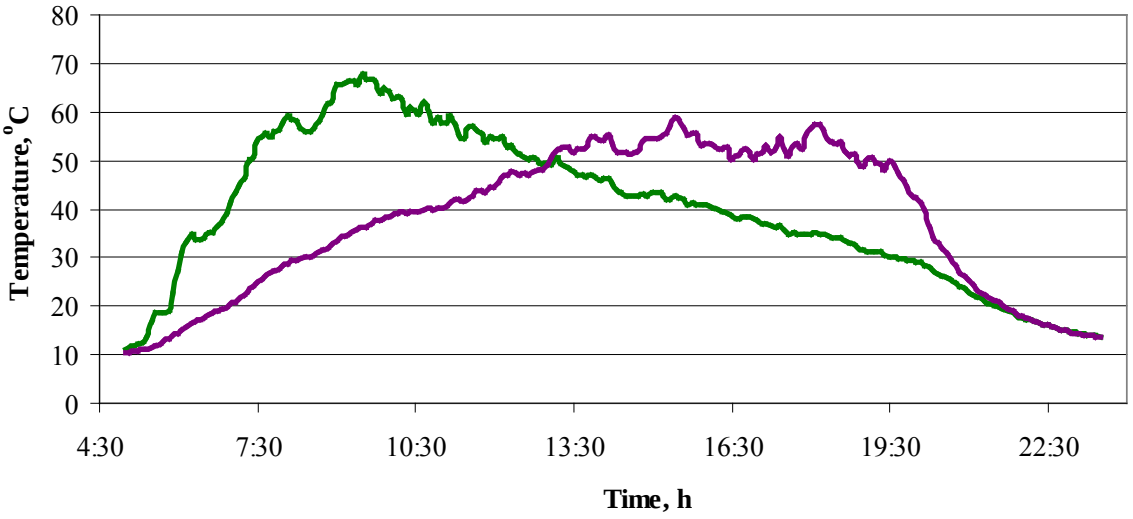

Fig. 5. Daily course of mean temperature at eastern (——) and western (——) sides of semi-spherical solar collector

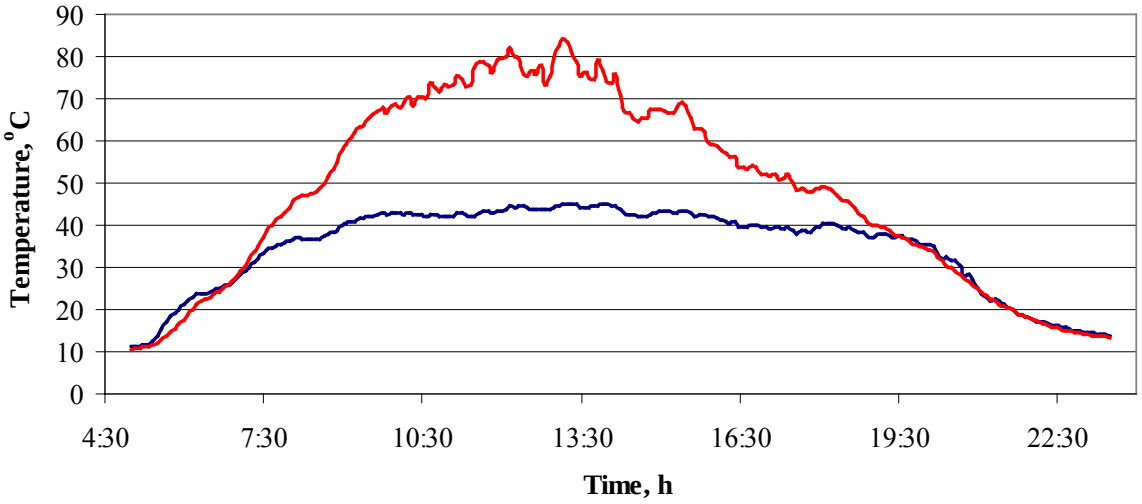

Fig. 6. Daily course of mean temperatures at northern ( ) and southern ( ) sides of semi-spherical solar collector

But at middle of day, when temperature of southern side reaches 80 ºC , temperature of northern side reaches 40 ºC. There is no s pot on the surface of the semi-spherical solar collector, which never gets warm.

3.3. Energy gain from semi-spherical solar collector

Daily energy gain from semi-spherical solar collector has been calculated from Eq. (1). Results are shown in Fig. 7. There is daily energy gain from semi-spherical solar collector compared with daily sum of solar energy, measured with pyranometer. A linear coherence can be observed, with coefficient of determination R^2= 0.87.

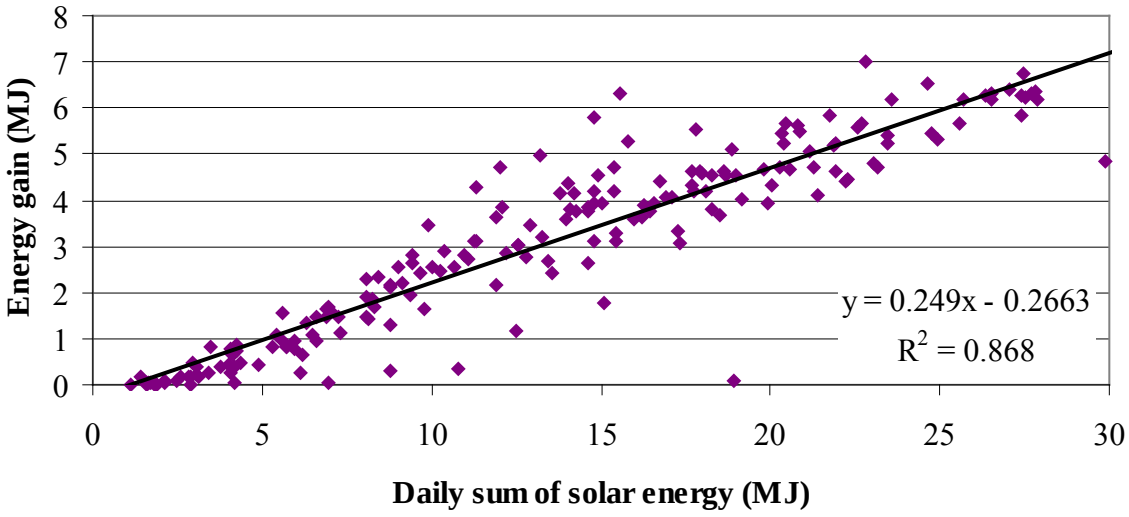

Fig. 7. Daily energy gain from semi-spherical solar collector via daily sum of solar energy, measured with pyranometer from 1 August to 31 October 2009 and from 1 Jun to 30 August 2010.

The slope of the best-fit line (0.25) in this case characterises efficiency of collector. It can be increased using up-to-date materials in the construction of the collector.

4. Discussion and conclusions

Obtained results suggest that semi-spherical solar collector can be appropriate for use of solar energy in Latvia and other countries with similar geographic and climatic conditions. Daily course of surface temperature suggests that semi-spherical solar collector better than common flat plate collector collects solar energy at morning and at evening.

The strong linear coherence between daily energy gain from solar collector and daily sum of solar energy can suggest on independence of work of semispherical solar collector on other circumstances. It can also be because the semi-spherical solar collector uses solar energy evenly all day. However this question needs to be studied additionally, as well as difference between maximal temperatures at eastern and western sides of semi-spherical solar collector.

Other result of this work is method of calculation of received energy of some surface, including impact of clouds. This method is rather simple, precise and not need many input data. This method is usable not only for solar collectors, but also for solar cells, also possible at several forms for better receiving of solar energy. Further study would be interesting on impact of several forms of clouds.

References

[1] L. Kancevica, J. Navickas, E. Ziemelis, I. Ziemelis, Increase of the Efficiency of Solar Collectors, Proceedings of the Second International Scientific Conference "Biometrics and Information Technologies in Agriculture: Research and Development", Lithuanian University of Agriculture, 2006, pp. 89-92.

[2] I. Ziemelis, U. Iljins, J. Navickas, Economical Comparison of Some Parameters of Flat-Plate Solar Collectors, Proceedings of the International Research Conference "The Role of Chemistry and Physics in the Development of Agricultural Technologies", Lithuanian University of Agriculture, 2004, pp. 23 – 25.

[3] I.Pelece, Influence of nebulosity on use of solar energy in Latvia, Proceedings of the International Scientific Conference "Engineering for rural development", 2008, Latvia University of Agriculture, pp. 28-33.

[4] I. Pelece, U. Iljins, I. Ziemelis, Theoretical calculation of energy received by semi-spherical solar collector, Proceedings of the International Scientific Conference "Engineering of Agricultural Technologies", Lithuanian University of Agriculture, 2008, Vol. 6. pp. 263-269.

[5] U. Iljins, I. Ziemelis, I. Pelece, E.Ziemelis. Spherical solar collector. (In Latvian: Saules enerģijas kolektoriekārta ar sfērisko enerģijas kolektoru un tās pielietojumi) *Patent LV 13550 B* Riga: Patenti un precu zimes 5/2007 p.637

[6] J. Zagars, I. Vilks. Astronomy for high schools. (In Latvian: Astronomija augstskolām) Riga: LU 2005.

[7] I. Pelece, U. Iljins, I. Ziemelis, Forecast of energy received by solar collectors, Proceedings of the International Scientific Conference „Applied Information and Communication Technologies". - Jelgava: LLU, 2008. - lpp. 62-67.

[8] A. T. Young, Air mass and refraction, Applied Optics, 1994, Vol. 33, pp. 1108–1110.

[9] S. Younes, T. Muneer, Improvements in solar radiation models based on cloud data, Building Serv. Eng. Res. Technol., 2006 Vol. 27, pp. 41-54.

The effectivity of a hybrid solar distillator directly combined with a solar cell

Kazuo Murase[1,*], Tin Yao[1], Toki Aoyagi[1], Keishi Okuyama[1]

[1] *Chuo University,1-13-27,Kasuga,Bunkyo-ku, Tokyo, Japan*
[*] *Corresponding author .Tel :+81(3)3817-1912, Fax :+81(3)3817-1895; email: hmurase@kc.chuo-u.ac.jp*

Abstract: Solar energy is one of the most promising natural and renewable energy resources. A solar membrane distillator hybridized with a photovoltaic cell supplies with both water and energy which are indispensable for human life and industry and contributes to effective utilization of renewable energy, especially solar energy. The effectivity of a hybrid solar membrane distillator was experimentally and numerically verified. The dependence of cell temperature on conversion efficiency was unrecognized in this work because of an amorphous Si module. However the hybrid solar distillator contributed to the stable standard conversion efficiency of a cell. Relationship between solar intensity and distillate productivity is almost identifiably approximated for the membrane distillator even if with or without a photovoltaic cell. This work indicated of the effectivity of a hybrid solar distillator with a photovoltaic cell.

Keywords: *Hybrid solar distillator, Solar cell, Membrane distillation, PTFE membrane*

Nomenclature

C_P : *Specific heat* ..... *J/(kg·K)*
D: Distillate productivity..... $kg/(m^2 \cdot s)$
e: Porosity of PTFE membrane..... *[-]*
FF: Fill Factor ..... *[-]*
I: Solar intensity..... W/m^2
I_{SC} : *Short Circuit Current* ..... *A*
k: Thermal conductivity..... *W/(m·K)*
l: Thickness of partition..... *m*
L: Length of hybrid distillator..... *m*
P: Saturated vapor pressure..... *Pa*
P_{MAX} : *Maximum Power*..... *W*
q_I: *Heat flux from solar energy*..... W/m^2
q_L: *Latent heat flux* ..... W/m^2
q_R: *Radiative heat flux* ..... W/m^2
q_S: *Sensitive heat flux*..... W/m^2
q_U: *Overall heat flux* ..... W/m^2
R: Gas constant..... $Pa \cdot m^3/(mol \cdot K)$
T: Temperature ..... *K*
u: Water velocity ..... *m/s*
U: Overall heat transfer coefficient..... $W/(m^2 \cdot K)$
V_{OC}: *Open Circuit Voltage*..... *[V]*
z: Interval ..... *m*
Geek
α: Absorptivity of partition..... *[-]*
Γ: Diffusion coefficient of vapor into air ..... m/s^2
δ: Membrane thickness..... *m*
ε: Emissivity of partition ..... *[-]*
ρ: Density ..... kg/m^3
σ: Stefan-Boltzmann constant ..... $W/(m^2K^4)$
η: Conversion efficiency..... *[%]*

1. Introduction

Water and energy are indispensable for human life and our industry. However arid regions and demand for water sources have been year by year expanding in the world with drastic increases in industrialization. The consumption of natural resources, particularly fossil fuel, for generating the huge energy causes environmental problems such as global warming. Therefore we should aggressively utilize inexhaustible natural resources such as ocean for water and solar energy as one of renewable energy. Utilization of renewable energy for desalination is one of the promising technologies for simultaneously resolving energy and water problems and for the soft global process as reviewed in reference [1].

Desalination is one of chemical separation processes which remove salt from seawater or saline or brackish water. Practical desalination processes are classified in thermal and non-thermal processes. Thermal processes utilize phase-change process, evaporation and

condensation, to produce to distillated water such as Multi-stage flash, Vapor compression and solar still. Non-thermal processes are membrane separation processes such as Reverse osmosis and Electrodialysis. Only Membrane Distillation (MD) is classified into both thermal and membrane process. MD has the advantages of high selectivity of separation, lower temperature or pressure operation and the high-mass transfer rate as reviewed in reference [2]. A solar driven membrane distillation is suitable for the combination of desalination process and utilization of renewable energy [3].

On other hands solar energy is one of the most promising and all ranged renewable energy according to the rapid and diverse development of a solar cell. However the maximum conversion efficiency of a cell is below at most 35% in spite of the active research of a new type of solar cell. The low efficiency results from the independent reuse of solar energy that is solar ray or solar heat. Therefore several hybrid photovoltaic–thermal systems have been researched in order to improve the conversion efficiency due to the dependence of cell temperature [4] or recover waste heat [5-7].

We have been developing a flat type of solar distillator for environmental problem of the global warming by irrigation [8-10]. The flat type of a membrane distillator has the easy combination with other processes due to supporting the water surface with a membrane. In order to effectively utilize solar energy in both energy sources, solar ray and heat, a new solar membrane distillator directly hybridized with a solar cell was set up not in conventional desalination process [11] but in solar distillator unified with a solar cell. A double glass solar cell manufactured by KANEKA Co.LTd and a wide PTFE membrane by NITTO DENKO were selected for the direct hybridization. The effectivity of our hybrid solar membrane distillator was experimentally and numerically investigated. .

2. Experimental set-up

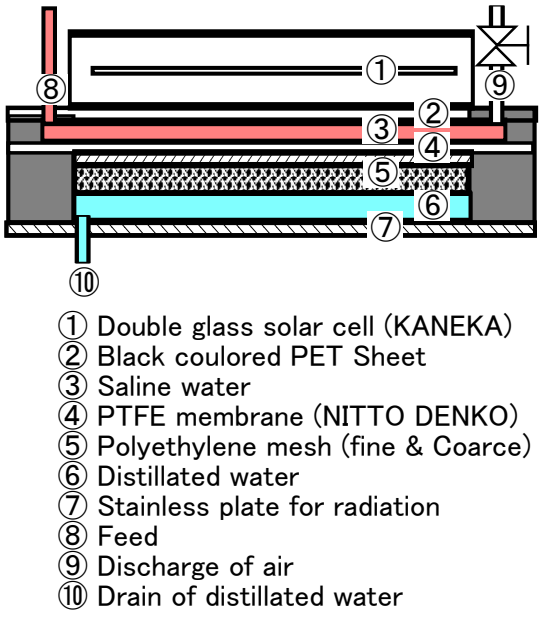

Figure 1. A schematic cross section hybrid solar distillator

Figure 1 schematically shows the cross section of a flat-type hybrid solar distillator combined with a solar cell. The double glass solar sell (manufactured by KANEKA Co.Ltd, Amorphous Si, 1.1cm in thickness, 0.98m in length, 0.95m in width) is put on a flat-type membrane distillator. The I-V Curve Tracer (EKO INSTRUMENTS, MP-160) was used to investigate dynamic fundamental characteristics of a cel l, the Open Circuit Voltage, Short Circuit Current, Conversion Efficiency and Fill Factor of solar cell. A flat-type of membrane distillator composed of a solar absorber of black colored PET sheet (1.88mm in thickness), saline water (2mm in thickness), PTFE (Poly Tera Fluoro Ethylene) membrane (NITTO-DENKO Co.Ltd,NTF-5200,1μm in porε diαmεtεr,85μm in thickness and 80% in void fraction), diffusion gap of water vapor supported with fine and coarse types of polyethylene meshes (5mm in thickness)and radiator of stainless plate(2.2mm in thickness). The hybrid distillator was tilted at the lower angle, 2 deg., for the stable water flow and set up at the outdoor situation in JAPAN. The intensity of solar energy measured with a pyranometer (EKO Instruments Co. Ltd. Model MS-42). Distillate productivity and

partitions temperatures obtained with cupper-constantan thermocouples were respectively recorded per one hour and one minute. The water volume heated through the cell was keeping at the constant value without the outlet of water. Each dynamic characteristics of separately solar cell, membrane distillator and the hybrid membrane distillator was independently measured in order to estimate the effectivity of the hybridization at the different weather conditions during the summer season in Japan

The Photovoltaic performance, particularly Conversion efficiency (η), was evaluated by I-V curve tracer (EKO Instruments Co. Ltd. Model MP-160) on the basis of experimental data of Open Circuit Voltage (V_{OC}), Short Circuit Current (I_{SC}), Maximum Power (P_{MAX}), Fill Factor (FF).

3. Numerical simulation

3.1. Heat and mass balances

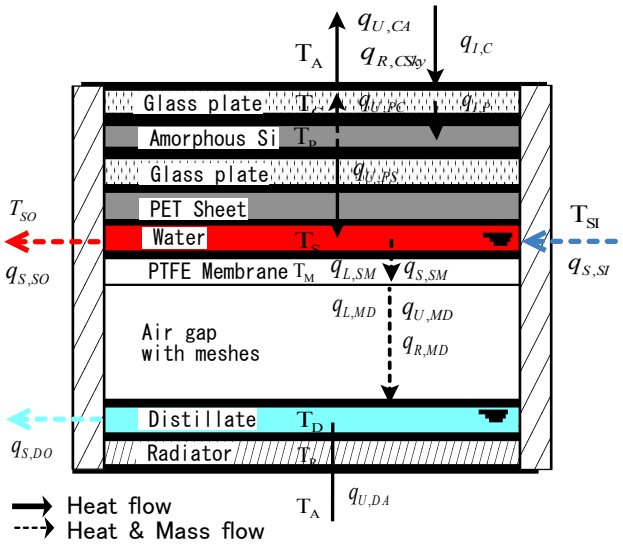

Figure 2. Heat and mass flow of a hybrid distillator

Figure 2 s hows flows of heat and mass transfer for the simulation model of a hybrid solar distillator. This model was constituted on the following assumptions ;

1. Temperature gradients in the flow direction are negligible.
2. Heat transfers with respect to PET sheet, PTFE membrane and radiator are approximated as overall heat transfer coefficients due to only heat conduction.
3. Temperature polarization across the PTFE membrane is negligible.
4. The mesh spacer within the air gap between the PTFE membrane and the radiator has no effect on the heat and mass transfer.

Energy balances for each partition are presented as follow:

Glass cover [T_C] $$:: \rho_C C_{P,C} \ell_C \frac{dT_C}{dt} = q_{I,C} + q_{U,PC} - q_{U,CA} - q_{R,CSky} \quad (1)$$

Amorphous Si [T_P] $$:: \rho_P C_{P,P} \ell_P \frac{dT_P}{dt} = q_{I,P} - q_{U,PC} - q_{U,PS} \quad (2)$$

Saline Water [T_S] $$: \rho_S C_{P,S} \ell_S \left(\frac{dT_S}{dt} + u_S \frac{dT_S}{dx} \right) = q_{U,PS} - q_{S,SM} + q_{S,SI} - q_{S,SO} \quad (3)$$

PTFE Membrane [T_M] $$: \rho_M C_{P,M} \ell_M \frac{dT_M}{dt} = q_{S,SM} - q_{L,MD} - q_{U,MD} - q_{R,MD} \quad (4)$$

Distillated Water [T_D] $: \rho_D C_{P,D} \ell_D \left(\frac{dT_D}{dt} + u_D \frac{dT_D}{dx} \right) = q_{L,MD} + q_{U,MD} + q_{R,MD} - q_{U,DR}$ (5)

Radiator [T_R] $: \rho_R C_{P,R} \ell_R \frac{dT_R}{dt} = q_{U,MR} - q_{U,RA}$ (6)

Distillate productivity is evaluated the following expression [12]

$$D = \Gamma \frac{\pi}{RT_{av}} \frac{1}{\left(\delta / e^{3.6} + z\right)} \frac{P_S - P_D}{P_{BM}}$$

3.2. Numerical analysis

Heat and mass transfer Equations.(1)-(7) were numerically simulated by Runge-Kutta method for estimating dynamic characteristics during one day and compared with experimental data in the open air situation. The temperature gradients along the flow direction may be negligible due to some partitions with high thermal conductivities. The initial or static conditions were estimated by simulated data at the steady state.

4. Results and discussion

4.1. Dynamic characteristics of solar cell

4.1.1. Effect of hybridization on conversion efficiency (η)

Conversion efficiency of photovoltaic cell (η) can βe estimated by the following expression.

$$\eta = \frac{P_{\max}}{P_{in}} = \frac{V_{OC} I_{SC} FF}{P_{in}} \times 100[\%] \quad (8)$$

Figures 3-(a),(b) show profiles of generated power by a photovoltaic cell and conversion efficiency (η) averaged for one hour in case of (a) exclusive solar cell (11.Augus.2010) and (b) hybridized cell (26.August.2010). In spite of the lower solar intensity per a day Fig. 3(b) shows the higher peak power and average conversion efficiency as shown in Table 1, which is list up each averaged values from 7:00 to 18:00.

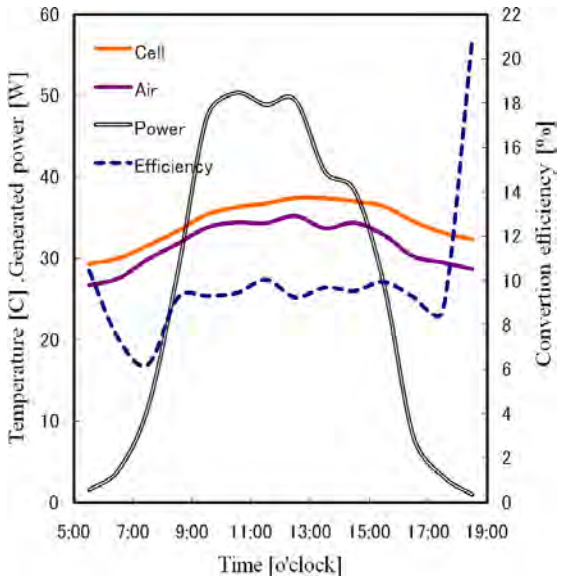

(a) Exclusive solar cell
[I=20.4MJ/(m^2·d),11.August.2010]

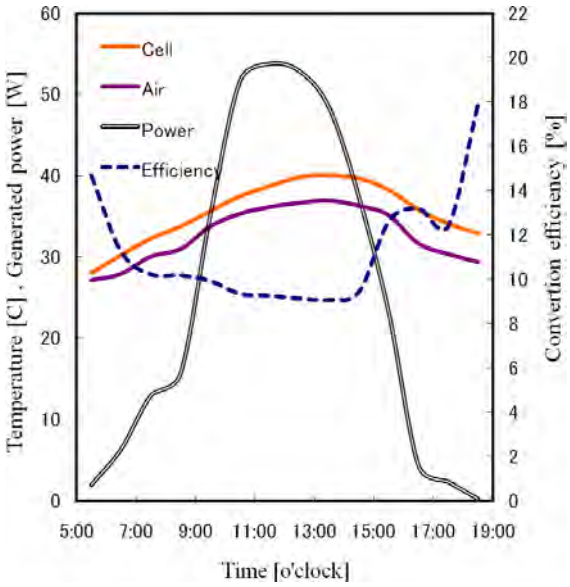

(b) Hybridized cell
[I=19.0MJ/(m^2·d), 26.August.2010]

Figures 3. Profiles of generated power and conversion efficiency for one day

Table 1 Each characteristic value averaged for 10 hours from 7:00 to 18:00

	Efficiency(η)	Power(P)	$T_{Cell\text{-}terminal}$	T_{Air}
(a) Exclusive solar cell	9.13	32.13	35.36	32.76
(b) Hybridized cell	10.42	30.7	36.85	33.96

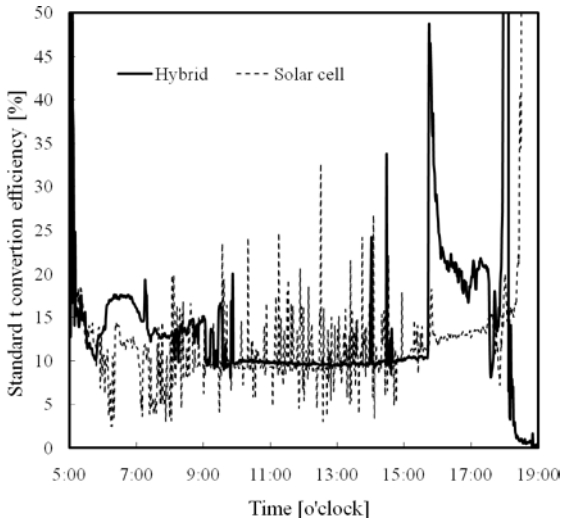

Figure 4. Detailed profiles of standard conversion efficiency

The conversion efficiency at the standard condition of solar irradiation (1kW/m^2) and of cell temperature (25C) is generally available for the public evaluation due to the free dependency of cell temperature. Figure 4 shows detailed profiles of standard conversion efficiency in two cases. Hybridization compresses fluctuation of standard conversion efficiency due to the steady water. In this work water has no flow along the PET sheet and was supplied only for the volume of evaporated water vapor due to the closed outlet of water. Solar intensity inherently has a fluctuated profile due to the presence of variable weather conditions such as cloud, indirect intensity, wind and so on.

4.2. Dynamic characteristics of membrane distillation

4.2.1. Effect of hybridization on temperature profiles of each partition

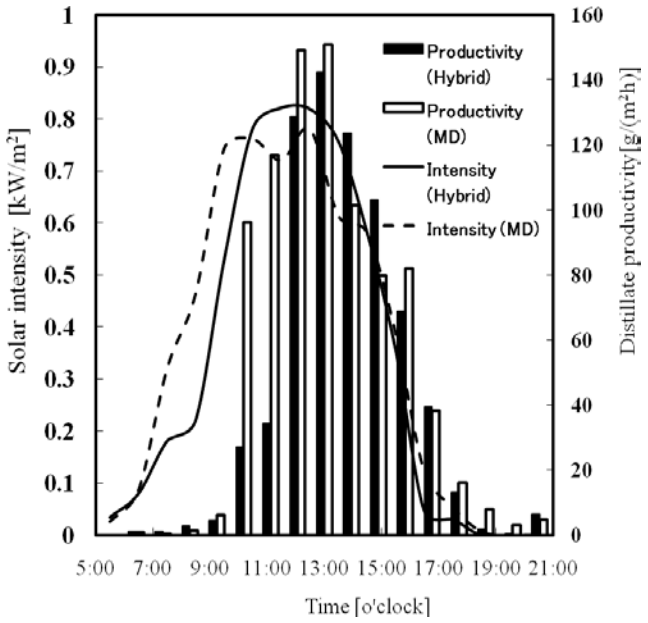

Figure 5. Effect of hybridization on distillate productivity for one hour

Figure 5 shows profiles of distillate productivity per one hour in two cases of hybrid distillator and membrane distillator without a photovoltaic cell. Table 2 lists up experimental data with total distillate productivity per a day in cases of MD with and without a cell. In spite of the less solar intensity by 20% i, the decrease of distillate productivity n case of the hybridized MD was settled within the less range of 7%.

Figures 6-(a),(b) indicate that hybridization increases the temperature difference between PET sheet and distillate partition. The temperature on PET sheet almost equals to that of evaporated water. The distillate productivity only depends on t he temperature difference between evaporated vapor and condensed water .

Table 2 Total distillate productivity per a day in cases of MD with and without a cell

	Solar intensity [MJ/(m^2・d)]	Distillate productivity[kg/(m^2・d)]
MD without a cell	20.4	0.855
Hybridized cell	19.0	0.691

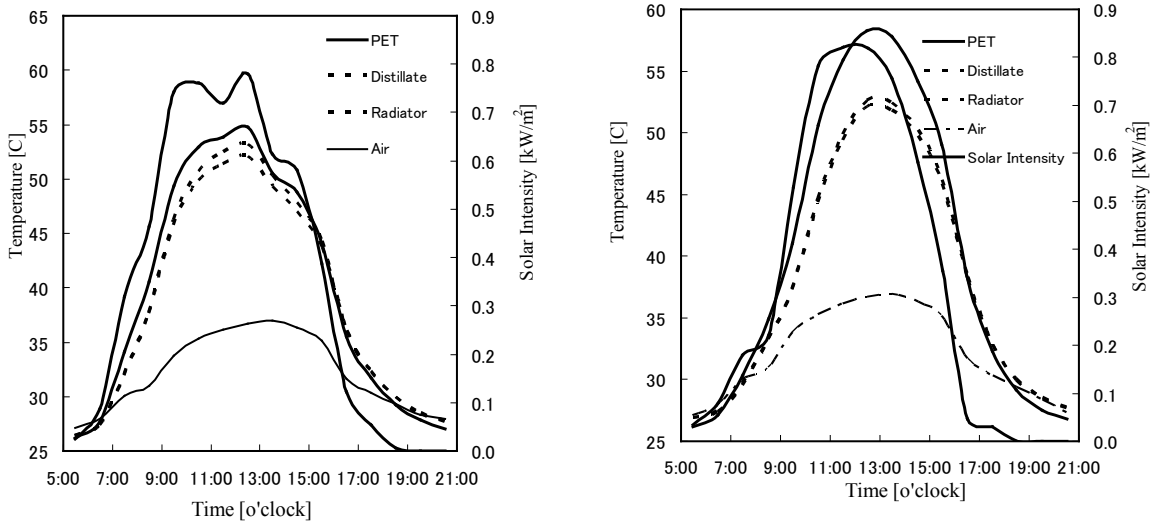

(a) MD without a cell *(b) MD with a cell (Hybrid)*

Figures 6. Temperature distributions in two types of Membrane Distillators (MD)

4.2.2. Numerical results

Figures 7-(a),(b) show profiles of dynamic distillate productivity by numerical simulation in two cases of membrane distillator with and without a photovoltaic cell. Experimental solar intensity and air temperature were used as the weather parameters. The peak value of distillate productivity is underestimated because productivity in Fig.7-(a) was calculated by the hybrid simulation model. Both profiles of productivity in Figs.7-(a),(b) were correspondingly traced by the model. However experimental times at the peak productivity were shifted by two hours from that of solar intensity. The calculated productivity has a response of no time lags for solar intensity due to the negligible temperature gradient along the water flow. The assumption will be invalid in case of operational conditions of water flow. The larger specific heat of water and thickness of spacer mesh than other partitions result in the time lag.

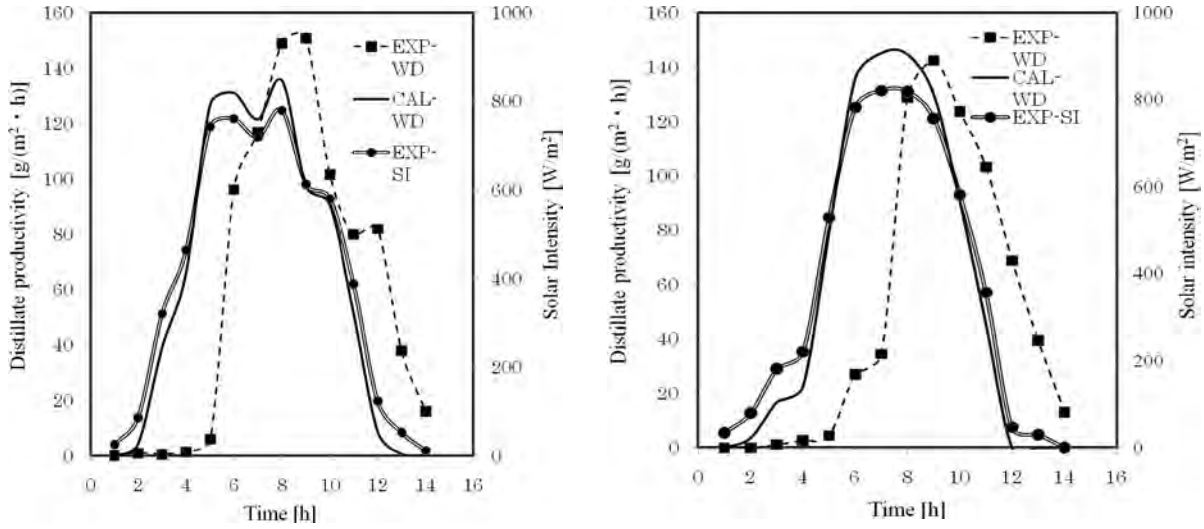

(a) MD without a cell *(b) MD with a cell (Hybrid)*

Figures 7. Numerical prediction of distillate productivity

4.2.3. Effect of hybridization on distillate productivity

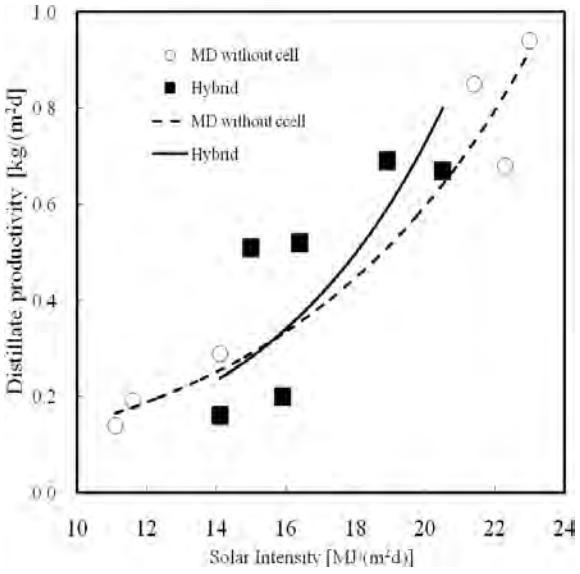

Figure 8. Effect of solar intensity on distillate productivity

Figure 8 shows the effect of solar intensity on distillate productivity for one day. Experimental data were intensively obtained at the summer season in Japan due to the less solar intensity than other arid lands. Approximated curves with experimental relationship between solar intensity and distillate productivity for membrane distillators even if with or without a photovoltaic cell were almost identifiable. The results indicate the effectivity of a hybrid solar membrane distillator directly with a photovoltaic cell even if for the increasing thermal resistances. The productivity is not necessarily desirable in comparison with our previous report [8]. The improvements of hybridization and process flow of water are required.

5. Conclusions

A solar membrane distillator hybridized with a photovoltaic cell supplies with both water and energy which are indispensable for human life and industry and contribute to effective utilization of renewable energy. The effectivity of a hybrid solar membrane distillator was experimentally and numerically verified.

The dependence of cell temperature on conversion efficiency was unrecognized in this work because of an amorphous Si module. However the hybrid solar distillator contributed to the stable standard conversion efficiency of a cell. An amorphous Si module is suitable for the comparatively higher temperature condition.

Relationship between solar intensity and distillate productivity is almost identifiably approximated for the membrane distillator even if with or without a photovoltaic cell. .The performance of distillate productivity is not necessarily desirable. The improvements of hybridization and process flow of water should be required.

Acknowledgements

The authors would like to thank Mr. Takuji Nomura, KANEKA Co LTD, and Mr. Hajime Oya, NITTO DENKO CO.LTD, respectively for their support of a Photovoltaic cell and a PTFE membrane.

References

[1] S.A.Kalogirou, Prog. Energy Combustion Sci.31, 2005, pp.242-281.

[2] M.Khayet, Adv. Colloid Interface Sci., 2010.(in press)

[3] H.Chang et al, Renewable energy 35, 2010 pp.2714-2722.

[4] E.Skoplaki et al. , Solar Energy Materials & solar cells 92, 2008, pp.1393-1402

[5] T.T.Chow et al. ,Solar energy 801, 2006, pp.298-306

[6] R.M.da Silva and J.L.M.Fernandes, Solar energy 12, 2010 pp.1985-1996

[7] A.Tiwari and M.S.Sodha, Renewable energy 31, 2006, pp.2460-2474

[8] K.Murase et al., Bulletin Society of Sea Water Sci. Japan 54, 2000, pp. 30-36

[9] K.Murase et al., Desalination and Water Treatment 9, 2009, pp. 96- 104

[10] K.Murase et al., Proc. WC IDA (DB09-099), 2009, Dubai

[11] S.Kumar and A.Tiwari, Energy Conversion and Management 51, 2010, pp.1219-1229

[12] H.Kurokawa et al., Kagaku Kogaku Ronbunnshu 14, 1988, pp.330-336

Comparative Energy and Exergy Analysis of Various Passive Solar Distillation Systems

Ragh Vendra Singh[1], Rahul Dev[2,*], M. M. Hasan[1], G. N. Tiwari[2]

[1]*Department of Mechanical Engineering, Jamia Milia Islamia, Jamia Nagar, New Delhi-110025, India.*
[2] *Centre for Energy Studies, Indian Institute of Technology, Delhi, Hauz khas, New Delhi-110016, India.*
** Corresponding author. Tel: +91 9968344470, Fax: +91 11 26591251, E-mail: rahuldsurya@yahoo.com*

Abstract: In this communication, a comparative energy and exergy analysis of various conventional solar distillation systems has been presented. The study includes passive solar distillation systems such as single and double slope solar stills. In a single slope solar still category, three solar stills with inclination angles 15º, 30º and 45º and a 15º inclined single slope multi wick solar still have been considered. Whereas one double slope solar stills and one double slope multi wick solar still, both inclined at 15º with east-west orientation, have been considered in double slope solar still category. The embodied energy is an important factor which depends on locally available materials and their manufacturing technologies. Materials like concrete, wood, steel etc are considered to calculate the embodied energy for the solar still equivalent to the fibre reinforced plastic after deriving the formulae. It has been found that the energy, exergy and embodied energy of single slope solar still are found higher than that of double slope solar still. Those materials which have lower thermal conductivity and low embodied energy than that of FRP such as concrete, PVC, wood can replace the FRP to save the embodied energy for similar performance. The metals have high embodied energy hence these can not be considered in terms of embodied energy despite the use of insulation.

Keywords: *Solar distillation, Water purification, Energy, Exergy, Embodied energy.*

Nomenclature

A_s *area of solar still*..... m^2
$I(t)$ *solar intensity* ..... W/m^2
$\dot{E}x_{evap}$ *exergy output*……..…… W/m^2
$\dot{E}x_{in}$ *exergy input*……..…… W/m^2
$K_{material}$ *thermal conductivity of material*. W/mK
K_{metal} *thermal conductivity of metal*……... W/mK
K_{FRP} *thermal conductivity of FRP*…..…… W/mK
L *latent heat of vaporization*..... *kJ/kg-K*
$l_{material}$ *thickness of material*……..…… *m*
l_{metal} *thickness of metal*……..…… *m*
$l_{Styrofoam}$ *thickness of Styrofoam*……..…… *m*
$\dot{m}_{ew}$ *hourly distillate collected*..... kg/m^2-*h*
$\dot{q}_{ew}$ *heat utilized in evaporation of water*… W/m^2
T_a *ambient temperature*..... *K*
T_s *sun temperature*..... *K*

1. Introduction

A solar distillation is a water purification technology. Saline/brackish water can be purified using solar energy. This technology works on the principles of greenhouse effect and hydrological cycle. The use of solar energy to produce potable water is a key factor in context of water & air pollution, global warming, energy security and climate change because most of other water purification technologies use conventional sources of energy such as coal, oil, gas etc [1]. A solar still is a device used for solar distillation in which impure or saline water is fed to obtain distilled water. It is a box type structure made of some materials such as fibre reinforced plastic (FRP), wood, concrete, or steel with insulation. It is covered with a simple window glass through which the solar radiation passes to incident on the water surface. A small amount of reflection heat losses and absorption take place at the glass cover and the water. A major part of incident solar radiation is absorbed by the basin liner. This heat is transferred to the saline water by convection as top heat loss and to the ambient as bottom heat loss. Heat transfer from the water to the glass cover take place by three mechanisms: evaporation, convection and radiation. Vapour leaves most of contaminants and microbes

through thermal diffusion on the basin liner. Further the vapour undergoes film type condensation at the inner surface of the glass cover because of inclination of glass cover, adhesion, cohesion between condensed water molecules, and gravity. The condensed water trickles down to a trough which guides it into a container placed otuside [2]. Researchers have worked to improve the performances of solar stills by suggesting its various designs, materials and operating conditions for different weather conditions. Tiwari and Tiwari [3] have reported that the yield from a single slope passive solar still may vary from 0.5 to 1.2 kg/m^2/day (in winter) and 1.0 to 2.5 kg/m^2/day (in summer) for Delhi, India. Tiwari [4] has found the efficiency of the single slope solar still 25.8, 19.7, 22.8 % at glass cover inclinations 15°, 30° and 45° respectively for the summer climatic condition of Delhi, India. Malik et al. [2] have shown that overall efficiency of a passive solar still is achieved with least water mass in the basin.

Energy and exergy analysis of solar stills have been presented by various researcher such as Dunkle [5], Cooper [6], Tsilingiris [7], and Dwivedi [8, 9] etc. A group of improved heat and mass transfer correlations in basin type solar stills has been developed by Hongfei et. al. [10]. Torchia- Núñez et al. [11] have found that for same exergy input a basin, brine and passive solar still have exergy efficiencies of 12.9%, 6%, and 5% respectively. Dev and Tiwari [12, 13] developed the characteristic equation for single and double slope passive solar stills. In ideal solar still, the instantaneous loss efficiency is minimum (for zero depth of water mass) as analyzed by Cooper [6]. Rubio et al. [14, 15] have studied asymmetries in various temperatures and amount of distillate for a double slope passive solar still (DSPSS) and proposed mathematical models, one in terms of lumped parameters and another for controlled temperatures of glass cover and basin. Dwivedi and Tiwari [8, 9] have reported that the thermal efficiency for single and double slope solar still varies from 22.6% to 31.3% and 25.4% to 34.3% respectively at 0.01 m water depth. Similarly, the average exergy efficiency for single and double slope solar still is 0.65% and 0.82% respectively. The exergy efficiency of single and double slope solar still varies from 0.18 to 1.25% and 0.13 to 1.16% respectively. Tiwari and Yadav [16] have shown that a single slope distiller gives better performance than a double slope for cold climatic conditions whereas a double slope distiller gives better performance than a single slope for summer climatic conditions irrespective of either basin type or multi-wick type. It has also been reported that the concrete basin solar still gives better performance than the FRP single and double slope stills because of the probability of leakage of vapour in the FRP stills was more than for the concrete still. Sakthivel and Shanmugasundaram [17] have shown that the efficiency of single slope solar still using the black granite gravel reaches up to 52% maximum which is 8% higher than the conventional single slope solar still. Singh and Tiwari [18] have studied double effect multi-wick solar stills to increase the still efficiency by utilizing the latent heat released by the vapor at first effect. Kumar and Anand [19] have studied shown that a tubular multiwick solar still gives distillate output of about 8%, 13%, and 18% more than tubular, simple multi-wick and conventional basin type solar stills respectively.

The embodied energy is an important factor which depends on locally available materials and their manufacturing technologies. Hence, on the basis of literature survey the performance of the solar stills on the basis of energy, exergy and materials have been analyzed in this paper.

2. Solar distillation systems

Passive solar distillation systems such as single and double slope solar stills have been taken. In a single slope solar still category, three solar stills with inclination angles 15º, 30º and 45º

(Fig. 1a, 1b) and a 15º inclined single slope multi wick solar still have been considered. Whereas one double slope solar stills and one double slope multi wick solar still both inclined at 15º with east-west orientation, have been considered in double slope solar still category (Fig. 1c, 1d). All these experimental setup have been installed at Solar Energy Park, I.I.T. Delhi, New Delhi, India (28°35´ N, 77°12´ E, altitude 216 m from mean sea level). The single slope solar still works on same principle as given above.

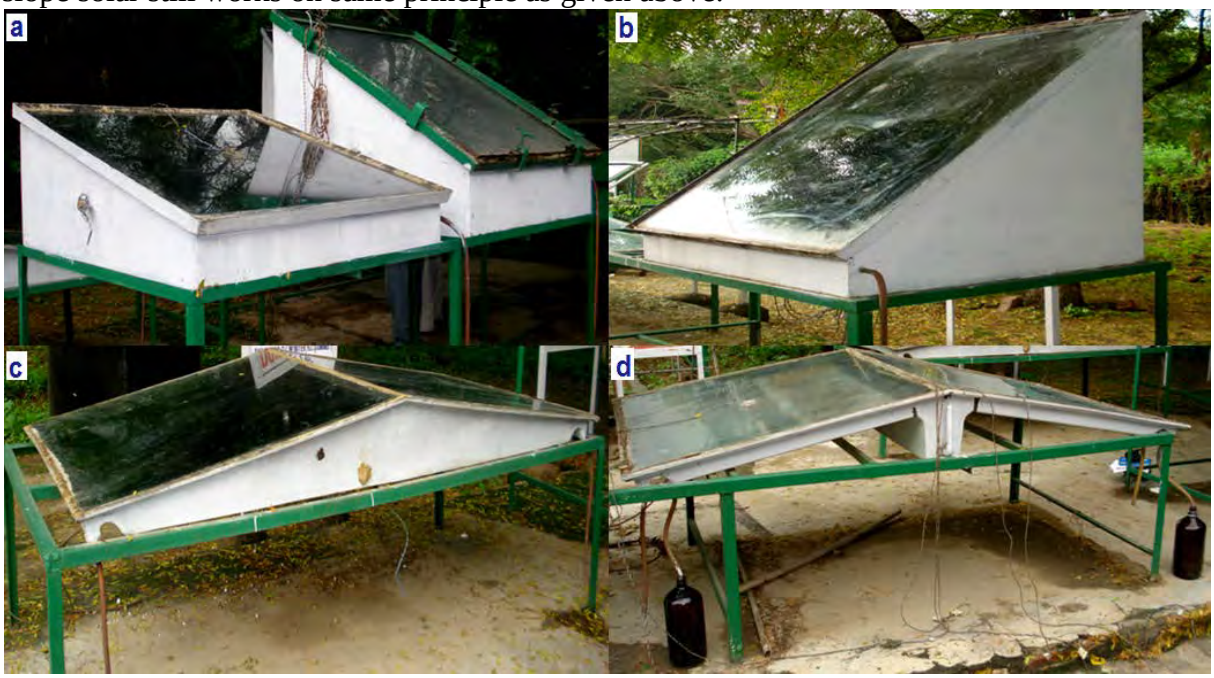

Fig. 1 Various solar stills: (a) Single slope solar still inclined at 15º and 30º with orientation towards south, (b) Single slope solar still inclined at 45º with orientation towards south, (c) Double slope solar still inclined at 15º with orientation towards east-west, (d) Double slope multi-wick solar still inclined at 15º with orientation towards east-west.

A schematic diagram of double slope passive solar still has been shown in Fig. 1c. Two simple window glasses have been placed over the walls of the solar still at inclination angle 15° facing east and west directions. To absorb higher amount of solar radiation, an inside surface of the solar still has been painted black in color. An inlet through the rear wall has been provided to feed the brackish/underground water in to the basin of the solar still. And two troughs are provided at inside of each short wall of the solar still to collect the distilled water. The orientation of the solar still has been kept east-west to receive solar radiation for maximum hours of sunshine. When the sun lies in the east direction then higher temperature difference occur at west side due to low glass temperature which yield higher amount of distillate at this side and vice versa except at the time of noon when both the glass covers have almost the same temperature.

In the single and double slope multi-wick solar still, water is fed from water reservoir through the multiple porous absorbers (black jute cloth) at a slow rate for fast evaporation. The saline water goes upwards due to capillary action in the jute cloths and forms a thin water layer. The solar radiation, after transmission through the glass covers, strikes this water film and heats the water. The water evaporates and condenses at the inner surface of the glass cover by releasing latent heat of vaporization. The condensed water is collected through the drainages for distilled water. A double slope multi-wick solar still, as shown in Fig. 1d, is a

development over the single slope multi-wick solar still similar to double slope solar still, Malik et al. [2]. The specifications of these solar stills are given in Table 1.

Table 1. Design specifications of solar stills which are installed at Solar Energy Park, Centre for Energy Studies, IIT Delhi, New Delhi, India.

Sr. No.	Specifications	Single slope solar still			
		Conventional			Multi-wick
		Type 1	Type 2	Type 3	Type 4
1	Area of basin (m^2)	1 × 1	1 × 1	1 × 1	1.1 × 1.14
2	Height of south wall (m)	0.06	0.15	0.15	0.06
3	Height of north wall (m)	0.26	0.74	1.15	0.25
4	Angle of inclination (°)	15	30	45	15
5	Size of glass (m^2)	1.02 × 1	1.02 × 1.2	1.02 × 1.44	1.02 × 1.14
6	Quantity of glass	1	1	1	1
7	Putty (kg)	1	1	1.5	1
8	Paint (kg)	0.5	0.8	1	0.5
9	Iron stand (kg)	5	20	18	17
10	Metal (kg)	0.2	0.2	0.2	nil
11	Jute cloth (m^2)	…	…	…	4 × 1

Sr. No.	Specifications	Double slope solar still	
		Conventional	Multi-wick
		Type 5	Type 6
1	Area of basin (m^2)	2 × 1	2 ×(1.1 × 1.14)
2	Height at ends (m)	0.25	0.05
3	Central height (m)	0.45	0.25
4	Angle of inclination at both sides (°)	15	15
5	Size of glass (m^2)	1.02 × 1.02	1.02 × 1.14
6	Quantity of glass	2	2
7	Putty (kg)	3	3
8	Paint (kg)	1	1
9	Iron stand (kg)	35	30
10	Metal (kg)	0.2	0.5
11	Black Jute cloth (m^2)	…	8 × 1

3. Mathematical expressions

Following are the mathematical expression used for the analysis of energy and exergy of considered solar still systems.
The thermal efficiency of a passive solar still can be calculated by the following formula [1]:

$$\eta_i = \frac{\dot{m}_{ew} \times L}{A_s \times I(t) \times 3600} \times 100 \qquad (1)$$

Exergy efficiency of a passive solar still can be calculated by the following formula [20]:

$$\eta_{EX} = \frac{\dot{E}x_{evap}}{\dot{E}x_{in}} \times 100 \qquad (2)$$

where,

$$\dot{E}x_{evap} = \sum_{i=1}^{24}\left(1 - \frac{T_a}{T_w}\right) \times \dot{q}_{ew} \quad ; \quad \dot{q}_{ew} = A_s.h_{ew}.\left(T_w - T_{gi}\right)$$

and

$$\dot{E}x_{in} = \dot{E}x_{sun} = A_s \times I(t) \times \left[1 - \frac{4}{3} \times \left(\frac{T_a}{T_s}\right) + \frac{1}{3} \times \left(\frac{T_a}{T_s}\right)^4\right]$$

Equivalent thickness of materials for same performance as FRP has in case of solar still:

$$l_{material} = \frac{K_{material}}{K_{FRP}} \times l_{FRP} \qquad (3)$$

Thickness of Styrofoam for insulation (when solar still is made of any metal and overall thermal conductivity is equivalent to FRP):

$$l_{Styrofoam} = \frac{K_{Styrofoam}.\left(K_{Metal}.l_{FRP} - K_{FRP}.l_{Metal}\right)}{K_{Metal}.K_{FRP}} \qquad (4)$$

4. Results and discussion

On the basis of literature survey and Eqs. (1, 2) it has been observed that energy, exergy efficiencies and embodied energy of single slope solar still remain higher in comparison to that of the double slope solar still. Dev and Tiwari [12,13] have found better performances at water depth 0.01 m and an inclination angle 30º for single slope passive solar still. They have also developed the characteristic equation of single and double slope passive solar still and suggested the sum of instantaneous gain and loss efficiencies ($\eta=\eta_i + \eta_{iL}$) remain lower than maximum efficiency under ideal i.e. 60%. Although, it can be seen that the energy efficiency can reach up to 60% maximum but because of several factor such as heat loss through vapor leakage and improper insulation, time lag in production, inclination angle, water depth etc, it does not attain such value. Similarly, the exergy efficiency which is measured for the source temperature i.e. sun temperature 6000 K , remain always very much lower than the energy efficiency because of the energy input by the sun is not fully utilized in evaporation process of the water in the solar still.

The design specifications (Table 1), properties of various materials (Table 2 which consists of probable materials for solar still), Eqs. (3) and (4) have been used to get total embodied energy for the solar still by considering metals, concrete, PVC, wood etc. equivalent to that of

FRP (i.e. to keep the productivity of the solar still same as of FRP). The metals have been found large thickness due to their conductivities but these metals (thickness 1 mm) can be considered with insulation of Styrofoam as shown in Table 2. One can see that steel which is very high energy intensive material can not be recommended as a material to make the solar still despite the use of insulation. The thicknesses of materials such as concrete, wood, and PVC have been found very near to the thickness of the FRP. Materials such as glass window and country fired bricks have more thickness which can not be considered.

Table 2. Various manufacturing materials of solar still, their thermal conductivities, embodied energy, density and thickness with and without insulation material.

Material	**Conductivity at 25 °C** (W/mK)	**Embodied energy** (MJ/kg) **(In India)**	**Density** (kg/m^3)	**Thickness of material without insulation** (m)	**Thickness of insulation** $l_{styrofoam}$ (m) **(for l_{metal}=1 mm)**
Copper	401	112	8930	5.7	0.0005
Steel	16.3	42	7860	0.232	0.0005
G.I. sheet	80	50.8	7860	1.14	0.0005
Aluminium	250	260	2600	3.56	0.0005
Concrete	0.42	2.4	2200	0.006	------
Country fired brick (22x10.5x6.5 cm^3 - delivered at 30 km)	1.31	7.9	286	0.018	------
Simple window glass	0.96	15.9	2600	0.014	------
Polystyrene expanded	0.03	117	640	0.001	------
Wood	0.17	1.8	850	0.0025	------
PVC	0.19	115	1410	0.003	------
Styrofoam (for insulation only)	0.033	100	35	------	------
FRP	0.351	92.2	1800	0.005	------
Paint	------	90	6.1	------	------
Jute cloth	------	55	-----	------	------

Note: Embodied energy values based on several international-local sources may vary.

The embodied energies of conventional single slope solar stills made of FRP, concrete, PVC, and wood are found and given in Table (3). The percentage increase in the embodied energy compared of other solar stills compared to that of single slope solar still inclined at 15°, with south wall height 0.06 m has also been given in same table which changes similarly irrespective of material used. The embodied energy double slope solar still, and double slope multi-wick solar still have been found to be 3070 MJ and 2323 MJ respectively when only FRP is considered. On the basis of this one can observe that the embodied energy of double slope solar stills including the multi-wick solar still are less energy intensive in comparisons to single slope solar stills (1361 MJ) and single multi-wick solar still (1495 MJ). One can see in Table 3, wood is found most suitable in terms of embodied energy but it degrades soon in comparison to other materials in terms of life. The PVC can be a better option over FRP in

terms of embodied energy and weight. According to previous studies [3, 4], single slope solar still inclined at 30° is suitable as per the latitude of Delhi. The total embodied energy for this solar still including glass, paint has been found 2587 MJ (FRP), 369 MJ (concrete), 1498 MJ (PVC), 292 MJ (wood). Similarly for double slope multi-wick solar still inclined at 15°, total embodied energy including glass, paint and fabric have been found 2875 MJ (FRP), 640 MJ (concrete), 1773 MJ (PVC), 562 MJ (wood).

Table 3. Embodied energy of single slope solar still for different materials such as FRP, Concrete, Steel, Wood.

Solar still	Specifications	Embodied energy (MJ)							
		FRP	Concrete	PVC	Wood	% increase	Glass	Paint	Fabric
Single slope	15°, with south wall height = 0.06 m	1361	52	718	6	----	168	28	----
	15°, with south wall height = 0.15 m	1776	68	937	8	30	168	45	----
	30°	2306	88	1217	11	70	208	73	----
	45°	2987	114	1576	14	120	245	90	----
	15°, Multi-wick	1495	57	790	6.6	10	226	45	27.5
Double slope	15°	3070	117	1615	13.5	125	345	90	----
	15°, Multi-wick	2323	88	1221	10.2	70	407	90	55

5. Conclusions

1. On the basis of above analysis and literature survey, the energy, exergy and embodied energy of single slope solar still are found higher than that of double slope solar still.
2. Those materials which have lower thermal conductivity and low embodied energy than that of FRP such as concrete, PVC, wood can replace the FRP to save the embodied energy for similar performance.
3. The metals have high embodied energy hence these can not be considered in terms of embodied energy despite the use of insulation.
4. PVC material has been found to be better in terms of embodied energy in comparison to other materials.

On the basis of above study, the similar analysis can be recommended for other materials such as glass, steel, aluminum, copper, bricks, and other advance materials, as the research in the field of materials science is progressing, to have a material of less embodied energy, light in weight, good insulator and portable in comparison to FRP as well which should be easily available in less price.

References

[1] G.N. Tiwari, A.K. Tiwari, Solar distillation practice for water desalination systems, Anshan Publication, UK Edition, 2008, pp. 1-40.

[2] M.A.S. Malik, G.N. Tiwari, A. Kumar, M.S. Sodha, Solar Distillation, Pergamon Oxford, 1982, pp. 1-35.

[3] A.K. Tiwari, G.N. Tiwari, Effect of the condensing cover's slope on internal heat and mass transfer in distillation: an indoor simulation, Desalination 180, 2005, pp. 73-88.

[4] A.K. Tiwari, Annual performance of solar stills for different inclinations of condensing covers and water depths. PhD Thesis, Centre for Energy Studies, IIT Delhi, New Delhi, India, 2006.

[5] R.V. Dunkle, Solar Water Distillation: The Roof Type Still and a Multiple Effect Diffusion Still, Int. Development in Heat Transfer. ASME proceedings, 1961(part5), pp. 895-902.

[6] P.I. Cooper, The maximum efficiency of single-effect solar stills, Solar Energy 15, 1973, pp. 205-214.

[7] P.T. Tsilingiris, Modeling heat and mass transport phenomena at higher temperatures in solar distillation systems – The Chilton–Colburn analogy , Solar Energy 84, 2010, pp. 308-317.

[8] V.K. Dwivedi, G.N. Tiwari, Annual energy and exergy analysis of single and double slope passive solar stills, Applied Science Research 3(3), 2008, pp. 225-241.

[9] V.K. Dwivedi, Performance study of various designs of solar still. PhD Thesis: Centre for Energy Studies, IIT Delhi, New Delhi, India: 2009.

[10] Z. Hongfei, Z. Xiaoyan, Z. Jing, W. Yuyuan, A group of improved heat and mass transfer correlations in solar stills, Energy Convers. Mgmt. 43, 2002, pp. 2469-2478.

[11] J. C. Torchia- Núñez, M. A. Porta-Gándara, J.G. Cervantes-de Gortari, Exergy analysis of a passive solar still, Renewable energy 33(4), 2008, pp. 608-616.

[12] R. Dev, G.N. Tiwari, Characteristic equation of a passive solar still, Desalination 245, 2009, pp. 246-265.

[13] R. Dev, H.N. Singh, G.N. Tiwari, Characteristic equation of double slope solar still, Desalination 267, 2011, pp. 261-266.

[14] E. Rubio, M.A. Porta, J.L. Fernanadez, Cavity geometry influence on mass flow rate for single and double slope solar stills. Applied Thermal Engineering 20, 2000, pp. 1105-1111.

[15] E. Rubio, J.L. Fernandez, M.A. Porta-Gandara, Thermal performance of the condensing cover in a triangular solar still, Renewable Energy 29, 2004, pp. 895-906.

[16] G.N. Tiwari, Y.P. Yadav, comparative designs and long term performance of various designs of solar distillery, Energy Convers. Mgmt 27(3), 1987, pp. 327-333.

[17] M. Sathivel, S. Shanmugasundaram, Effect of energy storage medium (black granite gravel) on the performance of a solar still, Int. J. of Energy Research 32, 2008, pp. 68-92.

[18] A.K. Singh, G.N. Tiwari, Performance study of double effect distillation in a multiwick solar still. Energy Convers. Mgmt 33 (3), 1992, pp. 207-214.

[19] A. Kumar, J.D. Anand, Modelling and performance of a tubular multiwick solar still. Energy 17 (11), 1992, pp. 1067-1071.

[20] A. Hepbasli, A key review on exergetic analysis and assessment of renewable energy resources for a sustainable future, Renewable and Sustainable Energy Reviews 12, 2008, pp. 593–661.

Simulation of a solar assisted combined heat pump-Organic Rankine Cycle-system

Stefan Schimpf[1,*], Karsten Uitz[2], Roland Span[1]

[1] *Ruhr-Universität Bochum, Thermodynamics, Bochum, Germany*
[2] *SIMAKA Energie- und Umwelttechnik GmbH, Argenbühl, Germany*
** Corresponding author. Tel: +49 2343226390, Fax: +49 2343214163, E-mail: s.schimpf@thermo.rub.de*

Abstract: In conventional collector systems for the supply of domestic hot water and space heating the collectors come to a standstill during summer whenever the maximum temperature in the storage tank is reached. The resulting excess heat can be harnessed by a combined heat pump-Organic Rankine Cycle-system. The aim of this work is to simulate such a system in order to determine the optimum operating conditions and impacts on power requirement and cost. For this purpose models for collector, storage tank, heat pump and geothermal heat exchanger are implemented. First results indicate that the isentropic efficiency of the scroll expander has the largest influence on the ORC-revenue. For a system consisting of 12 m² flat-plate collector area with an expansion efficiency of $\eta_{s,\exp} = 0.7$ the power requirement for space heating and domestic hot water is reduced by 3.6%, whereas the costs decrease by 42 € or 12.3% respectively compared to a conventional system. The results suggest that an installation is more reasonable in larger dwelling units like hotels, senior citizens' homes and multiple family dwellings.

Keywords: *Solar Heating, Organic Rankine Cycle, Heat pump.*

Nomenclature

A_c	collector aperture area	m²	
c	coefficients of the characteristic line of the collector		
$c_{p,CF}$	isobaric heat capacity of collector fluid	kJ/kgK	
COP	coefficient of performance of the heat pump		
C_{tot}	total electricity costs	€	
$E_{HP,DHW}$	electricity consumed by the heat pump for domestic hot water	kWh	
$E_{HP,SH}$	electricity consumed by the heat pump for space heating	kWh	
E_{ORC}	electricity generated in the ORC	kWh	
E_{tot}	total consumed electricity	kWh	
F'	collector efficiency factor		
G_b	beam radiation	W/m²	
G_d	diffuse radiation	W/m²	
h	enthalpy	kJ/kg	
K_θ	incidence angle modifier		
$\dot{m}_{ex}$	external mass flow	kg/s	
$\dot{m}_{ex}$	mass flow between nodes	kg/s	
n_{ser}	number of collectors in series		
$\dot{q}$	specific heat flow	W/m²	
q_{cond}	specific heat of condensation	kJ/kg	
q_{in}	supplied specific heat	kJ/kg	
$\dot{Q}_{DHW}$	heat transferred to the generation of domestic hot water	W	
$\dot{Q}_{Loss}$	heat loss of a node	W	
$\dot{Q}_\lambda$	conductive heat flow across nodes	W	
t_{ORC}	operating time in ORC mode	h	
T_a	ambient temperature	°C	
T_{ground}	temperature of the ground	°C	
T_{DHW}	temperature of domestic hot water	°C	
T_{SH}	space heating flow temperature	°C	
T_{in}	collector inlet temperature	°C	
T_m	mean collector temperature	°C	
T_{ORC}	scroll expander inlet temperature	°C	
T_{out}	collector outlet temperature	°C	
$w_{t,comp}$	specific work for compression	kJ/kg	
$w_{t,exp}$	specific work of expansion	kJ/kg	
$\dot{V}$	volume flow	l/h	
$\dot{V}_{str}$	volume flow per collector string	l/h	
β	collector slope		
$\eta_{s,c}$	isentropic compression efficiency		
$\eta_{s,p}$	isentropic pump efficiency		
$\eta_{s,exp}$	isentropic expansion efficiency		
ρ_{CF}	density of the collector fluid	kg/m³	
$(\tau\alpha)_n$	normal transmittance absorptance product		

1. Introduction

The application of ground coupled heat pumps and solar combisystems providing both space heating and domestic hot water is a proven technology. In these conventional systems the collectors come to a standstill whenever the maximum temperature in the storage tank is

reached. However The resulting excess heat can be harnessed in an Organic Rankine Cycle (ORC). The domestic application of an ORC driven by solar heat has been a topic of interest in recent years [1]-[5]. In contrast in this study a scroll expander is applied as expansion device. Advantages of the use of a scroll expander are that no valves have to be used and that their low costs are low because of mass production. The performance of a scroll expander as the expansion device of a Rankine cycle has been investigated by [6]-[8]. In the ORC the working fluid of the heat pump is evaporated by solar heat and is afterwards expanded through the scroll compressor of the heat pump which in this case operates as a scroll expander. When the fluid condenses heat is recharged into the ground increasing the coefficient of performance of the heat pump and potentially reducing the necessary borehole depth. Upgraded controls and a pump for the ORC are the only additionally required investments compared to conventional systems. A schematic drawing of the combined heat pump-ORC system is given in Fig. 1.

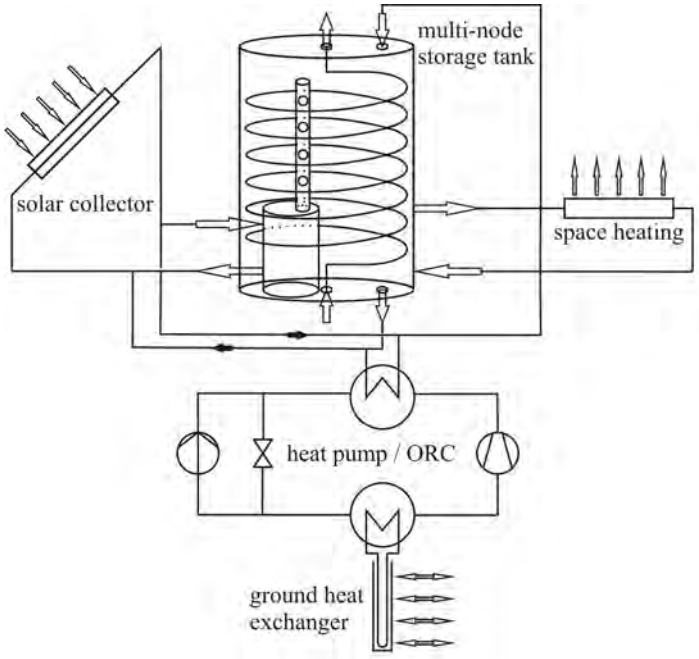

Fig. 1. Schematic drawing of the combined heat pump-ORC system.

2. Modelling of the components of the combined system

In order to simulate a combined system models for the solar collector, storage tank, heat pump, Organic Rankine Cycle and geothermal heat exchanger are required. The flat-plate collector has been modelled dynamically by use of a one-node model which is given in the European norm EN 12975 [9]. Dynamic modelling is necessary because the heat capacity of the collector strongly influences the ORC-revenues due to varying heating-up periods for different operating temperatures. The following differential equation Eq. (1) describes the thermal behaviour of a flat-plate collector.

$$\dot{q} = F'(\tau\alpha)_{en} K_{\theta b}(\theta) G_b + F'(\tau\alpha)_{en} K_{\theta d}(\theta) G_d - c_1 (T_m - T_a) - c_2 (T_m - T_a)^2 - c_5 dT_m/dt \quad (1)$$

The beam and diffuse radiation on the sloped collector have been calculated by means of the algorithms of the European Solar Radiation Atlas [10]. If the collector is feeding the storage tank the volume flow is fixed to a constant value. However if it is operating in ORC mode the volume flow is adjusted to keep a constant temperature. In this case the differential term in

Eq. (1) is zero and for hourly irradiation data the process can be considered stationary. The resulting volume flow can be calculated by equating Eq. (1) and Eq. (2).

$$\dot{q} = \rho_{CF} \cdot c_{p,CF} \cdot \dot{V} \cdot \left(T_{out} - T_{in}\right) / A_C \tag{2}$$

The storage tank installed in the combined system is a multi-node storage tank with stratification device. The stratification system ensures the layering of solar heated water at different temperatures which allows for the use of low-temperature solar heat in a solar combisystem. For each time step a mass and an energy balance have to be solved. It has to be considered that a mass flow also accounts for an energy flow throughout via mixing. The mass and energy flows in a node are depicted in Fig. 2.

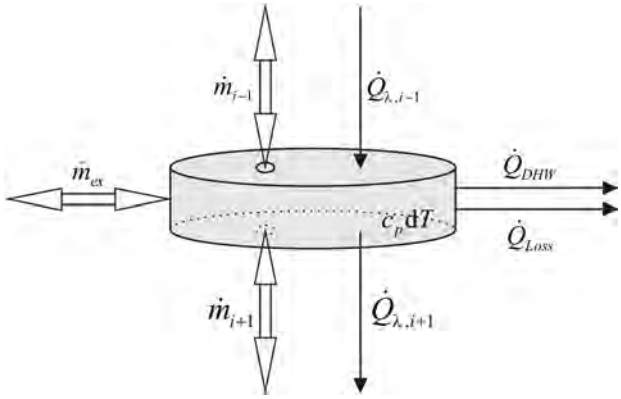

Fig. 2. Mass and energy flow in a node.

Mass flows between adjacent nodes ($\dot{m}_{i-1}, \dot{m}_{i+1}$) result from external flows ($\dot{m}_{ex}$) of the collector, heat pump or floor heating which are either supplied or removed. The terms $\dot{Q}_{\lambda,i-1}$ and $\dot{Q}_{\lambda,i+1}$ describe the heat conduction between adjacent nodes whereas $\dot{Q}_{DHW}$ marks the heat flow from the node to the coiled tube heat exchanger in which the domestic hot water is generated. $\dot{Q}_{Loss}$ indicates the heat loss from the storage tank to the ambient. The mass flows are first converted into equivalent heat flows, afterwards the set of differential equations is solved for each node.

All thermodynamic properties required for the simulation of the ORC and the heat pump are calculated with the software Refprop [11]. The terminal temperature differences in heat exchangers are set to 5 K. For the calculation of the COP of the heat pump the upper and lower pressure are the saturation pressures belonging to the temperatures T_{ground} and T_{SH} in case of floor heating or T_{DHW} in case of the generation of domestic hot water. The suction gas is overheated by 3 K (1a) and afterwards compressed (2a). The compression is assumed to be adiabatic with an isentropic efficiency of $\eta_{s,c} = 0.6$. Subsequently the refrigerant condenses (3a) and transfers heat to the floor or water heating system. The refrigerant leaves the condenser as saturated liquid so no subcooling is performed. To complete the cycle the pressure is relieved by an expansion valve (4a). The COP of the described process can be calculated with Eq. (3).

$$COP = \frac{q_{cond}}{w_{t,comp}} = \frac{\left|h_{3a} - h_{2a}\right|}{h_{2a} - h_{1a}} \tag{3}$$

For the calculation of the thermal efficiency of the ORC the pressure levels are given through the temperatures T_{ground} and T_{ORC}. The fluid is compressed by a pump with an isentropic

efficiency of $\eta_{s,p} = 0.6$ (2b). Afterwards the fluid is evaporated by heat transfer from the collector fluid (3b). The saturated vapour is expanded in the scroll expander (4b). By default the isentropic efficiency of the expansion is set to $\eta_{s,\exp} = 0.5$ which is in good agreement with Peterson et al. [6]. Downstream of the expander the refrigerant is condensed and subcooled by 2 K (1b). The thermal efficiency of this cycle can be calculated as

$$\eta_{ORC} = \frac{w_{t,\exp}}{q_{in}} = \frac{|h_{4b} - h_{3b}|}{h_{2b} - h_{1b}}. \quad (4)$$

To model the ground heat exchanger a short time step model is required because the thermal response of the ground is critical for the description of condensation in ORC mode. With the analytical approach of Lamarche and Beauchamp [12] an hourly calculation, which is in good agreement with the short time-step g functions developed numerically by Yavuzturk and Spitler [13], is achieved.

3. Simulation and optimisation of the combined system

In this work a combined heat pump-ORC system has been simulated which is installed in a single family house. The house has a total floor space of 167 m² and a transmission heat loss of 148.2 W/K. Both values are characteristically for a l ow-energy consumption house fulfilling the German KfW 70 standard. For this type of building a heat pump with a heating output of 5 kW is sufficient. The simulations were carried out with the refrigerant R134a as working fluid of heat pump and ORC. The simulated system comprises a multi-node storage tank with a volume of 700 l. Six south orientated flat-plate collectors with an aperture area of 2 m² each are installed in the system. The working fluid of the collectors is a 20/80 propylene glycol-water mixture. The characteristics of both storage tank and collector represent those of commercially available products. Hourly data for the ambient temperature and solar radiation for the climatological station Weihenstephan (48° 24' N, 11° 42' E) are taken from the European Solar Radiation Atlas [10]. It is assumed that at 6:30, 7:30, 18:30 and 19:30 in each case 50 l of hot water with a temperature of 45 °C are generated in the coiled tube heat exchanger passing through the storage tank.

The aim of the simulation is to find the optimum configuration of the combined system. For the optimisation the number of collectors in series, the volume flow per string of collectors, the collector slope and the expander inlet temperature of the ORC are varied. The range of these parameters is given in Table 1.

Table 1. Modified parameters for the optimization of the combined system and their range of values.

Parameter	Range of simulated values
Number of collectors in series n_{ser}	1 – 3
Volume flow per string of collectors $\dot{V}_{str}$	20 – 80 l/h
Collector slope β	15 – 55 °
Expander inlet temperature T_{ORC}	60 – 90 °C

Chen et al. [5] simulated a small scale solar-driven carbon dioxide power system and mention the importance of the expansion efficiency as the power output decreases by 60% for an isentropic efficiency of 50% instead of 85%. Wang et al. [7] managed to increase the expansion efficiency from 50% to 70% by using a compliant expander instead of a kinematically constrained one. In this work it is therefore investigated in how far the efficiency of the expansion influences the ORC output and the overall performance of the

combined system. For this purpose additional simulations have been done with efficiencies of $\eta_{s,\exp} = 0.6$ and $\eta_{s,\exp} = 0.7$ instead of the default value of $\eta_{s,\exp} = 0.5$.

The output values of the simulation are the electricity consumption of the heat pump for space heating and domestic hot water as well as the power generated in the scroll expander and the power consumption of the pump of the ground loop in the ORC. The power input of the ground loop pump is assumed to be 60 W and has to be subtracted from the power output of the scroll expander. For the financial evaluation electricity costs are set to 0.2 €/kWh whereas the generated power yields 0.3301 €/kWh under the current German feed-in tariff. All components have been simulated for one year with a time step of one minute except for the ground heat exchanger, which has been calculated on hourly basis. All simulations were performed using Microsoft Visual Basic for Applications scripts

4. Results

The results of the simulation show that the energetic optimum of the combined system is reached for collector slopes between 25° and 35°. The optimum is therefore found for slopes up to 23.4° lower than the rule of thumb of Duffie and Beckmann [14] proposing surface slopes equal to the latitude. This effect can be explained with the fact that in summer the total irradiation on slopes which are tilted to a lesser extent is higher. This relation which favours the ORC together with the influence of the volume flow on the power output of the ORC and the operating time in ORC mode are displayed in Fig. 3 for a connection of three collectors in series and an expander inlet temperature of 70 °C. The decrease of the ORC power output with increasing volume flow per collector string is due to the shorter operating time in ORC mode. With increasing volume flow lower collector outlet temperatures are achieved and thus the ORC starting temperature is reached less often.

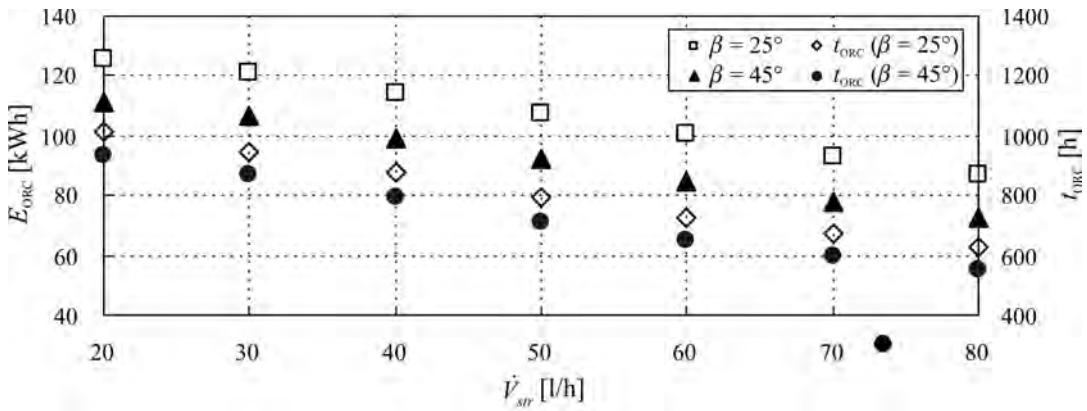

Fig. 3. Influence of the operating time in ORC mode t_{ORC}, the volume flow per collector string $\dot{V}_{str}$ and the collector slope β on the ORC power output E_{ORC} for a connection of three collectors in series and an expander inlet temperature of 70 °C.

The influence of the array configuration, either parallel connection or connection in series, and the specific volume flow per m² aperture area on the system performance is outlined in Table 2 for a collector slope of 25° and an expander inlet temperature of 70 °C. Different array configurations (A, B, C) with the same specific volume yield similar output values. The ORC power output is an exception because it decreases with the number of collectors connected in series. The total electricity demand of the combined system however is almost constant. If the volume flow per collector string is held constant and the number of collectors in series is increased (A, D, E) the electricity consumption of the heat pump for space heating $E_{HP,SH}$ rises. To reach T_{SH} a rather low irradiance is required and the operating time in space

heating mode is quite high. As a consequence the operating time is rising to a lesser extent than the solar gain is dropping because of the lower volume flow. In contrast the electricity consumption of the heat pump for the generation of domestic hot water is reduced and the ORC power output is increased because higher operating temperatures are reached more often and faster for smaller specific volume flows.

Table 2. The effect of the array configuration and the specific volume flow per m² aperture area on the annual electricity consumption of the heat pump for space heating $E_{HP,SH}$ and domestic hot water $E_{HP,DHW}$ as well as the ORC power output E_{ORC} and the total power consumption E_{tot} for a collector slope of 25° and an expander inlet temperature of 70 °C.

Case	n_{ser}	$\dot{V}_{str}$ [l/h]	$\dot{V}_{str}/(n_{ser}\cdot A_c)$ [l/m²h]	$E_{HP,SH}$ [kWh]	$E_{HP,DHW}$ [kWh]	E_{ORC} [kWh]	E_{tot} [kWh]
A	1	20	10	1261.6	611.2	113.4	1759.4
B	2	40	10	1260.1	612.4	102.8	1769.7
C	3	60	10	1258.7	599.2	100.3	1757.6
D	2	20	5	1303.6	598.0	123.5	1778.1
E	3	20	3.33	1354.1	536.5	125.9	1764.7

For the cases A, B and C given in Table 2 the influence of the isentropic expansion efficiency on the expander power output has been investigated. The results are illustrated in Fig. 4 together with the thermal efficiency of an Organic Rankine Cycle with the assumptions made in section 3, an evaporation temperature of 70 °C and a condensing temperature of 20 °C. If the power consumed by the ground loop pump is subtracted from the values depicted in Fig. 4 the same values for the power output of the ORC as in Table 2 are obtained for $\eta_{s,\exp} = 0.5$.

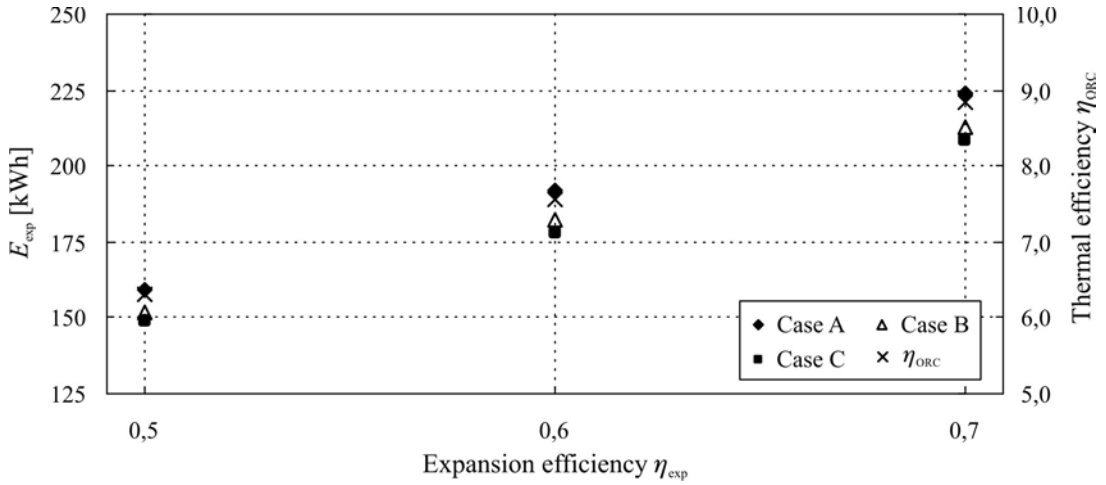

Fig. 4. Influence of the expansion efficiency $\eta_{s,exp}$ on the thermal efficiency of the ORC η_{ORC} and the expander power output E_{exp} for different array configurations with the same specific volume flow.

Fig. 4 shows that the thermal efficiency of the ORC η_{ORC} is the only variable influencing the expander output power. If the efficiency of the expansion is increased by ten percentage points the expander output power and η_{ORC} grow by about 20%. This result is in agreement with the course determined by Chen et al. [5]. With rising thermal efficiency a negligible lower amount of heat is recharged into the ground which would influence the electricity consumption of the heat pump. As the thermal efficiency has no effect on the operating time of the ORC, the power consumption of the ground loop pump remains constant. The results of the simulation reveal that all output values except for the power output remain almost unaffected by the expansion efficiency which has been expected.

Finally the optimised system configurations for each expander efficiency are compared with a conventional system from an energetic and financial point of view. The conventional system is simulated using the methods and assumptions presented in section 2 and section 3 just without the ORC mode. The simulation results for each optimised system and the conventional system are outlined in Table 3.

Table 3. Comparison of the electricity consumption and cost of a conventional solar combisystem and optimised system configurations of the combined heat pump-ORC system for different isentropic scroll expander efficiencies.

$\eta_{s,exp}$	n_{ser}	$\dot{V}_{str}$ [l/h]	β [°]	T_{ORC} [°C]	E_{tot} [kWh]	ΔE_{tot} [%]	ORC-revenue [€]	Total costs C_{tot} [€]	ΔC_{tot} [%]
-	2	30	35	-	1729.3	-	-	346.1	-
0.5	1	40	35	60	1717.4	-0.7	30.2	328.6	-5.1
0.6	1	40	25	60	1693.0	-2.1	41.2	319.1	-7.8
0.7	1	30	25	60	1665.1	-3.6	53.7	308.6	-10.8
0.5	1	30	25	60	1719.5	-0.6	35.8	326.3	-5.7
0.6	3	20	25	70	1727.3	-0.1	61.9	316.3	-8.6
0.7	3	20	25	70	1689.9	-2.3	74.2	303.9	-12.3

The results indicate that the energetic and financial optima are reached for different system configurations. The relative cost savings exceed the energy savings which is due to the fact that 1 kWh generated electricity equals 1.65 kWh consumed electricity because of the feed-in tariff. The energetic optima are reached for a parallel connection of collectors. The rather low energy savings can be explained with the fact that in the combined system the storage tank is charged with less solar heat than in a conventional system. However the combined system is still superior in comparison. For higher expansion efficiencies the array configurations with the lowest specific volume flow become attractive from a financial standpoint as a consequence of the greater ORC revenues.

5. Conclusion

In this work annual simulations of a solar assisted combined heat-pump ORC system have been performed. The results indicate that this system is superior to a conventional solar combisystem from an energetic and financial standpoint. The annual savings strongly depend on the efficiency of the expansion. For a small combined system with a flat-plate collector area of 12 m² the relative energetic savings range from 0.7% ($\eta_{s,exp} = 0.5$) to 3.6% ($\eta_{s,exp} = 0.7$). The absolute monetary savings are about 20 € for $\eta_{s,exp} = 0.5$. They rise to 42 € for an increased efficiency of $\eta_{s,exp} = 0.7$. It therefore seems possible to cover the additional costs that arise from an ORC pump and advanced controls. As the costs for the controls are independent of the system size an application of the combined system is more reasonable in larger dwelling units like hotels, senior citizens' homes and multiple dwelling houses. Experimental studies to evaluate the efficiency of the scroll compressor in expansion mode are required. The results of this study concerning collector slope and volume flow can also be transferred to future works regarding solar-driven Organic Rankine Cycles.

Acknowledgements

The authors would like to thank the Federal Ministry of Economics and Technology for financially supporting this work.

References

[1] J L. Wolpert; S. B. Riffat, Solar-powered Rankine system for domestic applications, Applied Thermal Engineering 16, 1996, pp. 281-289.

[2] C.-H. Kuo; W.-J. Yang; N. Arai; K. Mori, Solar-powered organic Rankine system for domestic electric-power generation, Energy and the environment: Proceedings of the Second Trabzon International Energy and Environment Symposium, 1999, pp. 67-74.

[3] A. Delgado-Torres; L. Garcia-Rodriguez, Analysis and optimization of the low-temperature solar organic Rankine cycle (ORC), Energy Conversion and Management 51, 2010, pp. 2846-2856.

[4] X. R. Zhang; H. Yamaguchi; K. Fujima; M. Enomoto; N. Sawada, Theoretical analysis of a thermodynamic cycle for power and heat production using supercritical carbon dioxide, Energy 32, 2007, pp. 591-599.

[5] Y. Chen; W. Pridasawas; P. Lundqvist, Dynamic simulation of a solar-driven carbon dioxide transcritical power system for small scale combined heat and power production, Solar Energy 84, 2010, pp. 1103-1110.

[6] R. B. Peterson; H. Wang; T. Herron, Performance of a small-scale regenerative Rankine power cycle employing a scroll expander, Proceedings of the Institution of Mechanical Engineers/ Part A, Journal of power and energy 222, 2008, pp. 271-282.

[7] H. Wang; R. B. Peterson; T. Herron, Experimental performance of a compliant scroll expander for an organic Rankine cycle, Proceedings of the Institution of Mechanical Engineers/ Part A, Journal of power and energy 223, 2009, pp. 863-872.

[8] T. Saitoh; N. Yamada; S. Wakashima, Solar Rankine Cycle System Using Scroll Expander, Journal of Environment and Engineering 2, 2007, pp. 708-718.

[9] EN 12975, T hermal solar systems and components - Solar collectors - Part 2: Test methods, 2006.

[10] K. Scharmer; J. Greif, The European solar radiation atlas, Les Presses de L'École des Mines, 1st Edition, 2000.

[11] E. W. Lemmon; M. O. McLinden; M. L. Huber, NIST Reference Fluid Thermodynamic and Transport Properties – REFPROP. NIST Standard Reference Database 23, Version 8, 2002.

[12] L. Lamarche; B. Beauchamp, A fast algorithm for the simulation of GCHP systems, ASHRAE Transactions 113, 2007, 470-476.

[13] C. Yavuzturk; J. D. Spitler, A short time step response factor model for vertical ground loop heat exchangers, ASHRAE Transactions 105, 1999, 475-485.

[14] J. A. Duffie; W. A. Beckman, Solar Engineering of Thermal Processes, Jon Wiley & Sons, 2nd Edition, 1980, pp. 98-101.

Optimisation of Low Temperature Difference Solar Stirling Engines using Genetic Algorithm

Kwanchai Kraitong, Khamid Mahkamov*

*School of Computing, Engineering and Information Sciences, Northumbria University, Newcastle upon Tyne, NE1 8ST, UK**
**Corresponding author. Tel:+44 191 2274739, Fax: +44 191 2437630, Email: khamid.mahkamov@northumbria.ac.uk*

Abstract: This paper presents results of theoretical investigations on the determination of optimal design parameters of a Low Temperature Difference (LTD) Solar Stirling Engine using optimisation method based on Genetic algorithms. The developed thermodynamic mathematical model of the engine takes into account hydraulic and mechanical losses in the engine's working process and this model was coupled to the optimisation algorithm. A set of such design parameters as the stroke of the displacer and diameter and stroke of the power piston and the thickness of the regenerator placed in the displacer have been considered as variables. The engine's performance parameter such as the brake power is used as the objective function of the optimisation algorithm. The GA code is implemented in MATLAB. The accuracy of the optimal design engine's performance is examined using 3D CFD modelling of the working process of the engine. The set of design parameters obtained from the optimisation procedure provides the noticeable improvement of the engine's performance compared with the performance of the original LTD Solar Stilring engine with the same operating condition.

Keywords: *LTD Stirling engine, Second-order mathematical model, Mechanical losses, CFD, Genetic algorithm.*

Nomenclature

C_p *specific heat at constant pressure..J·kg^{-1}K^{-1}*
C_v *specific heat at constant volume ...J·kg^{-1}K^{-1}*
D_p *diameter of piston.....m*
D_D *diameter of displacer.....m*
f *frequency.....Hz*
H_d *thickness of regenerator.....m*
m *mass of the gas in the control volume..... kg*
maxvalue maximum fitness value in the value map
$\dot{m}_i$ *inlet mass flow rate.....kg·s^{-1}*
$\dot{m}_o$ *outlet mass flow rate.....kg·s^{-1}*
P_b *brake power.....W*
P_c *pressure in the compression space.....Pa*
P_{c1} *pressure in the compression space in the displacer chamber.....Pa*
P_{c2} *pressure in compression space in the piston cylinder.....Pa*
P_e *pressure in the expansion space.....Pa*
P_i *indicated power.....W*
Q *heat transfer rate.....W*
T *total crank torque..... N·m*
T_b *frictional torque of the rolling bearing. N·m*
T_i *inlet temperature.....K*
T_o *outlet temperature.....K*
T_p *piston crank torque..... N·m*
t *time..... sec*
Value…… fitness value
V_c *volume of the compression space.....m^3*
V_{c1} *volume of the compression space in the displacer chamber..... m^3*
V_{c2} *volume of the compression space in the piston cylinder..... m^3*
V_{dc} *dead volume of the compression space...m^3*
V_{de} *dead volume of the expansion space.....m^3*
V_e *volume of the expansion space.....m^3*
V_{SP} *swept volume of the piston .....m^3*
V_{SD} *swept volume of the displacer.....m^3*
W *work.....J*
W_b *cyclic brake work.....J*
W_c *work of the compression space.....J*
W_e *work of the expansion space.....J*
x *current displacement of the piston.....m*
x_0 *stroke of the piston.....m*
y *current displacement of the displace.....m*
y_0 *stroke of the displacer .....m*
Z_D *stroke of displacer.....m*
Z_p *stroke of piston.....m*
θ *piston crank angle.....rad*
φ *displacement phase angle of the piston.. rad*
k, ε *turbulent kinetic energy and dissipation turbulent kinetic energy.....m^2·s^{-2}*

1. Indroduction

Low Temperature Difference (LTD) Stirling engines, though provide low electricity production, can be used as solar energy and waste heat recovery system due to their simple design and low cost production [1]. There is an interest towards development of LTD Stirling engines for deployment in rural areas of developing countries for production of power on the small scale. Because of this reason, numerous studies have been conducted for determination of optimal design parameters of LTD Stirling engines. Several thermodynamic mathematical models have been used for the determination of the optimum power and efficiency of such engines [2-7]. Furthermore, a considerable work was done on the development of optimisation algorithms for conventional high temperature engines [8, 9]. The search method which uses the Genetic algorithm (GA) code coupled to the mathematical model accounting for heat and mechanical losses using the theorem of forced work was presented by Altman in [9]. This work presents the determination of optimal design parameters of a LTD Stirling engine using GA optimization method, coupled to the second-order model of the engine, which takes into account hydraulic and mechanical losses, developed by Kraitong and Mahkamov [10]. Additionally, 3D CFD simulations using CFD FLUENT software were performed to calibrate results of the optimization calculations.

2. Physical model

Figure 1a represents a schematic diagram of the kinematical gamma LTD Stirling engine. The main components of the LTD Stirling engine are the power piston and displacer with corresponding cylinders, the hot and cold plates, , the regenerator placed inside the displacer and the drive mechanism with the flywheel. In this paper, a twin-power piston LTD Stirling engine, see Fig. 1b, manufactured by Kongtragool and Wongwises [11] is used in numerical investigations. This engine consists of two power pistons and one displacer with the built-in regenerator. The regenerator is made of coarse stainless steel mesh placed in the casing perforated at its top and bottom. Table 1 presents data on the physical dimensions of this Stirling engine.

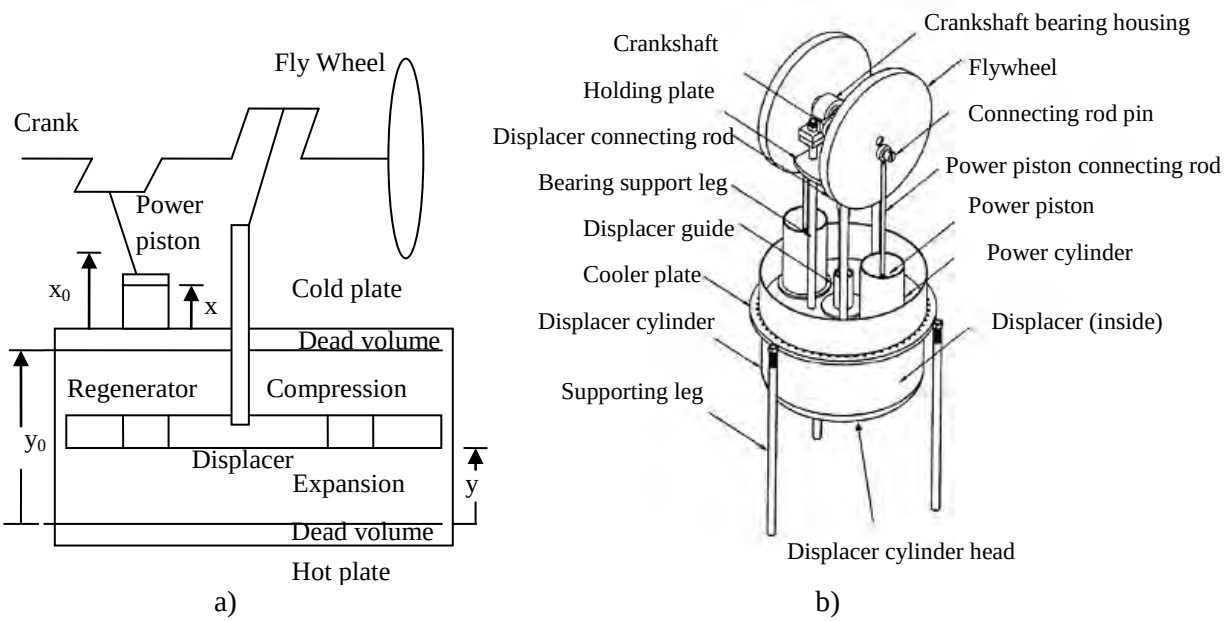

Fig. 1. a) A Schematic diagram of the kinematic gamma LTD Stirling engine and b) The physical characteristic of the twin power piston LTD Stirling from Kongtragool and Wongwises [11].

Table 1. Dimensions of the LTD Stirling engine manufactured by Kongtragool and Wongwises [11]

The geometric data of a twin power piston LTD Stirling engine	Value
working piston stroke (m)	0.0826
working piston diameter(m)	0.083
working piston swept volume (m^3)	893.8×10^{-6}
displacer piston stroke (m)	0.0795
displacer piston diameter (m)	0.32
displacer piston swept volume (m^3)	6393.8×10^{-6}
swept volume ratio	7.15
displacement phase angle of the pistons (°)	90

3. Modelling Procedure

3.1. Thermodynamic modelling

The second-order mathematical model taking into account the pressure drop and the mechanical losses developed by Kraitong and Mahkamov [10] was used for the performance prediction of the engine. This model is the modification of that developed by Timoumi et al. [7] and Urieli [12]. The equations of energy and mass conservation for each control volume are expressed as follows:

$$C_v \frac{d(mT)}{dt} = dQ - \frac{dW}{dt} - \dot{m}_o C_p T_o + \dot{m}_i C_p T_i \quad (1)$$

$$\frac{dm}{dt} = \dot{m}_o - \dot{m}_i \quad (2)$$

Work done by the working gas inside the compression space and the expansion space can be calculated as $\frac{dW_c}{dt} = P_c \frac{dV_c}{dt}$ and $\frac{dW_e}{dt} = P_e \frac{dV_e}{dt}$, respectively.

Volumes of the compression and expansion spaces are expressed as

$$V_c = V_{dc} + \frac{V_{SP}}{2}\left(1 + \cos(\theta - \varphi)\right) + \frac{V_{SD}}{2}\left(1 - \cos\theta\right) \quad (3)$$

$$V_e = V_{de} + \frac{V_{SD}}{2}\left(1 + \cos\theta\right) \quad (4)$$

where $V_{SP} = \pi \frac{D_p^2}{4} Z_p$ and $V_{SD} = \pi \frac{D_D^2}{4} Z_D$.

In order to determine the brake cyclic power, the kinetic motion equations of the mechanical transmission system of the reciprocating engine proposed by Guzzomi et al. [13,14] were used. The determination of the frictional forces in the sealing rings of the displacer rod is carried out using methodology described in [15]. These results were used to calculate the torque induced by the pistons (T_p). The brake cyclic work and the brake cyclic power, therefore, are calculated as

$$T = \Sigma T_p \tag{5}$$

$$W_b = \oint \left(\frac{dW_b}{dt} \right) dt = \int_0^{\tau} \left((T - T_b) \frac{d\theta}{dt} \right) dt \tag{6}$$

$$P_b = W_b f \tag{7}$$

For numerical calculations, the cycle was split into 1000 time-steps and calculations were performed until the pressure and temperature curves converged and the overall heat balance in the system was reached.

3.2. CFD modelling

To achieve better understanding of the working process of the LTD Stirling engine and obtain more accuracy in the performance prediction, 3D CFD modeling using the standard k-ε turbulence model for a compressible flow was carried out to investigate the work of the engine. Commercial CFD software, FLUENT was used to perform CFD simulations of the working process of the engine. During the simulations the movement of pistons was taken into account and the regenerator of the engine was treated as a homogeneous porous medium. The subroutines describing displacements of the pistons and the displacer were written and then connected to the main body of the programme. The cycle was divided into equal 500 time-steps and calculations were performed using a high performance computer. The average gas temperature and pressure in each engine's working space were monitored during calculations in order to determine whether the steady-state condition was reached in the simulated operation of the engine.

3.3. Optimisation modelling

Genetics algorithm is a stochastic optimisation method based on the mechanism of natural selection for survival as the procedure in order to obtain optimal results [16]. The real-valued GA or the continuous GA is applied in this work for the quantitative limitation and the reduction of the computing time [17]. The structure of the continuous GA of the LTD Stirling engine is represented in Fig. 2.

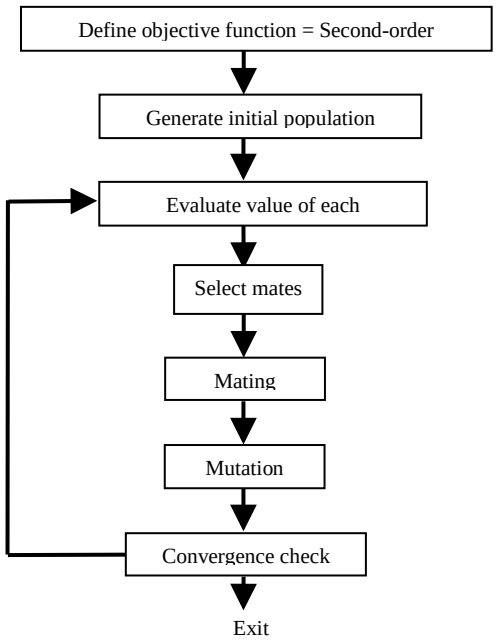

Fig. 2. The structure of the continuous GA of the LTD Stirling engine.

Several original engine design and operational parameters, namely the diameter of the displacer of 0.32 m, the engine speed of 46.5 rpm, the solar irradiation of 5097 W/m^2 created using a solar simulator and the cooler surface temperature of 307 K, are accepted to be fixed as constant values in this work. There are only four engine design parameters are defined as variables. These are the diameter and the stroke of the power piston, the stroke the displacer and the thickness of the regenerator:

$$Chromosome = (D_p; Z_p; Z_D; H_d) \quad (6)$$

The upper and the lower bound of each variable are as follows;
$0.02 < D_p < 0.13$; D_p is diameter of piston (m)
$0.04 < Z_p < 0.3$; Z_p is stroke of piston (m)
$0.04 < Z_D < 0.3$; Z_D is stroke of displacer (m)
$0.01 < H_d < 0.2$; H_d is thickness of regenerator (m)

The above boundaries are defined based on the practical manufacturing and design considerations. The maximum diameter of the piston is limited by the diameter of the cold plate which is equal to the fixed displacer diameter. The range of the displacer stroke to be investigated is typical for displacers of LTD Stirling engines [18]. Only one of the engine's performances, namely the brake power, is defined to be the chromosome value because the heat source is solar energy which is assumed to be cost-free. The the brake power of the engine obtained using the developed second-order mathematical model is used as the objective function:

$$Brakepower = f(chromosome) = f(D_p; Z_p; Z_D; H_d) \quad (7)$$

In GA, there is no effect of the guessed initial chromosomes on the convergence of the solution, thus the initial population is created by using the absolutely random procedure. A generated initial population is in the matrix formation of various chromosomes. The size of the population effects the convergence in the optimization procedure. The number of chromosomes between 30 and 100 is the typical size to operate GA [19]. In this study, the number of chromosomes in a generation of 30 is used. The chromosome value which is the brake power is evaluated by the fitness function for locating in the value map of each generation [20]:

$$Fitnessvalue = \frac{1}{1 + maxvalue - value} \quad (8)$$

The fitness value of each chromosome is descending order to determine survival chromosomes for the next generation. The number of survival chromosomes is defined by the selection rate of 0.5 from the weighted random pairing selection and the rank weighting technique [17]. The single point crossover is used for the mating process that the parents are operated by the reproduction operator to produce some offsprings for the next generation. Fittest chromosomes of the ranking are randomly selected to be the parents for the reproduction operation. The second operator of the reproduction called the mutation is used as a tool to avoid finding only the local solution. The mutation rate of 0.2, though probably is high, results in the gradual convergence and ensures that the global maximum is not missed out in during simulations [17].

Finally, the new generation is produced and the population of new design parameters in this generation is then evaluated by the developed thermodynamic model and the fitness function is checked for the ranking until the solution found satisfying the termination condition. The maximum number of generation in the computing process of 80 is defined to obtain the convergence of this algorithm. The optimisation code was modified from [19] and implemented in MATLAB. In this case, the continuous GA was used to obtain the optimal design parameters for the performance's improvement of an original LTD Stirling engine. Simulations were, thus, conducted for the same operating condition. A set of optimal design parameters from the numerical simulations was then used to create the engine mesh for the 3D CFD simulation to more accurately predict the engine power.

4. Results from optimisation cacluations

The modelling of the engine with the SM15-matrix regenerator was performed for the constant solar flux of 5097 W/m^2, the cooler surface temperature of 307 K, the engine speed of 46.5 rpm with air at 1 bar pressure used as a working fluid. Figure 3 represents the best brake power for each generation. The best brake power first sharply increases and then gradually reaches the convergence with its value of 1.515 W. The design parameters of this generation are presented in Table 2. The corresponding indicated power is 1.668 W.

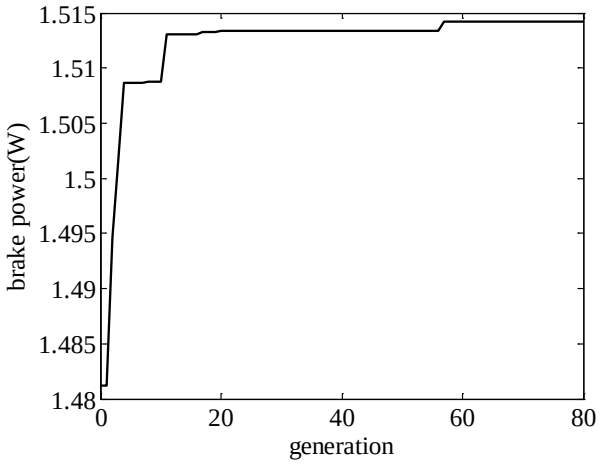

Fig. 3. The best brake power of each generation as the function of generations.

Table 2. The first set of optimal engine design parameters obtained from optimisation simulation.

Optimal engine design parameters	Value
working piston stroke (m)	0.228
working piston diameter(m)	0.065
displacer piston stroke (m)	0.074
displacer thickness (m)	0.056

However, it could be seen that the stroke of the power piston of 0.228 m which is much longer than the stroke of the displacer of 0.074 m. This may be unsuitable for the practical engine. Thus, the power piston and displacer strokes were fixed at 0.1 m and a new set the optimisation simulations with two variables were run. Optimal engine parameters from the second run are presented in Table 3 and the maximum brake and indicated power is 1.346 W and 1.47 W, respectively. There is only 11% reduction in power when compared with the results of the first optimization run.

Table 3. The second set of optimal engine design parameters is obtained from optimisation simulation.

Optimal engine design parameters	Value
working piston stroke (m)	0.1
working piston diameter(m)	0.1
displacer piston stroke (m)	0.095
displacer thickness (m)	0.058

Finally, two engines with optimal engine parameters shown in Tables 2 and 3 were modelled using 3D CFD simulation. The indicated power of the first and the second engine calculated from P-V diagrams which are shown in Fig. 4a and Fig. 4b are 1.427 W and 1.352 W, respectively. 3D CFD modelling results demonstrate that the second-order thermodynamic model used in oprimisation procedure has an adequate accuracy in the prediction of the engine performance.

5. Conclusion

The developed second-order mathematical model of the LTD Stirling engine was developed which accounts for hydraulic and heat losses in the working process and mechanical losses in the engine. This model was used with GA optimisation code. As a result of optimization simulations a set of design parameters for the engine was obtained which provides a considerable improvement in the performance. Results obtained using the developed second-order thermodynamic model were calibrated using 3D CFD modeling technique. The optimisation procedure developed in his work can be applied to improve the design of a wide range of Stirling engines, including high temperature ones.

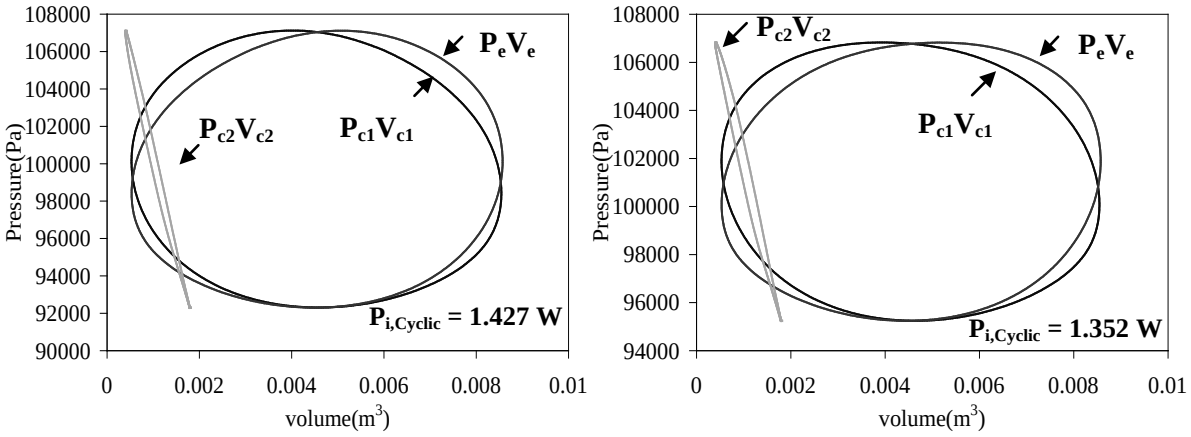

Fig. 4. 3D CFD modeling results: a) P-V diagrams for the first optimal parameters set obtained using and b) P-V diagrams for the second optimal parameters set

6. Acknowledgements

This work is a part of a PhD study which is supported by the Ministry of Science and Technology of the Royal Thai Government. Authors also would like to thank Professor Somchai Wongwises and Assistant Professor Bancha Kongtragool for providing data on their twin power piston LTD Stirling engine.

References

[1] B. Kongtragool, S. Wongwises, A review of solar-powered Stirling engines and low temperature differential Stirling engines, Renewable and Sustainable Energy Reviews, 2003, pp. 131–154.

[2] L. Erbay, H. Yavuz, Analysis of the Stirling heat engine at maximum power conditions, Energy 22, 1996, pp. 645–650.

[3] S. Hsu, F. Lin, J. Chiou, Heat-transfer aspects of Stirling power generation using incinerator waste energy, Renewable Energy 28, 2003, pp. 59–69.

[4] A. Tavakolpour, A. Zomorodian, A. Golneshan, Simulation, construction and testing of a two-cylinder solar Stirling engine powered by a flat-plate solar collector without regenerator, Renewable Energy 33, 2008, pp. 77–87.

[5] N. Martaj, L. Grosu, P. Rochelle, Exergetical analysis and design optimisation of the Stirling engine, Int. J. of Exergy 3, 2006, pp. 45–46.

[6] B. Orunov, V. T. Krykov, A. P. Korobkov, K. Mahkamov, D. Djumanov, The first stage of the development of a small Stirling tri-generation power unit, Proceeding of 12th international Stirling engine conference, 2005, pp. 416–423.

[7] Y. Timoumi, I. Tlili, S. Nasrallah, Design and performance optimization of GPU 3 Stirling engines, Energy URL doi:10.1016/j.energy.2008.02.005.

[8] Y. C. Hsieh, T. C. Hsu, J. S. Chiou, Integration of a free-piston Stirling engine and a moving grate incinerator, Renewable Energy 33, 2008, pp. 48–54.

[9] A. Altman, SNAPpro: Stirling numerical analysis program, URL http://home.comcast.net/snapburner/SNAPpro ISEC 2004.pdf, 2004.

[10] K. Kraitong, K. Mahkamov, Thermodynamic and CFD Modelling of Low Temperature Difference Stirling engines, Proceeding of 14th international Stirling engine conference, 2009.

[11] B. Kongtragool, S.Wongwises, Performance of a twin power piston low temperature differential Stirling engine powered by a solar simulator, Solar Energy 81, 2007, pp. 884-895.

[12] I. Urieli, Stirling Cycle Machine Analysis, URL http://www.ent.ohiou.edu/ urieli/stirling/me422.html>, 2008.

[13] D. C. Hesterman, B. J. Stone, A systems approach to the torsional vibration of multi-cylinder reciprocating engines and pumps, Proc. IMechE 208, 1994, pp. 395–408.

[14] A. L. Guzzomi, D. C. Hesterman, B. J. Stone, The effect of piston friction on engine block dynamics, Proc. IMechE 221, 2007, pp. 227–289.

[15] K. Mahkamov, D. Ingham, Analysis of the Working Process and Mechanical Losses in a Stirling Engine for a Solar Power Unit, J. of Solar Energy Engineering 121, 1999, pp. 121–127.

[16] D. E. Goldberg, Genetic Algorithms in Search, Optimization & Machine Learning, Addison-Wesley Publishing Company, USA, 1989, ISBN 0- 201-15767-5.

[17] R. L. Haupt, S. E. Haupt, Practical Genetic Algorithm, John Wiley & Sons, USA, Edition 2nd, 2004, ISBN 0-471-45565-2.

[18] J. R. Senft, An Introduction to Low Temperature Differential Stirling Engines, Moriya Press, USA, 2007, ISBN-13: 978-0965245517.

[19] A. M. S. Zalzala, P. J. Fleming, Genetic Algorithms in Engineering Systems, The Institution of Electrical Engineers, UK, 1997, ISBN 0-85296- 902-3.

[20] S. Elisaveta, B. Natasha, BASIC-A genetic algorithm for engineering problems solution, Computers and Chemical Engineering 30, 2006, pp. 1293–1309.

Performance Prediction and Experimental Analysis of a Solar Liquid Desiccant Air Conditioner

S. Alizadeh[1,*], H.R. Haghgou[1]

[1]*Department of Energy, Materials & Energy Research Centre, P. O. Box 14155-4777, Tehran, Iran*
[*]*Corresponding author. Tel: +98 261 620 4131, Fax: +98261 6201888, E-mail: shahab_alizadeh@hotmail.com*

Abstract: In a liquid desiccant air conditioner developed at Materials & Energy Research Centre (MERC), dehumidification of the outside air is achieved through a packed-bed heat and mass exchanger, using lithium chloride solution as the desiccant. The dry air thus obtained is evaporative cooled inside a cooling pad and directed into the conditioned space. The dilute solution from the dehumidification process is concentrated in a scavenger air regenerator using hot water from flat plate solar collectors. Carryover of the desiccant particles has been avoided by using eliminators, such as demister or filter.

In this paper the experimental results obtained from testing the prototype of the liquid desiccant absorber unit in a simulated Persian Gulf summer has been presented and compared with a previously developed model for the packed-bed. The comparison reveals that good agreement exists between the experiments and model predictions. The inaccuracies are well within the measuring errors of the temperature, humidity and the air and solution flow rates. The above tests further reveal that the unit would have a satisfactory performance in controlling the air temperature and humidity if installed on a commercial site of about 200 m^2 area in a hot and humid climate.

A commercialization study was performed for the solar operated liquid desiccant air conditioner (LDAC) and compared with the conventional vapour compression system. The study reveals that the operating cost of an LDAC is significantly lower than its conventional counterpart. The costs would further reduce if a storage system was used to store the concentrated solution of liquid desiccant. A simple payback of five years was determined for the solar components of the liquid desiccant system in this study.

Keywords: *Liquid desiccant, Dehumidification, Packed-bed, Solar regeneration.*

1. Introduction

Much work has so far been conducted in the area of air dehumidification using liquid desiccant and a cross-flow or a packed-bed type heat and mass exchanger, as the dehumidifier [1]. The use of the solar liquid desiccant air dehumidification / cooling system appears to be promising in hot and humid locations of Iran, such as the Persian Gulf region, due to high availability of solar energy. Figure 1 shows a schematic diagram of the solar air conditioner.

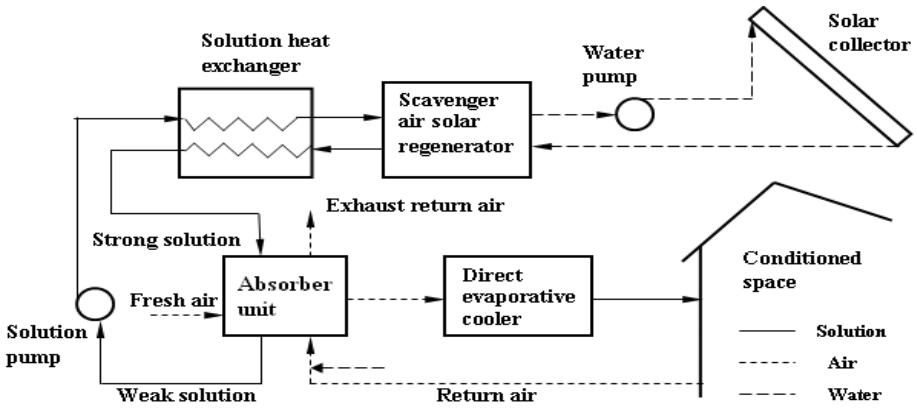

Figure 1. schematic diagram of a liquid desiccant solar air conditioner

Outside air is dehumidified in the absorber unit using a strong solution of lithium chloride and cooled within a direct evaporative cooler before it is introduced into the conditioned space. The dilute solution thus obtained is concentrated in a scavenger air solar regenerator using hot water from flat plate solar collectors. A solution heat exchanger, as indicated in the figure, is used for heat recovery between the strong and weak solutions. Return air from conditioned space has also been used to take some heat out of the outside air as shown in Figure 1.

Considerable laboratory experiments, computational analysis and design work has been carried out on a liquid desiccant system at the Sustainable Energy Centre of the University of South Australia [2-6], and the Queensland University of Technology [7, 8]. These involved modelling and experimental work on both cross flow and packed-bed dehumidifier as the absorber unit as well as the solar regenerator [9]. In the packed-bed system used in this study, different packing materials are considered, which include the polymer type usually used in cooling tower applications and the counter flow type with a layer of wick applied to the heat exchanger surfaces to reduce the carry over of the desiccant particles into the conditioned space, as well as to increase the dehumidification efficiency of the air conditioning unit.

In a solar liquid desiccant system the weak desiccant can be concentrated, stored and used at a later time; therefore, energy is stored as concentrated solution in the system rather than thermal. The system provides the options of using the solar LDAC either as a packaged roof top air conditioner for domestic or commercial use or as an air handler unit in commercial applications such as conditioning large volumes of ventilation air. The LDAC could also be used for space heating in winter due to the property of desiccants to provide heat when wetted and, thereby, indirectly heat the supply air.

2. Testing the conditioner prototype

In the experimental tests carried out on the developed LDAC, dehumidification and cooling are both achieved within the absorber unit by using liquid desiccant and the cool air from the conditioned space, respectively. A photograph of the absorber unit showing the system main components is demonstrated in Figure 2.

Figure 2. The LDAC packed-bed dehumidification unit as viewed from the MERC Energy Laboratory.

This 20 kW unit has an overall dimensions of approximately 1.3 × 1.5 × 1.8 m. The conditioner casing is made from an insulating material to protect the system from heat transfer with the environment. The packing material is incorporated vertically inside the dehumidification tower with the weak solution container at the bottom. The conditioner prototype was optimized for the air and solution flow rates, further reducing electrical power consumed by the unit.

Preliminary tests have been carried out on the system with water to ensure a smooth operation of the unit. These involved running the air conditioner at variable fan speeds by reducing the applied voltage from 220 to 110 V. The air velocity on the supply and exhaust sides of the conditioner and on a face area of approximately 0.15 m^2 was measured. The power consumed by the fan during the system operation was also measured and recorded.

Two sets of experiments were carried out with liquid desiccant. In the first set of the experiments, the absorber unit was tested with desiccant only sprayed into the outside air, while the direct evaporative cooler was inactivated. The experiments were aimed to investigate the air temperature rise due to condensation of the air moisture content, and reduction in the air relative humidity. The process of dehumidification / cooling of the outside air for these two experiments are shown on the psychrometric chart in Figure 3. The dashed line on this figure represents the test with desiccant only.

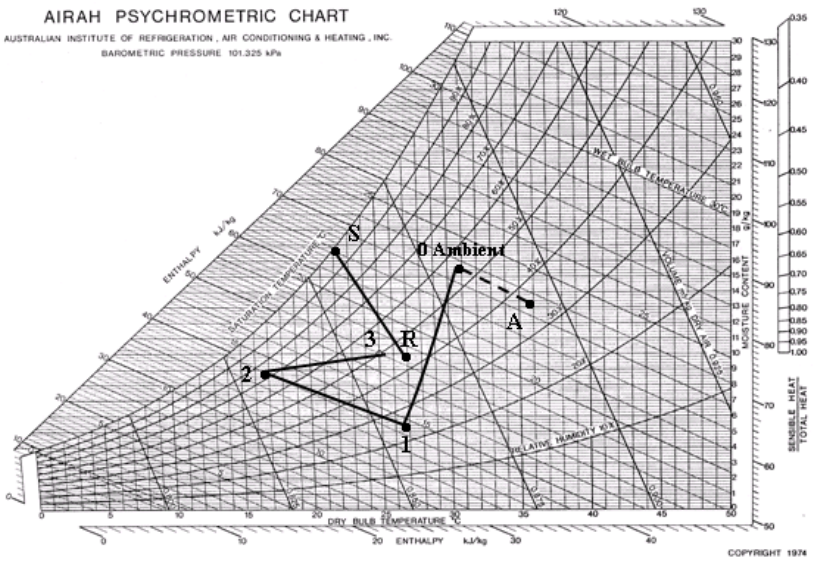

Figure 3. Psychrometric paths for the tests with: (a) desiccant only (dashed line); and (b) desiccant followed by evaporating cooling of the air. (Supply air: 0-1-2-3; Return air: R-S)

In the second set, the system was operated with the evaporative cooler activated, while lithium chloride solution was sprayed into the outside air. The test was to investigate the effect of dehumidification and direct evaporative cooling on the supply air. The process of dehumidification / cooling of the outside air for the above two experiments are shown on the psychrometric chart in Figure 3. The dashed line on this figure represents the test with desiccant only.

Following each set of experiments with liquid desiccant, the concentration of the dilute solution was measured, using a conductivity meter. A plot of conductivity-concentration as

indicated in Figure 4 was then produced for diluted samples and for several conductivity measurements. The plot was used to determine the subsequent values of concentration for new desiccant solutions, using a correction factor to be accounted for higher concentration values. The weak solution obtained from the dehumidification process in the above experiments was regenerated in a scavenger air solar regenerator. This will be described in section 4.

In Figure 5, the effect of air flow rate on the air temperature and relative humidity of the outside air has been studied. The air temperature and relative humidity on this figure are denoted by T_{bp} and H_{bp}, respectively, which are the air conditions before entering the packed-bed column. As seen from the figure a substantial reduction in the air relative humidity is achieved after it passes through the packed-bed column, which is due to the spray of the desiccant solution over the packing material. In Figure 5, values of the air temperature and relative humidity, following the dehumidification process, are denoted as T_{ap} and H_{ap}, respectively.

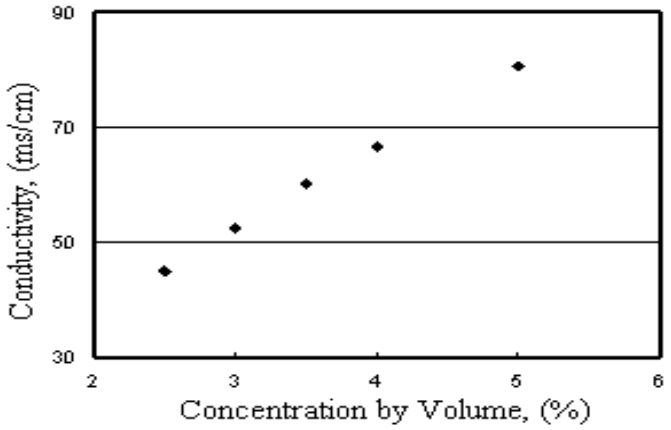

Figure 4. Conductivity-concentration chart for the lithium chloride solution.

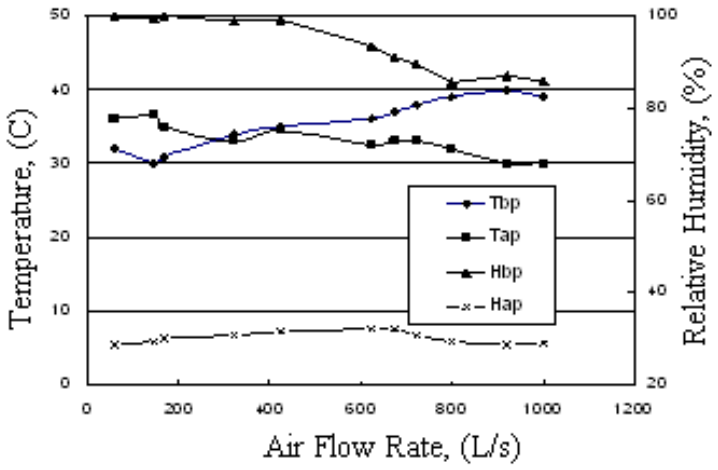

Figure 5. The effect of air flow rate on dehumidification process of the outside air.

In Figure 6 the experimental values of the temperature and humidity after the packing are compared with the predictions obtained from a developed model for the packed-bed. As can be seen from the figure there is good agreement between the data obtained from theory and experiment.

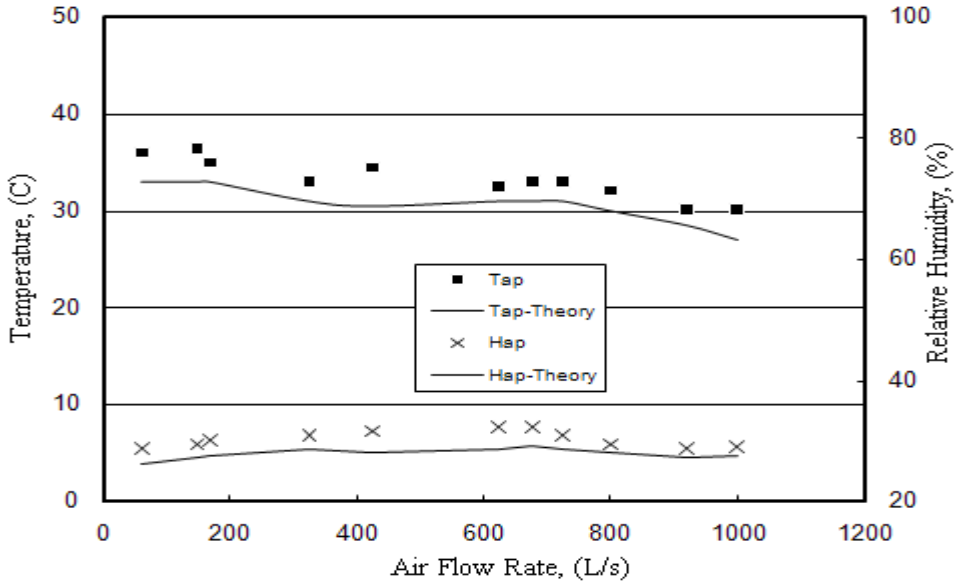

Figure 6. Comparison between the results obtained from the model and experiment.

3. Discussion of the test results

In the tests with desiccant only, the air dehumidification by liquid desiccant is an adiabatic (constant enthalpy) process; therefore, no heat is added or removed from the air during the process. However, according to Figure 3, for an adiabatic dehumidification the air dry bulb temperature increases as the relative humidity reduces. This is due to the heat generated in the process as a result of water vapour condensation in the air. The air wet bulb temperature as seen in Figure 3, remains constant.

The results from the tests with evaporative cooler and desiccant prove a satisfactory performance of the unit in a tightly control of the air temperature and humidity if installed on a commercial site of approximately 200 m^2 area in a hot and humid climate. This will maintain the building air conditions within the comfort zone (dry bulb temperature of about 25 °C and 50% relative humidity). The results of the tests further reveal that there are optimum values of air and solution flow rates, where the conditioner performance is enhanced.

To quantify the confidence level of the experimental data, the results of an uncertainty analysis are presented in Table 1 for the experimental values obtained from testing the conditioner prototype. In this analysis, the fixed errors are assumed to be calculated and accounted for via calibration against known standards. Hence, the remaining error is solely due to the precision error. The precision errors were determined by statistical means or from data provided by equipment manufacturers or by the best estimate based on experimental observations. Since the prototype testing of the absorber unit was under many uncontrolled environmental conditions, the results are quite acceptable.

The results obtained from the demonstration system in this study have been used in a solar liquid desiccant pilot plant project currently ongoing at MERC. The system was built and installed within the Fluid Mechanics Laboratory at Babol University of Technology, a hot and humid location on the Caspian Sea in the north of Iran. The system, which is also used for heating during the winter, is now being tested and monitored for a full year operation. Similar

equipment will also be installed and tested on the Persian Gulf region in southern part of the country, where the temperature and humidity are very high during most of the year.

Table 1. Experimental results obtained from the conditioner test and the uncertainty values.

Conditioner performance parameters	Measured values	Precision errors	Uncertainty values %
Supply and return air flow rates, L/s	1000	100	10
supply air temperature °*C*	15.2	1	6.7
supply air humidity ratio, kg/kg	0.0094	0.0005	5.3
Solution flow rate, L/min	3	0.2	6.8
Exit solution concentration, (*wt* %)	0.412	0.008	2
Effectiveness, %	82	5	6.1
Latent cooling, kW	16.7	0.5	3.3
Sensible cooling, kW	3.3	0.1	3.1
electrical energy used, kW	3	0.1	3.3
Total cooling, kW	20	0.6	3
Electrical COP	7	0.2	2.8

4. Performance of the solar regenerator

The concentration of dilute solution in this study is carried out in a scavenger air regenerator, using hot water from flat plate solar collectors. Both the scavenger air and the weak solution are preheated within the regenerator; however, solution regeneration will be more effective when preheating the air than preheating the solution [9]. It is notable that the lithium chloride desiccant can be concentrated using solar energy or other low grade heat at temperatures as low as 40 °C. The flat plate solar collectors used in this study can produce hot water at about 85 °C in summer.

In a scavenger air regenerator the weak solution is sprayed over a column of packed-bed (see Figure 7). Polymer pall rings, spheres or other polymer based materials are used as a packed-bed to increase the contact area between the solution and the scavenger air, which facilitates the regeneration process. A stream of outside air is passed through the column, using a fan, in a counter current operation to pick up the water evaporated from the solution, and the hot moist air is, subsequently, exhausted from top of the column. A mist eliminator, as shown in Figure 6, is used at the top of the regenerator column to prevent the carryover of the desiccant particles. Gas or electricity could be used as a back up for the regenerator during the peak cooling hours.

Eliminators, such as demister, are used to avoid carryover of desiccant into the environment. Alternative method in preventing the carryover is the use of indirect cooling, in which the supply air does not contact the desiccant [10]. The latter could also be used to produce potable water from the atmospheric air in remote areas when a cross flow plate heat exchanger is used. The water can either be used for human consumption or returned to the conditioner for evaporative cooling of the air.

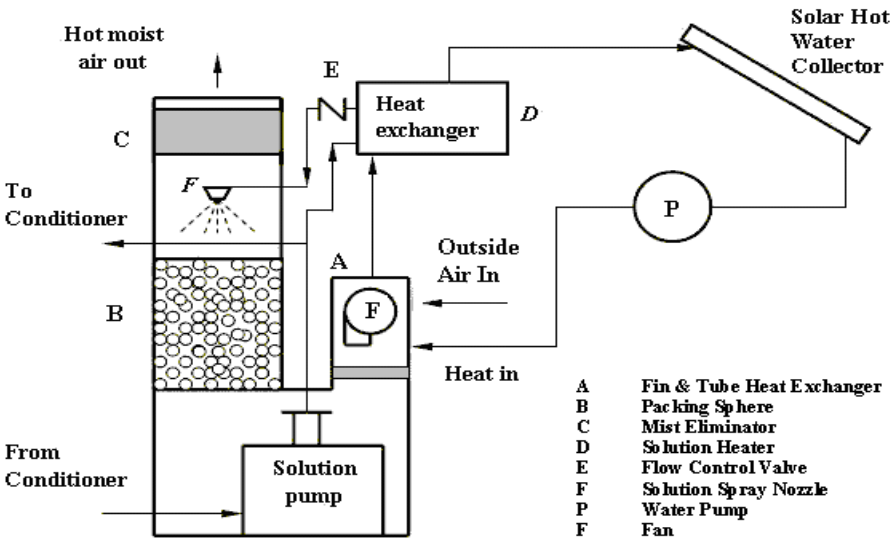

Figure 7. Schematic of the scavenger air solar regenerator.

5. Commercialization strategy for a solar LDAC

An LDAC, in which the carryover of the desiccant has been eliminated, creates new opportunities for solar cooling. A commercialization strategy has been proposed in this study for a solar operated LDAC and compared with conventional vapour compression systems. Based on the computer modelling results obtained from the system simulation for a building in the Persian Gulf region, the operating costs of an LDAC is significantly lower than its conventional counterpart. This study further reveals that using the solar operated LDAC with a storage system for the concentrated solution, will result in considerable savings in operating costs when compared with the equivalent gas-fired liquid desiccant system. A simple payback of five years was determined for solar components of the system in this study.

A 30 kW capacity, packaged roof-top LDAC delivering 1.5 m^3/s of outside air could be used in domestic applications as well as the commercial. The unit uses a storage system and 100 m^2 of flat plate solar collector to dehumidify and cool 500 m^2 of a residential building in the Persian Gulf region. Compared with the conventional unit, an annual saving of $2,500 with a payback of less than 5 years was determined for the solar LDAC in this application.

6. Conclusion

In this paper the performance of a solar LDAC developed at MERC, using packed-bed for air dehumidification, and a scavenger air regenerator was studied. It was found that the solar liquid desiccant system is an efficient and cost effective alternative to the conventional air conditioner. Elimination of carryover of the desiccant particles within the absorber unit in this study was performed through the cooling pad of the direct evaporative cooler, which acts as a filter, as well as evaporative cooling of the supply air. Using the indirect cooling technique, the unit could produce potable water from the atmospheric air in remote areas.

Experimental results obtained from prototype testing of the LDAC absorber unit indicates that the unit has a satisfactory performance in controlling the temperature and humidity when installed on a commercial site of about 200 m^2 area located on the Persian Gulf region. The tests further reveal that the experiments are in good agreement with a previously developed model for the packed-bed and that the conditioner unit can have an effectiveness of about 82% when used with liquid desiccant. The maximum electrical energy utilization of the unit,

which was determined through the above experiments, is 3 kW with an electrical COP of about 7.

For domestic roof-top applications, it was determined that a 30 kW capacity LDAC could dehumidify and cool 500 m^2 of a residential building on the Persian Gulf with an annual saving of $2,500 and a payback of less than 5 years.

References

[1] Y.J. Dai and H.F. Zhang, Numerical simulation and theoretical analysis of heat and mass transfer in a cross flow liquid desiccant air dehumidifier packed with honeycomb paper, Energy Conversion and Management, 2004, pp. 1343-1356.

[2] W.Y. Saman and S. Alizadeh, Modelling and performance analysis of a cross-flow type plate heat exchanger for dehumidification / cooling, Solar Energy, 2001, pp. 361-372.

[3] W.Y. Saman and S. Alizadeh, Design and Optimization of a Liquid Desiccant Solar Air Conditioner Using Cross Flow Type Plate Heat Exchanger, ISES 2001 Solar World Congress, 2001, Adelaide, Australia.

[4] W.Y. Saman and S. Alizadeh, An experimental study of a cross-flow type plate heat exchanger for dehumidification / cooling. Solar Energy, 2002, pp. 59-71.

[5] S. Alizadeh and W.Y. Saman, Modeling and performance analysis of a forced-flow solar collector / regenerator using liquid desiccant, Solar Energy, 2002, pp. 143-154.

[6] S. Alizadeh and W.Y. Saman, An experimental study of a forced-flow solar collector / regenerator using liquid desiccant, Solar Energy, 2002, pp. 345-362.

[7] S. Alizadeh, and K.Y. Khouzam, "A Study into the Potential of Using Liquid Desiccant Solar Air-Conditioner with Gas Backup in Brisbane – Queensland", Proceedings of 42th Australian and New Zealand Solar Energy Society, December 1-3, 2004, Perth, W.A.

[8] S. Alizadeh and K. Khouzam, Economical and environmental study of a liquid desiccant solar air conditioner for Queensland, Australia, Proceedings of the ISES Solar World Congress, Orlando, Florida, U.S.A, 6-12 August, 2005.

[9] S. Alizadeh, Development of a dehumidification/ indirect evaporative cooling system using liquid desiccant, PhD thesis, School of Advanced Manufacturing and Mechanical Engineering, the University of South Australia, Mawson Lakes Campus, S.A., 2002, Australia.

[10] J. L. McNab and P. McGregor, Dual indirect cycle air conditioner uses heat concentrated desiccant and energy recovery in a polymer plate heat exchanger, 21st IIR International Congress of Refrigeration, August 17-22, 2003, Washington DC, USA.

Investigation on radiative load ratio of chilled beams on performances of solar hybrid adsorption refrigeration system for radiant cooling in subtropical city

K.F. Fong*, C.K. Lee, T.T. Chow

Building Energy and Environmental Technology Research Unit, School of Energy and Environment & Division of Building Science and Technology, City University of Hong Kong, Hong Kong, China
** Corresponding author. Tel: +852 3442 8724, Fax: +852 3442 9716, E-mail: bssquare@cityu.edu.hk*

Abstract: The effectiveness of solar adsorption system for space conditioning would be enhanced through radiant ceiling cooling, since a higher chilled water temperature can be supplied. In such provision, desiccant dehumidification should be involved in order to cater for the latent cooling load. A solar hybrid adsorption refrigeration system is therefore formulated. In this study, the effect of radiative load ratio *R* of active chilled beams (ACB) and passive chilled beams (PCB) for the solar hybrid adsorption refrigeration system was investigated. Through the year-round dynamic simulation, it was found that the performances, like solar fraction and primary energy consumption, of the system with ACB or PCB would be improved along with the decrease of *R* from 0.3 to 0.1. At the same *R*, the system with PCB would have better performances than that with ACB. With suitable design and control, the solar hybrid adsorption refrigeration system with PCB at low *R* would be more technically feasible for office use in the subtropical climate.

Keywords: *Radiant cooling, Radiative load ratio, Adsorption refrigeration, Solar air-conditioning, High temperature cooling*

1. Introduction

To promote the low energy buildings in the hot and humid places, strategic use of renewable energy in air-conditioning would certainly contribute to sustainable design. Solar air-conditioning is getting popular in the European countries [1,2]. Through the approach of high temperature cooling, the energy performance of chiller can be enhanced by using higher chilled water supply temperature for radiant cooling. As the latent cooling load cannot be effectively handled in such provision, a separate desiccant dehumidification is necessary [3,4]. In fact, it would be effective to hybridize the adsorption refrigeration, radiant cooling and desiccant dehumidification, driven by solar energy for building space conditioning. In the previous study [5], this solar hybrid adsorption refrigeration system would have much less annual primary energy consumption than the conventional vapour compression air-conditioning system for office application. In this study, it is to investigate more deeply about the effect of chilled beams on the performances of the solar hybrid adsorption refrigeration system in the subtropical city.

The common chilled beams include the active chilled beams (ACB) and passive chilled beams (PCB), which are mounted at the ceiling level but not for structural purpose. ACB have finned coils, in which chilled water flows inside. ACB make use of forced convection for cooling through induction, so they are connected with a supply air stream that is mechanically driven. PCB also have finned coils inside, but they rely on natural convection rather than forced convection. Therefore, their performances would be affected by the radiative load ratio, which is the proportion of radiative to total (i.e. radiative and convective) cooling capacity of the chilled beams. In this study, the effect of the radiative load ratio *R* on the year-round performances of the solar hybrid adsorption refrigeration system was evaluated for the office application. Two types of offices were involved, a typical office and a high-tech

office, where the latter is featured with a much higher internal heat gains due to different electrical facilities of information technology and office automation.

Fig. 1 illustrates the design of solar hybrid adsorption refrigeration system with ACB serving an office. Solar energy is collected to supply to the adsorption refrigeration and the desiccant dehumidification through regenerative water and desiccant water respectively. Auxiliary heaters are involved whenever the required driving temperatures are not sufficient. The adsorption chiller provides chilled water to the chilled beams for sensible cooling, it also furnishes the chilled water to the supply air coil for supporting the desiccant dehumidification. The chilled beam valve and the supply air valve are used to control the required chilled water flow rate to the respective equipment. For the system with ACB, supply air fan is needed for induction of indoor air. However for PCB, no supply and return air fans, and the associated air ducts are required.

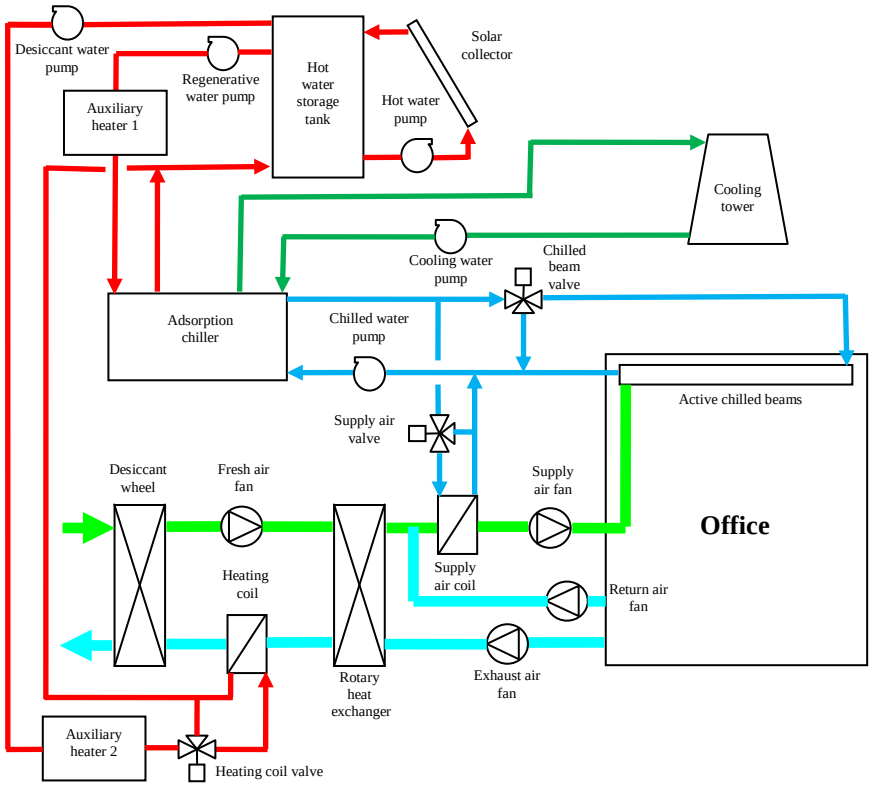

Fig. 1. Solar hybrid adsorption refrigeration system for active chilled beams.

2. Methodology

In this study, year-round dynamic simulation was applied for the solar hybrid adsorption refrigeration system. Generally the entire system model was built on the component-based simulation platform TRNSYS [6], and the validated component models of adsorption chiller [7] and desiccant wheel [8] were used. The models of ACB and PCB were developed from the empirical information of the manufacturers [9,10]. The other system components, including the office building zone, solar collector, storage tank, auxiliary heaters, rotary heat exchanger, water coils, cooling tower, pumps, fans and valves were based on those of TRNSYS and the component library TESS [11]. Different radiative load ratios were adjusted at the TRNSYS multizone building model. The indoor design conditions were set at 25.5°C and 60%RH. The floor area was 196 m^2 with 24 occupants and daily working schedule

between 08:00 to 18:00. The fresh air amount was based on 10 litres/s per occupant. The subtropical city Hong Kong (22.32°N and 114.17°E) was used, and the year-round dynamic simulation was carried out with the typical meteorological year for Hong Kong [12]. The major simulation parameters of the solar hybrid adsorption refrigeration system are summarized in Table 1.

Table 1. Values of major simulation parameters of solar hybrid absorption refrigeration system.

Fresh air stream		
Fresh air mass flow rate ($kg \cdot s^{-1}$)		0.288
Fresh air fan power (kW)		0.277
Exhaust air stream		
Exhaust air mass flow rate ($kg \cdot s^{-1}$)		0.259
Exhaust air fan power (kW)		0.166
Rotary heat exchanger		
Temperature effectiveness of rotary heat exchanger		0.8
Rotary heat exchanger power consumption (kW)		0.1
Desiccant wheel		
Mass per unit length of matrix material in desiccant wheel ($kg \cdot m^{-1}$)		0.003
Mass per unit length of silica gel in desiccant wheel ($kg \cdot m^{-1}$)		0.005
Half height or width of air channel (m)		0.0015
Outer diameter of desiccant wheel (m)		0.6
Effective area ratio of desiccant wheel		0.744
Fraction of wheel area for regeneration		0.5
Length of desiccant wheel (m)		0.2
Desiccant wheel speed (rph)		13
Number of discretization segments along the air channel length		20
Number of time steps for one revolution of the desiccant wheel		360
Desiccant wheel power consumption (kW)		0.1
Adsorption Chiller	**Typical**	**High-tech**
Number of stages per chiller	2	
Mass of metal in adsorption/desorption chamber per stage (kg)	60	80
Mass of silica gel in adsorption/desorption chamber per stage (kg)	30	40
Mass of metal in condenser coil per stage (kg)	75	90
Mass of metal in evaporator coil per stage (kg)	75	90
Maximum adsorbate intake in Freundlich equation	0.552	
Exponent in Freundlich equation	1.6	
Ratio of initial absorbrate intake to maximum abosrbrate intake	0.7	
Adsorption/desorption period (s)	360	

Cooling water system	**Typical**	**High-tech**
Cooling tower air volume flow rate ($m^3 \cdot s^{-1}$)	2.640	3.333
Cooling tower fan power (kW)	0.812	1.026
Cooling water mass flow rate ($kg \cdot s^{-1}$)	0.7	0.8
Cooling water pump power (kW)	0.138	0.168
Chilled water system	**Typical**	**High-tech**
Chilled water mass flow rate ($kg \cdot s^{-1}$)	1.05	1.3
Chilled water pump power (kW)	0.207	0.277
Hot water system	**Typical**	**High-tech**
Hot water mass flow rate ($kg \cdot s^{-1}$)	2.55	3.15
Hot water pump power (kW)	0.200	0.294
Desiccant water pump flow rate ($kg \cdot s^{-1}$)	0.15	
Desiccant water pump power (kW)	0.011	
Regenerative water pump flow rate ($k\ g \cdot s^{-1}$)	1.2	1.5
Regenerative water pump power (kW)	0.145	0.184
Chilled beams	**Typical**	**High-tech**
Model of ACB used	DID600B-L-2-M/3000x3000 [9]	
Numbers of ACB used	24	32
Model of PCB used	36CBPB14 [10]	
Numbers of PCB used	42	54
Supply air stream (ACB only)	**Typical**	**High-tech**
Supply air mass flow rate (kg·s-1)	1.008	1.344
Supply air fan power (kW)	0.258	0.345
Return air stream (ACB only)	**Typical**	**High-tech**
Return air mass flow rate (kg·s-1)	0.72	1.056
Return air fan power (kW)	0.092	0.135

3. Results and discussion

3.1. Performance indicators

A number of performance indicators were used in this study, including solar fraction *SF*, coefficient of performance *COP* and primary energy consumption *PE*, as determined below.

$$SF = \frac{Q_{sol}}{Q_{sol} + (Q_{aux1} + Q_{aux2})} \quad (1)$$

where Q_{sol} is the solar thermal gain, Q_{aux1} and Q_{aux2} are the heat output from Auxiliary Heaters 1 and 2 respectively.

$$COP = \frac{Q_e}{Q_g} \quad (2)$$

where Q_e is the refrigeration effect of absorption chiller and Q_g is the heat input to generator of absorption chiller.

$$PE = PE_p + PE_f + PE_{aux} \quad (3)$$

where PE_p is the primary energy consumption of pumps, PE_f is the primary energy consumption of fans, cooling tower, desiccant wheel and rotary heat exchanger, PE_{aux} is the primary energy consumption of auxiliary heaters.

In addition, the annually averaged room conditions, including zone temperature T_z and zone humidity RH_z, were also examined.

3.2. Solar fraction and coefficient of performance

Table 2 summarizes the annually averaged performances of the solar hybrid adsorption refrigeration system with different types of chilled beams for typical and high-tech offices. Generally the system could maintain satisfactory indoor conditions for both types of offices. The results of the typical office shows that the annually averaged *SF* of the system with PCB would become better, increased by 10.9% along with *R* decreased from 0.3 to 0.1, while that with ACB could be increased by 3.9%. Similarly for the high-tech office, the annually averaged *SF* of the system with PCB was raised by 15.6% for *R* from 0.3 to 0.1, and that with ACB by 6.4%. *SF* decreased with an increase of *R*, it was because the radiative load had less effect in reducing the zone air temperature. Hence, with a higher radiative load ratio, the zone air temperature would drop slower, meaning that the running hour of the chiller would increase. As such, the regenerative heat required was larger and resulted in a lower *SF*. For *COP*, although it was slightly increased with the rise of *R*, the change was minimal for both types of offices. At the same *R*, PCB had higher *COP* than ACB. The main reason was due to a higher chilled water supply temperature would be offered by the PCB, and the regenerative heat demand could be reduced.

Table 2. Annually averaged performance of solar hybrid adsorption refrigeration system.

Office	Chilled beams	*R*	*SF*	*COP*	T_z (°C)	RH_z (%)
Typical	ACB	0.1	0.689	0.548	25.02	53.12
	ACB	0.2	0.675	0.548	25.07	52.94
	ACB	0.3	0.663	0.548	25.13	52.80
	PCB	0.1	0.791	0.557	25.29	53.14
	PCB	0.2	0.754	0.558	25.39	53.09
	PCB	0.3	0.713	0.559	25.51	52.95
High-tech	ACB	0.1	0.568	0.546	25.19	52.51
	ACB	0.2	0.553	0.546	25.25	52.33
	ACB	0.3	0.534	0.547	25.33	52.07
	PCB	0.1	0.659	0.554	25.45	53.00
	PCB	0.2	0.616	0.554	25.56	52.87
	PCB	0.3	0.570	0.557	25.71	52.57

Fig. 2 illustrates the annual profiles of *SF* of the solar hybrid adsorption refrigeration system using ACB and PCB for both typical and high-tech offices at various *R*. The changing patterns were similar, with high *SF* from November to February and low *SF* from May to September. The former period was typical short autumn and winter in subtropical climate, while the latter was typical long summer. As compared between Fig. 2(a) and 2(b), the *SF* profiles of the typical office were generally higher than those of the high-tech offices, since the cooling demand of the typical office was lower and the involvement of auxiliary heaters would be less.

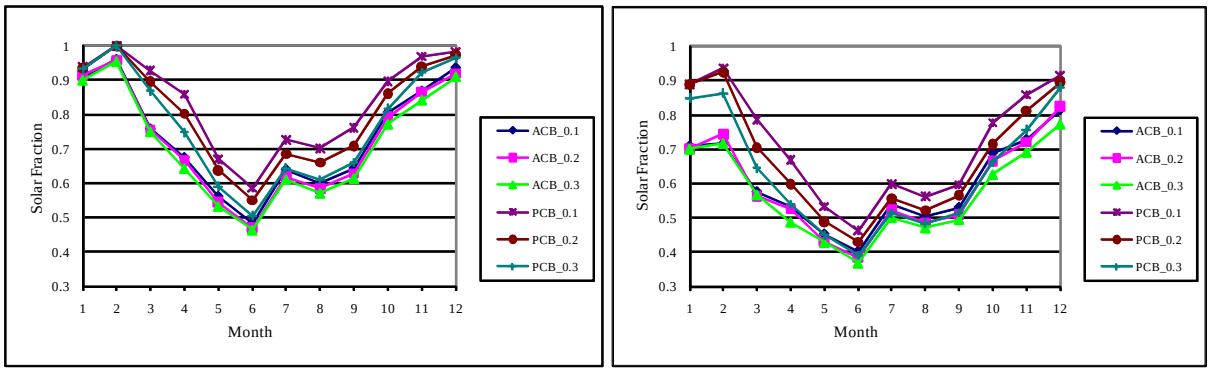

(a) Typical office *(b) High-tech office*

Fig. 2. Annual SF profiles solar hybrid adsorption refrigeration system.

Fig. 3 presents the annual profiles of *COP* of the adsorption chiller for ACB and PCB for typical and high-tech offices at various *R*. Generally the *COP* was higher in the winter months, while lower in the summer months. However the variation range of *COP* was narrow and maintained within about 10% even for different scenarios, since the chiller was supported by auxiliary heating. As compared between the chiller for the typical office and that for the high-tech office, although the latter *COP* was higher in the winter months, it was lower in the summer months. As a whole, the adsorption chiller for the high-tech office had lower annually averaged *COP* already shown in Table 2.

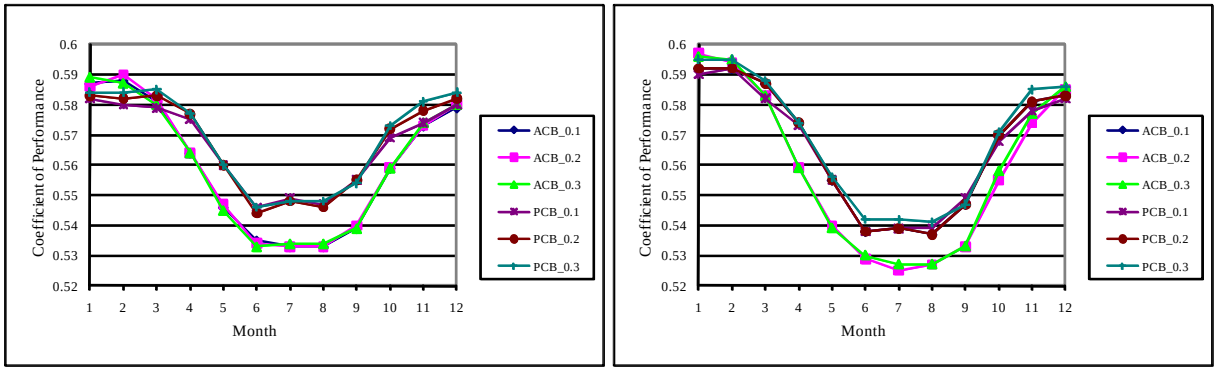

(a) Typical office *(b) High-tech office*

Fig. 3. Annual COP profiles of adsorption chiller of solar hybrid system.

3.3. Primary energy consumption

Table 3 summarizes the annual primary energy consumption of the solar hybrid adsorption refrigeration system with ACB and PCB for both typical and high-tech offices. The results of the typical office shows that the *PE* of the system with PCB would become less, reduced by 25.5% along with the decrease of *R* from 0.3 to 0.1, while that with ACB could be reduced by

8.0% only. Similarly for the high-tech office, the *PE* of the system with PCB was trimmed by 25.6% for *R* from 0.3 to 0.1, and that with ACB by 9.6%. These changing patterns were directly related to those of *SF*, since higher *SF* of the solar hybrid adsorption refrigeration system indicated less demand of auxiliary heating, thus leading to lower *PE*. At the same *R*, PCB could have less *PE* than ACB, up to 36.4% and 31.0% for typical office and high-tech office respectively. This was because the *SF* of the system with PCB was better than that with ACB, as discussed in Section 3.2, and the PE_{aux} of the system with PCB was less. In addition, the system with PCB did not have the additional supply and return air fans, so the PE_f of PCB was only about half of that of ACB.

Table 3. Annual energy performance of solar hybrid adsorption refrigeration system.

Office	Chilled beams	*R*	*PE* (kWh)	PE_p (kWh)	PE_f (kWh)	PE_{aux} (kWh)
Typical	ACB	0.1	60,943	19,466	8,232	33,247
	ACB	0.2	63,687	19,910	8,236	35,543
	ACB	0.3	66,212	20,155	8,238	37,820
	PCB	0.1	38,786	15,454	4,355	18,977
	PCB	0.2	44,764	16,588	4,361	23,815
	PCB	0.3	52,024	17,769	4,374	29,882
High-tech	ACB	0.1	94,371	26,124	9,670	58,578
	ACB	0.2	98,591	26,411	9,673	62,507
	ACB	0.3	104,398	26,971	9,676	67,751
	PCB	0.1	65,073	21,423	4,392	39,258
	PCB	0.2	75,309	22,871	4,402	48,036
	PCB	0.3	87,459	24,168	4,410	58,882

Fig. 4 presents the annual profiles of *PE* of the system with ACB and PCB for the two types of offices. Obviously the *PE* variation followed the seasonal change, and the system serving the high-tech office would demand higher *PE*. For the same type of chilled beams, higher *R* would require higher *PE*.

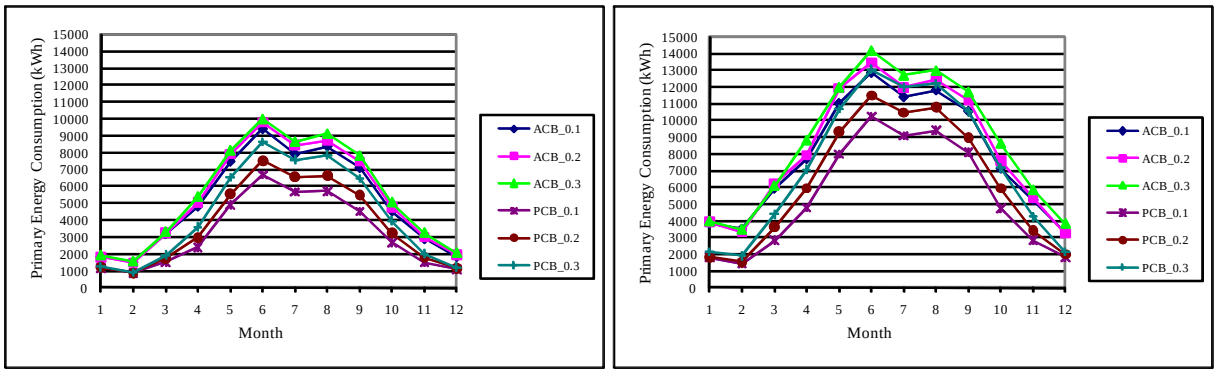

(a) Typical office *(b) High-tech office*

Fig. 4. Annual PE profiles of solar hybrid adsorption refrigeration system.

4. Conclusion

Through the year-round study of the solar hybrid adsorption refrigeration system using the two types of chilled beams, the effect of *R* on the system performances was investigated,

particularly the *SF* and the *PE*. It was found that the system with either ACB or PCB could have higher *SF* and lower *PE* when *R* was decreased from 0.3 to 0.1. Although both ACB and PCB could provide satisfactory indoor conditions for the typical and high-tech offices, the PCB had better annually averaged *SF* and total *PE* at the same *R*. As the conventional *R* of ACB is 0.1 or less, and that of PCB is between 0.1 and 0.2, suitable equipment selection and control provision of the solar hybrid adsorption refrigeration system would be technically feasible for office use in the hot and humid city. Through appropriate system design and year-round evaluation of solar air-conditioning, this would certainly help to determine a solution for reduction of carbon footprint of buildings in the subtropical climate.

Acknowledgement

The work described in this paper was fully supported by a grant from City University of Hong Kong (Strategic Research Grant, Project No. 7008037).

References

[1] H-M. Henning, Solar-Assisted Air-Conditioning in Buildings, A Handbook for Planners. Springer-Verlag Wien New York, 2004.

[2] U. Eicker, Solar Technologies for Buildings. Chichestor: Wiley, 2003.

[3] D. Song, T. Kim, S. Song, S. Hwang, S. Leigh, Performance evaluation of a radiant floor cooling system integrated with dehumidified ventilation, Applied Thermal Engineering, 28, 2008, pp. 1299-1311.

[4] J.L. Niu, L.Z. Zhang, H.G. Zuo, Energy savings potential of chilled-ceiling combined with desiccant cooling in hot and humid climates, Energy and Buildings, 34, 2002, pp. 487-495.

[5] K.F. Fong, C.K. Lee, T.T. Chow, Z. Lin, L.S. Chan, Solar hybrid air-conditioning system for high temperature cooling in subtropical city. Renewable Energy, 35(11), 2010, pp. 2439-2451.

[6] TRNSYS 16, a TRaNsient SYstem Simulation program. The Solar Energy Laboratory, University of Wisconsin-Madison, June 2006.

[7] S.H. Cho and J.N. Kim, Modeling of a silica gel/water adsorption-cooling system, Energy, 17, 1992, pp. 829-839.

[8] X.J. Zhang, Y.J. Dai and R.Z. Wang, A simulation study of heat and mass transfer in a honeycombed rotary desiccant dehumidifier, Applied Thermal Engineering, 23, 2003, pp. 989-1003.

[9] TROX Active Chilled Beams, Type DID600B-L-2-M/3000x3000, TROX Technik, TROX GmbH, July 2006.

[10] Carrier Product Data, Active and Passive Chilled Beams, model 36CBPB14, Carrier Corporation, 2008.

[11] TESS Component Libraries – Version 2.0. The Thermal Energy System Specialists, Nov 2004.

[12] A.L.S. Chan, T.T. Chow, S.K.F. Fong and J.Z. Lin, Generation of a typical meteorological year for Hong Kong, Energy Conversion and Management, 47, 2006, pp. 87-96.

A hybrid solar-gas air conditioning system based on adsorption and chilled water storage

Antonio P. F. Leite[1,*], Douglas B. Riffel[2], Celina M.C. Ribeiro[1], Francisco A. Belo[1], Paulo V.S.R. Domingos[1], Daniel Sarmento[1], Manoel B. Soares[1], Leonaldo J. L. Nascimento[1]

[1] *Solar Energy Laboratory, Federal University of Paraiba, Joao Pessoa-PB, Brazil*
[2] *Mechanical Engineering Department, Federal University of Sergipe, Aracaju-SE, Brazil*
** Corresponding author. Tel: +55 83 32 16 71 27, Fax: +55 83 32 16 77 24, E-mail: antpralon@yahoo.com.br*

Abstract: This paper presents constructive aspects and preliminary experimental results of an adsorptive chiller as part of a 20 kW central air conditioning unit for providing thermal comfort in a set of rooms that comprises an area of 110 m^2. Some simulation results of the air conditioner regeneration system are also presented. The cooling system is basically made up of a cold-water storage tank – supplied by an activated carbon-methanol chiller, and a hot-water storage tank – fed by a field of high efficient solar collectors with complementary heat by natural gas. The adsorber – a compact heat exchanger containing the activated carbon – was conceived and constructed in four modules, in order to allow heat and mass recovery. Other components are the same existing on conventional central air conditioners, as a condenser, an evaporator and a cooling tower. Constructive details of the collector's field, the adsorbers and the regenerating storage component are shown. The solar system is a 120 m^2 collection area field composed by 76 units of a flat plate collector covered with a high efficient transparent insulation. Results obtained from a multi-objective optimization based on a statistic modeling shown that – for a specific cooling power of 120 W/kg of adsorbent – the chiller's COP can reach 0.6. With this COP value, and considering the mean value of the total daily irradiation in João Pessoa (7º8'S, 34º50'WG), we can expected a solar energy cover fraction of 70%, for a typical summer day. This scenario is expected for the following operation temperatures: 30°C for the condenser, 7°C for the evaporator and 105°C at the start of the regeneration process. For an acclimatization period of 8 hours (9 to 17 h), the main dimensioning parameters were: 504 kg of activated carbon, 180 liters of methanol, 7,000 liters of hot water, 10,300 liters of chilled water with its temperature varying in the fan-coil from 1°C to 14°C.

Keywords: *Solar-gas adsorptive chiller, Thermal storage, Numerical simulation.*

1. Introduction

The simplicity of operation and minimal requires of maintenance of the adsorption chiller are certainly the major advantages compared to conventional liquid chiller (vapor compression) and to absorption chiller.

The scope of this technology involves besides the sectors of commerce and service, also the industrial, and it becomes possible the large-scale use of 'trigeneration' (combined heat, power and cooling).

The system consists basically of 3 components: an activated carbon–methanol adsorption chiller (water-cooling unit), a chilled water storage tank and an air–water heat exchanger (fan-coil). The schematic diagram of the system operation is shown in Fig.1.

The adsorption chiller is made up of the following main devices: four adsorbers (heat exchangers porous media/liquid), disposed in a parallel-series arrangement, one hot water storage tank supplied by solar energy and natural gas, two air condensers, one evaporator, and accessories such as valves and circulation pumps.

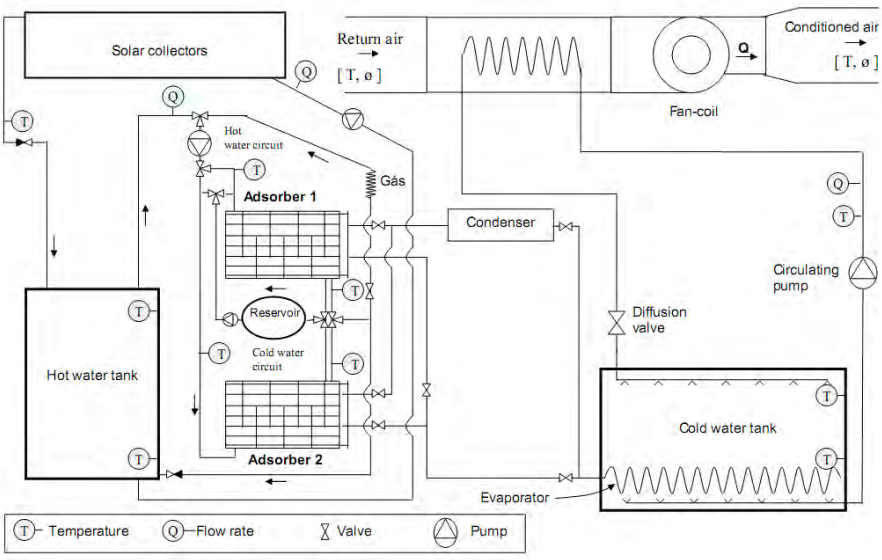

Fig.1. Scheme operation of the adsorption chiller fed by solar energy and natural gas, with thermal storage of chilled water (1).

2. Methodology

For dimensioning the adsorptive air conditioning system, we used a detailed study of individual components by means of a computer simulation program, using initially the analysis of each component and then the entire integrated system.

The computational simulation, called ADSOL, was carried out using the calculation program in the Simulink interface, with functions created in Matlab® to simulate the operation of the solar collectors field connected to the hot water storage tank and the adsorption chiller (2). For the collectors and the chiller, empirical correlations and simple methods of energy balance were used. For the storage tank, the function was based on the finite volume method.

The simulation of the complete system aims to determine the seasonal variations of different operating parameters such as the temperature, the efficiency of solar collectors, the coefficient of performance (COP) and the specific cooling power (SCP). With these data it is possible to adjust the operating times and other parameters of the system operation.

2.1. Solar collectors

For modeling the field of solar collectors it was used the quadratic efficiency collector Eq.(1) (3), which estimates the average efficiency of a solar collector at a given time, from the temperature difference between the collector (T) and the environment (T_{env}) and from the solar radiation (Rad) at that moment. The constants a_0, a_1 and a_2 depend on the characteristics of the collector, as the overall coefficient of thermal loss to the environment and the relationship between the transparent and the total area. It also takes into account the arrangement of the collectors (parellel-series) that was disposed in two sets of 38 collectors each one.

$$\eta = a_0 - a_1 \frac{T - T_{env}}{Rad} - a_2 \frac{(T - T_{env})^2}{Rad} \qquad (1)$$

The Eq.(2) represents a simple energy balance for each collector:

$$T_i = T_{i-1} + \frac{\eta A \cdot Rad}{\dot{V}_{col} c_p \rho} \quad (2)$$

Where, *Ti* is the temperature of the i-th collector in serie, *A* is the transparent area, $\dot{V}_{col}$ is the water flow in each collector in parallel, c_p is the specific heat of the water and ρ is the density of the water (properties taken in the inlet temperature).

2.2. Adsorption chiller

The adsorption chiller operation was simulated using a model developed by Riffel et al. (4). It was investigated statistically the results of the dynamic model of the adsorber in order to obtain the optimum project parameters, taking into account the best operating points and the influence of seven variables (temperature and mass flow of hot water, cycle length, number of tubes, number of fins, fin thickness and material of manufacture) (5). The results showed that all variables are statistically significant and interdependent. In other words, a change in one variable affects directly the other one. This demonstrates the importance of using statistical modeling for this analysis. As a main result, we observed that the COP is highly dependent on the number of fins, the material and the cycle length. The inner surface of the adsorber, exchange heat with water from a hot or cold source, depending on the phase of the cycle. The adsorbent occupies the space delimited by the external wall of the tube and the corrugated fins. The adsorbent bed operates under vacuum for getting the required thermodynamic properties of the working fluid (the methanol). The micropores of the adsorbent medium has a diameter smaller than 2 nm. In the case of specific cooling power (SCP), the most important variables were the number of fins, the number of tubes and the hot water temperature.

The Eq.(3) represents an energy balance for the water that flows in the adsorber. Losses in the pipeline and the delayed response in thermal heat exchanger (adsorber) were not considered.

$$T_{out} = T_{in} - \frac{SCP}{COP} \cdot \frac{m_{ads}}{\dot{V}_{ad} c_p \rho} \quad (3)$$

Where, T_{out} and T_{in} are, respectively, the water temperatures at the exit and entry of the adsorbers, m_{ads} is the total mass of adsorbent (activated carbon), and $\dot{V}_{ad}$ is the water flow in the adsorber.

2.2. Hot water tank

The geometry of the hot water storage tank is cylindrical, with is connected at the bottom and the top, with the solar collectors and the adsorbers. For calculating the heat exchanges in the tank the finite volume method was used and it was considered a stratified tank with one-dimensional heat transfer. The stratification occurs in layers of increasing density and decreasing temperature. This method presents a numerical solution that enables problem solving under any initial conditions and it consists in dividing the tank into a finite number of longitudinal nodes of same temperature and volume. Thus, we obtained the equations of the heat and mass transfers for each volume, applying the respective boundary conditions. The solution of the equations is performed by implicit formulation and the method of matrix inversion. The model of the hot water tank was developed by Riffel (2), by changing only the response of simulation to provide temperature values in both the base and on top of the tank.

3. Description of the central air conditioning unit

The air conditioning system is based on an adsorption cycle with heat recovery, in which the steps of regeneration and production of refrigeration effect occur simultaneously, i.e., the adsorbers (I and II, in Fig. 1) work in alternated way; when one is the adsorbing phase, the other is in the desorbing phase (1). The adsorber model takes into account the geometry of the finned-tube liquid-adsorbent heat exchanger. It is based on the activated carbon-methanol pair and is responsible for cooling the water that is accumulated in the tank. The working fluid is the methanol, which flows through a compact heat exchanger evaporator, where the water is cooled. The conditioned air is obtained by changing heat with the stored chilled water and the air process through a fan-coil, and then it is distributed in the set rooms by a pipelines network. The regeneration is made by solar thermal energy produced by a highly efficient solar collectors field that is stored in a water tank, and, from this main tank to the adsorptive chiller, an additional heat is supplied by the combustion of natural gas.

4. Constructive aspects of the central air conditioning unit

4.1. Regeneration system

The regeneration system comprises a f ield of flat solar collectors with high efficiency**,** coupled to a thermal storage tank. The water previously heated by the solar energy will get the process temperature of 105°C with the help of a small gas heater.

4.1.1. Solar collectors

The solar collectors are flat and static. The outer surface of the collectors is painted nonselective matte black, and a Teflon film is placed between the absorbing surface and the glass cover plate (Fig. 2) (6, 7).

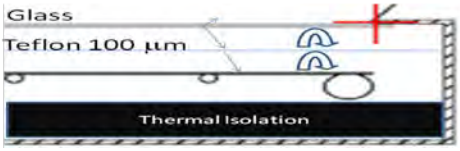

Fig. 2. Scheme of TIM cover.

The field of collectors was installed in a parallel-series arrangement, in two symmetrical blocks, each consisting of 38 units of a commercial flat collectors of 1.58 m^2 each, covering a total collection area of 120 m^2, installed on the roof titled 9^o facing to the South (Fig. 3), which corresponds to the average value for the six hottest months in João Pessoa (7°8′S, 34°50′WG), whose climate is typically hot and humid (8).

Fig. 3. Field of flat plate collectors with TIM coverage installed on the LES/UFPB.

4.1.2. Hot-water storage tank

As showed in a previous article (9), the required cylindrical hot water tank for providing the minimum gas consumption was obtained from simulations to be around 7m^3 of capacity, by comparing the volumes from 1m^3 to 9m^3 during 24 hours. It was built in steel, with 2.074m of diameter and 2.50m of height, insulated with 50mm thick polyurethane foam.

4.1.3. Adsorptive chiller

As result from simulations carried outd by Riffel (4, 5), we have determined the characteristics of the adsorber, as shown in Table 1.

Table 1. Characteristics of the adsorber.

Dimensions	668mm x 330.2mm x 19mm
Number of flat tubes	27
Row number of fins	28
Tube external diameter	12.7mm
Tube internal diameter	10.9mm
Fin width	19mm
Fin thinckness	0.3mm
Fin pitch	1.8mm
Heat transfer area (fin side)	4.175m²

4.1.4. Condenser and evaporator

The equations related to the condenser and evaporator where widely described and experimentally validated on a previous paper (10). They are a finned-tube heat exchanger. From the simulation data, the evaporator must operate continuously (i.e., during the 24 hours a day) to ensure the storage of chilled water required by the heat exchanger air-water (fan-coil) and thus provide the design temperature for the inlet air of the rooms. For the evaporator we selected a compact plate heat exchanger, manufactured by CIAT (French), for a wide power range (2 to 200 kW) (11). The equipment will be adapted for the required operating conditions, to ensure that the outlet methanol is completely superheated.

4.1.5 Natural gas heater

The natural gas heater model GWH 300DE-GN - BOSH, will heat the water from the hot water tank until the temperature of 105°C to ensure the regeneration. The simulation program calculates the total amount of natural gas need to be consumed in one day.

5. Results

For the simulation we have taken some considerations concerning some system parameters. The chilled water temperature is considered constant and equal to 7^{o}C and the cold water temperature is taken 5^{o}C above ambient temperature. The mass of the adsorbent (activated carbon) is considered equal to 116 kg for each adsorber, and the adsorber water flow is equal to 0.1L/s. The simulation results were obtained considering a typical summer day in Joao Pessoa, represented by the data of January 1, 2010 (10).

The water flow in each set of collectors in parallel arrangement was examined for different volumetric flows (0.1L/s, 0.2L/s, 0.3L/s, 0.4L/s and 0.5L/s) to verify which of them provides the lower gas consumption while the system reach a regeneration temperature. They are presented in different response curves generated for periods of 24 hours.

The volumetric rate flow through the solar collectors field was measured to compare this value with those obtained in the simulation. The measure was made with an ultrasonic flow meter, mark FMS, model UFM170. The volumetric flow rate is considered constant and the average of six measured values was about 0.71L/s.

5.1. Figures

The Fig. 5 shows the daily consumption of natural gas, for the water collector flow between 0.1L/s and 0.5L/s.

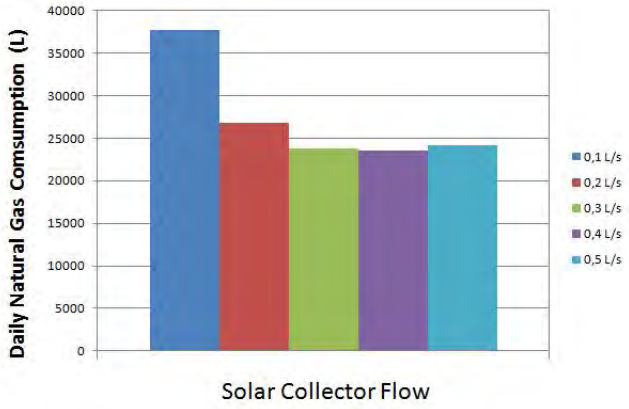

Fig. 5. Daily consumption of natural gas.

Taking into account the simulation results of Fig. 5, we can see that the solar collectors water flow of 0.4L/s gives the minimum consumption of natural gas. Thus, other results based on this flow rate are shown in Figs. 6 and 7.

The Fig. 6 shows the average water temperature in the hot water tank, during a whole day. The curves show that, at around 7am it was obtained the minimum temperature, of 58°C, corresponding to the maximum gas flow of 0.037L/s. The need of gas decreases with the temperature rise. Due to the thermal inertia, until the maximum temperature at 16:10h (86.2°C) the gas flow increases, and then it decreases following the same tendency of the temperature.

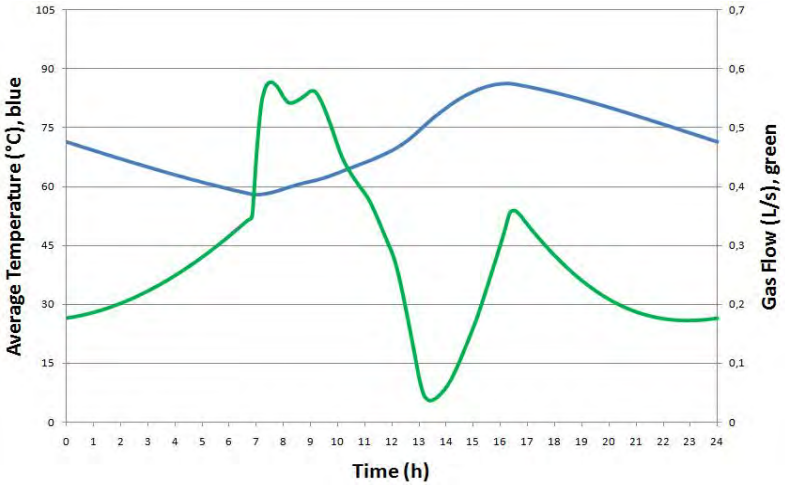

Fig.6 Average hot water temperature and the corresponding natural gas flow for the solar collector flow rate of 0.4L/s, during a day.

The Fig. 7 shows the solar collector temperatures (blue) and the temperatures of the bottom and the top (red and green) of the storage water tank, obtained with a water flow rate of 0.4L/s. We can see that there is an agreement between the temperature curves in the collectors

and on the top and the bottom of the storage tank. Due to the thermal inertia, the temperature at the bottom of the tank remains almost constant until around 8am, when it begins to increase, reaching its maximum at 16:20 and then starts to decrease.

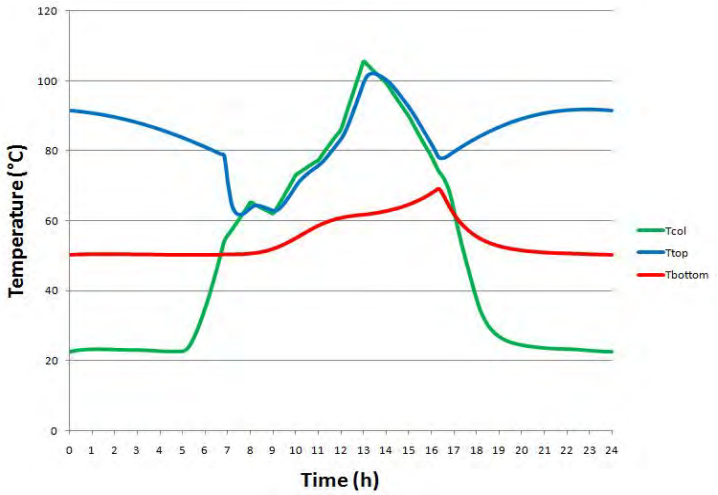

Fig.7. Thermal response of the system to the real situation, for a water flow rate of 0.4L/s, during a day.

6. Conclusion

We have presented the main parameters of a central air conditioning unit based on t he adsorption of methanol in activated carbon and a hybrid regeneration system, projected to provide until 70% of the required heat by solar energy, the complementary heat by natural gas. A simulation program was developed and we have obtained from it an optimal volume of the storage hot water of 7,000 liters. It was found that 0.4L/s is the flow rate through the solar collectors field that gives the minimum consumption of gas, and the water pump should be regulated to obtain the ideal volumetric flow.

6.1. The current stage of the project

The solar collectors are installed and connected to the hot water storage tank; to compensate the thermal inertia of it a small tank of 500 liters was built and connected to the main one for providing the process regeneration temperature (105oC) with aid of the gas heater and. An equipment for analyzing the heat losses from the storage tank was also built.

The 4 adsorber modules were made, and a test bench is now under construction. The chilled water storage tanks were manufactured and their hydraulic connections installed. The air–water heat exchanger unit (fan-coil) and their pipelines network are already installed in a set of rooms.

Acknowledgements

The authors would like to thank CNPq (CT-Petro/CNPq 15/2007) and FAPITEC/SE (FUNTEC 02/2009) for the grant support, CNPq for the post-PhD scholarship to the third author and, CAPES for PhD scholarship to the first author and for post-PhD scholarship to the second author.

References

[1] A.P.F. Leite, F.A. Belo, M.M. Martins, D.B. Riffel, Central air conditioning based on adsorption and solar energy, Applied Thermal Engineering, Volume 31, Issue 1, January 2011, Pages 50-58, ISSN 1359-4311.

[2] D.B. Riffel, A.P.F. Leite, F.A. Belo, Simulação do aporte térmico de coletores solares planos em um tanque cilíndrico estratificado. In: I Congresso Brasileiro de Energia Solar, Fortaleza, CE, 2007.

[3] J.A. Duffie and W.A. Beckman, Solar Engineering of Thermal Processes, J. Wiley & Sons, 1980.

[4] D.B. Riffel, Estudo Teórico e Experimental da Dinâmica e da Otimização de Refrigeradores Térmicos por Adsorção, Tese de Doutorado (Eng. Mecânica), PPGEM/UFPB, 2008.

[5] D.B. Riffel, U. Wittstadt, F.P. Schmidt, T. Nunez, F.A. Belo, A.P.F. Leite, F. Ziegler, Transient modeling of an adsorber using finned-tube heat exchanger, International Journal of Heat and Mass Transfer, Volume 53, Issues 7-8, March 2010, Pages 1473-1482, ISSN 0017-9310.

[6] A.P.F. Leite, F.A. Belo, M.B. Grilo, R.R.D. Andrade, Avaliação experimental de um adsorvedor multitubular coberto com material isolante transparente, Anais do V I Congresso Iberoamericano de Engenharia Mecânica (CIBEM6), Coimbra, Portugal, 15-18 Oct., 2003, Vol. I, pp. 253-258.

[7] A.P.F. Leite, F.A. Belo, M.B. Grilo, R.R.D. Andrade, F. Meunier, An improved multi-tubular solar collector applied to adsorption refrigeration, Proc. ISES Solar World Congress, Orlando, Florida, USA, 6-12 Aug., 2005.

[8] P.V.S. Domingos, D.B. Riffel, A.C.R. Veloso, C.M.C. Ribeiro, F.A. Belo, A.P.F. Leite, Simulação numérica do sistema de regeneração de um ar condicionado solar por adsorção baseado em um campo de coletores planos de alta eficiência, IV Conferência Latino Americana de Energia Solar (IV ISES_CLA) y XVII Simposio Peruano de Enegía Solar (XVII-SPES), Cuzco, Peru, 1-5.11.2010.

[9] R.R.D. de Andrade, M.M. Machado, A. Lourenço, F.A. Belo, A.P.F. Leite, Avaliação experimental de uma cobertura isolante composta por material transparente para uso em coletor solar, V Congresso Nacional de Engenharia Mecânica – COBEM 2008, 25 a 28 de agosto, Salvador/Bahia, Brasil.

[10] D.B. Riffel, F.A. Belo, A.P.F. Leite, Otimização de chiller adsortivo solar por modelagem estatística, Climatização & Refrigeração, Abril de 2010, pags. 38 a 45.

[11] D.B. Riffel, F.A. Belo, A.P.F. Leite, Heat and mass recovery in an activated carbon-methanol adsorptive chiller, Proceedings of COBEM 2009 - 20th International Congress of Mechanical Engineering, November 15-20, 2009, Gramado, RS, Brazil.

Performance analysis of the solar-thermal assisted air-conditioning system installed in an office building

Masaya Okumiya[1,*], Takuya Shinoda[1], Makiko Ukai[1], Hideki Tanaka[2], Mika Yoshinaga[3], Kazuyuki Kato[4], Toshiharu Shimizu[4]

[1] *Nagoya University,Nagoya,Japan*
[2] *Chubu University,Kasugai,Japan*
[3] *Meijyo University,Nagoya,Japan*
[4] *Tohogas Co. Ltd.,Nagoya,Japan*

** Corresponding author. Tel: +81 527894653, Fax: +81 527893773,*
E-mail:okumiya@davinci.nuac.nagoya-u.ac.jp

Abstract: In this study, performance of the solar-thermal assisted air-conditioning system installed in an office building is investigated. In this paper, firstly the results of field measurements in winter (heating) and summer (cooling) are presented. Efficiency and performance of equipments which constitutes a system are investigated. Also the utilization efficiency of solar energy and the solar fraction are estimated for winter/summer season. In addition to analysis of field measurement data, system simulation of performance was conducted in this paper. Simulation program using in this study was developed as the tool for Life Cycle Energy Management of HVAC system. In this paper mathematical model of each equipment are presented as well as how to model total system . Although there are some limitations of solar system simulation with 1 hour time step, the calculation result was well in agreement in an actual measurement.

Keywords: *Solar-thermal assisted air-conditioning system, Field measurement, Simulation*

Nomenclature

Ac area of collector..... m2
C fluid thermal capacity rate ratio ……..……..-
Cmax higher capacity rate of heat exchanger in two side..... kW /C
Cmin lower thermal capacity rate of flow medium in two side ..... kW /C
C1 thermal capacity rate of fluid at primary side..... kW /C
C2 thermal capacity rate of fluid at secondary side..... kW /C
FE water flow rate through collector..... kg/h
G gas consumption of absorption machine in cooling ..... kW
J solar radiation kW/m2
N number of transfer units .....-
Qc collected heat ..... kW
Qhex actual heat exchange rate ..... kW
Qhexmax ideal maximum heat exchange ratekW
q load ratio of absorption machine in cooling .....-
Ta outdoor air temperature.....C
Tc,out collector outlet water temperature C
Tc,in collector inlet water temperature C
T1,in inlet water temperature of heat exchanger in primary side.....C
T1,out outlet water temperature of heat exchanger in primary side.....C
T2,in inlet water temperature of heat exchanger in secondary side C
T2,out outlet water temperature of heat exchanger in secondary side C
U heat loss coefficient of collctor.....kW/m^2·s^{-1}
UA overall heat transfer coefficient .....kW /C
Wmax higher flow rate of heat exchanger in two side.....kW /C
Wmin lower flow rate of heat exchanger in two side.....kW /C

α absorption rate of collector..... -
ε heat exchanger effectiveness ..... -
η thermal efficiency of collector..... -
τ transmittance of collector cover glass.....-
ω specific dissipation of turbulent kinetic energy.....s^{-1}

1. Introduction

Practical use of renewable energy is necessary for CO2 emissions reduction, especially, possibility of energy conversion by using solar thermal is high, and it is considered to be one of the effective means.

Although the solar-thermal-conversion air conditioning system combined with the absorption refrigerating machine was proposed at 1970's in Japan[1)2)], remarkable spread after that was not seen because of solar heat collection at high temperature having been difficult. Also there was not high performance thermal driven chiller (absorption machine) for effective use solar thermal energy.

In this paper, the actual proof examination of the air conditioning system which combined the solar collector and the gas absorption chiller/heater which can use solar heat is presented. The actual proof examination started from Jan. 2010 in Tsu City, Mie for the purpose to demonstrate effectiveness of solar HVAC system. Firstly the outline of building and system was described. Then performance of system in winter and summer season is presented and discussed. Furthermore the system simulation for solar system was intoroduced and possibility to represent the behavior of system is discussed.

2. Outline of Object Building and System

A building is 2,400m2 of total area and 4 stories. The appearance is shown in Fig. 1. The layout of equipments on roof is shown in Fig. 2, and specification of equipments is shown in Table 1. The appearance of two type of collector is shown in Fig.3. The system flow of diagram and outline of control are shown in Fig. 4.

3. Result of Actual Proof Examination

3.1 Thermal efficiency of collector

Fig. 5 shows the change of amount of heat collection Qc and thermal efficiency calculated by following equation.

$$Qc = (Tc,out - Tc,in) * FE \quad (1)$$

$$\eta = Qc/ (J * Ac) \quad (2)$$

Fig.1 Appearance of building

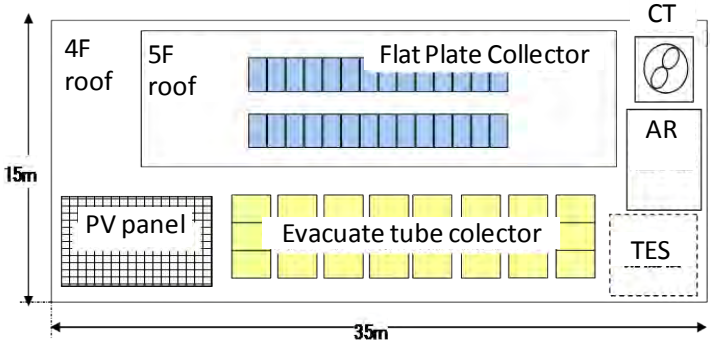

Fig.2 Layout of equipments on roof

Fig.3 Appearance of collectors

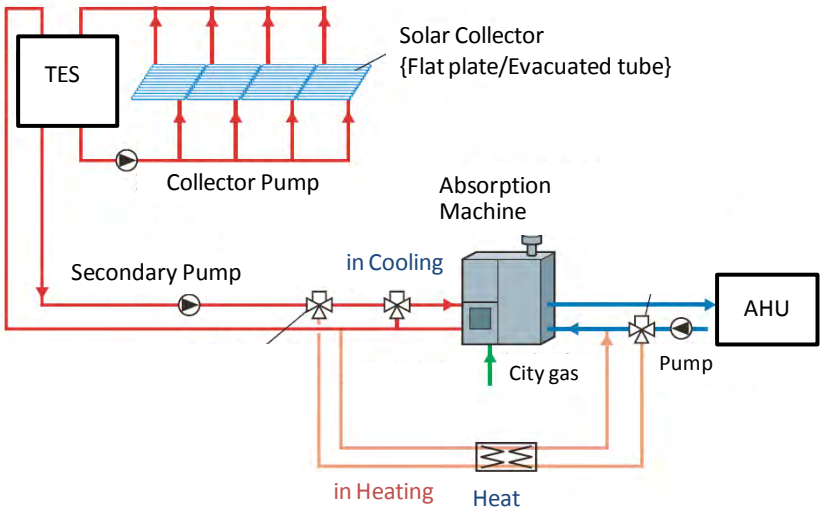

Fig. 4 System diagram of solar heating/cooling system

Table 1 Specification of equipments

Solar	Total are 139m^2	Flat plate
Collector	Medium : Water	2.0m^2 x 28
	Tilted angle : 25°	Evacuated tube
	Angle of direcstion : SSW30°	4.1m^2 x 20
Absorption	Three stage	
Machine	Cooling 527kW Heating 290kW	
TES	4.9m^3	

Fig. 6 shows daily solar irradiance and amount of heat collected in March 2010. Total amount of solar insolation was 16,800kWh and total amount of heat collected was 5,870kWh. Thermal efficiency of solar collector in March was 35%.

Thermal efficiency is plotted as a function of {(Tc,out+Tc,in)/2-Ta}/I in Fig.7. At the high collecting temperature (at large value of (Tc,out+Tc,in)/2-Ta), efficiency of flat plate collector decrease while that of evacuate tube type heat pipe stable. It means evacuate tuype heat pipe collector is suitable for "Solar cooling" where absorption machine require relatively high temperature heat source water.

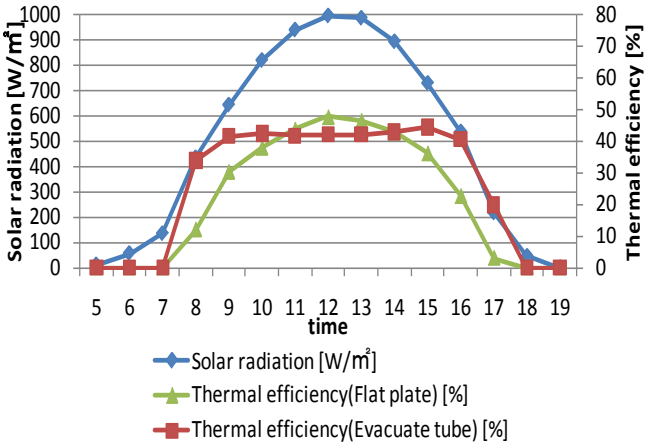

Fig.5 Collected heat and thermal efficiency of collector

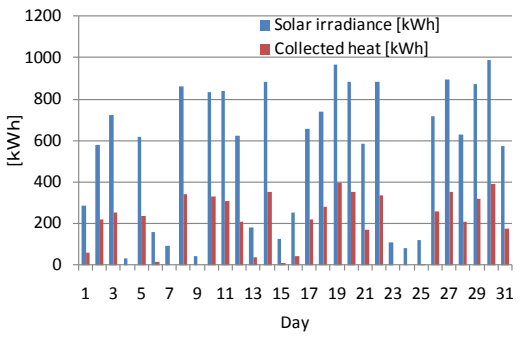

Fig.6 Daily solar irradiance and amount of heat collected (March, 2010)

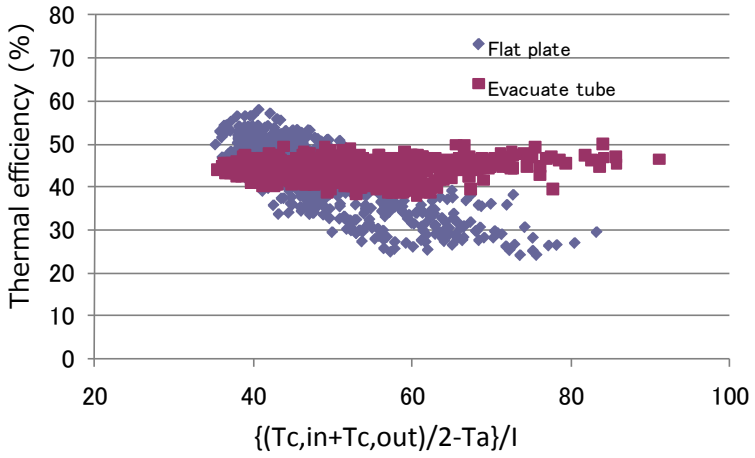

Fig.7 Plot of thermal efficiency as function of {(Tc,in+Tc,out)/2-Ta}/I

3.2 System performance in winter (heating)

Fig. 8 shows daily amount of solar heat and gas energy consumed for heating. Monthly solar fraction calculated by following equation was 19%. Seasonal performance of the system is shown in Table 2. Solar heat utilization efficiency is 72% and solar fraction is 13.1 for heating season. Also ratio of pump energy to amount of collected heat is 12%.

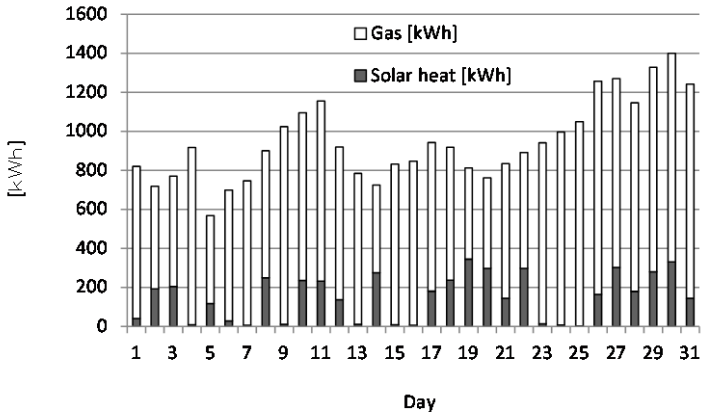

Fig.8 Daily amount of solar heat and gas energy consumed for heating

Table 2 Performance of system in heating season

		Feb.	Mar.	Apr.	Total
Collected heat	kWh	4,543	5,873	3,807	13,223
Heat delivered to heat exchanger	kWh	3,426	4,701	2,155	10,282
Heat loss	kWh	1,117	1,172	1,652	3,941
Pump energy (primary)	kWh	629	786	328	1,743
Solar fraction	%	8.3	16.0	25.5	13.1

3.3 System performance in summer (cooling)

Fig. 9 shows seasonal performance of the system for summer. Solar heat utilization efficiency changes among 78 to 89%. The highest heat utilization efficiency was seen in August. Fig. 10 shows . Monthly solar fraction calculated by following equation changes among 16 to 18%. In August, the coefficient of performance for system (System COP) and the saving rate of gas consumption were 1.4 and 0.1 respectively.

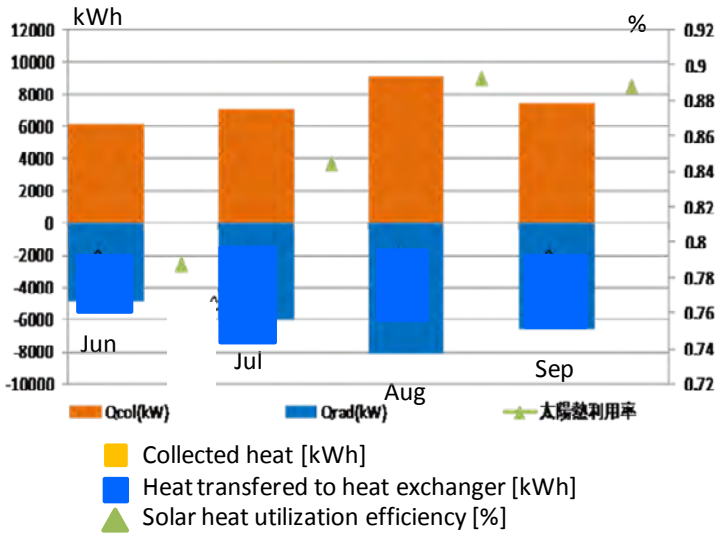

Fig. 9 Heat collected and transferred to absorption machine

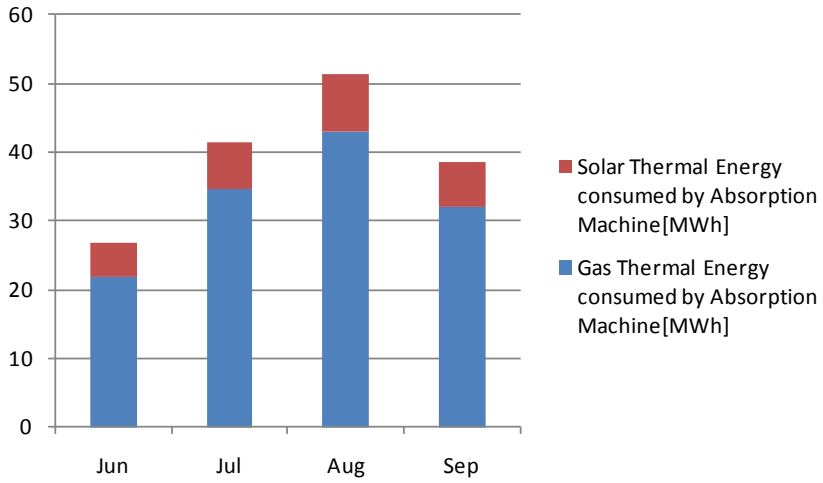

Fig. 10 Monthly amount of solar thermal energy and gas energy consumed for absorption machine

4. Simulation

In this paper, simulation of the performance of system in winter was conducted using LCEM tool. LCEM tool was developed by the basis of editorial supervision of Ministry of Land, Infrastructure and transportation, Japan for life cycle energy management of HVAC system.

4.1 Outline of Analysis Model

A part of LCEM tool Ver.3.02 was improved, and the simulation model was built. It consists of two models of the heat collection system shown in Fig. 11 and the air-conditioning system shown in Fig. 12. Two models are combined via interface.

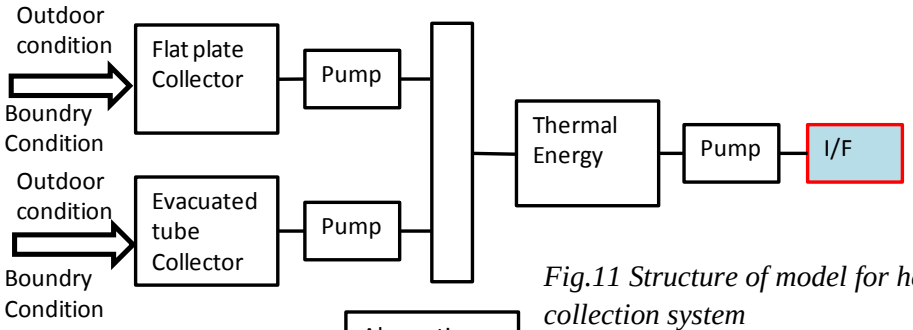

Fig.11 Structure of model for heat collection system

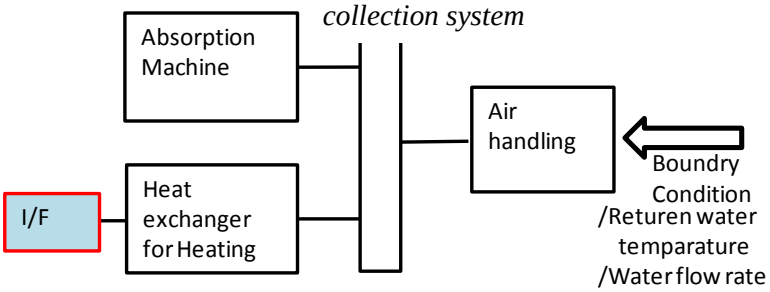

Fig,12 Structure of model for solar air-conditioning system

4.2 Collector Object

Heat collected by solar collector Qc (kW) is calculated by the following equations.

$$Qc = \eta * J * Ac \qquad (3)$$

Moreover, thermal efficiency of solar collector is expressed with the following equations.

$$\eta = \tau*\alpha - U*\triangle t/J$$

$$\triangle t = (Tc,in+Tc,out) / 2 - Ta \qquad (4)$$

The following characteristic were used in this simulation.

$$\text{Flat plate collector: } \eta = 0.578-0.00493\triangle t/J \qquad (5)$$

$$\text{Vacuum-tube type: } \eta = 0.496-0.00156\triangle t/J \qquad (6)$$

4.3 Thermal Storage Tank Object

The characteristic of thermal storage tank was assumed as complete mixed.

4.4 Pump Object

The energy consumed by pump is calculated using pump efficiency, water flow rate and head of piping system. Efficiency of pump is set constant in the object used in his paper. LCEM tool cannot make the model of the differential gap in the ON-OFF control of a pumps.

4.5 Heat Exchanger Object

The heat exchanger object used in this paper are as follows.

$$Qhex = C1* (T1\ in-T1out) = C2* (T2\ out-T2in) = \varepsilon*Qhexmax \qquad (7)$$

$$Qhexmax = Cmin* (T1\ in-T2in) \qquad (8)$$

$$\varepsilon = [1-exp\ \{-N\ (1-C)\}] /[1-Cexp\ \{-N\ (1-C)\}] \qquad (9)$$

$$N = UA/Cmin \quad (10)$$

$$C = Cmin/Cmax \quad (11)$$

$$Cmin = 4.186 * Wmin/60 \quad (12)$$

$$Cmax = 4.186 * Wmax/60 \quad (13)$$

4.6 Absorption Chiller/Heater Object

The amount of gas consumption is assumed as the function of the load factor (q), and was modeled by the following formulas.

In case of 0% <q< 25%

$$G = 1.2 * q/100 * 25.8 \quad (14)$$

In case of 25%<q<40%

$$G = (-0.013 * q + 1.533) * q/100 * 25.8 \quad (15)$$

In case of 40%<q<100%

$$G = q/100 * 25.8 \quad (16)$$

The differential gap in ON-OFF of absorption machine can not be expressed by LCEM tool and the outlet temperature was set to constant value of 55 degrees C.

5. Simulation Result

In this section simulation results for heating operation are shown. Fig. 13 shows the comparison between measurement and simulation for flat plate collector and evacuated heat pipe. Fig. 14 shows the heat collected and delivered to heat exchanger. Also fig.14 shows temperature in thermal storage tank. Fig. 15 shows the change of output of absorption machine. From these figures, it can be concluded that simulation results using LCEM tool shows good agreement with an actual measurement. However there are limitations of simulation as follows.

Time interval of calculation

In this study, 1 hour of time interval for calculation is applied. The system is controlled by the shorter time interval. Therefore, calculation result of collected heat at end of operation (evening) is overestimated. Also output of absorption machine (operate as boiler in heating) is overestimated when heat load is small. In this situation, absorption machine repeats operation and stop at short time step. However, this action cannot be expressed by simulation.

Simplified model

In this study, components in the system are modeled simply, for example heat loss from storage tank was neglected. This kind of simplification effects on the accuracy of simulation.

6. Conclusion

The system performance for the 1st year has been grasped by field measurements. Also system simulation for heating season was conducted by using LCEM tool. The simulation for cooling season will be conducted from now on. Although the system demonstrated good performance, improvement of operation should be conducted based on the results of field

measurements and simulation. Also simulation program will be revised to reduce the limitation which was mentioned in this paper.

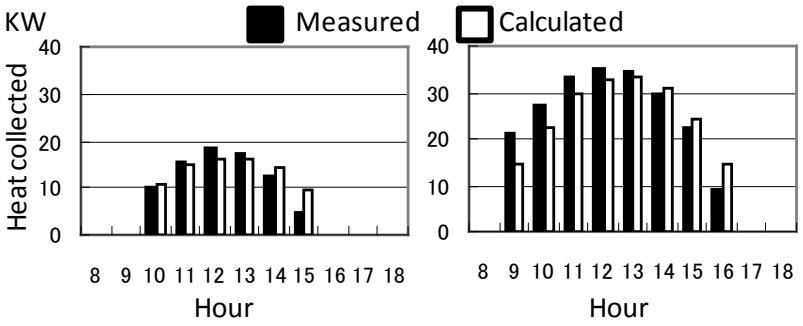

Fig. 13 Comparison collected heat by collector between measurement and simulation

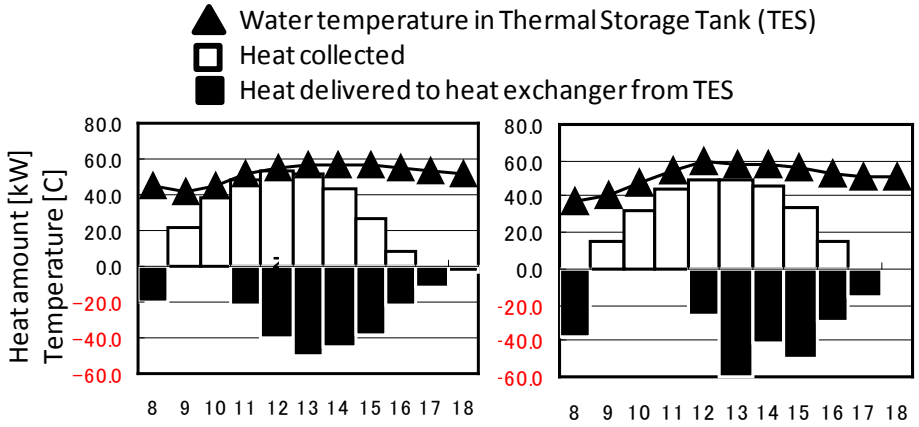

Fig.14 heat collected, heat delivered to heat exchanger and water temperature in thermal storage tank

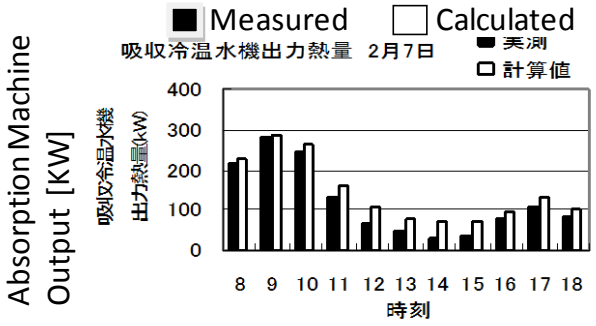

Fig. 15 Comparison of output of absorption between measurement and simulation

References

[1] N.Nakahara, K.Okada, H.Niwa, Study on System Applications of CPC Solar Collectors Part 4-Actual Operating Results of Solar Facilities for Chita Citizen's Hospital, SHASE Transactoin, No.33, 1987,pp61-73 (in Japanese).

[2] New Energy and Industrial Technology Development Organization, Japan, Design Guide for Solar Architectyre, 2001 (in Japanese)

Characterization of nanostructure black nickel coatings for solar collectors

Z.Ghasempour, S.M. Rozati*

Physics Department, University of Guilan, Rasht,41335.Iran
** Corresponding author. Tel: +98131220912 Fax: +98 1313220066, E-mail: smrozati@guilan.ac.ir*

Abstract: In this research, black nickel coatings have been deposited on brass, copper and steel substrates by electrodeposition method. The physical properties of solar absorber black nickel coatings on different metallic surfaces have been investigated. The effect of different metallic substrates including brass, copper and steel with presence of bright nickel middle layer and without its presence on optical and structural properties of deposited layers have been studied. These coatings characterized by scanning electron microscopy (SEM), X-ray diffraction (XRD) and energy-dispersive X-ray analysis (EDAX). For investigation of optical properties of deposited layers, UV-VIS-NIR spectrophotometer was used.

Keywords: *Electroplating, Black nickel, Bright nickel*

1. Introduction

The use of selective coatings has been widely established as an industrial application which used to absorb solar thermal energy. Demands for design and construction of solar absorber plates to achieve reduced energy consumption and its applications in the areas of electrical energy, heating and cooling systems lead to the development of growing of black nickel coatings [1]. Fundamental properties of black nickel coatings are currently excessively studied because of their potential application in numerous fields such as electronic devices, opto-electronic, optics, biotechnology, human medicine, solar energy conversion and etc [2]. Black nickel is one of the most commonly used solar selective coatings in solar collector systems for the efficient conversion of solar energy into thermal energy [3]. Such coatings are identified by high solar absorptance (α>95%) and low thermal emittance (ε<40%). Considering all studied cases selected for selective solar absorber coating, black nickel plates due to lower consumption of requirement electrical energy also electroplating in large scale for production and development in the industry are considered as one of the most appropriate coatings [4]. There are different methods for the deposition of black nickel coatings, including Chemical vapor deposition (CVD), sputtering, spray pyrolysis[5], electroless[6], pulse plating[7] and electrodeposition [8,9]. Among these methods, because of simple setup, low cost process of coating in industrial scale, easy control of production processes and high speed production, the electroplating method attracted special attention.

Electroplating of metallic films is one of the appropriate techniques to obtaining absorber coatings with selective optical properties for solar collectors. Electrical current and reclamation agents that are used in this process are cheap and this good economic sense to develop this approach. By using this method, optical coatings with suitable properties for solar absorber plate's applications with large scale are provided.

Electroplating is a process in which by using electrical current, a thin layer of metal is deposited on the surface of another metal. Figure 1 shows the schematic of electroplating system in hull cell. The presence of the bright nickel middle layer causes changes in the optical properties, including absorptance and emittance, of the films.

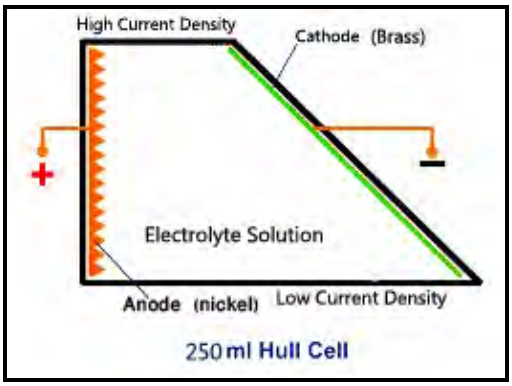

Fig. 1. The schematic of electroplating system in hull cell

2. Methodology

Black nickel coatings have been deposited on three different substrates namely brass, copper and stainless steel by electroplating method. Before deposition at First, the desired metal plates in dimensions of 7 × 1 0 cm perfectly polished and then thoroughly washed with distilled water. After that all substrates were degreased with a hot commercial alkaline solution followed by rinsing in distilled water. Finally they are placed in the chloride electrolyte solution for black nickel plating. All the coating process is carried out in hull cell. The Quality of black nickel coatings depend on the electrolyte solution composition and its concentration, electrodes, solution pH, bath temperature, current density and (deposition) duration (time). Therefore to obtain optimum optical properties for black nickel coatings, deposition parameters have to be optimized. In this type of coating, the soluble nickel metal used as a anode with 99% purity. Direct current passes between two electrodes in a conducting solution of nickel salts. The chemical bath for black nickel deposition consisted of a mixture of distilled water, nickel, zinc, tin and ammonium chloride with potassium thiociyanate. By flowing the current through the electrolyte, one of the electrodes (anode) is dissolved in the solution and the other electrode (cathode) is covered by a black nickel layer. In the electrolyte solution Ni positive ions (Ni^{++}) present so as the electrical current flows through the electrolyte, positive ions by absorbing two electrons on the surface of cathode are converted to nickel metal and deposited on the cathode surface. Reverse reaction occurs at the anode. So with the consumption of nickel in the cathode, the nickel ions are provided by anode. The concentrations of additives were varied to improve the optical performance. After numerous tests the best conditions for strongly adherent and durable black nickel coating, as mentioned in table 1, were obtained as follow: solution with pH 4.2, electrolyte bath temperature 65°C, plating time 10 min and current density 0.1 A/dm^2.
The effect of different substrate metals including brass, copper and stainless steel without the presence of the middle bright nickel layer and with the presence of it, on the optical and structural properties of the black nickel coatings have been investigated. Changes in the physical as well as optical properties of black nickel coatings are measured. SEM and XRD analysis are carried out by Philips PW3710 and Philips XL 30; the absorption spectra of coatings and emittance spectra are measured by carry 500 and Jasco FTIR respectively.

Table 1: Optimum conditions of coating

Current density	Temperature	pH	anode	cathode	Deposition time
0.1 A/dm^2	65℃	4.2	Nickel metal	Brass plate	10 minute

3. Results

3.1. Evaluation of optical properties, absorption analysis

Absorption spectrum curves of the black nickel coatings for various wavelengths depending on the metal substrate; including brass, copper and steel with and without bright nickel middle layer are presented in Fig.1-a and Fig.1-b. As can be seen from the graphs below, the black nickel coating has high absorption coefficient. The results from Graphs show that by changing the substrate, the absorption spectrum will change. The highest absorption is related to the coating layer on brass substrate without bright nickel and lowest absorption is belonged to the coating layer on stainless steel substrate with present of bright nickel.

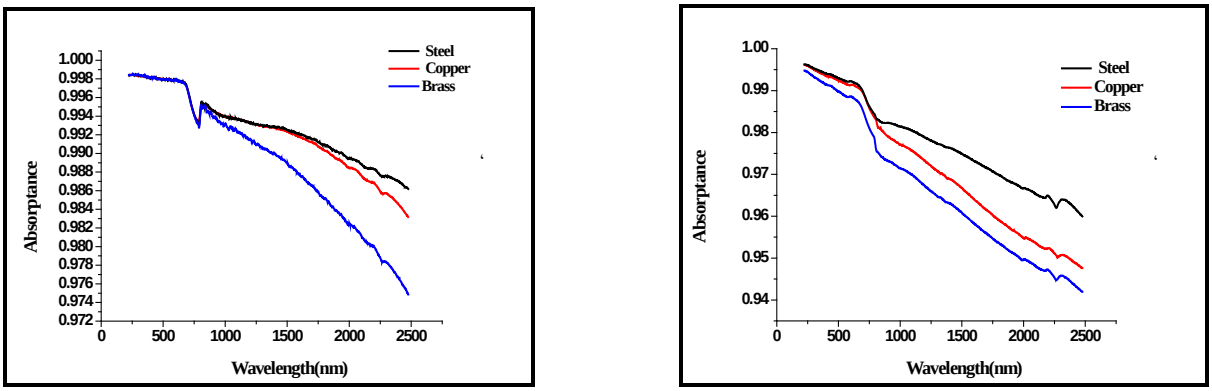

Figure (1 – a) absorption spectrum of black nickel on brass, copper and steel substrates without bright nickel, as a function of wavelength. Figure (1 – b) absorption spectrum of black nickel coating on copper, brass and steel substrates with bright nickel as a function of wavelength.

3.2. Emittance analysis

Below figure shows the result of emittance. By comparing the results the lowest emittance is belonged to the brass substrate and highest emittance is belonged to the steel substrate.

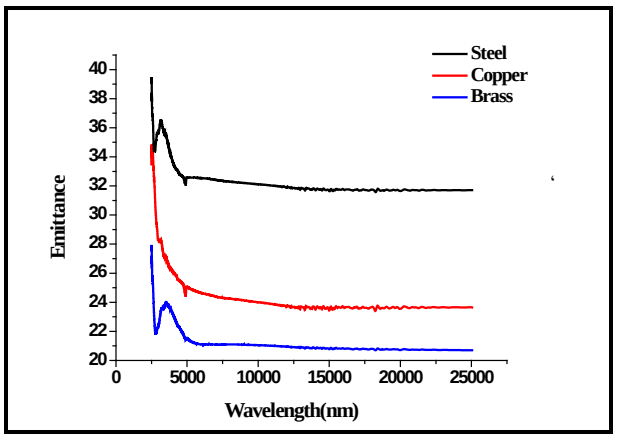

Figure (2) emittance spectrum of black nickel on brass, copper and steel substrates without bright nickel, as a function of wavelength.

3.3. SEM analysis

Scanning Electron Microscopy (SEM) Images of nano black nickel coatings prepared from nickel chloride bath with and without the presence of bright nickel middle layer. fig 3-a and 3-b shows the image of black nickel coating on brass substrate without and with bright nickel middle layer respectively.

By comparing the images of SEM it can be distinguished that layers with bright nickel have larger grains in comparison with layers without bright nickel. Since layers without bright nickel have a higher absorptance spectra so as result when grain size increase absorbtance spectra decrees.

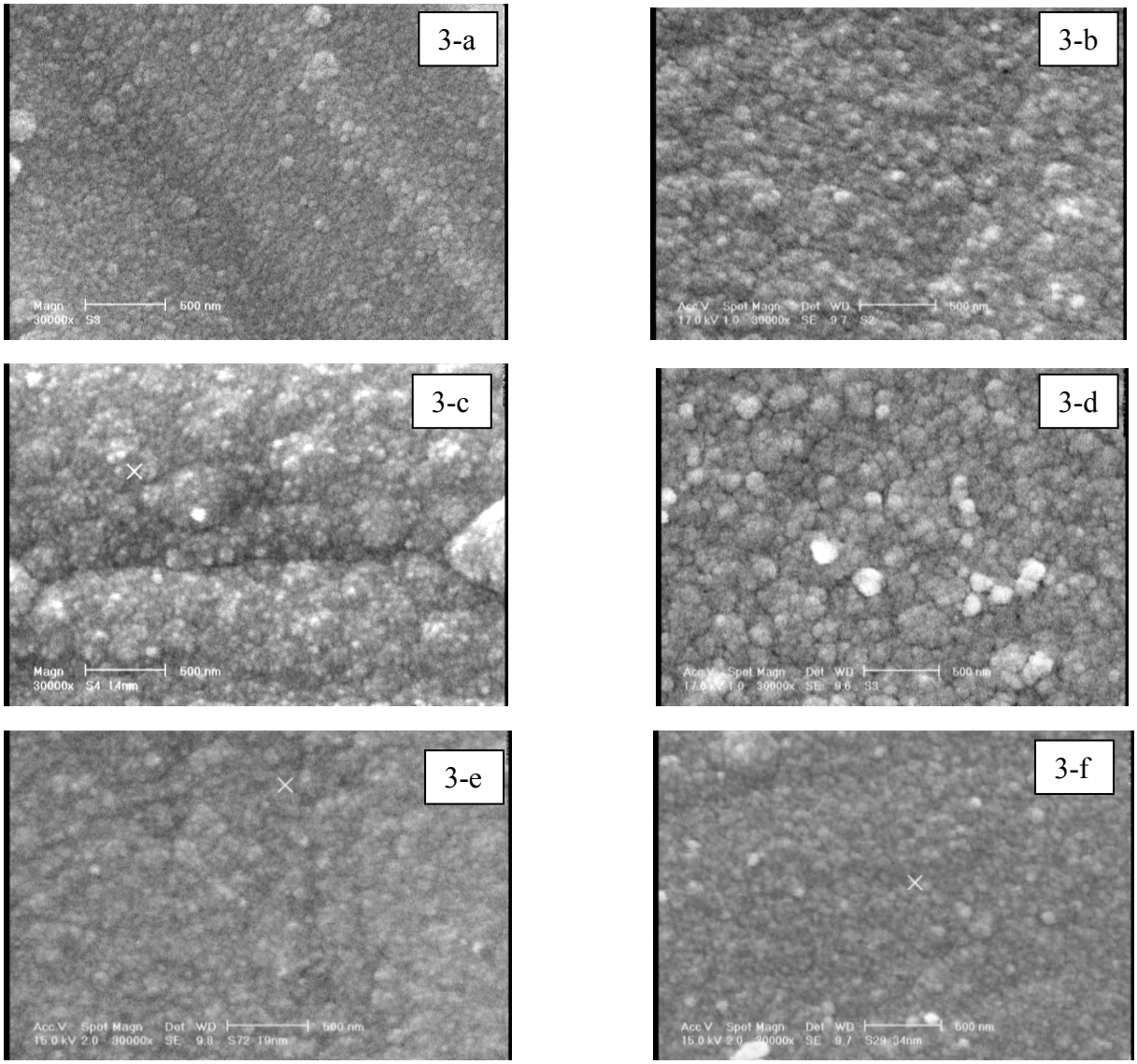

Figure 3: (SEM) Images of the black nickel coating
a) SEM image of a black nickel coating without bright nickel layer on the brass substrate b) SEM image of a black nickel coating on the brass substrate with bright nickel layer c) SEM image of a black nickel coating without nickel layer on the steel substrate d) SEM image of a black nickel coating With the bight nickel layer on stainless steel e) SEM image of a black nickel coating on copper without the bright nickel layer f) SEM image of a black nickel coating on copper with bright nickel layer

3.4. Results of X-ray diffraction and elemental analysis(EDAX)

Figure 4-a and 4-c show X-ray diffraction pattern of electrodeposited black nickel coatings on brass substrate. Two different structures clearly can be seen with and without the presence of bright nickel. Without presence of bright nickel there was no peak related to crystalline nickel and only the peaks belong to brass substrate have grown. While with regard to the 4-b, the presence of Ni element in the deposited films is provided by elemental analysis EDAX. The major difference between two structures can be recognized in fig 4-c. In XRD analysis of layer deposited in the presence of bright nickel the preferred orientations (111), (200) and (220) belong to nickel can be seen.

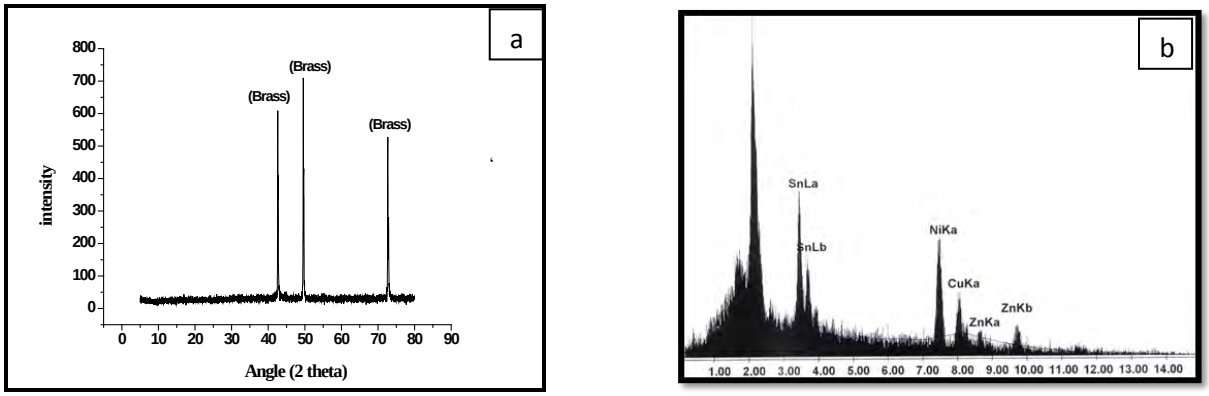

Figure 4– a, b X-ray diffraction pattern and elemental analysis black nickel coating without bright nickel

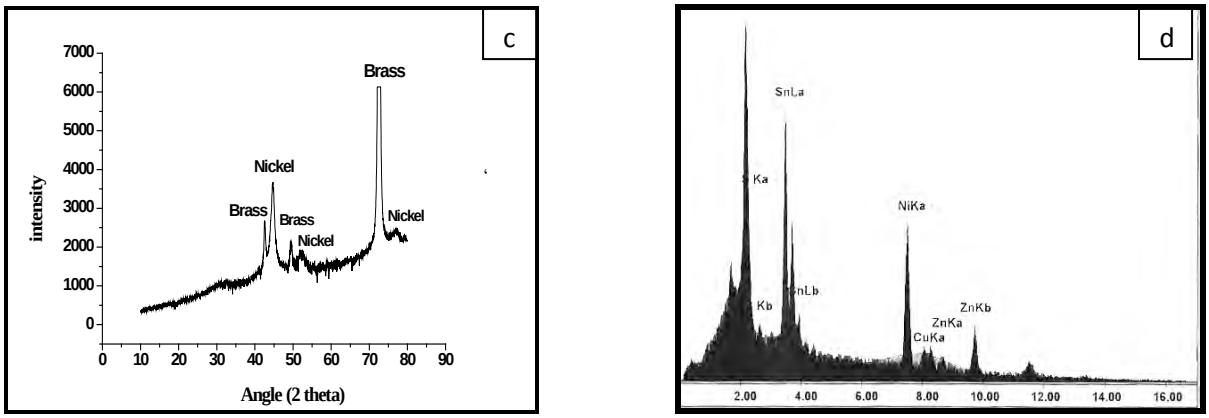

Figure 4–c, d X-ray diffraction pattern and elemental analysis black nickel coating with bright nickel

In order to identify the predominant nickel phase in the deposited films, it is necessary to investigate the coatings using X-ray diffractometer. Fig. shows the typical XRD pattern for the bright nickel substrate coated with black nickel films. This result is in good agreement with result of EDAX analysis.

4. Conclusion

The black nickel coatings with high absorption coefficient are suitable for solar applications. The coatings are very adhesive and have good thermal stability, with high absorption coefficient. SEM images show the relationship between absorption spectra with fine diameter of spherical particles, so that the layer of black nickel deposited on brass substrate without bright nickel coating have very small spherical particles and consequently optical properties of selected increases. Conversely, with the presence of bright nickel layer the particle size increases and absorption spectrum decreases. The highest absorption is for layer deposited on

brass without bright nickel and low absorption spectrum associated with the nickel coating on steel with bright nickel middle layer. EDAX analysis indicates presence of nickel on formed films. X-ray diffraction analyses show that electrodeposited films have polycrystalline structure and black nickel films were mainly consisting of metallic nickel. This result is matched with result of EDAX analysis. The presence of bright nickel middle layer cues the growth of nickel structure in orientation of (111), (200) and (220).

References

[1] K. N. Srinivasan, N. V. Shanmugam, M. Selvam, S. John, B. A. Shenol, Nickel-black solar absorber coatings, Energy Convers 24, 1984, pp. 255-258.

[2] S. R. Rajagopalan, K. S. Indari, K. S. G. Doss, An explanation for the black colour of black nickel, Journal of Electroanalytical Chemistry, 1965, pp. 465-472

[3] P. K. Gogna, K. L. Chopra, Structure-dependent thermal and optical properties of black nickel coatings, Thin Solid Films 57, 1979, pp. 299-302.

[4] M. Koltun, G.Gukhmen, A.Gavrilina, Stable selective coating black nickel for solar collector surfaces, Solar Energy Materials and Solar Cells 33, 1994, pp. 41-44

[5] M. Madhusudana and H. K. Sehgal, Spray-deposited black nickel selective absorber surfaces for solar thermal conversion, Applied Energy 10, 1982, pp. 65-74.

[6] S. John, N. V. Shanmugam, K. N. Srinivasan, M. Selvam and B. A. Shenoi, Blackening of electroless nickel deposits for solar energy applications, Surface Technology 20, 1983, pp. 331– 338.

[7] G. Devaraj and S. Guruviah, Pulse plating, Materials Chemistry and Physics 25, 1990, pp. 439-461

[8] S. Shawki, S. Mikhail, Black nickel coatings for solar collectors, Materials and Manufactoring Processes 15, 2000, pp. 737-746.

[9] S. N. Patel, O. T. Inal, A. J. Singh, A. Scherer, Optimization and thermal degradation study of black nickel solar collector coatings, Solar Energy Materials 11, 1985, pp. 381-399.

Investigations of heating process and absorber materials in air heating collector

Aivars Aboltins*, Janis Palabinskis

Institute of Agricultural Machinery, Latvia University of Agriculture , Cakstes bulv. 5, Jelgava ,LV-3001, Latvia
**Corresponding author. Tel: +371 29134846, Fax: +371 46 13211001, E-mail:aivars.aboltins@llu.lv*

Abstract: The research had two aims-1 st. determine the airflow temperature distribution depending on the thickness of the collector air channel and collector length, where the absorber is a steel tinplate ; 2 nd. search non-traditional (utilized) materials (slices of black coloured beer cans, different size black colour seed boxes made of polypropylene) that could be used as absorbents of air heating solar collectors
0.1x0.5x1.0 meters long flat-plate collectors (FPC) for experimental research into the materials of solar air heating collector were built. The air velocity at the experiments was v=0.9 m/s, covered material - polystyrol plate**.** We used the sun following collectors, which guarantees perpendicular location of the plane of absorber from the flow of sun irradiance.
From the experimental data were obtained an analytical expressions that describe the solar radiation and collector air channel size influence to the flowing air temperature in FPC using steel tinplate absorber.
The panel of black colored slices of beer cans can be used for air heating solar collectors as absorber. The experimental data show the temperature difference in outlet of sun following collector reaches up to 10-11 degree with sun irradiance 1000 W/m^2 at different weather conditions. It is a little more better than the best seed boxes.

Keywords: *Solar Collector, Air, Temperature, Absorber*

1. Introduction

The greatest advantage of solar energy comparing with other forms of energy is that it is clean and can be supplied without environmental pollution. Over the past century, fossil fuels provided most of our energy, because it was much cheaper and more convenient than energy from alternative energy sources, and until recently, environmental pollution has been of little concern. The limited reserves of fossil fuels cause a situation in which the price of fuels will accelerate as the reserves are decreasing.

Solar energy is used to heat and cool buildings (both actively and passively), dry products, heat water for domestic and industry use, heat swimming pools, generate electricity, for chemistry applications and many more operations [1].

The application of solar energy is completely dependent on solar radiation, a low-grade and fluctuating energy source. An intrinsic difficulty in using solar energy is caused by the wide variation in the solar radiation intensity. The availability of solar irradiance depends not only on the location, but also on the season. Extreme differences are experienced between summer and winter, and from day to day.

In general, solar water and solar air heaters are flat-plate collectors (FPCs), consisting of an absorber, a transparent cover, and backward insulation. Despite the similarity in designs, the different modes of operations and different properties of the heat transfer medium greatly affect the thermal performance and electric energy consumption for forcing the heat transfer medium a through the collector. Solar water heaters are operated as a closed-loop system whereas, in most cases, solar air heaters are operated in the open-loop mode.

The performance of solar air heaters is mainly influenced by meteorological parameters (direct and diffuse radiation, ambient temperature, wind speed), design parameters (type of collector, collector materials) and flow parameters (air flow rate, mode of flow). The principal requirement of these designs is a large contact area between the absorbing surface and air.

The efficiency of solar collector depending on the collector covered materials (polyvinylchloride film, cell polycarbonate PC, translucent roofing slate) [2-5], absorbers (black colored wood, steel-thin plate etc.), with different air velocities in collector was investigated [6-9]. The main efficiency parameter of solar collector is the air heating degree and it we chose as a criterion of efficiency.

The plane of FPC absorber is perpendicular to the flow of sun irradiance at sun following collector therefore this type is more powerful than stationary collector. The sun rays fall under angle to collector plane (it means it falls under angle to covered material) and it gives more reflection.

For manufacturing of collectors it is important to know their thickness and its effect on the temperature distribution of heated air. As one of the best absorbers is a tin plate in the middle of collector, then it is interesting to know how heated air temperature changes above and below the plate.

There is a need to test the various, cheap, easily available materials in an absorbent material for manufacturing of solar collectors.

2. Methodology

In the laboratory a *0.1×0.5×1.0* meters long experimental solar collectors were constructed for research into the properties of absorber materials. The air velocity at the experiments was v=0.9 m/s. Our investigations are devoted the sun following collectors, which guarantees perpendicular location of the plane of absorber from flow of the sun irradiance (Fig.1).

In the experiments, the collector covered material was a polystyrol plate. This material has gained immense popularity due to such properties as safety, mechanical crashworthiness, translucence and high UV radiation stability. The covered material - polystyrol plate reduced irradiance by 12-15 %.

The experimental data are recorded by means of an electronic metering and recording equipment of temperature, irradiance and lighting REG [10]. It is equipped with 16 temperature transducers and metering sensors of solar irradiance and lighting. The reading time of the data can be programmed from 1 to 99 minutes (1 minute in our case).
The recorded data are stored in the REG memory (there is a place for 16,384 records) and in case of need it is transferred to a computer for archiving with further processing. For evaluation and analysis of the results software REG – 01 has been developed, which is meant for transfer to the computer and processing of the recorded data. The information is stored in the form of a table and in case of need it is depicted as a graph.

The air heating experiments by this collector were made at different weather conditions. The solar irradiance measuring instrument is a pyranometer. The data of sun irradiance are dependent on clouds, shadows and we aligned the experimental data with the method of least squares using Eq. (1) [11].

$$\overline{y_i} = \frac{1}{35}[17y_i + 12(y_{i-1} + y_{i+1}) - 3(y_{i-2} + y_{i+2})] \quad (1)$$

where $\overline{y_i}$ - aligned data, y_i - experimental data, i- index.

Fig. 1. Sun following collector at work

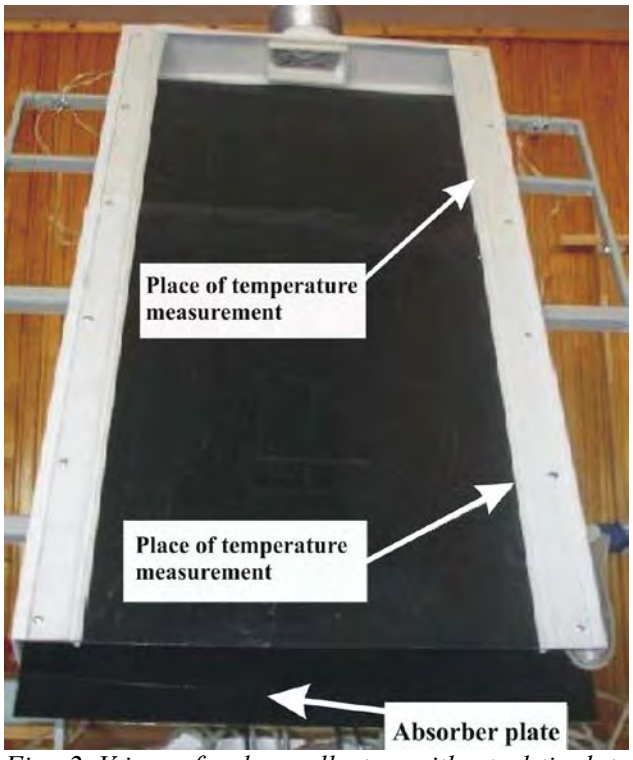

Fig. 2. View of solar collector with steel-tinplate absorber in middle.

3. Results

At first we researched a situation when the absorber (black coloured steel-thin plate) is put at the bottom and middle of the collector (Fig.2). Using the experimental results and statistical processing data we received correlation between the distance from absorber, sun irradiance to absorber plate and air temperature change in the collector. We got expressions for air temperature changing over steel-thin plate absorber in FPC at 35cm and 60cm from inlet.

The temperature change ΔT over absorber at 0.35 m distance from input can be expressed with Eq. (2);

$$\Delta T = 3.8 \cdot 10^{-3} \cdot R + 21.3 \cdot y - 318.5 \cdot y^2 - 4.6 \cdot 10^{-3} \cdot R \cdot y \ , \quad (2)$$

where y-distance from absorber,(m), R- sun radiation (W / m^2).

Close connection of this expression and the experimental data shows coefficient of determination $\eta^2 = 0.804$ in temperature increase domain $\Delta T \in (0;3)\ ^{O}C$.

The temperature change ΔT over absorber at 0.60 m from inlet we can be expressed with Eq.(3);

$$\Delta T = 1.57 + 0.011 \cdot R - 4.15 \cdot 10^{-6} \cdot R^2 - 34.8 \cdot y + 369.8 \cdot y^2 - 0.021 \cdot R \cdot y \qquad (3)$$

with coefficient of determination $\eta^2 = 0.855$.

The visual interpretation of expressions (2), (3) is shown in Fig.3-4.as contour plot .

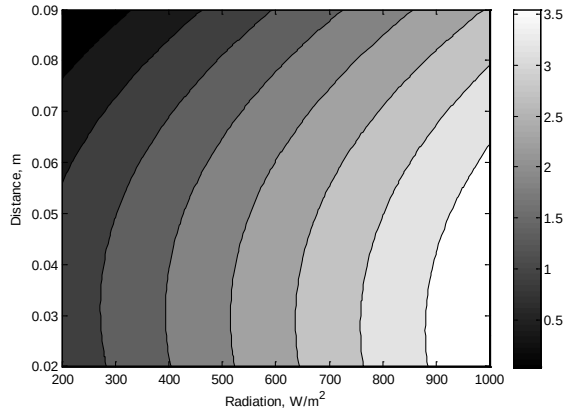

Fig. 3. Plot of air temperature increase ΔT depending on distance over absorber y (m) and radiation R (W/m^2) at 0.35 m from inlet

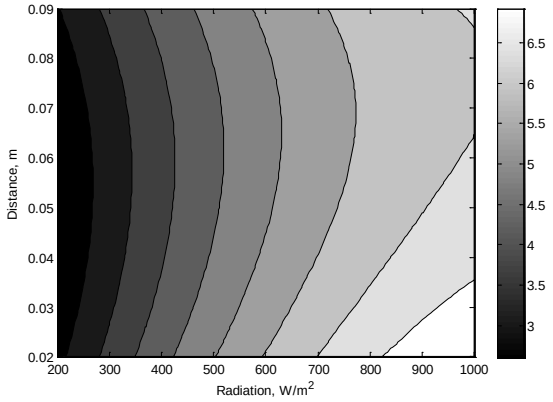

Fig. 4. Contour plot of air temperature increase ΔT depending on distance y(m) over absorber and radiation of sun R (W/m^2) at 0.6 m from inlet.

The temperature change ΔT in the collector length over absorber (steel-tinplate) put in the middle of the air channel can be expressed with Eq. (4);

$$\Delta T = 0.0073 \cdot R - 5.4 \times 10^{-6} R^2 + 17 \cdot x - 25.6 \cdot x^2 + 0.028 \cdot R \cdot x \ , \qquad (4)$$

where x-length of collector,(m). Coefficient of determination $\eta^2 = 0.98$ in temperature increase domain $\Delta T \in (0;18)\ ^{O}C$.

The temperature change ΔT in the collector under absorber can be expressed with Eq.(5) ($\Delta T \in (0;10)\ ^{O}C$):

$$\Delta T = 4.2 \cdot x - 4.9 \cdot x^2 - 2.8 \times 10^{-3} \cdot R + 3.4 \times 10^{-6} R^2 + 0.012 \cdot R \cdot x \ , \qquad (5)$$

with coefficient of determination $\eta^2 = 0.955$.

The graphical interpretation of these expressions is shown in Fig.5, Fig.6.

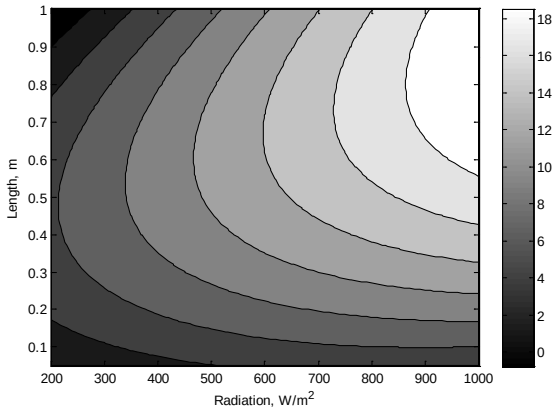

Fig. 5. Air temperature increase ΔT over steel-tinplate absorber depending on collector length x (m) and radiation R (W / m^2)

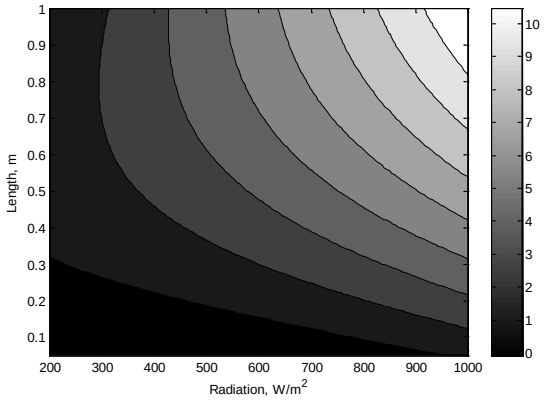

Fig. 6. Air temperature increase ΔT under steel-tinplate absorber depending on collector length x (m) and radiation R (W / m^2)

Second we tested new absorber materials which can be used in hand made air heated solar collectors. These materials must be cheap, light and simple use. We made panels with different size black seed boxes which were made of polypropylene (Fig.1, Fig.8) and a panel with coloured slices of beer cans (Fig.7, Fig.1) . These slices help to mix the air flow in the collector and rise the outlet air temperature.

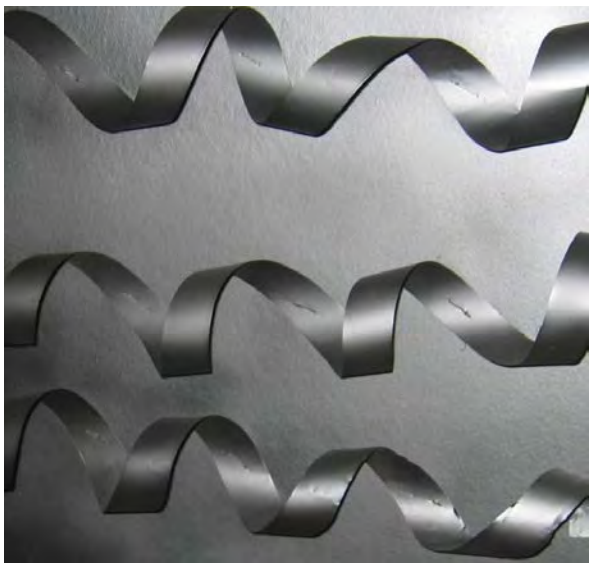

Fig.7 Black coloured slices of beer cans as absorbers of air collector

Fig.8 The panel of 13 seed boxes as absorbers of air collector

Air heating level is not highly dependent on ambient temperature. Much more it is influenced by solar radiation. Experimental results which was made in 7.September 2010. showed it (Fig.9).

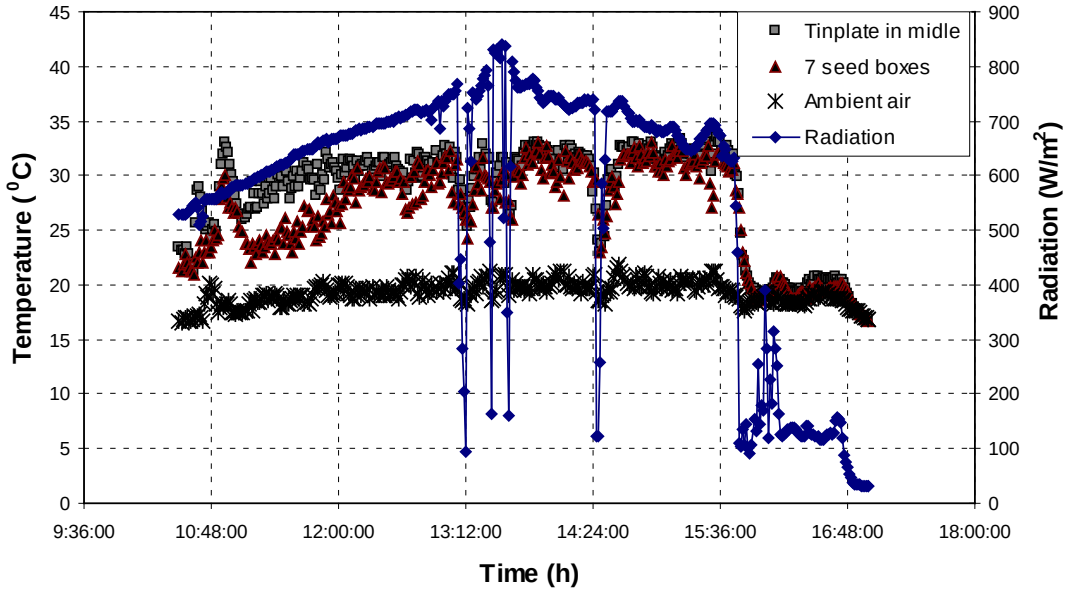

Fig.9 Ambient air, collectors(with tinplate, seed boxes absorbers) outlet temperatures and solar radiation changes (10:30 -17:00 o'clock).

Ambient air heating degree serves as the main effectiveness of collectors at the same size collectors with the same fan power. Comparing the absorbers with 7 seed boxes in line (the best variant of seed boxes [8]) and the absorber panel with slices at the same weather conditions we can see that the absorber panel with slices of cans gives little bit better results (temperature increases at the outlet of collector) than the variant of seed boxes Fig.10. The air inflow temperature equal with ambient air temperature and it changed from 17 ^0C to 25 ^0C during the experiment.

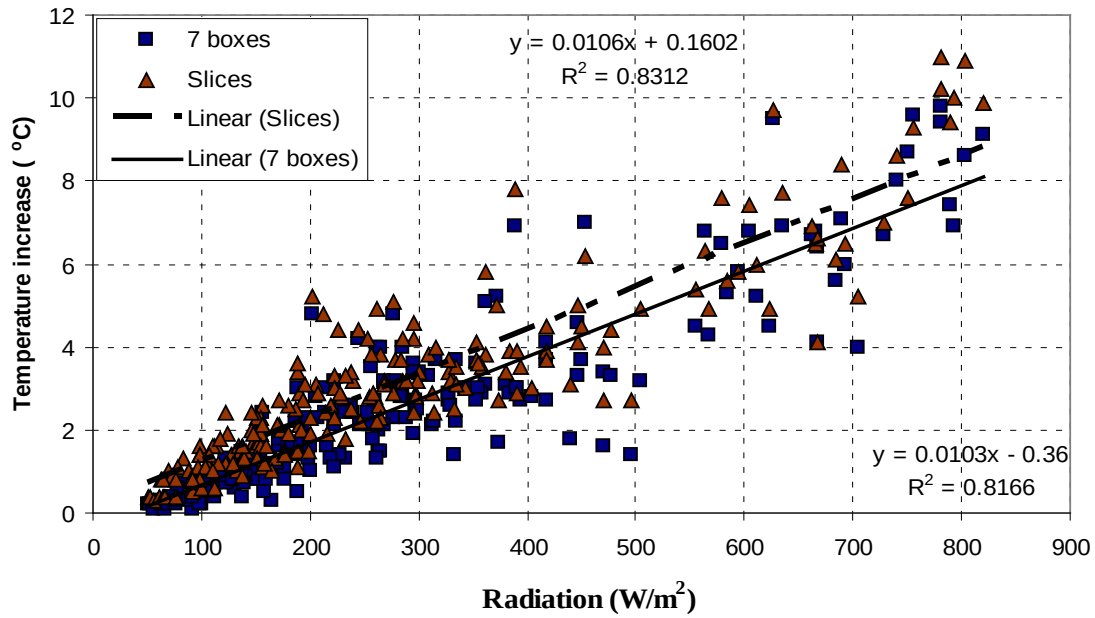

Fig.10 Air heating temperature difference with black coloured slices and 7 element seed boxes in line depending upon solar irradiance in sun following collector (11:00 -18:00 o'clock).

The experimental data show very good linear correlation between solar radiation and air-heating degree (correlation coefficient greater than 0.9).

The efficiency of solar air collectors is influenced both by the design and air circulation and by the properties of the material used for cover, absorber and insulation. The efficiency of this absorber material can be explained by the type of absorber which mix the air flow in thickness and width of the collector area. It is important because without air mix, air exchange at corners and near sides of the collector does not take place.

4. Conclusions

1. The theoretical expressions for air temperature which are changing over steel-thin plate absorber in FPC at 35cm and 60cm from inlet are obtained. These expressions show temperature distribution depending on the distance to the absorbent tin plate and radiation.

2. Using experimental data processing temperature distribution above and below the absorbent sheet according to the length of the collector and solar radiation was obtained.

3. Absorber black colored slices of beer cans can be used for air heating solar collectors. The experimental data show that the temperature difference in outlet of sun following collector reaches up to 9-11 degree with sun irradiance 1000 W/m^2 at different weather conditions.

4. Air solar collectors due to their physical and mechanical properties are suitable in Latvia for heating the air. At favorable weather conditions the heating degree of ambient air reaches more than 10 degrees at exit with the absorber length 1 m and air velocity v=0.9 m/s.

References

[1] S. Kalogirou Solar energy engineering: processes and systems, Academic Press Elsevier Inc. 2009.

[2] A.Lauva, A. Aboltins, J. Palabinskis, N. Karpova-Sadigova Comparative studies of the solar material collector, Proceedings of the 5th International Scientific Conference "Engineering for Rural Development ", 2006, pp.90-94

[3] A.Aboltins**,** J.Palabinskis**,** A.Lauva, J.Skujans, U.Iljins The material investigations of solar collector, Proceedings of the 6th International Scientific Conference "Engineering for Rural Development ", 2007, pp. 18-23

[4] J. Palabinskis, A. Aboltins, A. Lauva, N. Karpova-Sadigova The comparative material investigations of solar collector, Agronomy Research, Vol. 6 „ Engineering of Agricultural Technologies", 2008, pp.255-261

[5] J. Palabinskis, A. Lauva, A. Āboltiņš, N. Karpova-Sadigova. Movable Air Solar Collector and its Efficiency, 7th International Scientific Conference „ Engineering for Rural Development", 2008, pp 51 - 56

[6] A. Aboltins**,** J. Palabinskis**,** A. Lauva, G. Rušķis The investigations of air solar collector efficiency, Proceedings of the 8th International Scientific Conference "Engineering for Rural Development ", 2009, pp.176-181

[7] A. Aboltins**,** J. Palabinskis**,** A. Lauva, G. Rušķis The steel-thin plate absorbers investigations in air solar collector, Proceedings of the 8th International Scientific Conference "Engineering for Rural Development ", 2009, pp.182-187

[8] A.Aboltins**,** J.Palabinskis**,** G. Rušķis Usage of different materials in air heated solar collectors, Proceedings of the 9th International Scientific Conference "Engineering for Rural Development ", 2010, pp.67-72

[9] A. Aboltins, J. Palabinskis, G. Rušķis. The investigations of heating process in solar heating collector, Agronomy Research, Vol. 8 „Biosystems Engineering", 2010, pp.5 - 11

[10] REG Tehniskais apraksts un lietošanas pamācība (REG Technical description and using instruction), 2004, (in Latvian).

[11] Веденяпин Г.В. Общая методика экспериментального исследования и обработки опытных данных (The general methology of experimental research and treatment of experimental data). Колос, М.,1967, (in Russian)

Characterization of black chrome films prepared by electroplating technique

S. Jafari, S. M. Rozati*

Physics Department, University of Guilan, Rasht 41335, Iran
** Corresponding author. Tel: +98 1313220912, Fax: +98 1313220066, E-mail: smrozati@guilan.ac.ir*

Abstract: The surface and optical properties of black chrome films prepared by two different electrochemical baths were characterized. The black chrome films have been deposited on bright nickel substrates by electroplating technique. The surface morphology and phase structure of the films were investigated by using scanning electron microscopy (SEM) and X-ray diffraction (XRD), respectively. The chemical composition of prepared films was determined by energy-dispersive x-ray analysis (EDS). The spectral reflectance was also measured in the UV-Vis-NIR and IR regions. From the SEM analysis, it was found that prepared films by the first chemical bath is denser with nano size grains and by the second chemical bath they become porous, with micro sized grains. The XRD results show that in both cases chrome is the main chemical component in the films. The films prepared by second chemical bath have better optical properties than the films prepared by first chemical bath.

Keywords: *Black chrome, Electroplating, Solar collector.*

1. Introduction

The growing energy demand through out the world has attached great important to the study of renewable source [1]. The cost and effective utilization of solar energy and conversion of that into thermal energy requires an efficient solar coating as having high solar absorptance (>0.9) in the visible region and very low thermal emittance (<0.1) in the infrared to minimize the radiation heat loss [2, 3]. This property is named selectivity [4]. The higher the selectivity value, the better the thermodynamical efficiency of the solar energy collectors [1]. Other necessary properties of a practical solar selective coating are ease and availability of application, low cost and long-term durability under solar radiation [5]. Black chrome is one of the most commonly used solar selective coatings in solar collector systems for the efficient conversion of solar energy into thermal energy. A variety of deposition techniques such as chemical oxidation, CVD, spray, sputtering and electroplating are available for preparation of solar selective surfaces. Of the above techniques, electroplating is attractive due to its simplicity, low cost and large area involved [2]. Electroplating of metallic films is one the appropriate techniques for obtaining absorber coatings with selective optical properties for solar collectors. Electroplated black chrome is one of the most widely used solar absorber, mainly due to its high absorptance, good stability in a wide rang of oxidizing/reducing environments and high thermal resistance [3]. Coatings used as solar selective surface in solar collectors have low thicknesses, therefore these coatings cannot protect the substrate against atmospheric corrosion and thermal oxidation. For solving this problem bright nickel coating before black chrome deposition is recommended [6]. Nickel under coat before black chrome deposition decreases thermal emissivity and increases thermal resistance of black chrome coatings [3].

2. Experimental method

Electroplating is an electrodeposition process for producing a dense, uniform, and adherent coating, usually of a metal or an alloy, upon a conductive surface by the act of electric current. The core part of the electroplating process is the electrolytic cell (electroplating unit). In the electrolytic cell a current is passed through a bath containing electrolyte, the anode, and

the cathode. The workpiece to be plated is the cathode (negative terminal). The anode, however, can be one of the two types: sacrificial anode (dissolvable anode) and permanent anode (inert anode). The sacrificial anodes are made of the metal that is to be deposited. The permanent anodes can only complete the electrical circuit, but cannot provide a source of fresh metal to replace what has been removed from the solution by deposition at the cathode. Electrolyte is the electrical conductor in which current is carried by ions rather than by free electrons (as in a metal). Electrolyte completes an electric circuit between two electrodes. Upon application of electric current, the positive ions in the electrolyte will move toward the cathode and negatively charged ions toward the anode. This migration of ions through the electrolyte constitutes the electric current in that part of the circuit. The migration of electrons into the anode through the wiring and an electric generator and then back to the cathode constitutes the current in the external circuit. The metallic ions of the salt in the electrolyte carry a positive charge and are thus attracted to the cathode. When they reach the negatively charged workpiece, it provides electrons to reduce those positively charged ions to metallic form, and then the metal atoms will be deposited onto the surface of negatively charged workpiece [7].

Black chrome electroplates are obtained by replacing the sulphate ion in conventional chrome plating baths by fluoride, silicofluoride, acetate, borate, nitrate or sulphamate ions. Care should be taken to ensure complete removal of the sulphate ions; these are deleterious to the bath. The substances introduced in to the bath as catalysts can be divided into three groups, acetate baths, floride-catalysed baths and nitrates and other catalysts. In the fluoride or mixed catalyst plating baths a higher plating efficiency, a harder, more corrosion and wear-resistance deposit is obtained. The fluoride is commonly added as the SiF_6^{2-} ion in amount of 2-3g/l. this chemistry provides better substrate activation for plating on bright nickel [8].

The deposition of black chrome was carried out on bright nickel plated brass substrates in an electrochemical bath by electroplating technique. The brass substrates of 0.1 mm thickness were cut in strips of 5.5 cm × 6.5 cm for electroplating of bright nickel. The brass substrates were pretreated by different cleaning procedure. Mechanical polishing was done with a grinding paper No.2000, followed by rinsing in distilled water. Then substrates were cleaned in a hot commercial alkaline cleaner, followed by rinsing in distilled water and activated in an aqueous 10 vol% H_2SO_4 solution, followed by rinsing in distilled water. Then bright nickel deposited on prepared brass substrates by electroplating technique. The chemical bath for bright nickel deposition consists of nickel sulphate ($NiSO_4$), nickel chloride ($NiCL_2$) and boric acid (H_3BO_3). The bright nickel deposition carried out in 0.5A/dm^2 current density for 5 min in 50 °C-60 °C temperatures. Nickel metal with 99.9% purity used as anode for bright nickel deposition and brass substrate was used as cathode. Prior to the deposition of black chrome, the prepared bright nickel substrates were cleaned in a hot commercial alkaline cleaner, followed by rinsing in distilled water and activated in an aqueous 10 vol% H_2SO_4 solution. Following activation the plates were thoroughly rinsed in distilled water to remove all trace sulphate. Then black chrome was deposited on bright nickel substrates. The deposition conditions to get black chrome were optimized by varying the chemical bath composition, current density and plating time. In this paper, two chemical baths were used for electroplating to comparison of surface and optical properties of these surfaces and selecting the better films.

The first bath for black chrome deposition consists of chromic acid, acetic acid and barium acetate (acetate bath). Electrodeposition carried out in 3A/dm^2 current density for 180 seconds in 50 °C temperature. The second bath for black chrome deposition consists of chromic acid,

fluorosilicic acid and barium carbonate (floride-catalysed bath). Deposition carried out in 6A/dm2 current density for 120 seconds in 25 °C temperature. Several experiments were done to prove the reproducibility of the samples.

Details of the optimized plating processes used in this study are given in table 1.

Table 1. Experimental electrodeposition parameters.

Bath	Composition	Temperature (°C)	Current density (A/dm^2)	Plating time (s)
First	Chromic acid (CrO_3) Acetic acid (CH_3COOH) Barium acetate ($Ba(CH_3COO)_2$)	50	3	180
Second	Chromic acid (CrO_3) Fluorosilicic acid (H_2SiF_6) Barium carbonate ($BaCO_3$)	25	6	120

Barium compounds such as the carbonate, acetate or hydroxide are usually added to black chrome plating solutions. Their role is to precipitate any sulphate ions from solution, and apart from possible complexation of the carbonate ion with Cr (III), they are not expected to significantly affect black chrome electrochemistry [9].
For the black chrome deposition Pb-Sb alloy, which contains only 2-5% Sb, was used as the anode(the permanent anode) and bright nickel substrate used as cathode. After deposition the samples were cleaned in distilled water and air dried at room temperature. Surface morphology of the coatings was characterized with scanning electron microscopy (SEM), manufactured by Philips, XL30 model. The X-ray diffraction (XRD) analysis was done using a PW1840 diffractometer. The normal spectral reflectance of the electrodeposited black chrome coating in UV-Vis-NIR and IR regions was recorded using a Cary 500 Scan UV-Vis-NIR spectrophotometer and FTIR Jasco, respectively.

3. Results and discussion

3.1. SEM analysis

Fig. 1 gives the scanning electron microscopy (SEM) of magnification 15000× for black chrome films prepared from two different baths. Figure 1 shows that the surface morphology of films deposited from different bath composition are different. From the SEM analysis it was found that the black chrome films achieved from the first bath is denser with nano size grains but films deposited from the second bath they become porous, with micro sized grains.

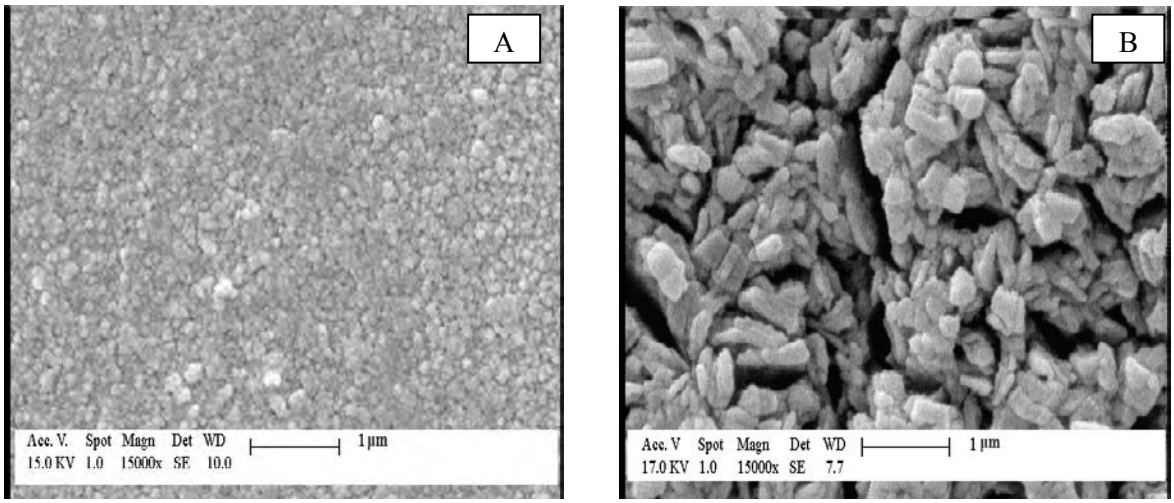

Fig. 1. The SEM images of black chrome films deposited on bright nickel substrates from two different baths. A: first bath, B: second bath.

3.2. EDS analysis

Fig. 2 a nd Table 2 show the chemical composition of black chrome deposited from two different baths. The data indicate that films prepared from both baths have contained chrome in their composition. Wight percentage of chrome in films prepared from the second bath is more than of the films prepared from the first bath.

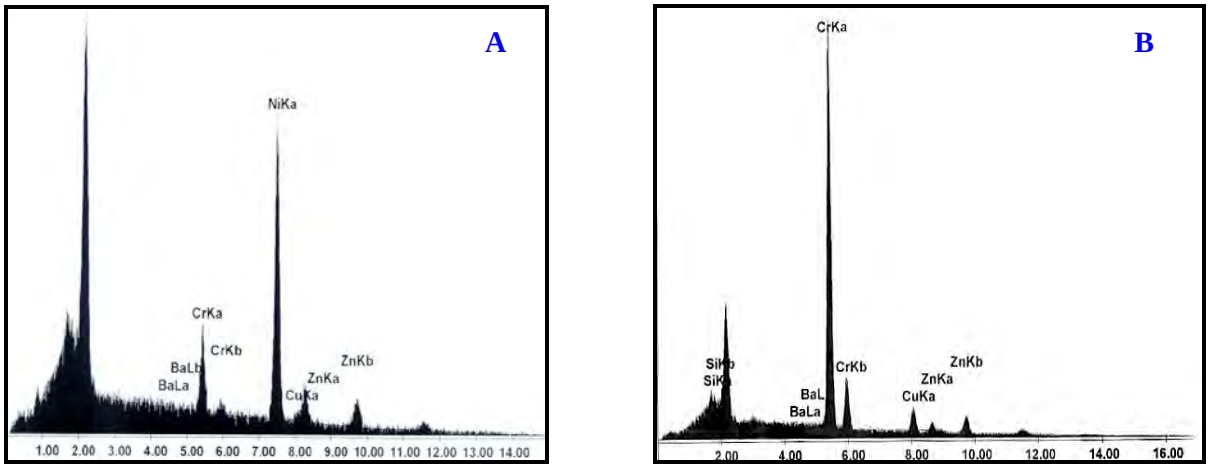

Fig. 2. The EDS spectrum for black chrome films deposited d on bright nickel substrate from two different baths. A: First bath, B: Second bath.

Table 2. The EDS analysis of black chrome deposited from two different baths.

Elements	Wt.% first bathe	Wt.% second bath
Cr	8.38	62.62
Ni	84.23	12.50
Cu	4.58	12.80
Zn	1.65	8.53
Si	-	1.92
Ba	1.16	1.63

3.3. XRD analysis

In order to identify the predominant chrome phase in the deposited films, it is necessary to investigate the coatings using X-ray diffractometer. Fig. 3 shows the XRD patterns for the bright nickel substrate coated with black chrome films. It is possible to detect that the bulk structure of the black chrome films were mainly consist of metallic chrome with the crystallographic plane (110) perpendicular to the substrate [6, 7]. As can be seen from Fig. 3, the different compositions of chrome are obtained in these two films prepared from two different baths.

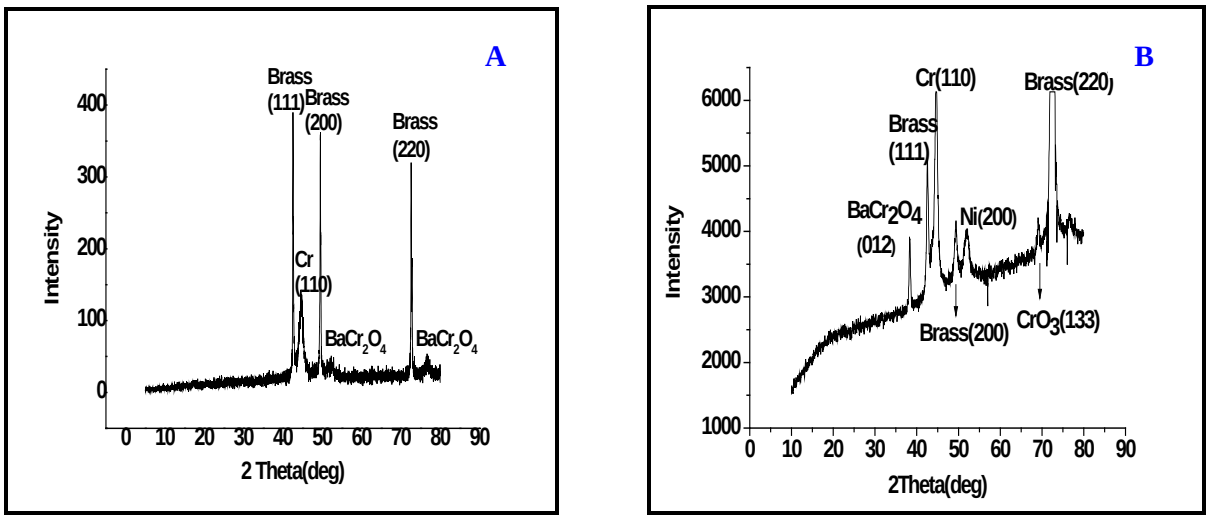

Fig. 3. The XRD patterns for black chrome films deposited on bright nickel substrate from two different baths. A: First bath, B: Second bath.

3.4. Spectral reflectance

The influence of two different electrochemical baths on the selective absorber properties of black chrome films are given in Figs. 4 and 5. Figs. 4 and 5 shows the spectral reflectance in the UV-Vis-NIR and IR regions for black chrome deposited on b right nickel substrates prepared from two different baths respectively. From figure 4 it is evident that the spectral reflectance in UV-Vis-NIR region is below 12% for black chrome films deposited on bright nickel prepared from both baths, indicating that in this spectral region the solar absorptance is quite high [2]. Spectral reflectance for black chrome films prepared from the second bath is less than of films prepared from the first bath, hence, its absorption is higher. This difference is probably due to the rougher surface and chemical composition of these samples which enhances the absorption of the radiation and can explain the high absorptance level of this material. Hence, using of second bath is recommended to get good solar selective black chrome coating in the UV-Vis-NIR region. Fig. 5 indicates that the spectral reflectance of black chrome films in the IR (2.5μm-20μm) region, and hence the emissivity of them. From Fig. 5 it is evident that films prepared from the second bath have lower thermal emittance. It can be seen in the figure 5 that by using of the first bath spectral reflectance is reduced and hence increases the thermal emittance of films will increase.

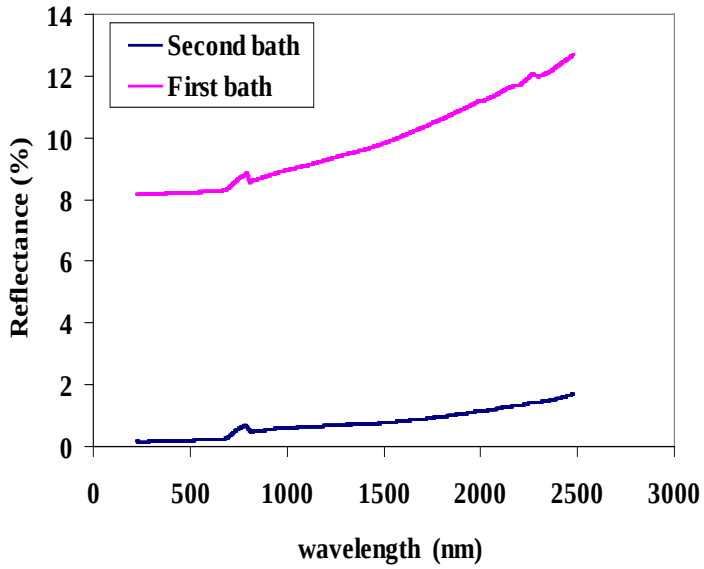

Fig. 4. The Spectral reflectance in the UV-Vis-NIR region for black chrome films deposited on bright nickel substrates from two different baths.

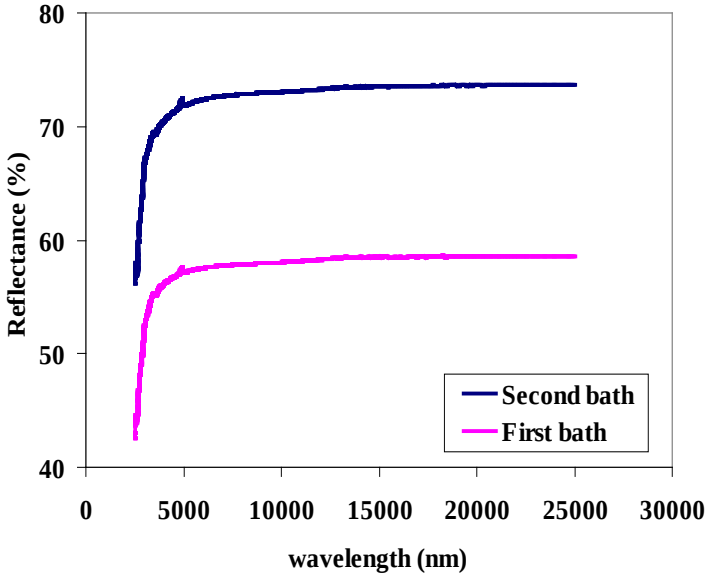

Fig. 5. The Spectral reflectance in the IR region for black chrome films deposited on bright nickel substrates from two different baths.

4. Conclusion

The black chrome films were prepared by electroplating technique from two different baths on bright nickel substrates. SEM analysis shows that films prepared from first bath is denser with nano size grains while films prepared from the second bath become porous, with micro sized grains. The EDS analysis results indicate the presence of chrome on films prepared from both baths. The chrome amount in the films prepared from second bath is higher than one. XRD analysis shows that structure of black chrome films from both baths were mainly consist of metallic chrome with (110) orientation. Black chrome films have good optical properties for solar energy absorption. The spectral reflectance in the UV-Vis-NIR and IR regions shows that films prepared from the second bath have higher absorption and lower emittance, Hence these films are better for using in solar collectors.

References

[1] M. Aguilar, E. Barrera, M. Palomar-Pardave, L. Huerta, S. Muhl, Characterization of black and white chromium electrodeposition films: surface and optical properties, Journal of Non-Crystalline Solids 329, 2003, pp. 31-38.

[2] J. Quintana, P. J. Sebastian, The influence of various substrate treatments on morphology and selective absorber characteristics of electrochemical black chrome, Solar Energy Materials and Solar Cells 33, 1994, pp. 465-474.

[3] Z. Abdel Hamid, Electrodeposition of black chromium from environmentally electrolyte based on trivalent chromium salt, Surface & Coating Technology 203, 2009, pp. 3442-3449.

[4] M. R. Bayati, M. H. Shariat, K. Janghorban, Design and chemical composition and optimum working conditions for trivalent black chromium electroplating bath used for solar thermal collectors, Renewable Energy 30, 2005, pp. 2163-2178.

[5] G. E. Mcdonald, Spectral reflectance properties of black chrome for use as a solar selective coating, Solar Energy 17, 1975, pp. 119-122.

[6] M. Daryabegy, A. R. Mahmoodpoor, Method of manufacturing absorbing layers on copper for solar applications (I), Renewable Energy Organization of Iran 2, 2006, pp. 35-39.

[7] H. Lou, Y. Huang, Electroplating, Encyclopedia of Chemical Processing, DOI: 10.1081, pp. 1-10.

[8] N. Vasudevan, V. K. William Grips and Indira Rajagopalan, The present status of black chromium plating, Surface Technology 14, 1981, pp. 119-132.

[9] P. M. Driver, An electrochemical approach to the characterization of black chrome selective surfaces, Solar Energy Materials 14, 1981, pp. 179-202.

Selective solar absorber coating research at the CSIR (South Africa)

K.T. Roro[1*], N.Tile[1,2], B. Yalisi[1,2], M. De Gama[1], T. Wittes[1], T. Roberts[1], A. Forbes[1,2]

[1]*CSIR-National Laser Centre, P.O. Box 395, Pretoria 0001, South Africa*
[2] *School of Physics, University of KwaZulu Natal, Private Bag X54001, Durban 5000, South Africa*
** Corresponding author. Tel: +27128413794, Fax: +27128413152, E-mail: KRoro@csir.co.za*

Abstract: A sol-gel technique has been established at a laboratory scale for low cost production of high efficient selective solar absorbers comprising a composite material of nano-structured carbon in a nickel oxide matrix. In order for these materials to be applied in real world scenarios it is necessary to extensively scale up the fabrication process to allow large area coatings. This can be done by adapting this sol-gel technique to large area deposition.
In this project, we are undertaking research and development activities for three-years to make a 'Lab to Large scale' transition in order to eventually integrate into existing solar collectors for low cost domestic water heating in a rural area for social good.
A spray coating technique has been used to deposit these C/NiO coatings on aluminum substrates. Preliminary optical results have shown absorptance of up to 90 %. The preparation and characterization as well as the process towards developing a large-area solar selective coating for low cost domestic heating will be discussed.

Keywords: *Sol-gel, Carbon-nickel oxide, Selective solar absorbers, Large-area.*

Nomenclature

α_{sol}	*normal solar absorptance*	I_{sol}	*direct normal solar irradiance*
ε_{ther}	*normal thermal emittance*	I_P	*Plank black body distribution*
R	*reflectance*		

1. Introduction

Hot water is required to maintain adequate sanitation and health. Often, water has to be boiled in order to make it safe for drinking. In rural Africa, the traditional fuel used for heating water is firewood, which produces smoke and is generally unsafe. Access to energy from fossil fuels such as oil, gas, and coal, by expanding grid electricity is either impractical or too expensive in these countries. There is therefore a clear need for low-cost and environmental friendly means of water heating.

Solar energy is a promising alternative energy source that can address these challenges. It is a resource readily available in every country around the world, and is not a threat to the environment through pollution or to the climate through greenhouse gas emission. As a matter of fact, most African countries have around 325 days of strong sunlight a year, on average, more than 6 kWh energy per square meter a day [1]. Solar thermal energy is a technology for harnessing solar energy for thermal energy (heat). Solar thermal collectors for water heating use a spectrally selective surface that absorb sunlight and convert it to heat. High performing selective surfaces already exist in the market, but most of these products are produced using complicated manufacturing process and are expensive. The spectral selective surfaces are the most costly component of a solar thermal collector [2]. This means that if one reduces the price of selective solar absorbers one can hopefully reduce the cost of a solar thermal collector.

A sol-gel technique has been established at a laboratory scale for low cost production of high efficient selective solar absorbers comprising a composite material of nano-structured carbon in a nickel oxide matrix [3,4]. These coatings were deposited using a spin coater. Some of the

advantages of this novel technique to fabricate carbon-metal oxide composite coatings are that it is simple and easy to control, utilizes readily available chemicals, does not require sophisticated equipments, the coatings can be deposited at ambient pressure conditions, and the process is low in material consumption. Therefore, the method is very promising for developing countries and could hopefully reduce the production costs for spectrally selective absorbers [5]. In order for these materials to be applied in real world scenarios it is necessary to extensively scale up the fabrication process to allow large area coatings. However, the spin coating process cannot be used for large area coatings. To succeed as a useful manufacturing technique, the specific deposition approach must be highly scalable while still producing films with the quality of laboratory deposition methods, e.g., spin coating. Spray deposition is historically scalable to large areas, and may also be applicable to deposit these C/NiO composite coatings. Thus, large area coating can be done by adapting this sol-gel technique to large area deposition.

In this study, we will demonstrate the preparation of sol-gel C/NiO nanocomposite coatings with reasonable optical properties on aluminum substrates by spray-coating technique and show the dependence of variation of the optical properties on different deposition process parameter.

2. Experimental

The absorbing films were coated on rough highly reflecting aluminum substrates. The substrates were cut into a 55 × 55 mm^2 size and cleaned before deposition. The pre-cleaning process involved cleaning the substrates with aqueous detergent and distilled water in order to remove the grease. Due to poor adhesion to the aluminum surfaces (uncleaned or cleaned with soap and water), the substrates were etched. The pre-cleaned substrates were thoroughly rinsed and dipped in a phosphoric acid bath at 60 °C for about 30 minutes or in an HCl bath kept at room temperature to remove the protective oxide layer. They were then thoroughly rinsed using distilled water to remove the acid. Finally they were blown dry with a N_2 and coated immediately.

The preparation of the solution was adopted from a previous experiment [4]. The NiO precursor solution was prepared by dissolving an appropriate quantities of nickel acetate [($NiAc_2$), $Ni(CH_3COO)_2.4H_2O$] in 50 ml of absolute ethanol [(EtOH), CH_3CH_2OH] followed by magnetic stirring at room temperature. An amount of diethanolamine [(DEA), $NH(CH_2CH_2OH)_2$] was added as a chelating agent. For the carbon precursor, sucrose was dissolved in doubly distilled water in the mass ratio 1:1 prior to mixing with the matrix precursor solutions. After a period of stirring appropriate quantity of polyethylene glycol[(PEG), $HO(CH_2CH_2O)nH$], a structure directing template, was added to the NiO matrix precursor sol. The oxide and carbon precursor solutions were mixed and stirred again. The resultant solution was then further stirred until the formation of a sol. The final solution was poured into the spray gun and a conventional air compressor is used to eject the solution on top of the pre-cleaned aluminum substrates. The schematic representation of the spray deposition used during this study is shown in Fig. 1. A relatively low pressure (30-90 kpa) was used during deposition in order to ensure a fine atomization while preventing blowing off the droplets already deposited on the substrate. The distance of the spray gun from the substrate was kept at 50 cm. In order to vary the thickness of the coatings, number of passes of the spray gun across the substrate was varied.

Once the substrates were spray coated, the samples were put into a tube furnace for pyrolysis and crystallization. The furnace temperature was raised to 450 °C at a rate of

20 °C min^{-1}, maintained at that temperature for 60 minutes, and then left to cool to room temperature naturally. Nitrogen gas was continuously flown through the furnace throughout the heat treatment in order to maintain an inert atmosphere.

The near-normal spectral reflectance of the samples was measured in the 0.3-2.5 μm wavelength range with a Perkin Elmer Lambda 900 spectrophotometer. A spectralon sample was used for reference spectrum measurements. A Bruker Tensor 27 spectrophotometer with a gold mirror reference was used to measure near normal reflectance in the 2.5–20.0 μm wavelength range. The reflectance measurements were used to calculate solar absorptance, α, and the thermal emittance, ε, of the samples at 100 ° C using Eqs (1) and (2), respectively [6]:

$$\alpha_{sol} = \frac{\int_{0.3}^{2.5} I_{sol}(\lambda)(1-R(\lambda))d\lambda}{\int_{0.3}^{2.5} I_{sol}(\lambda)d\lambda} \quad (1)$$

$$\varepsilon_{ther} = \frac{\int_{2.5}^{20} I_P(\lambda)(1-R(\lambda))d\lambda}{\int_{2.5}^{20} I_P(\lambda)d\lambda} . \quad (2)$$

The thermo-gravimetric analysis (TGA) was done on Perkin-Elmer TGA 4000 t hermo-gravimetric analyzer. Approximately 100 mg final mixture of C/NiO precursor solution was placed in open 190 μl alumina pan and heated from 25 °C to 980 °C at a heating rate of 5 °C min^{-1} in N_2 atmosphere (flow rate 50 ml min^{-1}). The differential scanning calorimeter (DSC) results were collected on Mettler Toledo DSC 1 instrument. The surface morphology of the coatings was investigated using a ZEISS ULTRA plus FEG-SEM scanning electron microscopy. The Energy Dispersive Spectroscopy (EDS) analysis was done using a JEOL-JSM 7500F Scanning Electron Microscope. Raman spectra were collected using a Raman spectroscopy (Jobin-Yvon T64000 spectroscope), equipped with an Olympus BX-40 microscope attachment. An Ar^+ laser (514.5 nm) with energy setting 1.2 mW from a Coherent Innova Model 308 was used as an excitation source.

3. Results

In order to determine the optimal temperature of heat treatment, the C/NiO precursor solution was thermally analyzed by TGA and DSC techniques. Figure 2 displays a typical TGA and DSC curves for the C/NiO precursor solution. It can be seen from the figure that the DSC curve shows 1 endothermic peak at 83 °C and 4 exothermic peak at 210 °C, 262 °C, 342 °C and 436 °C. TGA curve exhibit four weight loss stages: 53 % the initial weight loss occurred

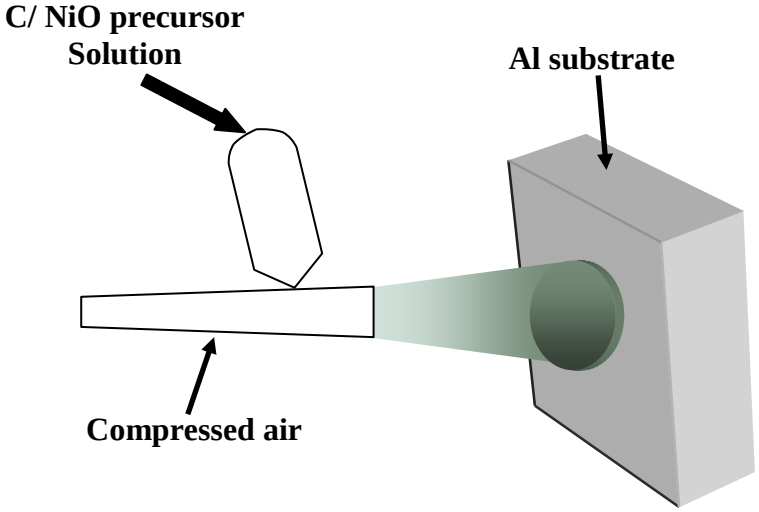

Fig. 1. A schematic diagram of the spray deposition technique used to deposit C/NiO nanocomposite coatings on Al surface.

31 and 57 °C, 10 % between 75 and 144 °C, 15 % between 144 and 295 and the final weight loss (13 %) between 295 and 341. The first weight loss was likely due to the evaporation of ethanol whereas the second and third was probably due to desorption of moisture and desorption of organic molecules, respectively. The fourth weight loss was most likely due to carbonization. Above 450 °C no noticeable weight loss has occurred. This stabilization of weight loss is accompanied by a distinct DSC exothermic peak at 437 °C which indicates the crystallization of the composite material. It is therefore decided to anneal the samples at temperatures between 450 °C to 550 °C . This choice has also been accompanied by the improvement of the optical absorption for samples heat treated in this temperature range (not shown).

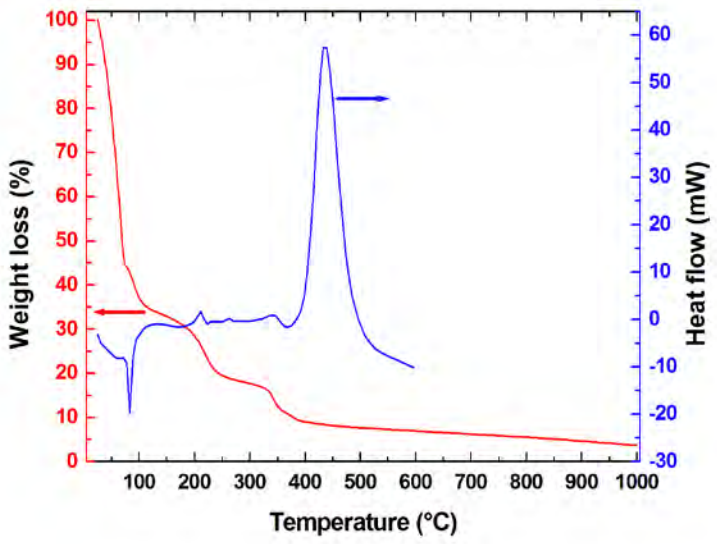

Fig. 2. Typical TGA and DSC spectra for C/NiO precursor solution.

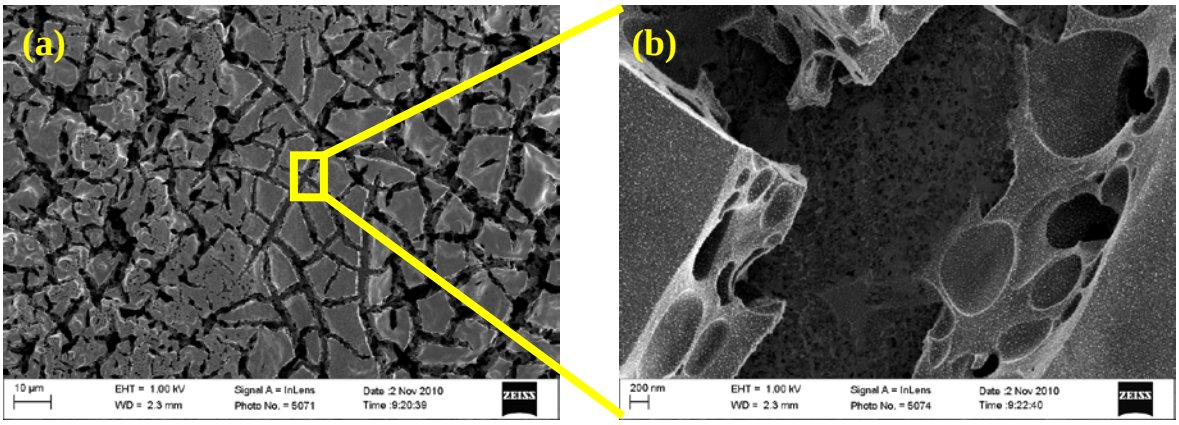

Fig. 3. (a) FE-SEM images of C/NiO nanocomposite coated on aluminum substrate, (b) enlarged image.

Figure 3 (a) depicts a typical SEM image of a C/NiO composite coating. The higher magnification image is shown in Fig. 3(b). As can be seen from Fig. 3 (a), the surface of the coating is uniform and cracked. The enlarged image (Fig 3(b)) shows that the coatings are porous. It is believed that the porosity of this film can produce high absorptance by multiple reflections [7]. The size distribution of the spherical particles in the coating is between 10 and 20 nm.

The composition of C/NiO composites was investigated using EDS (Fig. 4(a)). It reveals the presence of C, O, and Ni, which confirms the existence of NiO nanoparticles in the coating. The Al signal originates from the substrate used for coating. The presence of carbon in these films is further evidenced by Raman studies conducted on these coatings. Figure 4(b) shows a typical Raman spectrum of the C/NiO nanocomposite. The D band at ~ 1350 cm^{-1} originates from amorphous carbon and structural defects; the G band at ~ 1580 cm^{-1} is attributed to graphite structures, stems from tangential shearing mode of the carbon atoms [8-10]. The G' band at ~ 2700 cm^{-1} is an overtone of the D band which indicates the long range graphite ordering. Higher order Raman modes are also visible in the region 2920- 3220 cm^{-1}.

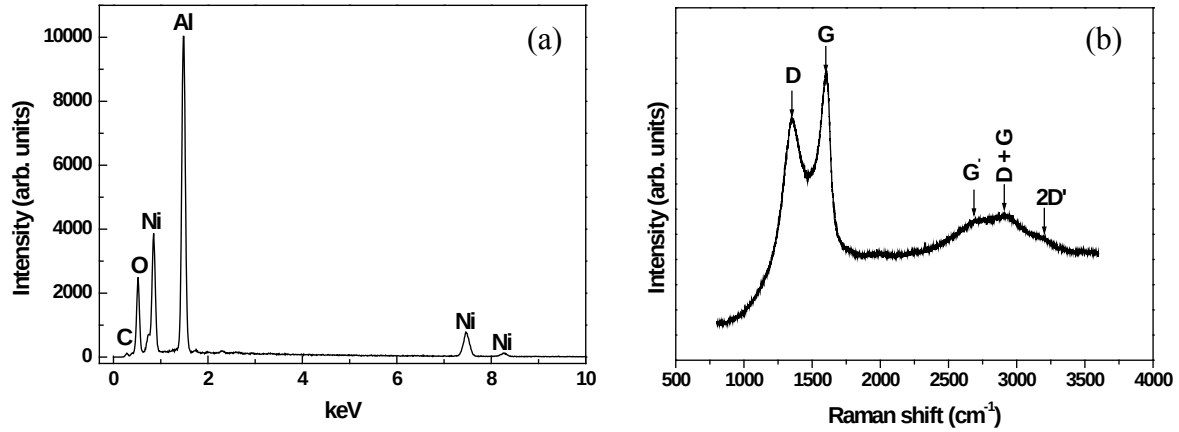

Fig. 4. (a) A typical EDS spectrum for C/NiO nanocomposite coated on aluminum substrate, (b) Raman spectra of the C/NiO nanocomposite coating.

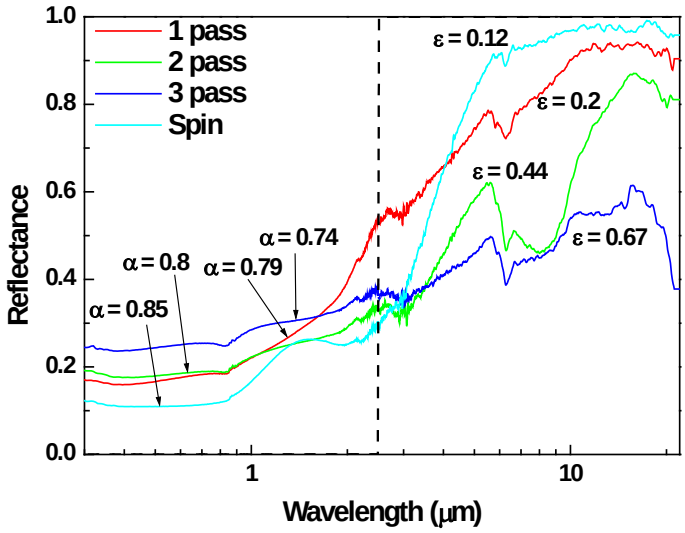

Fig. 5. The near normal reflectance spectra of C/NiO nanocomposite deposited with different passes on aluminum substrate etched with H_3PO_4. The spectrum for spin coated samples is also included for comparison. The broken line represents the reflectance spectrum for an ideal selective solar absorber.

Figure 5 shows the reflectance spectra of spray deposited samples with different passes, together with a spin coated sample as a reference. The dips in the spectra at about 6.3 μm are due to water absorption (O–H bending vibrations at 1,600 cm^{-1}) [11,12]. The O–H bending vibrations for the spray deposited samples are much stronger than the spin coated samples. This implies that spray coated samples have higher emittance (lower reflectance) values.

The reflectance spectra of the C/NiO nanocomposite deposited on a luminum substrate cleaned with HCl are presented in Fig. 6. It can be seen from the figure that the O–H mode vibrations are also present in this C–NiO samples. Although the solar absorptance values for some of the samples cleaned using HCl are better than the spin coated sample, they are highly emitting.

4. Discussion

The main reason for film cracking is due to film shrinkage because of solvent out gassing during the heat treatment [13]. Although it is minor, the thermal expansion rate difference between the coatings and the aluminum substrate can also contribute to the cracking during the cooling process [13]. According to Borström *et al.* [14], film homogeneity and propensity of film cracking is very important for solar absorbing thin films. The durability of the coatings will be severely affected due to infiltration of water and subsequent degradation of aluminum substrates. This clearly suggests that further study is necessary in order to reduce these cracks.

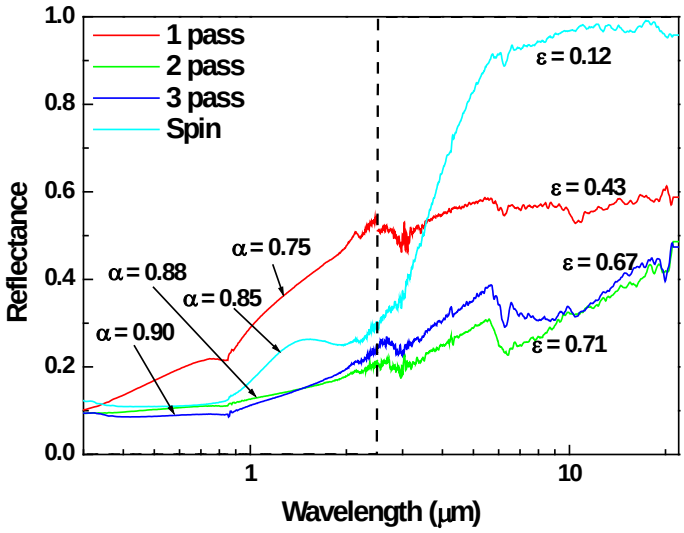

Fig. 6. The near normal reflectance spectra of C/NiO nanocomposite deposited with different passes on aluminum substrate etched with HCl. The spectrum for spin coated samples is also included for comparison. The broken line represents the reflectance spectrum for an ideal selective solar absorber.

In an effort to increase the absorptance of this single layer we have pretreated the substrate surface by etching with H_3PO_4 and HCl. It is well known that the solar absorptance of selective absorber coatings can be enhanced by producing a textured surface [13]. The surface texturing of the aluminum surface with HCl enhanced the absorptance of the coating considerably (Fig. 6). However, the emittance of these coatings becomes worse. The magnitude of the surface roughness accompanying the pretreatment has to be much smaller than the peak thermal radiation wave length and comparable to the solar wavelength [14].

The production cost for a 1 μm thick coating material for a lab scale is estimated to be R 0.35/m^2 ($ 0.05 / m^2). This price can change significantly if the precursor materials are purchased in bulk. All other additional production costs and heat treatment were not estimated. The price for aluminium substrate is R61.76/m^2 ($ 8.6/m^2). This implies that the material cost for the coating is very small compared to the substrate price. The material cost for a 100 nm thick coating for Ni-Alumina coatings were estimated to be 0.14 €/ m^2 (R 1.4 / m^2) [2]. It should be noted that the additional costs and heat treatment as well as transfer efficiency of the paint during spraying might slightly increase the cost.

Further research will focus on the optimization of the spray process parameters and the study of the durability of these coatings.

5. Conclusion

Spray deposition method was adapted for large-area deposition of sol-gel prepared C/NiO nanocomposite coatings on aluminum substrate for selective solar absorber application. The coatings were made possible by using conventional air compressor. The number of passes was varied in order to optimize the thickness of the coatings. The performance of the sprayed samples was compared with the spin coated. The preliminary results have shown that the sprayed samples have comparable solar absorption properties with the spin coated suggesting that the sol-gel synthesized and sprayed C/NiO composite films is very encouraging.

The properties of these coatings will, however, require further developments before it could be integrated into an existing solar collector for low cost domestic water heating in a rural area for social good.

References

[1] G. Legros, I. Havet, N. Bruce, S. Bonjour, The energy access situation in developing countries, UNDP-WHO, 2009.

[2] T. Boström, E. Wäckelgård, G. Westin, Solar Energy 74, 2003, 497-503.

[3] G. Katumba, G. Makiwa, T. R. Baisitse, L. Olumekor, A. Forbes, and E. Wäckelgård, phys. stat. sol. (c) **5**, No. 2, 2008, 549–551.

[4] G. Katumba, L. Olumekor, A. Forbes, G. Makiwa, B. Mwakikunga, J. Lu, E. Wäckelgård, Sol. Energy Mater. Sol. Cell. 92, 2008,1285– 1292.

[5] T. Boström, G. Westin, E. Wäckelgård, Sol. Energy Mater. Sol. Cell. 91, 2007, 38-43.

[6] J. A. Duffie and W. A. Beckman, Solar Engineering of Thermal Processes, JohnWiley & Sons, New York, NY, USA, 1980.

[7] C. E. Kennedy, "Technical Report: Review of Mid-to-High-temperature Solar Selective Absorber Materials," National Renewable Energy Laboratory, prepared under Task No. CP02.2000, NREL/TP-520-31267, 2002.

[8] O. Lourie, H.D. Wagner, J. Mater. Res. 13, 2000, 2418.

[9] A.M. Rao, A. Jorio, M.A. Pimenta, M.S.S. Dantas, R. Saito, G. Dresselhous, and M.S. Dresselhaus, Phys. Rev. Lett. 84, 2000, 1820.

[10] A. Jorio, G. Dresselhaus, M.S. Dresselhaus, M. Souza, M.S.S. Danatas, M.A. Pimenta, A.M. Rao, R. Saito, C. Liu, H.M. Cheng, Phys. Rev. Lett. 85, 2000, 2617.

[11] G. Katumba, J. Lu, L. Olumekor, G. Westin, E. Wäckelgård, J. Sol–Gel Sci. Technol. 36, 2005, 33-43.

[12] A.V. Rao, R.R. Kalesh, G.M. Pajonk, J. Mater. Sci. 38, 2003,4407.

[13] T. Boström, S. Valizadeh, J. Lu, J. Jensen, G. Westin, E. Wäckelgård, J. Non-Cryst. Solids, 2010, doi:10.106/j.jnoncrysol.2010.09.023

[14] S. Sakka (Ed.), Handbook of Sol-gel Science and Technology, kluwer Academic Publishers, New York, 2005

[15] W.F. Bogaerts and C.M. Lampert, J. Mater. Sci. 18, 1983, 2847.

[16] F. Jahan, B.E. Smith, J. Mater. Sci. 5, 1986, 905-906.

Steel-Tinplate as a solar wall panel and its effectiveness

G. Ruskis*, A. Aboltins, J. Palabinskis

Institute of Agricultural Machinery, Latvia University of Agriculture, Cakstes blvd. 5, Jelgava, LV-3001, Latvia
** Corresponding author. Tel: +371 29490286, Fax: +371 63020762, E-mail:* guntisruskis@inbox.lv

Abstract: The aims of the research, was to investigate black colored steel-tinplate use for absorber and covered material of collector and compare the efficiency of three types of air heating collectors. This heated air we can exploited for drying of agricultural produce, room ventilation and room heating and etc.
0.1∗0.5∗1.0 meters long flat-plate collector (FPC) for experimental research was built. Air velocity at the experiments was v=0.9 m/s. We used the sun following collectors. The experimental data were measured and recorded in the electronic equipment (REG). The experiments were carried out in September 2010 at the same weather conditions.
Collectors of insulated and un-insulated surfaces with steel-tinplate absorber as covering material warmed ambient air up to 10-12 and 5-6 degrees corresponding (at irradiance 800 W/m^2). This difference indicates the great importance of insulating the collector body. It can explain with intensify heat exchange between absorber and ambient air which reduce efficiency of collector. There was good correlation with irradiance and air heating degree.
Our investigations showed that more effective FPC was collector with absorber tinplate at middle of collector body. At favorable weather conditions the heating degree of ambient air at the outlet reaches 6-8 degrees more that at the outlet of insulated collector covered by steel-tinplate.

Keywords: *Solar Energy, Air Heating, Collector, Solar Wall, Absorber.*

1. Introduction

Under Kyoto targets, the European Commission member states and stakeholders identified and developed a range of cost-effective measures to reduce emissions. The new package sets a range of ambitious targets to be met by 2020, including improvement of energy efficiency by 20%, increasing the market share of renewable to 20%. In a renewable energy-intensive scenario, global consumption of renewable resources reaches a level equivalent to 318 EJ ($E = 10^{18}$) per annum of fossil fuels by 2050, but it is less than 0.01% of solar energy reaching the earth's surface each year [1].

Solar energy is used to heat and cool buildings (both actively and passively), drying production, heat water for domestic and industry use, heat swimming pools, generate electricity, for chemistry applications and many more operations [1].

One of the solar energy uses is a solar wall. Solar wall system is simple, effective, inexpensive, ecological, building integrated into any solution [2-3]. This system, raising the temperature of indoor air for 5 - 25 degrees above the outside air temperature, allowing to save 20 - 70% of fuel energy while supplying the area with fresh air.

This system successfully used around the world since 1977, when the Canadian government subsidized the eco-system tests. Solar wall missions are located in North America, Europe and Asia - a total of more than 25 countries worldwide.

There is no need for heat ventilation at the expense of the economy, because the system provides fresh air circulation, while the walls of the building do not overheat in the summer, because the system acts as a coolant. In many countries, is increasing interest in solar wall panels use. Solar wall panels use is discussed a lot in works of Italian climates [4].

Using solar collectors efficiency studies [5], the idea was to use steel-tinplate absorber as a solar panel on the wall. Steel-tinplate absorber can be used on the roof, thereby providing ventilation and heating in early spring and autumn, with the heat and fresh air, and drying the products with heated air in the summer.

Our aim was to find the collector's (the adsorbent is used as a coating material) efficiency of insulation using and warm-up stage of air.

2. Methodology

The aim of the research was to investigate black colored steel-tinplate use for absorber and covered material of collector and compare the efficiency of three types of air heating collectors: collectors with insulated and un-insulated surfaces with covered material - steel-tinplate and classical collector with covered material - polystyrol plate and absorber black colored steel-tinplate in middle. View of flat-plate collector (FPC) when the absorber (black colored steel-tinplate) is put in the middle of the collector is shown in Fig.1. In the second case, absorber placed collector coverage place, it means at the top of collector.

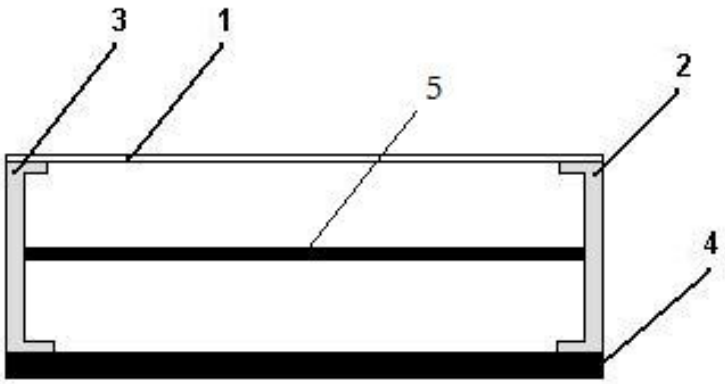

Fig. 1. Schema of solar collector frontal view: 1 – covered material; 2, 3 – side surface /plastic/; 4 – floor of collector; 5 – absorber (steel-tinplate)

In the experiments, the collector covered material was a polystyrol plate. This material has gained immense popularity due to such properties as safety, mechanical crashworthiness, translucence and high UV radiation stability.

In the laboratory a *0.1∗ 0.5∗1.0* meters long experimental solar collector was constructed for research into the properties of absorber materials. Air velocity at the experiments was v=0.9 m/s. Our investigations devoted the sun following collectors, which guarantees perpendicular location of plane of absorber from flow of sun radiation.

Experimental data is recorded by means of an electronic metering and recording equipment of temperature, radiation and lighting (REG) [6]. It is equipped with 16 temperature transducers and metering sensors of solar radiation and lighting. Solar radiation measuring instrument was the pyranometer. The isolated collector was made by the collector surfaces faced with cellular plastic 2 cm plates.

We compare three equal sizes FPC: collectors of insulated and un-insulated surfaces with absorber steel-tinplate as a covering material and classic collector with the covering material polystyrene plate and absorber tinplate in the middle of collector. Experiments were made in

September 2010 in different weather conditions at different atmospheric air temperatures. To assess different absorbers influence was made comparatively research at similar weather conditions. Inflow air temperature in collector is equal to the ambient air temperature. Ambient air temperature was changing from 13ºC to 18ºC in our experiments.

The data of sun radiation are depended from clouds, shadows and we aligned experimental data with method of least squares using Eq. (1). [7]

$$\overline{y_i} = \frac{1}{35}[17y_i + 12(y_{i-1} + y_{i+1}) - 3(y_{i-2} + y_{i+2})] \qquad (1)$$

Where $\overline{y_i}$ - aligned data, y_i - experimental data, i - ordinal number.

3. Results

Using the experimental results and statistical processing data we received a relation between the length of the collector, sun radiation to absorber plate and air temperature exchange in the collector.

We research situation when absorber (steel-tinplate) puts at top of collector (Fig. 2). To compare insulated and un-insulated collectors with steel-tinplate as a covering material we can see that at the same weather conditions for insulated collector is warming up air to 3 degree up (at radiation 800 W/m^2) than collector with un-insulated surfaces (Fig. 3).

Fig. 2. Sun collector comparatively research in experiment.

We can see that the solar radiation changes significantly affect the passing air temperature. This effect does not happen instantly, but with a delay of 3-5 minutes. It should be noted that the un-insulated collector efficiency is highly influenced by wind speed, which cools the surface of the collector body.

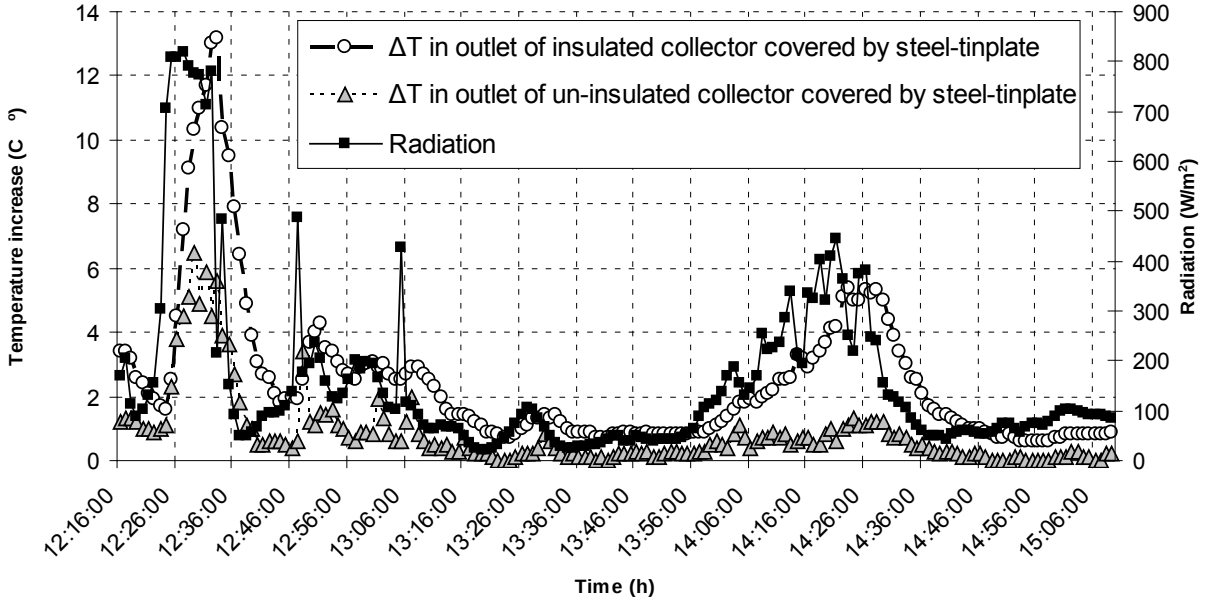

Fig. 3. Temperature difference in outlet of collector with steel-tinplate covering material for insulated and un-insulated surfaces comparing with sun radiation.

As you can see in Fig. 4, near little sun radiation are not visible constitutive air heating, but increasing sun radiation is growing air heating level and you can see that collector with absorber steel-tinplate at middle of collector body is more powerful than collector with steel-tinplate absorber as covering material. Air heating level is not highly dependent on ambient temperature. Much more it is influenced by solar radiation and insulation. If the collector is covered with the steel tinplate then this collector efficiency is highly influenced by environmental conditions, especially wind and ambient air temperature. These conditions reduces absorber own temperature. In the classic collectors whose effects are much smaller (Fig. 4)

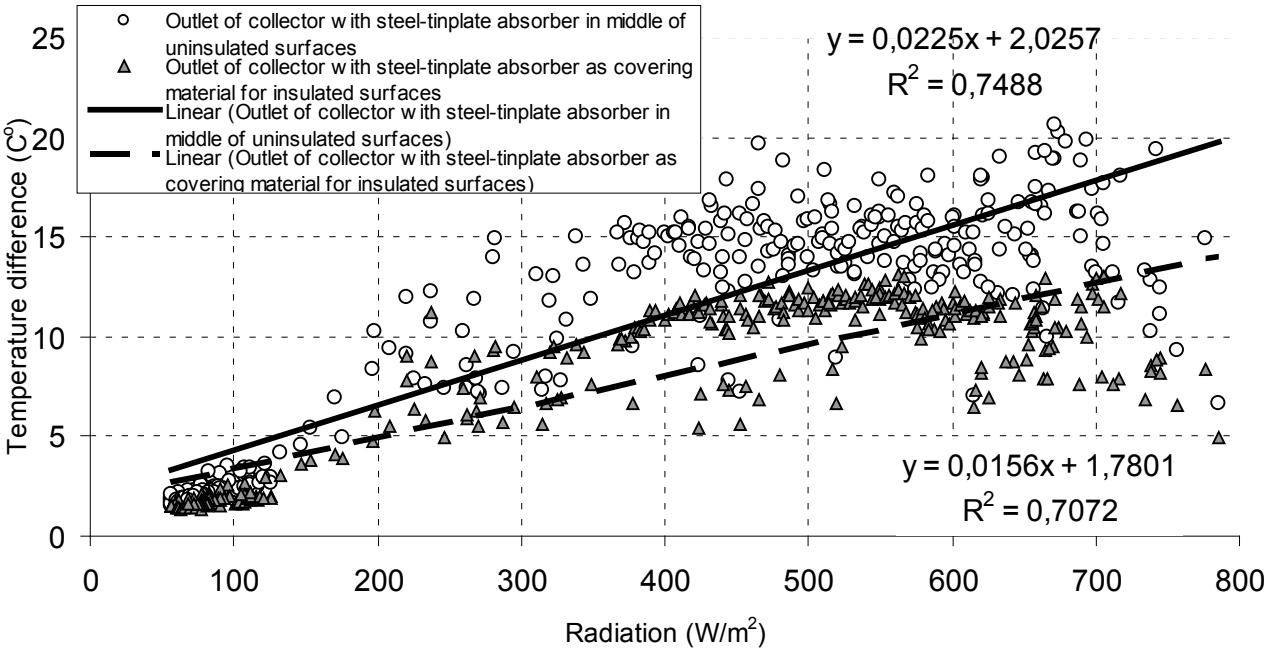

Fig. 4. Temperature difference in outlet of collector (with absorber tinplate at middle of collector body and with steel-tinplate absorber as covering material) comparing with sun radiation.

Near little sun radiation are not visible constitutive air heating, but increasing sun radiation is growing air heating level and you can see that collector with absorber steel-tinplate at middle of collector body is more powerful than collector with steel-tinplate absorber as covering material.

Using the experimental results and statistical processing data we received a relation between the air temperature exchange under the steel-thin plate absorber in the collector, length of the collector and sun radiation to absorber plate.

The temperature change ΔT under tinplate can be expressed with the Eq. (2).

$$\Delta T = 1.3 \cdot 10^{-2} x \cdot R - 4.8 \cdot 10^{-3} R - 1.9 \cdot 10^{-6} R^2 - 0.3x + 0.68x^2, \qquad (2)$$

Where x – length of collector (m); R – sun radiation (W·m^{-2}).
Coefficient of determination is $\eta^2 = 0.771$. The graphical interpretation of Eq. (2) is shown in Fig.3.

In Fig. 5. you can see contour plot of air temperature (under absorbent) increase dependence on length of collector and sun radiation for un-insulated collector with absorber with steel-tinplate as a covering material.

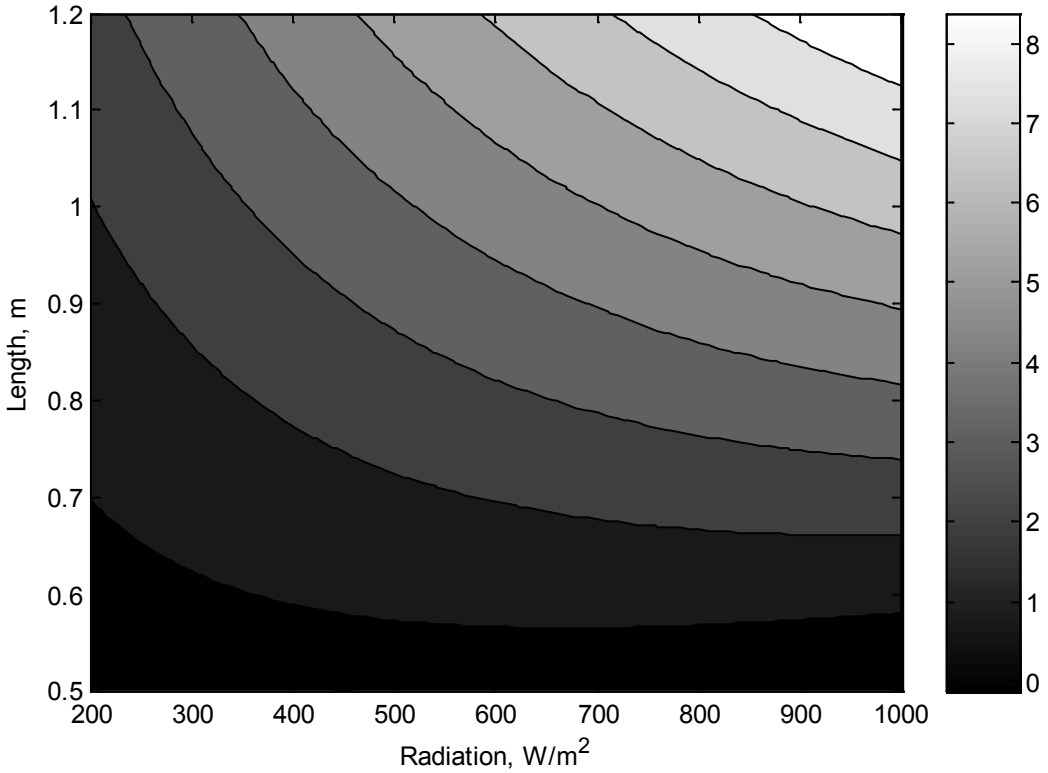

Fig. 5. Contour plot of air temperature (under tin plate) increase dependence on length of the collector and sun radiation.

4. Conclusions

1. Collectors of insulated and un-insulated surfaces with steel-tinplate absorber as covering material warmed ambient air up to 10-12 and 5-6 degrees corresponding (at irradiance 800 W/m^2). This difference indicates the great importance of insulating the collector body.

2. Use of isolation for collector construction dose not give inportant role if there is no wind to cool collector.

3. Using the experimental results and data statistical processing we received a relation between the air temperature exchange under the steel-thin plate absorber in the collector, length of the collector and sun radiation to absorber plate.

4. At favorable weather conditions the heating degree of ambient air at the outlet of collector with absorber tinplate at middle of collector body reaches 6-8 degrees more that at the outlet of insulated collector covered by steel-tinplate.

5. Our investigations showed that steel-tinplate absorber use as covered material of flat-plate collector for ventilated air heating is possible in Latvia.

References

[1]. S. Kalogirou, Solar energy engineering: processes and systems, Academic Press Elsevier Inc., 2009.

[2]. Solar Buildings: http://www.nrel.gov/docs/fy99osti/24499.pdf

[3]. Solar wall: http://solarwall.com/en/products/solarwall-air-heating/uses-and-applications/agriculture.php

[4]. F. Stazi, C. Di Perna, C. Filiaci, and A. Stazi, The Solar Wall in the Italian Climates, World Academy of Science, Engineering and Technology 37, 2008, pp. 31 – 39.

[5]. A. Aboltins**,** J. Palabinskis**,** A. Lauva, G. Rušķis, The steel–thin plate absorbers investigations in air solar collector, Proceedings of the 8th International Scientific Conference "Engineering for Rural Development", 2009, pp. 182 – 187.

[6]. REG 2004 Tehniskais apraksts un lietošanas pamācība (Technical description and using instruction), pp. 11. (in Latvian)

[7]. Веденяпин Г.В. Общая методика экспериментального исследования и обработки опытных данных (The general methology of experimental research and treatment of experimental data). Колос, М., 1967. (in Russian)

Nano structure black cobalt coating for solar absorber

G.Toghdori[1], S.M.Rozati[1*], N. Memarian[1], M.Arvand[2], M.H.Bina[3]

[1]*Department of Physics, University of Guilan, Rasht42335, Iran*
[2]*Department of Chemistry, University of Guilan, Rasht42335, Iran*
[3]*Department of Materials Engineering, Esfahan University of Technology, Esfahan, Iran*
** Corresponding author. Tel: +981313220912, Fax: +981313220066 E-mail: smrozati@guilan.ac. ir*

Abstract: Black cobalt thin films on bright nickel plated on brass and copper substrates were prepared by the electrodeposition method. The Influence of substrate metal and heat treatment process on the surface morphology and absorptance of samples was investigated. Surface morphology and spectral reflectance of films were measured by scanning electron microscopy and spectrophotometer in the visible and near-IR region of spectrum respectively. Scanning electron microscopy images showed that the black cobalt films have porous structure. The absorptance of prepared films is over than 90%, which makes them suitable for using as solar absorbers.

Keywords: *electroplating, black cobalt, solar absorber coating, black coating.*

Nomenclature (Optional)

T	*Temperature ..... °C*
t	*Time .....s*
α	*Solar Absorptance*
ε	*Thermal Emittance*

1. Introduction

The preparative aspects of cobalt oxide thin films have been a subject of investigations by various workers because of their numerous applications in various fields of technology. They are attractive in application to solar thermal energy collectors as selective absorbing layers [1]. Spectrally selective surfaces exhibiting high values of solar absorptance α and low values of thermal emittance (ε) improve the thermal performance of solar collectors by reducing the radiative heat loss component [2]. Such surfaces are employed as receiver coatings in flat plate evacuated tube and concentrating collectors and may under stagnation conditions in the latter application, experience temperatures of 500˚C. Many surface coating types have been developed which have potential for application as selective absorbers [3]. An attractive aim of selective surface research studies is the development of a single coating type which could be used for all solar collector designs. For successful industrial development such a coating would not only possess favourable optical properties but also would be readily reproducible, durable, thermally stable and inexpensive to produce. Selective solar absorber coating in solar thermal systems, working under moderate concentrations, experience operating temperatures in the rang 300-500˚C. Cobalt oxide coatings [4] are proposed as potential candidates for this use. However, little is known about their stability and the modes of degradation when operated at high temperatures. It is well known that the metal substrate microstructure strongly influences the grain size and morphology of the in-situ grown film [5]. It is also well known that the microstructure of electrodeposits varies markedly with deposition parameters and that various impurities from the plating bath may be incorporated into the deposit [5].

A general class of absorber coatings is those formed by chemical “conversion” processes. The previous works on the electrochemical preparation of cobalt oxides can be divided in to two groups: direct and indirect. In the former, a solution is prepared by dissolution of the chemical components that allow the directly preparation of black cobalt on the substrate at the cathode in the electrolysis process [6]. On the latter the formation of cobalt oxide is

accomplished in two steps, i.e. first the metallic cobalt is deposited on the substrate and secondly, the cobalt is oxidized to black cobalt through chemical or thermal oxidation [6]. Because of its optical, semiconducting, magnetic and electrochemical properties, black cobalt is a promising material among transition metal oxides, which renders it attractive for solar photochemical applications and electrochemical devices as a counter electrode [7]. Today, although there are six physical mechanisms of solar absorptance [8]. It is recognized that one of the most efficient solar absorber films base their optical properties on its microstructural volume and surperficial parameters. However, in spite of all the existing mechanisms, the textured surfaces are the most dependent of the surface morphology than whatever other material is. These materials show a high solar absorptance by multiple reflection of the incident radiation among dendrites that are approximately two microns apart, while the long-wavelength thermal emittance is rather unaffected by texture. Several techniques, such as chemical conversion and thermal oxidation of metallic films and electrodeposition, are currently used to achieve such spectrally selective, black-metal, solar absorber surfaces [9]. However, the desired characteristics of the metallic coating could be better controlled by directed electrodeposition. In this paper electrodeposition of cobalt photothermal material, suitable for using in solar energy collection, has been studied.

2. Experimental Details

Black cobalt thin films on bright nickel plated on brass and copper substrates were prepared by the electrodeposition method. The core part of the electroplating process is the electrolytic cell. In the electrolytic cell a current is passed through a bath containing electrolyte, the anode and the cathode. The workpiece to be plated is the cathode (substrate). The Anode is a metal which is coating on the cathode surface. Electrolyte is the electrical conductor in which current is carried by ions rather than by free electrons (as in a metal). When a direct electric current passes through an electrolyte, chemical reactions (Oxidation/Reduction) take place at the solution. Reduction takes place at the cathode, and oxidation takes place at the anode. Electrolyte completes an electric circuit between two electrodes. Upon application of electric current, the positive ions in the electrolyte will move toward the cathode and the negatively charged ions toward the anode. The metallic ions of the salt in the electrolyte carry a positive charge and are thus attracted to the cathode. When they reach the negatively charged workpiece, it provides electrons to reduce those positively charged ions to metallic form, and then the metal atoms will be deposited onto the surface of the negatively charged workpiece.
Brass and copper plates were thoroughly degreased and cleaned, then subjected to a 1-min acid etch in 5% sulphuric acid prior to bright nickel deposition. According to watts bath [10] bright nickel deposition was carried out under the conditions mentioned in table 1. A piece of nickel metal with 99.9% purity was used as anode.

Table 1: Deposition condition and bath composition for deposition of bright nickel.

Composition bath		Current density	Temperature
Nickel sulphate	250 gl^{-1}	0.5 A/dm^2	70°C [11]
Nickel chloride	50 gl^{-1}		
Boric acid	50 gl^{-1}		

After bright nickel plating, the panels were rinsed with distilled water. Finally black cobalt deposition was carried out under the conditions described in table2 according to McDonald electrolyte bath [6]. The anode was cobalt metal with 99.9% purity and bright nickel plated brass and copper was used as cathode.

Table 2: Deposition condition and bath composition for deposition of black cobalt.

Composition bath		Current density	Temperature	pH
Cobalt sulphate	400 gl^{-1}	3 A/dm^2	30˚C	4
Cobalt chloride	50 gl^{-1}			
Cobalt nitrate	4 gl^{-1}			
Boric acid	40 gl^{-1}			

The cobalt sulphate is the main source of cobalt ions, the cobalt chloride helps to improve the conductivity of electrolyte solution and the boric acid is a leveling agent. Cobalt nitrate was added to the bath to obtain a black layer on the sample.
The films deposited on brass substrate and bright nickel plated brass substrate annealed in the air environment at temperature 400 ˚C for 20 Min to study their physical properties after heat-treatment. The absorptance was calculated from the equation 1-R, in the visible region [12]. Where R is the room temperature reflectance measuremement. Reflectance in the visible region was determined with a Carry 500 spectrophotometer. The morphology of the surfaces is detected by scanning electron microscope (SEM) model Philips XL30.

3. Results and Discussion

3.1. SEM Analysis

Figure 1 depicts the surface morphology of black cobalt films deposited on different bright nickel plated substrates. Fig.1.a is for a brass substrate and Fig.1.b belongs to a copper substrate. It is obvious that the crystal structure of black cobalt film deposited shows a porous structure. There is no evident difference between the morphology of films deposited on different substrates. While by changing the substrate metal the porous sizes have changed from micro, for copper substrate, to nano-sized porous structure for brass substrate. Figure 2 shows the surface morphology of black cobalt films deposited on brass substrate, (a) before heat-treatment and (b) after heat-treatment. From figures 1 and 2 it is clear that the films deposited on brass substrates after annealing had more cracks on the surface and the porosity of the structure was increased. By comparing fig.1a and fig.2a it is evidence that the presence of bright nickel middle layer causes a more uniform structure without any crack in the surface of electrodeposited black cobalt films on brass substrate. In addition by using the bright nickel middle layer the porosity of structure increased. This porous structure results enhanced the absorptance in coatings and makes these layers suitable for solar absorber application.

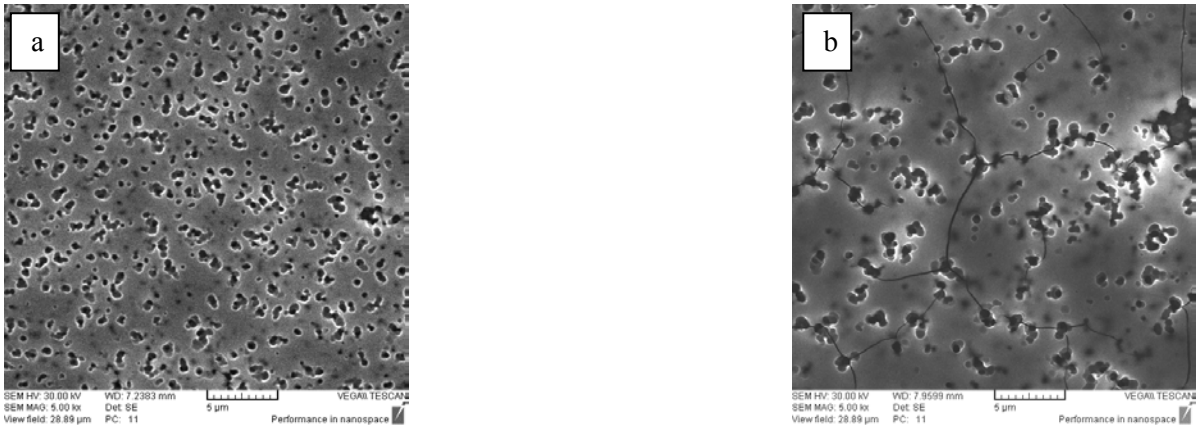

Fig. 1. The surface morphology of black cobalt film deposited on bright nickel-plated substrates (a) for brass substrate (b) for copper substrate.

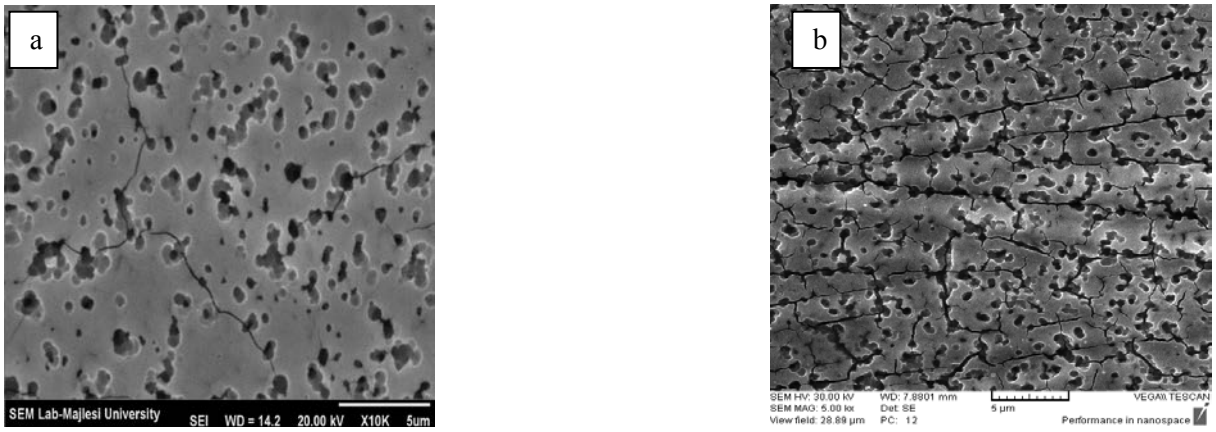

Fig. 2. The surface morphology of black cobalt films deposited on brass substrate (a) before annealing (b) after annealing.

3.2. EDAX Analysis

Figure 3 and table 3 show the elements in electrodeposited cobalt film on brass substrate by EDAX analysis. These Data expressed that the main elements in black cobalt coating, is cobalt metal.

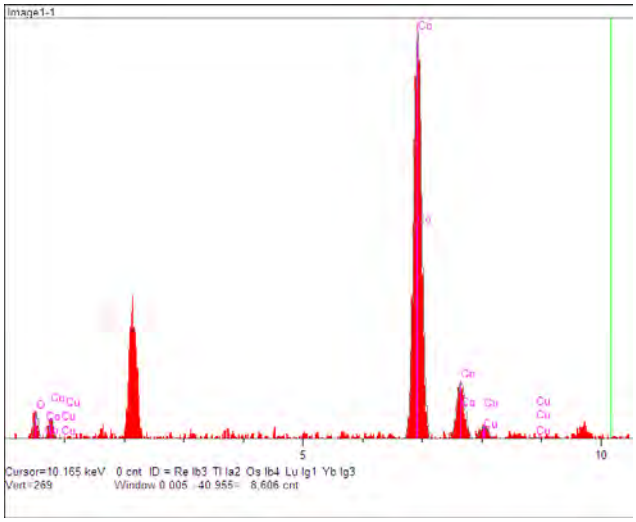

Fig. 3. EDAX of black cobalt as-deposited on brass substrate.

Table 3. The elemental concentration of black cobalt film deposited on brass substrate.

Intensity(c/s)	Conc. (Wt %)	Element
14.11	4.648	O
420.67	90.610	Co
13.34	4.742	Cu

3.3. Solar Absorptance Analysis

The changes in absorptance of layers by the wavelength for bright nickel-plated brass and copper substrates are shown in Fig.4. And the films absorptance of black cobalt films deposited on brass substrate before heat treatment and after heat treatment in visible region of wavelength are shown in Fig.5. The optimal solar absorptance was 98%-99.55% at wavelength range 400-1200 nm for the as-deposited films and films after heat treatment.

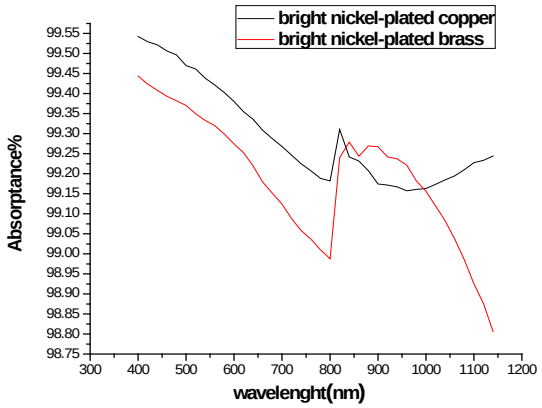

Fig. 4. The relationship between the absorptance and wavelength of black cobalt films deposited on different substrates.

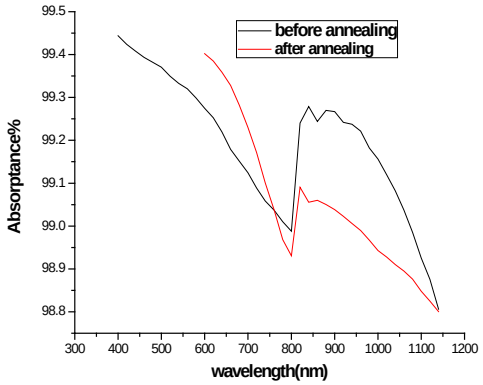

Fig. 5. The relationship between the absorptance and wavelength of black cobalt deposited on brass substrate (a) before heat treatment (b) after heat- treatment.

4. Conclusions

Black cobalt coatings on bright nickel plated on brass and copper substrate were prepared by the electrodeposition method. The influence of heat treatment on optical absorption and surface morphology of black cobalt films deposited on brass substrates has been studied. Heat treatment of black cobalt films deposited on br ass substrates caused cracks in the surface structure. Heat treatment of black cobalt deposited on br ass caused a slight decrease in an absorption in the near-IR region. Due to high absorption in visible region the best substrate for a black cobalt solar absorber coating is bright nickel-plated on copper substrate.

References

[1] B. Pejova, A. Isahi, M. Najdoski and I. Grozdanov, Fabrication and characterization of nanocrystalline cobalt oxide thin films, Material Research Bulletin 36, 2001, pp. 161-170.

[2] A.R. Shashikala, A.K. Sharma and D.R. Bhandari, Solar selective black nickel-cobalt coatings on aluminum alloys, Solar energy materials & Solar cells 91, 2007, pp. 629-635.

[3] M. G. Hutchins, P.J. Wright and P.D. Grebenik, Coparision of different of black cobalt selective solar absorber surfaces, Solar energy materials 16, 1987, pp. 113-131.

[4] C.Choudhury and H.K. Sehgal, High temperature degradation in cobalt oxide selective absorber, Solar energy 30, 1983, pp. 291-292.

[5] S.C. Kwon, D.L. Douglass, The Selective Solar Properties of oxide films grown In-Situ on cobalt and cobalt alloys, Solar Energy Materials 11, 1984, pp.299-310.

[6] E. Barrera, I. Gonzalez and T. Viveros, A new cobalt electrodeposit bath for solar absorber, Solar energy materials and solar cells 51, 1998, pp. 69-82.

[7] Z. Abdel Hamid, A. Abdel Aal and P. Schmuki, Nanostructured black cobalt coating for solar absorbers, Surf. Interface Anal 40, 2008, pp. 1493-1499.

[8] C. E. Barrera, L. Salgado, U. Morales and I. Gonzalez, Solar Absorptance of black cobalt and black cobalt-silver films and its relation with roughness coefficient, Renewable Energy 24, 2001, pp. 357-364.

[9] E. Barrera, M. P. Pardave, N. Batina and I. Gonzalez, Formation Mechanisms and Characterization of black and white cobalt Electrodeposition onto Stainless Steel, Journal of Electrochemical Society 147, 2000, pp. 1787-1796.

[10] T.M.Chang, M.Sone, A.Shibata, C.Ishiyama, Y.Higo, Bright nickel film deposited by supercritical carbon dioxide emulsion using additive-free watts bath, Electrochimica Acta 55, 2010, pp. 6469-6475.

[11] B. Gaida, Electroplating (Question and Answers), by La librairie de Traitenents de Surface, first, 1983, pp.167-187.

[12] G. McDonald, A Preliminary study of a solar selective coating system using a black cobalt oxide for high temperature solar collectors, Thin Solid Films 72, 1980, pp. 83-87.

Combining the radiative, conductive and convective heat flows in and around a skylight

Martin Fält*, Ron Zevenhoven

Thermal and Flow Engineering, Department of Chemical Engineering, Åbo Akademi University, Turku, 20500, Finland
** Corresponding author. Tel: +358 2 215 4441, Fax: +358 2 215 4792, E-mail: martin.falt@abo.fi*

Abstract: Normal skylights bring light into the spaces located below them. By the use of infrared radiation (IR) transmissive polymer films and IR-emitting and absorbing gases, an advanced version of the skylight may supply cooling and thermal insulation to the room located below it. This novel radiative skylight can, in its cooling mode, lead heat from the room below, to the cool skies located above the skylight. When cooling is no longer needed or attainable this connection will be cut, thus providing the room with an optimal amount of thermal resistance. This article is a progress report on the modeling of the skylight. The main work is done to combine the different heat transfer methods into one single model by the use of the commercial program Comsol 4.1. The results show that a cooling effect of 100 W/m^2 is achievable when the skylight is compared to a similar skylight containing only air.

Keywords: *Radiative cooling, heat transfer in participating media, skylight.*

1. Introduction

Skylights are popular in building technology due to their ability to bring light into a space. However, as they light up a space, they also heat it up. T his heat can be unwanted and therefore, has to be removed. This article will present the results from a numerical modeling of a skylight, which can function either as a radiative cooler or as a thermal insulator. Radiative cooling is a passive cooling method that connects a warm object located e.g. on top of a building to a lower sky temperature through heat radiation; one could describe it as an inverse solar collector [1].

The improved skylight contains a quantity of gas that is active in radiative heat transfer (i.e. a participating gas), and a cooling or insulating effect is achieved by controlling the circulating motion of this gas. The use of gases in the spaces between windows has been studied mainly with the goal of increasing thermal resistance by replacing air with a gas having lower conductive properties. Another option is to use gases that absorb and emit thermal radiation and thus decrease the radiative heat transfer through the window [2]. The use of such gases, which are active in radiative heat transfer, has also been studied for radiative cooling purposes; these studies show that cooling is also attainable during the day [3–5]. However, a window or a skylight that combines the three functions is a novel idea.

2. Methodology

The skylight model, whose design and function is described in [6], was designed at the authors' laboratory at Åbo Akademi University to determine its performance as a passive cooler and a thermal insulator. As shown in Figure 1, it consists of three windows. The outer and the inner window are made of an IR-transmitting polymer, τ=0.19, and the middle window is made of silica glass, which is highly reflective to IR radiation at all wavelengths, ρ=0.9. The spaces between these windows contain a greenhouse gas that acts as the system´s heat carrier. The walls are assumed to be thermally insulated and to have an absorptivity of α=0.9. Heat that originates directly from the sun is not incorporated into this model as both

the windows and the gas are assumed not to absorb short wave heat radiation in the interval of 0.1–3μm.

When the skylight is set in its cooling mode, heat is transferred to the gas through the lower window (Glass 1) by radiation, conduction, and convection from the room below. The heated gas rises to the upper compartment due to the decrease in the gases´ density. In the upper space, the gas is cooled by radiative heat transfer through the upper polymer window (Glass 2) and the "atmospheric window" to the colder air masses in the upper atmosphere. There also exists a forced convective heat transfer between the upper part of the skylight and its surroundings. The effect of this heat transfer depends on the temperature of the surroundings; for the modeled cases, it is cooling.

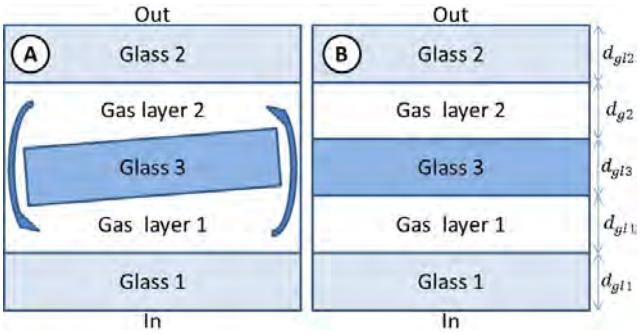

Fig. 1.Skylight in cooling mode "A" and in insulating mode "B"

When the greenhouse gas cools, its density increases, and it flows down to the lower part of the skylight. This convective heat flow is induced by the slightly tilted middle window. The angel of the tilt and the width of glass 3 has been chosen according to Fig. 2 so as to decrease the formation of hindering Bérnard cells (convective swirls).

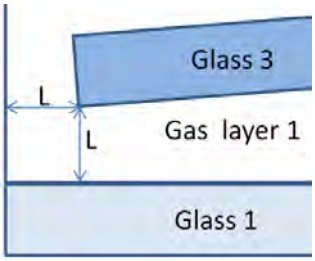

Fig. 2. Detail of the skylight in cooling mode

Then when no c ooling is needed, the connection between the two gas spaces is cut, thus changing the task of the roof components from a passive radiative cooler to a thermal insulator. The weather parameters that are used in this modeling are average values for the months of February and July for year 2008 in Helsinki, Finland. The data for February is used to model when a skylight with a maximal amount of thermal resistance is needed and the data for July is used to model when cooling is needed. The data was procured from the Finnish meteorological institute, and it is presented in Table 1.

Table 1. Average weather data for two months in 2008 for Helsinki Finland.

Unit	February	July
$T_{ambient}$ [°C]	0.73	17.62
T_{sky}[°C]	-7.51	3.67
v_{wind} [m/s]	4.13	3.20

Modeling natural convection induced by heat radiation is, however, somewhat tricky; an attempt to do this was made by the author in [6]. It has also been shown that the wavelength dependency is crucial for calculating radiative heat transfer in participating media [7].

The exponential wide-band method is used in this paper to calculate the gases absorptivity and emissivity, which are assumed to be equal [8]. The studied gas is chosen to be CO_2 which absorptivity is calculated to be, α=0.19, as an isothermal and a gray value (no wave length dependency). In future work the gas absorptivity will be treated as temperature and wavelength dependent variable.

3. Results

The results from the modeling are given in Table 2 where the total heat transfers from the room to the skylight are presented. This data is calculated by the Comsol model in W/m as the model is 2 dimensional. These results are in turn squared to get them into a more comfortable unit of W/m^2. These results are from the last time step of a 1000 second long dynamic simulation. The reason for solving this problem as a time dependent instead of a stationary problem is to avoid unstable equilibrium points. The time of 1000 seconds was assumed to be a time period long enough for the heat flows to stabilize. However, some of the simulations seem not to have stabilized.

Table 2 shows that a cooling capacity 98 W/m^2 can be obtained during the summer by this design, when comparing the cooling case with CO_2 to the insulating case with air. The table also shows that if the skylight is set in its insulating mode for the winter an unnecessary heat loss of 80 W/m^2 would be achieved. This same effect is also achieved if the skylight is filled with air. A reason to this could be that the simulations were not simulated for a long enough time.

Table 2. Average heat transfer for two months in 2008 for Helsinki, Finland.

[W/m^2]	Summer Cooling	Winter Insulating	Summer Insulating	Winter Cooling
CO_2	117	966	88	883
Air	15	983	19	655

Nonetheless, if the gas in the cooling skylight would be replaced with air instead of the greenhouse gas, CO_2 in this case, is it obvious that the cooling would drop by as much as 85%. The reason for this is that air does not absorb or emit heat radiation and cannot therefore be directly cooled down by the sky. If the winter insulating cases are then compared to each other is the skylight with the CO_2 at α=0.19 a somewhat better thermal insulator than the skylight containing air. The reason for this is that CO_2 is a better conductive insulator than air; however, CO_2 is a better transfer medium for convective heat than air and therefore works better in the cooling mode.

So for the skylight to work as attended is it important to choose the thickness of the skylight correctly. The skylight should be thin enough to prevent convective air movement to form when the skylight is in the insulating mode but thick enough that a convective heat flow can occur between the two compartments when the skylight is in its cooling mode. The thickness of 10 cm has shown to give good results and is therefore used in this study; the width of the skylight is 0.5 m. While then observing Fig.3-a to Fig. 4-b it becomes obvious that the figures presented are not in scale; these distortions allow the figures to be more easily understood without taking too much space.

3.1. Skylight filled with CO_2

3.1.1. Cooling mode

The goal in the cooling mode is to get the gas inside the skylight to move from the lower compartment to the upper one. This movement should in turn transfer heat from the room to the sky. When observing the simulation results in Fig. 3-a and Fig. 3-b one can observe that this flow is taking place. Additionally, the gas that is moving around in the skylight, as pictured in Fig. 3-a, is clearly cooled down by radiative heat exchange between the sky and the skylight. This is certain as the temperature of this gas flow is lower than that of both the temperature of the room and the temperature of the ambient.

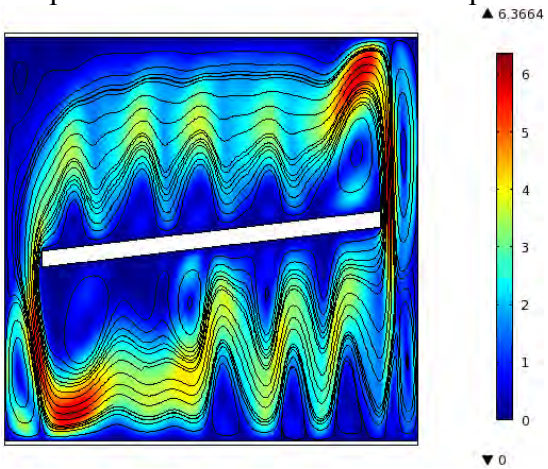

Fig. 3-a. Velocity profile in [cm/s] for cooling mode during summer[*]

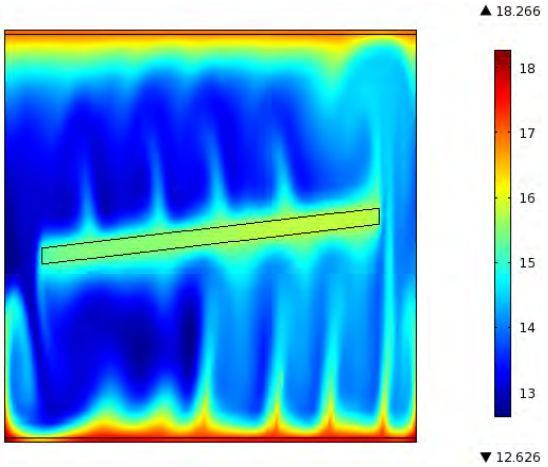

Fig. 3-b. Temperature profile in [°C] for cooling mode during summer[*]

3.1.2. Insulating mode

As mentioned above, for the insulating case to work optimally, the gas movement in the skylight should be kept to a minimum. This, however, is only partially achieved as clear Bérnard cells can be seen in the lower part of the skylight, with also some minor circles in the upper compartment. This suggests that more work could be done to find an optimal depth for the skylight. An interesting phenomenon can be seen in Fig. 4-b where the lowest temperature is achieved in the lower part of the upper compartment. This has to do w ith the high reflectivity of the middle glass window.

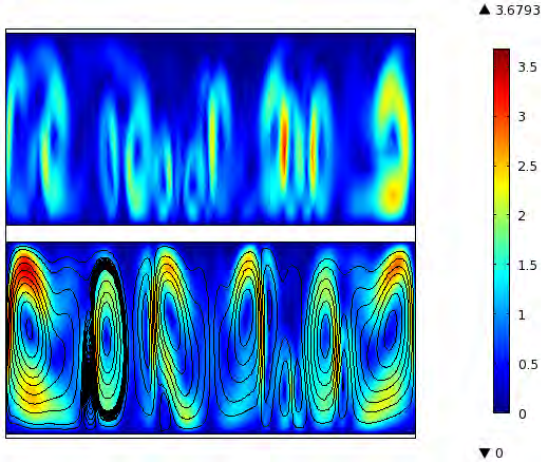

Fig. 4-a. Velocity profile in [cm/s] for insulating mode during winter[*]

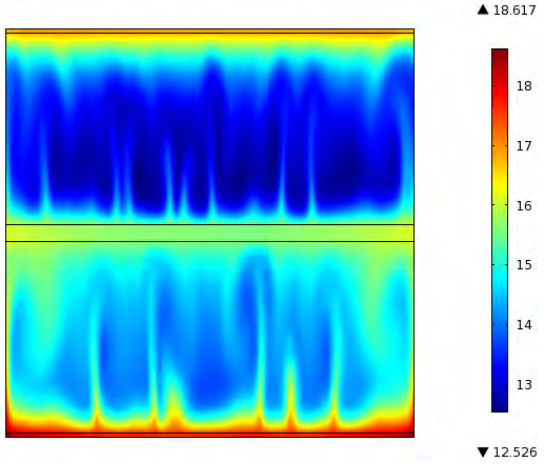

Fig. 4-b. Temperature profile in [°C] for insulating mode during winter[*]

[*] Note that the figures are not in scale.

3.2. Skylight filled with air

For comparison, the same analyses as presented in chapter 3.1, have also been made for a skylight filled with air.

3.2.1. Cooling mode

Even though the skylight is filled with air, a flow pattern is formed between the two compartments; this shown in Fig. 5-a. However, the flow velocities are somewhat slower in Fig. 5-a. than in Fig. 3-a. Furthermore, the temperature profile presented in Fig. 5-b shows that temperatures do not reach lower temperatures than that of the ambient and thus the air is not cooled by the sky.

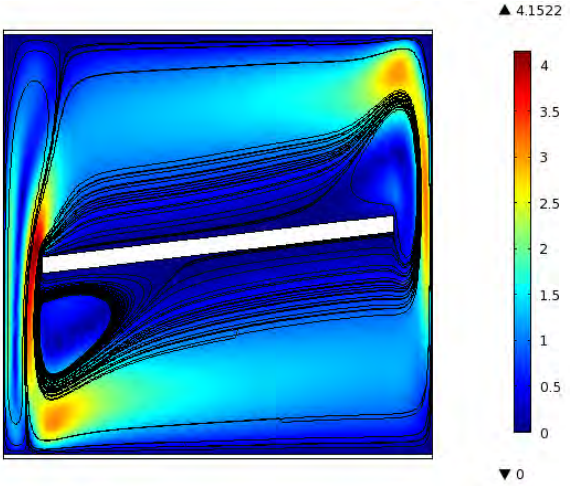

Fig. 5-a. Velocity profile in [cm/s] for cooling mode during summer†

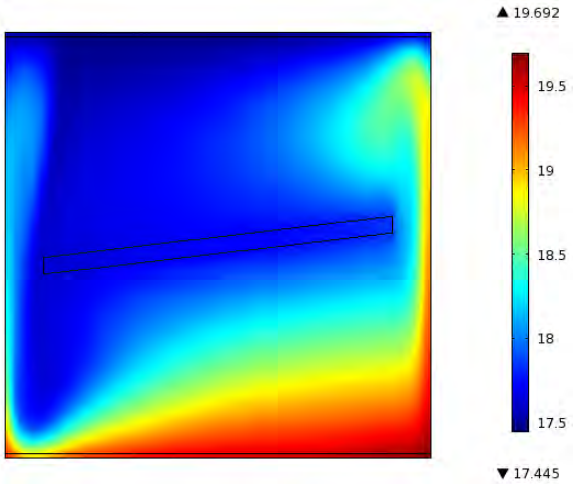

Fig. 5-b. Temperature profile in [°C] for cooling mode during summer†

3.2.2. Insulating mode

Interestingly the air filled skylight has the worst insulating properties. The main reason for this is the high air velocities that are presented in Fig. 6-a; another could one could be that the simulation time of 1000 seconds was too short. The temperature profile presented in Fig. 6-a reinforces that temperatures below the ambient are not achievable in a skylight filled with air.

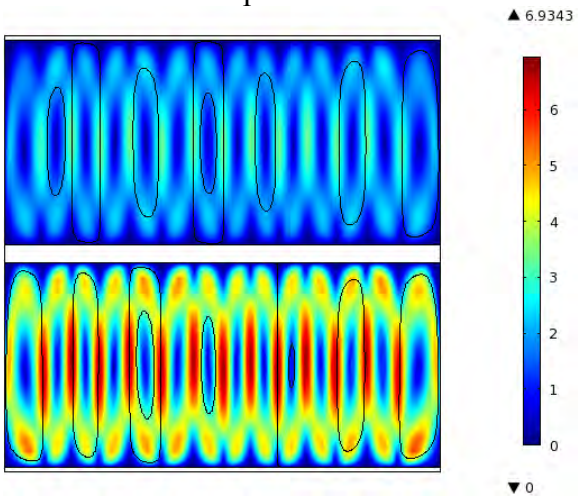

Fig. 6-a. Velocity profile in [cm/s] for insulating mode during winter†

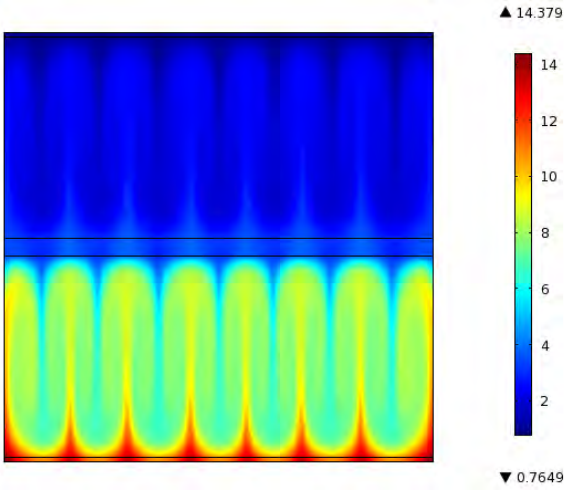

Fig. 6-b. Temperature profile in [°C] for insulating mode during winter†

† Note that the figures are not in scale.

4. Summary and Conclusions

This article presents an idea for using a regulated skylight to control heat flow in and out of a space located below. The concept was evaluated using a commercial multiphysics program Comsol.

This study shows that cooling effects of up to 100 W/m^2 are achievable under normal summertime conditions in southern Finland. However, improvements to the design could still be made and thus increase this cooling effect. These improvements would be a result from a careful analysis and optimization of the difference in heat transfer between the two skylight modes. Further improvements to the modeling would be to run Comsol parallel with Matlab so that wavelength dependency could be incorporated into the model, as it is an important factor for radiative heat exchange in participating media. The method chosen for calculating the wavelength dependency would be the exponential wide-band model.

If this system was successfully implemented, savings could be achieved by reducing the use of conventional cooling methods. Unfortunately, window materials that possess the necessary transmission properties typically have poor mechanical properties.

An experimental setup is being designed to assess the modeling results and to study different combinations of materials.

Acknowledgment

This work is funded by Maj and Tor Nessling Foundation projects 2009301, 2010362 and 2011285 “Solar heat engineering and carbon dioxide: energy recovery using a greenhouse gas”, and the Foundation for Åbo Akademi University.

References

[1] E. Erell, Y. Etzion, Radiative cooling of buildings with flat-plate solar collectors, Build. Environ. 35, 2000, pp. 297 – 305.

[2] M. Rubin, Calculating Heat Transfer Through Windows, Int. J. Energy Res. 6, 1982, pp. 341 – 349.

[3] T.S. Eriksson, C.G. Granqvist, J. Karlsson, Transparent thermal insulation with infrared-absorbing gases, Solar Energy Materials. 16, 1987, pp. 243 – 253.

[4] E.M. Lushiku, T.S. Eriksson, A. Hjortsberg, C.G. Granqvist, Radiative cooling to low temperatures with selectively infrared-emitting gases, Solar & Wind Technology. 1, 1984, pp. 115 – 121.

[5] C.G. Granqvist, Radiative cooling to low temperatures general considerations and applications to selectively emitting SiO films, J. Appl. Phys. 52, 1981, pp. 4205 – 4220.

[6] M. Fält, R. Zevenhoven, Radiative cooling in northern Europe using a roof window, Proc. of ES2010, Phoenix, AZ, May, 2010, paper 90192.

[7] G. Rey Colomer, Numerical methods for radiative heat transfer, 2006, pp. 1–161.

[8] R. Siegel, J.R. Howell, Thermal Radiation Heat Transfer, 3rd ed., Hemisphere Pub. Corp., Washington, D.C., 1992 pp. 562 – 567.

Development of a solar intermittent refrigeration system for ice production

G. Moreno-Quintanar, W. Rivera*, R. Best

Centro de Investigación en Energía, Universidad Nacional Autónoma de México
A.P.34, 62580 Temixco, Mor., México
** Corresponding author: Tel. +52 5556229740, E-mail address: wrgf@cie.unam.mx*

Abstract: A solar powered intermittent absorption refrigeration system has been developed at the Centro de Investigación en Energía of the Universidad Nacional Autónoma de México. The system was evaluated with the ammonia/lithium nitrate/water (NH3/LiNO3/H2O) mixture. The system was designed to produce up to 8 kg/day of ice. The system consists of a Compound Parabolic Concentrator (CPC) with a cylindrical receiver acting as the generator/absorber, a condenser, an evaporator and an expansion valve. The system operates exclusively with solar energy and no moving parts are required. Evaporator temperatures as low as - 11°C were obtained for a period of time up to 8 hours. Coefficients of performance as high as 0.098 were obtained. These coefficients were 24% higher than those obtained with the same system operating with the binary ammonia/lithium nitrate (NH3/LiNO3) mixture previously reported in the literature. The results showed that the developed system seems to be a good alternative for refrigeration in zones where electricity is not available.

Keywords: *solar cooling, absorption systems, ice production, ammonia/lithium nitrate/water.*

Nomenclature

A	concentrator aperture area ..... m^2	Q_R	heat received from solar radiation..... MJ
Cp	heat capacity ..... $J\ kg^{-1}\ K^{-1}$	T	temperature ..... K
COP_S	solar coefficient of performance …….....	t	time ..... s
G	solar radiation ..... $W\ m^{-2}$	ρ	density ..... $kg \cdot m^{-3}$
H	insolation ..... $MJ\ m^{-2}$	ν	specific volume ..... $m^3 \cdot kg^{-1}$
h_{fus}	heat of fusion of ice ..... $kJ\ kg^{-1}$	m	mass..... kg
Q_{EV}	cooling capacity ..... MJ		

1. Introduction

Solar refrigeration is a useful application in areas of the world with high insolation levels where there is a demand for cooling and there is not electricity to supply conventional power systems.

Although the basic concepts of solar refrigeration appeared since about five decades, to date there are only a limited number of developed systems reported in the open literature, some of the most important works are the following. Erhard et al. [1] reported the performance of a solar refrigeration system operating with $NH_3/SrCl_2$. The main part of the device is an absorber/desorber unit which is mounted inside a concentrating solar collector in which the heat of absorption is transported out of the solar collector by means of two horizontally working heat pipes. The overall efficiency defined as the cooling capacity to the solar radiation received by the solar collectors of the cooling system varied from 0.05 to 0.08. Wang et al. [2] published the results of a combined adsorption heating and cooling system which operated with activated carbon/methanol. The system was tested with electric heating and it was found that with 61 MJ heating it was able produce up to 9 kg ice were made. The calculated Coefficient of Performance (COP) which is defined as the cooling capacity to the heat supplied to the generator of the system

was 0.0591. Li et al. [3] published the experimental study on dynamic performance of a flat-plate solar solid-adsorption refrigeration for ice maker operating with activated carbon/methanol. The experimental results showed that this machine can produce 4–5 kg of ice after receiving 14–16 MJ of radiation energy with a surface area of 0.75 m^2, while producing 7–10 kg of ice after receiving 28–30 MJ of radiation energy with 1.5 m^2. Hildbrand et al. [4] reported the results of the performance of an adsorptive solar refrigerator built in Yverdon-les-Bains, Switzerland operating with the adsorption pair silicagel + water. Cylindrical tubes function as both the adsorber system and the solar collector. The condenser is air-cooled and the evaporator contains 40 l of water that can freeze. The results showed that the gross solar coefficient of performance defined by the authors varied between 0.1 and 0.25 with a mean value of 0.16. Khattab [5] presented the description an operation of a novel solar-powered adsorption refrigeration system operating with activated carbon/methanol. The system consisted of a modified glass tube having a generator (sorption bed) at one end and a combined evaporator and condenser at the other end and a simple arrangement of plane reflectors to heat the generator. The daily ice production was 6.9 and 9.4 kg/m^2 and the net solar COP was 0.136 and 0.159 for cold and hot climate respectively. Li et al. [6] developed a no valve, flat plate solar ice maker on the basis of previous research achievements. The system operated again with activated carbon/methanol. The authors reported that the no valve solar ice maker prototype was approached to practical application of mass production from view of cost and techniques. Rivera et al [7] published a paper about the development of a solar intermittent system operating with the ammonia/lithium nitrate mixture. The authors reported that solar coefficients of performance as high as 0.08 can be obtained whit the developed system

From the literature review it is clear that although has been relevant research on developing solar refrigeration systems the most of them have been focused in adsorption systems which have in general low coefficients of performance. Because of this in the present paper the system developed previously by Rivera [7] was evaluated but using now the ternary mixture ammonia/lithium nitrate/water with the purpose to increase the mixture conductivity and to decrease the mixture viscosity trying to increase the system efficiency. Physical and thermodynamic properties of the ternary mixture were taken from Libotean et al [8,9].

2. System description

The system was designed to operate with the ammonia/lithium nitrate/water mixture for a maximum capacity of 8 kg of ice/day. It consists of a compound parabolic collector CPC with a cylindrical receiver acting as the generator/absorber, a condenser, a storage tank, an expansion valve, a capillary tube, an evaporator and a (see Fig. 1). The system operates exclusively with solar energy and no moving parts are required.

During the day, the ammonia/lithium nitrate/water mixture in the generator-absorber is heated by the solar radiation incident on the CPC until it reaches the saturation temperature. Then the ammonia is partially evaporated from the solution. Due to the increase of the temperature and consequently of the pressure of the solution in the cylindrical receiver of the CPC, the ammonia vapor goes to the condenser, where it is condensed by water and then it is stored in the tank. In the night, the temperature and pressure in the generator-absorber decreases because of the decreases of the ambient temperature and the ammonia liquid passes through the expansion valve (which is opened manually) decreasing its pressure and temperature, producing the refrigerant

effect in the evaporator. After the ammonia has absorbed heat from the water stored in the trays inside the evaporator, the pressure in this component increases. In this way, the pressures are inverted in the components in natural way, and the ammonia vapor returns to the generator-absorber where it is absorbed by the strong solution. About 7 o´clock in the morning, after the ice has been produced and the ammonia has been absorbed by the solution stayed in the cylindrical receiver of the CPC, the expansion valve is closed and the ice removed from the trays leaving the system ready for a new cycle.

The CPC is made out of an aluminum sheet with a reflectance of 0.85. The cylindrical receptor is covered with a selective black paint with a range of emittance from 0.25 to 0.49 and absorptance from 0.88 to 0.94; it resists temperatures higher than 300°C. The CPC's concentration ratio is 3.3, with a half-angle of 11.54° and an aperture area of 2.54 m^2. The condenser is a heat exchanger composed of a helicoidal aluminum coil, immersed in a water store. The water inside of the condenser is continuously recirculated by a pump that is connected to a cooling system. It is important to mention that the pump is used just in order to keep the condenser temperature fixed eliminating the system variability with regard to the ambient temperature, however, this pump it is not necessary in normal operating conditions. Furthermore the cooling system and the pump are used exclusively to control the temperature of cooling water for experimental purposes. The cylindrical storage tank has a capacity of 8.5 L; a tube to measure the level is connected to the tank. Leaving the tank, there are two expansion devices: the capillary tube and the needle valve. Only one of these expansion devices is used during the evaporation process. The capillary tube is recommended because it permits the automation of the evaporation process. The evaporator is a heat exchanger that consists of a coil inside an insulated metal container with a front door, in which the ice is produced. The coil is horizontally distributed along five levels, each one bearing an aluminum tray. Water to be frozen is contained in these trays. Fig. 2 shows a photograph of the developed system.

In order to evaluate the system, 14 thermistors, 7 wall thermocouples, 5 pressure transducers, 2 manometers, 1 level tube (placed in the storage tank) and 1 pyranometer were used (see Fig. 1).

3. Evaluation parameters

Five main parameters were used in order to evaluate the experimental system: (i) the amount of the ammonia produced in the generator, (ii) the insolation, (iii) the solar energy received by the CPC, (iv) the cooling capacity and (v) the solar coefficient of performance.

The amount of the ammonia produced in the generator can be obtained as:

$$m_{NH_3} = \rho v_{NH_3} \quad (1)$$

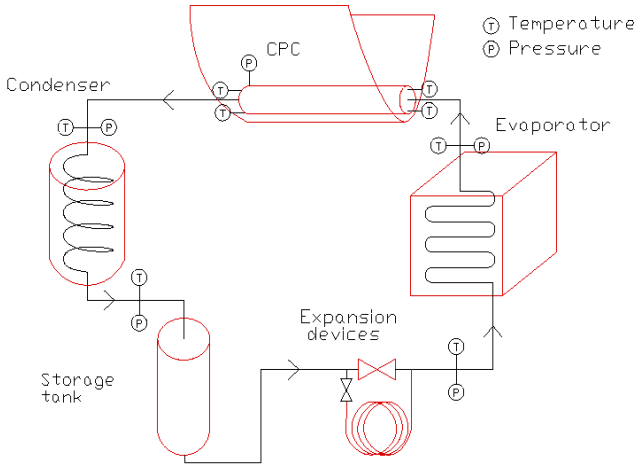

Fig. 1. Schematic diagram of the solar intermittent absorption refrigeration system.

Fig. 2. Photograph of the solar intermittent absorption refrigeration system developed.

The energy received from the solar radiation is calculated as the sum of the contributions of the product of the irradiation, the time and the aperture area.

$$Q_R = \sum_{i=1}^{n} G_i t A \tag{3}$$

The cooling capacity is the sum of the sensible heat to reduce the water temperature from ambient to 0°C plus the heat of fusion of ice

$$Q_{EV} = m_{H_2O}\,(h_{fus} + C_p \Delta T) \quad (4)$$

Finally, the solar coefficient of performance is defined as the cooling capacity in the evaporator to the energy received from the solar radiation.

$$COP_S = \frac{Q_{EV}}{Q_R} \quad (5)$$

4. Results

In order to experimentally evaluate the solar refrigeration system operating the two mixtures, more than 40 tests runs were carried out mainly during summer time, however, only 18 were taken in the analysis since in the others the solar radiation was considerably low (lower than 14MJ) because of long cloudy skies periods (normally higher than 2 hours).

During the experimental test runs, the main evaluating parameters such: temperatures, solar radiation and pressures were logged every 15 seconds.

Fig. 3 shows the maximum pressure reached in the cylindrical receiver against the maximum solution temperature reached during the generation stage. It can be observed that the pressure increases slightly win the increment of the solution temperature. The solution temperatures varied from 87°C to 112°C, meanwhile the pressures varied from 13 bar to 16.1 bar.

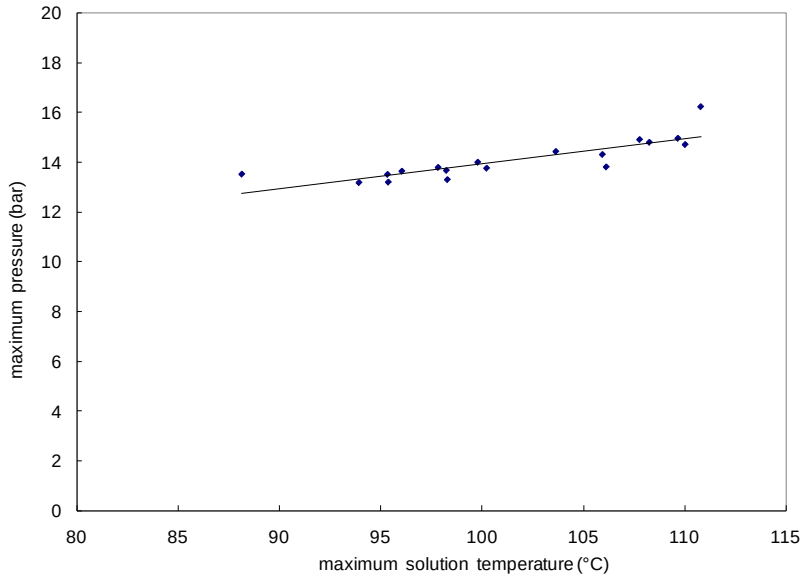

Fig. 3. Maximum pressure against maximum solution temperature for the solar system.

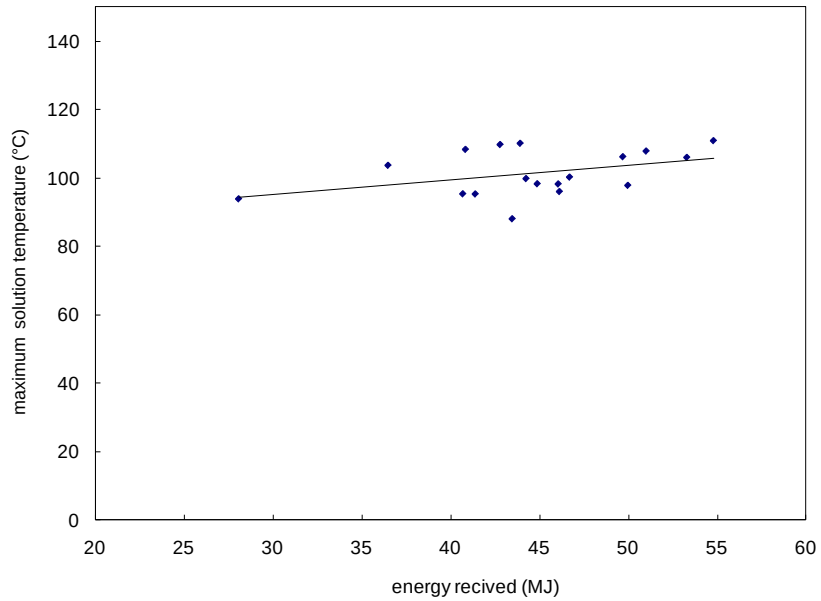

Fig. 4. Maximum solution temperature against the energy received by the CPC.

Fig. 4 shows the maximum temperature reached by the solution during the generation stage as function of the energy received by the CPC during the sunshine hours. In this figure it can be seen that there is a considerable data dispersion between these two parameters, however, it can be observed as it was expected that the solution temperature increases with the energy received by the CPC. It can be observed that the energy received by the CPC varied considerably from about 27 MJ to 56 MJ which is almost two times the minimum value. The high difference that exist among the energy received values is related with the cloudy of each day, since the solar radiation was almost the same since the most of the values (16 of the total) were obtained during the same season (summer).

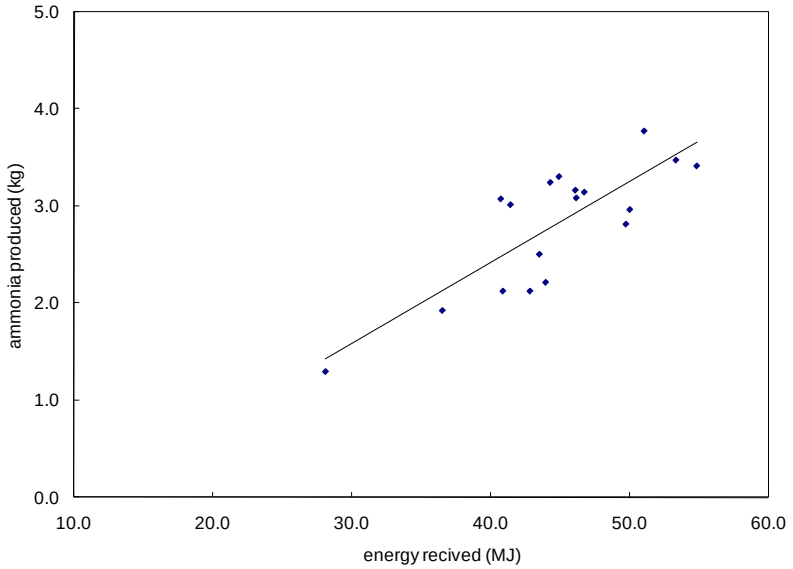

Fig. 5. Ammonia produced during the generation stage against the energy received.

In Fig. 5 it can be seen that the amount of ammonia produced (measured after the sunshine hours in the level tube placed in the condensate tank) increases considerably with the increase of the energy received by the CPC. The amount of ammonia produced varied from 1.3 kg at an energy received of 28.2 MJ to 3.8 kg at an energy received of 50 MJ. From this figure and from the explained in Fig. 4 that the amount of refrigerant produced (ammonia) is very dependent of the solar radiation received by the CPC.

In Fig. 6 it can be seen the solar coefficient of performance against the cooling capacity. It can be observed that the solar coefficient of performance increases considerably with and increases of the cooling capacity. The solar coefficient of performance varied from 0.06 at a cooling capacity of 1.7 MJ to a 0.098 at a cooling capacity of 4 MJ.

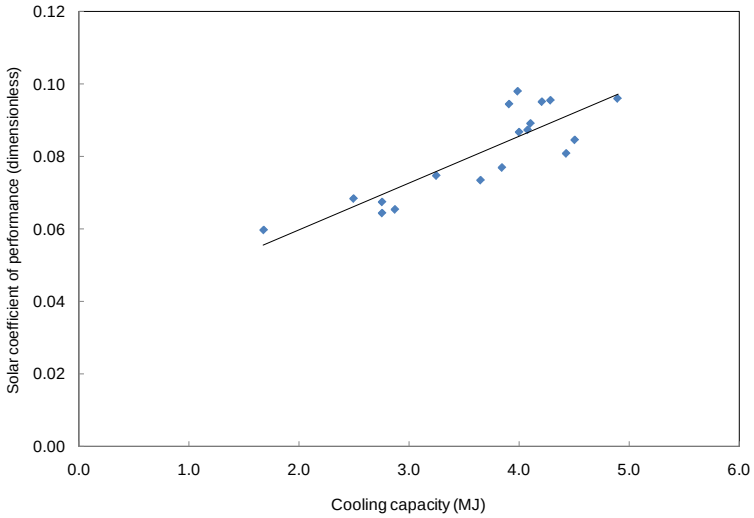

Fig. 6. Solar coefficient of performance against cooling capacity.

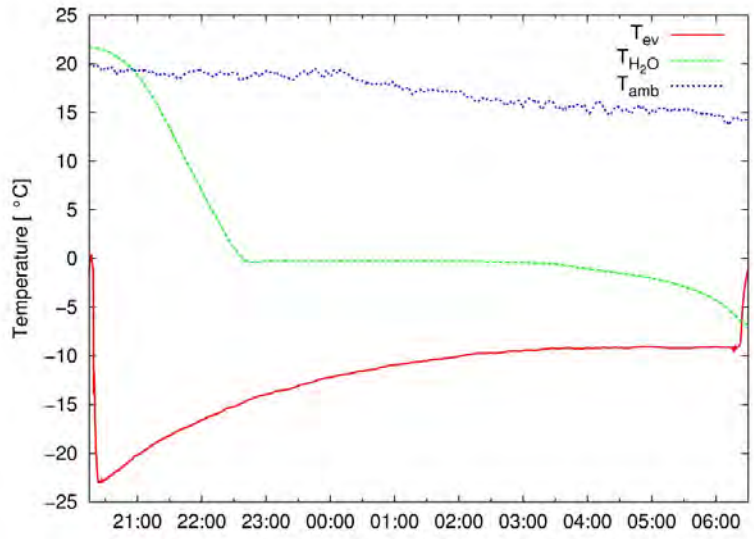

Fig. 7. Evaporator, water and ambient temperatures against time.

In Figure 7 it can be seen that the evaporator temperature was lower than -11°C for a period

higher than 8 hours. Also it can be seen how the water temperature decreases from the ambient temperature to 0°C and remains constant while the ice is been produced.

5. Conclusions

A solar intermittent refrigeration system for ice production has been evaluated with the ammonia/lithium nitrate/water mixtures at the Centro de Investigación en Energía of the UNAM. Evaporator temperatures as low as - 11°C were obtained for a period of time up to 8 hours. The solar coefficient of performance reached values up to 0.098, which is 24% higher than the maximum obtained previously by Rivera [7] operating the system with the ammonia/lithium nitrate mixture.

Acknowledgments

The authors would like to thank to PAPIIT-UNAM project number IN110706-2 to sponsor the present research and to Dr. Victor Hugo Gómez Espinoza for his invaluable help.

References

[1] A. Erhard, K. Spindler, T. Hahne, Test and simulation of a solar powered solid sorption cooling machine, Int. J. Refrigeration 21(2), 1998, pp. 133-141.

[2] R. Z. Wang, Y. X. Xu, J. Y. Wu, M. Li, H. B. Shou, Research on a combined adsorption heating and cooling system, Applied Thermal Engineering 22, 2002, pp. 603–617.

[3] M. Li, R. Z. Wang, Y. X. Xu, J. Y. Wu, A.O. Dieng, Experimental study on dynamic performance analysis of a flat-plate solar solid-adsorption refrigeration for ice maker, Renewable Energy 27, 2002, pp. 211–221.

[4] C.Hildbrand, P Dind, M. Pons, F. Buchter, A new solar powered adsorption refrigerator with high performance. Solar Energy 77, 2004, pp. 311–318.

[5] N. M. Khattab, A novel solar-powered adsorption refrigeration module, Applied Thermal Engineering 24, 2004, pp. 2747–2760.

[6] M. Li, C. J. Sun, R. Z Wang, W. D Cai, Development of no valve solar ice maker, Applied Thermal Engineering 2004;24:865–872.

[7] W. Rivera, G. Moreno-Quintanar, C. O Rivera, R. Best, F. Martínez, Evaluation of a solar intermittent refrigeration system for ice production operating with ammonia/lithium nitrate, Solar Energy 85(1), 2011, pp. 38-45.

[8] S. Libotean, D. Salavera, M. Valles, J. Esteve, A. Coronas, Vapor-liquid equilibrium of ammonia+lithium nitrate+water and ammonia+lithium nitrate solution from (293.15 to 353.15) K, Journal Chemical and Engineering Data 52, 2007, pp. 1050–1055.

[9] S. Libotean, D. Salavera, M. Valles, J. Esteve, A. Coronas, Densities, viscosities, and heat capacities of ammonia + lithium nitrate and ammonia + lithium nitrate + water solutions between (293.15 to 353.15) K, Journal Chemical and Engineering Data 53, 2008, pp. 2383–2393.

Development of Model Solar Kitchen with Green Energy for Demonstration and Application in Rural Areas

Sanjib Kumar Rout

C.V. Raman College of Engineering, Bidyanagar, Mahura, Janla, Bhubaneswar-752054, India
**Telephone: 91-674 2460043/2460093, FAX- 91-674246009, Email-sanjibrout.1@gmail.com*

Abstract: The paper demonstrates how effectively hoteliers and corporate can architect and utilize both solar thermal and green gas energy for the production of zero carbon foot print food products. It involves the usage of shefflers, solar parabolic reflectors, solar ovens, solar cookers, solar dryers, solar water heaters, biomass gasifiers, biogas plant, etc which have been suitably designed and placed architecturally in the green kitchen premises to harvest maximum solar thermal green energy for effective production of low and zero carbon foot print food products with minimal loss of nutritional value. Further, the digested slurry of biogas plant is used as humus rich fertilizer for spice garden spread around the green kitchen to beautify the ambient. Replacement of conventional energy partially by green and thermal energy reduces the energy cost substantially. It not only cuts down the cost of fuel but also maintains a clean environment in canteen area and its surroundings in addition to providing nutritious food. The methods developed in this project may also be implemented in vast rural mass and community centre for cost effective and hygienic food production.

Keywords*: Fossil fuel, Carbon foot print, Green canteen, Solar energy, Biomass energy*

1. Introduction:

Today, India is growing with an average GDP growth of 8.9% per annum, which signifies the tremendous growth of its economy. Massive investment are being laid out by the Government and private sectors for the development of small and large manufacturing software industries and in service sectors like education, healthcare, hotels and real estates. These are being constructed throughout the country and environment becomes a concern everywhere. Our Government is enforcing norms to ensure that all these projects remain as much greener as possible. In any corporate offices, hotels, schools and colleges, quantity kitchen is mandatory to support their employees, students and customers so that they can avail nutritional food [1]. A survey has been conducted with some hotels and schools located in the rural part of Odisha State of our Country about the greenery of their kitchen and about their waste disposal. Today most of these industries, corporate offices, hotels and motels are very much aware of the energy saving equipment but have least ideas to make their environment green by applying the cheapest and easiest methods of non-conventional energy [2]. We tried to collect the feedback to understand their knowledge about energy saving devices, carbon emission, carbon footprint products and application of non-conventional energy for quantity kitchen.

It is a matter of concern of rural hotels and schools where food is prepared for more than 500 people per day with all conventional fuel and equipment. Our survey found most of these organizations trying to project their awareness by using energy efficient electrical and ceramic appliances, low-cost wood and coal steamers and also by disposing the food waste in isolated places without making the assessment how much damage is made to the environment [3].

The aim of this project is to develop a model green kitchen to demonstrate an effective and cheaper prototype which shall

1. Reduce carbon dioxide emission to a substantial level by the application of solar thermal reflectors, ovens and driers [4].
2. Establish a convenient waste management system and through it produce methane in order to utilize it in the kitchen [5] and to generate bio-fertilizer for its easy utilization in the spice garden.
3. Produce zero carbon footprint food products with higher nutritional value.
4. Reduce the total operational cost by at least 40% of the conventional one.

2. Materials and Methodology

2.1. Materials for green kitchen and its layout

A green kitchen attached to a 500 person capacity quantity kitchen was established at C.V. Raman College of Engineering, Bhubaneswar, India as per the layout shown in Fig. 1.

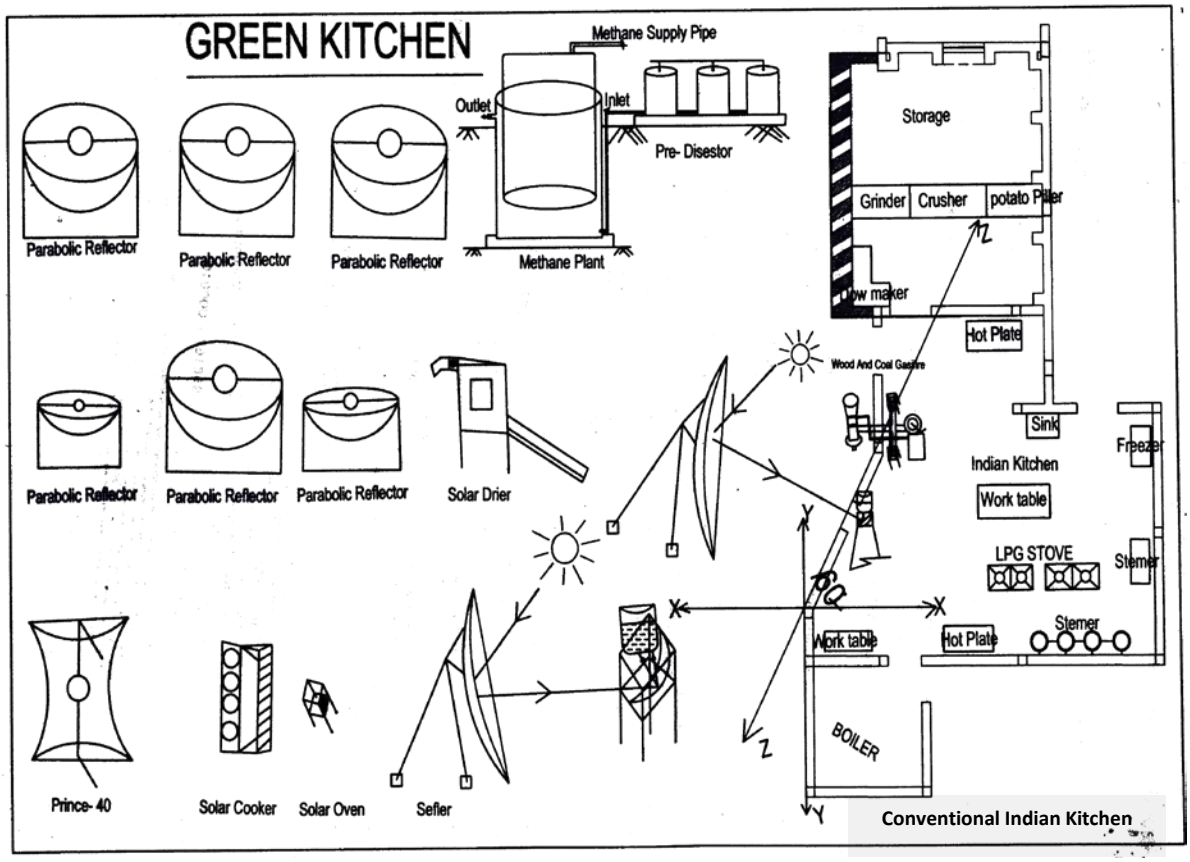

Fig. 1 Layout of green kitchen

Devices like solar reflectors of parabolic type, Schefflers, solar dyers, solar oven [6], solar water heaters, biomass gasifier and a food waste digester methane plant were installed. All these equipments have been installed by taking the following points into consideration:

1. The conventional kitchen wall facing the Scheffler was in east-west direction
2. Sheffler foundation was done taking latitudinal angle into consideration[7]
3. Thermal reflectors were located where maximum sun-light is available [8]
4. Schefflers fixed focus concentrator
5. Methane plant was installed near the conventional kitchen wall with less sun-light

From the survey conducted, it was realized that the small, medium and large hotels and motels of the locality had expressed serious concern regarding the effective utilization of solar thermal equipments in quantity food preparation and found that the food waste disposal outside the kitchen boundary as the most easiest and cheapest way. By way of this disposal, they were ignorant about the emission of methane gas to the atmosphere which has more than 20 time green house effect than that of carbon dioxide gas. They were also very much doubtful to accept the concept of the reduction fuel consumption by the food waste.

The layout of solar and green energy devices as shown Fig. 1 was designed for the demonstration to hoteliers and corporate to observe as well as analysed how the green kitchen effective and convenient for the reduction of cost of food production. This project had taken all the observations and experiments considering 78,000 Lux intensity of sun light as a reference during the month of August to December, the winter season. In a sunny day of the period green kitchen was able to cook grains, vegetables, meats and produce hot water continuously for more than six hours in a day from 9 hour morning to 15 hour evening. During summer the Lux intensity of sun light might rise for the locality as per temperature weather relationship curve, shown in Fig. 2 [7].

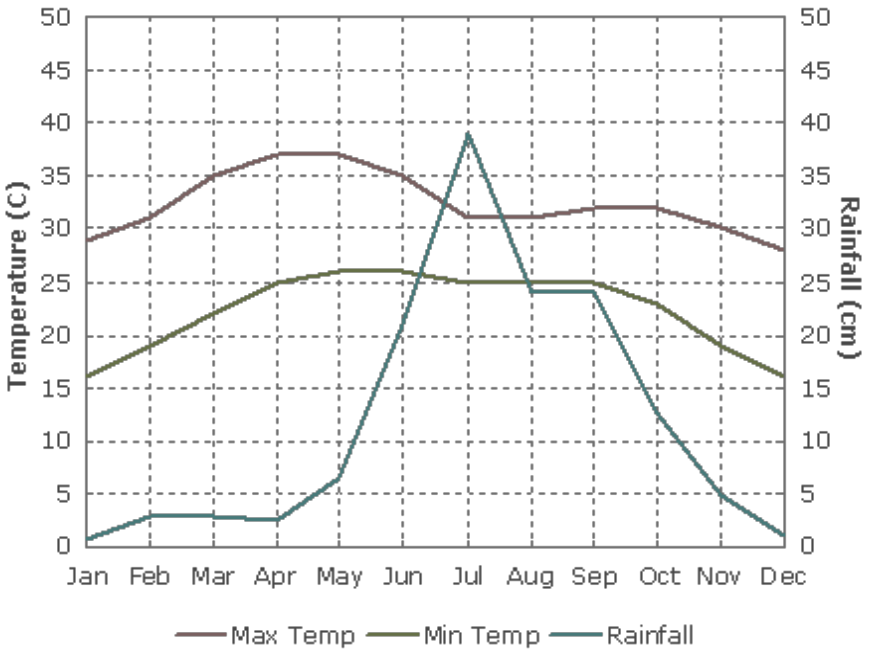

Fig. 2 Relationship of atmospheric temperature, average rain fall vs season

2.2. Methods adopted for the installation of green energy devices

The details of green energy devices are presented in Fig. 3 along with specification and cost.

Sl. No.	Name of equipment	Photograph	Cost of the equipment (in Indian Rupees)
01	Scheffler – 1		80,000
02	Scheffler – 2		1,20,000
03	Parabolic reflector-1		37,000
04	Parabolic reflector-2		32,000
05	Solar drier		10,000
06	Solar oven		3,000
07	Solar water heater	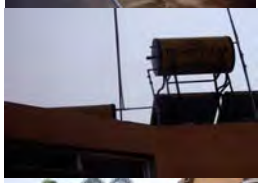	1,00,000
08	Methane plant		5,00,000
09	Biomass gassifier		10,000
			8,92,000

Fig. 3 The detailed specification and cost of green energy devices

2.3. Theoretical background for the installation of Scheffler

The installation of Scheffler-1 disc above the ground was taken as 5.2 m and the distance of the receiver from the disc centre as 3.8 m while the height of the receiver above the ground was evaluated using the equation 1.

$$Y = B-\{X*\sin(A)\} \quad \text{-------} \quad (1)$$

where, Y = height of the receiver, B = height of the disc above the ground, X = distance of receiver from disc centre and, A = latitudinal angle at any place
In order to keep the focal line constant, orientation of scheffler was adjusted with a programmable motor fitted device as per the movement of the solar rays on earth.

2.4. Basic principles of the installation of other solar devices

2.4.1. Parabolic Reflector

Both parabolic reflectors shown in Fig. 3 (Sl. No. 1 & 2 - Schefflers) and (Sl. No. 3 & 4 – Prince-40) [9] were installed to receive full sun rays and get concentrated on fixed focal centre through reflection where the cooker was placed with blacken surface to absorb maximum thermal energy. Here also the orientation of reflectors were adjusted with a programmable motor fitted device as per the movement sun rays

2.4.2. Solar dryer

The solar dryer was designed on the principle of green house glass where high frequency solar radiation got absorbed through inclined glass surface by the food materials but longer wavelength radiations reflected out. Moisture content was continuously ventilated. The inclination angle was experimentally evaluated to receive maximum temperature.

2.5. Methane Plant

The cellulosic materials comprising both vegetable waste and food waste of the canteen are predigested aerobically. The digested slurry with high biological oxygen was an aerobically digested to methane rich biogas which was purified by the separation of carbon dioxide gas. The high calorific methane rich gas was found to produce $0.6x10^{-3}$ m^3 of methane gas per kg of cellulosic waste on dry basis. The digested effluent was found to be rich in P_2O_5 with small quantity of K_2O and Nitrogen ingredients to act as ideal fertilizer for spice garden making the hotel environment greener, beautiful and profitable.

2.6. Biomass gasifier

Waste dry biomass collected by locals was fired in the special designed oven and thermal energy was fire through exhaust fan drive in a special designed energy efficient oven to utilize its maximum thermal energy by the cooking vessel.

3. Results and Discussion

3.1. Cost analysis of equipments

The cost of all equipments utilized in the project with respect to the cost in Indian market are worked out and compared with the conventional devices adopted by hoteliers, etc. on the basis of preparing food for 500 consumers as given in Table 1.

Table 1: Equipments used in a conventional kitchen to prepare food for 500 persons

Sl. No.	**Name of the equipment**
01	Cooking Range 4 Burner (LPG)
02	Cooking range High Pressure
03	Convection oven
04	Griddle
05	Stock Pot Burner
06	Deep fat fryer (2 Comp.) 5 Ltr.
07	Potato Peeler Heavy Duty
08	Dough mixer
09	Steamer compartment with boiler
10	Tandoor (Gas/coal)
11	Thawing tub
12	Vegetable slicer
13	Chapatti Puffer cum holplate
14	Aluminium steamer idli
15	Deep freezer
16	Vegetable steamer big
17	Hot dog roller

The conventional Indian quantity kitchen cost is around Rs. 25 Lakhs. This is three times the cost of the green kitchen. Making a simple comparison of the total cost of a green kitchen and a quantity kitchen we have found that the former is 30% less.

3.2. Cost saving analysis

In this exercise, we have tried to calculate the savings of fossil fuel per day by utilizing all these green equipments for preparing the following items:
a. Preparation of rice, b. Preparation of vegetables, c. Preparation of meat, d. Preparation of grains. In this total exercise (Table 2), it is calculated in a sunny day by utilizing this green kitchen. Fig. 2 shows the atmospheric temperature and rain fall profile in a year at the surveyed place.

Table 2: Saving of fossil fuel, its cost and environmental benefits by the implementation of solar thermal devices and methane gas plant for 500 people per meal

Sl. no.	Recipe	Quantity		Ambience of light (Lux)	Total time taken (Min.)	Quantity of savings of		
		Ingredient	Water (Lit.)			Fossil fuel(kg)	CO_2 (kg)	Cost (Rs.)
01	Cooked rice	Raw rice (60 kg)	144	78,000	72	9.6	29	288
02	Vegetables	Vegetables (75 kg)	60	78,000	69	12	36	360
03	Grains	Dal (25 kg)	90	78,000	108	6.75	18	180
04	Meat	Chicken (70 kg)	252	78,000	108	16.8	50	504

To prepare two meals in a day for 500 people the employed boiler consumes about 40 kg fire woods. On the other hand, upon employing gasifier it reduces 50 % of fire wood (20 kg) consumption in addition to 20 kg equivalent of CO_2 emission.
Approximately 120 kg of food waste is produced daily from the canteen emitting CH_4 and CO_2 as green house gases to the environment. Methane (CH_4) has 21 times stronger green house effect than CO_2. By generating bio gas out of this food wastes and considering all losses into account about 4 lakhs Indian rupees is saved in compensation to LPG consumption.

3.3. Application in spice garden

In most of the hotels, motels and corporate we have seen they spent a substantial amount of money in manure to keep their garden attractive and flowering. In our project we have introduced a concept of organic spice garden which we have demonstrated by doing a beautiful green landscape and planting 63 varieties of spices in the garden as an alternative to traditional rock and flower garden. In this food waste plant which we have installed that contains digested effluent which is being utilized in this spice garden to grow healthy and produce organic spices which can be reutilize in kitchen by using all the food wastes in the system.

We are yet to calculate the total value of spices generated in 1.5 acres of land in one year which can be worked out in the next year.

3.4. Theoretical background for architect

Green kitchen can be installed very conveniently at low installation cost if it is planned during the construction of the project. Architect should have fundamental knowledge about the geographical location of the place for installation of thermal reflectors because they can adjust the floor level of the kitchen to an operational height which cannot be done with an established kitchen. We have given an example of 4 places and shown a calculation as per equation (1) conveying the idea of geographical location of the place is important to install the thermal reflectros as shown in Fig. 4.

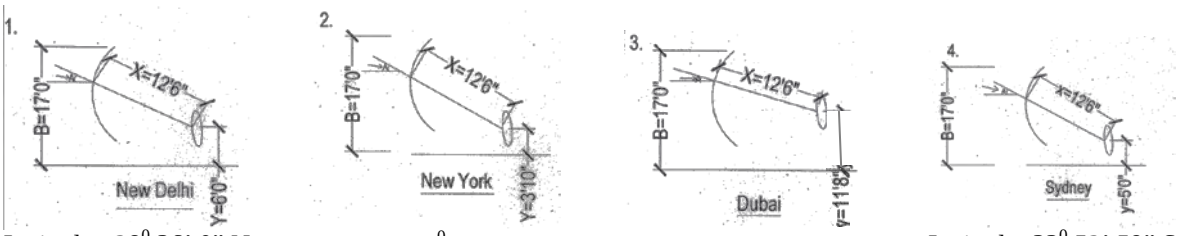

Latitude - 28^0 36’ 0” N
Y = 6.017’ or 6’0”

Latitude -40^0 42’ 51” N
Y = 3.847’ or 3’10”

Latitude -25^0 15’ 8” N
Y = 11.668’ or 11’8”

Latitude -33^0 52’ 59” S
Y = 5.089’ or 5’0”

Fig. 4: Diagram showing the angle of incidence of solar ray on Scheffler and its height from the ground at different location

This study shows if the architect is aware of these factors then will keep in mind so that the reflector can be installed at a convenient height for operation. Apart from reflector the architecture should workout for disposal of waste from methane plant in such a way that it will not have any negative impact on the environment and kitchen surroundings, so that the waste can be easily pumped to the green kitchen site.

4. Conclusion

The C.V. Raman College of Engineering, Bhubaneswar, India has successfully installed a composite 500 students green kitchen project for demonstration to hoteliers, corporate that how effectively to produce low and zero carbon foot print food products and also to incorporate this concept during design stage. On total in a year (operation of 6 months) using this green kitchen, around 4.8 lakh Indian rupees is saved than the conventional method of cooking along with a reduction of about 48,000 kg of green house gas emission to the environment. 50 % utilization of green kitchen in an annum, it has been evaluated that the total investment is fully recovered in a year in addition to providing tremendous safety to the environment. The methods developed in this project may also be demonstrated to vast rural mass and community centre for cost effective and hygienic food production.

References

[1] Blaine P. Friedlander Jr. Sweden, Researchers at school of Medicine, New York, Dr Vlassara, National Academy of Sciences, Proceedings from World Conference of Advances in Solar Cooking & The Times of India (14th Nov. 2002)

[2] Suhatme S.P., Solar energy principles of thermal collection and storage, New Delhi: Tata McGraw-Hill; 1996

[3] Parkin G.F., Own W.F., Fundamentals of anaerobic digestion of waste water sludge, J. Environ. Eng.-ASCE 112, 1986, pp. 867-920

[4] Alexopoulos, S., Hoffschmidt, B Solar tower power plant in Germany and future perspectives of the development of the technology in Greece and Cyprus, Renewable Energy 35, 2010, pp. 1352-1356

[5] Standard methods for the examination of water and wastewater. 19th ed. Washington, DC: APHA-AWWA-WEF; 1995

[6] Mullick S.C., Kandpal T.C. and Subhod Kumar, Thermal test procedure for paraboloid concentrator solar cooker, Solar Energy 46, 1991, pp. 139-144

[7] Chung T.M., A study of luminous efficacy of daylight in Hong Kong, Energy Buildings 19, 1992, 45

[8] Temps R.C., Coulson KL. Solar radiation incident upon slopes of different orientations, Sol Energy 19, 1977, pp. 179-84

[9] Ajay Chandak: Paraboloidal Solar Concentrator with Square / Rectangular Sections: Patent Application no. 581/MUM/2008 with Indian Patent Office.

Volume 15

Wind Energy Applications

Wind energy resources of the South Baltic Sea

Charlotte Hasager[1,*], Jake Badger[1], Ferhat Bingöl[1], Niels-Erik Clausen[1], Andrea Hahmann[1], Ioanna Karagali[1], Merete Badger[1] Alfredo Peña[1]

[1] *Risø National Laboratory for Sustainable Energy, DTU, Roskilde, Denmark*
** Corresponding author. Tel: +45 46775014, Fax: +45 46775970, E-mail: cbha@risoe.dtu.dk*

Abstract: The wind resources of the South Baltic Sea in the area between latitude 54 and 58 degrees North and longitude 10 to 22 degrees East are quantified from state-of-the-art methods using a combination of long-term and short-term mesoscale modeling output and satellite-based methods. The long-term overall statistics based on the NCEP/NCAR re-analysis dataset will be used in combination with more than one year of real time simulations using the Weather Research and Forecasting (WRF) mesoscale model operated at Risø DTU. The satellite Synthetic Aperture Radar (SAR) ocean wind maps and scatterometer ocean wind maps from QuikSCAT will be used to evaluate the wind resource calculation. The advantage of including SAR wind maps for evaluation is the finer spatial detail. In some regions, the mesoscale model may not fully resolve the wind-producing atmospheric structures. The satellites, however, only provides information at 10 m above sea level, whereas the mesoscale model provide results at several heights.

Keywords: *Offshore wind, mesoscale model, satellite data*

1. Introduction

The wind energy resources in the South Baltic Sea are not known in much detail despite the fact that several wind farms are being planned at sea. The existing wind farms are located typically less than 10 km offshore whereas most new wind farms are planned further offshore, up to 80 km. There are plans to construct more than 12GW installed wind farm capacity in the South Baltic Sea. The countries Denmark, Sweden and Germany already have installed offshore wind farms whereas Poland, Russia (Kaliningrad), and the Baltic countries have plans to do so. The web-site http://www.4coffshore.com/windfarms/ provides a listing and map of existing and planned offshore wind farms. It is important to know the wind climate in the planning phase of wind farms, as the expected annual energy production will be proportional to the expected financial benefit of the investment.

The European Wind Atlas[1] covers land areas http://www.windatlas.dk/Europe/Index.htm whereas the corresponding offshore atlas http://www.windatlas.dk/Europe/oceanmap.html covers sea. It is seen that the Baltic Sea is not fully covered. Furthermore, information gained since year 1999, in particular, from satellite Earth observation and from atmospheric mesoscale modeling jointly provides a new opportunity to map the wind resource with higher spatial detail.

The main objective is to provide a new wind atlas for the South Baltic Sea using available satellite images and mesoscale modeling. The results will be evaluated to meteorological data.

The satellite Earth observations used in the South Baltic wind atlas include scatterometer wind vectors from the SeaWinds instrument on-board the QuikSCAT satellite collected from 1999 to 2009 by NASA, and Synthetic Aperture Radar (SAR) data from the Advanced SAR (ASAR) on-board the satellite Envisat collected from 2002 to present by the European Space Agency (ESA).

In the South Baltic Sea a new approach to the numerical wind atlas method[2] based on mesoscale modeling is used. The mesoscale model used for the South Baltic is the Weather

Research and Forecasting (WRF) mesoscale model developed jointly by several US agencies. Additional refinement of the results will be with the microscale model Wind Atlas Analysis and Applications Program (WAsP)[3] developed at Risø DTU. The Weibull distribution scale (A) and shape (k) parameters and energy density are some of the outputs, see[1].

The results from satellite and mesoscale modeling are compared, as well as comparison to meteorological masts. The project is on-going. It is approximately mid-term in regard to finalizing the wind atlas, thus the proceedings paper presents work in progress. The investigated area is shown in Fig. 1. The project is related to the South Baltic Offshore Wind Energy Regions (OFF.E.R.) project with partners from Sweden, Germany, Poland, Lithuania and Denmark. The area and team is indicated in Fig. 1.

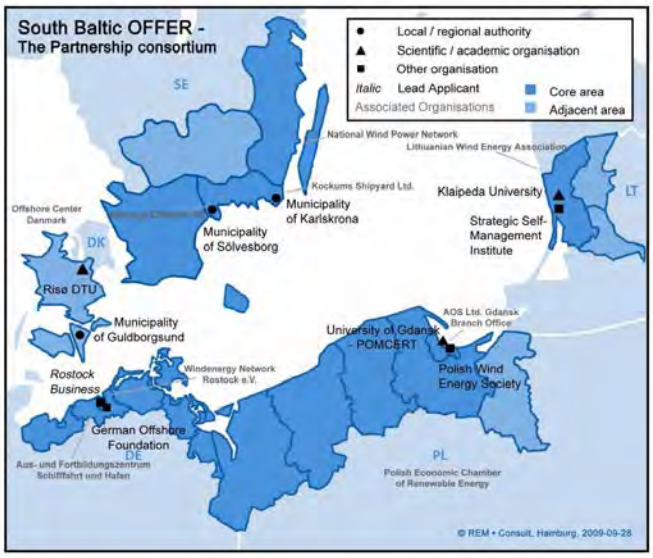

Fig. 1. South Baltic Sea highlighting regions and partners in the South Baltic OFF.E.R. project.

2. Methodology

2.1. Wind profile, meso- and microscale modeling, and satellite remote sensing

The use of satellite remote sensing is motivated by the fact that only satellites provide spatial observations of ocean winds. Meteorological masts observe winds in the local area in which they are located. Meteorological masts are costly to operate. In some cases access to data is restricted. Thus available offshore meteorological mast data in the South Baltic Sea is limited. The advantage of meteorological masts is that observations typically are collected at several heights, and therefore the vertical wind profile can be quantified. It is well known that the wind profile in its simplest form at low heights is logarithmic and that the wind profile in non-neutral atmospheric stratification and at higher heights deviates from the logarithmic profile [4-8]. For wind resource estimation, the most important level is hub-height where the wind turbines harvest the energy.

Satellite ocean winds are mapped at 10 m above sea level. It is clear that wind turbine hub-height is higher, say 80 to 100 m. Thus the satellite-based results have to be extrapolated to higher levels. One option is to use WAsP for the vertical extrapolation. Another option is to use the numerical wind atlas. The latter method is applied in the present context. The advantage of mesoscale modeling is that in such models the advection of air is effectively accounted for through modeling over long distances. In contrast, microscale models account for influences only at shorter distances. In enclosed seas such as the Baltic Sea, the surrounding lands are expected to influence winds over long distances.

2.2. Satellite techniques

The techniques of scatterometer and SAR wind retrievals are presented first. Similarities of the two satellites used – QuikSCAT and Envisat – are that they both map any area at specific local times as both satellites are in sun-synchronous polar orbits. For QuikSCAT the local mapping time is around 6 a.m and 6 p.m. while for Envisat it is around 9 a.m. and 9 p.m. in the South Baltic Sea. Both satellites carry microwave radars, i.e. active instruments sending and receiving microwave signals. Microwave radar works day and night and in all weather conditions. The microwaves penetrate cloud, rain and fog. For QuikSCAT though, rain gives rise to problems in case of heavy rain and therefore rain flags are added to the data such that the user can avoid using rain-affected data.

The physical principle of retrieving oceans winds is similar for scatterometer and SAR. The wind over ocean constantly modulates the sea surface creating capillary and short gravity waves. These very short waves are generated near-instantaneously and decay at the same rate, but appear to be in balance at all times to the mean wind speed as observed at 10 m. The Geophysical Model Function (GMF) that describe the relationship between the backscattered normalized radar cross section is found to be non-linearly proportional to the wind speed, as a function on slant range and relative wind direction in regard to the viewing geometry. For further details on ocean wind mapping see references for scatterometer [9-11] and SAR [12-14]. The nominal accuracy on wind speed is within 2 m s^{-1} for wind speeds between 3 and 25 m s^{-1}.

To highlight major differences between scatterometer and SAR the following may be noted: Scatterometer provides medium spatial resolution, around 25 km by 25 km grid size whereas SAR provides high spatial resolution, around 1 km by 1 km grid size. The resolutions here refer to the final wind results (not the raw sampling which has much higher spatial resolution).

The swath of QuikSCAT was very wide, 1800 km, and this means that most of the globe was mapped twice per day for the 10 years of active observations. This results in roughly 7300 individual ocean wind maps in the South Baltic Sea. The archive is freely available, e.g. from Remote Sensing Systems (http://www.remss.com/qscat/) as so-called level 3 products. This means as gridded geo-coded products of wind speed and wind direction.

In contrast, Envisat ASAR has a swath of 400 km in the so-called wide swath mode (WSM). The sampling in WSM provides a possibility of mapping any location in the South Baltic around 10 times per month. From simple calculation the data could amount to roughly 1000 samples everywhere on the globe. However, Envisat ASAR was and is not always mapping, as the mapping is based 'on demand', typical for science or for commercial activity, and also, the on-board data storage and downlink cannot handle continued operation. The archive at ESA (http://earth.esa.int/EOLi) provide gateway to check the actual data availability. In the present work around 3000 WSM wind maps are used, meaning roughly 400 available samples in each grid cell. For SAR-based wind mapping the raw data are retrieved by Risø DTU and processed into wind maps using the Johns Hopkins University Applied Physics Laboratory software ANSWRS[15].

Finally, an important difference between scatterometer and SAR is that while scatterometer observes the ocean surface from several angles using multiple antennae or rotating antenna (as for QuikSCAT), SAR only views the surface from one direction. This basic difference means that only scatterometer provides both wind speed and direction through the GMF. In order to map wind speed from SAR it is necessary first to estimate the wind direction, and use this *a*

priori information in the GMF. In our case we use the wind direction from the global atmospheric model by the US Navy, the so-called NOGAPS model. Further detail in[12].

2.3. Statistical-dynamical downscaling

The long-term overall statistics based on the NCEP/NCAR re-analysis dataset 1980-2009 will be used in combination with nearly two years of real time simulations using the WRF mesoscale model operated at Risø DTU. The usual procedure at Risø DTU for calculating wind resource with the numerical wind atlas method involves, as a first step, the definition of a set of wind classes. The set of wind classes represent the different wind conditions (wind speed, direction and atmospheric stability) defined from long term, large scale atmospheric reanalysis datasets.

The wind classes are based on geostrophic wind and potential temperature at 0, 1500, 3000, 5500 m above sea level. The wind classes are defined by the distribution of wind speed, direction and stability at one point. For the South Baltic wind atlas the area of interest is large. It is therefore of interest to see how well wind classes defined at one point manages to represent the large scale climate over this large area. There are two issues: 1) do wind classes represent the large scale wind climate well over the entire region of interest; 2) to what extent can a single wind class describe the wind in the region at any given time.

The WRF model is triple nested to the inner domain over Denmark with a 2 km by 2 km grid resolution for the weather forecasts, but the outer grid at an 18 km by 18 km grid covers most of the South Baltic. The weather forecasts plus some additional simulations at higher resolution will be used as basis in the statistical-dynamical downscaling.

3. Results

3.1. Satellite results

Results from the study area using QuikSCAT are shown in Fig. 2. The results are based on all available ocean wind maps from RSS without rain-flag from 10 years, 1999 to 2009. The results are maps of the Weibull A and k parameters. Weibull A is seen to vary from 8.0 to 8.5 m s^{-1} in the South Baltic Sea, and Weibull k is seen to vary from 1.9 to 2.3. Near the coastlines the white area indicates that data are not available.

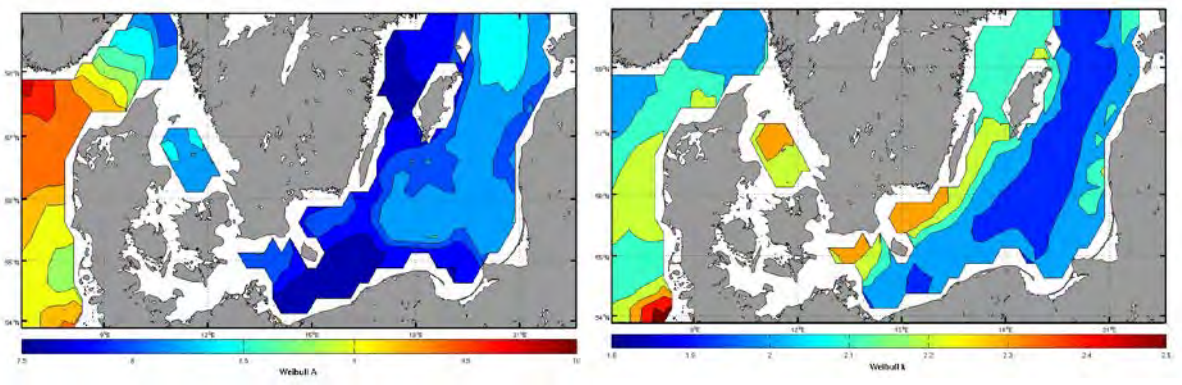

Fig. 2 Weibull A ranging from 7.5 (blue) to 10.0 (red) m $s^{-1}$and Weibull k ranging from 1.8 (blue) to 2.5 (red) in the South Baltic and Danish Seas observed from 10 years of QuikSCAT ocean wind maps. Domain size is 7° to 22° East and 53° to 59° North.

Results from the study area using Envisat ASAR are shown in Fig. 3. The upper panel shows the number of wind maps, the middle panel the mean wind speed, and the lower panel the

energy density. In most of the area there are more than 400 samples. The mean wind speed varies from around 5 m s^{-1} to nearly 11 m s^{-1}. Finally, the energy density varies from 400 to nearly 1200 W m^{-2}. In particular near the coastlines, the energy density is seen to be low. High energy density is found in the open sea.

3.2. Wind class results

Four sets of wind classes were defined, all based on the large scale conditions at 16.25E 56.25N. The sets, named SB1, SB2, SB3, SB4, contain 134, 84, 84, 36 wind classes respectively, see Fig. 4. Sets SB1, SB2, SB4 differ in that a different number of wind classes are allowed for each direction sector (14, 7, 3 respectively) but in each sector the wind speed range of each wind class varies so as to get obtain wind classes with approximately equal frequency of occurrence. Set SB3 uses 7 wind classes per sector, but the wind speed range is fixed and this the frequency of each wind classes varies within each sector.

The first question is, how well do the wind classes represent the large-scale wind climate over the South Baltic. This is answer is: The 134 wind classes of set SB1 capture the wind power in the large scale climate quite accurately with only a small error of less than 3% in the mean of the wind cubed. Whereas the 36 wind classes of set SB4 do more poorly, with an error in the region of 14% in the mean of the wind cubed. Wind classes sets SB2 and SB3 give an error in the region of 5% on the mean of the wind cubed.

The second question concerns to what extent it can be expected that a single wind class, at any given time is influencing the area of interest. The probability of a single wind class acting over a region rapidly drops off when moving away from 16.25E 56.25N. We may conclude that occasions where the same wind class influences large parts of the region of interest happen very rarely. By selecting periods where the wind classes are persistent the probability of locations experiencing the wind class is increased. However, it is not thought that persistency filtering is sufficiently powerful for the South Baltic domain. In conclusion, the variability means that an approach where several wind classes acting more locally, as opposed to acting over the whole domain, will have to be defined and used for the downscaling.

4. Discussion

Satellite wind maps from QuikSCAT provide twice daily 10 year results at 25 km by 25 km resolution. The WRF statistical-dynamical downscaling will provide 30 year results at 5 km by 5 km resolution. Envisat ASAR provides results at 1 km by 1 km resolution. The challenge of using different sources of information is the reliability of each. Comparisons between SAR and three meteorological masts in the North Sea[16] show good agreement, less than 5% error on mean wind speed, Weibull A and k. Comparisons between SAR and meteorological masts in the South Baltic Sea show similar agreement for mean wind speed, but less good agreement for Weibull A and k[17]. Mesoscale model results typically range between 10 to 15% uncertainty. Thus combining satellite wind maps and mesoscale modeling is expected to provide an accurate wind atlas for the South Baltic Sea.

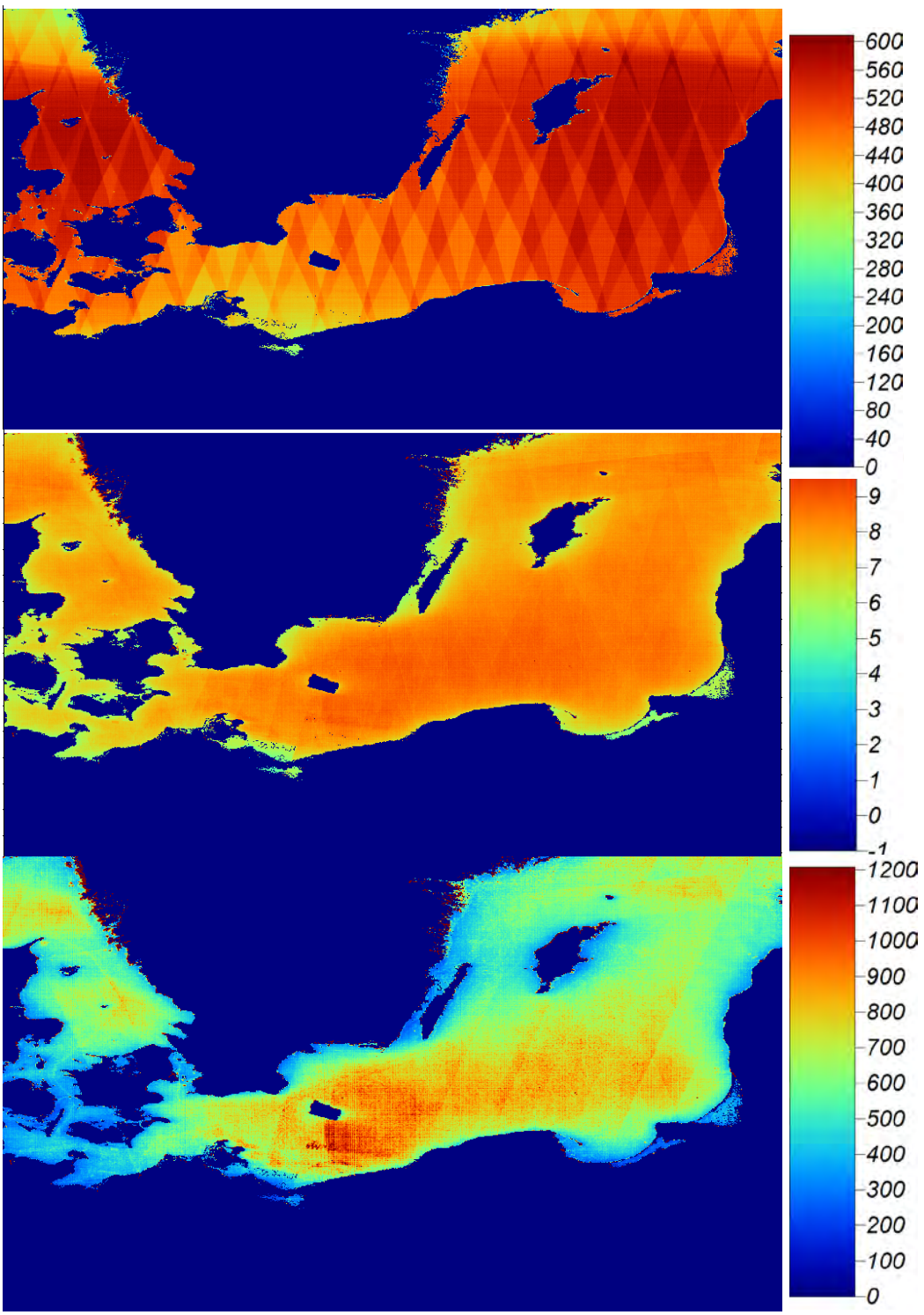

Fig. 3 Envisat ASAR wind maps: (Top) Number of wind speed maps use; (Middle)Mean wind speed in m s^{-1}; (Bottom) Wind energy density in W m^{-2} for the South Baltic Sea. Domain size is 10° to 22° East and 52° to 59° North.

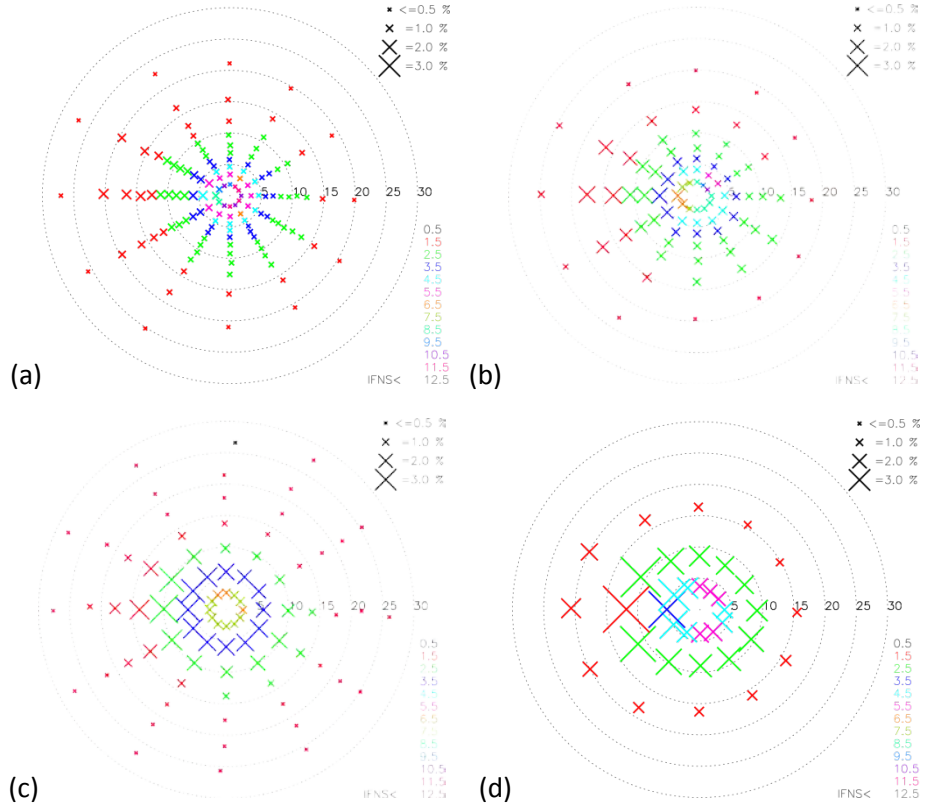

Fig. 4 Four sets of wind classes (a) SB1, (b) SB2, (c) SB3 and (d) SB4. Each cross represents a forcing wind speed (distance from the centre of the diagram) and direction. The speed scale is in m s^{-1}. The colours indicate the inverse Froude number squared (IFNS).

5. Conclusion

The wind atlas for the South Baltic Sea is in progress using satellite remote sensing and mesoscale modeling. The final results will be compared to available meteorological data to estimate the uncertainty of the results. The analysis will be completed in Spring 2011.

Acknowledgements

We acknowledge support from South Baltic OFF.E.R and satellite data from ESA and RSS.

References

[1] I. Troen,; E. L.Petersen, European Wind Atlas; Risø National Laboratory: Roskilde, 1989.

[2] H.Frank; O. Rathmann; N. Mortensen; L. Landberg The Numerical Wind Atlas, the KAMM/WAsP Method;Risø-R-1252(EN); Roskilde, Denmark, 2001.

[3] N. Mortensen; D. N. Heathfield; L. Landberg; O. Rathmann; I. Troen; E.L.Petersen Wind Atlas Analysis and Wind Atlas Analysis and Application program:WAsP 7.0 Help Facility;ISBN 87-550-2667-2; Risø National Laboratory: Roskilde, 2000.

[4] A. Sathe; S.E. Gryning, A. Peña, Comparison of the Atmospheric Stability and Wind Profiles at two Wind Farm Sites over a long marine fetch in the North Sea. Wind Energy **2010,** (in press).

[5] A. Peña; C.B. Hasager, S.E. Gryning; M.Courtney; I. Antoniou; T. Mikkelsen. Offshore wind profiling using light detection and ranging measurements. Wind Energy **2009,** 12, 105-124.

[6] C.B.Hasager; A. Peña; M.B.Christiansen; P.Astrup;M.Nielsen;F.Monaldo;D.Thompson; P.Nielsen.Remote sensing observation used in offshore wind energy. IEEE Journal of Selected Topics in Applied Earth Observations and Remote Sensing **2008,** 1 (1), 67-79.

[7] A.Peña; S.E.Gryning. Charnock's roughness length model and non-dimensional wind profiles over the sea. Boundary-Layer Meteorology **2008,** 128, 191-203.

[8] A.Peña; S.E.Gryning; C.B.Hasager. Measurements and Modelling of the Wind Speed Profile in the Marine Atmospheric Boundary Layer. Boundary-Layer Meteorology **2008,** 129 (3), 479-495.

[9] W.T.Liu;W.Tang Equivalent neutral wind; National Aeronautics and Space Administration, Jet Propulsion Laboratory, California Institute of Technology, National Technical Information Service, distributor: 1996.

[10] H.Hersbach; A.Stoffelen;S.de Haan.An improved C-band scatterometer ocean geophysical model function:CMOD5. J. Geophysical Research **2007,** 112 (C03006).

[11] A.Stoffelen; D.L.T.Anderson. Wind retrieval and ERS-1 scatterometer radar backscatter measurements. Advance Space Research **1993,** 13, 53-60.

[12] M.B.Christiansen;C.B.Hasager;D.R.Thompson;F.Monaldo.Ocean winds from synthetic aperture radar. In Ocean remote Sensing: Recent Techniques and Applications., Niclos, R., Caselles, V., Eds.; Research Singpost Editorial: 2008; pp 31-54.

[13] R.C.Beal; G.S.Young;F. Monaldo; D.R.Thompson; N.S.Winstead; C.A.Schott High resolution wind monitoring with Wide Swath SAR: A user's guide; U.S. Department of Commerce: Washington, DC, 2005.pp. 1-155.

[14] F.Monaldo;D.R.Thompson;N.S.Winstead;W.Pichel;P.Clemente-Colón;M.B.Christiansen. Ocean wind field mapping from synthetic aperture radar and its application to research and applied problems. Johns Hopkins Apl. Tech. Dig. **2005,** 26, 102-113.

[15] F.Monaldo. The Alaska SAR demonstration and near-real-time synthetic aperture radar winds. John Hopkins APL Technical Digest **2000,** 21, 75-79.

[16] M.Badger; J.Badger;M.Nielsen;C.B.Hasager;A.PeñaWind class sampling of satellite SAR imagery for offshore wind resource mapping. J. Applied Meteorology and Climatology **2010,** 49,12,2474-2491.

[17] Hasager, C. B.; Badger, M.; Peña, A.; Larsén, X. G. SAR-Based Wind Resource Statistics in the Baltic Sea. Remote Sensing **2011,** 3,1,117-144.

The wind energy potential in the coasts of Persian Gulf used in design and analysis of a horizontal axis wind turbine

Mehdi Reiszadeh[1], Sadegh Motahar[2,*]

[1]*Islamic Azad University, Shahreza Branch, Shahreza, Iran*
[2] *Department of Mechanical Engineering, Isfahan University of Technology, Isfahan, Iran*
** Corresponding author. Tel: +98 9133219887, Fax: +98 3212239037, E-mail: smotahar@me.iut.ac.ir*

Abstract: There are many wind synoptic stations installed all over Iran. One of these stations in the coasts of Persian Gulf is Bardekhun station in Bushehr province. The goal of this study is to assess the wind energy potential of this region and to design a proper horizontal axis wind turbine for this site. The one-year measured hourly time-series wind speed data are extracted from measurements at a height of 10m, 30m and 40m above the ground level. The Weibull distribution gives the mean wind speed of 4.50 m/s, 5.36 m/s and 5.83 m/s and the power density per year of 125 W/m^2, 196 W/m^2 and 253 W/m^2 respectively for these heights. According to these results, a small wind turbine can be installed in the height of 30m and 40m. A MATLAB code using the blade-element-momentum theory has been developed to design and analyze the three-blade wind turbine rotor. After calculation of geometrical parameters of rotor blade, the rotor power coefficient versus rotor tip speed ratio is evaluated. The energy produced per year by this wind turbine using the Weibull distribution for wind speed will be 155MWh.

Keywords: *Wind potential, Weibull distribution, Wind turbine, produced energy*

1. Introduction

Annual growth in energy consumption and global warming are two important reasons for considering wind as an efficient and clean source of energy. Iran (Persia) is exposed to the continental streams from Asia, Europe, Africa, Indian and Atlantic Pacific. The first vertical axes and drag type windmills on record were built by the Persians in approximately 900 AD [1]. According to the research and studies, it has been estimated that the wind energy potential in Iran is more than 10000 MW for electricity production [2]. There are two wind farm producing electricity in Iran: a 70MW power plant in Manjil and a 28MW power plant in Binalood. Since Iran has many windy regions, utilization of this type of energy would not only be possible but also economically feasible. The Ministry of Energy has serious programs for the evaluation of the wind energy potential in the country. At the first stage, the country's wind energy potential evaluation is performed for a wide range of the country. At the second stage, after the exact investigation on the wind potential, the Iran's wind atlas is prepared. To prepare the wind atlas, 53 wind synoptic stations have been installed all over Iran [3]. These stations record wind data every 10 min. Also, the effects of thunderstorms and turbulences on wind stream are considered in the results.

In the recent years, many researchers have studied the wind energy potential in Iran. Mostafaeipour and Abarghooei [4] investigated the wind energy potential in Manjil area in the north of Iran. They reported it is one of the best locations in the world for installing wind turbine. Mostafaeipour [5] utilized wind speed data over a period of almost 13 years between 1992 and 2005 from 11 stations in Yazd province to assess the wind power potential at these sites. The results showed that most of the stations have annual average wind speed of less than 4.5 m/s which is considered as unacceptable for installation of the wind turbines. Keyhani et al [6] used the statistical data of eleven years wind speed measurements of the capital of Iran, Tehran to find out the wind energy potential. They concluded that the site studied is not suitable for electric wind application in a large-scale and the wind potential of the region can be adequate for non-grid connected electrical and mechanical applications, such as wind

generators for local consumption, battery charging, and water pumping. Mostafaeipour [7] performed an analysis of offshore wind speed in global scale and also studied feasibility of introducing this technology for harnessing wind in Persian Gulf, Caspian Sea, Urmia Lake and Gulf of Oman. He suggested that policy makers to invest and pay more attentions toward harnessing renewable energy sources like offshore wind in Persian Gulf and Gulf of Oman in southern parts of Iran.

This paper presents a study of the wind energy potential in the Bardekhun station. Knowledge of the wind speed distribution is a very important factor to evaluate the wind potential in the windy areas. The Weibull distribution is the best one, with an acceptable accuracy level. A stall-regulated horizontal wind turbine with nominal power of 50kW is designed for this wind station. A MATLAB code was written based on the BEM theory. This code utilizes a generalized rotor design procedure in determining the final blade shape and performance iteratively considering drag, tip losses, and ease of manufacture.

2. Site description and the wind data

This site is located in the vicinity of Deyer port in Bushehr province in the coasts of Persian Gulf. It is situated in the latitude of 27°98' N, the longitude of 51°49' W and the altitude of 4m. Its distance from capital city of Iran, Tehran, is about 1330 km. A well known wind in this region is North Wind which has effect on the architectural and environmental design of buildings. The one-year measured hourly time-series wind speed data, from January 1, 2007 to December 31, 2007 are extracted from Renewable Energy Organization of Iran, SUNA [2].

3. Wind data analysis

3.1. Weibull distribution

Statistical analysis can be used to determine the wind energy potential of a given site and to estimate the wind energy output at this site [1]. This type of analysis relies on the use of the probability density function, *p(U)*, of wind speed. One way to define the probability density function is that the probability of a wind speed occurring between U_a and U_b is given by:

$$p(U_a \le U \le U_b) = \int_{U_a}^{U_b} p(U)dU \tag{1}$$

Where U is wind speed and $\int_0^\infty p(U)dU = 1$.

In general, Rayleigh and Weibull probability density functions are used in wind data analysis. The Rayleigh distribution uses one parameter, the mean wind speed ($\overline{U}$). Determination of the Weibull probability density function requires knowledge of two parameters: k, shape factor and c, scale factor. Both these parameters are a function of wind speed, U, and standard deviation of wind speed, σ_U. The Weibull probability density function is given by:

$$p(U) = \left(\frac{k}{c}\right)\left(\frac{U}{c}\right)^{k-1} \exp\left[-\left(\frac{U}{c}\right)^{k}\right] \tag{2}$$

The cumulative distribution function of the speed U gives us the fraction of time (probability) that the wind speed is equal or lower than U. the cumulative distribution *F (U)* is given by:

$$F(U) = 1 - \exp\left[-\left(\frac{U}{c}\right)^{k}\right] \tag{3}$$

The parameters *c* and *k* are calculated based on the following empirical formulas [1, 8]:

$$k = \left(\frac{\sigma_U}{\overline{U}}\right)^{-1.086}, \frac{c}{\overline{U}} = \frac{k^{2.6674}}{0.184 + 0.816k^{2.73855}} \tag{4}$$

Annual energy produced by a wind turbine with performance curve $P_w(U)$ is [1, 9]:

$$\overline{P_w} = 365 \times 24 \int_0^{\infty} p(U)P_w(U) = 365 \times 24 \times \sum_{i=1}^{N_B} \frac{1}{2}(U_{i+1} - U_i)\left(p(U_{i+1})P_w(U_{i+1}) + p(U_i)P_w(U_i)\right) \tag{5}$$

3.2. Power density

The wind power per unit area, or wind power density, is proportional to the density of the air (for standard conditions sea-level, 15°C, the density of air is 1.225 kg/m^3), the area swept by the rotor (or the rotor diameter squared for a conventional horizontal axis wind machine) and the cube of the wind velocity. The average wind power density is:

$$\frac{\overline{P}}{A} = \frac{1}{2}\rho \int_0^{\infty} U^3 p(U)dU \tag{6}$$

4. Wind turbine aerodynamic design

The primary aerodynamic factors affecting the blade design are: design rated power and rated wind speed, design tip speed ratio, solidity, airfoil, number of blades, rotor power control (stall or variable pitch), rotor orientation (upwind or downwind of the tower) [1]. The analysis here uses momentum theory and blade element theory. Momentum theory refers to a control volume analysis of the forces at the blade based on the conservation of linear and angular momentum. Blade element theory refers to an analysis of forces at a section of the blade, as a function of blade geometry. The results of these approaches can be combined into what is known as strip theory or blade-element- momentum (BEM) theory. This theory can be used to relate blade shape to the rotor's ability to extract power from the wind. The analysis in this paper covers a simple optimum blade design including wake rotation and an infinite number of blades. This blade design can be used as the start for a general blade design analysis. The forces on the blades of a wind turbine can also be expressed as a function of lift and drag coefficients and the angle of attack. In this analysis, the blade is assumed to be divided into *N* sections (or elements) [1, 9].

5. Results and discussions

5.1. Wind energy potential

The data collected for an interval of 10 min have been used to analyze the wind energy potential of this site. All measurements in the wind station are recorded using the cup anemometer at a height of 10m, 30m and 40m above the ground level.

5.1.1. Wind speed distribution

The most critical factor influencing the power developed by a wind energy conversion system is the wind speed. Due to the cubic relationship between speed and power, even a small variation in the wind speed may result in significant change in power.

Results of wind data analysis at three different heights have been summarized in Table 1.The mean wind speed, mean cubic wind speed, standard deviation of wind data and the Weibull distribution parameters for each height are calculated. Maximum wind speed per year and its occurrence time can be used in control and structural analysis of wind turbines. These results obtained for one-year measured data.

Table 1. Results of wind data analysis at different heights

	Height		
	40m	30m	10m
Mean wind speed (m/s)	5.83	5.36	4.50
Mean cubic wind speed (m/s)	7.50	6.96	6.00
Standard deviation	3.313	3.042	4.506
Max. wind speed per year (m/s)	33 (11/4/2007 23:50)	31.1 (11/4/2007 23:50)	28.2 (15/3/2007 11:00)
Weibull distribution constants	k=1.848 c=6.568	k=1.850 c=6.037	k=1.737 c=5.058

The corresponding average wind speeds and best fits to the Weibull distribution at 30m and 40m height in comparison with the distribution of measured data are shown in Fig.1. The Weibull scale and shape factors can be found in Table 1 at each height. As shown in Fig. 1(a), the Weibull distribution function reaches the top point at about 4.00 m/s with a value of about 13.54%, however the Weibull distribution function in Fig. 1(b) reaches the top point at about 4.00 m/s with the value of frequency equal to 12.39%.

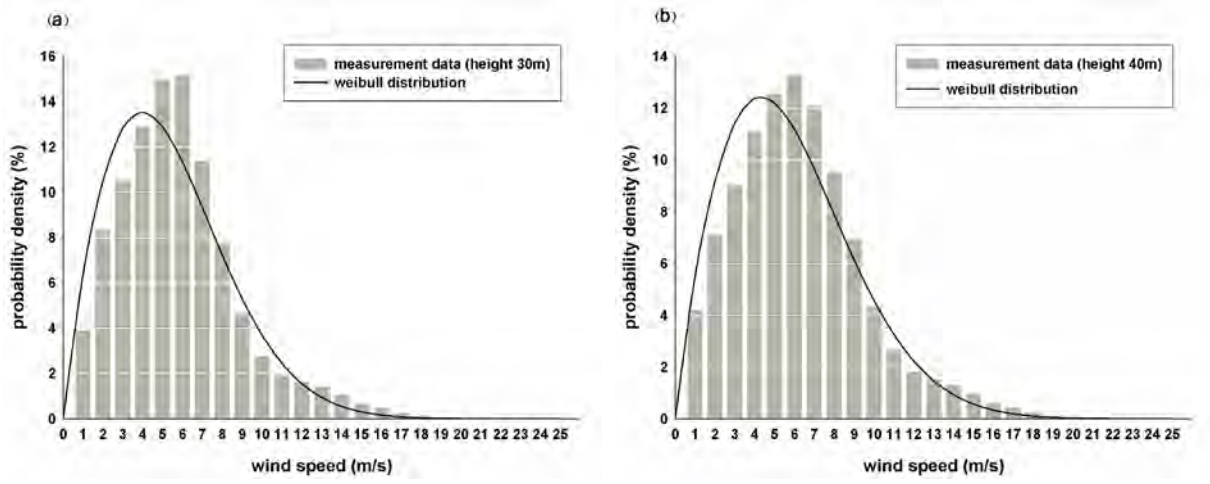

Fig. 1. Weibull probability distribution function at (a) 30m (b) 40m

Fig. 2(a) illustrated the Weibull distribution function at the height of 10m. The distribution of measured data can be seen in this figure. The Weibull distribution reaches to the maximum

frequency of 15.61% at the wind speed around 3.00m/s. The cumulative distribution functions at three given heights are shown in Fig. 2(b). According to this figure, the cumulative density at 40m gets up to 56.50% for mean wind speed of 5.83m/s. This probability is 52.62% and 50.47% for mean wind speed of 5.36m/s and 4.50m/s at 30m and 10m heights, respectively.

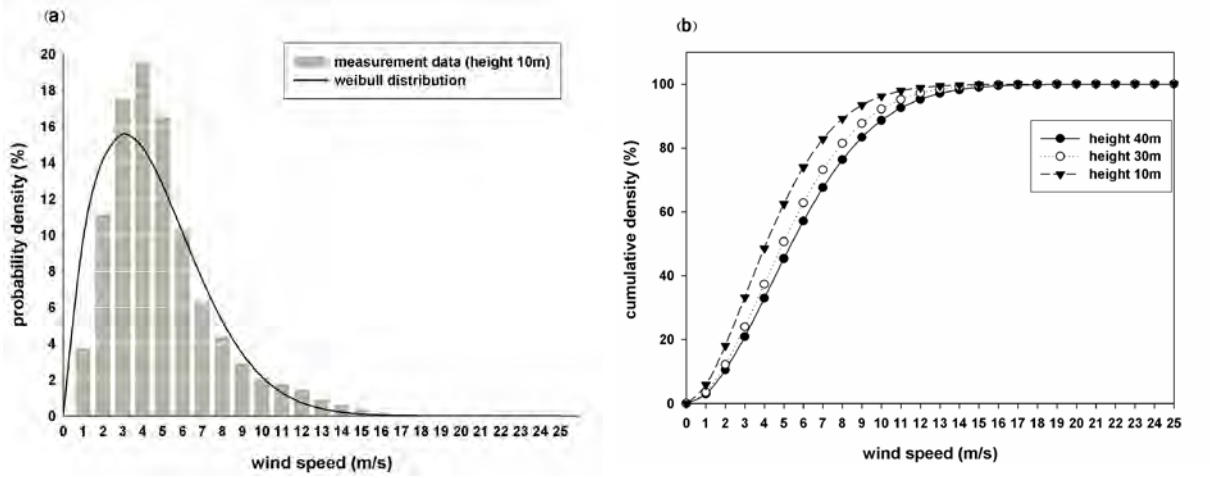

Fig. 2. (a) Weibull probability distribution function at 10m (b) Cumulative function at three heights

5.1.2. Estimation of monthly wind potential

The monthly distribution of the wind speed measured between January 1, 2007 and December 31, 2007 is plotted in Fig. 3(a). It can be seen from this figure, the wind speeds vary between 3.34 and 7.52 m/s. According to these results, the average speed for 10 m is 4.50 m/s. This is below the minimum speed, 5.0 m/s, required for effective wind turbines, but it is enough for water pumping applications. The monthly average wind power density at height of 40m is illustrated in Fig. 3(b). The wind potential of a site, i.e. average power density, which is proper to run a wind turbine, is qualitatively estimated based on the following [1]: $\overline{P}/A$<100 W/m^2 is a poor potential, $\overline{P}/A\approx$400 W/m^2, is a good potential, and $\overline{P}/A$>700 W/m^2 is a great potential. Here, there is a poor potential in October, September and August, because the power density is near to 100 W/m^2 in these months. For the reminders of the year, there is a reasonable potential.

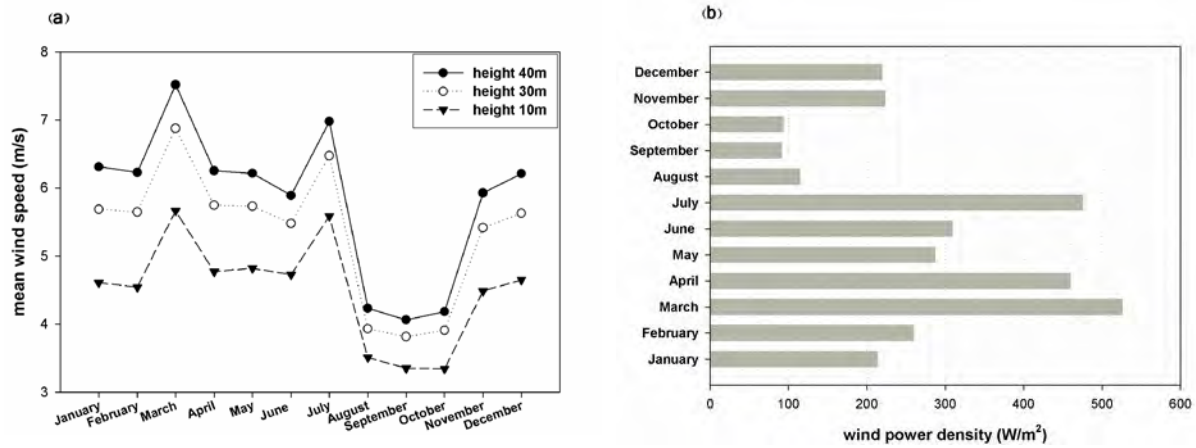

Fig.3. (a) Monthly average wind speed at three heighs (b) Monthly power density at 40m

5.1.3. Wind potential in the site

If annual average wind speeds are known for a certain site, the average wind power density can be found over these regions. Fig. 4 illustrates the power densities per year at three heights. These power densities are drawn for measured data and for the Weibull distribution function. The Weibull distribution function illustrates power density per year a little lower than measured data. The wind power density per year at height of 10m is suitable for water pumping, because it is not actually a good potential. The power density at height of 40m and 30m are more reasonable. A proper wind turbine can be run by the wind at these heights. In the next section, a wind turbine designed and proposed for installation at 40m.

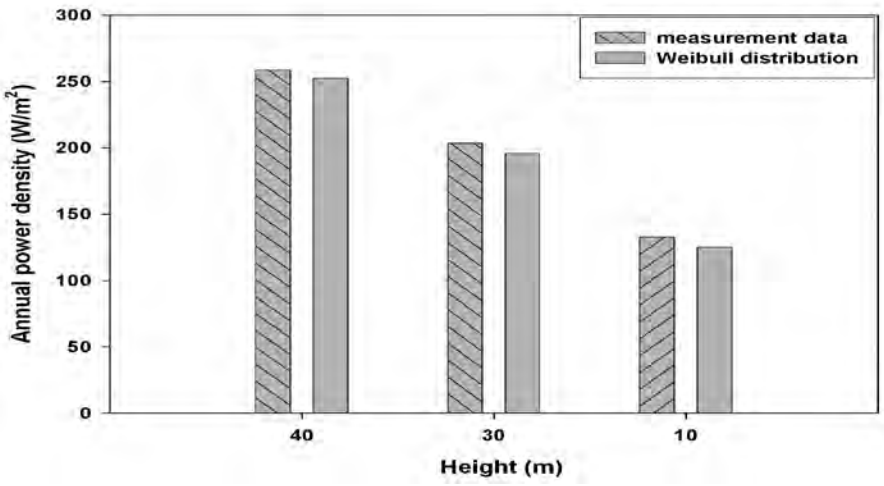

Fig.4. power density per year at three heights

5.2. Wind turbine design and performance results

In order to utilize the wind energy potential for the mentioned site, a power of 50kW is needed at 7.50m/s wind speed (mean cubic wind speed at 40m height). For this purpose, a 3-blade, stall-regulated and upwind horizontal axis wind turbine (HAWT) has been designed based on the BEM theory. The blade has NACA 4415 airfoil and has a tip speed ratio of λ=6.

5.2.1. Blade geometry

To develop the maximum possible power coefficient (C_p) requires suitable blade geometry. The geometrical parameters for blade design are shown in Table 2. Assume the mechanical efficiency and the overall rotor power coefficient are 0.99 and 0.40, respectively. With these assumptions, the radius of rotor will be R=13m. The blade is divided into *N* elements (usually 10-20). The first column, r/R, is fraction of rotor radius. The straight line connecting the leading and trailing edges is the chord line of the airfoil, and the distance from the leading to the trailing edge measured along the chord line is designated as the chord, *c*, of the airfoil (second column in Table 2). The section pitch angle (θ_p) is the angle between the chord line and the plane of rotation. $\theta_{p,0}$ is the blade pitch angle at the tip. The relative wind is the vector sum of the wind velocity at the rotor and the wind velocity due to rotation of the blade. The angle between the chord line and the relative wind is the angle of relative wind ($\varphi = \theta_p + \alpha$).The blade twist angle is the difference between section pitch angle and the blade pitch angle at the tip, i.e. $\theta_T = \theta_p - \theta_{p,0}$. The design aerodynamic condition occurs when C_d/C_L is at a minimum for each blade section. The aerodynamic properties of the airfoil at each section, i.e. C_L-α (lift coefficient vs. angle of attack) and C_d-α (drag coefficient vs. angle of attack) can be obtained from the empirical curves.

Table 2. Blade design of a 26m-diameter Rotor

r/R	Chord (m)	Twist angle (degree)	Angle of relative wind (degree)	Section pitch (degree)
0.0500	2.0091	42.5590	48.8672	42.8672
0.1000	2.6631	33.0493	39.3575	33.3575
0.1500	2.6778	25.7003	32.0085	26.0085
0.2000	2.4742	20.2288	26.5370	20.5370
0.2500	2.2268	16.1518	22.4600	16.4600
0.3000	1.9939	13.0615	19.3696	13.3697
0.3500	1.7907	10.6673	16.9753	10.9756
0.4000	1.6174	8.7717	15.0793	9.0799
0.4500	1.4704	7.2405	13.5474	7.5488
0.5000	1.3453	5.9818	12.2870	6.2900
0.5500	1.2380	4.9307	11.2330	5.2389
0.6000	1.1450	4.0412	10.3374	4.3494
0.6500	1.0634	3.2794	9.5639	3.5876
0.7000	0.9903	2.6201	8.8820	2.9283
0.7500	0.9225	2.0443	8.2625	2.3525
0.8000	0.8558	1.5373	7.6712	1.8455
0.8500	0.7825	1.0876	7.0541	1.3958
0.9000	0.6856	0.6861	6.2952	0.9943
0.9500	0.5029	0.3255	4.9618	0.6338

5.2.2. HAWT performance curves

The Betz limit, $C_{P,max} = 0.59$, is the maximum theoretically possible rotor power coefficient. In practice three effects lead to a decrease in the maximum achievable power coefficient: rotation of the wake behind the rotor, finite number of blades and associated tip losses, and non-zero aerodynamic drag [1]. Although the blade has been designed for optimum operation at a specific design tip speed ratio, the performance of the rotor over all expected tip speed ratios needs to be determined. The results are usually presented as a graph of power coefficient versus tip speed ratio, called a C_P-λ curve, as shown in Fig. 5(a). The maximum value of C_P in C_P-λ curve, Fig. 5(a), is 0.4586 at λ=6. C_P-λ curves can be used in wind turbine design to determine the rotor power for any combination of wind and rotor speed. They provide immediate information on the maximum rotor power coefficient and optimum tip speed ratio.

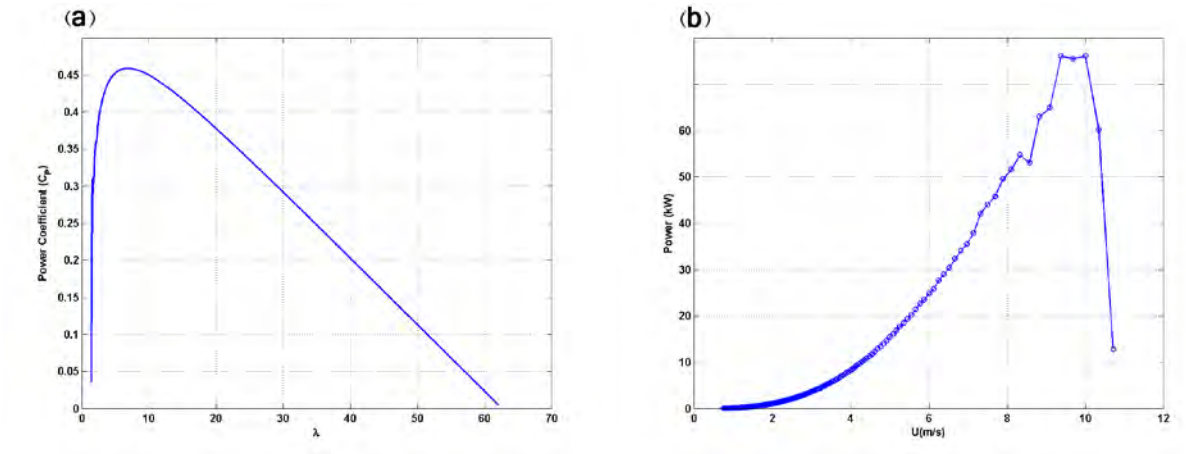

Fig. 5 (a) C_P-λ curve (b) Rotor power vs. wind speed

Fig. 5(b) illustrates the power produced by the wind turbine in various wind speeds. In order to estimate the energy captured per year by this wind turbine, $p(U)$ and $P_w(U)$ are obtained from Fig. 1(b) and Fig. 5(b) respectively and are put in the Eq. (5). So, the energy of the wind turbine per year will be 155 MWh.

6. Conclusions

In this study, a site in the coasts of Persian Gulf was evaluated for wind potential. Statistical analysis of wind data at three heights, 10m, 30m and 40m, showed that there is a promising wind potential for installing wind turbine at height of 30 and 40m. The power density per year at these two heights was 253 and 196 W/m^2, respectively. In the second part of paper, a 50kW horizontal axis wind turbine was designed for installing at 40m. The energy produced per year by this turbine was 155MWh. The wind potential in this coastal region can be utilized for both water pumping and electricity generation by small wind turbine. It might be suitable for the rural parts of Bushehr.

References

[1] J.F. Manwell, J.G. McGowan, A.L. Rogers, Wind Energy Explained: Theory, Design and Application, John Wiley & Sons Ltd, 2002.

[2] Renewable Energy Organization of Iran, http://www.suna.org.ir/ .

[3] M. Ameri, M. Ghadiri and M. Hosseini, Recent Advances in the Implementation of Wind Energy in Iran, The 2nd Joint International Conference on S ustainable Energy and Environment (SEE 2006), Bangkok, Thailand, November 2006.

[4] A. Mostafaeipour and H. Abarghooei, Harnessing wind energy at Manjil area located in north of Iran, Renewable and Sustainable Energy Reviews, 12(6), 2008, pp. 1758-1766.

[5] A. Mostafaeipour, Feasibility study of harnessing wind energy for turbine installation in province of Yazd in Iran, Renewable and Sustainable Energy Reviews, 14, 2010, pp.93-111.

[6] A. Keyhani, M . Ghasemi-Varnamkhastia, M . Khanalia, and R. Abbaszadeh, An assessment of wind energy potential as a power generation source in the capital of Iran, Tehran, Energy, 35(1), 2010, pp. 188-201.

[7] A. Mostafaeipour, Feasibility study of offshore wind turbine installation in Iran compared with the world, Renewable and Sustainable Energy Reviews, 14(7), 2010, pp. 1722-1743.

[8] A. Balouktsis, D. Chassapis and T.D. Karapantsios, A nomogram method for estimating the energy produced by wind turbine generators, Solar Energy, 72(3), 2002, pp. 251-259.

[9] T. Burton, D. Sharpe, N. Jenkins and E. Bossanyi, Wind Energy Handbook, John Wiley & Sons Ltd, 2001.

Measurements of the wind energy resource in the Latvia

P. Shipkovs[1]*, V. Bezrukov[1], V. Pugachev[1], Vl. Bezrukovs[2], V. Silutins[3]

[1] *Institute of Physical Energetics (IPE), Riga, Latvia,*
[2] *Ventspils University College (VUC), Ventspils, Latvia*
[3] *Encom Ltd, Riga,Latvia*
** Corresponding author. Phone/Fax: +37167553537, e-mail: shipkovs@edi.lv*

Abstract: In the Baltic countries interest to the renewable energy is growing. Government support and availability of large unpopulated areas on the coast makes attractive use of these lands for the placement of large wind power plants (WPP). For successful implementation of planned projects reliable information about distribution of the resource of wind energy is needed. Researches in this area are carried out by collaboration IPE with VUC. The paper presents the results of years-long observations on the density fluctuations of wind energy at heights of 10 to 60 *m* in the area in the Baltic Sea coast in the north and the south-west of Latvia. The velocity observations from 2004 till 2010 years have been obtained by measurements complex of the LOGGER 9200 Symphonie type. The results presented in the form of tables, bar charts and graphs. The graphs of seasonal fluctuations of wind speed have been obtained for the heights up to 60 *m* by measurements over the period of 2007 – 2010. The histograms have been composed for the relative frequency of repetition of wind speed. The wind speed distribution on heights up to 60 *m* was analysed and coefficients of approximating functions for the two areas with different terrain types were calculated. Extrapolation results of the distribution curves of wind velocity and density mean values on heights up to 150 *m* were shown.

Keywords: *Wind energy, Measurement of wind speed, Wind speed approximation at 150 m, Wind energy density fluctuation, Acoustic noise level*

1. Introduction

The availability of large unpopulated coastal areas and the developed infrastructure of electric power networks in the Baltic countries make attractive the use of these areas for siting large wind power plants (WPP). In the coastal territories of western Estonia, in the Ida-Virumaa region at the site of the former shale quarries the construction of WPPs is planned whose power will be over 600 *MW*. Further it is also planned to start offshore WPP construction. In Latvia, projects on the construction of 450 *MW* coastal WPPs have been approved; there are also projects as to the construction of a 900 *MW* wind park offshore. In Lithuania, the total power of wind parks in 2010 has made up 200 *MW*, with 1000 *MW* to be reached; after 2020 it is planned to start works in the offshore territories. In Latvia, planned preparation of the infrastructure is going on: construction of thermal power plants and of the transmission line "Kurzeme Arc" (by 2017), which would allow for construction of a ~900 *MW* WPP in the sea near Liepaja (by 2020). The governmental support is confirmed by working out administrative and legislative regulations as well as by creating a favourable tariff policy that would encourage the construction of large WPPs. At the same time, for the territory of the Baltic countries there are no databases of long-term measurements of wind speeds at different heights that can be used to compose an atlas of wind energy resource distribution in this region. The systematic long-term measurements of wind speeds in Latvia since 2007, taking into account the wind speed distribution on several levels, have been carried out in the two sites: on the south-west coast of the Baltic Sea in the Ventspils region and on the north of the country in the Ainaži region in 35 *km* from the shore [1]. The places where the metrological masts are situated are shown on the map of Fig. 1 by black stars. On the same map, by dark grey colour the regions are indicated which, according to the forecasts of meteorological observations and being territorially remote from populated areas, could be promising for siting WPPs.

Fig. 1. The coastal map of Baltic countries with the places of interest for siting WPPs indicated.

2. Research on the cyclic behaviour of wind energy fluctuations

The measurements of wind speed were carried out using certified sensors of wind speed of the NRG #40 type and sensors indicating the direction of the air stream of the NRG #200P type. The sensors are arranged on metallic masts with the height of 53 and 60 *m* above the ground. The periodicity of the information read-out from the sensors at all the height levels was 10 *s*. For storing information an NRG LOGGER Symphonie complex was employed, which has independent supply from batteries and is able to store information from nine sensors in the memory card during a year.

In the observation period a database has been built up containing the wind speed values at heights of 10, 20, 30, 40 , 50 and 60 *m*, wind temperature and direction in two regions in the Latvian territory. At the present time, the database contains more than 3'000'000 records of measurements. To compare the wind energy flow levels on the sea shore in the Ventspils region and in the area remote from the sea in the Ainaži region, in Table 1 average wind speed values, V_a, are given, with standard deviations *SD*, and the wind energy density values, P_d, W/m^2. Dark colour in the table corresponds to a larger value of wind speed or energy density for the month.

The charts of seasonal fluctuations of average wind speed *V* (*m/s*) for the measurement period *T* (*a month*) at the heights 20, 30, 40, 50 *m* in the Ventspils region and 10, 30, 50, 60 *m* in the Ainaži region are shown in Figs. 2 and 3. The results of wind speed measurements taken in the Ventspils and Ainaži regions are systematized and presented in the form of histogram in Figs. 4 and 5. The envelope of the histogram shows the wind speed *V* distribution in the relative frequency of repetition *F*, which corresponds to the relation $F = \frac{T_V}{T} \cdot 100\%$, where T_V is the total duration of wind with the speed *V* in the whole measurement period *T* for the heights 20, 30, 40, 50 *m* in the Ventspils region and 10, 30, 50, 60 *m* in the Ainaži region.

Table 1. Distribution of average wind speed values with standard deviations and corresponding power density values at the height 50 (m) in the observation period.

		Ventspils			Ainaži		
Year	**Month**	V_a, (m/s)	SD, (m/s)	P_d, (W/m^2)	V_a, (m/s)	SD, (m/s)	P_d, (W/m^2)
2009	April	4.27	0.78	76.92	4.48	0.72	85.53
	May	4.82	0.97	93.59	4.58	0.81	93.10
	June	4.80	0.99	95.32	4.56	0.84	97.48
	July	4.28	0.83	77.96	3.87	0.65	57.99
	August	4.37	0.80	73.82	4.14	0.67	64.92
	September	5.04	1.03	113.19	4.61	0.74	83.86
	October	4.78	1.07	151.59	5.00	0.79	139.02
	November	4.97	1.12	103.52	4.73	0.79	84.99
	December	4.23	0.88	81.45	3.98	0.63	66.16
2010	January	3.60	0.67	56.48	3.01	0.43	47.71
	February	3.58	0.74	47.95	3.32	0.48	43.83
	March	4.88	1.08	105.12	4.91	0.81	107.57
	April	3.71	0.80	52.75	4.14	0.71	68.58
	May	4.02	0.88	68.15	4.16	0.77	75.45
	June	4.36	0.91	88.80	4.23	0.79	78.83
	July	4.02	0.76	55.71	3.42	0.61	38.88
	August	4.09	0.81	67.83	3.88	0.68	63.92
	September	4.99	1.02	116.10	4.81	0.70	107.69
	October	4.98	0.99	120.17	5.08	0.78	120.79
	Average:	**4.41**	**0.90**	**86.65**	**4.26**	**0.71**	**80.33**

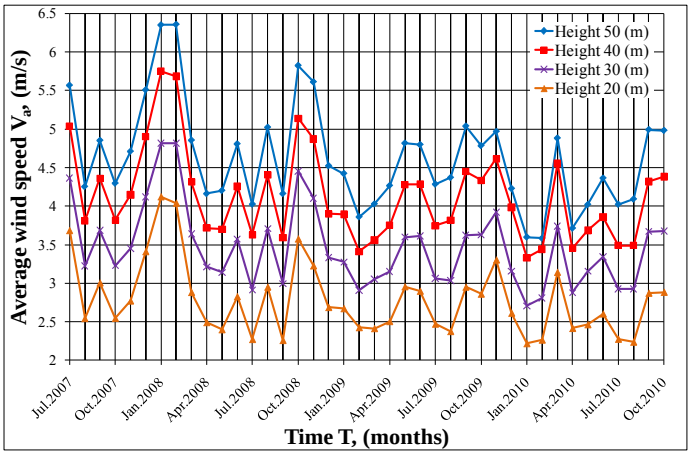

Fig. 2. Average wind speed values V_a in period T (2007/2010) at heights 10, 30, 40 and 50 (m) in the Ventspils region.

The histogram allows determination of the wind energy flow density, which is calculated by the equation:

$$P_d = \rho \frac{V_{a.c.}^3}{2} = \rho \frac{\sum_{n=0}^{n} V_n^3 F_n}{2 \cdot 100}, \qquad (1)$$

where $V_{a.c.}$ – is the average cubic wind speed, *m/s*,

$\rho = 1.23\ kg/m^3$ – is the air density at atmosphere pressure *101.325 kPa* and temperature *15° C*,

V_n – is the wind speed, *m/s*,

F_n – is the relative frequency of repetition, %, corresponding to wind speed V_n and determined by curves on the histograms of Figs. 4.

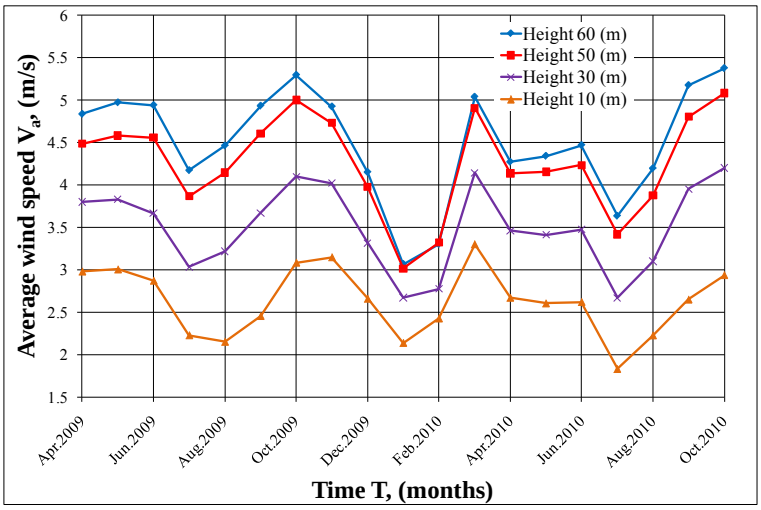

Fig.3. Average wind speed values V_a in period T (2009/2010) at heights 10, 30, 50 and 60 (m) in the Ainaži region.

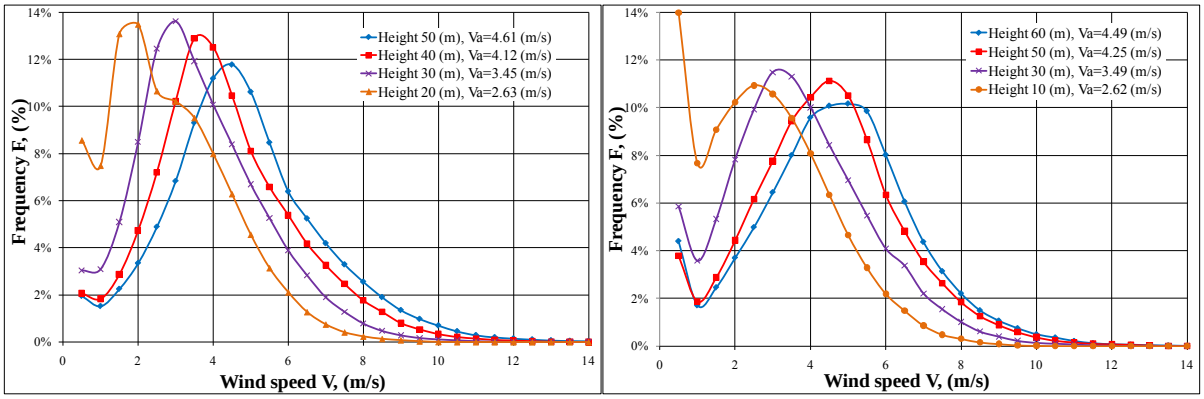

Fig. 4 (left). Distribution of wind speed in relative frequency of repetition F= f(V) at heights 10, 30, 40 and 50 (m) in the Ventspils region and Fig. 4 (right). Distribution of wind speed in relative frequency of repetition F= f(V) at heights 20, 30, 50 and 60 (m) in the Ainaži region.

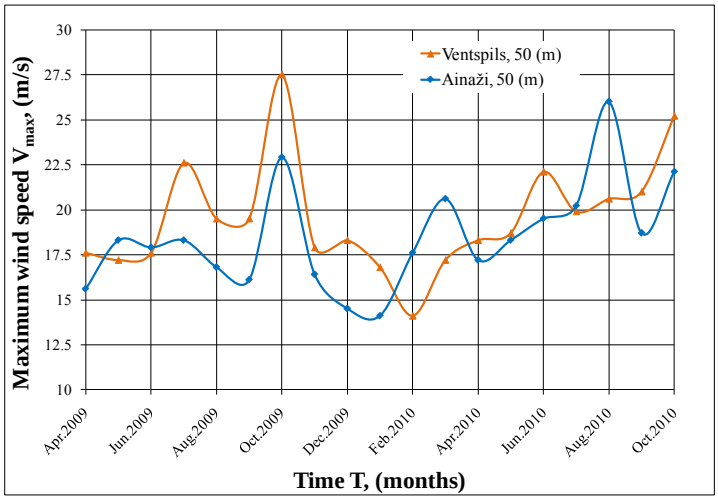

Fig.5. The maximum values of separate wind gusts, V (m/s), with duration 10 (s) in the regions Ventspils and Ainaži, at height 50 (m) above the ground level in the period of 2009/2010.

From analysis of statistical data for 2009/2010 shown in Fig. 5 it follows that in the coastal zone winds are gustier, whereas farther from shore their speeds are more uniform. The maximum value for separate wind gusts lasting not less than 10 *s* in the Ventspils region is not much higher than in Ainaži, with the situation changing in individual months. In January of 2005 the wind gusts in the Ventspils region at a height of 50 *m* reached 34.1 *m/s*.

3. Approximating functions for calculation of the wind speed and wind energy density up to 150 m

The distribution curves of the average wind speed V_a *(m/s)* in height *h (m)* above the ground level in the regions Ventspils and Ainaži obtained based on the data accumulated for a long time are presented in Fig. 6. The measured values of wind speed in the Ventspils region are shown by two curves. Curve 1 corresponds to the average wind speed values in the period of 2007/2010, curve 2 – to the average wind speed values in the period of 2009/2010, and curve *3* – to the distribution of the average wind speed in the Ainaži region in the period of 2009/2010.
Analysis of the distribution curves in Fig.6 obtained for the average wind speed V_a shows that the wind speed distribution in height up to 30 *m* is to a considerable extent determined by the topography of the terrain. In the Ventspils region it is represented by 8 - 10 *m* high tract of forest, whereas in the Ainaži region – an open plain remote from the sea. The points on the curves corresponding to the measured values of wind speed at a height over 30 *m* could be well approximated by the exponential function of the form:

$$V_a = kh^{\alpha}. \qquad (2)$$

For the curves of Fig. 7 the following values for approximating functions have been obtained:

For curve *1* – $V_a = 1.19\ h^{0.37}$, the coefficient of determination $R^2 = 0.9941$;
For curve *2* – $V_a = 1.11\ h^{0.37}$, the coefficient of determination $R^2 = 0.9937$;
For curve *3* – $V_a = 1.02\ h^{0.37}$, the coefficient of determination $R^2 = 0.9977$,

hereafter R^2 – reveals how close is modelled approximation function to actual measured values, most reliable when is at or near 1.

Fig. 7 shows curves *1, 2, 3* for measured values of the average wind speed V_a *(m/s)*, calculated using the corresponding values of approximating functions and extrapolated up to the height *h* of 150 *m*. From analysis of the distribution of the average cubic wind speed depending on the height above the surface $V_{a.c.} = f(h)$ for curves *1, 2, 3* the following coefficients and exponents have been obtained for approximating function in Eq. (2):

For curve *1* – $V_{a.c.} = 1.69\ h^{0.31}$, the coefficient of determination $R^2 = 0.9877$;
For curve *2* – $V_{a.c.} = 1.61\ h^{0.31}$, the coefficient of determination $R^2 = 0.9883$;
For curve *3* – $V_{a.c.} = 1.59\ h^{0.29}$, the coefficient of determination $R^2 = 0.9994$.

With due regard for the relationship in Eq. (1) the distribution curves for the average cubic wind speed values in height $V_{a.c.} = f(h)$ are calculated up to the height of 150 *m* and are presented in Fig. 8 (left). Correspondingly, the distribution curves for the wind energy density $P_d = f(h)$ are presented in Fig. 8 (right). For calculation of the wind energy density in the coastal area and in the regions remote from the coast by 30 - 40 *km* the following functions have been used:

For curve *1* – $P_d = 3.17\ h^{0.93}$ the coefficient of determination $R^2 = 0.9874$;
For curve *2* – $P_d = 2.64\ h^{0.94}$, the coefficient of determination $R^2 = 0.9882$;
For curve *3* – $P_d = 2.57\ h^{0.88}$, the coefficient of determination $R^2 = 0.9995$.

For flat territories typical of the Baltic countries the approximating function Eq. (2) could be reduced to the form more convenient for the use as shown in the Eq. (3) & Eq. (4):

$$V_{a.h} = V_{a.h_1}\left(\frac{h}{h_1}\right)^{\alpha}, \quad (3)$$

$$V_{a.h} = V_{a.h_1}\left(\frac{h - h_0}{h_1 - h_0}\right)^{\alpha} \quad (4)$$

where $V_{a.h}$ – is the calculated value of the average wind speed *(m/s)* at height *h*, *(m)*;

$V_{a.h_1}$– is the measured value of the average wind speed *(m/s)* at height h_1, *(m)* for a flat area;

h_0 – is the height of the surface relief at the installation point of the measuring set,

α – is the approximation coefficient (depending on the remoteness from the sea shore is 0.37 – 0.31).

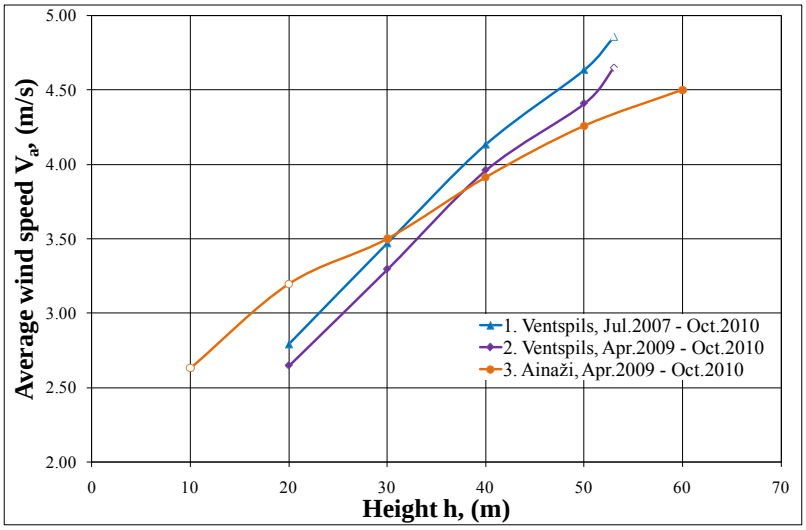

Fig. 6. The curves of the average wind speed vs. height V_a = f(h) in the Ventspils and Ainaži regions obtained by measurements.

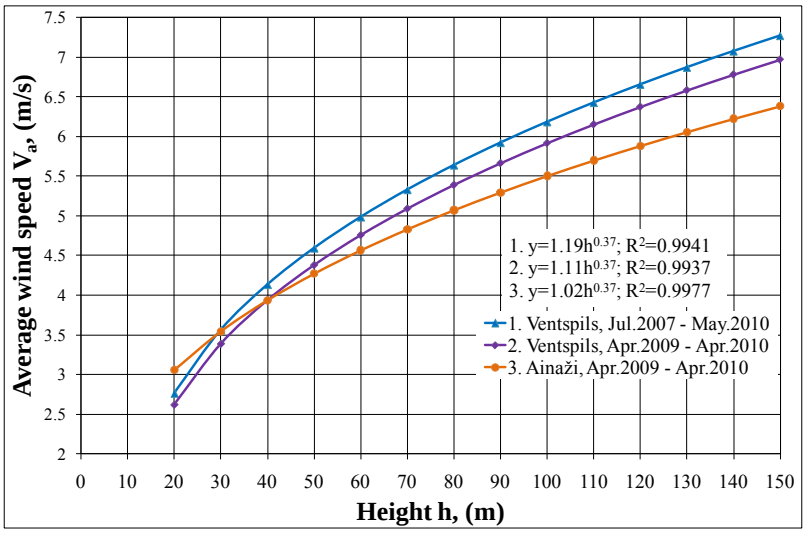

Fig. 7. The curves of the average wind speed vs. height V_a = f(h) in the Ventspils and Ainaži regions extrapolated up to the height of 150 (m).

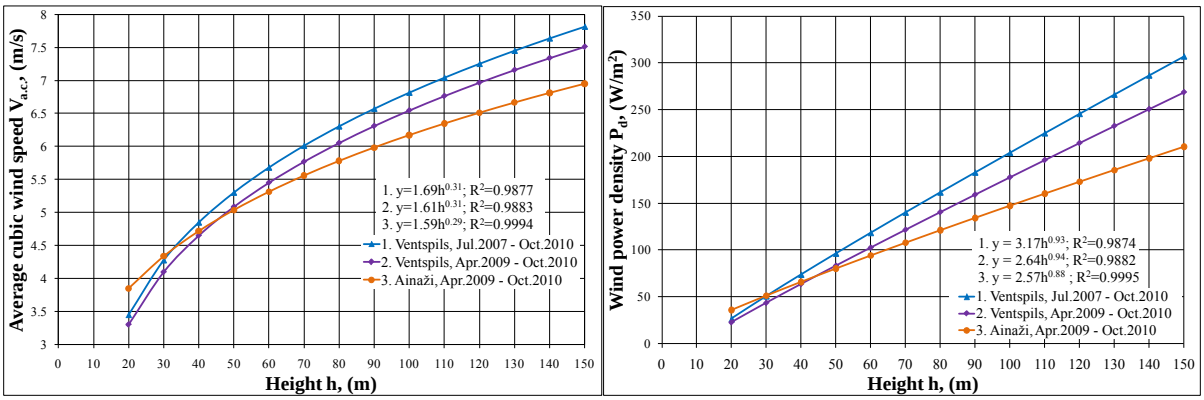

Fig. 8 (left). The curves of the average cubic wind speed vs. height $V_{a.c.}$ = f(h) in the Ventspils and Ainaži regions extrapolated up to the height of 150 (m). Fig. 8 (right). The curves of the wind energy density vs. height P_d = f(h) in the Ventspils and Ainaži regions extrapolated up to the height of 150 (m).

4. Estimation of the acoustic noise level distribution around a WPP

One of the negative aspects of WPP operation is emission of low-frequency noise that acts on humans and disturb comfortable life conditions. Calculations allow to define a zone of noise influence on environment and to determine if the planned projects are in accordance with requirements of the Law of Republic of Latvia, which establishes acceptance standards of noise level in populated areas. In compliance with the sanitary norms in Latvia the noise level accepted at the places of permanent residence of people must not exceed 40 *dB(A).* This means that the construction of WPPs in the proximity of settlements is not allowed.

Fig. 9. The map of noise level distribution around a WPP consisting of 32 generators with the total power of 80.0 (MW) in the territory 8000x5000 (m).

Figure 9 s hows the map of noise level distribution in the territory surrounding a WPP consisting of 32 generators with the total power of 80.0 *MW* in the Ainaži region. The maximum value of the noise level in the WPP territory is 50.14 *dB(A),* the noise level of a generator being 99.0 *dB(A)* [3].

5. Conclusions

1. Availability of large unpopulated areas on the coasts of the Baltic countries, along with the developed infrastructure of electric power networks, makes attractive the use of these lands for siting large wind power plants (WPPs).

2. During long-term observations a statistical database has been accumulated on the distribution of speeds and directions of winds at different heights: 10, 20, 30, 40, 50 and 60 *m* in the Ventspils and Ainaži regions on the Baltic Sea shore.

3. The graphs of seasonal fluctuations of wind speed have been obtained for the heights up to 60 *m* by measurements over the period of 2007 - 2010.

4. The histograms have been composed for the relative frequency of repetition of wind speed over the period of 2007 - 2010.

5. The values of approximating functions have been obtained allowing for the calculations of the wind speed at a height up to 150 *m* above the ground level in coastal zones of the Baltic Sea and in a territory remote from the sea by 35 *km*.

6. The wind speed measurements are noticeably affected by the terrain features, therefore to raise the precision at determination of approximating functions it is worthwhile to dispose the measuring sensors at a height over 30 *m* above the surface level.

7. During the period of observations it has been revealed that in 2009 the average yearly wind speed on the Baltic Sea shore decreased 5% with respect to 2007. To compose the atlas of the wind energy resources it is necessary to investigate the period of cyclic yearly fluctuations of the wind speed.

8. The maximum values obtained for separate wind gusts lasting not less than 10 *s* are not much higher in the Ventspils region than in Ainaži. In January 2005 the wind gusts at a height of 50 *m* in the Ventspils region reached 34.1 *m/s.*

9. In the places of WPP location the level of acoustic noise can be higher than 50.14 *dB(A),* while in compliance with the sanitary norms the noise level allowable for residential areas must not exceed 40 *dB(A).*

References

[1] V. Bezrukov, V. Pugachov, P. Shipkovs, G. Kashkarova, Vl. Bezrukovs „Investigation of the wind energy potential in the Baltic region". SCW2005, ISES Solar World Congress, August 6 – 12, Orlando, US, - 6 pp.

[2] P. Shipkovs, V. Bezrukov, V. Pugachev, Vl. Bezrukovs, V. Silutins, Research of the wind energy resource distribution in the Baltic region, World Renewable Energy Congress XI 23-30 September 2010, Abu Dhabi, UEA, pp.1931 – 1936.

[3] P. Shipkovs, V. Bezrukov, Vl. Pugachov, Vl. Bezrukovs, S. Orlova „Measurements and utilization of wind energy on the Baltic Sea coast". The 10th World Renewable Energy Congress – WREC X, 19-25 July, 2008, Glasgow, Scotland, CD proceedings 2398 – 2403.

Using meteorological wind data to estimate turbine generation output: a sensitivity analysis

M. L. Kubik[1,*], P. J. Coker [2], C. Hunt[3]

[1] *Technologies for Sustainable Built Environments, University of Reading, United Kingdom*
[2] *School of Construction Management and Engineering, University of Reading, United Kingdom*
[3] *AES, Richmond upon Thames, United Kingdom*
** Corresponding author. Tel: +44 (0)118 378 4670, E-mail: m.kubik@pgr.reading.ac.uk*

Abstract: Various studies investigating the future impacts of integrating high levels of renewable energy make use of historical meteorological (met) station data to produce estimates of future generation. Hourly means of 10m horizontal wind are extrapolated to a standard turbine hub height using the wind profile power or log law and used to simulate the hypothetical power output of a turbine at that location; repeating this procedure using many viable locations can produce a picture of future electricity generation. However, the estimate of hub height wind speed is dependent on the choice of the wind shear exponent α or the roughness length z_0, and requires a number of simplifying assumptions. This paper investigates the sensitivity of this estimation on generation output using a case study of a met station in West Freugh, Scotland. The results show that the choice of wind shear exponent is a particularly sensitive parameter which can lead to significant variation of estimated hub height wind speed and hence estimated future generation potential of a region.

Keywords: *Wind shear exponent, Wind profile, Renewable energy, Variability, Intermittency*

Nomenclature

α	*wind shear coefficient*..... *dimless*	k	*von Karman constant*.....*dimless*
u_1	*horizontal velocity component at* z_1 .....ms^{-1}	z_0	*surface roughness factor*.....*m*
u_2	*horizontal velocity component at* z_2 .....ms^{-1}	z_1	*vertical measurement height 1* .....*m*
u_*	*friction velocity*.....ms^{-1}	z_2	*vertical measurement height 2* .....*m*

1. Introduction

Various influential studies investigating the impacts of the variability of renewable resources begin with meteorological (met) station data, as this is often readily available over a wide geographic area [1-3]. Alternative studies instead rely on statistical methods, e.g. [4], have direct access to wind farm generation data, e.g. [5], or take a black box approach and consider the impact of wind at a system level, based upon industry forecasts and policy targets, e.g. [6].

A typical weather station will log hourly mean horizontal wind and gust speeds at a standard height of 10m, which may be extrapolated to estimate the wind speed at a standard wind turbine height. By applying a wind turbine power curve, the wind speed can be converted into a hypothetical generation output, and repeating this process to a greater number of turbines and to a wider geographical area can give insight into how a future involving a high penetration of renewable energy may look.

Two common analytical models are used to map the wind velocity profile with height, and hence allow the calculation of horizontal wind speed at a certain elevation over the earth's surface: the log law and the power law [7]. In reality, the complex and dynamic nature of the atmospheric boundary layer means that one single profile will not provide a consistently reliable extrapolation of wind speed from one height to another. The variables in the log and power laws therefore are particularly important to consider when performing the kind of future resource study suggested above. This paper investigates precisely this sensitivity by

carrying out a resource analysis of hourly mean wind data for a met station in West Freugh, Scotland, in the same manner that other influential resource studies [1-3] have used.

First, the relevant background literature and the methodology used in this research are presented, with particular focus given to the assumptions made in the analysis. The findings of the research are then discussed, the implications identified, and avenues for future research are highlighted.

2. Background literature

There are two main analytical models used to extrapolate wind speeds to greater heights: the log law and the power law. In general, the two models have been shown to perform equivalently in shear extrapolation predictions on average, although at any particular site one model may be better than another [8]. However, for either approach, large errors in the predictions are common and this error is exacerbated further when energy production is estimated. This section introduces the theory and assumptions behind these two approaches, and indicates some of the previous work into better understanding and applying them.

2.1. The Logarithmic Law

The log law's origins lie in boundary layer fluid mechanics and atmospheric research [7]. For determining the horizontal velocity u at a height z is commonly expressed

$$u(z) = \left(\frac{u_*}{k}\right)\ln\left(\frac{z}{z_0}\right) \tag{1}$$

Where u_* is the friction velocity, k is the von Karman constant and z_0 is a measure of surface roughness known as the roughness length; u_* and k are generally determined from a graph of experimental data [9].

There are cases where wind velocity u_1 is known at a reference height z_1, and required at another z_2, in which case it can be derived from equation 1 that

$$u_2 = u_1 \frac{\ln(z_2) - \ln(z_1)}{\ln(z_1) - \ln(z_0)} \tag{2}$$

This is a simpler expression to solve, as it eliminates the need to calculate the friction velocity and von Karman constant, which can be difficult to estimate in the atmosphere. A neutral wind profile is assumed [9], where convection is negligible, the lapse rate (the fall of temperature in the troposphere with height) is nearly adiabatic and stratification is nearly hydrostatically neutral (i.e. there is no *vertical* wind flow in the atmosphere without excitation).

Seasonal variations in local terrain characteristics can have a profound influence the on estimation of z_0 (due to changes in foliation, vegetation, snow cover etc.). Table 1 extracts some guideline roughness lengths for different types of terrain as given in the European Wind Atlas [10].

Table 1- Typical Surface Roughness Lengths z_0

Terrain	z_0 (m)
Water areas (lakes, fjords, open sea)	0.0001
Airport runway areas	0.01
Airport areas with buildings and trees	0.02
Farmland with very few buildings and trees	0.03
Farmland with closed appearance	0.10
City	1.00

2.2. The Power Law

The power law [9] is an empirical equation, expressed

$$u_2 = u_1\left(\frac{z_2}{z_1}\right)^{\alpha} \tag{3}$$

Where α is the wind shear coefficient or power exponent, an empirically derived constant applied over the height range that the power law is applied. Calculating the wind shear coefficient becomes trivial if the wind speeds at two heights are known, as equation 3 may be rearranged in terms of α

$$\alpha = \frac{\ln(u_2) - \ln(u_1)}{\ln(z_2) - \ln(z_1)} \tag{4}$$

The exponent α is a dynamic value that is dependent upon the stability of the atmosphere. The wind shear exponent may be taken as constant for a given height in a given height range, but a different α should be chosen depending on the height range over which the power law is applied [9]. For neutral stability conditions, α is approximately 1/7, or 0.143 (this rule of thumb is known as the "1/7^{ths} power law"), regarded as a reasonable but conservative estimate [11]. However, various site specific studies have found that the coefficient is actually greater, and that this leads to underestimation of the energy resource available [12-14].

2.3. Usage of the two laws

Each method requires knowledge of a wind speed at a reference height, and one further coefficient: a roughness length z_0 in the case of the log law and a wind shear coefficient α in the case of the power law. Both may be calculated using on site measurements, but the power law is common engineering practice [15] favoured by the wind industry and consultants, as the wind shear coefficient is a dynamic value that varies according to a large number of factors including time of day, season, atmospheric stability and regional topography [11]. The log law on the other hand is only valid under certain assumptions regarding atmospheric stability, and actual profiles may deviate from the log law. In the wind industry the two methods are generally checked where possible to ensure that they provide similar results [15].

Unlike wind developers, many researchers do not have the resources to conduct field investigations (for example, by erecting weather masts) to determine the horizontal wind characteristics at likely development sites, and instead rely upon available 10m met station data and shear profile extrapolation for their models, often over a large height range and assuming one constant annual value.

3. Methodology

Meteorological data for this study was obtained from the British Atmospheric Data Centre MIDAS database for a station located at West Freugh airfield, Scotland. A wider number of sites were considered, but this site was chosen because it provided a reliable and continuous data set. Five years (2005-2009) of Hourly Climate Messages (HCM) were chosen over Synoptic (SYNOP) data for analysis, as the latter relies on a 10min wind sample to produce an hourly average. HCM readings sample continuously to produce an hourly average mean wind at a standard height of 10m. The readings were recorded to the nearest knot, but converted to SI units for analysis.

The literature identified that the log and power law extrapolations were each dependent on a single parameter: the surface roughness z_0 and the wind shear coefficient α respectively. Four surface roughness lengths were selected for analysis using Table 1, based upon an understanding of the site topography (i.e. an airfield with building and trees being the best description, and hence the starting point) and similarly, a range of four shear coefficients were also selected, using the $1/7^{th}$ power law as a starting point. Both sets of parameters were selected to represent a realistic spread of values that an analyst might take for the site [15].

A Vestas V80 2MW wind turbine power curve was used for calculation of generation output, with an assumed hub height of 60m. The generation outputs were calculated each year for each of the extrapolated profiles of 10m wind speed, producing an apparent indication of the site's annual capacity factor, energy production, zero generation hours and the proportion of time when a hypothetical turbine would be producing no power output.

4. Results

Annual capacity factors, based upon wind speed extrapolation to 60m, are shown in Figure 1, with all other results summarised in Table 2. A sample week (from June 2005) has been extracted from the analysis and used to illustrate the change in estimated 60m wind speed and generation outputs under each law; this is shown in Figure 2.

Figure 3 maps the profile of wind speed with height from a starting height of z_1=10m, using the log and power law with the variables specified in the methodology. A typical wind speed of u_1=5ms^{-1} was a chosen to illustrate this behaviour. The extrapolated wind speeds at z=60m are emphasised for discussion, as this was the height of interest in this study.

Table 2 - Summary of mean values attained under log and power law

5 year average	power law (α)				log law (z_0)			
	0.100	0.143	0.200	0.300	0.010	0.020	0.030	0.100
Capacity Factor	0.266	0.307	0.364	0.463	0.293	0.306	0.314	0.348
Zero prod hrs	1777	1779	1785	1468	1778	1779	1779	1782
% non gen time	20.4%	20.4%	20.5%	16.9%	20.4%	20.4%	20.4%	20.5%
Total GWh	4.623	5.348	6.344	8.057	5.105	5.320	5.470	6.053

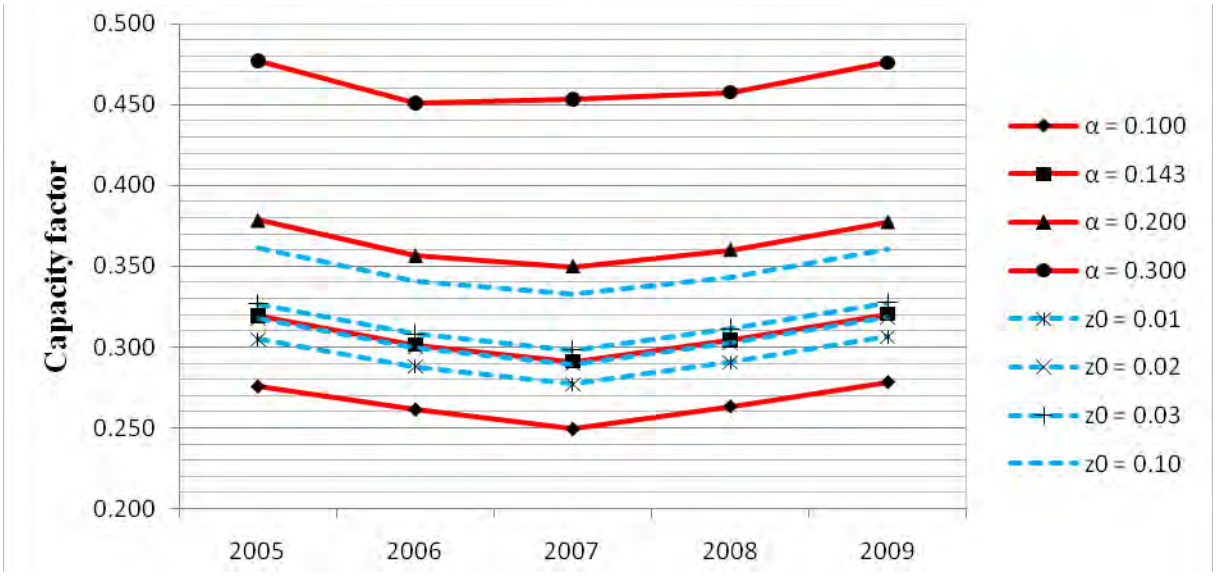

Figure 1 - Graph of extrapolated annual capacity factors

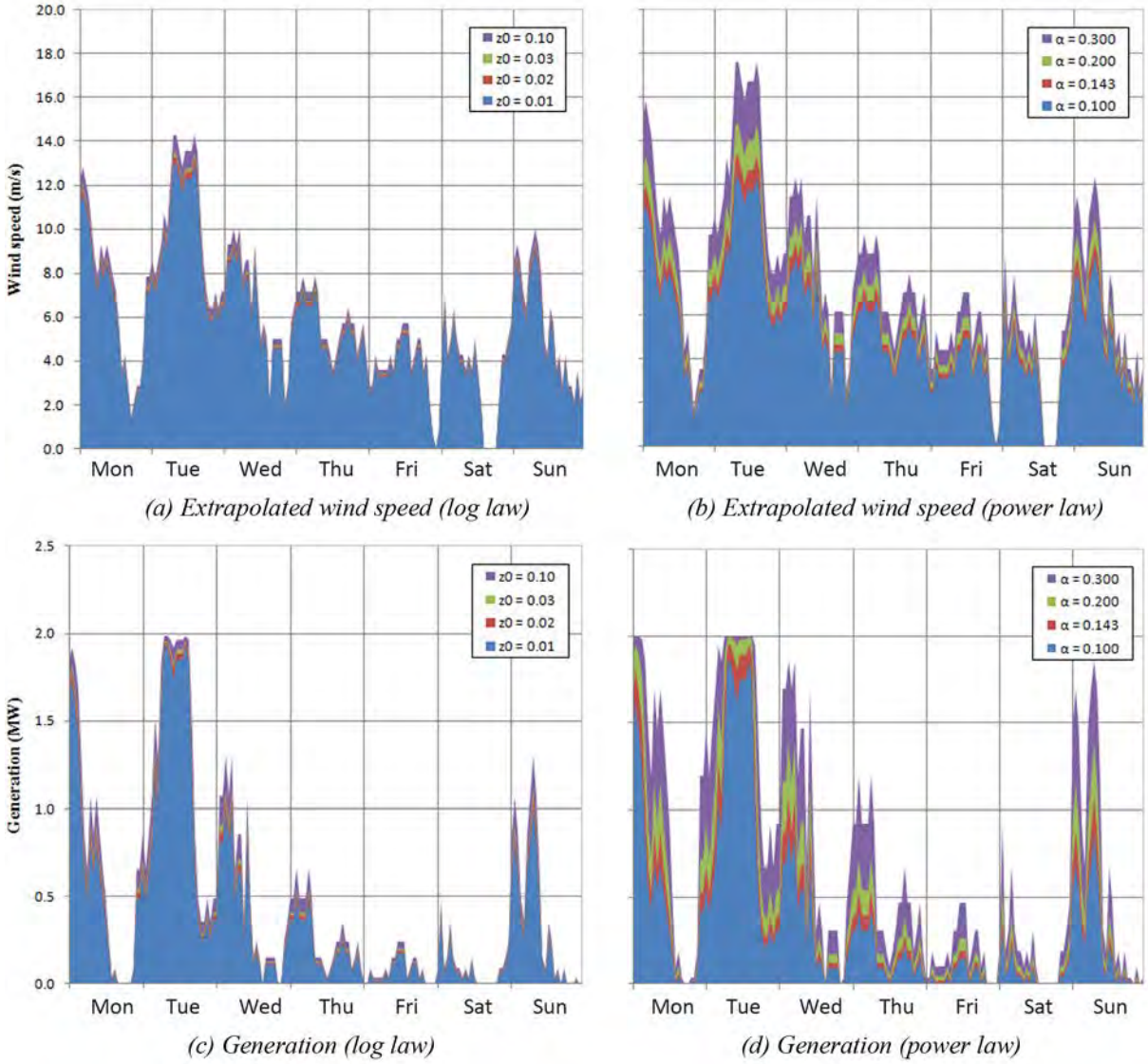

Figure 2 - Sample week of wind extrapolation and estimated generation using the log and power law

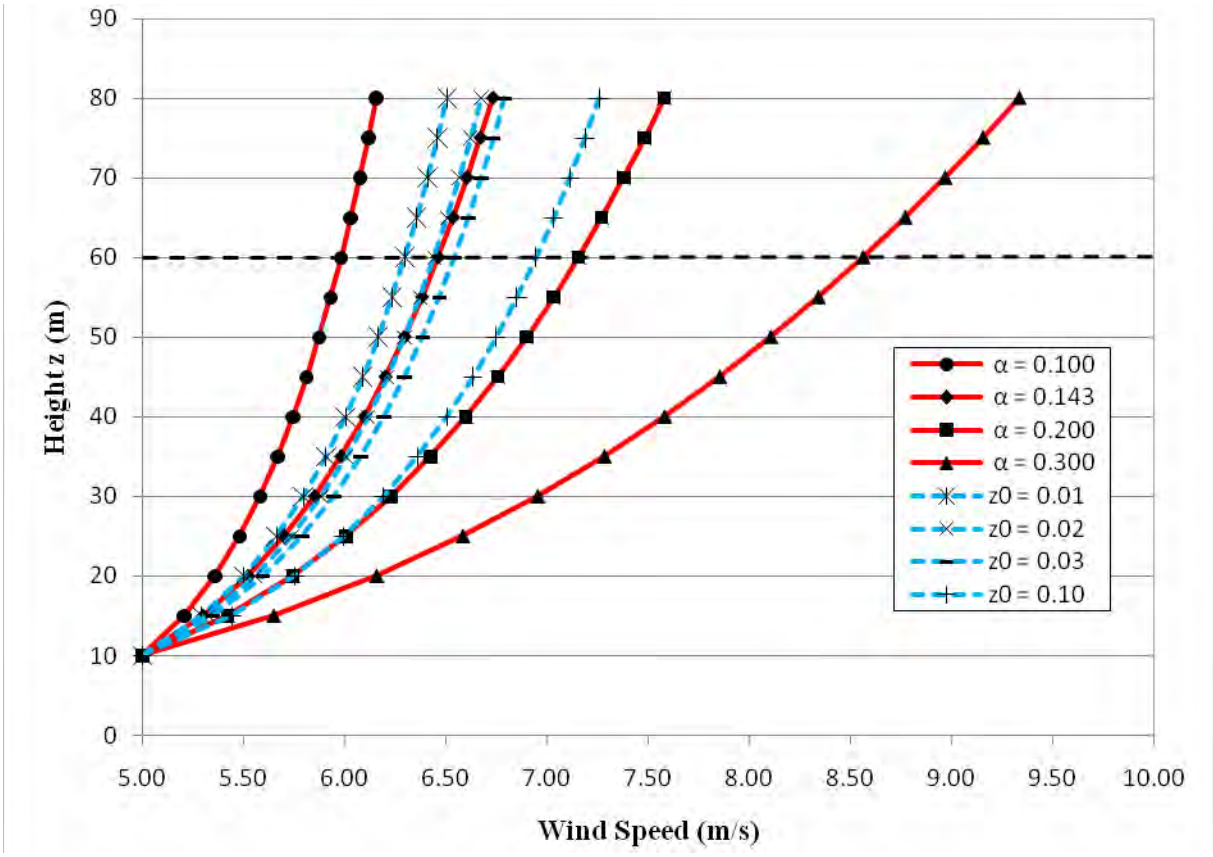

Figure 3- Graph illustrating the wind shear profiles under various log and power law parameters

5. Discussion

It is clear that the base case parameter choices (z_0 = 0.02m and α = 0.143) follow a near identical profile (Figure 3), and hence produce very similar capacity factor estimates and total amounts of energy annually (Table 2). T his is to be expected, as both represent neutral stability conditions. The parameter values in this study were selected to represent the realistic values an analyst might take for the West Freugh site, as discussed earlier in the methodology. Through these choices a wider range of surface roughnesses than shear coefficients were applied (a percentage change of 1000% in z_0 and 300% in α respectively, from the lowest to highest values). Regardless of this disparity, which would be expected to favour a tighter knit set of results for the power law, Figure 3 shows that the range of extrapolated wind speeds at 60m was in fact considerably larger for the power law than the log law (0.65ms^{-1} and 2.58ms^{-1} respectively). This trend is also clearly observed in Figure 2(a) and (b); in the former, the wind speeds for each series are banded close together, in the latter they are considerably more widespread.

Figure 2 also very clearly illustrates the variable nature of the wind resource and the importance that it has on the output of a wind turbine. The sensitivity of the power output is pronounced for different shear coefficients, though relatively similar generation profiles are produced for the range of surface roughnesses, as shown in Figure 2(c) and (d). This is similarly observed in the clustered nature of the log law annual capacity factors in Figure 1, compared to a considerably wider range for the power law.

The reason for the pronounced difference in generation outputs, observed particularly strongly using the power law, is that wind turbine power is related to the cube of wind speed, so a

difference in the wind speed error becomes far more significant in a generation calculation. This is best illustrated with an example; the mean 60m wind speed calculated for West Freugh in 2005, using $\alpha = 0.100$ and $\alpha = 0.200$, together with the limits of one standard deviation, is overlain onto a Vestas V80 power curve in Figure 4. As the cumulative energy generated is calculated by integrating under the area of the curve, it is clearly illustrated how a small change in mean wind speed estimate equates to a significantly larger area under the curve, and hence a large change in total generated energy.

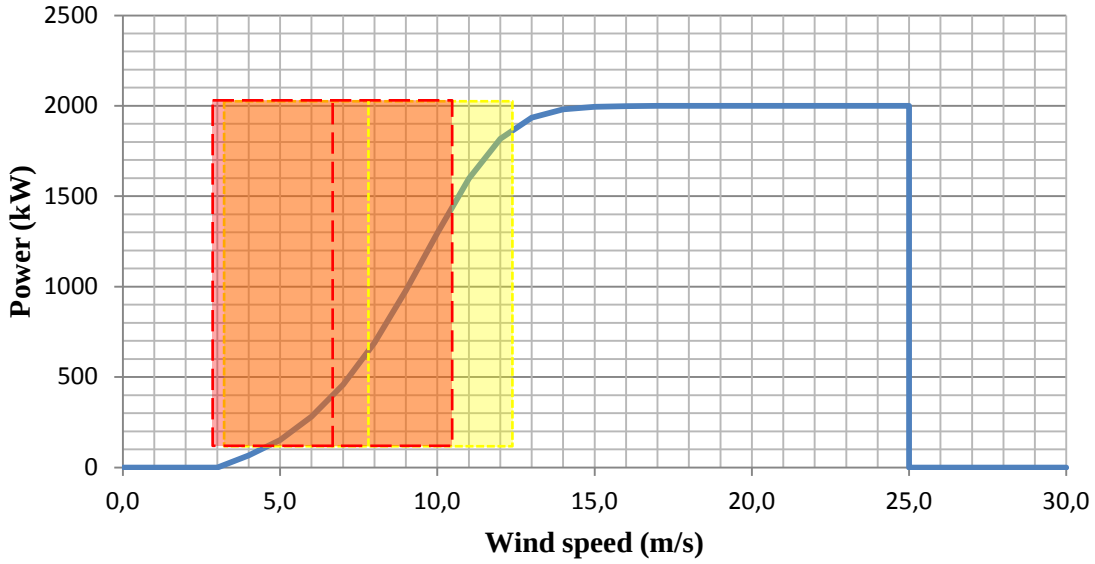

Figure 4- Vestas V80 power curve, annotated. The long red dashes indicate the mean wind and range of one standard deviation for α=0.100, and the short yellow dashes for α=0.200.

6. Conclusions

It is clear from the results that the wind shear coefficient is a more sensitive parameter than surface roughness, and that an equivalent percentage change to each value will impact the wind speed and generation estimates more robustly than when using the log law. However, if properly used, the power law can provide a more accurate idea of the renewable energy output of a particular site or area than the log law, which requires neutral stability conditions to be scientifically exact.

This study is not suggesting that either the power or log laws are intrinsically good or bad, but rather highlights the importance of the quality of information that goes into a model. It is important that there is a good understanding of the site before attempting to apply a single parameter to characterise the system, particularly as in reality the wind shear coefficient is a dynamic value dependant on a large number of parameters.

In order to understand the accuracy of using a single wind shear for the power law model, it is important to compare this theoretical generation data to the output for a real wind farm. Without this information, a critical analysis of this type of approach to future resource estimate cannot be made. Another interesting topic for future research will be to look into how different wind turbine designs, with different power curve characteristics, may change the energy yield of a site. Both of these are aspects of research that the authors intend to investigate in future studies.

Acknowledgements

The authors wish to thank James Cox of Pöyry Energy Consulting for clarifying aspects of the methodology used in their energy models. They also extend their thanks to Lauren Wheatley of AES, and to Thomas Campbell and Richard Mardon of Your Energy Ltd., for their business insight regarding the appraisal of wind sites.

References

[1] Pöyry, *Impact of intermittency: how wind variability could change the shape of the British and Irish electricity markets*. 2009.

[2] G. Sinden, "Characteristics of the UK wind resource: Long-term patterns and relationship to electricity demand," *Energy Policy*, vol. 35, no. 1, pp. 112-127, Jan. 2007.

[3] SKM, "Growth scenarios for UK renewables generation and implications for future developments and operation of electricity networks," BERR Publication URN 08/1021, Jun-2008.

[4] P. Meibom et al., *Final Report for All Island Grid Study Work-stream 2(b): Wind Variability Management Studies*. Roskilde, Denmark: Risø National Laboratory, 2007.

[5] ESB, *The Impact of Wind Power Generation in Ireland*. ESB National Grid, 2004.

[6] B. Klusmann and U. Ziller, *Power supply 2020 - how to reach a modern energy economy*. Bundersverband Erneuerbare Energie, 2009.

[7] J. F. Manwell, J. G. McGowan, and A. L. Rogers, *Wind Energy Explained: Theory, Design and Application*. John Wiley and Sons, 2010.

[8] M. R. Elkinton, A. L. Rogers, and J. G. McGowan, "An Investigation of Wind-shear Models and Experimental Data Trends for Different Terrains," *Wind Engineering*, vol. 30, no. 4, pp. 341-350, May. 2006.

[9] H. Panofsky and J. Dutton, *Atmospheric Turbulence: models and methods for engineering applications*. Pennsylvania State University: John Wiley and Sons, 1984.

[10] WAsP, "WAsP 9 documentation: The roughness of a terrain." [Online]. Available: http://www.wasp.dk. [Accessed: 22-Nov-2010].

[11] P. Gipe, *Wind power: renewable energy for home, farm, and business*. Chelsea Green Publishing, 2004.

[12] M.H. Albadi and E.F. El-Saadany, "The Effects of Wind Profile on Thermal Units Generation Costs," presented at the Power Systems Conference and Exposition, 2009. PSCE '09. IEEE/PES, Seattle, WA, pp. 1-6, 2009.

[13] D. Sisterson, B. Hicks, R. Coulter, and M. Wesely, "Difficulties in using power laws for wind energy assessment," *Solar Energy*, vol. 31, no. 2, pp. 201-204, 1983.

[14] M. W. Tennis, S. Clemmer, and J. Etherington, *Assessing Wind Resources A Guide for Landowners, Project Developers and Power Suppliers*. Union of Concerned Scientists, 1999.

[15] L. Wheatley, T. Campbell, and R. Mardon, "Personal Communication with AES and Your Energy Ltd.," 2010.

Wind speed and power characteristics at different heights for a wind data collection tower in Saudi Arabia

Alam Md. Mahbub[2], Shafiqur Rehman[1,2,*], Josua Meyer[2], Luai M. Al-Hadhrami[1]

[1]*Center for Engineering Research, Research Institute, King Fahd University for Petroleum and Minerals, Dhahran-31261, Saudi Arabia*
[2]*Mechanical and Aeronautical Engineering Department, University of Pretoria, Pretoria, South Africa*
** Corresponding author: Tel: 966 3 8603802, Fax: 966 3 8603996, E-mail: srehman@kfupm.edu.sa*

Abstract: Generating energy with clean and renewable sources of energy has become imperative due to the present days' energy crisis and growing environmental consciousness. The objective of the present study is to assess the wind power, wind shear exponent, air turbulence intensity, energy yield, plant capacity factor and effect of hub height on energy yield and PCF for the site under consideration. To achieve the set objectives, wind speed measurements at different height made during the evaluation period were utilized. The site under consideration was found to be feasible for developing grid connected wind farms in the area with annual energy yield of 11.75GWh with plant capacity factor of 48.8% from one wind turbine of 2.75MW rated power with a hub height of 100m from Vestas.

Keywords: *Wind Energy, Saudi Arabia, Plant Capacity Factor, Wind Speed, Weibull Parameters, Wind Shear, Wind Turbulence*

1. Introduction

The adverse effect of climate change such as tsunami, floods, forest fires, have become common in the recent years due to alarmingly increasing pollution levels and increasing global population and thereof increasing power demands. Each megawatt of electricity generated using fossil fuel adds around half a ton of green house gases equivalent CO_2 in to the atmosphere. The accumulating effect of fast depletion of fossil fuels, alarmingly rising environmental pollution levels, and at the same time gradually emerging awareness of environmental degradation has given rise to the use of renewable sources of energy such as wind, solar, small and large hydro, geothermal, tidal, and bio-energy. Of these clean sources, the rapid development in wind energy conversion technology has made it an alternative to conventional energy systems in recent years. Wind energy is the fastest growing source of energy and is getting worldwide attention due to the technological advances for harnessing the wind power and its competitive cost of production compared to other traditional means. In order to conserve the conventional energy resources and to address the environmental problems, the wind power utilization is the answer to these problems. The worldwide wind power installed capacity is increasing rapidly due to new projects being commissioned in different parts of the world. United States of America (USA) is leading the world with regard to global wind power installed capacity. The other countries contributing towards wind power sectors are Germany, Spain, Denmark, India, China, United Kingdom, Egypt, and others.

Various wind speed and wind power characteristics studies have been reported in and around the Middle East region. Some of these studies include Marafia and Ashour [1] for offshore/onshore wind power project development in Qatar; El-Osta and Kalifa [2] for a proposed 6 MW wind farm in Zwara, Libya; Al-Nassar et. al. [3] showed that the annual mean wind speed in Kuwait lied in the range of 3.7 to 5.5 m/s with mean; Hrashyat [4] reported wind resource assessment of the south western region of Jordan; Elamouri and Amar [5] for Tunisia; Ucar and Balo [6] for Manisa, Turkey; Bagiorgas et. al [7] for Western Greece; Shahta and Hanitsch [8] studied the technical and economic assessment of wind power for Hurghada in Egypt; Toğrul and Kizi [9] for Bishkek, Kyrgyzstan; Jowder [10] reported wind resource assessment for Bahrain; and Himri et. al [11] provided review of

renewable energy in general and the wind in particular for Algeria. Sahin and Bilgili [12] studied the wind characteristics of Belen-Hatay province of Turkey using hourly wind speed records between years 2004 and 2005.

The work on wind resource assessment in Saudi Arabia dates back to 1986, when Ansari et. al [13] used hourly wind speed data to develop a Wind Atlas for Saudi Arabia. In Saudi Arabia, work on wind speed data analysis such as Weibull parameter determination and distribution, wind speed prediction using different methods such as auto-regression and neural network, wind power generation cost determination, and so on has been reported in the literature. Rehman et. al. [14] presented the Weibull parameters for ten anemometer locations in Saudi Arabia and found that the wind speed was well represented by Weibull distribution function. Rehman and Halawani [15] presented the statistical characteristics of wind speed and diurnal variation. The autocorrelation coefficients were found to be matching with the actual diurnal variation of the hourly mean wind speed for most of the locations used in the study. Some of the other studies include Rehman et. al [16], Rehman and Aftab [17] and Rehman et. al [18].

The objective of the present study is to assess the wind power, wind shear exponent, air turbulence intensity, energy yield, plant capacity factor and effect of hub height on energy yield and PCF for the site under consideration.

2. Site, equipment and Data Description

The 40 meter tall tower was installed at Juaymah power plant, a site located in the eastern part of Saudi Arabia. The latitude, longitude and altitude of the measurements site were 26°47' N, 49˚53' E and near sea level, respectively. The data was collected for a period of 33 months stretching from July 01 2006 to April 01, 2009. The area is surrounded by government and private industries and power plants which are connected to the national electric grid. In order to assess the wind potential at the site, an instrumented 40 m tall wind tower, was installed. The meteorological data (wind speeds, wind direction, air temperature, relative humidity, surface station pressure, global solar radiation) were collected for a period of more than two years. The details of the equipment installed at the site are provided in Table 1.

Table 1. Details of the equipment installed at an isolated village.

Item Description	**Technical Information**
Wind speed sensor, NRG#40 Three cup anemometer	AC sine wave, Accuracy: 0.1 m/s, Range: 1-96 m/s Output: 0-125 HZ, Threshold: 0.78 m/s
Wind direction vane, NRG#200P Potentiometer	Accuracy: 1%, Range: 360^o Mechanical, Output: 0-Exc. Voltage, Threshold: 1 m/s, Dead band: Max - 8^o and Typical 4^o
Temperature sensor #110S Integrated circuit	Accuracy: ±1.1 ^{o}C, Range: -40 ^{o}C to 52.5 ^{o}C, Output: 0 – 2.5 volts DC, Operating temperature range: -40 ^{o}C to 52.5 ^{o}C
Barometric pressure sensor BP20	Accuracy: ±15 mb, Range: 150 – 1150 mb, Output: Linear voltage
Relative humidity sensor RH-5 Polymer resistor	Accuracy: ±5%, Range: 0 – 95 % Output: 0 – 5 volts, Operating temperature range: -40 ^{o}C to 54 ^{o}C
Pyranometer Li-Cor #LI-200SA Global solar radiation	Accuracy: 1%, Range: 0 – 3000 W/m^2 , Output: Voltage DC, Operating temperature range: -40 ^{o}C to 65 ^{o}C

3. Results and Discussion

This section provides detailed wind data analysis including calculation of site wind exponent and air turbulent intensity, wind energy yield and cost of energy. Over entire period of data collection the mean wind speeds at 10, 20, 30 and 40 meters AGL were 4.14, 4.84, 5.34 and 5.65 m/s respectively. The climatic parameters like average ambient temperature, relative humidity, barometric pressure, air density, wind shear exponent, roughness, and roughness class were 26.1°C, 17.3%, 1014 mbar, 1.181 kg/m3, 0.228, 0.239, 2.72, respectively.

3.1. Annual, seasonal and diurnal behavior of mean wind speed

The annual mean wind speeds build up a confidence on the amount of energy that could be generated and also provide future trends. In present case, the annual mean wind at 10, 20, 30 and 40 meters above ground level (AGL) were 4.1, 4.8, 5.3 and 5.6m/s, respectively, in the year 2007 and 4.2, 4.9, 5.4 and 5.8m/s, in the year 2008. This shows an increased of about 2% in wind speed in the year 2008 compared to that in 2007. The maximum wind speeds observed during these two years at 10, 20, 30 and 40 meters AGL were 15.9m/s, 17.8m/s, 18.4m/s and 19.5m/s, respectively. The prevailing wind direction was found to be NNW and NW during the data collection period.

Knowledge of monthly variation of wind speed provides confidence on the availability of energy in different months of the year. Monthly changes in wind speed at 10meters AGL, over entire data collection period, are shown in Fig. 2. Highest wind speed was observed in June while lowest in August at all the heights of wind speed measurements. At 40m AGL, the monthly mean wind speed always remained above 5.5m/s except during August to October, which means that a wind turbine with cut-in-speed of 3.5m/s can produce energy during all the months of the year at this site.

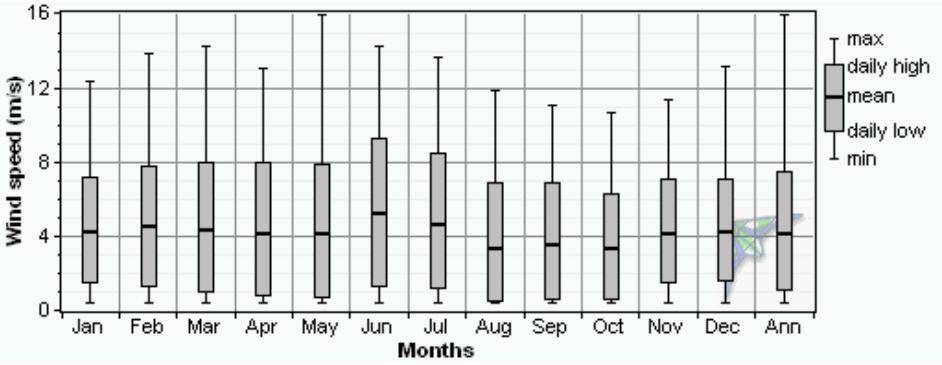

Fig. *1. Seasonal variation of mean wind speed at 10 meters AGL.*

Fig. 3 shows the variation of half hourly mean wind speed at different heights during entire data collection period. It is evident from this figure that as the height of wind measurements increases the wind speed range decreases. At 40m AGL, the half hourly mean wind speed varied from 4.7m/s to 7.0m/s (range=2.3m/s) while at 20m from 3.7m/s to 6.7m/s (range=3.0m/s). At 40m AGL, the wind speed was found above 5.2m/s for most of the time except between 8 P.M. and 12 mid night. This implies that power of the wind can be harnessed during entire day at the measurement site using a wind turbine with cut-in-speed of 3.5m/s and hub height greater than or equal to 40m.

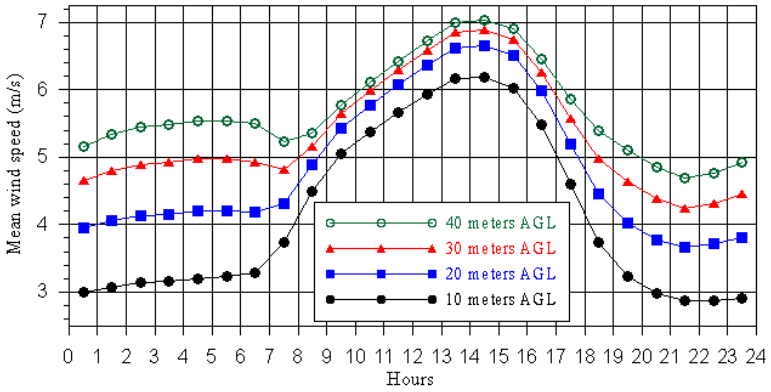

Fig. 2. Diurnal variation of hourly mean wind speed at Juaymah.

3.2. Wiebull parameters and wind frequency analysis

Wiebull distribution function is most widely used function for modeling the wind speed around the globe. The scale factor (c) of the Weibull distribution is related to the average wind speed at different heights and is calculated using the maximum likelihood method. Similarly, the Weibull (k) value is the dimensionless shape factor of the Weibull distribution. This factor reflects the breadth of the distribution. The variation of both scale and shape parameters with measurement heights is shown in Figs. 3 and 4 respectively. Since the wind speed increases with height, hence the scale parameter too follow the trend as can be seen from Fig. 3. The shape parameter also increases with height as shown in Fig. 4. This implies that as height increases, the shape of the distribution tends to be tight which implies less variation in the wind speed. The line of best fit show high values of coefficient of determination (~95%), as given in these figures. The scale parameter increases by about 0.058m/s for each meter increase in measurement height while the shape parameter increases by 0.0157 per meter.

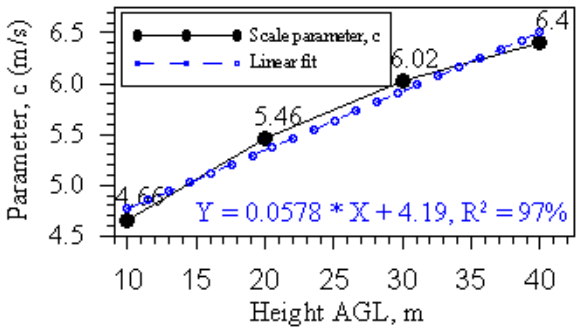

Fig. 3. Variation of scale parameter, c, with measurement height.

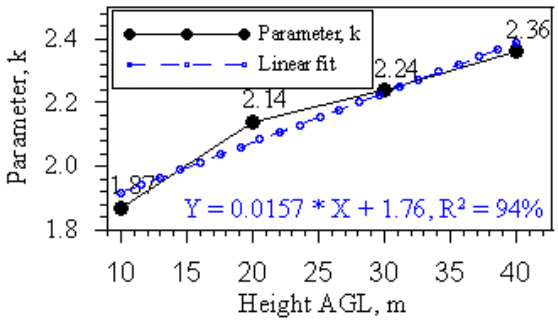

Fig. 4. Variation of shape parameter, k, with measurement height.

Wind speed frequency distribution in different wind speed bins is a very important parameter from energy yield estimation point of view. As the height of wind speed measurement increase, the percent frequency of occurrence of higher winds also increases, as shown in Figures 5(a) and 5(b) at 10 and 40meters AGL. The percent frequencies of 55%, 71%, 78% and 82% at 10, 20, 30 and 40 meters AGL, respectively, were found above 3.5 m/s. An increase of 10 meters in height (from 10 to 20 meters) of the wind speed measurements resulted in an increase of about 16% in the availability of wind speed above 3.5m/s while further increase of 10m in height results only 7% increase in frequency. This analysis confirms that a wind turbine with cut-in-speed of 3.5m/s or more could produce energy for 82% of time at the site of measurements. It is very evident from Figs. 5(a) and 5(b) that as the height increases, the Weibull function fit becomes increasingly better and the wind speed fluctuation also becomes less and less due to decrease in wind turbulence at higher altitudes.

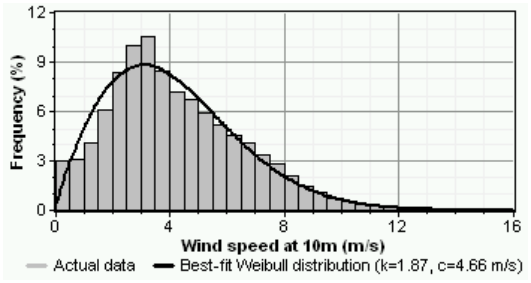

Fig. 5(a). Wiebull fit and frequency distribution of wind speed at 10 meters AGL.

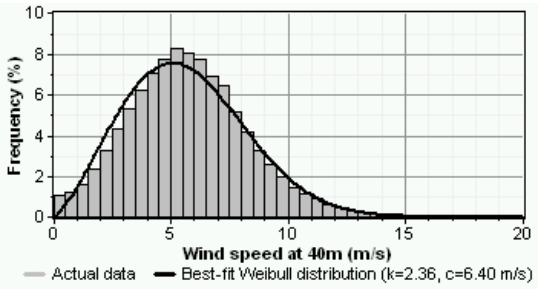

Fig. 5(b). Wiebull fit and frequency distribution of wind speed at 40 meters AGL.

3.3. *Air density and wind power density variation*

In this study, the measured values of air pressure and the temperature were used to calculate the local air density values at Juaymah measurement site. During diurnal cycle, the air density was found to vary between a minimum of 1.159 kg/m^3 during 13:00-14:00 hours and a maximum of 1.201 kg/m^3 during 04:00-05-00 hours. Higher values were noticed during nighttime and lower during day time due to corresponding lower and higher temperatures and air pressure. Around the year, highest mean air density of 1.236 kg/m^3 was obtained in the month of January which characterized by low temperature and relatively high air pressure. On the other hand, lowest air density of 1.136 kg/m3 was recorded in the month of July which is known for high temperature and relatively low air pressure. The mean wind power density values calculated using the local air density and the cube of wind speed during the data collection period at 10, 20, 30 and 40m AGL were 84.7, 119.1, 154.2 and 180.32 W/m^2, respectively. An increase of about 12% was noticed in wind power density in the year 2008 compared to that in 2007 at all measurement heights. The seasonal trends of wind power density values at different heights are depicted in Fig. 6 which indicative of highest values in June and lowest in October.

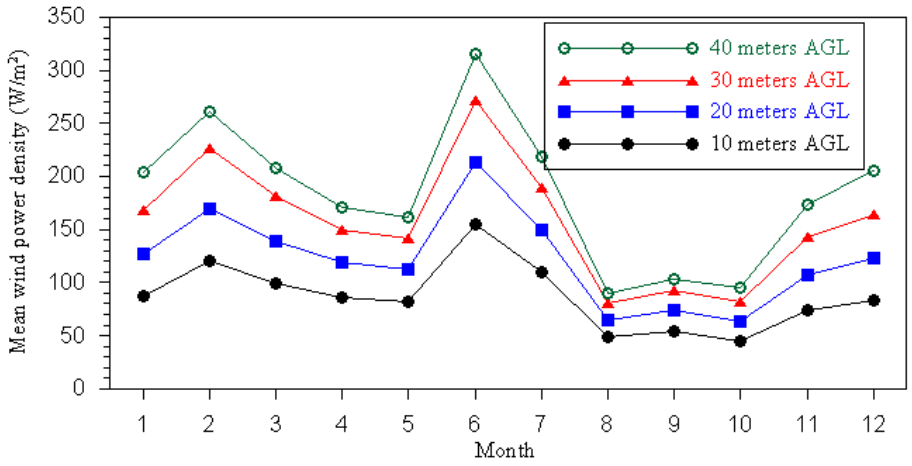

Fig. 6. Seasonal variation of wind power density at different measurement heights.

3.4. Wind shear exponent and turbulence analysis

The power law exponent is a number that characterizes the wind shear, which is the change in wind speed with height above ground. The wind shear exponent (WSE) obtained using all the data values was 0.273 while 0.269 and 0.279 for the data of years 2007 a nd 2008, respectively. Higher values of WSE (~0.285) were observed from October to January and relatively lower (~0.265) during rest of the months with lowest in September. The WSE values are very much dependent on the meteorological changes that take place during 24 hours of day as demonstrated in Fig. 7. It is clear from this figure that higher values of WSE (~0.4) were observed from 7 PM to 7AM and lower (~0.1) from 8:30 AM to 4:30 PM. For precise estimation of wind speed at higher altitudes, different values of WSE during day and

nighttime could be used. The overall surface roughness was estimated as 1.124 m with highest of 1.386 m in October and lowest 0.995 m in June.

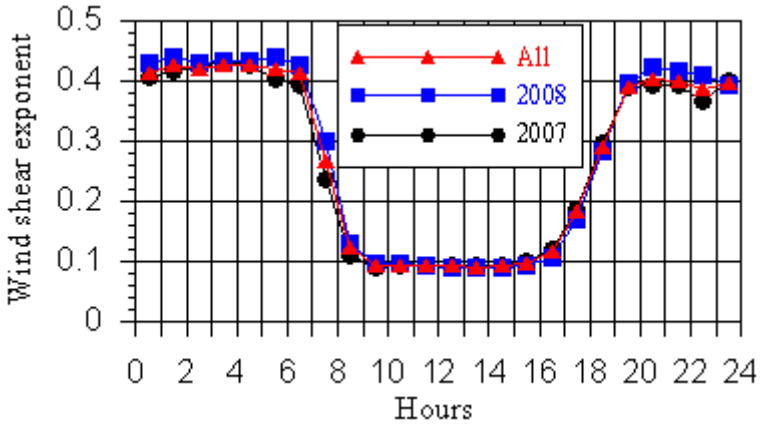

Fig. 7. Diurnal variation of wind shear exponent at Juaymah.

Wind turbulence intensity is critical parameter and dictates the durability or the operational life of the wind turbines. It is highly site dependent and should be well understood before any real time installation. According to International Electrotechnical Commission (IEC, IEC Standard 61400-1) there are standard category A and B values of the turbulence intensities. Any value between these two or below is said to be safe for the normal operation of the wind turbine. The characteristic turbulence intensity, which is another important parameter, is defined as the sum of mean turbulence intensity and the standard deviation of mean turbulence intensity in a wind speed bin. The overall mean turbulence intensity values over entire period of data collection were 0.172, 0.142, 0.127 and 0.122 at 10, 20, 30 and 40m AGL, respectively. The mean turbulence intensity decreases with increasing height AGL as the near ground turbulence effects minimize with height. The mean turbulence intensity along with IEC and characteristic turbulence values is given in Fig. 8. It is evident from this figure that the mean turbulence intensity at the site of measurements is much below even the category C of IEC limits and hence will be safe for normal operating life of the turbines.

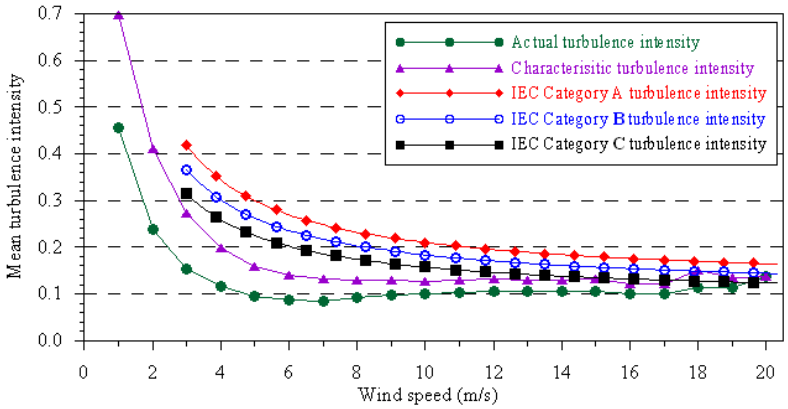

Fig. 8. Varitaion of mean turbulence intensity with wind speed.

3.5. Wind energy yield analysis

For energy yield estimation, a three bladed wind turbine of 2.75MW rated power with rotor diameter of 100m from Vestas was chosen. The net energy yield was calculated by considering the down time, array, soiling and other losses as 4, 5, 1 and 4%, respectively. For energy yield estimation, three hub heights of 60, 80 and 100 meters were considered. The

Annual average wind speed at 60, 80 and 100m AGL was found to be 6.3, 6.8 and 7.2m/s, respectively. The chosen wind turbine could produce average net power of 1,103; 1,239 and 1,341kW corresponding to wind speed at hub heights of 60, 80 and 100m; respectively. Furthermore, the annual net energy equivalent to 9,664; 10,851 and 11,747MWh could be produced with an average plant capacity factor (PCF) of 40.1, 45.0 and 48.8% corresponding to hub heights of 60, 80 and 100m, respectively, from the chosen wind turbine. On an average, the rated power could be produced for only 4% of the time during the year with a hub height of 100m. There will be certain times when the wind turbine will have zero output. It is evident that on annual basis, only 3.6% of the times there will be no power with a hub height of 100m and around 3.9% of the times for 60m hub height. Since wind is an intermittent source of energy, one has to bear with this type of situation.

4. Conclusions

The analysis of the measured data showed that the annual average wind speeds were 4.1, 4.8, 5.3 and 5.7 m/s at 10, 20, 30 and 40m AGL, respectively. The prevailing wind direction was found to be NNW and NW during measurement period. Highest wind speed was observed in June while minimum in August and October at all the heights of wind speed measurements. During entire data collection period, the average wind power density values at 10, 20, 30 and 40m AGL were 85.5, 119.1, 154.2 and 180.3W/m^2, respectively.

The wind shear exponent (WSE) obtained using all the data values was 0.273 while 0.269 and 0.279 for the data of 2007 and 2008, respectively. No definite seasonal trend could be noticed in the values of WSE. The overall mean turbulence intensity values over entire period of data collection were 0.172, 0.142, 0.127 and 0.122 at 10, 20, 30 and 40m AGL, respectively.

The monthly average minimum energy of 526, 600 and 661MWh was generated in August while a maximum of 1,034; 1,127 and 1,192MWh in June corresponding to hub heights of 60, 80 and 100m, respectively. The monthly mean plant capacity factor (PCF) varied between 25.7 and 52.2% for 60m hub height, 29.3 and 57.0% for 60m and between 32.3 and 60.2% for 100m hub height in the months of August and June, respectively.

References

[1] A.H. Marafia, and H.A., Ashour, Economics of off-shore/on-shore Wind Energy Systems in Qatar, Renewable Energy, 28, 2003, pp. 1953-1963.

[2] W. El-Osta, , and Y. Kalifa, Prospects of Wind Power Plants in Libya: A Case Study, Renewable Energy, 28: 2003, pp. 363-371.

[3] W. Al-Nassar, , S. Alhajraf, A. Al-Enizi, L. Al-Awadhi, Potential Wind Power Generation in the State of Kuwait, Renewable Energy, 30, 2005, pp. 2149-2161.

[4] E.S. Hrayshat, Wind Resource Assessment of the Jordanian Southern Region. Renewable Energy, 32, 2007, pp. 1948-1960.

[5] M. Elamouri, and F.B. Amar, Wind Energy Potential in Tunisia, Renewable Energy, 33(4), 2008, pp. 758-768.

[6] A. Ucar and F. Balo, A seasonal analysis of wind turbine characteristics and wind power potential in Manisa, Turkey, International Journal of Green Energy, 5, 2008, pp. 466–479.

[7] H. S. Bagiorgas, G. Mihalakakou, and D. Matthopoulos, A Statistical Analysis of Wind Speed Distributions in the Area of Western Greece, 5(1 & 2), 2008, pp. 120 – 137.

[8] A.S.A. Shahta and R. Hanitsch, Electricity Generation and Wind Potential Assessment at Hurghada, Egypt, Renewable Energy, 33, 2008, pp. 141-148.

[9] İ. T. Toğruland and M.İ. Kizi, Determination of Wind Energy Potential and Wind Speed Data in Bishkek, Kyrgyzstan, International Journal of Green Energy, 5(3), 2008, pp. 157 – 173.

[10] F.A.L. Jowder, Wind Power Analysis and Site Matching of Wind Turbine Generators in Kingdom of Bahrain, Applied Energy, 86, 2009, pp. 538–545.

[11] Y. Himri, A.S. Malik, A.B. Stambouli, S. Himri, and B. Draoui, Review and use of the Algerian Renewable Energy for Sustainable Development, Renewable and Sustainable Energy Reviews, 13, 2009, pp. 1584-1591.

[12] B. Sahin and M. Bilgili, Wind Characteristics and Energy Potential in Belen-Hatay, Turkey, International Jopurnal of Green Energy, 6(2), 2009, pp. 157–172.

[13] J. Ansari, I.K. Madni, and H. Bakhsh, Saudi Arabian Wind Energy Atlas, KACST, Riyadh, Saudi Arabia, 1986, pp. 1-27.

[14] S. Rehman, T.O. Halawani and T. Husain, Weibull Parameters for Wind Speed Distribution in Saudi Arabia, Solar Energy, 53(6), 1994, pp. 473-479.

[15] S. Rehman and T.O. Halawani, Statistical Characteristics of Wind in Saudi Arabia, Renewable Energy, 4(8), 1994, pp. 949-956.

[16] S. Rehman, T.O. Halawani and M. Mohandes, Wind Power Cost Assessment at Twenty Locations in the Kingdom of Saudi Arabia. Renewable Energy, 28, 2003, pp. 573-583.

[17] S. Rehman and A. Aftab, Assessment of Wind Energy Potential for Coastal Locations of the Kingdom of Saudi Arabia, Energy, 29, 2004, pp. 1105-1115.

[18] S. Rehman, I. El-Amin, F. Ahmad, S.M. Shaahid, A.M. Al-Shehri and J.M. Bakhashwain, Wind Power Resource Assessment for Rafha, Saudi Arabia, Renewable and Sustainable Energy Reviews,11, 2007, pp. 937-950.

A wind tunnel method for screening the interaction between wind turbines in planned wind farms

Mats Sandberg[1,*], Hans Wigö[1], Leif Claesson[1], Mathias Cehlin[1]

[1] *University of Gävle, Gävle, Sweden*
** Corresponding author. Tel: +46 26648139, Fax: +46 648181, E-mail: msg@HiG.se*

Abstract: The energy captured by wind farms is reduced if there is an interaction between the individual turbines. In the paper a novel method for studying the interaction between wind turbines is presented. It is based on recording the static pressure on ground in a wind tunnel provided with wind turbine models.
The assumption is that the pressure distribution at ground reflects the pressure distribution at hub height. The pressure distribution at hub height is a result of the flow in the vicinity of the turbine.
The pressure at ground is recorded with a pressure plate provided with 400 pressure taps. The wind turbine model is a porous disk giving a non rotating wake.
At first the pressure response to one wind turbine is recorded. This is the reference case giving the characteristics of a non disturbed wind turbine. Its region of influence can therefore be determined. This provides important information on how to avoid any interaction between turbines. A nearby turbine should not be placed within the region of influence. In the paper we show how the pressure response varies with different distances between two turbines. The agreement between the static pressure on ground and at hub height has been tested by recording the static pressure at hub height with a small Prandtl tube.

Keywords: *Wind farms, Wind tunnel, Pressure distribution on ground, Pressure distribution at hub height, Region of influence*

1. Introduction

To benefit of economies of scale, wind turbines are arranged in wind farms. As wind energy capacity expands, the size of individual wind farms continues to increase requiring tens to hundreds of wind turbines typically arranged in a large array. While organizing wind turbines in wind farms help in reducing the cost of energy production they introduce another problem, aerodynamic interaction. One of the research challenges is to accurately model interactions between the individual turbines to accurately predict power output before wind farm construction. In a wind farm with *N* turbines the wind farm efficiency is defined as

$$\eta_A = \frac{E_{A_i}}{E_T N} \qquad (1)$$

Where E_A is the annual energy captured by the wind farm and E_T is the annual energy captured by one isolated turbine. If there were no aerodynamic interaction the energy captured by the wind farm would be NE_T and the efficiency would subsequently be 100 %. Figure 1 shows a wind turbine with rotor diameter *D*. Array losses can be reduced by optimization of the downwind spacing and the cross wind spacing.

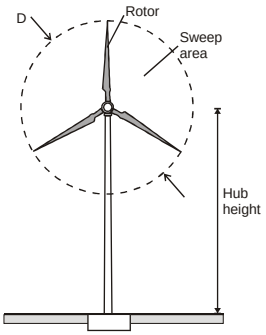

Fig. 1. Definition of some concepts

Behind a wind turbine there is rotating wake with a velocity deficit with respect to the approaching free wind U_∞. If we set the reference pressure (static pressure) in the undisturbed wind to zero there is an under pressure in the wake (compare Figure 5). After a relatively short distance there is pressure recovery. However the velocity deficit goes on for a long distance behind the turbine.

With a too short distance between wind turbines the wind turbines upstream will lower the exposed wind speed of the turbines downstream. Subsequently the power generated by the wind farm will be reduced. This calls for the need of methods for predicting the risk of interaction. Providing such methods in the planning process is the purpose of this research. The importance of accurate design models increases since the turbines gets larger and larger by time. If there is an interaction between wind turbines one can minimize the loss in power generated by suitable control of the wind turbines [1].

It is extremely difficult to predict the power output from wind farms, due to atmospheric turbulence, wind shear, changes in wind directions, wake effect from neighboring turbines etc. In recent times, CFD (Computational Fluid Dynamics) simulations have been performed on wind turbines. Recent wake studies based on CFD using various turbulence models have been presented by e.g. Ivanell [2], Sørensen et al. [3], and Wußow et al.[4]. CFD methods for simulating wake flows and wake interactions need to resolve many different length scales, ranging from the thickness of the blade boundary layer to the distance between the turbines. Hence, there are still limitations in CFD to simulate an entire park, due to computer limitations.

1.1. Basic assumption behind the method

Our approach for studying the aerodynamic interaction between individual wind turbines is based on the assumption that with a plain ground the static pressure distribution on the ground reflects the pressure distribution at hub .Aand the pressure distribution at the hub height reflects the air flow pattern at this height. For natural ventilation the relation between the static pressure in air and on the ground has been explored in [5]. The results were encouraging and are the impetus for this work.

2. Methodology

2.1. Wind tunnel

The experiments were conducted in the atmospheric boundary layer wind tunnel at University of Gävle. The pertinent details of the wind tunnel are shown in Figure 2. Within the empty wind tunnel there is a pressure gradient, see Fig 9. To equalize the pressure within the wind tunnel with the ambient pressure the wind tunnel is provided with a slot of width 6 cm located 255 cm downstream of the centre of the turning table. The slot is running along the whole perimeter of the wind tunnel.

During the tests the wind speed at half height in the test section was about 20 m/s.

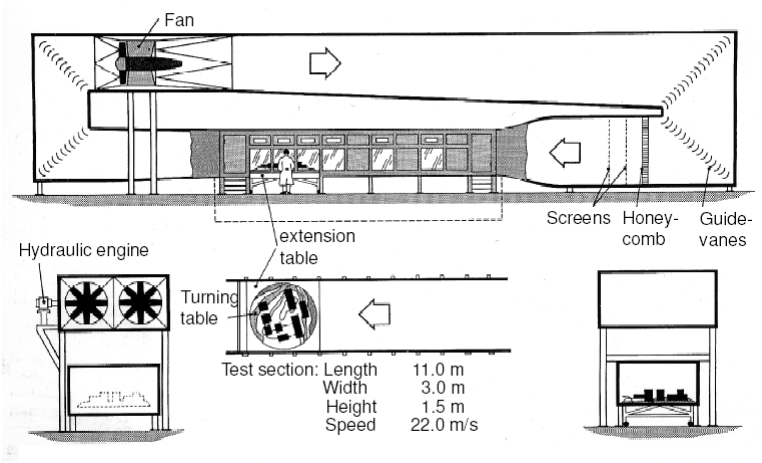

Fig. 2. Atmospheric boundary layer wind tunnel

2.2. Wind turbine model

The wind turbine model used in this study was in scale 1:2000 and had a diameter of 45 mm and the hub height was 45 mm. This corresponds to a wind turbine with 90 meters diameter and a hub height of 90 meters. In the model the rotor where replaced by a porous disc, which was used to simulate the wake behind the wind turbine Medici & Alfredsson [6] .The disc porosity was 42% and the corresponding drag coefficient was 0.85. This value of the drag coefficient is approximately the same as the value obtained for a turbine at high tip speed ratios.

2.3. Technique for measurement of static pressure at hub height and on the ground

The static pressure at hub height (45mm above ground in the wind tunnel) was measured with a Prandtl tube of 3 mm diameter. The static pressure on ground was measured with a pressure plate provided with 400 pressure taps organized in a quadratic pattern with a distance of 37 mm between the centers of the taps, see Figure 3. The pressure was recorded with a pressure transducer connected to a scanner valve. Measuring the pressure in all 400 pressure taps takes about 5 hours

Figure 4 shows the wind tunnel with one wind turbine model placed on the pressure plate. In this picture the wind tunnel was provided with roughness elements and spires to generate a turbulent boundary layer.

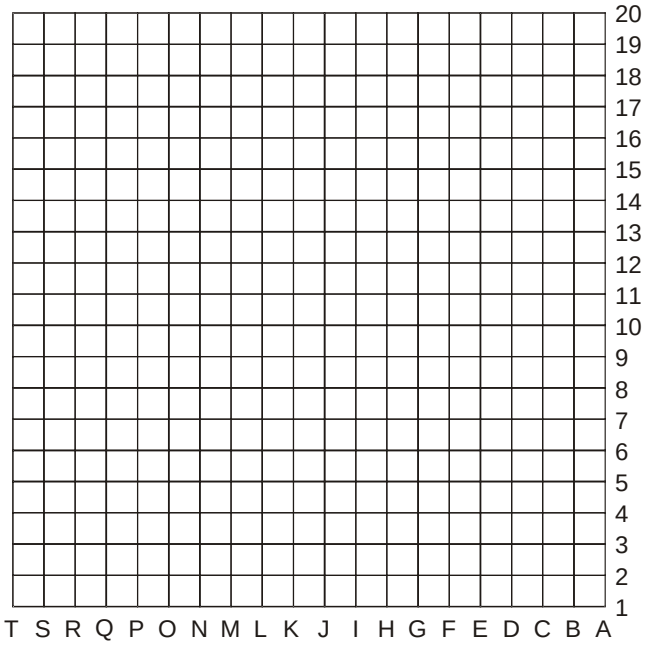

Fig. 3 Notation for the pressure plate

Fig. 4 Wind tunnel with one wind turbine model placed on the pressure plate along line 10 in Fig.3

To eliminate the effect of the pressure gradient along the wind tunnel a measurement was first made with an empty wind tunnel. These data were then subtracted from the pressure readings obtained with a turbine model present.

3. Results

3.1. Pressure response on ground due to one wind turbine

To begin with one wind turbine was placed on the pressure plate along line 10 in Figure 3 and the pressure was recorded. Figure 5 shows the recorded pressure (raw data) quantified as a pressure coefficient.

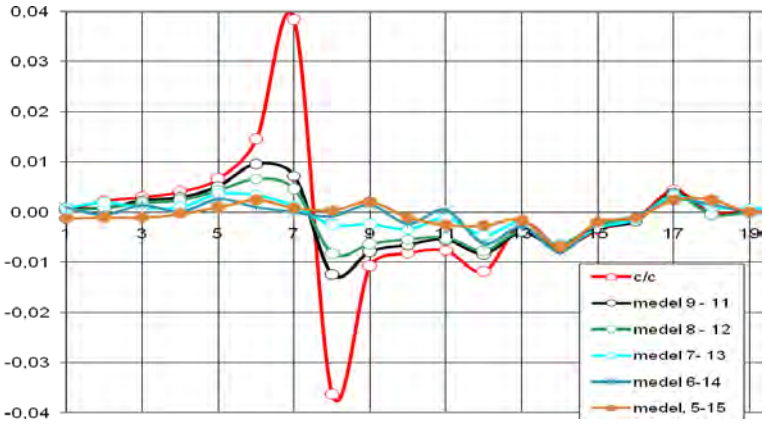

Fig. 5. Recorded pressure coefficients at different positions with one wind turbine on the pressure plate. (medel = average).

The pressure is shown as the pressure distribution along line 10 (center line) in Figure 3.. The pressures in the surroundings are shown as the mean value of the lines 9-11, 8-12, 7-13, 6-14 and 5-15 respectively .

Upwind the pressure reflects the deceleration of the flow when approaching the disk. The highest pressure corresponds to the stagnation pressure on a solid disk. Then there is an acceleration of the flow when passing through the openings of the disk. After reaching the minimum pressure in the wake the static pressure is recovered relatively fast.

3.2. The region of influence of one wind-turbine

The gray area in Figure 6 shows the region of influence, of a wind turbine located on the center line.

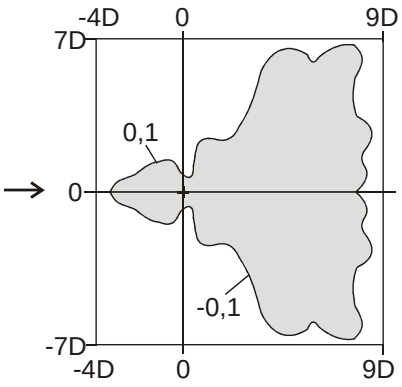

Fig. 6. Region of influence from one wind turbine located at the cross based on static pressure readings on the pressure plate. The pressure has been normalized with the highest pressure..

The region of influence on the upwind side is defined by the line representing 10% of the highest pressure (0.1 line) an on the downwind side by the line representing -10% of the highest pressure (-0.1 line). The pressure has been normalized with the highest pressure which occurs just before the wind turbine.

3.3. An example of interaction between wind turbines

The interaction between two wind turbines was explored by placing two wind turbines with a separation distance of 6.66 D. The wind turbines were located along the center line.
Figure 7 shows the response from one isolated wind turbine which is the reference case.

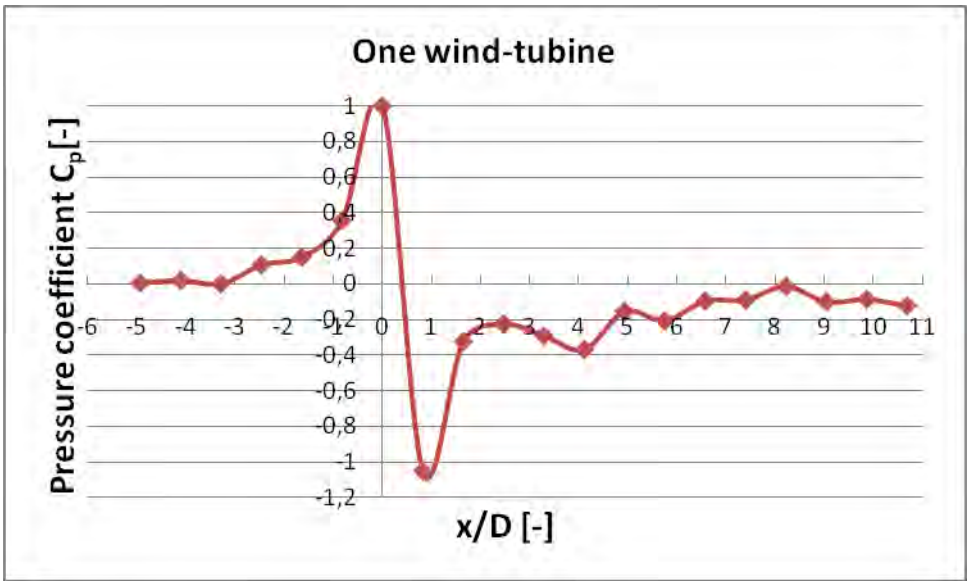

Fig. 7. One undisturbed wind turbine.

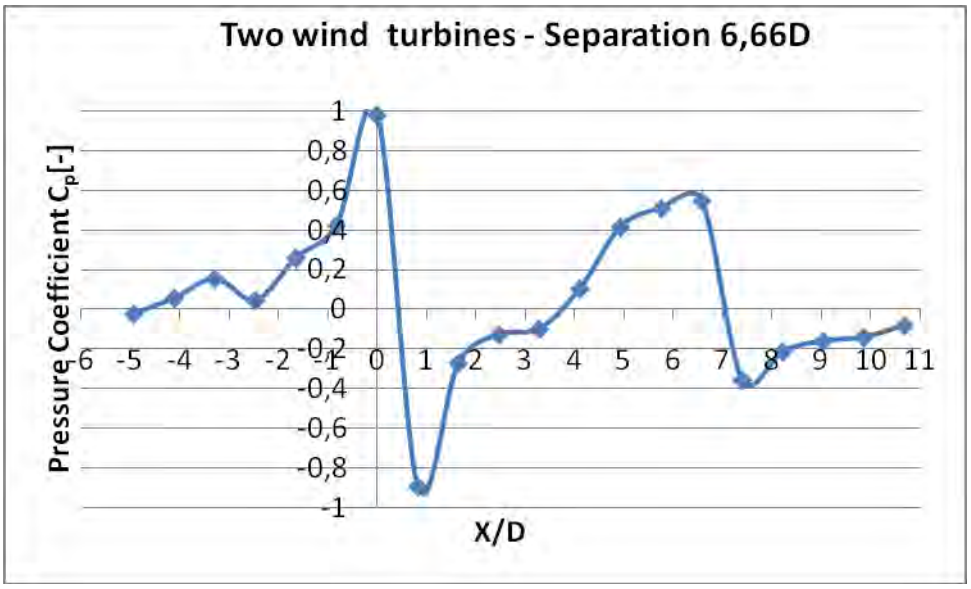

Fig.8 Two wind turbines

By comparing the pressure response of the undisturbed wind turbine in Figure 7 with the pressure response of the wind turbine located downstream in Figure 8 one sees clearly that the wind turbine located downstream is disturbed by the one located upstream.

3.4. Comparison between static pressure at hub height and on the plate

Our method is bases on that that there is a close relationship between the static pressure at hub height and on ground. This has benne tested by measuring the static pressure at hub height with a Prandtl tube. The result is shown in Figure 9.

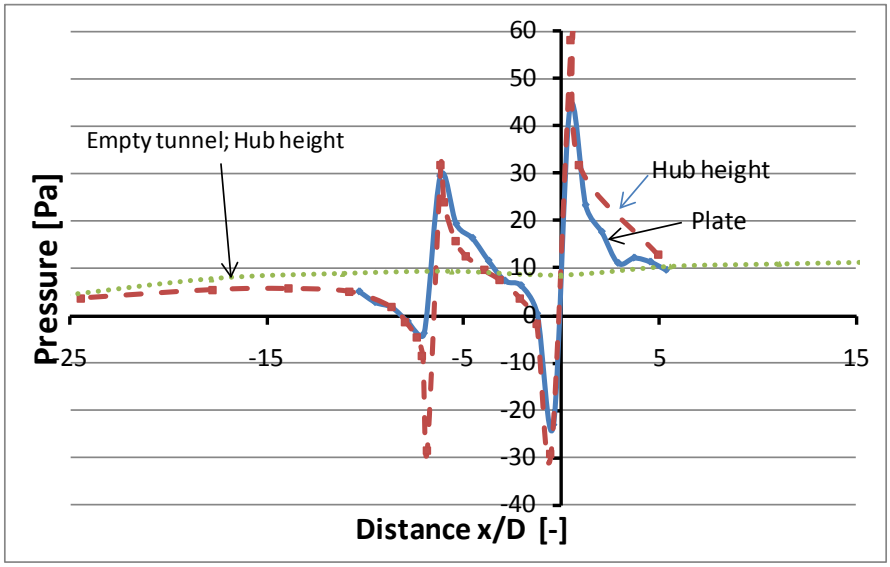

Fig.9 Static pressure at hub height and on ground (pressure plate).

There is a god correspondence between the pressures at the two levels.

4. Discussion

There is a clear response in the static pressure on the pressure plate due the presence of wind turbine models. This makes it possible to quantitatively explore the interaction between wind turbines. There is also a good correspondence between the static pressure on the ground (pressure plate) and the static pressure at hub height recorded with a Prandtl tube. Downstream of a wind turbine there is a relatively fast recovery of the static pressure. Therefore the response in static pressure may underestimate the length of the wake in terms of the velocity recovery. This will be explored by measuring the total pressure at hub height and to in detail investigate the velocity field in the wake region with Particle Image Velocimetry.

5. Conclusions

This is a new method, which is fast and economic, for exploring the interaction qualitatively between wind turbines. The next step is to develop it into a quantitative method that makes prediction of energy production possible.

References

[1] Johnson K. E. and Naveen T (2009). "Wind farm control: addressing the aerodynamic interaction among wind turbines". 2009 American Control Conference, St. Louis,MO,USA, June 10-12.

[2] Ivanell, S. (2009) "Numerical Computations of Wind Turbine Wakes". Doctoral dissertation, KTH, Sweden.

[3] Sørensen, J. N., Mikkelsen, R. & Troldborg, N. (2007) "Simulation and modelling of turbulence in wind farms". In EWEC 2007:Milan, European Wind Energy Association.

[4] Wußow, S., Sitzki, L. & Hahm, T. (2007) "3D simulation of the turbulent wake behind a wind turbine". Journal of physics: Conference series, The science of making torque from wind **75** 012033.

[5] Kobayashi T, Sandberg M, Kotani H, Claesson L, (2010) Experimental investigation and CFD analysis of cross-ventilated flow through single room detached house model *Building and Environment* 45pp. pp. 2723-2734

[6] Medici, D. and Alfredsson, P. H. (2005). Wind turbine near wakes and comparisons to the wake behind a disc. ASME Conference, January 2005, Reno, Nevada. AIAA-2005-0595

Site Matching Of Offshore Wind Turbines - A Case Study

Pravin B Dangar[1]*, Santosh H Kaware[2], Dr.P.K.Katti[3]

Department of Electrical Engineering
Dr Babasaheb Ambedkar Technological University,Lonere,Raigad ,Maharashtra ,India
Corresponding author. Tel : 9867055282 , E-mail: pravindangar@rediffmail.com,

Abstract: The stress on demand and supply gap of electricity has lead the globe to face acute problems. Further use of fossil fuel based energies for improved life and development have lead to adverse environmental effects, like climate change. Offshore wind farms have great potential as sustainable energy source. This accentuates to focus attention on technical issues such as selection, requirements, characteristics and power production from wind turbine. This paper presents a methodology developed for selection of optimum windmill for a specific site based on capacity factor approach by proper analysis of wind data. Offshore wind data for the purpose is obtained from, INCOIS Hyderabad- India for a particular site under proposal in India. The wind data is used to generate mean wind speeds for a typical day in a month by using MATLAB program. The windmill with the highest average capacity factor is the optimum one and to be recommended. The results of said analysis are presented. Such analysis at the planning and development stages of installation will enable the wind power developer or the power utilities to make a judicious choice of potential site and wind turbine generator system from the available potential sites and wind turbine generators respectively.

Keywords: *Offshore wind, Climate change, Capacity factor, Wind data.*

1. Introduction

A Number of potential wind power sites are available all over the world. Of these, not all sites have wind turbine generators installed. The observation with the existing wind farms shows that some of the wind power plants have performed poorly probably due to improper site matching. Hence there arises a n eed for a systematic approach toward the problem of optimum siting of wind turbine generators. [4] The production of electricity by a wind turbine generator at a specific site depends upon many factors. These factors include the mean wind speed of the site and the speed characteristics of the wind turbine itself namely, cut-in, rated, and furling wind speeds including the hub height. Commercially many models of wind turbine generators available, with similar MW and KW ratings. Each of these wind turbines has their own specifications and speed parameters. These speed parameters affect the capacity factor at a given specific site, and subsequently affect the choice of optimum wind turbine generator for the site. In this paper the method to determine capacity factor of different offshore wind turbine under different tower heights, rated wind speeds, is discussed for Mumbai offshore region.

1.1. Capacity Factor

It compares the plant's actual production over a given period of time with mean wind speed the amount of power the plant would have produced if it had run at rated wind speed for the same amount of time and hence can be defined as ;

- The ratio of average power output to the rated power output [1]
- An indicator of how much energy a particular wind turbine makes in a particular place.

$$C.F. = (Pa / Pr) \quad (1)$$

2. Methodology

2.1. Offshore Wind Turbine Site Matching Based On Capacity Factors

The methodology for the selection of the optimum windmill for a specific site is developed the flowchart is shown in Fig 1. The selection is based on the capacity factors (CF) of the available windmills. The long term wind speed data recorded at different hours of the day for many years is used. The particular steps used to determine C F for the mean wind speeds for at different hours of the day are generated with the manufacturer's specifications. The windmill with the highest capacity factor for the specific site is the optimum one and to be recommended.

- Step1: Calculation of Mean Wind Speeds

  The mean wind speed for a typical day of a month need to be generated by averaging all the recorded wind speeds for regular interval of long term data of the wind speeds for the site to be considered.
- Methodology Of Determination Of Capacity Factor

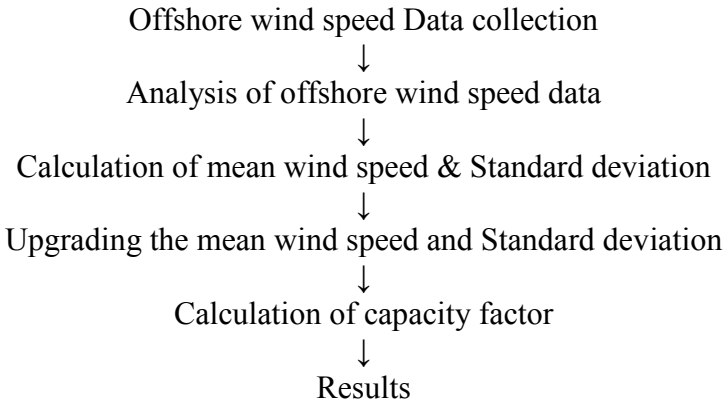

Fig 1 Methodology for determination of capacity factor

The mean wind speed is then calculated using the equation below

$$V_i = \left(\frac{\sum_{j=1}^{N_j} V_j^{\,3}}{N_j} \right)^{1/3} \qquad (2)$$

Where

V_j =observed wind speed
N_j =number of wind speed observations
V_i =mean wind speed

- Step 2 Upgrading the Mean Wind Speed

$$V_z = V_i \left(\frac{Z}{Z_i} \right)^x \qquad (3)$$

Where

V_z= mean wind speed at projected height, Z

V_i= mean wind speed at reference height, Z_i
Z= projected height (or hub height)
x=power law exponent depends upon the roughness of the surface. For open land, x is usually taken as 1/7.

- Step 3 Generation of the Wind Speed Probability Density Functions

$$f(v)=\left(\frac{v}{C_i^{\,2}}\right)\exp\left(-\left(\frac{v}{2C_i^{\,2}}\right)\right) \tag{4}$$

Where

$C_i = v_i/1.253$
v= wind speed
The Weibull probability density function is represented by

$$f(v)=\left(\frac{k}{c}\right)\cdot\left(\frac{v}{c}\right)^{k-1}\exp\left(-\left(\frac{v}{c}\right)^{k}\right) \tag{5}$$

Where;

c=scale factor, unit of speed
k=shape factor, dimensionless
v=wind speed
The Weibull parameters c and k can be found using the following acceptable approximations

$$k=\left(\frac{\sigma}{v}\right)^{-1.086} \qquad 1\le k\le 10$$

$$c=\frac{v}{\Gamma\left(1+\frac{1}{k}\right)}$$

In both the probability density functions, the wind speed v will be the mean wind speed V_Z, calculated at hub height from equation (3)

- Step 4 Calculation of Capacity Factors

The average power output from a wind turbine is the power produced at each wind speed multiplied by fraction of the time that wind speed is, experienced integrated over all possible wind speeds. In integral form the equation is [2,4]

$$P_a=\int_0^{\infty} P_w\cdot f(v)\cdot dv \tag{6}$$

Capacity factor can be defined as the ratio between average power output given by equation (6) and rated power of the wind turbine P_r can be obtained from the manufacturer's details. In equation(6) the power at various wind speeds can obtained from the following equation

$$P_w = \begin{cases} P \cdot \dfrac{v^k - v_c^{\,k}}{v_R^{\,k} - v_c^{\,k}} & for\ v_c \le v \le v_R \\ P & for\ v_R \le v \le v_f \\ 0 & elsewhere \end{cases} \quad (7)$$

Where

P is the rated electrical power,
v_c is the cut in wind speed,
v_R is the rated wind speed
v_f is the cut off wind speed
k is the Weibull shape parameter defined under the equation(5), the relationship betweenpower and wind speed is as under,

$$P = \frac{1}{2} C_p \cdot \rho \cdot A \cdot v^3 \eta$$

For which considering value of air density factor ρ = 3.485 P/T

Where P=101.3 kpa and T=273K the power equation thus can be written as

$P=0.646\ C_p .\ A\ .\ v^3.\eta$ (8)

Thus the capacity factor defined above can be expressed as

$$CF = \frac{1}{P_r} \int P(v) \cdot f(v) \cdot dv \quad (9)$$

- Step 5 Choice of the Optimum Wind Turbine Based on Capacity Factor
  The capacity factors of different turbines are computed from the wind speeds (v_c, v_R, v_f) and rated power data obtained from manufacturer details. Now detailed table for the capacity factor for each turbine is prepared from which it can be clear that certain turbine will have a maximum value of capacity factor. This becomes the candidate which can produce the optimal power for the chosen site and wind data. [4, 5, 6]

3. Computation and Results

3.1. Data Analysis:

The wind speed data that is obtained from Indian National Centre for Ocean Information Services (INCOIS) has been first arranged on the hourly basis. The mean wind speed and standard deviation on the hourly basis and daily basis is computed. The results of computed mean wind speed data has been presented year wise for the year 1998 and 2005 respectively in Figure 2 to 5.

3.2. Computation Of Capacity Factor

The capacity factor of a machine indicates the ability to generate the mechanical energy by utilizing the wind power. This solely depends upon how the wind speed utilized to spin the rotor of turbine. The mean wind speed data that has been obtained from INCOISIS is used to determine the hub height wind speed as per the equation 3 . Further wind turbine data of the

selected machine is used for the computation of capacity factor for each of the machine the details of which are shown in table 1.the computation of capacity factor has been carried out by using MATLAB program.

Table 1. Offshore wind turbine specification

Company Name	Power Rating MW	Cut in wind Speed (m/s)	Rated wind speed (m/s)	Cut out wind speed (m/s)	Rotor diameter in meter	Turbine Height in meter
RE Power	5	3	11.4	25	126	90
GE	3.6	3.5	14	27	111	90
Vestas	3	3.5	15	25	90	90
Vestas	3	3	12	25	112	94

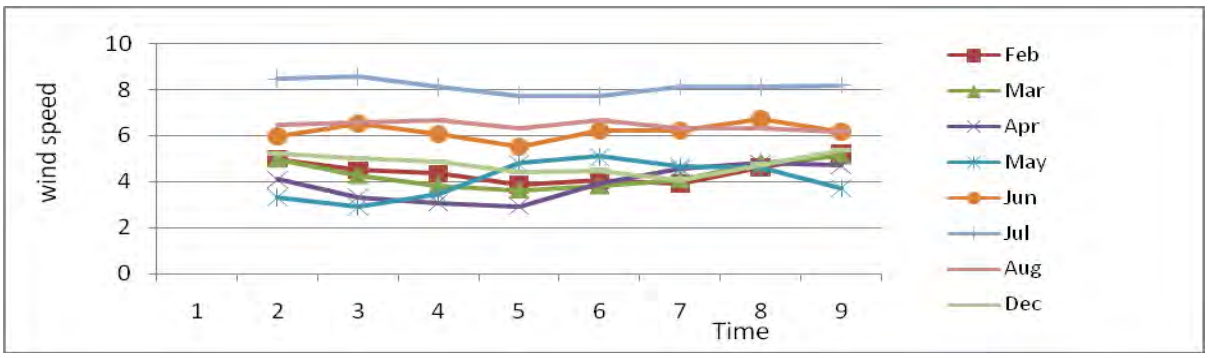

Fig .2 Hourly average mean wind speed of the year 1998

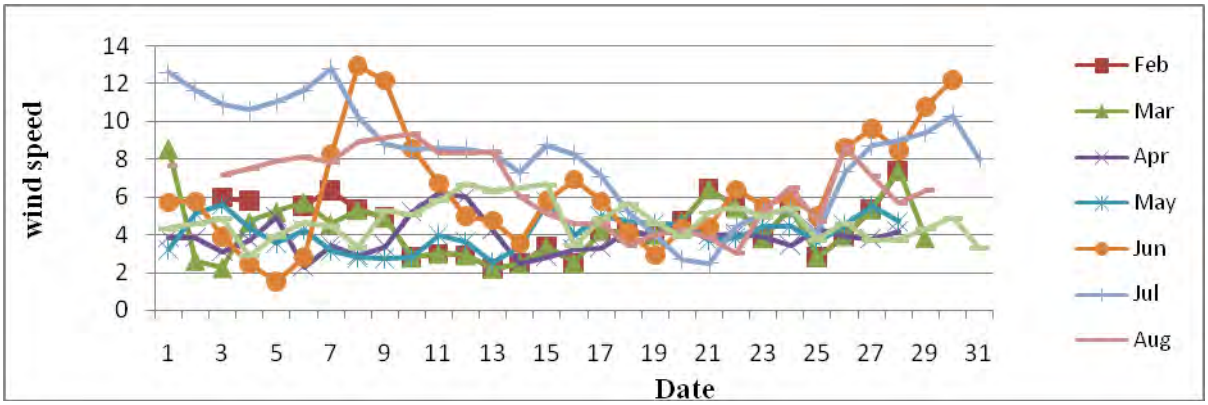

Fig 3 Monthly Average wind speed of the year 1998

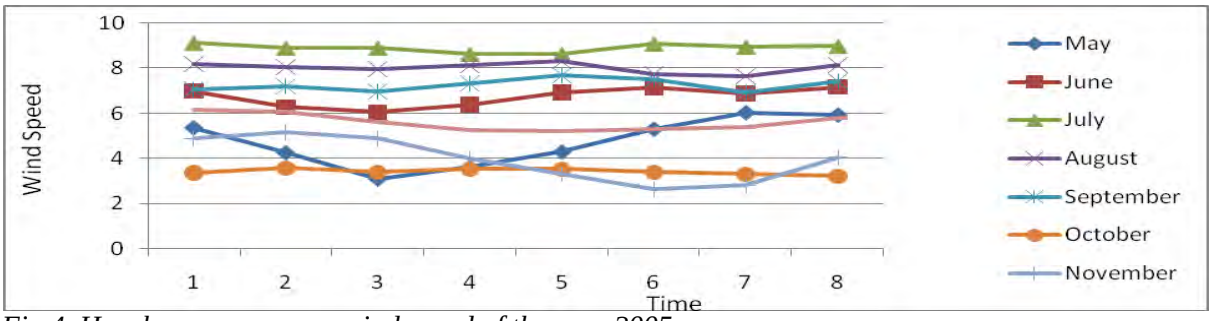

Fig.4. Hourly average mean wind speed of the year 2005

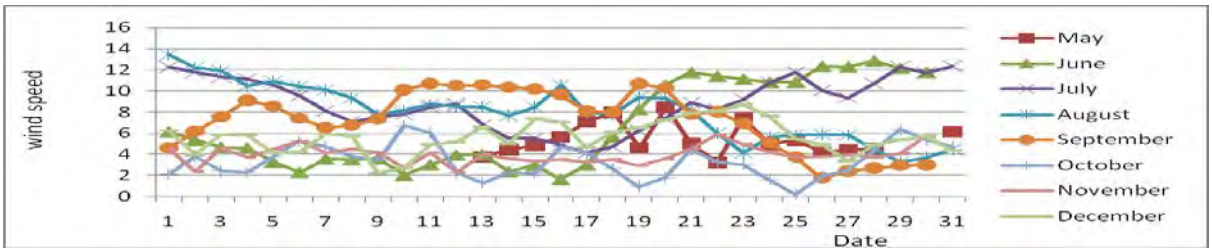

Fig .5. Monthly average wind speed of the year 2005

The graphical representation of monthly capacity factor for the selected machine for the respective years has been presented in Fig 6 and 7. Finally the annual capacity factors for the selected machine have been presented in tabular and graphically in table 2 and Fig.8. From the result available the machine with optimal capacity factor that is RE Power 5 MW and Vestas 112/3.0 MW has been recommended.

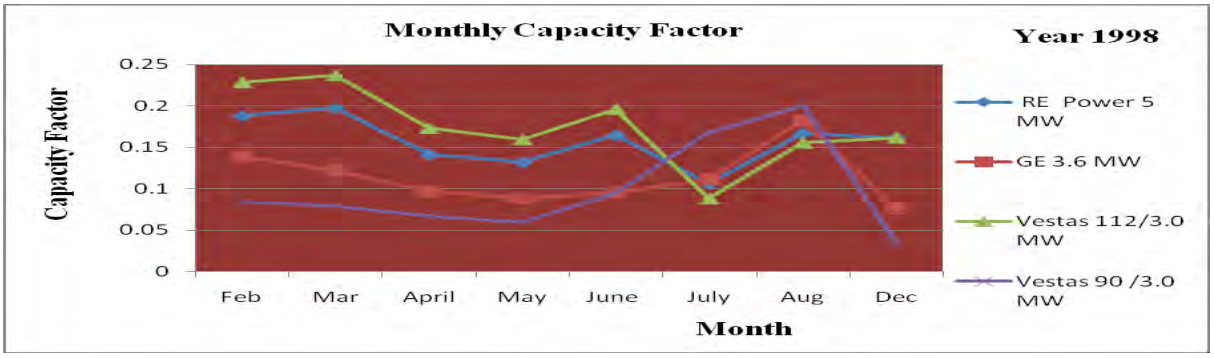

Fig.6. Monthly Capacity factor for the year 1998

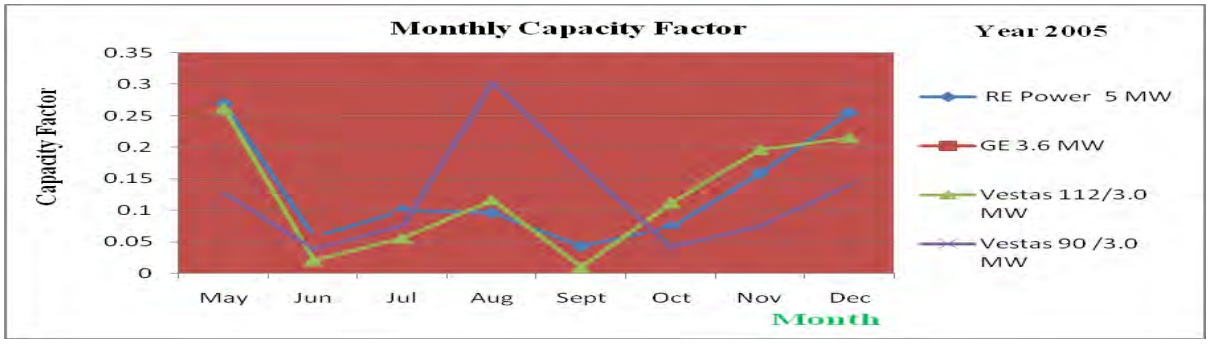

Fig.7. Monthly Capacity Factor for the year 2005

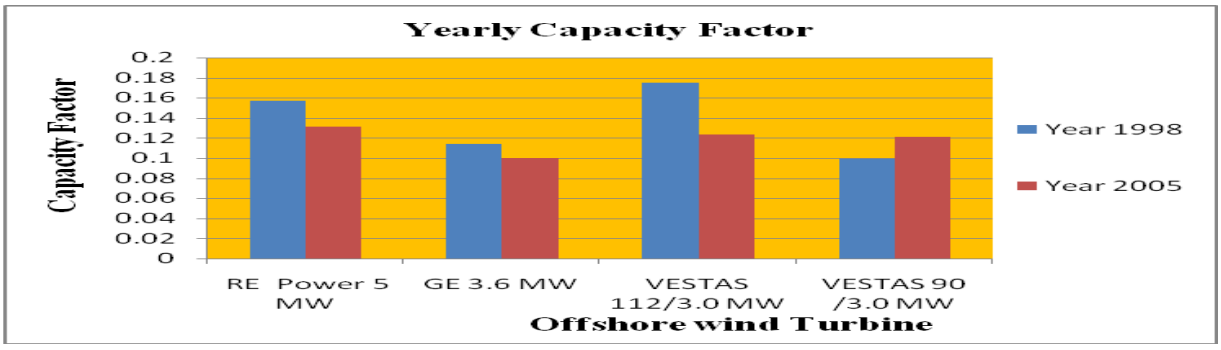

Fig. 8 Average annual capacity factor

Table 2. Yearly average capacity factors

Hub Height		90 m	90 m	94 m	90 m
Buoy ID	Year	RE Power 5 MW	GE 3.6 MW	Vestas 112/3.0 MW	Vestas 90 /3.0 MW
SWO2	1998	0.15727643	0.1142502	0.175344331	0.098867349
SWO2	2005	0.13160839	0.1001096	0.123371867	0.121234018

The typical disposition of the selected wind turbines for the proposed site used in this work as mentioned has been presented in Fig. 9 and 10 respectively for RE power and Vestas machines. This will give an effective feel of how a wind form may appear if installed on an offshore site.

Fig.9. RE Power 5 MW offshore wind turbine layout for 50MW

Fig.10. Vestas 112/3.0 MW offshore wind turbine layout for 50MW

3.3. Conclusions

The paper presents a methodology for assessment of offshore wind data and the capacity factor of wind turbines for their suitability to be used for harnessing offshore wind energy in a better fashion as depicted by the results. This not only helps to choose a better turbine but also to maximize the system performance. Further the illustration presented for a specific site in Konkan region of Maharashtra exemplifies the suitability of method presented.

Acknowledgement

The authors acknowledge thankfully the support extended by Indian National Centre for Ocean Information Services,(INCOIS) Hyderabad for providing necessary offshore wind data for Mumbai (India) offshore area, Department of Electrical Engineering, and Dr. Babasaheb Ambedkar Technological University, Lonere, Dist: Raigad, Maharashtra (India) for their financial support during the work.

References

[1] Jeffrey Logan and Stan Mark Kaplan Wind Power in the United States: Technology, Economic, and Policy Issues June 20, 2008 Specialists in Energy Policy Resources, Science, and Industry Division. pp 1-53

[2] Pradeep.K.Katti, Dr.Mohan K Khedkar, Generation capacity Assessment of Distribute Resources Based on Weather Model for Integrated Operation, International conference CERA -2005, IIT Roorke India . pp1-6

[3] Ziyad M. Salameh lrianto Safari ,Optimum Windmill- Site Matching . IEEE Transactions on Energy Conversion, Vol. 7, No. 4, December 1992. pp 669-676

[4] Suresh H. Jangamshetti, and V. Guruprasada Rau, Optimum Siting Of Wind Turbine Generators , IEEE Transactions on Energy Conversion ,Vol 16, No. 1, March 2001,pp 8-13

[5] Tai-Her Yeh and Li Wang A Study on Generator Capacity for Wind Turbines Under Various Tower Heights and Rated Wind Speeds Using Weibull Distribution , IEEE Transactions on Energy Conversion, Vol. 23, No. 2, June 2008,pp-592-602

[6] Suresh H. Jangamshetti, and Dr. V. Guruprasada Rau, Site matching of wind turbine Generators : A case study, IEEE Transactions on Energy Conversion, Vol. 14, No. 4, December 1999 pp- 1537-1543

[7] Bogdas S.Borowy,Ziyad M Salame Methodology for Optimally Sizing the Combination of a Battery Bank and PV Array in a Wind/PV Hybrid System IEEE Transactions on Energy Conversion, Vol. 11, No. 2, June 1996 pp 367-375

Experimental and Fluid-dynamic Analysis of a Micro Wind Turbine in Urban Area

Marco Milanese[1,*], Arturo de Risi[1], Domenico Laforgia[1]

[1] *Department of Engineering for Innovation – University of Salento, Lecce, Italy*
** Corresponding author. Tel: +39 0832297760, Fax: +39 0832297777, E-mail: marco.milanese@unisalento.it*

Abstract: In urban areas, the evaluation of the energy outcome of a horizontal axis micro wind turbine depends on several factors such as mean wind velocity, location, turbulence, etc. To maximize the micro wind turbine efficiency it is important to define the best location. The present paper focuses on the definition of common rules for micro siting in urban areas.

In this work, the efficiency of a 1 kWp horizontal-axis wind turbine has been evaluated, by means of CFD and experimental data. The numerical results have been compared with the experimental data collected over a period of time of three years, by using a measurement equipment installed on the roof of the Engineering building at the University of Salento. The results have shown that horizontal axis wind turbines suffer from wake effect due to buildings, therefore best sites in urban area have to be identified by a careful fluid dynamic analysis aimed at evaluating all causes that can reduce significantly the performance of the generator.

Keywords: *Micro wind turbine, best location, experimental and fluid-dynamic analysis*

1. Introduction

In the last years, prices of oil have achieved strong variations on international markets. These occurrences have underlined the very important role of energy as fundamental factor for human activity [1,2,3]. In this scenario, small/micro wind generators are gaining an important role due to both the low environmental impact and the possibility to avoid big electrical networks.

Several authors have studied the topic of microgeneration, by taking into account both technical and social aspects [4,5,6]. Kelleher e Ringwood [7] developed software to estimate the economic performance of small/micro solar and wind plants. Watson [8] carried out studies about the microgeneration management techniques considering power supply issues. Besides, in order to estimate micro wind turbine performance several studies have been carried out by using computational fluid dynamic models (CFD), since they can show an exhaustive draft about the wind flow around the micro turbine in any meteorological conditions, allowing saving time and costs [9,10].

For evaluating the economic convenience about the installation of a micro wind turbine in urban area, it is important to calculate positive and negative effects of buildings or other obstacles on the aerogenerator performance. For this reason, the present work focuses on the best siting of small horizontal-axis wind turbines in urban area. Particularly, an aerogenerator has been installed on the roof of the Engineering building at the University of Salento and monitored over a period of time of three years.

During experimental testes it was observed a perpetual transient condition of the microturbine that reduces its performance. Then CFD simulations have been carried out to fully understand the relationship between the aerogenerator performance measured under several meteorological conditions and the shape of the building where the plant is installed. In this way, a useful rule for best placing of horizontal-axis wind turbines in urban areas has been obtained.

2. Experimental setup and numerical model

2.1. Description of the experimental setup

In this work, an experimental apparatus has been developed for monitoring the performance of a horizontal axis micro wind turbine (1 kWp).

Anemometer, PLC, analogic/digital conversion unit, web server, voltage transducers and current transducers composed the measurement apparatus. Table 1 reports the main technical specifications of the experimental setup.

Table 1. Mean technical features of the plant

Elements	Technical features
Aerogenerator	- power: 1 kWp - cut-in velocity: 2.5 m/s - Electric generator: 24 VDC (alternator + rectifier) - n. 4 batteries: Trojan T105, 6VDC - inverter: 24 VDC-220 VAC - fiberglass rotor: D=2.5 m - Pole: 9 m
voltage transducer	R_M 0.47 Ω - Precision T_A=25 °C 0.7%
current transducer	V_{OUT} 0÷10 V - Precision T_A=25 °C 1%
anemometer	optical encoder (precision +0.3m/s up to 3m/s, ±1% over 3m/s)
PLC	8 input-PNP,NPN /8 output-Transistor PNP, interface RS232 COM-Port
analogical/digital conversion unit	8 analogical input 12 bit
Web-server	Ethernet - 10 Mbit/s

The whole system was controlled by a PLC that acquires and processes several signals and monitors all parameters under investigation. Besides the measures were viewable in real time on an Internet web site and stored on a remote hard disk.

2.2. CFD Model

In order to study the wind microturbine performance, a 3D model of the building has been drawn, as Fig. 1 shows. The total height from the ground of the aerogenerator is equal to 20 m.

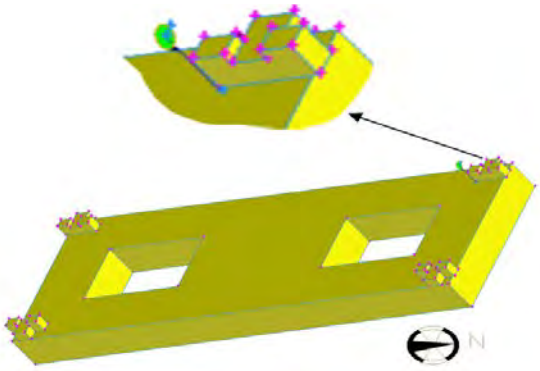

Fig. 1. 3D model of the building where the aerogenerator has been installed.

The fluid dynamic simulation domain has been obtained by subtracting the building volume to a parallelepiped sufficiently large to consider undisturbed fluid-dynamic conditions on the boundary.

For meshing the volume, tetrahedral elements whose size was in the range between 0.2 and 2 m have been used. The computational cell size has been selected to reduce the maximum computational error and to obtain grid-independent solutions.
The mesh sensitivity analysis has been performed by comparing the results from several simulations carried out with different mesh resolutions.

Table 2. Sensitivity analysis results

Cells (n)	Mean wind velocity close to the aerogenerator (m/s)	Variation (%)
579'596	7.93	-
1'084'494	8.16	2.8%
2'552'154	8.26	4.1%

As Table 2 shows, by incrementing the number of cells from 579'596 to 2'552'154 the mean wind velocity close to the aerogenerator changes within 4.1% and this difference outcomes equal to 1.3% switching the number of cells from 1'084'494 to 2'552'154. So it is reasonable to use the denser grid, since further incrementing the number of cells, advantages shouldn't be enough to justify the relative increment of calculation time.

Numerical simulations have been carried out by using FLUENT software and studying eight wind directions with an angular difference equal to 45° and wind velocity within the range 4÷8 m/s. This range has been fixed by taking into account the following considerations:

- Up to 4 m/s, the electric power is lower than 5% of the nominal power and the data statistical dispersion is much large with respect to the measured values: this issue does not allow to do a comparison between experimental and numerical data;
- Over 8 m/s, there are not enough data (less than 2%).

Turbulence has been evaluated using the standard k-ε turbulence model.

3. Discussion of results

3.1. Measured data analysis

The aerogenerator was installed on the roof of the Engineering building at the University of Salento. The following coordinates individuate the exact location: 40°20'03" N, 018°06'51" E and 35 m with respect to the mean sea level.

The wind microturbine has been monitored over a period of three years (2005, 2006 and 2007), measuring several parameters: wind velocity and direction, electric current, voltage and generated power. All parameters have been registered each 10 minutes.
For modeling wind data the Weibull function has been used in accord with following equation.

$$P(v < v_i < v + dv) = P(v > 0)\frac{k}{c}\left(\frac{v_i}{c}\right)^{k-1} \exp\left(-\left(\frac{v_i}{c}\right)^{k}\right)dv \quad (1)$$

Where c is the scale parameter, k is the shape factor, v_i is a generic wind velocity value, dv is the wind velocity increment, $P(v<v_i<v+dv)$ is the probability to register a wind velocity within the range v e $v+dv$ and $P(v>0)$ is the probability to register a wind velocity major to zero.

Weibull function is completely defined if c and k are known: these coefficients have been calculated by using the modified maximum probability method and considering a wind velocity step equal to 0.1 m/s. Table 3 reports the values of c and k for the period under

investigation (2005÷2007), whereas Fig. 2 shows the comparison between experimental data and the Weibull curve.

Table 3. Weibull function parameters for the period under investigation (2005÷2007)

Year	*k*	*c* (m/s)	Most probable velocity (m/s)	Mean velocity (m/s)	Standard deviation (m/s)
2005	1.658	3.457	1.98	3.09	1.91
2006	1.649	3.420	1.94	3.06	1.90
2007	1.669	3.444	1.99	3.08	1.89
Mean values	1.659	3.440	1.97	3.08	1.90

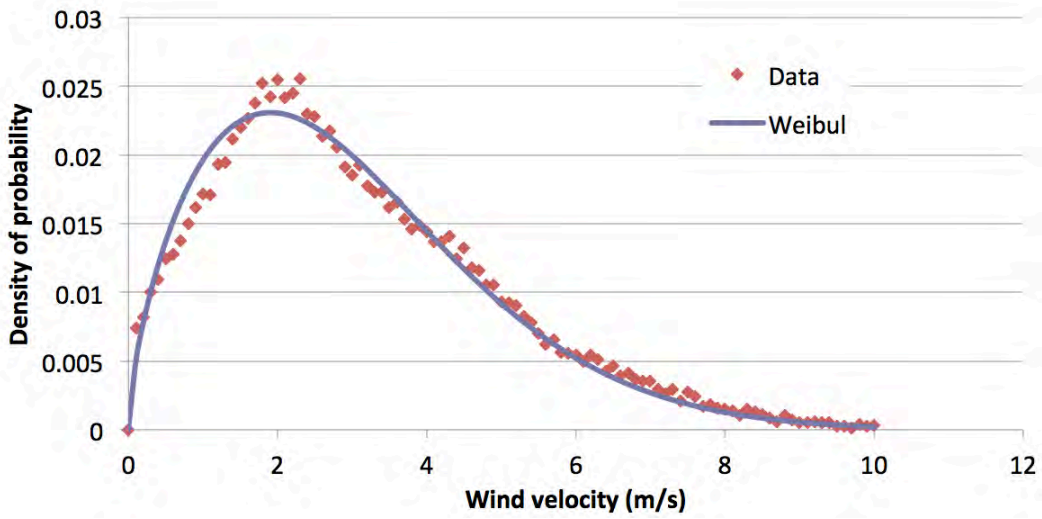

Fig. 2. Comparison between experimental data and the Weibull curve.

The anemometric analysis shows that the mean wind velocity at 20 m from the ground is equal to 3.08 m/s. This value is comparable with the aerogenerator cut-in velocity (2.5 m/s) and so it demonstrates that the site does not have a good wind potential. Nevertheless it is important to remark that at 35 m from the ground the mean wind velocity is equal to 4.9 m/s as the Wind Atlas of Apulia Region [11] shows. In other words, the mean wind velocity has to be halved going from 20 m to 35 m of height from the ground: this issue is common to many sites in urban area and it represents a big problem in order to achieve good performance from micro wind turbines.

Over experimentation time, more parameters have been measured as voltage, current and electric power. These data have been organized and analysed as function of wind direction. In this way it has been possible to study the influence of the shape of the building on the aerogenerator performance.

Fig. 3 shows the measured electric power for wind direction North as a function of wind velocity. Besides it is possible to see the comparison between the mean electric power (best fit of the measures of power - red curve) and the nominal electric power (orange curve). Particularly, for wind velocity up to 3 m/s the mean power curve is higher than nominal one, within 3 and 4 m/s the two curves are about similar and over 4 m/s the mean power curve is lower with respect to the nominal one. Moreover it is possible to observe a noticeable variability of measures due to the irregularity of wind velocity in the site under investigation.

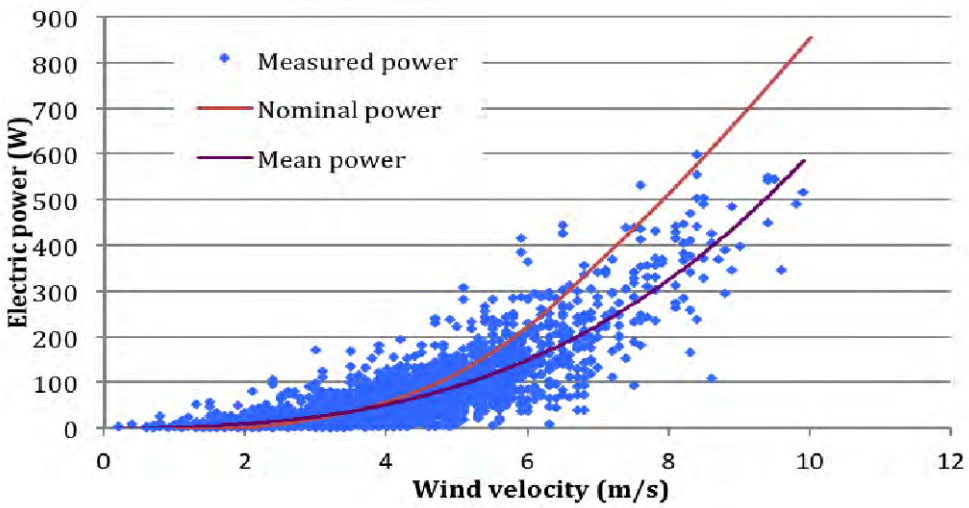

Fig. 3. Electric power output as function of wind velocity (wind direction North). The blue points indicate the measures of power, the red curve indicates the mean power (best fit of the measures) and the orange curve indicates the nominal power.

In order to complete the experimental data analysis, the measured electric power has been examined for each wind direction as Fig. 4 shows.

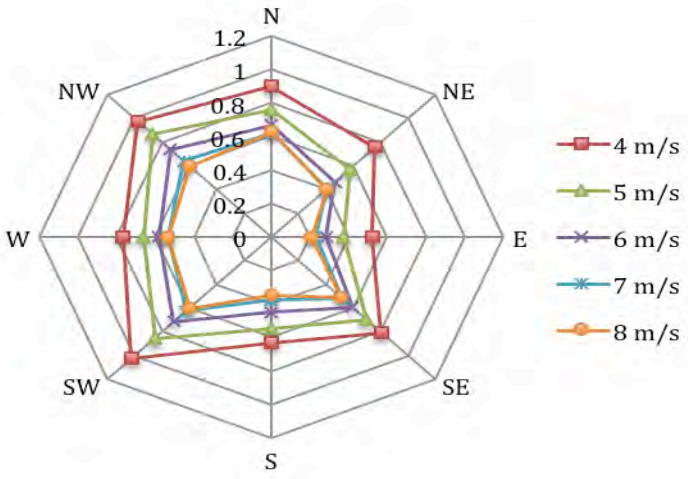

Fig. 4. Ratio between measured electric power and seminal electric power as function of wind direction and intensity

Fig. 4 demonstrates that electric power is very influenced by the wind direction, or in other words, this parameter strictly correlate with the intensity of the wake due to the shape of the building. These effects are more evident by observing the ratio between mean power and nominal power that decreases for high values of wind velocity and for all the considered directions.

3.2. CFD analysis

To fully understand the fluid-dynamic phenomena that influence the wind turbine performance several numerical simulations have been carried out by using the software FLUENT. All results are reported next.

The CFD post-processing analysis was developed taking into account for each wind direction four sections of the calculation domain. Particularly, three sections were positioned

transversely to the wind direction (the first one was placed ten meters forward the building, the second one close to the aerogenerator and the third one ten meter rear the building) and one longitudinal section was placed parallel to the wind direction. This section is very interesting because it shows the flow evolution along the building.

Numerical simulations have been carried out considering the wind velocity within the range 4÷8 m/s like to experimental analysis. Fig. 5 shows the results along the longitudinal sections for wind directions N-S (North is the prevalent wind direction), in the case of wind velocity equal to 6 m/s (mean velocity within the range 4÷8 m/s). It is important to notice that in the other cases under investigation (wind velocity equal to 4, 5, 7 and 8 m/s and other wind directions) the results are qualitatively similar to the case shown next.

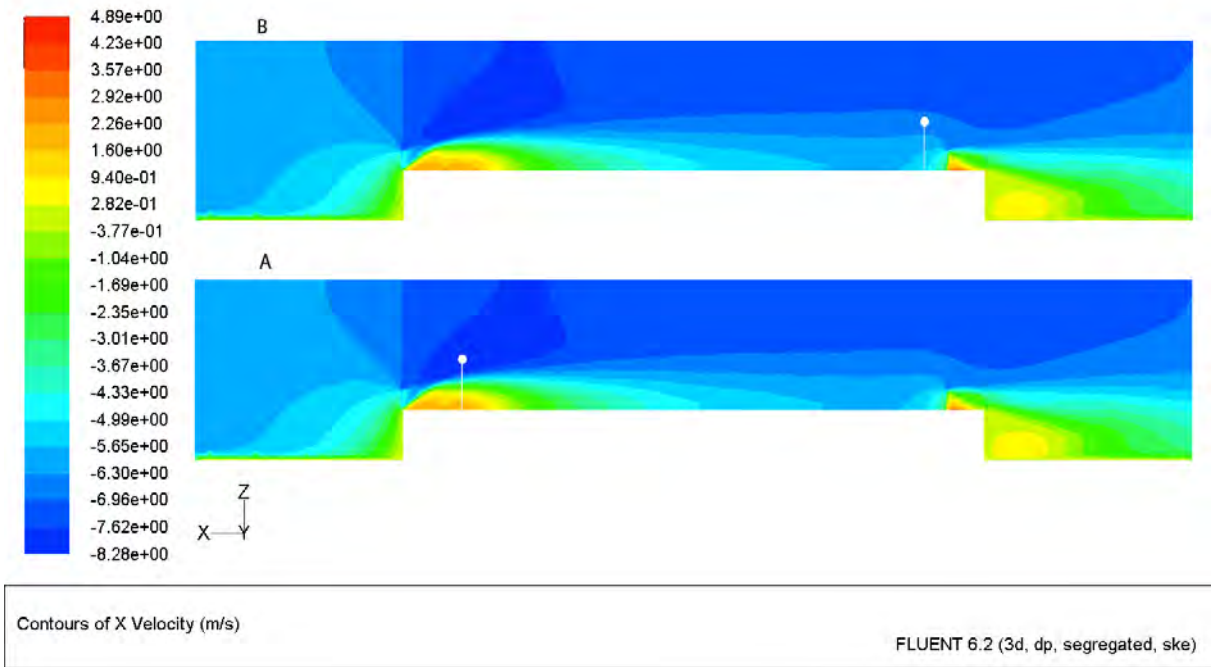

Fig. 5. Contours of X wind velocity: wind intensity on the boundary: 6 m/s; wind direction: North (A) and South (B); the pole is sketched by a line and a white circle

As the contours of X wind velocity demonstrate (Fig. 5), close to the aerogenerator there is a very strong vorticity phenomenon, whereas above this area the wind velocity rise quickly over to 8 m/s, against an inlet wind velocity equal to 6 m/s.

These results allow achieving a possible understanding of the experimental results reported in Fig. 3 and Fig. 4: the building generates an increment both of wind velocity and of vorticity influencing the aerogenerator performance; in fact the electric power results meanly lower than the nominal one, due to the strong vorticity, but in some cases the higher values of wind velocity results in a higher electric power output with respect to the nominal one. For example, under meteorological condition with wind velocity equal to 6 m/s the maximum measure of electric power matches the nominal power curve for a wind intensity equal to 8 m/s, as the analysis of Fig. 3 and Fig. 5 reveals.

Changing wind direction from North to South (Fig. 5B), the wind velocity distributions are similar to the previous case (wind direction North - Fig. 5A), with an opposite relative position of the aerogenerator.

According to experimental results, the longitudinal sections North-South show bigger wind intensity when the direction is North and so also the experimental electric power results bigger than the case South.

Another important consideration can be done taking into account the results shown in Fig. 3. As it is described before, for wind velocity up to 3 m/s the mean power curve is higher than nominal one: in this case the wind intensification effects due to the building are predominant on the vorticity. Instead, when the wind rises over to 4 m/s the vorticity generated by the wake of the building becomes prevalent on t he wind intensification effects, cutting the aerogenerator performance.

To define the best location for the horizontal axis micro wind turbine has to be take into account the turbulence intensity, defined as the ratio of the magnitude of the root mean square turbulent fluctuations to the reference velocity:

$$I = \frac{\sqrt{\frac{2}{3}k_e}}{v_{ref}} \qquad (2)$$

where k_e is the turbulence kinetic energy and v_{ref} is the mean velocity magnitude for the flow. Fig. 6 shows the comparison between the contours of X wind velocity and turbulence intensity. This evaluation allows defining the best location for the horizontal axis micro wind turbine in urban area. In fact, by overlapping areas of higher X velocity with areas of lower turbulence intensity it is possible to individuate an area where the aerogenerator can gives maximum performance.

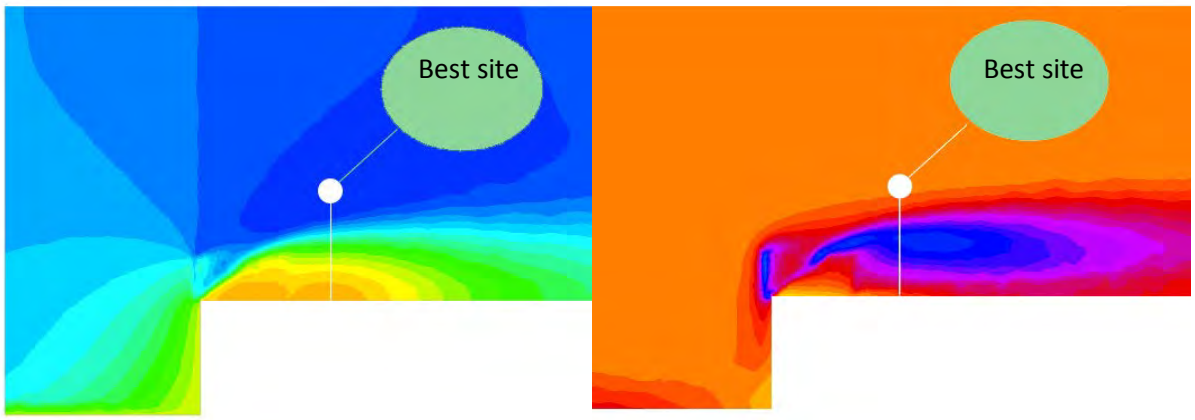

Fig. 6. Comparison between contours of X wind velocity and turbulence intensity. The pole is sketched by a line and a white circle. The best site in sketched by a green ellipse

4. Conclusions

This work focuses on experimental and numerical analysis about the electric power generation from a 1 kW horizontal-axis aerogenerator installed on the roof of the Engineering building at the University of Salento in urban area. Particularly the influence of the building on the micro wind turbine performance has been studied.

Experimental data were collected over a p eriod of time of three years during which it w as observed a perpetual transient condition of the microturbine that reduces its performance. Then to fully understand this occurrence and in order to value the performance of the

horizontal axis wind turbine, several CFD calculations have been carried out, taking into account different meteorological conditions. Numerical simulations calculated wind velocity fields and turbulence intensity above the building due to fluid-dynamic effects.

The experimental and numerical results of this study reveal that the siting of the horizontal-axis micro wind turbine on a building should allow to exploit bigger wind intensity, but often this advantage is neglected from turbulence phenomena; in fact, in the case under investigation, the measured aerogenerator efficiency appears lesser in comparison with the nominal performance curve. But, the best site can be found by crossing the contours of wind velocity with the turbulence intensity fields. In this way it is possible to localize an area (best location) where the aerogenerator can gives maximum performance.

In conclusion, the result presented in the present investigation showed that horizontal axis wind turbines suffer from wake effect due to buildings, therefore best sites in urban area have to be identified by a careful fluid dynamic analysis aimed at evaluating all causes that can reduce significantly the performance of the generator.

References

[1] T. Devezas, D. LePoire, J.C.O. Matias and A.M.P Silva, Energy scenarios: Toward a new energy paradigm, Futures, 40(1), 2008, pp. 1-16.

[2] H. Schiffer, WEC energy policy scenarios to 2050, Energy Policy, 36(7), 2008, pp. 2464-2470.

[3] V.D.Z. Bob and G. Reyen, Climate sensitivity uncertainty and the necessity to transform global energy supply, Energy, 2006, pp. 2571-2587.

[4] G.J. Dalton, D.A. Lockington, T.E. Baldock, Feasibility analysis of stand-alone renewable energy supply options for a large hotel, Renewable Energy, 33(7), 2008, pp. 1475–1490.

[5] R. Sauter, J. Watson, Strategies for the deployment of micro-generation: implications for social acceptance, Energy Policy, 35(5), 2007, pp. 2770–2779.

[6] S.R. Allen, G.P. Hammond, M.C. McManus, Prospects for and barriers to domestic micro-generation: a United Kingdom perspective, Applied Energy, 85(6), 2008, pp. 528–544.

[7] J. Kelleher, J.V. Ringwood, A computational tool for evaluating the economics of solar and wind microgeneration of electricity, Energy, 34, 2009, pp. 401–409.

[8] J. Watson, Co-provision in sustainable energy systems: the case of micro-generation, Energy Policy, 32(17), 2004, pp. 1981–1990.

[9] J. He, C.C.S. Song, Evaluation of pedestrian winds in urban area by numerical approach, Journal of Wind Engineering and Industrial Aerodynamics, 81, 1999, pp. 295-309.

[10] G.T. Johnson, L.J. Hunter, Urban wind flows: wind tunnel and numerical simulations—a preliminary comparison, Environmental Modelling & Software, 13, 1998, pp. 279–286.

[11] L. Tornese, A. de Risi, D. Laforgia, Atlante eolico della Regione Puglia, 2008, Graficazerottanta.

Adjustment of $k-\omega$ SST turbulence model for an improved prediction of stalls on wind turbine blades

Tawit Chitsomboon*, Chalothorn Thamthae

School of Mechanical Engineering, Institute of Engineering,
Suranaree University of Technology, Nakornratchasima, Thailand
** Corresponding author. Tel: +66 044 224414, Fax: +66 044 224413, E-mail: tabon@sut.ac.th*

Abstract: The eddy viscosity in the buffer zones of the turbulent boundary layers was limited to investigate its effects on the points of incipient separation for flows over wind turbine airfoils. The $k-\omega$ SST turbulence model was used as the base model within the framework of a finite volume CFD scheme. Flows over two different wind turbine airfoils were computed and compared with experimental results. Much improvements in the lift and drag coefficients in the stall regions were observed when compared with the results of the original turbulence model.

Keywords: *Turbulence model, $k-\omega$ SST turbulence model, Airfoil stall prediction, Stall in wind turbine*

1. Introduction

Practical flows over wind turbine blades at large angles of attack are very complicated, thus difficult to predict accurately by numerical methods. The difficulties stem from the fact that the boundary layers separate from the blade's suction surfaces due to adverse pressure gradients and its interaction with turbulence. Several investigations have been conducted by various researchers to compute these separated flows; the results have been hitherto only partially successful. Some investigations have over-predicted the lift coefficients [1-3] while some have under-predicted them [4-6]. Moreover, all computations missed the characteristic dips and rises of the lift coefficients in the regions right after the onsets of stalls [1-8]. The reasons for the inaccurate numerical predictions were invariably attributable to the inaccuracies incurred by the turbulence models used in the computations.

Early computations employed the $k-\varepsilon$ turbulence model [9] but later on the $k-\omega$ turbulence model [10] became more acceptable; at present the $k-\omega$ SST model [11-12] seems to be more preferable among wind turbine researchers. This model utilizes both the $k-\varepsilon$ and the $k-\omega$ models under a strategy of a blending function. Like it predecessors this model employs the fully turbulent flow condition as its basic assumption, i.e. the flow devoid of a transition region. The performances of this model in the predictions of separated flows over airfoils were only partially satisfactory since substantial inaccuracies of the lift and drag coefficients predictions were still prevailed in the stall regimes [1-8].

In particular, the $k-\omega$ SST turbulence model had been demonstrated to over-predict the lift coefficients beyond the stall points [1,5,6,8]. It is believed by the authors that these over-predictions were due to the fact that the turbulence levels (hence, turbulent eddy viscosities) in the boundary layers were too high, thus enhancing a momentum transfers to the near wall regions which helped the boundary layer to push through the adverse pressure gradient regions more easily than otherwise. The resulting delayed separation then caused the low pressure on the suction side to spread over more area than normal which thus increased the lift. The turbulence levels that were too high, in turn, were caused by the fully turbulent assumptions that were employed in the turbulence model.

To this end, it should be noted that the buffer zone which bridges the laminar sub-layer and the log-law region in a boundary layer is very important to the physic of turbulence in the boundary layer. This zone is very difficult to model numerically. A small 'model error' in this relatively thin region could induce a large overall error.

The objective of this study was to improve the accuracy of the numerical prediction of separated flows on airfoils by an adjustment of the turbulence intensity in the buffer zones of turbulent boundary layers. The $k-\omega$ SST turbulence model [11,12] will be used as the basis for this investigation.

2. Methodology

In order to limit the eddy viscosities in the regions from the buffer zones to the log-law zone a damping function f_{SST} is proposed. The limited eddy viscosity for the $k-\omega$ SST model thus becomes,

$$\mu_t = f_{SST} \min\left[\frac{\rho k}{\omega}; \frac{a_1 \rho k}{SF_2}\right] \tag{1}$$

The damping function f_{SST} was defined as a function of y^+ (a scaled normal distance from the wall),

$$f_{SST} = f \ (<1.0) \quad ; \quad a \le y^+ \le b \tag{2}$$

$$f_{SST} = 1 \quad ; \quad y^+ < a,\ y^+ > b \tag{3}$$

For simplicity, the damping function was initially defined as a step function as shown in Figure 1 (solid line). Later, it was modified to be a continuous function. The constant a was set in the range 5-30 and the constant b was set in the range 50-300 for a parametric study. The values selected correspond to the edges of the buffer zone and the log law zone of a turbulent boundary layer.

The CFD code used in this study was the FLUENT Code [13]. The computational mesh was an O-type extending approximately to 35 chord lengths away from the airfoil and 250 points were employed along airfoil surfaces. The first cell at any surface point was sized such that $y^+ \le 2$ whereas grids away from it were expanded at a rate less than 20%. This grid system was found to be suitable for a RANS simulation of turbulent boundary layer flows [14,15].

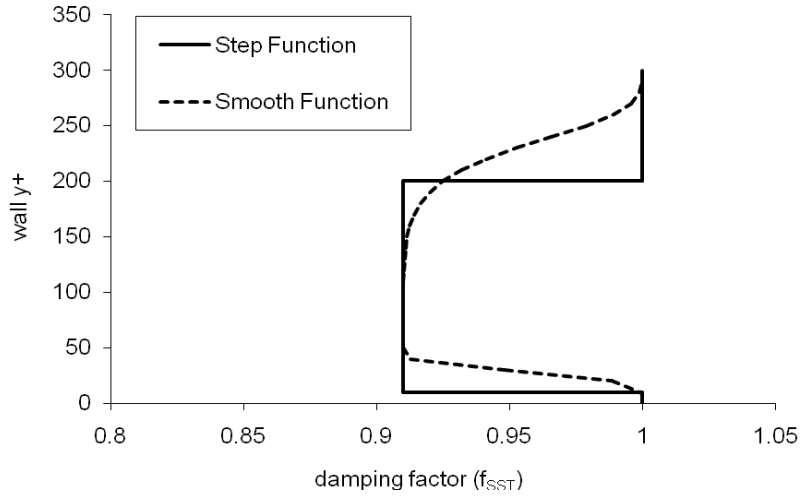

Fig. 1 Example of the step damping function and the hyperbolic (smooth) damping function.

Computations of flows over NREL's S809 airfoil [16] and NACA 63-215 [17] were conducted. An initially parametric study was performed to find out as to how sensitive a boundary layer would respond to changes in the values of a, b and f, using the step function. For this purpose, only some values of angles of attack, namely: 9^o, 11^o, 15^o and 20^o were selected; these are critical points on the lift curve of the S809 airfoil.

3. Results

Figure 2 compares the various computed results with the experimental data at angles of attack 9^o and 11^o. It can be seen that the lifts are quite sensitive to small changes in the values of a, b and f. Actually, several numerical experiments had been performed to weed out the unreasonable ones; only the more meaningful results are demonstrated here.

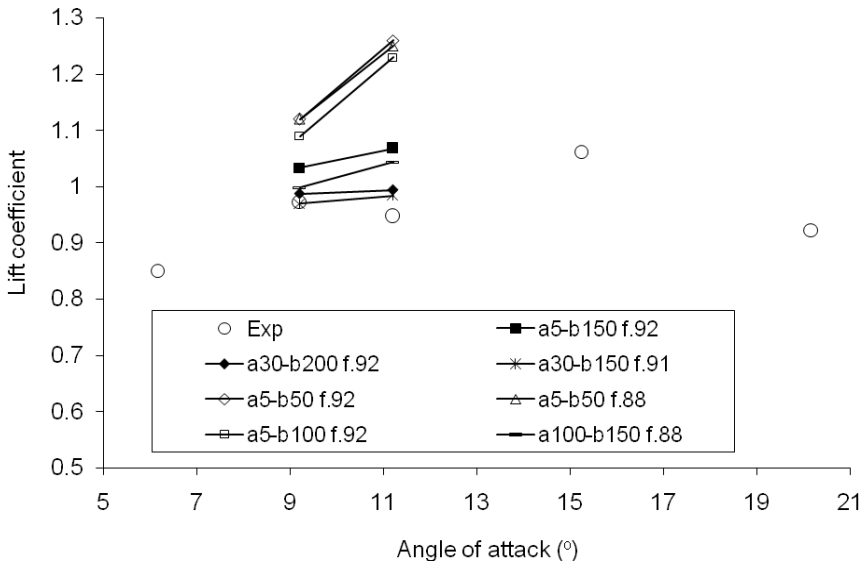

Fig.2 Effects of a, b and f in the step damping function on the lift coefficients.

After getting the feel for the sensitivity of the response, more numerical experiments were performed; the results of which are shown in Fig. 3 wherein it is observed that the characteristic dip and rise of the lift distributions are captured. The value of f a and b in the

ranges 0.90-0.91, 5-10 and 100-200, respectively, were found to be acceptable. Note that the range of acceptable f is very narrow.

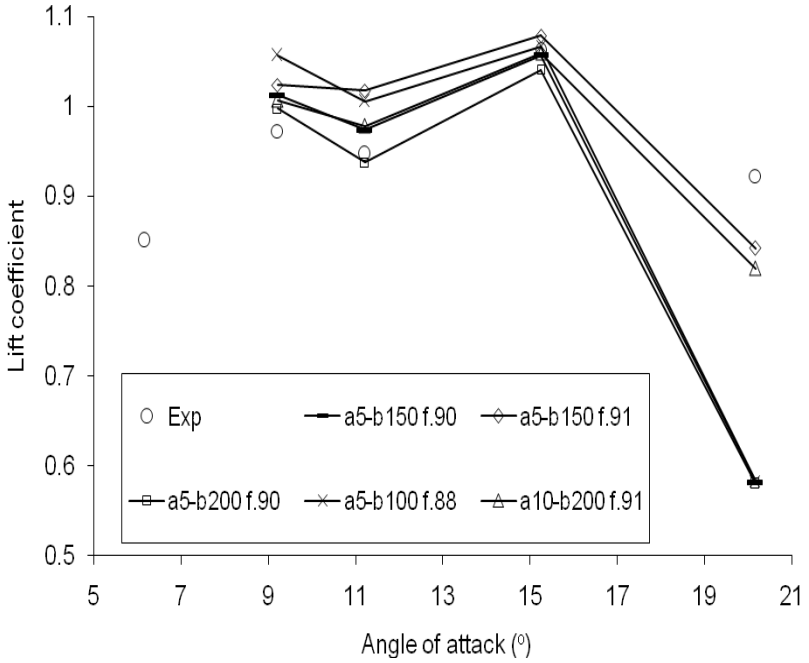

Fig. 3 Effects of a, b and f in the step damping function on lift at high angles of attack.

From the knowledge and experience gained in the parametric study of the step damping function, a continuous function is now proposed as,

$$f_{SST} = 0.1 + \{1 - 0.1\tanh[(0.03y^+)^4]\} \times \{0.9 + 0.1\tanh[(0.005y^+)^8]\} \qquad (4)$$

This damping function is the product of two hyperbolic functions; it was designed (by trial and error) for a rapid rise in the buffer zone and a gradual decrease in the log-law zone, as shown in Fig. 1 (dash line.)

Figure 4 compares the experimental results for lift on the S809 airfoil [16] to three computations, namely: 1) the present model by using the continuous damping function (denoted as SST+), 2) the 2-equation $k-\omega$ SST model (denoted as SST) and 3) the 4-equation $k-\omega$ SST turbulence model with transition [8] (denoted as SST-T.) This last turbulence model is an enhanced version of its 2-equation counterpart wherein a model for transition to turbulence is also incorporated. It is clearly seen that, in the stall region, the SST+ results compare much more favorably to the experiment than those of the other two models. The improvements are not only in a quantitative manner but also in a qualitatively manner, notably the dip and rise of the distribution right after the incipient point of stall at about 10 degree angle of attack. Drag coefficient plot, shown in Fig. 5, also indicates that SST+ results are superior to other models.

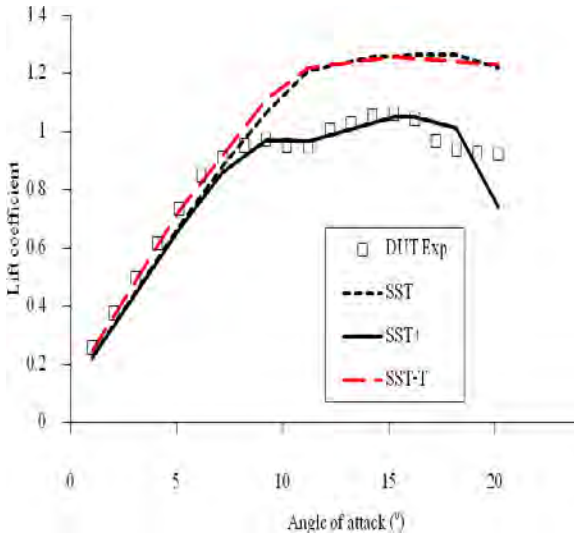

Fig. 4 Lift predictions on S809 airfoil using present and original turbulence models

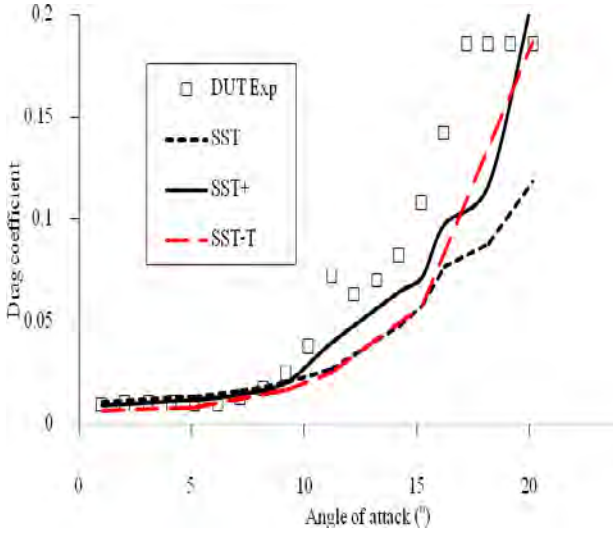

Fig. 5 Drag predictions on S809 airfoil using present and original turbulence models.

It is evident that in the low angle of attack region where the flow is still attached, SST-T gives best results but from the stall point onward SST-T exhibits over-predictions much in the same trend as SST. This perhaps is due to the fact that when flows separate on the suction side there is no transition regions left to give an advantage point to SST-T.

The predicted pressure distributions on the S809 airfoil surfaces at 14^o and 20^o angles of attack are shown in Figs. 6 and 7, respectively. The figures confirm that SST+ gives better overall agreements to the experiment than SST and SST-T. Specifically, the points of separation predicted by SST+ agree better with the experimental results; this is the main reason why it can predict aft-stall lift coefficients more accurately.

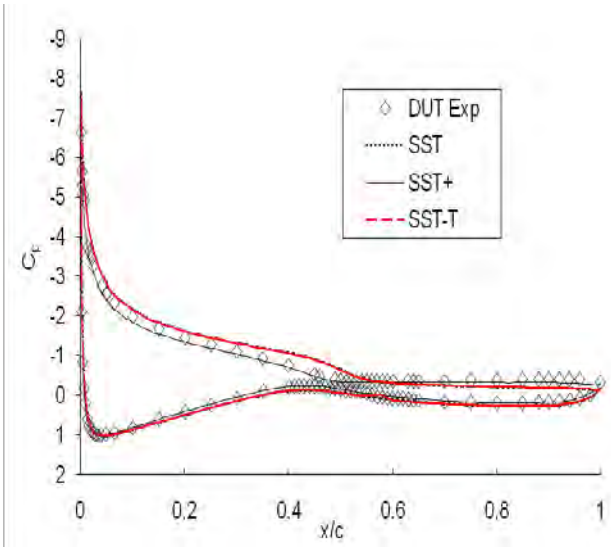

Fig.6 Comparison of pressure distributions on S809 airfoil at 14^o angle of attack

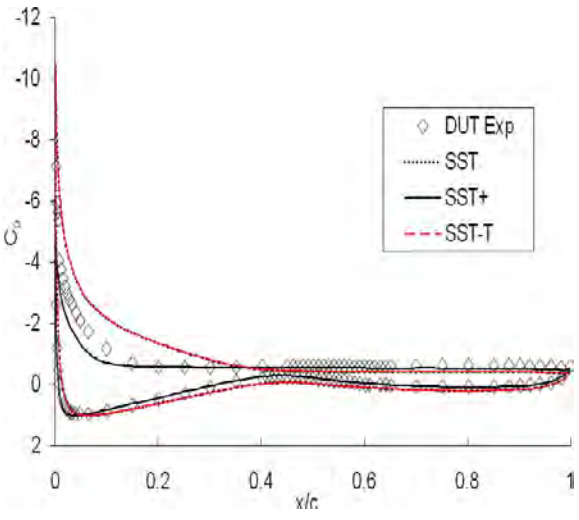

Fig.7 Comparisons of pressure distributions on S809 airfoil at 20^o angle of attack

The incipient of separations can be noticed as the point where the pressure distributions on the suction side are leveled off. Again, SST and SST-T give almost identical results.

To verify that the improved results obtained by the adjustment made to the buffer zone was not specific to an airfoil, flows over another airfoil, the NACA 63-215 [17] were solved under similar conditions. The results are shown in Figs. 8 and 9. Again, SST+ gives much better results than the original models, both quantitatively and qualitatively.

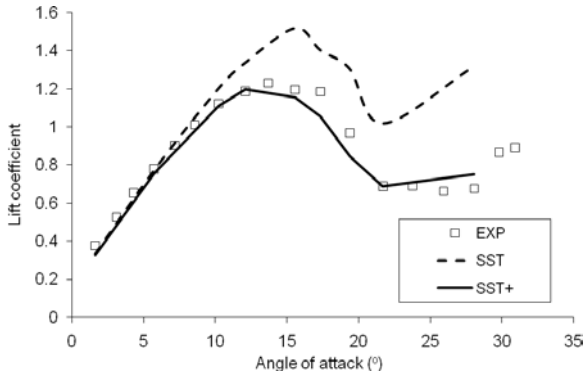

Fig.8 Comparison of lift between modified and original turbulence model.

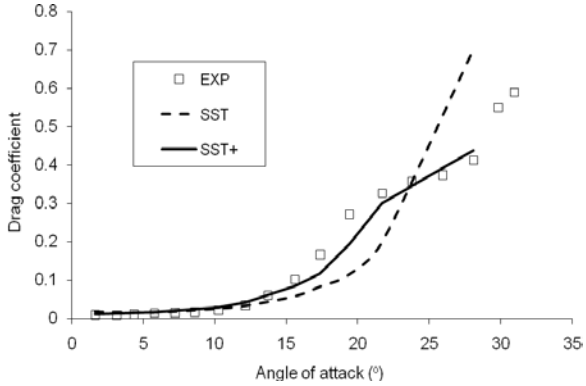

Fig.9 Comparison of drag between modified and original turbulence model.

4. Discussion and Conclusions

It could perhaps be reasoned that the improvements in lift and drag predictions over airfoils after stall were caused by the eddy viscosities in the buffer zones being reduced to about the right levels so as to compensate for the overall collective effects of the transition regions upstream that were neglected by the fully-developed turbulence model. In addition, compensations were also automatically provided for the local phenomena occurring within the buffer zones.

It has been evident that the behavior of a turbulent boundary layer over an airfoil is very sensitive to events in the buffer zone. A small change in the levels of turbulence intensity in the buffer zone could produce a dramatic change in the overall response of the separated flows on airfoils resulting in large changes on lift and drag.

By limiting the turbulence intensities (eddy viscosities) in the narrow buffer zones of turbulent boundary layers by about 10% together with the use of the $k-\omega$ SST turbulence model, this investigation has demonstrated that predictions of lifts and drags (after stall) on two independent airfoils were much improved. The improvements were evidently due to the reductions in the delay of incipient separation points which in turn were caused by the boundary layer being less energetic since the eddy viscosities (hence momentum transfers) were limited.

References

[1] P. Catalano and M. Amato, An evaluation of RANS turbulence modeling for aerodynamics, Aerospace Science and Technology 7, 2003, pp. 493-509.

[2] D.J. Mavriplis, Three-dimensional high-lift analysis using a parallel unstructured multigrid solver. AIAA Paper 98-2619, June 1998.

[3] C.L. Rumsey, T.B. Gatski, Recent turbulence model advances applied to multi element airfoil computations, J Aircraft 38(5), 2001, pp. 904–10

[4] Wolfe, W.P. and Ochs, S.S. "CFD Calculations of S809 Aerodynamic Characteristics," AIAA-97-0973, *Proceeding 35th AIAA Aerospace Sciences Meeting and Exhibit*, Reno 1997

[5] Bertagnolio, F., Sørensen, N.N., and Johansen, J. (2006, December). Status for the Two-Dimensional Navier-Stokes Solver EllipSys2D. Risø-R-1282(EN), Risø National Laboratory

[6] Chow, R. and van Dam, C.P., Computational Investigations of Deploying Load Control Microtabs on a Wind Turbine Airfoil, AIAA-2007-1018

[7] Rumsey, C.L., Ying, S.X., (2002). Prediction of high lift: review of present CFD capability. Progress in Aerospace Sciences 38: pp. 145–180

[8] Langtry, R.B., Gola, J., and Menter, F.R. (2006). Predicting 2D airfoil and 3D wind turbine rotor performance using a transition model for general CFD codes. 44th AIAA Aerospace Sciences Meeting and Exhibit, Reno 2006, AIAA 2006-0395

[9] Jones, W. P., and Launder B. E., The prediction of Laminarization with a Two-Equation Model of Turbulence, International Journal of Heat and Mass Transfer, Vol. 15, 1972, pp. 301-314

[10] Wilcox, D. C., (1993).Turbulence Modeling for CFD. DCW Industries, Inc., 5354 Palm Drive, La Cafiada, Calif.

[11] Menter, F.R. (1993). Zonal two equation $k-\omega$ turbulence models for aerodynamic flows. AIAA Paper 93-2906

[12] Menter, F.R. (1994, Nov). Two-equation eddy viscosity turbulence models for engineering applications. AIAA J 32:1299-1310.

[13] Fluent 6.3 User manual

[14] Franck Bertagnolio, Niels S_rensen and Jeppe Johansen, Status for the Two-Dimensional Navier-Stokes Solver EllipSys2D, Risø–R–1282(EN)

[15] Cummings, R.M., Forsythe, J.R., Morton, S.A., and Squires, K.D., (2003). Computational challenges in high angle of attack flow prediction. Progress in Aerospace Sciences, 39:369–384. doi:10.1016/S0376-0421(03)00041-1

[16] Somers, D.M., (1997). Design and experimental results for the S809 airfoil. Airfoils Inc., State College, PA. NREL/SR-440-6918

[17] Bertagnolio F., Sørensen N N., Johansen J., and Fuglsang P. (2001). Wind Turbine Airfoil Catalog, Risø-R-1280(EN), Risø National Laboratory, August 2001

Acknowledgements

This research was supported by the Royal Golden Jubilee Ph.D. program of the Thailand Research Fund. The authors are thankful to Prof. J.N. Sørensen of the Technological University of Denmark for his collaboration through the RGJ Ph.D. program.

Impact of ambient turbulence on performance of a small wind turbine

William D. Lubitz[1,*]

[1] *University of Guelph, Guelph, Ontario, Canada*
** Corresponding author. Tel: +1 519 824 4120 x54387, Fax: +1 519 836 0227, E-mail: wlubitz@uoguelph.ca*

Abstract: High resolution measurements of wind speed and energy generation from an instrumented Bergey XL.1 small wind turbine were used to investigate the effect of ambient turbulence levels on wind turbine energy production. It was found that ambient turbulent intensity impacts energy production, but that the impact is different at different wind speeds. At low wind speeds, increased turbulence appeared to increase energy production from the turbine. However, at wind speeds near the turbine furling speed, elevated turbulence resulted in decreased energy production, likely to turbulent gusts initiating furling events. Investigation of measurements recorded at 1 Hz showed a time lag of one to two seconds between a change in wind speed and the resulting change in energy production. Transient changes in wind speed of only one second duration did not impact energy production, however, longer duration changes in wind speed were tracked reasonably well by energy production.

Keywords: *Small Wind Turbine, Turbulence, Gusts, Wind Energy*

1. Introduction

Turbulence in the approaching wind can have a significant impact on the power output of wind turbines. This is particularly important for smaller wind turbines, which in practice are often located near buildings, trees and other obstacles. Some small wind turbine installations may experience inflow turbulence intensity many times greater than an open field site.

Current power curve representations do not account for the impact of turbulence on small turbine energy production. For example, curves based on IEC 16400-12-1 are statistical averages of power measurements binned by wind speed, whereby the variance of the data is lost [1]. This approach cannot properly account for site-varying levels of turbulence [2]. IEC 16400-12-1 does not specifically limit turbulence levels of measurements used in power curves, and the resulting power curves provide no guidance on how differing levels of turbulence will affect the power production of the turbine. It can be argued that the effect of site specific turbulence levels in large turbines is manageable, however small turbines may be tested under this or a similar standard while experiencing a wider range of ambient turbulence levels, creating an immediate need to address the impact of site turbulence and provide useful information in the context of the wind turbine power curve.

Ambient turbulence and wind direction variance both have significant impacts on small wind turbines. The smaller masses and length scales of small wind turbines mean that the impacts of turbulence on small turbines will be different from utility scale turbines [3]. Elevated turbulence levels can result in lower wind energy production and greater mechanical stresses on turbine components [4]. The smaller size, gustier operating environment and passive yaw systems associated with small turbines mean they are much more likely to be operating in a yawed state when the turbine cannot align itself to gusting winds [5]. The power output of a horizontal axis wind turbine falls rapidly when the turbine is not aligned to the wind, with a cos^2 dependence on relative wind angle [6]. Elevated turbulence intensity has been found to be the most important factor in reducing turbine structure fatigue life [4], and turbulence intensity impacts furling behaviour [7].

The effect of turbulence on power output is more difficult to generalize, since turbulent gusts impact wind alignment, airfoil performance and furling/power limiting. A small turbine tested in a high turbulence intensity environment was found to temporarily shut down more often due to high gust speeds exceeding limits [8]. Smith [9] used long term small wind turbine performance measurements collected at the National Renewable Energy Laboratory (NREL) to produce power curves and estimate annual energy production (AEP) for seven small wind turbines at varying levels of observed turbulence intensity. The small wind turbines showed a 9% to 32% difference between AEP at the best and worst turbulence levels. Most of the turbines had lower AEP in both the extreme high and low turbulence levels, although one (Skystream) exhibited a trend of increasing AEP with increasing turbulence intensity..

The goal of this study was to determine the impact of varying turbulence conditions on the performance of a representative small wind turbine. High resolution (1 minute and 1 Hz) data from a Bergey XL.1 1 kW capacity horizontal axis wind turbine were analyzed to explore the impact of turbulence on turbine power output.

2. Methodology

A Bergey XL.1 small wind turbine was used in this study. The Bergey XL.1 is an upwind, horizontal axis SWT with a rated capacity of 1.0 kW. It consists of a three blade, 2.5 m diameter fixed-blade rotor directly coupled to a variable speed permanent magnet alternator. This turbine was chosen due to its mechanical and control system simplicity, and because it has been the subject of a wide body of prior studies documenting its performance and operation [10-13].

The Bergey XL.1 was mounted on an 18 m tall, 0.114 m diameter galvanized steel tubular tilt-up tower. An additional 18 m tall, 0.152 m diameter tubular tilt-up tower was installed 13.4 m to the north of the turbine tower to serve as a meteorological mast for obtaining reference measurements of hub-height wind speed.

NRG 40C cup anemometers and one R.M. Young 81000 three-dimensional sonic anemometer were used for this study. The sonic anemometer was mounted on a short arm such that it's sensing volume was 20 cm directly below the rotor disk when the wind was from the prevailing direction of southwest. One NRG 40C and an NRG 200S wind direction sensor were located at the top of the reference mast 1 m above hub-height on separate 1.53 m booms. All NRG 40C anemometers used in this study were manufactured during the initial months of 2009 and calibrated by Otech Engineering (Davis, CA, USA). These calibrations were verified in the University of Guelph wind tunnel before experiment installation.

Power from the turbine was measured by tracking the voltage across a 2180 W, 2.0 Ω dynamic breaking resistor that dissipated the turbine's electrical power output. The 2.0 Ω resistance was selected to mimic the turbine's intended operation as part of a battery charging system under high load, while keeping the parameters needed to characterize electrical performance to a minimum. Additional sensors were installed to measure the yaw angle and rotor speed of the turbine. Ziter [14] gives further details of the experimental equipment.

The turbine and meteorological tower were installed at a representative SWT site on a farm in Oxford County, southwestern Ontario (43°18'N, 80°33'W). The collocated towers were installed in a field (grass, approximately 0.1 m tall) open for several hundred meters to the west and predominantly open to the north and southwest as well. The prevailing wind was from the southwest. Low rise buildings and trees to the east were all more than 100 m distant.

Other potentially significant obstacles included a small cluster of trees located 160 m to the northwest and a barn located almost 200 m to the southwest. Potentially disturbed direction sectors were determined according to IEC 61400-12-1 criteria [1]. Data from disturbed sectors were not used.

3. Results

3.1. One Minute Data

Fig. 1 shows the overall measured XL.1 power curve, based on binning and averaging of 1 minute averaging period, air density-corrected data from undisturbed sectors. The study turbine exhibited a cut-in speed of 4 m/s, and began furling at 9 m/s. Note that because a constant 2.0 Ω load was used, these power curves are not comparable to the manufacturer's or other power curves measured using a grid connection or battery charging controller. The reduced energy generation above 9 m/s for the study turbine is believed to be due to the addition of a nacelle anemometer and solar panel on the tail boom (that were not used in this study), which resulted in earlier furling than would otherwise occur.

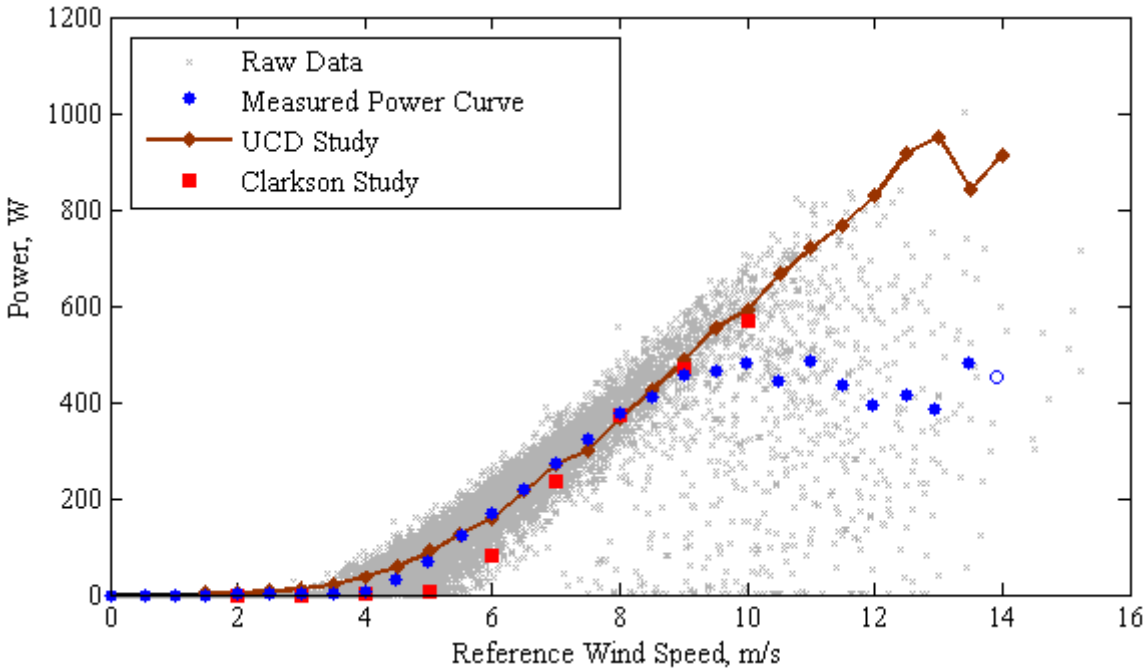

Figure 1. Measured Bergey XL. 1 power curve using a 2 Ω resistive load, with comparisons to UCD [12] and Clarkson [10] XL.1 power curves also measured with a 2.0 Ω load.

Next, the data from the turbine was divided into three categories based on turbulence intensity (which is the standard deviation of the wind speed divided by the mean wind speed during the 1 minute averaging period). The median turbulence intensity for the entire dataset was 0.173. Low turbulence intensity was classified as turbulence intensity less than 0.14. Turbulence intensity greater than 0.18 was considered high. Turbulence intensity between these two values was classified as intermediate. Figure 2 shows the number of observations in each wind speed bin and turbulence category.

Figure 3 shows the percentage difference between the overall power curve and three power curves derived from the categorized data. Low turbulence intensity consistently results in reduced power output (approximately -2%) between 4 m/s and 7 m/s, corresponding roughly to the operating range above cut-in and below the beginning of furling. The results for the

case of high turbulence are less consistent, with the percent increase in power output varying between 0% and +4% in the wind speed bins between 4 m/s and 7 m/s. This variability is likely due to the reduced number of high turbulence intensity observations in individual bins, compared to low turbulence observations. The intermediate differences are almost a mirror image of the low turbulence differences in Figure 3, again supported that these make up most of the observations.

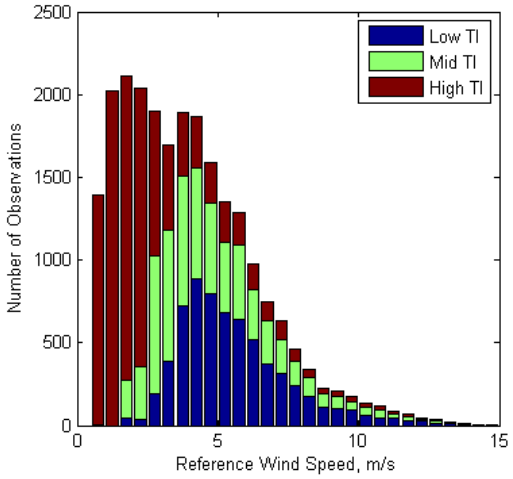

Figure 2. Number of observations by turbulence level and wind speed bin.

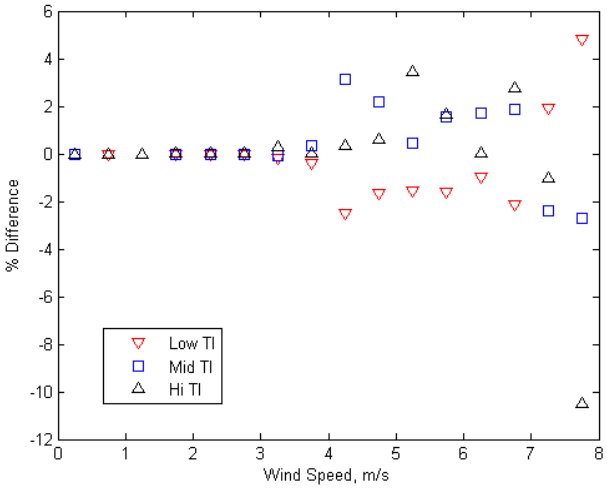

Figure 3. Percent difference between stratified and overall power curves.

The impacts of turbulence on furling were more pronounced. Figure 4 shows the wind percent difference between each of the three stratified turbulence power curves and the overall power curve, over the full range of available data. It is apparent that low turbulence intensity results in increased energy production, likely due to a reduction in intermittent furling and associated hunting. It should be noted that significant variability between bins is likely due to the small number of observations in each bin (Figure 2) at the higher wind speeds.

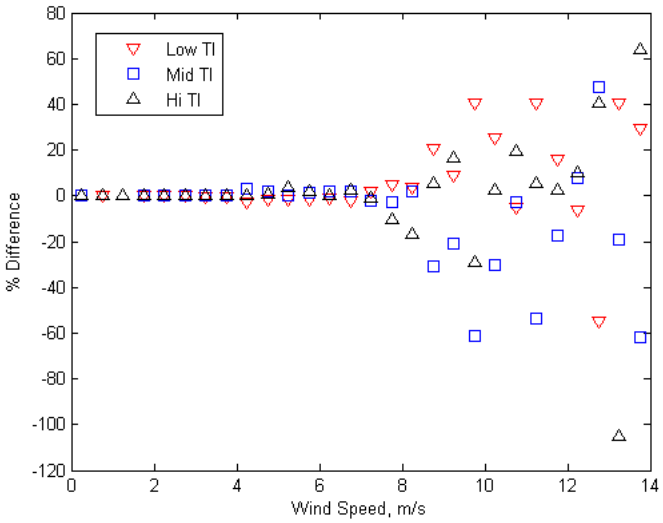

Figure 4. Percent difference between stratified and overall power curves.

Some impact of turbulence was noted at intermediate wind speeds above the cut-in wind speed. The effects of turbulence were found to be most pronounced at wind speeds approaching the furling speed of the turbine, and gusting was observed to cause intermittent

furling and consequently significant hunting and off-axis orientation, reducing power generation.

3.2. One Second Data: Transient Effects

The one second data from the turbine allows direct observation of the turbine response to variations in wind speed. Figure 4 shows 100 seconds of energy production and wind speed. Note that the wind speed shown is that measured by the sonic anemometer immediately below the rotor disk. A prior study [14] found the magnitude of this wind speed to be higher than the reference wind speed, however, turbulence levels were consistent between the two anemometers, and the sonic anemometer is a much closer indication of the wind experienced by the turbine rotor than the reference wind speed, which is over 13 m horizontally distant from the turbine.

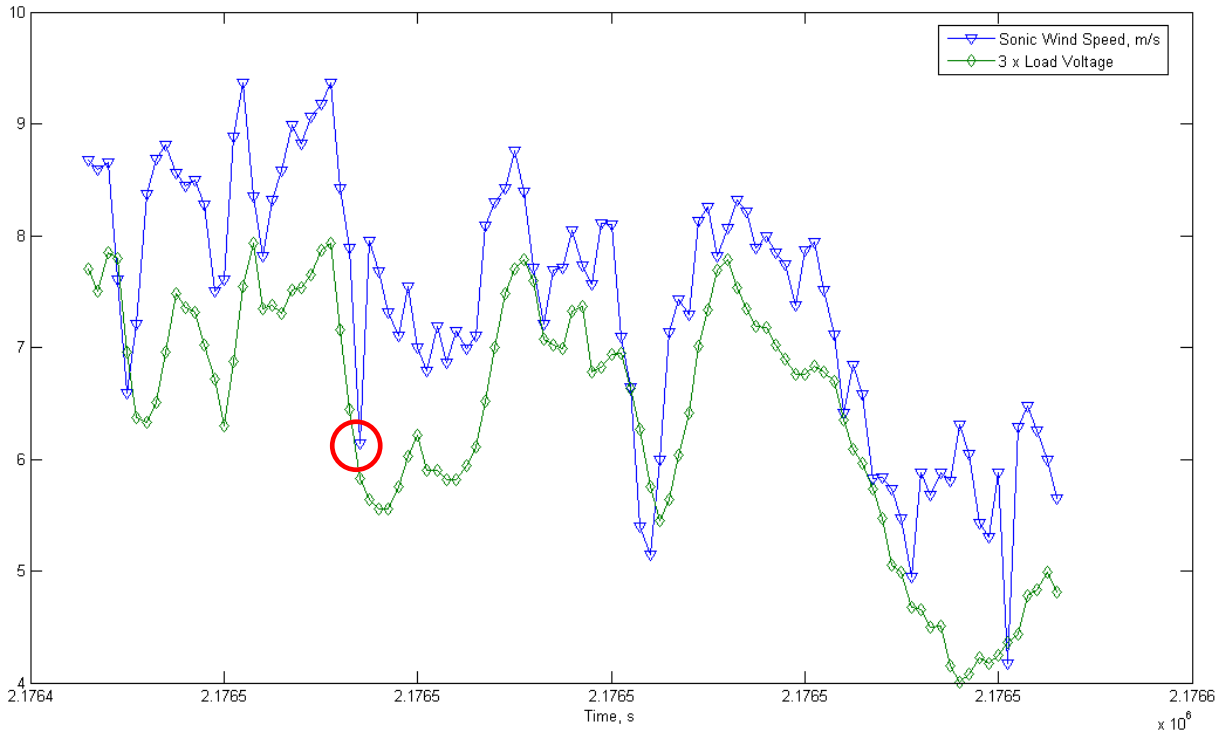

Figure 4. Example of 1 second sonic anemometer wind speed measurements and turbine energy production as measured by voltage across the resistor.

It is apparent that the turbine energy production is approximately one to two seconds delayed relative to the wind at the rotor disk, however, the rate of change and duration of wind speed perturbations appears to influence this. The circle in figure 4 s hows a transient gust of approximately one second duration that is not apparent in turbine energy production. However, changes in wind speed with time constants of many seconds are reasonably well tracked by energy production, factoring in the one to two second delay.

4. Discussion

The UC Davis turbine shown in Figure 1 is mounted on a 9 m mast on the roof of a 3 storey building that contains a penthouse and other roof top infrastructure, on a campus surrounded by other buildings and trees. It would be expected that this turbine would experience higher

ambient turbulence than the Clarkson turbine or the one in this study. With that in mind, it is interesting to note that the UC Davis turbine appears to have a lower cut-in wind speed (at about 3 m/s) than the 4 m/s overall cut-in speed observed for our own turbine, and the 5 m/s cut-in speed of the Clarkson turbine.

Very high turbulence levels resulted in overall decreased performance. It should be noted there are inherent limitations in using a single value of turbulence intensity, which combines all turbulence scales in a single measurement, as the only measure of wind speed variability. It was observed that turbulence impacts depended on the time scale of the turbulence: due to inertia, the turbine had difficulty responding to short time scale turbulence events. This could lead to reduced power output. However longer time period gust events that could be tracked by the turbine would be expected to result in greater overall performance when data was averaged, due to the non-linearity of turbine response to wind speed.

Applying a power curve produced at one level of ambient turbulence to a site with different ambient turbulence is likely to introduce significant errors in site-specific predictions of power output. The results of this study suggest that including additional turbulence information in the performance evaluation of small wind turbines could result in more accurate characterization turbine performance.

5. Conclusions

Measured data from a small wind turbine showed that turbulence has a range of impacts on a small wind turbine. Specifically,

- Turbulence levels had a small but noticeable impact on overall power output at wind speeds between cut-in and furling.
- Low turbulence levels resulted in increased power output at wind speeds associated with furling, likely due delayed onset of furling because of the presence of fewer gusts above the mean wind speed.
- Turbine energy production lagged changes in wind speed by one to two seconds. While changes in wind speed occurring over many seconds were reasonably well tracked by energy production, transient events of approximately one second duration were not tracked by energy production.

The results found here were broadly in agreement with other studies of the impact of turbulence on small wind turbines. The interaction of turbine with turbulent winds is complex and will vary depending on turbine characteristics.

References

[1] International Electrotechnical Commission (IEC), “Wind Turbines – Part 12-1: Power Performance Measurements of Electricity Producing Wind Turbines, Ed. 1.0,” International Standard, IEC 61400-12-1. Geneva Switzerland, Dec. 2005.

[2] Gottschall, J. and Peinke, J., Stochastic Modelling of a Wind Turbine's Power Output with Special Respect to Turbulent Dynamics, J. Physics: Conf. Series, 75 (1), 2007.

[3] Bertenyi, T., Wickens, C., and McIntosh, S., Enhanced Energy Capture Through Gust Tracking in the Urban Wind Environment, *29th ASME Wind Energy Symposium*, Orlando, FL, USA. Jan. 4–7 2010.

[4] V. Riziotis, and Voutsinas, S., Fatigue Loads on Wind Turbines of Different Control Strategies Operating in Complex Terrain, J. Wind Eng. & Ind. Aero. 85, 2000, pp. 211–240.

[5] Larwood, S., Wind Turbine Wake Measurements in the Operating Region of a Tail Vane, 39th AIAA Aerospace Sciences Meeting, Reno, Nevada, USA. Jan. 8–11 2001.

[6] Pedersen, T., On Wind Turbine Power Performance Measurements at Inclined Airflow, Wind Energy, Vol. 7, 2004, pp. 163–176.

[7] Corbus, D. and Prascher, D., Analysis and Comparison of Test Results from the Small Wind Research Turbine Test Project, Tech. Rep. NREL/CP-500-36891, NREL, Nov. 2004.

[8] Van Dam, J., Meadors, M., Link, H., and Migliore, P., Power Performance Test Report for the Southwest Windpower AIR-X Wind Turbine, Tech. Rep. TP-500-34756, NREL, Sept. 2003.

[9] J. Smith, Effects of Turbulence Intensity on the Performance of Small Wind Turbines. Small Wind Conference, Stevens Point, WI, USA. June 14-15, 2010.

[10] Humiston, C., and Viser, K., "Full Scale Aerodynamic Effects of Solidity and Blade Number on Small Horizontal Axis Wind Turbines," Proceedings of World Wind Energy Conference, Cape Town, South Aftrica, 2003.

[11] Klemen, M. A., 2004, "Bergey XL. 1 Power Curve," North Dakota State University [online database], http://www.ndsu.nodak.edu/ndsu/klemen/Bergey_XL.1_Power_Curve.htm [cited 11 November 2009].

[12] Seitzler, M., "The Electrical and Mechanical Performance Evaluation of a Roof-Mounted, One-Kilowatt Wind Turbine," Report CWEC-2009-003. California Wind Energy Collaborative, University of California, Davis. Davis CA, USA. 2009.

[13] Summerville, B. Small Wind Turbine Performance in Western North Carolina, Report. Appalachian State University, Boone, NC, 2005. http://www.wind.appstate.edu/reports/researcharticlesmallwindperformanceBJS.pdf. [cited 5 July 2010.]

[14] Ziter, B., Alternative Methods of Estimating Hub-Height Wind Speed for Small Wind Turbine Performance Evaluation. MASc Thesis, School of Engineering, University of Guelph, ON,Canada. May, 2010.

Feasibility study of 6.6MW wind farm in Greek mainland

George C. Bakos

Democritus University of Thrace, Dept. of Electrical and Computer Engineering, Xanthi, Greece
**Corresponding author. Tel: +30 2541079725, Fax: +30 2541079734, E-mail: bakos@ee.duth.gr*

Abstract: Wind energy has the advantage of being a priority sector of the Greek government. Greece has a considerable potential for electricity generation from wind not only in the island area but also in mainland. This paper deals with the current status of wind energy in Greece and the presentation of technical and economical feasibility of a 6.6MW wind farm applied to a potential wind farm site located in Greek mainland (Rentina-Karditsa). Wind speed, prevailing wind direction and temperature measurements are performed for a period of one (1) year (from 11/5/2009 to 11/5/2010). For economic consideration two different technological scenarios based on capacity factor (CF) are investigated and compared with respect to net present value (NPV), internal rate of return (IRR) and payback period (PBP) criteria. The profitability analysis shows that larger installed capacity with larger rated power wind turbines present higher IRR of the investment. The sensitivity analysis backs up the findings.

Keywords: *Renewable energy, Wind energy, Wind farm techno-economic assessment, RES legislation*

1. Introduction

Recently, there has been a considerable expansion of distributed generation (DG) technologies, thanks to progress in reliability, in competitiveness and operation know-how and incentive policies adopted by many developed countries. The presence of DG facilities brings benefits both to the electric power system and the total energy system. With DGs energy can be generated directly where it is consumed. As a consequence, transmission and distribution networks are less charged; safety operation margins increase, and transmission costs and power losses are reduced. The spread of DG technologies enhances supply safety in the energy field by reducing dependence on fossil fuels [1-4].

Wind power is driving growth in the renewables sector and represents a huge investment potential in Greece. The superb wind resources in Greece are among the most attractive in Europe, with a profile of more than 8 m/s and/or 2,500 wind hours in many parts of the country. Capacity increased by an average of 30% annually between 1990 and 2003 and almost 30% of total capacity was installed in the period of 2003-2004. It is estimated that in addition to the 1200-plus MW operating currently at wind farms, a further 7,500 MW will be installed by 2020. A detailed presentation of current and future wind farm installations on Greek islands is given in Ref. [5].

Electricity from Renewable Energy Sources, High Efficiency Cogeneration of Heat and Power and Other Devices». The main scope of the Law 3468 is to establish an adequate legislative and regulatory framework in order to support investments in renewable energy sources (RES) and High Efficiency cogeneration of heat and power (HE-CHP) energy sectors and eventually increase the penetration of these resources in the energy mix of the country. Aiming at conveying to the Hellenic legislation Directive 2001/77/EC of the European Parliament and of the Council of 27 September 2001 on the «Promotion of Electricity Produced from RES in the Internal Electricity Market», the National target is set to a 20.1% RES contribution on the total electricity production by 2010 while for 2020 the target is 29%. In the internal electricity market, the production of electricity from RES and HE-CHP are promoted in priority over other means of power production with specific regulations and principles. Until 2020, in Greece to achieve the target set by EC, the remaining RES

contribution to total electricity (excluding the large hydro) should be 58,37% wind, 2,73% Small Hydro, 2,73% biomass, 1,94% solar thermal, 22,95% photovoltaic energy (PV) and 11,28% other technologies.

On 4 June 2010, the Hellenic Parliament approved Law 3851 referring to "*Acceleration of RES growing facing climate change and other legislation related to Ministry of Environment, Energy and Climate Change subjects*". Law 3851/10 was published in the Official Gazette of the Hellenic Republic and is in effect since then. The main scope of New Law 3851 is the increased utilisation of the vast renewable energy resource of the country together with complying with the environmental targets of the Kyoto protocol. The attraction of large scale energy investments is also envisaged, in parallel with simplification measures for the necessary licensing procedures.

Wind energy has the advantage of being a priority sector of the Greek government. Greece has a considerable potential for electricity generation from wind not only in the island area but also in mainland. This paper deals with the current status of wind energy in Greece and the presentation of technical and economical feasibility of a 6.6MW wind farm applied to a potential wind farm site located in Greek mainland (Rentina-Karditsa). For economic consideration two different technological scenarios based on CF are investigated and compared with respect to NPV, IRR and PBP criteria. The profitability analysis shows that larger installed capacity with larger rated power wind turbines present higher IRR of the investment. The sensitivity analysis backs up the findings.

2. Case study: 6.6 MW wind farm in Greek mainland

The proposed wind farm site is located in the Prefecture of Thessaly (Karditsa-Rentina) in the heart of Greek mainland. The site, known to local people as “Lepouchi”, covers an area of 200.000 m^2 (Photos 1, 2) and is situated 3km from Rentina village. It is near to Rentina-Fourna national road and therefore quite favorable for wind turbines transportation. However, an improvement of an existing 500m forest road would be required to provide easy access to wind farm site. The proposed site is almost a flat-shrubbery area with presence of rocks, suitable for placement of tower foundations, roadways and crane pads. It is also favorable from the environmental point of view due to absence of wildlife, noise and visual issues. However, an important drawback is its distance (25km) from the nearest electrical substation (situated at Makrakomi-Lamia). The excessive cost associated with electrical issues is considered in economic analysis and affected the economic performance of proposed wind farm installation.

2.1. Analysis of wind power generation input parameters

The data was collected for the period from 11/5/2009 to 11/5/2010 with availability 98,7%. The wind speed data was the major parameter for wind energy generation and utmost care was taken in its collection. Two cup anemometers (one as primary and the other as auxiliary), wind direction vanes, temperature sensor and humidity sensor, certified according to ISO 17025:2005, were installed within the wind farm area (latitude 39º 05’ 02,4’’ and longitude 21º 56’ 46,8’’) placed on the top of a 30m metallic pole. A data recorder STYLITIS 40/41 (SYMMETRON) and a PV 10Wp/12V connected to a lead battery 12V/12Ah were also used.

Wind Speed

Significant variations in seasonal or monthly average wind speed are common over most parts of Greece. In the proposed site, the monthly average wind speed (Table 1) is high during

November-February and reaches a maximum of 7,5m/s because of South-West winds. The annual average wind speed is estimated 6m/s ($\pm 0{,}26$m/s) at wind turbine height of 80m.

Fig 1: Geographic location of wind farm site

Fig 2: Wind farm site

Table 1: Monthly average wind speed

Month	Average Wind Speed (m/s)	Data Availability (%)
January	7,3	96,1
February	7,5	97,0
March	5,3	96,0
April	4,4	100,0
May	4,0	98,0
June	5,0	100,0
July	4,0	95,0
August	2,9	100,0
September	2,9	100,0
October	5,2	95,7
November	5,9	97,1
December	7,4	95,2

Relative Humidity

The relative humidity of air depends on the amount of water vapor in the air, which in turn affects the air density. Moist air is less dense than dry air since water molecules is lighter than either a nitrogen molecule or an oxygen molecule, which are the major constituents of dry air. As the relative humidity increases air density decreases. The air density also depends on temperature and pressure and is given as follows:

$$air density = D\left(\frac{273{,}15}{T}\right)\left[\frac{B - 0{,}3783e}{760}\right] \qquad (1)$$

where D is the density of dry air at standard atmospheric temperature (25 C) and pressure (100kPa) (D=1,168kg/ m^3), T is the absolute temperature in Kelvin, B is the barometric pressure in torr and e is the vapour pressure of the moist air in torr. For the proposed site of wind farm installation, the mean yearly temperature is 10,4C and the monthly variation of relative humidity for the given period is between 50% and 70%.

Generation Hours

The generation hour is the period in which the wind turbine produces electric power from the energy available in the wind:

Generation hour = total number of hours in a year – (low wind hours + wind turbine maintenance hours + turbine breakdown hours + grid maintenance hours + grid breakdown hours)

Wind power generation hour is directly governed by the design of wind turbine, especially the cut-in and cut-out speed of wind turbines. A lesser cut-in speed and higher cut-out speed significantly improves the generation hours. Reduction in stoppage hours of wind turbine due to uncontrollable factors such as grid unavailability and mechanical breakdown improves the wind power generation. Periodic maintenance of turbine and grid are unavoidable and if done during off-seasonal period (when the average wind speed is below the cut-in speed) reduces energy loss and increases the total energy generation of wind turbine.

2.2. Wind farm energy generation

In order to calculate the wind farm energy generation is essential to perform the wind flow calculations. This is carried out using the *MS3D3H/3R* model which is integrated to *WindFarm* code. Then the *WindRose* code was used to estimate the total energy production for different capacity wind turbines. Net energy production is calculated using the energy losses related to wind turbine availability due to technical reasons (such as wind turbine malfunction, stoppage time for maintenance etc), wake and transmission losses. Two different technological scenarios were investigated where different capacity wind turbines were proposed.

Technological Scenario I (TS-I)

Four (4) wind turbines VESTAS V82 – 1,65MW were considered forming a 6.6MW wind farm. Table 2 shows the yearly total energy production per wind turbine, the wind direction and wake losses. Figs. 3-4 show the yearly energy yield (net) and the changes of energy yield due to wake losses per turbine respectively. It was calculated that gross energy production of 12,77GWh/year would be delivered to the grid resulting to 1930 generation hours and CF of 22,1%.

Table 2: Yearly total energy production per wind turbine, the wind direction and wake losses (TS-I)

TOTAL ENERGY YIELD			
Wind Turbine Identifier	Base Yield GWh	Wake Losses % Loss	Total Yield GWh
1	3.63	-1.44%	3.58
2	3.34	-1.76%	3.28
3	3.32	-2.01%	3.25
4	3.23	-1.14%	3.19
Total	13.52	-1.59%	13.30

TOTAL ENERGY YIELD			
Wind Direction	Base Yield GWh	Wake Losses % Loss	Total Yield GWh
0	0.24	-21.17%	0.19
22.5	0.38	-1.99%	0.38
45	0.28	0.00%	0.28
67.5	0.03	0.00%	0.03
90	0.02	0.00%	0.02
112.5	0.03	-4.52%	0.03
135	0.06	-15.74%	0.05
157.5	0.10	-32.59%	0.07
180	0.28	-16.77%	0.23
202.5	1.08	-0.83%	1.07
225	1.74	0.00%	1.74
247.5	2.97	0.00%	2.97
270	5.38	0.00%	5.38
292.5	0.70	-2.09%	0.69
315	0.13	-12.34%	0.11
337.5	0.08	-31.80%	0.06
Total	13.52	-1.59%	13.30

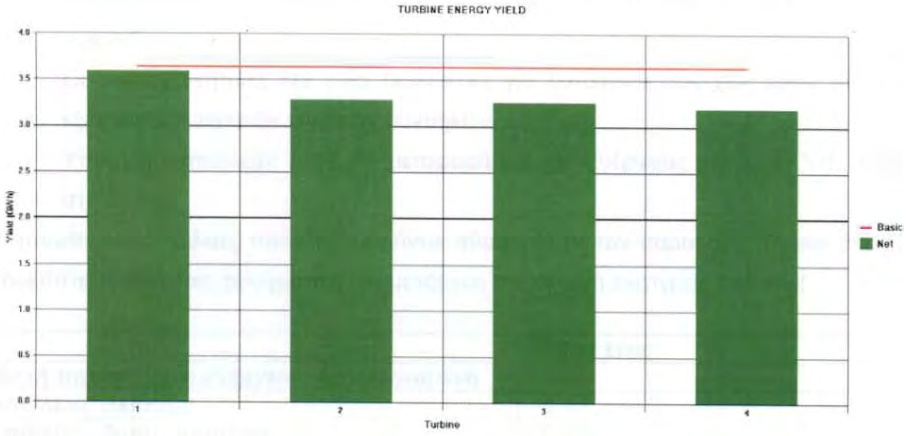

Fig. 3: Yearly net energy yield per turbine (TS-I)

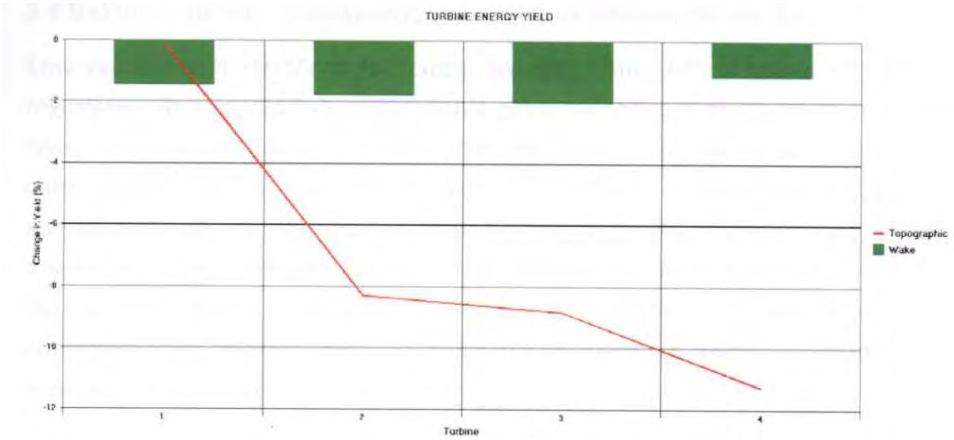

Fig. 4: Wake losses per turbine (TS-I)

Technological Scenario II (TS-II)

Four (4) wind turbines VESTAS V100 – 1,8MW were considered forming a 7.2 MW wind farm. Table 3 shows the yearly total energy production per wind turbine, the wind direction and wake losses. Figs. 5-6 show the yearly energy yield (net) and the changes of energy yield due to wake losses per turbine respectively. It was calculated that gross energy production of

17,30GWh/year would be delivered to the grid corresponding to 2400 generation hours and CF of 27,4%.

Table 3: Yearly total energy production per wind turbine, the wind direction and wake losses (TS-II)

TOTAL ENERGY YIELD

Wind Turbine Identifier	Base Yield GWh	Wake Losses % Loss	Total Yield GWh
1	4.85	-1.88%	4.76
2	4.58	-2.49%	4.47
3	4.55	-2.83%	4.42
4	4.45	-1.54%	4.38
Total	18.43	-2.18%	18.03

TOTAL ENERGY YIELD

Wind Direction	Base Yield GWh	Wake Losses % Loss	Total Yield GWh
0	0.40	-22.71%	0.31
22.5	0.64	-3.26%	0.62
45	0.48	0.00%	0.48
67.5	0.08	0.00%	0.08
90	0.04	0.00%	0.04
112.5	0.06	-4.37%	0.06
135	0.10	-17.22%	0.09
157.5	0.17	-35.90%	0.11
180	0.41	-18.47%	0.33
202.5	1.42	-1.51%	1.40
225	2.18	0.00%	2.18
247.5	3.76	0.00%	3.76
270	7.31	0.00%	7.31
292.5	1.04	-3.17%	1.01
315	0.20	-13.86%	0.17
337.5	0.15	-34.90%	0.10
Total	18.43	-2.19%	18.03

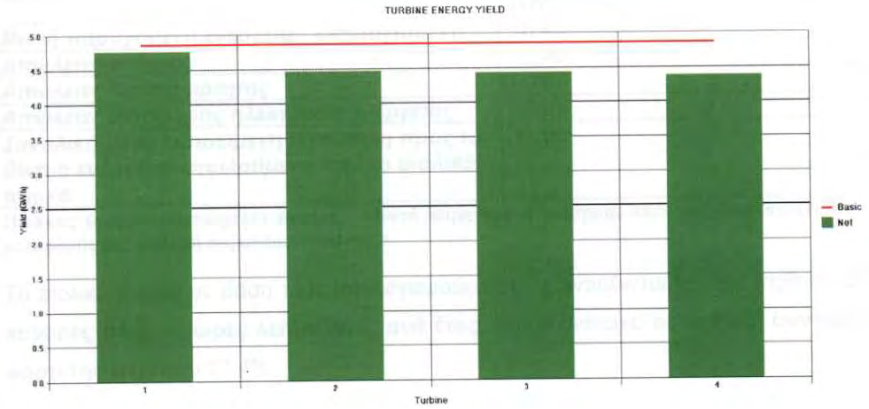

Fig. 5: Yearly net energy yield per turbine (TS-II)

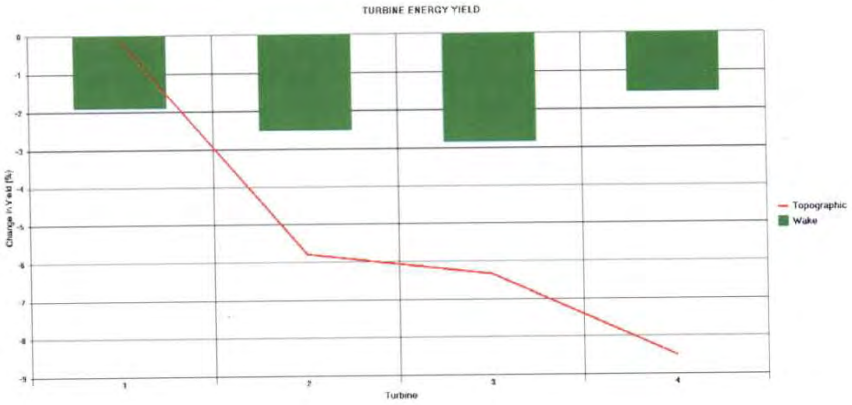

Fig. 6: Wake losses per turbine (TS-II)

2.3 A systematic economic assessment

The analytical technoeconomic general model is the computerized renewable energy technologies (RETs) assessment tool 'RETScreen' [6] which is used for preliminary evaluation of the technical feasibility and financial viability of potential grid-connected wind

installations anywhere in the world. For Greece in particular, it takes into account the prevailing Greek national development and energy laws, the government's subsidy and the prices applicable for buying or selling energy to the PPC by the electric energy producer.

For the technological scenarios TS-I and TS-II, different economic and financial feasibility indices are calculated such as the year-to-positive cash flow, IRR, ROI and NPV. The results of the installed wind power plants are shown in Figs. 6-7 respectively. The initial capital cost for TS-I is 8.500.000€ and for TS-II is 9.500.000€. The owner covers 25% of initial cost and the rest 75% is provided as a loan by private banks (10-year period and interest rate of 6%). The owner also decided to use the extra bonus 20% increase of feed-in tariff provided by Law 3851/2010 (i.e. 105€/MWh).

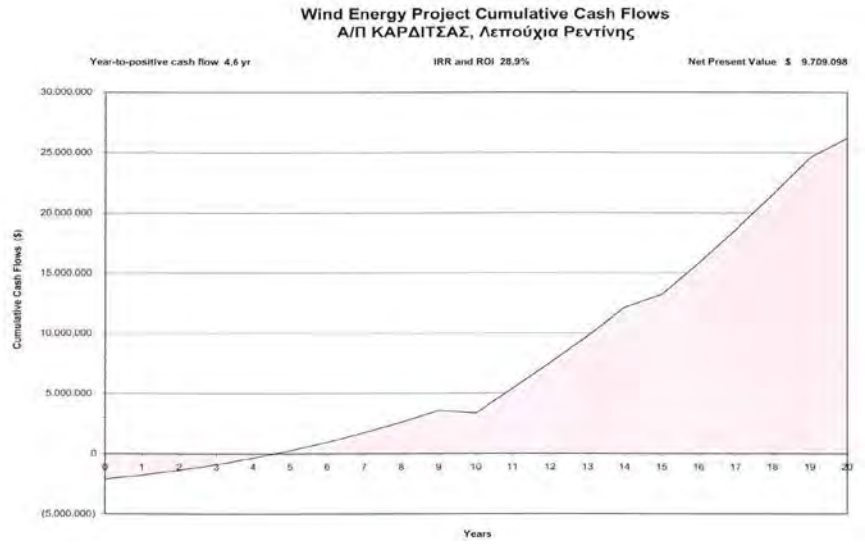

Fig. 6: Wind farm economic analysis (TS-I)

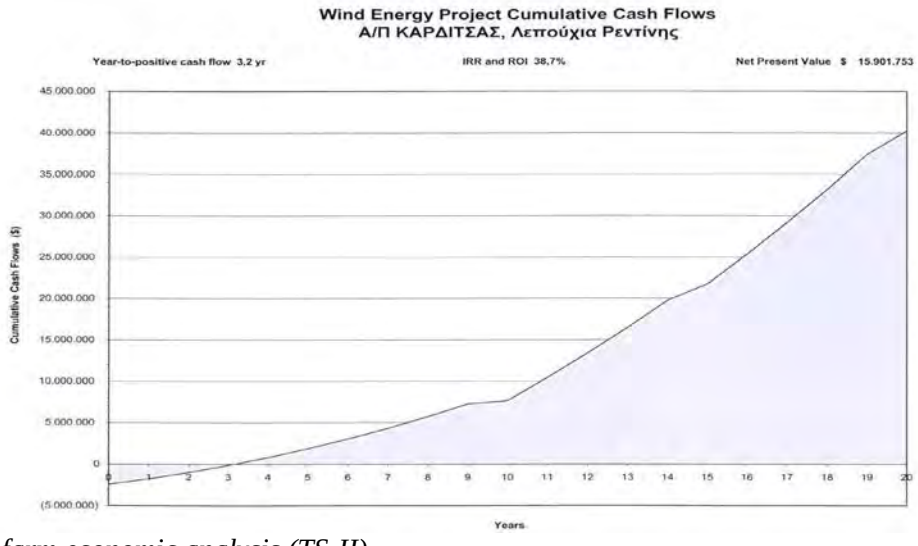

Fig. 7: Wind farm economic analysis (TS-II)

3. Conclusions

Two different technological scenarios were investigated and cash flow economic analysis was performed under the new legislation for RES penetration in Greece. From the results shown in Figs 5-6, it is concluded that Technological Scenario I [four (4) wind turbines VESTAS V82-1.65MW and installed capacity of 6.6MW] constitutes the less profitable investment in comparison to technological Scenario II [larger wind farm of 7.2MW consisted of four (4)

VESTAS V100-1.8MW]. This is due to increased performance of wind turbines in TS-II which compensates for the increased initial cost of the investment. For the particular wind farm installation in the Greek mainland, it was found that larger installed capacity with larger rated power wind turbines presented higher IRR of the investment. Furthermore, the PBP is 7,5 years and 6,2 years for TS-I and TS-II respectively. The results show that the implementation of wind farms in Greek mainland could present a profitable investment despite the fact that the sites are not so favorable compared to the islands. However, the experience of the implementation of wind farms in Greece emphasised the necessity for a simplified licensing procedure and a better coordination through institutions for Environmental Approvals.

The question becomes apparent: where does Greece go from here? According to Greek Ministry of Development, a wind total of 7500MW (including offshore) is planned to be installed until 2020 (while 4000MW of them until 2014). This capacity is limited due to grid stability, due to suggestions from Regulatory Authority for Energy (RAE) for possible excessive charging of consumers and due to public opposition in large scale wind farm installation, particularly in Greek islands. In order to achieve the goal of 7500MW, the Hellenic Parliament approved recently Law 3851 regarding RES electricity. According to this legislation, wind projects can get an extra bonus 20% increase of feed-in tariff, providing that the owner will not apply for a grant to the Greek State. This policy mechanism designed to promote mature wind projects for immediate connection to the grid. Also, the Hellenic State is planning to upgrade the existing grid to overcome grid stability problems and to offer more benefits to local people (such as discounted electricity bills) in order to overcome their opposition.

The main conclusion is that, with respect to electricity supply, wind farm applications will continue to play the most important role in Greece. The country high wind potential through out the year, the increasing environmental sense of Greek population, the elimination of time consuming license procedures, noticed during the implementation of first wind farm installations in Greece, and the improved financial incentives will increase the wind penetration in Greek electricity market.

References

[1] Tsikalakis A.G. and Hatziargyriou N.D. (2007) Environmental benefits of distributed generation with and without emissions trading, Energy Policy 35, pp.3395-3409

[2] Dicorato M. et al (2007) Environmental-constrained energy planning using energy-efficiency and distributed-generation facilities, Renewable Energy (In Press).

[3] Meyer I. Niels (2003) Distributed generation and the problematic deregulation of energy markets in Europe, International Journal of Sustainable Energy Vol. 23, No. 4, pp. 217-221.

[4] Deepak Sharma (2003) The multidimensionality of electricity reform – an Australian perspective, Energy Policy 31, pp. 1093-1102.

[5] Centre of Renewable Energy Sources (CRES), www.cres.gr.

[6] Retscreen Manual (2000), Energy Diversification Research Laboratory (CEDRL), Canada.

Optimal spatial allocating of wind turbines taking externalities into account

Jürgen Meyerhoff[1], Martin Drechsler[2,*]

[1] *Technische Universität Berlin, Berlin,Germany Germany*
[2] *UFZ – Helmholtz Centre for Environmental Research, Leipzig, Germany*
** Corresponding author. Tel: +49 3412351713, Fax: +49 3412351473, E-mail: martin.drechsler@ufz.de*

Abstract: Wind power is one of the most promising options for producing energy in a climate-friendly manner. However, besides its environmental benefits wind power generation causes externalities such as impacts on humans and biodiversity. All studies conducted so far show that these externalities can be substantial. The question is how this knowledge translates into a welfare-optimal spatial allocation of turbines that needs to consider both production and external costs. We present a modeling approach for the determination of the welfare-optimal spatial allocation of wind turbines (WT) and apply it to the planning region West Saxony in Germany. The approach combines choice experiments, a non-market valuation method used to measure externalities of wind power, and spatially explicit ecological-economic modeling within an optimization framework. Optimal is understood here as producing a given amount of wind power at lowest social costs. Social costs comprise (i) externalities measured by the (monetized) impact of WT on biodiversity, the distance of the WT to settlements, the height of the WT and size of wind farms, and (ii) the construction and operating costs associated with the WT. We show that the social costs of wind power production can be reduced substantially if externalities are taking into account.

Keywords: *choice experiment, externality, modeling, spatial allocation, welfare-optimal, wind power.*

1. Introduction

Wind power belongs to the most efficient renewable energy sources and constitutes an important component of the energy mix in many countries. In future, wind power is going to expand further to help meeting ambitious energy and climate policy goals. However, despite its doubtless advantages, wind power generation comes along with considerable negative externalities that lead to conflicts with other important policy goals, including human health and biodiversity conservation. Human health is affected because of the shade and noise effects produced by wind turbines (WT) [1]. Visual impacts of WT on landscapes have been considered by [2,3]. Biodiversity is affected especially through increased mortality and habitat loss for birds and bats [4,5]. External costs of wind power have been quantified, e.g., by [6-8]; see [9] for an overview.

The quality and extent of the monetary and non-monetary externalities of wind power considerably depend on the characteristics of the sites selected for wind power development. One the one hand the unit cost of wind-generated electricity depends on the energy produced per year and this depends on the local wind conditions. On the other hand, WT erected in the vicinity of settlements or bird habitats increase the impact on humans and birds. Different sites available for the installation of a WT will have different pros and cons in terms of wind power production costs and external costs. Since the pros and cons of wind power generation vary in space, they can be balanced and conflicts with other policy goals be mitigated through the appropriate spatial allocation of the WT. In the present article we propose a welfare-economic approach that determines the spatial allocation in a way that the social cost of producing a given amount of wind power is minimized. The mentioned balance of the pros and cons is reflected by the fact that the social cost is calculated as the sum of the production cost (e.g., installation and operating costs) and the external costs. The latter comprise the

monetized impacts on human health, biodiversity, etc. and depend on the preferences of the people, i.e. on how they value these impacts.

Despite their advantages such as their analytical clarity and rootedness in economic theory, welfare-economic approaches have been rarely used to optimize the spatial allocation of land use in general, and WT in particular. An example that goes into this direction is found in [10] which explores trade-offs between wind power production and the conservation of two animal species. However, since the analysis does not include any information about social preferences, it cannot determine the welfare-optimal allocation of WT. The above-mentioned studies [6-9] on the other hand, provide the necessary information about social preferences but do not include any assessment or modeling of how the valued impacts depend on the spatial allocation of the WT. As a consequence, they too cannot determine the welfare-optimal spatial allocation. This lack has recently been criticized [11]. The two approaches, spatially explicit modeling of impacts and the economic valuation of impacts have complementary strengths and weaknesses and combining them allows overcoming the weaknesses. In the present paper we follow this route to determine the welfare-optimal spatial allocation of WT in a study region in Germany. For this region we investigate a number of policy relevant questions: (i) how do society's preferences affect the welfare-optimal allocation of WT, (ii) what is the trade-off between the production and the external costs of wind power production, and (iii) what are the consequences of ignoring external cost in the planning of landscapes for wind power production.

The paper is structured as follows. In section 2 we will outline the modeling approach and present the study region. In section 3 we apply the modeling approach to the study region and present the results in section 4. Section 5 discusses the results and draws conclusions for policy design.

2. Methodology

2.1. The modeling approach

The objective of the analysis is to allocate WT in the study region such that a given level of electricity $E_{\min}$ is produced per year at minimal social cost C. The social cost of wind power supply is composed of the production costs C_p and external costs C_e. To determine external costs we define attributes that capture the relevant externalities as identified through stakeholder interviews (see section 3.1 below). The attributes are quantified through spatially explicit models and valued through choice experiments. In the present case the attributes comprise: the loss rate (L) of important species, the minimum distance of WT to settlements (D), the height of the installed WT (H) and the size of wind parks (S). The attributes D, H and S consider the impact of WT on the landscape and ultimately human inhabitants. The disturbance of humans by the noise of a WT depends, among others, on the height of the WT and its distance to the settlement areas. Attribute H considers that WT technologies with different heights may by installed. Attribute S considers that WT may be allocated in larger or smaller wind parks. The production cost and attribute L depend on the time frame. We consider a time frame of 20 years, which is about the life time of a WT, so C_p measures production costs over 20 years and L measures species decline within 20 years. The analysis is carried out in several steps. First we construct the social cost function

$$C = C_p + C_e(L, D, H, S) \qquad (1)$$

where C_e are the external costs associated with the attributes *L*, *D*, *H* and *S*. They are determined through choice experiments (see section 3.1). We further identify the sites that are physically and legally suitable for the installation of a WT. Given these potential sites, WT allocation strategies are formed as described above, considering that the energy target $E_{\min}$ must be fulfilled. For each allocation strategy we determine the associated attributes C_p, *L*, *D*, *H* and *S* and determine the social cost *C*. For given energy target $E_{\min}$, the welfare-optimal allocation of WT, i.e. the allocation that minimizes *C*, is determined through numerical optimization.

2.2. Application of the modeling approach

The approach is applied to the Planning Region West Saxony in Germany that is a part of the Free State of Saxony. The region has about 500,000 households (2005) and covers an area of around 4,300km². Due to its topography the region is fairly suited for wind power production but at the same time belongs to the core distributional area of the endangered Red Kite (*Milvus milvus*). Red Kites have been frequently observed to be killed by WT. The Red Kite therefore forms the focal bird species in our analysis and *L* measures the rate by which the Red Kite population declines as a consequences of the presence of WT in the region [12]. Below we go through the steps of the modeling approach.

2.2.1. Construction of the external cost function through choice experiments

We consider an external cost function which is the sum of the partial external costs $C_y(y)$ associated with the attributes $y \in \{L,D,H,S\}$:

$$C_e(L,D,H,S) = \sum_{y\in\{L,D,H,S\}} C_y(y) \cdot \sum_{t=1}^{T} (1+r)^{-t} \qquad (2)$$

The partial external cost $C_y(y)$ represents the cost for a single year. Since we are considering a time span of T=20 years, we have to aggregate the costs over these 20 years. We discount the external costs at annual rate *r*. We assume that $C_y(y)$ has the shape $C_y(y)=a_y/(y-b_y)+g_y$ (which can describe concave or convex increases or decreases of C_y with *y*) and carry out choice experiments (CE) [13] to determine the parameters a_y, b_y and g_y for all $y \in \{L,D,H,S\}$. CE are based on the assumption that the utility to consumers of any good (i.e., also public goods such as a landscape) is derived from its attributes or characteristics. Due to this focus CE are particularly useful for valuing multidimensional changes. In a CE, respondents are asked to make comparisons among environmental alternatives characterized by a variety of attributes and the levels of these. Typically, respondents are offered multiple choices during the survey, each presenting alternative designs of the environmental change in question and the option to choose the status quo. The record of choices serves as a basis to estimate the respondents' willingness to pay. Changes in welfare due to a marginal change in a given attribute are calculated using the MWTP. It is defined as the maximum amount of income a person will pay in exchange for an improvement in the level of a given attribute provided and can be identified as the difference in C_y associated with the change in *y*.

In the present study we consider the four different attributes *L*, *D*, *H* and *S* with three levels for each attribute to characterize changes in the environment. They are combined to choice sets using an experimental design that allows determination of the independent influence of the attributes on respondents' choices (details of the CE can be found in [9]). The choices of 353 randomly chosen inhabitants from the study region were considered.

2.2.2. Specifying the decision space and modeling the attributes

We start our analysis by identifying which parts in the landscape are physically and legally qualified for the allocation of WT with the help of a geographical information system (GIS) of the region. Broadly speaking, these are open areas distant enough from infrastructure, settlements and nature conservation areas. The analysis focuses on two WT technologies k=1,2. The k=1 type has a hub height of 78m and rotor diameter of 82m, yielding a nominal power of 2MW, while the k=2 type has a hub height of 105m and a rotor diameter of 90m, yielding a nominal power of 3MW. The suitable parts of the landscape are subsequently filled with a grid of points with each point in the grid representing a potential site for the allocation of a WT, taking technical minimum distances between individual WT into account. The number of potential sites is N=1098. Allocation scenarios are defined by deciding for each potential WT site i=1,…,N whether it should contain a WT of type 1 or type 2 or no WT.

The energy yield E_{ik} for each site i and WT type k is calculated by using the technical parameters of the WT and the relevant frequency distribution of wind speeds observed at the spatial location and altitude of the WT hub (for further details see [12]). The wind speed data were obtained from Eurowind GmbH (Köln, Germany). The total energy E_{tot} produced per year in the region is obtained by summing E_{ik} over all installed WT.

The production cost $C_{p,k}$ (over a time frame of 20 years) associated with a WT of type k comprises the construction and operating costs. The construction costs are composed of selling prices, taken from the companies' price lists, and a 10 percent mark-up to cover on-site construction costs, including grid connection. Annual operating costs are typically estimated at five percent of the construction costs (information provided by interviewed WT operators).

Ecological externalities are partly taken into account by prohibiting the erection of WT in areas protected by nature conservation laws. However, protected areas are by no means sufficient to reach the ambitious goals of biodiversity policy. So the impacts of WT on biodiversity have to be considered even if the WT are installed outside the protected areas. We consider L, the percentage of the regional Red Kite population that is lost due to WT over the modeling time frame of 20 years. We model this loss rate as the sum of "marginal" loss rates l_i over all sites i=1,…,N that contain a WT. We assume that the contribution l_i of site i to L is determined by the probability of an individual of the focal species being found at the site. This depends, e.g., on how close the site is to a nest, whether the site is located within a migratory bird route, etc. In the case of Red Kites we assume that l_i is a declining function of the distances of site i to known nests (i.e., WT close to a nest cause a higher collision risk for the Red Kite with the WT than WT at more distance to a nest).

The modeling of the remaining three attributes is straightforward. Attribute D represents the minimum distance of WT to settlements, considering all settlements and installed WT in the region. Attribute H is modeled as the average over the heights of all installed WT in the region. To determine attribute S we apply the wind park method [14] that clusters all WT into wind parks. S is then the average size of those wind parks.

3. Results

3.1. Construction of the social cost function

The choice experiments yield the following MWTP (in Euros per household per month)[1]: 2.13 for an improvement in the Red Kite loss rate L from 10% to 5% per 20 years; -2.18 for a worsening in L from 10% to 15%; 3.18 for an increase in the settlement distance D from 800m to 1100m; and 3.94 for an increase in D from 800m to 1500m. Changes in the other two attributes, H and S, did not lead to a statistically significant MWTP.

The partial cost functions $C_y(y)$ (eq. 2) are fitted to these measured MWTP to obtain the external cost function $C_e(L,D)$ shown in Fig. 1. One can see that external costs increase with increasing externalities, i.e. with increasing Red Kite loss rate L and decreasing settlement distance D.

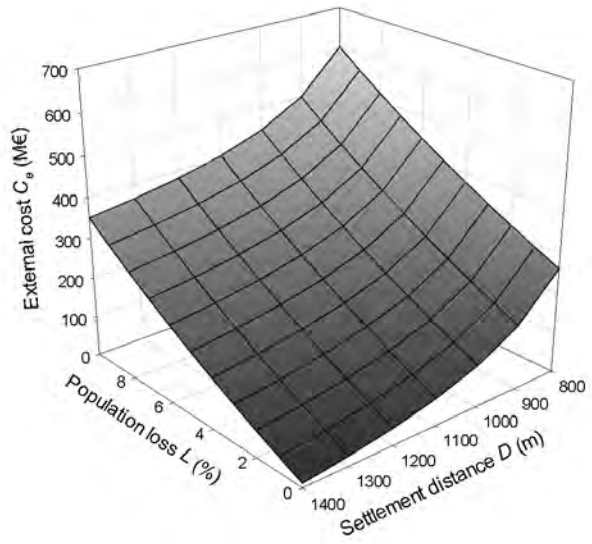

Fig. 1. External cost $C_e=C_L+C_D$ for the study region as a function of Red Kite loss rate L and settlement distance D, considering a time frame of 20 years with annual discount rate r=3%.

3.2. Evaluation of the attributes

Figure 2a shows the production cost C_p (over 20 years, discounted to the present year) for all potential WT sites i in the region. One can see that the production costs are lowest in the south, centre and east, and highest in the north east, which reflects relatively high wind speeds and large energy outputs E_{ik} in the south, centre and east and low wind speeds and energy outputs in the north east.

The external costs are determined by the settlement distance D and the Red Kite loss rate L which is the sum of the impacts l_i associated with each WT site i. The impacts for all potential WT sites are shown in Fig. 2b. We find that the l_i are relatively uncorrelated to the production costs, so there are both "low-conflict" WT sites that have low (high) production costs and low (high) impact on the Red Kite and "high-conflict" sites with low (high) production costs and high (low) impact on the Red Kite.

[1] The conditional logit reveals that only the attributes L and D have a significant influence on respondents' choices among the alternatives presented on the choice sets. Thus, only for these attributes MWTPs are calculated. See [9] for more details on the analysis of the choice experiments.

3.3. The welfare-optimal allocation of WT

The task is to allocate WT to the potential sites i=1,…,N so that the energy target E_{min}=690 GWh per year is achieved at minimal social cost where social cost is given by the sum of production costs (cf. Fig. 2a) and external costs (Fig. 1). The resulting optimal WT allocation scenario is characterized by the following welfare-optimal levels of the attributes: the optimal Red Kite population loss rate is L*=1.2 percent within 20 years, the optimal settlement distance is D*=1,025m and the optimal production cost amounts to C_p*=730 million Euros (sum over 20 years, present value, discounted at 3% per year). Altogether, a number of 122 large WT types but no small WT are installed.

To understand the trade-offs between production and external costs we determined the optimal allocation of WT under the assumption that the MWTP for avoiding externalities are reduced to one tenth of the observed values (cf. section 3.1). By assuming that society places little value to the externalities of the WT (L and D) this scenario considers mainly the production costs, and WT are allocated so that the total production cost (C_p) for reaching the energy target E_{min} are minimized. Consequently, the 690 GWh per year can be produced at a production cost of only C_p*=690 million Euros. While production costs are reduced, the optimal levels of the externalities are increased in this scenario: L* increases to 2.6 percent within 20 years and D* reduces to 800m. That means that the price for reducing the production cost is an increase in the external costs. According to Fig.1, increasing L from 1.2 to 2.6 and reducing D from 1025m to 800m increases the external cost by about 210 million Euros. So altogether, ignoring the externalities saves 40 million Euros of production costs but raises external costs by 210 million Euros and on net raises social cost by 170 million Euros.

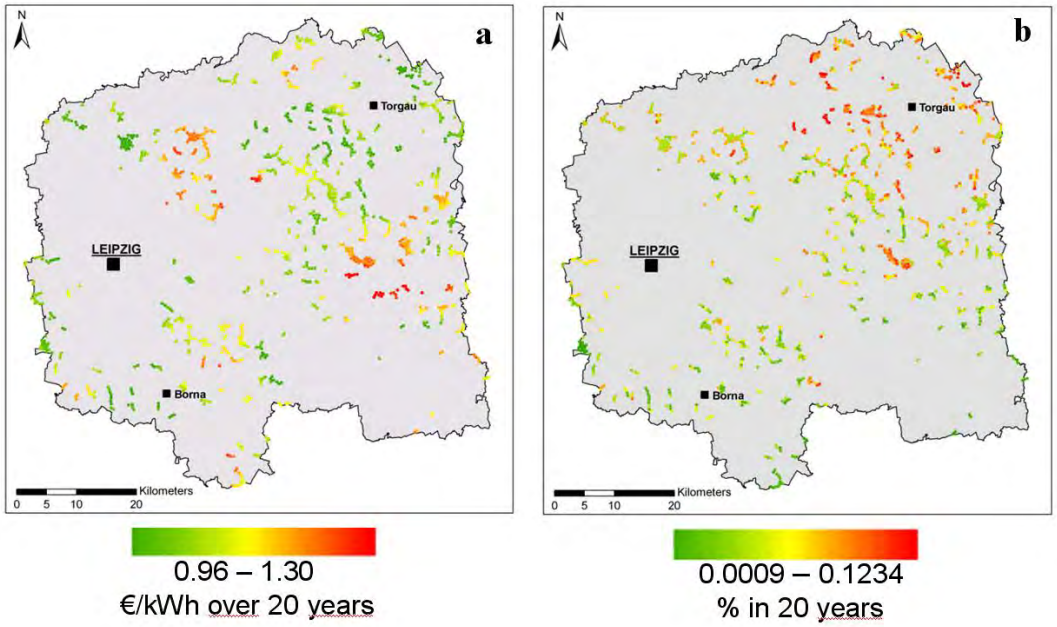

Fig. 2. a: Present value cost of producing 1 kWh over 20 years for each WT site, represented by color scale; b: contribution to Red Kite loss (l_i: see text) of each potential WT site i, represented by color scale. Small WT (k=1) are installed at sites between 750m and 1000m from settlements, large WT (k=2) at larger distances > 1000m.

4. Discussion and Conclusions

Wind power is one of the most promising options for producing energy in a climate-friendly manner. However, it causes negative externalities in terms of adverse impacts on humans and

biodiversity. To alleviate the conflict between the positive impact of wind power on climate policy and its negative externalities, wind turbines (WT) should be allocated so that social costs (i.e., the sum of wind power production costs plus external costs) are minimized with regard to the desired climate-friendly energy target. Determining such an allocation ex ante requires the combination of different methods, including economic modeling of the production costs, modeling of the non-monetary external effects, monetary valuation of these external effects, and numerical optimization.

The goal is to reach a certain energy target in a concrete region ($E_{\min}$) in a welfare-optimal manner, i.e. at lowest social costs. To do this, we explored trade-offs between production costs and externalities by combining choice experiments and spatially explicit modeling. It turned out that in the study region the distance of WT to settlements and the impact on a focal species, the Red Kite, represent significant externalities of wind power supply. On the other hand wind park size and height of the turbines are not. The welfare-optimal allocation balances production costs and externalities and minimizes the sum of production costs and external costs. When determining the welfare-optimal allocation of WT in our study region in Germany it turned out that ignoring the externalities and minimizing only the production costs would reduce the production costs by about five percent from 730 million Euros to 690 million Euros but increase the external cost by 210 million Euros each compared to the welfare optimum. Altogether, ignoring the externalities would increase social cost by 210-(730-690)=170 million Euros.

The magnitude of the chosen energy target reflects the importance of producing energy in a climate friendly manner. The optimal magnitude should be chosen such that the regional social costs of wind power production are outweighed by the benefits accruing from reduced CO2 emission. Determining the "globally" optimal level of the energy target, however, was beyond the scope of this study and is a matter of future research.

The numbers obtained in the analysis depend on several assumptions. In the assessment of the impacts of WT on the Red Kite, e.g., we ignored options of on-site management that make sites unattractive for the Red Kite and would thus reduce the modeled collision risk. Moreover, the search range of Red Kites is not circular. Information on the search behavior of Red Kites, however, is difficult to obtain and requires sophisticated field observations. If this information was at hand it could be easily fed into the model.

In the establishment of the external cost function (C_e, eq. (2)) we assumed that it is separable and can be written as the sum of partial costs. This ignores the possibility of interactions so that the marginal willingness to pay for the reduction of one externality depends on the level of another externality. In the choice experiments we searched for such interactions but did not find any significant ones. If they are significant, interactions can be considered by an appropriate adaptation of the shape of C_e.

With regard to the production costs we ignored the spatial variation of grid connection costs. These very much depend on the distance of a site to the next feed in station, and also on whether a solitary WT or a wind park is connected. Generally connection costs per WT decrease with increasing size of a wind park (economy of scale). Taking these factors into account would require detailed knowledge about the present power grid and even more, assumptions how allocation of WT and expansion of the power grid co-evolve. Since the evolution of power grids and the installation of new smart technologies to make existing

power grids effective for renewable energies are currently a hot topic it may be interesting to further explore this issue in future.

Acknowledgements

The authors thank the German Ministry for Education and Research for funding the research project "Conflicts of interest over wind power" [Nachhaltige Landnutzung im Spannungsfeld umweltpolitisch konfligierender Zielsetzungen am Beispiel der Windenergiegewinnung] (Grant No. 01UN0601A, B) as a part of the fona Programme "Economics for Sustainability [Wirtschaftswissenschaften für Nachhaltigkeit] (WIN)". The views expressed in this paper are the responsibility of the authors alone. In addition we thank the West Saxony Regional Planning Office for the constructive cooperation and commentary.

References

[1] E. Hau, Wind Turbines. Fundamentals, Technology, Application, Economics. Springer, Berlin/Heidelberg, Germany, 2006.

[2] C.L. Krause, Our visual landscape: Managing the landscape under special consideration of visual aspects. Landscape and Urban Planning 54, 2001, pp. 239-254.

[3] B. Möller, Changing wind-power landscapes: regional assessment of visual impact on land use and population in Northern Jutland, Denmark. Applied Energy 83, 2006, pp. 477-494.

[4] H. Hötker, K.M. Thomsen, H. Jeromin, H., Impacts on biodiversity of exploitation of renewable energy sources: the example of birds and bats – facts, gaps in knowledge, demands for further research, and ornithological guidelines for the development of renewable energy exploitation. Michael-Otto-Institut im NABU, Bergenhusen, Germany, 2006 (http://www.batsandwind.org/pdf/impacts%20on%20biodiversity%20of%20renewable%20energy.pdf).

[5] J. Bright, R. Langston, R. Bullman, R., Evans, S. Gardener, J. Pearce-Higgins, Map of bird sensitivities to wind farms in Scotland: A tool to aid planning and conservation, Biological Conservation 141, 2008, pp. 2342-2356.

[6] B. Álvarez-Farizo, N. Hanley, Using conjoint analysis to quantify public preferences over the environmental impacts of wind farms. An example from Spain, Energy Policy 30, 2002, pp. 107-116.

[7] K. Ek, Quantifying the environmental impacts of renewable energy: The case of Swedish wind power, in: D. Pearce D. (Ed.), Environmental Valuation in Developed Countries: Case Studies. Edward Elgar, Cheltenham, 2006, pp. 181-210.

[8] A. Dimitropoulos, A. Kontoleon, Assessing the determinants of local acceptability of wind farm investment: a choice experiment in the Greek Islands. University of Cambridge, UK, Department of Land Economics, Environmental Economy and Policy Research Working Paper No. 35.2008.

[9] J. Meyerhoff, C. Ohl, V. Hartje, Landscape externalities from onshore wind power. Energy Policy 38, 2010, pp. 82-92.

[10] M.J. Punt, R.A. Groeneveld, E.C. van Ierland, J.H. Stel, Spatial planning of offshore wind farms: a windfall to marine environmental protection? Ecological Economics 69, 2009, pp. 93-103.

[11] J. Ladenburg, Onshore and offshore locations for wind power development – what does the public prefer and should it matter? Modern Energy Review 1, 2009, pp. 32-34.

[12] M. Eichhorn, M. Drechsler, Spatial trade-offs between wind power production and bird collision avoidance in agricultural landscapes, Ecology and Society 15, 2010 [online] URL: http://www.ecologyandsociety.org/vol15/iss2/art10/.

[13] J.J. Louviere, D.A. Hensher, J.D. Swait, Stated Choice Methods. Analysis and Application. Cambgridge University Press. Cambridge, 2000.

[14] M. Schmitt, F. Dosch, E. Bergmann, Flächeninanspruchnahme durch Windkraftanlagen. Berichte aus Forschung und Praxis. Raumforschung und Raumordnung 64/5, 2006, pp. 405-412.

Opportunities for co-utilization of infrastructures for wind energy generation

Tarja Ketola[1]

[1] *Industrial Management Unit, University of Vaasa, Finland*
Tel: +358 44 0244 389, E-mail: tarja.ketola@uwasa.fi

Abstract: The co-utilization opportunities of different infrastructures for wind energy generation will be investigated in this paper. Information is derived from previous research and discussions with Finnish wind energy companies as well as with authorities, environmental organizations and local inhabitants in the Ostrobothnia region of Finland. Wind power can be built in areas where there are already other business activities. These co-utilization areas include harbours, industrial sites, roads, railways and existing masts and towers. Moreover, both natural and cultivated environments have vast co-utilization potentials for wind energy offshore, near shore and onshore like in fields, forests and swamps and on hills and islands. The environmental and socio-cultural considerations are of crucial importance when planning co-utilization in natural environments, and very important also in cultivated environments. Industrial areas are the least environmentally and socio-culturally vulnerable, but the potential partners there are businesses that demand substantial financial benefits from co-utilization cooperation, hence making the economic considerations decisive. Co-utilization projects can mitigate or prevent many undesirable environmental, socio-cultural and economic impacts of wind turbines, if they are holistically and carefully planned. Furthermore, wind turbines as structures can serve numerous environmentally, socio-culturally and economically beneficial purposes.

Keywords: *Wind energy, Co-utilization, Infrastructure, Life cycle assessment, Social acceptance*

1. Introduction

Wind turbines can be short, medium-sized and tall, are they can be located off shore, near shore and on shore. They have a variety of environmental, social, cultural and economic impacts, both positive and negative, which depend on the areas they are built in.

Wind turbines can be built in areas where there are already other business activities, and not only in locations where no other human activities take place. These co-utilization areas include e.g. harbours, industrial sites, roads, railways and existing masts and towers. Wind turbines and wind farms can also be built in cultivated environments, i.e. on fields and fallows. In addition, natural environments, such as forests, fields of flowers, arctic hills, swamps, islands and offshore sea areas, are increasingly used as wind farm building sites.

The environmental and socio-cultural considerations of wind turbines are of crucial importance when planning co-utilization in natural environments, and very important also in cultivated environments. Industrial areas are the least environmentally and socio-culturally vulnerable, but the potential partners there are businesses that demand substantial financial benefits from co-utilization cooperation, hence making the economic considerations decisive.

The starting point of this research is the compiling of a sustainability assessment, i.e. an environmental, social, cultural and economic life cycle assessment (LCA) of wind turbines from previous economic and environmental impact and social acceptance studies on wind power and discussions with Finnish wind energy companies and their interest groups. The opportunities for co-utilization will then be mapped in cooperation with Finnish wind energy companies and their interest groups. Wind turbines as structures can serve numerous environmentally, socio-culturally and economically beneficial purposes.

2. Methodology

This is an exploratory study, which derives its information from previous research[1,2,3,4,5,6,7,8] and discussions with wind energy companies, authorities, environmental groups and local inhabitants of Ostrobothnia at a wind energy seminar organized by the Regional Council of Ostrobothnia in Vaasa, Finland, on 30 September 2010, to discuss regional wind power planning. The author of this paper is a member of the CLEEN WIPO research group with 26 Finnish wind energy companies and seven Finnish research institutes. This research group is currently planning a major research project to enhance wind power (WIPO) building and exports. The CLEEN Ltd is the Finnish energy and environment strategic centre for science, technology and innovation with 44 shareholders (major Finland-based companies and national research institutes) established in 2008 to facilitate and coordinate research in the field of energy and environment. This paper analyses current knowledge of wind power impacts and co-utilization, and maps out some research cooperation possibilities for the WIPO project.

3. Results

Table 1 compiles environmental, social, cultural and economic impacts of wind turbines.

Table 1. Environmental, social, cultural and economic impacts of wind turbines.

Environmental impacts	**Social impacts**	**Cultural impacts**	**Economic impacts**
POSITIVE: +Renewable, natural energy production method +Rescue nature from harmful options +Hardly any CO_2 or other emissions +Hardly any hazards to humans or nature +Compensate within 3-6 months the energy used during their whole life-cycle +Nearly all parts of turbines are recyclable	POSITIVE: +Boost local employment: planning, construction & maintenance +Boost entrepreneurship +Boost research & development +Farmers: can lease land, generate small-scale power for their farms and become large-scale wind power producers	POSITIVE: +Traditional; long experience from windmills +Use and upkeep of local knowhow +Could be integrated into contemporary culture, like windmills were: parts of cultural heritage	POSITIVE: +Plenty of business opportunities +Innovation opportunities for many businesses +Major growth opportunities home & abroad +Low maintenance costs +Give nations a great chance to improve their energy self-sufficiency in the most renewable and least harmful way +Help meet CO_2 targets
NEGATIVE: -Wind turbine construction and infrastructure building on natural sites disturb flora and fauna, damage their habitats, and destroy forest, flower field and sea bottom ecosystems, diminishing biodiversity -Propellers and power lines are hazardous to birds, bats and insects -Radar impacts on bats disturb their orienteering - CO_2 & other emissions from parts production and transportation -Noise causes danger (cannot hear predators) and stress to animals	NEGATIVE: -Cause "not in my backyard" (NIMBY) syndrome -Cyclic noise causes stress & stress-related illnesses to humans -Hinder visibility -May spoil visual landscape -Cause light and shadow reflections -May cause accidents to people -May impact real estate values and prices	NEGATIVE: -May upset current cultural landscapes	NEGATIVE: -Local resistance inhibits or slows down investments -Require often many permits and environmental impact assessments (EIAs) with long, exhaustive application procedures -Winds change, challenging even energy supply -Possible radar impacts on military monitoring sensors and air & sea monitoring radars

Table 2 maps co-utilization opportunities of wind turbines in different areas and elaborates on the way they decrease malignant and increase benign environmental, social, cultural and/or economic impacts of wind power.

Table 2. Some co-utilization opportunities of wind turbines.

Co-utilization	**Benefits for environmental, social, cultural and/or economic impacts**
Industrial sites, warehouse areas, harbours	+Infrastructures are already in place; hence there is no need to cause ecological harm by building them. +Usually far away from natural sites and residential areas; hence propeller noise does not disturb nature or humans. +Visual disturbance is minimized by already spoilt scenery and long distance to natural and residential sites. +Require fewer permits & no environmental impact assessments (EIAs). +Wind power generation can be integrated into the site's business operations, thereby giving both energy & financial benefits to companies. +Easy to supply energy to cities and residential areas because of the established grid and power line connections. +Companies on the site can invent multiuse purposes for wind turbines. +The jungle of turbines of wind farms can breed novel business ideas. +Rebuilding power lines underground prevents birds, bats and insects from flying into them.
Roadsides and railway banks	+Propellers' noise is hidden by traffic. +Visual disturbance is lessened by already spoilt asphalt, metal and concrete constructions. +Turbines have tall towers that can be used for traffic control, other surveillance and storage. +Wind energy generation by roads and railways could allow recharging the batteries of electric cars and novel electric trains during the journey. +The jungle of turbine masts can inspire novel means of transportation (e.g. postmodern Tarzans). +Wind farms in public areas will attract extreme sports enthusiasts with their creative inventions. +Building power lines underground prevents birds, bats and insects from flying into them.
Masts and towers	+Radio masts, telecommunication masts and many different kinds of towers can act also as wind turbines. +Possible added negative environmental, social, cultural and economic impacts of attaching propellers to these masts and towers can be easily analyzed and minimized, taking the special characteristics of the location into account. +Both the infrastructure and the turbine trunks are ready-made. +These second-hand wind turbine masts and towers save plenty of steel, fibreglass and metal-plastic composites normally needed to build the turbine trunks. +The trunks could serve also as habitats and nesting places for animals, particularly if they are covered by moss, lichen and other plants. +Building power lines underground prevents birds, bats and insects from flying into them.

Farm fields and fallows	+Little ecological disturbance or damage, as farm fields are typically monocultures with diminished biodiversity. +Farming and wind power generation can be done simultaneously. +Farmers earn either from leasing land and doing turbine maintenance, from generating the energy they need through small-scale wind power, or from becoming large-scale wind power producers and sellers. +Social nuisance is minimized: farmers who benefit do not suffer from the NIMBY syndrome and tolerate the visual harm and noise stress caused by the turbines. +Distance to neighbours is often quite long. +Building power lines underground prevents birds, bats and insects from flying into them.
Swamps	+Swamps that are already in commercial peat energy production are suitable for wind power generation, as they have already been ruined ecologically, socially, culturally and visually, and are plagued by noise from heavy work machinery. +Building power lines underground prevents birds, bats and insects from flying into them. -However, swamps still in their natural state should not be disturbed or damaged by wind power developments, which would destroy their fragile ecosystems and biodiversity once and for all.
Islands	+Wind turbines could be built on the hilly centre of an island with fishermen and/or summer residency, so that they will not disturb the coastal fishermen's houses, summer cottage owners, tourists or nature. +The island's commercial activities (shops, bank, post-office, car battery recharge, etc.) could also be built in the centre. +Building power lines underground prevents birds, bats and insects from flying into them.
Offshore (and near-shore) areas	+The adverse ecological impacts of dredging, building infrastructure and setting up turbines in marine ecosystems can be mitigated by turning the concrete and steel foundations into artificial reefs by erosion protection. +The reefs would attract fish, plants and other marine life, and could develop into holistic ecosystems, thereby preserving biodiversity. +Blocks built from rocks of different sizes can muffle turbine noise that drives fish away. Strong fish populations enhance fishing as a natural livelihood of the area. +Near-shore and offshore wind farms can be built to accommodate research platforms for marine life, weather and tidal energy research. +Shark nets could possibly be attached to the below sea-level turbine constructions of near-shore wind farms. +Building power lines underwater prevents birds from flying into them.

4. Discussion and Conclusions

There are many co-utilization places for wind turbines in which they would not cause much environmental, social or cultural harm and could be made economically profitable.

Industrial sites, warehouse areas, harbours, roadsides and railway banks are environmentally, socially, culturally and economically best places for wind turbines. There they do not damage

nature or disturb humans; their building expenses are low because of the ready-made infrastructures, and profit opportunities are great due to the easy supply of energy to local businesses and residents.

Using existing, i.e. second-hand, masts and towers in these areas would cut down the turbine construction expenses to the minimum and save plenty of unrenewable building material.

Farm fields and fallows are also environmentally, socially, culturally and economically rather benign areas to build wind turbines since they are monocultures, lie often away from residential areas, and wind power generation provides several livelihood opportunities for farmers.

Swamps exploited for peat energy production, are already environmentally, socially and culturally ruined, and therefore, would not suffer much from wind turbines, which would add to the high profits derived from peat energy production. Untouched swamps should be left alone.

Islands are often ecologically valuable areas, but islands with a commercial centre in the middle would not be too much hurt by wind turbines, if they were also built in the centre, which would leave the ecologically fragile and socially important coastal areas untouched.

Offshore wind farm building has several environmentally damaging impacts, but they could be mitigated by turning the concrete and steel foundations into artificial reefs, which would attract fish and other marine life. This could lead also to a beneficial effect on the livelihoods of fishermen. Offshore wind farm platforms could be used by researchers. Near-shore wind farms are more malignant environmentally, socially and culturally, but could possibly be used e.g. for attaching shark nets to.

There are some areas where the malignant environmental, social, cultural and/or economic impacts outweigh the benign ones.

Arctic hills have plenty of space and plenty of wind. In wintertime the colour of wind turbines and snow is synchronized, making a visual match. However, infrastructure building and turbine construction rape virgin land. Moreover, reindeer herders oppose arctic wind farms because they endanger the winter pastures of reindeer. And ultimately, since climate change causes trees to migrate north, plenty of space must be left for the arrival of trees.

Forests of any kind are not suitable or economically profitable places as trees muffle wind. Furthermore, infrastructure building, turbine construction and propeller noise cause such massive disturbance and damage to flora, fauna, soil, rocks, and to the whole forest ecosystem that wind turbines should not be built in forests.

Wind power should not be built in nature protection areas or bird and other animal sanctuaries, on the migration routes of birds, fish and sea mammals, or on environmental or cultural heritage sites. An ample buffer zone between these areas and wind farms should be reserved to prevent any environmental, social or cultural disturbance against these most valuable assets of the humankind.

The findings of this research are based on previous studies of the impacts of wind turbines (which themselves have taken account of hundreds of studies) and on the partially conflicting views of wind energy companies, authorities, environmental organizations and local inhabitants of the Ostrobothnia region of Finland gathered together at a wind power seminar.

This study adds to the knowledge of previous wind turbine impact research through the empirical study. The most important value of this research comes from exploring and mapping out novel empirical findings for a new research area of co-utilization impacts of wind power.

This research has not critically evaluated any of the conflicting views of the seminar participants but listed them all as positive and negative impacts of wind turbines and their co-utilization. The number of participants at the wind power seminar was 63, which is not a representative sample of the population of the city of Vaasa (59,633 inhabitants on 31.10.2010) or the Ostrobothnia region (about 1 million inhabitants during the early 2000s). Those who attended the seminar were more interested in wind power than an average citizen of the city or region, but the participants (wind energy companies, authorities, environmental organizations and local inhabitants) represented the different views and perspectives to wind power development well enough to give a rather balanced account of the positive and negative impacts of wind turbines and their co-utilization.

Similar studies could be conducted at other wind power seminars and at wind farm planning meetings collecting together people with different backgrounds and interests. New issues to address and ideas to solve them would no doubt emerge in such gatherings as wind farms become more widespread and people gain more experience on their impacts.

5. Recommendations

Co-utilization is an effective way of enhancing the social acceptance of wind power. Participation at every stage of the planning process in close cooperation with the wind energy companies tends to make local people, farmers, environmental organizations, authorities and businesses adopt a very positive attitude towards wind power. They appreciate the wind energy companies' respect for their expertise and creativity in mapping out co-utilization possibilities and planning continuous cooperation.

The active involvement in the projects and the resulting structures in turbines that for example, protect nature or collect data, satisfy the needs of most local people, environmental organizations and authorities. Farmers and companies want also business opportunities from co-utilization. The others often shy away from the profit-maximizing limited liability type market economy in co-utilization, but show great interest in socio-culturally beneficial co-op type co-utilization. This poses both an opportunity and challenge for the limited liability type wind energy companies: can they set limits to their short-term profit greed in order to secure long-term survival and success?

These issues are worth contemplating, as wind power is one of the few energy businesses that are strongly supported by environmental organizations. One of the most radical environmental organizations, Greenpeace, estimates that 20 per cent of the world's energy could be produced by wind power by 2030.[6] Such encouragement should be taken advantage of by solving the negative environmental, social, cultural and economic impacts of wind power through co-utilization and other measures.

References

[1] European Environment Agency, Europe's onshore and offshore wind energy potential, An assessment of environmental and economic constraints, EEA Technical Report 6/2009. EEA, 2009.

[2] European Wind Energy Association, Wind at work: wind energy and job creation in the EU, EWEA, 2009.

[3] P. Hokkanen, Kansalaisosallistuminen ympäristövaikutusten arviointimenettelyssä (In Finnish) (Citizen participation in the environmental impact assessment procedure), Acta Universitatis Tamperensis 1285, University of Tampere Press, 2007.

[4] J. Koistinen, Tuulivoimaloiden linnustovaikutukset, Suomen ympäristö 721 (In Finnish), (The bird population impacts of wind power plants, Finland's environment 721), Finland's Ministry of the Environment, 2004.

[5] S. Korpinen, V. Pohjanheimo, K. Auvinen, A. Mäkinen, WWF Suomen kanta tuulivoimasta Suomessa (In Finnish) (WWF Finland's position in wind power in Finland), Worldwide Fund for Nature Finland, 2007.

[6] S. Teske, A. Zervos, C. Lins, J. Muth, Energy (r)evolution: a sustainable world energy outlook, Greenpeace International and European Renewable Energy Council (EREC), 2010.

[7] V. Varho, Calm or storm? Wind power actors' perceptions of Finnish wind power and its future, Environmentalica Fennica 25, Helsinki University Printing House, 2007.

[8] E. Weckman, Tuulivoimalat ja maisema, Suomen ympäristö 5 (In Finnish) (Wind power plants and the landscape, Finland's environment 5), Finland's Ministry of the Environment, 2006.

Optimal Layout for Wind Turbine Farms

Koby Attias[1,*], Shaul P. Ladany[1],

[1]*Ben- Gurion University, Beer-Sheva, Israel*
**Corresponding author. Tel: 972-52-5250815, Fax:972-77-2101037, E-mail:yattias@elta.co.il*

Abstract: A general discrete model was formulated for the expected Net Present Value (NPV) of the profit and for the expected yield of the investment (Internal Rate of Return - IRR) to be derived from rectangular grid shaped wind-turbine farms. The model considers the wind shade in the downwind direction and the effect of the wake behind the turbine, the joint wind-direction wind-velocity probability distribution, as well as the various relevant cost and revenue factors. It was assumed that the wind-turbines are identical and of equal heights, and are spaced equally along the axes of the rectangle, but not necessarily at the same equal distance at both axes. Using the model, the optimal layout that maximizes the expected NPV and/or IRR was derived numerically for a given data set, in stages, determining the optimal number of turbines in a row and the associated optimal distance in-between them, and also the optimal number of turbines in a column and the optimal distance in-between them. Sensitivity analysis has shown that minor changes in the parameters do not affect the selection of the optimal layout.

***Keywords**: wind energy, optimal layout, wind farms*

1. Introduction

The harvesting of wind energy is centuries old as manifested by the middle-age wind mills in Europe. Heier [1] describes how the use of wind energy to generate electricity started in 19th century, but only the oil crisis of October 1973 provided the strong impact. The understanding and use of wind energy has been investigated by Lindley et al.[2], and are summarized by Manwell et al. [3]and Burton et al. [4]. Plans for actions to increase the use of wind energy were introduced by Milborrow et al. [5] , and the success is evidenced by travelers in Denmark and North Western parts of Germany where thousands of wind-turbines have been installed in recent years. The performance of wind farms were evaluated by Haack [6], while the integration of wind power into general power systems is discussed by Ackermann [7]and Heier [1].

Obviously, the erection of multiple wind-turbines in windfarms necessitates the determination of their layout. Bossanyi et al.[8], has dealt with the issue of investigating the efficiency of different layouts and even for designing aerodynamically optimal layouts. However, they did not integrate the economic and financial optimization of windfarms with the aerodynamic aspects. Yet the methods of operational research and operations management determine such optimizations using the maximization of the expected profit as the objective function. For example, see Ladany [9] and [10] in which the optimal layout of urban gasoline-stations was determined.

Hence, the aim of this paper is to develop a model to determine economically optimal layouts for windfarms (i.e. the number of turbines and their setting), which include the aerodynamic interactions between the turbines, the various cost factors and the particular wind regime. Section 2 presents the model; Section 3 considers the aerodynamic interaction between the turbines; Section 4 describes the optimization procedure; Section 5 shows a numerical example; Section 6 offers the conclusions.

Searching through Tables 2 & 3, it is possible to detect solutions that provide the best combination of N_{PV}'s and I_r's, although each is less than its maximum value. For example, for

a layout of I=4, J=6 (24 turbines), with the turbines separated with x=100 m and y=300 m, provides an N_{PV}=$21.5 million, and an I_r=19.7%, which is the authors recommend "optimal solution."

1.1. Aim of this paper

The aim of this paper is to explore and searching a model. By Using the model, we got the optimal layout that maximizes the expected NPV and/or IRR was derived numerically for a given data set, in stages,

2. The model

Consider a rectangular grid layout (see Figure 1) of I x J wind-turbines of equal size and height, 2 adjacent turbines separated by the distance x in one direction and y in the other direction (obviously the minimum of x & y is more than the diameter of the turbine's rotor).

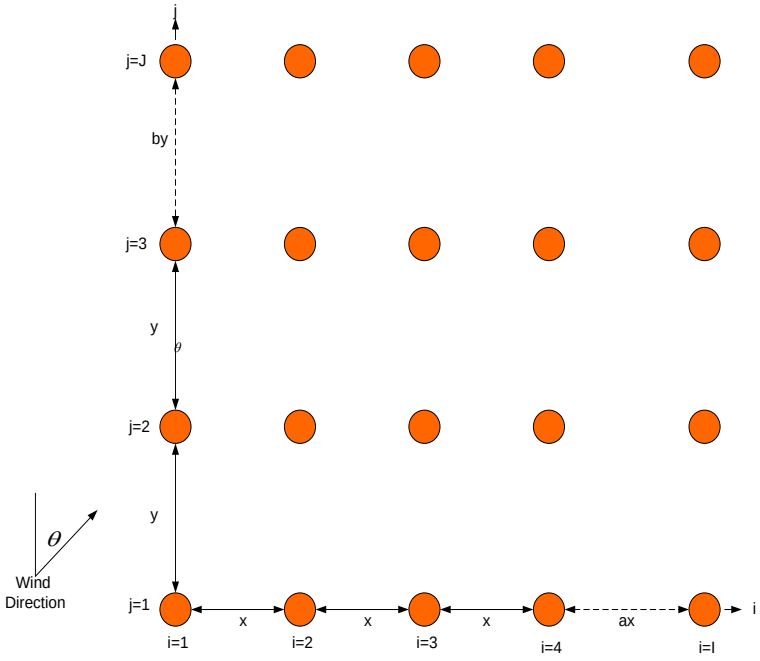

Figure 1: Location of turbine i, j in a rectangular grid layout of I x J turbines

When the wind blows in direction θ with a nominal velocity of V(θ), the effective wind velocity in front of the turbine at position i, j (which takes into account the aerodynamic interaction between the turbines, the wake affect – see the discussion in section 4) is Vij(θ, x, y).

Vij(θ, x, y) is obviously a function of V(θ), and it is developed in section 4. The effective wind velocity incident on 'turbine i, j' is Vij(θ, x, y), so the electrical power generated by the 'turbine i, j' is: eij(θ, x, y) [kwh]:

$$e_{ij}(\theta,x,y) = 0.5\rho V^3_{ij}(\theta,x,y)\cdot BC_pN_m \qquad (1)$$

where ρ is the air density [kg/m3], B is the swept rotor area [m2], Cp is the rotor efficiency coefficient (capacity factor) [%/100], Nm is the efficiency for converting the rotor mechanical power to electricity [%/100].

When the joint probability of the nominal wind velocity and its angle of incidence θ is defined as p (Vθ, θ), the expected annual energy to be generated by turbine i, j is

$$E(e \mid x, y)_{ij} = \sum_{v_\theta, \theta} e_{ij}(\theta, x, y) \cdot p(V_\theta, \theta) \tag{2}$$

while the total expected energy to be generated by the whole farm, T(x, y), is

$$T(x, y) = \sum_{i=1}^{I} \sum_{j=1}^{J} E(e \mid x, y)_{ij} \tag{3}$$

If the lifetime of a turbine is L, then K is the total investment in the windfarm (including the cost of turbines, installations and land cost), F is the net revenue from the selling electricity from the windfarm, r is the appropriate financial interest rate, H is the total operating time per period(for example operating time is: 24 h/d X 328.5 d/y =7884 h/y , and maintenance days are= 365-328.5=36.5d/y), P is the unit sale price of electricity , M is the cost of operation and maintenance of the windfarm per period, the Net Present Value, NPV, of the profit to be derived from the farm is

$$N_{pv}(x, y) = -K + \sum_{k=1}^{L} \frac{H \cdot T(x, y) \cdot P - M}{(1 + r)^{k-1}} = -K + \sum_{k=1}^{L} \frac{F}{(1 + r)^{k-1}} \tag{4}$$

Where $H \cdot T(x, y) \cdot P - M$ =F
The Internal Rate of Return (IRR) on the investment, Ir (x, y) is the value of the interest rate, r, that results in
NPV (x, y) =0.

3. The aerodynamic interaction between the turbines

Since a wind-turbine generates electricity from the energy in the wind, the wind leaving the turbine has less energy content than the wind arriving in front of the turbine. Therefore a wind-turbine will always cast a wind shadow in the downwind direction. This is described as the wake behind the turbine, which is quite turbulent and has an average down-wind speed slower than the wind arriving in front of the turbine.

With effective yawing, we assume the direction of the wind is always perpendicular to the front of the turbine. Hence, the diameter of the turbine is considered always perpendicular to the wind's direction. Nybore [11] has shown that behind the turbine the wind creates a cone-sloped wake which extends 4.5º to the sides, as shown in Figure 2, (i.e. creating a truncated cone with a 9º head-angle.)

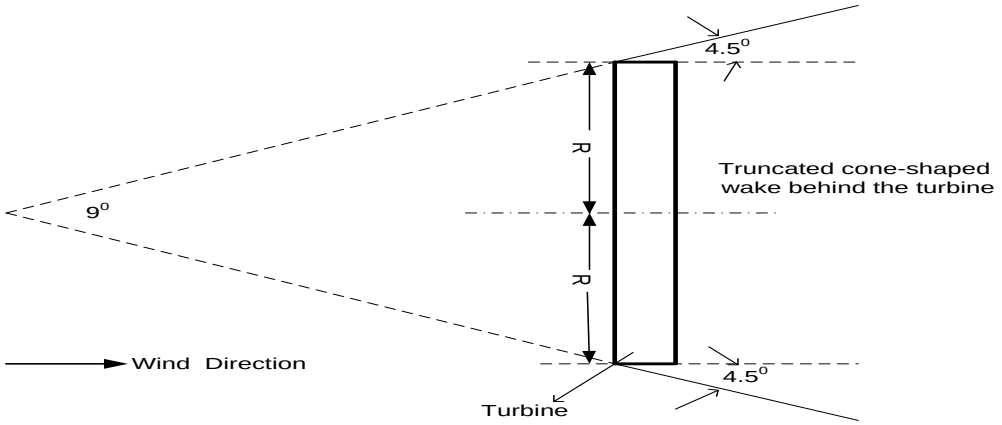

Figure 2: A 2-dimensional representation (top view) of the cone-shaped wake created by the wind behind the turbine

In a windfarm, 'turbine i, j' might or might not be affected by the wake created by another turbine positioned in front of it (in relation to the direction of the wind.) Moreover, the effect might be partial or complete. As a result, we distinguish 4 different states for the wind velocity hitting 'turbine i, j', as shown in Figure 3.

Adapting the findings of Nybore [11] to the notation required for dealing with a grid shaped farm, the wind velocity onto 'turbine i, j', when the general wind velocity in direction θ is V(θ), and the grids are separated by the distances x and y, is:

For state (a) when 'turbine i, j', is not affected by the wake of another turbine m, n ,

$$V_{ij}(\theta, x, y) = V(\theta) \quad (5)$$

Where m, n are the coordinates on the grid of another turbine in front of 'turbine i, j'. m might be less, equal or more than i, and likewise n might be less, equal or more than j, but (m, n) ≠ (i, j).

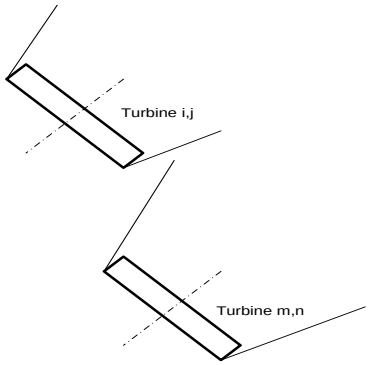

(a) Turbine i, j not affected by the wake of another turbine m, n

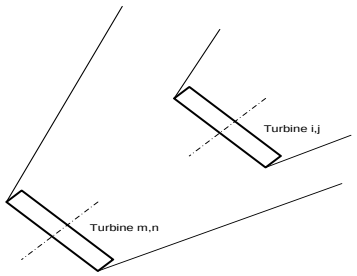

(b) Turbine i, j fully affected by the wake of another turbine m, n

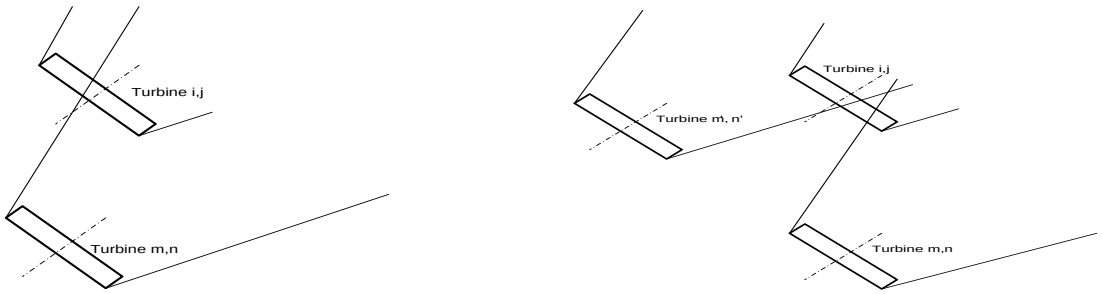

(c) Portion of turbine i, j is affected by the wake of another turbine m, n

(d) Portion of turbine i, j is affected simultaneously by the wake of turbine m, n and of turbine m', n'

Figure 3: Top view of the 4 states in which turbine i, j can be affected by the wake

For state (b) when turbine i, j is fully affected by the wake of turbine m, n,

$$V_{ij}(\theta,x,y) = V(\theta)\cdot\{1-[1-\frac{V_{mn}(\theta,x,y)}{3V(\theta)}]\cdot[\frac{R}{R+0.078d}]^2\} \quad (6)$$

where
R is the radius of the turbine's rotor, and
d is the distance between the centers of turbine i, j and turbine m, n (See fig. 4)
Note: This formula was developed by engineer Niels Otto Jensen from Risoe.

The wind in the wake $V_{ij}(\theta,x,y)$ is related to the surrounding free wind $V(\theta)$, the downwind distance (d meters), the rotor radius (R meters) and the spreading angle of the wind (about 4.5^0) . The factor 0.078 is called the constant of spreading, its corresponds to a spreading angle of about 4.5^0

For state (c) (when a portion (either a major or a minor portion) of turbine i, j is affected by the wake of another turbine m, n), Nybore's [11] equation is adjusted to the prevailing conditions:

$$V_{ij}(\theta,x,y) = V(\theta)\frac{A_{ij}}{\Pi R^2}\cdot\{1-[1-\frac{V_{mn}(\theta,x,y)}{3V(\theta)}]\cdot[\frac{R}{R+0.078d}]^2\} + V(\theta)[\frac{\Pi R^2 - A_{ij}}{\Pi R^2}], \quad (7)$$

where
Aij is the area of intersection between the area of the rotor of turbine i, j and the cross-section (at turbine i, j) of the wake cone affected by turbine m, n.

For state (d) when a portion of turbine i, j is simultaneously affected by the wakes of turbine m, n and also of turbine m', n', Nybore's[11] equation is further adjusted:

$$\begin{aligned} V_{ij}(\theta,x,y) = {} & V(\theta)\frac{A_{ij}}{\Pi R^2}\cdot\{1-[1-\frac{V_{mn}(\theta,x,y)}{3V(\theta)}]\cdot[\frac{R}{R+0.078d}]^2\} \\ & + V(\theta)\frac{A_{i'j'}}{\Pi R^2}\cdot\{1-[1-\frac{V_{m'n'}(\theta,x,y)}{3V(\theta)}]\cdot[\frac{R}{R+0.078d'}]^2\} + V(\theta)[\frac{\Pi R^2 - A_{ij} - A_{i'j'}}{\Pi R^2}], \end{aligned} \quad (8)$$

where
$A_{i'j'}$ is the area of intersection between the area of the rotor of turbine i, j and the cross-section (at turbine i, j) of the wake cone affected by turbine m', n', and
d' is the distance between the centers of turbine i, j and turbine m', n'.
d is the distance between the centers of turbine i, j and turbine m, n.

For states (c) and (d), A_{ij} is depicted in Figure 4.

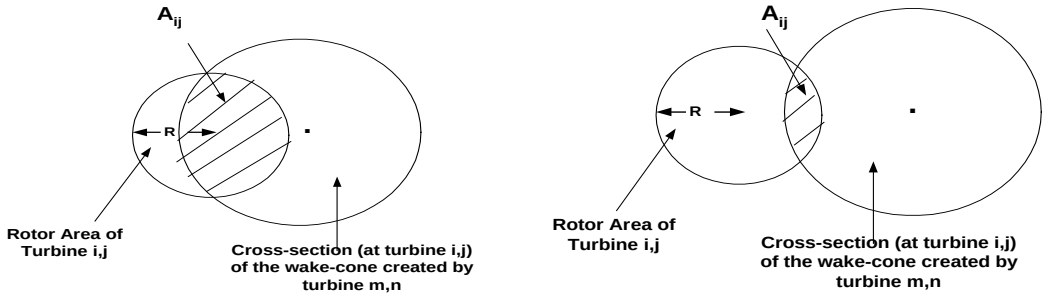

(a) Major portion of turbine i, j is affected (b) Minor part of turbine i, j is affected

Figure 4: Front view of the intersection (shaded) of the rotor area of turbine i, j, and of the cross-section (at turbine i, j) of the wake-cone affected by turbine m, n.

While the occurrence of state (d) in itself is very rare, theoretical situations exist in which in state (d) the cross-section (at turbine i, j) of the wake-cone created by turbine m, n and of turbine m', n' partially overlap while intersecting the rotor area of turbine i, j . Such other states can be dealt with by adjusting Nybore's [11] formula similarly to equation (8).

4. The optimization procedure

The optimization is performed in a sequential manner. An initial minimal sized layout with least possible number of turbines, (J=1, I=1) is selected and its NPV and Ir are calculated. At the second stage the number of turbines is increased, say to J=1, I=2, then numerically the value of x is searched that maximizes NPV, x1, and separately the value of x is searched that maximizes Ir, x2, retaining the resulting maximal NPV and Ir values. At the 3rd step, the number of turbines is further increased, say to J=2, I=2, the combination of values of x and y that maximize N_{PV}, (x_1, y_1), and that maximize IRR, (x_2, y_2), are evaluated, retaining the obtained maximal values of N_{PV} & I_r. The number of turbines is further increased, and the optimal outcomes of x & y for each layout are evaluated, and the corresponding maximal values of N_{PV} & I_r are retained.

5. Numerical example

To demonstrate the use of the model, a realistic set of data was assumed:
L= 20 y, R= 18 m, ρ = 1.225 kg/m^3, H= 7884 h/y (24 h/d X 328.5 d/y =7884 h/y),
P= 0.05 $/kWh, capacity of turbine=600kWh
C_p= 0.4, N_m= 0.95, and r=5% /y.
Total investment in the windfarm $K=I\cdot J\cdot\{C_T+C_I+C_L[(I-1)x\cdot(J-1)y]\}$, (9)
Where (cost in US dollar, $US)
C_T=cost per turbine=450,000$
C_I=cost per turbine installation=100,000$
C_L=cost of land per turbine=10$/m^2
Cost of operation&maintenance of the windfarm per turbine $M=0.015\cdot C_T\cdot I\cdot J$, $/y (10)

The results of the optimization procedure with the objective to maximize N_{pv} are presented in Table 2. The table provides for each combination of values of I x J the maximal achievable N_{pv}, and the values of x and y that generated this N_{pv}. In addition, the value of I_r generated by these values of x and y is also listed. Table 3 lists similar results, providing for each

combination of I x J the maximal achievable I_r, and the values of x and y that generated this I_r. In addition, the value of N_{pv} generated by these values of x and y is also presented .

Table 2: Optimal results of x and y (for any given I x J) for maximal N_{PV}, and I_r

Parameter	**J- Turbines in Column**	**I-Number of Turbines in Row**				
		2	**3**	**4**	**5**	**6**
x (m)	**2**	300	300	300	300	300
y (m)		100	100	100	100	100
N_{PV} (M$)		4.6	6.5	8.5	10.4	12.4
I_r (%)		27.7	25.3	24.4	23.9	23.5
x (m)	**5**	100	100	100	100	100
y (m)		300	300	500	500	500
N_{PV} (M$)		10.6	14.3	18.8	21.9	25.6
I_r (%)		24.1	21.3	17.9	17.2	16.8
x (m)	**6**	100	100	100	100	100
y (m)		300	300	300	500	500
N_{PV} (M$)		12.6	17.1	21.5	25.9	* **30.3**
I_r (%)		23.9	21.0	19.7	16.9	16.4

* Optimal results

Table 3: Optimal results of x and y (for any given I x J) for maximal I_r, and N_{PV}

Parameter	**J- Turbines in Column**	**I-Number of Turbines in Row**				
		2	**3**	**4**	**5**	**6**
x (m)	**2**	300	300	300	300	300
y (m)		100	100	100	100	100
N_{PV} (M$)		4.6	6.5	8.5	10.4	12.4
I_r (%)		* **27.7**	25.3	24.4	23.9	23.5
x (m)	**5**	100	100	100	100	300
y (m)		300	300	300	300	100
N_{PV} (M$)		10.6	14.3	18.0	21.4	24.3
I_r (%)		24.1	21.3	19.9	19.0	18.1
x (m)	**6**	100	100	100	100	100
y (m)		300	300	300	300	300
N_{PV} (M$)		12.6	17.1	21.5	25.6	28.9
I_r (%)		23.9	21.0	19.7	18.8	17.9

From Table 2, it is evident that maximal Net Present Value, N_{PV} of $ 30.3 million can be achieved for I=6 and J=6 (36 turbines), each one separated x=100 m on the x direction, and y=500 m on the y direction. However, this solution provides only an I_r=16.4%. On the other hand, Table 3 shows that a maximal rate of return, I_r of 27.7% is attainable with I=2 and J=2, the turbines being apart, in x=300 m on the x direction, and y=100 m on the y direction. The disadvantage of this high rate of return is that it generates only a Net Present Value of $4.6 million. If the decision would be done by an investment company, they should opt for the largest possible rate of return on their its investments in any given project. However, a power-generating company that is not diversifying its investments in many different types of projects with different level of risks, it would decide on a project that generates a large N_{PV} while satisfying at least a minimal level of I_r. Searching through Tables 2 & 3, it is possible to detect solutions that provide the best combination of N_{PV}'s and I_r's, although each is less than its maximum value. For example, for a layout of I=4, J=6 (24 turbines), with the turbines separated with x=100 m and y=300 m, provides an N_{PV}=$21.5 million, and an I_r=19.7%, which is the authors recommend "optimal solution."

6. Conclusions

The developed model optimizes windfarm layouts on flat ground or over water for both economic and aerodynamic criteria. Although there are other criteria (e.g. visual impact) to consider, the model performance is an advance for economic optimization. The model with its accompanying computer program, can handle different wind-regimes and all the different combinations of cost and technical parameters for rectangular layouts, of which single-line layouts are special cases. Even the seeming dependence of the solution on the initial selection of the directions of the perpendicular axes can be eliminated, by repeating the calculations for different directions of the axes, and by selecting the layout that has the axis given by the "recommended optimal solution" Furthermore, the computer program can be adjusted, for layouts that are not rectangles, but also parallelograms.

References

[1] Heier, Siegfried, Grid Integration of Wind Energy Conversion Systems, 2nd ed., John Wiley & Sons, Inc., New York, N.Y., 2004.

[2] Lindley, D. et al., "The Effect of Terrain and Construction Method on the Flow over Complex Terrain Models in a Simulated Atmospheric Boundary Layer," in Proceedings of the Third B.W.E.A. Wind Energy Conference, edited by Musgrove,P.J., Cranfield, U.K., April 1981, pp.198-199.

[3] Manwell, J.F., Mcgowan, J.G. and Rogers, A.L., Wind Energy Explained, John Wiley & Sons, Inc., New York, N.Y., 2002

[4] Burton, Tony, Sharpe, David, Jenkines, Nick and Bossanyi, Ervin, Wind Energy Handbook, John Wiley & Sons, Inc., New York, N.Y. 2001.

[5] Milborrow, David ,Garrad, Andrew and Madsen, Birger, A Plan for Action in Europe:Wind Energy –The Facts, European Wind Energy Association(EWEA) European Communities, 1999, pp. 133-134.

[6] Haac, Barry N. An Examination of Small Wind Electric Systems in Michigan, Department of Geography, University of Michigan,1977, pp.27.

[7] Ackermann, Tomas, Wind Power in Power Systems, John Wily& Sons, Inc., New York, N.Y.,2004.

[8] Bossani, E.A.et al., "The Efficiency of Wind Turbine Clusters," in Third International Symposium on Wind Energy Systems, edited by Stephens,H.S., and Stapleton, C.A. , Cranfield, U.K., August 1980, pp.403-406.

[9] Ladany, Shaul P., "Optimal Layout for Urban Gasoline Stations ," in Gilad, I.E.& M. '98, Haifa 1998, pp.45-49.

[10] Ladany, Shaul P ., and Li, Jingwen, "Layout Design for Urban Service Facilities," Communications in Dependability and Quality Management, Vol.5, No.2, 2002, pp.16-30.

[11] Nybore, Claus, The WindFarm-Planning Windphysics, The Danish Centre for Renewable Energy, Copenhagen, 1988, pp. 1-29.

What do we really know? A meta-analysis of studies into public responses to wind energy

Ian D. Bishop[1,*]

[1] *University of Melbourne, Melbourne, Australia*
** Corresponding author. Tel: +61 383444180, Fax: +61 393472916, E-mail: i.bishop@unimelb.edu.au*

Abstract: There have now been many studies about the public response to wind energy infrastructure. This includes at least 31 papers already published in 2010. There remains however a large gap between the knowledge required for effective planning and the agreed understanding of visual and other impact levels, and the influence of planning and communication processes There is only limited agreement on some basic impact variables: numbers of turbines, amelioration with distance, role of design and so forth. There is no consensus on what methods should be used to assess acceptability or to design for acceptable outcomes. This means that, in many countries, there is no societal consensus about the acceptability of wide spread deployment of wind energy systems. This paper reviews recent studies in environmental, especially visual, impact and other aspects of the process that shape public response. These deal with issues and measures including both local and regional impacts, willingness-to-pay, validity of visual simulations and the use of virtual environments in design. The response of any individual and, cumulatively, of the community is a combination of affective and cognitive factors. Both are complex in character. Affective response involves primarily aesthetic appreciation but may be influenced by deep-seated philosophical attitudes to renewable energy in the context of global environmental issues. Cognitive responses overlay with the affective response in relation to global issues but also draw heavily on local factors of noise concerns, tourism effects and health issues. Cognitive responses are also dependent on personal circumstance and experiences and perceptions of the reasonableness of the planning process. These different aspects may be applied independently to infrastructure design, planning and evaluation but are often combined inappropriately in multi-factorial studies. A diversity of approaches in the literature are analyzed for their capacity to contribute to effective discrimination of the factors behind public responses to wind farm developments, to agreement on the key elements affecting local responses, and preferred approaches to planning and design. A combination of such meta-analysis and computational innovation in mapping and visualisation may provide the opportunity for integration of these advances in knowledge such that a systematic, objective, comprehensive and acceptable approach to wind energy infrastructure planning and design is feasible and achievable.

Keywords: *Wind energy, Visual impact, Affective response, Cognitive response*

1. Introduction

There has recently been a very rapid expansion of the literature on public responses to wind energy development and the visual landscape effects in particular. Between 2000 and 2006 there were 2-3 papers per year, in 2007 this jumped to 10, in 2009 to 15 and in 2010 over 30 papers were published on the topic. Some of these deal with aesthetic theory, some with impact mapping, some with experiments seeking to determine key impact variables and their relative importance, others deal with specific wind farm developments and the impact mapping, often linked to public consultation, which went with them. Given this surge of interest, provoked by the rapid expansion of the wind energy industry, it is time to ask what have we collectively learned from this research and how it makes for better planning.

While there is a high cross citation rate amongst these papers, there is also a wide diversity of approaches and research questions which means that there are as yet few definitive answers. The first stage of analysis of these contributions must therefore be to determine the research questions being asked and their relationship to each other. Key topics are:

- development of better tools or procedures for public engagement early in the planning process [1-5]

- understanding of relative significance of key design variables such as distance, contrast, colour, movement [6-8], number of turbines [9-11], size of turbines [10, 12] whether on-shore or off-shore [13] and the existing quality of the host landscape [14]
- understanding of non-design variables such as conservation value of location or the planning process [15, 16], broad social attitudes to wind energy [17, 18] or behaviour (e.g. recreation) when exposed to wind energy facilities [19, 20]
- more systematic analysis tools which respect multiple criteria in either site selection [21-25], impact assessment [8, 11, 26-28], historical changes in the landscape [29] or regional or national level impacts [30]
- responses to visual simulations [31]
- use of interactive virtual environments to facilitate interactive design [32]
- changing attitudes as a result of familiarity [16, 33]
- deep convictions about nature, landscapes and seascapes [34] and cultural ecosystem services [35]
- understanding the relationships between stakeholders in environmental conflicts [36]
- willingness-to-pay studies encompassing some of the other variables (such as distance) [13, 37-39]
- project evaluations including environmental externalities [40, 41]
- the NIMBY effect - or not? [18, 42-46]

This review will focus on just a small section of this wide range. That section is the attempt to establish some firm knowledge about how various design and planning variables contribute to expectations and responses to wind farm development. The analysis considers the variables in terms of the provoked affective and cognitive responses [47] since there are clear indications that both are at play in the public response. There is also a distinction to be made between responses to simulated wind energy developments, responses to proposed developments and responses to completed projects [16, 33]. It should also be noted that most studies consider several aspects of impact and response, in the list above and in the Tables below I have tended to focus on my perception of the main findings in each.

2. Findings from the literature

2.1. Affective Response to Wind Energy

As we experience the landscape we form impressions - such as beautiful or inspiring or unpleasant - without be conscious of any thinking behind those impressions. These responses have a high level of commonality within cultures and, in some respects, between cultures. They are largely unaffected by personal experiences, even familiarity with the landscape has been shown to have limited influence [48]. These apparently innate impressions are referred to as affective responses and have been attributed to evolutionary influences by some authors [49]. Because affective responses are relatively consistent across the population, we are in position to built a body of knowledge about typical responses and use these in spatially explicit landscape assessment and impact studies.

In the case of responses to wind energy infrastructure, we can consider our perceptions of the aesthetics of the developments as an affective response. Something we find intrudes on our enjoyment of landscape or something that adds elegance and interest to the view. Some people may have a positive response in certain landscape types and a negative response in a different landscape type, or the response may be influenced by the layout of the wind farm relative to the landscape, the number of turbines, their distance and so forth. However, we can expect similar sets of responses in different populations and similar dominant response types

allowing development of an empirical framework for impact estimation. As mentioned, the key variables have been analyzed in a number of papers [6-13]. Some of the key findings are summarised in Table 1. These are separated into effects of on-shore and offshore installations, as there is limited comparative work. A review of related work [13] concluded that there was less impact from off-shore installation (reflected in greater willingness-to-pay to adopt that option) but the relative impacts of off- and on-shore infrastructure are not yet well defined and the preference for offshore is disputed in at least one recent review [50].

Studies in affective response typically use scenic beauty, visual quality or a similar phrase as a key reported measure - with some examples of willingness-to-pay and choice experiments. Several of the papers studied multiple variables but disentangling these is sometimes difficult. In addition, there are some clear disagreements in findings in several places - including in relation to important considerations like distance and size. Some studies that considered the size of wind farms (numbers of turbines) did so in the context of fixed total power output. In this situation mixed results were reported [12] with some communities preferring more distributed production while other saw benefit in greater concentration. However, this is more of a reasoned factor than a purely aesthetic one and leads us into the next section.

Table 1. Some key finding relating to aesthetic responses to wind energy infrastructure

Variable Increasing	On-Shore Impact	Off-shore Impact
Distance	- linear decline to at least 12 km [6]	- linear decline to ~12 km [7]
	- limited distance effect [14]	- decline with distance [38]
Number of turbines	- increase with number, size and proximity until turbines occupy 15% of view, then constant [8]	no known studies
	- impact proportional to number of windmills [10]	
	- between 2 and 8 turbines best accepted [9]	
Colour/contrast	- increase with contrast [6, 7]	- increase with contrast [7]
	- increase to 1563 CIELAB points then constant [8]	
Size of turbines	-one 5MW turbine has more impact than same from smaller units [10]	no known studies
	- least important attribute [12]	
	- smaller turbines require less compensation [15]	
Movement	no known studies	- less when blades moving especially at low distances [7]
Visual complexity	- fractality introduced by [8], simpler structures preferred	no known studies
Continuity	- bumps in outline envelope not preferred [8]	no known studies
Host landscape	- effect is negative on landscapes of higher scenic quality but a positive on landscapes of lower quality [14]	- greater distance offshore preferred [38]

2.2. Cognitive Response to Wind Energy

It has been argued that the more visceral affective response ('the heart') is indeed conditioned by a rapid evolution driven cognitive response ('the head'). Whatever the truth of this, there are clearly a number of variables in human responses to wind turbines that require more sustained or deeper consideration than the aesthetic, or are dependent on knowledge or experience, and these are generally referred to as the cognitive factors. These may include specifically beliefs about nature, concerns about real estate values and trust in the planning process. Table 2 seeks to summarise findings on issues of this kind. Again, there are studies that were conducted in relation to on-shore installations and others where the focus was offshore, but these are not separated explicitly in this Table. Among the differences is the noise issue (which is in part aesthetic but of more sustained character and believed by some to induce specific negative health impacts hence applied with other cognitive factors here) that applies almost exclusively to on-shore facilities. The second is an argument, recently summarised [50], that off-shore turbines turn quintessentially natural [34] and often sublime sea or ocean views into industrial landscapes. On-shore facilities, on the other hand, are typically in locations long altered by human activities in the form of agricultural and transportation infrastructure.

Studies involving primarily cognitive variables use a range of measures that seem very similar but this similarity could be misleading. Acceptability is not the same as willingness-to-accept compensation, for example. General 'attitude' to wind infrastructure may be different again because of a range of factors reviewed in the environmental economics literature [51].

Table 2. Some key finding relating to cognitive responses to wind energy infrastructure. The variable of column 1 is measured by the measure in column 2. Column 3 indicates the way in which the response measure depends on the variable.

Variable	Response Measure	Findings
protected site [15]	willingness to accept compensation	avoid protected sites
planning with local representatives [15]	willingness to accept compensation	engage locally
prior experience with off-shore wind farms [16]	attitude to visual impacts	experience with more distance farm leads to more positive attitude
local electricity shortages [17]	acceptability	local needs on island suggested as positive contributor
small scale introduction [17]	acceptability	suggested as positive contributor
open-minded, international contacts [17]	acceptability	suggested as positive contributor
the developers, poor local communications [18, 44]	acceptability	suggested as negative contributor
occasional beach use [19]	stated attitude to offshore infrastructure	more positive attitude
regular year-round beach use [19]	stated attitude to offshore infrastructure	more negative attitude
living with wind farm [33]	range of beliefs on benefits, visual qualities, energy security	more awareness of benefits, greater acceptance

3. Discussion and Conclusion

The research methods used in trying to increase our understanding of the many variables introduced in the literature include attitude surveys, observational methods, willingness-to-pay (or be paid) studies, choice experiments and so forth. The entities on which people are asked to comment include real wind farms (post construction), hypothetical wind farms, visually simulated wind farms and abstract concepts in renewable energy. Nearly all the reported results are the outcome of research by professional people and have been peer reviewed.

Despite the breadth and depth of our investigations we do not yet know all the answers. We cannot yet predict what the response to a particular wind farm proposal will be (although many people would be willing to guess), if compensation is a possibility we do not know how to quantify it or spatially distribute it. We don't know what distribution of turbines across the landscape (to meet specific power needs) will have the least visual impact: should we have bigger but fewer turbines? Bigger but fewer farms?

Yet, some points are fairly clear:

- aesthetic impacts are less the further the viewer is from the turbines (although we have no clear idea of the shape of the distance-impact curve)
- contrast with the surroundings and background should be low
- farms should not be located in highly valued landscapes
- the distribution and design of the turbines should have regard for aesthetic factors such as complexity and continuity
- protected sites should be avoided
- less dissent arises through "involvement of the local population in the siting procedure, transparent planning processes, and a high information level" [18].
- familiarity with existing small scale projects is likely to increase later acceptance of further projects

A number of the studies mentioned were multi-factorial and sought to determine the relative significance of a range of contributing variables. If we accept the premise that responses to wind turbines are of two distinct kinds, one largely independent of culture, education, wealth and personal experience (the affective) and one heavily dependent on the circumstances of an affected community, then it is probably unwise to be mixing these together in our research studies. We need to know more about both, but putting both together into a single study can muddy the waters and fail to give a clear answer on either variable type. Once we have deeper knowledge about the aesthetics, for example, then we might combine this with other factors in a more comprehensive study.

In addition, and briefly mentioned above, there have been important attempts to create geographic information system based tools for prediction of visual, and other, impacts [52]. These have a significant potential role to play in relation to initial site selection and design and should complement systems based on wind potential mapping and other engineering factors. Finally, these can be supplemented but interactive collaborative design systems, such as [32], which can help to create the knowledge, participation and sense of involvement which are just as critical to the outcome as the planning and design itself.

References

[1] G. Higgs, R. Berry, D. Kidner and M. Langford, Using IT approaches to promote public participation in renewable energy planning: Prospects and challenges, Land Use Policy, 25, 2008, pp.596-607.

[2] A. Simao, P.J. Densham and M. Haklay, Web-based GIS for collaborative planning and public participation: An application to the strategic planning of wind farm sites, Journal of Environmental Management, 90, 2008, pp.2027-2040.

[3] M. Portman, Involving the public in the impact assessment of offshore renewable energy facilities, Marine Policy, 33, 2009, pp.332.

[4] G. Munda and G. Gamboa, The problem of windfarm location: A social multi-criteria evaluation framework, Energy Policy, 35, 2007, pp.1564-1583.

[5] D. Robb, Thoughtful planning reaps widespread support for New York wind project, Power Engineering, 107, 2003, pp.36-40.

[6] I.D. Bishop, Determination of thresholds of visual impact: the case of wind turbines, Environment and Planning B: Planning and Design, 29, 2002, pp.707-718.

[7] I.D. Bishop and D.R. Miller, Visual assessment of off-shore wind turbines: The influence of distance, contrast, movement and social variables, Renewable Energy, 32, 2007, pp.814-831.

[8] A.D. Torres-Sibille, V.A. Cloquell-Ballester, V.A. Cloquell-Ballester and R. Darton, Development and validation of a multicriteria indicator for the assessment of objective aesthetic impact of wind farms, Renewable & Sustainable Energy Reviews, 13, 2009, pp.40-55.

[9] N. Daugarrd, Acceptability Study of Wind Power in Denmark, Energy Centre Denmark, Copenhagen, 1997.

[10] T. Tsoutsos, A. Tsouchlaraki, M. Tsiropoulos and M. Serpetsidakis, Visual impact evaluation of a wind park in a Greek island, Applied Energy, 86, 2009, pp.546-553.

[11] T. Tsoutsos, A. Tsouchlaraki, M. Tsiropoulos and J. Kaldellis, Visual impact evaluation methods of wind parks: Application for a Greek Island, Wind Engineering, 33, 2009, pp.83-92.

[12] J. Meyerhoff, C. Ohl and V. Hartje, Landscape externalities from onshore wind power, Energy Policy, 38, 2010, pp.82-92.

[13] J. Ladenburg, Stated public preferences for on-land and offshore wind power generation - A review, Wind Energy, 12, 2009, pp.171-181.

[14] A. Lothian, Scenic perceptions of the visual effects of wind farms on South Australian landscapes, Geographical Research, 46, 2008, pp.196-207.

[15] A. Dimitropoulos and A. Kontoleon, Assessing the determinants of local acceptability of wind-farm investment: A choice experiment in the Greek Aegean Islands, Energy Policy, 37, 2009, pp.1842-1854.

[16] J. Ladenburg, Visual impact assessment of offshore wind farms and prior experience, Applied Energy, 86, 2009, pp.380-387.

[17] J.K. Kaldellis, Social attitude towards wind energy applictions in Greece, Energy Policy, 2003, pp.8.

[18] S. Krohn and S. Damborg, On Public Attitudes Towards Wind Power, Renewable Energy, 16, 1999, pp.954-960.

[19] J. Ladenburg, Attitudes towards offshore wind farms-The role of beach visits on attitude and demographic and attitude relations, Energy Policy, 38, 2010, pp.1297-1304.

[20] M.B. Lilley, J. Firestone and W. Kempton, The effect of wind power installations on coastal tourism, Energies, 3, 2010, pp.1-22.

[21] S.M.J. Baban and T. Parry, Developing and applying a GIS-assisted approach to locating wind farms in the UK, Renewable Energy, 24, 2000, pp.59-71.

[22] I.J. Ramirez-Rosado, E. Garcia-Garrido, L.A. Fernancez-Jimenez, P.J. Zorzano-Santamaria, C. Monteiro and V. Miranda, Promotion of new wind farms based on a decision support system, Renewable Energy, 33, 2007, pp.558-566.

[23] P. Lejeune and C. Feltz, Development of a decision support system for setting up a wind energy policy across the Walloon Region (southern Belgium), Renewable Energy, In Press, Corrected Proof, 2010,

[24] M. Petri and S. Lombardo, Renewable energy sources: The case of wind farms analysis, in O. Gervasi and B. Murgante (ed), Computational Science and Its Applications - Iccsa 2008, Pt 1, Proceedings, 2008, pp.111-125

[25] L.I. Tegou, H. Polatidis and D.A. Haralambopoulos, Environmental management framework for wind farm siting: Methodology and case study, Journal of Environmental Management, 91, 2010, pp.2134-2147.

[26] B. Alvarez-Farizo and N. Hanley, Using conjoint analysis to quantify public preferences over the environmental impacts of wind farms. An example from Spain, Energy Policy, 30, 2002, pp.107-116.

[27] J.P. Hurtado, J. Fernandez, J.L. Parrondo and E. Blanco, Spanish method of visual impact evaluation in wind farms, Renewable & Sustainable Energy Reviews, 8, 2004, pp.483-491.

[28] B. Moller, Changing wind-power landscapes: regional assessment of visual impact on land use and population in Northern Jutland, Denmark, Applied Energy, 83, 2006, pp.477-494.

[29] B. Moller, Spatial analyses of emerging and fading wind energy landscapes in Denmark, Land Use Policy, 27, 2010, pp.233-241.

[30] M. Rodrigues, C. Montanes and N. Fueyo, A method for the assessment of the visual impact caused by the large-scale deployment of renewable-energy facilities, Environmental Impact Assessment Review, 30, 2010, pp.240-246.

[31] R. Phadke, Steel forests or smoke stacks: The politics of visualisation in the Cape Wind controversy, Environmental Politics, 19, 2010, pp.1-20.

[32] I.D. Bishop and C. Stock, Using collaborative virtual environments to plan wind energy installations, Renewable Energy, 35, 2010, pp.2348-2355.

[33] D.C. Eltham, G.P. Harrison and S.J. Allen, Change in public attitudes towards a Cornish wind farm: Implications for planning, Energy Policy, 36, 2008, pp.23-33.

[34] K. Gee, Offshore wind power development as affected by seascape values on the German North Sea coast, Land Use Policy, 27, 2010, pp.185-194.

[35] K. Gee and B. Burkhard, Cultural ecosystem services in the context of offshore wind farming: A case study from the west coast of Schleswig-Holstein, Ecological Complexity, 7, 2010, pp.349-358.

[36] M.I. Gonzalez and B. Estevez, Participation, communication and negotiation in environmental conflicts: Offshore wind energy in the Trafalgar Sea area, Arbor-Ciencia Pensamiento Y Cultura, 181, 2005, pp.377-392.

[37] P.A. Groothuis, J.D. Groothuis and J.C. Whitehead, Green vs. green: Measuring the compensation required to site electrical generation windmills in a viewshed, Energy Policy, 36, 2008, pp.1545.

[38] J. Ladenburg and A. Dubgaard, Willingness to pay for reduced visual disamenities from offshore wind farms in Denmark, Energy Policy, 35, 2007, pp.4059-4071.

[39] G. Riddington, D. McArthur, T. Harrison and H. Gibson, Assessing the Economic Impact of Wind Farms on Tourism in Scotland: GIS, Surveys and Policy Outcomes, International Journal of Tourism Research, 12, 2010, pp.237-252.

[40] D. Moran and C. Sherrington, An economic assessment of windfarm power generation in Scotland including externalities, Energy Policy, 35, 2007, pp.2811-2825.

[41] J. Munksgaard and A. Larsen, Socio-economic assessment of wind power-lessons from Denmark, Energy Policy, 26, 1998, pp.85-93.

[42] C.R. Jones and J.R. Eiser, Understanding 'local' opposition to wind development in the UK: How big is a backyard?, Energy Policy, 38, 2010, pp.3106-3117.

[43] W. Roper and N. Campeau, Renewable energy production issues with the Cape Cod offshore wind energy programme, International Journal of Environmental Technology and Management, 6, 2006, pp.405-420.

[44] M. Wolsink, Wind power and the NIMBY-myth: institutional capacity and the limited significance of public support, Renewable Energy, 21, 2000, pp.49-64.

[45] M. Wolsink, Planning of renewables schemes: Deliberative and fair decision-making on landscape issues instead of reproachful accusations of non-cooperation, Energy Policy, 35, 2007, pp.2692-2704.

[46] M. Wolsink, Wind power implementation: The nature of public attitudes: Equity and fairness instead of 'backyard motives', Renewable & Sustainable Energy Reviews, 11, 2007, pp.1188-1207.

[47] S. Kaplan, Aestethics, affect and cognition: Environmental preference from an evolutionary perspective, Environment and Behavior, 19, 1987, pp.3 - 32.

[48] J.D. Wellman and G.J. Buyhoff, Effects of Regional Familiarity on Landscape Preferences, Env. and Behav., 1980, pp.105-110.

[49] J.H. Appleton, The Experience of Landscape, John Wiley, 1975.

[50] C. Haggett, Understanding public responses to offshore wind power, Energy Policy, 2011,

[51] A.M. Freeman, The measurement of environmental and resource values: theory and methods, Resources for the Future, 2nd edition, 2003.

[52] M. Rodrigues, C. Montañés and N. Fueyo, A method for the assessment of the visual impact caused by the large-scale deployment of renewable-energy facilities, Environmental Impact Assessment Review, 30, 2010, pp.240-246.

Economic assessment of wind power uncertainty

Viktoria Gass[1,*], Franziska Strauss[1], Johannes Schmidt[1], Erwin Schmid[1]

[1] *Department of Economics and Social Sciences, University of Natural Resources and Life Sciences, Feistmantelstrasse 4, A-1180 Vienna, Austria*
** Corresponding author. Tel: +43 1476543594, Fax: +43 1476543692, E-mail: v.gass@students.boku.ac.at*

Abstract: Wind energy has been the fastest growing and most promising renewable energy source in terms of profitability in recent years. However, one major drawback of wind energy is the variability in production due to the stochastic nature of wind. The article presents statistical simulation methods to incorporate risks from stochastic wind speeds into profitability calculations. We apply the Measure-Correlate-Predict Method (MCP) within the variance ratio method to generate long-term wind velocity estimates for a potential wind energy site in Austria. The bootstrapping method is applied to generate wind velocities for the economic life-time of a wind turbine. The internal rate of return is used as profitability indicator. We use the Conditional Value at Risk approach (CVaR) to derive probability levels for a certain internal rate of returns, as the CVaR is a reliable risk measure even if return distributions are not normal. In contrast to other scientific publications, our methodology can be generally applied, because we do not rely on estimated distributions for wind speed predictions, but on measured wind speed distributions, which are usually readily available. In addition, the CVaR has not been applied as a measure of risk for wind site evaluation before and it does not rely on any specific function regarding the profitability distribution.

Keywords: *Wind power, Bootstrapping, Measure-Correlate-Predict Method, Conditional Value at Risk, Internal Rate of Return*

1. Introduction

Wind energy was the fastest growing renewable energy resource in the European Union (EU) in the last decade. The annual installed capacity has risen from 814 MW in 1996 to 10,163 MW in 2009 [1]. In 2009, approx. € 13 billion, including € 1.5 billion offshore were invested in wind energy in the EU [1]. In this respect, the wind power capacity shall reach approx. 80 GW by 2010 becoming the renewable energy technology after hydro power with the highest installed capacity in the EU [1]. In 2009, approx. 5.4% of the electricity consumption was produced with wind energy in the EU. It is projected that the contribution of wind energy to total electricity consumption within the EU is increasing to approx. 15.5% in 2020 [2]. The stochastic nature of wind leads to fluctuations in wind energy production. The literature concerning wind speed uncertainty can be divided, for instance, into literature focusing on uncertainty in wind energy output and on economic profitability. With respect to uncertainty in wind energy output, Kwon [3] has elaborated a numerical procedure for evaluating the uncertainty caused by wind variability and power performance using probability models in order to assess the risk of power output deviations. He conducted a case study analysis to show that the standard deviation of the annual energy output normalized by the average value of power output is approx. 11%, which can cause investments to be unprofitable. Tindal et al. [4] have compared the predicted annual power production with the actual power production. Their dataset included 510 wind farms across Europe and the US. They showed that the actual wind power output is 93.3% of predicted wind power output. According to the authors, a major reason for this deviation is the rather poor quality of wind speed measurements which have been conducted before the installation of wind turbines.

A number of articles have statistically analysed wind speed data by assessing the wind energy potential in a certain region (e.g.[5], [6], [7], [8], [9], [10], [11]).The economic potential and profitability have been identified by applying traditional methods of financial analysis such as

the Net Present Value approach, the Internal Rate of Return approach, or the Life Cycle Cost Analysis approach.

Morthorst [12], for example, analysed whether there is a relationship between the expected profitability of a wind turbine and the annual increase in installed capacity in Denmark. He used the net internal rate of return approach (after tax) as a measure for profitability. Kaldellis et al. [13] conducted a sensitivity analysis in order to show the impact of different parameters on the economic viability and attractiveness of a wind energy plant. However, Montes and Martin [14] argue that statistical simulation methods should be used to account for and assess the economic risk resulting from the variability in wind speed.
Some authors analyze the wind energy potential of a specific site by using either Monte Carlo simulations for predicting wind speeds or by using the wind speed measurement data directly if sufficient measurement data are available [15], [3], [16], [9], [17]. However, Monte Carlo simulations require assumptions with respect to the distribution of the wind speeds. Consequently, Carta et al. [18] concluded that not every wind regime can be accurately described with known probability distributions.

The following article presents an approach that accounts for the uncertainty of wind speed in profitability assessments. The approach can easily be applied for any actual and potential wind energy site without specifying the distributions of wind speed. The article is structured as follows: Section 2 presents the methodology. Section 3 presents a case study analysis in which the methodology has been applied to and section 4 discusses the results and draws major conclusions from the methodology and analysis.

2. Methodology

Our approach consists of generating long-term wind speed data for a potential wind energy site (‘target site’) where only short time series of wind measurement data are available using the Measure-Correlate-Predict Algorithm (MCP) with wind speed data from a reference site. A bootstrapping procedure is applied to compute wind speed data for the economic life-time of the wind turbine. The internal rate of return approach is used as profitability index. The bootstrapping procedure allows more accurately reflecting the distribution of the wind regime in the predicted wind speeds than methods currently applied in the scientific literature on wind energy production. Furthermore, the bootstrapping procedure can be applied to any wind regime. As a measure of risk we use the Conditional Value at Risk approach (‘CVaR’). The CVaR can be uniformly applied and is not only appropriate if returns are normally distributed. The CVaR also provides information at which probability level a certain internal rate of return can be expected.

2.1. Assessment of the wind energy potential at a specific site

Wind speed measurement data are usually collected at a specific site (target site) through a period of one year or less. Wind speed frequency distributions are computed from the data in order to estimate a probability density function. Several probability density functions have been used in the literature, but the two-parametric Weibull and the one-parametric Rayleigh distribution, which is a special case of the Weibull distribution, are usually used to predict wind speeds [3], [13], [16], [15]. The two-paramteric Weibull probability density function is given by the following equation [9]:

$$f(V) = \frac{k}{c}\left(\frac{V}{c}\right)^{k-1} exp\left\{-\left(\frac{V}{c}\right)^{k}\right\},\ 0 < V < \infty \qquad (1)$$

where c and k are the scale and shape parameters and V the wind speed. The shape parameter k is usually between 1.5 and 3.0. If the value of the shape parameter is 2.0, the distribution is called Rayleigh distribution. The probability density function of the Rayleigh distribution is shown in Eq. 2 [9]:

$$f(V) = \frac{2V}{c^2} exp\left\{-\left(\frac{V}{c}\right)^k\right\} \quad (2)$$

A review carried out by Carta et al. [18] shows that the two-parametric Weibull distribution has several advantages compared to other probability density functions proposed in the scientific literature. However, not every wind speed regime can be described by a probability distribution. We applied the bootstrapping procedure as it does not require any assumptions on the distribution of the wind speed [18] [19]. However, long-term wind measurement data are needed for the target site. As already indicated, wind measurement data are usually collected through a period of one year or less. We apply the Measure-Correlate-Predict (MCP) algorithm to estimate long-term wind speed data for a target site using wind data from a reference site. We use long-term wind data from a closely located meteorological station at the reference site. According to [21], the MCP algorithm in the form of the Variance Ratio Method gives consistent and reliable estimates of wind speeds. The relationship between the wind speed data at the reference site and the wind speed at the target site can be expressed by the following equation [21]:

$$\widehat{V_t} = \left(\mu_t - \left(\frac{\sigma_t}{\sigma_r}\right)\mu_r\right) + \left(\frac{\sigma_t}{\sigma_r}\right)V_r \ , \quad (3)$$

where $\widehat{V_t}$ is the predicted long-term wind speed at the target site, V_r is the long-term wind speed at the reference site and μ_t, μ_r, σ_t and σ_r are the mean and the standard deviation of the target and the reference site, respectively. If wind measurements have not been conducted at hub height, the measured wind speeds have to be adjusted to hub height. We apply the following equation [10]

$$V_{hub} = V_m \frac{\ln\left(\frac{h_{hub}}{z}\right)}{\ln\left(\frac{h_m}{z}\right)} \quad (4)$$

where V_{hub} defines the wind speed at hub height, V_m the wind speed at measurement height, h_{hub} and h_m are the height of the hub and the measurement facility, and z is the roughness length [22]. The respective surface roughness at a specific site strongly depends on the terrain conditions.

The actual power output $P(V)$ of a wind turbine can be expressed by the following equation [9]:

$$P(V) = \int_{V_{in}}^{V_n} \frac{1}{2}\, cp \cdot \rho \cdot V^3 \cdot \pi \cdot \left(\frac{D}{2}\right)^2 + \int_{v_n}^{V_{out}} P_t \quad (5)$$

where V_n defines the rated wind speed, V_{in} the cut-in wind speed, cp the capacity factor, ρ the air mass density, V the wind speed, D the rotor diameter, V_{out} the cut-out wind speed and $P_t$the rated power output. A wind turbine starts generating power at the cut-in wind speed (V_{in}). From the cut-in wind speed to the rated wind speed (V_n), the power generated continuously increases up to the nominal power of the wind turbine. The turbine produces

constantly electricity at its rated power from the rated wind speed to the cut-out wind speed (V_{out}).

2.2. Profitability Calculations

The economic evaluation of investment projects is usually based on the Discounted Cash Flow (DCF) approach [23]. The approach provides information about the value of a project based on the present value of the cash flows that the project can be expected to generate in the future (cash in- and outflows). In the case of wind energy, cash inflows result from the electricity sold and cash outflows are investment and operating expenses. Operating expenses are mainly maintenance costs, personnel expenses, insurance costs, land lease, etc [24]. Cash in- and outflows are discounted to reflect the time and risk preferences of the decision maker associated with the cash flows. The DCF method comprises the following steps:
- estimating future cash flow for a certain discrete projection period, and
- discounting these cash flows to the present value at a rate of return that considers the relative risk of achieving the cash flows and the time value of money.

The financial attractiveness of wind energy investment projects is usually measured by the NPV and/ or the internal rate of return (IRR) [11], [12], [20], [25]. Investors are usually interested in the maximum NPV for a preferred discount rate of future cash flows. The IRR provides the discount rate at which NPV is equal to zero such that it can also be defined as the return that the project is going to generate considering cash out- and in- flows. A project can be stated to be economically viable, if the IRR is at least above the risk free rate or, if the NPV is equal or greater than zero. Equation 10 defines the IRR [23]:

$$NPV = 0 = CF_o + \frac{CF_1}{(1+IRR)^1} + \frac{CF_2}{(1+IRR)^2} + \cdots + \frac{CF_n}{(1+IRR)^n} = \sum_{t=0}^{n} \frac{CF_t}{(1+IRR)^t}, \quad (8)$$

where CF_t is the cash flow in the corresponding year.

2.3. The Conditional Value at Risk (CVaR)

We apply the CVaR as a measure of risk. Since the Value at Risk (VaR) as well as the variance as risk measures provide only reliable results if the underlying events are normally distributed [26], CVaR does not require a normal distribution of events and considers especially the tails of the underlying distribution [26]. The CVaR and the VaR are closely related, therefore we describe the VaR first. The VaR states that with probability β the expected value will not be lower than a certain threshold α. The CVaR focuses on the tails of the distribution and averages the values which fall short of threshold α depending on the probability level β. Therefore, the CVaR is a more conservative risk measure.

3. Case study analysis

The wind measurement data from a wind turbine site in Styria, which is in operation since 2005, have been used in our case study analysis. The data consist of hourly mean wind speeds as well as of hourly mean power output for the years 2006 to 2008. The hourly mean wind speeds of the year 2007 have been used as target site data. The data from a meteorological station (reference station) includes daily mean wind speeds for the years 1990 to 2009. Therefore, the calculations are based on daily mean wind speeds using the daily average of hourly wind speed measurement data of the target site. We use data from 2007 for the application of the MCP method. The different wind velocities are shown in Fig. 1, where Fig.

1a shows the daily mean wind velocities at the target site for the year 2007 and Fig. 1b shows the daily mean wind velocities at the reference site for the year 2007.

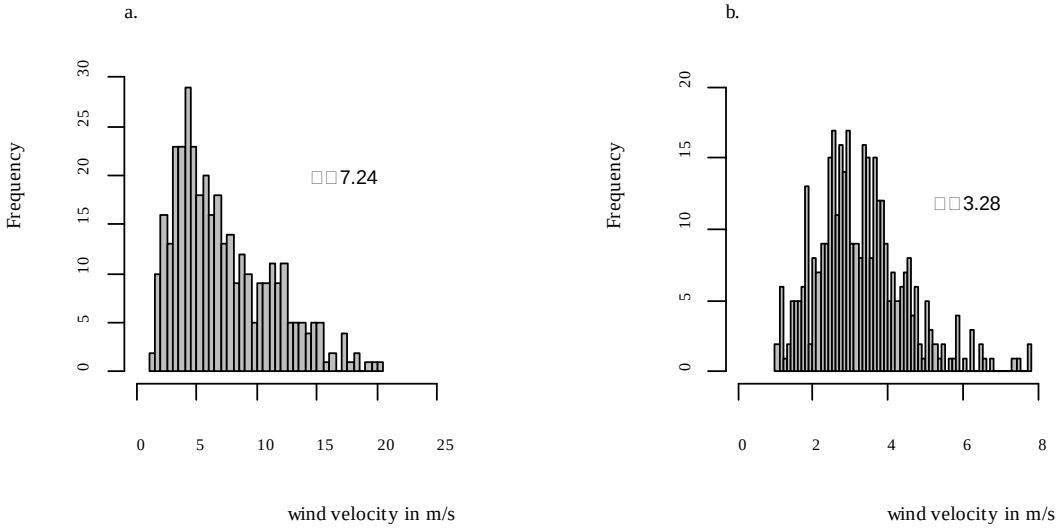

Fig. 1. Histogram of daily mean wind velocities: a. daily mean wind velocities at the target site for the year 2007; b. daily mean wind velocities at the reference site for the year 2007.

The correlation equation of the hourly mean wind velocity at the target site and the hourly mean wind velocity of the reference site derived from Eq. (3) is as follows:

$$\widehat{V_t} = -3.7507 + 3.3065\, V_r \qquad (9)$$

The long term wind velocities at the target site are estimated on the basis of the slope and the intercept of the Eq. (9). However, before applying the MCP method, the wind speed at the reference station has to be extrapolated from the anemometer to hub height using Eq. (4). As the target site is located in mountainous area, the correlation between the target and the reference site is low (0.2120). According to the utility manager (oral communication), the reference station has been used to evaluate the target station before deciding on the construction of the wind park. Therefore, we also use the same reference station in our case study analysis. The daily wind measurement data at the reference site record a period of 20 years such that long-term daily mean wind velocities are computed for this period with the MCP method.

Currently, the feed-in tariffs are guaranteed for a period of 13 years in Austria. Therefore, we assume that a potential investor requires a certain return of investment within the period in which he or she receives a guaranteed electricity price. Our calculations concerning the profitability assessment are based on a 13 year period of predicted daily mean wind velocities. Seasonal differences are reflected in the bootstrapping procedure, which has been repeated 1000 times. Consequently, several trajectories are obtained both for the wind speeds and the power outputs. The trajectories are also used in the statistical evaluations revealing information that are relevant for investment decisions.

The energy power output is derived for a 1.3 MW wind turbine with a turbine diameter (D) of 62 m, a cut-in wind speed (V_{in}) of 4 m/s, a cut-out wind speed (V_{out}) of 25 m/s, and a rated wind speed (V_n) of 13 m/s, respectively. The capacity factor (cp), which is defined as the ratio of the energy generated to nominal energy generation is 0.4. The air mass density (ρ) corresponds to 1.27 kg/m^3. The wind turbine starts producing power at a wind speed of 4

m/s and reaches its rated wind speed at 13 m/s. The daily generated electricity production can be computed by multiplying the computed power output with 24 (hours of a day). The daily generated electricity production is then added up to annual generated electricity production as profitability calculations are conducted on annual time steps.

The histogram of the daily and annual generated electricity in kWh is shown in Fig. 2a and Fig. 2b, which follows a normal distribution according to the central limit theorem. The theorem states that the probabilities of events generated with the sum of independent, identical distributed random variables X approximate to a normal distribution for a sufficiently large number of events. The central limit theorem indicates that the distribution of $\sum X_i$ for an increasing n approaches always the $N(n\mu; \sigma\sqrt{n})$ distribution.

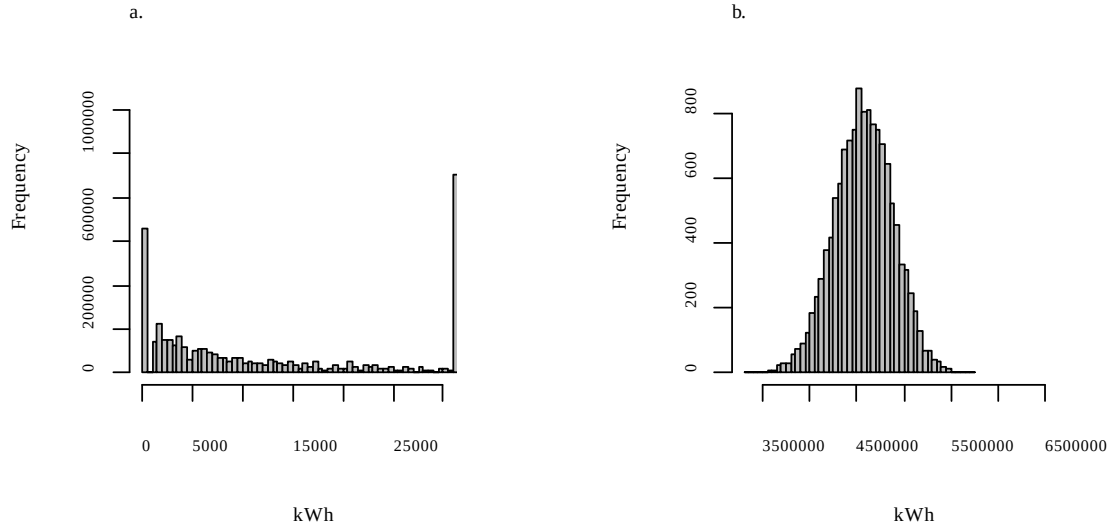

Fig. 2. a. Histogram of the daily generated electricity in kWh; b. Histogram of the annual generated electricity in kWh .

The annual Free Cash Flows (FCF) can be derived from the annual generated electricity. The cash inflows result from the generated electricity, which is sold at the guaranteed feed-in tariff that currently amounts to 0.0753 €/kWh in Austria. The cash outflows are the investment costs for the wind turbine, which are € 1.5 mil. per MW installed according to the provider of the wind measurement data. The operating costs are amounting to 0.020 €/kWh. Further corporate tax payments have to be considered when calculating the FCFs (current corporate tax rate is 25% in Austria). It is assumed that demolition costs at the end of the lifetime equal the revenue which can be generated out of selling the steel from the wind turbine. The internal rate of return has been calculated from the computed annual FCF. A standard criterion for investment decisions is the hurdle rate. It reflects a discounting rate at which the investments provide a positive cash flow. If a negative NPV results out of discounting the FCF with the hurdle rate, the underlying investment will most likely not be approved by the management. Consequently, an investment can be approved if the IRR exceeds the hurdle rate. The resulting probability density functions are shown for different risk aversion levels in Fig. 3. The IRR will be not lower than 7.94% at a probability level of β = 90% according to the probability density function of the IRR shown in Fig. 3 a. If the hurdle rate for an investor is above 7.94% then an investor shall not decide against the investment. However, the investor might realize an IRR above 9.19% with a 10% probability. Fig. 7b shows the resulting IRRs for a 95%- probability level.

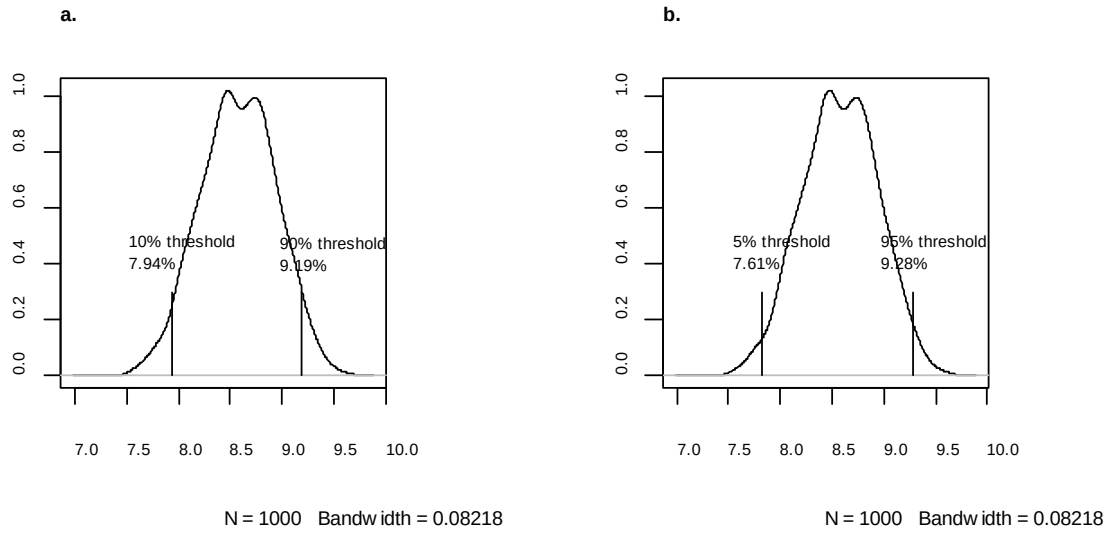

Fig. 3. Probability density functions of the IRR and the CVaR. a. Probability density function of the IRR with the threshold levels of 10% and 90%; b. Probability density function of the IRR with the threshold levels of 5% and 95%.

4. Concluding Remarks

We have developed a methodology to better assess the profitability of a wind energy site in the presence of wind speed uncertainty. Our approach can be applied to any wind regime. We apply statistical simulation methods to close the gap in the scientific literature on wind energy production [14]. Neither the bootstrapping method to predict wind speeds nor the conditional value at risk approach have been applied for investment assessments in combination with wind site evaluations. We have combined and applied these methods for a case study analysis. For a 1.5 MW wind turbine with investment costs of € 1.5 mil. per MW and operating expenses of 0.020 €/kWh, the IRR with a probability of 95% will not be lower than approx. 7.61% for the case study wind energy site. With a 5% probability, however, an investor can achieve an IRR of 9.28%.

References:

[1] EWEA. Wind in power 2009 European statistics. 2010.

[2] EREC European Renewable Energy Council. Renewable Energy Technology Roadmap 20% by 2020. 2008.

[3] Kwon S. Uncertainty analysis of wind energy potential assessment. Applied Energy. 2010;87:856-865.

[4] Tindal A, Harman K, Johnson C, Schwarz A, Garrad A, Hassan G. Validation of GH energy and uncertainty perdictions by comparison to actual production. AWEA Wind Resource and Project Energy Assessment Workshop, Portland2007.

[5] Keyhani A, Ghasemi-Varnamkhasti M, Khanali M, Abbaszadeh R. An assessment of wind energy potential as a power generation source in the capital of Iran, Tehran. Energy. 2010;35:188-201.

[6] Ramachandra T. Wind energy potential assessment in Uttara Kannada district of Karnataka, India. Renewable Energy. 1997;10:585-611.

[7] Ramachandra T, Shruthi B. Wind energy potential mapping in Karnataka, India, using GIS. Energy Conversion and Management. 2005;46:1561-1578.

[8] Rehman S. Wind power cost assessment at twenty locations in the kingdom of Saudi Arabia. Renewable Energy. 2003;28:573-583.

[9] Arslan O. Technoeconomic analysis of electricity generation from wind energy in Kutahya, Turkey. Energy. 2010;35:120-131.

[10] Hoogwijk M. Assessment of the global and regional geographical, technical and economic potential of onshore wind energy. Energy Economics. 2004;26:889-919.

[11] Voivontas D. Evaluation of Renewable Energy potential using a GIS decision support system. Renewable Energy. 1998;13:333-344.

[12] Morthorst P. Capacity development and profitability of wind turbines. Energy Policy. 1999;27:779-787.

[13] Kaldellis JK, Gavras TJ. The economic viability of commercial wind plants in Greece A complete sensitivity analysis. Energy Policy. 2000;28:509-517.

[14] Montes G, Martin E. Profitability of wind energy: Short-term risk factors and possible improvements. Renewable and Sustainable Energy Reviews. 2007;11:2191-2200.

[15] Correia P, Ferreira de Jesus J. Simulation of correlated wind speed and power variates in wind parks. Electric Power Systems Research. 2010;80:592-598.

[16] Friedman PD. Evaluating economic uncertainty of municipal wind turbine projects. Renewable Energy. 2010;35:484-489.

[17] Akdag SA, Güler Ö. Evaluation of wind energy investment interest and electricity generation cost analysis for Turkey. Applied Energy. 2010;87:2574-2580.

[18] Carta J, Ramírez P, Velázquez S. A review of wind speed probability distributions used in wind energy analysis: Case studies in the Canary Islands. Renewable and Sustainable Energy Reviews. 2009;13:933-955.

[19] Efron B. Bootstrap Methods: Another Look at the Jackknife. The Annals of Statistics. 1979;7:1-26.

[20] Burton T, Sharpe D, Jenkins N, Bossanyi E. Handbook of wind energy. Chichester, England: John Wiley & Sons, Ltd.; 2001.

[21] Rogers A, Rogers J, Manwell J. Comparison of the performance of four measure-correlate-predict algorithms. Journal of Wind Engineering and Industrial Aerodynamics. 2005;93:243-264.

[22] Silva J, Ribeiro C, Guedes R. Roughness Length Classification of Corine Land Cover Classes. MEGAJOULE-Consultants; 2007.

[23] Khatib H. Economic evaluation of projects in the electricity supply industry: The Institiution of Engineering and Technology, London, UK; 2003.

[24] Blanco MI. The economics of wind energy. Renewable and Sustainable Energy Reviews. 2009;13:1372-1382.

[25] Talavera D, Nofuentes G, Aguilera J. The internal rate of return of photovoltaic grid-connected systems: A comprehensive sensitivity analysis. Renewable Energy. 2010;35:101-111.

[26] Rockafellar R, Uryasev S. Conditional value-at-risk for general loss distributions. Journal of Banking & Finance. 2002;26:1443-1471.

Economics of DC wind collection grid as affected by cost of key components

Georgios Stamatiou[1,*], Kailash Srivastava[2], Muhamad Reza[2], Pericle Zanchetta[1]

[1] *University of Nottingham, Nottingham, UK*
[2] *ABB Corporate Research, Västerås, Sweden*
** Corresponding author. +30 6976276783, E-mail: geostamatiou@gmail.com*

Abstract: Using High Voltage Direct Current (HVDC) transmission lines to connect offshore wind parks to the onshore power grid has been proven technically advantageous to AC solutions and more cost-effective for relatively long transmission distances (>70km).The concept of applying DC technology can be expanded to the collection grid. DC collection grid offshore wind parks can be developed only if several key components currently nonexistent are available. The technical challenges involved can result in the unpredictability of their costs. This paper investigates the effect the uncertainty of the key components' cost can have on the overall economic performance of DC collection grid offshore wind parks. Results for a wide cost range are presented and corresponding cost boundaries which secure the economic viability of such parks were determined.

Keywords: *DC grid, Offshore Wind park, Techno-economics, DC/DC.*

1. Introduction

In the future the size of offshore wind farms and the distance to shore are expected to increase, thereby leading to higher losses in the AC collection grid and AC transmission. DC technologies can provide lower losses and use cheaper cables than their AC counterparts, thereby compensating for the increased cost of the necessary power electronic devices. HVDC transmission systems have already been proven technically advantageous and cost-effective over AC transmission for distances longer than 60-70 km according to [1], and applying DC technologies not only to the transmission system but also to the collection grid of offshore wind parks could prove additionally effective according to [2].

Key components refer to those components that are not at present available in the market but are needed to realize DC collection grids. According to [3], the following components are identified as key components: DC Circuit Breaker and DC/DC Converter which includes the Medium Frequency Transformer. DC breakers for high power applications have not been constructed and DC/DC converters are not currently available for high power rating beyond 1 or 2 MW [6]. Lundberg in [10] conducts a techno-economic analysis on DC wind parks but omits the cost of DC switchgear and underestimates the cost range of the DC/DC converters, neglecting their challenging nature.

This paper investigates the effect of cost uncertainties of key components on the economic viability of offshore DC wind collection grid. Four different wind park layouts are considered. Initial assumptions on the key components' costs are made and using a cost-benefit programming tool, cost evaluation scenarios take place by altering the cost of the key components. Finally, cost boundaries are defined, beyond which any DC collection grid layout is not economically competitive.

2. Key components

2.1. DC Circuit breaker

Realising DC collection grid for offshore wind farms requires the existence of switching and protection devices specifically designed for DC grids. DC Circuit breakers are a characteristic example. Figure 1 (a) presents a typical DC grid. A capacitor is required to stabilize the

voltage and reduce the voltage ripple at the DC side of the converter. Due to this capacitor, the system can be described by an equivalent constant voltage source V_{Grid} and grid impedance L_{Grid} as in Figure 1 (b). When a short-circuit occurs, all of the grid voltage is applied across the equivalent resistance. As a result, there is a large and constant voltage across the inductance, leading to a constant and steep rate of rise of the current. Therefore, the fault current reaches dangerously high values quite quickly. Decreasing the rate of rise of the current implies the forced application of voltage across the circuit breaker so that the voltage drop across the inductance is decreased. Additionally in contrast to an AC system, a DC system by definition does not have current zero crossings, which could aid for the safe interruption of the fault current.

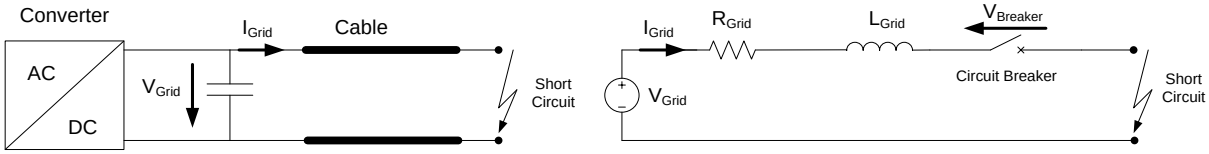

(a) (b)

Figure 1. a) Representation of DC grid under short circuit condition b) Equivalent circuit of a DC grid under short circuit conditions

Therefore a high-power DC breaker must a) be able to act very rapidly to avoid extremely high currents and b) Allow active turn-off.

2.2. DC/DC Converter

The requirement for transforming voltages in a high-power DC grid is one of the major challenges towards the realization of DC power networks including DC collection grid. Different topologies for DC/DC converters have been developed using medium or high-frequency AC link as discussed in [4], based on the general model of Figure 2. A galvanic isolated DC/DC converter consists of an inverter at the input side, an AC link consisting of a transformer and an inverter at the output side to transform back to DC. The voltage at the endpoints of the transformer does not need to be sinusoidal or at 50-60Hz. Hence the frequency of the alternating voltage can be equal to the switching frequency and a rectangular waveform of such frequency can be applied to the transformer. The AC link is based on a medium/high frequency transformer, resulting in galvanic isolation which is important for security reasons in high power applications.

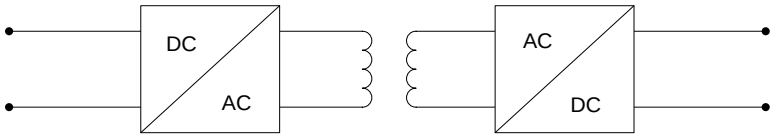

Figure 2. General topology of a galvanic isolated DC/DC converter

The overall dimensions of such a transformer are significantly reduced due to the higher operating frequency, resulting in a compact DC/DC converter. The transformer can be single or three phase. The transformer can be single or three phase with the latter being more advantageous for high-power applications [5].

2.3. Medium Frequency Transformer

As mentioned in section 2.2, the fundamental component of a high power DC/DC converter is the medium frequency transformer, which is also the most challenging to construct for high power applications. The non-sinusoidal excitation of the core and the use of high-frequency components require sophisticated approach methods. The material and the design of the core of the transformer are of utmost importance. Traditional low frequency-high voltage-high power transformers use laminated cores. However, this concept cannot be applied to medium frequency transformers. Increasing the frequency leads to excessive losses and the insulation between the core sheets will lead to a reduced thermal conductivity of the core [3].

3. Methodology

3.1. Layouts

For the scope of this paper, four different offshore wind park layouts where investigated: "Small DC", "Large DC", "Series DC" and "AC/DC". These designs are thoroughly presented in [10] and [7]. All of them have a DC transmission link and DC collection grid with the notable exception of the AC/DC which has an AC collection grid. AC is currently the only technology used in the collection grid of wind parks and therefore, AC/DC layout is used as a benchmark for the rest fully DC wind park designs. It is important to mention that the turbines in all DC collection grids, the turbines consist of a Permanent magnet generator coupled to a rectifier and then to a DC/DC converter while the turbines of the AC/DC park consist of a Doubly Fed Induction Generator (DFIG) connected to a transformer.

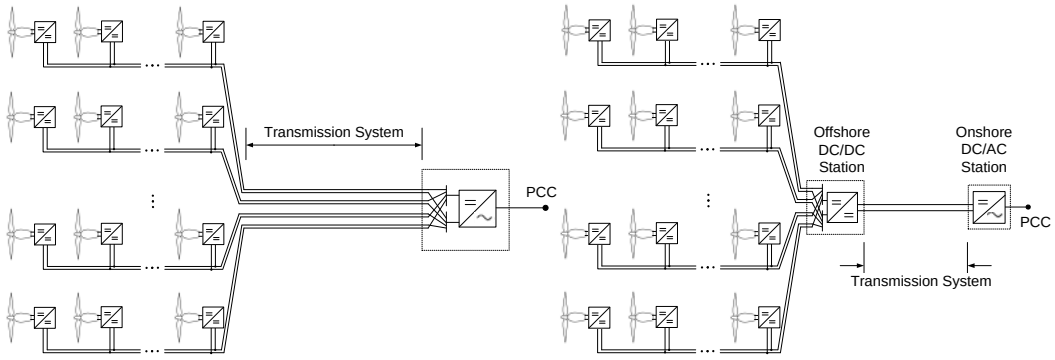

Figure 3. a) Small DC offshore wind park b) Large DC offshore wind park

The small DC layout presented in Figure 3 (a) has DC feeders of Medium Voltage (MV) which are extended to the onshore inverter, located just before the Point of Common Coupling (PCC) to the main grid. Figure 3 (b) presents the Large DC layout which resembles the Small DC but uses a large offshore DC/DC converter on a platform, to achieve High Voltage DC (HVDC) on the transmission system, resulting in decreased transmission losses. The Series DC layout is featured in Figure 4 (a). The turbines have a MV DC output and are connected in series, resulting in HVDC along each feeder and also on the transmission line, without the need of an additional offshore DC/DC converter. The AC/DC layout is depicted in Figure 4 (b), having a conventional AC collection grid and an HVDC transmission system.

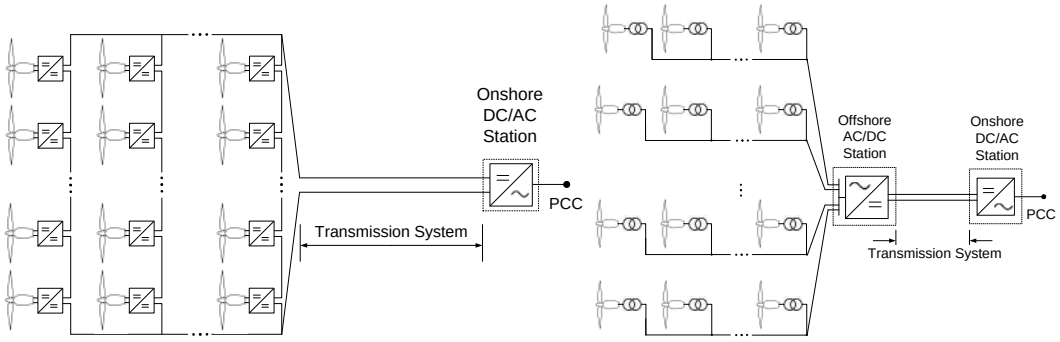

Figure 4. a) Series DC offshore wind park b) AC/DC offshore wind park

3.2. Energy Cost

The minimum cost of energy production for any desired wind farm project is described by the Energy Cost and is given in currency units per kWh delivered to the PCC. Its calculation is given by equation (1):

$$\text{Energy Cost} = \frac{\text{Total capital cost} \cdot \dfrac{\mathrm{r}(1+\mathrm{r})^{N}}{(1+\mathrm{r})^{N}-1} + \text{O\&M}}{\text{Average power production} \cdot \mathrm{T}} \qquad (1)$$

where O&M is the total annual Operation and Maintenance costs, r is the interest rate, N is the lifetime of the wind farm in years and T is the average operational hours per year in the form of T=24·365 hours·0.95, where the last term expresses a park availability of 95% annually. Ideally, a project should have the lowest energy cost possible.

3.3. Cost-Benefit Tool

A Cost-Benefit programming tool was developed in order to calculate the Energy Cost. It consists of sets of function/script in Matlab environment while the management of input and output information is provided by dedicated Microsoft Office Excel files. Every desired offshore wind park is represented by a dedicated Excel file, containing all the important technical and economical parameters that precisely describe its unique configuration. The tool imports this information and after performing a sequence of calculations, determines the Energy Cost according to equation (1).

3.3.1. Energy yield Calculation

The determination of the Energy Cost requires the calculation of the average power production of the wind parks. This is done by considering every wind park as a complex model consisting of interconnected elements. The components which have been modeled are the wind turbines, transformer, DC/DC converter, HVDC station and cables (AC and DC). The modeling details are available in [7]. The power at PCC is calculated for a given instantaneous wind speed and to describe the variations in the wind speed over time, a density function is used and in particular the Weibull distribution $f(w)$ described in [8], were w is the wind speed in m/s, as the ideal representation of real measured wind data. Using the probability density function, the average power can be generally calculated as:

$$P_{average} = \int_0^{\infty} P(w) \cdot f(w) \cdot dw \qquad (2)$$

where P(w) is the power at PCC for wind speed of w m/s.

3.3.2. Capital and maintenance costs

Wind park related cost data was obtained from published sources. A lot of information was available in [9] and [10]. The gathered data is referred in [7] regarded the following: Wind turbine (different for AC and DC grid), foundations, transformer, HVDC stations, cables (AC and DC), cable installation, offshore platform, DC/DC converters (according to type of usage) and switchgear (for AC). No resource was found on DC switchgear and due to the challenging construction, we assumed that setting its cost as double the AC switchgear. Additionally, Lundberg in [10] claims that since a DC/DC converter contains approximately the same amount of semiconductors as an AC/DC converter of the same rating, it is reasonable to have the same cost as the latter, namely 1 SEK/VA. However, regarding the complexities involved in the construction of DC/DC converters, such a cost was not considered adequate. A more careful and trustworthy approach was adopted. The converters on the turbines of the Series DC layout were considered at 3 SEK/VA owing to the high insulation requirements. The high power converters used in the offshore platform of the Large DC were considered at 2 SEK/VA because of the complex construction and the DC/DC converters on the turbines of the Small and Large DC schemes cost 1.5 SEK/VA due to the complexities involved.

In order to calculate the O&M costs, the components which require maintenance were gathered in three sets of related components: "Turbine", "Collection grid" and "Transmission system". According to literature sources, O&M can be taken as a certain percentage of the capital cost. Therefore the corresponding “Turbine O&M”, “Collection grid O&M” and “Transmission system O&M” were defined as 4%, 2% and 0.5% percentages respectively, of the total capital costs of the three initial sets.

3.4. Simulation considerations and assumptions

For each of the four suggested layouts, three different power capacities were considered: a) 160 MW, b) 500 MW and c) 1200 MW. Regarding the design considerations, the collection grid voltage was set at 30kV DC for DC grids and 30kV AC for the AC grids. Additionally the HVDC transmission links were rated at ±150kV for the 160 and 500 MW cases and ±320kV for the 1200 MW. Finally each feeder of the collection grid consisted of 10 turbines in all cases. The design peculiarity of the 1200 MW Series DC requested the need for 32kV DC at the exit of the turbines’ DC/DC converters and 20 turbines per feeder. Finally, every wind park was simulated for transmission distances in the range of 0-200km. Additionally, several assumptions were made as in Table 1.

Table 1. Simulation assumption

Parameter	Assumption
Wake effect	Neglected
Cable inventory	Maximum 4 different cables per model
Turbine's power rating	2MW
Turbine power curve	Same for DFIG (before transformer) and FPCG (before DC/DC converter)
Weibull shape factor	k=2
Converter loss curve	Same for HVDC and DC/DC
Interest rate	7% per annum
Life cycle	25 years
Average wind speed	10 m/s for all cases and all transmission distances

4. Results

4.1. Cost of DC/DC converters

In order to determine how sensitive the economic viability of the DC collection grid is with respect to the DC/DC converter cost, all costs were kept unchanged and the DC/DC converter cost was altered. Assuming that the cost proportion between the 3 different kinds of DC/DC converters as described in 3.3.1 remains always fixed, the following concept is followed: all of these values are multiplied by a common percentage representing the cost fluctuation i.e. a 50% percentage means that the new costs are half the original ones.

Figure 5 presents the results in Energy Cost terms for all layouts of the 160 MW power rating, for percentages of 50%, 100% and 300%. For a specific power capacity, the energy cost curves of the Large DC, Series DC and AC/DC seem to be parallel. This happens because these three layouts share the same transmission lines and increasing the distance will only increase the length of the cables. As a result, all three layouts will experience the same amount of capital and O&M cost increase and therefore energy cost increase. The order of the energy cost curves is defined by the costs with no transmission line involved. This is the energy cost at 0 km of distance. The Small DC differs in a great degree because it features multiple transmission cables and for increasing distance, the huge capital and O&M cost as well as excessive transmission system losses, force the energy cost to increase at a steep rate. As expected, the energy cost curve of the AC/DC layout remains the same in all three scenarios as it contains no DC/DC converters. On the contrary, the energy cost of the Small DC, Large DC and Series DC increase for increasing percentage (more expensive converters). As observed in the figure and also confirmed in [7], the Small DC rarely has the smallest energy cost and when this happens, it is only for distances less than 2-3 km. Additionally, its energy cost increases almost exponentially due to the large number of costly transmission lines and increased losses. Therefore, Small DC is of no interest for offshore development where distances are expected to be in the order of 10s to 100s of km and as a result, it will not be depicted again in the following figures.

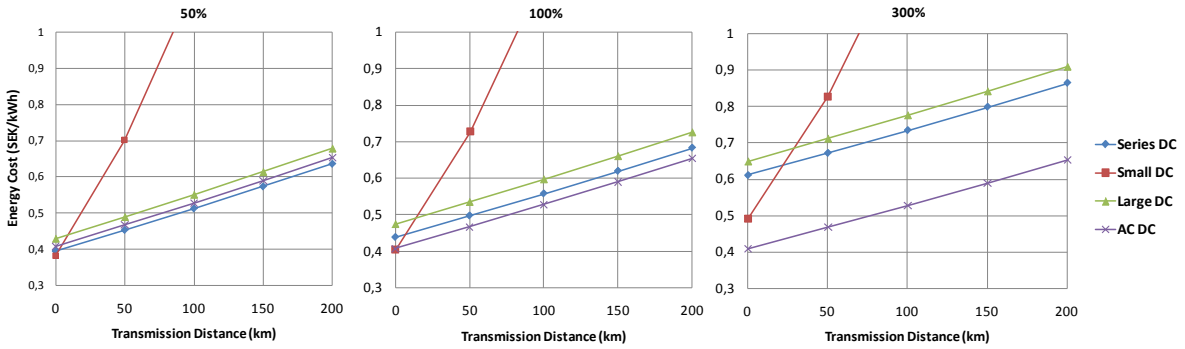

Figure 5. Energy cost curves of 160MW layouts for DC/DC cost percentages of 50%, 100% and 300%

For very small percentages, the Series DC has the smallest energy cost in all distances with the AC/DC following. For increasing percentage, AC/DC remains constant with the Series DC moving upwards until they coincide for a certain percentage. After this, the AC/DC maintains the smallest energy cost for all distances, and effectively all DC collection grid layouts have been ruled out of the competition. In every case, the Large DC has always higher energy cost than both the Series DC and the AC/DC. Therefore, only AC/DC and Series DC are considered as competitive layouts. This break-even percentage is different for each of the three power ratings and the findings are presented in Table 1.

Table 2. Break-even DC/DC cost percentages for each power rating

Wind park Power rating	Break-even percentage
160 MW	67%
500 MW	94%
1200MW	145%

If the results from all layouts and capacities are presented in the same graph as in Figure 6, it can be seen that for the basic scenario of 100% percentage, the AC/DC technology has the lowest energy cost up to a distance of ~100km, with the Series DC having the lowest energy cost for any greater distance. It was observed that by decreasing the DC/DC converter cost, the AC/DC technology was the most cost-benefit solution for smaller distances until it was eventually not competitive at all, with the Series DC being the cheapest for all distances. Reversely, for increasing converter cost the dominance of the Series DC is shifted to higher distances until a certain point when AC/DC has the lowest energy cost for all distances within the range of 0-200km.

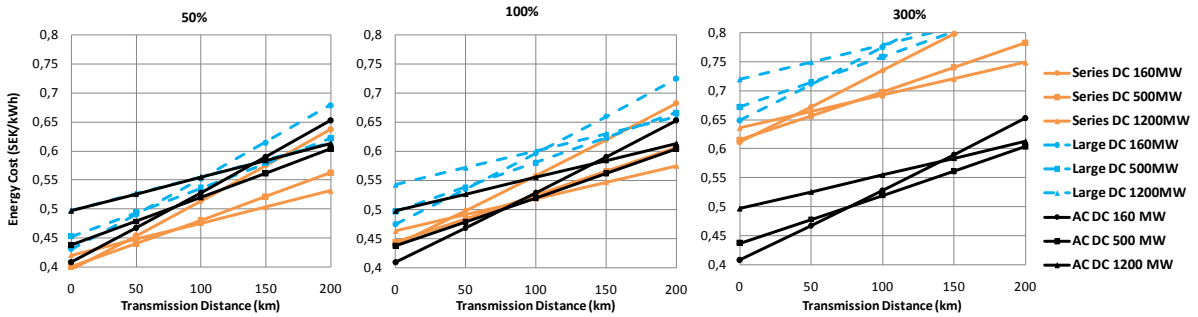

Figure 6. Energy Cost curves of Series DC, Large DC and AC/DC for DC/DC cost percentages of 50%, 100% and 300%.

It was determined that these two percentages are the break-even values for the 160MW and 1200MW as in Table 2. Therefore, for a percentage lower than 67%, the Series DC is the technology with the lowest energy cost for all distances, then AC/DC begins to be the cheapest up to certain distances, and when the percentage exceeds 145%, the AC/DC is the cheapest overall with no DC collection grid layout being competitive any more. The general conclusion is that if DC collection grid is to be regarded as a future solution for offshore wind parks for distances up to 200km, Series DC is the most cost-benefit wise interesting approach and the cost of the DC/DC converters must not exceed 145% of the originally assumed costs described in Table 1. When the cost percentage is less than 67%, Series DC (therefore DC collection grid) is the best solution in all distances.

4.2. DC switchgear cost

The same concept as before was followed in the case of the DC switchgear cost were the uncertainties in the DC breaker cost are involved. The original cost was multiplied by a percentage and break-even costs were determined as in Table 3. It is interesting to notice that no break-even percentage was evaluated for the 160MW case, meaning that AC/DC has always the lowest energy cost for all distances, no matter how cheap the DC switchgear gets.

When all the results are compared, the Series DC remains competitive until the percentage regarding the cost of the DC switchgear exceeds 378% and the AC/DC technology features the lowest energy cost for all 200km. This margin is high due to the smaller contribution of

Table 3. Break-even DC switchgear cost percentages for each power rating

Wind park Power rating	Break-even percentage
160 MW	Nonexistent
500 MW	54%
1200MW	378%

the DC switchgear to the overall capital costs, compared to the DC/DC converters. Even if the percentage drops to 0%, AC/DC will still be the most competitive for distances up to 60km.

5. Conclusions

Under the circumstances where offshore wind farms are growing in the capacity and distance from shore, DC wind collection grid along with DC transmission can be the most cost effective solution. However, any development of such designs depends on the presence of currently unavailable components, namely DC/DC converters and DC circuit breakers, and also on their expected costs. Specifically, the cost of DC/DC converters must be quite close to the suggested values of this paper while there is a lot more margin for the DC circuit breaker's cost. Any future research aiming to materialise the needed key components must be done with respect to the indicated cost boundaries and general findings of this paper.

References

[1] P. Bresesti, W. L. Kling, R. L. Hendriks, and R. Vailati, “HVDC connection of offshore wind farms to the trans-mission system,” IEEE Trans. Energy Conv., vol. 22, no. 1, pp. 37-43, Mar. 2007

[2] Macken, K.J.P.; Driesen, J.L.J.; Belmans, R.J.M., "A DC Bus System for connecting offshore wind turbines with utility system," European Wind Energy Conference 2001, Copenhagen, Denmark, 2-6 July 2001, pp. 1030-1035.

[3] Christoph Meyer, “Key Components for Future Offshore DC Grids” PhD thesis submitted to Electrical Engineering Department, RWTH Aachen.

[4] Ranganathan, V.T., Ziogas, P.D. Stefanovic, V.R., “A regulated DC-DC voltage source converter using high frequency link,” IEEE Transaction on Industry Application (IAS) 18 (1982), No. 3, pp. 279-287.

[5] Jacob, J.H.A.M., “Multi-phase Series Resonant DC/DC Converters,” Aachen Germany, RWTH Aachen University, Aachener Beitrage des ISEA Band 42, PhD Thesis 2006.

[6] Engel, B., Victor, M., Bachman, G., Falk, A., “15kV/16.7 Hz energy Supply System with Medium Frequency Transformer and 6.5 kV IGBTs in Resonant Operation,” European Power Electronics Conference (EPE), Toulouse, France, September 2003.

[7] Georgios Stamatiou, "Techno-Economical Analysis of DC Collection Grid for Offshore Wind Parks", MSc. Thesis, University of Nottingham, 2010, http://hermes.eee.nottingham.ac.uk/mcf/Thesis.pdf

[8] http://www.weibull.com/AccelTestWeb/weibull_distribution.htm

[9] B. Van Eeckhout,” The economic value of VSC HVDC compared to HVAC for offshore wind farms,” Master Thesis submitted to Katholik University of Leuven.

[10] Stefan Lundberg, ”Performance comparison of wind park configurations,” Chalmers University of Technology, 2003.

Study of transient stability for parallel connected inverters in Microgrid system works in stand-alone

F. Andrade[1,*], J. Cusido[2], L. Romeral[1], J. J. Cárdenas[1]

[1] *Universitat Politécnica de Catalunya, Barcelona, Spain*
[2] *CTM Centre Tecnològic, Manresa, Spain*
** Tel: +34937398510, Fax: +34937398016, E-mail: fabio.andrade@mcia.upc.edu*

Abstract: Distributed generators systems and Microgrid are becoming more important to increase the renewable energy penetration in the public utility. This paper presents a mathematical model for connected inverters in Microgrid systems with large range variations in operating conditions. No-lineal tools and computer simulations, phase-plane trajectory analysis, method of Lyapunov and bifurcations analysis for evaluate the limits of the small signal models are used, and conclusion suggested utilizing models that can permit to analysis of the system when subjected to a severe transient disturbance such as loss a large load or loss of generation. The study of transient stability for Microgrid systems in stand-alone of the utility grid is useful to improve the design of Microgrid's architecture.

Keywords: *Microgrid model, Transient Stability, Parallel Inverters, Method of Lyapunov.*

1. Introduction

Distributed generators systems and Microgrid are becoming more important to increase the renewable energy penetration in the public utility [1-2]. Thus, the use of intelligent power interfaces between the electrical photovoltaic generation source and the grid is required. These interfaces have a final stage consisting of dc/ac inverters, which can be classified in current source inverters (CSI) and voltage-source inverters (VSI). In order to inject current to the grid, CSI are commonly used, while in island or autonomous operation, VSI are needed to maintain the voltage stability [3-5].

A Microgrid can be operated either in grid connected mode or in stand-alone mode. In grid connected mode, most of the system level dynamics are established by the public utility, this is due to the relatively small size of local generators. In stand-alone mode, the system dynamics are established by micro generators themselves [6]. This paper presents an analysis of transient stability of power systems for parallel connected inverter in a Microgrid under autonomous operation.

The power inverters do not present the natural relations between frequency and active output power, neither between output voltage and reactive output power. Therefore, in order to reach stable operation, when the inverters are connected in parallel, these inherent operating conditions must be established by the inverter's control system [7].

Previous analysis of stability of stand-alone systems have been done by means of small signal models [5, 8], either assuming an ideal inverter or considering power inverter with a high switching frequency and their closed-loop inner controllers. Simulation and experimental result show that the systems work well when there is a small perturbation, but when the perturbation is bigger, the system could be in unstable operation.

The small signal analysis works with root locus plots Bode diagrams, Nyquist plots, etc., researching the desired dynamic behaviour of the systems. On the contrary, this paper works with no-lineal tools for large signal analysis supported by computer simulations. It is used

phase-plane trajectory analysis and method of Lyapunov to evaluate the limits of the small signal models. It is suggested the utilization of models that allow to analyze the system when it is subjected to a s evere transient disturbance such as loss of large loads or loss of generation.

2. A Microgrid Study

Fig 1 shows the circuit diagram of the Microgrid systems in stand-alone considered in this paper. This system configuration was studied by Duminda, in [8]. It was considered small signal modeling. For simplicity, the system has two inverter connected, but it can be extended for n-number of inverters.

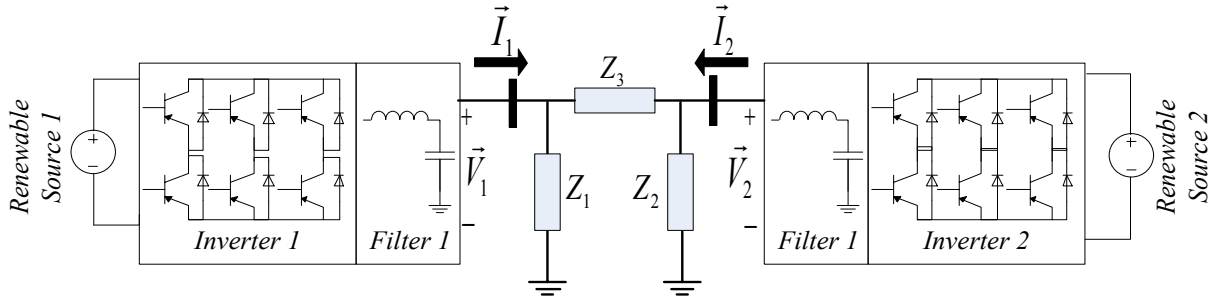

Fig. 1. Parallel connected inverters in Microgrid system works in stand-alone.

The Distributed Generator (DG) considered consists of a power DC renewable source, a three-leg inverter and an output LC filter. By assuming the renewable energy source as an ideal source form, the DC bus dynamics can be neglected. Each DG presents a PWM controller with a current and voltage loop and a PQ controller. The PQ controller must autonomously respond effectively to system changes without communication, only with local variables. Commonly, the PQ controller uses the droop curves (*f vs P* and *V vs Q*) and a filter with a cut-off frequency of approximately a decade smaller than a grid frequency. The task of the PQ controller is to imitate the governor of a synchronous generator. This artificial droop control scheme can be expressed as follows

$$\omega = \omega_0 - k_p P \qquad V = V_0 - k_v Q \tag{1}$$

Where P and Q are filtered with a low pass filter with cut-off frequency ω_f, the equations of these filters in the Laplace domain can be expressed as:

$$P(s) = \frac{\omega_f}{s+\omega_f} P_i(s) \qquad Q(s) = \frac{\omega_f}{s+\omega_f} Q_i(s) \tag{2}$$

P_i and Q_i are instantaneous power and are calculated from the measured output voltage and output current as in

$$P_i(s) = V_d I_d + V_q I_q \qquad Q_i(s) = V_d I_q - V_q I_d \tag{3}$$

2.1. A mathematical model of the each voltage source inverter

Considering (1), (2) and working in the time domain,

$$\dot{\omega} = -\omega_f \omega - k_p \omega_f + P_i \tag{4}$$

$$\dot{V} = -\omega_f V - k_v \omega_f + Q_i \tag{5}$$

The inverters are modeled in a common reference frame (d-q), fig. 2. Each voltage vector has an angle δ_i with respect to the d-axes.

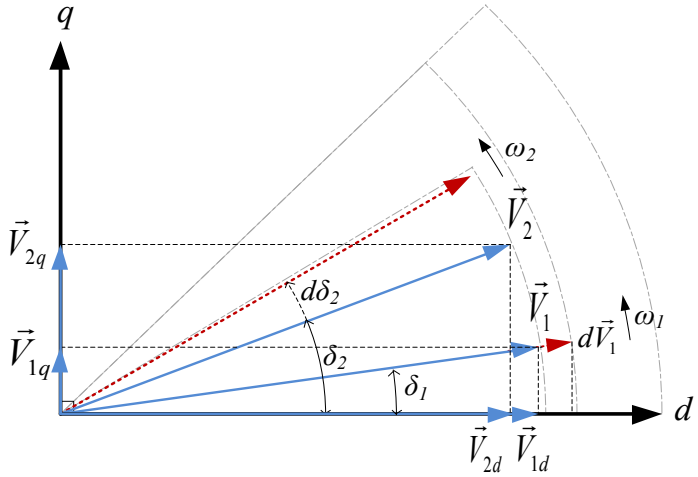

Fig. 2. Voltage vectors in reference d-q frame.

The vector V can be represented as $\vec{V} = V_d + jV_q$ Where

$$V_d = V\cos(\delta) \qquad V_q = V\sin(\delta) \qquad \delta = \arctan\left(\frac{V_q}{V_d}\right) \tag{6}$$

From (4) and fig. 2 it is shown that ω_i changes in response to the real power flow and modifies the angle δ_i. Thus, from (6) it can be expressed

$\omega = \dot{\delta} = \frac{\dot{V}_q V_d - \dot{V}_d V_q}{V_d^{\,2} + V_q^{\,2}}$ Considering $|V| = \sqrt{V_d^{\,2} + V_q^{\,2}}$ and the expressions (4), (5) and (6) it can be obtained the state equation (7) which describe the behavior of each inverter.

$$\begin{cases} \dot{\omega} = \omega_f \omega - k_p \omega_f P \\ \dot{V}_d = -\omega_f V_d - \omega V_q - \dfrac{k_p \omega_f V_d}{|V|} Q \\ \dot{V}_q = \omega V_d - \omega_f V_q - - \dfrac{k_v \omega_f V_q}{|V|} Q \end{cases} \tag{7}$$

2.2. Combined model of all the inverters and network model

In previous section the mathematical model of an individual inverter on a common reference d-q frame was discussed. Let us consider a system with two inverters connected to a network, as shown in fig. 1. The state equation for two inverters is

$$\begin{cases} \dot{\omega}_1 = \omega_{f1}\omega_1 - k_{p1}\omega_{f1}P_1 \\ \dot{V}_{d1} = -\omega_{f1}V_{d1} - \omega_1 V_{q1} - \dfrac{k_{p1}\omega_{f1}V_{d1}}{|V_1|}Q_1 \\ \dot{V}_{q1} = \omega_1 V_{d1} - \omega_{f1}V_{q1} - -\dfrac{k_{v1}\omega_{f1}V_{q1}}{|V_1|}Q_1 \\ \dot{\omega}_2 = \omega_{f2}\omega_2 - k_{p2}\omega_{f2}P_2 \\ \dot{V}_{d2} = -\omega_{f2}V_{d2} - \omega_2 V_{q2} - \dfrac{k_{p2}\omega_{f2}V_{d2}}{|V_2|}Q_2 \\ \dot{V}_{q2} = \omega_2 V_{d2} - \omega_{f2}V_{q2} - -\dfrac{k_{v2}\omega_{f2}V_{q2}}{|V_2|}Q_2 \end{cases} \tag{8}$$

The network in the fig. 1 is described by the nodal admittance matrix equation

$$\begin{bmatrix} \vec{I}_1 \\ \vec{I}_2 \end{bmatrix} = \begin{bmatrix} Y_1 + Y_3 & -Y_3 \\ -Y_3 & Y_2 + Y_3 \end{bmatrix} \begin{bmatrix} \vec{E}_1 \\ \vec{E}_2 \end{bmatrix} \rightarrow \begin{bmatrix} I_{1d} \\ I_{1q} \\ I_{2d} \\ I_{2q} \end{bmatrix} = \begin{bmatrix} G_{11} & -B_{11} & -G_{12} & B_{12} \\ B_{11} & G_{11} & -B_{12} & -G_{12} \\ G_{12} & B_{12} & G_{22} & -B_{22} \\ -B_{12} & -G_{12} & B_{22} & G_{22} \end{bmatrix} \begin{bmatrix} V_{d1} \\ V_{q1} \\ V_{d2} \\ V_{q2} \end{bmatrix} \tag{9}$$

Considering the active and reactive power equations (3) and (9),

$$\begin{bmatrix} P_1 \\ Q_1 \\ P_2 \\ Q_2 \end{bmatrix} = \begin{bmatrix} V_{d1} & V_{q1} & 0 & 0 \\ -V_{q1} & V_{d1} & 0 & 0 \\ 0 & 0 & V_{d2} & V_{q2} \\ 0 & 0 & -V_{q2} & V_{d2} \end{bmatrix} \begin{bmatrix} G_{11} & -B_{11} & -G_{12} & B_{12} \\ B_{11} & G_{11} & -B_{12} & -G_{12} \\ G_{12} & B_{12} & G_{22} & -B_{22} \\ -B_{12} & -G_{12} & B_{22} & G_{22} \end{bmatrix} \begin{bmatrix} V_{d1} \\ V_{q1} \\ V_{d2} \\ V_{q2} \end{bmatrix} \tag{10}$$

Which the above equation, combined with (8), gives the whole system equations

$$\begin{cases} \dot{X}_1 = \alpha_1 X_1 - \alpha_2\sqrt{X_2^2 + X_3^2} - \alpha_3 \dfrac{(X_2X_5 + X_3X_6)}{\sqrt{X_2^2 + X_3^2}} + \alpha_4 \dfrac{(X_3X_5 - X_2X_6)}{\sqrt{X_2^2 + X_3^2}} \\ \dot{X}_2 = \alpha_1 X_2 - X_1X_3 - \alpha_5 X_2\sqrt{X_2^2 + X_3^2} - \alpha_6 X_2 \dfrac{(X_2X_5 + X_3X_6)}{\sqrt{X_2^2 + X_3^2}} + \alpha_7 X_2 \dfrac{(X_3X_5 - X_2X_6)}{\sqrt{X_2^2 + X_3^2}} \\ \dot{X}_3 = \alpha_1 X_3 - X_1X_2 - \alpha_5 X_3\sqrt{X_2^2 + X_3^2} - \alpha_6 X_3 \dfrac{(X_2X_5 + X_3X_6)}{\sqrt{X_2^2 + X_3^2}} + \alpha_7 X_3 \dfrac{(X_3X_5 - X_2X_6)}{\sqrt{X_2^2 + X_3^2}} \\ \dot{X}_4 = \beta_1 X_4 - \beta_2\sqrt{X_5^2 + X_6^2} - \beta_3 \dfrac{(X_2X_5 + X_3X_6)}{\sqrt{X_5^2 + X_6^2}} + \beta_4 \dfrac{(X_3X_5 - X_2X_6)}{\sqrt{X_5^2 + X_6^2}} \\ \dot{X}_5 = \beta_1 X_5 - X_4X_6 - \beta_5 X_5\sqrt{X_5^2 + X_6^2} - \beta_6 X_5 \dfrac{(X_2X_5 + X_3X_6)}{\sqrt{X_5^2 + X_6^2}} + \beta_7 X_5 \dfrac{(X_3X_5 - X_2X_6)}{\sqrt{X_5^2 + X_6^2}} \\ \dot{X}_6 = \beta_1 X_6 - X_4X_5 - \beta_5 X_6\sqrt{X_5^2 + X_6^2} - \beta_6 X_6 \dfrac{(X_2X_5 + X_3X_6)}{\sqrt{X_5^2 + X_6^2}} + \beta_7 X_6 \dfrac{(X_3X_5 - X_2X_6)}{\sqrt{X_5^2 + X_6^2}} \end{cases} \tag{11}$$

Where

$\alpha_1 = -\omega_{f1};\ \alpha_2 = k_{p1}G_{11}\omega_{f1};\ \alpha_3 = k_{p1}G_{12}\omega_{f1};\ \alpha_4 = k_{p1}B_{12}\omega_{f1};\ \alpha_5 = k_{v1}B_{11}\omega_{f1};\ \alpha_6 = k_{v1}B_{12}\omega_{f1};\ \alpha_7 = k_{v1}G_{12}\omega_{f1}$

$\beta_1 = -\omega_{f2};\ \beta_2 = k_{p2}G_{22}\omega_{f2};\ \beta_3 = k_{p2}G_{12}\omega_{f2};\ \beta_4 = k_{p2}B_{12}\omega_{f2};\ \beta_5 = k_{v2}B_{22}\omega_{f2};\ \beta_6 = k_{v2}B_{12}\omega_{f2};\ \beta_7 = k_{v2}G_{12}\omega_{f2}$

3. Study of Stability for the Microgrid

In this section it is constructed a Lyapunov function for the Microgrid system and obtained the respective eigenvalues for the A matrix of lineal system.

3.1. Lyapunov's method

One of the main impediments for the application of Lyapunov's method to physical systems is the lack of formal procedures to construct the Lyapunov function for the differential equations describing the given physical system [10]. A function *V(X)* is called a Lyapunov function of the system *f(X)* where *f(0)=0* if it fulfills the following properties [11]:

i. $V(0) = 0$

ii. $V(X) > 0$ for all X

iii. $\frac{d}{dt}V(X) \le 0$ along all trajectories of the system

Then the point *X=0* is locally stable.

It is proposed to construct the Lyapunov function by using the set of representative variables for each generator. By following this principle, firstly it is chosen the square frequency variables (X1 and X4) divided into the working frequency to obtain "per unit" values and secondly it is used the dq voltage of each generator divided by the module of voltage; this method is repeated for every generator of the Microgrid. Finally, every term of the obtained Lyapunov function are multiplied by a different constant. These constants must be chosen to fulfill the iii property.

$$V(X) = \frac{AX_1^2}{\omega_k} + B\frac{X_2^2 + X_3^2}{\sqrt{X_2^2 + X_3^2}} + \frac{CX_4^2}{\omega_k} + D\frac{X_5^2 + X_6^2}{\sqrt{X_5^2 + X_6^2}} \tag{12}$$

The above equation fulfills (i) and (ii) properties as can be seen by inspection. Condition (iii) can be shown as

$$\frac{\partial V(X)}{\partial X_1}\dot{X}_1 + \frac{\partial V(X)}{\partial X_2}\dot{X}_2 + \frac{\partial V(X)}{\partial X_3}\dot{X}_3 + \frac{\partial V(X)}{\partial X_4}\dot{X}_4 + \frac{\partial V(X)}{\partial X_5} + \dot{X}_5 + \frac{\partial V(X)}{\partial X_6}\dot{X}_6 \le 0 \tag{13}$$

Hence,

$$\begin{aligned} AX_1\dot{X}_1 + B\left(X_2^2 + X_3^2\right)^{1/2} X_2\dot{X}_2 + C\left(X_2^2 + X_3^2\right)^{1/2} + DX_3\dot{X}_3 + CX_4\dot{X}_4 + \\ + E\left(X_5^2 + X_6^2\right)^{1/2} X_5\dot{X}_5 + F\left(X_5^2 + X_6^2\right)^{1/2} X_6\dot{X}_6 \le 0 \end{aligned} \tag{14}$$

Then the Lyapunov function (12) and the mathematical model (11) are simulated in MATLAB/Simulink for reaching the best values of every constant and the region where the Lyapunov function is valid and the system is stable. A first study it is used A=C; B=E and C=F.

3.2. Eigenvalues of lineal system

Considering the system of the figure 1 and the nonlineal model in (11) and applying Taylor's series around the operating point at this model, it can be obtained the state-space equations of the small-signal model. This is acceptable if variations around the operating point are assumed to be small; therefore, the small signal lineal model is $\left[\dot{\tilde{X}}\right]=[A]\left[\tilde{X}\right]$.

Finally the systems with parameters presented on Table I, the initial active and reactive output powers zero, and initial vectors V1 y V2 in phase, the A matrix values are

$$A=\begin{bmatrix} -37.7 & -0.466 & -0.936 & 0 & 0.157 & 0.944 \\ 0 & -36.57 & -0.217 & 0 & -0.94 & 0.157 \\ 154.5 & 0 & 0 & 0 & 0 & 0 \\ 0 & 0.097 & -0.956 & -37.7 & -0.34 & -0.97 \\ 0 & -0.954 & 0.097 & -9.86 & -36.5 & -2.42 \\ 0 & -0.061 & 0.006 & 154.9 & -2.32 & -0.15 \end{bmatrix}$$

And the respective eigenvalues are $\lambda_1=0;\ \lambda_2=-10.8;\ \lambda_3=-26.9;\ \lambda_4=-35.7\ \lambda_5=-37.7;\ \lambda_6=-37.5;$
According to [8] only the nonzero eigenvalues are important for the stability studies. The system has five negative real eigenvalues, and then it is a stable point.

Table I. System parameters.

Variable	Value	unit
Line transmission (Z_3)	0.5+3i	Ω
Local load (Z_1)	13+6i	Ω
Local load (Z_2)	25+13i	Ω
Cut-off freq. of measuring filter (ω_f)	37.7	rd/s
Frequency droop coefficient (k_p)	0.0005	rd/s/W
Frequency droop coefficient (k_v)	0.0005	V/VAR
Nominal frequency	377	rd/s

4. Simulation Results

The methodology used is as follows; firstly of all the Microgrid system is implemented be means of the power electronics toolbox of Matlab/SIMULINK, the system parameters for simulation are shown in table I. Secondly, the simulated values of every state variable in the operating point are used to find the A matrix values and its eigenvalues. This eigenvalues are used to determinate the stability of the system. After that, it is utilized the set of equation (11) to verified the model and then the values of the state variables and its derivatives are used to evaluate the Lyapunov function. Finally it is studied the Lyapunov function and it is determined the region of stability of the system.

The fig 3 shows the PQ power simulation by means of the Power electronic toolbox. This was repeated with a different line inductor values (from 8mH to 0.5mH with step of 0.5mH). For each simulation the values of state variables at the operating point were saved and these were used to study the small signal stability.

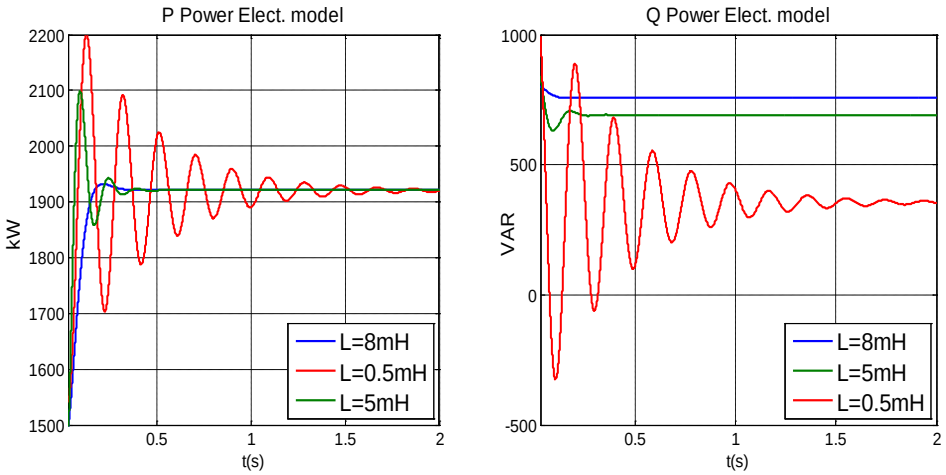

Fig. 3. Simulation results of a DG Microgrid system by means of Power Electronics tools

The fig 4 shows the PQ power simulation by means of nonlineal model of the Microgrid systems obtained in 2.2. It can be seen the same behavior in both transient and steady state values. As explained previously, the line inductance was varied for the nonlineal model. The values of state variables were used to validate the Lyapunov function.

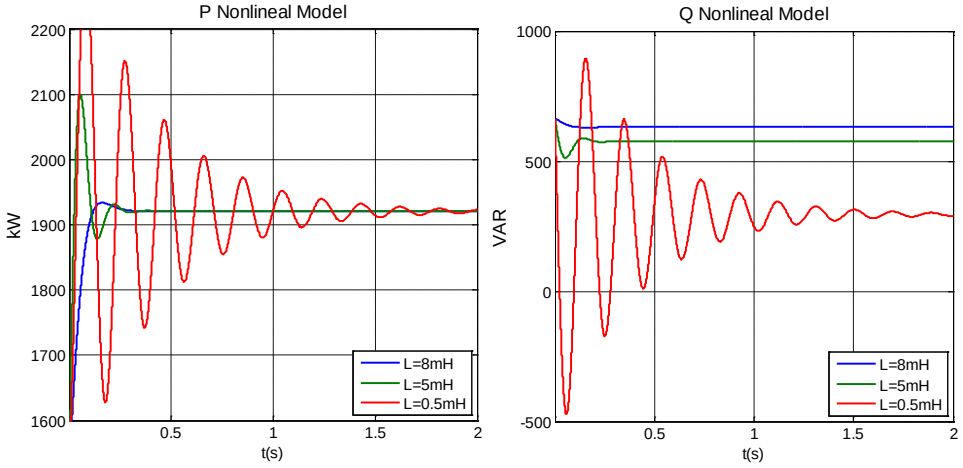

Fig. 4. Simulation results of a DG Microgrid system by means of Nonlineal model.

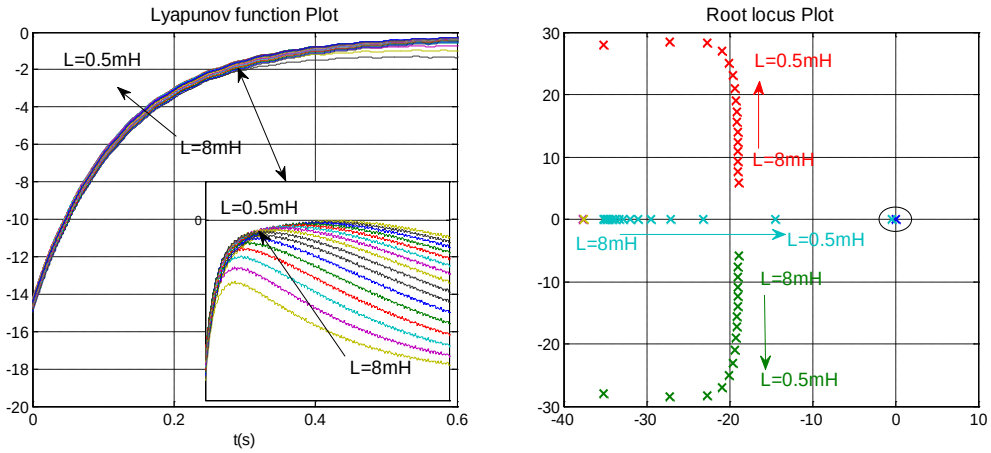

Fig. 5. Study of stability by means of Lyapunov function and root locus plot.

Fig 5 shows the study of stability by using the Lyapunov function and the root locus plot. They can be seen how the stability is affected when the line inductance decrease. The transient stability analysis by a Lyapunov method evaluate all variations starting in around a stable point that converge to it, therefore it can determine the lowest value of V(X) on the surface $\dot{V}(X) = 0$ and by this way the region of asymptotic stability is determined. The small signal stability analysis by a root locus plot shows how the roots are moved when the line inductor decreases, but cannot give an "a priori" region of asymptotic stability.

5. Conclusions

In this paper, a nonlinear state-space model of a Microgrid is presented. The model includes the most important dynamics. This modeling method is able to be extended to n-generators. The model has been analyzed by means of both stability studies Lyapunov function and root locus plot. A general methodology to find a valid Lyapunov function for non linear stability analysis has been presented. Using that Lyapunov function the region of asymptotic stability can be determined. These tools will allow the design of Microgrid systems with loads, generators and storage systems assuring the global stability of the system.

References

[1] A. G. Madureira, Coordinated voltage support in distribution networks with distributed generation and microgrids, IET Renewable Power Generation, 2009, pp. 439 – 454.

[2] P. N. Vovos, Centralized and Distributed Voltage Control: Impact on D istributed Generation Penetration, IEEE Transactions on Power Systems, 2007, pp. 476 – 483.

[3] C. L. Chen, State-space modeling, analysis, and implementation of paralleled inverters for microgrid applications, Applied Power Electronics Conference and Exposition (APEC), 2010, pp. 619 – 626.

[4] A. Arulampalam, Control of power electronic interfaces in distributed generation microgrids, International Journal of Electronics, 2004, pp. 503 – 523.

[5] N. Pogaku, Modeling, Analysis and Testing of Autonomous Operation of an Inverter-Based Microgrid, IEEE Transactions on Power Electronics, 2007, pp. 613 – 625.

[6] N. L. Soultanis, A Stability Algorithm for the Dynamic Analysis of Inverter Dominated Unbalanced LV Microgrids, IEEE Transactions on Power Systems, 2007, pp. 294 – 304.

[7] J. Guerrero, A wireless controller to enhance dynamic performance of parallel inverters in distributed generation system, IEEE Transactions on Power Electronics, 2004.

[8] P. Duminda, Stability Analysis of Microgrids with Constant Power Loads, Sustainable ICSET 2008. IEEE International Conference on Energy Technologies, 2008.

[9] E.A.A. Coelho, Small-Signal Stability for Parallel-Connected Inverters in Stand-Alone AC Supply Systems, IEEE Transactions on Industry Applications, 2002, pp. 533 – 542.

[10] A. Bacciotti, Liapunov Function and Stability in Control Theory, Springer, 2nd edition, 2005, pp. 27 – 80.

[11] H. Khalil, Nonlinear Systems. Prentice Hall, 2nd edition, 1996.

Optimal Design of a Small Permanent Magnet Wind Generator for Rectified Loads

Jawad Faiz[1,*], Nariman Zareh [1]

[1]*Center of Excellence on Applied Electromagnetic Systems, School of Electrical and Computer Engineering, University of Tehran, Tehran, Iran*
** Corresponding author. Tel: +98 61114223, Fax: +98 88533029, E-mail: jfaiz@ut.ac.ir*

Abstract: This paper presents an optimal design procedure for a small permanent magnet wind generator which supplies a full-bridge diode rectified load. The aim is to improve the output voltage waveform of the generator. An electromagnetic-thermal design algorithm is proposed based on an analytical model of a surface-mounted permanent magnet generator. A comprehensive combined model, consisting of design program and simulation of the designed generator under rectified load, is utilized. Design variables are optimized over their appropriate limits using a genetic algorithm. The results indicate the improvement of the output voltage waveform.

Keywords: *Wind Generator, Permanent Magnet Machine, Optimal Design*

Nomenclature

U	*rated wind velocity……..m/s*	D	*air gap diameter……..m*
U_{mean}	*dominant mean velocity of wind..m/s*	$B_{sat\text{-}s}$, $B_{sat\text{-}r}$	*stator, rotor saturated flux density... T*
β	*pitch angle……..rad.*	P	*pole numbers*
R	*blade radius……m*	K_{w1}	*winding factor*
ω_r	*shaft angular speed……rad/s*	C_φ	*flux conical factor*
$C_p(\lambda,\beta)$	*turbine aerodynamic efficiency.… %*	K_c	*carter coefficient*
η_{gen}	*efficiency of generator……%*	p_{rl}	*normalized rotor leakage peamability*
P_{gen}	*rated output electrical power ….....W*	K_s	*stator lamination factor*
n_s	*rotation speed……rpm*	τ_s	*stator slot pitch (πD/S)*
SML_{pk}	*peak specific magnetic loading…..T*	THD_v	*voltage time harmonic distortion*
SEL_{pk}	*specific electric loading……A/m*	K	*shape parameter*
h_{sy},h_{ry}	*stator and rotor yoke height…....m*	$\lambda(\omega_r R/U)$	*tip speed ratio*
w_s	*stator slot width (τ_s-w_t)……..m*	μ_r	*relative permeability*

1. Introduction

Permanent magnet generator (PMG) is a self-excited system and it can be a proper choice to coupling it to wind turbine. The output of the generator can charge the batteries or supply inverter or both [1]. There are different techniques to connect a DC bus (with power electronics devices) to the PMG [2]. Utilization of rectified loads distorts the output voltage waveform of the PMG leading to a low quality power delivered to the load. A proper operation of the generator under such conditions requires a precise design optimization of the PMG. Such design needs an appropriate modeling and comprehensive design algorithm.

Details of PMG design for direct coupling to a wind turbine has been given in [3] in which four configurations including radial-flux, axial-flux, cross-field-flux and claw-pole generators have been compared based on the air gap flux density, copper losses, PM weakening and the system cost. This comparison indicates that a radial-flux, internal-PM is a proper choice for designing a 400 kW generator. Application of different configurations of PMG for wind turbine has been proposed in [4] and 60 configurations has been compared based on the torque density and also cost per developed torque function. It shows a radial-flux PMG using surface-mounted Ferrite PMs has a better performance compared with the internal PM

version. In [5], the axial-flux and radial-flux PMGs, for direct driven wind turbine, have been optimized based on the cost per developed torque objective function. The results indicate that the radial-flux machines have lower cost and torque density. In [6], two types of radial-flux PMG (internal- and surface-mounted PM) with inner rotor structures for direct coupling to wind turbine are analyzed and compared. The electromagnetic behavior of generators and optimal shape of the PMs have been estimated by finite element method (FEM). The results indicate lower torque ripples in the surface-mounted PMG. Design and performance analysis of an ironless axial-flux PMG have been proposed in [7] and [8]. The particular ironless machine configuration leads to a longer effective air gap of the machine. Also a multi-variable optimization algorithm based on the design parameters for improvement of the PMG performance of the machine has been introduced. Finally, a prototype 3.5 kW machine has been built and tested in which noise, cogging torque and copper losses have been reduced in expense of heavier machine. In [9], a small radial- and axial-flux wind generators have been optimally designed using an optimization algorithm based on population growth which tries to maximize annual energy gaining from variable speed wind turbine-generator. However, thermal analysis of the PMG has been neglected.

In recent years application of power electronics components in variable speed drives and controlling output of generators has been increased. Therefore, a reliable, economical design and satisfactory operation of these machines are crucial. This paper considers the electromechanical conversion of wind energy. Electromagnetic design procedure of a surface-mounted radial-flux PMG and its thermal model are proposed. A comprehensive combined model consisting of the generator design routine and simultaneous simulation of the typical design in the presence of a rectified load is introduced and impact of this type of load upon the distortion of the output voltage waveform of the generator is studied. Finally, the design optimization procedure is proposed to achieve a near sinusoidal output voltage waveform.

2. Electromechanical Conversion of Wind Energy

Wind speed is modeled as a continuous stochastic variable. The probability of the occurrence of a define wind velocity can be expressed by a probability density function. Comparisons of the measured wind speeds show that if the time interval is long enough, the Weibull distribution function is suitable to describe the wind velocity [10, 11]:

$$f(U) = \frac{k}{c}\left(\frac{U}{c}\right)^{k-1} e^{-\left(\frac{U}{c}\right)^{k}} \tag{1}$$

where k=2 and c is the magnification parameter ($2U_{mean}/\sqrt{\pi}$). *A portion of the wind energy transmitted* to the shaft is converted into mechanical energy by blades of the turbine and its efficiency depends on the blades profile, and air density. Wind energy converted into mechanical energy (P_{shaft}) is:

$$P_{shaft} = 0.5\rho_{air}\pi R^2 U^3 \left(0.51\left(\frac{116}{\lambda_1} - 0.4\beta - 5\right)e^{-\frac{21}{\lambda_1}} + 0.006\lambda\right) \tag{2}$$

Nowadays most horizontal three-blade turbines are designed as such that their operating point are placed in the range of 5 to 7 m/s. In this case, turbine operates with maximum $C_p(\lambda,\beta)$ between 0.35 and 0.45 [9]. R and ω_r can be determined as follows:

$$R = \sqrt{\frac{P_{gen}}{\frac{1}{2}\rho_{air}\pi U^3 C_P \eta_{gen}}}$$

$$\omega_r = \sqrt{\frac{\frac{1}{2}\rho_{air}\pi\lambda^2 U^5 C_P \eta_{gen}}{P_{gen}}} \tag{3}$$

(4)

Eqns. (3) and (4) can be used as a guide for estimation of *R* and *U* in the design process of the small wind generator.

3. Design of PMG

Low-Carbon soft-steel is used in the rotor and silicon-steel laminations in the stator of PMG. The slot has semi-closed shape. The PM (NdFeB) pieces are mounted on the external surface of the rotor. The apparent power of the air gap of a radial-flux generator (S_g) versus the main dimensions of the machine is as follows [12]:

$$S_g = \frac{1}{2}\pi^2 . K_{w1} . D^2 L . n_s . SML_{pk} . SEL_{pk} \tag{5}$$

Product D^2L determines the capability of the energy absorbed by the turbine:

$$D^2 L = \frac{\varepsilon P_{gen}}{0.5\pi^2 . K_{W1} . n_s . SML_{pk} . SEL_{pk} . \cos\varphi} \tag{6}$$

where $\varepsilon = E_f / V_a$. Ratio $K_L = L/D$ is chosen in the range of 0.14 and 0.50 based on the main design and available backgrounds [12-14]. Therefore, diameter and stack length are evaluated using this ratio. In choosing *D* a particular attention must be paid to the required *P* and a proper pole pitch. On the other hand, in order to reduce the overhang copper losses and its additional expense, *D* must be limited as possible.

3.1. Magnetic Design

The generator pole numbers, PM dimensions, stator and rotor dimensions are determined in this stage.

Air gap Flux Density: The air gap flux density is limited by saturation level of the stator teeth. An appropriate value for SML_{pk} is 0.9 T. This can hold a relative balance between the magnetic circuit saturation and power absorption capability of PMG [15, 16].
Generator Poles Number: Frequency range of small PMGs is between 10 and 70 Hz or 30 and 80 Hz [9]. Therefore, the rated frequency of the generator can be chosen in the range of 45-65 Hz and P is then calculated. Conventional PM machines have normally low P and the pole pitch is considerably larger than the PM pitch; therefore, the pole arc to PM arc ratio (α) is not so crucial. However, in wind PMG, P is high and pole pitch and PM pitch are comparable and suggested range is between 0.67 and 0.77 [14].
PM Dimensions: Operating point of the magnetic circuit can be determined by intersection of the PM demagnetization curve and load line of the magnetic circuit. The slope of the load line shows the resistance of the PM against demagnetizing. A security margin in a surface-mounted PMG is guaranteed by choosing PC≥6. The PM length is estimated as follows [13]:

$$l_m = (PC - p_{rl}\mu_r) . C_\phi K_c l_g \tag{7}$$

p_{rl} is typically between 0.05 and 0.2 [15]. As seen, the required length of PM for providing the excitation flux depends on the air gap length. The air gap length in this design is taken to be about 0.01*D*.
Dimensions of Stator and Rotor: To prevent the saturation of the PMG yoke, a special attention must be paid to the dimensions and cross-section of the yoke. Assume a define stack length for PMG; the height of the yoke is evaluated as follows [17]:

$$h_{sy} > \frac{\alpha \pi D}{4pK_s} \cdot \frac{B_g}{B_{sat-s}} \tag{8}$$

$$h_{ry} > \frac{\alpha \pi (D - 2l_{m)}}{4p} \cdot \frac{B_g}{B_{sat-r}} \tag{9}$$

In order to be ensuring about non-saturated teeth of the stator, the following constraint must be held [17]:

$$w_t > \frac{\tau_s}{K_s} \cdot \frac{B_g}{B_{sat-s}} \tag{10}$$

In most electrical machines w_s is taken to be almost equal to the tooth width as such that $0.5<w_s/\tau_s<0.6$ [18]. However, if $w_s=w_t=0.5\tau_s$, the product of the electric and magnet loading approaches its peak value, and this maximizes the power absorption capability of PMG. Therefore, in a PMG with equal slot and tooth width, the non-saturation condition is as follows:

$$B_g < \frac{1}{2} . K_s . B_{sat-s} \tag{11}$$

3.2. Electrical Design

SEL_{pk} of a PMG is limited by the slot filling factor, slot height and stator conductors current density. The typical range of SEL_{pk} for a PMG is 1000 to 4000 A/m [9]. For low-voltage PMGs, the slot filling factor is in the range of 0.3 and 0.5 and current density of the stator conductors is between 3 and 8 A/mm^2. Of course, for higher current density up to 10 A/mm^2, class F insulation for windings and a proper cooling system are suggested [16]. For given SEL_{pk}, filling factor and conductor current density in a radial PMG with elliptic slots, the slot height is as follows [9]:

$$h_s = \frac{SEL_{pk}}{\sqrt{2} . J . K_{sf} . (1 - w_t / \tau_s)} \tag{12}$$

3.3. Thermal Modeling of PMG

Thermal analysis of any electrical machine is a crucial stage of the design process. Different models, depending on the required precision and complexity, have been so far proposed for thermal analysis of the PM machines. Here, an equivalent thermal-resistance network is used [18] to estimate the temperature distribution over 8 different points of PMG. To use the model, the corresponding losses of any node are calculated and by applying the losses to the resistance network, the temperature rise of the above-mentioned points are evaluated. A particular attention must be paid to the temperature rise of the PM and winding in PMG. Conducting resistance between any two-node is used to complete the 8 points in the equivalent thermal model of the motor as seen in Fig. 1. Computation procedure for the resistances is complicated and it is necessary to take into account the precise heat flow, heat convection, internal heat generation sources, different materials and dimensions of the PMG. To simplify the model, heat transfer between the PMG and cooling environment is considered assuming a mean temperature for the cooling material (15 degrees).

Two nodes have been assigned to the stator, one node to the yoke and one node to the tooth. In the full-load PMG, windings are the main source of the generated heat. Two nodes are considered in the model, one for the conductors in the slots and one for the end windings. Prediction of the PMs temperature rise is important in the thermal modeling of the PMG,

therefore one node is assigned to the PMs. Estimation of the temperature rise of PMG by n+1 thermal networks need to solve n related equations. These equations are extracted from $\theta = G^{-1}P_d$ [18], where P_d is the dissipated losses vector corresponding to any node and θ is the temperature rise vector. Thermal resistances model for forming the thermal conduction matrix G is as follows:

$$G = \begin{bmatrix} \sum_{i=1}^{n} \frac{1}{R_{1,i}} & -\frac{1}{R_{1,2}} & \cdots & -\frac{1}{R_{1,n}} \\ -\frac{1}{R_{2,1}} & \sum_{i=1}^{n} \frac{1}{R_{2,i}} & & -\frac{1}{R_{2,n}} \\ \vdots & \vdots & \ddots & \vdots \\ -\frac{1}{R_{n,1}} & -\frac{1}{R_{n,2}} & \cdots & \sum_{i=1}^{n} \frac{1}{R_{n,i}} \end{bmatrix} \quad (13)$$

This model is used in the final stage of the electromagnetic design of PMG temperature constraints are maximum permissible temperature of winding=120°C, and PM=100°C. If these constraints are satisfied, the design will be completed; otherwise the design process returns to the initial stage of the design routine and necessary modifications for the current density and magnetic flux density are made in order to decrease the heat and thus losses.

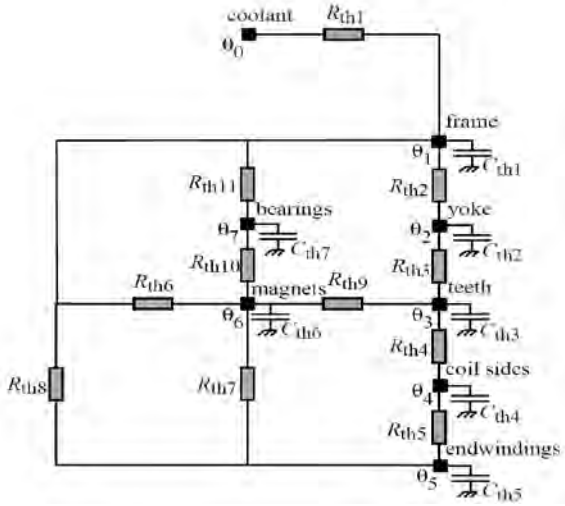

Fig. 1. Equivalent circuit of thermal model of PMG [18]

3.4. Cost Estimation for PMG Manufacturing

The cost of manufacturing a machine in an industrial plant is under influence of many factors such as identical built machines every year, technology and automation level used, organizing the product process, expense of the skilled labor, and quality of materials used. Since, here it is not possible to take into account all the above-mentioned factors in a mathematical model for cost estimation, a logical procedure is followed and the active materials of the machine are considered to evaluate the cost index and express it as a function of the dimensions of the PMG. The active materials of a PMG consist of PM, copper and iron used in the rotor and stator. Therefore, the cost index of a PMG is approximated as follows:

$$C_{total} = C_{PM}.\rho_{PM}.V_{PM} + C_{cu}.\rho_{cu}.V_{cu} + C_{fe}.\rho_{fe}.V_{fe} \quad (14)$$

where ρ is the density, V is the volume and C is the unit weight cost of the materials. The cost of each material includes: Iron 1.65 €, PM 50 € and Copper 3.1 €.

3.5. Synthetic Simulation Model

To study the impact of a rectified load upon the PMG operation, a synthetic comprehensive system consisting of simultaneous generator design routine and simulation has been proposed and applied. In this system, first the design routine calculates characteristics of the generator based on the proposed voltage, power, power factor and frequency; then turbine-generator-rectifier set included in Simulink receives the required data such as flux-linkage under each pole, resistance, inductance and poles number. At the end of simulation process, voltage waveform and performance characteristics of generator are determined. In this system, generator design algorithm is programmed. At the end of design routine, system model consisting of turbine, generator and rectifier system are implemented.

A 3 kW, 220 V, 50 Hz optimally designed PMG based on efficiency [9] is re-designed here in the presence of a nominal rectified load. The generator voltage waveform has been presented in Fig. 2. The results show that the harmonic distortion index of the voltage waveform is 15.5% which indicates the low quality output power of the PMG.

3.6. Optimization

As shown in Fig. 2, rectified load distorts the output voltage waveform and a genetic algorithm is implemented to improve the output voltage waveform. For this a fitness function based on the THD_v reduction is defined as follows:

$$Fitness\ Function = \frac{1}{THD_v} \tag{15}$$

Test designs on the wind PMG are obtained and the corresponding fitness functions are evaluated, then new design is generated by combining the best previous results. The PM residual flux density, ratio between the stack length and air gap diameter, PM arc, number of slot per pole per phase, magnetic permeance coefficient, specific electrical loading and current density are taken as design variables.

Also the range of variables values has been restricted to reasonable limits as shown in Table 1. Fig. 3 shows the obtained voltage waveforms based on the objective function of (15). Table 2 summarizes the design details of two generators. Referring to the obtained results in the design with optimal voltage, THD of voltage improves 9%. The induced voltage is Ldi/dt, and THD can be reduced by decreasing the number of winding turns.

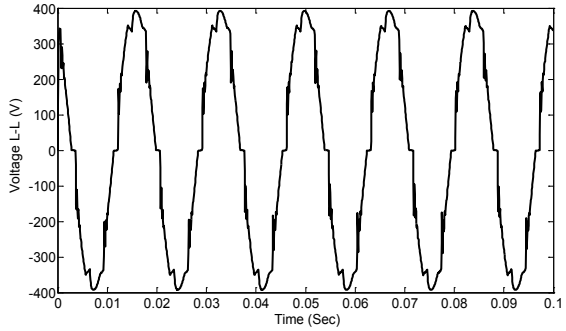

Fig. 2. Non-optimal induced line voltage of a generator under rectified load

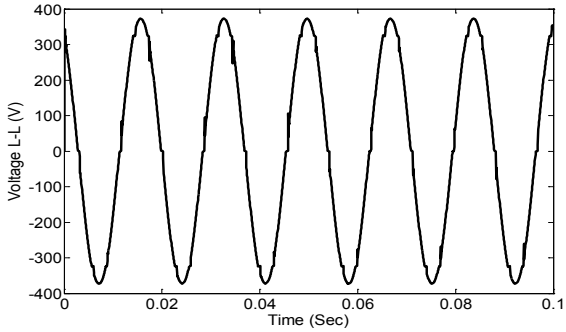

Fig. 3. Optimal induced line voltage of generator under rectified load

Also contribution of the PM arc in the pole of PMG rises in order to compensate the back-emf. Following these improvements, voltage distortion is reduced, but considering the increase *SEL* and *SML*, the magnetic loading is decreased to provide the required power. Consequents of these changes are: rising the iron losses due to the increase of the air gap flux

density, increasing the cost due to increase of PM volume, decreasing copper losses due to lower number of winding turns and resistance. Since the losses distribution in the optimal design of the PMG is subject to the change of the temperature rise of the six above-mentioned points, the PMG are in the permissible ranges

Table 1. Constraints of variables in optimization routine.

Parameter	Symbol	Value
PM residual density (T)	B_r	1-1.4
PM arc (ºElec)	A	90-170
Current density (A/mm^2)	J	3-8
Specific electrical loading (kA/m)	SEL	10-40
Air gap width to diameter ratio	k_L	0.2-1
Slot No./pole/phase	Q	1-2
Magnetic permeance coefficient	PC	5-16

Table 2. Comparison of design and performance of a 3 kW, 220 V and 60 Hz PMG with optimal efficiency and voltage in presence of rectified load (U=12 m/s).

Parameter	Symbol	Optimal Efficiency	Optimal Voltage
Shaft speed (rpm)	N_m	440/66	440/66
Generator stack length (m)	L	0.1437	0.164
Air gap diameter (m)	D	0.1437	0.232
PM arc (elec. Deg.)	A	144	157.5
PM height (m)	l_m	0.01	0.0183
PM residual flux density (T)	B_s	1.2	1.25
Phase winding no. of turns	N_{ph}	N_{ph}	176
No. of slots/phase/pole	q	1	2
Air gap length (m)	l_g	0.0011	0.0012
Winding diameter (m)	D_{cond}	0.0011	0.0013
Copper losses/Iron losses (W)	P_{cu}/P_{fe}	95.9/80.8	56.5/136.6
Power factor	Pf	91	93
Efficiency (%)	η	94.18	93.1
Air gap flux density (T)	B_g	0.72	0.79
Specific electric loading (kA/m)	SEL	30	10
Winding current density (A/mm^2)	J	5	3.64
THDv (%)	-----	15.5	5.7
Materials cost (€)	Cost	249.9	776.4
Stator winding resistance (Ω)	R_s	2.55	1.27
Stator winding leakage inductance (H)	L_l	0.003	0.00064
Stator winding mutual inductance (H)	L_m	0.005	0.0011

4. Conclusion

In this paper a comprehensive electromagnetic-thermal design algorithm for a wind PMG was presented. A combined model consisting of simultaneous generator design program and simulation in the presence of a rectified load was used to study the impact of this type of load upon the induced voltage distortion. Base on the presented model and genetic algorithm optimization routine, specifications of an optimal generator for improvement of the induced output voltage waveform of the PMG were obtained which leads to 9% decrease of the harmonic distortion index.

References

[1] L. Hansen, F. Blaabjerg, Conceptual survey of Generators and Power Electronics for Wind Turbines, Riso National Laboratory Report, December 2001.

[2] .Baroudi, V.Dinavahi, A.Knight, A Review of Power Converter topologies for Wind Generators, IEEE Conference on Renewable Energies, Canada, Sep. 2005.

[3] E. Spooner, A.C. Williamson, Direct-coupled, Permanent-magnet Generators for Wind Turbine Applications, IEE Proc. B, Electr. Power Appl., Vol. 143, pp. 1-8, Jan. 1996.

[4] M.R. Dubois, H. Polinder, J.A. Ferreira, Comparison of Generator Topologies for Direct-drive Wind Turbines, ICEM 92, pp. 761-765, Manchester, UK, 1992.

[5] M.R. Dubois, H. Polinder, J.A. Ferreira, Axial and Radial-Flux Permanent Magnet Generators for Direct-Drive Wind Turbines, EWEC, Copenhagen, Denmark, 2001.

[6] S. A. Papathanassiou, A. G. Kladas, M. P. Papadopoulos, Direct-Coupled Permanent Magnet Wind Turbine Design Considerations, European Wind Energy Conference (EWEC'99), Nice, France, 1999.

[7] N.F. Lombard, Design and Evaluation of an Ironless Stator Axial Flux PM Machine, M. Eng. Thesis, University of Stellenbosch, Matieland, South Africa, 1997.

[8] N. F. Lombard, M. J. Kamper, Analysis and Performance of an Ironless Stator Axial Flux PM Machine, IEEE Trans. Energy Conversion, Vol. 14, pp.1051-1056, Dec. 1999.

[9] M.A.Khan, Contributions to Permanent Magnet Wind Generator Design Including the Application of Soft Magnetic Composites, PhD. Thesis, University of Cape Town, 2006.

[10] M. R. Patel, Wind and Solar Power Systems, CRC Press,1999.

[11] Andreas Petersson, Analysis, Modeling and Control of Doubly-Fed Induction Generators for Wind Turbines, Ph.D. Dissertation, Chalmers University of Technology, 2005.

[12] M.A.Khan, P.Pillay, Design of a PM Wind, Optimized for Energy Capture over a Wide Operating Range, IEEE Conference on Electrical Machines and Drives, Spain, 2005.

[13] P. Lampola, J. Perho, Electromagnetic Analysis of a Low-Speed Permanent-Magnet Wind Generator, IEE Opportunity and Advances in International Power Generation Conf., pp. 55-58, 1996.

[14] N. Bianchi and A. Lorenzoni, Permanent Magnet Generators for Wind Power Industry: An Overall Comparison with Traditional Generators, IEE Opportunity and Advances in International Power Generation Conf., pp.49-54, 1996.

[15] T. J. E. Miller, Brushless Permanent-Magnet and Reluctance Motor Drives, New York: Oxford University Press, 1989.

[16] G. R. Slemon, Design of Permanent Magnet AC Motors for Variable Speed Drives, Tutorial Course of IEEE-IAS Annual Meeting,, Michigan: IEEE, 1991.

[17] S. Huang, J. Luo, F. Leonardi, and T. A. Lipo, A General Approach to Sizing and Power Density Equations for Comparison of Electrical Machines, IEEE Trans. Ind. Applications, vol. 34, pp. 92-97, Jan. / Feb. 1998.

[18] J. Lindstrom, Thermal Model of a P ermanent-Magnet Motor for a Hybrid Electric Vehicle, Ph.D. Thesis, Dept. of Electric Power Engineering, Chalmers University of Technology, Sweden, 1999.

Storage of Renewable Electricity through Hydrogen Production

Christoph Stiller[1], Patrick Schmidt[1], Jan Michalski[1,*]

[1] *Ludwig-Bölkow-Systemtechnik GmbH, Daimlerstr. 15, 85521 Munich/Ottobrunn, Germany*
** Corresponding author. Tel: +49 8960811041, E-mail:christoph.stiller@LBST.de*

Abstract: With more than 20 GW of installed wind power capacity installed in Northern Germany and more to come when offshore wind power expands, there are periods when the available wind power exceeds the grid capacity or even the electricity demand in reach. This excess wind power could be utilised for the electrolytic production of hydrogen, which can be stored and used as a transportation fuel, feedstock for the chemical industry, for re-electrification or for natural gas (NG) pipeline injection.
Based on the potential availability of excess wind power for hydrogen production and in view of the expected build-out, the paper drafts and discusses the economic framework and modalities of hydrogen production. Potential usages are discussed in general and specially for Northern Germany, where a hydrogen demand of 320 mill. Nm^3 was identified by 2020 for industry and transportation.
With some initial incentives, electrolytic hydrogen production can be made competitive by 2020. It is concluded that Northern Germany is an ideal region for the production of hydrogen from renewables due to the its high wind power density, its geologic conditions allowing for cavern storage, its industrial demand for hydrogen and also its pioneering role in hydrogen fuelled road transportation.

Keywords: *Hydrogen, Storage, Electrolysis.*

1. Introduction

With the increasing renewable power capacity, especially wind power, installed in many countries, there will be periods when the available power exceeds the capacity of the grid or even the demand in reach. This excess electricity may be eliminated by cutting down renewable power feed-in or, more advantageously, by adding additional temporal demand through electricity storage devices. In countries without excessive potential for pumped hydro storage, the storage technology with the highest energetic potential is offered by hydrogen. Hydrogen can be produced from electricity by water electrolysis and stored inexpensively in underground salt caverns where geologic conditions are suitable, or at higher costs in aboveground pressure vessels or liquid dewars. The hydrogen can be used for power generation when renewable generation is low, but also as a transportation fuel, as a feedstock for the chemical industry or other purposes. Therewith, hydrogen not only makes renewable electricity storable over long periods but also creates cross-links to other energy-intensive sectors.

This paper presents the main results of a recent study on the potentials of hydrogen production from wind power in Northern Germany [1], where more than 20 GW of wind power capacity are installed today and there will be tremendous increases in the coming years due to the expansion of offshore wind power. It will first review the current framework of the German electricity generation. Then, based on the expected electricity generation and demand, the amount of excess power available for hydrogen production will be estimated. This will be followed by a discussion of operation models for hydrogen electrolysis, rounded off by a discussion of required storage demand and possible uses and costs of the hydrogen.

2. General framework of the German electricity generation

Since 1990, electricity production in Germany has only increased by about 0.8% p.a. on average, and almost the entire surplus has been covered by renewable electricity [2].

Due to the age structure of the power plant park and in view of the previously planned nuclear phase-out, currently a large number of new fossil power plant projects (especially hard coal) are in the planning phase; yet, it needs to be mentioned that the realization of many projects is becoming ever more uncertain, partly due to the postponement of the nuclear phase-out but also due to decreasing public acceptance for infrastructure projects [3].

The share of renewables for electricity production in Germany has increased from 10 to 15% in only three years (2005-2008), and for 2011 the Transmission System Operators (TSOs) expect a total of 112 TWh renewable electricity, representing almost 20% of overall production [4]. Highest shares are being achieved in the North (e.g., in Schleswig-Holstein, renewable energy generation, mainly wind power, exceeds 40% of the electricity demand). Specifically in regions with high intermittent renewable capacities installed, already today grid capacity issues occur and wind turbine power need to be cut off temporarily in order not to cause grid breakdown (regulated in the renewable energy law as "feed-in management") [5]. Further extensive renewable potentials lie within repowering of onshore wind farms and the build-out of offshore wind energy use in the North and Baltic Sea.

By 2020, according to the "Lead scenario 2009" [6], 33 GW from onshore and 9 GW from offshore wind power are expected to be fed into the German grid. The offshore feed-in is expected to grow to 24 GW by 2030. Since all offshore capacity is landed in Northern Germany (mainly in Schleswig-Holstein and Lower Saxony) where also the density of onshore generation is high, this will at times cause massive excess power production. This implies grid reinforcement and extension to transmit the power to neighboring regions; however, even Germany-wide power production may exceed the demand and export capacities at times of low load and high wind.

Possible remedies are the temporal shift of loads by demand-side management and battery electric vehicles; however, potentials are limited both with respect to quantities and time periods over which the loads can be bridged [7]. Therefore, large-scale electricity storage will be urgently required in order to more easily integrate the further increase in intermittent renewable electricity generation into the grid.

3. Availability of excess power for hydrogen production

In order to analyse the potentials of hydrogen production from excess renewable electricity, the quantities of power surplus have to be estimated. In this sense "excess power/electricity" will be defined as the portion of power/electricity which cannot be utilised in times of high generation (renewable+fossil+nuclear) and low demand as well as export capacities of a region. In such cases the renewable generation will have to be cut off in order to assure grid stability. The quantity of excess power production depends mainly on the following four factors:

- Installed capacity of intermittent renewables, especially wind power. The feed-in of photovoltaics is less relevant in this context as it provides electricity during daytime where demand is comparatively high.
- Installed capacity of conventional power plants, especially base load plants. In particular, lignite and nuclear power plants are operated at high load also in times of high winds increasing the excess power. For example, during the night of October 4th, 2009, high wind volume and low electricity demand resulted in the negative spot market price of 0.50 €/kWh. Since at this time German nuclear power plants still operated at an average load of 77%, lignite at 65%, hard coal at 12% and natural gas at

9% [8] we assume this capacity utilization as the minimum practical part load of conventional plants during situations with excess electricity.

- Electricity demand and demand profile of the region. In general, the excess electricity can be reduced either by demand-side management or by an increased demand for a given level of power supply.
- Export capacity to neighbour regions. This is not only limited by the available transfer capacities, but also by the fact that adjacent regions are meteorologically linked. In this sense, excess wind power generation may occur not only in Northern Germany but also in other regions with own wind parks. In consequence, extension of grid capacity alone is not always effective to reduce excess power.

For the calculation of the excess power, specific assumptions regarding the capacity of energy generation per type and demand curves had to be made. The minimum generation of dispatchable power plants was derived from the estimated available capacity and the minimum part load numbers mentioned above. Onshore wind power curves were based on scaled Germany-wide production curves of the reference year 2008. Wind speed data from FINO platforms in the North and Baltic Sea were used in order to calculate the offshore power curves based on the characteristics of a 5 MW turbine. To estimate the electricity demand, hourly data from 2008 provided by UCTE / ENTSOE [9] were scaled to the respective future demand. Due to metrological linkages between adjacent regions, electricity export to neighbour countries was not considered as a way to use excess electricity. From the comparison of resulting generation and demand, the excess power generation could be estimated as shown in Figure 1.

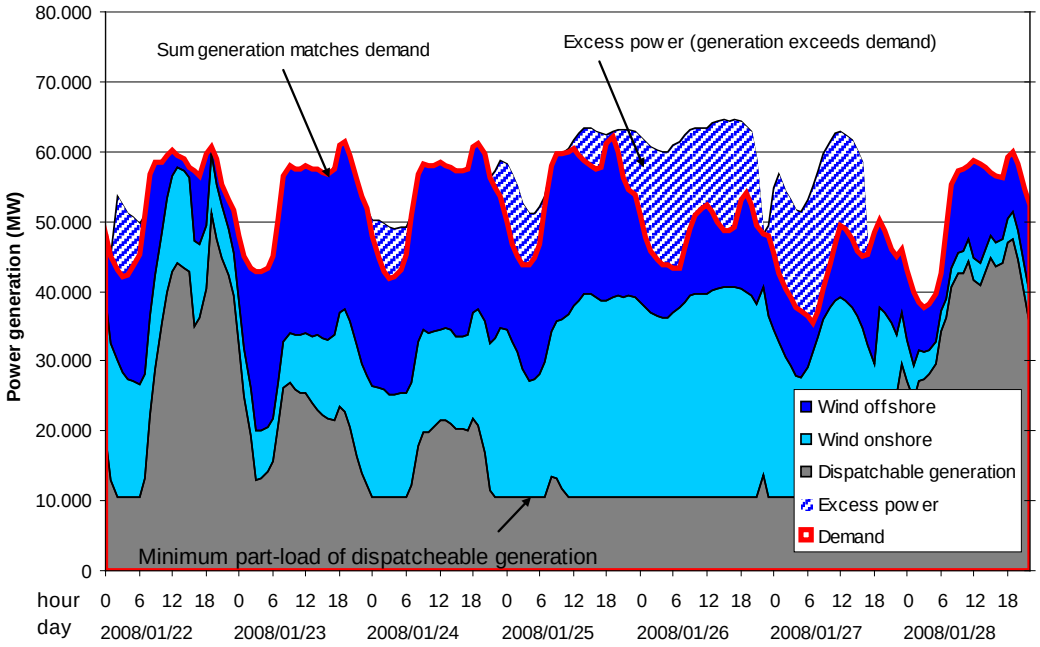

Fig. 1. Methodology to determine excess power (1 week displayed)

With this methodology, the excess electricity was estimated for different scenarios based on the generation and demand projections of the "Lead scenario 2009" [6]. Two variations from the lead scenario were considered: a scenario where 15 GW nuclear generation capacity would remain online (compensated by lower capacities of hard coal and natural gas), and an extreme scenario where the 2008 values for fossil and nuclear generation capacity and demand were frozen and the onshore and offshore generation capacity ramped up as in the

Lead scenario (33 GW onshore + 9 GW offshore by 2020, and 36 GW onshore + 24 GW offshore by 2030). Figure 2 shows the resulting excess power generation per year in Germany until 2030. In the lead scenario, only up to 9 TWh of excess electricity accrue until 2030 due to the consequent phase-out of fossil power plants. Retaining nuclear capacities will strongly increase excess electricity, and assuming that the power plant park of 2008 is retained while ramping up renewables, huge amounts of excess electricity will accrue until 2030. According to this estimation, by 2020 between 1.1 and 13 TWh of electricity (corresponding to 1.1-13% of overall wind power generation) cannot be used when they accrue and will therefore be available for energy storage in the form of hydrogen. For comparison, other authors with similar approaches have concluded that for whole Europe, 16 to 260 TWh excess power would accrue by 2020 [10]. Wietschel et al. [11] found that for Germany, 9 TWh excess power would accrue with 38.3 GW wind power installed, increasing to 28 TWh with 48.3 GW wind power installed.

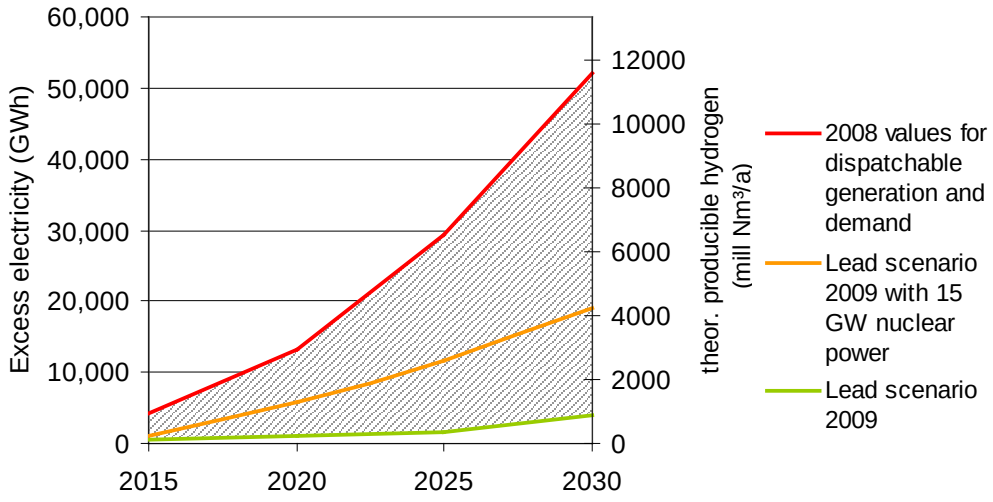

Fig. 2. Resulting excess power generation in Germany through 2030

4. Operation model for hydrogen production

Northern Germany is generally an ideal location for hydrogen production from renewables and large-scale storage due to the high concentration of wind power capacity and the geologic conditions facilitating the construction of underground salt caverns suitable for hydrogen storage. With the aim to develop a sound operation strategy for hydrogen production based on the use of excess electricity while at the same time unstraining the grid in the most economic way, the location of electrolysers as well as the economics of purchasing electricity (i.e. the connection to the electricity market) are the main criteria to be addressed.

In general there are three major options for the allocation of electrolysers: directly at the larger on- and offshore wind farms, at the end user location (e.g., an industrial sites or a hydrogen refuelling station) or at grid hubs of the high or ultra-high voltage grid in the areas with the highest wind loads and the heaviest loads on the grid (e.g., along the west coast of Schleswig-Holstein). Placement directly at the wind farms helps to unstrain the electric grid regionally and super-regionally, but hydrogen production is dispersed and the distribution to the consumers is comparatively complex, especially from offshore locations. Placement directly at the consumer site omits the transportation of hydrogen, but does not unstrain the electric grid between the wind farm and the consumer. Furthermore, access to large-scale storage caverns for longer-term storage of hydrogen cannot be provided easily in either of the distributed placement strategies. Therefore we assume that placing larger electrolysis plants at

grid hubs in areas with high wind power capacity is most beneficial, since this concept effectively unstrains the electric grid and allows for access to large-scale storage and efficient distribution of the produced hydrogen. The maximum electrolysis capacity installed at the grid hubs should be limited to a certain share of the upstream wind power. Figure 3 shows the scheme of a large-scale hydrogen storage plant (re-electrification by either CCGT or fuel cell is optional).

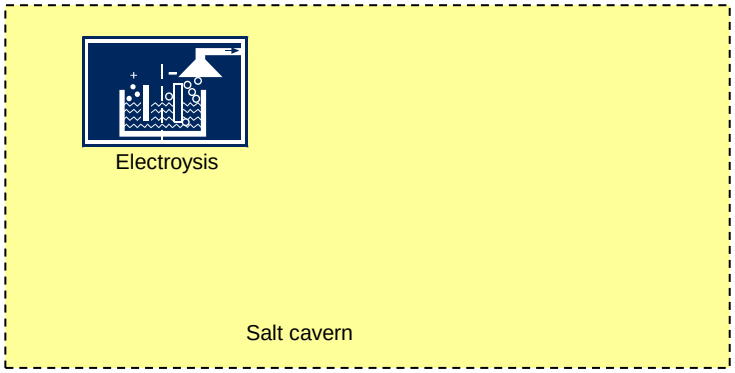

Fig. 3. Scheme of a hydrogen storage plant with optional re-electrification

As a price basis for the required electricity, either the feed-in tariffs for renewable electricity, or the day-ahead spot market hourly price curve of the European Energy Exchange (EEX) are reasonable. The latter can be interpreted either as purchasing the power at the EEX or directly from the wind farm operators, who otherwise would trade at EEX. Today, most wind power is fed in according to the fixed feed-in tariffs regulated by the German Renewable Energy Law. However, it can be expected that by 2020 the fixed feed-in tariffs will have been changed into market premiums, and most wind power will be directly traded at the spot market. Moreover, the spot market price represents the balance between electricity demand and supply: in times of low demand and high renewable energy generation the spot market price will be low, and vice versa. Hence, taking the spot market price as a base for electricity purchases ensures the operation of electrolysers in a way which indirectly unstrains the grid by using the excess electricity at low costs. As a simple operation strategy, electrolysers may be operated at full load during hours when the price is below a certain threshold, and may be kept in warm stand-by mode when the price is above the threshold. The number of operation hours per year and the average electricity price paid then depend on the price threshold set.

Further revenues for hydrogen producers can result from control reserve, since electrolysers represent a controllable load within the power grid. An electrolyser can be turned off or switched on upon request in order to provide positive or negative control reserve. The provision of the so-called “minute reserve” is tendered jointly by the transmission system operators (TSO) in Germany in 4-hour blocks for the following day. It is important to mention that the pure provision of control power (without actually being called) is already compensated by a per-MW rate. While tendering for control reserve brings additional revenues to the hydrogen production, it also increases the administration effort; since the control reserve is awarded at 10:00 AM for the next day, and the day-ahead spot market auction is at noon, the operator has to rely on a forecast of the spot market price in order to

decide whether the electrolyser should be operated during every 4 hour block (i.e. tender positive control reserve), or not (i.e. tender negative control reserve). Once control reserve has been awarded, the electrolyser must be operated according to the plan, even if electricity prices differ from the forecast. Therefore and due to the implication to operate in 4-hour blocks, the average electricity price levels will be somewhat higher if control reserve is to be provided.

A further benefit for the hydrogen producers can be achieved by directly utilising stranded wind power from turbines which otherwise would need to be temporarily cut down due to local grid restrictions (so-called "feed-in management"), provided that there are no grid restrictions between the wind turbines and the electrolysers. However, the TSOs are obliged to reinforce the power grid in order to avoid such events; hence, the potential benefits from this strategy are limited and uncertain.

5. Required storage demand, options for usage of the hydrogen, and costs

A strategy as described above will lead to a variable electrolyser utilisation with a tendency to higher production in the winter time with high wind power feed-in. In order to optimally level out the seasonal variations in production and facilitate a constant delivery of hydrogen to the end customers we found that a hydrogen storage capacity of approximately 700 full load hours is needed. If the hydrogen consumption can be adapted to the availability (higher consumption in winter than in summer), the storage capacity can be lower; on the other hand, if the hydrogen consumption is inflexible and peaks in summer, the storage capacity will need to be higher. Generally, the economic optimum of design storage capacity will be a trade-off between storage costs and timely flexibility of electrolysis operation (leading to savings in electricity costs). In the case of large-scale storage in salt caverns, the storage only contributes a minor part to the overall costs; however, if storage in e.g. aboveground pressure vessels or liquid hydrogen dewars is chosen, then the costs will be a multiple of the electrolysis costs.

A viable use of the renewable hydrogen is the partial or complete substitution of hydrogen generated from natural gas for uses in chemical and process industry. Besides saving fossil primary energy for hydrogen production by reforming, this has the potential to reduce the greenhouse gas emissions of the industries, improving their carbon footprint and avoiding costs of CO_2 certificates. Furthermore, hydrogen-powered road transportation will be an emerging market in the mid term. Offering renewable hydrogen at the refuelling stations to be erected is an interesting option, especially when considering the fact that the consumers might prefer "green hydrogen" and could also be forced by legislation (California has already implemented a law that 33% of all hydrogen for transportation will need to be renewable).

By screening the hydrogen consuming industry and using estimates on the hydrogen demand for road transportation, we have identified a demand potential of about 320 mill. Nm^3 hydrogen from wind power in the federal states Hamburg and Schleswig-Holstein by 2020 [1]. Based on lower heating value, this represents an energy of 960 GWh, which equals about 4.5% of the overall industrial final energy use in this region today. For the production and distribution of the hydrogen, about 1.55 TWh of electricity would be needed per year that could be predominantly supplied from excess electricity. The use of the this amount of renewable hydrogen in industry and transportation in Hamburg and Schleswig-Holstein instead of fossil hydrogen would save about 320.000 tons of CO_2-equivalent emissions. Beyond this, there might be potential to export renewable hydrogen, e.g. as a transportation fuel to other regions in Europe.

Based on current technology, the specific costs of hydrogen production from wind energy in Schleswig-Holstein including distribution will, depending on quantity and location of the consumption, amount to 0.42-0.75 €/Nm³ by 2020 (0.14-0.25 €/kWh of lower heating value). This is about 0.12-0.32 €/Nm³ more than the cheapest supply from fossil energy sources today. However, in the case of an incentive-supported early implementation of electrolytic hydrogen production, hydrogen from wind energy can become competitive by 2020, mainly through the rise of fossil energy prices and the cost reduction potentials of electrolysis.

A further use of the hydrogen could be used for power generation (so-called re-electrification) in combined cycle gas turbines or fuel cells. Re-electrification is a way to stabilise the electric grid by not only taking away power in times of excess renewable electricity but also providing backup power to compensate lack of renewable generation, e.g. in times of low wind. Co-firing gas turbines with natural gas at flexible shares is technically feasible. Also, the injection of hydrogen into the natural gas grid to substitute a certain part of the natural gas is possible. Almost all NG end users can tolerate hydrogen fractions up to 5% by volume (representing 1.6% by energy) without modifications. From the NG grid perspective, mainly the process gas chromatographs will have to be modified in order to detect hydrogen. In a future scenario, also up to 20% by volume hydrogen could be admixed to natural gas [12].

6. Conclusion

The paper showed that due to the ongoing build-out of intermittent renewable generation capacity and limited part-load ability of dispatchable power plants, significant amounts of excess electricity will accrue in the German electricity system in the future. This excess energy may be used to generate hydrogen, which can then be economically stored in large-scale salt caverns and utilized in industry and transportation sector or for electricity generation at times of low feed-in of renewables. An operation model based on central electrolysis plants at grid hubs, the spot market as a price basis for electricity purchases and a threshold-price strategy can yield minimum overall hydrogen production costs and at the same time facilitate effective unstraining of the grid.

Northern Germany is an ideal region for the production of hydrogen from renewables due to the its high wind power density, its geologic conditions allowing for cavern storage, its industrial demand for hydrogen and also its pioneering role in hydrogen fuelled road transportation (Berlin, Hamburg). Hydrogen storage is the only technology that can provide sufficient storage potential (multi-TWh) in Germany for a fully renewable electricity system. With some initial incentives, electrolytic hydrogen production can be made competitive within some years after the start of its deployment.

References

[1] C. Stiller, P. Schmidt, J. Michalski, R. Wurster, U. Albrecht, U. Bünger, M. Altmann, Potenziale der Wind-Wasserstoff-Technologie in der Freien und Hansestadt Hamburg und in Schleswig-Holstein. A study commissioned by Wasserstoffgesellschaft Hamburg e.V., Free and Hanseatic city of Hamburg (represented by the Administration of Urban Development and Environment), and the federal state of Schleswig-Holstein (represented by the Ministry of Science, Economics and Transport). Ludwig-Bölkow-Systemtechnik, March 2010. Available at: http://www.h2hamburg.de/index.php?page=download.

[2] M. Reichmuth, G. Schröder, R. Pohl, A. Scheuermann, A. Schiffler, A. Weber, Jahresprognose 2011 zur deutschlandweiten Stromerzeugung aus regenerativen

Kraftwerken. Available at: http://www.eeg-kwk.net/cps/rde/xbcr/eeg_kwk/2010-10-12-IE-EEG-Jahresprognose2011.pdf

[3] Hamburger Abendblatt, 11 December 2009: Climate protectors cheer: No power plant in Lubmin (in German: "Klimaschützer jubeln: Kein Kraftwerk in Lubmin"). http://www.abendblatt.de/wirtschaft/article1304949/Klimaschuetzer-jubeln-Kein-Kraftwerk-in-Lubmin.html

[4] Arbeitsgemeinschaft Energiebilanzen e.V.: Electricity generation by energy carriers 1990 to 2008 (in TWh) Germany, Status 27 May 2009; http://www.ag-energiebilanzen.de/viewpage.php?idpage=65

[5] Act Revising the Legislation on Renewable Energy Sources in the Electricity Sector and Amending Related Provisions – Renewable Energy Sources Act (EEG 2009) –official document, Federal Law Gazette (Bundesanzeiger) 2008 I No. 49, Bonn, 31 October 2008, p. 2074.

[6] German Federal Ministry for the Environment, Nature Conservation and Nuclear Safety: Lead scenario 2009. http://www.bmu.de/files/pdfs/allgemein/application/pdf/leitszenario2009.pdf

[7] M. Klobasa, Nachfrageseitige Regelungsmöglichkeiten im Energiesystem; in: EnInnov 08, 10. Symposium Energieinnovation. Energiewende: 13.-15. Februar 2008; TU Graz: Verlag der TU Graz, 2008; ISBN: 978-3-902465-94-8, pp. 89-90

[8] EEX Transparency data, power plant information (visited October 2009); available at: http://www.eex.com/en/Transparency/Power%20plant%20information

[9] European Network of Transmission System Operators for Electricity: Hourly load values of a specific country for a specific month; available at: http://www.entsoe.eu/index.php?id=92, visited October 2009

[10] C. Hoffmann, M. Greiner, L. Von Bremen, K. Knorr, S. Bofinger, M. Speckmann, K. Rohrig, Design of transport and storage capacities for a future European power supply system with a high share of renewable energies. IRES Conference 2008, Berlin, 24-25 November 2008.

[11] M. Wietschel, U. Hasenauer, N. Juncà Vicens, M. Klobasa, P. Seydel, Ein Vergleich unterschiedlicher Speichermedien für überschüssigen Windstrom. Zeitschrift für Energiewirtschaft 30 (2006) 2, pp. 103-114.

[12] J. Hüttenrauch, G. Müller-Syring, Zumischung von Wasserstoff zum Erdgas. Energie-Wasser-Praxis 10/2010, pp. 68-71; available at: http://www.gat-dvgw.de/fileadmin/gat/newsletter/pdf/pdf_2010/03_2010/internet_68-71_Huettenrauch.pdf

Combined cycle plants as support for wind power

N. Afonso Moreira[1*], A. Borges[1], A. Machado[2]

[1] *CITAB – Universidade de Trás-os-Montes e Alto Douro, Vila Real, Portugal*
[2] *Sonorgás – Departamento de I&D, Vila Real, Portugal*
** Tel: +351 932 505 044, E-mail: nam@utad.pt*

Abstract: The growing interest in diversifying the energy sources used, the major environmental objectives established, and the need to reduce the current European energy dependence, have been causing a growing and significant increase in betting on renewable energy sources. Thus recent years have witnessed a continuous increase of installed power from sources like solar, biomass, photovoltaic, wind, Biofuels, biogas among other.
The integration of renewable energy is mainly in the production of electrical power, in which has already a significant contribution. In the group of renewable energy sources used for the production of electrical power wind is the source that has registered further progress, and is also expected, that represents in the future, large part of the electric energy produced by renewable energy sources.

Although the wind helps to meet many of the problems, it's also presents some disadvantages, or constraints. Among the best-known disadvantages associated with wind, as noise and visual impact, stands out as the major technical problems the flashing of its production. The inability to predict the production of wind, leads to problems in securing demand, as well as in network integrity.

In this scenario the Combined Cycle Gas Turbine (CCGT) stands out as a great complement to wind power. Their ability to quickly put into operation, as well as the advantages that technology and fuel used presents, makes it the optimal solution to integrate with the wind energy.

Keywords: *Combined cycle plants, wind power,*

1. Introduction

In the last decade it has been attended an increasing interest on renewable energy sources. This trend is mainly in response to the increased consumption of fossil fuels, to the problem of security of supply and still to tackle the environmental problems caused by such consumption. Alternative power plants, as the solar, biomass and wind energy are the great trends. However in the majority of the cases the alternative energies are incapable to support, alone, the existing demand, forcing then, a combination with other fossil fuels like natural gas, oil, etc.

Natural gas emerged as the best fuel to be used in partnership with renewable. Its combustion gives low emission levels of pollutants, ash free, the content of carbon monoxide (the most responsible for acid rain) is practically zero and the levels of NO_x formed are well below the values of any other fossil fuel. Additional in its combustion, CO_2 emissions (responsible for the greenhouse effect) are much lower than other fuels, may even make the comparison between the products of combustion and respiration of the human (CO_2 and H_2O). For this reasons natural gas is the best option to use in support to renewable energy.

Since 1990 gross electricity generation from renewable energy sources (RES) in Europe grew significantly. Among new renewable (excluding large hydropower), wind power has the largest addition to renewable energy capacity. One of the main disadvantages of wind power is that wind is very unpredictable. Strength can vary from none to storm force. Therefore, wind turbines are unable to produce a continuous amount of electricity during the time, creating problems with network stability, and uncertainty regarding the availability of energy.

The combination of natural gas combined cycle plants and wind power is a good answer to grid stability problems and makes the whole system more secure. Gas is used as a back-up to overcome the intermittency of wind power.

2. Renewable energy policies in Europe

In the last decade, the number of countries that exploit renewable energy production has increased exponentially, and wind energy has been highlighted as a promising and attractive option among the other renewable energy sources.

Renewable have a long history of European policies and associated measures. Since 1986 the European Commission has listed among its objectives the promotion of community renewable energy [1]. In 1997 set the goal of achieving a target of 12% renewable energy by 2010. Most recent measurements, as the document "AN ENERGY POLICY FOR EUROPE" [2], published in 2007, amends the targets for 20% integration of renewable energy by 2020 and 10% integration of renewable energy in the transport.

2.1. European policies for wind power

The 20% target means that more than one-third of the EU's electricity will come from renewable sources in 2020 – up from 16% in 2006. By 2020, wind energy is expected to have overtaken hydropower as the EU's largest source of renewable electricity (Table 1).

Table 1. Renewable contribute to EU electricity consumption in 2020 [3].

Type of energy	2005	2020 - Targets	
	TWh	TWh	%
Wind	70,5	477	34,8
Hydro	346,9	384	28
Photovoltaic	1,5	180	13,1
Biomass	80	250	18,3
Geothermal	5,4	31	2,3
Solar thermal elect.	---	43	3,1
Ocean	---	5	0,4

To achieve this objective, the EU adopted a new Renewable Directive in April 2009, which set individual targets for each member state. In response to the Directive 2009/28/EC [4] member countries in 2010 presented its National Action Plan for Renewable Energy [5]. This plan sets national targets for 2020 relating to the share of energy from renewable sources consumed in transport, power generation and heating and cooling (Figure 1).

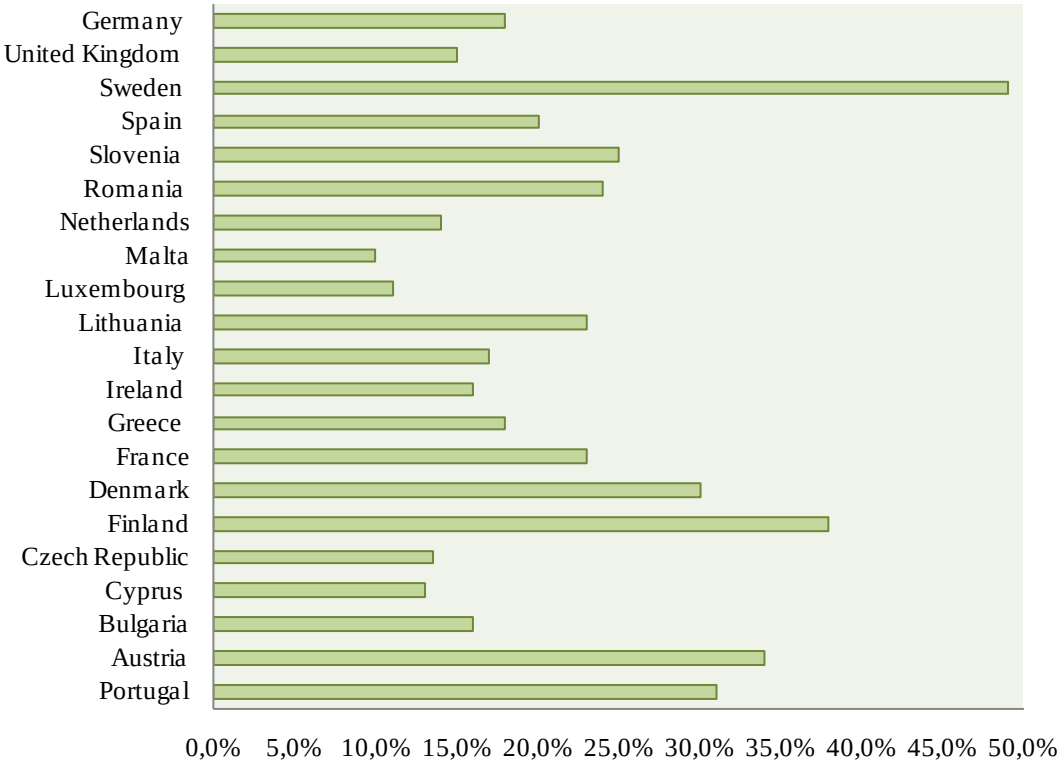

Fig. 1. Targets for Renewable Energy inclusion in final energy consumption in 2020.

With few exceptions, the field of electric energy production is the sector which foresees a greater share of energy produced by renewable energy sources. Wind energy stands out as a renewable energy source with greater participation (figure 2), and on average, excluding countries like the Czech Republic and Finland that does not estimates wind power production, the average of European countries to integrate wind power in 2020, as estimated targets, is approximately 42.3%.

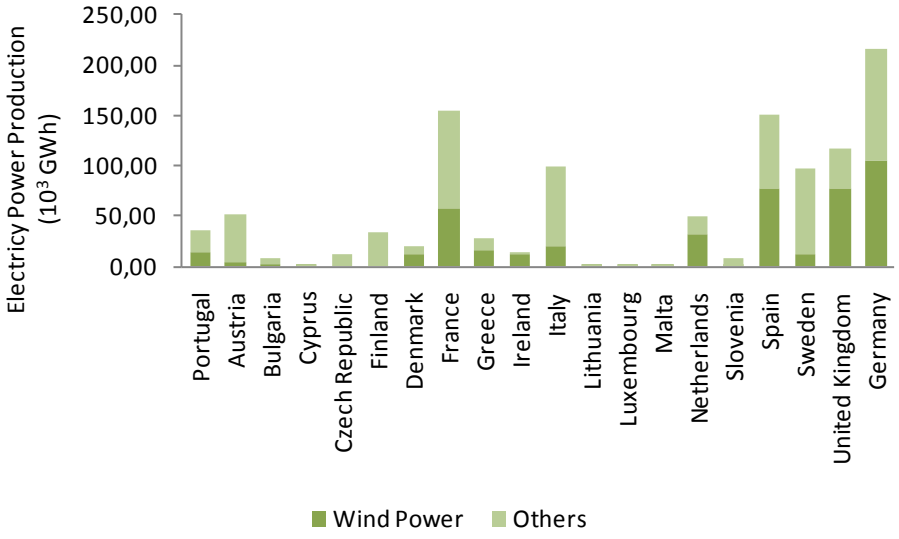

Fig. 2. Targets for Wind Power and others in electricity power production.

2.2. European wind energy tariffs

In most EU member states electricity utilities now buy electricity generated from renewable sources produced by individuals and companies. Prices paid for 'self-produced' electricity is called a feed-in tariff.

Table 2. Fee-in tariffs on member state in 2010 (€/kWh) [6].

Member state	Windpower 'On-shore'	Wind power 'Off-shore'	Solar PV	Biomass	Hydro
Austria	0.073	0.073	0.29 - 0.46	0.06 -0.16	n/a
Belgium	n/a	n/a	n/a	n/a	n/a
Bulgaria	0.07 - 0.09	0.07 - 0.09	0.34 - 0.38	0.08 - 0.10	0.045
Cyprus	0.166	0.166	0.34	0.135	n/a
Czech Republic	0.108	0.108	0.455	0.077 - 0.103	0.081
Denmark	0.078	0.078	n/a	0.039	n/a
Estonia	0.051	0.051	0.051	0.051	0.051
Finland	n/a	n/a	n/a	n/a	n/a
France	0.082	0.31 - 0.58	n/a	0.125	0.06
Germany	0.05 - 0.09	0.13 - 0.15	0.29 - 0.55	0.08 - 0.12	0.04 - 0.13
Greece	0.073	0.073	0.29 - 0.46	0.06 -0.16	n/a
Hungary	n/a	n/a	n/a	n/a	n/a
Ireland	0.07 - 0.09	0.07 - 0.09	0.34 - 0.38	0.08 - 0.10	0.045
Italy	0.166	0.166	0.34	0.135	n/a
Latvia	0.108	0.108	0.455	0.077 - 0.103	0.081
Lithuania	0.078	0.078	n/a	0.039	n/a
Luxembourg	0.051	0.051	0.051	0.051	0.051
Malta	n/a	n/a	n/a	n/a	n/a

The rates of remuneration for wind energy are generally among the lowest rates of pay for electric energy produced by renewable sources in EU countries. The exceptions are Estonia, Latvia and Lithuania who practice the same tariffs for electricity produced by renewable energy sources, and Denmark, where the remuneration of the energy produced by wind is greater than the produced from biomass.

3. Development of installed capacity and production of wind and combined cycle plants power

During 2009, 10,526 MW of wind power was installed across Europe, of which 10,163 MW in EU countries. This represents growth in the EU of approximately 15, 5% compared with the values of installed power in 2008 (figure 3).

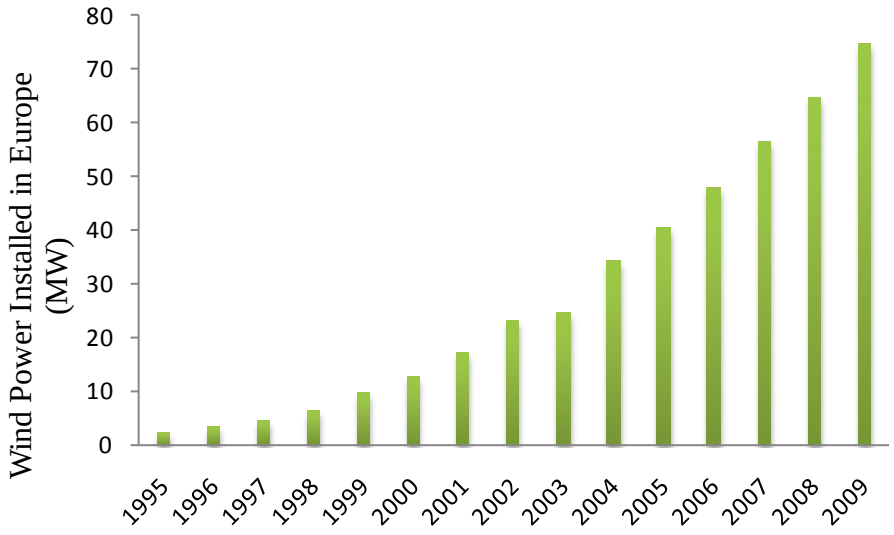

Fig. 3. Wind Power Installed in Europe [7].

The facilities in Europe are characterized by a continuous development in mature markets like Spain and Germany, along with countries like Italy, France and the UK. In 2007, production of electrical power through the wind reached a value of 104.3 GWh in the European Union [8].

Spain is the second EU country with the highest installed capacity of wind power. In 2009 it had an installed capacity of 18 GW, double the number counted in 2005 (figure 4).

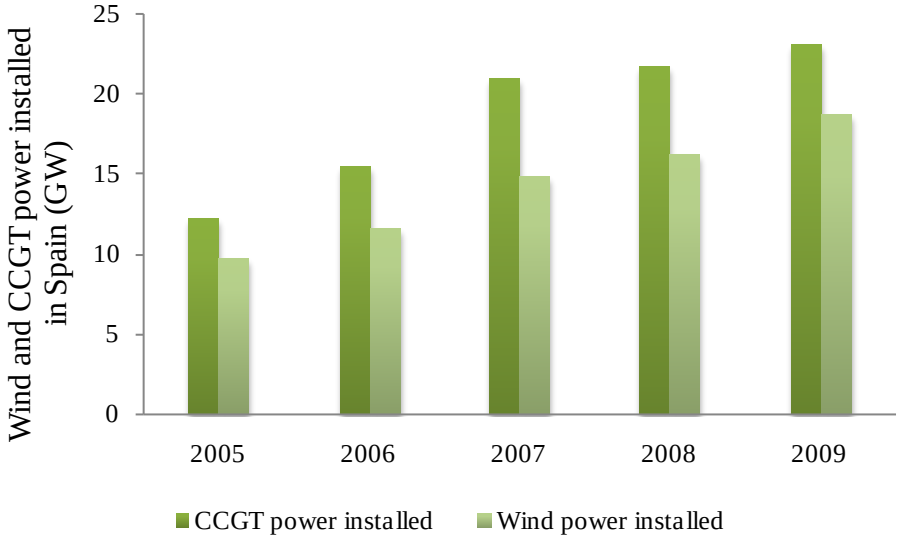

Fig. 4. CCGT and Wind Power Installed in Spain [10].

Many of the world`s electric utilities and independent power producers are turning to gas turbine combined-cycle power technology for new capacity. The major reasons for the predominance of this technology are high efficiency, moderate capital cost, low environmental impact, favorable natural gas prices and short construction schedules. Recent advances in gas turbine technology allow for a combined-cycle efficiency of almost 60 percent. The turbines used in Combined Cycle Plants are commonly fuelled with natural gas, which is found in abundant reserves in several countries. Natural gas is becoming the fuel of

choice for private investors and consumers because it is more versatile than coal or oil and can be used in 90% of energy applications.

In the last decade, most countries concentrated their power generation investments in gas-fired power plants, especially combined-cycle gas turbines (CCGT). The document "European Energy and Transport - Trends to 2030" [9], indicates that the CCGT plants accounted for about 51% of total investment in power plants combined, between 2005 and 2010. Also according to the estimates presented in this document, in 2030 the CCGT plants will reach a total installed capacity of 145 GW in Europe.

A country that reflects the growing interest and increasing investment in CCGT plants is Spain. In 2005 Spain had a total installed capacity of 12 GW of CCGT, in 2009 reached 23 GW, which represents an increase of 88% (figure 4).

4. Correlation Analysis

Although wind energy has many advantages, like being a renewable source of energy, not emissions of greenhouse gases, among other well-known advantages, also has considerable disadvantages. The disadvantages more marked are the related to visual and noise pollution caused by the same; however to technical level the biggest disadvantage of wind power is the intermittency of production. That is, wind does not present a continues production, as it is not possible to predict in advance with will be its real production.

For this reason, it is necessary to resort to so-called support system. The support system is a complementary system to the wind power, than is able to put into operation that is, to produce electrical power, in case of failure of electric power generation by wind energy, ensuring availability to demand.

The most common support systems used to support wind power plants are Combined Cycle Gas Turbine. This choice is justified by the use of a fuel that although is a fossil fuel, has great advantages when compared to the other, as well as the highly effective technology applied.

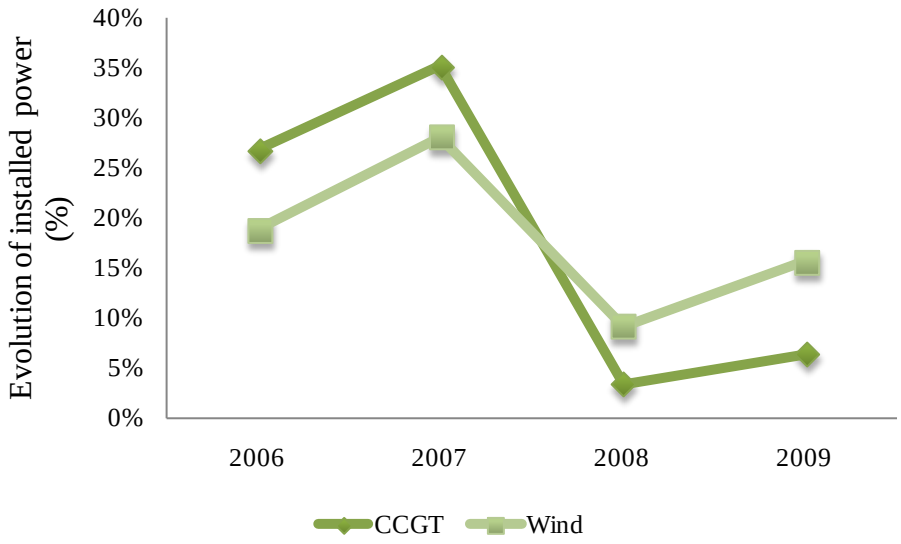

Fig. 5. CCGT and Wind evolution of installed power in Spain [10].

As we can see by the analysis of figure 5, the evolution of installed power to CCGT and wind power is very similar. Both forms of energy have a significant increase of installed power to the scheduled between 2006/07 and 2008/09, and both show a decrease in the growth of installed capacity in 2008.

In the year 2007, which corresponded to the years where there was a greater increase of installed power, CCGT reached a total installed capacity of 20 GW, corresponding to an increase of 5.5 GW compared to the previous period, and the energy wind power grew by 3.2 GW, reaching a total of 14.8 GW.

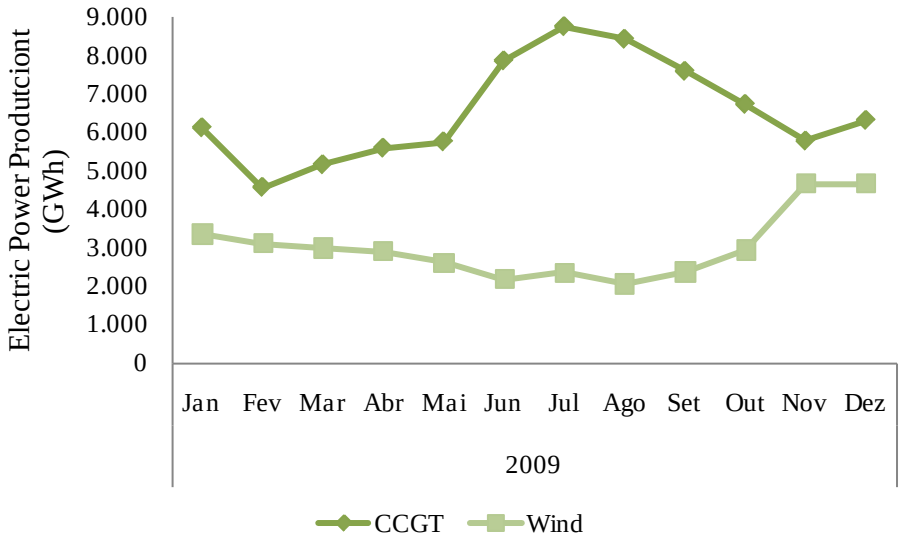

Fig. 6. CCGT and Wind electric power production in Spain [11].

As we can see by the analysis of the previous figure (Fig. 6) the electricity produce by CCGT follows the production of electric power by wind. That is, whenever there is a decrease in wind generation, the CCGT start working to remedy this breach. With the increase of electricity generation by wind, CCGT production decreases.

Thus the intermittency of electricity generation by wind does not because failures in the availability of energy and do not create problems in the network integrity.

5. Development Perspectives

According to estimates the installed capacity of wind power will tend to continue to increase. The figures for Europe are that the production of electricity by wind power to reach 477 TWH in 2020.

Assuming that the trends are maintained, the increase in installed capacity of CCGT will also maintain its growth trend, and is also expected that due to the development of technology associated with CCGT this increase will be even higher than expected. With current technology, the CCGT are already the best option to serve to support the production of other renewable energy sources, specifically through the production of wind energy.

References

[1] Official Journal C 241, 09/25/1986 p. 0001 - 0003;

[2] COM (2007) 1 final; 2007;

[3] European Renewable Technology Roadmap 2008;

[4] Directive 2009/28/EC of the European Parliament and the Council of 23 April 2009

[5] http://ec.europa.eu/energy/renewables/transparency_platform/action_plan_en.htm

[6] Price for Renewable Energies in Europe; Report 2009; European Renewable Energies Federation.

[7] Wind in power - 2009 European statistics; The European Wind Energy Association; February 2010

[8] European Environment Agency; 2008

[9] European Energy and Transport - Trends to 2030; European Commission; Directorate-General for Energy and Transport; 2007.

[10] El sistema eléctrico espanõl; RED ELÉCTRICA DE ESPANÃ; 2010

[11] Boletin Mensual; RED ELÉCTRICA DE ESPANÃ; 2010

Learning a wind farm power curve with a data-driven approach

Antonino Marvuglia[1,*], Antonio Messineo[2]

[1] *CRP Henri Tudor/CRTE, 66 rue de Luxembourg, L-4002 Esch/Alzette, Luxembourg*
[2] *Faculty of Engineering & Architecture, Kore University of Enna, Italy*
**Corresponding author. Tel: +352 425991652, Fax: +352 425991555, E-mail: antonino.marvuglia@tudor.lu*

Abstract: Improving the performance of prediction algorithms is one of the priorities in the wind energy research agenda of the scientific community. In a very simplistic approach, short-term predictions of wind power production at a given site could be generated by passing forecasts of meteorological variables (namely wind speed) through the so-called wind farm power curve, which links the wind speed to the power that is produced by the whole wind farm. However, the estimation of this conversion function is indeed a challenging task, because it is nonlinear and bounded, in addition to being non-stationary due for example to changes in the site environment and seasonality. Even for a single wind turbine the measured power at different wind speeds is generally different to the rated power, since the operating conditions on site are generally different to the conditions under which the turbine was calibrated (the wind speed on site is not uniform horizontally across the face of the turbine; the vertical wind profile and the air density are different than during the calibration; the wind data available on site are not always measured at the height of the turbine's hub).

The recent developments in data mining and evolutionary computation (EC) offer promising approaches to modelling the power curves of turbines. In this paper we use a self-supervised neural network called GMR (Generalized Mapping Regressor) to learn the relationship between the wind speed and the generated power in a whole wind farm. GMR is an incremental self-supervised neural network which can approximate every multidimensional function or relation presenting any kind of discontinuity. The approach used is a data driven one, in the sense that the relationship is learned directly from the data, without using any explicit physical or mathematical relationship between input and output space. The model is potentially applicable to any site, provided that a statistically consistent amount of wind and power data is available. The methodology allows the creation of a non-parametric model of the power curve that can be used as a reference profile for on-line monitoring of the power generation process, as well as for power forecasts.

The results obtained with the proposed approach are compared with another state-of-the-art data mining algorithm (namely, a feedforward Multi Layer Perceptron) showing that the algorithm provides fair performances if a suitable pre-processing of the input data is accomplished.

Keywords: *Wind farm, Power curve, Data-driven, Neural network, Machine learning*

1. Introduction

An interesting aspect of current research on wind power generation is the definition and implementation of accurate models to predict the energy output of a whole wind farm, rather than single wind turbines. In power systems a traditional generator is usually described as 'dispatchable', whereas wind generation is often referred to as 'non dispatchable'. Even though wind power generation has reached maturity in power systems, it is often still considered as a negative load because it is less predictable than thermal generation [1; 2].
Accurate wind power forecasting and prediction reduces the risk of uncertainty and allows for better grid planning and integration of wind into power systems.

There has been much debate and discussion in relation to the costs associated with wind power integration. A common conclusion is that as the levels of wind power penetration increase additional system balancing is required. Wind power forecasting and prediction tools are therefore invaluable because they enable better dispatch, scheduling and unit commitment of thermal generators, hydro plant and energy storage plant and more competitive market trading as wind power ramps up and down. Overall they reduce the financial and technical risk of uncertainty of wind power production for all electricity market participants.

Researchers have applied different methodologies in studying wind farms. In [3] the author built a model to predict the power produced by a wind farm using the data from the weather prediction model (HIRLAM) and the local weather model (WASP). In [4] a regression and a neural network (NN) model are compared in order to estimate a turbine's power curve. A novel approach for the analysis and modelling of wind vector fields was introduced by Goh et al. [5] and developed by Mandic et al. [6]. In these papers the wind vector is represented as a complex-valued quantity and wind speed and direction are modelled simultaneously. In [7] a new algorithm based on fuzzy logic was applied to estimate wind turbine power curve. In [8] a variety of different approaches have been used to build prediction models and characterize power curves of a wind farm by a nonlinear parametric model. In [9] parametric and non-parametric models have been applied for the same task and results have been compared. An extensive review of the existing wind speed and related generated power forecasting approaches can be found in [10].

The key issue addressed in this paper is the estimation of the relationship between the wind speed and a wind farm power output. This relationship is expressed as a power curve, which has a logistic function shape. However, as discussed in [8], the experimental power curve of a wind turbine (and of an entire wind farm as well) is not an ideal logistic function. All regions outside of the logistic curve represent either power losses or power gains. The presence of outliers and abnormal values might be due to several reasons: the presence of values of wind speed close to the cut-in or the cut-out speed of the installed wind turbines; environmental issues (blades affected by dirt, bugs and ice); shut-down due to maintenance or energy curtailment; control system issues; sensors malfunctions; pitch control malfunctions; unsuitable blade pitch angle setting; blade damage [8; 11]. Finally, the measured powers at different wind speeds are generally different than the rated power also because the operating conditions on site are generally different than the conditions under which the turbine was calibrated (the wind speed on site is not uniform horizontally across the face of the turbine; the vertical wind profile and the air density are different during the operation phase than during the calibration; the wind data on site are not always measured at the height of the turbine's hub). Moreover, due to the nonlinearity of the wind farm power curve, the uncertainty in its estimation dramatically amplifies the uncertainty contained in the wind speed forecasts. If the model of a power curve reflecting a normal status was available, the abnormal status of a turbine could be monitored and detected by this model.

The main motivation of this paper lies in the detection of the abnormalities of the wind turbines (and as a consequence also wind farms as a whole) power curve. The recent developments in data mining and evolutionary computation (EC) offer promising approaches to modelling turbines power curves. In this paper we use a self-supervised neural network called GMR (Generalized Mapping Regressor) [12; 13] to learn the relationship between the wind speed and the power generated in a wind farm. GMR is an incremental self-supervised neural network which can approximate every multidimensional function or relation presenting any kind of discontinuity. The approach used is a data driven approach, in the sense that the relationship is learned directly from the data, without using any explicit physical or mathematical relationship between input and output space. The methodology allows the creation of a non-parametric model of the power curve that can be used as a reference profile for on-line monitoring of the power generation process, as well as for power forecasts.

2. Methodology

GMR is an incremental self-organizing neural network with chains (second layer weights) among neurons. The basic idea of GMR is to transform the function approximation problem

into a pattern recognition problem under an unsupervised framework. Hence, a coarse-to-fine covering strategy of the mapping is used. Suppose we want to model the mapping relationship between a set of inputs **x** and a set of outputs **y**. GMR algorithm works transforming the data mapping problem *f*: $\mathbf{x} \rightarrow \mathbf{y}$ into a pattern recognition problem in the augmented space *Z* represented by vectors $\mathbf{z} = [\mathbf{x}^T \ \mathbf{y}^T]^T$, which are the inputs of GMR. In this space, the branches of the mapping become clusters which have to be identified.
The algorithm comprises four phases (training, linking, merging, and recalling) which are schematized in Fig. 1.

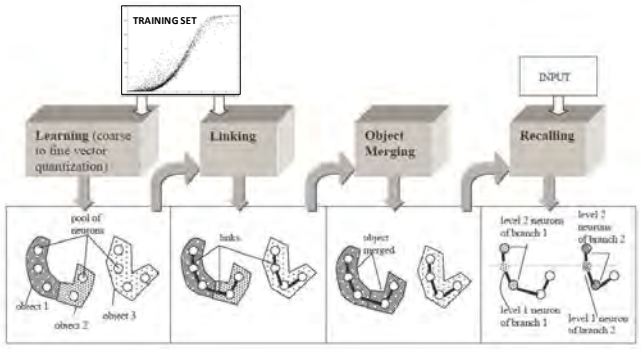

Fig. 1. The four phases of the GMR algorithm.

The ***training phase*** concerns the *vector quantization* of the *Z* space. The aim of vector quantization is, in practice, the reduction of the original data set to a small representative set of prototype vectors that are easier to manage [14]. During training, the augmented space is recovered by either creating neurons or adapting their weights according to the novelty of the input data. At the presentation of each input belonging to the training data set (TS), there are two possibilities: either creation of a new neuron (whose weight vector is equal to the input vector) or adaptation of the weight vector of the closest neuron (in input/weight space). Given a threshold ρ (*vigilance threshold*), a new neuron is created if the hyperspheres of radius ρ, centered in the already created weight vectors, do not contain the input. The parameter ρ is very important: it determines the resolution of training. Learning can be divided into two sub-phases: *coarse quantization* and *fine quantization*. The vigilance threshold used in the coarse quantization phase (ρ_1) is higher than the one used in the fine quantization, ρ_2. In general, the first epoch (i.e. presentation of the entire TS) defines the number of neurons needed for mapping and the others adapt their weights for a better approximation. The neurons thus obtained identify the *objects*, which are compact sets of data in *Z*. The resulting neurons are called *object neurons*. In the second sub-phase, at first a pre-processing is required for labelling each neuron with the list of the input data which had the neuron as winner (i.e. whose weight vector is the closest to the input vector); it can be accomplished by presenting all data (*production phase*) to GMR and recording the corresponding winning neurons. At the end, for each neuron a list of the inputs for which it won is stored. This list represents the *domain* of the object neuron. Every list is considered as the TS for a subsequent training which takes place separately (and in parallel) for each object domain. At the end, the neural network is made up of the neurons generated by the secondary learning phases (*final neurons*), labelled as belonging to an object by the corresponding object neuron.

The next phase is the ***linking phase***. Neurons' linking is accomplished by computing the second layer weights, which are discrete and equal to zero in the absence of a link. A link is computed at the presentation of each piece of data from the TS. The technique used in this paper to perform the linking phase exploits the direction of the principal component of the domain data (i.e. the direction corresponding to the highest eigenvalue of the autocorrelation matrix of the domain data) [12]. This direction is here referred to as domain *principal*

direction (PD). For each data point, the weights are sorted according to the Euclidean distance from it, and the winning neuron is determined. It is then linked to another neuron chosen in a subset of neurons (*candidate neurons*). The subset was here determined by defining in advance a number *k* of nearest neighbours of the input. Then, for each candidate, the absolute value of the scalar product between its PD and the winner's PD is evaluated. The winner is linked to the candidate yielding the maximum scalar product (i.e., the candidate whose PD is closest in direction to the winner's PD). This approach is justified by the fact that clusters with similar shapes have to be connected.

In the ***merging phase***, GMR checks whether different objects are linked. If they are, the objects are merged. The ***recalling phase*** replaces the neurons in the reduced manifold with Gaussians representing the domain. Their parameters are estimated by the maximum likelihood (ML) technique. This phase is essentially a process of Gaussian labelling followed, if required, by an interpolation step. A more detailed description of GMR is contained in [12].

3. Results

The data used for the case study refer to a wind farm (whose location is not disclosed for confidentiality reasons) and the available data set comprises a wind speed time series (one whole year) measured by an anemometer located at 50 m above the ground level (a.g.l.), as well as the power produced by each of the wind turbines, collected by a SCADA (Supervisory Control and Data Acquisition) systems at the wind farm. Since the aim of the study was modelling the power curve of the wind farm as a whole, the sum of the power produced by all the turbines was used for the application of the proposed algorithm. A training and a test set containing respectively 90% and 10% of the entire time series available (randomly selected across the whole data set) were created. In order to speed up the training, a sampling of one datum out of three was then made on the training set (TS), so to select a smaller subset (that was used as the actual TS). Before starting the training phase, the data which had been clearly recorded erroneously, due to a malfunctioning of the SCADA system, were filtered out (namely, data with an abscissa greater than the cut-in speed of the wind turbines and with a null ordinate). The remaining data were normalized in the interval [–1; +1] and denoised using the Kernel Principal Component Analysis (KPCA) technique with a bandwidth of the Gaussian kernel $\sigma = 0.4$. KPCA is a *generically nonlinear* signal processing technique; it is often used for denoising in image applications [15]. The denoised TS used to train GMR contains 2828 observations. A test data set containing 876 observations has been used in the recalling phase. Figure 2 shows the data before (a) and after (b) the normalization and denoising procedure. The data showed in Fig. 2(a) have been previously rescaled, only for visualization purposes, in order to protect data confidentiality.

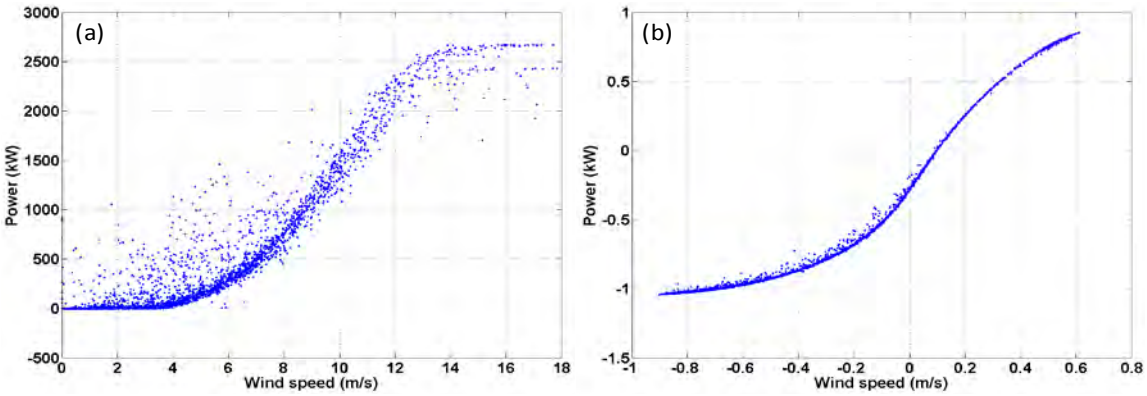

Fig. 2. Training set data before (a) and after (b) normalization and denoising.

A number of nearest neighbours k=4 was used during the linking phase. In the rough phase the vigilance threshold was set to $\rho_1 = 0.5$ and in the fine tuning phase $\rho_2 = 0.025$ was used. The number of final neurons is 101 and the number of object neurons is 26. During the recalling phase, GMR was used both without interpolation and with Gaussian interpolation. Figure 3 shows the results of the linking and merging phases of GMR. A zoom of the part of the curve contained in the dashed box is showed in the upper left and lower right corners of Fig. 3(b). In the lower right corner different objects are represented with different symbols to improve readability.

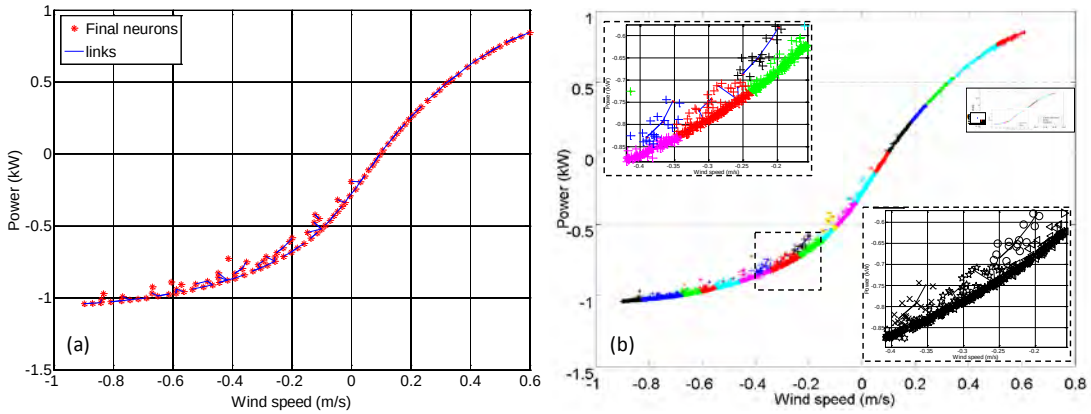

Fig. 3. Results of the linking (a) and merging (b) phases of GMR.

The same TS used for the GMR model was also used to train a feedforward Multi Layer Perceptron (MLP). The learning algorithm used is backpropagation with momentum [16]. The network has two layers of neurons, the hidden layer with 10 and the output layer with 1 neuron (since the output is mono-dimensional). A logistic sigmoid function and a linear function were respectively used as the activation function of the first and the second layer.
Figure 4 shows the results of the modelling obtained both on the TS and test set data, with the two models, while Table 1 summarizes their prediction accuracy.

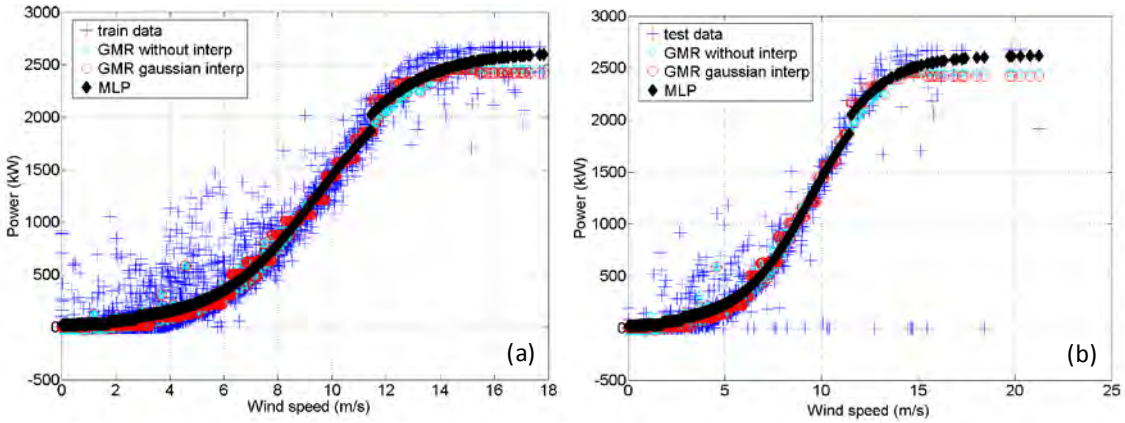

Fig. 4. Results of the GMR and MLP predictions on the training set (a) and the test set (b).

Their performances have been assessed computing the mean absolute error (MAE) and the symmetric mean absolute percentage error (sMAPE), using the test set data. The respective standard deviations (Std dev, in Table 1) have also been computed.
The sMAPE measure computes the absolute error in percent between the absolute value of the actual observation y_t and the absolute value of the forecast $\hat{y}_t$ across all observations t of the test set of size n [17]:

$$sMAPE = \frac{1}{n}\sum_{t=1}^{n}\frac{|y_t - \hat{y}_t|}{(|y_t| + |\hat{y}_t|)/2} * 100 \quad (1)$$

The MAE of MLP is worse than the one of the two GMR models, because GMR recognizes that the "thickness" of the data cloud around the average logistic sigmoid trend actually contains some information content and it is not just due to noise (see the links in Fig. 3(a)), whereas the MLP follows the average trend of the data, thus finding a smooth curve profile.

Table 1. Prediction accuracy of the models applied (GMR and MLP).

	MLP	GMR gaussian interp	GMR without interp
MAE (kW)	1990.60	436.11	458.63
Std dev of AE (kW)	2515.40	918.34	906.40
sMAPE (%)	68.03	64.19	68.35
Std dev of sMAPE (%)	76.25	73.73	76.40
minimum AE	71.79	1.02	0.47
maximum AE	9159.40	8585.10	8585.10

3.1. On-line monitoring by residual approach and control charts

Once the two non-parametric models mentioned above have been trained, they can be used to characterize the wind farm power in normal conditions, and therefore they can serve as an on-line wind farm power generation profile. The residual control chart techniques (statistical quality control) [18] are used to analyze residuals between model predicted power and observed power. The control chart approach allows the residuals and their variations to be monitored, thus detecting abnormal conditions of a turbine.

The means of the residuals obtained on the TS (μ_{Train}) and the test set (μ_{Test}), as well as their standard deviations (σ_{Train}; σ_{Test}) were computed. Once μ_{Train} and σ_{Train} are known, the upper and lower control limits of the control chart can be computed and used to detect the anomalies. Control limits for the control chart can then be derived using Eq. (2) [18]:

$$UCL_1 = \mu_{Train} + \eta\frac{\sigma_{Train}}{\sqrt{N_{Test}}}; \quad LCL_1 = \mu_{Train} - \eta\frac{\sigma_{Train}}{\sqrt{N_{Test}}} \quad (2)$$

N_{Test} is the number of points in the test data set, but it can be adjusted to make the control chart less sensitive to the data variability and thus reduce the risk of false alarms. The parameters in Eq. (2) could be adjusted dynamically, based on ope rations of individual turbines. In the application described in this paper, N_{Test} was set equal to 10, while η was set to the widely used value $\eta = 3$ [9]. If μ_{Test} is above UCL_1 or below LCL_1, the power generation process at the generic sampling time $y_{TestSet} = [y(i), \hat{y}(i)]$ is considered to be deficient (or "out-of-control"), otherwise it is not considered abnormal, i.e. it is considered "in-control". Similarly, the control limits for σ^2_{Test} can also be calculated to detect out-of-control points, using control limits defined as a function of the variance of σ^2_{Train} [8; 9; 18].
Figure 5 shows the out-of-control points detected in the TS by GMR and the MLP on the basis of the limits defined by Eq. (2). Out of the 876 points of the test set, GMR detected 183 out-of-control points, while the MLP network detected 136 of them. It is possible to notice that GMR in this case is more conservative in the part of the curve closer to the cut-off wind speed. This is due to the choice of the parameters η and N_{Test}, but also to the fact that the MLP model tends to find a smooth solution, passing between the two data clouds in the last part of

the curve, whereas GMR remains closer to a constant value of the output power for wind speeds equal to or higher than the cut off speed, as it should be in case of ideal functioning of the turbines. It is also possible to notice that GMR detects some of the points above the left tail of the curve as "in-control" points, while MLP labels them as "out-of-control". This is due to the fact that GMR finds some links and, as a consequence, some branches of the mapping, also in this zone of the space (see Fig. 3). This is reasonable and in line with the results found in [9] using a parametric model and a non-parametric model based on the k-nearest neighbour (k-NN) algorithm. In fact, one of the main advantages of GMR, compared with feedforward neural networks, lays into the fact that, while for many functional (i.e. single-valued) approximation problems feedforward network can work well by minimizing a sum-of-squares error function, they can actually give rise to high imprecision in presence of multi-valued mappings, or mappings whose structure varies for different regions of the input space. The prominent feature of GMR is its capability to output all the solutions and their corresponding mapping branches.

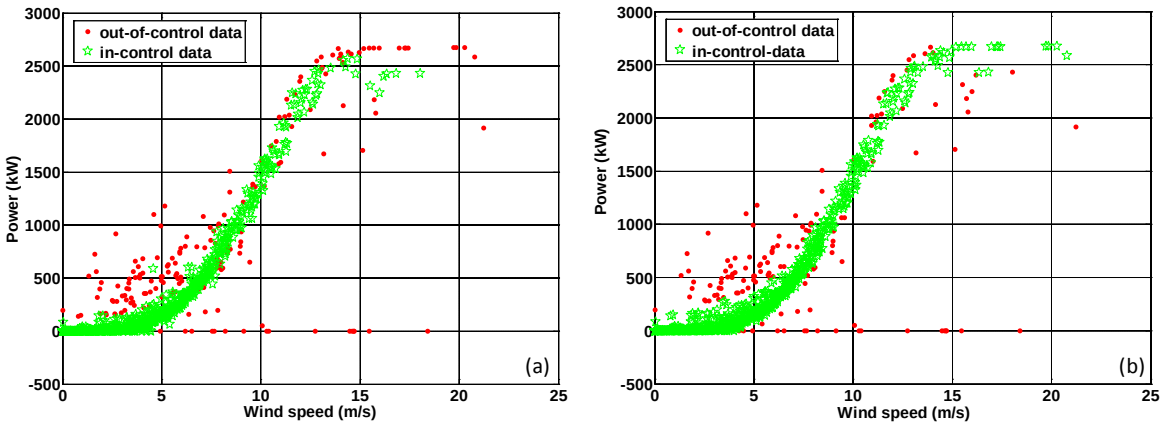

Fig. 5. Data (within the test set) detected as "in-control" and "out-of-control" according to the limits defined in Eq. (2), using GMR with Gaussian interpolation (a) and MLP (b).

4. Conclusions

The paper presents an application of a data-driven technique for mapping the power curve of a whole wind farm and shows its utilization for the creation of quality control charts. The results obtained with the proposed methodology are compared with those obtained with a "traditional" non-parametric method: a MLP neural network. A few other applications have already been presented in the literature, dealing with the same topic. The originality of this paper is twofold: on one hand, its application to the modelling of the power curve of an entire wind farm, instead of a single wind turbine; on the other hand, the utilization of GMR, which is an incremental self-organizing competitive neural network with adaptive linking among neurons, able to approximate every kind of mapping (function or relation) in both senses, i.e. $M(x,y): x \in \Re^m \leftrightarrow y \in \Re^n$. The models can be used as the reference power curve (on-line profile) for monitoring the performances of a w ind farm as a whole. In a real, on-line application, the models will be updated using the most current operational data.

The case study here presented demonstrated that the control chart approach produces satisfactory results in monitoring power curves. In future research, other data mining algorithms will be assessed for enhancing accuracy of non-parametric models. In particular, the application of Bayesian networks will be considered to identify links between anomalies and the specific reasons causing them, which is not possible simply using control charts.

References

[1] R.M.G. Castro, A.F.M. Ferreira, A comparison between chronological and probabilistic methods to estimate wind power capacity credit, IEEE Trans Pow Syst 16(4), 2001, pp. 904-909.

[2] P. Børre Eriksen, T. Ackermann, H. Abildgaard, P. Smith, W. Winter, J. Rogríguez García, System operation with high wind penetration, IEEE Pow Energ Magazine, November/December 2005.

[3] L. Landberg, Short-term prediction of the power production from wind farms, Journal of Wind Engineering and Industrial Aerodynamics 80(1-2), 1998, pp. 207–220.

[4] S. Li, D.C. Wunsch, E. O'Hair, M.G. Giesselmann, Comparative analysis of regression and artificial neural network models for wind turbine power curve estimation, J Solar Energ Engineering 123(4), 2001, 327–332.

[5] S.L. Goh, M. Chen, D.H. Popović, K. Aihara, D. Obradovic, D.P. Mandic, Complex-valued estimation of wind profile, Renew Energ 31, 2006, pp. 1733–1750.

[6] D.P. Mandic, S. Javidi, S.L. Goh, A. Kuhc, K. Aihara, Complex-valued prediction of wind profile using augmented complex statistics, Renew Energ 34, 2009, 196–201.

[7] T. Üstütaş, A.D Şahin, Wind turbine power curve estimation based on cluster center fuzzy logic modelling, Journal of Wind Engineering and Industrial Aerodynamics 96, 2008, pp. 611–620.

[8] A. Kusiak, H. Zheng, Z. Song. Models for monitoring wind farm power, Renew Energ 34, 2009, pp. 583–590.

[9] A. Kusiak, H. Zheng, Z. Song, On-line monitoring of power curves, Renew Energ 34, 2009, pp. 1487–1493.

[10] M. Lei, L. Shiyan, J. Chuanwen, L. Hongling, Z. Yan, A Review on the Forecasting of Wind Speed and Generated Power, Renew Sust Energ Rev 13(4), 2009, pp. 915-920.

[11] B. Bell, Individual wind turbine and overall power plant performance verification, San Diego, CA, 2008.

[12] Cirrincione G, Cirrincione M, Lu C, Van Huffel S. A novel neural approach to inverse problems with discontinuities (the GMR neural network), Proceedings of 2003 Int. J Conf Neural Networks (IJCNN'03), Portland, Oregon, pp. 3106–3111.

[13] C. Lu, The Generalised Mapping Regressor (GMR) neural network for inverse discontinuous problems, MSc Thesis, 2000, Katholieke Universiteit Leuven (Belgium).

[14] R.M. Gray, Vector quantization, IEEE ASSP Magazine 4(2), 1984, pp. 4–29.

[15] A.R. Teixeira, A.M. Tomé, K. Stadlthanner, E.W. Lang. KPCA denoising and the pre-image problem revisited, Digit Signal Process 18, 2008, pp. 568–580.

[16] M.T. Hagan, H.B. Demuth, M.H. Beale, Neural network design, PWS Publishing, 1996.

[17] S. Haykin, Neural Networks – A Comprehensive Foundation, Prenctice Hall, Upper Saddle River, 1999.

[18] D.C. Montgomery, Introduction to statistical quality control, John Wiley & Sons, New York, 5th ed. 2005.

Dynamic stall for a Vertical Axis Wind Turbine in a two-dimensional study

R. Nobile[1,*], M. Vahdati[1], J. Barlow[1], A. Mewburn-Crook[2]

[1] *University of Reading, Reading, UK*
[2] *Wind Dam Renewables Ltd, Swansea, UK*
***** *Corresponding author. Tel: +44 1183784666, E-mail: r.nobile@reading.ac.uk*

Abstract: The last few years have proved that Vertical Axis Wind Turbines (VAWTs) are more suitable for urban areas than Horizontal Axis Wind Turbines (HAWTs). To date, very little has been published in this area to assess good performance and lifetime of VAWTs either in open or urban areas. At low tip speed ratios (TSRs<5), VAWTs are subjected to a phenomenon called 'dynamic stall'. This can really affect the fatigue life of a VAWT if it is not well understood. The purpose of this paper is to investigate how CFD is able to simulate the dynamic stall for 2-D flow around VAWT blades. During the numerical simulations different turbulence models were used and compared with the data available on the subject. In this numerical analysis the Shear Stress Transport (SST) turbulence model seems to predict the dynamic stall better than the other turbulence models available. The limitations of the study are that the simulations are based on a 2-D case with constant wind and rotational speeds instead of considering a 3-D case with variable wind speeds. This approach was necessary for having a numerical analysis at low computational cost and time. Consequently, in the future it is strongly suggested to develop a more sophisticated model that is a more realistic simulation of a dynamic stall in a three-dimensional VAWT.

Keywords: *Vertical Axis Wind Turbine (VAWT), Urban Area, Computational Fluid Dynamics (CFD), Dynamic Stall, Turbulence Model*

Nomenclature

N	*number of rotor blades*	λ	*tip speed ratio* $(\Omega R/ U_\infty)$
c	*airfoil/blade chord* ..... *mm*	θ	*azimuth angle* ..... *deg*
t	*thickness of the blade* ..... *mm*	α	*angle of attack* ..... *deg*
s	*span of the blade* ..... *mm*	V	*relative wind speed* ..... *m/s*
R_r	*radius of rotor* ..... *mm*	ω	*rotational speed* ..... *rad/s*
R_m	*radius of central mast* ..... *mm*	*PIV*	*Particle Image Velocimetry* .....
U_∞	*undisturbed velocity* ..... *m/s*	Ω	*rotation frequency/vorticity* ..... *rad/s*

1. Introduction

In the last few decades, the production of electricity from wind turbines has seen a rapid growth in many countries around the world. The major drivers are the recent need to reduce CO_2 emissions into the atmosphere and meet the growing demand for electricity [1]. One promising alternative for the future generation of electricity is the installation and integration of wind turbines in the built environment combined with other alternative sustainable systems [2], [3]. The benefits are mainly generation of electricity on the site where it is needed with reduction in transmission losses and cable costs [3].

In the late 1970s and early 1980s, very little research was conducted on V AWTs on understanding the aerodynamics and flow interaction between blades during the operation of a wind turbine [4]. Recently, the progress of small wind turbines in the built environment has been mainly focused on Horizontal Axis Wind Turbines (HAWTs) rather than Vertical Axis Wind Turbines (VAWTs). But several studies have shown that VAWTs are more suitable for urban areas than HAWTs [3], [5], [6], [7]. The advantages are mainly: omni-directional without a yaw control, better aesthetics to integrate into buildings, more efficient in turbulent environments and lower sound emissions [8]. In addition there is some research speculating

that VAWTs are appropriate for large scale of 10 MW or more, as VAWTs can operate mechanically better than HAWTs [9], [10]. They can withstand high winds due to their aerodynamic stall behaviour [5]. Generally, the aerodynamic analysis of a VAWT is very complicated, as the blades are called on to operate in unsteady flow, pitching relative to the mean flow and cutting the stream tube twice [5]. One important aspect to consider during the operation of a VAWT at low wind speeds is the generation of a phenomenon called dynamic stall. The phenomenon is mainly characterised by the development of vortices that will interact with the airfoil of the blades and have a substantial impact on the design and power generation of the wind turbine [11].

The main purpose of this work is to understand how ANSYS CFX 12.0 is able to approach the development of dynamic stall around the blades of a VAWT. Also, the final objective of the numerical study is to make a contribution in the field of dynamic stall as many straight-bladed VAWTs are called to operate. In this paper a number of simulations are explored to understand static and dynamic stall around the rotor of a 3 straight-bladed VAWT. To reduce time and memory costs a 2 -D case is explored for all numerical simulations. The Computational Fluid Dynamics (CFD) Software used was ANSYS CFX 12.0. Here, the three turbulence models analysed were the k-ε model, the standard k-ω model and the SST (Shear Stress Transport) model. The numerical simulations were studied for different tip speed ratios and compared with the small amount of experimental data available in literature.

2. Methodology

In order to understand the physics involved during dynamic stall of a straight-bladed vertical Darrieus wind turbine, a 2-D rotor is proposed and analysed. This 2-D approach is adopted for reducing time and computational costs. The airfoil analysed, for the VAWT, is a NACA 0018 and its characteristics are listed in Table 1. The rotor is composed of 3 blades and a central mast. The solid model of the rotor was generated with ProEngineer 4.0 and imported into ANSYS CFX 12.0.

Table 1: Properties of the rotor

NACA0018					
Cord c (mm)	Thickness t (mm)	Span s (mm)	Rotor Radius R_r (mm)	Number Blades N	Mast Radius R_m (mm)
490	88.2	50	3000	3	75

The mesh, as shown in Figure 1, is mainly composed of three sub-domains: one fixed sub-domain outside the rotor, one dynamic sub-domain around the blades of the rotor and one fixed sub-domain for the remaining part of the rotor. The mesh was generated by adopting a Sweep Method with one element deep and the total number of elements is 4.58×10^5, as listed in Table 2.

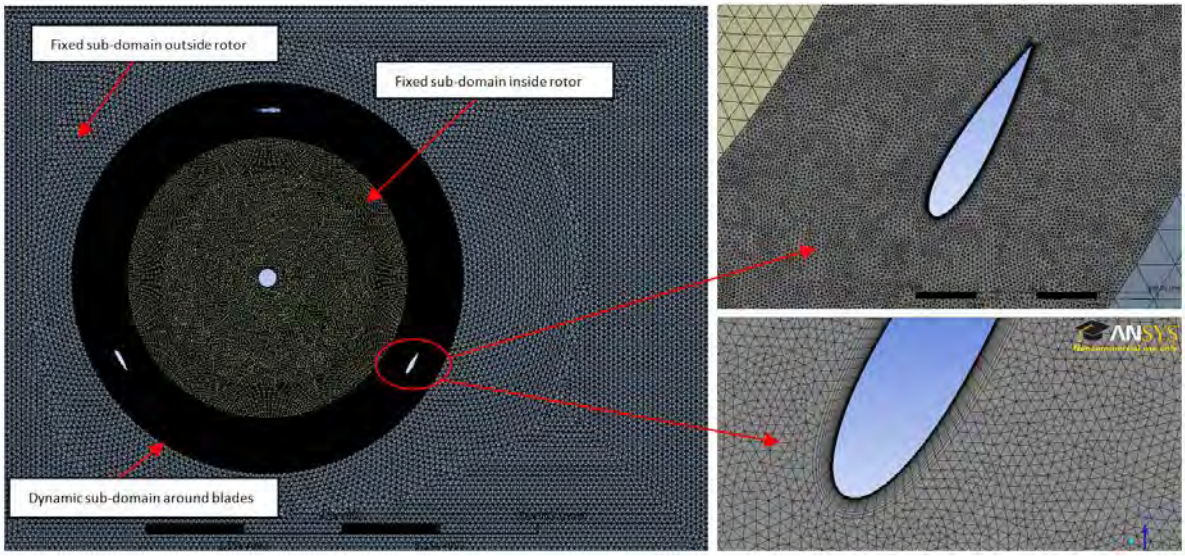

Fig. 1. Mesh for the 2-D rotor

Table 2. Sub-domain properties

Sub-domain	Number of elements
1) Fixed sub-domain outside rotor	$20*10^3$
2) Dynamic sub-domain around blades	$42*10^4$
3) Fixed sub-domain inside rotor	$18*10^3$
Total number of elements	$4.58*10^5$

All sub-domains were meshing by using only triangle elements, as they are more appropriate for simulations involved fluids [12]. The mesh around the blades of the rotor, which is a wake development region, was refined through the use of the facing sizing and inflation options available in ANSYS 12.0. In this region, the use of prism elements is able to capture boundary layer effects more effectively and efficiently. The three different meshes were linked together with the use of domain interfaces. Symmetrical boundaries were used for the top and bottom parts of the 2-D model with no-slip boundary conditions at the two sides. An opening boundary was chosen for the output and a constant wind speed of 6 m/s, with a turbulence intensity of 5%, was defined for the inlet. The two wall sides were placed at 4c from the diameter of the blades respectively. The outlet and inlet were placed 4c and 10c away respectively. Table 3 gives a summary of the parameters employed in the four different cases where different time steps and tip speed ratios (TSRs) were defined. For all transient simulations a total time was defined to give enough time for the flow to develop around the blades of the rotor. Finally, the residual target, in the convergence criteria, was set to be 10^{-4}.

Table 3. Input data for the four cases analysed

Simulation Case	Tip speed ratio	Angular speed (rad/s)	Time for one rotation (s)	Angle of attack (deg.)	Time Step Simulation (s)
Case 1	$\lambda_1=2.3$	$\omega_1=4.7$	$t_1=1.33$	$-30\leq\alpha_1\leq30$	0.0037
Case 2	$\lambda_2=3.0$	$\omega_2=6.0$	$t_2=1.05$	$-21\leq\alpha_1\leq21$	0.0029
Case 3	$\lambda_3=4.0$	$\omega_3=8.0$	$t_3=0.78$	$-15\leq\alpha_1\leq15$	0.0022
Case 4	$\lambda_4=5.0$	$\omega_4=10$	$t_4=0.63$	$-12\leq\alpha_1\leq12$	0.0017

The effect of different TSRs are presented and discussed in the conclusions section of this paper.

2.1. Dynamic Stall

Although VAWTs have several advantages over HAWTs, the aerodynamics around the blades is very complicated [11]. VAWTs, during their operation, are called to work under both static and dynamic stall conditions. Consequently, the blades are subjected to cyclic forces due to the variation of incidence angle of the blade relative to the wind direction [13]. Although the presence of dynamic stall at low TSRs can have a positive impact on the power generation of a wind turbine, the formation of vortices can generate other problems such as vibrations, noise and reduction of fatigue life of the blades due to unsteady forces [13]. Larsen et al. [14] show that dynamic stall is mainly characterised by flow separations at the suction side of the airfoil. This can be summarised in four crucial stages: 1) Leading edge separation starts, 2) Vortex build-up at the leading edge, 3) Detachment of the vortex from leading edge and build-up of trailing edge vortex, 4) Detachment of trailing edge vortex and breakdown of leading edge vortex. The sequence of these four flow events will generate unsteady lift, drag and pitching moment coefficients with a large range of flow hysteresis dependent on the angle of attack [15]. The expression of the angle of attack α adopted for the simulation, without induction factor, is given by Eq. (1):

$$\alpha = \arctan\left(\frac{\sin\theta}{\lambda - \cos\theta}\right) \tag{1}$$

where θ is the azimuth angle and λ the TSR. In this study, as shown in Table 3, four different cases are analysed with different parameters that are highly dependent on the TSRs.

2.2. Turbulence Models

Wang et al. [16] show that the most popular turbulence models, adopted in the CFD community, are mainly Direct Numerical Simulation (DNS), Large Eddy Simulation (LES) and Reynolds-Averaged Navier-Stokes (RANS). The DNS method today requires a large amount of computing resources and time. The LES method is more appropriate for 3-D simulations. Therefore, the only method adopted for this 2-D numerical study was the RANS method. The three RANS turbulence methods analysed, due to low computational costs, are: the standard k-ω model, the standard k-ε model and the SST model. A more detailed description about the turbulence methods can be found in the book by Wilcox [17].

3. Results

In this section of the paper a number of numerical simulations are analysed for different TSRs. The numerical simulations obtained during the present study are mainly compared with the study carried out by Wang et al. [16], as this previous numerical study showed a good agreement with experimental data. However, it should be point out few differences between the two numerical studies. The main differences are summarised and listed in Table 4.

In this numerical study, a number of cycles of the rotor were calculated at different TSRs until a periodic solution was achieved. The total time was set to be 4s to give enough time for the rotor to reach a period state in all four cases.

Table 4. Main differences between the two numerical methods

Present Study	Wang et al. Study
ANSYS CFX	FLUENT
Rotor with 3 blades and central mast	Single pitching blade
Free-stream turbulence intensity 5%	Free-stream turbulence intensity 0.25%
Variable time step with angular velocity	Constant time step
Triangle elements	Quadrilateral elements
$\alpha=\arctan(\sin\theta/\lambda-\cos\theta)$	$\alpha=10^0+15^0\sin(\omega t)$
Wake interactions	No wake interaction
No converged steady state	Initial input from converged steady state

In Fig. 2 and Fig. 3, the left side, show graphically the results obtained for this numerical analysis, while the right side compare the CFD results of Wang et al. with experimental data by Lee and Gerontakos [18]. Furthermore, Fig. 2 and 3 show how the lift and the drag coefficients, C_l and C_d, are affected by different angles of attack and TSRs. The curve shapes are in good agreement with the experimental data obtained by Lee and Gerontakos. Here, the final results are more realistic and less fluctuating than the CFD simulation conducted by Wang et al [16]. Also, a strong instability at high angles of attack is observed and is thought to be due to the deep dynamic stall that is typical for low TSRs. However, the few exceptions are the absence of a second peak on the curves due to the presence of a trailing edge vortex and the lack of intersection points between upstroke and downstroke paths that are seen in the experimental graphs on the right.

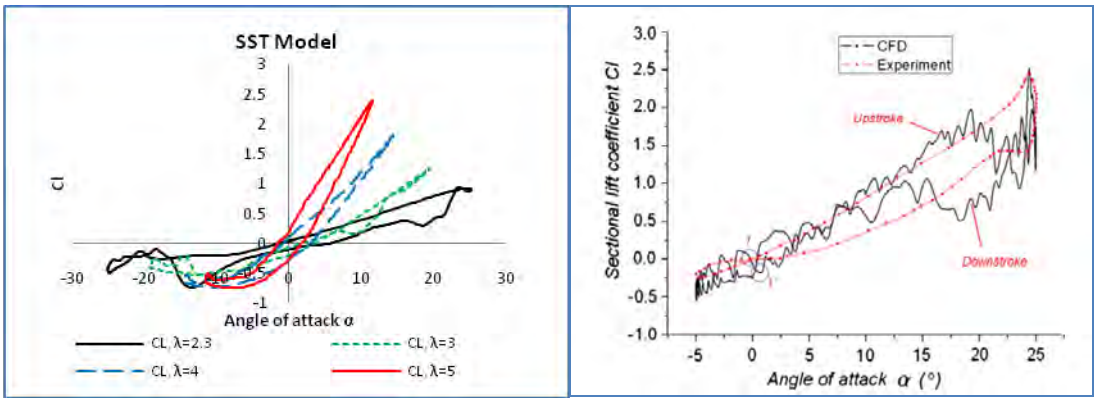

Fig. 2. Lift coefficient C_L for the two numerical studies and experimental data

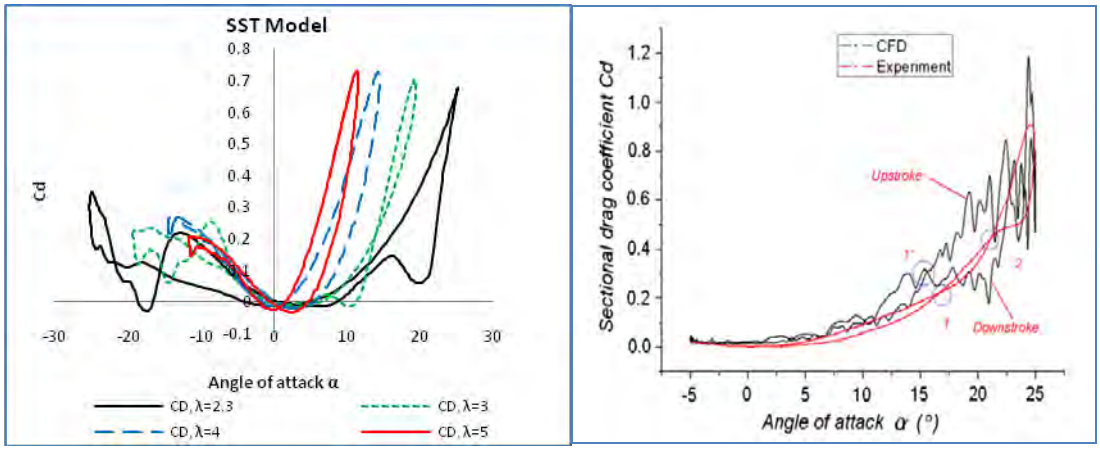

Fig. 3. Drag coefficient C_D for the two numerical studies and experimental data

However, the development of several peaks, especially for negative angle of attacks and low TSRs can be associated with the development of upstream wakes that will interact with the downstream blades. Also the presence of a central mast will generate several wakes that will affect the flow downstream. The different hysteresis loops in Fig. 2 and 3, show clearly the development of two phenomena called dynamic and static stall. Dynamic stall typically will develop at high angle of attacks for $\lambda<4$ and is characterised by its fluctuating nature, while static stall will take place at low angle of attacks for $\lambda \geq 4$ with smoother curves and less intersection points. One important consideration is that the range of angle of attack is different from the experimental data obtained by Lee and Gerontatos. This is mainly due to the use of Eq. (1) instead of using $\alpha=10^0+15^0\sin(\omega t)$ that is typically adopted for the case of a pitching motion single blade.

Finally, the numerical results are analysed by comparing the evolution of the shed vorticity with the experimental data available in the field of dynamic stall. Fig. 4 shows the vorticity field at $\theta=120^0$ for the three turbulence methods adopted in this numerical study. The SST method shows a good agreement with the experimental data obtained by Ferreira et al. [19] and Wang et al. [16] than the k-ω and k-ε methods that are more dissipative. This turbulence method is able to show the generation of specific vortices at the leading and trailing edges respectively. A more detailed explanation will be given in the next section for the SST method, as the results best agreeing with experiments

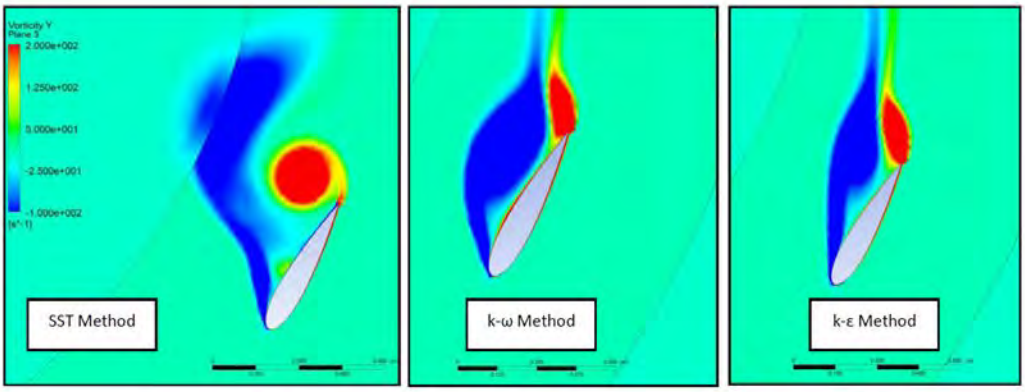

Fig. 4. Vorticity field for θ=120º for the three different turbulence methods

3.1. SST Results

In this section only the SST method is analysed in its several stages during a complete revolution of the rotor when a periodic solution is achieved. Fig. 5 clearly shows the several stages involved through dynamic stall for a TSR of 2.3 at different azimuth angles θ. This specific TSR was chosen because it corresponds to the case with deep stall. Fig.5 shows that for an azimuth angle θ between 180^0 and 240^0 the flow is almost attached to the blade. Then at an angle of $\theta=260^0$ a leading edge vortex will start to develop and expand until 280^0. Also, in this stage there is the generation of a trailing edge vortex that will detach at approximately 300^0. Afterwards, there is a progressive reattachment of the flow to the blade with leading and trailing edge vortices moving downstream. At $\theta=360^0$ there is again the presence of a second small leading and trailing edge vortices that will disappear between 20^0 and 40^0. Then the development of a third leading edge vortex will take place at 60^0 followed by a trailing edge vortex at 80^0. Finally, the flow will start to become laminar and to reattach to the blade until the same dynamics will start again from the beginning stage. From the final results it can be stated that the SST model shows a good agreement with the four stages related to dynamic

stall mentioned above. Furthermore, this 2-D study has the advantages of showing how the two kinds of vortices will move down and eventually affect the physics of the blades that are called to work downstream.

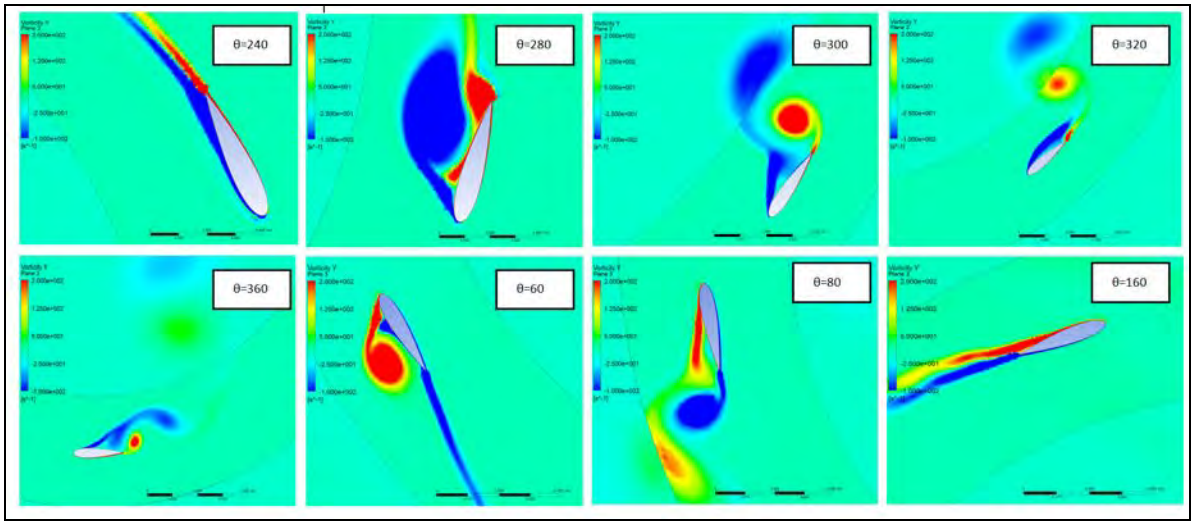

Fig. 5: Vorticity field at different azimuthal angles θ for the SST model at λ=2.3

4. Conclusions

A numerical analysis of the physics involved during dynamic stall of a rotor of a straight-bladed VAWT, composed of 3 bl ades with profile NACA0018, was conducted at four different TSRs. In this study three RANS turbulence models have been explored for the four cases analysed. The lift and drag coefficients are in good agreement with the study carried by Wang et al, but a number of differences have been found between the two studies. The most relevant are the absence of a second peak on the curves due to the development of the trailing edge vortex and the lack of intersection points at high TSRs. But at low TSRs there is an increase in the number of intersection points especially for negative angles of attacks that can be related to deep dynamic stall. This instability is mainly associated with the development of upstream wakes from upstream blades and mast that interact with the downstream blades. In this numerical study, the analysis has proved the presence of two different phenomena called dynamic and static stall that are highly depended on the TSRs adopted. In here the SST model is examined in terms of vorticity distributions around the blades. In general the method shows more reasonable accuracy with some existing wind tunnel experiments than the k-ε and k-ω turbulence methods that seem to be more dissipative. Also, the method is able to show the main four phases involved during dynamic stall. But one important observation for the SST method is the presence of single-vortices instead of having several small vortices that are typically found around the airfoil for PIV dynamic stall tests. A better improvement can be achieved in the future investigation of a 3-D case where the LES and the DES methods are strongly recommended. The two methods will take into consideration the 3-D nature of the vortices developed during dynamic stall. In general this paper gives a substantial contribution to the aerodynamics involved at different TSRs and angles of attack for a 2-D rotor with central mast. This is necessary because the development of dynamic stall in VAWTs can have a substantial impact on both the design and power generation of a wind turbine.

References

[1] K. Pope et al., Effects of stator vanes on power coefficients of a zephyr vertical axis wind

turbine, Renewable Energy, 2009, pp. 1-9.

[2] J. Knight, Urban wind power: Breezing into town, Nature, vol. 430, no. 6995, 2004, pp. 12-13.

[3] S. Mertens, Wind energy in the built environment: concentrator effects of buildings. TU Delft, 2006, pp. 3-14.

[4] R. Howell, N. Qin, J. Edwards, and N. Durrani, Wind tunnel and numerical study of a small vertical axis wind turbine, Renewable Energy, vol. 35, 2010, no.2, pp. 412-422.

[5] A. Mewburn-Crook, The Design and development of an augmented vertical wind turbine, School of Mechanical, Aeronatical and Production Engineering, 1990, pp. 1-59

[6] S. Stankovic, N. Campbell, and A. Harries, Urban Wind Energy. Earthscan, 2009.

[7] C. J. Ferreira, G. van Bussel, and G. van Kuik, 2D CFD simulation of dynamic stall on a Vertical Axis Wind Turbine: verification and validation with PIV measurements, presented at the 45th AIAA Aerospace Sciences Meeting and Exhibit, 2007, pp. 1-11.

[8] C. Hofemann, C. J. Simao Ferreira, G. J. Van Bussel, G. A. Van Kuik, F. Scarano, and K. R. Dixon, 3D Stereo PIV study of tip vortex evolution on a VAWT, 2008, pp. 1-8.

[9] G. Marsh and S. Peace, Tilting at windmills: Utility-scale VAWTs: towards 10MW and beyond? , Refocus, vol. 6, no. 5, 2005, pp. 37-42.

[10] G. Marsh, Wind turbines: How big can they get? , Refocus, vol. 6, no. 2, 2005. , pp. 22-28.

[11] C. J. Simão Ferreira, A. van Zuijlen, H. Bijl, G. van Bussel, and G. van Kuik, Simulating dynamic stall in a two-dimensional vertical-axis wind turbine: verification and validation with particle image velocimetry data, Wind Energy, vol. 13, no. 1, 2010, pp. 1-17.

[12] ANSYS Meshing: Application Introduction, ANSYS, 2009.

[13] N. Fujisawa and S. Shibuya, "Observations of dynamic stall on Darrieus wind turbine blades," Journal of Wind Engineering and Industrial Aerodynamics, vol. 89, no. 2, 2001, pp. 201-214.

[14] J. Larsen, S. Nielsen, and S. Krenk, Dynamic stall model for wind turbine airfoils, Journal of Fluids and Structures, vol. 23, no. 7, 2007, pp. 959-982.

[15] J. A. Ekaterinaris and M. F. Platzer, Computational prediction of airfoil dynamic stall, Progress in Aerospace Sciences, vol. 33, no. 11, 1998, pp. 759-846.

[16] S. Wang, D. B. Ingham, L. Ma, M. Pourkashanian, and Z. Tao, Numerical investigations on dynamic stall of low Reynolds number flow around oscillating airfoils, Computers & Fluids, vol. 39, no. 9, 2010, pp. 1529-1541.

[17] D. C. Wilcox, Turbulence Modeling for CFD. DCW industries La Canada, 2006.

[18] T. Lee and P. Gerontakos, Investigation of flow over an oscillating airfoil, Journal of Fluid Mechanics, vol. 512, 2004, pp. 313-341.

[19] C. J. Simão Ferreira, A. van Zuijlen, H. Bijl, G. van Bussel, and G. van Kuik, Simulating dynamic stall in a two-dimensional vertical-axis wind turbine: verification and validation with particle image velocimetry data, Wind Energy, vol. 13, no. 1, 2010, pp. 1-17.

Simulation and technical comparison of different wind turbine power control systems

Mojtaba Tahani[1], Iman Rahbari [2,*], Samira Memarian[2], Saeedeh Mirmahdian[3]

[1] *Iran University of Science and Technology, Tehran, Iran*
[2] *Semnan University, Semnan, Iran*
[3]*Islamic Azad University of Arak, Arak, Iran*
** Corresponding author. Tel: +989128021976, E-mail: rahbarii2@asme.org*

Abstract: wind as a significant renewable source of energy along with different ways for its optimum utilization is attended. At this paper, initially different types of wind turbine power control systems are introduced briefly, then advantages and disadvantages of them, are evaluated in practical and theoretical aspects. At the following, governing generated power formulation is proved briefly, then the effective parameters on power, e.g. wind velocity, wind temperature are studied and simulated in MATLAB software. Then practical data from an actual stall control wind turbine entered and related curves are investigated. Based on these data, performance of an actual pitch control wind turbine is estimated and related curves are investigated. At the following, using Weibull theory, real power-time curve and estimated power-time curve, monthly produced energy of turbines are estimated. And finally Specific Power Performance (SPP) is defined and shown that pitch control system produced energy more than stall control system at the same rotor swept area.

Keywords: *Wind Turbine, Power Control System, Pitch Control, Stall Control*

1. Introduction

The human progresses in various scientific and industrial fields have increased the need to generate energy and to investigate its various resources. Providing this energy from fossil sources like oil and gas is not reasonable because of various reasons such as environmental pollutions, reduction of reservoir of these resources and the next generation's requirements for them. These facts along with economic problems and the increment of fuel cost have encouraged the researchers in various countries to pay more attention to renewable energies. Therefore, the wind, as one of the renewable energy resources, and its optimal exploitation methods, have been noticed so that the predictions indicate that in 2020 the portion of wind in generating the energy required for human activities will be more than 375 TWh. The design of wind turbines depends on the conditions of the location they are installed, and most of them are designed to generate power with the minimum possible cost at low wind speeds. Thus, if the wind speed exceeds a specified limit, some of the important parts of turbine may be harmed. The designers use various control systems to prevent these harms and also to optimal exploitation of turbines. The most important control systems are stall control, pitch control, and yaw control, from which the pitch control is the most common system [1 to 3] .

Of course, some researches were also performed to design other control systems. One of them is "control of wind turbine using memory based method" by Song [4]. Using this method, the turbine chooses the optimal power control method based on the previous experienced conditions. Another new method was also presented in the paper titled as "multi variable control strategy for variable speed variable pitch" by Bakhezzar et al. [5] . Using the doubly fed induction generator to control the voltage induced by rotor in the generator has been noticed by the researchers in the recent years. Fernandez and Garcia investigated this subject in a paper titled as "comparative study on doubly fed induction generator (DFIG) wind turbines operating with power regulation" [6] . Modeling and controlling this type of generators were performed by Hee Song Ko [7] .

In this paper, the control systems of wind turbines were investigated comprehensively. In addition to theoretical facts, technical and empirical points were also involved. Furthermore, the power generated by different control systems was compared in this study. The effect of local conditions of the place considered for installing the turbine, such as wind blowing conditions, on the selection of the appropriate control system was also discussed in this paper.

2. Investigation of generated power

The one-dimensional BEM theory was used to investigate the power generation of wind turbines [3] . Based on this theory, the rotor of wind turbine can be modeled as an ideal impenetrable disk. Because there is no friction between air and the rotor, and the wake flow speed has no rotational component. The shape of stream lines thorough the rotor will be similar to figure (1). This disk decreases the speed from V_0 at the upstream to u at the rotor plate, and to u_1 at the back of rotor. At normal speeds, the flow can be assumed incompressible, and the speed and pressure variations can be assumed as shown in figure (1) .

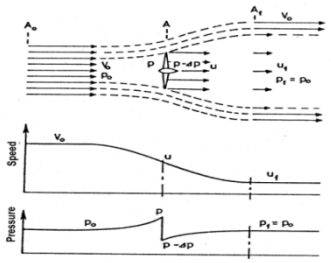

Fig. 1. Demonstration of streamlines, axial speed and pressure up- downstream of rotor.

Using axial momentum equation, it can be proved that:

$$u = \frac{1}{2}(V_0 + u_2) \tag{1}$$

Also, the usable power in a cross section area equal to the area swept by rotor (A) is:

$$P_{avail} = \frac{1}{2}\rho A V_0^3 \tag{2}$$

The dimensionless power coefficient is obtained by dividing the power by the usable power:

$$C_P = \frac{P}{\frac{1}{2}\rho V_0^3 A} \tag{3}$$

And finally, the induction factor is defined as:

$$u = (1-a)V_0 \tag{4}$$

It can be observed that for $a = 1/3$, $C_{P,\max} = 16/27$.

3. Investigation of power control systems

3.1. Stall control systems

Blade design of this type of turbines is so that they naturally control the power generated by turbine. These rotors with constant pitch are designed to operate near the optimal tip speed in moderate winds. In turbines with this type of control system, an asynchronous generator is often used by which the rotor rotational speed is kept approximately constant. A rotating tip located at the end of the rotor is usually used as the aerodynamic brake. This device which is activated by centrifugal force, is subjected against the wind flow with a 90° angle, and limits the rotor momentum by applying the opposite torque due to the drag force.

3.2. Pitch control systems

In a turbine with pitch control system, all blades can rotate about the root, and thus, the attack angle changes simultaneously throughout the rotor length. One of the most conventional mechanical mechanisms of the rotor pitch control contains a piston inserted inside the turbine main shaft. This piston changes the rotor pitch by its reciprocating movement using a mechanism installed forward the turbine hub. Obviously, the lift coefficient has a direct relation with the attack angle [1] . Therefore, decreasing the attack angle reduces the lift force and the power. Thus, pitch control system can control the output power by rotating the rotors. Also, referring the power curve of this type of turbines, it is obviously found that since the rotors can rotate slowly, the power curve is smoother and the power peaks are reduced [3] . To overcome the problem caused by great peaks in power for high speeds in a wind turbine with pitch control system, a system named as "OptiSlip" produced by Vestas was used.

From technical point of view, using pitch control mechanisms to control power necessitates the use of very strong hydraulic systems to generate and transfer very high pressures (120 Bar for medium wind turbines, and even more for greater turbines). Providing this hydraulic system affects the turbine total price. In places with high air turbulence, the pitch control system should operate harder. This results in overheating the hydraulic oil, and finally, lengthy turbine stops by safety system. This reduces the turbine productivity.

3.3. Active stall control systems

There is another method which uses the combination of pitch and stall control systems. In this system, to achieve the maximum efficiency at low wind speeds the rotors are repositioned like a wind turbine controlled by pitch. At high speeds, the rotors are rotated slowly against the wind to get stall. With this type of control, a smoother limited power is achieved compared with pitch control turbines. Combining both systems facilitates the required stops in emergency cases and restarting wind turbines compared with stall control. This type of system is less common today [2] .

3.4. Yaw control systems

In this control system, instead of limiting the output power using pitch or stall controls, the turbine yaw is controlled. The machines which use pitch and stall control systems usually have yaw control. This system receives the data related to wind flow direction from the turbine wind gauge and tries to turn the nacelle so that the maximum air flow rate enters the rotor disk. In a machine controlled by yaw system, at high wind speeds, the rotor turns against the wind direction to reduce the air flow rate in rotor, and thus, the generated power decreases.

4. Study procedure

4.1. Weibull distribution method theory and its application in estimating the available wind electricity energy generation

Considering the random nature of wind with long-term measurements in various time periods, Weibull Density Function was used to compute the wind energy [8] .

$$F(V) = \frac{k}{c}\left(\frac{V}{c}\right)^{k-1} e^{-\left(\frac{V}{c}\right)^{k}} \tag{5}$$

F (v), the cumulative distribution function, is:

$$F(V) = 1 - e^{-\left(\frac{V}{c}\right)^{k}} \tag{6}$$

Where V is the wind speed, c and k are scale parameter and shape parameter, respectively. These parameters can be computed using "Maximum likelihood" method with iteration from the following equations:

$$k = \left(\frac{\sum_{i=1}^{n} V_i^{k} Ln(V_i)}{\sum_{i=1}^{n} V_i^{k}} - \frac{\sum_{i=1}^{n} Ln(V_i)}{n} \right)^{-1} \tag{7}$$

$$c = \left(\frac{1}{n}\sum_{i=1}^{n} V_i^{k}\right)^{\frac{1}{k}} \tag{8}$$

Where V_i , is the speed at time period i and n is the number of the wind non-zero speeds. The continuous distribution of wind flow in the studied region is obtained using Weibull curve. The generated energy is estimated by combining this curve and the power curve of wind turbines. The energy of a wind turbine in a month is investigated by following equations:

$$E_{Month} = N_0 \int_{V_{Cut-In}}^{V_{Cut-Out}} P(u)\, f(u)\, du \tag{9}$$

Where N_0 is 744 hours/month, f(u) is Weibull function and P(u) is power curve.

4.2. Location of study

Location of the present study was Paskulan wind farm in Manjil, a city in Iran. Its pressure can be assumed about 1 Atmosphere with a good precision. The average air temperature during the test period was $13.67^{\circ}\mathrm{C}$. Therefore, the average air density was $1.231\,\mathrm{kg/m^3}$.

4.3. Wind blow condition

Since the wind patterns of a region repeat annually, the Weibull curve obtained in March 2003 [9] can be used to estimate the wind condition in March 2009 with a good accuracy. Based on this curve, weibull shape parameter (k) was 1.68, weibull scale parameter (A) was 11.7 m/s and average wind velocity was 10.4 m/s. As mentioned before, stall and pitch control

systems are more applicable compared with the other control systems. Thus, in the following was concentrated on the sample turbines with these two control system types.

First, based on Eq. (3), the effective parameters on the power generated by turbine considering the weather conditions of the studied region were simulated in MATLAB software for two turbines with different control systems.

The first turbine is of 550 kW type and was made by NEG-MICON Company. It uses stall control system. The second turbine is of V47-660 kW type and was made by Vestas Company. It uses pitch control system and is equipped with OptiSlip. The power curves of above turbines for the ideal case and for the air conditions of the mentioned wind farm were shown in figures (2).

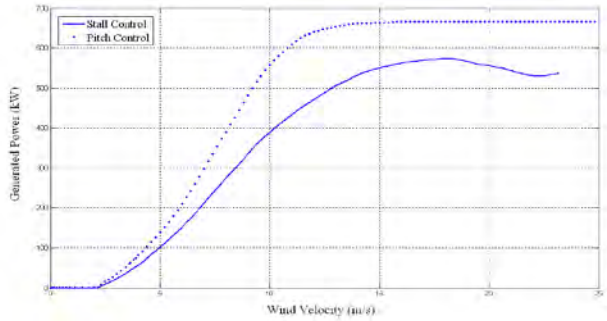

Fig. 2. Ideal power curve wind turbines.

For 550 kW wind turbine, it's obvious that maximum generated power, is 550 KW occurs at 18 m/s. Power curve after reaching to maximum point, will be decreased. In the following, this curve will be compared with practical curve. For 660 kW wind turbine, it can be obviously observed that the power generated by the turbine is uniform compared with the past and remains constant after reaching the maximum value. This maximum power value occurs at speed of 15 m/s.

In the following, the power generated by 550 kW turbine is investigated in the real mode. The values used in this section were recorded by the logger located on these turbines. This system measures and records the turbine generated power data, wind speed, wind temperature, and some other parameters with 10 minute time intervals, And during the studied time period 4463 time intervals were recorded that, the turbine was active only during 1501 intervals. During the other intervals, the turbine was in stop mode due to maintenance and blowing wind with very high speeds (cut-out), or other unforeseen characters. In figure (3), the real generated power was shown versus the active times.

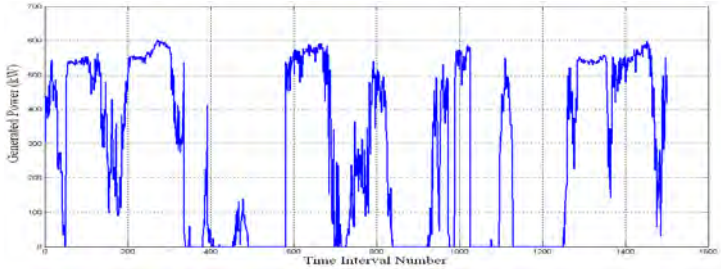

Fig. 3. Demonstration of Power vs. Time intervals for stall control wind turbine in real mode.

The power curve for active time intervals was shown in figure (4).

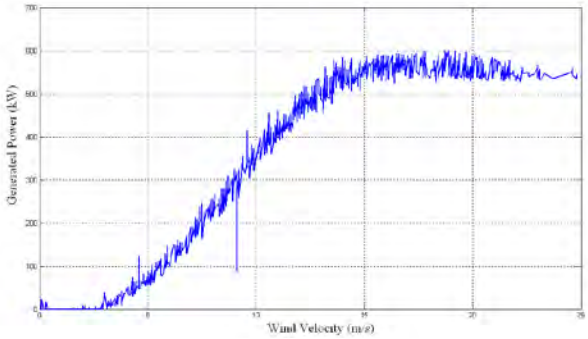

Fig. 4. Demonstration of Power curve for stall control wind turbine in real mode.

Comparing figures (2) and (4) reveals that there is a marked difference between the power generated in real mode and the power computed in ideal mode obtained with constant power values presented by the manufacturer and based on the weather conditions of the studied location.

The reason of this difference is that the turbine characteristics presented by the manufacturer (such as power coefficient and power curve based on standard DIN ISO 2533) are related to the generated power of 550 kW, but in fact, the turbine maximum mechanical power is 600 kW (about 10% more than the nominal power), and it was observed that with turbine optimum operation, this maximum value of power is exploitable.

The percentage error curve versus the wind speed was shown in figure (5).

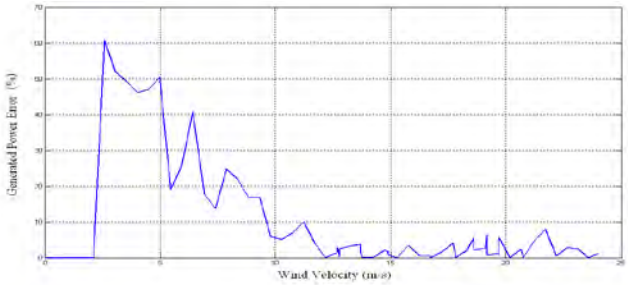

Fig. 5. The percentage error curve versus the wind speed for stall control wind turbine.

As shown in this figure, at speeds lower than 2.5 m/s the turbine does not start to operation to generate remarkable power, thus, there is no percentage error. At near cut-in speeds, the percentage error is very high. The reason is the small value of generated power; therefore, it's not noticeable. It can be observed that the percentage error reduces with increasing speed and remains lower than 10% after the speed of 10 m/s.

Based on equation (9) and using trapezoidal numerical integrating method for the studied time period, 224110 kWh of energy generation was estimated.

By computing the area under the power-real time curve by trapezoidal numerical integrating method, the real power generated during this time period reached 68672.9 kWh. Considering the fact that turbine was active only in 1/3 of the time period, if assumed the turbine will operate in such a way this time interval, estimated energy using this method and Weibull function has 9.758 % variations. Now assume the pitch regulated turbine installed in the previous location and subjected to the previous wind conditions. Assuming that the turbine

stop time, due to periodical repairs or possible malfunctions and not generating power at speeds more than cut-in value, is equal to the corresponding value of stall controlled turbine, and the turbine operates in ideal conditions, the power-time curve of this turbine was estimated by figure (6).

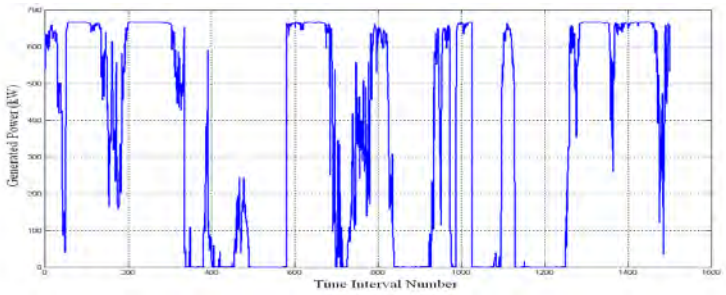

Fig. 6. Estimated Power Vs. Time intervals for pitch control wind turbine.

Comparing figures (6) and (3) obviously reveals that the variations of the power generated by pitch controlled turbine are very smaller than the corresponding values of stall controlled turbine. By numerical integrating in this period, it was found that 90670 kWh of energy is exploitable from this turbine.

Based on Weibull theory and using equation (6) and trapezoidal numerical integrating method for the studied time period, 299690 kWh of energy generation was estimated.

Considering the fact that the turbine was active during 1/3 of the period, the estimated value by Weibull theory has a good consistency with the value estimated using power curve. If assumed the turbine will operate in such a way this time interval, estimated energy using this method and Weibull function has 11.1634 % variations.

By defining Specific Power Performance (SPP) as follows, the value of this parameter for pitch controlled and stall controlled turbines were presented in table (1).

$$SPP = \frac{Generated\ Energy \quad (Kwh)}{Rotor\ Swept\ Area \quad (m^2)} \tag{10}$$

Table 1. Specific Power Performance for various turbines

Type of Power Control system	Rotor Swept Area	SPP based on Weibull function	SPP based on power-time curve
Stall Control	1325 m^2	169.13	154.1
Pitch Control	1735 m^2	172.73	155.38

As it can be observed, the value of Specific Power Performance for wind turbines using pitch control system is about 0.8 - 2.13% greater than the corresponding value of the wind turbines using stall control system.

5. Conclusion

In this study, the governing generated power formulation was first proved. Then, the types of power control systems were investigated theoretically and practically. It was found that selecting the appropriate power control system for optimum exploitation of turbine depends on the conditions of the intended location to install the turbine. It's possible that using pitch

control system results in turbine failures due to the numerous times of operation; and thus, it reduces the turbine efficiency. Then, Weibull theory for estimating the energy generated by turbine was introduced and investigated. Then, power curves of two different wind turbines under the wind conditions of the studied region sketched using MATLAB. Then, the practical values of energy and power generated by stall controlled turbine were obtained and investigated based on the data received from the turbine installed in the region. Then, the power and energy generated by pitch controlled turbine were estimated. Finally, by defining Specific Power Performance and comparing two different control systems, it was found that SPP Value for pitch controlled turbine is about 0.8-2.13% greater than the corresponding value of stall controlled turbine. In choosing the appropriate wind turbine for installation in a site, this low difference along with more prices also should be considered.

References

[1] Erich Hau, Wind turbines, fundamentals, technologies, applications, economics, Springer, 2nd Edition, 2005, pp. 73 – 88.

[2] Thomas Ackermann, Wind power in power system, John Wiley and Sons, 2005, pp. 13-20.

[3] Martin O. L. Hansen, Aerodynamics of wind turbine, EarthScan, 2008, pp. 39 – 48.

[4] Y. D. Song, Control of wind turbines using memory based method, journal of wind engineering and industrial aerodynamics 85, 2000, pp. 263-275.

[5] B. Boukhezzar, L. Lupu, H.Siguerdidjane, M. Hand, Multivariable control strategy for variable speed variable pitch wind turbine, Renewable energy journal 32, 2007, pp. 1273–1287.

[6] L. M. Fernandez, C. A. Garcia, Comparative study on performance of control systems for doubly fed induction generator (DFIG) wind turbines operating with power regulation, Energy journal 33, 2008, pp. 1438 – 1452.

[7] Hee - Song Ko, Gi- Gab Yoon, Won Pyo Hong, Modeling and control of a DFIG based variable speed wind turbine, Electric power research 78, pp. 1841 – 1849.

[8] Eyad S. Hrayshat, Wind availability and its potentials for electricity generation in Ta. la, Jordan, Renewable and Sustainable Energy Reviews Journal 9, 2005, pp. 111- 117.

[9] M. Sharifi, Application of Weibull function in estimation of produced energy by wind turbines in Iran, Proceedings of 21st International Power System Conference 2003, 2190-2197.